VOLUME 26
1988
ACC. NOS N88-10001 TO N88-30583

STAR
AN ABSTRACT JOURNAL

Scientific and Technical Aerospace Reports

Annual Index 1988

Part One
SUBJECT

PRODUCED BY THE
SCIENTIFIC AND TECHNICAL
INFORMATION
DIVISION

NASA

NATIONAL AERONAUTICS AND SPACE ADMINISTRATION

WHAT YOU CAN DO FOR *STAR*

All users of this abstract service are urged to forward reports to be considered for announcement in *STAR*. This will aid NASA in its efforts to provide the fullest possible coverage of all scientific and technical publications that might support aeronautics and space research and development. If you have prepared relevant reports (other than those that you will transmit to NASA, DoD, or DOE through the usual contract- or grant-reporting channels), please send them for consideration to the NASA Scientific and Technical Information Facility, P.O. Box 8757, BWI Airport, Maryland 21240.

Reprints of journal articles, book chapters, and conference papers are also welcome. These will be considered for announcement in *STAR's* companion journal, *International Aerospace Abstracts*.

You may specify a particular source to be included in a report announcement if you wish; otherwise the report will be placed on public sale at the National Technical Information Service. Copyrighted publications will be announced but not distributed or sold.

PURCHASE OF *STAR*

The semimonthly issues are available to registered users on annual subscription for $99.00 from the NASA Scientific and Technical Information Facility, ATTN: Registration Services, P.O. Box 8757, BWI Airport, MD 21240. *STAR* is publically available on annual subscription for $99.00 from the Superintendent of Documents, U.S. Government Printing Office, Washington, DC 20402.

PUBLISHED BY:

UNITED STATES GOVERNMENT
NATIONAL AERONAUTICS AND SPACE ADMINISTRATION
SCIENTIFIC AND TECHNICAL INFORMATION DIVISION
Scientific and Technical Aerospace Reports, Volume 26, is prepared by the NASA Scientific and Technical Information Facility operated for the National Aeronautics and Space Administration by RMS Associates.

The Administrator of the National Aeronautics and Space Administration has determined that the publication of this periodical is necessary in the transaction of the public business required by law of this Agency. Use of funds for printing this periodical has been approved by the Director of the Office of Management and Budget through March 22, 1989.

US ISSN 0036-8741

SPECIAL NOTICE

The abstract sections of the semimonthly *STAR* journals can be bound separately. Individual abstracts can be located readily by means of the page numbers given at each entry, e.g., p 1753. To assist the user in binding *STAR* Volume 26, four (4) title pages are included in the back of Part 1 of the Annual Index.

For sale by the Superintendent of Documents, U.S. Government Printing Office
Washington, D.C. 20402

VOLUME 26 NUMBERS 1-24

Scientific and Technical Aerospace Reports

Annual Index (Part I) January - December 1988

TABLE OF CONTENTS

Page

PART I

Introduction iii
Subject Index A-1

PART II

Introduction iii
Personal Author Index B-1
Corporate Source Index C-1
Contract Number Index D-1
Report/Accession Number Index E-1

INTRODUCTION

WHAT STAR ANNUAL INDEXES ARE

This Annual Index is an edited consolidation of the indexes to the individual issues of *Scientific and Technical Aerospace Reports (STAR)* for the calendar year 1988 (Volume 26 Numbers 1 through 24). For the convenience of the user, it is divided into two parts, each bound separately. Part I contains the Subject Index. Part II contains the Personal Author Index, Corporate Source Index, Contract Number Index, and Report/Accession Number Index. The Annual Index supersedes the semimonthly indexes previously issued during 1988.

Each entry in this index includes a group of identifying numbers in the following form: 12 p 1680 N88-20043. The first two digits (12) identify the issue in which the document was announced. The "p" and the four digits that follow (1680) refer to the page number, in the designated issue, on which the abstract of the document appears. The next group of numbers (N88-20043) is the NASA Accession Number, a unique identification number assigned by NASA to each document that was acquired, indexed, and announced in *STAR* during the year.

In addition to these identifying numbers each entry in the Subject Index contains a title, or title and title extension. Each entry in the Personal Author and Corporate Source Indexes contains the title of the document.

At the beginning of each index in this cumulation, a typical listing is illustrated with each of its elements identified to assist the reader in using the different types of index entries.

HOW TO USE THE SUBJECT INDEX

Subject terms in this cumulative index are arranged alphabetically, and are supplemented with cross-references which are intended to serve as directions that will enable the user to modify, enlarge, or narrow his search in accordance with his specific interest. The subject headings have been selected from the latest revison of the *NASA Thesaurus*. Two types of cross-references are used:

1. Use (U) references direct the user to alternate headings under which materials on the subject may be found. For example:

   ANNULAR JETS
   U ANNULAR FLOW
   U JET FLOW
   COLUMBIUM
   U NIOBIUM

2. Narrower Term (NT) references refer the user to more specific headings in the same subject area, under which additional material on the subjects may be found. For example:

   EMISSION
   NT ELECTRON EMISSION
   NT NEUTRON EMISSION
   NT THERMAL EMISSION

Finally, a searcher should use the titles and title extensions in the index to narrow further his quest for particular items. This is because subject terms can readily refer to more than one class of document. For example:

CATHODES
Cesium plasma cathodes as sources of high intensity electron beams
Cathode material testing in electrochemical half cells

This illustrates a case where two references on different topics are listed under the same subject term.

HOW TO USE THE PERSONAL AUTHOR INDEX

All personal authors identified in the abstract-section citations in the individual *STAR* issues appear in this index. Differences in transliteration schemes may require multiple searching of the index for variants of an author's name. For example:

EMELIANOV, M. D.
YEMELYANOV, M. D.

HOW TO USE THE CORPORATE SOURCE INDEX

The corporate source index entries are abridged versions of the corporate sources used in the abstract-section citations in the individual issue supplements. The corporate source supplementary (organizational component) does not appear in the index. For example:

PRINCETON UNIV., N.J. DEPT. OF CHEMICAL ENGINEERING.
(Corporate source at citation)
PRINCETON UNIV., N.J.
(Corporate source index entry)

HOW TO USE THE CONTRACT NUMBER INDEX

All contract numbers that are identified in the abstract-section citations in the individual *STAR* issues appear in this index. Changes by agencies in the style in which contract numbers are presented may require multiple searching for variants. For example:

AF 33(615)-67-C-1758
F33615-67-C-1758

HOW TO USE THE REPORT/ACCESSION NUMBER INDEX

All report numbers that have been assigned by the corporate source, monitoring activity, or cataloging activity appear in this index. Variations in initial input may result in different report number series. For example:

TP-924
ONERA-TP-924

A COMPREHENSIVE INFORMATION SERVICE

The National Aeronautics and Space Administration makes the results of worldwide research and development activities in aeronautics, space, and supporting disciplines promptly available to participants in its program. NASA's scientific and technical information system now contains over two million documents, which are abstracted, indexed, and obtained through retrieval and dissemination services. These services which include the abstract journal, *Scientific and Technical Aerospace Reports (STAR),* are described fully in a bulletin, *The NASA Scientific and Technical Information System... and How to Use It,* available at no charge from the NASA Scientific and Technical Information Facility, P.O. Box 8757, B.W.I. Airport, Maryland 21240.

AVAILABILITY OF DOCUMENTS

Information concerning the availability of documents announced in the *STAR* issues covered in this index is found in the introduction to the most currently issued semimonthly issue.

PUBLIC COLLECTIONS OF NASA DOCUMENTS

DOMESTIC: NASA and NASA-sponsored documents and a large number of aerospace publications are available to the public for reference purposes at the library maintained by the American Institute of Aeronautics and Astronautics, Technical Information Service, 555 West 57th Street, 12th Floor, New York, New York 10019

EUROPEAN: An extensive collection of NASA and NASA-sponsored publications is maintained by the British Library Lending Division, Boston Spa, Wetherby, Yorkshire, England for public access. The British Library Lending Division also has available many of the non-NASA publications cited in *STAR*. European requesters may purchase facsimile copy or microfiche of NASA and NASA-sponsored documents, those identified by both the symbols # and * from ESA - Information Retrieval Service European Space Agency, 8-10 rue Mario-Nikis, 75738 Paris CEDEX 15, France.

FEDERAL DEPOSITORY LIBRARY PROGRAM

In order to provide the general public with greater access to U.S. Government publications, Congress established the Federal Depository Library Program under the Government Printing Office (GPO), with 50 regional depositories responsible for permanent retention of material, inter-library loan, and reference services. At least one copy of nearly every NASA and NASA-sponsored publication, either in printed or microfiche format, is received and retained by the 50 regional depositories. A list of the regional GPO libraries, arranged alphabetically by state, appears on the inside back cover. These libraries are *not* sales outlets. A local library can contact a Regional Depository to help locate specific reports, or direct contact may be made by an individual.

Typical Subject Index Listing

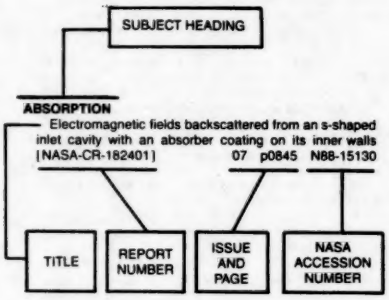

The subject heading is the key to the subject content of the document. Titles, issues, page numbers, report numbers, and accession numbers of pertinent documents are provided under each subject heading. When the title is insufficiently descriptive of the document content, a title extension has been added, separated by three hyphens. The report number helps to indicate the type of document cited (e.g., NASA report, translation, NASA contractor report). The issue and page identify the *STAR* issue in which the document was announced and the page number on which the citation appears. The accession number denotes the number by which the citation is identified on that page. The titles are arranged under each subject heading in ascending accession number order. The subject headings have been selected from the latest revision of the *NASA Thesaurus* (NASA SP-7064).

A

A STARS
Generation and propagation of sound waves in a collapsing or anti-collapsing star with uniform density
[DE87-703034] 15 p2151 N88-22839

A-300 AIRCRAFT
The European Airbus A-300 10 p1309 N88-17824

A-320 AIRCRAFT
The A320 Airbus program
[SNIAS-872-111-105] 05 p0529 N88-13215
Electrical flight commands in transport aircraft
[SNIAS-872-111-108] 05 p0551 N88-13361
Overall description of the computer aided design and manufacturing systems associated with the A320 program at Aerospatiale and its partners
[SNIAS-872-111-104] 05 p0635 N88-13883
Presentation of SIGMA (Interactive Assisted Geometry System). A computer assisted shape design program developed at the Aerospatiale Aircraft Division
[SNIAS-872-111-110] 05 p0635 N88-13884
The use of simulation in the development of the Airbus 12 p1702 N88-20188
Design and implementation of contact ultrasonic sensors to assess internal damage
[I-177/87] 21 p2906 N88-27247
New generation of integrated monitoring systems for modern aircraft 22 p3035 N88-28015

ABEL FUNCTION
A construction of simple Abelian varieties
[ZW-8702] 05 p0642 N88-13929
Class of N-associative rings
[PB87-230421] 06 p0769 N88-14724
Theory of the generalized Abel integral equations
[ETN-88-91086] 09 p1229 N88-17362
On generalized lie-like algebras
[PREPRINT-574] 14 p1968 N88-21748
Retrieval of temperature and concentration profiles from a limited number of absorption measurements 21 p2947 N88-27501

ABERRATION
Aberrations: Their effect on off-axis beam steering
[AD-A189601] 13 p1840 N88-21008

ABILITIES
Exploiting auxiliary information about items in the estimation of Rasch item difficulty parameters
[AD-A184383] 03 p0372 N88-12341
Intelligent tutoring systems as tools for investigating individual differences in learning 09 p1204 N88-17216
Modeling incorrect responses to multiple-choice items with multilinear formula score theory
[AD-A187887] 11 p1522 N88-19090
Visual recognition training: Effectiveness of computer graphics
[AD-A188302] 12 p1669 N88-19997
A comparison of the Army's Project A: Cognitive and psychomotor tests to analogous Air Force and Navy tests
[AD-A188636] 12 p1670 N88-20002
Optimizing feedback utilization in motor skill training
[AD-A191559] 18 p2552 N88-25146
Skilled memory and expertise: Mechanisms of exceptional performance
[AD-A193829] 22 p3133 N88-28628

ABLATION
Time-resolved ablation measurements of imploding targets
[DE87-014464] 02 p0178 N88-11111
The Rayleigh-Taylor instability in ablatively accelerated targets with 1, 1/2 and 1/4 micrometers laser light
[AD-A185945] 07 p0858 N88-15208
Molecular dynamics of laser ablation of a polymer coating
[DE88-004337] 13 p1750 N88-20466
Analytic solutions to dynamic equations of plasma armature railguns
[DE88-006842] 15 p2023 N88-22057
Self-similar expansions in ion beam fusion 16 p2278 N88-23635
Spectroscopic study of heliotron E plasmas: Stark profile, CXR, poloidal rotation and carbon coating 17 p2441 N88-24523
Use of a two-stage light-gas gun as an injector for electromagnetic railguns
[DE88-007200] 18 p2469 N88-24657
Systematics of excimer laser ablation: Thin film preparation of high T(sub c) material
[DE88-010569] 19 p2675 N88-25909
Why plasma armature railguns don't work (and what can be done about it)
[DE88-007900] 20 p2763 N88-26384
Absorption characteristics of Si3N4 ablation layer plasma 20 p2783 N88-26504

ABLATIVE NOSE CONES
Experimental investigation of hypersonic aerodynamics
[NASA-CR-182973] 18 p2458 N88-24591

ABM
U APOGEE BOOST MOTORS

ABNORMALITIES
Correlation between EEG abnormal activity and aircraft accidents: A long term observation 21 p2984 N88-27719
Detection of latent epilepsy in aircrew candidates 21 p2984 N88-27720

ABORT TRAJECTORIES
The effects of RCS jet firing on the isolated Orbiter and mated coast phases of the glide return to launch site maneuver at Mach number 6 (IA302B)
[NASA-CR-180223] 20 p2766 N88-26403

ABORTED MISSIONS
Destruction test of small scaled solid propellant motors
[ISAS-R-620] 03 p0278 N88-11752
RB-ARD: A proof of concept rule-based abort 08 p1065 N88-16435

ABRASION
Abrasion resistant porous silica antireflective coatings
[DE88-006230] 14 p1894 N88-21308
Stressed fabric abrasion test procedure for urethane coated fabric fuel tanks
[AD-A196327] 24 p3356 N88-29982

ABRASION RESISTANCE
Anti-abrasion protection with highly organized materials
[DE87-014238] 01 p0029 N88-10187
Coatings for Advanced Heat Engines Workshop: Book of abstracts
[DE87-012623] 02 p0180 N88-11121
Indentation damage in ceramics
[AD-A184688] 03 p0294 N88-11844
Synthesis and structure property studies of toughened epoxy resins via functionalized polysiloxanes. Friction and wear studies
[AD-A188258] 11 p1462 N88-18718
Abrasion and impact resistant coatings
[DE88-003562] 13 p1750 N88-20464
Study of the friction and wear-related properties of ceramic superconductors
[DE88-011844] 21 p3024 N88-27950

ABRASIVES
Some speculations on the mechanisms of abrasive grinding and polishing
[DE87-014242] 02 p0181 N88-11126
Surface conditioning products as tools for corrosion removal and corrosion prevention 17 p2320 N88-23856

ABSOLUTE ZERO
Zero temperature quark matter equation of state
[DE88-003408] 10 p1422 N88-18496

ABSORBERS
Toward a comprehensive theory for the sweeping of trapped radiation by inert orbiting matter
[NASA-CR-182584] 11 p1569 N88-19395
Comprehensive model for laser instability in a CO2 laser with gaseous saturable absorber 14 p1979 N88-21808

ABSORBERS (EQUIPMENT)
Fiber optics refractometer for absorption machines
[DE88-002296] 07 p0932 N88-15662
Variable response load limiting device
[NASA-CASE-LAR-12801-1] 17 p2346 N88-23982

ABSORBERS (MATERIALS)
NT ANTIRADAR COATINGS
NT RADAR ABSORBERS
Heat and mass transfer in laminar wavy film absorption with the presence of non-absorbable gases 21 p2947 N88-27502

ABSORPTION
Electromagnetic fields backscattered from an s-shaped inlet cavity with an absorber coating on its inner walls
[NASA-CR-182401] 07 p0845 N88-15130
Determination of aquo-complexes of chromium and iron in chromium plating and polishing solutions by ion chromatography
[AD-A190168] 15 p2039 N88-22148
Sources and levels of background noise in the NASA Ames 40- by 80-foot wind tunnel
[NASA-TM-100077] 17 p2395 N88-24239

ABSORPTION BANDS
U ABSORPTION SPECTRA

ABSORPTION COEFFICIENT
U ABSORPTIVITY

ABSORPTION COOLING
Technical evaluation of a solar-powered absorption cooling system (LiBr-H2O)
[PB87-108254] 04 p0463 N88-12867
Design and development of absorption heat pumps
[DE88-900082] 04 p0466 N88-12885
Self operating absorption cooling system using solar energy: Small power experimental plant
[DE88-900194] 07 p0874 N88-15299
Thermal energy storage by means of an absorption cycle
[ETN-88-91614] 09 p1186 N88-17108

ABSORPTION CROSS SECTIONS
Absorption, scattering, and thermal radiation by conductive fibers
[AD-A186105] 07 p0842 N88-15106
Absolute rate measurements of two-photon process of gases, liquids, and solids
[DE88-003800] 10 p1407 N88-18391
Rotational structure and absorption cross sections from 300 to 190 K of the Schumann-Runge bands
[AERONOMICA-ACTA-A-318-1987] 15 p2036 N88-22131
Ultraviolet absorption cross sections of methylbromide at stratospheric temperatures
[AERONOMICA-ACTA-A-320-1987] 15 p2036 N88-22132
Temperature dependence of ultraviolet absorption cross sections of chlorofluoroethanes
[AERONOMICA-ACTA-A-325-1987] 18 p2482 N88-24726
Nucleon-nucleus interaction data base: Total nuclear and absorption cross sections
[NASA-TM-4053] 20 p2852 N88-26935
Studies of HZE particle interactions and transport for space radiation protection purposes
[NASA-TM-101159] 20 p2886 N88-27142
Ultraviolet absorption cross sections of chloro- and chlorofluoromethanes at stratospheric temperatures
[AERONOMICA-ACTA-A-324-1988] 23 p3231 N88-29228
Aeronomic problems of molecular oxygen photodissociation. Part 2: Theoretical absorption cross sections of the Schumann-Runge bands at 79 K
[AERONOMICA-ACTA-A-331-1988] 24 p3344 N88-29907

ABSORPTION SPECTRA
NT FRAUNHOFER LINES
NT HERZBERG BANDS
Picosecond CO2 laser interactions with polyatomic molecules
[DE87-012072] 01 p0051 N88-10327
DSA RuO2/TiO2 electrode modeled by ion implantation: An in situ characterization by photoacoustic and photocurrent spectroscopy
[DE87-009129] 02 p0245 N88-11545
Photoluminescence studies of GaAs/AlAs superlattices
[DE87-013817] 02 p0245 N88-11548
Spectroscopy and nonthermal processes 02 p0252 N88-11594
A mode-locked ruby laser with chlorophyll d as saturable absorber 03 p0327 N88-12064
Investigations of extragalactic hydroxyl 03 p0389 N88-12441
Far infrared Fourier transform spectroscopy of semiconductors
[DE88-000188] 04 p0499 N88-13072
Titanium oxide absorption and spot sizes in II Peg, HR 1099 and UX Ari 04 p0508 N88-13126
A flash spectrum of Cl I, C I, N I, and Ni II absorption in 31 Cygni: A direct observation of the reversing layer 04 p0513 N88-13158
Sensitivity of the H alpha line to expansion, geometrical extent and temperature gradient in the G and K supergiant chromospheres 04 p0514 N88-13159
IUE observations of the hybrid K3 II star Iota Aurigae and constraints on the outer atmospheric structure 04 p0515 N88-13171
Pure dephasing of a vibrational adbond
[AD-A185222] 05 p0609 N88-13740
Proceedings of the Third Airborne Imaging Spectrometer Data Analysis Workshop
[NASA-CR-181552] 05 p0611 N88-13755
Preliminary results from an investigation of AIS-1 data over an area of epithermal alteration: Plateau, Northern Queensland, Australia 05 p0613 N88-13768
Causes of spurious features in spectral reflectance data 05 p0614 N88-13769
Automatic continuum analysis of reflectance spectra 05 p0614 N88-13770
Analysis of airborne imaging spectrometer data for the Ruby Mountains, Montana, by use of absorption-band-depth images 05 p0614 N88-13771
Mapping hydrothermally altered rocks in the Northern Grapevine Mountains, Nevada and California with the airborne imaging spectrometer 05 p0614 N88-13772
Analysis of SO2 signals in SBUV/TOMS data 05 p0618 N88-13794
Comparison of ground based and TOMS measurements of SO2 from volcanic emissions 05 p0618 N88-13795
A critical review of measurements of water vapor absorption in the 840 to 1100 cm(-1) spectral region
[NASA-CR-182361] 06 p0742 N88-14565
Use of lasers with F sub A(II)-color center KCl:Li crystals in the intraresonator laser spectroscopy method 06 p0769 N88-14729
Laboratory measurements of the ozone absorption coefficient in the wavelength region 339 to 362 nm at different temperatures
[NOTA-INTERNA-882] 07 p0878 N88-15324
Intracavity spectrum analyzer with NaF:F2(+):F3(-) crystal laser for long-wave IR wave band 07 p0919 N88-15584
Characterization of Er,Cr:YSGG
[AD-A185885] 07 p0932 N88-15659
Literature survey relating to the absorption properties of ozone in the near ultraviolet
[ESRO-SM-81] 09 p1190 N88-17129
Memory effects on infrared adsorbate spectra
[AD-A186976] 09 p1253 N88-17512
Guided-wave approaches to spectrally selective energy absorption
[NASA-CR-182532] 10 p1320 N88-17892
Absolute rate measurements of two-photon process of gases, liquids, and solids
[DE88-003800] 10 p1407 N88-18391
Simulation of infrared spectra
[AD-A187881] 11 p1453 N88-18658
Growth and characteristics of materials for tunable lasers in the near infrared spectral region
[NASA-CR-182501] 11 p1491 N88-18901
Laser raman studies related to liquid propellants: Structural characteristics inferred from the nitrate anion spectra
[AD-A188462] 12 p1612 N88-19641
Study of the vibrational modes of subsurface oxygen on Al (111) using diode laser infrared reflection-absorption spectroscopy
[AD-A188322] 12 p1632 N88-19769
Influence of nonlinear spectroscopic effects on atmospheric propagation of intense laser radiation at 10.6 microns wavelength 13 p1789 N88-20705
Effect of Mg impurity on local vibrations of U-centers in LiF lattice 14 p1969 N88-21753
Infrared reflection-absorption spectroscopy of hyperfine layers on surfaces of semiconductors and dielectrics 14 p1969 N88-21755
Single-laboratory evaluation of SW-846 methods 7090/7091 determination of beryllium by flame and furnace atomic absorption spectrophotometry
[PB88-171434] 16 p2175 N88-22963
A sup 57 Fe Mossbauer study of the superconductor YBa sub 2 (Fe sub x Cu sub 1-x) sub 3 O sub y
[DE88-701543] 16 p2282 N88-23661
Selective radiation absorption in aluminized composite propellant combustion 19 p2630 N88-25598
Absorption characteristics of Si3N4 ablation layer plasma 20 p2783 N88-26504
Raman and absorption spectrophotometric studies of selected lanthanide, californium-doped lanthanide, and actinide trihalides in the solid state
[DE88-008234] 20 p2874 N88-27061
Detection of absorption lines in the spectra of X-ray bursts from X1608-52
[ISAS-RN-360] 20 p2887 N88-27143
The 1985-86 measurements with the tunable diode laser absorption spectrometer
[PB88-214002] 23 p3231 N88-29226
Absorption spectra and energy levels of Gd(3+), Nd(3+) and Cr(3+) in the garnet Gd3Sc2Ga3O12
[AD-A193634] 23 p3292 N88-29599

ABSORPTION SPECTROSCOPY
Calorimetric Absorption Spectroscopy (CAS): A new method for the characterization of the optical properties of semiconductor systems
[ETN-87-90407] 01 p0098 N88-10645
Intracavity absorption spectroscopy with ring traveling-wave dye laser 03 p0300 N88-11890
Study of interactional effects in the chemisorbed layer by Infrared Reflection Absorption Spectroscopy (IRAS)
[DE88-001808] 06 p0680 N88-14164
Latitude coverage of observations of the middle atmosphere by solar absorption spectrometry from a heliosynchronous orbit
[AERONOMICA-ACTA-A-316-1987] 06 p0742 N88-14566
L2,3 XANES of the high T sub c superconductor YBa2Cu3O7 with variable oxygen content
[NOTA-INTERNA-888] 06 p0788 N88-14837
Lyman-alfa/OH-resonance-absorbtion measurements and simulation calculations for the investigation of the induction behavior of methane/ethane/oxygen mixtures in reflected shock waves
[ETN-88-90806] 07 p0831 N88-15042
Increasing time resolution of picosecond absorption spectrometer by selection of length of laser light pulses 07 p0919 N88-15579
Energy transfer studies with lasers
[DE88-004864] 10 p1337 N88-17991
Hot corrosion in gas turbines: A new, unique and informative technique is EASE (Electronic Absorption Spectroscopy Experiments)
[AD-A188503] 12 p1583 N88-19470
Resonance energy transfer between carbon monoxide and oxygen molecules using dye laser intracavity absorption spectroscopy
[AD-A188488] 12 p1689 N88-20104
Infrared absorption spectroscopy and chemical kinetics of free radicals
[DE88-006536] 15 p2033 N88-22112
Diode laser spectroscopy of chemical moieties at surfaces
[AD-A190710] 15 p2036 N88-22127
Merit of Hadamard transform active absorption spectrometer described 15 p2053 N88-22232
Statistical fine structure in inhomogeneously broadened absorption lines in solids
[AD-A190341] 16 p2174 N88-22957
Methods and possibilities of biological action spectroscopy 16 p2272 N88-23597
Measurement of atmospheric OH with laser differential optical absorption spectroscopy (LDOAS) 18 p2539 N88-25068
Tropospheric OH measurements by long path absorption with rapid spectral concordance 18 p2539 N88-25069
Isothermal measurement and thermal desorption using SAW devices 19 p2671 N88-25881
Laser spectoscopy of plasmas
[AD-A193009] 20 p2861 N88-26991

ABSORPTIVE INDEX
U ABSORPTIVITY

ABSORPTIVITY
Direct Absorption Receiver (DAR) systems assessment
[DE87-012277] 02 p0196 N88-11222
Enhancement of surface-atmosphere fluxes by desert-fringe vegetation through reduction of surface albedo and of soil heat flux
[NASA-CR-181442] 02 p0197 N88-11231
Laboratory evaluation and application of microwave absorption properties under simulated conditions for planetary atmospheres
[NASA-CR-181466] 02 p0254 N88-11606
Precise measurement of refractive index and absorption coefficient of near millimeter wave and far infrared materials
[AD-A184538] 03 p0293 N88-11840
Double-effect absorption heat pump, phase 3
[PB87-232195] 03 p0317 N88-12005
Thermal stress in the edge cladding of Nova glass laser disks
[DE88-000425] 04 p0448 N88-12780
Optical probe
[EP-PATENT-0-210-869-A1] 05 p0650 N88-13984
Laboratory measurements of the ozone absorption coefficient in the wavelength region 339 to 362 nm at different temperatures
[NOTA-INTERNA-882] 07 p0878 N88-15324
Instability of strong-absorption domain in semiconductor 08 p1077 N88-16495
Literature survey relating to the absorption properties of ozone in the near ultraviolet
[ESRO-SM-81] 09 p1190 N88-17129
Effect of translucence of engineering ceramics on heat transfer in diesel engines
[DE88-003732] 10 p1305 N88-17804
Photoacoustic measurements of atmospheric aerosol absorption coefficients at ultraviolet, visible and infrared wavelengths 11 p1512 N88-19036
Experimental research on skin reflection, transmission, absorption of light rays 16 p2187 N88-23039
Behavior, physiology and energy deposition in rats chronically exposed to 2450 MHz radiation
[PB88-171418] 16 p2237 N88-23363
Influence of refractive index and solar concentration on optical power absorption in slabs
[NASA-TM-4056] 19 p2726 N88-26190
Storage of thermal energy by means of an absorption cycle
[PB88-190814] 21 p2966 N88-27619
Atmospheric nitrogen oxides: Their detection and chemistry
[PB88-193057] 21 p2970 N88-27642
The effect of particle properties on radiative heat transfer 24 p3350 N88-29941

ABSTRACTS
Center for Electronics and Electrical Engineering Technical Progress Bulletin covering center programs, October to December 1986 with 1987 CEEE events calendar
[PB87-226890] 02 p0168 N88-11058

Center for Electronics and Electrical Engineering technical publication announcements covering center programs, July to September 1986 with 1987 CEEE events calendar
[PB87-223442] 02 p0168 N88-11059
FY 1985 scientific and technical reports, articles, papers and presentations
[NASA-TM-86521] 04 p0501 N88-13083
Strategic management of research and development: A literature search
[NASA-CR-182337] 06 p0790 N88-14847
USSR Space Life Sciences Digest index to issues 10-14
[NASA-CR-3922(17)] 07 p0883 N88-15361
The Shock and Vibration Digest, Volume 20, No. 1 08 p0975 N88-15897
USSR Space Life Sciences Digest, issue 14
[NASA-CR-3922(16)] 08 p1045 N88-16317
AGARD reports: A quarterly listing, 1 July through September 30, 1987
[AD-A186572] 08 p1093 N88-16579
NASA JSC neural network survey results 09 p1205 N88-17220
Engine structures: A bibliography of Lewis Research Center's research for 1980-1987
[NASA-TM-100842] 17 p2350 N88-24002
USSR Space Life Sciences Digest, Issue 17
[NASA-CR-3922(20)] 17 p2381 N88-24155
The Shock and Vibration Digest, volume 20, no. 4 17 p2391 N88-24214
Infinite dimensional dynamical systems and their finite dimensional analogues
[AD-A192041] 18 p2563 N88-25216
USSR space life sciences digest, issue 18
[NASA-CR-3922(21)] 19 p2707 N88-26096
Reports of planetary geology and geophysics program, 1987
[NASA-TM-4041] 20 p2885 N88-27133
Aerospace applications studies, 1971-1987
[AGARD-R-759] 21 p2889 N88-27147
Bibliography of Lewis Research Center technical publications announced in 1987
[NASA-TM-100910] 22 p3162 N88-28832
Nineteenth Lunar and Planetary Science Conference. Press abstracts
[NASA-CR-183037] 24 p3440 N88-30473

ABUNDANCE
Quasi-thermal models 02 p0253 N88-11600
Carbon abundances and C12/C13 ratios in M giants 04 p0515 N88-13167
Infrared excesses of barium stars 04 p0516 N88-13174
Galactic interstellar abundance surveys with IUE and IRAS 04 p0522 N88-13206
Abundance and distribution of ultramafic microbreccia in Moses Rock Dike: Quantitative application of AIS data 05 p0613 N88-13766
Primordial nucleosynthesis during the keV era
[DE88-002233] 08 p1104 N88-16623
Spectroscopic determinations of surface gravities of giant stars, and ultraviolet observations of RR Lyrae and X Arietis 11 p1569 N88-19391
Effects of galactic chemical evolution on thorium/neodymium cosmochronology
[DE88-003829] 11 p1570 N88-19397
HNC: A detector to study ultraheavy cosmic rays 12 p1713 N88-20252
Ground-based column abundance measurements of atmospheric hydroxyl
[NASA-CR-182676] 14 p1944 N88-21598
The relationship between low activity comets and more active comets 14 p1997 N88-21904
On the interpretation of the 3 micron emission feature in the spectrum of Comet Halley: Abundances in Comet Halley and in interstellar matter 14 p2002 N88-21935
On the forbidden red lines of oxygen in comets 14 p2006 N88-21963
Para-ortho abundance ratio of molecular hydrogen in NGC2023
[ISAS-RN-352] 18 p2573 N88-25286
Review of the theoretical changes of surface chemistry during massive star evolution
[SER-C-PREPUBL-FASC-17] 18 p2593 N88-25411
Fine-scale traverses in cumulate rocks, Stillwater Complex: A lunar analogue study
[NASA-CR-183066] 20 p2823 N88-26747
Probing the possibility of a (12)C/(13)C abundance gradient from observations of interstellar CH+
[DE88-008908] 20 p2884 N88-27125
Detection of abundant molecular gas in the UV-excess quasar Mrk 1014 22 p3164 N88-28842
An upper limit on the primordial He4 abundance from speckle interferometric observations of muon Cassiopeiae 23 p3298 N88-29641
Mars: Near-infrared comparative spectroscopy during the 1986 opposition 23 p3301 N88-29658

AC (CURRENT)
U ALTERNATING CURRENT

AC GENERATORS
Study of free-piston Stirling engine driven linear alternators
[NASA-CR-181425] 01 p0055 N88-10355
The ac power system testbed
[NASA-CR-175068] 03 p0309 N88-11948
Computer-aided modeling and prediction of performance of the modified Lundell class of alternators in space station solar dynamic power systems
[NASA-CR-182538] 11 p1507 N88-19000
Design of a superconducting alternator for space-based power generation 17 p2412 N88-24340

ACCELERATED LIFE TESTS
Improved cathode life testing
[REPT-3189-T] 02 p0168 N88-11056
Time-temperature-stress capabilities of composite materials for advanced supersonic technology application
[NASA-CR-178272] 06 p0677 N88-14144
Developing an accelerated endurance test for greases: A status report
[AD-A185963] 07 p0836 N88-15072
Robust prediction and interpolation for vector stationary processes, 2d enriched version
[AD-A185875] 07 p0865 N88-15247
Technical applications of solar energy. Project: Selective coatings
[BMFT-FB-T-86-213] 14 p1943 N88-21591
Examination of temperature effects on gate-to-drain avalanche breakdown in GaAs MESFETs (Metal-Semiconductor Field Effect Transistors) by measuring light emission under RF drive
[AD-A189634] 15 p2141 N88-22778
Development of a slip-ring system for energy transfer in space conditions. Space flight qualification and extended life tests
[BMFT-FB-W-86-019] 16 p2169 N88-22932
Brief evaluation of the alloy 17-4-PH (Z5 CNU 17-04). Semifinished product: 205 mm dia forged roller, test reports
[DF/NH-3616/84] 17 p2322 N88-23866
A statistical treatment of accelerated life test data for copper-water heat pipes 20 p2783 N88-26509
Analysis of debris from accelerated life test of the Hughes five-year Vuilleumier cryocooler
[AD-A193101] 21 p2931 N88-27400
Development of a test method to determine potential peroxide content in turbine fuels. Part 2
[AD-A192244] 23 p3199 N88-29042
Performance Prediction for Coatings. Proceedings of a Workshop
[AD-A188973] 24 p3354 N88-29966
Prediction of degradation of polymeric coating materials 24 p3354 N88-29970
Alternative immersion accelerated testing of coating systems for Naval shoreline facilities 24 p3355 N88-29977

ACCELERATION (PHYSICS)
NT ANGULAR ACCELERATION
NT DECELERATION
NT ELECTRON ACCELERATION
NT HIGH GRAVITY ENVIRONMENTS
NT IMPACT ACCELERATION
NT PARTICLE ACCELERATION
NT PLASMA ACCELERATION
NT SPIN REDUCTION
NT TRANSVERSE ACCELERATION
Acceleration to hypervelocities using minimum energy concepts
[DE87-011796] 01 p0089 N88-10583
Flame acceleration and transition to detonation in channels
[DE87-014193] 03 p0284 N88-11786
Fiber-optic accelerometer investigation
[AD-A185359] 05 p0584 N88-13561
Separable orthogonal coordinates and particle creation for an accelerating observer
[DE87-703358] 05 p0657 N88-14029
Steady waves in a nonlinear theory of viscoelasticity
[AD-A185548] 06 p0723 N88-14448
On a possibility of ion acceleration up to high energies in a high-current electron beam
[DE88-700532] 07 p0931 N88-15657
Looking for new gravitational forces with antiprotons
[DE88-003154] 09 p1192 N88-17142
Considerations of acceleration effects in relativistic kinematics 09 p1260 N88-17553
Research and development of surface skimming bulk wave devices for sensor applications
[AD-A187504] 11 p1470 N88-18766
Reference position vector 12 p1577 N88-19432
Fighter design for human load limits 12 p1580 N88-19451
Lower bounds on acceleration estimation accuracy
[AD-A188383] 12 p1619 N88-19681
Parametric study of acceleration-induced stresses and frequency changes in doubly-rotated crystal resonators
[AD-A189261] 13 p1761 N88-20532
An experimental investigation of decelerating flow about two-dimensional cambered plates
[DE88-006598] 13 p1766 N88-20567
Impact shock generator from explosively driven plates
[DE88-003596] 14 p1918 N88-21452
Analysis of head response to torso acceleration. Volume 1: Development of performance requirements
[PB88-156757] 14 p1953 N88-21640
Centrifugal acceleration of ions in the polar magnetosphere
[NASA-TM-101148] 17 p2374 N88-24120
Effects of Coriolis acceleration on the vibrations of spinning structures 18 p2522 N88-24966
Study of the structure of turbulence in accelerating transitional boundary layers
[AD-A191698] 19 p2663 N88-25837
Dynamics explorer data analysis
[NASA-CR-181428] 19 p2691 N88-25996
Gone with the solar wind: A study of protons accelerated by interplanetary shocks 19 p2743 N88-26283
An investigation of soft launch and instability breakup with a two-stage light gas gun
[DE88-010371] 21 p2901 N88-27218
Characterization of accelerating pipe flow
[AD-A193065] 21 p2943 N88-27481
Stochastic geologic effects on near-field ground motions in alluvium
[AD-A192315] 21 p2972 N88-27652
A study of mechanisms producing astrophysical jets
[AD-A194100] 23 p3300 N88-29649
Models of cerebral-body perfusion and cerebral chemical transport
[AD-A194945] 24 p3407 N88-30283

ACCELERATION STRESSES (PHYSIOLOGY)
Fighter design for human load limits 12 p1580 N88-19451
Liquid ventilation: New data and possible use in space medicine 12 p1654 N88-19908
Macaca rhesus tolerance to +Gz accelerations 19 p2704 N88-26080
Evoked potential analysis of impact acceleration experiments 21 p2981 N88-27708
EEG indices of G-induced Loss Of Consciousness (G-LOC) 21 p2982 N88-27709

ACCELERATION TOLERANCE
F-16 control stick response during +Gz-induced loss of consciousness
[AD-A184107] 04 p0400 N88-12491
Measurement and modification of sensorimotor system function during visual-motor performance
[AD-A186351] 07 p0889 N88-15387
Human and animal hypovolemic reactions to increasing +Gz accelerations 07 p0890 N88-15395
Karyometric evaluation of neuronal reactions of rat cerebral cortex to the combined effect of ionizing radiation, longitudinal accelerations and vibration 07 p0890 N88-15396
Improvement of human tolerance to head-pelvis (+Gz) accelerations by increasing hydration 10 p1364 N88-18153
Effect of cardioactive compounds on rat myocardium actomyosin following exposure to accelerations 10 p1365 N88-18161
Fighter design for human load limits 12 p1580 N88-19451
Analysis of head response to torso acceleration. Volume 2: Description of data retrieval, analysis and display software
[PB88-156765] 15 p2104 N88-22536
Macaca rhesus tolerance to +Gz accelerations 19 p2704 N88-26080
Significance of sensory signal phase mismatch in mechanisms of motion sickness development 20 p2830 N88-26787
Physiological monitoring methodology in the USAFSAM centrifuge 21 p2924 N88-27356
Detection of acceleration (+Gz) induced blackout by matched-filtering of visual evoked potentials 21 p2982 N88-27710
Variation of carotid flow under load, studied by the Doppler echo method — acceleration tolerance
[REPT-1149] 23 p3240 N88-29282

ACCELERATORS
The impact of new computer technology on accelerator control
[DE87-014021] 02 p0219 N88-11378
GOLD: Integration of model-based control systems with artificial intelligence and workstations
[DE88-000506] 04 p0483 N88-12976

GOLD: Integration of model-based control systems with artificial intelligence and workstations
[DE88-000706] 04 p0483 N88-12977
An improved data reduction procedure for accelerometer centrifuge data 12 p1577 N88-19436
ACCELEROMETERS
NT STRAIN GAGE ACCELEROMETERS
Requirements for the calibration of mechanical shock transducers
[PB87-227591] 03 p0325 N88-12054
Fiber-optic accelerometer investigation
[AD-A185359] 05 p0584 N88-13561
Design and test of a spacecraft instrument shock isolator 08 p0998 N88-16044
An integration test for accelerometer evaluation 09 p1178 N88-17054
A quantitative method for evaluating sensor layouts 09 p1178 N88-17056
Strategic placement of accelerometers to measure forces by the sum of weighted accelerations
[DE88-002262] 10 p1333 N88-17968
Research and development of surface skimming bulk wave devices for sensor applications
[AD-A187504] 11 p1470 N88-18766
Thirteenth Biennial Guidance Test Symposium, volume 1
[AD-A185782] 12 p1576 N88-19427
Robotics applications in the testing of inertial sensors 12 p1577 N88-19433
GRADIO three-axis electrostatic accelerometers 12 p1645 N88-19849
Concept of an Opto-electronic Accelerometer System (OAS) 12 p1645 N88-19852
Surface wave accelerometer
[ETN-88-92000] 16 p2210 N88-23192
The optical accelerometer: A novel sensor for vertical flight guidance 18 p2518 N88-24935
Air loading effects on a capacitively sensed membrane supported silicon accelerometer 19 p2672 N88-25886
Wave structures in thermospheric density from satellite electrostatic triaxial accelerometer measurements
[AD-A194134] 23 p3233 N88-29240
ACCEPTABILITY
Automatically generated acceptance test: A software reliability experiment
[NASA-CR-181667] 17 p2347 N88-23984
Electromagnetic characterization and acceptance test of the electromagnetic pulse (EMP) simulator SPERANS
[FOA-C-30476-4.2] 22 p3071 N88-28230
ACCEPTANCE
U ACCEPTABILITY
ACCEPTOR MATERIALS
Wittig synthesis of conductive segmented block polymer compositions
[AD-A184018] 03 p0295 N88-11850
Excimer laser-assisted deposition of GaAs, AlAs and (Al,Ga)As from Lewis acid-base adducts
[AD-A184588] 03 p0329 N88-12081
Donor acceptor polymerization chemistry as a vehicle to low energy cure matrix resins
[AD-A190119] 15 p2044 N88-22179
Modeling the primary events of photosynthesis using chlorophyll containing fixed distance donor-acceptor molecules
[DE88-010033] 20 p2831 N88-26793
ACCESS CONTROL
The varieties of capabilities in Flex
[RSRE-MEMO-4042] 01 p0078 N88-10500
Usage analysis of user files in UNIX
[NASA-CR-181561] 05 p0633 N88-13868
Channel access protocols for multihop packet radio networks
[AD-A186074] 07 p0842 N88-15105
Media independent interface
[NASA-CR-172033] 08 p1066 N88-16446
Media independent interface. Interface control document
[NASA-CR-172032] 08 p1067 N88-16447
On proving register atomicity
[CWI-CS-R8707] 13 p1818 N88-20862
Two queues with alternating service and switching times
[CWI-OS-R8712] 13 p1831 N88-20949
Impact of blocking policies in closed, exponential and symmetrical ring networks
[FUB-8-1986] 14 p1960 N88-21693
Protection and security mechanisms in the SMITE capability computer
[RSRE-MEMO-4117] 17 p2384 N88-24167
Computer resource management technology program (PE 64740F). Task no. 9: Advanced user authentication
[PB88-183066] 18 p2555 N88-25163
L-band and SHF multiple access schemes for the MSAT system 19 p2650 N88-25734
Using common subexpressions to optimize multiple queries
[DE88-008210] 20 p2844 N88-26877
A state-of-the-art survey of low-cost security in local area networks
[NPL-DITC-113/88] 22 p3141 N88-28678
Formal specification of a secure document control system for SMITE
[RSRE-88002] 23 p3245 N88-29309
Performance analysis of FDDI
[NASA-CR-183206] 24 p3413 N88-30321
ACCESSORIES
Stability analysis of a rigid body with a flexible attachment using the energy-casimir method
[AD-A185646] 06 p0723 N88-14449
Software modifications to total data reporting accessory for metabolic measurement cart
[AD-A193641] 22 p3132 N88-28823
ACCIDENT INVESTIGATION
NT AIRCRAFT ACCIDENT INVESTIGATION
Detection of hyperventilation of parachutists
[DFVLR-FB-87-11] 01 p0075 N88-10482
Aircraft accident reports: Brief format, US Civil and Foreign Aviation, Issue Number 4 of 1986 accidents
[PB87-916906] 06 p0666 N88-14086
Aircraft accident report: Grand Canyon Airlines, Inc., and Helitech, Inc., midair collision over Grand Canyon National Park, June 18, 1986
[PB87-910403] 06 p0666 N88-14087
Aircraft accident/incident, Newark, New Jersey, November 13, 1986
[NTSB/AAR-87/04-SUMM] 10 p1276 N88-17639
Space shuttle accident: NASA's actions to address the Presidential Commission report
[PB88-135306] 15 p2024 N88-22059
ACCIDENT PREVENTION
Detection of hyperventilation of parachutists
[DFVLR-FB-87-11] 01 p0075 N88-10482
Report of the helicopter human factors working group — accident prevention
[CAA-PAPER-87007] 03 p0351 N88-12274
Protected areas with enhanced bird-aircraft collision risk in the Federal Republic of Germany
[GEOPHYSBDBW-FM-209] 11 p1437 N88-18576
Rotorcraft TCAS (traffic alert and collision avoidance system) evaluation: Group 3 results
[AD-A191719] 18 p2461 N88-24614
ACCIDENTS
NT BIRD-AIRCRAFT COLLISIONS
NT LOSS OF COOLANT
Cost savings possible with Air Force conversion to JP-8 as its primary fuel
[AD-A183784] 01 p0030 N88-10192
Measurements of gas velocities and temperatures in a large open pool fire
[DE87-005853] 03 p0261 N88-11641
Structural analysis of a bolted joint concept for the space shuttle's solid rocket motor casing
[NASA-TM-89092] 04 p0407 N88-12531
Visualization of an aircraft accident based on digital flight data recorder information 05 p0538 N88-13278
Aircraft accident report: Grand Canyon Airlines, Inc., and Helitech, Inc., midair collision over Grand Canyon National Park, June 18, 1986
[PB87-910403] 06 p0666 N88-14087
Post-Challenger evaluation of space shuttle risk assessment and management
[NASA-CR-182461] 12 p1705 N88-20202
Potential off-normal events and associated radiological source terms for the compact ignition tokamak: Fusion Safety Program
[DE88-004112] 13 p1842 N88-21024
Chronic stress as a factor in aircraft mishaps 16 p2239 N88-23376
Acute stress 16 p2239 N88-23377
Critical nuclear launch issues: A perspective from the State of Florida 17 p2423 N88-24412
A novel plant protection strategy for transient reactors 17 p2425 N88-24423
Evaluation of UN fuel pin failure modes and motion of fuel during severe accidents for reactors in space 17 p2425 N88-24424
Reactor core coolability with reduced power levels 17 p2425 N88-24425
Analysis of a nuclear orbital transfer vehicle reentry accident 17 p2425 N88-24426
Health and environmental consequences of the Chernobyl nuclear power plant accident
[DOE/ER-0332] 19 p2689 N88-25985
Book analysis. Challenger: A major malfunction
[AD-A192458] 20 p2764 N88-26388
The role and the place of insurance of large space projects 22 p3161 N88-28826
ACCLIMATIZATION
NT ALTITUDE ACCLIMATIZATION
NT COLD ACCLIMATIZATION
NT HEAT ACCLIMATIZATION
Physicochemical correlates of human adaptation to extreme environments 06 p0750 N88-14607
Medical problems related to altitude in: Human performance physiology and environmental medicine at terrestrial extremes, chapter 14
[AD-A188340] 12 p1666 N88-19989
Acute mountain sickness at 4500 m is not altered by repeated eight-hour exposures to 3200-3550 m normobaric hypoxic equivalent
[AD-A188358] 12 p1666 N88-19990
ACCOMMODATION
Evaluation of a cryogenic refrigerator for cooling focal plane instrumentation. Appendix B: Accommodation study — satellite instruments
[BAE-TP-8095-VOL-2] 05 p0572 N88-13486
Gradiometer accommodation on board a drag-free satellite 12 p1645 N88-19850
ACCOUNTING
A general approach to error propagation
[DE87-014287] 02 p0224 N88-11412
A comparison of the Cray-2 performance before and after the installation of memory pseudo-banking
[NASA-CR-177462] 09 p1215 N88-17287
Monitoring the usage of a computer system
[DE88-004310] 15 p2106 N88-22542
Financial reporting: NASA (National Aeronautics and Space Administration) can improve compliance with GAO (General Accounting Office) standards and treasury requirements
[PB88-172523] 18 p2587 N88-25373
Aircraft avionics and missile system installation cost study. Volume 2: Appendices F and G
[AD-A195372] 24 p3325 N88-29801
ACCRETION
U DEPOSITION
ACCRETION DISKS
Gravitational accretion of hot dark matter 03 p0388 N88-12439
X-ray pulsars: Accretion flow deceleration 03 p0390 N88-12451
Disk accretion during the early stages of stellar evolution 04 p0505 N88-13106
The contribution of accretion luminosity to the infrared spectra of T Tauri stars: A possible test 04 p0518 N88-13183
EXOSAT guest observer program. Binary parameters of the X-ray Pulsar 4U1626-67
[NASA-CR-182374] 06 p0802 N88-14905
ACCUMULATIONS
Ultra-low power digital filter
[AD-A184485] 03 p0310 N88-11959
ACCUMULATORS
NT DUST COLLECTORS
NT SOLAR COLLECTORS
Wet deposition and snowpack monitoring operations and quality assurance manual
[PB87-212817] 01 p0064 N88-10413
The use of alloy 117 as a liquid metal current collector
[AD-A185740] 06 p0698 N88-14281
Performance of a small, graphite electrode, multistage depressed collector with a 500-W, continuous wave, 4.8- to 9.6-GHz traveling wave tube
[NASA-TP-2788] 07 p0848 N88-15146
A dynamic model for the aft accumulator in the TE SP-100 system 17 p2414 N88-24354
ACCURACY
NT GEODETIC ACCURACY
NT GEOMETRIC ACCURACY
Impact of turbulence modeling on numerical accuracy and efficiency of compressible flow simulations
[NASA-TM-88333] 02 p0173 N88-11088
Performance and operating envelope of imaging and scattering particle sizing instruments
[NASA-CR-180859] 03 p0323 N88-12042
Dynamic positioning at sea using the global positioning system
[AD-A184453] 04 p0397 N88-12476
Optimization of dilatometer test procedures
[DE87-014998] 04 p0447 N88-12769
Accuracy potential of non-metric cameras in close-range photogrammetry 04 p0463 N88-12862
Lower bounds on bearing accuracy for closely spaced sources
[AD-A184258] 04 p0486 N88-12997
Contribution to the improvement of the guidance accuracy of automatic pilots
[ETN-88-90607] 05 p0551 N88-13360
Operating envelopes of particle sizing instrumentation used for icing research
[NASA-CR-180870] 05 p0586 N88-13573
Timing variation in dual loop benchmarks
[AD-A185697] 06 p0707 N88-14338

Robot accuracy improvement through kinematic parameter identification 06 p0712 N88-14363
Limiting accuracy of scatterometer determination of wind speed over ocean from satellite 08 p1007 N88-16107
Successful mixed formulation for axisymmetric shell analysis employing discontinuous stress fields of the same order as the displacement field [DE88-700021] 09 p1178 N88-17052
The accuracy of the radiation parameterization in mesoscale models [DFVLR-IB-553-85/11] 09 p1190 N88-17133
The empirical accuracy of uncertain inference models 09 p1208 N88-17243
On precision and accuracy (bias) statements for measurement procedures [DE88-004434] 10 p1402 N88-18359
Total Variation Diminishing (TVD) schemes of uniform accuracy [NASA-TM-100552] 11 p1436 N88-18566
Effects of stress on judgement and decision making in dynamic tasks [AD-A188203] 11 p1523 N88-19092
Lower bounds on acceleration estimation accuracy [AD-A188383] 12 p1619 N88-19681
Measuring accuracy of 3-dimensional bodies by the GOMER-1 device [DE87-703230] 12 p1628 N88-19744
Cramer-Rao bounds on the accuracy of location and velocity estimations using CCD optical sensors [AD-A188481] 12 p1629 N88-19748
Experience with and ways to upgrade accuracy of hydromagnetic surveys in ocean 13 p1787 N88-20692
Density measurements on solids and liquids [PB88-164934] 15 p2036 N88-22129
Effect of friction and control parameters on the tracking accuracy of a target seeker [AD-A190010] 15 p2056 N88-22257
Analysis of a range estimator which uses MLS angle measurements [NASA-CR-182896] 16 p2160 N88-22884
Accuracy versus convergence rates for a three dimensional multistage Euler code [NASA-CR-181665] 16 p2261 N88-23519
Mapping from LANDSAT and SPOT satellite imagery 17 p2352 N88-24018
Limits of accuracy and range of laser radars 18 p2517 N88-24934
DMSP-SSM/1 NASA algorithm validation using primarily LANDSAT and secondarily DMSP and/or AVHRR visible and thermal infrared satellite imagery [NASA-CR-182979] 18 p2532 N88-25024
Portable implementation of a generic exponential function in Ada [DE88-007699] 19 p2715 N88-26117
Basic research for the geodynamics program [NASA-CR-183149] 21 p2973 N88-27662
Global-scale temperature changes to August 1987 and a comparison of satellite and conventional data 22 p3125 N88-28572
Another approach for forecasting forecast skill 22 p3126 N88-28580
Experimental 30-day forecasts from several spectral general circulation models 22 p3126 N88-28582
Dependence of medium range forecast errors upon the large-scale initial state 22 p3126 N88-28585
Aerodynamic data accuracy and quality: Requirements and capabilities in wind tunnel testing [AGARD-AR-254] 23 p3173 N88-28893
Accuracy of satellite data navigation [AD-A195877] 24 p3322 N88-29787
Precision measurement of the Fresnel drag coefficient using a ring laser [AD-A196025] 24 p3366 N88-30043
Increasing accuracy in evaluating vector of state under conditions of incomplete observability of expanded system 24 p3448 N88-30511

ACEE PROGRAM
Department of Housing and Urban Development-Independent Agencies Appropriations for fiscal year 1988, Friday, 10 April 1987: National Aeronautics and Space Administration 03 p0386 N88-12425
SR-7A aeroelastic model design report [NASA-CR-174791] 23 p3179 N88-28928

ACETIC ACID
Changes in functional parameters of animals during long-term inhalation of acetic acid 07 p0895 N88-15423
Effect of long-term inhalation of acetic acid vapor on some functional parameters of man 19 p2705 N88-26084

ACETONE
Characterization of catalysts with metal-support effects and of the species adsorbed on their surfaces [DE87-014636] 04 p0414 N88-12564
Boundary layer flow visualization for flight testing 17 p2297 N88-23742
Liquid-phase oxidation of acetone with hydrogen peroxide on oxide catalysts 19 p2706 N88-26091

ACETONITRILE
Electrochemistry in near-critical and supercritical fluids. 6: The electrochemistry of ferrocene and phenazine in acetonitrile between 25C and 300C [AD-A192171] 18 p2482 N88-24723

ACETYL COMPOUNDS
Process for the preparation of acyl halides [GB-PATENT-2-133-792-A] 01 p0020 N88-10124
The photochemistry of some possible cometary CN parent species 14 p1997 N88-21905

ACETYLENE
Ethynylated aromatics as high temperature matrix resins [NASA-TM-89829] 11 p1450 N88-18640
Polymerization of fluorinated diacetylenes [AD-A188051] 11 p1462 N88-18716
The photochemistry of some possible cometary CN parent species 14 p1997 N88-21905
Large ionic species in sooting acetylene and benzene flames 24 p3348 N88-29932

ACHONDRITES
Ureilites are not igneous differentiates 24 p3441 N88-30477

ACID BASE EQUILIBRIUM
Acid-base equilibrium and some rat blood parameters following exposure to hyperbaric oxygenation 07 p0894 N88-15420

ACID RAIN
Spatial characterization of acid rain stress in Canadian Shield Lakes [NASA-CR-181136] 01 p0067 N88-10430
Spatial characterization of acid rain stress in Canadian Shield Lakes [NASA-CR-180577] 01 p0067 N88-10431
Simulation of global wet and dry deposition of nitric acid in a three-dimensional chemistry-transport model [DE87-009847] 09 p1188 N88-17116
Acid rain: Delays and management changes in the Federal research program [GAO/RCED-87-89] 19 p2690 N88-25988
Acid Precipitation: A current awareness bulletin [DE88-007987] 20 p2821 N88-26738
Atmospheric science issues in Congress 22 p3125 N88-28573
Regional environmental studies using national data bases and GIS (Geographic Information System) [DE88-008368] 23 p3230 N88-29225

ACIDITY
Photon stimulated desorption from oxidized Al(110) [DE88-002209] 06 p0787 N88-14828

ACIDS
NT ACETIC ACID
NT ACRYLIC ACID
NT AMINO ACIDS
NT BORIC ACIDS
NT CARBOXYLIC ACIDS
NT CHROMIC ACID
NT DEOXYRIBONUCLEIC ACID
NT DICARBOXYLIC ACIDS
NT GLUTAMIC ACID
NT GLUTAMINE
NT HYDROCHLORIC ACID
NT HYDROFLUORIC ACID
NT NICOTINIC ACID
NT NITRIC ACID
NT NUCLEIC ACIDS
NT PHOSPHORIC ACID
NT RIBONUCLEIC ACIDS
NT SULFONIC ACID
NT SULFURIC ACID
NT THYMINE
Synthesis of novel acid electrolytes for phosphoric acid fuel cells [PB87-221305] 01 p0066 N88-10426
Compilation and analysis of air quality data in support of acid deposition research [DE87-014428] 02 p0196 N88-11226
Wear of iron and nickel in corrosive liquid environments [NASA-TM-100246] 03 p0289 N88-11817
Corrosion strength of niobium and its alloys [DE87-703693] 04 p0416 N88-12578
Electroformation: Principle electrochemical process of electrodeposition and electroformation of copper [INPE-4374-NTE/274] 08 p0969 N88-15863
Copper electroforming from acid sulfate baths: Preliminary studies [INPE-4375-RPE/554] 08 p0969 N88-15864
Active sites and roles of solid acid base catalysts [NASA-TT-20333] 24 p3345 N88-29909

ACOUSTIC ATTENUATION
NT SHOCK WAVE ATTENUATION
Active minimisation of acoustic fields. A review of research into the active control of sound undertaken at ISVR from 1983 to 1986 [ISVR-TR-146] 01 p0091 N88-10593
AFAR (Azores Fixed Acoustic Range) measurements of intensity and intensity moments [AD-A184431] 03 p0355 N88-12237
Theoretical and practical aspects of the functional absorber method of arranging sound absorbing panels [BBC-RD-1987/15] 05 p0648 N88-13955
Attenuation of ultrasonic waves in nonmagnetized magnetic fluids 09 p1234 N88-17396
Measured and calculated acoustic attenuation rates of tuned resonator arrays for two surface impedance distribution models with flow [NASA-TP-2766] 09 p1241 N88-17440
High frequency acoustic underwater communication with low probability of being traced [REPT-4-87] 09 p1242 N88-17447
Silencium resonators (Silators) for the attenuation and elimination of sound [MBB-Z-546/83] 10 p1312 N88-17841
An application of dimensionless Eigenvalues to underwater acoustic ducts [AD-A188167] 11 p1542 N88-19219
Sound propagation through a turbulent atmosphere: Experimental techniques and data analysis [AD-A188891] 12 p1688 N88-20094
Overground Excess Sound Attenuation (ESA). Volume 1: Experimental study for flat grassy terrains [AD-A191289] 16 p2265 N88-23549
Reflection of sound in open ended ducts [PB88-103478] 21 p3012 N88-27870
Acoustic propagation in the lower atmosphere [ISL-R-126/87] 21 p3013 N88-27878
Experiments on the dissipation of sound by separated flow at an edge [ISVR-TR-151] 23 p3279 N88-29522
A comparison of simple analytical models for representing propeller aircraft structural and acoustic responses [ISVR-TR-153] 23 p3279 N88-29523

ACOUSTIC COMBUSTION
U COMBUSTION STABILITY

ACOUSTIC DUCTS
An application of dimensionless Eigenvalues to underwater acoustic ducts [AD-A188167] 11 p1542 N88-19219

ACOUSTIC EMISSION
Fracture mode research of boron aluminum composite materials by Acoustic Emission (AE) [NAL-TR-927] 02 p0142 N88-10891
An acoustic emission digital data acquisition workstation [DE87-012425] 02 p0191 N88-11191
Transply crack density detection by acousto-ultrasonics [NASA-TM-100224] 03 p0279 N88-11758
Development of an acoustic emission monitor and monitoring techniques for long-term monitoring of U-0.8Ti electron-beam weldments for postweld cracking [DE88-000819] 04 p0453 N88-12804
Contribution of acoustic analysis to assess damage in fluid storage tanks under high pressure --- composite materials, filament winding [SNIAS-872-430-119] 05 p0559 N88-13407
The Shock and Vibration Digest, Volume 19, No. 12 05 p0610 N88-13746
Experimental studies on acoustic emission monitoring of crack propagation in offshore structures: A literature survey 05 p0610 N88-13748
Acoustic emissions at an open crack [DE88-001504] 05 p0611 N88-13751
Theory of transient thermal self-focusing of sound beams 09 p1234 N88-17401
Nonlinear and diffraction effects in sound beams with random transverse structure 09 p1235 N88-17402
Laboratory studies related to in-flight acoustic emission monitoring [AD-A186714] 09 p1242 N88-17445
The acoustic-electric field analysis of multilayered surface acoustic wave devices [ETN-88-91592] 09 p1242 N88-17446
Acoustic emission-microstructural relations in ferritic steels. Part 3: The effect of inclusion content [AERE-R-12041] 10 p1341 N88-18015
Acoustic emission measurements of PWR weld materials with inserted defects [AERE-R-12386] 10 p1341 N88-18016
Institute for Materials Science and Engineering, nondestructive evaluation: Technical activities 1987 [PB88-153655] 10 p1342 N88-18020

STA-2A NDT testing
[NASA-CR-179301] 11 p1497 N88-18937
Ultrasonic measurements research: Progress in 1987
[AD-A188506] 12 p1687 N88-20092
Application of ISRM testing methods to fracture toughness testing of graphite 13 p1747 N88-20446
A study of the dynamics of high temperature brittle intergranular fracture by acoustic emission
[AERE-R-12479] 13 p1780 N88-20650
Study of strength characteristics of glass-reinforced plastic by acoustic emissions method 14 p1885 N88-21268
Acoustic emission frequency discrimination
[NASA-CASE-MSC-20467-1] 17 p2342 N88-23966
Frequency Analysis of Acoustic Emission - Application to machining and welding
[DE88-701478] 18 p2570 N88-25262
An analysis of the efficiency and directivity of the sound generated by a moving laser source
[AD-A192220] 20 p2849 N88-26914
On the possibility of the soliton description of acoustic emission during plastic deformation of crystals
[DE88-701878] 20 p2876 N88-27075
Acoustic emission calibration instrumentation
[DE88-010817] 21 p2951 N88-27528
Application of pattern recognition techniques to the identification of aerospace acoustic sources
[NASA-CR-183116] 21 p3013 N88-27877
Proceedings of the French-German Colloquium on Helicopter Detection
[ISL-R-104/87] 22 p3147 N88-28723
Acoustic direction finding of flying helicopters 22 p3148 N88-28728
Examples of the application of acoustics for the detection and classification of targets 22 p3143 N88-28729
The development of acoustic emission for structural integrity monitoring of aircraft
[AD-A196264] 24 p3427 N88-30398

ACOUSTIC EXCITATION
Active control of jet flowfields
[AD-A186736] 08 p0989 N88-15989
Characteristics of thermooptical sound excitation in metals 08 p1076 N88-16486
Performance of linear vertical antenna in refractive multimode waveguide 08 p1076 N88-16489
On the correlation of plume centerline velocity decay of turbulent acoustically excited jets
[NASA-TM-100193] 09 p1114 N88-16681
Coupled FE and HIE method for exterior acoustics of axisymmetric shells — finite element (FE) Helmholtz integral equation (HIE)
[ARE-TM(UHA)-87506] 09 p1243 N88-17448
Transient sound radiation from infinite thin plate
[ARE-TM(UHA)-87508] 09 p1243 N88-17449
Acoustic radiation from line- and point-loaded plates: Uniformly asymptotic solutions
[AD-A189367] 13 p1834 N88-20669
Enhanced viscous flow drag reduction using acoustic excitation
[NASA-CR-182734] 15 p2062 N88-22295
Acoustically excited heated jets. 1: Internal excitation
[NASA-CR-4129-PT-1] 17 p2298 N88-23751
Acoustically excited heated jets. 2: In search of a better understanding
[NASA-CR-4129-PT-2] 17 p2299 N88-23752
Acoustically excited heated jets. 3: Mean flow data
[NASA-CR-4129-PT-3] 17 p2299 N88-23753

ACOUSTIC FATIGUE
Abrasion and impact resistant coatings
[DE88-003562] 13 p1750 N88-20464

ACOUSTIC FREQUENCIES
NT AUDIO FREQUENCIES
Describing the source created by turbulent flow over orifices and louvers
[AD-A190254] 15 p2130 N88-22706

ACOUSTIC GENERATORS
U SOUND GENERATORS

ACOUSTIC IMPEDANCE
Development of a new method of measuring the characteristic impedance and complex wave number of a porous acoustic material
[AD-A185038] 05 p0646 N88-13957
Measured and calculated acoustic attenuation rates of tuned resonator arrays for two surface impedance distribution models with flow
[NASA-TP-2766] 09 p1241 N88-17440
Evaluation of a multi-point method for determining acoustic impedance
[NASA-TM-100637] 20 p2849 N88-26913
Arctic ice attenuation model study
[AD-A193382] 22 p3146 N88-28715

ACOUSTIC INSTABILITY
Low-disturbance wind tunnels 07 p0811 N88-14937
Characterizing particle combustion in a Rijke burner
[AD-A186157] 08 p0966 N88-15847
Propagation of acoustic disturbances in transonic flow fields of lifting wings
[DFVLR-FB-88-13] 21 p3013 N88-27880

ACOUSTIC LEVITATION
Single mode levitation and translation
[NASA-CASE-NPO-16675-1-CU] 17 p2395 N88-24241
Program for the feasibility of developing a high pressure acoustic levitator
[NASA-CR-182154] 20 p2782 N88-26498
Combustion studies of acoustically suspended liquid droplets
[AD-A193892] 23 p3192 N88-29998

ACOUSTIC MEASUREMENT
NT NOISE MEASUREMENT
Investigation of the suitability of the 8ft x 6ft transonic wind-tunnel for aeroacoustic research on propellers
[RAE-TM-AERO-2093] 01 p0008 N88-10041
A new method for determining acoustic properties of the seabed from the ambient noise field in the ocean
[RAE-TR-86035] 01 p0090 N88-10590
Experimental study of the propagation of an acoustic wave in the low atmosphere
[ISL-R-111/86] 02 p0231 N88-11454
AFAR (Azores Fixed Acoustic Range) measurements of intensity and intensity moments
[AD-A184431] 03 p0355 N88-12237
Development of an acoustic echosounder for detection of lower level atmospheric turbulence
[AD-A184877] 05 p0626 N88-13831
Measuring the annoyance of aircraft noise
[AD-A185494] 06 p0777 N88-14770
Transient classifier systems and man-machine interface research
[AD-A186213] 07 p0899 N88-15446
Comprehensive inflight vibration and acoustic testing 08 p0999 N88-16052
Wind tunnel investigations of periodic vortex separation on rough-surface circular cylinders using acoustic measuring methods
[DFVLR-FB-87-24] 09 p1112 N88-16665
Recommendations for organising the calibration of pure-tone audiometers
[NPL-AC-112] 09 p1167 N88-16999
Payload bay atmospheric vent airflow testing at the Vibration and Acoustic Test Facility
[NASA-TM-100460] 11 p1437 N88-18572
The estimation of target trajectory parameters from Closest Point of Approach (CPA) time measurements in a field of acoustic sensors
[FB-3-87] 11 p1439 N88-18586
Acoustic measurements from a rotor blade-vortex interaction noise experiment in the German-Dutch Wind Tunnel (DNW)
[NASA-TM-4024] 11 p1542 N88-19218
Analysis of in-flight acoustic data for a twin-engined turboprop airplane
[NASA-CR-178389] 11 p1543 N88-19220
Application of ISRM testing methods to fracture toughness testing of graphite 13 p1747 N88-20446
Method for determination of the wind velocity and direction
[NASA-TT-20233] 13 p1802 N88-20769
Survey of acoustic techniques for monitoring El Nino
[PB88-157615] 13 p1804 N88-20783
Measurement and analysis of the noise radiated by low Mach numbers centrifugal blowers
[AD-A189226] 13 p1833 N88-20966
Method for determining the coordinates of sound sources by means of a sound measurement system
[NASA-TT-20242] 13 p1834 N88-20972
Method for determining artillery position
[NASA-TT-20238] 13 p1834 N88-20973
Space time processing, environmental-acoustic effects
[AD-A190764] 15 p2130 N88-22708
Acoustic propagation in the low atmosphere. Experimental study and modeling by the radius method
[ISL-CO-247/86] 15 p2131 N88-22713
Simulated measurement of power flow in structures near to simple sources and simple boundaries
[NASA-TM-89124] 19 p2722 N88-26166
Sound power measurements in situ using a reference sound source
[PB88-182571] 20 p2849 N88-26910
Evaluation of a multi-point method for determining acoustic impedance
[NASA-TM-100637] 20 p2849 N88-26913
Acoustic propagation in the lower atmosphere
[ISL-R-126/87] 21 p3013 N88-27878
Application of acoustic-Doppler current profiler and expendable bathythermograph measurements to the study of the velocity structure and transport of the Gulf Stream
[NASA-CR-183188] 22 p3129 N88-28605

ACOUSTIC MICROSCOPES
Imaging subtle microstructural variations in ceramics with precision ultrasonic velocity and attenuation measurements
[NASA-TM-100129] 07 p0867 N88-15257
Cryogenic acoustic microscopy
[AD-A187274] 10 p1299 N88-17767
Interface control using low frequency (3 to 20 MHz) acoustic microscopy
[REPT-48-411/F] 21 p2959 N88-27577
Application of nondestructive testing techniques to materials testing
[AD-A195718] 24 p3381 N88-30138

ACOUSTIC PROPAGATION
Application of ray theory to propagation of low frequency noise from wind turbines
[NASA-CR-178367] 03 p0373 N88-12349
Compressor large bandwidth noise emission mechanisms
[ETN-88-91177] 05 p0646 N88-13959
The acoustic source created by turbulent flow over orifices and louvers
[REPT-97674] 06 p0776 N88-14784
Model-scale sound propagation experiment
[NASA-TM-100602] 15 p2130 N88-22709
Acoustic propagation in the low atmosphere. Experimental study and modeling by the radius method
[ISL-CO-247/86] 15 p2131 N88-22713
Study of the convergence of a finite difference scheme for acoustic propagation in the atmosphere in a parabolic approximation. Statistical calculation of the sound field in the presence of kinematic turbulence
[ONERA-RS-8/3641-PY-160-P] 17 p2394 N88-24235
The calculation of casually constrained optima in the active control of sound
[ISVR-TR-147] 17 p2395 N88-24237
Investigation of intensity and phase fluctuations of an acoustic wave after crossing thermal turbulence
[ETN-88-92542] 17 p2395 N88-24238
Linear and nonlinear acoustic wave propagation in the atmosphere
[NASA-CR-4157] 18 p2571 N88-25268
Sound propagation over uneven ground and irregular topography
[NASA-CR-182956] 20 p2849 N88-26911
Acoustic propagation in the lower atmosphere
[ISL-R-126/87] 21 p3013 N88-27878

ACOUSTIC PROPERTIES
NT ACOUSTIC IMPEDANCE
NT ACOUSTIC INSTABILITY
NT ACOUSTIC SCATTERING
NT ACOUSTIC VELOCITY
NT REVERBERATION
NT SOUND INTENSITY
First article test noise survey of the A/F32T-9 large turbo fan engine enclosed noise suppressor system, Sky Harbor IAP (International Airport), Phoenix, Arizona
[AD-A183799] 01 p0090 N88-10588
Development of a new method of measuring the characteristic impedance and complex wave number of a porous acoustic material
[AD-A185038] 05 p0646 N88-13957
Aerodynamic and acoustic characteristics of an advanced propeller under take-off and landing conditions
[NAL-TR-935] 09 p1243 N88-17453
The temporal and spatial acoustical response of a point-driven fluid-loaded plate
[AD-A188504] 12 p1636 N88-19794
Low frequency ocean ambient noise: Measurements and theory
[AD-A191188] 16 p2237 N88-23362
Acoustic characteristics of 1/20-scale model helicopter rotors
[NASA-CR-177355] 16 p2265 N88-23548
Remote sensing of acoustic properties of shallow water sediments: A review
[AD-A192107] 18 p2570 N88-25267
Ray scattering from a collection of ice keels
[AD-A191757] 19 p2722 N88-26163
The acoustic field scattered from some approximate pressure release materials
[AD-A194768] 23 p3278 N88-29515

ACOUSTIC RADIATION
U SOUND WAVES

ACOUSTIC SCATTERING
NT REVERBERATION
Underwater acoustic backscatter from a model of arctic ice open leads and pressure ridges
[AD-A184693] 03 p0354 N88-12234
On a boundary data operator and generalized exterior Robin problems for the Helmholtz equation
[AD-A185124] 05 p0640 N88-13915

Research on acoustical scattering, diffraction catastrophes, optics of bubbles, photoacoustics, and acoustical phase conjugation
[AD-A185785] 06 p0776 N88-14761
Acoustic scattering from composite wind-wave surfaces 3: Forward scatter intensities and spatial coherence at low and high frequencies and small grazing angles for Bubble-free regimes
[AD-A185908] 07 p0881 N88-15345
Ultrasonic testing of near-surface zones using scattered signals
[ETN-88-90813] 07 p0929 N88-15642
Acoustic backscattering from bottom sediment at normal incidence in the laboratory
[AD-A186905] 09 p1242 N88-17443
Comparison of the rough surface reflection coefficient with specularly scattered acoustic data
[AD-A187086] 09 p1242 N88-17444
Scattering of impulsive acoustic waves by a semi-infinite crack in the plane interface of a half-space and a layer
[PB88-126396] 10 p1405 N88-18377
Inversion of parabolic and paraboloidal projections
[AD-A187538] 10 p1405 N88-18380
Estimation of sea surface wave spectra using acoustic tomography
[AD-A187837] 11 p1516 N88-19057
Observations of the upper ocean using a multi-beam Doppler sonar
[AD-A188896] 12 p1649 N88-19878
Sound propagation through a turbulent atmosphere: Experimental techniques and data analysis
[AD-A188891] 12 p1688 N88-20094
Ray scattering from a collection of ice keels
[AD-A191757] 19 p2722 N88-26163
Quantitative particle characterization by scattered ultrasound 20 p2848 N88-26908
Studying materials using acoustic waves
[AD-A192234] 20 p2850 N88-26915
The covariance of scalar fields scattered by pressure-release randomly rough surfaces
[AD-A192489] 22 p3146 N88-28714
Arctic ice attenuation model study
[AD-A193382] 22 p3146 N88-28715
The acoustic field scattered from some approximate pressure release materials
[AD-A194768] 23 p3278 N88-29515
Reflection and scattering of acoustic rays computed for parabolic ice keel models
[AD-A193898] 23 p3278 N88-29517

ACOUSTIC SOUNDING
Remote acoustic sounding of ferromanganese nodules 06 p0727 N88-14471
Nonlinear acoustic parameter and its application in ultrasonic imaging 14 p1902 N88-21364
Remote sensing of temperature profiles. Performance test of PASS
[DE88-753108] 20 p2826 N88-26768

ACOUSTIC STABILITY
U FREQUENCY STABILITY

ACOUSTIC VELOCITY
Noncontact temperature measurements of hot steel bodies using an electromagnetic acoustic transducer (EMAT)
[DE88-000560] 04 p0446 N88-12765
Coupled acoustic and ocean thermodynamic model
[AD-A184357] 04 p0472 N88-12911
A modified version of the phase sensitive technique for measurements of absolute sound velocity in solids
[DE88-002303] 10 p1405 N88-18378
Ultrasonic-velocity studies of composite and heterogeneous materials
[AD-A189000] 12 p1604 N88-19595
On the possibility of high velocity deflagration front propagation by radiative energy transfer
[AD-A189022] 12 p1613 N88-19645
Target localization in an inhomogeneous medium
[AD-A190008] 15 p2130 N88-22703
Low frequency ocean ambient noise: Measurements and theory
[AD-A191188] 16 p2237 N88-23362
Operational noise data for CH-47D and AH-64 army helicopters
[AD-A191059] 18 p2570 N88-25263
Evaluation of the biot coefficients
[AD-A191643] 18 p2570 N88-25265
The high pressure sound velocity and equation of state of aqueous solutions of hydroxylammonium nitrate and triethanolammonium nitrate
[AD-A191740] 18 p2570 N88-25266
Thermophysical properties of argon
[DE88-010376] 19 p2613 N88-25509
Dynamics and stability of combustion driven self oscillations in presence of various frequencies. Extensive stability criteria
[ETN-88-92123] 20 p2771 N88-26432
Ultrasonic studies of stresses and plastic deformation in steel during tension and compression
[AD-A192308] 21 p2912 N88-27280
Metal halide optical glasses
[AD-A193794] 23 p3198 N88-29032
Calculation of non-stationary aerodynamic forces in the near sonic range
[NASA-TT-20310] 24 p3322 N88-29782

ACOUSTIC VIBRATIONS
U SOUND WAVES

ACOUSTICS
NT AEROACOUSTICS
NT GEOMETRICAL ACOUSTICS
NT MAGNETOACOUSTICS
NT PSYCHOACOUSTICS
NT UNDERWATER ACOUSTICS
Activities report of the Institute of Sound and Vibration Research
[ETN-87-90685] 01 p0090 N88-10589
Design, construction, activation, and operation of a high intensity acoustic test chamber 02 p0137 N88-10864
A digital control system for high level acoustic noise generation 02 p0138 N88-10865
Nonsteady-state vibrations in acoustic medium of elastic elliptical shell subjected to instantaneously applied uniform pressure 02 p0160 N88-11000
Evaluation of a scale-model experiment to investigate long-range acoustic propagation
[NASA-TP-2748] 02 p0230 N88-11450
A hybrid numerical technique for predicting the aerodynamic and acoustic fields of advanced turboprops
[NASA-CR-174926] 03 p0374 N88-12352
Excitation of natural oscillations of a boundary layer by an external acoustic field 04 p0425 N88-12634
Nonlinear acoustics
[AD-A184271] 04 p0488 N88-13004
Development of an acoustic echosounder for detection of lower level atmospheric turbulence
[AD-A184877] 05 p0626 N88-13831
Application of Vandermonde decomposition to directional and modal analysis of broadband transients
[AD-A185007] 05 p0646 N88-13956
Longitudinal mode combustion instabilities in air breathing engines 06 p0680 N88-14166
JPRS report: Science and technology. USSR: Physics and mathematics
[JPRS-UPM-87-008] 06 p0769 N88-14727
Dependence of acoustical characteristics of laser-induced breakdown in dielectric materials on shape of inelastic region 06 p0774 N88-14753
Acoustical phase conjugation
[PREPRINT-561] 06 p0777 N88-14768
Development of rotorcraft interior noise control concepts. Phase 2: Full scale testing, revision 1
[NASA-CR-172594-REV-1] 06 p0777 N88-14769
Study on arc sound in TIG and plasma welding processes and the possibility of its application in practice
[PB87-143947] 07 p0863 N88-15238
On the convergence of the p-version of the boundary element Galerkin method
[AD-A186198] 07 p0910 N88-15514
Solid mechanics research for quantitative non-destructive evaluation
[AD-A186599] 08 p0993 N88-16010
JPRS report: Science and technology. USSR: Physics and mathematics
[JPRS-UPM-87-010] 08 p1075 N88-16485
Recent Langley helicopter acoustics contributions 09 p1109 N88-16646
The assessment of the sound insulation requirements for a large broadcasting studio, using a scale model: Theoretical considerations
[BBC-RD-1987/20] 09 p1155 N88-16921
Qualification by analysis of IUS plume deflectors 09 p1179 N88-17063
JPRS report: Science and technology. USSR: Physics and mathematics
[JPRS-UPM-87-009] 09 p1233 N88-17395
Investigation of thermoacoustic heat transport using a thermoacoustic couple
[AD-A186889] 09 p1242 N88-17442
Acoustic backscattering from bottom sediment at normal incidence in the laboratory
[AD-A186905] 09 p1242 N88-17443
The acoustic-electric field analysis of multilayered surface acoustic wave devices
[ETN-88-91592] 09 p1242 N88-17446
Wind turbine acoustics research bibliography with selected annotation
[NASA-TM-100528] 09 p1243 N88-17450
Bearing detection in the presence of two sources of varying coherence using the complex cepstrum
[NASA-CR-181605] 09 p1243 N88-17451
Speech recognition: Acoustic-phonetic knowledge acquisition and representation
[AD-A187293] 10 p1320 N88-17893
An application of dimensionless Eigenvalues to underwater acoustic ducts
[AD-A188167] 11 p1542 N88-19219
Linear and nonlinear acoustics with nonuniform entropy in combustion chambers 12 p1607 N88-19609
The temporal and spatial acoustical response of a point-driven fluid-loaded plate
[AD-A188504] 12 p1636 N88-19794
Structural-acoustic interior noise modeling and analysis from experimental data
[PB88-141775] 12 p1687 N88-20088
Three-dimensional scattering of impulsive acoustic waves by a semi-infinite crack in the plane interface of a half space and a layer
[PB88-146998] 12 p1687 N88-20089
A study of methods to predict and measure the transmission of sound through the walls of light aircraft
[NASA-CR-182656] 12 p1687 N88-20090
Acoustic phonons, surface plasmons and surface acoustic plasmons in a superlattice and their nonreciprocal device applications
[AD-A188918] 12 p1698 N88-20163
Invariant characteristics of acoustic field in stratified ocean 13 p1788 N88-20698
Survey of acoustic techniques for monitoring El Nino
[PB88-157615] 13 p1804 N88-20783
Flow/acoustic interaction in duct inflow
[AD-A189264] 13 p1833 N88-20967
Mixing fuel particles for space combustion research using acoustics
[NASA-TM-100295] 14 p1872 N88-21186
Additional peak of light scattering by sound under conditions of acoustic instability 14 p1968 N88-21752
Nondestructive evaluation by acousto-ultrasonics 15 p2082 N88-22412
Flaw characterization in structural ceramics using scanning laser acoustic microscopy 15 p2082 N88-22415
Nondestructive evaluation of sintered ceramics 15 p2083 N88-22416
Mechanisms mediating perception of complex acoustic patterns
[AD-A189765] 15 p2102 N88-22520
Mechanisms mediating the perception of complex acoustic patterns
[AD-A190112] 15 p2130 N88-22705
Space time processing, environmental-acoustic effects
[AD-A190764] 15 p2130 N88-22708
Thin superconducting film characterization by surface acoustic waves
[AD-A190417] 15 p2143 N88-22791
Applications research studies of microtubules
[AD-A190855] 16 p2182 N88-23005
Utilization of dense packed planar acoustic echosounders to identify turbulence structure in the lowest levels of the atmosphere
[AD-A191006] 16 p2233 N88-23335
Advanced turboprop aircraft flyover noise: Annoyance to counter-rotating-propeller configurations with an equal number of blades on each rotor, preliminary results
[NASA-TM-100612] 16 p2265 N88-23547
Control of combustion and acoustically coupled fluid dynamic instabilities 17 p2318 N88-23843
The exact calculation of quadrupole sources for some incompressible flows
[NASA-TM-100623] 17 p2395 N88-24240
Acoustic convective system
[NASA-CASE-NPO-17278-1-CU] 18 p2498 N88-24818
Identification and acoustic characterization of seamounts
[AD-A192204] 18 p2548 N88-25123
Remote sensing of acoustic properties of shallow water sediments: A review
[AD-A192107] 18 p2570 N88-25267
Effects of Mach number on acoustic-vortex interactions in a ramjet 19 p2625 N88-25573
Acousto-ultrasonic input-output characterization of unidirectional fiber composite plate by P waves
[NASA-CR-4162] 19 p2678 N88-25923
Local free-space mapping and path guidance for mobile robots
[AD-A192970] 20 p2810 N88-26674
Acoustic diffraction by an absorbing finite strip in a moving fluid
[PB88-191382] 20 p2849 N88-26912
An analysis of the efficiency and directivity of the sound generated by a moving laser source
[AD-A192220] 20 p2849 N88-26914
Studying materials using acoustic waves
[AD-A192234] 20 p2850 N88-26915

Robust methods for array signal processing
[AD-A192854] 21 p3012 N88-27871
Publications on acoustics research at the Langley Research Center during 1980-1986
[NASA-TM-100590] 21 p3013 N88-27881
Development of a nitrile rubber for dynamic damping
[AD-A194060] 22 p3058 N88-28145
Theory of acoustoplasticity and ultrasonic measurements of residual stresses
22 p3067 N88-28326
Computer-controlled measurements of nonlinear standing waves
[AD-A193840] 22 p3147 N88-28717
Large aperture multi-dimensional laser radar testbed
[AD-A193447] 23 p3218 N88-29155
Asymptotic modal analysis and statistical energy analysis
[NASA-CR-183077] 23 p3278 N88-29514
ASKA-acoustics: Theory and applications --- vibro acoustics
[FFA-TN-1988-13] 23 p3279 N88-29519
Overview of computational vibro acoustics. State of the art and future development
[FFA-TN-1988-17] 23 p3279 N88-29521

ACOUSTO-OPTICS
Discussion on the modelling and processing of signals from an acousto-optic spectrum analyzer
[AD-A185639] 06 p0694 N88-14257
Research on acoustical scattering, diffraction catastrophes, optics of bubbles, photoacoustics, and acoustical phase conjugation
[AD-A185785] 06 p0776 N88-14761
A continued study of optical sound generation and amplification
[AD-A188362] 12 p1691 N88-20116
Bathymetric hazard survey test
[AD-A189150] 13 p1803 N88-20775
Solid-state ring laser with acoustooptical phase nonreciprocity of opposing waves
14 p1970 N88-21761
The effect of internal relaxation on optoacoustic conversion in liquids
[AD-A191307] 16 p2176 N88-22970
Fast acting optical beam detection and deflection system
[AD-A192161] 18 p2521 N88-24954
A high dynamic range acousto-optic image correlator for real-time pattern recognition
[DE88-007933] 19 p2726 N88-26191
Studies of coherent beam processing concepts, phase 1
[AD-A194749] 22 p3083 N88-28306
Approximate and numerical methods in acousto-optics. Part 1: Normal incidence of the light
[AD-A194294] 22 p3152 N88-28755
Acoustic-optical detector of gravitational waves based on high-quality crystals
[DE88-702459] 23 p3232 N88-29232
Acoustooptic processing of two-dimensional signals using temporal and spatial integration
[AD-A194803] 24 p3359 N88-29999

ACQUISITION
NT DATA ACQUISITION
NT TARGET ACQUISITION
Speech recognition: Acoustic-phonetic knowledge acquisition and representation
[AD-A185897] 07 p0840 N88-15097
Systems integrated human engineering on the Navy's rapid acquisition of manufactured parts/test and integration facility 09 p1206 N88-17226
Avionics acquisition, trends and future approaches
12 p1702 N88-20184
Performance of a rapid carrier acquisition circuit for satellite ground terminal modems
[RSRE-TEST-REPORT-87/CC3/2]
22 p3071 N88-28227
Artificial intelligence software acquisition program, volume 2
[AD-A194239] 22 p3141 N88-28680
Estimating reliability with discrete growth models
[AD-A193845] 22 p3143 N88-28692
Artificial intelligence software acquisition program, volume 1
[AD-A194104] 23 p3267 N88-29447
Scattering impulse response synthesis using random noise illumination: Initial concept evaluation
[AD-A195086] 24 p3364 N88-30034

ACRYLATES
Interactions in miscible polymer blends
[AD-A193824] 22 p3058 N88-28144
Dissolution rates of polymers and copolymers based on methyl, ethyl and butyl methacrylate
[AD-A194713] 23 p3197 N88-29027

ACRYLIC ACID
Polyacrylic acid electrolyte-modified zinc phosphate conversion coatings for corrosion protection of steel
[DE88-004878] 19 p2617 N88-25527

ACRYLIC RESINS
High-molecular compounds (selected articles)
[AD-A184668] 03 p0293 N88-11842
Polymer material for heat sensors
06 p0676 N88-14142
Group contribution analysis of the damping behavior of homopolymers, statistical copolymers and interpenetrating polymer networks based on acrylic, vinyl and styrenic mers
[AD-A185904] 07 p0836 N88-15070
The adhesive bonding of thermoplastic composites
[AD-A190994] 16 p2173 N88-22953
Modification of polymers by photografting processes
17 p2323 N88-23871
Polyacrylic acid electrolyte-modified zinc phosphate conversion coatings for corrosion protection of steel
[DE88-004878] 19 p2617 N88-25527
Interactions in miscible polymer blends
[AD-A193824] 22 p3058 N88-28144

ACRYLONITRILES
Interfacial shear strength of pitch and high strain pan fibers in an epoxy matrix
[AD-A185966] 07 p0826 N88-15011
Method of obtaining of fire resistant polyacrylonitrile fiber or cloth from it
[AD-A185941] 07 p0836 N88-15071

ACTINIDE SERIES
NT LAWRENCIUM
NT NEPTUNIUM
NT PLUTONIUM ISOTOPES
NT PLUTONIUM 238
NT THORIUM
NT URANIUM
NT URANIUM ISOTOPES
NT URANIUM 238

ACTINIDE SERIES COMPOUNDS
NT CALIFORNIUM COMPOUNDS
NT URANIUM COMPOUNDS
NT URANIUM FLUORIDES
Bulk superconductivity in La2CuO4
[DE88-002509] 09 p1254 N88-17516

ACTINOMETERS
NT ADVANCED VERY HIGH RESOLUTION RADIOMETER
NT DICKE RADIOMETERS
NT INFRARED DETECTORS
NT INFRARED RADIOMETERS
NT INFRARED SCANNERS
NT INFRARED SPECTROMETERS
NT INFRARED SPECTROPHOTOMETERS
NT MICROWAVE RADIOMETERS
NT RADIOMETERS
NT SOLAR SPECTROMETERS
NT SPECTROHELIOGRAPHS
NT SPECTROPHOTOMETERS
NT SPECTRORADIOMETERS
NT TOTAL OZONE MAPPING SPECTROMETER
NT ULTRAVIOLET SPECTROMETERS
NT ULTRAVIOLET SPECTROPHOTOMETERS

ACTIVATION
Oxide-bound transition metal complexes for methane activation
[PB88-169719] 14 p1887 N88-21277
Determination of Tafel constants in nonlinear polarization curves
[AD-A192335] 21 p2912 N88-27282
The design of methane activation catalysts
[DE88-002265] 23 p3199 N88-29043

ACTIVATION (BIOLOGY)
Influence of general vertical vibration on relationships between mediators in various segments of brain
06 p0751 N88-14613
Toward a mathematical formalism of performance, task difficulty, and activation 16 p2239 N88-23372
Effect of microgravity on lymphocyte activation --- Spacelab D1 mission 22 p3061 N88-28163

ACTIVATION ANALYSIS
NT NEUTRON ACTIVATION ANALYSIS

ACTIVATION ENERGY
Flammability limits in cocurrent smoldering combustion
[DE87-014102] 03 p0284 N88-11785
Precipitation in alumina-rich spinel: A transformation-toughened ceramic single crystal
[DE87-012380] 06 p0785 N88-14815
Insights into the mechanisms of chemical reactions: Reaction paths for chemical reactions
[DE88-003041] 10 p1297 N88-17755
Diffusion studies in amorphous NiZr alloys
[DE88-003009] 10 p1301 N88-17781
Novel catalysts for methane activation
[DE88-003637] 13 p1738 N88-20390
Kinetics of polymer decomposition
[DE88-005500] 13 p1749 N88-20460
Dissolution rates of polymers and copolymers based on methyl, ethyl and butyl methacrylate
[AD-A194713] 23 p3197 N88-29027

ACTIVE CONTROL
Flutter suppression and gust load alleviation. Part 1: Results of phase 1 to 3. Part 2: Description of the Garteur model
[MBB/LKE-292/S/PUB/191] 01 p0007 N88-10038
Augmenting the control of a flexible manipulator with passive mechanical damping 01 p0055 N88-10350
Active minimisation of acoustic fields. A review of research into the active control of sound undertaken at ISVR from 1983 to 1986
[ISVR-TR-146] 01 p0091 N88-10593
A preliminary investigation into the feasibility of implementing a direct sideforce control system on the Astra Hawk by means of an active control surface --- aircraft control
[ETN-87-90924] 02 p0126 N88-10795
Investigation of control law for active flutter suppression
[NASA-TT-20126] 02 p0130 N88-10818
Active control of helicopter vibration using multiloop self-adaptive control 03 p0264 N88-11660
Minimisation of helicopter vibration through active control of structural response 03 p0264 N88-11662
Modeling and control of large flexible vehicles in the atmosphere and space
[AD-A185368] 05 p0555 N88-13377
Cartesian path control of a two-degree-of-freedom robot manipulator
[NASA-CR-182331] 05 p0639 N88-13908
Design verification and fabrication of active control systems for the DAST ARW-2 high aspect ratio wing, part 1
[NASA-CR-177959-PT-1] 06 p0669 N88-14101
Design verification and fabrication of active control systems for the DAST ARW-2 high aspect ratio wing. Part 2: Appendices
[NASA-CR-177959-PT-2] 06 p0669 N88-14102
Active control of flexural vibrations in beams
06 p0794 N88-14866
Handling qualities of a wide-body transport airplane utilizing Pitch Active Control Systems (PACS) for relaxed static stability application
[NASA-TP-2482] 07 p0821 N88-14987
Active control of jet flowfields
[AD-A186736] 08 p0989 N88-15989
Analytical study of the effect of early warning on optimal shock isolation 08 p0998 N88-16047
Sensitivity of active vibration control to structural changes and model reduction 10 p1284 N88-17683
Active control technology with adaptive control concept in the aircraft construction
[MBB/LKE-294/S/PUB/295] 10 p1313 N88-17845
La Recherche Aerospatiale, bimonthly bulletin, number 1987-2, 237/March-April
[ESA-TT-1074] 11 p1433 N88-18550
An application of active surface heating for augmenting lift and reducing drag of an airfoil
[NASA-TM-100563] 11 p1436 N88-18570
Structural design requirements for aircraft incorporating active control technology 12 p1580 N88-19453
Active vibration control of a cantilevered beam with three elastic coordinates
[AD-A188824] 12 p1636 N88-19797
Control augmented structural synthesis
[NASA-CR-4132] 13 p1721 N88-20290
Practical considerations for structural control: System uncertainty, system time delay and truncation of small control forces
[PB88-163738] 14 p1933 N88-21528
Sensitivity of control-augmented structure obtained by a system decomposition method
[NASA-TM-100535] 14 p1954 N88-21647
Instrumentation to provide an active control capability for distributed parameter systems
[AD-A190043] 15 p2076 N88-22375
Active control and system identification of rotordynamic structure 16 p2218 N88-23230
Integrated Application of Active Controls (IAAC) technology to an advanced subsonic transport project: Program review
[NASA-CR-3880] 17 p2301 N88-23763
Vibration and control of flexible rotor supported by magnetic bearings
[NASA-TM-100688] 17 p2345 N88-23977
The calculation of casually constrained optima in the active control of sound
[ISVR-TR-147] 17 p2395 N88-24237
Low authority control of large space structures using a constrained threshold control formulation
18 p2472 N88-24667

Experimental study of active vibration control
[AD-A191454] 18 p2526 N88-24989
Vibration protection of inelastic structures by means of active and passive control 18 p2528 N88-25001
Analysis of a closed-kinematic chain robot manipulator
[NASA-CR-183031] 18 p2561 N88-25206
Active control of 2-D instability waves on an axisymmetric body
[AD-A191578] 19 p2663 N88-25835
Active phase compensation system for fiber optic holography
[NASA-TM-101295] 20 p2805 N88-26641
Direct-solution techniques for viscous flows and their control
[AD-A194775] 23 p3211 N88-29114
A comparison of simple analytical models for representing propeller aircraft structural and acoustic responses
[ISVR-TR-153] 23 p3279 N88-29523

ACTIVE GALACTIC NUCLEI
Image sharpening observations of active galactic nuclei 01 p0098 N88-10643
Spherical models of QSO/AGN emission line clouds 06 p0806 N88-14921
The radio structure of active nuclei in edge-on spiral and Seyfert galaxies 09 p1264 N88-17576
Prediction and analysis of basic gravitational microlensing phenomena 11 p1550 N88-19272
Speckle imaging of active galactic nuclei: NGC 1068 and NGC 4151 18 p2592 N88-25407
Activities in astrophysics
[INPE-4582-PRE/1316] 24 p3456 N88-30570

ACTIVE GALAXIES
NT RADIO GALAXIES
NT SEYFERT GALAXIES
The imaging of extra-galactic low-energy gamma-ray sources prospects, techniques, and instrumentation
[NASA-CR-182536] 12 p1713 N88-20251
Variable spectra of active galaxies
[NASA-CR-182694] 13 p1853 N88-21091

ACTIVE GLACIERS
U GLACIERS

ACTIVE MAGNETO PARTICLE TRACER EXPLORERS
U AMPTE (SATELLITES)

ACTIVE VOLCANOES
U VOLCANOES

ACTIVITY (BIOLOGY)
Biophysical applications of solid state and tritium NMR
[DE88-005328] 13 p1808 N88-20806
Biological processes in the water column of the South Atlantic bight: Zooplankton responses
[DE88-004811] 14 p1951 N88-21630
Methods and possibilities of biological action spectroscopy 16 p2272 N88-23597

ACTIVITY CYCLES (BIOLOGY)
Pharmacological resetting of the Circadian sleep-wake cycle
[AD-A186194] 07 p0889 N88-15385
Biological rhythms, sleep, and wakefulness in prolonged confinement 19 p2696 N88-26022

ACTS
Communication satellite technology trends 01 p0015 N88-10088
An examination of the Advanced Communications Technology Satellite (ACTS) and its application to the Defense Data Network (DDN)
[AD-A184003] 03 p0276 N88-11742
A laser communication experiment utilizing the ACT satellite and an airborne laser transceiver
[NASA-TM-100792] 11 p1492 N88-18910
Space communication link propagation data for selected cities within the multiple beam and steerable antenna coverage areas of the advanced communications technology satellite
[NASA-TM-100861] 16 p2191 N88-23070
Service offerings and interfaces for the ACTS network of Earth stations
[NASA-TM-100809] 18 p2471 N88-24663
Experiments applications guide: Advanced Communications Technology Satellite (ACTS)
[NASA-TM-100265] 22 p3048 N88-28082
A statistical rain attenuation prediction model with application to the advanced communication technology satellite project. 1: Theoretical development and application to yearly predictions for selected cities in the United States
[NASA-CR-179498] 23 p3205 N88-29077

ACTUATION
Wind-tunnel investigation of actuated forebody strakes for yaw control at high angles of attack 17 p2299 N88-23754

ACTUATOR DISKS
Calculation of the damage of highly loaded gas turbine disks under real flight conditions
[ETN-87-90416] 01 p0007 N88-10036
Linear and nonlinear theories of flow through an actuator disk --- windpowered pumps
[R-803-A] 03 p0316 N88-11995

ACTUATORS
Minimisation of helicopter vibration through active control of structural response 03 p0264 N88-11662
On the root locus method applied to flexural vibration control systems 03 p0320 N88-12022
An evaluation plan of bus architectures and protocols using the NASA Ames intelligent redundant actuation system
[NASA-CR-177458] 04 p0398 N88-12482
Design of feedback control systems for stable plants with saturating actuators
[NASA-CR-182613] 12 p1681 N88-20050
Design of a linear actuator and breadboard test result --- far IR telescope 14 p1877 N88-21217
Photoelastic model tests of the Dornier linear actuator --- far IR telescope 14 p1877 N88-21218
Fine adjustment mechanism for FIRST 14 p1878 N88-21219
A joint actuator design for a robotic manipulator 14 p1879 N88-21232
The 22nd Aerospace Mechanisms Symposium
[NASA-CP-2506] 14 p1924 N88-21468
The 15-meter diameter hoop/column antenna surface control actuator system 14 p1924 N88-21469
High output paraffin actuators: Utilization in aerospace mechanisms 14 p1924 N88-21470
Servo-actuator control for sampled-data feedback disturbance rejection --- helicopters
[ESA-TT-1002] 16 p2163 N88-22903
Evaluation of a high-torque backlash-free roller actuator 16 p2219 N88-23239
The LDCM actuator for vibration suppression
[NASA-CR-182898] 17 p2335 N88-23940
Linear force device
[NASA-CASE-MSC-20549-2] 18 p2516 N88-24927
Toggle release
[NASA-CASE-MSC-21354-1] 18 p2523 N88-24969
SRB/SLEEC (Solid Rocket Booster/Shingle Lap Extendible Exit Cone) feasibility study, volume 2. Appendix A: Design study for a SLEEC actuation system
[NASA-CR-178974] 23 p3187 N88-28965
Semiconductor bridge (SCB) igniter studies. 1: Comparison of SCB and hot-wire pyrotechnic actuators
[DE88-008802] 23 p3200 N88-29046
Thermocouple for heating and cooling of memory metal actuators
[NASA-CASE-NPO-17068-1-CU] 23 p3217 N88-29151
Feasibility study of a microprocessor controlled actuator test mechanism
[AD-A194654] 23 p3249 N88-29337
Sensor and actuator selection for large space structure control
[AD-A194912] 24 p3333 N88-29842
A standard architecture for controlling robots
[AD-A195929] 24 p3423 N88-30371

ACUITY
NT VISUAL ACUITY

ADA (PROGRAMMING LANGUAGE)
Data Management Working Group report 01 p0016 N88-10097
Petri nets as a support to symbolic execution of concurrent Ada programs
[REPT-87-007] 01 p0082 N88-10529
Praxis: The programming language: An advanced overview
[DE87-014319] 02 p0220 N88-11388
ADAMEASURE: An implementation of the Halstead and Henry metrics
[AD-A184005] 03 p0365 N88-12299
PROVER: A first-order logic system in Ada
[DE88-000220] 04 p0479 N88-12951
A review and analysis of Fortran 8x
[DE88-001320] 04 p0479 N88-12955
An Ada graphical tool to support software development
[DE87-014854] 05 p0636 N88-13891
A plan for collecting ada software development cost, schedule and environment data
[AD-A185905] 07 p0902 N88-15460
Version description document for the Ada compiler validation capability (version 1.9) (for microcomputer)
[AD-A186390] 07 p0903 N88-15471
Can space station software be specified through Ada?
07 p0925 N88-15622
Ada (trade name) compiler validation summary report. Systems designers' PLC SD Ada-plus VAX/VMS x MC68020. Version 2B.00. Host: VAX 8600. Target: Motorola MC68020. Completion of on-site testing
[AD-A186571] 08 p1053 N88-16356
The Ada compiler: On the design and implementation of an Ada compiler
[ETN-88-91594] 09 p1215 N88-17284
Rationale for the design of the Ada (tradename) programming language
[AD-A187106] 09 p1217 N88-17297
Implementation of elementary functions in Ada
[CWI-NM-R8709] 09 p1218 N88-17303
Design and implementation of elementary functions in Ada
[CWI-NM-R8710] 09 p1218 N88-17304
Description of a limited VAX-Ada program support environment developed within UDP division version 1.0
[ARE-TM(UDP)-87103] 09 p1219 N88-17308
Contributions to a numerical library in Ada
[NPL-DITC-98/87] 09 p1219 N88-17309
Occam/Ada parallel programming system
[ISAL-IDI1-87-11] 09 p1219 N88-17312
The implementation and use of Ada on distributed systems with high reliability requirements
[NASA-CR-182481] 09 p1221 N88-17326
Factors causing unexpected variations in Ada benchmarks
[AD-A187231] 10 p1388 N88-18291
VAXELN experimentation: Programming a real-time clock and interrupt handling using VAXELN Ada 1.1
[AD-A188100] 11 p1525 N88-19107
Applicability of Ada (trademark) tasking for avionics executives
[AD-A188827] 12 p1578 N88-19445
Design method for Ada programs
[ESA-CR(P)-2528] 14 p1958 N88-21671
Ada tasking in Ten15
[RSRE-MEMO-4074] 14 p1958 N88-21676
Examination of the effects of using Ada (trade name) in flight control software
[AD-A189679] 14 p1959 N88-21683
Ada (Trademark) compiler validation summary report. ALSYS: AlsyCOMP-013, V2.0 HOST: IBM PC AT. Target: IBM 370 3084Q
[AD-A189640] 15 p2106 N88-22548
Ada user library
[FOA-C-20657-2.7] 16 p2246 N88-23418
Proposal for standard mathematical packages in Ada
[CWI-NM-R8718] 16 p2249 N88-23439
Simulation: A simulation system in Ada
[FOA-A-20043-2.7] 17 p2385 N88-24176
Dialog design: General requirements and analysis of an Ada system --- user interface design
[FOA-C-20691-2.7] 17 p2385 N88-24177
New York TRACON demonstration of program recoding requirements analysis document
[DOT/FAA/CT-87/34] 18 p2462 N88-24622
Beyond Ada: Generating Ada code from equational specifications
[AD-A191866] 18 p2557 N88-25176
Portable implementation of a generic exponential function in Ada
[DE88-007699] 19 p2715 N88-26117
Ada (trade name) compiler validation summary report: Verdix Corporation VAda-010-03315, version 5.5 MicroVAX 2 host ISBC 386/20P Intel target
[AD-A193226] 21 p2997 N88-27774
Ada (trade name) compiler validation summary report: Verdix corporation VAda-010-13125, version 5.41 Sun Microsystems Sun-3/160 host microbar GPC68020 target
[AD-A193415] 21 p2997 N88-27777
Ada (trade name) compiler validation summary report: Verdix Corporation VAda-010-0101, version 5.41 VAX-11/750
[AD-A193414] 22 p3136 N88-28645
Ada (trade name) compiler validation summary report: Verdix Corporation VAda-010-03205, version 5.42 MicroVAX 2 host and national DB32000 (NS32032 target
[AD-A193485] 23 p3247 N88-29326
Level 1 Ada/SQL (Structured Query Language) database language interface user's guide
[AD-A194480] 23 p3249 N88-29335

ADAPTATION
NT ACCLIMATIZATION
NT ALTITUDE ACCLIMATIZATION
NT COLD ACCLIMATIZATION
NT DARK ADAPTATION
NT HEAT ACCLIMATIZATION
NT LIGHT ADAPTATION
System adaptivity and the modelling of stereotypes --- human-computer interaction
[NPL-DITC-91/87] 01 p0077 N88-10494
Wall interference tests of a CAST 10-2/DOA 2 airfoil in an adaptive-wall test section
[NASA-TM-4015] 02 p0122 N88-10772
The role of adaptive supplemental visual cuing in flight simulation
[AD-A185932] 07 p0822 N88-14992
Long-term adaptation of the otolith organs 07 p0886 N88-15375

Physiological and immunological aspects of human adaptation to temperature elevation in a closed environment 07 p0895 N88-15424
Adaptive finite difference methods in fluid dynamics 08 p0985 N88-15958
General biological character of adaptive capacity of mammalian metabolism in response to diverse and extreme environmental factors 08 p1047 N88-16324
Group adaptation and individual adjustment in antarctica: A summary of recent research [AD-A186605] 08 p1051 N88-16347
Adaptive finite element methods for parabolic systems in one- and two-space dimensions [AD-A186534] 08 p1073 N88-16475
Brain potentials and personality: A new look at stress susceptibility [AD-A186931] 09 p1199 N88-17189
Physiological and ecological implications of coupled heat- and water-transport mechanisms of endotherms and vegetation [DE88-004170] 10 p1352 N88-18081
Polar worker adaptability to Antarctic high altitudes 10 p1366 N88-18165
NASA Workshop on Biological Adaptation [NASA-TM-89468] 10 p1368 N88-18174
Analysis and synthesis of adaptive neural elements [AD-A187047] 10 p1395 N88-18316
Human adaptation to various hypercapnic conditions in relation to salivary electrolyte dynamics and renal function 12 p1664 N88-19977
A multiple model adaptive tracking algorithm against airborne targets [AD-A190619] 15 p2057 N88-22263
Adaptive neural network architecture [AD-A190114] 15 p2104 N88-22533
Implementation of a distributed adaptive routing algorithm on the Intel iPSC (Intel Personal Super-Computer) [AD-A189849] 15 p2109 N88-22567
Development of adaptive grid schemes based on Poisson grid generators [AD-A190953] 16 p2262 N88-23528
Adaptive segmentation evaluation [AD-A190965] 16 p2274 N88-23609
Adaptive local grid refinement in computational fluid mechanics [AD-A192215] 18 p2510 N88-24890
Method of assessing changes in biorhythmological structure of human physiological functions 19 p2706 N88-26088
The human element in space: Lessons from Antarctica [AD-A193440] 21 p2988 N88-27741
Adaptive identification by systolic arrays [AD-A193532] 23 p3266 N88-29444
An adaptive overlapping local grid refinement method for two-dimensional parabolic systems [AD-A193560] 23 p3271 N88-29464
On adaptive cell-averaging CFAR (Constant False-Alarm Rate) radar signal detection [AD-A196286] 24 p3360 N88-30009

ADAPTIVE CONTROL
NT ACTIVE CONTROL
NT LEARNING MACHINES
NT MODEL REFERENCE ADAPTIVE CONTROL
NT SELF ADAPTIVE CONTROL SYSTEMS

A method for the calculation of transonic flows for the control of adaptive wind tunnels [ETN-87-90411] 01 p0003 N88-10015
Model adaptation and imbalance compensation in rotors with active magnetic bearings [ETN-87-90440] 01 p0056 N88-10361
Adaptive control of hydraulic devices [FB-1/85] 01 p0084 N88-10543
Improvements to the adaptive maneuvering logic program [NASA-CR-3985] 03 p0262 N88-11648
Minimisation of helicopter vibration through active control of structural response 03 p0264 N88-11662
Adaptive control of Large Space Structure (LSS) [ISAS-R-621] 03 p0276 N88-11740
Correction of inertial navigation system drift errors for an autonomous land vehicle using optical radar terrain data [AD-A184973] 05 p0544 N88-13311
A Multipurpose Adaptive Controller (MAC) for real time digital regulation [REPT-87-028] 06 p0762 N88-14673
Dynamics, control and sensor issues pertinent to robotic hands for the EVA retriever system 06 p0796 N88-14876
Pulsed plasma arc welding process with double closed-loop adaptive penetration control system [PB87-143780] 07 p0863 N88-15236
Solid modelling for the manipulative robot arm (power) and adaptive vision control for space station missions 08 p1061 N88-16409
Adaptive proximate time-optimal servomechanisms 09 p1175 N88-17043
Real-time artificial intelligence issues in the development of the adaptive tactical navigator 09 p1211 N88-17260
Systolic array adaptive beamforming [AD-A187496] 10 p1385 N88-18269
Adaptive control of a manipulator with a flexible link [NASA-CR-181637] 11 p1476 N88-18807
An evaluation in a modern wind tunnel of the transonic adaptive wall adjustment strategy developed by NPL in the 1940's [NASA-CR-181623] 12 p1575 N88-19417
Speed control of a missile with throttleable ducted rocket propulsion 12 p1597 N88-19561
A wind tunnel model with dynamic control [BU-352] 13 p1724 N88-20310
Estimation-correlation, modeling, and identification in adaptive array processors [AD-A189130] 13 p1757 N88-20512
Adaptive algorithms for HF antenna arrays [AD-A189329] 13 p1761 N88-20534
Wall interference assessment and corrections for transonic adaptive wall airfoil data 14 p1863 N88-21129
Flexiwall 3 SO: A second order predictive strategy for rapid wall adjustment in two-dimensional compressible flow [NASA-CR-181662] 15 p2015 N88-22018
Model selection for the multiple model adaptive algorithm for in-flight simulation [AD-A189715] 15 p2016 N88-22022
Multivariable control law design for the AFTI/F-16 with a failed control surface using a parameter-adaptive controller [AD-A189848] 15 p2020 N88-22040
Multiple model parameter adaptive control for in-flight simulation [AD-A190568] 15 p2021 N88-22044
Optimal control and identification of space structures [AD-A190033] 15 p2025 N88-22065
Moving-bank multiple model adaptive estimation applied to flexible spacestructure control [AD-A190761] 15 p2026 N88-22071
Aerofoil testing in a self-streamlining flexible walled wind tunnel [NASA-CR-4128] 16 p2156 N88-22865
Automatic control of robot motion [AD-A191012] 16 p2215 N88-23218
Accurate positioning of long, flexible ARM's (Articulated Robotic Manipulator) 16 p2219 N88-23243
Contribution to the adaptive dynamic control of a robot manipulator [LAAS-87-350] 16 p2255 N88-23475
Genetic algorithms for adaptive real-time control in space systems 17 p2388 N88-24195
Generalized predictive control of multivariable systems [OUEL-1640/86] 17 p2391 N88-24209
An adaptive load-following control system for a space nuclear power system 17 p2406 N88-24307
Accurate multigrid solution of the Euler equations on unstructured and adaptive meshes [NASA-CR-181679] 18 p2460 N88-24608
Parameter-adaptive model-following for in-flight simulation [AD-A190567] 18 p2467 N88-24645
Kinematics, dynamics and control of a closed chain mechanism manipulator 18 p2523 N88-24967
Robust adaptive regulation without persistent excitation [NASA-TM-100571] 18 p2561 N88-25204
The experimental verification of wall movement influence coefficients for an adaptive walled test section [NASA-CR-181681] 19 p2598 N88-25439
Empty test section streamlining of the transonic self-streamlining wind tunnel fitted with new walls [NASA-CR-181680] 19 p2598 N88-25442
Adaptive residual mode filter control of distributed parameter systems for large space structure applications 19 p2719 N88-26143
Experiments in adaptive control of a very flexible one link manipulator 20 p2842 N88-26885
Asymptotically efficient adaptive allocation schemes for controlled Markov chains: Finite parameter space [AD-A192228] 20 p2846 N88-26893
An h-p adaptive finite element method for steady compressible flow 21 p2941 N88-27467
Control of free-flying space robot manipulator systems [NASA-CR-183104] 21 p2957 N88-27563
Unified multilevel adaptive finite element methods for elliptic problems [DE88-011938] 21 p3007 N88-27840
Dual adaptive control: Design principles and applications [NASA-CR-177485] 22 p3038 N88-28038
Experimental investigations for the generation of phase modes for adaptive antennas [REPT-10-87] 23 p3205 N88-29074
Adaptive computational methods for aerothermal heating analysis [NASA-CR-181635] 23 p3212 N88-29115
Motion planning with obstacles and dynamic constraints 23 p3222 N88-29175
Identification and control of time-varying flexible structures: An artificial intelligence approach 23 p3265 N88-29437
Computer-Aided-Control Engineering (CACE) primitives for robust and adaptive control systems, phase 1 [AD-A192446] 23 p3265 N88-29439
Topics in adaptive control and inference [AD-A194718] 23 p3266 N88-29443
Adaptive identification by systolic arrays [AD-A193532] 23 p3266 N88-29444
Adaptive mesh generation for viscous flows using Delaunay triangulation [NASA-CR-181699] 24 p3316 N88-29749
Supersonic wall adaptation in the rubber tube test section of the DFVLR Goettingen [IB-222-87-A-08] 24 p3330 N88-29824
Adaptive control in positioning a rigid-flexible robot arm [AD-A195194] 24 p3422 N88-30367

ADAPTIVE CONTROL SYSTEMS
U ADAPTIVE CONTROL

ADAPTIVE FILTERS
Estimation filters with adaptive scanning time for flying target tracking [ETN-87-90401] 01 p0036 N88-10232
An adaptive lattice algorithm for spectral line estimation [AD-A184970] 05 p0634 N88-13876
A generalization of order statistic filters: The alpha-trimmed linear filter [AD-A186125] 07 p0842 N88-15107
An adaptive filtering technique for removing periodic noise from modal response data [DE88-002347] 10 p1322 N88-17903
A Gram-Schmidt space-time adaptive canceller using adaptive lattice filters [AD-A189684] 14 p1959 N88-21684
Active control of 2-D instability waves on an axisymmetric body [AD-A191578] 19 p2663 N88-25835
Sidelobe level of an adaptive array using the SMI (Sampled Matrix Inversion) algorithm [AD-A193131] 21 p2932 N88-27409
CryoSQUID: A SQUID-based magnetic field sensor [AD-A194237] 23 p3239 N88-29275
Topics in adaptive control and inference [AD-A194718] 23 p3266 N88-29443

ADAPTIVE OPTICS
Performances of an Actively Stabilized Stellar Interferometer (ASSI): Faint magnitudes, low fringe contrast measurements and operationality 01 p0097 N88-10641
Wavefront error sensing [NASA-CR-181504] 03 p0321 N88-12030
Develop techniques for ion implantation of (lead-lanthanum-zirconate-titanate) for adaptive optics [DE88-000642] 05 p0650 N88-13986
Research in the optical sciences [AD-A192175] 18 p2575 N88-25297

ADDITION RESINS
NT ACRYLIC RESINS
NT VINYL COPOLYMERS

ADDITIVES
NT ADMIXTURES
NT ANTIKNOCK ADDITIVES
NT ANTIOXIDANTS
NT OIL ADDITIVES
NT PLASTICIZERS
NT PROPELLANT ADDITIVES
NT PROPELLANT BINDERS
NT SOLID ROCKET BINDERS

Effect of high-temperature annealing on the microstructure and thermoelectric properties of GaP doped SiGe [NASA-TM-100164] 01 p0029 N88-10188
The effect of additives on the reactivity of palladium surfaces for the chemisorption and hydrogenation of carbon monoxide: A surface science and catalytic study [DE87-014685] 02 p0145 N88-10909
Polymer modified binders for bituminous or asphaltic paving layers [PC-5] 02 p0153 N88-10958

Boundary lubrication. Experiments with boundary lubrication and plain bearings at +60...-60 deg C temperatures
[DE87-752869] 02 p0180 N88-11124
Slip casting and extruding shapes of rhenium with metal oxide additives. Part 2: Development of grain stabilized rhenium parts for resistojets
[NASA-CR-180851] 03 p0278 N88-11749
Mechanical properties of an acicular ferrite steel microalloyed to niobium and vanadium
[DE87-703547] 04 p0415 N88-12574
Partial substitution of vanadium by niobium in AISI H13 steel
[DE87-703548] 04 p0415 N88-12575
Analysis of free cutting brass by A.C. polarography
[PD-MT-8728] 04 p0417 N88-12587
Investigation of fuel additive effects on sooting flames
[AD-A186403] 07 p0829 N88-15026
Diagonal and off-diagonal disorder in doped quantum wells
[INPE-4255-PRE/1128] 08 p1089 N88-16556
Effects of additives on fire properties of polyethylene
[AD-A187064] 09 p1146 N88-16871
IRAC test report. Gallium doped silicon band 2: Read noise and dark current
[NASA-TM-87813] 09 p1159 N88-16945
Electron Spin Resonance (ESR) measurements on intermediate-valence Cer compounds doped with paramagnetic ions: CeOs2:Gd ion and CePd3:Mn-ion
[ETN-88-91081] 09 p1256 N88-17526
Silicon and indium doping of GaAs: Measurements of the effect of doping on mechanical behavior and relation with dislocation formation
[DE88-003862] 11 p1554 N88-19303
A review of approaches to the study of turbulence modification by means of non-Newtonian additives
[AD-A188799] 12 p1627 N88-19734
Lattice relaxation of the DX centers in Ga/sub 1-x/Al/sub x/As and of the pressure-induced deep donors in GaAs
[DE88-005452] 13 p1848 N88-21061
Development of a laboratory test for multiport injector deposits: Approaches 1 and 2
[AD-A190697] 15 p2048 N88-22203
Improved properties of SiGe/GaP alloys
[NASA-CASE-NPO-17259-1-CU] 18 p2585 N88-25358
Grain boundary structure in Ni3Al
[DE88-009164] 20 p2773 N88-26444
Alternate/modified binders for airfield pavements
[AD-A192781] 21 p2899 N88-27206
Processing and additive effects of ZrO2 on microstructure and dielectric porperties of BaTiO3 ceramics
[AD-A193126] 21 p2917 N88-27316
Relative flow rates of explosive powders
[DE88-010767] 21 p2923 N88-27350
Numerical calculations of dopent diffusion involving flashlamp heating of silicon 21 p2929 N88-27384
Influence of dispersed additives reinforcement on the wear reinforcement mechanisms of the alumina-steel couple. Macroscopic and structural aspects
[ECL-88-01] 22 p3059 N88-28148

ADDRESSING

Protection and security mechanisms in the SMITE capability computer
[RSRE-MEMO-4117] 17 p2384 N88-24167

ADDUCTS

Excimer laser-assisted deposition of GaAs, AlAs and (Al,Ga)As from Lewis acid-base adducts
[AD-A184586] 03 p0329 N88-12081

ADENOSINE TRIPHOSPHATE

Electron cytochemical detection of Ca(2)+-ATPase in protonema of moss funaria hygrometrica (H e d w.) under hypogravitation 06 p0749 N88-14602
Myosin Ca sup (2+), Mg sup (2+)-adenosine triphosphatase activity in ray myocardium following 30-day expose to 1.1 and 2.0 G 10 p1362 N88-18141

ADENOSINES

NT ADENOSINE TRIPHOSPHATE
Role of adenosine analogs and growth hormone in waking and sleep
[AD-A187897] 11 p1519 N88-19070

ADHEROMETERS

U ADHESION TESTS

ADHESION

Adhesion properties of polyelectrolyte-chemisorbed zinc phosphate conversion coatings
[DE87-012489] 01 p0029 N88-10186
Variational and nonvariational theory of frictionless adhesive contact between bodies
[REPT-87-11] 01 p0054 N88-10345
The effect of sulfur and zirconium Co-doping on the oxidation of NiCrAl
[NASA-TM-100209] 02 p0150 N88-10940
Ion plating: Fundamental processing studies and synthesis of high performance coatings
[AD-A184766] 03 p0303 N88-11908
Interfacial strength deveiopment in thermoplastic resins and fiber-reinforced thermoplastic composites
[NASA-CR-181525] 04 p0411 N88-12549
Tribological studies on high speed steel cutting tools
[DE88-002550] 07 p0864 N88-15246
Mechanical properties of steel-to-steel adhesive bonds
[PB88-111299] 08 p0971 N88-15877
Effect of peel angle on peel force
[AD-A186117] 08 p0972 N88-15878
Adhesion, friction and micromechanical properties of ceramics
[NASA-TM-100782] 10 p1305 N88-17801
Adhesion of vapour phase deposited ultra-thin polyimide films on polycrystalline silver
[AD-A187930] 10 p1306 N88-17810
Adhesion of PVD titanium coatings to beryllium substrates
[DE88-005147] 11 p1463 N88-18721
Factors affecting the sticking of insects on modified aircraft wings
[NASA-CR-182615] 12 p1575 N88-19421
Generalized Levinson's theorem and quantum sticking coefficients at O K
[AD-A189371] 12 p1699 N88-20171
Interfacial adhesion: Theory and experiment
[NASA-TM-100830] 13 p1742 N88-20417
Development of a torsion balance for adhesion measurements
[NASA-TM-100799] 13 p1748 N88-20454
Mechanical design of a ultrahigh gravity UHV facility to launch and recover a low-speed projectile tested on board KC 135 14 p1877 N88-21216
Laser enhanced adhesion of copper films to sapphire substrates
[DE88-006802] 15 p2038 N88-22144
Fracture toughness of silicon nitride-silicon nitride joints bonded with oxynitride glass
[DE88-005548] 15 p2043 N88-22172
Development of a high-temperature resistant (700 F), corrosion-preventive organic coating
[AD-A191407] 16 p2182 N88-23009
Interface characterization of Cu-Cu and Cu-Ag-Cu low temperature solid state bonds
[AD-A191015] 16 p2283 N88-23667
Adhesion between polystyrene and polymethylmethacrylate
[AD-A192050] 18 p2492 N88-24785
Environmental integrity of coating/metal interface
[AD-A192184] 18 p2492 N88-24786
The adherence of nickel oxide on nickel during high temperature oxidation
[DE88-011194] 20 p2774 N88-26450
Reducing adhesion and agglomeration within a cloud of combustible particles
[NASA-TM-100902] 20 p2788 N88-26539
An IETS (Inelastic Electron Tunneling Spectroscopy) study of surface reactions applicable to adhesion
[AD-A192274] 21 p2909 N88-27261
Improved adhesion for SiO2 particles in silica substrates using helium-ion irradiation
[DE88-008915] 21 p2920 N88-27332
Plasma treatment of polymers for improved adhesion
[DE88-011623] 21 p2921 N88-27334
Dry adhesive friction of elastomers: A study of the fundamental mechanical aspects
[ETN-88-92903] 23 p3198 N88-29036
Ultrasonic detection of diffusion and adhesion loss 24 p3354 N88-29967
Semi-microdroplet assay for cell adhesion molecules
[NASA-CR-183139] 24 p3406 N88-30274
Scanning electron microscopy study of adhesion in sea urchin blastulae
[NASA-CR-183136] 24 p3406 N88-30275

ADHESION TESTS

Study of surface treatment before bonding of light alloys
[DCQ/L-48-287/F] 06 p0682 N88-14181
Composite/metal jointing technology for vehicle weight reduction
[DE88-900228] 08 p0992 N88-16005
Mechanical design of a ultrahigh gravity UHV facility to launch and recover a low-speed projectile tested on board KC 135 14 p1877 N88-21216
The use of micromachined structures for the management of mechanical properties and adhesion of thin films 19 p2674 N88-25899
Study of surface treatments before adhesive bonding of light alloys --- aircraft industry
[ETN-88-92743] 21 p2916 N88-27308
Adhesion of hydrated silicate films
[DE88-011250] 21 p2920 N88-27333
Semi-microdroplet assay for cell adhesion molecules
[NASA-CR-183139] 24 p3406 N88-30274

ADHESIVE BONDING

Pressure sensitive adhesives
[EP-PATENT-0-183-495-A1] 01 p0026 N88-10164
Polyitaconic acid macromolecule primer for adhesive bonding and corrosion control of aluminum
[DE87-013306] 01 p0027 N88-10173
Effect of adhesive layers on impact damage and dynamic response in composite laminates 02 p0141 N88-10887
Durability (lifetime) predictions adhesively bonded structures
[AD-A184069] 03 p0335 N88-12110
Influence of bonding shop moisture on metal-honeycomb junctions bonded with ultra-thin adhesive films
[SNIAS-872-422-112] 05 p0558 N88-13399
Water disbondment characterization of organic Coating/metal substrate systems
[AD-A184847] 05 p0567 N88-13454
Computation of bonded assemblies. Elastoplastic adhesives, first part
[SNIAS-NT-18926/AQET] 05 p0569 N88-13467
First International Week of Adhesive Bonding and Assembling
[SNIAS-872-430-106] 05 p0569 N88-13468
Flexibilized copolyimide adhesives
[NASA-TM-89303] 05 p0570 N88-13474
Bending of a bonded beam as a test method for adhesive properties
[AD-A184813] 05 p0609 N88-13736
Study of surface treatment before bonding of light alloys
[DCQ/L-48-287/F] 06 p0682 N88-14181
Study of selection criteria for adhesives used in aircraft structure bonding
[ETN-88-91619] 08 p0971 N88-15875
Synthesis of high molecular weight peptide polymers and copolymers containing L-dope residues
[AD-A186462] 08 p0973 N88-15887
Composite/metal jointing technology for vehicle weight reduction
[DE88-900228] 08 p0992 N88-16005
Adhesive bond strengths on aluminium alloys as a function of surface topographies and their wetting properties
[ARE-TM(UMM)-87403] 09 p1148 N88-16880
The failure and fracture analysis of adhesive bonds
[ETN-87-90713] 09 p1181 N88-17077
A finite element analysis of adhesively bonded composite joints including geometric nonlinearity, nonlinear viscoelasticity moisture diffusion and delayed failure
[AD-A187455] 10 p1296 N88-17747
The effect on initial bond strength and durability of a Phosphoric Acid Dip (PAD) following chromic acid anodising of aluminum
[ARE-TM(UMM)-87402] 10 p1300 N88-17772
New scientific findings on the morphology of aluminum oxide layers, serving as an adhesive basis
[MBB-Z-137/86] 10 p1312 N88-17840
Theoretical analysis of adhesive fracture and crack-damage interactions 10 p1343 N88-18030
Cavitation in model elastomeric composites
[AD-A187401] 11 p1447 N88-18625
Finite element analysis of adhesively bonded composite joints including geometric nonlinearity, nonlinear viscoelasticity, moisture diffusion and delayed failure
[PB88-147822] 11 p1451 N88-18648
Shelf life degradation of selected anaerobic threadlocking adhesives at various storage temperatures
[AD-A187712] 11 p1461 N88-18711
An interdisciplinary approach to predictive modeling of structural adhesive bonding: Factors affecting the durability of titanium/epoxy bonds
[AD-A189503] 12 p1611 N88-19636
Detection of bondline delaminations in multilayer structures with lossy components
[NASA-CR-182716] 14 p1883 N88-21256
Increasing strength of graphite/epoxy bolted joints by introducing an adhesively bonded metallic insert
[FFA-TN-1987-45] 15 p2088 N88-22442
The adhesive bonding of thermoplastic composites
[AD-A190994] 16 p2173 N88-22953
A modified sulphuric acid anodising process used as a pretreatment for the adhesive bonding of aluminum alloys
[ARE-TM(UMM)-87410] 16 p2177 N88-22974
Evaluation of a thermoplastic polyimide (422) for bonding GR/PI composite
[NASA-TM-100584] 16 p2182 N88-23003
Polyitaconic acid macromolecule primer for adhesive bonding and corrosion control of aluminum 17 p2319 N88-23849

Water based primers for structural adhesive bonding of aircraft 17 p2321 N88-23862
Thermographic detection of buried debonds [AD-A192115] 18 p2475 N88-24880
Calculation of assemblies bonded with quasi-elastic adhesives [REPT-47-632/F] 18 p2493 N88-24793
Study of surface treatments before adhesive bonding of light alloys --- aircraft industry [ETN-88-92743] 21 p2916 N88-27308
Adhesion of hydrated silicate films [DE88-011250] 21 p2920 N88-27333
Chemistry of adhesion at the polyimide-metal interface [AD-A194647] 22 p3058 N88-28143
A study of the floating roller peel test for adhesives [AD-A194114] 23 p3198 N88-29034
Criteria for matrix dominated failure [AD-A196263] 24 p3341 N88-29887
Method of attaching strain gauges to various materials [NASA-CASE-LAR-13797-1] 24 p3376 N88-30108

ADHESIVES
NT PASTES
Pressure sensitive adhesives [EP-PATENT-0-183-495-A1] 01 p0026 N88-10164
Low extractable wipers for cleaning space flight hardware 02 p0137 N88-10863
Contribution to the study of composite materials and their damage [NASA-TT-20107] 02 p0143 N88-10897
Process for the production of a thermoplastic elastomer composition [EP-PATENT-0-202-782-A2] 05 p0569 N88-13465
Flexibilized copolyimide adhesives [NASA-TM-89303] 05 p0570 N88-13474
High temperature adhesive [PB87-109229] 06 p0683 N88-14186
Viscoelastic properties of EA951 adhesive: A source of creep deformations of a strongback [DE88-001581] 06 p0685 N88-14197
Effect of peel angle on peel force [AD-A186117] 08 p0972 N88-15878
Composite/metal jointing technology for vehicle weight reduction [DE88-900228] 08 p0992 N88-16005
Evaluation of high temperature structural adhesives for extended service, phase 5 [NASA-CR-178176] 09 p1149 N88-16884
Initial adhesive screening of novel polyamide-imides and their copolymers [NASA-TM-100641] 20 p2779 N88-26481
Conductivity mechanism and operating behavior of electrically conductive adhesives on the example of a power transistor [ETN-88-92355] 21 p2940 N88-27464
A study of the floating roller peel test for adhesives [AD-A194114] 23 p3198 N88-29034
Criteria for matrix dominated failure [AD-A196263] 24 p3341 N88-29887
Predicting the durability of adhesives and coatings by remote detection of hidden defects and coating-thickness irregularities: A theoretical and numerical study 24 p3355 N88-29972
Primerless RTV silicones [BDX-613-3807] 24 p3356 N88-29980

ADI METHODS
U ALTERNATING DIRECTION IMPLICIT METHODS

ADIABATIC CONDITIONS
Monte Carlo simulation of primitive atom-transfer reactions in solution [AD-A183977] 03 p0375 N88-12360
Adiabatic diesel engine component development: Reference engine for on-highway applications [NASA-CR-179531] 03 p0386 N88-12426
Adiabatic supernova expansion into the circumstellar medium [DE87-014241] 03 p0387 N88-12433
Variation of wave action: Modulations of the phase shift for strongly nonlinear dispersive waves with weak dissipation. A new adiabatic invariant involving the modulated phase shift for strongly nonlinear, slowly varying, and weakly damped oscillators. The modulated phase shift for weakly dissipated nonlinear oscillatory waves of the Korteweg-de vries type [AD-A185630] 06 p0765 N88-14702
Model for plasma equilibrium configuration evolution in a tokamak with adiabatic compression [DE88-700354] 07 p0936 N88-15684
Review of the state of the art and projected technology of low heat rejection engines [PB88-131255] 11 p1496 N88-18934
On stress collapse in adiabatic shear bands [AD-A187185] 11 p1498 N88-18942
Adiabatic representation of three-body problem in hyperspherical coordinates. Statement of the problem [DE88-701162] 15 p2126 N88-22678
Analysis for high compressible supersonic flow in converging nozzle [IPPJ-860] 16 p2157 N88-22869

ADIABATIC DEMAGNETIZATION COOLING
Research on high-specific-heat dielectrics [AD-A187248] 11 p1461 N88-18710

ADIABATIC EQUATIONS
Adiabetic formation of large-scale models of the atmosphere 14 p1935 N88-21541

ADIPOSE TISSUES
Role of body fat in the prediction of the metabolic response for immersion in cold water [AD-A186914] 09 p1198 N88-17182
Prediction of physical fitness: Estimated percent body fat using body circumferences versus weight-height measures [AD-A190233] 15 p2103 N88-22526

ADJOINTS
The adjoint process in stochastic optimal control [AD-A189720] 15 p2116 N88-22605

ADJUSTING
Method for joint adjustment of satellite and surface geodetic networks 08 p1007 N88-16105
Possibilities for on-line surge suppression by fast guide vane adjustment in axial compressors 10 p1283 N88-17674
The significance of orientation unknowns in station and net adjustments 11 p1506 N88-18994
Fine adjustment mechanism for FIRST 14 p1878 N88-21219

ADJUSTMENT
U ADJUSTING

ADMINISTRATION
U MANAGEMENT

ADMITTANCE
U ELECTRICAL IMPEDANCE

ADMIXTURES
Structure of stably stratified atmospheric surface layer in presence of heat-releasing admixture 04 p0462 N88-12856
Development of an equation of state for computation of supercompressibility factors, critical flow factors and other properties for wet, sour natural gases, synthetic gases and admixtures [PB88-202676] 20 p2798 N88-26602

ADRENAL GLAND
Effect of external electrostatic field on catecholamine secretion by rat adrenals 10 p1366 N88-18166
Hypothalamic-pituitary-adrenal responses to short duration high intensity cycle exercise [AD-A192597] 21 p2985 N88-27727

ADRENALINE
U EPINEPHRINE

ADRENERGICS
Distinctions and mechanisms of effects of epinephrine and norepinephrine on cardiac pumping function under hypokinetic conditions 07 p0891 N88-15399
Propranolol and the compensatory circulatory responses to orthostasis at high altitude [AD-A192675] 22 p3131 N88-28618

ADRIATIC SEA
Preliminary report of hydrological measurements carried out in the southern Adriatic Sea: Palma 86 campaign [PREPRINT-555] 06 p0748 N88-14597

ADSORBENTS
Characterization and fundamental studies on CuO sorbent materials to determine attrition mechanisms on substrate gamma alumina [DE88-003674] 13 p1749 N88-20456

ADSORPTION
NT CHEMISORPTION
Kinetics of CO adsorption on nickel using time resolved vibration spectroscopy [ETN-87-90615] 03 p0289 N88-11814
Study of field adsorption using pulsed-laser field ion microscopy [DE88-000310] 03 p0330 N88-12085
Characterization of catalysts with metal-support effects and of the species adsorbed on their surfaces [DE87-014636] 04 p0414 N88-12564
The structure of adsorbed sulfur and carbon on molybdenum and rhenium single crystal surfaces, and their influence on carbon monoxide and hydrocarbon chemisorption [DE88-001393] 04 p0499 N88-13073
Pure dephasing of a vibrational adbond [AD-A185222] 05 p0609 N88-13740
Extending the range of Low Energy Electron Diffraction (LEED) surface structure determination: Co-adsorbed molecules, incommensurate overlayers and alloy surface order studied by new video and electron counting LEED techniques [DE88-001401] 06 p0786 N88-14820
Coverage dependence of adsorbate-substrate bond lengths: Chlorine and caesium adsorbed on silver single crystals [PB87-125142] 06 p0788 N88-14833
Use of hydrophilic polymer coatings for control of electroosmosis and protein adsorption 07 p0925 N88-15620
Memory effects on infrared adsorbate spectra [AD-A186976] 09 p1253 N88-17512
Proceedings of the 19th DOE/NRC Airborne Waste Management and Air Cleaning Conference [NUREG/CP-0086-VOL-2] 11 p1509 N88-19019
Scanning tunneling microscopy of silver, gold, and aluminium monomers and small clusters on graphite [DE88-003871] 11 p1562 N88-19349
In-situ vibrational spectroscopy of specifically adsorbed azide on silver electrodes [AD-A188511] 12 p1605 N88-19600
Some applications of surface Raman and infrared spectroscopies to mechanistic electrochemistry involved adsorbed species [AD-A188777] 12 p1606 N88-19602
Electrosorptive detection based on double-layer capacitance for selective anion monitoring in ion chromatography. Part 1: Mercury electrodes [AD-A188780] 12 p1606 N88-19603
FTIR (Fourier Transform Infrared) and FTNMR (Fourier Transform Nuclear Magnetic Resonance) study of organophosphorus surface reactions [AD-A188337] 12 p1609 N88-19625
Electrosorptive detection of simple organic compounds in liquid chromatography [AD-A188757] 13 p1736 N88-20376
Measuring thin film properties using SAW (Surface Acoustic Wave) devices: Diffusivity and surface area [DE88-002216] 13 p1834 N88-20970
Recent progress in structure determination by LEED (Low-Energy Electron Diffraction) measure the properties of the deep donors (DX-cent) [DE88-003851] 13 p1846 N88-21048
Millimeter-wave pulse distortion by a single adsorption line simulating the terrestrial atmosphere [PB88-161237] 14 p1906 N88-21388
Mass transfer mechanisms for water adsorbed on silica gel [DE88-005993] 15 p2032 N88-22107
Molecular dynamics of materials possessing high energy content [AD-A190034] 15 p2034 N88-22118
Dilution refrigerator with non-valve adsorption system of sup 3/He circulation [DE88-700974] 15 p2050 N88-22209
Theory of the dissociation dynamics of small molecules on metal surfaces: Finite temperature studies [DE88-006495] 15 p2132 N88-22716
Anomalies in the heat-capacity signatures of submonolayer adsorbates with attractive lateral interactions [AD-A190736] 15 p2147 N88-22817
UV-Laser reactions of molecular adsorbates [AD-A190796] 16 p2212 N88-23201
Preferential surface adsorption in miscible blends of polystyrene and poly(vinyl methyl ether) [AD-A191451] 18 p2490 N88-24769
The electrokinetic behavior of calcium oxalate monohydrate in macromolecular solutions [NASA-TM-101144] 18 p2493 N88-24791
Heat pump augmented radiator for low-temperature space applications [DE88-008369] 20 p2765 N88-26393
Fundamental optical studies of competitive adsorption and thin film phenomena [DE88-008780] 20 p2875 N88-27068
Theory of the dissociation dynamics of small molecules on metal surfaces: Finite temperature studies [DE88-007763] 21 p3013 N88-27882
Modification of YBa2Cu3O(7-x) ceramics by adsorbed water and other gases [DE88-011518] 22 p3057 N88-28140
Correlations between wettability and structure in monolayers of alkanethiols adsorbed on gold [AD-A194348] 23 p3191 N88-28991

ADSORPTIVITY
Coadsorption of H2O and CO2 on the Martian surface 23 p3307 N88-29702

ADVANCED COMMUNICATIONS TECHNOLOGY SAT
U ACTS

ADVANCED VERY HIGH RESOLUTION RADIOMETER
AVHRR/HIRS (Advanced Very High Resolution Radiometer/High Resolution Infra-Red Sounder) operational method for satellite based sea surface temperature determination [PB88-107594] 06 p0708 N88-14340

Sea surface current estimates off central California as derived from enhanced AVHRR (Advanced Very High Resolution Radiometer) infrared images
[AD-A186867] 09 p1194 N88-17155
General determination of Earth surface type and cloud amount using multispectral AVHRR data
[NOAA-TR-NESDIS-39] 11 p1506 N88-18997
Pre-launch calibration of channels 1 and 2 of the advanced very high resolution radiometer
[PB88-157169] 14 p1913 N88-21427
The absolute radiometric calibration of the advanced very high resolution radiometer
[NASA-CR-182755] 14 p1941 N88-21584
Calibration and processing of AVHRR data for temperature estimation
[INPE-4493-PRE/1257] 15 p2095 N88-22485
Navigation system from AVHRR data from NOAA series satellites 17 p2359 N88-24054
DMSP-SSM/1 NASA algorithm validation using primarily LANDSAT and secondarily DMSP and/or AVHRR visible and thermal infrared satellite imagery
[NASA-CR-182979] 18 p2532 N88-25024
An objective technique for Arctic cloud analysis using multispectral AVHRR (Advanced Very High Resolution Radiometer) satellite imagery
[AD-A194732] 23 p3235 N88-29250

ADVANCED X RAY ASTROPHYSICS FACILITY
U X RAY ASTROPHYSICS FACILITY

ADVANCING GLACIERS
U GLACIERS

ADVECTION
A study of numerical methods for hyperbolic conservation laws with stiff source terms
[NASA-TM-100075] 10 p1399 N88-18343
Coherent structure-reflective turbulent viscous flow modeling
[AD-A188339] 13 p1765 N88-20556
Open cell associated with warm advection 17 p2351 N88-24010
A zoomable and adaptable hidden fine-mesh approach to solving advection-dispersion equations
[DE88-006174] 21 p3004 N88-27816

AE-C SATELLITE
U EXPLORER 51 SATELLITE

AE-D SATELLITE
U EXPLORER 54 SATELLITE

AE-E SATELLITE
U EXPLORER 55 SATELLITE

AERIAL EXPLOSIONS
Australian structures response evaluation: Ground shock and air blast measurements for site investigation survey
[MRL-TN-526] 20 p2813 N88-26685

AERIAL IMAGERY
U AERIAL PHOTOGRAPHY

AERIAL PHOTOGRAPHY
Matching segments from a map and an aerial image using relaxation techniques
[SNIAS-872-422-103] 05 p0620 N88-13809
Application of remote sensing to agricultural field trials
[ISBN-90-6754-089-7] 06 p0729 N88-14483
Model-based building verification in aerial photographs
[AD-A186010] 07 p0870 N88-15278
The aerophotogrammetric determination of Earth surface deformations
[SER-C-321] 07 p0872 N88-15288
Photogrammetric principles for combining remote sounding and three-dimensional mapping 08 p1012 N88-16135
Three-dimensional image generation from an aerial photograph
[AD-A188039] 11 p1503 N88-18979
Automatic knowledge acquisition for aerial image interpretation
[AD-A188616] 12 p1638 N88-19810
A texture analysis approach to computer vision for identification of roads in aerial photographs
[AD-A189340] 12 p1639 N88-19815
Marginal Ice Zone Experiment (MIZEX) 1984 VARAN-S data set
[ETN-88-92032] 14 p1950 N88-21625
Updating land-use of the Sao Jose dos Campos municipality through remote sensing data
[INPE-4479-RPE/562] 16 p2287 N88-23693
Latin American Symposium on Remote Sensing, 4th Brazilian Remote Sensing Symposium and 6th SELPER Plenary Meeting, volume 1 17 p2352 N88-24013
Remote sensing techniques in the estimation of the area cultivated with beans, corn, and castor beans in the Irece County (Bahia State) 17 p2358 N88-24045
Structure and dynamics of vegetation in the middle semi-arid tropics. Quixaba's Caatinga (PE): Terrain analysis of MSS/LANDSAT data 17 p2358 N88-24049
Remote sensing and structural rupture: Application examples in the study of tectonics 17 p2359 N88-24050
Analysis and interpretation of image lithostructure: An application of the multiconcept in the metamorphic belt of Sul de Santana da Boa Vista (RS) 17 p2359 N88-24051
Tornado tracks in Southwestern Brazil, Eastern Paraguay, and Northwestern Argentina 17 p2362 N88-24071
Interpretation of MSS/LANDSAT data for evaluation of physical distribution of mangroves in Cananeia-Iguape (SP) 17 p2363 N88-24072
Low altitude remote sensing data in the implementation of a mathematical model for the planning of urban equipment networks 17 p2363 N88-24074
Evaluation of the mangrove area at the Piaui River (SE) through remote sensing 17 p2365 N88-24086
The 35 mm vertical aerial photographs for mapping stands of bracatinga in different age classes 17 p2366 N88-24087
The breaked anticlines, cuesta and crest homoclines, ortoclinal valleys, and other forms of relief on maps delineated with the help of remote sensing imagery 17 p2366 N88-24089
Stereoscopic photographs, ground and aerial, of trees used in the arborization of Curitiba (PR) 17 p2366 N88-24091
Preliminary study on the application of digital processing of TM-LANDSAT data in the mapping of apple orchards in Fraiburgo (SC) 17 p2367 N88-24093
Characteristics of drainage determinations in aerial photographs and relief determination on different scales planialtimetric charts for three soils in the state of Sao Paulo 17 p2367 N88-24095
Criteria for planimetric and altimetric correction of maps restituted from aerial photographs in 1:100,000 scale 17 p2367 N88-24097
National Meeting on Remote Sensing Applied to Municipal Planning 19 p2681 N88-25939
Application of remote sensing in the conservation of natural areas: Ribeira Valley 19 p2683 N88-25949
Use of remote sensing in the study of superficial formation certifying the development of integrated economy-case example: Rio Claro (SP) region 19 p2683 N88-25950
Application of 35mm EM aerial reconnaissance photographic format of the municipality of Ubatuba (SP) 19 p2684 N88-25953
Aerial photography as an instrument of atmospheric analysis: Maps of the middle atmosphere and its dynamics, Baixada Santista (SP) 19 p2684 N88-25955
Aerial photography as an instrument of municipal and regional planning: Metropolitan area of Sao Paulo (SP) 19 p2684 N88-25957
New duplicating paper with high resolution for aerial photography
[PB87-228706] 19 p2685 N88-25962
Automatic line network extraction from aerial imagery of urban areas through knowledge based image analysis
[AD-A193067] 21 p2965 N88-27615
Automatic line network extraction from aerial imagery of urban areas through knowledge-based image analysis
[AD-A192399] 23 p3227 N88-29208

AERIAL RECONNAISSANCE
Earth resources: A continuing bibliography with indexes (supplement 56)
[NASA-SP-7041(56)] 10 p1347 N88-18051
Hydrographic data from the OPTOMA (Ocean Prediction Through Observation, Modeling and Analysis) program: OPTOMA 23, 9-19 November 1986
[AD-A189868] 15 p2099 N88-22506
Air-to-air radar flight testing
[AGARD-AG-300-VOL-7] 21 p2932 N88-27406

AEROACOUSTICS
Investigation of the suitability of the 8ft x 6ft transonic wind-tunnel for aeroacoustic research on propellers
[RAE-TM-AERO-2093] 01 p0008 N88-10041
Noise of a model high speed counterrotation propeller at simulated takeoff/approach conditions (F7/A7)
[NASA-TM-100206] 01 p0091 N88-10592
Fluctuating pressure loads under high speed boundary layers
[NASA-TM-100517] 05 p0647 N88-13962
Flow induced pulsations in pipe systems
[ETN-88-91367] 06 p0702 N88-14307
NASA/Army Rotorcraft Technology. Volume 2: Materials and Structures, Propulsion and Drive Systems, Flight Dynamics and Control, and Acoustics
[NASA-CP-2495-VOL-2] 09 p1106 N88-16632
A decade of aeroacoustic research at NASA Ames Research Center 09 p1109 N88-16648
Aeroacoustic research programs at the Army Aviation Research and Technology Activity 09 p1109 N88-16649
An experimental investigation of the chopping of helicopter main rotor tip vortices by the tail rotor. Part 2: High speed photographic study
[NASA-CR-177457] 09 p1114 N88-16678
Investigation of aeroacoustic mechanisms by remote thermal imaging
[DE88-002612] 15 p2021 N88-22046
Aerodynamic noise of wind turbines
[PB88-165188] 16 p2265 N88-23546
Research investigation of helicopter main rotor/tail rotor interaction noise
[NASA-CR-4143] 19 p2722 N88-26165
Outdoor sound propagation, its implications for unattended ground sensors
[FEL-1986-64] 20 p2850 N88-26917
The influence of surface rounding on trailing edge noise
[AD-A193387] 21 p3012 N88-27876
Acoustic propagation in the lower atmosphere
[ISL-R-126/87] 21 p3013 N88-27878
The role of acoustic resonances in unsteady turbomachinery aerodynamics
[PNR90455] 22 p3147 N88-28720

AEROASSIST
Aeroassisted-vehicle design studies for a manned Mars mission
[NASA-TM-100031] 03 p0271 N88-11700
Aeroassisted manned transfer vehicle (TAXI) for advanced Mars Transportation: NASA/USRA 1987 Senior Design Project
[NASA-CR-181478] 03 p0275 N88-11736
An analysis of the effect of aeroassist maneuvers on orbital transfer vehicle performance
[NASA-TM-89117] 06 p0672 N88-14116
Effect of transition aerodynamics on aeroassist flight experiment trajectories
[NASA-TM-100546] 11 p1446 N88-18620
Aeroassisted orbit transfer vehicle trajectory analysis
[NASA-TM-89138] 12 p1599 N88-19575
Aeroassist flight experiment guidance Quiet Time
[NASA-TM-100556] 14 p1881 N88-21244
Orbital transfer vehicle: Concept definition and system analysis study
[NASA-CR-179315] 15 p2024 N88-22060

AEROBIOLOGY
Project Explorer takes its second step: GAS-608 in engineering development 10 p1288 N88-17707

AEROBRAKING
Aeroassisted-vehicle design studies for a manned Mars mission
[NASA-TM-100031] 03 p0271 N88-11700
Aeroassisted manned transfer vehicle (TAXI) for advanced Mars Transportation: NASA/USRA 1987 Senior Design Project
[NASA-CR-181478] 03 p0275 N88-11736
New concepts for atmospheric braking deceleration in planetary atmosphere entry
[SNIAS-CAS-DECE-P003-DPAA] 16 p2168 N88-22923

AEROCAPTURE
A technique for capture analysis of low thrust missions in a planetary system
[AD-A188934] 12 p1594 N88-19544
A design study of onboard navigation and guidance during aerocapture at Mars
[NASA-CR-172053] 18 p2469 N88-24654

AERODYNAMIC AXIS
U AERODYNAMIC BALANCE

AERODYNAMIC BALANCE
The effects of rotor unbalance on the vertical response of a soft-mounted block 08 p1000 N88-16057

AERODYNAMIC BRAKES
NT DRAG CHUTES
NT LEADING EDGE FLAPS
NT TRAILING EDGE FLAPS
NT VORTEX FLAPS
NT WING FLAPS

AERODYNAMIC BUZZ
U FLUTTER

AERODYNAMIC CENTER
U AERODYNAMIC BALANCE

AERODYNAMIC CHARACTERISTICS
NT AERODYNAMIC BALANCE
NT AERODYNAMIC DRAG
NT AERODYNAMIC STABILITY
NT INTERFERENCE DRAG
NT INTERFERENCE LIFT
NT JET LIFT
NT LIFT
NT STATIC AERODYNAMIC CHARACTERISTICS
NT SUPERSONIC DRAG
NT ZERO LIFT
Integration of dynamic, aerodynamic and structural optimization of helicopter rotor blades
[NASA-CR-181441] 01 p0002 N88-10012
Diagnosis of flow channel in aircraft gas-turbine engines on basis of vibration spectrum characteristics 02 p0159 N88-10993

An experimental evaluation of advanced rotorcraft airfoils in the NASA Ames eleven-foot transonic wind tunnel
[NASA-CR-166587] 03 p0261 N88-11640
Improvements to the adaptive maneuvering logic program
[NASA-CR-3985] 03 p0262 N88-11648
An aerodynamic performance evaluation of the NASA/Ames Research Center advanced concepts flight simulator
[NASA-TM-89659] 03 p0268 N88-11685
Fin gaps and body slots of guided projectiles: Effects, data correlation and modeling
[AD-A184440] 03 p0270 N88-11698
Technical evaluation report on the Fluid Dynamics Panel Symposium on aerodynamic and related hydrodynamic studies using water facilities
[AGARD-AR-225] 03 p0312 N88-11968
A hybrid numerical technique for predicting the aerodynamic and acoustic fields of advanced turboprops
[NASA-CR-174926] 03 p0374 N88-12352
Planform effects on the supersonic aerodynamics of multibody configurations
[NASA-TP-2762] 04 p0393 N88-12454
A method for the efficient calculation of elastic rotor blade dynamic response in forward flight
04 p0394 N88-12460
An integrated study of structures, aerodynamics and controls on the forward swept wing X-29A and the oblique wing research aircraft
[NASA-CR-181548] 04 p0399 N88-12486
Calculation of aerodynamic characteristics of three-dimensional finite span wings in potential incompressible flow 04 p0425 N88-12631
Conical wing with maximum lift-to-drag ratio in supersonic gas flow 04 p0425 N88-12633
Aerodynamics of Hypersonic Lifting Vehicles
[AGARD-CP-428] 05 p0529 N88-13219
The drag of slender axisymmetric cones in rarefied hypersonic flow 05 p0531 N88-13229
Low Reynolds number influence on aerodynamic performance of hypersonic lifting vehicles
05 p0531 N88-13230
Hypersonic airbreathing propulsion: Evolution and opportunities 05 p0531 N88-13231
Hypersonic aerodynamics: Applications for HOTOL
05 p0535 N88-13252
A perspective of computational fluid dynamics
05 p0538 N88-13279
Computational methods for problems in aerodynamics and large space structure using parallel and vector architectures
[AD-A185401] 05 p0541 N88-13294
An experimental investigation of the aerodynamics of a NACA 64A010 airfoil-flap combination with and without flap oscillations. Part 1: Steady-state characteristics
[NASA-TM-88217] 05 p0542 N88-13305
Nonlinear lift control at high speed and high angle of attack using vortex flow technology
05 p0545 N88-13319
Aircraft dynamics: Aerodynamic aspects and wind tunnel techniques 05 p0545 N88-13320
Full-envelope aerodynamic modeling of the Harrier aircraft
[NASA-TM-88376] 05 p0552 N88-13363
Vortical Flows Research Program of the Fluid Dynamics Research Branch
[NASA-TM-88332] 05 p0582 N88-13549
On the parabolized Navier-Stokes equations without sublayer assumptions
[AD-A186127] 07 p0849 N88-15152
Chemical reactions in turbulent mixing flows
[AD-A186141] 07 p0849 N88-15153
A note on the aerodynamic design of thin parallel-sided aerofoil sections
[ARL-AERO-TM-388] 09 p1114 N88-16877
A flight-test methodology for identification of an aerodynamic model for a V/STOL aircraft
[NASA-TM-100067] 09 p1117 N88-16894
Aerodynamic and acoustic characteristics of an advanced propeller under take-off and landing conditions
[NAL-TR-935] 09 p1243 N88-17453
Investigation of the influence of wind shear on the aerodynamic characteristics of aircraft using a vortex-lattice method 10 p1274 N88-17619
The aerodynamic design optimisation of a forward swept wing fighter aircraft
[CAR-87-18] 11 p1433 N88-18553
Aerodynamic characteristics of wings designed with a combined-theory method to cruise at a Mach number of 4.5
[NASA-TP-2799] 12 p1575 N88-19420
Australian aerodynamic design codes for aerial tow bodies
[AD-A189048] 13 p1715 N88-20258
Nonaxisymmetric body supersonic, aerodynamic prediction
[AD-A189338] 13 p1716 N88-20259
A correlation study of X-29A aircraft and associated analytical development
[NASA-CR-183103] 13 p1722 N88-20296
Lateral and longitudinal stability and control parameters for the space shuttle discovery as determined from flight test data
[NASA-TM-100555] 13 p1724 N88-20309
Investigation into the effects of flap end modifications on the performance of a wing with a single slotted flap
[BU-357] 14 p1866 N88-21148
Oscillating airfoils: Achievements and conjectures
[AD-A190490] 15 p2014 N88-22008
Improvements to tilt rotor performance through passive blade twist control
[NASA-TM-100583] 15 p2086 N88-22434
Design method for laminar flow control of two-dimensional airfoils in incompressible flow. Numerical study of LFC design concepts
[DE88-751809] 16 p2155 N88-22859
The structure of sonic underexpanded turbulent air jets in still air
[AD-A190856] 16 p2157 N88-22870
Propfan model wind tunnel aeroelastic research results 16 p2220 N88-23246
High Reynolds number tests of a Douglas DLBA 032 airfoil in the Langley 0.3-meter transonic cryogenic tunnel
[NASA-TM-87663] 17 p2296 N88-23734
Boundary layer flow visualization for flight testing
17 p2297 N88-23742
Natural laminar flow and airplane stability and control
17 p2298 N88-23747
The exact calculation of quadrupole sources for some incompressible flows
[NASA-TM-100623] 17 p2395 N88-24240
Experiment investigation on longitudinal characteristics of the forward swept wing
[AD-A191553] 18 p2456 N88-24582
High speed and high angle of attack aerodynamic characteristics of winged space vehicle
[ISSN-0285-6808] 18 p2459 N88-24599
Numerical solutions of the Euler equations for the flow field around counter-rotating propellers
19 p2636 N88-25638
Influence of wind shear on the aerodynamic characteristics of airplanes
[NASA-TP-2827] 20 p2755 N88-26344
Airbus 1987: Success in Europe
[ETN-88-92099] 20 p2758 N88-26364
Surface disturbances produced by low-level, subsonic B-1 aircraft
[AD-A192257] 20 p2824 N88-26752
Wind tunnel tests of elliptical missile body configurations at Mach numbers 0.4 to 5.0
[AD-A193525] 22 p3038 N88-28040
Effects of independent variation of Mach and Reynolds numbers on the low-speed aerodynamic characteristics of the NACA 0012 airfoil section
[NASA-TM-4074] 23 p3170 N88-28879
Aerodynamic data accuracy and quality: Requirements and capabilities in wind tunnel testing
[AGARD-AR-254] 23 p3173 N88-28893
Technology for pressure-instrumented thin airfoil models
[NASA-CR-4173] 23 p3180 N88-28933
Interactive plotting of NASTRAN aerodynamic models using NPLOT and DISSPLA
[AD-A194115] 23 p3226 N88-29204
Aircraft dynamics: Aerodynamic aspects and wind tunnel techniques 24 p3313 N88-29731
Survey on nonlinear effects 24 p3317 N88-29757
Semi-empirical methods for conventional and unconventional missiles 24 p3318 N88-29758
Air intake aerodynamics 24 p3318 N88-29762
A new computational capability for ramjet projectiles
[AD-A196061] 24 p3327 N88-29812

AERODYNAMIC CHORDS
U AIRFOIL PROFILES

AERODYNAMIC COEFFICIENTS
International Conference on the Aerodynamics at Low Reynolds Numbers between 10(4) and 10(6)
[ONRL-7-023-C] 01 p0002 N88-10010
Investigations of separated flow states on wings of medium aspect ratio taking into account the wind tunnel interference problem
[ETN-87-90437] 01 p0003 N88-10016
An experimental evaluation of advanced rotorcraft airfoils in the NASA Ames eleven-foot transonic wind tunnel
[NASA-CR-166587] 03 p0261 N88-11640
Improvements to the adaptive maneuvering logic program
[NASA-CR-3985] 03 p0262 N88-11648
Semiempirical method for prediction of aerodynamic forces and moments on a steadily spinning light airplane
[NASA-TM-4009] 04 p0393 N88-12456
Aerodynamic sensitivities from subsonic, sonic and supersonic unsteady, nonplanar lifting-surface theory
[NASA-TM-100502] 04 p0394 N88-12459
Numerical calculations of the flowfield around propellers 05 p0536 N88-13261
Characteristics of a separating confluent boundary layer and the downstream wake
[NASA-TM-100046] 06 p0704 N88-14323
Computer program for the calculation of the profile-vortices interactions (two dimensional inviscid incompressible flow with point singularities)
[ISL-R-124/86] 08 p0987 N88-15982
Friction drag reduction (a speculative essay)
[INPE-4278-PRE/1150] 08 p0988 N88-15985
Experimental rotordynamic coefficient results for honeycomb seals
[NASA-CR-182440] 08 p0993 N88-16007
Wind tunnel modeling techniques
[KU-SFB-210/E/33] 09 p1121 N88-16711
Investigation of the influence of wind shear on the aerodynamic characteristics of aircraft using a vortex-lattice method 10 p1274 N88-17619
Finite element calculations for aerodynamic coefficients of a 3-dimensional body in subsonic flow using Green's function method
[NASA-TM-100208] 13 p1718 N88-20272
Constructing Gloved wings for aerodynamic studies
[NASA-TM-100440] 14 p1863 N88-21128
Data processing method for high angle of attack testing with rolling angle 14 p1864 N88-21134
New definition of pressure-center coefficient of reentry craft with asymmetrical configuration
14 p1864 N88-21138
New airfoil sections for straight bladed turbine
[DE88-701075] 14 p1942 N88-21588
Submunitions simulations, volume 2
[TR-CR-RD-SS-87-7-VOL-2] 19 p2641 N88-25669
A preliminary investigation of drag reduction and mechanism for a blunt body of revolution with slanted base
[NASA-TT-20349] 24 p3317 N88-29753
Accuracy criteria for evaluating supersonic aerodynamic coefficient predictions 24 p3317 N88-29756
Computational aerodynamic analysis for a range-limited 25mm training round
[AD-A185270] 24 p3320 N88-29772

AERODYNAMIC CONFIGURATIONS
NT WING NACELLE CONFIGURATIONS
Problem and solution formulations for the generation of 3D block-structured grids --- aircraft design
[NLR-MP-86020-U] 01 p0005 N88-10028
The aerothermodynamic environment for holes in hypersonic configurations
[DE87-014651] 02 p0121 N88-10767
Aerodynamic design and performance of a bent-axis geometry vehicle
[DE87-013726] 02 p0124 N88-10786
An aerodynamic performance evaluation of the NASA/Ames Research Center advanced concepts flight simulator
[NASA-TM-89659] 03 p0268 N88-11685
Numerical simulation of the hypersonic flow around lifting vehicles 05 p0532 N88-13234
Lifting bodies: An attractive aerodynamic configuration choice for hypervelocity vehicles
05 p0534 N88-13248
General aerodynamic-aerothermodynamic concepts for Hermes 05 p0535 N88-13251
Numerical analysis of supersonic flows using panel method 05 p0537 N88-13266
Tip aerodynamics from wind tunnel test of semi-span wing
[NASA-TM-88253] 05 p0540 N88-13290
Fundamentals of fighter aircraft design
05 p0544 N88-13316
Nonlinear aerodynamic wing design
[NASA-CR-3950] 06 p0665 N88-14079
Large-Scale Advanced Prop-Fan (LAP) blade design
[NASA-CR-174790] 06 p0668 N88-14097
Design verification and fabrication of active control systems for the DAST ARW-2 high aspect ratio wing, part 1
[NASA-CR-177959-PT-1] 06 p0669 N88-14101
Design verification and fabrication of active control systems for the DAST ARW-2 high aspect ratio wing. Part 2: Appendices
[NASA-CR-177959-PT-2] 06 p0669 N88-14102
Aerodynamic design of first stage turbines for small aero engines 06 p0713 N88-14370
Aerodynamic testing of small turbines
06 p0713 N88-14371
Langley Symposium on Aerodynamics, volume 1
[NASA-CP-2397] 07 p0809 N88-14926

Computational fluid dynamics overview
07 p0809 N88-14927
Finite-volume scheme for transonic potential flow about airfoils and bodies in an arbitrarily shaped channel
07 p0809 N88-14928
Application of a full potential method for analysis of complex aircraft geometries 07 p0809 N88-14930
Three-dimensional unsteady flow elicited by finite wings and complex configurations
[AD-A186464] 08 p0951 N88-15770
An overview of key technology thrusts at Bell Helicopter Textron 09 p1111 N88-16657
Burst vortex/boundary layer interaction
[NASA-CR-182510] 10 p1268 N88-17583
The intelligent wing. Aerodynamic development direction for future passenger aircraft
[MBB-UT-006/87] 10 p1313 N88-17848
Aerodynamic aspects of the configurational systems layout of a dispenser
[MBB-UA-1047/87] 10 p1315 N88-17863
A performance index approach to aerodynamic design with the use of analysis codes only
[NASA-TP-2805] 11 p1433 N88-18552
Analysis of shear-layer probe data for holes in hypersonic configurations
[DE88-003992] 11 p1435 N88-18564
Computer program for conceptual tandem rotor helicopter design
[AD-A187832] 11 p1439 N88-18584
Generation of surface grids through elliptic partial differential equations for aircraft and missile configurations
[AD-A186631] 11 p1535 N88-19169
A multigrid full potential transonic code for arbitrary configurations — aircraft 11 p1539 N88-19195
A review of technologies applicable to low-speed flight of high-performance aircraft investigated in the Langley 14- x 22-foot subsonic tunnel
[NASA-TP-2796] 13 p1717 N88-20264
New definition of pressure-center coefficient of reentry craft with asymmetrical configuration
14 p1864 N88-21138
An investigation into the effect of canard location on the aerodynamics of the close-coupled canard configuration
[BU-361] 14 p1866 N88-21149
Designs of profiles for cascades
[NASA-TT-20161] 15 p2067 N88-22326
Experimental investigation of the hypersonic flow over a six finned configuration
[AD-A190870] 16 p2157 N88-22871
Qualification of a water tunnel for force measurements on aeronautical models 16 p2200 N88-23128
An experimental study to determine the flow and the subsonic static and dynamic stability characteristics of aircraft operating at high angles-of-attack
16 p2201 N88-23129
It's time to reinvent the general aviation airplane
17 p2294 N88-23726
Full potential methods for analysis/design of complex aerospace configurations
[NASA-CR-3982] 17 p2296 N88-23736
Preliminary aerodynamic design considerations for advanced laminar flow aircraft configurations
17 p2297 N88-23746
Flight testing a V/STOL aircraft to identify a full-envelope aerodynamic model
[NASA-TM-100996] 17 p2301 N88-23762
Multi-body aircraft with an all-movable center fuselage actively controlling fuselage pressure drag
[NASA-CASE-LAR-13511-1] 17 p2301 N88-23765
An analytic model for aerodynamic shapes
[AD-A191573] 18 p2456 N88-24583
Wind tunnel investigation of wing and control panel loads at transonic and supersonic speeds on some schematic cruciform missile configurations
[FFA-TN-1986-43] 18 p2457 N88-24585
Incompressible Euler solution on a multiblock grid around a car configuration
[FFA-TN-1987-65] 18 p2457 N88-24586
Summary of low-speed wind tunnel results of several high-speed counterrotation propeller configurations
[NASA-TM-100945] 18 p2458 N88-24597
High speed and high angle of attack aerodynamic characteristics of winged space vehicle
[ISSN-0285-6808] 18 p2459 N88-24599
Actuated forebody strakes
[NASA-CASE-LAR-13983-1] 18 p2464 N88-24628
Application of advanced grid generation techniques for flow field computations about complex configurations
[NASA-CR-183049] 18 p2515 N88-24922
Aerodynamics of lifting bodies with combined transverse and longitudinal curvature 19 p2598 N88-25436
A low speed wind tunnel investigation of Reynolds number effects on a 60-deg swept wing configuration with leading and trailing edge flaps
[NASA-CR-181684] 19 p2598 N88-25441
Proceedings of the 5th NAL Symposium on Aircraft Computational Aerodynamics
[NAL-SP-8] 19 p2635 N88-25630
Numerical simulations of aerodynamic contribution of flows about a space-plane-type configuration
19 p2635 N88-25632
Aerodynamic simulation for complete ASKA aircraft configuration 19 p2637 N88-25641
Numerical simulation of viscous flows over transonic aircraft configurations 19 p2637 N88-25642
Calculations of unsteady aerodynamics for a full aircraft configuration using boundary element method
19 p2637 N88-25643
Ludwig Prandtl collected treatises on applied mechanics, hydro- and aerodynamics, part 1
[NASA-TT-20316] 20 p2752 N88-26337
Wind tunnel tests of the influence of airfoil-thickness on normal force and pitching moment of two slender wings at transonic and supersonic Mach numbers
[DFVLR-FB-88-17] 21 p2893 N88-27171
AGARD standard aeroelastic configurations for dynamic response. 1: Wing 445.6
[AGARD-R-765] 21 p2896 N88-27193
Wind tunnel tests of elliptical missile body configurations at Mach numbers 0.4 to 5.0
[AD-A193525] 22 p3038 N88-28040
Delta wing configurations 23 p3167 N88-28860
Complex configurations 23 p3167 N88-28861
Transport-type configurations
23 p3169 N88-28867
Combat aircraft 23 p3169 N88-28868
Three dimensional grid generation for complex configurations: Recent progress
[AGARD-AG-309] 23 p3245 N88-29313
Component adaptive grid generation for aircraft configurations 23 p3246 N88-29316
Experience with three dimensional composite grids
23 p3247 N88-29324
Space shuttle phase B wind tunnel model and test information. Volume 3: Launch configuration
[NASA-CR-178416-VOL-3-PT-2]
24 p3315 N88-29744
Space shuttle phase B wind tunnel model and test information. Volume 1: Booster configuration
[NASA-CR-178414-VOL-1-PT-1]
24 p3315 N88-29745
Special Course on Missile Aerodynamics
[AGARD-R-754] 24 p3317 N88-29755
Prediction of dynamic derivatives
24 p3318 N88-29761
Next generation missile design
24 p3319 N88-29766

AERODYNAMIC DRAG
NT SUPERSONIC DRAG
The contraction of satellite orbits under the influence of air drag. Part 8: Orbital lifetime in an oblate atmosphere, when perigee distance is perturbed by odd zonal harmonics in the geopotential
[RAE-TR-86069-PT-8] 01 p0010 N88-10058
Planform effects on the supersonic aerodynamics of multibody configurations
[NASA-TP-2762] 04 p0393 N88-12454
Numerical study of supersonic flow around blunt bodies with extended needle nose 04 p0425 N88-12635
Studies of unsteadiness in boundary layers
[AD-A185662] 06 p0703 N88-14315
Investigation of the feasibility of an analytical method of accounting for the effects of atmospheric drag on satellite motion 07 p0923 N88-15608
Full scale and wind tunnel surface pressure measurements on the T.R.R.L. spray dispersion programme vehicles
[REPT-8623] 09 p1114 N88-16676
Transonic wind tunnel calibration 1986: Force measurements on three ONERA-C5 models and three half sphere cylinder calibration bodies in the F+W transonic test section
[F+W-FO-1854] 09 p1122 N88-16714
Verification of a micro-thrusting model to maintain satellites in low orbit
[AD-A186874] 09 p1133 N88-16793
Wind tunnel studies of circulation control elliptical airfoils 10 p1270 N88-17598
Preliminary design of the ORION attitude control system
[AD-A187179] 10 p1292 N88-17729
Determination of the drag of missiles with variable lateral acceleration possibility
[REPT-FM15] 10 p1310 N88-17831
Flight tests of external modifications used to reduce blunt base drag
[NASA-TM-100433] 13 p1719 N88-20279
Frozen orbit analysis in the Martian system
[AD-A189574] 13 p1856 N88-21106
Comparison of pressure distributions on model and full-scale NACA 64-621 airfoils with ailerons for wind turbine application
[NASA-TM-100802] 14 p1943 N88-21593
Computational fluid dynamics drag prediction: Results from the Viscous Transonic Airfoil Workshop
[NASA-TM-100095] 15 p2014 N88-22009
Zero-lift drag predictions in supersonic flow for complex configurations 15 p2054 N88-22246
Boundary layer measurements using hot-film sensors
17 p2297 N88-23743
Calibration of averaging total pressure flight wake rake and natural-laminar-flow airfoil drag certification
[NASA-CR-181630] 19 p2599 N88-25443
Theoretical and experimental investigations of a vortex drag behind a wing profile with spoiler
[ISL-PU-309/87] 21 p2892 N88-27169
A preliminary investigation of drag reduction and mechanism for a blunt body of revolution with slanted base
[NASA-TT-20349] 24 p3317 N88-29753

AERODYNAMIC FORCES
NT AERODYNAMIC DRAG
NT AERODYNAMIC INTERFERENCE
NT AERODYNAMIC LOADS
NT BLAST LOADS
NT GUST LOADS
NT INTERFERENCE LIFT
NT JET LIFT
NT LIFT
NT SUPERSONIC DRAG
NT WING LOADING
NT ZERO LIFT
Semiempirical method for prediction of aerodynamic forces and moments on a steadily spinning light airplane
[NASA-TM-4009] 04 p0393 N88-12456
Numerica calculation in the Laplace domain for subsonic unsteady aerodynamic forces acting on a finite wing
05 p0535 N88-13256
Computational methods for problems in aerodynamics and large space structure using parallel and vector architectures
[AD-A185401] 05 p0541 N88-13294
Calculated unsteady aerodynamics of wings
[AD-A189608] 12 p1574 N88-19415
Unsteady aerodynamics of a Wortmann FX-63-137 wing in a fluctuating wind field
[AD-A190128] 15 p2013 N88-22006
Influence of unsteady aerodynamic forces on dynamic response of variable sweep aircraft
15 p2054 N88-22245
Measurements of aerodynamic forces on unsteadily moving bluff parachute canopies
16 p2202 N88-23137
Reduced order models for nonlinear aerodynamics
16 p2220 N88-23248
Nonlinear programming extensions to rational function approximation methods for unsteady aerodynamic forces
[NASA-TP-2776] 18 p2463 N88-24623
A characteristic method for calculating the generalized flat flutter aerodynamic forces
[NASA-TT-20300] 19 p2598 N88-25438
Contamination and distortion of steady flow field induced by discrete frequency disturbances in aircraft gas engines
[AD-A195440] 24 p3370 N88-30069

AERODYNAMIC HEAT TRANSFER
Calculation of aerodynamic heat transfer for blunt-nosed thin wings at different angles of attack at supersonic speeds
[NASA-TT-20127] 02 p0123 N88-10776

AERODYNAMIC HEATING
NT SHOCK HEATING
Thermal stress analysis of space shuttle orbiter subjected to reentry aerodynamic heating
[NASA-TM-88286] 01 p0061 N88-10389
The aerodynamics of supersonic parachutes
[DE87-014846] 04 p0395 N88-12464
Parachute materials
[DE87-014845] 04 p0411 N88-12550
Atmospheric entry heating of cosmic dust
06 p0794 N88-14865
High-temperature properties of ceramic fibers and insulations for thermal protection of atmospheric entry and hypersonic cruise vehicles
[NASA-TM-100059] 10 p1295 N88-17743
Trajectory characteristics and heating of hypervelocity projectiles having large ballistic coefficients
[NASA-TP-2614] 12 p1574 N88-19412
Fluid-thermal-structural study of aerodynamically heated leading edges
[NASA-TM-100579] 13 p1783 N88-20666
Nuclear-powered space debris sweeper
17 p2418 N88-24380

Aerodynamic heating of missiles
24 p3319 N88-29764
AERODYNAMIC INTERFERENCE
A transonic model representation for two-dimensional wall interference assessment
[NLR-TR-86026-U] 01 p0001 N88-10006
Wall interference tests of a CAST 10-2/DOA 2 airfoil in an adaptive-wall test section
[NASA-TM-4015] 02 p0122 N88-10772
A 0.15-scale study of configuration effects on the aerodynamic interaction between main rotor and fuselage
[NASA-CR-166577] 04 p0395 N88-12462
Computation of nacelle interference using boundary element method 05 p0537 N88-13267
Determination of the drag of missiles with variable lateral acceleration possibility
[REPT-FM15] 10 p1310 N88-17831
An investigation into the effect of canard location on the aerodynamics of the close-coupled canard configuration
[BU-361] 14 p1866 N88-21149
Porous wind tunnel corrections for counterrotation propeller testing
[NASA-TM-100873] 15 p2015 N88-22019
Multi-body aircraft with an all-movable center fuselage actively controlling fuselage pressure drag
[NASA-CASE-LAR-13511-1] 17 p2301 N88-23765
Submunitions simulations, volume 2
[TR-CR-RD-SS-87-7-VOL-2] 19 p2641 N88-25669
The present status and the future of missile aerodynamics
[NASA-TM-100063] 24 p3320 N88-29773
AERODYNAMIC LIFT
U LIFT
AERODYNAMIC LOADS
NT BLAST LOADS
NT GUST LOADS
Stability of mechanical joints in launching vehicles: Local and global stationary values of energy density
03 p0270 N88-11696
Numerical optimization of conical flow waveriders including detailed viscous effects
05 p0533 N88-13245
Aeroelastic analysis of modern transport aircraft
05 p0550 N88-13352
Wing divergence of trimmed aircraft
05 p0550 N88-13354
Measurement of model deformation in wind tunnels
05 p0551 N88-13358
Crack growth prediction in 3D structures under aeronautical-type spectrum loadings
05 p0602 N88-13688
Static force and moment test of the Holloman narrow-gage rocket sled at Mach numbers from 3.5 to 5.5
[AD-A186291] 07 p0822 N88-14995
A review of research in rotor loads
09 p1106 N88-16629
Loads and aeroelasticity division research and technology accomplishments for FY 1987 and plans for FY 1988
[NASA-TM-100534] 09 p1114 N88-16680
X-wing potential for Navy applications
10 p1271 N88-17604
Cornering characteristics of the main-gear tire of the space shuttle orbiter
[NASA-TP-2790] 11 p1438 N88-18583
Some aspects of aircraft dynamic loads due to flow separation
[AGARD-R-750] 11 p1439 N88-18588
Testing of a one-bladed 30-meter-diameter rotor on the DOE/NASA Mod-O wind turbine
[NASA-TM-100274] 11 p1509 N88-19014
Calculated unsteady aerodynamics of wings
[AD-A189606] 12 p1574 N88-19415
Workshop on Design Loads for Advanced Fighters
[AGARD-R-746] 12 p1579 N88-19449
The development of manoeuvre load criteria for agile aircraft 12 p1579 N88-19450
Structural design requirements for aircraft incorporating active control technology 12 p1580 N88-19453
The relationship between operational flight manoeuvre parameters and design parameters
12 p1580 N88-19454
Manoeuvres by default, by demand and by design
12 p1580 N88-19455
Design loads for Swedish military aircraft in a twenty years' perspective 12 p1580 N88-19456
Nonaxisymmetric body supersonic, aerodynamic prediction
[AD-A189338] 13 p1716 N88-20259
Calculation of the distributed loads on the blades of individual multiblade propellers in axial flow using linear and nonlinear lifting surface theories
[NASA-TT-20173] 13 p1719 N88-20278
Determination of canopy loads for a light aircraft by wind tunnel testing and computer modelling
[BU-353] 14 p1869 N88-21167
A numerical model of unsteady, subsonic aeroelastic behavior
[NASA-TM-101126] 16 p2156 N88-22862
The 2-D and 3-D time marching transonic potential flow method for propfans 16 p2220 N88-23245
Certification aspects of airplanes which may operate with significant natural laminar flow 17 p2298 N88-23749
An initial investigation into methods of computing transonic aerodynamic sensitivity coefficients
[NASA-CR-183061] 20 p2752 N88-26332
In-flight load measurements of the Robot-X canards
[AD-A193428] 21 p2895 N88-27187
Unsteady flow past an NACA 0012 airfoil at high angles of attack
[AD-A194650] 23 p3172 N88-28886
Stress intensity factors for cracked metallic structures under rapid thermal loading
[AD-A191219] 23 p3193 N88-29004
Matching P.S.D.: Design loads
24 p3312 N88-29720
A summary of methods for establishing airframe design loads from continuous gust design criteria
24 p3312 N88-29721
Status review of atmosphere turbulence and aircraft response 24 p3312 N88-29726
A summary of atmospheric turbulence measurements with specially-equipped aircraft in the US
24 p3312 N88-29727
Calculation of non-stationary aerodynamic forces in the near sonic range
[NASA-TT-20310] 24 p3322 N88-29782
Empirical flutter prediction method
[AD-A195699] 24 p3327 N88-29810
AERODYNAMIC MOMENTS
U STABILITY DERIVATIVES
AERODYNAMIC NOISE
NT BLADE SLAP NOISE
Rotorcraft flight research with emphasis on rotor systems 09 p1111 N88-16656
Laboratory studies related to in-flight acoustic emission monitoring
[AD-A186714] 09 p1242 N88-17445
Measurement and analysis of the noise radiated by low Mach numbers centrifugal blowers
[AD-A189226] 13 p1833 N88-20966
Structureborne noise measurements on a small twin-engine aircraft
[NASA-CR-4137] 16 p2265 N88-23545
Aerodynamic noise of wind turbines
[PB88-165188] 16 p2265 N88-23546
Analytical modeling of the structureborne noise path on a small twin-engine aircraft
[NASA-CR-4136] 17 p2394 N88-24233
First article noise survey of the A/F32T-9 large turbo fan engine enclosed noise suppressor system, far-field noise, Ellsworth AFB, South Dakota
[AD-A191938] 19 p2602 N88-25457
Research investigation of helicopter main rotor/tail rotor interaction noise
[NASA-CR-4143] 19 p2722 N88-26165
Theory of sound production by vortex-airfoil interaction
[AD-A193386] 21 p3012 N88-27875
The influence of surface rounding on trailing edge noise
[AD-A193387] 21 p3012 N88-27876
Noise generation and boundary layer effects in vortex-airfoil interaction and methods of digital hologram analysis for these flow fields
[AD-A194191] 23 p3171 N88-28883
AERODYNAMIC STABILITY
On the prediction of the aeroelastic behavior of lifting systems due to flow separation
[ESA-TT-1043] 03 p0259 N88-11633
Effects of the installation and operation of jet-exhaust yaw vanes on the longitudinal and lateral-directional characteristics of the F-14 airplane
[NASA-TP-2769] 04 p0393 N88-12455
Predictions of F-111 TACT aircraft buffet response and correlations of fluctuating pressures measured on aluminum and steel models and the aircraft
[NASA-CR-4069] 05 p0529 N88-13218
Analysis and test evaluation of the dynamic response and stability of three advanced turboprop models at low forward speed
[NASA-CR-175026] 06 p0668 N88-14096
Flap-lag-torsion aeroelastic stability of a circulation control rotor in forward flight 10 p1271 N88-17600
An application of eigenspace methods to symmetric flutter suppression
[NASA-CR-181618] 10 p1284 N88-17684
Special flight mechanical features of the bearingless helicopter rotor
[MBB-FM-315/O] 10 p1309 N88-17825
A correlation study of X-29A aircraft and associated analytical development
[NASA-CR-183103] 13 p1722 N88-20296
Unsteady aerodynamics of a Wortmann FX-63-137 wing in a fluctuating wind field
[AD-A190128] 15 p2013 N88-22006
Preliminary airworthiness evaluation of the UH-60A with Advanced Digital Optical Control System (ADOCS)
[AD-A190674] 15 p2018 N88-22030
The application of linear maximum likelihood estimation of aerodynamic derivatives for the Bell-205 and Bell-206
[AD-A191279] 16 p2161 N88-22894
Stability and control methodology for conceptual aircraft design. Volume 1: Methodology manual
[AD-A191314] 16 p2164 N88-22906
Actuated forebody strakes
[NASA-CASE-LAR-13983-1] 18 p2464 N88-24628
Integrated Technology Rotor Methodology Assessment Workshop
[NASA-CP-10007] 21 p2889 N88-27148
A comparison of the various helicopter mathematical models used in the methodology assessment
21 p2889 N88-27149
A comparison of theory and experiment for aeroelastic stability of a hingeless rotor model in hover
21 p2889 N88-27150
A comparison of theory and experiment for coupled rotor-body stability of a hingeless rotor model in hover under simulated vacuum conditions
21 p2889 N88-27151
A comparison of theory and experiment for coupled rotor-body stability of a hingeless rotor model in hover
21 p2889 N88-27152
A comparison of theory and experiment for the aeroelastic stability of a bearingless model rotor in hover
21 p2890 N88-27153
A comparison of theory and experiment for coupled rotor body stability of a bearingless rotor model in hover and forward flight 21 p2890 N88-27154
The importance of steady and dynamic inflow on the stability of rotor-body systems 21 p2890 N88-27156
Effects of static equilibrium and higher-order nonlinearities on rotor blade stability in hover
21 p2890 N88-27157
Aeroelastic modeling of rotor blades with spanwise variable elastic axis offset: Classic issues revisited and new formulations 21 p2890 N88-27158
Comparison of experimental rotor damping data-reduction techniques 21 p2891 N88-27159
Comparison of experimental coupled helicopter rotor/body stability results with a simple analytical model
21 p2891 N88-27160
Aeromechanical stability analysis of COPTER
21 p2891 N88-27161
The present status and the future of missile aerodynamics
[NASA-TM-100063] 24 p3320 N88-29773
AERODYNAMIC STALLING
Measurements and calculations of aerodynamic torques for a vertical-axis wind turbine
[DE88-001783] 04 p0465 N88-12876
Unsteady stall penetration experiments at high Reynolds number
[AD-A186120] 07 p0814 N88-14958
The development of CFD methods for rotor applications 09 p1105 N88-16627
Investigation of dynamic stall using LDV (Laser Doppler Velocimetry): Mean flow studies
[AD-A187629] 10 p1272 N88-17611
Modeling of limit cycle stall flutter oscillations
12 p1583 N88-19472
Effect of spatial inlet temperature and pressure distortion on turbofan engine stability
[NASA-TM-100850] 14 p1868 N88-21162
Performance optimization of a cruise missile using dynamic-stall induced lift augmentation
[AD-A190497] 15 p2017 N88-22027
Development of aeroelastic analysis methods for turborotors and propfans, including mistuning
16 p2219 N88-23244
Application of Navier-Stokes analysis to stall flutter
16 p2220 N88-23249
Stall flutter analysis of propfans
16 p2221 N88-23256
Preliminary aerodynamic design considerations for advanced laminar flow aircraft configurations
17 p2297 N88-23746
E3 10C compressor test analysis of high-speed post-stall data
[NASA-CR-179521] 23 p3179 N88-28929
AERODYNAMIC VEHICLES
U AIRCRAFT

AERODYNAMICS
NT AEROTHERMODYNAMICS
NT ROTOR AERODYNAMICS
NT SUPERSONICS
NT UNSTEADY AERODYNAMICS
Aeronautical engineering: A continuing bibliography with indexes (supplement 218)
[NASA-SP-7037(218)] 01 p0001 N88-10002
The Green's function method for fully unsteady aerodynamics around three-dimensional bodies and its application to flutter analysis
[UTIAS-298] 03 p0260 N88-11639
Modeling XV-15 tilt-rotor aircraft dynamics by frequency and time-domain identification techniques
03 p0263 N88-11657
New aerodynamic design of the fenestron for improved performance 03 p0264 N88-11664
The Proceedings of the Symposium on Mechanics for Space Flight
[ISAS-SP-5] 03 p0317 N88-12006
Aeronautical engineering: A continuing bibliography with indexes (supplement 219)
[NASA-SP-7037(219)] 04 p0396 N88-12470
Proceedings of the 4th NAL Symposium on Aircraft Computational Aerodynamics
[NAL-SP-7] 05 p0535 N88-13253
Unsteady aerodynamics of an oscillating cascade in a compressible flow field
[NASA-TM-100219] 05 p0549 N88-13346
Aeronautical engineering: A continuing bibliography with indexes (supplement 220)
[NASA-SP-7037(220)] 06 p0663 N88-14065
Development of an unsteady wake theory appropriate for aeroelastic analyses of rotors in hover and forward flight
[NASA-CR-182357] 06 p0664 N88-14075
Development of transonic speed cascade design method using Euler code and inverse solution
06 p0676 N88-14139
Aeronautical engineering. A continuing bibliography with indexes, supplement 221
[NASA-SP-7037(221)] 08 p0949 N88-15758
Unsteady three-dimensional flow separation
[NASA-CR-182412] 08 p0949 N88-15761
Realization of the immediate objectives of the Aero-Gas Dynamics and Vibration Laboratory (LAGG) at the National Center for Research, Science and Technology (PUSPIPTEK) at Serpong, Java (Indonesia), Project TTA-79
[GG/QPR-10] 08 p1092 N88-16572
Aeronautical engineering: A continuing bibliography with indexes (supplement 223)
[NASA-SP-7037(223)] 09 p1111 N88-16661
Computational unsteady aerodynamics for aeroelastic analysis
[NASA-TM-100523] 09 p1112 N88-16668
Method of iterative coupling between periodic aerodynamic and dynamic fields
[PB87-169934] 09 p1113 N88-16669
Mach number effects on transonic aeroelastic forces and flutter characteristics
[NASA-TM-100547] 09 p1113 N88-16675
Methods for evaluating the quality and reliability of aerodynamic software programs
[PB87-169793] 09 p1219 N88-17314
Application of empirical and linear methods to VSTOL powered-lift aerodynamics
[NASA-TM-100048] 10 p1267 N88-17581
Fixed wing CCW aerodynamics with and without supplementary thrust deflection
10 p1272 N88-17607
Supersonic aerodynamics of delta wings
[NASA-TP-2771] 10 p1273 N88-17615
A research program on the aerodynamics of a highly loaded turbine stage 10 p1280 N88-17655
Design and aerodynamic performance of a small mixed-flow gas generator turbine
10 p1281 N88-17662
Aerodynamic performance of a scale-model, counter-rotating unducted fan 10 p1282 N88-17666
Numerical methods for propeller aerodynamics and acoustics at DFVLR 10 p1282 N88-17668
Analysis of highspeed propellers aerodynamics
10 p1282 N88-17669
Effect of transition aerodynamics on aeroassist flight experiment trajectories
[NASA-TM-100546] 11 p1446 N88-18620
Aeronautical engineering: A cumulative index to a continuing bibliography
[NASA-SP-7037(222)] 12 p1574 N88-19416
JPRS report: Science and technology. Europe and Latin America
[JPRS-ELS-88-001] 12 p1614 N88-19649
Aeronautical engineering: A continuing bibliography with indexes (supplement 224)
[NASA-SP-7037(224)] 13 p1715 N88-20254
Australian aerodynamic design codes for aerial tow bodies
[AD-A189048] 13 p1715 N88-20258
Activities report of the Lille Institute of Fluid Mechanics
[ETN-88-91983] 13 p1771 N88-20597
Activities report of the Aerodynamics Department
[ETN-88-91979] 14 p1862 N88-21123
Aeronautical engineering: A continuing bibliography with indexes (supplement 225)
[NASA-SP-7037(225)] 14 p1863 N88-21126
Aeronautical engineering: A continuing bibliography with indexes (supplement 226)
[NASA-SP-7037(226)] 16 p2155 N88-22857
Oil flow patterns on a series of capsule-type re-entry vehicles at hypersonic speeds
[DE88-751805] 16 p2155 N88-22858
Aerofoil testing in a self-streamlining flexible walled wind tunnel
[NASA-CR-4128] 16 p2156 N88-22865
Computer tomography and hybrid optical/digital methods for aerodynamic measurements
[AD-A190909] 16 p2157 N88-22872
Aircraft flight dynamics research in past decade reviewed 16 p2186 N88-23031
Aerodynamic and Related Hydrodynamic Studies Using Water Facilities
[AGARD-CP-413] 16 p2200 N88-23125
Application of high speed holography to aerodynamic and hydrodynamic three-dimensional velocimetry
16 p2203 N88-23144
Use of water towing tanks for aerodynamics and hydrodynamics 16 p2204 N88-23149
A new laminar water tunnel to study the transition process in a blasius layer and in a separation bubble and a new tool for industrial aerodynamics and hydrodynamic research 16 p2204 N88-23150
Reduced order models for nonlinear aerodynamics
16 p2220 N88-23248
Modal forced response of propfans in yawed flow
16 p2221 N88-23253
Joint University Program for Air Transportation Research, 1986
[NASA-CP-2502] 17 p2293 N88-23715
The effects of inlet turbulence and rotor/stator interactions on the aerodynamics and heat transfer of a large-scale rotating turbine model. Part 4: Aerodynamic data tabulation
[NASA-CR-179469] 17 p2339 N88-23956
Aeronautical engineering: A continuing bibliography with indexes (supplement 227)
[NASA-SP-7037(227)] 18 p2456 N88-24578
Some rotorcraft applications of computational fluid dynamics
[NASA-TM-100066] 18 p2459 N88-24601
A decade of computer simulations for space shuttle aerodynamics
[NASA-TM-100990] 18 p2459 N88-24603
Nonlinear programming extensions to rational function approximation methods for unsteady aerodynamic forces
[NASA-TP-2776] 18 p2463 N88-24623
Nonlinear flying quality parameters based on dynamic inversion
[AD-A192146] 18 p2464 N88-24627
Internal fluid dynamics within a nonspinning partially liquid-filled shell due to burster rupture
[AD-A191055] 18 p2507 N88-24874
NAS: The first year
[NASA-TM-101006] 18 p2560 N88-25196
Aerodynamics of lifting bodies with combined transverse and longitudinal curvature 19 p2598 N88-25436
Aerodynamic focusing of particles and heavy molecules
[DE88-007145] 19 p2598 N88-25440
Aerodynamic analysis of natural laminar flow airfoil
19 p2634 N88-25624
Accurate, productive aerodynamic simulation on patched mesh systems
[AD-A192040] 19 p2714 N88-26110
Ludwig Prandtl collected treatises on applied mechanics, hydro- and aerodynamics, part 2, IV interfaces and resistance
[NASA-TT-20315] 20 p2752 N88-26338
A two-point aerodynamic model for identification
20 p2786 N88-26526
Parametric estimation of aerodynamic nonlinearities in rolling moment due to sideslip using maximum likelihood method 20 p2786 N88-26528
Aeronautical engineering: A continuing bibliography with indexes
[NASA-SP-7037(229)] 21 p2891 N88-27163
Analysis of experimental data for cast 10-2/DOA2 supercritical airfoil at high Reynolds numbers
[AD-A192827] 21 p2892 N88-27166
An experimental study of the effect of pitch rate on delta wing aerodynamics and stability
[NASA-CR-183159] 21 p2893 N88-27173
Design of a mechanism to control wind tunnel turbulence 21 p2926 N88-27370
Aerodynamics of Hypersonic Lifting Vehicles: Fluid Dynamics Panel AGARD Symposium
[AGARD-AR-246] 21 p2943 N88-27480
Aeronautical engineering: A continuing bibliography with indexes
[NASA-SP-7037(228)] 22 p3037 N88-28031
Three-dimensional zonal grids about arbitrary shapes by Poisson's equation
[NASA-TM-101018] 22 p3039 N88-28042
The role of acoustic resonances in unsteady turbomachinery aerodynamics
[PNR90455] 22 p3147 N88-28720
Theoretical aerodynamics, transonic flow
[AD-A196247] 24 p3321 N88-29777

AEROELASTIC RESEARCH WINGS
Analytic investigation of helicopter rotor blade appended aeroelastic devices
[NASA-CR-166525] 03 p0266 N88-11676
Prediction of wing aeroelastic effects on aircraft life and pitching moment characteristics
05 p0551 N88-13356

AEROELASTICITY
The history of aeroelasticity research in Germany from the beginning until 1945 --- airframes
[DFVLR-MITT-86-25] 01 p0001 N88-10003
Analytical modeling of helicopter static and dynamic induced velocity in GRASP
[NASA-TM-100026] 02 p0123 N88-10777
AGARD standard aeroelastic configurations for dynamic response. Candidate configuration I.-wing 445.6
[NASA-TM-100492] 02 p0192 N88-11202
On the prediction of the aeroelastic behavior of lifting systems due to flow separation
[ESA-TT-1043] 03 p0259 N88-11633
Linearized aeroelastic analysis of a wind turbine with a two-bladed rotor
[ETN-87-90600] 03 p0347 N88-12192
The effect of mass, wind angle and erection technique on the aeroelastic behaviour of a cable-stayed bridge model
[NAE-AN-46] 04 p0455 N88-12819
Numerica calculation in the Laplace domain for subsonic unsteady aerodynamic forces acting on a finite wing
05 p0535 N88-13256
Aeroelasticity and optimization in fighter aircraft design
05 p0546 N88-13324
Aeroelastic analysis of modern transport aircraft --- European Airbus
[SNIAS-872-111-102] 05 p0546 N88-13329
Velocity scaled aeroelastic testing of an unducted fan
[GTL-191] 05 p0548 N88-13337
Static Aeroelastic Effects on High Performance Aircraft
[AGARD-CP-403] 05 p0550 N88-13348
Examples of static aeroelastic effects on present combat aircraft projects 05 p0550 N88-13349
Trends in aeroelastic analysis of combat aircraft
05 p0550 N88-13350
Static aeroelastic considerations in the definition of design loads for fighter airplanes
05 p0550 N88-13351
Static aeroelastic effects on the flutter of a supercritical wing 05 p0550 N88-13353
The use of aeroelastic wind tunnel models to prove structural design 05 p0551 N88-13355
Prediction of wing aeroelastic effects on aircraft life and pitching moment characteristics
05 p0551 N88-13356
Influence of the static deformation on a wing in the unsteady aerodynamic 05 p0551 N88-13357
Solution procedure for the Navier-Stokes equations applied to rotors 05 p0579 N88-13533
A numerical model of unsteady, subsonic aeroelastic behavior
[NASA-TM-100487] 06 p0663 N88-14064
Modern wing flutter analysis by computational fluid dynamics methods
[NASA-TM-100531] 07 p0816 N88-14965
Unsteady transonic algorithm improvements for realistic aircraft applications
[NASA-TM-100516] 08 p0949 N88-15760
NASA/Army Rotorcraft Technology. Volume 1: Aerodynamics, and Dynamics and Aeroelasticity
[NASA-CP-2495-VOL-1] 09 p1105 N88-16625
Rotorcraft aeroelastic stability
09 p1106 N88-16631
Rotorcraft flight research with emphasis on rotor systems 09 p1111 N88-16656
Computational unsteady aerodynamics for aeroelastic analysis
[NASA-TM-100523] 09 p1112 N88-16668

Mach number effects on transonic aeroelastic forces and flutter characteristics
[NASA-TM-100547] 09 p1113 N88-16675
Loads and aeroelasticity division research and technology accomplishments for FY 1987 and plans for FY 1988
[NASA-TM-100534] 09 p1114 N88-16680
Experimental study on the effect of fiber orientation on flutter characteristics of high-aspect-ratio transport wing
[NAL-TR-936] 09 p1120 N88-16708
Flap-lag-torsion aeroelastic stability of a circulation control rotor in forward flight 10 p1271 N88-17600
Prediction of aeroelastic response of a model X-wing rotor 10 p1271 N88-17603
Using frequency-domain methods to identify XV-15 aeroelastic modes
[NASA-TM-100033] 10 p1277 N88-17646
The application of modern aeroelastic developments for future projects
[MBB-UT-007/87] 10 p1313 N88-17850
Vibration and flutter characteristics of the SR7L large-scale propfan
[NASA-TM-100272] 10 p1344 N88-18036
A discretization of the integral equation for the time dependent linearized subsonic potential flow over a wing
[AD-A188534] 12 p1574 N88-19411
Unsteady transonic small-disturbance theory including entropy and vorticity effects
[NASA-TM-100568] 12 p1575 N88-19418
Structural design requirements for aircraft incorporating active control technology 12 p1580 N88-19453
Design of an aeroelastic composite wing wind tunnel model
[AD-A188855] 12 p1582 N88-19466
An experimental investigation of the flap-lag-torsion aeroelastic stability of a small-scale hingeless helicopter rotor in hover
[NASA-TP-2546] 13 p1715 N88-20257
Application of a nonisentropic full potential method to AGARD standard airfoils
[NASA-TM-100560] 13 p1716 N88-20263
Aeroelastic models in aircraft design
[MBB/LKE-294/S/PUB/249] 13 p1722 N88-20298
Activities report of the Structures Department
[ETN-88-91986] 13 p1783 N88-20672
Scale model development for aeroelasticity studies
[ETN-88-91887] 14 p1868 N88-21164
Shape sensitivity analysis of wing static aeroelastic characteristics
[NASA-TP-2808] 15 p2018 N88-22031
A numerical model of unsteady, subsonic aeroelastic behavior
[NASA-TM-101126] 16 p2156 N88-22862
Lewis Structures Technology, 1988. Volume 1: Structural Dynamics
[NASA-CP-3003-VOL-1] 16 p2217 N88-23226
Development of aeroelastic analysis methods for turborotors and propfans, including mistuning
16 p2219 N88-23244
The 2-D and 3-D time marching transonic potential flow method for propfans 16 p2220 N88-23245
Aeroelastic forced response analysis of turbomachinery 16 p2220 N88-23247
Vibration and flutter analysis of the SR-7L large-scale propfan 16 p2221 N88-23254
Unsteady pressure and structural response measurements of an elastic supercritical wing
[NASA-TM-100591] 17 p2299 N88-23756
Control law parameterization for an aeroelastic wind-tunnel model equipped with an active roll control system and comparison with experiment
[NASA-TM-100593] 17 p2308 N88-23807
Aircraft aeroelasticity and structural dynamics research at the NASA Langley Research Center: Some illustrative results
[NASA-TM-100627] 18 p2459 N88-24598
Integrated Technology Rotor Methodology Assessment Workshop
[NASA-CP-10007] 21 p2889 N88-27148
A comparison of theory and experiment for aeroelastic stability of a hingeless rotor model in hover
21 p2889 N88-27150
A comparison of theory and experiment for coupled rotor-body stability of a hingeless rotor model in hover
21 p2889 N88-27152
A comparison of theory and experiment for the aeroelastic stability of a bearingless model rotor in hover
21 p2890 N88-27153
Effects of static equilibrium and higher-order nonlinearities on rotor blade stability in hover
21 p2890 N88-27157
Aeroelastic modeling of rotor blades with spanwise variable elastic axis offset: Classic issues revisited and new formulations 21 p2890 N88-27158
Comparison of experimental rotor damping data-reduction techniques 21 p2891 N88-27159
Comparison of experimental coupled helicopter rotor/body stability results with a simple analytical model
21 p2891 N88-27160
Aeromechanical stability analysis of COPTER
21 p2891 N88-27161
Aeroelastic characteristics of the AH-64 bearingless tail rotor 21 p2891 N88-27162
AGARD standard aeroelastic configurations for dynamic response. 1: Wing 445.6
[AGARD-R-765] 21 p2896 N88-27193
Prediction of the aeroelastic behavior of tuned blades. Application to aircraft engines
[ISAL-87-0046] 21 p2897 N88-27199
Nonlinear stochastic interaction in aeroelastic structures
[AD-A193427] 21 p2961 N88-27589
Experimental investigation of propfan aeroelastic response in off-axis flow with mistuning
[NASA-TM-101320] 22 p3089 N88-28344
SR-7A aeroelastic model design report
[NASA-CR-174791] 23 p3179 N88-28928
Application of unsteady aerodynamic methods for transonic aeroelastic analysis
[NASA-TM-100665] 24 p3317 N88-29754
History of aeroelasticity in Germany from the beginning to 1945
[ESA-TT-1082] 24 p3319 N88-29767
Recent advances in transonic computational aeroelasticity
[NASA-TM-100663] 24 p3321 N88-29778
Aeroelastic response of metallic and composite propfan models in yawed flow
[NASA-TM-100964] 24 p3326 N88-29807

AEROEMBOLISM
Space cabin atmosphere and extracurricular sortie --- embolisms 19 p2696 N88-26023

AEROLOGY
Statistical structure of temperature field over South Pacific Ocean 06 p0726 N88-14465
Acoustic propagation in the lower atmosphere
[ISL-R-126/87] 21 p3013 N88-27878

AEROMAGNETO FLUTTER
U FLUTTER

AERONAUTICAL ENGINEERING
Aeronautical engineering: A continuing bibliography with indexes (supplement 218)
[NASA-SP-7037(218)] 01 p0001 N88-10002
Color display programming for aviation
[DFVLR-MITT-87-03] 01 p0006 N88-10031
USSR Report: Engineering and Equipment
[JPRS-UEQ-87-007] 02 p0157 N88-10985
On the occasion of the 50th anniversary of the death of Professor Hugo Junkers
[MBB/LW-3016/S/PUB/201] 02 p0257 N88-11627
Status of titanium alloys R and D described
03 p0298 N88-11876
JPRS Report: Science and Technology. China
[JPRS-CST-87-033] 03 p0326 N88-12062
Aeronautical engineering: A continuing bibliography with indexes (supplement 219)
[NASA-SP-7037(219)] 04 p0396 N88-12470
JPRS report: Science and technology. Japan
[JPRS-JST-87-025] 04 p0403 N88-12502
USSR report: Engineering and equipment
[JPRS-UEQ-87-008] 04 p0423 N88-12621
Fundamentals of fighter aircraft design
05 p0544 N88-13316
Astronautics and aeronautics, 1978: A chronology
[NASA-SP-4023] 05 p0662 N88-14062
Aeronautical engineering: A continuing bibliography with indexes (supplement 220)
[NASA-SP-7037(220)] 06 p0663 N88-14065
Low frequency VLBI in space using GAS-Can satellites: Report on the May 1987 JPL Workshop
[NASA-CR-182362] 06 p0801 N88-14904
Aeronautical engineering. A continuing bibliography with indexes, supplement 221
[NASA-SP-7037(221)] 08 p0949 N88-15758
Aeronautical engineering: A continuing bibliography with indexes (supplement 223)
[NASA-SP-7037(223)] 09 p1111 N88-16661
Impact and promise of NASA aeropropulsion technology 09 p1118 N88-16698
Aeronautical engineering: A cumulative index to a continuing bibliography
[NASA-SP-7037(222)] 12 p1574 N88-19416
Research and technology, 1987
[NASA-TM-100323] 12 p1713 N88-20253
Aeronautical engineering: A continuing bibliography with indexes (supplement 224)
[NASA-SP-7037(224)] 13 p1715 N88-20254
Aeronautics and space report of the President: 1986 activities 13 p1852 N88-21087
Aeronautical engineering: A continuing bibliography with indexes (supplement 225)
[NASA-SP-7037(225)] 14 p1863 N88-21126
External tank gamma ray imaging telescope study. Final review, phase 2
[NASA-CR-179320] 15 p2150 N88-22834
Research and technology
[NASA-TM-100172] 15 p2153 N88-22851
Aeronautical engineering: A continuing bibliography with indexes (supplement 226)
[NASA-SP-7037(226)] 16 p2155 N88-22857
The use of the NRC/NAE water facilities in Canadian aeronautical research and development
16 p2201 N88-23132
The ONERA water tunnels test possibilities for flow visualization in aeronautical and Naval domains
16 p2202 N88-23139
Aeronautical engineering: A continuing bibliography with indexes (supplement 227)
[NASA-SP-7037(227)] 18 p2456 N88-24578
NASA history data book. Volume 1: NASA resources 1958-1968
[NASA-SP-4012-VOL-1] 18 p2596 N88-25428
The role of computational fluid dynamics in aeronautical engineering (5). Improvements and applications of implicit TVD finite volume code 19 p2638 N88-25653
Flight research and testing
[NASA-TM-100439] 20 p2758 N88-26361
Aeronautical engineering: A continuing bibliography with indexes
[NASA-SP-7037(229)] 21 p2891 N88-27163
Aeronautical engineering: A continuing bibliography with indexes
[NASA-SP-7037(228)] 22 p3037 N88-28031
Development and design of windtunnel and test facility for RPV (Remote Piloted Vehicle) enhancement devices
[AD-A194842] 24 p3329 N88-29822

AERONAUTICS
Langley aerospace test highlights, 1987
[NASA-TM-100595] 15 p2153 N88-22853
NASA historical data book. Volume 2: Programs and projects 1958-1968
[NASA-SP-4012-VOL-2] 18 p2596 N88-25429
NASA historical data book. Volume 3: Programs and projects 1969-1978
[NASA-SP-4012-VOL-3] 18 p2596 N88-25430
Activities report of the Department of Aerospace Engineering
[ETN-88-91607] 24 p3460 N88-30582

AERONOMY
Computer simulation procedure for designing airborne aerometric monitoring programs
[DE88-011896] 21 p2975 N88-27674
Aeronomic problems of the molecular oxygen photodissociation. Part 3: Solar spectral irradiances in the region of the O2 Herzberg continuum, Schumann-Runge bands and continuum
[AERONOMICA-ACTA-A-332-1988]
24 p3343 N88-29897
Aeronomic problems of molecular oxygen photodissociation. Part 2: Theoretical absorption cross sections of the Schumann-Runge bands at 79 K
[AERONOMICA-ACTA-A-331-1988]
24 p3344 N88-29907
Aeronomic problems of molecular oxygen photodissociation. Part 4: The various parameters for the Herzberg continuum
[AERONOMICA-ACTA-A-333-1988]
24 p3352 N88-29955

AEROPHYSICS
U ATMOSPHERIC PHYSICS

AEROSOLS
NT FOG
Aerosol sensor: Real time determination of aerosol mass size distributors using filtering quartz oscillators
[ETN-87-90397] 01 p0049 N88-10311
Comparison of three aerosol sampling techniques and the differences in the nitrate determined by each
[DE87-011456] 03 p0348 N88-12200
Plume mechanics and aerosol growth processes
[AD-A184467] 04 p0442 N88-12742
Thermophoresis of spherical aerosol particle at arbitrary Knudsen numbers 04 p0461 N88-12850
Theory of heat and moisture exchange between finely disperse storm-generated spray and turbulent air flow
04 p0461 N88-12851
Multiwave laser soundings of atmospheric aerosol: Experimental research (review)
04 p0461 N88-12852
Structure of stably stratified atmospheric surface layer in presence of heat-releasing admixture
04 p0462 N88-12856
Altered and enhanced iodargyrite with bismuth triiodide for use in precipitation enhancement operations
[AD-A185229] 05 p0561 N88-13419
Comparison of ground based and TOMS measurements of SO2 from volcanic emissions
05 p0618 N88-13795

Short-term in vitro screening studies related to the inhalation toxicology of potentially toxic aerosols
[AD-A184815] 05 p0629 N88-13845
Airborne particulate matter in spacecraft
[NASA-CP-2499] 06 p0753 N88-14623
Nonuniformity of electromagnetic field at Lambda = 10.6 micron wavelength inside atmospheric aerosol particles 06 p0772 N88-14743
Aerosol optical depth and ratios of diffuse-sky to total solar irradiance measured from aircraft following the eruption of El Chichon
[PB88-100789] 07 p0878 N88-15326
Atmospheric heating from optical absorption by aerosols
[DE88-002654] 07 p0878 N88-15327
Atmospheric science 07 p0883 N88-15357
Mechanisms of cloud layer formation in Venusian atmosphere 08 p1004 N88-16087
Mesoscale aerosol clouds 08 p1013 N88-16140
Characteristics and climatic relevance of the atmospheric aerosol components 08 p1017 N88-16164
An aureolar radiometer for the determination of aerosol size distribution 08 p1018 N88-16174
Aerosol size distribution from measurements of the radiance in the solar aureole 08 p1019 N88-16176
Remote measurement of aerosol stream velocity with continuous-wave CO2-laser 08 p1079 N88-16506
Aerosols in Martian Atmosphere and Natural Dust Observation (AMANDO). Proposal for the Mars orbiter balloon and rover to study the Martian atmosphere, its thermal content, and its interaction with the soil
[IFSI-87-9] 08 p1100 N88-16619
Comparison of UNL laser imaging and sizing system and a phase/Doppler system for analyzing sprays from a NASA nozzle
[NASA-CR-182437] 09 p1161 N88-16956
Design and characteristics of a liquid aerosol generator
[AD-A186942] 09 p1174 N88-17034
Radon Research Program, FY-1987
[DE88-002633] 09 p1188 N88-17120
Induced turbulence in aerosol-loaded atmospheres , Jun. 1987
[DE87-014724] 09 p1192 N88-17141
Statistics of breakdown centers appearing during propagation of laser radiation through turbulent atmosphere 09 p1236 N88-17411
Christiansen effect in infrared spectra of soil-derived atmospheric dusts
[AD-A187071] 09 p1248 N88-17479
Meteorological and aerosol measurements from the NOAA WP-3D aircraft during WATOX-86, January 4-9, 1986
[PB88-120860] 10 p1352 N88-18079
Measurement of combustion aerosol size distributions with multistage inertial impactors
[DE88-751101] 11 p1454 N88-18669
Optical characterization of tropospheric aerosols
[AD-A187839] 11 p1511 N88-19029
Photoacoustic measurements of atmospheric aerosol absorption coefficients at ultraviolet, visible and infrared wavelengths 11 p1512 N88-19036
Air quality and human performance, chapter 16
[AD-A188335] 12 p1666 N88-19988
Fibrous glass aerosols: A literature review
[AD-A188420] 12 p1672 N88-20008
Vertical structure of Venusian cloud layer at landing sites of Vega-1 and Vega-2 vehicles 13 p1725 N88-20317
Roentgenoradiometric analysis of aerosol in Venusian clouds by Vega-1 and Vega-2 automatic interplanetary stations 13 p1726 N88-20319
Determining chemical composition of aerosol in Venusian cloud layer on Vega-1 automatic interplanetary station using Malakhit mass spectrum analyzer 13 p1726 N88-20321
Observations on electrostatic effects in a filter test system
[AD-A188797] 13 p1736 N88-20378
Application of laser-induced fluorescence in an atmospheric-pressure boron-seeded flame
[AD-A189631] 14 p1889 N88-21287
Combined aerodynamic size, charge-to-mass, and velocity measurements of aerosol particles
[ST-REPT-VOL-5-NO-4] 14 p1944 N88-21599
Corrections for differential scattering by aerosols in the measurement of ozone by DIAL --- differential absorption lidar (DIAL)
[NPL-QU-78] 14 p1945 N88-21603
Optical properties of Southern Hemisphere aerosols: Report of the joint CSIRO/NASA study
[NASA-CR-179287] 14 p1945 N88-21605
Analysis of meteorological conditions and haze distribution for the Second Arctic Gas and Aerosol Sampling Program (AGASP 2), March-April 1986
[PB88-164140] 14 p1948 N88-21618
Aerosol lidar for environment protection and meteorology
[DFVLR-FB-87-43] 14 p1982 N88-21828
Study of mean free path effects on growth of ultrafine metallic aerosols
[AD-A190206] 15 p2039 N88-22149
The optical properties of aerosols
[AD-A191420] 16 p2176 N88-22972
Understanding CO2 and climate
[PB88-167655] 16 p2234 N88-23341
SAGE 1 and SAM 2 measurements of 1 micron aerosol extinction in the free troposphere
[NASA-CR-182945] 17 p2374 N88-24121
High-energy laser-assisted imaging through vaporizing aerosols
[DE88-007911] 18 p2521 N88-24957
Information analysis of integral equations in remote sensing of atmospheric aerosols 18 p2532 N88-25022
SAM 2 data user's guide
[NASA-RP-1200] 18 p2543 N88-25094
Aerodynamic focusing of particles and heavy molecules
[DE88-007145] 19 p2598 N88-25440
Laser-RDX aerosol pyrolysis with matrix isolation of unstable intermediates 19 p2632 N88-25614
Composite, meso-gamma scale diagnostic modeling
[DE88-008189] 19 p2689 N88-25983
Studies of the mechanisms and rates with which nitrogen species are incorporated into cloud water and precipitation
[PB88-193065] 20 p2826 N88-26764
Cloud simulation warm cloud experiments: Droplet growth and aerosol scavenging
[AD-A192944] 21 p2974 N88-27666
Interpretation of the polarimetric observations of Jupiter
[DE88-702414] 21 p3031 N88-27991
South Pole lidar: Brief description of the instrument
[NOTA-INTERNA-907] 22 p3083 N88-28308
IR (infrared) sky radiance distributions in the marine boundary layer
[AD-A193683] 22 p3119 N88-28531
Stratocumulus and cloud-free reflectance from multi-spectral satellite measurements
[AD-A193899] 22 p3128 N88-28599
Real-time measurements of the size fractionation of ambient black carbon aerosols at elevated humidities
[DE88-010870] 23 p3215 N88-29138
High energy and high intensity laser effects on aerosols: Changes in droplet morphology, surrounding temperature and vapor concentration
[AD-A193825] 23 p3220 N88-29164
Forty-eight-inch lidar aerosol measurements taken at the Langley Research Center, May 1974 to December 1987
[NASA-RP-1209] 23 p3232 N88-29234
European validation of SAGE-2 aerosol profiles
[AERONOMICA-ACTA-A-327-1988] 23 p3234 N88-29243
Microphysical processes in cloud layers of Venus 24 p3448 N88-30522
Possibilities of determining vertical profiles of microphysical characteristics of stratospheric aerosol using space measurements of transparency and solar halo 24 p3449 N88-30526
Volatiles on Mars
[NASA-CR-183113] 24 p3456 N88-30571

AEROSPACE ENGINEERING
NT AERONAUTICAL ENGINEERING
Numerical simulation system 04 p0404 N88-12511
Astronautics and aeronautics, 1978: A chronology
[NASA-SP-4023] 05 p0662 N88-14062
NAL news updated: FY87 business plan, developments 06 p0675 N88-14135
Research and technology objectives and plans. Summary, Fiscal Year 1986
[NASA-TM-87504] 06 p0800 N88-14894
Activities report in aircraft design and astronautics
[ETN-88-90618] 07 p0809 N88-14925
Investigation of design concepts for large space structures to support military applications
[AD-A186098] 07 p0824 N88-15000
Internal fluid mechanics research on supercomputers for aerospace propulsion systems
[NASA-TM-100289] 07 p0854 N88-15188
FY87 scientific and technical reports, articles, papers, and presentations
[NASA-TM-100318] 08 p1093 N88-16578
Environment assisted degradation mechanisms in aluminum-lithium alloys
[NASA-CR-182482] 10 p1301 N88-17782
Messerschmitt-Boelkow-Blohm: A company with a tradition 10 p1316 N88-17866
JPRS report: Science and technology. Europe and Latin America
[JPRS-ELS-88-003] 11 p1468 N88-18754
JPRS report: Science and technology. China
[JPRS-CST-87-029] 11 p1468 N88-18755
JPRS report. Science and technology: Europe and Latin America
[JPRS-ELS-87-054] 12 p1573 N88-19406
JPRS report. Science and technology: Europe and Latin America
[JPRS-ELS-87-055] 12 p1686 N88-20086
JPRS report: Science and technology. USSR: Space
[JPRS-USP-88-002] 13 p1724 N88-20312
JPRS report: Science and technology. China
[JPRS-CST-88-003] 13 p1755 N88-20495
JPRS report: Science and technology. China
[JPRS-CST-87-030] 13 p1756 N88-20501
Aeronautics and space report of the President: 1986 activities 13 p1852 N88-21087
Wave propagation and dynamics of lattice structures
[AD-A190611] 15 p2025 N88-22069
JPRS report: Science and technology. Japan
[JPRS-JST-88-001] 15 p2051 N88-22218
JPRS report: Science and technology. Japan
[JPRS-JST-87-029] 15 p2052 N88-22228
Life and reliability of rotating disks 15 p2085 N88-22428
JPRS report: Science and technology. Japan
[JPRS-JST-87-030] 16 p2185 N88-23026
JPRS report: Science and technology. China
[JPRS-CST-88-009] 16 p2186 N88-23030
A low dimensional dynamical system for the wall layer 16 p2194 N88-23088
Technology development program for twenty-first century aerospace vehicles 17 p2302 N88-23768
Soviet spacecraft engineering research
[FASAC-TAR-3090] 17 p2311 N88-23823
Effects of spatial resolution in CARS measurements
[PB88-121900] 18 p2482 N88-24727
Marine techniques: R and D axes, identification of areas of common interest with space techniques 19 p2629 N88-26047
Aerospace applications studies, 1971-1987
[AGARD-R-759] 21 p2889 N88-27147
Damping characteristics of metal matrix composites
[AD-A193144] 21 p2904 N88-27233
The 1988 Goddard Conference on Space Applications of Artificial Intelligence
[NASA-CP-3009] 24 p3415 N88-30330
Activities report of the Department of Aerospace Engineering
[ETN-88-91607] 24 p3460 N88-30582

AEROSPACE ENVIRONMENTS
NT EARTH ORBITAL ENVIRONMENTS
NT INTERPLANETARY SPACE
NT INTERSTELLAR SPACE
TIROS-N/NOAA A-J space environment monitor subsystem
[PB87-203998] 01 p0015 N88-10083
The combined release and radiation effects satellite, a joint NASA/DOD program 02 p0135 N88-10851
High temperature metal matrix composites for future aerospace systems
[NASA-TM-100212] 02 p0149 N88-10938
Effects of long term storage on aerospace nickel cadmium cell performance 02 p0165 N88-11035
Space Environment Technology --- conference
[ISBN-2-85428-170-5] 03 p0271 N88-11702
Irradiations. Accumulated doses. Heavy ions --- space environment 03 p0272 N88-11708
Low Earth orbit environmental effects on the space station photovoltaic power generation systems
[NASA-TM-100230] 03 p0387 N88-12429
Mechanistic studies of polymeric samples exposed aboard STS 8
[NASA-CR-182364] 06 p0686 N88-14202
Comparative anatomic analysis of seedling organs of pisum sativum (fabaceae) cultivated under space flight conditions 06 p0749 N88-14603
Airborne particulate matter in spacecraft
[NASA-CP-2499] 06 p0753 N88-14623
Space environmental effects on polymeric materials
[NASA-CR-182418] 07 p0838 N88-15082
Exobiology and life science 07 p0883 N88-15358
Resolution of holograms produced by the fluid experiment system and the holography ground system 07 p0923 N88-15609
Space environmental effects on polymeric materials
[NASA-CR-182454] 09 p1148 N88-16879
Space station integrated wall damage and penetration damage control. Task 5: Space debris measurement, mapping and characterization system
[NASA-CR-179281] 10 p1285 N88-17688

USSR Space Life Sciences Digest, issue 15
[NASA-CR-3922(18)] 10 p1368 N88-18175
Radiation and temperature effects on the time-dependent response of T300/934 graphite/epoxy
[NASA-CR-182603] 11 p1451 N88-18646
Oxidation and protection of fiberglass-epoxy composite masts for photovoltaic arrays in the low Earth orbital environment
[NASA-TM-100839] 11 p1465 N88-18734
Microgravity and Materials Processing Facility study (MMPF): Requirements and Analyses of Commercial Operations (RACO) preliminary data release
[NASA-CR-179309] 11 p1466 N88-18742
Study of industry requirements that can be fulfilled by combustion experimentation aboard space station
[NASA-CR-180854] 11 p1566 N88-19377
Space utilization plans 15 p2051 N88-22219
Microgravity robotics technology program
[NASA-TM-100898] 16 p2215 N88-23219
EnviroNET: An interactive space-environment information resource
[NASA-TM-101137] 17 p2309 N88-23812
Space spider crane
[NASA-CASE-LAR-13411-1-SB] 17 p2312 N88-23828
Turbomachinery in space 17 p2408 N88-24321
Electromagnetic damping and vibration isolation of space structures
[AD-A191492] 18 p2471 N88-24665
Technologies applicable to space tethers
[NASA-CR-183055] 19 p2606 N88-25471
Application of AI to space systems 19 p2634 N88-25626
Evaluation of the ion trap mass spectrometer for potential application in the space station
[DE88-008940] 19 p2674 N88-25902
Microgravity science and applications bibliography, 1987 revision
[NASA-TM-4067] 22 p3062 N88-28171
Optimization of low gravity materials processing experiments using expert systems 23 p3252 N88-29361

AEROSPACE INDUSTRY
NT AIRCRAFT INDUSTRY
Aerospace research at the National Aerospace Laboratory (NLR)
[ETN-87-90821] 01 p0107 N88-10697
Implementation of finite element quality assurance in a commercial industrial organisation
[PNR90393] 02 p0183 N88-11137
Fundamentals of fighter aircraft design 05 p0544 N88-13316
Requirements and recommendations for the development of theoretical codes and experimental facilities in the near future 05 p0546 N88-13327
Measurements in an electromagnetic test laboratory
[SNIAS-872-430-102] 05 p0575 N88-13507
Operational groups at the Aerospatiale Aircraft Division
[SNIAS-872-111-107] 05 p0658 N88-14036
Activities report in aircraft design and astronautics
[ETN-88-90618] 07 p0809 N88-14925
Wind shear detection. Forward-looking sensor technology
[NASA-CP-10004] 07 p0817 N88-14970
The appropriate use of contract types in development contracts (a systems approach with emphasis on the European space sector)
[ESA-STR-222] 08 p1092 N88-16573
The ESA centralized management system for satellite electronic test and checkout instrumentation 09 p1124 N88-16731
European industrial consortia, for space projects: Their origins, development and possible evolution 09 p1128 N88-16765
Research, development, and growth strategy 10 p1309 N88-17820
Cooperation know-how in high-tech products
[MBB-Z-101/86] 10 p1311 N88-17833
The prospects of space utilization
[MBB-UR-931/86] 10 p1314 N88-17856
Messerschmitt-Boelkow-Blohm: A company with a tradition 10 p1316 N88-17866
Messerschmitt-Boelkow-Blohm: Biography and history of a company 10 p1316 N88-17867
Messerschmitt-Boelkow-Blohm, the company today. Data, numbers and facts 10 p1316 N88-17868
JPRS report: Science and Technology. Europe and Latin America
[JPRS-ELS-88-002] 10 p1316 N88-17870
A comparison of projection methods in the forecasting of overhead costs for seven government aerospace contractors
[AD-A187572] 10 p1425 N88-18514
The judgement and evaluation of long-term investments demonstrated by means of a civil aircraft program 12 p1701 N88-20180
Time and cost reduction through computer integrated manufacture 12 p1703 N88-20191
Acceleration of prototype development and reduction of cost by multidisciplinary integration 12 p1704 N88-20199
Quality and productivity drive innovation and improvement at United Technologies Aerospace Operations, Inc.
[NASA-CR-182944] 18 p2525 N88-24983
Air Force technical objective document, FY89
[AD-A193110] 21 p2896 N88-27194
Managing and controlling change
[PNR90419] 22 p3159 N88-28801
Aircraft airframe cost estimating relationships: Study approach and conclusions
[R-3255-AF] 24 p3324 N88-29795
Study on industrial organization for European Ground Support Equipment (EGSE) to support European space programs. Volume 1: Technical reports
[SD-RP-AI-009-VOL-1] 24 p3435 N88-30446
Study on industrial organization for European Ground Support Equipment (EGSE) to support European space programs. Volume 2: Technical reports
[SD-RP-AI-009-VOL-2] 24 p3435 N88-30448

AEROSPACE MEDICINE
NT AVIATION PSYCHOLOGY
NT SPACE PSYCHOLOGY
Aerospace medicine and biology: A continuing bibliography with indexes
[NASA-SP-7011(303)] 02 p0217 N88-11367
Summary report of the history and events pertinent to the Civil Aeromedical Institute's evaluation of providing smoke/fume protective breathing equipment for airline passenger use
[AD-A184499] 03 p0261 N88-11645
Motion and space sickness 04 p0404 N88-12510
JPRS report: Science and technology. USSR: Life sciences
[JPRS-ULS-87-009] 04 p0473 N88-12915
Study of certain biological characteristics of bacteria during the French-Soviet CYTOS-2 space experiment 04 p0473 N88-12917
Aerospace medicine and biology: A continuing bibliography with indexes
[NASA-SP-7011(304)] 04 p0474 N88-12922
Human respiratory responses during high performance flight
[AGARD-AG-312] 04 p0474 N88-12923
JPRS report: Science and technology. USSR: Life sciences
[JPRS-ULS-87-011] 06 p0749 N88-14601
Electron cytochemical detection of Ca(2)+-ATPase in protonema of moss funaria hygrometrica (H e d w.) under hypogravitation 06 p0749 N88-14602
Comparative anatomic analysis of seedling organs of pisum sativum (fabaceae) cultivated under space flight conditions 06 p0749 N88-14603
Aerospace medicine and biology: A continuing bibliography with indexes (supplement 305)
[NASA-SP-7011(305)] 06 p0752 N88-14616
JPRS report: Science and technology. USSR: Space Biology and Aerospace Medicine, volume 21, no. 3, May - June 1987
[JPRS-USB-88-001] 07 p0889 N88-15389
JPRS report: Science and technology. USSR: Space Biology and Aerospace Medicine, volume 21, no. 4, July - August 1987
[JPRS-USB-88-002] 07 p0893 N88-15412
Use of bifidumbacterin for correction of intestinal dysbacteriosis 07 p0895 N88-15427
Bibliography of space biology and medicine 07 p0897 N88-15435
JPRS report: Science and technology. USSR: Space
[JPRS-USP-87-006] 08 p1001 N88-16063
Space biology and medicine 08 p1006 N88-16096
USSR Space Life Sciences Digest, issue 14
[NASA-CR-3922(16)] 08 p1045 N88-16317
USSR report: Life sciences. Biomedical and behavioral sciences
[JPRS-UBB-86-022] 08 p1046 N88-16318
Preliminary evaluation of a micro-based repeated measures testing system
[NASA-CR-172038] 08 p1048 N88-16331
Aerospace medicine and biology: A continuing bibliography with indexes (supplement 307)
[NASA-SP-7011(307)] 08 p1049 N88-16332
Sudden in-flight incapacitation in general aviation
[AD-A187044] 09 p1115 N88-16682
JPRS Report: Science and Technology. USSR: Space Biology and Aerospace Medicine, volume 21, no. 5, September - October 1987
[JPRS-USB-88-003] 10 p1359 N88-18122
Medical and psychological problems of assuring flight safety under present conditions 10 p1359 N88-18123
Isotope methods of determining distribution and movement of blood in the body 10 p1362 N88-18138
Discrete adaptation to sensory conflict 10 p1363 N88-18146
JPRS Report: Science and Technology. USSR: Space Biology and Aerospace Medicine, volume 21, no. 6, November - December 1987
[JPRS-USB-88-004] 10 p1364 N88-18150
Present stage of space medicine 10 p1364 N88-18151
Improvement of human tolerance to head-pelvis (+Gz) accelerations by increasing hydration 10 p1364 N88-18153
Aerospace medicine and biology: A cumulative index to a continuing bibliography (supplement 306)
[NASA-SP-7011(306)] 10 p1369 N88-18180
Aerospace medicine and biology: A continuing bibliography with indexes (supplement 308)
[NASA-SP-7011(308)] 10 p1369 N88-18183
JPRS report: Science and technology. USSR: Life sciences
[JPRS-ULS-88-001] 11 p1520 N88-19079
Summary of Payload Integration Plan (PIP) for Starlab-1 flight experiment, enclosure 3
[NASA-TM-89713] 11 p1522 N88-19086
Full scale architectural simulation techniques for space stations 12 p1651 N88-19887
Life science techonology --- space applications 12 p1653 N88-19900
Liquid ventilation: New data and possible use in space medicine 12 p1654 N88-19908
Medilab: A project of a medical laboratory in space 12 p1660 N88-19946
Gastric emptying assessment by echography after a stress (rotating chair) 12 p1661 N88-19955
USSR report: Life sciences. Biomedical and behavioral sciences
[JPRS-UBB-87-008] 12 p1662 N88-19966
Selected aspects of triazolam in relation to aviator performance in naval flight operations
[AD-A189322] 12 p1667 N88-19996
Aerospace medicine and biology: A continuing bibliography with indexes (supplement 309)
[NASA-SP-7011(309)] 13 p1810 N88-20814
USSR Space Life Sciences Digest, issue 16
[NASA-CR-3922(19)] 15 p2101 N88-22515
Aerospace medicine and biology: A continuing bibliography with indexes (supplement 310)
[NASA-SP-7011(310)] 16 p2238 N88-23369
USSR Space Life Sciences Digest, issue 17
[NASA-CR-3922(20)] 17 p2381 N88-24155
Aerospace medicine and biology: A continuing bibliography with indexes (supplement 311)
[NASA-SP-7011(311)] 17 p2382 N88-24161
Aerospace medicine and biology: A continuing bibliography with indexes (supplement 312)
[NASA-SP-7011(312)] 18 p2551 N88-25141
JPRS report: Science and technology. USSR: Space Biology and Aerospace Medicine, volume 22, no. 1, January - February 1988
[JPRS-USB-88-005] 19 p2702 N88-26069
Results of medical research conducted in 1985 during long-term spaceflights 19 p2702 N88-26070
USSR space life sciences digest, issue 18
[NASA-CR-3922(21)] 19 p2707 N88-26096
JPRS report: Science and technology. USSR: Life sciences
[JPRS-ULS-88-009] 20 p2829 N88-26785
Does dihydroergotamine used in therapeutical doses influence the physical and psychomotor performance of young pilots or other traffic drivers subjected to hypotonia?
[ETN-88-92136] 20 p2832 N88-26799
Aerospace medicine and biology: A continuing bibliography with indexes (supplement 313)
[NASA-SP-7011(313)] 20 p2832 N88-26800
Electric and Magnetic Activity of the Central Nervous System: Research and Clinical Applications in Aerospace Medicine
[AGARD-CP-432] 21 p2977 N88-27683
Simulator sickness in the AH-64 Apache combat mission simulator
[AD-A193419] 21 p2988 N88-27739
Aerospace Medicine and Biology: A continuing bibliography with indexes (supplement 314)
[NASA-SP-7011(314)] 21 p2988 N88-27742
Activities report in aerospace medicine
[ETN-88-92906] 23 p3240 N88-29283
Central serous chorioretinopathy in USAF aviators: A review
[AD-A195697] 24 p3407 N88-30280

Aerospace medicine and biology: A continuing bibliography with indexes (supplement 315)
[NASA-SP-7011(315)] 24 p3407 N88-30281

AEROSPACE PLANES
NT HOTOL LAUNCH VEHICLE
NT X-30 VEHICLE
National aero-space plane: A technology development and demonstration program to build the X-30
[GAO/NSIAD-88-122] 17 p2301 N88-23764
Review of convectively cooled structures for hypersonic flight
[NASA-TM-87740] 17 p2310 N88-23817
Heat transfer in aerospace propulsion
[NASA-TM-100874] 17 p2339 N88-23957
A system status monitor for the National Aerospace Plane
[AD-A190681] 18 p2463 N88-24624
Guidance and control strategies for aerospace vehicles
[NASA-CR-183032] 18 p2467 N88-24644
High speed and high angle of attack wind tunnel test results of the winged space vehicle C-2
[ISAS-RN-623] 20 p2751 N88-26329
Ascent guidance for a winged boost vehicle
[NASA-CR-172083] 24 p3334 N88-29846
A study of the critical factors controlling the synthesis of ceramic matrix composites from preceramic polymers
[AD-A195405] 24 p3340 N88-29681

AEROSPACE SAFETY
Report of the helicopter human factors working group --- accident prevention
[CAA-PAPER-87007] 03 p0361 N88-12274
Civil aeronautics
[ETN-88-90616] 05 p0543 N88-13309
Safety philosophy, policy, and requirements for manned spaceflight. Volume 1: Executive summary
[HEG-0886/1036-VOL-1] 08 p0962 N88-15826
Parachute for in-flight training on parachute ejection
[REPT-87-11] 18 p2458 N88-24593

AEROSPACE SCIENCES
Trends in research and development in the Netherlands. The influence of national science policy between 1973 and 1986
[B8701588] 08 p1094 N88-16580
Activities report in aerospace
[ETN-88-91978] 14 p1991 N88-21886
USSR Space Life Sciences Digest, issue 16
[NASA-CR-3922(19)] 15 p2101 N88-22515
NASA scientific and technical publications: A catalog of Special Publications, Reference Publications, Conference Publications, and Technical Papers, 1987
[NASA-SP-7063(02)] 15 p2149 N88-22830
Issues and recommendations associated with distributed computation and data management systems for the space sciences
[NASA-CR-183026] 20 p2881 N88-27108
JPRS report: Science and technology. USSR: Space
[JPRS-USP-88-001] 24 p3444 N88-30498

AEROSPACE SYSTEMS
Design of a condenser-boiler for a binary mercury-organic Rankine cycle solar dynamic space power system
[AD-A184188] 03 p0348 N88-12198
An approach to implementing state space searches on heterogeneous systems of multiprocessors
[DE88-001321] 04 p0482 N88-12967
Initial dynamic load estimates during configuration design 05 p0593 N88-13621
AGARD: The NATO Advisory Group for Aerospace Research and Development
[AD-A185062] 05 p0662 N88-14063
Maximum entropy/optimal projection design synthesis for decentralized control of large space structures
[AD-A186359] 07 p0824 N88-15003
An inference engine for embedded diagnostic systems 08 p1056 N88-16367
KBS V and V as related to automation of space station subsystems: Rationale for a KBS lifecycle 08 p1057 N88-16375
Case-based reasoning for space applications: Utilization of prior experience in knowledge-based systems 08 p1065 N88-16433
Relating service doctrine to space system requirements
[AD-A186620] 08 p1074 N88-16483
AGARD reports: A quarterly listing, 1 July through September 30, 1987
[AD-A186572] 08 p1093 N88-16579
Verification of a micro-thrusting model to maintain satellites in low orbit
[AD-A186874] 09 p1133 N88-16793
Multipurpose corrosion inhibitors for aerospace materials in Naval environments
[AD-A186728] 09 p1143 N88-16853
High-resolution Real-Time Radiography (RTR) system design
[AD-A187107] 09 p1186 N88-16992
Dynamic stress at critical locations of a structure as a criterion for mathematical model modification 09 p1180 N88-17066
Advanced decision aiding techniques applicable to space 09 p1209 N88-17250
The evolution of naval warfare technology and the impact of space systems
[AD-A186900] 09 p1233 N88-17392
A strategy for space warfare
[AD-A186658] 09 p1233 N88-17394
AFAL (Air Force Astronautics Laboratory) technical objective document FY89
[AD-A187861] 11 p1567 N88-19378
Hot corrosion in gas turbines: A new, unique and informative technique is EASE (Electronic Absorption Spectroscopy Experiments)
[AD-A188508] 12 p1583 N88-19470
Activities report of the Systems Department
[ETN-88-91987] 13 p1756 N88-20505
Vapor-mist for lightweight high voltage space insulation systems
[DE87-011704] 13 p1762 N88-20538
Compatibility in space reactor fuel systems
[DE88-005698] 13 p1839 N88-21004
JPRS report: Science and technology. China
[JPRS-CST-87-023] 14 p1863 N88-21130
On the danger of redundancies in some aerospace mechanisms 14 p1925 N88-21475
Technologies applicable to space tethers
[NASA-CR-183055] 19 p2606 N88-25471
Application of AI to space systems 19 p2634 N88-25626
Army space systems for terrestrial applications
[AD-A192735] 21 p2965 N88-27613
Electronic combat roadmap for space
[AD-A194282] 22 p3146 N88-28709
Intelligent test integration system 23 p3254 N88-29371
Sensor and actuator selection for large space structure control
[AD-A194912] 24 p3333 N88-29842

AEROSPACE TECHNOLOGY TRANSFER
Spinoff, 1987
[NASA-TM-89652] 02 p0250 N88-11577
AGARD: The NATO Advisory Group for Aerospace Research and Development
[AD-A185062] 05 p0662 N88-14063
Cooperation know-how in high-tech products
[MBB-Z-101/86] 10 p1311 N88-17833
Langley aerospace test highlights, 1987
[NASA-TM-100595] 15 p2153 N88-22853

AEROSPACE VEHICLES
NT AEROSPACE PLANES
NT FLEXIBLE SPACECRAFT
NT HOTOL LAUNCH VEHICLE
NT X-30 VEHICLE
Computational methods for problems in aerodynamics and large space structure using parallel and vector architectures
[AD-A185401] 05 p0541 N88-13294
Guidance and control strategies for aerospace vehicles
[NASA-CR-181579] 05 p0643 N88-13935
Hypervelocity Technology (HVT) crew escape 09 p1214 N88-17280
Rainfall rates and drop-size distributions for environmental testing
[AD-A191342] 16 p2236 N88-23354
Study of the influence of metallurgical factors on fatigue and fracture of aerospace structural materials
[AD-A192909] 20 p2774 N88-26452
Knowledge-based fault diagnosis on future space vehicles 23 p3254 N88-29374
Dynamics of articulated aerospace structures
[AD-A195685] 24 p3324 N88-29794
Automated early fatigue damage sensing system
[AD-A195717] 24 p3382 N88-30143

AEROSTATICS
Static Aeroelastic Effects on High Performance Aircraft
[AGARD-CP-403] 05 p0550 N88-13348

AEROSTATS
U AIRSHIPS

AEROTHERMOCHEMISTRY
Summary of discussions at the Ninth Meeting of the Sandia Cooperative Group on the Aerothermochemistry of Turbulent Combustion
[DE88-002281] 06 p0680 N88-14165
Summary of discussions at the Tenth Meeting of the Sandia Cooperative Group on the Aerothermochemistry of Turbulent Combustion
[DE88-008467] 21 p2910 N88-27269

AEROTHERMODYNAMICS
The aerothermodynamic environment for holes in hypersonic configurations
[DE87-014851] 02 p0121 N88-10767
Aerothermal modeling program, phase 2 02 p0185 N88-11149
A 3-D Euler solution for hypersonic Mach numbers 05 p0533 N88-13240
Aerothermodynamics research at NASA Ames 05 p0533 N88-13242
The off-design performance of hypersonic waveriders 05 p0533 N88-13244
General aerodynamic-aerothermodynamic concepts for Hermes 05 p0535 N88-13251
HOST turbine heat transfer program summary
[NASA-TM-100280] 06 p0704 N88-14320
Computational fluid dynamics and aerothermodynamics
[NASA-CR-182490] 09 p1166 N88-16989
Shock wave/turbulent boundary layer interaction in high-Reynolds-number hypersonic flows
[AD-A188029] 11 p1434 N88-18555
Assessment, development and application of combustor aerothermal models
[NASA-TM-100290] 12 p1582 N88-19469
Activities report of the Toulouse Research Center
[ETN-88-91988] 13 p1850 N88-21077
Aerothermal tests of quilted dome models on a flat plate at a Mach number of 6.5
[NASA-TP-2804] 15 p2067 N88-22325
Review and assessment of the HOST turbine heat transfer program 15 p2086 N88-22431
Experimental measurements of heat transfer from an iced surface during artificial and natural cloud icing conditions
[AIAA-PAPER-88-1352] 17 p2293 N88-23718
Application of integrated fluid-thermal-structural analysis methods
[NASA-TM-100625] 17 p2350 N88-24001
Analysis of gas turbine test cell number 1, Lemoore Naval Air Station, California
[AD-A192870] 20 p2762 N88-26380
Adaptive computational methods for aerothermal heating analysis
[NASA-CR-181636] 23 p3212 N88-29115
Numerical models for analytical predictions of combustor aerothermal performance characteristics 24 p3349 N88-29935
Impact of ETO propellants on the aerothermodynamic analyses of propulsion components
[NASA-TM-101303] 24 p3374 N88-30094

AFC (CONTROL)
U AUTOMATIC FREQUENCY CONTROL

AFCS (CONTROL SYSTEM)
U AUTOMATIC FLIGHT CONTROL

AFFINITY
NT ELECTRON AFFINITY

AFRICA
Desertification in the Sahelian and Sudanian Zones of West Africa
[PB87-217063] 03 p0345 N88-12183
Environmental processes and spectral reflectance characteristics associated with soil erosion in desert fringe regions
[NASA-CR-182332] 05 p0620 N88-13811
Northern Hemisphere circulation and the principal components of subsequent summer patterns in North America and West Africa 13 p1801 N88-20765
Using space photography of the Earth in the classroom: Drought in Africa
[NASA-CR-182948] 19 p2685 N88-25960
Westward moving atmospheric wave disturbances over the African tropics: Dynamic and energetic aspects
[MITT-57] 20 p2827 N88-26774
Monitoring of agricultural production in West Africa. The need to integrate different satellite platforms 22 p3096 N88-28383
Modes of interannual climate variability and Sahel rainfall anomalies 22 p3121 N88-28547
ENSO, sea-surface temperatures and African rainfall 22 p3122 N88-28550
Sub-Saharan rainfall anomalies and global sea-surface temperature relationships for the recent fifteen year (1970-1984) period 22 p3122 N88-28552
Simulation studies of the influence of sea-surface temperature anomalies on the Sahelian circulation and rainfall 22 p3122 N88-28553
An observational study of interaction between large scale tropical cumulus convection and the equatorial circulation anomalies 22 p3124 N88-28564

AFRICAN RIFT SYSTEM
Geologic results obtained from the use of SPOT imagery along plate boundaries: Examples in the East African rift and of the northern-Caribbean collision 22 p3105 N88-28437

AFTERBODIES
Comparison of wind tunnel and flight test afterbody and nozzle pressures for a twin-jet fighter aircraft at transonic speeds
[NASA-TP-2588] 02 p0121 N88-10765
Effect of empennage arrangement on single-engine nozzle/afterbody static pressures at transonic speeds
[NASA-TP-2753] 02 p0122 N88-10771
A calculation method for the propulsive jet and its aerodynamic interaction with an afterbody
[ESA-TT-1039] 03 p0259 N88-11632
A dynamic model for the aft accumulator in the TE SP-100 system 17 p2414 N88-24354
Variable Mach number wall jets for control/propulsion on hypervelocity projectiles/interceptors: Tests with an existing model
[AD-A192845] 21 p2892 N88-27167
AFTERBURNERS
U AFTERBURNING
AFTERBURNING
Kinetic mechanisms for ionization and afterburning suppression
[AD-A189219] 13 p1737 N88-20383
High performance turbofan afterburner systems 24 p3347 N88-29922
AGB STARS
U ASYMPTOTIC GIANT BRANCH STARS
AGE DETERMINATION
U CHRONOLOGY
AGE FACTOR
Drosophila geotaxis as a tool for the study of aging 10 p1288 N88-17706
Age, alcohol, and simulated altitude: Effects on performance and breathalyzer scores
[AD-A190642] 15 p2103 N88-22531
Biological patterns of growth in postnatal ontogenesis of lower primates 19 p2705 N88-26087
AGE HARDENING
U PRECIPITATION HARDENING
AGGLOMERATION
Measurement of agglomerate strength distributions in agglomerated powders
[DE87-013605] 01 p0090 N88-10591
Comparison of calculated and measured ignition times for boron agglomerates 19 p2624 N88-25563
Reducing adhesion and agglomeration within a cloud of combustible particles
[NASA-TM-100902] 20 p2788 N88-26539
AGGREGATES
Planetary science 07 p0883 N88-15356
Cometary nucleus as aggregate of planetesimals
[ISAS-RN-364] 19 p2741 N88-26275
AGING (BIOLOGY)
Drosophila geotaxis as a tool for the study of aging 10 p1288 N88-17706
Biological patterns of growth in postnatal ontogenesis of lower primates 19 p2705 N88-26087
AGING (MATERIALS)
NT AGING (METALLURGY)
Rheological and aging characterization of elastomers
[DE87-009598] 02 p0151 N88-10944
Pyrotechnic component development at Sandia National Laboratory
[DE87-006899] 02 p0154 N88-10967
PRAAGE: An interactive IBM-PC code for unreliability/aging analysis
[DE87-012124] 04 p0453 N88-12803
Theoretical bases of polymer photodegradation and photooxidation
[AD-A186533] 08 p0974 N88-15889
Evaluation of bituminous materials used in pavement recycling projects at Tyndall, MacDill, and Hurlburt Air Force Bases
[AD-A188068] 10 p1317 N88-17871
Effects of thermal and thermo-mechanical treatments on the mechanical properties of centrifugally cast alloy 718
[AD-A188195] 11 p1458 N88-18690
Experimental and mathematical investigation of response characteristics and aging phenomena in safety fuse elements
[ETN-88-91478] 11 p1480 N88-18832
Aging properties of cable polmers (2)
[NASA-TT-20228] 13 p1752 N88-20479
Partial discharges and the electrical aging of cross linked polyethene (XLPE) cable insulation
[EUT-86-E-160] 14 p1892 N88-21300
Pressure induced ageing of polymers 14 p1929 N88-21504
Effect of moisture level in PBXW-109(E) (plastic-bonded explosive) mixes on the aging of the cured explosive
[AD-A190200] 15 p2048 N88-22202
Elementary characterization of Fibredux 913 CTS 5 34 percent preimpregnated carbon-epoxy from Ciba Geigy
[M-484300] 16 p2171 N88-22941
Investigation of the long term effects of aging on carbon epoxy composites exposed naturally to the weather under cyclic loads. (Results of sampling after 2.5 years). Test report M1-641300
[CEAT-39/M/79-C-M1-641300] 17 p2316 N88-23834
Aging of carbon fibers
[SNPE-NT-10/86/CRB/NP] 18 p2479 N88-24707
Evaluation of the chromium oxide arc spraying treatment on solar energy collectors
[ETN-88-92564] 18 p2537 N88-25053
High temperature resins for injection. High temperature pre-impregnated
[RC-648676] 20 p2780 N88-26486
Aging of CFRP due to longterm storage in heated air
[DFVLR-FB-88-05] 21 p2922 N88-27345
Degradation of fiber composites during storage
[FOA-C-20702-2.6] 22 p3051 N88-28102
Prediction of long-term creep in polypropylene from short-term tests
[NPL-DMA(A)-156] 22 p3088 N88-28337
Stress corrosion of ceramic materials
[AD-A191979] 23 p3195 N88-29016
Development of a test method to determine potential peroxide content in turbine fuels. Part 2
[AD-A192244] 23 p3199 N88-29042
AGING (METALLURGY)
The aging behavior of types 308 and 308CRE stainless steels and its effect on mechanical properties
[DE87-012541] 04 p0417 N88-12590
Influence of microstructure and aging condition on the fatigue crack propagation in age hardened aluminium alloys 05 p0599 N88-13659
Role of interstitials and precipitates in initiation and propagation of I.C.F. cracks in austenitic stainless steels 06 p0718 N88-14411
Shear failure in round bar tensile tests of Al-Zn-Mg-Cu alloys
[PB87-143632] 07 p0869 N88-15271
Kinetics and mechanism of thermal aging embrittlement of duplex stainless steels
[DE88-002987] 08 p0969 N88-15866
Long-term-aging embrittlement of cast duplex stainless steels: Mechanism and kinetics
[DE88-002929] 09 p1145 N88-16861
Long-term aging of cast stainless steels: Mechanisms and resulting properties
[DE88-002888] 09 p1145 N88-16864
Characterization of duplex stainless steel by TEM (Transmission Electron Microscopy), SANS (Small-Angle Neutron Scattering) and APFIM (Atom-Probe Field Ion Microscopy) techniques
[DE88-002916] 09 p1145 N88-16865
Aging degradation of cast stainless steels: Effects on mechanical properties
[DE88-003053] 09 p1145 N88-16866
Effect of low-temperature aging on the mechanical properties of cast stainless steels
[DE88-002872] 10 p1300 N88-17774
Brief evaluation of the alloy 17-4-PH (Z5 CNU 17-04). Semifinished product: 205 mm dia forged roller, test reports
[DF/NH-3616/84] 17 p2322 N88-23866
On the reversion phenomena of Cu-3 percent Ti alloys
[NASA-TT-20170] 18 p2488 N88-24762
On the abnormal phenomena observed in the electrical resistivity measurement during the decomposition process of saturated Cu-Fe alloys
[NASA-TT-20183] 18 p2507 N88-24869
Aging behavior of Au-based ohmic contacts to GaAs
[NASA-CR-182146] 19 p2662 N88-25831
AGREEMENTS
High resolution satellite imagery simulation --- treaty verification
[FOA-C-30462-3.3,9.3] 05 p0620 N88-13810
The impact of independent research and development regulations on companies not required to negotiate advanced independent research and development agreements
[AD-A190007] 15 p2147 N88-22818
Department of Defense Statement on the Balanced Technology Initiative to the Committee on Armed Services, United States Senate, 100th Congress, second session
[AD-A191841] 18 p2588 N88-25378
Monitoring space weaponry: Detection and verification issues
[DE88-008726] 20 p2847 N88-26900
AGRICULTURAL AIRCRAFT
AN-30M cloud-seeding airplane in international exhibition 06 p0725 N88-14456
AGRICULTURE
A comparative thematic mapping analysis of SPOT data: The Vientiane Plain (Laos) 03 p0343 N88-12168
SPOT: A tool for agricultural statistics 03 p0344 N88-12170
JPRS report: Science and technology. USSR: Life sciences
[JPRS-ULS-87-009] 04 p0473 N88-12915
Application of remote sensing to agricultural field trials
[ISBN-90-6754-089-7] 06 p0729 N88-14483
Crop forecasting in Brazil: A short history of productivity models
[INPE-4150-PRE/1056] 12 p1637 N88-19801
USSR report: Life sciences. Biomedical and behavioral sciences
[JPRS-UBB-87-010] 12 p1651 N88-19889
USSR report: Life sciences. Biomedical and behavioral sciences
[JPRS-UBB-87-008] 12 p1662 N88-19966
Food Irradiation Newsletter, Vol. 11, No. 1
[DE88-700808] 12 p1671 N88-20004
Global mixed-layer natural and anthropogenic fluxes 13 p1807 N88-20803
Assessment of crop loss from air pollutants: Meteorology-atmospheric chemistry and long range transport
[PB88-146857] 15 p2089 N88-22448
Thailand in maps. Application of the mapping system THEMAK2 for specific purpose atlas preparation 16 p2226 N88-23295
Earth resources: A continuing bibliography with indexes (issue 57)
[NASA-SP-7041(57)] 16 p2229 N88-23314
Estimation of an area cultivated with wheat from LANDSAT data through a two-phase sampling method 17 p2357 N88-24041
National Meeting on Remote Sensing Applied to Municipal Planning 19 p2681 N88-25939
Mapping of land use in Sao Jose dos Campos municipality by remote sensing, an aid for the elaboration of its PDDI 19 p2681 N88-25940
Technique to obtain the agricultural ownership limits by satellite imagery, to approve control, and to accompany agricultural activity 19 p2682 N88-25943
The use of satellite imagery for municipal conditions in rural recording in Pereira Barreto (SP) 19 p2682 N88-25944
The impact of hemp production on the development of the municipalities of Araras, Leme, Santa Cruz da Conceicao and Pirassununga 19 p2683 N88-25948
Application of interactive graphic system (CAD/CAM) in the determination of process evolution in land use in the Ribeirao Preto municipality 19 p2684 N88-25956
Water resources and agricultural land use investigations in northeastern Gujarat (India) 22 p3091 N88-28355
Application of SPOT to agricultural information systems in temperate regions 22 p3093 N88-28369
On the modes of growing-season precipitation over central North America 22 p3124 N88-28567
Study of the spectral response of soybeans
[INPE-4592-PRE/1322] 24 p3387 N88-30174
AGRISTARS PROJECT
Potential use of SPOT satellite data for the national resources inventory 22 p3093 N88-28370
Monitoring of agricultural production in West Africa. The need to integrate different satellite platforms 22 p3096 N88-28383
AGROMETEOROLOGY
Nowcasting for the national economy needs 02 p0199 N88-11241
Automatic data acquisition system utilizing microcomputers: Automatic Meteorological Stations (AMS)
[INPE-4215-PRE/1096] 12 p1646 N88-19859
LANDSAT TM and agrometeorological data for wheat yield estimation at the farm level
[INPE-4591-PRE/1321] 24 p3388 N88-30180
AH-64 HELICOPTER
Apache for the battlefield of today and the 21st century 03 p0265 N88-11670
Operational noise data for CH-47D and AH-64 army helicopters
[AD-A191059] 18 p2570 N88-25263
Aeroelastic characteristics of the AH-64 bearingless tail rotor 21 p2891 N88-27162
Test of an 0.8-scale model of the AH-64 Apache in the NASA Langley full-scale wind tunnel
[AD-A196129] 24 p3319 N88-29768
AILERONS
Comparison of pressure distributions on model and full-scale NACA 64-621 airfoils with ailerons for wind turbine application
[NASA-TM-100802] 14 p1943 N88-21593
AIR
NT ALVEOLAR AIR
NT HIGH TEMPERATURE AIR
Fuel-injector/air-swirl characterization 02 p0185 N88-11150
Dilution jet mixing program, phase 3 02 p0185 N88-11153

Flame acceleration and transition to detonation in channels
[DE87-014193] 03 p0284 N88-11786
Millimeter-wave studies of moist air
[AD-A184681] 03 p0306 N88-11935
The atomic weight and isotopic composition of oxygen and their variation in nature
[DE87-014397] 04 p0413 N88-12558
On the meteor trail spectra 06 p0737 N88-14533
Fuel-injector/air-swirl characterization
[NASA-CR-180864] 07 p0820 N88-14985
A rapid method for the computation of equilibrium chemical composition of air to 15000 K
[NASA-TP-2792] 09 p1140 N88-16830
NF85: A three-dimensional, air-dynamics computer code for analyzing explosions in structures
[DE88-005085] 10 p1331 N88-17953
J85-21 fuel nozzle atomization tests
[AD-A189394] 12 p1613 N88-19647
Two-dimensional electron fluid computer calculations of nanosecond pulse, low pressure microwave air breakdown in a rectangular waveguide and their verification by experimental measurement
[DE88-004407] 12 p1618 N88-19678
Ion content and infrared absorption of moist atmospheric air
[AD-A188839] 12 p1643 N88-19838
An interferometric investigation of the diffraction of planar shock waves over a half-diamond cylinder in air
[UTIAS-322] 13 p1768 N88-20575
Observation of anomalous low J-value Stokes and anti-Stokes lines in stimulated rotational Raman scattering over long air paths
[DE88-003756] 14 p1911 N88-21418
Simplified curve fits for the transport properties of equilibrium air
[NASA-CR-178411] 18 p2513 N88-24911
Numerical simulation of ignition of hydrogen jet in hot air 19 p2637 N88-25647
Air loading effects on a capacitively sensed membrane supported silicon accelerometer 19 p2672 N88-25886
Heat and mass transfer in laminar wavy film absorption with the presence of non-absorbable gases 21 p2947 N88-27502

AIR BEARINGS
U GAS BEARINGS

AIR BLASTS
U AERIAL EXPLOSIONS

AIR BREATHING ENGINES
NT CONVERTIBLE FAN-SHAFT ENGINES
NT GAS TURBINE ENGINES
NT J-57 ENGINE
NT JET ENGINES
NT RAMJET ENGINES
NT SUPERSONIC COMBUSTION RAMJET ENGINES
NT TURBOFAN ENGINES
NT TURBOJET ENGINES
NT TURBOPROP ENGINES
Longitudinal mode combustion instabilities in air breathing engines 06 p0680 N88-14166

AIR CARGO
Aircraft accident reports, brief format, US civil and foreign aviation. Issue number 1: 1986 accidents
[PB87-916903] 02 p0123 N88-10781

AIR CONDITIONING
Life-cycle cost analysis of residential heat pumps and alternative HVAC (Heating, Ventilating and Air-Conditioning) systems
[DE88-003701] 07 p0839 N88-15090
Use of a general control simulation program to evaluate HVAC control stability
[DE88-000476] 08 p0975 N88-15896
Research on fluid dynamic energy separation
[DE88-002776] 10 p1339 N88-18001
Enhanced emergency smoke venting
[DOT/FAA/CT-88/22] 20 p2756 N88-26350

AIR CONDITIONING EQUIPMENT
Plant Growth Module (PGM) conceptual design 05 p0631 N88-13855
Experimental studies of heat and mass exchange in parallel-passage rotary desiccant dehumidifiers for solar cooling applications
[DE88-001119] 10 p1350 N88-18069
Perspectives in microclimate cooling involving protective clothing in hot environments
[AD-A188370] 12 p1671 N88-20007
Pressurizing systems and air conditioning systems
[MBB/LKE-312/S/PUB/246] 13 p1812 N88-20828
The effects of different combinations of inlet air conditions used for cooling as measured on a heated manikin
[AD-A191116] 18 p2552 N88-25151

AIR COOLING
The influence of high free stream turbulence, intensive cooling and wake on the external heat transfer of convectively cooled gas turbine blades
[ETN-87-90432] 01 p0056 N88-10360
National Aerospace Laboratory experiment 04 p0404 N88-12509
Cooling electronic equipment at simulated high altitude in hypobaric chambers
[AD-A185196] 05 p0584 N88-13560
Portable, ambient air microclimate cooling in simulated desert and tropic conditions
[AD-A186457] 08 p1050 N88-16338
Perspectives in microclimate cooling involving protective clothing in hot environments
[AD-A188370] 12 p1671 N88-20007
Acoustic convective system
[NASA-CASE-NPO-17278-1-CU] 18 p2498 N88-24818
The effects of different combinations of inlet air conditions used for cooling as measured on a heated manikin
[AD-A191116] 18 p2552 N88-25151
Computational study on thermal efficiency of ceramic gas turbine
[DE88-753114] 20 p2809 N88-26667
Study on the heat resisting and cooling property of the ceramics-metal hybrid stator vanes
[DE88-753117] 20 p2810 N88-26668

AIR CURRENTS
NT JET STREAMS (METEOROLOGY)
NT MERIDIONAL FLOW
NT VERTICAL AIR CURRENTS
Cross flow in the Alps and flat foehn during the experiment MERKUR --- mesoscale experiment 08 p1013 N88-16142
Study of passages of cross-equatorial current during southern monsoon 14 p1900 N88-21347

AIR CUSHION VEHICLES
U GROUND EFFECT MACHINES

AIR DATA SYSTEMS
Proceedings of the 14th Symposium on Aircraft Integrated Monitoring Systems
[DFVLR-MITT-88-04] 22 p3033 N88-28001
German Air Force requirements for the on-board life monitoring system (OLMOS) on Tornado 22 p3033 N88-28007
Event monitoring functions introduced by the Onboard Life Monitoring System (OLMOS) into a German aircraft 22 p3034 N88-28008
Onboard Life Monitoring System (OLMOS), hardware equipment onboard and on ground 22 p3034 N88-28009
A solution to improve a military aircraft's Onboard-Checkout-And-Monitoring-System (OCAMS) 22 p3034 N88-28013
Japan Air Line's Aircraft Integrated Monitoring System (AIMS) activities 22 p3034 N88-28014
New generation of integrated monitoring systems for modern aircraft 22 p3035 N88-28015
Proposal for the on-board part of a future aircraft integrated monitoring system 22 p3035 N88-28016
Planning for AIMS on the next generation 7J7 aircraft 22 p3035 N88-28017
Faultfinder: A diagnostic expert system with graceful degradation for onboard aircraft applications 22 p3035 N88-28018
The Sundstrand B747-400 data management unit 22 p3035 N88-28021
The use of AIMS data for operational and research purposes in atmospheric sciences 22 p3036 N88-28025
On-board data processing of navigation data at high latitudes in Antarctica 22 p3036 N88-28027
Interface techniques and systems for standard aircraft data buses 22 p3036 N88-28028
A guide to good magnetic tape management practice for MODAS users --- modular airborne data acquisition system (MODAS)
[RAE-TM-IT-212] 22 p3162 N88-28834

AIR DEFENSE
NT ANTIMISSILE DEFENSE
Automation strategy and results for an airbase command and control information system
[NLR-MP-86031-U] 01 p0035 N88-10223
A piloted simulation investigating handling qualities and performance requirements of a single-pilot helicopter in air combat employing a helmet-driven turreted gun
[AD-A186878] 09 p1116 N88-16689
MOAOPS and BOOM-MAP computer programs for sonic boom research, volume 1
[AD-A189548] 12 p1574 N88-19414
Aircrew training devices: Utility and utilization of advanced instructional features, phase 4
[AD-A188418] 12 p1670 N88-20000
Simulation of effect of anti-radar stealth principle 13 p1755 N88-20496
Task listing: Visually assisted and visually dependent tasks for fighter aircraft
[AD-A191041] 16 p2244 N88-23404
Modeling and evaluation of variable structure organizations
[AD-A191947] 18 p2588 N88-25381
Proposal for a new aggressor aircraft
[AD-A194311] 22 p3041 N88-28056
Inflight rearming
[AD-A193564] 23 p3176 N88-28909
Typical weather months in the past (1973-1983) in Central Europe
[AD-A194701] 23 p3235 N88-29249
Integration of LANTIRN (Low Altitude Navigation and Targeting Infrared for Night) into operational fighter training
[AD-A194906] 24 p3325 N88-29799
LANTIRN simulator training in the F-16C
[AD-A195201] 24 p3330 N88-29826

AIR DROP OPERATIONS
Developmental airdrop testing techniques and devices
[AGARD-AG-300-VOL-6] 04 p0398 N88-12481
Control systems for platform landings cushioned by air bags
[AD-A196154] 24 p3358 N88-29996

AIR DUCTS
Reflection of sound in open ended ducts
[PB88-103478] 21 p3012 N88-27870

AIR FILTERS
Comparison of three aerosol sampling techniques and the differences in the nitrate determined by each
[DE87-011456] 03 p0348 N88-12200
Computer code simulations of explosions in flow networks and comparison with experiments
[DE88-001946] 05 p0573 N88-13491
Characteristics of pressure loss during filtration using a porous ceramic filter
[DE88-752547] 20 p2798 N88-26604

AIR FLOW
NT AIR CURRENTS
NT JET STREAMS (METEOROLOGY)
NT MERIDIONAL FLOW
NT VERTICAL AIR CURRENTS
Boundary layer profile investigations downstream of an aero-engine intake anti-icing air exhaust slot
[PNR90378] 02 p0171 N88-11080
The generation of nearly isotropic turbulence by means of grids
[PNR90411] 02 p0172 N88-11084
The air flow on hills from models and experiments
[BMFT-FB-T-86-175] 02 p0198 N88-11236
On the role of snow in the redistribution of precipitation by small scale topography 02 p0203 N88-11267
A real-data numerical study and four-dimensional data assimilation application for mesobeta-scale flow in complex terrain 02 p0212 N88-11329
On the scheme dependency of the three-dimensional Euler solutions 03 p0318 N88-12010
National Aerospace Laboratory experiment 04 p0404 N88-12509
Practical application of two-dimensional viscous flow computation 05 p0535 N88-13257
The development and evaluation of three-dimensional models of cold flow in internal combustion engines
[DE88-900077] 05 p0589 N88-13594
Controlled ecological life support systems: Development of a plant growth module 05 p0630 N88-13854
Foam generation and air entrainment near a free surface
[AD-A185986] 07 p0848 N88-15149
Typhoon structural evolution
[AD-A186090] 07 p0879 N88-15333
Portable, ambient air microclimate cooling in simulated desert and tropic conditions
[AD-A186457] 08 p1050 N88-16338
Preliminary experiments on surface flow visualization in the cryogenic wind tunnel by use of condensing or freezing gases
[NASA-CR-181634] 11 p1442 N88-18602
Perspectives in microclimate cooling involving protective clothing in hot environments
[AD-A188370] 12 p1671 N88-20007
Air-jet spoiler
[BU-364] 13 p1722 N88-20299
Control of structure in turbulent flows: Bifurcating and blooming jets
[AD-A189607] 13 p1766 N88-20562
The pressure drag and momentum flux during a cold frontal passage over the Alps 13 p1800 N88-20763
Determination of canopy loads for a light aircraft by wind tunnel testing and computer modelling
[BU-353] 14 p1869 N88-21167

Visualization of the air flowing through a dynamic model of the vocal folds
[ISVR-TR-154] 14 p1952 N88-21634
The development of a microanemometer. New possibilities for measuring very low air velocities
[ETN-88-92244] 16 p2210 N88-23191
The role of vortex structure in tropical cyclone motion
[AD-A190961] 16 p2235 N88-23351
Acoustic convective system
[NASA-CASE-NPO-17278-1-CU] 18 p2498 N88-24818
Noise generation by air bubbles in water: An experimental study of creation and splitting
[AD-A192063] 19 p2664 N88-25839
A numerical study of the test time in a hypersonic shock tunnel
[AD-A194057] 23 p3172 N88-28888
A calculation of the turbulent boundary layer on a slender ellipsoid at low incidence
[FFA-TN-1988-02] 23 p3213 N88-29126
Nozzle airflow influences on fuel patternation 24 p3346 N88-29916

AIR FREIGHT
U AIR CARGO

AIR INLETS
U AIR INTAKES

AIR INTAKES
NT ENGINE INLETS
NT SUPERSONIC INLETS
The role of computation fluid dynamics in aeronautical engineering (4). The development and applications of implicit TVD finite volume code 05 p0536 N88-13259
Calibration of the ARL (Aeronautical Research Laboratories) rain and icing facility
[AD-A186776] 09 p1121 N88-16710
Details of low speed intake test facility at the Warton (United Kingdom) 2.7m x 2.1m wind tunnel
[AXM-127] 14 p1870 N88-21174
Equipment for mass flow measurements in the low-speed wind tunnel at DFVLR in Brunswick, West Germany
[DFVLR-MITT-88-02] 21 p2900 N88-27212

AIR JETS
Experimental study of three-dimensional turbulent jet-solid boundary interaction 01 p0046 N88-10293
The numerical simulation of the mesoscale characteristics associated with Baiu front. Part 1: Structure, low-level jet and radiation characteristics 02 p0203 N88-11272
Interaction of the cold conveyor belt with polar jet streaks
[AD-A186774] 09 p1192 N88-17145
Air-jet spoiler
[BU-364] 13 p1722 N88-20299
The structure of sonic underexpanded turbulent air jets in still air
[AD-A190856] 16 p2157 N88-22870

AIR LAND INTERACTIONS
Validation of a three dimensional numerical model of the sea breeze in complex terrain 02 p0211 N88-11325
An introduction to the parameterization of land-surface processes 14 p1937 N88-21554
Continental surface processes and water cycle 14 p1937 N88-21555
Sensitivity of general circulation models to surface processes 14 p1937 N88-21556

AIR LAUNCHING
Automatic routing module 09 p1210 N88-17251
Store separation and missile firing from aircraft: Experimental methods for trajectory projection
[NASA-TT-20214] 11 p1439 N88-18589

AIR LOCKS
HERMES Program: Airlock swimming pool tests 12 p1591 N88-19525

AIR MASSES
Operational practice of an air mass transformation model 02 p0208 N88-11308
Development and testing of an air-mass transformation trajectory model 02 p0209 N88-11309
Model calculations of the behavior of orographically influenced cold fronts 08 p1015 N88-16155
Parametric methodologies of cloud vertical transport for acid deposition models
[PB88-191374] 20 p2825 N88-26762
Energy budget and ground temperatures in hot regions
[AD-A196298] 24 p3404 N88-30268

AIR NAVIGATION
NT ALL-WEATHER AIR NAVIGATION
NT AREA NAVIGATION
NT NAP-OF-THE-EARTH NAVIGATION
Generating diagnostic knowledge from a structural and functional description 02 p0129 N88-10813
Proceedings of a Workshop on Innovative Solutions for Safety in Air Transportation
[ILR-MITT-178(1987)] 11 p1437 N88-18573
Activities report in air traffic control
[ETN-88-91092] 11 p1438 N88-18581
Integrated avionics reliability 17 p2294 N88-23723
A comparison of integrated and separate systems for flight control and navigation 17 p2303 N88-23779
A positioning system based on NAVSAT
[NLR-MP-87018-U] 20 p2757 N88-26358
Electrical load and power source capacity report for the C-130 aircraft Self Contained Navigation System (SCNS): LSI model 6216A, 6216B, 6216C, revision
[AD-A193079] 21 p2895 N88-27186
Observed track-keeping performance of DC10 aircraft equipped with the Collins AINS-70 area navigation system: Karlsruhe and Masstricht UACs (Upper Area Control centres)
[EEC-202] 24 p3323 N88-29788
Integration of LANTIRN (Low Altitude Navigation and Targeting Infrared for Night) into operational fighter training
[AD-A194906] 24 p3325 N88-29799

AIR POLLUTION
NT GLOBAL AIR POLLUTION
NT INDOOR AIR POLLUTION
NBS (National Bureau of Standards) research reports (April 1987)
[PB87-210258] 01 p0018 N88-10111
Investigations of the dispersion of spontaneously released heavy gases
[WA-81] 01 p0066 N88-10427
Carbon monoxide (CO) concentration in the air as a purity parameter
[INPE-4232-PRE/1107] 01 p0067 N88-10429
An instrument for the quasi-continuous determination of atmospheric soot content
[DFVLR-FB-87-04] 01 p0068 N88-10433
Investigation of large scale impact of air pollution components on forest ecosystems in Bavaria, West Germany
[DFVLR-FB-87-17] 01 p0068 N88-10434
Mid infrared LHS system packaging using flexible waveguides
[NASA-CR-181192] 01 p0093 N88-10607
Opportunities for nowcasting air pollution episodes and accidental toxic and radioactive releases 02 p0210 N88-11317
Real-time evaluation and prediction of coastal dispersion near the SW tip of Africa --- effluents 02 p0210 N88-11318
Aircraft engine exhaust plume dynamics
[AD-A184238] 04 p0400 N88-12488
Emerging environmental constraints on the use of gasoline and diesel fuel and tradeoffs associated with the use of alternative fuels
[DE87-011504] 04 p0422 N88-12614
The use of TOMS data for tropospheric ozone studies 05 p0616 N88-13784
AN-30M cloud-seeding airplane in international exhibition 06 p0725 N88-14456
On-site meteorological program guidance for regulatory modeling applications
[PB87-227542] 06 p0731 N88-14498
Pollution from motor vehicles and aircraft at Stapleton International Airport (abbreviated report), revision 2
[AD-A185916] 07 p0875 N88-15307
Use of back air trajectories in interpreting atmospheric chemistry data: A review and bibliography
[PB88-102108] 07 p0876 N88-15312
Fuel nitrogen conversion in a supercharged spark ignition engine
[DE88-003739] 08 p0974 N88-15893
A review of methanol vehicles and air quality impacts
[DE88-002846] 08 p1023 N88-16194
Current issues in atmospheric change
[NASA-CR-182406] 08 p1039 N88-16287
Estimation of aerial deposition and foliar uptake of xenobiotics: Assessment of current models
[DE88-000993] 09 p1188 N88-17117
A comparison of multi-layer meso-alpha MLAM model results with surface and aircraft observations from CAPTEX
[DE88-000549] 09 p1188 N88-17118
Model investigations of atmospheric ammonia scavenging
[DE88-002337] 09 p1194 N88-17153
The role of repowering in America's power generation future
[DOE/FE-0096] 10 p1351 N88-18076
Meteorological and aerosol measurements from the NOAA WP-3D aircraft during WATOX-86, January 4-9, 1986
[PB88-120860] 10 p1352 N88-18079
The role of analytical chemistry in assessing atmospheric effects of combustion
[DE88-003909] 10 p1352 N88-18082
Developments in National Weather Service meteorological data collection programs as related to EPA (Environmetal Protection Agency) air pollution models
[PB88-130240] 10 p1356 N88-18104
Using SIR (Scientific Information Retrival) system for data management during a field program
[DE88-001555] 10 p1424 N88-18508
Computer architecture for research in meteorology and atmospheric chemistry
[PB88-145313] 11 p1510 N88-19020
Optimal sampling to provide user-specific climate information 11 p1515 N88-19051
Proceedings of the Forest-Atmosphere Interaction Workshop
[CONF-8510250] 12 p1641 N88-19824
Air quality and human performance, chapter 16
[AD-A188335] 12 p1666 N88-19988
Computer simulation of tropospheric chemistry
[JUEL-2144] 13 p1798 N88-20756
Carbon dioxide and climate 14 p1936 N88-21545
Assessment of crop loss from air pollutants: Meteorology-atmospheric chemistry and long range transport
[PB88-146857] 15 p2089 N88-22448
A theoretical model of the washout of trace gases by raindrops in the atmosphere 17 p2375 N88-24125
Air pollution: Ozone attainment requires long-term solutions to solve complex problems
[PB88-167275] 18 p2538 N88-25060
Ozone in the atmosphere 18 p2539 N88-25064
Motor vehicles as sources of compounds important to tropospheric and stratospheric ozone
[PB88-195219] 18 p2540 N88-25076
Photointerpretation with instrumentation for evaluation of environmental impact: Mata Atlantica in Cubatao 19 p2683 N88-25946
Study of evolution of vegetal cover and slide scars in the Cubatao municipality-Sao Paulo 19 p2683 N88-25947
A primer on greenhouse gases
[DE88-007576] 19 p2689 N88-25981
Composite, meso-gamma scale diagnostic modeling
[DE88-008189] 19 p2689 N88-25983
Pollutant formation in heterogeneous mixtures of fuel drops and air
[DOE/CE-50052/H1] 19 p2689 N88-25986
Sulfur dioxide-hydrogen peroxide relationships in clean air, clouds, and precipitation
[DE88-008352] 19 p2690 N88-25990
Overview of the PRECP (processing of emissions by clouds and precipitation) Program
[DE88-008205] 20 p2822 N88-26741
An efficient model for changes of global climate and composition of the atmosphere due to human activities
[ETN-88-92359] 20 p2827 N88-26775
National air toxics information clearinghouse: NATICH data base users guide for data viewing, February 1988
[PB88-197470] 21 p2970 N88-27645
National ambient Volatile Organic Compounds (VOCs) data base update, documentation
[PB88-195631] 21 p2971 N88-27646
Photochemical oxidant formation: Overview of current knowledge and emerging issues
[PB88-195235] 21 p2971 N88-27647
Foliar nitrate reductase: A marker for assimilation of atmospheric nitrogen oxides
[DE88-010453] 21 p2971 N88-27648
Atmospheric science issues in Congress 22 p3125 N88-28573
Effects of air polution on human exercise performance
[AD-A192680] 22 p3131 N88-28617
The 1985-86 measurements with the tunable diode laser absorption spectrometer
[PB88-214002] 23 p3231 N88-29226
Investigation of the large-scale impact of air pollution components on forest ecosystems in Bavaria
[ESA-TT-1087] 24 p3390 N88-30187

AIR PURIFICATION
Operation of an experimental algal gas exchanger for use in a CELSS 03 p0358 N88-12255
Non-conventional approaches to food processing in CELSS, 1. Algal proteins: Characterization and process optimization 03 p0358 N88-12256
Preliminary experimental results of gas recycling subsystems except carbon dioxide concentration 03 p0359 N88-12261
Airborne particulate matter in spacecraft
[NASA-CP-2499] 06 p0753 N88-14623
Proceedings of the 19th DOE/NRC Airborne Waste Management and Air Cleaning Conference
[NUREG/CP-0086-VOL-1] 11 p1509 N88-19018

Proceedings of the 19th DOE/NRC Airborne Waste Management and Air Cleaning Conference
[NUREG/CP-0086-VOL-2] 11 p1509 N88-19019

AIR QUALITY

Carbon monoxide (CO) concentration in the air as a purity parameter
[INPE-4232-PRE/1107] 01 p0067 N88-10429
Compilation and analysis of air quality data in support of acid deposition research
[DE87-014428] 02 p0196 N88-11226
Aircraft engine exhaust plume dynamics
[AD-A184238] 04 p0400 N88-12488
Airborne particulate matter in spacecraft
[NASA-CP-2499] 06 p0753 N88-14623
Pollution from motor vehicles and aircraft at Stapleton International Airport (abbreviated report), revision 2
[AD-A185916] 07 p0875 N88-15307
Impacts of world development on selected characteristics of the atmosphere: An integrative approach. Volume 1: Main report
[DE88-001495] 07 p0875 N88-15309
Impacts of world development on selected characteristics of the atmosphere: An integrative approach. Volume 2: Appendices
[DE88-001496] 07 p0875 N88-15310
A review of methanol vehicles and air quality impacts
[DE88-002846] 08 p1023 N88-16194
Evaluation of regional-scale air quality models: Chairmen reports from four workshops
[DE88-001397] 10 p1352 N88-18080
Tropospheric ultraviolet radiation: Assessment of existing data and effect on ozone formation
[PB88-130133] 10 p1354 N88-18095
Air quality and human performance, chapter 16
[AD-A188335] 12 p1666 N88-19988
Air pollution: Ozone attainment requires long-term solutions to solve complex problems
[PB88-167275] 18 p2538 N88-25060
NOAA (National Oceanic and Atmospheric Administration) Meteorology Division support to the Environmental Protection Agency
[PB88-179866] 19 p2689 N88-25980
Sulfur dioxide-hydrogen peroxide relationships in clean air, clouds, and precipitation
[DE88-006352] 19 p2690 N88-25990
Meteorological aspects of wet deposition in Southern Finland
[FMI-3] 19 p2693 N88-26007
Regional environmental studies using national data bases and GIS (Geographic Information System)
[DE88-008368] 23 p3230 N88-29225

AIR SAMPLING

Detection of vapors of flammable liquids in air by atmospheric sampling mass spectrometry/mass spectrometry
[DE88-000030] 02 p0196 N88-11227
Comparison of three aerosol sampling techniques and the differences in the nitrate determined by each
[DE87-011456] 03 p0348 N88-12200
Method for sampling of methyl salicylate vapor in air using passivated stainless steel syringes and analysis by gas chromatography
[AD-A187838] 11 p1447 N88-18624
Proceedings of the 19th DOE/NRC Airborne Waste Management and Air Cleaning Conference
[NUREG/CP-0086-VOL-2] 11 p1509 N88-19019
Optimal sampling to provide user-specific climate information 11 p1515 N88-19051
Fibrous glass aerosols: A literature review
[AD-A188420] 12 p1672 N88-20008
Aircraft emissions characterization: TF41-A2, TF30-P103 and TF30-P109 engines
[AD-A192053] 18 p2466 N88-24638

AIR SEA ICE INTERACTIONS

Report of the second session of the working group on sea ice and climate
[WCP-128] 06 p0745 N88-14580

AIR SEA INTERACTIONS

U AIR WATER INTERACTIONS

AIR SICKNESS

U MOTION SICKNESS

AIR START

Propulsion analysis and application potential of air breathing combined propulsion for ballistic space transporter
[ETN-88-92369] 21 p2903 N88-27227

AIR TO AIR MISSILES

Advances in Air-Launched Weapon Guidance and Control
[AGARD-CP-431] 12 p1596 N88-19553
Effects of closing speed uncertainty on optimal guidance 12 p1597 N88-19556
Guidance and control of air-launched armaments: An aeroengineer's perspective 12 p1597 N88-19557
Future air-to-air training for the RF-4
[AD-A194363] 23 p3240 N88-29284
Approximations and implementations of nonlinear filtering schemes
[AD-A194685] 23 p3271 N88-29462

AIR TO AIR REFUELING

Aircraft refueling demonstrator using a microbot alpha 2 robot 21 p2926 N88-27367
Low altitude: A new dimension in air refueling
[AD-A193819] 23 p3176 N88-28910

AIR TO AIR ROCKETS

U AIR TO AIR MISSILES

AIR TO SURFACE MISSILES

A study into the effects and viability of applying lateral force control to an air to ground rocket
[ETN-87-90925] 02 p0131 N88-10821
Advances in Air-Launched Weapon Guidance and Control
[AGARD-CP-431] 12 p1596 N88-19553
Guidance and control of air-launched armaments: An aeroengineer's perspective 12 p1597 N88-19557
The use of hardware-in-the-loop-techniques in the development of a modern air-to-surface missile system 12 p1597 N88-19562

AIR TRAFFIC

Activities report in flight and space travel
[ISSN-0070-3966] 14 p2012 N88-22000
FAA (Federal Aviation Administration) technical center: Mission and role in natinal airspace system plan implementation
[PB88-169818] 18 p2460 N88-24609

AIR TRAFFIC CONTROL

Knowledge Based Concepts and Artificial Intelligence: Applications to Guidance and Control
[AGARD-LS-155] 02 p0128 N88-10806
An expert system for aircraft conflict resolution in dense airspaces 02 p0129 N88-10810
A rule-based system for arrival sequencing and scheduling in air traffic control 02 p0129 N88-10815
Nowcasting for the national economy needs 02 p0199 N88-11241
Experimental use of artificial intelligence for (future) ATC systems
[PB87-106449] 04 p0482 N88-12970
Flightpath reconstruction and systematic radar error estimation from multiradar range-azimuth measurements
[NLR-MP-85064-U] 06 p0693 N88-14251
FAA air traffic control operations concepts. Volume 1: ATC background and analysis methodology
[AD-A185979] 07 p0818 N88-14973
FAA air traffic control operations concepts. Volume 2: ACF/ACCC (Area Control Facility/Area Control Computer Complex) terminal and en route controll ers
[AD-A185980] 07 p0818 N88-14974
FAA air traffic control operations concepts. Volume 3: ISSS (Initial Sector Suite System) en route controllers
[AD-A185981] 07 p0818 N88-14975
FAA air traffic control operations concepts. Volume 4: TAAS (Terminal Advanced Automation System) terminal controllers
[AD-A185982] 07 p0818 N88-14976
FAA air traffic control operations concepts. Volume 5: ATCT/TCCC (Airport Traffic Control Tower/Tower Control Computer Complex) tower controllers
[AD-A185983] 07 p0818 N88-14977
Chicago's O'Hare Runway Configuration Management System (RCMS). Volume 2: Users guide
[AD-A186222] 08 p0953 N88-15783
Cockpit data management
[NASA-CR-178407] 11 p1438 N88-18579
Cockpit data management
[NASA-CR-178407-SUPPL] 11 p1438 N88-18580
Activities report in air traffic control
[ETN-88-91092] 11 p1438 N88-18581
Air traffic control
[FAA-ORDER-7110.65E] 12 p1576 N88-19426
Estimates of potential increases in airport capacity through ATC (Air Traffic Control) system improvements in the airport and terminal areas
[AD-A188533] 12 p1578 N88-19444
Activities report in civil aeronautics
[ETN-88-91344] 13 p1715 N88-20255
A method and measures to evaluate trackers for air traffic control
[NLR-TR-86072-U] 13 p1720 N88-20287
Electronics and communications in air traffic control: The Presidential Address
[ETN-88-92057] 14 p1865 N88-21146
Aircraft accident report: North Star Aviation, Inc., PA-32 RT-300, N39614 and Alameda Aero Club Cessna 172, N75584, Oakland, California, March 31, 1987
[PB87-910412] 15 p2016 N88-22021
An evaluation of the effects of high visual taskload on the separate behaviors involved in complex monitoring performance
[AD-A190641] 15 p2105 N88-22538
Integrated multisensor navigation systems 17 p2294 N88-23722
Space based radar application to air traffic control 17 p2399 N88-24262
FAA (Federal Aviation Administration) technical center: Mission and role in natinal airspace system plan implementation
[PB88-169818] 18 p2460 N88-24609
Optimization of the dilation characteristic on the control jurisdiction of an area control facility
[AD-A191720] 18 p2461 N88-24615
World-wide aeronautical satellite communications 19 p2644 N88-25688
Statistical properties of real time events in an ATC (Air Traffic Control) system
[PB88-118781] 20 p2756 N88-26353
Analysis of ATCRBS (Air Traffic Control Radar Beacon System), mode select (Mode S) in combat operations
[AD-A193140] 22 p3040 N88-28050
Fine resolution errors in secondary surveillance radar altitude reporting
[RSRE-87019] 23 p3175 N88-28906

AIR TRAFFIC CONTROLLERS (PERSONNEL)

An expert system for aircraft conflict resolution in dense airspaces 02 p0129 N88-10810
A rule-based system for arrival sequencing and scheduling in air traffic control 02 p0129 N88-10815
FAA air traffic control operations concepts. Volume 1: ATC background and analysis methodology
[AD-A185979] 07 p0818 N88-14973
Air traffic control
[FAA-ORDER-7110.65E] 12 p1576 N88-19426
The program Kennedy Approach as an experimental design of a dynamic computerized air traffic control test
[DFVLR-FB-87-50] 16 p2159 N88-22881

AIR TRANSPORTATION

Issues in air transport and airport management
[PB87-204509] 02 p0124 N88-10782
V/STOL aircraft configurations and opportunities in the Pacific Basin
[NASA-TM-100005] 03 p0261 N88-11644
Airline safety: A comparative analysis
[AD-A185358] 05 p0543 N88-13308
Digest of the annual report of the Lufthansa German Airlines
[ISSN-0415-603X] 08 p0952 N88-15779
TECOM's research efforts in the dynamic environments 08 p0999 N88-16048
Proceedings of a Workshop on Innovative Solutions for Safety in Air Transportation
[ILR-MITT-178(1987)] 11 p1437 N88-18573
Activities report in civil aeronautics
[ETN-88-91344] 13 p1715 N88-20255
FAA aviation forecasts fiscal years 1988-1999
[AD-A191711] 18 p2455 N88-24576

AIR WATER INTERACTIONS

NT AIR SEA ICE INTERACTIONS
Study on propagation and inverse scattering --- sea studies
[ESA-CR(P)-2394] 01 p0063 N88-10405
Contribution of bubbles and waves to air-sea CO2 flux, with implications for remote sensing
[PB87-203980] 01 p0073 N88-10467
Vertical profiles of wind-induced current --- North Sea
[IOS-238] 02 p0193 N88-11207
Properties of the atmospheric boundary layer above a subtropical oceanic front
[AD-A184006] 03 p0351 N88-12215
Influence of stratification in near-surface water layer on intensity of gas exchange between atmosphere and water 04 p0459 N88-12841
Studies of thin surface films aim at seeing deep ocean processes 04 p0460 N88-12847
Theory of heat and moisture exchange between finely disperse storm-generated spray and turbulent air flow 04 p0461 N88-12851
Interactions between the Asian monsoons, the tropical Pacific and the southern hemisphere extratropics 04 p0470 N88-12907
Reactions of porphyrins in surfactant assemblies, microemulsions and in solutions
[AD-A184797] 05 p0560 N88-13412
Estimation of marine boundary layer depth and relative humidity with multispectral satellite measurements
[AD-A184881] 05 p0620 N88-13804
Influence of gas exchange between ocean and atmosphere on formation of atmospheric pressure field 06 p0726 N88-14467
Acoustic scattering from composite wind-wave surfaces 3: Forward scatter intensities and spatial coherence at low and high frequencies and small grazing angles for Bubble-free regimes
[AD-A185908] 07 p0881 N88-15345
The ocean heat budget
[AD-A186130] 07 p0881 N88-15346
WOCE Core Project 2 Planning Meeting: The Southern Ocean
[WCP-138] 07 p0882 N88-15348

Report of the Workshop on Space Systems Possibilities for a Global Energy and Water Cycle Experiment
[WCP-137] 09 p1193 N88-17147
Moving ionospheric perturbations induced by wave trains propagating through ocean 09 p1239 N88-17427
NASA Oceanic Processes Program
[NASA-TM-4025] 10 p1357 N88-18109
Numerical simulations of the California current: Filament formation as related to baroclinic instability
[AD-A187573] 10 p1358 N88-18115
On the barotropic model of the ocean circulation
[AD-A188148] 10 p1358 N88-18118
Variation of the wind stress related to frontal passages during FASINEX (Frontal Air-Sea Interaction Experiment) 1986
[AD-A187180] 11 p1514 N88-19042
Numerical simulation of the ocean front response to the mesoscale atmospheric forcing
[INPE-4473-TDL/324] 12 p1648 N88-19866
Estimates of ocean-atmosphere thermal interaction in Gulf Stream energy-active test range in winter of 1984 13 p1785 N88-20679
Sample models of steady and low frequency circulations in the tropical atmosphere, with application to tropical air-sea interactions 13 p1801 N88-20764
Dynamics of the Oceanic Surface Mixed Layer
[AD-A188348] 13 p1804 N88-20785
Structures and fluxes in a deep convecting mixed layer 13 p1804 N88-20786
On the zonal momentum balance at the equator 13 p1805 N88-20788
The mixed layer of the western equatorial Pacific Ocean
[HIG-1861] 13 p1805 N88-20789
Unsteady shallowing mixed layer 13 p1805 N88-20791
Some effects of heating on the wind-driven velocity in the upper ocean 13 p1805 N88-20792
Mixed-layer shear related to wind stress in the central equatorial Pacific 13 p1805 N88-20793
Wind forcing and observed oceanic wavenumber spectra 13 p1806 N88-20797
Energy and momentum fluxes through the sea surface 13 p1806 N88-20798
Radiative processes affecting ocean mixed-layer heat content and their monitoring from satellite 13 p1806 N88-20800
The Hapex-Mobilhy program 14 p1938 N88-21560
Equatorial dynamics and ocean-atmosphere coupling 14 p1936 N88-21565
An improved wind input source term for third generation ocean wave modeling
[KNMI-WR-87-8] 14 p1950 N88-21624
Mass, heat and nutrient fluxes in the Atlantic Ocean determined by inverse methods
[NASA-CR-180535] 14 p1950 N88-21626
Changes in the California current system observed off northern California during July-August 1986
[AD-A190027] 15 p2100 N88-22510
Noise generation by air bubbles in water: An experimental study of creation and splitting
[AD-A192083] 19 p2664 N88-25839
US participation in the TOGA (Tropical Ocean and the Global Atmosphere) Program: A research strategy
[DE88-010986] 19 p2681 N88-25936
A study of the dynamics of the Intertropical Convergence Zone (ITCZ) in a symmetric atmosphere-ocean model
[NASA-TM-86220] 19 p2693 N88-26005
Physical oceanography and tracer chemistry of the southern ocean
[DE88-006852] 20 p2828 N88-26779
Air-sea interaction in the vicinity of a land-sea boundary in the presence of upwelling 21 p2973 N88-27861
Zonal wind observations at Christmas Island (2 deg N, 157 deg W) during the 1986-1987 El-Nino 22 p3120 N88-28539
Atlantic SST variability and high latitude climate fluctuations 22 p3122 N88-28551
Simulation studies of the influence of sea-surface temperature anomalies on the Sahelian circulation and rainfall 22 p3122 N88-28553
Recent secular changes in the wintertime circulation of the Southern Hemisphere 22 p3122 N88-28555
On the energy source of 1982-83 ENSO episode simulated by the NCAR community climate model 22 p3122 N88-28556
Some evidence for a Northern Hemispheric extratropic trigger mechanism of ENSO events 22 p3123 N88-28558
A system for determination of wind fields from cloud tracks: INPE experiment
[INPE-4492-PRE/1256] 22 p3128 N88-28594
Genesis of Atlantic lows experiment NASA electra boundary layer flights data report
[NASA-TM-100703] 22 p3128 N88-28597
Observational/numerical study of the upper ocean response to hurricanes
[AD-A193592] 22 p3128 N88-28598
A bulk model for the unstable planetary boundary layer over the sea. A sensitivity investigation
[DM-51] 22 p3129 N88-28600
Doppler radar analysis of coastal marine atmospheric boundary layer structure during a cold air outbreak
[AD-A196023] 24 p3403 N88-30261
Analysis of environmental parameters from the Panama City tower radar experiment
[AD-A194994] 24 p3404 N88-30264

AIRBORNE EQUIPMENT
NT AIRBORNE/SPACEBORNE COMPUTERS
Airborne lidar experiments at the Savannah River Plant
[NASA-TM-4007] 02 p0194 N88-11209
Efficiency analysis of airborne Electronic CounterMeasures (ECM) systems
[AD-A184606] 03 p0306 N88-11934
Definition and use of sensors for measuring electrical conductivity in thunderclouds
[ESA-TT-1047] 03 p0352 N88-12222
Study of an airborne Doppler radar: Project Asterix
[BLL-MO-TRANS-1667-(9022.552)] 04 p0432 N88-12675
Airborne Visible/Infrared Imaging Spectrometer (AVIRIS). A description of the sensor, ground data processing facility, laboratory calibration, and first results
[NASA-CR-182365] 06 p0705 N88-14325
A system overview of the Airborne Visible/Infrared Imaging Spectrometer (AVIRIS) 06 p0705 N88-14326
First results from the Airborne Visible/Infrared Imaging Spectrometer (AVIRIS) 06 p0707 N88-14335
BARS-1M meteorological complex carried on IL-18 airplane 06 p0725 N88-14458
Uses of airborne laser Chayka-1 for probing water, land surfaces 06 p0725 N88-14461
Airborne tracking sunphotometer apparatus and system
[NASA-CASE-ARC-11622-1] 06 p0730 N88-14492
Helicopters as test carriers for avionics systems (HETAS)
[DFVLR-IB-112-85/18] 09 p1116 N88-16692
Airborne Wind Shear Detection and Warning Systems: First Combined Manufacturers' and Technologists' Conference
[NASA-CP-10006] 10 p1273 N88-17616
Airborne Doppler lidar detection of wind shear. Results of performance analysis 10 p1275 N88-17627
Forward looking wind shear detection 10 p1275 N88-17629
Crew interface with windshear systems 10 p1275 N88-17631
Feasibility study for a 2nd generation system for airborne maritime pollution surveillance
[ETN-88-92108] 15 p2092 N88-22466
Users guide to CAESAR
[BCRS-87-04] 16 p2228 N88-23306
Preparation and execution of calibration measurements for handling of airborne SAR data (AGRISAR)
[ETN-88-92338] 17 p2333 N88-23926
Airborne and spaceborne radar images for geologic and environmental mapping in the Amazon rain forest, Brazil 17 p2353 N88-24021
Trajectory measurement of the Fokker 100 aircraft during autoland testing
[NLR-MP-86010-U] 20 p2758 N88-26366
Computer simulation procedure for designing airborne aerometric monitoring programs
[DE88-011696] 21 p2975 N88-27674
Maintenance support for military aircraft by intelligent on-board maintenance data panel 22 p3034 N88-28012
On experiences with two hot-wire instruments for measuring the liquid water content in clouds
[ESA-TT-1085] 23 p3236 N88-29255
Airborne radar technology for windshear detection
[NASA-CR-183203] 23 p3236 N88-29257

AIRBORNE LASERS
A study of the performance of airborne laser radar systems and techniques
[ETN-87-90928] 02 p0179 N88-11117
Atmospheric backscatter at 10.6 microns; a compendium of measurements made outside the United Kingdom by the airborne LATAS coherent laser radar velocimeter
[RSRE-87002] 12 p1631 N88-19763

AIRBORNE SURVEILLANCE RADAR
Airborne bistatic radar applications
[ETN-87-90930] 02 p0163 N88-11020
A study of the performance of airborne laser radar systems and techniques
[ETN-87-90928] 02 p0179 N88-11117
Air-to-air radar flight testing
[AGARD-AG-300-VOL-7] 21 p2932 N88-27406

AIRBORNE/SPACEBORNE COMPUTERS
Data Management Working Group report 01 p0016 N88-10097
A129 advanced solutions for meeting today's combat helicopter requirement 03 p0265 N88-11669
Electrical flight commands in transport aircraft
[SNIAS-872-111-108] 05 p0551 N88-13361
Study of fault tolerant techniques for satellite data handling
[FTT/REP/0001/SAAB] 05 p0632 N88-13860
AVIRIS onboard data handling and control 06 p0706 N88-14332
The feasibility of using TAE as the UIL for the space station and for other internal NASA tasks and projects 07 p0925 N88-15618
Modeling of architecture of a problem-oriented on-board processor 08 p1008 N88-16114
An inference engine for embedded diagnostic systems 08 p1056 N88-16367
Embedded expert system for space shuttle main engine maintenance 08 p1058 N88-16382
ESSAA: Embedded system safety analysis assistant 08 p1060 N88-16396
Intelligent man/machine interfaces on the space station 08 p1063 N88-16418
Space languages 08 p1063 N88-16420
Knowledge representation by connection matrices: A method for the on-board implementation of large expert systems 08 p1065 N88-16434
Prototype space station automation system delivered and demonstrated at NASA 08 p1066 N88-16442
Applications of expert systems for satellite autonomy 08 p1066 N88-16443
Introducing new technology into onboard handling systems 09 p1124 N88-16733
Verifying shuttle onboard software using expert systems 09 p1207 N88-17237
Airworthiness considerations 10 p1276 N88-17636
An expert system to support the verification/validation of flight-critical software
[MBB-UT-102/87] 10 p1314 N88-17852
The RVD mission: The on-board data processing requirements 12 p1586 N88-19495
Advances in Air-Launched Weapon Guidance and Control
[AGARD-CP-431] 12 p1596 N88-19553
Computer aided tactics for air combat 12 p1597 N88-19559
The use of hardware-in-the-loop-techniques in the development of a modern air-to-surface missile system 12 p1597 N88-19562
Microprocessors in space instrumentation
[RR-321] 14 p1955 N88-21655
Architecture and role of the Sensor Subsystem in future aircraft weapon systems 17 p2302 N88-23770
Development of a generic architecture 17 p2303 N88-23774
Test philosophy of the EH101 integrated avionic 17 p2303 N88-23775
Modeling of functional specifications for onboard software: Experience with the Rafale avionics system 17 p2303 N88-23777
The avionics software architecture impact on system architecture 17 p2303 N88-23778
Design for interoperability (interchangeability) 17 p2305 N88-23789
Development of an airborne facility for advanced avionics research 17 p2307 N88-23801
Workshops for the design of avionics systems and the development of onboard software 17 p2307 N88-23802
A timing evaluator for C programs generated by the model system
[AD-A191204] 17 p2385 N88-24174
Development of an airborne facility for advanced avionics research
[NLR-MP-87012-U] 20 p2760 N88-26368
A cockpit natural language study - selected transcripts
[AD-A192972] 20 p2834 N88-26808
Airborne remote operated device
[DE88-010324] 21 p2895 N88-27188
Aircraft component health monitoring: An effective approach 22 p3033 N88-28006
Event monitoring functions introduced by the Onboard Life Monitoring System (OLMOS) into a German aircraft 22 p3034 N88-28008
Reliable onboard computing for critical space systems
[RR-670-I] 22 p3135 N88-28641
Computers in weapons systems: A look at the F-15
[AD-A194498] 23 p3178 N88-28920
Feasibility study of a microprocessor controlled actuator test mechanism
[AD-A194654] 23 p3249 N88-29337

Knowledge-based fault diagnosis on future space vehicles 23 p3254 N88-29374
An expert systems application to space base data processing 23 p3256 N88-29384
Development and demonstration of an on-board mission planner for helicopters
[NASA-CR-177482] 24 p3328 N88-29817

AIRBUS
U EUROPEAN AIRBUS

AIRCRAFT
Steering mechanism --- vehicles
[EP-PATENT-0-181-700-A1] 01 p0053 N88-10338
Bibliography of icing on aircraft (status 1987)
[DFVLR-MITT-87-18] 16 p2158 N88-22876

AIRCRAFT ACCIDENT INVESTIGATION
Aircraft accident/incident summary reports: Unalaska, Alaska, September 25, 1985; Jenkinsburg, Georgia, September 29, 1985; Boston, Massachusetts, December 15, 1985; Dekalb, Texas, December 31, 1985; and Erie, Pennsylvania, February 21, 1986
[PB87-910408] 02 p0123 N88-10780
Aircraft accident reports, brief format, US civil and foreign aviation. Issue number 1: 1986 accidents
[PB87-916903] 02 p0123 N88-10781
Aircraft accident reports: Brief format, US Civil and Foreign Aviation, Issue Number 5 of 1986 accidents
[PB87-916907] 08 p0952 N88-15780
Aircraft accident reports: Brief format, US Civil and Foreign Aviation, Issue Number 7 of 1986 accidents
[PB87-916909] 08 p0952 N88-15781
Aircraft accident reports: Brief format, US Civil and Foreign Aviation, Issue Number 8 of 1986 accidents
[PB87-916910] 08 p0953 N88-15782
Aircraft accident/incident summary reports, Des Moines, Iowa, November 25, 1985; Chicago, Illinois, August 10, 1986
[PB88-910411] 09 p1115 N88-16685
Aircraft accident report: Midair collision of Cessna-340A, N8716K, and North American SNJ-4N, N711SQ, Orlando, Florida, May 1, 1987
[PB88-910402] 13 p1720 N88-20282
Aircraft accident reports, brief format, US civil and foreign aviation, issue number 10 of 1986 accidents
[PB87-916912] 15 p2016 N88-22020
Aircraft accident report: North Star Aviation, Inc., PA-32 RT-300, N39614 and Alameda Aero Club Cessna 172, N75584, Oakland, California, March 31, 1987
[PB87-910412] 15 p2016 N88-22021
Aircraft accident report: Midair collision of US Army U-21A, Army 18061 and Sachs Electric Company Piper PA-31-350, N60SE, Independence, Missouri, January 20, 1987
[PB88-910401] 16 p2159 N88-22877
Aircraft accident/incident summary reports: Modena, Pennsylvania, March 17, 1986; Redwater, Texas, April 4, 1986
[PB88-910403] 16 p2159 N88-22878
Aircraft accident/incident, Copperhill, Tennessee, February 22, 1986
[PB88-910407] 18 p2461 N88-24612
Aircraft accident report: Northwest Airlines, Inc., McDonnell Douglas DC-9-82, N312RC, Detroit Metropolitan Wayne County Airport, Romulus, Michigan, August 16, 1987
[PB88-910406] 19 p2601 N88-25449
Aircraft accident report: Air New Orleans, DBA continental express flight 962 British Aerospace 3101 (Jetstream 31), N331CY, New Orleans International Airport, Kenner, Louisiana, May 26, 1987
[PB88-910408] 19 p2601 N88-25450
Aircraft accident report: Joe Foster Excavating, Inc., Bell 206B, N49606, in-flight collision with trees, Alamo, California, August 3, 1986
[PB88-910405] 20 p2755 N88-26345
Aircraft accident report: Midair collision of SkyWest Airlines Swearingen METRO 2, N163SW, and Mooney M20, N6485U, Kearns, Utah, January 15, 1987
[PB88-910404] 20 p2755 N88-26346
The role played by FDRs in understanding the windshear phenomenon 22 p3036 N88-28023
Centralized class A flight mishap investigation
[AD-A194397] 24 p3322 N88-29786

AIRCRAFT ACCIDENTS
NT BIRD-AIRCRAFT COLLISIONS
Aircraft accidents
[JB-84] 01 p0004 N88-10020
Full-scale transport controlled impact demonstration program
[NASA-TM-89642] 01 p0004 N88-10021
Summary report of the history and events pertinent to the Civil Aeromedical Institute's evaluation of providing smoke/fume protective breathing equipment for airline passenger use
[AD-A184499] 03 p0261 N88-11645
Aircraft fire safety research 04 p0406 N88-12526
Airline safety: A comparative analysis
[AD-A185358] 05 p0543 N88-13308
Aircraft accident reports: Brief format, US Civil and Foreign Aviation, Issue Number 4 of 1986 accidents
[PB87-916906] 06 p0666 N88-14086
Annual review of aircraft accident data: US air carrier operations calendar year 1985
[PB88-135843] 10 p1276 N88-17638
Aircraft accident/incident, Newark, New Jersey, November 13, 1986
[NTSB/AAR-87/04-SUMM] 10 p1276 N88-17639
Aircraft accident report: Midair collision of Cessna-340A, N8716K, and North American SNJ-4N, N711SQ, Orlando, Florida, May 1, 1987
[PB88-910402] 13 p1720 N88-20282
Aircraft accident report: Midair collision of US Army U-21A, Army 18061 and Sachs Electric Company Piper PA-31-350, N60SE, Independence, Missouri, January 20, 1987
[PB88-910401] 16 p2159 N88-22877
Peak Acceleration Device (PAD)
[AD-A191639] 18 p2461 N88-24611
Improved procedure for impact probability computation of aircraft crash based on Balfanz model
[JUEL-SPEZ-425] 21 p2894 N88-27176
Correlation between EEG abnormal activity and aircraft accidents: A long term observation
21 p2984 N88-27719
Smoke hoods: Net safety benefit analysis --- aircraft accidents
[CAA-PAPER-87017] 23 p3174 N88-28898
Visual related accidents/incidents
23 p3242 N88-29293
Failure analysis for gas turbines
[NLR-MP-87037-U] 24 p3326 N88-29808

AIRCRAFT ANTENNAS
A conformal aircraft phased array antenna for airplane-satellite communication in the L band
[ESA-TT-1057] 03 p0305 N88-11926
Air gap testing using Trailing Wire Antenna (TWA) waveform
[AD-A187639] 11 p1477 N88-18812
MSAT-X phased array antenna adaptions to airborne applications 19 p2647 N88-25713
Airborne measurement of low frequency atmospheric noise ALFAN 1
[AD-A193056] 21 p2931 N88-27405

AIRCRAFT BASES
U MILITARY AIR FACILITIES

AIRCRAFT BRAKES
NT TRAILING EDGE FLAPS
NT WING FLAPS
Aircraft and ground vehicle friction correlation test results obtained under winter runway conditions during joint FAA/NASA Runway Friction Program
[NASA-TM-100506] 11 p1438 N88-18582

AIRCRAFT CABINS
U AIRCRAFT COMPARTMENTS

AIRCRAFT CARRIERS
Simulator evaluation of lineup visual landing aids for night carrier landing
[AD-A191212] 18 p2468 N88-24648
Multiple-Purpose Subsonic Naval Aircraft (MPSNA): Multiple Application Propfan Study (MAPS)
[NASA-CR-175104] 23 p3177 N88-28917

AIRCRAFT COMMUNICATION
Optimizing HF antenna systems on the Dolphin and Sea Hawk helicopters
[AD-A186552] 09 p1152 N88-16901
Information transfer in the National Airspace System
10 p1275 N88-17634
Electronics and communications in air traffic control: The Presidential Address
[ETN-88-92057] 14 p1865 N88-21146
Operation and performance of an integrated helicopter communication system 17 p2305 N88-23787
Developing a global aeronautical satellite system
19 p2644 N88-25687
World-wide aeronautical satellite communications
19 p2644 N88-25688
Design, development and trials of an airline passenger telephone system 19 p2646 N88-25704
Performance of the ICAO standard core service modulation and coding techniques
19 p2648 N88-25723
Development of an 8000 bps voice codec for AvSat
19 p2653 N88-25755
Airborne measurement of low frequency atmospheric noise ALFAN 1
[AD-A193056] 21 p2931 N88-27405

AIRCRAFT COMPARTMENTS
Test results and predictions for the response of near-ceiling sprinkler links in a full-scale compartment fire
[NBSIR-87/3633] 01 p0033 N88-10209
Research simulators for helicopters
03 p0263 N88-11656
Aircraft fire safety research 04 p0406 N88-12526
A hybrid fibreglass-CFRP cloth for new furnishings --- aircraft cabins
[SNIAS-872-111-109] 05 p0558 N88-13396
Development of rotorcraft interior noise control concepts. Phase 3: Development of noise control concepts
[NASA-CR-178172] 06 p0776 N88-14762
Man rating the b-1B molecular sieve oxygen generation system
[AD-A186275] 07 p0899 N88-15447
Analysis of in-flight acoustic data for a twin-engined turboprop airplane
[NASA-CR-178389] 11 p1543 N88-19220
Pressurizing systems and air conditioning systems
[MBB/LKE-312/S/PUB/246] 13 p1812 N88-20828
Aircraft interior noise reduction by alternate resonance tuning
[NASA-CR-182540] 20 p2849 N88-26909
Analysis of the transmission of sound into the passenger compartment of a propeller aircraft using the finite element method
[FFA-TN-1988-15] 23 p3279 N88-29520
A field study on soft contact lens wear in USAF military transport aircraft
[AD-A195962] 24 p3407 N88-30285

AIRCRAFT CONFIGURATIONS
Intergration effects of D-shaped, underwing, aft-mounted, separate-flow, flow-through nacelles on a high-wing transport
[NASA-TM-4018] 02 p0122 N88-10773
Civil applications of high-speed rotorcraft and powered-lift aircraft configurations
[NASA-TM-100035] 03 p0261 N88-11643
Planform effects on the supersonic aerodynamics of multibody configurations
[NASA-TP-2762] 04 p0393 N88-12454
A 0.15-scale study of configuration effects on the aerodynamic interaction between main rotor and fuselage
[NASA-CR-166577] 04 p0395 N88-12462
Analytical method for generating computational grids about complete aircraft configurations
05 p0540 N88-13287
Navier-Stokes simulation of transonic transportation aircraft configurations. 1: Flow-field simulation over wing-fuselage combinations 05 p0540 N88-13288
Computation of transonic flows with nacelle simulation
[SNIAS-872-111-117] 05 p0542 N88-13300
A simulation study of the flight dynamics of elastic aircraft. Volume 2: Data
[NASA-CR-4102-VOL-2] 08 p0959 N88-15813
Predicting dynamic separation characteristics of general configurations
[AD-A186689] 09 p1116 N88-16691
An examination of the impact of potential advances in component technology for future military engines
10 p1279 N88-17650
The aerodynamic design optimisation of a forward swept wing fighter aircraft
[CAR-87-18] 11 p1433 N88-18553
Presentation of Class 1 designs for a family of commuter airplanes
[NASA-CR-182563] 11 p1439 N88-18587
Generation of surface grids through elliptic partial differential equations for aircraft and missile configurations
[AD-A186631] 11 p1535 N88-19169
A multigrid full potential transonic code for arbitrary configurations --- aircraft 11 p1539 N88-19195
Steady and unsteady transonic small disturbance analysis of realistic aircraft configurations
[NASA-TM-100557] 13 p1717 N88-20269
CODAC (Cockpit Oriented Display of Aircraft Configurations) version 1.4 user's guide
[NASA-CR-181650] 13 p1718 N88-20273
Configuration management issues and objectives for a real-time research flight test support facility
[NASA-TM-100437] 13 p1813 N88-20832
Oscillating airfoils: Achievements and conjectures
[AD-A190490] 15 p2014 N88-22008
Trends in Computational Fluid Dynamics (CFD) for aeronautical 3D steady applications: The Dutch situation
[NLR-MP-86074-U] 15 p2015 N88-22017
The application of linear maximum likelihood estimation of aerodynamic derivatives for the Bell-205 and Bell-206
[AD-A191279] 16 p2161 N88-22894
Water facilities in retrospect and prospect: An illuminating tool for vehicle design
16 p2200 N88-23126
Flow visualization study of vortex manipulation on fighter configurations at high angles of attack
16 p2201 N88-23130

Aircraft aeroelasticity and structural dynamics research at the NASA Langley Research Center: Some illustrative results
[NASA-TM-100627] 18 p2459 N88-24598
Applications of the Navier-Stokes equations to wings and complex configurations using a zonal approach
[NASA-TM-100080] 18 p2459 N88-24602
Actuated forebody strakes
[NASA-CASE-LAR-13983-1] 18 p2464 N88-24628
Computational design of low aspect ratio wing-winglet configurations for transonic wind-tunnel tests
[NASA-CR-183021] 18 p2464 N88-24630
Application of advanced grid generation techniques for flow field computations about complex configurations
[NASA-CR-183049] 18 p2515 N88-24922
Calculation of aerodynamic characteristics of airplane configurations at high angles of attack
[NASA-CR-4182] 23 p3172 N88-28891
Three dimensional grid generation for complex configurations: Recent progress
[AGARD-AG-309] 23 p3245 N88-29313
Lessons learned in the mesh generation for PN/S calculations 23 p3245 N88-29314
Component adaptive grid generation for aircraft configurations 23 p3246 N88-29316
Generation of multiple block grids for arbitrary 3D geometries 23 p3246 N88-29317
Grid generation on and about a cranked-wing fighter aircraft configuration 23 p3246 N88-29318
Grid generation for an advanced fighter aircraft 23 p3246 N88-29319
Algebraic grid generation for fighter type aircraft 23 p3246 N88-29320
Composite grid generation for aircraft configurations with the EAGLE code 23 p3246 N88-29321
Analytical surfaces and grids 23 p3247 N88-29322
Mesh generation for industrial application of Euler and Navier Stokes solvers 23 p3247 N88-29323
Grid generation around transport aircraft configurations using a multi-block structured computational domain 23 p3247 N88-29325
Recent advances in transonic computational aeroelasticity
[NASA-TM-100663] 24 p3321 N88-29778
Generation of surface grids through elliptic partial differential equations for aircraft and missile configurations
[AD-A195639] 24 p3424 N88-30378

AIRCRAFT CONSTRUCTION
U AIRCRAFT STRUCTURES

AIRCRAFT CONSTRUCTION MATERIALS
NT AIRFRAME MATERIALS
The fatigue properties of aerospace steels under constant amplitude and flight-by-flight simulated loading
[BAE-MSM-R-GEN-0566] 01 p0059 N88-10377
Review of investigations of aeronautical fatigue in the Federal Republic of Germany
[LBF-S-178] 02 p0192 N88-11201
The use of aeroelastic wind tunnel models to prove structural design 05 p0551 N88-13355
A hybrid fibreglass-CFRP cloth for new furnishings — aircraft cabins
[SNIAS-872-111-109] 05 p0558 N88-13396
Paints required for aeronautical construction
[SNIAS-872-551-102] 05 p0569 N88-13470
Flammability test on aircraft seats equipped with fire barrier fabrics for the Porcher company
[CEAT-M5-525200] 06 p0666 N88-14084
Time-temperature-stress capabilities of composite materials for advanced supersonic technology application
[NASA-CR-178272] 06 p0677 N88-14144
Study of the evolution of short cracks in fatigue analysis — aircraft construction materials
[DCQ/L-46-555] 06 p0722 N88-14442
Roughness and waviness requirements for laminar flow surfaces 07 p0813 N88-14953
Moisture plotting of carbon fiber composite in flight operations
[MBB-UT-119/87] 09 p1138 N88-16823
Multipurpose corrosion inhibitors for aerospace materials in Naval environments
[AD-A186728] 09 p1143 N88-16853
Modern materials for light constructions — aircraft
[MBB-Z-136/86] 10 p1312 N88-17839
Viscoelastic behavior of a polyetheretherketone (PEEK) composite
[AD-A189545] 13 p1734 N88-20068
Environmental effects on the post-impact compressive strength of CFC
[RAE-TM-MAT-STR-1088] 14 p1884 N88-21258
Experimental comparison of lightning simulation techniques to CV-580 airborne lightning strike measurements
[AD-A190576] 15 p2098 N88-22496
Elementary characterization of Fibredux 913 CTS 5 34 percent preimpregnated carbon-epoxy from Ciba Geigy
[M-484300] 16 p2171 N88-22941
Investigation into the operation of the new special drills for drilling holes in thin components made of composite materials — aircraft components
[LR-519] 16 p2215 N88-23215
Detection sensitivity in thick assemblies — eddy currents, light alloys, aircraft construction materials
[REPT-48-912/F] 16 p2216 N88-23221
Application of the ONERA model to the life estimation under fatigue cracking of a Al-Li alloy. Parameter identification and test-experiment comparison under FALSTAFF loading
[ONERA-RT-32/7169-RY-063-R] 16 p2222 N88-23264
Crack retardation under load spectra. Experimental study and numerical simulation using the simplified K constant model — light alloys, aircraft construction materials
[ONERA-RT-30/7169-RY-054-R] 16 p2222 N88-23266
Certification aspects of airplanes which may operate with significant natural laminar flow 17 p2298 N88-23749
Characterization of the 2219 Cegedur alloy. Data acquisition of the fracture mechanics — aircraft construction materials
[REPT-48-442/F] 18 p2487 N88-24751
Characterization of 7090 and 7091 profiles made with Cegedur powder — powder metallurgy, aircraft construction materials
[REPT-48-441/F] 18 p2487 N88-24752
Aluminum alloy
[NASA-CASE-LAR-13924-1-CU] 18 p2487 N88-24753
Energy dissipation in a rolling aircraft tire
[NASA-CR-182978] 19 p2676 N88-25913
Prediction of fatigue life of notched specimens under aircraft loading and importance of the relative method in the case of local strain approach, part 2
[TAE-595-PT-2] 19 p2680 N88-25934
Factors affecting strength in composite materials used for aircraft
[DT-212/87] 21 p2907 N88-27248
The composite aeroengine
[PNR90451] 22 p3045 N88-28070

AIRCRAFT CONTROL
NT HELICOPTER CONTROL
Measurements in the functional mock up test of the NAL QSTOL aircraft control system
[NAL-TR-928] 02 p0126 N88-10793
A survey of aircraft integrated control technology
[AR-004-561] 02 p0126 N88-10794
A preliminary investigation into the feasibility of implementing a direct sideforce control system on the Astra Hawk by means of an active control surface — aircraft control
[ETN-87-90924] 02 p0126 N88-10795
The application of emulation techniques in the analysis of highly reliable, guidance and control computer systems 02 p0127 N88-10798
Knowledge Based Concepts and Artificial Intelligence: Applications to Guidance and Control
[AGARD-LS-155] 02 p0128 N88-10806
Overview of AGARD Lecture Series No. 155: Knowledge-based concepts and artificial intelligence applications to guidance and control 02 p0128 N88-10807
AI expert system technology issues for guidance and control applications 02 p0128 N88-10808
Application of knowledge-based techniques to aircraft trajectory generation and control 02 p0129 N88-10811
Towards the unmanned cockpit 02 p0129 N88-10812
Approach trajectory planning system for maximum concealment
[NASA-TM-88258] 02 p0227 N88-11435
Mission-oriented flying qualities criteria for helicopter design via in-flight simulation 03 p0263 N88-11652
Effects of the installation and operation of jet-exhaust yaw vanes on the longitudinal and lateral-directional characteristics of the F-14 airplane
[NASA-TP-2769] 04 p0393 N88-12455
An integrated study of structures, aerodynamics and controls on the forward swept wing X-29A and the oblique wing research aircraft
[NASA-CR-181548] 04 p0399 N88-12486
Structural optimization in the design process — aircraft
[SNIAS-872-111-115] 05 p0535 N88-13885
Flaps-up takoff performance of the OV-1D aircraft with YT53-L-704 engine installed
[AD-A185960] 07 p0819 N88-14979
Fiber optics for controls 08 p0958 N88-15798
A flight-test methodology for identification of an aerodynamic model for a V/STOL aircraft
[NASA-TM-100067] 09 p1117 N88-16694
Aircraft flight test trajectory control
[NASA-CR-179428] 09 p1120 N88-16707
Proceedings of the Circulation-Control Workshop, 1986
[NASA-CP-2432] 10 p1268 N88-17586
The impact of circulation control on rotary aircraft controls systems 10 p1271 N88-17601
A potential flight evaluation of an upper-surface-blowing/circulation-control-wing concept 10 p1272 N88-17609
Airborne Wind Shear Detection and Warning Systems: First Combined Manufacturers' and Technologists' Conference
[NASA-CP-10006] 10 p1273 N88-17616
Investigation of the influence of wind shear on the aerodynamic characteristics of aircraft using a vortex-lattice method 10 p1274 N88-17619
Simulator investigation of wind shear recovery techniques 10 p1275 N88-17630
Active control technology with adaptive control concept in the aircraft construction
[MBB/LKE-294/S/PUB/295] 10 p1313 N88-17845
Workshop on Design Loads for Advanced Fighters
[AGARD-R-746] 12 p1579 N88-19449
Structural design requirements for aircraft incorporating active control technology 12 p1580 N88-19453
The relationship between operational flight manoeuvre parameters and design parameters 12 p1580 N88-19454
Output aiming control
[AD-A188463] 12 p1583 N88-19473
Rotorcraft flight-propulsion control integration: An eclectic design concept
[NASA-TP-2815] 12 p1584 N88-19475
F-16 simulator for man-in-the-loop testing of aircraft control systems (SIMTACS)
[AD-A189675] 14 p1870 N88-21178
Design of an integrated control system for flutter margin augmentation and gust load alleviation, tested on a dynamic windtunnel model
[PB88-149885] 15 p2020 N88-22038
Expanded envelope concepts for aircraft control-element failure detection and identification
[NASA-CR-181664] 16 p2160 N88-22886
Conceptual final paper on the preliminary design of an oblique flying wing SST
[NASA-CR-182879] 16 p2161 N88-22891
Stability and control methodology for conceptual aircraft design. Volume 1: Methodology manual
[AD-A191314] 16 p2164 N88-22906
Joint University Program for Air Transportation Research, 1986
[NASA-CP-2502] 17 p2293 N88-23715
Investigation of air transportation technology at Princeton University, 1986 17 p2294 N88-23724
Flight penetration of wind shear: Control strategies 17 p2294 N88-23727
Natural laminar flow and airplane stability and control 17 p2298 N88-23747
Wind-tunnel investigation of actuated forebody strakes for yaw control at high angles of attack 17 p2299 N88-23754
Optimization of the dilation characteristic on the control jurisdiction of an area control facility
[AD-A191720] 18 p2461 N88-24615
Actuated forebody strakes
[NASA-CASE-LAR-13983-1] 18 p2464 N88-24628
Overview of NASA research in fiber optics for aircraft controls
[NASA-TM-100919] 19 p2603 N88-25458
Influence of wind shear on the aerodynamic characteristics of airplanes
[NASA-TP-2827] 20 p2755 N88-26344
Propfan test assessment testbed aircraft stability and control/performance 1/9-scale wind tunnel tests
[NASA-CR-182121] 20 p2757 N88-26360
Low-speed wind-tunnel test of a STOL supersonic-cruise fighter concept
[NASA-TM-4050] 20 p2761 N88-26374
Nonlinear identification of an aircraft for the direct calculation of an anticipatory control 20 p2787 N88-26535
Investigations of aircraft control with jet spoilers
[ISL-R-112/87] 21 p2898 N88-27202
Computer system for the primary fly-by-wire control of civil transport aircraft (experimental system)
[FBW-TB-2086/86] 21 p2898 N88-27204
Optimal control of the wing rock phenomenon 21 p2927 N88-27373
High performance forward swept wing aircraft
[NASA-CASE-ARC-11636-1] 23 p3177 N88-28914

Variable wing camber control systems for the future Airbus program
[MBB-UT-104/88] 23 p3180 N88-28932
Comparison of the influence of different gust models on structural design 24 p3312 N88-29722
Pilot modeling 24 p3314 N88-29736
Pilot modeling applications 24 p3314 N88-29737
Advances in flying qualities: Concepts and criteria for a mission oriented flying qualities specification 24 p3314 N88-29739
A second look at MIL prime flying qualities requirements 24 p3314 N88-29740
The role of simulation in flying qualities and flight control system related development 24 p3315 N88-29742
Angle of attack and sideslip estimation using an inertial reference platform
[AD-A194876] 24 p3319 N88-29769
A fiber optic collective flight control system for helicopters
[AD-A195406] 24 p3328 N88-29818
Controlled degradation of resolution of high-quality flight simulator images for training effectiveness evaluation
[AD-A196189] 24 p3330 N88-29823
Numerical simulation of nozzle flows
[AD-A195144] 24 p3369 N88-30064
Four-axis side-arm flight control simulator investigation
[AD-A196026] 24 p3409 N88-30294
Prediction and measurement of human pilot dynamic characteristics in a manned rotorcraft simulation
[NASA-CR-183246] 24 p3410 N88-30297

AIRCRAFT DESIGN
NT HELICOPTER DESIGN
International Conference on the Aerodynamics at Low Reynolds Numbers between 10(4) and 10(6)
[ONRL-7-023-C] 01 p0002 N88-10010
Design principles and practices for implementation of MIL-STD-1760 in aircraft and stores
[AD-A183724] 01 p0005 N88-10027
Problem and solution formulations for the generation of 3D block-structured grids --- aircraft design
[NLR-MP-86020-U] 01 p0005 N88-10028
Aerospace research at the National Aerospace Laboratory (NLR)
[ETN-87-90821] 01 p0107 N88-10697
Ensuring the service life of designs (experience in aircraft construction) 02 p0157 N88-10986
On the occasion of the 50th anniversary of the death of Professor Hugo Junkers
[MBB/LW-3016/S/PUB/201] 02 p0257 N88-11627
Rotorcraft Design for Operations
[AGARD-CP-423] 03 p0262 N88-11649
The influence of operational requirements on LHX concept formulation 03 p0262 N88-11650
Design requirements for future commercial operations 03 p0262 N88-11651
Mission-oriented flying qualities criteria for helicopter design via in-flight simulation 03 p0263 N88-11652
MBB simulation facilities applied for rotorcraft research 03 p0263 N88-11655
Impacts of rotor hub design criteria on the operational capabilities of rotorcraft systems 03 p0264 N88-11663
New aerodynamic design of the fenestron for improved performance 03 p0264 N88-11664
Rotorcraft designs for the year 2000 03 p0264 N88-11665
Apache for the battlefield of today and the 21st century 03 p0265 N88-11670
The EH-101 integrated project: A naval, utility and commercial helicopter system 03 p0265 N88-11672
Flight propulsion control integration for V/STOL aircraft
[NASA-TM-100226] 03 p0267 N88-11680
Flap-lag equations of motion of rigid, articulated rotor blades with three hinge sequences
[NASA-TM-100023] 04 p0401 N88-12495
A reliability concept for optimizing aircraft design 04 p0423 N88-12622
Renewed interest in airships for industry use discussed 04 p0424 N88-12628
The A320 Airbus program
[SNIAS-872-111-105] 05 p0529 N88-13215
Validation elements of the computation methods and measurement techniques for high lift aerodynamic systems
[SNIAS-872-111-101] 05 p0541 N88-13299
Special Course on Fundamentals of Fighter Aircraft Design
[AGARD-R-740] 05 p0544 N88-13315
Fundamentals of fighter aircraft design 05 p0544 N88-13316
Mission requirements and aircraft sizing 05 p0545 N88-13317
Design of wings and wing/body configurations for transonic and supersonic speeds 05 p0545 N88-13318
Aircraft dynamics: Aerodynamic aspects and wind tunnel techniques 05 p0545 N88-13320
Fundamentals of fighter aircraft design: Engine intake and afterbody 05 p0545 N88-13322
Aeroelasticity and optimization in fighter aircraft design 05 p0546 N88-13324
Materials for fighter aircraft 05 p0546 N88-13325
Requirements and recommendations for the development of theoretical codes and experimental facilities in the near future 05 p0546 N88-13327
Aeroelastic analysis of modern transport aircraft --- European Airbus
[SNIAS-872-111-102] 05 p0546 N88-13329
Damage considerations in sizing aircraft cells. Life predictions
[SNIAS-872-111-116] 05 p0546 N88-13330
Static Aeroelastic Effects on High Performance Aircraft
[AGARD-CP-403] 05 p0550 N88-13348
Static aeroelastic considerations in the definition of design loads for fighter airplanes 05 p0550 N88-13351
The use of aeroelastic wind tunnel models to prove structural design 05 p0551 N88-13355
Surface treatment problems found in new aircraft designed using structural composites
[SNIAS-872-111-113] 05 p0558 N88-13397
Utilization of a high rate vector computer in computational fluid mechanics for aeronautics
[ETN-88-91171] 05 p0581 N88-13547
Overall description of the computer aided design and manufacturing systems associated with the A320 program at Aerospatiale and its partners
[SNIAS-872-111-104] 05 p0635 N88-13883
Presentation of SIGMA (Interactive Assisted Geometry System). A computer assisted shape design program developed at the Aerospatiale Aircraft Division
[SNIAS-872-111-110] 05 p0635 N88-13884
Structural optimization in the design process --- aircraft
[SNIAS-872-111-115] 05 p0635 N88-13885
Operational groups at the Aerospatiale Aircraft Division
[SNIAS-872-111-107] 05 p0658 N88-14036
Damage tolerance of stiffened-skin structures: Prediction and experimental verification
[NLR-MP-86041-U] 06 p0667 N88-14091
A simulation study of the flight dynamics of elastic aircraft. Volume 1: Experiment, results and analysis
[NASA-CR-4102] 06 p0669 N88-14099
NAL news updated: FY87 business plan, developments 06 p0675 N88-14135
Activities report in aircraft design and astronautics
[ETN-88-90618] 07 p0809 N88-14925
Langley Symposium on Aerodynamics, volume 1
[NASA-CP-2397] 07 p0809 N88-14926
Application of a full potential method for analysis of complex aircraft geometries 07 p0809 N88-14930
Viscous vortex flows 07 p0810 N88-14934
Flight research on natural laminar flow 07 p0813 N88-14950
Design and experimental evaluation of a swept supercritical Laminar Flow Control (LFC) airfoil 07 p0813 N88-14951
The NASA aircraft icing research program 08 p0957 N88-15803
Overview of NASA PTA propfan flight test program 08 p0957 N88-15805
NASA/Army Rotorcraft Technology. Volume 2: Materials and Structures, Propulsion and Drive Systems, Flight Dynamics and Control, and Acoustics
[NASA-CP-2495-VOL-2] 09 p1106 N88-16632
NASA's rotorcraft icing research program 09 p1108 N88-16641
Rotorcraft flight-propulsion control integration 09 p1108 N88-16643
Aeroacoustic research programs at the Army Aviation Research and Technology Activity 09 p1109 N88-16649
NASA/Army Rotorcraft Technology. Volume 3: Systems Integration, Research Aircraft, and Industry
[NASA-CP-2495-VOL-3] 09 p1110 N88-16650
Integrated diagnostics 09 p1111 N88-16655
McDonnell Douglas Helicopter Company independent research and development: Preparing for the future 09 p1111 N88-16660
Testing of a schematic transport plane model in several European windtunnels
[PB87-170270] 09 p1113 N88-16671
The wind tunnel as a yardstick for aircraft design
[NLR-MP-85032-U] 09 p1121 N88-16712
Computational fluid dynamics and aerothermodynamics
[NASA-CR-182490] 09 p1166 N88-16989
Development of vertical takeoff aircraft with turbojet engines in Germany 10 p1309 N88-17822
Variable sweep wings 10 p1309 N88-17823
The European Airbus A-300 10 p1309 N88-17824
Purposes and tasks of high-performance aircraft construction
[MBB/LK-S/PUB/296] 10 p1312 N88-17842
Presentation of Class 1 designs for a family of commuter airplanes
[NASA-CR-182563] 11 p1439 N88-18587
Counter-Rotating Integrated Shrouded Propfan (CRISP): The MTU propfan program --- Motoren und Turbinen Union (MTU)
[ETN-88-91023] 11 p1441 N88-18597
Chinese 7760 CAD/CAMM software system introduced 11 p1468 N88-18756
Aerodynamic characteristics of wings designed with a combined-theory method to cruise at a Mach number of 4.5
[NASA-TP-2799] 12 p1575 N88-19420
Workshop on Design Loads for Advanced Fighters
[AGARD-R-746] 12 p1579 N88-19449
The development of manoeuvre load criteria for agile aircraft 12 p1579 N88-19450
Changes in USAF structural loads requirements 12 p1580 N88-19452
Structural design requirements for aircraft incorporating active control technology 12 p1580 N88-19453
The relationship between operational flight manoeuvre parameters and design parameters 12 p1580 N88-19454
Manoeuvres by default, by demand and by design 12 p1580 N88-19455
Design loads for Swedish military aircraft in a twenty years' perspective 12 p1580 N88-19456
Determination of design loads for modern combat aircraft 12 p1580 N88-19457
Interaction between structural considerations and system design in advanced flight controls 12 p1580 N88-19458
Manned simulation: Helpful means to determine and improve structural load criteria 12 p1581 N88-19459
Use of demonstration/validation prototypes: Impact on total development costs and times 12 p1703 N88-20194
The design of aircraft using the decision support problem technique
[NASA-CR-4134] 13 p1721 N88-20291
How to generate equal probability design load conditions --- aircraft design
[NLR-TR-86060-U] 13 p1722 N88-20295
Aeroelastic models in aircraft design
[MBB/LKE-294/S/PUB/249] 13 p1722 N88-20298
Activities report in aeronautics and astronautics
[ETN-88-91332] 13 p1859 N88-21115
Computer aided design of aircraft structures
[ETN-88-91353] 14 p1867 N88-21154
The NASA integrated test facility and its impact on flight research
[NASA-TM-100418] 14 p1870 N88-21177
Trends in Computational Fluid Dynamics (CFD) for aeronautical 3D steady applications: The Dutch situation
[NLR-MP-86074-U] 15 p2015 N88-22017
Activities report in aerospace
[ETN-88-91566] 16 p2155 N88-22856
The initial calculation of range and mission fuel during conceptual design --- aircraft design
[LR-525] 16 p2161 N88-22889
Basic design of a flight director system for NAL STOL research aircraft
[DE88-751806] 16 p2162 N88-22897
Stability and control methodology for conceptual aircraft design. Volume 1: Methodology manual
[AD-A191314] 16 p2164 N88-22906
Water facilities in retrospect and prospect: An illuminating tool for vehicle design 16 p2200 N88-23126
The use of the NRC/NAE water facilities in Canadian aeronautical research and development 16 p2201 N88-23132
It's time to reinvent the general aviation airplane 17 p2294 N88-23726
Full potential methods for analysis/design of complex aerospace configurations
[NASA-CR-3982] 17 p2296 N88-23736
Laminar Flow Aircraft Certification
[NASA-CP-2413] 17 p2296 N88-23737
Boundary-layer stability and airfoil design 17 p2296 N88-23738
High-flaps for natural laminar flow airfoils 17 p2296 N88-23739
Computational wing design studies relating to natural laminar flow 17 p2297 N88-23740
Preliminary aerodynamic design considerations for advanced laminar flow aircraft configurations 17 p2297 N88-23746

Multi-body aircraft with an all-movable center fuselage actively controlling fuselage pressure drag
[NASA-CASE-LAR-13511-1] 17 p2301 N88-23765
Sensitivity analysis and multidisciplinary optimization for aircraft design: Recent advances and results
[NASA-TM-100630] 17 p2302 N88-23766
The specification and design of a future maritime reconnaissance aircraft 17 p2303 N88-23772
A structured approach to weapon system design 17 p2303 N88-23773
Acta aeronautica et astronautica sinica (selected articles)
[AD-A191552] 18 p2455 N88-24575
A transonic small disturbance wing design methodology 18 p2457 N88-24590
Class 2 design update for the family of commuter airplanes
[NASA-CR-182681] 18 p2464 N88-24629
Current fire safety design aspects of commuter aircraft
[DOT/FAA/CT-87/32] 19 p2600 N88-25448
Proceedings of the 5th NAL Symposium on Aircraft Computational Aerodynamics
[NAL-SP-8] 19 p2635 N88-25630
Numerical calculation of supersonic flow by the PNS equations 19 p2636 N88-25636
Aerodynamic simulation for complete ASKA aircraft configuration 19 p2637 N88-25641
Calculations of unsteady aerodynamics for a full aircraft configuration using boundary element method 19 p2637 N88-25643
An initial investigation into methods of computing transonic aerodynamic sensitivity coefficients
[NASA-CR-183061] 20 p2752 N88-26332
Flight research and testing
[NASA-TM-100439] 20 p2758 N88-26361
Flight Mechanics Panel Symposium on Rotorcraft Design for Operations: Technical evaluation report
[AGARD-AR-243] 20 p2758 N88-26362
A new method for the estimation of aircraft inertia characteristics 20 p2787 N88-26530
Concept development of a Mach 3.0 high-speed civil transport
[NASA-TM-4058] 21 p2895 N88-27182
Supersonic transport/hypersonic transport (SST/HST) development
[REPT-881-111-101] 21 p2896 N88-27192
Development of direct-inverse 3-D methods for applied transonic aerodynamic wing design and analysis
[NASA-CR-183127] 22 p3037 N88-28033
Complex configurations 23 p3167 N88-28861
Transport-type configurations 23 p3169 N88-28867
Combat aircraft 23 p3169 N88-28868
Variable Sweep Transition Flight Experiment (VSTFE)-parametric pressure distribution boundary layer stability study and wing glove design task
[NASA-CR-3992] 23 p3173 N88-28894
A contribution to the quantitative analysis of the influence of design parameters on the optimal design of passenger aircraft
[ETN-88-92979] 23 p3176 N88-28912
Critical joints in large composite primary aircraft structures. Volume 2: Technology demonstration test report
[NASA-CR-172587] 23 p3177 N88-28915
Critical joints in large composite primary aircraft structures. Volume 3: Ancillary test results
[NASA-CR-172588] 23 p3177 N88-28916
Vision through aircraft transparencies 23 p3242 N88-29294
The Flight of Flexible Aircraft in Turbulence: State-of-the-Art in the Description and Modelling of Atmospheric Turbulence
[AGARD-R-734-ADD] 24 p3311 N88-29717
Current and proposed gust criteria and analysis methods: An FAA overview 24 p3311 N88-29718
Matching P.S.D.: Design loads 24 p3312 N88-29720
A summary of methods for establishing airframe design loads from continuous gust design criteria 24 p3312 N88-29721
Comparison of the influence of different gust models on structural design 24 p3312 N88-29722
Measured and predicted responses of the Nord 260 aircraft to the low altitude atmospheric turbulence 24 p3312 N88-29723
A review of measured gust responses in the light of modern analysis methods 24 p3312 N88-29724
Aircraft dynamics: Aerodynamic aspects and wind tunnel techniques 24 p3313 N88-29731
Compression pylon
[NASA-CASE-LAR-13777-1] 24 p3323 N88-29789

AIRCRAFT DETECTION
Acta aeronautica et astronautica sinica (selected articles)
[AD-A191552] 18 p2455 N88-24575
Surface disturbances produced by low-level, subsonic B-1 aircraft
[AD-A192257] 20 p2824 N88-26752
Proceedings of the French-German Colloquium on Helicopter Detection
[ISL-R-104/87] 22 p3147 N88-28723
Acoustic detection of helicopters: Experiments 22 p3148 N88-28727
Examples of the application of acoustics for the detection and classification of targets 22 p3148 N88-28729
Detection of helicopters using ground-controlled microphones 22 p3148 N88-28730
Correlation method and sensors adapted to the environment 22 p3149 N88-28732
Acoustic-seismic helicopter detection 22 p3149 N88-28734
Helicopter Warning Sensor (HWS) 22 p3149 N88-28735
The VHF experimental radar LARA. A long-wavelength radar for helicopter detection 22 p3149 N88-28738
The radar detection of hovering helicopters 22 p3150 N88-28739

AIRCRAFT ENERGY EFFICIENCY PROGRAM
U ACEE PROGRAM

AIRCRAFT ENGINES
NT CONVERTIBLE FAN-SHAFT ENGINES
NT HELICOPTER ENGINES
NT TF-30 ENGINE
NT TF-34 ENGINE
Noise emission of civil and military aero-engines. Sources of generation and measures for attenuation
[ETN-87-91021] 01 p0091 N88-10595
Turbines with counterrotating runners for aircraft power plants 02 p0158 N88-10992
Diagnosis of flow channel in aircraft gas-turbine engines on basis of vibration spectrum characteristics 02 p0159 N88-10993
Transmission efficiency in advanced aerospace powerplant
[PNR90391] 02 p0182 N88-11133
The use of Kevlar on aero-engine fan containment casings
[PNR90410] 02 p0182 N88-11134
Development of heat flux sensors for turbine airfoils 02 p0184 N88-11143
The flight evaluation of an advanced engine display and monitoring system 03 p0264 N88-11659
A129 advanced solutions for meeting today's combat helicopter requirement 03 p0265 N88-11660
Crack initiation and propagation due to cyclic thermal gradients — aircraft turbine blades
[ESA-TT-1023] 03 p0336 N88-12114
Aircraft engine exhaust plume dynamics
[AD-A184238] 04 p0400 N88-12488
Aircraft classification by type of propulsive devices. Determination of type and number of carrying solutions 04 p0424 N88-12626
Dynamics of reverse flows at pump inlet 04 p0425 N88-12636
Calculation of the tribological properties of surfaces by semi-empirical methods
[AD-A184283] 04 p0450 N88-12791
A numerical investigation on wing/nacelle interferences 05 p0535 N88-13258
Correlation of air pressure drop and flame arrestor characteristics for explosion suppression materials
[AD-A184960] 05 p0548 N88-13340
Performance of supersonic impingement radial turbines 06 p0712 N88-14367
Conclusions from a research program on mixed flow gas generator turbines 06 p0713 N88-14368
Aerodynamic design of first stage turbines for small aero engines 06 p0713 N88-14370
Flaps-up takoff performance of the OV-1D aircraft with YT53-L-704 engine installed
[AD-A185960] 07 p0819 N88-14979
Pollution from motor vehicles and aircraft at Stapleton International Airport (abbreviated report), revision 2
[AD-A185916] 07 p0875 N88-15307
Technology developments for a compound cycle engine 09 p1107 N88-16637
Small gas turbine engine technology 09 p1107 N88-16638
Creep and fatigue research efforts on advanced materials 09 p1119 N88-16701
Turbine engine monitoring systems: Can they benefit component improvement program management?
[AD-A186992] 09 p1120 N88-16706
Calibration of the ARL (Aeronautical Research Laboratories) rain and icing facility
[AD-A186776] 09 p1121 N88-16710
Development of a shell system for DS moulds at RR precision casting facility — directional solidification (DS)
[PNR90400] 09 p1151 N88-16893
Advanced Technology for Aero Gas Turbine Components
[AGARD-CP-421] 10 p1279 N88-17647
The coming revolution in turbine engine technology 10 p1279 N88-17648
Optimisation of military compressors for weight and volume 10 p1279 N88-17649
An examination of the impact of potential advances in component technology for future military engines 10 p1279 N88-17650
Specification of an engine and its components starting from a consideration of aircraft missions 10 p1279 N88-17651
Application of highly loaded single-stage mixed-flow compressors in small jet-engines 10 p1280 N88-17652
A research program on the aerodynamics of a highly loaded turbine stage 10 p1280 N88-17655
Design and aerodynamic performance of a small mixed-flow gas generator turbine 10 p1281 N88-17662
Development of a plenum chamber burner system for an advanced VTOL engine 10 p1281 N88-17664
Aerodynamic performance of a scale-model, counter-rotating unducted fan 10 p1282 N88-17666
Gear systems for advanced turboprops 10 p1282 N88-17667
Ceramic bearings for use in gas turbine engines
[NASA-TM-100288] 10 p1340 N88-18007
Sampling intervals
[AD-A189445] 12 p1573 N88-19408
Elevated temperature crack growth studies of advanced titanium aluminides
[AD-A189025] 12 p1608 N88-19618
Optimizing powerplant design and development cycles 12 p1701 N88-20183
Engine flow simulation for wind tunnel testing at NLR
[NLR-MP-87011-U] 13 p1723 N88-20305
Aircraft corrosion problems and research in the Netherlands
[NLR-MP-86066-U] 13 p1744 N88-20427
Investigation of the misfueling of reciprocating piston aircraft engines
[NASA-TP-2803] 14 p1865 N88-21144
Research as part of the Air Force in aero propulsion technology (AFRAPT) program
[AD-A190336] 15 p2019 N88-22036
AFRAPT (Air Force Research in Aero Propulsion Technology) trainee program
[AD-A190525] 15 p2035 N88-22123
Lewis Structures Technology, 1988. Volume 2: Structural Mechanics
[NASA-CP-3003-VOL-2] 15 p2077 N88-22382
Structural analyses of engine wall cooling concepts and materials 15 p2081 N88-22405
Engine structures: A bibliography of Lewis Research Center's research for 1980-1987
[NASA-TM-100842] 17 p2350 N88-24002
Prediction of the aeroelastic behavior of tuned blades. Application to aircraft engines
[ISAL-87-0046] 21 p2897 N88-27199
Engine condition monitoring civil requirements: A British Airways view 22 p3033 N88-28002
Background to the UK military requirements for engine usage, condition and maintenance management systems 22 p3033 N88-28004
Recent advances in engine health management 22 p3033 N88-28005
Aircraft component health monitoring: An effective approach 22 p3033 N88-28006
The design and testing of aero engines to minimise hazard from birds
[PNR90436] 22 p3040 N88-28049
Applications of fatigue analyses: Aircraft engines
[PNR90439] 22 p3044 N88-28066
Trends in civil aircraft propulsion
[PNR90441] 22 p3044 N88-28067
Future trends in aviation propulsion
[PNR90443] 22 p3044 N88-28068
RB211 developments
[PNR90444] 22 p3045 N88-28069
The composite aeroengine
[PNR90451] 22 p3045 N88-28070
A review of non-contacting displacement measurement techniques used to monitor the movement of rotor blades in gas turbine aero engines
[PNR90457] 22 p3045 N88-28071
Holographic interferometry for flow visualization studies in high speed fans
[PNR90459] 22 p3045 N88-28072
Use of penetrating radiations for the dynamic examination of aero gas turbines
[PNR90470] 22 p3045 N88-28073
AGARD engine disc cooperative test programme
[AGARD-R-766] 23 p3179 N88-28926

Developing the Rolls-Royce Tay
[PNR90447] 24 p3327 N88-29809
Fuel effects on flame radiation and hot-section durability 24 p3347 N88-29925
Contamination and distortion of steady flow field induced by discrete frequency disturbances in aircraft gas engines
[AD-A195440] 24 p3370 N88-30069

AIRCRAFT EQUIPMENT
NAVSIM 2: A computer program for simulating aided-inertial navigation for aircraft
[NASA-CR-177438] 04 p0398 N88-12478
Lightning discharge protection rod
[NASA-CASE-LAR-13470-1] 06 p0666 N88-14083
Information transfer in the National Airspace System 10 p1275 N88-17634
Electrical/pneudraulic design considerations
[AD-A188097] 12 p1581 N88-19462
Equipment test methods for externally produced electromagnetic transients
[RAE-TM-FS(F)-457] 14 p1865 N88-21140
Recommended test specification for the electromagnetic compatibility of aircraft equipment
[RAE-TM-FS(F)-510] 14 p1867 N88-21155
Basic design studies for the realization of liquid crystal display systems in aircraft
[VA-87-001] 16 p2163 N88-22900
Aircraft field degradation and electromagnetic compatibility
[PB88-183975] 19 p2602 N88-25456
Tactical Rubidium Frequency Standard (TRFS), volume 1
[AD-A192981] 20 p2805 N88-26640
A cockpit natural language study - selected transcripts
[AD-A192972] 20 p2834 N88-26808
Electrical load and power source capacity report for the C-130 aircraft Self Contained Navigation System (SCNS): LSI model 6216A, 6216B, 6216C, revision
[AD-A193079] 21 p2895 N88-27186
The Flight of Flexible Aircraft in Turbulence: State-of-the-Art in the Description and Modelling of Atmospheric Turbulence
[AGARD-R-734] 24 p3312 N88-29725
A summary of atmospheric turbulence measurements with specially-equipped aircraft in the US 24 p3312 N88-29727
Standard fatigue specimens for fastener evaluation --- aircraft components
[FFA-TN-1987-68] 24 p3384 N88-30157

AIRCRAFT FUEL SYSTEMS
Pumping systems and flow interfaces for rapid response electronic reheat controls 10 p1282 N88-17665

AIRCRAFT FUELS
Correlation of air pressure drop and flame arrestor characteristics for explosion suppression materials
[AD-A184960] 05 p0548 N88-13340
Study of electrostatic modulation of fuel sprays to enhance combustion performance in an aviation gas turbine
[AD-A184967] 05 p0548 N88-13341
Effects of aviation fluids on fiber composite material
[FOA-C-20674-2.6] 08 p0965 N88-15840
Large-Scale Advanced Prop-Fan (LAP)
[NASA-CR-182112] 13 p1723 N88-20306
Aviation turbine fuels from tar sands bitumen and heavy oils. Part 3: Laboratory sample production
[AD-A189278] 13 p1753 N88-20484
Feasibility of producing jet fuel from GPGP (Great Plains Gasification Plant) by-products
[DE88-010233] 20 p2781 N88-26492
Biodegradation of JP-5 aviation fuel by subsurface microbial communities
[AD-A192743] 20 p2781 N88-26493
Combustion and fuels in gas turbine engines
[AGARD-CP-422] 24 p3345 N88-29910

AIRCRAFT GUIDANCE
The application of emulation techniques in the analysis of highly reliable, guidance and control computer systems 02 p0127 N88-10798
Knowledge Based Concepts and Artificial Intelligence: Applications to Guidance and Control
[AGARD-LS-155] 02 p0128 N88-10806
Overview of AGARD Lecture Series No. 155: Knowledge-based concepts and artificial intelligence applications to guidance and control 02 p0128 N88-10807
Some data processing requirements for precision Nap-Of-the-Earth (NOE) guidance and control of rotorcraft
[NASA-CR-177453] 04 p0401 N88-12493
Contribution to the improvement of the guidance accuracy of automatic pilots
[ETN-88-90607] 05 p0551 N88-13360
Simulator investigation of wind shear recovery techniques 10 p1275 N88-17630
Airworthiness considerations 10 p1276 N88-17636
Commonality in the design and production of the H-423 (F3) and H-770 (F-15) RLG inertial navigation systems 12 p1577 N88-19431
Flight simulations of MLS interception procedures applicable to laterally segmented approach paths
[NLR-MP-86037-U] 13 p1721 N88-20288
Joint University Program for Air Transportation Research, 1986
[NASA-CP-2502] 17 p2293 N88-23715
Investigation of air transportation technology at Princeton University, 1986 17 p2294 N88-23724
Optics: Perspectives for Measurement Techniques and Signal Processing for Flight Guidance --- conference
[DFVLR-MITT-87-21] 18 p2516 N88-24928
Laboratory tests of laser gyroscopes for future utilization in multifunction systems for precision navigation and flight guidance 18 p2517 N88-24932
Limits of accuracy and range of laser radars 18 p2517 N88-24934
The optical accelerometer: A novel sensor for vertical flight guidance 18 p2518 N88-24935

AIRCRAFT HAZARDS
Test results and predictions for the response of near-ceiling sprinkler links in a full-scale compartment fire
[NBSIR-87/3633] 01 p0033 N88-10209
Aircraft fire safety research 04 p0406 N88-12526
TOMS and the NOAA/FAA volcano support plan 05 p0618 N88-13796
NASA wind shear model: Summary of model analyses 10 p1273 N88-17617
Response of wind shear warning systems to turbulence with implication of nuisance alerts 10 p1274 N88-17618
Forward looking wind shear detection 10 p1275 N88-17629
Crew interface with windshear systems 10 p1275 N88-17631
Aviation weather: Status of FAA's (Federal Aviation Administration's) new hazardous weather detection and dissemination systems
[PB88-115910] 11 p1513 N88-19041
Lapwings and birdstrikes. The biology of the lapwing Vanellus vanellus in relation to the birdstrike hazard it presents
[CAA-PAPER-87015] 14 p1865 N88-21142
An experimental and theoretical study of the ice accretion process during artificial and natural icing conditions
[NASA-CR-182119] 14 p1865 N88-21143
Heat transfer from a negatively buoyant wall jet
[NBS/GCR-88/541] 15 p2050 N88-22208
In-flight measurement of ice growth on an airfoil using an array of ultrasonic transducers
[AIAA-PAPER-87-0178] 17 p2293 N88-23717
Experimental measurements of heat transfer from an iced surface during artificial and natural cloud icing conditions
[AIAA-PAPER-86-1352] 17 p2293 N88-23718
National plans for aircraft icing and improved aircraft icing forecasts and associated warning services 18 p2546 N88-25113
Flight-management strategies for escape from microburst encounters
[NASA-TM-4057] 19 p2603 N88-25461
Intelligent guidance and control for wind shear encounter
[NASA-CR-183060] 20 p2755 N88-26347
Extinguishing agent for magnesium fire, phases 5 and 6
[AD-A192436] 21 p2930 N88-27398
TDWR (Terminal Doppler Weather Radar) PRF (Pulse Repetition Frequency) selection criteria
[AD-A193089] 21 p2932 N88-27407
Extreme gusts distribution 24 p3314 N88-29734

AIRCRAFT INDUSTRY
Purposes and tasks of high-performance aircraft construction
[MBB/LK-S/PUB/296] 10 p1312 N88-17842
The use of simulation in the development of the Airbus 12 p1702 N88-20188
Prototype manufacturing techniques for reducing cost, schedule, and technical risk 12 p1702 N88-20189
Activities report in aerospace
[ETN-88-91566] 16 p2155 N88-22856
FAA aviation forecasts fiscal years 1988-1999
[AD-A191711] 18 p2455 N88-24576
Class 2 design update for the family of commuter airplanes
[NASA-CR-182681] 18 p2464 N88-24629
China's acquisition and use of foreign aviation technology
[AD-A194827] 24 p3440 N88-30471

AIRCRAFT INSTRUMENTS
NT AUTOMATIC PILOTS
NT FLIGHT RECORDERS
Boeing 727 MLS (Microwave Landing System) terminal instrument procedures (TERPS) approach data collection and processing, data report
[AD-A185523] 06 p0667 N88-14090
Quantifying some information processing aspects of the pilot's instrument crosscheck
[AD-A186114] 07 p0898 N88-15443
A comparison of keyboard designs for cockpit applications
[AD-A187775] 12 p1581 N88-19460

AIRCRAFT INTERIORS
U AIRCRAFT COMPARTMENTS

AIRCRAFT LANDING
NT CRASH LANDING
NT DITCHING (LANDING)
Global positioning satellite-based automatic landing system and wind estimated feedback for the AH-64 helicopter 02 p0124 N88-10784
A rule-based system for arrival sequencing and scheduling in air traffic control 02 p0129 N88-10815
Additional investigations in landing process of aircraft: Test distributions
[DFVLR-MITT-87-13] 09 p1115 N88-16686
An investigation of classical dynamic scaling techniques applied to an oleo-pneumatic landing gear strut
[AD-A187664] 13 p1721 N88-20292
Simulator evaluation of lineup visual landing aids for night carrier landing
[AD-A191212] 18 p2468 N88-24648
Additional investigations into the aircraft landing process: Test distributions
[ESA-TT-1099] 23 p3177 N88-28913

AIRCRAFT MAINTENANCE
A project of an intelligent system to help on-line trouble shooting --- aircraft maintenance
[SNIAS-872-111-106] 05 p0529 N88-13216
Design and control of repairs of carbon fiber lift augmentation flaps in the ATR42 aircraft
[SNIAS-872-111-112] 05 p0529 N88-13217
Simulated service test behavior of various internal and external coatings applied on CF6-50 first stage turbine blades
[NLR-MP-86018-U] 05 p0549 N88-13343
Investigation of the nature and concentration of vapor and mist during the cleaning of aircraft
[PML-1985-29] 05 p0623 N88-13817
Damage tolerance of stiffened-skin structures: Prediction and experimental verification
[NLR-MP-86041-U] 06 p0667 N88-14091
Field evaluation of interactive simulation for maintenance training: SH-3 helicopter electro-mechanical bladefold system
[AD-A185923] 07 p0821 N88-14991
Supportability in aircraft systems through technology and acquisition strategy applications
[AD-A186465] 08 p0949 N88-15759
A model for estimating depot maintenance costs for Air Force fighter and attack aircraft
[AD-A187097] 09 p1105 N88-16624
IMIS: Integrated Maintenance Information System. A maintenance information delivery concept 09 p1203 N88-17207
Knowledge based jet engine diagnostics 09 p1203 N88-17210
Tutoring electronic troubleshooting in a simulated maintenance work environment 09 p1204 N88-17215
Army maintenance: Actions to reduce the likelihood of helicopter gear failures
[PB88-135256] 11 p1433 N88-18551
Sampling intervals
[AD-A189445] 12 p1573 N88-19408
The design of aircraft using the decision support problem technique
[NASA-CR-4134] 13 p1721 N88-20291
Development of a flexible and economic helicopter engine monitoring system
[PB88-165147] 16 p2160 N88-22887
Development of a high-temperature resistant (700 F), corrosion-preventive organic coating
[AD-A191407] 16 p2182 N88-23009
Preventing aircraft corrosion by predictive corrosion modeling 17 p2321 N88-23863
Composite repair of cracked aluminum alloy aircraft structure
[AD-A190514] 18 p2455 N88-24573
Predictive corrosion modeling, volume 1
[AD-A191229] 18 p2485 N88-24739
Proceedings of the 14th Symposium on Aircraft Integrated Monitoring Systems
[DFVLR-MITT-88-04] 22 p3033 N88-28001

Background to the UK military requirements for engine usage, condition and maintenance management systems
22 p3033 N88-28004
Recent advances in engine health management
22 p3033 N88-28005
Tornado: Airframe fatigue life monitoring
22 p3034 N88-28011
Maintenance support for military aircraft by intelligent on-board maintenance data panel
22 p3034 N88-28012
A solution to improve a military aircraft's Onboard-Checkout-And-Monitoring-System (OCAMS)
22 p3034 N88-28013
Proposal for the on-board part of a future aircraft integrated monitoring system 22 p3035 N88-28016
Development of a maintenance data bus monitor and recorder 22 p3036 N88-28022
The impact of increased aircraft reliability on maintenance facility design
[AD-A194395] 22 p3042 N88-28057

AIRCRAFT MANEUVERS
Global positioning satellite-based automatic landing system and wind estimated feedback for the AH-64 helicopter 02 p0124 N88-10784
Improvements to the adaptive maneuvering logic program
[NASA-CR-3985] 03 p0262 N88-11648
Developmental airdrop testing techniques and devices
[AGARD-AG-300-VOL-6] 04 p0396 N88-12481
Trends in aeroelastic analysis of combat aircraft
05 p0550 N88-13350
Overlooked potential of systems with Markovian coefficients
[NLR-MP-86049-U] 05 p0552 N88-13366
Langley Symposium on Aerodynamics, volume 1
[NASA-CP-2397] 07 p0809 N88-14926
Unsteady stall penetration experiments at high Reynolds number
[AD-A186120] 07 p0814 N88-14958
Rotorcraft flight-propulsion control integration
09 p1108 N88-16643
Rotorcraft handling-qualities design criteria development 09 p1109 N88-16645
Predicting dynamic separation characteristics of general configurations
[AD-A186689] 09 p1116 N88-16691
Future fighter maneuverability for air combat
[MBB/LKE-1/S/PUB/120] 10 p1312 N88-17843
MOAOPS and BOOM-MAP computer programs for sonic boom research, volume 1
[AD-A189548] 12 p1574 N88-19414
Workshop on Design Loads for Advanced Fighters
[AGARD-R-746] 12 p1579 N88-19449
The development of manoeuvre load criteria for agile aircraft 12 p1579 N88-19450
Fighter design for human load limits
12 p1580 N88-19451
The relationship between operational flight manoeuvre parameters and design parameters
12 p1580 N88-19454
Manoeuvres by default, by demand and by design
12 p1580 N88-19455
Design loads for Swedish military aircraft in a twenty years' perspective 12 p1580 N88-19456
Manned simulation: Helpful means to determine and improve structural load criteria 12 p1581 N88-19459
Task listing: Visually assisted and visually dependent tasks for fighter aircraft
[AD-A191041] 16 p2244 N88-23404
Full potential methods for analysis/design of complex aerospace configurations
[NASA-CR-3982] 17 p2296 N88-23736
Flight-management strategies for escape from microburst encounters
[NASA-TM-4057] 19 p2603 N88-25461
Flight simulator: Field of view utilized in performing tactical maneuvers
[AD-A192412] 20 p2782 N88-26379
Structural dynamics of maneuvering aircraft
[AD-A192376] 23 p3176 N88-28908
Variation of carotid flow under load, studied by the Doppler echo method --- acceleration tolerance
[REPT-1149] 23 p3240 N88-29282
An interim comparison of operational CG records in turbulence on small and large civil aircraft
24 p3313 N88-29729

AIRCRAFT MODELS
Improvements to the adaptive maneuvering logic program
[NASA-CR-3985] 03 p0262 N88-11648
Measurement of model deformation in wind tunnels
05 p0551 N88-13358
Aeroelastic models in aircraft design
[MBB/LKE-294/S/PUB/249] 13 p1722 N88-20298
Activities report of the Lille Institute of Fluid Mechanics
[ETN-88-91983] 13 p1771 N88-20597
Measurements on a helicopter rotor
[R-764-S] 14 p1861 N88-21119
Design, simulation and laboratory testing of an inertial system for measuring the attitude and narrow-spaced motions
[DFVLR-FB-87-42] 14 p1912 N88-21426
User's manual for LINEAR, a FORTRAN program to derive linear aircraft models
[NASA-TP-2768] 14 p1967 N88-21740
Model selection for the multiple model adaptive algorithm for in-flight simulation
[AD-A189715] 15 p2016 N88-22022
K-pulse estimation from incomplete multiple-frequency scattering data and target identification
[AD-A190827] 16 p2190 N88-23061
Nonlinear flying quality parameters based on dynamic inversion
[AD-A192146] 18 p2464 N88-24627
A two-point aerodynamic model for identification
20 p2786 N88-26526
Estimation of aircraft parameters using filter error methods and extended Kalman filter
[DFVLR-FB-88-15] 23 p3176 N88-28911
Interactive plotting of NASTRAN aerodynamic models using NPLOT and DISSPLA
[AD-A194115] 23 p3226 N88-29204
Analysis of the transmission of sound into the passenger compartment of a propeller aircraft using the finite element method
[FFA-TN-1988-15] 23 p3279 N88-29520
A comparison of simple analytical models for representing propeller aircraft structural and acoustic responses
[ISVR-TR-153] 23 p3279 N88-29523
Computer programs for generation of NASTRAN and VIBRA-6 aircraft models
[AD-A195467] 24 p3323 N88-29792

AIRCRAFT NOISE
NT BLADE SLAP NOISE
NT JET AIRCRAFT NOISE
NT SONIC BOOMS
Noise of a model high speed counterrotation propeller at simulated takeoff/approach conditions (F7/A7)
[NASA-TM-100206] 01 p0091 N88-10592
Noise levels from propeller-driven aircraft measured at ground level and at 1.2 m above the ground
[NPL-AC-110] 01 p0091 N88-10594
Noise emission of civil and military aero-engines. Sources of generation and measures for attenuation
[ETN-87-91021] 01 p0091 N88-10595
Results of the 1986 NASA/FAA/DFVLR main rotor test entry in the German-Dutch wind tunnel (DNW)
[NASA-TM-100507] 04 p0487 N88-13003
Aircraft interior noise reduction by alternate resonance tuning
[NASA-CR-181530] 04 p0488 N88-13005
Development of rotorcraft interior noise control concepts. Phase 3: Development of noise control concepts
[NASA-CR-178172] 06 p0776 N88-14762
Development of rotorcraft interior noise control concepts. Phase 2: Full scale testing, revision 1
[NASA-CR-172594-REV-1] 06 p0777 N88-14769
Measuring the annoyance of aircraft noise
[AD-A185494] 06 p0777 N88-14770
Recent Langley helicopter acoustics contributions
09 p1109 N88-16646
Identification and proposed control of helicopter transmission noise at the source
09 p1109 N88-16647
A decade of aeroacoustic research at NASA Ames Research Center 09 p1109 N88-16648
Aeroacoustic research programs at the Army Aviation Research and Technology Activity
09 p1109 N88-16649
Laboratory studies related to in-flight acoustic emission monitoring
[AD-A186714] 09 p1242 N88-17445
Supersonic and subsonic aircraft noise effects on animals: A literature survey
[AD-A186922] 10 p1404 N88-18373
Sound transmission through the walls of light aircraft: An investigation of structure-borne noise in a Handley Page 137 Jetstream 3 aircraft
[NASA-CR-182509] 10 p1405 N88-18376
Comparison of two transonic noise prediction formulations using the aircraft noise prediction program
[NASA-CR-181609] 12 p1688 N88-20095
Activities report of the Physics Department
[ETN-88-91985] 13 p1833 N88-20964
Noise assessment of unsuppressed TF-34-GE-100A engine at Warfield ANG, Baltimore, Maryland
[AD-A189966] 15 p2129 N88-22702
Structureborne noise measurements on a small twin-engine aircraft
[NASA-CR-4137] 16 p2265 N88-23545
Advanced turboprop aircraft flyover noise: Annoyance to counter-rotating-propeller configurations with an equal number of blades on each rotor, preliminary results
[NASA-TM-100612] 16 p2265 N88-23547
Analytical modeling of the structureborne noise path on a small twin-engine aircraft
[NASA-CR-4136] 17 p2394 N88-24233
Advisory circular: Noise certification handbook
[FAA-AC-36-4B] 17 p2394 N88-24234
Research investigation of helicopter main rotor/tail rotor interaction noise
[NASA-CR-4143] 19 p2722 N88-26165
Simulated measurement of power flow in structures near to simple sources and simple boundaries
[NASA-TM-89124] 19 p2722 N88-26166
Helicopter main-rotor noise: Determination of source contributions using scaled model data
[NASA-TP-2825] 20 p2848 N88-26907
Application of pattern recognition techniques to the identification of aerospace acoustic sources
[NASA-CR-183116] 21 p3013 N88-27877
Aeroacoustic investigation on the noise from ultralight aircraft
[DFVLR-FB-88-03] 21 p3013 N88-27879
Aircraft noise: A review
[PNR90450] 22 p3147 N88-28719
Aircraft noise prediction program propeller analysis system IBM-PC version user's manual version 2.0
[NASA-CR-181689] 24 p3428 N88-30399

AIRCRAFT NOISE PREDICTION
U NOISE PREDICTION (AIRCRAFT)

AIRCRAFT PARTS
Operational load measurements on service helicopters
03 p0263 N88-11658
Lewis materials research and technology: An overview
09 p1119 N88-16699
High temperature polymer matrix composites
09 p1119 N88-16700
Validation of GEMACS (General Electromagnetic Model for the Analysis of Complex Systems) for modeling lightning-induced electromagnetic fields
[AD-A188822] 12 p1620 N88-19687
Design and test of a new coaxial air joints
[DE88-751808] 16 p2164 N88-22908
Simulation of moisture diffusion of fiber reinforced components of aircraft for general air transportation
[IFL-IB-87-05] 21 p2907 N88-27253
Stress corrosion of C ring specimen in salt spray tests
[I-186/87] 21 p2916 N88-27307

AIRCRAFT PERFORMANCE
NT HELICOPTER PERFORMANCE
Helicopter (performance) management
03 p0264 N88-11666
Analytic investigation of helicopter rotor blade appended aeroelastic devices
[NASA-CR-166525] 03 p0266 N88-11676
The A320 Airbus program
[SNIAS-872-111-105] 05 p0529 N88-13215
Aircraft dynamics: Aerodynamic aspects and wind tunnel techniques 05 p0545 N88-13320
Techniques for performance optimisation in cruise and manoeuverability 05 p0545 N88-13321
Requirements and recommendations for the development of theoretical codes and experimental facilities in the near future 05 p0546 N88-13327
Aeroelastic analysis of modern transport aircraft
05 p0550 N88-13352
Influence of Environmental Factors on Aircraft Wing Performance
[VKI-LS-1987-03] 08 p0951 N88-15771
The influence of wind shear, downdraft, and turbulence in aircraft performance 08 p0952 N88-15773
The potential influence of rain on airfoil performance
08 p0952 N88-15774
Effects of wing simulated ground frost on aircraft performance 08 p0952 N88-15775
Effects of aircraft deicing/antiicing fluids on airfoil characteristics 08 p0952 N88-15776
Low altitude windshear threat to commercial aircraft
08 p0952 N88-15777
Effects of enviromentally imposed roughness on airfoil performance 08 p0952 N88-15778
Directions in propulsion control
08 p0956 N88-15799
SWAN: An expert system with natural language interface for tactical air capability assessment
09 p1210 N88-17253
Development of vertical takeoff aircraft with turbojet engines in Germany 10 p1309 N88-17822
Variable sweep wings 10 p1309 N88-17823
Purposes and tasks of high-performance aircraft construction
[MBB/LK-S/PUB/296] 10 p1312 N88-17842

Flight testing of fighter aircraft
[MBB/LKE-62/S/PUB/292] 10 p1312 N88-17844
Performance survey of airfoil profiles
[ETN-88-91093] 11 p1436 N88-18568
Investigations of the laminar-turbulent boundary layer transition for the improvement of the performance of powered glider aircraft profiles
[ETN-88-91094] 11 p1436 N88-18569
Aircraft and ground vehicle friction correlation test results obtained under winter runway conditions during joint FAA/NASA Runway Friction Program
[NASA-TM-100506] 11 p1438 N88-18582
Structural shape optimization in multidisciplinary system synthesis
[NASA-TM-100538] 12 p1614 N88-19650
Aquila remotely piloted vehicle: Its potential battlefield contribution still in doubt
[PB88-120241] 13 p1721 N88-20289
Development of a real-time aeroperformance analysis technique for the X-29A advanced technology demonstrator
[NASA-TM-100432] 14 p1866 N88-21151
Performance improvements of an F-15 airplane with an integrated engine-flight control system
[NASA-TM-100431] 14 p1867 N88-21159
Parametric study of supersonic STOVL flight characteristics
[NASA-CR-177330] 16 p2161 N88-22893
Airplane runway performance monitoring system
[NASA-CASE-LAR-13854-1-CU] 18 p2462 N88-24621
Method for prediction and determination of takeoff performance for vectored thrust vehicles
[AD-A191809] 18 p2463 N88-24626
Propfan test assessment testbed aircraft stability and control/performance 1/9-scale wind tunnel tests
[NASA-CR-182121] 20 p2757 N88-26360
Proceedings of the 14th Symposium on Aircraft Integrated Monitoring Systems
[DFVLR-MITT-88-04] 22 p3033 N88-28001
Japan Air Line's Aircraft Integrated Monitoring System (AIMS) activities 22 p3034 N88-28014
The exploitation of Aircraft Integrated Monitoring System (AIMS) data in height-keeping studies for aircraft operating above FL 290 22 p3036 N88-28026
High performance forward swept wing aircraft
[NASA-CASE-ARC-11636-1] 23 p3177 N88-28914
Measured and predicted responses of the Nord 260 aircraft to the low altitude atmospheric turbulence 24 p3312 N88-29723
Status review of atmosphere turbulence and aircraft response 24 p3312 N88-29726
Aircraft dynamics: Aerodynamic aspects and wind tunnel techniques 24 p3313 N88-29731

AIRCRAFT PILOTS
Application of knowledge-based techniques to aircraft trajectory generation and control 02 p0129 N88-10811
Human respiratory responses during high performance flight
[AGARD-AG-312] 04 p0474 N88-12923
Sitting posture of helicopter pilots of the Royal Netherlands Air Force; preliminary recommendations
[IZF-1986-16] 05 p0631 N88-13857
Does the knife open perspectives for the myopic pilot?
[ETN-87-90166] 09 p1199 N88-17187
Sitting posture of pilots in the Boelkow 105c helicopter
[IZF-1986-22] 09 p1202 N88-17202
Crew interface with windshear systems 10 p1275 N88-17631
Trends in the distribution of tasks between commercial pilots and flight control systems
[MBB-UT-008/87] 10 p1314 N88-17851
Realtime pilot model parameter identification
[AD-A188873] 12 p1584 N88-19476
Selected aspects of triazolam in relation to aviator performance in naval flight operations
[AD-A189322] 12 p1667 N88-19996
Relationship of encoding speed and memory tests to flight training performance
[AD-A190670] 15 p2105 N88-22539
Personality, attitudes, and pilot training performance: Preliminary analysis
[AD-A193102] 21 p2991 N88-27746
Stress/fatigue and the ARNG (Army National Guard) aviator
[AD-A194184] 22 p3132 N88-28621
Central serous chorioretinopathy in USAF aviators: A review
[AD-A195697] 24 p3407 N88-30280

AIRCRAFT POWER SOURCES
U AIRCRAFT ENGINES

AIRCRAFT POWER SUPPLIES
Aerospace energy systems laboratory: Requirements and design approach
[NASA-TM-100423] 17 p2390 N88-24206

AIRCRAFT PRODUCTION
Advanced organic composite materials for aircraft structures: Future program
[NASA-CR-181467] 06 p0678 N88-14155
Product planning in civil aircraft construction
[MBB-UT-002/87] 10 p1313 N88-17849
The application of modern aeroelastic developments for future projects
[MBB-UT-007/87] 10 p1313 N88-17850
Flight Vehicle Development Time and Cost Reduction
[AGARD-CP-424] 12 p1700 N88-20173
Risk reduction cost avoidance for full scale development begins with concept formulation 12 p1700 N88-20174
Development savings through parametric modeling of program costs 12 p1700 N88-20175
Picking winners: Parametric cost estimating and project management 12 p1700 N88-20176
Parametric study of the total cost of aircraft modernization in terms of development and equipment series costs 12 p1700 N88-20177
The increased time and cost of development: Causes and (some) remedies 12 p1701 N88-20178
The judgement and evaluation of long-term investments demonstrated by means of a civil aircraft program 12 p1701 N88-20180
Development cost reduction using integrated CAE-CAD-CAM techniques 12 p1701 N88-20182
Structural materials: The changing scene 12 p1703 N88-20190
Schedule and cost control of development 12 p1704 N88-20196
People, procedures, performance: The keys to improving the development environment 12 p1704 N88-20197
The effects of two Carlucci initiatives concurrency and streamlining, on the test and evaluation phase of system acquisitions 12 p1704 N88-20198
Acceleration of prototype development and reduction of cost by multidisciplinary integration 12 p1704 N88-20199
Organization of helicopter development activities with a view toward reduction of costs and cycles 12 p1704 N88-20200
The influence of infrastructure on the costs and timescales of collaborative programmes 12 p1704 N88-20201
Activities report in aerospace
[ETN-88-91566] 16 p2155 N88-22856

AIRCRAFT PRODUCTION COSTS
Advanced composite airframe program: Today's technology 09 p1107 N88-16636
Product planning in civil aircraft construction
[MBB-UT-002/87] 10 p1313 N88-17849

AIRCRAFT RELIABILITY
Ensuring the service life of designs (experience in aircraft construction) 02 p0157 N88-10986
Reliability of finite element methods in North America
[AGARD-R-748] 02 p0184 N88-11139
The Shock and Vibration Digest, Volume 19, No. 11 03 p0265 N88-11673
Airworthiness of long-life jet transport structures 03 p0265 N88-11674
Damage tolerance of stiffened-skin structures: Prediction and experimental verification
[NLR-MP-86041-U] 06 p0667 N88-14091
Preliminary airworthiness evaluation of a UH-1 equipped with a terrain mapping receiver antenna
[AD-A186274] 07 p0819 N88-14980
Airworthiness considerations 10 p1276 N88-17636
An evaluation of perceptions of form, fit, function (F3) standardization on the Standard Inertial Navigation Unit (STD INU) program
[AD-A188955] 12 p1579 N88-19446
The development of manoeuvre load criteria for agile aircraft 12 p1579 N88-19450
Preliminary airworthiness evaluation of the UH-60A equipped with the XM-139 VOLCANO mine dispensing system
[AD-A190604] 15 p2018 N88-22029
Preliminary airworthiness evaluation of the UH-60A with Advanced Digital Optical Control System (ADOCS)
[AD-A190674] 15 p2018 N88-22030
Airworthiness and flight characteristics test of a ski assembly for the UH-60A Black Hawk helicopter
[AD-A191414] 16 p2162 N88-22895
Semi-Markov adjunction to the Computer-Aided Markov Evaluator (CAME)
[NASA-CR-181645] 19 p2678 N88-25924
The impact of increased aircraft reliability on maintenance facility design
[AD-A194395] 22 p3042 N88-28057
The Flight of Flexible Aircraft in Turbulence: State-of-the-Art in the Description and Modelling of Atmospheric Turbulence
[AGARD-R-734-ADD] 24 p3311 N88-29717
Current and proposed gust criteria and analysis methods: An FAA overview 24 p3311 N88-29718
Re-assessment of gust statistics using CAADRP data 24 p3313 N88-29732
Acquisition of gust statistics from AIDS-recorded data 24 p3313 N88-29733
Preliminary airworthiness evaluation of the UH-60A/ESSS (External Stores Support System) with HELLFIRE launcher installed
[AD-A196187] 24 p3323 N88-29793
The development of acoustic emission for structural integrity monitoring of aircraft
[AD-A196264] 24 p3427 N88-30398

AIRCRAFT SAFETY
Some approaches to the design of high integrity software 02 p0127 N88-10799
Reliability of finite element methods in North America
[AGARD-R-748] 02 p0184 N88-11139
Experimental evidence for modifying the current physical model for ice accretion on aircraft surfaces
[NASA-TM-87184] 04 p0397 N88-12473
Airline safety: A comparative analysis
[AD-A185358] 05 p0543 N88-13308
Theoretical analysis of the electrical aspects of the basic electro-impulse problem in aircraft de-icing applications
[NASA-CR-180845] 05 p0543 N88-13310
Corrosion in avionics and associated equipment; cause, effect and prevention 05 p0547 N88-13335
A flow visualization study of the leading edge separation bubble on a NACA 0012 airfoil with simulated glaze ice
[NASA-CR-180846] 07 p0816 N88-14966
Sudden in-flight incapacitation in general aviation
[AD-A187044] 09 p1115 N88-16682
Annual review of aircraft accident data: US air carrier operations calendar year 1985
[PB88-135843] 10 p1276 N88-17638
Aircraft accident/incident, Newark, New Jersey, November 13, 1986
[NTSB/AAR-87/04-SUMM] 10 p1276 N88-17639
Aviation weather: Status of FAA's (Federal Aviation Administration's) new hazardous weather detection and dissemination systems
[PB88-115910] 11 p1513 N88-19041
The development of manoeuvre load criteria for agile aircraft 12 p1579 N88-19450
Atmospheric electrical modeling in support of the NASA F-106 storm hazards project
[NASA-CR-181639] 13 p1799 N88-20758
Proceedings of the Workshop on the Assessment of Crew Workload Measurements Methods, Techniques and Procedures. Volume 1: Preliminary Selection of Measures
[AD-A189004] 13 p1812 N88-20827
Equipment test methods for externally produced electromagnetic transients
[RAE-TM-FS(F)-457] 14 p1865 N88-21140
Activities report in flight and space travel
[ISSN-0070-3966] 14 p2012 N88-22000
Soft-ground aircraft arresting systems
[AD-A190838] 16 p2165 N88-22912
Variable response load limiting device
[NASA-CASE-LAR-12801-1] 17 p2346 N88-23982
Study of benefits of passenger protective breathing equipment from analysis of past accidents
[DOT/FAA/CT-88/03] 18 p2461 N88-24610
Development of a multipurpose smart recorder for general aviation aircraft
[NASA-CR-168353] 18 p2465 N88-24637
Current fire safety design aspects of commuter aircraft
[DOT/FAA/CT-87/32] 19 p2600 N88-25448
Enhanced emergency smoke venting
[DOT/FAA/CT-88/22] 20 p2756 N88-26350
Corrosion in aircraft structures. Part 1: Text
[LR-527-PT-1] 20 p2775 N88-26458
Corrosion in aircraft structures. Part 2: Figures
[LR-527-PT-2] 20 p2775 N88-26459
The Flight of Flexible Aircraft in Turbulence: State-of-the-Art in the Description and Modelling of Atmospheric Turbulence
[AGARD-R-734-ADD] 24 p3311 N88-29717

AIRCRAFT SPECIFICATIONS
The European Airbus A-300 10 p1309 N88-17824

AIRCRAFT SPIN
Contribution to the numerical solution of airplane spin motion
[ETN-88-92368] 21 p2896 N88-27190

AIRCRAFT STABILITY
Decoupling and stabilization of speed and height in F4 Phantom aircraft using output feedback
[ETN-87-90926] 02 p0125 N88-10787
Local-optimal control in systems with delay 04 p0424 N88-12627
Examples of static aeroelastic effects on present combat aircraft projects 05 p0550 N88-13349

Integration of a supersonic unsteady aerodynamic code into the NASA FASTEX system
[NASA-CR-182329] 06 p0663 N88-14068
General Rotorcraft Aeromechanical Stability Program (GRASP) version 1.03: User's manual
[NASA-TM-100043] 09 p1219 N88-17313
Some aspects of aircraft dynamic loads due to flow separation
[AGARD-R-750] 11 p1439 N88-18586
A flight test investigation into flow separation and structural response for a transport aircraft at buffet onset
[RAE-TR-87006] 14 p1867 N88-21156
The effects of torque response and time delay on rotorcraft vertical axis handling qualities
[AD-A189873] 15 p2017 N88-22023
Influence of unsteady aerodynamic forces on dynamic response of variable sweep aircraft
15 p2054 N88-22245
Natural laminar flow and airplane stability and control
17 p2298 N88-23747
Propfan test assessment testbed aircraft stability and control/performance 1/9-scale wind tunnel tests
[NASA-CR-182121] 20 p2757 N88-26360
Low-speed wind-tunnel test of a STOL supersonic-cruise fighter concept
[NASA-TM-4050] 20 p2761 N88-26374
High performance forward swept wing aircraft
[NASA-CASE-ARC-11636-1] 23 p3177 N88-28914
A second look at MIL prime flying qualities requirements 24 p3314 N88-29740

AIRCRAFT STRUCTURES
NT AIRFRAMES
NT FUSELAGES
NT PLASTIC AIRCRAFT STRUCTURES
The influence of load cycle reconstitution on fatigue behaviour
[ARL-STRUC-R-424] 02 p0192 N88-11198
A reliability concept for optimizing aircraft design
04 p0423 N88-12622
Aircraft dynamic response calculation based on discrete-continual model 04 p0424 N88-12624
Aircraft classification by type of propulsive devices. Determination of type and number of carrying solutions
04 p0424 N88-12626
Materials for fighter aircraft 05 p0546 N88-13325
Surface treatment problems found in new aircraft designed using structural composites
[SNIAS-872-111-113] 05 p0558 N88-13397
Philosophy and practice of nondestructive tests of composite material structures at Aerospatiale Aquitaine
[SNIAS-872-430-105] 05 p0559 N88-13400
Measurement and control of damage in composite materials: Nondestructive controls by thermography, holography, and radiography
[SNIAS-872-430-110] 05 p0559 N88-13403
Structural optimization in the design process — aircraft
[SNIAS-872-111-115] 05 p0635 N88-13885
Damage tolerance of stiffened-skin structures: Prediction and experimental verification
[NLR-MP-86041-U] 06 p0667 N88-14091
Numerical simulation of flight body circumference flow
06 p0676 N88-14137
Study of surface treatment before bonding of light alloys
[DCQ/L-48-287/F] 08 p0682 N88-14181
Study of selection criteria for adhesives used in aircraft structure bonding
[ETN-88-91619] 08 p0971 N88-15875
Experimental study on the effect of fiber orientation on flutter characteristics of high-aspect-ratio transport wing
[NAL-TR-936] 09 p1120 N88-16708
Evaluation of high temperature structural adhesives for extended service, phase 5
[NASA-CR-178176] 09 p1149 N88-16884
Modern materials for light constructions — aircraft
[MBB-Z-136/86] 10 p1312 N88-17839
Purposes and tasks of high-performance aircraft construction
[MBB/LK-S/PUB/296] 10 p1312 N88-17842
The application of modern aeroelastic developments for future projects
[MBB-UT-007/87] 10 p1313 N88-17850
Sound transmission through the walls of light aircraft: An investigation of structure-borne noise in a Handley Page 137 Jetstream 3 aircraft
[NASA-CR-182509] 10 p1405 N88-18376
High performance composites research at NASA-Langley
[NASA-TM-100518] 11 p1450 N88-18642
Automatic riveting machine for spherically-formed airframe structures
[ETN-88-91024] 11 p1495 N88-18924
Factors affecting the sticking of insects on modified aircraft wings
[NASA-CR-182615] 12 p1575 N88-19421
Changes in USAF structural loads requirements
12 p1580 N88-19452
Manoeuvres by default, by demand and by design
12 p1580 N88-19455
Advanced durability analysis. Volume 1: Analytical methods
[AD-A188341] 12 p1635 N88-19789
Structural materials: The changing scene
12 p1703 N88-20190
Standardized environmental fatigue sequence for the evaluation of composite components in combat aircraft (ENSTAFF = ENvironmental fatSTAFF)
[LBF-FB-179] 13 p1722 N88-20300
European approaches in standard spectrum development — aircraft load spectra
[NLR-MP-87007-U] 13 p1782 N88-20661
Activities report of the Structures Department
[ETN-88-91986] 13 p1783 N88-20672
Activities report in aeronautics and astronautics
[ETN-88-91332] 13 p1859 N88-21115
Computer aided design of aircraft structures
[ETN-88-91353] 14 p1867 N88-21154
A flight test investigation into flow separation and structural response for a transport aircraft at buffet onset
[RAE-TR-87006] 14 p1867 N88-21156
A study of damage tolerance in curved composite panels
[AD-A190617] 15 p2029 N88-22092
Activities report in aerospace
[ETN-88-91566] 16 p2155 N88-22856
Design studies of primary aircraft structures in ARALL laminates
[LR-520] 16 p2160 N88-22888
User's manual for EULER3DS
[AD-A191048] 16 p2208 N88-23177
Investigation into the operation of the new special drills for drilling holes in thin components made of composite materials — aircraft components
[LR-519] 16 p2215 N88-23215
Structureborne noise measurements on a small twin-engine aircraft
[NASA-CR-4137] 16 p2265 N88-23545
Fuel containment, lightning protection and damage tolerance in large composite primary aircraft structures
[NASA-CR-3875] 17 p2317 N88-23839
Water based primers for structural adhesive bonding of aircraft 17 p2321 N88-23862
Analytical modeling of the structureborne noise path on a small twin-engine aircraft
[NASA-CR-4136] 17 p2394 N88-24233
Simulated measurement of power flow in structures near to simple sources and simple boundaries
[NASA-TM-89124] 19 p2722 N88-26166
Sensitivity to crack initiation in thick assemblies. Test report 48-444
[REPT-48-444] 20 p2758 N88-26365
Corrosion in aircraft structures. Part 1: Text
[LR-527-PT-1] 20 p2775 N88-26458
Corrosion in aircraft structures. Part 2: Figures
[LR-527-PT-2] 20 p2775 N88-26459
Design manual for impact damage tolerant aircraft structure, addendum
[AGARD-AG-238-ADD] 21 p2895 N88-27185
Design and implementation of contact ultrasonic sensors to assess internal damage
[I-177/87] 21 p2906 N88-27247
Nonlinear vibrations of periodically stiffened plates
21 p2963 N88-27598
Critical joints in large composite primary aircraft structures. Volume 2: Technology demonstration test report
[NASA-CR-172587] 23 p3177 N88-28915
Critical joints in large composite primary aircraft structures. Volume 3: Ancillary test results
[NASA-CR-172588] 23 p3177 N88-28916
Asymptotic modal analysis and statistical energy analysis
[NASA-CR-183077] 23 p3278 N88-29514
A comparison of simple analytical models for representing propeller aircraft structural and acoustic responses
[ISVR-TR-153] 23 p3279 N88-29523
Dynamics of articulated aerospace structures
[AD-A195685] 24 p3324 N88-29794
Aircraft airframe cost estimating relationships: Study approach and conclusions
[R-3255-AF] 24 p3324 N88-29795

AIRCRAFT SURVIVABILITY
Efficiency analysis of airborne Electronic CounterMeasures (ECM) systems
[AD-A184606] 03 p0306 N88-11934
SWAN: An expert system with natural language interface for tactical air capability assessment
09 p1210 N88-17253
A computer graphics simulation of the endgame in aircraft combat survivability
[AD-A187826] 11 p1541 N88-19214
Threat expert system technology advisor
[NASA-CR-177479] 24 p3328 N88-29816

AIRCRAFT TIRES
Aircraft and ground vehicle friction correlation test results obtained under winter runway conditions during joint FAA/NASA Runway Friction Program
[NASA-TM-100506] 11 p1438 N88-18582
Static mechanical properties of 30 x 11.5 - 14.5, type 8 aircraft tires of bias-ply and radial-belted design
[NASA-TP-2810] 14 p1867 N88-21157
Energy dissipation in a rolling aircraft tire
[NASA-CR-182978] 19 p2676 N88-25913
A critical speed study for aircraft bias ply tires
[AD-A193616] 22 p3084 N88-28313

AIRCRAFT WAKES
NT PROPELLER SLIPSTREAMS
NT SLIPSTREAMS
Dispersion in the wake of aircraft: An investigation of the effects of a ground plane on trailing vortices. Literature survey
[IC-AERO-REP-86-04] 01 p0003 N88-10014
Predicting dynamic separation characteristics of general configurations
[AD-A186689] 09 p1116 N88-16691
Propulsive performance of a lifting flapping wing
17 p2295 N88-23733
Laser-Doppler measurements of turbulence structures in free streams behind flat and rotation symmetrical profiles
[ETN-88-92336] 21 p2948 N88-27510

AIRCREWS
U FLIGHT CREWS

AIRDROPS
Control systems for platform landings cushioned by air bags
[AD-A196154] 24 p3358 N88-29996

AIRFIELD SURFACE MOVEMENTS
A new look at the use of linear methods to predict aircraft dynamic response to taxi over bomb damaged and repaired airfields 09 p1180 N88-17069
Airport surface traffic automation study
[AD-A194553] 23 p3181 N88-28934

AIRFIELDS
U AIRPORTS

AIRFOIL CHARACTERISTICS
U AIRFOILS

AIRFOIL OSCILLATIONS
NT WING OSCILLATIONS
A natural low frequency oscillation in the wake of an airfoil near stalling conditions
[NASA-TM-100213] 02 p0123 N88-10779
Active feedback interaction with a shear layer
[AD-A188525] 12 p1573 N88-19410
Wing flutter calculations with the CAP-TSD unsteady transonic small disturbance program
[NASA-TM-100580] 12 p1575 N88-19419
Application of a nonisentropic full potential method to AGARD standard airfoils
[NASA-TM-100560] 13 p1716 N88-20263
Development of drive mechanism for an oscillating airfoil 14 p1926 N88-21482
Unsteady flow field measurements using LDV (Laser Doppler Velocimetry)
[AD-A189907] 15 p2083 N88-22298
Control and use of unsteady flows: Insect use of various wing kinematics and related pressure measurements using a pitching airfoil 21 p2926 N88-27366
Liquid crystals for unsteady surface shear stress visualization
[DE88-010570] 21 p2951 N88-27527

AIRFOIL PROFILES
NT WING PROFILES
NT WING SPAN
A critical assessment of wind tunnel results for the NACA 0012 airfoil
[NASA-TM-100019] 03 p0260 N88-11636
Breakdown of the conservative potential equation
07 p0809 N88-14929
Computer program for the calculation of the profile-vortices interactions (two dimensional inviscid incompressible flow with point singularities)
[ISL-R-124/86] 08 p0987 N88-15982
Flow field measurements using hotwire anemometry
[AD-A187029] 09 p1160 N88-16951
The further development of circulation control airfoils
10 p1270 N88-17594
Circulation control STOL aircraft design aspects
10 p1272 N88-17610
Performance survey of airfoil profiles
[ETN-88-91093] 11 p1496 N88-18568

Investigations of the laminar-turbulent boundary layer transition for the improvement of the performance of powered glider aircraft profiles
[ETN-88-91094] 11 p1436 N88-18569
An experimental-computational investigation of transonic shock wave-turbulent boundary layer interaction in a curved test section
[CWI-NM-R8716] 14 p1909 N88-21408
New airfoil sections for straight bladed turbine
[DE88-701075] 14 p1942 N88-21588
High Reynolds number, low Mach number, steady flow field calculations over a NACA 0012 airfoil using Navier-Stokes and interactive boundary layer theory
[AD-A189871] 15 p2013 N88-22005
Computational fluid dynamics drag prediction: Results from the Viscous Transonic Airfoil Workshop
[NASA-TM-100095] 15 p2014 N88-22009
Designs of profiles for cascades
[NASA-TT-20161] 15 p2067 N88-22326
Short duration flow establishment on a profile in a Water-Ludwieg-Tunnel 16 p2201 N88-23134
Computation of flow around NACA0012 airfoil at high angle of attack 19 p2636 N88-25640
Parallelization on a multiprocessor system of a solution method for the unsteady Navier-Stokes equations at high Reynolds numbers
[ONERA-NT-1987-8] 20 p2803 N88-26632
Treatment of the separated flow around profiles (nonviscous, incompressible, two dimensional flow) by the singularities method
[ISL-R-106/87] 20 p2803 N88-26633
Wind tunnel tests of the influence of airfoil-thickness on normal force and pitching moment of two slender wings at transonic and supersonic Mach numbers
[DFVLR-FB-88-17] 21 p2893 N88-27171
Theory of sound production by vortex-airfoil interaction
[AD-A193386] 21 p3012 N88-27875
The influence of surface rounding on trailing edge noise
[AD-A193387] 21 p3012 N88-27876
An efficient patched grid Navier-Stokes solution for multiple bodies, phase 1
[AD-A194166] 23 p3211 N88-29110
Effects of precipitation on wind turbine performance
[DE88-001144] 23 p3228 N88-29211

AIRFOIL SECTIONS
U AIRFOIL PROFILES

AIRFOIL THICKNESS
U AIRFOIL PROFILES

AIRFOILS
NT AEROELASTIC RESEARCH WINGS
NT AILERONS
NT ARROW WINGS
NT BEARINGLESS ROTORS
NT CAMBERED WINGS
NT CIRCULATION CONTROL AIRFOILS
NT CIRCULATION CONTROL ROTORS
NT CRUCIFORM WINGS
NT DELTA WINGS
NT FIXED WINGS
NT FLAPS (CONTROL SURFACES)
NT JET FLAPS
NT LAMINAR FLOW AIRFOILS
NT LEADING EDGE FLAPS
NT LOW ASPECT RATIO WINGS
NT OBLIQUE WINGS
NT PROPELLER BLADES
NT RIGID ROTORS
NT ROTARY WINGS
NT SLENDER WINGS
NT SPOILERS
NT SUPERCRITICAL AIRFOILS
NT SUPERCRITICAL WINGS
NT SUPERSONIC AIRFOILS
NT SWEPT FORWARD WINGS
NT SWEPT WINGS
NT SWEPTBACK WINGS
NT TABS (CONTROL SURFACES)
NT THIN AIRFOILS
NT THIN WINGS
NT TILTING ROTORS
NT TRAILING EDGE FLAPS
NT UPPER SURFACE BLOWN FLAPS
NT VARIABLE SWEEP WINGS
NT VORTEX FLAPS
NT WING FLAPS
NT WINGS
NT X WING ROTORS
Analyses and assessments of span wise gust gradient data from NASA B-57B aircraft
[NASA-CR-178288] 01 p0002 N88-10007
The structure of separated flow regions occurring near the leading edge of airfoils including transition
[NASA-CR-181434] 01 p0002 N88-10011
Wall interference tests of a CAST 10-2/DOA 2 airfoil in an adaptive-wall test section
[NASA-TM-4015] 02 p0122 N88-10772
Development of heat flux sensors for turbine airfoils 02 p0184 N88-11143
Film cooling heat transfer on a turbine airfoil 02 p0186 N88-11156
Measurement of airfoil heat transfer coefficients on a turbine stage 02 p0186 N88-11158
Coolant passage heat transfer with rotation 02 p0186 N88-11160
Thermal barrier coating life prediction model development 02 p0190 N88-11183
Thermal barrier coating life prediction model development 02 p0190 N88-11185
Local heat/mass transfer and pressure drop in a two-pass rib-roughened channel for turbine airfoil cooling
[NASA-CR-179635] 03 p0322 N88-12039
Theoretical and practical aspects of multigrid methods in boundary element calculations
[NLR-MP-85021-U] 03 p0370 N88-12328
Investigation of low-speed turbulent separated flow around airfoils
[NASA-CR-177450] 04 p0396 N88-12471
NCSU code: Validation and extension on NAL's UNIVAC 1100/60 system
[PD-FM-8716] 04 p0476 N88-12931
Measurement of velocity and vorticity fields in the wake of an airfoil in periodic pitching motion
[NASA-TP-2780] 04 p0487 N88-13002
Computation of dynamic stall of NACA0012 airfoil by block pentadiagonal matrix scheme 05 p0535 N88-13255
Practical application of two-dimensional viscous flow computation 05 p0535 N88-13257
The role of computation fluid dynamics in aeronautical engineering (4). The development and applications of implicit TVD finite volume code 05 p0536 N88-13259
Application of discrete vortex method to analysis of separated flow around aerofoils 05 p0537 N88-13268
Navier-Stokes analysis of laminar flow control of a two-dimensional airfoil 05 p0540 N88-13286
A swept wing panel in a low speed flexible walled test section
[NASA-CR-4106] 05 p0540 N88-13292
The development of a computer code (U2DIIF) for the numerical solution of unsteady, inviscid and incompressible flow over an airfoil
[AD-A185033] 05 p0541 N88-13293
Computation of rime ice accretion on airfoils
[FFA-TN-1987-08] 05 p0542 N88-13301
An experimental investigation of the aerodynamics of a NACA 64A010 airfoil-flap combination with and without flap oscillations. Part 1: Steady-state characteristics
[NASA-TM-88217] 05 p0542 N88-13305
Measurement of local convective heat transfer coefficients from a smooth and roughened NACA-0012 airfoil: Flight test data
[NASA-TM-100284] 05 p0582 N88-13552
Potential flow around two-dimensional airfoils using a singular integral method
[NASA-CR-182345] 06 p0664 N88-14070
Investigation of viscous/inviscid interaction in transonic flow over airfoils with suction 06 p0664 N88-14074
A zonal approach for the solution of coupled Euler and potential solutions of flows with complex geometries
[AD-A185465] 06 p0702 N88-14310
Characteristics of a separating confluent boundary layer and the downstream wake
[NASA-TM-100046] 06 p0704 N88-14323
Computational fluid dynamics overview 07 p0809 N88-14927
Finite-volume scheme for transonic potential flow about airfoils and bodies in an arbitrarily shaped channel 07 p0809 N88-14928
A multistage time-stepping scheme for the thin-layer Navier-Stokes equations 07 p0810 N88-14932
Boundary layer transition 07 p0811 N88-14942
Separated flow 07 p0812 N88-14944
Advanced natural laminar flow airfoil with high lift to drag ratio 07 p0812 N88-14947
Airfoil large eddy breakup devices for turbulent drag reduction 07 p0814 N88-14956
Unsteady stall penetration experiments at high Reynolds number
[AD-A186120] 07 p0814 N88-14956
A flow visualization study of the leading edge separation bubble on a NACA 0012 airfoil with simulated glaze ice
[NASA-CR-180846] 07 p0816 N88-14966
An experimental mapping of the flow field behind a glaze ice shape on a NACA 0012 airfoil
[NASA-CR-180847] 08 p0950 N88-15766
Three-dimensional unsteady flow elicited by finite wings and complex configurations
[AD-A186464] 08 p0951 N88-15770
Effects of enviromentally imposed roughness on airfoil performance 08 p0952 N88-15778
Theoretical and experimental studies of the transonic flow field and associated boundary conditions near a longitudinally-slotted wind-tunnel wall
[NASA-CR-181169] 08 p0959 N88-15815
Experimental investigation of shock-induced disturbances on transonic airfoils
[DFVLR-FB-87-28] 09 p1112 N88-16666
A note on the aerodynamic design of thin parallel-sided aerofoil sections
[ARL-AERO-TM-388] 09 p1114 N88-16677
Navier-Stokes solutions for laminar incompressible flow over a NACA 0012 airfoil and a backward facing step
[FFA-TN-1987-50] 09 p1162 N88-16966
Well-posedness and spectral estimation for infinite dimensional systems
[AD-A187621] 10 p1401 N88-18354
Pressure distributions from high Reynolds number transonic tests of an NACA 0012 airfoil in the Langley 0.3-meter transonic cryogenic tunnel
[NASA-TM-100526] 11 p1435 N88-18565
High Reynolds number transonic tests on a NACA 0012 airfoil in the Langley 0.3-meter transonic cryogenic tunnel
[NASA-TM-100527] 11 p1436 N88-18571
Status of the special-purpose airfoil families
[DE88-001124] 11 p1506 N88-18998
A generalisation of Hall's scheme for solving the Euler equations for two-dimensional flows 11 p1537 N88-19188
Application of a nonisentropic full potential method to AGARD standard airfoils
[NASA-TM-100560] 13 p1716 N88-20263
On the Kutta condition for flows around lifting airfoils and wings
[DFVLR-FB-87-40] 13 p1717 N88-20268
Constructing Gloved wings for aerodynamic studies
[NASA-TM-100440] 14 p1863 N88-21128
Wall interference assessment and corrections for transonic adaptive wall airfoil data 14 p1863 N88-21129
Comparison of pressure distributions on model and full-scale NACA 64-621 airfoils with ailerons for wind turbine application
[NASA-TM-100802] 14 p1943 N88-21593
High Reynolds number, low Mach number, steady flow field calculations over a NACA 0012 airfoil using Navier-Stokes and interactive boundary layer theory
[AD-A189871] 15 p2013 N88-22005
Oscillating airfoils: Achievements and conjectures
[AD-A190490] 15 p2014 N88-22008
Aerofoil testing in a self-streamlining flexible walled wind tunnel
[NASA-CR-4128] 16 p2156 N88-22865
An integral equation for the linearized supersonic flow over a wing
[AD-A191408] 16 p2158 N88-22875
The transonic wind tunnel (TWB) at DFVLR, Brunswick (Federal Republic of Germany)
[DFVLR-MITT-88-01] 16 p2164 N88-22909
Reduced order models for nonlinear aerodynamics 16 p2220 N88-23248
Application of Navier-Stokes analysis to stall flutter 16 p2220 N88-23249
In-flight measurement of ice growth on an airfoil using an array of ultrasonic transducers
[AIAA-PAPER-87-0178] 17 p2293 N88-23717
High Reynolds number tests of a Douglas DLBA 032 airfoil in the Langley 0.3-meter transonic cryogenic tunnel
[NASA-TM-87663] 17 p2296 N88-23734
Boundary-layer stability and airfoil design 17 p2296 N88-23738
Wind tunnel testing of low-drag airfoils 17 p2297 N88-23741
Flight experiences with laminar flow 17 p2297 N88-23744
Preliminary aerodynamic design considerations for advanced laminar flow aircraft configurations 17 p2297 N88-23746
Natural laminar flow and airplane stability and control 17 p2298 N88-23747
Passive shock wave-boundary layer control for the Bell FX69-H-098 airfoil 18 p2457 N88-24588
Prediction of laminar and turbulent flows past single and twin airfoils 18 p2457 N88-24589
Two dimensional hyperbolic grid generation
[VKI-TN-162] 18 p2511 N88-24897
Characteristics of merging shear layers and turbulent wakes of a multi-element airfoil
[NASA-TM-100053] 18 p2511 N88-24900

Manipulation of the structure of a turbulent boundary layer 18 p2512 N88-24901
Computational Fluid Mechanics
[NASA-CR-183022] 18 p2514 N88-24915
A characteristic method for calculating the generalized flat flutter aerodynamic forces
[NASA-TT-20300] 19 p2598 N88-25438
Finite element analysis of incompressible viscous flow around multi-element aerofoils 19 p2635 N88-25634
Wall interference assessment/correction of data from tests of a CAST 10-2/DOA 2 airfoil in the Langley 0.3-m transonic cryogenic tunnel 20 p2751 N88-26331
Improved potential flow computational methods with Euler corrections for airfoil and wing/body design
[AD-A192303] 20 p2752 N88-26334
Effects of numerical dissipation on finite-volume solutions of compressible flow problems
[AD-A193173] 21 p2944 N88-27485
Investigation of viscous/inviscid interaction in transonic flow over airfoils with suction
[NASA-CR-183112] 21 p2945 N88-27490
Determination of the local heat-transfer characteristics on glaze ice accretions on a cylinder and a NACA 0012 airfoil 21 p2946 N88-27500
An experimental investigation of two 15 percent-scale wind tunnel fan-blade designs
[NASA-TM-88256] 22 p3046 N88-28076
Thermal barrier coating life-prediction model development
[NASA-CR-179507] 22 p3058 N88-28142
Computational tools for simulation methodologies 23 p3168 N88-28865
Effects of independent variation of Mach and Reynolds numbers on the low-speed aerodynamic characteristics of the NACA 0012 airfoil section
[NASA-TM-4074] 23 p3170 N88-28879
Noise generation and boundary layer effects in vortex-airfoil interaction and methods of digital hologram analysis for these flow fields
[AD-A194191] 23 p3171 N88-28883
Unsteady flow past an NACA 0012 airfoil at high angles of attack
[AD-A194650] 23 p3172 N88-28886
The effects of inlet turbulence and rotor/stator interactions on the aerodynamics and heat transfer of a large-scale rotating turbine model. Volume 3: Heat transfer data tabulation 65 percent axial spacing
[NASA-CR-179488] 23 p3180 N88-28930
The use of hot-film technique for boundary layer studies on a 21 percent thick airfoil
[NAE-AN-45] 24 p3321 N88-29781
The effects of inlet turbulence and rotor/stator interactions on the aerodynamics and heat transfer of a large-scale rotating turbine model. Volume 2: Heat transfer data tabulation. 15 percent axial spacing
[NASA-CR-179467] 24 p3326 N88-29804
Studies of gas turbine heat transfer airfoil surface and end-wall cooling effects
[AD-A195165] 24 p3326 N88-29805

AIRFRAME MATERIALS
Composite structural materials
[NASA-CR-181416] 02 p0190 N88-11186

AIRFRAMES
The history of aeroelasticity research in Germany from the beginning until 1945 --- airframes
[DFVLR-MITT-86-25] 01 p0001 N88-10003
Reduced complexity structural modeling for automated airframe synthesis
[NASA-CR-177440] 04 p0393 N88-12453
Fundamentals of fighter aircraft design: Engine intake and afterbody 05 p0545 N88-13322
Advanced composite airframe program: Today's technology 09 p1107 N88-16636
Durability and damage tolerance of aluminum castings
[AD-A186444] 10 p1341 N88-18013
Aircraft corrosion problems and research in the Netherlands
[NLR-MP-86066-U] 13 p1744 N88-20427
A study of damage tolerance in curved composite panels
[AD-A190617] 15 p2029 N88-22092
Propulsion and airframe aerodynamic interactions of supersonic V/STOL configurations. Volume 4: Summary
[NASA-CR-177343-VOL-4] 16 p2157 N88-22868
Design manual for impact damage tolerant aircraft structure, addendum
[AGARD-AG-238-ADD] 21 p2895 N88-27185
Tornado: Airframe fatigue life monitoring 22 p3034 N88-28011
Crash simulation calculations and component idealization for an airframe. Computer code KRASH 79
[ETN-88-92971] 23 p3174 N88-28899
Stress intensity factors for cracked metallic structures under rapid thermal loading
[AD-A191219] 23 p3193 N88-29004
A summary of methods for establishing airframe design loads from continuous gust design criteria 24 p3312 N88-29721
Aircraft airframe cost estimating relationships: Study approach and conclusions
[R-3255-AF] 24 p3324 N88-29795
Evaluation of bond testing equipment for inspection of Army advanced composite airframe structures
[AD-A195795] 24 p3341 N88-29885

AIRGLOW
NT GEOCORONAL EMISSIONS
NT NIGHTGLOW
The nonlinear thermodynamics of meteors, noctilucent clouds, enhanced airglow and global atmospheric circulation 06 p0738 N88-14538
Vehicle glow observed on the SONDA 3
[INPE-4297-PRE/1168] 12 p1600 N88-19581
Ground-based facility for spectrophotometric studies of the airflow and aurora
[AP-29] 22 p3119 N88-28532

AIRLINE OPERATIONS
Issues in air transport and airport management
[PB87-204509] 02 p0124 N88-10782
Civil aeronautics
[ETN-88-90616] 05 p0543 N88-13309
Digest of the annual report of the Lufthansa German Airlines
[ISSN-0415-603X] 08 p0952 N88-15779
Analysis of bird strikes to UK registered aircraft 1985 (civil aircraft over 5700 kg maximum weight
[CAA-PAPER-87012] 09 p1115 N88-16684
Annual review of aircraft accident data: US air carrier operations calendar year 1985
[PB88-135843] 10 p1276 N88-17638
Estimates of potential increases in airport capacity through ATC (Air Traffic Control) system improvements in the airport and terminal areas
[AD-A188533] 12 p1578 N88-19444
Engine condition monitoring civil requirements: A British Airways view 22 p3033 N88-28002
RB211 developments
[PNR90444] 22 p3045 N88-28069

AIRPORT PLANNING
Issues in air transport and airport management
[PB87-204509] 02 p0124 N88-10782
Measuring airport landside capacity
[PB88-102637] 06 p0670 N88-14107
Analyses of heliport system plans
[DOT/FAA/PM-87/31] 17 p2308 N88-23810
FAA aviation forecasts fiscal years 1988-1999
[AD-A191711] 18 p2455 N88-24576
Airport surface traffic automation study
[AD-A194553] 23 p3181 N88-28934

AIRPORT SECURITY
Aviation security: FAA (Federal Aviation Administration) needs preboard passenger screening performance standards
[PB87-216800] 02 p0124 N88-10783

AIRPORT TOWERS
FAA air traffic control operations concepts. Volume 3: ISSS (Initial Sector Suite System) en route controllers
[AD-A185981] 07 p0818 N88-14975
FAA air traffic control operations concepts. Volume 4: TAAS (Terminal Advanced Automation System) terminal controllers
[AD-A185982] 07 p0818 N88-14976
FAA air traffic control operations concepts. Volume 5: ATCT/TCCC (Airport Traffic Control Tower/Tower Control Computer Complex) tower controllers
[AD-A185983] 07 p0818 N88-14977

AIRPORTS
NT HELIPORTS
First article test noise survey of the A/F32T-9 large turbo fan engine enclosed noise suppressor system, Sky Harbor IAP (International Airport), Phoenix, Arizona
[AD-A183799] 01 p0090 N88-10588
ZEUS: A knowledge-based expert system that assists in predicting visibility at airbases
[AD-A184197] 05 p0626 N88-13829
Measuring airport landside capacity
[PB88-102637] 06 p0670 N88-14107
Measuring the annoyance of aircraft noise
[AD-A185494] 06 p0777 N88-14770
Pollution from motor vehicles and aircraft at Stapleton International Airport (abbreviated report), revision 2
[AD-A185916] 07 p0875 N88-15307
NASA wind shear model: Summary of model analyses 10 p1273 N88-17617
Radar backscatter from airports and surrounding areas 10 p1274 N88-17623
Radar returns from ground clutter in vicinity of airports 10 p1274 N88-17624
Status of FAA terminal Doppler weather radar programs 10 p1275 N88-17632
The advanced low-level windshear alert system operational demonstration results, Summer, 1987, Denver Stapleton International Airport 10 p1275 N88-17633
Evaluation of bituminous materials used in pavement recycling projects at Tyndall, MacDill, and Hurlburt Air Force Bases
[AD-A188068] 10 p1317 N88-17871
Micro PAVER concept and development airport pavement management system
[AD-A187360] 11 p1441 N88-18598
Estimates of potential increases in airport capacity through ATC (Air Traffic Control) system improvements in the airport and terminal areas
[AD-A188533] 12 p1578 N88-19444
Noise assessment of unsuppressed TF-34-GE-100A engine at Warfield ANG, Baltimore, Maryland
[AD-A189966] 15 p2129 N88-22702
Microwave landing system mathematical modeling study for Midway Airport Runway 22L, Chicago, Illinois
[AD-A191721] 18 p2462 N88-24616
An analysis of time and space requirements for aircraft turnrounds
[TT-8705] 24 p3322 N88-29783

AIRSHIPS
A heat transfer model for a heated helium airship
[AD-A183786] 03 p0259 N88-11629
Renewed interest in airships for industry use discussed 04 p0424 N88-12628

AIRSPACE
Information transfer in the National Airspace System 10 p1275 N88-17634

AIRSPEED
An observer approach to the estimation of helicopter airspeed
[DFVLR-FB-87-13] 01 p0005 N88-10029
Decoupling and stabilization of speed and height in F4 Phantom aircraft using output feedback
[ETN-87-90926] 02 p0125 N88-10787
MOAOPS and BOOM-MAP computer programs for sonic boom research, volume 1
[AD-A189548] 12 p1574 N88-19414

AIRWORTHINESS
U AIRCRAFT RELIABILITY

AIRWORTHINESS REQUIREMENTS
U AIRCRAFT RELIABILITY

ALABAMA
Hypocenters (1977-1984) around the Richton Dome and the Melvin, Alabama, 1978 earthquake
[DE87-014336] 03 p0351 N88-12214

ALARMS
U WARNING SYSTEMS

ALASKA
Solar Energy Meteorological Research and Training Site, Alaska
[DE87-013706] 01 p0069 N88-10440
Coastal winds of the southeast Alaska Peninsula
[PB87-206173] 02 p0215 N88-11354
Thematic mapper study of Alaskan ophiolites
[NASA-CR-182554] 11 p1504 N88-18984
Alaska Loran C probe test results
[AD-A189131] 13 p1720 N88-20284
Influence of the Yukon River on the Bering Sea
[NASA-CR-182802] 17 p2376 N88-24126

ALBEDO
NT EARTH ALBEDO
Estimating scattered and absorbed radiation in plant canopies by remote sensing
[NASA-CR-181390] 02 p0193 N88-11205
Enhancement of surface-atmosphere fluxes by desert-fringe vegetation through reduction of surface albedo and of soil heat flux
[NASA-CR-181442] 02 p0197 N88-11231
Preliminary estimation of color inhomogeneities on the surface of Venus according to the television images obtained by the VENERA-13 and VENERA-14 automated space probes
[NASA-TT-20114] 02 p0254 N88-11608
Estimation of broadband planetary albedo from operational narrowband satellite measurements
[PB88-107644] 07 p0945 N88-15748
Research project on CO-induced climate change
[DE88-002352] 08 p1023 N88-16193
Higher frequency ambient noise in the arctic ocean
[AD-A192203] 18 p2547 N88-25122
Ultraviolet geometric albedo of Uranus
[NASA-CR-183099] 20 p2885 N88-27136
Differences in radiation budget parameters over Asia in relation to contrasting Indian monsoons 22 p3125 N88-28574
Energy budget and ground temperatures in hot regions
[AD-A196298] 24 p3404 N88-30268

ALCOHOLS
NT ETHYL ALCOHOL
NT GLYCOLS
NT ISOPROPYL ALCOHOL

NT METHYL ALCOHOL
NT PHENOLS
NT POLYVINYL ALCOHOL
Compendium of significant events in the recent development of alcohol fuels in the United States
[DE87-013355] 01 p0032 N88-10202
Preparation of polymer polyols
[EP-PATENT-0-162-589-A1] 01 p0102 N88-10665
Experimental and theoretical study of condensation in multicomponent mixtures
[DE88-002715] 07 p0830 N88-15033
Status of alcohol fuels utilization technology for highway transportation: A 1986 perspective. Volume 2: Compression ignition engines
[DE88-006059] 13 p1753 N88-20485
Comparison of isopropyl alcohol and trichloroethylene in removing solder flux
[DE88-005556] 14 p1889 N88-21288
Age, alcohol, and simulated altitude: Effects on performance and breathalyzer scores
[AD-A190642] 15 p2103 N88-22531

ALDEHYDES
NT FORMALDEHYDE
Characterization of catalysts with metal-support effects and of the species adsorbed on their surfaces
[DE87-014636] 04 p0414 N88-12564

ALDOSTERONE
Effects of anti-g suit inflation on renin and aldosterone response physical exercise 12 p1659 N88-19944
Plasma cortisol, renin and aldosterone during an intense heat acclimation program
[AD-A189387] 13 p1809 N88-20810

ALERTNESS
An evaluation of the effects of high visual taskload on the separate behaviors involved in complex monitoring performance
[AD-A190641] 15 p2105 N88-22538
Pupil measures of alertness and mental load 16 p2239 N88-23378
Physiological measures and mental-state assessment 16 p2242 N88-23392
The application of non-stationary data analysis techniques in the identification of changes in the electroencephalogram associated with the onset of drowsiness 21 p2978 N88-27688

ALEUTIAN ISLANDS (US)
Geological evolution and analysis of confirmed or suspected gas hydrate localities. Volume 10: Basin analysis, formation and stability of gas hydrates of the Aleutian Trench and the Bering Sea
[DE88-001008] 10 p1346 N88-18048

ALFVEN WAVES
U MAGNETOHYDRODYNAMIC WAVES

ALGAAS
U ALUMINUM GALLIUM ARSENIDES

ALGAE
NT BLUE GREEN ALGAE
NT CHLORELLA
NT MICROCYSTIS
Controlled Ecological Life Support System: Regenerative Life Support Systems in Space
[NASA-CP-2480] 03 p0357 N88-12251
Biomass recycle as a means to improve the energy efficiency of CELSS algal culture systems 03 p0358 N88-12254
Operation of an experimental algal gas exchanger for use in a CELSS 03 p0358 N88-12255
Non-conventional approaches to food processing in CELSS, 1. Algal proteins: Characterization and process optimization 03 p0358 N88-12256
Sunlight supply and gas exchange systems in microalgal bioreactor 03 p0359 N88-12258
Research on a solar biotechnology based on the culture of photosynthetic cells
[DE88-900129] 10 p1359 N88-18120
Ecological algal system in microgravity conditions: Preliminary results 12 p1655 N88-19915
Regenerative life support system research
[NASA-CR-182606] 12 p1671 N88-20006
An outdoor test facility for the large-scale production of microalgae
[DE88-001146] 21 p2984 N88-27723
The biological clock of Chlamydomonas reinhardii in space 22 p3061 N88-28162

ALGAL BLOOM
U ALGAE

ALGEBRA
NT ADJOINTS
NT AUTOMORPHISMS
NT BANACH SPACE
NT BINOMIALS
NT CANONICAL FORMS
NT CUBIC EQUATIONS
NT DETERMINANTS
NT DYADICS
NT EIGENVALUES
NT EIGENVECTORS
NT GROUP THEORY
NT HERMITIAN POLYNOMIAL
NT HESSIAN MATRICES
NT HILBERT SPACE
NT LIE GROUPS
NT LINEAR EQUATIONS
NT LINEAR TRANSFORMATIONS
NT MATRICES (MATHEMATICS)
NT NONLINEAR EQUATIONS
NT NONLINEAR EVOLUTION EQUATIONS
NT POLYNOMIALS
NT QUADRATIC EQUATIONS
NT RICCATI EQUATION
NT STATE VECTORS
NT STIFFNESS MATRIX
NT STRESS TENSORS
NT TENSORS
NT VECTOR SPACES
NT VECTORS (MATHEMATICS)
NT VORTICITY
A system of three-dimensional complex variables
[NASA-TM-88318] 05 p0645 N88-13951
Fast algorithms for structural optimization and least squares
[AD-A185766] 06 p0724 N88-14452
Embedding topological median algebras in products of dendrons
[PB88-100888] 06 p0767 N88-14713
Class of N-associative rings
[PB87-230421] 06 p0769 N88-14724
Scientific data manipulation in a relational database system
[PB87-124400] 06 p0791 N88-14850
Stability analysis of finite difference schemes for hyperbolic systems, and problems in applied and computational linear algebra
[AD-A185824] 07 p0908 N88-15499
Algebraic specification of process algebra, including two examples
[PB88-106729] 07 p0912 N88-15531
Annotated algebraic specification of the static semantics of pool
[PB88-106695] 07 p0912 N88-15533
Recent developments in the numerical solution of differential/algebraic systems
[DE88-001885] 07 p0912 N88-15535
Prospectus for the development of a linear algebra library for high-performance computers
[DE88-003715] 08 p1068 N88-16457
Strong convergence and convergence rates of approximating solutions for algebraic Riccati equations in Hilbert spaces
[AD-A186190] 08 p1072 N88-16464
Symbolic, algebraic, and numeric solutions to heat conduction problems using Green's functions 09 p1165 N88-16987
An algebraic approach to a calculus of functional differences: Fixed differences and integrals
[AD-A187079] 09 p1227 N88-17346
An applicative programmer's approach to matrix algebra, lessons for hardware and software 10 p1382 N88-18251
The impact of hierarchical memory systems on linear algebra algorithm design
[DE88-003574] 10 p1385 N88-18274
Programming methodology and performance issues for advanced computer architectures
[DE88-003098] 10 p1387 N88-18287
Leapfrog variants of iterative methods for linear algebra equations
[NASA-CR-181616] 10 p1398 N88-18332
Vector bundles over real algebraic varieties
[PB88-126677] 10 p1398 N88-18335
A new approach for shaping of dual-reflector antennas
[NASA-CR-182581] 11 p1476 N88-19806
Generating the states of a probabilistic system
[AD-A187896] 11 p1540 N88-19208
Supporting valid time: An historical algebra
[AD-A187740] 11 p1565 N88-19368
An evaluation of historical algebras
[AD-A188350] 12 p1684 N88-20067
New representation for kinematics of manipulator
[DE88-751446] 14 p1917 N88-21445
Tutorial on GAMS (Generalized Algebraic Modeling System): A modeling language for optimization
[AD-A189867] 15 p2109 N88-22568
Design of an algorithm to translate nested relational algebra queries to GENESIS trace manager commands
[AD-A190502] 15 p2112 N88-22581
Numerical solution of nonlinear algebraic equations in stiff ODE solving
[DE88-006634] 15 p2118 N88-22622
About disequations simplification
[RR-645-I-IMAG-55-LIFIA] 15 p2119 N88-22624
Research on algebraic manipulation
[AD-A190149] 15 p2120 N88-22634
The algebraic structure of convolutional codes
[AD-A190280] 15 p2120 N88-22635
Complexity of some problems in module algebra
[PB88-165386] 15 p2122 N88-22648
Super Virasoro algebra and solvable supersymmetric quantum field theories
[DE88-752299] 15 p2127 N88-22681
A new block solver for large, full, unsymmetric, complex systems of linear algebraic equations
[AD-A190590] 16 p2256 N88-23483
Mahler's method in transcendence theory 17 p2393 N88-24227
Nonlinear conformal transformations and Clifford algebras
[PB87-225942] 19 p2719 N88-26147
Flexible valued algebras of four-dimensions
[ETN-88-92382] 21 p3008 N88-27844
Algebraic grid generation for fighter type aircraft 23 p3246 N88-29320
Composite grid generation for aircraft configurations with the EAGLE code 23 p3246 N88-29321
Polynomial definition of discrete field points of map of diffusion equation, part 1
[AD-A193697] 23 p3271 N88-29467

ALGORITHMS
NT PARSING ALGORITHMS
NT SIMPLEX METHOD
Feature selection applied to radar target identification
[AD-A183880] 01 p0034 N88-10215
Simulations using the pseudo-current algorithm
[DE87-012403] 01 p0040 N88-10255
Accurate, stable, explicit solution of the parabolized Navier-Stokes equations 01 p0043 N88-10276
Development of response models for the Earth Radiation Budget Experiment (ERBE) sensors. Part 4: Preliminary nonscanner models and count conversion algorithms
[NASA-CR-178295] 01 p0050 N88-10317
Description of NCAR (National Center for Atmospheric Research) Community Climate Model (CCM1)
[PB87-203782] 01 p0072 N88-10462
Fronts propagating with curvature dependent speed: Algorithms based on Hamilton-Jacobi formulations
[NASA-CR-178382] 01 p0077 N88-10495
Study, design and evaluation of data reduction by encoding or information extraction. Part 3: Algorithm design --- multispectral satellite imagery
[NLR-TR-85094-L-PT-3] 01 p0079 N88-10503
Study, design and evaluation of data reduction by encoding or information extraction. Part 4: Performance demonstration --- multispectral satellite imagery
[NLR-TR-85094-L-PT-4] 01 p0079 N88-10504
Study, design and evaluation of data reduction by encoding or information extraction. Part 5: Algorithm implementation aspects --- multispectral satellite imagery
[NLR-TR-85094-L-PT-5] 01 p0079 N88-10505
A nonmythical generalization of Dekker's algorithm and its ramifications --- mutually exclusive processes
[CS-8702] 01 p0080 N88-10513
The box method for linear programming. Part 1: Basic theory
[DE87-011029] 01 p0080 N88-10515
A graphical tool for observing the behavior of parallel logic programs
[DE87-011467] 01 p0080 N88-10516
A look at the evolution of mathematical software for dense matrix problems over the past fifteen years
[DE87-011485] 01 p0081 N88-10517
Adaptive line of sight algorithms
[DE87-014275] 01 p0081 N88-10523
EVA reference manual
[DE87-014073] 01 p0082 N88-10526
Strategies for concurrent processing of complex algorithms in data driven architectures
[NASA-CR-181435] 01 p0082 N88-10527
Development of a line-drawing algorithm
[CS-8701] 01 p0082 N88-10530
Digital algorithms for the control and dynamic decoupling of industrial robot axes
[ETN-87-90441] 01 p0084 N88-10546
Computing the bounded region determined by finitely many lines in the plane
[CS-8703] 01 p0086 N88-10558
S-step iterative methods for symmetric linear systems
[DE87-010819] 01 p0086 N88-10559
Parallel computation of a domain decomposition method
[DE87-011444] 01 p0086 N88-10560
PROGRESS: A program for robust regression analysis on the IBM PC
[REPT-85-14] 01 p0088 N88-10576
Numerical computation of transonic potential flow about 3-dimensional inlets
[NAL-TR-924] 02 p0122 N88-10770

Automated detection of severe thunderstorms using geosynchronous infrared data 02 p0201 N88-11257
Statistical remote sensing algorithm development: A complementary process to mesoscale numerical models 02 p0206 N88-11292
Numerical simulation of Tokamaks: Ideal MHD equilibrium and stability [DE87-013452] 02 p0218 N88-11373
A preliminary taxonomy of visible surface algorithms [DE87-013559] 02 p0220 N88-11386
Concurrent algorithms for transient nonlinear FE analysis [NASA-CR-181455] 02 p0221 N88-11389
Using MINOS (Modular In-core Nonlinear Optimization System) as a subroutine for decomposition [DE87-013086] 02 p0221 N88-11390
Projection-space iterative interpolation for limited-angle tomography in parallel- and fan-beam geometry, part 1 [DE87-013965] 02 p0221 N88-11391
Weighted decoding of block codes and some topics on decoding complexity [ENST-87E005] 02 p0221 N88-11394
Finite elements for 2D elliptic equations with moving nodes [DE87-013501] 02 p0224 N88-11410
Iterative solution of a nonlinear system arising in phase change problems [DE87-014672] 02 p0226 N88-11426
BIMOND3: Monotone piecewise bicubic Hermite interpolation code [DE87-014612] 02 p0229 N88-11442
QUICKSILVER: A 3D, electromagnetic, PIC code [DE87-013013] 02 p0245 N88-11547
Efficient numerical approaches for predicting supersonic flows with viscous/inviscid interaction 03 p0260 N88-11637
An antenna array processing system for multiple source bearing estimation 03 p0305 N88-11927
Application of an upwind algorithm to the parabolized Navier-Stokes equations 03 p0316 N88-12000
An algorithmic approach to crustal deformation analysis [NASA-CR-181497] 03 p0349 N88-12203
Study of microburst detection performance during 1985 in Memphis, Tennessee [AD-A184013] 03 p0354 N88-12231
SBNR (Signed Binary Number Representations) digital signal processor architecture [AD-A184603] 03 p0364 N88-12290
Token execution strategies for distributed algorithms: Simulation studies [AD-A184792] 03 p0365 N88-12294
Algorithms and hardware for efficient image smoothing [TR-149] 03 p0365 N88-12296
End of year report for parallel vision algorithm design and implementation [AD-A184327] 03 p0366 N88-12301
The structure-mapping engine: Algorithm and examples [AD-A184042] 03 p0368 N88-12315
Numerical solution of bound constrained problems [DE88-000653] 03 p0371 N88-12334
Solution of the two-dimensional Euler equations on unstructured triangular meshes 04 p0396 N88-12469
Two dimensional path planning with obstacles and shadows [AD-A184075] 04 p0397 N88-12474
Autonomous Land Vehicle (ALV) planning and navigation system [AD-A184243] 04 p0397 N88-12475
GPS vertical axis performance enhancement for helicopter precision landing approach [NASA-CR-177443] 04 p0397 N88-12477
New feedback design methodologies for large space structures: A multi-criterion optimization approach 04 p0408 N88-12535
On M-ARY sequential hypotheses testing for the classification of radar signals [AD-A184094] 04 p0430 N88-12666
Design of source coders and joint source/channel coders for noisy channels [NASA-CR-181547] 04 p0432 N88-12678
A simplified procedure for correcting both errors and erasures of a Reed-Solomon code using the Euclidean algorithm 04 p0435 N88-12698
On the VLSI design of a pipeline Reed-Solomon decoder using systolic arrays 04 p0436 N88-12700
A modern control theory based algorithm for control of the NASA/JPL 70-meter antenna axis servos 04 p0436 N88-12706
Programmable Logic Arrays (PLA's) design for testability [PB87-102935] 04 p0438 N88-12718
Studies of pressure-velocity coupling schemes for analysis of incompressible and compressible flows [NASA-CR-181526] 04 p0443 N88-12748
Optimization of explicit time-stepping algorithms and Stream-Function-Coordinate (SFC) concept for fluid dynamics problems 04 p0445 N88-12762
Tracking through turbulence at the Tonopah Test Range [DE88-001448] 04 p0446 N88-12766
An algorithmic approach to crustal deformation analysis 04 p0468 N88-12891
Coupled acoustic and ocean thermodynamic model [AD-A184357] 04 p0472 N88-12911
Comparing barrier algorithms [NASA-CR-178377] 04 p0476 N88-12934
A tight upper bound for the speed-up of parallel best-first branch-and-bound algorithms [AD-A184246] 04 p0477 N88-12939
A characterization of separating pairs and triplets in a graph [AD-A184278] 04 p0477 N88-12941
Numerical studies of the dual HEMT/algorithm development and numerical studies of Schrodinger's equation [AD-A184471] 04 p0478 N88-12946
Statistical inference: Computer oriented algorithmic approach [DE87-013874] 04 p0478 N88-12948
Methods for design and evaluation of integrated hardware/software systems for concurrent computation [NASA-CR-181522] 04 p0479 N88-12953
Parallelization of hydrocodes on the Intel Hypercube, part 2 [DE88-001591] 04 p0480 N88-12957
Development of the non-equilibrium reactive chemical transport code CHMTRNS [DE88-000682] 04 p0481 N88-12964
On operator splitting for unsteady boundary value problems [AD-A184281] 04 p0484 N88-12981
A comparison of adaptive refinement techniques for elliptic problems [DE88-000805] 04 p0485 N88-12987
The finite element method for electronic structure [DE88-001708] 04 p0485 N88-12989
Driving mechanism of unsteady separation shock motion in hypersonic interactive flow 05 p0530 N88-13226
Numerical prediction of turbulent flows in dump diffusers 05 p0537 N88-13265
Programming techniques for high-speed processing of large scale numerical simulation on supercomputers 05 p0537 N88-13269
Vectorizing the FFTs on supercomputer SX system 05 p0537 N88-13270
Tridiagonal approximate factorization method: A preconditioning technique for solving nonsymmetric linear systems suitable to supercomputers 05 p0537 N88-13271
MODTRAN: A moderate resolution model for LOWTRAN [AD-A185384] 05 p0574 N88-13503
Model-based motion estimation and its application to restoration and interpolation of motion pictures [AD-A185054] 05 p0584 N88-13558
Free Lagrange reconnection algorithms for hydrocodes using a quadrilateral mesh [DE88-001580] 05 p0611 N88-13752
Automatic continuum analysis of reflectance spectra 05 p0614 N88-13770
Learning a color algorithm from examples [AD-A184385] 05 p0632 N88-13862
Approximating multivariate normal orthant probabilities using the Clark algorithm [AD-A184855] 05 p0634 N88-13873
An adaptive lattice algorithm for spectral line estimation [AD-A184970] 05 p0634 N88-13876
Indirect solution of static problems using concurrent vector processing computers [DE87-012105] 05 p0636 N88-13889
The maximum likelihood estimator method of image reconstruction: Its fundamental characteristics and their origin [DE88-000462] 05 p0636 N88-13892
Research and development of finite elements and iterative algorithms for elliptic partial differential equations [DE88-001381] 05 p0643 N88-13934
Restoration of particle pitch angle distribution functions by a maximum entropy algorithm [ATR-86(7098)-3] 05 p0648 N88-13969
Molecular dynamics studies of aromatic hydrocarbon liquids [DE88-001473] 05 p0648 N88-13973
Supercomputing at Florida State University (FSU) [DE87-013900] 05 p0654 N88-14009
Range imagery algorithms for the detection of obstacles by autonomous vehicles [AD-A185421] 05 p0659 N88-14045
A fully redundant double difference algorithm for obtaining minimum variance estimates from GPS observations [NASA-CR-182363] 06 p0667 N88-14089
Study of synthetic aperture radar data compression and encoding. Part 3: Performance evaluation of speckle suppression and data compression algorithms [NLR-TR-85085-L-PT-3] 06 p0692 N88-14248
Study of synthetic aperture radar data compression and encoding. Part 4: Algorithm implementation aspects [NLR-TR-85085-L-PT-4] 06 p0692 N88-14249
On real-time systems using local area networks [AD-A185475] 06 p0694 N88-14256
Vectorization of a multigrid method for the compressible Navier-Stokes equations [PB87-230496] 06 p0698 N88-14284
Computational methods for complex flowfields [AD-A185793] 06 p0703 N88-14317
Fast algorithms for structural optimization and least squares [AD-A185766] 06 p0724 N88-14452
Numerical modeling of troposphere-induced gravity wave propagation 06 p0735 N88-14522
Report of the International Satellite Cloud Climatology Project (ISCCP) workshop on cloud algorithms in the polar regions [WCP-131] 06 p0745 N88-14581
Optimal pre-scheduling of problem remappings [NASA-CR-178378] 06 p0756 N88-14633
Parallel algorithms for unconstrained and constrained nonlinear optimization [PB87-230454] 06 p0756 N88-14634
Parallel algorithms for polynomials [PB87-226304] 06 p0756 N88-14635
Algorithms and programming tools for image processing on the MPP:3 [NASA-CR-182349] 06 p0757 N88-14641
A computer decision-making process for the elimination of noise from data [AD-A185746] 06 p0759 N88-14659
Parallel pivoting combined with parallel reduction [NASA-CR-178422] 06 p0760 N88-14662
Adaptive grid for polyhedral visibility in object space: An implementation [PB88-100938] 06 p0760 N88-14663
A Multipurpose Adaptive Controller (MAC) for real time digital regulation [REPT-87-028] 06 p0762 N88-14673
Scanline algorithms on a grid [PB88-103379] 06 p0766 N88-14710
Digital signal processing algorithms for automatic voice recognition 06 p0793 N88-14862
Some vision algorithms 06 p0795 N88-14871
An engineering study of hybrid adaptation of wind tunnel walls for three-dimensional testing [NASA-CR-178374] 07 p0814 N88-14957
Experimental design of a piloted helicopter off-axis-tracking simulation using a helmet mounted display [AD-A186228] 07 p0820 N88-14982
Catalog of compartment fire model algorithms and associated computer subroutines [PB88-110861] 07 p0839 N88-15087
Study of synthetic aperture radar data compression and encoding. Part 2: SAR image speckle suppression and data compression algorithms [NLR-TR-85085-L-PT-2] 07 p0843 N88-15116
Multipath time-delay estimation via the EM algorithm [PB88-106851] 07 p0845 N88-15124
Multitasked embedded multigrid for three-dimensional flow simulation [NASA-CR-182398] 07 p0852 N88-15173
An efficient algorithm for computing the crossovers in satellite altimetry [NASA-CR-182389] 07 p0871 N88-15286
Middle atmospheric wind measurements using a medium frequency radar [AD-A185931] 07 p0879 N88-15330
Improvements in profiler wind estimates using smoothed data in the spectrum finder algorithm [PB88-102181] 07 p0881 N88-15342
Parallel algorithms for computer vision on the connection machine [AD-A185842] 07 p0901 N88-15456
Program translation via abstraction and reimplementation [AD-A185845] 07 p0901 N88-15458
Investigation and implementation of an algorithm for computing optimal search paths [AD-A185927] 07 p0902 N88-15461
A multicut algorithm for two-stage stochastic linear programs [AD-A186148] 07 p0903 N88-15466

Image processing language development
[AD-A186251] 07 p0903 N88-15467
Tracking procedure for non-normally distributed measurement errors
[AD-A186287] 07 p0903 N88-15468
Parallel LU-factorization algorithms for dense matrices
[DE88-002179] 07 p0904 N88-15478
Algorithm and program for recognition of compactly positioned vertices of events for the HPD minimum guidance system
[DE88-700542] 07 p0905 N88-15482
Monte Carlo photon transport on vector and parallel supercomputers
[DE88-002503] 07 p0905 N88-15486
Simplified self-tuning control algorithms
[OUEL-1657/86] 07 p0907 N88-15494
An O(n3L) interior point algorithm for convex quadratic programming
[AD-A186001] 07 p0909 N88-15504
Correctness proofs for systolic algorithms: Palindromes and sorting
[PB88-106075] 07 p0912 N88-15534
Investigation of candidate data structures and search algorithms to support a knowledge based fault diagnosis system 07 p0923 N88-15606
Monte Carlo simulation of triangulated random surfaces in grand canonical ensemble
[DE88-700378] 07 p0941 N88-15718
Unsteady transonic algorithm improvements for realistic aircraft applications
[NASA-TM-100516] 08 p0949 N88-15760
Attitude determination of artificial satellites through joint application of static and dynamic optimal estimation techniques
[INPE-4415-TDL/306] 08 p0963 N88-15832
Numerical arc segmentation algorithm for a radio conference-NASARC (version 2.0) technical manual
[NASA-TM-100160] 08 p0977 N88-15910
The design and implementation of surface acoustic wave devices for linear FM and a new non-linear FM pulse compression technique for radar applications
[AD-A186741] 08 p0980 N88-15922
Assessment of VAS-derived products created by a simultaneous algorithm on a convectively active day
[AD-A186158] 08 p1054 N88-16359
Orbital navigation, docking and obstacle avoidance as a form of three dimensional model-based image understanding 08 p1061 N88-16406
Iterative-deepening heuristic search for optimal and semi-optimal resource allocation 08 p1062 N88-16410
The power of neural nets 08 p1064 N88-16430
A data structure and algorithm for fault diagnosis 08 p1065 N88-16432
A parallel algorithm for the general LU-factorization
[DE88-002177] 08 p1066 N88-16444
A note on the partitioning shortest path algorithm
[CWI-OS-R8703] 08 p1067 N88-16451
Short data length effects in an asymptotically efficient ARMA (AutoRegressive Moving Average) spectral estimator
[AD-A186561] 08 p1068 N88-16458
Adaptive exponential stabilization of a first order continuous-time system
[CWI-OS-R8705] 08 p1069 N88-16461
Control variate selection for multiresponse simulation
[AD-A186637] 08 p1069 N88-16463
High performance VLSI algorithms and architectures for digital signal processing 09 p1155 N88-16926
Numerical arc segmentation algorithm for a radio conference-NASARC, version 2.0: User's manual
[NASA-TM-100161] 09 p1156 N88-16928
Mesospheric dynamics and chemistry from SME data
[NASA-CR-182465] 09 p1191 N88-17139
Implementing clips on a parallel computer 09 p1211 N88-17259
Vision technology/algorithms for space robotics applications 09 p1212 N88-17267
Calibration of neural networks using genetic algorithms, with application to optimal path planning 09 p1214 N88-17277
Supercomputers for solving PDE (Partial Differential Equations) problems
[AD-A186583] 09 p1215 N88-17283
Nested transactions, conflict-based locking, and dynamic atomicity
[AD-A187033] 09 p1217 N88-17294
Multicolor numbering of irregular triangular meshes
[AD-A186559] 09 p1217 N88-17298
Algorithm design for scientific computation for highly parallel multiprocessor systems
[AD-A186713] 09 p1217 N88-17299
Algorithms for transitive reduction of an acyclic graph
[PB87-162822] 09 p1220 N88-17317
A comparison of algorithms for the analysis of images generated by two-dimensional electrophoresis
[DE88-003730] 09 p1220 N88-17319
A fast bottom-up algorithm for computing the cut sets of noncoherent fault trees
[DE88-003741] 09 p1220 N88-17320
A raster scan algorithm for generating visible parametric surfaces
[DE88-003222] 09 p1220 N88-17321
Multiple-object motion estimation by maximal matching of 3-D point and line features 09 p1220 N88-17322
Acceleration techniques for decoupling algorithms in semiconductor simulation
[DE88-003593] 09 p1221 N88-17323
A parallel block cyclic reduction algorithm for the fast solution of elliptic equations
[DE88-003595] 09 p1221 N88-17324
A state space approach to the problem of adaptive pole assignment
[CWI-OS-R8704] 09 p1224 N88-17339
Experiments with the back propagation algorithm: A systematic look at a small problem
[RSRE-MEMO-4049] 09 p1224 N88-17340
On line search termination criteria for and convergence of conic algorithms for minimization
[DE88-002844] 09 p1227 N88-17351
Advances in reliable numerical computation: A summary — conference
[NPL-DITC-102/87] 09 p1229 N88-17367
Navier-Stokes simulation of wind-tunnel flow using LU-ADI factorization algorithm
[NASA-TM-100042] 10 p1268 N88-17584
Formulation methods of rigid multibody systems for large space structures and some results of computer simulation
[NAL-TR-942] 10 p1293 N88-17730
Designing variable-length codes with good error-recovery properties
[BBC-RD-1987/19] 10 p1317 N88-17876
Recursive forward dynamics for multiple robot arms moving a common task object
[NASA-CR-182526] 10 p1340 N88-18008
The arithmetic cube and its associated algorithms 10 p1374 N88-18195
Hardware implementation for special functions. An application for combat simulation 10 p1374 N88-18197
Role of broadcasting in multiprocessor systems 10 p1374 N88-18201
The mapping of parallel algorithms to reconfigurable parallel architectures 10 p1376 N88-18209
A comparative study of heurstic algorithms for task assignment in distributed computing systems 10 p1376 N88-18211
Distributed control of large parallel computers 10 p1376 N88-18215
Strategies for concurrent processing of complex algorithms 10 p1379 N88-18236
Investigations on the usefulness of the Massively Parallel Processor for study of electronic properties of atomic and condensed matter systems
[NASA-CR-182514] 10 p1383 N88-18259
Parameter identification and sensitivity analysis for a robotic manipulator arm
[NASA-CR-181608] 10 p1385 N88-18272
The impact of hierarchical memory systems on linear algebra algorithm design
[DE88-003574] 10 p1385 N88-18274
PSolve: A concurrent algorithm for solving sparse systems of linear equations
[DE88-003584] 10 p1386 N88-18275
Introduction to a system for implementing neural net connections on SIMD architectures
[NASA-CR-181612] 10 p1386 N88-18279
Graph transformation algorithms for array memory optimization in applicative languages
[DE88-004727] 10 p1387 N88-18283
Experiences with serial and parallel algorithms for channel routing using simulated annealing
[NASA-CR-182530] 10 p1388 N88-18289
Semantics of EqL
[AD-A188151] 10 p1389 N88-18297
Implementation and analysis of a Navier-Stokes algorithm on parallel computers
[NASA-CR-181614] 10 p1390 N88-18301
A parallel quasi-Newton method for partially separable large scale minimization
[DE88-003592] 10 p1393 N88-18309
Performance studies of a parallel processor for large linear programming problems
[PB88-121611] 10 p1393 N88-18310
Application of a multigrid method to a buoyancy-induced flow problem
[DE88-003961] 10 p1397 N88-18326
Quasigroup approach to solution of linear algebraic equation systems
[DE88-700595] 10 p1398 N88-18330
Straightening and the Stanley decomposition for the (2;n)-nilpotent vectorfield
[PB88-126685] 10 p1398 N88-18336
The hybrid Monte Carlo Algorithm and the chiral transition
[DE88-004305] 10 p1399 N88-18341
A computer simulation study of an expert system for walking machine motion planning
[AD-A187907] 11 p1438 N88-18577
Further results on finite-state codes 11 p1472 N88-18782
New mode switching algorithm for the JPL 70-meter antenna servo controller 11 p1474 N88-18791
A hydrodynamic analysis of fluid flow between meshing spur gear teeth
[AD-A187671] 11 p1482 N88-18844
Three-dimensional flow fields past reentry vehicles 11 p1484 N88-18858
A new computational technique for generating algorithms, with application to the solution of the time-dependent incompressible Navier-Stokes equations 11 p1485 N88-18864
Real-time kinematic and dynamic analysis and adaptive model following control of manipulator arms 11 p1495 N88-18927
Symmetries in nonlinear control systems and their applications 11 p1496 N88-18929
Contour-to-grid interpolation with nonlinear finite elements: A feasibility study
[AD-A188108] 11 p1503 N88-18980
A spectral method for computing complete synthetic seismograms
[AD-A187663] 11 p1510 N88-19024
Ground clutter processing for wind measurements with airport surveillance radars
[AD-A187708] 11 p1514 N88-19044
Visual integration and detection of discontinuities: The key role of intensity edges
[AD-A188012] 11 p1520 N88-19076
Approaches to the automatic generation and control of finite element meshes 11 p1526 N88-19113
A hierarchical structure for automatic meshing and adaptive FEM analysis 11 p1527 N88-19119
Digital control of the Czochralski growth of Gallium arsenide-controller software reference manual
[AD-A187210] 11 p1528 N88-19127
The roll back chip: Hardware support for distributed simulation using time warp
[AD-A187823] 11 p1529 N88-19132
Performance measurements of distributed simulation strategies
[AD-A187824] 11 p1529 N88-19133
A theory of program correctness, and algorithms for proofs
[ANL-87-4] 11 p1531 N88-19146
An exact pseudo polynomial algorithm for the 0-1 linear diophantine equation
[INPE-4289-PRE/1160] 11 p1531 N88-19148
Algorithmic alternatives
[DE88-003905] 11 p1531 N88-19149
A tool for the analysis of quasi-Newton methods with application to unconstrained minimization
[DE88-005783] 11 p1532 N88-19153
A shared memory algorithm and proof for the alternative construct in CSP (Communicating Sequential Processes)
[AD-A187820] 11 p1533 N88-19156
Two new frameworks for learning
[AD-A187723] 11 p1534 N88-19162
Learning functions from examples
[AD-A187725] 11 p1534 N88-19163
Implementation of multigrid in SOLA algorithm — fluid flow 11 p1538 N88-19191
Solution of a rotating Navier-Stokes problem by a nonlinear multigrid algorithm 11 p1538 N88-19194
Application of the multigrid technique to the pressure-correction equation for the SIMPLE algorithm — Semi-Implicit Method for Pressure Linked Equations (SIMPLE) 11 p1539 N88-19196
Discretizations for multigrid methods 11 p1539 N88-19198
Estimation in linear models with censored data
[AD-A187209] 11 p1540 N88-19203
Generating the states of a probabilistic system
[AD-A187896] 11 p1540 N88-19208
Connection between general observers and Lanczos potential
[DE88-700139] 11 p1563 N88-19354
A traveling-salesman-based approach to aircraft scheduling in the terminal area
[NASA-TM-100062] 12 p1576 N88-19424
Calibration of a ring laser gyro inertial navigation system 12 p1576 N88-19428

Realtime pilot model parameter identification
[AD-A188873] 12 p1584 N88-19476
Preliminary orbit determination algorithms: Application to the Brazilian satellite
[INPE-4411-NTE/276] 12 p1594 N88-19546
Identification of microwave line-of-sight multipath components 12 p1616 N88-19665
Optimum filters and smoothers design for carrier phase and frequency tracking
[NASA-CR-182654] 12 p1618 N88-19679
An efficient numerical algorithm for solving scattering and inverse scattering problems of electromagnetic waves
[AD-A188479] 12 p1619 N88-19684
Evaluating the performance of the LPC (Linear Predictive Coding) 2.4 kbps (kilobits per second) processor with bit errors using a sentence verification task
[AD-A188573] 12 p1620 N88-19686
A numerical study of automated dynamic relaxation for nonlinear static tensioned structures
[AD-A188372] 12 p1635 N88-19790
An intelligent allocation algorithm for parallel processing
[NASA-CR-182648] 12 p1675 N88-20014
Computer architecture for efficient algorithmic executions in real-time systems: New technology for avionics systems and advanced space vehicles
[NASA-CR-182650] 12 p1675 N88-20016
Some questions of using coding theory and analytical calculation methods on computers
[DE88-700905] 12 p1676 N88-20021
A variant of the ISODATA algorithm for application to agricultural targets
[INPE-4436-PRE/1235] 12 p1676 N88-20023
Research on algorithms for nonlinear programming
[AD-A188326] 12 p1677 N88-20024
Analysis, estimation, and control for perturbed and singular systems and for systems subject to discrete events
[AD-A188496] 12 p1677 N88-20026
Experimental analysis of algorithms
[AD-A188528] 12 p1677 N88-20028
Research on automatic verification of finite-state concurrent systems
[AD-A188618] 12 p1677 N88-20029
An emulation tool for simulating matrix operations on an SIMD (Single Instruction Multiple Data stream) multiprocessor
[AD-A188654] 12 p1678 N88-20030
Analysis of simulated annealing type algorithms
[AD-A189382] 12 p1679 N88-20037
MOBICALC: An integrated and interactive system for development of administrative models
[INPE-4335-TDL/291] 12 p1679 N88-20038
A computer code for the solution of large scale network reliability analysis problems
[AD-A188455] 12 p1680 N88-20042
Support for concurrent computing environments
[AD-A188498] 12 p1680 N88-20043
OPS83: Style guide for high performance
[AD-A188505] 12 p1681 N88-20051
Method of reduction of polynomially nonlinear equations to linear equations
[DE88-700922] 12 p1683 N88-20064
Further refinement and applications of the mixed computational algorithm for plane elastic contact problems
[AD-A188308] 12 p1683 N88-20065
Object-oriented design in numerical linear algebra
[AD-A189427] 12 p1685 N88-20073
Task allocation for efficient performance of a decentralized organization
[AD-A188699] 12 p1705 N88-20204
Development of a dependency theory toolbox for database design
[AD-A188872] 12 p1707 N88-20216
Analysis of pre-flight modulator voltage calibration data for the Voyager plasma science experiment
[NASA-CR-182577] 12 p1710 N88-20236
An L-U implicit multigrid algorithm to solve the Euler equations for transonic flow in rotating turbomachinery passages 13 p1718 N88-20270
A method and measures to evaluate trackers for air traffic control
[NLR-TR-86072-U] 13 p1720 N88-20287
Material parameter measurements at high temperatures
[NASA-CR-182707] 13 p1739 N88-20397
Adaptive control of scientific balloon-borne gondola attitude 13 p1755 N88-20497
Statistical signal processing using a class of iterative estimation algorithms
[AD-A189050] 13 p1757 N88-20511
Adaptive algorithms for HF antenna arrays
[AD-A189329] 13 p1761 N88-20534
Systems near the onset and in the well-developed regimes of turbulence
[DE88-005365] 13 p1786 N88-20565
Finite element methods for quasi-prismatic bodies with application to gears 13 p1779 N88-20644
Numerical modeling of wave migration of seismic data 13 p1786 N88-20684
Stratospheric trace gas distributions from fair infrared thermal emission spectroscopy 13 p1797 N88-20749
A new algorithm for general multiobjective optimization
[NASA-TM-100536] 13 p1813 N88-20830
The physical structure of concurrent problems and concurrent computers
[DE88-005812] 13 p1814 N88-20835
Parallel image compression
[NASA-CR-180758] 13 p1814 N88-20837
Broadband correlation analysis
[AD-A188732] 13 p1814 N88-20839
On relaxation algorithms based on Markov random fields
[AD-A189043] 13 p1814 N88-20840
Passive DF: A tutorial, part 1
[NASA-CR-182669] 13 p1815 N88-20846
Two dimensional uncorrelated bias in fix algorithms
[NASA-CR-182683] 13 p1815 N88-20847
Preconditioned conjugate gradient algorithms and software for solving large sparse linear systems
[DE88-002180] 13 p1816 N88-20849
Conic algorithms for unconstrained minimization with special consideration of problems with large sparse Hessians: A summary of research performed
[DE88-002549] 13 p1816 N88-20850
Algorithms with conic termination for nonlinear optimization
[DE88-005893] 13 p1816 N88-20851
Method to evaluate image-recovery algorithms based on task performance
[DE88-005382] 13 p1816 N88-20853
Experimental verification of a finite-difference time-domain thin slot algorithm
[DE88-005572] 13 p1817 N88-20859
Approximation algorithms for scheduling unrelated parallel machines
[CWI-OS-R8714] 13 p1817 N88-20861
Verification of a systolic algorithm for string comparison
[CWI-CS-R8734] 13 p1819 N88-20873
Interpolation algorithms for digital terrain models
[INPE-4373-PRE/1196] 13 p1820 N88-20877
Spectral element methods: Algorithms and architectures
[NASA-CR-182701] 13 p1820 N88-20878
A report on the study of algorithms to enhance vector computer performance for the discretized one-dimensional time-dependent heat conduction equation: EPIC research, phase 1
[DE88-005642] 13 p1820 N88-20880
An implementation of the OPS5 language for computers compatible with IBM-PC
[INPE-4291-PRE/1162] 13 p1821 N88-20882
On the design of parallel numerical methods in message passing and shared memory environments
[DE88-003566] 13 p1822 N88-20888
An amoeba replicated service organisation — Amoeba operating system
[CWI-CS-R8723] 13 p1822 N88-20892
Robustifying the Kalman filter
[AD-A189240] 13 p1825 N88-20907
A study of data compactation using numerical methods
[INPE-4317-TDL/284] 13 p1828 N88-20929
Local search for constrained routing problems --- traveling salesman
[CWI-OS-R8711] 13 p1830 N88-20948
Passive autonomous infrared sensor technology
[AD-A188698] 13 p1839 N88-21005
Optics for large telescope 13 p1840 N88-21014
On the role of complete reducibility in general competitive equilibrium models
[DE88-005893] 13 p1851 N88-21083
JPRS report: Science and technology. China
[JPRS-CST-87-023] 14 p1863 N88-21130
Finite element explicit algorithm for solving temporal temperature fields 14 p1899 N88-21339
Advances in contact algorithms and their application to tires
[NASA-TP-2781] 14 p1922 N88-21456
Modeling the viscoplastic behavior of Inconel 718 at 1200 F 14 p1929 N88-21502
Classification of small image areas by digital correlation for the connection of different images in photogrammetry and long-range reconnaissance
[ETN-88-91506] 14 p1940 N88-21578
Development and testing of the gust front algorithm
[AD-A189722] 14 p1949 N88-21622
Verification of an algorithm for log-time sorting by square comparison
[CWI-CS-R8729] 14 p1956 N88-21656
Multiextremal optimization via adaptive partition algorithms
[REPT-87-44] 14 p1957 N88-21664
On the design of some systolic algorithms
[CS-8705] 14 p1957 N88-21666
Monte Carlo modified method for Green function. Algorithm and computer code for calculations in equal mass many-body system
[DE88-701114] 14 p1957 N88-21667
A parallel algorithm for computing the singular value decomposition of a matrix
[DE88-007059] 14 p1958 N88-21673
Identification of nonlinear output-affine systems using an orthogonal least squares algorithm
[RR-313] 14 p1958 N88-21678
A prediction-error estimation algorithm for nonlinear output-affine systems
[RR-314] 14 p1959 N88-21679
Identification of nonlinear rational systems using a prediction-error estimation algorithm
[RR-317] 14 p1959 N88-21680
A Gram-Schmidt space-time adaptive canceller using adaptive lattice filters
[AD-A189684] 14 p1959 N88-21684
Implementing embedded artificial intelligence rules within algorithmic programming languages
[NASA-CR-178393] 14 p1959 N88-21686
Parallel algorithms for mapping pipelined and parallel computations
[NASA-CR-181655] 14 p1960 N88-21687
A state-space approach to super-optimal H sup infinity control problems
[OUEL-1690/87] 14 p1962 N88-21702
An orthogonal parameter estimation algorithm for nonlinear stochastic systems
[RR-307] 14 p1966 N88-21736
Model selection for the multiple model adaptive algorithm for in-flight simulation
[AD-A189715] 15 p2016 N88-22022
Moving-bank multiple model adaptive estimation applied to flexible spacestructure control
[AD-A190761] 15 p2026 N88-22071
Identification of a star field from a spinning satellite
[CNES-NT-120] 15 p2026 N88-22074
A multiple model adaptive tracking algorithm against airborne targets
[AD-A190819] 15 p2057 N88-22263
Motion sickness: Quantitative, algorithmic malaise indication in real time
[AD-A189674] 15 p2101 N88-22518
The visit problem: Visibility graph-based solution
[DE88-000343] 15 p2108 N88-22556
Consistent estimates of autoregressive parameters for autoregressive moving average models
[RR-663-I] 15 p2109 N88-22564
Implementation of a distributed adaptive routing algorithm on the Intel iPSC (Intel Personal Super-Computer)
[AD-A189849] 15 p2109 N88-22567
Memory efficient evaluations of nonlinear stochastic equations and C3 applications
[AD-A189872] 15 p2110 N88-22569
An analysis of multiple grain CHiP architectures
[AD-A189942] 15 p2110 N88-22570
Extension of computer based algorithms by operator analysis
[NASA-CR-182798] 15 p2111 N88-22575
Transformations of concurrent algorithms for highly parallel systems: A one year project summary report
[AD-A190236] 15 p2111 N88-22576
Design and implementation of VLSI prime factor algorithm processor
[AD-A190483] 15 p2112 N88-22580
Design of an algorithm to translate nested relational algebra queries to GENESIS trace manager commands
[AD-A190502] 15 p2112 N88-22581
SEARCH: An interactive computer program for optimizing two-variable, unconstrained experiments or simulation
[AD-A190593] 15 p2112 N88-22583
Cholesky downdating on a hypercube
[DE88-006780] 15 p2113 N88-22586
Implementation and performance analysis of parallel assignment algorithms on a hypercube computer
[AD-A190678] 15 p2115 N88-22600
Finding texture boundaries in images
[AD-A190554] 15 p2117 N88-22609
Multi-disciplinary techniques for understanding time-varying space-based imagery
[AD-A190711] 15 p2117 N88-22610
Development and application of the p-version of the finite element method
[AD-A190036] 15 p2120 N88-22633

The algebraic structure of convolutional codes
[AD-A190280] 15 p2120 N88-22635
Non-rigid motion and Regge calculus
[AD-A190387] 15 p2121 N88-22640
Trust regions and projected gradients
[DE88-005829] 15 p2122 N88-22646
Structural decomposition of multiple time scale Markov processes
[AD-A189739] 15 p2123 N88-22657
Approximation methods for the identification and control of distributed parameter systems
[AD-A190201] 15 p2124 N88-22662
Target localization in an inhomogeneous medium
[AD-A190008] 15 p2130 N88-22703
Expanded envelope concepts for aircraft control-element failure detection and identification
[NASA-CR-181664] 16 p2160 N88-22886
Numerical arc segmentation algorithm for a radio conference: A software tool for communication satellite systems planning
[NASA-TM-100789] 16 p2167 N88-22919
Algorithms and architectures for acoustic phonetical detection of continuous speech
[ENST-87E016] 16 p2189 N88-23054
Strategies for concurrent processing of complex algorithms in data driven architectures
[NASA-CR-181657] 16 p2193 N88-23083
Test code for the assessment and improvement of Reynolds stress models 16 p2197 N88-23105
Fast algorithms for Euler and Navier-Stokes simulations
[AD-A190897] 16 p2208 N88-23175
Multigrid for structures analysis
16 p2218 N88-23232
Parallel computer methods for eigenvalue extraction
16 p2218 N88-23233
Microgravity manipulator demonstration
16 p2219 N88-23242
Results of the testing of the segmentation program on RESEDA
[BCRS-87-01] 16 p2228 N88-23304
Validate algorithms for the determination of rainfall rates from SSM/I microwave satellite imagery
[AD-A191337] 16 p2236 N88-23353
Efficient and fast data compression codes for discrete sources with memory
[ETN-88-92233] 16 p2246 N88-23420
HIFI: A design method for implementing signal processing algorithms on VLSI processor arrays
[ETN-88-92238] 16 p2247 N88-23421
Synthesis and simulation of systolic algorithms
[ETN-88-92183] 16 p2247 N88-23423
Correctness proofs for systolic algorithms: A palindrome recognizer
[CWI-CS-R8747] 16 p2248 N88-23434
A very simple construction for atomic multiwriter register
[CWI-CS-R8751] 16 p2249 N88-23436
A queueing network model for analyzing a class of branch and bound algorithms on a master-slave architecture
[CWI-OS-R8717] 16 p2249 N88-23441
Approximate agreement
[AD-A191030] 16 p2251 N88-23455
Fast Algorithm Simulation and Test (FAST) facility
[AD-A191183] 16 p2252 N88-23457
On 2-D versus 3-D: Sine of squared angular error and weighted perpendicular fixing
[NASA-CR-182899] 16 p2252 N88-23458
Algorithms and intuition
[NASA-CR-182900] 16 p2252 N88-23459
Compilation of preprints
[AD-A191245] 16 p2252 N88-23460
An algorithm for random access communication over a noisy channel
[AD-A191315] 16 p2252 N88-23461
Simulation of FELIN logics. Polynomials roots simultaneous computation algorithms
[ETN-88-92182] 16 p2253 N88-23464
Parallelization of Gauss-Seidel algorithms as an example of parallel iterative equation solving
[REPT-87-76] 16 p2254 N88-23471
Parallel artificial intelligence search techniques for real time applications
[AD-A190683] 16 p2255 N88-23473
Systolic algorithm for matrix-vector multiplication
[PB88-165394] 16 p2256 N88-23484
Computation of a complete elliptic integral of the first kind using q-expansion 16 p2257 N88-23490
New stable, vectorisable Kalman filter algorithms based on orthogonal transformations
[DFVLR-FB-87-52] 16 p2258 N88-23494
Formal solution of differential linear systems in the proximity of a singularity
[ETN-88-92190] 16 p2258 N88-23495
Approximation and representation of explicit surfaces in the presence of singularities
[ETN-88-92191] 16 p2258 N88-23496
Convergence qualification of partition algorithms in global optimization
[REPT-87-61] 16 p2259 N88-23505
Algorithm for accounting the conditions in infinity for two-dimensional magnetostatics problems
[DE88-701673] 16 p2264 N88-23541
Adaptive segmentation evaluation
[AD-A190965] 16 p2274 N88-23609
Automated database design technology and tools
[NASA-CR-182875] 16 p2286 N88-23687
A three dimensional assignment method in the time space
[REPT-87-49] 16 p2287 N88-23690
Experimental evaluation of algorithms for connected speech recognition using hidden Markov models
[RSRE-MEMO-4099] 17 p2333 N88-23928
An efficient parallel algorithm for the simulation of three-dimensional compressible transition on a 20 processor Flex/32 multicomputer
[NASA-CR-178340] 17 p2337 N88-23943
Shape detection in remote sensing through graph isomorphism 17 p2354 N88-24028
Digital processing of infrared and visible images from the GOES satellite and its integration with meteorological radar data 17 p2360 N88-24057
Generation of thematic maps for updating aeronautical pilot charts utilizing LANDSAT-TM images
17 p2361 N88-24062
Low altitude remote sensing data in the implementation of a mathematical model for the planning of urban equipment networks 17 p2363 N88-24074
Research on enhancing the utilization of digital multispectral data and geographic information systems in global habitability studies
[NASA-CR-182799] 17 p2368 N88-24101
Cloud cover determination in polar regions from satellite imagery
[NASA-CR-182906] 17 p2375 N88-24123
The multi-disciplinary design study: A life cycle cost algorithm
[NASA-CR-4156] 17 p2385 N88-24172
On the efficient implementation of the fast multipole algorithm
[AD-A191167] 17 p2385 N88-24173
Parallel processors and nonlinear structural dynamics algorithms and software
[NASA-CR-182925] 17 p2387 N88-24187
Genetic algorithms for adaptive real-time control in space systems 17 p2388 N88-24195
An algorithm for super-optimal H sup inf design: The 2-block case
[OUEL-1711/87] 17 p2391 N88-24210
A control technique for improved robot performance
17 p2391 N88-24212
Small particle bed reactors: Sensitivity to Brayton cycle parameters 17 p2435 N88-24487
A feedback linearization approach to spacecraft control using momentum exchange devices
[NASA-CR-172057] 18 p2472 N88-24668
Dynamics of a flexible orbiting platform with MRMS
[ISSN-0285-6808] 18 p2473 N88-24673
Geodesy by radio interferometry: Optimization of wet path delay algorithms using microwave radiometer data
[PB88-167739] 18 p2498 N88-24820
Delay-doppler radar imaging
[AD-A191509] 18 p2499 N88-24826
A method for discrimination of radar targets using complex natural resonances
[AD-A191848] 18 p2500 N88-24832
Information and stochastic systems
[AD-A192167] 18 p2501 N88-24838
Identification of cascaded microwave circuits with moderate reflections using reflections and transmission measurements
[PB88-171921] 18 p2503 N88-24849
Fast algorithm development for large-eddy simulation of circular-jet turbulence
[AD-A192044] 18 p2509 N88-24887
SOLA-DM: A numerical solution algorithm for transient three-dimensional flows
[DE88-007159] 18 p2514 N88-24913
The coordination of multiple robotic manipulators
[AD-A190869] 18 p2522 N88-24963
Dynamic response of plates to moving loads: Structural impedance and finite element methods
18 p2528 N88-25000
Advanced development of the boundary element method for elastic and inelastic thermal stress analysis
18 p2529 N88-25002
Multishaker modal testing
[NASA-CR-179355] 18 p2530 N88-25010
DMSP-SSM/I NASA algorithm validation using primarily LANDSAT and secondarily DMSP and/or AVHRR visible and thermal infrared satellite imagery
[NASA-CR-182979] 18 p2532 N88-25024
Analysis of lightning field changes during active thunderstorms in Florida 18 p2545 N88-25103
A multiprocessor data flow accelerator module
[DE88-007587] 18 p2554 N88-25161
Multi-sensor integration on the NCUBE hypercube computer
[DE88-007472] 18 p2554 N88-25162
A mixed-integer linear programming problem which is efficiently solvable
[AD-A191028] 18 p2556 N88-25168
Decomposition of linear programs using parallel computation
[AD-A191718] 18 p2556 N88-25173
An electrostatic potential comparator
[AD-A192051] 18 p2557 N88-25177
A centered projective algorithm for linear programming
[AD-A192100] 18 p2557 N88-25178
Making progress during a stall in the simplex algorithm
[DE88-007120] 18 p2558 N88-25182
An improved simulated annealing algorithm for standard cell placement
[NASA-CR-182952] 18 p2558 N88-25183
Algorithms and software for solving finite element equations on serial and parallel architectures
[NASA-CR-183027] 18 p2559 N88-25191
Gram-Schmidt implementation of a linearly constrained adaptive array
[AD-A191651] 18 p2560 N88-25198
Robot navigation using simple sensor fusion
[DE88-006184] 18 p2561 N88-25203
A concurrent neural network algorithm for the traveling salesman problem
[DE88-006981] 18 p2562 N88-25208
Algorithms and data structures for an expanded family of matroid intersection problems
[AD-A191482] 18 p2562 N88-25213
A primal-dual algorithm for the computation of the minimum of a convex function on the intersection of convex functions, and its application in data analysis
[RR-638-M] 18 p2563 N88-25217
Multigrid methods for elliptic Partial Differential Equations (PDEs)
[CWI-NM-R8722] 18 p2566 N88-25242
A constraint algorithm for maintaining rigid bonds in molecular dynamics simulations of large molecules
[AD-A191663] 18 p2572 N88-25277
Dendritic growth in the presence of convection
18 p2580 N88-25328
Modem for the land mobile satellite channel
19 p2649 N88-25727
Rearrangement procedures in regenerative multibeammobile communications satellites with frequency reuse 19 p2650 N88-25735
Speech coding at 4800 bps for mobile satellite communications 19 p2652 N88-25749
A 4.8 kbps code-excited linear predictive coder
19 p2652 N88-25750
Robust vector quantization for noisy channels
19 p2653 N88-25754
Analysis and improvement of the vector quantization in SELP (Stochastically Excited Linear Prediction)
19 p2653 N88-25756
The solution of the Elrod algorithm for a dynamically loaded journal bearing using multigrid techniques
[NASA-TM-100941] 19 p2666 N88-25854
Automatic calibration of space based manipulators and mechanisms
[NASA-CR-182804] 19 p2676 N88-25912
A concurrent on-board vision system for a mobile robot
[DE88-007475] 19 p2676 N88-25914
Model-based computed tomography for nondestructive evaluation: An overview and proposal
[DE88-010600] 19 p2679 N88-25926
Updating of municipal official register of real estate through the geographical information system
19 p2684 N88-25952
Algorithmic generation of feasible system architectures
[AD-A191722] 19 p2713 N88-26106
Intermediate level computer vision processing algorithm development for the content addressable array parallel processor
[AD-A192086] 19 p2714 N88-26111
Automatic routing in symbolic IC design environment
19 p2714 N88-26112
Efficient parallel algorithm for the connected component problem and its implementation on the DPP84 (Delft Parallel Processor)
[PB87-225959] 19 p2715 N88-26118

An extension of the Hopfield-Tank model for solution of the multiple traveling salesmen problem
[DE88-006377] 19 p2715 N88-26122
Hybrid simulations
[DE88-009125] 19 p2715 N88-26123
Distributed mathematics in a heterogeneous environment
[DE88-009128] 19 p2716 N88-26124
Gaussian techniques on shared-memory multiprocessors
[DE88-010594] 19 p2716 N88-26126
QR factorization of a dense matrix on a hypercube multiprocessor
[DE88-009187] 19 p2716 N88-26129
Fault diagnosis in distributed computer networks
[AD-A192406] 19 p2718 N88-26140
SLAPP: A special multiprocessor array for signal processing and linear algebra
[AD-A191587] 19 p2719 N88-26146
Some supraconvergent schemes for hyperbolic equations on irregular grids
[DE88-009113] 19 p2720 N88-26151
Calculating the self-intersections of Bezier curves
[AD-A192371] 19 p2721 N88-26156
Digital control of the czochralski growth of gallium arsenide. System reference manual. Valid for Czochralski growth controller software version 2.4
[AD-A191997] 19 p2732 N88-26227
Simple 2-D navigation for wheeled vehicles
[DE88-007115] 20 p2756 N88-26351
Microwave image understanding and its application to radar cross section management
20 p2788 N88-26542
Multi-target tracking algorithms for cluttered environments 20 p2789 N88-26543
A random access algorithm for environments with capture and limited feedback capabilities
[AD-A192233] 20 p2790 N88-26552
Effects of atmospheric model layering on LOWTRAN 6 calculations of 8-12 micrometers near-horizon sky radiances
[AD-A192969] 20 p2791 N88-26559
Improved 3-D turbomachinery CFD algorithm
[NASA-CR-179364] 20 p2801 N88-26619
Parallelization on a multiprocessor system of a solution method for the unsteady Navier-Stokes equations at high Reynolds numbers
[ONERA-NT-1987-8] 20 p2803 N88-26632
Optimization of performance criteria with bounded joint velocities for robots with one degree of redundancy
[DE88-003915] 20 p2810 N88-26670
An assessment of modelling techniques for the finite element analysis of reinforced concrete plate and shell structures
[AD-A192263] 20 p2814 N88-26697
Image pyramid motion detection applied to sea ice
20 p2817 N88-26713
Computer science research, 1987: Computation Directorate
[DE88-008637] 20 p2834 N88-26812
Tuning a major part of a clustering algorithm
[AD-A191446] 20 p2836 N88-26821
SEGMERGE: A scanline visible surface algorithm with adaptive span selection and inexpensive antialiasing
[DE88-009186] 20 p2836 N88-26826
Computing small singular values of bidiagonal matrices with guaranteed high relative accuracy: LAPACK working note number 3
[DE88-008465] 20 p2837 N88-26829
A practical shifted Adams algorithm
[DE88-008573] 20 p2837 N88-26830
Conditions for finite convergence of algorithms for nonlinear programs and variational inequalities
[AD-A192355] 20 p2838 N88-26834
A matroid algorithm and its application to the efficient solution of two optimization problems on graphs, revision
[AD-A192709] 20 p2838 N88-26838
A new trajectory following polynomial-time algorithm for the linear programming problem
[REPT-87-87] 20 p2840 N88-26848
Algorithm for generating the minimal cycle basis of a graph
[PB88-126610] 20 p2846 N88-26891
A new approach to machine-based perception of monocular images
[DE88-002418] 20 p2853 N88-26942
Methods for indirect imaging through the atmosphere
[ONERA-NT-1987-4] 20 p2884 N88-27124
Processing and analysis of images transmitted by Vega space probes over Halley's comet
[ETN-88-92291] 20 p2885 N88-27131
Three-dimensional scene analysis using stero based imaging
[AD-A193120] 21 p2894 N88-27178
Automatic omega station and LOP (Line Of Position) selection
[AD-A193302] 21 p2894 N88-27179
Numerical optimization, system theoretic and software tools for the integrated design of flexible structures and their control systems
[AD-A192927] 21 p2895 N88-27183
The integration of decision support problems into feature modeling based design 21 p2927 N88-27372
Optimal control of the wing rock phenomenon
21 p2927 N88-27373
Calibration and data reduction techniques for the AFGL infrared array spectrometer 21 p2927 N88-27374
Creating aspect graphs for use in object recognition
21 p2928 N88-27379
Optical interconnections for digital image coding
21 p2928 N88-27381
TDWR (Terminal Doppler Weather Radar) PRF (Pulse Repetition Frequency) selection criteria
[AD-A193089] 21 p2932 N88-27407
Sidelobe level of an adaptive array using the SMI (Sampled Matrix Inversion) algorithm
[AD-A193131] 21 p2932 N88-27409
A numerically efficient digital matched filter for periodic and windowed periodic radar waveforms
[AD-A193132] 21 p2932 N88-27410
Effects of numerical dissipation on finite-volume solutions of compressible flow problems
[AD-A193173] 21 p2944 N88-27485
Higher order vortex methods with rezoning
[DE88-010777] 21 p2947 N88-27505
Dexterous hands: Optimizing grasp by design and planning 21 p2958 N88-27572
A lubrication study of engine bearings
21 p2958 N88-27574
Three-dimensional aspects of fatigue crack closure
[AD-A192296] 21 p2960 N88-27581
Photon limited image processing in the space-time domain
[AD-A193142] 21 p2972 N88-27655
Validate algorithms for the determination of rainfall rates from SSM/I microwave satellite imagery
[AD-A192299] 21 p2974 N88-27664
Full analysis of a powerful window random access algorithm
[AD-A192437] 21 p2995 N88-27763
Synchronizable series expressions. Part 2: Overview of the theory and implementation
[AD-A192783] 21 p2996 N88-27768
Distributed algorithms for probabilistic solution of computational vision problems
[AD-A193150] 21 p2997 N88-27773
Computer aided design for linear control State Variable System (SVS)
[AD-A193282] 21 p2997 N88-27775
Verification of flight software written in C using ACSL
[DE88-006100] 21 p2998 N88-27779
The sub-implicit method: New multiprocessor algorithms for old implicit codes
[DE88-011345] 21 p2999 N88-27785
Maximum entropy signal restoration with linear programming
[DE88-011740] 21 p2999 N88-27787
A hidden-surface removal algorithm for structures defined by triangular and rectangular surface patches
[DFVLR-MITT-88-03] 21 p3000 N88-27792
Performability analysis: Measures, an algorithm and a case study
[AD-A192477] 21 p3001 N88-27800
A modular proof of correctness for a network synchronizer
[AD-A192726] 21 p3002 N88-27802
Improving the performance of AI algorithms
[AD-A192848] 21 p3003 N88-27809
Parallel quasi-Newton methods for unconstrained optimization
[AD-A193250] 21 p3003 N88-27812
Parallel solutions to geometric problems on the scan model of computation
[AD-A192321] 21 p3004 N88-27819
Finding minimum-cost circulations by successive approximation
[AD-A192724] 21 p3005 N88-27824
Finding minimum-cost circulations by canceling negative cycles
[AD-A192727] 21 p3005 N88-27825
Numerical optimization
[AD-A193032] 21 p3005 N88-27827
A review of parallel methods for solving sets of linear equations and their application within optimisation algorithms
[AD-A193137] 21 p3006 N88-27830
The computation of stationary distributions on Markov chains through perturbations
[AD-A193191] 21 p3009 N88-27855
A comparison of generators for pseudo-random normal deviates
[DE88-011711] 21 p3010 N88-27859
Robust methods for array signal processing
[AD-A192854] 21 p3012 N88-27871
Satellite attitude determination using a CCD (Charge-Coupled-Device) star camera
[AD-A192662] 22 p3046 N88-28080
Efficient multiplication algorithms over the finite fields GF(q sup m), where q equals 3,5
22 p3066 N88-28191
A wideband, high-resolution spectrum analyzer
22 p3066 N88-28194
Surface tension and viscosity with Lagrangian hydrodynamics on a triangular mesh
[AD-A194120] 22 p3075 N88-28258
Interferometric tomography of continuous fields with incomplete projections
[NASA-CR-183181] 22 p3081 N88-28295
Applications of an exponential finite difference technique
[NASA-TM-100939] 22 p3084 N88-28312
An analytical investigation of geared system dynamics containing spur and helical gears
22 p3085 N88-28317
Parameter identification of material constants in a composite shell structure
[DE88-008115] 22 p3086 N88-28326
A systolic array for efficient execution of the Faddeev algorithm
[DE88-011330] 22 p3135 N88-28635
VAXGAP: A code for the routine analysis of gamma-ray pulse-height spectra on a VAX computer
[DE88-011702] 22 p3137 N88-28648
Importance sampling for stochastic simulations
[AD-A193585] 22 p3138 N88-28654
A fast algorithm for the numerical evaluation of conformal mappings
[AD-A193903] 22 p3138 N88-28658
Rational Newton algorithms to compute formal solutions of linear differential equations in an irregular singular point
[RR-704-M] 22 p3140 N88-28670
Random pseudo-polynomial algorithms and exact problems
[REPT-87-014] 22 p3140 N88-28672
Fitting an ellipse to data
[NPL-DITC-95/87] 22 p3143 N88-28693
Second order differential equations in the complex domain
[RR-674-M] 22 p3144 N88-28695
Random number generation
[USIP-87-15] 22 p3145 N88-28707
Time minimal computation of feedback control schemes for optimal guidance problems used in space flight
[ETN-88-92969] 23 p3184 N88-28953
An overview of technology for spoken interaction with machines
[AD-A194153] 23 p3202 N88-29058
Random-access algorithms for environments with capture
[AD-A194303] 23 p3203 N88-29060
Automatic classification of digitally modulated signals
[AD-A194623] 23 p3203 N88-29064
Hierarchical organization for large, dynamic radio networks
[AD-A193942] 23 p3204 N88-29067
An efficient patched grid Navier-Stokes solution for multiple bodies, phase 1
[AD-A194166] 23 p3211 N88-29110
Vortex dynamics of coherent and chaotic structures (including algorithms for computer simulations and diagnosis)
[AD-A193580] 23 p3212 N88-29117
Analysis of the effect of faulty spares on the performance of diagnostic algorithms in reliable systems
[AD-A193526] 23 p3223 N88-29186
The gradient method for interface tracking
[AD-A194477] 23 p3248 N88-29334
Some learnability results for analogical generation
[AD-A193669] 23 p3250 N88-29342
An algorithm for determining the location of points in computer simulations
[AD-A193713] 23 p3250 N88-29343
A fast parametric maximum flow algorithm, revision
[AD-A194026] 23 p3250 N88-29345
Faster algorithms for the shortest path problem
[AD-A194031] 23 p3250 N88-29347
Faster scaling algorithms for network problems
[AD-A194032] 23 p3251 N88-29348
Analyst-centered models for systems design, analysis, and development 23 p3253 N88-29364
Mathematical algorithms for approximate reasoning
23 p3262 N88-29418

Optimisation algorithms for highly parallel computer architectures. The performance of the truncated Newton, conjugate gradient algorithm in FORTRAN and Ada
[AD-A193940] 23 p3265 N88-29435
The complexity of AI algorithms
[AD-A193494] 23 p3265 N88-29438
MACSYMA program for the painleve test of nonlinear ordinary and partial differential equations
[AD-A194293] 23 p3270 N88-29458
On Wiener-Masani's algorithm for finding the generating function of multivariate stochastic processes
[NASA-CR-182905] 23 p3273 N88-29481
SDI (Strategic Defense Initiative) battle management/C3 (Command, Control and Communications) algorithms technology program plan
[AD-A194357] 23 p3275 N88-29495
A streamwise upwind algorithm for the Euler and Navier-Stokes equations applied to transonic flows
[NASA-TM-101019] 24 p3316 N88-29751
An improved spherical earth diffraction algorithm for SEKE
[AD-A195847] 24 p3360 N88-30005
Transient interaction of electromagnetic pulses in dielectrics and microwave biophysics
[AD-A195687] 24 p3360 N88-30008
Reducing the parallel solution time of sparse circuit matrices using reordered Gaussian elimination and relaxation
[AD-A195152] 24 p3366 N88-30045
LANDSAT-TM data to map flooded areas
[INPE-4594-PRE/1324] 24 p3387 N88-30177
Validate algorithms for the determination of rainfall rates from SSM/I microwave satellite imagery
[AD-A195428] 24 p3404 N88-30270
Algorithms for nonlinear least-squares problems
[AD-A196071] 24 p3411 N88-30305
Range data description based on multiple characteristics 24 p3419 N88-30351
Statistical analysis of the LMS (Last Mean Squares) and modified stochastic gradient
[AD-A195497] 24 p3424 N88-30376
Kalman filter-based algorithms for estimating depth from image sequences
[AD-A195818] 24 p3424 N88-30380
Reconstruction of multidimensional signals from multiple level threshold crossings
[AD-A195561] 24 p3425 N88-30383
Design and performance analysis of a relational replicated database system
[AD-A196290] 24 p3437 N88-30456
The guide star catalog
[NASA-CR-183253] 24 p3452 N88-30547

ALIGNMENT
NT SELF ALIGNMENT
An optoelectronic alignment telescope for straightness measurements
[ETN-87-90383] 01 p0093 N88-10609
Recognizing rigid objects by aligning them with an image
[AD-A184253] 03 p0368 N88-12318
Carbon-fiber reinforced plastics 04 p0403 N88-12506
Optical alignment of Centaur's inertial guidance system
[NASA-TM-88844] 04 p0405 N88-12515
Alignment and assembly tool for very large diameter cylinders
[NASA-CASE-MFS-28001-2] 06 p0711 N88-14360
Development and study of fibre-optic link lines on the basis of the KEM-8-4PD, KEM-8-4PR quantum-electronic modules
[DE88-700372] 07 p0932 N88-15663
Demonstration of efficient full aperture Type 1/Type 2 third harmonic conversion on Nova
[DE88-003834] 14 p1914 N88-21438
Particle beam alignment system for single event upset-Van de Graaf experiments
[AD-A189695] 15 p2132 N88-22721
Thermal compensating mount
[NASA-CASE-LAR-13794-1] 18 p2519 N88-24942
Precise beam alignment He-Ne laser tubes
[PB87-228334] 19 p2675 N88-25906
Precise rotational alignment of X-ray transmission diffraction gratings
[DE88-010599] 21 p2911 N88-27273

ALIPHATIC HYDROCARBONS
NT ACETYLENE
NT ALKANES
NT ALKENES
NT BUTADIENE
NT BUTANES
NT BUTENES
NT CETANE
NT ETHANE
NT ETHYLENE
NT METHANE
NT OXYACETYLENE
NT PARAFFINS
NT POLYBUTADIENE
NT PROPANE
NT PROPYLENE
NT VINYLIDENE

ALKALI HALIDES
NT CESIUM IODIDES
NT SODIUM CHLORIDES
NT SODIUM FLUORIDES

ALKALI METALS
NT CESIUM
NT LIQUID LITHIUM
NT LIQUID POTASSIUM
NT LIQUID SODIUM
NT LITHIUM
NT LITHIUM ISOTOPES
NT POTASSIUM
NT RUBIDIUM
NT RUBIDIUM ISOTOPES
NT SODIUM
NT SODIUM VAPOR
Valence bond cluster studies of alkali metal/semiconductor bonding
[AD-A184276] 04 p0496 N88-13054
Tetrahedral carbon and interstitial electrons in Li cluster: CLi4 and (LiCH3)4
[AD-A184277] 04 p0496 N88-13055
Solar pumped, alkali vapor laser
[AD-A187156] 09 p1170 N88-17016
Clusters: Link between molecules and solids
[AD-A188170] 11 p1543 N88-19224
Kinetic mechanisms for ionization and afterburning suppression
[AD-A189219] 13 p1737 N88-20383
AMTEC electrode development 17 p2409 N88-24324
Thermochemical analysis of mass transfer in a NB-1ZR-potassium heat pipe 17 p2412 N88-24346
Review of alkali metal and refractory alloy compatibility for Rankine cycle applications 17 p2428 N88-24447
Alkali metal thermoelectric converter design for space power systems applications 17 p2437 N88-24499
A capillary pumped SHE/AMTEC system 17 p2437 N88-24500
High power density electrodes for AMTEC 17 p2437 N88-24501
Performance of vapor-fed sodium heat engine/AMTEC systems 17 p2437 N88-24502
C-CAMP: A closed cycle alkali metal power system
[DE88-009715] 19 p2688 N88-25975
A fundamental understanding of the interfacial compatibility in hybrid material systems
[AD-A192921] 21 p2909 N88-27264
Model for bimetallic interfaces, part 2
[DE88-702672] 22 p3157 N88-28787

ALKALIES
NT LITHIUM HYDROXIDES
NT SODIUM HYDROXIDES
DTA/DSC studies of phase equilibria in binary mixtures of barium carbonate with alkali carbonates
[DE87-001195] 02 p0194 N88-11213
Mechanisms of intergranular attack and stress corrosion cracking of alloy 600 by high-temperature caustic solutions containing impurities
[DE87-012820] 10 p1300 N88-17773
The band systems of alkali vapors
[NASA-TT-20206] 10 p1417 N88-18462

ALKALINE BATTERIES
A new concept in an electrically rechargeable zinc-air alkaline battery
[DE88-003858] 13 p1762 N88-20539
Alkaline fuel cell performance investigation
[NASA-TM-100937] 21 p2909 N88-27267
Regenerative fuel cell energy storage system for a low earth orbit space station
[NASA-CR-174802] 24 p3389 N88-30184

ALKALINE EARTH METALS
Group 2A metastable collision complexes: Spectroscopy and behavior in intense radiation fields
[AD-A186737] 08 p1082 N88-16524
Evaluation and compilation of thermodynamic properties of high temperature chemical species
[AD-A187509] 11 p1452 N88-18654
Electronic energy transfer processes in the alkali/alkaline earth metal vapors
[AD-A190035] 15 p2034 N88-22119
Thermochemistry and high temperature thermodynamic properties of rare earth-alkaline earth-copper oxide superconductors
[DE88-005976] 15 p2140 N88-22770
Multiphoton ionization of alkaline earth atoms in an intense laser field
[DE88-008078] 21 p3014 N88-27884

ALKALINE EARTH OXIDES
NT BARIUM OXIDES
NT BERYLLIUM OXIDES
NT CALCIUM OXIDES
NT MAGNESIUM OXIDES
Activated metal oxide surfaces as highly basic and reducing environments
[AD-A184958] 05 p0561 N88-13417

ALKALINITY
Corrosion strength of niobium and its alloys
[DE87-703693] 04 p0416 N88-12578

ALKALOIDS
NT ATROPINE
NT CAFFEINE
NT ERGOTAMINE
NT MORPHINE

ALKANES
NT BUTANES
NT CETANE
NT ETHANE
NT METHANE
NT PARAFFINS
NT PROPANE
Organic molecules on meteoritic solid substrates
[NASA-CR-181570] 05 p0560 N88-13411
Photolytic formation of free radicals and their effect on hydrocarbon pyrolysis chemistry in a concentrated solar environment
[DE88-004129] 13 p1794 N88-20730

ALKENES
NT BUTENES
NT ETHYLENE
NT PROPYLENE
NT VINYLIDENE
Chemical activation of molecules by metals: Experimental studies of electron distributions and bonding
[DE88-004465] 10 p1407 N88-18393
Photolytic formation of free radicals and their effect on hydrocarbon pyrolysis chemistry in a concentrated solar environment
[DE88-004129] 13 p1794 N88-20730
Evaluation of the acute toxicity of a synthetic polyalphaolefin-based hydraulic fluid
[AD-A190412] 15 p2045 N88-22184

ALKYL COMPOUNDS
Separation of anionic from nonionic alkoxy compounds using silica gel
[GB-PATENT-2-140-415-A] 01 p0020 N88-10122
Surface catalytic degradation study of two linear perfluoropolyalkylethers at 345 C
[NASA-TP-2774] 04 p0410 N88-12543
Improved perfluoroalkylether fluid development
[NASA-CR-180872] 08 p0967 N88-15851
The performance of perfluoropolyalkylether oils under boundary lubrication conditions
[AD-A191057] 17 p2323 N88-23869
A study of solvent effects on the synthesis of pure component and composite ceramic powders by metal alkoxide hydrolysis
[DE88-008381] 20 p2777 N88-26470

ALKYLATION
Evaluation of direct methane conversion to higher hydrocarbons and oxygenates
[DE88-003812] 15 p2049 N88-22204

ALKYNES
NT ACETYLENE
NT OXYACETYLENE

ALL-WEATHER AIR NAVIGATION
Rotor SAR (ROSAR): A new high-resolution all-weather vision method for helicopters
[MBB-UA-1046/87] 10 p1314 N88-17855

ALLOCATIONS
NT RESOURCE ALLOCATION
An allotment planning concept and related computer software for planning the fixed satellite service at the 1988 space WARC
[NASA-TM-100244] 03 p0308 N88-11944
Architecture for dynamic task allocation in a man-robot symbiotic system
[DE87-013872] 03 p0362 N88-12277
Engineering calculations for the Delta S method of solving the orbital allotment problem
[NASA-CR-182372] 06 p0671 N88-14110
Dynamic function allocation in fighter cockpits
[AD-A185397] 09 p1201 N88-17199
Task allocation in a distributed computing system 09 p1206 N88-17230
Allocation of database files across parallel stores for efficient processing of partial-match queries
[AD-A188196] 11 p1565 N88-19371
An intelligent allocation algorithm for parallel processing
[NASA-CR-182648] 12 p1675 N88-20014

On two-stage allocation procedures for selection problems
[AD-A190766] 15 p2126 N88-22675
Topics in adaptive control and inference
[AD-A194718] 23 p3266 N88-29443

ALLOYING
De-alloying
[DE87-012488] 01 p0022 N88-10139
A study of surface tension driven segregation in monotectic alloy systems
[NASA-CR-182894] 16 p2178 N88-22983
Ion beam alloying of aluminum for corrosion resistance 17 p2321 N88-23860
Shape memory alloys: New materials for future engineering
[NASA-TT-20193] 20 p2775 N88-26455

ALLOYS
NT ALUMINUM ALLOYS
NT ANTIMONY ALLOYS
NT ASTROLOY (TRADEMARK)
NT AUSTENITIC STAINLESS STEELS
NT BAINITIC STEEL
NT BEARING ALLOYS
NT BERYLLIUM ALLOYS
NT BINARY ALLOYS
NT BORON ALLOYS
NT BRASSES
NT BRONZES
NT CARBON STEELS
NT CAST ALLOYS
NT CHROMIUM ALLOYS
NT CHROMIUM STEELS
NT COBALT ALLOYS
NT COPPER ALLOYS
NT EUTECTIC ALLOYS
NT FERRITIC STAINLESS STEELS
NT GERMANIUM ALLOYS
NT GOLD ALLOYS
NT HASTELLOY (TRADEMARK)
NT HEAT RESISTANT ALLOYS
NT HIGH STRENGTH ALLOYS
NT HIGH STRENGTH STEELS
NT INCONEL (TRADEMARK)
NT INDIUM ALLOYS
NT IRON ALLOYS
NT LEAD ALLOYS
NT LIGHT ALLOYS
NT LIQUID ALLOYS
NT LITHIUM ALLOYS
NT LOW CARBON STEELS
NT MAGNESIUM ALLOYS
NT MANGANESE ALLOYS
NT MARAGING STEELS
NT MARTENSITIC STAINLESS STEELS
NT MOLYBDENUM ALLOYS
NT MONOTECTIC ALLOYS
NT NICKEL ALLOYS
NT NICKEL STEELS
NT NIMONIC ALLOYS
NT NIOBIUM ALLOYS
NT NITINOL ALLOYS
NT QUATERNARY ALLOYS
NT RARE EARTH ALLOYS
NT REFRACTORY METAL ALLOYS
NT RHENIUM ALLOYS
NT SHAPE MEMORY ALLOYS
NT SILICON ALLOYS
NT SILVER ALLOYS
NT SOLDERS
NT STAINLESS STEELS
NT STEELS
NT TANTALUM ALLOYS
NT TELLURIUM ALLOYS
NT TERNARY ALLOYS
NT THALLIUM ALLOYS
NT TIN ALLOYS
NT TITANIUM ALLOYS
NT TUNGSTEN ALLOYS
NT URANIUM ALLOYS
NT VANADIUM ALLOYS
NT ZINC ALLOYS
NT ZIRCONIUM ALLOYS
A physical metallurgical basis for heat-affected zone and base-plate properties of a microalloyed HSLA steel
[AD-A180200] 01 p0022 N88-10137
De-alloying
[DE87-012488] 01 p0022 N88-10139
Equations for determining CVD tungsten-rhenium alloy composition and plating rate
[DE87-006831] 01 p0024 N88-10152
Formation of amorphous alloys by solid state reactions
[DE87-013175] 02 p0146 N88-10918
Investigation of the structure of coatings of self fluxing alloys fused by laser energy
[BLL-M-37301-(5828.4)] 02 p0148 N88-10930
Elevated temperature strain gages 02 p0184 N88-11144
Creep fatigue life prediction for engine hot section materials (isotropic): Third year progress review 02 p0188 N88-11173
Life prediction and constitutive models for engine hot section anisotropic materials program 02 p0188 N88-11175
Effects of surface chemistry on hot corrosion life 02 p0189 N88-11180
Modelling and theories of alloy phase behavior
[DE87-014399] 03 p0287 N88-11804
A fundamental study of the mechanical and microstructural response of elevated temperature PM aluminum-titanium alloys 03 p0289 N88-11819
Ultra-fine grained alloy material
[AD-A184500] 03 p0290 N88-11820
Progress in the development of niobium alloyed high speed steel
[DE87-703549] 04 p0415 N88-12576
An expert system for materials design
[DE88-000191] 04 p0483 N88-12974
The mechanism by which sigma-phase forms in Fe-Cr-Ni system alloys
[BLL-M-37380-(5828.4)] 05 p0564 N88-13437
Corrosion resistance of sintered alloy steels
[BLL-M-37363-(5828.4)] 05 p0564 N88-13438
Projects within the Center for Advanced Materials
[PB88-123054] 06 p0677 N88-14143
Study of the embedded atom method of atomistic calculations for metals and alloys
[DE88-002798] 07 p0835 N88-15065
Rare earth elements in heat treatable steels
[PB87-144002] 08 p0968 N88-15858
Mechanisms of intergranular attack and stress corrosion cracking of alloy 600 by high-temperature caustic solutions containing impurities
[DE87-012820] 10 p1300 N88-17773
Transmission electron microscopy studies of titanium-containing braze/alumina seals
[DE88-005243] 10 p1303 N88-17792
Strength and structure of Ga sub 1-xIn sub xAs alloys
[AD-A188092] 10 p1303 N88-17795
Electronic structure of random alloys and the theory of ordering processes
[DE88-004476] 10 p1407 N88-18394
Tight binding theory of semiconductors 10 p1415 N88-18447
Corrosion performance of high damping alloys in 3.5 percent sodium chloride environment
[AD-A188048] 11 p1457 N88-18687
Institute for Materials Science and Engineering, Metallurgy: Technical activities 1987
[PB88-157722] 11 p1460 N88-18702
National Center for Small-Angle Scattering Research: Reports on measurements carried out by users of the facilities of the NCSASR, December 1, 1985-September 30, 1987
[DE88-003754] 11 p1462 N88-18719
Electron paramagnetic resonance studies of Mn(2+) in 2-6 semiconductor alloys 11 p1560 N88-19340
Electronic structure and phase stability of alloys
[DE88-004574] 11 p1562 N88-19350
JPRS report: Science and technology. USSR: Materials science
[JPRS-UMS-87-009] 14 p1884 N88-21261
Electrical resistivities of some compound forming liquid metal alloys
[PB88-145172] 15 p2037 N88-22137
Bithermal fatigue: A simplified alternative to thermomechanical fatigue 15 p2064 N88-22424
Protective coatings on metals, volume 10
[PB88-174461] 16 p2181 N88-23000
Noncontact temperature measurement: Requirements and applications for metals and alloys research 17 p2328 N88-23899
Predictive corrosion modeling, volume 1
[AD-A191229] 18 p2485 N88-24739
Effect of size of precipitates on recrystallization temperatures in Cu-Cr, Cu-Zr, and Cu-Zr-Cr alloys
[NASA-TT-20166] 18 p2489 N88-24763
On quench sensitivity of Cu-Cr alloys
[NASA-TT-20174] 18 p2489 N88-24765
Solid-state combustion synthesis of ceramics and alloys in reduced gravity
[NASA-CR-4163] 19 p2608 N88-25479
Plastic deformation and roughness of free metal surfaces
[PB88-195621] 20 p2772 N88-26439
EXAFS studies of the microstructure of semiconductor alloys, defects and semiconductor-metal interfaces 20 p2868 N88-27031
Non-equilibrium phases and phase diagrams
[DE88-008896] 20 p2980 N88-27098
On the systematics of phase transformation in metallic alloys
[DE88-008041] 21 p2913 N88-27288
Theoretical predictions of precipitate shapes in cubic alloys
[DE88-010856] 21 p2914 N88-27291
Oxidation-erosion of metals and alloys: Models, verification, and prediction
[DE88-010016] 21 p2915 N88-27300
Refractory metal alloys and composites for space power systems
[NASA-TM-100946] 21 p2916 N88-27310
Thermal conductivity of isotopically pure semiconductors, superlattices, semiconductor alloys and semiconductors as a function of temperature; control of the segregation coefficient in LEC crystal growth; and photo-Hall measurements of GaAs 21 p2927 N88-27375
Significance of the local electrode potential within pits, crevices and cracks
[AD-A192482] 21 p2935 N88-27432
Study of the erosion corrosion of alloys and coatings
[AD-A194337] 22 p3055 N88-28128
Equipment for the pressure welding of metals and alloys utilising the effects of superplasticity
[RAE-TRANS-2162] 22 p3055 N88-28129
The VPE-hydride technique with alloy source: Equilibrium analysis
[AD-A194036] 22 p3157 N88-28784
Influence of local volume forces on surface relaxation of pure metals and alloys: Applications to Ni, Al, Ni3Al
[DE88-702718] 23 p3195 N88-29014

ALLUVIUM
Stochastic geologic effects on near-field ground motions in alluvium
[AD-A192315] 21 p2972 N88-27652

ALMUCANTAR
U ELEVATION ANGLE

ALOHA SYSTEM
Spatial distribution of traffic in a cellular mobile data network
[EUT-87-E-168] 14 p1904 N88-21378
L-band and SHF multiple access schemes for the MSAT system 19 p2650 N88-25734
Integrated voice/data protocols for satellite channels 19 p2651 N88-25739

ALOUETTE SATELLITES
Alouette-ISIS program summary
[NASA-CR-180747] 08 p1023 N88-16195

ALPHA DECAY
Modeling of irradiation-induced amorphization in a titanate ceramic
[DE87-014751] 03 p0292 N88-11833

ALPHA PARTICLES
Feasibility of alpha particle measurement in a magnetically confined plasma by CO2 laser Thomson scattering
[DE88-000039] 02 p0241 N88-11522
Theoretical plasma physics
[DE88-001475] 04 p0492 N88-13029
Slowing down tail enhanced, neoclassical and classical alpha particle fluxes in tokamak reactors
[DE88-001930] 06 p0783 N88-14806
Long-term-aging embrittlement of cast duplex stainless steels: Mechanism and kinetics
[DE88-002929] 09 p1145 N88-16861
Influence of fast alpha diffusion and thermal alpha buildup on Tokamak reactor performance
[DE88-003661] 09 p1251 N88-17496
Problems in modeling TF ripple loss of fast alphas from a tokamak reactor
[DE88-000612] 11 p1553 N88-19296
Simulation of nuclear collisions at high energies in the frames of quark-gluon string model
[DE88-700914] 12 p1690 N88-20113
The calibration of photographic and spectroscopic films: The response of 2aO film to small dosages of alpha particles from 3/10th's rad to 8 rads at energy levels 153 MeV, 79 MeV and 47 MeV
[NASA-CR-177830] 13 p1773 N88-20608
Spectroscopic data relevant to alpha particle diagnostics 17 p2442 N88-24527
Infrared and far-infrared laser development for plasma diagnostics at Oak Ridge National Laboratory
[DE88-007262] 19 p2674 N88-25904
Design and calibration of a two-channel low-noise heterodyne receiver for use in a CO2 laser Thomson scattering alpha particle diagnostic
[DE88-007866] 19 p2728 N88-26201
A CO2 laser Thomson scattering diagnostic for fusion product alpha particle measurement
[DE88-007683] 20 p2857 N88-26965
The distribution of some chemical elements between dissolved and particulate phases in the ocean
[DE88-010181] 21 p2977 N88-27682

Measure of hydrogen concentration profile in materials by resonant nuclear reactions
[DE88-702599] 23 p3193 N88-28999

ALPHA RADIATION
U ALPHA PARTICLES

ALPHABETS
Errors associated with Russian name transliteration
[DE87-011717] 02 p0248 N88-11566

ALPHANUMERIC CHARACTERS
NT BINARY DIGITS
NT DIGITS
Comparison of alphanumeric data entry methods for advanced helicopter cockpits
[AD-A186934] 09 p1201 N88-17201
A comparison of two chord keyboard coding systems for alphanumeric data entry
[AD-A189230] 13 p1813 N88-20834

ALPINE METEOROLOGY
The 54-hours continuous post-frontal precipitation north of the Alpine mountain barrier, 22-25 August 1975
02 p0203 N88-11268
Study of isolated convective clouds in the lower Alps in summer 1984, using radar and a simple Weinstein numerical model
[ESA-TT-1061] 03 p0353 N88-12224
Research work at the Meteorological Institute of the University of Munich (Federal Republic of Germany)
[MITT-56] 08 p1013 N88-16141
Cross flow in the Alps and flat foehn during the experiment MERKUR --- mesoscale experiment
08 p1013 N88-16142
Energy balance and discharge of an Alpine glacier, illustrated by Mount Vernagtferner in the Oetzal Alps, Tyrol 08 p1014 N88-16145
Results of the experiment MERKUR: Structural change of a weak cold front in the sphere of influence of the Alps --- mesoscale experiment 08 p1014 N88-16146
Vertical sounding of th air layer close to a glacier on Mount Vernagferner in the Oetzal Alps, Tyrol (experiment LUZIVER 1983) 08 p1015 N88-16152
Simulation of a lee cyclogenesis using a numerical model 08 p1016 N88-16162
Simulations of thermally induced winds and cross flow situations
[MITT-57] 09 p1193 N88-17148
An analytical method for the determination of the average horizontal wind velocities across two-dimensional hills
[ISBN-3-923624-06-9] 11 p1515 N88-19048
The German Front Experiment 1987: Experimental design
[DFVLR-MITT-87-24] 16 p2234 N88-23343

ALPS MOUNTAINS (EUROPE)
Energy balance and discharge of an Alpine glacier, illustrated by Mount Vernagtferner in the Oetzal Alps, Tyrol 08 p1014 N88-16145
Results of the experiment MERKUR: Structural change of a weak cold front in the sphere of influence of the Alps --- mesoscale experiment 08 p1014 N88-16146
Statistics of two-dimensional structure elements of mountainous ranges (mosaic model) for calculating three-dimensional reflection functions
[DFVLR-FB-87-33] 09 p1185 N88-17099
The Monte Generoso-Zimmerwald (Switzerland) baseline from satellite laser ranging data using various analysis techniques
[LR-533] 14 p1940 N88-21576
The German Front Experiment 1987: Experimental design
[DFVLR-MITT-87-24] 16 p2234 N88-23343
SPOT image exploitation for glacial mass balance fluctuation monitoring in the French Alps
22 p3090 N88-28350

ALTERATION
U REVISIONS

ALTERNATING CURRENT
Evaluation of stand-alone inverters for remote applications
[DE87-010957] 01 p0040 N88-10257
Comparison of costs and benefits for dc and ac transmission
[DE87-008774] 02 p0167 N88-11052
Output power enhancement of AC Raman free-electron laser
[DE88-000503] 04 p0449 N88-12786
Sliding charge density waves and related problems
[AD-A186720] 09 p1157 N88-16934
The theory and implementation of a high quality pulse width modulated waveform synthesiser applicable to voltage FED inverters
[ETN-87-90712] 09 p1157 N88-16937
Application of ac-impedance method on determination of corrosion rate of metals
[DE88-750307] 10 p1300 N88-17771
Advanced capacitor development
[AD-A189985] 15 p2059 N88-22276
AC impedance analysis of corrosion fatigue in naval aircraft alloys
[AD-A190822] 17 p2322 N88-23865
Some equivalent circuit models for AC impedance analysis of pyrite/solution interface
[DE88-010574] 21 p2939 N88-27452

ALTERNATING CURRENT GENERATORS
U AC GENERATORS

ALTERNATING DIRECTION IMPLICIT METHODS
A finite-element alternating method for two-dimensional Mode-1 crack configurations
[NASA-TM-100616] 16 p2224 N88-23276

ALTERNATIVES
Compendium of significant events in the recent development of alcohol fuels in the United States
[DE87-013355] 01 p0032 N88-10202
Alternative fuels: Information on DOD's (Department of Defense's) methanol vehicle program
[PB87-213328] 02 p0156 N88-10976
Application of electronic fuel injection to the optimum engine for methanol utilization
[PB87-201950] 02 p0180 N88-11120
A systems analysis of fire suppression alternatives for the US space station
[AD-A189847] 15 p2025 N88-22064

ALTERNATORS (GENERATORS)
U AC GENERATORS

ALTIMETERS
NT LASER ALTIMETERS
NT RADIO ALTIMETERS
The global positioning system as an aid to the testing of inertial navigation units (volume 1, addendum 1)
[AD-A185783] 12 p1578 N88-19443
Integrated multisensor navigation systems
17 p2294 N88-23722

ALTIMETRY
NT SATELLITE ALTIMETRY
Considering refraction in leveling with laser plane
04 p0462 N88-12857
Tidal estimation in the Pacific with application to SEASAT altimetry
[NASA-TM-100694] 13 p1803 N88-20780
Criteria for planimetric and altimetric correction of maps restituted from aerial photographs in 1:100,000 scale
17 p2367 N88-24097

ALTITUDE
NT FLIGHT ALTITUDE
NT HIGH ALTITUDE
NT LOW ALTITUDE
NT SEA LEVEL
Analysis of the inter-layer independence of stellar scintillometer profiles of Cn2
[AD-A189372] 12 p1645 N88-19854
A model of the ionosphere in the altitude interval 50 to 4000 km. Part 1: Atomic ions (H(+), He(+), N(+), O(+))
[DFVLR-FB-88-11-PT-1] 23 p3233 N88-29241

ALTITUDE ACCLIMATIZATION
Differentiation of hemopoietic stem cells during adaptation to high altitude 07 p0893 N88-15410
Mononuclear phagocytes during adaptation of essentially healthy people to high altitudes
07 p0896 N88-15432
Biorhythmic aspects of intercontinental Antarctic adaptation 08 p1046 N88-16321
Dexamethasone as prophylaxis for acute mountain sickness: Effect of dose level
[AD-A185848] 08 p1047 N88-16325
Status of microcirculation in high-altitude blood loss
12 p1663 N88-19973
Depressed sweating during exercise at altitude
[AD-A192603] 22 p3130 N88-28609
Human acclimatization and physical performance at high altitude
[AD-A192651] 22 p3130 N88-28611
Influence of altitude and caffeine during rest and exercise on plasma levels of proenkephalin peptide F
[AD-A192659] 22 p3131 N88-28616
Biomedical aspects of military operations at high altitude
[AD-A192677] 22 p3132 N88-28619
Alterations in upper extremity motor function in soldiers during acute high altitude exposure
[AD-A192676] 23 p3238 N88-29272

ALTITUDE CONTROL
Magnetic emissions testing of the space station engineering model resistojet
[NASA-TM-100788] 10 p1292 N88-17728
The exploitation of Aircraft Integrated Monitoring System (AIMS) data in height-keeping studies for aircraft operating above FL 290 22 p3036 N88-28026

ALTITUDE SICKNESS
Dexamethasone as prophylaxis for acute mountain sickness: Effect of dose level
[AD-A185848] 08 p1047 N88-16325
Medical problems related to altitude in: Human performance physiology and environmental medicine at terrestrial extremes, chapter 14
[AD-A188340] 12 p1666 N88-19989
Acute mountain sickness at 4500 m is not altered by repeated eight-hour exposures to 3200-3550 m normobaric hypoxic equivalent
[AD-A188358] 12 p1666 N88-19990
Human acclimatization and physical performance at high altitude
[AD-A192651] 22 p3130 N88-28611
Alterations in cutaneous vasomotor regulation during acute and chronic hypoxia
[AD-A192653] 22 p3131 N88-28612
Biomedical aspects of military operations at high altitude
[AD-A192677] 22 p3132 N88-28619
Alterations in upper extremity motor function in soldiers during acute high altitude exposure
[AD-A192676] 23 p3238 N88-29272

ALTITUDE SIMULATION
Cooling electronic equipment at simulated high altitude in hypobaric chambers
[AD-A185196] 05 p0584 N88-13560
Oxygen transport during exercise at extreme simulated altitude: Operation Everest 2
[AD-A185720] 06 p0752 N88-14620
Operation Everest 2: Comparison of four instruments for measuring blood oxygen saturation
[AD-A186456] 08 p1049 N88-16337
Altitude simulation testing of Ariane's second-stage engine 09 p1126 N88-16747
Experimental evaluation of turning vane designs for high-speed and coupled fan-drive corners of 0.1-scale model of NASA Lewis Research Center's proposed altitude wind tunnel
[NASA-TP-2681] 10 p1285 N88-17686
Age, alcohol, and simulated altitude: Effects on performance and breathalyzer scores
[AD-A190642] 15 p2103 N88-22531
Techniques utilized in the simulated altitude testing of a 2D-CD vectoring and reversing nozzle
[NASA-TM-100872] 19 p2604 N88-25464
Analysis of clinical symptoms of human decompression sickness during altitude chamber studies
19 p2703 N88-26074

ALTITUDE TESTS
Measured performance of the heat exchanger in the NASA icing research tunnel under severe icing and dry-air conditions
[NASA-TM-100116] 04 p0451 N88-12796
Techniques utilized in the simulated altitude testing of a 2D-CD vectoring and reversing nozzle
[NASA-TM-100872] 19 p2604 N88-25464

ALTITUDE TOLERANCE
Effect of pyrocetam on mouse resistance to hypoxic hypoxia 2-3 months after exposure to X-radiation
07 p0895 N88-15425
Operation Everest 2: Alterations in the immune system at high altitude
[AD-A188011] 11 p1520 N88-19075
Analysis of clinical symptoms of human decompression sickness during altitude chamber studies
19 p2703 N88-26074

ALU (COMPUTER COMPONENTS)
U ARITHMETIC AND LOGIC UNITS

ALUMINA
U ALUMINUM OXIDES

ALUMINATES
Conductivity studies on hydroxide ion conductors in the Li-Al-O-H system at intermediate temperatures
[AD-A185714] 06 p0697 N88-14279
Phase behavior in the Li-Al-O-H system at intermediate temperatures
[AD-A185732] 06 p0697 N88-14280

ALUMINIDES
Advances in processing techniques for nickel aluminides
[DE87-014571] 05 p0566 N88-13449
Development of iron aluminides
[AD-A185190] 05 p0568 N88-13461
Elevated temperature crack growth studies of advanced titanium aluminides
[AD-A189025] 12 p1608 N88-19618
Chemical compatibility between silicon carbide and a nickel aluminide
[DE88-006188] 18 p2479 N88-24708
Hot isostatic pressing of nickel aluminide powders
[DE88-009677] 19 p2617 N88-25525
Nickel aluminides: A new family of nickel + aluminum alloys featuring simple composition, low density, excellent oxidation resistance and high yield strength that increases with temperature
[DE88-010692] 20 p2776 N88-26481

A fundamental understanding of the interfacial compatibility in hybrid material systems
[AD-A192921] 21 p2909 N88-27264
ALUMINIZING
U ALUMINUM COATINGS
ALUMINUM
Large-strain softening of aluminum at elevated temperature
[DE87-011559] 01 p0024 N88-10153
Observations of localized grain boundary dislocations in series of (001) and (110) symmetrical tilt boundaries in aluminum
[DE87-014011] 01 p0025 N88-10156
Polyitaconic acid macromolecule primer for adhesive bonding and corrosion control of aluminum
[DE87-013306] 01 p0027 N88-10173
Relation between shock strength and strain-rate plasticity at maximum deviatoric stress
[DE87-011736] 01 p0061 N88-10390
Accurate ab initio calculations which demonstrate a 3 Pi u ground state for Al2
[NASA-TM-89302] 01 p0102 N88-10666
A simulation study of interfaces in Ni, Al and Ni3Al with and without boron
[DE87-013156] 01 p0102 N88-10667
Mathematical modelling of solar ultraviolet radiation induced optical degradation in anodized aluminum
02 p0135 N88-10846
Factors determining the morphology of precipitation in aluminum-germanium and aluminum-silicon alloys
[DE87-014682] 03 p0287 N88-11806
The infiltration kinetics of aluminum in silicon carbide compacts
[AD-A184682] 03 p0290 N88-11823
Aluminum oxynitride spinel (ALON): A review
[AD-A184753] 03 p0294 N88-11845
Defect characterization in quartz and related materials
[AD-A184754] 03 p0294 N88-11846
Carbon-fiber reinforced aluminum
04 p0403 N88-12507
Data base on the high heat flux behaviour of metals and carbon materials for plasma facing components: Experiments at the 10 MW neutral beam injection test stand of the IPP Nagoya
[IPPJ-AM-53] 04 p0492 N88-13031
Microstructural change of Al on H implantation
[IPPJ-847] 04 p0493 N88-13036
Plasticity of aluminum and iron at high shear strain rate and high pressure 05 p0563 N88-13430
X-ray analysis of polycrystalline aluminium subjected to fatigue cycling
[NAL-TM-MT-8706] 05 p0564 N88-13434
The growth of persistent slip bands
05 p0597 N88-13648
Temperature dependent mechanical properties of an alumina fiber reinforced aluminum composite
06 p0677 N88-14147
Bending properties of aluminum base composite with CVD-fiber
[PB87-130678] 06 p0678 N88-14156
The effect of temperature on fatigue crack initiation from aluminosilicate inclusions 06 p0720 N88-14427
Chromic acid anodizing of aluminum foil
[NASA-CR-178417] 07 p0837 N88-15077
J-estimation procedure based on moire interferometry data
[AD-A185965] 07 p0867 N88-15258
Nb3Al formation in sputter-deposited Nb/Al multi-layer samples
[DE88-003192] 08 p0970 N88-15868
Investigation on diffusion reaction brazing of aluminium
[PB87-143358] 08 p0992 N88-16001
The effect on initial bond strength and durability of a Phosphoric Acid Dip (PAD) following chromic acid anodising of aluminum
[ARE-TM(UMM)-87402] 10 p1300 N88-17772
Investigation of materials for inert electrodes in aluminum electrodeposition cells
[DE88-003380] 10 p1323 N88-17906
Strategic placement of accelerometers to measure forces by the sum of weighted accelerations
[DE88-002262] 10 p1333 N88-17968
Durability and damage tolerance of aluminum castings
[AD-A186444] 10 p1341 N88-18013
Evaluation and compilation of thermodynamic properties of high temperature chemical species
[AD-A187509] 11 p1452 N88-18654
Dynamical properties of aluminium from experimental dispersion relations
[DE88-700240] 11 p1459 N88-18697
Study of the vibrational modes of subsurface oxygen on Al (111) using diode laser infrared reflection-absorption spectroscopy
[AD-A188322] 12 p1632 N88-19769
X-ray source model for Z-pinch aluminum plasmas
[AD-A189509] 12 p1696 N88-20148
The effect of microstructure on the fatigue crack growth resistance of nickel base superalloys
[AD-A189526] 13 p1741 N88-20414
Aluminum-air battery development
[DE88-006617] 13 p1762 N88-20542
Aluminum-air battery development
[DE88-006618] 13 p1762 N88-20543
Development of a manufacturing unit for selective coating of solar absorbers made out of aluminum
[BMFT-FB-T-86-204] 14 p1942 N88-21590
Fabrication and electrical characterization of multilevel aluminum interconnects used to achieve silicon-hybrid wafer-scale integration
[AD-A190519] 15 p2060 N88-22282
Polyitaconic acid macromolecule primer for adhesive bonding and corrosion control of aluminum
17 p2319 N88-23849
The variation of torsional ductility of high-purity aluminum with temperature and strain rate
[DE88-005618] 18 p2487 N88-24755
Plate response analysis using shock tube
[AD-A190828] 18 p2526 N88-24987
A numerical study of Rayleigh-Taylor instability in aluminum and steel plates
[DE88-010475] 20 p2774 N88-26449
A finite element analysis for the hydroforming of aluminum
[DE88-008050] 20 p2784 N88-26516
Crystallization of aluminum hydroxide in the aluminum-air battery: Literature review, crystallizer design and results of integrated system tests
[DE88-010510] 20 p2797 N88-26594
Ultraviolet-visible spectroscopy of laser-produced aluminum plasmas
[AD-A193004] 20 p2860 N88-26990
Electronic and geometric structure of silver and palladium on aluminum (111) in monoatomic surface layers
[ETN-88-92120] 20 p2879 N88-27093
Evaluation of explosive bonding for patching aluminum with aluminum
[AD-A193303] 21 p2913 N88-27285
Nuclear magnetic resonance spectrometer
[AD-A192928] 21 p2950 N88-27523
Growth and characterization of CuGaS2, CuAlS2 and CuGa0.9Al0.1S2 single crystals
[AD-A192963] 21 p3021 N88-27930
The 2D Rydberg series in Al I
[NASA-TM-101189] 22 p3150 N88-28740
Initiation of explosive molten aluminum-water interactions at wet or underwater surfaces
[DE88-004686] 23 p3194 N88-29006
Relation between strength, creep and relaxation behavior in Cu and Al at room temperature
[ETN-88-92982] 23 p3195 N88-29015
Muon-spin rotation experiment (micro + SR) on aluminum and indium after low temperature electron irradiation
[ETN-88-92985] 23 p3294 N88-29617
Fatigue crack growth characteristics of ARALL (trademark)-1
[AD-A196185] 24 p3341 N88-29889
High frequency GaAlAs modulator and photodetector for phased array antenna applications
[NASA-TM-101328] 24 p3367 N88-30048
Development of graded reference radiographs for aluminum welds, phase 1
[AD-A195594] 24 p3381 N88-30140
ALUMINUM ALLOYS
Contribution to the study of the Ti-Al phase diagram by conventional and high resolution electron microscopy
[ESA-TT-1021] 01 p0023 N88-10143
Evaluation of cracking in aluminum cylinders
[PB87-201398] 01 p0024 N88-10149
Crack propagation behavior of the materials StE 460 and AlMg 4.5Mn
[FD-1/1986] 01 p0058 N88-10373
Monte Carlo calculations for the simulation of channeling experiments on irradiated aluminum alloys. Calculation of angle-dependent efficiency curves
[HMI-B-433] 01 p0092 N88-10597
An investigation of the high strain rate deformation of SiCw/2124 Al composite
[OUEL-1675/87] 02 p0142 N88-10895
Development of a pilot plant for the production of rapidly solidified aluminum alloy powders
[BMFT-FB-T-86-153] 02 p0146 N88-10914
Study of the microscopic mechanisms of cyclic deformation. Development of a new approach: The case of aluminum
[ISAL-87-0003] 02 p0149 N88-10936
Coating life prediction 02 p0189 N88-11181
Corrosion resistance of silver-plated carbon-aluminum composite 03 p0285 N88-11793
A fundamental study of the mechanical and microstructural response of elevated temperature PM aluminum-titanium alloys 03 p0289 N88-11819
Gas tungsten arc welding of Al-10Fe-5Ce
[AD-A184202] 03 p0334 N88-12104
Corrosion behavior of P/M mechanically alloyed IN-9052.1: An electro-chemical investigation
[AD-A184191] 04 p0414 N88-12567
Weldability of 2219-T851 and 2519-T87 aluminum armor alloys for use in Army vehicle systems
[AD-A184296] 04 p0451 N88-12792
Investigation by differential scanning calorimetry of microstructure in a superplastic Al-Mg-Zr alloy
[AD-A184902] 05 p0564 N88-13439
A fundamental study of P/M processed elevated temperature aluminum alloys
[AD-A185393] 05 p0565 N88-13445
Phase diagram and thermochemical properties of the Al-Cu system
[ETN-88-91015] 05 p0566 N88-13447
An investigation of unipolar arcing at atmospheric pressure in aluminum 2024 and aluminum coated glass slides
[AD-A184903] 05 p0577 N88-13521
The effect of ion beam mixed Ni-Al surface layers on PSB extrusion morphology in fatigued nickel
05 p0598 N88-13652
The evolution of local mechanical properties of Al 2219-T851 during fatigue 05 p0598 N88-13653
Cyclic deformation of an extruded AlMgSi alloy
05 p0598 N88-13654
Closure behavior under constant effective stress intensity loading conditions 05 p0598 N88-13656
Growth of short fatigue cracks in a squeeze formed aluminum alloy 05 p0598 N88-13658
Influence of microstructure and aging condition on the fatigue crack propagation in age hardened aluminium alloys 05 p0599 N88-13659
Fatigue crack growth behavior of A356-T6 cast aluminum alloy 05 p0599 N88-13660
Behavior of short cracks in a 2024 aluminum alloy sheet tested at several stress ratios 05 p0600 N88-13669
The effect of microstructure on the surface crack length: Crack depth relationship for short cracks
05 p0600 N88-13670
On the role of crack tip shielding in influencing the behavior of long and small fatigue cracks in aluminum-lithium alloy 2090 05 p0600 N88-13671
The influence of microstructure and residual stresses on the initiation and propagation of short surface cracks on AlMgSi1 05 p0601 N88-13674
An experimental study of closure behavior of naturally initiated small cracks 05 p0601 N88-13676
Propagation of small fatigue cracks in 2024-T3 aluminum alloy 05 p0601 N88-13678
Fatigue crack retardation in aluminium alloys
05 p0602 N88-13681
Observations on the effect of overloads on fatigue crack growth 05 p0602 N88-13684
Crack growth in contrasting titanium alloys under the conjoint action of high and low cycle fatigue
05 p0602 N88-13686
Variable amplitude fatigue crack growth in aluminum alloys 2090-T8E41 and 7075-T651
05 p0602 N88-13687
Effects of MN dispersoids on near threshold fatigue crack growth in 2134 type alloys
05 p0603 N88-13692
Fatigue mechanisms in ARALL, a fatigue resistant hybrid aluminum aramid composite material
05 p0605 N88-13711
A comparison of plastic work energy and external input for fatigue crack propagation 05 p0607 N88-13722
X-ray fatigue failure prediction based on plasticity response to microcracks 05 p0607 N88-13725
Environmentally assisted fatigue crack growth
05 p0608 N88-13731
Fatigue crack growth 05 p0608 N88-13734
Characterization of the microstructures of various materials
[AD-A184961] 05 p0655 N88-14017
Study of surface treatment before bonding of light alloys
[DCQ/L-48-287/F] 06 p0682 N88-14181
The effect of shear lips on fatigue crack growth in Al-2024 sheet material 06 p0718 N88-14408
Study of the evolution of short cracks in fatigue analysis — aircraft construction materials
[DCQ/L-48-555] 06 p0722 N88-14442
Effect of overload ratios on fatigue crack growth behavior in Ti-6Al-4V alloy
[PB87-147062] 07 p0833 N88-15055
Study on the square wave alternating plasma arc welding for aluminum alloys
[PB87-143772] 07 p0863 N88-15239

Examination of the physical processes associated with the keyhole region of variable polarity plasma arc welds in aluminum alloy 2219
07 p0927 N88-15634
X-ray measurements of phason distortion in ion-implanted Al-Mn
[DE87-014566] 07 p0937 N88-15694
Investigation of microstructural factors that cause low fracture toughness in silicon carbide whisker/Al alloy composites
[AD-A186443] 09 p1137 N88-16817
Multipurpose corrosion inhibitors for aerospace materials in Naval environments
[AD-A186728] 09 p1143 N88-16853
Adhesive bond strengths on aluminium alloys as a function of surface topographies and their wetting properties
[ARE-TM(UMM)-87403] 09 p1148 N88-16880
Micro-mechanisms of deformation in SiC/Al composites
[AD-A188282] 10 p1296 N88-17749
Environment assisted degradation mechanisms in aluminum-lithium alloys
[NASA-CR-182482] 10 p1301 N88-17782
Corrosion behavior of sputter-deposited aluminum-based alloys exposed to chloride solutions
[AD-A187262] 10 p1303 N88-17794
The metallurgical database of Aladin: An alloy de sign system
[AD-A187724] 11 p1457 N88-18682
Study of the effects of metallurgical factors on the growth of fatigue microcracks
[AD-A188475] 12 p1608 N88-19615
Development of metastable processing paths for high temperature alloys
[AD-A188682] 12 p1608 N88-19617
Thermal-mechanical fatigue testing of a titanium-aluminide alloy
[AD-A189555] 12 p1609 N88-19620
Composites strengthening
[AD-A189258] 13 p1734 N88-20364
Threshold fatigue crack growth in Ti-6Al-2Sn-4Zr-6Mo
[AD-A189560] 13 p1741 N88-20415
A calorimetric determination of the enthalpy of formation and a description of the defect structure of the ordered beta-phase /Ni, Cu/ /1-x/ Al/x/
[NASA-TT-20157] 13 p1745 N88-20434
Processing of glass to aluminum (low melting metals) seals via an injection molding technique
[DE88-004689] 13 p1751 N88-20468
Processing, physical metallurgy and creep of NiAl + Ta and NiAl + Nb alloys
[NASA-CR-182113] 14 p1890 N88-21295
Electron diffraction evidence for the ordering of excess nickel atoms by relation to stoichiometry in nickel-rich beta'-NiAl formation of a nickel-aluminum (Ni2Al) superlattices
[NASA-TT-20177] 14 p1890 N88-21297
Diffusion welding of aluminomagnesium alloys to ceramics
14 p1898 N88-21333
The effect of strain rate on the strength and ductility of SiCw/2124 Al composite
[OUEL-1692/87] 14 p1924 N88-21466
Effect of loading conditions on environment-sensitive fracture
[BR102697] 14 p1934 N88-21533
Joints in fiber-reinforced aluminum alloys
[NASA-TT-20160] 15 p2031 N88-22104
Processing, microstructure, and mechanical properties of silicon carbide particulate reinforced aluminum alloys
[AD-A188981] 15 p2037 N88-22136
The effective fracture toughness of aluminum at rapid heating rates
[AD-A189745] 15 p2038 N88-22146
The age hardening response of thermomechanically processed Al-Mg-Li alloys
[AD-A189870] 15 p2039 N88-22147
Investigation and synthesis of high temperature and increased stiffness RSP aluminum alloys
[AD-A190407] 15 p2039 N88-22151
Response of aluminum alloys to erosive particle impacts
[DE88-005910] 15 p2041 N88-22159
The corrosion resistance of an aluminum alloy coated with polysilazane derived ceramics
[AD-A190703] 15 p2046 N88-22189
Aluminum-air battery development
[DE88-006620] 15 p2061 N88-22287
A modified sulphuric acid anodising process used as a pretreatment for the adhesive bonding of aluminum alloys
[ARE-TM(UMM)-87410] 16 p2177 N88-22974
Fatigue crack growth under full-scale cyclic plasticity
[DFVLR-FB-87-48] 16 p2222 N88-23263
Environment effects on crack propagation with tensile stress
[GKSS-87/E/46] 16 p2223 N88-23267
Stress corrosion cracking properties of Al-Li alloys
17 p2320 N88-23853
AC impedance analysis of corrosion fatigue in naval aircraft alloys
[AD-A190822] 17 p2322 N88-23865
Strain hardening at large strains in aluminum alloys
[DE88-007415] 18 p2484 N88-24737
Improving knowledge of the corrosion behavior of aluminum alloys of the 7XXX series
[REPT-48-451/F] 18 p2486 N88-24750
Characterization of the 2219 Cegedur alloy. Data acquisition of the fracture mechanics --- aircraft construction materials
[REPT-48-442/F] 18 p2487 N88-24751
Aluminum alloy
[NASA-CASE-LAR-13924-1-CU]
18 p2487 N88-24753
Martensitic transformation and microstructures in sintered NiAl alloys
[NASA-TT-20178] 18 p2488 N88-24761
Rapidly solidified lightweight durable disk material
[AD-A191697] 18 p2491 N88-24775
Nondestructive evaluation methods for determination of thermal history and mechanical properties of aluminum-lithium alloys
[DE88-007352] 19 p2615 N88-25516
Effect of Zr or Cr content on the fracture toughness of the high purity Al-Zn-Mg alloys
[NASA-TT-20294] 19 p2616 N88-25518
Extended ductility of Al and alpha-Fe alloys through dynamic recovery mechanisms
[DE88-008679] 19 p2616 N88-25522
Prediction of fatigue life of notched specimens under aircraft loading and importance of the relative method in the case of local strain approach, part 2
[TAE-595-PT-2] 19 p2680 N88-25934
Precipitation study by electrical resistivity measurement in Ni-Al alloys
[DE88-701877] 20 p2773 N88-26440
Grain boundary structure in Ni3Al
[DE88-009164] 20 p2773 N88-26444
Optimizing superplastic response in lithium containing aluminum-magnesium alloys
[AD-A192217] 20 p2774 N88-26451
Fatigue of lithium-aluminum alloys: An example of localization of the plastic deformation
[ETN-88-92309] 20 p2775 N88-26456
Analysis of the perforation of monolithic and simple laminate aluminium targets as a test of analytical deformation models
[MRL-R-1111] 20 p2813 N88-26686
A fundamental understanding of the interfacial compatibility in hybrid material systems
[AD-A192921] 21 p2909 N88-27264
A method for determining the solubility of hydrogen in molten aluminum-lithium alloys
[DE88-009807] 21 p2910 N88-27270
Thermomechanical processing of Al alloy 2090 for grain refinement and superplasticity
[AD-A192333] 21 p2912 N88-27281
Analysis of grain refinement and superplasticity in aluminum-magnesium alloys
[AD-A193029] 21 p2912 N88-27283
Processing and properties of advanced aluminum alloys
[AD-A193224] 21 p2912 N88-27284
Constant amplitude fatigue life data for notched and unnotched annealed Ti-6Al-4V sheet
[AD-A193420] 21 p2913 N88-27287
Study of surface treatments before adhesive bonding of light alloys --- aircraft industry
[ETN-88-92743] 21 p2916 N88-27308
Study of feasibility and optimization conditions of laser treatments: Application of the local recrystallization of aluminum
[ISAL-87-0048] 21 p2916 N88-27309
Kinetic of oxidation to air of a Fe-Al-Mn alloy system at 600-800(sup 0)C temperature range
[DE88-702309] 21 p2920 N88-27330
Influence of microstructure and microdamage processes on fracture at high loading rates
[AD-A192957] 21 p2960 N88-27583
Stress relaxation of a titanium (Ti-6Al-4V) threaded joint
[DE86-010102] 21 p2961 N88-27590
Stress corrosion evaluation of powder metallurgy aluminum alloy 7091 with the breaking load test method
22 p3053 N88-28115
Corrosion of aluminium alloys by IRFNA
[AD-A194319] 22 p3055 N88-28127
Study of fatigue cracks in aluminum alloys. Influence of microstructure
[REPT-48-553] 22 p3056 N88-28134
A fundamental study of P/M processed elevated temperature aluminum alloys
[AD-A192958] 23 p3194 N88-29005
An investigation into the metallurgical aspects of joining rapidly-solidified aluminum alloys
[AD-A194677] 23 p3194 N88-29009
Structural relationship between icosahedral and Frank-Kasper phases of Al-Li-Cu
[AD-A193768] 23 p3195 N88-29011
Passive damping concepts for free and forced member and grillage vibration
[NASA-CR-183114] 23 p3225 N88-29196
Some effects of nitrates on the tensile properties of Al 7075-T7351
[AD-A195118] 24 p3354 N88-29965

ALUMINUM ARSENIDES

Photoluminescence studies of GaAs/AlAs superlattices
[DE87-013817] 02 p0245 N88-11548
Excimer laser-assisted deposition of GaAs, AlAs and (Al,Ga)As from Lewis acid-base adducts
[AD-A184588] 03 p0329 N88-12081
Photoluminescence studies of InGaAlAs quaternary alloys
[DE88-007197] 20 p2874 N88-27062
Investigations on the MBE (Molecular Beam Epitaxy) growth and properties of Al(sub y)Ga(sub y)In(sub 1-x-y)AsInP and InGaAs-InAlAs superlattices
[DE88-009105] 21 p3022 N88-27941

ALUMINUM BORON COMPOSITES

Fracture mode research of boron aluminum composite materials by Acoustic Emission (AE)
[NAL-TR-927] 02 p0142 N88-10891
Analytical and experimental characterization of damage processes in composite laminates
[AD-A187221] 10 p1296 N88-17746
Structure and strength of boron-aluminum composites
14 p1885 N88-21264
Influence of heat treatment on the properties of boroaluminum
14 p1886 N88-21270

ALUMINUM CARBIDES

Research and development on high strength ceramic heaters discussed
04 p0404 N88-12508

ALUMINUM COATINGS

Ion plating for corrosion control
[AD-A185061] 05 p0565 N88-13442
Studies on hot-dip zinc-aluminum coated sheet steels
[ETN-88-92217] 15 p2042 N88-22166

ALUMINUM COMPOUNDS

NT ALUMINATES
NT ALUMINIDES
NT ALUMINUM ARSENIDES
NT ALUMINUM CARBIDES
NT ALUMINUM FLUORIDES
NT ALUMINUM NITRIDES
NT ALUMINUM OXIDES
NT ALUMINUM SILICATES
NT ANDESITE
NT SAPPHIRE

Application of sol-gel procedures to ceramic composites
[ETN-88-92741] 21 p2921 N88-27338

ALUMINUM FLUORIDES

High temperature solar electrothermal processing-3. Zinc from zinc oxide at 1200-1675K using a non-consumable anode
[AD-A186600] 09 p1141 N88-16836

ALUMINUM GALLIUM ARSENIDES

Numerical studies of the dual HEMT/algorithm development and numerical studies of Schrodinger's equation
[AD-A184471] 04 p0478 N88-12946
Resonant level lifetime in GaAs/ AlGaAs double-barrier structures
[AD-A185376] 05 p0655 N88-14020
Radiant power degradation of silicon-doped gallium arsenide and gallium aluminum arsenide infrared light-emitting diodes
[AD-A186726] 09 p1157 N88-16935
AlGaAs heterojunction lasers
[NASA-CR-4119] 09 p1171 N88-17020
Superlattice photodetectors
[AD-A186956] 09 p1253 N88-17511
The physics of very small structures
[AD-A187672] 11 p1556 N88-19311
Comparison of low temperature photoluminescence of bulk MBE (Molecular Beam Epitaxy) grown AlGaAs and GaAs using a graphite generated dimer versus a standard tetramer arsenic group-V source
[DE88-004939] 11 p1558 N88-19329
Pressure-dependent DLTS (Deep Level Transient Spectroscopy) experiments on Si-doped AlGaAs
[DE88-003842] 13 p1846 N88-21047
Optical nonlinearities in GaAs/GaAlAs multiple quantum wells fabricated by metalorganic chemical vapor deposition for use in optical signal processing
[AD-A191558] 18 p2582 N88-25337

Nonlinear optical properties and subpicosecond dynamics of excitons and electron-hole plasmas in multiple quantum well structures
[AD-A191926] 19 p2727 N88-26196
Far-infrared studies of doped AlGaAs/GaAs multiple-quantum-well structures
20 p2862 N88-26998
Electro-optical studies of Al(x)Ga(1-x)As/GaAs coupled quantum wells 20 p2862 N88-26999
Quantum wells and bulk AlGaAs under hydrostatic pressure 20 p2862 N88-27000
Ultrafast physics in semiconductor microstructures
[AD-A193300] 21 p3022 N88-27936
A high frequency GaAlAs travelling wave electro-optic modulator at 0.82 micrometers
[NASA-TM-100970] 22 p3073 N88-28240
Spectroscopic studies with multiple quantum well materials with applications to optical signal processing at room temperature
[AD-A194171] 24 p3429 N88-30409

ALUMINUM GRAPHITE COMPOSITES
Effect of interface on mechanical properties of graphite/201 aluminum composites
05 p0606 N88-13717
Interface characteristics and the mechanical properties of metal matrix composites
[AD-A186441] 08 p0966 N88-15845
Elastoplastic response of unidirectional graphite/aluminum under combined tension-compression cyclic loading
[CCMS-88-01] 11 p1451 N88-18647
A piecewise quadratic strength tensor theory for composites
[AD-A190929] 16 p2173 N88-22952
Temperature-dependent tensile and shear response of graphite/aluminum
[NASA-CR-182914] 19 p2609 N88-25484

ALUMINUM NITRIDES
Ceramic substrates for semiconductor applications reported: AlN substrates 19 p2633 N88-25621
AlN substrate applications 19 p2634 N88-25622
Low temperature film growth of the oxides of zinc, aluminum and vanadium (and related systems, oxides of gold and germanium, nitrides of aluminum and tungsten) by reactive sputter deposition
[AD-A193497] 23 p3191 N88-28986

ALUMINUM OXIDES
NT SAPPHIRE
Toughening of alpha-alumina: Preliminary results
[DE87-702776] 01 p0028 N88-10178
Studies of alumina additions in zirconia - magnesia
[DE87-703500] 04 p0419 N88-12602
T.E.M. study of boehmite gels and of their transformation into alpha-alumina
[SNIAS-872-430-121] 05 p0656 N88-14023
Temperature dependent mechanical properties of an alumina fiber reinforced aluminum composite
06 p0677 N88-14147
The effect of texture on the crack growth resistance of alumina
[NASA-TM-100250] 06 p0686 N88-14206
The dc conductivity studies of an hydroxide ion conductor at intermediate temperatures
[AD-A186044] 07 p0847 N88-15142
Static and dynamic determination of aluminum oxide toughness
[PB87-146999] 07 p0869 N88-15275
Tunable Al2O3:Ti3+ -laser with optical pumping
09 p1237 N88-17415
The influence of the heating procedure on the oxidation behaviour of NiAl studied by XPS
[AERE-R-12498] 10 p1300 N88-17776
The migration of grain boundaries in ceramic materials with particular reference to the sintering process
[DE88-004085] 10 p1306 N88-17808
New scientific findings on the morphology of aluminum oxide layers, serving as an adhesive basis
[MBB-Z-137/86] 10 p1312 N88-17840
The soft/hard wet anodization of aluminum oxide and its use in a thin film multilayered capacitor
[AD-A187575] 10 p1325 N88-17919
Deactivation of alumina based catalysts
11 p1455 N88-18673
Study of adherent oxide scales
[AD-A187368] 11 p1456 N88-18680
The YAlO(sub 3):Er laser
[PB88-130877] 11 p1493 N88-18911
Preparation and characterization of thin films of alumina by metalorganic chemical vapor deposition
[AD-A186366] 12 p1608 N88-19614
Contact and current noise in beta alumina and Nasicon ceramics
[AD-A189168] 12 p1611 N88-19635
Characterization and fundamental studies on CuO sorbent materials to determine attrition mechanisms on substrate gamma alumina
[DE88-003674] 13 p1749 N88-20456
Recommendations on developing polycrystalline alumina fiber 13 p1756 N88-20502
Analytically modeling the carbothermic reduction of alumina in a thermal plasma
[DE88-005535] 13 p1841 N88-21020
Crack resistance of multilayer ceramic-based composite material 14 p1885 N88-21265
Oxide-bound transition metal complexes for methane activation
[PB88-169719] 14 p1887 N88-21277
Nonlinearly tunable wideband emission of infrared radiation by Al2O3:Ti laser 14 p1970 N88-21758
Microwave sintering of alumina-SiC composites at 2.45 and 60 GHz
[DE88-006455] 15 p2030 N88-22095
Processing defects and strength of alumina substrates
[W-10/87] 15 p2087 N88-22441
The kinetics of contact noise in NaBeta alumina
[AD-A190651] 15 p2130 N88-22707
Synthesis and characterization of high-T(sub c) screen-printed Y-Ba-Cu-O films on alumina
[NASA-TM-100860] 15 p2146 N88-22805
High-strength ceramic based on tetragonal ZrO2 with Al2O3 admixture 16 p2180 N88-22996
Thermal conductivity of hard anodized coatings on aluminum
[AD-A191755] 18 p2492 N88-24784
Effect of process conditions on aluminum oxide thin film used in pH ISFET 19 p2673 N88-25892
The protonic Beta double prime aluminas: Preparation, stability, conductivity and structure
[DE88-008442] 20 p2768 N88-26415
Application of controlled interfacial pore structures to kinetic studies in alumina
[DE88-010884] 21 p2919 N88-27326
Preparation and characterization of ceramic materials based on Al2O3 reinforced with a ZrO2 dispersion
[ISAL-87-0041] 21 p2922 N88-27340
Comparison of sol-gel procedures for zircon and alumina
[REPT-881-430-108] 21 p2922 N88-27342
Study of the erosion corrosion of alloys and coatings
[AD-A194337] 22 p3055 N88-28128
Influence of dispersed additives reinforcement on the wear reinforcement mechanisms of the alumina-steel couple. Macroscopic and structural aspects
[ECL-88-01] 22 p3059 N88-28148
Laser crystallized silicon films on alumina ceramic substrates and application to thin film c-Si solar cells
[PB88-131966] 22 p3116 N88-28515
The high temperature creep deformation of Si3N4-6Y2O3-2Al2O3
[NASA-CR-183204] 23 p3190 N88-28981
Low temperature film growth of the oxides of zinc, aluminum and vanadium (and related systems, oxides of gold and germanium, nitrides of aluminum and tungsten) by reactive sputter deposition
[AD-A193497] 23 p3191 N88-28986
Al2O3-TiO2 and Al2TiO5 ceramic materials
[SNIAS-881-430-122] 23 p3199 N88-29038

ALUMINUM SILICATES
NT ANDESITE
The effect of temperature on fatigue crack initiation from aluminosilicate inclusions
[PNR90377] 02 p0154 N88-10962
Structure and mechanical properties of metal matrix composites made using semi-solid processes: The case of the system Al-Si/SiC
[ETN-88-92299] 17 p2316 N88-23836
Mechanical and structural characterization of aluminum ceramic fibers
[ETN-88-92168] 17 p2323 N88-23870

ALVEOLAR AIR
Biofeedback control of alveolar carbon dioxide tension to eliminate hypocapnia in man in the presence of hypoxia 07 p0892 N88-15405
Breath-by-breath measurement of alveolar gas exchange 12 p1653 N88-19905

ALVEOLI
Breath-by-breath measurement of alveolar gas exchange 12 p1653 N88-19905
Liquid ventilation: New data and possible use in space medicine 12 p1654 N88-19908

AMAZON REGION (SOUTH AMERICA)
Project CODEAMA/FUNCATE (test-area of Barreirinha-AM): Field report
[INPE-4500-RPE/563] 15 p2090 N88-22455
Surface CO results from the ABLE-2B expedition to Amazonia
[INPE-4501-PRE/1258] 15 p2093 N88-22469
Surface ozone and ozonesounding results from the ABLE-2B expedition to Amazonia
[INPE-4523-PRE/1275] 15 p2095 N88-22484
Aerodynamic aspects of the Amazon Forest
[INPE-4445-TDL/313] 15 p2098 N88-22501
Detection, monitoring and analysis of some environmental effects of fires in the Amazon region through utilization of NOAA and LANDSAT satellite imagery and aircraft data
[INPE-4503-TDL/326] 16 p2230 N88-23322
Oxidation and reduction rates for organic carbon in the Amazon mainstream tributary and floodplain, inferred from distributions of dissolved gases
[NASA-CR-182943] 18 p2538 N88-25062
Recent measurements of ozone in the Amazon forests
[INPE-4494-PRE/1258] 24 p3389 N88-30185

AMBIENCE
Vertical directionality of ambient noise at 32 deg N as a function of longitude: Tape number 86180
[AD-A193228] 21 p3012 N88-27872

AMBIENT TEMPERATURE
GAS eleven node thermal model (GEM)
10 p1289 N88-17712
Polymeric electrolytes for ambient temperature lithium batteries
[DE88-004896] 13 p1763 N88-20547
Ambient temperature secondary lithium batteries using LiAl lithium insertion anodes
[DE88-008394] 20 p2793 N88-26574

AMBIPOLAR DIFFUSION
Evolution of poloidal variation of impurity density and ambipolar potential in rotating tokamak plasma, part 2
[DE88-009882] 19 p2731 N88-26218

AMBIT
U FIELD THEORY (PHYSICS)

AMBULANCES
Satellite communications experiment for the Ontario air ambulance service 19 p2646 N88-25705

AMIDES
NT POLYIMIDES
NT UREAS
A 13C and 15N solid state NMR characterization of aramid-containing nylon-6 polymers synthesized by in situ polymerization of caprolactam with benzoyl caprolactam derivatives
[AD-A187067] 09 p1147 N88-16872
Synthesis and characterization of 1,2-cyclobutenedicarboxamides: Thermally generated polymers and Diels-Alder adducts
[AD-A188591] 12 p1611 N88-19633

AMINES
NT DIAMINES
NT EPINEPHRINE
NT ERGOTAMINE
NT GUANIDINES
NT NOREPINEPHRINE
NT SEROTONIN
NT TETRYL
High-molecular compounds (selected articles)
[AD-A184668] 03 p0293 N88-11642
Studies on syntheses of amine-carboxyboranes (boron analogues of amino acids) and derivatives
[AD-A184838] 05 p0557 N88-13386
Thermally stable aromatic structures from acyclic precursors. 1. Para polyphenylene model compounds from 3-Dimethyl amino hex-5-EN-1-YNES
[AD-A185300] 05 p0568 N88-13462
Modification of polymers by photografting processes
17 p2323 N88-23871
Aromatic cyclotriphosphazenes
[NASA-CASE-ARC-11428-3] 18 p2477 N88-24692
Structural study of impregnating resins of TGMDA/DDS type
[ETN-88-92167] 20 p2780 N88-26488

AMINO ACIDS
NT GLUTAMIC ACID
NT GLUTAMINE
Observing effect of laser radiation of low-frequency Raman scattering of light 06 p0772 N88-14742
A program for the study of skeletal muscle catabolism following physical trauma
[AD-A189771] 15 p2102 N88-22521
Studies of model ion channels in defect-free multibilayers of phospholipids
[AD-A188740] 16 p2238 N88-23365
Fast atom bombardment study on interaction of anticodonic nucleotides and their cognate amino acid
[ISAS-RN-355] 20 p2850 N88-26918
Precise ultraviolet absorbance study of the interaction of amino acids and mononucleosides in aqueous solution
[ISAS-RN-356] 21 p2908 N88-27256

AMMONIA
NT LIQUID AMMONIA

Ruthenium catalysts and their use in ammonia production
[GB-PATENT-2-136-704-A] 01 p0020 N88-10123
JPRS report: Science and technology. China
[JPRS-CST-87-031] 03 p0299 N88-11880
XeCl excimer laser induced multiphoton ionization of ammonia molecule 03 p0299 N88-11883
Model investigations of atmospheric ammonia scavenging
[DE88-002337] 09 p1194 N88-17153
Human blood glutamic acid level with exposure to high ambient concentrations of ammonia 10 p1361 N88-18134
Electrochemistry in near-critical and supercritical fluids. 5: The dimerization of quinoline and acridine radical anions and dianions in ammonia from -70 C to 150 C
[AD-A190858] 16 p2175 N88-22967
Microwave spectroscopy and gravitational collapse 18 p2594 N88-25413
Interaction of vinylidene fluoride: Tetrafluoroethylene copolymer with ammonia
[NASA-TT-20292] 19 p2620 N88-25542
Employment of porous polytetrafluoroethylene Membrane with a hydrophilic and hydrophobic stratal structure for construction of an enzyme electrode
[NASA-TT-20296] 19 p2620 N88-25543

AMMONIUM COMPOUNDS
NT AMMONIUM NITRATES
NT AMMONIUM PERCHLORATES
Development of microencapsulated DNBM quaternary ammonium inhibitors for paints 17 p2319 N88-23851

AMMONIUM NITRATES
An infra-red investigation of HAN (Hydroxylammonium Nitrate)-based liquid propellants
[AD-A187226] 10 p1307 N88-17815
The burning of HAN-based (hydroxylammonium nitrate) liquid propellants
[DE88-006863] 18 p2494 N88-24800
Electrical ignition of HAN-based liquid propellants
[AD-A191349] 18 p2495 N88-24801
The high pressure sound velocity and equation of state of aqueous solutions of hydroxylammonium nitrate and triethanolammonium nitrate
[AD-A191740] 18 p2570 N88-25266
Titrimetric analysis of HAN-based liquid propellants
[AD-A196225] 24 p3357 N88-29990

AMMONIUM PERCHLORATES
Equilibrium calculations of ionization in tracer flames
[PB87-104154] 04 p0412 N88-12555
A general qualitative study of point and extended defects and their interactions in non-metallic systems
[AD-A191687] 19 p2618 N88-25532
Descriptive characterization of propellant particles
[AD-A195176] 24 p3356 N88-29985

AMMONOLYSIS
Process for preparing transition metal nitrides and transition metal carbonitrides and their reaction intermediates
[DE88-000849] 06 p0679 N88-14162

AMMUNITION
NT INCENDIARY AMMUNITION
Control and stabilization mechanisms of submunitions
[DFVLR-IB-111-86/9] 03 p0259 N88-11630
Thermoplastic elastomers as LOVA (Low Vulnerability Ammunition) binders
[AD-A184350] 04 p0419 N88-12599
Calculation evaluation of the boundary conditions of autoinflammation of propulsive charges
[PB87-139044] 08 p0974 N88-15890
Real time AI expert system for robotic applications 08 p1061 N88-16408
Dependence of the expectancy of hitting on the number of spread shots. Determination of the expectancy of hitting using a spread salvo
[REPT-FM6] 10 p1310 N88-17829
Splinter generator
[MBB-UA-1048/87] 11 p1491 N88-18897

AMOEBA
How does Physarum polycephalum perceive and use gravity? 12 p1655 N88-19918

AMORPHOUS MATERIALS
NT AMORPHOUS SILICON
Construction and characterization of amorphous-silicon test structures
[DE87-013595] 01 p0029 N88-10182
Formation of amorphous alloys by solid state reactions
[DE87-013175] 02 p0146 N88-10918
EXELFS (Extended Electron Energy Loss Fine Structure) of amorphous and crystalline SiC
[DE87-013551] 02 p0151 N88-10948
Corrosion-resistant amorphous metallic coatings: Engineering development
[NASA-CR-181487] 03 p0287 N88-11802
Modeling of irradiation-induced amorphization in a titanate ceramic
[DE87-014751] 03 p0292 N88-11833
Microstructure of amorphous and crystalline zirconium alloys rapidly solidified
[DE87-703700] 05 p0564 N88-13432
Structural investigations of some metallic glasses
[ECN-198] 06 p0686 N88-14203
Structural relaxation and mechanical properties of amorphous Fe-Zr alloys 07 p0840 N88-15094
Study of molecular mobility of noncrystaline polymer alloys of different compatibility using mechanical spectrometry
[ISAL-87-0032] 09 p1149 N88-16883
Diffusion studies in amorphous NiZr alloys
[DE88-003009] 10 p1301 N88-17781
The soft/hard wet anodization of aluminum oxide and its use in a thin film multilayered capacitor
[AD-A187575] 10 p1325 N88-17919
Laboratory amorphous carbon: A possible analog of cometary dust 14 p2009 N88-21981
Fast ion conducting glasses
[AD-A191412] 16 p2183 N88-23010
Long-time tunneling in amorphous metals at helium temperatures
[DE88-701150] 16 p2281 N88-23654
Electrodeposition of amorphous Ni-Cr-P alloys
[DE88-006868] 19 p2616 N88-25521
Hydrogenated amorphous silicon-germanium alloys
[DE88-001147] 19 p2620 N88-25546
Study of Staebler-Wronsky degradation effect in a Si:H based P-I-N solar cells
[NASA-CR-182564] 19 p2687 N88-25970
Glass forming ranges of amorphous alloys
[DE88-007897] 20 p2772 N88-26438
Plasma deposition: Investigations on a new approach
[ETN-88-92619] 20 p2861 N88-26992
Formation of metastable structures and amorphous phases in Cu-W alloys using the triod sputtering technique
[DE88-009051] 21 p2915 N88-27298
PECVD of amorphous nickel--phosphorus films
[DE88-011088] 21 p2915 N88-27299
Influence of the interface on the crystallization of amorphous Ge in Pb/Ge multilayers
[DE88-010072] 22 p3156 N88-28776

AMORPHOUS SEMICONDUCTORS
NT AMORPHOUS SILICON
Amorphous or microcrystalline semiconductor memory device
[EP-PATENT-0-162-529-A1] 01 p0026 N88-10167
Preparation of amorphous silicon semiconductors
[GB-PATENT-2-176-054-A] 05 p0656 N88-14022
Defects and disorder in amorphous and damaged silicon
[AD-A192277] 20 p2879 N88-27089
Influence of the temperature-dependence of recombination life-time of free carriers in amorphous semiconductors on thermostimulated photocurrent spectra
[DE88-702728] 23 p3293 N88-29609
Thermostimulated conductivity in amorphous semiconductors with non-exponential density of localized states
[DE88-702737] 23 p3293 N88-29612
Ultrafast processes and spectroscopy with free electron lasers
[AD-A195248] 24 p3379 N88-30126

AMORPHOUS SILICON
Detection of minimum-ionizing particles in hydrogenated amorphous silicon
[DE88-002769] 07 p0837 N88-15081
Research on high-efficiency, stacked, multijunction, amorphous silicon alloy thin-film solar cells
[DE88-001108] 13 p1793 N88-20723
Progress of amorphous silicon based solar cells and modules
[DE88-004666] 13 p1794 N88-20733
Investigations of the origins of metastable, light-induced changes in hydrogenated amorphous silicon
[DE88-001117] 13 p1846 N88-21051
Defects and disorder in amorphous and damaged silicon
[AD-A192277] 20 p2879 N88-27089
Amorphous silicon solar cells using a metal substrate
[PB88-131941] 21 p2968 N88-27628
Rapid thermal annealing of silicon layers amorphized by ion implantation
[DE88-702307] 23 p3290 N88-29591

AMPERAGE
U ELECTRIC CURRENT

AMPHIBIA
NT FROGS
Limb regeneration in amphibians, a suitable model for investigations of the effects of weightlessness as regards evolution and modifications 07 p0885 N88-15369
Changes in the morphological and molecular biological processes during early embryo development in amphibians under micro-g conditions 07 p0885 N88-15371
Embryonic development of the newt Cynops pyrrhogaster in very weak magnetic fields
[ISAS-RN-357] 19 p2702 N88-26068

AMPHIBOLES
Origin of SNC kaersutitic amphibole: Experimental data 23 p3306 N88-29693
Reappraisal of the geology of Kangimut Sammisoq, Ameralik Fjord, Southern West Greenland: Crustal structure and interpretation of isotopic data 24 p3398 N88-30234

AMPLIFICATION
NT POWER GAIN
NT SOUND AMPLIFICATION
NT WAVE AMPLIFICATION
Gain evaluation for an idealized curtain array antenna
[PB87-210290] 02 p0161 N88-11006
Investigation of two laser beam coupling and amplification in Ce-doped SBN single crystals 03 p0327 N88-12069
Increased gain of channel intensifier tubes by pulsed biasing
[DE88-000512] 04 p0490 N88-13019
A focussed MCP (microchannel plate) image intensifier type for high speed gating
[DE88-000480] 05 p0583 N88-13555
Narrow linewidth gain measurements in a KrF excimer amplifier pumped longitudinally by a high-power electron beam
[DE88-001365] 05 p0586 N88-13575
Signal processing studies program optical signal amplification, volume 2
[AD-A188054] 10 p1320 N88-17896
Signal processing studies program optical signal amplification, volume 1
[AD-A188055] 10 p1321 N88-17897
A cause of divergence in the Kalman gain equation 12 p1578 N88-19438
Some measurements of height gain at V.H.F. 12 p1617 N88-19671
Solid-state travelling wave amplifiers based on multi-stream instability
[AD-A189566] 12 p1624 N88-19718
Fiber-coupled external-cavity semiconductor high power laser
[AD-A188454] 13 p1774 N88-20611
Wavelength scaling of lithium-like recombination scheme for X-UV gain production --- X-ray lasers
[ETN-88-92002] 13 p1778 N88-20634
Effect of off-axis radiation in amplified spontaneous emission
[DE88-007001] 14 p1915 N88-21440
Amplification of signals in fiber optics using the stimulated Raman effect
[AD-A190281] 15 p2133 N88-22727
Analysis and design of gain scheduled control systems
[NASA-CR-182867] 16 p2163 N88-22904
Model for pulse amplification by a gaseous laser amplifier
[DE88-011729] 20 p2808 N88-26657
On the small signal gain of free electron lasers in the low-current regime
[DFVLR-FB-88-10] 21 p2955 N88-27552
Optoelectronic gain control of a microwave single stage GaAs MESFET amplifier
[NASA-CR-182201] 24 p3368 N88-30055

AMPLIFICATION FACTOR
U AMPLIFICATION

AMPLIFIER DESIGN
Phase 2 development of a 12 GHz MMIC FET amplifier
[IM-I86-1010] 01 p0038 N88-10240
Construction of a 60 GHz Traveling Wave Tube (TWT) for intersatellite link on geostationary orbit (ISL/TWT)
[BMFT-FB-W-86-015] 16 p2192 N88-23076

AMPLIFIERS
NT BROADBAND AMPLIFIERS
NT CYCLOTRON RESONANCE DEVICES
NT DISTRIBUTED AMPLIFIERS
NT FLUID AMPLIFIERS
NT LIGHT AMPLIFIERS
NT MICROWAVE AMPLIFIERS
NT PARAMETRIC AMPLIFIERS
NT PHOTOMULTIPLIER TUBES
NT POWER AMPLIFIERS
NT PREAMPLIFIERS
NT TRANSISTOR AMPLIFIERS
NT TRAVELING WAVE AMPLIFIERS
NT VOLTAGE AMPLIFIERS
Traveling-wave maser closed-cycle refrigerator data acquisition and display system 04 p0437 N88-12708
Power density measurements in the near field of the DSS 13 26-meter antenna 04 p0437 N88-12711

Narrow linewidth gain measurements in a KrF excimer amplifier pumped longitudinally by a high-power electron beam
[DE88-001365] 05 p0586 N88-13575
Integrated photo-responsive metal oxide semiconductor circuit
[NASA-CASE-GSC-12782-1] 06 p0695 N88-14271
Conceptual designs of a 50 NM FEL (Free-Electron Laser) oscillator and a 20-40 NM SASE (Self-Amplified Spontaneous Emission) amplifier
[DE88-003150] 10 p1334 N88-17974
New generation imager system
[NASA-CR-180464] 10 p1408 N88-18398
Design and fabrication of advanced hybrid circuits for high energy physics
[DE88-004392] 11 p1479 N88-18825
Ballistic deficits in pulse shaping amplifiers
[DE88-003908] 11 p1481 N88-18840
Pulse-train amplification of subnanosecond near-transform-limited KrF laser pulses
[DE88-004460] 12 p1631 N88-19764
Phase preservation cleanup in a double-pass Raman amplifier SBS (Stimulated Brillouin Scattering) conjugator
[AD-A189428] 13 p1761 N88-20536
Advanced components for spaceborne infrared astronomy
[NASA-CR-177470] 13 p1772 N88-20601
Wiggler taper optimization for free-electron-laser amplifiers with moderate space-charge effects
[DE88-003758] 13 p1775 N88-20618
Generating squeezed microwave radiation with a Josephson parametric amplifier
14 p1978 N88-21805
Characterization of a 30-GHz IMPATT solid state amplifier
[NASA-TM-100876] 18 p2503 N88-24847
Aurora status and plans
[DE88-006476] 18 p2521 N88-24955
Reducing sensitivity to errors in free electron laser amplifiers
[DE88-007017] 18 p2522 N88-24960
Thermionic integrated circuit program
[DE88-010119] 19 p2662 N88-25833
A 2.3-GHz low-noise cryo-FET amplifier
22 p3066 N88-28195
Theoretical and experimental study of a mode-converting coupler for application to a harmonic gyrotron amplifier
[AD-A193760] 22 p3081 N88-28294

AMPLITUDE DESTRIBUTION ANALYSIS
Four-wave mixing used in optical amplitude encoding
03 p0376 N88-12366
Near optimal blind deconvolution
[REPT-87-016] 15 p2123 N88-22655

AMPLITUDE MODULATION
Four-wave mixing used in optical amplitude encoding
03 p0376 N88-12366
Fast autotuning of a hydrogen maser by cavity Q modulation 04 p0436 N88-12707
Axial anisotropy of the intensity of the cosmic ray nuclear component
[IFSI-87-7] 05 p0662 N88-14061
Phase phenomena in parametric generators and amplifiers of ultrashort light pulses
07 p0918 N88-15576
Magnet strength fluctuations in the SSC (Superconducting Super Collider) lattice. Part 2: Frequency modulation
[DE88-006491] 15 p2141 N88-22774
A study on the co- and adjacent channel protection requirements for mobile satellite ACSSB modulation
19 p2650 N88-25732
Basic causes of amplitude modulation in climatic/weather parameters
[DE88-702743] 23 p3236 N88-29254

AMPLITUDE PROBABILITY ANALYSIS
U AMPLITUDE DISTRIBUTION ANALYSIS

AMPLITUDES
NT PULSE AMPLITUDE
NT SCATTERING AMPLITUDE
The giant spot on II Peg in 1986
04 p0508 N88-13120
Fatigue 87, volume 1
[AD-A184045] 05 p0597 N88-13645
A dislocation model for fatigue crack propagation under variable amplitude loading 05 p0602 N88-13683
The how and why of variable amplitude testing
05 p0603 N88-13690
Regional wave attenuation and seismic moment from the inversion of NORESS spectra
[AD-A187399] 11 p1510 N88-19023
Envelope and phase statistics for non-Gaussian noise and resulting error probabilities for digital communications systems 12 p1617 N88-19672
Passive DF: A tutorial, part 1
[NASA-CR-182669] 13 p1815 N88-20846
Constant amplitude fatigue life data for notched and unnotched annealed Ti-6Al-4V sheet
[AD-A193420] 21 p2913 N88-27287

AMPTE (SATELLITES)
A fluid simulation of the AMPTE lithium gas releases in the solar wind
[TRITA-EPP-87-06] 05 p0661 N88-14056
Nature and the nonlinear evolution of electrostatic waves associated with the AMPTE (Active Magnetosphere Particle Tracer Explorers) solar wind releases
[AD-A185471] 06 p0806 N88-14920
AMPTE-UKS ion observations at a quasi-parallel bow shock 08 p1095 N88-16589
An unusual magnetopause encounter by AMPTE-UKS
08 p1097 N88-16602
Observations of small scale structures using data from the wave experiment on the AMPTE-UKS spacecraft
08 p1099 N88-16612
Deployable booms and antennas on AMPTE-IRM
14 p1874 N88-21198
Magnetic cavity formation at Comet Halley and at the AMPTE Li release 14 p1996 N88-21898
Observation of nonlinear wave decay processes in the solar wind by the AMPTE IRM plasma wave experiment
[AD-A191409] 16 p2290 N88-23713
Attitude and orbit control for the AMPTE-UKS (Active Magnetospheric Particle Tracer Explores-UK Subsatellite): Evaluation of the in-flight performance
[PB87-225199] 19 p2604 N88-25467
Plasma of earth's magnetosphere ring currents. Model compared with results of AMPTE/CCE experiment
24 p3447 N88-30515

ANAEROBES
A process study of the biothermal conversion of water hyacinths to methane
[DE88-000554] 06 p0730 N88-14488
Shelf life degradation of selected anaerobic threadlocking adhesives at various storage temperatures
[AD-A187712] 11 p1461 N88-18711

ANALOG CIRCUITS
DEDALE: An expert system for analog circuit maintenance 02 p0128 N88-10809

ANALOG COMPUTERS
Specification for IBM/IBM compatible 3480 tape cartridge
[NASA-TM-100702] 17 p2384 N88-24168

ANALOG DATA
Statistical very short-range forecasting via analogues
02 p0206 N88-11290
The design and testing of an analog optical communication link capable of the simultaneous transmission of four frequency division multiplexed audio signals
[AD-A184695] 03 p0307 N88-11936
Signal chain for the Airborne Visible/Infrared Imaging Spectrometer (AVIRIS) 06 p0706 N88-14331
Massively parallel implementations of theories for apparent motion
[AD-A185841] 07 p0901 N88-15455
Emerging technologies program 3-5: Microslectronics Panel report
[AD-A189463] 12 p1624 N88-19716
Visual display representation of multidimensional systems: The effect of information correlation and display integrality
[AD-A188655] 12 p1672 N88-20010
An overview of the development of a linear broadband analog fiber-optic link
[DE88-008668] 20 p2854 N88-26945

ANALOG SIMULATION
Modeling of environmentally-induced transients within satellites. Part 2: Discharge coupling transients
03 p0273 N88-11722
Modelling of a hydraulic motor and servo-valve to produce a desired system response using analogue and digital compensation techniques
[ETN-88-92079] 14 p1899 N88-21337
Development of a hybrid simulator for robotic manipulators
[AD-A193119] 21 p2956 N88-27557

ANALOG TO DIGITAL CONVERTERS
Digital to analog and analog to digital conversion using pulse duration modulation
[ETN-87-90415] 01 p0078 N88-10499
Measurements in the functional mock up test of the NAL QSTOL aircraft control system
[NAL-TR-928] 02 p0126 N88-10793
Digitization functions in computer graphics
[ETN-88-91363] 05 p0635 N88-13887
Life sciences flight experiments microcomputer
06 p0792 N88-14857
Multilayer holographic functional element in analog-digital converter 07 p0921 N88-15593
Method for set-up for researching signal curve development
[NASA-TT-20235] 13 p1760 N88-20526
Fast analog-to-digital converter
[DE88-701488] 15 p2106 N88-22543
Mass digitization of topographic-cartographic information 16 p2226 N88-23288
Digitizing the traffic network of JOG 250 by scanning --- JOG 250 map 18 p2533 N88-25029
Tests for the automatic pattern recognition of building surfaces by the TK 50 18 p2533 N88-25030
Development of a mobile satellite communication unit
19 p2646 N88-25701
Baseband assembly analog-to-digital converter board
22 p3067 N88-28201
Multichannel data transmission through a fiber optic cable
[AD-A193842] 22 p3070 N88-28221

ANALOGIES
Geometrically nonlinear rod mechanism analogy of axisymmetrically loaded spherical shells based on a comprehensive approach to the stability of circular arches
[ETN-87-90419] 01 p0062 N88-10398
Analogical inference and analogical access
[AD-A184345] 03 p0369 N88-12321
Similarity networks as a knowledge representation for space applications 08 p1062 N88-16411
Some learnability results for analogical generation
[AD-A193669] 23 p3250 N88-29342

ANALOGS
Studies on syntheses of amine-carboxyboranes (boron analogues of amino acids) and derivatives
[AD-A184838] 05 p0557 N88-13386
Infinite dimensional dynamical systems and their finite dimensional analogues
[AD-A192041] 18 p2563 N88-25216
Space station habitability recommendations based on a systematic comparative analysis of analogous conditions
[NASA-CR-3943] 18 p2587 N88-25372
Superconductive analogue of spin glasses
[DE88-702059] 19 p2733 N88-26233
Operational multifield analog forecasting of US seasonal temperatures for non-winter seasons
22 p3127 N88-28592
Rifts of deeply eroded Hawaiian basaltic shields: A structural analog for large Martian volcanoes
24 p3443 N88-30494

ANALYSIS (MATHEMATICS)
NT ABEL FUNCTION
NT ANALYTIC FUNCTIONS
NT APPROXIMATION
NT ASYMPTOTES
NT ASYMPTOTIC SERIES
NT BANACH SPACE
NT BESSEL FUNCTIONS
NT BIHARMONIC EQUATIONS
NT BINARY INTEGRATION
NT BOREL SETS
NT BORN APPROXIMATION
NT BORN-OPPENHEIMER APPROXIMATION
NT BOUNDARY INTEGRAL METHOD
NT BURGER EQUATION
NT CALCULUS
NT CALCULUS OF VARIATIONS
NT CAUCHY INTEGRAL FORMULA
NT CAUCHY-RIEMANN EQUATIONS
NT CHEBYSHEV APPROXIMATION
NT COLLINEARITY
NT COMBINATIONS (MATHEMATICS)
NT COMBINATORIAL ANALYSIS
NT COMPLEX VARIABLES
NT COMPUTATIONAL CHEMISTRY
NT COMPUTATIONAL FLUID DYNAMICS
NT CONFORMAL MAPPING
NT CONJUGATE GRADIENT METHOD
NT CONTINUITY (MATHEMATICS)
NT CONVOLUTION INTEGRALS
NT COPLANARITY
NT COSINE SERIES
NT CUBIC EQUATIONS
NT DELTA FUNCTION
NT DIFFERENCE EQUATIONS
NT DIFFERENTIAL EQUATIONS
NT EINSTEIN EQUATIONS
NT ELLIPTIC DIFFERENTIAL EQUATIONS
NT ELLIPTIC FUNCTIONS
NT ENTIRE FUNCTIONS
NT ERROR ANALYSIS
NT EULER-CAUCHY EQUATIONS
NT EXISTENCE THEOREMS
NT EXPONENTIAL FUNCTIONS
NT EXTREMUM VALUES
NT FAST FOURIER TRANSFORMATIONS
NT FINITE DIFFERENCE THEORY
NT FINITE ELEMENT METHOD
NT FINITE VOLUME METHOD
NT FLUX VECTOR SPLITTING

NT FOKKER-PLANCK EQUATION
NT FOURIER ANALYSIS
NT FOURIER TRANSFORMATION
NT FOURIER-BESSEL TRANSFORMATIONS
NT FREDHOLM EQUATIONS
NT FUNCTION SPACE
NT FUNCTIONAL ANALYSIS
NT GAUSS EQUATION
NT GREEN'S FUNCTIONS
NT HALF PLANES
NT HALF SPACES
NT HANKEL FUNCTIONS
NT HARMONIC ANALYSIS
NT HARTREE APPROXIMATION
NT HELMHOLTZ VORTICITY EQUATION
NT HILBERT SPACE
NT HILBERT TRANSFORMATION
NT HYPERBOLIC DIFFERENTIAL EQUATIONS
NT HYPERBOLIC FUNCTIONS
NT HYPERGEOMETRIC FUNCTIONS
NT HYPERPLANES
NT INTEGRAL CALCULUS
NT INTEGRAL EQUATIONS
NT INTEGRAL TRANSFORMATIONS
NT INTERPOLATION
NT ITERATION
NT ITERATIVE SOLUTION
NT J INTEGRAL
NT JACOBI MATRIX METHOD
NT KERNEL FUNCTIONS
NT LAGUERRE FUNCTIONS
NT LAPLACE TRANSFORMATION
NT LEAST SQUARES METHOD
NT LEBESGUE THEOREM
NT LIAPUNOV FUNCTIONS
NT LIMITS (MATHEMATICS)
NT LINEAR EQUATIONS
NT LIOUVILLE THEOREM
NT LIPSCHITZ CONDITION
NT LOGARITHMS
NT MAXIMA
NT MEAN SQUARE VALUES
NT MEASURE AND INTEGRATION
NT MEROMORPHIC FUNCTIONS
NT MINIMA
NT MONTE CARLO METHOD
NT NEUMANN PROBLEM
NT NEWTON METHODS
NT NEWTON-RAPHSON METHOD
NT NONLINEAR EQUATIONS
NT NONLINEAR EVOLUTION EQUATIONS
NT NUMERICAL ANALYSIS
NT NUMERICAL INTEGRATION
NT ORTHOGONAL FUNCTIONS
NT PADE APPROXIMATION
NT PARABOLIC DIFFERENTIAL EQUATIONS
NT PARTIAL DIFFERENTIAL EQUATIONS
NT PARTICLE IN CELL TECHNIQUE
NT PARTITIONS (MATHEMATICS)
NT PERIODIC FUNCTIONS
NT PERMUTATIONS
NT PHASE-SPACE INTEGRAL
NT POISSON EQUATION
NT POWER SERIES
NT QUADRATIC EQUATIONS
NT RAYLEIGH-RITZ METHOD
NT REAL VARIABLES
NT RELAXATION METHOD (MATHEMATICS)
NT RICCATI EQUATION
NT RITZ AVERAGING METHOD
NT RUNGE-KUTTA METHOD
NT SERIES (MATHEMATICS)
NT SINGULAR INTEGRAL EQUATIONS
NT SINGULARITY (MATHEMATICS)
NT SPHERICAL HARMONICS
NT STURM-LIOUVILLE THEORY
NT TANGENTS
NT TAYLOR SERIES
NT TRIGONOMETRIC FUNCTIONS
NT TRUNCATION ERRORS
NT VECTOR ANALYSIS
NT VLASOV EQUATIONS
NT VOLTERRA EQUATIONS
NT VORTICITY
NT VORTICITY EQUATIONS
NT WALSH FUNCTION
NT WEIERSTRASS FUNCTIONS
NT WEIGHTING FUNCTIONS
NT ZONAL HARMONICS

Transactions of the 4th Army Conference on Applied Mathematics and Computing
[AD-A183544] 01 p0085 N88-10547

Mathematics applied to nuclear geophysics
[INPE-4234-PRE/1109] 01 p0086 N88-10561

Summaries of the FY 1987 applied mathematical sciences research program
[DE87-014447] 02 p0225 N88-11416

A collection of test problems for ordinary differential equation solvers which have provisions for rootfinding
[DE88-000045] 02 p0226 N88-11428

Mathematical techniques for system realization and identification
[AD-A186352] 07 p0915 N88-15557

Strong representation of weak convergence
[AD-A186433] 07 p0916 N88-15563

Numerical resolution of the equations of three-dimensional stable compressible transonic flows
[PB87-168415] 09 p1113 N88-16673

Practical applicability of exact and approximate forms of the randomization test for two independent samples
[AD-A186815] 09 p1231 N88-17381

The mathematization of the military sciences
[MBB-Z-139/87] 10 p1311 N88-17834

International Conference on Industrial and Applied Mathematics
[AD-A188251] 11 p1483 N88-18851

Cumulative reports and publications through December 31, 1987
[NASA-CR-181624] 11 p1524 N88-19099

A unified approach for digital image processing problems: Mathematical morphology
[INPE-4311-TDL/278] 11 p1537 N88-19183

Analysis of simulated annealing type algorithms
[AD-A189382] 12 p1679 N88-20037

Analiticity in fourth order wave equations
[DE88-700837] 12 p1686 N88-20080

Research in applied mathematics ralated to identification of noisy systems
[AD-A189355] 13 p1825 N88-20908

Computation and graphics in mathematical research
[DE88-005796] 13 p1831 N88-20953

Aero/structural tailoring of engine blades (AERO/STAEBL)
[NASA-CR-180805] 14 p1959 N88-21682

Nonlinear analysis and optimal design of dynamic mechanical systems for spacecraft application
[AD-A190644] 15 p2026 N88-22070

The analysis of non-linear dynamic behavior (including snap-through) of postbuckled plates by simple analytical solution
[NASA-TM-89165] 15 p2087 N88-22439

Symmetry and global bifurcation in nonlinear solid mechanics
[AD-A190521] 15 p2121 N88-22642

Analytical sensor redundancy assessment
[NASA-CR-182892] 16 p2163 N88-22901

Analytical orbit propagation of artificial satellites
[INPE-4454-TDL/315] 16 p2166 N88-22915

Generalizing the structure of explanations in explanation-based learning
[AD-A191327] 16 p2256 N88-23481

On 1/n-expansion and wave functions
[DE88-701639] 16 p2260 N88-23509

Application of chaos theory to 1/f noise
[AD-A191150] 17 p2334 N88-23935

Activities of the Institute for Computer Applications in Science and Engineering (ICASE)
[NASA-CR-181666] 17 p2384 N88-24166

Analytical modeling of the structureborne noise path on a small twin-engine aircraft
[NASA-CR-4136] 17 p2394 N88-24233

On a class of functionals invariant under a Z(sup n) action
[AD-A193474] 23 p3269 N88-29451

Finite element analysis of steady and transiently moving/rolling nonlinear viscoelastic structure. Part 1: Theory
[NASA-CR-179886] 23 p3273 N88-29480

Theoretical aerodynamics, transonic flow
[AD-A196247] 24 p3321 N88-29777

ANALYSIS OF VARIANCE

A heteroscedastic hierarchical model
[AD-A184256] 03 p0372 N88-12340

Annotated computer output for split plot design: GENSTAT ANOVA
[AD-A187120] 10 p1385 N88-18271

The statistical characterization of tensile strengths for a nuclear-type graphite 13 p1746 N88-20440

Exact tests for variance component models with unequal cell frequencies in the last stage
[AD-A191645] 18 p2568 N88-25253

ANALYTIC FUNCTIONS

NT ENTIRE FUNCTIONS

A system of three-dimensional complex variables
[NASA-TM-88318] 05 p0645 N88-13951

Using Clifford algebras for the geometry of a tube domain (and its corresponding bounded domain) in the complexified Minkowski space of arbitrary dimension
[REPT-87-64] 16 p2264 N88-23540

N=2 supergravity in superspace: Solution to the constraints
[DE88-702135] 19 p2741 N88-26272

N=2 supergravity in superspace: The invariant action
[DE88-702136] 19 p2741 N88-26273

Holomorphic geometry of interacting string
[DE88-702714] 23 p3295 N88-29627

Track performance considerations for monopulse radars
[AD-A196232] 24 p3360 N88-30007

ANALYTIC GEOMETRY

NT CATENARIES
NT CIRCUMFERENCES
NT CONICS
NT ELLIPSES
NT OBLATE SPHEROIDS
NT PARABOLAS
NT PROLATE SPHEROIDS
NT QUADRANTS
NT S CURVES
NT TANGENTS
NT TORUSES

Steps into a geometer's workbench
[CWI-CS-R8726] 13 p1819 N88-20870

Geometry and graphics applied to robotics
[CWI-CS-R8727] 13 p1824 N88-20903

ANALYTICAL CHEMISTRY

The development of a new and novel Hadamard transform infrared spectrometer for analytical chemistry
[DE87-014804] 02 p0175 N88-11094

A prototype expert system for separation science
[DE87-013542] 03 p0371 N88-12333

Atomic and molecular gas phase spectrometry
[AD-A187562] 11 p1452 N88-18655

Analytical Chemistry Division
[DE88-701236] 16 p2174 N88-22956

ANALYZERS

NT ENGINE ANALYZERS
NT SIGNAL ANALYZERS

Multi-channel communications system analyzer
[AD-A184756] 03 p0307 N88-11937

Multichannel scaling analyzer
[DE88-700541] 07 p0905 N88-15481

A comparison of measurements from the A/E35U-3 and PWMA (Portable Wear Metal Analyzer) spectrometers
[AD-A186855] 09 p1177 N88-17047

Diagnostics for research in atomization and turbulent two-phase flows
[AD-A187338] 11 p1482 N88-18843

Some applications of surface Raman and infrared spectroscopies to mechanistic electrochemistry involved adsorbed species
[AD-A188777] 12 p1606 N88-19602

Hercules: A power analyzer for MOS VLSI circuits
[AD-A188702] 12 p1623 N88-19706

A production-quality UNIX Very High Speed Integrated Circuit (VHSIC) Hardware Description Language (VHDL) subset analyzer
[AD-A188832] 12 p1623 N88-19710

Instrumentation for the characterization and development of millimeter wave components compatible with monolithic integration
[AD-A189724] 15 p2059 N88-22275

FLOSIN: A fluid loop analyzer for SINDA 15 p2066 N88-22321

Two papers on a symbolic analyzer for MOS (Metal-Oxide Semiconductors) circuits
[AD-A188817] 15 p2139 N88-22761

Computer-aided writing
[AD-A192516] 20 p2838 N88-26837

An investigation of the uses of time domain capable vector network analyzers as a diagnostic for helix traveling-wave circuits
[AD-A192460] 21 p2935 N88-27430

Calibration of the portable wear metal analyzer
[AD-A192971] 21 p2950 N88-27524

ANATOMY

NT ADRENAL GLAND
NT ALVEOLI
NT AORTA
NT ARM (ANATOMY)
NT ARTERIES
NT AUTONOMIC NERVOUS SYSTEM
NT BONE MARROW
NT BONES
NT BRAIN
NT CAPILLARIES (ANATOMY)
NT CARDIAC VENTRICLES
NT CARDIOVASCULAR SYSTEM
NT CENTRAL NERVOUS SYSTEM
NT CEREBELLUM
NT CEREBRAL CORTEX
NT CEREBRUM
NT CHEMORECEPTORS
NT CIRCULATORY SYSTEM
NT COCHLEA

NT COLLAGENS
NT CORNEA
NT EAR
NT EFFERENT NERVOUS SYSTEMS
NT EYE (ANATOMY)
NT FINGERS
NT FOVEA
NT GASTROINTESTINAL SYSTEM
NT GLOTTIS
NT GRAVIRECEPTORS
NT HAND (ANATOMY)
NT HEAD (ANATOMY)
NT HEART
NT HIPPOCAMPUS
NT HUMAN BODY
NT HYPOTHALAMUS
NT INTESTINES
NT JOINTS (ANATOMY)
NT KIDNEYS
NT LARYNX
NT LEG (ANATOMY)
NT LIMBS (ANATOMY)
NT LIVER
NT LUNGS
NT MIDDLE EAR
NT MUSCLES
NT MUSCULOSKELETAL SYSTEM
NT MYOCARDIUM
NT NECK (ANATOMY)
NT NERVES
NT NERVOUS SYSTEM
NT OCULOMOTOR NERVES
NT OTOLITH ORGANS
NT PHOTORECEPTORS
NT PITUITARY GLAND
NT PROPRIOCEPTORS
NT PUPILS
NT RESPIRATORY SYSTEM
NT RETINA
NT SEMICIRCULAR CANALS
NT SENSE ORGANS
NT SKIN (ANATOMY)
NT SKULL
NT SPINAL CORD
NT SPLEEN
NT STOMACH
NT SYMPATHETIC NERVOUS SYSTEM
NT TESTES
NT THALAMUS
NT TIBIA
NT TORSO
NT VEINS
NT VESTIBULES
NT WRIST

ANDES MOUNTAINS (SOUTH AMERICA)
SPOT imagery as an aid to understanding volcanism and tectonics: Examples from the Chilean Andes and the Tibetan Plateau 22 p3103 N88-28427

ANDESITE
Does subduction zone magmatism produce average continental crust 24 p3394 N88-30214

ANDROMEDA GALAXY
Stars, gas and dust in the Andromeda galaxy
[B8679680] 16 p2289 N88-23708

ANECHOIC CHAMBERS
Anechoic Chamber test of the Electromagnetic Measurement System ground test unit
[DE87-012998] 01 p0035 N88-10226
New main reflector, subreflector and dual chamber concepts for compact range applications
[NASA-CR-181506] 04 p0402 N88-12498
Acoustic characteristics of 1/20-scale model helicopter rotors
[NASA-CR-177355] 16 p2265 N88-23548
Almond test body --- for microwave anechoic chambers
[NASA-CASE-LAR-13747-1] 18 p2502 N88-24845

ANELASTICITY
Anelastic behaviour of materials under multiaxial strains. Part 3: Order-disorder transition, Shoek effect and Poisson's ratio in AISI-1080 steel
[DE87-703087] 02 p0191 N88-11193
Effect of hydrogen, deuterium and oxygen on the anelastic properties of refractory alloys
[DE88-007349] 18 p2484 N88-24736

ANEMIAS
Hypoxic hypoxia as a stimulus of erythropoiesis in vivo and in vitro 07 p0885 N88-15373
Role of hemoglobin affinity for oxygen in efficiency of blood respiratory function 07 p0892 N88-15406
Hemolysis in runners as evidenced by low serum haptoglobin: Implications for preflight monitoring of astronauts
[NASA-TM-100304] 11 p1518 N88-19067

ANEMOMETERS
NT HOT-FILM ANEMOMETERS
NT HOT-WIRE ANEMOMETERS
NT LASER ANEMOMETERS
Measurement of gas flow velocities near obstacles: Analysis and optimization of an optical barrier velocimeter. Associated signal processing
[ESA-TT-1056] 03 p0315 N88-11991
Comparative testing of wind measuring equipment. Part 1: Inventory and selection
[R-814-D-PT-1] 03 p0325 N88-12053
Simulating high-resolution vertical plane array wind characteristics using lower-spatial-resolution wind measurements
[DE88-005626] 13 p1800 N88-20761
The development of a microanemometer. New possibilities for measuring very low air velocities
[ETN-88-92244] 16 p2210 N88-23191
Thermal remote anemometer system
[NASA-CASE-LAR-13508-1] 17 p2342 N88-23962
A microcomputer based frequency-domain processor for laser Doppler anemometry
[NASA-TM-100998] 20 p2803 N88-26634

ANEMOMETRY
U VELOCITY MEASUREMENT

ANGLE OF ATTACK
Calculation of aerodynamic heat transfer for blunt-nosed thin wings at different angles of attack at supersonic speeds
[NASA-TT-20127] 02 p0123 N88-10776
Optimum take-off run of aircraft on ground airfields 04 p0423 N88-12623
Low speed wind tunnel investigation of propeller slipstream aerodynamic effects on different nacelle/wing combinations. Part 1: Total forces and moments and pressure distributions on nacelle/wing at different angles of attack and yaw and at different thrust coefficients
[FFA-TN-1987-22] 05 p0542 N88-13302
Predicting dynamic separation characteristics of general configurations
[AD-A186689] 09 p1116 N88-16691
Measurement of forces and moments on, and velocity about a body of revolution with an attached fin at angles of attack
[AD-A187796] 11 p1433 N88-18554
Modeling of limit cycle stall flutter oscillations 12 p1583 N88-19472
Surface flow visualization of separated flows on the forebody of an F-18 aircraft and wind-tunnel model
[NASA-TM-100436] 14 p1863 N88-21127
Data processing method for high angle of attack testing with rolling angle 14 p1864 N88-21134
An experimental study to determine the flow and the subsonic static and dynamic stability characteristics of aircraft operating at high angles-of-attack 16 p2201 N88-23129
Flow visualization study of vortex manipulation on fighter configurations at high angles of attack 16 p2201 N88-23130
Investigation on the movement of vortex burst position with dynamically changing angle of attack for a schematic deltawing in a watertunnel with correlation to similar studies in windtunnel 16 p2204 N88-23152
Experiments to investigate the vortices shed from a submarine-like body of revolution 16 p2205 N88-23156
Wind-tunnel investigation of actuated forebody strakes for yaw control at high angles of attack 17 p2299 N88-23754
Computation of flow around NACA0012 airfoil at high angle of attack 19 p2636 N88-25640
High speed and high angle of attack wind tunnel test results of the winged space vehicle C-2
[ISAS-RN-623] 20 p2751 N88-26329
The effect of a turbulent airstream on a vertically-launched missile at high angles of attack
[AD-A192408] 20 p2758 N88-26363
Calculation of aerodynamic characteristics of airplane configurations at high angles of attack
[NASA-CR-4182] 23 p3172 N88-28891
Angle of attack and sideslip estimation using an inertial reference platform
[AD-A194876] 24 p3319 N88-29769
Computer programs for calculation of sting pitch and roll angles required to obtain angles of attack and sideslip on wind tunnel models
[NASA-TM-100659] 24 p3329 N88-29820

ANGLES (GEOMETRY)
NT ANGLE OF ATTACK
NT BRAGG ANGLE
NT DIHEDRAL ANGLE
NT ELEVATION ANGLE
NT LEADING EDGE SWEEP
NT SWEEP ANGLE
NT SWEEPBACK
Effects of free stream turbulence, Reynolds number and incidence angle on axial turbine cascade performance 05 p0548 N88-13339
The effect of collision angle on mach reflection
[AD-A185798] 06 p0704 N88-14319
Acoustic scattering from composite wind-wave surfaces 3: Forward scatter intensities and spatial coherence at low and high frequencies and small grazing angles for Bubble-free regimes
[AD-A185908] 07 p0881 N88-15345
An investigation of oblique hypervelocity impact 07 p0927 N88-15629
The angular reflectance signature of the canopy hot spot in the optical regime
[DE88-005385] 11 p1505 N88-18991
Reduction of erosion in elbows due to flow modifications, phase 1
[DE88-001028] 13 p1769 N88-20584
A symmetric set of Euler angles and oblique orientation space sections
[DE88-005317] 13 p1847 N88-21056
Universal precision sine bar attachment
[NASA-CASE-MFS-28253-1] 18 p2523 N88-24971
Joint angle sensors for closed-loop control 19 p2673 N88-25891

ANGULAR ACCELERATION
Laser gyroscopes using the rate-bias technique 18 p2517 N88-24930

ANGULAR CORRELATION
Perturbed angular correlations in zirconia ceramics
[DE88-004117] 11 p1464 N88-18731
Angular position measurements at high temperatures and high radiation environments 17 p2434 N88-24479

ANGULAR DISTRIBUTION
Analysis of relativistic nucleus-nucleus interactions in emulsion chambers 07 p0926 N88-15624
Mode pattern of field generated by parametric radiator in acoustic waveguide 08 p1076 N88-16488
Equation of gravitational-gyroscopic waves: Angular potential and its applications 08 p1079 N88-16504
Research relative to angular distribution of snow reflectance/snow cover characterization and microwave emission
[NASA-CR-182733] 14 p1941 N88-21582
Angular resolved energy analysis of (69)Ga+ ions from a gallium liquid metal ion source
[AERE-R-12649] 15 p2139 N88-22760
Angular radiation models for Earth-atmosphere system. Volume 1: Shortwave radiation
[NASA-RP-1184] 21 p2976 N88-27677

ANGULAR MOMENTUM
Angular momentum evolution of young stars 04 p0504 N88-13099
Post-zero-age main sequence rotation 04 p0504 N88-13100
Relation of wave energy and momentum with the plasma dispersion relation in an inhomogeneous plasma
[DE88-002305] 08 p1084 N88-16530
Application of state-multipole Heisenberg equations to Raman excitation dynamics
[DE88-003828] 10 p1335 N88-17977
State-to-state dynamics of molecular energy transfer
[DE88-003282] 10 p1406 N88-18382
Positron-annihilation 2D-ACAR studies of disordered and defected alloys
[DE88-003118] 10 p1416 N88-18454
Parametric dependence in the equilibrium dynamics of rotating structures
[AD-A187817] 11 p1498 N88-18945
Modelling and control of an annular momentum control device
[NASA-CR-4138] 13 p1754 N88-20491
Collective rotation of molecules driven by the angular momentum of light in a nematic film
[FUB-6-1988] 15 p2131 N88-22714
Nutational stability of a satellite equipped with an active magnetic momentum wheel 20 p2784 N88-26513
Mass transfer instabilities due to angular momentum flows in close binaries --- stars
[MPE-PREPRINT-113] 22 p3165 N88-28849
Atmospheric angular momentum and length of day
[AD-A194505] 23 p3233 N88-29238

ANGULAR MOTION
U ANGULAR VELOCITY

ANGULAR RESOLUTION
CERGA high angular resolution optical network --- astronomical interferometry 01 p0096 N88-10633
Diagnostics of solar coronal loops at interferometric angular resolution 01 p0098 N88-10642
Galactic nuclei and quasars at high angular resolution 01 p0098 N88-10644
New results from high angular resolution observations of alpha Ori 04 p0514 N88-13161
The angular diameter of alpha Scorpii in the near-infrared Ca II triplet 04 p0514 N88-13162

Analysis of a range estimator which uses MLS angle measurements
[NASA-CR-182896] 16 p2160 N88-22884

ANGULAR VELOCITY
Spin-up and spin-down on the way to the main sequence 04 p0518 N88-13181
Investigation of the spin stability of the NPS (Naval Postgraduate School) mini-satellite (Orion)
[AD-A187781] 11 p1445 N88-18613
A LQG regulator for the angular motion of the rotor at a tuned gyroscope
[INPE-4280-PRE/1152] 12 p1631 N88-19759
Automatic feedback control of a rigid body for finite displacements 18 p2473 N88-24674

ANHYDRIDES
NT PEROXIDES
Synthesis of energetic materials
[AD-A189115] 13 p1753 N88-20482

ANIMALS
NT AMOEBA
NT AMPHIBIA
NT ARTEMIA
NT BIRDS
NT CATS
NT CHICKENS
NT DOGS
NT DROSOPHILA
NT FISHES
NT FROGS
NT HUMAN BEINGS
NT INSECTS
NT INVERTEBRATES
NT MAMMALS
NT MICE
NT MOLLUSKS
NT MONKEYS
NT PARAMECIA
NT PRIMATES
NT RATS
NT SEA URCHINS
NT SNAILS
NT VERTEBRATES
NT WATERFOWL
A plethysmograph for measuring pulmonary ventilation in small animals
[AD-A184978] 05 p0629 N88-13846
Space station accommodations for life sciences research facilities. Phase 1: Conceptual design and programmatics studies for Missions SAAX0307, SAAX0302 and the transition from SAAX0307 to SAAX0302. Volume 2: Study results
[NASA-CR-179244] 08 p0962 N88-15829
Supersonic and subsonic aircraft noise effects on animals: A literature survey
[AD-A186922] 10 p1404 N88-18373
Five New South Wales barrier lagoons: Their macrobenthic fauna and seagrass communities 11 p1517 N88-19059
Space station accommodations for life sciences research facilities: Phase A conceptual design and programmatics studies for Missions SAAX0307, SAAX0302 and the transition from SAAX0307 to SAAX0302. Volume 1: Executive summary
[NASA-CR-179267] 12 p1599 N88-19571
Animal research on the Space Station 12 p1662 N88-19964
A neuronal model of classical conditioning
[AD-A188378] 12 p1670 N88-19999
A cardiostimulant protein from the Australian Red Waratah Sea anemone, Actinia tenebrosa 18 p2550 N88-25138
USAF hyperbaric animal transfer chamber system
[AD-A193633] 23 p3237 N88-29265

ANIMATION
NT COMPUTER ANIMATION

ANIONS
Separation of anionic from nonionic alkoxy compounds using silica gel
[GB-PATENT-2-140-415-A] 01 p0020 N88-10122
The mechanism of stereo regulation during anionic polymerization of polar monomers
[AD-A186530] 08 p0973 N88-15888
A simple interpretation of the Fe2(-) photoelectron spectrum
[NASA-CR-182553] 11 p1543 N88-19225
Electrosorptive detection based on double-layer capacitance for selective anion monitoring in ion chromatography. Part 1: Mercury electrodes
[AD-A188780] 12 p1606 N88-19603
Electronic structure and stability of small cation and anion hydrogen clusters 16 p2267 N88-23562

ANISOTROPIC FLUIDS
Study of one-dimensional spectral dynamic equations of the Reynolds stresses in homogeneous anisotropic turbulence: Application to split-spectrum modeling 16 p2196 N88-23095
Modeling scalar flux and the energy and dissipation equations 16 p2196 N88-23096

ANISOTROPIC MEDIA
NT ANISOTROPIC FLUIDS
Mechanics of anisotropic media. Study of the boundary conditions --- stratified composites
[SNIAS-872-430-112] 05 p0559 N88-13404
Time-domain reciprocity theorems for electromagnetic fields in dispersive media
[PB88-126925] 10 p1319 N88-17886
Subroutines for solving the equation of diffusion in media with anisotropic properties
[DE88-700743] 11 p1536 N88-19179
An improved boundary force method for analyzing cracked anisotropic materials
[NASA-TM-101495] 24 p3340 N88-29879

ANISOTROPIC PLATES
A refined nonlinear analysis of laminated composite plates and shells
[AD-A184436] 04 p0454 N88-12811
Postbuckling of laminated anisotropic panels
[NASA-TM-100509] 08 p0994 N88-16011
The buckling and vibration of composite plates using the Levy method considering shear deformation and rotary inertia
[AD-A189743] 15 p2076 N88-22374
On the calculation of stresses in pin-loaded anisotropic plates
[ETN-88-92239] 16 p2222 N88-23261
On the calculation of stresses in pin-loaded anisotropic plates
[LR-529] 16 p2223 N88-23268

ANISOTROPIC SHELLS
A refined nonlinear analysis of laminated composite plates and shells
[AD-A184436] 04 p0454 N88-12811

ANISOTROPY
NT ELASTIC ANISOTROPY
Life prediction and constitutive models for engine hot section anisotropic materials program 02 p0188 N88-11175
Deviatoric constitutive relationship for anisotropic materials
[AD-A184332] 03 p0295 N88-11854
Experimental perspectives on heavy electron metals
[DE87-014766] 04 p0416 N88-12583
Structure of thermotropic polyesters with large substituents
[AD-A184086] 04 p0418 N88-12595
Velocity scaled aeroelastic testing of an unducted fan
[GTL-191] 05 p0548 N88-13337
Molecular and supramolecular orientation in conducting polymers
[DE88-000533] 05 p0569 N88-13472
Axial anisotropy of the intensity of the cosmic ray nuclear component
[IFSI-87-7] 05 p0662 N88-14061
Nonlinear relaxation and ergodicity breakdown in random anisotropy spin glasses
[PREPRINT-565] 06 p0764 N88-14693
Dipole component of relict radiation determined from Relikt experiment data 08 p1002 N88-16070
Nonequilibrium ionization of pregalactic plasma and lessening of relic radiation anisotropy 08 p1002 N88-16071
The role of anisotropy in the long range reconnaissance of the albedo of land surfaces 08 p1017 N88-16169
The anisotropy of reflected solar radiation over several types of land surface 08 p1018 N88-16171
Transversely anisotropic curved optical fibres: Variational analysis of a nonstandard Eigenproblem
[PB88-112966] 08 p1083 N88-16528
An analytical study of the effects of transverse shear deformation and anisotropy on natural vibration frequencies of laminated cylinders
[NASA-TM-100554] 10 p1295 N88-17739
Bias, internal stress and substrate effects on the microstructure and properties of PVD-wear resistant coatings
[AERE-R-12360] 10 p1304 N88-17798
The mechanism of anisotropic silicon etching and its relevance for micromachinings
[MBB-UA-1013/86] 10 p1311 N88-17838
The physics of metallic superlattices: An experimental point of view
[DE88-003080] 10 p1416 N88-18452
A sky temperature survey at 19.2 GHz using a balloon borne Dicke radiometer for anisotropy tests of the cosmic microwave background 11 p1571 N88-19403
Brillouin scattering from collective spin waves in magnetic superlattices
[DE88-005347] 12 p1697 N88-20154
Observations of the large scale anisotropy in the cosmic background radiation at 3 mm
[INPE-4425-PRE/1229] 12 p1712 N88-20249
Anisotropy of microstructural eddy motion in surface layer during calm 13 p1784 N88-20677
Electrical characteristics of MBE (Molecular Beam Epitaxyl)-grown GaAs/sub 1-x/Sb/sub x on InP and correlation with film microstructure
[DE88-003841] 13 p1847 N88-21053
Early reheating and cosmic strings 13 p1855 N88-21103
A model of the anisotropic structure of the neutral gas coma of a comet 14 p1999 N88-21918
Anisotropic emission from comets: Fans versus jets. 1: Concept and modeling 14 p2001 N88-21927
Anisotropic emission from comets: Fans versus jets. 2: Periodic Comet Tempel 2 14 p2001 N88-21928
Improvements to tilt rotor performance through passive blade twist control
[NASA-TM-100583] 15 p2086 N88-22434
Electrical anisotropy of layered semiconductor ZrSe2 16 p2257 N88-23488
Shape stability in composites 18 p2479 N88-24706
Changes in seismic velocity and apparent attenuation due to isotropic and anisotropic scattering: Results from physical modeling 19 p2691 N88-25997
Peturbational analysis of the curved anisotropic optical fiber for the birefringence due to the geometry
[PB88-171848] 19 p2726 N88-26189
Stress concentration around circular hole in a composite material specimen representative of the X-29A forward-swept wing aircraft
[NASA-CR-179435] 20 p2814 N88-26694
Anisotropic characteristic lengths in single crystal YBa2Cu3O(sub 7-Delta)
[DE88-009959] 20 p2877 N88-27080
Anisotropy of the lower critical field in YBa2Cu3O(sub 7-Delta)
[DE88-009971] 20 p2877 N88-27081
Probabilistic anisotropic failure criteria for composite materials
[AD-A193046] 21 p2904 N88-27232
An anisotropic continuum damage model for creep-dominated, multiaxial loading histories 21 p2964 N88-27608
On plasma stability under anisotropic random electric field influence
[DE88-702422] 21 p3019 N88-27918
Investigation of magnetic anisotropy and spin wave modes in transition metal multilayers
[DE88-009007] 22 p3154 N88-28765
Anisotropic constitutive modeling for nickel-base single crystal superalloys
[NASA-CR-182157] 24 p3353 N88-29961

ANNEALING
NT LASER ANNEALING
NT PULSE HEATING
Effect of high-temperature annealing on the microstructure and thermoelectric properties of GaP doped SiGe
[NASA-TM-100164] 01 p0029 N88-10188
Hydrogen annealing of P(sub) b and E prime defect centers in oxidized silicon wafers
[DE87-014293] 02 p0152 N88-10951
Defect characterization in quartz and related materials
[AD-A184754] 03 p0294 N88-11846
Dynamics of atoms in low-symmetry systems
[AD-A184318] 03 p0375 N88-12361
On the stressing of annealed NITINOL: The electrical resistance and calorimetric effects
[AD-A184485] 04 p0414 N88-12569
Threshold stress for fatigue crack initiation from a small crack 05 p0601 N88-13675
Structural characterization of ion implanted beta-SiC thin films
[DE87-014567] 05 p0656 N88-14027
Ion mixing and surface modification in metal-semiconductor systems
[DE88-001702] 06 p0786 N88-14823
Effect of high pressure oxygen loading on the superconductivity of La2CuO4
[DE88-002108] 06 p0787 N88-14827
Kinetics and mechanism of thermal aging embrittlement of duplex stainless steels
[DE88-002987] 08 p0969 N88-15866
Influence of post-anneal cooling treatments on suppression of cryogenic intergranular fracture in experimental Ni-free high-Mn austenitic steels
[DE88-002766] 09 p1145 N88-16863
Neutron- and X-ray-small angle scattering with Fe-base metallic glasses
[DE88-002538] 09 p1147 N88-16876
Forward-biased current annealing of radiation damaged gallium arsenide and silicon solar cells
[AD-A186904] 09 p1186 N88-17105
Growth of HgZnTe layers by LPE technique
[AD-A186723] 09 p1255 N88-17520

X-ray diffraction study of thermotropic liquid crystalline polyesters and diester model compounds
[AD-A186788] 09 p1255 N88-17521
Low temperature reactivity of chars towards oxygen, appendix E2
[DE88-004088] 10 p1298 N88-17760
Experiences with serial and parallel algorithms for channel routing using simulated annealing
[NASA-CR-182530] 10 p1388 N88-18289
High temperature processing of superconducting Y1Ba2Cu3O6.9
[DE88-003002] 10 p1416 N88-18449
Improved magnetization for YBa2Cu3O/sub 7-delta annealed in oxygen above 1000 C
[DE88-003934] 10 p1418 N88-18469
Processing relationships in YBa2Cu3O(7-x) superconductors
[DE88-005137] 11 p1559 N88-19330
Radiation response of thin oxides grown by rapid thermal oxidation and rapid thermal annealing techniques
[DE88-003632] 11 p1561 N88-19347
An in situ annealing study of lead implanted single crystal calcium titanate
[DE88-005435] 11 p1562 N88-19351
Analysis of simulated annealing type algorithms
[AD-A189382] 12 p1679 N88-20037
Study of defects in metals by positron annihilation
[DE88-701042] 13 p1745 N88-20432
Optical study of germanium, germanium plus arsenic, and germanium plus gallium implants in gallium arsenide
[AD-A189600] 13 p1845 N88-21045
Structure and strength of boron-aluminum composites
14 p1885 N88-21264
Dynamical optimization techniques for the calculation of electronic structure in solids
[DE88-006010] 15 p2140 N88-22766
The effect of elevated temperature on irradiated MOS devices 17 p2406 N88-24308
A study on the precipitation and reversion behaviors of Cu-0.3 percent Cr alloy by the step annealing method
[NASA-TT-20169] 18 p2489 N88-24764
An improved simulated annealing algorithm for standard cell placement
[NASA-CR-182952] 18 p2558 N88-25183
Electrical study of metal/group 3-5 semiconductor interfaces: Comparison with the atomic-level studies
20 p2874 N88-27059
NDP (Neutron Depth Profiling) evaluations of boron-implanted compound semiconductors
[AD-A192306] 21 p2934 N88-27425
Short pulse X-ray diffraction studies of shocked and annealed crystals using the JANUS research laser
[DE88-011329] 23 p3288 N88-29579
An HVEM study of displacement cascade damage in Nb3Sn at 13 K
[DE88-009997] 23 p3289 N88-29584
Rapid thermal annealing of silicon layers amorphized by ion implantation
[DE88-702307] 23 p3290 N88-29591

ANNIHILATION REACTIONS
NT POSITRON ANNIHILATION
Basic physics program for a low energy antiproton source in North America
[DE88-003148] 08 p1082 N88-16522
Event classification in (anti)neutrino experiments using an Internal Picket Fence-External Muon Identifier (IPF-EMI) detector system
[NIKHEF-H/87-6] 09 p1245 N88-17457
Beta limitation of matter-antimatter boundary layers
[TRITA-EPP-87-11] 09 p1250 N88-17490
A study of the magnetic field annihilation process in the magnetosphere and some geotechnical applications
[DE88-004165] 10 p1355 N88-18096
Nuclear structure at intermediate energies
[DE88-002796] 10 p1407 N88-18390
Advanced space propulsion study - antiproton and beamed power propulsion
[AD-A189218] 13 p1732 N88-20355
Proton/antiproton yields W(+/-)boson gamma X as a test of the quark charges
[NIKHEF-H/87-11] 13 p1836 N88-20987
New limits on charged Higgs boson mass with CELLO at Petra (Italy) and status of the neutral Higgs boson search
[NOTA-INTERNA-897] 14 p1980 N88-21817
Annihilation momentum density of positrons trapped at vacancy-type defects in metals and alloys
[DE88-005936] 15 p2144 N88-22797
Prospects for antiproton production and propulsion
16 p2267 N88-23556
Stable, heavy, neutral particles in the sun and in toponium decay 17 p2452 N88-24568
Research in theoretical particle physics
[DE88-008230] 20 p2851 N88-26927
Study of the production of Ko mesons in proton antiproton interactions at 630 GeV
[NOTA-INTERNA-908] 21 p3015 N88-27892

ANNOTATIONS
Annotated algebraic specification of the static semantics of pool
[PB88-106695] 07 p0912 N88-15533

ANNUAL VARIATIONS
Spatial characterization of acid rain stress in Canadian Shield Lakes
[NASA-CR-181136] 01 p0067 N88-10430
Spatial characterization of acid rain stress in Canadian Shield Lakes
[NASA-CR-180577] 01 p0067 N88-10431
Theoretical and lidar studies of the seasonal and nocturnal variations of the mesospheric sodium layer at Urbana, Illinois 01 p0068 N88-10435
Atlas of wide-field-of-view outgoing longwave radiation derived from Nimbus 7 Earth radiation budget data set - November 1978 to October 1985
[NASA-RP-1186] 01 p0070 N88-10451
Short reference year
[PB87-107470] 03 p0352 N88-12221
Environmental processes and spectral reflectance characteristics associated with soil erosion in desert fringe regions
[NASA-CR-182332] 05 p0620 N88-13811
The lower thermosphere wind regime from simultaneous observations over Euroasia (Colim, Dushanbe, Frunze)
06 p0733 N88-14510
On the interconnection of dynamic processes in the lower thermosphere with meteorological phenomena in the tropostratosphere 06 p0734 N88-14512
Characteristics of atmospheric disturbances with a quasi-two day period 06 p0734 N88-14515
Lower thermosphere wind regime according to radiometeor measurements in Kazan
06 p0736 N88-14526
Density variations of meteor flux along the Earth's orbit 06 p0739 N88-14545
Structural peculiarities of the Quadrantid meteor shower 06 p0740 N88-14552
The global climate system: Autumn 1984 to spring 1986
[CSM-R84/86] 06 p0745 N88-14583
Neurophysiological analysis of hypothalamic regulation mechanisms of primary sleep and hypobiosis
06 p0751 N88-14611
Seasonal cycling of sulfur and iron in porewaters of a Delaware salt marsh
[NASA-CR-182385] 07 p0876 N88-15311
The solar radiation incident at the top of the atmosphere of Uranus and Neptune
[AERONOMICA-ACTA-A-317-1987]
07 p0878 N88-15323
SEQUAL (seasonal Equatorial Atlantic) meteorological data from Moorings S2, S5 and S6 (March 1983 - March 1985)
[PB88-108048] 07 p0880 N88-15337
Long-term variation of total ozone
[INPE-4307-PRE/1173] 08 p1023 N88-16192
Effect of storage thermal behavior in seasonal storage solar heating systems
[PB88-114236] 10 p1350 N88-18067
Spatial-temporal variability of North Pacific sea surface temperature anomaly patterns 11 p1516 N88-19058
Seasonal variations and excitation mechanisms of the equatorially trapped waves 13 p1798 N88-20751
Computer simulation of tropospheric chemistry
[JUEL-2144] 13 p1798 N88-20756
Northern Hemisphere circulation and the principal components of subsequent summer patterns in North America and West Africa 13 p1801 N88-20765
Analysis of winter season precipitation bands over the Southern Plains 14 p1947 N88-21609
Seasonal variation for structural strength value
[PB88-169248] 16 p2222 N88-23260
Latitudinal and seasonal variation of the cloud characteristic parameters and their effects on the cloud classification 17 p2351 N88-24005
Sea ice kinematics: Space and time scales
[AD-A191162] 17 p2376 N88-24128
Examples of ice pack rigidity and mobility characteristics determined from ice motion
[AD-A191163] 17 p2377 N88-24129
The seasonal exchange of carbon dioxide between the atmosphere and the terrestrial biosphere: Extrapolation from site-specific models to regional models
[DE88-007870] 20 p2822 N88-26740
Circulation statistics from seasonal and perpetual January and July simulations with the NCAR (National Center for Atmospheric Research) Community Climate Model (CCM1):R15
[PB88-192620] 20 p2823 N88-26748
The 1985 Meteorological Yearbook of Ispra (27th)
[PB88-125729] 20 p2828 N88-26777
Following the seasonal evolution of a natural environment in a humid tropical region. Preliminary Evaluation of SPOT (PEPS) number 186: Bangui, Central Africa 22 p3093 N88-28368
Variations in spectral reflectance signature in healthy stands of pine and spruce
[FOA-C-30468-3.1] 22 p3116 N88-28512
Proceedings of the Twelfth Annual Climate Diagnostics Workshop
[PB88-191747] 22 p3119 N88-28534
Indian monsoon rainfall: 1986-1987
22 o3120 N88-28536
Zonal wind observations at Christmas Island (2 deg N, 157 deg W) during the 1986-1987 El-Nino
22 p3120 N88-28539
Intraseasonal variability in atmospheric surface pressure and relationship to polar motion
22 p3120 N88-28540
The dynamics and thermodynamics of a 30-60 day oscillation 22 p3121 N88-28543
Complex EOF analysis of intraseasonal tropical wind fluctuations 22 p3121 N88-28544
Some diagnostic results concerning the tropical 40-50 day oscillation 22 p3121 N88-28546
Tropospheric biennial variability and its relationship to the southern oscillation 22 p3121 N88-28549
Recent secular changes in the wintertime circulation of the Southern Hemisphere 22 p3122 N88-28555
Northern Hemisphere 700 mb teleconnections based on half-monthly mean anomaly data stratified by season and by sign 22 p3123 N88-28561
Interannual variability of 850 mb temperatures during the Northern Hemisphere winter
22 p3123 N88-28562
The active layer of the upper Atlantic Ocean
22 p3124 N88-28566
Operational multifield analog forecasting of US seasonal temperatures for non-winter seasons
22 p3127 N88-28592
Observed normal mode structure of low frequency oscillations 22 p3128 N88-28595

ANNULAR DUCTS
Determination of the dynamic parameters of annular clearances with turbulent flow and incompressible media
[ETN-87-90434] 01 p0047 N88-10303
Use of a local heat source for determining temperature of inlet heat section in ring channels
[DE88-700332] 07 p0854 N88-15187
Entrance and exit region friction factor models for annular seal analysis
[NASA-CR-183084] 19 p2678 N88-25921

ANNULAR FLOW
Experimental and theoretical studies of vertical annular liquid jets
[DE87-013907] 01 p0047 N88-10299
The numerical and analytical study of bifurcation and multicellular flow instability due to natural convection between narrow horizontal isothermal cylindrical annuli at high Rayleigh numbers
[AD-A186113] 07 p0849 N88-15151
An experimental investigation of straight and curved annular wall jets
[NASA-CR-182546] 11 p1434 N88-18557
Experimental and numerical study of liquid distribution in dispersive-annular flow
[DE88-700844] 14 p1909 N88-21406
Interaction of a two-dimensional bluff body and incompressible jet and annulus flows
[AD-A190503] 15 p2064 N88-22310
Investigation of annular flow at high evaporation rates in view of liquid film cooling
[DFVLR-FB-88-08] 21 p2949 N88-27517

ANNULAR NOZZLES
Wake interaction effects on the transition process on turbine blades
[AD-A188020] 10 p1332 N88-17962

ANNULAR PLATES
A finite element procedure for interference-fit and cold-working problems with limited yielding
[AR-004-517] 04 p0485 N88-12992
Analysis of annular microstrip antennas for hyperthermic applicators
[PB88-181508] 19 p2643 N88-25679

ANNULAR SUSPENSION AND POINTING SYSTEM
Synchronous response modelling and control of an annular momentum control device
[NASA-CR-4166] 24 p3358 N88-29995

ANNULI
The numerical and analytical study of bifurcation and multicellular flow instability due to natural convection between narrow horizontal isothermal cylindrical annuli at high Rayleigh numbers 10 p1328 N88-17937
Embedded minimal sufaces with an infinite number of ends
[DE88-006429] 15 p2126 N88-22680

Nonlinear elliptic problems with critical exponent in shrinking annuli
[W-02/87] 23 p3273 N88-29477

ANODES
NT CELL ANODES
Impedance of passive lithium anodes in SOCl2 solutions under low-field polarization
[DE88-000922] 04 p0439 N88-12728
Internal reforming development for solid oxide fuel cells
[DE87-006518] 04 p0464 N88-12871
Investigation of materials for inert electrodes in aluminum electrodeposition cells
[DE88-003380] 10 p1323 N88-17906
Anodic behavior of Ni-P and Ni-Cr-P metallic glasses
[DE88-005334] 11 p1463 N88-18722
Aluminum-air battery development
[DE88-006617] 13 p1762 N88-20542
Generation of high brightness ion beam from insulated anode PED 16 p2278 N88-23637
Research on anode plasma behavior of flashover pulsed ion sources 16 p2279 N88-23640
Time-resolved spectroscopic measurement of anode plasma in magnetically-insulated diode 16 p2279 N88-23641
Study on the flashover ion diode with cryogenic anode 16 p2279 N88-23642
Sulfur-tolerant anode materials
[DE88-001034] 18 p2537 N88-25054
Ambient temperature secondary lithium batteries using LiAl lithium insertion anodes
[DE88-008394] 20 p2793 N88-26574

ANODIC COATINGS
Corrosion behavior of high density tungsten alloys
[AD-A187108] 09 p1143 N88-16852
The soft/hard wet anodization of aluminum oxide and its use in a thin film multilayered capacitor
[AD-A187575] 10 p1325 N88-17919
An interdisciplinary approach to predictive modeling of structural adhesive bonding: Factors affecting the durability of titanium/epoxy bonds
[AD-A189503] 12 p1611 N88-19636
ONR Far East Scientific Bulletin, volume 12, number 3, July-September 1987
[AD-A188554] 13 p1851 N88-21081
AC impedance analysis of corrosion fatigue in naval aircraft alloys
[AD-A190822] 17 p2322 N88-23865
Thermal conductivity of hard anodized coatings on aluminum
[AD-A191755] 18 p2492 N88-24784

ANODIZING
Mathematical modelling of solar ultraviolet radiation induced optical degradation in anodized aluminum 02 p0135 N88-10846
Chromic acid anodizing of aluminum foil
[NASA-CR-178417] 07 p0837 N88-15077
The effect on initial bond strength and durability of a Phosphoric Acid Dip (PAD) following chromic acid anodising of aluminum
[ARE-TM(UMM)-87402] 10 p1300 N88-17772
A modified sulphuric acid anodising process used as a pretreatment for the adhesive bonding of aluminum alloys
[ARE-TM(UMM)-87410] 16 p2177 N88-22974

ANOMALIES
NT GEOTHERMAL ANOMALIES
NT GRAVITY ANOMALIES
NT MAGNETIC ANOMALIES
BRASILSAT A2: Ground and in-orbit anomalies 02 p0164 N88-11032
Effects of long term storage on aerospace nickel cadmium cell performance 02 p0165 N88-11035
Test summary for advanced H2 cycle NI-CD cell 02 p0165 N88-11040
Anomalies in gauge theories
[DE87-014087] 02 p0229 N88-11444
Covariant Lorentz anomalies in higher dimensional space
[DE87-753021] 02 p0230 N88-11448
Chiral U(1) anomaly in D = 4 super Yang-Mills theory coupled to supergravity
[DE87-753022] 02 p0252 N88-11591
Analytical average model of studies on orbital resonance 03 p0269 N88-11689
On air-drag perturbation of transit satellite and selection of parameters in orbit improvement 03 p0269 N88-11691
Electrostatic discharges in geostationary orbit: The case of Telecom 1 03 p0275 N88-11733
The interpretation of crustal dynamics data in terms of plate motions and regional deformation near plate boundaries
[NASA-CR-181475] 03 p0349 N88-12205
Failure control techniques for the SSME
[NASA-CR-179224] 04 p0409 N88-12537
J = O Task Force
[DE88-001326] 04 p0450 N88-12788
On the interannual variability of South American climate and the Southern Oscillation 04 p0470 N88-12905
Anomalous phonon behavior of superconductor Y-Ba-Cu-O
[DE87-703401] 05 p0654 N88-14010
Role of anomalous currents in formation of ocean surface temperature field 06 p0727 N88-14474
Anomalies in electromagnetic absorption of circularly polarized ultrasonic waves by tungsten within Doppler-shifted cyclotron resonance range 06 p0775 N88-14756
Anomalous scaling laws in multifractal objects
[NOTA-INTERNA-883] 07 p0916 N88-15565
Variations of tropical circulation and associated rainfall anomalies, during 2 years of contrast
[INPE-4359-TDL/300] 08 p1039 N88-16286
Space shuttle main engine anomaly data and inductive knowledge based systems: Automated corporate expertise 08 p1060 N88-16398
A generalized description of the anomalous Doppler resonance and the stabilizing role of ion dynamics
[INPE-4384-PRE/1204] 08 p1081 N88-16513
F-layer polar cap arcs
[AD-A186592] 09 p1190 N88-17127
Persistence characteristics of 500 mb blocking and zonal flows in the mid-latitudes of the Northern and Southern Hemispheres 10 p1353 N88-18088
Spatial-temporal variability of North Pacific sea surface temperature anomaly patterns 11 p1516 N88-19058
NAVARES: A prototype expert system for NAVSTAR anomaly resolution
[AD-A189491] 12 p1600 N88-19579
Ion content and infrared absorption of moist atmospheric air
[AD-A188839] 12 p1643 N88-19838
SUSY anomaly in quantum-mechanical systems
[DE88-700890] 12 p1899 N88-20170
Anomalous shock sensitivity/density relationship for RDX-polyethylene wax and related formulations from MRL Small Scale Gap Test (SSGT) measurements
[MRL-R-1099] 13 p1739 N88-20399
Sample models of steady and low frequency circulations in the tropical atmosphere, with application to tropical air-sea interactions 13 p1801 N88-20764
Computerised measurement of human horizontal smooth pursuit eye movements 13 p1811 N88-20819
Sea surface temperatures of winter 1982-83 and their effect on atmospheric circulation 14 p1936 N88-21546
Aerodynamic aspects of the Amazon Forest
[INPE-4445-TDL/313] 15 p2098 N88-22501
Tropical circulations and the associated rainfall anomalies during two contrasting years
[INPE-4506-PRE/1261-REV] 15 p2098 N88-22502
Recent developments in the path integral approach to anomalies
[DE87-703032] 15 p2118 N88-22616
Anomalies in the vegetation in the Alto Xingu - MT 17 p2357 N88-24043
Remote sensing and structural rupture: Application examples in the study of tectonics 17 p2359 N88-24050
Electrical conduction in thin film carbons
[AD-A191726] 18 p2491 N88-24780
Anomalous temperature-dependent negative magnetoresistance in pregraphitic carbons
[AD-A191725] 19 p2619 N88-25535
Electron tunneling in junctions doped with semiconductors and metals 19 p2734 N88-26236
A severe spacecraft-charging event on SCATHA in September 1982
[AD-A193007] 20 p2765 N88-26396
Drift wave vortices and anomalous transport
[DE88-009562] 20 p2859 N88-26982
The 1986-87 Pacific warm episode: Oceanic and Atmospheric features 22 p3120 N88-28535
Modes of interannual climate variability and Sahel rainfall anomalies 22 p3121 N88-28547
Tropospheric biennial variability and its relationship to the southern oscillation 22 p3121 N88-28549
Sub-Saharan rainfall anomalies and global sea-surface temperature relationships for the recent fifteen year (1970-1984) period 22 p3122 N88-28552
Simulation studies of the influence of sea-surface temperature anomalies on the Sahelian circulation and rainfall 22 p3122 N88-28553
Northern Hemisphere 700 mb teleconnections based on half-monthly mean anomaly data stratified by season and by sign 22 p3123 N88-28561
An observational study of interaction between large scale tropical cumulus convection and the equatorial circulation anomalies 22 p3124 N88-28564
Factors influencing summer temperatures and precipitation in the southwest 22 p3124 N88-28565
Global-scale temperature changes to August 1987 and a comparison of satellite and conventional data 22 p3125 N88-28572
The impact of the El Nino event on the ECMWF model performance 22 p3125 N88-28576
Determination of most probable predicted 50 kPa pattern by empirical orthogonal functions 22 p3128 N88-28593
Global gauge anomaly of classical groups in even dimension
[DE88-008572] 22 p3158 N88-28797
One equatorial anomaly in nighttime ionospheric F region 24 p3447 N88-30517
Evolutionary helium and CNO anomalies in the atmospheres and winds of massive hot stars
[NASA-CR-183254] 24 p3452 N88-30550

ANORTHOSITE
The tectonic setting of Archean anorthosites 24 p3397 N88-30231
Crustal underplating in the North American Craton: Evidence from the Petrogenesis of anorthositic rocks in the Middle Proterozoic Midcontinent Rift System 24 p3400 N88-30252

ANTARCTIC ENVIRONMENT
U ICE ENVIRONMENTS

ANTARCTIC OCEAN
Physical oceanography and tracer chemistry of the southern ocean
[DE88-006852] 20 p2828 N88-26779

ANTARCTIC REGIONS
NT ROSS ICE SHELF
Antarctic field tests of SARSAT personal locater beacons
[NASA-TM-4008] 01 p0063 N88-10403
Contributions to geodesy, photogrammetry, and cartography. Series 2, number 45
[ISSN-0469-4244] 01 p0065 N88-10416
Digital Name Data Base Antarctic as a component of a landscape data base of the Antarctic 01 p0065 N88-10419
Kinetics investigations of atmospheric chemical reactions
[PB87-213351] 01 p0069 N88-10439
Human adaptation to isolated and confined environments
[NASA-CR-181502] 03 p0357 N88-12248
TOMS: The Antarctic ozone hole and ozone trends 05 p0615 N88-13775
USSR report: Earth sciences
[JPRS-UES-87-004] 06 p0725 N88-14455
Ferromanganese nodules of Antarctic sector in Pacific Ocean 06 p0727 N88-14472
A review of atmospheric ozone and current thinking on the Antarctic ozone hole
[AD-A185608] 06 p0732 N88-14501
The distribution of evaporitic weathering products on Antarctic meteorites 06 p0798 N88-14888
WOCE Core Project 2 Planning Meeting: The Southern Ocean
[WCP-138] 07 p0882 N88-15348
Biorhythmic aspects of intercontinental Antarctic adaptation 08 p1046 N88-16321
Group adaptation and individual adjustment in antarctica: A summary of recent research
[AD-A186605] 08 p1051 N88-16347
Physical and structural characteristics of Weddell Sea pack ice
[AD-A188189] 10 p1358 N88-18119
Observations and analyses of summer whistlers at the Great Wall Station of Antarctica 11 p1469 N88-18759
Feasibility report: Operation of light air cushion vehicle at McMurdo Sound, Antarctica
[AD-A189057] 13 p1755 N88-20494
The 1987 Airborne Antarctic Ozone Experiment: The Nimbus-7 TOMS data atlas
[NASA-RP-1201] 13 p1791 N88-20714
Activities and objectives of the Polar Research Board
[DE88-004543] 13 p1797 N88-20747
Radon-222 in the Antarctic Peninsula
[INPE-4486-PRE/1251] 15 p2092 N88-22468
Ionospheric research in Antarctica
[INPE-4521-PRE/1273] 16 p2232 N88-23331
Changes in the Antarctic atmosphere due to the reduction of stratospheric ozone
[ETN-88-92565] 18 p2540 N88-25074
ECC (Electrochemical Concentration Cell) ozonesonde observations at South Pole, Antarctica during 1987
[PB88-202015] 21 p2970 N88-27644
On-board data processing of navigation data at high latitudes in Antarctica 22 p3036 N88-28027
South Pole lidar: Brief description of the instrument
[NOTA-INTERNA-907] 22 p3083 N88-28308

Topography of an Antartic ice stream
22 p3092 N88-28361
An evaluation of SPOT imagery for Earth science studies in the Antarctic. Preliminary Evaluation Program (PEPS) 269 for SPOT
22 p3103 N88-28430
Changes in stratospheric ozone: Observations and theories
[AERONOMICA-ACTA-A-334-1988]
24 p3390 N88-30188
Antarctic Meteorite Newsletter, Volume 11, Number 2, August 1988
[NASA-TM-89801] 24 p3457 N88-30573

ANTARCTICA
U ANTARCTIC REGIONS

ANTENNA ARRAYS
NT LINEAR ARRAYS
NT STEERABLE ANTENNAS
The application of group radiators for the determination of tension crack corrosion
[BAM-06264] 01 p0022 N88-10141
Gain evaluation for an idealized curtain array antenna
[PB87-210290] 02 p0161 N88-11006
A conformal aircraft phased array antenna for airplane-satellite communication in the L band
[ESA-TT-1057] 03 p0305 N88-11926
An antenna array processing system for multiple source bearing estimation 03 p0305 N88-11927
Analysis of the ICE combiner for multiple antenna arraying 04 p0436 N88-12704
The use of coaxial transmission line elements in log-periodic dipole arrays
[AD-A184864] 05 p0574 N88-13499
An evaluation of equivalent models for design of rectangular microstrip antennas
[FOA-C-30451-3.2] 08 p0977 N88-15905
Investigation of design considerations for Telemetry, Tracking and Command (TT and C) antenna system on Naval Postgraduate School Orion mini-satellite
[AD-A187130] 10 p1291 N88-17718
Compensation of relector antenna surface distortion using an array feed
[NASA-TM-100286] 11 p1476 N88-18805
Deformations in VLBI antennas
[NASA-TM-100696] 11 p1502 N88-18970
Large-aperture sparse array antenna systems of moderate bandwidth for multiple emitter location
[AD-A188409] 12 p1619 N88-19683
Investigation of surface wave blindness in microstrip phased array antennas
[AD-A189326] 12 p1621 N88-19696
Estimation-correlation, modeling, and identification in adaptive array processors
[AD-A189130] 13 p1757 N88-20512
Adaptive algorithms for HF antenna arrays
[AD-A189929] 13 p1761 N88-20534
Conformal microstrip slot antenna and antenna array
[AD-A189623] 15 p2055 N88-22252
Case study of active array feed compensation with sidelobe control for reflector surface distortion
[NASA-TM-100287] 16 p2192 N88-23073
Gram-Schmidt implementation of a linearly constrained adaptive array
[AD-A191651] 18 p2560 N88-25196
An adaptive array antenna for mobile satellite communications 19 p2647 N88-25710
MSAT mobile electronically steered phased array antenna development 19 p2647 N88-25711
MSAT-X phased array antenna adaptions to airborne applications 19 p2647 N88-25713
Simple, low-profile, circularly polarized arrays
19 p2647 N88-25716
Antenna technology for advanced mobile communication systems 19 p2651 N88-25743
A microstrip array feed for MSAT spacecraft reflector antenna 19 p2652 N88-25747
Active feed array compensation for reflector antenna surface distortions
[NASA-TM-100826] 19 p2654 N88-25762
Array trade-off study using multilayer parasitic subarrays
[NASA-TM-101321] 22 p3070 N88-28222
A novel method to correct radiation pattern distortion of conformal antennas
[AD-A193675] 23 p3204 N88-29066
Development of a general software package for the analysis and synthesis of planar antenna arrays for space applications
[S-247-02] 24 p3359 N88-30000
High frequency GaAlAs modulator and photodetector for phased array antenna applications
[NASA-TM-101328] 24 p3367 N88-30048

ANTENNA COMPONENTS
NT ANTENNA FEEDS
NT DIPLEXERS
Gain evaluation for an idealized curtain array antenna
[PB87-210290] 02 p0161 N88-11006
Studies of the structural dynamic behavior of satellite antenna system
[AD-A185526] 06 p0673 N88-14121
Development of a magnetically suspended, tetrahedron-shaped antenna pointing system
14 p1926 N88-21478
Features and applications of the integrated composites analyzer (ICAN) code 15 p2078 N88-22391
Sidelobe level of an adaptive array using the SMI (Sampled Matrix Inversion) algorithm
[AD-A193131] 21 p2932 N88-27409

ANTENNA COUPLERS
NT DIPLEXERS

ANTENNA DESIGN
Study of advanced satellite concept using a multifeed reconfigurable antenna
[ESA-CR(P)-2406-VOL-1] 01 p0013 N88-10073
Study of advanced satellite concept using a multifeed reconfigurable antenna. Detailed report on mission definition, coverage analysis and performance requirements, antenna geometry
[ITS-TR-014.C/85] 01 p0013 N88-10074
Study of advanced satellite concept using a multifeed reconfigurable antenna. Detailed report on Polarization Sensitive Reflector (PSR) and offset parabolic antennas, Appendix 1
[ESA-CR(P)-2406-VOL-3] 01 p0013 N88-10075
Study of advanced satellite concept using a multifeed reconfigurable antenna. Appendix 3 : Feeding network, final performance analysis, study of reconfiguration possibilities
[ITS-TR-032/85] 01 p0014 N88-10076
Telemetry, Tracking, and Control Working Group report 01 p0016 N88-10096
Mechanical properties characterization of composite sandwich materials intended for space antenna applications
[NASA-TM-88893] 01 p0020 N88-10121
Realization of a conical four-part antenna for the scanning of interference fields
[REPT-13-86] 01 p0034 N88-10216
Shape optimization of linear antennas
[ETN-87-90413] 01 p0036 N88-10233
Data Relay Satellite antenna subsystem study
[ESA-CR(P)-2435-VOL-2] 02 p0162 N88-11014
Study of antenna configuration for Data Relay Satellite (DRS) user spacecraft
[A5/516/86] 02 p0162 N88-11018
DRS (Data Relay Satellite) antenna subsystem study
[ESA-CR(P)-2435-VOL-1] 02 p0162 N88-11019
New main reflector, subreflector and dual chamber concepts for compact range applications
[NASA-CR-181506] 04 p0402 N88-12498
Band 2 VHF antenna for home construction
[BBC-RD-1987/13] 04 p0432 N88-12677
Capacitive resonant transducer for the Frascati gravitational antenna
[IFSI-86-9] 05 p0578 N88-13528
Studies of the structural dynamic behavior of satellite antenna system
[AD-A185526] 06 p0673 N88-14121
Theory of displaced phase center antenna for space based radar applications
[PB87-229837] 06 p0690 N88-14227
National Aeronautics and Space Administration (NASA)/American Society for Engineering Education (ASEE) Summer Faculty Fellowship Program, 1987. Volume 2
[NASA-CR-172009-VOL-2] 06 p0796 N88-14874
Automatic antenna switching design for Extra Vehicular Activity (EVA) communication system
06 p0797 N88-14883
Interaction between a module cluster and a plasma in a magnetic field
[PB87-148276] 07 p0934 N88-15675
An evaluation of equivalent models for design of rectangular microstrip antennas
[FOA-C-30451-3.2] 08 p0977 N88-15905
A simplified approach to axisymmetric dual-reflector antenna design
[NASA-TP-2797] 09 p1111 N88-16662
European developments in antenna technology
09 p1123 N88-16725
Multisurface control mechanism for a deployable antenna: Far Infrared and Submillimeter Space Telescope (FIRST) technology study
[RP-FA-D003] 09 p1135 N88-16807
Optimizing HF antenna systems on the Dolphin and Sea Hawk helicopters
[AD-A186552] 09 p1152 N88-16901
Study of dual beam antenna systems for the data relay satellite, volume 1
[S-272-02-VOL-1] 09 p1152 N88-16905
Study of dual beam antenna systems for the data relay satellite. Volume 2: Executive summary
[S-272-03-VOL-2] 09 p1153 N88-16906
Study on a double reflector compact range — satellite antennas
[S-201-05] 09 p1153 N88-16908
Evaluation of CWMS (Continuous-Wave Measurement System) single-wire dipole antenna
[DE88-003979] 09 p1155 N88-16920
Investigation of design considerations for Telemetry, Tracking and Command (TT and C) antenna system on Naval Postgraduate School Orion mini-satellite
[AD-A187130] 10 p1291 N88-17718
User's guide for the HF (High Frequency) broadcast antenna design and validation summary programs
[PB88-116124] 10 p1317 N88-17875
Capacitor analysis for RF antennas
[DE88-004178] 10 p1318 N88-17883
Observation model and parameter partials for the JPL VLBI parameter estimation software MASTERFIT-1987
[NASA-CR-182524] 10 p1427 N88-18523
Improved backfire antenna using circular dipole
11 p1468 N88-18757
The characteristics of two broadband (2 MHz to 10 MHz) switched vee antennas
[AD-A187874] 11 p1471 N88-18770
The Telecommunications and Data Acquisition Report
[NASA-CR-182545] 11 p1471 N88-18774
An optimal structure for a 34-meter millimeter-wave center-fed BWG antenna: The Cross-Box concept
11 p1472 N88-18778
A 2.3-GHz maser at Usuda, Japan, for TDRSS-orbiting VLBI experiment 11 p1472 N88-18779
A noise-adding radiometer for the Parkes antenna
11 p1473 N88-18788
X-band system performance of the very large array
11 p1473 N88-18789
DSS 14 64-meter antenna S- and X-band efficiency and system noise temperature calibrations, September 1987
11 p1473 N88-18790
New mode switching algorithm for the JPL 70-meter antenna servo controller 11 p1474 N88-18791
Optical links in the angle-data assembly of the 70-meter antennas 11 p1474 N88-18792
Seventy-meter antenna performance predictions: GTD analysis compared with traditional ray-tracing methods
11 p1474 N88-18793
A new approach for shaping of dual-reflector antennas
[NASA-CR-182581] 11 p1476 N88-18806
Deformations in VLBI antennas
[NASA-TM-100696] 11 p1502 N88-18970
Large-aperture sparse array antenna systems of moderate bandwidth for multiple emitter location
[AD-A188409] 12 p1619 N88-19683
Aerospatiale unfurlable reflector and associated mechanisms 14 p1875 N88-21203
Multiple-beam ground station reflector antenna system: A preliminary study
[EUT-87-E-171] 14 p1904 N88-21379
Optically interconnected phased arrays
[NASA-TM-100855] 14 p1908 N88-21400
The 15-meter diameter hoop/column antenna surface control actuator system 14 p1924 N88-21469
Short experiment study of four-wire helical antennas (half turn half wave)
[CNES-CT/DRT/TIT/AN-249-T]
15 p2058 N88-22266
Simple, low-profile, circularly polarized arrays
19 p2647 N88-25716
Omni-directional L-band antenna for mobile communications 19 p2648 N88-25717
The 15-meter antenna performance optimization using an interdisciplinary approach 19 p2652 N88-25746
Technologies for antenna shape and vibration control
19 p2652 N88-25748
A role for high frequency superconducting devices in free space power transmission systems
[NASA-TM-100971] 19 p2662 N88-25830
Radar cross section studies/compact range research
[NASA-CR-183124] 20 p2792 N88-26565
Experiments applications guide: Advanced Communications Technology Satellite (ACTS)
[NASA-TM-100265] 22 p3048 N88-28082
Strawman Optical Reception Development Antenna (SORDA) 22 p3065 N88-28187
DSS 13 microprocessor antenna controller
22 p3066 N88-28192
An 8.4-GHz dual maser front end for Parkes reimplementation 22 p3066 N88-28197
X-band noise temperature near the Sun at a 34-meter high efficiency antenna 22 p3067 N88-28200
Investigations on multiport antennas for polarimetric and modal field scanning
[REPT-5-87] 23 p3205 N88-29073
Experimental investigations for the generation of phase modes for adaptive antennas
[REPT-10-87] 23 p3205 N88-29074

Development of a multiport-hybrid-mode exciter for use in antennas for polarimetric field measurements
[REPT-12-87] 23 p3205 N88-29075
Development of a general software package for the analysis and synthesis of planar antenna arrays for space applications
[S-247-02] 24 p3359 N88-30000
Fields and waves 24 p3363 N88-30025
A 30/20 GHz multibeam array antenna suitable for future high rate TDMA European satellite networks
[ETN-88-93079] 24 p3365 N88-30037

ANTENNA FEEDS
Study of advanced satellite concept using a multifeed reconfigurable antenna
[ESA-CR(P)-2406-VOL-1] 01 p0013 N88-10073
Study of advanced satellite concept using a multifeed reconfigurable antenna. Detailed report on mission definition, coverage analysis and performance requirements, antenna geometry
[ITS-TR-014.C/85] 01 p0013 N88-10074
Study of advanced satellite concept using a multifeed reconfigurable antenna. Detailed report on Polarization Sensitive Reflector (PSR) and offset parabolic antennas, Appendix 1
[ESA-CR(P)-2406-VOL-3] 01 p0013 N88-10075
Study of advanced satellite concept using a multifeed reconfigurable antenna. Appendix 3 : Feeding network, final performance analysis, study of reconfiguration possibilities
[ITS-TR-032/85] 01 p0014 N88-10076
An analysis of simplified feed architectures for MMIC (Monolithic Microwave Integrated Circuit) T/R (Transmit/Receive) module arrays
[AD-A185474] 06 p0697 N88-14275
Compensation of relector antenna surface distortion using an array feed
[NASA-TM-100286] 11 p1476 N88-18805
Modification of parabolic dish antenna pattern using two symmetrically placed circular flat plates
[AD-A189543] 13 p1758 N88-20517
Development of 20 GHz monolithic transmit modules
[NASA-CR-182134] 17 p2445 N88-24539
A MININEC model of the miniloop antenna
[AD-A191759] 18 p2500 N88-24830
Active feed array compensation for reflector antenna surface distortions
[NASA-TM-100826] 19 p2654 N88-25762

ANTENNA FIELDS
U ANTENNA RADIATION PATTERNS

ANTENNA RADIATION PATTERNS
NT SIDELOBES
Study of advanced satellite concept using a multifeed reconfigurable antenna. Appendix 3 : Feeding network, final performance analysis, study of reconfiguration possibilities
[ITS-TR-032/85] 01 p0014 N88-10076
Realization of a conical four-part antenna for the scanning of interference fields
[REPT-13-86] 01 p0034 N88-10216
Effects on electromagnetic wave propagation at frequencies over 10 GHz due to inhomogeneities of the complex refraction index
[REPT-86-025] 01 p0036 N88-10228
NBS (National Bureau of Standards) calibration procedures for horizontal dipole antennas (25 to 1000 MHz)
[PB87-210233] 03 p0305 N88-11922
New main reflector, subreflector and dual chamber concepts for compact range applications
[NASA-CR-181506] 04 p0402 N88-12498
Overestimation of on-axis power dehsity by the Fraunhofer (far-field) approximation
[AD-A186399] 07 p0843 N88-15111
The ESTEC Mini Compact Antenna Test Range
[ESA-CR(P)-2475] 08 p0977 N88-15907
Diagnostic concept of the resonance cone technique and its application in ground and space experiments 08 p1027 N88-16222
Resonance cones in nonthermal plasmas: Laboratory experiments 08 p1027 N88-16223
Performance of linear vertical antenna in refractive multimode waveguide 08 p1076 N88-16489
A simplified approach to axisymmetric dual-reflector antenna design
[NASA-TP-2797] 09 p1111 N88-16662
Exact image principle in electromagnetic field computation
[EL-57] 09 p1153 N88-16907
Modification of parabolic dish antenna pattern using two symmetrically placed circular flat plates
[AD-A189543] 13 p1758 N88-20517
Multiple-beam ground station reflector antenna system: A preliminary study
[EUT-87-E-171] 14 p1904 N88-21379
Exact image method for Gaussian beam problems involving a planar interface
[NASA-CR-182702] 14 p1905 N88-21380
Short experiment study of four-wire helical antennas (half turn half wave)
[CNES-CT/DRT/TIT/AN-249-T] 15 p2058 N88-22266
Analysis and experiments concerning the performance and calibration of compact antenna-test ranges
[PB88-169263] 16 p2188 N88-23047
Analysis and experiments concerning the performance and calibration of compact antenna-test ranges
[ISBN-9-09-001727-5] 16 p2188 N88-23048
Determination of characteristic radiation properties of a torus antenna: Integral equation method
[DFVLR-FB-87-46] 16 p2188 N88-23049
A diagnostic technique used to obtain cross range radiation centers from antenna patterns
[NASA-CR-182903] 16 p2192 N88-23071
A MININEC model of the miniloop antenna
[AD-A191759] 18 p2500 N88-24830
Analysis of annular microstrip antennas for hyperthermic applicators
[PB88-181508] 19 p2643 N88-25679
An adaptive array antenna for mobile satellite communications 19 p2647 N88-25710
Evaluation of vertical monopole antennas with elevated radials
[DE88-008339] 19 p2654 N88-25760
Active feed array compensation for reflector antenna surface distortions
[NASA-TM-100826] 19 p2654 N88-25762
Antenna heights for the optimum utilization of the oceanic evaporation duct. Part 3: Results from the Mediterranean measurements, volume 2
[AD-A192311] 20 p2791 N88-26554
Antenna heights for the optimum utilization of the oceanic evaporation duct. Part 1: Results from the Pacific measurements. Part 2: Results from the Key West measurements, volume 1
[AD-A192358] 20 p2791 N88-26555
Analytical approximation of a distorted reflector surface defined by a discrete set of points
[NASA-TM-101323] 21 p2934 N88-27424
Polynomials with restricted coefficients and their applications
[AD-A192589] 23 p3202 N88-29055
A novel method to correct radiation pattern distortion of conformal antennas
[AD-A193675] 23 p3204 N88-29066
Application of sampling techniques to near-field far-field transformation
[ESA-CR(P)-2546] 24 p3359 N88-30002
The focal plane reception pattern calculation for a paraboloidal antenna with a nearby fence
[NASA-TM-100691] 24 p3365 N88-30039

ANTENNAS
NT AIRCRAFT ANTENNAS
NT BACKFIRE ANTENNAS
NT DIPOLE ANTENNAS
NT DIRECTIONAL ANTENNAS
NT FURLABLE ANTENNAS
NT GRAVITATIONAL WAVE ANTENNAS
NT HELICAL ANTENNAS
NT HOOP COLUMN ANTENNAS
NT LOG PERIODIC ANTENNAS
NT LOOP ANTENNAS
NT MICROSTRIP ANTENNAS
NT MICROWAVE ANTENNAS
NT MONOPOLE ANTENNAS
NT OMNIDIRECTIONAL ANTENNAS
NT PARABOLIC ANTENNAS
NT PLASMA ANTENNAS
NT RADIO ANTENNAS
NT REFLECTOR ANTENNAS
NT SATELLITE ANTENNAS
NT SLOT ANTENNAS
NT SPACECRAFT ANTENNAS
NT STEERABLE ANTENNAS
NT TWO REFLECTOR ANTENNAS
NT WAVEGUIDE ANTENNAS
Numerical modeling: Integral equation method 03 p0304 N88-11919
Experiments: Test range facilities, part 2 03 p0305 N88-11921
Low-frequency VLBI in space and interstellar refraction
[PB87-127643] 06 p0696 N88-14267
Preliminary airworthiness evaluation of a UH-1 equipped with a terrain mapping receiver antenna
[AD-A186274] 07 p0819 N88-14980
Treatment of small wire loops in the method of moments code NEC (Numerical Electromagnetics Code)
[DE88-002995] 07 p0846 N88-15136
Optimizing HF antenna systems on the Dolphin and Sea Hawk helicopters
[AD-A186552] 09 p1152 N88-16901
Space-time processing of field produced by moving source 09 p1234 N88-17399
The design of impedance- matching networks for broadband antennas
[AD-A187600] 10 p1320 N88-17895
The coaxial colinear antenna: Theoretical and experimental models 11 p1475 N88-18803
Optically controlled phased-array antenna technology for space communication systems
[NASA-TM-100852] 11 p1476 N88-18809
The complex point spread function of the RSRE SAR (Synthetic Aperture Radar)
[AD-A189011] 12 p1621 N88-19693
The evaluation and selection of a 5th ground antenna site for the global positioning system
[AD-A189495] 13 p1720 N88-20286
Electromagnetic scattering from and natural resonances of the circular strip 13 p1759 N88-20523
Optical RF distribution links for MMIC phased array antennas
[NASA-TM-100841] 13 p1764 N88-20555
Optically interconnected phased arrays
[NASA-TM-100855] 14 p1908 N88-21400
Nonlinear wave and diffusion equations
[AD-A191421] 16 p2265 N88-23544
Practical VLF/LF radio test system
[AD-A191768] 18 p2500 N88-24831
IGUANA: Interactive graphics utility for automated NEC analysis
[AD-A191760] 18 p2556 N88-25174
The new MININEC (version 3): A mini-numerical electromagnetic code
[AD-A191778] 19 p2642 N88-25675
Adaptive interference techniques for mobile antennas 19 p2647 N88-25714
On 3-5 transistors for MM-wave applications
[AD-A191580] 19 p2661 N88-25825
Antenna heights for the optimum utilization of the oceanic evaporation duct. Part 3: Results from the Mediterranean measurements, volume 2
[AD-A192311] 20 p2791 N88-26554
Antenna heights for the optimum utilization of the oceanic evaporation duct. Part 1: Results from the Pacific measurements. Part 2: Results from the Key West measurements, volume 1
[AD-A192358] 20 p2791 N88-26555
A model for insulated wires in the method of moments code NEC (Numerical Electromagnetics Code)
[DE88-008920] 20 p2794 N88-26577
The feasibility of the disturbance accommodating controller for precision antenna pointing 22 p3064 N88-28182
HPM (High Power Microwave) simulation fidelity studies
[DE88-012229] 22 p3068 N88-28209
Improvements in techniques of microwave thermography
[AD-A193620] 23 p3239 N88-29276

ANTHRACENE
Statistical fine structure in the inhomogeneously broadened electronic origin of pentacene in p-terphenyl
[AD-A191211] 16 p2176 N88-22968
Electronic and ionic transport in polymers
[AD-A191642] 18 p2490 N88-24772

ANTHROPOMETRY
Physiological determinants of load bearing capacity
[AD-A184977] 05 p0629 N88-13848

ANTIAIRCRAFT MISSILES
Dependence of the expectancy of hitting on the number of spread shots. Determination of the expectancy of hitting using a spread salvo
[REPT-FM6] 10 p1310 N88-17829
Investigation of several spread shot conditions
[REPT-TR-164] 10 p1310 N88-17830
POLYPHEM, a universal defensive missile with optical waveguides guidance
[MBB-UA-1045/87] 10 p1315 N88-17862

ANTIBIOTICS
Study of certain biological characteristics of bacteria during the French-Soviet CYTOS-2 space experiment 04 p0473 N88-12917
Antibiotic activity in space, results and hypothesis 12 p1660 N88-19952
The Antibio experiment --- Spacelab D1 mission 22 p3060 N88-28159

ANTICLINES
The breaked anticlines, cuesta and crest homoclines, ortoclinal valleys, and other forms of relief outcrops delineated with the help of remote sensing imagery 17 p2366 N88-24089
Diapirs of the Mediterranean ridge: The tectonic regime of an incipient accreted terrane 24 p3396 N88-30224

ANTICLINORIA
U ANTICLINES
ANTICONVULSANTS
Carbamates, atropine, and diazepam: Effects on performance in the running rat
[AD-A188009] 11 p1517 N88-19062
ANTICYCLONES
Synoptic perturbations and climate
08 p1016 N88-16158
ANTIFERROMAGNETISM
Experimental perspectives on heavy electron metals
[DE87-014766] 04 p0416 N88-12583
A mechanism for symmetry breaking in antiferromagnetic Heisenberg systems
[ETN-88-91320] 05 p0657 N88-14031
Structural properties of high-T/sub c/ oxide super conductors
[DE88-002974] 08 p1090 N88-16563
Comparison between muon spin rotation and neutron scattering studies on the 3-dimensional magnetic ordering of La2CuO(4-y) 17 p2396 N88-24244
Ground state properties and electronic structure of high T sub c superconductors
[DE88-007485] 18 p2585 N88-25360
Self energy corrections to the ab initio band structures: Chromium
[DE88-701825] 21 p3020 N88-27927
Static and dynamic behavior of a quasi one-dimensional Heisenberg antiferromagnet in the long-range ordered state. A nuclear magnetic resonance study performed with a He3-He4 dilution refrigerator
[B8705564] 23 p3281 N88-29533
Theory of superconductivity in oxides
[AD-A195647] 24 p3433 N88-30432
Theoretical model of high temperature superconductors
[DE88-702707] 24 p3434 N88-30441
ANTIFRICTION BEARINGS
NT BALL BEARINGS
NT ROLLER BEARINGS
Corrosion-wear process under rolling-sliding motion
[AD-A189603] 13 p1778 N88-20635
On the computation of stationary deterministic behavior of nonlinear dynamic systems with applications to rotor-bearing structures
[ETN-88-92241] 16 p2214 N88-23213
ANTIGENS
A solid phase enzyme-linked immunosorbent assay for the antigenic detection of Legionella pneumophila (serogroup 1): A compliment for the space station diagnostic capability 06 p0795 N88-14868
ANTIGRAVITY
Non-minimal interaction of gravity with other physical fields: An overview
[DE87-703362] 05 p0624 N88-13819
ANTIKNOCK ADDITIVES
Detailed kinetic modeling of autoignition chemistry
[DE87-013226] 03 p0283 N88-11782
ANTIMATTER
NT ANTINEUTRINOS
NT ANTINUCLEONS
NT ANTIPARTICLES
NT ANTIPROTONS
NT POSITRONS
A matter-antimatter propulsion system for manned interstellar flight
[DE87-013311] 02 p0141 N88-10885
Solid antimatter
[PB87-166146] 09 p1259 N88-17549
Antimatter: Its history and its properties
[DE88-004308] 10 p1423 N88-18498
Proceedings of the Cooling, Condensation, and Storage of Hydrogen Cluster Ions Workshop
[AD-A189857] 16 p2266 N88-23555
Atomic processes in matter-antimatter interactions
[DE88-008911] 19 p2723 N88-26172
ANTIMISSILE DEFENSE
Mathematical models for the S.D.I.
[AD-A184667] 03 p0373 N88-12345
Investigation of design concepts for large space structures to support military applications
[AD-A186098] 07 p0824 N88-15000
Feasibility of software built-in test for SDI (Strategic Defense Initiative) applications
[AD-A185750] 07 p0917 N88-15572
The impact of deployment rates on the effectiveness of strategic defenses
[AD-A186907] 09 p1233 N88-17393
Signal and data processing for IR sensors
10 p1374 N88-18199
Strategic Defense Initiative Program: Status of space surveillance and tracking system
[PB88-150438] 14 p1967 N88-21739
Real-time stressed channel simulator
[AD-A190223] 15 p2025 N88-22067
Constellation sizing for modest directed energy platforms
[DE88-007033] 15 p2070 N88-22343
MPD (magnetoplasmadynamic) thruster advanced pumping system concepts
[AD-A190513] 15 p2138 N88-22756
The Oak Ridge National Laboratory strategic defense initiative shield optimization program
[DE88-006946] 19 p2721 N88-26160
The Oak Ridge National Laboratory strategic defense initiative shield optimization program: Executive summary
[DE88-008016] 20 p2847 N88-26899
SDI: Myth or reality
[DE88-009121] 20 p2847 N88-26901
The strategic defense initiative: Strategic implications
[AD-A192341] 20 p2847 N88-26902
Future SDI (Strategic Defense Initiative) decision making
[AD-A192794] 21 p3010 N88-27860
Comparative analysis of the space power architecture studies
[NASA-TM-100977] 22 p3049 N88-28090
SDI (Strategic Defense Initiative): A policy analysis
[AD-A194240] 23 p3275 N88-29493
Strategic defense initiative architecture dataflow modeling technique version 1.5
[AD-A194356] 23 p3275 N88-29494
SDI (Strategic Defense Initiative) battle management/C3 (Command, Control and Communications) algorithms technology program plan
[AD-A194357] 23 p3275 N88-29495
SDI (Strategic Defense Initiative). Where do we go from here
[AD-A194544] 23 p3275 N88-29497
Nonlinear analysis of non-neutral plasmas
[AD-A192506] 23 p3284 N88-29556
Report to congress on the strategic defense system architecture
[AD-A195476] 24 p3426 N88-30393
ANTIMISSILE MISSILES
A simulation of post boost vehicle deployment of multiple reentry vehicles
[DE88-009537] 20 p2764 N88-26391
Looking beyond the strategic defense initiative
[AD-A195079] 24 p3427 N88-30394
ANTIMISTING FUELS
Antimisting kerosene: Low temperature degradation and blending
[NASA-CR-182725] 20 p2781 N88-26495
ANTIMONIDES
NT INDIUM ANTIMONIDES
ANTIMONY ALLOYS
MBE growth of InAsSb strained-layer superlattices
[DE88-000365] 05 p0654 N88-14011
Nonlinear absorption of CO2 laser radiation in p-type InSb
[DE88-004055] 11 p1492 N88-18906
Electrical characteristics of MBE (Molecular Beam Epitaxyl)-grown GaAs/sub 1-x/Sb/sub x on InP and correlation with film microstructure
[DE88-003841] 13 p1847 N88-21053
The influence of solute segregation on the dislocation structure of small and large angle (001) twist boundaries in Fe-Sb alloys
[DE88-009166] 22 p3155 N88-28770
ANTIMONY COMPOUNDS
NT INDIUM ANTIMONIDES
Activities of As, Sb, Bi and Pb in copper mattes and their effects on impurity elimination
[TKK-V-A10(1988)] 15 p2041 N88-22165
ANTINEUTRINOS
Wrong helicity events induced by the CERN-SPS wide band muonic (anti)neutrino beam
[NIKHEF-H/87-2] 06 p0779 N88-14779
Properties of nuclei and elementary particles at low and intermediate energies
[DE88-001913] 09 p1244 N88-17456
Event classification in (anti)neutrino experiments using an Internal Picket Fence-External Muon Identifier (IPF-EMI) detector system
[NIKHEF-H/87-6] 09 p1245 N88-17457
ANTINUCLEONS
Theoretical studies in few-body intermediate energy physics
[DE88-004101] 12 p1689 N88-20106
ANTIOXIDANTS
Experimental study of protective effect of antioxidant enzymes-superoxide dismutase and catalase-when using intermittent toxic modes of hyperbaric oxygenation
19 p2707 N88-26094
ANTIPARTICLES
NT ANTINEUTRINOS
NT ANTINUCLEONS
NT ANTIPROTONS
NT POSITRONS
Formation and reactivity of small hydrogen cluster ions
16 p2267 N88-23560
Infrared spectroscopy of H3(+)
16 p2268 N88-23565
The role of electron-ion recombination in bulk antimatter production
16 p2268 N88-23567
First capture of antiprotons in an ion trap and the possibility of antihydrogen
16 p2268 N88-23569
Magnetic traps for an anti-hydrogen gas
16 p2269 N88-23572
Production of heavy antinuclei: Review of experimental results
16 p2269 N88-23574
Atomic processes in matter-antimatter interactions
[DE88-008911] 19 p2723 N88-26172
ANTIPROTONS
A program to study antiprotons in the cosmic rays: Arizona collaboration
[NASA-CR-180702] 01 p0120 N88-10764
Experimental studies of elementary particle interactions at high energies
[DE88-000804] 05 p0648 N88-13971
Basic physics program for a low energy antiproton source in North America
[DE88-003148] 08 p1082 N88-16522
Looking for new gravitational forces with antiprotons
[DE88-003154] 09 p1192 N88-17142
Nuclear structure at intermediate energies
[DE88-002796] 10 p1407 N88-18390
Initial operation of the Tevatron collider
[FNAL-TM-1449] 11 p1547 N88-19252
Advanced space propulsion study - antiproton and beamed power propulsion
[AD-A189218] 13 p1732 N88-20355
Prospects for antiproton production and propulsion
16 p2267 N88-23556
First capture of antiprotons in an ion trap and the possibility of antihydrogen 16 p2268 N88-23569
The cluster ion approach to the condensation and storage of antihydrogen 16 p2269 N88-23575
Analysis of containerless condensation of polyatomic hydrogen ions, with emphasis on H3(+,-) association channels and a future workshop to study related topics
16 p2269 N88-23576
ANTIRADAR COATINGS
Radar ECCM's new area: Anti-STEALTH and anti-ARM 03 p0299 N88-11881
ANTIREFLECTION COATINGS
On 1064 nm and 350 nm laser damage thresholds of high index oxide films deposited from organic solutions and sols
[DE88-001636] 07 p0859 N88-15217
Abrasion resistant porous silica antireflective coatings
[DE88-006230] 14 p1894 N88-21308
Oxide optical coatings prepared by metal-organic vapor deposition
[DE88-006809] 15 p2043 N88-22175
Optical coatings for high average power XeF lasers
[DE88-011356] 20 p2807 N88-26656
Improved adhesion for SiO2 particles in silica substrates using helium-ion irradiation
[DE88-008915] 21 p2920 N88-27332
Survey of material for an infrared-opaque coating
[NASA-TM-88204] 22 p3153 N88-28757
ANTISHIP MISSILES
Utilization of dynamic characteristics of materials to optimize military explosive charges. Application to antiship devices
[SNIAS-872-320-101] 05 p0610 N88-13743
ANTISTATIC DEVICES
U STATIC DISCHARGERS
ANTISUBMARINE WARFARE
Investigation and implementation of an algorithm for computing optimal search paths
[AD-A185927] 07 p0902 N88-15481
ANTISUBMARINE WARFARE AIRCRAFT
NT P-3 AIRCRAFT
ANTITANK MISSILES
An investigation of steep descent guidance for terminally-guided sub-munitions
12 p1596 N88-19555
ANXIETY
Selecting the right crew for future space stations: An analysis of selection research on offshore divers, aviation pilots and other high risk groups in Scandinavia
19 p2696 N88-26021
AO-1 AIRCRAFT
U OV-1 AIRCRAFT
AORTA
Morphometric analysis of rat aorta endothelium during long-term hypokinesia 07 p0894 N88-15417
APATITES
U MINERALS
APERTURES
NT SYNTHETIC APERTURES

An excitation-term modification for a certain class of electromagnetic aperture-coupling problems
[DE88-000260] 04 p0437 N88-12713
Overestimation of on-axis power density by the Fraunhofer (far-field) approximation
[AD-A186399] 07 p0843 N88-15111
Aberrations: Their effect on off-axis beam steering
[AD-A189601] 13 p1840 N88-21008
Demonstration of efficient full aperture Type 1/Type 2 third harmonic conversion on Nova
[DE88-003834] 14 p1914 N88-21438
Experimental determination of the coefficients of the hydraulic resistance of apertures in the rotary disks
[AD-A190627] 15 p2066 N88-22317
Improvements in techniques of microwave thermography
[AD-A193620] 23 p3239 N88-29276

APL (PROGRAMMING LANGUAGE)
Report outline of a programming variable and application through example
[INPE-4211-PRE/1092] 01 p0081 N88-10521

APNEA
U RESPIRATION

APOGEE BOOST MOTORS
ESA Bulletin No. 8
[ETN-87-90513] 09 p1122 N88-16718
A European apogee boost motor for GEOS
09 p1123 N88-16719

APPENDAGES
NT ARM (ANATOMY)
NT FINGERS
NT HAND (ANATOMY)
NT LEG (ANATOMY)
An experimental investigation of appendage-flat plate junction flow. Volume 2. Elliptical nose appendage data base
[AD-A184974] 05 p0580 N88-13539
Numerical calculation of appendage, flat plate junction flow
[AD-A186371] 07 p0850 N88-15158

APPLICATION
U UTILIZATION

APPLICATIONS OF MATHEMATICS
Toward a mathematical formalism of performance, task difficulty, and activation 16 p2239 N88-23372

APPLICATIONS PROGRAMS (COMPUTERS)
NT NASTRAN
Integration of dynamic, aerodynamic and structural optimization of helicopter rotor blades
[NASA-CR-181441] 01 p0002 N88-10012
Collection and analysis of specific ELINT Signal Parameters
[NASA-CR-181419] 01 p0033 N88-10213
High-efficiency silicon solar cells: Numerical modeling, transient measurements, efficiency goals, and v-shaped grooves
[DE87-012842] 01 p0066 N88-10423
A study of carbon monoxide distribution determinations for a global transport model
[NASA-CR-181423] 01 p0067 N88-10432
A reference guide for IGVIEW: An IGES-compatible geometry system
[DE87-013441] 01 p0083 N88-10534
An interactive computer program for materials analysis by means of ion scattering
[MRL-R-1040] 01 p0091 N88-10596
RE-1000 free-piston Stirling engine hydraulic output system description
[NASA-TM-100185] 01 p0108 N88-10700
Recent advances in structural dynamics of large space structures
[NASA-TM-100513] 02 p0138 N88-10867
Computer simulation of thermal modeling of primary lithium cells 02 p0163 N88-11022
Pinhole occulter experiment
[NASA-CR-179206] 02 p0235 N88-11481
Vectorization of MHD equilibrium and stability codes
[DE87-753013] 02 p0240 N88-11516
Limit of possible operation of crescent and bean shaped Tokamaks
[IPPJ-837] 02 p0242 N88-11532
A heat transfer model for a heated helium airship
[AD-A183786] 03 p0259 N88-11629
Improvements to the adaptive maneuvering logic program
[NASA-CR-3985] 03 p0262 N88-11648
Analytic investigation of helicopter rotor blade appended aeroelastic devices
[NASA-CR-166525] 03 p0266 N88-11676
Electromagnetic scattering by a thick strip on a half-space
[PB87-227096] 03 p0306 N88-11928
Bearing loads in slider crank mechanisms
[PB87-216495] 03 p0332 N88-12089
Issues in image processing software development for a multi-user, multi-programming environment
[DE88-000358] 03 p0365 N88-12298
Stochastic model of the NASA/MSFC ground facility for large space structures with uncertain parameters: The maximum entropy approach
[NASA-CR-181489] 03 p0372 N88-12343
A hybrid numerical technique for predicting the aerodynamic and acoustic fields of advanced turboprops
[NASA-CR-174926] 03 p0374 N88-12352
Solution of the two-dimensional Euler equations on unstructured triangular meshes
04 p0394 N88-12469
An integrated study of structures, aerodynamics and controls on the forward swept wing X-29A and the oblique wing research aircraft
[NASA-CR-181548] 04 p0399 N88-12486
Microgravity nucleation and particle coagulation experiments support
[NASA-CR-181540] 04 p0423 N88-12618
Higher order theory analysis of a modified free-edge delamination specimen 04 p0455 N88-12820
Applications of the hybrid automated reliability predictor
[NASA-TP-2760] 04 p0475 N88-12928
The ISI (Information Sciences Institute) grapher: A portable tool for displaying graphs pictorially
[AD-A184354] 04 p0478 N88-12944
Methods for design and evaluation of integrated hardware/software systems for concurrent computation
[NASA-CR-181522] 04 p0479 N88-12953
Monocrystal sputtering by the computer simulation code ACOCT
[IPPJ-848] 04 p0493 N88-13035
Cosmological applications of singular hypersurfaces in general relativity 04 p0521 N88-13202
Experiences using the Mark IV supersonic hypersonic arbitrary body program 05 p0534 N88-13249
Practical application of two-dimensional viscous flow computation 05 p0535 N88-13257
The role of computation fluid dynamics in aeronautical engineering (4). The development and applications of implicit TVD finite volume code
05 p0536 N88-13259
Practical and modern simulation by systematic connection of the LU-ADI code and the solution adaptive grid program 05 p0536 N88-13260
Development of the computer program for turbulent boundary layers 05 p0536 N88-13264
Numerical analysis of supersonic flows using panel method 05 p0537 N88-13266
Computation of nacelle interference using boundary element method 05 p0537 N88-13267
Computer graphics for computational aerodynamics
05 p0538 N88-13276
A numerical study of the effects of curvature and convergence on dilution jet mixing
[NASA-TM-89878] 05 p0549 N88-13347
MODTRAN: A moderate resolution model for LOWTRAN
[AD-A185384] 05 p0574 N88-13503
Integration of a supersonic unsteady aerodynamic code into the NASA FASTEX system
[NASA-CR-182329] 06 p0663 N88-14068
Transonic Navier-Stokes computations of strake-generated vortex interactions for a fighter-like configuration 06 p0664 N88-14073
Documentation of computer programs for optimization and simulation of multicarrier SAW-based demodulator
[PB87-134532] 06 p0693 N88-14252
Virtual image processor: A prototype implementation
[AD-A185560] 06 p0758 N88-14652
Interactive nonlinear least squares program
[PB88-109855] 06 p0760 N88-14661
Computational fluid dynamics overview
07 p0809 N88-14927
Research study for materials/properties test results database
[NASA-CR-178923] 07 p0861 N88-15222
Accomplishments at NASA Langley Research Center in rotorcraft aerodynamics technology
09 p1105 N88-16626
Comprehensive rotorcraft analysis methods
09 p1106 N88-16630
A jet in a crossflow
[NASA-CR-182469] 09 p1113 N88-16674
Numerical modeling of multidimensional flow in seals and bearings used in rotating machinery
[NASA-TM-100779] 09 p1165 N88-16988
Algorithm design for scientific computation for highly parallel multiprocessor systems
[AD-A186713] 09 p1217 N88-17299
SURE reliability analysis: Program and mathematics
[NASA-TP-2764] 09 p1231 N88-17380
Two-phase reduced gravity experiments for a space reactor design
[DE86-015530] 09 p1247 N88-17475
Data reduction and analysis of HELIOS plasma wave data
[NASA-CR-182466] 09 p1264 N88-17572
Vibration and flutter characteristics of the SR7L large-scale propfan
[NASA-TM-100272] 10 p1344 N88-18036
Evaluation of surface energy and radiation balance systems on the Konza Prairie
[NASA-CR-182534] 10 p1355 N88-18097
SAGE: The Clemson University Systolic Array Generating Engine 10 p1379 N88-18235
Parameter identification and sensitivity analysis for a robotic manipulator arm
[NASA-CR-181608] 10 p1385 N88-18272
Benchmarks of neutral beam injection codes for stellarators
[DE88-003786] 10 p1412 N88-18428
On the stability of the supersonic boundary layer
11 p1435 N88-18561
Documentation for computer code NACL
[LBL-21859] 11 p1531 N88-19145
ZAP user's manual
[LBL-21270] 11 p1546 N88-19248
Predictive wall adjustment strategy for two-dimensional flexible walled adaptive wind tunnel: A detailed description of the first one-step method
[NASA-CR-181635] 12 p1573 N88-19409
Calculation of flow about posts and powerhead model
[NASA-CR-179305] 12 p1625 N88-19722
Analysis of pre-flight modulator voltage calibration data for the Voyager plasma science experiment
[NASA-CR-182577] 12 p1710 N88-20236
Dynamics of high-speed mechanisms with elastic members 13 p1779 N88-20643
Computer software for the computation of the scattered field and the optical microscope image of line objects patterned in thick layers
[PB88-153705] 13 p1814 N88-20838
Accuracy requirements and benchmark experiments for CFD validation
[NASA-TM-100087] 14 p1911 N88-21423
Monolithic ceramic analysis using the SCARE program
15 p2081 N88-22409
Continuous fiber ceramic matrix composites for heat engine components 15 p2082 N88-22411
Numerical arc segmentation algorithm for a radio conference: A software tool for communication satellite systems planning
[NASA-TM-100789] 16 p2167 N88-22919
Thermoviscoelastic characterization and predictions of Kevlar/epoxy composite laminates
[NASA-CR-182878] 16 p2172 N88-22946
Two-equation low-Reynolds-number turbulence modeling of transitional boundary layer flows characteristic of gas turbine blades
[NASA-CR-4145] 16 p2209 N88-23185
POPEYE: A production rule-based model of multitask supervisory control (POPCORN)
16 p2240 N88-23384
Development of Electromagnetic PIC code for LIB diode 16 p2276 N88-23622
Stability requirement FOT ignition and high gain implosion = 2-D simulation for high neutron yield experiment = 16 p2278 N88-23633
The application of Rutherford backscattering for analyzing multilayered structure change induced by pulsed ion beam bombardment 16 p2278 N88-23638
Numerical simulation of scramjet inlet flow fields
[NASA-TP-2517] 17 p2296 N88-23735
Testing complex avionics software: A practical experience 17 p2306 N88-23794
Theoretical studies of Resonance Enhanced Stimulated Raman Scattering (RESRS) of frequency doubled Alexandrite laser wavelength in cesium vapor
[NASA-CR-182871] 17 p2317 N88-23841
Electromagnetic scattering from nonlinear anisotropic cylinders 17 p2333 N88-23930
Manual for obscuration code with space station applications
[NASA-CR-178099] 17 p2334 N88-23931
Numerical modelling of flows using phoenics
17 p2339 N88-23955
Theory of neutron moisture probes and interpretation of measurements in complex soil and water systems
17 p2342 N88-23965
A proposal of adaptation of a knowledge-based scene analysis model to some remote sensing problems
17 p2354 N88-24026
The SAGE geographic analysis system
17 p2361 N88-24063
COMTAL vision one/20 programming processor system from the VAX 11/780 17 p2364 N88-24079

A control technique for improved robot performance
17 p2391 N88-24212
Novel silicon Schottky barrier infrared imaging arrays
17 p2439 N88-24510
A benchmark for galactic cosmic ray transport codes
[NASA-TM-101157] 17 p2453 N88-24571
Prediction of laminar and turbulent flows past single and twin airfoils 18 p2457 N88-24589
Dynamics of a flexible orbiting platform with MRMS
[ISSN-0285-6808] 18 p2473 N88-24673
Shape stability in composites
18 p2479 N88-24706
Kinematics, dynamics and control of a closed chain mechanism manipulator 18 p2523 N88-24967
Dynamic response of plates to moving loads: Structural impedance and finite element methods
18 p2528 N88-25000
Advanced development of the boundary element method for elastic and inelastic thermal stress analysis
18 p2529 N88-25002
Automated cartographic generalization for linear map features 18 p2532 N88-25021
Computer and model changes at National Meteorological Center (NWC) 18 p2547 N88-25116
SYMBL: A new Boolean compiler
18 p2554 N88-25160
The Environment for Application Software Integration and Execution (EASIE), version 1.0. Volume 3: Program execution guide
[NASA-TM-100575] 18 p2558 N88-25184
Phase diagrams in materials science and the use of the computer in their calculation
[PB88-155262] 18 p2586 N88-25364
The development of a user friendly thermodynamic code for the personal computer 19 p2623 N88-25559
Development of a generic combustion stability code for liquid propellant rocket engines
19 p2626 N88-25576
Anatomy of group burning mode transitions in spray group combustion 19 p2626 N88-25578
A computer program for performance prediction of tripropellant rocket engines with tangential slot injection
19 p2627 N88-25581
Boundary layer simulator (BLIMPJ) improvement
19 p2627 N88-25582
Analysis of microwave burner measurement system using a microwave network analysis computer program
19 p2631 N88-25604
Solid rocket motor performance: A workshop report
19 p2631 N88-25607
Evaluation of techniques for direct measurement of burning rates in nozzleless motors
19 p2631 N88-25609
On the NAL numerical simulator system
19 p2635 N88-25631
Rarefied gas numerical wind tunnel 3. Universal code for three dimensional bodies 19 p2637 N88-25644
The new MININEC (version 3): A mini-numerical electromagnetic code
[AD-A191778] 19 p2642 N88-25675
Semi-Markov adjunction to the Computer-Aided Markov Evaluator (CAME)
[NASA-CR-181645] 19 p2678 N88-25924
Prediction of fatigue life of notched specimens under aircraft loading and importance of the relative method in the case of local strain approach, part 2
[TAE-595-PT-2] 19 p2680 N88-25934
Improved method for stress and compatibility analysis of multicomponent rotating systems
[NASA-TM-100884] 19 p2680 N88-25935
The impact of disorganized occupation of urban sub-basins: Sub-basin of the Cabucu River, metropolitan area of Sao Paulo (SP) 19 p2682 N88-25945
Updating of municipal official register of real estate through the geographical information system
19 p2684 N88-25952
MM4 (Penn State/NCAR (National Center for Atmospheric Research)) mesoscale model version 4 documentation
[PB88-173232] 19 p2688 N88-25979
BOLETIM: An expert system for weather forecasting
[INPE-4538-TDL/329] 19 p2693 N88-26011
Stability of spheromak against current driven modes: Effects of flux hole on stability
[IPPJ-868] 19 p2730 N88-26211
Intelligent guidance and control for wind shear encounter
[NASA-CR-183060] 20 p2755 N88-26347
Determination of Tafel constants in nonlinear polarization curves
[AD-A192335] 21 p2912 N88-27282

APPROACH
NT INSTRUMENT APPROACH
Noise of a model high speed counterrotation propeller at simulated takeoff/approach conditions (F7/A7)
[NASA-TM-100206] 01 p0091 N88-10592
GPS vertical axis performance enhancement for helicopter precision landing approach
[NASA-CR-177443] 04 p0397 N88-12477
Effect of motion cues during complex curved approach and landing tasks: A piloted simulation study
[NASA-TP-2773] 04 p0398 N88-12480

APPROACH CONTROL
Report of safety survey: Human integration of approach charts
[DOT/FAA/PM-87/15] 01 p0076 N88-10438
Approach trajectory planning system for maximum concealment
[NASA-TM-88258] 02 p0227 N88-11435
The role of adaptive supplemental visual cuing in flight simulation
[AD-A185932] 07 p0822 N88-14992
Space vehicle approach velocity judgments under simulated visual space conditions
[NASA-TM-89437] 11 p1523 N88-19094
Flight simulations of MLS interception procedures applicable to laterally segmented approach paths
[NLR-MP-86037-U] 13 p1721 N88-20288

APPROPRIATIONS
Budget reimbursements: The National Aeronautics and Space Administration's reimbursable work
[PB87-207296] 01 p0107 N88-10696
Department of Housing and Urban Development, and Certain Independent Agencies Appropriations, 1988, Part 2
[S-HRG-100-106-PT-2] 03 p0385 N88-12423
The 1988 National Aeronautics and Space Administration (NASA) authorization
[GPO-76-600] 06 p0792 N88-14854
Department of Housing and Urban Development independent agencies appropriations for 1989. Part 7: National Aeronautics and Space Administration
[GPO-85-166] 16 p2286 N88-23689
Department of Defense statement on defense agency research and development to the Subcommittee on Defense of the Committee on Appropriations, United States House of Representatives, 100th Congress, second session
[AD-A191840] 18 p2588 N88-25377
The Department of Defense report on the merit review process for competitive selection of university research projects and an analysis of the potential for expanding the geographic distribution of research for the Committees on Appropriations, United States Congress
[AD-A191842] 18 p2588 N88-25379

APPROXIMATION
NT BORN APPROXIMATION
NT BORN-OPPENHEIMER APPROXIMATION
NT CHEBYSHEV APPROXIMATION
NT FINITE DIFFERENCE THEORY
NT FINITE ELEMENT METHOD
NT HARTREE APPROXIMATION
NT LEAST SQUARES METHOD
NT MEAN SQUARE VALUES
NT NEWTON METHODS
NT NEWTON-RAPHSON METHOD
NT PADE APPROXIMATION
NT PARTICLE IN CELL TECHNIQUE
NT RAYLEIGH-RITZ METHOD
NT RELAXATION METHOD (MATHEMATICS)
NT RITZ AVERAGING METHOD
Correction to a single higher order theory of elastic plates
[ETN-87-90676] 01 p0062 N88-10397
Approximate polynomial preconditioning applied to biharmonic equations on vector supercomputers
[NASA-TM-100217] 01 p0087 N88-10563
Wake shield 03 p0298 N88-11871
Relaxation effect of stark split levels for two-level system interacting with symmetrical strong resonant bichromatic field 03 p0299 N88-11882
Polynomial compensation, inversion, and approximation of discrete time linear systems
[NASA-TM-100027] 03 p0372 N88-12344
Finite deformations of shell with rigid inclusion
04 p0426 N88-12639
Solution of three-dimensional inverse problem of gravimetry in contact surfaces class by local corrections method 04 p0460 N88-12848
An adaptive subdivision method with crack prevention for rendering beta-spline objects
[AD-A184249] 04 p0477 N88-12940
Back-of-the-envelope problems
[AD-A184105] 04 p0484 N88-12980
Tridiagonal approximate factorization method: A preconditioning technique for solving nonsymmetric linear systems suitable to supercomputers
05 p0537 N88-13271
Master plots for predicting the case-depth in laser surface treatments
[PB87-221875] 05 p0586 N88-13574
Approximating multivariate normal orthant probabilities using the Clark algorithm
[AD-A184855] 05 p0634 N88-13873
Stability properties of spline approximations for retarded systems
[PB87-220919] 05 p0639 N88-13910
Numerical and analytical methods in nonlinear partial differential equations
[AD-A185210] 05 p0641 N88-13918
Approximate solutions for the momentum transport in turbulent flows in narrow rod array bundles using the finite element method
[ETN-88-90810] 06 p0701 N88-14306
Errors in retrieving hydrological fields and fields of their differential characteristics by method of approximation by orthogonal functions 06 p0727 N88-14475
Distributed infimum approximation
[PB87-234969] 06 p0764 N88-14695
Diffusion first passage times: Approximations and related differential equations
[AD-A185592] 06 p0765 N88-14700
Stochastic approximation and large deviations: General results for w.p.l. Convergence
[AD-A185818] 06 p0768 N88-14721
Relativistic stellar pulsations 06 p0801 N88-14902
Error assessments of widely-used orbit error approximations in satellite altimetry
[NASA-CR-182390] 07 p0823 N88-14998
On the approximation of the output process of multi-user random access communication networks
[AD-A186197] 07 p0842 N88-15108
Overestimation of on-axis power density by the Fraunhofer (far-field) approximation
[AD-A186399] 07 p0843 N88-15111
Bounding the expectation of convex functions with limited distribution information
[AD-A186147] 07 p0910 N88-15512
Estimation and testing in truncated and nontruncated linear median-regression models
[AD-A186317] 07 p0911 N88-15522
On stochastic optimality of policies in first passage problems
[AD-A186293] 07 p0915 N88-15554
Propagation of radiation along a constricting optical waveguide 07 p0920 N88-15590
The application of vector diffraction to the scalar anomalous diffraction approximation of Van de Hulst
[AD-A185930] 07 p0929 N88-15643
A semianalytical solution of the heat conduction equation for several boundary conditions
08 p1014 N88-16148
Short data length effects in an asymptotically efficient ARMA (AutoRegressive Moving Average) spectral estimator
[AD-A186561] 08 p1068 N88-16458
Strong convergence and convergence rates of approximating solutions for algebraic Riccati equations in Hilbert spaces
[AD-A186190] 08 p1072 N88-16464
A study of the free energy of the Lenz-Ising model using the cluster variation method of Morita
[AD-A186023] 08 p1073 N88-16476
Approximation of noncorrelated reflections in problem of sound propagation through waveguide with rough boundary 08 p1076 N88-16487
Active and passive remote sensing of ice
[AD-A186685] 09 p1195 N88-17162
Applications of nonlinear systems theory to control design
[NASA-CR-182485] 09 p1231 N88-17377
Random truncation models and Markov processes
[CWI-MS-R8702] 09 p1232 N88-17389
Fully Lagrangian Renormalized Approximation theory of fluid turbulence
[DE88-004960] 10 p1330 N88-17952
Explicit approximations for strictly nonlinear oscillators with slowly varying parameters with applications to free electron lasers
[DE88-004116] 10 p1336 N88-17984
A unified framework for approximation in inverse problems for distributed parameter systems
[NASA-CR-181621] 10 p1400 N88-18346
Eigenvalue problems
[AD-A188069] 10 p1401 N88-18356
Advances in calculating macroionic solution structure
[DE88-003799] 10 p1409 N88-18406
The application of the hybrid iterative method to scattering by perfectly conducting bodies of revolution
11 p1475 N88-18802
Approximate method for predicting the permanent set in a beam in vacuo and in water subject to a shock wave 11 p1500 N88-18957
Accurate efficient evaluation of Bessel transform: Programs and error analysis
[AD-A187718] 11 p1536 N88-19174

WKBJ method and strained coordinates for high frequency inertial wave filtering
[INPE-4214-PRE/1095] 11 p1537 N88-19186
Core-core and core-valence correlation
[NASA-CR-182552] 11 p1544 N88-19226
Theoretical studies of the potential surface for the F - H2 greater than HF + H reaction
[NASA-CR-182551] 11 p1557 N88-19319
Approximation algorithms for scheduling unrelated parallel machines
[CWI-OS-R8714] 13 p1817 N88-20861
Predicting oscillatory finite difference solutions to the heat equation: A comparative study of the coefficient and matrix methods
[AD-A189591] 13 p1825 N88-20911
What do multistep methods approximate
[PB88-148838] 13 p1828 N88-20932
Nonstationary solution in random vibration theory
[PB88-163746] 14 p1933 N88-21529
The NPL data approximation subroutine library: Cu rrent and planned facilities
[NPL-DITC-104/87] 14 p1959 N88-21681
On the Edgeworth expansion and the bootstrap approximation for a Studentized U-statistic
[CWI-MS-R8708] 14 p1965 N88-21728
Deterministic approximations of probability inequalities
[REPT-87-43] 14 p1966 N88-21732
A posterior error estimation in a finite element method for parabolic partial differential equations
[AD-A190296] 15 p2120 N88-22636
An approximation technique for solving a system of Fredholm integral equations for asymmetric detector response functions
[AD-A190577] 15 p2121 N88-22645
Constructive version of the approximation induction principle
[PB88-165477] 15 p2122 N88-22647
Approximations in extreme value theory
[AD-A189817] 15 p2124 N88-22659
Approximation methods for the identification and control of distributed parameter systems
[AD-A190201] 15 p2124 N88-22662
Extreme value for dependent sequences via the Stein-Chen method of poisson approximation
[AD-A190325] 15 p2125 N88-22668
Efficiency of some computational techniques for electromagnetic scattering problems
[PB88-148895] 16 p2187 N88-23043
On local approximations of the pressure-strain term in turbulence models 16 p2197 N88-23102
Approximation and representation of explicit surfaces in the presence of singularities
[ETN-88-92191] 16 p2258 N88-23496
Jacobi polynomials as generalized Faber polynomials
[CWI-PM-R8706] 16 p2258 N88-23498
An approximation theory for the identification of nonlinear distributed parameter systems
[NASA-CR-181658] 16 p2260 N88-23510
Introduction to nilpotent approximation filtering
[CWI-PM-R8709] 16 p2262 N88-23524
Complex space monofilar approximation of diffraction currents on a conducting half plane
[NASA-CR-182883] 16 p2273 N88-23605
A new collocation-type method for the numerical solution of Hammerstein equations 17 p2393 N88-24226
An evaluation of energy-independent heavy ion transport coefficient approximations
[NASA-TM-101158] 17 p2397 N88-24251
Nonlinear programming extensions to rational function approximation methods for unsteady aerodynamic forces
[NASA-TP-2776] 18 p2463 N88-24623
A feedback linearization approach to spacecraft control using momentum exchange devices
[NASA-CR-172057] 18 p2472 N88-24668
Axisymmetric viscid-inviscid interaction by a frozen vorticity approximation
[AD-A191743] 18 p2509 N88-24885
Construction of approximations to acoustic Green's functions for nonhomogeneous oceans using transmutation
[PB88-185384] 18 p2548 N88-25126
Open or closed curves by regularized B-splines
[RR-652-M] 18 p2563 N88-25218
A mixed min-max control problem governed by integral equations 18 p2564 N88-25228
Numerical solution of linear integral equations with random forcing terms 18 p2565 N88-25237
On a biorthogonal system associated with uniform asymptotic expansions
[CWI-AM-R8709] 18 p2566 N88-25240
Galerkin approximation for inverse problems for nonautonomous nonlinear distributed systems
[NASA-CR-181676] 18 p2567 N88-25246
Optimal discrete-time LQR problems for parabolic systems with unbounded input: Approximation and convergence
[NASA-CR-181673] 18 p2567 N88-25247
Curvature of blended rolled edge reflectors at the shadow boundary contour
[NASA-CR-182974] 18 p2576 N88-25300
Non equilibrium expansion of a radiating gas in a channel of varying section
[DE88-702063] 19 p2665 N88-25845
Solution of Faddeev-Yakubovsky differential equations by the finite-dimensional approximation method for four spinless particles in the 1+3 scattering problem
[DE87-702983] 19 p2719 N88-26145
Semi-discrete approximations to nonlinear systems of conservation laws; consistency and L(infinity)-stability imply convergence
[NASA-CR-181683] 19 p2721 N88-26157
Finite element approximation to a model problem of transonic flow
[DE88-701835] 20 p2752 N88-26333
L(sub infinity symbol)-approximations of complex functions and robust controllers for large flexible space structures
[PB88-186226] 20 p2764 N88-26390
Finite-dimensional approximation for optimal fixed-order compensation of distributed parameter systems
[NASA-CR-181674] 20 p2843 N88-26873
Prolongation, restriction and coarse grid approximation in a three-dimensional cell-centered multigrid method
[REPT-88-02] 20 p2846 N88-26889
Analytical approximation of a distorted reflector surface defined by a discrete set of points
[NASA-TM-101323] 21 p2934 N88-27424
A fast vortex code for computing 2-D flow in a box
[DE88-011732] 21 p2946 N88-27498
Approximation problems of the Hilbert transform to identify minimum phase linear systems
[FUB-42-1986] 21 p2999 N88-27790
Modeling and approximate performance analysis of multiuser computer systems
[ETN-88-92137] 21 p3002 N88-27806
Approximations of stochastic equations driven by predictable processes
[AD-A192714] 21 p3005 N88-27823
Finding minimum-cost circulations by successive approximation
[AD-A192724] 21 p3005 N88-27824
Asymptotic of Peanokerns of finite fixed order
[ETN-88-92381] 21 p3008 N88-27843
Approximations and optimal control for the pathwise average cost per unit time and discounted problems for wideband noise driven systems
[AD-A192712] 21 p3008 N88-27847
Evaluation of quantum mechanics path integrals by the approximations exact on a class of polynomial functionals
[DE88-702434] 21 p3011 N88-27865
Perturbation expansions generated by an approximate propagator
[DE88-702435] 21 p3011 N88-27866
Steady-state approximations in Raman excitation equations
[DE88-011759] 21 p3014 N88-27889
Approximate and numerical methods in acousto-optics. Part 1: Normal incidence of the light
[AD-A194294] 22 p3152 N88-28755
Stability of semidiscrete approximations for hyperbolic initial-boundary-value problems: Stationary modes
[NASA-TM-100994] 23 p3270 N88-29455
Canonical forms in the control of DPS
[AD-A194671] 23 p3270 N88-29461
Approximations and implementations of nonlinear filtering schemes
[AD-A194685] 23 p3271 N88-29462
Finding minimum-cost circulations by successive approximation
[AD-A194028] 23 p3272 N88-29469
Numerical modelling of premixed flames in gaseous media 24 p3350 N88-29944
Approximation of viscoelastic stresses from Newtonian turbulent kinematics
[AD-A194317] 24 p3371 N88-30077
Automatic qualitative analysis of ordinary differential equations using piecewise linear approximations
[AD-A196310] 24 p3424 N88-30379
Convergence of Galerkin approximations for operator Riccati equations: A nonlinear evolution equation approach
[NASA-CR-181706] 24 p3425 N88-30386
Image focusing in space and time
[AD-A195839] 24 p3429 N88-30410

APPROXIMATION METHODS
U APPROXIMATION

APSIDES
NT PERIGEES
NT PERIHELIONS

APT (PICTURE TRANSMISSION)
U AUTOMATIC PICTURE TRANSMISSION

APTITUDE
A comparison of the Army's Project A: Cognitive and psychomotor tests to analogous Air Force and Navy tests
[AD-A188636] 12 p1670 N88-20002
Properties of some Bayesian scoring procedures for computerized adaptive tests
[AD-A189925] 15 p2124 N88-22660
Validity of the academic aptitude composite of the Air Force Officer Qualifying Test (AFOQT)
[AD-A194753] 23 p3240 N88-29286
Reliability and construct validity of reaction time, inspection time and machine-paced tests of cognitive speed
[AD-A193779] 23 p3241 N88-29289

AQUARID METEOROIDS
Results of observations of the Eta Aquarid and Orionid meteor showers in 1980-1984 06 p0740 N88-14548
The structure of the Halley meteor stream and the orbital history of the comet 14 p2008 N88-21975

AQUATIC PLANTS
NT PHYTOPLANKTON

AQUEOUS SOLUTIONS
Reduction of CO2 to methanol and methane by photo and dark reactions on semiconductor and metal electrodes
[PB87-226825] 02 p0156 N88-10975
Organic molecules on meteoritic solid substrates
[NASA-CR-181570] 05 p0560 N88-13411
Coagulation in stirred tanks
[B8711373] 05 p0562 N88-13420
Observing effect of laser radiation of low-frequency Raman scattering of light 06 p0772 N88-14742
Excess thermodynamic properties of aqueous electrolytes to high temperatures and pressures
[DE88-001768] 07 p0940 N88-15712
Precipitation of surfactants and surfactant mixtures in aqueous solutions
[DE88-003333] 10 p1298 N88-17763
A review of pitting corrosion in high temperature aqueous solutions
[DE88-003547] 10 p1302 N88-17787
An experimental investigation of the hydrodynamic and heat-transfer behavior of aqueous foam in laminar tube flow
[DE88-004954] 11 p1483 N88-18855
The influence of strain on hydrogen entry, transport, and embrittlement of a high strength steel in aqueous sodium chloride solution
[AD-A189302] 12 p1608 N88-19619
Velocity and concentration fields over a crystal growing in a water solution. Experimental study and numerical simulation 14 p1987 N88-21856
Corrosion and fatique properties of FeCrB/Si metallic glass wires in aqueous environments
17 p2320 N88-23855
The high pressure sound velocity and equation of state of aqueous solutions of hydroxylammonium nitrate and triethanolammonium nitrate
[AD-A191740] 18 p2570 N88-25266
Precise ultraviolet absorbance study of the interaction of amino acids and mononucleosides in aqueous solution
[ISAS-RN-356] 21 p2908 N88-27256

AQUICULTURE
Aquarack: Aims and Possible Research Projects
[DFVLR-MITT-87-01] 01 p0073 N88-10469
The Aquarack as a potential instrument for basic research work in space biology: Inventory and scientific dispositions 01 p0073 N88-10470
Investigations of the survey of the reproductive biology of Xiphophorus in an Aquarack
01 p0074 N88-10471
The usefulness of microalgal structures as an element of closed ecological systems like Aquarack and CELSS --- Controlled Ecological Life Support System (CELSS)
01 p0074 N88-10476
Use of SPOT images for coastal development and inventory of aquacultural sites in New Caledonia (ALIAS project). First results 03 p0344 N88-12175
SPOT: A tool to aid preselection of sites favorable for aquiculture. Evaluation and perspectives of the Preliminary Evaluation Program for SPOT (PEPS) ALIAS Caledonie
22 p3108 N88-28456

AQUIFERS
Field experience with aquifer thermal energy storage
[DE88-007075] 18 p2538 N88-25058

ARABSAT
Prevention of radiation induced degradations and of electrostatic perturbations on the Arabsat spacecraft in flight results 03 p0275 N88-11734

ARC CLOUDS
Convective scale interaction: Arc cloud lines and the development and evolution of deep convection
[NASA-CR-181469] 02 p0215 N88-11357
ARC DISCHARGES
Introduction to the problem of environmentally induced discharges 03 p0273 N88-11717
Modeling of environmentally-induced transients within satellites. Part 2: Discharge coupling transients 03 p0273 N88-11722
In-flight diagnosis: Analysis of spurious events --- spacecraft 03 p0274 N88-11724
Low-current behavior and current chopping of vacuum arcs
[ISBN-90-9001649-X] 05 p0578 N88-13529
Some investigations of electrical discharges at the surfaces of solid cathodes immersed in aqueous electrolyte solutions
[PB87-168209] 09 p1159 N88-16946
Arcs in cesium seeded noble gases resulting from a magnetically induced electric field
[EUT-87-E-177] 13 p1843 N88-21028
Study of surface discharges
[ONERA-12/7236-PY] 15 p2026 N88-22073
Arcing and rf signal generation during target irradiation by a high-energy, pulsed neutral particle beam
[DE88-007169] 18 p2471 N88-24664
Multiply stripped ion generation in the metal vapor vacuum arc
[DE88-008418] 19 p2725 N88-26179
ARC HEATING
Rocket nozzle thermal shock tests in an arc heater facility 02 p0133 N88-10832
Spectroscopic investigations and measurements of certain ARC jet parameters 06 p0796 N88-14877
Upgrading of NASA-Ames high-energy hypersonic facilities: A Study
[NASA-CR-182475] 09 p1122 N88-16717
Numerical investigations in three-dimensional internal flows
[NASA-CR-183108] 23 p3210 N88-29106
ARC JET ENGINES
A low-power arcjet cyclic lifetest
[NASA-TM-100233] 03 p0278 N88-11748
Advanced electric propulsion and space plasma contactor research
[NASA-CR-180862] 06 p0674 N88-14126
Performance-limiting factors in MPD thrusters
[AD-A185605] 06 p0674 N88-14128
Arcjet thruster research and technology
[NASA-CR-180865] 10 p1293 N88-17732
An experimental investigation of an arcjet thruster exhaust using Langmuir probes
[NASA-TM-100258] 14 p1883 N88-21253
MPD (magnetoplasmadynamic) thrust chamber flow dynamics
[AD-A189940] 15 p2137 N88-22751
Advanced electric propulsion research
[NASA-CR-182130] 16 p2170 N88-22937
Arcjet thruster research and technology, phase 1
[NASA-CR-182107] 17 p2314 N88-23830
Electric propulsion options for the SP-100 reference mission 17 p2404 N88-24296
Status of high power electric propulsion technology 17 p2428 N88-24443
Performance and long duration test of a 30 kw thermal arcjet engine
[AD-A190962] 18 p2474 N88-24677
Evaluation of the communications impact of a low power arcjet thruster
[NASA-TM-100926] 18 p2475 N88-24682
An extended life and performance test of a low-power arcjet
[NASA-TM-100942] 18 p2476 N88-24687
Arcjet power supply and start circuit
[NASA-CASE-LEW-14374-1] 23 p3181 N88-28939
Performance and lifetime assessment of MPD arc thruster technology
[NASA-TM-101293] 24 p3336 N88-29860
Unified study of plasma/surface interactions for space power and propulsion
[AD-A195971] 24 p3338 N88-29870
ARC LAMPS
Arc lamp power supply using a voltage multiplier
[NASA-CASE-LAR-13202-1] 17 p2335 N88-23942
ARC MELTING
Growth and deformation mechanisms of refractory alloy hybrid materials
[AD-A190492] 15 p2039 N88-22152
Evaporation characteristics of elements during vacuum arc remelting of alloy A-286 15 p2055 N88-22248
ARC SPRAYING
Evaluation of the chromium oxide arc spraying treatment on solar energy collectors
[ETN-88-92564] 18 p2537 N88-25053
ARC WELDING
NT GAS TUNGSTEN ARC WELDING
NT PLASMA ARC WELDING
A physical metallurgical basis for heat-affected zone and base-plate properties of a microalloyed HSLA steel
[AD-A180200] 01 p0022 N88-10137
Process and equipment capabilities materials joining laboratory, 1987
[DE87-014534] 02 p0180 N88-11122
The nature of metallurgical reactions in underwater welding
[AD-A184464] 04 p0414 N88-12568
Optical seam tracking in robotic arc welding
[VTT-RR-463] 06 p0713 N88-14376
Study on the cryogenic toughness of stainless steel weld metals
[PB87-143830] 07 p0834 N88-15057
Synchronous multi-image high speed photography of welding arc by optical fibers
[PB87-143939] 07 p0857 N88-15202
Electronic imaging technique for welding and other high-luminosity processes
[DE88-002199] 07 p0862 N88-15227
Microcomputer controlled arc welding power source: Its steady state and transient performance
[PB87-143921] 07 p0863 N88-15233
MIG welding with pulsed wire feed
[PB87-143582] 07 p0863 N88-15234
Study of welding arc control in China
[PB87-143350] 07 p0863 N88-15235
Study on arc sound in TIG and plasma welding processes and the possibility of its application in practice
[PB87-143947] 07 p0863 N88-15238
A numerical thermal model of the rapid solidification parameters in the capacitor discharge welding process
[DE88-002206] 07 p0864 N88-15244
Submerged arc flux welding with CaF2-CaO-SiO2 fluxes: Possible electrochemical effects on weld metal
[DE88-003107] 08 p0992 N88-16004
A detailed microstructural examination of the cause of HAZ cracking in type 316 steel
[AERE-R-12428] 10 p1301 N88-17777
A generalized method for automatic downhand and wirefeed control of a welding robot and positioner
[NASA-TP-2807] 10 p1316 N88-17869
Microstructural characterization of HSLA-100 GMA-weldments
[AD-A187782] 11 p1457 N88-18683
Microstructural characterization of the heat affected zone of HSLA (High Strength Low Alloy)-100 steel GMA (Gas Metal Arc)-weldment
[AD-A187825] 11 p1457 N88-18686
Ensuring higher stability of immersed-arc welding of structural aluminum alloys and magnesium alloys 14 p1898 N88-21331
The effect of surface tension in the weld pool on seam formation when welding thin sheet with light rays 14 p1898 N88-21334
Welding torch gas cup extension
[NASA-CASE-MFS-29252-1] 17 p2345 N88-23980
Trailer shield assembly for a welding torch
[NASA-CASE-MFS-29260-1] 18 p2524 N88-24972
Ultrasonic and video computerized data acquisition for automated welding
[DE88-006741] 19 p2677 N88-25918
Physical-chemical reactions at welding arc/molten pool interfaces
[DE88-007717] 20 p2808 N88-26862
ARC length control for plasma welding
[NASA-CASE-MSC-20900-1] 24 p3380 N88-30131
ARCHAEOLOGY
Subsurface morphology and geoarchaeology revealed by spaceborne and airborne radar 17 p2353 N88-24022
Utilization of LANDSAT-TM, for aiding in the localization of archeological sites in the state of Sao Paulo 17 p2362 N88-24069
ARCHES
Reinforced concrete arches under blast and shock environments 09 p1180 N88-17065
ARCHITECTURE
Maximum entropy/optimal projection design synthesis for decentralized control of large space structures
[AD-A186359] 07 p0824 N88-15003
Helicopter crashworthiness research program 09 p1107 N88-16635
Finely grained parallelism in an applicative architecture 10 p1383 N88-18256
Introduction to a system for implementing neural net connections on SIMD architectures
[NASA-CR-181612] 10 p1386 N88-18279
Space Station Human Factors Research Review. Volume 3: Space Station Habitability and Function: Architectural Research
[NASA-CP-2426-VOL-3] 12 p1650 N88-19883
Space station architectural elements model study
[REPT-31799] 12 p1650 N88-19885
Real-time stressed channel simulator
[AD-A190223] 15 p2025 N88-22067
A direct-execution parallel architecture for the Advanced Continuous Simulation Language (ACSL)
[NASA-CR-182809] 15 p2115 N88-22602
Space station architectural elements and issues definition study
[NASA-CR-3941] 18 p2587 N88-25371
Comparative analysis of the space power architecture studies
[NASA-TM-100977] 22 p3049 N88-28090
Microsupercomputers: Design and implementation
[AD-A194712] 22 p3135 N88-28638
The triangle: A multiprocessor architecture for fast curve and surface generation
[AD-A195882] 24 p3414 N88-30324
Report to congress on the strategic defense system architecture
[AD-A195476] 24 p3426 N88-30393
Monte-Carlo estimation of the influence of plant architecture parameters on spectral brightness 24 p3450 N88-30533
ARCHITECTURE (COMPUTERS)
Digital system bus integrity
[NASA-CR-181446] 01 p0006 N88-10030
The varieties of capabilities in Flex
[RSRE-MEMO-4042] 01 p0078 N88-10500
Strategies for concurrent processing of complex algorithms in data driven architectures
[NASA-CR-181435] 01 p0082 N88-10527
A unified approach to parallel computation: Performance evaluation and architecturally independent parallel programming
[DE87-012519] 01 p0084 N88-10540
Fault tolerant considerations and methods for guidance and control systems
[AGARD-AG-289] 02 p0126 N88-10796
An expert system for aircraft conflict resolution in dense airspaces 02 p0129 N88-10810
An embedded multiprocessor computer for proof-of-principle testing of exploratory systems concepts
[DE87-012735] 02 p0218 N88-11372
Benchmarking the Connection Machine
[DE87-013500] 02 p0218 N88-11374
Memory systems for single bus multiprocessor architecture. Application to the SCOM system
[ENST-86E022] 02 p0219 N88-11379
Multi-processor architectures for artificial intelligence processing
[OUEL-1671/87] 02 p0219 N88-11380
Some 2-D WSI array architectures --- wafer scale integration (WSI)
[OUEL-1672/87] 02 p0219 N88-11381
Implementation of preconditioned s-step conjugate gradient methods on a multiprocessor system with memory hierarchy
[DE87-014401] 02 p0222 N88-11400
Summaries of the FY 1987 applied mathematical sciences research program
[DE87-014447] 02 p0225 N88-11416
Methodology of performance evaluation of real time distributed systems
[ENST-87D003] 02 p0228 N88-11440
The warp computer: Architecture, implementation, and performance
[AD-A184329] 03 p0363 N88-12286
SBNR (Signed Binary Number Representations) digital signal processor architecture
[AD-A184603] 03 p0364 N88-12290
Layering central authentication on the interactive services of an existing homogeneous distributed system
[DE87-011544] 03 p0366 N88-12304
Delft parallel processor 84/16
[PB87-226254] 03 p0366 N88-12305
Interfacing distributed operating systems
[AD-A184489] 03 p0366 N88-12306
Network reconstitution protocol
[AD-A184755] 03 p0367 N88-12309
A survey of artificial neural systems
[AD-A184759] 03 p0368 N88-12312
An object-oriented architecture for intelligent tutoring systems
[AD-A184790] 03 p0368 N88-12314
Low-level vision on warp and the apply programming model
[AD-A184330] 03 p0369 N88-12320
Implementation of the Runge-Kutta-Fehlberg method for solution of ordinary differential equations on a parallel processor
[AD-A184660] 03 p0370 N88-12331
Autonomous Land Vehicle (ALV) planning and navigation system
[AD-A184243] 04 p0397 N88-12475

An evaluation plan of bus architectures and protocols using the NASA Ames intelligent redundant actuation system
[NASA-CR-177458] 04 p0398 N88-12482
Programmable real-time digital video image processing
[PB87-104162] 04 p0430 N88-12661
On the VLSI design of a pipeline Reed-Solomon decoder using systolic arrays 04 p0436 N88-12700
Research in VLSI (Very Large Scale Integration) systems
[AD-A184089] 04 p0438 N88-12721
Center for Supercomputing Research and Development (CEDAR)
[DE88-000807] 04 p0475 N88-12930
Methods for design and evaluation of integrated hardware/software systems for concurrent computation
[NASA-CR-181522] 04 p0479 N88-12953
Parallelization of hydrocodes on the Intel Hypercube, part 2
[DE88-001591] 04 p0480 N88-12957
Utilization of a high rate vector computer in computational fluid mechanics for aeronautics
[ETN-88-91171] 05 p0581 N88-13547
Test and evaluation of the transputer in a multi-transputer system
[AD-A184969] 05 p0631 N88-13859
Arrays for discrete Fourier transform
[REPT-87-019] 05 p0632 N88-13861
XCUT: A rule-based expert system for the automated process planning of machined parts
[DE87-011638] 05 p0639 N88-13905
On real-time systems using local area networks
[AD-A185475] 06 p0694 N88-14256
Fast algorithms for structural optimization and least squares
[AD-A185766] 06 p0724 N88-14452
Objects architecture: A comprehensive design approach for real-time, distributed, fault-tolerant, reactive operating systems
[AD-A185476] 06 p0755 N88-14631
A taxonomy of analytical computer performance models for computer design
[AD-A185561] 06 p0755 N88-14632
Set of multi-process primitives for stack based machines
[PB87-234381] 06 p0756 N88-14636
Benchmarking and evaluation of hardware description languages for design of VLSI systems
[PB87-134557] 06 p0758 N88-14648
Wide-area communication under Amoeba
[PB87-234431] 06 p0760 N88-14665
Computer architectures for artificial intelligence
[PB87-123824] 06 p0761 N88-14671
National Aeronautics and Space Administration (NASA)/American Society for Engineering Education (ASEE) Summer Faculty Fellowship Program, 1987. Volume 2
[NASA-CR-172009-VOL-2] 06 p0796 N88-14874
A general architecture for intelligent training systems 06 p0796 N88-14875
Fault-tolerant computer architecture based on INMOS transputer processor 06 p0797 N88-14880
Study of communication options in a distributed data handling system and survey of advanced man machine communications schemes. Work package 1: Interprocess communication
[ESA-CR(P)-2447] 07 p0843 N88-15114
Reliability modelling for fault-tolerant parallel processor
[AD-A185867] 07 p0900 N88-15451
An interactive visual interface for Fastbus diagnostics
[DE88-002569] 07 p0900 N88-15453
UNITY: A framework for study of parallel programming problem-solving
[AD-A185616] 07 p0906 N88-15490
Image understanding by Image-Seeking Adaptive Networks (ISAN)
[AD-A186214] 07 p0906 N88-15492
Integration of symbolic and algorithmic hardware and software for the automation of space station subsystems
[NASA-TM-89705] 07 p0907 N88-15497
Correctness proofs for systolic algorithms: Palindromes and sorting
[PB88-106075] 07 p0912 N88-15534
Modeling of architecture of a problem-oriented on-board processor 08 p1008 N88-16114
An easy-to-use diagnostic system development shell 08 p1055 N88-16366
A distributed architecture for intelligent monitoring and anomaly diagnosis of the Hubble Space Telescope 08 p1057 N88-16379
Development of a task-level robot programming and simulation system 08 p1058 N88-16387
A multiprocessing architecture for real-time monitoring 08 p1059 N88-16390
Application of parallel distributed processing to space based systems 08 p1059 N88-16393
Knowledge-based simulation 08 p1061 N88-16404
Similarity networks as a knowledge representation for space applications 08 p1062 N88-16411
Conceptual information processing: A robust approach to KBS-DBMS integration 08 p1063 N88-16422
Neural networks as a possible architecture for the distributed control of space systems 08 p1064 N88-16431
A learning apprentice for software parts composition 08 p1065 N88-16436
Information handling architecture and software for CIM (Computer Integrated Manufacturing)
[PB88-105820] 08 p1067 N88-16453
Prospectus for the development of a linear algebra library for high-performance computers
[DE88-003715] 08 p1068 N88-16457
High performance VLSI algorithms and architectures for digital signal processing 09 p1155 N88-16926
First Annual Workshop on Space Operations Automation and Robotics (SOAR 87)
[NASA-CP-2491] 09 p1203 N88-17206
Design of a neural network simulator on a transputer array 09 p1205 N88-17221
Communications patterns in a symbolic multiprocessor
[AD-A186896] 09 p1215 N88-17282
Supercomputers for solving PDE (Partial Differential Equations) problems
[AD-A186583] 09 p1215 N88-17283
High performance data buses: Progress and evolution
[DE88-002570] 09 p1215 N88-17285
Rationale for the design of the Ada (tradename) programming language
[AD-A187106] 09 p1217 N88-17297
A multithreaded processor architecture for parallel symbolic computation
[AD-A187034] 09 p1222 N88-17327
A type-oriented approach to knowledged-based systems
[MA-47] 09 p1222 N88-17329
Horizontal estimation and information fusion in multitarget and multisensor environments
[AD-A186935] 09 p1224 N88-17336
Proceedings of the Workshop on Future Directions in Computer Architecture and Software
[AD-A184949] 10 p1373 N88-18191
Some further observations about reduced instruction set computers 10 p1373 N88-18192
An empirical analysis of the Lilith instruction set 10 p1373 N88-18193
High-performance CPU implementation of the nebula instruction set architecture 10 p1373 N88-18194
The arithmetic cube and its associated algorithms 10 p1374 N88-18195
Automatically reconfigurable computer architecture 10 p1375 N88-18204
A large-grain dataflow architecture 10 p1375 N88-18207
A distributed system architecture based on macro dataflow model 10 p1376 N88-18210
Future directions in computer architecture and software: The year 2000 10 p1377 N88-18218
An investigation of parallelism in rule based systems 10 p1377 N88-18223
A parallel computer based on cube connected cycles 10 p1378 N88-18227
Performance evaluation of a loop interconnection structure 10 p1378 N88-18229
Aspects of a multiprocessor architecture 10 p1379 N88-18232
Strategies for concurrent processing of complex algorithms 10 p1379 N88-18236
Parallel architectures for logic programming 10 p1380 N88-18241
Real time artificial intelligence architecture 10 p1380 N88-18242
Future directions in computer architecture 10 p1383 N88-18257
Future directions in computer architecture and software workshop 10 p1383 N88-18258
A performance analysis of architectural scalability
[DE88-003537] 10 p1383 N88-18261
Emerging supercomputer architectures
[DE88-003539] 10 p1384 N88-18262
Supercomputer performance: The theory, practice, and results
[DE88-004697] 10 p1384 N88-18266
Systolic array adaptive beamforming
[AD-A187496] 10 p1385 N88-18269
MICRO system for control, acquisition and processing of experimental data
[DE88-700724] 10 p1386 N88-18278
Using program structure to achieve prefetching for cache memories
[DE88-003599] 10 p1387 N88-18282
CUEMAP: A tool for generating hierarchical charts and dataflow diagrams
[DE88-004778] 10 p1387 N88-18284
Programming methodology and performance issues for advanced computer architectures
[DE88-003098] 10 p1387 N88-18287
Implementation and analysis of a Navier-Stokes algorithm on parallel computers
[NASA-CR-181614] 10 p1390 N88-18301
A framework for evaluating computer architectures to support systems with security requirements, with applications
[AD-A187082] 10 p1392 N88-18303
An Ethernet local area network controller with supporting operating system software
[DE88-003534] 10 p1392 N88-18304
Dynamic processor self-scheduling for general parallel nested loops
[DE88-003572] 10 p1393 N88-18311
Parallel garbage collection on a virtual memory system
[DE88-003567] 10 p1396 N88-18317
The implementation of artificial intelligence in control systems
[DE88-003497] 10 p1396 N88-18318
Performance and evaluation at the Center for Supercomputing Research and Development
[DE88-003563] 10 p1417 N88-18456
Center for Supercomputing Research and Development
[DE88-003564] 10 p1418 N88-18466
Fuzzy logic inference processor for real time control: A second generation full custom design
[AD-A188155] 11 p1471 N88-18773
A comparison of VLSI architectures for time and transform domain decoding of Reed-Solomon codes 11 p1472 N88-18783
Modules of nanosecond logic electronics system with computer control
[DE88-700190] 11 p1479 N88-18828
Computer architecture for research in meteorology and atmospheric chemistry
[PB88-145313] 11 p1510 N88-19020
Optical symbolic processor for expert system execution
[AD-A187882] 11 p1525 N88-19103
Measurement and analysis of memory conflicts on vector multiprocessors
[AD-A188206] 11 p1525 N88-19104
Modular CAMAC system, 2
[DE88-700237] 11 p1525 N88-19106
Feasibility study of generating plans and strategies for software testing by knowledge based system
[AD-A187834] 11 p1529 N88-19134
Parallel processing in nonlinear programming
[INPE-4298-PRE/1169] 11 p1533 N88-19158
Object recognition on a systolic array
[AD-A187726] 11 p1534 N88-19164
Performance of a multigrid method on parallel architecture 11 p1539 N88-19200
Theory and practice of fault tolerance in distributed systems
[AD-A187559] 11 p1540 N88-19204
Optical computing research
[AD-A187862] 11 p1549 N88-19264
VSLI design generators
[AD-A188706] 12 p1623 N88-19707
Architecture with parallel processing for incremental computation
[INPE-4326-PRE/1178] 12 p1675 N88-20012
Efficient parallel architecture for highly coupled real-time linear system applications
[NASA-CR-182649] 12 p1675 N88-20015
Computer architecture for efficient algorithmic executions in real-time systems: New technology for avionics systems and advanced space vehicles
[NASA-CR-182650] 12 p1675 N88-20016
BLITZ: Blitzen's micron-code assembly language design document, version 1.0
[TR88-14] 12 p1676 N88-20019
An emulation tool for simulating matrix operations on an SIMD (Single Instruction Multiple Data stream) multiprocessor
[AD-A188654] 12 p1678 N88-20030
A laboratory facility for research in parallel computation
[AD-A188499] 12 p1680 N88-20044
Northeast Artificial Intelligence Consortium (NAIC) administrative matters and ancillary functions, volume 1
[AD-A189466] 12 p1682 N88-20055
NAVLAB: An autonomous navigation testbed
[AD-A189049] 13 p1720 N88-20283

Architecture specification for PAVE PILLAR avionics
[AD-A188722] 13 p1723 N88-20303
Analysis for architecture for image processing
[INPE-4294-PRE/1165] 13 p1791 N88-20715
Spectral element methods: Algorithms and architectures
[NASA-CR-182701] 13 p1820 N88-20878
Distributed transaction processing and the Camelot system
[AD-A188614] 13 p1821 N88-20885
A simulation study of a parallel processor with unbalanced loads
[AD-A189573] 13 p1822 N88-20887
On the design of parallel numerical methods in message passing and shared memory environments
[DE88-003566] 13 p1822 N88-20888
Locality, communication and interconnect length in multicomputers
[CWI-CS-R8708] 13 p1822 N88-20890
Soar: An architecture for general intelligence
[AD-A188742] 13 p1823 N88-20898
Towards a tribology information system: The results of a Planning Workshop held at the National Bureau of Standards, July-August 1985
[PB88-168604] 14 p1918 N88-21448
Activities and operations of the Advanced Computing Research Facility, October 1986-October 1987
[DE88-006223] 14 p1955 N88-21653
Proposal for a parallel system with image processing applications
[INPE-4293-PRE/1164] 14 p1961 N88-21696
Adaptive neural network architecture
[AD-A190114] 15 p2104 N88-22533
Parallel memory addressing using coincident optical pulses
[AD-A189767] 15 p2106 N88-22547
Multiple-transform pipelines for image coding
[REPT-87-038] 15 p2108 N88-22561
An analysis of multiple grain CHiP architectures
[AD-A189942] 15 p2110 N88-22570
Transformations of concurrent algorithms for highly parallel systems: A one year project summary report
[AD-A190236] 15 p2111 N88-22576
Inference engine for expert systems
[INPE-4465-TDL/321] 15 p2113 N88-22590
Modeling a parallel architecture for image processing
[RR-646-I] 15 p2114 N88-22593
Simulation of fault tolerance in a hypercube arrangement of discrete processors
[AD-A189682] 15 p2114 N88-22594
The modeling, simulation and comparison of interconnection networks for parallel processing
[AD-A190571] 15 p2115 N88-22599
Design and implementation of a parallel computer for expert system applications
[DE88-005288] 15 p2115 N88-22601
Concurrent algorithms for a mobile robot vision system
[DE88-005850] 15 p2117 N88-22614
High speed transcendental elementary function architecture in support of the Vector Wave Equation (VWE)
[AD-A189746] 15 p2119 N88-22627
Space-variant optical systems
[AD-A189967] 15 p2133 N88-22724
Application of new technologies to DTIC document processing
[AD-A189778] 15 p2148 N88-22823
A methodolgy, based on analytical modeling, for the design of parallel and distributed architectures for relational database query processors
[AD-A189844] 15 p2149 N88-22825
New generation knowledge processing, volume 1
[AD-A190165] 15 p2149 N88-22826
Algorithms and architectures for acoustic phonetical detection of continuous speech
[ENST-87E016] 16 p2189 N88-23054
Strategies for concurrent processing of complex algorithms in data driven architectures
[NASA-CR-181657] 16 p2193 N88-23083
Parallel computer methods for eigenvalue extraction
16 p2218 N88-23233
Microgravity manipulator demonstration
16 p2219 N88-23242
Fundamentals of microprocessor-based design: A tutorial, second edition
[DE88-006761] 16 p2244 N88-23406
Design of high yield microprocessors
[ETN-88-92184] 16 p2245 N88-23410
Synthesis and simulation of systolic algorithms
[ETN-88-92183] 16 p2247 N88-23423
Intelligent systems interconnection: What should come after open systems interconnection?
[CWI-CS-R8742] 16 p2253 N88-23465
New generation knowledge processing, volume 2
[AD-A190166] 16 p2285 N88-23681
Architecture and role of the Sensor Subsystem in future aircraft weapon systems 17 p2302 N88-23770
Rapid prototyping of complex avionic system architectures 17 p2302 N88-23771
Development of a generic architecture
17 p2303 N88-23774
Test philosophy of the EH101 integrated avionic
17 p2303 N88-23775
The avionics software architecture impact on system architecture 17 p2303 N88-23778
A software life cycle support environment
17 p2306 N88-23800
Evolution of a family of image processing systems at INPE 17 p2361 N88-24065
Integration of symbolic and algorithmic hardware and software for the automation of space station subsystems
17 p2387 N88-24190
TALOS: A distributed architecture for intelligent monitoring and anomaly diagnosis of the Hubble Space Telescope 17 p2388 N88-24193
Models and metrics for software management and engineering
[NASA-CR-182953] 17 p2389 N88-24200
A five-layer Open Systems Interconnection (OSI) implementation 17 p2390 N88-24204
Adaptive local grid refinement in computational fluid mechanics
[AD-A192215] 18 p2510 N88-24890
Tutorial on computer control
[DE88-006185] 18 p2554 N88-25157
The -mdoc macro package: A software tool to support computer documentation standards
[DE88-000500] 18 p2559 N88-25188
Algorithms and software for solving finite element equations on serial and parallel architectures
[NASA-CR-183027] 18 p2559 N88-25191
Network architecture for OPS5
[DE88-002802] 18 p2560 N88-25194
The ATF (Advanced Toroidal Facility) Data M Management System
[DE88-007265] 18 p2589 N88-25385
SAMS: The synchronization and monitoring system for ATF (Advanced Toroidal Facility) data acquisition provides unified data access for ATF data acquisition
[DE88-007268] 18 p2589 N88-25386
Signal processing computational needs
[AD-A191756] 19 p2642 N88-25674
Algorithmic generation of feasible system architectures
[AD-A191722] 19 p2713 N88-26106
Multidimensional nodal transport methods for multiple-instruction multiple-data distributed memory machines
[DE88-004732] 19 p2713 N88-26108
Intermediate level computer vision processing algorithm development for the content addressable array parallel processor
[AD-A192086] 19 p2714 N88-26111
Effective communication between a microVAX and a specialized high-speed subprocessor
[DE88-007967] 19 p2714 N88-26115
Logic and fault simulation on the Mach1000 hardware accelerator
[DE88-009794] 19 p2717 N88-26130
Analysis and synthesis of decision-making organizations
[AD-A191948] 19 p2738 N88-26258
The UMAC simulator 20 p2834 N88-26811
Research in VLSI computer systems
[AD-A192915] 20 p2835 N88-26816
Design of high performance microcomputers for numerical data processing
[ETN-88-92371] 20 p2835 N88-26818
The scaled-sized model: A revision of Amdahl's law
[DE88-008114] 20 p2844 N88-26875
An investigation of performance improvement in knowledge-based control systems
21 p2928 N88-27382
Computational fluid dynamics on parallel processors
[AD-A192397] 21 p2941 N88-27469
A demonstration of retro-traverse using a semi-autonomous land vehicle
[DE88-009851] 21 p2957 N88-27568
Assessing and enhancing human performance: Utility of a workstation network
[AD-A192840] 21 p2991 N88-27743
MINIAC: A small embedded computer
[DE88-008142] 21 p2994 N88-27757
Research into the architecture of CAD based robot vision systems
[AD-A193330] 21 p2997 N88-27776
Software engineering guidelines for RASP and ANDECS: Requirements and architectural design
[DFVLR-MITT-88-07] 21 p3000 N88-27793
FORTRAN 77 implementation of abstract datatype models
[DFVLR-MITT-88-08] 21 p3000 N88-27794
Image processing using a parallel architecture
[AD-A192833] 21 p3002 N88-27803
Notes on operating system requirements for the next millennium
[DE88-010712] 21 p3002 N88-27805
Neural network research: A personal perspective
[AD-A192717] 21 p3003 N88-27808
Parallel quasi-Newton methods for unconstrained optimization
[AD-A193250] 21 p3003 N88-27812
What have we learnt from using real parallel machines to solve real problems
[DE88-011227] 22 p3135 N88-28636
Configuration control in compiler construction
[AD-A193916] 22 p3135 N88-28639
Survey of neural net paradigms for specification of discrete networks
[AD-A192682] 22 p3141 N88-28674
Dynamic resource allocation in a hierarchical multiprocessor system: A preliminary study
[NASA-CR-183177] 22 p3141 N88-28675
Method for Veterbi decoding of large constraint length convolutional codes
[NASA-CASE-NPO-17310-1-CU]
23 p3183 N88-28946
Hierarchical organization for large, dynamic radio networks
[AD-A193942] 23 p3204 N88-29067
Systolic array fault tolerance performance analysis
[AD-A193521] 23 p3244 N88-29306
Nanosequencer digital logic controller
[NASA-CASE-NPO-16116-2] 23 p3245 N88-29310
Solving the symmetric tridiagonal eigenvalue problem on the hypercube
[AD-A193905] 23 p3250 N88-29344
Issues on the use of meta-knowledge in expert systems 23 p3252 N88-29357
DAISY-DAMP: A distributed AI system for the dynamic allocation and management of power
23 p3254 N88-29373
ARGES: An expert system for fault diagnosis within space-based ECLS systems 23 p3255 N88-29380
SCARES: A Spacecraft Control Anomaly Resolution Expert System 23 p3256 N88-29381
Programming model for distributed intelligent systems
23 p3257 N88-29390
Blackboard architectures and their relationship to autonomous space systems 23 p3261 N88-29414
Validation of expert systems 23 p3262 N88-29416
Semantic based man-machine interface for real-time communication 23 p3262 N88-29421
Networking and AI systems: Requirements and benefits 23 p3263 N88-29425
Expert system technology as a data processing tool
23 p3263 N88-29427
A performance study of the hypercube architecture
[AD-A194361] 23 p3264 N88-29433
Optimisation algorithms for highly parallel computer architectures. The performance of the truncated Newton, conjugate gradient algorithm in FORTRAN and Ada
[AD-A193940] 23 p3265 N88-29435
Adaptive identification by systolic arrays
[AD-A193532] 23 p3266 N88-29444
Strategic defense initiative architecture dataflow modeling technique version 1.5
[AD-A194356] 23 p3275 N88-29494
A multiprocessor avionics system for an unmanned research vehicle
[AD-A194806] 24 p3325 N88-29800
N-version software demonstration for digital flight controls
[NASA-CR-181483] 24 p3328 N88-29815
Acoustooptic processing of two-dimensional signals using temporal and spatial integration
[AD-A194803] 24 p3359 N88-29999
A model for architectural comparison
[AD-A195993] 24 p3411 N88-30302
The design of an intelligent multidisk control module for VME bus based systems
[AD-A195587] 24 p3411 N88-30303
Scheme86: A system for interpreting SCHEME
[AD-A195931] 24 p3413 N88-30319
Automated satellite control in Ada
24 p3416 N88-30336
MOORE: A prototype expert system for diagnosing spacecraft problems 24 p3418 N88-30343
A standard architecture for controlling robots
[AD-A195929] 24 p3423 N88-30371
Architecture for optical digital computers
[AD-A195477] 24 p3430 N88-30416
Integrating information systems in a major decentralized international organization, volume 7
[AD-A195856] 24 p3439 N88-30468

ARCS
Numerical arc segmentation algorithm for a radio conference: A software tool for communication satellite systems planning
[NASA-TM-100789] 16 p2167 N88-22919
ARCTIC ENVIRONMENTS
U ICE ENVIRONMENTS
ARCTIC OCEAN
Eastern - western Arctic Sea ice analysis 1986
[AD-A184016] 03 p0355 N88-12235
Physical and structural characteristics of Weddell Sea pack ice
[AD-A188189] 10 p1358 N88-18119
Predictions and studies with a one-dimensional ice/ocean model
[AD-A189158] 13 p1803 N88-20776
Microwave and structural properties of saline ice
[AD-A189307] 13 p1803 N88-20779
Higher frequency ambient noise in the arctic ocean
[AD-A192203] 18 p2547 N88-25122
Arctic ice island and sea ice movements and mechanical properties
[DE88-004267] 20 p2829 N88-26782
Arctic ice attenuation model study
[AD-A193382] 22 p3146 N88-28715
Sea ice processes
[AD-A193980] 23 p3237 N88-29262
ARCTIC REGIONS
On the surging potential of polar ice streams. Antarctic surges: A clear and present danger
[DE87-013980] 02 p0216 N88-11363
Underwater acoustic backscatter from a model of arctic ice open leads and pressure ridges
[AD-A184693] 03 p0354 N88-12234
Huurre expedition to the North Pole in 1984
[PB87-220935] 04 p0462 N88-12858
Disturbance and recovery of Arctic Alaskan tundra terrain. A review of recent investigations
[AD-A184442] 04 p0467 N88-12887
USSR report: Earth sciences
[JPRS-UES-87-004] 06 p0725 N88-14455
A 1,000-watt solar power unit for Far North
06 p0728 N88-14481
Neogene paleoclimate in Pacific Ocean subarctic region determined from study of diatoms
08 p1010 N88-16125
Rocket experiments and payloads for Super CAMP --- Cold Arctic Mesopause Project (CAMP)
08 p1034 N88-16271
Physical and structural characteristics of Weddell Sea pack ice
[AD-A188189] 10 p1358 N88-18119
Activities and objectives of the Polar Research Board
[DE88-004543] 13 p1797 N88-20747
Analysis of meteorological conditions and haze distribution for the Second Arctic Gas and Aerosol Sampling Program (AGASP 2), March-April 1986
[PB88-164140] 14 p1948 N88-21618
Real-time environmental Arctic monitoring (R-TEAM)
[AD-A189948] 15 p2099 N88-22508
An investigation of Soviet capabilities in extended range arctic ice forecasting
[AD-A191082] 17 p2376 N88-24127
Sea ice kinematics: Space and time scales
[AD-A191162] 17 p2376 N88-24128
Higher frequency ambient noise in the arctic ocean
[AD-A192203] 18 p2547 N88-25122
A modal approach to Arctic noise modelling with implied vertical coherence
[AD-A192966] 20 p2850 N88-26916
Arctic ice attenuation model study
[AD-A193382] 22 p3146 N88-28715
The spatial and temporal variability of the arctic atmospheric boundary layer and its effect on electromagnetic (EM) propagation
[AD-A193958] 23 p3204 N88-29068
An objective technique for Arctic cloud analysis using multispectral AVHRR (Advanced Very High Resolution Radiometer) satellite imagery
[AD-A194732] 23 p3235 N88-29250
Reflection and scattering of acoustic rays computed for parabolic ice keel models
[AD-A193898] 23 p3278 N88-29517
AREA
Computer modeling for surface properties of carbon fibers 21 p2928 N88-27383
Determination of the specific area of liquid gas and the velocity of weak pressure waves in aqueous foams
[NASA-TT-20347] 24 p3373 N88-30087
AREA NAVIGATION
Observed track-keeping performance of DC10 aircraft equipped with the Collins AINS-70 area navigation system: Karlsruhe and Masstricht UACs (Upper Area Control centres)
[EEC-202] 24 p3323 N88-29788
ARGON
NT ARGON ISOTOPES
Comparative tests of high temperature creep-rupture behavior of the austenitic CrNi steel DIN W.NR.1.4970 in argon and steam
[KFK-4261] 01 p0063 N88-10402
Extreme ultraviolet beam-foil spectroscopy of highly ionized neon and argon
[AD-A185197] 05 p0561 N88-13418
Rovibrational spectroscopy of ArCO van der Waals complex
[DE88-004291] 10 p1406 N88-18387
Two-photon (VUV and visible) resonant ionization spectroscopy of atoms and molecules
[DE88-004332] 10 p1407 N88-18388
Electron stimulated desorption and coherent electron scattering
[AD-A189091] 13 p1835 N88-20978
Kinetics of slow electrons in excimer laser with electron-beam pumping 14 p1970 N88-21760
Question on the measurement of the metal work function in an electron spectrometer by the secondary-electron emission threshold method
[NASA-TT-20190] 16 p2178 N88-22979
Thermophysical properties of argon
[DE88-010376] 19 p2613 N88-25509
ARGON ISOTOPES
Prospects for large dynamic range isotope analysis using photon burst mass spectrometry
[DE88-009110] 19 p2613 N88-25505
ARGON LASERS
Photocurrent generation from basic metals, utilizing a short pulsed ArF excimer laser
[AD-A184928] 05 p0587 N88-13579
Mirrors for high-power continuous-wave Ar-lasers
09 p1235 N88-17404
Psychophysical, biochemical and histological studies of spectrally selective photic damage to primate retina
[AD-A188115] 11 p1517 N88-19063
Resonator coupling of two ring cavity, argon-ion lasers
[AD-A189558] 13 p1775 N88-20616
Doubly periodic output from a dye laser pumped by a free-running argon laser
[DE88-005027] 13 p1778 N88-20633
The interaction of small particles with laser beams
[AD-A190716] 15 p2072 N88-22354
Design and preliminary evaluation of an underwater laser-based imaging system
[DE88-010560] 19 p2675 N88-25908
ARGON PLASMA
Investigations on an RF plasma related to plasma etching
[ETN-88-91366] 06 p0784 N88-14809
Laser thermal propulsion
[AD-A186407] 07 p0933 N88-15666
Electron temperature measurements in an argon/cesium plasma diode
[AD-A188835] 12 p1695 N88-20141
Modeling of atomic processes in X-ray laser plasmas
[AD-A194118] 23 p3286 N88-29567
Energy conversion measurements in laser-sustained argon plasmas for application to rocket propulsion
[AD-A194931] 24 p3337 N88-29861
ARGOS SYSTEM
Mini-station for VHF reception: Argos system simplified description
[INPE-4551-NTE/279] 19 p2655 N88-25764
ARGUMENTS (MATHEMATICS)
U INDEPENDENT VARIABLES
ARIANE LAUNCH VEHICLE
Telemetry conditioning units for the European launcher Ariane 01 p0012 N88-10068
Study of advanced satellite concept using a multifeed reconfigurable antenna
[ESA-CR(P)-2406-VOL-1] 01 p0013 N88-10073
Study of advanced satellite concept using a multifeed reconfigurable antenna. Detailed report on mission definition, coverage analysis and performance requirements, antenna geometry
[ITS-TR-014.C/85] 01 p0013 N88-10074
Study of advanced satellite concept using a multifeed reconfigurable antenna. Appendix 3 : Feeding network, final performance analysis, study of reconfiguration possibilities
[ITS-TR-032/85] 01 p0014 N88-10076
Introduction to local area network design on Ariane 5 and future launchers
[SNIAS-872-422-102] 05 p0635 N88-13886
Aerodynamic design and test performance of supersonic turbines for the Vulcain rocket engine
06 p0713 N88-14373
Ariane localization technique by Data Relay Satellite (DRS)
[SES/ENG/TN-548/86] 09 p0961 N88-15821
The TV-SAT/TDF/TELE-X pyrotechnical system
[CNES-87/CT/DRT/TVE/IL/358]
08 p0974 N88-15891
Ariane 4, long version: Pressure distribution measurements on two models of different scale of the Ariane 4 nose fairings in the transonic tunnel of F+W Emmen (Switzerland) with varying tunnel configurations. Comparison with measurements taken at Modane (France) and with calculations after the Euler method
[F+W-TF-1878] 09 p1122 N88-16716
Launch vehicle vibration: Measures taken to avoid pogo on ESA's Ariane launch vehicle
09 p1123 N88-16727
ESA Bulletin No. 15: Ariane, the European launcher for the 1980's
[ESA-BULLETIN-NO-15] 09 p1125 N88-16741
The Ariane launcher and its progress
09 p1125 N88-16742
Ariane launch performance 09 p1125 N88-16743
Increased performance for Ariane
09 p1125 N88-16744
SYLDA: A dual-launch system for Ariane
09 p1125 N88-16745
The Ariane launch base 09 p1126 N88-16746
Altitude simulation testing of Ariane's second-stage engine 09 p1126 N88-16747
Mechanical in-flight environment of Ariane payloads
09 p1126 N88-16748
Dynamic tests of the Ariane launch vehicle
09 p1126 N88-16749
Integration testing of the propulsion system of Ariane's first stage 09 p1126 N88-16751
Stage separation testing of Ariane
09 p1126 N88-16752
The HM-7 engine of Ariane's third stage
09 p1126 N88-16753
The Ariane fairing and its separation systems
09 p1126 N88-16754
ESA Bulletin No. 25
[ISSN-0376-4265] 09 p1128 N88-16767
The Ariane-3 program 09 p1128 N88-16771
Ariane 4 pyrotechnics system: Definition of the chains and pyrotechnic devices
[CNES-88/CT/DRT/TVE/IL/25]
17 p2310 N88-23816
Reaching for the skies: The Ariane family story and beyond. An introduction to Europe's successful series of space transportation systems
[ESA-BR-42] 22 p3048 N88-28078
The Ariane line 22 p3161 N88-28828
The Ariane 5 program management specifications
22 p3162 N88-28829
Ariane 5, HERMES and European vehicles for space station servicing
[SNIAS-881-422-102] 23 p3183 N88-28943
Simulation of Vulcain engine operation at low inlet pressure
[ETN-88-93083] 24 p3339 N88-29875
ARID LANDS
Remote Sensing-Arid Lands Workshop, Page, Arizona, June 10-12, 1986
[DE87-012368] 01 p0064 N88-10412
The use of SPOT images for water resources surveys. The examples of the Kasserine area (Tunisia) and the Jebel Amour (Algeria) 03 p0345 N88-12179
Desertification in the Sahelian and Sudanian Zones of West Africa
[PB87-217063] 03 p0345 N88-12183
Semi-arid ecosystem development as a function of resource processing and allocation
[DE88-000890] 07 p0875 N88-15308
Improved canopy reflectance modeling and scene inference through improved understanding of scene pattern
[NASA-CR-182488] 10 p1347 N88-18049
Preliminary analyses of SPOT HRV multispectral products for arid and temperate environments
22 p3099 N88-28407
ARIP (IMPACT PREDICTION)
U COMPUTERIZED SIMULATION
U IMPACT PREDICTION
ARITHMETIC
NT FLOATING POINT ARITHMETIC
Implementation of a digital optical matrix-vector multiplier using a holographic look-up table and residue arithmetic
[NASA-CR-180431] 01 p0078 N88-10496
A programmable global system for the manipulation of residue numbers
[ETN-88-91476] 11 p1530 N88-19139
ARITHMETIC AND LOGIC UNITS
The arithmetic cube and its associated algorithms
10 p1374 N88-18195
The design of ultra high-speed numeric intensive systems (having fault tolerant and load balancing capabilities) 10 p1374 N88-18196

Fast serial input-serial output pipelined inner product units
[REPT-87-031] 11 p1530 N88-19142

ARIZONA
A Workshop on Desert Processes, September 24-28, 1984: Report on the conference
[AD-A184599] 03 p0345 N88-12184

ARM (ANATOMY)
Determination of the effect of walking on the forced convective heat transfer coefficient using an articulated mannikin
[AD-A186452] 08 p1049 N88-16335
Free boundary problems arising in the control of a flexible robot arm
[AD-A189124] 12 p1634 N88-19781
A three dimensional non-singular modelling of rigid manipulators
[AD-A189707] 15 p2116 N88-22604

ARMATURES
Exact solutions to the governing dynamic equations of plasma armature electromagnetic railguns
[DE87-014442] 01 p0011 N88-10063
The method of rigid armature flux orientation for the field-oriented control of highly dynamic drives with synchronous machines
[ETN-87-90405] 01 p0042 N88-10269
On the glitches in the force transmitted by an electrodynamic exciter to a structure
05 p0594 N88-13624
A laboratory railgun for terminal ballistics and arc armature research studies
[AD-A187225] 11 p1442 N88-18603
Structural integrity of metallic armature rail guns
[AD-A188735] 13 p1728 N88-20333
Analytic solutions to dynamic equations of plasma armature railguns
[DE88-006842] 15 p2023 N88-22057
Fundamental limits to the velocity of solid armatures in railguns 18 p2469 N88-24656
Why plasma armature railguns don't work (and what can be done about it)
[DE88-007900] 20 p2763 N88-26384
Plasma armature formation in high-pressure, high-velocity hydrogen
[DE88-008347] 20 p2857 N88-26967

ARMED FORCES
NT ARMED FORCES (FOREIGN)
NT ARMED FORCES (UNITED STATES)
NT NAVY
Land campaign force assessment. Methods used in Central-Europe-study
[FOA-C-10288-9.3] 06 p0768 N88-14723

ARMED FORCES (FOREIGN)
Corrosion in avionics and associated equipment; cause, effect and prevention 05 p0547 N88-13335
Soviet military power, 1987 13 p1858 N88-21114
Fire retardant coatings for military equipment: A review
[MRL-R-1104] 19 p2619 N88-25540

ARMED FORCES (UNITED STATES)
Military needs and forecast, 2
01 p0015 N88-10087
Cost savings possible with Air Force conversion to JP-8 as its primary fuel
[AD-A183784] 01 p0030 N88-10192
Transactions of the 4th Army Conference on Applied Mathematics and Computing
[AD-A183544] 01 p0085 N88-10547
Turbine engine supportability study for Army Aviation Systems Command (AVSCOM)
[DE88-002339] 07 p0820 N88-14984
Relating service doctrine to space system requirements
[AD-A186620] 08 p1074 N88-16483
Brain potentials and personality: A new look at stress susceptibility
[AD-A186931] 09 p1199 N88-17189
IMIS: Integrated Maintenance Information System. A maintenance information delivery concept
09 p1203 N88-17207
Evaluating software testing methods to reduce testing duplication in US Army communications equipment acquisition
[AD-A186961] 09 p1216 N88-17292
Sampling intervals
[AD-A189445] 12 p1573 N88-19408
Digital Topographic Support System (DTSS)
[AD-A188304] 12 p1638 N88-19808
Soft maps for US Army electronic map background applications
[AD-A188427] 12 p1638 N88-19809
Implementing information systems/office automation in an Air Force environment
[AD-A188956] 12 p1707 N88-20218
An overview of the army GIS (Geographic Information Systems) Research Program
[AD-A189711] 14 p1992 N88-21871
The Engineer Studies Center guide to research and data collection
[AD-A189971] 16 p2285 N88-23680
Defense Small Business Innovation Research Program (SBIR). Volume 3: Air Force abstracts of phase 1 awards, 1987 17 p2448 N88-24548
Management and the executive
[AD-A190778] 18 p2587 N88-25374
Department of Defense Statement on the Technology Base to the Subcommittee on Defense Industry and Technology of the Committee on Armed Services, United States Senate, 100th Congress, second session
[AD-A191839] 18 p2588 N88-25376
The Army's role in space: Support for the battlefield commander
[RAND-P-7396] 19 p2721 N88-26159
Army space systems for terrestrial applications
[AD-A192735] 21 p2965 N88-27613
Stress/fatigue and the ARNG (Army National Guard) aviator
[AD-A194184] 22 p3132 N88-28621
Tactical air force night/adverse weather training
[AD-A194243] 22 p3133 N88-28625
Stress and the military pilot
[AD-A194313] 22 p3133 N88-28626
Proposed improvements to the USAF flight screening program
[AD-A194506] 23 p3240 N88-29285
Validity of the academic aptitude composite of the Air Force Officer Qualifying Test (AFOQT)
[AD-A194753] 23 p3240 N88-29286
Reliability and construct validity of reaction time, inspection time and machine-paced tests of cognitive speed
[AD-A193779] 23 p3241 N88-29289
SSTS (Space Surveillance and Tracking System): The importance of early test and evaluation organizational participation
[AD-A193745] 23 p3276 N88-29499
Centralized class A flight mishap investigation
[AD-A194397] 24 p3322 N88-29786

ARMOR
Weldability of 2219-T851 and 2519-T87 aluminum armor alloys for use in Army vehicle systems
[AD-A184296] 04 p0451 N88-12792
Numerical simulations of impact tests on a rigid wall --- armor steel
[SNIAS-872-320-102] 05 p0610 N88-13744
Short fiber reinforced thermoplastic composites for armor applications: Interfacial bonding
[DE88-004007] 10 p1295 N88-17742
Crack arrest fracture toughness of armor steels
[AD-A187711] 11 p1456 N88-18681
Hydrogen induced cracks in armor steel weldments fabricated with austenitic filler alloys
[AD-A188733] 13 p1740 N88-20406
Texture profile in thermomechanically processed 2-inch-thick 5 Ni-steel armor plate
[AD-A189275] 13 p1741 N88-20410
Fit evaluation of female body armor
[AD-A188721] 14 p1953 N88-21638
Armoured vehicle track elastomers: Research and development at MRL
[MRL-GD-0012] 19 p2620 N88-25541
Ballistic evaluation of applique armours: Presentation and interpretation of ballistic data
[MRL-TN-527] 19 p2635 N88-25629

AROMATIC COMPOUNDS
Ethynylated aromatics as high temperature matrix resins
[NASA-TM-89829] 11 p1450 N88-18640

ARRAYS
NT ANTENNA ARRAYS
NT LINEAR ARRAYS
NT PHASED ARRAYS
NT SOLAR ARRAYS
NT STEERABLE ANTENNAS
NT SYNTHETIC ARRAYS
NT SYSTOLIC ARRAYS
Methodology for control and operation of wind arrays in utility systems
[DE87-013129] 01 p0039 N88-10248
The fundamentals of photovoltaic system electrical design
[DE87-009061] 02 p0194 N88-11214
Some 2-D WSI array architectures --- wafer scale integration (WSI)
[OUEL-1672/87] 02 p0219 N88-11381
Programmable Logic Arrays (PLA's) design for testability
[PB87-102935] 04 p0438 N88-12718
Chemically modified microelectrode arrays. New kinds of electronic devices
[AD-A184389] 04 p0439 N88-12724
Arrays for discrete Fourier transform
[REPT-87-019] 05 p0632 N88-13861
Low frequency VLBI in space using GAS-Can satellites: Report on the May 1987 JPL Workshop
[NASA-CR-182362] 06 p0801 N88-14904
Thin film electret boundary layer transition detector: A feasibility study
[AD-A185675] 07 p0856 N88-15199
Strong laws of large numbers for arrays of orthogonal random variables
[AD-A186159] 07 p0910 N88-15513
A study of the TCAS 2 collision avoidance system mounted on a Boeing 737 aircraft
[NASA-CR-182457] 09 p1116 N88-16687
IRAC test report. Gallium doped silicon band 2: Read noise and dark current
[NASA-TM-87813] 09 p1159 N88-16945
A combined cosmic ray muon spectrometer and high energy air shower array
[DE88-003057] 09 p1264 N88-17574
A deep-water OBS (Ocean Bottom Seismometer) array with real-time telemetry
[AD-A187404] 10 p1357 N88-18112
Massive fine-grain parallelism in array computation: A data flow solution 10 p1382 N88-18254
Implementing dynamic arrays: A challenge for high-performance machines
[AD-A188142] 11 p1533 N88-19157
Piezoelectric polymer tactile sensor arrays for robotics
[AD-A188852] 12 p1634 N88-19780
Phase transitions in two-dimensional superconducting arrays in a transverse magnetic field
[INPE-4457-RPE/559] 12 p1697 N88-20157
Control strategies and hardware used in solar thermal applications
[DE88-004631] 13 p1794 N88-20731
Simulating high-resolution vertical plane array wind characteristics using lower-spatial-resolution wind measurements
[DE88-005626] 13 p1800 N88-20761
GADL: A gate array description language
[EUT-87-E-165] 14 p1907 N88-21396
Electromagnetic sensor arrays for nondestructive evaluation and robot control
[AD-A190210] 15 p2056 N88-22260
Coupled high power waveguide laser research
[AD-A189800] 15 p2071 N88-22345
Today's photovoltaic systems: An evaluation of their performance
[DE88-006926] 15 p2090 N88-22457
Self-checking logic arrays
[RR-656-I] 15 p2106 N88-22545
A computer model investigation of a half square log-periodic array
[AD-A190955] 16 p2190 N88-23062
Derivative arrays, geometric control theory and realizations of linear descriptor systems
[AD-A190882] 16 p2260 N88-23513
Spectral radiation measurement using a photodiode array as receiver 16 p2271 N88-23591
Joint services electronics program
[AD-A191749] 18 p2504 N88-24853
Null steering applications of polynomials with unimodular coefficients
[AD-A191087] 18 p2562 N88-25211
The XRD (X-Ray Diode) array, the grazing incidence spectrometer and the X-ray imaging came.a on PBFA 2
[DE88-007282] 19 p2728 N88-26200
Development of 30 micrometers extrinsic silicon multiplexed infrared detector array
[NASA-CR-177446] 22 p3082 N88-28301
Recent advances in optical spectroscopy using high performance array detectors
[AD-A194219] 22 p3152 N88-28753
Natural convection immersion cooling of an array of simulated chips in an enclosure filled with dielectric liquid
[AD-A193594] 23 p3207 N88-29088
SQUID (superconducting quantum interference device) arrays for simultaneous magnetic measurements: Calibration and source localization performance
[AD-A193815] 23 p3216 N88-29143
Nonlinear dynamics of coupled oscillator arrays
[AD-A194888] 24 p3367 N88-30053
Development of a unit cell for a Ge:Ga detector array
[NASA-CR-177445] 24 p3375 N88-30100
Tolerances for phase locking of semiconductor laser arrays
[AD-A195974] 24 p3378 N88-30120

ARRESTING GEAR
Analysis of head response to torso acceleration. Volume 1: Development of performance requirements
[PB88-156757] 14 p1953 N88-21640

Soft-ground aircraft arresting systems
[AD-A190838] 16 p2165 N88-22912

ARRHYTHMIA
Vagal tone as an index of mental state
16 p2239 N88-23373
Estimating the cost of mental loading in a bimodal divided-attention task: Combining reaction time, heart-rate variability and signal-detection theory
16 p2241 N88-23385

ARRIVALS
On the direction of arrival estimation
[AD-A186031] 07 p0914 N88-15546

ARROW WINGS
Parametric flutter studies of an arrow-wing configuration: Some early results
[NASA-TM-100608] 19 p2599 N88-25444

ARSENIC
Comparison of low temperature photoluminescence of bulk MBE (Molecular Beam Epitaxy) grown AlGaAs and GaAs using a graphite generated dimer versus a standard tetramer arsenic group-V source
[DE88-004939] 11 p1558 N88-19329
Optical study of germanium, germanium plus arsenic, and germanium plus gallium implants in gallium arsenide
[AD-A189600] 13 p1845 N88-21045
Raman characterization of AsF5-intercalated vapor grown graphite fibers
[AD-A191709] 18 p2491 N88-24778

ARSENIC COMPOUNDS
NT ALUMINUM ARSENIDES
NT ALUMINUM GALLIUM ARSENIDES
NT ARSENIDES
NT GALLIUM ARSENIDES
NT INDIUM ARSENIDES
The first gallium-arsenic compound containing a single Ga3As unit: Isolation and crystal structure of ((thf)Br2Ga)3As (thf = tetrahydrofuran)
[AD-A187457] 11 p1555 N88-19309

ARSENIDES
NT ALUMINUM ARSENIDES
NT ALUMINUM GALLIUM ARSENIDES
NT GALLIUM ARSENIDES
NT INDIUM ARSENIDES
Chemical vapor deposition of B6P and B6As films
[DE87-009288] 02 p0151 N88-10942
The synthesis and characterization of some rare earth arsenides
[AD-A186445] 08 p0965 N88-15839
Non-linear materials (TAS)
[AD-A189197] 12 p1633 N88-19775
Activities of As, Sb, Bi and Pb in copper mattes and their effects on impurity elimination
[TKK-V-A10(1988)] 15 p2041 N88-22165
Recent data on Si:As impurity band conduction multiplexed arrays
[AD-A191752] 18 p2582 N88-25340

ARTEMIA
Effect of spaceflight factors on biological material flown aboard Cosmos-1514 biosatellite
10 p1364 N88-18154

ARTERIES
NT AORTA
Distinctive changes in arterial pressure and blood flow in common carotid artery of monkeys flown aboard Cosmos-1514 biosatellite 07 p0892 N88-15404
Operation Everest 2: Comparison of four instruments for measuring blood oxygen saturation
[AD-A186456] 08 p1049 N88-16337
Hemodynamic effects of beta-adrenergic blocking with obsidan in clinostatic and orthostatic positions
10 p1367 N88-18171
Models of cerebral-body perfusion and cerebral chemical transport
[AD-A194945] 24 p3407 N88-30283

ARTHROPODS
NT ARTEMIA
NT DROSOPHILA
NT INSECTS

ARTIFICIAL CLOUDS
NT BARIUM ION CLOUDS
NT CHEMICAL CLOUDS

ARTIFICIAL GRAVITY
Preliminary analysis of an integrated logistics system for OSSA payloads. Volume 4: Supportability analysis of the 1.8m centrifuge 12 p1584 N88-19481
Analysis of a rotating advanced-technology space station for the year 2025
[NASA-CR-178345] 12 p1600 N88-19580
Some operational aspects of a rotating advanced-technology space station for the year 2025
[NASA-CR-181617] 20 p2765 N88-26397

ARTIFICIAL INTELLIGENCE
NT EXPERT SYSTEMS
Space Station Mission Planning System (MPS) development study. Volume 1: Executive summary
[NASA-CR-179202] 01 p0009 N88-10047
Space Station Mission Planning System (MPS) development study. Volume 2
[NASA-CR-179200] 01 p0009 N88-10048
Space Station Mission Planning Study (MPS) development study. Volume 3: Software development plan
[NASA-CR-179203] 01 p0009 N88-10049
A methodology for dynamic task allocation in a man-machine system
[DE87-007373] 01 p0077 N88-10492
Workshop on AI (Artificial Intelligence) and Simulation (2nd) held in Seattle, Washington on 14 July 1987
[AD-A183736] 01 p0084 N88-10542
Language modelling for automatic speech recognition: A review
[RSRE-MEMO-4038] 01 p0084 N88-10544
Multimedia sensory systems for the solution of the error recovery problem --- robots
[REPT-87-010] 01 p0084 N88-10545
Application of knowledge-based techniques to aircraft trajectory generation and control
02 p0129 N88-10811
Multi-processor architectures for artificial intelligence processing
[OUEL-1671/87] 02 p0219 N88-11380
Semantic network processing systems --- artificial intelligence
[OUEL-1677/87] 02 p0223 N88-11401
Robotics and Intelligent Systems Program
[DE87-014561] 02 p0223 N88-11404
Knowledge acquisition issues encountered during the development of an estimating expert system
[DE87-013320] 02 p0248 N88-11568
Diagnostics aid for mass spectrometer trouble-shooting
[DE88-000350] 03 p0324 N88-12049
The user's guide to the BACK system --- knowledge representation
[KIT-42] 03 p0367 N88-12310
A survey of artificial neural systems
[AD-A184759] 03 p0368 N88-12312
Antithesis: A study in clause combining and discourse structure
[AD-A184789] 03 p0368 N88-12313
An object-oriented architecture for intelligent tutoring systems
[AD-A184790] 03 p0368 N88-12314
The structure-mapping engine: Algorithm and examples
[AD-A184042] 03 p0368 N88-12315
Performance evaluation of artificial intelligence systems
[AD-A184054] 03 p0368 N88-12316
Potential applications of expert systems and operations research to space station logistics functions
[NASA-CR-180473] 03 p0372 N88-12342
Advanced techniques for the storage and use of very large, heterogeneous spatial databases. The representation of geographic knowledge: Toward a universal framework --- relations (mathematics)
[NASA-CR-181517] 03 p0385 N88-12421
A tight upper bound for the speed-up of parallel best-first branch-and-bound algorithms
[AD-A184246] 04 p0477 N88-12939
Experimental use of artificial intelligence for (future) ATC systems
[PB87-106449] 04 p0482 N88-12970
An expert system for materials design
[DE88-000191] 04 p0483 N88-12974
A model of functional knowledge and insight
[AD-A184113] 04 p0483 N88-12975
GOLD: Integration of model-based control systems with artificial intelligence and workstations
[DE88-000506] 04 p0483 N88-12976
GOLD: Integration of model-based control systems with artificial intelligence and workstations
[DE88-000706] 04 p0483 N88-12977
A project of an intelligent system to help on-line trouble shooting --- aircraft maintenance
[SNIAS-872-111-106] 05 p0529 N88-13216
Towards building a team of intelligent robots
[NASA-CR-181538] 05 p0589 N88-13595
Collision-free motion of two robot arms in a common workspace
[CSE-87-00002] 05 p0589 N88-13596
Dealing with unanticipated events in autonomous navigation
[DE88-000590] 05 p0590 N88-13602
ZEUS: A knowledge-based expert system that assists in predicting visibility at airbases
[AD-A184197] 05 p0626 N88-13829
Diagnostic reasoning in digital systems
[NASA-CR-181564] 05 p0633 N88-13871
Behavioral Architecture Robot Control System (BARCS): A new way of building robots
[REPT-87-036] 05 p0638 N88-13902
LISP: A language for stratified design
[AD-A185606] 06 p0759 N88-14654
A computer decision-making process for the elimination of noise from data
[AD-A185746] 06 p0759 N88-14659
USSR report: Cybernetics, computers and automation technology
[JPRS-UCC-86-014] 06 p0761 N88-14669
Artificial intelligence systems
06 p0761 N88-14670
Computer architectures for artificial intelligence
[PB87-123824] 06 p0761 N88-14671
Genie inference engine rule writer's guide
[AD-A185709] 06 p0762 N88-14675
A general architecture for intelligent training systems
06 p0796 N88-14875
Dynamics, control and sensor issues pertinent to robotic hands for the EVA retriever system
06 p0796 N88-14876
Tools and technologies for expert systems: A human factors perspective 06 p0797 N88-14882
Development of a prototype H-46 helicopter diagnostic expert system
[AD-A186077] 07 p0809 N88-14924
Expert system study for spacecraft management
[TL-2699-ISS-1] 07 p0824 N88-15004
Improved input representation for enhancement of neural network performance
[DE88-001830] 07 p0907 N88-15496
Proceedings of the Second International Symposium on Methodologies for Intelligent Systems: Colloquia program
[DE88-001490] 07 p0907 N88-15498
Expert system technology 07 p0926 N88-15628
DoD Gateway Information System (DGIS) common command language: The first prototyping and the decision for artificial intelligence
[AD-A185950] 07 p0942 N88-15725
Directions in propulsion control
08 p0956 N88-15799
A knowledge-based object recognition system for applications in the space station
[NASA-CR-182411] 08 p0989 N88-15991
Deriving descriptions of the mind
[AD-A186647] 08 p1052 N88-16349
Methodology for testing and validating knowledge bases 08 p1055 N88-16364
Clips as a knowledge based language
08 p1055 N88-16365
MTK: An AI tool for model-based reasoning
08 p1056 N88-16372
KBS V and V as related to automation of space station subsystems: Rationale for a KBS lifecycle
08 p1057 N88-16375
Monitoring of space station life support systems with miniature mass spectrometry and artificial intelligence
08 p1057 N88-16376
Automatic mathematical modeling for space application 08 p1060 N88-16402
Knowledge-based simulation
08 p1061 N88-16404
Rapid prototyping and AI programming environments applied to payload modeling 08 p1061 N88-16405
Iterative-deepening heuristic search for optimal and semi-optimal resource allocation
08 p1062 N88-16410
Similarity networks as a knowledge representation for space applications 08 p1062 N88-16411
Discovery and problem solving: Triangulation as a weak heuristic 08 p1062 N88-16412
Planning and scheduling for robotic assembly
08 p1062 N88-16416
Intelligent man/machine interfaces on the space station 08 p1063 N88-16418
Space languages 08 p1063 N88-16420
The intelligent user interface for NASA's advanced information management systems
08 p1063 N88-16424
An AI approach for scheduling space-station payloads at Kennedy Space Center 08 p1064 N88-16425
Neural network based speech synthesizer: A preliminary report 08 p1064 N88-16429
The power of neural nets 08 p1064 N88-16430
Neural networks as a possible architecture for the distributed control of space systems
08 p1064 N88-16431
Application of artificial intelligence to impulsive orbital transfers 08 p1066 N88-16439
Substructure discovery in executed action sequences
[AD-A186446] 08 p1069 N88-16462
Tutoring electronic troubleshooting in a simulated maintenance work environment
09 p1204 N88-17215
An intelligent tutor for the space domain
09 p1204 N88-17217

Neural network based architectures for aerospace applications 09 p1204 N88-17218
NASA JSC neural network survey results 09 p1205 N88-17220
Design of a neural network simulator on a transputer array 09 p1205 N88-17221
Cooperative analysis expert situation assessment research 09 p1206 N88-17228
Teaching artificial neural systems to drive: Manual training techniques for autonomous systems 09 p1207 N88-17238
A situation-response model for intelligent pilot aiding 09 p1208 N88-17241
A human performance modelling approach to intelligent decision support systems 09 p1208 N88-17242
Artificial Intelligence (AI), Operations Research (OR), and Decision Support Systems (DSS): A conceptual framework 09 p1209 N88-17245
Range and mission scheduling automation using combined AI and operations research techniques 09 p1209 N88-17249
Robotic air vehicle. Blending artificial intelligence with conventional software 09 p1210 N88-17252
A conceptual framework for intelligent real-time information processing 09 p1211 N88-17257
Real-time artificial intelligence issues in the development of the adaptive tactical navigator 09 p1211 N88-17260
Implementation of a robotic flexible assembly system 09 p1212 N88-17265
System integration of a Telerobotic Demonstration System (TDS) testbed 09 p1212 N88-17266
Mathematical structures for speech recognition [AD-A187063] 09 p1217 N88-17295
Horizontal estimation and information fusion in multitarget and multisensor environments [AD-A186935] 09 p1224 N88-17336
Parallel architectures for logic programming 10 p1380 N88-18241
Real time artificial intelligence architecture 10 p1380 N88-18242
Analysis and synthesis of adaptive neural elements [AD-A187047] 10 p1395 N88-18316
Parallel garbage collection on a virtual memory system [DE88-003567] 10 p1396 N88-18317
The implementation of artificial intelligence in control systems [DE88-003497] 10 p1396 N88-18318
The representation of knowledge within model-based control systems [DE88-004863] 10 p1396 N88-18319
Visual integration and detection of discontinuities: The key role of intensity edges [AD-A188012] 11 p1520 N88-19076
Research in knowledge representation for natural language communication and planning assistance [AD-A187355] 11 p1522 N88-19087
Effects of stress on judgement and decision making in dynamic tasks [AD-A188203] 11 p1523 N88-19092
TYPICAL: A knowledge representation system for automated discovery and inference [AD-A187483] 11 p1533 N88-19160
The choice of learning strategy in an autonomous system [AD-A187707] 11 p1534 N88-19161
Two new frameworks for learning [AD-A187723] 11 p1534 N88-19162
Learning functions from examples [AD-A187725] 11 p1534 N88-19163
Error detection and recovery for robot motion planning with uncertainty [AD-A187746] 11 p1534 N88-19165
Concepts and nomenclature in the world modeling system (a lesson in applied metaphysics) [AD-A188246] 11 p1534 N88-19166
Optical computing research [AD-A187862] 11 p1549 N88-19264
Autonomous Liquid Encapsulated Czochralski (LEC) growth of single crystal GaAs by intelligent digital control [AD-A187211] 11 p1555 N88-19305
Robotic intelligence issues for space manipulator monitoring, control programming 12 p1588 N88-19504
Mobile robot activity model for autonomous free flying platforms 12 p1588 N88-19507
Low cost mobile robot [AD-A188507] 12 p1633 N88-19778
A knowledge acquisition tool for the intelligent processing of materials [AD-A188982] 12 p1679 N88-20036
Knowledge-based system analysis and control [AD-A188163] 12 p1681 N88-20049
OPS83: Style guide for high performance [AD-A188505] 12 p1681 N88-20051
Learning by experimentation [AD-A188912] 12 p1681 N88-20053
Physics for robots [AD-A189056] 12 p1682 N88-20054
Northeast Artificial Intelligence Consortium (NAIC) administrative matters and ancillary functions, volume 1 [AD-A189466] 12 p1682 N88-20055
The integration of artificial intelligence techniques to improve the effectiveness of electronic countermeasure strategies in a tactical environment [AD-A189483] 12 p1682 N88-20056
Towards a solution to the proper integration of a logic programming system and a large knowledge based management system [AD-A188949] 12 p1705 N88-20207
Intelligent control of robot manipulators in hazardous environments [DE88-003305] 13 p1778 N88-20638
An implementation of the OPS5 language for computers compatible with IBM-PC [INPE-4291-PRE/1162] 13 p1821 N88-20882
The use of an automated flight test management system in the development of a rapid-prototyping flight research facility [NASA-TM-100435] 13 p1823 N88-20896
Mathematic modeling of visual perception problems [INPE-4355-PRE/1186] 13 p1823 N88-20897
Soar: An architecture for general intelligence [AD-A188742] 13 p1823 N88-20898
Knowledge retrieval as specialized inference [AD-A189042] 13 p1823 N88-20899
A Darwinian approach to artificial neural systems [DE87-013184] 13 p1824 N88-20900
Quality enhancement with machine intelligence [DE88-005639] 13 p1824 N88-20901
Aspects and applications of primary processing of visual information [INPE-4290-PRE/1161] 13 p1841 N88-21015
Application of expert systems in project management decision aiding [NASA-CR-180762] 13 p1850 N88-21074
Implementing embedded artificial intelligence rules within algorithmic programming languages [NASA-CR-178393] 14 p1959 N88-21686
Representing knowledge in two distinct descriptions: Extensional vs. intensional [CWI-CS-R8728] 14 p1961 N88-21699
Perfect knowledge and beyond — chess endgames [REPT-87-37] 14 p1967 N88-21738
Comparative analysis [AD-A190556] 15 p2065 N88-22313
Instrumentation for scientific computing in neural networks, information science, artificial intelligence and applied mathematics [AD-A189981] 15 p2106 N88-22549
A probabilistic approach to low-level vision [AD-A189041] 15 p2107 N88-22553
An intelligent simulation model generator [REPT-87-053] 15 p2109 N88-22562
Inference engine for expert systems [INPE-4465-TDL/321] 15 p2113 N88-22590
Memory-based expert systems [AD-A190203] 15 p2116 N88-22606
Synapses that compute motion [AD-A190389] 15 p2116 N88-22607
Multi-disciplinary techniques for understanding time-varying space-based imagery [AD-A190711] 15 p2117 N88-22610
Discrete event simulation in the artificial intelligence environment [DE88-004296] 15 p2117 N88-22613
Multivariate analysis and its application [AD-A189983] 15 p2124 N88-22661
Rigidity and smoothness of motion [AD-A190555] 15 p2128 N88-22694
ROVER: A prototype active vision system [AD-A189246] 15 p2133 N88-22722
Autonomous control system for Czochralski growth of LEC GaAs [AD-A189726] 15 p2141 N88-22779
The Scientific and Technical Information Network (STINET). Foundation for evolution [AD-A189750] 15 p2148 N88-22822
Data base design and implementation [AD-A190414] 15 p2149 N88-22827
Extending problem solver capabilities through case-based inference [AD-A191332] 16 p2243 N88-23401
Design as a formal, knowledge engineered activity [CWI-CS-R8744] 16 p2248 N88-23431
Knowledge engineering in design [CWI-CS-R8745] 16 p2248 N88-23432
STRUTEX: A prototype knowledge-based system for initially configuring a structure to support point loads in two dimensions [NASA-TM-100613] 16 p2250 N88-23448
Parallel artificial intelligence search techniques for real time applications [AD-A190683] 16 p2255 N88-23473
Automatic control of an industrial process and computer aided process control by means of an expert system [LAAS-88-004] 16 p2255 N88-23476
Parallelism in a Prolog knowledge base machine [ETN-88-92187] 16 p2255 N88-23477
Capitalizing on failure through case-based inference [AD-A190927] 16 p2255 N88-23480
Rule-based fault-tolerant flight control 17 p2294 N88-23725
Fiber waveguide sensors for intelligent materials [NASA-CR-183028] 17 p2343 N88-23968
A proposal of adaptation of a knowledge-based scene analysis model to some remote sensing problems 17 p2362 N88-24068
Linguistic definition of generic models in computer vision [RSRE-MEMO-4110] 17 p2386 N88-24182
MTK: An AI tool for model-based reasoning 17 p2387 N88-24189
Simultaneous use of artificial intelligence and Petri nets: Application to the monitoring of a fabrication plan [LAAS-87-354] 17 p2390 N88-24207
Notes on artificial intelligence. Part 1: Technical forecast [FOA-C-30448-3.3-PT-1] 17 p2390 N88-24208
Energy optimal trajectory planning for robot manipulators and autonomous vehicles 17 p2437 N88-24497
A system status monitor for the National Aerospace Plane [AD-A190681] 18 p2463 N88-24624
Timesharing performance as an indicator of pilot mental workload [NASA-CR-182807] 18 p2552 N88-25150
A computational model of motor behavior [AD-A191179] 18 p2553 N88-25152
LispSEI: The programmer's manual [AD-A191632] 18 p2556 N88-25172
Representation and decision mechanisms in artificial intelligence [AD-A191083] 18 p2560 N88-25197
The ISI (Information Sciences Institute) grapher manual [AD-A192198] 18 p2561 N88-25200
Modeling of geometric reasoning for robot programming [ETN-88-92290] 18 p2561 N88-25202
Robot navigation using simple sensor fusion [DE88-006184] 18 p2561 N88-25203
Application of flight systems methodologies to the validation of knowledge-based systems [NASA-TM-100442] 18 p2561 N88-25207
Automatic discovery of optimal classes [NASA-TM-101174] 18 p2566 N88-25238
JPRS report: Science and technology. Japan [JPRS-JST-88-005] 19 p2633 N88-25619
Application of AI to space systems 19 p2634 N88-25626
The development of an intelligent interface to a computational fluid dynamics flow-solver code [NASA-TM-100908] 19 p2716 N88-26127
An expert system model using predicate transition nets [AD-A191953] 19 p2718 N88-26141
Modeling and evaluation of expert systems in decisionmaking organizations [AD-A191951] 19 p2739 N88-26260
A cockpit natural language study - selected transcripts [AD-A192972] 20 p2834 N88-26808
Direct manipulation and the design of user interfaces [PB88-126354] 20 p2834 N88-26810
SIMS: Single Interface to Multiple Systems [AD-A192264] 20 p2837 N88-26832
Building an artificial intelligence capability at Los Alamos [DE88-009155] 20 p2842 N88-26866
Expert system application education proj-ct [NASA-CR-183089] 20 p2843 N88-26867
Narrative domain implementation [AD-A192265] 20 p2843 N88-26868
NEXT: An expert system development tool to support engineering design [NLR-MP-86070-U] 20 p2843 N88-26871
Qualitative reasoning for physicists [PB88-116298] 20 p2848 N88-26906
Challenge equality problems in lattice theory [DE88-010094] 20 p2876 N88-27072
EXSAT: Expert system to configure telecommunication satellites [SNIAS-881-440-101] 21 p2902 N88-27223
Mitsubishi Electric Advance (R and D Edition), Volume 41 [PB88-194162] 21 p2929 N88-27388

Computer-Aided Engineering (CAE) for engineering design 21 p2929 N88-27390
The MELCOM PSI 2 AI workstation 21 p2930 N88-27395
Motor-response learning at a process control panel by an autonomous robot
[DE88-005055] 21 p2955 N88-27554
Block Oriented Simulation System (BOSS)
[NASA-CR-182947] 21 p2995 N88-27760
Synchronizable series expressions. Part 2: Overview of the theory and implementation
[AD-A192783] 21 p2996 N88-27768
The programmer's apprentice project: A research overview
[AD-A192784] 21 p2996 N88-27769
Improving the performance of AI algorithms
[AD-A192848] 21 p3003 N88-27809
Faultfinder: A diagnostic expert system with graceful degradation for onboard aircraft applications 22 p3035 N88-28018
Heat exchanger demonstration expert system 22 p3066 N88-28193
Artificial intelligence software acquisition program, volume 2
[AD-A194239] 22 p3141 N88-28680
Stereo and eye movement
[AD-A193588] 22 p3142 N88-28681
Loglisp programming system users manual
[AD-A193933] 22 p3142 N88-28682
Connectionist models and artificial intelligence
[RR-684-I-IMAG-66-LIFIA] 22 p3142 N88-28684
Uncertainty analysis in automatic robot programming
[RR-695-I-IMAG-68-LIFIA] 22 p3142 N88-28685
Motion planning for legged locomotion systems on uneven terrain 23 p3221 N88-29170
Automatic line network extraction from aerial imagery of urban areas through knowledge-based image analysis
[AD-A192399] 23 p3227 N88-29208
Artificial intelligence applied to process signal analysis 23 p3252 N88-29359
DAISY-DAMP: A distributed AI system for the dynamic allocation and management of power 23 p3254 N88-29373
Intelligent resource management for local area networks: Approach and evolution 23 p3256 N88-29385
Distributed cooperating processes in a mobile robot control system 23 p3256 N88-29386
Programming model for distributed intelligent systems 23 p3257 N88-29390
AI and simulation: What can they learn from each other 23 p3257 N88-29391
Reasoning about fault diagnosis for the space station common module thermal control system 23 p3258 N88-29395
Intelligent interface design and evaluation 23 p3260 N88-29405
The concurrent common Lisp development environment 23 p3263 N88-29422
AI tools in computer based problem solving 23 p3263 N88-29424
Networking and AI systems: Requirements and benefits 23 p3263 N88-29425
Radial basis functions, multi-variable functional interpolation and adaptive networks
[RSRE-MEMO-4148] 23 p3265 N88-29436
Identification and control of time-varying flexible structures: An artificial intelligence approach 23 p3265 N88-29437
The complexity of AI algorithms
[AD-A193494] 23 p3265 N88-29438
A model of information growth 23 p3265 N88-29440
Artificial intelligence software acquisition program, volume 1
[AD-A194104] 23 p3267 N88-29447
Design of a feeling-thinking machine
[AD-A194107] 23 p3267 N88-29448
Active explanation reduction: An approach to the multiple explanations problem
[AD-A194127] 23 p3276 N88-29501
Distributed knowledge base systems for diagnosis and information retrieval
[AD-A193107] 23 p3296 N88-29633
Corner extraction from radar images
[AD-A194857] 24 p3362 N88-30020
Path planning and path following for the Amsterdam autonomous cart
[FVI-86-22] 24 p3380 N88-30133
The design of an intelligent multidisk control module for VME bus based systems
[AD-A195587] 24 p3411 N88-30303
Quality measures and assurance for AI (Artificial Intelligence) software
[NASA-CR-4187] 24 p3411 N88-30304
Reification without evaluation
[AD-A195928] 24 p3414 N88-30326
The 1988 Goddard Conference on Space Applications of Artificial Intelligence
[NASA-CP-3009] 24 p3415 N88-30330
An intelligent training system for space shuttle flight controllers 24 p3415 N88-30331
Artificial intelligence costs, benefits, risks for selected spacecraft ground system automation scenarios 24 p3416 N88-30332
A shared-world conceptual model for integrating space station life sciences telescience operations 24 p3416 N88-30333
Artificial intelligence in a mission operations and satellite test environment 24 p3416 N88-30334
Automated satellite control in Ada 24 p3416 N88-30336
Contingency rescheduling of spacecraft operations 24 p3416 N88-30337
Knowledge based tools for Hubble Space Telescope planning and scheduling: Constraints and strategies 24 p3417 N88-30338
The proposal entry processor: Telescience applications for Hubble Space Telescope science operations 24 p3417 N88-30339
Candidate functions for advanced technology implementation in the Columbus mission planning environment 24 p3417 N88-30340
A rule-based systems approach to spacecraft communications configuration optimization 24 p3417 N88-30341
MOORE: A prototype expert system for diagnosing spacecraft problems 24 p3418 N88-30343
Low level image processing techniques using the pipeline image processing engine in the flight telerobotic servicer 24 p3418 N88-30346
Autonomous image data reduction by analysis and interpretation 24 p3418 N88-30347
Parallel and distributed computation for fault-tolerant object recognition 24 p3419 N88-30350
The second generation intelligent user interface for the crustal dynamics data information system 24 p3419 N88-30352
Spacelab data processing facility (SLDPF) Quality Assurance (QA)/Data Accounting (DA) expert systems: Transition from prototypes to operational systems 24 p3420 N88-30353
Automated cataloging and characterization of space-derived data 24 p3420 N88-30354
A design for a ground-based data management system 24 p3420 N88-30355
Automatic mathematical modeling for real time simulation system 24 p3420 N88-30356
A simulation engine: Combining an expert system with a simulation language 24 p3421 N88-30358
Verification and validation of rulebased systems for Hubble Space Telescope ground support 24 p3421 N88-30361
The need for a comprehensive expert system development methodology 24 p3421 N88-30362
The combinatorics of object recognition in cluttered environments using constrained search
[AD-A196224] 24 p3422 N88-30364
Study of software requirements and artificial intelligence techniques for robotics
[TL-3333] 24 p3422 N88-30365
Research on problem-solving systems
[AD-A195154] 24 p3423 N88-30370
Knowledge based simulation: An artificial intelligence approach to system modeling and automating the simulation life cycle
[AD-A195838] 24 p3423 N88-30372
Theories of comparative analysis
[AD-A196328] 24 p3427 N88-30395
Optical symbolic computing
[AD-A195690] 24 p3429 N88-30406
Information retrieval systems evolve-advances for easier and more successful use 24 p3438 N88-30462

ARTIFICIAL RESPIRATION
U RESUSCITATION

ARTIFICIAL SATELLITES
NT ACTS
NT ALOUETTE SATELLITES
NT AMPTE (SATELLITES)
NT ARABSAT
NT ASTRONOMICAL SATELLITES
NT AZUR SATELLITE
NT BIOSATELLITES
NT COLUMBUS SPACE STATION
NT COMMUNICATION SATELLITES
NT COS-B SATELLITE
NT COSMIC BACKGROUND EXPLORER SATELLITE
NT COSMOS SATELLITES
NT COSPAS
NT DIRECT BROADCAST SATELLITES
NT DMSP SATELLITES
NT DYNAMICS EXPLORER 1 SATELLITE
NT ERS-1 (ESA SATELLITE)
NT ESA SATELLITES
NT EUROPEAN COMMUNICATIONS SATELLITE
NT EXOSAT SATELLITE
NT EXPLORER SATELLITES
NT EXPLORER 47 SATELLITE
NT EXPLORER 51 SATELLITE
NT EXPLORER 54 SATELLITE
NT EXPLORER 55 SATELLITE
NT FRENCH SATELLITES
NT GAMMA RAY OBSERVATORY
NT GEODETIC SATELLITES
NT GEOPHYSICAL SATELLITES
NT GEOPOTENTIAL RESEARCH MISSION
NT GEOS SATELLITES (ESA)
NT GEOS 2 SATELLITE
NT GEOSAT SATELLITES
NT GOES SATELLITES
NT HEAO 2
NT HELIOS SATELLITES
NT HELIOS 1
NT HELIOS 2
NT HIPPARCOS SATELLITE
NT HUBBLE SPACE TELESCOPE
NT INFRARED ASTRONOMY SATELLITE
NT INFRARED SPACE OBSERVATORY (ISO)
NT INTERCOSMOS SATELLITES
NT INTERNATIONAL SUN EARTH EXPLORER 3
NT INTERNATIONAL SUN EARTH EXPLORERS
NT ISIS SATELLITES
NT IUE
NT L-SAT
NT LAGEOS (SATELLITE)
NT LANDSAT SATELLITES
NT LANDSAT 5
NT MAGSAT SATELLITES
NT MARECS MARITIME SATELLITES
NT MARISAT SATELLITES
NT MARITIME SATELLITES
NT METEOROLOGICAL SATELLITES
NT METEOSAT SATELLITE
NT MIR SPACE STATION
NT NAVIGATION SATELLITES
NT NAVSTAR SATELLITES
NT NIMBUS 7 SATELLITE
NT NOAA SATELLITES
NT NOAA 7 SATELLITE
NT PASSIVE SATELLITES
NT PEGASUS SATELLITES
NT PROGNOZ SATELLITES
NT ROSAT MISSION
NT SAGE SATELLITE
NT SALYUT SPACE STATION
NT SARSAT
NT SAS
NT SCATHA SATELLITE
NT SCIENTIFIC SATELLITES
NT SEASAT SATELLITES
NT SHUTTLE PALLET SATELLITES
NT SOLAR MESOSPHERE EXPLORER
NT SOLAR POWER SATELLITES
NT SPACE INFRARED TELESCOPE FACILITY
NT SPACE STATION POLAR PLATFORMS
NT SPACE STATIONS
NT SPOT (FRENCH SATELLITE)
NT SYNCHRONOUS SATELLITES
NT TETHERED SATELLITES
NT TIROS N SERIES SATELLITES
NT TIROS SATELLITES
NT UK SATELLITES
NT X RAY ASTROPHYSICS FACILITY
The combined release and radiation effects satellite, a joint NASA/DOD program 02 p0135 N88-10851
Evaluation and certification of heater assemblies developed for thermal vacuum acceptance testing 02 p0136 N88-10853
Design, construction, activation, and operation of a high intensity acoustic test chamber 02 p0137 N88-10864
Computational method for orbit improvement for short arc observations of artificial satellites 03 p0269 N88-11690
Estimates of satellite EHF communication outages due to attenuation by rain
[AD-A183969] 03 p0307 N88-11941
Satellite autonomous navigation with SHAD (Stellar Horizon Atmospheric Dispersion)
[AD-A184988] 05 p0544 N88-13313
MAXIE 1 (Magnetospheric Atmospheric X-ray Imaging Experiment) Program
[AD-A185878] 07 p0877 N88-15317
Supportability in aircraft systems through technology and acquisition strategy applications
[AD-A186465] 08 p0949 N88-15759

An evaluation of semianalytical satellite theory against long arcs of real data for highly eccentric orbits
[AD-A185825] 08 p0960 N88-15819
Attitude determination of artificial satellites through joint application of static and dynamic optimal estimation techniques
[INPE-4415-TDL/306] 08 p0963 N88-15832
Attitude dynamics for satellites stabilized through spin
[INPE-4403-NTE/275] 08 p0963 N88-15833
SAMSS: An in-progress review of the Spacecraft Assembly, Maintenance, and Servicing Study
08 p0981 N88-15930
Development of on-orbit fluid gaging techniques
08 p0982 N88-15936
Selection of efficient correcting motor for an artificial Earth satellite 08 p1007 N88-16102
Space applications in geography
08 p1007 N88-16104
Applications of expert systems for satellite autonomy
08 p1066 N88-16443
Verification of a micro-thrusting model to maintain satellites in low orbit
[AD-A186874] 09 p1133 N88-16793
Formulation methods of rigid multibody systems for large space structures and some results of computer simulation
[NAL-TR-942] 10 p1293 N88-17730
Five-diagonal weighting scheme for geoidal profiles
[AD-A188033] 10 p1347 N88-18054
Project SKYLITE: A design exploration
[AD-A187906] 11 p1511 N88-19030
Optimal selection of global positioning system set to minimize emitter location errors
[AD-A189559] 12 p1579 N88-19447
Customer concerns regarding satellite servicing
12 p1587 N88-19503
Analysis of the sensitivity of the attitude control system of an artificial satellite
[INPE-4285-PRE/1157] 12 p1599 N88-19573
Electromagnetic modeling of a control valve
[INPE-4140-PRE/1048] 12 p1622 N88-19700
Zoom versus full-field sensitivity at the ETS (Experimental Test System)
[AD-A188162] 12 p1628 N88-19742
Dynamics of small and large scale irregularities at sub-auroral latitudes
[AD-A189052] 12 p1645 N88-19853
Utilization of strapdown inertial and non-inertial sensors in determination of satellite attitude by Kalman filters
[INPE-4313-TDL/280] 13 p1731 N88-20349
Aeronautics and space report of the President: 1986 activities 13 p1852 N88-21087
Comparison of methods for the calculation of thermal contact resistance of the first Brazilian satellite
[NASA-TT-20180] 14 p1880 N88-21239
MAXIE 1
[AD-A189688] 14 p1882 N88-21247
Numerical orbit propagation methods for earth artificial satellites
[INPE-4405-RPE/556] 15 p2023 N88-22053
Chronology of China's successful satellite launchings
15 p2053 N88-22234
Analytical orbit propagation of artificial satellites
[INPE-4454-TDL/315] 16 p2166 N88-22915
Review of power requirements for satellite remote sensing systems 17 p2419 N88-24387
Design considerations for the ORION satellite: Structure, propulsion and attitude control subsystems for a small, general purpose spacecraft
[AD-A193837] 22 p3048 N88-28086
The 44/20 GHz ground terminal
[AD-A194002] 23 p3204 N88-29069
Long haul communications in the HF spectrum utilizing high speed modems
[AD-A194683] 24 p3360 N88-30003
DATATRAN: Datum transformation software
[AD-A195723] 24 p3387 N88-30175
Space systems cost study
[AD-A196024] 24 p3439 N88-30469
Orbital evolution of distant artificial earth satellites
24 p3445 N88-30506
Families of periodic solutions in problem of solid body rotation at triangular libration point in restricted three-body problem 24 p3446 N88-30508

ARTILLERY
Method for determining artillery position
[NASA-TT-20238] 13 p1834 N88-20973
Method for determining artillery position
[NASA-TT-20237] 13 p1834 N88-20974
Method for determining artillery position
[NASA-TT-20236] 14 p1979 N88-21813

ARTS
NT ABILITIES
NT COMPUTER ANIMATION
NT GRAPHIC ARTS

ARYABHATA
U INDIAN SPACECRAFT

ARYL COMPOUNDS
U AROMATIC COMPOUNDS

ASBESTOS
Environmental projects. Volume 4: Asbestos survey
[NASA-CR-182527] 10 p1353 N88-18083

ASCENT
NT CLIMBING FLIGHT
Analysis of clinical symptoms of human decompression sickness during altitude chamber studies
19 p2703 N88-26074

ASCENT PROPULSION SYSTEMS
Propulsion analysis and application potential of air breathing combined propulsion for ballistic space transporter
[ETN-88-92369] 21 p2903 N88-27227
Ascent guidance for a winged boost vehicle
[NASA-CR-172083] 24 p3334 N88-29846

ASCENT TRAJECTORIES
A study to evaluate STS heads-up ascent trajectory performance employing a minimum-Hamiltonian optimization strategy
[NASA-TP-2793] 08 p0960 N88-15820
Optimal thrust vector control of coplanar orbital evasive maneuvers
[AD-A189544] 13 p1730 N88-20346
Wind measurements by electromagnetic probes
[NASA-TM-4066] 23 p3236 N88-29256
Ascent guidance for a winged boost vehicle
[NASA-CR-172083] 24 p3334 N88-29846

ASHES
TOMS and the NOAA/FAA volcano support plan
05 p0618 N88-13796
Energy efficient continuous flow ash lockhopper
[NASA-CASE-NPO-16985-1-CU] 18 p2497 N88-24814

ASIA
Conceptual models of Baiu front and Baiu frontal disturbances in multiscale characteristics --- East Asia
02 p0203 N88-11271
The numerical simulation of the mesoscale characteristics associated with Baiu front. Part 1: Structure, low-level jet and radiation characteristics
02 p0203 N88-11272
Tropical and monsoonal studies
[AD-A188387] 14 p1947 N88-21611

ASPECT RATIO
NT HIGH ASPECT RATIO
NT LOW ASPECT RATIO
Investigations of separated flow states on wings of medium aspect ratio taking into account the wind tunnel interference problem
[ETN-87-90437] 01 p0003 N88-10016
On tokamak equilibrium
[DE87-014811] 02 p0239 N88-11507
The effect of microstructure on the surface crack length: Crack depth relationship for short cracks
05 p0600 N88-13670
Experimental model of halo plasma observed in small-aspect FRC plasma
[INPE-4159-PRE/1061] 08 p1085 N88-16534
Conceptual design of a radio-frequency driven compact tokamak
[INPE-4364-PRE/1190] 08 p1085 N88-16535
High Rayleigh number convection in rectangular enclosures with differentially heated vertical walls and aspect ratios between zero and unity
[NASA-TM-100277] 12 p1628 N88-19739
The aspect ratio dependence of the attractor dimension in Taylor-Couette flow
[AD-A196297] 24 p3369 N88-30065

ASPHALT
A laboratory study of asphalt concrete mix designs for high-contact pressure aircraft traffic
[AD-A185753] 06 p0670 N88-14106
Comparative study of nondestructive pavement testing, MacDill Air Force Base, Florida
[AD-A186082] 07 p0822 N88-14993
Investigation of the inter-relationship between base pavement stiffness and asphalt overlay compaction
[DOT/FAA/ES-88/1] 14 p1869 N88-21170

ASPHALTENES
Application of high performance liquid chromatography to the fast determination of bitumen generic composition
[PC-2] 02 p0145 N88-10911

ASPIRATION
U VACUUM

ASSAULTING
U ATTACKING (ASSAULTING)

ASSAYING
Experience of developing an integrated nondestructive assay system
[DE88-003149] 09 p1184 N88-17092
Methods and techniques of NDA (nondestructive assay)
[DE88-009145] 20 p2812 N88-26682

ASSEMBLIES
NT SUBASSEMBLIES
NT TAIL ASSEMBLIES
Fast shock tube assemblies
[DE87-011732] 01 p0008 N88-10042
The effect of different packagings on the vibration behavior and the coupling factors of steam turbine blading
[ETN-87-90425] 01 p0056 N88-10357
Reactions of porphyrins in surfactant assemblies, microemulsions and in solutions
[AD-A184797] 05 p0560 N88-13412
Computation of bonded assemblies. Elastoplastic adhesives, first part
[SNIAS-NT-18926/AQET] 05 p0569 N88-13467

ASSEMBLING
NT ORBITAL ASSEMBLY
Space Assembly, Maintenance, and Servicing Study (SAMSS) 01 p0015 N88-10089
Space station assembly/servicing capabilities
01 p0016 N88-10100
Structural Assembly Demonstration Experiment (SADE)
[NASA-CR-179205] 02 p0138 N88-10868
Experimental assembly of structures in EVA: Hardware morphology and development issues
02 p0139 N88-10872
Access flight hardware design and development
02 p0139 N88-10873
Marshall Space Flight Center's role in EASE/ACCESS mission management 02 p0139 N88-10875
Research and development at the Marshall Space Flight Center Neutral Buoyancy Simulator
02 p0139 N88-10878
A synopsis of the EVA training conducted on EASE/ACCESS for STS-61-B 02 p0140 N88-10879
Results of the ACCESS experiment
02 p0140 N88-10880
Overview of crew member energy expenditure during Shuttle Flight 61-B EASE/ACCESS task performance
02 p0140 N88-10882
Design and assembly sequence analysis of option 3 for CETF reference space station
[NASA-TM-100503] 05 p0553 N88-13369
RETE experiment Assembly, Integration, and Verification (AIV) activities
[IFSI-87-6] 05 p0555 N88-13380
Planning and scheduling for robotic assembly
08 p1062 N88-16416
Implementation of a robotic flexible assembly system
09 p1212 N88-17265
Robotic assembly and testing of rotary solenoids
[BDX-613-3663] 11 p1480 N88-18834
The space station assembly phase: Flight telerobotic servicer feasibility, volume 1
[NASA-CR-182689] 13 p1731 N88-20351
The space station assembly phase: Flight telerobotic servicer feasibility. Volume 2: Methodology and case study
[NASA-CR-182690] 13 p1731 N88-20352
Recognizing and locating partially occluded planar objects for assembly routines
[LAAS-87-360] 16 p2247 N88-23422
Assembly Test Article (ATA)
[NASA-CR-179361] 21 p2903 N88-27226
Study of the assembly, integration and verification programs of telecommunication satellites applicable to other satellite programs
[MATRA-100/CC/MLG/031/87] 24 p3334 N88-29847

ASSEMBLY
Alignment and assembly tool for very large diameter cylinders
[NASA-CASE-MFS-28001-2] 06 p0711 N88-14360

ASSEMBLY LANGUAGE
High-speed assembly language (80386/80387) programming for laser spectra scan control and data acquisition providing improved resolution water vapor spectroscopy
[NASA-CR-4117] 08 p1053 N88-16355
Efficient instruction level simulation of computers
[AD-A187821] 11 p1529 N88-19130

ASSESSMENTS
NT DAMAGE ASSESSMENT
NT TECHNOLOGY ASSESSMENT
Land campaign force assessment. Methods used in Central-Europe-study
[FOA-C-10288-9.3] 06 p0768 N88-14723

ASSIGNMENT
U ALLOCATIONS

ASSIMILATION
A real-data numerical study and four-dimensional data assimilation application for mesobeta-scale flow in complex terrain 02 p0212 N88-11329
Assimilation of meteorological observations 14 p1936 N88-21544

ASSOCIATION REACTIONS
Overview of hydrogen clusters 16 p2267 N88-23557
Associative two-body condensation in laser-cooled sodium and hydrogen 16 p2267 N88-23559
Formation and reactivity of small hydrogen cluster ions 16 p2267 N88-23560
Analysis of containerless condensation of polyatomic hydrogen ions, with emphasis on H3(+,-) association channels and a future workshop to study related topics 16 p2269 N88-23576

ASSOCIATIONS
U ORGANIZATIONS

ASSOCIATIVE PROCESSING (COMPUTERS)
The associative memory ME7
[ESA-TT-1033] 01 p0079 N88-10506
Estimation of the position and orientation of objects using associative memories
[ESA-TT-1034] 01 p0079 N88-10507
General potential surfaces and neural networks
[AD-A184484] 03 p0367 N88-12311
Optical Conceptual Computing and Associative Memory (OCCAM)
[AD-A190030] 15 p2107 N88-22550
Rapid feature extraction via the radon transform
[AD-A190032] 15 p2110 N88-22573
Optical computing based on neuronal models
[AD-A191481] 18 p2575 N88-25293
Optical data processing
[AD-A193024] 20 p2839 N88-26841
Content-addressable memory storage by neural networks: A general model and global Liapunov method
[AD-A192716] 21 p3002 N88-27807

ASSURANCE
Implementation of finite element quality assurance in a commercial industrial organisation
[PNR90393] 02 p0183 N88-11137
ESTEC's product assurance activities 09 p1125 N88-16739
Quality assurance of ceramic materials and gas turbine components
[IZFP-850303-TW] 11 p1465 N88-18735
Case study: The Hermes program product assurance 22 p3162 N88-28831

ASTEROID BELTS
NT ASTEROIDS
On the possible origin of meteoroid generating asteroid orbits 06 p0740 N88-14553

ASTEROID CAPTURE
Design study for asteroidal exploitation 03 p0389 N88-12445

ASTEROID MISSIONS
Design study for asteroidal exploitation 03 p0389 N88-12445
The comet rendezvous asteroid flyby mission 14 p2005 N88-21956

ASTEROIDS
Design study for asteroidal exploitation 03 p0389 N88-12445
Speckle interferometry of asteroids
[NASA-CR-180438] 15 p2151 N88-22843

ASTHMA
Mathematical modelling of the heat and water vapour transport in the human respiratory tract 17 p2382 N88-24160

ASTRO MISSIONS (STS)
IPS guidestar selection for stellar mode (ASTRO)
[NASA-TM-100336] 21 p2894 N88-27181

ASTROBIOLOGY
U EXOBIOLOGY

ASTRODYNAMICS
The kinematics of late-type supergiants
[SER-C-PREPUBL-FASC-28] 24 p3454 N88-30560

ASTROLOY (TRADEMARK)
The effect of temperature on fatigue crack initiation from aluminosilicate inclusions 06 p0720 N88-14427

ASTROMASTS
U LONGERONS

ASTROMETRY
Test of the Hipparcos payload in the Liege vacuum facility focal 02 p0135 N88-10850
Phase-coherent astrometric interferometry
[AD-A184428] 04 p0439 N88-12725
An astrometric search for a stellar companion to the sun 04 p0520 N88-13195
Performance considerations for the astrometric telescope facility on the phase 1 space station
[NASA-TM-100040] 06 p0800 N88-14898
Preparation of photometric measurements on a million stars in the framework of the satellite project HIPPARCOS/TYCHO
[ETN-88-91502] 13 p1853 N88-21093
Apparent brightness of stars and lasers 22 p3065 N88-28188
An upper limit on the primordial He4 abundance from speckle interferometric observations of muon Cassiopeiae 23 p3298 N88-29641

ASTRONAUT LOCOMOTION
Results of research with biological satellites 08 p1006 N88-16097

ASTRONAUT MANEUVERING EQUIPMENT
NT MANNED MANEUVERING UNITS
Personnel occupied woven envelope robot 23 p3260 N88-29408

ASTRONAUT PERFORMANCE
Results of the ACCESS experiment 02 p0140 N88-10880
EASE (Experimental Assembly of Structures in EVA) overview of selected results 02 p0140 N88-10881
Overview of crew member energy expenditure during Shuttle Flight 61-8 EASE/ACCESS task performance 02 p0140 N88-10882
Implications of shiftwork in space for human physiology experiments 12 p1659 N88-19942
Hypnosis: Possible applications for cosmonauts 12 p1665 N88-19984
NASA-Ames workload research program 17 p2380 N88-24151

ASTRONAUT TRAINING
A synopsis of the EVA training conducted on EASE/ACCESS for STS-61-B 02 p0140 N88-10879
The relationship between preflight underwater training and space motion sickness 19 p2696 N88-26025
Marintek's ocean basin, a training facility for extravehicular activity? 19 p2698 N88-26041

ASTRONAUTICS
Soviet space transport systems 13 p1727 N88-20328
Activities report of the Department of Aerospace Engineering
[ETN-88-91607] 24 p3460 N88-30582

ASTRONAUTS
NT ORBITAL WORKERS
Radiation effects in space
[DE87-012529] 01 p0075 N88-10479
Assessment of intercompartment fluid shifts by blood densitometry in astronauts 12 p1661 N88-19958
Studies of the vestibulo-ocular reflex on STS 4, 5 and 6
[NASA-TM-100461] 12 p1666 N88-19987
Incorporation of privacy elements in space station design
[NASA-CR-182748] 14 p1881 N88-21242
Design, development and evaluation of Stanford/Ames EVA prehensors
[NASA-CR-182688] 15 p2105 N88-22540
An investigation of conformable antennas for the astronaut backpack communication system
[NASA-CR-182908] 17 p2333 N88-23929
Bi-stem gripping apparatus
[NASA-CASE-MFS-28185-1] 17 p2345 N88-23979
Human performance issues arising from manned space station missions
[NASA-CR-3942] 18 p2553 N88-25156
Selection of isolated space crews 19 p2697 N88-26028

ASTRONOMICAL CATALOGS
Rigorous compilation of the Northern International Reference Stars (NIRS) 03 p0387 N88-12431
Catalogue of chromospherically active binaries 04 p0520 N88-13192
Catalog of infrared observations. Part 1: Data
[NASA-RP-1196-PT-1-ED-2] 07 p0944 N88-15738
Color-magnitude diagrams of star clusters in the Magellanic clouds from wide-field electronography. Part 3: NGC 1841
[PUBL-SER-C-FASC-14] 07 p0944 N88-15740
Catalog of infrared observations. Part 2: Appendixes
[NASA-RP-1196-PT-2-ED-2] 08 p1099 N88-16615
Global properties of star formation in spiral galaxies 14 p1994 N88-21883
Far infrared supplement: Catalog of infrared observations, second edition
[NASA-RP-1205] 24 p3452 N88-30545
A new determination of the Geneva photometric passbands and their absolute calibration
[SER-C-PREPUBL-FASC-26] 24 p3452 N88-30546
The guide star catalog
[NASA-CR-183253] 24 p3452 N88-30547

ASTRONOMICAL MAPS
Long-baseline astrometric interferometers
[AD-A188474] 12 p1713 N88-20250
Solar microwave radiation maps measured at Metsaehovi Radio Research Station in 1978-1979
[PB88-127543] 13 p1857 N88-21108
The guide star catalog
[NASA-CR-183253] 24 p3452 N88-30547

ASTRONOMICAL MODELS
NT DENSITY WAVE MODEL
NT STELLAR MODELS
On the degree of generality of inflationary solutions in cosmological models with a scalar field
[DE87-703079] 02 p0251 N88-11586
Cosmology with decaying vacuum energy
[DE88-000698] 03 p0389 N88-12443
A re-examination of the corona-wind dividing line: Diagnostics of non-coronal atmospheres 04 p0504 N88-13101
The acceleration of winds by MHD waves in open magnetic structures 04 p0506 N88-13109
Large scale solar and stellar magnetic fields 04 p0507 N88-13117
Comments on H. Arp The persistent problem of spiral galaxies
[TRITA-EPP-87-05] 05 p0660 N88-14052
The archiving of meteor research information 06 p0732 N88-14505
Neutron stars observations as astrophysical probes 06 p0800 N88-14896
Mars: High resolution VLA observations at wavelengths of 2 and 6 cm and derived properties 06 p0804 N88-14909
Spherical models of QSO/AGN emission line clouds 06 p0806 N88-14921
Number count-redshift relation in a perturbed Friedmann universe
[DE88-750302] 07 p0945 N88-15743
HEAO-1 observations of gamma-ray bursts 07 p0947 N88-15756
Comparative analysis of ultraviolet observations of Halley's comet on ASTRON astrophysical station before and after perihelion 08 p1004 N88-16086
Magnetic field of planet Uranus: Predictions, measurements, interpretations 08 p1005 N88-16094
Observations and modeling of the prominence/corona transition region 08 p1094 N88-16585
Beta limitation of matter-antimatter boundary layers
[TRITA-EPP-87-11] 09 p1250 N88-17490
Prediction and analysis of basic gravitational microlensing phenomena 11 p1550 N88-19272
Spectral images and multi-component models of the chromospheres of AR Lacertae 11 p1568 N88-19384
The TempIS Project: Performance analysis of temporal queries
[AD-A188354] 12 p1706 N88-20213
Models of recombination lines in radio H2 regions
[INPE-4302-TDL/277] 12 p1710 N88-20232
Data analysis of an observation of the quasar 3C 273 in the high-energy X-ray range, and the significance for astrophysical models
[ETN-88-91493] 14 p1993 N88-21878
Radiation transport in planetary nebulae
[ETN-88-91500] 14 p1993 N88-21880
Time dependent MHD models for the cometary magnetosphere 14 p1997 N88-21900
Cometary MHD and chemistry: Application to Halley 14 p2000 N88-21922
Crustal models of the evolving comet nucleus 14 p2005 N88-21953
Three approaches to the modeling of Comet Halley's motion over long periods of time 14 p2010 N88-21992
The thermal evolution of the jets in SS433 --- galactic object
[MPE-PREPRINT-107] 16 p2289 N88-23705
Stochasticity in elliptical galaxies
[SER-C-PREPUBL-FASC-20] 17 p2450 N88-24556
On the magnetic structure and energy balance of EUV-emitting plasma in the quiet Sun 17 p2452 N88-24567
Observation of a point source in Cygnus constellation with the underground detector at Frejus (France)
[PITHA-87/02] 20 p2684 N88-27122
Gamma radiation from center of the galaxy of the order of MeV values
[MPE-207] 21 p3032 N88-27999
On the dynamics of the metagalaxy
[TRITA-EPP-88-05] 22 p3166 N88-28852
Clustering of galaxies and clusters of galaxies in a decaying-particle cosmological model with a massive decay product
[DE88-753434] 23 p3298 N88-29642
Molecular hydrogen in galaxies 23 p3299 N88-29645
The interaction of Io with the plasma torus 23 p3308 N88-29704

Workshop on the Origins of Solar Systems
[NASA-CR-183025] 24 p3451 N88-30536
Comparisons of solar nebula models
24 p3451 N88-30539
The atmospheres of the earth and the other planets: Origin, evolution and composition
24 p3452 N88-30544

ASTRONOMICAL OBSERVATORIES
NT ASTRONOMICAL SATELLITES
NT GAMMA RAY OBSERVATORY
NT HEAO 2
NT HUBBLE SPACE TELESCOPE
NT INFRARED ASTRONOMY SATELLITE
NT INFRARED SPACE OBSERVATORY (ISO)
NT IUE
NT ROSAT MISSION
NT SAS
NT SPACE INFRARED TELESCOPE FACILITY
NT X RAY ASTROPHYSICS FACILITY
Ground-based optical interferometry
01 p0096 N88-10631
Activities report in astronomy
[ISSN-0531-4496] 01 p0108 N88-10701
A near-earth optical communications terminal with a corevolving planetary sun shield
04 p0434 N88-12693
Automatic telescope operations
04 p0519 N88-13190
LDR structural experiment definition
[NASA-TM-100618] 17 p2312 N88-23826

ASTRONOMICAL PHOTOGRAPHY
A search for X-ray luminous late type stars in NIPSS data
04 p0511 N88-13143
Further development of a stellar camera following the rotation-modulation-collimator principle for balloon-borne observations in the X-ray range
[ETN-88-91496] 14 p1913 N88-21428
Study of the ionic and neutral species in the coma of Comet Halley with an image intensifier camera
14 p2006 N88-21962
Memoirs of the Faculty of Science, Kyoto University. Series of Physics, Astrophysics, Geophysics and Chemistry, volume 37, no. 2
[ISSN-0368-9689] 16 p2287 N88-23694
Narrow-band photographic observations of the HII Region S296 in Canis Major 16 p2288 N88-23696
Dust and C2-contents in the coma of Halley's Comet (1966III)
16 p2288 N88-23697
Photographic observations of the large scale features of Comet Halley 16 p2288 N88-23698
Methods for indirect imaging through the atmosphere
[ONERA-NT-1987-4] 20 p2884 N88-27124
Satellite attitude determination using a CCD (Charge-Coupled-Device) star camera
[AD-A192662] 22 p3046 N88-28080

ASTRONOMICAL PHOTOMETRY
NT STELLAR SPECTROPHOTOMETRY
Extragalactic VLBI objects: Candidates for optical interferometry?
01 p0094 N88-10616
Automatic telescope operations
04 p0519 N88-13190
A processing method and results of meteor shower radar observations
06 p0736 N88-14539
The Valec fireball and predicted meteorite fall
06 p0739 N88-14547
Conception and realization of components for a microchannel-plate detector, and testing of the detector system in the laboratory and in astronomical use
[ETN-88-91495] 11 p1491 N88-18809
Memoirs of the Faculty of Science, Kyoto University. Series of Physics, Astrophysics, Geophysics and Chemistry, volume 37, no. 2
[ISSN-0368-9689] 16 p2287 N88-23694
Method of digital surface photometry of galaxies and its application to the edge-on galaxy NGC 5907
16 p2287 N88-23695
Surface photometric investigations for spiral galaxies of large dimension structures in edge-on gemetry
[ETN-88-92126] 21 p3030 N88-27985

ASTRONOMICAL SATELLITES
NT GAMMA RAY OBSERVATORY
NT HEAO 2
NT HUBBLE SPACE TELESCOPE
NT INFRARED ASTRONOMY SATELLITE
NT INFRARED SPACE OBSERVATORY (ISO)
NT IUE
NT SAS
NT SPACE INFRARED TELESCOPE FACILITY
NT X RAY ASTROPHYSICS FACILITY
An autonomous, closed-loop pointing system for use with satellite optics
[DE87-012011] 02 p0235 N88-11483
Infrared astronomy: Why and how?
09 p1123 N88-16722
Integrated focal plane star sensor
[OG-RT/86-0156] 09 p1262 N88-17562
Observation model and parameter partials for the JPL VLBI parameter estimation software MASTERFIT-1987
[NASA-CR-182524] 10 p1427 N88-18523
Deep space target location with Hubble Space Telescope (HST) and Hipparcos data
[NASA-CR-182520] 10 p1427 N88-18524
Study of a safe attitude for the Infrared Space Observatory (ISO) during perigee pass
[SNIAS-881-440-113] 23 p3185 N88-28954
Far infrared spectroscopy telescope (FIRST) inflatable thermal shield, phase 1
[SR/FIS/108(87)CZ] 24 p3453 N88-30552

ASTRONOMICAL SPECTROSCOPY
Microcomputer control of spectroscopic instruments
[ATR-86(8431)-4] 03 p0326 N88-12058
A 23 hour EXOSAT observation of the X-ray pulsar 1E2259+586 and the associated supernova remnant G109.1-1.0
[MPE-PREPRINT-99] 14 p1994 N88-21882
The observability of carbon monoxide in planetary nebulae
[ETN-88-91498] 14 p2011 N88-21994
Multiple object redshift determinations in clusters of galaxies using OCTOPUS
[INPE-4528-PRE/1278] 15 p2150 N88-22835
Fabry-Perot etalons as prefilters for astronomical far infrared Fourier transform spectroscopy
[MPE-205] 16 p2273 N88-23603
A spectroscopic study of absorption and emission features of interstellar dust components
[B8681462] 16 p2289 N88-23706
The high-throughput X-ray spectroscopy mission E6889478 MN513835 --- ESA program
[ESA-SP-1092] 17 p2450 N88-24554
Radial velocities monitoring of a sample of barium and S stars using CORAVEL: Towards an evolutionary link between barium and S stars?
[SER-C-PREPUBL-FASC-19] 18 p2593 N88-25410
Analysis of emission features in IRAS LRS spectra
21 p2928 N88-27380
The high-throughput X-ray spectroscopy mission: The mission-science report
[ESA-SP-1097] 24 p3453 N88-30557

ASTRONOMICAL TELESCOPES
U TELESCOPES

ASTRONOMY
NT GAMMA RAY ASTRONOMY
NT INFRARED ASTRONOMY
NT RADIO ASTRONOMY
NT SPACEBORNE ASTRONOMY
NT ULTRAVIOLET ASTRONOMY
NT X RAY ASTRONOMY
NT X RAY BINARIES
NT X RAY SOURCES
Activities report in astronomy
[ISSN-0531-4496] 01 p0108 N88-10701
National Science Foundation
[PB87-228375] 03 p0384 N88-12410
Method for determining atmospheric temperature profiles from observations of astronomical refraction of stars
08 p1013 N88-16139
On the time delay of the ultrahigh-energy radiation signal from the source Cygnus X-3
[DE88-700649] 10 p1431 N88-18547
Research and technology, 1987
[NASA-TM-100323] 12 p1713 N88-20253
Advice for astronomical research
[ISBN-9-03-460977-4] 16 p2289 N88-23703
Computing basic solar and lunar data from the Air Almanac
[AD-A190777] 16 p2290 N88-23710
NASA thesaurus: Astronomy vocabulary
[NASA-SP-7069] 17 p2450 N88-24553
Digital image processing from speckle interferograms by correlation methods: Application in atmospheric optics, astronomy, and biology
[ETN-88-92125] 20 p2855 N88-26953
Reports of planetary astronomy, 1988
[NASA-TM-4063] 22 p3163 N88-28835
Amateur astronomy in the space age
[RAE-TM-SS-4] 22 p3163 N88-28836
On the dynamics of the metagalaxy
[TRITA-EPP-88-05] 22 p3166 N88-28852
Automated generation of spacecraft activity plans
23 p3258 N88-29396
Catalog of open clusters and associated interstellar matter
[NASA-RP-1202] 23 p3300 N88-29652
Activities report in astronomy
[ISSN-0531-4496] 24 p3451 N88-30535
Workshop on the Origins of Solar Systems
[NASA-CR-183025] 24 p3451 N88-30536

ASTROPHYSICS
NT NUCLEAR ASTROPHYSICS
NT SOLAR PHYSICS
NT STELLAR PHYSICS
USSR report: Space
[JPRS-USP-87-003] 01 p0009 N88-10050
X-ray astronomy instruments to operate on Mir station
01 p0009 N88-10052
Institute of Geophysics and Planetary Physics at Lawrence Livermore National Laboratory
[DE87-014618] 02 p0251 N88-11583
Calibration on the Sun for stellar magnetic fields
04 p0506 N88-13113
Variations of the vertical and horizontal velocities of the small-scale structures and the physical problems related to overshoot layers 04 p0507 N88-13115
Photon counting image sensor development for astronomical applications
[NASA-CR-181507] 05 p0660 N88-14049
Astrophysics observatory in Byurakan
[AD-A185144] 05 p0660 N88-14050
Neutron stars observations as astrophysical probes
06 p0800 N88-14896
Interface between astrophysical datasets and distributed database management systems (DAVID)
[NASA-CR-182394] 07 p0942 N88-15731
Nonlinear, relativistic Langmuir waves in astrophysical magnetospheres
[NASA-CR-182422] 08 p1024 N88-16197
An introduction to nuclear astrophysics
[DE88-002761] 08 p1100 N88-16618
Quark matter in astrophysics and cosmology
[DE88-003406] 10 p1429 N88-18534
Measurements of astrophysical reaction rates for radioactive samples
[DE88-004309] 10 p1429 N88-18537
An adaptive grid finite difference method for time-dependent Magnetohydrodynamic (MHD) flows and its astrogeophysical applications
11 p1553 N88-19294
Photohydrodynamical processes near compact objects
11 p1589 N88-19390
Research and technology, 1987
[NASA-TM-100323] 12 p1713 N88-20253
Physics of condensed matter at extreme conditions
[DE88-006232] 13 p1832 N88-20958
Very high energy gamma ray astrophysics
[DE88-005821] 13 p1854 N88-21095
Particle cosmology comes of age
[DE88-006998] 15 p2151 N88-22844
Memoirs of the Faculty of Science, Kyoto University. Series of Physics, Astrophysics, Geophysics and Chemistry, volume 37, no. 2
[ISSN-0368-9689] 16 p2287 N88-23694
Narrow-band photographic observations of the HII Region S296 in Canis Major 16 p2288 N88-23696
Research and Technology, 1987, Goddard Space Flight Center
[NAS 1.15:101097] 17 p2453 N88-24572
Research in particle and gamma-ray astrophysics
[NASA-CR-183111] 20 p2887 N88-27146
The classical nova outburst
[DE88-009138] 21 p3030 N88-27987
A study of mechanisms producing astrophysical jets
[AD-A194100] 23 p3300 N88-29649
A coded mask telescope for observations of X and gamma ray sources in the southern sky
[INPE-4580-PRE/1314] 24 p3453 N88-30551
Research in particle and gamma-ray astrophysics
[NASA-CR-183126] 24 p3455 N88-30566
Activities in astrophysics
[INPE-4582-PRE/1316] 24 p3456 N88-30570

ASYMMETRY
Two classes of preconditioners computed using block matrix factorization techniques
[DE88-001313] 04 p0485 N88-12988
Asymmetry and variations of solar limb darkening along the diameter defined by diurnal motion in April 1981
04 p0506 N88-13111
Dynamic behavior of dissymmetric rotor bearings modelled with a periodic coefficient large system
05 p0596 N88-13640
Geometric nonlinear analysis of asymmetric thin-walled members
[PB87-133856] 06 p0723 N88-14446
Solar Dynamics and G-modes
[NASA-CR-180737] 06 p0805 N88-14911
The effect of asymmetric heating on flow stability and heat transfer for flow in a vertical tube
[DE88-003242] 07 p0855 N88-15193
Typhoon structural evolution
[AD-A186090] 07 p0879 N88-15333
Calculation of symmetric and asymmetric vortex seperation on cones and tangent ogives based on discrete vortex models
[NASA-CR-4122] 08 p0950 N88-15768
Evaluation of magnetic coordinates in finite-beta, asymmetric plasmas
[DE88-003665] 10 p1412 N88-18424

Asymmetric double Langmuir probe for fast and automatic measurements of plasma temperature
[DE88-004773] 10 p1414 N88-18436
Multiple scattering from nonspherical targets
[AD-A189939] 15 p2133 N88-22723
Stable, heavy, neutral particles in the sun and in toponium decay 17 p2452 N88-24568
Employment of porous polytetrafluoroethylene Membrane with a hydrophilic and hydrophobic stratal structure for construction of an enzyme electrode
[NASA-TT-20296] 19 p2620 N88-25543
Three-dimensional vortex interactions
[AD-A194066] 23 p3172 N88-28889

ASYMPTOTES
Asymptotic error bounds for power approximations to multinomial tests of fit
[MEMO-640] 08 p1072 N88-16470
On 1/n-expansion and wave functions
[DE88-701639] 16 p2260 N88-23509
Asymptotics for a system of nonlinearly coupled wave equations with an application to the galloping oscillations of overhead transmission lines
[REPT-87-78] 17 p2348 N88-23991
The two isotropic asymptotes of fiber composites
[AD-A192305] 21 p2904 N88-27231

ASYMPTOTIC GIANT BRANCH STARS
Neutron capture nucleosynthesis in low mass AGB stars 04 p0517 N88-13178
AGB (Asymptotic Giant Branch): Star evolution
[DE88-001829] 07 p0945 N88-15742
Asymptotic giant branch populations in composite stellar systems 13 p1854 N88-21098

ASYMPTOTIC METHODS
An asymptotic theory for a class of initial-boundary value problems for weakly nonlinear wave equations with an application to a model of the galloping oscillations of overhead transmission lines
[REPT-87-12] 01 p0086 N88-10556
Parallel computation of a domain decomposition method
[DE87-011444] 01 p0086 N88-10560
Asymptotics of the effective potentials and wave functions of a three-body problem in suitable coordinates
[DE87-703323] 03 p0370 N88-12326
Extrema of skewed stable processes
[AD-A185422] 05 p0642 N88-13925
Asymptotic normality of poly-t densities with Bayesian applications
[AD-A185718] 06 p0768 N88-14719
Sound propagation over uneven ground and irregular topography
[NASA-CR-182352] 06 p0776 N88-14763
Detecting and interval estimation about a slope change point
[AD-A186030] 07 p0909 N88-15509
Maximum likelihood principle and model selection when the true model is unspecified
[AD-A186027] 07 p0914 N88-15544
A note on extended quasi-likelihood
[AD-A186318] 07 p0915 N88-15555
Short data length effects in an asymptotically efficient ARMA (AutoRegressive Moving Average) spectral estimator
[AD-A186561] 08 p1068 N88-16458
Numerical analysis of motion of solid bodies in atmosphere 08 p1079 N88-16505
Steady ship waves at low Froude numbers, part 2
[AD-A176805] 09 p1160 N88-16953
On some asymptotics of laminar flow in a coiled pipe 10 p1328 N88-17936
Joint moments of the maximum in a critical branching process
[AD-A188157] 11 p1541 N88-19209
Extrema of Gaussian process by simulation 11 p1541 N88-19211
Analysis, estimation, and control for perturbed and singular systems and for systems subject to discrete events
[AD-A188496] 12 p1677 N88-20026
Steps into a geometer's workbench
[CWI-CS-R8726] 13 p1819 N88-20870
Estimation of convolution tails
[AD-A190323] 15 p2125 N88-22666
Asymptotically efficient adaptive allocation schemes for controlled Markov chains: Finite parameter space
[AD-A192228] 20 p2846 N88-26893
A simple explanation of the Stokes phenomenon
[AD-A193253] 21 p3006 N88-27832
Asymptotic normality of minimum L1-norm estimates in linear models
[AD-A193399] 21 p3006 N88-27835
Thickness effects on the stability of shell like structures 23 p3224 N88-29192
An asymptotic evaluation of the tail of a multiple symmetric alpha-stable integral
[AD-A194570] 23 p3270 N88-29460
Asymptotic modal analysis and statistical energy analysis
[NASA-CR-183077] 23 p3278 N88-29514

ASYMPTOTIC PROPERTIES
Asymptotically stable all-pass transfer functions: Canonical form, parametrization and realization
[PB87-123972] 06 p0763 N88-14684
AGB (Asymptotic Giant Branch): Star evolution
[DE88-001829] 07 p0945 N88-15742
Adaptive exponential stabilization of a first order continuous-time system
[CWI-OS-R8705] 08 p1069 N88-16461
A state space approach to the problem of adaptive pole assignment
[CWI-OS-R8704] 09 p1224 N88-17339

ASYMPTOTIC SERIES
Concurrent algorithms for transient nonlinear FE analysis
[NASA-CR-181455] 02 p0221 N88-11389
Elastodynamic ray theory and asymptotic methods for direct and inverse scattering problems 03 p0335 N88-12108
Asymptotic form of stationary solutions of the Navier-Stokes equations for large Reynolds numbers 04 p0459 N88-12838
Asymptotic analysis of a turbulent boundary layer in a strong adverse pressure gradient
[AD-A185406] 05 p0581 N88-13543
Diffusion first passage times: Approximations and related differential equations
[AD-A185592] 06 p0765 N88-14700
Testing and interval estimation in a change-point model allowing at most one change
[AD-A185525] 06 p0767 N88-14716
Parameter estimation for the Dirichlet-Multinomial Distribution (DMD) using supplementary beta-binomial data
[AD-A186335] 07 p0911 N88-15524
Maximum likelihood principle and model selection when the true model is unspecified
[AD-A186027] 07 p0914 N88-15544
Variable selection in logistic regression
[AD-A186032] 07 p0914 N88-15547
On the asymptotic joint distributions of the eigenvalues of random matrices which arise under components of covariance model
[AD-A186387] 07 p0915 N88-15558
Dynamic observers as asymptotic limits of recursive filters: Special cases
[AD-A187578] 10 p1397 N88-18324
Asymptotic expansions for large deviation probabilities in the strong law of large numbers
[AD-A187432] 10 p1402 N88-18361
Estimation of the probability of a long time to the first entrance to a state in a semi-Markov model
[AD-A188960] 12 p1685 N88-20074
Survival analysis using additive risk models
[AD-A189053] 13 p1825 N88-20906
Acoustic radiation from line- and point-loaded plates: Uniformly asymptotic solutions
[AD-A189367] 13 p1834 N88-20969
On the Edgeworth expansion and the bootstrap approximation for a Studentized U-statistic
[CWI-MS-R8708] 14 p1965 N88-21728
On 2-D versus 3-D: Sine of squared angular error and weighted perpendicular fixing
[NASA-CR-182899] 16 p2252 N88-23458
Asymptotic theory for weighted least squares estimators in Aalen's additive risk model
[AD-A191085] 18 p2562 N88-25210
On a biorthogonal system associated with uniform asymptotic expansions
[CWI-AM-R8709] 18 p2566 N88-25240
Asymptotic of Peanokerns of finite fixed order
[ETN-88-92381] 21 p3008 N88-27843
Statistical analysis of dyadic stationary processes
[AD-A193057] 21 p3009 N88-27853
Joint asymptotic distribution of marginal quantiles and quantile functions in samples from a multivariate population
[AD-A193385] 21 p3010 N88-27856
Asymptotic orders of reachability in perturbed linear systems
[AD-A192718] 22 p3143 N88-28688
Mathematical problems of nonlinear wave propagation and of waves in heterogeneous media
[AD-A195970] 24 p3368 N88-30057

ASYNCHRONOUS MOTORS
Study on the dynamics of executive electromechanism with thyristor commutator for cryogenic systems
[DE87-703209] 12 p1622 N88-19702
Industrial electric motors and controllers
[PB88-139589] 14 p1907 N88-21394

ATHODYDS
U RAMJET ENGINES

ATLANTIC OCEAN
An illustrative example of the nowcasting challenge 02 p0199 N88-11243
Summary of 1987 Atlantic tropical cyclone activity and verification of author's seasonal forecast 02 p0215 N88-11356
On the interannual variability of South American climate and the Southern Oscillation 04 p0470 N88-12905
Tectonics and magmatism of Walvis Ridge and Discovery Rise (Atlantic Ocean) 06 p0726 N88-14463
Geophysical-geomorphological statistical regionalization of North Atlantic 06 p0726 N88-14466
Tectonics of sedimentary cover and basement of Labrador Sea 06 p0726 N88-14468
Mathematical-cartographic modeling of economic utilization of Atlantic Ocean 06 p0726 N88-14469
Hydrochemical structure of Gulf Stream frontal zone waters 06 p0727 N88-14476
Modes of surface circulation and climate over the tropical Atlantic, Eastern Pacific, and Indian Oceans 06 p0742 N88-14564
Annual data summary and climatological evaluation, CERC (Coastal Engineering Research Center) field research facility, 1985, volume 2, appendix C
[AD-A185894] 07 p0881 N88-15344
Nature of Western Pacific transition zone 08 p1010 N88-16122
New data on structure of earth's crust and seismicity of basins in Atlantic and Indian Oceans 08 p1010 N88-16123
Hurricane climatology for the Atlantic and Gulf coasts of the United States
[PB88-114657] 08 p1039 N88-16288
Annual data summary and climatological evaluation CERC (Coastal Engineering Research Center) field research facility, 1985. Volume 1. Main text and appendixes A and B
[AD-A186442] 08 p1039 N88-16289
Predictability of ice concentration in the high-latitude North Atlantic from statistical analysis of SST (Sea Surface Temperature) and ice concentration data
[AD-A186621] 08 p1045 N88-16315
Hydrographic and current measurements in the North-East Atlantic Ocean. Data report on F.S. Meteor cruises 69/5 and 69/6, October to November 1984
[REPT-166] 09 p1196 N88-17164
Analysis of low frequency current fluctuations in the North-East Atlantic Ocean
[REPT-170] 09 p1196 N88-17165
Meteorological and aerosol measurements from the NOAA WP-3D aircraft during WATOX-86, January 4-9, 1986
[PB88-120860] 10 p1352 N88-18079
Trace element geochemistry of the South Atlantic Bight
[DE88-003515] 10 p1356 N88-18108
Current velocity and hydrographic observations in the Straits of Florida, the Caribbean Sea and offshore of the Antillean Archipelago: Subtropical Atlantic climate studies (STACS) 1984 and 1985
[PB88-149299] 12 p1649 N88-19874
Propagation of subsurface salinity maximum in tropical Atlantic 13 p1786 N88-20686
The use of a barotropic finite element model for the study of circulation on the continental shelf of the southeast coast of Brazil
[INPE-4401-PRE/1218] 13 p1802 N88-20774
Oceanographic export system development, year 1
[AD-A189134] 14 p1950 N88-21623
Current velocity and hydrographic observations in the Straits of Florida, the Caribbean Sea and offshore of the Antillean Archipelago: Subtropical Atlantic Climate Studies (STACS) 1986
[PB88-160767] 14 p1951 N88-21628
Forecast of Atlantic seasonal hurricane activity for 1988 15 p2098 N88-22500
SeaSoar profiles in the Iceland-Scotland area, May 1987
[IOS-253] 18 p2548 N88-25124
Determination of mesoscale variability of sea surface temperature and attenuation in the North Atlantic from satellite measurement
[REPT-162] 18 p2548 N88-25127
Meteorological satellite product support and research for project GALE
[NASA-CR-180989] 19 p2727 N88-28193
Interannual variability in the Atlantic and Indian Oceans and its relationship to the southern oscillation 22 p3121 N88-28548
Atlantic SST variability and high latitude climate fluctuations 22 p3122 N88-28551

Sub-Saharan rainfall anomalies and global sea-surface temperature relationships for the recent fifteen year (1970-1984) period 22 p3122 N88-28552
Low frequency variability of SST and its relationship to atmospheric forcing 22 p3122 N88-28554
The active layer of the upper Atlantic Ocean 22 p3124 N88-28566

ATMOSPHERE EXPLORER C
U EXPLORER 51 SATELLITE

ATMOSPHERE EXPLORER D
U EXPLORER 54 SATELLITE

ATMOSPHERE EXPLORER E
U EXPLORER 55 SATELLITE

ATMOSPHERES
MAXIE 1
[AD-A189686] 14 p1882 N88-21247

ATMOSPHERIC ABSORPTION
U ATMOSPHERIC ATTENUATION

ATMOSPHERIC ATTENUATION
An instrument for the quasi-continuous determination of atmospheric soot content
[DFVLR-FB-87-04] 01 p0068 N88-10433
Development of a climatic map of rainfall attenuation for Europe
[REPT-372] 02 p0216 N88-11359
Experimental study of the propagation of an acoustic wave in the low atmosphere
[ISL-R-111/86] 02 p0231 N88-11454
Estimates of satellite EHF communication outages due to attenuation by rain
[AD-A183969] 03 p0307 N88-11941
Absorption of far IR-radiation by H2O-N2 complexes under atmospheric conditions 04 p0462 N88-12655
Method of determining atmospheric moisture content by measurement of upward radiation intensity in near IR 08 p1007 N88-16106
Radiation absorption in the infrared spectral range: A comparison between laboratory measurements and theoretical calculation illustrated by a H2O 2.7 micrometer 08 p1018 N88-16170
Literature survey relating to the absorption properties of ozone in the near ultraviolet
[ESRO-SM-81] 09 p1190 N88-17129
Remote sensing of atmospheric optical thickness and sea-water attenuation when submerged: Wavelength selection and anticipated errors
[AD-A187609] 11 p1548 N88-19262
MM-wave propagation and application in military communication systems 12 p1617 N88-19669
Distortion of wideband carbon dioxide laser radar waveforms due to atmospheric dispersion and absorption
[AD-A188687] 12 p1632 N88-19771
Calibration of the solar radiation estimation method by satellites
[INPE-4349-PRE/1185] 12 p1646 N88-19861
Atmospheric attenuation of near infrared radiation propagating through fog 14 p1899 N88-21342
Corrections for differential scattering by aerosols in the measurement of ozone by DIAL — differential absorption lidar (DIAL)
[NPL-QU-78] 14 p1945 N88-21603
Space communication link propagation data for selected cities within the multiple beam and steerable antenna coverage areas of the advanced communications technology satellite
[NASA-TM-100861] 16 p2191 N88-23070
Study of the convergence of a finite difference scheme for acoustic propagation in the atmosphere in a parabolic approximation. Statistical calculation of the sound field in the presence of kinematic turbulence
[ONERA-RS-6/3641-PY-160-P] 17 p2394 N88-24235
Atmospheric propagation of laser beams
[AD-A191447] 18 p2520 N88-24952
Development and validation of transmission measurements techniques of image contrast, utilizing existing IR imagers
[AD-A191471] 18 p2541 N88-25079
Ground level hydroxyl (OH) concentration measurements by long path differential optical laser absorption
[ETN-88-92124] 20 p2855 N88-26952
An evaluation of two millimeter wave propagation models for horizontal atmospheric attenuation at 70-115 GHZ
[AD-A192699] 21 p2931 N88-27403
Sound propagation at low altitude 22 p3148 N88-28725
Evaluation of atmospheric effects for operational tactical decision aid
[AD-A194205] 23 p3232 N88-29236
European validation of SAGE-2 aerosol profiles
[AERONOMICA-ACTA-A-327-1988] 23 p3234 N88-29243

ATMOSPHERIC BOUNDARY LAYER
The air flow on hills from models and experiments
[BMFT-FB-T-86-175] 02 p0198 N88-11236
Forecasting boundary layer clouds and fog: A review of operational numerical models 02 p0208 N88-11307
Evaluation of a mesoscale prediction system with surface weather observations and comparison with a large-scale prediction system 02 p0210 N88-11319
Development and testing of a vertically-nested regional prediction system — weather forecasting 02 p0210 N88-11322
A preliminary demonstration of the use of boundary-layer models of flow in complex terrain for high resolution surface wind forecasting 02 p0212 N88-11330
Visualization of the flow field around a generic destroyer model in a simulated turbulent atmospheric boundary layer
[AD-A184658] 03 p0320 N88-12023
Properties of the atmospheric boundary layer above a subtropical oceanic front
[AD-A184006] 03 p0351 N88-12215
A model for the convective atmospheric boundary layer during the winter in the Khartoum Region (Sudan)
[R-822-A] 03 p0353 N88-12225
Heat and moisture transport in the atmospheric boundary layer
[AD-A184222] 04 p0470 N88-12904
Estimation of marine boundary layer depth and relative humidity with multispectral satellite measurements
[AD-A184881] 05 p0620 N88-13804
A method to obtain a wind model for the boundary layer in a representative tropical region
[R-818-D] 06 p0743 N88-14569
Facilities for research and weather observations on the 213 m tower at Cabauw (Netherlands) and at remote locations
[KNMI-WR-87-5] 06 p0746 N88-14587
A semianalytical solution of the heat conduction equation for several boundary conditions 08 p1014 N88-16148
Wind tunnel modeling techniques
[KU-SFB-210/E/33] 09 p1121 N88-16711
Correction of the wind field measured by the NCAR electra during FASINEX (Frontal Air-Sea Interaction Experiment) for inertial navigation system drifts
[AD-A187780] 11 p1514 N88-19045
Similarity theories and microturbulence in the atmospheric mixed layer 13 p1806 N88-20802
Modeling surface exchanges: The soil +vegetation-atmosphere continuum 14 p1937 N88-21553
An introduction to the parameterization of land-surface processes 14 p1937 N88-21554
Continental surface processes and water cycle 14 p1937 N88-21555
Sensitivity of general circulation models to surface processes 14 p1937 N88-21556
Unsteady aerodynamics of a Wortmann FX-63-137 wing in a fluctuating wind field
[AD-A190128] 15 p2013 N88-22006
Spectral measurements in a disturbed boundary layer over snow
[AD-A190217] 15 p2097 N88-22494
Ground level hydroxyl (OH) concentration measurements by long path differential optical laser absorption
[ETN-88-92124] 20 p2855 N88-26952
Genesis of Atlantic lows experiment NASA electra boundary layer flights data report
[NASA-TM-100703] 22 p3128 N88-28597
The spatial and temporal variability of the arctic atmospheric boundary layer and its effect on electromagnetic (EM) propagation
[AD-A193958] 23 p3204 N88-29068
The surface evaporative duct height product: An evaluation
[AD-A195918] 24 p3392 N88-30199
Doppler radar analysis of coastal marine atmospheric boundary layer structure during a cold air outbreak
[AD-A196023] 24 p3403 N88-30261

ATMOSPHERIC CHEMISTRY
A study of carbon monoxide distribution determinations for a global transport model
[NASA-CR-181423] 01 p0067 N88-10432
Diagnostics of atmospheric chemistry through ozone measurement
[INPE-4230-PRE/1105] 01 p0068 N88-10437
Kinetics investigations of atmospheric chemical reactions
[PB87-213351] 01 p0069 N88-10439
Status of the solar and infrared radiation submodels in the LLNL 1-D and 2-D chemical-transport models
[DE87-014320] 01 p0069 N88-10441
Description of the Mountain Cloud Chemistry Program version of the PLUVIUS MOD 5.0 reactive storm simulation model
[DE87-012846] 01 p0070 N88-10450
The combined release and radiation effects satellite, a joint NASA/DOD program 02 p0135 N88-10851
Production of NO by galactic cosmic rays and lightning
[DE87-014613] 02 p0197 N88-11230
The effects of minor trace gases on the transfer of thermal infrared radiation through the Earth's atmosphere 04 p0468 N88-12893
Scientific and Operational Requirements for TOMS Data
[NASA-CP-2497] 05 p0615 N88-13774
The use of TOMS data for tropospheric ozone studies 05 p0616 N88-13784
The polar ionosphere and interplanetary field
[AD-A185386] 05 p0624 N88-13822
First flight of the ATMOS instrument during the Spacelab 3 Mission, April 29 through May 6, 1985
[NASA-CR-182360] 06 p0728 N88-14482
Use of lasers with F sub A(II)-color center KCl:Li crystals in the intraresonator laser spectroscopy method 06 p0769 N88-14729
Nonuniformity of electromagnetic field at Lambda = 10.6 micron wavelength inside atmospheric aerosol particles 06 p0772 N88-14743
Use of back air trajectories in interpreting atmospheric chemistry data: A review and bibliography
[PB88-102108] 07 p0876 N88-15312
Characteristics and climatic relevance of the atmospheric aerosol components 08 p1017 N88-16164
Investigations of the influence of chemical reactions of the vertical flow of gaseous and particulate compounds 08 p1017 N88-16165
The sodium layer at 69 N latitude in wintertime 08 p1027 N88-16218
Lidar metal density measurements in the upper atmosphere 08 p1027 N88-16219
Current issues in atmospheric change
[NASA-CR-182406] 08 p1039 N88-16287
Measurement of vertical distributions of halogenated hydrocarbons in the stratosphere
[ETN-88-91065] 09 p1191 N88-17135
Investigation of OH reaction products. Excimer laser photolysis/slab laser fluorescence under tropospheric conditions
[REPT-8] 09 p1191 N88-17137
Mesospheric dynamics and chemistry from SME data
[NASA-CR-182465] 09 p1191 N88-17139
Model investigations of atmospheric ammonia scavenging
[DE88-002337] 09 p1194 N88-17153
Gas phase pulse radiolysis
[DE88-002981] 10 p1296 N88-17751
Evaluation of regional-scale air quality models: Chairmen reports from four workshops
[DE88-001397] 10 p1352 N88-18080
The role of analytical chemistry in assessing atmospheric effects of combustion
[DE88-003909] 10 p1352 N88-18082
Initial results with the LLNL 2-D chemical-radiative-transport model of the troposphere and stratosphere
[DE88-004355] 11 p1512 N88-19033
Reports and contributions of the Max-Planck Institute of Chemistry (Otto Hahn Institute)
[REPT-1/87] 11 p1570 N88-19398
Ion content and infrared absorption of moist atmospheric air
[AD-A188839] 12 p1643 N88-19838
Evaluation of chemical and atmospheric sciences research
[AD-A188468] 12 p1687 N88-20091
Gas-chromatographic analysis of products of thermal reactions of aerosol in Venusian cloud layer on Vega-1 and Vega-2 automatic interplanetary stations 13 p1725 N88-20318
Roentgenoradiometric analysis of aerosol in Venusian clouds by Vega-1 and Vega-2 automatic interplanetary stations 13 p1726 N88-20319
Effect of nitrogen dioxide release on thermosphere 13 p1789 N88-20704
Activities report in meteorology
[AR-86-87] 13 p1798 N88-20755
Computer simulation of tropospheric chemistry
[JUEL-2144] 13 p1798 N88-20756
Local meteorological processes and air mass origin during a cloud chemical field experiment on Areskutan, Sweden, in summer 1986
[AP-28] 14 p1948 N88-21615
Observational and theoretical studies of greenhouse climate effects
[DE88-006237] 14 p1948 N88-21621

The role of water in the thermal balance of the coma
14 p1999 N88-21916
Atmospheric carbon dioxide and the global carbon cycle: The key uncertainties
[DE88-005059] 15 p2092 N88-22465
Effect of vibrational excitation on rate parameters of atmospheric reactions
[AD-A190464] 15 p2094 N88-22477
Surface ozone and ozonesounding results from the ABLE-2B expedition to Amazonia
[INPE-4523-PRE/1275] 15 p2095 N88-22484
Study of polyatomic dynamics in the atmosphere
[AD-A190964] 16 p2233 N88-23334
A theoretical model of the washout of trace gases by raindrops in the atmosphere 17 p2375 N88-24125
Ozone in the atmosphere 18 p2539 N88-25064
Laboratory experiments on atmospheric OH reactions
18 p2539 N88-25066
Effect of carbohydrate oxidation on the tropospheric HOx-system 18 p2539 N88-25067
Measurement of atmospheric OH with laser differential optical absorption spectroscopy (LDOAS)
18 p2539 N88-25068
Tropospheric OH measurements by long path absorption with rapid spectral concordance
18 p2539 N88-25069
Determination of tropospheric H concentrations by a double-pulsed UV laser method
18 p2539 N88-25070
Tropospheric OH measurement by Laser Induced Fluorescence (LIF) 18 p2540 N88-25071
Development of continuous wave laser frequency modulation of OH in tropospheric concentrations range
18 p2540 N88-25073
A primer on greenhouse gases
[DE88-007576] 19 p2689 N88-25981
Sulfur dioxide-hydrogen peroxide relationships in clean air, clouds, and precipitation
[DE88-006352] 19 p2690 N88-25990
The rate of volcanism on Venus
[NASA-CR-183039] 19 p2742 N88-26281
The solar flare of 18 August 1979: Incoherent scatter radar data and photochemical model comparisons
[DE88-007616] 19 p2743 N88-26286
Overview of the PRECP (processing of emissions by clouds and precipitation) Program
[DE88-008205] 20 p2822 N88-26741
Studies of the mechanisms and rates with which nitrogen species are incorporated into cloud water and precipitation
[PB88-193065] 20 p2826 N88-26764
Ground level hydroxyl (OH) concentration measurements by long path differential optical laser absorption
[ETN-88-92124] 20 p2855 N88-26952
Atmospheric nitrogen oxides: Their detection and chemistry
[PB88-193057] 21 p2970 N88-27642
Large-eddy simulations of concentration fluctuations
[DE88-009480] 21 p2973 N88-27660
Low density real gas flows about hypersonic vehicles
[AD-A194251] 22 p3075 N88-28253
Investigations into the properties, conditions and effects of the ionosphere
[AD-A194245] 22 p3118 N88-28528
Photochemistry of ionospheric D-region with injection of nitrogen oxides 24 p3444 N88-30499

ATMOSPHERIC CIRCULATION

NT ZONAL FLOW (METEOROLOGY)

A baroclinic wavy basic state model: Description and preliminary experiments
[KNMI-WR-87-1] 01 p0068 N88-10436
Description of NCAR (National Center for Atmospheric Research) Community Climate Model (CCM1)
[PB87-203782] 01 p0072 N88-10462
Detailed analysis of a mesoscale convective complex situation in the Carpathian Basin (Europe)
02 p0207 N88-11296
Operational practice of an air mass transformation model 02 p0208 N88-11308
Development and testing of an air-mass transformation trajectory model 02 p0209 N88-11309
An isentropic coordinate model used in a mesoscale data assimilation system 02 p0212 N88-11333
Convective scale interaction: Arc cloud lines and the development and evolution of deep convection
[NASA-CR-181469] 02 p0215 N88-11357
Heat and moisture transport in the atmospheric boundary layer
[AD-A184222] 04 p0470 N88-12904
Systematic stratospheric-tropospheric exchange viewed from isentropic coordinates 05 p0615 N88-13777
Insights into the general circulation of the lower stratosphere from TOMS 05 p0616 N88-13780
Lower-stratospheric/upper-tropospheric exchange processes associated with tropical cyclones as observed by TOMS 05 p0616 N88-13782
Environmental and convective influence on tropical cyclone development versus non-development
[AD-A185231] 05 p0627 N88-13835
Global atmospheric circulation statistics: Four year averages
[NASA-TM-100690] 05 p0628 N88-13842
Atmosphere dynamics in the equatorial meteor zone
06 p0733 N88-14508
Circulation in the mesosphere and lower thermosphere during the MAP (Middle Atmosphere Program)/WINE (Winter in the Northern Europe) period
06 p0734 N88-14514
On connection between evolution of troposphere fronts and changes of circulation regime in meteor zone
06 p0735 N88-14519
The nonlinear thermodynamics of meteors, noctilucent clouds, enhanced airglow and global atmospheric circulation 06 p0738 N88-14538
Interim review of the possibilities and opportunities for the ONR tropical cyclone motion research initiative
[AD-A185679] 06 p0746 N88-14592
The global balance of dynamic vorticity in relation to heat sources and sinks 07 p0876 N88-15316
Thunderstorms with snow: A comprehensive, empirical study of their occurrence, development and structure
[AD-A185929] 07 p0879 N88-15329
Middle atmospheric wind measurements using a medium frequency radar
[AD-A185931] 07 p0879 N88-15330
Feasibility studies of optical processing of image bandwidth compression schemes
[AD-A186073] 07 p0932 N88-15660
Orographically influenced cold fronts in a spectral approach 08 p1016 N88-16161
Numerical simulation of the flow about New Zealand
08 p1017 N88-16163
Long-term variation of total ozone
[INPE-4307-PRE/1173] 08 p1023 N88-16192
Research project on CO-induced climate change
[DE88-002352] 08 p1023 N88-16193
Large-scale dynamics of the mean flow breakdown in the stratosphere and mesosphere during the winter 1983/84 08 p1028 N88-16228
Variations of tropical circulation and associated rainfall anomalies, during 2 years of contrast
[INPE-4359-TDL/300] 08 p1039 N88-16286
Meteosat tracks Karman vortex streets in the atmosphere 09 p1128 N88-16770
Simulation of global wet and dry deposition of nitric acid in a three-dimensional chemistry-transport model
[DE87-009847] 09 p1188 N88-17116
Numerical investigation of orographically enhanced instability
[AD-A186841] 09 p1189 N88-17125
The effects of a geomagnetic storm on thermospheric circulation
[AD-A186638] 09 p1190 N88-17128
Numerical simulation of thermally generated mountain-foreland circulation
[DFVLR-FB-87-30] 09 p1190 N88-17132
Interaction of the cold conveyor belt with polar jet streaks
[AD-A186774] 09 p1192 N88-17145
Development of a physically-based general circulation model parameterization of clouds and their radiative interactions
[DE88-004060] 09 p1194 N88-17154
Persistence characteristics of 500 mb blocking and zonal flows in the mid-latitudes of the Northern and Southern Hemispheres 10 p1353 N88-18088
Application of satellite data in observational and theoretical studies of the evolving structure of baroclinic waves
[NASA-CR-179277] 10 p1354 N88-18091
Northern winter circulations for the period 1974-1983
[AD-A187779] 11 p1511 N88-19028
Analysis of quasi-geostrophic forcing during the AIMCS (Airborne Investigations of Mesoscale Convective System) Project. Volume 1: Discussion
[PB88-133095] 12 p1646 N88-19860
Sound propagation through a turbulent atmosphere: Experimental techniques and data analysis
[AD-A188891] 12 p1688 N88-20094
Negative viscosity in global circulations
13 p1786 N88-20685
Low-order spectral models of atmospheric circulation: A survey
[CWI-AM-R8705] 13 p1797 N88-20748
Seasonal variations and excitation mechanisms of the equatorially trapped waves 13 p1798 N88-20751
Model validation research: Comparison of simulated and observed climate patterns for the past 18,000 years
[DE88-004945] 13 p1800 N88-20759
Sample models of steady and low frequency circulations in the tropical atmosphere, with application to tropical air-sea interactions 13 p1801 N88-20764
Northern Hemisphere circulation and the principal components of subsequent summer patterns in North America and West Africa 13 p1801 N88-20765
Planetary scale barotropic spectral model
13 p1801 N88-20766
Study of passages of cross-equatorial current during southern monsoon 14 p1900 N88-21347
Introduction to the dynamics of the ocean and the atmosphere 14 p1935 N88-21537
The atmosphere as a component of the climate system: Structure and variability 14 p1935 N88-21540
Adiabetic formation of large-scale models of the atmosphere 14 p1935 N88-21541
Representation of physical processes in global atmospheric models 14 p1935 N88-21542
Parameterization of radiation in a general circulation model 14 p1935 N88-21543
Sea surface temperatures of winter 1982-83 and their effect on atmospheric circulation
14 p1936 N88-21546
Lidar active remote sensing. Applications to the atmosphere 14 p1936 N88-21547
Wind and buoyancy driven ocean circulation
14 p1938 N88-21564
Tropical and monsoonal studies
[AD-A188387] 14 p1947 N88-21611
Stellar scintillometer atmospheric optical turbulence profiling experiment: A qualitative comparison of two identical instruments at AMOS (Air Force Maui Optical Station), 1985
[AD-A190589] 15 p2094 N88-22479
Aerodynamic aspects of the Amazon Forest
[INPE-4445-TDL/313] 15 p2098 N88-22501
Tropical circulations and the associated rainfall anomalies during two contrasting years
[INPE-4506-PRE/1261-REV] 15 p2098 N88-22502
Ocean general circulation models: Report on proceedings of a meeting of ocean and climate modelers
[DE88-005530] 15 p2099 N88-22504
Utilization of dense packed planar acoustic echosounders to identify turbulence structure in the lowest levels of the atmosphere
[AD-A191006] 16 p2233 N88-23335
Global atmospheric circulation statistics, 1000-1 mb
[PB88-168240] 16 p2234 N88-23340
Nonlinear normal mode initialization of the NCAR (National Center for Atmospheric Research) CCM (Community Climate Model)
[PB88-171814] 16 p2235 N88-23347
The role of vortex structure in tropical cyclone motion
[AD-A190961] 16 p2235 N88-23351
Geostrophic flow in the central Bering Sea, Fall 1986 and Summer 1987
[PB88-174354] 16 p2237 N88-23360
Open cell associated with warm advection
17 p2351 N88-24010
A system for determination of wind fields using geostationary meterological satellites
17 p2360 N88-24056
On regime selection in global atmospheric flow
17 p2374 N88-24119
Cloud cover determination in polar regions from satellite imagery
[NASA-CR-182906] 17 p2375 N88-24123
Analysis of a six-component barotropic spectral model: Chaotic motion, predictability and vacillation — atmospheric circulation
[CWI-AM-R8710] 18 p2542 N88-25090
Cluster analysis of multiple planetary flow regimes
[NASA-CR-182931] 18 p2594 N88-25418
US participation in the TOGA (Tropical Ocean and the Global Atmosphere) Program: A research strategy
[DE88-010986] 19 p2681 N88-25938
ECMWF (European Centre for Medium Range Weather Forecasts) global analyses 1979-1986: Circulation statistics and data evaluation
[PB88-178165] 19 p2692 N88-26001
Tracer water transport and subgrid precipitation variation within atmospheric general circulation models
[NASA-CR-182897] 20 p2823 N88-26745
Circulation statistics from seasonal and perpetual January and July simulations with the NCAR (National Center for Atmospheric Research) Community Climate Model (CCM1):R15
[PB88-192620] 20 p2823 N88-26748
Photon limited image processing in the space-time domain
[AD-A193142] 21 p2972 N88-27655
Intercomparison of NMC (National Meteorological Center) and ECMWF (European Centre for Medium Range Weather Forecasts) global analyses: 1980-1986
[PB88-196548] 21 p2974 N88-27668

Surface energy balance of three general circulation models: Current climate and response to increasing atmospheric CO2
[DE88-010967] 21 p2975 N88-27673
Beaufort sea mesoscale circulation study: Hydrography helicopter operations, April 1987
[PB88-203658] 21 p2976 N88-27681
The 1986-87 Pacific warm episode: Oceanic and Atmospheric features 22 p3120 N88-28535
The observed dynamical structure of low frequency variabilities 22 p3120 N88-28541
Climatology of various synoptic systems over the tropical North Pacific 22 p3121 N88-28542
The dynamics and thermodynamics of a 30-60 day oscillation 22 p3121 N88-28543
Aspects of the 30-60 day oscillation in a GCM simulation 22 p3121 N88-28545
Some diagnostic results concerning the tropical 40-50 day oscillation 22 p3121 N88-28546
Low frequency variability of SST and its relationship to atmospheric forcing 22 p3122 N88-28554
Recent secular changes in the wintertime circulation of the Southern Hemisphere 22 p3122 N88-28555
On the energy source of 1982-83 ENSO episode simulated by the NCAR community climate model 22 p3122 N88-28556
Variations in the atmosphere associated with the 11-year solar cycle 22 p3122 N88-28557
Some evidence for a Northern Hemispheric extratropic trigger mechanism of ENSO events 22 p3123 N88-28558
Persistence of North Pacific Sea surface temperature and atmospheric flow patterns 22 p3123 N88-28559
On the impact of low-latitude anomalous forcing on local and remote circulation: Winters(DJF) 1978/79 to 1986/87 22 p3123 N88-28560
Northern Hemisphere 700 mb teleconnections based on half-monthly mean anomaly data stratified by season and by sign 22 p3123 N88-28561
An observational study of interaction between large scale tropical cumulus convection and the equatorial circulation anomalies 22 p3124 N88-28564
Factors influencing summer temperatures and precipitation in the southwest 22 p3124 N88-28565
Another approach for forecasting forecast skill 22 p3126 N88-28580
Theoretical and practical limits of predictability of the NMC medium-range model 22 p3127 N88-28586
On climate prediction for India 22 p3127 N88-28590
Characteristics of regression equations for specifying monthly precipitation amounts over the United States from the field of concurrent mean 700 mb heights 22 p3127 N88-28591
Observed normal mode structure of low frequency oscillations 22 p3128 N88-28595
Development of an adjustable buoyancy balloon tracer of atmospheric motion. Phase 3: Refinement of the operational prototype system
[PB88-190764] 23 p3231 N88-29230
Atmospheric angular momentum and length of day
[AD-A194505] 23 p3233 N88-29238
Regional intercomparisons of General Circulation Model predictions and historical climate data: CO2
[DE88-010416] 23 p3235 N88-29248

ATMOSPHERIC COMPOSITION

NT ATMOSPHERIC MOISTURE
NT IONOSPHERIC COMPOSITION

NBS (National Bureau of Standards) research reports (April 1987)
[PB87-210258] 01 p0018 N88-10111
Carbon monoxide (CO) concentration in the air as a purity parameter
[INPE-4232-PRE/1107] 01 p0067 N88-10429
An instrument for the quasi-continuous determination of atmospheric soot content
[DFVLR-FB-87-04] 01 p0068 N88-10433
Diagnostics of atmospheric chemistry through ozone measurement
[INPE-4230-PRE/1105] 01 p0068 N88-10437
Kinetics investigations of atmospheric chemical reactions
[PB87-213351] 01 p0069 N88-10439
Airborne lidar studies of Arctic polar stratospheric clouds 01 p0069 N88-10443
Contribution of bubbles and waves to air-sea CO2 flux, with implications for remote sensing
[PB87-203980] 01 p0073 N88-10467
ECC (Electrochemical Concentration Cell) ozonesonde observations at South Pole, Antarctica during 1986
[PB87-207502] 02 p0197 N88-11228
Stratospheric particles: Synchrotron X-ray fluorescence determination of trace element contents
[DE87-012482] 02 p0198 N88-11234
Convective cross section analysis
[PB87-204566] 02 p0216 N88-11361
Spectroscopic and retrieval studies in support of SCRIBE (Stratospheric Cryogenic Interferometer Balloon Experiment)
[AD-A184037] 03 p0351 N88-12216
Preliminary experimental results of gas recycling subsystems except carbon dioxide concentration 03 p0359 N88-12261
Spacecraft Fire Safety
[NASA-CP-2476] 04 p0406 N88-12520
Inerting and atmospheres 04 p0406 N88-12524
Fire-related medical science 04 p0406 N88-12525
Spacecraft material flammability testing and configurations 04 p0407 N88-12529
OH(A-X) fluorescence from photodissociative excitation of HO2 at 157.5 nm
[NASA-CR-181580] 05 p0563 N88-13429
TOMS: The Antarctic ozone hole and ozone trends 05 p0615 N88-13775
October lower stratospheric Antarctic temperature and total ozone from 1979-1985 05 p0615 N88-13776
Photochemical ozone overburden correction 05 p0615 N88-13778
Analysis of the breakdown of the Antarctic circumpolar vortex using TOMS ozone data 05 p0615 N88-13779
Insights into the general circulation of the lower stratosphere from TOMS 05 p0616 N88-13780
Lower-stratospheric/upper-tropospheric exchange processes associated with tropical cyclones as observed by TOMS 05 p0616 N88-13782
Volcanic eruption detection with TOMS 05 p0618 N88-13793
Analysis of SO2 signals in SBUV/TOMS data 05 p0618 N88-13794
Comparison of ground based and TOMS measurements of SO2 from volcanic emissions 05 p0618 N88-13795
Use of satellite data in volcano monitoring 05 p0618 N88-13797
Complementary information between UV and IR for remote sensing of total ozone 05 p0619 N88-13800
First flight of the ATMOS instrument during the Spacelab 3 Mission, April 29 through May 6, 1985
[NASA-CR-182360] 06 p0728 N88-14482
A review of atmospheric ozone and current thinking on the Antarctic ozone hole
[AD-A185608] 06 p0732 N88-14501
Lidar investigations of M-zone 06 p0741 N88-14558
Description of data on the Nimbus 7 LIMS map archive tape: Water vapor and nitrogen dioxide
[NASA-TP-2761] 06 p0744 N88-14572
Use of back air trajectories in interpreting atmospheric chemistry data: A review and bibliography
[PB88-102108] 07 p0876 N88-15312
Hydrogen chloride measurements in launch-vehicle exhaust clouds
[DE87-011552] 08 p0964 N88-15837
Mechanisms of cloud layer formation in Venusian atmosphere 08 p1004 N88-16087
Atmosphere of Venus in north polar area based on radio transmission data from Venera-15 and Venera-16 spacecraft 08 p1005 N88-16090
Characteristics and climatic relevance of the atmospheric aerosol components 08 p1017 N88-16164
Lidar metal density measurements in the upper atmosphere 08 p1027 N88-16219
An advanced visible-UV spectrometer for atmospheric composition measurements 08 p1029 N88-16231
Current issues in atmospheric change
[NASA-CR-182406] 08 p1039 N88-16287
A rapid method for the computation of equilibrium chemical composition of air to 15000 K
[NASA-TP-2792] 09 p1140 N88-16830
An infrared grating spectrometer for GIRL
[ETN-88-91071] 09 p1167 N88-16997
Concept, construction, and experimental testing of a polychromator for a Raman lidar for the simultaneous telemetering of carbon dioxide and water vapor, relative to oxygen
[GKSS-87/E/20] 09 p1191 N88-17134
Model investigations of atmospheric ammonia scavenging
[DE88-002337] 09 p1194 N88-17153
Tropospheric ultraviolet radiation: Assessment of existing data and effect on ozone formation
[PB88-130133] 10 p1354 N88-18095
Gas-phase photoelectron spectroscopy of metals and metal oxides of importance in the upper atmosphere
[AD-A187771] 11 p1511 N88-19027
The influence of atmospheric thermal tides on diurnal variations in chemical constituents in the mesosphere 11 p1512 N88-19035
Vega-1 and Vega-2 automatic stations: Functioning of landing modules in Venusian atmosphere 13 p1725 N88-20313
Research on absorption of UV radiation in Venusian atmosphere from Vega-1 and Vega-2 landing modules 13 p1725 N88-20316
Gas-chromatographic analysis of products of thermal reactions of aerosol in Venusian cloud layer on Vega-1 and Vega-2 automatic interplanetary stations 13 p1725 N88-20318
Chemical composition and structure of Venusian clouds determined from results of roentgenoradiometric experiments carried out by landing modules of Vega-1 and Vega-2 automatic interplanetary stations 13 p1726 N88-20320
Effect of nitrogen dioxide release on thermosphere 13 p1789 N88-20704
An automated ozone photometer
[NASA-TM-100064] 14 p1908 N88-21404
Lidar active remote sensing. Applications to the atmosphere 14 p1936 N88-21547
Report of Atmospheric-Canopy Exchange Panel
[DE88-004478] 14 p1944 N88-21597
Ground-based column abundance measurements of atmospheric hydroxyl
[NASA-CR-182676] 14 p1944 N88-21598
Analysis of meteorological conditions and haze distribution for the Second Arctic Gas and Aerosol Sampling Program (AGASP 2), March-April 1986
[PB88-164140] 14 p1948 N88-21618
Assessment of crop loss from air pollutants: Meteorology-atmospheric chemistry and long range transport
[PB88-146857] 15 p2089 N88-22448
Surface CO results from the ABLE-2B expedition to Amazonia
[INPE-4501-PRE/1258] 15 p2093 N88-22469
Study of polyatomic dynamics in the atmosphere
[AD-A190964] 16 p2233 N88-23334
Understanding CO2 and climate
[PB88-167655] 16 p2234 N88-23341
Information analysis of integral equations in remote sensing of atmospheric aerosols 18 p2532 N88-25022
Oxidation and reduction rates for organic carbon in the Amazon mainstream tributary and floodplain, inferred from distributions of dissolved gases
[NASA-CR-182943] 18 p2538 N88-25062
Trace gas measurements in the troposphere using tunable diode lasers 18 p2540 N88-25072
Stratospheric positive ion composition measurements and acetonitrile detection: A consistent picture
[AERONOMICA-ACTA-A-326-1987] 18 p2542 N88-25084
A primer on greenhouse gases
[DE88-007576] 19 p2689 N88-25981
Diagnostic studies of the HxOy-NzOy-O3 photochemical system using data from NASA GTE field expeditions
[NASA-CR-183038] 19 p2689 N88-25984
Meteorological aspects of wet deposition in Southern Finland
[FMI-3] 19 p2693 N88-26007
Physiological effects on man of long duration confinement in a carbon dioxide enriched environment 19 p2695 N88-26017
Measurement of HO2 and other trace gases in the stratosphere using a high resolution far-infrared spectrometer at 28 KM
[NASA-CR-180400] 20 p2821 N88-26737
Wavenumber spectra from THIR 6.7 micron water vapor data 20 p2824 N88-26756
An efficient model for changes of global climate and composition of the atmosphere due to human activities
[ETN-88-92359] 20 p2827 N88-26775
Space infrared telescope facility project
[NASA-CR-183058] 20 p2883 N88-27121
Ultraviolet geometric albedo of Uranus
[NASA-CR-183099] 20 p2885 N88-27136
ECC (Electrochemical Concentration Cell) ozonesonde observations at South Pole, Antarctica during 1987
[PB88-202015] 21 p2970 N88-27644
National air toxics information clearinghouse: NATICH data base users guide for data viewing, February 1988
[PB88-197470] 21 p2970 N88-27645
National ambient Volatile Organic Compounds (VOCs) data base update, documentation
[PB88-195631] 21 p2971 N88-27646
Photochemical oxidant formation: Overview of current knowledge and emerging issues
[PB88-195235] 21 p2971 N88-27647
Atmospheric deposition of nitrate to the ocean surface 23 p3231 N88-29227
Forty-eight-inch lidar aerosol measurements taken at the Langley Research Center, May 1974 to December 1987
[NASA-RP-1209] 23 p3232 N88-29234

Laboratory evaluation and application of microwave absorption properties under simulated conditions for planetary atmospheres
[NASA-CR-182443] 23 p3300 N88-29653
Recent measurements of ozone in the Amazon forests
[INPE-4494-PRE/1258] 24 p3389 N88-30185
Recent observations of carbon monoxide in the Amazon Rain Forest
[INPE-4478-PRE/1245] 24 p3390 N88-30186

ATMOSPHERIC CONDITIONS
U METEOROLOGY

ATMOSPHERIC CONDUCTIVITY
The influence of conductivities consistent with field-aligned currents on high-latitude convection patterns
[TRITA-EPP-88-02] 22 p3119 N88-28533

ATMOSPHERIC CORRECTION
The absolute radiometric calibration of the advanced very high resolution radiometer
[NASA-CR-182755] 14 p1941 N88-21584
Atmospheric corrections for in-flight satellite radiometric calibration
[AD-A196124] 24 p3391 N88-30194

ATMOSPHERIC DENSITY
Models of high spatial frequency thermal blooming instabilities
[DE87-014280] 01 p0052 N88-10330
Mesoscale density variability in the mesosphere and thermosphere: Effects of vertical flow accelerations
06 p0736 N88-14529
Aerosol optical depth and ratios of diffuse-sky to total solar irradiance measured from aircraft following the eruption of El Chichon
[PB88-100789] 07 p0878 N88-15326
Investigation of the feasibility of an analytical method of accounting for the effects of atmospheric drag on satellite motion 07 p0923 N88-15608
Atmosphere of Venus in southern polar area
08 p1005 N88-16088
Atmosphere of Venus in south polar area based on radio transmission data 08 p1005 N88-16089
Density flows at the mountain edge
08 p1016 N88-16156
Improved resolution atmospheric density measurements based on simulations 08 p1027 N88-16221
A method of atmospheric density measurements during space shuttle entry using ultraviolet-laser Rayleigh scattering
[NASA-TM-100056] 15 p2069 N88-22337
A survey of denser-than-air atmospheric dispersion models
[DE88-006626] 15 p2092 N88-22467
Three-dimensional temperature fields in the atmosphere up to 50 km altitude
[ETN-88-92150] 18 p2542 N88-25089
Wave structures in thermospheric density from satellite electrostatic triaxial accelerometer measurements
[AD-A194134] 23 p3233 N88-29240
Approximation of atmospheric density by Chebyshev polynomials in predicting motion of low artificial earth satellites 24 p3445 N88-30503

ATMOSPHERIC DIFFUSION
Opportunities for nowcasting air pollution episodes and accidental toxic and radioactive releases
02 p0210 N88-11317
Real-time evaluation and prediction of coastal dispersion near the SW tip of Africa --- effluents
02 p0210 N88-11318
A computer code to calculate line by line atmospheric transmission spectra on a microcomputer
[NASA-TM-100686] 05 p0554 N88-13372
Atmospheric diffusion at coastal site in presence of sea-breeze
[DE88-700038] 07 p0876 N88-15314
Development of an atmospheric diffusion evaluation method incorporating topographical effects. Part 1: Literature review of atmospheric diffusion models incorporating terrain effects
[DE88-753104] 20 p2822 N88-26742
Wind tunnel study of atmospheric diffusion in unstable stratified boundary layer. Part 2: Characteristic scale and diffusion
[DE88-753109] 20 p2823 N88-26749
Global vertical mass transport by clouds: A two-dimensional model study
[CM-74] 24 p3391 N88-30192

ATMOSPHERIC EFFECTS
Analysis of free molecular effects on the attitude of satellites in geostationary transfer orbit. Part 2: Force and torque measurement in free molecular wind tunnel tests
[DFVLR-IB-222-86-A/07] 01 p0014 N88-10078
Object-dependent atmospheric influence on LANDSAT recordings 01 p0065 N88-10420
Computational method for orbit improvement for short arc observations of artificial satellites
03 p0269 N88-11690
The atmosphere of Mars and optical communications
04 p0434 N88-12692
Considering refraction in leveling with laser plane
04 p0462 N88-12857
The effect of environment on low cycle fatigue properties in HSLA steel 05 p0605 N88-13705
Fatigue crack propagation in Al-Zn-Mg bicrystals and its dependence on the environment
05 p0605 N88-13707
Environmental fracture toughness and static fatigue crack propagation of silica glass
05 p0606 N88-13716
Environmentally assisted fatigue crack growth
05 p0608 N88-13731
AIS-2 radiometry and a comparison of methods for the recovery of ground reflectance
05 p0611 N88-13757
Calibrating AIS images using the surface as a reference 05 p0612 N88-13760
Causes of spurious features in spectral reflectance data 05 p0614 N88-13769
Results on the low elevation angle propagation experiment, part 1
[TUD-R-328] 06 p0693 N88-14250
Induced turbulence in aerosol-loaded atmospheres, Jun. 1987
[DE87-014724] 09 p1192 N88-17141
User's guide for the HF (High Frequency) broadcast antenna design and validation summary programs
[PB88-116124] 10 p1317 N88-17875
The role of analytical chemistry in assessing atmospheric effects of combustion
[DE88-003909] 10 p1352 N88-18082
Proceedings of the Forest-Atmosphere Interaction Workshop
[CONF-8510250] 12 p1641 N88-19824
Analysis of spectral reflectance characteristics of targets under satellites and automatic cloud recognition
13 p1755 N88-20498
The spreading and mixing of dense gas clouds in still air
[KNMI-WR-87-12] 16 p2230 N88-23320
The effects of solar cycle and latitude dependence on the formation of ionospheric C layer
[INPE-4342-TDL/293] 16 p2232 N88-23332
Spectral measurements for correcting LANDSAT data for atmospheric effects 17 p2353 N88-24020
Spectral measurements for correcting LANDSAT data for atmospheric effects 17 p2362 N88-24066
Analysis of the parameters responsible for the variations of the illumination conditions in the LANSAT data
17 p2362 N88-24070
Evaluation of atmospheric effects for operational tactical decision aid
[AD-A194205] 23 p3232 N88-29236

ATMOSPHERIC ELECTRICITY
NT AURORAL ELECTROJETS
NT EQUATORIAL ELECTROJET
NT IONOSPHERIC CURRENTS
F-layer polar cap arcs
[AD-A186592] 09 p1190 N88-17127
The growth potential of corona discharges from aircraft flying in precipitation
[AD-A190507] 15 p2094 N88-22478
Atmospheric Science and Remote Sensing Laboratory
[NASA-CR-179290] 16 p2236 N88-23355
Finite element simulation of the atmosphere's electromagnetic response to charge perturbations associated with lightning 17 p2375 N88-24124

ATMOSPHERIC EMISSION
U AIRGLOW

ATMOSPHERIC ENTRY
NT HYPERSONIC REENTRY
NT REENTRY
NT SPACECRAFT REENTRY
Guidance and control strategies for aerospace vehicles
[NASA-CR-181579] 05 p0643 N88-13935
Atmospheric entry heating of cosmic dust
06 p0794 N88-14865
A simplified streamline swallowing procedure for the windward meridian of axisymmetric blunt bodies
[AD-A188413] 12 p1626 N88-19732
Guidance and control strategies for aerospace vehicles
[NASA-CR-183032] 18 p2467 N88-24644
A design study of onboard navigation and guidance during aerocapture at Mars
[NASA-CR-172053] 18 p2469 N88-24654
Investigation of the validity of the non-rotating planet assumption for three-dimensional earth atmospheric entry
[AD-A194877] 24 p3331 N88-29829

ATMOSPHERIC HEAT BUDGET
Climatology and space observations
[ISBN-2-85-428179-9] 14 p1935 N88-21536
Introduction to the dynamics of the ocean and the atmosphere 14 p1935 N88-21537
Parameterization of radiation in a general circulation model 14 p1935 N88-21543
Carbon dioxide and climate 14 p1936 N88-21545
The Earth radiation budget and its spatial and temporal variations 14 p1936 N88-21548
The role of radiation transfer in climate modification
14 p1936 N88-21549
Continental surface processes and water cycle
14 p1937 N88-21555
Sensitivity of general circulation models to surface processes 14 p1937 N88-21556

ATMOSPHERIC HEATING
Possible dynamical mechanisms for the Martian polar warming phenomenon
[NASA-CR-181454] 02 p0254 N88-11605
Structure of stably stratified atmospheric surface layer in presence of heat-releasing admixture
04 p0462 N88-12856
Flux tube dynamics and solar/stellar redshift measurements 04 p0503 N88-13095
Observational constraints and evidence for saturation
04 p0503 N88-13097
Heating of stellar chromospheres and coronae: Evidence for non-magnetic basal heating
04 p0503 N88-13098
Atmospheres of stars in the limits of thin and thick convection zones: The M dwarfs
04 p0505 N88-13104
Magnetic flux tubes as sources of wave generation
04 p0505 N88-13108
Statistical properties of small high-velocity events in the solar transition region 04 p0506 N88-13112
Atmospheric heating from optical absorption by aerosols
[DE88-002654] 07 p0878 N88-15327
The role of anabatic winds in the heating of valleys
08 p1014 N88-16144
The role of water in the thermal balance of the coma
14 p1999 N88-21916
Extratropical response to tropical heating as a function of period of model integrations
22 p3125 N88-28577
Observed normal mode structure of low frequency oscillations 22 p3128 N88-28595
Ionosonde studies of field-aligned irregularities during high-power HF heating at Arecibo
[AD-A195848] 24 p3401 N88-30256

ATMOSPHERIC IMPURITIES
U AIR POLLUTION

ATMOSPHERIC IONIZATION
NT AURORAL IONIZATION
Satellite environment: Polar orbits
03 p0272 N88-11713
Elementary process and meteor train spectra
06 p0732 N88-14504
Meteor matter interaction with the Earth's atmosphere and the ionospheric E-region structure
06 p0738 N88-14537
Meteor velocity distribution and an optimum monitoring mathematical model 06 p0739 N88-14546
TOTAL: A new instrument to study turbulent parameters in the mesosphere and lower thermosphere
08 p1029 N88-16234
Theoretical plasma physics research of active space experiments
[AD-A192075] 18 p2577 N88-25309

ATMOSPHERIC LASERS
Atmospheric backscatter at 10.6 microns; a compendium of measurements made outside the United Kingdom by the airborne LATAS coherent laser radar velocimeter
[RSRE-87002] 12 p1631 N88-19763
Distortion of wideband carbon dioxide laser radar waveforms due to atmospheric dispersion and absorption
[AD-A188687] 12 p1632 N88-19771
Atmospheric propagation of laser beams
[AD-A191447] 18 p2520 N88-24952

ATMOSPHERIC LOADING
U POLLUTION TRANSPORT

ATMOSPHERIC MODELS
NT REFERENCE ATMOSPHERES
A study of carbon monoxide distribution determinations for a global transport model
[NASA-CR-181423] 01 p0067 N88-10432
A baroclinic wavy basic state model: Description and preliminary experiments
[KNMI-WR-87-1] 01 p0068 N88-10436
Description of NCAR (National Center for Atmospheric Research) Community Climate Model (CCM1)
[PB87-203782] 01 p0072 N88-10462

Contribution of bubbles and waves to air-sea CO2 flux, with implications for remote sensing
[PB87-203980] 01 p0073 N88-10467
The air flow on hills from models and experiments
[BMFT-FB-T-86-175] 02 p0198 N88-11236
Mesoscale Analysis and Forecasting: Incorporating Nowcasting
[ESA-SP-282] 02 p0199 N88-11239
On the role of snow in the redistribution of precipitation by small scale topography 02 p0203 N88-11267
Conceptual models of Baiu front and Baiu frontal disturbances in multiscale characteristics — East Asia
02 p0203 N88-11271
A one-dimensional model of thermally-driven coastal front evolution 02 p0204 N88-11274
The role of low-level cooling in a conceptual model of the Australian summertime cool change: Implications for very-short-range forecasting 02 p0204 N88-11275
On the interaction between radar and satellite image nowcasting systems and mesoscale numerical models
02 p0204 N88-11277
Satellite imagery and conceptual models in mesoscale forecasting 02 p0205 N88-11282
Simplified models for use in an operational short range forecasting system 02 p0206 N88-11289
The studies of physical models on hailstorms and their applications in nowcasting 02 p0207 N88-11300
Forecasting boundary layer clouds and fog: A review of operational numerical models
02 p0208 N88-11307
Operational practice of an air mass transformation model 02 p0208 N88-11308
Development and testing of an air-mass transformation trajectory model 02 p0209 N88-11309
Two-dimensional numerical modeling of the life cycle of fog 02 p0209 N88-11311
The Norwegian mesoscale Numerical Weather Prediction (NWP) system 02 p0210 N88-11320
Preliminary results from real data experiments with the NRL mesoscale numerical model
02 p0211 N88-11323
Validation of a three dimensional numerical model of the sea breeze in complex terrain
02 p0211 N88-11325
The mesoscale numerical model for heavy rainfall forecasting in Yangtze River Valley, China
02 p0211 N88-11326
The impact on short-term precipitation forecast skill of time-dependent lateral and lower boundary conditions within a meso-beta numerical cloud prediction model
02 p0211 N88-11327
Mesoscale analysis and nowcasting via a numerical model coupled with satellite sounder data
02 p0211 N88-11328
A preliminary demonstration of the use of boundary-layer models of flow in complex terrain for high resolution surface wind forecasting 02 p0212 N88-11330
An isentropic coordinate model used in a mesoscale data assimilation system 02 p0212 N88-11333
Strategies for using mesoscale data in an operational mesoscale model 02 p0212 N88-11335
Methods of incorporating satellite data into mesoscale numerical forecast models 02 p0212 N88-11336
Toward optimizing the use of data for operational mesoscale forecasting at the National Meteorological Center 02 p0213 N88-11337
Assimilation of high resolution TOVS data into a mesoscale NWP model — numerical weather prediction (NWP) 02 p0213 N88-11338
Impact of a direct assimilation of satellite-inferred precipitation rates into a regional meteorological model
02 p0213 N88-11342
Initialization experiments with the NMC nested grid model — National Meteorological Center (NMC)
02 p0213 N88-11343
The future of data in mesoscale numerical models
02 p0214 N88-11344
Simulation of mesoscale satellite sounder data from a mesoscale numerical model 02 p0214 N88-11345
The challenge of using mesoscale data in mesoscale numerical models 02 p0214 N88-11346
The challenge of using mesoscale data in mesoscale numerical models: A position paper
02 p0214 N88-11347
Comments on the challenge of using mesoscale data in mesoscale numerical models
02 p0214 N88-11348
Four-dimensional initialization of mesoscale models
02 p0214 N88-11349
Windfield simulations from a hierarchy of nested meso- and micrometeorological models
02 p0215 N88-11351
Documentation of the regional climate model based on FITNAH
[DFVLR-MITT-87-07] 02 p0216 N88-11358
Thermal atmospheric models
02 p0253 N88-11599
Quasi-thermal models 02 p0253 N88-11600
M dwarfs: Theoretical work 02 p0253 N88-11602
A model for the convective atmospheric boundary layer during the winter in the Khartoum Region (Sudan)
[R-822-A] 03 p0353 N88-12225
Structure of stably stratified atmospheric surface layer in presence of heat-releasing admixture
04 p0462 N88-12856
Banded ion morphology 04 p0468 N88-12892
User's guide to NCAR (National Center for Atmospheric Research) CCM1
[PB87-224366] 04 p0469 N88-12899
A review of parameterizations of microphysical processes in clouds for application in models of regional atmospheric deposition
[DE88-000451] 04 p0471 N88-12909
Application of dynamic atmosphere models to the analysis of angular diameter observations of Mira variables 04 p0515 N88-13168
Analysis of geophysical data bases and models for spacecraft interactions
[AD-A184809] 05 p0555 N88-13375
MODTRAN: A moderate resolution model for LOWTRAN
[AD-A185384] 05 p0574 N88-13503
Ozone, jet streaks and severe weather
05 p0616 N88-13781
Application of TOMS data to weather analysis models
05 p0617 N88-13787
The polar ionosphere and interplanetary field
[AD-A185386] 05 p0624 N88-13822
On-site meteorological program guidance for regulatory modeling applications
[PB87-227542] 06 p0731 N88-14498
A method to obtain a wind model for the boundary layer in a representative tropical region
[R-818-D] 06 p0743 N88-14569
Integrated systems with applications to the multi-phases of the ephemerides, physics and methematics of the upper atmosphere
[AD-A185748] 06 p0743 N88-14570
An Earth radiation budget climate model
[NASA-CR-182368] 06 p0744 N88-14578
Report of the second session of the CAS/JSC working group on numerical experimentation — weather forecasting
[WMO/TD-168] 06 p0745 N88-14579
A survey study of energy distribution in component stars of Algol-type binary systems 06 p0801 N88-14901
Dynamics Explorer guest investigator
[NASA-CR-181494] 07 p0878 N88-15325
An introduction to single point closure methodology
08 p0986 N88-15973
Turbulence models for practical applications
08 p0986 N88-15974
Examples of turbulence-model applications
08 p0987 N88-15975
Direct and large eddy simulation of turbulence. Summary of the state of art 1987 08 p0987 N88-15977
Synoptic perturbations and climate
08 p1016 N88-16158
Numerical modeling of radiation fog
08 p1017 N88-16166
Research project on CO-induced climate change
[DE88-002352] 08 p1023 N88-16193
A comparison of multi-layer meso-alpha MLAM model results with surface and aircraft observations from CAPTEX
[DE88-000549] 09 p1188 N88-17118
Numerical investigation of orographically enhanced instability
[AD-A186841] 09 p1189 N88-17125
The effects of a geomagnetic storm on thermospheric circulation
[AD-A186638] 09 p1190 N88-17128
The accuracy of the radiation parameterization in mesoscale models
[DFVLR-IB-553-85/11] 09 p1190 N88-17133
Simulations of thermally induced winds and cross flow situations
[MITT-57] 09 p1193 N88-17148
A Lagrangian model of dry thermals
[DM-50] 09 p1193 N88-17150
Development of an engineering model atmosphere for Mars
[NASA-CR-182462] 09 p1263 N88-17568
Theoretical and observational problems with Holes in the far UV dayglow
[AD-A188190] 10 p1355 N88-18100
Minimum Energy Routing through Interactive Techniques (MERIT) modeling
[NASA-CR-182535] 10 p1356 N88-18105
A spherical, non-LTE, blanketed model stellar atmosphere for Phi Cas (FOIa)
10 p1428 N88-18528
Computer architecture for research in meteorology and atmospheric chemistry
[PB88-145313] 11 p1510 N88-19020
Initial results with the LLNL 2-D chemical-radiative-transport model of the troposphere and stratosphere
[DE88-004355] 11 p1512 N88-19033
The influence of atmospheric thermal tides on diurnal variations in chemical constituents in the mesosphere
11 p1512 N88-19035
An analytical method for the determination of the average horizontal wind velocities across two-dimensional hills
[ISBN-3-923624-06-9] 11 p1515 N88-19048
Model of limited area of 5 layers for numerical weather forcasting
[INPE-4324-RPE/551] 11 p1516 N88-19053
Comparison of simulation modeling and satellite techniques for monitoring ecological processes
[NASA-CR-182592] 12 p1641 N88-19825
Enhancements to the atmospheric transmittance/radiance program FASCODE
[AD-A188863] 12 p1643 N88-19839
National Severe Storms Laboratory, fiscal year 1987
[PB88-140108] 12 p1647 N88-19863
Spatial and temporal monitoring of the Jovian atmosphere 12 p1711 N88-20240
A polarimetric rain backscatter model developed for coherent polarization diversity radar applications
13 p1759 N88-20520
Low-order spectral models of atmospheric circulation: A survey
[CWI-AM-R8705] 13 p1797 N88-20748
Dynamical modeling of marine boundary layer convection 13 p1797 N88-20750
Computer simulation of tropospheric chemistry
[JUEL-2144] 13 p1798 N88-20756
Model validation research: Comparison of simulated and observed climate patterns for the past 18,000 years
[DE88-004945] 13 p1800 N88-20759
Sample models of steady and low frequency circulations in the tropical atmosphere, with application to tropical air-sea interactions 13 p1801 N88-20764
Similarity theories and microturbulence in the atmospheric mixed layer 13 p1806 N88-20802
Model of Jovian F region ionosphere
[NASA-CR-182587] 13 p1855 N88-21105
Millimeter-wave properties of the atmosphere: Laboratory studies and propagation modeling
[PB88-164215] 14 p1905 N88-21387
Climatology and space observations
[ISBN-2-85-428179-9] 14 p1935 N88-21536
Adiabetic formation of large-scale models of the atmosphere 14 p1935 N88-21541
Representation of physical processes in global atmospheric models 14 p1935 N88-21542
Parameterization of radiation in a general circulation model 14 p1935 N88-21543
Assimilation of meteorological observations
14 p1936 N88-21544
Carbon dioxide and climate 14 p1936 N88-21545
Sea surface temperatures of winter 1982-83 and their effect on atmospheric circulation
14 p1936 N88-21546
The role of radiation transfer in climate modification
14 p1936 N88-21549
Net radiative flux at the Earth surface: Estimation from satellite observations 14 p1936 N88-21550
Satellite estimations of the solar radiation flux at the surface 14 p1936 N88-21551
Satellite retrieval of cloud cover parameters and the International Satellite Cloud Climatology Program (ISCCP) 14 p1937 N88-21552
An introduction to the parameterization of land-surface processes 14 p1937 N88-21554
Sensitivity of general circulation models to surface processes 14 p1937 N88-21556
The Hapex-Mobilhy program 14 p1938 N88-21560
Nonlinear normal mode initialization of a limited area model using nonstationary Rossby modes — numerical weather forecasting
[KNMI-WR-87-10] 14 p1947 N88-21614
A model of the anisotropic structure of the neutral gas coma of a comet 14 p1999 N88-21918
Derivation of consistent surface fixed fields for use in a global NWP model
[AD-A190131] 15 p2093 N88-22475
A study on electric fields and conductivity associated with electrified clouds in the region of South America
[INPE-4487-TDL/325] 15 p2096 N88-22486

Ocean general circulation models: Report on proceedings of a meeting of ocean and climate modelers
[DE88-005530] 15 p2099 N88-22504
WAVFLD: A program to compute ionospheric height gain functions and field strengths at VLF
[AD-A191159] 16 p2191 N88-23066
Nonlinear normal mode initialization of the NCAR (National Center for Atmospheric Research) CCM (Community Climate Model)
[PB88-171814] 16 p2235 N88-23347
Chemical kinetics and photochemical data for use in stratospheric modeling evaluation Number 8
[NASA-CR-182919] 17 p2351 N88-24012
On regime selection in global atmospheric flow
17 p2374 N88-24119
Cloud cover determination in polar regions from satellite imagery
[NASA-CR-182906] 17 p2375 N88-24123
The precipitation of energetic heavy ions into the upper atmosphere of Jupiter
[NASA-TM-101155] 17 p2452 N88-24565
Changes in the Antarctic atmosphere due to the reduction of stratospheric ozone
[ETN-88-92565] 18 p2540 N88-25074
Brunt-Doppler ducting of buoyancy waves in a temperature- and wind-stratified atmosphere
18 p2542 N88-25086
Analysis of a six-component barotropic spectral model: Chaotic motion, predictability and vacillation --- atmospheric circulation
[CWI-AM-R8710] 18 p2542 N88-25090
Photochemical and thermal modeling in the early atmosphere of the earth
[NASA-CR-183029] 18 p2543 N88-25093
Adaptive grid refinement for numerical weather prediction
[AD-A192172] 18 p2544 N88-25101
Bracknell Meteorological Office
18 p2545 N88-25107
Applications products of aviation forecast models
18 p2546 N88-25109
Comparative verification between GEM model and official aviation terminal forecasts
18 p2546 N88-25115
Computer and model changes at National Meteorological Center (NWC) 18 p2547 N88-25116
MM4 (Penn State/NCAR (National Center for Atmospheric Research)) mesoscale model version 4 documentation
[PB88-173232] 19 p2688 N88-25979
NOAA (National Oceanic and Atmospheric Administration) Meteorology Division support to the Environmental Protection Agency
[PB88-179866] 19 p2689 N88-25980
A study of the dynamics of the Intertropical Convergence Zone (ITCZ) in a symmetric atmosphere-ocean model
[NASA-TM-86220] 19 p2693 N88-26005
Verification of regional climates of GISS GCM. Part 1: Winter
[NASA-TM-100695] 19 p2694 N88-26012
Effects of atmospheric model layering on LOWTRAN 6 calculations of 8-12 micrometers near-horizon sky radiances
[AD-A192969] 20 p2791 N88-26559
Rocket measurements within a polar cap arc: Ionospheric modelling
[AD-A192381] 20 p2824 N88-26754
Diffusion of slight solar induced disturbances in the middle atmosphere
[MITT-53] 20 p2825 N88-26758
The NASA Marshall engineering thermosphere model
[NASA-CR-179359] 20 p2825 N88-26760
Influence of stable stratification on atmospheric turbulence: An experimental contribution
[ETN-88-92292] 20 p2827 N88-26772
Photochemical oxidant formation: Overview of current knowledge and emerging issues
[PB88-195235] 21 p2971 N88-27647
Approximate analytical formulae for electron density and collision frequency in the natural and nuclear-disturbed ionosphere and inner magnetosphere
[AD-A193129] 21 p2972 N88-27654
Development of radiation and cloud parameterization programs for AFGL (Air Force Geophysics Laboratory) global models
[AD-A193369] 21 p2973 N88-27658
Air-sea interaction in the vicinity of a land-sea boundary in the presence of upwelling 21 p2973 N88-27661
Surface energy balance of three general circulation models: Current climate and response to increasing atmospheric CO2
[DE88-010967] 21 p2975 N88-27673
Another approach for forecasting forecast skill
22 p3126 N88-28580
A bulk model for the unstable planetary boundary layer over the sea. A sensitivity investigation
[DM-51] 22 p3129 N88-28600
Atmospheric deposition of nitrate to the ocean surface
23 p3231 N88-29227
A model of the ionosphere in the altitude interval 50 to 4000 km. Part 1: Atomic ions (H(+), He(+), N(+), O(+))
[DFVLR-FB-88-11-PT-1] 23 p3233 N88-29241
A model of the ionosphere in the altitude interval 50 to 4000 km. Part 2: Molecular ions (N2(+), NO(+), O2(+)) and electron density
[DFVLR-FB-88-12-PT-2] 23 p3234 N88-29242
Snapshots of high-latitude electrodynamics using Viking and DMSP/F7 observations
[TRITA-EPP-88-01] 23 p3234 N88-29244
Investigations on the entropy of cloudy air
[ESA-TT-1060] 23 p3234 N88-29245
Global vertical mass transport by clouds: A two-dimensional model study
[CM-74] 24 p3391 N88-30192
Ionosonde studies of field-aligned irregularities during high-power HF heating at Arecibo
[AD-A195848] 24 p3401 N88-30256
Cloud/mesoscale model development and application studies
[AFGL-TR-87-0219] 24 p3404 N88-30269
Using nonstationary models of the atmosphere to describe satellite drag 24 p3445 N88-30502
Model representation of electron concentration distribution in outer middle-latitude ionosphere using data from Intercosmos-19 artificial earth satellite
24 p3447 N88-30513

ATMOSPHERIC MOISTURE

Diagnosing short term changes in temperature and moisture profiles from single Doppler radar
02 p0200 N88-11251
Structure and modification of winter mountain clouds in the Sierra Nevada: Nowcasting/forecasting the onset of supercooled liquid water 02 p0202 N88-11263
Effects of the large scale motion and horizontal inhomogeneity of the moist static instability on development of the mesoscale convective systems in the midlatitudes 02 p0207 N88-11297
The effect of enhanced conventional and VAS moisture analysis on RAFS short-range precipitation forecasts --- Regional Analysis and Forecasting System (RAFS)
02 p0215 N88-11352
Lidar-radiometric method for determining liquid-water content of cirrus clouds 04 p0461 N88-12854
Influence of bonding shop moisture on metal-honeycomb junctions bonded with ultra-thin adhesive films
[SNIAS-872-422-112] 05 p0558 N88-13399
Investigation of effect of silver compounds on microflora in water reclaimed from atmospheric moisture condensate in a closed environment 07 p0892 N88-15407
Method of determining atmospheric moisture content by measurement of upward radiation intensity in near IR
08 p1007 N88-16106
Characteristics and climatic relevance of the atmospheric aerosol components
08 p1017 N88-16164
Report of the Workshop on Space Systems Possibilities for a Global Energy and Water Cycle Experiment
[WCP-137] 09 p1193 N88-17147
Determination of atmospheric moisture structure from high resolution MAMS radiance data
11 p1515 N88-19049
Climatology and space observations
[ISBN-2-85-426179-9] 14 p1935 N88-21536

ATMOSPHERIC OPTICS

Object-dependent atmospheric influence on LANDSAT recordings 01 p0065 N88-10420
An instrument for the quasi-continuous determination of atmospheric soot content
[DFVLR-FB-87-04] 01 p0068 N88-10433
Effect of clarifying the atmosphere in relation to quasi-monochromatic CO2 laser radiation
06 p0709 N88-14348
Aerosol optical depth and ratios of diffuse-sky to total solar irradiance measured from aircraft following the eruption of El Chichon
[PB88-100789] 07 p0878 N88-15326
Influence of nonlinear spectroscopic effects on atmospheric propagation of intense laser radiation at 10.6 microns wavelength 13 p1789 N88-20705
Activities report of the Division of Optical Technology
[FOA-C-30477-3] 18 p2576 N88-25299

ATMOSPHERIC PHYSICS

NT CLOUD PHYSICS
Morphology of the Earth's environment
03 p0272 N88-11706
Ionosphere and plasmasphere
03 p0272 N88-11709
USSR report: Earth sciences
[JPRS-UES-86-006] 04 p0458 N88-12831
Analysis of geophysical data bases and models for spacecraft interactions
[AD-A184809] 05 p0555 N88-13375
USSR report: Earth sciences
[JPRS-UES-87-004] 06 p0725 N88-14455
Polar Geophysical Institute's studies of magnetosphere, ionosphere 06 p0728 N88-14480
Integrated systems with applications to the multi-phases of the ephemerides, physics and methematics of the upper atmosphere
[AD-A185748] 06 p0743 N88-14570
The ocean heat budget
[AD-A186130] 07 p0881 N88-15346
USSR report: Earth sciences
[JPRS-UES-87-003] 08 p1009 N88-16119
Electrodynamics of the high latitude middle atmosphere 08 p1028 N88-16225
Rayleigh lidar observations of gravity wave activity in the stratosphere and lower mesosphere
[NASA-CR-182384] 09 p1189 N88-17123
AFGL (Air Force Geophysics Laboratory) fiscal year 1988 Air Force technical objectives document
[AD-A187701] 11 p1503 N88-18977
Enhancements to the atmospheric transmittance/radiance program FASCODE
[AD-A188863] 12 p1643 N88-19839
Analysis of the inter-layer independence of stellar scintillometer profiles of Cn2
[AD-A189372] 12 p1645 N88-19854
Evaluation of chemical and atmospheric sciences research
[AD-A188468] 12 p1687 N88-20091
JPRS report: Science and technology. USSR: Earth sciences
[JPRS-UES-88-001] 13 p1784 N88-20674
Activities report in meteorology
[AR-86-87] 13 p1798 N88-20755
Plasmapause formation
[AERONOMICA-ACTA-A-319-1987] 15 p2138 N88-22759
NOAA-ERL-ARL (National Oceanic and Atmospheric Administration-Environmental Research Laboratories-Air Resources Laboratory) solar UV radiation and climate research project: Program description
[PB88-169396] 16 p2233 N88-23339
Theoretical plasma physics research of active space experiments
[AD-A192075] 18 p2577 N88-25309
Atmospheric Lidar Experiment In Space (ALEXIS)
[DFVLR-MITT-88-10] 22 p3118 N88-28526
Investigations into the properties, conditions and effects of the ionosphere
[AD-A194245] 22 p3118 N88-28528
Atmospheric science issues in Congress
22 p3125 N88-28573
Investigations of magnetosphere-ionosphere coupling relevant to operational systems
[AD-A195972] 24 p3391 N88-30195

ATMOSPHERIC PRESSURE

KR+ laser excitation of NH2 in atmospheric pressure flames
[AD-A183421] 01 p0050 N88-10322
Detection of CO2-induced climate change
[DE87-013127] 01 p0071 N88-10457
Regime dependent analysis experiments --- sea level pressure field 02 p0209 N88-11314
Mesoscale surface field analysis from routine observations --- pressure, wind fields
02 p0209 N88-11315
High resolution determination of true surface winds at sea from wind and pressure data
02 p0210 N88-11316
An improved method of analyzing surface geostrophic winds and pressure 02 p0212 N88-11334
On the interannual variability of South American climate and the Southern Oscillation 04 p0470 N88-12905
An investigation of unipolar arcing at atmospheric pressure in aluminum 2024 and aluminum coated glass slides
[AD-A184903] 05 p0577 N88-13521
An analysis of tropopause pressure and total ozone correlations 05 p0617 N88-13789
The use of TOMS-modified VAS data for large-scale NWP 05 p0618 N88-13791
Cosmic ray NM-64 neutron monitor data 14, Rome, Italy, January - December 1985
[IFSI-87-8] 05 p0661 N88-14060
Influence of gas exchange between ocean and atmosphere on formation of atmospheric pressure field
06 p0726 N88-14467
Observations of a midlatitude squall line boundary layer wake
[AD-A185609] 06 p0748 N88-14589

Atmosphere of Venus in southern polar area
08 p1005 N88-16088
Atmosphere of Venus in south polar area based on radio transmission data
08 p1005 N88-16089
The structure and dynamics of monsoon depressions
10 p1355 N88-18102
Moscow USSR. Limited surface observations climatic summary (LISOCS), parts A-F
[AD-A188080] 11 p1514 N88-19046
Application of laser-induced fluorescence in an atmospheric-pressure boron-seeded flame
[AD-A189631] 14 p1889 N88-21287
Premixed turbulent flame propagation
[AD-A192955] 21 p2909 N88-27265
Intraseasonal variability in atmospheric surface pressure and relationship to polar motion
22 p3120 N88-28540
Observed normal mode structure of low frequency oscillations
22 p3128 N88-28595

ATMOSPHERIC RADIATION
NT AIRGLOW
NT AURORAL ARCS
NT AURORAS
NT DAYGLOW
NT GEOCORONAL EMISSIONS
NT IONOSPHERIC NOISE
NT NIGHTGLOW
NT SKY RADIATION
NT STRATOSPHERE RADIATION
NT TROPOSPHERIC RADIATION
NT WHISTLERS
The accuracy of the radiation parameterization in mesoscale models
[DFVLR-IB-553-85/11] 09 p1190 N88-17133
Microscopic control of metallization stability
[AD-A187553] 10 p1421 N88-18487
Radon-222 in the Antarctic Peninsula
[INPE-4486-PRE/1251] 15 p2092 N88-22468
Estimation of total Outgoing Longwave Radiation (OLR) flux from geostationary meteorological satellite infrared window radiance
17 p2351 N88-24006
Observations of wave number dependent spectral line ratio fluctuations in the atmospheric emissions
[IRF-PREPRINT-101] 18 p2542 N88-25085
Radiation safety in commercial air traffic
[NASA-TM-101156] 19 p2600 N88-25447
Review of methods for remote sensing of atmospheric emissions from stationary sources
[PB88-190483] 20 p2821 N88-26739
A control program for global radiation measurements
[KNMI-TR-100] 20 p2824 N88-26757

ATMOSPHERIC REFRACTION
NT RADIO WAVE REFRACTION
Microwave refractive index structure function profiles (Cn2) measured from a small aircraft
[AD-A184343] 04 p0431 N88-12670
Use of electron beam instruments to determine fluctuations in vertical refraction partial angle
04 p0461 N88-12853
Considering refraction in leveling with laser plane
04 p0462 N88-12857
Satellite autonomous navigation with SHAD (Stellar Horizon Atmospheric Dispersion)
[AD-A184988] 05 p0544 N88-13313
An investigation of millimeter wave propagation in the atmosphere: Measurement program
[AD-A184837] 05 p0574 N88-13498
Method for determining atmospheric temperature profiles from observations of astronomical refraction of stars
08 p1013 N88-16139
An evaluation of the impact of variable temporal and spatial data resolution upon IREPS (Integrated Refractive Effects Prediction System)
[AD-A187764] 11 p1470 N88-18769
Propagation in longitudinally varying ducts, with emphasis on guiding to antiguiding transitions
12 p1615 N88-19658
The correlation between methodological and low-level angle-of-arrival measurements
12 p1617 N88-19668
The spatial and temporal variability of the arctic atmospheric boundary layer and its effect on electromagnetic (EM) propagation
[AD-A193958] 23 p3204 N88-29068

ATMOSPHERIC SCATTERING
NT TROPOSPHERIC SCATTERING
Study on propagation and inverse scattering --- sea studies
[ESA-CR(P)-2394] 01 p0063 N88-10405
Statistical model of interaction of electromagnetic waves with natural objects being sensed
08 p1008 N88-16112
Atmospheric backscatter at 10.6 microns; a compendium of measurements made outside the United Kingdom by the airborne LATAS coherent laser radar velocimeter
[RSRE-87002] 12 p1631 N88-19763
Ozone sonde and Dobson spectrometer data obtained during the MAP/GLOBUS 1983 campaign over Western Europe
[BPT-5/87] 13 p1802 N88-20771
Temporal analysis of the changes in Parque Estadual de Jacupiranga vegetation through digital treatment of LANDSAT imagery
17 p2367 N88-24094

ATMOSPHERIC SHELLS
U ATMOSPHERIC STRATIFICATION

ATMOSPHERIC SOUNDING
GOES observations for the FIRE/SRB Wisconsin experiment region from October 11 through November 2, 1986
[NASA-TM-100485] 01 p0071 N88-10453
Parachute characteristics of Titan descent modules --- planetary probe
[BF-3/86-B] 02 p0122 N88-10774
Thunderstorm nowcasting using Doppler radar and soundings
02 p0200 N88-11248
Diagnosing short term changes in temperature and moisture profiles from single Doppler radar
02 p0200 N88-11251
VAS products as indices of thunderstorms and severe local storm potential --- Visible and Infrared Spin Scan Radiometer Atmospheric Sounder (VAS)
02 p0201 N88-11253
Horizontal shape matching applied to VAS data --- Visible and Infrared Spin Scan Radiometer Atmospheric Sounder (VAS)
02 p0201 N88-11254
Analysis of thickness fields retrieved from NOAA-7 observations through the 3I (Improved Initialization Inversion) method. Interest for weather forecasting
02 p0201 N88-11255
Assimilation of high resolution TOVS data into a mesoscale NWP model --- numerical weather prediction (NWP)
02 p0213 N88-11338
A VAS-numerical model impact study using the Gal-Chen variational approach --- Visible Infrared Spin-Scan Radiometer Atmospheric Sounder (VAS)
02 p0213 N88-11339
High latitude problems to be studied by incoherent scatter radars
[DMI-GEOPHYS-PAPERS-R-77]
03 p0350 N88-12211
Spectroscopic and retrieval studies in support of SCRIBE (Stratospheric Cryogenic Interferometer Balloon Experiment)
[AD-A184037] 03 p0351 N88-12216
Multiwave laser soundings of atmospheric aerosol: Experimental research (review)
04 p0461 N88-12852
Development of a data analysis system for the detection of lower level atmospheric turbulence with an acoustic sounder
[AD-A184972] 05 p0624 N88-13821
Development of an acoustic echosounder for detection of lower level atmospheric turbulence
[AD-A184877] 05 p0626 N88-13831
Statistical structure of temperature field over South Pacific Ocean
06 p0726 N88-14465
Latitude coverage of observations of the middle atmosphere by solar absorption spectrometry from a heliosynchronous orbit
[AERONOMICA-ACTA-A-316-1987]
06 p0742 N88-14566
Facilities for research and weather observations on the 213 m tower at Cabauw (Netherlands) and at remote locations
[KNMI-WR-87-5] 06 p0746 N88-14587
High-spatial-resolution TOVS observations for the FIRE/SRB Wisconsin experiment region from October 14 through November 2, 1986
[NASA-TM-100522] 06 p0747 N88-14593
Vertical sounding of th air layer close to a glacier on Mount Vernagfermer in the Oetzal Alps, Tyrol (experiment LUZIVER 1983)
08 p1015 N88-16152
Telescope design for Michelson Interferometer for Passive Atmospheric Sounding (MIPAS) B
08 p1017 N88-16167
Proceedings of the 8th ESA Symposium on European Rocket and Balloon Programs and Related Research
[ESA-SP-270] 08 p1024 N88-16201
The German scientific balloon and sounding rocket program
08 p1024 N88-16202
The French balloon and sounding rocket space program
08 p1025 N88-16203
The Norwegian scientific balloon and sounding rocket program 1987-1990
08 p1025 N88-16204
The Swedish sounding rocket and balloon program
08 p1025 N88-16205
Swiss scientific balloon and sounding rocket experiments 1985-1987
08 p1025 N88-16206
New techniques for rocket and balloon-borne instrumentation for investigations of the structure, dynamics and electrodynamics of the middle atmosphere
08 p1027 N88-16220
An advanced visible-UV spectrometer for atmospheric composition measurements
08 p1029 N88-16231
In-situ stratospheric water vapor measurements on board long duration balloons
08 p1029 N88-16232
TOTAL: A new instrument to study turbulent parameters in the mesosphere and lower thermosphere
08 p1029 N88-16234
Developments in instrumental techniques for observations of magnetospheric and ionospheric shaped charge releases
08 p1031 N88-16248
The Cryogenic Infrared Spectrometer and Telescope for the Atmosphere (CRISTA) experiment on Astro-SPAS
08 p1034 N88-16270
Rocket experiments and payloads for Super CAMP --- Cold Arctic Mesopause Project (CAMP)
08 p1034 N88-16271
Future developments of auroral D-region research using the EISCAT VHF incoherent scatter radar
08 p1035 N88-16278
Assessment of VAS-derived products created by a simultaneous algorithm on a convectively active day
[AD-A186158] 08 p1054 N88-16359
Technical assessment of the joint CSIRO/Bureau of Meteorology proposal for a geostationary imager/sounder over the Australian region
[RTP-15] 09 p1135 N88-16811
Report of the Workshop on Space Systems Possibilities for a Global Energy and Water Cycle Experiment
[WCP-137] 09 p1193 N88-17147
Analysis of quasi-geostrophic forcing during the AIMCS (Airborne Investigations of Mesoscale Convective Systems) Project. Volume 2: Results for June 14 through July 16, 1984
[PB88-123807] 10 p1354 N88-18092
Roys and radiosondes in the region
[INPE-4362-PRE/1188] 13 p1796 N88-20743
Lidar active remote sensing. Applications to the atmosphere
14 p1936 N88-21547
Aerosol lidar for environment protection and meteorology
[DFVLR-FB-87-43] 14 p1982 N88-21828
Coordinated Auroral Experiments using Scatter And Rocket investigations (CAESAR investigations)
[MPAE-W-47-87-13] 15 p2096 N88-22487
A multivariate variational objective analysis-assimilation method. Part 1: Development of the basic model
[NASA-CR-182651] 15 p2097 N88-22491
Geochemistry of the middle and lower atmosphere: Environmental impact through the deterioration of the ozone layer
[INPE-4477-PRE/1241] 16 p2230 N88-23321
Ozonesonde observations at Lauder, New Zealand during the Spring and early Summer of 1986
[PB88-173273] 16 p2232 N88-23328
Spectroradiometry in meteorology
16 p2272 N88-23599
Tiros operational vertical sounder (TOVS) and radiosonding in the region
17 p2360 N88-24059
Stratospheric positive ion composition measurements and acetonitrile detection: A consistent picture
[AERONOMICA-ACTA-A-326-1987]
18 p2542 N88-25084
MRS-3000 meteorological rocket probe for the MMR-06 dart integrated meteorological rocket system
[NASA-TT-20303] 19 p2693 N88-26010
High latitude ionospheric radio studies
[AD-A192270] 20 p2824 N88-26753
Influence of stable stratification on atmospheric turbulence: An experimental contribution
[ETN-88-92292] 20 p2827 N88-26772
Components of an atmospheric lidar system
[AD-A193366] 21 p2953 N88-27539
ECC (Electrochemical Concentration Cell) ozonesonde observations at South Pole, Antarctica during 1987
[PB88-202015] 21 p2970 N88-27644
The use of AIMS data for operational and research purposes in atmospheric sciences
22 p3036 N88-28025
South Pole lidar: Brief description of the instrument
[NOTA-INTERNA-907] 22 p3083 N88-28308
European validation of SAGE-2 aerosol profiles
[AERONOMICA-ACTA-A-327-1988]
23 p3234 N88-29243
Microwave instrument for planetary mission (Titan/CASSINI mission orbiter spacecraft)
[BAE-CS/TP-8359] 24 p3375 N88-30102
Spaceborne lidar: Development of a laboratory test system
[BF-R-66.090-1] 24 p3378 N88-30118
Possibilities of determining vertical profiles of microphysical characteristics of stratospheric aerosol using space measurements of transparency and solar halo
24 p3449 N88-30526

ATMOSPHERIC STRATIFICATION
Analysis of thickness fields retrieved from NOAA-7 observations through the 3I (Improved Initialization Inversion) method. Interest for weather forecasting
02 p0201 N88-11255
General theory of radio propagation through a stratified atmosphere
[PB87-226197] 04 p0430 N88-12662
Structure of stably stratified atmospheric surface layer in presence of heat-releasing admixture
04 p0462 N88-12856
Systematic stratospheric-tropospheric exchange viewed from isentropic coordinates 05 p0615 N88-13777
Mechanisms of cloud layer formation in Venusian atmosphere 08 p1004 N88-16087
Atmosphere of Venus in north polar area based on radio transmission data from Venera-15 and Venera-16 spacecraft 08 p1005 N88-16090
Distribution of electron concentration in nighttime atmosphere of Venus based on radio transmission data
08 p1005 N88-16092
Chemical composition and structure of Venusian clouds determined from results of roentgenoradiometric experiments carried out by landing modules of Vega-1 and Vega-2 automatic interplanetary stations
13 p1726 N88-20320
Influence of stable stratification on atmospheric turbulence: An experimental contribution
[ETN-88-92292] 20 p2827 N88-26772
ATMOSPHERIC TEMPERATURE
NT AURORAL TEMPERATURE
NT IONOSPHERIC TEMPERATURE
A device for measuring fast temperature fluctuations --- atmospheric temperature
[KNMI-TR-92] 01 p0070 N88-10449
Detection of CO2-induced climate change
[DE87-013127] 01 p0071 N88-10457
Diagnosing short term changes in temperature and moisture profiles from single Doppler radar
02 p0200 N88-11251
Mesoscale MOS forecast support for 1988 winter Olympics ski events --- model output statistics (MOS)
02 p0209 N88-11312
Short range forecast of the daily maximum temperature 02 p0209 N88-11313
Spectroscopic and retrieval studies in support of SCRIBE (Stratospheric Cryogenic Interferometer Balloon Experiment)
[AD-A184037] 03 p0351 N88-12216
Contributions of lidar measurements to the study of long term variations of the middle atmosphere
[ETN-88-91237] 05 p0625 N88-13824
Statistical structure of temperature field over South Pacific Ocean 06 p0726 N88-14465
Influence of gas exchange between ocean and atmosphere on formation of atmospheric pressure field
06 p0726 N88-14467
Particle-gas temperature differentials resulting from time-dependent radiative-conductive heat flux divergences in the tenuous dust-laden atmosphere of mars
[AD-A185888] 07 p0945 N88-15747
Atmosphere of Venus in southern polar area
08 p1005 N88-16088
Atmosphere of Venus in south polar area based on radio transmission data 08 p1005 N88-16089
Method for determining atmospheric temperature profiles from observations of astronomical refraction of stars 08 p1013 N88-16139
Development of a Doppler wind lidar system for atmospheric wind measurements
08 p1027 N88-16217
Revised uniform summary of surface weather observations. Parts A-F: Carswell AFB, Texas
[AD-A186820] 09 p1192 N88-17144
Statistical studies of low frequency oscillations in satellite-observed stratospheric temperatures
10 p1353 N88-18086
Air temperature shield tests
[AD-A187459] 11 p1514 N88-19043
Moscow USSR. Limited surface observations climatic summary (LISOCS), parts A-F
[AD-A188080] 11 p1514 N88-19046
Thermal structure of Venusian Atmosphere determined from results of measurements from Vega-2 landing module 13 p1725 N88-20315
Roys and radiosondes in the region
[INPE-4362-PRE/1188] 13 p1796 N88-20743
A study of satellite emission computed tomography
[AD-A189567] 13 p1797 N88-20745
Tropic heat MR (Meteorological Recorder) meteorological data (April 1984 - June 1985)
[PB88-161286] 14 p1948 N88-21620
Ultraviolet absorption cross sections of methylbromide at stratospheric temperatures
[AERONOMICA-ACTA-A-320-1987]
15 p2036 N88-22132
Tiros operational vertical sounder (TOVS) and radiosonding in the region 17 p2360 N88-24059
Three-dimensional temperature fields in the atmosphere up to 50 km altitude
[ETN-88-92150] 18 p2542 N88-25089
Effects of moderate cold and heat stress on the potential work performance of industrial workers. Part 6: The effects of increasing vapour pressure at four air temperatures on the performance and physiology of white females
[PB88-124854] 18 p2550 N88-25137
Satellite remote sensing of the wet bulb globe temperature heat stress index, phase 2
[AD-A192798] 20 p2818 N88-26717
Our climate in danger
[DE88-701824] 20 p2822 N88-26743
An efficient model for changes of global climate and composition of the atmosphere due to human activities
[ETN-88-92359] 20 p2827 N88-26775
Investigations on Mie and Rayleigh scattering as basis for the development of Rayleigh temperature lidars with aid of Michelson interferometry
[GKSS-87/E/62] 21 p2976 N88-27675
Proceedings of the Twelfth Annual Climate Diagnostics Workshop
[PB88-191747] 22 p3119 N88-28534
The 1986-87 Pacific warm episode: Oceanic and Atmospheric features 22 p3120 N88-28535
Prolonged periods of above-normal temperatures in Canada, 1986/87 22 p3120 N88-28538
Atlantic SST variability and high latitude climate fluctuations 22 p3122 N88-28551
Northern Hemisphere 700 mb teleconnections based on half-monthly mean anomaly data stratified by season and by sign 22 p3123 N88-28561
Interannual variability of 850 mb temperatures during the Northern Hemisphere winter
22 p3123 N88-28562
Urbanization: Its detection and effect in the United States climate record 22 p3125 N88-28571
Global-scale temperature changes to August 1987 and a comparison of satellite and conventional data
22 p3125 N88-28572
DERF forecasts of thickness
22 p3126 N88-28579
Some screening experiments in objective prediction of monthly mean temperature over the United States during the winter season 22 p3127 N88-28589
Operational multifield analog forecasting of US seasonal temperatures for non-winter seasons
22 p3127 N88-28592
Determination of most probable predicted 50 kPa pattern by empirical orthogonal functions
22 p3128 N88-28593
Soot and radiation in a gas turbine combustor
[AD-A191991] 23 p3179 N88-28924
Energy budget and ground temperatures in hot regions
[AD-A196298] 24 p3404 N88-30268
ATMOSPHERIC TIDES
Meteor observation by the Kyoto meteor radar
06 p0733 N88-14507
Variations of the semi-diurnal tidal wind in the meteor region with periods of about 27 and 13.5 days
06 p0734 N88-14516
Tidal activity in the meteor zone over Budrio, Italy
06 p0734 N88-14517
Some aspects of metallic ion chemistry and dynamics in the mesosphere and thermosphere
06 p0737 N88-14534
Solar tides in the upper equatorial thermosphere: A comparison between AE-E data and the NCAR thermospheric general circulation model
[AD-A186160] 08 p1023 N88-16196
ATMOSPHERIC TURBULENCE
NT CLEAR AIR TURBULENCE
NT GUSTS
NT LOW LEVEL TURBULENCE
The atmosphere of Mars and optical communications
04 p0434 N88-12692
Development of a data analysis system for the detection of lower level atmospheric turbulence with an acoustic sounder
[AD-A184972] 05 p0624 N88-13821
Development of an acoustic echosounder for detection of lower level atmospheric turbulence
[AD-A184877] 05 p0626 N88-13831
Introduction to the Modeling of Turbulence
[VKI-LS-81-06] 08 p0986 N88-15972
An introduction to single point closure methodology
08 p0986 N88-15973
Turbulence models for practical applications
08 p0986 N88-15974
Examples of turbulence-model applications
08 p0987 N88-15975
Numerical implementation and performance of Reynolds stress closures in finite volume computations of recirculating and strongly swirling flows
08 p0987 N88-15976
Observational evidence for saturation of gravity waves and the production of turbulence in the mesosphere
08 p1028 N88-16229
TOTAL: A new instrument to study turbulent parameters in the mesosphere and lower thermosphere
08 p1029 N88-16234
VAWT (Vertical-Axis Wind Turbine) stochastic loads produced by atmospheric turbulence
[DE88-001355] 09 p1187 N88-17110
Statistics of breakdown centers appearing during propagation of laser radiation through turbulent atmosphere 09 p1236 N88-17411
Comparison of a few methods of restoring images distorted by atmospheric turbulence
[ESA-TT-1065] 09 p1248 N88-17481
Response of wind shear warning systems to turbulence with implication of nuisance alerts
10 p1274 N88-17618
Similarity theories and microturbulence in the atmospheric mixed layer 13 p1806 N88-20802
Effect of atmospheric turbulence on the bit error probability of a space to ground near infrared laser communications link using binary pulse position modulation and an avalanche photodiode detector
[NASA-TM-100699] 14 p1873 N88-21189
JPRS report: Science and technology. China
[JPRS-CST-87-042] 14 p1899 N88-21338
Intermittency of atmospheric turbulence--applicatin of Lyapunov exponents and fractional dimension
14 p1900 N88-21348
Stellar scintillometer atmospheric optical turbulence profiling experiment: A qualitative comparison of two identical instruments at AMOS (Air Force Maui Optical Station), 1985
[AD-A190589] 15 p2094 N88-22479
The potential impact on atmospheric ozone and temperature of increasing trace gas concentrations
[NASA-CR-182965] 17 p2373 N88-24112
Study of the convergence of a finite difference scheme for acoustic propagation in the atmosphere in a parabolic approximation. Statistical calculation of the sound field in the presence of kinematic turbulence
[ONERA-RS-8/3641-PY-160-P]
17 p2394 N88-24235
Aircraft/lidar turbulence comparison
18 p2546 N88-25111
Influence of stable stratification on atmospheric turbulence: An experimental contribution
[ETN-88-92292] 20 p2827 N88-26772
Atmospheric turbulence research at DFVLR
[AGARD-R-752] 21 p2975 N88-27669
Performance analysis of a noncoherently combined large aperture optical heterodyne receiver
22 p3065 N88-28189
The Flight of Flexible Aircraft in Turbulence: State-of-the-Art in the Description and Modelling of Atmospheric Turbulence
[AGARD-R-734-ADD] 24 p3311 N88-29717
Current and proposed gust criteria and analysis methods: An FAA overview 24 p3311 N88-29718
Flight test equipment for the on-board measurement of wind turbulence 24 p3311 N88-29719
Measured and predicted responses of the Nord 260 aircraft to the low altitude atmospheric turbulence
24 p3312 N88-29723
The Flight of Flexible Aircraft in Turbulence: State-of-the-Art in the Description and Modelling of Atmospheric Turbulence
[AGARD-R-734] 24 p3312 N88-29725
Status review of atmosphere turbulence and aircraft response 24 p3312 N88-29726
A summary of atmospheric turbulence measurements with specially-equipped aircraft in the US
24 p3312 N88-29727
The NAE atmospheric research aircraft
24 p3313 N88-29730
Extreme gusts distribution 24 p3314 N88-29734
A digital simulation technique for the Dryden atmospheric model
[NASA-TT-20342] 24 p3404 N88-30266
Microphysical processes in cloud layers of Venus
24 p3448 N88-30522
ATMOSPHERIC WINDOWS
Filling of the atmospheric transmission window due to emission from very high rotational levels of NO and O3
[AD-A194670] 23 p3233 N88-29239
Molecular line shape effects on atmospheric window absorption
[AD-A196316] 24 p3342 N88-29894
ATMOSPHERICS
NT WHISTLERS

ATOLL REEFS
U CORAL REEFS
ATOMIC BATTERIES
U RADIOISOTOPE BATTERIES
ATOMIC BEAMS
High intensity 5 eV O-atom exposure facility for material degradation studies 02 p0135 N88-10847
Materials preparation and longevity in hyperthermal atomic oxygen 03 p0297 N88-11862
Atomic beam studies of the interaction of hydrogen with transition metal surfaces
[DE88-000208] 05 p0648 N88-13970
Atomic beam study of crystalline order and precipitation in nickel based alloys
[ETN-88-91994] 18 p2177 N88-22975
Laboratory experiments of relevance to the space station environment 18 p2592 N88-25402
Fast atom bombardment study on interaction of anticodonic nucleotides and their cognate amino acid
[ISAS-RN-355] 20 p2850 N88-26918
ATOMIC CLOCKS
On-orbit frequency stability analysis of the GPS NAVSTAR 8 rubidium clock and NAVSTARs 9 and 10 cesium clocks
[AD-A184984] 05 p0544 N88-13312
Study and construction of a compact hydrogen maser with a high-degree of frequency stability
[PB87-151122] 07 p0859 N88-15216
Atomic clocks research: An overview
[AD-A185567] 07 p0930 N88-15648
Ultrahigh coherent semiconductor lasers and their applications to Rb atomic clock 14 p1976 N88-21789
Tactical Rubidium Frequency Standard (TRFS), volume 2
[AD-A191190] 18 p2503 N88-24850
Quartz crystal resonators and oscillators for frequency control and timing applications
[AD-A193310] 21 p2937 N88-27443
A three-dimensional model of the gas-cell atomic frequency standard
[AD-A193218] 21 p3011 N88-27868
ATOMIC COLLISIONS
Proceedings of the Workshop on Opportunities for Atomic Physics Using Slow, Highly-Charged Ions
[DE87-013991] 02 p0231 N88-11457
Final (n,l) state-resolved electron capture by multiply charged ions from neutral atoms
[IPPJ-AM-54] 04 p0492 N88-13030
Monocrystal sputtering by the computer simulation code ACOCT
[IPPJ-848] 04 p0493 N88-13035
Total and partial cross sections for electron capture for C(q+) (q=6-2) and O(q+) (q=8-2) ions in collisions with H, H2 and He atoms
[IPPJ-AM-56] 09 p1252 N88-17501
Correlated processes in atomic collisions
[DE88-003508] 10 p1406 N88-18383
Negative-energy quanta
[DE88-700904] 12 p1689 N88-20101
Memoirs of the Faculty of Science, Kyoto University. Series of Physics, Astrophysics, Geophysics and Chemistry, volume 37, no. 2
[ISSN-0368-9689] 16 p2287 N88-23694
Theoretical studies of dynamics combustion
[DE88-007565] 19 p2611 N88-25495
Theoretical atomic and molecular physics
[DE88-007122] 19 p2724 N88-26175
Atomic physics of strongly correlated systems
[DE88-007789] 19 p2724 N88-26177
Recoil saturation of the self-energy in atomic systems
[DE88-010450] 20 p2851 N88-26930
ATOMIC ENERGY
U NUCLEAR ENERGY
ATOMIC ENERGY LEVELS
The influence of polymer structure on triplet luminescence
[DE87-014431] 02 p0152 N88-10952
Migration and transfer of triplet energy in selected polymer systems
[DE87-014432] 02 p0152 N88-10953
Wavelengths of the 3p-3d transitions of the Co- and Fe-like ions: The effects of electron correlation
[DE88-000219] 04 p0498 N88-13067
The angular diameter of alpha Scorpii in the near-infrared Ca II triplet 04 p0514 N88-13162
Localization of Cu 3d levels in the high Tc superconductor YBa2Cu3O approximately 7 by Cu2p X-ray photoelectron spectroscopy
[NOTA-INTERNA-887] 07 p0939 N88-15710
Nuclear excitation via the motion of electrons in a strong laser field
[AD-A187166] 09 p1171 N88-17017
Light absorption by an atom moving inside a spherical box
[AD-A187241] 10 p1407 N88-18395
Systematics on neutron-induced isomeric cross-section ratios at 14.5 MeV
[ECN-200] 14 p1980 N88-21815
Electronic energy transfer processes in the alkali/alkaline earth metal vapors
[AD-A190035] 15 p2034 N88-22119
Stark effect in intense field. Perturbation theory and 1/n-expansion
[DE87-702947] 16 p2266 N88-23550
ATOMIC EXCITATIONS
The study of excited oxygen molecule gas species production and quenching on thermal protection system materials
[NASA-CR-172027] 02 p0233 N88-11470
Low-power photolytically pumped lasers
[DE88-002448] 08 p0991 N88-15998
New branch of solid-state physics 08 p1079 N88-16508
Resonance excitation in gamma gamma collisions at LEP200
[NIKHEF-H/87-3] 08 p1081 N88-16514
Kinetic studies following state-selective laser excitation
[DE88-004094] 10 p1335 N88-17981
Nuclear transitions induced by atomic excitations
[DE88-004311] 11 p1545 N88-19239
Quantum Monte Carlo study of the MIES associated with H2(X 1 sigma g +) and H2(B 1 sigma u +) 16 p2268 N88-23564
Density diagnostics by hydrogen line intensity ratios: Excitation cross section between excited states 17 p2441 N88-24522
Cascade fluorescences from laser-excited lithium atom for plasma diagnostics 17 p2442 N88-24526
Distorted-wave-method calculation of electron-impact excitation of atomic ions 17 p2443 N88-24532
Monte Carlo investigation of hot photoexcited electron relaxation in GaAs 19 p2659 N88-25805
High-speed phenomena in GaAs multiple-quantum-wells 19 p2660 N88-25812
Excitation of single-mode glass fiber by partially coherent sources
[ETN-88-92121] 20 p2854 N88-26951
ATOMIC EXPLOSIONS
U NUCLEAR EXPLOSIONS
ATOMIC GASES
U MONATOMIC GASES
ATOMIC INTERACTIONS
NT ATOMIC COLLISIONS
A simple interpretation of the Fe2(-) photoelectron spectrum
[NASA-CR-182553] 11 p1543 N88-19225
Competing interactions in metallic superlattices
[DE88-005344] 13 p1847 N88-21057
Contribution to the study of order effects in the Ising model framework: Ground states and phase diagrams
[ONERA-NT-1987] 20 p2880 N88-27095
Determination of quantum corrections for electrical conductivity mechanism of three dimensional, perturbed copper coatings. Weak localization and electron-electron interaction
[ETN-88-92378] 21 p2941 N88-27466
ATOMIC MASS
U ATOMIC WEIGHTS
ATOMIC PHYSICS
Proceedings of the Workshop on Opportunities for Atomic Physics Using Slow, Highly-Charged Ions
[DE87-013991] 02 p0231 N88-11457
Atomic physics with highly charged ions
[DE88-000894] 05 p0648 N88-13972
Theoretical atomic and molecular physics
[DE88-001625] 05 p0649 N88-13974
Application of ECR ion source beams in atomic physics
[DE88-003767] 10 p1406 N88-18384
Research and technology, 1987
[NASA-TM-100323] 12 p1713 N88-20253
Simulation code for ICF including radiative energy transfer 16 p2277 N88-23627
Finite ion-relaxation and nonequilibrium radiation effects on laser-driven implosions 16 p2276 N88-23636
Atomic processes in matter-antimatter interactions
[DE88-008911] 19 p2723 N88-26172
Theoretical atomic and molecular physics
[DE88-007122] 19 p2724 N88-26175
Atomic physics of strongly correlated systems
[DE88-007789] 19 p2724 N88-26177
Modeling of atomic processes in X-ray laser plasmas
[AD-A194118] 23 p3286 N88-29567
ATOMIC RECOMBINATION
NT OXYGEN RECOMBINATION
Nascent vibrational/rotational distribution produced by hydrogen atom recombination
[AD-A193005] 20 p2852 N88-26933
ATOMIC SPECTRA
Atomic frequency standards for ultra-high-frequency stability 04 p0433 N88-12685
Hydrogen and deuterium in the local interstellar medium 04 p0521 N88-13204
Atomic and molecular gas phase spectrometry
[AD-A187562] 11 p1452 N88-18655
Theory of two-photon emission from atomic inner shells
[AD-A187742] 11 p1543 N88-19223
Single-laboratory evaluation of SW-846 methods 7090/7091 determination of beryllium by flame and furnace atomic absorption spectrophotometry
[PB88-171434] 16 p2175 N88-22963
Array detectors for plasma spectrochemistry
[AD-A194220] 22 p3052 N88-28105
The electromagnetic spectrum: The information mine
[AD-A194316] 22 p3069 N88-28215
Determination of impurities in silicon carbide by ICP AES (inductively coupled plasma atomic emission spectrometry) after coprecipitation with lanthanum hydroxide
[NASA-TT-20332] 23 p3193 N88-29003
Modeling of atomic processes in X-ray laser plasmas
[AD-A194118] 23 p3286 N88-29567
ATOMIC STRUCTURE
Some electronic factors influencing superconductivity in some rare-Earth-like elements and the beginning of rare-Earth series
[DE87-702582] 01 p0102 N88-10668
Electronic structure of crystalline NaSn
[DE87-702583] 01 p0102 N88-10669
Elastic moduli of copper under compression
[DE87-013137] 02 p0147 N88-10922
Small-Angle Neutron Scattering (SANS) from polymers and colloids
[DE87-013548] 02 p0151 N88-10946
Dynamics of atoms in low-symmetry systems
[AD-A184318] 03 p0375 N88-12361
Interatomic Auger rates for the sodium fluoride crystal
[DE87-013012] 03 p0382 N88-12401
Experimental perspectives on heavy electron metals
[DE87-014766] 04 p0416 N88-12583
The finite element method for electronic structure
[DE88-001708] 04 p0485 N88-12989
Nuclear techniques in studies of condensed matter
[NASA-RP-1195] 04 p0489 N88-13015
Tetrahedral carbon and interstitial electrons in Li cluster: CLi4 and (LiCH3)4
[AD-A184277] 04 p0496 N88-13055
Atomic and electronic structure of surfaces and chemisorbed layers
[DE87-014987] 04 p0498 N88-13065
Wavelengths of the 3p-3d transitions of the Co- and Fe-like ions: The effects of electron correlation
[DE88-000219] 04 p0498 N88-13067
The role of electronic structure calculation in mechanistic analysis of electron transfer reactions in the liquid phase
[DE87-014395] 05 p0647 N88-13963
Structural investigations of some metallic glasses
[ECN-198] 06 p0686 N88-14203
Electronic band structure and photoemission: A review and projection
[DE88-002236] 06 p0787 N88-14829
Study of the embedded atom method of atomistic calculations for metals and alloys
[DE88-002798] 07 p0835 N88-15065
Embedded cluster models for electronic structure and energetics of complex oxides
[DE88-003097] 07 p0938 N88-15702
Soft X-ray absorption and emission spectra and the electronic structure of the Ba2YCu3O/sub 7-x/ superconductor
[DE88-002609] 08 p1090 N88-16559
Structural properties of high-T/sub c/ oxide super conductors
[DE88-002974] 08 p1090 N88-16563
Activities report in nuclear physics
[ETN-88-91609] 09 p1245 N88-17458
Electronic and chemical structure of 3-5/metal and Si/metal interfaces
[AD-A186579] 09 p1254 N88-17518
Electronic structure calculations and binding analyses for selected binary and ternary metal hydrides
[ETN-88-91087] 09 p1256 N88-17527
Surface and interface electronic structure
[DE88-003363] 09 p1258 N88-17545
Insights into the mechanisms of chemical reactions: Reaction paths for chemical reactions
[DE88-003041] 10 p1297 N88-17755
Investigations on the usefulness of the Massively Parallel Processor for study of electronic properties of atomic and condensed matter systems
[NASA-CR-182514] 10 p1383 N88-18259
Energy-related atomic and molecular structure and scattering studies
[DE88-004246] 10 p1406 N88-18386

Semiempirical studies of atomic structure
[DE88-004096] 10 p1407 N88-18392
Electronic structure of random alloys and the theory of ordering processes
[DE88-004476] 10 p1407 N88-18394
The electronic structure of YBa2Cu3O/sub 7-delta/ above and below T/sub c/
[DE88-003495] 10 p1420 N88-18479
Calculations of rate constants for the three-body recombination of H2 in the presence of H2
[NASA-CR-182548] 11 p1454 N88-18664
Gas-phase photoelectron spectroscopy of metals and metal oxides of importance in the upper atmosphere
[AD-A187771] 11 p1511 N88-19027
A simple interpretation of the Fe2(-) photoelectron spectrum
[NASA-CR-182553] 11 p1543 N88-19225
Atomic-scale simulation in materials science
[DE88-005204] 11 p1544 N88-19230
Symmetry and equivalence restrictions in electronic structure calculations
[NASA-TM-89252] 11 p1557 N88-19320
Spatial distribution of carbon and native defects in large-diameter bulk grown GaAs
[DE88-003870] 11 p1562 N88-19348
Electronic properties of semiconductor inversion layers in sub-micron structures
[AD-A188635] 12 p1698 N88-20161
Tungsten-carbon multilayer system studied with X-ray scattering
[DE88-005749] 13 p1735 N88-20373
Model catalyst studies of SMSI (Strong Metal/Support interactions) and the role of D-electrons in chemisorption and catalysis
[DE88-004518] 13 p1738 N88-20393
Properties of reactively sputtered WNx films Zhao, X. -A.
[AD-A188711] 13 p1835 N88-20976
Theoretical studies on the electronic structure and properties of complex ceramic crystals and glasses
[DE88-005837] 13 p1846 N88-21049
Research on stable processible conducting polymers for electronic applications
[AD-A190246] 15 p2044 N88-22180
Dynamical optimization techniques for the calculation of electronic structure in solids
[DE88-006010] 15 p2140 N88-22768
First-principles calculations of quasiparticle energies at surfaces and interfaces: Semiconductor surface-state spectra and band offsets
[DE88-006340] 15 p2141 N88-22773
Experimental studies on electronic properties of HgTe/CdTe and Hg sub 1-z Cd sub x Te/CdTe heterostructures and superlattices
[AD-A189826] 15 p2142 N88-22783
Electronic structure of matter at high compression: Isostructural transitions and approach of the Fermi-gas limit
[MPQ-124] 16 p2266 N88-23551
The H5(+) potential energy hypersurface: Characterization of ten distinct energetically low-lying stationary points 16 p2267 N88-23561
Electronic structure and stability of small cation and anion hydrogen clusters 16 p2267 N88-23562
Point defects in irradiated silicates
17 p2408 N88-24319
The theory of random alloys
[DE88-006408] 18 p2487 N88-24756
Silicon-sapphire waveguides
[AD-A191754] 18 p2504 N88-24854
Electronic structure, elementary excitations, optical and transport properties of semiconductor superlattices
[AD-A190795] 18 p2581 N88-25333
Transition probabilities in OH A 2 sigma + - X 2 pi i: Bands with v prime = 0 and 1, v double prime = 0 to 4
[NASA-CR-182946] 18 p2584 N88-25353
Ground state properties and electronic structure of high T sub c superconductors
[DE88-007485] 18 p2585 N88-25360
Electronic structure of Zintl phase compounds by nonlinear optimization
[DE88-009998] 19 p2613 N88-25508
Half collision studies of inelastic energy transfer processes
[DE88-008096] 19 p2724 N88-26178
Calculation of the line shapes of radiators immersed in plasma 19 p2729 N88-26210
All-electron local density theory of electronic structure and superconductivity in YBa2Cu3O7 and YBa2Cu3O6
[DE88-009944] 19 p2735 N88-26246
Structural and magnetic properties of Fe impurities in YBa2Cu3O(sub 7-delta)
[DE88-009961] 19 p2735 N88-26247
The electronic structure of condensed molecular systems
[DE88-007823] 20 p2851 N88-26923
Piezoelectric effects in strained layer superlattices
20 p2863 N88-27002
Electronic structure of quantum-well states revealed under high pressures 20 p2870 N88-27036
Ordering transitions of ternary alloys A(1-x)B(x)C
20 p2873 N88-27054
Discrete variational methods and their application to electronic structures
[DE88-702215] 21 p3014 N88-27888
Probing the electronic and defect structure of perovskite superconductors
[DE88-008349] 21 p3022 N88-27939
The 2D Rydberg series in Al I
[NASA-TM-101189] 22 p3150 N88-28740
Atomistic simulation of silicon grain boundaries
[DE88-009925] 22 p3155 N88-28771
Influence of local volume forces on surface relaxation of pure metals and alloys: Applications to Ni, Al, Ni3Al
[DE88-702718] 23 p3195 N88-29014
Possible mechanism for high-temperature superconductivity in the BaSr-La(Y)-CuO systems
[DE88-702060] 23 p3288 N88-29576
Band electronic structures and crystal packing forces
[DE88-010247] 23 p3289 N88-29585

ATOMIC THEORY
NT HEISENBERG THEORY

ATOMIC WEIGHTS
The atomic weight and isotopic composition of nitrogen and their variation in nature
[DE87-012867] 02 p0144 N88-10902
The atomic weight and isotopic composition of oxygen and their variation in nature
[DE87-014397] 04 p0413 N88-12558
Measurement of Beta-decay energies of short-lived neutron-rich nuclei in the vicinity of mass number between 101 and 106, and A = 109
[ETN-88-92376] 21 p3014 N88-27890
Diamond like carbon coatings: Categorization by atomic number density
[NASA-CR-174895] 22 p3059 N88-28151

ATOMIZATION
U ATOMIZING

ATOMIZERS
Calculation on film preparation and film motion of a swirl atomizer
[DFVLR-FB-87-25] 09 p1162 N88-16962
Laboratory scale inert gas atomizer for producing rapidly solidified powders
[DE88-006734] 18 p2497 N88-24812
Analysis of the flow through double swirl airblast atomizers 24 p3351 N88-29949

ATOMIZING
NT GAS ATOMIZATION
NT LIQUID ATOMIZATION
Study of electrostatic modulation of fuel sprays to enhance combustion performance in an aviation gas turbine
[AD-A184967] 05 p0548 N88-13341
Military jet fuels, 1944-1987
[AD-A186752] 09 p1150 N88-16890
Design and characteristics of a liquid aerosol generator
[AD-A186942] 09 p1174 N88-17034
J85-21 fuel nozzle atomization tests
[AD-A189394] 12 p1613 N88-19647
Atomization in a turbulent shear layer: Preliminary measurements 19 p2624 N88-25565
Liquid Engine Jet Atomization Workshop report
19 p2627 N88-25584
Pulsed spray structure and atomisation techniques
[AD-A192280] 20 p2800 N88-26614
Small-droplet spray measurements with a scattered-light scanner
[NASA-TM-100973] 20 p2806 N88-26645

ATOMS
NT HELIUM ATOMS
NT HYDROGEN ATOMS
NT METASTABLE ATOMS
NT NEUTRAL ATOMS
NT NITROGEN ATOMS
NT OXYGEN ATOMS
Theory of atoms in strong, pulsed electromagnetic fields. 2: A free electron and a harmonically bound electron
[DE87-012571] 01 p0035 N88-10225
Field ion microscope studies of surface reconstructions
[DE87-014644] 02 p0147 N88-10924
Quantum-mechanical aspects of classically chaotic driven systems
[DE87-013152] 02 p0178 N88-11106
Quantum electrodynamics based on self-energy: Spontaneous emission in cavities
[DE87-703071] 02 p0232 N88-11461
Materials preparation and longevity in hyperthermal atomic oxygen 03 p0297 N88-11862
Theory of atomic additivity in molecular hyperpolizabilities 03 p0297 N88-11867
Production of atom flows at materials evaporation by laser radiation
[DE87-703327] 03 p0328 N88-12074
Theory of multiphoton ionization of atoms by strong, short pulsed lasers
[DE88-000963] 05 p0588 N88-13588
Photoionization of atoms and ions: Application of time-dependent response method within the density functional theory
[AD-A185686] 07 p0930 N88-15649
Correlation effects on double electron capture in highly-charged, low-energy ion-atom collisions
[DE87-013179] 07 p0930 N88-15651
Status of cross section data for photon scattering by atoms
[DE87-011281] 08 p1081 N88-16517
Depth of origin of sputtered atoms: Experimental and theoretical study of Cu/Ru(0001)
[DE88-002848] 08 p1082 N88-16520
Light absorption by an atom moving inside a spherical box
[AD-A187241] 10 p1407 N88-18395
Electron tunneling microscopy
[AD-A187426] 11 p1452 N88-18652
Atomistic simulation of low-energy beam deposition
[DE88-004344] 11 p1544 N88-19228
Laser measurements of state-resolved Ga and in atom sticking and desorption on metal and semiconductor surfaces
[AD-A187644] 11 p1555 N88-19310
Theory of laser cooling and spectroscopy of harmonically trapped single atoms
[AD-A189576] 13 p1775 N88-20617
Spontaneous decay and atomic fluorescence near a metal surface of an absorbing dielectric
[AD-A187508] 13 p1835 N88-20975
Optical cooling and trapping 14 p1974 N88-21782
Macroscopic quantum jumps in a single atom
14 p1975 N88-21784
Squeezed states of light 14 p1976 N88-21791
Clusters of transition metal atoms
[AD-A191265] 16 p2270 N88-23579
Theoretical calculations of XeF ground state kinetics
[AD-A191398] 16 p2270 N88-23580
Sources of polarized ions and atoms
[DE88-010910] 20 p2852 N88-26931
Multiphoton ionization of alkaline earth atoms in an intense laser field
[DE88-008078] 21 p3014 N88-27884
Soot and radiation in a gas turbine combustor
[AD-A191991] 23 p3179 N88-28924
Infrared detection using Rydberg atoms
[AD-A194308] 23 p3191 N88-28990
Cooperative effects and intrinsic optical bistability in collections of atoms
[AD-A193993] 23 p3280 N88-29530
Modeling of atomic processes in X-ray laser plasmas
[AD-A194118] 23 p3286 N88-29567
Cluster beam studies
[AD-A195182] 24 p3434 N88-30443

ATP
U ADENOSINE TRIPHOSPHATE

ATROPHY
Investigation of rat skeletal muscles following short-term spaceflight aboard Cosmos-1667 biosatellite
10 p1365 N88-18157
Evaluation of the endogenous glucocorticoid hypothesis of denervation atrophy
[NASA-CR-182848] 17 p2381 N88-24157

ATROPINE
Carbamates, atropine, and diazepam: Effects on performance in the running rat
[AD-A188009] 11 p1517 N88-19062
Low doses of atropine sulfate impair retention of a well-learned spatial task
[AD-A194065] 23 p3237 N88-29266

ATTACHMENTS
U ACCESSORIES

ATTACK AIRCRAFT
NT AH-64 HELICOPTER
NT B-1 AIRCRAFT
NT B-57 AIRCRAFT
NT B-70 AIRCRAFT
NT BOMBER AIRCRAFT
NT F-4 AIRCRAFT
NT F-14 AIRCRAFT
NT F-15 AIRCRAFT
NT F-16 AIRCRAFT
NT F-18 AIRCRAFT
NT F-27 AIRCRAFT
NT F-106 AIRCRAFT
NT F-111 AIRCRAFT
NT FIGHTER AIRCRAFT

NT HARRIER AIRCRAFT
NT MIG AIRCRAFT
NT MIRAGE AIRCRAFT
NASA supersonic STOVL propulsion technology program
[NASA-TM-100227] 06 p0668 N88-14093
A model for estimating depot maintenance costs for Air Force fighter and attack aircraft
[AD-A187097] 09 p1105 N88-16624
Task listing: Visually assisted and visually dependent tasks for fighter aircraft
[AD-A191041] 16 p2244 N88-23404

ATTACKING (ASSAULTING)
A strategy for space warfare
[AD-A186658] 09 p1233 N88-17394
Computer aided tactics for air combat 12 p1597 N88-19559
Task listing: Visually assisted and visually dependent tasks for fighter aircraft
[AD-A191041] 16 p2244 N88-23404
Determination of the hydroperoxide potential of jet fuels
[AD-A195975] 24 p3357 N88-29991

ATTENTION
Effects of divided attention on identity and semantic priming
[AD-A184289] 03 p0357 N88-12250
Latency differences and effects of selective attention to gratings in the central and right visual fields: 2
[DE87-014730] 04 p0473 N88-12918
Research on visual information processing with special reference to oculomotor behavior in the areas of exploration, recognition and search
[AD-A186598] 08 p1051 N88-16346
Visual evoked potentials
[AD-A187942] 11 p1519 N88-19071
Two attentional models of classical conditioning: Variations in CS effectiveness revisited
[AD-A187697] 11 p1522 N88-19088
Construction of a multidimensional questionnaire to determine interindividual differences in controlling attention
[DFVLR-FB-87-45] 14 p1952 N88-21637
Selective mechanisms in auditory and bimodal signal processing
[AD-A190529] 15 p2103 N88-22530
Vagal tone as an index of mental state 16 p2239 N88-23373
Probe-evoked event-related potential techniques for evaluating aspects of attention and information processing 16 p2240 N88-23379
Estimating the cost of mental loading in a bimodal divided-attention task: Combining reaction time, heart-rate variability and signal-detection theory 16 p2241 N88-23385
Attention, effort, and fatigue: Neuropsychological perspectives 16 p2241 N88-23387
Processing deficits in monitoring analog and digital displays: Implications for attentional theory and mental-state estimation research 16 p2241 N88-23389
Eye and head response to an attention cue in a dual task paradigm
[AD-A191052] 16 p2551 N88-25143
A model for visual attention
[AD-A193061] 21 p2991 N88-27744
Divided attention revisited: Selection based on location or pitch
[AD-A193814] 22 p3133 N88-28627
Visual motion perception and visual attentive processes
[AD-A193640] 23 p3241 N88-29288
Central adrenergic receptors as mediators of central response to stress: Study with Positron Emission Tomography (PET)
[AD-A194947] 24 p3407 N88-30284
Comparative aspects of multiple processes of attention
[AD-A195805] 24 p3408 N88-30291

ATTENUATION
NT ACOUSTIC ATTENUATION
NT ATMOSPHERIC ATTENUATION
NT MICROWAVE ATTENUATION
NT RADIO ATTENUATION
NT SHOCK WAVE ATTENUATION
NT SIDELOBE REDUCTION
NT WAVE ATTENUATION
Radiation-induced transient attenuation of optical fibers at 800 and 1300 nm
[DE87-013165] 02 p0235 N88-11485
A statistical rain attenuation prediction model with application to the advanced communication technology satellite project. Part 2: Theoretical development of a dynamic model and application to rain fade durations and tolerable control delays for fade countermeasures
[NASA-TM-100242] 03 p0308 N88-11945
Ferromagnetic mitigation of electromagnetic pulse affects
[AD-A185685] 06 p0694 N88-14258
Chapter 2: Threshold for Raman conversion of FEL laser pulses in the atmosphere
[DE88-002470] 07 p0859 N88-15215
Theory of transient thermal self-focusing of sound beams 09 p1234 N88-17401
Formulation of a general technique for predicting pneumatic attenuation errors in airborne pressure sensing devices
[NASA-TM-100430] 13 p1723 N88-20302
Phase velocity and attenuation of plane elastic waves in a particle-reinforced composite medium
[AD-A189414] 13 p1734 N88-20366
Some models for rain and cloud attenuation of millimeter waves
[PB88-160809] 14 p1948 N88-21616
Fog, rain and aerosol attenuation in the atmosphere
[AD-A190867] 16 p2235 N88-23350
Theoretical basis for an experimental test with regard to the origin of VHF (Very High Frequency) radiation from natural lightning
[DE88-007535] 18 p2544 N88-25102
Determination of mesoscale variability of sea surface temperature and attenuation in the North Atlantic from satellite measurement
[REPT-162] 18 p2548 N88-25127
Propagation measurements for an Australian land mobile satellite system 19 p2645 N88-25697
Influence of scattering on seismic waves: Physical mechanisms contributing to attenuation in the crust
[AD-A191699] 19 p2690 N88-25992
Changes in seismic velocity and apparent attenuation due to isotropic and anisotropic scattering: Results from physical modeling 19 p2691 N88-25997
Poloidal field measurements using laser enhanced attenuation of an energetic lithium beam
[DE88-008360] 20 p2856 N88-26963
A statistical rain attenuation prediction model with application to the advanced communication technology satellite project. 1: Theoretical development and application to yearly predictions for selected cities in the United States
[NASA-CR-179498] 23 p3205 N88-29077
Finite-difference simulations of Rayleigh-wave scattering by shallow heterogeneity
[AD-A194961] 24 p3402 N88-30259

ATTENUATION COEFFICIENTS
Transport coefficients close to the mobility edge and nonlinear sigma model composite operators --- electron transport
[PREPRINT-541] 06 p0777 N88-14767
The analytical exponential decay coefficient of the submarine light field
[AD-A187215] 11 p1548 N88-19261
Remote sensing of acoustic properties of shallow water sediments: A review
[AD-A192107] 18 p2570 N88-25267
Metal halide optical glasses
[AD-A193794] 23 p3198 N88-29032

ATTENUATORS
NT POTENTIOMETERS (RESISTORS)
NT RESISTORS
NT THERMISTORS

ATTITUDE (INCLINATION)
NT PITCH (INCLINATION)
NT ROLL
NT SATELLITE ORIENTATION
NT YAW
Observations of localized grain boundary dislocations in series of (001) and (110) symmetrical tilt boundaries in aluminum
[DE87-014011] 01 p0025 N88-10156
Long-term adaptation of the otolith organs 07 p0886 N88-15375
Attitude determination of artificial satellites through joint application of static and dynamic optimal estimation techniques
[INPE-4415-TDL/306] 08 p0963 N88-15832
Numerical simulations of buoyancy driven flows in cylinders and cavities for vapor crystal growth 14 p1987 N88-21854
Minimal parameter solution of the orthogonal matrix differential equation
[NASA-TM-4043] 17 p2383 N88-24165
Improvement of head-up display standards. Volume 2: Evaluation of head-up displays to enhance unusual attitude recovery
[AD-A194601] 23 p3178 N88-28921

ATTITUDE CONTROL
NT DIRECTIONAL CONTROL
NT LATERAL CONTROL
NT LONGITUDINAL CONTROL
NT SATELLITE ATTITUDE CONTROL
NT THRUST VECTOR CONTROL
Attitude Control Working Group report 01 p0016 N88-10099
Improvements to the precision pan and tilt head
[RSRE-MEMO-3998] 01 p0057 N88-10365
Predictive momentum management for a space station measurement and computation requirements
[NASA-CR-172026] 02 p0138 N88-10866
USSR Report: Engineering and Equipment
[JPRS-UEQ-87-007] 02 p0157 N88-10985
Equal-modulus vector programmed frequency control of minimally redundant structure of powered, single-degree-of-freedom gyroscopes for spacecraft attitude control system 02 p0159 N88-10994
Effect of void gas lying between fluid slugs in nutation dampers 03 p0319 N88-12015
On the root locus method applied to flexural vibration control systems 03 p0320 N88-12022
Attitude dynamics for satellites stabilized through spin
[INPE-4403-NTE/275] 08 p0963 N88-15833
Analysis, design, construction and testing of a reaction wheel model for space applications
[INPE-4358-TDL/299] 08 p0963 N88-15834
Guidance of high-altitude sounding rockets using the S19 and Spinning Rocket Altitude Control (SPINRAC) systems 08 p1034 N88-16273
Development of a coupled expert system for the spacecraft attitude control problem 09 p1205 N88-17223
A fiber optic gyro strapdown reference system for guided weapons 12 p1597 N88-19560
Analysis of the sensitivity of the attitude control system of an artificial satellite
[INPE-4285-PRE/1157] 12 p1599 N88-19573
Separation dynamics for the last stage of a launch vehicle and satellite
[INPE-4281-PRE/1153] 12 p1601 N88-19582
Electromagnetic modeling of a control valve
[INPE-4140-PRE/1048] 12 p1622 N88-19700
Characterization of integrated photovoltaic detectors for MECB solar sensors
[INPE-4408-PRE/1221] 12 p1630 N88-19754
Laser gyro attitude control system feasibility
[AD-A189368] 13 p1720 N88-20285
Utilization of strapdown inertial and non-inertial sensors in determination of satellite attitude by Kalman filters
[INPE-4313-TDL/280] 13 p1731 N88-20349
A feedback double path compensating control structure for the attitude control of a flexible spacecraft
[INPE-4464-PRE/1239] 14 p1880 N88-21240
Multivariable control law design for the AFTI/F-16 with a failed control surface using a parameter-adaptive controller
[AD-A189848] 15 p2020 N88-22040
Three axis attitude control system
[NASA-CASE-GSC-12970-1] 17 p2308 N88-23808
Attitude control laws for gas-jet spacecraft 18 p2467 N88-24643
Attitude and orbit control for the AMPTE-UKS (Active Magnetospheric Particle Tracer Explores-UK Subsatellite): Evaluation of the in-flight performance
[PB87-225199] 19 p2604 N88-25467
Spacecraft applications of advanced global positioning system technology
[NASA-CR-172063] 20 p2757 N88-26359
Spacecraft applications of advanced global positioning system technology
[NASA-CR-172055] 21 p2894 N88-27180
Airborne remote operated device
[DE88-010324] 21 p2895 N88-27188
Simulation of attitude and maneuvers for the Brazilian spin-stabilized satellite
[INPE-4271-PRE/1143] 22 p3046 N88-28079
SIRTF nod maneuvers
[NASA-TM-101007] 22 p3048 N88-28085
Angle of attack and sideslip estimation using an inertial reference platform
[AD-A194876] 24 p3319 N88-29769
Synchronous response modelling and control of an annular momentum control device
[NASA-CR-4166] 24 p3358 N88-29995
Robust design of distributed controllers for large flexible space structures
[NASA-CR-183202] 24 p3380 N88-30134
MOORE: A prototype expert system for diagnosing spacecraft problems 24 p3418 N88-30343

ATTITUDE GYROS
Equal-modulus vector programmed frequency control of minimally redundant structure of powered, single-degree-of-freedom gyroscopes for spacecraft attitude control system 02 p0159 N88-10994
Advanced gyros in spacecraft control. Digital capture loops for dry tuned gyros
[LITEF-120046] 08 p0962 N88-15827

Design, simulation and laboratory testing of an inertial system for measuring the attitude and narrow-spaced motions
[DFVLR-FB-87-42] 14 p1912 N88-21426

ATTITUDE INDICATORS
Calibration of attitude control sensors
02 p0159 N88-10995

ATTITUDE STABILITY
NT DIRECTIONAL STABILITY
NT GYROSCOPIC STABILITY
NT LATERAL STABILITY
NT LONGITUDINAL STABILITY

ATTRACTION
Weak convergence of sums of moving averages in the alpha-stable domain of attraction
[AD-A186430] 07 p0912 N88-15529

ATTRITION (MATERIALS)
U COMMINUTION

AUDIO EQUIPMENT
NT MICROPHONES
Acoustic backscattering from bottom sediment at normal incidence in the laboratory
[AD-A186905] 09 p1242 N88-17443

AUDIO FREQUENCIES
Complementary satellite sound broadcasting systems: A NASA assessment for the Voice of America
[NASA-TM-100300] 10 p1321 N88-17899
Performance of single and multiple system AM stereo decoder receivers
[PB88-168307] 15 p2057 N88-22265
Auditory pattern memory: Mechanisms of tonal sequence discrimination by human observers
[AD-A190337] 15 p2104 N88-22534
Use of optical disk technology at the Air Command and Staff College
[AD-A192424] 21 p3027 N88-27969
Divided attention revisited: Selection based on location or pitch
[AD-A193814] 22 p3133 N88-28627

AUDIO SIGNALS
A digital audio link to the Channel Islands in the UHF television band: Preliminary experimental results
[BBC-RD-1987/9] 02 p0161 N88-11011

AUDIO VISUAL EQUIPMENT
U TRAINING DEVICES
U VISUAL AIDS

AUDIOLOGY
Activities report of the Institute of Sound and Vibration Research
[ETN-87-90685] 01 p0090 N88-10589
Further investigation of tests for susceptibility to noise-induced hearing loss
[ISVR-TR-149] 14 p1952 N88-21633

AUDIOMETRY
Recommendations for organising the calibration of pure-tone audiometers
[NPL-AC-112] 09 p1167 N88-16999
Auditory evoked magnetic fields in man
[PB88-193446] 20 p2831 N88-26796

AUDITORY PERCEPTION
Recognition of isolated non-speech sounds
[AD-A184600] 03 p0306 N88-11933
Speech recognition: Acoustic-phonetic knowledge acquisition and representation
[AD-A185897] 07 p0840 N88-15097
Long-term adaptation of the otolith organs
07 p0886 N88-15375
Morphology and development of the inner ear of Anurans 07 p0886 N88-15378
Computing support for basic research in perception and cognition
[AD-A186192] 07 p0897 N88-15437
Further investigation of tests for susceptibility to noise-induced hearing loss
[ISVR-TR-149] 14 p1952 N88-21633
Mechanisms mediating perception of complex acoustic patterns
[AD-A189765] 15 p2102 N88-22520
Complex sound processing: An interdisciplinary approach
[AD-A189782] 15 p2102 N88-22523
Perception of complex auditory patterns
[AD-A190218] 15 p2102 N88-22524
Auditory perception of complex sounds
[AD-A190528] 15 p2103 N88-22529
Mechanisms mediating the perception of complex acoustic patterns
[AD-A190112] 15 p2130 N88-22705
Motor theory of auditory perception
[AD-A192095] 18 p2550 N88-25136
Contra- and ipsilateral auditory stimuli produce different activation patterns at the human auditory cortex: A neuromagnetic study
[PB88-181490] 19 p2708 N88-26098
Demodulation processes in auditory perception
[AD-A193421] 21 p2988 N88-27740
Divided attention revisited: Selection based on location or pitch
[AD-A193814] 22 p3133 N88-28627

AUDITORY SIGNALS
Multipath time-delay estimation via the EM algorithm
[PB88-106851] 07 p0845 N88-15124
Complex sound processing: An interdisciplinary approach
[AD-A189782] 15 p2102 N88-22523
Auditory perception of complex sounds
[AD-A190528] 15 p2103 N88-22529
Selective mechanisms in auditory and bimodal signal processing
[AD-A190529] 15 p2103 N88-22530
Auditory pattern memory: Mechanisms of tonal sequence discrimination by human observers
[AD-A190337] 15 p2104 N88-22534
Time-frequency representations for speech signals
[AD-A188661] 18 p2498 N88-24819
Motor theory of auditory perception
[AD-A192095] 18 p2550 N88-25136

AUDITORY STIMULI
Further investigation of tests for susceptibility to noise-induced hearing loss
[ISVR-TR-149] 14 p1952 N88-21633
Complex sound processing: An interdisciplinary approach
[AD-A189782] 15 p2102 N88-22523
Auditory pattern memory: Mechanisms of tonal sequence discrimination by human observers
[AD-A190337] 15 p2104 N88-22534
Motor theory of auditory perception
[AD-A192095] 18 p2550 N88-25136
Contra- and ipsilateral auditory stimuli produce different activation patterns at the human auditory cortex: A neuromagnetic study
[PB88-181490] 19 p2708 N88-26098
Auditory evoked magnetic fields in man
[PB88-193446] 20 p2831 N88-26796
The interaction of thalamo-cortical systems in the 40 Hz following response 21 p2979 N88-27694
Divided attention revisited: Selection based on location or pitch
[AD-A193814] 22 p3133 N88-28627
Human auditory and visual continuous evoked potentials 23 p3238 N88-29269

AUGER EFFECT
Interatomic Auger rates for the sodium fluoride crystal
[DE87-013012] 03 p0382 N88-12401

AUGER SPECTROSCOPY
Auger electron spectroscopy of oxidized titanium overlayers: Speciation of homogeneous and heterogeneous samples
[KFK-4221] 02 p0146 N88-10913
Metal modification for improved glass-ceramic to metal seals: 1. Auger results on ion implantation and vapor deposition films
[DE88-005244] 10 p1339 N88-18006
The intergranular segregation of boron in substoichiometric Ni3Al
[DE88-004783] 11 p1462 N88-18720
An electron spectroscopic investigation of high-temperature superconducting oxides
[DE88-003807] 11 p1558 N88-19325
An interpretation of the ethylenic, carbidic, and graphite auger lineshapes of chemisorbed carbon species
[AD-A189092] 13 p1736 N88-20379
Quantitative AES: The establishment of a standard reference spectrum for the accurate determination of spectrometer transmission functions
[NPL-DMA(A)-151] 14 p1887 N88-21279
Auger electron spectroscopy of contrast-forming layers on metals
[NASA-TT-20182] 16 p2178 N88-22980
Initial stages of molecular beam heteroepitaxial growth in GaAs-(Ca,Sr)F2 and GaAs/Si systems
[LAAS-87-355] 16 p2281 N88-23658
Interface characterization of Cu-Cu and Cu-Ag-Cu low temperature solid state bonds
[AD-A191015] 16 p2283 N88-23667
Application of Auger electron spectroscopy to the study of trace element effects on weldability
[DE88-010457] 21 p2915 N88-27301

AUGMENTATION
NT STABILITY AUGMENTATION
NT THRUST AUGMENTATION
Optical sizing of soot in gas turbine combustors and exhaust augmentor tubes
[AD-A183785] 01 p0006 N88-10034
Method estimating integral mean value of enhancement factor and path latitude for whistlers below magnetic latitude 10 deg 03 p0300 N88-11885
Improvements to a UHF rebroadcast television link suffering tidal fading: Countisbury UHF relay station
[BBC-RD-1987/14] 05 p0573 N88-13495
Software enhancements and modifications to Program FDTD executable on the Cray X-MP computer
[DE88-001877] 07 p0904 N88-15476
Improved input representation for enhancement of neural network performance
[DE88-001830] 07 p0907 N88-15496
Enhancement of computer system for applications software branch 07 p0923 N88-15610
New technique for enhancing helium production in ferritic materials
[DE88-003048] 09 p1142 N88-16847
Suppression of the mass enhancement in CeB6 in high magnetic fields
[DE88-002946] 09 p1241 N88-17439
Observation of enhanced electric field in an RF-plugged sheet plasma in the RFC-XX-M open-ended machine
[IPPJ-857] 09 p1252 N88-17503
Design for performance enhancement in feedback control systems with multiple saturating nonlinearities
[NASA-CR-182614] 11 p1535 N88-19168
Investigations into shock-induced enhancement of mixing and combustion in supersonic burners
[AD-A189609] 12 p1607 N88-19608
Sensitivity of control-augmented structure obtained by a system decomposition method
[NASA-TM-100535] 14 p1954 N88-21647
Real-time flight test data distribution and display
[NASA-TM-100424] 15 p2022 N88-22050
Theoretical studies of Resonance Enhanced Stimulated Raman Scattering (RESRS) of frequency-doubled Alexandrite laser wavelength in cesium vapor
[NASA-CR-182870] 15 p2036 N88-22133
Data management and language enhancement for generalized set theory computer language for operation of large relational databases
[NASA-CR-182868] 16 p2250 N88-23446
Enhanced backscattering from rough surfaces
[AD-A191089] 16 p2274 N88-23610
Saturation and the limit of jet mixing enhancement by single frequency plane wave excitation: Experiment and theory
[NASA-TM-100882] 17 p2295 N88-23732
Application of its transformation in color enhancement of LANDSAT imagery 17 p2365 N88-24082
Enhancement of volume H(-) production by vibrationally pre-exciting the hydrogen molecules
[DE88-010783] 20 p2853 N88-26937
Vapor Compression Distillation Subsystem (VCDS) component enhancement, testing and expert fault diagnostics development, volume 2
[NASA-CR-172076] 21 p2994 N88-27755

AURIGA CONSTELLATION
A flash spectrum of Cl I, C I, N I, and Ni II absorption in 31 Cygni: A direct observation of the reversing layer
04 p0513 N88-13158

AURORAL ACTIVITY
U AURORAS

AURORAL ARCS
Electrodynamics of midnight sector of auroral oval in period of slight disturbance 08 p1003 N88-16077
Characteristics of particle acceleration at high latitude
08 p1026 N88-16210
First results from the Viking associated Aureld-VIP rocket and EISCAT campaign — auroras; Swedish satellite
08 p1026 N88-16211
CAESAR investigations — Coordinated Auroral Experiment using Scatter And Rockets (CAESAR)
08 p1031 N88-16249
EISCAT measurements of ion velocities during Coordinated Auroral Experiment using Scatter And Rockets (CAESAR) campaign 08 p1031 N88-16251
Remote and in-situ plasma measurements during the Coordinated Auroral Experiment using Scatter And Rockets (CAESAR) flight 08 p1032 N88-16252
Low frequency electrostatic waves observed on board the Coordinated Auroral Experiment using Scatter And Rockets (CAESAR) 2 payload 08 p1032 N88-16253
A multiple-satellite observation of the high-latitude auroral activity on 11 January 1983
[AD-A175170] 09 p1189 N88-17122
Coordinated Auroral Experiments using Scatter And Rocket investigations (CAESAR investigations)
[MPAE-W-47-87-13] 15 p2096 N88-22487
Dynamics explorer data analysis
[NASA-CR-181428] 19 p2691 N88-25996

AURORAL ELECTROJETS
Simultaneous observation of upward moving field aligned energetic electrons and ions on auroral zone field lines
[IRF-PREPRINT-102] 16 p2231 N88-23326

AURORAL IONIZATION
Spectrophotometric remote sensing of the diffuse aurora
[AD-A188599] 12 p1643 N88-19837

AURORAL SPECTROSCOPY
Auroral X-ray images during a pulsation event
08 p1026 N88-16214
Ground-based facility for spectrophotometric studies of the airflow and aurora
[AP-29] 22 p3119 N88-28532
AURORAL TEMPERATURE
Support for FY87 midlatitude electron-density calibration campaign
[AD-A190174] 15 p2094 N88-22476
AURORAL ZONES
Electric field measurements on Viking: First results
[TRITA-EPP-87-04] 05 p0625 N88-13826
Balloon measurement of magnetic field during substorms in auroral zone 08 p1026 N88-16213
Future developments of auroral D-region research using the EISCAT VHF incoherent scatter radar
08 p1035 N88-16278
Preliminary results from the dc electric field experiment on Viking — Swedish satellite
[TRITA-EPP-87-03] 09 p1190 N88-17130
On the conjugacy of the aurora: High and low latitudes
[AD-A193008] 20 p2824 N88-26755
AURORAS
NT AURORAL ARCS
Relativistic electron precipitations in a pulsating aurora
04 p0468 N88-12894
Viking quick look plots: A short description — Swedish satellite 06 p0692 N88-14243
Polar Geophysical Institute's studies of magnetosphere, ionosphere 06 p0728 N88-14480
Dynamics Explorer guest investigator
[NASA-CR-181494] 07 p0878 N88-15325
Holes in OI 130 nm emission fields of upper atmosphere during day 08 p1004 N88-16082
Viking: The first Swedish satellite
08 p1025 N88-16207
Global views of the aurora from the Viking satellite — Swedish satellite 08 p1025 N88-16208
Instantaneous pictures of the high-latitude electrodynamics using Viking and DMSP/F7 observations — Swedish satellite
08 p1025 N88-16209
Report on ground-based activity at Andoya (Norway) in relation to the Aureid-VIP high rocket and to the Viking satellite — Swedish satellite 08 p1026 N88-16212
Auroral X-ray images during a pulsation event
08 p1026 N88-16214
First results of balloon-borne X-ray and electric field observations near the footprint of the Viking satellite
08 p1026 N88-16215
A new technique for rocket and space-borne investigations of time-dependant auroral morphology
08 p1030 N88-16241
Wave acceleration of auroral electrons
08 p1031 N88-16245
Acceleration of auroral particles by magnetic field-aligned electric fields 08 p1031 N88-16246
Observations of field-aligned current structures during the Coordinated Auroral Experiment using Scatter And Radar (CAESAR) flight 2 08 p1031 N88-16250
AURIO: A proposal for flying auroral imaging observatory on the Polar Platform in the Space Station/Columbus program 08 p1034 N88-16268
The rocket and scatter experiment ROSE: Presentation of the scientific payload 08 p1034 N88-16269
Microphysics of the auroral acceleration region of other regions of the magnetosphere 08 p1096 N88-16592
Acceleration/heating processes on auroral field lines as observed by the Viking spacecraft
08 p1096 N88-16596
Low frequency waves and small scale solitary structures observed by Viking — Swedish satellite; auroras
08 p1099 N88-16611
Acceleration of auroral particles by magnetic field-aligned electric fields
[TRITA-EPP-87-08] 09 p1190 N88-17131
Spectrophotometric remote sensing of the diffuse aurora
[AD-A188599] 12 p1643 N88-19837
Dynamics of small and large scale irregularities at sub-auroral latitudes
[AD-A189052] 12 p1645 N88-19853
Waves and static electric fields in the auroral acceleration region 12 p1646 N88-19856
On the acceleration of electrons and positive ions in the same direction along magnetic field lines by parallel electric fields
[IRF-PREPRINT-103] 15 p2096 N88-22488
A proposal for the establishment of a center of excellence in theoretical geoplasma research
[AD-A189742] 16 p2231 N88-23327
The Jovian aurora: Electron or ion precipitation
[NASA-TM-101153] 17 p2452 N88-24566
Dynamics Explorer-2 measurements during an isolated auroral substorm
[AD-A191202] 18 p2543 N88-25091
Superthermal electron processes in the upper atmosphere of Uranus: Aurora and electroglow
[NASA-TM-101150] 18 p2594 N88-25417
Dynamics explorer data analysis
[NASA-CR-181428] 19 p2691 N88-25996
Investigation of the Sun-aligned F-region walls and related phenomena in the auroral latitude range
[AFGL-TR-87-0248] 19 p2692 N88-26000
High latitude ionospheric radio studies
[AD-A192270] 20 p2824 N88-26753
The low-latitude auroral boundary: Steady-state and time-dependent representations
[AD-A193200] 21 p2972 N88-27656
On the dynamics of the auroral ionosphere during the breakup of a substorm
[AD-A193368] 21 p2972 N88-27657
Snapshots of high-latitude electrodynamics using Viking and DMSP/F7 observations
[TRITA-EPP-88-01] 23 p3234 N88-29244
Five channel auroral photometer
[REPT-112] 24 p3375 N88-30101
Structural dynamics of high-latitude magnetosphere determined from solar electron data
24 p3444 N88-30500
X- and gamma-ray background observations in Antarctic
[INPE-4583-PRE/1317] 24 p3459 N88-30578
AUSTENITE
Fatigue, fracture and strain hardening of high carbon hardened alloy steel
[AD-A186101] 07 p0831 N88-15043
Sliding-wear properties of retained austenite in carburized layer
[PB87-149092] 07 p0833 N88-15054
The effect of deformation rate on JBK-75 stainless steel forgings
[DE88-001696] 07 p0834 N88-15061
The influence of grain boundary chemistry and structure on the intergranular attack and intergranular stress corrosion cracking of austenitic alloys
[DE88-002436] 07 p0835 N88-15063
Response of Fe-Cr-Mn austenitic alloys to thermal aging neutron irradiation
[DE88-003415] 10 p1302 N88-17785
Hydrogen induced cracks in armor steel weldments fabricated with austenitic filler alloys
[AD-A188733] 13 p1740 N88-20406
Ultrasonic studies of stresses and plastic deformation in steel during tension and compression
[AD-A192308] 21 p2912 N88-27280
Kinetic of martensitic transformations induced by hydrogen in the austenite
[DE88-701623] 23 p3194 N88-29007
AUSTENITIC STAINLESS STEELS
Development of creep resistant austenitic stainless steels for advanced steam cycle superheater application
[DE87-012929] 01 p0023 N88-10147
Comparative tests of high temperature creep-rupture behavior of the austenitic CrNi steel DIN W.NR.1.4970 in argon and steam
[KFK-4261] 01 p0063 N88-10402
Study of stainless steel time-temperature sensitization diagrams, part 1
[ETN-87-90762] 03 p0289 N88-11815
Effect of helium on irradiation creep in an austenitic stainless steel
[DE87-013754] 03 p0290 N88-11824
Modified 14Cr-16Ni stainless steels with improved creep resistance at 700 C due to tailored precipitate microstructures
[DE87-014788] 03 p0290 N88-11825
Influence of some parameters on the stress corrosion of a ABNT 304 stainless steel in MgCl/sub 2/
[DE87-703707] 04 p0416 N88-12580
Method for the ultrasonic inspection of the soundness of the metal in weld joints in two-ply pipes
[BLL-CE-TRANS-8265-(9022.09)]
04 p0453 N88-12805
Ultrasonic method of inspecting austenitic weld joints in nuclear power station equipment
[BLL-CE-TRANS-8281-(9022.09)]
04 p0453 N88-12806
Welded joint fatigue of a AISI 304 L type stainless steel
[DE87-703530] 05 p0592 N88-13607
Role of interstitials and precipitates in initiation and propagation of L.C.F. cracks in austenitic stainless steels
06 p0718 N88-14411
Elevated temperature fatigue crack propagation
06 p0720 N88-14424
Sliding-wear properties of retained austenite in carburized layer
[PB87-149092] 07 p0833 N88-15054
Evolution of radiation-induced voids and dislocations at low temperature
[DE88-700350] 07 p0939 N88-15704
Effects of a regenerating heat treatment on the creep behavior and the lifetime during creep test loading
[ETN-88-91063] 09 p1144 N88-16855
Influence of post-anneal cooling treatments on suppression of cryogenic intergranular fracture in experimental Ni-free high-Mn austenitic steels
[DE88-002766] 09 p1145 N88-16863
The role of composition and microstructure gradients on weld metal properties and behavior
[DE88-004956] 10 p1303 N88-17791
Thermal fatigue of stainless steel
[DE88-004146] 11 p1458 N88-18694
Properties to seals made with Li2O-Al2O3-SiO2-glass ceramics and aluminum-containing austenitic stainless steels
[DE88-004688] 12 p1633 N88-19776
The fatigue behavior of ferritic and austenitic steels at elevated temperatures
[DE88-006304] 13 p1744 N88-20431
Improved glass-ceramic to metal seals in actuator and detonator applications with an aluminum-containing austenitic stainless steel
[DE88-004691] 13 p1749 N88-20458
Investigation of the use of horizontally polarised shear waves for TOFD studies on austenitic steel
[AERE-R-12145] 13 p1780 N88-20649
Fracture toughness characterization of SA508 and Sa533B RPB steels
[CISE-3908] 14 p1889 N88-21292
Effect of protective coatings on high-temperature fatigue of heat-resistant alloys 14 p1895 N88-21314
Dependence of hydrogen embrittlement of austenitic stainless steels on structural state of grain boundaries
14 p1896 N88-21316
Reduced-activation austenitic stainless steels: The Fe-Cr-C system
[DE88-008091] 20 p2773 N88-26442
Helium induced degradation in the weldability of an austenitic stainless steel
[DE88-009062] 20 p2773 N88-26443
Controlling phase formation and stability to improve the high temperature creep resistance of austenitic stainless steels
[DE88-011401] 21 p2914 N88-27293
AUSTRALIA
The role of low-level cooling in a conceptual model of the Australian summertime cool change: Implications for very-short-range forecasting 02 p0204 N88-11275
Australian East Coast cyclones 3: Case study of the storm of August 1986 02 p0204 N88-11276
Analysis of the reliability of Royal Australian Air force non-destructive inspection
[AD-A186979] 09 p1177 N88-17049
Mesoscale coastal ocean dynamics
11 p1517 N88-19060
Sixteenth AINSE Plasma Physics Conference. Conference handbook
[DE88-700825] 11 p1552 N88-19290
Recommended replacements for tetryl in Australian production fuzes and related ordnance
[MRL-R-1089] 13 p1754 N88-20489
Some properties of Australian produced explosive composition H-6
[MRL-TN-525] 13 p1754 N88-20490
Fire retardant coatings for military equipment: A review
[MRL-R-1104] 19 p2619 N88-25540
Propagation measurements for an Australian land mobile satellite system 19 p2645 N88-25697
AUTOCLAVES
The 700 F properties of autoclave cured PMR-2 composites
[NASA-TM-100923] 18 p2480 N88-24712
AUTOCLAVING
Determination of lumped-mass thermal properties associated with autoclave curing of graphite/epoxy composites 21 p2925 N88-27364
AUTOCOLLIMATORS
U COLLIMATORS
AUTOCORRELATION
The circular serial autocorrelation computer program
[AD-A184795] 03 p0365 N88-12295
Autocorrelation of control points on 11-band multispectral imagery
[AD-A188185] 10 p1348 N88-18056
The display of multivariate information: The effects of auto- and cross-correlation, reliability and heterogeneity
[AD-A191070] 16 p2243 N88-23398
Picosecond optical autocorrelation experiments on fast photodetectors 19 p2659 N88-25802

AUTOIONIZATION
Two-laser resonance enhanced photoionization spectrum of gas phase benzene
03 p0300 N88-11889
Correlation effects on double electron capture in highly-charged, low-energy ion-atom collisions
[DE87-013179] 07 p0930 N88-15651
Photoionization dynamics of excited molecular states
[DE88-002982] 09 p1246 N88-17468
Theoretical studies of atomic transitions
[DE88-004719] 10 p1407 N88-18389
Contributions of autoionizing resonances to the electron collisional excitation rates for Be-like ions
[AD-A190924] 18 p2572 N88-25275
Autoionization for lower level detrapping in X-ray lasers
[AD-A195845] 24 p3379 N88-30123
AUTOMATA THEORY
USSR report: Cybernetics, computers and automation technology
[JPRS-UCC-86-014] 06 p0761 N88-14669
Management of complex information in support of evolving autonomous expert systems
[AD-A186680] 09 p1224 N88-17337
Connectionist models and artificial intelligence
[RR-684-I-IMAG-66-LIFIA] 22 p3142 N88-28684
A proof of the Kahn principle for input/output automata
[AD-A194454] 23 p3248 N88-29333
The complexity of AI algorithms
[AD-A193494] 23 p3265 N88-29438
AUTOMATIC CONTROL
NT ACTIVE CONTROL
NT ADAPTIVE CONTROL
NT AUTOMATIC FLIGHT CONTROL
NT AUTOMATIC FREQUENCY CONTROL
NT AUTOMATIC LANDING CONTROL
NT CASCADE CONTROL
NT DYNAMIC CONTROL
NT FEEDBACK CONTROL
NT FEEDFORWARD CONTROL
NT LEARNING MACHINES
NT LINEAR QUADRATIC GAUSSIAN CONTROL
NT LINEAR QUADRATIC REGULATOR
NT MODEL REFERENCE ADAPTIVE CONTROL
NT NUMERICAL CONTROL
NT OFF-ON CONTROL
NT OPTIMAL CONTROL
NT SELF ADAPTIVE CONTROL SYSTEMS
NT SELF ALIGNMENT
NT SEQUENTIAL CONTROL
NT TIME OPTIMAL CONTROL
Test results and predictions for the response of near-ceiling sprinkler links in a full-scale compartment fire
[NBSIR-87/3633] 01 p0033 N88-10209
Hardware fault insertion and instrumentation system: Mechanization and validation
[NASA-CR-181445] 01 p0078 N88-10497
Optimization of a controlled two-server maintenance system
[INPE-4202-PRE/1083] 01 p0107 N88-10694
Synthesizing controllers for uncertain systems by a quantitative pole-placement
[PB87-195590] 02 p0223 N88-11403
Real time analysis of the results from mechanized ultrasonic testing
[DE87-752511] 03 p0334 N88-12107
CNET (Chief of Naval Education and Training) Program Automated Tracking System (CPATS): A comprehensive study
[AD-A184694] 03 p0385 N88-12418
Some data processing requirements for precision Nap-Of-the-Earth (NOE) guidance and control of rotorcraft
[NASA-CR-177453] 04 p0401 N88-12493
Failure control techniques for the SSME
[NASA-CR-179224] 04 p0409 N88-12537
Robust statistical methods for automated outlier detection 04 p0433 N88-12681
GOLD: Integration of model-based control systems with artificial intelligence and workstations
[DE88-000506] 04 p0483 N88-12976
On the next generation of reliability analysis tools
[NASA-CR-178380] 04 p0487 N88-13000
Ground vehicle convoying
[DE88-000360] 04 p0502 N88-13088
Automatic telescope operations
04 p0519 N88-13190
Automated design of controlled diffusion blades
[NASA-TM-100251] 05 p0542 N88-13304
Study of welding arc control in China
[PB87-143350] 07 p0863 N88-15235
Study on arc sound in TIG and plasma welding processes and the possibility of its application in practice
[PB87-143947] 07 p0863 N88-15238
Intelligent controllers
[DE88-001862] 07 p0904 N88-15475
Modelling of clustering effects in point processes: An application to failures in SPC-systems (stored program control-systems)
[PB87-149241] 07 p0904 N88-15480
Integration of symbolic and algorithmic hardware and software for the automation of space station subsystems
[NASA-TM-89705] 07 p0907 N88-15497
Investigation of candidate data structures and search algorithms to support a knowledge based fault diagnosis system 07 p0923 N88-15606
Microprocessor control and networking for the amps breadboard 07 p0924 N88-15615
NASA (National Aeronautics and Space Administration) ADP (Automated Data Processing) system: Information on the automated mission and the payload tracking system
[PB88-104989] 07 p0942 N88-15730
Advancing automation and robotics technology for the space station and for the US economy: Submitted to the United States Congress October 1, 1987
[NASA-TM-100777] 08 p0959 N88-15816
Advancing automation and robotics technology for the space station and for the US economy: Submitted to the United States Congress May 15, 1987
[NASA-TM-89811] 08 p0959 N88-15817
Advancing automation and robotics technology for the space station and for the US economy: Submitted to the United States Congress October 1, 1986
[NASA-TM-89190] 08 p0960 N88-15818
Preliminary evaluation of a micro-based repeated measures testing system
[NASA-CR-172038] 08 p1048 N88-16331
Integration of symbolic and algorithmic hardware and software for the automation of space station subsystems
08 p1056 N88-16373
KBS V and V as related to automation of space station subsystems: Rationale for a KBS lifecycle
08 p1057 N88-16375
Artificial intelligence and space power systems automation 08 p1058 N88-16381
Prototype space station automation system delivered and demonstrated at NASA 08 p1066 N88-16442
Hydrogen maser
[PB87-171617] 09 p1172 N88-17025
Computer control of a microgravity mammalian cell bioreactor 09 p1197 N88-17172
First Annual Workshop on Space Operations Automation and Robotics (SOAR 87)
[NASA-CP-2491] 09 p1203 N88-17206
Teaching artificial neural systems to drive: Manual training techniques for autonomous systems
09 p1207 N88-17238
Autonomous control procedures for shuttle rendezvous proximity operations 09 p1208 N88-17244
Automatic routing module 09 p1210 N88-17251
A conceptual framework for intelligent real-time information processing 09 p1211 N88-17257
Implementation of a robotic flexible assembly system
09 p1212 N88-17265
System integration of a Telerobotic Demonstration System (TDS) testbed 09 p1212 N88-17266
Regulation of nonlinear and generalized linear systems
[AD-A186706] 09 p1224 N88-17338
A smart, mapping, charting and geodesy control generator, phase 1
[AD-A188184] 10 p1347 N88-18055
A collaborative program of research in engineering sciences
[DE88-003383] 10 p1423 N88-18504
Robotic assembly and testing of rotary solenoids
[BDX-613-3663] 11 p1480 N88-18834
Toward automatic finite element analysis
11 p1527 N88-19120
Autonomous Liquid Encapsulated Czochralski (LEC) growth of single crystal GaAs by intelligent digital control
[AD-A187211] 11 p1555 N88-19305
Calibration of a ring laser gyro inertial navigation system 12 p1576 N88-19428
Research on flow control
[AD-A189014] 12 p1627 N88-19736
Automatic data acquisition system utilizing microcomputers: Automatic Meteorological Stations (AMS)
[INPE-4215-PRE/1096] 12 p1646 N88-19859
The automated symbolic derivation of state equations for dynamic systems
[DE88-005222] 12 p1683 N88-20060
RIAR automated research and management systems
[DE88-700934] 12 p1706 N88-20209
AVSCOM'S modifications to Teledyne Systems Company's air-to-air fire control system simulation model
[AD-A189136] 13 p1722 N88-20294
Analysis of spectral reflectance characteristics of targets under satellites and automatic cloud recognition
13 p1755 N88-20498
The evaluation of automatic barometers, illustrated by the Nakaasa barometer
[KNMI-TR-95] 13 p1774 N88-20610
The use of an automated flight test management system in the development of a rapid-prototyping flight research facility
[NASA-TM-100435] 13 p1823 N88-20896
The automated symbolic derivation of state equations for dynamic systems
[DE88-000968] 13 p1830 N88-20945
Development and flight test of an experimental maneuver autopilot for a highly maneuverable aircraft
[NASA-TP-2618] 14 p1867 N88-21153
An automated ozone photometer
[NASA-TM-100064] 14 p1908 N88-21404
Autonomous control system for Czochralski growth of LEC GaAs
[AD-A189726] 15 p2141 N88-22779
The necessity of automation in Brazil
[INPE-4346-PRE/1183] 15 p2150 N88-22832
A computational procedure for automated flutter analysis 16 p2220 N88-23250
Automatic control of an industrial process and computer aided process control by means of an expert system
[LAAS-88-004] 16 p2255 N88-23476
Automated database design technology and tools
[NASA-CR-182875] 16 p2286 N88-23687
Operation and performance of an integrated helicopter communication system 17 p2305 N88-23787
Development of an airborne facility for advanced avionics research 17 p2307 N88-23801
A design analysis for an automated robotic workpiece manipulator 17 p2344 N88-23975
Integration of symbolic and algorithmic hardware and software for the automation of space station subsystems
17 p2387 N88-24190
Connecting remote systems for demonstration of automation technologies 17 p2387 N88-24191
Knowledge based system verification and validation as related to automation of space station subsystems: Rationale for a knowledge based system lifecycle
17 p2387 N88-24192
Automatic program generation from specifications using PROLOG 17 p2388 N88-24196
An optimal disturbance rejection control system for multimegawatt space nuclear power systems
17 p2436 N88-24495
Energy optimal trajectory planning for robot manipulators and autonomous vehicles 17 p2437 N88-24497
A general approach for automating source code verification
[AD-A191461] 18 p2556 N88-25170
Development of the field-induced electron injection and impact ionization (F4I) technique for radiation hardness testing of MOS (Metal-Oxide-Semiconductor) gate insulators
[AD-A192114] 18 p2583 N88-25345
Technical feasibility study of applying auto-control methods to plating process solutions
[DE88-008014] 19 p2641 N88-25670
Technical instructions for a control operating system of the gas flow installation for the solid fuel combustion chamber
[LR-507] 20 p2788 N88-26537
Automated measurement of crack length and load line displacement at elevated temperature
[AGARD-R-751] 20 p2814 N88-26695
Feasibility study of a microprocessor controlled actuator test mechanism
[AD-A194654] 23 p3249 N88-29337
Second Conference on Artificial Intelligence for Space Applications
[NASA-CP-3007] 23 p3251 N88-29351
Space station as a vital focus for advancing the technologies of automation and robotics
[IAF-86-62] 23 p3251 N88-29352
Machine vision for real time orbital operations
23 p3253 N88-29367
Automatic object recognition
23 p3254 N88-29368
Failure modes and effects analysis automation
23 p3254 N88-29370
A plan for time-phased incorporation of automation and robotics on the US space station
23 p3255 N88-29377
Software development without languages
23 p3257 N88-29392
Utilization of artificial intelligence techniques for the Space Station power system 23 p3261 N88-29412
Spray automated balancing of rotors: Methods and materials
[NASA-CR-182151] 24 p3330 N88-29825

Artificial intelligence costs, benefits, risks for selected spacecraft ground system automation scenarios
24 p3416 N88-30332
Automated space vehicle control for rendezvous proximity operations 24 p3416 N88-30335
An automated computerized vision technique for determination of three-dimensional object geometry
24 p3419 N88-30348

AUTOMATIC CONTROL VALVES
NT PRESSURE REGULATORS

AUTOMATIC DATA PROCESSING
U DATA PROCESSING

AUTOMATIC FLIGHT CONTROL
NT AUTOMATIC LANDING CONTROL
Assessment of software quality for the AIRBUS A310 automatic pilot 02 p0128 N88-10804
Design verification and fabrication of active control systems for the DAST ARW-2 high aspect ratio wing. Part 2: Appendices
[NASA-CR-177959-PT-2] 06 p0669 N88-14102
Study on a unidirectional ring laser gyro. Part 1: Proposition of the principle and studies on the components
[NAL-TR-933] 09 p1169 N88-17010
Expert system applications in spacecraft subsystem controllers 09 p1210 N88-17254
Automatic flight control system for modern helicopters
12 p1597 N88-19558
Preliminary airworthiness evaluation of the UH-60A with Advanced Digital Optical Control System (ADOCS)
[AD-A190674] 15 p2018 N88-22030
Automation tools for demonstration of goal directed and self-repairing flight control systems
[NASA-CR-179433] 19 p2715 N88-26121
Automatic landing by computer vision
[ETN-88-92991] 23 p3175 N88-28905

AUTOMATIC FREQUENCY CONTROL
State of tuning
[NASA-TT-20195] 18 p2561 N88-25205

AUTOMATIC LANDING CONTROL
Trajectory measurement of the Fokker 100 aircraft during autoland testing
[NLR-MP-86010-U] 20 p2758 N88-26366
Automatic landing by computer vision
[ETN-88-92991] 23 p3175 N88-28905

AUTOMATIC PATTERN RECOGNITION
U PATTERN RECOGNITION

AUTOMATIC PICTURE TRANSMISSION
A low cost automatic Earth observation satellite tracking ground receiving station 17 p2309 N88-23815

AUTOMATIC PILOTS
Assessment of software quality for the AIRBUS A310 automatic pilot 02 p0128 N88-10804
Towards the unmanned cockpit
02 p0129 N88-10812
A linear quadratic Gaussian with loop transfer recovery proximity operations autopilot for spacecraft
[NASA-CR-172028] 02 p0227 N88-11433
Contribution to the improvement of the guidance accuracy of automatic pilots
[ETN-88-90607] 05 p0551 N88-13360
Reduced order optimal command applied to longitudinal automatic pilots
[SNIAS-872-111-114] 05 p0552 N88-13362
An autopilot design for the United States Marine Corps' airborne remotely operated device
[AD-A186379] 07 p0820 N88-14983
Integrated autopilot/autothrottle based on a total energy control concept: Design and evaluation of additional autopilot modes
[NASA-CR-4131] 13 p1724 N88-20308
Development and flight test of an experimental maneuver autopilot for a highly maneuverable aircraft
[NASA-TP-2818] 14 p1867 N88-21153
Low altitude: A new dimension in air refueling
[AD-A193819] 23 p3176 N88-28910

AUTOMATIC ROCKET IMPACT PREDICTORS
U COMPUTERIZED SIMULATION
U IMPACT PREDICTION

AUTOMATIC TEST EQUIPMENT
Rivista Tecnica Selenia, volume 10, number 2
[ETN-87-90763] 01 p0011 N88-10064
The ISA test system: A catalog of automatic support facilities 01 p0012 N88-10067
Ultrasonic examination of high performance polymer composites
[DRIC-T-7862] 01 p0027 N88-10170
Automated microwave dielectric constant measurement
[AD-A184182] 04 p0431 N88-12667
Survey of electronic measurement needs below 10 MHz
[PB88-110366] 07 p0844 N88-15121
Computer aided testing procedure for stress corrosion cracking investigations
[GKSS-86/E/63] 11 p1460 N88-18706
Rocketdyne automated dynamics data analysis and management system 11 p1499 N88-18954
Systems for the 21st century
17 p2302 N88-23769
Automated measurement of crack length and load line displacement at elevated temperature
[NLR-MP-87049-U] 20 p2816 N88-26706
Results of the use of an automated electrical measuring instrument calibration system
[SNIAS-881-430-107] 23 p3217 N88-29146

AUTOMATIC WEATHER STATIONS
Very short range statistical forecasting of automated weather observations
[AD-A190803] 16 p2235 N88-23349

AUTOMATION
Technology requirements for telerobotic satellite servicing in space 12 p1592 N88-19536
Principles of lazy and incremental program generation
[CWI-CS-R8749] 16 p2249 N88-23435
Automation of surface observations program
18 p2545 N88-25106
Enumeration, comments and discussion concerning papers presented during the Conference on Computer Applications in Production and Engineering (CAPE) 87
[NLR-MP-87015-U] 20 p2839 N88-26844
Advanced manufacturing management current and forthcoming technologies
[PNR90445] 22 p3159 N88-28802

AUTOMOBILE ENGINES
Japanese industrial research on lean combustion: A case study: International Research Monitoring Program
[DE87-013839] 02 p0144 N88-10904
Development of a light duty gas engine for cogeneration service
[PB87-221297] 02 p0180 N88-11119
Application of electronic fuel injection to the optimum engine for methanol utilization
[PB87-201950] 02 p0180 N88-11120
Automotive Stirling engine: Mod 2 design report
[NASA-CR-175106] 02 p0250 N88-11578
Hot piston ring tests
[NASA-TM-100256] 06 p0729 N88-14486
Advanced Gas Turbine (AGT) Technology Development Project, ceramic component developments
[NASA-CR-180871] 12 p1709 N88-20229
Advanced Gas Turbine (AGT) technology development project
[NASA-CR-180891] 12 p1709 N88-20230
Motor vehicles as sources of compounds important to tropospheric and stratospheric ozone
[PB88-195219] 18 p2540 N88-25076
The influence of foreign particles on bearing metals
[NASA-TT-20155] 20 p2775 N88-26454
Phase 1 results from the Stirling-powered vehicle project
[NASA-TM-100978] 21 p3029 N88-27980
Testing of a variable-stroke Stirling engine
[NASA-TM-100899] 24 p3440 N88-30472

AUTOMOBILE FUELS
Alternative fuels: Information on DOD's (Department of Defense's) methanol vehicle program
[PB87-213328] 02 p0156 N88-10976
Detailed kinetic modeling of autoignition chemistry
[DE87-013226] 03 p0283 N88-11782
Models for conducting economic analysis of alternative fuel vehicles
[AD-A184028] 03 p0334 N88-12103
Technical highlights of the Alternative Fuels Utilization Program
[DE88-005064] 15 p2049 N88-22205

AUTOMOBILES
NT ELECTRIC AUTOMOBILES
Steering mechanism — vehicles
[EP-PATENT-0-181-700-A1] 01 p0053 N88-10338
Identifying areas of leading edge Japanese science and technology: Patent activity and citation analysis using US POC (Patent Office Classification) classification
[PB87-204095] 02 p0249 N88-11575
A simulation study of a speed control system for autonomous on-road operation of automotive vehicles
[AD-A184030] 03 p0362 N88-12279
Computational study of three-dimensional wake structures
[REPT-2] 05 p0539 N88-13281
Applications of fatigue analyses: Transportation
05 p0608 N88-13733
Development, features of roller rocker arm reported
06 p0689 N88-14219
Report to Congress on the Automotive Technology Development Program
[DE88-003742] 07 p0864 N88-15242
Experimental investigation on the bending fatigue performance of gas carbonitrided and carburized gears
[PB87-147997] 08 p0992 N88-16003
Ergonomics of car controls for disabled people, phase 1. Part 1: Chapters 1-7. Part 2: Appendices. Part 3: References
[ISBN-0-947767-82-7] 09 p1202 N88-17204
JPRS report: Science and technology. Japan
[JPRS-JST-87-026] 16 p2184 N88-23018
Present, future of automotive hybrid IC applications discussed 16 p2185 N88-23024
The integration of digital maps in vehicle navigation systems 16 p2225 N88-23286
Incompressible Euler solution on a multiblock grid around a car configuration
[FFA-TN-1987-65] 18 p2457 N88-24586
Navigation system for land vehicles
[NASA-CASE-LAR-13322-1] 18 p2462 N88-24620
Digital maps for an electronic traffic guide
18 p2534 N88-25033
Unified methods of accelerated laboratory tests of the preparations for temporary protection of cars
[NASA-TT-20298] 21 p2921 N88-27336
A demonstration of retro-traverse using a semi-autonomous land vehicle
[DE88-009851] 21 p2957 N88-27568

AUTOMORPHISMS
A construction of simple Abelian varieties
[ZW-8702] 05 p0642 N88-13929
Mathematical morphology: An algebraic approach
[CWI-AM-R8707] 16 p2258 N88-23497

AUTONOMIC NERVOUS SYSTEM
NT SYMPATHETIC NERVOUS SYSTEM
Motion and space sickness 04 p0404 N88-12510
Direct interaction between autonomic nerves and the immune system
[AD-A188576] 12 p1667 N88-19991

AUTONOMOUS NAVIGATION
Dynamic image interpretation for autonomous vehicle navigation
[AD-A184043] 03 p0262 N88-11647
The 3-D world modeling for an autonomous robot
[DE87-013878] 03 p0333 N88-12102
A simulation study of a speed control system for autonomous on-road operation of automotive vehicles
[AD-A184030] 03 p0362 N88-12279
Autonomous Land Vehicle (ALV) planning and navigation system
[AD-A184243] 04 p0397 N88-12475
Expert robots in nuclear plants
[DE87-014839] 04 p0452 N88-12800
Satellite autonomous navigation with SHAD (Stellar Horizon Atmospheric Dispersion)
[AD-A184988] 05 p0544 N88-13313
Dealing with unanticipated events in autonomous navigation
[DE88-000590] 05 p0590 N88-13602
Range imagery algorithms for the detection of obstacles by autonomous vehicles
[AD-A185421] 05 p0659 N88-14045
A demonstration of autonomous navigation and machine vision using the HERMIES-2B robot
[DE88-002298] 07 p0862 N88-15228
Proceedings of Image Understanding Workshop, volume 2
[AD-A186104] 07 p0902 N88-15464
Real-time artificial intelligence issues in the development of the adaptive tactical navigator
09 p1211 N88-17260
An overview of vision-based navigation for autonomous land vehicles 1986
[AD-A188186] 10 p1276 N88-17640
A computer simulation study of an expert system for walking machine motion planning
[AD-A187907] 11 p1438 N88-18577
Search problems in mission planning and navigation of autonomous aircraft
[NASA-CR-182666] 12 p1579 N88-19448
Low cost mobile robot
[AD-A188507] 12 p1633 N88-19778
NAVLAB: An autonomous navigation testbed
[AD-A189049] 13 p1720 N88-20283
Local free-space mapping and path guidance for mobile robots
[AD-A192970] 20 p2810 N88-26674
A feasibility study in path planning using optimization techniques
[AD-A193030] 21 p2894 N88-27177
Three-dimensional scene analysis using stero based imaging
[AD-A193120] 21 p2894 N88-27178
A demonstration of retro-traverse using a semi-autonomous land vehicle
[DE88-009851] 21 p2957 N88-27568
Assessments of maneuverability with the TeleOperated Vehicle (TOV)
[AD-A191584] 21 p2993 N88-27751

AUTONOMY
An autonomous, closed-loop pointing system for use with satellite optics
[DE87-012011] 02 p0235 N88-11483
Expert system study for spacecraft management
[TL-2699-ISS-1] 07 p0824 N88-15004
Intelligent Mobile Autonomous System (IMAS)
[AD-A193181] 21 p3003 N88-27811
Study of standard generic approach for spacecraft (S/C) autonomy and automation (phase 3). Book A: Autonomy concept description
[ESA-CR(P)-2555-VOL-1] 23 p3185 N88-28955
Study of standard generic approach for spacecraft (S/C) autonomy and automation (phase 3). Book B: Autonomy concept application example
[ESA-CR(P)-2555-VOL-2] 23 p3185 N88-28956
Study of standard generic approach for spacecraft (S/C) autonomy and automation (phase 3). Book C: Autonomy concept summary
[ESA-CR(P)-2555-VOL-3] 23 p3185 N88-28957
Knowledge elicitation for an operator assistant system in process control tasks 23 p3253 N88-29366
Expert systems for MSFC power systems 23 p3255 N88-29375
Blackboard architectures and their relationship to autonomous space systems 23 p3261 N88-29414
Path planning and path following for the Amsterdam autonomous cart
[FVI-86-22] 24 p3380 N88-30133
Integrating information systems in a major decentralized international organization, volume 7
[AD-A195856] 24 p3439 N88-30468

AUTOPILOTS
U AUTOMATIC PILOTS

AUTORADIOGRAPHY
High resolution electron and ion microscopy
[AERE-R-12502] 10 p1297 N88-17754
Optimization of the southern electrophoretic transfer method
[DE88-004527] 10 p1299 N88-17765

AUTOREGRESSIVE PROCESSES
Least squares linear lags and limited memory filters
[NASA-CR-178381] 03 p0372 N88-12339
Application of lattice filtering techniques to CW measured time domain data
[AD-A184351] 04 p0431 N88-12671
Identifiability of multivariate ARMA models
[AD-A187394] 10 p1400 N88-18350
Identification of microwave line-of-sight multipath components 12 p1616 N88-19665
Application of the NARMAX method to nonlinear frequency response estimation
[RR-319] 14 p1964 N88-21721
Parametric methods of analysing linear and nonlinear systems
[RR-318] 14 p1967 N88-21741
Consistent estimates of autoregressive parameters for autoregressive moving average models
[RR-663-I] 15 p2109 N88-22564
Autoregressive moving average modeling of radar target signatures
[AD-A194612] 22 p3069 N88-28218
Strong law for mixing sequence
[AD-A193615] 23 p3274 N88-29490

AUXILIARY EQUIPMENT (COMPUTERS)
U PERIPHERAL EQUIPMENT (COMPUTERS)

AUXILIARY POWER SOURCES
NT FISSION ELECTRIC CELLS
NT NUCLEAR AUXILIARY POWER UNITS
NT SNAP
NT SNAP 19
NT SPACE POWER REACTORS
Design and testing of a small radial turbine for auxiliary power units 10 p1281 N88-17661

AUXILIARY PROPULSION
An 8-cm ion thruster characterization
[NASA-CR-180819] 01 p0017 N88-10106
Auxiliary propulsion system flight package
[NASA-CR-180828] 02 p0141 N88-10886
Auxiliary propulsion technology for advanced Earth-to-orbit vehicles
[NASA-TM-100237] 06 p0674 N88-14127
Component data base for space station resistojet auxiliary propulsion
[NASA-CR-180834] 10 p1293 N88-17731
A cyclic ground test of an ion auxiliary propulsion system: Description and operational considerations
[NASA-TM-100870] 17 p2313 N88-23829
Successful completion of a cyclic ground test of a mercury ion auxiliary propulsion system
[NASA-TM-101351] 24 p3339 N88-29873

AV-8A AIRCRAFT
U HARRIER AIRCRAFT

AV-8B AIRCRAFT
U HARRIER AIRCRAFT

AVAILABILITY
Resilient procedures: A structured replication approach 10 p1381 N88-18245

AVALANCHE DIODES
V-band IMPATT power amplifier
[NASA-CR-180711] 01 p0042 N88-10267
Optically tuned MM-wave IMPATT source
[AD-A185250] 05 p0577 N88-13523
Optical communication with semiconductor laser diodes
[NASA-CR-182464] 09 p1154 N88-16918
Superlattice photodetectors
[AD-A186956] 09 p1253 N88-17511
Effect of atmospheric turbulence on the bit error probability of a space to ground near infrared laser communications link using binary pulse position modulation and an avalanche photodiode detector
[NASA-TM-100699] 14 p1873 N88-21189
Examination of temperature effects on gate-to-drain avalanche breakdown in GaAs MESFETs (Metal-Semiconductor Field Effect Transistors) by measuring light emission under RF drive
[AD-A189634] 15 p2141 N88-22778
Study for the determination of general and specific properties of wide energy-band gap HgCdTe in the 1 to 2 micrometer wavelength range
[AD-A191091] 17 p2334 N88-23934
Characterization of a 30-GHz IMPATT solid state amplifier
[NASA-TM-100876] 18 p2503 N88-24847

AVALANCHES
Gas flow effects in pulse avalanche discharge XeCl excimer lasers 03 p0328 N88-12070

AVERAGE
NT MEAN
Causes of spurious features in spectral reflectance data 05 p0614 N88-13769
Weak convergence of sums of moving averages in the alpha-stable domain of attraction
[AD-A186430] 07 p0912 N88-15529
Weighted averaging method for image smoothing reported 14 p1901 N88-21352

AVHRR
U ADVANCED VERY HIGH RESOLUTION RADIOMETER

AVIATION
U AERONAUTICS

AVIATION METEOROLOGY
Meteorological systems support to critical shuttle requirements on the Eastern Test Range — STS 02 p0205 N88-11281
Study of microburst detection performance during 1985 in Memphis, Tennessee
[AD-A184013] 03 p0354 N88-12231
Eighth Session of the Commission for Aeronautical Meteorology (abridged)
[WMO-673] 06 p0745 N88-14585
Characterization of meteorological phenomena influencing aircraft operations 08 p0951 N88-15772
AEV local verification for aviation, precipitation and temperature programs: AV, REL, TEM (September 1987 revision)
[PB88-115662] 10 p1355 N88-18101
Power spectral density analysis of wind-shear turbulence for related flight simulations
[NASA-CR-182721] 13 p1802 N88-20773
Meteorological and Environmental Inputs to Aviation Systems
[NASA-CP-2498] 18 p2545 N88-25105
Automation of surface observations program 18 p2545 N88-25106
Bracknell Meteorological Office 18 p2545 N88-25107
Special observations 18 p2545 N88-25108
Applications products of aviation forecast models 18 p2546 N88-25109
General-aviation's view of progress in the aviation weather system 18 p2546 N88-25110
Objective detection and forecasting of Clear-Air Turbulence (CAT): A status report 18 p2546 N88-25114
Comparative verification between GEM model and official aviation terminal forecasts 18 p2546 N88-25115
Denver ARTCC evaluation of PROFS (Prototype Regional Observations and Forecast System) mesoscale weather products 18 p2547 N88-25117
The Federal Aviation Administration/Massachusetts Institute of Technology (FAA/MIT) Lincoln Laboratory Doppler weather radar program 18 p2547 N88-25118

AVIATION PSYCHOLOGY
Some aspects of sociopsychological screening of flying school applicants 07 p0890 N88-15392
JPRS report: Science and technology. USSR: Space Biology and Aerospace Medicine, volume 21, no. 4, July - August 1987
[JPRS-USB-88-002] 07 p0893 N88-15412
New US book on aviation psychology reviewed 07 p0896 N88-15433
Temperament Structure Scales (TSS). Test manual
[ESA-TT-1069] 09 p1201 N88-17197

AVIATORS
U AIRCRAFT PILOTS

AVIONICS
Digital system bus integrity
[NASA-CR-181446] 01 p0006 N88-10030
The ISA test system: A catalog of automatic support facilities 01 p0012 N88-10067
AI expert system technology issues for guidance and control applications 02 p0128 N88-10808
Soviet aviation technology's state of the art SU-27 fighter
[AD-A184121] 03 p0259 N88-11628
The flight evaluation of an advanced engine display and monitoring system 03 p0264 N88-11659
Helicopter (performance) management 03 p0264 N88-11666
The Avionics Flight Evaluation System (AFES) of the DFVLR
[ESA-TT-1037] 03 p0266 N88-11677
Assessment of existing specifications against the design-philosophy for grounding and inter-unit wiring (EMCR 20/85)
[EMCR-22/85] 03 p0310 N88-11956
Electronic system reliability and effectiveness
[AD-A184522] 03 p0311 N88-11961
Workshop on Avionics Corrosion Control
[AGARD-R-733] 05 p0547 N88-13331
Avionic corrosion 05 p0547 N88-13332
Corrosion of electronic components 05 p0547 N88-13333
US Naval Air Force avionic and electrical system corrosion prevention and control maintenance 05 p0547 N88-13334
Avionics and corrosion 05 p0547 N88-13336
Error propagation in a digital avionic mini processor
[NASA-CR-181565] 05 p0633 N88-13872
Diagnostic emulation: Implementation and user's guide
[NASA-CR-178391] 06 p0756 N88-14638
Supportability in aircraft systems through technology and acquisition strategy applications
[AD-A188465] 08 p0949 N88-15759
Avionics systems integration technology 09 p1110 N88-16654
Helicopters as test carriers for avionics systems (HETAS)
[DFVLR-IB-112-85/18] 09 p1116 N88-16692
Neural network based architectures for aerospace applications 09 p1204 N88-17218
Helicopter activities in Germany
[MBB-UD-487/86] 10 p1314 N88-17853
Navigation recovery block design description
[NASA-CR-182473] 10 p1342 N88-18022
Applicability of Ada (trademark) tasking for avionics executives
[AD-A188827] 12 p1578 N88-19445
An evaluation of perceptions of form, fit, function (F3) standardization on the Standard Inertial Navigation Unit (STD INU) program
[AD-A188955] 12 p1579 N88-19446
Computer architecture for efficient algorithmic executions in real-time systems: New technology for avionics systems and advanced space vehicles
[NASA-CR-182650] 12 p1675 N88-20016
Avionics acquisition, trends and future approaches 12 p1702 N88-20184
Reducing time required for the development of avionic systems 12 p1702 N88-20185
Architecture specification for PAVE PILLAR avionics
[AD-A188722] 13 p1723 N88-20303
Advanced avionics system analysis. Modular avionics cost benefit study formulation
[AD-A189019] 14 p1867 N88-21158
General aviation activity and avionics survey: 1986 data
[AD-A189986] 15 p2013 N88-22003
Reliability analysis within a Computer Aided Engineering (CAE) infrastructure
[NLR-MP-86059-U] 15 p2074 N88-22369
Information systems for quality. Experience at the Nerviano Aeritalia plant. Avionic systems and equipment group
[ETN-88-92274] 15 p2148 N88-22821
Rapid prototyping of complex avionics system architectures
[ETN-88-92275] 16 p2162 N88-22898
The use of rule induction to assist in the diagnosis of avionic circuit board defects
[ETN-88-92077] 16 p2162 N88-22899

Digital avionics design and reliability analyzer
[NASA-CR-181641] 16 p2254 N88-23472
Joint University Program for Air Transportation Research, 1986
[NASA-CP-2502] 17 p2293 N88-23715
Integrated avionics reliability 17 p2294 N88-23723
Integrated Application of Active Controls (IAAC) technology to an advanced subsonic transport project: Program review
[NASA-CR-3880] 17 p2301 N88-23763
The Design, Development and Testing of Complex Avionics Systems
[AGARD-CP-417] 17 p2302 N88-23767
Technology development program for twenty-first century aerospace vehicles 17 p2302 N88-23768
Systems for the 21st century 17 p2302 N88-23769
Rapid prototyping of complex avionic system architectures 17 p2302 N88-23771
The specification and design of a future maritime reconnaissance aircraft 17 p2303 N88-23772
A structured approach to weapon system design 17 p2303 N88-23773
Development of a generic architecture 17 p2303 N88-23774
Test philosophy of the EH101 integrated avionic 17 p2303 N88-23775
Systems engineering technique 17 p2303 N88-23776
Modeling of functional specifications for onboard software: Experience with the Rafale avionics system 17 p2303 N88-23777
The avionics software architecture impact on system architecture 17 p2303 N88-23778
A comparison of integrated and separate systems for flight control and navigation 17 p2303 N88-23779
Development and testing of a predictive methodology for optimization of man-machine interface in future avionics systems 17 p2304 N88-23780
Crewstation Information and Development System (CIDS) 17 p2304 N88-23781
Managing advanced avionic system design 17 p2304 N88-23783
Psychosensory cockpit ergonomics, advantages of intelligent information systems 17 p2304 N88-23784
Advanced development of a cockpit automation design support system 17 p2304 N88-23785
Design and development of an avionics system adapted to helicopter missions 17 p2305 N88-23786
Operation and performance of an integrated helicopter communication system 17 p2305 N88-23787
Designing for design effectiveness of complex avionics systems 17 p2305 N88-23788
Design for interoperability (interchangeability) 17 p2305 N88-23789
The electromagnetic threat to future avionic systems 17 p2305 N88-23790
The integration, characterisation and trialling of a modern complex airborne radar 17 p2305 N88-23791
Experience in the integration of human engineering effort with avionics systems development 17 p2305 N88-23793
Testing complex avionics software: A practical experience 17 p2306 N88-23794
A look toward the future of complex avionics systems development using the USAF Test Pilot School's avionics systems test training aircraft 17 p2306 N88-23797
Software engineering for the British Aerospace Experimental Aircraft Programme (EAP) 17 p2306 N88-23798
Avionics systems: Development method and computer tools 17 p2306 N88-23799
Development of an airborne facility for advanced avionics research 17 p2307 N88-23801
Workshops for the design of avionics systems and the development of onboard software 17 p2307 N88-23802
Coherent functional development: Key to successful future system integration 17 p2307 N88-23803
Development of complex avionics systems: Experience from French military programs 17 p2307 N88-23804
User's guide to the Fault Inferring Nonlinear Detection System (FINDS) computer program
[NASA-CR-178410] 18 p2462 N88-24619
Development of an airborne facility for advanced avionics research
[NLR-MP-87012-U] 20 p2760 N88-26368
A cockpit natural language study - selected transcripts
[AD-A192972] 20 p2834 N88-26808
Air Force technical objective document, FY89
[AD-A193110] 21 p2896 N88-27194
Computation of ECM (Electronic Counter-Measures) war reserve materiel spare requirements
[AD-A193301] 21 p2897 N88-27195
The impact of increased aircraft reliability on maintenance facility design
[AD-A194395] 22 p3042 N88-28057
Avionic and electrical system corrosion prevention and control maintenance 22 p3054 N88-28119
Electronic failure analysis-corrosion of avionics 22 p3054 N88-28122
Avionics system design for high energy fields: A guide for the designer and airworthiness specialist
[NASA-CR-181590] 23 p3178 N88-28919
Aircraft avionics and missile system installation cost study. Volume 1: Technical report and appendices A through E
[AD-A194605] 23 p3178 N88-28923
Avionic expert systems 23 p3253 N88-29365
Contribution of expert systems to avionics advance. Application on AS30 laser weapon system
[SNIAS-881-320-103] 23 p3267 N88-29449
The OFP (Operational Flight Program) update cycle needs you
[AD-A194910] 24 p3325 N88-29798
Aircraft avionics and missile system installation cost study. Volume 2: Appendices F and G
[AD-A195372] 24 p3325 N88-29801

AVOIDANCE
NT COLLISION AVOIDANCE
Windshear training aid. Volume 1: Overview, pilot guide, training program
[PB88-127196] 10 p1276 N88-17637

AXAF
U X RAY ASTROPHYSICS FACILITY

AXES (COORDINATES)
U COORDINATES

AXES (REFERENCE LINES)
NT AXES OF ROTATION
NT EARTH AXIS

AXES OF ROTATION
NT EARTH AXIS
Resources, confusions and compatibility in dual axis tracking: Displays, controls and dynamics
[AD-A185871] 07 p0898 N88-15440
Data acquisition and analysis system for the Sandia 34-meter Vertical Axis Wind Turbine
[DE88-002417] 09 p1187 N88-17112
Study on a rotor speed control system for a horizontal axis windmill
[NAL-TR-931] 10 p1349 N88-18062

AXIAL COMPRESSION LOADS
Elastoplastic response of unidirectional graphite/aluminum under combined tension-compression cyclic loading
[CCMS-88-01] 11 p1451 N88-18647
Fracture criterion of reactor graphite under multiaxial stresses 13 p1746 N88-20442
Local delamination buckling in layered structures 18 p2480 N88-24711

AXIAL COMPRESSORS
U TURBOCOMPRESSORS

AXIAL FLOW
Experimental study of interacting vortex rings 03 p0318 N88-12007
Gas dynamic characteristics in past axial flow CO2 laser 03 p0327 N88-12067
Application of modified loss and deviation correlations to transonic axial compressors
[AGARD-R-745] 05 p0549 N88-13344
Highlights from a research program on a very highly loaded axial gas generator turbine 06 p0713 N88-14369
Computation of secondary flows in an axial multistage compressor 10 p1284 N88-17681
Boundary effects on the drag of a cylinder in axial motion at low Reynolds number 13 p1768 N88-20578
Supersonic axial-flow fan flutter 16 p2221 N88-23255
Hydrogen turbines for space power systems: A simplified axial flow gas turbine model 17 p2419 N88-24385
Solid rocket motor aft field joint flow field analysis
[NASA-CR-179288] 18 p2474 N88-24675
Experimental investigation of propfan aeroelastic response in off-axis flow with mistuning
[NASA-TM-101320] 22 p3089 N88-28344
Nonequilibrium flow of a radiating gas in a vertical channel with axial temperature variation
[DE88-702535] 23 p3212 N88-29120
Studies of unsteady axial-compressor functioning 24 p3380 N88-30129

AXIAL FLOW COMPRESSORS
U TURBOCOMPRESSORS

AXIAL FLOW PUMPS
NT TURBINE PUMPS
High Reynolds number pump facility for cavitation research
[AD-A189310] 13 p1765 N88-20558
Rotor self-lubricating axial stop
[NASA-CASE-MFS-28273-1] 17 p2344 N88-23974

AXIAL FLOW TURBINES
Modal testing of a very flexible 110 m wind turbine structure
[DE88-003796] 10 p1351 N88-18072
Visualization of flows in turbomachinery
[AD-A189927] 15 p2063 N88-22299
Visualisation of the flow at the tip of a high speed axial flow turbine rotor
[AD-A189928] 15 p2063 N88-22300
Visualisation of the flow at the tip of a high speed axial flow turbine rotor: An assessment of flow visualisation techniques and the requirement of the experimental turbine
[AD-A189929] 15 p2063 N88-22301
Experimental vibration damping characteristics of the third-stage rotor of a three-stage transonic axial-flow compressor
[NASA-TM-100948] 18 p2466 N88-24642
Hydrogen turbines for space power systems: A simplified axial flow gas turbine model
[DE88-009585] 19 p2677 N88-25920

AXIAL LOADS
NT AXIAL COMPRESSION LOADS
The use of Hencky's equations for the estimation of multiaxial elastic-plastic notch stresses and strains
[FB-3/1986] 01 p0060 N88-10383
Stress-strain analysis and life predictions of a notched shaft under multiaxial loading
[FB-5/1986] 01 p0060 N88-10384
Application of fracture mechanics theory in the reliability analysis of structural ceramics in multiaxial loading 03 p0335 N88-12113
Analysis and testing of predamaged shell structures 04 p0428 N88-12653
Micromechanics of fatigue crack initiation under axial and torsional loadings 06 p0719 N88-14413
Residual stress effect on stability of axially loaded columns
[PB87-143889] 08 p0996 N88-16032
An experimental and numerical study of notch sensitivity of ARALL laminates
[CCMS-88-04] 11 p1450 N88-18644
Fracture criterion of reactor graphite under multiaxial stresses 13 p1746 N88-20442
Notch sensitivity of graphite materials for VHTR 13 p1747 N88-20447
Cyclic uniaxial and biaxial hardening of type 304 stainless steel modeled by the viscoplasticity theory based on overstress 14 p1931 N88-21514
Damage models for delamination and transverse fracture
[AD-A189652] 15 p2029 N88-22088
Numerical and experimental research on propagation of elastic stress waves in conical shell under axial impulsive loading 15 p2053 N88-22238
JPRS report: Science and technology. USSR: Materials science
[JPRS-UMS-88-006] 16 p2179 N88-22988
Effect of uniaxial compression on physical and mechanical properties of ferroelectric ceramic material 16 p2180 N88-22993
Effects of axial load on elastomeric isolation bearings
[PB88-179015] 16 p2223 N88-23269
Integrated polysilicon tactile sensor 19 p2669 N88-25863
Forces and moments on a slender, cavitating body
[DE88-007208] 21 p2945 N88-27491
Stress relaxation of a titanium (Ti-6Al-4V) threaded joint
[DE88-010102] 21 p2961 N88-27590
Development of a biaxial test system for thin-walled metal tubes using tensile-compressive axial load and internal-external pressure
[DE88-011279] 21 p2962 N88-27592
An experimental and analytical evaluation of a biaxial test for determining shear properties of composite materials
[NASA-CR-182928] 21 p2962 N88-27593
An anisotropic continuum damage model for creep-dominated, multiaxial loading histories 21 p2964 N88-27608
Failure analysis of quasi-isotropic composite laminates with free edges under off-axis loading 22 p3049 N88-28092
Determination of multiaxial flow surfaces at elevated temperatures using the concept of dissipation potential
[ORNL/TM-10787] 24 p3383 N88-30149

AXIAL MODES
Generating soft X-ray spectra using the SPEED pentaxial diode
[DE87-013591] 01 p0098 N88-10647
Aerodynamic design and performance of a bent-axis geometry vehicle
[DE87-013726] 02 p0124 N88-10786

Permanent magnet excitation of axial flow synchronous machines with high rotation moment
[ETN-88-92385] 20 p2796 N88-26592

AXIAL STRAIN
On the relations between cyclic contraction ratio, flow stress, and deformation mechanisms in bainitic CrMoV steels
[VTT-36] 01 p0025 N88-10158
Fatigue oxidation interaction in low cycle fatigue
06 p0719 N88-14420
Effect of uniaxial stress on the Raman spectra of graphite fibers
[AD-A191730] 18 p2492 N88-24783
Uniaxial tensile strain measurement for ceramic testing at elevated temperature: Requirements, problems and solutions
[DE88-008090] 19 p2621 N88-25550

AXIAL STRESS
Ion-implantation-induced stress in glasses: Variation of damage mode efficiency with changes in glass structure
[DE87-013523] 01 p0028 N88-10175
Life prediction of steel cords
06 p0715 N88-14386
An investigation of the failure response of laminates under biaxial stress
[AD-A190039] 15 p2029 N88-22090
J-integral measurement using moire interferometry
[AD-A193751] 23 p3226 N88-29202

AXIOMS
Using design axioms and topology to model database semantics
[CWI-CS-R8711] 13 p1818 N88-20863
Algebra of Communicating Processes (ACP)tau: A universal axiom system for process specification
[CWI-CS-R8725] 13 p1819 N88-20869
A convergence theorem in process algebra
[CWI-CS-R8733] 13 p1827 N88-20920
Pairwise complete regularity as a separation axiom
[REPT-87-57] 16 p2264 N88-23539
Fixpoint representations of characteristic sets of linear-time temporal formulas
[CWI-CS-R8754] 20 p2840 N88-26849

AXISYMMETRIC BODIES
Numerical study of supersonic flow around blunt bodies with extended needle nose 04 p0425 N88-12635
The drag of slender axisymmetric cones in rarefied hypersonic flow 05 p0531 N88-13229
Hypersonic static and dynamic stability of axisymmetric shapes: A comparison of prediction methods and experiment 05 p0534 N88-13246
The role of computation fluid dynamics in aeronautical engineering (4). The development and applications of implicit TVD finite volume code
05 p0536 N88-13259
Development of the computer program for turbulent boundary layers 05 p0536 N88-13264
Rarefied gas numerical wind tunnel. 2: Two-dimensional and axially symmetric bodies 05 p0538 N88-13273
Coupled FE and HIE method for exterior acoustics of axisymmetric shells --- finite element (FE) Helmholtz integral equation (HIE)
[ARE-TM(UHA)-87506] 09 p1243 N88-17448
A simplified streamline swallowing procedure for the windward meridian of axisymmetric blunt bodies
[AD-A188413] 12 p1626 N88-19732
Nonaxisymmetric body supersonic, aerodynamic prediction
[AD-A189338] 13 p1716 N88-20259
Static performance of an axisymmetric nozzle with post-exit vanes for multiaxis thrust vectoring
[NASA-TP-2800] 13 p1719 N88-20280
Active control of 2-D instability waves on an axisymmetric body
[AD-A191578] 19 p2663 N88-25835
Influence of rear body geometry on the velocity characteristics of the near wake
[ISL-R-113/87] 20 p2753 N88-26339

AXISYMMETRIC DEFORMATION
U AXIAL STRAIN

AXISYMMETRIC FLOW
NT ANNULAR FLOW
Effect of empennage arrangement on single-engine nozzle/afterbody static pressures at transonic speeds
[NASA-TP-2753] 02 p0122 N88-10771
Numerical analysis of axisymmetric flow with H2-O2 reactions 05 p0538 N88-13272
Method of calculations for flow of ideal gas through plane and axisymmetric nozzles with broken-line contour
06 p0771 N88-14737
New techniques in computational aerodynamics
[AD-A186719] 09 p1112 N88-16664
Numerical simulation of axisymmetric turbulent flow in combustors and diffusors
[NASA-CR-4115] 10 p1268 N88-17582
On the interaction of Tollmein-Schlichting waves in axisymmetric supersonic flows
[NASA-CR-181619] 10 p1331 N88-17955
Visualisation of the flow at the tip of a high speed axial flow turbine rotor
[AD-A189928] 15 p2063 N88-22300
An investigation of ducted propellers in axisymmetric shear flow 16 p2202 N88-23136
Initial condition effect on pressure waves in an axisymmetric jet
[NASA-TM-100915] 16 p2209 N88-23184
Saturation and the limit of jet mixing enhancement by single frequency plane wave excitation: Experiment and theory
[NASA-TM-100882] 17 p2295 N88-23732
Solid rocket motor aft field joint flow field analysis
[NASA-CR-179288] 18 p2474 N88-24675
Nonaxisymmetric viscous lower branch modes in axisymmetric supersonic flows
[NASA-CR-181687] 21 p2891 N88-27164
Velocity measurements and flow visualization in turbulent three-dimensional supersonic flows using oxygen flow tagging
[AD-A192551] 21 p2892 N88-27165
Coupled experimental and theoretical investigations of instability, chaos and turbulence in an axisymmetric jet flow
[AD-A192943] 21 p2942 N88-27476
Fellowships in hypersonic aerodynamics
[AD-A194265] 23 p3172 N88-28885

AXISYMMETRY
U SYMMETRY

AXLES
U SHAFTS (MACHINE ELEMENTS)

AZIDES (INORGANIC)
In-situ vibrational spectroscopy of specifically adsorbed azide on silver electrodes
[AD-A188511] 12 p1605 N88-19600

AZIDES (ORGANIC)
Polyazidoesters as energetic polymers and copolymer components with fluoro derivatives
[AD-A194236] 23 p3199 N88-29039

AZIMUTH
Optical alignment of Centaur's inertial guidance system
[NASA-TM-88844] 04 p0405 N88-12515
An optimal structure for a 34-meter millimeter-wave center-fed BWG antenna: The Cross-Box concept
11 p1472 N88-18778
The orientation of global satellite networks
11 p1506 N88-18996
Analysis of a range estimator which uses MLS angle measurements
[NASA-CR-182896] 16 p2160 N88-22884
Small scale mixing in the initial region of a jet
[AD-A193500] 23 p3192 N88-28994

AZO COMPOUNDS
NT HMX
NT RDX

AZOLES
NT CARBAZOLES
NT PYRROLES
Ordered polymers for space applications
[AD-A188460] 12 p1610 N88-19630

AZULENE
Energy transfer studies with lasers
[DE88-004864] 10 p1337 N88-17991
The effect of oriented defects on long-range ordering of hydrocarbon films: Azulene on Pt(111)
[AD-A196089] 24 p3344 N88-29904

AZUR SATELLITE
AZUR, the first German research satellite 625-A, 1964-1969 10 p1310 N88-17827

B

B STARS
A helium flare on the active G5 dwarf Kappa Ceti
04 p0519 N88-13189
Consistent spherical Nonlocal Thermal Equilibrium (NLTE) models for objects with B-star-like luminosities
[ETN-88-90601] 06 p0800 N88-14897
A spherical, non-LTE, blanketed model stellar atmosphere for Phi Cas (FOIa)
10 p1428 N88-18528
The effects of rotation on the winds from hot stars
11 p1569 N88-19393

B-1 AIRCRAFT
Surface disturbances produced by low-level, subsonic B-1 aircraft
[AD-A192257] 20 p2824 N88-26752

B-57 AIRCRAFT
Analyses and assessments of span wise gust gradient data from NASA B-57B aircraft
[NASA-CR-178288] 01 p0002 N88-10007

B-70 AIRCRAFT
An experimental investigation of dynamic ground effect
[NASA-CR-4105] 04 p0394 N88-12458

BAC AIRCRAFT
NT VC-10 AIRCRAFT

BACILLUS
Growth and differentiation of Bacillus subtilis under microgravity conditions 22 p3060 N88-28158

BACK INJURIES
Sitting posture of pilots in the Boelkow 105c helicopter
[IZF-1986-22] 09 p1202 N88-17202

BACKFIRE ANTENNAS
Improved backfire antenna using circular dipole
11 p1468 N88-18757

BACKGROUND NOISE
The assessment of the sound insulation requirements for a large broadcasting studio, using a scale model: Practical details
[BBC-RD-1987/21] 10 p1318 N88-17878
Determination of distributed resistance of base of bipolar transistors measuring noise spectral densities
[DE88-700197] 11 p1479 N88-18829
Stellar scintillometer atmospheric optical turbulence profiling experiment: A qualitative comparison of two identical instruments at AMOS (Air Force Maui Optical Station), 1985
[AD-A190589] 15 p2094 N88-22479
Sources and levels of background noise in the NASA Ames 40- by 80-foot wind tunnel
[NASA-TM-100077] 17 p2395 N88-24239
Effect of hypoxia on speech recognition in noise
[AD-A193943] 23 p3240 N88-29280

BACKGROUND RADIATION
Quantification of the background signal to solar neutrino detection from cosmogenic activation of the atmosphere
[DE87-013830] 01 p0119 N88-10762
Particle physics and cosmology
[DE87-005400] 03 p0387 N88-12432
Dipole component of relict radiation determined from Relikt experiment data 08 p1002 N88-16070
The origin of the diffuse X-ray background and the formation of galaxies and voids
10 p1428 N88-18527
A sky temperature survey at 19.2 GHz using a balloon borne Dicke radiometer for anisotropy tests of the cosmic microwave background 11 p1571 N88-19403
An attempt to measure the diffuse brightness of the sky at submillimeter wavelengths
12 p1710 N88-20233
Measurements of the cosmic background radiation
[NASA-CR-182637] 12 p1712 N88-20248
Observations of the large scale anisotropy in the cosmic background radiation at 3 mm
[INPE-4425-PRE/1229] 12 p1712 N88-20249
Specification for an infrared satellite surveillance system for the detection of aircraft
[AD-A189592] 13 p1797 N88-20746
A low-frequency measurement of the spectrum of the cosmic microwave background radiation
13 p1858 N88-21112
A map of the cosmic background radiaton at 3 millimeters
[INPE-4529-PRE/1279] 15 p2152 N88-22850
The two-dimensional one component plasma in a doubly periodic background: Exact results
[AD-A191260] 16 p2280 N88-23650
Sky radiance distributions for thermal imaging backgrounds
[AD-A191135] 17 p2373 N88-24115

BACKSCATTERING
Investigation of lidar backscatter including depolarization and higher scattering orders
[ETN-87-90431] 01 p0052 N88-10334
Airborne lidar studies of Arctic polar stratospheric clouds 01 p0069 N88-10443
Underwater acoustic backscatter from a model of arctic ice open leads and pressure ridges
[AD-A184693] 03 p0354 N88-12234
Measurement of cirrus cloud optical properties by high spectral resolution lidar 04 p0470 N88-12906
Large bandwidth ground scattering model --- radar scattering
[FOA-C-30458-3.2] 05 p0576 N88-13511
Electromagnetic wave probing of Earth's environment
[NASA-CR-182358] 06 p0690 N88-14232
The inverse back scattering problem for the Schroedinger equation in two space dimensions
[AD-A185603] 06 p0765 N88-14701
Research on acoustical scattering, diffraction catastrophes, optics of bubbles, photoacoustics, and acoustical phase conjugation
[AD-A185785] 06 p0776 N88-14761
Backscatter from a periodic rough surface at near grazing incidence
[NASA-CR-182397] 07 p0845 N88-15128

Electromagnetic fields backscattered from an s-shaped inlet cavity with an absorber coating on its inner walls
[NASA-CR-182401] 07 p0845 N88-15130
Design of the Backscatter Spectroscopy System for the Nova Laser Facility
[DE88-001880] 07 p0859 N88-15214
A backscatter lidar proposed for the second German Spacelab mission 08 p1018 N88-16173
Backscattering signal analysis concerning a three-dimensional object configuration on the basis of object motion
[ESA-TT-1044] 09 p1154 N88-16915
Focused ultrasonic backscatter technique for near-surface flaw detection in structural ceramics
[DE88-003112] 09 p1183 N88-17091
Acoustic backscattering from bottom sediment at normal incidence in the laboratory
[AD-A186905] 09 p1242 N88-17443
Composition and thickness of multilayer foils using MeV ion-beam techniques
[DE88-004360] 11 p1448 N88-18629
Backscatter from flaws in fiber-reinforced composites 11 p1450 N88-18639
Backscattering from three dimensional conducting bodies
[AD-A187570] 11 p1470 N88-18788
Depolarized infrared reflectance from dry and wetted surfaces
[AD-A188213] 11 p1492 N88-18903
Atmospheric backscatter at 10.6 microns; a compendium of measurements made outside the United Kingdom by the airborne LATAS coherent laser radar velocimeter
[RSRE-87002] 12 p1631 N88-19783
Observations of the upper ocean using a multi-beam Doppler sonar
[AD-A188896] 12 p1649 N88-19878
A polarimetric rain backscatter model developed for coherent polarization diversity radar applications 13 p1759 N88-20520
Radial track of moving objects determined by HF backscatter technique 14 p1901 N88-21354
Corrections for differential scattering by aerosols in the measurement of ozone by DIAL --- differential absorption lidar (DIAL)
[NPL-QU-78] 14 p1945 N88-21603
Space-time structure of ultrashort light pulses formed during stimulated backscattering of laser beam 14 p1972 N88-21767
Enhanced backscattering from rough surfaces
[AD-A190995] 16 p2190 N88-23063
Enhanced backscattering from rough surfaces
[AD-A191089] 16 p2274 N88-23610
The application of Rutherford backscattering for analyzing multilayered structure change induced by pulsed ion beam bombardment 16 p2278 N88-23638
Radar penetration in the Amazonian rain forest 17 p2358 N88-24044
Multiple scattering of waves in discrete random media
[AD-A191068] 18 p2499 N88-24623
Radio-wave scintillations and ionospheric irregularities at high latitudes
[AD-A192140] 18 p2501 N88-24837
Center for thin film studies
[AD-A191996] 19 p2732 N88-26226
Sources of scattering in vegetarian and other surfaces and objects
[NASA-CR-182975] 20 p2816 N88-26710
ZT imaging system for layered thin wall structures
[AD-A195466] 24 p3352 N88-29954
The effect of equatorial ionospheric irregularities on the performance of a south-looking OTH-B (Over-The-Horizon-Backscatter) radar
[AD-A195090] 24 p3362 N88-30018
Measurement and interpretation of North Atlantic Ocean marine radar sea scatter
[AD-A196239] 24 p3364 N88-30036
Spaceborne lidar: Development of a laboratory test system
[BF-R-66.090-1] 24 p3378 N88-30118

BACKWARD FACING STEPS

Numerical solution of turbulent flow past a backward facing step using a nonlinear K-epsilon model
[NASA-CR-178421] 07 p0854 N88-15189
Navier-Stokes solutions for laminar incompressible flow over a NACA 0012 airfoil and a backward facing step
[FFA-TN-1987-50] 09 p1162 N88-16966
Modeling the stability of a turbulent premixed flame, downstream from a step by a Lagrangian method 24 p3350 N88-29943

BACKWARD WAVES

JPRS report: Science and technology. China
[JPRS-CST-87-034] 03 p0301 N88-11897
New physical explanation of phase-conjugate waves produced in backward stimulated scattering 03 p0302 N88-11900

BACTERIA

NT BACILLUS
NT ESCHERICHIA
NT PSEUDOMONAS
NT STAPHYLOCOCCUS
Application of photosynthetic N(2)-fixing cyanobacteria to the CELSS program 03 p0358 N88-12257
Study of certain biological characteristics of bacteria during the French-Soviet CYTOS-2 space experiment 04 p0473 N88-12917
Investigation of effect of silver compounds on microflora in water reclaimed from atmospheric moisture condensate in a closed environment 07 p0892 N88-15407
Possible use of plasmids for study of effect of space flight factors on biological objects 08 p1046 N88-16319
Analysis of gases in the earth's crust
[PB88-141619] 10 p1354 N88-18093
Antibiotic activity in space, results and hypothesis 12 p1660 N88-19952
Production and turnover of suspended organic detritus in the coastal water of the southeastern continental shelf
[DE88-005118] 14 p1951 N88-21631
Saccharification of cellulose by combined fungal and bacterial preparations 17 p2316 N88-23833
The synthesis of polyphenylene from a CIS-dihydrocatechol biologically produced monomer 18 p2478 N88-24699
Biodegradation of JP-5 aviation fuel by subsurface microbial communities
[AD-A192743] 20 p2781 N88-26493
Genetic effects of low level microwave radiation
[AD-A192687] 21 p2984 N88-27722

BACTERIAL DISEASES

A solid phase enzyme-linked immunosorbent assay for the antigenic detection of Legionella pneumophila (serogroup 1): A compliment for the space station diagnostic capability 06 p0795 N88-14868
Use of bifidumbacterin for correction of intestinal dysbacteriosis 07 p0895 N88-15427

BACTERIOLOGY

Study of certain biological characteristics of bacteria during the French-Soviet CYTOS-2 space experiment 04 p0473 N88-12917

BAFFLES

Computational studies of wave-shaping in a blast simulator by perforated plates in the driver
[AD-A188200] 11 p1483 N88-18850

BAGS

NT GAS BAGS

BAINITIC STEEL

On the relations between cyclic contraction ratio, flow stress, and deformation mechanisms in bainitic CrMoV steels
[VTT-36] 01 p0025 N88-10158
Activities report in metal manufacturing
[ISSN-0524-7705] 07 p0839 N88-15086
On the relations between cyclic contraction ratio flowstress and deformation mechanisms in bainitic CrMoV steels
[DE87-753043] 08 p0968 N88-15856

BALANCE

Energy balance in laser-irradiated vaporizing droplets
[DE88-000525] 04 p0449 N88-12782
A GaAs MESFET balanced mixer with very low intermodulation
[AD-A184848] 05 p0655 N88-14015
An empirical investigation of load indices for load balancing applications
[AD-A185763] 06 p0724 N88-14451
Functional development of gravity receptors in insects and amphibians 07 p0886 N88-15376
An analysis of DREO's (Defence Research Establishment Ottawa) analog rebalance loops for the CSG-2 (Canadian Strapdown Gyroscope) tuned-rotor gyroscope
[AD-A188577] 12 p1629 N88-19749
The effect of sting interference at low speeds on the drag coefficient of an ellipsoidal body using a magnetic suspension and balance system
[NASA-CR-181611] 13 p1718 N88-20274
Development of a torsion balance for adhesion measurements
[NASA-TM-100799] 13 p1748 N88-20454
Stability of uncapsulated weight cells with thin film elongation measurement bands under influence of humidity, temperature and operation voltage
[ETN-88-92383] 21 p2951 N88-27531

BALANCE EQUATIONS

U EQUATIONS

BALANCING

Balancing strain gauge bridges
[GB-PATENT-2-129-567-A] 01 p0048 N88-10307
Model adaptation and imbalance compensation in rotors with active magnetic bearings
[ETN-87-90440] 01 p0056 N88-10361
Botany Facility: Considerations and analyses of the balancing system philosophy proposed for the BF centrifuge
[SIRA-A/7373/WP110/PWF001] 17 p2378 N88-24139
Spray automated balancing of rotors: Methods and materials
[NASA-CR-182151] 24 p3330 N88-29825

BALL BEARINGS

Investigation of instability, dynamic forces, and effect of dynamic loading on strength of cages for the bearings in the high pressure oxygen turbopumps for the space shuttle main engine
[NASA-CR-178970] 06 p0714 N88-14378
Mechanisms of rolling contact spalling
[NASA-CR-179243] 06 p0714 N88-14380
Models for steady and nonsteady Coulomb torque in ball bearings 14 p1876 N88-21208
Ball bearings with chemical vapor deposition (CVD)-TiC coated components 14 p1876 N88-21210
Experience with duplex bearings in narrow angle oscillating applications 14 p1926 N88-21484
On the torque and wear behavior of selected thin film MOS2 lubricated gimbal bearings 14 p1926 N88-21485
Titanium carbide coatings for aerospace ball bearings 14 p1927 N88-21486
Two gimbal bearing case studies: Some lessons learned 14 p1927 N88-21487
Investigation of rolling contact fatigue of ball bearings
[NASA-TT-20196] 19 p2678 N88-25922
Evaluation of transfer films of Salox M on 440C for HPOTP bearing cage applications, task 119
[NASA-CR-179020] 23 p3223 N88-29184

BALLISTIC MISSILES

Rocket and airjet propulsion for ballistic and aerodynamic space probes
[REPT-TR-527] 10 p1310 N88-17826
Where directed energy stands in strategic defense
[DE88-005092] 10 p1403 N88-18365

BALLISTIC RANGES

Design and implementation of the ESL compact range underhung bridge crane
[NASA-CR-182396] 07 p0862 N88-15231

BALLISTIC TRAJECTORIES

Ballistic Single Stage Carrier Vehicle (BETA): A single stage reusable ballistic space shuttle concept
[MBB-UR-949/70] 10 p1310 N88-17828
Trajectory characteristics and heating of hypervelocity projectiles having large ballistic coefficients
[NASA-TP-2614] 12 p1574 N88-19412
Motion in a random gyrotropic environment in D dimensions
[PB87-170650] 12 p1685 N88-20079
Aerodynamic possibilities for the realization of trajectory corrections
[ISL-CO-251/86] 14 p1862 N88-21120
Distribution of neutral gas molecules at large distances from Halley's comet 14 p1999 N88-21914

BALLISTICS

NT HYDROBALLISTICS
NT INTERIOR BALLISTICS
NT TERMINAL BALLISTICS
High pressure strand burn rate tests of polyvinylnitrate/nitramine propellants
[AD-A184178] 04 p0422 N88-12615
Composite materials applications program at the US Army Ballistic Research Laboratory: Work in progress 04 p0428 N88-12651
An ultra-high-speed cinematographic method for the study of wakes in hypersonic ballistic ranges 05 p0531 N88-13228
Production of flows for aeroballistic investigation in the shock tubes of the Franco-German Research Institute (ISL), Saint-Louis (France)
[ISL-R-113/86] 05 p0541 N88-13295
Optoelectronic measurement methods for ballistic experiments
[PB87-110706] 05 p0583 N88-13554
Computer simulations of ballistic experiments
[DE87-005835] 07 p0862 N88-15226
Critical analysis of the dynamic behavior laws for metallic materials --- ballistics
[ISL-NB-401/86] 08 p0969 N88-15862
A continuous oxidizer regression model for the combustion of composite solid propellants
[AD-A186742] 08 p0974 N88-15894
Study on cineradiography
[ISL-R-120/86] 08 p0990 N88-15994
Ballistic deficits in pulse shaping amplifiers
[DE88-003908] 11 p1481 N88-18840

A simplified computer code for reduction to burning rates of closed bomb pressure-time data (MINICB)
[AD-A189112] 13 p1736 N88-20380
Experimental investigation of hypersonic aerodynamics
[NASA-CR-182973] 18 p2458 N88-24591
Ballistic transport and hot electron spectroscopy in Tunneling Hot Electron Transfer Amplifier (THETA)
19 p2659 N88-25808
Contact force history and dynamic response due to the impact of a soft projectile
[NASA-TM-100961] 20 p2811 N88-26679
Proof-of-principle high speed electronic imaging system, phase 2
[AD-A193798] 23 p3181 N88-28937
Combustion diagnostics of propellant with new grain geometries
[AD-A194944] 24 p3342 N88-29895

BALLISTOCARDIOGRAPHY
Cardiac contractility in weightlessness according to spatial ballistocardiography 07 p0890 N88-15393
Ballistocardiography in weightlessness research
11 p1521 N88-19080

BALLOON FLIGHT
Large balloon development and trans-Mediterranean flights 08 p1030 N88-16239
Instrumentation utilisation for risk control in safety operations --- balloons and rockets
08 p1030 N88-16240
Contribution of stratospheric balloon flights in space biology 08 p1033 N88-16266
Future plans for the NASA suborbital program
08 p1034 N88-16267
Results of the 1987 NASA/JPL balloon flight solar cell calibration program
[NASA-CR-182617] 12 p1574 N88-19413
On the dynamic behavior of balloon during its launch; application of panel method and extension to unsteady problem
[ISAS-RN-622] 20 p2751 N88-26330
Development of an adjustable buoyancy balloon tracer of atmospheric motion. Phase 3: Refinement of the operational prototype system
[PB88-190764] 23 p3231 N88-29230

BALLOON SOUNDING
Balloon-based infrared solar occultation measurements of stratospheric O3, H2O, HNO3 and CFC-12
[NOAA-TR-NESDIS-34] 01 p0068 N88-10438
Spectroscopic and retrieval studies in support of SCRIBE (Stratospheric Cryogenic Interferometer Balloon Experiment)
[AD-A184037] 03 p0351 N88-12216
The German scientific balloon and sounding rocket program 08 p1024 N88-16202
The French balloon and sounding rocket space program 08 p1025 N88-16203
The Norwegian scientific balloon and sounding rocket program 1987-1990 08 p1025 N88-16204
The Swedish sounding rocket and balloon program
08 p1025 N88-16205
Swiss scientific balloon and sounding rocket experiments 1985-1987 08 p1025 N88-16206
Balloon measurement of magnetic field during substorms in auroral zone 08 p1026 N88-16213
First results of balloon-borne X-ray and electric field observations near the footprint of the Viking satellite
08 p1026 N88-16215
How ground-based observations contribute to rocket, balloon and space shuttle experiments: Experience from the past and outlook for the future
08 p1026 N88-16216
New techniques for rocket and balloon-borne instrumentation for investigations of the structure, dynamics and electrodynamics of the middle atmosphere 08 p1027 N88-16220
In-situ stratospheric water vapor measurements on board long duration balloons 08 p1029 N88-16232
Aerosols in Martian Atmosphere and Natural Dust Observation (AMANDO). Proposal for the Mars orbiter balloon and rover to study the Martian atmosphere, its thermal content, and its interaction with the soil
[IFSI-87-9] 08 p1100 N88-16619
Stratospheric positive ion composition measurements and acetonitrile detection: A consistent picture
[AERONOMICA-ACTA-A-326-1987]
18 p2542 N88-25084

BALLOON-BORNE INSTRUMENTS
Balloon-based infrared solar occultation measurements of stratospheric O3, H2O, HNO3 and CFC-12
[NOAA-TR-NESDIS-34] 01 p0068 N88-10438
Forecasting and nowcasting cumulus convection with soundings released from a storm-intercept vehicle
02 p0202 N88-11262
Max '91: Flare research at the next solar maximum
[NASA-TM-89700] 06 p0806 N88-14919
A new liquid helium-cooled Fabry-Perot spectrometer used in a far infrared astronomical balloon experiment
08 p1028 N88-16224
An advanced visible-UV spectrometer for atmospheric composition measurements 08 p1029 N88-16231
Justification and prospects of observations of interstellar, far-infrared emission lines, using a small-sized balloon-borne telescope 08 p1032 N88-16254
PRONAOS: A submillimeter facility --- astronomical balloon 08 p1032 N88-16255
Solar ultraviolet spectrum obtained from a balloon gondola 08 p1032 N88-16258
Contribution of stratospheric balloon flights in space biology 08 p1033 N88-16266
Balloon-borne three-meter telescope for far-infrared and submillimeter astronomy
[NASA-CR-182310] 09 p1262 N88-17565
Mars Lander/Rover vehicle development: An advanced space design project for USRA and NASA/OAST
[NASA-CR-182571] 12 p1709 N88-20227
Further development of a stellar camera following the rotation-modulation-collimator principle for balloon-borne observations in the X-ray range
[ETN-88-91496] 14 p1913 N88-21428
Far-infrared (120-300 micron) observations of the Carina Nebula 14 p1993 N88-21876
Balloon-borne three-meter telescope for far-infrared and submillimeter astronomy
[NASA-CR-182924] 17 p2449 N88-24550
Utilization of the IR telescope gimbaling system as a stabilized pointing platform for balloon payloads. Volume 1: Technical results
[NASA-CR-179339] 18 p2522 N88-24962
Estimation of balloon position from wind data
[DE88-008968] 19 p2597 N88-25434
Modeling, designing and simulating a pointing control system for balloon-borne solar experiments
[NASA-TM-100337] 22 p3082 N88-28300

BALLOONING MODES
Limit of possible operation of crescent and bean shaped Tokamaks
[IPPJ-837] 02 p0242 N88-11532
Ballooning modes or Fourier modes in a toroidal plasma?
[AD-A184299] 04 p0491 N88-13022

BALLOONS
NT HIGH ALTITUDE BALLOONS
NT JIMSPHERE BALLOONS
Proceedings of the 8th ESA Symposium on European Rocket and Balloon Programs and Related Research
[ESA-SP-270] 08 p1024 N88-16201
Operational activity and improvements in the services and facilities of the balloon launch centers in France
08 p1030 N88-16238
Large balloon development and trans-Mediterranean flights 08 p1030 N88-16239
Balloon-borne three-meter telescope for far-infrared and submillimeter astronomy
[NASA-CR-182310] 09 p1262 N88-17565
Adaptive control of scientific balloon-borne gondola attitude 13 p1755 N88-20497
Utilization of the IR telescope gimbaling system as a stabilized pointing platform for balloon payloads. Volume 1: Technical results
[NASA-CR-179339] 18 p2522 N88-24962

BALLS
Film thicknesses in circular elastohydrodynamic contacts
[PB87-123725] 06 p0710 N88-14354

BALMER SERIES
Excess emission in the wings of the Hydrogen Balmer lines during a flare on the late-type dMe star YZ CMi
04 p0511 N88-13146

BANACH SPACE
NT HILBERT SPACE
Spectral and structural properties of nonnegative reducible operators in Banach relations
[ETN-87-90402] 01 p0089 N88-10581
Spectral dilation of L(B,H)-valued measures and its application to stationary dilation for Banach space valued processes
[NASA-CR-182388] 07 p0913 N88-15536
Series representations of infinitely divisible random vectors and a generalized shot noise in Banach spaces
[AD-A186429] 07 p0918 N88-15574
Series representations of infinitely divisible random vectors and a generalized shot noise in banach spaces
[AD-A186502] 08 p1073 N88-16474
Some aspects of control for semilinear distributed parameter systems
[INPE-4147-PRE/1054] 08 p1075 N88-16484
Feedback stabilization of distributed systems
[AD-A187111] 09 p1222 N88-17328
Perturbation theory for dual semigroups 2. Time-dependent perturbations in the sun-reflexive case
[PB88-113097] 09 p1230 N88-17369
Critical values of functionals on Banach surfaces
[DE88-702735] 23 p3272 N88-29472

BAND STRUCTURE OF SOLIDS
Electronic band structure and photoemission: A review and projection
[DE88-002236] 06 p0787 N88-14829
The band systems of alkali vapors
[NASA-TT-20206] 10 p1417 N88-18462
Electronic structure of matter at high compression: Isostructural transitions and approach of the Fermi-gas limit
[MPQ-124] 16 p2266 N88-23551
Non-effective-mass matching in superlattices
20 p2872 N88-27049
Self energy corrections to the ab initio band structures: Chromium
[DE88-701825] 21 p3020 N88-27927
Study of superconducting properties in some many valley semiconductors
[DE88-702325] 23 p3291 N88-29593

BANDGAP
U ENERGY GAPS (SOLID STATE)

BANDPASS FILTERS
NT TRACKING FILTERS
Implementation of an FIR band pass filter using a bit-slice processor
[AD-A184895] 05 p0634 N88-13875
Computer aided filter design
[AD-A193959] 23 p3208 N88-29093
Band pass with cavity resonators by use of three oscillation types
[ETN-88-92984] 23 p3209 N88-29096

BANDSTOP FILTERS
A notch filter instrument for measuring ELF (Extremely Low Frequency) MSK (Minimum Shift Keying) signals
[AD-A193324] 21 p2933 N88-27414
Confirmation of slow-waves in a crosstie overlay coplanar waveguide and its application to band-reject gratings and reflectors
[AD-A194981] 24 p3361 N88-30011

BANDWIDTH
NT BROADBAND
NT NARROWBAND
NT SPECTRAL LINE WIDTH
Bandwidth efficient block codes for M-ary PSK modulation
[NASA-CR-181543] 04 p0437 N88-12712
Performance optimization of electronic networks in the frequency domain
[PB87-123873] 04 p0438 N88-12720
Feasibility studies of optical processing of image bandwidth compression schemes
[AD-A186073] 07 p0932 N88-15660
Considerations concerning the basic bandwidth reduction of high definition television systems (HDTV) component signals, based on psychophysiological properties of the eye
[IRT-B-83/87] 09 p1153 N88-16909
Large-aperture sparse array antenna systems of moderate bandwidth for multiple emitter location
[AD-A188409] 12 p1619 N88-19683
High speed, bandpass sampling of digital communications waveforms
[AD-A189842] 15 p2056 N88-22254
Monolithic phase shifter study
[AD-A190213] 15 p2059 N88-22278
A fiber optic beamforming processor for wideband direction finding
[AD-A194862] 24 p3428 N88-30404
Ultra-wideband direction finding using a fiber optic beamforming processor
[AD-A194861] 24 p3430 N88-30413

BANG-BANG CONTROL
U OFF-ON CONTROL

BARANY CHAIR
Gastric emptying assessment by echography after a stress (rotating chair) 12 p1661 N88-19955

BARCHANS
U DUNES

BARDEEN APPROXIMATION
U BARRIER LAYERS
U ELECTRICAL PROPERTIES
U SURFACE PROPERTIES

BARIUM
Magnetic anomalies in the rare earth oxide superconductors GdBa2Cu3O(7-x) and YbBa2Cu3O(7-x)
[AD-A190713] 15 p2144 N88-22793
Synthesis and characterization of high-T(sub c) screen-printed Y-Ba-Cu-O films on alumina
[NASA-TM-100860] 15 p2146 N88-22805
High temperature superconductivity
[AD-A190259] 16 p2281 N88-23655
Effects of 67.5 MeV electron irradiation on Y-Ba-Cu-O and Gd-Ba-Cu-O high-temperature superconductors
[AD-A191271] 16 p2283 N88-23669

Radial velocities monitoring of a sample of barium and S stars using CORAVEL: Towards an evolutionary link between barium and S stars?
[SER-C-PREPUBL-FASC-19] 18 p2593 N88-25410
Electron irradiation effects in YBa2Cu3O7-Delta single crystals
[DE88-010050] 20 p2878 N88-27085
Generation of Adlam-Allen waves by plasma release experiments in the solar wind
[PB88-106000] 20 p2886 N88-27140

BARIUM COMPOUNDS
NT BARIUM OXIDES
NT BARIUM TITANATES
DTA/DSC studies of phase equilibria in binary mixtures of barium carbonate with alkali carbonates
[DE87-001195] 02 p0194 N88-11213
Resistivity of EuBa2(Cu/sub 1-y/Zn/sub y/)3O/sub x/ as a ffunction of temperature, magnetic field, pressure and Zn concentration
[DE87-014740] 04 p0499 N88-13069
Effect of a weak magnetic field on high temperature superconductivity in Y-Ba-Cu-O ceramics
[DE88-702192] 19 p2733 N88-26235
All-electron local density theory of electronic structure and superconductivity in YBa2Cu3O7 and YBa2Cu3O6
[DE88-009944] 19 p2735 N88-26246
Anharmonic model for high-Tc superconductors
[DE88-702196] 21 p3020 N88-27924
Superconducting properties of LaBa2Cu3O(sub x) and YBa2Cu3O(sub y)
[DE88-012038] 21 p3024 N88-27952
Magnetic phase transitions in 90-K superconductors Ho1Ba2Cu3O(7-delta) and Gd1Ba2Cu3O(7-delta) observed by ZF-muon(+)SR
[DE88-752611] 23 p3290 N88-29588

BARIUM ION CLOUDS
Deployable booms and antennas on AMPTE-IRM
14 p1874 N88-21198

BARIUM OXIDES
High temperature stability of superconducting YBa2Cu3O subx as characterized by X-ray diffraction
[DE88-001856] 06 p0787 N88-14824
Atomic-level studies of superconducting YBa2Cu3O sub 7-x
[DE88-002522] 06 p0788 N88-14831
Low field characterization of YBa2Cu3O sub 7-delta single crystals
[DE88-002895] 07 p0938 N88-15700
Fabrication of YBa2Cu3O7 superconducting ceramics
[DE88-003012] 07 p0938 N88-15701
Magnetic investigations of superconductive, polycrystalline (RE)1Ba2Cu3O(7-x) compounds (RE = Y, Gd, Ho, Dy)
[DE88-002537] 08 p1090 N88-16558
Soft X-ray absorption and emission spectra and the electronic structure of the Ba2YCu3O/sub 7-x/ superconductor
[DE88-002609] 08 p1090 N88-16559
High temperature superconductivity research at Argonne National Laboratory
[DE88-003055] 09 p1258 N88-17541
The structure and properties of twin boundaries in superconducting YBa2Cu3O7
[DE88-003864] 10 p1418 N88-18468
Improved magnetization for YBa2Cu3O/sub 7-delta annealed in oxygen above 1000 C
[DE88-003934] 10 p1418 N88-18469
Freestanding films of YBa2Cu3O/sub 6.9/
[DE88-003995] 10 p1419 N88-18471
Grain boundaries, planar defects and superconducting properties of YBa2Cu3O7
[DE88-003477] 10 p1419 N88-18475
Superconductivity and phase stability in the heavy rare earth quaternary compounds RBa2Cu3O7 (R = Ho, Er, Tm, Yb, Lu)
[DE88-003478] 10 p1419 N88-18476
Superconducting properties and structural characterization of high T/sub c/ oxides
[DE88-003479] 10 p1420 N88-18477
Penetration depth measurements of YBa2Cu3O/sub 7-delta/ at 4 MHz
[DE88-003493] 10 p1420 N88-18478
The electronic structure of YBa2Cu3O/sub 7-delta/ above and below T/sub c/
[DE88-003495] 10 p1420 N88-18479
Simulation and processing of high resolution images of defects and interfaces in superconducting YBa2Cu3O7
[DE88-003856] 10 p1420 N88-18480
High-resolution X-ray microstructural study of single crystals of YBa2Cu3O/sub 7-y/
[DE88-004856] 10 p1421 N88-18484
Atom probe microanalysis of superconducting YBa2Cu3O(sub 7-x)
[DE88-003203] 11 p1557 N88-19322
Processing relationships in YBa2Cu3O(7-x) superconductors
[DE88-005137] 11 p1559 N88-19330
Mass transport and chemical demixing of Y-Ba-Cu-O compounds during sintering in temperature gradients
[DE88-004887] 12 p1696 N88-20151
Properties of superconductors with strong electron-phonon interaction 14 p1974 N88-21779
Ordered structures in YBa2Cu3O/sub 7-y/, La2Cu3O/sub 7-y/, La/sub 2-x/Sr/sub x/CuO/sub 4-par. delta/ and related perovskites
[DE88-006461] 14 p1987 N88-21851
Melt processing ceramic YBa2Cu3O(sub 6.9)
[DE88-007039] 15 p2047 N88-22199
Superconductivity and the tailoring of lattice parameters of the compound YBa2Cu3O(sub x)
[DE88-005904] 15 p2140 N88-22769
High temperature superconductors in the La(sub 1+x)Ba(sub 2-x)Cu O(sub y system
[DE88-006367] 15 p2145 N88-22802
Material degradation in a barium hydroxide latent heat storage pilot unit
[DFVLR-FB-87-49] 16 p2175 N88-22961
A sup 57 Fe Mossbauer study of the superconductor YBa sub 2 (Fe sub x Cu sub 1-x) sub 3 O sub y
[DE88-701543] 16 p2282 N88-23661
Vacancy ordering in the basal plane of YBa2Cu3O(sub)z
[DE88-004572] 18 p2583 N88-25348
Mass spectrometric high temperature measurements of the barium oxide-zirconium dioxide system and the determination of thermodynamic data for barium zirconate. Clarification of the counter-stopping capacity of coated particles for solid fission products by zirconium dioxide addition
[NASA-TT-20187] 19 p2611 N88-25496
Effects of grain boundary composition on properties of YBa2Cu3O/sub 7-x/
[DE88-007679] 20 p2875 N88-27064
The superconducting transition in oxygen deficient YBa2Cu3O(sub 7-Delta)
[DE88-009957] 20 p2877 N88-27079
Anisotropic characteristic lengths in single crystal YBa2Cu3O(sub 7-Delta)
[DE88-009959] 20 p2877 N88-27080
Anisotropy of the lower critical field in YBa2Cu3O(sub 7-Delta)
[DE88-009971] 20 p2877 N88-27081
Preparation of high-T(sub)c Y1Ba2Cu3O(sub 7-Delta) superconducting thin films by MBE (Molecular-Beam-Epitaxy) techniques
[DE88-009999] 20 p2877 N88-27082
Oxygen vacancy ordering and superconductivity in YBa2Cu3O(sub 7-x)
[DE88-010005] 20 p2877 N88-27083
Pure metallic bridge and point-contact tunneling into single- and polycrystal YBa2Cu3O(sub 7-y)
[DE88-010030] 20 p2878 N88-27084
Phase transformations and thermodynamic behavior of the YBa2Cu3O(sub)x system via EMF measurements
[DE88-010054] 20 p2878 N88-27086
Ceramic processing of high-T(sub)c superconductors
[DE88-010090] 20 p2878 N88-27087
Compilation of NRL publications on high temperature superconductivity
[AD-A189137] 21 p3019 N88-27921
Thermodynamics of oxygen-vacancy ordering in YBa2Cu3O(sub z)
[DE88-009816] 21 p3022 N88-27940
Preparation and characterization of isotopic oxygen-enriched yttrium barium copper oxide
[DE88-010939] 22 p3154 N88-28766
High Tc superconducting HoBa2Cu(sub 1-x)Fe(sub x)3O(sub 7-y)
[DE88-008909] 22 p3155 N88-28768
Superconducting properties of oxygen deficient YBa2Cu3O(sub 7-delta)
[DE88-009969] 22 p3155 N88-28774
Effect of neutron irradiation on critical magnetization current in single crystal YBa2Cu3O(sub 7-delta)
[DE88-009970] 22 p3156 N88-28775
Effects of metal substitutions (Fe and Ga) in YBa2Cu3O7 on its superconducting properties and microstructures
[DE88-007393] 23 p3287 N88-29572
Possible mechanism for high-temperature superconductivity in the BaSr-La(Y)-CuO systems
[DE88-702060] 23 p3288 N88-29576
Preparation of superconducting YBa2Cu3O(sub 7-x) films by magnetron sputtering
[DE88-009977] 23 p3289 N88-29583

BARIUM TITANATES
Determination of the origin of self-pumped phase conjugation in barium titanate
[AD-A184697] 03 p0377 N88-12372
Manufacturing of a barium titanate with high dielectric coefficient by decomposition of precipitates of double oxalates
[ISAL-IDI1-88-02] 21 p2911 N88-27278

BAROCLINIC INSTABILITY
Numerical model of Rayleigh instability and spin-off eddies on fronts 13 p1788 N88-20696

BAROCLINIC WAVES
A baroclinic wavy basic state model: Description and preliminary experiments
[KNMI-WR-87-1] 01 p0068 N88-10436
Application of satellite data in observational and theoretical studies of the evolving structure of baroclinic waves
[NASA-CR-179277] 10 p1354 N88-18091
Westward moving atmospheric wave disturbances over the African tropics: Dynamic and energetic aspects
[MITT-57] 20 p2827 N88-26774
Rossby waves in mid-latitude oceans
24 p3405 N88-30273

BAROCLINITY
A study of finite difference and finite element vertical discretization schemes for baroclinic prediction equations
[AD-A186617] 08 p1040 N88-16291
North Pacific Ocean. Subtropical front north of Hawaii, R/V Thomas G. Thompson: 7 January - 10 February 1974. CTD data report
[AD-A186565] 08 p1044 N88-16310
North Pacific Ocean. Subarctic front central Pacific, R/V Thomas G. Thompson: 8 September - 9 October 1975. CTD data report
[AD-A186567] 08 p1044 N88-16312
North Pacific Ocean. Northwest Pacific Transition Zone, R/V Thomas G. Thompson: 19 March - 1 May 1971. STD data report
[AD-A186568] 08 p1044 N88-16313
North Pacific Ocean. Gulf of Alaska, R/V Thomas G. Thompson: 1 February - 8 March 1967. STD data report
[AD-A186569] 08 p1045 N88-16314
North Pacific Ocean. Central Pacific Transition Zone, R/V Thomas G. Thompson: 25 March - 3 May 1968. STD data report
[AD-A186570] 09 p1195 N88-17160
Sampling strategies for Monte-Carlo forecasting methods 22 p3126 N88-28583

BAROMETERS
The evaluation of automatic barometers, illustrated by the Nakaasa barometer
[KNMI-TR-95] 13 p1774 N88-20610

BAROMETRIC PRESSURE
U ATMOSPHERIC PRESSURE

BAROTROPIC FLOW
Properties of the atmospheric boundary layer above a subtropical oceanic front
[AD-A184006] 03 p0351 N88-12215
Mesoscale eddy dynamics by the method of point vortices 04 p0463 N88-12863
The role of vortex structure in tropical cyclone motion
[AD-A190961] 16 p2235 N88-23351
Analysis of a six-component barotropic spectral model: Chaotic motion, predictability and vacillation — atmospheric circulation
[CWI-AM-R8710] 18 p2542 N88-25090
Cluster analysis of multiple planetary flow regimes
[NASA-CR-182931] 18 p2594 N88-25418

BAROTROPISM
NT PLANETARY WAVES
On the barotropic model of the ocean circulation
[AD-A188148] 10 p1358 N88-18118
The use of a barotropic finite element model for the study of circulation on the continental shelf of the southeast coast of Brazil
[INPE-4401-PRE/1218] 13 p1802 N88-20774

BARRED GALAXIES
Kinematics and dynamics of barred spiral galaxies
03 p0388 N88-12440

BARRELS (CONTAINERS)
Numerical computations of natural convection heat transfer in irregular geometries
[DE88-002358] 07 p0852 N88-15178

BARRICADES
U BARRIERS

BARRIER LAYERS
Ytterbium monolayer diffusion barriers at Hg(1-x)Cd(x)Te/Al junctions
[AD-A188013] 10 p1299 N88-17768
Calculating depletion region carrier concentrations with capacitance-voltage measurements and etching
[AD-A189630] 15 p2141 N88-22777
A review of diffusion barrier technology for application in SP-100 fuel pins 17 p2410 N88-24328
Fabrication of SP-100 fuel barrier structures by chemical vapor deposition 17 p2416 N88-24371

A 10 microns photoexcited avalanche gain due to electron impact ionization from GaAs quantum well superlattices 20 p2867 N88-27026
Resonant tunneling in InGaAs-InP double-barrier structures and superlattices 20 p2871 N88-27047
Containment of a silicone fluid free surface in reduced gravity using barrier coatings
[NASA-TM-101314] 24 p3371 N88-30072

BARRIERS
Flammability test on aircraft seats equipped with fire barrier fabrics for the Porcher company
[CEAT-M5-525200] 06 p0666 N88-14084
Macroscopic quantum effects in a Josephson tunnel junction
[DE88-002239] 06 p0787 N88-14830
Verification of obstacle accountability areas using a simple mathematical model. Part 1: Description of general model and application for a specific case --- engine failure at takeoff
[NLR-TR-85069-U] 09 p1115 N88-16683
A program for the calculation of radio-wave transmission loss over the spherical earth and over obstacles 12 p1616 N88-19662

BARS
NT ELASTIC BARS
Exact finite element method analysis of viscoelastic tapered structures to transient loads 05 p0595 N88-13632
Bar code document accountability system performance update
[DE88-002256] 06 p0791 N88-14849
On the dissipative response due to discontinuous strains in bars of unstable elastic material
[AD-A188114] 11 p1498 N88-18947
Delamination stresses in semicircular laminated composite bars
[NASA-TM-4026] 13 p1735 N88-20375
Vibration frequencies of tapered bars with nonclassical boundary conditions
[NASA-CR-183059] 20 p2813 N88-26688
Wide range stress intensity factor expression for an edge-cracked round bar bend specimen
[AD-A196285] 24 p3382 N88-30147

BARYCENTER
U CENTER OF GRAVITY

BARYONS
Scalar densities and baryon mass differences in lattice QCD with Wilson fermions
[PREPRINT-544] 06 p0778 N88-14773
BRYNTRN: A baryon transport computer code, computation procedures and data base
[NASA-TM-4037] 16 p2290 N88-23714

BASALT
Petrogenesis of basalts from the Archean Matachewan Dike Swarm Superior Province of Canada 06 p0796 N88-14878

BASE FLOW
Influence of base modifications on in-flight base drag in the presence of jet exhaust for Mach numbers from 0.7 to 1.5
[NASA-TP-2802] 11 p1488 N88-18881
Efficient, high resolution computations of projectile and missile flow fields
[AD-A191086] 16 p2158 N88-22873
Study of a system for reducing base drag by controlling vortices
[REPT-87/43] 17 p2295 N88-23730

BASE PRESSURE
Empirical formulas for the base pressure of missile bodies with a central propulsive jet
[ESA-TT-1046] 03 p0270 N88-11694
Base pressure measurements on a missile body with cruciform tail
[ESA-TT-1062] 03 p0270 N88-11695
Flight and wind-tunnel measurements showing base drag reduction provided by a trailing disk for high Reynolds number turbulent flow for subsonic and transonic Mach numbers
[NASA-TP-2638] 06 p0701 N88-14299
Flight tests of external modifications used to reduce blunt base drag
[NASA-TM-100433] 13 p1719 N88-20279
An experimental investigation of rocket ramjet nozzle assembly base pressures
[AD-A189714] 15 p2027 N88-22076

BASES
Improved description of base dynamics in the modeling of bipolar transistors
[PB88-181516] 19 p2732 N88-26229
Active sites and roles of solid acid base catalysts
[NASA-TT-20333] 24 p3345 N88-29909

BASES (CHEMICAL)
NT ALKALIES
NT ATROPINE
NT CAFFEINE
NT ERGOTAMINE
NT LITHIUM HYDROXIDES
NT MORPHINE
NT PYRIDINES
NT QUINOLINE
NT SODIUM HYDROXIDES
NT URACIL

BASES (FOUNDATIONS)
U FOUNDATIONS

BASIC (PROGRAMMING LANGUAGE)
Computer program in BASIC language for computation of spectrochemical analytical data
[DE88-701229] 15 p2032 N88-22106

BASINS
U STRUCTURAL BASINS

BASINS (CONTAINERS)
Marintek's ocean basin, a training facility for extravehicular activity? 19 p2698 N88-26041

BATCH PROCESSING
Scale-up of a batch-type chemical powder preparation process for high field varistor fabrication
[DE88-006601] 13 p1762 N88-20541
MVS (Multiple Virtual Storage) batch computing and data management at ANL
[DE88-007342] 19 p2718 N88-26137
Fabrication of bulk superconducting ceramics
[DE88-009956] 22 p3155 N88-28773

BATHING
Analysis of water recovered after being used for washing by men and women 10 p1361 N88-18135
The effects of normal and therapeutic baths on the central vascular organs of persons with healthy hearts, as measured by X-ray
[NASA-TT-20252] 13 p1811 N88-20818

BATHOLITHS
Pluton emplacement and magmatic arc construction: A model from the Patagonian batholith 24 p3393 N88-30206
Genesis of archean granitoids in the Pilbara block and implications for crustal growth 24 p3394 N88-30210

BATHS
A rapid electrochemical technique for determining the current efficiency for cadmium plating
[AD-A193679] 22 p3056 N88-28130

BATHYMETERS
Airborne electromagnetic sounding of sea ice thickness and sub-ice bathymetry
[AD-A188939] 12 p1649 N88-19879
Bathymetric hazard survey test
[AD-A189150] 13 p1803 N88-20775
Inversion algorithms for geophysical problems
[AD-A189252] 13 p1815 N88-20845
The representation of the sea-bottom in deep sea areas by the Digital Terrain Model (DTM) program TASH 16 p2226 N88-23293
To relate measurements of gravity and geoid anomalies over the oceans to near surface density distributions
[AD-A192168] 18 p2547 N88-25120
Identification and acoustic characterization of seamounts
[AD-A192204] 18 p2548 N88-25123
Bathymetry estimation by analyzing swell on SPOT images 19 p2701 N88-26062
Study of the Arachon (France) underwater delta using Thematic Mapper data 19 p2702 N88-26064
Evaluation of the contribution of SPOT in the framework of the mineral exploration program of the Aitutaki Atoll (Cook Islands). Preliminary study of the impact of the passage of Hurricane Sally 22 p3109 N88-28483

BATHYMETRY
U BATHYMETERS

BATHYTHERMOGRAPHS
JEDA (Joint Environmental Data Analysis) Center report on tropical Pacific subsurface thermal data management, 1986
[PB88-140090] 12 p1649 N88-19875
Editing master oceanographic observation data set 4
[AD-A188405] 12 p1649 N88-19876
Expendable conductivity, temperature and depth system (XCTD) development program
[AD-A192182] 18 p2547 N88-25121
Application of acoustic-Doppler current profiler and expendable bathythermograph measurements to the study of the velocity structure and transport of the Gulf Stream
[NASA-CR-183188] 22 p3129 N88-28605

BATTERIES
U ELECTRIC BATTERIES

BATTERY CHARGERS
Overcharge protection in Li-alloy/metal disulfide cells
[DE87-011364] 01 p0041 N88-10260
A novel class of positive electrodes for rechargeable batteries
[DE88-004559] 13 p1763 N88-20545
Development of a total electric vehicle drive system
[DE88-900367] 14 p1917 N88-21446
GTE battery management system: State of charge indicator evaluation
[DE88-006800] 15 p2058 N88-22272
Aircraft battery state of charge and charge control system
[AD-A194979] 24 p3367 N88-30052

BATTERY SEPARATORS
U SEPARATORS

BAYES THEOREM
Comparing hard and soft prior bounds in geophysical inverse problems
[NASA-CR-181557] 05 p0624 N88-13820
A unified mathematical approach to image analysis
[AD-A185719] 06 p0765 N88-14703
Asymptotic normality of poly-t densities with Bayesian applications
[AD-A185718] 06 p0768 N88-14719
A three-parameter generalisation of the beta-binomial distribution with applications
[AD-A185733] 06 p0768 N88-14720
On determining the weight for obtaining a large number of items
[AD-A186181] 07 p0915 N88-15553
A prototype of pilot knowledge evaluation by an intelligent CAI (Computer-Aided Instruction) system using a Bayesian diagnostic model
[AD-A186080] 08 p1054 N88-16358
De Finetti's approach to group decision making
[AD-A188074] 11 p1536 N88-19177
Signal-filter design and system performance for polarimetric radar
[AD-A189257] 13 p1758 N88-20514
Admissibility in fair Bayes prediction problems. Part 1: General theory
[CWI-MS-R8703] 14 p1965 N88-21725
Sequential tests for the drift of a Wiener process with a smooth prior and the heat equation
[AD-A190322] 15 p2121 N88-22638
Properties of some Bayesian scoring procedures for computerized adaptive tests
[AD-A189925] 15 p2124 N88-22660
Admissible Bayes tests for structural relationship
[AD-A190326] 15 p2125 N88-22669
Empirical and hierarchical Bayes competitors of preliminary test estimators in two sample problems
[AD-A190327] 15 p2125 N88-22670
On two-stage allocation procedures for selection problems
[AD-A190766] 15 p2126 N88-22675
Bayesian solutions to a 2 x 2 decision matrix using interval scaled payoffs with an application to foreign policy decisions
[AD-A190863] 16 p2260 N88-23511
Knowledge acquisition tool implementation
[AD-A190415] 18 p2555 N88-25164
Automatic discovery of optimal classes
[NASA-TM-101174] 18 p2566 N88-25238
An application of the Bayesian method to the estimation and forecast of system hardware components MTBF 22 p3068 N88-28211
Topics in adaptive control and inference
[AD-A194718] 23 p3266 N88-29443
Selecting the best binomial population: Parametric empirical Bayes approach
[AD-A193341] 23 p3269 N88-29450
Easy Bayes estimation for Rasch-type models
[AD-A193628] 23 p3274 N88-29491
Dirichlet prior in Bayesian estimation of item response curves
[AD-A195311] 24 p3426 N88-30392

BAYESIAN STATISTICS
U BAYES THEOREM

BAYS (STRUCTURAL UNITS)
Redistribution of particulates in shuttle bay during launch 02 p0133 N88-10837
Centaur G Prime modal test 09 p1181 N88-17075
Payload bay atmospheric vent airflow testing at the Vibration and Acoustic Test Facility
[NASA-TM-100460] 11 p1437 N88-18572
Moving-bank multiple model adaptive estimation applied to flexible spacestructure control
[AD-A190761] 15 p2026 N88-22071
FEB structural analysis, revision H
[AD-A192302] 20 p2814 N88-26698

BAYS (TOPOGRAPHIC FEATURES)
NT DELAWARE BAY (US)
Tide- and wind-forced currents in Buzzards Bay, Massachusetts
[PB88-110580] 07 p0882 N88-15350
Continental shelf processes affecting the oceanography of the South Atlantic Bight
[DE88-004102] 09 p1196 N88-17166
Biological processes in the water column of the South Atlantic bight: Zooplankton responses
[DE88-004811] 14 p1951 N88-21630

Relevance of a thematic map (SPOT data) with regards to the real flora and structure of the vegetation covering of salt marshes (Mont Saint Michel Bay, France)
22 p3109 N88-28468

BCC LATTICES
U SODY CENTERED CUBIC LATTICES

BEACONS
NT RADAR BEACONS
NT RADIO BEACONS
COSPAS/SARSAT 406-MHz emergency beacon digital controller
[NASA-TM-100859] 20 p2792 N88-26566

BEADS
Examination of the physical processes associated with the keyhole region of variable polarity plasma arc welds in aluminum alloy 2219 07 p0927 N88-15634
Unsteady flow about cambered plates
[AD-A191226] 17 p2337 N88-23945
Analysis of a feed device for the pneumatic transport of noncohesive particles
[VKI-TM-44] 24 p3369 N88-30062

BEAM CURRENTS
Use of polarimetry to measure the current profile in MTX
[DE87-013835] 02 p0237 N88-11495
Stabilized X-ray generator power supply
[DE88-700297] 07 p0830 N88-15034
Neutral beam propagation through the atmosphere
[AD-A188984] 12 p1691 N88-20115
Requirements for neutral beam current drive in tokamaks
[DE88-006180] 20 p2859 N88-26980
A millimeter-wave tunneLadder TWT
[NASA-CR-182184] 22 p3072 N88-28239

BEAM INJECTION
Improvement of energy confinement of neutral beam heated plasma by lower hybrid current drive in JT-60
[DE87-752963] 02 p0239 N88-11509
Two dimensional neutral transport analysis in tokamak plasma
[DE87-752984] 02 p0239 N88-11510
Transport analysis of OH and NBI heated discharges in JT-60
[DE87-752985] 02 p0239 N88-11511
Reactivity for DT plasma with beam-induced tail in magnetic confinement system
[DE87-753017] 02 p0240 N88-11517
Fusion reactivity enhancement due to ion tail formation by beam and ion cyclotron heating
[DE87-753018] 02 p0240 N88-11518
Volume produced H(-),D(-) ion source for proton accelerator and thermo-nuclear fusion research by sheet plasma (III)
[IPPJ-838] 02 p0242 N88-11531
Effects of injection of free electron lasers on axial velocity spread of beams 03 p0299 N88-11878
Negative ion beams for heating and current-drive in NET
[AD-A184390] 04 p0489 N88-13012
Coherent emission from relativistic beam-plasma interactions 04 p0493 N88-13039
Method of plasma diagnostics by a heavy ion beam for the T-15 tokamak
[DE88-700342] 07 p0935 N88-15678
Simple model for hot ion plasmas
[DE88-750045] 07 p0936 N88-15688
Electrostatic VLF emission determined from rocket and satellite experiments 08 p1002 N88-16068
Absorption of cyclotron radiation in skin layer in Araks experiment 08 p1003 N88-16076
Preliminary injector, accelerator, and beamline design for rf-linac-driven XUV free-electron lasers
[DE88-003185] 10 p1336 N88-17983
The numerical simulation of accelerator components
[DE87-011597] 10 p1412 N88-18423
Benchmarks of neutral beam injection codes for stellarators
[DE88-003786] 10 p1412 N88-18428
Effects of X irradiation and high field electron injection on the electrical properties of rapid thermal oxides
[DE88-002642] 10 p1417 N88-18461
Corpuscular plasma diagnostics complex on a tokamak with a strong field
[DE88-701576] 16 p2279 N88-23646
Ion temperature profile measurement using charge exchange recombination spectroscopy on JIPP T-IIU
17 p2440 N88-24518
Spectroscopic measurements of ion temperature, rotation speed and beam deposition profile on DIII-D
17 p2440 N88-24519
Spectroscopic study of heliotron E plasmas: Stark profile, CXR, poloidal rotation and carbon coating
17 p2441 N88-24523
REFLEX: An energy deposition code that models the effects of electron reflection during electron beam heating tests
[DE88-009789] 19 p2726 N88-26186
Pseudospark switches
[DE88-702227] 23 p3207 N88-29085
Initial operation and edge plasma studies in ATF (Advanced Toroidal Facility)
[DE88-011400] 23 p3285 N88-29562

BEAM INTERACTIONS
Transverse focussing using plasma wake fields
[DE87-011503] 01 p0099 N88-10652
Investigation of two laser beam coupling and amplification in Ce-doped SBN single crystals
03 p0327 N88-12069
Coherent emission from relativistic beam-plasma interactions 04 p0493 N88-13039
Atomic beam studies of the interaction of hydrogen with transition metal surfaces
[DE88-000208] 05 p0648 N88-13970
Experimental research of electron beam instability on the Doppler anomalous effect
[DE88-700565] 07 p0932 N88-15658
Two dimensional simulations of multipass beam breakup
[CEBAF-PR-87-008] 11 p1547 N88-19254
Observation of anomalous low J-value Stokes and anti-Stokes lines in stimulated rotational Raman scattering over long air paths
[DE88-003756] 14 p1911 N88-21418
Crossed molecular beam studies of substitution and exchange reactions
[DE88-006322] 14 p1980 N88-21814
Gamma rays from Cygnus X-1: Modeling and nonthermal pair production
[DE88-006830] 18 p2596 N88-25426

BEAM SPLITTERS
Advances in X-ray optics, 1987
[DE88-003298] 11 p1549 N88-19268
Soft X-ray beamsplitters and highly dispersive multilayer mirrors for use as soft X-ray laser cavity components
[DE88-004003] 11 p1549 N88-19270
Space infrared telescope facility wide field and diffraction limited array camera (IRAC)
[NASA-CR-182704] 13 p1853 N88-21092
Detecting squeezed states by cross-correlation
14 p1978 N88-21806
Modulated-splitting-ratio fiber-optic temperature sensor
[NASA-TM-101332] 22 p3042 N88-28062
Four-frame gated optical imager with 120-ps resolution
[DE88-011735] 22 p3080 N88-28288

BEAM SWITCHING
Investigations on beam quality of high frequency excited CO2 high performance lasers
[ETN-88-92363] 21 p2954 N88-27550

BEAM WAVEGUIDES
A millimeter-wave tunneLadder TWT
[NASA-CR-182184] 22 p3072 N88-28239
Analytical and experimental studies of beam waveguide absorbers for structural damping
[AD-A195085] 24 p3382 N88-30144

BEAMS (RADIATION)
NT ATOMIC BEAMS
NT ELECTRON BEAMS
NT ION BEAMS
NT LASER BEAMS
NT LIGHT BEAMS
NT MOLECULAR BEAMS
NT NEUTRAL BEAMS
NT NEUTRINO BEAMS
NT NEUTRON BEAMS
NT PARTICLE BEAMS
NT PHONON BEAMS
NT PHOTON BEAMS
NT PROTON BEAMS
NT RADAR BEAMS
NT RELATIVISTIC ELECTRON BEAMS
The nature of beamstrahlung
[DE87-012837] 02 p0234 N88-11474
Interactive Design of Accelerators (IDA)
[DE87-013298] 02 p0234 N88-11476
Determination of the origin of self-pumped phase conjugation in barium titanate
[AD-A184697] 03 p0377 N88-12372
Phenomena at a focus in a laser system
[AD-A185442] 05 p0588 N88-13585
Current status of high power microwave effects and simulation
[DE87-004112] 06 p0751 N88-14615
Investigation of the performance of a novel double crystal X-ray monochromator measurements
[PB87-125167] 06 p0788 N88-14834
Cage mode propagation experiments
[AD-A186019] 07 p0841 N88-15100
Microsecond beam propagation in air
[DE88-002221] 07 p0845 N88-15127
Explosive absorption of laser beam of finite diameter
07 p0921 N88-15597
Analysis of the decomposition of transparent polymer materials (blocks) under the action of laser beams in free generation mode
[AD-A187090] 09 p1147 N88-16873
Theory of transient thermal self-focusing of sound beams 09 p1234 N88-17401
Nonlinear and diffraction effects in sound beams with random transverse structure 09 p1235 N88-17402
A ring model of the lasertron
[DE88-004656] 10 p1323 N88-17908
Correcting ray field failures caused by focusing in an inhomogeneous duct: A critical look at the Gaussian beam method 12 p1616 N88-19663
Multipass beam breakup in recirculating linacs
[CEBAF-PR-87-007] 12 p1690 N88-20111
Multimode-waveguide laser beam deflector
[DE88-006222] 13 p1776 N88-20622
Practical constraints on sources for pulsed beam lithographies
[DE88-006594] 13 p1776 N88-20623
Studies of compound states of negative ions using laser beams
[DE88-004708] 13 p1777 N88-20627
Aberrations: Their effect on off-axis beam steering
[AD-A189601] 13 p1840 N88-21008
Observation of anomalous low J-value Stokes and anti-Stokes lines in stimulated rotational Raman scattering over long air paths
[DE88-003756] 14 p1911 N88-21418
Optical cooling and trapping 14 p1974 N88-21782
Laser cooling of neon metastable states
14 p1975 N88-21785
Quantum nondemolition detection and squeezing in optical fibers 14 p1976 N88-21793
Variable-energy positron studies on liquids and liquid-solid interfaces
[DE88-006356] 15 p2033 N88-22109
The interaction of small particles with laser beams
[AD-A190716] 15 p2072 N88-22354
Ultrasonic beam distortion in transversely isotropic media
[DE88-005937] 15 p2129 N88-22699
Optical switching and control techniques using nonlinear optical wave mixing
[AD-A190467] 15 p2134 N88-22730
TDWR (Terminal Doppler Weather Radar) clutter residue map generation and usage
[AD-A191148] 16 p2235 N88-23352
Fast acting optical beam detection and deflection system
[AD-A192161] 18 p2521 N88-24954
Heavy ion fusion system assessment: Final focus and transport model
[LBL-23040] 19 p2725 N88-26183
Electron-acoustic waves in a beam-plasma system
[DE88-702053] 19 p2729 N88-26207
Time-Optimal Adaptive Shaped Torque (TOAST) technical note
[AD-A192719] 20 p2843 N88-26869
Distortion functions
[DE88-752634] 21 p3015 N88-27896
Guided radiation beams in free electron lasers
[AD-A194525] 22 p3082 N88-28305
Beam optics test stand
[AD-A193901] 23 p3216 N88-29144

BEAMS (SUPPORTS)
NT BOX BEAMS
NT CANTILEVER BEAMS
NT CURVED BEAMS
NT I BEAMS
NT TIMOSHENKO BEAMS
An experimental and theoretical study of the bending behavior of Kevlar 49/epoxy beams and rings
[DE87-010430] 01 p0061 N88-10394
Assessment of structural integrity from forced vibration testing
[DE87-014642] 02 p0191 N88-11195
Shape optimization of damping layers
05 p0595 N88-13635
An examination of chaotic motion for the buckled beam 05 p0597 N88-13644
Optimal control of large space structures via generalized inverse matrix
[NASA-CR-182336] 05 p0639 N88-13907
Beam and column buckling under directed loading
[PB87-124004] 06 p0722 N88-14436
Buckling of braced monosymmetric cantilevers: Timoshenko energy approach
[PB87-133849] 06 p0723 N88-14445
Effects of fabrication on the fatigue capacity of welded steel structures
[PB87-144226] 08 p0995 N88-16021

FABSTRAN: A computer program for frame and beam static and transient response analysis (nonlinear)
[ARE-TR-86205] 09 p1182 N88-17079
Composite materials for rail transit systems
[NASA-CR-178401] 10 p1294 N88-17738
Strategic placement of accelerometers to measure forces by the sum of weighted accelerations
[DE88-002262] 10 p1333 N88-17968
Robust controller design for flexible structures
[AD-A187217] 10 p1340 N88-18009
Some aspects of the mechanics and mechanisms of dynamic brittle fracture 10 p1343 N88-18028
Piezoelectric laminates for torsional and bending model control: Theory and experiment 10 p1343 N88-18029
Experimental set-up and mathematical modeling of H-shaped beam type structure
[AD-A187196] 11 p1466 N88-18743
Approximate method for predicting the permanent set in a beam in vacuo and in water subject to a shock wave 11 p1500 N88-18957
The Euler-Bernoulli beam equation with boundary energy dissipation
[AD-A189517] 13 p1765 N88-20560
Component mode synthesis using experimental modes enhanced by mass loading
[DE88-006097] 13 p1781 N88-20657
Finite element methodology for nonlinear free and harmonic forced vibrations of beam and plate structures 13 p1782 N88-20663
Design graphs for the first two bending Eigenvibration forms of rotating beams consisting of two beam points
[IW-86006R] 13 p1783 N88-20670
The X-beam as a deployable boom for the space station 14 p1925 N88-21473
Motion synchronization of a mechanism to deploy and restow a truss beam 14 p1925 N88-21474
Creep rupture analysis of a beam resting on high temperature foundation 14 p1930 N88-21509
Stabilization and control problems in structural dynamics
[AD-A190197] 15 p2073 N88-22361
Coupled bending-torsion steady-state response of pretwisted, nonuniform rotating beams using a transfer-matrix method
[NASA-TM-100596] 15 p2086 N88-22435
Bi-stem gripping apparatus
[NASA-CASE-MFS-28185-1] 17 p2345 N88-23979
Dynamic characteristics of a vibrating beam with periodic variation in bending stiffness
[NASA-TP-2697] 17 p2348 N88-23988
Space station architectural elements model study
[NASA-CR-4027] 18 p2464 N88-24632
Estimation and control of distributed models for certain elastic systems arising in large space structures
[AD-A192120] 18 p2472 N88-24666
On the bending response of Kevlar 49/epoxy beams and rings
[DE88-006824] 18 p2530 N88-25012
Mobile remote manipulator system for a tetrahedral truss
[NASA-CASE-MSC-20985-1] 20 p2765 N88-26398
Optimal design of viscoelastic structures 21 p2959 N88-27579
Coupled thermal vibrations of beams with temperature-dependent properties 21 p2963 N88-27601
Tripping of stiffened plates using a refined beam theory
[AD-A193989] 22 p3087 N88-28333
Damage initiation in the short beam shear test of composite materials using stiffness reduction
[AD-A194880] 24 p3340 N88-29883
Vibrational power flow analysis of rods and beams
[NASA-CR-183166] 24 p3383 N88-30151

BEAMSHAPING
U COLLIMATION

BEARING (DIRECTION)
Lower bounds on bearing accuracy for closely spaced sources
[AD-A184258] 04 p0486 N88-12997
Visual attention effects on discrimination of line orientation and line arrangement
[AD-A187013] 09 p1200 N88-17190
Bearing detection in the presence of two sources of varying coherence using the complex cepstrum
[NASA-CR-181605] 09 p1243 N88-17451
Composite ceramic superconducting filaments for superconducting cable
[AD-A187833] 11 p1556 N88-19312
A comparison of terrain association and resection as methods of position location
[AD-A189480] 13 p1790 N88-20710
Method for determining artillery position
[NASA-TT-20236] 14 p1979 N88-21813
Determination of beam orientation of optical diagnostics of excited 200-MeV hydrogen atoms resulting from photodetachment of H(-)ions
[AD-A189976] 14 p1981 N88-21823
Relative orientation
[AD-A190385] 15 p2089 N88-22449
Deflection of a circular liquid jet on a flat plate perpendicular to the flow direction
[NASA-TT-20279] 16 p2207 N88-23173

BEARING ALLOYS
The influence of foreign particles on bearing metals
[NASA-TT-20155] 20 p2775 N88-26454

BEARINGLESS ROTORS
An overview of key technology thrusts at Bell Helicopter Textron 09 p1111 N88-16657
Special flight mechanical features of the bearingless helicopter rotor
[MBB-FM-315/O] 10 p1309 N88-17825
Testing of a tail rotor system in a fiber composite type of construction
[MBB-UD-472/86] 10 p1314 N88-17854
Comprehensive analysis of helicopters with bearingless rotors
[NASA-CR-182537] 10 p1390 N88-18300
Design, manufacture and spin test of high contact ratio helicopter transmission utilizing Self-Aligning Bearingless Planetary (SABP)
[NASA-CR-4155] 18 p2524 N88-24975
A comparison of theory and experiment for the aeroelastic stability of a bearingless model rotor in hover 21 p2890 N88-27153
A comparison of theory and experiment for coupled rotor body stability of a bearingless rotor model in hover and forward flight 21 p2890 N88-27154
A comparison of theory and flight test of the BO 105/BMR in hover and forward flight 21 p2890 N88-27155
Aeromechanical stability analysis of COPTER 21 p2891 N88-27161
Aeroelastic characteristics of the AH-64 bearingless tail rotor 21 p2891 N88-27162

BEARINGS
NT ANTIFRICTION BEARINGS
NT BALL BEARINGS
NT FOIL BEARINGS
NT GAS BEARINGS
NT JOURNAL BEARINGS
NT MAGNETIC BEARINGS
NT ROLLER BEARINGS
Composite bearing materials containing solid lubricant in filamentary form, stages 3 and 4
[IRD-87/2] 01 p0054 N88-10344
Boundary lubrication. Experiments with boundary lubrication and plain bearings at +60...-60 deg C temperatures
[DE87-752869] 02 p0180 N88-11124
Bearing loads in slider crank mechanisms
[PB87-216495] 03 p0332 N88-12089
Coatings for high-temperature bearings and seals
[NASA-TM-100249] 05 p0567 N88-13453
Dynamic behavior of dissymmetric rotor bearings modelled with a periodic coefficient large system 05 p0596 N88-13640
Developing an accelerated endurance test for greases: A status report
[AD-A185963] 07 p0836 N88-15072
Evaluation of load tracks and wear of two sets of bearings from space shuttle main engine high pressure oxygen turbopumps
[NASA-CR-178969] 07 p0861 N88-15223
A variational formulation of a hydrodynamic lubrication problem
[MEMO-642] 08 p0987 N88-15979
Results of NASA/Army transmission research 09 p1108 N88-16640
Self-lubricating coatings for high-temperature applications 09 p1119 N88-16703
Numerical modeling of multidimensional flow in seals and bearings used in rotating machinery
[NASA-TM-100779] 09 p1165 N88-16988
Optimal design and parameter identification of flexible rotor-bearing systems 10 p1339 N88-18002
Numerical and analytical study of fluid dynamic forces in seals and bearings
[NASA-TM-100268] 11 p1485 N88-18867
Computer-aided design analysis of 57-mm, angular-contact, cryogenic turbopump bearings
[NASA-TP-2816] 11 p1496 N88-18933
Ply-level failure analysis of a graphite/epoxy laminate under bearing-bypass loading
[NASA-TM-100578] 13 p1735 N88-20372
Performance of elastomeric bearings
[PB88-159470] 14 p1918 N88-21450
The 22nd Aerospace Mechanisms Symposium
[NASA-CP-2506] 14 p1924 N88-21468
Mode 2 fracture mechanics 15 p2083 N88-22418
Active control and system identification of rotordynamic structure 16 p2218 N88-23230
Effects of axial load on elastomeric isolation bearings
[PB88-179015] 16 p2223 N88-23269
The flying characteristics of the membrane slider bearing 18 p2522 N88-24965
The 000 stage equipment bearing performance with a lower viscosity lubricant
[DE88-011827] 21 p2957 N88-27566

BEAT
U SYNCHRONISM

BEAT FREQUENCIES
Energy cascading in the beat-wave accelerator
[DE87-014727] 03 p0377 N88-12374
Heating efficiency of beat wave excitation in a density gradient
[AD-A193066] 21 p3017 N88-27905

BEAUFORT SEA (NORTH AMERICA)
Examples of ice pack rigidity and mobility characteristics determined from ice motion
[AD-A191163] 17 p2377 N88-24129
MIZPAC (marginal ice zone Pacific) 84-86 CTD (Conductivity, Temperature, Depth) data report
[AD-A192478] 21 p2976 N88-27679
Beaufort sea mesoscale circulation study: Hydrography helicopter operations, April 1987
[PB88-203658] 21 p2976 N88-27681

BED REST
Prevention of disuse osteoporosis: Effect of sodium fluoride during five weeks of bed rest
[NASA-CR-172018] 01 p0075 N88-10483
Regulation of calcium metabolism during prolonged antiorthostatic hypokinesia
[NASA-TT-20219] 11 p1521 N88-19085
P-31 Magnetic Resonance Spectroscopy (MRS) of limb muscles during bedrest with exercise countermeasures 12 p1656 N88-19925
Some reflections on the standardization of bed-rest procedures for weightlessness simulation (cardiovascular and endocrine apsects) 12 p1662 N88-19961
Noninvasive examination of bones during long-term hypokinesia 19 p2704 N88-26077
Physiology of prolonged bed rest
[NASA-TM-101010] 22 p3130 N88-28607
Interplanetary travel: Is gravity needed to close the loop
[NASA-TM-101013] 22 p3132 N88-28622

BEDROCK
NT BATHOLITHS
Preliminary estimation of color inhomogeneities on the surface of Venus according to the television images obtained by the VENERA-13 and VENERA-14 automated space probes
[NASA-TT-20114] 02 p0254 N88-11608
Structure of Southwestern Michipicoten Greenstone Belt, Ontario: Evidence for Archean accretion 24 p3397 N88-30228

BEDS (PROCESS ENGINEERING)
Theoretical prediction of single phase turbulent flow distribution in particulate bed reactors 17 p2419 N88-24386

BEER LAW
The analytical exponential decay coefficient of the submarine light field
[AD-A187215] 11 p1548 N88-19261

BEHAVIOR
NT HUMAN BEHAVIOR
Assessment of fatigue in aviation crews
[AD-A184129] 03 p0356 N88-12245
Supertracks: The building blocks of chaos
[DE88-001513] 04 p0522 N88-13207
Quantifying some information processing aspects of the pilot's instrument crosscheck
[AD-A186114] 07 p0898 N88-15443
Innovation and creativity: A critical linkage
[DE88-003309] 10 p1426 N88-18515
Experiments concerning gravisensitivity of protozoa 12 p1660 N88-19949
Describing constraints on a digital circuit's behavior
[AD-A189200] 13 p1761 N88-20531
An evaluation of the effects of high visual taskload on the separate behaviors involved in complex monitoring performance
[AD-A190641] 15 p2105 N88-22538
Program profiling in Cedar
[AD-A190883] 16 p2250 N88-23449
The behavior of drop-containing turbulent eddies
[AD-A191669] 18 p2509 N88-24883
Behavioral response of rats exposed to high-power microwave radiation
[AD-A192199] 18 p2548 N88-25128
Motor theory of auditory perception
[AD-A192095] 18 p2550 N88-25136
Modeling and evaluation of variable structure organizations
[AD-A191947] 18 p2588 N88-25381

Anomalous temperature-dependent negative magnetoresistance in pregraphitic carbons
[AD-A191725] 19 p2619 N88-25535
Behavioral, psychological and demographic predictors of physical fitness
[AD-A192697] 21 p2986 N88-27733
The dynamic behavior of a turbulent boundary layer subjected to a shock-induced separation
[AD-A194164] 22 p3075 N88-28252
Optical bistable behavior of a planar quasi-waveguide interferometer made with a conjugated organic polymer film
[AD-A194349] 22 p3152 N88-28756
Elastic behavior of a rubber layer bonded between two rigid spheres
[AD-A193698] 23 p3198 N88-29030

BELGIUM
Analysis of SPOT multispectral data concerning a border zone between two geographical regions in southern Belgium 22 p3100 N88-28411

BELL AIRCRAFT
NT UH-1 HELICOPTER
NT XV-15 AIRCRAFT

BELLMAN THEORY
Normed Bellman equation with degenerate diffusion coefficients and its application to differential equations
[AD-A190319] 15 p2120 N88-22637

BELTRAMI FLOW
Weak interactions and local order in strong turbulence 09 p1159 N88-16948

BENCHES
U SEATS

BEND TESTS
Investigation on ductile fracture behavior of 3-inch diameter Type 304 stainless steel pipe with a circumferential through-wall crack
[DE87-753016] 02 p0191 N88-11196
Crack initiation studies in hydrogen embrittled spring steel strip 05 p0605 N88-13710
An optical interferometry technique to evaluate closure along a crack front 05 p0607 N88-13726
Experimental investigation on the bending fatigue performance of gas carbonitrided and carburized gears
[PB87-147997] 08 p0992 N88-16003

BENDING
NT ELASTIC BENDING
An experimental and theoretical study of the bending behavior of Kevlar 49/epoxy beams and rings
[DE87-010430] 01 p0061 N88-10394
Aerodynamic design and performance of a bent-axis geometry vehicle
[DE87-013726] 02 p0124 N88-10786
Hardening of metal during production of bent shapes
[BLL-M-37250-(5828.4)] 02 p0148 N88-10928
Generalized hybrid variational principle, corresponding finite element model 03 p0301 N88-11895
Compactness of quasi-conforming element spaces, convergence of quasi-conforming element method 03 p0301 N88-11896
Analysis and testing of predamaged shell structures 04 p0428 N88-12653
Kinematic formulation of finite elements for plate bending 04 p0455 N88-12821
Crack growth prediction in 3D structures under aeronautical-type spectrum loadings 05 p0602 N88-13688
Bending properties of aluminum base composite with CVD-fiber
[PB87-130678] 06 p0678 N88-14156
Developments in electronics ceramics reported 06 p0684 N88-14192
Life prediction of steel cords 06 p0715 N88-14386
Multiaxial fatigue failure criterion: A new approach 06 p0719 N88-14418
Bending analysis of thin plates with openings
[PB87-143400] 07 p0869 N88-15274
Study of the temperature dependence of the mechanical characteristics of the steels GX 5 CrNi 13 4 and GGG 40 in tensile and bending tests
[DE88-001469] 09 p1143 N88-16850
Piezoelectric laminates for torsional and bending model control: Theory and experiment 10 p1343 N88-18029
Benchmark computation and finite element performance evaluation for a rhombic plate bending problem
[AD-A187402] 10 p1345 N88-18041
Mechanisms in thermal mechanical forming of plates
[AD-A187797] 11 p1466 N88-18744
Mathematical modeling of the postbuckling behavior of structural elements 11 p1500 N88-18960
An efficient Mindlin finite strip plate element based on assumed strain distribution 15 p2081 N88-22407
Coupled bending-torsion steady-state response of pretwisted, nonuniform rotating beams using a transfer-matrix method
[NASA-TM-100596] 15 p2086 N88-22435
Non-rigid motion and Regge calculus
[AD-A190387] 15 p2121 N88-22640
Effects of axial load on elastomeric isolation bearings
[PB88-179015] 16 p2223 N88-23269
Dynamic characteristics of a vibrating beam with periodic variation in bending stiffness
[NASA-TP-2697] 17 p2348 N88-23988
On the bending response of Kevlar 49/epoxy beams and rings
[DE88-006824] 18 p2530 N88-25012
MHD bending waves in a current sheet
[NASA-TM-101149] 18 p2579 N88-25323
Static analysis of thin plates using the finite strip-element method 19 p2679 N88-25931
Vertical ship motions and sea loads considering nonlinear effects
[TAE-592] 20 p2784 N88-26515
Improved finite strip Mindlin plate bending element using assumed shear strain distributions
[NASA-TM-100928] 23 p3225 N88-29195

BENDING DIAGRAMS
Design graphs for the first two bending Eigenvibration forms of rotating beams consisting of two beam points
[IW-86006R] 13 p1783 N88-20670

BENDING FATIGUE
Bending of a bonded beam as a test method for adhesive properties
[AD-A184813] 05 p0609 N88-13736
Experimental investigation on the bending fatigue performance of gas carbonitrided and carburized gears
[PB87-147997] 08 p0992 N88-16003

BENDING MOMENTS
Computation of the tensile and bending restraint intensities of welded specimens by finite element method
[PB87-143798] 08 p0995 N88-16024
The Euler-Bernoulli beam equation with boundary energy dissipation
[AD-A189517] 13 p1765 N88-20560

BENDING VIBRATION
Dynamic characteristics of a vibrating beam with periodic variation in bending stiffness
[NASA-TP-2697] 17 p2348 N88-23988

BENDS (PHYSIOLOGY)
U DECOMPRESSION SICKNESS

BENZENE
Detailed mechanism of benzene oxidation
[NASA-TM-100202] 03 p0282 N88-11775
Two-laser resonance enhanced photoionization spectrum of gas phase benzene 03 p0300 N88-11889
Detailed mechanism of toluene oxidation and comparison with benzene
[NASA-TM-100261] 05 p0563 N88-13428
Ordered polymers for space applications
[AD-A188460] 12 p1610 N88-19630
Size effects in the electrical resistivity of benzene-derived carbon fibers
[AD-A191708] 18 p2491 N88-24777
Microstructure of thin intercalated benezene derived graphite fibers
[AD-A191724] 19 p2618 N88-25534
Large ionic species in sooting acetylene and benzene flames 24 p3348 N88-29932

BERING SEA
Navarin Basin Ice Drift Program
[PB88-104021] 06 p0748 N88-14599
Geostrophic flow in the central Bering Sea, Fall 1986 and Summer 1987
[PB88-174354] 16 p2237 N88-23360
Influence of the Yukon River on the Bering Sea
[NASA-CR-182802] 17 p2376 N88-24126

BERNOULLI EQUATION
U BERNOULLI THEOREM

BERNOULLI THEOREM
Subcritical branching processes in a two state random environment, and a percolation problem on trees
[PB87-230439] 06 p0762 N88-14677
A Prohorov bound for a Poisson process and a Bernoulli process
[CWI-MS-R8701] 09 p1232 N88-17388

BERNSTEIN ENERGY PRINCIPLE
ICRF launcher studies
[DE88-001710] 04 p0495 N88-13046
Ion Bernstein modes in current-carrying plasmas 21 p3017 N88-27903

BERYLLIUM
Shielding analysis of a small compact space nuclear reactor
[AD-A185566] 06 p0779 N88-14784
Phenomenological model of superconductivity of heavy fermions in U(sub 1-x)ThsubxBesub13 09 p1238 N88-17423
Evaluation and compilation of thermodynamic properties of high temperature chemical species
[AD-A187509] 11 p1452 N88-18654
Adhesion of PVD titanium coatings to beryllium substrates
[DE88-005147] 11 p1463 N88-18721
Single-laboratory evaluation of SW-846 methods 7090/7091 determination of beryllium by flame and furnace atomic absorption spectrophotometry
[PB88-171434] 16 p2175 N88-22963
Contributions of autoionizing resonances to the electron collisional excitation rates for Be-like ions
[AD-A190924] 18 p2572 N88-25275
Studies of internal stresses and surface roughness of sputtered Be and BeB films
[DE88-011737] 22 p3086 N88-28327

BERYLLIUM ALLOYS
High velocity erosion of metal interfaces
[DE87-013937] 01 p0025 N88-10155
Joining of dissimilar materials with the pulsed Nd-YAG laser
[DE88-003757] 11 p1458 N88-18693

BERYLLIUM COMPOUNDS
NT BERYLLIUM OXIDES

BERYLLIUM OXIDES
Gas core reactors for direct nuclear propulsion 17 p2428 N88-24442

BESSEL FUNCTIONS
NT HANKEL FUNCTIONS
Frozen-field, rigid-beam, uniform-conductivity-channel tracking force calculation
[DE87-012510] 02 p0190 N88-11190
Accurate efficient evaluation of Bessel transform: Programs and error analysis
[AD-A187718] 11 p1536 N88-19174
Expressing mathematical subroutines constructively
[AD-A190559] 15 p2121 N88-22644
Distributions of quadratic forms
[AD-A190224] 15 p2124 N88-22663
Exact image theory for the problem of dielectric/magnetic slab
[NASA-CR-182865] 16 p2189 N88-23055
On the nucleonics component of cosmic radiation, in the atmosphere
[DE88-702493] 22 p3166 N88-28854

BETA FACTOR
Beta limitation of matter-antimatter boundary layers
[TRITA-EPP-87-11] 09 p1250 N88-17490
Formation of high-Beta plasmas in various modes of operation in TPE-2 12 p1693 N88-20132
Flux coordinate studies of elongated plasmas at high Beta 12 p1694 N88-20134
Shear Alfven spectrum of analytic high-Beta equilibria 12 p1694 N88-20136

BETA INTERACTIONS
U WEAK INTERACTIONS (FIELD THEORY)

BETA PARTICLES
Nuclear beta decay after Les Houches
[DE87-014921] 04 p0489 N88-13011
Double beta decay and nuclear structure
[DE88-001966] 07 p0931 N88-15652
Theory of double beta decay
[DE88-002285] 07 p0931 N88-15653
Plasma separation process. Betacell (BCELL) code, user's manual
[DE88-006955] 20 p2859 N88-26981
Measurement of Beta-decay energies of short-lived neutron-rich nuclei in the vicinity of mass number between 101 and 106, and A = 109
[ETN-88-92376] 21 p3014 N88-27890

BETATRONS
Betatron oscillations in a free electron laser
[DE88-004859] 10 p1337 N88-17990
Optical guiding in the separable beam limit
[AD-A192452] 21 p2952 N88-27534
Distortion functions
[DE88-752634] 21 p3015 N88-27896

BIAS
NT RESPONSE BIAS
Increased gain of channel intensifier tubes by pulsed biasing
[DE88-000512] 04 p0490 N88-13019
Conditionally unbiased bounded influence robust regression with applications to generalized linear models
[AD-A186319] 07 p0915 N88-15556
On precision and accuracy (bias) statements for measurement procedures
[DE88-004434] 10 p1402 N88-18359
Simultaneous estimation and detection of bias shifts for inertial navigation systems 12 p1576 N88-19429
Homogenizing surface and satellite observations of cloud. Aspects of bias in surface data
[AD-A188523] 12 p1648 N88-19869

Two dimensional uncorrelated bias in fix algorithms
[NASA-CR-182683] 13 p1815 N88-20847
Bias reduction when there is no unbiased estimate
[AD-A189407] 13 p1829 N88-20937
Min-max bias robust regression
[AD-A191345] 16 p2263 N88-23529
A critical speed study for aircraft bias ply tires
[AD-A193616] 22 p3084 N88-28313
Urbanization: Its detection and effect in the United States climate record 22 p3125 N88-28571
Systematic behavior of NMC medium range forecasts and the effect of model changes 1985-87 22 p3125 N88-28575
Two biased estimation techniques in linear regression: Application to aircraft
[NASA-TM-100649] 23 p3274 N88-29489

BIBLIOGRAPHIES
Aeronautical engineering: A continuing bibliography with indexes (supplement 218)
[NASA-SP-7037(218)] 01 p0001 N88-10002
Standard reference data publications, 1985-1986
[PB87-210241] 01 p0021 N88-10128
Earth resources: A continuing bibliography with indexes (issue 55)
[NASA-SP-7041(55)] 01 p0065 N88-10415
Problems in integrating geographic data
[DE87-012880] 01 p0106 N88-10689
A physico-chemical study of some areas of fundamental significance to biophysics
[DE87-013457] 02 p0217 N88-11365
Aerospace medicine and biology: A continuing bibliography with indexes
[NASA-SP-7011(303)] 02 p0217 N88-11367
Using bibliographic databases in technology transfer
[NASA-CR-181403] 02 p0222 N88-11399
Current experiments in elementary particle physics
[DE87-013961] 02 p0231 N88-11456
Publications and final reports on contracts and grants, 1986 (National Environmental Satellite, Data and Information Service)
[PB87-220810] 03 p0352 N88-12218
Health hazards of video display terminals. A comprehensive, annotated bibliography on a critical issue of workplace health and safety with sources for obtaining items and list of terminal suppliers
[RSI-IAS-4] 03 p0355 N88-12240
Aeronautical engineering: A continuing bibliography with indexes (supplement 219)
[NASA-SP-7037(219)] 04 p0396 N88-12470
Internal reforming development for solid oxide fuel cells
[DE87-006518] 04 p0464 N88-12871
Aerospace medicine and biology: A continuing bibliography with indexes
[NASA-SP-7011(304)] 04 p0474 N88-12922
Research papers and publications (1981-1987): Workload research program
[NASA-TM-100016] 04 p0474 N88-12924
Literature review of solid lubrication mechanisms
[AD-A185010] 05 p0567 N88-13456
Aeronautical engineering: A continuing bibliography with indexes (supplement 220)
[NASA-SP-7037(220)] 06 p0663 N88-14065
Aerospace medicine and biology: A continuing bibliography with indexes (supplement 305)
[NASA-SP-7011(305)] 06 p0752 N88-14616
Precipitation in alumina-rich spinel: A transformation-toughened ceramic single crystal
[DE87-012380] 06 p0785 N88-14815
University program management information system, fiscal year 1985
[NASA-TM-88381] 06 p0790 N88-14846
Bibliographic relationships: Toward a conceptual structure of bibliographic information used in cataloging 06 p0791 N88-14852
Bibliography of textbooks on fibre reinforced plastics (212 books)
[PB87-146080] 07 p0827 N88-15017
Annotated bibliography on reliable system design
[PB88-109848] 07 p0866 N88-15254
USSR Space Life Sciences Digest index to issues 10-14
[NASA-CR-3922(17)] 07 p0883 N88-15361
Bibliography of space biology and medicine 07 p0897 N88-15435
A summary of the Naval Postgraduate School research program
[AD-A186362] 07 p0942 N88-15727
Index of USA-CERL publications for October 1984 - June 1987
[AD-A186375] 07 p0942 N88-15728
NASA patent abstracts bibliography: A continuing bibliography. Section 1: Abstracts (supplement 32)
[NASA-SP-7039(32)-SECT-1-ABST] 07 p0943 N88-15732
Catalog of infrared observations. Part 1: Data
[NASA-RP-1196-PT-1-ED-2] 07 p0944 N88-15738
Aeronautical engineering. A continuing bibliography with indexes, supplement 221
[NASA-SP-7037(221)] 08 p0949 N88-15758
Aerospace medicine and biology: A continuing bibliography with indexes (supplement 307)
[NASA-SP-7011(307)] 08 p1049 N88-16332
Aeronautical engineering: A continuing bibliography with indexes (supplement 223)
[NASA-SP-7037(223)] 09 p1111 N88-16661
Publications of the exobiology program for 1986: A special bibliography
[NASA-TM-4029] 09 p1203 N88-17205
Wind turbine acoustics research bibliography with selected annotation
[NASA-TM-100528] 09 p1243 N88-17450
Earth resources: A continuing bibliography with indexes (supplement 56)
[NASA-SP-7041(56)] 10 p1347 N88-18051
Aerospace medicine and biology: A cumulative index to a continuing bibliography (supplement 306)
[NASA-SP-7011(306)] 10 p1369 N88-18180
Aerospace medicine and biology: A continuing bibliography with indexes (supplement 308)
[NASA-SP-7011(308)] 10 p1369 N88-18183
Recent progress in the dynamic applications of piezoelectric crystals 10 p1417 N88-18460
NASA patent abstracts bibliography: A continuing bibliography. Section 2: Indexes (supplement 32)
[NASA-SP-7039(32)-SECT-2] 10 p1425 N88-18511
Spacecraft fire detection and extinguishment: A bibliography
[NASA-CR-180880] 11 p1444 N88-18612
Cumulative reports and publications through December 31, 1987
[NASA-CR-181624] 11 p1524 N88-19099
Aeronautical engineering: A cumulative index to a continuing bibliography
[NASA-SP-7037(222)] 12 p1574 N88-19416
The Shock and Vibration Digest, volume 20, no. 3 12 p1635 N88-19786
Aeronautical engineering: A continuing bibliography with indexes (supplement 224)
[NASA-SP-7037(224)] 13 p1715 N88-20254
Aerospace medicine and biology: A continuing bibliography with indexes (supplement 309)
[NASA-SP-7011(309)] 13 p1810 N88-20814
Aeronautical engineering: A continuing bibliography with indexes (supplement 225)
[NASA-SP-7037(225)] 14 p1863 N88-21126
Management: A bibliography for NASA managers
[NASA-SP-7500(22)] 14 p1991 N88-21867
Artificial neural networks: An introduction with an annotated bibliography
[DE88-007003] 15 p2116 N88-22603
Aeronautical engineering: A continuing bibliography with indexes (supplement 226)
[NASA-SP-7037(226)] 16 p2155 N88-22857
Enhanced backscattering from rough surfaces
[AD-A190995] 16 p2190 N88-23063
Earth resources: A continuing bibliography with indexes (issue 57)
[NASA-SP-7041(57)] 16 p2229 N88-23314
Aerospace medicine and biology: A continuing bibliography with indexes (supplement 310)
[NASA-SP-7011(310)] 16 p2238 N88-23369
Engine structures: A bibliography of Lewis Research Center's research for 1980-1987
[NASA-TM-100842] 17 p2350 N88-24002
Aerospace medicine and biology: A continuing bibliography with indexes (supplement 311)
[NASA-SP-7011(311)] 17 p2382 N88-24161
Aeronautical engineering: A continuing bibliography with indexes (supplement 227)
[NASA-SP-7037(227)] 18 p2456 N88-24578
Electromagnetic field penetration into structures
[AD-A192127] 18 p2501 N88-24836
Bibliography of Soviet laser developments, number 83, May - June 1986
[AD-A190969] 18 p2520 N88-24950
Aerospace medicine and biology: A continuing bibliography with indexes (supplement 312)
[NASA-SP-7011(312)] 18 p2551 N88-25141
Management and the executive
[AD-A190778] 18 p2587 N88-25374
NASA patent abstracts bibliography: A continuing bibliography. Section 1: Abstracts
[NASA-SP-7039(33)] 18 p2590 N88-25388
Wind tunnel wall interference (January 1980 - May 1988): A selected, annotated bibliography
[NASA-TM-4061] 19 p2604 N88-25466
Ocean, Wave, and Tidal Energy Systems: Current abstracts
[DE88-008299] 19 p2687 N88-25973
Proceedings of the Workshop on the Assessment of Crew Workload Measurement Methods, Techniques and Procedures. Volume 2: Library references
[AD-A191209] 19 p2710 N88-26101
A bibliography and author index for electrical discharges in vacuum (1897-1986)
[DE88-008744] 20 p2794 N88-26579
Aerospace medicine and biology: A continuing bibliography with indexes (supplement 313)
[NASA-SP-7011(313)] 20 p2832 N88-26800
Aeronautical engineering: A continuing bibliography with indexes
[NASA-SP-7037(229)] 21 p2891 N88-27163
Technology for large space systems: A bibliography with indexes (supplement 18)
[NASA-SP-7046(18)] 21 p2901 N88-27214
Photovoltaic Energy. Electricity from Sunlight: A current awareness bulletin
[DE88-008289] 21 p2969 N88-27634
Aerospace Medicine and Biology: A continuing bibliography with indexes (supplement 314)
[NASA-SP-7011(314)] 21 p2988 N88-27742
Aeronautical engineering: A continuing bibliography with indexes
[NASA-SP-7037(228)] 22 p3037 N88-28031
Microgravity science and applications bibliography, 1987 revision
[NASA-TM-4067] 22 p3062 N88-28171
The anatomy of the gyroscope
[AGARD-AG-313] 22 p3079 N88-28287
Bibliography on tropical rain forests and the global carbon cycle. Volume 1: An introduction to the literature
[DE88-010761] 22 p3118 N88-28523
Bibliography of Lewis Research Center technical publications announced in 1987
[NASA-TM-100910] 22 p3162 N88-28832
Literature review: Validity and potential usefulness of psychomotor ability tests for personnel selection and classification
[AD-A193558] 23 p3241 N88-29287
Multicriteria integer programming for problems involving linear and nonlinear utility functions
[AD-A194530] 23 p3249 N88-29336
Topics in adaptive control and inference
[AD-A194718] 23 p3266 N88-29443
Bibliography of Soviet laser developments, number 88, March - April 1987
[AD-A195978] 24 p3378 N88-30116
Aerospace medicine and biology: A continuing bibliography with indexes (supplement 315)
[NASA-SP-7011(315)] 24 p3407 N88-30281
Publications of the Jet Propulsion Laboratory 1987
[NASA-CR-181198] 24 p3436 N88-30453

BICARBONATES
U CARBONATES

BICRYSTALS
Fatigue crack propagation in Al-Zn-Mg bicrystals and its dependence on the environment 05 p0605 N88-13707
Fatigue crack growth and fracture of copper-bismuth bicrystals 06 p0715 N88-14385
Free energy calculation via MD (molecular dynamics): Methodology and application to bicrystals
[DE88-002902] 09 p1256 N88-17532
Molecular dynamics study of high-temperature grain-boundary stability in a (100) sigma = 29 bicrystal model
[DE88-002955] 09 p1258 N88-17546

BIDIRECTIONAL REFLECTANCE
Cloud cover determination in polar regions from satellite imagery
[NASA-CR-181544] 04 p0471 N88-12908
Summary of along-track data from the Earth radiation budget satellite for several major desert regions
[NASA-RP-1197] 13 p1802 N88-20772
Determination and application of bidirectional solar-optical properties of fenestration systems
[DE88-010364] 20 p2820 N88-26727
Angular radiation models for Earth-atmosphere system. Volume 1: Shortwave radiation
[NASA-RP-1184] 21 p2976 N88-27677
Comparison of the bidirectional reflectance distribution function of various surfaces
[NASA-TM-101317] 22 p3153 N88-28760

BIFURCATION (MATHEMATICS)
U BRANCHING (MATHEMATICS)

BIG BANG COSMOLOGY
Particle physics and cosmology
[DE87-005400] 03 p0387 N88-12432
New cosmological scenario
[DE87-703357] 04 p0520 N88-13198
Cosmology in the plasma universe
[TRITA-EPP-87-07] 05 p0660 N88-14053
Big Bang Nucleosynthesis: Accelerator tests and can (UC OMEGA)(sub B) really be large
[DE88-003405] 11 p1570 N88-19396

Particle physics and cosmology
[DE88-004944] 13 p1854 N88-21096

BIGHTS
U BAYS (TOPOGRAPHIC FEATURES)

BIHARMONIC EQUATIONS
Approximate polynomial preconditioning applied to biharmonic equations on vector supercomputers
[NASA-TM-100217] 01 p0087 N88-10563
Grid generation for an advanced fighter aircraft
23 p3246 N88-29319

BIMETALS
Model for bimetallic interfaces, part 2
[DE88-702672] 22 p3157 N88-28787

BINARY ALLOYS
Electronic structure of crystalline NaSn
[DE87-702583] 01 p0102 N88-10669
Superconductivity of pseudobinary compounds A15 (V-Cr)3Si, (V-MO)3Si, Mo3(Si-Re), bombarded with fast neutrons 03 p0285 N88-11792
Structural analysis using X-ray scattering and neutron scattering on binary amorphous (Co,Cu)Ti alloys
[ETN-88-91487] 11 p1459 N88-18699
Processing, structure and properties of heavily deformed in situ composites
[AD-A189611] 13 p1742 N88-20416
Erosion in dual-phase microstructures
[DE88-004507] 13 p1743 N88-20421
On the theory of the conversion of metallic mixed phases. 5: Fluctuations and nucleation in sub-cooled phases
[NASA-TT-20249] 14 p1890 N88-21296
Fundamental studies on high temperature deformation recrystallization, and grain growth of two-phase materials
[AD-A189725] 15 p2038 N88-22145
Corrosion and electrochemical behavior of binary magnesium alloys
[AD-A190624] 15 p2040 N88-22154

BINARY CODES
Bandwidth efficient block codes for M-ary PSK modulation
[NASA-CR-181543] 04 p0437 N88-12712
Parallel binary and parallel coded decimal time code formats
[AD-A190126] 17 p2384 N88-24170

BINARY DATA
SBNR (Signed Binary Number Representations) digital signal processor architecture
[AD-A184603] 03 p0364 N88-12290
Distributed fault tolerant embeddings of binary trees in hypercubes
[AD-A192929] 20 p2839 N88-26840
Use of a coherent square wave reference to demodulate BPSK (Binary Phase Shift Keying) carriers and a visual indicator of the quality of received QPSK (Quadrature Phase Shift Keying) carriers
[AD-A193528] 23 p3204 N88-29065

BINARY DIGITS
Extraction and evaluation of Boolean relations for the solution of linear programs in 0-1 variables, volume 1
[ENST-86E023-VOL-1] 02 p0227 N88-11430
Extraction and evaluation of Boolean relations for the solution of linear programs in 0-1 variables, volume 2
[ENST-86E023-VOL-2] 02 p0227 N88-11431

BINARY INTEGRATION
Very thin VLSI-layouts (Very Large Scale Integration-Layouts) of complete binary trees
[PB88-100847] 06 p0789 N88-14841
Analysis of binarized Hartley phase-only filter performance with respect to stochastic noise
[DE88-007604] 18 p2519 N88-24945

BINARY MIXTURES
NT EUTECTIC ALLOYS
NT EUTECTICS
DTA/DSC studies of phase equilibria in binary mixtures of barium carbonate with alkali carbonates
[DE87-001195] 02 p0194 N88-11213
Thermodynamic properties for natural gas binaries
[PB87-226833] 04 p0500 N88-13074
Laval nozzle flow of a binary, retrograde mixture
[MPIS-1/1987] 11 p1488 N88-18682
Exciton relaxation phenomena in a disordered system
14 p1978 N88-21802

BINARY STARS
NT CATACLYSMIC VARIABLES
NT DWARF NOVAE
NT ECLIPSING BINARY STARS
NT NEMESIS (STAR)
NT X RAY BINARIES
Binary Star Explorer 01 p0095 N88-10624
The nucleus of LT-5: An unusual triple system? --- planetary nebula
[PUBL-SER-C-FASC-11] 03 p0388 N88-12436
Differential B and V light curves of the bright BY Draconis star HD80715 04 p0509 N88-13130
Asynchronous rotation in close binary systems with circular orbits 04 p0509 N88-13131
PG 0308 + 096: A short-period white dwarf + dM binary with strongly modulated H-alpha emission
04 p0509 N88-13132
The Parkes radio survey of active chromosphere stars
04 p0511 N88-13141
IRAS and near IR observations of active binaries
04 p0518 N88-13186
Radio emission from RS CVn binaries: A 5 GHz VLA survey of 93 systems 04 p0519 N88-13191
Catalogue of chromospherically active binaries
04 p0520 N88-13192
A survey study of energy distribution in component stars of Algol-type binary systems 06 p0801 N88-14901
Mapping stellar surface features
09 p1262 N88-17564
The formation of single millisecond pulsars in globular clusters
[MPE-PREPRINT-97] 10 p1428 N88-18525
Very high energy gamma ray astrophysics
[DE88-005821] 13 p1854 N88-21095
The X-ray properties of AM Her stars
[MPE-PREPRINT-106] 16 p2289 N88-23704
A model for the X-ray binary 4U1820-30
[NASA-TM-101143] 17 p2451 N88-24562
Colliding stellar winds in the eclipsing Wolf-Rayet binary V444 Cygni
[NASA-CR-182937] 17 p2451 N88-24563
Duplicity in the solar neighborhood. Part 3: New spectroscopic elements for nine solar-type binary stars
[SER-C-PREPUBL-FASC-18-PT-3]
18 p2592 N88-25405
EXOSAT observations of Hercules X-1
[MPE-PREPRINT-119] 22 p3164 N88-28641
Mass transfer instabilities due to angular momentum flows in close binaries --- stars
[MPE-PREPRINT-113] 22 p3165 N88-28849
An upper limit on the primordial He4 abundance from speckle interferometric observations of muon Cassiopeiae 23 p3298 N88-29641
Binary star measurements using digital speckle interferometer of 6-m telescope
24 p3448 N88-30521
Duplicity in the solar neighborhood: Part 4: Spectroscopic orbits for four dwarf M stars
[SER-C-PREPUBL-FASC-21] 24 p3454 N88-30561
Duplicity in the solar neighborhood: Part 5: Spectroscopic orbit for the nearby double-lined solar-type star HR 8581
[SER-C-PREPUBL-FASC-23] 24 p3455 N88-30562
Activities in astrophysics
[INPE-4582-PRE/1316] 24 p3456 N88-30570

BINARY SYSTEMS (DIGITAL)
U DIGITAL SYSTEMS

BINARY SYSTEMS (MATERIALS)
NT BINARY ALLOYS
NT BINARY MIXTURES
NT EUTECTIC ALLOYS
NT EUTECTICS
Investigation of the deformation behavior of ferritic two-phase Fe-Ni-Al alloys with high concentrations of the intermetallic (Fe, Ni)Al phase at high temperatures
[ETN-87-90605] 03 p0288 N88-11812
The correlation between microstructure and thermomechanical properties of two-phase materials and porous sintered materials
[KFK-4205] 03 p0292 N88-11835
Retention processes in supercritical fluid chromatography
[DE88-000079] 04 p0413 N88-12559
Thermodynamic properties of supercritical mixtures
[DE88-000809] 04 p0413 N88-12562
Boundary effects on the drag of an oscillating sphere: Applications to the magnetic sphere rheometer. Attenuation and dispersion of acoustic waves in nematic liquid crystals 04 p0488 N88-13007
Electronic structure calculations and binding analyses for selected binary and ternary metal hydrides
[ETN-88-91087] 09 p1256 N88-17527
Demixing of aqueous polymer two-phase systems in low gravity
[NASA-TM-101141] 18 p2496 N88-24809

BINDERS (ADHESIVES)
U ADHESIVES

BINDERS (MATERIALS)
NT PROPELLANT BINDERS
NT SOLID ROCKET BINDERS
Polymer modified binders for bituminous or asphaltic paving layers
[PC-5] 02 p0153 N88-10958
Thermoplastic elastomers as LOVA (Low Vulnerability Ammunition) binders
[AD-A184350] 04 p0419 N88-12599
The use of NMR imaging to measure porosity and binder distributions in green-state and partially sintered ceramics
[DE88-003099] 08 p0972 N88-15881
Mechanism of and particle size effects on shock sensitivity of heterogeneous pressed explosives: Preliminary assessment of binderless RDX in fuze trains
[MRL-R-1077] 09 p1150 N88-16892
Thermoplastic elastomers as LOVA binders
[AD-A186563] 10 p1304 N88-17797
NMR (Nuclear Magnetic Resonance) imaging for detecting binder/plasticizers in green-state structural ceramics
[DE88-003111] 10 p1304 N88-17800
High yield synthesis of B4C/BN ceramic materials by pyrolysis of polymeric Lewis base adducts of decaborane(14)
[AD-A188154] 11 p1462 N88-18717
Increasing the rate at which ceramic castings undergo preliminary heat-treatment in an ultra-high frequency magnetic field 14 p1886 N88-21275
Effect of moisture level in PBXW-109(E) (plastic-bonded explosive) mixes on the aging of the cured explosive
[AD-A190200] 15 p2048 N88-22202
Determination of binder distributions in green-state ceramics by NMR imaging
[DE88-009990] 20 p2778 N88-26474
Alternate/modified binders for airfield pavements
[AD-A192781] 21 p2899 N88-27206

BINDING
Relativistic corrections for one- and two-photon matrix elements of weakly-bound systems
[NOTA-INTERNA-884] 07 p0929 N88-15645
Electronic structure calculations and binding analyses for selected binary and ternary metal hydrides
[ETN-88-91087] 09 p1256 N88-17527
Tight binding theory of semiconductors
10 p1415 N88-18447

BINOCULAR VISION
Biorhythms of binocular vision
20 p2830 N88-26788

BINOMIALS
A three-parameter generalisation of the beta-binomial distribution with applications
[AD-A185733] 06 p0768 N88-14720
Selecting the best binomial population: Parametric empirical Bayes approach
[AD-A193341] 23 p3269 N88-29450
Relaxed heaps: An alternative to fibonacci heaps
[AD-A194030] 23 p3272 N88-29470

BIOASSAY
DNA damage and repair in human skin in situ
[DE87-014288] 03 p0356 N88-12241
Superoxide dismutase assays
[AD-A183972] 03 p0356 N88-12242
Methods of quantifying and enhancing reactive oxygen apecies production 21 p2924 N88-27357
Genetic effects of low level microwave radiation
[AD-A192687] 21 p2984 N88-27722

BIOASTRONAUTICS
Lung function in simulated microgravity
12 p1654 N88-19907

BIOCHEMISTRY
NT BIOGEOCHEMISTRY
NT ENZYMOLOGY
NT PHYSIOCHEMISTRY
JPRS report: Science and technology. USSR: Life sciences
[JPRS-ULS-87-009] 04 p0473 N88-12915
JPRS report: Science and technology. USSR: Life sciences
[JPRS-ULS-87-011] 06 p0749 N88-14601
Human physical fields 06 p0750 N88-14609
A learning model as a basis for investigations of the effects of gravity on the learning processes and memory formulation 07 p0886 N88-15374
Experiments with rats flown aboard Cosmos-1667 biosatellite (main objectives, conditions and results)
07 p0893 N88-15414
Acid-base equilibrium and some rat blood parameters following exposure to hyperbaric oxygenation
07 p0894 N88-15420
Changes in functional parameters of animals during long-term inhalation of acetic acid
07 p0895 N88-15423
Neurochemical changes in hibernation
08 p1046 N88-16322
Biophysical and biochemical mechanisms in synaptic transmitter release
[AD-A187059] 09 p1199 N88-17184
Molecular mechanisms of neuronal responsivity
[AD-A187061] 09 p1199 N88-17185
Project Explorer takes its second step: GAS-608 in engineering development 10 p1288 N88-17707
Human blood glutamic acid level with exposure to high ambient concentrations of ammonia
10 p1361 N88-18134
New book on metabolic aspects of spaceflight stress
10 p1367 N88-18172

USSR report: Life sciences. Biomedical and behavioral sciences
[JPRS-UBB-87-010] 12 p1651 N88-19889
Survival under space vacuum: Biochemical aspects 12 p1657 N88-19930
USSR report: Life sciences. Biomedical and behavioral sciences
[JPRS-UBB-87-008] 12 p1662 N88-19966
Improved methods for high resolution electron microscopy
[DE88-005731] 13 p1774 N88-20609
JPRS report: Science and technology. USSR: Life sciences
[JPRS-ULS-88-004] 13 p1810 N88-20815
Technology '87: Research and Development Laboratory Technology Transfer Program
[DE88-003142] 13 p1852 N88-21084
Diagnostic studies of the HxOy-NzOy-O3 photochemical system using data from NASA GTE field expeditions
[NASA-CR-183038] 19 p2689 N88-25984
JPRS report: Science and technology. USSR: Life sciences
[JPRS-ULS-88-009] 20 p2829 N88-26785
Regulatory biochemical and metabolic responses in photoreceptors
[AD-A192898] 20 p2831 N88-26794
Methods of quantifying and enhancing reactive oxygen species production 21 p2924 N88-27357

BIOCONTROL SYSTEMS
Motion sickness: Quantitative, algorithmic malaise indication in real time
[AD-A189674] 15 p2101 N88-22518
The biomorphic model of the human operator controlling a single or a double integrator
[LR-505] 16 p2243 N88-23402

BIOCONVERSION
ECUT (Energy Conversion and Utilization Technologies) program: Biocatalysis Project
[NASA-CR-182917] 17 p2370 N88-24110

BIODEGRADATION
Shelf life degradation of selected anaerobic threadlocking adhesives at various storage temperatures
[AD-A187712] 11 p1461 N88-18711
Degradation of jet and missile fuels by aquatic microbial communities
[AD-A188065] 11 p1465 N88-18737
Biodegradation of JP-5 aviation fuel by subsurface microbial communities
[AD-A192743] 20 p2781 N88-26493

BIODYNAMICS
Facilitory effects of voluntary movements on vestibulomotor reaction 12 p1664 N88-19976
Analysis of head response to torso acceleration. Volume 2: Description of data retrieval, analysis and display software
[PB88-156765] 15 p2104 N88-22536
Using IMSL mathematical and statistical computer subroutines in physiological and biomechanical research
[AD-A192594] 21 p2995 N88-27765
Hierarchical structure in polymeric solids and its influence on properties
[AD-A194720] 23 p3197 N88-29029

BIOELECTRIC POTENTIAL
Electroencephalographic changes during equilibrium test in the presence of rhythmic photic interference 19 p2703 N88-26075

BIOELECTRICITY
Local human skin potential: Spatial distribution, magnitude and origin
[DE87-012882] 01 p0075 N88-10480
Critical phenomena and electromagnetic effects in biological membranes
[AD-A188156] 11 p1518 N88-19064
Changes in blood conductivity during immersion 12 p1663 N88-19969
Brain activity during tactical decision-making. Part 2: Probe-evoked potentials and workload
[AD-A188688] 12 p1667 N88-19994
Studies of the intact human brain: Implications for performance 21 p2977 N88-27684
CEEG dynamic brain mapping: A new method to evaluate brain function in different psychological and drug conditions 21 p2977 N88-27685
Fourth generation neurocognitive pattern analysis system 21 p2977 N88-27686
The application of non-stationary data analysis techniques in the identification of changes in the electroencephalogram associated with the onset of drowsiness 21 p2978 N88-27688
Neurophysiological patterns of operational fatigue: Preliminary results 21 p2981 N88-27703
Fighter pilot performance during airborne and simulator missions: Physiological comparisons 21 p2981 N88-27704
Event-related and steady potential changes in the brain related to workload during tracking 21 p2981 N88-27705
Neurophysiological precursors of accurate visuomotor performance 21 p2981 N88-27706
The neuroelectric selection of Naval aviation personnel: An evaluation 21 p2981 N88-27707
Evoked potential analysis of impact acceleration experiments 21 p2981 N88-27708
EEG indices of G-induced Loss Of Consciousness (G-LOC) 21 p2982 N88-27709
Detection of acceleration (+Gz) induced blackout by matched-filtering of visual evoked potentials 21 p2982 N88-27710
Electroencephalographic correlates of pilot performance: Simulation and in-flight studies 21 p2982 N88-27711
Motion evoked vestibular potentials 21 p2982 N88-27712
Measurement and classification of the mode of action of antidepressant drugs 21 p2983 N88-27714
Measurement of electrical activity in the CNS with cortical evoked potentials and EEG: Efficacy profiles of drugs using factor analysis 21 p2983 N88-27715
An approach to studying the effects of psychostimulants on cerebral electrical activity in the non-human primate 21 p2983 N88-27716
Spontaneous cerebral electrical activity during prolonged hypoglycemia: A quantitative study in humans 21 p2983 N88-27717
Correlation between EEG abnormal activity and aircraft accidents: A long term observation 21 p2984 N88-27719
Cytochrome electron transfer and biomolecular electronics
[AD-A195482] 24 p3406 N88-30277

BIOENGINEERING
NT ANTHROPOMETRY
NT BALLISTOCARDIOGRAPHY
NT BIOINSTRUMENTATION
NT BIOMETRICS
NT BIOTELEMETRY
NT BODY MEASUREMENT (BIOLOGY)
NT ECHOCARDIOGRAPHY
NT ELECTROCARDIOGRAPHY
NT ELECTROENCEPHALOGRAPHY
NT ELECTRORETINOGRAPHY
NT MAGNETOCARDIOGRAPHY
NT PLETHYSMOGRAPHY
ECUT (Energy Conversion and Utilization Technologies) program: Biocatalysis Project
[NASA-CR-182917] 17 p2370 N88-24110

BIOFEEDBACK
NT SENSORY FEEDBACK
Biofeedback control of alveolar carbon dioxide tension to eliminate hypocapnia in man in the presence of hypoxia 07 p0892 N88-15405
The effects of increased cognitive demands on autonomic self-regulation: An indicator of parallel processing in the brain 21 p2925 N88-27362

BIOGENESIS
U BIOLOGICAL EVOLUTION

BIOGENY
Exobiology and life science 07 p0883 N88-15358

BIOGEOCHEMISTRY
Biogeochemical cycling in the ocean. Part 1: Introduction to the effects of upwelling along the west coast of North America
[NASA-TM-88230] 07 p0882 N88-15349
International geosphere-biosphere program: A study of global change
[PB88-142393] 11 p1510 N88-19021
Global mixed-layer natural and anthropogenic fluxes 13 p1807 N88-20803

BIOGRAPHY
On the occasion of the 50th anniversary of the death of Professor Hugo Junkers
[MBB/LW-3016/S/PUB/201] 02 p0257 N88-11627
Messerschmitt-Boelkow-Blohm: Biography and history of a company 10 p1316 N88-17867

BIOINSTRUMENTATION
NT BIOTELEMETRY
High polymer sensor materials discussed 06 p0676 N88-14140
Vital signs rate meter
[AD-A187015] 09 p1198 N88-17183
Clinical applications of computerized thermography 17 p2330 N88-23915
Electrical and chemical sensors for biological cell research 19 p2669 N88-25866
Silver multi-layers for planar Ag/AgCl reference electrodes 19 p2672 N88-25883

BIOLOGICAL ACTIVITY
U ACTIVITY (BIOLOGY)

BIOLOGICAL ANALYSIS
U BIOASSAY

BIOLOGICAL CELLS
U CELLS (BIOLOGY)

BIOLOGICAL CLOCKS
U RHYTHM (BIOLOGY)

BIOLOGICAL EFFECTS
NT DESYNCHRONIZATION (BIOLOGY)
NT JET LAG
Master index for the carbon dioxide research state-of-the-art report series
[DE87-012757] 01 p0072 N88-10459
The photophysics and chemistry of PAH (Polycyclic Aromatic Hydrocarbons) compounds
[DE87-014455] 02 p0153 N88-10954
Photocatalytic electrochemistry at a biological-membrane metal-colloid interface
[DE87-009122] 02 p0166 N88-11041
Aerospace medicine and biology: A continuing bibliography with indexes
[NASA-SP-7011(303)] 02 p0217 N88-11367
Aerospace medicine and biology: A continuing bibliography with indexes
[NASA-SP-7011(304)] 04 p0474 N88-12922
TOMS as a monitor of the ultraviolet radiation environment: Applications to photobiology 05 p0617 N88-13785
Research for electric energy systems
[DE88-001733] 06 p0695 N88-14265
Aerospace medicine and biology: A continuing bibliography with indexes (supplement 305)
[NASA-SP-7011(305)] 06 p0752 N88-14616
Semi-arid ecosystem development as a function of resource processing and allocation
[DE88-000890] 07 p0875 N88-15308
Biogeochemical cycling in the ocean. Part 1: Introduction to the effects of upwelling along the west coast of North America
[NASA-TM-88230] 07 p0882 N88-15349
JPRS report: Science and technology. USSR: Space Biology and Aerospace Medicine, volume 21, no. 3, May - June 1987
[JPRS-USB-88-001] 07 p0889 N88-15389
Karyometric evaluation of neuronal reactions of rat cerebral cortex to the combined effect of ionizing radiation, longitudinal accelerations and vibration 07 p0890 N88-15396
Nystagmometric distinctions of individuals regularly exposed to vibration 07 p0891 N88-15401
Distinctive changes in arterial pressure and blood flow in common carotid artery of monkeys flown aboard Cosmos-1514 biosatellite 07 p0892 N88-15404
Investigation of energy metabolism of biological systems in weightlessness 07 p0893 N88-15409
Third Soviet-French Symposium on Space Cytology 07 p0893 N88-15411
Simulation of effect on biological systems of impact wave from heavy charged particle track 07 p0896 N88-15429
New book on space ecology reviewed 07 p0897 N88-15434
Possible use of plasmids for study of effect of space flight factors on biological objects 08 p1046 N88-16319
Zero gravity and living organism 08 p1046 N88-16320
Aerospace medicine and biology: A continuing bibliography with indexes (supplement 307)
[NASA-SP-7011(307)] 08 p1049 N88-16332
Rapid hypothermia subsequent to oral nicotinic acid and immersion in warm (30C) water
[AD-A186458] 08 p1050 N88-16339
Radon Research Program, FY-1987
[DE88-002633] 09 p1188 N88-17120
Kinetic toxic aspect of potential use of sulfur hexafluoride in closed environments 10 p1362 N88-18142
Effect of external electrostatic field on catecholamine secretion by rat adrenals 10 p1366 N88-18166
Aerospace medicine and biology: A cumulative index to a continuing bibliography (supplement 306)
[NASA-SP-7011(306)] 10 p1369 N88-18180
Aerospace medicine and biology: A continuing bibliography with indexes (supplement 308)
[NASA-SP-7011(308)] 10 p1369 N88-18183
The ESA facility Biorack 12 p1652 N88-19897
Survival under space vacuum: Biochemical aspects 12 p1657 N88-19930
Cellular effects of heavy ions: Experimental results and theoretical approaches --- space radiation 12 p1658 N88-19933
Radiation problems in manned space flight with a view to the Space Station 12 p1658 N88-19934
Effects of cosmic heavy ion radiation and space microgravity on plant systems 12 p1658 N88-19936
Organs and tissues regeneration in amphibia under the space flight conditions 12 p1660 N88-19951

Biorack experiments in Spacelab D-1 and TML-1: Further developments in gravitational biology
12 p1661 N88-19953
Nitrogen's biological effect on oxygen transport through hematoparenchymal barrier 12 p1662 N88-19967
Effects of whole-body irradiation with low-intensity microwaves on morphological, functional and cytochemical characteristics of leukocytes 12 p1663 N88-19971
Aerospace medicine and biology: A continuing bibliography with indexes (supplement 309)
[NASA-SP-7011(309)] 13 p1810 N88-20814
Protection against laser damage to human body reviewed 15 p2053 N88-22237
Behavior, physiology and energy deposition in rats chronically exposed to 2450 MHz radiation
[PB88-171418] 16 p2237 N88-23363
Aerospace medicine and biology: A continuing bibliography with indexes (supplement 310)
[NASA-SP-7011(310)] 16 p2238 N88-23369
Spectroradiometry in industrial safety
16 p2272 N88-23600
Aerospace medicine and biology: A continuing bibliography with indexes (supplement 311)
[NASA-SP-7011(311)] 17 p2382 N88-24161
A cardiostimulant protein from the Australian Red Waratah Sea anemone, Actinia tenebrosa
18 p2550 N88-25138
Aerospace medicine and biology: A continuing bibliography with indexes (supplement 312)
[NASA-SP-7011(312)] 18 p2551 N88-25141
Extremely Low Frequency (ELF) communications program: Non-ionizing electromagnetic radiation literature evaluation and assessment, 1966-1987 literature review
[AD-A192024] 19 p2642 N88-25677
Effect of long-term inhalation of acetic acid vapor on some functional parameters of man
19 p2705 N88-26084
Validation of maximum permissible concentration of urea in reclaimed potable water and evaluation of its biological effect 19 p2705 N88-26086
Interaction of biological systems with static and ELF electric and magnetic fields
[DE88-007951] 20 p2831 N88-26792
Aerospace medicine and biology: A continuing bibliography with indexes (supplement 313)
[NASA-SP-7011(313)] 20 p2832 N88-26800
Aerospace Medicine and Biology: A continuing bibliography with indexes (supplement 314)
[NASA-SP-7011(314)] 21 p2988 N88-27742
Physiological effects of extremely low frequency electric and magnetic fields
[DE88-752814] 22 p3132 N88-28620
Study of biological effects and radiation protection to future European manned space flights
[DGT-33061] 23 p3281 N88-29535
Bioeffects of electromagnetic waves
24 p3364 N88-30032
Aerospace medicine and biology: A continuing bibliography with indexes (supplement 315)
[NASA-SP-7011(315)] 24 p3407 N88-30281

BIOLOGICAL EVOLUTION
Analysis of laser extracted volatiles in carbonaceous chondrites 06 p0793 N88-14861
Publications of the exobiology program for 1986: A special bibliography
[NASA-TM-4029] 09 p1203 N88-17205
The evolution of glutathione metabolism in phototrophic microorganisms
[NASA-CR-182902] 19 p2695 N88-26015
LSU scientists discover evidence of large meteorite impacts on the early earth 24 p3441 N88-30480

BIOLOGICAL MODELS
U BIONICS

BIOLOGICAL MODELS (MATHEMATICS)
A functional interpretation of the logistic equation
[REPT-87-037] 05 p0645 N88-13946
A theoretical concept for state changes and shape changes in weightlessness 07 p0884 N88-15365
Random truncation models and Markov processes
[CWI-MS-R8702] 09 p1232 N88-17389
Regulation of hemodynamics upon imitation of the transition to weightlessness (mathematical modeling)
13 p1810 N88-20817
Validation of mathematical model predictions of immersion survival times
[IAM-652] 14 p1952 N88-21635
Further development of a mathematical model for the specification of immersion clothing insulation
[IAM-653] 14 p1954 N88-21644
Models describing muscle behavior and control
[LR-522] 16 p2238 N88-23368
The biomorphic model of the human operator controlling a single or a double integrator
[LR-505] 16 p2243 N88-23402

BIOLOGICAL RHYTHM
U RHYTHM (BIOLOGY)

BIOLOGY
JPRS report: Science and technology. China
[JPRS-CST-88-003] 13 p1755 N88-20495

BIOLUMINESCENCE
Varifront 3 expedition data report (USNS DE STEIGUER CRUISE 1202-82). Bioluminescence, hydrographic, nutrient, and satellite data from the Gulf of California (November-December 1981)
[AD-A185011] 05 p0620 N88-13805

BIOMAGNETISM
An innovative workstation 08 p1063 N88-16421
Auditory evoked magnetic fields in man
[PB88-193446] 20 p2831 N88-26796
SQUID (superconducting quantum interference device) arrays for simultaneous magnetic measurements: Calibration and source localization performance
[AD-A193815] 23 p3216 N88-29143
Methods and instrumentation for biomagnetism
[AD-A193811] 23 p3239 N88-29278

BIOMASS
Wheat production in controlled environments
[UAES-PAPER-3324] 03 p0361 N88-12270
Design concepts for bioreactors in space
09 p1198 N88-17179
Vegetation mapping using high resolution MSS (multispectral scanner) data: Canopy reflectance and shadow problems encountered and possible solutions
[DE88-004273] 14 p1939 N88-21574
The use of SLAR and SIRA imagenes for the classification of forest typen in tropical rain forests
17 p2356 N88-24036
Production costs of hydrocarbon fuels from biomass
[DE88-006667] 18 p2495 N88-24804
Proceedings of the 1987 Biomass Thermochemical Conversion Contractors' Review Meeting
[DE88-006730] 18 p2535 N88-25041
An advanced extruder-feeder biomass liquefaction reactor system 18 p2535 N88-25042
Molecular-beam, mass-spectrometric studies of wood vapor and model compounds over HZSM-5 catalyst
18 p2535 N88-25044
Low-temperature thermochemical conversion of high moisture biomass feedstocks 18 p2536 N88-25047
Evaluation of the grassy biomass in the Sahelian zone in the South Tamesna region (Niger): Prospects and limits of use of SPOT data 22 p3092 N88-28359
Study of the spectral response of soybeans
[INPE-4592-PRE/1322] 24 p3387 N88-30174

BIOMASS ENERGY PRODUCTION
Biomass recycle as a means to improve the energy efficiency of CELSS algal culture systems
03 p0358 N88-12254
A process study of the biothermal conversion of water hyacinths to methane
[DE88-000554] 06 p0730 N88-14488
Alternative Energy in the Midwest: Research and Applications. Conference Proceedings, Rosemont, Illinois, March 19-20, 1987
[PB88-142278] 11 p1509 N88-19015
Proceedings of the 1987 Biomass Thermochemical Conversion Contractors' Review Meeting
[DE88-006730] 18 p2535 N88-25041
An advanced extruder-feeder biomass liquefaction reactor system 18 p2535 N88-25042
Low pressure entrained flow pyrolysis of biomass to produce liquid fuels 18 p2535 N88-25043
Molecular-beam, mass-spectrometric studies of wood vapor and model compounds over HZSM-5 catalyst
18 p2535 N88-25044
Upgrading pyrolysis vapors to aromatic gasoline with zeolite catalysis at atmospheric pressure
18 p2536 N88-25045
Low-temperature thermochemical conversion of high moisture biomass feedstocks 18 p2536 N88-25047
Technical and economic evaluation of emerging biomass pyrolysis processes for gasoline production
18 p2536 N88-25048
Bench-scale studies on fluid-bed pyrolysis of wood using different contact gases 18 p2536 N88-25049
An outdoor test facility for the large-scale production of microalgae
[DE88-001146] 21 p2984 N88-27723

BIOMECHANICS
U BIODYNAMICS

BIOMEDICAL DATA
Human respiratory responses during high performance flight
[AGARD-AG-312] 04 p0474 N88-12923
USSR report: Life sciences. Biomedical and behavioral sciences
[JPRS-UBB-87-010] 12 p1651 N88-19889
Results of medical research conducted in 1985 during long-term spaceflights 19 p2702 N88-26070
Use of principal component method for analysis of multidimensional quantitative data in biomedical investigations 19 p2706 N88-26089
Biomedical aspects of military operations at high altitude
[AD-A192677] 22 p3132 N88-28619

BIOMETRICS
NT ANTHROPOMETRY
NT BALLISTOCARDIOGRAPHY
NT BODY MEASUREMENT (BIOLOGY)
NT ECHOCARDIOGRAPHY
NT ELECTROCARDIOGRAPHY
NT ELECTROENCEPHALOGRAPHY
NT ELECTRORETINOGRAPHY
NT MAGNETOCARDIOGRAPHY
NT PLETHYSMOGRAPHY
Air quality and human performance, chapter 16
[AD-A188335] 12 p1666 N88-19988
Mental-State Estimation, 1987
[NASA-CP-2504] 16 p2239 N88-23370
An overview of current approaches and future challenges in physiological monitoring
16 p2239 N88-23371
Toward a mathematical formalism of performance, task difficulty, and activation 16 p2239 N88-23372
Vagal tone as an index of mental state
16 p2239 N88-23373
Challenges of physiological monitoring in a Navy operational setting 16 p2239 N88-23374
Attention, effort, and fatigue: Neuropsychological perspectives 16 p2241 N88-23387
C3 generic workstation: Performance metrics and applications 16 p2242 N88-23397
Computer resource management technology program (PE 64740F). Task no. 9: Advanced user authentication
[PB88-183066] 18 p2555 N88-25163
Method for measuring absolute linear parameters of chromosomes 19 p2707 N88-26095

BIONICS
Multiaperture optical system research
[AD-A188211] 11 p1549 N88-19267
Complex sound processing: An interdisciplinary approach
[AD-A189782] 15 p2102 N88-22523

BIOPHYSICS
NT HEALTH PHYSICS
NT PUBLIC HEALTH
A physico-chemical study of some areas of fundamental significance to biophysics
[DE87-013457] 02 p0217 N88-11365
JPRS report: Science and technology. USSR: Life sciences
[JPRS-ULS-87-013] 06 p0750 N88-14608
Biophysical and biochemical mechanisms in synaptic transmitter release
[AD-A187059] 09 p1199 N88-17184
Long term synaptic plasticity and learning in neuronal networks
[AD-A186834] 09 p1199 N88-17188
Evaluation of spare room in cerebrospinal system using noninvasive methods 10 p1361 N88-18137
Two-dimensional static otolith model
10 p1367 N88-18167
Critical phenomena and electromagnetic effects in biological membranes
[AD-A188156] 11 p1518 N88-19064
USSR report: Life sciences. Biomedical and behavioral sciences
[JPRS-UBB-87-008] 12 p1662 N88-19966
Biophysical applications of solid state and tritium NMR
[DE88-005328] 13 p1808 N88-20806
JPRS report: Science and technology. USSR: Life sciences
[JPRS-ULS-88-004] 13 p1810 N88-20815
Synapses that compute motion
[AD-A190389] 15 p2116 N88-22607
JPRS report: Science and technology. USSR: Life sciences
[JPRS-ULS-88-009] 20 p2829 N88-26785
Transient interaction of electromagnetic pulses in dielectrics and microwave biophysics
[AD-A195687] 24 p3360 N88-30008

BIOPOLYMER DENATURATION
Estimations of gravitational effects on thermal denaturation process in a bidpolymer
03 p0318 N88-12013

BIOPOLYMERS
NT CARBONIC ANHYDRASE
NT CATALASE
NT CHOLINESTERASE
NT CYTOCHROMES
NT DEOXYRIBONUCLEIC ACID
NT ENZYMES
NT FIBRINOGEN
NT HEMOGLOBIN
NT NUCLEIC ACIDS
NT PROTEINS
NT RIBONUCLEIC ACIDS

Estimations of gravitational effects on thermal denaturation process in a biopolymer
03 p0318 N88-12013
Calculation of far infrared absorption in B poly(dA).poly(dT)
[AD-A193128] 21 p2918 N88-27318

BIOPROCESSING
Space Bioreactor Science Workshop
[NASA-CP-2485] 09 p1196 N88-17168
Design concepts for bioreactors in space
09 p1198 N88-17179
Cell culture experiments planned for the space bioreactor 09 p1198 N88-17180
Cell cultures in space: From basic research to biotechnology 2 12 p1660 N88-19948
French evaluation of Japanese biosensors
16 p2184 N88-23020
Separation of biological materials in microgravity
[NASA-TM-101142] 17 p2331 N88-23916

BIOREACTORS
Sunlight supply and gas exchange systems in microalgal bioreactor 03 p0359 N88-12258
Space Bioreactor Science Workshop
[NASA-CP-2485] 09 p1196 N88-17168
Suspension cell culture in microgravity and development of a space bioreactor 09 p1196 N88-17169
Space bioreactor: Design/process flow
09 p1197 N88-17170
Bioreactor design concepts 09 p1197 N88-17171
Computer control of a microgravity mammalian cell bioreactor 09 p1197 N88-17172
Shear and mixing effects on cells in agitated microcarrier tissue culture reactors 09 p1197 N88-17173
Some process control/design considerations in the development of a microgravity mammalian cell bioreactor 09 p1197 N88-17174
Nutrient requirements and other factors involved in the culture of human kidney cells on microcarrier beads
09 p1197 N88-17176
Potential use of the bioreactor to determine effects of microgravity and other environmental parameters on growth of hybridoma cells 09 p1198 N88-17178
Design concepts for bioreactors in space
09 p1198 N88-17179
Aspects of bioregenerative life support systems
12 p1655 N88-19917

BIOREGENERATION
U REGENERATION (PHYSIOLOGY)

BIOREGENERATIVE LIFE SUPPORT SYSTEMS
U CLOSED ECOLOGICAL SYSTEMS

BIORHYTHMS
U RHYTHM (BIOLOGY)

BIOSATELLITES
Space biology and medicine 08 p1006 N88-16096

BIOSENSORS
U BIOINSTRUMENTATION

BIOSIMULATION
U BIONICS

BIOSPHERE
Remote sensing of the biosphere
[NASA-CR-182382] 07 p0871 N88-15281
New book on space ecology reviewed
07 p0897 N88-15434
International geosphere-biosphere program: A study of global change
[PB88-142393] 11 p1510 N88-19021
The seasonal exchange of carbon dioxide between the atmosphere and the terrestrial biosphere: Extrapolation from site-specific models to regional models
[DE88-007870] 20 p2822 N88-26740

BIOSYNTHESIS
Synthesis of high molecular weight peptide polymers and copolymers containing L-dope residues
[AD-A186462] 08 p0973 N88-15887
Life sciences experiments on stratospheric balloons and sounding rockets 08 p1033 N88-16252

BIOT METHOD
Evaluation of the biot coefficients
[AD-A191643] 18 p2570 N88-25265

BIOTECHNOLOGY
Preliminary study of a biotechnology research facility for microgravity, executive summary
[MATRA-EPT/AS/VT209/246/NT]
01 p0032 N88-10204
JPRS report: Science and technology. USSR: Life sciences
[JPRS-ULS-87-012] 03 p0355 N88-12238
Biotechnology in western Europe
[PB88-105887] 07 p0883 N88-15360
Safety guidelines and procedures for bioscience-based industry and other applied microbiology
[PB87-140521] 08 p1045 N88-16316
Space Bioreactor Science Workshop
[NASA-CP-2485] 09 p1196 N88-17168
Advanced utilization of solar energy: Utilization for biotechnology
[DE88-770031] 12 p1640 N88-19819
USSR report: Life sciences. Biomedical and behavioral sciences
[JPRS-UBB-87-010] 12 p1651 N88-19889
BIOTEX, a project for biotechnological basic experiments under microgravity — Spacelab
12 p1652 N88-19899
Cell cultures in space: From basic research to biotechnology 2 12 p1660 N88-19948
USSR report: Life sciences. Biomedical and behavioral sciences
[JPRS-UBB-87-008] 12 p1662 N88-19966
JPRS report: Science and technology. USSR: Life sciences
[JPRS-ULS-88-002] 12 p1665 N88-19982
JPRS report: Science and technology. USSR: Life sciences
[JPRS-ULS-88-004] 13 p1810 N88-20815
JPRS report: Science and technology. Japan
[JPRS-JST-88-001] 15 p2051 N88-22218
JPRS report: Science and technology. Japan
[JPRS-JST-87-026] 16 p2184 N88-23018
French evaluation of Japanese biosensors
16 p2184 N88-23020
North Carolina Biomolecular Engineering and Materials Applications Center (NC-BEMAC)
[AD-A190923] 16 p2237 N88-23364
Non-contact temperature measurements for biotechnology discipline working group
17 p2329 N88-23904
Proceedings of the American Society for Composites
[AD-A189861] 18 p2477 N88-24693
Carbon matrix composites prospective roles for biotechnology 18 p2477 N88-24694
Current and future molecular structures of aerospace organic matrix resins 18 p2477 N88-24695
Industrial perspective on current and future needs in aerospace matrix resin chemistry
18 p2477 N88-24696
Applications of biotechnology to synthetic chemistry for aerospace matrix resins development
18 p2478 N88-24697
The application of hydrocarbon bioconversion technology to aerospace materials production
18 p2478 N88-24698
Ecological risk factors related to environmental uses of genetically engineered organisms
[DE88-006674] 18 p2549 N88-25132
Research and development programs on advanced structural ceramics in Korea 19 p2633 N88-25620

BIOTELEMETRY
An innovative workstation 08 p1063 N88-16421

BIOTITE
An integrated study of the Alto Paranaiba Kimberlite Province, Minas Gerais, Brazil: A possible tool for diamond exploration 17 p2355 N88-24031
The petrogenesis of oceanic kimberlites and included mantle megacrysts: The Malaitan alnoite
24 p3397 N88-30232

BIPOLAR TRANSISTORS
On the choice of a element low-noise preamplifier on bipolar transistors
[DE88-700639] 10 p1322 N88-17904
Development of a planar heterojunction bipolar transistor for very high speed logic
[AD-A188137] 11 p1478 N88-18820
Determination of distributed resistance of base of bipolar transistors measuring noise spectral densities
[DE88-700197] 11 p1479 N88-18829
Microelectronic applications of the conductor-thin insulator-semiconductor (CIS) structure
11 p1560 N88-19341
Technology development of a planar BiPolar transistor
[AD-A188761] 12 p1623 N88-19708
Solid-state travelling wave amplifiers based on multi-stream instability
[AD-A189566] 12 p1624 N88-19718
Quartz oscillator analysis
[DE88-005886] 13 p1764 N88-20550
Neutron effects on the electrical and switching characteristics of NPN bipolar power transistors
17 p2431 N88-24483
Joint services electronics program research in electronics
[AD-A192206] 18 p2504 N88-24857
Improved description of base dynamics in the modeling of bipolar transistors
[PB88-181516] 19 p2732 N88-26229
Resonant tunneling transistors and resonant tunneling hot electron spectroscopy 20 p2866 N88-27018

BIPOLARITY
Small scale bipolar nickel-hydrogen testing
[NASA-TM-100936] 18 p2538 N88-25059

BIPROPELLANTS
U LIQUID ROCKET PROPELLANTS

BIRD-AIRCRAFT COLLISIONS
Analysis of bird strikes to UK registered aircraft 1985 (civil aircraft over 5700 kg maximum weight
[CAA-PAPER-87012] 09 p1115 N88-16684
Protected areas with enhanced bird-aircraft collision risk in the Federal Republic of Germany
[GEOPHYSBDBW-FM-209] 11 p1437 N88-18576
Lapwings and birdstrikes. The biology of the lapwing Vanellus vanellus in relation to the birdstrike hazard it presents
[CAA-PAPER-87015] 14 p1865 N88-21142
The design and testing of aero engines to minimise hazard from birds
[PNR90436] 22 p3040 N88-28049

BIRDS
NT CHICKENS
NT WATERFOWL
Compilation of 1986 annual reports of the Navy ELF (Extremely Low Frequency) communications system ecological monitoring program, volume 3
[AD-A184563] 03 p0306 N88-11932
Lapwings and birdstrikes. The biology of the lapwing Vanellus vanellus in relation to the birdstrike hazard it presents
[CAA-PAPER-87015] 14 p1865 N88-21142
Motor theory of auditory perception
[AD-A192095] 18 p2550 N88-25136
Survey for least bell's vireo in riparian habitat on Vandenberg Air Force Base, Santa Barbara County, California
[NASA-TM-100984] 20 p2822 N88-26744

BIREFRINGENCE
NT KERR ELECTROOPTICAL EFFECT
Improper ferroelectricity: A theoretical and experimental study
[AD-A184614] 03 p0381 N88-12397
Spectral contents readout of birefringent sensors
[NASA-CR-179430] 13 p1784 N88-20673
Multiple scattering of polarized light in cirrus clouds
13 p1801 N88-20768
Peturbational analysis of the curved anisotropic optical fiber for the birefringence due to the geometry
[PB88-171848] 19 p2726 N88-26189
Theory of acoustoplasticity and ultrasonic measurements of residual stresses
22 p3087 N88-28328

BISMUTH
Fatigue crack growth and fracture of copper-bismuth bicrystals 06 p0715 N88-14385

BISMUTH COMPOUNDS
NT BISMUTH OXIDES
NT BISMUTH SULFIDES
Altered and enhanced iodargyrite with bismuth triiodide for use in precipitation enhancement operations
[AD-A185229] 05 p0561 N88-13419
Photorefractive damage mechanism in electro-optic materials
[AD-A194560] 23 p3282 N88-29543

BISMUTH OXIDES
Holographically correcting synthetic aperture aberrations
[AD-A189510] 12 p1692 N88-20123
Properties of superconductors with strong electron-phonon interaction 14 p1974 N88-21779

BISMUTH SULFIDES
Activities of As, Sb, Bi and Pb in copper mattes and their effects on impurity elimination
[TKK-V-A10(1988)] 15 p2041 N88-22165

BISTABLE CIRCUITS
Applications of optical computing to problems with symbolic computations
[AD-A189772] 15 p2106 N88-22548
Optical bistable behavior of a planar quasi-waveguide interferometer made with a conjugated organic polymer film
[AD-A194349] 22 p3152 N88-28756

BISTATIC RADAR
U MULTISTATIC RADAR

BISTATIC REFLECTIVITY
Active and passive remote sensing of ice
[AD-A186685] 09 p1195 N88-17162

BIT ERROR RATE
Program description of FIBRAM: A radiation attenuation model for optical fibers
[PB87-230686] 06 p0690 N88-14229
Implementation of encoders and decoders for Reed-Solomon codes
[PB88-126628] 10 p1387 N88-18286
Digital bit error rate estimator for telemetry links
[INPE-4351-TDL/295] 12 p1598 N88-19583
Evaluating the performance of the LPC (Linear Predictive Coding) 2.4 kbps (kilobits per second) processor with bit errors using a sentence verification task
[AD-A188573] 12 p1620 N88-19686

Effect of atmospheric turbulence on the bit error probability of a space to ground near infrared laser communications link using binary pulse position modulation and an avalanche photodiode detector
[NASA-TM-100699] 14 p1873 N88-21189
Direct bit detection receiver noise performance analysis for 32-PSK and 64-PSK modulated signals
[AD-A190009] 15 p2056 N88-22256
The bit-error rate performance of a satellite microwave matrix switch
[NASA-TM-100285] 16 p2167 N88-22920
Interleaver design for trellis-coded differential 8-PSK modulation with non-coherent detection
19 p2648 N88-25719
An error floor in tone calibrated transmission
19 p2649 N88-25729
Error performance of voice band data signals with an overloaded delta modulator
[FEL-1987-05] 20 p2792 N88-26562
A new code for Galileo 22 p3065 N88-28186

BIT SYNCHRONIZATION
Direct bit detection receiver performance analyses for 8-DPSK (Differential Phase Shift Keyed) modulated signals operating with improper carrier phase synchronization
[AD-A193839] 22 p3070 N88-28220

BITS
Digital video bit-rate reduction: DPCM for sub-Nyquist PAL
[BBC-RD-1987/16] 05 p0573 N88-13494
Direct bit detection receiver noise performance analysis for 32-PSK and 64-PSK modulated signals
[AD-A190009] 15 p2056 N88-22256

BITUMENS
Application of high performance liquid chromatography to the fast determination of bitumen generic composition
[PC-2] 02 p0145 N88-10911
Colloidal structure of bitumens. Relationship between composition-structure behavior
[PC-4] 02 p0146 N88-10912
Polymer modified binders for bituminous or asphaltic paving layers
[PC-5] 02 p0153 N88-10958
Aviation turbine fuels from tar sands bitumen and heavy oils. Part 2: Laboratory sample production
[AD-A185744] 06 p0687 N88-14211
Evaluation of bituminous materials used in pavement recycling projects at Tyndall, MacDill, and Hurlburt Air Force Bases
[AD-A188068] 10 p1317 N88-17871
Aviation turbine fuels from tar sands bitumen and heavy oils. Part 3: Laboratory sample production
[AD-A189278] 13 p1753 N88-20484
Turbine fuels from tar sands bitumen and heavy oil. Volume 2, phase 3: Process design specifications for a turbine fuel refinery charging San Ardo heavy crude oil
[AD-A190120] 16 p2183 N88-23011

BIVARIATE ANALYSIS
On the extreme points of the set of all 2xn bivariate positive quadrant dependent distributions with fixed marginals and some applications
[AD-A186316] 07 p0911 N88-15521
Measuring the dependence between two point processes through confidence intervals for the second order distribution
[AD-A186735] 08 p1074 N88-16481
An APL function for bivariate normal probabilities
[AD-A186535] 09 p1232 N88-17382

BL LACERTAE OBJECTS
Relativistic jet models for the BL Lacertae object Mrk 421 during three epochs of observation
[NASA-TM-89727] 13 p1853 N88-21090

BLACK AND WHITE PHOTOGRAPHY
Use of SPOT panchromatic imagery to update forest maps of northern Quebec, Canada
03 p0344 N88-12172
Application of 35mm EM aerial reconnaissance photographic format of the municipality of Ubatuba (SP)
19 p2684 N88-25953

BLACK BODY RADIATION
Numerical calculations of dopent diffusion involving flashlamp heating of silicon 21 p2929 N88-27384
Overview and future direction for blackbody solar-pumped lasers
[NASA-TM-100621] 21 p2955 N88-27553

BLACK BRANT SOUNDING ROCKETS
Past, present and future role of Black Brant rocket systems to support international space science programs 08 p1034 N88-16272

BLACK HOLES (ASTRONOMY)
Photohydrodynamical processes near compact objects
11 p1569 N88-19390

BLACK SEA
Geological evolution and analysis of confirmed or suspected gas hydrate localities. Volume 2: Basin analysis, formation and stability of gas hydrates in the Black Sea
[DE88-001052] 18 p2532 N88-25023

BLACKOUT (PHYSIOLOGY)
F-16 control stick response during +Gz-induced loss of consciousness
[AD-A184107] 04 p0400 N88-12491
Detection of acceleration (+Gz) induced blackout by matched-filtering of visual evoked potentials
21 p2982 N88-27710

BLADDERS (MECHANICS)
U DIAPHRAGMS (MECHANICS)

BLADE SLAP
U BLADE-VORTEX INTERACTION

BLADE SLAP NOISE
Helicopter main-rotor noise: Determination of source contributions using scaled model data
[NASA-TP-2825] 20 p2848 N88-26907

BLADE TIPS
Modeling and measurement of heat transfer on turbine blade tips 01 p0006 N88-10032
Heat transfer in the tip region of a rotor blade simulator 02 p0186 N88-11159
The physics and mathematical description of the Achilles heel of stationary wind turbine aerodynamics: The tip flow
[R-812-D] 03 p0260 N88-11635
Calculation of helicopter rotor blade/vortex interaction by Navier-Stokes procedures
[NASA-CR-177441] 05 p0540 N88-13291
Aerodynamic design of first stage turbines for small aero engines 06 p0713 N88-14370
An experimental investigation of the chopping of helicopter main rotor tip vortices by the tail rotor. Part 2: High speed photographic study
[NASA-CR-177457] 09 p1114 N88-16678
Inflow measurements made with a laser velocimeter on a helicopter model in forward flight. Volume 4: Tapered planform blades at an advance ratio of 0.15
[NASA-TM-100544] 16 p2156 N88-22863
Recent advances in capacitance type of blade tip clearance measurements
[NASA-TM-101291] 19 p2603 N88-25460
Investigation of helicopter rotor blade/wake interactive impulsive noise
[NASA-CR-177435] 23 p3171 N88-28882
Computational methods for the problems of the tip vortex
[NASA-CR-181438] 24 p3320 N88-29775

BLADE-VORTEX INTERACTION
Results of the 1986 NASA/FAA/DFVLR main rotor test entry in the German-Dutch wind tunnel (DNW)
[NASA-TM-100507] 04 p0487 N88-13003
Calculation of helicopter rotor blade/vortex interaction by Navier-Stokes procedures
[NASA-CR-177441] 05 p0540 N88-13291
Lift distribution and velocity field measurements for a three-dimensional, steady blade/vortex interaction
[NASA-TM-100013] 07 p0815 N88-14962
The development of CFD methods for rotor applications 09 p1105 N88-16627
Recent Langley helicopter acoustics contributions
09 p1109 N88-16646
An experimental investigation of the chopping of helicopter main rotor tip vortices by the tail rotor. Part 2: High speed photographic study
[NASA-CR-177457] 09 p1114 N88-16678
Acoustic measurements from a rotor blade-vortex interaction noise experiment in the German-Dutch Wind Tunnel (DNW)
[NASA-TM-4024] 11 p1542 N88-19218
Advancing-side directivity and retreating-side interactions of model rotor blade-vortex interaction noise
[NASA-TP-2784] 15 p2131 N88-22710
Theory of sound production by vortex-airfoil interaction
[AD-A193386] 21 p3012 N88-27875
Transonic blade-vortex interactions
22 p3037 N88-28035
Investigation of helicopter rotor blade/wake interactive impulsive noise
[NASA-CR-177435] 23 p3171 N88-28882

BLADES
Euler solution of multiblade rotor flow
[NASA-TM-100014] 06 p0704 N88-14322
A multistage mesh generator for solving the average-passage equation system
[NASA-CR-179539] 08 p0951 N88-15769
Vibration and flutter characteristics of the SR7L large-scale propfan
[NASA-TM-100272] 10 p1344 N88-18036
Analysis of rotating flexible blades using MSC/NASTRAN 16 p2222 N88-23259
Cascades with harmonically oscillating blades in supersonic flow
[NASA-TT-20323] 19 p2599 N88-25446

BLANKETS (FUSION REACTORS)
Technical evaluation of major candidate blanket systems for fusion power reactor
[DE87-752989] 02 p0239 N88-11512
Physics modeling support contract
[DE88-004039] 10 p1335 N88-17980
MHD (magnetohydrodynamic) thermal hydraulic analysis of three-dimensional liquid metal flows in fusion blanket ducts
[DE88-009929] 19 p2731 N88-26219
Blanket technology experiments at Argonne National Laboratory
[DE88-010006] 19 p2731 N88-26220
Reactor applications of the Compact Fusion Advanced Rankine (CFAR) cycle for a D-T tokamak fusion reactor
[DE88-011351] 22 p3153 N88-28762

BLASIUS FLOW
A new laminar water tunnel to study the transition process in a blasius layer and in a separation bubble and a new tool for industrial aerodynamics and hydrodynamic research 16 p2204 N88-23150

BLAST LOADS
Composite materials applications program at the US Army Ballistic Research Laboratory: Work in progress
04 p0428 N88-12651
A summary of experimental results on square plates and stiffened panels subjected to air-blast loading
09 p1178 N88-17057
Mechanical impact: Theoretical simulation and correlation 09 p1179 N88-17060
Misty picture weather-watch and microbarograph project: Experiments 9412-14-18
[DE88-003949] 11 p1514 N88-19047
Buckling of blast loaded cylinder
[AD-A190124] 15 p2076 N88-22376

BLASTOFF
U ROCKET LAUNCHING

BLEED-OFF
U PRESSURE REDUCTION

BLENDS
U MIXTURES

BLINDNESS
NT FLASH BLINDNESS
Maps for the blind and methods of their production
16 p2227 N88-23298

BLOCH BAND
Bloch oscillations in small Josephson junctions: Their manifestation in switching effects
14 p1969 N88-21756

BLOCK DIAGRAMS
A new state space model for the NASA/JPL 70-meter antenna servo controls 04 p0436 N88-12702

BLOCKING
Adaptive line of sight algorithms
[DE87-014275] 01 p0081 N88-10523
Persistence characteristics of 500 mb blocking and zonal flows in the mid-latitudes of the Northern and Southern Hemispheres 10 p1353 N88-18088
Impact of blocking policies in closed, exponential and symmetrical ring networks
[FUB-8-1986] 14 p1960 N88-21693

BLOCKS
Analysis of the decomposition of transparent polymer materials (blocks) under the action of laser beams in free generation mode
[AD-A187090] 09 p1147 N88-16873
A new block solver for large, full, unsymmetric, complex systems of linear algebraic equations
[AD-A190590] 16 p2256 N88-23483

BLOOD
NT FIBRINOGEN
Scotopic sensitivity with 10 percent oxygen
[AD-A183973] 03 p0356 N88-12243
An assessment of clinical chemical sensing technology for potential use in space station health maintenance facility
[NASA-CR-172013] 04 p0475 N88-12926
Oxygen transport during exercise at extreme simulated altitude: Operation Everest 2
[AD-A185720] 06 p0752 N88-14620
Physiological and biochemical aspects of toxic effects of oxidants in man's environment (air, water)
07 p0890 N88-15391
Cosmonauts' hormonal responses after brief spaceflights 07 p0890 N88-15394
Role of hemoglobin affinity for oxygen in efficiency of blood respiratory function 07 p0892 N88-15406
Operation Everest 2: Comparison of four instruments for measuring blood oxygen saturation
[AD-A186456] 08 p1049 N88-16337
Significance of nutrition to change in human carbohydrate and lipid metabolism under emotional stress 19 p2703 N88-26073

BLOOD CELLS
NT ERYTHROCYTES
NT LEUKOCYTES
NT LYMPHOCYTES
Blood redistribution in man with lower body negative pressure 07 p0891 N88-15397

BLOOD CIRCULATION
NT BRAIN CIRCULATION
NT CORONARY CIRCULATION
NT PERIPHERAL CIRCULATION
NT PULMONARY CIRCULATION
Polycythemia and hydration status: Effects on blood volume and thermoregulation during exercise-heat stress [AD-A185946] 07 p0888 N88-15383
Human and animal hypovolemic reactions to increasing +Gz accelerations 07 p0890 N88-15395
Blood redistribution in man with lower body negative pressure 07 p0891 N88-15397
Human metabolism and peripheral circulation during antiorthostatic hypokinesia 07 p0891 N88-15398
Distinctive changes in arterial pressure and blood flow in common carotid artery of monkeys flown aboard Cosmos-1514 biosatellite 07 p0892 N88-15404
Changes in regional and central hemodynamics during seven-day water immersion 07 p0895 N88-15421
Exercise thermoregulation after prolonged wakefulness [AD-A186224] 08 p1048 N88-16327
Late radiation damage in bone, bone marrow and brain vasculature, with particular emphasis upon fractionation models [DE87-753039] 08 p1048 N88-16330
Effect of spaceflight factors on primate's blood circulation 10 p1359 N88-18124
Isotope methods of determining distribution and movement of blood in the body 10 p1362 N88-18138
Comparative evaluation of orthostatic stability following immersion in horizontal and vertical positions 10 p1363 N88-18143
Effect of antiorthostatic position and different illumination on sensitivity of skin in upper half of the body to ultraviolet radiation 10 p1363 N88-18145
Improvement of human tolerance to head-pelvis (+Gz) accelerations by increasing hydration 10 p1364 N88-18153
Effect of exogenous cardiosynchronized counterpulsation on human regional and central hemodynamics 10 p1366 N88-18163
Response of coronary blood flow to step changes in plasma protein concentration in the isolated rat heart 12 p1651 N88-19892
Load and control of the cardiocirculatory system in weightlessness 12 p1656 N88-19922
Neuro-reflex mechanisms of circulation regulation in simulated microgravity 12 p1656 N88-19923
Physiological reactions upon controlled changes of blood distribution in humans 12 p1656 N88-19924
Nitrogen's biological effect on oxygen transport through hematoparenchymal barrier 12 p1662 N88-19967
Status of microcirculation in high-altitude blood loss 12 p1663 N88-19973
Effects of intense, time-constrained mental effort on hemodynamics and cardiovascular function 12 p1664 N88-19975
The effects of normal and therapeutic baths on the central vascular organs of persons with healthy hearts, as measured by X-ray [NASA-TT-20252] 13 p1811 N88-20818
Contribution of ultrasonic Doppler detection of circulating bubbles to human interventions under the sea and in space 19 p2697 N88-26029
Human hemodynamics during water immersion as related to position during submersion 19 p2703 N88-26071
Hemostasis parameters of individuals with neurocirculatory dystonia submitted to dry immersion 19 p2703 N88-26072
Respiration and oxygen tension in the blood of animals exposed to high pressures 20 p2830 N88-26790
The impact of hyperthermia and hypohydration on circulation, strength, endurance and health [AD-A192657] 22 p3131 N88-28615
Propranolol and the compensatory circulatory responses to orthostasis at high altitude [AD-A192675] 22 p3131 N88-28618
Variation of carotid flow under load, studied by the Doppler echo method --- acceleration tolerance [REPT-1149] 23 p3240 N88-29282

BLOOD COAGULATION
Role of carbon dioxide in correction of coagulation hemostasis under hypoxic conditions 10 p1365 N88-18160
Changes in hemostasis system of animals under conditions of granulocytopoiesis inhibition under effect of decreased barometric pressure 12 p1651 N88-19890
Distinctive features in blood clotting and fibrinolytic properties under effect of epinephrine in presence of hypoxia and hypercapnia 19 p2705 N88-26082
Hemorrhages and hemostasis in guinea pigs exposed to radiation at high altitude 19 p2705 N88-26083

BLOOD FLOW
Studies of the processing of single words using positron tomographic measures of cerebral blood flow change [AD-A184058] 03 p0356 N88-12244
Assessment of intercompartment fluid shifts by blood densitometry in astronauts 12 p1661 N88-19958
Potential applications of computational fluid dynamics to biofluid analysis [NASA-TM-100089] 14 p1911 N88-21422

BLOOD PLASMA
Polycythemia and hydration status: Effects on blood volume and thermoregulation during exercise-heat stress [AD-A185946] 07 p0888 N88-15383
Human and animal hypovolemic reactions to increasing +Gz accelerations 07 p0890 N88-15395
Role of testing total gas (O2 and CO2) tension of blood plasma in the study of human gas homeostasis 07 p0894 N88-15419
Response of coronary blood flow to step changes in plasma protein concentration in the isolated rat heart 12 p1651 N88-19892
Assessment of intercompartment fluid shifts by blood densitometry in astronauts 12 p1661 N88-19958
Changes in blood conductivity during immersion 12 p1663 N88-19969
Plasma cortisol, renin and aldosterone during an intense heat acclimation program [AD-A189387] 13 p1809 N88-20810
Hemostasis parameters of individuals with neurocirculatory dystonia submitted to dry immersion 19 p2703 N88-26072
Plasma volume expansion in rats: Effects on thermoregulation and exercise [AD-A192656] 22 p3130 N88-28606
Influence of altitude and caffeine during rest and exercise on plasma levels of proenkephalin peptide F [AD-A192659] 22 p3131 N88-28616

BLOOD PRESSURE
NT HYPERTENSION
NT LOWER BODY NEGATIVE PRESSURE
Distinctive changes in arterial pressure and blood flow in common carotid artery of monkeys flown aboard Cosmos-1514 biosatellite 07 p0892 N88-15404

BLOOD VESSELS
NT AORTA
NT ARTERIES
NT CAPILLARIES (ANATOMY)
NT VEINS

BLOOD VOLUME
Polycythemia and hydration status: Effects on blood volume and thermoregulation during exercise-heat stress [AD-A185946] 07 p0888 N88-15383
Human and animal hypovolemic reactions to increasing +Gz accelerations 07 p0890 N88-15395
Blood redistribution in man with lower body negative pressure 07 p0891 N88-15397
Distinctive changes in arterial pressure and blood flow in common carotid artery of monkeys flown aboard Cosmos-1514 biosatellite 07 p0892 N88-15404
Is ANF implied in the right attenuated renal response to central hypervolemia? 12 p1659 N88-19945
Plasma cortisol, renin and aldosterone during an intense heat acclimation program [AD-A189387] 13 p1809 N88-20810
Leg volume change under Lower Body Negative Pressure (LBNP) in dependence on stratification [DFVLR-FB-87-47] 16 p2238 N88-23367
Validation of a modified one-step rebreathing technique for non-invasive measurement of submaximal cardiac output [AD-A192852] 21 p2987 N88-27735
Plasma volume expansion in rats: Effects on thermoregulation and exercise [AD-A192656] 22 p3130 N88-28606
Alterations in cutaneous vasomotor regulation during acute and chronic hypoxia [AD-A192653] 22 p3131 N88-28612

BLOWDOWN WIND TUNNELS
The 0.6m x 0.6m trisonic test section (TMK) of DFVLR in Cologne-Porz, Federal Republic of Germany (status 1986) [ESA-TT-1052] 03 p0267 N88-11681
The vertical test section (VMK) of DFVLR in Cologne-Porz, Federal Republic of Germany (status 1986) [ESA-TT-1053] 03 p0267 N88-11682
The design and preliminary calibration of a boundary-layer flow channel [NASA-CR-178399] 04 p0394 N88-12457
The 30 x 30 inch wind tunnel [IC-AERO-87-01] 14 p1869 N88-21168
The transonic wind tunnel (TWB) at DFVLR, Brunswick (Federal Republic of Germany) [DFVLR-MITT-88-01] 16 p2164 N88-22909

BLOWERS
An experimental comparison of two designs of mercury propellant tank for use with an electric propulsion engine [RAE-TR-75109] 01 p0018 N88-10109
Measurement and analysis of the noise radiated by low Mach numbers centrifugal blowers [AD-A189226] 13 p1833 N88-20966

BLOWING
NT SPANWISE BLOWING
Experimental investigations on blunt bodies and corner configurations in hypersonic flow 05 p0530 N88-13225
Dimensions of ignition zones in blow-outs of combustible gases from rectangular and circular ports 07 p0918 N88-15577
An aerodynamic comparison of blown and mechanical high lift airfoils 10 p1272 N88-17606
Numerical study of delta wing leading edge blowing [NASA-CR-183101] 20 p2752 N88-26335

BLUE GREEN ALGAE
NT MICROCYSTIS
The usefulness of microalgal structures as an element of closed ecological systems like Aquarack and CELSS --- Controlled Ecological Life Support System (CELSS) 01 p0074 N88-10476
Food production and gas exchange system using blue-green alga (spirulina) for CELSS 03 p0358 N88-12253

BLUFF BODIES
Computational study of three-dimensional wake structures [REPT-2] 05 p0539 N88-13281
Wakes of two dimensional bluff bodies in subsonic flow. Influence of a separating plate and of a pulsed injection of momentum [IMFL-4200-86/75] 05 p0541 N88-13297
Separated flow 07 p0812 N88-14944
Numerical solutions of three-dimensional Navier-Stokes equations for closed-bluff bodies [NASA-CR-182359] 09 p1166 N88-16990
Experimental study of two-dimensional vortex patterns for impulsively started bodies in comparison with other configurations 11 p1435 N88-18562
Research on flow around bluff bodies, flow induced vibrations 14 p1864 N88-21135
Interaction of a two-dimensional bluff body and incompressible jet and annulus flows [AD-A190503] 15 p2064 N88-22310
Oscillating flow over bluff bodies in a U-shaped water tunnel 16 p2201 N88-23131
Measurements of aerodynamic forces on unsteadily moving bluff parachute canopies 16 p2202 N88-23137
Incompressible Euler solution on a multiblock grid around a car configuration [FFA-TN-1987-65] 18 p2457 N88-24586
Vortex methods for separated flows [NASA-TM-100068] 20 p2753 N88-26342

BLUNT BODIES
Calculation of aerodynamic heat transfer for blunt-nosed thin wings at different angles of attack at supersonic speeds [NASA-TT-20127] 02 p0123 N88-10776
Numerical study of supersonic flow around blunt bodies with extended needle nose 04 p0425 N88-12635
Experimental investigations on blunt bodies and corner configurations in hypersonic flow 05 p0530 N88-13225
The effects of sweep and bluntness on a glancing shock wave turbulent boundary layer interaction 05 p0531 N88-13227
A spatial marching technique for the inviscid blunt body problem 05 p0533 N88-13239
The role of computation fluid dynamics in aeronautical engineering (4). The development and applications of implicit TVD finite volume code 05 p0536 N88-13259
Studies of unsteadiness in boundary layers [AD-A185662] 06 p0703 N88-14315
The simulation of three-dimensional viscous supersonic flow past blunt bodies with a hybrid implicit/explicit finite difference method [DFVLR-FB-87-32] 08 p0950 N88-15765
Hypersonic blunt body computations including real gas effects [NASA-TM-100074] 10 p1400 N88-18344
A simplified streamline swallowing procedure for the windward meridian of axisymmetric blunt bodies [AD-A188413] 12 p1626 N88-19732
Nonaxisymmetric body supersonic, aerodynamic prediction [AD-A189338] 13 p1716 N88-20259
Flight tests of external modifications used to reduce blunt base drag [NASA-TM-100433] 13 p1719 N88-20279

Interaction of a two-dimensional bluff body and incompressible jet and annulus flows
[AD-A190503] 15 p2064 N88-22310
Numerical study of unsteady viscous hypersonic blunt body flows with an impinging shock
[NASA-TM-100096] 15 p2122 N88-22650
High-resolution shock-capturing schemes for inviscid and viscous hypersonic flows
[NASA-TM-100097] 15 p2122 N88-22651
Relaxation scheme for compressible flows
19 p2640 N88-25663
The modified-fluid-in-cell method to which adaptive mesh and multigrid were applied
19 p2640 N88-25664
Navier-Stokes code NS3D for blunt bodies. Part 1: Analysis, results and verification
[DE88-010105] 19 p2666 N88-25855
A preliminary investigation of drag reduction and mechanism for a blunt body of revolution with slanted base
[NASA-TT-20349] 24 p3317 N88-29753

BMC
U BONE MINERAL CONTENT

BO-105 HELICOPTER
Test equipment with fiber optic data bus and laser gyro strapdown system LTN-90 for the helicopter BO-105
[ESA-TT-1038] 01 p0005 N88-10025
Sitting posture of pilots in the Boelkow 105c helicopter
[IZF-1986-22] 09 p1202 N88-17202
Helicopter main-rotor noise: Determination of source contributions using scaled model data
[NASA-TP-2825] 20 p2848 N88-26907

BODIES OF REVOLUTION
NT CONCENTRIC SPHERES
NT CONICAL BODIES
NT CYLINDRICAL BODIES
NT FALLING SPHERES
NT PARABOLIC BODIES
NT ROTATING CYLINDERS
NT ROTATING SPHERES
NT SLENDER CONES
NT SPHERES
NT TORUSES
Solution of geometrically nonlinear problem for reinforced shell of revolution having arbitrary shape
04 p0426 N88-12637
Similar solutions for viscous hypersonic flow over a slender three-fourths-power body of revolution
[NASA-TM-100205] 04 p0443 N88-12752
Numerical analysis of motion of solid bodies in atmosphere 08 p1079 N88-16505
Measurement of forces and moments on, and velocity about a body of revolution with an attached fin at angles of attack
[AD-A187796] 11 p1433 N88-18554
The Hamiltonian structure of nonlinear elasticity: The convective representation of solids, rods, and plates
[AD-A187200] 11 p1498 N88-18943
The effect of sting interference at low speeds on the drag coefficient of an ellipsoidal body using a magnetic suspension and balance system
[NASA-CR-181611] 13 p1718 N88-20274
Experiments to investigate the vortices shed from a submarine-like body of revolution
16 p2205 N88-23156
The use of fins to reduce the pressure drop in a rotating cavity with a radial flow
[PNR90465] 22 p3079 N88-28282
A preliminary investigation of drag reduction and mechanism for a blunt body of revolution with slanted base
[NASA-TT-20349] 24 p3317 N88-29753

BODY CENTERED CUBIC LATTICES
Computer simulations of knock-on processes in bcc Ta crystal
[DE87-752980] 02 p0246 N88-11554
Computer simulation of pencil glide in B.C.C. metals
[DE88-001802] 07 p0834 N88-15062

BODY FLUIDS
NT BLOOD
NT CEREBROSPINAL FLUID
NT FIBRINOGEN
NT SALIVA
NT URINE
Effect of spaceflight factors on primate hydration homeostasis 10 p1360 N88-18126
The precision of limits on bodily fluids when using beta-expectation inner tolerance limits
[AD-A187966] 10 p1369 N88-18185
Fluid volume changes in astronauts: How they fit our understanding of physiology 12 p1655 N88-19919
Estimation of body fluid shift by electrical impedance in various postures 12 p1661 N88-19956
Use of principal component method for analysis of multidimensional quantitative data in biomedical investigations 19 p2706 N88-26089

BODY KINEMATICS
Numerical solution of multibody systems in space applications 14 p1875 N88-21200

BODY MEASUREMENT (BIOLOGY)
NT ANTHROPOMETRY
Estimating the cost of mental loading in a bimodal divided-attention task: Combining reaction time, heart-rate variability and signal-detection theory
16 p2241 N88-23385
Physiological measures and mental-state assessment
16 p2242 N88-23392
Improvements in techniques of microwave thermography
[AD-A194613] 23 p3203 N88-29062
Improvements in techniques of microwave thermography
[AD-A193620] 23 p3239 N88-29276

BODY SWAY TEST
Electroencephalographic changes during equilibrium test in the presence of rhythmic photic interference
19 p2703 N88-26075

BODY TEMPERATURE
Human thermoregulatory model for whole body immersion in water at 20 and 28 C
[AD-A185052] 05 p0629 N88-13849
Infradian biorhythms of human vital signs
06 p0750 N88-14606
Biorhythmic aspects of intercontinental Antarctic adaptation 08 p1046 N88-16321
Influence of skeletal muscle glycogen on passive rewarming after hypothermia
[AD-A186451] 08 p1049 N88-16334
Rapid hypothermia subsequent to oral nicotinic acid and immersion in warm (30C) water
[AD-A186458] 08 p1050 N88-16339
Role of body fat in the prediction of the metabolic response for immersion in cold water
[AD-A186914] 09 p1198 N88-17182
The role of hydration on peripheral response to cold
[AD-A186448] 09 p1199 N88-17186
Vestibular response to caloric stimulation during orbital flight 12 p1658 N88-19939
Plasma cortisol, renin and aldosterone during an intense heat acclimation program
[AD-A189387] 13 p1809 N88-20810

BODY TEMPERATURE (NON-BIOLOGICAL)
U TEMPERATURE

BODY TEMPERATURE REGULATION
U THERMOREGULATION

BODY WEIGHT
Operation Everest 2: Nutrition and body composition
[AD-A186449] 08 p1049 N88-16333
Variability in intake and dehydration in young men during a simulated desert walk
[AD-A192654] 22 p3131 N88-28613

BODY-WING AND TAIL CONFIGURATIONS
Design of wings and wing/body configurations for transonic and supersonic speeds
05 p0545 N88-13318
Investigation of the influence of wind shear on the aerodynamic characteristics of aircraft using a vortex-lattice method 10 p1274 N88-17619
The determination of the topological structure of skin friction lines on a rectangular wing-body combination
[NASA-CR-4168] 20 p2753 N88-26343

BODY-WING CONFIGURATIONS
Numerical simulation of the hypersonic flow around lifting vehicles 05 p0532 N88-13234
Vortex formation over delta, double-delta and wave rider configurations at supersonic speeds
05 p0533 N88-13243
The RAE experimental data-base for missiles at high Mach number and its use in assessing CFD methods
05 p0534 N88-13250
Low speed wind tunnel investigation of propeller slipstream aerodynamic effects on different nacelle/wing combinations. Part 1: Total forces and moments and pressure distributions on nacelle/wing at different angles of attack and yaw and at different thrust coefficients
[FFA-TN-1987-22] 05 p0542 N88-13302
Compressible Euler solution on a multiblock grid around a wing-fuselage configuration
[FFA-TN-1987-46] 05 p0542 N88-13303
Transonic Navier-Stokes computations of strake-generated vortex interactions for a fighter-like configuration 06 p0664 N88-14073
Aerodynamic and propeller performance characteristics of a propfan-powered, semispan model
[NASA-TM-86705] 06 p0667 N88-14092
Testing of a schematic transport plane model in several European windtunnels
[P887-170270] 09 p1113 N88-16671
Design of an aeroelastic composite wing wind tunnel model
[AD-A188855] 12 p1582 N88-19466
Transonic Navier-Stokes computations of strake-generated vortex interactions for a fighter-like configuration
[NASA-TM-100009] 15 p2014 N88-22010
Laser velocimeter measurements in a wing-fuselage type juncture
[NASA-TM-100588] 15 p2014 N88-22012
A transonic small disturbance wing design methodology 18 p2457 N88-24590
Improved potential flow computational methods with Euler corrections for airfoil and wing/body design
[AD-A192303] 20 p2752 N88-26334
VSAERO analysis of tip planforms for the free-tip rotor
[NASA-CR-177487] 22 p3038 N88-28036
Analytical surfaces and grids
23 p3247 N88-29322

BOEING AIRCRAFT
NT BOEING 737 AIRCRAFT
NT BOEING 747 AIRCRAFT
NT C-135 AIRCRAFT
NT CH-46 HELICOPTER
Prototype manufacturing techniques for reducing cost, schedule, and technical risk 12 p1702 N88-20189
Planning for AIMS on the next generation 7J7 aircraft
22 p3035 N88-28017

BOEING MILITARY AIRCRAFT
U MILITARY AIRCRAFT

BOEING 737 AIRCRAFT
Simulation of an enhanced TCAS 2 system in operation
[NASA-CR-181545] 04 p0398 N88-12479
A study of the TCAS 2 collision avoidance system mounted on a Boeing 737 aircraft
[NASA-CR-182457] 09 p1116 N88-16687

BOEING 747 AIRCRAFT
Acquisition of gust statistics from Aircraft Integrated Data Systems (AIDS) recorded data
[NLR-MP-86048-U-ISS-2] 06 p0745 N88-14586
The intelligent QAR and its cost effective role in new generation AIMS — quick access recorder (QAR); aircraft integrated monitoring systems (AIMS)
22 p3035 N88-28020
The Sundstrand B747-400 data management unit
22 p3035 N88-28021
RB211 developments
[PNR90444] 22 p3045 N88-28069

BOGOLIUBOV THEORY
Bogolyubov transformation in relativistic theory of gravitation
[DE88-701592] 16 p2232 N88-23329

BOGS
U MARSHLANDS

BOHR THEORY
Inelastic two composite particle systems scattering at high energy
[DE88-701841] 20 p2851 N88-26928

BOILERS
Design of a condenser-boiler for a binary mercury-organic Rankine cycle solar dynamic space power system
[AD-A184188] 03 p0348 N88-12198
Proceedings of the 1987 International Symposium on Condensing Heat Exchangers
[DE88-005230] 13 p1766 N88-20564

BOILING
NT FILM BOILING
NT NUCLEATE BOILING
Review of nucleation and incipient boiling under pool and forced convection conditions
08 p0982 N88-15938
A model for stationary and dynamic impression of undercooled boiling in coupled thermohydraulic and neutron physics calculations of nuclear reactors
[IKE-6-171] 09 p1247 N88-17472
Prediction of high-temperature thermodynamic properties of mixed electrolyte solutions including solubility equilibria, vapor pressure depression and boiling point elevation
[DE88-006344] 13 p1849 N88-21069
Analysis and interpretation of low gravity boiling experiments in the KC-135 17 p2432 N88-24466
Ammonia boiling in long tubes. Heat transfer and charge loss in vertical and horizontal tubes
[NASA-TT-20313] 19 p2667 N88-25858
Investigation on refrigerant R12 critical boiling point in narrow flow pipes considered as model fluid
[ETN-88-92374] 20 p2802 N88-26626
Effects of surface tension and contact angle on sensible heating and boiling incipience in dielectric falling films
[DE88-007057] 21 p2945 N88-27492

BOILING WATER REACTORS
The dishomogeneity of the degree of sensitization in large recirculation pipes in Boiling Water Reactor (BWR) power plants
[CISE-3955] 09 p1247 N88-17473

BOLIDES
The end height of fireball as a function of their residual kinetic energy 06 p0737 N88-14535
The Valec fireball and predicted meteorite fall 06 p0739 N88-14547

BOLKOW AIRCRAFT
NT BO-105 HELICOPTER

BOLOGRAMS
U BOLOMETERS

BOLOMETERS
An adiabatic demagnetization cooled bolometer system for millimeter continuum astronomy 07 p0943 N88-15735
Preparing the Alcator C bolometer system for use on MTX (Microwave Tokamak Experiment) [DE88-006724] 15 p2134 N88-22733

BOLTED JOINTS
Structural analysis of a bolted joint concept for the space shuttle's solid rocket motor casing [NASA-TM-89092] 04 p0407 N88-12531
Nonlinear axial stiffness characteristics of axisymmetric bolted joints 04 p0452 N88-12799
Behavior of bolted joints in composite laminates 06 p0677 N88-14148
Device for measuring hole elongation in a bolted joint [NASA-CASE-LAR-13453-1] 06 p0712 N88-14361
Comparison of the strength of single and multiple bolted joints in CFRP [PB87-123766] 06 p0722 N88-14438
Experimental and theoretical investigation of mechanically fastened composites [AD-A185896] 07 p0826 N88-15008
Simplified procedures for designing composite bolted joints [NASA-TM-100281] 07 p0828 N88-15020
Experimental investigation of damping characteristics of bolted structural connections for plates and shells [AD-A186075] 07 p0867 N88-15259
Detection sensitivity in thick assemblies --- eddy currents, light alloys, aircraft construction materials [REPT-48-912/F] 16 p2216 N88-23221
Experimental investigation of the effects of underwater exposure on the damping characteristics of bolted structural connections for plates and shells [AD-A194486] 23 p3226 N88-29200
Clevis joint for deployable space structures [NASA-CASE-LAR-13898-1] 24 p3380 N88-30130

BOLTS
Joints in carbon fibre reinforced composites [BR99969] 01 p0019 N88-10114
Fastening high resistance bolts in real assemblies [CRIF-MT-171] 07 p0861 N88-15221
Increasing strength of graphite/epoxy bolted joints by introducing an adhesively bonded metallic insert [FFA-TN-1987-45] 15 p2088 N88-22442
On the calculation of stresses in pin-loaded anisotropic plates [ETN-88-92239] 16 p2222 N88-23261
Bearing-bypass material system test [NASA-CASE-LAR-13458-1] 17 p2342 N88-23967
FEB structural analysis, revision H [AD-A192302] 20 p2814 N88-26698

BOLTZMANN DISTRIBUTION
A moment approach to modeling negative ion sources [AD-A188858] 12 p1691 N88-20114
Para-ortho abundance ratio of molecular hydrogen in NGC2023 [ISAS-RN-352] 18 p2573 N88-25286
Extension of Boltzmann's theory to a liquid [DE88-009153] 20 p2880 N88-27097
Boltzmann equation approach to two-phase flow turbulence [AD-A196153] 24 p3373 N88-30086

BOLTZMANN TRANSPORT EQUATION
The physics of charge separation preceding lightning strokes in thunderclouds [NASA-CR-178371] 01 p0071 N88-10452
Boltzmann-Fokker-Planck calculations using standard discrete-ordinates codes [DE88-005393] 11 p1537 N88-19185
Simulation of the plasma interaction with thin dust clouds 11 p1552 N88-19291
The development of KENO and the calculation of differential parameters with KENO [DE88-006176] 18 p2555 N88-25166
On microphysical principles of thermofluid dynamics [ETN-88-92095] 20 p2801 N88-26620
Feedback control of a hyperbolic partial-differential equation with viscoelastic damping [AD-A192896] 21 p3003 N88-27810

BOMB CALORIMETERS
Determination of the melting and decomposition points of different materials in an oxygen stream [INFORME-I-158/86] 09 p1142 N88-16844

BOMBER AIRCRAFT
NT B-1 AIRCRAFT
NT B-57 AIRCRAFT
NT B-70 AIRCRAFT
Store separation of nuclear weapons [DE87-010778] 02 p0124 N88-10785
Use of demonstration/validation prototypes: Impact on total development costs and times 12 p1703 N88-20194
A study of Radar Cross Section (RCS) characteristics and their application in future weapon systems [ETN-88-92081] 14 p1906 N88-21390
Pilot report: AFTI (Advanced Fighter Technology Integration) F-111 [AD-A192937] 21 p2895 N88-27184
The Soviet Stealth fighter: Check or checkmate [AD-A195200] 24 p3323 N88-29791
Human factors report on information management requirements for next-generation manned bombers [AD-A195870] 24 p3409 N88-30296

BOMBS (ORDNANCE)
A simplified computer code for reduction to burning rates of closed bomb pressure-time data (MINICB) [AD-A189112] 13 p1736 N88-20380
Descriptive characterization of propellant particles [AD-A195176] 24 p3356 N88-29985

BOMBS (PRESSURE GAGES)
U PRESSURE GAGES

BOMBS (SAMPLERS)
U SAMPLERS

BOND GRAPHS
An interactive-graphics method for dynamic system modelling, applying consistency rules 09 p1181 N88-17072

BONDING
NT ADHESIVE BONDING
NT CERAMIC BONDING
NT EXPLOSIVE WELDING
NT INERTIA BONDING
NT METAL BONDING
NT METAL-METAL BONDING
NT REACTION BONDING
NT RESIN BONDING
Low-pressure eutectic bonding of depleted uranium to copper [DE87-014625] 02 p0181 N88-11128
Bond character at a silicon/copper surface [AD-A184167] 03 p0295 N88-11851
Superconductivity as a synchronous spatial alternation of valence bonds [AD-A184208] 03 p0382 N88-12405
Tool and process for miniature explosive joining of tubes [NASA-CASE-LAR-13662-1] 06 p0711 N88-14359
Mechanical properties of steel-to-steel adhesive bonds [PB88-111299] 08 p0971 N88-15877
Tight binding theory of semiconductors 10 p1415 N88-18447
Interfacial adhesion: Theory and experiment [NASA-TM-100830] 13 p1742 N88-20417
An investigation of the infrared emission spectra of carbon condensates 14 p1886 N88-21272
Fracture toughness of silicon nitride-silicon nitride joints bonded with oxynitride glass [DE88-005548] 15 p2043 N88-22172
The inspection of electronic metallurgical bonds [AD-A192197] 18 p2486 N88-24745
Molecular characterization of structure and bonding in thin film materials [DE88-006811] 18 p2584 N88-25351
Fracture physics of delamination of composite materials [AD-A192021] 19 p2609 N88-25482
Molecular orbital studies of the bonding in heavy element organometallics: Progress report [DE88-007765] 19 p2723 N88-26168
Effect of the matrix on the creep-behavior of carbon-carbon composite [AD-A193211] 21 p2905 N88-27235
An IETS (Inelastic Electron Tunneling Spectroscopy) study of surface reactions applicable to adhesion [AD-A192274] 21 p2909 N88-27261
Method for maintaining precise suction strip porosities [NASA-CASE-LAR-13638-1] 23 p3201 N88-29051
Evaluation of bond testing equipment for inspection of Army advanced composite airframe structures [AD-A195795] 24 p3341 N88-29885

BONE DEMINERALIZATION
Prevention of disuse osteoporosis: Effect of sodium fluoride during five weeks of bed rest [NASA-CR-172018] 01 p0075 N88-10483
Histomorphometric analysis of rat bones after spaceflight aboard Cosmos-1667 biosatellite 10 p1360 N88-18128
NASA Workshop on Biological Adaptation [NASA-TM-89468] 10 p1368 N88-18174
Disuse condition stimulates bone resorption in organ culture 12 p1656 N88-19926
Noninvasive examination of bones during long-term hypokinesia 19 p2704 N88-26077
Effect of different doses of alpha-hydroxydimethyl-gamma-aminopropylidene phonate on rat bones 19 p2704 N88-26078

BONE MARROW
Late radiation damage in bone, bone marrow and brain vasculature, with particular emphasis upon fractionation models [DE87-753039] 08 p1048 N88-16330

BONE MINERAL CONTENT
Disuse condition stimulates bone resorption in organ culture 12 p1656 N88-19926
An in vitro model system to study the effect of microgravity and loading conditions on the mineralization and resorption of skeletal tissues 12 p1657 N88-19927
Use of diphosphonates to correct disorders in calcium metabolism and mineral composition of bone tissue with 60-day hypokinesia in rats [NASA-TT-20220] 13 p1809 N88-20807
Noninvasive examination of bones during long-term hypokinesia 19 p2704 N88-26077
Effect of different doses of alpha-hydroxydimethyl-gamma-aminopropylidene phonate on rat bones 19 p2704 N88-26078

BONES
NT SKULL
NT TIBIA
Histomorphometric analysis of rat bones after spaceflight aboard Cosmos-1667 biosatellite 10 p1360 N88-18128
Morphological study of early changes in rat bones in simulated weightlessness 10 p1365 N88-18158

BOOLEAN ALGEBRA
NT BOOLEAN FUNCTIONS
Search rearrangement backtracking often requires exponential time to verify unsatisfiability [AD-A186121] 07 p0909 N88-15511
A graph separator theorem and its application to Gaussian elimination to optimize Boolean expressions for parallel evaluation [AD-A188527] 14 p1962 N88-21706
Two papers on a symbolic analyzer for MOS (Metal-Oxide Semiconductors) circuits [AD-A188617] 15 p2139 N88-22761

BOOLEAN FUNCTIONS
Extraction and evaluation of Boolean relations for the solution of linear programs in 0-1 variables, volume 1 [ENST-86E023-VOL-1] 02 p0227 N88-11430
Extraction and evaluation of Boolean relations for the solution of linear programs in 0-1 variables, volume 2 [ENST-86E023-VOL-2] 02 p0227 N88-11431
The geometry of the Karnaugh map --- Boolean expressions [ETN-87-90961] 02 p0227 N88-11432
A complexity transform for NP-complete problems [OUEL-1708/87] 14 p1962 N88-21703
A graph separator theorem and its application to Gaussian elimination to optimize Boolean expressions for parallel evaluation [AD-A188527] 14 p1962 N88-21706
Technology mapping from Boolean expressions to standard cells [EUT-87-E-174] 14 p1963 N88-21709
SYMBL: A new Boolean compiler 18 p2554 N88-25160
Investigation of the potential impact of new photonic materials on optical processing systems 21 p2924 N88-27359

BOOMS (EQUIPMENT)
Pinhole occulter experiment [NASA-CR-179206] 02 p0235 N88-11481
Development of the Extendable and Retractable Mast (ERM), Design phase 2. Volume 1 --- spacecraft payloads [RP-2010-0000-DS/09] 11 p1467 N88-18750
Some highlights on ROSAT mechanisms 14 p1874 N88-21195
The CTM program of masts and the CTM engineering model --- spacecraft mechanism 14 p1874 N88-21196
Deployable/retrievable boom: One application to tethered satellite 14 p1874 N88-21197
Deployable booms and antennas on AMPTE-IRM 14 p1874 N88-21198
The EURECA antenna deployment and retraction mechanisms 14 p1878 N88-21225
Required operational capacity for a 7-1/2 ton capacity, Air Mobile Crane (AMC) [AD-A192023] 19 p2601 N88-25451

BOOST
U ACCELERATION (PHYSICS)
BOOSTER RECOVERY
A two stage launch vehicle for use as an advanced space transportation system for logistics support of the space station
[NASA-CR-182572] 11 p1443 N88-18606
BOOSTER ROCKET ENGINES
NT APOGEE BOOST MOTORS
NT SPACE SHUTTLE BOOSTERS
A two stage launch vehicle for use as an advanced space transportation system for logistics support of the space station
[NASA-CR-182572] 11 p1443 N88-18606
BOOSTERS (EXPLOSIVES)
A study of diverging detonation in high-explosive systems
[DE87-006070] 01 p0031 N88-10194
BORANES
Dynamics of production and oxidation of boranes
[AD-A188988] 12 p1606 N88-19605
BORATES
Structure of sol-gel-derived inorganic polymers. 2: Silicates and borates
[DE87-013068] 01 p0027 N88-10172
BORAZON (TRADEMARK)
U BORON NITRIDES
BOREHOLES
Cryogenic cell --- neutron borehole logging
[GB-PATENT-2-139-745-A] 01 p0048 N88-10308
Geophysical diffraction tomography for imaging isolated subsurface inclusions
[DE88-003918] 11 p1505 N88-18990
Evaluation of a miniature horizontal pendulum tilt transducer 12 p1577 N88-19435
Theoretical and numerical solution of the forward-scattering problem in a circularly cylindrical configuration
[PB88-173489] 16 p2189 N88-23056
Finite elements for the computation of three-dimensional electromagnetic fields in inhomogeneous media (revised)
[PB88-173471] 16 p2190 N88-23057
Reaming experiments for the lethality test system
[DE88-007902] 20 p2763 N88-26383
BOREL SETS
Volume functions in the general theory of relativity
[ETN-87-90406] 01 p0089 N88-10582
BORES
U CAVITIES
BORESCOPES
U ENDOSCOPES
BORIC ACIDS
Boronium complexes as polymer catalysts
[GB-PATENT-2-161-475-A] 01 p0026 N88-10166
BORIDES
NT TITANIUM BORIDES
A synthetic plasma source
[TRITA-EPP-86-15] 05 p0652 N88-13995
High-current density, high-brightness electron beams from large-area lanthanum hexaboride cathodes
[AD-A187700] 11 p1477 N88-18813
The relationship of the chemical bonding topology of high critical temperature copper oxide superconductors to that of the chevrel phases and the ternary lanthanide rhodium borides
[AD-A189255] 13 p1845 N88-21042
The combustion synthesis of boride composites
[DE88-005474] 15 p2028 N88-22084
Boron-containing organosilane polymers and ceramic materials thereof
[NASA-CASE-ARC-11649-1-SB] 23 p3199 N88-29040
BORN APPROXIMATION
Inversion of parabolic and paraboloidal projections
[AD-A187538] 10 p1405 N88-18380
Seismic inversion by a RMS (Root-Mean-Square) Born approximation in the space-time domain
[PB88-165402] 15 p2131 N88-22711
Born-type reconstruction of material parameters of an inhomogeneous, lossy dielectric slab from reflected-field data
[PB88-188958] 18 p2569 N88-25261
Time-domain far-field scattering of plane electromagnetic waves by a penetrable object in the Born approximation
[PB87-176129] 24 p3365 N88-30040
BORN-MAYER EQUATION
U BORN APPROXIMATION
BORN-OPPENHEIMER APPROXIMATION
Systematic studies of molecular vibrational anharmonicity and vibration-rotation interaction by self-consistent-field higher derivative methods: Applications to asymmetric and symmetric top and linear polyatomic molecules
[DE87-014691] 02 p0232 N88-11485
BORON
NT BORON ISOTOPES
A simulation study of interfaces in Ni, Al and Ni3Al with and without boron
[DE87-013156] 01 p0102 N88-10667
Analytical electron microscopy characterization of boron in sintered alpha-SiC
[DE87-012532] 02 p0142 N88-10889
Influence of boron on porosity in nickel-base superalloy castings 03 p0299 N88-11877
Studies on syntheses of amine-carboxyboranes (boron analogues of amino acids) and derivatives
[AD-A184836] 05 p0557 N88-13386
Basic energy sciences research in the Metals and Ceramics Division of Oak Ridge National Laboratory
[DE87-013538] 06 p0681 N88-14171
Evaluation and compilation of thermodynamic properties of high temperature chemical species
[AD-A187509] 11 p1452 N88-18654
The intergranular segregation of boron in substoichiometric Ni3Al
[DE88-004783] 11 p1462 N88-18720
Feasibility studies of the growth of 3-5 compounds of boron by MOCVD
[NASA-CR-181622] 11 p1561 N88-19343
The unique characteristics of the structure of composite materials made on a base of sphalerite-analogous boron nitride 14 p1886 N88-21273
The structure of the boron-hydrogen complex in silicon
[DE88-005433] 15 p2144 N88-22795
Comparison of calculated and measured ignition times for boron agglomerates 19 p2624 N88-25563
Grain boundary structure in Ni3Al
[DE88-009164] 20 p2773 N88-26444
NDP (Neutron Depth Profiling) evaluations of boron-implanted compound semiconductors
[AD-A192306] 21 p2934 N88-27425
Paramagnetic point defects in boron-implanted HgO.7CdO.3Te
[AD-A193276] 21 p3021 N88-27934
BORON ALLOYS
Investigations of crystallization velocity and boron diffusion in glassy iron-boron alloys and of activity coefficients of boron in crystalline iron-boron alloys
[ETN-87-90613] 03 p0381 N88-12393
BORON CARBIDES
Analytical electron microscopy characterization of boron in sintered alpha-SiC
[DE87-012532] 02 p0142 N88-10889
Shielding analysis of a small compact space nuclear reactor
[AD-A185566] 06 p0779 N88-14784
Wire-cut electrical discharge machinability of ceramics
[AD-A186989] 09 p1146 N88-16870
High yield synthesis of B4C/BN ceramic materials by pyrolysis of polymeric Lewis base adducts of decaborane(14)
[AD-A188154] 11 p1462 N88-18717
Microdesigning of lightweight/high strength ceramic materials
[AD-A188526] 12 p1610 N88-19631
The combustion synthesis of boride composites
[DE88-005474] 15 p2028 N88-22084
Electrical properties of materials for elevated temperature resistance strain gage application
[NASA-CR-182214] 24 p3376 N88-30106
BORON CHLORIDES
Advanced B and Al combustion kinetics over wide temperature ranges
[AD-A190752] 15 p2036 N88-22128
BORON COMPOUNDS
NT BORANES
NT BORATES
NT BORIC ACIDS
NT BORIDES
NT BORON CARBIDES
NT BORON CHLORIDES
NT BORON HYDRIDES
NT BORON NITRIDES
NT BORON OXIDES
NT BORON PHOSPHIDES
NT TITANIUM BORIDES
Boron-containing organosilane polymers and ceramic materials thereof
[NASA-CASE-ARC-11649-1-SB] 23 p3199 N88-29040
BORON FIBERS
Analytical and experimental characterization of damage processes in composite laminates
[AD-A187221] 10 p1296 N88-17746
BORON HYDRIDES
NT BORANES
New synthetic approaches to boron hydride transformations
[AD-A193872] 22 p3052 N88-28108
BORON ISOTOPES
Studies of boron implantation through photochemically deposited SiO2 films on Hg(sub 1-x)Cd(sub x)Te
[SD-TR-87-26] 19 p2621 N88-25548
BORON NITRIDES
Investigation of BN CO2 wave guide laser 03 p0302 N88-11905
High yield synthesis of B4C/BN ceramic materials by pyrolysis of polymeric Lewis base adducts of decaborane(14)
[AD-A188154] 11 p1462 N88-18717
A segmented calorimeter for low-energy particle beams in space
[DE88-001806] 13 p1838 N88-20997
Hermetic coating of optical fibers
[AD-A189886] 15 p2044 N88-22177
BORON OXIDES
Application of laser-induced fluorescence in an atmospheric-pressure boron-seeded flame
[AD-A189631] 14 p1889 N88-21287
BORON PHOSPHIDES
Chemical vapor deposition of B6P and B6As films
[DE87-009288] 02 p0151 N88-10942
BORON REINFORCED MATERIALS
NT ALUMINUM BORON COMPOSITES
NT BORON-EPOXY COMPOSITES
Fracture mode research of boron aluminum composite materials by Acoustic Emission (AE)
[NAL-TR-927] 02 p0142 N88-10891
Joints in fiber-reinforced aluminum alloys
[NASA-TT-20160] 15 p2031 N88-22104
BORON-EPOXY COMPOSITES
Composite repair of cracked aluminum alloy aircraft structure
[AD-A190514] 18 p2455 N88-24573
BOROSILICATE GLASS
Homogeneity of glasses: Experiment WL-IHF-05 in D1 mission --- Spacelab
[ETN-88-92339] 21 p2924 N88-27353
BOSE GEOMETRY
Method of two-time Green functions in molecular hydrodynamics of superfluid liquid 06 p0771 N88-14735
BOSE-EINSTEIN STATISTICS
U QUANTUM STATISTICS
BOSON FIELDS
Searches for forces weaker than gravity
[DE88-003579] 13 p1832 N88-20959
BOSONS
NT ALPHA PARTICLES
NT KAONS
NT MESON RESONANCE
NT MESONS
NT MUONS
NT PHOTONS
NT PIONS
W decays
[NOTA-INTERNA-877] 05 p0648 N88-13966
Vector boson pair production in e(+)e(-) collisions
[PREPRINT-549] 06 p0778 N88-14774
Single weak gauge boson production at CLIC
[PREPRINT-550] 06 p0778 N88-14775
Searches for forces weaker than gravity
[DE88-003579] 13 p1832 N88-20959
Proton/antiproton yields W(+/-)boson gamma X as a test of the quark charges
[NIKHEF-H/87-11] 13 p1836 N88-20987
New limits on charged Higgs boson mass with CELLO at Petra (Italy) and status of the neutral Higgs boson search
[NOTA-INTERNA-897] 14 p1980 N88-21817
Einstein metrics and Brans-Dicke superfields
[DE88-006992] 15 p2146 N88-22809
Involution-dependent constants and the cancellation of divergences in the 1-loop open string amplitude
[DE88-006537] 15 p2146 N88-22811
Stable, heavy, neutral particles in the sun and in toponium decay 17 p2452 N88-24568
Superfluidity of a two dimensional Boson Coulomb gas
[DE88-009827] 19 p2735 N88-26244
Production of pi(0) mesons and charged hadrons in nu bar neon and nu neon charges current interactions
[MPI-PAE/EXP.EL.188] 22 p3150 N88-28743
The ground state of the bosonic string
[USIP-88-01] 22 p3151 N88-28746
The Hilbert space of the closed bosonic string
[USIP-88-04] 22 p3151 N88-28747
Open bosonic string in background electromagnetic field
[DE88-702140] 23 p3201 N88-29053
The Hilbert space of the open bosonic string
[USIP-88-02] 23 p3295 N88-29628
BOTANY
NT GEOBOTANY
Exobiology and botany facilities for EURECA
12 p1652 N88-19898

Botany Facility pre-phase C/D. Core payload for EURECA, volume 2
[BF-RP-ER-015-VOL-2] 17 p2377 N88-24130
Life Support Subsystem (LSS). Concept for the Botany Facility — EURECA
[TN-RB524-107/86] 17 p2377 N88-24131
Impact of control errors on the volume/weight demand of the Ventilation and Dryer (VAD) concept — EURECA Botany Facility
[TN-RB524-006/87] 17 p2377 N88-24132
Summary of the activities performed during the Botany Facility (BF) predevelopment phase for the Life Support S/S (LSS)
[TB-RB524-002/87] 17 p2378 N88-24133
Botany Facility. Thermal Control (TC) subsystem test report on experiment container of laboratory model and breadboard centrifuge
[BF-TN-ER-061/86] 17 p2378 N88-24135
Botany Facility: Test report on breadboard tests for the determination of the heat transfer at the glass disk and of the temperature distribution in the fluorescent tube
[BF-TN-ER-053] 17 p2378 N88-24136
Botany Facility: Breadboarding results of the illumination system
[SIRA-A/7373/WP110/MAC003] 17 p2378 N88-24137
Botany Facility: Magnetic fluid seal considerations for the centrifuge
[SIRA-A/7373/WP110/MAC004] 17 p2378 N88-24138
Botany Facility: Considerations and analyses of the balancing system philosophy proposed for the BF centrifuge
[SIRA-A/7373/WP110/PWF001] 17 p2378 N88-24139
Botany Facility: The problems of plant fixation
[SIRA-A/7373/WP220/RJS/001] 17 p2379 N88-24140
Botany Facility: Problems of water supply, plant nutrients and soil in the Botany Facility
[SIRA-A/7373/WP220/RJS/003] 17 p2379 N88-24141
Supply and distribution of plant nutrients in the Botany Facility
[SIRA-A/7373/WP220/RJS/004] 17 p2379 N88-24142
EURECA Botany Facility. Technical note: Removal of phytotoxins
[SIRA-A/7373/WP220/RJS/005] 17 p2379 N88-24143
Botany Facility pre-phase C/D. Core payload for EURECA, volume 1
[BF-RP-ER-015-VOL-1] 17 p2379 N88-24144

BOUNDARIES
NT FLUID BOUNDARIES
NT FREE BOUNDARIES
NT GRAIN BOUNDARIES
NT LIQUID-LIQUID INTERFACES
NT LIQUID-SOLID INTERFACES
NT LIQUID-VAPOR INTERFACES
Some investigations of electrical discharges at the surfaces of solid cathodes immersed in aqueous electrolyte solutions
[PB87-168209] 09 p1159 N88-16946
Image chunking: Defining spatial building blocks for scene analysis
[AD-A187072] 09 p1200 N88-17191
Boundary stabilization of thin elastic plates
[AD-A187123] 10 p1343 N88-18025
Numerical studies of propagation of Lg waves across ocean continent boundaries using the Representation Theorem (RT) 10 p1353 N88-18085
Probability bounds for M-Skorohod oscillations
[AD-A187981] 10 p1404 N88-18371
Finding texture boundaries in images
[AD-A190554] 15 p2117 N88-22609
The theory of flotation
[NASA-TT-20278] 16 p2207 N88-23172
Transmitting boundary for finite-difference calculations with finite modeling of an infinite medium
[AD-A191441] 18 p2570 N88-25264
Curvature of blended rolled edge reflectors at the shadow boundary contour
[NASA-CR-182974] 18 p2576 N88-25300
On the use of convergent beam electron diffraction for identification of antiphase boundaries in GaAs grown on Si
[DE88-008220] 18 p2585 N88-25362
Seismic body waves and the earth's inner core
[DE88-007395] 19 p2691 N88-25994
Physical mechanisms in shock-induced turbulent separated flow
[AD-A193165] 21 p2944 N88-27484
Computational boundary conditions for the incompressible Navier-Stokes equations in channels and pipes
[AD-A193356] 21 p2944 N88-27487
The low-latitude auroral boundary: Steady-state and time-dependent representations
[AD-A193200] 21 p2972 N88-27856
Indian Ocean validation
[AD-A194458] 23 p3175 N88-28902

BOUNDARY ELEMENT METHOD
Calculation of the eigenvibrations of axisymmetric fluid configurations with a singularity method, taking into account surface tension effects under reduced gravity
[ETN-87-90438] 01 p0048 N88-10304
Characteristics and boundary elements for three dimensional nonstationary Navier Stokes flows
[PREPRINT-1051] 02 p0172 N88-11086
An integral equation analysis of inelastic shells 03 p0336 N88-12118
Theoretical and practical aspects of multigrid methods in boundary element calculations
[NLR-MP-85021-U] 03 p0370 N88-12328
Computation of nacelle interference using boundary element method 05 p0537 N88-13267
Significance of foundation-soil separation in dynamic soil-structure interaction 05 p0596 N88-13641
Studies on fluid-structural vibration using boundary element method
[PB87-129508] 06 p0699 N88-14291
Boundary element analysis for dynamic loading of a circular plate on an elastic medium
[CI-86] 06 p0722 N88-14443
On the convergence of the p-version of the boundary element Galerkin method
[AD-A186198] 07 p0910 N88-15514
Boundary elements combined with singular fields for three-dimensional cracked solids
[RAE-TR-87038] 09 p1183 N88-17088
A viscoelastic BEM (Boundary Element Method) for modeling oxidation
[AD-A187490] 11 p1452 N88-18653
An analysis of large deformation axisymmetric inelastic problems by finite element and boundary element methods 13 p1782 N88-20664
Three-dimensional mesh-generation and plotting routines for use with a boundary element program (BIE3D)
[AD-A188079] 14 p1958 N88-21675
A note on the analyticity of the Neumann Kernel and an associated quadrature problem in two-dimensional boundary element methods
[ETN-88-92054] 14 p1964 N88-21719
Boundary element method for three-dimensional magnetostatic fields in terms of vector variables
[EL-61] 15 p2122 N88-22649
Calculations of unsteady aerodynamics for a full aircraft configuration using boundary element method 19 p2637 N88-25643
Boundary element method for contact heat transfer
[DE88-011013] 20 p2800 N88-26613
Time-domain boundary element analysis of dynamic near-tip fields for impact-loaded collinear cracks
[AD-A192930] 20 p2815 N88-26700
Off-boundary approach to the boundary element method
[AD-A192931] 20 p2815 N88-26701
Parallel implementation of the boundary element method
[DE88-011846] 21 p3007 N88-27839
An improved boundary force method for analyzing cracked anisotropic materials
[NASA-TM-101495] 24 p3340 N88-29879

BOUNDARY INTEGRAL METHOD
A user's guide for BIE3D: A boundary integral equation computer program for three-dimensional elastostatic analysis
[RAE-TM-MAT-STR-1078] 01 p0079 N88-10509
Boundary integral technique for performing analysis of two-dimensional volumes of revolution
[DE87-013053] 01 p0082 N88-10524
Numerical modeling: Finite methods 03 p0304 N88-11918
Boundary integral analysis of flow and deformation of long bubbles in capillaries
[DE88-002110] 10 p1326 N88-17927
Boundary-integral-equation method for computing the three-dimensional flow of groundwater
[PB88-126891] 10 p1330 N88-17951
Fast Poisson solver on irregular regions by boundary integral-based domain decomposition methods
[DE88-003583] 10 p1399 N88-18340
Three-dimensional mesh-generation and plotting routines for use with a boundary element program (BIE3D)
[AD-A188079] 14 p1958 N88-21675
A note on the analyticity of the Neumann Kernel and an associated quadrature problem in two-dimensional boundary element methods
[ETN-88-92054] 14 p1964 N88-21719
A new boundary integral equation formulation for elastodynamic and elastostatic crack analysis
[AD-A192967] 20 p2815 N88-26702

BOUNDARY LAYER CONTROL
Investigations on a transonic airfoil with a 30 mm wide perforation/cavity arrangement
[ESA-TT-1072] 03 p0260 N88-11634
Navier-Stokes analysis of laminar flow control of a two-dimensional airfoil 05 p0540 N88-13286
Study of the effect of mass transfer on a transonic boundary layer. Application to flow relaminarization
[ETN-88-91169] 05 p0541 N88-13296
Structural tests and development of a laminar flow control wing surface composite chordwise joint
[NASA-CR-172462] 06 p0663 N88-14066
Turbulence, turbulence control, and drag reduction
[AD-A185643] 06 p0665 N88-14080
Numerical simulation of a controlled boundary layer 07 p0810 N88-14933
Wind tunnel wall interference 07 p0811 N88-14938
Boundary layer transition 07 p0811 N88-14942
Separated flow 07 p0812 N88-14944
Vortex dynamics 07 p0812 N88-14945
Overview of the Langley viscous drag reduction program 07 p0812 N88-14946
Flight research on natural laminar flow 07 p0813 N88-14950
Design and experimental evaluation of a swept supercritical Laminar Flow Control (LFC) airfoil 07 p0813 N88-14951
Laminar flow integration: Flight tests status and plans 07 p0813 N88-14952
Roughness and waviness requirements for laminar flow surfaces 07 p0813 N88-14953
Secondary subharmonic instability of boundary layers with pressure gradient and suction
[NASA-CR-4112] 07 p0848 N88-15148
Control of vortical separation on conical bodies 10 p1267 N88-17580
Reduction of tilt rotor download using circulation control 10 p1271 N88-17605
Structure of shear flow turbulence and its control
[AD-A187909] 11 p1482 N88-18846
Research on flow control
[AD-A189014] 12 p1627 N88-19736
Development of disturbances in swept wing flows
[NASA-CR-182675] 13 p1768 N88-20574
The NASA Langley Laminar-Flow-Control (LFC) experiment on a swept, supercritical airfoil: Design overview
[NASA-TP-2809] 14 p1861 N88-21117
Application of hybrid laminar flow control to global range military transport aircraft
[NASA-CR-181638] 14 p1862 N88-21124
Control of laminar flow around of the wing in free-air conditions
[AD-A187479] 15 p2013 N88-22004
Modifications to the Langley 8-foot transonic pressure tunnel for the laminar flow control experiment
[NASA-TM-4032] 15 p2021 N88-22047
Investigation of boundary layer disturbances caused by periodic heating of a thin ribbon
[AD-A190572] 15 p2065 N88-22314
Design method for laminar flow control of two-dimensional airfoils in incompressible flow. Numerical study of LFC design concepts
[DE88-751809] 16 p2155 N88-22859
An assessment of the drag reduction properties of riblets and the penalties of off-design conditions
[RAE-TM-AERO-2113] 17 p2295 N88-23731
Boundary-layer stability and airfoil design 17 p2296 N88-23738
Wind tunnel testing of low-drag airfoils 17 p2297 N88-23741
Operational considerations for laminar flow aircraft 17 p2298 N88-23748
Pressure distributions from subsonic tests of an advanced laminar-flow-control wing with leading- and trailing-edge flaps
[NASA-TM-4040-PT-1] 17 p2300 N88-23758
Passive shock wave-boundary layer control for the Bell FX69-H-098 airfoil 18 p2457 N88-24588
A new method of calculating the boundary layer characteristics downstream of manipulators. Part 1: Boundary layer integral parameters
[PNR90455] 22 p3078 N88-28279
A new method of calculating the boundary layer characteristics downstream of manipulators. Part 2: Skin friction and net drag reduction
[PNR90456] 22 p3078 N88-28280

Boundary layer simulation and control in wind tunnels
[AGARD-AR-224] 23 p3167 N88-28857
High-aspect-ratio wings 23 p3167 N88-28859
Techniques for boundary layer tripping and control 23 p3168 N88-28863
Environmental effects on transition and boundary layer characteristics 23 p3170 N88-28876
A mapping of the viscous flow behavior in a controlled diffusion compressor cascade using laser Doppler velocimetry and preliminary evaluation of codes for the prediction of stall
[AD-A194490] 23 p3211 N88-29112
Pressure distributions from subsonic tests of an advanced laminar-flow-control wing with leading- and trailing-edge flaps
[NASA-TM-4040-PT-2] 24 p3321 N88-29776

BOUNDARY LAYER EQUATIONS
Breakdown of steady and unsteady interacting boundary layers
[NLR-MP-86047-U] 01 p0045 N88-10284
Development and testing of a vertically-nested regional prediction system --- weather forecasting 02 p0210 N88-11322
Introduction to Computational Fluid Dynamics
[VKI-LS-1987-02] 06 p0701 N88-14300
Boundary layer equations and methods of solution 06 p0701 N88-14302
Three-dimensional structure of boundary layers in transition to turbulence
[AD-A185466] 06 p0702 N88-14311
The numerical and analytical study of bifurcation and multicellular flow instability due to natural convection between narrow horizontal isothermal cylindrical annuli at high Rayleigh numbers
[AD-A186113] 07 p0849 N88-15151
Pseudo-stationary oblique-shock-wave reflections in low gamma gases: Isobutane and sulphur hexafluoride
[UTIAS-TN-267] 13 p1768 N88-20576
General fuselage coordinates for the calculation of three-dimensional boundary layers
[MBB/LKE-122/S/PUB/244] 13 p1771 N88-20596
The sensitivity of boundary layer instability growth rates to compliant wall properties
[AD-A190433] 15 p2064 N88-22309
Composite reduced Navier-Stokes procedures for flow problems with strong pressure interactions
[AD-A191127] 18 p2508 N88-24875
Transient particle deposition in a boundary layer of impulsive flow over a flat plate
[AD-A191537] 18 p2508 N88-24880
Cross stream differencing for integral boundary layer equations
[AD-A191744] 18 p2509 N88-24886
Boundary layer solutions for the free-edge problem in composite laminates 21 p2904 N88-27229
A study of the vortex sheet method for solving the Prandtl boundary layer equations
[DE88-011346] 22 p3074 N88-28249

BOUNDARY LAYER FLOW
NT BOUNDARY LAYER SEPARATION
NT REATTACHED FLOW
NT SECONDARY FLOW
NT SEPARATED FLOW
Measurement techniques in low-speed turbulent flows: A report on EUROMECH 202
[NLR-MP-86036-U] 01 p0045 N88-10283
Breakdown of steady and unsteady interacting boundary layers
[NLR-MP-86047-U] 01 p0045 N88-10284
Numerical solution of Euler equations for compressible fluids by the finite element method, volume 3
[ETN-87-90650] 02 p0170 N88-11070
Boundary layer profile investigations downstream of an aero-engine intake anti-icing air exhaust slot
[PNR90378] 02 p0171 N88-11080
Vertical profiles of wind-induced current --- North Sea
[IOS-238] 02 p0193 N88-11207
Theoretical analysis of primary instabilities in three dimensional boundary layer flows
[ESA-TT-1063] 03 p0315 N88-11992
Visualization of the flow field around a generic destroyer model in a simulated turbulent atmospheric boundary layer
[AD-A184658] 03 p0320 N88-12023
The design and preliminary calibration of a boundary-layer flow channel
[NASA-CR-178399] 04 p0394 N88-12457
Total linearisation method for solving viscous free boundary flow problems by the finite element method
[PB87-222337] 04 p0441 N88-12737
Active and passive plume distribution models in the convective boundary layer using a large eddy simulation model
[KNMI-TR-90] 05 p0581 N88-13546
Combined riblet and lebu drag reduction system
[NASA-CASE-LAR-13286-1] 06 p0664 N88-14071
Characteristics of a separating confluent boundary layer and the downstream wake
[NASA-TM-100046] 06 p0704 N88-14323
Upwind relaxation algorithms for Euler/Navier-Stokes equations 07 p0810 N88-14931
Vortex dynamics 07 p0812 N88-14945
Computational design of natural laminar flow wings for transonic transport application 07 p0813 N88-14948
On the parabolized Navier-Stokes equations without sublayer assumptions
[AD-A186127] 07 p0849 N88-15152
A method for the approximate calculation of the skin friction coefficient of horizontal wavy plates
[VKI-TN-160] 07 p0851 N88-15172
Acta Aerodynamica Sinica (selected articles)
[AD-A185723] 08 p0949 N88-15757
Numerical simulation of heat transfer turbulence, volume 2
[AD-A185130] 08 p0983 N88-15947
Numerical simulation of turbulent spots in channel and boundary layer flows 08 p0983 N88-15948
A theory for turbulent curved wall jets 10 p1269 N88-17590
The further development of circulation control airfoils 10 p1270 N88-17594
Boundary-layer and wake measurements on a swept, circulation-control wing 10 p1270 N88-17597
Boundary integral analysis of flow and deformation of long bubbles in capillaries
[DE88-002110] 10 p1326 N88-17927
Shock wave/turbulent boundary layer interaction in high-Reynolds-number hypersonic flows
[AD-A188029] 11 p1434 N88-18555
Radial mixing in turbomachines
[AD-A188028] 11 p1482 N88-18847
Effects of waves on the boundary layer of a surface-piercing flat plate: Experiment and theory
[AD-A188356] 12 p1626 N88-19731
A simplified streamline swallowing procedure for the windward meridian of axisymmetric blunt bodies
[AD-A188413] 12 p1626 N88-19732
The design and use of a temperature-compensated hot-film anemometer system for boundary-layer flow transition detection on supersonic aircraft
[NASA-TM-100421] 13 p1723 N88-20304
Numerical experiments on the stability of controlled boundary layers
[NASA-CR-181649] 13 p1771 N88-20591
General fuselage coordinates for the calculation of three-dimensional boundary layers
[MBB/LKE-122/S/PUB/244] 13 p1771 N88-20596
Surface flow visualization of separated flows on the forebody of an F-18 aircraft and wind-tunnel model
[NASA-TM-100436] 14 p1863 N88-21127
Boundary-layer and wake measurements on a swept, circulation-control wing
[NASA-TM-89426] 15 p2014 N88-22013
Visualization of flows in turbomachinery
[AD-A189927] 15 p2063 N88-22299
Cavitation inception in rectangular two-dimensional slots
[AD-A190677] 15 p2066 N88-22318
Theoretical investigation of secondary instability of three-dimensional boundary-layer flows with application to the DFVLR-F5 model wing
[DFVLR-FB-87-44] 15 p2068 N88-22330
Shear-layer structures in near-wall turbulence 16 p2198 N88-23110
Conditionally-averaged structures in wall-bounded turbulent flows 16 p2198 N88-23112
Nonlinear wave interactions in swept wing flows
[NASA-CR-4142] 16 p2206 N88-23160
Solution of the compressible Navier-Stokes equations of motion by Chebyshev polynomials for laminar shock-boundary layer flow
[AD-A191033] 16 p2208 N88-23176
Simulation of laminar-turbulent transition in the vicinity of a wall
[AD-A191380] 16 p2208 N88-23180
Two-equation low-Reynolds-number turbulence modeling of transitional boundary layer flows characteristic of gas turbine blades
[NASA-CR-4145] 16 p2209 N88-23185
Single phase liquid immersion cooling of discrete heat sources in a vertical channel
[AD-A191224] 17 p2337 N88-23944
Unsteady flow about cambered plates
[AD-A191226] 17 p2337 N88-23945
Surface curvature and pressure gradient effects on turbulent flow: An assessment based on numerical solution of the Reynolds equations 17 p2338 N88-23954
Transient particle deposition in a boundary layer of impulsive flow over a flat plate
[AD-A191537] 18 p2508 N88-24880
Hypersonic turbulent wall boundary layer computations
[NASA-CR-182147] 18 p2514 N88-24917
Correlations of velocity and temperature fluctuations in the stagnation-point flow of circular cylinder in turbulent flow
[NASA-TM-100930] 19 p2597 N88-25435
Boundary layer development as a function of chamber pressure in the NASA Lewis 1030:1 area ratio rocket nozzle
[NASA-TM-100917] 19 p2664 N88-25841
The heat transfer and fluid dynamics of concave surface curvature
[AD-A193064] 21 p2943 N88-27479
A simple, analytic 3-dimensional downburst model based on boundary layer stagnation flow
[NASA-TM-100632] 22 p3042 N88-28058
Flow dynamics stimulated by hairpin-like vortices in initially laminar boundary layers
[AD-A194253] 22 p3075 N88-28254
Noise generation and boundary layer effects in vortex-airfoil interaction and methods of digital hologram analysis for these flow fields
[AD-A194191] 23 p3171 N88-28883
The use of hot-film technique for boundary layer studies on a 21 percent thick airfoil
[NAE-AN-45] 24 p3321 N88-29781

BOUNDARY LAYER NOISE
U AERODYNAMIC NOISE
U BOUNDARY LAYERS

BOUNDARY LAYER PLASMAS
The formation of boundary layers by the entry of low-energy electrons and energetic ions into the Earth's magnetosphere 08 p1095 N88-16590
Fundamental studies on MPD thrusters
[AD-A190307] 15 p2137 N88-22753
Plasma behavior in the boundary layer near a railgun surface
[DE88-008889] 21 p3017 N88-27909

BOUNDARY LAYER SEPARATION
Calculation of three-dimensional stationary turbulent boundary layer on root section of wing ignoring compressibility 04 p0424 N88-12630
Numerical simulation of unsteady separated flows
[AD-A184132] 04 p0442 N88-12741
Study of the effect of mass transfer on a transonic boundary layer. Application to flow relaminarization
[ETN-88-91169] 05 p0541 N88-13296
Delta wing in incompressible flow. Experimental study in F2
[ONERA-RT-36/1147-AN-249-G] 05 p0541 N88-13298
Vortical Flows Research Program of the Fluid Dynamics Research Branch
[NASA-TM-88332] 05 p0582 N88-13549
Post stall behavior in axial-flow compressors
[AD-A185712] 06 p0665 N88-14081
Separated flow 07 p0812 N88-14944
Advanced natural laminar flow airfoil with high lift to drag ratio 07 p0812 N88-14947
Design and experimental evaluation of a swept supercritical Laminar Flow Control (LFC) airfoil 07 p0813 N88-14951
Three-dimensional unsteady flow elicited by finite wings and complex configurations
[AD-A186464] 08 p0951 N88-15770
High-speed inlet research program and supporting analyses 08 p0958 N88-15811
A computationally efficient modelling of laminar separation bubbles
[NASA-CR-182417] 08 p0984 N88-15949
Wind tunnel investigations of periodic vortex separation on rough-surface circular cylinders using acoustic measuring methods
[DFVLR-FB-87-24] 09 p1112 N88-16665
Burst vortex/boundary layer interaction
[NASA-CR-182510] 10 p1268 N88-17583
A theory for turbulent curved wall jets 10 p1269 N88-17590
Pressure distributions and oil-flow patterns for a swept circulation-control wing 10 p1270 N88-17596
Experimental research on swept shock wave/boundary layer interactions
[AD-A187250] 10 p1331 N88-17957
Effects of waves on the boundary layer of a surface-piercing flat plate: Experiment and theory
[AD-A188356] 12 p1626 N88-19731
Interaction between two-dimensional sonic jets and supersonic flow to model heat addition in a supersonic combustor
[AD-A189572] 13 p1716 N88-20261
Coherent structure-reflective turbulent viscous flow modeling
[AD-A188339] 13 p1765 N88-20556
A flight test investigation into flow separation and structural response for a transport aircraft at buffet onset
[RAE-TR-87008] 14 p1867 N88-21156

Unsteady flow about cambered plates
[AD-A191226] 17 p2337 N88-23945
Accounting for the effects of unsteady, separated boundary layers in transonic two dimensional calculations
[ONERA-RT-30/3064-RY-063-R] 17 p2338 N88-23952
Instability of laminar separation bubbles: Causes and effects
[AD-A191168] 18 p2508 N88-24876
Computation of the turbulent boundary layer downstream of vortex generators
[AD-A191544] 18 p2508 N88-24881
Experimental study of unsteady separating turbulent boundary layers
[AD-A192997] 21 p2943 N88-27477
Physical mechanisms in shock-induced turbulent separated flow
[AD-A193165] 21 p2944 N88-27484
Study of three-dimensional transonic flow separations
[AD-A193018] 22 p3037 N88-28032
The dynamic behavior of a turbulent boundary layer subjected to a shock-induced separation
[AD-A194164] 22 p3075 N88-28252
Missiles, fuselage and similar bodies 23 p3167 N88-28858
Empirical tools for simulation methodologies 23 p3168 N88-28866
Calculation of aerodynamic characteristics of airplane configurations at high angles of attack
[NASA-CR-4182] 23 p3172 N88-28891
A study of the effect of random input motion on low Reynolds number flows
[AD-A195559] 24 p3316 N88-29747
The effects of incoming boundary layer thickness on unsteady shock-induced turbulent separations induced by cylinders
[AD-A196190] 24 p3368 N88-30060

BOUNDARY LAYER STABILITY

Experience about the application and valuation of roughness strips for boundary layer transition control in wind tunnel tests in the high-speed range
[ESA-TT-1028] 01 p0044 N88-10278
Theoretical analysis of primary instabilities in three dimensional boundary layer flows
[ESA-TT-1063] 03 p0315 N88-11992
Time-dependent hypersonic viscous interactions
[AD-A185764] 06 p0665 N88-14082
Low-disturbance wind tunnels 07 p0811 N88-14937
Boundary layer transition 07 p0811 N88-14942
Advanced natural laminar flow airfoil with high lift to drag ratio 07 p0812 N88-14947
Laminar flow integration: Flight tests status and plans 07 p0813 N88-14952
Secondary subharmonic instability of boundary layers with pressure gradient and suction
[NASA-CR-4112] 07 p0848 N88-15148
Calculation evaluation of the boundary conditions of autoinflammation of propulsive charges
[PB87-139044] 08 p0974 N88-15890
Oscillating airfoils: Achievements and conjectures
[AD-A190490] 15 p2014 N88-22008
The sensitivity of boundary layer instability growth rates to compliant wall properties
[AD-A190433] 15 p2064 N88-22309
Investigation of boundary layer disturbances caused by periodic heating of a thin ribbon
[AD-A190572] 15 p2065 N88-22314
Theoretical investigation of secondary instability of three-dimensional boundary-layer flows with application to the DFVLR-F5 model wing
[DFVLR-FB-87-44] 15 p2068 N88-22330
Spectral measurements in a disturbed boundary layer over snow
[AD-A190217] 15 p2097 N88-22494
Boundary-layer stability and airfoil design 17 p2296 N88-23738
Wind tunnel testing of low-drag airfoils 17 p2297 N88-23741
Cross stream differencing for integral boundary layer equations
[AD-A191744] 18 p2509 N88-24886
Active control of 2-D instability waves on an axisymmetric body
[AD-A191578] 19 p2663 N88-25835
Stability and drag reduction in a boundary layer with microbubbles
[AD-A191975] 23 p3209 N88-29099
A singular perturbation analysis of the weakly nonlinear evolution of long and short water waves and waves in boundary layers 23 p3209 N88-29102

BOUNDARY LAYER TRANSITION

The structure of separated flow regions occurring near the leading edge of airfoils including transition
[NASA-CR-181434] 01 p0002 N88-10011
Excitation of natural oscillations of a boundary layer by an external acoustic field 04 p0425 N88-12634
Numerical optimization of conical flow waveriders including detailed viscous effects 05 p0533 N88-13245
Hypersonic static and dynamic stability of axisymmetric shapes: A comparison of prediction methods and experiment 05 p0534 N88-13246
JPRS report: Science and technology. Japan
[JPRS-JST-87-028] 06 p0675 N88-14130
Visible boundary layer transition points through flight tests 06 p0675 N88-14136
Three-dimensional structure of boundary layers in transition to turbulence
[AD-A185466] 06 p0702 N88-14311
Low-disturbance wind tunnels 07 p0811 N88-14937
Flow diagnostics and visualization in wind tunnels and flight 07 p0811 N88-14940
Boundary layer transition 07 p0811 N88-14942
Advanced natural laminar flow airfoil with high lift to drag ratio 07 p0812 N88-14947
Computational design of natural laminar flow wings for transonic transport application 07 p0813 N88-14948
Natural laminar flow nacelle for transport aircraft 07 p0813 N88-14949
Design and experimental evaluation of a swept supercritical Laminar Flow Control (LFC) airfoil 07 p0813 N88-14951
Roughness and waviness requirements for laminar flow surfaces 07 p0813 N88-14953
Thin film electret boundary layer transition detector: A feasibility study
[AD-A185675] 07 p0856 N88-15199
Wake interaction effects on the transition process on turbine blades
[AD-A188020] 10 p1332 N88-17962
Investigations of the laminar-turbulent boundary layer transition for the improvement of the performance of powered glider aircraft profiles
[ETN-88-91094] 11 p1436 N88-18569
Structure of shear flow turbulence and its control
[AD-A187909] 11 p1482 N88-18846
Development of disturbances in swept wing flows
[NASA-CR-182675] 13 p1768 N88-20574
Preliminary in-flight boundary layer transition measurements on a 45 deg swept wing at Mach Numbers between 0.9 and 1.8
[NASA-TM-100412] 13 p1772 N88-20598
Turbulent transfer of momentum and heat in boundary layer of fluid beyond an obstacle. 1: Hydrodynamic characteristics 13 p1787 N88-20690
Propagation of artificial disturbances immersed in thick turbulent boundary layer 14 p1864 N88-21136
Control of laminar flow around of the wing in free-air conditions
[AD-A187479] 15 p2013 N88-22004
The sensitivity of boundary layer instability growth rates to compliant wall properties
[AD-A190433] 15 p2064 N88-22309
Theoretical investigation of secondary instability of three-dimensional boundary-layer flows with application to the DFVLR-F5 model wing
[DFVLR-FB-87-44] 15 p2068 N88-22330
Inflectional instabilities in the wall region of bounded turbulent shear flows 16 p2199 N88-23114
Two-equation low-Reynolds-number turbulence modeling of transitional boundary layer flows characteristic of gas turbine blades
[NASA-CR-4145] 16 p2209 N88-23185
Experimental study of bypass transition in a boundary layer
[NASA-TM-100913] 16 p2209 N88-23186
Boundary layer measurements using hot-film sensors 17 p2297 N88-23743
Natural laminar flow and airplane stability and control 17 p2298 N88-23747
Certification aspects of airplanes which may operate with significant natural laminar flow 17 p2298 N88-23749
Crossflow vorticity sensor
[NASA-CASE-LAR-13436-1-CU] 17 p2300 N88-23759
Boundary layer transition
[CERT-OA-37/5018-AYD] 18 p2458 N88-24595
Numerical simulation of transition to turbulence in plane Poiseuille flow by a spectral method 19 p2640 N88-25661
Study of the structure of turbulence in accelerating transitional boundary layers
[AD-A191698] 19 p2663 N88-25837
Boundary layer development as a function of chamber pressure in the NASA Lewis 1030:1 area ratio rocket nozzle
[NASA-TM-100917] 19 p2664 N88-25841
Numerical simulation studies of laminar-turbulent transition in the plan channel 19 p2665 N88-25850
Turbulence transition in a circular pipe 20 p2782 N88-26503
Empirical tools for simulation methodologies 23 p3168 N88-28866
Missiles, fuselages and similar bodies 23 p3169 N88-28869
Introduction and critical flow phenomena 23 p3169 N88-28870
Boundary layer development and transition 23 p3169 N88-28871
Classical separation, trailing-edge flows and buffeting 23 p3170 N88-28874
Environmental effects on transition and boundary layer characteristics 23 p3170 N88-28876
Boundary layer manipulation 23 p3170 N88-28877
Variable Sweep Transition Flight Experiment (VSTFE)-parametric pressure distribution boundary layer stability study and wing glove design task
[NASA-CR-3992] 23 p3173 N88-28894
On the generation of mean flows by the interaction of Goertler vortices and Tollmien-Schlichting waves in curved channel flows
[NASA-CR-181690] 24 p3315 N88-29743
Techniques used in the F-14 variable-sweep transition flight experiment
[NASA-TM-100444] 24 p3374 N88-30093

BOUNDARY LAYERS

NT ATMOSPHERIC BOUNDARY LAYER
NT COMPRESSIBLE BOUNDARY LAYER
NT HYPERSONIC BOUNDARY LAYER
NT INCOMPRESSIBLE BOUNDARY LAYER
NT LAMINAR BOUNDARY LAYER
NT PLANETARY BOUNDARY LAYER
NT SUPERSONIC BOUNDARY LAYERS
NT THERMAL BOUNDARY LAYER
NT THREE DIMENSIONAL BOUNDARY LAYER
NT TURBULENT BOUNDARY LAYER
NT TWO DIMENSIONAL BOUNDARY LAYER
Vortex/boundary-layer interactions: Data report, volume 1
[NASA-CR-181462] 02 p0121 N88-10768
Vortex/boundary-layer interactions: Data report, volume 2
[NASA-CR-181463] 02 p0122 N88-10769
Numerical simulation of a supersonic chemically reacting mixing layer 02 p0143 N88-10900
The four spot time-of-flight laser anemometer 02 p0184 N88-11145
Heat transfer in a real engine environment 02 p0186 N88-11155
Film cooling heat transfer on a turbine airfoil 02 p0186 N88-11156
Flow field measurements in a 90 degree turning duct 02 p0186 N88-11157
A flash spectrum of Cl I, C I, N I, and Ni II absorption in 31 Cygni: A direct observation of the reversing layer 04 p0513 N88-13158
Numerical simulation of boundary layers. Part 3: Turbulence and relaminarization in sink flows
[NASA-TM-88220] 06 p0698 N88-14283
An investigation of the effects of the propeller slipstream on a wing boundary layer 06 p0700 N88-14293
Experimental investigation of heterogeneous compressible shear layers 06 p0700 N88-14294
Studies of unsteadiness in boundary layers
[AD-A185662] 06 p0703 N88-14315
Modern concept concerning transport of bottom sediments in abyssal regions of world ocean 06 p0728 N88-14478
Observations of a midlatitude squall line boundary layer wake
[AD-A185609] 06 p0746 N88-14589
Spectral methods: Analysis and applications to flow problems
[AD-A186265] 07 p0850 N88-15156
Consistent boundary conditions for Reduced Navier-Stokes (RNS) scheme applied to 3-dimensional internal viscous flows
[NASA-CR-180874] 08 p0950 N88-15762
Friction drag reduction (a speculative essay)
[INPE-4278-PRE/1150] 08 p0988 N88-15985
Influence of the wall boundary layer on force measurements on half models in the transonic wind tunnel
[F+W-TF-1876] 09 p1122 N88-16715
Use of boundary-layer method for problem of sound propagation through channel with variable cross-section containing stream of fluid 09 p1233 N88-17396
Beta limitation of matter-antimatter boundary layers
[TRITA-EPP-87-11] 09 p1250 N88-17490
Free-surface flow phenomena ahead of a two-dimensional body in a viscous fluid 10 p1329 N88-17944
Experimental research on swept shock wave/boundary layer interactions
[AD-A187250] 10 p1331 N88-17957

On the stability of the supersonic boundary layer
11 p1435 N88-18561
Analysis of shear-layer probe data for holes in hypersonic configurations
[DE88-003992] 11 p1435 N88-18564
Thermal cracking and variable properties effects on free boundary layer diffusion flames
[NBS/GCR-88/542] 12 p1614 N88-19652
Effects of waves on the boundary layer of a surface-piercing flat plate: Experiment and theory
[AD-A188356] 12 p1626 N88-19731
A finite-amplitude analysis of the buoyant instability of a highly viscous film over a less viscous half-space
13 p1769 N88-20581
Dynamical modeling of marine boundary layer convection 13 p1797 N88-20750
Proceedings of the Seminar on Hydrodynamics and Crystal Growth
[ETN-88-92025] 14 p1987 N88-21853
Transport processes during directional solidification and crystal growth: Scaling and experimental study
14 p1988 N88-21857
High Reynolds number, low Mach number, steady flow field calculations over a NACA 0012 airfoil using Navier-Stokes and interactive boundary layer theory
[AD-A189871] 15 p2013 N88-22005
Coherent structure 16 p2199 N88-23117
Coherent structures and modeling: Some background comments 16 p2199 N88-23120
High Reynolds number tests of a Douglas DLBA 032 airfoil in the Langley 0.3-meter transonic cryogenic tunnel
[NASA-TM-87663] 17 p2296 N88-23734
Boundary layer measurements using hot-film sensors
17 p2297 N88-23743
Unsteady flow about cambered plates
[AD-A191226] 17 p2337 N88-23945
A formulation for the boundary-layer equations in general coordinates
[NASA-TM-100079] 18 p2459 N88-24600
Flame spread mechanisms over PMMA surfaces
[NASA-TT-20284] 19 p2612 N88-25500
Ignition and flammability characteristics of solid fuel ramjets 19 p2626 N88-25575
Boundary layer simulator (BLIMPJ) improvement
19 p2627 N88-25582
Numerical investigation of acoustic energy exchange through flow turning 19 p2629 N88-25593
Investigation of Rossby-number similarity in the neutral boundary layer using large-eddy simulation
[DE88-008910] 19 p2666 N88-25851
A domain decomposition method for boundary layer problems
[DE88-008917] 19 p2666 N88-25852
Prediction of continental shelf sediment transport using a theoretical model of the wave-current boundary layer
[AD-A192272] 20 p2829 N88-26783
Solution of the Orr-Sommerfeld equation for the Blausius boundary-layer documentation of program ORRBL and a test case
[NASA-CR-4169] 20 p2841 N88-26858
The diffusion of vorticity from a plane boundary
[AD-A192706] 21 p2942 N88-27474
IR (infrared) sky radiance distributions in the marine boundary layer
[AD-A193683] 22 p3119 N88-28531
Shock boundary layer interaction
23 p3170 N88-28873
Three-dimensional laser Doppler velocimeter studies of flow in a 90 deg curved duct having a square cross-section 23 p3209 N88-29101
Polynomial definition of discrete field points of map of diffusion equation, part 1
[AD-A193697] 23 p3271 N88-29467
Temperature profile construction methods: An evaluation
[AD-A195919] 24 p3403 N88-30262

BOUNDARY LUBRICATION
The performance of perfluoropolyalkylether oils under boundary lubrication conditions
[AD-A191057] 17 p2323 N88-23869
Perfluoropolyalkylether lubricants under boundary conditions: Iron catalysis of lubricant degradation
[AD-A193241] 21 p2956 N88-27560
Evaluation of transfer films of Salox M on 440C for HPOTP bearing cage applications, task 119
[NASA-CR-179020] 23 p3223 N88-29184

BOUNDARY VALUE PROBLEMS
NT CAUCHY PROBLEM
NT DIRICHLET PROBLEM
NT NEUMANN PROBLEM
Inhomogeneous conditions at open boundaries for wave propagation problems
[AD-A183847] 01 p0033 N88-10214
An exact theory of elastic plates
[ETN-87-90675] 01 p0062 N88-10396
Regularity properties of a doubly degenerate equation in hydrology
[REPT-87-07] 01 p0064 N88-10409
An asymptotic theory for a class of initial-boundary value problems for weakly nonlinear wave equations with an application to a model of the galloping oscillations of overhead transmission lines
[REPT-87-12] 01 p0086 N88-10556
Computing the bounded region determined by finitely many lines in the plane
[CS-8703] 01 p0086 N88-10558
Effect of dissipation on propagation of spherical detonation shock wave 02 p0159 N88-10998
Analysis of thickness fields retrieved from NOAA-7 observations through the 3I (Improved Initialization Inversion) method. Interest for weather forecasting
02 p0201 N88-11255
Strategies for using mesoscale data in an operational mesoscale model 02 p0212 N88-11335
Toward optimizing the use of data for operational mesoscale forecasting at the National Meteorological Center 02 p0213 N88-11337
Initialization experiments with the NMC nested grid model --- National Meteorological Center (NMC)
02 p0213 N88-11343
Four-dimensional initialization of mesoscale models
02 p0214 N88-11349
Preconditioned iterative methods applied to singularly perturbed elliptic boundary value problems: Volume 2
[DE87-014337] 02 p0225 N88-11415
The method of lines for time dependent free boundary problems
[DE87-013929] 02 p0226 N88-11423
IMPSOR: A fully vectorized FORTRAN code for three dimensional moving boundary problems with Dirichlet or Neumann boundary conditions
[DE87-014964] 02 p0226 N88-11427
A collection of test problems for ordinary differential equation solvers which have provisions for rootfinding
[DE88-000045] 02 p0226 N88-11428
Stability of semidiscrete approximations for hyperbolic initial-boundary-value problems: An eigenvalue analysis
[NASA-TM-88328] 02 p0227 N88-11434
Numerical modeling: Finite methods
03 p0304 N88-11918
Dynamics of the von Karman vortex street
03 p0316 N88-11998
The diffusion-convection vortex method for solving two-dimensional incompressible Navier-Stokes equation
03 p0317 N88-12001
Nonlinear thermoviscoelastic analysis of metallic plane curved beams 03 p0336 N88-12119
Numerical solution of bound constrained problems
[DE88-000653] 03 p0371 N88-12334
Numerical prediction of propeller performance by vortex lattice method
[UTIAS-TN-265] 04 p0400 N88-12489
Three-dimensional, free-Lagrange hydrodynamics
[DE88-000494] 04 p0443 N88-12749
Analytical studies of axially symmetric motion of an incompressible viscous fluid between two concentric rotating spheres 04 p0444 N88-12757
Higher order theory analysis of a modified free-edge delamination specimen 04 p0455 N88-12820
On operator splitting for unsteady boundary value problems
[AD-A184281] 04 p0484 N88-12981
Solution of some 3-D viscous and inviscid supersonic flow problems by finite-volume space-marching schemes
05 p0532 N88-13235
Numerical experiments with hypersonic flows beneath a cone-delta-wing combination 05 p0532 N88-13238
Development of an integrated BEM approach for hot fluid structure interaction
[NASA-CR-181577] 05 p0556 N88-13384
Mechanics of anisotropic media. Study of the boundary conditions --- stratified composites
[SNIAS-872-430-112] 05 p0559 N88-13404
An examination of chaotic motion for the buckled beam 05 p0597 N88-13644
On a boundary data operator and generalized exterior Robin problems for the Helmholtz equation
[AD-A185124] 05 p0640 N88-13915
Guidance and control strategies for aerospace vehicles
[NASA-CR-181579] 05 p0643 N88-13935
Boundary layer equations and methods of solution
06 p0701 N88-14302
Modified quantum mechanics of small composite systems
[NIKHEF-H/87-1] 06 p0790 N88-14845
Stability analysis of finite difference schemes for hyperbolic systems, and problems in applied and computational linear algebra
[AD-A185824] 07 p0908 N88-15499
Perturbative coherence in field theory
[DE88-700366] 07 p0941 N88-15717
A semianalytical solution of the heat conduction equation for several boundary conditions
08 p1014 N88-16148
Adaptive finite element methods for parabolic systems in one- and two-space dimensions
[AD-A186534] 08 p1073 N88-16475
Equation of gravitational-gyroscopic waves: Angular potential and its applications 08 p1079 N88-16504
An initial investigation into methods of computing transonic aerodynamics sensitivity coefficients
[NASA-CR-182444] 09 p1112 N88-16663
Investigation of iterative and spectral Galerkin techniques for solving electromagnetic boundary value problems 09 p1155 N88-16925
Steady ship waves at low Froude numbers, part 2
[AD-A176805] 09 p1160 N88-16953
A guide to the transient three phase porous flow model implemented in the two-dimensional CRAY-TENSOR code: Physics, numerics, and code description
[DE88-003709] 09 p1165 N88-16983
A quasi-three-dimensional calculation procedure for the prediction of flow and heat transfer in heat exchanger passages 09 p1165 N88-16985
Feedback stabilization of distributed systems
[AD-A187111] 09 p1222 N88-17328
Note on boundary stabilization of wave equations
[AD-A187113] 09 p1227 N88-17348
Boundary value problems for ordinary differential equations with multiple turning points
[CWI-AM-R8701] 09 p1228 N88-17354
Numerical solutions of two moving boundary problems by both finite difference and finite element methods with applications
[DE88-002867] 09 p1230 N88-17374
An experimental investigation of pressure driven three-dimensional turbulent boundary layers
10 p1327 N88-17934
Free-surface flow phenomena ahead of a two-dimensional body in a viscous fluid
10 p1329 N88-17944
The h-p version of the finite element method for problems with nonhomogeneous essential boundary condition
[AD-A187356] 10 p1400 N88-18348
Boundary value problems for differential and functional differential equations
[AD-A187378] 10 p1400 N88-18349
On an overdetermined Neumann problem
[AD-A187451] 10 p1401 N88-18352
Time delays and boundary feedback stabilization in one-dimensional viscoelasticity, appendices A through H
[AD-A187534] 10 p1401 N88-18353
Integral equations with modified fundamental solutions for exterior boundary value problems from electromagnetic wave theory
[ETN-88-91483] 11 p1475 N88-18800
On the dissipative response due to discontinuous strains in bars of unstable elastic material
[AD-A188114] 11 p1498 N88-18947
Spatial-temporal variability of North Pacific sea surface temperature anomaly patterns 11 p1516 N88-19058
Parallel pseudospectral domain decomposition techniques
[NASA-CR-181629] 11 p1524 N88-19101
Estimates of green tensors for certain boundary value problems
[NASA-TT-20203] 11 p1535 N88-19172
Accurate boundary conditions for exterior problems in gas dynamics
[NASA-TM-100807] 11 p1537 N88-19182
Accelerating the computation of steady state solutions for non-equilibrium, chemically reacting flow fields
12 p1625 N88-19724
Mesoscale monitoring of the soil freeze/thaw boundary from orbital microwave radiometry
[NASA-CR-182659] 12 p1645 N88-19855
Error questions in the computation of solution manifolds of parametrized equations
[AD-A188648] 12 p1684 N88-20068
Study of inhomogeneously filled cylindrical resonant cavities by the finite integration technique
[PB88-133707] 12 p1697 N88-20156
Predicting oscillatory finite difference solutions to the heat equation: A comparative study of the coefficient and matrix methods
[AD-A189591] 13 p1825 N88-20911
Convergence of Runge-Kutta methods on classes of stiff initial value problems
[CWI-NM-R8717] 13 p1827 N88-20924
Double layer polarization of nonconducting spheroidal particles and its application to Kerr effect
[ISSN-0208-5658] 13 p1832 N88-20960
Solutions for direct and indirect problems in free surface flows
[REPT-87-35] 14 p1909 N88-21409

Nonlinear normal mode initialization of a limited area model using nonstationary Rossby modes — numerical weather forecasting
[KNMI-WR-87-10] 14 p1947 N88-21614
A spline collocation method for integral equations of the first kind with logarithmic singularity — boundary value problems
[REPT-87-39] 14 p1963 N88-21712
On a class of similarity solutions of the equation u sub t = (absolute value of u sup m-1 u sub x) sub x with m greater than -1
[REPT-87-54] 14 p1963 N88-21713
Some maximum norm estimates for the finite element method applied to nonlinear two dimensional boundary value problems
[ETN-88-91505] 14 p1964 N88-21715
Boundary stabilization of the reaction-diffusion equation with unilateral conditions
[RR-315] 14 p1964 N88-21720
Global spatial periodic solutions to the Ginzburg-Landau equations
[DE88-006424] 15 p2119 N88-22623
Numerical methods for singularly perturbed differential equations with applications
[AD-A189786] 15 p2119 N88-22628
Pointwise stabilization for coupled quasilinear and linear wave equations
[AD-A190031] 15 p2120 N88-22632
Sequential tests for the drift of a Wiener process with a smooth prior and the heat equation
[AD-A190322] 15 p2121 N88-22638
Stopping rules and observed significance levels
[AD-A190320] 15 p2124 N88-22664
Some numerical methods for the computation of capillary free boundaries governed by the Navier-Stokes equations
[REPT-87-69] 16 p2206 N88-23167
Modeling and estimation of a low degree geopotential model from terrestrial gravity data
[NASA-CR-182808] 16 p2232 N88-23330
Continuous decoupling transformations for linear boundary value problems
[ETN-88-92248] 16 p2258 N88-23493
Spectral analysis in the linear geodetic boundary value problem
[B8735056] 16 p2259 N88-23502
Algorithm for accounting the conditions in infinity for two-dimensional magnetostatics problems
[DE88-701673] 16 p2264 N88-23541
Nonlinear wave and diffusion equations
[AD-A191421] 16 p2265 N88-23544
Analysis for fuel implosion in ICF target and pellet gain 16 p2276 N88-23620
Parameter estimation for boundary value problems by integral equations of the second kind
[NASA-CR-181660] 17 p2332 N88-23918
The calculation of transonic flow over the shuttle orbiter using slender body theory 18 p2460 N88-24606
Computation and characteristics of pulsatile multi-bifurcation flow 18 p2483 N88-24729
Nonlinear waves
[AD-A192148] 18 p2510 N88-24889
Duct flow nonuniformities for Space Shuttle Main Engine (SSME)
[NASA-CR-179338] 18 p2511 N88-24899
Advanced development of the boundary element method for elastic and inelastic thermal stress analysis 18 p2529 N88-25002
NFEARS: A nonlinear adaptive finite element solver, part 1
[AD-A191823] 18 p2563 N88-25215
Solving time-dependent two-dimensional eddy current problems
[NASA-TM-100875] 18 p2566 N88-25239
Stability and convergence of the Peaceman-Rachford ADI method for initial-boundary value problems
[CWI-NM-R8724] 18 p2566 N88-25243
On bunch lengthening using the fourth harmonic cavity in the NSLS VUV ring
[DE88-007392] 18 p2574 N88-25288
Characterization of a modified Rijke burner for measurement of distributed combustion 19 p2628 N88-25587
Static analysis of thin plates using the finite strip-element method 19 p2679 N88-25931
Modelling and forecasting deep ocean and near surface mesoscale eddies: Hindcasting and forecasting with, and coupling a surface boundary layer model to, the Harvard quasigeostrophic model 19 p2694 N88-26013
Initial value problems for nonlinear heat equations
[DE88-702021] 19 p2737 N88-26251
Vortex methods for separated flows
[NASA-TM-100068] 20 p2753 N88-26342
Vibration frequencies of tapered bars with nonclassical boundary conditions
[NASA-CR-183059] 20 p2813 N88-26688
Off-boundary approach to the boundary element method
[AD-A192931] 20 p2815 N88-26701
Thermo-viscoelastic analysis of composite materials, volume 1
[NASA-CR-183048-VOL-1] 21 p2904 N88-27230
Investigation of viscous/inviscid interaction in transonic flow over airfoils with suction
[NASA-CR-183112] 21 p2945 N88-27490
Initial boundary value problems of nonlinear wave equations in an exterior domain
[DE88-701883] 21 p3026 N88-27962
Development of direct-inverse 3-D methods for applied transonic aerodynamic wing design and analysis
[NASA-CR-183127] 22 p3037 N88-28033
Optimum-Path-to-Go guidance of command adjusted trajectory projectiles
[AD-A193377] 22 p3040 N88-28051
Non-reflecting boundary conditions for computations of unsteady flows in turbomachines
[PNR90469] 22 p3079 N88-28284
Regularity of solutions for nonlinear degenerate elliptic boundary value problems
[DE88-702646] 22 p3146 N88-28710
The influence of numerical boundary conditions on transonic flow
[DFVLR-FB-88-06] 23 p3172 N88-28890
Computation of the eigenvalues for perturbations of Poiseuille flow using a two-point boundary value method
[AD-A193479] 23 p3210 N88-29104
Nonlinear dynamic analysis and optimal control of shallow shells 23 p3224 N88-29191
Thickness effects on the stability of shell like structures 23 p3224 N88-29192
Stability of semidiscrete approximations for hyperbolic initial-boundary-value problems: Stationary modes
[NASA-TM-100994] 23 p3270 N88-29455
Canonical forms in the control of DPS
[AD-A194671] 23 p3270 N88-29461
Stability and convergence in the numerical solution of stiff initial value problems
[B8681480] 23 p3272 N88-29474
Nonlinear elliptic problems with critical exponent in shrinking annuli
[W-02/87] 23 p3273 N88-29477
Elliptic equations with nearly critical growth
[W-16-87] 23 p3273 N88-29478
The acoustic field scattered from some approximate pressure release materials
[AD-A194768] 23 p3278 N88-29515
Theory of filtering and control with application to control of large space structures
[AD-A195500] 24 p3335 N88-29851
Initial value problems in viscoelasticity
[AD-A196052] 24 p3382 N88-30145
Stability, stochastic stationarity and generalized Lyapunov equations for two-point boundary-value descriptor systems
[AD-A195645] 24 p3425 N88-30385
Multiple solutions and bifurcation for a class of nonlinear Sturm-Liouville eigenvalue problems on an unbounded domain
[AD-A195954] 24 p3426 N88-30389

BOW SHOCK WAVES
U BOW WAVES
U SHOCK WAVES

BOW WAVES
Slow-mode shocks in the earth's magnetosphere
[DE88-000483] 04 p0468 N88-12895
On the numerical simulation of three-dimensional hypersonic flow 05 p0532 N88-13237
The off-design performance of hypersonic waveriders 05 p0533 N88-13244
AMPTE-UKS ion observations at a quasi-parallel bow shock 08 p1095 N88-16589
On the start up of supersonic underexpanded jets — Mach disks 11 p1435 N88-18563
To what extent is mass loading responsible for the Venus bowshock precursor?
[NASA-TM-89307] 12 p1711 N88-20239
The foreshock region upstream from the Comet Halley bow shock 14 p1995 N88-21893

BOX BEAMS
Design procedures for fiber composite box beams
[NASA-TM-100296] 09 p1133 N88-16828

BOXES (CONTAINERS)
Cage mode propagation experiments
[AD-A186019] 07 p0841 N88-15100
FEB (Multifilter Electronics Box) lifting device analysis, revision A
[AD-A192313] 21 p2935 N88-27427

BRACKETS
Mechanical design of the ac bracket package for the RETE experiment
[IFSI-87-4] 05 p0555 N88-13379
Partially braced inelastic beam buckling experiments
[PB87-133831] 06 p0723 N88-14444
Locking hinge
[NASA-CASE-MSC-21056-1] 17 p2312 N88-23827

BRAGG ANGLE
Distributed feedback effects in lasers and high gain laser instabilities in optically pumped CH3F 03 p0329 N88-12079
Models for electromagnetic scattering from the sea at extremely low grazing angles
[AD-A190472] 15 p2057 N88-22261

BRAIN
NT CEREBELLUM
NT CEREBRAL CORTEX
NT CEREBRUM
NT HIPPOCAMPUS
NT HYPOTHALAMUS
NT THALAMUS
Latency differences and effects of selective attention to gratings in the central and right visual fields: 2
[DE87-014730] 04 p0473 N88-12918
Influence of general vertical vibration on relationships between mediators in various segments of brain 06 p0751 N88-14613
Dimensional analysis of nonlinear oscillations in brain, heart and muscle
[DE87-014749] 06 p0751 N88-14614
Model based monitoring of human sleep stages
[ISBN-90-9001448-9] 06 p0752 N88-14618
Brain morphogenesis in rats developing in weightlessness 07 p0894 N88-15415
Evoked brain activity and personnel performance
[AD-A185922] 07 p0897 N88-15436
Neurochemical changes in hibernation 08 p1046 N88-16322
Effects of extreme hypoxia on phospholipid metabolism in subcellular structures of rat brain 08 p1046 N88-16323
Late radiation damage in bone, bone marrow and brain vasculature, with particular emphasis upon fractionation models
[DE87-753039] 08 p1048 N88-16330
Changing the layers of mind
[AD-A186648] 08 p1052 N88-16350
An innovative workstation 08 p1063 N88-16421
Knowledge representation by connection matrices: A method for the on-board implementation of large expert systems 08 p1065 N88-16434
Probabilistic neural networks: In or out of equilibrium
[DE88-002907] 09 p1201 N88-17198
Development and experimentation of an eye/brain/task testbed 09 p1205 N88-17219
Effect of exogenous cardiosynchronized counterpulsation on human regional and central hemodynamics 10 p1366 N88-18163
Center for nonlinear dynamics of the brain
[AD-A187245] 11 p1518 N88-19068
Three-dimensional computer graphics brain-mapping project
[AD-A187202] 11 p1528 N88-19126
Effects of intense, time-constrained mental effort on hemodynamics and cardiovascular function 12 p1664 N88-19975
Protection from stress 12 p1664 N88-19978
Risk of hypertension and functional cerebral laterality in oil expedition works in far north 12 p1665 N88-19980
Brain activity during tactical decision-making. Part 2: Probe-evoked potentials and workload
[AD-A188688] 12 p1667 N88-19994
Neurocognitive predictions of performance
[AD-A188323] 12 p1669 N88-19998
Neurophysiological predictors of quality of performance 16 p2242 N88-23391
The event-related brain potential as an index of information processing and cognitive activity: A program of basic research
[AD-A191244] 16 p2243 N88-23400
Role of opioid peptides in pathogenesis of vestibulovegetative disorders 19 p2704 N88-26079
Effect of low-frequency whole-body vertical vibration on the serotoninergic system of the brain and spinal cord 19 p2704 N88-26081
Effect of weightlessness on brain development (results of flight of pregnant rats on Kosmos-1514 biosatellite and study of subsequent development of their progeny on earth 20 p2829 N88-26786
Studies of the intact human brain: Implications for performance 21 p2977 N88-27684
CEEG dynamic brain mapping: A new method to evaluate brain function in different psychological and drug conditions 21 p2977 N88-27685
Fourth generation neurocognitive pattern analysis system 21 p2977 N88-27686

Normative developmental equations for the EEG and their sensitivity to neurological and psychiatric disorders
21 p2977 N88-27687
Squid instrumentation for neuromagnetic study of complex brain activity
21 p2978 N88-27691
Electric and magnetic brain activity related to cognitive performance
21 p2979 N88-27692
Neuromagnetic evidence of place mechanisms for frequency and intensity coding in the human auditory cortex
21 p2979 N88-27693
A study of sources in the human brain associated with stereopsis
21 p2979 N88-27695
Event-related brain potentials as indices of mental workload and attentional allocation
21 p2979 N88-27696
Using ERPS to study human information processing
21 p2980 N88-27698
Cognitive task demands as reflected in physiological measures
21 p2980 N88-27699
The effect of endogenous alpha on hemispheric asymmetries and the relationship of frontal theta to sustained attention
21 p2980 N88-27701
Fighter pilot performance during airborne and simulator missions: Physiological comparisons
21 p2981 N88-27704
Event-related and steady potential changes in the brain related to workload during tracking
21 p2981 N88-27705
EEG indices of G-induced Loss Of Consciousness (G-LOC)
21 p2982 N88-27709
Motion evoked vestibular potentials
21 p2982 N88-27712
The effect of mild hypoxia on the vestibular evoked response
21 p2982 N88-27713
An approach to studying the effects of psychostimulants on cerebral electrical activity in the non-human primate
21 p2983 N88-27716
Spontaneous cerebral electrical activity during prolonged hypoglycemia: A quantitative study in humans
21 p2983 N88-27717
Correlation between EEG abnormal activity and aircraft accidents: A long term observation
21 p2984 N88-27719
Cognitive and neural bases of skilled performance
[AD-A193392] 21 p2992 N88-27747
Content-addressable memory storage by neural networks: A general model and global Liapunov method
[AD-A192716] 21 p3002 N88-27807
New method for the study of spontaneous brain activity
[AD-A193813] 22 p3132 N88-28624
SQUID (superconducting quantum interference device) arrays for simultaneous magnetic measurements: Calibration and source localization performance
[AD-A193815] 23 p3216 N88-29143
Methods and instrumentation for biomagnetism
[AD-A193811] 23 p3239 N88-29278
Design of a feeling-thinking machine
[AD-A194107] 23 p3267 N88-29448
Central adrenergic receptors as mediators of central response to stress: Study with Positron Emission Tomography (PET)
[AD-A194947] 24 p3407 N88-30284

BRAIN CIRCULATION

Fast dynamic studies with PC384-7B; system improvements and development of an automated blood sampling system — tomography
[USIP-87-05] 01 p0075 N88-10481
Studies of the processing of single words using positron tomographic measures of cerebral blood flow change
[AD-A184058] 03 p0356 N88-12244
Change in functional activity of cortical brain structures and their blood supply in alert rabbits in response to rocking
04 p0473 N88-12916
Circulatory response of males 45-52 years of age to antiorthostatic hypokinesia
07 p0894 N88-15416
Models of cerebral-body perfusion and cerebral chemical transport
[AD-A194945] 24 p3407 N88-30283

BRAIN DAMAGE

Neuropeptides in experimental head injury
[AD-A186067] 11 p1520 N88-19077
Three-dimensional computer graphics brain-mapping project
[AD-A187202] 11 p1526 N88-19126

BRAKES

Preloaded brake disc
[NASA-CASE-MSC-21132-1] 23 p3223 N88-29181

BRAKES (FOR ARRESTING MOTION)

NT AIRCRAFT BRAKES
NT DRAG CHUTES
NT LEADING EDGE FLAPS
NT TRAILING EDGE FLAPS
NT VORTEX FLAPS
NT WING FLAPS

Developing an accelerated endurance test for greases: A status report
[AD-A185963] 07 p0836 N88-15072
Aerodynamic and thermal modeling of electromagnetic brakes. Evaluation of convective exchange coefficients and friction losses in the rough wall channels
[ISAL-ITC1-87-02] 16 p2215 N88-23214

BRAKING

Flaps-up takoff performance of the OV-1D aircraft with YT53-L-704 engine installed
[AD-A185960] 07 p0819 N88-14979

BRANCHING (MATHEMATICS)

NT PERIOD DOUBLING
Fully developed turbulence via Feigenbaum's period-doubling bifurcations
[DE88-000242] 04 p0441 N88-12739
Application of the Von Karman equation to the bifurcation theory
[NOTA-INTERNA-891] 05 p0642 N88-13927
Transient periodic behavior related to a saddle-node bifurcation
[ETN-88-91321] 05 p0642 N88-13928
Tutorial on elementary bifurcation theory
[DE87-014849] 05 p0642 N88-13932
Subcritical branching processes in a two state random environment, and a percolation problem on trees
[PB87-230439] 06 p0762 N88-14677
Global bifurcation of periodic solutions with symmetry
[AD-A185881] 07 p0908 N88-15501
Local bifurcation control
[AD-A187435] 10 p1324 N88-17915
Joint moments of the maximum in a critical branching process
[AD-A188157] 11 p1541 N88-19209
Problems in fluid dynamics
[NASA-CR-182678] 14 p1909 N88-21410
Bifurcations in unsteady aerodynamics-implications for testing
[NASA-TM-100083] 15 p2015 N88-22014
Symmetry and global bifurcation in nonlinear solid mechanics
[AD-A190521] 15 p2121 N88-22642
Research in nonlinear partial differential equations and bifurcation theory
[AD-A190986] 16 p2260 N88-23514
Generalized Jordan chains and two bifurcation theorems of Krasnoselskii
[AD-A192353] 21 p3008 N88-27845
Bifurcations of periodic solutions of non-integrable Hamiltonians with two degrees of freedom: Numerical and analytical results
[DE88-702747] 23 p3272 N88-29473

BRANCHING (PHYSICS)

W decays
[NOTA-INTERNA-877] 05 p0648 N88-13966
The numerical and analytical study of bifurcation and multicellular flow instability due to natural convection between narrow horizontal isothermal cylindrical annuli at high Rayleigh numbers
10 p1328 N88-17937
Systematics on neutron-induced isomeric cross-section ratios at 14.5 MeV
[ECN-200] 14 p1980 N88-21815
Gluino branching ratio effects on the search for supersymmetry
[PREPRINT-572] 14 p1981 N88-21821

BRASSES

Analysis of free cutting brass by A.C. polarography
[PD-MT-8728] 04 p0417 N88-12587
Materials dependence of deformation texture development in various deformation modes
[DE88-004312] 14 p1922 N88-21457

BRAVAIS CRYSTALS

Equilibria, lattices and chaotic dynamics of point vortices
04 p0444 N88-12758

BRAYTON CYCLE

The Goddard Space Flight Center mechanical cooler program
08 p0983 N88-15944
Design features of small Brayton cycles for autonomous underwater vehicles
[AD-A187799] 11 p1506 N88-18999
Gas-cooled reactor power systems for space
[DE88-005220] 11 p1545 N88-19240
Comparison of entropy generation and conventional design methods for heat exchangers
[AD-A190256] 15 p2064 N88-22306
Speculations on future opportunities to evolve Brayton powerplants aboard the space station
17 p2396 N88-24258
Characteristics of the closed Brayton cycle for dynamic isotope power systems
17 p2422 N88-24401
Dynamic isotope power system critical component verification
17 p2425 N88-24421
SNAP-DYN: Proven technology for wear-term, higher power in space
17 p2425 N88-24422
The closed Brayton cycle: An energy conversion system for near-term military space missions
17 p2435 N88-24488
The effect of operating temperature and turbine blade cooling on Brayton cycle space power systems
17 p2435 N88-24489
A combined Rankine/Brayton pulse power cycle
17 p2435 N88-24490
Energy conversion system optimization study for multimegawatt space nuclear power application
17 p2436 N88-24492
Advanced energy system program
[PB88-183025] 19 p2686 N88-25965

BRAZIL

Impacts of world development on selected characteristics of the atmosphere: An integrative approach. Volume 1: Main report
[DE88-001495] 07 p0875 N88-15309
Actual performance and economic feasibility of residential solar water heaters
[INPE-4399-RPE/555] 08 p1023 N88-16191
Conditions and mechanisms of the process of technological innovation in Brazil: The role of research institutes
[INPE-4175-TDL/274] 11 p1567 N88-19383
Crop forecasting in Brazil: A short history of productivity models
[INPE-4150-PRE/1056] 12 p1637 N88-19801
Mapping of the mangroves of the Guanabarra Bay through the utilization of remote sensing techniques
[INPE-3942-TDL/229] 12 p1637 N88-19804
High altitude chemical release systems for project BIME (Brazilian Ionospheric Modification Experiments) project IMS (Ionospheric Modification Studies) project PIIE (Polar Ionospheric Irregularities Experiment) project polar arcs
[AD-A188299] 12 p1642 N88-19833
The use of a barotropic finite element model for the study of circulation on the continental shelf of the southeast coast of Brazil
[INPE-4401-PRE/1218] 13 p1802 N88-20774
Radon-222 in the Antarctic Peninsula
[INPE-4486-PRE/1251] 15 p2092 N88-22468
The necessity of automation in Brazil
[INPE-4346-PRE/1183] 15 p2150 N88-22832
The 1985 mutual phenomena of Jupiter's satellites observed in Brazil
[INPE-4526-PRE/1276] 15 p2152 N88-22848

BRAZILIAN SPACE PROGRAM

BRASILSAT A2: Ground and in-orbit anomalies
02 p0164 N88-11032
Vehicle glow observed on the SONDA 3
[INPE-4297-PRE/1168] 12 p1600 N88-19581
Multilayer thermal insulation tests
[INPE-4475-PRE/1243] 12 p1626 N88-19729
Report of the participation in the International Training Course: Remote Sensing in Village Forestry
[INPE-4476-NTE/278] 12 p1637 N88-19802
Solar cell experiment on the first satellite of the Brazilian complete space mission
[INPE-4248-PRE/1121] 14 p1880 N88-21238
INPE position paper on the CCSDS standardized method of link budget computation
[INPE-4533-NTE/279] 15 p2148 N88-22820

BRAZING

Process and equipment capabilities materials joining laboratory, 1987
[DE87-014534] 02 p0180 N88-11122
Low-pressure eutectic bonding of depleted uranium to copper
[DE87-014625] 02 p0181 N88-11128
Investigation on diffusion reaction brazing of aluminium
[PB87-143368] 08 p0992 N88-16001
Transmission electron microscopy studies of titanium-containing braze/alumina seals
[DE88-005243] 10 p1303 N88-17792
Technology for pressure-instrumented thin airfoil models
[NASA-CR-4173] 23 p3180 N88-28933

BREADBOARD MODELS

Design, manufacture and testing of an elegant breadboard model communications processor
[D/2244] 01 p0034 N88-10217
Coherent infrared detection, volume D — CO2 laser intersatellite data link
[ESA-CR(P)-2392-VOL-2] 01 p0034 N88-10219
Microprocessor control and networking for the amps breadboard
07 p0924 N88-15615
High-resolution Real-Time Radiography (RTR) system design
[AD-A187107] 09 p1166 N88-16992
Design of a linear actuator and breadboard test result — far IR telescope
14 p1877 N88-21217
Docking/berthing subsystem: Design and breadboard test
14 p1879 N88-21233

Mid infrared multichannel focal plane breadboard --- pushbroom sensors
[RT-87/014] 14 p1982 N88-21827
Nondestructive evaluation of large scale composite components
[AD-A190998] 16 p2173 N88-22954
Botany Facility. Thermal Control (TC) subsystem test report on experiment container of laboratory model and breadboard centrifuge
[BF-TN-ER-061/86] 17 p2378 N88-24135
Botany Facility: Test report on breadboard tests for the determination of the heat transfer at the glass disk and of the temperature distribution in the fluorescent tube
[BF-TN-ER-053] 17 p2378 N88-24136
Botany Facility: Breadboarding results of the illumination system
[SIRA-A/7373/WP110/MAC003] 17 p2378 N88-24137
MSAT mobile electronically steered phased array antenna development 19 p2647 N88-25711
AC power system breadboard
[NASA-CR-179369] 22 p3049 N88-28091
Biosample: Preservation, handling and observation system synthesis and breadboarding --- Spacelab
[ESA-CR(P)-2609] 24 p3336 N88-29857
Breadboard RL10-2B low-thrust operating mode (second iteration) test report
[NASA-CR-182160] 24 p3338 N88-29867
The dc power control for a liquid-fed resistojet
[NASA-TM-101326] 24 p3338 N88-29869

BREAKAWAY
U BOUNDARY LAYER SEPARATION

BREAKDOWN
Dependence of acoustical characteristics of laser-induced breakdown in dielectric materials on shape of inelastic region 06 p0774 N88-14753

BREAKERS (ELECTRIC)
U CIRCUIT BREAKERS

BREAKING
Buckling and breakdown problems in structural mechanics. Failure of prestressed double-walled containers or rings
[MBB-UR-E-956/87] 13 p1783 N88-20671
Stress corrosion evaluation of powder metallurgy aluminum alloy 7091 with the breaking load test method 22 p3053 N88-28115

BREAKWATERS
Breaking wave forces on vertical cylinders
[RR-CE71] 03 p0338 N88-12126
Technology Reports of Kyushu University, volume 61, no. 2
[ISSN-0023-2718] 16 p2256 N88-23485

BREATHING
Life in a hyperbaric environment. A new O2-H2 breathing mixture for industrial diving 19 p2695 N88-26019

BREATHING APPARATUS
NT OXYGEN MASKS
Summary report of the history and events pertinent to the Civil Aeromedical Institute's evaluation of providing smoke/fume protective breathing equipment for airline passenger use
[AD-A184499] 03 p0261 N88-11645
A plethysmograph for measuring pulmonary ventilation in small animals
[AD-A184978] 05 p0629 N88-13846
Man rating the b-1B molecular sieve oxygen generation system
[AD-A186275] 07 p0899 N88-15447
Acute mountain sickness at 4500 m is not altered by repeated eight-hour exposures to 3200-3550 m normobaric hypoxic equivalent
[AD-A188358] 12 p1666 N88-19990
Study of benefits of passenger protective breathing equipment from analysis of past accidents
[DOT/FAA/CT-88/03] 18 p2461 N88-24610

BRECCIA
Abundance and distribution of ultramafic microbreccia in Moses Rock Dike: Quantitative application of AIS data 05 p0613 N88-13766

BREEDER REACTORS
NT EXPERIMENTAL BREEDER REACTOR 2
NT LIQUID METAL FAST BREEDER REACTORS
Three dimensional Monte Carlo simulation of molecular movement and heat radiation in vacuum devices: Computer code MOVAK3D --- fusion reactors
[KFK-4292] 09 p1246 N88-17471
Outlook for the fusion hybrid and tritium-breeding fusion reactors
[PB88-149281] 13 p1843 N88-21029
Development of fast breeder reactors in China 16 p2186 N88-23032

BREMSSTRAHLUNG
Generating soft X-ray spectra using the SPEED pentaxial diode
[DE87-013591] 01 p0098 N88-10647
LLE Review, volume 30
[DE87-014469] 02 p0178 N88-11109
The Hermes-3 program
[DE87-012132] 02 p0234 N88-11473
The nature of beamstrahlung
[DE87-012837] 02 p0234 N88-11474
Relativistic plasma concentration measuring by Bremsstrahlung
[DE88-700560] 07 p0936 N88-15685
Spectrophotometric remote sensing of the diffuse aurora
[AD-A188599] 12 p1643 N88-19837
Measurements of Z(sub eff) profile with a visible bremsstrahlung continuum detector array 17 p2443 N88-24529
Spectral modelling of the soft gamma ray repeater
[DE88-007027] 17 p2453 N88-24570
Intense ion beam diagnostics for particle beam fusion experiments on PBFA 2
[DE88-007279] 18 p2577 N88-25308
Bremsstrahlung from high Z impurities in hot plasmas
[DE88-011755] 20 p2861 N88-26994
Proof of the feasibility of coherent and incoherent schemes for pumping a gamma-ray laser
[AD-A193856] 23 p3220 N88-29165
X- and gamma-ray background observations in Antarctic
[INPE-4583-PRE/1317] 24 p3459 N88-30578

BRIDGES (STRUCTURES)
The effect of mass, wind angle and erection technique on the aeroelastic behaviour of a cable-stayed bridge model
[NAE-AN-46] 04 p0455 N88-12819
Design and implementation of the ESL compact range underhung bridge crane
[NASA-CR-182396] 07 p0862 N88-15231
Deformation induced cracking in steel girder bridges and retrofit guidelines
[PB88-102710] 07 p0868 N88-15265
Dynamic analysis of plane frames by microcomputer 11 p1531 N88-19143
Propagation modeling for land mobile satellite systems 19 p2645 N88-25694
Multi-metallic galvanic corrosion
[AD-A195995] 24 p3353 N88-29963

BRIDGMAN METHOD
Numerical analysis of Marangoni convection in Bridgman method 03 p0319 N88-12014
MCT crystal growth
[NASA-CR-179297] 11 p1557 N88-19318
Analysis of low gravity tolerance of model experiments for space station: Preliminary results for directional solidification
[NASA-CR-182657] 12 p1614 N88-19648

BRIGHTNESS
Compact electron storage rings
[DE87-013301] 02 p0234 N88-11477
Eyesight trainer for pilots 03 p0355 N88-12239
The closest solar analogs in the bright star catalogue 04 p0506 N88-13110
Performance characteristics of magnesium-sodium nitrate flares in oxygen-nitrogen atmospheres
[AD-A185274] 05 p0570 N88-13476
AIS-2 spectra of California wetland vegetation 05 p0613 N88-13763
Monte Carlo method calculation of spectral brightness coefficient of vegetation cover as function of illumination conditions 08 p1008 N88-16113
Bright source lasers and experiments at very high irradiance
[DE88-004317] 10 p1337 N88-17988
Relaxing the brightness constancy assumption in computing optical flow
[AD-A187437] 10 p1410 N88-18410
An attempt to measure the diffuse brightness of the sky at submillimeter wavelengths 12 p1710 N88-20233
Research on influence of individual sea water components on spectral brightness coefficient of outgoing radiation 13 p1785 N88-20682
IUE program SUGSD: Varability time scale of H Ly-alpha from Uranus
[NASA-CR-182706] 13 p1856 N88-21107
The absolute total magnitudes of periodic comets and their variations 14 p1994 N88-21887
Comparison of active regions on the nucleus of Comet Halley 14 p2004 N88-21948
Comparison of Halley's monochromatic comae with others 14 p2006 N88-21965
Dynamic properties of human brightness perception
[ETN-88-92243] 16 p2238 N88-23366
Generation of high brightness ion beam from insulated anode PED 16 p2278 N88-23637
Study on the flashover ion diode with cryogenic anode 16 p2279 N88-23642
Dust and C2-contents in the coma of Halley's Comet (1986III) 16 p2288 N88-23697
Mapping soil and rock variation from satellite images in the Sahel 17 p2354 N88-24023
Space station contamination study: Assessment of contaminant spectral brightness 18 p2591 N88-25395
Apparent brightness of stars and lasers 22 p3065 N88-28188
Preliminary analysis of recent 2.2-4.2 micrometers telescopic observations of Elysium, Mars: Implications for crystallinity and hydration state of surface materials 23 p3306 N88-29692
Astron observations of supernova 1987A in large magellanic cloud 24 p3445 N88-30504

BRIGHTNESS DISCRIMINATION
Laser flash effects on chromatic discrimination in monkeys
[AD-A187703] 11 p1517 N88-19061

BRIGHTNESS DISTRIBUTION
Observations of the brightness temperature distribution of the quiet solar corona at decametric wavelengths 01 p0114 N88-10729
Doppler snapshots 04 p0508 N88-13125
Application of correlation method of reception of direct and reflected cosmic radiation to study of plasmaspheres of planet and distribution of radiation brightness 08 p1004 N88-16085
Comparative analysis of ultraviolet observations of Halley's comet on ASTRON astrophysical station before and after perihelion 08 p1004 N88-16086
Some periodicities in motion of Halley's Comet relative to center of mass 13 p1726 N88-20324
Spectral reflective characteristics of sea surface 13 p1784 N88-20676

BRIGHTNESS TEMPERATURE
Observations of the brightness temperature distribution of the quiet solar corona at decametric wavelengths 01 p0114 N88-10729
Mars: High resolution VLA observations at wavelengths of 2 and 6 cm and derived properties 06 p0804 N88-14909
LANDSAT thematic mapper radiometric calibration study
[NASA-CR-182410] 07 p0872 N88-15287
Statistical studies of low frequency oscillations in satellite-observed stratospheric temperatures 10 p1353 N88-18086
Mesoscale monitoring of the soil freeze/thaw boundary from orbital microwave radiometry
[NASA-CR-182659] 12 p1645 N88-19855
Validate algorithms for the determination of rainfall rates from SSM/I microwave satellite imagery
[AD-A188769] 16 p2233 N88-23337
The NBS scale of radiance temperature 17 p2328 N88-23897

BRILLOUIN EFFECT
Stimulated Mandelstam-Brillouin scattering during forward scattering of light 08 p1078 N88-16499
Brillouin scattering from collective spin waves in magnetic superlattices
[DE88-005347] 12 p1697 N88-20154
Phase preservation cleanup in a double-pass Raman amplifier SBS (Stimulated Brillouin Scattering) conjugator
[AD-A189428] 13 p1761 N88-20536
Experimental studies of elastic properties of crystals by Brillouin scattering
[DE88-005923] 14 p1986 N88-21848
Brillouin scattering and transmission electron microscopy studies of radiation-induced elastic softening, disordering and amorphization of intermetallic compounds
[DE88-005927] 14 p1987 N88-21850
Computer modeling of time dependent SBS (Stimulated Brillouin Scattering) in two and three dimensions
[DE88-008922] 19 p2720 N88-26150

BRILLOUIN ZONES
Positron-annihilation 2D-ACAR studies of disordered and defected alloys
[DE88-003118] 10 p1416 N88-18454
Center for thin film studies
[AD-A191996] 19 p2732 N88-26226
Calculation of far infrared absorption in B poly(dA).poly(dT)
[AD-A193128] 21 p2918 N88-27318

BRINES
Porosity influence on the strength and elasticity of first-year sea ice
[AD-A184493] 03 p0354 N88-12233
Geochemistry of freezing brines, low-temperature properties of sodium chloride
[AD-A185751] 06 p0680 N88-14168
The effect of H2S concentration and pH on hydrogen permeation in AISI 410 stainless steel in 5 percent NaCl
[NPL-DMA(A)-148] 14 p1890 N88-21293

The effect of H2S concentration and pH on the cracking resistance of AISI 410 stainless steel in 5 percent brine
[NPL-DMA(A)-149] 14 p1890 N88-21294

BRITISH COLUMBIA
Longer-duration post-frontal precipitation at Vancouver International Airport, 1953-1983
02 p0203 N88-11269

BRITTLE MATERIALS
Strength and toughness of a brittle material
[VTT-RR-479] 09 p1183 N88-17089
A fractal analysis of brittle fracture
[AD-A188334] 12 p1635 N88-19788
Bimodular behavior and crack closure in compression in a brittle material
[AD-A191267] 18 p2224 N88-23275
Loading rate sensitivity of open hole composites in compression
[NASA-TM-100834] 19 p2610 N88-25490
Size effects in linear elastic fracture mechanics
21 p2964 N88-27609

BRITTLENESS
A probabilistic model of brittle crack formation
[AD-A184423] 03 p0338 N88-12129
Effects of stress-relieving on the mechanical properties and the structure of specimens of high-temperature fine-grained structural steels heat-treated to simulate welding
[BLL-CE-TRANS-8258-(9022.09)]
04 p0417 N88-12586
Evaluation method of the brittle fracture strength in structurally stress-concentrated regions
[PB87-129490] 06 p0721 N88-14435
New mechanism of the high temperature (reversible) temper brittleness of alloy steels
[PB87-143954] 07 p0833 N88-15056
The development of test methodology for testing glassy materials 07 p0927 N88-15633
Some aspects of the mechanics and mechanisms of dynamic brittle fracture 10 p1343 N88-18028
Brittle to ductile transition to cleavage fracture
[DE88-004074] 10 p1420 N88-18481
A fractal analysis of brittle fracture
[AD-A188334] 12 p1635 N88-19788
A study of the dynamics of high temperature brittle intergranular fracture by acoustic emission
[AERE-R-12479] 13 p1780 N88-20650
Guidelines for estimation and characterization of the thermo-mechanical properties of new optical materials
[DE88-004359] 13 p1840 N88-21010
The Nordic J-R curve round robin test program --- reactor steel
[VTT-RR-510] 14 p1923 N88-21459
High-performance polymeric materials
[AD-A190708] 15 p2046 N88-22190
Strength and microstructure of ceramics
[AD-A190712] 15 p2046 N88-22191
Fracture technology for brittle materials
15 p2083 N88-22417
Bimodular behavior and crack closure in compression in a brittle material
[AD-A191267] 18 p2224 N88-23275
Some design considerations for ceramic components in heat engine applications 17 p2323 N88-23875
Rapidly solidified lightweight durable disk material
[AD-A191697] 18 p2491 N88-24775
Self-consistent model for the brittle response of solids
18 p2528 N88-24999
Ductile-brittle transition of cutting behavior in diamond turning of single crystal Si
[DE88-008890] 20 p2809 N88-26664

BROADBAND
Design and analysis of a broadband TM(sub 01) mode generator in cylindrical waveguide
[DE87-011308] 01 p0036 N88-10243
Experiments: Test range facilities, part 2
03 p0305 N88-11921
Lewis Information Network (LINK): Background and overview
[NASA-TM-100162] 03 p0305 N88-11925
NBS (National Bureau of Standards) wideband sampling wattmeter
[PB87-210324] 03 p0323 N88-12041
Band 2 VHF antenna for home construction
[BBC-RD-1987/13] 04 p0432 N88-12677
Broadband linear polarization and chromospheric CaII H and K line emission in late-type main sequence stars
04 p0511 N88-13140
Application of Vandermonde decomposition to directional and modal analysis of broadband transients
[AD-A185007] 05 p0646 N88-13956
A study of rotor broadband noise mechanisms and helicopter tail rotor noise 06 p0777 N88-14766
Design, production, and characterization of broadband optical waveguides
[DFVLR-FB-85-52] 06 p0780 N88-14791
Determination of cloud base height and emissivity from downwelling angular radiances
[AD-A185985] 07 p0879 N88-15331
Estimation of broadband planetary albedo from operational narrowband satellite measurements
[PB88-107844] 07 p0945 N88-15748
Crosstalk analysis of a broadband data communications system
[DE88-003652] 09 p1156 N88-16927
Signal processing for an optical wide band data transmission system
[DE88-003854] 10 p1319 N88-17888
Wide band data transmission system using optical fibers
[DE88-004555] 10 p1319 N88-17889
The design of impedance- matching networks for broadband antennas
[AD-A187600] 10 p1320 N88-17895
Low-noise cryogenically cooled broad-band microwave preamplifiers
[DE88-004561] 10 p1324 N88-17912
Nonlinear optics with broad-band lasers
[DE88-005026] 10 p1337 N88-17992
CARS measurements of combustion. 2: Gas species concentration measurements
[NAL-TR-940] 11 p1453 N88-18663
Distortion of wideband carbon dioxide laser radar waveforms due to atmospheric dispersion and absorption
[AD-A188687] 12 p1632 N88-19771
Bragg-cell receiver study
[NASA-CR-182684] 13 p1761 N88-20535
Broadband correlation analysis
[AD-A188732] 13 p1814 N88-20839
Optimal and conventional space-time processing in flow noise
[AD-A189104] 13 p1833 N88-20965
New wide-band transducer developed
14 p1901 N88-21353
Nonlinearly tunable wideband emission of infrared radiation by Al2O3:Ti laser 14 p1970 N88-21758
A very wide frequency band pulsed/IF radar system
[NASA-CR-182669] 16 p2190 N88-23059
A mixed-modem solution for sensitive data segregation on a broadband network
[DE88-001765] 19 p2718 N88-26139
Approximations and optimal control for the pathwise average cost per unit time and discounted problems for wideband noise driven systems
[AD-A192712] 21 p3008 N88-27847
SERI standard broadband format: A solar and meteorological data archival format
[DE88-001145] 21 p3028 N88-27975
Effects of tectonic release on broadband regional distance bodywaves
[AD-A194247] 22 p3119 N88-28529
On broadband matching of multiport electrical networks with applications
[AD-A194224] 23 p3207 N88-29086
The effect of equatorial ionospheric irregularities on the performance of a south-looking OTH-B (Over-The-Horizon-Backscatter) radar
[AD-A195090] 24 p3362 N88-30018
Scattering impulse response synthesis using random noise illumination: Initial concept evaluation
[AD-A195086] 24 p3364 N88-30034
A fiber optic beamforming processor for wideband direction finding
[AD-A194862] 24 p3428 N88-30404
Ultra-wideband direction finding using a fiber optic beamforming processor
[AD-A194861] 24 p3430 N88-30413

BROADBAND AMPLIFIERS
Wide band gyrotron traveling wave amplifier analysis
[AD-A194269] 23 p3216 N88-29139

BROADCASTING
Monitoring of harmful interference to the HF (High Frequency) broadcasting service. 3: Results of the June 1986 coordinated monitoring period
[PB87-210274] 01 p0036 N88-10229
HF (High Frequency) broadcasting planning model: A comparison of two versions
[PB87-210282] 01 p0036 N88-10230
The criterion of equal integrated quality: An improved method of planning DBS systems
[BBC-RD-1987/10] 02 p0161 N88-11012
Theory and methods for design of pulse shapes for broadcast teletext
[CRC-1405] 02 p0162 N88-11013
Band 2 VHF antenna for home construction
[BBC-RD-1987/13] 04 p0432 N88-12677
Improvements to a UHF rebroadcast television link suffering tidal fading: Countisbury UHF relay station
[BBC-RD-1987/14] 05 p0573 N88-13495
SAHAYOG: A testbed for load sharing under failure
[AD-A186615] 08 p1069 N88-16460
The assessment of the sound insulation requirements for a large broadcasting studio, using a scale model: Theoretical considerations
[BBC-RD-1987/20] 09 p1155 N88-16921
Experimental Radio Data System (RDS): A survey of reception reliability in the UK
[BBC-RD-1987/17] 09 p1155 N88-16922
Future television systems: Comparison of sequent ial and interlaced scanning
[BBC-RD-1987/18] 09 p1155 N88-16923
User's guide for the HF (High Frequency) broadcast antenna design and validation summary programs
[PB88-116124] 10 p1317 N88-17875
The assessment of the sound insulation requirements for a large broadcasting studio, using a scale model: Practical details
[BBC-RD-1987/21] 10 p1318 N88-17878
Complementary satellite sound broadcasting systems: A NASA assessment for the Voice of America
[NASA-TM-100300] 10 p1321 N88-17899
Role of broadcasting in multiprocessor systems
10 p1374 N88-18201
Datacast: The transmission system
[BBC-RD-1988/1] 14 p1905 N88-21385
Performance study of a unipole antenna with conventional and elevated radial wire ground screens
[AD-A193283] 21 p2933 N88-27413

BROKEN SYMMETRY
Abrikosov vortex motion and elementary pinning force in a SNS Josephson junction
[DE87-013607] 01 p0105 N88-10683
Spontaneous symmetry breaking in N=2 supergravity
[DE87-702749] 01 p0109 N88-10704
Spontaneous symmetry breaking in N=3 supergravity
[DE87-702753] 01 p0109 N88-10705
A mechanism for symmetry breaking in antiferromagnetic Heisenberg systems
[ETN-88-91320] 05 p0657 N88-14031
Breaking of supersymmetry degeneracy and phenomenological conditions
[PREPRINT-559] 06 p0790 N88-14843
Chiral symmetry breaking in finite quantum electrodynamics
[DE88-700860] 12 p1699 N88-20169
Diffraction theory in QCD and beyond
[DE88-005958] 13 p1837 N88-20992
Measurement of the sup 4He(gamma, p)sup 3H total cross section and charge symmetry
[NOTA-INTERNA-902] 14 p1981 N88-21820
Research in theoretical particle physics
[DE88-008230] 20 p2851 N88-26927

BROMIDES
NT POTASSIUM BROMIDES
Technical evaluation of a solar-powered absorption cooling system (LiBr-H2O)
[PB87-108254] 04 p0463 N88-12867
Organic metal (ET)4Hg3Br8A quasi-two-dimensional superconductor 14 p1974 N88-21778
Ultraviolet absorption cross sections of methylbromide at stratospheric temperatures
[AERONOMICA-ACTA-A-320-1987]
15 p2036 N88-22132

BROMINATION
The effect of bromination of carbon fibers on the coefficient of thermal expansion of graphite fiber-epoxy composites
[NASA-TM-100236] 02 p0143 N88-10899
Improving the interlaminar shear strength of carbon fiber-epoxy composites through carbon fiber bromination
[NASA-TM-100248] 07 p0827 N88-15018
Brominated graphite fibers and method of producing the same
[NASA-CASE-LEW-14698-1] 24 p3341 N88-29888

BROMINE
NT BROMINE ISOTOPES

BROMINE COMPOUNDS
NT BROMIDES
NT POTASSIUM BROMIDES
Impact on ozone attainment of CFC (chlorofluorocarbon) controls used to prevent future depletion of stratospheric ozone
[PB88-195177] 19 p2690 N88-25989

BROMINE ISOTOPES
Development and applications of new technical advances to problems of fluid/electrolyte/mineral imbalance in military personnel
[AD-A186437] 07 p0889 N88-15388

BROMINE 82
U BROMINE ISOTOPES

BROMINE 87
U BROMINE ISOTOPES

BRONZES
Progress toward a crystal streak camera using tungsten bronze crystals for the electrooptic material
[DE87-013110] 03 p0323 N88-12044

The effects of various conductor components on Nb3Sn filament prestrain in cable-in-conduit conductors
[DE88-003956] 11 p1479 N88-18824

BROWNIAN MOVEMENTS
Detecting and interval estimation about a slope change point
[AD-A186030] 07 p0909 N88-15509
Green's function for a ball
[AD-A186239] 07 p0910 N88-15516
Decoupling identities and predictable transformations in exchangeability
[AD-A186013] 07 p0913 N88-15540
Remark on the multiple Wiener integral
[AD-A186015] 07 p0913 N88-15541
Techniques in linear and nonlinear partial differential equations
[AD-A187109] 09 p1227 N88-17347
Filtering of jump processes
[AD-A189701] 15 p2123 N88-22656

BRUCETON TEST
U STATISTICAL TESTS

BRYOPHYTES
Electron cytochemical detection of Ca(2)+-ATPase in protonema of moss funaria hygrometrica (H e d w.) under hypogravitation 06 p0749 N88-14602

BUBBLE CHAMBERS
Scanning and measuring peculiarities with high-space resolution objects recorded at the Gabor holograms
[DE88-700373] 07 p0857 N88-15203
Analysis of relativistic nucleus-nucleus interactions in emulsion chambers 07 p0926 N88-15624
Optical system of laser illuminated streamer chamber
[DE88-702127] 18 p2577 N88-25306

BUBBLE MEMORY DEVICES
High density ion implanted contiguous disk bubble technology
[AD-A190169] 15 p2143 N88-22789

BUBBLE TECHNIQUE
High density ion implanted contiguous disk bubble technology
[AD-A190169] 15 p2143 N88-22789

BUBBLES
The structure of separated flow regions occurring near the leading edge of airfoils including transition
[NASA-CR-181434] 01 p0002 N88-10011
An inviscid model of planar, separated flows of finite extent
[RAE-TR-86070] 01 p0044 N88-10279
The dynamics of bubble growth for Rayleigh-Taylor unstable interfaces
[AD-A184752] 03 p0321 N88-12027
Cosmological applications of singular hypersurfaces in general relativity 04 p0521 N88-13202
Heat transfer investigations in a slurry bubble column
[DE88-001445] 06 p0699 N88-14286
Bubble expansion and collapse studies
[DE88-002377] 06 p0699 N88-14290
New equilibrium forms of free surface of confined magnetic fluid 06 p0770 N88-14734
Research on acoustical scattering, diffraction catastrophes, optics of bubbles, photoacoustics, and acoustical phase conjugation
[AD-A185785] 06 p0776 N88-14761
A flow visualization study of the leading edge separation bubble on a NACA 0012 airfoil with simulated glaze ice
[NASA-CR-180846] 07 p0816 N88-14966
Foam generation and air entrainment near a free surface
[AD-A185986] 07 p0848 N88-15149
A computationally efficient modelling of laminar separation bubbles
[NASA-CR-182417] 08 p0984 N88-15949
Cavitation inception scale effects. 1. Nuclei distributions in natural waters. 2. Cavitation inception in a turbulent shear flow
[AD-A186553] 08 p0988 N88-15987
Experimental and theoretical study on cavitation inception and bubbly flow dynamics. Part 1: Design, development and operation of a cavitation susceptibility meter. Part 2: Linearized dynamics of bubbly and cavitating flows with bubble dynamics effects
[AD-A187133] 09 p1160 N88-16952
Boundary integral analysis of flow and deformation of long bubbles in capillaries
[DE88-002110] 10 p1326 N88-17927
Mechanistic model for void distribution in flashing flow
[DE88-002948] 10 p1326 N88-17928
Mass transport phenomena between bubbles and dissolved gases in liquids under reduced gravity conditions
[NASA-TM-100273] 11 p1455 N88-18672
Analytical and numerical analysis of finite amplitude Rayleigh-Taylor instability
[DE88-004056] 11 p1474 N88-18797
Optically stimulated sound from gas bubbles in water 12 p1686 N88-20087
Cavitation inception
[AD-A189220] 13 p1765 N88-20557
Some problems of the theory of bubble growth and condensation in bubble chambers
[NASA-TT-20232] 13 p1771 N88-20593
Detecting the gas bubbles in a liquid metal coolant by means of magnetic flowmeters
[DE88-701427] 15 p2062 N88-22294
The elliptic Sinh-Gordon equation and the construction of toroidal soap bubbles
[DE88-006426] 15 p2113 N88-22585
Generation and coalescence of bubbles and stability of foams under microgravity conditions
[BMFT-FB-W-86-020] 16 p2184 N88-23017
A new laminar water tunnel to study the transition process in a blasius layer and in a separation bubble and a new tool for industrial aerodynamics and hydrodynamic research 16 p2204 N88-23150
Some visualization studies on turbulent boundary layers using multiwire hydrogen bubble generation 16 p2204 N88-23153
Low frequency ocean ambient noise: Measurements and theory
[AD-A191188] 16 p2237 N88-23362
The structure and stability of spherically expanding flames 17 p2318 N88-23842
Instability of laminar separation bubbles: Causes and effects
[AD-A191168] 18 p2508 N88-24876
Dynamical properties of a collapsing spherical cavity 19 p2623 N88-25562
Noise generation by air bubbles in water: An experimental study of creation and splitting
[AD-A192063] 19 p2664 N88-25839
Contribution of ultrasonic Doppler detection of circulating bubbles to human interventions under the sea and in space 19 p2697 N88-26029
Stability and drag reduction in a boundary layer with microbubbles
[AD-A191975] 23 p3209 N88-29099
A multiple-scales partial solution of the pulse-forced Rayleigh-Piesset equation of cavitation bubble dynamics
[AD-A193733] 23 p3212 N88-29118
Fluid physics double rack --- Spacelab
[SD-TN-AI-012] 24 p3358 N88-29992
Studies on pressure response of gas bubbles contributions of condensed droplets in bubbles generated by a uniform nucleation
[NASA-TT-20343] 24 p3370 N88-30068

BUCKLING
NT CREEP BUCKLING
NT ELASTIC BUCKLING
NT THERMAL BUCKLING
Interactive buckling effects in stiffened FRP panels
[ARE-TM(UMS)-87204] 01 p0059 N88-10378
Buckling of viscoelastic columns 02 p0190 N88-11187
An analytical study of the effects of transverse shear deformation and anisotropy on buckling loads of laminated cylinders
[NASA-TM-100508] 05 p0557 N88-13387
An examination of chaotic motion for the buckled beam 05 p0597 N88-13644
Beam and column buckling under directed loading
[PB87-124004] 06 p0722 N88-14436
Distortional buckling formulae for thin-walled channel columns
[PB87-124012] 06 p0722 N88-14437
Partially braced inelastic beam buckling experiments
[PB87-133831] 06 p0723 N88-14444
Buckling of braced monosymmetric cantilevers: Timoshenko energy approach
[PB87-133849] 06 p0723 N88-14445
Contribution to the study of wrinkling in metal stamping
[ISAL-IDI1-87-08] 08 p0976 N88-15900
Postbuckling of laminated anisotropic panels
[NASA-TM-100509] 08 p0994 N88-16011
Accuracies of southwell and force/stiffness methods in the prediction of buckling strength of hypersonic aircraft wing tubular panels
[NASA-TM-88295] 09 p1183 N88-17090
Determination of the ultimate loads for corrugated-steel, barrel-type shell structures
[AD-A187716] 11 p1498 N88-18944
Mathematical modeling of the postbuckling behavior of structural elements 11 p1500 N88-18960
Buckling and breakdown problems in structural mechanics. Failure of prestressed double-walled containers or rings
[MBB-UR-E-956/87] 13 p1783 N88-20671
Unrestrained out-of-plane buckling of monosymmetric rings
[PB88-155213] 14 p1923 N88-21458
Postbuckling delamination of a stiffened composite panel using finite element methods
[NASA-CR-182803] 15 p2030 N88-22098
Cubic spline solution of symmetric buckling problems of clamped shallow spherical shells 15 p2053 N88-22239
The buckling and vibration of composite plates using the Levy method considering shear deformation and rotary inertia
[AD-A189743] 15 p2076 N88-22374
Buckling of blast loaded cylinder
[AD-A190124] 15 p2076 N88-22376
The analysis of non-linear dynamic behavior (including snap-through) of postbuckled plates by simple analytical solution
[NASA-TM-89165] 15 p2087 N88-22439
Local buckling and crippling of composite stiffener sections
[NASA-TM-101133] 17 p2317 N88-23840
Forced motion of initially stressed shells and plates 18 p2529 N88-25005
Three-dimensional analysis of a postbuckled embedded delamination
[NASA-TP-2823] 20 p2812 N88-26684
A study of fluid-structure problems 21 p2941 N88-27468
Nonlinear interaction between overall and local buckling of stiffened panels with symmetric cross-sections
[PB88-104054] 21 p2960 N88-27580
Adaptive finite element methods for shells
[AD-A193221] 21 p2960 N88-27585
Tripping of stiffened plates using a refined beam theory
[AD-A193989] 22 p3087 N88-28333

BUDGETING
High energy experimental physics
[DE87-013516] 03 p0376 N88-12363
CNET (Chief of Naval Education and Training) Program Automated Tracking System (CPATS): A comprehensive study
[AD-A184694] 03 p0385 N88-12418
Budget and programs for 1986 research
[IFSI-86-16] 05 p0660 N88-14048
Department of Defense statement on defense agency research and development to the Subcommittee on Defense of the Committee on Appropriations, United States House of Representatives, 100th Congress, second session
[AD-A191840] 18 p2588 N88-25377
Department of Defense Statement on the Balanced Technology Initiative to the Committee on Armed Services, United States Senate, 100th Congress, second session
[AD-A191841] 18 p2588 N88-25378
Economic impact of space flight activities in West Germany. Influence of allocations of Bundesministerium fuer Forschung und Technologie
[ETN-88-92106] 21 p2901 N88-27215

BUDGETS
Budget reimbursements: The National Aeronautics and Space Administration's reimbursable work
[PB87-207296] 01 p0107 N88-10696
Feasibility study of a carbon dioxide observational platform system. Volume 2: Programmatics
[NASA-CR-180404] 06 p0672 N88-14114
INPE position paper on the CCSDS standardized method of link budget computation
[INPE-4533-NTE/279] 15 p2148 N88-22820

BUFFER STORAGE
A review of the semiconductor storage of television signals. Part 2: Applications 1975-1986
[BBC-RD-1987/6] 02 p0161 N88-11009
Throughput analysis of a flow-contoured communication network with buffer space limitations
[CWI-OS-R8702] 08 p0977 N88-15908
Effective buffering schemes for performing matrix operations for numerical databases 21 p3027 N88-27968

BUFFERS
Effects of emission energy transient in periodic-pulse XeCl excimer laser of approximately 400 W average power 14 p1971 N88-21763

BUFFETING
On the prediction of the aeroelastic behavior of lifting systems due to flow separation
[ESA-TT-1043] 03 p0259 N88-11633
A modular BLSS simulation model 03 p0359 N88-12260
Predictions of F-111 TACT aircraft buffet response and correlations of fluctuating pressures measured on aluminum and steel models and the aircraft
[NASA-CR-4069] 05 p0529 N88-13218
Experimental investigation of shock-induced disturbances on transonic airfoils
[DFVLR-FB-87-28] 09 p1112 N88-16666

Some aspects of aircraft dynamic loads due to flow separation
[AGARD-R-750] 11 p1439 N88-18588
A flight test investigation into flow separation and structural response for a transport aircraft at buffet onset
[RAE-TR-87006] 14 p1867 N88-21156
Numerical method for unsteady viscous-inviscid interaction to calculate buffeting
[ONERA-RSF-02/3617-AY-008-A] 17 p2338 N88-23949
Classical separation, trailing-edge flows and buffeting 23 p3170 N88-28874

BUILDING MATERIALS
U CONSTRUCTION MATERIALS

BUILDING STRUCTURES
U BUILDINGS

BUILDINGS
Measuring the annoyance of aircraft noise
[AD-A185494] 06 p0777 N88-14770
A proposed metric for assessing the potential of community annoyance from wind turbine low-frequency noise emissions
[DE88-001113] 08 p1022 N88-16187
Experimental studies of heat and mass exchange in parallel-passage rotary desiccant dehumidifiers for solar cooling applications
[DE88-001119] 10 p1350 N88-18069
Computer assisted generalization of buildings for digital landscape models by classification methods 16 p2226 N88-23294

BULK MODULUS
Ground state properties and electronic structure of high T sub c superconductors
[DE88-007485] 18 p2585 N88-25360

BUMPY TORUSES
Long wavelength vortices of low frequency interchange modes
[IPPJ-844] 02 p0241 N88-11525

BUNA (TRADEMARK)
Fracture morphologies of carbon-black-loaded SBR (Styrene-Butadiene Rubber) subjected to low-cycle, high-stress fatigue
[DE88-006808] 16 p2181 N88-23002

BUNCHING
NT ELECTRON BUNCHING
A qualitative study of wake fields for very short bunches
[DE88-002565] 09 p1164 N88-16980

BUOYANCY
Numerical computations of natural convection heat transfer in irregular geometries
[DE88-002358] 07 p0852 N88-15178
A payload for investigating the influence of convection on GaAs crystal growth 10 p1288 N88-17702
Application of a multigrid method to a buoyancy-induced flow problem
[DE88-003961] 10 p1397 N88-18326
Wind and buoyancy driven ocean circulation 14 p1938 N88-21564
Heat transfer from a negatively buoyant wall jet
[NBS/GCR-88/541] 15 p2050 N88-22208
Direct numerical simulation of buoyantly driven turbulence 18 p2196 N88-23097
Brunt-Doppler ducting of buoyancy waves in a temperature- and wind-stratified atmosphere 18 p2542 N88-25086
Nonlinear equation of state effects and the momentum-dilution trade-off in a turbulent buoyant jet
[DE88-701839] 20 p2799 N88-26610
Development of an adjustable buoyancy balloon tracer of atmospheric motion. Phase 3: Refinement of the operational prototype system
[PB88-190764] 23 p3231 N88-29230

BUOYS
Navarin Basin Ice Drift Program
[PB88-104021] 06 p0748 N88-14599
SEQUAL (seasonal Equatorial Atlantic) meteorological data from Moorings S2, S5 and S6 (March 1983 - March 1985)
[PB88-108048] 07 p0880 N88-15337
A deep-water OBS (Ocean Bottom Seismometer) array with real-time telemetry
[AD-A187404] 10 p1357 N88-18112
Comparison of surface current determined from satellite-tracked buoy with shipboard wind data during the 4th Brazilian antarctic expedition, 10-14 March, 1986 17 p2354 N88-24024
Near surface current determined from INPE's satellite-tracked buoy, during 6-26 November, 1985 17 p2360 N88-24058
Descriptions of HF and VHF Loran-C buoys and evaluations as potential datum marker buoys
[AD-A192069] 18 p2462 N88-24618
Arctic ice island and sea ice movements and mechanical properties
[DE88-004267] 20 p2829 N88-26782
KOSPAS-SARSAT satellites used for ocean current study 24 p3450 N88-30534

BURGER EQUATION
Vectorization of the odd-even hopscotch scheme and the alternating direction implicit scheme for the two-dimensional Burgers' equations
[CWI-NM-R8720] 16 p2249 N88-23440

BURKINA
Evaluation of SPOT data for crop inventory and monitoring in Sudanian Africa. Example of Bane area (Burkina Faso) 22 p3096 N88-28388

BURN-IN
Burn-in with mixed populations
[AD-A194651] 22 p3085 N88-28321

BURNERS
Turbulent Bunsen burner flames
[ETN-87-90433] 01 p0021 N88-10134
Correlation of velocity and velocity-density turbulence in the exhaust of an atmospheric burner 02 p0185 N88-11147
Experimental verification of vapor deposition rate theory in high velocity burner rigs 02 p0189 N88-11179
Effects of surface chemistry on hot corrosion life 02 p0189 N88-11180
Oxygen enriched combustion system performance study
[DE88-001500] 05 p0562 N88-13424
Development of a plenum chamber burner system for an advanced VTOL engine 10 p1281 N88-17664
Investigations into shock-induced enhancement of mixing and combustion in supersonic burners
[AD-A189609] 12 p1607 N88-19608
Dual Stokes cars measurements in supersonic combusting flow 19 p2625 N88-25569
Evidences for distributed combustion 19 p2626 N88-25586
Characterization of a modified Rijke burner for measurement of distributed combustion 19 p2628 N88-25587
Nonlinear mechanisms of solid propellant combustion instability 19 p2628 N88-25588
Analysis of microwave burner measurement system using a microwave network analysis computer program 19 p2631 N88-25604
Dynamics and stability of combustion driven self oscillations in presence of various frequencies. Extensive stability criteria
[ETN-88-92123] 20 p2771 N88-26432
Flame stabilization in a reheat combustor 24 p3346 N88-29921

BURNING
U COMBUSTION

BURNING PROCESS
U COMBUSTION

BURNING RATE
High pressure strand burn rate tests of polyvinylnitrate/nitramine propellants
[AD-A184178] 04 p0422 N88-12615
Performance characteristics of magnesium-sodium nitrate flares in oxygen-nitrogen atmospheres
[AD-A185274] 05 p0570 N88-13476
A continuous oxidizer regression model for the combustion of composite solid propellants
[AD-A186742] 08 p0974 N88-15894
The correlation of HMX (cyclotetramethylenetetranitramine) particle characterization techniques to propellant burn rate
[AD-A187119] 09 p1140 N88-16833
Speed control of a missile with throttleable ducted rocket propulsion 12 p1597 N88-19561
A simplified computer code for reduction to burning rates of closed bomb pressure-time data (MINICB)
[AD-A189112] 13 p1736 N88-20380
Crack opening and extension in inert solid propellant. An experimental study
[AD-A189808] 15 p2048 N88-22201
Chemical kinetics of nitramine propellant combustion
[AD-A191556] 18 p2495 N88-24802
Effect of thickness on downward flame spread over paper
[NASA-TT-20282] 19 p2612 N88-25501
Measurement of burning rates of NOSOL-363 propellants under cross-flow and strand burner conditions using real-time X-ray radiography 19 p2623 N88-25560
Burning rate measurements of Non-Newtonian Liquid Propellant (NNLP) 19 p2623 N88-25561
Combustion rate limits of hydrogen plus hydrocarbon fuel: Air diffusion flames from an opposed jet burner technique 19 p2624 N88-25567
Anatomy of group burning mode transitions in spray group combustion 19 p2626 N88-25578
Effect of burn-path tortuosity on the burn rate of composite propellants 19 p2630 N88-25602
Analysis of microwave burner measurement system using a microwave network analysis computer program 19 p2631 N88-25604
Modeling and experimental measurements of solid propellant flame structure 19 p2631 N88-25605
Pressure differential scanning calorimetry (DSC) evaluation of solid rocket propellant burn rate mod 19 p2631 N88-25606
Evaluation of techniques for direct measurement of burning rates in nozzleless motors 19 p2631 N88-25609
Combustion diagnostics of propellant with new grain geometries
[AD-A194944] 24 p3342 N88-29895
Descriptive characterization of propellant particles
[AD-A195176] 24 p3356 N88-29985
Discovery of a low temperature form of TAGN (Triaminoguanidinium Nitrate)
[AD-A196059] 24 p3357 N88-29989

BURNOUT
Computer calculations of PIN diode limiter characteristics
[AD-A185563] 06 p0697 N88-14277
Investigation of fuel additive effects on sooting flames
[AD-A186403] 07 p0829 N88-15026

BURST TESTS
Hydroburst test of a carbon-carbon involute exit cone
[NASA-TP-2556] 06 p0671 N88-14112

BURSTS
NT GAMMA RAY BURSTS
NT RADIO BURSTS
NT SOLAR RADIO BURSTS
NT TYPE 3 BURSTS
Nowcasting microbursts using Doppler radar in a forecaster-computer environment 02 p0200 N88-11246
Three-wave parametric resonance in plasma of relativistic electron flux 14 p1972 N88-21772
Analysis of the coma outburst of Comet Halley, March 24 to 25 (UT), 1986 14 p2000 N88-21920
Outburst of Halley's comet 14 p2007 N88-21967
Prospects for large dynamic range isotope analysis using photon burst mass spectrometry
[DE88-009110] 19 p2613 N88-25505
Detection of absorption lines in the spectra of X-ray bursts from X1608-52
[ISAS-RN-360] 20 p2887 N88-27143
The hard X-ray burst spectrometer event listing 1980-1987
[NASA-TM-4036] 20 p2887 N88-27144

BURUNDI
Analysis of the multispectral content and of SPOT subscenes in two regions of Burundi. Lithologic and tectonic interpretations 22 p3105 N88-28439

BUS CONDUCTORS
Digital system bus integrity
[NASA-CR-181446] 01 p0006 N88-10030
Lightweight power bus for a baseload nuclear reactor in space 17 p2438 N88-24505

BUSINESS MANAGEMENT
U INDUSTRIAL MANAGEMENT

BUTADIENE
Polymerization of azaethylenes (imines) and aza-1,3-dienes: Potential reactive monomers
[AD-A194717] 23 p3197 N88-29028

BUTANES
The role of low temperature chemistry in the autoignition of n-butane
[DE88-002385] 07 p0829 N88-15031
Pseudo-stationary oblique-shock-wave reflections in low gamma gases: Isobutane and sulphur hexafluoride
[UTIAS-TN-267] 13 p1768 N88-20576
Dissolution rates of polymers and copolymers based on methyl, ethyl and butyl methacrylate
[AD-A194713] 23 p3197 N88-29027

BUTENES
Synthesis and characterization of 1,2-cyclobutenedicarboxamides: Thermally generated polymers and Diels-Alder adducts
[AD-A188591] 12 p1611 N88-19633
High-temperature thermosets derived from the Diels-Alder polymerization of bisbenzocyclobutenes and bimaleimides
[AD-A188800] 13 p1747 N88-20449

BUTT JOINTS
Plasma joining of metal matrix composites
[AD-A188559] 12 p1604 N88-19593

BUTYLENE
U BUTENES

BY-PRODUCTS
Production of jet fuels from coal derived liquids. Volume 1: Market assessment for liquid by-products from the Great Plains gasification plant
[AD-A184846] 05 p0570 N88-13475

CELSS Program Meeting 05 p0630 N88-13853
Controlled ecological life support systems: Development of a plant growth module 05 p0630 N88-13854
Upgrading pyrolysis vapors to aromatic gasoline with zeolite catalysis at atmospheric pressure 18 p2536 N88-25045
Feasibility of producing jet fuel from GPGP (Great Plains Gasification Plant) by-products [DE88-010233] 20 p2781 N88-26492

BYPASS RATIO
Experimental study of bypass transition in a boundary layer [NASA-TM-100913] 16 p2209 N88-23186

C

C (PROGRAMMING LANGUAGE)
Mixing Microsoft C and Microsoft FORTRAN program modules on the IBM Personal Computer [DE88-001947] 05 p0637 N88-13895
C-GKS, a C implementation of GKS, the graphical kennel system [CWI-CS-R8753] 16 p2249 N88-23438
VPC: A proposal for a vector parallel C programming language [AD-A190885] 16 p2251 N88-23451
A timing evaluator for C programs generated by the model system [AD-A191204] 17 p2385 N88-24174
FASTRUN phase sequencer descriptor language (PDL) [DE88-007966] 20 p2837 N88-26828

C STARS
U CARBON STARS

C-M DIAGRAM
U COLOR-MAGNITUDE DIAGRAM

C-130 AIRCRAFT
Electrical load and power source capacity report for the C-130 aircraft Self Contained Navigation System (SCNS): LSI model 6216A, 6216B, 6216C, revision [AD-A193079] 21 p2895 N88-27186

C-135 AIRCRAFT
Reduced-gravity two-phase flow experiments in the NASA KC-135 17 p2431 N88-24465
Analysis and interpretation of low gravity boiling experiments in the KC-135 17 p2432 N88-24466
The Marshall Space Flight Center KC-135 microgravity test program for FY84-86 [NASA-TM-4059] 22 p3056 N88-28136

CABIN ATMOSPHERES
NT SPACECRAFT CABIN ATMOSPHERES
Northwest Airlines flight experiments 05 p0617 N88-13786
Advancements in oxygen generation and humidity control by water vapor electrolysis [NASA-CR-172073] 22 p3134 N88-28633

CABLES
Development and study of fibre-optic link lines on the basis of the KEM-8-4PD, KEM-8-4PR quantum-electronic modules [DE88-700372] 07 p0932 N88-15663

CABLES (ROPES)
BASIC desk-top computer program for the three-dimensional static configuration of an extensible flexible cable in a uniform stream [AD-A184852] 05 p0609 N88-13737
The Shock and Vibration Digest, Volume 19, No. 12 05 p0610 N88-13746
Dynamics of cables and chains 05 p0610 N88-13747
Life prediction of steel cords 06 p0715 N88-14386

CAD (DESIGN)
U COMPUTER AIDED DESIGN

CADASTRAL MAPPING
The Systeme d'Analyse Geographique (SAGE) geographic analysis system 17 p2353 N88-24019
The SAGE geographic analysis system 17 p2361 N88-24063
Tests for the automatic pattern recognition of building surfaces by the TK 50 18 p2533 N88-25030
Recent developments in software and hardware by Scitex Co. --- computer aided mapping 18 p2535 N88-25038
Technique to obtain the agricultural ownership limits by satellite imagery, to approve control, and to accompany agricultural activity 19 p2682 N88-25943
Updating of municipal official register of real estate through the geographical information system 19 p2684 N88-25952
Aerial photography as an instrument of municipal and regional planning: Metropolitan area of Sao Paulo (SP) 19 p2684 N88-25957

CADMIUM
Effects of cadmium electrode properties on nickel-cadmium cell performance [AD-A191394] 16 p2193 N88-23081
A rapid electrochemical technique for determining the current efficiency for cadmium plating [AD-A193679] 22 p3056 N88-28130

CADMIUM COMPOUNDS
NT CADMIUM SELENIDES
NT CADMIUM SULFIDES
NT CADMIUM TELLURIDES

CADMIUM MERCURY TELLURIDES
U MERCURY CADMIUM TELLURIDES

CADMIUM NICKEL BATTERIES
U NICKEL CADMIUM BATTERIES

CADMIUM SELENIDES
Ultrafast physics in semiconductor microstructures [AD-A193300] 21 p3022 N88-27936

CADMIUM SULFIDES
Physico-chemical studies on copper sulfide behavior in the CdS-Cu2S solar cell [ETN-88-91068] 09 p1187 N88-17109
Investigation of the subsequent treatment and the stability of CuxS-CdS thin-film solar cells [ETN-88-91488] 11 p1507 N88-19006

CADMIUM TELLURIDES
Preparation and properties of evaporated CdTe films [DE87-012270] 02 p0195 N88-11216
Population inversion in gapless semiconductors as result of interband pumping 06 p0770 N88-14732
CdTe(110)-Mn interface reaction and the formation of non-equilibrium ternary semimagnetic semiconductor alloys [AD-A187593] 10 p1422 N88-18491
Metal contacts to cadmium telluride (CdTe) [AD-A188306] 12 p1698 N88-20159
CdZnTe as a wide-band-gap absorber for a tandem, thin-film solar cell [DE88-001114] 13 p1793 N88-20724
Research on single-crystal CdTe solar cells [DE88-001115] 13 p1793 N88-20725
Thin-film cadmium telluride solar cells [DE88-001107] 13 p1846 N88-21050
Electrical and optical properties of Hg/sub 1-x/Cd/sub x/Te doped layers grown by Liquid Phase Epitaxy (LPE) [DE88-701023] 16 p2281 N88-23653
MBE growth of HgTe/CdTe superlattices on Si(100) substrates 20 p2869 N88-27033
Type 3 - type 1 transition and strain effect in Hg(1-x)Cd(x)Te-CdTe and Hg(1-x)Zn(x)Te-CdTe superlattices 20 p2872 N88-27052
Tunnelling currents in reverse biased CMT photodiodes [RSRE-MEMO-4137] 23 p3209 N88-29097

CAFFEINE
Influence of altitude and caffeine during rest and exercise on plasma levels of proenkephalin peptide F [AD-A192659] 22 p3131 N88-28616

CAI
U COMPUTER ASSISTED INSTRUCTION

CALCITE
Kinetics of thermochemical gas-solid reactions important in the Venus sulfur cycle [NASA-CR-182963] 19 p2742 N88-26280

CALCIUM
NT CALCIUM ISOTOPES
Simultaneous, cospatial imaging of the Sun in cyanogen and singly-ionized calcium 04 p0507 N88-13114
The angular diameter of alpha Scorpii in the near-infrared Ca II triplet 04 p0514 N88-13162
Lidar metal density measurements in the upper atmosphere 08 p1027 N88-16219
High temperature superconductivity [AD-A190259] 16 p2281 N88-23655

CALCIUM CARBONATES
NT CALCITE
Characterization of the dimensions of colloidal calcium carbonate dispersions in toluene with neutron small-angle scattering [ECN-197] 06 p0680 N88-14167
Nucleation and growth of calcium carbonate crystals on surface-modified polyethylene and polystyrene [DE88-005126] 11 p1465 N88-18733

CALCIUM COMPOUNDS
NT CALCITE
NT CALCIUM CARBONATES
NT CALCIUM FLUORIDES
NT CALCIUM OXIDES
NT CALCIUM SILICATES
NT PEROVSKITES
Electron cytochemical detection of Ca(2)+-ATPase in protonema of moss funaria hygrometrica (H e d w.) under hypogravitation 06 p0749 N88-14602
An in situ annealing study of lead implanted single crystal calcium titanate [DE88-005435] 11 p1562 N88-19351

CALCIUM FLUORIDES
Submerged arc flux welding with CaF2-CaO-SiO2 fluxes: Possible electrochemical effects on weld metal [DE88-003107] 08 p0992 N88-16004
High temperature solar electrothermal processing-3. Zinc from zinc oxide at 1200-1675K using a non-consumable anode [AD-A186600] 09 p1141 N88-16836

CALCIUM ISOTOPES
The elastic scattering of intermediate energy protons from (40)Ca and (208)Pb 01 p0092 N88-10599

CALCIUM METABOLISM
Prevention of disuse osteoporosis: Effect of sodium fluoride during five weeks of bed rest [NASA-CR-172018] 01 p0075 N88-10483
Regulation of calcium metabolism during prolonged antiorthostatic hypokinesia [NASA-TT-20219] 11 p1521 N88-19085
Use of diphosphonates to correct disorders in calcium metabolism and mineral composition of bone tissue with 60-day hypokinesia in rats [NASA-TT-20220] 13 p1809 N88-20807

CALCIUM OXIDES
Submerged arc flux welding with CaF2-CaO-SiO2 fluxes: Possible electrochemical effects on weld metal [DE88-003107] 08 p0992 N88-16004
Nuclear magnetic ordering and paramagnetic relaxation of diatomic molecules in Ca (OH)2 [B8681469] 23 p3281 N88-29532

CALCIUM SILICATES
Development of highly porous calcium silicate hydrate materials with extremely low thermal conductivity [BMFT-FB-T-86-164] 02 p0150 N88-10941

CALCIUM 45
U CALCIUM ISOTOPES

CALCULATION
U COMPUTATION

CALCULATORS
Langlie Test Method Program for use with the HP-41CV/X calculator [DE88-001935] 06 p0687 N88-14210

CALCULUS
NT ASYMPTOTIC SERIES
NT COLLINEARITY
NT CONTINUITY (MATHEMATICS)
NT COPLANARITY
NT COSINE SERIES
NT FOURIER-BESSEL TRANSFORMATIONS
NT INTEGRAL CALCULUS
NT LIMITS (MATHEMATICS)
NT PADE APPROXIMATION
NT POWER SERIES
NT SERIES (MATHEMATICS)
NT TAYLOR SERIES
NT VECTOR ANALYSIS
NT VORTICITY
Formalizing reusable software components in the programmer's apprentice [AD-A185843] 07 p0901 N88-15457
Martingale representation and the Malliavin calculus [AD-A189721] 15 p2119 N88-22626
Non-rigid motion and Regge calculus [AD-A190387] 15 p2121 N88-22640
Filtering of jump processes [AD-A189701] 15 p2123 N88-22656
Unique normal forms for lambda calculus with surjective pairing [PB88-173539] 16 p2260 N88-23508
Practical higher-order functional and logic programming based on lambda-calculus and set-abstraction [AD-A193645] 23 p3271 N88-29466

CALCULUS OF VARIATIONS
A VAS-numerical model impact study using the Gal-Chen variational approach — Visible Infrared Spin-Scan Radiometer Atmospheric Sounder (VAS) 02 p0213 N88-11339
The method of lines for time dependent free boundary problems [DE87-013929] 02 p0226 N88-11423
The role of computation fluid dynamics in aeronautical engineering (4). The development and applications of implicit TVD finite volume code 05 p0536 N88-13259
A study of the free energy of the Lenz-Ising model using the cluster variation method of Morita [AD-A186023] 08 p1073 N88-16476
A substructure method for dynamic simulation of flexible mechanical systems with geometric nonlinearities 09 p1176 N88-17044
Studies in finite time thermodynamics [DE88-004531] 10 p1423 N88-18500
Total Variation Diminishing (TVD) schemes of uniform accuracy [NASA-TM-100552] 11 p1436 N88-18566
On exterior variational calculus [DE88-700861] 12 p1683 N88-20062

Inversion algorithms for geophysical problems
[AD-A189252] 13 p1815 N88-20845
Nonlinear differential equations
[DE88-006047] 13 p1828 N88-20933
The inverse power method for semilinear elliptic equations
[DE88-006427] 15 p2118 N88-22620
Discrete variational methods and their application to electronic structures
[DE88-702215] 21 p3014 N88-27888
On the distribution equations
[DE88-702217] 23 p3270 N88-29454
On the Nash point equilibria in the calculus of variations
[AD-A194959] 24 p3424 N88-30381

CALDERAS
Gravity and fault structures, Long Valley Caldera, California
[DE87-014117] 02 p0197 N88-11229
Mid-tertiary volcano-tectonic development of the Southwestern Cordillera of North America
06 p0797 N88-14879
A three-dimensional gravity model of the geologic structure of Long Valley caldera
[DE88-006331] 16 p2231 N88-23324
A core hole into the hydrothermal system of the Long Valley caldera
[DE88-006335] 16 p2231 N88-23325

CALENDARS
Calendar of selected aeronautical and space meetings
[AGARD-CAL-87/1] 05 p0657 N88-14033
Calendar of selected aeronautical and space meetings
[AGARD-CAL-88/1] 05 p0658 N88-14037

CALIBRATING
NT WIND TUNNEL CALIBRATION
Development of response models for the Earth Radiation Budget Experiment (ERBE) sensors. Part 2: Analysis of the ERBE integrating sphere ground calibration
[NASA-CR-178293] 01 p0049 N88-10316
Wet deposition and snowpack monitoring operations and quality assurance manual
[PB87-212817] 01 p0064 N88-10413
Spectrometric test of a linear array sensor
[NASA-TM-100676] 01 p0064 N88-10414
NBS (National Bureau of Standards) calibration services users guide: Fee schedule
[PB87-210654] 01 p0090 N88-10586
Monitored background radiometer
02 p0133 N88-10831
Calibration of attitude control sensors
02 p0159 N88-10995
The absolute radiometric calibration of space-based sensors 03 p0277 N88-11744
Mass transport by diffusion 03 p0297 N88-11864
NBS (National Bureau of Standards) calibration procedures for horizontal dipole antennas (25 to 1000 MHz)
[PB87-210233] 03 p0305 N88-11922
Requirements for the calibration of mechanical shock transducers
[PB87-227591] 03 p0325 N88-12054
NBS (National Bureau of Standards) measurement services: Radiometric standards in the vacuum ultraviolet
[PB87-227625] 03 p0325 N88-12055
Calibration standard for metallographic microscopes
[RFP-3956-REV] 03 p0326 N88-12057
Absolute and interband calibration --- SPOT
03 p0341 N88-12152
The correspondence of surface climate parameters with satellite and terrain data
[NASA-CR-181515] 03 p0346 N88-12185
Lyman alpha SMM/UVSP absolute calibration and geocoronal correction
[NASA-TM-100314] 03 p0389 N88-12446
The design and preliminary calibration of a boundary-layer flow channel
[NASA-CR-178399] 04 p0394 N88-12457
Performance optimization of electronic networks in the frequency domain
[PB87-123873] 04 p0438 N88-12720
Evaluation of the sensidyne toxic gas sensor for HF (Hydrogen Fluoride) vapor
[DE88-000647] 04 p0446 N88-12767
Accuracy potential of non-metric cameras in close-range photogrammetry 04 p0463 N88-12862
Radiometric calibration of the Earth observing system's imaging sensors
[NASA-CR-181542] 04 p0463 N88-12865
Calibration on the Sun for stellar magnetic fields
04 p0506 N88-13113
Development of response models for the Earth Radiation Budget Experiment (ERBE) sensors. Part 3: ERBE scanner measurement accuracy analysis due to reduced housekeeping data
[NASA-CR-178294] 05 p0583 N88-13553
Fabricate, calibrate and test a dosimeter for integration into the CRRES (Combined Release and Radiation Effects Satellite) satellite
[AD-A185439] 05 p0585 N88-13564
Improvement of modal scaling factors using mass additive technique 05 p0593 N88-13620
AIS-2 radiometry and a comparison of methods for the recovery of ground reflectance
05 p0611 N88-13757
Calibrating AIS images using the surface as a reference 05 p0612 N88-13760
Causes of spurious features in spectral reflectance data 05 p0614 N88-13769
Analysis of SO2 signals in SBUV/TOMS data
05 p0618 N88-13794
Media calibrations of the Doppler signal for a gravitational wave experiment --- interplanetary medium
[IFSI-86-13] 05 p0625 N88-13825
Area detectors for X-ray spectroscopy
[DE88-001429] 06 p0679 N88-14163
Picosecond cable calibrator: Beam Research Program
[DE88-002375] 06 p0695 N88-14266
Computer simulation of the L/sub 3/-edge densitometer
[DE88-001944] 06 p0705 N88-14324
Airborne Visible/Infrared Imaging Spectrometer (AVIRIS). A description of the sensor, ground data processing facility, laboratory calibration, and first results
[NASA-CR-182365] 06 p0705 N88-14325
Spectral and radiometric calibration of the Airborne Visible/Infrared Imaging Spectrometer
06 p0707 N88-14334
Robot accuracy improvement through kinematic parameter identification 06 p0712 N88-14363
Self calibration of motion and stereo vision for mobile robot navigation
[AD-A185602] 06 p0781 N88-14794
Calibration constants for the 1986 BGO crystals matrix
[NOTA-INTERNA-886] 07 p0856 N88-15197
LANDSAT thematic mapper radiometric calibration study
[NASA-CR-182410] 07 p0872 N88-15287
The results of the 1984/1985 Round-Robin Calibration of Reference Solar Cells for the Summit Working Group on Technology, Growth and Employment
[DE88-900215] 07 p0874 N88-15303
Problems and possible solutions involved in hard target calibration of coherent Doppler lidar
07 p0922 N88-15602
Research sensors 08 p0955 N88-15795
Optical measurement systems
08 p0955 N88-15796
High Resolution Picture Transmission (HRPT) data processing from NOAA series satellites
[INPE-4372-PRE/1195] 08 p0963 N88-15831
Temperature Metrology '86
[DE88-700236] 08 p0989 N88-15990
Calibration of the ARL (Aeronautical Research Laboratories) rain and icing facility
[AD-A186776] 09 p1121 N88-16710
Tensorial calibration. 2. Second order tensorial calibration
[AD-A186614] 09 p1167 N88-16994
Tensorial calibration. Part 1: First order tensorial calibration
[AD-A186708] 09 p1167 N88-16995
The superconducting gravimeter: Application, calibration, and further development
[SER-C-329] 09 p1167 N88-16998
Recommendations for organising the calibration of pure-tone audiometers
[NPL-AC-112] 09 p1167 N88-16999
Hydrogen maser
[PB87-171617] 09 p1172 N88-17025
Finite element analysis for the calculation of calibration curves of fracture mechanics specimen for semicircular surface cracks with several starting depths, for the crack depth measurement following the dc potential method
[GKSS-87/E/19] 09 p1183 N88-17086
Calibration of neural networks using genetic algorithms, with application to optimal path planning
09 p1214 N88-17277
Strong consistency of certain information theoretic criteria for model selection in calibration, discriminant analysis and canonical correlation analysis
[AD-A186584] 09 p1232 N88-17385
Error modeling and confidence interval estimation for inductively coupled plasma calibration curves
[AD-A186711] 09 p1250 N88-17488
Signal processing studies program optical signal amplification, volume 2
[AD-A188054] 10 p1320 N88-17896
Johnson noise thermometer for high radiation and high temperature environments
[DE88-003770] 10 p1323 N88-17911
A technique for low level, wide range CW microwave power meter calibrations
[DE88-004147] 10 p1333 N88-17966
NBS (National Bureau of Standards) measurement services: Spectral irradiance calibrations
[PB88-123781] 10 p1408 N88-18401
Source and event selection for radio-planetary frame-tie measurements using the Phobos Landers
11 p1471 N88-18775
Using ridge regression in systematic pointing error corrections 11 p1472 N88-18777
Phase calibration generator 11 p1473 N88-18785
DSS 14 64-meter antenna S- and X-band efficiency and system noise temperature calibrations, September 1987
11 p1473 N88-18790
Calibration of a Harwood DWT-1000 controlled-clearance piston gauge
[DE88-004496] 11 p1489 N88-18888
Calibration of beam power monitors for laser welding
[DE88-004687] 11 p1492 N88-18908
Thirteenth Biennial Guidance Test Symposium, volume 1
[AD-A185782] 12 p1576 N88-19427
Calibration of a ring laser gyro inertial navigation system 12 p1576 N88-19428
The complex point spread function of the RSRE SAR (Synthetic Aperture Radar)
[AD-A189011] 12 p1621 N88-19693
Zoom versus full-field sensitivity at the ETS (Experimental Test System)
[AD-A188162] 12 p1628 N88-19742
DIRBE External Calibrator (DEC)
[NASA-CR-180761] 12 p1631 N88-19760
Long term measurement network for FIFE
[NASA-CR-182491] 12 p1646 N88-19857
Ultrasonic measurements research: Progress in 1987
[AD-A188506] 12 p1687 N88-20092
Investigations of high resolution imaging through the Earth's atmosphere using speckle interferometry
[AD-A189295] 12 p1692 N88-20121
An attempt to measure the diffuse brightness of the sky at submillimeter wavelengths
12 p1710 N88-20233
Analysis of pre-flight modulator voltage calibration data for the Voyager plasma science experiment
[NASA-CR-182577] 12 p1710 N88-20236
The Joint NASA/Goddard-University of Maryland Research Program in Charged Particle and High Energy Photon Detector Technology
[NASA-CR-182612] 12 p1712 N88-20247
The imaging of extra-galactic low-energy gamma-ray sources prospects, techniques, and instrumentation
[NASA-CR-182536] 12 p1713 N88-20251
A low-frequency measurement of the spectrum of the cosmic microwave background radiation
13 p1858 N88-21112
NBS (National Bureau of Standards) measurement services. GOES (Geostationary Operational Environmental Satellite) time code dissemination: Description and operation
[PB88-168760] 14 p1880 N88-21235
Quantitative AES: The establishment of a standard reference spectrum for the accurate determination of spectrometer transmission functions
[NPL-DMA(A)-151] 14 p1887 N88-21279
Pre-launch calibration of channels 1 and 2 of the advanced very high resolution radiometer
[PB88-157169] 14 p1913 N88-21427
Calibration of a hot-wire/hot-film anemometer over a range of temperatures, velocities and pressures
[AD-A189717] 14 p1913 N88-21430
The Spring 1985 high precision baseline test of the JPL GPS-based geodetic system
[NASA-CR-182686] 14 p1940 N88-21577
The absolute radiometric calibration of the advanced very high resolution radiometer
[NASA-CR-182755] 14 p1941 N88-21584
High energy cosmic muons and the calibration of the L3 electromagnetic calorimeter
[NOTA-INTERNA-895] 14 p2011 N88-21999
A 150,000 pounds per square inch dynamic pressure calibrator
[AD-A190659] 15 p2069 N88-22335
Support for FY87 midlatitude electron-density calibration campaign
[AD-A190174] 15 p2094 N88-22476
Stellar scintillometer atmospheric optical turbulence profiling experiment: A qualitative comparison of two identical instruments at AMOS (Air Force Maui Optical Station), 1985
[AD-A190589] 15 p2094 N88-22479
Computer grading of extensometers (BS 3846)
[NPL-DMA(A)-152] 15 p2108 N88-22560
Design, fabricate, calibrate, test and deliver two satellite electron flux detectors
[AD-A190799] 16 p2169 N88-22930

Analysis and experiments concerning the performance and calibration of compact antenna-test ranges
[PB88-169263] 16 p2188 N88-23047
Analysis and experiments concerning the performance and calibration of compact antenna-test ranges
[ISBN-9-09-001727-5] 16 p2188 N88-23048
Enhanced backscattering from rough surfaces
[AD-A190995] 16 p2190 N88-23063
Radiation standards 16 p2272 N88-23592
Reflection standards for spectroradiometry. Realization and calibration 16 p2272 N88-23595
Preparation and execution of calibration measurements for handling of airborne SAR data (AGRISAR)
[ETN-88-92338] 17 p2333 N88-23926
A control technique for improved robot performance 17 p2391 N88-24212
Johnson noise thermometer for high-radiation and high-temperature environments 17 p2434 N88-24480
Intensity calibration of a VUV system by branching line pairs 17 p2443 N88-24533
Expendable conductivity, temperature and depth system (XCTD) development program
[AD-A192182] 18 p2547 N88-25121
Calibration of averaging total pressure flight wake rake and natural-laminar-flow airfoil drag certification
[NASA-CR-181630] 19 p2599 N88-25443
An error floor in tone calibrated transmission 19 p2649 N88-25729
Automatic calibration of space based manipulators and mechanisms
[NASA-CR-182804] 19 p2676 N88-25912
Design and calibration of a two-channel low-noise heterodyne receiver for use in a CO2 laser Thomson scattering alpha particle diagnostic
[DE88-007866] 19 p2728 N88-26201
Time-resolved doubly bent crystal X-ray spectrometer
[DE88-007899] 20 p2805 N88-26637
Microwave calibration system 2
[AD-A192976] 20 p2805 N88-26639
Fiber optic sensors with internal referencing
[NASA-TM-100893] 20 p2806 N88-26644
Surface disturbances produced by low-level, subsonic B-1 aircraft
[AD-A192257] 20 p2824 N88-26752
Calibration and data reduction techniques for the AFGL infrared array spectrometer 21 p2927 N88-27374
Calibration of the portable wear metal analyzer
[AD-A192971] 21 p2950 N88-27524
Acoustic emission calibration instrumentation
[DE88-010817] 21 p2951 N88-27528
Validate algorithms for the determination of rainfall rates from SSM/I microwave satellite imagery
[AD-A192299] 21 p2974 N88-27664
Test and calibration system for monitoring the Advanced Technologies Testing Aircraft System (ATTAS) data acquisition system 22 p3037 N88-28029
Apparent brightness of stars and lasers 22 p3065 N88-28188
A digitally implemented phase-locked loop detection scheme for analysis of the phase and power stability of a calibration tone 22 p3066 N88-28196
DSS 14 antenna calibrations for GSSR/VLA Saturn radar experiments 22 p3068 N88-28207
Calibration technique and study on metrological characteristics of a high-voltage inverse square-law function generator
[DE88-702101] 22 p3072 N88-28236
Calibration of a triple wire probe for turbulence measurements
[AD-A193956] 22 p3081 N88-28296
Calibration of quartz load cells: An in-situ procedure for instrumented falling weight impact machines
[NPL-DMA(A)-155] 22 p3081 N88-28297
Langley Research Center Metrology Program status for fiscal year 1987
[NASA-TM-100651] 22 p3086 N88-28324
Research and development objectives: Installation, startup, and test operation of a remote and program controlled measuring table for the calibration of EGRET experiment
[ETN-88-92105] 22 p3152 N88-28752
SQUID (superconducting quantum interference device) arrays for simultaneous magnetic measurements: Calibration and source localization performance
[AD-A193815] 23 p3216 N88-29143
Results of the use of an automated electrical measuring instrument calibration system
[SNIAS-881-430-107] 23 p3217 N88-29146
Development of an adjustable buoyancy balloon tracer of atmospheric motion. Phase 3: Refinement of the operational prototype system
[PB88-190764] 23 p3231 N88-29230
NBS (National Bureau of Standards) measurement services: The NBS photodetector spectral response calibration transfer program
[PB88-201595] 24 p3376 N88-30109
Atmospheric corrections for in-flight satellite radiometric calibration
[AD-A196124] 24 p3391 N88-30194
A new determination of the Geneva photometric passbands and their absolute calibration
[SER-C-PREPUBL-FASC-26] 24 p3452 N88-30546

CALIFORNIA
North Pacific Ocean. Tradewind region east of Hawaii, R/V Thomas G Thompson: 25 September - 1 November 1972. STD data report
[AD-A186566] 08 p1044 N88-16311
CTD observations in the coastal transition zone off northern California, 16-25 February 1987
[AD-A187283] 10 p1357 N88-18111
Numerical simulations of the California current: Filament formation as related to baroclinic instability
[AD-A187573] 10 p1358 N88-18115
Hydrographic data from the OPTOMA (Ocean Prediction Through Observation, Modeling and Analysis) program: OPTOMA 23, 9-19 November 1986
[AD-A189868] 15 p2099 N88-22506
Soil erosion and causative factors at Vandenberg Air Force Base, California
[NASA-TM-100981] 17 p2381 N88-24156
Survey for least bell's vireo in riparian habitat on Vandenberg Air Force Base, Santa Barbara County, California
[NASA-TM-100984] 20 p2822 N88-26744

CALIFORNIUM COMPOUNDS
Raman and absorption spectrophotometric studies of selected lanthanide, californium-doped lanthanide, and actinide trihalides in the solid state
[DE88-008234] 20 p2874 N88-27061

CALORIC REQUIREMENTS
Significance of nutrition to change in human carbohydrate and lipid metabolism under emotional stress 19 p2703 N88-26073

CALORIC STIMULI
Nystagmometric distinctions of individuals regularly exposed to vibration 07 p0891 N88-15401

CALORIMETERS
NT BOMB CALORIMETERS
Calorimetric Absorption Spectroscopy (CAS): A new method for the characterization of the optical properties of semiconductor systems
[ETN-87-90407] 01 p0098 N88-10645
Application of prediction of equilibrium to servo-controlled calorimetry measurements
[DE87-013745] 03 p0324 N88-12046
Simultaneous TG/DSC (thermogravimetry/Differential Scanning Calorimetry) and TG/MS (thermogravimetry/Mass Spectrometry) analyses of polymeric and energetic materials
[DE88-000727] 04 p0413 N88-12561
Investigation by differential scanning calorimetry of microstructure in a superplastic Al-Mg-Zr alloy
[AD-A184902] 05 p0564 N88-13439
An automated flow calorimeter for heat capacity and enthalpy measurements at elevated temperatures and pressures
[DE88-002357] 07 p0857 N88-15206
A calorimeter for measuring the neutral beam power reaching the plasma
[DE88-001412] 07 p0937 N88-15691
The high resolution spaghetti hadron calorimeter
[NIKHEF-H/87-7] 08 p0990 N88-15993
DSC (Differential Scanning Calorimeter) stability test for liquid propellants: A preliminary report
[AD-A187115] 09 p1150 N88-16888
Design and fabrication of advanced hybrid circuits for high energy physics
[DE88-004392] 11 p1479 N88-18825
High resolution hadron calorimetry
[NIKHEF-H/87-8] 13 p1773 N88-20605
Energy loss of particles in dense matter-calorimetry
[NIKHEF-H/87-12] 13 p1836 N88-20988
A segmented calorimeter for low-energy particle beams in space
[DE88-001806] 13 p1838 N88-20997
High energy cosmic muons and the calibration of the L3 electromagnetic calorimeter
[NOTA-INTERNA-895] 14 p2011 N88-21999
Calorimetric technique for measuring liquid helium flow rate
[DE88-701308] 16 p2200 N88-23123
Calorimetry applied to nucleus-nucleus collisions at ultrarelativistic energies
[DE88-006173] 18 p2573 N88-25282
Pressure differential scanning calorimetry (DSC) evaluation of solid rocket propellant burn rate mod 19 p2631 N88-25606

CALORIMETRY
U HEAT MEASUREMENT

CAM (MANUFACTURING)
U COMPUTER AIDED MANUFACTURING

CAMBER
NT WING CAMBER
Unsteady flow about cambered plates
[AD-A184725] 03 p0320 N88-12025
An experimental investigation of decelerating flow about two-dimensional cambered plates
[DE88-006596] 13 p1766 N88-20567
Discrete vortex analysis of unsteady flow about two-dimensional cambered plates
[DE88-006597] 14 p1909 N88-21407

CAMBERED WINGS
Aerodynamic characteristics of wings designed with a combined-theory method to cruise at a Mach number of 4.5
[NASA-TP-2799] 12 p1575 N88-19420

CAMERA SHUTTERS
Analysis of spectral reflectance characteristics of targets under satellites and automatic cloud recognition 13 p1755 N88-20498

CAMERA TUBES
NT IMAGE DISSECTOR TUBES
NT VIDICONS

CAMERAS
NT DIFFRACTION LIMITED CAMERAS
NT FAINT OBJECT CAMERA
NT FRAMING CAMERAS
NT HIGH SPEED CAMERAS
NT MULTISPECTRAL BAND CAMERAS
NT PINHOLE CAMERAS
NT STREAK CAMERAS
NT TELEVISION CAMERAS
Study of a payload for Columbus Polar Platform Earth observation demonstration mission, executive summary
[ESA-CR(P)-2412] 01 p0014 N88-10079
Use of a 35mm camera for remote surface cleanliness verification 02 p0133 N88-10835
Programmable 10 MHz optical fiducial system for hydrodiagnostic cameras
[DE87-013223] 02 p0175 N88-11091
Cineradiography
[DE87-013158] 03 p0324 N88-12045
Accuracy potential of non-metric cameras in close-range photogrammetry 04 p0463 N88-12862
The technical evolution of the Wilson camera: The beginnings (1895-1925)
[NOTA-INTERNA-876] 05 p0585 N88-13568
Electronic imaging technique for welding and other high-luminosity processes
[DE88-002199] 07 p0862 N88-15227
Object detection in images from outdoor scenes using evidential reasoning
[FOA-C-30461-3.3] 08 p1020 N88-16183
Space infrared telescope facility wide field and diffraction limited array camera (IRAC)
[NASA-CR-182704] 13 p1853 N88-21092
Cryogenic mechanism for ISO camera 14 p1878 N88-21221
Analysis of contamination data recorded by the IECM camera/photometer
[NASA-TM-100324] 14 p1882 N88-21246
Further development of a stellar camera following the rotation-modulation-collimator principle for balloon-borne observations in the X-ray range
[ETN-88-91496] 14 p1913 N88-21428
ROVER: A prototype active vision system
[AD-A189246] 15 p2133 N88-22722
An investigation of the crystalchemistry and thermochemistry of selected mineral systems
[AD-A189758] 15 p2142 N88-22781
An investigation into the precision of a digital camera
[B8735054] 16 p2210 N88-23193
Obtaining information on cloud particles by a commercial miniature camera
[DFVLR-MITT-87-19] 16 p2234 N88-23342
The modeling of error budget analysis and tolerance specifications for BRESEX multiband linear array CCD camera 17 p2355 N88-24029
The XRD (X-Ray Diode) array, the grazing incidence spectrometer and the X-ray imaging camera on PBFA 2
[DE88-007282] 19 p2728 N88-26200
Stress analysis using infrared thermography
[ETN-88-92169] 20 p2816 N88-26705
The FEL CCD-camera: Experimental system for camera and image processing research
[FEL-1987-34] 21 p2952 N88-27532
Satellite attitude determination using a CCD (Charge-Coupled-Device) star camera
[AD-A192662] 22 p3046 N88-28080
Four-frame gated optical imager with 120-ps resolution
[DE88-011735] 22 p3080 N88-28288

PLZT (Lead-Lathanium-Zirconium-Titanium) electro-optic photographic system
[AD-A193473] 23 p3215 N88-29137
Kalman filter-based algorithms for estimating depth from image sequences
[AD-A195818] 24 p3424 N88-30380
CAMOUFLAGE
A Workshop on Desert Processes, September 24-28, 1984: Report on the conference
[AD-A184599] 03 p0345 N88-12184
Cleanability of aircraft polyurethane topcoats
[AD-A193456] 23 p3170 N88-28878
CAMS
AVIRIS scan drive design and performance
06 p0706 N88-14330
CANADA
NT BRITISH COLUMBIA
Corrosion in avionics and associated equipment; cause, effect and prevention 05 p0547 N88-13335
Petrogenesis of basalts from the Archean Matachewan Dike Swarm Superior Province of Canada
05 p0796 N88-14878
Northern lights: The economic and practical potential of imported power from Canada
[DE88-006026] 15 p2093 N88-22473
Mobile satellite service for Canada
19 p2643 N88-25683
International and domestic regulator issues facing the Canadian MSAT system 19 p2644 N88-25692
An evaluation of the applicability of SPOT stereoscopic imagery to the Canada Land Use Monitoring Program (CLUMP) 22 p3099 N88-28403
Prolonged periods of above-normal temperatures in Canada, 1986/87 22 p3120 N88-28538
CANADIAN SPACE PROGRAM
The Canadian SPOT program
03 p0340 N88-12147
Canadian activities and goals in remote sensing of ocean colour and fluorescence from space
08 p1043 N88-16300
Multi-axis control of telemanipulators
12 p1593 N88-19539
System and concept design of the SSRMS latching end effector --- Space Station 14 p1875 N88-21204
CANADIAN SPACECRAFT
NT ALOUETTE SATELLITES
CANARD CONFIGURATIONS
Examples of static aeroelastic effects on present combat aircraft projects 05 p0550 N88-13349
An investigation into the effect of canard location on the aerodynamics of the close-coupled canard configuration
[BU-361] 14 p1866 N88-21149
Preliminary aerodynamic design considerations for advanced laminar flow aircraft configurations
17 p2297 N88-23746
Flow around a delta wing with or without a canard control surface (phi BA = 60 deg). Part 1: Hydrodynamic visualization in permanent regime
[ONERA-RT-10/2891-AN-101-A-PT-1]
21 p2892 N88-27170
In-flight load measurements of the Robot-X canards
[AD-A193428] 21 p2895 N88-27187
CANBERRA BOMBER
U B-57 AIRCRAFT
CANCELLATION
A Gram-Schmidt space-time adaptive canceller using adaptive lattice filters
[AD-A189684] 14 p1959 N88-21684
CANCER
DNA damage and repair in human skin in situ
[DE87-014288] 03 p0356 N88-12241
Analysis of annular microstrip antennas for hyperthermic applicators
[PB88-181508] 19 p2643 N88-25679
CANISTERS
U CANS
CANNONS
U GUNS (ORDNANCE)
CANONICAL FORMS
Canonical transformations and exact invariants for dissipative systems
[DE87-703663] 04 p0485 N88-12985
Asymptotically stable all-pass transfer functions: Canonical form, parametrization and realization
[PB87-123972] 06 p0763 N88-14684
Canonical coordinates for partial differential equations
[NASA-CR-182486] 11 p1535 N88-19170
Introduction to classical mechanics of systems with constraints, part 1
[DE88-701055] 13 p1832 N88-20957
Introduction to classical mechanics of systems with constraints, part 3
[DE88-701057] 13 p1850 N88-21073
Bogolyubov transformation in relativistic theory of gravitation
[DE88-701592] 16 p2232 N88-23329
Perturbation theory for dual semigroups. Part 4: The intertwining formula and the canonical pairing
[CWI-AM-R8802-PT-4] 18 p2569 N88-25258
Canonical construction of differential operators intertwining representations of real semisimple Lie groups
[DE88-701852] 20 p2845 N88-26882
Canonical forms in the control of DPS
[AD-A194671] 23 p3270 N88-29461
Canonical variables and canonical integrals for motion in near-circular orbits 24 p3446 N88-30512
CANOPIES
Resistance of canopy materials against chemicals
[PML-1985-22] 05 p0569 N88-13466
Determination of canopy loads for a light aircraft by wind tunnel testing and computer modelling
[BU-353] 14 p1869 N88-21167
Measurements of aerodynamic forces on unsteadily moving bluff parachute canopies
16 p2202 N88-23137
Vision through aircraft transparencies
23 p3242 N88-29294
CANOPIES (VEGETATION)
Moisture determinations in and under vegetation canopies. Part 2: Results after parameterization of the CLOUD model
[FEL-1986-63] 01 p0064 N88-10410
Estimating scattered and absorbed radiation in plant canopies by remote sensing
[NASA-CR-181390] 02 p0193 N88-11205
Proceedings of the Third Airborne Imaging Spectrometer Data Analysis Workshop
[NASA-CR-181552] 05 p0611 N88-13755
The use of airborne imaging spectrometer data to determine experimentally induced variation in coniferous canopy chemistry 05 p0612 N88-13761
Toward detecting California shrubland canopy chemistry with AIS data 05 p0613 N88-13764
Analysis of airborne imaging spectrometer data for the Ruby Mountains, Montana, by use of absorption-band-depth images 05 p0614 N88-13771
Application of remote sensing to agricultural field trials
[ISBN-90-6754-089-7] 06 p0729 N88-14483
Monte Carlo method calculation of spectral brightness coefficient of vegetation cover as function of illumination conditions 08 p1008 N88-16113
Detection of soil erosion with Thematic Mapper (TM) satellite data within Pinyon-Juniper woodlands
[NASA-CR-182476] 09 p1185 N88-17103
Improved canopy reflectance modeling and scene inference through improved understanding of scene pattern
[NASA-CR-182488] 10 p1347 N88-18049
The angular reflectance signature of the canopy hot spot in the optical regime
[DE88-005385] 11 p1505 N88-18991
Proceedings of the Forest-Atmosphere Interaction Workshop
[CONF-8510250] 12 p1641 N88-19824
Remote sensing of earth terrain
[NASA-CR-182677] 13 p1790 N88-20711
Modeling surface exchanges: The soil-vegetation-atmosphere continuum
14 p1937 N88-21553
Report of Atmospheric-Canopy Exchange Panel
[DE88-004478] 14 p1944 N88-21597
Surface CO results from the ABLE-2B expedition to Amazonia
[INPE-4501-PRE/1258] 15 p2093 N88-22469
Use of energy emission for detecting the necessity of irrigation in wheat in field conditions
[INPE-4461-TDL/318] 16 p2229 N88-23315
Radar penetration in the Amazonian rain forest
17 p2352 N88-24015
Radar penetration in the Amazonian rain forest
17 p2358 N88-24044
Structure and dynamics of vegetation in the middle semi-arid tropics. Quixaba's Caatinga (PE): Terrain analysis of MSS/LANDSAT data 17 p2358 N88-24049
History of wildland fires on Vandenberg Air Force Base, California
[NASA-TM-100983] 18 p2549 N88-25134
The use of satellite imagery for municipal conditions in rural recording in Pereira Barreto (SP)
19 p2682 N88-25944
Study of evolution of vegetal cover and slide scars in the Cubatao municipality-Sao Paulo
19 p2683 N88-25947
Remote sensing technique applied to vegetation as an aid to municipal planning 19 p2683 N88-25951
Canopy reflectance modeling in a tropical wooded grassland
[NASA-CR-182981] 19 p2685 N88-25961
Hydrologic models for land-atmosphere retrospective studies of the use of LANDSAT and AVHRR data
[NASA-CR-182862] 20 p2818 N88-26716
Foliar nitrate reductase: A marker for assimilation of atmospheric nitrogen oxides
[DE88-010453] 21 p2971 N88-27648
CANS
Modal analyses of the Kernville diagnostic canister
[DE88-003268] 07 p0870 N88-15277
CRRES chemical release mechanisms
14 p1874 N88-21192
Optimization of mechanical/corrosion properties of Ti-CODE 12 plate and sheet. Part 2: Thermomechanical processing effects
[DE88-007493] 19 p2616 N88-25517
CANT
U SLOPES
CANTILEVER BEAMS
The matrix exponential in transient structural analysis
05 p0593 N88-13619
Bending of a bonded beam as a test method for adhesive properties
[AD-A184813] 05 p0609 N88-13736
Beam and column buckling under directed loading
[PB87-124004] 06 p0722 N88-14436
Active control of flexural vibrations in beams
06 p0794 N88-14866
A fiber-resin micromechanics analysis of the delamination front in a DCB specimen
[NASA-TM-100540] 10 p1294 N88-17737
Research and development of surface skimming bulk wave devices for sensor applications
[AD-A187504] 11 p1470 N88-18766
Active vibration control of a cantilevered beam with three elastic coordinates
[AD-A188824] 12 p1636 N88-19797
CANTILEVER MEMBERS
NT CANTILEVER BEAMS
Buckling of braced monosymmetric cantilevers: Timoshenko energy approach
[PB87-133849] 06 p0723 N88-14445
A parametric study of embedded cantilever retaining walls: The results of a finite element study
[RR-CE83] 24 p3383 N88-30152
CANTILEVER WINGS
U WINGS
CAPACITANCE
Development of a repetitive 1-MV, 22-kJ Marx generator
[DE87-011286] 01 p0038 N88-10242
Improper ferroelectricity: A theoretical and experimental study
[AD-A184614] 03 p0381 N88-12397
Polymer materials for pressure sensors
06 p0676 N88-14141
Extraction of MOS VLSI (Very-Large-Scale-Integrated) circuit models including critical interconnect parasitics
[AD-A185847] 08 p0979 N88-15914
Minimum necessary intensity of source of preionization for stabilization of a self-sustaining laser discharge with mean power raised by electron beam or X-rays
[PB87-178158] 09 p1171 N88-17024
Design of a charge sensitive preamplifier on high resistivity silicon
[DE88-003491] 10 p1323 N88-17907
Capacitive charge division in centroid finding cathode readouts in MWPCs
[DE88-003545] 10 p1333 N88-17969
Electrosorptive detection based on double-layer capacitance for selective anion monitoring in ion chromatography. Part 1: Mercury electrodes
[AD-A188780] 12 p1606 N88-19603
Recent advances in capacitance type of blade tip clearance measurements
[NASA-TM-101291] 19 p2603 N88-25460
Noise in piezoresistive and capacitive sensors
19 p2670 N88-25874
Air loading effects on a capacitively sensed membrane supported silicon accelerometer
19 p2672 N88-25886
Defects in high-mobility semiconductor systems
[AD-A192298] 20 p2879 N88-27090
Ice detector
[NASA-CASE-LAR-13776-1] 23 p3217 N88-29149
CAPACITANCE-VOLTAGE CHARACTERISTICS
Calculating depletion region carrier concentrations with capacitance-voltage measurements and etching
[AD-A189630] 15 p2141 N88-22777
CAPACITORS
Investigations into the design of multi-terawatt magnetic switches
[DE87-012014] 01 p0040 N88-10254
The role of hydrogen in radiation-induced defect formation in polysilicon gate MOS devices
[DE87-012374] 06 p0785 N88-14814

Radiation hardness evaluation of thin film ferroelectric capacitors
[DE88-001357] 07 p0848 N88-15147
A numerical thermal model of the rapid solidification parameters in the capacitor discharge welding process
[DE88-002206] 07 p0864 N88-15244
Capacitor analysis for RF antennas
[DE88-004178] 10 p1318 N88-17883
Pulsed current transformer for low inductive loads
[AD-A187224] 10 p1324 N88-17913
The soft/hard wet anodization of aluminum oxide and its use in a thin film multilayered capacitor
[AD-A187575] 10 p1325 N88-17919
Radiation response of thin oxides grown by rapid thermal oxidation and rapid thermal annealing techniques
[DE88-003632] 11 p1561 N88-19347
Advanced capacitor development
[AD-A189985] 15 p2059 N88-22276
The application of high temperature superconductors to space electrical power distribution components
[NASA-TM-100901] 16 p2171 N88-22939
Joint angle sensors for closed-loop control
19 p2673 N88-25891
High power pulse energy system concept
[AD-A192440] 21 p2935 N88-27429
Development of inductive storage pulsed power generators
[AD-A193878] 22 p3117 N88-28521
Stress corrosion of ceramic materials
[AD-A191979] 23 p3195 N88-29016
In-house capacitor technology program
[AD-A194804] 24 p3367 N88-30049

CAPE HATTERAS (NC)
Research on the physical oceanography of the Gulf Stream
[AD-A188512] 12 p1649 N88-19877

CAPE KENNEDY LAUNCH COMPLEX
Short-term forecasting of lightning based on the surface wind field at Kennedy Space Center
02 p0208 N88-11306
Short range forecasting of sea breeze generated thunderstorms at the Kennedy Space Center: A real-time experiment using a primitive equation mesoscale numerical model
02 p0211 N88-11324

CAPES (LANDFORMS)
NT CAPE HATTERAS (NC)

CAPILLARIES (ANATOMY)
Models of cerebral-body perfusion and cerebral chemical transport
[AD-A194945] 24 p3407 N88-30283

CAPILLARY CIRCULATION
U CAPILLARY FLOW

CAPILLARY FLOW
Experimental study of thermocapillary flows in a thin liquid layer with heat fluxes imposed on the free surface
[NASA-TM-100252] 04 p0445 N88-12763
Computation of free boundaries
[PB87-226023] 06 p0763 N88-14680
Study of helium transfer technology for STICCR: Fluid management
[NASA-CR-177463] 10 p1291 N88-17720
Continual capillary viscosimetry using extrusiograph techniques
[PB88-166293] 15 p2046 N88-22195
Instrumental aspects of capillary supercritical fluid chromatography
[ETN-88-92242] 16 p2174 N88-22960
Some numerical methods for the computation of capillary free boundaries governed by the Navier-Stokes equations
[REPT-87-69] 16 p2206 N88-23167
Liquid motions in partially filled containers: Preliminary results of the D-1 mission --- Spacelab
[NLR-MP-86042-U] 20 p2802 N88-26629
Polymeric heat pipe wick
[NASA-CASE-GSC-13019-1] 23 p3214 N88-29133

CAPILLARY TUBES
Boundary integral analysis of flow and deformation of long bubbles in capillaries
[DE88-002110] 10 p1326 N88-17927

CAPILLARY WAVES
NT BAROCLINIC WAVES
NT GRAVITY WAVES
NT RIPPLES
Dispersion equation for plane capillary-gravity wave on free surface of viscous incompressible fluid
04 p0459 N88-12842
Influence of surfactants on damping of gravity-capillary waves. 1: Frequency dependence
04 p0459 N88-12843

CAPTIVE TESTS
NT STATIC FIRING
NT STATIC TESTS

CAPTURE CROSS SECTIONS
U ABSORPTION CROSS SECTIONS

CAPTURE EFFECT
On symmetric TVD schemes
19 p2639 N88-25659

CARBAMATES (TRADENAME)
NT URETHANES
Carbamates, atropine, and diazepam: Effects on performance in the running rat
[AD-A188009] 11 p1517 N88-19062

CARBAZOLES
Research on stable processible conducting polymers for electronic applications
[AD-A190246] 15 p2044 N88-22180

CARBIDES
NT ALUMINUM CARBIDES
NT BORON CARBIDES
NT CHROMIUM CARBIDES
NT NIOBIUM CARBIDES
NT SILICON CARBIDES
NT TITANIUM CARBIDES
NT TUNGSTEN CARBIDES
Surface chemistry of transition metal carbides: A theoretical analysis
[AD-A184237] 03 p0291 N88-11829
JPRS report: Science and technology. Japan
[JPRS-JST-87-028] 06 p0675 N88-14130
Effects of ion implantation on cavitation erosion of a cobalt based metal/carbide alloy
[AD-A187239] 10 p1303 N88-17793
A comparison of uranium nitride and mixed carbide fuels swelling 17 p2435 N88-24485
Development of fine-grained carbide-particle hardened Hadfield manganese steels
[DE88-008919] 19 p2617 N88-25523

CARBOHYDRATE METABOLISM
NT HYPOGLYCEMIA
Significance of nutrition to change in human carbohydrate and lipid metabolism under emotional stress 19 p2703 N88-26073
Physiology of prolonged bed rest
[NASA-TM-101010] 22 p3130 N88-28607

CARBOHYDRATES
NT CELLULOSE
NT GLUCOSE
NT GLYCOGENS
NT NUCLEOSIDES
NT STARCHES
Manipulation of muscle glycogen concentrations using high and low carbohydrate diets and exercise
[AD-A187732] 11 p1519 N88-19069
Workshop on Atmospheric OH
[BPT-7/87] 18 p2538 N88-25063
Effect of carbohydrate oxidation on the tropospheric HOx-system 18 p2539 N88-25067

CARBON
NT CARBON 12
NT CARBON 13
Theory of the carbon phase diagram at high pressures and temperatures
[DE87-012245] 01 p0028 N88-10180
Materials preparation and longevity in hyperthermal atomic oxygen 03 p0297 N88-11862
Carbon abundances and C12/C13 ratios in M giants 04 p0515 N88-13167
The initiation and growth of fatigue cracks in carburised 9Cr1Mo steel 05 p0603 N88-13696
Studies of metal/carbon surface chemistry
[DE87-009545] 07 p0829 N88-15029
Non-steady group combustion of a cloud of char particles
[DE87-010773] 08 p0966 N88-15849
The influence of yellow substances on remote sensing of sea-water constituents from space 08 p1044 N88-16308
Total and partial cross sections for electron capture for C(q+) (q=6-2) and O(q+) (q=8-2) ions in collisions with H, H2 and He atoms
[IPPJ-AM-56] 09 p1252 N88-17501
Clusters: Link between molecules and solids
[AD-A188170] 11 p1543 N88-19224
Spectroscopic studies of a laser-produced carbon plasma in the near and extreme ultraviolet 11 p1553 N88-19292
Carbon residue studies of polyphenyl ethers and ester-based lubricants using a microcarbon residue tester
[AD-A188585] 12 p1611 N88-19632
Tungsten-carbon multilayer system studied with X-ray scattering
[DE88-005749] 13 p1735 N88-20373
An interpretation of the ethylenic, carbidic, and graphite auger lineshapes of chemisorbed carbon species
[AD-A189092] 13 p1736 N88-20379
Improved methods for high resolution electron microscopy
[DE88-005731] 13 p1774 N88-20609
Microprobe examination of composite materials produced by burning of Ti, Cr, C powders with powder of any one Fe-group metal 14 p1886 N88-21269
An investigation of the infrared emission spectra of carbon condensates 14 p1886 N88-21272
Laboratory amorphous carbon: A possible analog of cometary dust 14 p2009 N88-21981
Hermetic coating of optical fibers
[AD-A189886] 15 p2044 N88-22177
Characterization of precipitates in a niobium-zirconium-carbon alloy
[NASA-TM-100848] 16 p2178 N88-22981
Fracture morphologies of carbon-black-loaded SBR (Styrene-Butadiene Rubber) subjected to low-cycle, high-stress fatigue
[DE88-006808] 16 p2181 N88-23002
High temperature solid lubrication by catalytically generated carbon
[AD-A190804] 16 p2182 N88-23004
Interface characterization of Cu-Cu and Cu-Ag-Cu low temperature solid state bonds
[AD-A191015] 16 p2283 N88-23667
Krypton based adsorption type cryogenic refrigerator
[NASA-CASE-NPO-17334-1-CU] 17 p2331 N88-23917
Cryogenic regenerator including saran-carbon heat conduction matrix
[NASA-CASE-NPO-17291-1-CU] 17 p2337 N88-23946
Liquid carbon
[AD-A191707] 18 p2491 N88-24776
Electrical conduction in thin film carbons
[AD-A191726] 18 p2491 N88-24780
Electron-Rayleigh wave interaction in thin film carbons
[AD-A191727] 18 p2492 N88-24781
Anomalous temperature-dependent negative magnetoresistance in pregraphitic carbons
[AD-A191725] 19 p2619 N88-25535
Zero-dimensional calculation for ZT-H
[DE88-009175] 19 p2731 N88-26217
Carbon analysis in natural olivine crystals of deep origin
[NASA-TT-20311] 19 p2734 N88-26239
Reduced-activation austenitic stainless steels: The Fe-Cr-C system
[DE88-008091] 20 p2773 N88-26442
Carbon deposition model for oxygen-hydrocarbon combustion, volume 1
[NASA-CR-179375] 21 p2908 N88-27254
Carbon deposition model for oxygen-hydrocarbon combustion, volume 2
[NASA-CR-179376] 21 p2908 N88-27255
Refractory films from spin-cast carbon
[DE88-011251] 21 p2919 N88-27327
Erosion/redeposition modeling and calculations for carbon
[DE88-010382] 22 p3057 N88-28139
A study of the interaction of NO2 with carbon particles
[DE88-010778] 22 p3118 N88-28524
High spatial resolution observations of neutral atomic carbon in the molecular clouds M17 and W51
[MPE-PREPRINT-109] 22 p3164 N88-28846
Real-time measurements of the size fractionation of ambient black carbon aerosols at elevated humidities
[DE88-010870] 23 p3215 N88-29138

CARBON COMPOUNDS
NT ALUMINUM CARBIDES
NT BORON CARBIDES
NT CALCITE
NT CALCIUM CARBONATES
NT CARBIDES
NT CARBON DIOXIDE
NT CARBON MONOXIDE
NT CARBONATES
NT CHLOROCARBONS
NT CHROMIUM CARBIDES
NT FLUOROCARBONS
NT NIOBIUM CARBIDES
NT POLYCARBONATES
NT SILICON CARBIDES
NT TITANIUM CARBIDES
NT TUNGSTEN CARBIDES

CARBON CYCLE
Carbon dioxide and climate: Summaries of research in FY 1987
[DE88-000916] 06 p0744 N88-14574
Atmospheric carbon dioxide and the global carbon cycle: The key uncertainties
[DE88-005059] 15 p2092 N88-22465
Simulation analysis of moored fluorometer time series from the Mid-Atlantic Bight
[DE88-006066] 15 p2099 N88-22505
Bibliography on tropical rain forests and the global carbon cycle. Volume 1: An introduction to the literature
[DE88-010761] 22 p3118 N88-28523

CARBON DIOXIDE
Detection of CO2-induced climate change
[DE87-013127] 01 p0071 N88-10457
Testimony to the US Senate on the greenhouse effect
[DE87-013995] 01 p0071 N88-10458
Master index for the carbon dioxide research state-of-the-art report series
[DE87-012757] 01 p0072 N88-10459
Contribution of bubbles and waves to air-sea CO2 flux, with implications for remote sensing
[PB87-203980] 01 p0073 N88-10467
Reduction of CO2 to methanol and methane by photo and dark reactions on semiconductor and metal electrodes
[PB87-226825] 02 p0156 N88-10975
High temperature CO2 study: Anti-Stokes coherent Raman diffusion and infrared spectroscopy
[ESA-TT-1048] 03 p0282 N88-11777
Kinetics of CO adsorption on nickel using time resolved vibration spectroscopy
[ETN-87-90615] 03 p0289 N88-11814
Carbon dioxide treatment for scale removal and control in potable water systems
[AD-A184346] 04 p0412 N88-12556
Organic molecules on meteoritic solid substrates
[NASA-CR-181570] 05 p0560 N88-13411
Controlled ecological life support systems: Development of a plant growth module 05 p0630 N88-13854
Interpretation of our present terrestrial climatic record
[DE88-000223] 06 p0744 N88-14573
The carbon dioxide chaperon efficiency for the reaction H + O2 + M yields HO2 + M from ignition delay times behind reflected shock waves
[NASA-TM-100125] 07 p0830 N88-15036
Welding in high pressure CO2 atmosphere --- underwater welding
[PB87-144044] 07 p0862 N88-15232
Concept, construction, and experimental testing of a polychromator for a Raman lidar for the simultaneous telemetering of carbon dioxide and water vapor, relative to oxygen
[GKSS-87/E/20] 09 p1191 N88-17134
Mesospheric dynamics and chemistry from SME data
[NASA-CR-182465] 09 p1191 N88-17139
Energy transfer studies with lasers
[DE88-004864] 10 p1337 N88-17991
Role of carbon dioxide in correction of coagulation hemostasis under hypoxic conditions
10 p1365 N88-18160
Effects of breathing air containing contaminants such as CO2, CO and hydrocarbons at 1 and 5 atmospheres
[PB88-132915] 11 p1521 N88-19084
Solar-assisted hydrogen generation by photoelectrocatalysis
[PB88-160932] 12 p1605 N88-19597
Carbon dioxide and climate 14 p1936 N88-21545
Observational and theoretical studies of greenhouse climate effects
[DE88-006237] 14 p1948 N88-21621
Sublimation characteristics of H2O comet nucleus with CO2 impurities 14 p2010 N88-21988
Atmospheric carbon dioxide and the global carbon cycle: The key uncertainties
[DE88-005059] 15 p2092 N88-22465
A laser-based photoacoustic spectrometer for direct breath C-13O2/C-12O2 measurement
[DE88-004915] 15 p2101 N88-22516
A glossary for carbon dioxide and climate
[DE88-007885] 19 p2689 N88-25982
A shock-tube experiment on gases mixing processes associated with CO2/N2 mixing gasdynamic laser
[ISAS-RN-350] 20 p2797 N88-26598
The seasonal exchange of carbon dioxide between the atmosphere and the terrestrial biosphere: Extrapolation from site-specific models to regional models
[DE88-007870] 20 p2822 N88-26740
Catalytic activation of carbon dioxide by metal complexes
[AD-A192310] 21 p2909 N88-27262
Surface energy balance of three general circulation models: Current climate and response to increasing atmospheric CO2
[DE88-010967] 21 p2975 N88-27673
Validation of a modified one-step rebreathing technique for non-invasive measurement of submaximal cardiac output
[AD-A192852] 21 p2967 N88-27735
Regional intercomparisons of General Circulation Model predictions and historical climate data: CO2
[DE88-010416] 23 p3235 N88-29248
Miniature respiratory sensor
[AD-A193430] 23 p3243 N88-29300
Coadsorption of H2O and CO2 on the Martian surface
23 p3307 N88-29702

CARBON DIOXIDE CONCENTRATION
Master index for the carbon dioxide research state-of-the-art report series
[DE87-012757] 01 p0072 N88-10459
Carbon Dioxide observational platform system (CO-OPS) Feasibility Study
[NASA-CR-179225] 06 p0671 N88-14113
Carbon dioxide and climate: Summaries of research in FY 1987
[DE88-000916] 06 p0744 N88-14574
Model validation research: Comparison of simulated and observed climate patterns for the past 18,000 years
[DE88-004945] 13 p1800 N88-20759
Atmospheric carbon dioxide and the global carbon cycle: The key uncertainties
[DE88-005059] 15 p2092 N88-22465
Surface CO results from the ABLE-2B expedition to Amazonia
[INPE-4501-PRE/1258] 15 p2093 N88-22469
Understanding CO2 and climate
[PB88-167655] 16 p2234 N88-23341
Physiological effects on man of long duration confinement in a carbon dioxide enriched environment
19 p2695 N88-26017
Visual sensitivities under reduced oxygen
[AD-A195628] 24 p3406 N88-30279

CARBON DIOXIDE LASERS
Picosecond CO2 laser interactions with polyatomic molecules
[DE87-012072] 01 p0051 N88-10327
Feasibility of alpha particle measurement in a magnetically confined plasma by CO2 laser Thomson scattering
[DE88-000039] 02 p0241 N88-11522
Investigation of BN CO2 wave guide laser
03 p0302 N88-11905
Gas dynamic characteristics in past axial flow CO2 laser 03 p0327 N88-12067
Methods for a coherent CO2 laser heterodyne radar system
[ESA-TT-1035] 03 p0328 N88-12076
USSR report: Physics and mathematics
[JPRS-UPM-87-006] 06 p0708 N88-14344
Compensation of small-scale phase distortions by means of a Fourier phase corrector
06 p0708 N88-14345
Repetitively pulsed and continuous wave CO2 lasers pumped by a pulsed self-sustained discharge for thermal processing 06 p0709 N88-14346
Effect of clarifying the atmosphere in relation to quasi-monochromatic CO2 laser radiation
06 p0709 N88-14348
NO2 heterodyne frequency measurements with a tunable diode laser, a CO laser transfer oscillator and CO2 laser standards
[NASA-CR-182393] 06 p0710 N88-14353
Strategic Defense Initiative Organization/DARPA (Defense Advanced Research Projects Agency) workshop on laser propulsion. Volume 1: Executive summary
[DE87-003254] 06 p0768 N88-14722
Production-process CO2 laser with amplified pulse-repetition operation 06 p0771 N88-14739
Nonuniformity of electromagnetic field at Lambda = 10.6 micron wavelength inside atmospheric aerosol particles
06 p0772 N88-14743
Dynamic restructuring of pulsed CO2 laser frequency and multiple-peak generation in a cell with IR-absorbing gas in the resonator 07 p0919 N88-15580
Study of vibration relaxation in active medium of CO2-laser using phase-absorption method
07 p0919 N88-15582
Laser thermal propulsion
[AD-A186407] 07 p0933 N88-15666
Study of combination type CO2 laser welding system
[PB87-143764] 08 p0992 N88-16002
Remote measurement of aerosol stream velocity with continuous-wave CO2-laser 08 p1079 N88-16506
Continuously frequency-tunable high-pressure CO2-laser with plasmatic cathode
09 p1238 N88-17418
Airborne Doppler lidar detection of wind shear. Results of performance analysis 10 p1275 N88-17627
Experiments for the high resolution detection of moving targets using a CO2 laser radar
[MBB-UA-1044/87] 10 p1316 N88-17864
Operation of electron-beam controlled CO2 laser at 6 atmospheres 11 p1468 N88-18758
Nonlinear absorption of CO2 laser radiation in p-type InSb
[DE88-004055] 11 p1492 N88-18906
Coherent laser radar system theory
[AD-A188759] 13 p1774 N88-20612
Influence of nonlinear spectroscopic effects on atmospheric propagation of intense laser radiation at 10.6 microns wavelength 13 p1789 N88-20705
Characteristics of welds joining parts of high-strength pipe steels and produced by beam of continuous-wave CO2-laser 14 p1897 N88-21325
Laser technology: CO2 lasers and laser optics
[ETN-88-91469] 14 p1915 N88-21441
Comprehensive model for laser instability in a CO2 laser with gaseous saturable absorber
14 p1979 N88-21808
Laser processing-status, perspectives
15 p2050 N88-22211
Compound ceramic processing
15 p2050 N88-22212
Single crystal growth by laser CVD
15 p2050 N88-22213
Hard ceramic film by laser PVD
15 p2051 N88-22216
Coupled high power waveguide laser research
[AD-A189800] 15 p2071 N88-22345
Laser evaporation studies
[AD-A189815] 15 p2071 N88-22346
Engineering planetary lasers for interstellar communication
[NASA-CR-180780] 17 p2311 N88-23825
An optical preamplifier for detection of CO2 laser radiation
[AD-A190790] 18 p2520 N88-24949
High power axial flow CO2 laser
[ETN-88-91951] 18 p2521 N88-24959
Design of catalytic monoliths for closed-cycle carbon dioxide lasers
[NASA-CR-182983] 18 p2558 N88-25185
A two-wavelength infrared interferometer/polarimeter system for CIT (Compact Ignition Tokamak)
[DE88-007681] 18 p2579 N88-25321
Design and calibration of a two-channel low-noise heterodyne receiver for use in a CO2 laser Thomson scattering alpha particle diagnostic
[DE88-007866] 19 p2728 N88-26201
Alternative analysis of CO2-laser-produced plasma waves
[DE88-008434] 19 p2730 N88-26215
A CO2 laser Thomson scattering diagnostic for fusion product alpha particle measurement
[DE88-007683] 20 p2857 N88-26965
Investigations on beam quality of high frequency excited CO2 high performance lasers
[ETN-88-92363] 21 p2954 N88-27550
Transverse CO2 laser two-dimensional gain distributions
[AD-A196240] 24 p3378 N88-30119

CARBON DIOXIDE REMOVAL
Electrochemical carbon dioxide concentrator subsystem development
[NASA-CR-177411] 08 p1053 N88-16353
Advanced EMU electrochemically regenerable CO2 and moisture absorber module breadboard
[NASA-CR-172054] 21 p2993 N88-27754

CARBON DIOXIDE TENSION
NT HYPERCAPNIA
NT HYPOCAPNIA
Human adaptation to various hypercapnic conditions in relation to salivary electrolyte dynamics and renal function 12 p1664 N88-19977

CARBON FIBER REINFORCED PLASTICS
Joints in carbon fibre reinforced composites
[BR99969] 01 p0019 N88-10114
Theoretical investigation of stress concentrations in damaged carbon fibre reinforced plastic plate structures. Volume 1: Main text
[BR99872-VOL-1] 03 p0280 N88-11761
Theoretical investigation of stress concentrations in damaged carbon fibre reinforced plastic plate structures. Volume 2: Tables, figures and plates
[BR99873-VOL-2] 03 p0280 N88-11762
Investigation of reliability of strength values measured on CFRP test bars by statistical methods. Part 1: Probability distributions for strength analysis
[ESA-TT-1036] 03 p0336 N88-12115
Solar converging method 04 p0403 N88-12504
Carbon-fiber reinforced plastics
04 p0403 N88-12506
Design and control of repairs of carbon fiber lift augmentation flaps in the ATR42 aircraft
[SNIAS-872-111-112] 05 p0529 N88-13217
A hybrid fibreglass-CFRP cloth for new furnishings --- aircraft cabins
[SNIAS-872-111-109] 05 p0558 N88-13396
Determination of the fiber ratio in carbon fiber/resin composites by means of image analysis
[SNIAS-872-422-101] 05 p0558 N88-13398
Measurement and control of damage in composite materials: Nondestructive controls by thermography, holography, and radiography
[SNIAS-872-430-110] 05 p0559 N88-13403

Comparison of fire resistance of metallic and nonmetallic structures
[SNIAS-872-551-101] 05 p0572 N88-13489
Study of damage in carbon fiber-epoxy composite materials. Utilization to assess broken specimens
[DCQ/L-45-650/F] 06 p0678 N88-14152
Flaw effects: Behavior in operation of delamination in a crossed multilayer composite specimen
[DCQ/L-47-363/F] 06 p0678 N88-14153
Measurement of mechanical parameters to define damage criteria in delamination of crossed stratified layers
[DCQ/L-47-361/F] 06 p0678 N88-14154
Comparison of the strength of single and multiple bolted joints in CFRP
[PB87-123766] 06 p0722 N88-14438
Hybrid FEM (Finite Element Method) approach to stress distribution in the vicinity of a notch in non-homogeneous materials
[PB87-143392] 07 p0868 N88-15268
Effects of aviation fluids on fiber composite material
[FOA-C-20674-2.6] 08 p0965 N88-15840
The effect of thermal shock on carbon fiber epoxy composites
[FOA-C-20675-2.6] 08 p0965 N88-15841
Fatigue and damage tolerance design data for carbon fibre composites
[BAE-MSM-R-GEN-0454] 09 p1138 N88-16818
Moisture plotting of carbon fiber composite in flight operations
[MBB-UT-119/87] 09 p1138 N88-16823
Integrity control of carbon fiber reinforced plastics (CFRP) structural elements. Conclusion with respect to the control methodology of CFRP primary structures in manned space flight and the implications to the design, analysis and testing of CFRP structural elements, executive summary
[MBB-TR-RB517-014/85] 09 p1139 N88-16824
Mechanical properties of carbon fiber reinforced thermoplastic matrix composites
[NAL-TR-934] 09 p1139 N88-16827
Ultrasonic inspection of advanced CFRP structures by computer-controlled, pulse-echo technique
[ETN-88-91665] 09 p1177 N88-17051
To determine the stress distribution in the vicinity of GRP end pads where the specimen is held and loaded (CFC coupon specimens) --- glass reinforced plastic (GRP) carbon fiber composite (CFC)
[BAE-WST-R-RES-CFC-12023] 09 p1182 N88-17080
Further tests to determine the stress distribution in the vicinity of GRP end pads where the specimen is held and loaded (CFC coupon specimens) --- glass reinforced plastic (GRP) carbon fiber composite (CFC)
[BAE-WST-R-RES-CFC-12023-ADD-1] 09 p1182 N88-17081
Colloquium on damage mechanics of graphite/expoxy laminates during fatigue
[DFVLR-MITT-87-08] 11 p1448 N88-18630
Influence of different parameters on damage development --- carbon fiber reinforced plastics 11 p1448 N88-18632
Initiation and propagation of damage in notched unidirectional and multidirectional CFRE resin laminates 11 p1449 N88-18633
Statistical evaluation of experimental results from fatigue strength tests on CFRP composite materials 11 p1449 N88-18635
Damage mechanisms of CFRP riveted joints 11 p1449 N88-18636
Damage mechanisms and fatigue life prediction of graphite/epoxy laminates 11 p1449 N88-18637
Reinforcing of thermoplastic polycarbonate and polysulfone with carbon fibers: Production and characteristics of UD-compound objects
[NASA-TT-20158] 13 p1735 N88-20374
Studies of traverse impact damage in composite materials using a Hopkinson pressure-bar technique
[OUEL-1706/87] 14 p1883 N88-21255
An investigation of the mechanical properties of improved carbon fibre composite materials
[RAE-TR-86021] 14 p1884 N88-21259
Stress-strain behaviour of a bolt hole in carbon fibre composite plates
[BU-354] 14 p1923 N88-21460
Fractography of composite delamination
[NASA-CR-182757] 15 p2030 N88-22096
Elementary characterization of Fibredux 913 CTS 5 34 percent preimpregnated carbon-epoxy from Ciba Geigy
[M-484300] 16 p2171 N88-22941
Delamination analysis in crossed layer composites
[REPT-48-447/F] 16 p2171 N88-22942
Fatigue damage development of various CFRP-laminates
[NASA-TT-20247] 16 p2172 N88-22945
Investigation of the long term effects of aging on carbon epoxy composites exposed naturally to the weather under cyclic loads. (Results of sampling after 2.5 years). Test report M1-641300
[CEAT-39/M/79-C-M1-641300] 17 p2316 N88-23834
GARTEUR TP-037: Impact damage tolerance of carbon fiber and hybrid laminates
[RAE-TR-87057] 17 p2316 N88-23837
Elementary characterization of preimpregnated carbon epoxy T400H/DA0506 from STRUCTIL. Test report M6-577100
[CEAT-047426] 18 p2478 N88-24703
Detecting delaminations in CFRP specimens using X-ray techniques
[FFA-TN-1988-04] 18 p2479 N88-24704
High temperature resins for injection. High temperature pre-impregnated
[RC-648676] 20 p2780 N88-26486
Rocket motor case materials. An evaluation of new fibers for composites
[FOA-C-20696-2.1] 21 p2906 N88-27245
Determination of the glass transition temperature of cured composite materials
[DT-87/62-R] 21 p2906 N88-27246
Design and implementation of contact ultrasonic sensors to assess internal damage
[I-177/87] 21 p2906 N88-27247
Relation between the mechanical characteristics of carbon-resin composites and their impact strength
[REPT-48-284/F] 21 p2907 N88-27249
Aging of CFRP due to longterm storage in heated air
[DFVLR-FB-88-05] 21 p2922 N88-27345
Use of microwave measuring systems for the nondestructive control of resins and composites
[REPT-881-430-123] 21 p2959 N88-27576
Nondestructive tests and high performance composite structures
[SNIAS-881-430-119] 23 p3188 N88-28969
Investigations on the modification of structural reliability by substitution of aluminum by carbon fiber reinforced plastics in aircraft construction
[ILR-MITT-195] 24 p3339 N88-29877
Thermal stress analysis in PMR-15 carbon fibre laminates
[ETN-88-93123] 24 p3341 N88-29886
Rupture of carbon fiber reinforced plastics (T300-914) composite materials: influence of initial first ply failures on the fatigue behavior
[SNIAS-881-422-103] 24 p3342 N88-29892
Evaluation of the potential health hazards associated with the machining of carbon fiber composites
[AD-A194835] 24 p3408 N88-30286

CARBON FIBERS
Anti-abrasion protection with highly organized materials
[DE87-014238] 01 p0029 N88-10187
Electron beam irradiation effects on carbon fiber reinforced PEEK composite
[DE87-753001] 02 p0142 N88-10890
The effect of bromination of carbon fibers on the coefficient of thermal expansion of graphite fiber-epoxy composites
[NASA-TM-100236] 02 p0143 N88-10899
Composite structural materials
[NASA-CR-181416] 02 p0190 N88-11186
Carbon-fiber reinforced aluminum 04 p0403 N88-12507
Carbon fiber reinforced glass matrix composites for space based applications
[AD-A184355] 04 p0410 N88-12546
Study of zero CTE (Coefficients of Thermal Expansion) of graphite/epoxy composites
[DE87-013557] 04 p0412 N88-12554
The use of aeroelastic wind tunnel models to prove structural design 05 p0551 N88-13355
Interfacial shear strength of pitch and high strain pan fibers in an epoxy matrix
[AD-A185966] 07 p0826 N88-15011
Macroscopic distribution of fiber finish
[DCQ/L-48-283/F] 07 p0827 N88-15013
Improving the interlaminar shear strength of carbon fiber-epoxy composites through carbon fiber bromination
[NASA-TM-100248] 07 p0827 N88-15018
Effects of processing variables on the behavior of E-glass/913 and XAS carbon fibre/913 laminates subjected to hot/wet environmental conditions
[BR101940] 09 p1138 N88-16820
The strength of hybrid composites
[BR101991] 09 p1138 N88-16821
Effect of post-cure heat-treatment on static and fatigue behaviour of XAS-914C carbon fibre composite
[AD-A186943] 10 p1294 N88-17735
Structure and surface characterizations of high strength carbon fibers
[AD-A189642] 15 p2029 N88-22087
Interfacial structure-property relationships at the fiber-matrix interphase in advanced composites
[AD-A190649] 15 p2030 N88-22093
Thermal expansion behavior of randomly oriented short carbon fiber reinforced copper composites
[NASA-TT-20175] 15 p2031 N88-22099
Reciprocating sliding wear characteristics of copper-carbon fiber composites
[NASA-TT-20176] 15 p2031 N88-22100
Eddy current nondestructive inspection of graphite epoxy using ferrite cup core probes
[AD-A189823] 15 p2074 N88-22365
Thermal conductivity, electrical conductivity and specific heat of copper-carbon fiber composite
[NASA-TT-20172] 16 p2172 N88-22948
Surface and interfacial properties of carbon fibers
[NASA-CR-182890] 16 p2173 N88-22951
High-temperature thermal conductivity of a carbon-bonded carbon-fiber insulation 17 p2402 N88-24281
Aging of carbon fibers
[SNPE-NT-10/86/CRB/NP] 18 p2479 N88-24707
Size effects in the electrical resistivity of benzene-derived carbon fibers
[AD-A191708] 18 p2491 N88-24777
Photoconductivity in carbon fibers
[AD-A191728] 18 p2492 N88-24782
Effect of uniaxial stress on the Raman spectra of graphite fibers
[AD-A191730] 18 p2492 N88-24783
Influence of carbon fiber surface treatment
[ETN-88-92536] 18 p2492 N88-24787
Electronic and structural studies of carbon/carbon composites
[AD-A191729] 19 p2609 N88-25481
Observation of metallic conductivity in liquid carbon
[AD-A191723] 19 p2618 N88-25533
Microstructure of thin intercalated benezene derived graphite fibers
[AD-A191724] 19 p2618 N88-25534
Thermoplastic coating of carbon fibers
[NASA-CR-183067] 20 p2767 N88-26407
The crystallization of tough thermoplastic resins in the presence of carbon fibers
[NASA-CR-182984] 20 p2776 N88-26464
Effect of the matrix on the creep-behavior of carbon-carbon composite
[AD-A193211] 21 p2905 N88-27235
Effects of electron beam irradiation on mechanical properties at low and high temperature of fiber reinforced composites using PEEK as matrix material
[DE88-753134] 21 p2905 N88-27239
Fabrication of SiC fiber reinforced glass matrix by extrusion process and investigation of its mechanical properties
[ETN-88-92367] 21 p2906 N88-27244
Refractory fibers surface treatment
[REPT-47-803/F] 21 p2922 N88-27339
Computer modeling for surface properties of carbon fibers 21 p2928 N88-27383
Effects of applied stress and temperature on the nonlinear elastic properties of graphite fibers
[AD-A194469] 22 p3050 N88-28093
An investigation of some basic properties of hybrid composite materials
[AD-A194136] 23 p3189 N88-28975
A test for interfacial effects and stress transfer in ceramic matrix composites
[NASA-CR-182873] 24 p3340 N88-29880
Brominated graphite fibers and method of producing the same
[NASA-CASE-LEW-14698-1] 24 p3341 N88-29888
Transverse expansion of individual carbon and graphite filaments
[AD-A195073] 24 p3342 N88-29891
Evaluation of the potential health hazards associated with the machining of carbon fiber composites
[AD-A194835] 24 p3408 N88-30286

CARBON ISOTOPES
NT CARBON 12
NT CARBON 13

CARBON MONOXIDE
Carbon monoxide (CO) concentration in the air as a purity parameter
[INPE-4232-PRE/1107] 01 p0067 N88-10429
A study of carbon monoxide distribution determinations for a global transport model
[NASA-CR-181423] 01 p0067 N88-10432
The effect of additives on the reactivity of palladium surfaces for the chemisorption and hydrogenation of carbon monoxide: A surface science and catalytic study
[DE87-014685] 02 p0145 N88-10909
Surface chemistry of transition metal carbides: A theoretical analysis
[AD-A184237] 03 p0291 N88-11829

Characterization of catalysts with metal-support effects and of the species adsorbed on their surfaces
[DE87-014636] 04 p0414 N88-12564
K-CO on transition metals: A local ionic interaction
[AD-A184342] 04 p0496 N88-13056
The structure of adsorbed sulfur and carbon on molybdenum and rhenium single crystal surfaces, and their influence on carbon monoxide and hydrocarbon chemisorption
[DE88-001393] 04 p0499 N88-13073
The delta upsilon = 1 fundamental bands of carbon monoxide in late-type stars 04 p0517 N88-13177
Carbon monoxide and turbulence-chemistry interactions: Blowoff and extinction of turbulent diffusion flames
[AD-A186276] 07 p0828 N88-15025
Energy transfer studies with lasers
[DE88-004864] 10 p1337 N88-17991
Investigation of effects of short-term exposure to high concentrations of carbon monoxide on operator's psychophysiological functions 10 p1361 N88-18133
Effects of breathing air containing contaminants such as CO2, CO and hydrocarbons at 1 and 5 atmospheres
[PB88-132915] 11 p1521 N88-19084
Resonance energy transfer between carbon monoxide and oxygen molecules using dye laser intracavity absorption spectroscopy
[AD-A188488] 12 p1689 N88-20104
Determination of the content of CO(+) and H2O(+) ions in the tail of Comet Giacobini-Zinner and Comet Halley 14 p2006 N88-21964
The observability of carbon monoxide in planetary nebulae
[ETN-88-91498] 14 p2011 N88-21994
Kinetics of CO oxidation over a deactivated Rh(111) single crystal catalyst
[DE88-003000] 19 p2613 N88-25504
The response of ultrathin palladium gate sensors to hydrogen and carbon monoxide
19 p2672 N88-25885
Mechanism of the nitric oxide-carbon monoxide-oxygen reaction over a single crystal rhodium catalyst
[DE88-006274] 21 p2910 N88-27268
Effects of air pollution on human exercise performance
[AD-A192660] 22 p3131 N88-28617
Modelling of CO oxidation in dilution jet flows
24 p3351 N88-29947
Recent observations of carbon monoxide in the Amazon Rain Forest
[INPE-4478-PRE/1245] 24 p3390 N88-30186

CARBON MONOXIDE LASERS
NO2 heterodyne frequency measurements with a tunable diode laser, a CO laser transfer oscillator and CO2 laser standards
[NASA-CR-182393] 06 p0710 N88-14353

CARBON STARS
Analysis of the carbon star G77-61
[ETN-87-90422] 01 p0109 N88-10707
Basic properties and variability
02 p0252 N88-11593
Spectroscopy and nonthermal processes
02 p0252 N88-11594
Circumstellar chemistry 02 p0253 N88-11598
Thermal atmospheric models
02 p0253 N88-11599
Synthetic spectra for the N-type carbon star TX Psc
04 p0516 N88-13173
Water masers associated with 2 carbon stars: EU Andromedae and V778 Cygni 04 p0517 N88-13176
Low mass stars with mass loss and low-luminosity carbon star formation 06 p0801 N88-14900
Asymptotic giant branch populations in composite stellar systems 13 p1854 N88-21098

CARBON STEELS
NT LOW CARBON STEELS
A quantitative statistical model for cleavage fracture initiation in carbide strengthened steels
[ETN-87-90735] 01 p0025 N88-10157
Laminated ferrous composites based on ultrahigh carbon (UHC) steels
[AD-A184617] 03 p0280 N88-11764
Method for the ultrasonic inspection of the soundness of the metal in weld joints in two-ply pipes
[BLL-CE-TRANS-8265-(9022.09)]
04 p0453 N88-12805
Crack initiation studies in hydrogen embrittled spring steel strip 05 p0605 N88-13710
Fatigue thresholds of C,Mn steels in saline environments 06 p0717 N88-14403
Fatigue, fracture and strain hardening of high carbon hardened alloy steel
[AD-A186101] 07 p0831 N88-15043
Weldability of a leaded carbon steel
[PB88-110341] 07 p0861 N88-15225
Propagation of fatigue crack in the medium-carbon steel containg both martensite and ferrite
[PB87-143962] 07 p0869 N88-15273
Development of a constitutive equation for HSLA (High-Strength Low-Alloy)-100 at cryogenic temperatures
[AD-A189243] 13 p1740 N88-20408
Environmental integrity of coating/metal interface
[AD-A192184] 18 p2492 N88-24786
Diffusion and solubility of some interstitial impurities in deformed metals
[DE88-701859] 21 p2914 N88-27296
Multi-metallic galvanic corrosion
[AD-A195995] 24 p3353 N88-29963

CARBON 12
Carbon abundances and C12/C13 ratios in M giants
04 p0515 N88-13167
Probing the possibility of a (12)C/(13)C abundance gradient from observations of interstellar CH+
[DE88-008908] 20 p2884 N88-27125
Dispersion effects in elastic electron scattering from C12
[B8805297] 23 p3281 N88-29536

CARBON 13
Solid state C-13 NMR characterization of textiles: Qualitative and quantitative analysis
[AD-A184349] 04 p0419 N88-12598
Carbon abundances and C12/C13 ratios in M giants
04 p0515 N88-13167
Probing the possibility of a (12)C/(13)C abundance gradient from observations of interstellar CH+
[DE88-008908] 20 p2884 N88-27125

CARBON-CARBON COMPOSITES
Carbon-carbon composites and Aerospatiale. State of the art and prospects
[SNIAS-872-430-108] 05 p0559 N88-13401
Hydroburst test of a carbon-carbon involute exit cone
[NASA-TP-2556] 06 p0671 N88-14112
Stress rupture behavior of silicon carbide coated, low modulus carbon/carbon composites
[NASA-CR-180863] 06 p0678 N88-14150
Interface characteristics and the mechanical properties of metal matrix composites
[AD-A186441] 08 p0966 N88-15845
A study of the mechanical behavior of a 2-D carbon-carbon composite 11 p1449 N88-18638
Study of the mechanical behavior of a 2-D carbon-carbon composite
[NASA-CR-182594] 11 p1451 N88-18649
Nondestructive evaluation of carbon-carbon coatings
[AD-A189524] 13 p1748 N88-20453
Strength and failure rate of composite materials with carbon in ceramic matrix 16 p2180 N88-22995
Composite piston
[NASA-CASE-LAR-13435-1] 17 p2346 N88-23981
Electronic and structural studies of carbon/carbon composites
[AD-A191729] 19 p2609 N88-25481
Electrical resistivity of carbon-carbon composites
[AD-A193006] 20 p2768 N88-26410
High temperature testing of C/C (Carbon/Carbon) composites
[AD-A193012] 20 p2768 N88-26411
Effect of the matrix on the creep-behavior of carbon-carbon composite
[AD-A193211] 21 p2905 N88-27235
Studies in support of oxidation-resistant composite materials
[AD-A193320] 21 p2905 N88-27238
On the electrical properties of carbon/carbon composites densified by chemical deposit in vapor phase
[SNIAS-881-430-117] 21 p2907 N88-27252
Soot and radiation in a gas turbine combustor
[AD-A191991] 23 p3179 N88-28924
Spallation and dynamic fracture as an effect of laser induced shock-waves
[AD-A193513] 23 p3188 N88-28971
Ultrafine microstructure composites prepared by chemical vapor deposition
[AD-A193849] 23 p3189 N88-28973
Very high temperature materials for mechanical application
[SNIAS-881-430-106] 23 p3189 N88-28978
Creep of carbon yarn and carbon-carbon composites at high temperatures and high stresses
[AD-A195224] 24 p3340 N88-29878

CARBONACEOUS CHONDRITES
Analysis of laser extracted volatiles in carbonaceous chondrites 06 p0793 N88-14861
Noble gases, C,N, and Si isotopes in interstellar SiC form the Murchison carbonaceous chondrite
24 p3442 N88-30483

CARBONACEOUS MATERIALS
NT GRAPHITE
NT PYROLYTIC GRAPHITE

CARBONACEOUS METEORITES
Organic molecules on meteoritic solid substrates
[NASA-CR-181570] 05 p0560 N88-13411

CARBONACEOUS ROCKS
NT COAL
Effective use of principal component analysis with high resolution remote sensing data to delineate hydrothermal alteration and carbonate rocks 05 p0612 N88-13758

CARBONATES
NT CALCITE
NT CALCIUM CARBONATES
NT POLYCARBONATES
DTA/DSC studies of phase equilibria in binary mixtures of barium carbonate with alkali carbonates
[DE87-001195] 02 p0194 N88-11213
Determination of optimum electrolyte composition for molten carbonate fuel cells literature review
[DE88-001015] 10 p1348 N88-18058
Evaluation and compilation of thermodynamic properties of high temperature chemical species
[AD-A187509] 11 p1452 N88-18654
Composite ceramic superconducting filaments for superconducting cable
[AD-A187833] 11 p1558 N88-19312
Studies on the use of propylene carbonate as a high-voltage insulator
[DE88-011786] 22 p3057 N88-28141

CARBONIC ANHYDRASE
North Carolina Biomolecular Engineering and Materials Applications Center (NC-BEMAC)
[AD-A190923] 16 p2237 N88-23364

CARBONIZATION
Process for preparing transition metal nitrides and transition metal carbonitrides and their reaction intermediates
[DE88-000849] 06 p0679 N88-14162
Disclination structures in carbon and graphite
[AD-A191056] 17 p2322 N88-23868
Influence of carbon fiber surface treatment
[ETN-88-92536] 18 p2492 N88-24787

CARBONYL COMPOUNDS
Surface modification by metal deposition and laser irradiation 01 p0023 N88-10148
The spectroscopy and reaction kinetics of coordinatively unsaturated metal carbonyls
[AD-A190533] 15 p2035 N88-22124

CARBOXYL GROUP
High-molecular compounds (selected articles)
[AD-A184668] 03 p0293 N88-11842
Studies on syntheses of amine-carboxyboranes (boron analogues of amino acids) and derivatives
[AD-A184838] 05 p0557 N88-13386
The radiation sensitivity of select metal chelate polymers: Mechanistic changes at higher energies
[AD-A193467] 23 p3196 N88-29019

CARBOXYLATES
Carboxylate formation at the interface between a polyimide coating and cobalt 17 p2320 N88-23859

CARBOXYLIC ACIDS
NT ACETIC ACID
NT ACRYLIC ACID
NT DICARBOXYLIC ACIDS
NT NICOTINIC ACID
Organic molecules on meteoritic solid substrates
[NASA-CR-181570] 05 p0560 N88-13411

CARBURETORS
A study of the interaction of laser light with liquid propellant drops
[AD-A185117] 05 p0587 N88-13582

CARBURIZING
A theoretical analysis of the deactivation of metal surfaces upon carburization
[AD-A184556] 03 p0290 N88-11821
Wear of hard steel in rolling lubricated contact
[RP-699] 03 p0332 N88-12094
Sliding-wear properties of retained austenite in carburized layer
[PB87-149092] 07 p0833 N88-15054
Effects of ion implantation on cavitation erosion of a cobalt based metal/carbide alloy
[AD-A187239] 10 p1303 N88-17793
Surface fatigue life of CBN and vitreous ground carburized and hardened AISI 9310 spur gears
[NASA-TM-100960] 19 p2677 N88-25916

CARCINOGENS
Toxic effects of man-made mineral fibers with particular reference to ceramic fibers
[AD-A187949] 11 p1519 N88-19072

CARCINOMA
U CANCER

CARDIAC VENTRICLES
Diagnostic value of some load tests in evaluation of nonspecific electrocardiographic changes
07 p0895 N88-15426

CARDIOGRAPHY
NT BALLISTOCARDIOGRAPHY
NT ECHOCARDIOGRAPHY
NT ELECTROCARDIOGRAPHY
NT MAGNETOCARDIOGRAPHY
CARDIOLOGY
The use of heart rate in the prescription and evaluation of exercise programs
[AD-A186454] 08 p1049 N88-16336
Challenges of physiological monitoring in a Navy operational setting 16 p2239 N88-23374
CARDIOVASCULAR SYSTEM
NT AORTA
NT ARTERIES
NT CAPILLARIES (ANATOMY)
NT CARDIAC VENTRICLES
NT HEART
NT MYOCARDIUM
NT VEINS
Cardiac contractility in weightlessness according to spatial ballistocardiography 07 p0890 N88-15393
Changes in regional and central hemodynamics during seven-day water immersion 07 p0895 N88-15421
Diagnostic value of some load tests in evaluation of nonspecific electrocardiographic changes 07 p0895 N88-15426
The use of heart rate in the prescription and evaluation of exercise programs
[AD-A186454] 08 p1049 N88-16336
Respiratory and cardiovascular responses to cold stress following repeated cold water immersion
[AD-A186460] 08 p1050 N88-16340
Forecasting complications of cardiovascular disease in flight personnel 10 p1361 N88-18136
JPRS Report: Science and Technology. USSR: Space Biology and Aerospace Medicine, volume 21, no. 6, November - December 1987
[JPRS-USB-88-004] 10 p1364 N88-18150
Results of long-term electrocardiographic monitoring of cosmonauts 10 p1364 N88-18152
Effect of hypercapnic-hypoxic test on cariorespiratory parameters of individuals with neurocirculatory dystonia 10 p1367 N88-18169
Cardiovascular adaptation to zero-g during a long term flight (237 days) on board the Salyut 7 Soviet space station (1984) 12 p1655 N88-19920
Cardiac and peripheral circulation assessment by ultrasound on 3 astronauts during two 7-day space flights (1982 Salyut-7 - 1985 STS 51G) 12 p1656 N88-19921
Load and control of the cardiocirculatory system in weightlessness 12 p1656 N88-19922
Renal effects of anti-gravity suit inflation in man in relation to cardiovascular and hormonal changes 12 p1661 N88-19959
Effects of intense, time-constrained mental effort on hemodynamics and cardiovascular function 12 p1664 N88-19975
The effects of normal and therapeutic baths on the central vascular organs of persons with healthy hearts, as measured by X-ray
[NASA-TT-20252] 13 p1811 N88-20818
Cardiovascular effects of weightlessness and ground-based simulation
[NASA-TM-88314] 18 p2551 N88-25140
JPRS report: Science and technology. USSR: Space Biology and Aerospace Medicine, volume 22, no. 1, January - February 1988
[JPRS-USB-88-005] 19 p2702 N88-26069
Results of medical research conducted in 1985 during long-term spaceflights 19 p2702 N88-26070
Hemostasis parameters of individuals with neurocirculatory dystonia submitted to dry immersion 19 p2703 N88-26072
Models of cerebral-body perfusion and cerebral chemical transport
[AD-A194945] 24 p3407 N88-30283
CARDS
The effects of data structure on total time on test plots
[AD-A187628] 10 p1389 N88-18296
Optical memory cards: A comparison with other current technologies and potential military applications
[AD-A187287] 10 p1425 N88-18512
The mechanical properties of card measured by photographic Moire
[NPL-DMOM-87] 14 p1923 N88-21463
CARGO
NT AIR CARGO
Developmental airdrop testing techniques and devices
[AGARD-AG-300-VOL-6] 04 p0398 N88-12481
Analysis of shock and vibration environments for cargo on C9B transport aircraft 08 p0999 N88-16051
Centaur G Prime modal test 09 p1181 N88-17075
Steps toward lunar settlement
[DE88-009141] 21 p2900 N88-27213
CARGO AIRCRAFT
NT C-130 AIRCRAFT
NT C-135 AIRCRAFT
NT F-27 AIRCRAFT
General equilibrium characteristics of a dual-lift helicopter system
[NASA-TP-2615] 12 p1573 N88-19407
CARGO SPACECRAFT
Design study for asteroidal exploitation 03 p0389 N88-12445
STS propellant scavenging systems study. Part 2, volume 2: Cost and WBS/dictionary
[NASA-CR-179276] 10 p1290 N88-17717
CARIBBEAN REGION
Caribbean and Central America wind energy assessment
[DE88-005134] 11 p1507 N88-19002
The role of aviation technology in the Caribbean Basin
[NASA-CR-183069] 20 p2745 N88-26289
Geologic results obtained from the use of SPOT imagery along plate boundaries: Examples in the East African rift and of the northern-Caribbean collision 22 p3105 N88-28437
CARIBBEAN SEA
Current velocity and hydrographic observations in the Straits of Florida, the Caribbean Sea and offshore of the Antillean Archipelago: Subtropical Atlantic Climate Studies (STACS) 1986
[PB88-160767] 14 p1951 N88-21628
CAROTENE
Cross section of resonant Raman scattering of light by polyenes 07 p0920 N88-15591
CARPATHIAN MOUNTAINS (EUROPE)
Detailed analysis of a mesoscale convective complex situation in the Carpathian Basin (Europe) 02 p0207 N88-11296
CARRIER DENSITY (SOLID STATE)
First report on InGaAs hall device 14 p1903 N88-21372
Free carrier nonlinear optics 14 p1977 N88-21796
High density femtosecond excitation of nonthermal carrier distributions in intrinsic and modulation doped GaAs quantum wells 14 p1977 N88-21798
Dynamical aspects of carrier tunneling in semiconductor superlattices 14 p1977 N88-21799
Femtosecond studies in hot carrier relaxation in GaAs and AlGaAs 14 p1977 N88-21801
Development of a model procedure for the determination of volume diffusion lengths by transient measurements on monocrystal silicon solar cells
[ETN-88-92119] 20 p2821 N88-26733
Auger recombination in GaSb/AlSb-multi quantum well heterostructures 20 p2862 N88-27001
CARRIER FREQUENCIES
Performance of a rapid carrier acquisition circuit for satellite ground terminal modems
[RSRE-TEST-REPORT-87/CC3/2] 22 p3071 N88-28227
CARRIER INJECTION
The qualitative determination of high injection effects in flux-loaded P-I-N diodes using the recombination radiation measuring method
[ETN-88-91475] 11 p1560 N88-19336
Neutron radiation tolerance of Au-activated silicon 17 p2408 N88-24316
Direct subpicosecond measurement of carrier mobility of photoexcited electrons in GaAs 19 p2659 N88-25803
Longitudinally localized optical carrier injection for femtosecond transport studies 19 p2659 N88-25806
CARRIER LIFETIME
An investigation of the equivalent circuit and carrier lifetimes of Si/SiGe heterostructure p-n diodes for frequencies between 0.5 and 18.5 MHz
[FOA-C-30469-3.2] 09 p1256 N88-17529
Carrier lifetime versus ion-implantation dose in Silicon On Sapphire 19 p2658 N88-25791
Auger recombination in GaSb/AlSb-multi quantum well heterostructures 20 p2862 N88-27001
Control of carrier lifetime in PbTe nipi superlattices by external photoinjection 20 p2863 N88-27006
CARRIER MOBILITY
NT ELECTRON MOBILITY
NT HOLE MOBILITY
First report on InGaAs hall device 14 p1903 N88-21372
Radiation effects in silicon
[DE88-006642] 16 p2282 N88-23659
Direct subpicosecond measurement of carrier mobility of photoexcited electrons in GaAs 19 p2659 N88-25803
Picosecond carrier transport in GaAs quantum wells 19 p2660 N88-25813
High power storage system based on thin film solid ionics
[AD-A193623] 23 p3291 N88-29598
Temperature dependence of conductivity and of Hall coefficients for noble metal films
[ETN-88-92981] 23 p3294 N88-29616
CARRIER MODULATION
U MODULATION
CARRIER ROCKETS
U LAUNCH VEHICLES
CARRIER TO NOISE RATIOS
Optimized tracking of RF carriers with phase noise, including Pioneer 10 results 04 p0434 N88-12694
High frequency acoustic underwater communication with low probability of being traced
[REPT-4-87] 09 p1242 N88-17447
The relationship between vision carrier-to-noise ratio and picture signal-to-noise ratio in a System I television receiver
[BBC-RD-1987/23] 10 p1318 N88-17877
CARRIER TRANSPORT (SOLID STATE)
A flux analysis of the solar cells
[INPE-4247-PRE/1120] 08 p1022 N88-16186
Picosecond carrier transport in GaAs quantum wells 19 p2660 N88-25813
Carrier transport in semiconductor magnetic sensors under nonuniform fields 19 p2672 N88-25888
CARRIER WAVES
Optimum filters and smoothers design for carrier phase and frequency tracking
[NASA-CR-182654] 12 p1618 N88-19679
CARRINGTON ROTATION
U SOLAR ROTATION
CARTAN SPACE
Torsion as a source of expansion in a Bianchi type I universe in the self-consistent Einstein-Cartan theory of a perfect fluid with spin density
[AD-A184200] 03 p0322 N88-12037
Raychaudhuri equation in the self-consistent Einstein-Cartan theory with spin-density
[NASA-TM-101145] 17 p2447 N88-24546
Inflation in Einstein-Cartan theory with energy-momentum tensor with spin
[NASA-TM-101164] 17 p2447 N88-24547
Inevitable inflation in Einstein-Cartan theory with improved energy-momentum tensor with spin
[NASA-TM-101146] 18 p2586 N88-25365
CARTESIAN COORDINATES
Fundamentals of turbulence for turbulence modeling and simulation 03 p0312 N88-11971
Point processes in the plane
[AD-A186017] 07 p0913 N88-15542
Supporting valid time: An historical algebra
[AD-A187740] 11 p1565 N88-19368
COMESH: A corner mesh finite difference code to solve multigroup diffusion equations in multidimensions
[DE88-701248] 15 p2108 N88-22555
A multigrid approach for the solution of a nonlinear diffusion equation in a time-dependent area using Cartesian coordinates
[GMD-STUDIEN-122] 16 p2257 N88-23491
A formulation for the boundary-layer equations in general coordinates
[NASA-TM-100079] 18 p2459 N88-24600
QN3D: A 3-dimensional quasi-neutral hybrid particle-in-cell code with applications to the tilt mode instability in field reversed configurations 18 p2580 N88-25325
Spatial dynamics of deformable multibody systems with variable kinematic structure 20 p2813 N88-26687
Application of rectangular co-ordinates to the problem of laminar combined convection in a straight horizontal tube whose circumference is heated nonuniformly
[PDR/CFDU/IC/33] 22 p3076 N88-28263
CARTOGRAPHY
U MAPPING
CARTRIDGE ACTUATED DEVICES
U ACTUATORS
U EXPLOSIVE DEVICES
CARTS
Software modifications to total data reporting accessory for metabolic measurement cart
[AD-A193641] 22 p3132 N88-28623
CASCADE CONTROL
Closed-loop system analysis using Lyapunov stability theory 04 p0483 N88-12978
Description and analysis of a cascade control of fluid flow
[PB87-112686] 06 p0698 N88-14282
Robust design of cascade control
[REPT-88-006] 22 p3142 N88-28687
CASCADE FLOW
Experimental determination of the oscillatory forces on two turbine blade profiles
[ETN-87-90417] 01 p0007 N88-10037
Theoretical investigations of three turbine cascades using a two dimensional time marching procedure
[DFVLR-FB-87-02] 01 p0057 N88-10362

Navier-Stokes cascade analysis with a stiff Kappa-Epsilon turbulence solver
[NASA-TM-100218] 02 p0123 N88-10778
Numerical analysis of cascade flow solving Navier-Stokes equations 05 p0536 N88-13262
Inverse design method for two-dimensional transonic cascades 05 p0536 N88-13263
Effects of free stream turbulence, Reynolds number and incidence angle on axial turbine cascade performance 05 p0548 N88-13339
Unsteady aerodynamics of an oscillating cascade in a compressible flow field
[NASA-TM-100219] 05 p0549 N88-13346
Post stall behavior in axial-flow compressors
[AD-A185712] 06 p0665 N88-14081
The unsteady gas flow through stator and rotor of a turbomachine 10 p1281 N88-17660
Transonic blade design on rotational stream surfaces 10 p1282 N88-17671
Investigation of dihedral effects in compressor cascades 10 p1282 N88-17672
Flow patterns induced by vortices
[NAL-TR-932] 10 p1332 N88-17963
Mixed direct-inverse problem of transonic cascade 15 p2054 N88-22244
Effect of freestream turbulence on a two dimensional cascade, with different surface roughness, at high Reynolds number
[AD-A190615] 15 p2065 N88-22316
Designs of profiles for cascades
[NASA-TT-20161] 15 p2067 N88-22326
Theoretical investigations of three turbine cascades using a 2-D time marching procedure
[ESA-TT-1077] 16 p2207 N88-23170
Development of a method of calculating unstable flows of cascades separated at the leading edge
[PB87-228714] 19 p2598 N88-25437
Cascades with harmonically oscillating blades in supersonic flow
[NASA-TT-20323] 19 p2599 N88-25446
Numerical analysis of three dimensional cascade flow by solving Navier-Stokes equations 19 p2638 N88-25650
Application of computational fluid dynamics to design of compressor cascade 19 p2639 N88-25655
A Navier-Stokes solver for cascade flows
[NASA-CR-181682] 19 p2666 N88-25856
A Navier-Stokes study of cascade flow fields including inlet distortion and rotating stall
[AD-A193109] 21 p2943 N88-27483
Investigation of oscillating cascade aerodynamics by an experimental influence coefficient technique
[NASA-TM-101313] 22 p3039 N88-28041
Modeling of momentum transport of axially parallel turbulent flows in rod cascades
[ETN-88-92978] 23 p3214 N88-29131
Numerical solutions of unsteady inviscid transonic turbine cascade flows
[AD-A196111] 24 p3316 N88-29748
Aerodynamics in ground effect and predicted landing ground roll of a fighter configuration with a secondary-nozzle thrust reverser
[NASA-TP-2834] 24 p3317 N88-29752
Three-dimensional elliptic grid generation technique with application to turbomachinery cascades
[NASA-TM-101330] 24 p3372 N88-30078

CASCADE WIND TUNNELS
Hot-wire measurements of compressor blade wakes in a cascade wind tunnel
[AD-A194737] 23 p3181 N88-28936

CASCADES
On helicity fluctuations and the energy cascade in turbulence
[NASA-CR-178403] 03 p0321 N88-12028

CASCADES (FLUID DYNAMICS)
U FLUID DYNAMICS

CASCODE MOSFET
U FIELD EFFECT TRANSISTORS

CASES (CONTAINERS)
NT ROCKET ENGINE CASES
Structural frequency functions for an impulsive, distributed forcing function 05 p0594 N88-13627
Low temperature storage container for transporting perishables to space station
[NASA-CASE-MFS-28248-1] 18 p2498 N88-24817

CASKS
U BARRELS (CONTAINERS)

CASSEGRAIN OPTICS
Optical photometer for the Tirgo telescope
[IFSI-87-5] 05 p0650 N88-13985
Design, fabrication and delivery of a miniature Cassegrainian concentrator solar array system
[NASA-CR-179237] 06 p0730 N88-14493

CASSINI MISSION
Study of a Radio Relay Link (RRL). Cassini mission. Data package for final presentation
[ESA-CR(P)-2472] 07 p0847 N88-15138

CAST ALLOYS
Influence of boron on porosity in nickel-base superalloy castings 03 p0299 N88-11877
Fatigue crack growth behavior of A356-T6 cast aluminum alloy 05 p0599 N88-13660
Durability and damage tolerance of aluminum castings
[AD-A186444] 10 p1341 N88-18013
Effects of thermal and thermo-mechanical treatments on the mechanical properties of centrifugally cast alloy 718
[AD-A188195] 11 p1458 N88-18690
Processing, physical metallurgy and creep of NiAl + Ta and NiAl + Nb alloys
[NASA-CR-182113] 14 p1890 N88-21295

CASTING
NT CENTRIFUGAL CASTING
NT INVESTMENT CASTING
NT SLIP CASTING
Activities at government research laboratories reported 04 p0403 N88-12503
Development of advanced fiber reinforced ceramics
[DE88-000779] 04 p0420 N88-12604
Advances in processing techniques for nickel aluminides
[DE87-014571] 05 p0566 N88-13449
Cyclic deformation behaviour of cast irons with various graphite shapes in the temperature range 20 C less than or = T less than or = 500 C 06 p0715 N88-14384
Selection of polymer materials for manufacturing optical parts
[AD-A185898] 07 p0836 N88-15069
Fabrication of YBa2Cu3O7 superconducting ceramics
[DE88-003012] 07 p0938 N88-15701
Development of a shell system for DS moulds at RR precision casting facility — directional solidification (DS)
[PNR90400] 09 p1151 N88-16893
Materials development for JPL oxygen plant
[DE88-003067] 10 p1297 N88-17752
Cast iron-base alloy for cylinder/regenerator housing
[NASA-CR-182116] 12 p1608 N88-19613
SBIR-Long fluoride fiber
[AD-A188595] 13 p1754 N88-20492
Structure and mechanical properties of metal matrix composites made using semi-solid processes: The case of the system Al-Si/SiC
[ETN-88-92299] 17 p2316 N88-23836
Compositional redistribution during casting of Hg sub 0.8 Cd sub 0.2 Te alloys
[NASA-TM-101151] 17 p2326 N88-23893
Fabrication of reactor shields at the Y-12 plant 17 p2402 N88-24283
Fluid flow modeling in casting processes and its implications
[DE88-010009] 20 p2810 N88-26671
Spatial organization of homopolymer chains inside spherical polybutadiene domains of SB diblock copolymers
[AD-A193390] 21 p2918 N88-27321
Preliminary investigation of flow modeling during solid propellant processing
[AD-A196168] 24 p3357 N88-29987

CASTING SOLVENTS
U PLASTICIZERS

CASTINGS
NT INGOTS
Studies on estimation of nickel in zinc base die casting by D.C. polarography
[PD-MT-8729] 04 p0417 N88-12588
Hydrogen induced cracks in armor steel weldments fabricated with austenitic filler alloys
[AD-A188733] 13 p1740 N88-20406
Increasing the rate at which ceramic castings undergo preliminary heat-treatment in an ultra-high frequency magnetic field 14 p1886 N88-21275

CAT SCANNER
U COMPUTER AIDED TOMOGRAPHY

CATABOLISM
Long duration confinement of aquatic organisms in weightlessness (aquaspace) 07 p0887 N88-15380
A program for the study of skeletal muscle catabolism following physical trauma
[AD-A189771] 15 p2102 N88-22521

CATACLYSMIC VARIABLES
Ultraviolet observations of AM Her — cataclysmic variable
[MPE-PREPRINT-92] 02 p0250 N88-11581
The hard X-ray eclipse in the intermediate polar EX Hydrae
[MPE-PREPRINT-95] 02 p0251 N88-11582
The Parkes radio survey of active chromosphere stars 04 p0511 N88-13141
SW UMa and V426 Oph: EXOSAT surprises 19 p2740 N88-26269
EXO033319-2554.2: A 55-MG eclipsing AM Herculis binary
[MPE-PREPRINT-114] 22 p3163 N88-28838
Intermediate polars observed in Brazil in the last eight years
[INPE-4567-PRE/1308] 24 p3454 N88-30559
Activities in astrophysics
[INPE-4582-PRE/1316] 24 p3456 N88-30570

CATALASE
Experimental study of protective effect of antioxidant enzymes-superoxide dismutase and catalase-when using intermittent toxic modes of hyperbaric oxygenation 19 p2707 N88-26094

CATALOGS
Source hierarchy list. Volume 1: A through D
[AD-A185900] 07 p0941 N88-15722
Component data base for space station resistojet auxiliary propulsion
[NASA-CR-180834] 10 p1293 N88-17731
Catalog of open clusters and associated interstellar matter
[NASA-RP-1202] 23 p3300 N88-29652

CATALOGS (PUBLICATIONS)
NT ASTRONOMICAL CATALOGS
Source header list. Volume 1: A through K
[AD-A184000] 04 p0501 N88-13086
Bibliographic relationships: Toward a conceptual structure of bibliographic information used in cataloging 06 p0791 N88-14852
Catalog of compartment fire model algorithms and associated computer subroutines
[PB88-110861] 07 p0839 N88-15087
NASA scientific and technical publications: A catalog of Special Publications, Reference Publications, Conference Publications, and Technical Papers, 1987
[NASA-SP-7063(02)] 15 p2149 N88-22830
Report on the Second Catalog Interoperability Workshop
[NASA-TM-100701] 19 p2718 N88-26135

CATALYSIS
Catalytic processes for space station waste conversion
[NASA-CR-177423] 01 p0077 N88-10491
A surface science investigation of potential intermediates, catalysts, and promoters in the synthesis of higher alcohols by metals
[DE87-014188] 02 p0144 N88-10906
The effect of additives on the reactivity of palladium surfaces for the chemisorption and hydrogenation of carbon monoxide: A surface science and catalytic study
[DE87-014685] 02 p0145 N88-10909
Photocatalytic electrochemistry at a biological-membrane metal-colloid interface
[DE87-009122] 02 p0166 N88-11041
The applicability of the catalytic wet-oxidation to CELSS 03 p0360 N88-12264
Surface catalytic degradation study of two linear perfluoropolyalkylethers at 345 C
[NASA-TP-2774] 04 p0410 N88-12543
Surface mediated photocatalysis
[AD-A188882] 12 p1603 N88-19589
Chromatographic and related reactors
[AD-A188452] 12 p1605 N88-19599
The redox chemistry of some peroxo and superoxo metal ion complexes
[AD-A189159] 12 p1606 N88-19606
Model catalyst studies of SMSI (Strong Metal/Support Interactions) and the role of D-electrons in chemisorption and catalysis
[DE88-004518] 13 p1738 N88-20393
On copper peroxide
[NASA-TT-20263] 15 p2037 N88-22135
Improvements to Raney copper zinc methanol synthesis catalysts 17 p2318 N88-23844
ECUT (Energy Conversion and Utilization Technologies) program: Biocatalysis Project
[NASA-CR-182917] 17 p2370 N88-24110
A scientific basis for an alternate cathode architecture
[AD-A191498] 18 p2481 N88-24717
An improved external recycle reactor for determining gas-solid reaction kinetics
[NASA-TM-101160] 19 p2611 N88-25492
Catalytic activation of carbon dioxide by metal complexes
[AD-A192310] 21 p2909 N88-27262
Precursor chemistry and the structure of silica aerogels
[DE88-011253] 21 p2920 N88-27328
Perfluoropolyalkylether lubricants under boundary conditions: Iron catalysis of lubricant degradation
[AD-A193241] 21 p2956 N88-27560

CATALYSTS
NT ELECTROCATALYSTS

Ruthenium catalysts and their use in ammonia production
[GB-PATENT-2-136-704-A] 01 p0020 N88-10123
Boronium complexes as polymer catalysts
[GB-PATENT-2-161-475-A] 01 p0026 N88-10166
A surface science investigation of potential intermediates, catalysts, and promoters in the synthesis of higher alcohols by metals
[DE87-014188] 02 p0144 N88-10906
A life test of a 22-Newton (5-lbf) hydrazine rocket
[NASA-TM-100232] 03 p0278 N88-11750
A theoretical analysis of the deactivation of metal surfaces upon carburization
[AD-A184556] 03 p0290 N88-11821
Surface coatings and catalyst production by electrodeposition 03 p0297 N88-11863
Mass transport by diffusion 03 p0297 N88-11864
Characterization of catalysts with metal-support effects and of the species adsorbed on their surfaces
[DE87-014636] 04 p0414 N88-12564
Phase purity of NiCo2O4, a catalyst candidate for electrolysis of water
[NASA-TM-100239] 05 p0556 N88-13385
Activated metal oxide surfaces as highly basic and reducing environments
[AD-A184958] 05 p0561 N88-13417
Catalytic combustion of methane
[PB88-123112] 07 p0829 N88-15028
Studies of metal/carbon surface chemistry
[DE87-009545] 07 p0829 N88-15029
Model Cu/ZnO catalysts for methanol synthesis: The role of surface structure
[DE88-002354] 07 p0830 N88-15037
Studies of supported metal catalysts
[DE88-002546] 07 p0831 N88-15038
Deactivation of alumina based catalysts
11 p1455 N88-18673
Properties of lanthanide oxides as supports for transition metal catalysts
[DE88-004520] 11 p1456 N88-18678
Electron microscopy study of morphology and composition of a ferrisilicate catalyst
[DE88-005754] 11 p1562 N88-19352
Surface mediated photocatalysis
[AD-A188882] 12 p1603 N88-19589
Chromatographic and related reactors
[AD-A188452] 12 p1605 N88-19599
Novel catalysts for methane activation
[DE88-003637] 13 p1738 N88-20390
A new polymer-based hydrogen getter
[DE88-004538] 13 p1751 N88-20467
Evaluation of direct methane conversion to higher hydrocarbons and oxygenates
[DE88-003812] 15 p2049 N88-22204
Improvements to Raney copper zinc methanol synthesis catalysts 17 p2318 N88-23844
Catalytic ignition of hydrogen and oxygen propellants
[NASA-TM-100957] 18 p2476 N88-24689
Surface composition-reactivity relationships in heterogeneous catalysis
[DE88-006679] 18 p2480 N88-24714
Update of low temperature catalyst development
[DE88-007032] 18 p2480 N88-24715
Molecular-beam, mass-spectrometric studies of wood vapor and model compounds over HZSM-5 catalyst
18 p2535 N88-25044
Upgrading pyrolysis vapors to aromatic gasoline with zeolite catalysis at atmospheric pressure
18 p2536 N88-25045
Research on hydrotreating catalysts to hydrodeoxygenate biocrude oils
18 p2536 N88-25046
Sulfur-tolerant anode materials
[DE88-001034] 18 p2537 N88-25054
Liquid-phase oxidation of acetone with hydrogen peroxide on oxide catalysts 19 p2706 N88-26091
Alkaline fuel cell performance investigation
[NASA-TM-100937] 21 p2909 N88-27267
Preparation and development of advanced battery catalysts
[AD-A193208] 21 p2937 N88-27441
The design of methane activation catalysts
[DE88-002265] 23 p3199 N88-29043
Active sites and roles of solid acid base catalysts
[NASA-TT-20333] 24 p3345 N88-29909

CATALYTIC ACTIVITY
A review of methanol vehicles and air quality impacts
[DE88-002846] 08 p1023 N88-16194
Surface composition-reactivity relationships in heterogeneous catalysis
[DE87-003450] 09 p1140 N88-16834
Copper peroxide
[NASA-TT-20245] 14 p1888 N88-21282
Design of catalytic monoliths for closed-cycle carbon dioxide lasers
[NASA-CR-182983] 18 p2558 N88-25185
Production of powdered sodium hydride with large specific surface by the catalyzed reaction of molten sodium with hydrogen-1
[NASA-TT-20185] 20 p2776 N88-26462

CATCHMENT AREAS
U WATERSHEDS

CATECHOLAMINE
NT EPINEPHRINE
NT NOREPINEPHRINE

CATEGORIES
The distribution of evaporitic weathering products on Antarctic meteorites 06 p0798 N88-14888

CATENARIES
Strain gages in engineering geodesy
[SER-C-320] 01 p0048 N88-10309

CATHODE RAY TUBES
Generation of specific chromaticities on CRT monitors
[AD-A187739] 11 p1440 N88-18590
Human efficiency for visual detection of targets on CRT displays using a two-level multiple channel time history format
[AD-A188419] 12 p1670 N88-20001
Design and testing of a luminance and chrominance stabilization system for a computer-controlled color display
[AD-A191922] 18 p2554 N88-25159
Display system image quality
23 p3242 N88-29298
Use of color CRTs (Cathode Ray Tubes) in aircraft cockpit: A literature search, revision B
[AD-A195062] 24 p3324 N88-29797

CATHODES
NT CELL CATHODES
NT HOLLOW CATHODES
NT PHOTOCATHODES
NT THERMIONIC CATHODES
NT TUBE CATHODES
Synergism of electroplating and vacuum processes
[DE87-013496] 01 p0033 N88-10211
Plasma thruster development
[AD-A184173] 04 p0408 N88-12536
Raman scattering as a diagnostic technique for cathode characterization
[AD-A184434] 04 p0439 N88-12726
Some investigations of electrical discharges at the surfaces of solid cathodes immersed in aqueous electrolyte solutions
[PB87-168209] 09 p1159 N88-16946
Continuously frequency-tunable high-pressure CO2-laser with plasmatic cathode
09 p1238 N88-17418
Investigation of materials for inert electrodes in aluminum electrodeposition cells
[DE88-003380] 10 p1323 N88-17906
Capacitive charge division in centroid finding cathode readouts in MWPCs
[DE88-003545] 10 p1333 N88-17969
A novel class of positive electrodes for rechargeable batteries
[DE88-004559] 13 p1763 N88-20545
Theoretical model of the cathode spot on a unipolar arc
[AD-A190109] 15 p2059 N88-22277
Aluminum-air battery development
[DE88-006620] 15 p2061 N88-22287
A scientific basis for an alternate cathode architecture
[AD-A191498] 18 p2481 N88-24717
Basic processes of plasma propulsion
[AD-A192117] 18 p2577 N88-25310
Degradation of beam brightness by field emission from a cathode shroud
[DE88-008345] 20 p2794 N88-26576
Alkaline fuel cell performance investigation
[NASA-TM-100937] 21 p2909 N88-27267
Long-pulse, high-power vircator experiments
[DE88-011787] 21 p2940 N88-27458
Electrocatalytic reduction of oxygen on modified oxide surfaces
[NASA-TM-101333] 24 p3352 N88-29952

CATHODIC COATINGS
The influence of cathodic protection on erosion-corrosion of metals and model alloys
[AD-A191613] 18 p2485 N88-24742
Extinction behavior of low voltage switching arc under consideration of cathodic coatings and dynamic arc column
[ETN-88-92384] 20 p2796 N88-26591

CATIONS
Impedance of passive lithium anodes in SOCl2 solutions under low-field polarization
[DE88-000922] 04 p0439 N88-12728
Precipitation of surfactants and surfactant mixtures in aqueous solutions
[DE88-003333] 10 p1298 N88-17763
Study of cations in the precipation of Estacao Antartica Comandante Ferraz
[INPE-4377-PRE/1197] 12 p1644 N88-19843
Universal detection of ions by replacement-ion chromatography employing an anion-replacement method and an ultraviolet-visible spectrophotometric detector
[AD-A191326] 16 p2176 N88-22971
Electronic structure and stability of small cation and anion hydrogen clusters 16 p2267 N88-23562
Computer simulation of uphill diffusion in ternary ionic system
[NASA-TT-20194] 18 p2573 N88-25285
Possible mechanism for high-temperature superconductivity in the BaSr-La(Y)-CuO systems
[DE88-702060] 23 p3288 N88-29576

CATS
Emetic mechanism in acute radiation sickness
[AD-A194102] 23 p3238 N88-29267

CAUCHY INTEGRAL FORMULA
A quadrature formula for a double-pole singular integral
[PD-FM-8725] 04 p0485 N88-12990
A method for the numerical solution of random Cauchy singular integral equation 16 p2565 N88-25234

CAUCHY PROBLEM
Cauchy problem for linearized system of Navier-Stokes equations considering compressibility
04 p0459 N88-12837
Computation of flow past conical hypersonic wings using a second order Godunov method
05 p0533 N88-13241
The Eckhaus Partial Differential Equation (PDE) I psi t + psi xx + 2(psi/sq)x psi +2(/psi/) to the 4th power psi = 0
[PREPRINT-546] 06 p0763 N88-14686
A fast Riemann solver with constant covolume applied to the random choice method
[CAR-87-19] 09 p1231 N88-17375
Detection of signals in non-Gaussian correlated noise derived from Cauchy processes
[AD-A187488] 10 p1320 N88-17894
On the equivalence of four-dimensional self-duality equations to continual analog of the main chiral field problem
[DE88-700871] 12 p1686 N88-20083
Further extensions of the choquet-deny and deny theorems with applications in characterization theory
[AD-A193358] 21 p3006 N88-27834
Cauchy problem for the nonlinear Schroedinger equation
[DE88-702454] 21 p3011 N88-27867
Backlund transformations associated with a Riemann-Hilbert spectral problem
[PREPRINT-596] 22 p3146 N88-28712
A limiting viscosity approach to the Riemann problem for materials exhibiting change of phase
[AD-A193477] 23 p3210 N88-29103

CAUCHY-RIEMANN EQUATIONS
On the Fefferman class of metrics associated with a 3-dimensional Cauchy-Riemann (CR)-space
[PREPRINT-579] 14 p1991 N88-21865

CAUSTIC LINES
Analytical caustic surfaces
[NASA-TM-87805] 02 p0168 N88-11060

CAUSTICS
U ALKALIES

CAUSTICS (OPTICS)
Analytical caustic surfaces
[NASA-TM-87805] 02 p0168 N88-11060

CAVITATION
U CAVITATION FLOW

CAVITATION CORROSION
Simulated service test behavior of various internal and external coatings applied on CF6-50 first stage turbine blades
[NLR-MP-86018-U] 05 p0549 N88-13343
Effects of ion implantation on cavitation erosion of a cobalt based metal/carbide alloy
[AD-A187239] 10 p1303 N88-17793

CAVITATION FLOW
Investigations of creep cavitation in Type 304 stainless steel
[DE87-014198] 03 p0287 N88-11803
Some stochastic aspects of intergranular creep cavitation
[DE88-000065] 04 p0416 N88-12581
Gas diffusion studies in steady and nonsteady cavities
[AD-A185795] 06 p0704 N88-14318
Cavitation inception scale effects. 1. Nuclei distributions in natural waters. 2. Cavitation inception in a turbulent shear flow
[AD-A186553] 08 p0988 N88-15987

Experimental and theoretical study on cavitation inception and bubbly flow dynamics. Part 1: Design, development and operation of a cavitation susceptibility meter. Part 2: Linearized dynamics of bubbly and cavitating flows with bubble dynamics effects
[AD-A187133] 09 p1160 N88-16952
Effects of ion implantation on cavitation erosion of a cobalt based metal/carbide alloy
[AD-A187239] 10 p1303 N88-17793
The use of multigrid techniques in the solution of the Elrod algorithm for a dynamically loaded journal bearing
[NASA-CR-180873] 10 p1331 N88-17954
Cavitation inception
[AD-A189220] 13 p1765 N88-20557
High Reynolds number pump facility for cavitation research
[AD-A189310] 13 p1765 N88-20558
Cavitation inception in rectangular two-dimensional slots
[AD-A190677] 15 p2066 N88-22318
Modeling of cavitation phenomena in homogeneous flow in transitory regimes in pipes
[ISAL-IDI1-87-15] 17 p2337 N88-23948
Superplasticity: A fundamental investigation on deformation mechanism and cavitation phenomena
[AD-A191548] 18 p2485 N88-24741
Gas diffusion studies in steady and nonsteady cavities 18 p2512 N88-24902
Noise generation by air bubbles in water: An experimental study of creation and splitting
[AD-A192063] 19 p2664 N88-25839
Pulsed spray structure and atomisation techniques
[AD-A192260] 20 p2800 N88-26614
Forces and moments on a slender, cavitating body
[DE88-007208] 21 p2945 N88-27491
Cavitation inception in a turbulent shear flow
[DE88-011486] 21 p2946 N88-27497
A multiple-scales partial solution of the pulse-forced Rayleigh-Plesset equation of cavitation bubble dynamics
[AD-A193733] 23 p3212 N88-29118
An investigation of acoustic cavitation produced by pulsed ultrasound
[AD-A193523] 23 p3278 N88-29516
Beam combining by phase transition nonlinear media
[AD-A194116] 23 p3283 N88-29547
Studies on pressure response of gas bubbles contributions of condensed droplets in bubbles generated by a uniform nucleation
[NASA-TT-20343] 24 p3370 N88-30068

CAVITIES
Development of response models for the Earth Radiation Budget Experiment (ERBE) sensors. Part 2: Analysis of the ERBE integrating sphere ground calibration
[NASA-CR-178293] 01 p0049 N88-10316
Quantum electrodynamics based on self-energy: Spontaneous emission in cavities
[DE87-703071] 02 p0232 N88-11461
Investigations on a transonic airfoil with a 30 mm wide perforation/cavity arrangement
[ESA-TT-1072] 03 p0260 N88-11634
Inertial confinement fusion reactor cavity analysis
[DE88-000788] 04 p0492 N88-13028
Program to development an optical transistor and switch
[AD-A185666] 06 p0697 N88-14278
Gas diffusion studies in steady and nonsteady cavities
[AD-A185795] 06 p0704 N88-14318
Electromagnetic fields backscattered from an s-shaped inlet cavity with an absorber coating on its inner walls
[NASA-CR-182401] 07 p0845 N88-15130
Review of nucleation and incipient boiling under pool and forced convection conditions 08 p0982 N88-15938
Evaluation of spare room in cerebrospinal system using noninvasive methods 10 p1361 N88-18137
Cavitation in model elastomeric composites
[AD-A187401] 11 p1447 N88-18625
Investigation of a ray-mode representation of the Green's function in a rectangular cavity
[PB88-131677] 11 p1469 N88-18763
Structural-acoustic interior noise modeling and analysis from experimental data
[PB88-141775] 12 p1687 N88-20088
Tunable condensed-media laser with antiresonant ring cavity 14 p1971 N88-21764
Observation of energetic particles (E greater than 30 keV) by the Giotto experiment EPA in the magnetic cavity of Comet Halley 14 p1997 N88-21903
Observation of synchronously transient pumped mode-locking dye laser under negative cavity detuning 16 p2187 N88-23041
Research in electromagnetic shielding theory. Part1. Shielding by rectangular enclosures
[AD-A192681] 20 p2791 N88-26557
Rf cavity primer for cyclic proton accelerators
[DE88-010655] 20 p2853 N88-26938
A critical review of IR drops and electrode potentials within pits, crevices and cracks
[AD-A192481] 21 p2935 N88-27431
Thermo-mechanical cracking in coated media with a cavity by a moving asperity friction
[AD-A193311] 21 p2961 N88-27586
The use of fins to reduce the pressure drop in a rotating cavity with a radial flow
[PNR90465] 22 p3079 N88-28282
Solar energy absorption efficiency of an ellipsoidal receiver-reactor with specularly reflecting walls
[AD-A193726] 22 p3117 N88-28520
Navier-Stokes calculations of transonic flows past cavities
[NASA-CR-180484] 23 p3212 N88-29116
Effects on the resonant frequencies caused by loading a spherical cavity with a dielectric sphere
[AD-A193864] 23 p3277 N88-29511
Studies on pressure response of gas bubbles contributions of condensed droplets in bubbles generated by a uniform nucleation
[NASA-TT-20343] 24 p3370 N88-30068

CAVITY RESONATORS
Theoretical and experimental investigation of electron beam acceleration and sub-millimeter wave generation in cyclotron resonant cavities
[AD-A184806] 05 p0649 N88-13975
Initial operation of a high-power whispering-gallery-mode gyrotron
[DE88-002500] 07 p0857 N88-15207
High-sensitivity recording of weak reflected or scattered radiation by method of coherent intracavity reception with YAG:Nd(3+) laser 08 p1078 N88-16502
Photodetachment neutralizer development: Laser window design study. Volume 2: Window design details
[DE88-000783] 09 p1170 N88-17014
Measured and calculated acoustic attenuation rates of tuned resonator arrays for two surface impedance distribution models with flow
[NASA-TP-2766] 09 p1241 N88-17440
Measurement technique for characterization of the gyrotron
[INPE-4322-RPE/550] 12 p1630 N88-19758
Study of inhomogeneously filled cylindrical resonant cavities by the finite integration technique
[PB88-133707] 12 p1697 N88-20156
Progress in diagnostic techniques for SC cavities
[CEBAF-PR-88-003] 13 p1772 N88-20600
Resonator coupling of two ring cavity, argon-ion lasers
[AD-A189558] 13 p1775 N88-20616
Status of RF superconductivity at Argonne National Laboratory
[DE88-005913] 15 p2144 N88-22796
Fluxons and order in long Josephson junctions
[AD-A190879] 16 p2282 N88-23665
On bunch lengthening using the fourth harmonic cavity in the NSLS VUV ring
[DE88-007392] 18 p2574 N88-25288
Superconducting rf and beam-cavity interactions
[DE88-008598] 20 p2852 N88-26936
Rf cavity primer for cyclic proton accelerators
[DE88-010655] 20 p2853 N88-26938
Progress in diagnostic techniques for SC (superconducting) cavities
[DE88-008600] 20 p2876 N88-27077
Laser CO2/TEA frequency-stabilized by phase conjugation 22 p3082 N88-28303
Qualitative characteristics of open waveguide resonator spectra
[DE88-702387] 23 p3202 N88-29056
Band pass with cavity resonators by use of three oscillation types
[ETN-88-92984] 23 p3209 N88-29096
Free electron lasers with small period wigglers
[DE88-011627] 23 p3218 N88-29156

CCD
U CHARGE COUPLED DEVICES

CD-ROM
U OPTICAL DISKS
U READ-ONLY MEMORY DEVICES

CDC COMPUTERS
NT CDC CYBER 205 COMPUTER

CDC CYBER 205 COMPUTER
An efficient sparse matrix multiplication scheme for the CYBER 205 computer
[NASA-TM-4028] 10 p1390 N88-18302
Optimization of the real level 2 BLAS on the Cyber 205
[CWI-NM-R8715] 14 p1956 N88-21657
Solving bidiagonal systems of linear equations on the CDC CYBER 205
[CWI-NM-R8725] 18 p2558 N88-25187

CDMA
U CODE DIVISION MULTIPLE ACCESS

CEILINGS (ARCHITECTURE)
Test results and predictions for the response of near-ceiling sprinkler links in a full-scale compartment fire
[NBSIR-87/3633] 01 p0033 N88-10209

CEILOMETERS
U CLOUD HEIGHT INDICATORS

CELESTIAL BODIES
NT A STARS
NT ACHONDRITES
NT ACTIVE GALAXIES
NT ANDROMEDA GALAXY
NT AQUARID METEOROIDS
NT ASTEROID BELTS
NT ASTEROIDS
NT ASYMPTOTIC GIANT BRANCH STARS
NT B STARS
NT BARRED GALAXIES
NT BINARY STARS
NT BL LACERTAE OBJECTS
NT BLACK HOLES (ASTRONOMY)
NT BOLIDES
NT CARBON STARS
NT CARBONACEOUS CHONDRITES
NT CARBONACEOUS METEORITES
NT CATACLYSMIC VARIABLES
NT CEPHEID VARIABLES
NT CHONDRITES
NT COMET HEADS
NT COMET NUCLEI
NT COMET TAILS
NT COMETS
NT COOL STARS
NT CRAB NEBULA
NT DEIMOS
NT DISK GALAXIES
NT DOUBLE STARS
NT DWARF NOVAE
NT DWARF STARS
NT EARLY STARS
NT EARTH (PLANET)
NT ECLIPSING BINARY STARS
NT ELLIPTICAL GALAXIES
NT ENCKE COMET
NT EXTRAGALACTIC RADIO SOURCES
NT F STARS
NT FAINT OBJECTS
NT FLARE STARS
NT G STARS
NT GALACTIC CLUSTERS
NT GALAXIES
NT GAS GIANT PLANETS
NT GEMINID METEOROIDS
NT GIACOBINI-ZINNER COMET
NT GIANT STARS
NT GLOBULAR CLUSTERS
NT GRIGG-SKJELLERUP COMET
NT H II REGIONS
NT HALLEY'S COMET
NT HERBIG-HARO OBJECTS
NT HERCULES NOVA
NT HOT STARS
NT INFRARED SOURCES (ASTRONOMY)
NT INFRARED STARS
NT IO
NT IRON METEORITES
NT IRREGULAR GALAXIES
NT JUPITER (PLANET)
NT JUPITER SATELLITES
NT K STARS
NT LATE STARS
NT LOCAL GROUP (ASTRONOMY)
NT M STARS
NT MAGELLANIC CLOUDS
NT MAGNETIC STARS
NT MAIN SEQUENCE STARS
NT MARS (PLANET)
NT METEORITES
NT METEOROID SHOWERS
NT METEOROIDS
NT MICROMETEOROIDS
NT MILKY WAY GALAXY
NT MIRA VARIABLES
NT MOON
NT NATURAL SATELLITES
NT NEBULAE
NT NEMESIS (STAR)
NT NEPTUNE (PLANET)
NT NEUTRON STARS
NT NOVAE
NT O STARS
NT ORION NEBULA
NT ORIONID METEOROIDS
NT PERSEID METEOROIDS
NT PHOBOS
NT PLANETARY NEBULAE

NT PLANETARY RINGS
NT PRE-MAIN SEQUENCE STARS
NT PROTOPLANETS
NT PROTOSTARS
NT PULSARS
NT QUADRANTID METEOROIDS
NT QUASARS
NT RADIO GALAXIES
NT RADIO JETS (ASTRONOMY)
NT RADIO SOURCES (ASTRONOMY)
NT RADIO STARS
NT RED DWARF STARS
NT RED GIANT STARS
NT REFERENCE STARS
NT S STARS
NT SATURN RINGS
NT SATURN SATELLITES
NT SEYFERT GALAXIES
NT SOLAR SYSTEM
NT SPIRAL GALAXIES
NT SPORADIC METEOROIDS
NT STAR CLUSTERS
NT STARBURST GALAXIES
NT STARS
NT STELLAR SYSTEMS
NT SUBGIANT STARS
NT SUN
NT SUPERGIANT STARS
NT SUPERMASSIVE STARS
NT SUPERNOVA 1987A
NT SUPERNOVAE
NT T TAURI STARS
NT TAURID METEOROIDS
NT TEMPEL 2 COMET
NT TERRESTRIAL PLANETS
NT TITAN
NT TITANIA
NT URANUS (PLANET)
NT URANUS RINGS
NT URANUS SATELLITES
NT VARIABLE STARS
NT VENUS (PLANET)
NT VIRGO GALACTIC CLUSTER
NT WEST COMET
NT WHITE DWARF STARS
NT WOLF-RAYET STARS
NT X RAY BINARIES
NT X RAY STARS
NT ZODIACAL DUST

CELESTIAL GEODESY
New possibilities for using gravity data in developing geodetic coordinate systems 08 p1009 N88-16116
Study of modern instrumentation and methods for astronomic positioning in the field
[AD-A196173] 24 p3452 N88-30548

CELESTIAL MECHANICS
Propagation of random initial conditions in time 04 p0486 N88-12993
Periodic orbits around a satellite modelled as a triaxial ellipsoid
[AD-A190592] 15 p2022 N88-22051
A standard library for modeling satellite orbits on a microcomputer
[AD-A195759] 24 p3331 N88-29830

CELESTIAL OBSERVATION
U ASTRONOMY

CELL ANODES
Morphological changes in polymer electrolyte cells
[AD-A195821] 24 p3368 N88-30054

CELL CATHODES
New materials for electrochemical cells
[AD-A183659] 01 p0037 N88-10238

CELL DIVISION
Potential use of the bioreactor to determine effects of microgravity and other environmental parameters on growth of hybridoma cells 09 p1198 N88-17178
Gravisensing in lentil seedling roots grown in space (Spacelab D-1 mission) 12 p1654 N88-19911

CELLS (BIOLOGY)
NT BLOOD CELLS
NT EGGS
NT ERYTHROCYTES
NT EUKARYOTES
NT LEUKOCYTES
NT LYMPHOCYTES
NT NEURONS
NT PROKARYOTES
NT PROTOPLASTS
Superoxide dismutase assays
[AD-A183972] 03 p0356 N88-12242
Electron cytochemical detection of Ca(2)+-ATPase in protonema of moss funaria hygrometrica (H e d w.) under hypogravitation 06 p0749 N88-14602
Review of cytoskeleton research in cell differentiation and development
[AD-A185832] 07 p0882 N88-15353
Investigations of Paramecium cells analyzed under microgravity conditions 07 p0884 N88-15367
Possible use of plasmids for study of effect of space flight factors on biological objects 08 p1046 N88-16319
Zero gravity and living organism 08 p1046 N88-16320
Effects of extreme hypoxia on phospholipid metabolism in subcellular structures of rat brain 08 p1046 N88-16323
Space Bioreactor Science Workshop
[NASA-CP-2485] 09 p1196 N88-17168
Suspension cell culture in microgravity and development of a space bioreactor 09 p1196 N88-17169
Space bioreactor: Design/process flow 09 p1197 N88-17170
Computer control of a microgravity mammalian cell bioreactor 09 p1197 N88-17172
Shear and mixing effects on cells in agitated microcarrier tissue culture reactors 09 p1197 N88-17173
Some process control/design considerations in the development of a microgravity mammalian cell bioreactor 09 p1197 N88-17174
Plant cell technologies in space: Background, strategies and prospects 09 p1198 N88-17177
Potential use of the bioreactor to determine effects of microgravity and other environmental parameters on growth of hybridoma cells 09 p1198 N88-17178
Cell culture experiments planned for the space bioreactor 09 p1198 N88-17180
Histomorphometric analysis of rat bones after spaceflight aboard Cosmos-1667 biosatellite 10 p1360 N88-18128
Effect of weightlessness on replicative function of rat hepatocyte DNA 10 p1360 N88-18129
Morphological and functional state of the hypothalamo-hypophyseal neurosecretory system of rats flown aboard Cosmos-1667 10 p1365 N88-18156
Interactions of cultured human endothelial cells with polymeric surfaces
[PB88-112255] 10 p1369 N88-18178
Critical phenomena and electromagnetic effects in biological membranes
[AD-A188156] 11 p1518 N88-19064
Cell cultures in space: From basic research to biotechnology 2 12 p1660 N88-19948
Cyropreservation of isolated rat hepathocytes for future use in Spacelab experiments: Preliminary results 12 p1660 N88-19950
Electrical and chemical sensors for biological cell research 19 p2689 N88-25866
Genetic effects of low level microwave radiation
[AD-A192687] 21 p2984 N88-27722
Contraction behavior and protoplasmic streaming in the slime mold Physarum polycephalum (Physarum kinetics) --- Spacelab D1 mission 22 p3060 N88-28160

CELLULAR MATERIALS (NON BIOLOGICAL)
U FOAMS

CELLULOSE
Saccharification of cellulose by combined fungal and bacterial preparations 17 p2316 N88-23833

CEMENTS
Open-graded bases for airfield pavements
[AD-A184461] 04 p0402 N88-12500
A laboratory study of asphalt concrete mix designs for high-contact pressure aircraft traffic
[AD-A185753] 06 p0670 N88-14106
Development of strength in cements
[PB87-232971] 06 p0684 N88-14189
Comparative study of nondestructive pavement testing, MacDill Air Force Base, Florida
[AD-A186082] 07 p0822 N88-14993
Use of reinforced inorganic cement materials for spark wire and drift chamber wire frames
[NASA-CR-180759] 13 p1746 N88-20438
The effect of Ca(OH)2-treated ceramic microspheres on the mechanical properties of high-temperature lightweight cement composites
[DE88-004590] 13 p1749 N88-20457
Cement paste matrix composite materials center
[AD-A188657] 15 p2028 N88-22083

CENSORED DATA (MATHEMATICS)
Further studies in estimation of life distribution characteristics from censored data
[AD-A184862] 05 p0643 N88-13937
A modified kernel quantile estimator under censoring
[AD-A186364] 07 p0911 N88-15525
Estimation and comparison of changes in the presence of information right censoring by modeling the censoring process
[AD-A186320] 08 p1074 N88-16478
A generalized quantile estimator under censoring
[AD-A188280] 10 p1402 N88-18364
Estimation in linear models with censored data
[AD-A187209] 11 p1540 N88-19203
Survival analysis, or what to do with upper limits in astronomical surveys
[NASA-CR-182936] 17 p2449 N88-24551

CENTAUR LAUNCH VEHICLE
The 250AH/90A active lithium-thionyl chloride cell for Centaur-G application 02 p0163 N88-11023
Zero-G thermodynamic vent system for shuttle/Centaur 08 p0983 N88-15943
Centaur G Prime modal test 09 p1181 N88-17075
Centaur operations at the space station
[NASA-CR-179593] 19 p2606 N88-25473
Centaur operations at the space station: Cost and transportation analysis
[NASA-CR-182128] 24 p3332 N88-29835

CENTAUR VEHICLE
U CENTAUR LAUNCH VEHICLE

CENTER OF GRAVITY
Effect of permissible variations of center-of-gravity locations of cargo airplane on its mass 04 p0424 N88-12625
A new method for the estimation of aircraft inertia characteristics 20 p2787 N88-26530

CENTER OF MASS
Numerical analysis of motion of solid bodies in atmosphere 08 p1079 N88-16505
An improved data reduction procedure for accelerometer centrifuge data 12 p1577 N88-19436
Some periodicities in motion of Halley's Comet relative to center of mass 13 p1726 N88-20324

CENTER OF PRESSURE
Experimental research on center of pressure of slender body with two pointed ends 14 p1864 N88-21137
New definition of pressure-center coefficient of reentry craft with asymmetrical configuration 14 p1864 N88-21138

CENTERBODIES
Multi-body aircraft with an all-movable center fuselage actively controlling fuselage pressure drag
[NASA-CASE-LAR-13511-1] 17 p2301 N88-23765

CENTIMETER WAVES
Utilization of microwave measuring systems for nondestructive control of composite materials
[SNIAS-872-430-109] 05 p0559 N88-13402
Recent observations of the OH radio lines in comets 14 p1999 N88-21917

CENTRAL AMERICA
Geological evolution and analysis of confirmed or suspected gas hydrate localities. Volume 9: Formation and stability of gas hydrates of the Middle America Trench
[DE88-001007] 10 p1347 N88-18050
Caribbean and Central America wind energy assessment
[DE88-005134] 11 p1507 N88-19002

CENTRAL EUROPE
Land campaign force assessment. Methods used in Central-Europe-study
[FOA-C-10288-9.3] 06 p0768 N88-14723
Typical weather months in the past (1973-1983) in Central Europe
[AD-A194701] 23 p3235 N88-29249

CENTRAL NERVOUS SYSTEM
NT BRAIN
NT CEREBELLUM
NT CEREBRAL CORTEX
NT CEREBRUM
NT HIPPOCAMPUS
NT HYPOTHALAMUS
NT SPINAL CORD
NT THALAMUS
Functional plasticity of the nervous system of vertebrates 01 p0074 N88-10474
Discrete adaptation to sensory conflict 10 p1363 N88-18146
Combined effect of ionizing radiation and altered gas atmosphere on central nervous system 10 p1367 N88-18168
Neuropeptides in experimental head injury
[AD-A188067] 11 p1520 N88-19077
Models describing muscle behavior and control
[LR-522] 16 p2238 N88-23368
Vagal tone as an index of mental state 16 p2239 N88-23373
The N2-P3 complex of the evoked potential and human performance 16 p2241 N88-23388
Effect of different modes of voluntary control of breathing on human electroencephalogram with exposure to acute hypoxic hypoxia 19 p2707 N88-26093
Measurement and classification of the mode of action of antidepressant drugs 21 p2983 N88-27714
Measurement of electrical activity in the CNS with cortical evoked potentials and EEG: Efficacy profiles of drugs using factor analysis 21 p2983 N88-27715

CENTRAL PROCESSING UNITS
NT ARITHMETIC AND LOGIC UNITS

Design, manufacture and testing of an elegant breadboard model communications processor
[D/2244] 01 p0034 N88-10217
Study and design of a communication processor unit
[RIDU/TREP/1002/SAAB] 01 p0083 N88-10538
File usage analysis and resource usage prediction: A measurement-based study
[NASA-CR-181553] 05 p0633 N88-13867
Predictability of process resource usage: A measurement-based study of UNIX
[NASA-CR-181562] 05 p0633 N88-13869
High-performance CPU implementation of the nebula instruction set architecture 10 p1373 N88-18194
Implementation of a buddy failure recovery concept in the NOVAC system 10 p1375 N88-18205
Simulation: A simulation system in Ada
[FOA-A-20043-2.7] 17 p2385 N88-24176
Computers in weapons systems: A look at the F-15
[AD-A194498] 23 p3178 N88-28920
The LTPP communication processor --- Columbus and Hermes
[CL/CP/SES/FR/004] 24 p3415 N88-30328

CENTRIFUGAL CASTING
Effects of thermal and thermo-mechanical treatments on the mechanical properties of centrifugally cast alloy 718
[AD-A188195] 11 p1458 N88-18690

CENTRIFUGAL COMPRESSORS
Flow in Centrifugal Compressors --- conference
[VKI-LS-1987-01] 07 p0850 N88-15160
Measurements in centrifugal compressors 07 p0850 N88-15161
Centrifugal compressors 07 p0850 N88-15162
The technology of centrifugal compressors: A design approach and new goals for research 07 p0850 N88-15163
Identification and avoidance of instabilities in high performance turbomachinery 07 p0850 N88-15164
Blade vibration problems in centrifugal compressors. Fundamental considerations 07 p0851 N88-15165
Flow in volutes and the influence on the flow in centrifugal compressors 07 p0851 N88-15169
Numerical study of a centrifugal impeller response to a downstream static pressure perturbation 07 p0851 N88-15170
The Goddard Space Flight Center mechanical cooler program 08 p0983 N88-15944
The advantage of variable geometry for turbine engines at low power 10 p1280 N88-17653
Secondary flow measurements with L2F-technique in centrifugal compressors 10 p1283 N88-17676
Method for predicting performance limits of centrifugal compressors 10 p1283 N88-17677
Open-cycle centrifugal vapor-compression heat pump
[PB88-157391] 11 p1488 N88-18885

CENTRIFUGAL FORCE
Two-dimensional static otolith model 10 p1367 N88-18167
Measurement and analysis of the noise radiated by low Mach numbers centrifugal blowers
[AD-A189226] 13 p1833 N88-20966
Centrifugal acceleration of ions in the polar magnetosphere
[NASA-TM-101148] 17 p2374 N88-24120

CENTRIFUGAL PUMPS
Operating experiences and test results of six cold helium compressors
[DE87-012115] 02 p0157 N88-10962
Rotor dynamic behavior of centrifugal pumps 08 p0975 N88-15898
Ames Research Center cryogenics program 08 p0981 N88-15927
Open-cycle centrifugal vapor-compression heat pump
[PB88-157391] 11 p1488 N88-18885

CENTRIFUGES
NT HUMAN CENTRIFUGES
Plasma centrifuge development at INPE
[INPE-4243-PRE/1117] 08 p1087 N88-16546
An improved data reduction procedure for accelerometer centrifuge data 12 p1577 N88-19436
Control test and validation for a large diameter high stability centrifuge 12 p1577 N88-19437
Preliminary analysis of an integrated logistics system for OSSA payloads
[NASA-CR-4114] 12 p1584 N88-19477
Preliminary analysis of an integrated logistics system for OSSA payloads. Volume 4: Supportability analysis of the 1.8m centrifuge 12 p1584 N88-19481
Vacuum-arc plasma centrifuge experiment
[INPE-4509-PRE/1263] 15 p2138 N88-22758
Botany Facility. Thermal Control (TC) subsystem test report on experiment container of laboratory model and breadboard centrifuge
[BF-TN-ER-061/86] 17 p2378 N88-24135
Botany Facility: Magnetic fluid seal considerations for the centrifuge
[SIRA-A/7373/WP110/MAC004] 17 p2378 N88-24138
Botany Facility: Considerations and analyses of the balancing system philosophy proposed for the BF centrifuge
[SIRA-A/7373/WP110/PWF001] 17 p2378 N88-24139
Computation of flow and diffusion process in gas centrifuges
[ETN-88-92366] 21 p2949 N88-27514

CEPHEID VARIABLES
The pulsation modes of CO Aur
[PUBL-SER-C-FASC-10] 03 p0387 N88-12430
Membership of Cepheids and red giants in 8 open clusters: NGC 129, 6067, 6649, 6664, IC 4725, Ly 6, Ru 79
[PUBL-SER-C-FASC-13] 07 p0944 N88-15739
Near-infrared observations of cepheids: The distance to M33 15 p2152 N88-22846

CEPSTRAL ANALYSIS
Some properties of the Hilbert transform
[DE88-002465] 09 p1227 N88-17350
Bearing detection in the presence of two sources of varying coherence using the complex cepstrum
[NASA-CR-181605] 09 p1243 N88-17451

CERAMAL PROTECTIVE COATINGS
U CERMETS
U PROTECTIVE COATINGS

CERAMALS
U CERMETS

CERAMIC BONDING
Analysis of end stresses in glass-metal bimaterial strips
[DE87-007848] 05 p0610 N88-13750
Behavior of metal ceramic interfaces
[PB87-147500] 07 p0837 N88-15076
Composite piston
[NASA-CASE-LAR-13435-1] 17 p2346 N88-23981

CERAMIC COATINGS
Thermal barrier coating life prediction model development 02 p0190 N88-11185
Ceramic-ceramic shell tile thermal protection system and method thereof
[NASA-CASE-ARC-11641-1] 11 p1448 N88-18628
Titanium carbide coatings for aerospace ball bearings 14 p1927 N88-21486
The corrosion resistance of an aluminum alloy coated with polysilazane derived ceramics
[AD-A190703] 15 p2046 N88-22189
Evaluation of ceramic thermal barrier coatings for gas turbine engine components
[ETN-88-91947] 16 p2181 N88-22998
Recent advances in metallic/ceramic coatings for corrosion control in military applications 17 p2320 N88-23858
Vanadic hot corrosion of gas turbine blade coating materials 17 p2321 N88-23864
An investigation of ceramic coatings for protection of SiC from high-temperature corrosion
[DE88-007873] 18 p2493 N88-24790
Development of protective coatings for ceramic tubular components
[PB88-197165] 20 p2776 N88-26463
Effects of ceramic surfaces on autoignition in a constant volume combustion apparatus
[AD-A193055] 21 p2909 N88-27266

CERAMIC FIBERS
Processing and properties of SiC/Nicalon composites
[DE87-013885] 03 p0279 N88-11757
High-temperature properties of ceramic fibers and insulations for thermal protection of atmospheric entry and hypersonic cruise vehicles
[NASA-TM-100059] 10 p1295 N88-17743
High yield synthesis of B4C/BN ceramic materials by pyrolysis of polymeric Lewis base adducts of decaborane(14)
[AD-A188154] 11 p1462 N88-18717
Toxic effects of man-made mineral fibers with particular reference to ceramic fibers
[AD-A187949] 11 p1519 N88-19072
Contemporary ceramics and the new technological revolution 14 p1902 N88-21363
High-T(sub c) superconducting wire fabrication and testing
[DE88-005989] 15 p2144 N88-22798
Mechanical and structural characterization of aluminum ceramic fibers
[ETN-88-92168] 17 p2323 N88-23870
SiC fiber analysis 17 p2326 N88-23891
SiC fiber reinforced reaction-bonded Si3N4 composites 17 p2326 N88-23892
Development of materials for fabric radiators 17 p2429 N88-24448
Auger analysis of a fiber/matrix interface in a ceramic matrix composite
[NASA-TM-100892] 19 p2610 N88-25487
Studies in support of oxidation-resistant composite materials
[AD-A193320] 21 p2905 N88-27238

CERAMIC MATRIX COMPOSITES
Ceramic-Ceramic Composites Meeting in Belgium
[ONRL-7-020-R] 01 p0019 N88-10118
Structural reliability and damage tolerance of ceramic composites for high-temperature applications
[PB87-208310] 01 p0019 N88-10119
Carbon fiber reinforced glass matrix composites for space based applications
[AD-A184355] 04 p0410 N88-12546
Study of ceramic-fiber/ceramic sol-gel based matrix composites
[SNIAS-872-430-120] 05 p0569 N88-13469
Thermo-mechanical behavior of high temperature fiber composites 06 p0678 N88-14149
High temperature tensile testing of ceramic composites
[NASA-CR-180888] 08 p0990 N88-15996
Activities report of the Materials Department
[ETN-88-91984] 13 p1745 N88-20436
Contemporary ceramics and the new technological revolution 14 p1902 N88-21363
Fracture toughness testing of a ceramic matrix composite
[AD-A189846] 15 p2029 N88-22089
A test for interfacial effects and stress transfer in ceramic matrix composites
[NASA-CR-182758] 15 p2046 N88-22194
Continuous fiber ceramic matrix composites for heat engine components 15 p2082 N88-22411
Fracture technology for brittle materials 15 p2083 N88-22417
Strength and failure rate of composite materials with carbon in ceramic matrix 16 p2180 N88-22995
Ceramic matrix composites 17 p2325 N88-23888
Carbon matrix composites prospective roles for biotechnology 18 p2477 N88-24694
Auger analysis of a fiber/matrix interface in a ceramic matrix composite
[NASA-TM-100892] 19 p2610 N88-25487
Manufacturing of a ceramic-ceramic composite matrix using the sol-gel procedure
[ETN-88-92157] 20 p2768 N88-26414
Theoretical and experimental analysis of the toughening behavior of whisker reinforcement in ceramic matrix composites
[DE88-011841] 21 p2906 N88-27241
Contribution to the development of coated fiber ceramic insolation material
[ETN-88-92361] 21 p2906 N88-27243
Very high temperature materials for mechanical application
[SNIAS-881-430-106] 23 p3189 N88-28978
A test for interfacial effects and stress transfer in ceramic matrix composites
[NASA-CR-182873] 24 p3340 N88-29880
A study of the critical factors controlling the synthesis of ceramic matrix composites from preceramic polymers
[AD-A195405] 24 p3340 N88-29881
Processing technology research in composites
[AD-A195693] 24 p3341 N88-29890

CERAMIC NUCLEAR FUELS
Cermet-fueled reactors for advanced space applications
[DE88-005528] 13 p1839 N88-21002
Cermet fuel thermal conductivity 17 p2410 N88-24329
Monolithic fuel cell based power source for burst power generation 17 p2429 N88-24450

CERAMICS
NT CERAMIC NUCLEAR FUELS
X-ray tomography and nuclear magnetic resonance imaging applications for advanced ceramic materials
[DE87-011534] 01 p0027 N88-10171
Use of sol-gels in the application of ceramic oxide thin films
[DE87-013610] 01 p0028 N88-10176
Toughening of alpha-alumina: Preliminary results
[DE87-702776] 01 p0028 N88-10178
Physics and chemistry of packing fine ceramic powders
[DE87-013709] 01 p0029 N88-10183
Ceramic composites by chemical vapor infiltration
[DE87-009128] 01 p0029 N88-10185
Simple instrumentation for testing of ceramic superconductors
[DE87-013849] 01 p0103 N88-10672
Studies on surface chemical states of some metals and ceramics bombarded with energetic light-ions
[DE87-752975] 02 p0145 N88-10910

Needs assessment for NDT and characterization of ceramics: Assessment of inspection technology for green state and sintered ceramics
[DE87-013550] 02 p0151 N88-10947
Needs assessment for nondestructive testing and materials characterization for improved reliability in structural ceramics for heat engines
[DE88-000040] 02 p0153 N88-10957
Study of the micromechanical behavior of a SiO2-Al2O3-Li2O glass ceramic and its relation to the microstructure
[ISAL-ITC1-87-01] 02 p0153 N88-10960
Crack behavior in ceramic materials under static, slowly increasing, and cyclic loading conditions
[KFK-4209] 02 p0154 N88-10964
NDE (Nondestructive Evaluation) of advanced structural ceramics
[DE87-014417] 03 p0292 N88-11832
Modeling of irradiation-induced amorphization in a titanate ceramic
[DE87-014751] 03 p0292 N88-11833
The behavior of plastic, ceramic masses in compression tests
[ETN-87-90603] 03 p0292 N88-11836
High temperature characterization of ceramic materials
[REPT-NT-3403] 03 p0292 N88-11837
Structure and grain coarsening during the processing of engineering ceramics
[NASA-TM-100235] 03 p0293 N88-11838
Indentation damage in ceramics
[AD-A184686] 03 p0294 N88-11844
Aluminum oxynitride spinel (ALON): A review
[AD-A184753] 03 p0294 N88-11845
Investigation of BN CO2 wave guide laser
03 p0302 N88-11905
The Shock and Vibration Digest, Volume 19, No. 10
03 p0335 N88-12112
Application of fracture mechanics theory in the reliability analysis of structural ceramics in multiaxial loading
03 p0335 N88-12113
Adiabatic diesel engine component development: Reference engine for on-highway applications
[NASA-CR-179531] 03 p0386 N88-12428
JPRS report: Science and technology. Japan
[JPRS-JST-87-025] 04 p0403 N88-12502
Ceramics thin film 04 p0403 N88-12505
Research and development on high strength ceramic heaters discussed 04 p0404 N88-12508
Effect of time and temperature on transformation toughened zirconias
[AD-A184356] 04 p0419 N88-12600
Molecular engineering of ceramics
[DE88-000174] 04 p0420 N88-12603
Development of advanced fiber reinforced ceramics
[DE88-000779] 04 p0420 N88-12604
Ceramic technology for advanced heat engines project
[DE88-001520] 04 p0420 N88-12605
Real-time Raman detection of molecular changes in ceramics undergoing sliding friction
[DE88-000558] 04 p0421 N88-12609
Statistical process control applied to the liquid-fed ceramic melter process
[DE88-000271] 05 p0569 N88-13471
Process for preparing transition metal nitrides and transition metal carbonitrides and their reaction intermediates
[DE88-000849] 06 p0679 N88-14162
Ceramic technology for advanced heat engines
[PB87-232997] 06 p0683 N88-14188
JPRS report: Science and technology. Japan
[JPRS-JST-87-023] 06 p0684 N88-14191
Developments in electronics ceramics reported
06 p0684 N88-14192
Electron microscopy studies of tensile cyclic fatigue-tested silicon nitride ceramics
[DE88-001438] 06 p0685 N88-14196
Cyclic fatigue of ceramics at high temperatures
[PB87-127700] 06 p0685 N88-14200
Exploitation of the sol-gel route in processing of ceramics and composites
[AD-A185482] 06 p0686 N88-14204
Characterization of mechanical damage mechanisms in ceramic composite materials
[AD-A185549] 06 p0686 N88-14205
The effect of texture on the crack growth resistance of alumina
[NASA-TM-100250] 06 p0686 N88-14206
Hitachi develops ceramic superconducting device
06 p0688 N88-14214
The consequences of intergrain Josephson coupling in ceramic high-temperature superconductors
[DE87-013713] 06 p0785 N88-14816
Interface effects on the mechanical properties of ceramic composites
[AD-A185899] 07 p0826 N88-15009
Assessment of electroceramics research in Europe and the Middle East
[AD-A186377] 07 p0836 N88-15074
A comparison of film-based tomography and computed tomography for advanced ceramic materials
[DE88-003114] 07 p0837 N88-15079
Techniques for ceramic sintering using microwave energy
[DE88-001416] 07 p0837 N88-15080
Imaging subtle microstructural variations in ceramics with precision ultrasonic velocity and attenuation measurements
[NASA-TM-100129] 07 p0867 N88-15257
Fabrication of YBa2Cu3O7 superconducting ceramics
[DE88-003012] 07 p0938 N88-15701
Nondestructive characterization of ceramic composite whiskers with neutron diffraction and ultrasonic techniques
[DE88-003075] 08 p0965 N88-15844
Processing and interfacial analysis of glass-ceramic to metal seals
[DE88-002999] 08 p0971 N88-15873
The use of NMR imaging to measure porosity and binder distributions in green-state and partially sintered ceramics
[DE88-003099] 08 p0972 N88-15881
Steady-state deformation of some lithium ceramics
[DE88-003116] 08 p0972 N88-15882
Aeropropulsion '87. Session 1: Aeropropulsion Materials Research
[NASA-CP-10003-SESS-1] 09 p1118 N88-16697
Ceramics for engines 09 p1119 N88-16704
Microstructures and properties of SiC whisker-reinforced mullite composites
[DE88-002611] 09 p1139 N88-16826
Nondestructive evaluation of structural ceramics by photoacoustic microscopy
[NASA-CR-180858] 09 p1146 N88-16868
Wire-cut electrical discharge machinability of ceramics
[AD-A186989] 09 p1146 N88-16870
Image correlation on an IBM-PC for characterization of advanced ceramics
[DE88-002829] 09 p1149 N88-16885
LFCM (Liquid-Fed Ceramic Melter) vitrification technology
[DE88-003441] 09 p1149 N88-16887
Focused ultrasonic backscatter technique for near-surface flaw detection in structural ceramics
[DE88-003112] 09 p1183 N88-17091
Application of high temperature ceramic superconductors (CSC) to commercial tokamak reactors
[DE88-003973] 09 p1257 N88-17538
Fabrication and materials evaluation of high performance aligned ceramic fibre reinforced glass matrix composite
[AERE-R-12517] 10 p1294 N88-17736
Materials development for JPL oxygen plant
[DE88-003067] 10 p1297 N88-17752
Friction and wear of monolithic and fiber reinforced silicon-ceramics sliding against IN-718 alloy at 25 to 800 C in atmospheric air at ambient pressure
[NASA-TM-100294] 10 p1304 N88-17796
NMR (Nuclear Magnetic Resonance) imaging for detecting binder/plasticizers in green-state structural ceramics
[DE88-003111] 10 p1304 N88-17800
Adhesion, friction and micromechanical properties of ceramics
[NASA-TM-100782] 10 p1305 N88-17801
Tribology of ceramics: Report of the Committee on Tribology of Ceramics
[NASA-CR-182506] 10 p1305 N88-17802
Effect of translucence of engineering ceramics on heat transfer in diesel engines
[DE88-003732] 10 p1305 N88-17804
Fabrication, phase transformation studies and characterization of SiC-AlN-Al2OC ceramics
[DE88-004053] 10 p1306 N88-17807
The migration of grain boundaries in ceramic materials with particular reference to the sintering process
[DE88-004085] 10 p1306 N88-17808
Metal modification for improved glass-ceramic to metal seals: 1. Auger results on ion implantation and vapor deposition films
[DE88-005244] 10 p1339 N88-18006
Ceramic bearings for use in gas turbine engines
[NASA-TM-100288] 10 p1340 N88-18007
Fundamental studies of corrosion of nonoxide structural ceramics
[PB88-141536] 11 p1461 N88-18709
Research on high-specific-heat dielectrics
[AD-A187248] 11 p1461 N88-18710
High yield synthesis of B4C/BN ceramic materials by pyrolysis of polymeric Lewis base adducts of decaborane(14)
[AD-A188154] 11 p1462 N88-18717
Tribological properties of alumina-boria-silicate fabric from 25 to 850 C
[NASA-TM-100806] 11 p1464 N88-18726
Application of X-ray computed tomography to ceramic/ceramic composites
[DE88-002903] 11 p1464 N88-18728
Ceramic technology for advanced heat engines program data base
[DE88-003922] 11 p1464 N88-18730
Perturbed angular correlations in zirconia ceramics
[DE88-004117] 11 p1464 N88-18731
Ceramic decomposition under irradiation
[DE88-004327] 11 p1464 N88-18732
Quality assurance of ceramic materials and gas turbine components
[IZFP-850303-TW] 11 p1465 N88-18735
Slip casting of advanced ceramics and composites
[DE88-003424] 11 p1467 N88-18746
Prototype thin-film thermocouple/heat-flux sensor for a ceramic-insulated diesel engine
[NASA-TM-100798] 11 p1490 N88-18892
Review of the state of the art and projected technology of low heat rejection engines
[PB88-131255] 11 p1496 N88-18934
Reliability based analysis of contact problems
[NASA-CR-182117] 11 p1503 N88-18975
Composite ceramic superconducting filaments for superconducting cable
[AD-A187833] 11 p1556 N88-19312
Research briefing on high-temperature superconductivity
[PB88-133004] 11 p1561 N88-19344
The preparation of titanium nitride and titanium carbonitride by the preceramic polymer route
[AD-A188357] 12 p1610 N88-19626
Microdesigning of lightweight/high strength ceramic materials
[AD-A188526] 12 p1610 N88-19631
Contact and current noise in beta alumina and Nasicon ceramics
[AD-A189168] 12 p1611 N88-19635
Properties to seals made with Li2O-Al2O3-SiO2-glass ceramics and aluminum-containing austenitic stainless steels
[DE88-004688] 12 p1633 N88-19776
Basic research in ceramic and semiconductor science at selected Japanese laboratories, based on a September 1986 visit: Highlights, summary and overview and detailed notes from selected Japanese laboratories
[DOE/ER-0314] 12 p1696 N88-20150
Advanced Gas Turbine (AGT) Technology Development Project, ceramic component developments
[NASA-CR-180871] 12 p1709 N88-20229
A new process for synthesis of silicon nitride powders for advanced ceramics
[AD-A189354] 13 p1748 N88-20451
Development of a torsion balance for adhesion measurements
[NASA-TM-100799] 13 p1748 N88-20454
The effect of Ca(OH)2-treated ceramic microspheres on the mechanical properties of high-temperature lightweight cement composites
[DE88-004590] 13 p1749 N88-20457
Improved glass-ceramic to metal seals in actuator and detonator applications with an aluminum-containing austenitic stainless steel
[DE88-004691] 13 p1749 N88-20458
Ultrasonic characterization of non-uniform porosity distributions in SiC ceramic
[DE88-004814] 13 p1749 N88-20459
Interfacial chemistry-structure and fracture of ceramic composites
[DE88-005516] 13 p1750 N88-20461
PNL-1 improved ceramic composites through controlled fiber matrix interaction
[DE88-005680] 13 p1750 N88-20462
Abrasion and impact resistant coatings
[DE88-003562] 13 p1750 N88-20464
Advances in X-ray line profile analysis to determine microstructure information about ceramics
[DE88-003938] 13 p1750 N88-20465
Micromechanical and microstructural studies of ceramic superplasticity
[DE88-005793] 13 p1751 N88-20472
Recent developments in nondestructive evaluation for structural ceramics
[DE88-005889] 13 p1751 N88-20473
X-ray computed tomography for structural ceramic applications: Beam hardening corrections
[DE88-005891] 13 p1752 N88-20474
Processing of nanophase ceramics
[DE88-005985] 13 p1752 N88-20475

Theory and experiments of fracture in cyclic compression: Single phase ceramics, transforming ceramics and ceramic composites
[DE88-005792] 13 p1781 N88-20659
Fracture criteria for discontinuously reinforced metal matrix composites
[NASA-CR-182665] 13 p1782 N88-20662
Theoretical studies on the electronic structure and properties of complex ceramic crystals and glasses
[DE88-005837] 13 p1846 N88-21049
A hydroxycarbonate route to superconductor precursor powders
[DE88-003638] 13 p1846 N88-21052
ONR Far East Scientific Bulletin, volume 12, number 3, July-September 1987
[AD-A188554] 13 p1851 N88-21081
Fabric space radiators
[DE88-005569] 14 p1880 N88-21237
JPRS report: Science and technology. USSR: Materials science
[JPRS-UMS-87-009] 14 p1884 N88-21261
Crack resistance of multilayer ceramic-based composite material 14 p1885 N88-21265
A dense and strong ceramic material made from zirconium dioxide 14 p1886 N88-21274
Increasing the rate at which ceramic castings undergo preliminary heat-treatment in an ultra-high frequency magnetic field 14 p1886 N88-21275
Ceramic materials from preceramic organometallic copolymers
[DE88-006067] 14 p1892 N88-21301
Interface structure and properties of alumina/glass ceramic composites
[DE88-006219] 14 p1892 N88-21302
Processing, texture and mechanical properties of sintered silicon carbide
[NASA-TT-20253] 14 p1893 N88-21305
Effect of oxidation on strength and thermal stability of material based on Si3N4 14 p1896 N88-21319
Diffusion welding of aluminomagnesium alloys to ceramics 14 p1898 N88-21333
Interfacial structure-property relationships at the fiber-matrix interphase in advanced composites
[AD-A190649] 15 p2030 N88-22093
Specimen preparation techniques for the examination of ceramic and metal-matrix composites
[DE88-005157] 15 p2030 N88-22094
Thermal conductivity of oxide ceramics
[DE88-005842] 15 p2042 N88-22169
Ultrasonic characterization of ceramic joints
[DE88-005844] 15 p2043 N88-22173
Temperature-dependent conductivity of oxygen-depleted YBCO ceramics
[AD-A190340] 15 p2044 N88-22182
Transformation toughening of ceramics
[AD-A190399] 15 p2045 N88-22183
Stress corrosion of ceramic materials
[AD-A190501] 15 p2045 N88-22187
High-performance polymeric materials
[AD-A190708] 15 p2046 N88-22190
Strength and microstructure of ceramics
[AD-A190712] 15 p2046 N88-22191
High temperature corrosion of ceramics
[DE88-006567] 15 p2046 N88-22193
Hafnia-rich mixed oxide ceramics of the system HfO2-ZrO2-TiO2 for heaters and heat exchangers in electrothermal thrusters: The effects of titania on selected electrical and mechanical properties of Hafnia-rich mixed oxides in the system Hafnia-Zirconia-Titania, volume 1
[NASA-CR-182800-VOL-1] 15 p2047 N88-22197
Gamma-ray densitometry: Nondestructive analysis of density evolution during ceramic powder processing
[DE88-006671] 15 p2047 N88-22198
Melt processing ceramic YBa2Cu3O(sub 6.9)
[DE88-007039] 15 p2047 N88-22199
JPRS report: Science and technology. Japan
[JPRS-JST-88-002] 15 p2050 N88-22210
Compound ceramic processing 15 p2050 N88-22212
Hard ceramic film by laser PVD 15 p2051 N88-22216
Function of Japan Fine Ceramics Center described 15 p2052 N88-22227
JPRS report: Science and technology. Japan
[JPRS-JST-87-029] 15 p2052 N88-22228
Developments in ceramic superconducting materials 15 p2052 N88-22229
An evaluation of nondestructive methods for ceramic heat exchanger applications
[DE88-006731] 15 p2068 N88-22328
Monolithic ceramic analysis using the SCARE program 15 p2081 N88-22409
Whisker-reinforced ceramic composites for heat engine components 15 p2082 N88-22410
Nondestructive evaluation of sintered ceramics 15 p2083 N88-22416
Magnetic anomalies in the rare earth oxide superconductors GdBa2Cu3O(7-x) and YbBa2Cu3O(7-x)
[AD-A190713] 15 p2144 N88-22793
Synthesis and characterization of high-T(sub c) screen-printed Y-Ba-Cu-O films on alumina
[NASA-TM-100860] 15 p2146 N88-22805
Design and test of a new coaxial air joints
[DE88-751808] 16 p2164 N88-22908
JPRS report: Science and technology. USSR: Materials science
[JPRS-UMS-88-006] 16 p2179 N88-22988
Strength and cracking resistance of ceramics. Report 3: SiC ceramics 16 p2180 N88-22994
High-strength ceramic based on tetragonal ZrO2 with Al2O3 admixture 16 p2180 N88-22996
JPRS report: Science and technology. Japan
[JPRS-JST-87-026] 16 p2184 N88-23018
Government research on ceramics coating technology 16 p2184 N88-23019
Status, trends in research on internal combustion engines 16 p2185 N88-23027
Bimodular behavior and crack closure in compression in a brittle material
[AD-A191267] 16 p2224 N88-23275
Structural Ceramics
[NASA-CP-2427] 17 p2323 N88-23872
Ceramics for turbine engines 17 p2323 N88-23873
Friction and wear of ceramics 17 p2323 N88-23874
Some design considerations for ceramic components in heat engine applications 17 p2323 N88-23875
Nondestructive evaluation of structural ceramics 17 p2324 N88-23876
Fracture mechanics 17 p2324 N88-23877
Structural ceramics research 17 p2324 N88-23878
Nondestructive Evaluation (NDE) of structural ceramics by photoacoustic microscopy 17 p2325 N88-23884
Molten salt corrosion of SiC and Si3N4 17 p2325 N88-23885
Thermal cyclic durability testing of ceramic materials for turbine engines 17 p2325 N88-23886
Fractographic and microstructural evaluation of 3500-hour durability specimens 17 p2325 N88-23887
Polymer precursors for ceramic composites 17 p2326 N88-23890
Fabric radiators 17 p2427 N88-24435
Ceramic electrical insulator development for thermoelectric SACE power system 17 p2430 N88-24459
Apparatus for the measurement of resistivity of glasses and ceramics 17 p2431 N88-24460
Thrust chamber thermal barrier coating techniques
[NASA-TM-100933] 18 p2476 N88-24690
Role of cracks in the creep of structural polycrystalline ceramics
[AD-A191485] 18 p2490 N88-24770
Environmental effects on slow crack growth in silicon nitride
[DE88-007206] 18 p2494 N88-24795
The stress analysis of ceramic, polymeric, and metallic composite systems by the finite element method 18 p2529 N88-25004
Solid-state combustion synthesis of ceramics and alloys in reduced gravity
[NASA-CR-4163] 19 p2608 N88-25479
Metals and Ceramics Division
[DE88-006955] 19 p2618 N88-25530
Paramagnetic spins in oxygen-loaded ceramic La2CuO4/sub 4+delta/
[DE88-007114] 19 p2619 N88-25539
Assessment of opportunities for gas-fired sintering in the advanced ceramics and powdered metals industries
[PB88-197157] 19 p2620 N88-25545
Uniaxial tensile strain measurement for ceramic testing at elevated temperature: Requirements, problems and solutions
[DE88-006090] 19 p2621 N88-25550
An assessment of the state of the art in predicting the failure of ceramics
[DE88-006998] 19 p2621 N88-25551
JPRS report: Science and technology. Japan
[JPRS-JST-88-005] 19 p2633 N88-25619
Research and development programs on advanced structural ceramics in Korea 19 p2633 N88-25620
Ceramic substrates for semiconductor applications reported: AlN substrates 19 p2633 N88-25621
AlN substrate applications 19 p2634 N88-25622
Effect of a weak magnetic field on high temperature superconductivity in Y-Ba-Cu-O ceramics
[DE88-702192] 19 p2733 N88-26235
Application of electron microscopy for the analysis of the mechanical behavior of advanced ceramics
[DE88-005049] 20 p2777 N88-26469
A study of solvent effects on the synthesis of pure component and composite ceramic powders by metal alkoxide hydrolysis
[DE88-008381] 20 p2777 N88-26470
Observations on residual stresses in ceramic composites by neutron diffraction techniques
[DE88-009937] 20 p2778 N88-26472
Application of magnification xeroradiography to advanced ceramics
[DE88-009965] 20 p2778 N88-26473
Determination of binder distributions in green-state ceramics by NMR imaging
[DE88-009990] 20 p2778 N88-26474
The outlook for ceramics in heat engines, 1990-2010: Results of a worldwide Delphi survey
[DE88-010075] 20 p2778 N88-26475
Factors influencing the toughening behavior of whisker reinforced ceramics
[DE88-011396] 20 p2779 N88-26479
Fracture resistance of a TiB2 particle/SiC matrix composite at elevated temperature
[NASA-TM-100967] 20 p2779 N88-26482
Ceramic Technology for Advanced Heat Engines Program data base
[DE88-008954] 20 p2780 N88-26489
Characteristics of pressure loss during filtration using a porous ceramic filter
[DE88-752547] 20 p2798 N88-26604
Computational study on thermal efficiency of ceramic gas turbine
[DE88-753114] 20 p2809 N88-26667
Study on the heat resisting and cooling property of the ceramics-metal hybrid stator vanes
[DE88-753117] 20 p2810 N88-26668
Ceramic processing of high-T(sub)c superconductors
[DE88-010090] 20 p2878 N88-27087
Polymer-ceramic composites
[AD-A193244] 21 p2905 N88-27237
Studies in support of oxidation-resistant composite materials
[AD-A193320] 21 p2905 N88-27238
Theoretical and experimental analysis of the toughening behavior of whisker reinforcement in ceramic matrix composites
[DE88-011841] 21 p2906 N88-27241
Preparation and properties of new inorganic glasses and gel-derived solids
[AD-A192922] 21 p2917 N88-27315
Processing and additive effects of ZrO2 on microstructure and dielectric porperties of BaTiO3 ceramics
[AD-A193126] 21 p2917 N88-27316
Preparation and properties of high Q microwave dielectrics in the (CA, SR, BA) zirconate system
[AD-A193127] 21 p2918 N88-27317
Ceramic technology for advanced heat engines project
[DE88-008945] 21 p2919 N88-27323
Studies of dynamic contact of ceramics and alloys for advanced heat engines
[DE88-008996] 21 p2919 N88-27324
Effects of near interfacial microstructure on toughness and subcritical crack growth in ceramic/metal systems
[DE88-009842] 21 p2919 N88-27325
Data compilation for radiation damage on ceramic insulators. Revised with updated data and reviews
[DE88-753426] 21 p2920 N88-27329
Application of sol-gel procedures to ceramic composites
[ETN-88-92741] 21 p2921 N88-27338
Preparation and characterization of ceramic materials based on Al2O3 reinforced with a ZrO2 dispersion
[ISAL-87-0041] 21 p2922 N88-27340
Study of the friction and wear-related properties of ceramic superconductors
[DE88-011844] 21 p3024 N88-27950
Ceramic fabrication technology for high-T(sub)c materials
[DE88-012060] 21 p3024 N88-27953
The High Temperature Materials Laboratory: A new research and user facility at the Oak Ridge National Laboratory
[DE88-010792] 22 p3057 N88-28138
Modification of YBa2Cu3O(7-x) ceramics by adsorbed water and other gases
[DE88-011518] 22 p3057 N88-28140
Influence of dispersed additives reinforcement on the wear reinforcement mechanisms of the alumina-steel couple. Macroscopic and structural aspects
[ECL-88-01] 22 p3059 N88-28148
Optimization of nondestructive control of ceramic pieces for aeronautical turbines
[ETN-88-92884] 22 p3059 N88-28149

Development of sensors for ceramic components in advanced propulsion systems: Survey and evaluation of measurement techniques for temperature, strain and heat flux for ceramic components in advanced propulsion systems
[NASA-CR-182111] 22 p3081 N88-28299
Laser crystallized silicon films on alumina ceramic substrates and application to thin film c-Si solar cells
[PB88-131966] 22 p3116 N88-28515
Fabrication of bulk superconducting ceramics
[DE88-009956] 22 p3155 N88-28773
Ultrafine microstructure composites prepared by chemical vapor deposition
[AD-A193849] 23 p3189 N88-28973
A fundamental study of P/M processed elevated temperature aluminum alloys
[AD-A192958] 23 p3194 N88-29005
Stress corrosion of ceramic materials
[AD-A191979] 23 p3195 N88-29016
Wave and fracture phenomena in impacted ceramics
[AD-A192946] 23 p3196 N88-29020
Development of creep fracture modelling in ceramics
[PB88-202825] 23 p3196 N88-29021
The mechanical behavior of surface modified ceramics
[DE88-010564] 23 p3196 N88-29022
Sinterable ceramic powders from laser-heated gases
[AD-A194162] 23 p3197 N88-29024
The sol-gel synthesis of ceramics
[SNIAS-881-430-114] 23 p3199 N88-29037
Al2O3-TiO2 and Al2TiO5 ceramic materials
[SNIAS-881-430-122] 23 p3199 N88-29038
Boron-containing organosilane polymers and ceramic materials thereof
[NASA-CASE-ARC-11649-1-SB] 23 p3199 N88-29040
Development of planar geometry solid oxide fuel cell technology, phase 1
[PB88-210356] 23 p3229 N88-29215
Electron microscopy of ceramic superconductors
[DE88-006446] 23 p3288 N88-29580
Fluctuations of order parameters in the high T(sub c) superconductors
[DE88-702549] 23 p3292 N88-29603
A study of the critical factors controlling the synthesis of ceramic matrix composites from preceramic polymers
[AD-A195405] 24 p3340 N88-29881
Processing technology research in composites
[AD-A195693] 24 p3341 N88-29890
Polymer-ceramic composites
[AD-A195789] 24 p3356 N88-29983
Piezoelectric and electrostrictive materials for transducer applications, volume 1
[AD-A194957] 24 p3374 N88-30096

CEREBELLUM
Growth and differentiation of cells in organotypical rat embryo cerebellar culture developing in weightlessness 19 p2703 N88-26076

CEREBRAL CORTEX
Change in functional activity of cortical brain structures and their blood supply in alert rabbits in response to rocking 04 p0473 N88-12916
Large-scale neuronal circuits for selective storage and recognition of complex stimuli, a pilot study
[AD-A184134] 04 p0474 N88-12920
Sleep induced in cat by electric stimulation of acoustic and motor areas in brain cortex 06 p0751 N88-14612
Karyometric evaluation of neuronal reactions of rat cerebral cortex to the combined effect of ionizing radiation, longitudinal accelerations and vibration 07 p0890 N88-15396
Retinotopic mapping of the human visual system with magnetoencephalography
[AD-A189557] 13 p1810 N88-20811
A systems engineering based methodology for analyzing human electrocortical responses
[AD-A190809] 18 p2550 N88-25135
Growth and differentiation of cells in organotypical rat embryo cerebellar culture developing in weightlessness 19 p2703 N88-26076
Method for observing changes in functional state of human operator 20 p2830 N88-26789

CEREBROSPINAL FLUID
Evaluation of spare room in cerebrospinal system using noninvasive methods 10 p1361 N88-18137

CEREBRUM
NT CEREBRAL CORTEX
Studies of the processing of single words using positron tomographic measures of cerebral blood flow change
[AD-A184058] 03 p0356 N88-12244
Models of cerebral-body perfusion and cerebral chemical transport
[AD-A194945] 24 p3407 N88-30283

CERENKOV COUNTERS
A program to study antiprotons in the cosmic rays: Arizona collaboration
[NASA-CR-180702] 01 p0120 N88-10764
The application of an image intensifier to atmospheric Cerenkov gamma ray astronomy
[MPE-PREPRINT-115] 22 p3163 N88-28839

CERENKOV EFFECT
U CERENKOV RADIATION

CERENKOV RADIATION
Cerenkov radiation field analysis due to a passing electron beam
[AD-A184870] 05 p0649 N88-13976
Energy distribution of Cerenkov radiation for finite frequency intervals
[AD-A186901] 09 p1244 N88-17454
An analysis of whistler-mode radiation from the Spacelab-2 electron beam, revision
[AD-A188228] 11 p1552 N88-19287
The application of imaging to the atmospheric Cerenkov technique: Observations of the Crab nebula 20 p2884 N88-27126
Effects of charge distribution within a particle beam on the sub-Cerenkov radiation
[AD-A193992] 22 p3150 N88-28742
Diffraction transition radiation from periodic electron bunches
[AD-A193593] 23 p3280 N88-29528

CERIUM
Gas tungsten arc welding of Al-10Fe-5Ce
[AD-A184202] 03 p0334 N88-12104

CERIUM COMPOUNDS
NT CERIUM OXIDES
Heavy Fermions and coherence in Kondo lattices: Specific heat of low energy excitation in Cer systems
[ETN-88-91080] 09 p1255 N88-17525
Electron Spin Resonance (ESR) measurements on intermediate-valence Cer compounds doped with paramagnetic ions: CeOs2:Gd ion and CePd3:Mn-ion
[ETN-88-91081] 09 p1256 N88-17526
Coexisting static magnetic ordering and superconductivity in CeCu2.1Si2 found by muon spin relaxation 17 p2396 N88-24245
Static magnetic ordering of CeCu2.1Si2 found by muon spin relaxation 17 p2396 N88-24246

CERIUM OXIDES
Thermodynamic and conductivity studies of nonstoichiometric cerium dioxide by Coulometric titration: A simultaneous measurement
[DE88-003054] 08 p1091 N88-16566

CERMETS
Internal reforming development for solid oxide fuel cells
[DE87-006518] 04 p0464 N88-12871
Cermet-fueled reactors for advanced space applications
[DE88-005528] 13 p1839 N88-21002
Molybdenum-base cermet fuel development
[DE88-005529] 13 p1839 N88-21003
Technical applications of solar energy. Project: Selective coatings
[BMFT-FB-T-86-213] 14 p1943 N88-21591
Direct conversion of solar energy to thermal energy
[BMFT-FB-T-86-220] 14 p1943 N88-21592
Cermet fuel thermal conductivity 17 p2410 N88-24329
Molybdenum-base cermet fuel development 17 p2434 N88-24481

CERTIFICATION
Computerized certification of digital ultrasonic instrumentation
[DE88-000820] 04 p0488 N88-13008
Airworthiness considerations 10 p1276 N88-17636
Utility NDE personnel qualification/certification: Enhanced personnel qualification requirements for ASME (American Society for Mechanical Engineers) Code Section 11 examinations
[DE88-006748] 16 p2216 N88-23222
Laminar Flow Aircraft Certification
[NASA-CP-2413] 17 p2296 N88-23737
Certification aspects of airplanes which may operate with significant natural laminar flow 17 p2298 N88-23749
US civil airmen statistics, 1987
[AD-A191714] 18 p2455 N88-24577
Calibration of averaging total pressure flight wake rake and natural-laminar-flow airfoil drag certification
[NASA-CR-181630] 19 p2599 N88-25443
Zero/zero rotorcraft certification issues. Volume 1: Executive summary
[NASA-CR-177483-VOL-1] 19 p2602 N88-25453
Zero/zero rotorcraft certification issues. Volume 2: Plenary session presentations
[NASA-CR-177483-VOL-2] 19 p2602 N88-25454
Zero/zero rotorcraft certification issues. Volume 3: Working group results
[NASA-CR-177483-VOL-3] 19 p2602 N88-25455
Materials qualification in oceanology and the offshore industry 19 p2700 N88-26050
The design and testing of aero engines to minimise hazard from birds
[PNR90436] 22 p3040 N88-28049

CESIUM
Coverage dependence of adsorbate-substrate bond lengths: Chlorine and caesium adsorbed on silver single crystals
[PB87-125142] 06 p0788 N88-14833
Atomic clocks research: An overview
[AD-A185567] 07 p0930 N88-15648
Arcs in cesium seeded noble gases resulting from a magnetically induced electric field
[EUT-87-E-177] 13 p1843 N88-21028
Theoretical studies of Resonance Enhanced Stimulated Raman Scattering (RESRS) of frequency doubled Alexandrite laser wavelength in cesium vapor
[NASA-CR-182871] 17 p2317 N88-23841

CESIUM COMPOUNDS
NT CESIUM IODIDES
Suppression of the mass enhancement in CeB6 in high magnetic fields
[DE88-002946] 09 p1241 N88-17439

CESIUM HALIDES
NT CESIUM IODIDES

CESIUM IODIDES
Heterogeneous isotope exchange between solid cesium iodide and gaseous methyl iodide
[ETN-88-91085] 09 p1141 N88-16840

CESIUM IONS
Photoionization of atoms and ions: Application of time-dependent response method within the density functional theory
[AD-A185686] 07 p0930 N88-15649

CESIUM PLASMA
Electron temperature measurements in an argon/cesium plasma diode
[AD-A188835] 12 p1695 N88-20141

CESSNA MILITARY AIRCRAFT
U MILITARY AIRCRAFT

CETANE
Cetane scale evaluation and possible modification
[AD-A189730] 15 p2048 N88-22200
Diesel combustion fundamentals, phase 1, volume 1
[AD-A193831] 22 p3052 N88-28107

CEYLON
U SRI LANKA

CFRP
U CARBON FIBER REINFORCED PLASTICS

CH-113 HELICOPTER
U CH-46 HELICOPTER

CH-46 HELICOPTER
An independent evaluation of the CH-46 Safety Reliability and Maintainability Program (SR and M)
[AD-A186310] 07 p0817 N88-14971

CHAD
Using space photography of the Earth in the classroom: Drought in Africa
[NASA-CR-182948] 19 p2685 N88-25960

CHAINS
Trajectory control of robot manipulators with closed-kinematic chain mechanism
[NASA-TM-89305] 05 p0591 N88-13605
The Shock and Vibration Digest, Volume 19, No. 12 05 p0610 N88-13746
Dynamics of cables and chains 05 p0610 N88-13747
Distribution of chain ends inside the polybutadiene microspheres of SB diblock copolymers
[AD-A191257] 16 p2182 N88-23007
Kinematics, dynamics and control of a closed chain mechanism manipulator 18 p2523 N88-24967
Analysis of a closed-kinematic chain robot manipulator
[NASA-CR-183031] 18 p2561 N88-25206
Spatial organization of homopolymer chains inside spherical polybutadiene domains of SB diblock copolymers
[AD-A193390] 21 p2918 N88-27321

CHAIRS
U SEATS

CHALCOGENIDES
NT ALKALINE EARTH OXIDES
NT ALUMINUM OXIDES
NT ANHYDRIDES
NT BARIUM OXIDES
NT BERYLLIUM OXIDES
NT BISMUTH OXIDES
NT BISMUTH SULFIDES
NT BORON OXIDES
NT CADMIUM SELENIDES
NT CADMIUM SULFIDES
NT CADMIUM TELLURIDES

NT CALCIUM OXIDES
NT CARBON DIOXIDE
NT CARBON MONOXIDE
NT CERIUM OXIDES
NT CHROMIUM OXIDES
NT COBALT OXIDES
NT COPPER OXIDES
NT COPPER SELENIDES
NT COPPER SULFIDES
NT DIOXIDES
NT DISULFIDES
NT HAFNIUM OXIDES
NT HEMATITE
NT HYDROGEN PEROXIDE
NT HYDROGEN SULFIDE
NT IRON OXIDES
NT LANTHANUM OXIDES
NT LANTHANUM TELLURIDES
NT LEAD OXIDES
NT LEAD SULFIDES
NT LEAD TELLURIDES
NT LITHIUM OXIDES
NT MAGNESIUM OXIDES
NT MANGANESE OXIDES
NT MERCURY TELLURIDES
NT METAL OXIDES
NT MOLYBDENUM DISULFIDES
NT MOLYBDENUM OXIDES
NT MOLYBDENUM SULFIDES
NT NICKEL OXIDES
NT NIOBIUM OXIDES
NT NITROGEN DIOXIDE
NT NITROGEN OXIDES
NT NITROUS OXIDES
NT OXIDES
NT PEROXIDES
NT POLYSULFIDES
NT PYRITES
NT QUARTZ
NT RUTILE
NT SAPPHIRE
NT SELENIDES
NT SILICON DIOXIDE
NT SILICON OXIDES
NT SULFIDES
NT SULFUR DIOXIDES
NT TANTALUM OXIDES
NT TIN OXIDES
NT TIN TELLURIDES
NT TITANIUM OXIDES
NT VANADIUM OXIDES
NT YTTRIUM OXIDES
NT ZINC OXIDES
NT ZINC SELENIDES
NT ZINC SULFIDES
NT ZINC TELLURIDES
NT ZIRCONIUM OXIDES
Photoinduced low-temperature changes in optical losses in fiber optics based on chalcogenide glasses
06 p0770 N88-14731

CHALLENGER (ORBITER)
Structural analysis of a bolted joint concept for the space shuttle's solid rocket motor casing
[NASA-TM-89092] 04 p0407 N88-12531
Space shuttle accident: NASA's actions to address the Presidential Commission report
[PB88-135306] 15 p2024 N88-22059

CHANCE-VOUGHT MILITARY AIRCRAFT
U MILITARY AIRCRAFT

CHANGE DETECTION
High polymer sensor materials discussed
06 p0676 N88-14140
Real-time image difference detection using a polarization rotation spacial light modulator
[NASA-CASE-NPO-17144-1-CU]
18 p2576 N88-25305
Monitoring urban land cover changes at the urban fringe from SPOT HRV imagery in south-east England
22 p3099 N88-28406

CHANNEL CAPACITY
Coding for spread-spectrum communications networks
[AD-A185667] 07 p0844 N88-15119
Information and coding capacities of mismatched Gaussian channels
[AD-A190321] 15 p2124 N88-22665
Coding capacity of generalized additive channels
[AD-A190315] 15 p2127 N88-22685
Information capacity of Gaussian channels
[AD-A190316] 15 p2127 N88-22686
Conditions for information capacity of the discrete-time Gaussian channel to be increased by feedback
[AD-A190317] 15 p2127 N88-22687
Coding capacity of discrete-time Gaussian and nonGaussian channels
[AD-A190318] 15 p2127 N88-22688
On the capacity of channels with unknown interference
[AD-A191160] 16 p2191 N88-23067
Communications using channels formed by meteor bursts
[AD-A192088] 18 p2501 N88-24834
Information and stochastic systems
[AD-A192167] 18 p2501 N88-24838
Evaluation of CDMA system capacity for mobile satellite system applications 19 p2651 N88-25740

CHANNEL FLOW
NT OPEN CHANNEL FLOW
Reynolds number effects on the small scale structure of a turbulent channel flow 01 p0001 N88-10004
MHD (magnetohydrodynamics) channel development
[DE87-014126] 02 p0237 N88-11498
Structural characteristics of dean vortices in a curved channel
[AD-A184724] 03 p0320 N88-12024
The design and preliminary calibration of a boundary-layer flow channel
[NASA-CR-178399] 04 p0394 N88-12457
A numerical investigation on wing/nacelle interferences 05 p0535 N88-13258
High resolution simulation of turbulent flow in a channel
[AD-A186022] 07 p0848 N88-15150
Reynolds-stress and dissipation rate budgets in a turbulent channel flow
[NASA-TM-89451] 07 p0852 N88-15174
Numerical simulation of heat transfer turbulence, volume 2
[AD-A185130] 08 p0983 N88-15947
Numerical simulation of turbulent spots in channel and boundary layer flows 08 p0983 N88-15948
Weak interactions and local order in strong turbulence
09 p1159 N88-16948
Numerical and physical aspects of large eddy simulation of turbulent flows
[ETN-88-91611] 09 p1162 N88-16965
Use of boundary-layer method for problem of sound propagation through channel with variable cross-section containing stream of fluid 09 p1233 N88-17396
Instability and transition in curved channel flow
10 p1328 N88-17938
Wavenumber - frequency structure of turbulent flow in a channel from a direct simulation
[AD-A189079] 12 p1627 N88-19737
Investigation of supersonic chemically reacting and radiating channel flow
[NASA-CR-182726] 14 p1862 N88-21125
Stochastic estimation of conditional eddies in turbulent channel flow 16 p2194 N88-23087
Self similarity of two point correlations in wall bounded turbulent flows 16 p2195 N88-23089
Ejection mechanisms in the sublayer of a turbulent channel 16 p2195 N88-23090
Modeling scalar flux and the energy and dissipation equations 16 p2196 N88-23096
Modeling of turbulent transport as a volume process
16 p2196 N88-23099
On local approximations of the pressure-strain term in turbulence models 16 p2197 N88-23102
Test code for the assessment and improvement of Reynolds stress models 16 p2197 N88-23105
Shear-layer structures in near-wall turbulence
16 p2198 N88-23110
Conditionally-averaged structures in wall-bounded turbulent flows 16 p2198 N88-23112
Active layer model for wall-bounded turbulence
16 p2199 N88-23115
A variational finite element method for three-dimensional, steady, compressible, viscous flows
18 p2512 N88-24904
Theoretical analysis of laminar incompressible flow in slender channels
[VTH-LR-517] 18 p2513 N88-24909
Numerical simulation studies of laminar-turbulent transition in the plan channel 19 p2665 N88-25850
Computational boundary conditions for the incompressible Navier-Stokes equations in channels and pipes
[AD-A193356] 21 p2944 N88-27487
Unsteady water channel
[AD-A194231] 23 p3171 N88-28884
Computation of the eigenvalues for perturbations of Poiseuille flow using a two-point boundary value method
[AD-A193479] 23 p3210 N88-29104
The strong nonlinear interaction of Tollmien-Schlichting waves and Taylor-Goertler vortices in curved channel flow
[NASA-CR-181697] 24 p3311 N88-29716
On the generation of mean flows by the interaction of Goertler vortices and Tollmien-Schlichting waves in curved channel flows
[NASA-CR-181690] 24 p3315 N88-29743

CHANNEL NOISE
Performance analysis of coded frequency-hopped spread-spectrum systems with unknown interference
[AD-A186069] 07 p0841 N88-15103
Information capacity of Gaussian channels
[AD-A190316] 15 p2127 N88-22686
An algorithm for random access communication over a noisy channel
[AD-A191315] 16 p2252 N88-23461
Outliner resistant filtering and smoothing: 2D version
[AD-A193319] 21 p3012 N88-27874

CHANNELS
Channeling and dechanneling at high energy
[DE88-003989] 11 p1548 N88-19259
Pre-launch calibration of channels 1 and 2 of the advanced very high resolution radiometer
[PB88-157169] 14 p1913 N88-21427
A study of a meteor burst communication system
21 p2934 N88-27421

CHANNELS (DATA TRANSMISSION)
Test equipment with fiber optic data bus and laser gyro strapdown system LTN-90 for the helicopter BO-105
[ESA-TT-1038] 01 p0005 N88-10025
Digital bus unit engineering model: Design, manufacture and test
[MRM/TREP/1003/SAAB] 01 p0083 N88-10537
An evaluation plan of bus architectures and protocols using the NASA Ames intelligent redundant actuation system
[NASA-CR-177458] 04 p0398 N88-12482
Design of source coders and joint source/channel coders for noisy channels
[NASA-CR-181547] 04 p0432 N88-12678
Increased gain of channel intensifier tubes by pulsed biasing
[DE88-000512] 04 p0490 N88-13019
An exact analysis and performance of framed ALOHA with capture
[AD-A185006] 05 p0574 N88-13500
Channel access protocols for multihop packet radio networks
[AD-A186074] 07 p0842 N88-15105
Coding for spread-spectrum communications networks
[AD-A185667] 07 p0844 N88-15119
High performance data buses: Progress and evolution
[DE88-002570] 09 p1215 N88-17285
Multiple-bus interconnection for future multiprocessor systems 10 p1375 N88-18203
Experiences with serial and parallel algorithms for channel routing using simulated annealing
[NASA-CR-182530] 10 p1388 N88-18289
Air Force Institute of Technology (AFIT) Local Area Network (LAN) performance evaluation model: An analytic model for assessing the impact of changing LAN hardware and software configurations
[AD-A187191] 11 p1469 N88-18764
An application of dimensionless Eigenvalues to underwater acoustic ducts
[AD-A188167] 11 p1542 N88-19219
DATAC bus monitor 17 p2294 N88-23721
Design for interoperability (interchangeability)
17 p2305 N88-23789
Communications using channels formed by meteor bursts
[AD-A192088] 18 p2501 N88-24834
Selection and effects of channels in distributed communication and decision making tasks: A theoretical review and a proposed research paradigm
[AD-A191807] 18 p2587 N88-25375
A study on the co- and adjacent channel protection requirements for mobile satellite ACSSB modulation
19 p2650 N88-25732
Development of a maintenance data bus monitor and recorder 22 p3036 N88-28022
Interface techniques and systems for standard aircraft data buses 22 p3036 N88-28028
Multichannel data transmission through a fiber optic cable
[AD-A193842] 22 p3070 N88-28221
Coding for meteor-burst communications channel and side information for channels with block-interference
23 p3202 N88-29054
Optics and symbolic computing
[AD-A195119] 24 p3360 N88-30004
Performance of DS/SSMA communications in impulsive channels. Part 1: Correlation receivers
[AD-A195712] 24 p3362 N88-30021

CHAOS
Dimension densities for turbulent systems with spatially decaying correlation functions
[DE87-010119] 02 p0169 N88-11066
IR laser excitation in molecules: Chaos and diffusive energy growth
[DE87-013147] 02 p0178 N88-11105

Quantum-mechanical aspects of classically chaotic driven systems
[DE87-013152] 02 p0178 N88-11106
Special Course on Modern Theoretical and Experimental Approaches to Turbulent Flow Structure and its Modelling
[AGARD-R-755] 03 p0312 N88-11970
Dynamics and routes to chaos from quasiperiodicity 03 p0312 N88-11974
A deterministic approach to turbulence: Chaos in Rayleigh-Benard convection 03 p0313 N88-11975
Determination of fractal dimension, connection of space and temporal chaos and application to experimental results 03 p0313 N88-11977
Fully developed turbulence via Feigenbaum's period-doubling bifurcations
[DE88-000242] 04 p0441 N88-12739
Supertracks: The building blocks of chaos
[DE88-001513] 04 p0522 N88-13207
Chaos: Chto Delat? (What is to be done?)
[DE88-000513] 05 p0643 N88-13933
Theoretical investigations of chaotic dynamics
[AD-A186404] 07 p0867 N88-15261
Studies of nonlinear and chaotic phenomena in solid state systems
[DE88-002330] 09 p1254 N88-17515
Instabilities and chaos in a multimode, standing-wave, CW dye laser
[DE88-005028] 10 p1337 N88-17993
Travelling waves and chaos in double-diffusive convection 11 p1484 N88-18857
Chaos, mappings and spatial complexity in fluids 11 p1484 N88-18860
Relative chaos in stellar systems
[DE88-700148] 12 p1710 N88-20234
Stochastic and chaotic oscillations
[CWI-AM-R8704] 13 p1829 N88-20940
Chaotic diffusion across magnetic field in a model of electrostatic turbulent plasma
[PREPRINT-566] 14 p1985 N88-21839
Electrical resistivity as quantum chaos
[DE88-007026] 16 p2284 N88-23675
Application of chaos theory to 1/f noise
[AD-A191150] 17 p2334 N88-23935
Stationary, wave type, and chaos type convection in spherical symmetry geometries
[ETN-88-92358] 20 p2801 N88-26625
Coupled experimental and theoretical investigations of instability, chaos and turbulence in an axisymmetric jet flow
[AD-A192943] 21 p2942 N88-27476
Statistical description of stochastic dynamics
[AD-A192924] 21 p3009 N88-27852
Regular and chaotic motion of fluid particles in a two dimensional fluid
[PREPRINT-591] 22 p3078 N88-28278
Vortex dynamics of coherent and chaotic structures (including algorithms for computer simulations and diagnosis)
[AD-A193580] 23 p3212 N88-29117
Chaotic behaviour in quantum dynamics
[AD-A193936] 23 p3295 N88-29623
Pierce diode with external circuit. Part 3: Chaotic behavior
[AD-A194837] 24 p3365 N88-30041

CHAOTIC CLOUD PATTERNS
U CLOUDS (METEOROLOGY)

CHAPMAN SHEAR LAYER
U SHEAR LAYERS

CHAPMAN-JOUGET FLAME
U CHEMICAL EQUILIBRIUM
U DETONATION
U FLAME PROPAGATION

CHARACTER RECOGNITION
Application of new technologies to DTIC document processing
[AD-A189778] 15 p2148 N88-22823

CHARACTERISTIC EQUATIONS
U EIGENVALUES
U EIGENVECTORS

CHARACTERISTIC FUNCTIONS
U EIGENVALUES
U EIGENVECTORS

CHARACTERISTIC METHOD
U METHOD OF CHARACTERISTICS

CHARACTERIZATION
Mechanical properties characterization of composite sandwich materials intended for space antenna applications
[NASA-TM-88893] 01 p0020 N88-10121
Elevated temperature strain gages 02 p0184 N88-11144
Characterization and thermal conductivity of hot-pressed silicon carbide
[DKG-25] 03 p0292 N88-11834
Synthesis and characterization of block copolymers
[AD-A184405] 03 p0295 N88-11855
Perturbation and characterization of nonlinear processes
[DE87-014580] 03 p0369 N88-12322
The characterization of diagnostic tasks for engineering systems
[DE88-000093] 04 p0483 N88-12973
Molecular-level synthesis and characterization of metal-polymer interfaces
[AD-A184956] 05 p0567 N88-13455
Characterization of the microstructures of various materials
[AD-A184961] 05 p0655 N88-14017
Study of damage in carbon fiber-epoxy composite materials. Utilization to assess broken specimens
[DCQ/L-45-650/F] 06 p0678 N88-14152
Design, production, and characterization of broadband optical waveguides
[DFVLR-FB-85-52] 06 p0780 N88-14791
Characterization of meteorological phenomena influencing aircraft operations 08 p0951 N88-15772
Study of selection criteria for adhesives used in aircraft structure bonding
[ETN-88-91619] 08 p0971 N88-15875
Comparison of UNL laser imaging and sizing system and a phase/Doppler system for analyzing sprays from a NASA nozzle
[NASA-CR-182437] 09 p1161 N88-16956
System characterization in nonlinear random vibration 09 p1180 N88-17071
Fracture mechanics characterization of crack growth under creep and fatigue conditions
[W-2/87] 09 p1183 N88-17087
Automatic prober for the dc characterization of gallium arsenide devices. Part 1: The measurement facility
[AD-A187583] 11 p1560 N88-19337
Preparation and characterization of thin films of alumina by metalorganic chemical vapor deposition
[AD-A188366] 12 p1608 N88-19614
Development of a CCD characterization system
[INPE-4361-TDL/301] 12 p1623 N88-19712
Microstructure characterization with a pulsed laser ultrasonic source
[DE88-005207] 12 p1632 N88-19766
The synthesis, characterization and structural studies of In(C5H4Me) by X-ray diffraction and electron diffraction techniques and a reinvestigation of the crystalline state of In(C5H5) by X-ray diffraction studies
[AD-A189110] 13 p1844 N88-21038
Fracture toughness characterization of SA508 and Sa533B RPB steels
[CISE-3908] 14 p1889 N88-21292
Research relative to angular distribution of snow reflectance/snow cover characterization and microwave emission
[NASA-CR-182733] 14 p1941 N88-21582
Fabrication and characterization of semiconductor lasers of Pb(1-x)Sn(x)Te
[INPE-4253-PRE/1126] 15 p2072 N88-22357
Spectrum fatigue testing for materials characterization
[VTT-RR-502] 15 p2088 N88-22443
Synthesis and characterization of high-T(sub c) screen-printed Y-Ba-Cu-O films on alumina
[NASA-TM-100860] 15 p2146 N88-22805
Characterization of precipitates in a niobium-zirconium-carbon alloy
[NASA-TM-100848] 16 p2178 N88-22981
The integration, characterisation and trialling of a modern complex airborne radar 17 p2305 N88-23791
Mechanical and structural characterization of aluminum ceramic fibers
[ETN-88-92168] 17 p2323 N88-23870
High frequency ultrasonic characterization of sintered SiC
[NASA-TM-100825] 17 p2347 N88-23985
Aircraft emissions characterization: TF41-A2, TF30-P103 and TF30-P109 engines
[AD-A192053] 18 p2466 N88-24638
Elementary characterization of preimpregnated carbon epoxy T400H/DA0506 from STRUCTIL. Test report M6-577100
[CEAT-047426] 18 p2478 N88-24703
Characterization of a 30-GHz IMPATT solid state amplifier
[NASA-TM-100876] 18 p2503 N88-24847
A characteristic method for calculating the generalized flat flutter aerodynamic forces
[NASA-TT-20300] 19 p2598 N88-25438
GTAW characterization for weld penetration on 304L stainless steel
[DE88-010611] 20 p2810 N88-26672
Techniques for characterizing damage zones in composite materials 21 p2905 N88-27240
Preparation and characterization of ceramic materials based on Al2O3 reinforced with a ZrO2 dispersion
[ISAL-87-0041] 21 p2922 N88-27340

CHARACTERS
U SYMBOLS

CHARGE CARRIERS
NT FREE ELECTRONS
NT HOLES (ELECTRON DEFICIENCIES)
NT MINORITY CARRIERS
The role of hydrogen in radiation-induced defect formation in polysilicon gate MOS devices
[DE87-012374] 06 p0785 N88-14814
Improving the method of calculating electronic properties of narrow bandgap semiconductors 07 p0926 N88-15627
Interpretation of the temperature dependence of conductivity in superconducting oxides
[DE88-003028] 08 p1091 N88-16565
Growth of HgZnTe layers by LPE technique
[AD-A186723] 09 p1255 N88-17520
Electronic structure, charge transfer excitations and high temperature superconductivity
[DE88-003096] 10 p1416 N88-18453
New method of examining microononhomogeneity of local centers in high-resistivity semiconductor materials under scanning electron microscope 14 p1969 N88-21754
Free carrier nonlinear optics 14 p1977 N88-21796
Breathing mode lattice relaxation associated with carrier emission and capture by deep electronic levels in silicon
[DE88-003844] 14 p1985 N88-21842
Calculating depletion region carrier concentrations with capacitance-voltage measurements and etching
[AD-A189630] 15 p2141 N88-22777
Radiation effects in silicon
[DE88-006642] 16 p2282 N88-23659
Systematic variation of magnetic-field penetration depth in high-T(c) superconductors studied by muon spin relaxation 17 p2396 N88-24243
Picosecond optoelectronic sampling of electrical waveforms produced by an optically excited field effect transistor
[AD-A192384] 21 p2935 N88-27428
A study of electronic transport and breakdown in SiO2
[AD-A194258] 22 p3156 N88-28780

CHARGE COUPLED DEVICES
Photon counting image sensor development for astronomical applications
[NASA-CR-181507] 05 p0660 N88-14049
Vertical charge transport in junction charge-coupled devices
[ETN-88-91613] 09 p1255 N88-17523
New generation imager system
[NASA-CR-180464] 10 p1408 N88-18398
Development of a CCD characterization system
[INPE-4361-TDL/301] 12 p1623 N88-19712
Cramer-Rao bounds on the accuracy of location and velocity estimations using CCD optical sensors
[AD-A188481] 12 p1629 N88-19748
ROVER: A prototype active vision system
[AD-A189246] 15 p2133 N88-22722
Space-variant optical systems
[AD-A189967] 15 p2133 N88-22724
An investigation into the precision of a digital camera
[B8735054] 16 p2210 N88-23193
Users guide to CAESAR
[BCRS-87-04] 16 p2228 N88-23306
Novel silicon Schottky barrier infrared imaging arrays 17 p2439 N88-24510
Simple high speed camera with CCD-sensor
[MPIS-8/1987] 18 p2518 N88-24940
The FEL CCD-camera: Experimental system for camera and image processing research
[FEL-1987-34] 21 p2952 N88-27532
Satellite attitude determination using a CCD (Charge-Coupled-Device) star camera
[AD-A192662] 22 p3046 N88-28080
Array detectors for plasma spectrochemistry
[AD-A194220] 22 p3052 N88-28105
Molecular fluorescence measurements with a charge-coupled device detector
[AD-A194221] 22 p3080 N88-28291
High performance charge transfer device detectors
[AD-A194409] 23 p3192 N88-28993
Molecular fluorescence measurements with a charge-coupled device detector
[AD-A194437] 23 p3216 N88-29141

CHARGE DISTRIBUTION
The physics of charge separation preceding lightning strokes in thunderclouds
[NASA-CR-178371] 01 p0071 N88-10452
Capacitive charge division in centroid finding cathode readouts in MWPCs
[DE88-003545] 10 p1333 N88-17969
Application of ECR ion source beams in atomic physics
[DE88-003767] 10 p1406 N88-18384

Electron current effect on stability of plasma channel
16 p2276 N88-23625
Measurements of Z(sub eff) profile with a visible bremsstrahlung continuum detector array
17 p2443 N88-24529
The electrokinetic behavior of calcium oxalate monohydrate in macromolecular solutions
[NASA-TM-101144] 18 p2493 N88-24791
Analysis of lightning field changes during active thunderstorms in Florida 18 p2545 N88-25103
Effects of charge distribution within a particle beam on the sub-Cerenkov radiation
[AD-A193992] 22 p3150 N88-28742
Nuclear and ionic charge distribution experiment on ISEE-1 and ISEE-3
[NASA-CR-180776] 23 p3183 N88-28947
Charge composition of primary cosmic ray nuclei with z greater than or equal to 2 in energy region greater than or equal to 2 TeV 24 p3448 N88-30519

CHARGE EFFICIENCY
Real time charge efficiency monitoring for nickel electrodes in NiCd and NiH2 cells
02 p0165 N88-11038
Nickel hydrogen cell positive-electrode studies: Cobalt segregation in reducing environments
[AD-A193025] 20 p2796 N88-26587
Computer controlled procedures for traction battery power performance tests
[ETN-88-92352] 20 p2796 N88-26589
Results from life test in progress on eagle-picher nickel cadmium cells
[AD-A192816] 21 p2936 N88-27434

CHARGE EXCHANGE
NT RESONANCE CHARGE EXCHANGE
Interpretation of the temperature dependence of conductivity in superconducting oxides
[DE88-003028] 08 p1091 N88-16565
Modeling considerations for selected rf-plasma edge effects
[DE88-003285] 09 p1252 N88-17500
Charge exchange in low energy (keV) and hyperthermal energy (10-100 eV) ion scattering
[AD-A187643] 11 p1543 N88-19222
Pion nucleus single charge exchange reactions above the delta(1232) resonance
[LA-11004-T] 11 p1544 N88-19231
Ion temperature profile measurement using charge exchange recombination spectroscopy on JIPP T-IIU
17 p2440 N88-24518
Spectroscopic measurements of ion temperature, rotation speed and beam deposition profile on DIII-D
17 p2440 N88-24519
Spectroscopic study of heliotron E plasmas: Stark profile, CXR, poloidal rotation and carbon coating
17 p2441 N88-24523

CHARGE SEPARATION
U POLARIZATION (CHARGE SEPARATION)

CHARGE TRANSFER
Synthesis, NMR characterization and electrical properties of siloxane-based polymer electrolytes
[AD-A184184] 04 p0418 N88-12596
Final (n,l) state-resolved electron capture by multiply charged ions from neutral atoms
[IPPJ-AM-54] 04 p0492 N88-13030
Comparison of 2D memory SEU transport simulation with experiments
[ATR-86(8139)-2-REV-A] 05 p0656 N88-14025
Vertical charge transport in junction charge-coupled devices
[ETN-88-91613] 09 p1255 N88-17523
Electronic structure, charge transfer excitations and high temperature superconductivity
[DE88-003096] 10 p1416 N88-18453
Mode priming in an overmoded gyrotron oscillator
[AD-A189151] 13 p1772 N88-20602
Characteristics of the positive lighting flash
[DE88-005854] 13 p1800 N88-20760
The kinetics of charge-transfer reactions on passive lithium electrodes
[DE88-009256] 21 p2939 N88-27454
Array detectors for plasma spectrochemistry
[AD-A194220] 22 p3052 N88-28105
Molecular fluorescence measurements with a charge-coupled device detector
[AD-A194221] 22 p3080 N88-28291
Applications of charge transfer devices in spectroscopy
[AD-A194408] 23 p3192 N88-28992

CHARGE TRANSFER DEVICES
NT CHARGE COUPLED DEVICES
Applications of charge transfer devices in spectroscopy
[AD-A194408] 23 p3192 N88-28992
High performance charge transfer device detectors
[AD-A194409] 23 p3192 N88-28993

CHARGED PARTICLES
NT ALPHA PARTICLES
NT ANTIPROTONS
NT ARGON PLASMA
NT BETA PARTICLES
NT BOUNDARY LAYER PLASMAS
NT CESIUM PLASMA
NT COLD PLASMAS
NT COLLISIONAL PLASMAS
NT COLLISIONLESS PLASMAS
NT CONDUCTION ELECTRONS
NT COSMIC PLASMA
NT CYLINDRICAL PLASMAS
NT DENSE PLASMAS
NT DEUTERIUM PLASMA
NT DEUTERONS
NT ELECTRON PLASMA
NT ELECTRONS
NT ENERGETIC PARTICLES
NT EVEN-EVEN NUCLEI
NT FREE ELECTRONS
NT HEAVY NUCLEI
NT HELIUM PLASMA
NT HIGH ENERGY ELECTRONS
NT HIGH TEMPERATURE PLASMAS
NT HOT ELECTRONS
NT HYDROGEN PLASMA
NT HYPERNUCLEI
NT INNER RADIATION BELT
NT IONIZED GASES
NT LASER PLASMAS
NT MAGNETIC CLOUDS
NT MAGNETICALLY TRAPPED PARTICLES
NT METALLIC PLASMAS
NT NITROGEN PLASMA
NT NONEQUILIBRIUM PLASMAS
NT NONUNIFORM PLASMAS
NT NUCLEI (NUCLEAR PHYSICS)
NT ODD-ODD NUCLEI
NT OXYGEN PLASMA
NT PARTONS
NT PHOTOELECTRONS
NT PLASMA CLOUDS
NT PLASMA FOCUS
NT PLASMA JETS
NT PLASMA LAYERS
NT PLASMA SHEATHS
NT PLASMAS (PHYSICS)
NT POLARONS
NT POSITRONS
NT PROTONS
NT RADIATION BELTS
NT RADIO JETS (ASTRONOMY)
NT RELATIVISTIC ELECTRON BEAMS
NT RELATIVISTIC PLASMAS
NT ROTATING PLASMAS
NT SEMICONDUCTOR PLASMAS
NT SOLAR ELECTRONS
NT SOLAR PROTONS
NT SOLAR WIND
NT SPACE PLASMAS
NT SPHERICAL PLASMAS
NT STELLAR WINDS
NT STRONGLY COUPLED PLASMAS
NT THERMAL PLASMAS
NT TOROIDAL PLASMAS
NT TRITONS
TIROS-N/NOAA A-J space environment monitor subsystem
[PB87-203998] 01 p0015 N88-10083
On the interaction of a planar metal surface with a charge and with a molecule
[DE87-703083] 02 p0147 N88-10920
Heavy-particle collisions in the plasma edge
[DE87-012928] 02 p0237 N88-11493
Complex scattering dynamics and the integer quantum Hall effect
[DE87-011790] 02 p0243 N88-11536
A simplified approach to the dynamics of charged particles in the magnetosphere
03 p0273 N88-11718
Defect characterization in quartz and related materials
[AD-A184754] 03 p0294 N88-11846
Development and evaluation of a Monte Carlo code system for analysis of ionization chamber responses
[AD-A183970] 03 p0375 N88-12359
Future directions in interplays between particle and nuclear physics: Summary session
[DE87-011791] 04 p0489 N88-13013
Cosmic-ray nuclear event with an anomalously strong concentration of energy and particles in the central region
[DE87-703376] 04 p0526 N88-13213
An electric field meter based upon a new principle: A dummy displacement electrode. Application to aerospace vehicles
[SNIAS-872-422-106] 05 p0585 N88-13567
Mechanistic studies of polymeric samples exposed aboard STS 8
[NASA-CR-182364] 06 p0686 N88-14202
Research in elementary particle physics
[DE88-002130] 06 p0777 N88-14771
Optimization of charged particle acceleration rate over wave parameters in the scheme with acceleration by surface electromagnetic waves
[DE88-700320] 07 p0846 N88-15134
Atmospheric science 07 p0883 N88-15357
Multiply charged particles in primary cosmic rays with energy less than or equal to 2 TeV
07 p0921 N88-15596
Analysis of relativistic nucleus-nucleus interactions in emulsion chambers 07 p0926 N88-15624
Performance and optimization of direct implicit time integration schemes for use in electrostatic particle simulation codes
[DE88-003254] 10 p1406 N88-18381
Forces on neutral atoms due to electromagnetic fields
[AD-A187461] 10 p1408 N88-18396
Boltzmann-Fokker-Planck calculations using standard discrete-ordinates codes
[DE88-005393] 11 p1537 N88-19185
Presentations to the SuperHILAC Program Advisory Committee
[DE88-003853] 11 p1547 N88-19256
On (e,e'N) reactions
[CEBAF-PR-87-028] 12 p1690 N88-20109
Velocity and concentration measurements in flowing suspensions by nuclear magnetic resonance
[DE88-006225] 13 p1770 N88-20589
Modeling the effects of heavy charged particles on MOSFETs (Metal-Oxide-Semiconductor Field Effect Transistors)
[AD-A190575] 15 p2143 N88-22792
A proposal for the establishment of a center of excellence in theoretical geoplasma research
[AD-A189742] 16 p2231 N88-23327
Nonlinear dynamics of interaction between charged particles modulated beam and bounded plasma regular oscillations
[DE88-701681] 16 p2280 N88-23648
Color charge motion in non-Abelian fields
[DE88-701306] 19 p2642 N88-25672
Electron-positron physics at 1 TeV
[DE88-009019] 19 p2725 N88-26180
Mechanisms for particle acceleration: Possibilities and constraints
[PB88-102538] 19 p2725 N88-26184
JFET/SOS (Junction Field-Effect Transistor/Silicon-on-Sapphire) devices: Gamma-radiation-induced effects
[AD-A193001] 20 p2795 N88-26586
Charged pion production and projectile breakup in 85A MeV(sup)12C induced heavy ion reactions
[LUIP-8802] 20 p2850 N88-26920
Neoclassical diffusion due to trapping/detrapping orbits in stellarators
[DE88-008566] 20 p2857 N88-26968
Optical guiding in the separable beam limit
[AD-A192452] 21 p2952 N88-27534
Self-energies and the interactions of particles with surfaces
[DE88-010451] 21 p3014 N88-27885
Propagation of charged particle beams in the atmosphere
[AD-A193185] 21 p3014 N88-27887
Solar flares and magnetospheric particles: Investigations based upon the ONR-602 and ONR-804 experiments
[AD-A193396] 21 p3031 N88-27994
Difficulties with interpretation of underground muons from Cygnus X-3
[DE88-701645] 23 p3309 N88-29710

CHARGING
Chemical analysis of charged Li/SO(sub)2 cells
02 p0163 N88-11026

CHARM (PARTICLE PHYSICS)
An introduction to charm and heavy quark physics
[DE87-013589] 02 p0231 N88-11455
On charm decays: Present status and future goals
[DE87-013586] 03 p0375 N88-12356
High energy experimental physics
[DE87-013516] 03 p0376 N88-12363
A method for the analysis of heavy flavor decays
[NOTA-INTERNA-909] 22 p3150 N88-28744

CHARPY IMPACT TEST
Fractographic and microstructural aspects of fracture toughness testing in irradiated 304 stainless steel
[DE88-000795] 06 p0681 N88-14172

Aging degradation of cast stainless steels: Effects on mechanical properties
[DE88-003053] 09 p1145 N88-16866
Influence of neutron irradiation on the Charpy impact properties of V-15Cr-5Ti
[DE88-003430] 11 p1458 N88-18692
The effect of notch root radius on the determination of toughness in ultrahigh strength steel friction welds
[AD-A195952] 24 p3384 N88-30156

CHARRING
Non-steady group combustion of a cloud of char particles
[DE87-010773] 08 p0966 N88-15849
Low temperature reactivity of chars towards oxygen, appendix E2
[DE88-004088] 10 p1298 N88-17760

CHARTS
NT BOND GRAPHS
NT FLOW CHARTS
NT GRAPHS (CHARTS)
NT METEOROLOGICAL CHARTS
NT NAUTICAL CHARTS
Control charts when the observations are correlated
[AD-A186388] 07 p0866 N88-15253
Evaluation of a parallel chart parser
[AD-A189172] 14 p1959 N88-21685

CHASSIS
Corrosion control by composite material substitution with application to the M-939 5-ton truck
04 p0428 N88-12654
Articulated suspension system
[NASA-CASE-NPO-17354-1-CU]
18 p2524 N88-24973
Unified methods of accelerated laboratory tests of the preparations for temporary protection of cars
[NASA-TT-20298] 21 p2921 N88-27336

CHEBYSHEV APPROXIMATION
An adaptive pseudo-spectral method for reaction diffusion problems
[NASA-CR-178394] 02 p0224 N88-11414
A vectorized Poisson solver over a spherical shell and its application to the quasi-geostrophic omega-equation
[NASA-CR-4116] 08 p1039 N88-16285
Electromagnetic scattering from and natural resonances of the circular strip 13 p1759 N88-20523
A study of data compactation using numerical methods
[INPE-4317-TDL/284] 13 p1828 N88-20929
Solution of the compressible Navier-Stokes equations of motion by Chebyshev polynomials for laminar shock-boundary layer flow
[AD-A191033] 16 p2208 N88-23176
Approximate solution of random differential equation
18 p2565 N88-25233
A comparative study of Chebyshev acceleration and residue smoothing in the solution of nonlinear elliptic difference equations
[CWI-NM-R8723] 18 p2569 N88-25259
Solution of the Orr-Sommerfeld equation for the Blausius boundary-layer documentation of program ORRBL and a test case
[NASA-CR-4169] 20 p2841 N88-26858
Solution to the compressible Navier-Stokes equations of motion by Chebyshev polynomials with implicit time stepping
[AD-A194119] 22 p3075 N88-28257
Approximation of atmospheric density by Chebyshev polynomials in predicting motion of low artificial earth satellites 24 p3445 N88-30503

CHECKOUT
Design and implementation of a debugger for an abstract machine
[AD-A184691] 03 p0363 N88-12283
Software reliability perspectives
[NASA-CR-181523] 04 p0479 N88-12952
A project of an intelligent system to help on-line trouble shooting --- aircraft maintenance
[SNIAS-872-111-106] 05 p0529 N88-13216
The ESA centralized management system for satellite electronic test and checkout instrumentation
09 p1124 N88-16731
The KATE shell: An implementation of model-based control, monitor and diagnosis 09 p1210 N88-17255
Debugging FORTRAN on a shared memory machine
[DE88-003589] 10 p1386 N88-18276

CHECKOUT EQUIPMENT
U TEST EQUIPMENT

CHELATE COMPOUNDS
U CHELATES

CHELATES
Soluble metal chelate polymers of coordination numbers six, seven and eight
[AD-A185094] 05 p0568 N88-13458
Chromatographic and mass spectrometric separation and analysis
[AD-A190113] 16 p2174 N88-22958
Soluble metal chelate polymers of coordination numbers six, seven and eight
[AD-A192485] 21 p2917 N88-27314

CHEMICAL ANALYSIS
NT CHROMATOGRAPHY
NT ELECTROPHOTOMETRY
NT GAS ANALYSIS
NT GAS CHROMATOGRAPHY
NT LIQUID CHROMATOGRAPHY
NT MICROANALYSIS
NT NEUTRON ACTIVATION ANALYSIS
NT OZONOMETRY
NT POTENTIOMETRIC ANALYSIS
NT QUALITATIVE ANALYSIS
NT QUANTITATIVE ANALYSIS
NT SPECTROSCOPIC ANALYSIS
NT VOLUMETRIC ANALYSIS
Real time analysis of detonation products
[DE87-007453] 01 p0031 N88-10195
Theoretical approaches to chemical dynamics in highly compressed fluids
[DE87-012242] 01 p0046 N88-10296
The development of a new and novel Hadamard transform infrared spectrometer for analytical chemistry
[DE87-014804] 02 p0175 N88-11094
Multidimensional elemental analysis with the Sandia nuclear microprobe
[DE87-014158] 02 p0183 N88-11136
Multidimensional elemental analysis with the Sandia nuclear microprobe
[DE87-014158] 02 p0183 N88-11136
Mass spectroscopic facility 03 p0296 N88-11861
Thin films for geothermal sensing
[DE88-000154] 03 p0326 N88-12061
Simultaneous TG/DSC (thermogravimetry/Differential Scanning Calorimetry) and TG/MS (thermogravimetry/Mass Spectrometry) analyses of polymeric and energetic materials
[DE88-000727] 04 p0413 N88-12561
Analysis of free cutting brass by A.C. polarography
[PD-MT-8728] 04 p0417 N88-12587
An assessment of clinical chemical sensing technology for potential use in space station health maintenance facility
[NASA-CR-172013] 04 p0475 N88-12926
The analysis of metal finishing solutions by ion chromatography
[AD-A184812] 05 p0561 N88-13414
Chemical analysis for excimer laser systems
[DE88-001941] 05 p0589 N88-13591
Evaluation of AIS-2 (1986) data over hydrothermally altered granitoid rocks of the Singatse Range (Yerington) Nevada and comparison with 1985 AIS-1 data
05 p0613 N88-13767
Development of FTMS methods for the detection of trace chemical species and development of FTMS methods for the analysis of various chemical species
[AD-A185857] 07 p0828 N88-15023
Specific organic compounds in excreta
07 p0895 N88-15422
The effect of propane on atomic spectrometric signals in the direct current plasma
[DE88-002457] 07 p0934 N88-15676
The synthesis and characterization of some rare earth arsenides
[AD-A186445] 08 p0965 N88-15839
Study of selection criteria for adhesives used in aircraft structure bonding
[ETN-88-91619] 08 p0971 N88-15875
Improved silicon nitride for advanced heat engines
[NASA-CR-175006] 08 p0973 N88-15886
Vapor generation of fuels
[PB88-109897] 08 p0974 N88-15892
Operation Everest 2: Comparison of four instruments for measuring blood oxygen saturation
[AD-A186456] 08 p1049 N88-16337
Ion chromatography in the manufacture of multilayer circuit boards
[DE88-002428] 10 p1322 N88-17902
The role of analytical chemistry in assessing atmospheric effects of combustion
[DE88-003909] 10 p1352 N88-18082
Analysis of gases in the earth's crust
[PB88-141619] 10 p1354 N88-18093
Analysis of water recovered after being used for washing by men and women 10 p1361 N88-18135
Synthesis and characterization of 1,2-cyclobutenedicarboxamides: Thermally generated polymers and Diels-Alder adducts
[AD-A188591] 12 p1611 N88-19633
Critical comparison of moving average and cumulative summation control charts for trace analysis data
[AD-A188312] 12 p1705 N88-20203
Fuels combustion research
[AD-A189114] 13 p1736 N88-20381
Development and evaluation of supercritical fluid chromatography-mass spectrometry
[DE88-005122] 13 p1738 N88-20394
Improved methods for high resolution electron microscopy
[DE88-005731] 13 p1774 N88-20609
Plasma cortisol, renin and aldosterone during an intense heat acclimation program
[AD-A189387] 13 p1809 N88-20810
On the structure of pulsed plasma jets
13 p1843 N88-21030
Measurement of species concentrations in flames by laser-induced fluorescence
[DE88-007096] 14 p1889 N88-21286
Analysis of explosives. 1: Computer programs for processing of X-ray powder deffraction data
[PB88-156898] 14 p1894 N88-21309
Spatial and temporal distribution of precipitation chemistry across Maryland in 1984, volume 1
[PB88-148929] 14 p1943 N88-21595
Isotopic and chemical studies of early crustal metasedimentary rocks
[NASA-CR-182711] 14 p1944 N88-21601
Structure and surface characterizations of high strength carbon fibers
[AD-A189642] 15 p2029 N88-22087
Spectrographic detection of nitrogen impurity in helium
[DE88-752301] 15 p2033 N88-22111
On copper peroxide
[NASA-TT-20263] 15 p2037 N88-22135
NMR analysis of a fluorocarbon copolymer
[DE88-002364] 15 p2043 N88-22170
Simulation analysis of moored fluorometer time series from the Mid-Atlantic Bight
[DE88-006066] 15 p2099 N88-22505
The adhesive bonding of thermoplastic composites
[AD-A190994] 16 p2173 N88-22953
Analytical Chemistry Division
[DE88-701236] 16 p2174 N88-22956
Chromatographic and mass spectrometric separation and analysis
[AD-A190113] 16 p2174 N88-22958
Identification of hydroxypropyl starch hydrolysate components 17 p2315 N88-23832
Analysis of thermal and radiation effects in materials using the GEMAT process 17 p2408 N88-24318
Thermochemical analysis of mass transfer in a NB-1ZR-potassium heat pipe 17 p2412 N88-24348
Selective detection in gas chromatography
[AD-A191499] 18 p2481 N88-24718
Synthesis and characterization of new phosphazene polymers
[AD-A191508] 18 p2490 N88-24771
Geological evolution and analysis of confirmed or suspected gas hydrate localities. Volume 2: Basin analysis, formation and stability of gas hydrates in the Black Sea
[DE88-001052] 18 p2532 N88-25023
Fundamental studies of separation processes
[DE88-007487] 19 p2611 N88-25494
Alternate techniques for noble-gas detection
[DE88-009471] 19 p2613 N88-25507
Carbon analysis in natural olivine crystals of deep origin
[NASA-TT-20311] 19 p2734 N88-26239
Surface phases and their influence on metal-oxide interfaces
[DE88-007938] 20 p2769 N88-26420
Microchemical analysis of polycrystalline Ni3Al and other ordered alloys using the field-ion microscope atom probe
[DE88-011519] 21 p2914 N88-27294
The electromagnetic spectrum: The information mine
[AD-A194316] 22 p3069 N88-28215
Noncontact photo-thermal sensing
[AD-A195450] 24 p3344 N88-29905
Geochronological and lead-isotope evidences for rapid crust formation in middle-proterozoic time: The Labrador example 24 p3398 N88-30239
Lithospheric evolution of the Northern Arabian Shield: Chemical and isotopic evidence from basalts, xenoliths and granites 24 p3399 N88-30242
Evidence of the in situ decay of Al-26 in a Semarkona chondrule 24 p3441 N88-30479

CHEMICAL ATTACK
NT INTERGRANULAR CORROSION
Corrosion resistance of silver-plated carbon-aluminum composite 03 p0285 N88-11793
Resistance of canopy materials against chemicals
[PML-1985-22] 05 p0569 N88-13486
Corrosion of tungsten alloys in marine environments
17 p2320 N88-23854

CHEMICAL BONDS
NT HYDROGEN BONDS
Polymer chain segment orientation during stress relaxation
[DE87-013392] 01 p0027 N88-10174

Accurate ab initio calculations which demonstrate a 3 Pi u ground state for Al2
[NASA-TM-89302] 01 p0102 N88-10666
Bonding and coupling of C sub 1 fragments on metal surfaces
[AD-A184186] 03 p0295 N88-11852
Free radical detection and reactions in the decomposition of energetic materials
[AD-A184677] 03 p0296 N88-11858
The itinerant resonating-valence-bond model for superconductivity
[DE87-014794] 03 p0380 N88-12391
Superconductivity as a synchronous spatial alternation of valence bonds
[AD-A184208] 03 p0382 N88-12405
Topological aspects of infinite metal clusters and superconductors
[AD-A184104] 04 p0495 N88-13049
Measurement of the electron density and the attachment rate coefficient in silane/helium discharges
[AD-A184268] 04 p0496 N88-13051
Valence bond theory and superconductivity
[AD-A184274] 04 p0496 N88-13052
The chemical bond and superconductivity
[AD-A184275] 04 p0496 N88-13053
Valence bond cluster studies of alkali metal/semiconductor bonding
[AD-A184276] 04 p0496 N88-13054
Tetrahedral carbon and interstitial electrons in Li cluster: CLi4 and (LiCH3)4
[AD-A184277] 04 p0496 N88-13055
Effect of sidechain length and crosslinking on ionic conductivity in polyphosphazene solid electrolytes
[AD-A184419] 04 p0497 N88-13058
Pure dephasing of a vibrational adbond
[AD-A185222] 05 p0609 N88-13740
Reactions and bonding between glasses and titanium
[DE88-000603] 06 p0685 N88-14195
The tribological properties of MoS2 coatings in vacuum, low relative humidity and high relative humidity environments
[DE88-001611] 06 p0711 N88-14356
X-ray structure analyses and molecular mechanics analyses of dense energetic materials
[AD-A185462] 06 p0779 N88-14781
Coverage dependence of adsorbate-substrate bond lengths: Chlorine and caesium adsorbed on silver single crystals
[PB87-125142] 06 p0788 N88-14833
Diffraction by glasses with a layer structure
[DE88-003059] 07 p0837 N88-15078
Feasibility of a complex compound heat pump
[PB88-113022] 07 p0853 N88-15183
The Coupled Cluster Single and Double excitation (CCSD) method in quantum chemistry: An efficient formulation of the theory and application to closed shell molecular systems
[DE88-000475] 07 p0930 N88-15650
Cohesive energies of transition metal silicides and phosphides --- Knudsen effusion
[AD-A186691] 09 p1254 N88-17519
Copper oxidation states, vacancy ordering and their effect on high temperature superconductivity
[DE88-003079] 09 p1258 N88-17542
Basic research on macromolecular dynamics
[PB88-141643] 10 p1305 N88-17805
Rovibrational spectroscopy of ArCO van der Waals complex
[DE88-004291] 10 p1406 N88-18387
Chemical activation of molecules by metals: Experimental studies of electron distributions and bonding
[DE88-004465] 10 p1407 N88-18393
Coupling of vibrational modes of adsorbates: Application to field induced shifts for CO and CN on Cu(100)
[AD-A187891] 11 p1453 N88-18659
A simple interpretation of the Fe2(-) photoelectron spectrum
[NASA-CR-182553] 11 p1543 N88-19225
An interdisciplinary approach to predictive modeling of structural adhesive bonding: Factors affecting the durability of titanium/epoxy bonds
[AD-A189503] 12 p1611 N88-19636
Properties of molecular solids and fluids at high pressure and temperature
[DE88-004195] 13 p1738 N88-20391
Improved glass-ceramic to metal seals in actuator and detonator applications with an aluminum-containing austenitic stainless steel
[DE88-004691] 13 p1749 N88-20458
The relationship of the chemical bonding topology of high critical temperature copper oxide superconductors to that of the chevrel phases and the ternary lanthanide rhodium borides
[AD-A189255] 13 p1845 N88-21042
Vapor phase deposition and growth of polyimide films on copper
[AD-A189969] 15 p2044 N88-22178
Synthesis and properties of novel cluster phases
[DE88-006816] 16 p2175 N88-22964
Distribution of chain ends inside the polybutadiene microspheres of SB diblock copolymers
[AD-A191257] 16 p2182 N88-23007
Polyitaconic acid macromolecule primer for adhesive bonding and corrosion control of aluminum
17 p2319 N88-23849
Liquid carbon
[AD-A191707] 18 p2491 N88-24776
A constraint algorithm for maintaining rigid bonds in molecular dynamics simulations of large molecules
[AD-A191663] 18 p2572 N88-25277
Molecular orbital studies of the bonding in heavy element organometallics: Progress report
[DE88-007765] 19 p2723 N88-26168
Fundamental studies of elastomers
[DE88-009679] 20 p2778 N88-26471
Structural studies of (Ga,In)(As,P) alloys and (InAs) sub m (GaAs) sub n strained-layer superlattices by fluorescence-detected EXAFS 20 p2872 N88-27051
Structure of bound states in polynomial potentials
[DE88-702437] 21 p3007 N88-27837
Discrete variational methods and their application to electronic structures
[DE88-702215] 21 p3014 N88-27888
Deep level defects in semiconductors: Stress and pressure studies
[DE88-010855] 21 p3024 N88-27948
On the bond distance in methane
[NASA-CR-181436] 22 p3150 N88-28741
Hydrogen storage by molecular polyhydrides
[AD-A194207] 23 p3191 N88-28989
Potential induced structural transformations of the Au(100) and Au(111) surfaces
[DE88-005446] 23 p3287 N88-29571

CHEMICAL CLEANING
Chemical cleaning of metal surfaces in vacuum systems by exposure to reactive gases
[AD-A188586] 12 p1608 N88-19616
Ammonia cleanup of lithium containing components
17 p2403 N88-24287
Cleanability of aircraft polyurethane topcoats
[AD-A193456] 23 p3170 N88-28878

CHEMICAL CLOUDS
NT BARIUM ION CLOUDS
A fluid simulation of the AMPTE lithium gas releases in the solar wind
[TRITA-EPP-87-06] 05 p0661 N88-14056
A modeling analysis program for the JPL table mountain to sodium cloud data
[NASA-CR-182555] 11 p1570 N88-19400
High altitude chemical release systems for project BIME (Brazilian Ionospheric Modification Experiments) project IMS (Ionospheric Modification Studies) project PIIE (Polar Ionospheric Irregularities Experiment) project polar arcs
[AD-A188299] 12 p1642 N88-19833
CRRES chemical release mechanisms
14 p1874 N88-21192
Magnetic cavity formation at Comet Halley and at the AMPTE Li release 14 p1996 N88-21898

CHEMICAL COMPOSITION
NT CARBON DIOXIDE CONCENTRATION
NT STELLAR COMPOSITION
Optimizing the application of high temperature corrosion resistant aluminium-silicon-base coatings
[BLL-M-37222-(5828.4)] 01 p0018 N88-10112
Equations for determining CVD tungsten-rhenium alloy composition and plating rate
[DE87-006831] 01 p0024 N88-10152
The effect of RDX particle size on the shock sensitivity of cast PBX formulations. 2: Bimodal compositions
[DE87-009581] 01 p0031 N88-10198
Gases released by surface flashover of insulators
[DE87-013851] 01 p0039 N88-10249
Addition polyimide composition
[EP-PATENT-0-167-304-A1] 01 p0053 N88-10337
Contribution of bubbles and waves to air-sea CO2 flux, with implications for remote sensing
[PB87-203980] 01 p0073 N88-10467
The atomic weight and isotopic composition of nitrogen and their variation in nature
[DE87-012867] 02 p0144 N88-10902
Application of high performance liquid chromatography to the fast determination of bitumen generic composition
[PC-2] 02 p0145 N88-10911
A geometrical model for determining the physicochemical properties of ternary metallic systems
[BLL-M-37303-(5828.4)] 02 p0149 N88-10931
Study of the morphology of thermosetting matrices
[ONERA-RT-5/3346-M] 02 p0153 N88-10961
Composition, structure and chemistry of interstellar dust
[NASA-TM-88350] 02 p0253 N88-11603
Heavy element compositions and energy spectra of galactic and solar cosmic rays 03 p0272 N88-11714
Joining of silicon carbide reinforced ceramics
[DE87-014881] 03 p0294 N88-11847
JPRS report: Science and technology. China
[JPRS-CST-87-025] 03 p0300 N88-11888
The nature of metallurgical reactions in underwater welding
[AD-A184464] 04 p0414 N88-12568
Polymer composition --- cable insulation
[EP-PATENT-0-199-444-A1] 04 p0418 N88-12594
Raman scattering as a diagnostic technique for cathode characterization
[AD-A184434] 04 p0439 N88-12726
Nuclear techniques in studies of condensed matter
[NASA-RP-1195] 04 p0489 N88-13015
A mathematical model of high alloy nickel base high temperature alloys
[BLL-M-37381-(5828.4)] 05 p0564 N88-13436
Ion plating for corrosion control
[AD-A185061] 05 p0565 N88-13442
The use of airborne imaging spectrometer data to determine experimentally induced variation in coniferous canopy chemistry 05 p0612 N88-13761
Toward detecting California shrubland canopy chemistry with AIS data 05 p0613 N88-13764
High energy molecules of high symmetry
[AD-A185385] 05 p0647 N88-13965
Ferromanganese nodules of Antarctic sector in Pacific Ocean 06 p0727 N88-14472
Hydrochemical structure of Gulf Stream frontal zone waters 06 p0727 N88-14476
Progress in the measurement of salinity and oxygen at the Woods Hole Oceanographic Institution
[PB88-108089] 06 p0748 N88-14598
Atlas of atomic spectral lines of neptunium emitted by an inductively coupled plasma
[DE88-000640] 06 p0782 N88-14796
Metallurgical processes in multi-component rare earth-transition metal permanent magnet alloys
[AD-A186401] 07 p0832 N88-15045
Exobiology and life science 07 p0883 N88-15358
The use of chlorophyll fluorescence measurements from space for separating constituents of sea water
08 p1043 N88-16307
A rapid method for the computation of equilibrium chemical composition of air to 15000 K
[NASA-TP-2792] 09 p1140 N88-16830
The effects of fuel composition on ignition delay in homogeneous charge and direct injection compression ignition engines
[DE88-003691] 09 p1143 N88-16849
Influence of post-anneal cooling treatments on suppression of cryogenic intergranular fracture in experimental Ni-free high-Mn austenitic steels
[DE88-002766] 09 p1145 N88-16863
Electronic and chemical structure of 3-5/metal and Si/metal interfaces
[AD-A186579] 09 p1254 N88-17518
Application of inverse gas chromatography to fluidity studies
[DE88-002896] 10 p1296 N88-17750
The measurement of chemical compositon with high spatial resolution using a dedicated scanning transmission electron microscope
[AERE-R-12317] 10 p1297 N88-17753
Electrically conducting polymer-copper sulphide composite films, preparation by treatment of polymer-copper (2) acetate composites with hydrogen sulfide
[NASA-TT-20204] 10 p1305 N88-17803
Acoustic emission-microstructural relations in ferritic steels. Part 3: The effect of inclusion content
[AERE-R-12041] 10 p1341 N88-18015
Determination of optimum electrolyte composition for molten carbonate fuel cells literature review
[DE88-001015] 10 p1348 N88-18058
Normal and superconducting state properties of La2-xSr/sub x/CuO4
[DE88-003013] 10 p1416 N88-18450
Composition and thickness of multilayer foils using MeV ion-beam techniques
[DE88-004360] 11 p1448 N88-18629
S-glass analysis by X-ray spectroscopy
[DE88-004636] 11 p1454 N88-18666
Electron microscopy study of morphology and composition of a ferrisilicate catalyst
[DE88-005754] 11 p1562 N88-19352
Mass loss from evolved stars
11 p1569 N88-19394
Analysis of model fuels and their compatibility with selected elastomers, part 1
[AD-A188361] 12 p1612 N88-19639

High altitude chemical release systems for project BIME (Brazilian Ionospheric Modification Experiments) project IMS (Ionospheric Modification Studies) project PIIE (Polar Ionospheric Irregularities Experiment) project polar arcs
[AD-A186299] 12 p1642 N88-19833
Fast protonic conducting solid electrolytes
[AD-A186524] 12 p1698 N88-20160
Gas-chromatographic analysis of products of thermal reactions of aerosol in Venusian cloud layer on Vega-1 and Vega-2 automatic interplanetary stations 13 p1725 N88-20318
Roentgenoradiometric analysis of aerosol in Venusian clouds by Vega-1 and Vega-2 automatic interplanetary stations 13 p1726 N88-20319
Determining chemical composition of aerosol in Venusian cloud layer on Vega-1 automatic interplanetary station using Malakhit mass spectrum analyzer 13 p1726 N88-20321
Elemental composition of Venusian rocks in northeastern part of Terra Aphrodite (determined using data from Vega-2 landing module) 13 p1726 N88-20322
Content of natural radioactive elements in Venusian rocks determined using data from Vega-1 and Vega-2 stations 13 p1726 N88-20323
Results of infrared spectrometer experiment. 1: Infrared radiation of parent molecules in Halley's Comet 13 p1726 N88-20325
The effect of microstructure on the fatigue crack growth resistance of nickel base superalloys
[AD-A189526] 13 p1741 N88-20414
On the structure of pulsed plasma jets 13 p1843 N88-21030
Microprobe examination of composite materials produced by burning of Ti, Cr, C powders with powder of any one Fe-group metal 14 p1886 N88-21269
The unique characteristics of the structure of composite materials made on a base of sphalerite-analogous boron nitride 14 p1886 N88-21273
Ground-based column abundance measurements of atmospheric hydroxyl
[NASA-CR-182676] 14 p1944 N88-21598
Diversity and similarity of comets 14 p1994 N88-21885
Photometry of P/Halley (1982i): Is what we have learned useful for other comets? 14 p1998 N88-21909
Composition of cometary dust particles --- Halley 14 p2001 N88-21932
Isotopic composition of Halley dust 14 p2002 N88-21933
Nature of Comet Halley's organic grains inferred from infrared spectra 14 p2007 N88-21973
Segregation effects in welded stainless steels
[DE88-701224] 15 p2037 N88-22139
Stability of the high-temperature G-16 primer composition
[DE88-006201] 15 p2049 N88-22206
Understanding CO2 and climate
[PB88-167655] 16 p2234 N88-23341
A sup 57 Fe Mossbauer study of the superconductor YBa sub 2 (Fe sub x Cu sub 1-x) sub 3 O sub y
[DE88-701543] 16 p2282 N88-23661
Dust and C2-contents in the coma of Halley's Comet (1986III) 16 p2288 N88-23697
Identification of hydroxypropyl starch hydrolysate components 17 p2315 N88-23832
Hydrogen embrittlement susceptibility of high strength ESR 4340 steel alloys for ballistically resistant/tolerant components 17 p2319 N88-23848
Compositional redistribution during casting of Hg sub 0.8 Cd sub 0.2 Te alloys
[NASA-TM-101151] 17 p2326 N88-23893
Aging of carbon fibers
[SNPE-NT-10/86/CRB/NP] 18 p2479 N88-24707
Surface composition-reactivity relationships in heterogeneous catalysis
[DE88-006679] 18 p2480 N88-24714
Rapidly solidified lightweight durable disk material
[AD-A191697] 18 p2491 N88-24775
Geological evolution and analysis of confirmed or suspected gas hydrate localities. Volume 2: Basin analysis, formation and stability of gas hydrates in the Black Sea
[DE88-001052] 18 p2532 N88-25023
Selective radiation absorption in aluminized composite propellant combustion 19 p2630 N88-25598
The structure and properties of grain boundaries in B2 ordered alloys
[DE88-009890] 20 p2773 N88-26447
Nickel aluminides: A new family of nickel + aluminum alloys featuring simple composition, low density, excellent oxidation resistance and high yield strength that increases with temperature
[DE88-010692] 20 p2776 N88-26461
Physical-chemical reactions at welding arc/molten pool interfaces
[DE88-007717] 20 p2808 N88-26662
Fine-scale traverses in cumulate rocks, Stillwater Complex: A lunar analogue study
[NASA-CR-183066] 20 p2823 N88-26747
Effects of grain boundary composition on properties of YBa2Cu3O/sub 7-x/
[DE88-007679] 20 p2875 N88-27064
Defect characterization of the redox behavior and stability of conducting oxides
[DE88-010799] 20 p2878 N88-27088
Space infrared telescope facility project
[NASA-CR-183058] 20 p2883 N88-27121
Initial testing of the tunable diode laser absorption spectrometer for measuring HNO3 in diesel engine exhaust, stage 2
[PB88-193073] 21 p2970 N88-27641
The distribution of some chemical elements between dissolved and particulate phases in the ocean
[DE88-010181] 21 p2977 N88-27682
Structure of bound states in polynomial potentials
[DE88-702437] 21 p3007 N88-27837
Evolution of heavy-element abundances in the galactic halo and disk
[DE88-011736] 22 p3164 N88-28845
Surface composition of Mars: A Viking multispectral view 23 p3300 N88-29655
Elemental composition of the Martian surface 23 p3302 N88-29665
Lava flow-field morphology: A case study from Mount Etna, Sicily 23 p3303 N88-29676
How dirty is Mars' North Polar cap, and why isn't it black 23 p3303 N88-29677
Some probable characteristics of the Martian regolith 23 p3303 N88-29678
What SNC meteorites tell us about Martian magmatism 23 p3303 N88-29679
Spectral reflectance of SNC meteorites: Relationships to Martian surface composition 23 p3304 N88-29683
The surface composition of Mars from earthbased observations 23 p3306 N88-29696
Martian surface analogs: Laboratory spectral studies in the mid infrared 23 p3307 N88-29699
The characterizatin of combustion by fuel composition: Measurements in a small conventional combustor 24 p3346 N88-29920
The performance of a surrogate blend in simulating JP-4 in a spray-fueled combustor 24 p3347 N88-29926
The effect of particle properties on radiative heat transfer 24 p3350 N88-29941
Bibliography of Soviet laser developments, number 88, March - April 1987
[AD-A195978] 24 p3378 N88-30116
Archean crustal evolution of the northern North China Craton 24 p3398 N88-30235
The complexity, depth, and rapidity of processes that formed the lunar crust 24 p3398 N88-30237
Lithospheric evolution of the Northern Arabian Shield: Chemical and isotopic evidence from basalts, xenoliths and granites 24 p3399 N88-30242
Growth of planetary crusts 24 p3400 N88-30247
Non-atmospheric noble gases from CO(sub 2) well ga 24 p3441 N88-30476
Star formation and molecular clouds 24 p3451 N88-30537

CHEMICAL ELEMENTS

NT ALKALI METALS
NT ALKALINE EARTH METALS
NT ALUMINUM
NT AMORPHOUS SILICON
NT ARGON
NT ARGON ISOTOPES
NT ARSENIC
NT BARIUM
NT BERYLLIUM
NT BISMUTH
NT BORON
NT BORON ISOTOPES
NT BROMINE ISOTOPES
NT CADMIUM
NT CALCIUM
NT CALCIUM ISOTOPES
NT CARBON
NT CARBON 12
NT CARBON 13
NT CERIUM
NT CESIUM
NT CHLORINE
NT CHROMIUM
NT COBALT
NT COBALT 60
NT COPPER
NT DEUTERIUM
NT DYSPROSIUM
NT ERBIUM
NT EUROPIUM
NT FLUORINE
NT GADOLINIUM
NT GALLIUM
NT GERMANIUM
NT GOLD
NT HAFNIUM
NT HEAVY ELEMENTS
NT HELIUM
NT HELIUM ISOTOPES
NT HOLMIUM
NT HYDROGEN
NT HYDROGEN ISOTOPES
NT INDIUM
NT IODINE
NT IODINE ISOTOPES
NT IRIDIUM
NT IRIDIUM ISOTOPES
NT IRON
NT IRON ISOTOPES
NT IRON 57
NT ISOTOPES
NT KRYPTON
NT KRYPTON ISOTOPES
NT LANTHANUM
NT LAWRENCIUM
NT LEAD (METAL)
NT LEAD ISOTOPES
NT LIQUID HELIUM
NT LIQUID HELIUM 2
NT LIQUID HYDROGEN
NT LIQUID LITHIUM
NT LIQUID NITROGEN
NT LIQUID OXYGEN
NT LIQUID POTASSIUM
NT LIQUID SODIUM
NT LITHIUM
NT LITHIUM ISOTOPES
NT MAGNESIUM
NT MAGNESIUM ISOTOPES
NT MANGANESE
NT MERCURY (METAL)
NT MERCURY ISOTOPES
NT MERCURY VAPOR
NT MOLYBDENUM
NT NEODYMIUM
NT NEODYMIUM ISOTOPES
NT NEON
NT NEPTUNIUM
NT NICKEL
NT NIOBIUM
NT NIOBIUM ISOTOPES
NT NITROGEN
NT NITROGEN ISOTOPES
NT NUCLIDES
NT OSMIUM
NT OXYGEN
NT OXYGEN ISOTOPES
NT PALLADIUM
NT PHOSPHORUS
NT PLATINUM
NT PLATINUM ISOTOPES
NT PLUTONIUM ISOTOPES
NT PLUTONIUM 238
NT POTASSIUM
NT RADIOACTIVE ISOTOPES
NT RADON
NT RADON ISOTOPES
NT RARE EARTH ELEMENTS
NT RARE GASES
NT RHENIUM
NT RHENIUM ISOTOPES
NT RHODIUM
NT RUBIDIUM
NT RUBIDIUM ISOTOPES
NT RUTHENIUM
NT SAMARIUM ISOTOPES
NT SELENIUM
NT SILICON
NT SILVER
NT SODIUM
NT SODIUM VAPOR
NT STRONTIUM
NT SULFUR
NT TANTALUM
NT TELLURIUM
NT THORIUM
NT TIN
NT TITANIUM
NT TRITIUM
NT TUNGSTEN
NT URANIUM
NT URANIUM ISOTOPES
NT URANIUM 238
NT VANADIUM
NT XENON
NT YTTERBIUM

NT YTTRIUM
NT ZINC
NT ZIRCONIUM
Multidimensional elemental analysis with the Sandia nuclear microprobe
[DE87-014158] 02 p0183 N88-11136
Compilation of temperature factors of cubic elements
[PB88-108170] 21 p2908 N88-27260
Diamond like carbon coatings: Categorization by atomic number density
[NASA-CR-174895] 22 p3059 N88-28151

CHEMICAL ENERGY
NT ENERGY OF FORMATION
Application of solar technology to fuel production chemical processing, and thermochemical energy transport: Status and future
[DE87-014172] 03 p0346 N88-12189
Cohesive energies of transition metal silicides and phosphides --- Knudsen effusion
[AD-A186691] 09 p1254 N88-17519
Molecular collision processes in gases and at surfaces
[AD-A189518] 13 p1836 N88-20982
A chemical method for achieving acceleration of macroparticles to ultrahigh velocities
[DE88-006377] 15 p2128 N88-22695
Thermodynamic analysis of chemical heat storage system for heat pump
[DE88-753121] 20 p2820 N88-26728
Prediction of deep levels and equilibrium concentrations of defects in semiconductors 21 p3023 N88-27945

CHEMICAL ENGINEERING
Process for the preparation of acyl halides
[GB-PATENT-2-133-792-A] 01 p0020 N88-10124
A process for producing phenolic foams
[EP-PATENT-0-170-357-A1] 01 p0026 N88-10162
Novel conductive polymers
[EP-PATENT-0-182-548-A2] 01 p0026 N88-10163
Pressure sensitive adhesives
[EP-PATENT-0-183-495-A1] 01 p0026 N88-10164
Crosslinkable elastomeric materials
[EP-PATENT-0-181-735-A1] 01 p0026 N88-10165
Boronium complexes as polymer catalysts
[GB-PATENT-2-161-475-A] 01 p0026 N88-10166
Bulletin of the Yamagata University (Engineering), Volume 20, No. 1, January 1988
[ISSN-0085-634X] 07 p0839 N88-15091
Rust converters
[AD-A188767] 14 p1891 N88-21299

CHEMICAL EQUILIBRIUM
NT ACID BASE EQUILIBRIUM
Chemical equilibrium calculations for the high pressure and temperature dissociation of liquid nitrogen
[DE87-013788] 01 p0021 N88-10135
Study of improved methods for predicting chemical equilibria
[DE87-014647] 02 p0145 N88-10908
Study of improved methods for predicting chemical equilibria
[DE87-014647] 02 p0145 N88-10908
Equilibrium calculations of ionization in tracer flames
[PB87-104154] 04 p0412 N88-12555
A rapid method for the computation of equilibrium chemical composition of air to 15000 K
[NASA-TP-2792] 09 p1140 N88-16830
Stability and uniqueness in nonlinear continuum mechanics
[AD-A189616] 12 p1699 N88-20172
NNEPEQ: Chemical equilibrium version of the Navy/NASA Engine Program
[NASA-TM-100851] 14 p1868 N88-21161
Energy storage and transport by reversible chemical reactions
[DE88-900370] 14 p1942 N88-21587
Thermochemical analysis of mass transfer in a NB-1ZR-potassium heat pipe 17 p2412 N88-24346

CHEMICAL EVOLUTION
Analysis of laser extracted volatiles in carbonaceous chondrites 06 p0793 N88-14861
Effects of galactic chemical evolution on thorium/neodymium cosmochronology
[DE88-003829] 11 p1570 N88-19397
Isotopic and chemical studies of early crustal metasedimentary rocks
[NASA-CR-182711] 14 p1944 N88-21601
Diversity and similarity of comets 14 p1994 N88-21885

CHEMICAL EXPLOSIONS
NT GAS EXPLOSIONS
Hot-spot reaction in unsustained shocks
[DE87-011781] 01 p0044 N88-10277
Experimental measurements and numerical simulations of metal spallation by detonating solid explosives
[DE87-013227] 01 p0054 N88-10347
Misty picture weather-watch and microbarograph project: Experiments 9412-14-18
[DE88-003949] 11 p1514 N88-19047
Shock initiation studies on heterogeneous explosives
[DE88-008681] 21 p2923 N88-27351
Diode laser ignition of high explosives and pyrotechnics
[DE88-008771] 21 p2923 N88-27352

CHEMICAL EXTINGUISHERS
U FIRE EXTINGUISHERS

CHEMICAL FRACTIONATION
A prototype expert system for separation science
[DE87-013542] 03 p0371 N88-12333
Mathematical models of continuous flow electrophoresis: Electrophoresis technology
[NASA-CR-179241] 07 p0828 N88-15021
Fundamental studies of separation processes
[DE88-007487] 19 p2611 N88-25494

CHEMICAL FUELS
NT AIRCRAFT FUELS
NT ANTIMISTING FUELS
NT AUTOMOBILE FUELS
NT CRUDE OIL
NT DIESEL FUELS
NT GASOHOL (FUEL)
NT GASOLINE
NT HYDROCARBON FUELS
NT HYDROGEN FUELS
NT JET ENGINE FUELS
NT JP-4 JET FUEL
NT JP-5 JET FUEL
NT JP-8 JET FUEL
NT KEROSENE
NT LIQUEFIED NATURAL GAS
NT LIQUID FUELS
NT NATURAL GAS
NT SYNTHETIC FUELS
Technical instructions for a control operating system of the gas flow installation for the solid fuel combustion chamber
[LR-507] 20 p2788 N88-26537

CHEMICAL KINETICS
U REACTION KINETICS

CHEMICAL LASERS
Distributed feedback effects in lasers and high gain laser instabilities in optically pumped CH3F 03 p0329 N88-12079
Computer simulation of cw HF chemical laser unstable resonator performance
[AD-A185059] 05 p0587 N88-13581
An experimental study of CW HF chemical laser amplifier performance and zero power gain
[AD-A185241] 05 p0588 N88-13584
Nitrogen scale-up
[AD-A185702] 06 p0709 N88-14351
Feasibility of chemical lasers based on chain reaction involving hydrogen fluorination with thermal branching mechanism 09 p1238 N88-17420
A chemical precursor to optical damage. Studies by laser ionization mass spectrometry
[DE88-004321] 10 p1409 N88-18408
Project SKYLITE: A design exploration
[AD-A187906] 11 p1511 N88-19030
Effects of translational and rotational nonequilibrium on CW (Continuous Wave) chemical laser performance
[AD-A191425] 16 p2214 N88-23210
Overview of the SDI (Strategic Defense Initiative) Program in short wavelength chemical lasers
[DE88-007912] 21 p3010 N88-27861
Chemically-produced N2(A) to NO(X) energy transfer in a supersonic flow
[AD-A192501] 22 p3082 N88-28302
NF (a 1 delta) production in a supersonic flow using N2F4+H2 in a BCL-16 nozzle
[AD-A194478] 22 p3082 N88-28304
Frequency doubling at 1.315 micrometers
[AD-A193902] 23 p3208 N88-29092
Preliminary studies of NF3+H2 production of N2(A3 sigma(+)u) in a supersonic flow
[AD-A194479] 23 p3219 N88-29162
N2(A3epsilon u+) by reaction of N2F4+H2 in a supersonic flow
[AD-A194493] 23 p3219 N88-29163
Bibliography of Soviet laser developments, number 88, March - April 1987
[AD-A195978] 24 p3378 N88-30116

CHEMICAL PROPERTIES
NT ACIDITY
NT HEAT OF COMBUSTION
NT HEAT OF FORMATION
NT HEAT OF FUSION
NT LATENT HEAT
NT SALINITY
NT THERMOCHEMICAL PROPERTIES
Standard reference data publications, 1985-1986
[PB87-210241] 01 p0021 N88-10128
Products of the neutralization of hydrazine fuels with hypochlorite, 2
[DE87-011454] 01 p0030 N88-10193
Theoretical approaches to chemical dynamics in highly compressed fluids
[DE87-012242] 01 p0046 N88-10296
Chemical vapor deposition of B6P and B6As films
[DE87-009288] 02 p0151 N88-10942
Contrast between the chemical, structural and electronic properties of thin films of Cu and Ni on the Ru(0001) surface
[DE88-002360] 07 p0938 N88-15698
Chemical activation of molecules by metals: Experimental studies of electron distributions and bonding
[DE88-004465] 10 p1407 N88-18393
Utilization of the JANAF (Joint Army Navy Air Force) database for chemical thermodynamic calculations
[DE88-004571] 10 p1423 N88-18501
Properties of lanthanide oxides as supports for transition metal catalysts
[DE88-004520] 11 p1456 N88-18678
Characteristics and use of lubricating greases
[DE88-751103] 11 p1463 N88-18723
Structure of sol-gel silica
[DE88-006870] 15 p2033 N88-22114
Diode laser spectroscopy of chemical moieties at surfaces
[AD-A190710] 15 p2036 N88-22127
Chemical compatibility between silicon carbide and a nickel aluminide
[DE88-006188] 18 p2479 N88-24708
Pollutant formation in heterogeneous mixtures of fuel drops and air
[DOE/CE-50052/H1] 19 p2689 N88-25986
Synthesis of model polymers and related structures in support of vinyl monomer grafting studies
[DE88-010245] 20 p2778 N88-26476
Refractory Materials of Zirconate. Part 2: Synthesis and some properties of strontium, zirconate, calcium zirconate and barium zirconate
[NASA-TT-20186] 20 p2779 N88-26483
Scanning tunneling microscopy as a surface chemical probe
[AD-A192710] 21 p2909 N88-27263
Energy distribution and transfer in flowing hydrogen microwave plasmas 21 p3019 N88-27919
Growth and characterization of CuGaS2, CuAlS2 and CuGa0.9Al0.1S2 single crystals
[AD-A192963] 21 p3021 N88-27930
Thermodynamic data bases for multivalent elements: An example for ruthenium
[DE88-004395] 23 p3190 N88-28984
Laser induced chemical vapor epitaxial growth of gallium arsenide films
[AD-A194254] 23 p3291 N88-29595
Chemical and spectroscopic characterization of a suite of Mars soil analogs 23 p3302 N88-29667
Attenuated total reflectance FT-IR spectroscopy to measure interfacial reaction kinetics at silica surfaces
[AD-A196330] 24 p3344 N88-29908

CHEMICAL PROPULSION
NT HYBRID PROPULSION
Space station onboard propulsion system: Technology study
[NASA-CR-179233] 07 p0825 N88-15006
Prospects for antiproton production and propulsion 16 p2267 N88-23556
Comparison of a direct thrust nuclear engine, nuclear electric engine and a chemical engine for future space missions 17 p2418 N88-24379
Recent advances in low-thrust propulsion technology
[NASA-TM-100959] 18 p2589 N88-25260

CHEMICAL REACTIONS
NT ALKYLATION
NT AMMONOLYSIS
NT ASSOCIATION REACTIONS
NT ATOMIC RECOMBINATION
NT BROMINATION
NT CARBONIZATION
NT CHLORINATION
NT COPOLYMERIZATION
NT CRACKING (CHEMICAL ENGINEERING)
NT DESULFURIZING
NT DIELS-ALDER REACTIONS
NT ELECTROCHEMICAL OXIDATION
NT ENDOTHERMIC REACTIONS
NT EXOTHERMIC REACTIONS
NT FERMENTATION
NT FLUORINATION
NT HALOGENATION
NT HYDROCRACKING
NT HYDROGENATION
NT HYDROLYSIS
NT ION RECOMBINATION
NT METAL-WATER REACTIONS
NT NITRATION
NT NITRIDING
NT NITROGENATION

NT OXIDATION
NT OXIDATION-REDUCTION REACTIONS
NT OXYGEN RECOMBINATION
NT OXYGENATION
NT PHOSPHORYLATION
NT PHOTOCHEMICAL REACTIONS
NT PHOTOCHROMISM
NT PHOTODECOMPOSITION
NT PHOTOLYSIS
NT PHOTOOXIDATION
NT PHOTOSYNTHESIS
NT PYROHYDROLYSIS
NT PYROLYSIS
NT RADIOLYSIS
NT REDUCTION (CHEMISTRY)
NT RUSTING
NT SULFIDATION
NT THERMAL DECOMPOSITION
NT THERMAL DISSOCIATION
NT TITRATION

Overcharge protection in Li-alloy/metal disulfide cells
[DE87-011364] 01 p0041 N88-10260

Chemical analysis of charged Li/SO(sub)2 cells
02 p0163 N88-11026

Voltammetric investigation of porous silicon for integrated circuit applications
[DE87-009287] 02 p0166 N88-11042

Shock-chemistry in natural materials and evolution of planetary surfaces
[DE87-012737] 02 p0254 N88-11604

Superfluid He4 as a solar neutrino detector
[DE87-014477] 02 p0257 N88-11625

The calculation of thermal rate constants for gas-phase and heterogeneous reactions in combustion processes
[AD-A184435] 03 p0284 N88-11788

Stress corrosion cracking of high-strength steels in aqueous environments 03 p0289 N88-11818

Numerical simulation of internal combustion engine flows: Development and users guide for MAGIC radial-azimuthal version
[DE87-014453] 03 p0332 N88-12091

Development of the non-equilibrium reactive chemical transport code CHMTRNS
[DE88-000682] 04 p0481 N88-12964

Hypersonic laminar boundary layer: Parametric study for the representation of real gas effects
05 p0532 N88-13236

Numerical analysis of axisymmetric flow with H2-O2 reactions 05 p0538 N88-13272

Plasma joining of metal matrix composites
[AD-A184828] 05 p0557 N88-13390

Fabrication of composites by chemical vapor deposition
[DE87-014565] 05 p0559 N88-13408

Shock compression of solids as a physical-chemical-mechanical process
[DE88-001674] 05 p0563 N88-13427

Modeling the effect of sulfur on the threshold environmental cracking rate of steels in high temperature water 05 p0604 N88-13703

The role of electronic structure calculation in mechanistic analysis of electron transfer reactions in the liquid phase
[DE87-014395] 05 p0647 N88-13963

Numerical study of chemically reacting flows using an LU scheme
[NASA-CR-180882] 06 p0668 N88-14094

Reactions and bonding between glasses and titanium
[DE88-000603] 06 p0685 N88-14195

Nitrogen scale-up
[AD-A185702] 06 p0709 N88-14351

Ozone formation due to interaction of meteoroids with Earth's atmosphere 06 p0738 N88-14536

Studies of metal/carbon surface chemistry
[DE87-009545] 07 p0829 N88-15029

SRB combustion dynamics analysis computer program (CDA-1)
[NASA-CR-182404] 07 p0830 N88-15032

Surface chemistry of chemically sensitive field effect transistors
[AD-A185917] 07 p0847 N88-15139

Chemical reactions in turbulent mixing flows
[AD-A186141] 07 p0849 N88-15153

Mixing in variable density, isothermal turbulent flows and implications for chemically reacting turbulent flows
[PB88-110044] 07 p0852 N88-15176

The KIVA-2 computer program for transient multidimensional chemically reactive flows with sprays
[DE88-000502] 07 p0854 N88-15191

Biogeochemical cycling in the ocean. Part 1: Introduction to the effects of upwelling along the west coast of North America
[NASA-TM-88230] 07 p0882 N88-15349

Physiological and biochemical aspects of toxic effects of oxidants in man's environment (air, water)
07 p0890 N88-15391

Atomic oxygen effects on metals
07 p0924 N88-15617

Aeropropulsion '87. Session 3: Internal Fluid Mechanics Research
[NASA-CP-10003-SESS-3] 08 p0954 N88-15790

Chemical reacting flows 08 p0955 N88-15793

Structural study of the impregnating resins of the type TGMDA/DDS --- epoxy resins
[ETN-88-91616] 08 p0965 N88-15842

An analytical study of the hydrogen-air reaction mechanism with application to scramjet combustion
[NASA-TP-2791] 08 p0966 N88-15846

Processing and interfacial analysis of glass-ceramic to metal seals
[DE88-002999] 08 p0971 N88-15873

Investigations of the influence of chemical reactions of the vertical flow of gaseous and particulate compounds
08 p1017 N88-16165

Feasibility of chemical lasers based on chain reaction involving hydrogen fluorination with thermal branching mechanism 09 p1238 N88-17420

Gas phase pulse radiolysis
[DE88-002981] 10 p1296 N88-17751

Insights into the mechanisms of chemical reactions: Reaction paths for chemical reactions
[DE88-003041] 10 p1297 N88-17755

Precipitation of surfactants and surfactant mixtures in aqueous solutions
[DE88-003333] 10 p1298 N88-17763

The chemistry of the hypochlorite neutralization of hydrazine fuels
[DE88-002971] 10 p1307 N88-17812

Laser studies of the dynamics of free radical reactions
[DE88-004431] 10 p1337 N88-17989

Chemical activation of molecules by metals: Experimental studies of electron distributions and bonding
[DE88-004465] 10 p1407 N88-18393

Reactions of some thiol collectors at noble-metal and pyrite electrodes
[PB88-138318] 11 p1455 N88-18674

Voltammetric investigation of porous silicon for integrated circuit applications
[DE88-004024] 11 p1456 N88-18677

Gas phase reactions of electrons, negative ions and free-radicals with transition metal complexes
11 p1560 N88-19339

Thermodynamics of wetting by liquid metals
[DE88-003634] 11 p1563 N88-19360

Chromatographic and related reactors
[AD-A188452] 12 p1605 N88-19599

The redox chemistry of some peroxo and superoxo metal ion complexes
[AD-A189159] 12 p1606 N88-19606

Picosecond laser studies of excited state processes
[AD-A189606] 12 p1607 N88-19607

Thermal cracking and variable properties effects on free boundary layer diffusion flames
[NBS/GCR-88/542] 12 p1614 N88-19652

A new parabolized Navier-Stokes code for chemically reacting flow fields 12 p1625 N88-19721

MOPAC manual: A general molecular orbital package, fourth edition
[AD-A188623] 13 p1733 N88-20362

Combustion theory and related questions
[AD-A189160] 13 p1737 N88-20382

Kinetic mechanisms for ionization and afterburning suppression
[AD-A189219] 13 p1737 N88-20383

Potassium cuprate (3)
[NASA-TT-20246] 13 p1739 N88-20401

Scale-up of a batch-type chemical powder preparation process for high field varistor fabrication
[DE88-006601] 13 p1762 N88-20541

Experimental and theoretical constraints on the origin of mid-ocean ridge geothermal fluids
13 p1804 N88-20784

Solid-state electrochemical processes in dye films
[AD-A188756] 13 p1844 N88-21036

Investigation of supersonic chemically reacting and radiating channel flow
[NASA-CR-182726] 14 p1862 N88-21125

Copper peroxide
[NASA-TT-20245] 14 p1888 N88-21282

Techniques for studying fast reactions in liquids
[DE88-005917] 14 p1888 N88-21285

Energy storage and transport by reversible chemical reactions
[DE88-900370] 14 p1942 N88-21587

Numerical simulation of turbulent flames using vortex methods
[AD-A189813] 15 p2034 N88-22116

An investigation of flow structure, mixing and chemical reaction in combusting turbulent flows
[AD-A189980] 15 p2034 N88-22117

Investigation of combustion in large vortices
[AD-A190406] 15 p2035 N88-22121

AFRAPT (Air Force Research in Aero Propulsion Technology) trainee program
[AD-A190525] 15 p2035 N88-22123

Evaluation of direct methane conversion to higher hydrocarbons and oxygenates
[DE88-003812] 15 p2049 N88-22204

The numerical simulation of viscous flows with change of phase and chemical reaction
[DE88-003204] 15 p2062 N88-22292

Chemically reacting turbulent flow
[AD-A190522] 15 p2065 N88-22311

The kinetics of contact noise in NaBeta alumina
[AD-A190651] 15 p2130 N88-22707

Synthesis and properties of novel cluster phases
[DE88-006816] 16 p2175 N88-22964

Analysis of non-premixed turbulent reacting flows
16 p2196 N88-23100

Advanced chemical heat pumps using liquid-vapor reactions
[DE88-006760] 16 p2205 N88-23159

Energy transfer processes in free radicals: A collaborative experimental and theoretical investigation
[AD-A191264] 16 p2269 N88-23578

Preventing aircraft corrosion by predictive corrosion modeling 17 p2321 N88-23863

Chemical kinetics and photochemical data for use in stratospheric modeling evaluation Number 8
[NASA-CR-182919] 17 p2351 N88-24012

Chemical compatibility between silicon carbide and a nickel aluminide
[DE88-006188] 18 p2479 N88-24708

Electrochemistry in liquid crystals
[AD-A191554] 18 p2481 N88-24719

Analysis of molecular mixing and chemical reaction in mixing layer
[AD-A191600] 18 p2482 N88-24721

Structural study of the TGMDA-DDS system --- epoxy system
[ONERA-RT-4/3346-M] 18 p2493 N88-24792

Study of mixing and reaction in the field of a vortex
[AD-A191489] 18 p2508 N88-24878

Numerical solutions of the complete Navier-Stokes equations
[NASA-CR-183023] 18 p2514 N88-24914

Workshop on Atmospheric OH
[BPT-7/87] 18 p2538 N88-25063

Ozone in the atmosphere 18 p2539 N88-25064

Laboratory experiments on atmospheric OH reactions
18 p2539 N88-25066

Characterization of yttrium aluminum garnet/YAG/using 14 MeV neutron activation
[AD-A191925] 18 p2582 N88-25342

Surface interactions relevant to space station contamination problems 18 p2592 N88-25401

Theoretical studies of the chemical reactions involved in the ignition of nitramines 19 p2632 N88-25615

Direct simulations of chemically reacting turbulent mixing layers, part 2
[NASA-CR-180853] 19 p2667 N88-25857

The 1986 IEEE Solid-State Sensor Workshop
[AD-A190922] 19 p2668 N88-25860

Thin-membrane Lamb-mode acoustic oscillators for chemical detection 19 p2673 N88-25895

Kinetics of thermochemical gas-solid reactions important in the Venus sulfur cycle
[NASA-CR-182963] 19 p2742 N88-26280

The rate of volcanism on Venus
[NASA-CR-183039] 19 p2742 N88-26281

The protonic Beta double prime aluminas: Preparation, stability, conductivity and structure
[DE88-006442] 20 p2768 N88-26415

Structural study of impregnating resins of TGMDA/DDS type
[ETN-88-92167] 20 p2780 N88-26488

Freely expanding detonation products: Scaling of rate processes
[DE88-007827] 20 p2799 N88-26606

Physical-chemical reactions at welding arc/molten pool interfaces
[DE88-007717] 20 p2808 N88-26662

Ion and electron interactions of atmospheric importance
[AD-A192255] 20 p2824 N88-26751

On the chemistry of superconductivity
[DE88-010714] 20 p2880 N88-27096

A study of the interaction of diffusion flames with a vortex pair flowfield 21 p2908 N88-27258

Mechanism of the nitric oxide-carbon monoxide-oxygen reaction over a single crystal rhodium catalyst
[DE88-006274] 21 p2910 N88-27268

Numerical computation of space shuttle orbiter flow field
[NASA-CR-183193] 22 p3040 N88-28048

Modification of YBa2Cu3O(7-x) ceramics by adsorbed water and other gases
[DE88-011518] 22 p3057 N88-28140
A study of the interaction of NO2 with carbon particles
[DE88-010778] 22 p3118 N88-28524
Radiative heat transfer to chemically reacting flow between concentric rotating spheres
[DE88-702538] 22 p3119 N88-28525
Theoretical investigations of nitrocubane decomposition
[AD-A194556] 23 p3200 N88-29047
Method of dispensing reagent chemicals in space
[NASA-CASE-LAR-13607-1-CU] 23 p3200 N88-29048
Laser induced chemical vapor epitaxial growth of gallium arsenide films
[AD-A194254] 23 p3291 N88-29595
Computed potential energy surfaces for chemical reactions
[NASA-CR-183168] 24 p3342 N88-29893
Design criteria for extraction with chemical reaction and liquid membrane permeation
[NASA-TT-20352] 24 p3343 N88-29899
Gas phase combustion chemistry of nitramine propellants
[AD-A195082] 24 p3344 N88-29902
Attenuated total reflectance FT-IR spectroscopy to measure interfacial reaction kinetics at silica surfaces
[AD-A196330] 24 p3344 N88-29908
Recent observations of carbon monoxide in the Amazon Rain Forest
[INPE-4478-PRE/1245] 24 p3390 N88-30186

CHEMICAL REACTORS
Mechanistic model for void distribution in flashing flow
[DE88-002948] 10 p1326 N88-17928
Research on hydrotreating catalysts to hydrodeoxygenate biocrude oils 18 p2536 N88-25046
Low-temperature thermochemical conversion of high moisture biomass feedstocks 18 p2536 N88-25047
An improved external recycle reactor for determining gas-solid reaction kinetics
[NASA-TM-101160] 19 p2611 N88-25492
Integrated solar reforming for thermochemical energy transport
[DE88-005010] 19 p2686 N88-25967
C-CAMP: A closed cycle alkali metal power system
[DE88-009715] 19 p2688 N88-25975

CHEMICAL RELAXATION
U MOLECULAR RELAXATION

CHEMICAL RELEASE MODULES
The combined release and radiation effects satellite, a joint NASA/DOD program 02 p0135 N88-10851

CHEMICAL SHIFT
U CHEMICAL EQUILIBRIUM

CHEMICAL TESTS
NT CHEMICAL ANALYSIS
NT CHROMATOGRAPHY
NT ELECTROPHOTOMETRY
NT GAS ANALYSIS
NT GAS CHROMATOGRAPHY
NT LIQUID CHROMATOGRAPHY
NT MICROANALYSIS
NT NEUTRON ACTIVATION ANALYSIS
NT OZONOMETRY
NT POTENTIOMETRIC ANALYSIS
NT QUALITATIVE ANALYSIS
NT QUANTITATIVE ANALYSIS
NT SALT SPRAY TESTS
NT SPECTROSCOPIC ANALYSIS
NT VOLUMETRIC ANALYSIS
Viscosity measurements at high temperatures on a standard reference material supplied by BCR --- Bureau Communite de Reference (BCR)
[NPL-DMA(A)-146] 01 p0020 N88-10126
Material degradation in a barium hydroxide latent heat storage pilot unit
[DFVLR-FB-87-49] 16 p2175 N88-22961

CHEMICAL VAPOR DEPOSITION
U VAPOR DEPOSITION

CHEMICAL WARFARE
Advanced development waste processing unit for combat vehicles, phase 2
[AD-A193793] 23 p3243 N88-29302
Four-axis side-arm flight control simulator investigation
[AD-A196026] 24 p3409 N88-30294

CHEMILUMINESCENCE
Laser probes of natural gas ignition chemistry
[PB87-209599] 01 p0021 N88-10129
The kinetics and dynamics of iodine monofluoride formation in gas-phase collisions
[AD-A185715] 06 p0709 N88-14352
Methods of quantifying and enhancing reactive oxygen species production 21 p2924 N88-27357

CHEMISORPTION
Separation of anionic from nonionic alkoxy compounds using silica gel
[GB-PATENT-2-140-415-A] 01 p0020 N88-10122
Adhesion properties of polyelectrolyte-chemisorbed zinc phosphate conversion coatings
[DE87-012489] 01 p0029 N88-10186
The effect of additives on the reactivity of palladium surfaces for the chemisorption and hydrogenation of carbon monoxide: A surface science and catalytic study
[DE87-014685] 02 p0145 N88-10909
Ro-vibrational laser spectroscopy of ESD neutrals from chemisorbed species
[DE87-013011] 04 p0447 N88-12770
Atomic and electronic structure of surfaces and chemisorbed layers
[DE87-014987] 04 p0498 N88-13065
The structure of adsorbed sulfur and carbon on molybdenum and rhenium single crystal surfaces, and their influence on carbon monoxide and hydrocarbon chemisorption
[DE88-001393] 04 p0499 N88-13073
The influence of crack conditions on hydrogen uptake by steels 05 p0604 N88-13702
Oxygen chemisorption cryogenic refrigerator
[NASA-CASE-NPO-16734-1-CU] 06 p0689 N88-14223
Extending the range of Low Energy Electron Diffraction (LEED) surface structure determination: Co-adsorbed molecules, incommensurate overlayers and alloy surface order studied by new video and electron counting LEED techniques
[DE88-001401] 06 p0786 N88-14820
Surface composition-reactivity relationships in heterogeneous catalysis
[DE87-003450] 09 p1140 N88-16834
Low temperature reactivity of chars towards oxygen, appendix E2
[DE88-004088] 10 p1298 N88-17760
Coupling of vibrational modes of adsorbates: Application to field induced shifts for CO and CN on Cu(100)
[AD-A187891] 11 p1453 N88-18659
Laser-induced desorption determinations of surface diffusion on Rh(111)
[DE88-005159] 11 p1454 N88-18667
An interpretation of the ethylenic, carbidic, and graphite auger lineshapes of chemisorbed carbon species
[AD-A189092] 13 p1736 N88-20379
Model catalyst studies of SMSI (Strong Metal/Support Interactions) and the role of D-electrons in chemisorption and catalysis
[DE88-004518] 13 p1738 N88-20393
First-principles calculations of quasiparticle energies at surfaces and interfaces: Semiconductor surface-state spectra and band offsets
[DE88-006340] 15 p2141 N88-22773

CHEMONUCLEAR PROPULSION
U CHEMICAL PROPULSION
U NUCLEAR PROPULSION

CHEMORECEPTORS
Central adrenergic receptors as mediators of central response to stress: Study with Positron Emission Tomography (PET)
[AD-A194947] 24 p3407 N88-30284

CHEMOTHERAPY
Effect of different doses of alpha-hydroxydimethyl-gamma-aminopropylidene phonate on rat bones 19 p2704 N88-26078

CHICKENS
Combined effect of microwaves and ionizing radiation 07 p0893 N88-15413

CHILDREN
A study of the performance of automatic speech recognisers with speech impaired children
[RSRE-MEMO-4040] 01 p0076 N88-10486

CHILLING
U COOLING

CHIMES
U AUDITORY SIGNALS

CHINA
A review of the analysis forecasting and research about severe local storms in Guangdong province (China) 02 p0207 N88-11298
The mesoscale numerical model for heavy rainfall forecasting in Yangtze River Valley, China 02 p0211 N88-11326
JPRS report: Science and technology. China
[JPRS-CST-87-031] 03 p0299 N88-11880
JPRS report: Science and technology. China
[JPRS-CST-87-034] 03 p0301 N88-11897
LISP as a rapid prototyping environment: The chinese tutor
[AD-A184328] 03 p0369 N88-12319
JPRS report: Science and technology. China
[JPRS-CST-87-032] 03 p0376 N88-12365
Technology transfer to China
[PB87-223418] 04 p0502 N88-13087
An evaluation of effectiveness of PTFE (polytetrafluoroethylene) type friction reducers on reducing friction and wear
[AD-A187440] 10 p1340 N88-18010
JPRS report: Science and technology. China
[JPRS-CST-87-030] 13 p1756 N88-20501
Technology transfer to China. Volume 2: Working papers, part 1
[PB88-158704] 14 p1992 N88-21872
Technology transfer to China. Volume 2: Working papers, part 2
[PB88-158712] 14 p1992 N88-21873
Rate of slip on the Altin Dagh Fault (North Tibet, China) 22 p3102 N88-28420
Archean crustal evolution of the northern North China Craton 24 p3398 N88-30235

CHINA (COMMUNIST) MAINLAND
U CHINA

CHINESE PEOPLES REPUBLIC
U CHINA

CHINESE SPACE PROGRAM
JPRS report: Science and technology. China
[JPRS-CST-87-023] 14 p1863 N88-21130
PRC space satellite achievements highlighted 14 p1863 N88-21131

CHIPS (ELECTRONICS)
Low noise-low power monolithic multiplexing readout electronics for silicon strip detectors
[MPI-PAE/EXP.EL.178] 02 p0168 N88-11057
Ultra-low power digital filter
[AD-A184485] 03 p0310 N88-11959
Integrated circuit design
[AD-A184486] 03 p0311 N88-11960
The design plan of a VLSI single chip (255, 223) Reed-Solomon decoder 04 p0435 N88-12697
Research in VLSI (Very Large Scale Integration) systems
[AD-A184089] 04 p0438 N88-12721
Technology upgrade of a silicon compiler
[AD-A184873] 05 p0655 N88-14016
On systolic architectures for interpolation and integration 10 p1382 N88-18250
Cryocooler systems demonstration
[AD-A188025] 11 p1467 N88-18745
Fuzzy logic inference processor for real time control: A second generation full custom design
[AD-A188155] 11 p1471 N88-18773
RELIC: A reliability simulator for integrated circuits
[AD-A187493] 11 p1477 N88-18811
The roll back chip: Hardware support for distributed simulation using time warp
[AD-A187823] 11 p1529 N88-19132
Parts-R-Us
[AD-A188621] 12 p1622 N88-19705
Computer aided fast turnaround laboratory for research in VLSI (Very Large Scale Integration)
[AD-A189451] 12 p1624 N88-19715
Reliability analyses of a surface mounted package using finite element simulation
[AD-A189488] 12 p1624 N88-19717
Laser programming integrated circuits
[AD-A189590] 13 p1762 N88-20537
Gridless routing for generalized cell assemblies: Report and user manual
[EUT-87-E-180] 13 p1764 N88-20549
Modulatable thin film field emission space gun
[AD-A189279] 13 p1845 N88-21043
A new approach on test generation for array structures using the behavior of the system --- VLSI chips
[INF-87-27] 14 p1907 N88-21397
French Multiproject Chip (MPC) activity report, 1986
[RR-650-I] 15 p2059 N88-22273
An expert system for discrete component digital circuit design
[AD-A189680] 15 p2059 N88-22274
An analysis of multiple grain CHiP architectures
[AD-A189942] 15 p2110 N88-22570
Design and implementation of VLSI prime factor algorithm processor
[AD-A190483] 15 p2112 N88-22580
High density ion implanted contiguous disk bubble technology
[AD-A190169] 15 p2143 N88-22789
A 30 GHz monolithic receive module technology assessment
[NASA-CR-180825] 16 p2194 N88-23084
A five-layer Open Systems Interconnection (OSI) implementation 17 p2390 N88-24204
Development of 20 GHz monolithic transmit modules
[NASA-CR-182134] 17 p2445 N88-24539
Defect detection and classification in VLSI pattern inspection 18 p2507 N88-24871

An improved simulated annealing algorithm for standard cell placement
[NASA-CR-182952] 18 p2558 N88-25183
An integrated on-chip pressure sensor for accurate control applications 19 p2671 N88-25880
Natural convection immersion cooling of an array of simulated chips in an enclosure filled with dielectric liquid
[AD-A193594] 23 p3207 N88-29088
Reliability assessment of Surface Mount Technology (SMT)
[AD-A193759] 23 p3208 N88-29089
Design of a self-timed VLSI multicomputer communication controller
[AD-A194567] 24 p3361 N88-30014
Circuit design criteria for stable lateral inhibition neural networks
[AD-A195066] 24 p3366 N88-30046

CHIPS (MEMORY DEVICES)
MINIAC: A small embedded computer
[DE88-008142] 21 p2994 N88-27757

CHIRAL DYNAMICS
Light scattering by oriented and randomly dispersed chiral particles
[DE87-014758] 03 p0376 N88-12368
Determination of the neutral current chiral coupling constants u sublsq, u subrsq, d sublsq and d subrsq from an (anti)neutrino-deuterium experiment
[B8715857] 06 p0779 N88-14780
The hybrid Monte Carlo Algorithm and the chiral transition
[DE88-004305] 10 p1399 N88-18341
Comment on the Adler-Bardeen theorem and related problems
[DE88-751051] 10 p1403 N88-18367
On the equivalence of four-dimensional self-duality equations to continual analog of the main chiral field problem
[DE88-700871] 12 p1686 N88-20083
Chiral symmetry in the path-integral approach
[DE88-700833] 12 p1699 N88-20168
Chiral symmetry breaking in finite quantum electrodynamics
[DE88-700860] 12 p1699 N88-20169
N=2 supergravity in superspace: The invariant action
[DE88-702136] 19 p2741 N88-26273
Theoretical particle physics
[DE88-011499] 23 p3295 N88-29621

CHIRP
The chirped-pulse free-electron laser
[DE88-009289] 20 p2807 N88-26651

CHLORELLA
Environmental life support system technology study — space flight
[ESA-CR(P)-2432] 02 p0218 N88-11371

CHLORIDES
NT BORON CHLORIDES
NT COPPER CHLORIDES
NT DICHLORIDES
NT HYDROCHLORIC ACID
NT HYDROGEN CHLORIDES
NT LITHIUM CHLORIDES
NT MAGNESIUM CHLORIDES
NT SILVER CHLORIDES
NT SODIUM CHLORIDES
Process for the preparation of acyl halides
[GB-PATENT-2-133-792-A] 01 p0020 N88-10124
The 250AH/90A active lithium-thionyl chloride cell for Centaur-G application 02 p0163 N88-11023
Corrosion susceptibility study of candidate pin materials for ALTC (Active Lithium/Thionyl Chloride) batteries
[DE88-001449] 04 p0440 N88-12734
Corrosion behavior of sputter-deposited aluminum-based alloys exposed to chloride solutions
[AD-A187262] 10 p1303 N88-17794
Rare Gas Halide (RGH) kinetics
[AD-A192352] 20 p2770 N88-26425
Effect of thermal cycling on CSPL (Chloride Silent Power Ltd.) sodium/sulfur cells
[DE88-011205] 21 p2939 N88-27455
Post-test observations on CSPL (Chloride Silent Power Limited) cells
[DE88-011975] 21 p2940 N88-27461
Advanced calcium-thionyl chloride high-power battery
[AD-A194401] 22 p3072 N88-28238
Some effects of nitrates on the tensile properties of Al 7075-T7351
[AD-A195118] 24 p3354 N88-29965

CHLORINATION
Crossed molecular beam studies of substitution and exchange reactions
[DE88-006322] 14 p1980 N88-21814

CHLORINE
Coverage dependence of adsorbate-substrate bond lengths: Chlorine and caesium adsorbed on silver single crystals
[PB87-125142] 06 p0788 N88-14833
The spreading and mixing of dense gas clouds in still air
[KNMI-WR-87-12] 16 p2230 N88-23320
Electronic states of the Xe(sub n)HCl systems in gas and condensed phases
[AD-A193881] 23 p3192 N88-28997

CHLORINE COMPOUNDS
NT AMMONIUM PERCHLORATES
NT BORON CHLORIDES
NT CHLORIDES
NT CHLORINE FLUORIDES
NT CHLOROCARBONS
NT COPPER CHLORIDES
NT DICHLORIDES
NT HYDROCHLORIC ACID
NT LITHIUM CHLORIDES
NT LITHIUM PERCHLORATES
NT MAGNESIUM CHLORIDES
NT SILVER CHLORIDES
NT SODIUM CHLORIDES
Magnetic investigations of the one-dimensional Heisenberg magnet Gd2Cl3
[ETN-88-91083] 09 p1241 N88-17438
Decomposition of hypochlorite in the presence of copper in a homogeneous medium
[NASA-TT-20199] 13 p1740 N88-20403

CHLORINE FLUORIDES
Temperature dependence of ultraviolet absorption cross sections of chlorofluoroethanes
[AERONOMICA-ACTA-A-325-1987] 18 p2482 N88-24726

CHLOROAROMATICS
Crossed molecular beam studies of substitution and exchange reactions
[DE88-006322] 14 p1980 N88-21814

CHLOROCARBONS
The potential impact on atmospheric ozone and temperature of increasing trace gas concentrations
[NASA-CR-182965] 17 p2373 N88-24112
Impact on ozone attainment of CFC (chlorofluorocarbon) controls used to prevent future depletion of stratospheric ozone
[PB88-195177] 19 p2690 N88-25989
Ultraviolet absorption cross sections of chloro- and chlorofluoromethanes at stratospheric temperatures
[AERONOMICA-ACTA-A-324-1988] 23 p3231 N88-29226

CHLOROETHYLENE
Comparison of isopropyl alcohol and trichloroethylene in removing solder flux
[DE88-005556] 14 p1889 N88-21288

CHLOROPHYLLS
A mode-locked ruby laser with chlorophyll d as saturable absorber 03 p0327 N88-12064
Varifront 3 expedition data report (USNS DE STEIGUER CRUISE 1202-82). Bioluminescence, hydrographic, nutrient, and satellite data from the Gulf of California (November-December 1981)
[AD-A185011] 05 p0620 N88-13805
The use of chlorophyll fluorescence measurements from space for separating constituents of sea water. Volume 1: Summary
[ESA-CR(P)-2444-VOL-1] 07 p0873 N88-15294
The use of chlorophyll fluorescence measurements from space for separating constituents of sea water. Volume 2: Appendices
[ESA-CR(P)-2444-VOL-2] 07 p0873 N88-15295
Artificial photosynthesis using chlorophyll based carotenoid-quinone triads
[DE88-001660] 07 p0884 N88-15362
The use of chlorophyll fluorescence measurements from space for separating constituents of sea water
08 p1043 N88-16307
Remote determination of chlorophyll concentration in the ocean using an optical pulse radar
[NASA-TT-20301] 19 p2694 N88-26014
Mechanisms of photochemical energy conversion by chlorophyll
[DE88-008763] 20 p2819 N88-26725
Modeling the primary events of photosynthesis using chlorophyll containing fixed distance donor-acceptor molecules
[DE88-010033] 20 p2831 N88-26793

CHOICE
U SELECTION

CHOKES
Parametric study of choke flutter with a linear theory
10 p1283 N88-17673

CHOKES (RESTRICTIONS)
Geometric analysis of ensemble of solutions in two-phase flow and complete resolution of problem of choking
[DE88-001687] 04 p0445 N88-12764

CHOLESKY FACTORIZATION
Data traffic reduction schemes for sparse Cholesky factorizations
[NASA-CR-181626] 13 p1813 N88-20831
Cholesky downdating on a hypercube
[DE88-006780] 15 p2113 N88-22586

CHOLINESTERASE
Carbamates, atropine, and diazepam: Effects on performance in the running rat
[AD-A188009] 11 p1517 N88-19062
Low doses of atropine sulfate impair retention of a well-learned spatial task
[AD-A194065] 23 p3237 N88-29266

CHONDRITES
NT CARBONACEOUS CHONDRITES
NT CARBONACEOUS METEORITES
Stratospheric particles: Synchrotron X-ray fluorescence determination of trace element contents
[DE87-012482] 02 p0198 N88-11234
Organic molecules on meteoritic solid substrates
[NASA-CR-181570] 05 p0560 N88-13411
Cometary evolution: Clues from chondritic interplanetary dust particles 14 p2002 N88-21934
New type of primitive meteorite found in Antarctica 24 p3441 N88-30478
Nebular processes recorded in chondritic meteorites 24 p3451 N88-30541

CHONDRULE
Astrophysics and the solar nebula 07 p0883 N88-15355
Evidence of the in situ decay of Al-26 in a Semarkona chondrule 24 p3441 N88-30479
Physical processes and timescales in planet and small-body accretion 24 p3451 N88-30540

CHOPPERS (ELECTRIC)
U ELECTRIC CHOPPERS

CHROMATES
Recent advances in metallic/ceramic coatings for corrosion control in military applications 17 p2320 N88-23858

CHROMATOGRAPHY
NT GAS CHROMATOGRAPHY
NT LIQUID CHROMATOGRAPHY
Supercritical fluid chromatography/supersonic jet spectroscopy
[DE88-000297] 03 p0282 N88-11774
Retention processes in supercritical fluid chromatography
[DE88-000079] 04 p0413 N88-12559
The analysis of metal finishing solutions by ion chromatography
[AD-A184812] 05 p0561 N88-13414
High energy molecules of high symmetry
[AD-A185385] 05 p0647 N88-13965
Ion chromatography in the manufacture of multilayer circuit boards
[DE88-002428] 10 p1322 N88-17902
Electrosorptive detection based on double-layer capacitance for selective anion monitoring in ion chromatography. Part 1: Mercury electrodes
[AD-A188780] 12 p1606 N88-19603
Fuels combustion research
[AD-A189114] 13 p1736 N88-20381
Determination of aquo-complexes of chromium and iron in chromium plating and polishing solutions by ion chromatography
[AD-A190168] 15 p2039 N88-22148
Universal detection of ions by replacement-ion chromatography employing an anion-replacement method and an ultraviolet-visible spectrophotometric detector
[AD-A191326] 16 p2176 N88-22971
Supercritical fluid chromatography/supersonic jet spectroscopy
[DE88-007935] 19 p2614 N88-25511

CHROME
U CHROMIUM

CHROMIC ACID
Chromic acid anodizing of aluminum foil
[NASA-CR-178417] 07 p0837 N88-15077
The effect on initial bond strength and durability of a Phosphoric Acid Dip (PAD) following chromic acid anodising of aluminum
[ARE-TM(UMM)-87402] 10 p1300 N88-17772

CHROMIUM
The mechanism by which sigma-phase forms in Fe-Cr-Ni system alloys
[BLL-M-37380-(5828.4)] 05 p0564 N88-13437
Determination, by X-ray fluorescence, of platinum, palladium, ruthenium, iron and chromium in special steels
[PB87-132114] 06 p0683 N88-14183

Reaction mechanism of sulfur dioxide with single crystal cobalt and chromium and CoCrAlY coatings
[AD-A185989] 09 p1253 N88-17509
Microprobe examination of composite materials produced by burning of Ti, Cr, C powders with powder of any one Fe-group metal. 14 p1886 N88-21269
Secondary electron emission characteristics improved by ion implantation 14 p1903 N88-21370
On quench sensitivity of Cu-Cr alloys
[NASA-TT-20174] 18 p2489 N88-24765
Effect of Zr or Cr content on the fracture toughness of the high purity Al-Zn-Mg alloys
[NASA-TT-20294] 19 p2616 N88-25518
Superconductivity of Cr/V superlattices 20 p2874 N88-27057
Self energy corrections to the ab initio band structures: Chromium
[DE88-701825] 21 p3020 N88-27927
Absorption spectra and energy levels of Gd(3+), Nd(3+) and Cr(3+) in the garnet Gd3Sc2Ga3O12
[AD-A193634] 23 p3292 N88-29599
An experimental study of biaxial yield in modified 9Cr-1Mo steel at room temperature
[NASA-CR-175012] 24 p3385 N88-30164

CHROMIUM ALLOYS
NT ASTROLOY (TRADEMARK)
NT CHROMIUM STEELS
The effect of sulfur and zirconium Co-doping on the oxidation of NiCrAl
[NASA-TM-100209] 02 p0150 N88-10940
Investigation of creep crack growth in heat resistant tube steels
[ETN-87-90606] 03 p0288 N88-11813
A comparison of high damping shape memory alloys with Cu-Mn-based and Fe-Cr-based alloys
[AD-A184110] 04 p0414 N88-12566
Model for ultrasonic attenuation and elastic constant in chromium and its alloys
[DE87-703478] 04 p0415 N88-12570
Microstructure and magnetic properties of cobalt-chromium alloys
[DE88-002762] 07 p0835 N88-15064
Reaction mechanism of sulfur dioxide with single crystal cobalt and chromium and CoCrAlY coatings
[AD-A185989] 09 p1253 N88-17509
Response of Fe-Cr-Mn austenitic alloys to thermal aging neutron irradiation
[DE88-003415] 10 p1302 N88-17785
The role of composition and microstructure gradients on weld metal properties and behavior
[DE88-004956] 10 p1303 N88-17791
Study of adherent oxide scales
[AD-A187368] 11 p1456 N88-18680
High temperature oxidation studies on alloys containing dispersed phase particles and clarification of the mechanism of growth of SiO2
[AD-A188158] 11 p1457 N88-18688
Corrosion resistance of electrodeposited amorphous Ni-Cr-P alloys
[DE88-005116] 11 p1459 N88-18695
Anodic behavior of Ni-P and Ni-Cr-P metallic glasses
[DE88-005334] 11 p1463 N88-18722
Effect of P implantation on the corrosion behavior of Fe-Cr alloys
[DE88-005732] 15 p2040 N88-22158
Characterization of an explosively consolidated rapidly solidified Fe-16Ni-9Cr-5Mo-2Cu alloy powder
[DE88-006733] 15 p2041 N88-22162
Fundamental studies of beta phase decomposition modes in titanium alloys
[AD-A191495] 18 p2485 N88-24740
The precipitation processes of Cu-Zr-Cr alloys
[NASA-TT-20168] 18 p2488 N88-24758
High temperature embrittleness of Cu-Cr alloy
[NASA-TT-20184] 18 p2488 N88-24759
Electrodeposition of amorphous Ni-Cr-P alloys
[DE88-006868] 19 p2616 N88-25521
Reduced-activation austenitic stainless steels: The Fe-Cr-C system
[DE88-008091] 20 p2773 N88-26442
The T-T-T curve in Cu-Cr alloy
[NASA-TT-20167] 20 p2774 N88-26453

CHROMIUM CARBIDES
Sputtered silver films to improve chromium carbide based solid lubricant coatings for use to 900 C
[NASA-TM-100783] 08 p0973 N88-15885

CHROMIUM COMPOUNDS
NT CHROMATES
NT CHROMIC ACID
NT CHROMIUM CARBIDES
NT CHROMIUM OXIDES

CHROMIUM OXIDES
Point defect structure of Cr2O3
[AD-A187620] 11 p1556 N88-19317
Evaluation of the chromium oxide arc spraying treatment on solar energy collectors
[ETN-88-92564] 18 p2537 N88-25053

CHROMIUM STEELS
On the relations between cyclic contraction ratio, flow stress, and deformation mechanisms in bainitic CrMoV steels
[VTT-36] 01 p0025 N88-10158
Modified 14Cr-16Ni stainless steels with improved creep resistance at 700 C due to tailored precipitate microstructures
[DE87-014788] 03 p0290 N88-11825
Reduced-activation ferritic steels: A comparison with Cr-Mo steels
[DE88-000332] 03 p0290 N88-11826
Impact behavior of 9-Cr and 12-Cr ferritic steels after low-temperature irradiation
[DE88-000333] 03 p0291 N88-11827
Tensile properties of extrusion consolidated Type 304 SS rapidly solidified powders
[DE87-014875] 05 p0566 N88-13450
Low cycle fatigue life predictions of a 1CrMoV steel in terms of a J-controlled short crack growth model 05 p0599 N88-13665
the influence of temper embrittlement on fatigue crack growth in hydrogen 05 p0605 N88-13709
Influence of stress ratio R on fatigue threshold delta K(th) for 40Cr steel 06 p0718 N88-14405
The effect of non-metallic inclusions on fatigue and fatigue thresholds of 25Mn-5Cr-1Ni steel 06 p0718 N88-14410
Low-chromium reduced-activation ferritic steels
[DE88-009060] 19 p2617 N88-25524
Investigation of structure and surface state effect on hydrogen embrittlement of steels, under consideration of acoustic emission analysis
[ETN-88-92350] 20 p2775 N88-26457

CHROMOSOMES
Changes in the morphological and molecular biological processes during early embryo development in amphibians under micro-g conditions 07 p0885 N88-15371
Method for measuring absolute linear parameters of chromosomes 19 p2707 N88-26095
Genetic effects of low level microwave radiation
[AD-A192687] 21 p2984 N88-27722
Effects of pulsed and CW (Continuous Wave) 2450 MHz radiation on transformation and chromosomes of human lymphocytes in vitro
[AD-A193104] 21 p2987 N88-27736

CHROMOSPHERE
Quasi-thermal models 02 p0253 N88-11600
Active region flows 02 p0255 N88-11611
High-resolution continuum observations of the Sun 02 p0255 N88-11614
Simultaneous, cospatial imaging of the Sun in cyanogen and singly-ionized calcium 04 p0507 N88-13114
Spectroscopic monitoring of RS CVn stars at Kitt Peak using the Penn State fiber optic echelle 04 p0509 N88-13127
X-rays, color, and the Vaughan-Preston gap 04 p0510 N88-13135
Relations between chromospheric and coronal structure, flux-flux correlations and convective zone properties 04 p0510 N88-13136
Broadband linear polarization and chromospheric CaII H and K line emission in late-type main sequence stars 04 p0511 N88-13140
The onset of chromospheric activity among the A- and F- type stars 04 p0511 N88-13144
Sensitivity of the H alpha line to expansion, geometrical extent and temperature gradient in the G and K supergiant chromospheres 04 p0514 N88-13159
The Wilson-Bappu relationship: A barometric effect 04 p0516 N88-13170
Synthetic spectra for the N-type carbon star TX Psc 04 p0516 N88-13173
Chromospheric variability mechanisms affecting pre-main sequence stars 04 p0517 N88-13180
Chromospheric and coronal heating in a bias-free sample of K dwarfs 04 p0518 N88-13184
Catalogue of chromospherically active binaries 04 p0520 N88-13192
A comprehensive exploration of late-type stars in the far-ultraviolet 04 p0520 N88-13194
Hydrogen and deuterium in the local interstellar medium 04 p0521 N88-13204
Observations of the solar chromosphere in Kunming
[PB87-143319] 07 p0944 N88-15737
Proceedings of the 21st ESLAB Symposium on Small Scale Processes in the Chromosphere/Corona, Interplanetary Medium and Planetary Magnetospheres
[ESA-SP-275] 08 p1094 N88-16582
Gasflows in the transition region above sunspot 08 p1095 N88-16586
Flux tubes and loops in the solar chromosphere and corona 08 p1095 N88-16591
Spectral images and multi-component models of the chromospheres of AR Lacertae 11 p1568 N88-19384

CHRONOBIOLOGY
U RHYTHM (BIOLOGY)

CHRONOLOGY
NT GEOCHRONOLOGY
Astronautics and aeronautics, 1978: A chronology
[NASA-SP-4023] 05 p0662 N88-14062
Data-base of Antarctic pre-Pleistocene sediment cores
[PB88-124151] 10 p1354 N88-18094
Effects of galactic chemical evolution on thorium/neodymium cosmochronology
[DE88-003829] 11 p1570 N88-19397
Early reheating and cosmic strings 13 p1855 N88-21103
Chronology of KSC and KSC related events for 1987
[NASA-CR-182754] 14 p2012 N88-22002
Marshall Space Flight Center 1960-1985: 25th anniversary report
[NASA-TM-100328] 15 p2153 N88-22852
Chronology of early lunar crust 24 p3394 N88-30212
Lewis Cliff 86010, a unique Antarctic meteorite: Possible new clues to the early history of the solar system 24 p3442 N88-30482

CHRONOTRONS
U TIME LAG

CHUGGING
U COMBUSTION STABILITY

CINEFLUOROGRAPHY
U MOTION PICTURES
U RADIOGRAPHY

CINEMATOGRAPHY
Flow measurements in a water tunnel using a holocinematographic velocimeter 16 p2203 N88-23141

CINERADIOGRAPHY
U MOTION PICTURES
U RADIOGRAPHY

CIRCADIAN RHYTHMS
Sleep and wakefulness: Handbook for flight medical officers, second edition
[AGARD-AG-270(E)] 02 p0217 N88-11366
Effect of night watches and intermittent sleep on state of circadian rhythms of physiological functions of fishermen 06 p0750 N88-14610
Pharmacological resetting of the Circadian sleep-wake cycle
[AD-A186194] 07 p0889 N88-15385
Biorhythmic aspects of intercontinental Antarctic adaptation 08 p1046 N88-16321
Inflight simian circadian rhythms and temperature homeostasis aboard Cosmos-1514 biosatellite 10 p1359 N88-18125
Center for the study of rhythmic processes
[AD-A188204] 11 p1520 N88-19078
Implications of shiftwork in space for human physiology experiments 12 p1659 N88-19942
Desynchronization of heart rate and breathing frequency after transmeridional flight across three time zones 12 p1663 N88-19968
Biological rhythms, sleep, and wakefulness in prolonged confinement 19 p2696 N88-26022
Biorhythms of binocular vision 20 p2830 N88-26788
The biological clock of Chlamydomonas reinhardii in space 22 p3061 N88-28162

CIRCLES (GEOMETRY)
Numerical arc segmentation algorithm for a radio conference-NASARC (version 2.0) technical manual
[NASA-TM-100160] 08 p0977 N88-15910
Fitting a circle to radially suppressed data
[NPL-DITC-103/87] 17 p2392 N88-24223
Linear programming in R sup 3 and the skeleton and largest incircle of a convex polygon
[PB88-124664] 20 p2846 N88-26892

CIRCUIT BOARDS
Ion chromatography in the manufacture of multilayer circuit boards
[DE88-002428] 10 p1322 N88-17902
VAXELN experimentation: Programming a real-time clock and interrupt handling using VAXELN Ada 1.1
[AD-A188100] 11 p1525 N88-19107
The inspection of electronic metallurgical bonds
[AD-A192197] 18 p2486 N88-24745
Procedures for identification and handling of Printed Circuit Boards (PCBs)
[AD-A191177] 23 p3206 N88-29078
Natural convection immersion cooling of an array of simulated chips in an enclosure filled with dielectric liquid
[AD-A193594] 23 p3207 N88-29088

CIRCUIT BREAKERS
Measuring technical and mathematical investigation of multiple reignitions at the switching of a motor using vacuum circuit breakers
[ETN-87-90406] 01 p0042 N88-10270
A simple self-breaking 2 MV gas switch
[DE87-014346] 02 p0166 N88-11047
Low-current behavior and current chopping of vacuum arcs
[ISBN-90-9001649-X] 05 p0578 N88-13529
CIRCUIT DIAGRAMS
Extraction of MOS VLSI (Very-Large-Scale-Integrated) circuit models including critical interconnect parasitics
[AD-A185847] 08 p0979 N88-15914
Data acquisition and processing for surface plate calibration
[AD-A187264] 11 p1564 N88-19366
ECP (Electrical Circuitry Program): A proposed program for electrical circuitry analysis
[AD-A190494] 15 p2060 N88-22280
Defect detection and classification in VLSI pattern inspection 18 p2507 N88-24871
Rule-based circuit optimization for CMOS VLSI 22 p3137 N88-28649
CIRCUIT PROTECTION
The 8.4-GHz low-noise maser pump source assembly 04 p0436 N88-12705
Trip electrical circuit of the gyrotron
[INPE-4336-NTE/273] 12 p1622 N88-19701
Metal oxide varistor polarization from an initial transient
[AD-A189012] 12 p1623 N88-19711
CIRCUIT RELIABILITY
DEDALE: An expert system for analog circuit maintenance 02 p0128 N88-10809
An integrated pressure sensor for in-vivo use 10 p1333 N88-17965
A methodology for hardware verification based on logic simulation
[AD-A188553] 12 p1622 N88-19704
Time domain wave propagation in multilayered integrated circuits
[AD-A193821] 22 p3073 N88-28241
CIRCUITS
NT ANALOG CIRCUITS
NT BISTABLE CIRCUITS
NT COINCIDENCE CIRCUITS
NT COMPARATOR CIRCUITS
NT COUPLING CIRCUITS
NT DELAY CIRCUITS
NT DIGITAL ELECTRONICS
NT DIPLEXERS
NT DISCRIMINATORS
NT ELECTRIC BRIDGES
NT ENCAPSULATED MICROCIRCUITS
NT EQUIVALENT CIRCUITS
NT FLUIDIC CIRCUITS
NT FREQUENCY DISCRIMINATORS
NT GATES (CIRCUITS)
NT HYBRID CIRCUITS
NT INTEGRATED CIRCUITS
NT ITERATIVE NETWORKS
NT LARGE SCALE INTEGRATION
NT LINEAR CIRCUITS
NT LINEAR INTEGRATED CIRCUITS
NT LOGIC CIRCUITS
NT MAGNETIC CIRCUITS
NT MATRICES (CIRCUITS)
NT MICROWAVE CIRCUITS
NT MIXING CIRCUITS
NT OHMS LAW
NT PHASE DETECTORS
NT PHASE SHIFT CIRCUITS
NT POWER SUPPLY CIRCUITS
NT PRINTED CIRCUITS
NT RC CIRCUITS
NT SCALERS
NT SWITCHING CIRCUITS
NT TRANSISTOR CIRCUITS
NT TRIGGER CIRCUITS
NT VARACTOR DIODE CIRCUITS
NT VERY LARGE SCALE INTEGRATION
NT VHSIC (CIRCUITS)
An optically strobed sample and hold circuit
[DE87-011877] 01 p0038 N88-10245
A tutorial on Rogowski coil theory and operation
[DE88-000006] 02 p0230 N88-11449
Electromagnetic effects of a discharge on circuitry --- spacecraft 03 p0274 N88-11726
The Pierce diode with an external circuit. Part 1: Simulations in the linear regime
[DE88-000413] 04 p0440 N88-12731
Radiation performance of AlGaAs concentrator cells and expected performance of cascade structures
[NASA-TM-100145] 04 p0465 N88-12878
Diagnostic reasoning in digital systems
[NASA-CR-181564] 05 p0633 N88-13871
The numerical and analytic of implicit differential equations and their application to control and circuit problems
[AD-A185404] 05 p0641 N88-13922
Signal processing for an optical wide band data transmission system
[DE88-003854] 10 p1319 N88-17888
Ballistic deficits in pulse shaping amplifiers
[DE88-003908] 11 p1481 N88-18840
Electrophoretically deposited styrene-acrylate coatings for suppression of internal electromagnetic pulse effects
[DE88-003820] 12 p1609 N88-19621
Research on automatic verification of finite-state concurrent systems
[AD-A188618] 12 p1677 N88-20029
Analysis of induction motors based on the numerical solution of the magnetic field and circuit equations
[EL-59] 14 p1907 N88-21398
ECP (Electrical Circuitry Program): A proposed program for electrical circuitry analysis
[AD-A190494] 15 p2060 N88-22280
A fully abstract semantics for event-based simulation
[AD-A190560] 15 p2060 N88-22283
Electrical circuit modeling of reversed field pinches
[DE88-006942] 15 p2136 N88-22745
Compilation of preprints
[AD-A191245] 16 p2252 N88-23460
Use of magnetic materials in excimer laser circuits
[DE88-006449] 19 p2674 N88-25903
RCL model for the development of hysteresis in superconductors
[DE88-702061] 19 p2733 N88-26234
An investigation of the uses of time domain capable vector network analyzers as a diagnostic for helix traveling-wave circuits
[AD-A192460] 21 p2935 N88-27430
A fiber optic synchronous detector using sample-and-hold circuits
[DE88-010973] 21 p3016 N88-27899
A millimeter-wave tunneLadder TWT
[NASA-CR-182184] 22 p3072 N88-28239
The p-well or n-well CMOS technology for advanced SEU-hard SRAMs
[DE88-006845] 22 p3156 N88-28777
Arcjet power supply and start circuit
[NASA-CASE-LEW-14374-1] 23 p3181 N88-28939
Distortions in processed signals and their application in electronic design. Part 1: Basic and general formulations
[DE88-702731] 23 p3204 N88-29070
Distortions in processed signals and their application in electronic design. Part 3: An automated generator of communication jamming signals
[DE88-702733] 23 p3205 N88-29072
Power supply conditioning circuit
[NASA-CASE-NPO-17233-1-CU] 23 p3208 N88-29095
Confirmation of slow-waves in a crosstie overlay coplanar waveguide and its application to band-reject gratings and reflectors
[AD-A194981] 24 p3361 N88-30011
Reducing the parallel solution time of sparse circuit matrices using reordered Gaussian elimination and relaxation
[AD-A195152] 24 p3366 N88-30045
CIRCULAR CYLINDERS
Effect of viscosity on a vertical cylinder due to surface waves
[ETN-87-90960] 02 p0171 N88-11075
The hybrid wavefront resonance method 03 p0303 N88-11913
The diffusion-convection vortex method for solving two-dimensional incompressible Navier-Stokes equation 03 p0317 N88-12001
Wind tunnel investigations of periodic vortex separation on rough-surface circular cylinders using acoustic measuring methods
[DFVLR-FB-87-24] 09 p1112 N88-16665
A large strain thermomechanical forming model for elastic-viscoplastic behavior in metals 10 p1301 N88-17780
Time-resolved heat transfer measurements and analysis in the wage region of a cylinder in crossflow 10 p1328 N88-17939
Nonaxisymmetric body supersonic, aerodynamic prediction
[AD-A189338] 13 p1716 N88-20259
Body tensor formalism in finite deformation elasticity and application to the torsion of a circular cylinder 13 p1780 N88-20651
Theoretical and numerical solution of the forward-scattering problem in a circularly cylindrical configuration
[PB88-173489] 16 p2189 N88-23056
Finite elements for the computation of three-dimensional electromagnetic fields in inhomogeneous media (revised)
[PB88-173471] 16 p2190 N88-23057
Oscillating flow over bluff bodies in a U-shaped water tunnel 16 p2201 N88-23131
Correlations of velocity and temperature fluctuations in the stagnation-point flow of circular cylinder in turbulent flow
[NASA-TM-100930] 19 p2597 N88-25435
Liquid motions in partially filled containers: Preliminary results of the D-1 mission --- Spacelab
[NLR-MP-86042-U] 20 p2802 N88-26629
Natural frequencies and stability of circular cylindrical immiscible liquid systems
[LRT-WE-9-FB-3(1987)] 22 p3062 N88-28172
Heat transport in a parabolic tube of circular cross-section
[LRT-WE-9-FB-2(1988)] 22 p3078 N88-28274
The effects of incoming boundary layer thickness on unsteady shock-induced turbulent separations induced by cylinders
[AD-A196190] 24 p3368 N88-30060
CIRCULAR ORBITS
NT STATIONARY ORBITS
Canonical variables and canonical integrals for motion in near-circular orbits 24 p3446 N88-30512
CIRCULAR PLATES
Unsteady flow about cambered plates
[AD-A184725] 03 p0320 N88-12025
On the instability of thin circular shear layers 04 p0395 N88-12467
Vibration and parametric excitation in rotating asymmetric circular plates 04 p0456 N88-12823
Boundary element analysis for dynamic loading of a circular plate on an elastic medium
[CI-86] 06 p0722 N88-14443
Experimental investigation of the effects of underwater exposure on the damping characteristics of bolted structural connections for plates and shells
[AD-A194486] 23 p3226 N88-29200
CIRCULAR POLARIZATION
An investigation on Faraday rotators and quarter-wave plates of a 35 GHz radar signature system
[DFVLR-FB-87-14] 01 p0037 N88-10236
Relativistic electromagnetic waves in an electron-ion plasma
[NASA-CR-182421] 08 p1085 N88-16532
Mode priming in an overmoded gyrotron oscillator
[AD-A189151] 13 p1772 N88-20602
Polarization properties of SiO masers 13 p1858 N88-21113
Linear and circular polarization of Comet Halley light 14 p2009 N88-21982
Research on Faraday rotators and quarter-wave plates of a 35-GHz radar signature system
[ESA-TT-1081] 16 p2189 N88-23052
CIRCULAR TUBES
Numerical study of the entrance flow and its transition in a circular pipe (2) 03 p0318 N88-12011
CIRCULAR WAVEGUIDES
Analysis of electromagnetic wave propagation in slightly inhomogeneous hollow waveguides
[DFVLR-FB-87-23] 09 p1152 N88-16904
CIRCULATION
NT ATMOSPHERIC CIRCULATION
NT BLOOD CIRCULATION
NT BRAIN CIRCULATION
NT COASTAL CURRENTS
NT CONGESTION
NT CORONARY CIRCULATION
NT EL NINO
NT GULF STREAM
NT LOMONOSOV CURRENT
NT OCEAN CURRENTS
NT PERIPHERAL CIRCULATION
NT PULMONARY CIRCULATION
NT WATER CIRCULATION
NT WATER CURRENTS
NT ZONAL FLOW (METEOROLOGY)
Influence of the friction coefficients, the power and the flowrate on the two-phase flow instabilities in natural circulation
[DE88-700036] 08 p0983 N88-15946
Solidification with natural circulation
[DE88-011197] 22 p3074 N88-28248
Finding minimum-cost circulations by canceling negative cycles
[AD-A194027] 23 p3271 N88-29468
Finding minimum-cost circulations by successive approximation
[AD-A194028] 23 p3272 N88-29469
Experimental and analytical study of two-phase flow in zero gravity
[AD-A195223] 24 p3358 N88-29993

An analysis of results of a high-resolution world ocean circulation model
[AD-A195760] 24 p3405 N88-30272
CIRCULATION CONTROL AIRFOILS
NT CIRCULATION CONTROL ROTORS
Proceedings of the Circulation-Control Workshop, 1986
[NASA-CP-2432] 10 p1268 N88-17586
Navier-Stokes calculations and turbulence modeling in the trailing edge region of a circulation control airfoil
10 p1268 N88-17587
Wall jet analysis for circulation control aerodynamics. Part 1: Fundamental CFD and turbulence modeling concepts 10 p1269 N88-17588
Investigations of a circulation control airfoil flowfield using an advanced laser velocimeter
10 p1269 N88-17589
Evaluation of a research circulation control airfoil using Navier-Stokes methods 10 p1269 N88-17591
Navier-Stokes computations for circulation control airfoils 10 p1269 N88-17592
Wall jet analysis for circulation control aerodynamics. Part 2: Zonal modeling concepts for wall jet/potential flow coupling 10 p1269 N88-17593
The further development of circulation control airfoils
10 p1270 N88-17594
On the effect of leading edge blowing on circulation control airfoil aerodynamics 10 p1270 N88-17595
Pressure distributions and oil-flow patterns for a swept circulation-control wing 10 p1270 N88-17596
Boundary-layer and wake measurements on a swept, circulation-control wing 10 p1270 N88-17597
Wind tunnel studies of circulation control elliptical airfoils 10 p1270 N88-17598
An aerodynamic comparison of blown and mechanical high lift airfoils 10 p1272 N88-17606
Fixed wing CCW aerodynamics with and without supplementary thrust deflection
10 p1272 N88-17607
Development of circulation control technology for powered-lift STOL aircraft 10 p1272 N88-17608
A potential flight evaluation of an upper-surface-blowing/circulation-control-wing concept
10 p1272 N88-17609
Circulation control STOL aircraft design aspects
10 p1272 N88-17610
Boundary-layer and wake measurements on a swept, circulation-control wing
[NASA-TM-89426] 15 p2014 N88-22013
On the validation of a code and a turbulence model appropriate to circulation control airfoils
[NASA-TM-100090] 16 p2156 N88-22864
CIRCULATION CONTROL ROTORS
Proceedings of the Circulation-Control Workshop, 1986
[NASA-CP-2432] 10 p1268 N88-17586
Flap-lag-torsion aeroelastic stability of a circulation control rotor in forward flight 10 p1271 N88-17600
The impact of circulation control on rotary aircraft controls systems 10 p1271 N88-17601
Analysis of a fixed-pitch X-wing rotor employing lower surface blowing 10 p1271 N88-17602
Prediction of aeroelastic response of a model X-wing rotor 10 p1271 N88-17603
X-wing potential for Navy applications
10 p1271 N88-17604
Reduction of tilt rotor download using circulation control 10 p1271 N88-17605
Analysis of a fixed-pitch X-wing rotor employing lower surface blowing
[AD-A187379] 24 p3321 N88-29779
CIRCULATION DISTRIBUTION
On estimating the basin-scale ocean circulation from satellite altimetry. Part 1: Straightforward spherical harmonic expansion
[NASA-CR-182367] 07 p0882 N88-15352
Northern winter circulations for the period 1974-1983
[AD-A187779] 11 p1511 N88-19028
CIRCULATORY SYSTEM
NT AORTA
NT ARTERIES
NT CAPILLARIES (ANATOMY)
NT CARDIAC VENTRICLES
NT CARDIOVASCULAR SYSTEM
NT HEART
NT MYOCARDIUM
NT VEINS
Circulatory response of males 45-52 years of age to antiorthostatic hypokinesia 07 p0894 N88-15416
Oxidative enzyme activity in healthy subjects and individuals with neurocirculatory dystonia during graded exercise 10 p1367 N88-18170
Macaca rhesus tolerance to +Gz accelerations
19 p2704 N88-26080
CIRCUMFERENCES
Numerical simulation of flight body circumference flow
06 p0676 N88-14137
CIRCUMSTELLAR MATTER
U STELLAR ENVELOPES
CIRRUS CLOUDS
Lidar-radiometric method for determining liquid-water content of cirrus clouds 04 p0461 N88-12854
Measurement of cirrus cloud optical properties by high spectral resolution lidar 04 p0470 N88-12906
Galactic interstellar abundance surveys with IUE and IRAS 04 p0522 N88-13206
The collection of statistics on the frequency of cloud cover over North America
[AD-A190456] 15 p2097 N88-22495
The collection of statistics on the frequency of cloud cover over North America
[AD-A193093] 21 p2974 N88-27667
Cloud/mesoscale model development and application studies
[AFGL-TR-87-0219] 24 p3404 N88-30269
CITIES
A diffraction based theoretical model for prediction of UHF path loss in cities 12 p1616 N88-19661
Urban cartography: A book review
16 p2227 N88-23297
Remote sensing technique applied to vegetation as an aid to municipal planning 19 p2683 N88-25951
Application of 35mm EM aerial reconnaissance photographic format of the municipality of Ubatuba (SP)
19 p2684 N88-25953
Aerial photography as an instrument of municipal and regional planning: Metropolitan area of Sao Paulo (SP)
19 p2684 N88-25957
Spread of large tropical conurbations
22 p3098 N88-28398
Integration of SPOT data into a geocoded information system 22 p3098 N88-28400
Mapping and urban multi-experimental assessment of SPOT: Mapping results 22 p3112 N88-28483
Urbanization: Its detection and effect in the United States climate record 22 p3125 N88-28571
CIVIL AVIATION
Aircraft accident reports, brief format, US civil and foreign aviation. Issue number 1: 1986 accidents
[PB87-916903] 02 p0123 N88-10781
Civil applications of high-speed rotorcraft and powered-lift aircraft configurations
[NASA-TM-100035] 03 p0261 N88-11643
Design requirements for future commercial operations
03 p0262 N88-11651
The EH-101 integrated project: A naval, utility and commercial helicopter system 03 p0265 N88-11672
Airline safety: A comparative analysis
[AD-A185358] 05 p0543 N88-13308
Civil aeronautics
[ETN-88-90616] 05 p0543 N88-13309
Aircraft accident reports: Brief format, US Civil and Foreign Aviation, Issue Number 4 of 1986 accidents
[PB87-916906] 06 p0666 N88-14086
Aircraft accident report: Grand Canyon Airlines, Inc., and Helitech, Inc., midair collision over Grand Canyon National Park, June 18, 1986
[PB87-910403] 06 p0666 N88-14087
Eighth Session of the Commission for Aeronautical Meteorology (abridged)
[WMO-673] 06 p0745 N88-14585
Digest of the annual report of the Lufthansa German Airlines
[ISSN-0415-603X] 08 p0952 N88-15779
Aircraft accident reports: Brief format, US Civil and Foreign Aviation, Issue Number 5 of 1986 accidents
[PB87-916907] 08 p0952 N88-15780
Aircraft accident reports: Brief format, US Civil and Foreign Aviation, Issue Number 7 of 1986 accidents
[PB87-916909] 08 p0952 N88-15781
Aircraft accident reports: Brief format, US Civil and Foreign Aviation, Issue Number 8 of 1986 accidents
[PB87-916910] 08 p0953 N88-15782
Product planning in civil aircraft construction
[MBB-UT-002/87] 10 p1313 N88-17849
Minimum Energy Routing through Interactive Techniques (MERIT) modeling
[NASA-CR-182535] 10 p1356 N88-18105
JPRS report: Science and technology. Europe and Latin America
[JPRS-ELS-88-001] 12 p1614 N88-19649
The judgement and evaluation of long-term investments demonstrated by means of a civil aircraft program
12 p1701 N88-20180
Activities report in civil aeronautics
[ETN-88-91344] 13 p1715 N88-20255
Availability and cost estimate of a high naphthene, modified aviation turbine fuel
[NASA-TM-100823] 13 p1749 N88-20455
General aviation activity and avionics survey: 1986 data
[AD-A189986] 15 p2013 N88-22003
Aircraft accident reports, brief format, US civil and foreign aviation, issue number 10 of 1986 accidents
[PB87-916912] 15 p2016 N88-22020
JPRS report: Science and technology. Japan
[JPRS-JST-88-001] 15 p2051 N88-22218
Activities report of Lufthansa
[ISSN-0176-5086] 16 p2155 N88-22855
The challenges and opportunities of supersonic transport propulsion technology
[NASA-TM-100921] 17 p2307 N88-23806
Competitive assessment of the U.S. civil helicopter industry
[PB88-186325] 18 p2455 N88-24574
FAA aviation forecasts fiscal years 1988-1999
[AD-A191711] 18 p2455 N88-24576
US civil airmen statistics, 1987
[AD-A191714] 18 p2455 N88-24577
General-aviation's view of progress in the aviation weather system 18 p2546 N88-25110
Radiation safety in commercial air traffic
[NASA-TM-101156] 19 p2600 N88-25447
Trends in civil aircraft propulsion
[PNR90441] 22 p3044 N88-28067
An interim comparison of operational CG records in turbulence on small and large civil aircraft
24 p3313 N88-29729
Re-assessment of gust statistics using CAADRP data
24 p3313 N88-29732
An analysis of time and space requirements for aircraft turnrounds
[TT-8705] 24 p3322 N88-29783
Report to Congress on the effectiveness of the Civil Aviation Security Program
[AD-A195282] 24 p3322 N88-29784
CLADDING
Comparative tests of high temperature creep-rupture behavior of the austenitic CrNi steel DIN W.NR.1.4970 in argon and steam
[KFK-4261] 01 p0063 N88-10402
Thermal stress in the edge cladding of Nova glass laser disks
[DE88-000425] 04 p0448 N88-12780
Development of composite polymer-glass edge claddings for Nova laser disks
[DE88-002389] 07 p0860 N88-15220
Beneficial and detrimental effects of silica in the high temperature oxidation of 20Cr/25Ni/Nb stainless steel
[AERE-R-12667] 10 p1301 N88-17779
Effects of commercial cladding on the fracture behavior of pressure vessel steel plates
[DE88-004333] 10 p1303 N88-17790
Composite ceramic superconducting filaments for superconducting cable
[AD-A187833] 11 p1556 N88-19312
SBIR-Long fluoride fiber
[AD-A188595] 13 p1754 N88-20492
Development program for 1.93-micron lasers
[NASA-CR-4148] 16 p2212 N88-23198
Laser cladding of Ni, Nb and Mg alloys for improved environmental resistance at high temperature
[AD-A191274] 16 p2213 N88-23208
Parametric analyses of the TE SP-100 system performance 17 p2415 N88-24358
The application of high-rate biaxial testing to the design of containment vessels for radioisotope heat sources
17 p2426 N88-24428
SNAP fuel performance 17 p2435 N88-24484
CLARK Y AIRFOIL
U AIRFOIL PROFILES
CLASSICAL MECHANICS
NT ASTRODYNAMICS
NT CELESTIAL MECHANICS
NT KEPLER LAWS
NT ORBITAL MECHANICS
Institute for Computational Mechanics in Propulsion (ICOMP) first year summary
[NASA-TM-100225] 03 p0370 N88-12330
Composite mechanics for engine structures
[NASA-TM-100176] 04 p0411 N88-12552
Existence of absolutely closed universe
08 p1080 N88-16509
Institute for Computational Mechanics in Propulsion (ICOMP)
[NASA-TM-100790] 11 p1540 N88-19202
Introduction to classical mechanics of systems with constraints, part 1
[DE88-701055] 13 p1832 N88-20957
Introduction to classical mechanics of systems with constraints, part 2
[DE88-701056] 13 p1849 N88-21072
Introduction to classical mechanics of systems with constraints, part 3
[DE88-701057] 13 p1850 N88-21073

Galilei relativity principle in classical electrodynamics
[DE87-703203] 14 p1904 N88-21376
Singular Lagrangians. Classical dynamics and quantization. Lectures for young scientists
[DE88-701158] 15 p2146 N88-22806
On the quantization of constrained generalized dynamics
[DE88-702223] 23 p3277 N88-29505

CLASSIFICATIONS
NT HIERARCHIES
NT INDEXES (DOCUMENTATION)
Clustering by means of medoids
[REPT-87-03] 01 p0085 N88-10551
Theoretical Aspects of Target Classification
[AGARD-LS-152] 03 p0303 N88-11909
Theoretical aspects of target classification: Physical optics and radon transform methods
03 p0304 N88-11915
Parametrization in scattering models
03 p0304 N88-11916
Input signal shaping: K-pulse
03 p0304 N88-11917
Computer-controlled testing of visual-spatial ability
[AD-A183971] 03 p0357 N88-12249
Aircraft classification by type of propulsive devices. Determination of type and number of carrying solutions
04 p0424 N88-12626
Cloud cover determination in polar regions from satellite imagery
[NASA-CR-181544] 04 p0471 N88-12908
The classification problem of finite rings by computable means
[AD-A185869] 07 p0908 N88-15500
Membership of Cepheids and red giants in 8 open clusters: NGC 129, 6067, 6649, 6664, IC 4725, Ly 6, Ru 79
[PUBL-SER-C-FASC-13] 07 p0944 N88-15739
Estimation of broadband planetary albedo from operational narrowband satellite measurements
[PB88-107644] 07 p0945 N88-15748
The power of neural nets 08 p1064 N88-16430
Event classification in (anti)neutrino experiments using an Internal Picket Fence-External Muon Identifier (IPF-EMI) detector system
[NIKHEF-H/87-6] 09 p1245 N88-17457
Rapid underway sediment classification by electrical methods
[AD-A187477] 10 p1357 N88-18114
Radar descriptors for the classification of terrain features
[AD-A188145] 11 p1504 N88-18983
Multisource context classification methods in remote sensing 11 p1504 N88-18985
Environmental gradient analysis, ordination, and classification in environmental impact assessments
[AD-A187294] 11 p1509 N88-19016
Mathematical modeling of two-state classification technology transfer summary and user's guide
[DE88-003849] 11 p1526 N88-19110
Terrain classification from digital elevation data using slope and curvature information
[AD-A188940] 12 p1639 N88-19812
Asymptotic giant branch populations in composite stellar systems 13 p1854 N88-21098
Land-use classification in a region north-west of Wuerzburg (Federal Republic of Germany) using digital, multispectral LANDSAT 5 Thematic Mapper data
[DFVLR-FB-87-37] 14 p1940 N88-21579
Classification of comets recorded in ancient China (300 BC - 1800 AD) and statistics of type-1 tails
14 p2008 N88-21976
High temperature materials: What's available
[AERE-R-12632] 15 p2028 N88-22081
On categorizing sounds
[AD-A189784] 15 p2129 N88-22700
Computer assisted generalization of buildings for digital landscape models by classification methods
16 p2226 N88-23294
Software development for the reconstruction of source parameters using research and development arrays
[REPT-840445-TW] 16 p2246 N88-23417
Adaptive segmentation evaluation
[AD-A190965] 16 p2274 N88-23609
Latitudinal and seasonal variation of the cloud characteristic parameters and their effects on the cloud classification 17 p2351 N88-24005
The use of SLAR and SIRA imagenes for the classification of forest typen in tropical rain forests
17 p2356 N88-24036
Utilization of TM/LANDSAT images in the implanted forests mapping in the Mogi-Guacu Region (SP-Brazil)
17 p2357 N88-24042
Generation of thematic maps for updating aeronautical pilot charts utilizing LANDSAT-TM images
17 p2361 N88-24062
Study of methods of post-processing applied to a problem of standard classification
17 p2362 N88-24067
Research on enhancing the utilization of digital multispectral data and geographic information systems in global habitability studies
[NASA-CR-182799] 17 p2368 N88-24101
A method for discrimination of radar targets using complex natural resonances
[AD-A191848] 18 p2500 N88-24832
Automatic discovery of optimal classes
[NASA-TM-101174] 18 p2566 N88-25238
Mechanisms for particle acceleration: Possibilities and constraints
[PB88-102538] 19 p2725 N88-26184
Interpreting forest biome productivity and cover utilizing nested scales of image resolution and biogeographical analysis
[NASA-CR-183036] 20 p2817 N88-26711
Topics in quasicrystalliography
21 p3023 N88-27947
Discrimination methods of traditional fields in a humid tropical region (Shaba, Zaire) using digital classification on SPOT data 22 p3096 N88-28387
Accuracy of land use classification for SPOT image data 22 p3100 N88-28410
Rendering of surfaces from volume data
[AD-A193649] 22 p3143 N88-28689
Detection of helicopters using ground-controlled microphones 22 p3148 N88-28730
Spectral classification of Low Mass X-ray Binaries (LMXB) energy spectra with color-color diagrams
[MPE-PREPRINT-111] 22 p3163 N88-28837
Literature review: Validity and potential usefulness of psychomotor ability tests for personnel selection and classification
[AD-A193558] 23 p3241 N88-29287
Relief effect correction on LANDSAT imagery for forest applications using digital terrain models
[INPE-4611-PRE/1334] 24 p3388 N88-30179
Lava thicknesses: Implications for rheological and crustal development 24 p3443 N88-30490

CLASSIFYING
Transient classifier systems and man-machine interface research
[AD-A186213] 07 p0899 N88-15446
Method for determining the coordinates of sound sources by means of a sound measurement system
[NASA-TT-20242] 13 p1834 N88-20972

CLAYS
NT VERMICULITE
Surface mediated photocatalysis
[AD-A188882] 12 p1603 N88-19589
Chemical and spectroscopic characterization of a suite of Mars soil analogs 23 p3302 N88-29667

CLEAN ROOMS
Use of a 35mm camera for remote surface cleanliness verification 02 p0133 N88-10835
Design, construction, activation, and operation of a high intensity acoustic test chamber
02 p0137 N88-10864

CLEANERS
NT AIR FILTERS
Low extractable wipers for cleaning space flight hardware 02 p0137 N88-10863

CLEANING
NT BATHING
NT CHEMICAL CLEANING
NT HOUSEKEEPING (SPACECRAFT)
NT STERILIZATION
NT WASHING
Fourteenth Space Simulation Conference: Testing for a Permanent Presence in Space
[NASA-CP-2446] 02 p0132 N88-10829
Shear stress cleaning for surface deparliculation
02 p0134 N88-10838
Low extractable wipers for cleaning space flight hardware 02 p0137 N88-10863
Investigation of the nature and concentration of vapor and mist during the cleaning of aircraft
[PML-1985-29] 05 p0623 N88-13817
Gas cleaning at high temperatures and pressures for gas turbines
[DE88-751171] 11 p1440 N88-18593
Evaluation of solder flux solvents in a vapor-degreasing application for hybrid microcircuits
[BDX-613-3638] 11 p1468 N88-18752
Thermal oxide growth on silicon: Intrinsic stress and silicon cleaning effects
[AD-A189790] 13 p1736 N88-20377
In-situ reactive of X-ray optics by glow discharge
[DE88-009840] 20 p2854 N88-26947

CLEANLINESS
NT HOUSEKEEPING (SPACECRAFT)
Use of a 35mm camera for remote surface cleanliness verification 02 p0133 N88-10835
Redistribution of particulates in shuttle bay during launch 02 p0133 N88-10837
Cleanliness tests with the Omega Meter: A comparative study for solder flux removal
[DE88-004634] 11 p1460 N88-18704
Electronic failure analysis-corrosion of avionics
22 p3054 N88-28122

CLEAR AIR TURBULENCE
Northwest Airlines flight experiments
05 p0617 N88-13786
Infrared low-level wind shear work
10 p1275 N88-17628
Objective detection and forecasting of Clear-Air Turbulence (CAT): A status report
18 p2546 N88-25114
Utilization of a single clear-air Doppler radar beam to measure vertical divergence
[AD-A195543] 24 p3405 N88-30271

CLEARANCES
Recent advances in capacitance type of blade tip clearance measurements
[NASA-TM-101291] 19 p2603 N88-25460

CLEAVAGE
A quantitative statistical model for cleavage fracture initiation in carbide strengthened steels
[ETN-87-90735] 01 p0025 N88-10157
On cleavage in fatigue for rail steels
06 p0716 N88-14388
Influence of cleavage on fatigue propagation rates in a low carbon steel 06 p0716 N88-14389
Brittle to ductile transition to cleavage fracture
[DE88-004074] 10 p1420 N88-18481
Small-scale cleavage test of polymer products
[PB88-165360] 16 p2181 N88-23001

CLIMATE
Atlas of wide-field-of-view outgoing longwave radiation derived from Nimbus 7 Earth radiation budget data set - November 1978 to October 1985
[NASA-RP-1186] 01 p0070 N88-10451
Detection of CO2-induced climate change
[DE87-013127] 01 p0071 N88-10457
Testimony to the US Senate on the greenhouse effect
[DE87-013995] 01 p0071 N88-10458
Description of NCAR (National Center for Atmospheric Research) Community Climate Model (CCM1)
[PB87-203782] 01 p0072 N88-10462
Understanding passive cooling systems
[PB87-210464] 02 p0194 N88-11211
Development of a climatic map of rainfall attenuation for Europe
[REPT-372] 02 p0216 N88-11359
The correspondence of surface climate parameters with satellite and terrain data
[NASA-CR-181515] 03 p0346 N88-12185
On the interannual variability of South American climate and the Southern Oscillation 04 p0470 N88-12905
New method of estimating continentality of climate on global scale 06 p0725 N88-14460
The climatic wind regime in the lower thermosphere from meteor radar observations 06 p0733 N88-14506
Modes of surface circulation and climate over the tropical Atlantic, Eastern Pacific, and Indian Oceans
06 p0742 N88-14564
Report of the Joint Scientific Commitee Ad Hoc Working Group on Radiative Flux Measurements --- Earth radiation budget
[WCP-136] 06 p0742 N88-14567
Carbon dioxide and climate: Summaries of research in FY 1987
[DE88-000916] 06 p0744 N88-14574
Report of the second session of the working group on sea ice and climate
[WCP-128] 06 p0745 N88-14580
Report of the first session of the International Working Group on Data Management for the Global Precipitation Climatology project
[WCP-132] 06 p0745 N88-14582
The global climate system: Autumn 1984 to spring 1986
[CSM-R84/86] 06 p0745 N88-14583
Recent Colorado State University tropical cyclone research c* interest to forecasters
[AD-A185996] 07 p0879 N88-15332
Annual data summary and climatological evaluation, CERC (Coastal Engineering Research Center) field research facility, 1985, volume 2, appendix C
[AD-A185894] 07 p0881 N88-15344
Greatest volcanic eruptions in world during 17th-18th centuries and weather anomalies in Eurasian middle latitudes 08 p1012 N88-16134
Synoptic perturbations and climate
08 p1016 N88-16158
Characteristics and climatic relevance of the atmospheric aerosol components
08 p1017 N88-16164

Parameterization of radiative transfer in the Earth's atmosphere with specific applications to clouds
10 p1353 N88-18087
Optimal sampling to provide user-specific climate information 11 p1515 N88-19051
An investigation of terrain related variables for predicting the multipath fade depth distribution on terrestrial microwave lines 12 p1615 N88-19654
Refractive index, meteorology and fading in line-of-sight transmission paths 12 p1616 N88-19666
Worldwide distributions of shipboard surface meteorological observations for EM propagation analysis
[AD-A188771] 12 p1648 N88-19871
Predictions and studies with a one-dimensional ice/ocean model
[AD-A189158] 13 p1803 N88-20776
The World Climate Research Program
14 p1935 N88-21538
Observational and theoretical studies of greenhouse climate effects
[DE88-006237] 14 p1948 N88-21621
Seasonal variation for structural strength value
[PB88-169248] 16 p2222 N88-23260
Nonlinear normal mode initialization of the NCAR (National Center for Atmospheric Research) CCM (Community Climate Model)
[PB88-171814] 16 p2235 N88-23347
Our climate in danger
[DE88-701824] 20 p2822 N88-26743
Circulation statistics from seasonal and perpetual January and July simulations with the NCAR (National Center for Atmospheric Research) Community Climate Model (CCM1):R15
[PB88-192620] 20 p2823 N88-26748
Vegetation studies on Vandenberg Air Force Base, California
[NASA-TM-100985] 20 p2831 N88-26795
Proceedings of the Twelfth Annual Climate Diagnostics Workshop
[PB88-191747] 22 p3119 N88-28534
Prolonged periods of above-normal temperatures in Canada, 1986/87 22 p3120 N88-28538
Modes of interannual climate variability and Sahel rainfall anomalies 22 p3121 N88-28547
Simulation studies of the influence of sea-surface temperature anomalies on the Sahelian circulation and rainfall 22 p3122 N88-28553
Low frequency variability of SST and its relationship to atmospheric forcing 22 p3122 N88-28554
Persistence of North Pacific Sea surface temperature and atmospheric flow patterns 22 p3123 N88-28559
The relationship between polar sea ice and the position of the near equatorial convergence zone
22 p3123 N88-28563
Evaluation of global data sets for climate studies
22 p3124 N88-28569
Differences in radiation budget parameters over Asia in relation to contrasting Indian monsoons
22 p3125 N88-28574
Extratropical response to tropical heating as a function of period of model integrations
22 p3125 N88-28577
On climate prediction for India
22 p3127 N88-28590
Characteristics of regression equations for specifying monthly precipitation amounts over the United States from the field of concurrent mean 700 mb heights
22 p3127 N88-28591
Regional environmental studies using national data bases and GIS (Geographic Information System)
[DE88-008368] 23 p3230 N88-29225
Regional intercomparisons of General Circulation Model predictions and historical climate data: CO2
[DE88-010416] 23 p3235 N88-29248
Activities report of the World Meteorological Organization
[WMO-689] 24 p3404 N88-30265

CLIMATE CHANGE
Master index for the carbon dioxide research state-of-the-art report series
[DE87-012757] 01 p0072 N88-10459
Global environmental change research
[S-HRG-100-301] 03 p0348 N88-12199
On regime selection in global atmospheric flow
17 p2374 N88-24119
Geophysical monitoring for climatic change, number 15
[PB88-180146] 19 p2692 N88-26003

CLIMATOLOGY
NT MICROCLIMATOLOGY
NT PALEOCLIMATOLOGY
Venusian surface and crust 01 p0010 N88-10054
Cloud climatology derived from the AFGWC (Air Force Global Weather Central) 3D-nephanalysis for January and July 1979
[AD-A183686] 01 p0070 N88-10446
Documentation of NCAR (National Center for Atmospheric Research) CCM1 program modules
[PB87-213567] 03 p0352 N88-12220
Ocean model processor for climate studies
[PB87-224713] 03 p0353 N88-12226
Inventory of weather stations. Climatological data from Dutch stations, no. 26
[KNMI-150-26] 05 p0628 N88-13841
New method of estimating continentality of climate on global scale 06 p0725 N88-14460
Interpretation of our present terrestrial climatic record
[DE88-000223] 06 p0744 N88-14573
An Earth radiation budget climate model
[NASA-CR-182368] 06 p0744 N88-14578
CTD/02 measurements during 1984 and 1985 as part of the Equatorial Pacific Ocean Climate Studies (EPOCS)
[PB88-102082] 06 p0748 N88-14600
Recent Colorado State University tropical cyclone research of interest to forecasters
[AD-A185996] 07 p0879 N88-15332
Objective prediction of monthly mean surface temperature and climatological relationships to mid-tropospheric heights
[DE88-000908] 07 p0880 N88-15340
Annual data summary and climatological evaluation, CERC (Coastal Engineering Research Center) field research facility, 1985, volume 2, appendix C
[AD-A185894] 07 p0881 N88-15344
Research work at the Meteorological Institute of the University of Munich (Federal Republic of Germany)
[MITT-56] 08 p1013 N88-16141
Research project on CO-induced climate change
[DE88-002352] 08 p1023 N88-16193
Hurricane climatology for the Atlantic and Gulf coasts of the United States
[PB88-114657] 08 p1039 N88-16288
Annual data summary and climatological evaluation CERC (Coastal Engineering Research Center) field research facility, 1985. Volume 1. Main text and appendixes A and B
[AD-A186442] 08 p1039 N88-16289
Revised uniform summary of surface weather observations. Parts A-F: Carswell AFB, Texas
[AD-A186820] 09 p1192 N88-17144
US Navy climatic study of the Mediterranean Sea
[AD-A188264] 10 p1356 N88-18107
Moscow USSR. Limited surface observations climatic summary (LISOCS), parts A-F
[AD-A188080] 11 p1514 N88-19046
Wind energy resource survey of New Zealand: National resource assessment
[PB88-139365] 12 p1640 N88-19822
A paper on horizontal deformation in the frontogenesis in south Brazil
[INPE-4469-TDL/322] 12 p1647 N88-19867
JPRS report: Science and technology. USSR: Earth sciences
[JPRS-UES-88-001] 13 p1784 N88-20674
Sample models of steady and low frequency circulations in the tropical atmosphere, with application to tropical air-sea interactions 13 p1801 N88-20764
Predictions and studies with a one-dimensional ice/ocean model
[AD-A189158] 13 p1803 N88-20776
Climatology and space observations
[ISBN-2-85-428179-9] 14 p1935 N88-21536
Space projects for the 90's relevant to climatology
14 p1935 N88-21539
The atmosphere as a component of the climate system: Structure and variability 14 p1935 N88-21540
The Earth radiation budget and its spatial and temporal variations 14 p1936 N88-21548
The role of radiation transfer in climate modification
14 p1936 N88-21549
Satellite retrieval of cloud cover parameters and the International Satellite Cloud Climatology Program (ISCCP) 14 p1937 N88-21552
Continental surface processes and water cycle
14 p1937 N88-21555
The International Satellite Land-Surface Climatology Project (ISLSCP) 14 p1937 N88-21558
Hydrological models 14 p1937 N88-21559
The Hapex-Mobilhy program 14 p1938 N88-21560
Climatic summaries of ocean weather stations
[PB88-162920] 14 p1948 N88-21617
Current velocity and hydrographic observations in the Straits of Florida, the Caribbean Sea and offshore of the Antillean Archipelago: Subtropical Atlantic Climate Studies (STACS) 1986
[PB88-160767] 14 p1951 N88-21628
CTD/O2 data collected in 1985 and 1986 for EPOCS (Equatorial Pacific Ocean Climate Studies)
[PB88-160775] 14 p1951 N88-21629
A multivariate variational objective analysis-assimilation method. Part 1: Development of the basic model
[NASA-CR-182651] 15 p2097 N88-22491
Monthly mean global climatology of temperature, wind, geopotential height, and pressure for 0 - 120 km
[NASA-TM-100697] 15 p2099 N88-22503
NOAA-ERL-ARL (National Oceanic and Atmospheric Administration-Environmental Research Laboratories-Air Resources Laboratory) solar UV radiation and climate research project: Program description
[PB88-169396] 16 p2233 N88-23339
Understanding CO2 and climate
[PB88-167655] 16 p2234 N88-23341
Outline of the GPCP strategy
17 p2351 N88-24007
Research and Technology, 1987, Goddard Space Flight Center
[NAS 1.15:101097] 17 p2453 N88-24572
Territorial management program
19 p2682 N88-25942
A glossary for carbon dioxide and climate
[DE88-007885] 19 p2689 N88-25982
Last spring frosts and first autumn frosts in Finland
[FMI-8] 19 p2693 N88-26008
Verification of regional climates of GISS GCM. Part 1: Winter
[NASA-TM-100695] 19 p2694 N88-26012
An efficient model for changes of global climate and composition of the atmosphere due to human activities
[ETN-88-92359] 20 p2827 N88-26775
Evaluation of surface energy and radiation balance systems for FIFE
[NASA-CR-183118] 20 p2828 N88-26778
Development of radiation and cloud parameterization programs for AFGL (Air Force Geophysics Laboratory) global models
[AD-A193369] 21 p2973 N88-27658
Air-sea interaction in the vicinity of a land-sea boundary in the presence of upwelling 21 p2973 N88-27661
Intercomparison of NMC (National Meteorological Center) and ECMWF (European Centre for Medium Range Weather Forecasts) global analyses: 1980-1986
[PB88-196548] 21 p2974 N88-27668
Surface energy balance of three general circulation models: Current climate and response to increasing atmospheric CO2
[DE88-010967] 21 p2975 N88-27673
Space shuttle natural environment analysis
[NASA-CR-179337] 21 p2976 N88-27676
Proceedings of the Twelfth Annual Climate Diagnostics Workshop
[PB88-191747] 22 p3119 N88-28534
Climatology of various synoptic systems over the tropical North Pacific 22 p3121 N88-28542
Aspects of the 30-60 day oscillation in a GCM simulation 22 p3121 N88-28545
Evaluation of global data sets for climate studies
22 p3124 N88-28569
A method to adjust climatological time series for discontinuous inhomogeneities
22 p3124 N88-28570
Urbanization: Its detection and effect in the United States climate record 22 p3125 N88-28571
Systematic behavior of NMC medium range forecasts and the effect of model changes 1985-87
22 p3125 N88-28575
The impact of the El Nino event on the ECMWF model performance 22 p3125 N88-28576
DERF forecasts of thickness
22 p3126 N88-28579
Experimental 30-day forecasts from several spectral general circulation models 22 p3126 N88-28582
Dependence of medium range forecast errors upon the large-scale initial state 22 p3126 N88-28585
On climate prediction for India
22 p3127 N88-28590
Meteorological features during the marginal ice zone experiment from 20 March to 10 April 1987
[AD-A193960] 23 p3235 N88-29251
Episodic vs. epochal release of SO2 on Mars
23 p3305 N88-29688
Energy budget and ground temperatures in hot regions
[AD-A196298] 24 p3404 N88-30268

CLIMBING FLIGHT
Improvement of head-up display standards. Volume 2: Evaluation of head-up displays to enhance unusual attitude recovery
[AD-A194601] 23 p3178 N88-28921

CLINICAL MEDICINE
JPRS report: Science and technology. USSR: Life sciences
[JPRS-ULS-87-012] 03 p0355 N88-12238
JPRS report: Science and technology. USSR: Life sciences
[JPRS-ULS-87-009] 04 p0473 N88-12915

An assessment of clinical chemical sensing technology for potential use in space station health maintenance facility
[NASA-CR-172013] 04 p0475 N88-12926
JPRS report: Science and technology. USSR: Life sciences
[JPRS-ULS-87-013] 06 p0750 N88-14608
Diagnostic value of some load tests in evaluation of nonspecific electrocardiographic changes 07 p0895 N88-15426
Preliminary evaluation of a micro-based repeated measures testing system
[NASA-CR-172038] 08 p1048 N88-16331
Relationships between coronary heart disease risk factors and serum ionized calcium in Kennedy Space Center Cohort
[NASA-TM-100979] 10 p1368 N88-18177
Basic results of medical studies during prolonged manned flights on-board the Salyut-7/Soyuz-T orbital complex
[NASA-TT-20217] 10 p1369 N88-18182
Minutes of the meeting of the Indo-US Subcommission on Science and Technology (8th) held at Washington, D.C. on September 22-24, 1986
[PB88-130158] 10 p1423 N88-18503
Full scale architectural simulation techniques for space stations 12 p1651 N88-19887
Technology '87: Research and Development Laboratory Technology Transfer Program
[DE88-003142] 13 p1852 N88-21084
Lasers: Invention to application
[PB88-161583] 14 p1914 N88-21436
Clinical measurements using fiber optic sensors
[DE88-005624] 15 p2134 N88-22731
Clinical applications of computerized thermography 17 p2330 N88-23915
Design considerations for the development of an implantable sensor for the continuous measurement of glucose in the diabetic patient 17 p2382 N88-24159
Vanderbilt free electron laser project in biomedical and materials research
[AD-A195961] 24 p3378 N88-30121

CLOCKS
NT ATOMIC CLOCKS
The navigation experiment NAVEX: Experimental results of clock synchronization
[DFVLR-MITT-87-05] 03 p0271 N88-11701
Ultra-low power digital filter
[AD-A184485] 03 p0310 N88-11959
On real-time systems using local area networks
[AD-A185475] 06 p0694 N88-14256
Timing variation in dual loop benchmarks
[AD-A185697] 06 p0707 N88-14338
The navigation experment NAVEX: Experimental results of clock synchronization
[ESA-TT-1084] 09 p1132 N88-16791
VAXELN experimentation: Programming a real-time clock and interrupt handling using VAXELN Ada 1.1
[AD-A188100] 11 p1525 N88-19107
A survey of provably correct fault-tolerant clock synchronization techniques
[NASA-TM-100553] 13 p1823 N88-20894
An investigation of a distributed clock for local area networks with ring topology 18 p2516 N88-24924

CLOSED BASINS
U STRUCTURAL BASINS

CLOSED CYCLES
A comparison of open and closed multimegawatt space power and weapon systems
[DE87-012975] 01 p0089 N88-10579
A cold ejector for closed-cycle helium refrigerators 04 p0434 N88-12690
Traveling-wave maser closed-cycle refrigerator data acquisition and display system 04 p0437 N88-12708
Design features of small Brayton cycles for autonomous underwater vehicles
[AD-A187799] 11 p1506 N88-18999
Analysis of closed cycle megawatt class space power systems with nuclear reactor heat sources 17 p2413 N88-24351
Comparison of open and closed multimegawatt space power systems 17 p2414 N88-24353
Characteristics of the closed Brayton cycle for dynamic isotope power systems 17 p2422 N88-24401
Design of catalytic monoliths for closed-cycle carbon dioxide lasers
[NASA-CR-182983] 18 p2558 N88-25185
Analysis of a closed-kinematic chain robot manipulator
[NASA-CR-183031] 18 p2561 N88-25206
C-CAMP: A closed cycle alkali metal power system
[DE88-009715] 19 p2688 N88-25975
CryoSQUID: A SQUID-based magnetic field sensor
[AD-A194237] 23 p3239 N88-29275

CLOSED ECOLOGICAL SYSTEMS
Aquarack: Aims and Possible Research Projects
[DFVLR-MITT-87-01] 01 p0073 N88-10469
The Aquarack as a potential instrument for basic research work in space biology: Inventory and scientific dispositions 01 p0073 N88-10470
The usefulness of microalgal structures as an element of closed ecological systems like Aquarack and CELSS --- Controlled Ecological Life Support System (CELSS) 01 p0074 N88-10476
Catalytic processes for space station waste conversion
[NASA-CR-177423] 01 p0077 N88-10491
Environmental life support system technology study --- space flight
[ESA-CR(P)-2432] 02 p0218 N88-11371
Controlled Ecological Life Support System: Regenerative Life Support Systems in Space
[NASA-CP-2480] 03 p0357 N88-12251
Progress in European CELSS activities 03 p0358 N88-12252
Food production and gas exchange system using blue-green alga (spirulina) for CELSS 03 p0358 N88-12253
Biomass recycle as a means to improve the energy efficiency of CELSS algal culture systems 03 p0358 N88-12254
Operation of an experimental algal gas exchanger for use in a CELSS 03 p0358 N88-12255
Non-conventional approaches to food processing in CELSS, 1. Algal proteins: Characterization and process optimization 03 p0358 N88-12256
Application of photosynthetic N(2)-fixing cyanobacteria to the CELSS program 03 p0358 N88-12257
Sunlight supply and gas exchange systems in microalgal bioreactor 03 p0359 N88-12258
A review of recent activities in the NASA CELSS program 03 p0359 N88-12259
A modular BLSS simulation model 03 p0359 N88-12260
Preliminary experimental results of gas recycling subsystems except carbon dioxide concentration 03 p0359 N88-12261
Fundamental study on gas monitoring in CELSS 03 p0359 N88-12263
The applicability of the catalytic wet-oxidation to CELSS 03 p0360 N88-12264
A large-scale perspective on ecosystems 03 p0360 N88-12265
Design of an elemental analysis system for CELSS research 03 p0360 N88-12266
An overview of Japanese CELSS research activities 03 p0360 N88-12267
Utilization of potatoes in bioregenerative life support systems 03 p0360 N88-12269
Wheat production in controlled environments
[UAES-PAPER-3324] 03 p0361 N88-12270
The effect of radiation on the long term productivity of a plant based CELSS 03 p0361 N88-12271
Mass balances for a biological life support system simulation model 03 p0361 N88-12272
Controlled Ecological Life Support System. Design, Development, and Use of a Ground-Based Plant Growth Module
[NASA-CP-2479] 05 p0630 N88-13852
CELSS Program Meeting 05 p0630 N88-13853
Controlled ecological life support systems: Development of a plant growth module 05 p0630 N88-13854
Plant Growth Module (PGM) conceptual design 05 p0631 N88-13855
Controlled Ecological Life Support Systems (CELSS) conceptual design option study
[NASA-CR-177421] 06 p0754 N88-14625
Controlled Ecological Life Support Systems (CELSS) physiochemical waste management systems evaluation
[NASA-CR-177422] 06 p0754 N88-14626
Modeling the growth dynamics of four candidate crops for Controlled Ecological Life Support Systems (CELSS) 06 p0799 N88-14889
Space station accommodations for life sciences research facilities. Phase 1: Conceptual design and programmatics studies for Missions SAAX0307, SAAX0302 and the transition from SAAX0307 to SAAX0302. Volume 2: Study results
[NASA-CR-179244] 08 p0962 N88-15829
Electrochemical carbon dioxide concentrator subsystem development
[NASA-CR-177411] 08 p1053 N88-16353
Design concepts for bioreactors in space 09 p1198 N88-17179
Kinetic toxic aspect of potential use of sulfur hexafluoride in closed environments 10 p1362 N88-18142
Ecological algal system in microgravity conditions: Preliminary results 12 p1655 N88-19915
Closed system physiology: Role of oxygen in the development of wheat 12 p1655 N88-19916
Regenerative life support system research
[NASA-CR-182606] 12 p1671 N88-20006

CLOSED FAULTS
U GEOLOGICAL FAULTS

CLOSED LOOP SYSTEMS
U FEEDBACK CONTROL

CLOSING
New concepts for high current self-sustained diffuse discharge closing switches
[DE87-011678] 01 p0040 N88-10252

CLOSURE LAW
Homogeneous turbulence two-point closures and applications to one-point closures 03 p0312 N88-11973
Reynold stress closure in jet flows using wave models
[NASA-CR-182662] 12 p1628 N88-19741
EDQNM closure: A homogeneous simulation to support it. A quasi-homogeneous simulation to disprove it 16 p2195 N88-23091
Angular distribution of turbulence in wave space 16 p2195 N88-23093
Study of one-dimensional spectral dynamic equations of the Reynolds stresses in homogeneous anisotropic turbulence: Application to split-spectrum modeling 16 p2196 N88-23095
Reynolds stress models of homogeneous turbulence 16 p2197 N88-23106

CLOSURES
Conditional second order closure for turbulent shear flows
[AD-A185369] 05 p0581 N88-13542
Quick actuating closure and handling system 14 p1925 N88-21476
Development of a more general Reynolds stress closure for swirling flow
[AD-A195121] 24 p3374 N88-30092
Syntactic closures
[AD-A195921] 24 p3412 N88-30311

CLOTH
U FABRICS

CLOTHING
NT EXTRAVEHICULAR MOBILITY UNITS
NT FLIGHT CLOTHING
NT GLOVES
NT GOGGLES
NT PRESSURE SUITS
NT PROTECTIVE CLOTHING
NT SPACE SUITS
Loss of performance due to military clothing and equipment
[IZF-1986-13] 01 p0077 N88-10490
An investigation of some basic properties of hybrid composite materials
[AD-A194136] 23 p3189 N88-28975

CLOUD CHAMBERS
Microgravity nucleation and particle coagulation experiments support
[NASA-CR-181540] 04 p0423 N88-12618
The technical evolution of the Wilson camera: The beginnings (1895-1925)
[NOTA-INTERNA-876] 05 p0585 N88-13568

CLOUD COVER
Cloud climatology derived from the AFGWC (Air Force Global Weather Central) 3D-nephanalysis for January and July 1979
[AD-A183686] 01 p0070 N88-10446
GOES observations for the FIRE/SRB Wisconsin experiment region from October 11 through November 2, 1986
[NASA-TM-100485] 01 p0071 N88-10453
Operational cloud-clearing techniques of VAS radiance data --- Visible and Infrared Spin Scan Radiometer Atmospheric Sounder (VAS) 02 p0201 N88-11256
The impact on short-term precipitation forecast skill of time-dependent lateral and lower boundary conditions within a meso-beta numerical cloud prediction model 02 p0211 N88-11327
Development of the SPOT commercial service: Preliminary conclusions after six months of operations 03 p0340 N88-12144
Cloud cover determination in polar regions from satellite imagery
[NASA-CR-181544] 04 p0471 N88-12908
Mesoscale applications of high resolution imagery
[AD-A185039] 05 p0627 N88-13833
Modeling cloudy and clear interval length probabilities using space shuttle imagery
[AD-A185290] 05 p0627 N88-13837
Automated satellite cloud analysis: A multispectral approach to the problem of snow/cloud discrimination
[AD-A185672] 06 p0746 N88-14591
Application of satellite data in observational and theoretical studies of the evolving structure of baroclinic waves
[NASA-CR-179277] 10 p1354 N88-18091
General determination of Earth surface type and cloud amount using multispectral AVHRR data
[NOAA-TR-NESDIS-39] 11 p1506 N88-18997

Homogenizing surface and satellite observations of cloud. Aspects of bias in surface data
[AD-A188523] 12 p1648 N88-19869
Satellite estimations of the solar radiation flux at the surface 14 p1936 N88-21551
Satellite retrieval of cloud cover parameters and the International Satellite Cloud Climatology Program (ISCCP) 14 p1937 N88-21552
Revised Uniform Summary of Surface Weather Observations, Loring AFB, Maine, Parts A - F
[AD-A188201] 14 p1947 N88-21610
Some models for rain and cloud attenuation of millimeter waves
[PB88-160809] 14 p1948 N88-21616
The collection of statistics on the frequency of cloud cover over North America
[AD-A190456] 15 p2097 N88-22495
Use of energy emission for detecting the necessity of irrigation in wheat in field conditions
[INPE-4461-TDL/318] 16 p2229 N88-23315
Comparison of the solar radiation estimation method by satellites 17 p2360 N88-24055
Restrictions in activity monitoring through remote sensing 17 p2365 N88-24084
Cloud cover determination in polar regions from satellite imagery
[NASA-CR-182906] 17 p2375 N88-24123
Development of radiation and cloud parameterization programs for AFGL (Air Force Geophysics Laboratory) global models
[AD-A193369] 21 p2973 N88-27658
The collection of statistics on the frequency of cloud cover over North America
[AD-A193093] 21 p2974 N88-27667
A system for determination of wind fields from cloud tracks: INPE experiment
[INPE-4492-PRE/1256] 22 p3128 N88-28594

CLOUD DISPERSAL
Numerical simulation of near-surface environments and particulate clouds generated by large-area fires
[AD-A188375] 12 p1641 N88-19828

CLOUD GLACIATION
Conception and discussion of a model describing ice formation on various obstacles
[ONERA-NT-1986-6] 01 p0072 N88-10460
The dependence of the normalized ice accretion thickness on cloud-physical parameters
[DFVLR-FB-87-08] 01 p0072 N88-10464
Obtaining information on cloud particles by a commercial miniature camera
[DFVLR-MITT-87-19] 16 p2234 N88-23342
Standardized ice accretion thickness as a function of cloud physics parameters
[ESA-TT-1080] 16 p2234 N88-23346
Experimental measurements of heat transfer from an iced surface during artificial and natural cloud icing conditions
[AIAA-PAPER-86-1352] 17 p2293 N88-23718

CLOUD HEIGHT INDICATORS
Determination of cloud base height and emissivity from downwelling angular radiances
[AD-A185985] 07 p0879 N88-15331
The visioceilometer and its tactical applications
[AD-A188216] 12 p1647 N88-19866

CLOUD PHOTOGRAPHY
The importance of mesoscale waves in the upper troposphere for formation of cloud and precipitation areas 02 p0203 N88-11273
Report of the International Satellite Cloud Climatology Project (ISCCP) workshop on cloud algorithms in the polar regions
[WCP-131] 06 p0745 N88-14581
Meteosat tracks Karman vortex streets in the atmosphere 09 p1128 N88-16770
Obtaining information on cloud particles by a commercial miniature camera
[DFVLR-MITT-87-19] 16 p2234 N88-23342
Enhanced infra-red picture of LR-FAX for spring and autumn seasons 17 p2351 N88-24011

CLOUD PHYSICS
The dependence of the normalized ice accretion thickness on cloud-physical parameters
[DFVLR-FB-87-08] 01 p0072 N88-10464
Structure and modification of winter mountain clouds in the Sierra Nevada: Nowcasting/forecasting the onset of supercooled liquid water 02 p0202 N88-11263
Detailed analysis of a mesoscale convective complex situation in the Carpathian Basin (Europe) 02 p0207 N88-11296
Effects of the large scale motion and horizontal inhomogeneity of the moist static instability on development of the mesoscale convective systems in the midlatitudes 02 p0207 N88-11297
Cumulus and thunderstorm initiation by mountains 02 p0207 N88-11301
The impact on short-term precipitation forecast skill of time-dependent lateral and lower boundary conditions within a meso-beta numerical cloud prediction model 02 p0211 N88-11327
Definition and use of sensors for measuring electrical conductivity in thunderclouds
[ESA-TT-1047] 03 p0352 N88-12222
Study of isolated convective clouds in the lower Alps in summer 1984, using radar and a simple Weinstein numerical model
[ESA-TT-1061] 03 p0353 N88-12224
Computer modeling aids studies of precipitation formation 04 p0458 N88-12832
The application of doubly-truncated hydrometeor distributions to numerical cloud models
[AD-A185273] 05 p0627 N88-13836
Report of the International Satellite Cloud Climatology Project (ISCCP) workshop on cloud algorithms in the polar regions
[WCP-131] 06 p0745 N88-14581
Automated satellite cloud analysis: A multispectral approach to the problem of snow/cloud discrimination
[AD-A185672] 06 p0746 N88-14591
Thunderstorms with snow: A comprehensive, empirical study of their occurrence, development and structure
[AD-A185929] 07 p0879 N88-15329
Anthropogenic effects on the droplet formation process, and ion concentrations in droplets — clouds 08 p1018 N88-16175
Rocket experiments and payloads for Super CAMP — Cold Arctic Mesopause Project (CAMP) 08 p1034 N88-16271
Layered-capacitor method for dielectric bridge measurements. Algorithms for inversion and parameter fitting: Documentation, verification, data analysis
[PB88-131479] 11 p1505 N88-18989
Cloud physics studies in SCPP (Sierra Cooperative Pilot Project) from 1977-87
[PB88-136924] 11 p1516 N88-19054
Research and development to acquire and reduce melting layer cloud physics and evaluate a prototype M-meter
[AD-A188390] 12 p1648 N88-19873
Gas-chromatographic analysis of products of thermal reactions of aerosol in Venusian cloud layer on Vega-1 and Vega-2 automatic interplanetary stations 13 p1725 N88-20318
Bibliography of icing on aircraft (status 1987)
[DFVLR-MITT-87-18] 16 p2158 N88-22876
Standardized ice accretion thickness as a function of cloud physics parameters
[ESA-TT-1080] 16 p2234 N88-23346
Studies of the mechanisms and rates with which nitrogen species are incorporated into cloud water and precipitation
[PB88-193065] 20 p2826 N88-26764
Present status of artificial rain making
[DE88-701823] 20 p2826 N88-26769
Dynamic interaction of convective cumulus with large-scale environment
[MITT-55] 20 p2827 N88-26773
Cloud simulation warm cloud experiments: Droplet growth and aerosol scavenging
[AD-A192944] 21 p2974 N88-27666
Stratocumulus and cloud-free reflectance from multi-spectral satellite measurements
[AD-A193899] 22 p3128 N88-28599
Investigations on the entropy of cloudy air
[ESA-TT-1060] 23 p3234 N88-29245
An objective technique for Arctic cloud analysis using multispectral AVHRR (Advanced Very High Resolution Radiometer) satellite imagery
[AD-A194732] 23 p3235 N88-29250
Global vertical mass transport by clouds: A two-dimensional model study
[CM-74] 24 p3391 N88-30192
Microphysical processes in cloud layers of Venus 24 p3448 N88-30522

CLOUD SEEDING
Altered and enhanced iodargyrite with bismuth triiodide for use in precipitation enhancement operations
[AD-A185229] 05 p0561 N88-13419
AN-30M cloud-seeding airplane in international exhibition 06 p0725 N88-14456
Present status of artificial rain making
[DE88-701823] 20 p2826 N88-26769

CLOUDS
Aqueous-phase reactions in clouds
[DE88-005249] 01 p0069 N88-10445
A review of parameterizations of microphysical processes in clouds for application in models of regional atmospheric deposition
[DE88-000451] 04 p0471 N88-12909
Volcanic eruption detection with TOMS 05 p0618 N88-13793
Analysis of SO2 signals in SBUV/TOMS data 05 p0618 N88-13794
The determination of exhaust cloud dimensions from films of space shuttle launches
[NASA-CR-4103] 06 p0732 N88-14500
Mesoscale aerosol clouds 08 p1013 N88-16140
Three-dimensional trajectory analyses of two drop sizing instruments: PMS OAP and PMS FSSP
[NASA-CR-4113] 11 p1437 N88-18574
Numerical simulation of near-surface environments and particulate clouds generated by large-area fires
[AD-A188375] 12 p1641 N88-19828
Polar mesospheric cloud experiment
[AD-A188936] 12 p1648 N88-19872
Chemical composition and structure of Venusian clouds determined from results of roentgenoradiometric experiments carried out by landing modules of Vega-1 and Vega-2 automatic interplanetary stations 13 p1726 N88-20320
Determining chemical composition of aerosol in Venusian cloud layer on Vega-1 automatic interplanetary station using Malakhit mass spectrum analyzer 13 p1726 N88-20321
Synchronous measurements of effective photon path length in visible and near-IR spectral regions in real cloud systems 13 p1790 N88-20706
The spreading and mixing of dense gas clouds in still air
[KNMI-WR-87-12] 16 p2230 N88-23320
SAM 2 data user's guide
[NASA-RP-1200] 18 p2543 N88-25094
Overview of the PRECP (processing of emissions by clouds and precipitation) Program
[DE88-008205] 20 p2822 N88-26741
Studies of the mechanisms and rates with which nitrogen species are incorporated into cloud water and precipitation
[PB88-193065] 20 p2826 N88-26764
Cloud simulation warm cloud experiments: Droplet growth and aerosol scavenging
[AD-A192944] 21 p2974 N88-27666
Distribution of hydroxyl clouds in the galaxy
[DE88-702415] 22 p3164 N88-28844
On experiences with two hot-wire instruments for measuring the liquid water content in clouds
[ESA-TT-1085] 23 p3236 N88-29255

CLOUDS (METEOROLOGY)
NT ARC CLOUDS
NT BARIUM ION CLOUDS
NT CHEMICAL CLOUDS
NT CIRRUS CLOUDS
NT CONVECTION CLOUDS
NT CUMULUS CLOUDS
NT NOCTILUCENT CLOUDS
NT STRATOCUMULUS CLOUDS
NT STRATUS CLOUDS
Solar Energy Meteorological Research and Training Site, Alaska
[DE87-013706] 01 p0069 N88-10440
Airborne lidar studies of Arctic polar stratospheric clouds 01 p0069 N88-10443
Cloud climatology derived from the AFGWC (Air Force Global Weather Central) 3D-nephanalysis for January and July 1979
[AD-A183686] 01 p0070 N88-10446
Description of the Mountain Cloud Chemistry Program version of the PLUVIUS MOD 5.0 reactive storm simulation model
[DE87-012846] 01 p0070 N88-10450
The physics of charge separation preceding lightning strokes in thunderclouds
[NASA-CR-178371] 01 p0071 N88-10452
Estimation from satellite imagery of summertime rainfall over varied space and time scales
[PB87-203246] 01 p0071 N88-10454
Forecasting boundary layer clouds and fog: A review of operational numerical models 02 p0208 N88-11307
Measurements of vapor flux, liquid water contents, precipitation rates and riming in a Utah mountain cloud system
[PB87-224945] 04 p0469 N88-12900
Cloud cover determination in polar regions from satellite imagery
[NASA-CR-181544] 04 p0471 N88-12908
Tropical easterly jet located using TOMS data 05 p0616 N88-13783
BARS-1M meteorological complex carried on IL-18 airplane 06 p0725 N88-14458
Report of the International Satellite Cloud Climatology Project (ISCCP) workshop on cloud algorithms in the polar regions
[WCP-131] 06 p0745 N88-14581
Research project on CO-induced climate change
[DE88-002352] 08 p1023 N88-16193

Parameterization of radiative transfer in the Earth's atmosphere with specific applications to clouds
10 p1353 N88-18087
Homogenizing surface and satellite observations of cloud. Aspects of bias in surface data
[AD-A188523] 12 p1648 N88-19869
Martian Clouds Data Workshop
[NASA-CR-182431] 12 p1711 N88-20238
Analysis of spectral reflectance characteristics of targets under satellites and automatic cloud recognition
13 p1755 N88-20498
Local meteorological processes and air mass origin during a cloud chemical field experiment on Areskutan, Sweden, in summer 1986
[AP-28] 14 p1948 N88-21615
Latitudinal and seasonal variation of the cloud characteristic parameters and their effects on the cloud classification 17 p2351 N88-24005
A system for determination of wind fields using geostationary meterological satellites
17 p2360 N88-24056
The rate of volcanism on Venus
[NASA-CR-183039] 19 p2742 N88-26281
The patterns of tropical convection during the 1986-87 ENSO 22 p3120 N88-28537

CLUMPS
Simulation studies for surfaces and materials strength
[NASA-CR-181535] 04 p0412 N88-12557
Supersonic beam observations of semiconductor clusters
[AD-A184991] 05 p0655 N88-14018
Clusters of transition metal atoms
[AD-A191265] 16 p2270 N88-23579
Submillimeter and far infrared line observations of M17 SW: A clumpy molecular cloud penetrated by UV radiation
[NASA-CR-182866] 16 p2288 N88-23701

CLUSTER ANALYSIS
Clustering by means of medoids
[REPT-87-03] 01 p0085 N88-10551
Annotated computer output for illustrative examples of clustering using the mixture method and two comparable methods from SAS
[AD-A184687] 03 p0364 N88-12292
Simulation of the layer-growth dynamics in silver films: Dynamics of adatom clusters and vacancy clusters on Ag(100)
[DE87-014764] 03 p0380 N88-12390
A study of the free energy of the Lenz-Ising model using the cluster variation method of Morita
[AD-A186023] 08 p1073 N88-16476
Environmental gradient analysis, ordination, and classification in environmental impact assessments
[AD-A187294] 11 p1509 N88-19016
The coordination cluster theory for metallic solutions
[DE88-005934] 13 p1738 N88-20389
A likelihood based grouping method for multidimensional observations. An interactive method used on large transportation data bases
[REPT-87-74] 16 p2286 N88-23685
Cluster analysis of multiple planetary flow regimes
[NASA-CR-182931] 18 p2594 N88-25418
Tuning a major part of a clustering algorithm
[AD-A191446] 20 p2836 N88-26821
Mutually exclusive alternatives by clustering
[DE88-007707] 20 p2882 N88-27115
To the opportunities of cluster analysis of light curves of supernovae
[DE88-701642] 21 p3030 N88-27982

CLUSTERS
Physics and chemistry 07 p0883 N88-15359
Transition metal cluster chemistry
[AD-A188731] 13 p1740 N88-20405

CLUTTER
Detection of targets in the presence of clutter using target echo modulations caused by rotating structures
[REPT-12-86] 01 p0036 N88-10231
Theory of displaced phase center antenna for space based radar applications
[PB87-229837] 06 p0690 N88-14227
Active and passive remote sensing of ice
[AD-A186685] 09 p1195 N88-17162
Radar backscatter from airports and surrounding areas 10 p1274 N88-17623
Radar returns from ground clutter in vicinity of airports
10 p1274 N88-17624
The maximum entropy method for the analysis of radar echoes from hovering helicopters in clutter
[FB-2-87] 11 p1475 N88-18799
Ground clutter processing for wind measurements with airport surveillance radars
[AD-A187708] 11 p1514 N88-19044
Computation of LMS (Least-Mean-Square) and matched digital filters for optical clutter suppression
[AD-A188885] 12 p1687 N88-20093
Signal-filter design and system performance for polarimetric radar
[AD-A189257] 13 p1758 N88-20514
A preliminary assessment of thunderstorm outflow wind measurement with airport surveillance radars
[AD-A189064] 13 p1799 N88-20757
Analysis, suppression of land clutter characteristics reported 14 p1903 N88-21369
The effects of better environmental inputs in estimating sea clutter
[AD-A192058] 19 p2643 N88-25678
Multi-target tracking algorithms for cluttered environments 20 p2789 N88-26543
Method and apparatus for measuring distance
[NASA-CASE-MSC-20912-1] 20 p2793 N88-26568
Rivista Tecnica Selenia, volume 10, no. 3, 1987
[ETN-88-92717] 22 p3068 N88-28210
Non-Gaussian models for surface clutter
22 p3068 N88-28212
The effect of equatorial ionospheric irregularities on the performance of a south-looking OTH-B (Over-The-Horizon-Backscatter) radar
[AD-A195090] 24 p3362 N88-30018

CMOS
Integrated circuit design
[AD-A184486] 03 p0311 N88-11960
Dramatically improved radiation hardness for CMOS silicon gate integrated circuits even down to cryogenic temperatures
[AD-A184672] 03 p0381 N88-12398
A study of charged particles/radiation damage to VLSI device materials
[NASA-CR-172036] 05 p0577 N88-13518
New breakthrough in Chinese integrated circuits: Successful development of high-speed CMOS circuits
[AD-A185381] 05 p0578 N88-13525
Effect of the gate oxide thickness on the speed of MOS integrated circuits
[PB88-155783] 10 p1323 N88-17910
Latent failures and coverage in fault-tolerant systems. A VLSI CMOS circuit design technique to aid test generation
[AD-A187615] 10 p1325 N88-17921
High density CMOS technology
11 p1561 N88-19342
Shorts in self-checking circuits
[RR-657-I] 14 p1908 N88-21402
An optimal CMOS structure for the design of a cell library
[EUT-87-E-166] 14 p1985 N88-21841
French Multiproject Chip (MPC) activity report, 1986
[RR-650-I] 15 p2059 N88-22273
Design of the Detector 2: A CMOS gate array for the study of concurrent error detection techniques
[AD-A191247] 16 p2193 N88-23079
Microelectronics the next fifteen years
17 p2305 N88-23792
Joint services electronics program
[AD-A190239] 18 p2503 N88-24848
Hot carrier effects in CMOS field effect transistors at cryogenic temperatures 19 p2662 N88-25829
Silver multi-layers for planar Ag/AgCl reference electrodes 19 p2672 N88-25883
Rule-based circuit optimization for CMOS VLSI
22 p3137 N88-28649
The p-well or n-well CMOS technology for advanced SEU-hard SRAMs
[DE88-006845] 22 p3156 N88-28777
The effects of total dose on the SEU sensitivity of CMOS static RAMS --- single event upset (SEU), satellite components
[AERE-R-12779] 24 p3428 N88-30401
A system study with an infrared sensitive microelectronic image sensor
[FOA-C-30481-3.1] 24 p3429 N88-30407

CN EMISSION
JHK photometry of CN-rich field giants
04 p0516 N88-13175

COAGULATION
NT BLOOD COAGULATION
Coagulation in stirred tanks
[B8711373] 05 p0562 N88-13420
Astrophysics and the solar nebula
07 p0883 N88-15355
Molecular composites processing and properties, 1
[AD-A194113] 23 p3189 N88-28974

COAL
Production of jet fuels from coal derived liquids. Volume 1: Market assessment for liquid by-products from the Great Plains gasification plant
[AD-A184846] 05 p0570 N88-13475
Application of inverse gas chromatography to fluidity studies
[DE88-002896] 10 p1296 N88-17750
High-density jet fuels from coal syncrudes, appendix 4
[DE88-003132] 10 p1307 N88-17813
The role of repowering in America's power generation future
[DOE/FE-0096] 10 p1351 N88-18076
Character of five selected LANDSAT lineaments in southwestern Pennsylvania: Report of investigations, 1987
[PB88-133517] 11 p1505 N88-18988
Coal particle behaviour in a counter-current combustor
[TAE-606] 19 p2612 N88-25498
Experiments on densely-loaded non-Newtonian slurries in laminar and turbulent pipe flows
[DE88-010579] 20 p2800 N88-26612

COAL DERIVED LIQUIDS
Production of jet fuels from coal derived liquids. Volume 1: Market assessment for liquid by-products from the Great Plains gasification plant
[AD-A184846] 05 p0570 N88-13475
Development and evaluation of supercritical fluid chromatography-mass spectrometry
[DE88-005122] 13 p1738 N88-20394

COAL GASIFICATION
Low temperature reactivity of chars towards oxygen, appendix E2
[DE88-004088] 10 p1298 N88-17760

COAL LIQUEFACTION
High-density jet fuels from coal syncrudes, appendix 4
[DE88-003132] 10 p1307 N88-17813

COALESCENCE
U COALESCING

COALESCING
Atmospheric science 07 p0883 N88-15357
Loop coalescing: A compiler transformation for parallel machines
[DE88-003571] 10 p1392 N88-18307
Effects of irradiation on thermal coalescence of pores in real crystals
[DE88-701683] 16 p2282 N88-23663

COANDA EFFECT
Proceedings of the Circulation-Control Workshop, 1986
[NASA-CP-2432] 10 p1268 N88-17586
Design of supersonic Coanda jet nozzles
10 p1270 N88-17599

COARSENESS
Structure and grain coarsening during the processing of engineering ceramics
[NASA-TM-100235] 03 p0293 N88-11838

COASTAL CURRENTS
Current velocity and hydrographic observations in the Straits of Florida, the Caribbean Sea and offshore of the Antillean Archipelago: Subtropical Atlantic climate studies (STACS) 1984 and 1985
[PB88-149299] 12 p1649 N88-19874
The use of a barotropic finite element model for the study of circulation on the continental shelf of the southeast coast of Brazil
[INPE-4401-PRE/1218] 13 p1802 N88-20774
Influence of the Yukon River on the Bering Sea
[NASA-CR-182802] 17 p2376 N88-24126

COASTAL DUNES
U DUNES

COASTAL ECOLOGY
NOAA's (National Oceanic and Atmospheric Administration's) Northeast Monitoring Program (NEMP): A report on progress of the first five years (1979-84) and a plan for the future
[PB87-210100] 02 p0196 N88-11225
Contribution of SPOT data to the physiographic study of coastal environment: La Pointe d'Arcay and l'Anse de l'Aiguillon (France) 03 p0344 N88-12176
Mapping of the mangroves of the Guanabarra Bay through the utilization of remote sensing techniques
[INPE-3942-TDL/229] 12 p1637 N88-19804

COASTAL MARSHLANDS
U MARSHLANDS

COASTAL PLAINS
Use of SPOT images for coastal development and inventory of aquacultural sites in New Caledonia (ALIAS project). First results 03 p0344 N88-12175

COASTAL WATER
Satellite and synoptic studies of chemical fronts in the California current and coastal upwelling zone
[AD-A183909] 01 p0073 N88-10466
Coastal winds of the southeast Alaska Peninsula
[PB87-206173] 02 p0215 N88-11354
Marine minerals: Exploring our new ocean frontier
[PB87-217725] 02 p0216 N88-11364
Contribution of SPOT data to the physiographic study of coastal environment: La Pointe d'Arcay and l'Anse de l'Aiguillon (France) 03 p0344 N88-12176
Coastal dynamics of the mouth of the Saloum (Senegal) --- SPOT imagery 03 p0345 N88-12177
The use of chlorophyll fluorescence measurements from space for separating constituents of sea water. Volume 1: Summary
[ESA-CR(P)-2444-VOL-1] 07 p0873 N88-15294

The use of chlorophyll fluorescence measurements from space for separating constituents of sea water. Volume 2: Appendices
[ESA-CR(P)-2444-VOL-2] 07 p0873 N88-15295
An investigation of offshore circulation using satellite data and feature tracking techniques
[AD-A186271] 07 p0881 N88-15347
Biogeochemical cycling in the ocean. Part 1: Introduction to the effects of upwelling along the west coast of North America
[NASA-TM-88230] 07 p0882 N88-15349
Ocean colour applications in ocean dynamics and coastal processes 08 p1042 N88-16297
Circulation and exchange processes on the South Atlantic Bight Continental Shelf
[DE88-003330] 13 p1804 N88-20781
Mechanical properties of sea ice and sea ice deformation in the near-shore zone
[PB88-147889] 13 p1804 N88-20782
Mixed-layer fronts in the California current 13 p1805 N88-20794
Production and turnover of suspended organic detritus in the coastal water of the southeastern continental shelf
[DE88-005118] 14 p1951 N88-21631
Changes in the California current system observed off northern California during July-August 1986
[AD-A190027] 15 p2100 N88-22510
Numerical simulation of coastal upwelling phenomena in Cabo Frio (RJ) through a two layer finite element model
[INPE-4502-RPE/561] 16 p2237 N88-23361
Influence of the Yukon River on the Bering Sea
[NASA-CR-182602] 17 p2376 N88-24126
Contribution of spaceborne high resolution radiometers to mapping of precoastal depths 19 p2701 N88-26063
The monitoring of sediment transport, water circulation and mixing in estuaries and coastal waters 22 p3108 N88-28457
Evaluation of SPOT data for remote sensing of physical and biological properties of estuaries and coastal zones 22 p3108 N88-28458

COASTAL ZONE COLOR SCANNER
Update of NASA's ocean colour activities 08 p1042 N88-16295
NIMBUS-7 CZCS. Coastal Zone Color Scanner imagery for selected coastal regions. North America - Europe. South America - Africa - Antarctica. Level 2 photographic product
[NASA-CR-180755] 15 p2089 N88-22447

COASTS
A one-dimensional model of thermally-driven coastal front evolution 02 p0204 N88-11274
An hourly analysis, updating and short-range forecasting system --- numerical weather forecasting 02 p0206 N88-11288
Real-time evaluation and prediction of coastal dispersion near the SW tip of Africa --- effluents 02 p0210 N88-11318
Contribution of SPOT data to the physiographic study of coastal environment: La Pointe d'Arcay and l'Anse de l'Aiguillon (France) 03 p0344 N88-12176
Coastal dynamics of the mouth of the Saloum (Senegal) --- SPOT imagery 03 p0345 N88-12177
East coast gravity validation study
[AD-A184292] 03 p0351 N88-12217
Hurricane Elena storm surge data
[AD-A184573] 03 p0353 N88-12228
The development of low level coastal flow fields when solar radiation is blocked by smoke
[DE87-014348] 03 p0354 N88-12230
Varifront 3 expedition data report (USNS DE STEIGUER CRUISE 1202-82). Bioluminescence, hydrographic, nutrient, and satellite data from the Gulf of California (November-December 1981)
[AD-A185011] 05 p0620 N88-13805
Atmospheric diffusion at coastal site in presence of sea-breeze
[DE88-700038] 07 p0876 N88-15314
Hurricane climatology for the Atlantic and Gulf coasts of the United States
[PB88-114657] 08 p1039 N88-16288
Annual data summary and climatological evaluation CERC (Coastal Engineering Research Center) field research facility, 1985. Volume 1. Main text and appendixes A and B
[AD-A186442] 08 p1039 N88-16289
Nearshore wave transformation study of sites near Port Canaveral Inlet, Florida
[AD-A186965] 09 p1195 N88-17159
CTD observations in the coastal transition zone off northern California, 16-25 February 1987
[AD-A187283] 10 p1357 N88-18111
Numerical simulations of the California current: Filament formation as related to baroclinic instability
[AD-A187573] 10 p1358 N88-18115
A propagation campaign in a marine environment utilizing a digital system at 36 GHz 12 p1618 N88-19675
Relationships between remotely-sensed surface properties and subsurface structure in the ocean
[AD-A189317] 12 p1650 N88-19881
SPOT investigations of estuaries and coastal zones: An overview 22 p3107 N88-28455
The use of SPOT data in mapping coastal areas 22 p3108 N88-28461
Physiography and kinematics of the western coast of the province of Huelva (Andalousia, Spain) 22 p3109 N88-28465
Meteorological features during the marginal ice zone experiment from 20 March to 10 April 1987
[AD-A193960] 23 p3235 N88-29251
Doppler radar analysis of coastal marine atmospheric boundary layer structure during a cold air outbreak
[AD-A196023] 24 p3403 N88-30261

COATING
NT ANODIZING
NT ELECTROPLATING
NT ENCAPSULATING
NT METALLIZING
Molecular dynamics of laser ablation of a polymer coating
[DE88-004337] 13 p1750 N88-20466

COATINGS
NT ALUMINUM COATINGS
NT ANODIC COATINGS
NT ANTIRADAR COATINGS
NT ANTIREFLECTION COATINGS
NT CATHODIC COATINGS
NT CERAMIC COATINGS
NT ELECTROPLATING
NT ENAMELS
NT ENCAPSULATING
NT GLASS COATINGS
NT GLAZES
NT METAL COATINGS
NT METALLIZING
NT NICKEL COATINGS
NT PAINTS
NT PLASTIC COATINGS
NT PRIMERS (COATINGS)
NT PROTECTIVE COATINGS
NT REFRACTORY COATINGS
NT SPRAYED COATINGS
NT THERMAL CONTROL COATINGS
NT ZINC COATINGS
Synergism of electroplating and vacuum processes
[DE87-013496] 01 p0033 N88-10211
JPRS report: Science and technology. USSR: Materials science
[JPRS-UMS-87-006] 03 p0285 N88-11791
Consortium for Materials Development in Space. Technical section
[NASA-CR-181508] 03 p0296 N88-11859
Surface coatings and catalyst production by electrodeposition 03 p0297 N88-11863
Mass transport by diffusion 03 p0297 N88-11864
Advanced natural gas fueled engine development. Part 2: Materials investigation
[PB87-223160] 03 p0331 N88-12088
Long-range pulselength scaling of 351nm laser damage thresholds
[DE87-014754] 04 p0448 N88-12777
Thermomechanical cracking in coated media due to high speed asperity excitation
[AD-A184176] 04 p0454 N88-12809
Effectiveness of electrodeposited coatings in reducing atmospheric corrosion of copper substrates
[DE87-013651] 05 p0566 N88-13448
Raman microprobe characterization of dielectric films following high-energy pulsed laser irradiation
[DE88-000559] 05 p0588 N88-13587
Fatigue characteristics of ion treated surfaces 05 p0606 N88-13713
Fractographic study of fiber composites 06 p0677 N88-14146
Effects of hydrolysis on metallo-organic solution deposition of PZT films
[ATR-86(8443)-1] 06 p0679 N88-14160
The tribological properties of MoS2 coatings in vacuum, low relative humidity and high relative humidity environments
[DE88-001611] 06 p0711 N88-14356
Electromagnetic fields backscattered from an s-shaped inlet cavity with an absorber coating on its inner walls
[NASA-CR-182401] 07 p0845 N88-15130
Tribological studies on high speed steel cutting tools
[DE88-002550] 07 p0864 N88-15246
TiN coatings on M2 steel produced by plasma assisted chemical vapor deposition
[DE88-003189] 08 p0970 N88-15867
Sputtered silver films to improve chromium carbide based solid lubricant coatings for use to 900 C
[NASA-TM-100783] 08 p0973 N88-15885
Self-lubricating coatings for high-temperature applications 09 p1119 N88-16703
Organic coatings to improve the storageability and safety of pyrotechnic compositions
[AD-A187158] 09 p1150 N88-16889
Los Alamos optical materials reliability, maintainability, and exposure testing program
[DE88-001953] 10 p1409 N88-18404
Protecting old oil tanks made of steel against internal corrosion using organic coatings
[DE88-751089] 11 p1459 N88-18698
Electrochromic thin films
[DE88-751099] 11 p1559 N88-19334
Electrophoretically deposited styrene-acrylate coatings for suppression of internal electromagnetic pulse effects
[DE88-003820] 12 p1609 N88-19621
Investigations of surface coatings based on silicon and nitrogen: From amorphous Si to silicon nitride
[DE88-004995] 12 p1609 N88-19622
The influence of the fiber-matrix bond on the mechanical behavior of NICALON/SiC composites
[DE88-006155] 13 p1734 N88-20369
Optimization of binary pigment coatings
[AD-A189103] 13 p1748 N88-20450
PNL-1 improved ceramic composites through controlled fiber matrix interaction
[DE88-005680] 13 p1750 N88-20462
Causes of damage in multilayer dielectric coatings exposed to high average power visible laser radiation
[DE88-005363] 13 p1775 N88-20619
Fatigue damage modeling for coated single crystal superalloys 15 p2085 N88-22427
Present, future of automotive hybrid IC applications discussed 16 p2185 N88-23024
Thin film research diagnostics instrumentation
[AD-A191240] 16 p2213 N88-23207
Implications of the trapping-desorption and direct inelastic scattering channels on Dicke-narrowed lineshapes
[AD-A191410] 16 p2270 N88-23581
Boundary layer flow visualization for flight testing 17 p2297 N88-23742
Predictive corrosion modeling, volume 1
[AD-A191229] 18 p2485 N88-24739
Environmental integrity of coating/metal interface
[AD-A192184] 18 p2492 N88-24786
Design and demonstration of a system for the deposition of atomic-oxygen durable coatings for reflective solar dynamic power system concentrators
[NASA-CR-4158] 19 p2606 N88-25474
Thermoplastic coating of carbon fibers
[NASA-CR-183067] 20 p2767 N88-26407
Interface modification in Nicalon (trademark)/SiC composites
[DE88-009708] 20 p2767 N88-26409
The effects of Hertzian stress and test ambient on the friction coefficient of MsS2 coatings
[DE88-008118] 20 p2777 N88-26487
Characterization of coating wear phenomena in nitride and carbide coated tool inserts
[DE88-011196] 20 p2779 N88-26478
Contribution to the development of coated fiber ceramic insolation material
[ETN-88-92361] 21 p2906 N88-27243
PECVD of amorphous nickel--phosphorus films
[DE88-011088] 21 p2915 N88-27299
Radiative heat transfer and selective emission in planar slab coatings on hot emissive substrates
[AD-A193133] 21 p2918 N88-27319
Thermo-mechanical cracking in coated media with a cavity by a moving asperity friction
[AD-A193311] 21 p2961 N88-27586
Thin film coatings for space electrical power system applications
[NASA-TM-101325] 23 p3187 N88-28966
Thin film-residual stress assessment
[AD-A193205] 23 p3196 N88-29018
The diamond as a new electronic material
[NASA-TT-20354] 23 p3209 N88-29098
The acoustic field scattered from some approximate pressure release materials
[AD-A194768] 23 p3278 N88-29515
Iridium-coated rhenium thrusters by CVD
[NASA-TM-101309] 24 p3339 N88-29874
Ultrasonic detection of diffusion and adhesion loss 24 p3354 N88-29967
Photoacoustic Fourier transform infrared spectroscopy. An early detection technique for coatings degradation 24 p3354 N88-29968

Predicting the durability of adhesives and coatings by remote detection of hidden defects and coating-thickness irregularities: A theoretical and numerical study
24 p3355 N88-29972
An electrochemical impedance spectroscopy study of reactions at the metal/coating interface
24 p3355 N88-29975
Containment of a silicone fluid free surface in reduced gravity using barrier coatings
[NASA-TM-101314] 24 p3371 N88-30072

COAXIAL CABLES
Crosstalk in braided shield coaxial cables
01 p0035 N88-10224
The use of coaxial transmission line elements in log-periodic dipole arrays
[AD-A184864] 05 p0574 N88-13499
Picosecond cable calibrator: Beam Research Program
[DE88-002375] 06 p0695 N88-14266
Coaxial cable connector
[NASA-CASE-NPO-16764-1-CU]
06 p0696 N88-14270
Shielding effectiveness against electromagnetic interference
[DE88-003664] 07 p0846 N88-15131
Measurement of shielding effectiveness of different cable and shielding configurations by mode-stirred techniques
[PB88-155791] 10 p1319 N88-17885
The coaxial colinear antenna: Theoretical and experimental models 11 p1475 N88-18803
The preparation, assembly and mounting of RF coaxial cables
[ESA-PSS-01-718-ISSUE-1] 13 p1756 N88-20504
Power transmission studies for tethered SP-100
[NASA-TM-100864] 14 p1883 N88-21251

COAXIAL FLOW
Experimental study of interacting vortex rings
03 p0318 N88-12007
Numerical solutions of the complete Navier-Stokes equations
[NASA-CR-183023] 18 p2514 N88-24914

COAXIAL TRANSMISSION
U COAXIAL CABLES
U TRANSMISSION

COBALT
NT COBALT 60
Microstructure and magnetic properties of cobalt-chromium alloys
[DE88-002762] 07 p0835 N88-15064
Reaction mechanism of sulfur dioxide with single crystal cobalt and chromium and CoCrAlY coatings
[AD-A185989] 09 p1253 N88-17509
Studies of the electron spectrum with reference to the clean surfaces of iron, cobalt and nickel and their subsequent exposure to oxygen
11 p1459 N88-18700
Carboxylate formation at the interface between a polyimide coating and cobalt 17 p2320 N88-23859
Nickel hydrogen cell positive-electrode studies: Cobalt segregation in reducing environments
[AD-A193025] 20 p2796 N88-26587

COBALT ALLOYS
NT ASTROLOY (TRADEMARK)
Reaction mechanism of sulfur dioxide with single crystal cobalt and chromium and CoCrAlY coatings
[AD-A185989] 09 p1253 N88-17509
Effects of ion implantation on cavitation erosion of a cobalt based metal/carbide alloy
[AD-A187239] 10 p1303 N88-17793
New super alloys used in turbochargers
19 p2634 N88-25628

COBALT COMPOUNDS
NT COBALT OXIDES
Growth of high quality CoSi2/Si superstructures on Si(111) 20 p2869 N88-27034

COBALT ISOTOPES
NT COBALT 60

COBALT OXIDES
Phase purity of NiCo2O4, a catalyst candidate for electrolysis of water
[NASA-TM-100239] 05 p0556 N88-13385

COBALT 60
Evaluation of silicon-on-insulator MOS (Metal-Oxide-Semiconductor) transistor response to 10-keV X-ray and cobalt-60 irradiation
[DE88-006102] 23 p3206 N88-29082

COBE
U COSMIC BACKGROUND EXPLORER SATELLITE

COBOL
COBOL Analysis System (CAS) users manual
[PB88-171442] 16 p2250 N88-23445

COCHLEA
Assessment of cochlear damage after microwave irradiation
[AD-A193237] 21 p2987 N88-27737

COCKPIT SIMULATORS
Investigation of pilot behavior in a training program for assessing handling qualities using a ground simulator
[ESA-TT-999] 03 p0357 N88-12247
Status of NASA/Army rotorcraft research and development piloted flight simulation
09 p1110 N88-16651
An enumeration of research to determine the optimal design and use of Army flight training simulators
[AD-A191242] 18 p2468 N88-24649

COCKPITS
MBB simulation facilities applied for rotorcraft research 03 p0263 N88-11655
Helicopter (performance) management
03 p0264 N88-11666
Effects of combining vertical and horizontal information into a primary flight display
[NASA-TP-2783] 04 p0399 N88-12487
Advanced helicopter cockpit and control configurations for helicopter combat missions
[NASA-TM-100017] 07 p0821 N88-14988
An inexpensive real-time interactive three dimensional flight simulation system
[AD-A184868] 07 p0821 N88-14989
Dynamic function allocation in fighter cockpits
[AD-A185397] 09 p1201 N88-17199
Comparison of alphanumeric data entry methods for advanced helicopter cockpits
[AD-A186934] 09 p1201 N88-17201
Cockpit data management
[NASA-CR-178407] 11 p1438 N88-18579
Cockpit data management
[NASA-CR-178407-SUPPL] 11 p1438 N88-18580
A comparison of keyboard designs for cockpit applications
[AD-A187775] 12 p1581 N88-19460
User perceptions of side-arm flight control in rotary-wing aircraft
[AD-A188519] 12 p1672 N88-20009
CODAC (Cockpit Oriented Display of Aircraft Configurations) version 1.4 user's guide
[NASA-CR-181650] 13 p1718 N88-20273
Geometric modeling of flight information for graphical cockpit display
[AD-A190484] 15 p2021 N88-22043
Psychosensory cockpit ergonomics, advantages of intelligent information systems 17 p2304 N88-23784
Advanced development of a cockpit automation design support system 17 p2304 N88-23785
Software engineering for the British Aerospace Experimental Aircraft Programme (EAP)
17 p2306 N88-23798
Checklist interruption and resumption: A linguistic study
[NASA-CR-177460] 20 p2756 N88-26348
A cockpit natural language study - selected transcripts
[AD-A192972] 20 p2834 N88-26808
Cockpit and cabin crew coordination
[AD-A192445] 21 p2993 N88-27752
A cockpit natural language study: Vocabulary and grammar analyses
[AD-A193289] 21 p2993 N88-27753
Visual related accidents/incidents
23 p3242 N88-29293
General operational and training visual concerns
23 p3242 N88-29295
Night lighting and night vision goggle compatibility
23 p3242 N88-29297
Future visual environment and concerns
23 p3242 N88-29299
Use of color CRTs (Cathode Ray Tubes) in aircraft cockpit: A literature search, revision B
[AD-A195062] 24 p3324 N88-29797

COD (CRACKS)
U CRACK OPENING DISPLACEMENT

CODE DIVISION MULTIPLE ACCESS
Code division multiple access applied to fiber optic data transmission
[AD-A186873] 09 p1247 N88-17477
Mobilestar field test program
19 p2646 N88-25707
Comparison of CDMA and FDMA for the MobileStar(sm) system 19 p2649 N88-25724
Evaluation of CDMA system capacity for mobile satellite system applications 19 p2651 N88-25740

CODERS
Design of source coders and joint source/channel coders for noisy channels
[NASA-CR-181547] 04 p0432 N88-12678
Experience with Omega: Implementation of a prototype programming environment, part 6
[AD-A187080] 10 p1385 N88-18270
A hybrid transform/DPCM encoder for data compression
[DE87-014852] 13 p1758 N88-20518
Speech coding at 4800 bps for mobile satellite communications 19 p2652 N88-25749
A 4.8 kbps code-excited linear predictive coder
19 p2652 N88-25750
Real-time speech encoding based on Code-Excited Linear Prediction (CELP) 19 p2653 N88-25751
Development of an 8000 bps voice codec for AvSat
19 p2653 N88-25755

CODING
NT AMPLITUDE MODULATION
NT DECODING
NT DELTA MODULATION
NT DIFFERENTIAL PULSE CODE MODULATION
NT FREQUENCY MODULATION
NT FREQUENCY SHIFT KEYING
NT PHASE MODULATION
NT PHASE SHIFT KEYING
NT PULSE AMPLITUDE MODULATION
NT PULSE CODE MODULATION
NT PULSE DURATION MODULATION
NT PULSE MODULATION
NT PULSE POSITION MODULATION
NT REDUNDANCY ENCODING
NT SIGNAL ENCODING
Study, design, and evaluation of data reduction by encoding or information extraction. Part 1: Data generation analysis --- multispectral satellite imagery
[NLR-TR-85094-L-PT-1] 01 p0078 N88-10501
Study, design and evaluation of data reduction by encoding or information extraction. Part 2: Operational considerations --- multispectral satellite imagery
[NLR-TR-85094-L-PT-2] 01 p0079 N88-10502
Study, design and evaluation of data reduction by encoding or information extraction. Part 3: Algorithm design --- multispectral satellite imagery
[NLR-TR-85094-L-PT-3] 01 p0079 N88-10503
Study, design and evaluation of data reduction by encoding or information extraction. Part 4: Performance demonstration --- multispectral satellite imagery
[NLR-TR-85094-L-PT-4] 01 p0079 N88-10504
Study, design and evaluation of data reduction by encoding or information extraction. Part 5: Algorithm implementation aspects --- multispectral satellite imagery
[NLR-TR-85094-L-PT-5] 01 p0079 N88-10505
Computations of hypervelocity impact using the CTH shock wave physics code
[DE87-013067] 02 p0169 N88-11062
IMPSOR: A fully vectorized FORTRAN code for three dimensional moving boundary problems with Dirichlet or Neumann boundary conditions
[DE87-014964] 02 p0226 N88-11427
BIMOND3: Monotone piecewise bicubic Hermite interpolation code
[DE87-014612] 02 p0229 N88-11442
A relativistic Monte Carlo binary collision model for use in plasma particle simulation codes
[DE87-013287] 02 p0237 N88-11494
The evolution of HOBO
[DE87-014742] 03 p0313 N88-11980
Studies of the processing of single words using positron tomographic measures of cerebral blood flow change
[AD-A184058] 03 p0358 N88-12244
Los Alamos National Laboratory computer benchmarking 1986
[LA-10898-MS] 03 p0363 N88-12285
Development and evaluation of a Monte Carlo code system for analysis of ionization chamber responses
[AD-A183970] 03 p0375 N88-12359
Competition Analysis Model (CAM). Volume 2: Computer manual
[AD-A184017] 03 p0384 N88-12411
Tau ranging revisited 04 p0437 N88-12710
INS3D: An incompressible Navier-Stokes code in generalized three-dimensional coordinates
[NASA-TM-100012] 04 p0485 N88-12991
A computer code to process and plot laser altimetry data interactively on a microcomputer
[NASA-TM-100687] 05 p0554 N88-13371
A computer code to calculate line by line atmospheric transmission spectra on a microcomputer
[NASA-TM-100686] 05 p0554 N88-13372
Hanford Meteorological Station computer codes. Volume 5: The TOWER computer code
[DE88-001610] 05 p0628 N88-13843
Some distance problems in coding theory
[B8711398] 05 p0635 N88-13888
Numerical study of chemically reacting flows using an LU scheme
[NASA-CR-180882] 06 p0668 N88-14094
Correction method for Barker-coded modulation
06 p0691 N88-14240
Methods for reducing computational costs of typical finite element unsteady hydrodynamic models
[AD-A185499] 06 p0702 N88-14312

Evaluation of a satellite laser ranging technique using pseudonoise code modulated laser diodes
[NASA-CR-182347] 06 p0708 N88-14343
Local and global techniques for the tracking of periodic solutions of parameter-dependent functional differential equations
[AD-A185756] 06 p0766 N88-14704
Plasma parameters for alternate operating modes of TIBER-2
[DE88-001890] 06 p0783 N88-14802
Bar code document accountability system performance update
[DE88-002256] 06 p0791 N88-14849
Analysis and performance prediction of scramjet inlets utilizing a three-dimensional Navier-Stokes code
07 p0811 N88-14936
Modern wing flutter analysis by computational fluid dynamics methods
[NASA-TM-100531] 07 p0816 N88-14965
Performance analysis of coded frequency-hopped spread-spectrum systems with unknown interference
[AD-A186069] 07 p0841 N88-15103
Coding for spread-spectrum communications networks
[AD-A185667] 07 p0844 N88-15119
Treatment of small wire loops in the method of moments code NEC (Numerical Electromagnetics Code)
[DE88-002995] 07 p0846 N88-15136
User manual for ATILA, a finite-element code for modeling piezoelectric transducers
[AD-A185948] 07 p0847 N88-15141
Local versus global minima in visual pattern completion
[PB87-234803] 07 p0897 N88-15439
TeXting the FORMULARY: A collection of examples of the use of TeX to produce ruled tables and displayed equations
[AD-A185920] 07 p0921 N88-15598
Verification of FANTASTIC integrated code
07 p0924 N88-15613
Neural network based speech synthesizer: A preliminary report 08 p1064 N88-16429
Absorption of electron cyclotron waves by superthermal electron velocity distributions in tokamak plasmas
[INPE-4385-PRE/1205] 08 p1086 N88-16539
New techniques in computational aerodynamics
[AD-A186719] 09 p1112 N88-16664
Outlier resistant predictive source encoding for a Gaussian stationary nominal source
[AD-A186725] 09 p1232 N88-17387
A transonic-small-disturbance wing design methodology
[NASA-TP-2806] 10 p1273 N88-17614
Designing variable-length codes with good error-recovery properties
[BBC-RD-1987/19] 10 p1317 N88-17876
The design of trellis codes for fading channels
[NASA-CR-182523] 10 p1320 N88-17891
Orthogonal patterns in binary neural networks
[NASA-TM-100060] 10 p1396 N88-18320
A performance index approach to aerodynamic design with the use of analysis codes only
[NASA-TP-2805] 11 p1433 N88-18552
The Telecommunications and Data Acquisition Report
[NASA-CR-182545] 11 p1471 N88-18774
A labeling procedure for linear finite-state codes
11 p1472 N88-18781
Further results on finite-state codes
11 p1472 N88-18782
A comparison of VLSI architectures for time and transform domain decoding of Reed-Solomon codes
11 p1472 N88-18783
A simplified, general-purpose deep-space ranging correlator design 11 p1473 N88-18786
VAXELN experimentation: Programming a real-time clock and interrupt handling using VAXELN Ada 1.1
[AD-A188100] 11 p1525 N88-19107
Spire based speaker-independent continuous speech recognition using mixed feature sets
[AD-A188634] 12 p1620 N88-19688
A concatenated coded modulation scheme for error control
[NASA-CR-182639] 12 p1621 N88-19697
A new parabolized Navier-Stokes code for chemically reacting flow fields 12 p1625 N88-19721
Some questions of using coding theory and analytical calculation methods on computers
[DE88-700905] 12 p1676 N88-20021
Trajectory code studies, 1987
[DE88-006218] 13 p1728 N88-20335
A comparison of two chord keyboard coding systems for alphanumeric data entry
[AD-A189230] 13 p1813 N88-20834
MASPLT: A one-dimensional graphics post processor for wave propagation codes
[DE88-005506] 13 p1817 N88-20856
CSQPLT: A graphics post processor for multidimensional wave propagation codes
[DE88-005508] 13 p1817 N88-20858
An integrated data description language for coding design knowledge
[CWI-CS-R8731] 13 p1819 N88-20871
Accuracy requirements and benchmark experiments for CFD validation
[NASA-TM-100087] 14 p1911 N88-21423
Tabulation of Mie scattering calculation results for microwave radiative transfer modeling
[NASA-CR-4130] 14 p1947 N88-21612
Performance of data compression codes in channels with errors
[AD-A189667] 15 p2055 N88-22253
Status of electric vehicle simulation programs at the INEL: Summer 1987
[DE88-006745] 15 p2058 N88-22271
Selective mechanisms in auditory and bimodal signal processing
[AD-A190529] 15 p2103 N88-22530
Multiple-transform pipelines for image coding
[REPT-87-038] 15 p2108 N88-22561
The algebraic structure of convolutional codes
[AD-A190280] 15 p2120 N88-22635
Information and coding capacities of mismatched Gaussian channels
[AD-A190321] 15 p2124 N88-22665
Coding capacity of generalized additive channels
[AD-A190315] 15 p2127 N88-22685
OCR vision system, an alternative to bar code
[DE88-003761] 15 p2149 N88-22828
On the validation of a code and a turbulence model appropriate to circulation control airfoils
[NASA-TM-100090] 16 p2156 N88-22864
A computer model investigation of a half square log-periodic array
[AD-A190955] 16 p2190 N88-23062
Mass digitization of topographic-cartographic information 16 p2226 N88-23288
Efficient and fast data compression codes for discrete sources with memory
[ETN-88-92233] 16 p2246 N88-23420
Error control techniques for satellite and space communications
[NASA-CR-182886] 17 p2332 N88-23922
Preliminary 2-D shell analysis of the space shuttle solid rocket boosters
[NASA-TM-100515] 17 p2348 N88-23989
Parallel binary and parallel coded decimal time code formats
[AD-A190126] 17 p2384 N88-24170
The Lewis heat pipe code with application to SP-100 GES heat pipes 17 p2421 N88-24395
Analytic and numerical modeling of heat and material transport in electrical hypervelocity guns
[AD-A192178] 18 p2469 N88-24655
Joint services electronics program
[AD-A190239] 18 p2503 N88-24848
Adaptive local grid refinement in computational fluid mechanics
[AD-A192215] 18 p2510 N88-24890
Duct flow nonuniformities for Space Shuttle Main Engine (SSME)
[NASA-CR-179338] 18 p2511 N88-24899
Narrative compression coding for a channel with errors
[AD-A191577] 19 p2642 N88-25673
Trellis-coded CPM for satellite-based mobile communications 19 p2648 N88-25718
Interleaver design for trellis-coded differential 8-PSK modulation with non-coherent detection
19 p2648 N88-25719
Codes for QPSK modulation with invariance under 90 degrees rotation 19 p2648 N88-25720
Trellis-coded MPSK modulation techniques for MSAT-X(sup)1 19 p2648 N88-25721
Modulation and coding for fast fading mobile satellite communication channels 19 p2648 N88-25722
Performance of the ICAO standard core service modulation and coding techniques
19 p2648 N88-25723
A 4.8 kbps code-excited linear predictive coder
19 p2652 N88-25750
Sinusoidal transform coding 19 p2653 N88-25752
Analysis and improvement of the vector quantization in SELP (Stochastically Excited Linear Prediction)
19 p2653 N88-25756
The development of an intelligent interface to a computational fluid dynamics flow-solver code
[NASA-TM-100908] 19 p2716 N88-26127
A VLSI single-chip (225,223) Reed-Solomon encoder with interleaver
[NASA-CASE-NPO-17280-1-CU]
21 p2902 N88-27220
SARLAC: A relativistic electron beam code
[AD-A193134] 21 p2932 N88-27411
Numerical computation of space shuttle orbiter flow field
[NASA-CR-183193] 22 p3040 N88-28048
Efficient multiplication algorithms over the finite fields GF(q sup m), where q equals 3,5
22 p3066 N88-28191
Numerical modeling results for mode propagation in a wedge
[AD-A193998] 22 p3147 N88-28718
Fine resolution errors in secondary surveillance radar altitude reporting
[RSRE-87019] 23 p3175 N88-28906
Method for Veterbi decoding of large constraint length convolutional codes
[NASA-CASE-NPO-17310-1-CU]
23 p3183 N88-28946
Coding for meteor-burst communications channel and side information for channels with block-interference
23 p3202 N88-29054
An overview of technology for spoken interaction with machines
[AD-A194153] 23 p3202 N88-29058
Hierarchical organization for large, dynamic radio networks
[AD-A193942] 23 p3204 N88-29067
A computer program package for introductory one-dimensional digital signal processing applications
[AD-A194656] 23 p3249 N88-29338

COEFFICIENT OF FRICTION
A method for the approximate calculation of the skin friction coefficient of horizontal wavy plates
[VKI-TN-160] 07 p0851 N88-15172
Influence of the friction coefficients, the power and the flowrate on the two-phase flow instabilities in natural circulation
[DE88-700036] 08 p0983 N88-15946
Tribological properties of alumina-boria-silicate fabric from 25 to 850 C
[NASA-TM-100806] 11 p1464 N88-18726
Evaluation of centrifugal barrel tumbling process for impregnation of molybdenum disulfide powder lubricant
[BDX-613-3698] 11 p1464 N88-18727
Compressible friction coefficients in a simulated heat pipe
[AD-A188818] 12 p1627 N88-19735
The effects of Hertzian stress and test ambient on the friction coefficient of MoS2 coatings
[DE88-008118] 20 p2777 N88-26467

COEFFICIENTS
NT AERODYNAMIC COEFFICIENTS
NT ATTENUATION COEFFICIENTS
NT COEFFICIENT OF FRICTION
NT CORRELATION COEFFICIENTS
NT COUPLING COEFFICIENTS
NT DIFFUSION COEFFICIENT
NT DISCHARGE COEFFICIENT
NT FLOW COEFFICIENTS
NT HEAT TRANSFER COEFFICIENTS
NT INFLUENCE COEFFICIENT
NT IONIZATION COEFFICIENTS
NT NOZZLE THRUST COEFFICIENTS
NT RECOMBINATION COEFFICIENT
NT REGRESSION COEFFICIENTS
NT SCATTERING COEFFICIENTS
NT STRUCTURAL INFLUENCE COEFFICIENTS
NT VIRIAL COEFFICIENTS
NT WIGNER COEFFICIENT
Reactive sticking coefficients of silane on silicon
[DE88-000601] 05 p0570 N88-13473
Concentration coefficients of elements in ferromanganese nodules relative to ocean sediments
06 p0726 N88-14464
Estimation of broadband planetary albedo from operational narrowband satellite measurements
[PB88-107644] 07 p0945 N88-15748
Cornering characteristics of the main-gear tire of the space shuttle orbiter
[NASA-TP-2790] 11 p1438 N88-18583
Calibration of a ring laser gyro inertial navigation system 12 p1576 N88-19428
Determination of the partition coefficients of organophosphorus compounds using high-performance liquid chromatography
[AD-A189276] 13 p1737 N88-20385
Transformation coefficient in wave-field acceleration scheme
[DE88-700158] 13 p1757 N88-20507
Predicting oscillatory finite difference solutions to the heat equation: A comparative study of the coefficient and matrix methods
[AD-A189591] 13 p1825 N88-20911
Experimental determination of the coefficients of the hydraulic resistance of apertures in the rotary disks
[AD-A190627] 15 p2066 N88-22317

Solving singular systems using orthogonal functions
[AD-A190881] 16 p2260 N88-23512
Evaluation of the biot coefficients
[AD-A191643] 18 p2570 N88-25265
Polynomials with restricted coefficients and their applications
[AD-A192589] 23 p3202 N88-29055

COENZYMES
NT ADENOSINE TRIPHOSPHATE
NT GLUTATHIONE

COFFEE
SPOT applications on Columbia's coffee zone
22 p3097 N88-28395

COGENERATION
Development of a light duty gas engine for cogeneration service
[PB87-221297] 02 p0180 N88-11119
Development of fast breeder reactors in China
16 p2186 N88-23032
Design of nuclear heat, power co-generation plant detailed
16 p2186 N88-23033
Advanced energy system program
[PB88-183025] 19 p2686 N88-25965

COGNITION
Studies of the processing of single words using positron tomographic measures of cerebral blood flow change
[AD-A184058] 03 p0356 N88-12244
Effects of divided attention on identity and semantic priming
[AD-A184289] 03 p0357 N88-12250
Evoked brain activity and personnel performance
[AD-A185922] 07 p0897 N88-15436
Computing support for basic research in perception and cognition
[AD-A186192] 07 p0897 N88-15437
Cirrus: An automated protocol analysis tool
[AD-A186646] 08 p1052 N88-16348
Deriving descriptions of the mind
[AD-A186647] 08 p1052 N88-16349
Changing the layers of mind
[AD-A186648] 08 p1052 N88-16350
Intelligent tutoring systems as tools for investigating individual differences in learning
09 p1204 N88-17216
A hypertext writing environment and its cognitive basis
[AD-A188179] 10 p1389 N88-18298
Effects of stress on judgement and decision making in dynamic tasks
[AD-A188203] 11 p1523 N88-19092
The construction of a pedagogy to promote meaningful learning of strategies and tactics for solving problems of elementary combinatorics
[AD-A187928] 11 p1542 N88-19216
Night Vision: Current Research and Future Directions, symposium proceedings
[PB88-132006] 11 p1550 N88-19274
Effects of intense, time-constrained mental effort on hemodynamics and cardiovascular function
12 p1664 N88-19975
Neurocognitive predictions of performance
[AD-A188323] 12 p1669 N88-19998
A comparison of the Army's Project A: Cognitive and psychomotor tests to analogous Air Force and Navy tests
[AD-A188636] 12 p1670 N88-20002
Expert systems: Their impact on performance and cognitive strategies in diagnostic inference
[AD-A188518] 12 p1677 N88-20027
Management information systems design implications: The effect of cognitive style and information presentation on problem solving
[AD-A188850] 12 p1705 N88-20205
A personalized and prescriptive decision aid for choice from a database of options
[AD-A188726] 13 p1811 N88-20820
Mental models of mechanical systems: Individual differences in qualitative and quantitative reasoning
[AD-A189035] 13 p1812 N88-20823
Human problem solving in dynamic environments. Understanding and supporting operators in large-scale, complex systems
[AD-A189539] 13 p1812 N88-20826
Online aiding for human-computer interfaces
[AD-A189239] 13 p1815 N88-20842
Soar: An architecture for general intelligence
[AD-A188742] 13 p1823 N88-20898
Conflict resolution in cooperative systems
[AD-A190351] 15 p2104 N88-22535
Relationship of encoding speed and memory tests to flight training performance
[AD-A190670] 15 p2105 N88-22539
The N2-P3 complex of the evoked potential and human performance
16 p2241 N88-23388
Processing deficits in monitoring analog and digital displays: Implications for attentional theory and mental-state estimation research
16 p2241 N88-23389
Problem solving in a natural task as a function of experience
[AD-A191180] 16 p2243 N88-23399
The event-related brain potential as an index of information processing and cognitive activity: A program of basic research
[AD-A191244] 16 p2243 N88-23400
Capitalizing on failure through case-based inference
[AD-A190927] 16 p2255 N88-23480
Extracting information from problem solving experience
[AD-A191331] 16 p2286 N88-23688
Spatial cognition 17 p2380 N88-24152
Induction of models under uncertainty
[NASA-TM-101173] 17 p2394 N88-24230
A systems engineering based methodology for analyzing human electrocortical responses
[AD-A190809] 18 p2550 N88-25135
Performance effectiveness and the work/rest cycle
[AD-A191448] 18 p2551 N88-25145
Models of incremental concept formation
[AD-A191597] 18 p2552 N88-25147
A computational model of motor behavior
[AD-A191179] 18 p2553 N88-25152
Selection and effects of channels in distributed communication and decision making tasks: A theoretical review and a proposed research paradigm
[AD-A191807] 18 p2587 N88-25375
Generalization and the backward propagation neural network
[AD-A191634] 19 p2710 N88-26100
Direct manipulation and the design of user interfaces
[PB88-126354] 20 p2834 N88-26810
The effects of increased cognitive demands on autonomic self-regulation: An indicator of parallel processing in the brain
21 p2925 N88-27362
Electric and magnetic brain activity related to cognitive performance
21 p2979 N88-27692
The effects of hypoxia on P300 and reaction time
[DCIEM-87-RR-12] 21 p2979 N88-27697
Cognitive task demands as reflected in physiological measures
21 p2980 N88-27699
Event-related and steady potential changes in the brain related to workload during tracking
21 p2981 N88-27705
Cognitive and neural bases of skilled performance
[AD-A193392] 21 p2992 N88-27747
Conjunctive measurement theory: Cognitive research prospects
[AD-A193627] 23 p3239 N88-29277
Reliability and construct validity of reaction time, inspection time and machine-paced tests of cognitive speed
[AD-A193779] 23 p3241 N88-29289
Expertise and reasoning with possibility: An explanation of modal logic and expert systems
23 p3253 N88-29363
Advancement of latent trait theory
[AD-A194302] 24 p3408 N88-30289
Contributions to engineering models of human-computer interaction, volume 1
[AD-A195590] 24 p3409 N88-30295
The bounded rationality constraint: Experimental and analytical results
[AD-A195897] 24 p3413 N88-30318

COGNITIVE PSYCHOLOGY
Gender and cognitive style differences at the human-computer interface
[NPL-DITC-90/87] 01 p0077 N88-10493
Determinants of dual-task interference and resource theories in cognitive psychology
[DFVLR-FB-88-14] 21 p2992 N88-27748

COHERENCE
A fast bottom-up algorithm for computing the cut sets of noncoherent fault trees
[DE88-003741] 09 p1220 N88-17320
Bearing detection in the presence of two sources of varying coherence using the complex cepstrum
[NASA-CR-181605] 09 p1243 N88-17451
Vortex dynamics of coherent and chaotic structures (including algorithms for computer simulations and diagnosis)
[AD-A193580] 23 p3212 N88-29117

COHERENT ANTI-STOKES RAMAN SPECTROSCOPY
U RAMAN SPECTROSCOPY

COHERENT ELECTROMAGNETIC RADIATION
NT COHERENT LIGHT
NT LASER BEAMS
Fluctuations in frequency of coherent radio signals in solar plasma according to Venera-15 and Venera-16 data
08 p1003 N88-16079
Emission angles for soft X-ray coherent transition radiation
[AD-A186851] 09 p1151 N88-16896

COHERENT LIGHT
Effect of optical inhomogeneities on space coherence of radiation emitted by laser with unstable resonator
06 p0771 N88-14738
Problems and possible solutions involved in hard target calibration of coherent Doppler lidar
07 p0922 N88-15602
Excitation of single-mode glass fiber by partially coherent sources
[ETN-88-92121] 20 p2854 N88-26951
Studies of coherent beam processing concepts, phase 1
[AD-A194749] 22 p3083 N88-28306

COHERENT RADAR
Distortion of wideband carbon dioxide laser radar waveforms due to atmospheric dispersion and absorption
[AD-A188687] 12 p1632 N88-19771
Coherent laser radar system theory
[AD-A188759] 13 p1774 N88-20612
Preliminary study of a coherent radar
[BCRS-86-03] 16 p2189 N88-23051

COHERENT RADIATION
NT COHERENT ELECTROMAGNETIC RADIATION
NT COHERENT LIGHT
NT LASER BEAMS
Coherent infrared detection, volume B --- CO2 laser intersatellite data link
[ESA-CR(P)-2392-VOL-1] 01 p0034 N88-10218
Coherent infrared detection, volume D --- CO2 laser intersatellite data link
[ESA-CR(P)-2392-VOL-2] 01 p0034 N88-10219
Brightness and coherence of radiation from undulators and high-gain free electron lasers
[DE87-011093] 02 p0177 N88-11102
Generation of IR stimulated radiation, UV visible violet coherent radiation by two-photon resonance pumping in K vapor
03 p0301 N88-11892
Methods for a coherent CO2 laser heterodyne radar system
[ESA-TT-1035] 03 p0328 N88-12076
Center for X-Ray Optics, 1986
[DE88-000715] 04 p0449 N88-12783
Coherent emission from relativistic beam-plasma interactions
04 p0493 N88-13039
Coherence, propagation and fluctuations of light: A generalized ray approach
[DE88-001669] 06 p0780 N88-14786
Formation of high-coherence radiation in free-running mode ruby laser for pulse holography
08 p1077 N88-16497
Coherent VUV source at 130 nm: Theory and modeling
[DE88-003874] 11 p1549 N88-19269
Nonclassical lights 14 p1979 N88-21810
Particle acceleration to high energies and amplification of coherent radiation by electromagnetic interactions in plasmas
[DE88-701020] 15 p2135 N88-22737
Generation of tunable coherent radiation in 3 micrometers-5 micrometers region using semiconductor lasers in external cavities
[AD-A190860] 16 p2212 N88-23202
Long duration coherent Lyman-alpha sources
16 p2268 N88-23571
Fast acting optical beam detection and deflection system
[AD-A192161] 18 p2521 N88-24954
Progress toward a soft X-ray FEL
[DE88-007669] 19 p2675 N88-25905
Interferometric recording of holographic optical elements using partially coherent light
20 p2805 N88-26636

COHERENT SCATTERING
Acoustic scattering from composite wind-wave surfaces 3: Forward scatter intensities and spatial coherence at low and high frequencies and small grazing angles for Bubble-free regimes
[AD-A185908] 07 p0881 N88-15345
A search for medium energy gamma ray pulsars
11 p1568 N88-19385
Characteristics of coherent and incoherent waves in snow at microwave and millimeter wave frequencies
[AD-A188990] 12 p1620 N88-19692
Electron stimulated desorption and coherent electron scattering
[AD-A189091] 13 p1835 N88-20978
Image charge, coherent scattering, and symmetry effects in electron stimulated desorption: O(-) from O sub 2 condensed on metals
[AD-A189093] 13 p1835 N88-20979
Ionospheric radio and propagation: Waves in plasmas
24 p3364 N88-30030

COHERENT SOURCES
U COHERENT RADIATION
U RADIATION SOURCES
COHERENT TRANSMISSION
U COHERENT RADIATION
COHESION
An explanation of the fractography of near-threshold fatigue in FCC metals 06 p0716 N88-14395
A comparison of the effects of group dynamics on individuals assigned to integral and non-integral aircrews [AD-A186467] 08 p1051 N88-16345
Cohesive energies of transition metal silicides and phosphides — Knudsen effusion [AD-A186691] 09 p1254 N88-17519
COINCIDENCE CIRCUITS
Coincidence counting corrections under conditions used by A. DeVolpi [NPL-RS(EXT)-90] 17 p2393 N88-24224
Some unsolved problems in modelling self-timed circuits using Petri Nets, series B, number 2 [PB88-181466] 18 p2507 N88-24872
COLD ACCLIMATIZATION
Biorhythmic aspects of intercontinental Antarctic adaptation 08 p1046 N88-16321
Respiratory and cardiovascular responses to cold stress following repeated cold water immersion [AD-A186460] 08 p1050 N88-16340
Effects of moderate cold and heat stress on the potential work performance of industrial workers. Part 6: The effects of increasing vapour pressure at four air temperatures on the performance and physiology of white females [PB88-124854] 18 p2550 N88-25137
COLD CATHODE TUBES
NT PHOTOMULTIPLIER TUBES
An experimental and theoretical investigation of optogalvanic effects [AD-A189618] 12 p1625 N88-19720
COLD FLOW TESTS
The development and evaluation of three-dimensional models of cold flow in internal combustion engines [DE88-900077] 05 p0589 N88-13594
COLD FORMING
U COLD WORKING
COLD FRONTS
The combined use of diagnosed mesoscale frontogenesis and satellite imagery in forecasting squall line formation 02 p0201 N88-11258
Structure and modification of winter mountain clouds in the Sierra Nevada: Nowcasting/forecasting the onset of supercooled liquid water 02 p0202 N88-11263
The role of low-level cooling in a conceptual model of the Australian summertime cool change: Implications for very-short-range forecasting 02 p0204 N88-11275
Results of the experiment MERKUR: Structural change of a weak cold front in the sphere of influence of the Alps — mesoscale experiment 08 p1014 N88-16146
Model calculations of the behavior of orographically influenced cold fronts 08 p1015 N88-16155
Density flows at the mountain edge 08 p1016 N88-16156
Orographically influenced cold fronts in a spectral approach 08 p1016 N88-16161
Numerical investigation of orographically enhanced instability [AD-A186641] 09 p1189 N88-17125
Scientific Colloquium in Honor of Prof. Dr. Rer. Nat. Hermann L. Jordan [DFVLR-MITT-87-11] 09 p1240 N88-17432
The retardation of cold fronts at high mesoscale mountains 09 p1241 N88-17437
Variation of the wind stress related to frontal passages during FASINEX (Frontal Air-Sea Interaction Experiment) 1986 [AD-A187180] 11 p1514 N88-19042
Numerical simulation of the ocean front response to the mesoscale atmospheric forcing [INPE-4473-TDL/324] 12 p1648 N88-19868
The German Front Experiment 1987: Experimental design [DFVLR-MITT-87-24] 16 p2234 N88-23343
COLD GAS
The effect of heat transfer on the dispersion of cold dense gases [OUEL-1688/87] 02 p0171 N88-11076
Cold gas jet system for satellite attitude control-modeling and simulation [INPE-4279-PRE/1150] 12 p1601 N88-19583
COLD PLASMAS
Ionosphere and plasmasphere 03 p0272 N88-11709
Nonlinear, relativistic Langmuir waves in astrophysical magnetospheres [NASA-CR-182422] 08 p1024 N88-16197
Resonance cones in nonthermal plasmas: Laboratory experiments 08 p1027 N88-16223
Hydromagnetic cavity eigenmodes in a non-uniform plasma 08 p1098 N88-16610
Nonlinear resonance of two-dimensional ion layers [AD-A188890] 12 p1695 N88-20145
Experimental studies of plasma heating due to the parametric decay of a large amplitude pump into lower hybrid waves 13 p1841 N88-21017
Consistency between current ramp-up/recharging scenario by non-inductive current drive and dense and cold divertor plasma. Conceptual design study of FY86 FER [DE88-751438] 14 p1984 N88-21833
COLD PRESSING
Preparation of oxide superconductors [DE88-009136] 20 p2875 N88-27063
COLD SURFACES
Interaction of the cold conveyor belt with polar jet streaks [AD-A186774] 09 p1192 N88-17145
COLD TOLERANCE
The effects of acute cold exposure on exercise performance [AD-A192650] 22 p3130 N88-29610
Alterations in cutaneous vasomotor regulation during acute and chronic hypoxia [AD-A192653] 22 p3131 N88-29612
COLD TRAPS
Magnetic trapping of neutral atoms [AD-A188473] 12 p1689 N88-20103
Spontaneous force optical traps [AD-A196103] 24 p3377 N88-30114
COLD WALLS
U COLD SURFACES
U WALLS
COLD WATER
Rational considerations for modelling human thermoregulation during cold water immersion [AD-A186226] 08 p1048 N88-16329
Role of body fat in the prediction of the metabolic response for immersion in cold water [AD-A186914] 09 p1198 N88-17182
COLD WEATHER
Attitudes towards the cold: Effects on psychological mood and subjective reports of illness during cold weather training [AD-A194777] 23 p3239 N88-29274
COLD WEATHER TESTS
Huurre expedition to the North Pole in 1984 [PB87-220935] 04 p0462 N88-12858
Calibration of the ARL (Aeronautical Research Laboratories) rain and icing facility [AD-A186776] 09 p1121 N88-16710
Flight testing under extreme environmental conditions [AGARD-AG-300-VOL-8] 21 p2951 N88-27525
COLD WORKING
NT EXPLOSIVE FORMING
A finite element procedure for interference-fit and cold-working problems with limited yielding [AR-004-517] 04 p0485 N88-12992
Interrelation and measurement of formability, strengthening, and thermomechanical processing under metalworking conditions [DE88-002485] 08 p0967 N88-15850
Computed stress and strain distributions under interference fit and after coldworking [AD-A186950] 10 p1342 N88-18024
Effects of cold working on precipitation in age hardenable alloys: On the copper alloys [NASA-TT-20164] 16 p2177 N88-22973
Cold worked reinforcing bars in tensile test under high loading rate and low temperatures [DE88-752993] 21 p2964 N88-27610
COLLAGENS
Hierarchical structure in polymeric solids and its influence on properties [AD-A194720] 23 p3197 N88-29029
COLLAPSE
Radiation induced collapse of the crystalline structure [DE87-014407] 04 p0498 N88-13064
Bubble expansion and collapse studies [DE88-002377] 06 p0699 N88-14290
Generation and propagation of sound waves in a collapsing or anti-collapsing star with uniform density [DE87-703034] 15 p2151 N88-22839
Dynamical properties of a collapsing spherical cavity 19 p2623 N88-25562
COLLECTION
Techniques utilized in the simulated altitude testing of a 2D-CD vectoring and reversing nozzle [NASA-TM-100672] 19 p2604 N88-25484
The Hanford meteorological data collection system and data base [DE88-008632] 21 p2975 N88-27672
Cooperative effects and intrinsic optical bistability in collections of atoms [AD-A193993] 23 p3280 N88-29530
COLLECTORS
U ACCUMULATORS
COLLEGES
U UNIVERSITIES
COLLIMATION
Development of a computer model for missile simulation, or simulation of a kinetic coverage area for a collimation guided missile [FOA-C-20667-2.5] 08 p1067 N88-16450
Systolic array adaptive beamforming [AD-A187496] 10 p1385 N88-18269
Ion generator and ion application system [NASA-CASE-MFS-28122-1] 17 p2397 N88-24253
COLLIMATORS
Optical links in the angle-data assembly of the 70-meter antennas 11 p1474 N88-18792
COLLINEARITY
Time-domain boundary element analysis of dynamic near-tip fields for impact-loaded collinear cracks [AD-A192930] 20 p2815 N88-26700
Two biased estimation techniques in linear regression: Application to aircraft [NASA-TM-100649] 23 p3274 N88-29489
COLLISION AVOIDANCE
UK airmiss statistics [CAP-530] 03 p0261 N88-11642
Handling qualities criterion for very low visibility rotorcraft 03 p0263 N88-11654
Simulation of an enhanced TCAS 2 system in operation [NASA-CR-181545] 04 p0398 N88-12479
Towards building a team of intelligent robots [NASA-CR-181538] 05 p0589 N88-13595
Collision-free motion of two robot arms in a common workspace [CSE-87-00002] 05 p0589 N88-13596
A study of the TCAS 2 collision avoidance system mounted on a Boeing 737 aircraft [NASA-CR-182457] 09 p1116 N88-16687
Safe rendezvous approach to a space station by impulsive transfers and continuous thrust arcs 12 p1585 N88-19486
UK airmiss statistics [REPT-3/87] 14 p1865 N88-21141
Aircraft accident report: Midair collision of US Army U-21A, Army 18061 and Sachs Electric Company Piper PA-31-350, N60SE, Independence, Missouri, January 20, 1987 [PB88-910401] 16 p2159 N88-22877
UK airmiss statistics [CAA-1/87] 17 p2300 N88-23761
Orbital navigation, docking and obstacle avoidance as a form of three dimensional model-based image understanding 17 p2388 N88-24194
Nuclear-powered space debris sweeper 17 p2418 N88-24380
Rotorcraft TCAS (traffic alert and collision avoidance system) evaluation: Group 3 results [AD-A191719] 18 p2461 N88-24614
The avoidance of collisions for Newtonian bodies with hidden variables [RSRE-87013] 22 p3041 N88-28053
Fine resolution errors in secondary surveillance radar altitude reporting [RSRE-87019] 23 p3175 N88-28906
UK airmisses involving commercial air transport [CAA-1/88] 23 p3176 N88-28907
Airport surface traffic automation study [AD-A194553] 23 p3181 N88-28934
On the collision hazard of colocated geostationary satellites [DFVLR-FB-88-02] 23 p3184 N88-28952
COLLISION PARAMETERS
NT COLLISION RATES
Heavy-particle collisions in the plasma edge [DE87-012928] 02 p0237 N88-11493
Total and partial cross sections for electron capture for C(q+) (q=6-2) and O(q+) (q=8-2) ions in collisions with H, H2 and He atoms [IPPJ-AM-56] 09 p1252 N88-17501
Atomic data for hydrogens in collisions with electrons: Addenda [IPPJ-AM-55-ADD] 09 p1252 N88-17502
Study of the production of Ko mesons in proton antiproton interactions at 630 GeV [NOTA-INTERNA-908] 21 p3015 N88-27892
On the degenerate Ferrari-Ibanez solution for colliding plane gravitational waves [MATH-REPT-209] 23 p3296 N88-29630
COLLISION RATES
Helical ripple transport in stellarators at low collision frequency [DE88-006431] 13 p1843 N88-21031
Contributions of autoionizing resonances to the electron collisional excitation rates for Be-like ions [AD-A190924] 18 p2572 N88-25275

Approximate analytical formulae for electron density and collision frequency in the natural and nuclear-disturbed ionosphere and inner magnetosphere
[AD-A193129] 21 p2972 N88-27654

COLLISION WARNING DEVICES
U COLLISION AVOIDANCE
U WARNING SYSTEMS

COLLISIONAL PLASMAS
NT STRONGLY COUPLED PLASMAS
Computer models for kinetic equations of magnetically confined plasmas
[DE87-011571] 02 p0236 N88-11492
Variable collision frequency effects on hose and sausage instabilities in relativistic electron beams
[AD-A184206] 04 p0490 N88-13021
The effects of a dc electric field on the current driven ion cyclotron instability
[AD-A188877] 12 p1695 N88-20142
Parallel gradient effects on ICRH (Ion Cyclotron Resonance Heating) in tokamaks
[DE88-009038] 19 p2730 N88-26216
Modulational instability of electric helicons in a magnetized collisional plasma
[DE88-701885] 20 p2858 N88-26976

COLLISIONLESS PLASMAS
Computer models for kinetic equations of magnetically confined plasmas
[DE87-011571] 02 p0236 N88-11492
Particle injection and cosmic ray acceleration at collisionless parallel shocks
[DE88-000507] 04 p0430 N88-12665
A study of single and binary ion plasma expansion into laboratory-generated plasma wakes
[NASA-CR-4125] 10 p1412 N88-18427
Plasma theory and simulation
[DE88-003620] 10 p1414 N88-18437
A quadratic-form analysis of the collisionless tearing mode
[AD-A188886] 12 p1695 N88-20144
Helical ripple transport in stellarators at low collision frequency
[DE88-006431] 13 p1843 N88-21031

COLLISIONS
NT ATOMIC COLLISIONS
NT BIRD-AIRCRAFT COLLISIONS
NT COULOMB COLLISIONS
NT INELASTIC COLLISIONS
NT IONIC COLLISIONS
NT METEORITE COLLISIONS
NT MIDAIR COLLISIONS
NT MOLECULAR COLLISIONS
NT PARTICLE COLLISIONS
Heavy-particle collisions in the plasma edge
[DE87-012928] 02 p0237 N88-11493
The Conference on the Dynamics of Molecular Collisions held in Oglebay Park, Wheeling, West Virginia on 12-17 July 1987
[AD-A184690] 03 p0374 N88-12354
Analytic model of an imploding Z-pinch plasma colliding inelastically with a thin-shelled cylindrical target
[DE88-000051] 03 p0378 N88-12379
A study of the interaction of laser light with liquid propellant drops
[AD-A185117] 05 p0587 N88-13582
The effect of collision angle on mach reflection
[AD-A185798] 06 p0704 N88-14319
Tool and process for miniature explosive joining of tubes
[NASA-CASE-LAR-13662-1] 06 p0711 N88-14359
Analysis and interpretation of satellite fragmentation data 06 p0798 N88-14885
Electronic energy transfer processes in the alkali/alkaline earth metal vapors
[AD-A190035] 15 p2034 N88-22119
Colliding stellar winds in the eclipsing Wolf-Rayet binary V444 Cygni
[NASA-CR-182937] 17 p2451 N88-24563
The multistring model VENUS for ultrarelativistic heavy ion collisions
[DE88-007666] 18 p2573 N88-25284
Atomic processes in matter-antimatter interactions
[DE88-008911] 19 p2723 N88-26172
Approximate analytical formulae for electron density and collision frequency in the natural and nuclear-disturbed ionosphere and inner magnetosphere
[AD-A193129] 21 p2972 N88-27654

COLLOCATION
Domain decomposition preconditioners for the spectral collocation method
[NASA-CR-181620] 10 p1400 N88-18345
A spline collocation method for integral equations of the first kind with logarithmic singularity --- boundary value problems
[REPT-87-39] 14 p1963 N88-21712
Periodic response of nonlinear systems 16 p2217 N88-23228
A new collocation-type method for the numerical solution of Hammerstein equations 17 p2393 N88-24226
On the collision hazard of colocated geostationary satellites
[DFVLR-FB-88-02] 23 p3184 N88-28952

COLLOIDING
Colloidal structure of bitumens. Relationship between composition-structure behavior
[PC-4] 02 p0146 N88-10912

COLLOIDS
NT AEROSOLS
NT FOG
Small-Angle Neutron Scattering (SANS) from polymers and colloids
[DE87-013548] 02 p0151 N88-10946
Photocatalytic electrochemistry at a biological-membrane metal-colloid interface
[DE87-009122] 02 p0166 N88-11041
Colloidal stability of oxidized silicon particles in ethanolic and aqueous media
[DE87-014783] 05 p0562 N88-13421
Characterization of the dimensions of colloidal calcium carbonate dispersions in toluene with neutron small-angle scattering
[ECN-197] 06 p0680 N88-14167
Electron transfer to iron(3) oxide colloids
[DE88-002885] 10 p1416 N88-18448
Colloidal characterization of silicon nitride and silicon carbide 17 p2325 N88-23883
Preliminary investigation of flow modeling during solid propellant processing
[AD-A196168] 24 p3357 N88-29987

COLOMBIA
SPOT applications on Columbia's coffee zone 22 p3097 N88-28395

COLONIES
Remote sensing applied to integrated regional development programs 19 p2685 N88-25958

COLOR
NT WATER COLOR
Development of a line-drawing algorithm
[CS-8701] 01 p0082 N88-10530
Preliminary estimation of color inhomogeneities on the surface of Venus according to the television images obtained by the VENERA-13 and VENERA-14 automated space probes
[NASA-TT-20114] 02 p0254 N88-11608
Performance and preference with various VDT (Video Display Terminal) phosphors
[AD-A184085] 04 p0475 N88-12925
On color polynomials of Fibonacci graphs
[AD-A184133] 04 p0486 N88-12996
X-rays, color, and the Vaughan-Preston gap 04 p0510 N88-13135
The use of color in electronic maps. Part 1: Generation and analysis of color on the Gould/DeAnza image processing system
[IZF-1986-32] 05 p0635 N88-13882
Fast, colour displays of digital terrain elevation data
[AD-A185596] 06 p0729 N88-14485
Use of colour on electronic data displays (second study)
[PB87-126744] 06 p0754 N88-14627
Use of lasers with F sub A(II)-color center KCl:Li crystals in the intraresonator laser spectroscopy method 06 p0769 N88-14729
Total light flux and colour of solar corona
[PB87-143335] 07 p0946 N88-15754
Status and prospects of the Joint Research Commitee (JRC) work on the application of ocean colour monitoring from space 08 p1043 N88-16299
Canadian activities and goals in remote sensing of ocean colour and fluorescence from space 08 p1043 N88-16300
Research in Switzerland on ocean and inland-water colour monitoring 08 p1043 N88-16301
Image chunking: Defining spatial building blocks for scene analysis
[AD-A187072] 09 p1200 N88-17191
Multicolor numbering of irregular triangular meshes
[AD-A186559] 09 p1217 N88-17298
Color shadow methods of analyzing reconstructed wave front 09 p1236 N88-17407
Excimer plasma displays
[AD-A186731] 09 p1250 N88-17489
The Quick Response Multicolor Printer (QRMP) system
[AD-A188140] 11 p1504 N88-18982
Laser flash effects on chromatic discrimination in monkeys
[AD-A187703] 11 p1517 N88-19061
Graphics and flow visualization of computer generated flow fields
[NASA-CR-182679] 13 p1767 N88-20573
Application of its transformation in color enhancement of LANDSAT imagery 17 p2365 N88-24082
Evaluation of TM false color composites for crop discrimination 17 p2367 N88-24096
CIMAG2: The computer program to generate color images
[AD-A191847] 18 p2557 N88-25175
Color charge motion in non-Abelian fields
[DE88-701306] 19 p2642 N88-25672
Cleanability of aircraft polyurethane topcoats
[AD-A193456] 23 p3170 N88-28878
Use of color CRTs (Cathode Ray Tubes) in aircraft cockpit: A literature search, revision B
[AD-A195062] 24 p3324 N88-29797

COLOR (PARTICLE PHYSICS)
U QUANTUM CHROMODYNAMICS

COLOR CENTERS
400-nm photoluminescence of a color center in undoped YAG grown under reducing atmosphere
[DE88-001760] 07 p0858 N88-15213
Anisotropy of light absorption by color centers in waveguides produced on photochromic glasses by diffusion 14 p1896 N88-21320
Dependence of formation of radiative color centers in optical glass fibers on technological factors 14 p1896 N88-21321
Infrared absorption spectroscopy and chemical kinetics of free radicals
[DE88-006536] 15 p2033 N88-22112

COLOR CODING
Generation of specific chromaticities on CRT monitors
[AD-A187739] 11 p1440 N88-18590
Utilization of space color transformation, linear contrast and filtration for enhancement of colored digital images
[INPE-4310-PRE/1176] 14 p1983 N88-21831
Comparative utilization of analog and digital processes in the treatment of MSS-LANDSAT data for studying the national parks of Brazil
[INPE-4011-TDL/240] 15 p2090 N88-22456
Visual enhancement of digital color imagery utilizing transformation in color coordinates (IHS transformation)
[INPE-4482-PRE/1248] 16 p2273 N88-23606
Use of color CRTs (Cathode Ray Tubes) in aircraft cockpit: A literature search, revision B
[AD-A195062] 24 p3324 N88-29797

COLOR ENHANCEMENT
U COLOR CODING

COLOR PERCEPTION
U COLOR VISION

COLOR PHOTOGRAPHY
Conversational Analysis of Color Images (CAICOU): An interactive development system for the analysis of color images
[RR-641-I-IMAG-39-LIFIA] 17 p2342 N88-23964
Anomalies in the vegetation in the Alto Xingu - MT 17 p2357 N88-24043
Remote sensing techniques in the estimation of the area cultivated with beans, corn, and castor beans in the Irece County (Bahia State) 17 p2358 N88-24045

COLOR VISION
Learning a color algorithm from examples
[AD-A184385] 05 p0632 N88-13862
Psychophysical, biochemical and histological studies of spectrally selective photic damage to primate retina
[AD-A188115] 11 p1517 N88-19063
Running head: What color is it
[NASA-CR-182600] 11 p1551 N88-19280
Design and testing of a luminance and chrominance stabilization system for a computer-controlled color display
[AD-A191922] 18 p2554 N88-25159
Central serous chorioretinopathy in USAF aviators: A review
[AD-A195697] 24 p3407 N88-30280
Eye movements and spatial pattern vision
[AD-A195496] 24 p3408 N88-30290

COLOR-MAGNITUDE DIAGRAM
Color-magnitude diagrams of star clusters in the Magellanic clouds from wide-field electronography. Part 3: NGC 1841
[PUBL-SER-C-FASC-14] 07 p0944 N88-15740

COLORATION
U COLOR

COLORIMETRY
Color fluctuations in the inner coma of Comet Halley as measured from VEGA-2 14 p2000 N88-21925
Near-infrared imaging of Comet Halley: Discovery of a color gradient in the inner coma 14 p2009 N88-21980
Note on the double crystal method of measuring heat transfer coefficient
[OUEL-1710/87] 17 p2338 N88-23950
Spectral classification of Low Mass X-ray Binaries (LMXB) energy spectra with color-color diagrams
[MPE-PREPRINT-111] 22 p3163 N88-28837

COLUMBIUM
U NIOBIUM

COLUMBUS SPACE STATION
Metallurgy laboratory for Columbus, executive summary
[SNIAS-813-CA/TS] 02 p0157 N88-10980
Thermophysical Properties Measurement Facility (TPMF) --- Columbus space station
[ESA-CR(P)-2417] 02 p0157 N88-10981
A preliminary study of a fluid science laboratory for space station (Columbus). Part 4: Executive summary
[NLR-TR-87023-L-PT-4] 02 p0170 N88-11072
Considerations concerning a thermal joint for a deployable or steerable battery radiator for the Columbus Polar Platform
[NLR-TR-86055-U] 03 p0276 N88-11739
Commercial Opportunities for Remote Sensing with Polar Platforms
[ESA-SP-269] 03 p0339 N88-12131
Possible commercial use of the polar platforms --- Columbus 03 p0339 N88-12132
Payload configurations and serviceability --- Columbus Polar Platforms 03 p0339 N88-12133
Legal protection of the Polar Platform's users 03 p0339 N88-12135
Confidentiality of data --- Columbus Polar Platforms 03 p0339 N88-12136
X-band SAR for a European remote sensing payload 03 p0340 N88-12142
Astromag: A particle spectrometer for the Space Station
[PREPRINT-557] 06 p0707 N88-14336
Columbus pressurized module utilization study, executive summary
[CS-RP-AI-027] 07 p0825 N88-15005
Allowable gravity-levels for Spacelab, Columbus and EURECA --- materials science
[BF-R-66.525-2] 07 p0838 N88-15084
Docking/Berthing Subsystem (DBS). Development part 1: Latching analysis --- Columbus
[ESA-CR(P)-2479] 08 p0962 N88-15825
Scientific objectives and functional requirements of life sciences in the Space Station 08 p1033 N88-16264
AURIO: A proposal for flying auroral imaging observatory on the Polar Platform in the Space Station/Columbus program 08 p1034 N88-16268
Technical aspects of future ocean colour remote sensing 08 p1042 N88-16298
Polar platform element of Space Station: Mission objectives, European priorities, candidate instrumentation and selection procedure 09 p1129 N88-16779
Space station overview 09 p1129 N88-16780
Use of Space Station for space science 09 p1129 N88-16782
Microgravity payloads and missions for Space Station: Some issues affecting compatibility with other payloads 09 p1129 N88-16783
The Columbus program, an overview 09 p1130 N88-16784
Coorbiting Platform Utilization Study (CPLUS), executive summary --- Columbus
[SN-WP-4000-DOC-6609/85/F] 09 p1133 N88-16798
Columbus feasibility studies. Volume 1: Requirements and system concept
[ETN-88-91073] 09 p1134 N88-16799
Columbus feasibility studies. Volume 2: Element constituents, mechanical
[ETN-88-91074] 09 p1134 N88-16800
Columbus feasibility studies. Volume 3: Avionics, systems
[ETN-88-91075] 09 p1134 N88-16801
Columbus feasibility studies. Volume 5: Programmatics
[ETN-88-91076] 09 p1134 N88-16802
Model of space platform electromagnetic (EMC) configuration
[ESA-CR(P)-2500] 09 p1135 N88-16809
Study on long term evolution towards European manned space flight. Volume 1: Executive summary
[MBB-RA3-004/87-VOL-1] 10 p1266 N88-17689
Project management in astronautics: From Spacelab to Columbus
[MBB-URE-943/87] 10 p1315 N88-17858
Columbus feasibility studies. Volume 4: Integration, test, and operations
[ETN-88-90576] 11 p1445 N88-18614
Man-Tended Free Flyer operational design features 12 p1585 N88-19485
Mission profiles of the MTFF co-orbiting with the US Space Station 12 p1585 N88-19487
Cost-effective orbit transfer modes for satellite retrieval and servicing --- Space Station 12 p1586 N88-19489
Assembly of user systems at Space Station 12 p1586 N88-19490
Analysis of RVD operations in manned space missions 12 p1586 N88-19494
On a knowledge based assisted system for highly autonomous control of experiment-manipulators in the Man-Tended Free Flyer 12 p1588 N88-19505
Promising concepts for ground-to-orbit experiment teleoperation --- Columbus 12 p1590 N88-19518
Columbus Simulation Facility (CSF) 12 p1590 N88-19522
External payload servicing: Operational requirements and technology 12 p1593 N88-19541
Microgravity User Support Center (MUSC) for EURECA, Spacelab and Columbus missions 12 p1660 N88-19947
Animal research on the Space Station 12 p1662 N88-19964
Feasibility demonstration of a sensor for high-quality two-phase flow --- Space Station
[NLR-TR-87009-U] 13 p1767 N88-20569
System and concept design of the SSRMS latching end effector --- Space Station 14 p1875 N88-21204
Colombus feasibility studies, executive summary
[ETN-88-92334] 17 p2311 N88-23820
Study on long-term evolution towards European manned spaceflight. Volume 1: Executive summary
[ERNO-OX1-002/88-VOL-1] 24 p3330 N88-29827
Studies on rocket exhaust plumes and impingement effects related to the Columbus Space Station program: Executive summary
[DFVLR-IB-222-88-A-12] 24 p3337 N88-29862
The LTPP communication processor --- Columbus and Hermes
[CL/CP/SES/FR/004] 24 p3415 N88-30328
Candidate functions for advanced technology implementation in the Columbus mission planning environment 24 p3417 N88-30340
COLUMNS
Beam and column buckling under directed loading
[PB87-124004] 06 p0722 N88-14436
Distortional buckling formulae for thin-walled channel columns
[PB87-124012] 06 p0722 N88-14437
COLUMNS (SUPPORTS)
Buckling of viscoelastic columns 02 p0190 N88-11187
Residual stress effect on stability of axially loaded columns
[PB87-143889] 08 p0996 N88-16032
COMBAT
Loss of performance due to military clothing and equipment
[IZF-1986-13] 01 p0077 N88-10490
Improvements to the adaptive maneuvering logic program
[NASA-CR-3985] 03 p0262 N88-11648
Apache for the battlefield of today and the 21st century 03 p0265 N88-11670
Impact of flying qualities on mission effectiveness for helicopter air combat, volume 1
[NASA-CR-166568] 06 p0669 N88-14100
Advanced helicopter cockpit and control configurations for helicopter combat missions
[NASA-TM-100017] 07 p0821 N88-14988
A piloted simulation investigating handling qualities and performance requirements of a single-pilot helicopter in air combat employing a helmet-driven turreted gun
[AD-A186878] 09 p1116 N88-16689
Future fighter maneuverability for air combat
[MBB/LKE-1/S/PUB/120] 10 p1312 N88-17843
Hardware implementation for special functions. An application for combat simulation 10 p1374 N88-18197
Future directions in computer architecture 10 p1383 N88-18257
State of the art of natural language processing
[AD-A188112] 11 p1530 N88-19136
A computer graphics simulation of the endgame in aircraft combat survivability
[AD-A187826] 11 p1541 N88-19214
Manned simulation: Helpful means to determine and improve structural load criteria 12 p1581 N88-19459
Computer aided tactics for air combat 12 p1597 N88-19559
Predicting Air Combat Maneuvering (ACM) performance: Fleet fighter ACM readiness program grades as performance criteria
[AD-A191605] 19 p2710 N88-26099
Realistic planning scenarios
[AD-A191640] 19 p2740 N88-26267
Computation of ECM (Electronic Counter-Measures) war reserve materiel spare requirements
[AD-A193301] 21 p2897 N88-27195
Analysis of ATCRBS (Air Traffic Control Radar Beacon System), mode select (Mode S) in combat operations
[AD-A193140] 22 p3040 N88-28050
Proposal for a new aggressor aircraft
[AD-A194311] 22 p3041 N88-28056
Design guidelines for prevention of corrosion in combat and tactical vehicles
[AD-A194172] 22 p3055 N88-28126
Stress and the military pilot
[AD-A194313] 22 p3133 N88-28626
Electronic combat roadmap for space
[AD-A194282] 22 p3146 N88-28709
Future air-to-air training for the RF-4
[AD-A194363] 23 p3240 N88-29284
SDI (Strategic Defense Initiative) battle management/C3 (Command, Control and Communications) algorithms technology program plan
[AD-A194357] 23 p3275 N88-29495
COMBINATIONS (MATHEMATICS)
On perfect hash functions
[ENST-86D008] 01 p0087 N88-10565
COMBINATORIAL ANALYSIS
NT COMBINATIONS (MATHEMATICS)
NT PARTITIONS (MATHEMATICS)
NT PERMUTATIONS
An exact analysis and performance of framed ALOHA with capture
[AD-A185006] 05 p0574 N88-13500
Search rearrangement backtracking often requires exponential time to verify unsatisfiability
[AD-A186121] 07 p0909 N88-15511
The perfectly matchable subgraph polytope of an arbitrary graph
[AD-A185993] 07 p0913 N88-15539
Polyhedral combinatorics
[CWI-OS-R8701] 08 p1072 N88-16466
The construction of a pedagogy to promote meaningful learning of strategies and tactics for solving problems of elementary combinatorics
[AD-A187928] 11 p1542 N88-19216
Analysis of simulated annealing type algorithms
[AD-A189382] 12 p1679 N88-20037
The clique polytope of a graph
[MEMO-663] 14 p1963 N88-21710
Parallel computing in combinatorial optimization
[CWI-OS-R8720] 16 p2254 N88-23468
Algorithms and data structures for an expanded family of matroid intersection problems
[AD-A191482] 18 p2562 N88-25213
Challenge problems focusing on equality and combinatory logic: Evaluating automated theorem-proving programs
[DE88-010057] 20 p2844 N88-26879
The combinatorics of object recognition in cluttered environments using constrained search
[AD-A196224] 24 p3422 N88-30364
COMBINED STRESS
Estimation multiaxial elastic-plastic notch stresses and strains in combined loading
[FB-2/1986] 01 p0060 N88-10382
The use of Hencky's equations for the estimation of multiaxial elastic-plastic notch stresses and strains
[FB-3/1986] 01 p0060 N88-10383
Design procedures for fiber composite box beams
[NASA-TM-100296] 09 p1139 N88-16828
COMBUSTIBILITY
U FLAMMABILITY
COMBUSTIBLE FLOW
Flame driving of longitudinal instabilities in liquid fueled dump combustors
[AD-A183536] 01 p0006 N88-10033
European reacting flow research: A final assessment
[AD-A185833] 07 p0828 N88-15022
Effects of turbulence on stationary and non-stationary processes in C-systems
[AD-A186215] 07 p0849 N88-15154
Turbulence interactions in single- and multi-phase turbulent mixing and combustion processes
[AD-A187505] 10 p1332 N88-17960
Measurement of rate constants of elementary gas reactions of importance to upper atmosphere and combustion systems
[AD-A189432] 13 p1737 N88-20386
An investigation of flow structure, mixing and chemical reaction in combusting turbulent flows
[AD-A189980] 15 p2034 N88-22117
Advanced diagnostics for reacting flows
[AD-A190485] 15 p2035 N88-22122
Chemically reacting turbulent flow
[AD-A190522] 15 p2065 N88-22311
Ignition and flame spread of PMMA
[NASA-TT-20290] 20 p2771 N88-26431
Experimental research of combustion systems 21 p2927 N88-27371
Modeling and experimental study of a reactive flow confined with well injection 24 p3351 N88-29946
COMBUSTION
NT AFTERBURNING
NT DEFLAGRATION
NT EROSIVE BURNING
NT FUEL COMBUSTION

NT HYDROCARBON COMBUSTION
NT METAL COMBUSTION
NT NUCLEAR FUEL BURNUP
NT PROPELLANT COMBUSTION
NT SOLID PROPELLANT COMBUSTION
NT SOLID PROPELLANT IGNITION
NT SPONTANEOUS COMBUSTION
NT SUPERSONIC COMBUSTION
Laser probes of natural gas ignition chemistry
[PB87-209599] 01 p0021 N88-10129
Improved numerical methods for turbulent viscous recirculating flows 02 p0185 N88-11148
An adaptive pseudo-spectral method for reaction diffusion problems
[NASA-CR-178394] 02 p0224 N88-11414
Combustion control with smart sensors
[DE87-013688] 03 p0281 N88-11768
Flammability limits in cocurrent smoldering combustion
[DE87-014102] 03 p0284 N88-11785
Flame acceleration and transition to detonation in channels
[DE87-014193] 03 p0284 N88-11786
Numerical simulation of turbulent premixed combustion and decay of turbulent swirling flow
[DE87-014253] 03 p0284 N88-11787
Techniques for fire detection 04 p0406 N88-12521
Fire-related standards and testing 04 p0406 N88-12522
Fire-related medical science 04 p0406 N88-12525
Space station internal environmental and safety concerns 04 p0407 N88-12527
Microgravity combustion fundamentals 04 p0407 N88-12528
Ignition and combustion of metals in oxygen 04 p0407 N88-12530
Combustion related shear-flow dynamics in elliptic supersonic jets 05 p0531 N88-13232
Correlation of air pressure drop and flame arrestor characteristics for explosion suppression materials
[AD-A184960] 05 p0548 N88-13340
Turbulence generation in combustion
[AD-A184810] 05 p0561 N88-13413
A study of the interaction of laser light with liquid propellant drops
[AD-A185117] 05 p0587 N88-13582
Summary of discussions at the Ninth Meeting of the Sandia Cooperative Group on the Aerothermochemistry of Turbulent Combustion
[DE88-002281] 06 p0680 N88-14165
Mixing and combustion of pulsed gas jets
[PB88-112834] 06 p0680 N88-14169
Mixing and combustion of pulsed gas jets
[PB88-108014] 06 p0680 N88-14170
Catalytic combustion of methane
[PB88-123112] 07 p0829 N88-15028
Dimensions of ignition zones in blow-outs of combustible gases from rectangular and circular ports 07 p0918 N88-15577
An analytical study of the hydrogen-air reaction mechanism with application to scramjet combustion
[NASA-TP-2791] 08 p0966 N88-15846
The effect of microgravity on flame spread over a thin fuel
[NASA-TM-100195] 08 p0967 N88-15853
Diffusion description of flame propagation due to the translational motion of burning reaction products
[DE88-700676] 10 p1297 N88-17757
The role of analytical chemistry in assessing atmospheric effects of combustion
[DE88-003909] 10 p1352 N88-18082
Fire tests on loose-fill insulation materials
[DE88-751182] 11 p1467 N88-18748
Investigations into shock-induced enhancement of mixing and combustion in supersonic burners
[AD-A189609] 12 p1607 N88-19608
The effect of combustion gas flow on the rotational dynamics of a spinning solid fuel rocket 13 p1732 N88-20358
Combustion theory and related questions
[AD-A189160] 13 p1737 N88-20382
Uncertainties in hydrogen combustion
[DE88-005354] 13 p1739 N88-20395
Microprobe examination of composite materials produced by burning of Ti, Cr, C powders with powder of any one Fe-group metal 14 p1886 N88-21269
Kinetics of combustion of finely divided solid fuel in granules
[BLL-M-37626-(5828.4)] 14 p1888 N88-21283
Numerical simulation of turbulent premixed combustion and decay of turbulent swirling flow
[DE88-006588] 14 p1888 N88-21284
The combustion synthesis of boride composites
[DE88-005474] 15 p2028 N88-22084
Cetane scale evaluation and possible modification
[AD-A189730] 15 p2048 N88-22200
Premixed turbulent flame calculation 16 p2196 N88-23098
Soviet combustion research
[PB88-182324] 18 p2483 N88-24730
The thermodynamic properties of quinoline and isoquinoline
[DE88-001218] 18 p2484 N88-24735
Evaluation of manure as a feedstock for gas turbines 18 p2536 N88-25050
Solid-state combustion synthesis of ceramics and alloys in reduced gravity
[NASA-CR-4163] 19 p2608 N88-25479
Theoretical studies of dynamics combustion
[DE88-007565] 19 p2611 N88-25495
Measurement of the radiative properties of gas and oil flames
[NASA-TT-20299] 19 p2612 N88-25502
Atomization in a turbulent shear layer: Preliminary measurements 19 p2624 N88-25565
Recent advances in photochemical techniques for ignition and combustion enhancement 19 p2625 N88-25570
Anatomy of group burning mode transitions in spray group combustion 19 p2626 N88-25578
Modelling of premixed combustion using a thin flame sheet and the effect of the hydrodynamic instability
[DE88-009467] 20 p2770 N88-26423
Asynchronous optical sampling for laser-based combustion diagnostics in high pressure flames
[AD-A192920] 20 p2770 N88-26428
Pulsed spray structure and atomisation techniques
[AD-A192280] 20 p2800 N88-26614
Premixed turbulent flame propagation
[AD-A192955] 21 p2909 N88-27265
Summary of discussions at the Tenth Meeting of the Sandia Cooperative Group on the Aerothermochemistry of Turbulent Combustion
[DE88-008467] 21 p2910 N88-27269
Theoretical study and numerical simulation of flame fronts
[PB88-122932] 22 p3051 N88-28104
Diesel combustion fundamentals, phase 1, volume 1
[AD-A193831] 22 p3052 N88-28107
Particle sizing in combustion systems, using scattered laser light
[AD-A196231] 24 p3352 N88-29953
Optical measurements of soot and temperature profiles in premixed propane-oxygen flames
[NASA-TM-101343] 24 p3358 N88-29997

COMBUSTION CHAMBERS
NT DUMP COMBUSTORS
Optical sizing of soot in gas turbine combustors and exhaust augmentor tubes
[AD-A183785] 01 p0006 N88-10034
On the modelling of non-reactive and reactive turbulent combustor flows 02 p0169 N88-11061
Turbine Engine Hot Section Technology, 1985
[NASA-CP-2405] 02 p0184 N88-11140
Aerothermal modeling program, phase 2 02 p0185 N88-11149
Fuel-injector/air-swirl characterization 02 p0185 N88-11150
Combustor-diffuser interaction program 02 p0185 N88-11152
Dilution jet mixing program, phase 3 02 p0185 N88-11153
On the mixing of a row of jets with a confined crossflow 02 p0185 N88-11154
3D inelastic analysis methods for hot section components 02 p0187 N88-11164
3-D inelastic analysis methods for hot section components 02 p0187 N88-11165
SCRAM JET (Supersonic Combustion Ramjet) combustion experiments 04 p0404 N88-12512
Longitudinal mode combustion instabilities in air breathing engines 06 p0680 N88-14166
Recent advances in high temperature instrumentation for hot section applications
[NASA-TM-100282] 06 p0707 N88-14339
Nitrogen scale-up
[AD-A185702] 06 p0709 N88-14351
Effects of turbulence on stationary and non-stationary processes in C-systems
[AD-A186215] 07 p0849 N88-15154
Design of a solid fuel combustion chamber
[VTH-LR-447] 09 p1141 N88-16837
Investigation of the flow and combustion behavior in a solid fuel combustion chamber, including the measuring program
[VTH-LR-460] 09 p1141 N88-16838
Design of a gas mass flow control system for the gas inlet installation of a solid fuel combustion chamber
[VTH-LR-471] 09 p1141 N88-16839
Solid fuel combustion chamber
[VTH-LR-515] 09 p1141 N88-16842
Numerical simulation of axisymmetric turbulent flow in combustors and diffusors
[NASA-CR-4115] 10 p1268 N88-17582
Numerical simulation of diffuser/combustor dome interaction 10 p1281 N88-17663
Measurements of gas turbine combustor and engine augmentor tube sooting characteristics
[AD-A187831] 11 p1440 N88-18592
Unsteady heat transfer in turbine blade ducts: Focus on combustor sources
[NASA-TM-100815] 11 p1486 N88-18870
Error evaluation of some practical thermocouple probes for gas turbine combustor tests
[NAL-TR-938] 11 p1489 N88-18886
Assessment, development and application of combustor aerothermal models
[NASA-TM-100290] 12 p1582 N88-19469
Linear and nonlinear acoustics with nonuniform entropy in combustion chambers 12 p1607 N88-19609
Interaction between two-dimensional sonic jets and supersonic flow to model heat addition in a supersonic combustor
[AD-A189572] 13 p1716 N88-20261
Finite area combustor theoretical rocket performance
[NASA-TM-100785] 14 p1883 N88-21252
High-temperature combustor liner tests in structural component response test facility 15 p2077 N88-22383
Life assessment of combustor liner using unified constitutive models 15 p2077 N88-22384
Combustion of a double base fuel in the presence of inert gases
[INPE-4516-RPE/564] 16 p2170 N88-22936
Water flow visualisation of a ramrocket combustion chamber 16 p2202 N88-23138
An empirical model of the effects of curvature and convergence on dilution jet mixing
[NASA-TM-100896] 18 p2466 N88-24640
Thrust chamber thermal barrier coating techniques
[NASA-TM-100933] 18 p2476 N88-24690
Combustion behavior of the vitiator. Experimental results of a second test series
[VTH-LR-509] 18 p2484 N88-24734
Evaluation of manure as a feedstock for gas turbines 18 p2536 N88-25050
Low frequency pressure oscillations in a model ramjet combustor 19 p2625 N88-25571
The pressure field generated in a cold-flow side-dump ramjet combustor 19 p2625 N88-25572
Numerical grid generation and flow simulation in SSME thrust chamber 19 p2626 N88-25577
A multiple chamber volume-filling model for prediction of transient solid rocket motor ballistic performance 19 p2633 N88-25618
An efficient computational tool for ramjet combustor research
[DE88-010034] 20 p2760 N88-26369
Dynamics and stability of combustion driven self oscillations in presence of various frequencies. Extensive stability criteria
[ETN-88-92123] 20 p2771 N88-26432
Technical instructions for a control operating system of the gas flow installation for the solid fuel combustion chamber
[LR-507] 20 p2788 N88-26537
Effects of ceramic surfaces on autoignition in a constant volume combustion apparatus
[AD-A193055] 21 p2909 N88-27266
Investigation of annular flow at high evaporation rates in view of liquid film cooling
[DFVLR-FB-88-08] 21 p2949 N88-27517
Experimental validation of a zero-dimensional computer model for spark-ignition engines
[DE88-009034] 21 p2957 N88-27565
Application of laser diffraction techniques to particle sizing in solid propellant rocket motors
[AD-A193841] 22 p3049 N88-28089
A study of flame spreading and combustion phenomena of stick propellants
[AD-A193598] 22 p3052 N88-28106
Numerical investigations in three-dimensional internal flows
[NASA-CR-183108] 23 p3210 N88-29106
Preliminary studies of NF3+H2 production of N2(A3 sigma(+)u) in a supersonic flow
[AD-A194479] 23 p3219 N88-29162
Automatic data retrieval from rocket motor holograms
[AD-A195586] 24 p3337 N88-29864
Combustion and fuels in gas turbine engines
[AGARD-CP-422] 24 p3345 N88-29910
Comparison of the performance of a reverse flow annular combustion chamber under low and high pressure conditions 24 p3347 N88-29923
Flow characteristics of a model annular combustor 24 p3347 N88-29924

Particle size measurements in sooting combustion systems 24 p3348 N88-29931
Numerical models for analytical predictions of combustor aerothermal performance characteristics 24 p3349 N88-29935
Gas turbine combustion modeling 24 p3349 N88-29936
Three-dimensional gas turbine combustor modelling 24 p3349 N88-29937
Numerical modeling of combustion processes in gas turbines 24 p3350 N88-29939
Three-dimensional combustor predictors: A comparison of equilibrium and laminar flamelet chemistry models 24 p3350 N88-29940
The effect of particle properties on radiative heat transfer 24 p3350 N88-29941
Analysis of the flow through double swirl airblast atomizers 24 p3351 N88-29949
The behaviour of synthetic fuels in a small transparent combustor 24 p3351 N88-29950
A small annular combustor of high power density, wide operating range and low manufacturing cost 24 p3351 N88-29951
Transition mixing study empirical model report [NASA-CR-182139] 24 p3371 N88-30076

COMBUSTION CHEMISTRY
Development of many-body methods for flame chemistry and large molecule applications [AD-A184451] 03 p0284 N88-11789
Laser probes of propellant combustion chemistry [AD-A184854] 05 p0561 N88-13415
Detailed mechanism of toluene oxidation and comparison with benzene [NASA-TM-100261] 05 p0563 N88-13428
Carbon monoxide and turbulence-chemistry interactions: Blowoff and extinction of turbulent diffusion flames [AD-A186276] 07 p0828 N88-15025
Non-steady group combustion of a cloud of char particles [DE87-010773] 08 p0966 N88-15849
Combustion mechanisms [AD-A187979] 11 p1453 N88-18660
Combustion and performance characteristics of methanol plus higher alcohols in a spark ignition engine [PB88-147962] 14 p1918 N88-21451
Laser spectroscopy and dynamics of combustion intermediates [DE88-006541] 15 p2033 N88-22110
Theoretical studies of dynamics combustion [DE88-007565] 19 p2611 N88-25495
Minimum ignition energy measurements using laser induced spark initiation 19 p2632 N88-25610
Theoretical studies of the chemical reactions involved in the ignition of nitramines 19 p2632 N88-25615
Temperature and species profiles in propellant ignition and combustion 19 p2633 N88-25616
Experiments and modeling of multi-component fuel behavior in combustion [AD-A195011] 24 p3343 N88-29896
Gas phase combustion chemistry of nitramine propellants [AD-A195082] 24 p3344 N88-29902

COMBUSTION CONTROL
Combustion control with smart sensors [DE87-013688] 03 p0281 N88-11768
Study of industry requirements that can be fulfilled by combustion experimentation aboard space station [NASA-CR-180854] 11 p1566 N88-19377
Control of combustion and acoustically coupled fluid dynamic instabilities 17 p2318 N88-23843
A study of flame spreading and combustion phenomena of stick propellants [AD-A193598] 22 p3052 N88-28106

COMBUSTION EFFICIENCY
Performance and combustion characteristics of direct-injection stratified-charge rotary engines [NASA-TM-100134] 04 p0400 N88-12490
Study of electrostatic modulation of fuel sprays to enhance combustion performance in an aviation gas turbine [AD-A184967] 05 p0548 N88-13341
Oxygen enriched combustion system performance study [DE88-001500] 05 p0562 N88-13424
Small engine technology programs 08 p0956 N88-15801
An investigation into the feasibility of using a dual-combustion mode ramjet in a high Mach number tactical missile [AD-A186906] 09 p1119 N88-16705
Finite area combustor theoretical rocket performance [NASA-TM-100785] 14 p1883 N88-21252
Research as part of the Air Force in aero propulsion technology (AFRAPT) program [AD-A190336] 15 p2019 N88-22036
Advanced B and Al combustion kinetics over wide temperature ranges [AD-A190752] 15 p2036 N88-22128
Measurement data processing system based on personal computer: For scramjet combustion test [DE88-751807] 16 p2174 N88-22959
Characteristic time correlations to liquid fuel ramjet combustion efficiency 19 p2624 N88-25566
Mach 2 combustion characteristics of hydrogen/hydrocarbon fuel mixtures 19 p2625 N88-25568
Basic research in supersonic combustion 19 p2634 N88-25623
Atomization of alternative fuels 24 p3345 N88-29913
Spray performance of a vaporizing fuel injector 24 p3346 N88-29919
The characterizatin of combustion by fuel composition: Measurements in a small conventional combustor 24 p3346 N88-29920
High performance turbofan afterburner systems 24 p3347 N88-29922
Comparison of the performance of a reverse flow annular combustion chamber under low and high pressure conditions 24 p3347 N88-29923

COMBUSTION HEAT
U HEAT OF COMBUSTION

COMBUSTION INSTABILITY
U COMBUSTION STABILITY

COMBUSTION PHYSICS
Combustion in turbulent jets and buoyant flames [PB87-232674] 03 p0283 N88-11779
The calculation of thermal rate constants for gas-phase and heterogeneous reactions in combustion processes [AD-A184435] 03 p0284 N88-11788
Spacecraft Fire Safety [NASA-CP-2476] 04 p0406 N88-12520
Microgravity combustion fundamentals 04 p0407 N88-12528
Spacecraft material flammability testing and configurations 04 p0407 N88-12529
Combustion characteristics of gas turbine alternative fuels [NASA-TM-100247] 05 p0548 N88-13338
SRB combustion dynamics analysis computer program (CDA-1) [NASA-CR-182404] 07 p0830 N88-15032
The carbon dioxide chaperon efficiency for the reaction H + O2 + M yields HO2 + M from ignition delay times behind reflected shock waves [NASA-TM-100125] 07 p0830 N88-15036
Combustion mechanisms [AD-A187979] 11 p1453 N88-18660
A study of combustion and flow behaviour in solid-propellant rocket motors [UTIAS-280] 13 p1732 N88-20357
Advanced B and Al combustion kinetics over wide temperature ranges [AD-A190752] 15 p2036 N88-22128
Microgravity combustion discipline working group summary of requirements for noncontact temperature measurements 17 p2328 N88-23902
Requirements for temperature and species concentration measurements in microgravity combustion experiments 17 p2329 N88-23903
Laser Diagnostics for combustion temperature and species measurements 17 p2330 N88-23912
On the structure, propagation, extinction and stability of laminar premixed flames in dissociation equilibrium 18 p2483 N88-24728
Combustion of PMMA, PE and PS in a ramjet [VTH-LR-514] 18 p2484 N88-24733
CFD benefits, goals, stepping-stones and techniques. Proposals for the scientific programme of the European Reserch Centre on flow, turbulence and combustion --- computational fluid dynamics [CFDU/88/1] 18 p2510 N88-24894
Next-generation fire extinguishing agent. Phase 1: Suppression concepts [AD-A192279] 19 p2614 N88-25514
Driving of axial acoustic fields by side-wall stabilized premixed flames 19 p2629 N88-25592
Basic research in supersonic combustion 19 p2634 N88-25623
Study of the local behavior of a flame [ETN-88-92300] 20 p2771 N88-26433
A study of flame spreading and combustion phenomena of stick propellants [AD-A193598] 22 p3052 N88-28106
Soot and radiation in a gas turbine combustor [AD-A191991] 23 p3179 N88-28924
Combustion dynamics and thermal structure of a planar spray flame 23 p3190 N88-28985
Numerical modeling of combustion processes in gas turbines 24 p3350 N88-29939
Modeling the stability of a turbulent premixed flame, downstream from a step by a Lagrangian method 24 p3350 N88-29943
Modeling and experimental study of a reactive flow confined with well injection 24 p3351 N88-29946

COMBUSTION PRODUCTS
Real time analysis of detonation products [DE87-007453] 01 p0031 N88-10195
The equation of state of PETN detonation products [DE87-013796] 02 p0155 N88-10971
Experimental verification of vapor deposition rate theory in high velocity burner rigs 02 p0189 N88-11179
Laser probes of propellant combustion chemistry [AD-A184854] 05 p0561 N88-13415
Pulsed plasma jet igniters: Species measurements in methane combustion [DE88-001389] 05 p0562 N88-13422
Formation and destruction of nitrous oxide in lean, premixed combustion [DE88-001390] 05 p0562 N88-13423
Impacts of world development on selected characteristics of the atmosphere: An integrative approach. Volume 1: Main report [DE88-001495] 07 p0875 N88-15309
Ionic mechanisms of soot formation in flames [AD-A186195] 08 p0966 N88-15848
CARS measurements of combustion. 1: Precision of thermometry [NAL-TR-939] 10 p1299 N88-17769
The role of analytical chemistry in assessing atmospheric effects of combustion [DE88-003909] 10 p1352 N88-18082
Gas cleaning at high temperatures and pressures for gas turbines [DE88-751171] 11 p1440 N88-18593
Measurements of particulates in solid propellant rocket motors [AD-A187777] 11 p1446 N88-18621
Simulation of infrared spectra [AD-A187881] 11 p1453 N88-18658
Measurement of combustion aerosol size distributions with multistage inertial impactors [DE88-751101] 11 p1454 N88-18669
Fuels combustion research [AD-A189114] 13 p1736 N88-20381
Burning characteristics and flammability of PVC cables in groups [NASA-TT-20226] 14 p1893 N88-21303
Development of a laboratory test for multiport fuel injector deposits - evaluation of the Jet Fuel Thermal Oxidation Test apparatus (JFTOT) [AD-A191313] 16 p2183 N88-23015
Evaluation of manure as a feedstock for gas turbines 18 p2536 N88-25050
Measurement of particulate size in solid propellant rocket motors 19 p2630 N88-25599
Temperature and species profiles in propellant ignition and combustion 19 p2633 N88-25616
Freely expanding detonation products: Scaling of rate processes [DE88-007827] 20 p2799 N88-26606
Carbon deposition model for oxygen-hydrocarbon combustion, volume 1 [NASA-CR-179375] 21 p2908 N88-27254
Carbon deposition model for oxygen-hydrocarbon combustion, volume 2 [NASA-CR-179376] 21 p2908 N88-27255
Finite-rate water condensation in combustion-heated wind tunnels [NASA-TP-2833] 22 p3046 N88-28075
Automatic data retrieval from rocket motor holograms [AD-A195586] 24 p3337 N88-29864
Gas turbine smoke measurement: A smoke generator for the assessment of current and future techniques 24 p3348 N88-29930
Rates of formation of soot from hydrocarbon flames and its destruction 24 p3349 N88-29933
The influence of pressure on soot formation 24 p3349 N88-29934

COMBUSTION STABILITY
NT FLAME STABILITY
Flame driving of longitudinal instabilities in liquid fueled dump combustors [AD-A183536] 01 p0006 N88-10033
Longitudinal mode combustion instabilities in air breathing engines 06 p0680 N88-14166
European reacting flow research: A final assessment [AD-A185833] 07 p0828 N88-15022
Catalytic combustion of methane [PB88-123112] 07 p0829 N88-15028
Characterizing particle combustion in a Rijke burner [AD-A186157] 08 p0966 N88-15847
Basic instability mechanisms in chemically reacting subsonic and supersonic flows [AD-A190101] 15 p2034 N88-22120

Investigation of combustion in large vortices
[AD-A190406] 15 p2035 N88-22121
AFRAPT (Air Force Research in Aero Propulsion Technology) trainee program
[AD-A190525] 15 p2035 N88-22123
Control of combustion instabilities in ramjet motors
19 p2625 N88-25574
Development of a generic combustion stability code for liquid propellant rocket engines
19 p2626 N88-25576
Liquid Engine Jet Atomization Workshop report
19 p2627 N88-25584
The 24th JANNAF Combustion Meeting, volume 1
[AD-A190163] 19 p2627 N88-25585
Evidences for distributed combustion
19 p2628 N88-25586
Characterization of a modified Rijke burner for measurement of distributed combustion
19 p2628 N88-25587
Nonlinear mechanisms of solid propellant combustion instability 19 p2628 N88-25588
Propellant combustion response to oscillatory radiant heat flux 19 p2628 N88-25589
Motor test data comparisons with laboratory data and stability predictions 19 p2629 N88-25594
One person's view of velocity-coupled instability
19 p2629 N88-25595
Measurement of particulate size in solid propellant rocket motors 19 p2630 N88-25599
Basic research in supersonic combustion
19 p2634 N88-25623
Dynamics and stability of combustion driven self oscillations in presence of various frequencies. Extensive stability criteria
[ETN-88-92123] 20 p2771 N88-26432
Study of the local behavior of a flame
[ETN-88-92300] 20 p2771 N88-26433
Evaluation and improvement of liquid propellant rocket chugging analysis techniques. Part 1: A one-dimensional analysis of low frequency combustion instability in the fuel preburner of the space shuttle main engine
[NASA-CR-183106] 21 p2903 N88-27224
Evaluation and improvement of liquid propellant rocket chugging analysis techniques. Part 2: A study of low frequency combustion instability in rocket engine preburners using a heterogeneous stirred tank reactor model
[NASA-CR-182724] 21 p2903 N88-27225
Small scale mixing in the initial region of a jet
[AD-A193500] 23 p3192 N88-28994
High performance turbofan afterburner systems
24 p3347 N88-29922

COMBUSTION TEMPERATURE
Ignition and flame propagation in sprays
[AD-A184679] 03 p0283 N88-11781
Flow characteristics of a model annular combustor
24 p3347 N88-29924

COMBUSTION WAVES
U FLAME PROPAGATION

COMBUSTION WIND TUNNELS
Finite-rate water condensation in combustion-heated wind tunnels
[NASA-TP-2833] 22 p3046 N88-28075

COMBUSTORS
U COMBUSTION CHAMBERS

COMET HEADS
Spatial distribution of O(supra 1D) from Comet Halley
14 p1999 N88-21913

COMET NUCLEI
Dynamics of meteor streams
06 p0732 N88-14503
Results of infrared spectrometer experiment. 1: Infrared radiation of parent molecules in Halley's Comet
13 p1726 N88-20325
Results of infrared spectrometer experiment. 2: Infrared radiometry of nucleus of Halley's Comet
13 p1727 N88-20326
Calculation of the shape of the contact surface at Comet Halley 14 p1995 N88-21892
Plasma phenomena in the vicinity of the closest approach of VEGA-1, 2 spacecraft to the Comet Halley nucleus 14 p1996 N88-21899
Photometry of P/Halley (1982i): Is what we have learned useful for other comets? 14 p1998 N88-21909
Water vapor and hydroxyl distributions in the inner coma of Comet Halley measured by the VEGA-2 three channel spectrometer TKS 14 p1998 N88-21910
Narrow-band photometry of Comet P/Giacobini-Zinner at the time of ICE encounter 14 p1998 N88-21911
CCD-observations of gas and dust jets in the coma of Comet Halley 14 p1998 N88-21912
Analysis of the coma outburst of Comet Halley, March 24 to 25 (UT), 1986 14 p2000 N88-21920
Color fluctuations in the inner coma of Comet Halley as measured from VEGA-2 14 p2000 N88-21925
Anisotropic emission from comets: Fans versus jets. 1: Concept and modeling 14 p2001 N88-21927
Anisotropic emission from comets: Fans versus jets. 2: Periodic Comet Tempel 2 14 p2001 N88-21928
Comet P/Halley's near-nucleus jet activity
14 p2001 N88-21929
Dust photometry in the near nucleus region of Comet Halley from VEGA-2 observations
14 p2001 N88-21930
The dust around the nucleus of Comet Halley
14 p2003 N88-21942
The nucleus of Comet Halley
14 p2004 N88-21947
Comparison of active regions on the nucleus of Comet Halley 14 p2004 N88-21948
Reconstruction of the orientation and shape of the nucleus of Comet Halley 14 p2004 N88-21949
Estimates of masses, volumes and densities of short-period comet nuclei 14 p2004 N88-21950
Porosity and fractality of a cometary nucleus
14 p2004 N88-21951
Properties of the nucleus of P/Halley
14 p2004 N88-21952
Crustal models of the evolving comet nucleus
14 p2005 N88-21953
Simulation of cometary nuclei
14 p2005 N88-21954
Diversity of comets, synergic temperature effects and the stability of organic compounds in icy nuclei
14 p2005 N88-21955
Rosetta: A mission to sample the nucleus of a comet
14 p2005 N88-21958
Retrieving samples from comet nuclei
14 p2006 N88-21959
P/Halley activity in November 1985
14 p2006 N88-21966
Different trapping mechanisms of gases by water ice and their relevance for comet nuclei
14 p2007 N88-21970
On the periodic southward jets of Comet Halley before perihelion passage 14 p2008 N88-21978
Dust tail streamers and Halley's nucleus rotation
14 p2008 N88-21979
Near-infrared imaging of Comet Halley: Discovery of a color gradient in the inner coma
14 p2009 N88-21980
The light curve of P/Halley and the rotation of its nucleus 14 p2009 N88-21984
Temperature of the nucleus of Comet Halley
14 p2009 N88-21985
Consequences of the size determination of P/Halley by space probes on the scale of sizes of cometary nuclei
14 p2009 N88-21986
Physical-mechanical properties of matrices on the comet nuclei surface models 14 p2010 N88-21987
Sublimation characteristics of H2O comet nucleus with CO2 impurities 14 p2010 N88-21988
The splitting of Comet Halley 1986
14 p2010 N88-21989
Photographic observations of the large scale features of Comet Halley 16 p2288 N88-23698
The evolution of cometary activity
18 p2594 N88-25416
Cometary nucleus as aggregate of planetesimals
[ISAS-RN-364] 19 p2741 N88-26275
Study of comet nucleus gamma-ray spectrometer penetration system
[NASA-CR-177393] 20 p2883 N88-27120
Processing and analysis of images transmitted by Vega space probes over Halley's comet
[ETN-88-92291] 20 p2885 N88-27131

COMET TAILS
Comparative plasma tails of Venus and comets
01 p0116 N88-10742
Plasma-tail activity and the interplanetary medium at Halley's Comet during Armada Week: 6-14 March 1986
01 p0118 N88-10752
Occultation of compact radio sources by the ion tail of Halley's Comet 01 p0118 N88-10753
Analysis of the ICE combiner for multiple antenna arraying 04 p0436 N88-12704
The striae in the dust tails of great comets: A formal comparison of the goodness of fit by various theories, and a new proposal 14 p2002 N88-21937
The origin of low mass particles within and beyond the dust coma envelopes of Comet Halley
14 p2002 N88-21938
Plasma tail of Comet Halley in January 1986
14 p2006 N88-21960
Determination of the content of CO(+) and H2O(+) ions in the tail of Comet Giacobini-Zinner and Comet Halley 14 p2006 N88-21964
The dust tail of Comet Halley
14 p2008 N88-21974
Classification of comets recorded in ancient China (300 BC - 1800 AD) and statistics of type-1 tails
14 p2008 N88-21976
Dust tail streamers and Halley's nucleus rotation
14 p2008 N88-21979
Dust and C2-contents in the coma of Halley's Comet (1986III) 16 p2288 N88-23697
Photographic observations of the large scale features of Comet Halley 16 p2288 N88-23698

COMETARY ATMOSPHERES
Study of pickup of cometary ions in turbulent solar winds 01 p0113 N88-10725
The global interaction of comets with the solar wind
01 p0117 N88-10746
Solar wind effects on the outer ion coma of Comet Halley 01 p0117 N88-10750
The solar wind interaction with comets: A post encounter view 01 p0118 N88-10751
Plasma-tail activity and the interplanetary medium at Halley's Comet during Armada Week: 6-14 March 1986
01 p0118 N88-10752
Extended atmospheres of outer planet satellites and comets
[NASA-CR-181449] 10 p1430 N88-18540
A mass spectrometer evolved gas analysis experiment for in-situ analysis of cometary dust volatiles
13 p1854 N88-21097
Proceedings of the International Symposium on the Diversity and Similarity of Comets
[ESA-SP-278] 14 p1994 N88-21884
Variability of Comet Halley's coma: VEGA-1 and VEGA-2 magnetic field observations 14 p1995 N88-21891
Calculation of the shape of the contact surface at Comet Halley 14 p1995 N88-21892
Physical processes in the vicinity of the cometopause interpreted on the basis of plasma, magnetic field and plasma wave data measured on board VEGA-2 spacecraft --- Halley's comet 14 p1996 N88-21894
Plasma phenomena in the vicinity of the closest approach of VEGA-1, 2 spacecraft to the Comet Halley nucleus 14 p1996 N88-21899
Time dependent MHD models for the cometary magnetosphere 14 p1997 N88-21900
Halley's environments by the Japanese Suisei spacecraft 14 p1999 N88-21915
The role of water in the thermal balance of the coma
14 p1999 N88-21916
A model of the anisotropic structure of the neutral gas coma of a comet 14 p1999 N88-21918
Profiles of the major gas emissions and distribution of dust particles in the inner coma (0 to 10,000 km) of Comet Halley 14 p1999 N88-21919
Comparison of Halley's monochromatic comae with others 14 p2006 N88-21965
Interaction mechanisms of comets with the zodiacal dust cloud 14 p2008 N88-21977
Dust and C2-contents in the coma of Halley's Comet (1986III) 16 p2288 N88-23697
Modeling of a cometary dust coma
[ETN-88-92980] 23 p3300 N88-29651
Extended atmospheres of outer planet satellites and comets
[NASA-CR-183157] 24 p3457 N88-30572

COMETARY MAGNETOSPHERES
Time dependent MHD models for the cometary magnetosphere 14 p1997 N88-21900

COMETS
NT COMET HEADS
NT COMET NUCLEI
NT COMET TAILS
NT ENCKE COMET
NT GIACOBINI-ZINNER COMET
NT GRIGG-SKJELLERUP COMET
NT HALLEY'S COMET
NT TEMPEL 2 COMET
NT WEST COMET
STIP Symposium on Physical Interpretation of Solar/Interplanetary and Cometary Intervals
[NASA-CR-181201] 01 p0110 N88-10709
Was the eclipse comet of 1893 a disconnected coronal transient? 01 p0115 N88-10733
Solar wind-cometary interaction at the ionopause and associated phenomena 01 p0117 N88-10748
Exobiology and life science 07 p0683 N88-15358
Laser simulation of light and plasma action on comets and planets 09 p1237 N88-17413
Proceedings of the International Symposium on the Diversity and Similarity of Comets
[ESA-SP-278] 14 p1994 N88-21884
Diversity and similarity of comets
14 p1994 N88-21885
The absolute total magnitudes of periodic comets and their variations 14 p1994 N88-21887
Cometary magnitude distribution: The tabulated data
14 p1995 N88-21888

The comet flux and the 15 Myr galactic cycle
14 p1995 N88-21889
The relationship between low activity comets and more active comets
14 p1997 N88-21904
The photochemistry of some possible cometary CN parent species
14 p1997 N88-21905
Polarization of molecular fluorescence bands in comets: Recent observations and interpretation
14 p1998 N88-21907
Photodissociation lifetimes of CH and CD radicals in comets
14 p1998 N88-21908
Objective-prism spectra of the Comets Honda (1968 e), Hartley-Good (1985 l) and Halley
14 p2000 N88-21924
Cometary evolution: Clues from chondritic interplanetary dust particles
14 p2002 N88-21934
The striae in the dust tails of great comets: A formal comparison of the goodness of fit by various theories, and a new proposal
14 p2002 N88-21937
Similarity and diversity of the polarization of comets
14 p2003 N88-21940
Particles injected by comets
14 p2003 N88-21944
Diversity of comets, synergic temperature effects and the stability of organic compounds in icy nuclei
14 p2005 N88-21955
On the forbidden red lines of oxygen in comets
14 p2006 N88-21963
On the interpretation of the CH cometary spectrum
14 p2007 N88-21969
The role of hydrogen thermalization in shaping the Lyman-alpha coma --- comets
14 p2007 N88-21971
Classification of comets recorded in ancient China (300 BC - 1800 AD) and statistics of type-1 tails
14 p2008 N88-21976
Interaction mechanisms of comets with the zodiacal dust cloud
14 p2008 N88-21977
The mass loss rates of periodic comets
14 p2010 N88-21991
The evolution of cometary activity
18 p2594 N88-25416
Did the greenhouse effect kill the dinosaurs
24 p3442 N88-30484

COMFORT
Improvement of the construction of protective clothing for better wearability and comfort --- rainwear
[IZF-1986-26] 07 p0899 N88-15448
Habitability of the Space Station: From vehicle to living space
19 p2697 N88-26033
Study of human factors engineering criteria for Extra Vehicular Activity (EVA) systems, volume 2
[STF23-F87025-VOL-2] 24 p3409 N88-30293

COMMAND AND CONTROL
Automation strategy and results for an airbase command and control information system
[NLR-MP-86031-U] 01 p0035 N88-10223
Using concept mapping to define problems and identify key kernels during the development of a decision support system
[AD-A185636] 06 p0762 N88-14674
An approach to validation and verification of the communications load model with supporting user's guide
[AD-A185926] 07 p0840 N88-15098
Case-based reasoning for space applications: Utilization of prior experience in knowledge-based systems
08 p1065 N88-16433
Relating service doctrine to space system requirements
[AD-A186620] 08 p1074 N88-16483
POCC capabilities document. Payload support capabilities description: MCC, JSC POCC, remote POCC interface
[NASA-TM-89708] 09 p1260 N88-17555
Future directions in computer architecture
10 p1383 N88-18257
Fuzzy logic inference processor for real time control: A second generation full custom design
[AD-A188155] 11 p1471 N88-18773
Aircrew training devices: Utility and utilization of advanced instructional features, phase 4
[AD-A188418] 12 p1670 N88-20000
Variable speed optimal control of a wind turbine generator
[LAAS-87-358] 16 p2229 N88-23316
Decision aiding and coordination in decision-making organizations
[AD-A191950] 19 p2738 N88-26259
Real time data base management
[AD-A191758] 19 p2739 N88-26265
An evaluation methodology for dependable multiprocessors
[AD-A192799] 20 p2842 N88-26863
Launch operations to support future space forces
[AD-A192679] 20 p2881 N88-27107
A virtual statistical mechanical neural computer
[AD-A193962] 22 p3139 N88-28660
LO-CO-GRAF (low cost graphics): Generating maps to support command and control/crisis management using small computers
[AD-A193964] 22 p3139 N88-28661
Distributed cooperating processes in a mobile robot control system
23 p3256 N88-29386
Strategic defense initiative architecture dataflow modeling technique version 1.5
[AD-A194356] 23 p3275 N88-29494
Definition of common support equipment and space station interface requirements for IOC model technology experiments
[NASA-TM-100656] 24 p3336 N88-29856
The design of an intelligent multidisk control module for VME bus based systems
[AD-A195587] 24 p3411 N88-30303
Automated satellite control in Ada
24 p3416 N88-30336

COMMAND GUIDANCE
Reduced order optimal command applied to longitudinal automatic pilots
[SNIAS-872-111-114] 05 p0552 N88-13362
Optimum-Path-to-Go guidance of command adjusted trajectory projectiles
[AD-A193377] 22 p3040 N88-28051
Air Force Systems Command software independent verification and validation implementation analysis and guidance
[AD-A194309] 22 p3137 N88-28653

COMMAND LANGUAGES
NT QUERY LANGUAGES
DOD Gateway Information System (DGIS) common command language: Prolog knowledge base profile. Common command language report no. 3
[AD-A186150] 08 p1092 N88-16574
A robotic language for cooperative multi-robots
17 p2387 N88-24186

COMMAND MODULES
Optimization techniques applied to passive measures for in-orbit spacecraft survivability
[NASA-CR-179216] 04 p0408 N88-12532

COMMAND SYSTEMS
U COMMAND GUIDANCE

COMMAND-CONTROL
U COMMAND AND CONTROL

COMMERCE
An overview of remote sensing users' requirements
03 p0340 N88-12139
A study of federal technology transfer to the commercial sector
[AD-A187017] 09 p1262 N88-17560
Status of emerging technologies: An economic/technological assessment to the year 2000
[PB88-155775] 11 p1567 N88-19381
Safety study: Commercial emergency medical service helicopter operation
[PB88-917001] 12 p1575 N88-19422
Spin off businesses as mechanisms for transferring technologies
[DE88-005640] 13 p1852 N88-21085
Datacast: The transmission system
[BBC-RD-1988/1] 14 p1905 N88-21385
Technology transfer to China. Volume 2: Working papers, part 2
[PB88-158712] 14 p1992 N88-21873
International commercialization of remote sensing
[BCRS-87-14] 16 p2228 N88-23310

COMMERCIAL AIRCRAFT
NT A-300 AIRCRAFT
NT A-320 AIRCRAFT
NT BOEING 737 AIRCRAFT
NT BOEING 747 AIRCRAFT
NT DC 9 AIRCRAFT
NT EUROPEAN AIRBUS
NT VC-10 AIRCRAFT
Design requirements for future commercial operations
03 p0262 N88-11651
Design and control of repairs of carbon fiber lift augmentation flaps in the ATR42 aircraft
[SNIAS-872-111-112] 05 p0529 N88-13217
Airline safety: A comparative analysis
[AD-A185358] 05 p0543 N88-13308
A study of the utilization of advanced composites in fuselage structures of commercial aircraft
[NASA-CR-172405] 06 p0679 N88-14157
Low altitude windshear threat to commercial aircraft
08 p0952 N88-15777
Aircraft accident reports: Brief format, US Civil and Foreign Aviation, Issue Number 7 of 1986 accidents
[PB87-916909] 08 p0952 N88-15781
Presentation of Class 1 designs for a family of commuter airplanes
[NASA-CR-182563] 11 p1439 N88-18587
High performance composites research at NASA-Langley
[NASA-TM-100518] 11 p1450 N88-18642
First encounters of the close kind: The formation process of airline flight crews
[AD-A187977] 11 p1523 N88-19091
NASA advanced turboprop research and concept validation program
[NASA-TM-100891] 16 p2163 N88-22902
Manufacturing requirements
17 p2297 N88-23745
From turboprop aircraft to multi-engined jet aircraft Aircraft Integrated Monitoring Systems (AIMS)
22 p3033 N88-28003
Critical joints in large composite primary aircraft structures. Volume 1: Technical summary
[NASA-CR-3914] 23 p3190 N88-28983
Report to Congress on the effectiveness of the Civil Aviation Security Program
[AD-A195282] 24 p3322 N88-29784

COMMERCIAL AVIATION
U CIVIL AVIATION
U COMMERCIAL AIRCRAFT

COMMERCIAL ENERGY
Heat pump and appliance research
[PB88-102462] 07 p0853 N88-15184

COMMINUTION
Planetary science
07 p0883 N88-15356
Characterization and fundamental studies on CuO sorbent materials to determine attrition mechanisms on substrate gamma alumina
[DE88-003674] 13 p1749 N88-20456

COMMON BUSINESS ORIENTED LANGUAGE
U COBOL

COMMONALITY
Expert system development for commonality analysis in space programs
07 p0928 N88-15835
Study of reconfigurable payloads for direct broadcast satellites, summary
[DBS87-0004] 09 p1135 N88-16808
Presentation of Class 1 designs for a family of commuter airplanes
[NASA-CR-182563] 11 p1439 N88-18587
Presentation of structural component designs for the family of commuter airplanes
[NASA-CR-182568] 12 p1581 N88-19463
A class 2 weight assessment for the implementation of commonality and preliminary structural designs for the family of commuter airplanes
[NASA-CR-182565] 12 p1581 N88-19464
Advanced propfan analysis for the family of commuter airplanes
[NASA-CR-182566] 12 p1582 N88-19468
Presentation of flight control design and handling quality commonality by separate surface stability augmentation for the family of commuter airplanes
[NASA-CR-182567] 12 p1583 N88-19471
A cost analysis for the implementation of commonality in the family of commuter airplanes, revised
[NASA-CR-182569] 12 p1708 N88-20221
Class 2 design update for the family of commuter airplanes
[NASA-CR-182681] 18 p2464 N88-24629

COMMUNICATING
NT AIRCRAFT COMMUNICATION
NT INFORMATION DISSEMINATION
NT MESSAGES
NT VERBAL COMMUNICATION
Online aiding for human-computer interfaces
[AD-A189239] 13 p1815 N88-20842

COMMUNICATION
NT FACSIMILE COMMUNICATION
NT LINE OF SIGHT COMMUNICATION
NT OPTICAL COMMUNICATION
NT UNDERWATER COMMUNICATION
Meteor-burst communications: Is this what the Navy needs?
[AD-A184433] 04 p0431 N88-12672
The SUPRENUM communications subroutine library for grid-oriented problems
[DE88-000137] 04 p0479 N88-12950
Program description of FIBRAM: A radiation attenuation model for optical fibers
[PB87-230686] 06 p0690 N88-14229
An approach to validation and verification of the communications load model with supporting user's guide
[AD-A185926] 07 p0840 N88-15098
Algebraic specification of process algebra, including two examples
[PB88-106729] 07 p0912 N88-15531
Space languages
08 p1063 N88-16420
POCC capabilities document. Payload support capabilities description: MCC, JSC POCC, remote POCC interface
[NASA-TM-89708] 09 p1260 N88-17555
Helsinki University of Technology Communications Laboratory
[PB88-112974] 10 p1318 N88-17881
The design of trellis codes for fading channels
[NASA-CR-182523] 10 p1320 N88-17891

Future directions in computer architecture
10 p1383 N88-18257
Networking requirements and future alternatives
[NASA-TM-89711] 10 p1426 N88-18517
The design and implementation of the Technical Facilities Controller (TFC) for the Goldstone deep space communications complex 11 p1474 N88-18794
Optimum filters and smoothers design for carrier phase and frequency tracking
[NASA-CR-182654] 12 p1618 N88-19679
Lasers: Invention to application
[PB88-161583] 14 p1914 N88-21436
Research and technology
[NASA-TM-100172] 15 p2153 N88-22851
The relationship between group process and performance 17 p2448 N88-24549
Evaluation of the communications impact of a low power arcjet thruster
[NASA-TM-100926] 18 p2475 N88-24682
Communication training for aircrews: A review of theoretical and pragmatic aspects of training program design
[NASA-CR-177459] 20 p2756 N88-26349
A study of a meteor burst communication system
21 p2934 N88-27421
Coding for meteor-burst communications channel and side information for channels with block-interference
23 p3202 N88-29054
An OKQPSK modem incorporating numerically controlled carrier synthesis
[DE88-009536] 23 p3244 N88-29304
Dynamic analysis of computer and communications sytems: Semi-Markov approach
23 p3244 N88-29305
Barriers to Information Transfer and Approaches Toward Their Reduction
[AGARD-CP-430] 24 p3437 N88-30458
Linguistic and cultural barriers to the transfer of information 24 p3437 N88-30459
Political and economic barriers to information transfer
24 p3437 N88-30460

COMMUNICATION CABLES
NT BEAM WAVEGUIDES
NT CIRCULAR WAVEGUIDES
NT COAXIAL CABLES
NT OPTICAL FIBERS
NT OPTICAL WAVEGUIDES
NT PLASMAGUIDES
NT RECTANGULAR WAVEGUIDES
NT WAVEGUIDES
Soliton mode of propagation of light pulses through single-mode optical fibers and problems of its experimental realization 07 p0920 N88-15592
Failure-resistant Fibre-Optical Communication Line (i²OCL)
[DE88-700470] 10 p1408 N88-18400
Aging properties of cable polmers (2)
[NASA-TT-20228] 13 p1752 N88-20479
Burning characteristics and flammability of PVC cables in groups
[NASA-TT-20226] 14 p1893 N88-21303

COMMUNICATION EQUIPMENT
NT DIPLEXERS
NT RADIO RECEIVERS
NT SATELLITE TELEVISION
NT SUPERHETERODYNE RECEIVERS
NT TRANSMITTER RECEIVERS
Multi-channel communications system analyzer
[AD-A184756] 03 p0307 N88-11937
SBNR (Signed Binary Number Representations) digital signal processor architecture
[AD-A184603] 03 p0364 N88-12290
Automatic antenna switching design for Extra Vehicular Activity (EVA) communication system
06 p0797 N88-14883
Validation of a stochastic model to determine failure rates for communication-electronic systems
[AD-A186536] 08 p0980 N88-15920
Team problem solving: Effects of communication and function overlap
[AD-A187010] 09 p1152 N88-16898
Evaluating software testing methods to reduce testing duplication in US Army communications equipment acquisition
[AD-A186961] 09 p1216 N88-17292
Information and stochastic systems
[AD-A192167] 18 p2501 N88-24838
Digital communication transmitter and receiver test procedures
[AD-A191218] 20 p2788 N88-26540
Event-related brain potentials as indices of mental workload and attentional allocation
21 p2979 N88-27696
The Telecommunications and Data Acquisition Report
[NASA-CR-183131] 22 p3063 N88-28178
Doppler-corrected differential detection system
[NASA-CASE-NPO-16987-1-CU]
24 p3359 N88-30001

COMMUNICATION NETWORKS
NT ALOHA SYSTEM
NT LOCAL AREA NETWORKS
Design, manufacture and testing of an elegant breadboard model communications processor
[D/2244] 01 p0034 N88-10217
Study of a coding and modulation system for the V32 call of the CCITT
[ENST-87E007] 02 p0162 N88-11015
Modeling and performance evaluation of the DPS25 packet switching multiprocessor system --- communication networks
[ENST-87E009] 02 p0162 N88-11016
Contribution to the study of circuit switched networks: Modeling and numerical solutions
[LAAS-87-174] 02 p0162 N88-11017
The role of spread spectrum in packet radio networks
[AD-A184511] 03 p0306 N88-11929
The design and testing of an analog optical communication link capable of the simultaneous transmission of four frequency division multiplexed audio signals
[AD-A184695] 03 p0307 N88-11936
Multi-channel communications system analyzer
[AD-A184756] 03 p0307 N88-11937
Network reconstitution protocol
[AD-A184755] 03 p0367 N88-12309
Multicast gateway design considerations
[PB87-219960] 04 p0430 N88-12663
Heterogeneous multi-trunking queueing systems
[AD-A184255] 04 p0431 N88-12668
An interactive computer graphics network monitor for a tactical communications network
[AD-A184131] 04 p0477 N88-12938
Contribution to optimal flow in networks. A experimental multiprocessor for asynchronous iteration implementation
[LAAS-87-269] 05 p0576 N88-13510
Communications payload concepts for geostationary facilities
[NASA-TM-100154] 05 p0576 N88-13513
An evolutionary communications scenario for Mars exploration
[NASA-TM-100263] 05 p0576 N88-13515
Connecting RPC (Remote Procedure Call)-based distributed systems using wide-area networks
[PB87-234423] 05 p0658 N88-14041
Land mobile satellite transmission measurements at 869 MHz. A comparison of error probabilities for various message block durations and fade margins as a function of vegetation shadowing
[NASA-CR-179929] 06 p0693 N88-14255
On real-time systems using local area networks
[AD-A185475] 06 p0694 N88-14256
Wide-area communication under Amoeba
[PB87-234431] 06 p0760 N88-14665
Development of a graphical display on the DMS test bed 06 p0794 N88-14864
High data rate modem simulation for the space station multiple-access communications system
06 p0795 N88-14870
An approach to validation and verification of the communications load model with supporting user's guide
[AD-A185926] 07 p0840 N88-15098
On the approximation of the output process of multi-user random access communication networks
[AD-A186197] 07 p0842 N88-15108
Reliability and survivability of communication networks
[AD-A186248] 07 p0842 N88-15109
Round table on the future of satellite communications and broadcasting in Europe
[ESA-STR-221] 07 p0843 N88-15112
Coding for spread-spectrum communications networks
[AD-A185667] 07 p0844 N88-15119
Throughput analysis of a flow-contoured communication network with buffer space limitations
[CWI-OS-R8702] 08 p0977 N88-15908
Waiting times in discrete-time cyclic-service systems --- communication networks
[CWI-OS-R8707] 08 p0977 N88-15909
Approximating the size of a dynamically growing asynchronous distributed network
[AD-A187011] 09 p1152 N88-16899
Adaptive spread spectrum networks
[AD-A187154] 09 p1152 N88-16900
Transient electromagnetic scattering from heterogeneous lossy spheres
[AD-A186669] 09 p1152 N88-16903
An introduction to military satellite communications
[RSRE-MEMO-3976] 09 p1153 N88-16911
Communications patterns in a symbolic multiprocessor
[AD-A186896] 09 p1215 N88-17282
Terrestrial Propagation Characteristics in Modern Systems of Communications, Surveillance, Guidance and Control
[AGARD-CP-407] 12 p1614 N88-19653
MM-wave propagation and application in military communication systems 12 p1617 N88-19669
Spread spectrum radio networks
[AD-A188914] 12 p1620 N88-19689
Static and dynamic jamming of networks
[AD-A188921] 12 p1620 N88-19690
Evaluation of network communication multiprocessor fault tolerance
[INPE-4305-PRE/1171] 12 p1674 N88-20011
An intelligent allocation algorithm for parallel processing
[NASA-CR-182648] 12 p1675 N88-20014
Knowledge-based system analysis and control
[AD-A188163] 12 p1681 N88-20049
Design methodology for allocating data in a distributed database
[AD-A188826] 12 p1706 N88-20215
Alternative force structuring strategies for military satellite communication systems
[AD-A189492] 13 p1758 N88-20516
Human problem solving in dynamic environments. Understanding and supporting operators in large-scale, complex systems
[AD-A189539] 13 p1812 N88-20826
Spatial distribution of traffic in a cellular mobile data network
[EUT-87-E-168] 14 p1904 N88-21378
A packet-switched wide-area communication network simulator
[FUB-3-1986] 14 p1905 N88-21381
On-board processing for mobile satellite communications
[ESA-CR(P)-2519] 14 p1905 N88-21382
Real-time stressed channel simulator
[AD-A190223] 15 p2025 N88-22067
NASA and the challenge of ISDN: The role of satellites in an ISDN world
[NASA-CR-182749] 15 p2126 N88-22676
Discrete generalized networks: Application to integer constrained flow problems
[AD-A190823] 16 p2190 N88-23060
Multiple address facility for packet radio: An investigation of performance/complexity trade off
[AD-A191043] 16 p2190 N88-23064
Problems in integrated networks
[AD-A191391] 16 p2191 N88-23069
Near-real-time TOMS, telecommunications and meteorological support for the 1987 Airborne Antarctic Ozone Experiment
[NASA-CR-4133] 16 p2233 N88-23338
Alpha structure based B-HIVE multicomputer
[AD-A188708] 16 p2244 N88-23405
Reasoning about networks with many identical finite-state processes
[AD-A188743] 16 p2245 N88-23413
IPC for modular software requires a third party connect
[AD-A189199] 16 p2246 N88-23414
Modeling, filtering and control of stochastic processes --- communication networks
[ENST-87E021] 17 p2333 N88-23925
MSAT-X: A technical introduction and status report
[NASA-CR-182921] 17 p2334 N88-23933
Connecting remote systems for demonstration of automation technologies 17 p2387 N88-24191
Propagation management for no-acknowledge HF communications links 18 p2502 N88-24843
Human problem solving in complex dynamic environments
[AD-A190788] 18 p2551 N88-25142
The AMSC mobile satellite system
19 p2643 N88-25681
NASA's mobile satellite development program
19 p2643 N88-25682
Mobile satellite service for Canada
19 p2643 N88-25683
A satellite system for land-mobile communications in Europe 19 p2643 N88-25685
Developing a global aeronautical satellite system
19 p2644 N88-25687
World-wide aeronautical satellite communications
19 p2644 N88-25688
An overview of the OmniTRACS: The first operational mobile Ku-band satellite communications
19 p2644 N88-25689
International and domestic mobile satellite regulatory proceedings: A comparison of outcomes and discussion of implications 19 p2644 N88-25690
International and domestic regulator issues facing the Canadian MSAT system 19 p2644 N88-25692
Development of the network architecture of the Canadian MSAT system 19 p2645 N88-25702

System architecture for the Canadian interim mobile satellite system 19 p2646 N88-25703
Design mobile satellite system architecture as an integral part of the cellular access digital network 19 p2650 N88-25736
An access alternative for mobile satellite networks 19 p2651 N88-25737
Satellites at sea --- INMARSAT 19 p2700 N88-26054
The contribution of space to maritime activities 19 p2700 N88-26055
Analysis and synthesis of decision-making organizations [AD-A191948] 19 p2738 N88-26258
The performance of Eurocom error correction schemes for data communications [FEL-1987-56] 20 p2792 N88-26563
An integrated circuit for error protection in modern data communication systems conforming to Eurocom specifications [FEL-1987-48] 20 p2796 N88-26593
Extensible networks. Part 1: Principles and constructions [REPT-87-91-PT-1] 20 p2842 N88-26864
The MELMUX MX-7100 series high-speed digital multiplexers 21 p2930 N88-27396
Activities report of the Communications Department [ENST-88D003] 21 p2931 N88-27401
Utilization of a satellite communication system to protect the national communication network [FUB-33-1986] 21 p2934 N88-27423
The Frequency Division Multiple Access/Time Domain Multiplex (FDMA/TDM) system reviewed 22 p3069 N88-28214
Determination of satcom access power levels within the ground segment [RSRE-MEMO-4097] 22 p3070 N88-28226
Performance of a rapid carrier acquisition circuit for satellite ground terminal modems [RSRE-TEST-REPORT-87/CC3/2] 22 p3071 N88-28227
Hierarchical organization for large, dynamic radio networks [AD-A193942] 23 p3204 N88-29067
Performance analysis of k-ary n-cube interconnection networks [AD-A195542] 24 p3361 N88-30010
Design of a self-timed VLSI multicomputer communication controller [AD-A194567] 24 p3361 N88-30014
Comparative analysis of passive communications satellites employing the SHF and HF spectrum for use in a strategic role [AD-A194682] 24 p3362 N88-30019
Integrating images, applications, and communications networks, volume 5 [AD-A195854] 24 p3436 N88-30452

COMMUNICATION SATELLITES
NT ACTS
NT DIRECT BROADCAST SATELLITES
NT EUROPEAN COMMUNICATIONS SATELLITE
NT L-SAT
NT MARECS MARITIME SATELLITES
Communication satellite technology trends 01 p0015 N88-10088
Study of mobile communications payload for Columbus Polar Platforms [ITS-TR-056A/86] 01 p0034 N88-10220
Electrostatic discharges in geostationary orbit: The case of Telecom 1 03 p0275 N88-11733
An examination of the Advanced Communications Technology Satellite (ACTS) and its application to the Defense Data Network (DDN) [AD-A184003] 03 p0276 N88-11742
Engineering calculations for the Delta S method of solving the orbital allotment problem [NASA-CR-182372] 06 p0671 N88-14110
Propagation effects on satellite systems at frequencies below 10 GHz: A handbook for satellite systems design [NASA-RP-1108/2] 06 p0690 N88-14226
Numerical arc segmentation algorithm for a radio conference-NASARC (version 2.0) technical manual [NASA-TM-100160] 08 p0977 N88-15910
Communications satellite systems operations with the space station. Volume 3: Supplementary technical report [NASA-CR-180875] 09 p1133 N88-16794
Multicarrier demodulator design, volume 1 --- communication satellites [ESA-CR(P)-2468-VOL-1] 09 p1158 N88-16941
Multicarrier demodulator design. Volume 2: Executive summary --- communication satellites [ESA-CR(P)-2468-VOL-2] 09 p1158 N88-16942
Satellite interference analysis and simulation using personal computers [NASA-CR-182522] 10 p1319 N88-17890
High efficiency, long life traveling wave tubes for future communications satellites [NASA-TM-100837] 12 p1598 N88-19565
Communication satellites: Guidelines for a strategic plan [NASA-TM-89306] 12 p1599 N88-19569
PRC space satellite achievements highlighted 14 p1863 N88-21131
RF-switches: Application and design --- satellite communication 14 p1877 N88-21215
Qualification testing of the EUROSTAR Solar Array Drive Mechanism (SADM) 14 p1879 N88-21229
NASA and the challenge of ISDN: The role of satellites in an ISDN world [NASA-CR-182749] 15 p2126 N88-22676
Numerical arc segmentation algorithm for a radio conference: A software tool for communication satellite systems planning [NASA-TM-100789] 16 p2167 N88-22919
The bit-error rate performance of a satellite microwave matrix switch [NASA-TM-100285] 16 p2167 N88-22920
MSAT-X: A technical introduction and status report [NASA-CR-182921] 17 p2334 N88-23933
Experimental radio frequency link for Ka-band communications applications [NASA-TM-100824] 18 p2470 N88-24659
Simulations of the electrostatic charging of ESA communications satellites [ESA-STM-239] 18 p2472 N88-24670
Proceedings of the Mobile Satellite Conference [NASA-CR-182964] 19 p2643 N88-25680
The AMSC mobile satellite system 19 p2643 N88-25681
NASA's mobile satellite development program 19 p2643 N88-25682
Mobile satellite service for Canada 19 p2643 N88-25683
AUSSAT mobile satellite services 19 p2643 N88-25684
A satellite system for land-mobile communications in Europe 19 p2643 N88-25685
Developing a global aeronautical satellite system 19 p2644 N88-25687
An overview of the OmniTRACS: The first operational mobile Ku-band satellite communications 19 p2644 N88-25689
Mobile satellite services: International co-ordination, co-operation and competition 19 p2644 N88-25691
International and domestic regulator issues facing the Canadian MSAT system 19 p2644 N88-25692
Land mobile satellite propagation results 19 p2645 N88-25698
Development of a mobile satellite communication unit 19 p2646 N88-25701
System architecture for the Canadian interim mobile satellite system 19 p2646 N88-25703
Satellite communications experiment for the Ontario air ambulance service 19 p2646 N88-25705
Land mobile satellite demonstration system 19 p2646 N88-25706
The JPL MSAT mobile laboratory and the pilot field experiments 19 p2646 N88-25708
Technical characteristics of the OmniTRACS: The first operation mobile Ku-band satellite communications system 19 p2647 N88-25709
An adaptive array antenna for mobile satellite communications 19 p2647 N88-25710
MSAT mobile electronically steered phased array antenna development 19 p2647 N88-25711
MSAT-X electronically steered phased array antenna system 19 p2647 N88-25712
MSAT-X phased array antenna adaptions to airborne applications 19 p2647 N88-25713
Adaptive interference techniques for mobile antennas 19 p2647 N88-25714
The JPL mechanically steered antenna 19 p2647 N88-25715
Simple, low-profile, circularly polarized arrays 19 p2647 N88-25716
Codes for QPSK modulation with invariance under 90 degrees rotation 19 p2648 N88-25720
Modulation and coding for fast fading mobile satellite communication channels 19 p2648 N88-25722
Performance of the ICAO standard core service modulation and coding techniques 19 p2648 N88-25723
Comparison of CDMA and FDMA for the MobileStar(sm) system 19 p2649 N88-25724
An 8-DPSK TCM modem for MSAT-X 19 p2649 N88-25725
Modem for the land mobile satellite channel 19 p2649 N88-25727
Pilot-aided modulation for narrow-band satellite communications 19 p2649 N88-25728
A study on the co- and adjacent channel protection requirements for mobile satellite ACSSB modulation 19 p2650 N88-25732
A framework for implementing data services in multi-service mobile satellite systems 19 p2650 N88-25733
L-band and SHF multiple access schemes for the MSAT system 19 p2650 N88-25734
Rearrangement procedures in regenerative multibeammobile communications satellites with frequency reuse 19 p2650 N88-25735
Design mobile satellite system architecture as an integral part of the cellular access digital network 19 p2650 N88-25736
An access alternative for mobile satellite networks 19 p2651 N88-25737
An operational open-end file transfer protocol for mobile satellite communications 19 p2651 N88-25738
Integrated voice/data protocols for satellite channels 19 p2651 N88-25739
Evaluation of CDMA system capacity for mobile satellite system applications 19 p2651 N88-25740
Considerations for spacecraft design for MSAT 19 p2651 N88-25741
Antenna system for MSAT mission 19 p2651 N88-25742
Antenna technology for advanced mobile communication systems 19 p2651 N88-25743
Frequency addressable beams for land mobile communications 19 p2652 N88-25744
Large antenna experiments aboard the space shuttle: Application of nonuniform sampling techniques 19 p2652 N88-25745
A microstrip array feed for MSAT spacecraft reflector antenna 19 p2652 N88-25747
Technologies for antenna shape and vibration control 19 p2652 N88-25748
Real-time speech encoding based on Code-Excited Linear Prediction (CELP) 19 p2653 N88-25751
Mobile satellite communications in the Forest Service 19 p2654 N88-25757
Mobile satellite service in the United States 19 p2654 N88-25758
EXSAT: Expert system to configure telecommunication satellites [SNIAS-881-440-101] 21 p2902 N88-27223
Utilization of a satellite communication system to protect the national communication network [FUB-33-1986] 21 p2934 N88-27423
PSDE/SAT 2: Preliminary spacecraft configuration study, executive summary [ESA-CR(P)-2618] 24 p3333 N88-29840
Comparative analysis of passive communications satellites employing the SHF and HF spectrum for use in a strategic role [AD-A194682] 24 p3362 N88-30019

COMMUNICATION SYSTEMS
U TELECOMMUNICATION

COMMUNICATION THEORY
NT SYLLABLES
NT WORDS (LANGUAGE)
Embedded expert system for space shuttle main engine maintenance 08 p1058 N88-16382
The use and generation of illustrative examples in computer-based instructional systems 08 p1060 N88-16400
Intelligent man/machine interfaces on the space station 08 p1063 N88-16418
Interfacing the expert: Characteristics and requirements for the user interface in expert systems 08 p1063 N88-16419
Space languages 08 p1063 N88-16420
Activities report of the Department of Systems and Communications [ENST-87D004] 16 p2189 N88-23053
DAISY-DAMP: A distributed AI system for the dynamic allocation and management of power 23 p3254 N88-29373

COMMUNITIES
Remote sensing techniques applied to the study of metropolitan regions: The west sector of the Sao Paulo metropolitan area 19 p2681 N88-25941

COMMUTATION
Determination of the commutation and angle and load response for a continuous-current, single phase controlled rectifier [AD-A190602] 15 p2060 N88-22285
Reduced order modeling of grid-connected photovoltaic inverter systems [DE88-010603] 21 p2969 N88-27635

COMMUTATORS
Study on the dynamics of executive electromechanism with thyristor commutator for cryogenic systems [DE87-703209] 12 p1622 N88-19702

Loss evaluation of self-commutated power conditioner for battery energy storage system
[DE88-752075] 20 p2794 N88-26575
COMMUTER AIRCRAFT
U GENERAL AVIATION AIRCRAFT
U PASSENGER AIRCRAFT
COMPACT DISK READ-ONLY MEMORY DEVICES
U OPTICAL DISKS
U READ-ONLY MEMORY DEVICES
COMPACTING
Physics and chemistry of packing fine ceramic powders
[DE87-013709] 01 p0029 N88-10183
Effects of cure pressure on resin flow, voids, and mechanical properties
[AD-A184267] 03 p0295 N88-11853
A note on compactifications of products of semigroups
[CWI-PM-R8701] 08 p1072 N88-16469
Dynamic consolidation of metal powders
[AD-A192126] 18 p2485 N88-24744
Sintering of the heterogeneous MgO compacts
[DE88-010357] 20 p2767 N88-26408
Superconductor consolidation
[DE88-010938] 21 p3024 N88-27949
COMPACTNESS
U VOID RATIO
COMPANION STARS
NT NEMESIS (STAR)
COMPARATOR CIRCUITS
Timing for subnanosecond pulses
[DE88-701390] 16 p2192 N88-23074
COMPARATORS
Multi-channel communications system analyzer
[AD-A184756] 03 p0307 N88-11937
An electrostatic potential comparator
[AD-A192051] 18 p2557 N88-25177
Measurement of the thermal conductivity of dielectric thin solid films with a thermal comparator
[DE88-008468] 21 p3016 N88-27898
COMPARISON
Problem specifications and collated solutions of the two-phase numerical-benchmark exercise 1986-7 --- two phase flow
[CFDU/87/1] 01 p0047 N88-10300
Modeling of human judgement in multicriteria analysis using pairwise comparison
[REPT-87-01] 01 p0076 N88-10484
Comparison of measured temperatures, thermal stresses and creep residues with predictions on a built-up titanium structure
[NASA-TM-86814] 03 p0337 N88-12125
Glassy GeO2 obtained by the gel process
[NASA-TT-20125] 06 p0685 N88-14201
Calculations of the turbulent wake behind a slender self-propelled double-body and comparisons with experiment
[AD-A185661] 06 p0703 N88-14314
Summary of comparison between experimental and analytical (including empirical) results for initiation of crack growth for surface cracks
[DE88-001604] 06 p0721 N88-14433
Some performance comparisons for a fluid dynamics code
[PB88-113709] 07 p0852 N88-15175
A comparison of experimental and theoretical results for labyrinth gas seals with honeycomb stators
[NASA-CR-182441] 08 p0993 N88-16006
A performance comparison of the Cray-2 and the Cray X-MP
[NASA-CR-177461] 09 p1216 N88-17288
Evaluating software testing methods to reduce testing duplication in US Army communications equipment acquisition
[AD-A186961] 09 p1216 N88-17292
A comparison of fitting techniques for the cumulative average learning curves with historical lot cost data
[AD-A187127] 09 p1227 N88-17349
Supercomputer performance: The theory, practice, and results
[DE88-004697] 10 p1384 N88-18266
Parallels between control PDE's (Partial Differential Equations) and systems of ODE's (Ordinary Differential Equations)
[NASA-CR-182487] 10 p1398 N88-18331
A comparison of projection methods in the forecasting of overhead costs for seven government aerospace contractors
[AD-A187572] 10 p1425 N88-18514
A comparative assessment of US and UK explosives qualified as replacements for tetryl
[MRL-R-1094] 13 p1754 N88-20486
A comparison of terrain association and resection as methods of position location
[AD-A189480] 13 p1790 N88-20710
Stochastic comparisons of order statistics, with applications in reliability
[AD-A189408] 13 p1829 N88-20938
Comparison of pressure distributions on model and full-scale NACA 64-621 airfoils with ailerons for wind turbine application
[NASA-TM-100802] 14 p1943 N88-21593
Stellar scintillometer atmospheric optical turbulence profiling experiment: A qualitative comparison of two identical instruments at AMOS (Air Force Maui Optical Station), 1985
[AD-A190589] 15 p2094 N88-22479
Comparative analysis of multistage interconnection networks
[AD-A190436] 15 p2115 N88-22598
Groundwater sapping valleys: Experimental studies, geological controls and implications to the interpretation of valley networks on Mars
[NASA-CR-182718] 15 p2152 N88-22847
Qualification of a water tunnel for force measurements on aeronautical models 16 p2200 N88-23128
A comparative study of vortex flows in wind and water tunnels 16 p2204 N88-23151
Investigation on the movement of vortex burst position with dynamically changing angle of attack for a schematic deltawing in a watertunnel with correlation to similar studies in windtunnel 16 p2204 N88-23152
A description of an automated database comparison program
[NASA-TM-100609] 16 p2253 N88-23463
Comparison of a direct thrust nuclear engine, nuclear electric engine and a chemical engine for future space missions 17 p2418 N88-24379
Space station habitability recommendations based on a systematic comparative analysis of analogous conditions
[NASA-CR-3943] 18 p2587 N88-25372
Five-point form of the nodal diffusion method and comparison with finite-difference
[DE88-004141] 19 p2720 N88-26154
The influence of uncompensated solution resistance on the determination and standard electrochemical rate constants using cyclic voltammetry and some comparisons with AC voltammetry
[AD-A192825] 20 p2770 N88-26427
Comparison theorems and their use in the analysis of some nonlinear diffusion problems
[DE88-010032] 20 p2845 N88-26884
A comparison of generators for pseudo-random normal deviates
[DE88-011711] 21 p3010 N88-27859
Comparison of the bidirectional reflectance distribution function of various surfaces
[NASA-TM-101317] 22 p3153 N88-28760
Regional intercomparisons of General Circulation Model predictions and historical climate data: CO2
[DE88-010416] 23 p3235 N88-29248
A model for architectural comparison
[AD-A195993] 24 p3411 N88-30302
Design and performance analysis of a relational replicated database system
[AD-A196290] 24 p3437 N88-30456
Plasma of earth's magnetosphere ring currents. Model compared with results of AMPTE/CCE experiment 24 p3447 N88-30515
COMPARTMENTATION
U COMPARTMENTS
COMPARTMENTS
NT AIR LOCKS
NT AIRCRAFT COMPARTMENTS
NT ANECHOIC CHAMBERS
NT COMMAND MODULES
NT HYPERBARIC CHAMBERS
NT PRESSURE CHAMBERS
NT PRESSURIZED CABINS
NT REVERBERATION CHAMBERS
NT SPACECRAFT CABINS
NT TEST CHAMBERS
NT VACUUM CHAMBERS
Cryogenic cell --- neutron borehole logging
[GB-PATENT-2-139-745-A] 01 p0048 N88-10308
COMPATIBILITY
NT ELECTROMAGNETIC COMPATIBILITY
NT SYSTEMS COMPATIBILITY
Compatability of dispersion-strengthened platinum with resistojet propellants
[NASA-TP-2765] 04 p0409 N88-12538
Compatibility of explosives: A data base system
[PB87-234464] 06 p0687 N88-14208
Geographic application of the relational data base system Cantor
[PB87-120945] 06 p0791 N88-14851
Resources, confusions and compatibility in dual axis tracking: Displays, controls and dynamics
[AD-A185871] 07 p0898 N88-15440
Microgravity payloads and missions for Space Station: Some issues affecting compatibility with other payloads 09 p1129 N88-16783
Microgravity experiments in space: Compatibility with dynamic perturbing effects 09 p1241 N88-17435
High-temperature thermosets derived from the Diels-Alder polymerization of bisbenzocyclobutenes and bimaleimides
[AD-A188800] 13 p1747 N88-20449
Compatibility in space reactor fuel systems
[DE88-005698] 13 p1839 N88-21004
The PC/AT compatible computer as a mission control center display processor at Ames-Dryden Flight Research Facility
[NASA-TM-100426] 14 p1955 N88-21654
Chemical compatibility between silicon carbide and a nickel aluminide
[DE88-006188] 18 p2479 N88-24708
A compatible encapsulant for explosives
[DE88-007212] 18 p2495 N88-24806
Sulfur-tolerant anode materials
[DE88-001034] 18 p2537 N88-25054
Improved method for stress and compatibility analysis of multicomponent rotating systems
[NASA-TM-100884] 19 p2680 N88-25935
A fundamental understanding of the interfacial compatibility in hybrid material systems
[AD-A192921] 21 p2909 N88-27264
Capitalizing on experience with intelligence gateway software
[AD-A193362] 21 p3028 N88-27971
COMPENSATION
Polynomial compensation, inversion, and approximation of discrete time linear systems
[NASA-TM-100027] 03 p0372 N88-12344
Transport delay compensation for computer-generated imagery systems
[NASA-TM-100084] 10 p1277 N88-17645
Covariance analysis and post-processing of gravity compensation effects for aided multi-state navigation systems
[PAPER-87-13] 12 p1577 N88-19430
Case study of active array feed compensation with sidelobe control for reflector surface distortion
[NASA-TM-100287] 16 p2192 N88-23073
COMPENSATORS
Pinhole occulter experiment
[NASA-CR-179206] 02 p0235 N88-11481
Defect characterization in quartz and related materials
[AD-A184754] 03 p0294 N88-11846
Investigation, development, and application of optimal output feedback theory. Volume 3: The relationship between dynamic compensators and observers and Kalman filters
[NASA-CR-4107] 05 p0636 N88-13900
Design of a velocity and position control laboratory servo system
[AD-A186596] 08 p0990 N88-15997
A Prohorov bound for a Poisson process and a Bernoulli process
[CWI-MS-R8701] 09 p1232 N88-17388
Analysis and synthesis of two degrees of freedom control systems 11 p1495 N88-18928
Modelling of a hydraulic motor and servo-valve to produce a desired system response using analogue and digital compensation techniques
[ETN-88-92079] 14 p1899 N88-21337
Time-Optimal Adaptive Shaped Torque (TOAST) technical note
[AD-A192719] 20 p2843 N88-26869
COMPENSATORY TRACKING
Resources, confusions and compatibility in dual axis tracking: Displays, controls and dynamics
[AD-A185871] 07 p0898 N88-15440
COMPETITION
Space station: Leadership for the future
[NASA-PAM-509/8-87] 01 p0013 N88-10072
A role for national laboratories in enhancing economic competitiveness. The example of high-temperature superconductors: CNSS papers, No. 1
[DE87-013633] 03 p0379 N88-12386
New theory for competing interactions and microstructures in partially-ordered (liquid-crystalline) phases
[DE87-014739] 03 p0380 N88-12389
Competition Analysis Model (CAM). Volume 2: Computer manual
[AD-A184017] 03 p0384 N88-12411
Competing interactions in metallic superlattices
[DE88-005344] 13 p1847 N88-21057
Competition: Issued on establishing and using Federally funded research and development centers
[PB88-178884] 23 p3296 N88-29632
COMPILATION (COMPUTERS)
U COMPILERS

COMPILER PROGRAMS
U COMPILERS
COMPILERS
FORTRAN compiler performance benchmarks for the IBM personal computer
[LA-10883-MS] 03 p0363 N88-12284
Mixing Microsoft C and Microsoft FORTRAN program modules on the IBM Personal Computer
[DE88-001947] 05 p0637 N88-13895
Technology upgrade of a silicon compiler
[AD-A184873] 05 p0655 N88-14016
Microprocessor emulating the intermediate code for FORTRAN compiler
[DE88-700540] 07 p0900 N88-15452
Program translation via abstraction and reimplementation
[AD-A185845] 07 p0901 N88-15458
Version description document for the Ada compiler validation capability (version 1.9) (for microcomputer)
[AD-A186390] 07 p0903 N88-15471
Ada (trade name) compiler validation summary report. Systems designers' PLC SD Ada-plus VAX/VMS x MC68020. Version 2B.00. Host: VAX 8600. Target: Motorola MC68020. Completion of on-site testing
[AD-A186571] 08 p1053 N88-16356
The Ada compiler: On the design and implementation of an Ada compiler
[ETN-88-91594] 09 p1215 N88-17284
Types and effects towards the integration of functional and imperative programming
[AD-A186930] 09 p1216 N88-17290
Rationale for the design of the Ada (tradename) programming language
[AD-A187106] 09 p1217 N88-17297
Description of a limited VAX-Ada program support environment developed within UDP division version 1.0
[ARE-TM(UDP)-87103] 09 p1219 N88-17308
Programming language translation for multicomputers
10 p1381 N88-18244
Design for a TPL compiler system: A system for retargeting high level language programs
10 p1381 N88-18248
Factors causing unexpected variations in Ada benchmarks
[AD-A187231] 10 p1388 N88-18291
Loop coalescing: A compiler transformation for parallel machines
[DE88-003571] 10 p1392 N88-18307
Performance and evaluation at the Center for Supercomputing Research and Development
[DE88-003563] 10 p1417 N88-18456
Efficient instruction level simulation of computers
[AD-A187821] 11 p1529 N88-19130
Applicability of Ada (trademark) tasking for avionics executives
[AD-A188827] 12 p1578 N88-19445
Automatic restructuring of FORTRAN programs for parallel execution
[DE88-003585] 12 p1676 N88-20018
Building software systems economically with mechanized logic: Initial design proposal
[AD-A188791] 12 p1678 N88-20031
Higher levels of a silicon compiler
[EUT-86-E-163] 14 p1955 N88-21650
Iteration of transformation passes over attributed program trees --- compilers
[INF-87-28] 14 p1956 N88-21661
Ada tasking in Ten15
[RSRE-MEMO-4074] 14 p1958 N88-21676
Examination of the effects of using Ada (trade name) in flight control software
[AD-A189679] 14 p1959 N88-21683
Ada (Trademark) compiler validation summary report. ALSYS: AlsyCOMP-013, V2.0 HOST: IBM PC AT. Target: IBM 370 3084Q
[AD-A189640] 15 p2106 N88-22546
ONTIC: A knowledge representation system for mathematics
[AD-A190553] 15 p2121 N88-22643
Automatic layout generation of data processing sections of VLSI microprocessor-like circuits
[ETN-88-92185] 16 p2245 N88-23411
Silicon compilers: Application to the compilation of the control area
[ETN-88-92186] 16 p2247 N88-23425
A timing evaluator for C programs generated by the model system
[AD-A191204] 17 p2365 N88-24174
EPL (Equational Programing Language) system design: Intermediate processing steps
[AD-A191203] 18 p2556 N88-25169
Nebula support software
[AD-A192281] 20 p2837 N88-26833
Programmer-friendly LL(1) parser generator
[PB88-126933] 20 p2841 N88-26857
Ada (trade name) compiler validation summary report: Verdix Corporation VAda-010-03315, version 5.5 MicroVAX 2 host ISBC 386/20P Intel target
[AD-A193226] 21 p2997 N88-27774
Ada (trade name) compiler validation summary report: Verdix corporation VAda-010-13125, version 5.41 Sun Microsystems Sun-3/160 host microbar GPC68020 target
[AD-A193415] 21 p2997 N88-27777
Configuration control in compiler construction
[AD-A193916] 22 p3135 N88-28639
Ada (trade name) compiler validation summary report: Verdix Corporation VAda-010-0101, version 5.41 VAX-11/750
[AD-A193414] 22 p3136 N88-28645
Subset-logic programming: Application and implementation
[AD-A193647] 22 p3138 N88-28655
Modularity in the PASCAL model compiler
[NPL-DITC-111/88] 22 p3139 N88-28664
Loglisp programming system users manual
[AD-A193933] 22 p3142 N88-28682
The SMITE modular compilation system
[RSRE-MEMO-4145] 23 p3244 N88-29307
Ada (trade name) compiler validation summary report: Verdix Corporation VAda-010-03205, version 5.42 MicroVAX 2 host and national DB32000 (NS32032 target
[AD-A193485] 23 p3247 N88-29326
A computer program package for introductory one-dimensional digital signal processing applications
[AD-A194656] 23 p3249 N88-29338
COMPLEMENTARY METAL OXIDE SEMICONDUCTORS
U CMOS
COMPLEMENTS (MATHEMATICS)
On serial-input multipliers for two-complement numbers
[REPT-86-035] 11 p1536 N88-19181
COMPLETENESS
Introduction to logic programming
[CWI-CS-R8741] 16 p2248 N88-23430
COMPLEX COMPOUNDS
Topological aspects of infinite metal clusters and superconductors
[AD-A184104] 04 p0495 N88-13049
An investigation of metal complexes of some 2-substituted and 2,6-disubstituted pyridine N-oxides
11 p1460 N88-18701
The structure of the boron-hydrogen complex in silicon
[DE88-005433] 15 p2144 N88-22795
Synthesis and properties of novel cluster phases
[DE88-006816] 16 p2175 N88-22964
Catalytic activation of carbon dioxide by metal complexes
[AD-A192310] 21 p2909 N88-27262
Structure and function of the manganese complex involved in photosynthetic oxygen evolution determined by X-ray adsorption spectroscopy and electron paramagnetic resonance spectroscopy
[DE88-010360] 21 p2985 N88-27725
Functional study of the Si/SiO2 structures. Application to the implementation of an integrated ion sensor
[ECL-87-16] 22 p3073 N88-28246
Charge storage and switching phenomena in metal complexes
[AD-A193778] 23 p3192 N88-28996
Polymeric electrolytes
[AD-A193766] 23 p3198 N88-29031
COMPLEX SYSTEMS
Implementation and performance of a complex vision system on a systolic array machine
[AD-A184331] 04 p0482 N88-12971
Pattern-recognition software detecting the onset of failures in complex systems
[DE88-002861] 09 p1220 N88-17318
On the sensitivity of complex, internally coupled systems
[NASA-TM-100537] 13 p1813 N88-20829
KOMPOT Program complex for the calculation of spatial magnetostatic fields of electromagnetic systems
[DE88-701691] 16 p2192 N88-23072
Matched index laser anemometry systems for flow studies in complex geometries 16 p2203 N88-23145
A new block solver for large, full, unsymmetric, complex systems of linear algebraic equations
[AD-A190590] 16 p2256 N88-23483
Systems engineering technique
17 p2303 N88-23776
Accurate multigrid solution of the Euler equations on unstructured and adaptive meshes
[NASA-CR-181679] 18 p2460 N88-24608
Application of advanced grid generation techniques for flow field computations about complex configurations
[NASA-CR-183049] 18 p2515 N88-24922
Human problem solving in complex dynamic environments
[AD-A190788] 18 p2551 N88-25142
COMPLEX VARIABLES
NT ANALYTIC FUNCTIONS
NT BESSEL FUNCTIONS
NT CAUCHY INTEGRAL FORMULA
NT CONFORMAL MAPPING
NT ELLIPTIC FUNCTIONS
NT ENTIRE FUNCTIONS
NT EXPONENTIAL FUNCTIONS
NT HANKEL FUNCTIONS
NT HYPERBOLIC FUNCTIONS
NT HYPERGEOMETRIC FUNCTIONS
NT LAGUERRE FUNCTIONS
NT LIOUVILLE THEOREM
NT LOGARITHMS
NT MEROMORPHIC FUNCTIONS
NT ORTHOGONAL FUNCTIONS
NT SINGULARITY (MATHEMATICS)
NT SPHERICAL HARMONICS
Polynomials with restricted coefficients and their applications
[AD-A192589] 23 p3202 N88-29055
COMPLEXITY
NT TASK COMPLEXITY
Weighted decoding of block codes and some topics on decoding complexity
[ENST-87E005] 02 p0221 N88-11394
Diagonalisation methods in polynomial setting
[PB87-138616] 06 p0769 N88-14726
Machine models and simulations
[PB88-118690] 10 p1386 N88-18280
COMPLIANCE (ELASTICITY)
U MODULUS OF ELASTICITY
COMPLICATION
U COMPLEXITY
COMPONENT RELIABILITY
Fracture mechanism of fine grain graphite under high heat fluxes
[IPPJ-842] 02 p0242 N88-11527
The Shock and Vibration Digest, Volume 19, No. 11
03 p0265 N88-11673
The Shock and Vibration Digest, Volume 19, No. 10
03 p0335 N88-12112
PRAAGE: An interactive IBM-PC code for unreliability/aging analysis
[DE87-012124] 04 p0453 N88-12803
Extremum methods of structural analysis for system reliability assessment 04 p0456 N88-12824
Conservatism implications of shock test tailoring for multiple design environments 05 p0592 N88-13611
Small space reactor power systems for unmanned solar system exploration missions
[NASA-TM-100228] 05 p0660 N88-14054
Estimating system reliability: Monte Carlo methods, sensitivity and errors in input parameters
[AD-A186182] 07 p0865 N88-15248
How errors in component reliability affect system reliability
[AD-A186264] 07 p0865 N88-15249
Small engine technology programs
08 p0956 N88-15801
Results of NASA/Army transmission research
09 p1108 N88-16640
Ceramics for engines 09 p1119 N88-16704
A strategy for failure prediction
10 p1380 N88-18243
Design and dynamic testing of an instrumented spacecraft component 11 p1499 N88-18952
Random vibration (stress screening) of printed wiring assemblies 11 p1499 N88-18953
Optimal arrangement of components via pairwise rearrangements
[AD-A187633] 11 p1541 N88-19213
A computer code for the solution of large scale network reliability analysis problems
[AD-A188455] 12 p1680 N88-20042
Estimating system and component reliabilities under partial information on cause of failure
[AD-A189107] 13 p1780 N88-20653
Power components for the space station 20-kHz power distribution system
[NASA-TM-100866] 14 p1904 N88-21374
On the danger of redundancies in some aerospace mechanisms 14 p1925 N88-21475
Monolithic ceramic analysis using the SCARE program
15 p2081 N88-22409
Continuous fiber ceramic matrix composites for heat engine components 15 p2082 N88-22411
Cumulative fatigue damage models
15 p2084 N88-22422
Life and reliability of rotating disks
15 p2085 N88-22428

Incorporating reliability into the design of experimental fusion facilities
[DE88-006767] 16 p2275 N88-23618
Pioneer 10 and 11 RTG performance update 17 p2405 N88-24301
Dynamic isotope power system critical component verification 17 p2425 N88-24421
Small scale bipolar nickel-hydrogen testing
[NASA-TM-100936] 18 p2538 N88-25059
Determining system maintainability as a probability
[DE88-007722] 19 p2679 N88-25927
Probabilistic structural analysis to quantify uncertainties associated with turbopump blades
[NASA-TM-100278] 22 p3050 N88-28094
An application of the Bayesian method to the estimation and forecast of system hardware components MTBF 22 p3068 N88-28211

COMPONENTS
Commonality analysis as a knowledge acquisition problem 08 p1062 N88-16413
Vapor Compression Distillation Subsystem (VCDS) component enhancement, testing and expert fault diagnostics development, volume 2
[NASA-CR-172076] 21 p2994 N88-27755
Development of sensors for ceramic components in advanced propulsion systems: Survey and evaluation of measurement techniques for temperature, strain and heat flux for ceramic components in advanced propulsion systems
[NASA-CR-182111] 22 p3081 N88-28299

COMPOSITE MATERIALS
NT ALUMINUM BORON COMPOSITES
NT ALUMINUM GRAPHITE COMPOSITES
NT BORON REINFORCED MATERIALS
NT BORON-EPOXY COMPOSITES
NT CARBON FIBER REINFORCED PLASTICS
NT CARBON-CARBON COMPOSITES
NT CERAMIC MATRIX COMPOSITES
NT CERMETS
NT COMPOSITE PROPELLANTS
NT EPOXY MATRIX COMPOSITES
NT EUTECTIC COMPOSITES
NT FIBER COMPOSITES
NT GLASS FIBER REINFORCED PLASTICS
NT GRAPHITE-EPOXY COMPOSITES
NT GRAPHITE-POLYIMIDE COMPOSITES
NT LAMINATES
NT METAL MATRIX COMPOSITES
NT POLYMER MATRIX COMPOSITES
NT REINFORCED PLASTICS
NT RESIN MATRIX COMPOSITES
NT THREE DIMENSIONAL COMPOSITES
NT WHISKER COMPOSITES
Structures and Materials Working Group report 01 p0016 N88-10093
Ceramic-Ceramic Composites Meeting in Belgium
[ONRL-7-020-R] 01 p0019 N88-10118
Mechanical properties characterization of composite sandwich materials intended for space antenna applications
[NASA-TM-88893] 01 p0020 N88-10121
Ceramic composites by chemical vapor infiltration
[DE87-009128] 01 p0029 N88-10165
Anti-abrasion protection with highly organized materials
[DE87-014238] 01 p0029 N88-10187
Composite bearing materials containing solid lubricant in filamentary form, stages 3 and 4
[IRD-87/2] 01 p0054 N88-10344
An experimental and theoretical study of the bending behavior of Kevlar 49/epoxy beams and rings
[DE87-010430] 01 p0061 N88-10394
Contribution to the study of composite materials and their damage
[NASA-TT-20107] 02 p0143 N88-10897
Damping characteristics of a composite-reinforced stainless-steel tube
[DE87-012455] 02 p0191 N88-11192
Energy changes in transforming solids
[DE87-011257] 02 p0191 N88-11194
Composite materials in western Europe
[PB87-102943] 03 p0279 N88-11759
Effects of solvent exposures on poly(etheretherketone) (PEEK) and PEEK-fiberglass composites
[MLM-3405] 03 p0281 N88-11766
JPRS report: Science and technology. USSR: Materials science
[JPRS-UMS-87-006] 03 p0285 N88-11791
GSSR powder metallurgy research, production expanding 03 p0286 N88-11797
Joining of silicon carbide reinforced ceramics
[DE87-014881] 03 p0294 N88-11847
Fabrication and testing of fire resistant graphite composite panels
[NASA-CR-177397] 04 p0397 N88-12472
JPRS report: Science and technology. Japan
[JPRS-JST-87-025] 04 p0403 N88-12502
Activities at government research laboratories reported 04 p0403 N88-12503
Carbon-fiber reinforced aluminum 04 p0403 N88-12507
Failure analysis of composite structure materials
[AD-A184468] 04 p0410 N88-12548
Composite mechanics for engine structures
[NASA-TM-100176] 04 p0411 N88-12552
A creep measurement of unidirectional epoxy-fiberglass rod
[DE87-014812] 04 p0411 N88-12553
Thermoplastic elastomers as LOVA (Low Vulnerability Ammunition) binders
[AD-A184350] 04 p0419 N88-12599
Work-in-progress presented at the Army Symposium on Solid Mechanics, 1986: Lightening of the Force
[AD-A184791] 04 p0427 N88-12644
Composite materials applications program at the US Army Ballistic Research Laboratory: Work in progress 04 p0428 N88-12651
Damping characteristics of a composite-reinforced stainless-steel plate
[DE88-000303] 04 p0457 N88-12828
Materials for fighter aircraft 05 p0546 N88-13325
Fabrication of composites by chemical vapor deposition
[DE87-014565] 05 p0559 N88-13408
Bending of a bonded beam as a test method for adhesive properties
[AD-A184813] 05 p0609 N88-13736
Damping analysis of flexural waves in fluid-loaded single and constrained plates
[AD-A185116] 05 p0609 N88-13739
An element of a multilayer shell for the computation of composite structures
[ONERA-RT-14/3542-RY-051-R] 05 p0610 N88-13742
Development of an impact- and solvent-resistant thermoplastic composite matrix, phase 4
[NASA-CR-178413] 06 p0677 N88-14145
Behavior of bolted joints in composite laminates 06 p0677 N88-14148
Sintering and densification of particulate composites: Inclusion size and clustering
[DE88-002230] 06 p0685 N88-14199
Exploitation of the sol-gel route in processing of ceramics and composites
[AD-A185482] 06 p0686 N88-14204
Characterization of mechanical damage mechanisms in ceramic composite materials
[AD-A185549] 06 p0686 N88-14205
Interface effects on the mechanical properties of ceramic composites
[AD-A185899] 07 p0826 N88-15009
Composite reliability enhancement via preloading
[AD-A185938] 07 p0826 N88-15010
Characterization of microstructure in metallic and composite materials
[AD-A186193] 07 p0826 N88-15012
Simplified procedures for designing composite bolted joints
[NASA-TM-100281] 07 p0828 N88-15020
Thermoplastic elastomers as LOVA binders
[AD-A185864] 07 p0835 N88-15067
Thermoplastic elastomers as LOVA binders
[AD-A185865] 07 p0835 N88-15068
Contribution to modeling flexion fatigue damage in unidirectional composite materials
[ECL-87-12] 08 p0965 N88-15843
Nondestructive characterization of ceramic composite whiskers with neutron diffraction and ultrasonic techniques
[DE88-003075] 08 p0965 N88-15844
Transparent metal model study of the use of a cellular growth front to form aligned monotectic composite materials
[NASA-CR-182414] 08 p0969 N88-15861
Composite/metal jointing technology for vehicle weight reduction
[DE88-900228] 08 p0992 N88-16005
Failure modes of laminate structures
[DE88-002579] 08 p0996 N88-16033
Advanced composite airframe program: Today's technology 09 p1107 N88-16636
Recent Sikorsky R and D progress 09 p1111 N88-16659
Review of thermal properties of graphite composite materials
[NASA-TM-100049] 09 p1139 N88-16825
Finite element analysis of damaged cross-ply composite laminates
[CCMS-87-10] 09 p1139 N88-16829
Residual stiffness and strength of Kevlar/epoxy laminated impulsively loaded to 7.9 ktaps
[DE88-003724] 09 p1149 N88-16886
Automated Composites, First International Conference, September 10-12, 1986, University of Nottingham, England
[PB87-126199] 10 p1294 N88-17734
Composite materials for rail transit systems
[NASA-CR-178401] 10 p1294 N88-17738
Short fiber reinforced thermoplastic composites for armor applications: Interfacial bonding
[DE88-004007] 10 p1295 N88-17742
A finite element analysis of adhesively bonded composite joints including geometric nonlinearity, nonlinear viscoelasticity moisture diffusion and delayed failure
[AD-A187455] 10 p1296 N88-17747
The analysis of deformations and strains in composites by moire interferometry
[AD-A187482] 10 p1345 N88-18043
Ultrasonic characterization of layered composite systems 10 p1404 N88-18374
The effect of magnetic impurities and barriers on the magnetization and critical current of fine filament NbTi composites
[DE88-004443] 10 p1419 N88-18472
Quantitative non-destructive evaluation of porous composite materials based on ultrasonic wave propagation
[NASA-CR-182544] 11 p1447 N88-18627
High performance composites research at NASA-Langley
[NASA-TM-100518] 11 p1450 N88-18642
Analysis of composite laminates with matrix cracks
[CCMS-88-03] 11 p1451 N88-18645
Creep behavior of tungsten/niobium and tungsten/niobium-1 percent zirconium composites
[NASA-TM-100804] 11 p1460 N88-18707
Application of X-ray computed tomography to ceramic/ceramic composites
[DE88-002903] 11 p1464 N88-18728
Nucleation and growth of calcium carbonate crystals on surface-modified polyethylene and polystyrene
[DE88-005126] 11 p1465 N88-18733
Slip casting of advanced ceramics and composites
[DE88-003424] 11 p1467 N88-18746
The place for thermoplastic composites in structural components
[AD-A189149] 12 p1604 N88-19596
Experimental and analytical investigation on a proposed embedded fiber optic displacement sensor
[AD-A189030] 12 p1630 N88-19756
Comparison of ultrasonic flaw detection analysis for spherical composite test specimens using two data acquisition techniques
[DE88-005002] 12 p1634 N88-19782
The Shock and Vibration Digest, volume 20, no. 3 12 p1635 N88-19786
A continuum damage model for viscoelastic materials
[AD-A189426] 12 p1637 N88-19800
Compression of composite materials: A review
[AD-A189272] 13 p1734 N88-20365
Phase velocity and attenuation of plane elastic waves in a particle-reinforced composite medium
[AD-A189414] 13 p1734 N88-20366
The influence of the fiber-matrix bond on the mechanical behavior of NICALON/SiC composites
[DE88-006155] 13 p1734 N88-20369
Delamination stresses in semicircular laminated composite bars
[NASA-TM-4026] 13 p1735 N88-20375
The effect of Ca(OH)2-treated ceramic microspheres on the mechanical properties of high-temperature lightweight cement composites
[DE88-004590] 13 p1749 N88-20457
PNL-1 improved ceramic composites through controlled fiber matrix interaction
[DE88-005680] 13 p1750 N88-20462
Micromechanical and microstructural studies of ceramic superplasticity
[DE88-005793] 13 p1751 N88-20472
Theory and experiments of fracture in cyclic compression: Single phase ceramics, transforming ceramics and ceramic composites
[DE88-005792] 13 p1781 N88-20659
Activities report in aeronautics and astronautics
[ETN-88-91332] 13 p1859 N88-21115
Detection of bondline delaminations in multilayer structures with lossy components
[NASA-CR-182716] 14 p1883 N88-21256
JPRS report: Science and technology. USSR: Materials science
[JPRS-UMS-87-009] 14 p1884 N88-21261
Microprobe examination of composite materials produced by burning of Ti, Cr, C powders with powder of any one Fe-group metal 14 p1886 N88-21269

The unique characteristics of the structure of composite materials made on a base of sphalerite-analogous boron nitride 14 p1886 N88-21273
JPRS report: Science and technology. USSR: Materials science
[JPRS-UMS-87-007] 14 p1895 N88-21312
Phenomenological piercing characteristics of composite materials 14 p1895 N88-21315
Mathematical stress analysis of composite materials 14 p1900 N88-21349
Cement paste matrix composite materials center
[AD-A186657] 15 p2028 N88-22083
The combustion synthesis of boride composites
[DE88-005474] 15 p2028 N88-22084
Superplastic flow of mullite-zirconia composites
[DE88-005905] 15 p2028 N88-22085
Microplasticity phenomena in graphite/magnesium metal matrix composites
[DE88-006772] 15 p2029 N88-22086
Structure and surface characterizations of high strength carbon fibers
[AD-A189642] 15 p2029 N88-22087
An investigation of the failure response of laminates under biaxial stress
[AD-A190039] 15 p2029 N88-22090
A study of damage tolerance in curved composite panels
[AD-A190617] 15 p2029 N88-22092
Microwave sintering of alumina-SiC composites at 2.45 and 60 GHz
[DE88-006455] 15 p2030 N88-22095
Interlaminar fracture toughness of thermoplastic composites
[NASA-TM-100532] 15 p2030 N88-22097
Application of copper-carbon fiber composites to power semiconductor devices
[NASA-TT-20171] 15 p2031 N88-22101
Mechanical behaviour of particle filled thermoplastics
[PB88-169297] 15 p2047 N88-22196
Eddy current nondestructive inspection of graphite epoxy using ferrite cup core probes
[AD-A189823] 15 p2074 N88-22365
Biaxial experiments supporting the development of constitutive theories for advanced high-temperature materials 15 p2078 N88-22386
Structural analyses of engine wall cooling concepts and materials 15 p2081 N88-22405
Ultrasonic beam distortion in transversely isotropic media
[DE88-005937] 15 p2129 N88-22699
Towards a damage tolerance philosophy for composite materials and structures
[NASA-TM-100548] 16 p2173 N88-22949
A piecewise quadratic strength tensor theory for composites
[AD-A190929] 16 p2173 N88-22952
Nondestructive evaluation of large scale composite components
[AD-A190998] 16 p2173 N88-22954
New method of grafting crystals
16 p2180 N88-22992
Investigation of non-linear optical behavior of semiconductors for optical switching, volume 1
[AD-A191297] 16 p2274 N88-23611
Strain intensity factor approach for predicting the strength of continuously reinforced metal matrix composites
[NASA-TM-100617] 17 p2317 N88-23838
Local buckling and crippling of composite stiffener sections
[NASA-TM-101133] 17 p2317 N88-23840
Cryogenic regenerator including saran-carbon heat conduction matrix
[NASA-CASE-NPO-17291-1-CU]
17 p2337 N88-23946
Mixed-mode fracture of uniaxial fiber reinforced composites
[AD-A191629] 18 p2478 N88-24700
Interfacial shear phenomena in graphite epoxy composites under impact loading using dynamic moire interferometry
[DE88-006773] 18 p2479 N88-24709
Functional and mechanical analysis of continuous media-application to the study of elastic composites with periodic structure: Homogenization
[NASA-TT-20188] 18 p2480 N88-24710
The 700 F properties of autoclave cured PMR-2 composites
[NASA-TM-100923] 18 p2480 N88-24712
Status and prognosis for alternative engine materials
[NASA-TM-100903] 18 p2486 N88-24749
New polyisoimides: An approach to in situ rigid-rod polyimide formation
[AD-A191665] 18 p2490 N88-24773
High strength/sigh modulus aromatic heterocyclic ABA block copolymers
[AD-A191666] 18 p2491 N88-24774
Nondestructive testing using ultrahigh frequencies
[CERT-5/1333-MO] 18 p2526 N88-24984
Improved structural polymer alloys and composites
[AD-A192092] 19 p2619 N88-25536
Fire retardant coatings for military equipment: A review
[MRL-R-1104] 19 p2619 N88-25540
Effect of a weak magnetic field on high temperature superconductivity in Y-Ba-Cu-O ceramics
[DE88-702192] 19 p2733 N88-26235
Instability-related delamination growth of embedded and edge delaminations 20 p2767 N88-26406
Interface modification in Nicalon (trademark)/SiC composites
[DE88-009708] 20 p2767 N88-26409
A micromechanics model of the stiffness and strength of laminates with fiber waviness
[NASA-CR-181670] 20 p2768 N88-26413
Observations on residual stresses in ceramic composites by neutron diffraction techniques
[DE88-009937] 20 p2778 N88-26472
Stress concentration around circular hole in a composite material specimen representative of the X-29A forward-swept wing aircraft
[NASA-CR-179435] 20 p2814 N88-26694
Boundary layer solutions for the free-edge problem in composite laminates 21 p2904 N88-27229
Thermo-viscoelastic analysis of composite materials, volume 1
[NASA-CR-183048-VOL-1] 21 p2904 N88-27230
Probabilistic anisotropic failure criteria for composite materials
[AD-A193046] 21 p2904 N88-27232
Analysis of transverse strength of composites using percolation theory
[AD-A193204] 21 p2904 N88-27234
Far- and mid-infrared properties of metal-insulator composite materials
[AD-A193227] 21 p2905 N88-27236
Polymer-ceramic composites
[AD-A193244] 21 p2905 N88-27237
Techniques for characterizing damage zones in composite materials 21 p2905 N88-27240
Characterization of elastic-plastic properties of AS4/APC-2 thermoplastic composite
[NASA-CR-183145] 21 p2906 N88-27242
Preparation and properties of new inorganic glasses and gel-derived solids
[AD-A192922] 21 p2917 N88-27315
Application of sol-gel procedures to ceramic composites
[ETN-88-92741] 21 p2921 N88-27338
Effects of applied stress and temperature on the nonlinear elastic properties of graphite fibers
[AD-A194469] 22 p3050 N88-28093
Durability of continuous fiber reinforced metal matrix composites
[AD-A193868] 22 p3050 N88-28097
Micromechanics of composite laminate compression failures
[NASA-CR-183179] 22 p3050 N88-28098
A transversely isotropic thermoelastic theory
[NASA-TM-101302] 22 p3087 N88-28332
Mixed finite element methods to compute stress in a load composite specimen with holes: Numerical results
[ONERA-RT-37/4242-RY-062-R]
22 p3088 N88-28336
Laboratory feasibility study of a composite embedded fiber optic sensor for measurement of structural vibrations
[AD-A194270] 22 p3152 N88-28754
Molecular composites processing and properties, 1
[AD-A194113] 23 p3189 N88-28974
Microwave frequency nondestructive control
[CERT-2/1355-MO] 23 p3189 N88-28976
Finite Element Composite Analysis Program (FECAP) for a microcomputer
[NASA-TM-100670] 23 p3190 N88-28982
Creep of carbon yarn and carbon-carbon composites at high temperatures and high stresses
[AD-A195224] 24 p3340 N88-29878
An improved boundary force method for analyzing cracked anisotropic materials
[NASA-TM-101495] 24 p3340 N88-29879
ZT imaging system for layered thin wall structures
[AD-A195466] 24 p3352 N88-29954
Polymer-ceramic composites
[AD-A195789] 24 p3356 N88-29983
Piezoelectric and electrostrictive materials for transducer applications, volume 1
[AD-A194957] 24 p3374 N88-30096
Experimental aspects of using time-averaged holographic interferometry to detect barely visible impact damage in a graphite/epoxy composite plate
[AD-A194418] 24 p3375 N88-30097
Application of nondestructive testing techniques to materials testing
[AD-A195716] 24 p3381 N88-30138
An organometallic route to micron-sized whiskers of zinc sulfide
[AD-A195889] 24 p3430 N88-30414

COMPOSITE PROPELLANTS
A continuous oxidizer regression model for the combustion of composite solid propellants
[AD-A186742] 08 p0974 N88-15894
Laser ignition of nitramine composite propellants and crack propagation and branching in burning solid propellants
[AD-A189260] 13 p1753 N88-20483
Nonlinear mechanisms of solid propellant combustion instability 19 p2628 N88-25588
Selective radiation absorption in aluminized composite propellant combustion 19 p2630 N88-25598
Effect of burn-path tortuosity on the burn rate of composite propellants 19 p2630 N88-25602
Thermomechanical computations for GAP, a high energy binder for composite propellants
[FOA-C-20718-2.1] 24 p3357 N88-29988

COMPOSITE STRUCTURES
NT LAMINATES
Structures and Materials Working Group report
01 p0016 N88-10093
Compendium of post-failure analysis techniques for composite materials
[AD-A183783] 01 p0018 N88-10113
The analysis of moisture absorption in multi-layered media
[NPL-DMA(A)-147] 01 p0019 N88-10115
A mixed finite element method for the computation of stress in a composite with loaded holes
[ONERA-RT-34/4242-RY-054-R]
01 p0062 N88-10395
Models of degradation of stratified composite structures
[ONERA-RT-13/3542-RY-061-R]
02 p0142 N88-10892
Properties of Nb3Sn superconductor wires with composite cores
[KFK-4263] 02 p0246 N88-11557
Three-dimensional finite element based, interative approach for analysis of laminated composites
03 p0280 N88-11763
Durability (lifetime) predictions adhesively bonded structures
[AD-A184069] 03 p0335 N88-12110
Materials studies for magnetic fusion energy applications at low temperatures-X
[PB87-232575] 03 p0381 N88-12395
Failure analysis of composite structure materials
[AD-A184468] 04 p0410 N88-12548
Composite mechanics for engine structures
[NASA-TM-100176] 04 p0411 N88-12552
Corrosion control by composite material substitution with application to the M-939 5-ton truck
04 p0428 N88-12654
Characterization of thin layers for optics
[PB87-217949] 04 p0490 N88-13017
Surface treatment problems found in new aircraft designed using structural composites
[SNIAS-872-111-113] 05 p0558 N88-13397
Philosophy and practice of nondestructive tests of composite material structures at Aerospatiale Aquitaine
[SNIAS-872-430-105] 05 p0559 N88-13400
Measurement and control of damage in composite materials: Nondestructive controls by thermography, holography, and radiography
[SNIAS-872-430-110] 05 p0559 N88-13403
Mechanics of anisotropic media. Study of the boundary conditions --- stratified composites
[SNIAS-872-430-112] 05 p0559 N88-13404
Micromechanics of the degradation of composite materials
[SNIAS-872-430-113] 05 p0559 N88-13405
The structures of large wound propulsion shells --- carbon fiber composites filament winding
[SNIAS-872-430-118] 05 p0559 N88-13406
Design and test of high performance composite tubes for use in deep water drilling and production systems
[SNIAS-872-430-107] 05 p0572 N88-13487
High performance composite tubes for offshore applications
[SNIAS-872-430-116] 05 p0572 N88-13488
Strain-energy-release rate analysis of the end-notched flexure specimen using the finite-element method
[NASA-TM-100494] 05 p0608 N88-13735

Bending of a bonded beam as a test method for adhesive properties
[AD-A184813] 05 p0609 N88-13736
Structural tests and development of a laminar flow control wing surface composite chordwise joint
[NASA-CR-172462] 06 p0663 N88-14066
A study of the utilization of advanced composites in fuselage structures of commercial aircraft
[NASA-CR-172405] 06 p0679 N88-14157
Ceramic technology for advanced heat engines
[PB87-232997] 06 p0683 N88-14188
Study on utilization of advanced composites in fuselage structures of large transports
[NASA-CR-172406] 07 p0827 N88-15014
Impact of solids on composite materials
[NASA-CR-182395] 07 p0827 N88-15015
Delamination durability of composite materials for rotorcraft 09 p1107 N88-16634
Helicopter crashworthiness research program 09 p1107 N88-16635
Experimental study on the effect of fiber orientation on flutter characteristics of high-aspect-ratio transport wing
[NAL-TR-936] 09 p1120 N88-16708
Space station structures development
[NASA-CR-179261] 09 p1133 N88-16792
Sublaminate damage mechanisms in composite structures
[AD-A186807] 09 p1137 N88-16815
The strength of hybrid composites
[BR101991] 09 p1138 N88-16821
Integrity control of carbon fiber reinforced plastics (CFRP) structural elements. Conclusion with respect to the control methodology of CFRP primary structures in manned space flight and the implications to the design, analysis and testing of CFRP structural elements, executive summary
[MBB-TR-RB517-014/85] 09 p1139 N88-16824
Mechanical properties of carbon fiber reinforced thermoplastic matrix composites
[NAL-TR-934] 09 p1139 N88-16827
Ultrasonic inspection of advanced CFRP structures by computer-controlled, pulse-echo technique
[ETN-88-91665] 09 p1177 N88-17051
Rotorcraft weight trends in light of structural material characteristics
[AD-A186576] 10 p1276 N88-17642
A finite element analysis of adhesively bonded composite joints including geometric nonlinearity, nonlinear viscoelasticity moisture diffusion and delayed failure
[AD-A187455] 10 p1296 N88-17747
La Recherche Aerospatiale, bimonthly bulletin, number 1987-1, 236/January-February
[ESA-TT-1055] 11 p1433 N88-18549
Finite element analysis of adhesively bonded composite joints including geometric nonlinearity, nonlinear viscoelasticity, moisture diffusion and delayed failure
[PB88-147822] 11 p1451 N88-18648
Slip casting of advanced ceramics and composites
[DE88-003424] 11 p1467 N88-18746
Wave propagation in laminated composite plates
[AD-A188999] 12 p1604 N88-19594
The place for thermoplastic composites in structural components
[AD-A189149] 12 p1604 N88-19596
Standardized environmental fatigue sequence for the evaluation of composite components in combat aircraft (ENSTAFF = ENvironmental faISTAFF)
[LBF-FB-179] 13 p1722 N88-20300
A preliminary investigation of finite-element modeling for composite rotor blades
[NASA-TM-100559] 13 p1781 N88-20656
Hygrothermomechanical fiber composite fatigue: Computational simulation
[NASA-TM-100840] 14 p1884 N88-21257
Structural and material testing of a composite microlite wing model
[BU-355] 14 p1923 N88-21461
The effect of strain rate on the strength and ductility of SiCw/2124 Al composite
[OUEL-1692/87] 14 p1924 N88-21466
Thermally stable deployable structure 14 p1925 N88-21472
A study of damage tolerance in curved composite panels
[AD-A190617] 15 p2029 N88-22092
Postbuckling delamination of a stiffened composite panel using finite element methods
[NASA-CR-182803] 15 p2030 N88-22098
Features and applications of the integrated composites analyzer (ICAN) code 15 p2078 N88-22391
Computational simulation methods for composite fracture mechanics 15 p2079 N88-22396
Thermal stress in high temperature cylindrical fasteners
[NASA-TM-100611] 15 p2087 N88-22438
Experimental comparison of lightning simulation techniques to CV-580 airborne lightning strike measurements
[AD-A190576] 15 p2098 N88-22496
Towards a damage tolerance philosophy for composite materials and structures
[NASA-TM-100548] 16 p2173 N88-22949
A piecewise quadratic strength tensor theory for composites
[AD-A190929] 16 p2173 N88-22952
Nondestructive evaluation of large scale composite components
[AD-A190998] 16 p2173 N88-22954
Durability of compound cylinder under static internal-pressure repeat load of long duration 16 p2180 N88-22991
Investigation into the operation of the new special drills for drilling holes in thin components made of composite materials --- aircraft components
[LR-519] 16 p2215 N88-23215
A nonlinear computation for composite structures
[ONERA-RT-15/3542-RY-062-R] 16 p2222 N88-23265
Insert design handbook
[ESA-PSS-03-1202-ISSUE-1] 17 p2311 N88-23822
Composite piston
[NASA-CASE-LAR-13435-1] 17 p2346 N88-23981
Interaction of ultrasonic waves with composite plates
[AD-A191879] 18 p2478 N88-24702
Shape stability in composites 18 p2479 N88-24706
The stress analysis of ceramic, polymeric, and metallic composite systems by the finite element method 18 p2529 N88-25004
Microlaminate composite structures by low pressure plasma spray deposition
[DE88-006453] 19 p2610 N88-25488
The construction of composite grids for general three-dimensional regions 20 p2843 N88-26872
Balance of X-ray radioscopy application to nondestructive tests of composite materials
[SNIAS-881-430-110] 21 p2907 N88-27250
Two-dimensional sequential and concurrent finite element analysis of unstiffened and stiffened aluminum and composite panels with hole
[NASA-CR-183083] 22 p3086 N88-28325
Parameter identification of material constants in a composite shell structure
[DE88-008115] 22 p3086 N88-28326
Critical joints in large composite primary aircraft structures. Volume 2: Technology demonstration test report
[NASA-CR-172587] 23 p3177 N88-28915
Critical joints in large composite primary aircraft structures. Volume 3: Ancillary test results
[NASA-CR-172588] 23 p3177 N88-28916
Elastic wave dispersion in laminated composite plate
[AD-A192289] 23 p3188 N88-28967
Nondestructive tests and high performance composite structures
[SNIAS-881-430-119] 23 p3188 N88-28969
Effect of fiber diameter on the reliability of composites - automated laser diffraction implementation
[AD-A193524] 23 p3188 N88-28972
Critical joints in large composite primary aircraft structures. Volume 1: Technical summary
[NASA-CR-3914] 23 p3190 N88-28983
Damage initiation in the short beam shear test of composite materials using stiffness reduction
[AD-A194880] 24 p3340 N88-29883
Evaluation of bond testing equipment for inspection of Army advanced composite airframe structures
[AD-A195795] 24 p3341 N88-29885
Experimental aspects of using time-averaged holographic interferometry to detect barely visible impact damage in a graphite/epoxy composite plate
[AD-A194418] 24 p3375 N88-30097

COMPOSITES
U COMPOSITE MATERIALS

COMPOSITION (PROPERTY)
NT ATMOSPHERIC COMPOSITION
NT ATMOSPHERIC MOISTURE
NT CARBON DIOXIDE CONCENTRATION
NT CHEMICAL COMPOSITION
NT CONCENTRATION (COMPOSITION)
NT GAS COMPOSITION
NT IONOSPHERIC COMPOSITION
NT METEORITIC COMPOSITION
NT METEOROID CONCENTRATION
NT MOISTURE CONTENT
NT PLANETARY COMPOSITION
NT STELLAR COMPOSITION

COMPOUND HELICOPTERS
Rotorcraft designs for the year 2000 03 p0264 N88-11665

COMPRESSED GAS
NT HIGH PRESSURE OXYGEN
Shock wave compression and metallization of simple molecules
[DE88-008031] 20 p2851 N88-26925

COMPRESSIBILITY
Shock measurements on explosives in the supra compressive region
[DE87-008423] 01 p0031 N88-10196
Nonlinear and nonparallel stability problems
[AD-A186406] 07 p0850 N88-15159
Compression of composite materials: A review
[AD-A189272] 13 p1734 N88-20365
Unsteady flow field measurements using LDV (Laser Doppler Velocimetry)
[AD-A189907] 15 p2063 N88-22298
Effects of axial load on elastomeric isolation bearings
[PB88-179015] 16 p2223 N88-23269
Bimodular behavior and crack closure in compression in a brittle material
[AD-A191267] 16 p2224 N88-23275
Nickel hydroxide active material densities
[AD-A191411] 16 p2230 N88-23319
The effects of thin compressive films on indentation fracture toughness measurements
[AD-A192243] 20 p2779 N88-26480
Development of an equation of state for computation of supercompressibility factors, critical flow factors and other properties for wet, sour natural gases, synthetic gases and admixtures
[PB88-202676] 20 p2798 N88-26602
Quantitative particle characterization by scattered ultrasound 20 p2848 N88-26908
Temperature, moisture and strain rate effects on the compressive mechanical behavior of Nylon 6/6
[DE88-010734] 21 p2961 N88-27591
Survey on nonlinear effects 24 p3317 N88-29757
Compression pylon
[NASA-CASE-LAR-13777-1] 24 p3323 N88-29789

COMPRESSIBILITY EFFECTS
Investigation of dihedral effects in compressor cascades 10 p1282 N88-17672

COMPRESSIBLE BOUNDARY LAYER
Secondary instability of compressible boundary layer to subharmonic three-dimensional disturbances
[NASA-CR-4144] 16 p2200 N88-23122
Theoretical investigation of 3-D shock wave-turbulent boundary layer interactions, part 6
[AD-A191546] 18 p2509 N88-24882
Spatial stability of a compressible mixing layer
[NASA-CR-181671] 18 p2514 N88-24916
Compressible boundary layers --- atmospheric reentry
[CERT-OA-13/5005-AYD] 20 p2801 N88-26623

COMPRESSIBLE FLOW
NT TRANSONIC FLOW
Rayleigh-Taylor instability in compressible fluids
[DE87-013494] 01 p0047 N88-10297
Numerical solution of Euler equations for compressible fluids by the finite element method, volume 3
[ETN-87-90650] 02 p0170 N88-11070
Impact of turbulence modeling on numerical accuracy and efficiency of compressible flow simulations
[NASA-TM-88333] 02 p0173 N88-11088
JPRS report: Science and technology. China
[JPRS-CST-87-034] 03 p0301 N88-11897
Analysis of compressible flow on high-velocity jet penetration 03 p0302 N88-11898
A free-Lagrange method for 2-D compressible flows
[DE88-000216] 04 p0442 N88-12745
Studies of pressure-velocity coupling schemes for analysis of incompressible and compressible flows
[NASA-CR-181526] 04 p0443 N88-12748
TOPAZ: The transient one-dimensional pipe flow analyzer: An update on code improvements and increased capabilities
[DE88-001781] 04 p0443 N88-12751
Cauchy problem for linearized system of Navier-Stokes equations considering compressibility 04 p0459 N88-12837
An analysis of the compressible-viscous flow field around a 3D-oscillating wing 05 p0535 N88-13254
Computation of dynamic stall of NACA0012 airfoil by block pentadiagonal matrix scheme 05 p0535 N88-13255
Computations of compressible viscous flows over multiple-bodies 05 p0539 N88-13282
Relaxation method for the compressible Navier-Stokes equations using upwind schemes 05 p0539 N88-13283
Interferometric data for a shock-wave/boundary-layer interaction
[NASA-TM-88227] 05 p0543 N88-13306
Unsteady aerodynamics of an oscillating cascade in a compressible flow field
[NASA-TM-100219] 05 p0549 N88-13346

A note on the use of symmetric line Gauss-Seidel for the steady upwind differenced Euler equations
[AD-A185223] 05 p0580 N88-13540
Evolution of mean square magnetic vector potential in compressible, two-dimensional, magnetofluid turbulence
[AD-A184985] 05 p0651 N88-13990
Vectorization of a multigrid method for the compressible Navier-Stokes equations
[PB87-230496] 06 p0698 N88-14284
Experimental investigation of heterogeneous compressible shear layers 06 p0700 N88-14294
A direct calculation method for perturbation fields of moving bodies in compressible media at subsonic Mach numbers
[ETN-88-90808] 06 p0701 N88-14305
On the subgrid-scale modeling of compressible turbulence
[NASA-CR-178420] 06 p0702 N88-14309
Rayleigh-Taylor instability in compressible fluids
[DE88-002473] 07 p0852 N88-15179
Finite element methods for compressible flows 08 p0984 N88-15956
Turbulence modeling for compressible flows 08 p0987 N88-15978
Modeling the unsteady flow found in axial turbomachinery
[ECL-87-07] 08 p0987 N88-15980
New techniques in computational aerodynamics
[AD-A186719] 09 p1112 N88-16664
Numerical resolution of the equations of three-dimensional stable compressible transonic flows
[PB87-168415] 09 p1113 N88-16673
Dynamic modelling by finite element method of an elasto-acoustic beam with due consideration of flow and viscosity
[PB87-178166] 09 p1164 N88-16978
Lifting-surface theory of oscillating propellers in compressible flow
[NAL-TR-943] 10 p1273 N88-17613
A numerical study of unsteady two-dimensional subsonic compressible base flow 10 p1327 N88-17931
On the stability of the supersonic boundary layer 11 p1435 N88-18561
A hydrodynamic analysis of fluid flow between meshing spur gear teeth
[AD-A187671] 11 p1482 N88-18844
A simplified streamline swallowing procedure for the windward meridian of axisymmetric blunt bodies
[AD-A186413] 12 p1626 N88-19732
Compressible friction coefficients in a simulated heat pipe
[AD-A188818] 12 p1627 N88-19735
Computational technique for compressible vortex flows using the integral equation solution
[NASA-CR-182695] 13 p1718 N88-20271
Slip velocity method for three-dimensional compressible turbulent boundary layers
[NASA-TM-100586] 13 p1771 N88-20592
Splitting of inviscid fluxes for real gases
[NASA-TM-100856] 14 p1964 N88-21717
Flexiwall 3 SO: A second order predictive strategy for rapid wall adjustment in two-dimensional compressible flow
[NASA-CR-181662] 15 p2015 N88-22018
Turbulent reacting flows and supersonic combustion
[AD-A189690] 15 p2034 N88-22115
Theoretical model and numerical solution for compressible viscous vortex cores 15 p2054 N88-22243
Transient compressible flow in porous materials
[DE88-006685] 15 p2067 N88-22324
Analysis for high compressible supersonic flow in converging nozzle
[IPPJ-860] 16 p2157 N88-22869
Solution of the compressible Navier-Stokes equations of motion by Chebyshev polynomials for laminar shock-boundary layer flow
[AD-A191033] 16 p2208 N88-23176
Noncondensing round turbulent gas jets in liquids
[AD-A191191] 16 p2208 N88-23179
Laser Doppler anemometry
[NASA-TM-100072] 16 p2210 N88-23187
Detailed transient model of a liquid-metal heat pipe 17 p2412 N88-24345
Boundary layer transition
[CERT-OA-37/5018-AYD] 18 p2458 N88-24595
Compressible flow in a pie-shaped cylinder rotating about the vertex 18 p2460 N88-24604
Accurate multigrid solution of the Euler equations on unstructured and adaptive meshes
[NASA-CR-181679] 18 p2460 N88-24608
Internal fluid dynamics within a nonspinning partially liquid-filled shell due to burster rupture
[AD-A191055] 18 p2507 N88-24874
A variational finite element method for three-dimensional, steady, compressible, viscous flows 18 p2512 N88-24904
Numerical simulation of compressible homogeneous turbulence: Effects of fluid compressibility
[PB88-127154] 19 p2597 N88-25433
Relaxation scheme for compressible flows 19 p2640 N88-25663
The modified-fluid-in-cell method to which adaptive mesh and multigrid were applied 19 p2640 N88-25664
Experimental and analytical studies of compressible vortices 19 p2665 N88-25848
An h-p adaptive finite element method for steady compressible flow 21 p2941 N88-27467
Implicit finite-difference simulation of an internal flow on a hypercube
[AD-A192474] 21 p2942 N88-27471
Solution to the compressible Navier-Stokes equations of motion by Chebyshev polynomials with implicit time stepping
[AD-A194119] 22 p3075 N88-28257
Analysis method for the production of Reynolds stresses in compressible turbulent flow (fluid mechanics)
[NASA-TT-20330] 24 p3373 N88-30088
Development of a more general Reynolds stress closure for swirling flow
[AD-A195121] 24 p3374 N88-30092

COMPRESSIBLE FLUIDS
Rayleigh-Taylor instability in compressible fluids
[DE87-013494] 01 p0047 N88-10297
Effect of dissipation on propagation of spherical detonation shock wave 02 p0159 N88-10998
Dispersion equation for plane capillary-gravity wave on free surface of viscous incompressible fluid 04 p0459 N88-12842
Rayleigh-Taylor instability in compressible fluids
[DE88-002473] 07 p0852 N88-15179
A compressible vapor flux model for transient heat pipe analysis 17 p2412 N88-24343
Implicit finite-difference simulation of an internal flow in a nozzle: An example of a physical application on a hypercube
[AD-A192475] 21 p2942 N88-27472

COMPRESSING
NT PLASMA COMPRESSION
NT SPEECH BASEBAND COMPRESSION
Optimum size of staged flux compression generators
[DE87-011741] 01 p0038 N88-10244
Theoretical approaches to chemical dynamics in highly compressed fluids
[DE87-012242] 01 p0046 N88-10296
A new compression method with fast searching on large databases
[DE87-010986] 01 p0106 N88-10691
Design of source coders and joint source/channel coders for noisy channels
[NASA-CR-181547] 04 p0432 N88-12678
Shock compression of solids as a physical-chemical-mechanical process
[DE88-001674] 05 p0563 N88-13427
Threshold and crack-growth tests on pre-cracked specimens produced in cyclic compression 06 p0718 N88-14412
Theory and experiments of fracture in cyclic compression: Single phase ceramics, transforming ceramics and ceramic composites
[DE88-005792] 13 p1781 N88-20659
Parallel image compression
[NASA-CR-180758] 13 p1814 N88-20837
Dynamic range compression/expansion of light beams by photorefractive crystals
[NASA-CASE-NPO-17140-1-CU] 17 p2438 N88-24508
Dynamic shear band development in plane strain
[AD-A190915] 18 p2526 N88-24988
The electronic structure of condensed molecular systems
[DE88-007823] 20 p2851 N88-26923
Ultrasonic studies of stresses and plastic deformation in steel during tension and compression
[AD-A192308] 21 p2912 N88-27280
An endochronic rate-sensitive constitutive equation for metals, application to generalized creep and large deformations
[AD-A194167] 22 p3055 N88-28125
Nonlinear stress-strain and inelastic rebound with exponential stiffness
[AD-A195667] 24 p3384 N88-30159

COMPRESSION LOADS
NT AXIAL COMPRESSION LOADS
NT IMPACT LOADS
Cumulative fatigue and life prediction of fibre composites. Part 2: Experimental techniques and results
[BR101014] 02 p0142 N88-10894
Experimental molecular spectroscopy in shock-compressed materials
[DE87-013139] 02 p0144 N88-10903
Analysis and testing of predamaged shell structures 04 p0428 N88-12653
Shock compression of solids as a physical-chemical-mechanical process
[DE88-001674] 05 p0563 N88-13427
Effect of compressive portion of loading cycles on the near threshold fatigue closure behavior 06 p0717 N88-14398
Mixed mode fatigue crack growth using the Brasilian disc 06 p0719 N88-14416
A loading system for creep testing under constant compressive stress
[NASA-TT-20119] 06 p0722 N88-14441
Equation of state of condensed materials physical principles and applications
[NASA-TT-20007] 08 p0968 N88-15855
An in vitro model system to study the effect of microgravity and loading conditions on the mineralization and resorption of skeletal tissues 12 p1657 N88-19927
Geodetic measurement of deformation east of the San Andreas fault in Central California
[NASA-CR-182709] 13 p1798 N88-20754
Effect of uniaxial compression on physical and mechanical properties of ferroelectric ceramic material 16 p2180 N88-22993
Investigation of the effect of minimum loads and compression of load spectra on the prediction capacities of the ONERA crack model — wings
[ONERA-RTS-33/7169-RY-064-R] 18 p2527 N88-24994
Air loading effects on a capacitively sensed membrane supported silicon accelerometer 19 p2672 N88-25886
Compression creep of filamentary composites
[NASA-CR-182550] 20 p2798 N88-26601
Micromechanics of composite laminate compression failures
[NASA-CR-183179] 22 p3050 N88-28098
The effect of compression on individual pressure vessel nickel/hydrogen components
[NASA-TM-101312] 22 p3052 N88-28109
Load interaction effects on compression fatigue crack growth in ductile solids
[FFA-TN-1988-12] 22 p3089 N88-28342
Critical joints in large composite primary aircraft structures. Volume 3: Ancillary test results
[NASA-CR-172588] 23 p3177 N88-28916

COMPRESSION RATIO
Variable-compression-ratio pistons for high power output diesel engines 22 p3084 N88-28316

COMPRESSION TESTERS
U COMPRESSION TESTS

COMPRESSION TESTS
The behavior of plastic, ceramic masses in compression tests
[ETN-87-90603] 03 p0292 N88-11836
A loading system for creep testing under constant compressive stress
[NASA-TT-20119] 06 p0722 N88-14441
Compression of composite materials: A review
[AD-A189272] 13 p1734 N88-20365
Notch sensitivity of graphite materials for VHTR 13 p1747 N88-20447
An investigation of the mechanical properties of improved carbon fibre composite materials
[RAE-TR-86021] 14 p1884 N88-21259
Electronic structure of matter at high compression: Isostructural transitions and approach of the Fermi-gas limit
[MPQ-124] 16 p2266 N88-23551
Bearing-bypass material system test
[NASA-CASE-LAR-13458-1] 17 p2342 N88-23967
Fuel containment and damage tolerance in large composite primary aircraft structures. Phase 2: Testing
[NASA-CR-172519] 19 p2601 N88-25452
An experimental and analytical evaluation of a biaxial test for determining shear properties of composite materials
[NASA-CR-182928] 21 p2962 N88-27593
The effect of compression on individual pressure vessel nickel/hydrogen components
[NASA-TM-101312] 22 p3052 N88-28109

COMPRESSION WAVES
Observations of an ion acoustic oscillation near a pulsed sheath
[INPE-4386-PRE/1206] 08 p0979 N88-15915

COMPRESSIVE STRENGTH
Face compression yield strength of the copper-Inconel composite specimen
[DE87-011974] 01 p0019 N88-10116

Effects of cure pressure on resin flow, voids, and mechanical properties
[AD-A184267] 03 p0295 N88-11853
Effect of interface on mechanical properties of graphite/201 aluminum composites
05 p0606 N88-13717
Characterization of mechanical damage mechanisms in ceramic composite materials
[AD-A185549] 06 p0686 N88-14205
Effect of low velocity impact on compression strength of a quasi-isotropic laminate
[FFA-TN-1987-38] 09 p1138 N88-16822
Effect of post-cure heat-treatment on static and fatigue behaviour of XAS-914C carbon fibre composite
[AD-A186943] 10 p1294 N88-17735
Strength and structure of Ga sub 1-xIn sub xAs alloys
[AD-A188092] 10 p1303 N88-17795
Statistical considerations of graphite strength for assessing design allowable stresses
13 p1746 N88-20441
Effects of high temperature neutron irradiation on the physical, chemical and mechanical properties of fine-grained isotropic graphite 13 p1747 N88-20444
The effect of Ca(OH)2-treated ceramic microspheres on the mechanical properties of high-temperature lightweight cement composites
[DE88-004590] 13 p1749 N88-20457
Environmental effects on the post-impact compressive strength of CFC
[RAE-TM-MAT-STR-1088] 14 p1884 N88-21258
High-strength ceramic based on tetragonal ZrO2 with Al2O3 admixture 16 p2180 N88-22996
High strength/sigh modulus aromatic heterocyclic ABA block copolymers
[AD-A191666] 18 p2491 N88-24774
Fuel containment and damage tolerance in large composite primary aircraft structures. Phase 2: Testing
[NASA-CR-172519] 19 p2601 N88-25452
Properties of two composite materials made of toughened epoxy resin and high-strain graphite fiber
[NASA-TP-2826] 19 p2609 N88-25480
Loading rate sensitivity of open hole composites in compression
[NASA-TM-100634] 19 p2610 N88-25490
A micromechanics model of the stiffness and strength of laminates with fiber waviness
[NASA-CR-181670] 20 p2768 N88-26413
Compression creep of filamentary composites
[NASA-CR-182550] 20 p2798 N88-26601
Development of a biaxial test system for thin-walled metal tubes using tensile-compressive axial load and internal-external pressure
[DE88-011279] 21 p2962 N88-27592

COMPRESSOR BLADES

Advanced turboprop wing installation effects measured by unsteady blade pressure and noise
[NASA-TM-100200] 01 p0002 N88-10008
Automated design of controlled diffusion blades
[NASA-TM-100251] 05 p0542 N88-13304
Operation of gas turbine engines in dust-laden environments 10 p1280 N88-17654
Radial compressor design using an Euler solver
10 p1283 N88-17675
Secondary flow measurements with L2F-technique in centrifugal compressors 10 p1283 N88-17676
Design and testing of a front stage for an advanced high pressure compressor 10 p1283 N88-17679
Experimental investigation of a supercritical compressor rotor blade section 10 p1284 N88-17680
Computation of secondary flows in an axial multistage compressor 10 p1284 N88-17681
Aero/structural tailoring of engine blades (AERO/STAEBL)
[NASA-CR-180805] 14 p1959 N88-21682
Research on aero-thermodynamic distortion induced structural dynamic response of multi-stage compressor blading
[AD-A192169] 18 p2456 N88-24584
Hot-wire measurements of compressor blade wakes in a cascade wind tunnel
[AD-A194737] 23 p3181 N88-28936
Empirical flutter prediction method
[AD-A195699] 24 p3327 N88-29810

COMPRESSOR EFFICIENCY

Process support compressor motor electromagnetic design summary
[DE87-014359] 02 p0167 N88-11048
Small engine technology programs
08 p0956 N88-15801
Method for predicting performance limits of centrifugal compressors 10 p1283 N88-17677
Analysis of the performance of an air-water heat pump: Regulation of intrinsic performances
[DE88-900241] 10 p1349 N88-18061
Efficiency characteristics of speed modulated drives at predicted torque conditions for air-to-air heat pumps
[DE88-005846] 13 p1770 N88-20588
Experimental and theoretical study of the dynamic operational behavior of a three stage radial compressor
[ETN-88-92129] 20 p2811 N88-26676

COMPRESSOR ROTORS

Three-dimensional calculation in high subsonic axial compressor rotor and its comparison with L2F velocity measurement 03 p0300 N88-11886

COMPRESSORS

NT CENTRIFUGAL COMPRESSORS
NT SUPERCHARGERS
NT SUPERSONIC COMPRESSORS
NT TRANSONIC COMPRESSORS
NT TURBOCOMPRESSORS
Process support compressor motor electromagnetic design summary
[DE87-014359] 02 p0167 N88-11048
Design verification tests for an axial gap permanent magnet compressor motor
[DE87-014360] 02 p0167 N88-11049
Combustor-diffuser interaction program
02 p0185 N88-11152
XeCl excimer laser with magnetic compressor
03 p0299 N88-11879
Application of modified loss and deviation correlations to transonic axial compressors
[AGARD-R-745] 05 p0549 N88-13344
Compressor large bandwidth noise emission mechanisms
[ETN-88-91177] 05 p0646 N88-13959
Oxygen chemisorption cryogenic refrigerator
[NASA-CASE-NPO-16734-1-CU] 06 p0689 N88-14223
Tests of cold helium compressors at Fermilab
[DE88-002837] 07 p0862 N88-15230
Air Force cryocooler development for spacecraft
08 p0983 N88-15945
Computation of secondary flows in an axial multistage compressor 10 p1284 N88-17681
RF pulse compression development
[DE88-004818] 11 p1479 N88-18826
Free-piston Stirling engine diaphragm-coupled heat-actuated heat pump component technology program, phase 1B
[DE88-003653] 11 p1483 N88-18854
Experimental vibration damping characteristics of the third-stage rotor of a three-stage transonic axial-flow compressor
[NASA-TM-100948] 18 p2466 N88-24642
Forced response unsteady aerodynamics in a multistage compressor 18 p2512 N88-24903
Application of computational fluid dynamics to design of compressor cascade 19 p2639 N88-25655
Fluid dynamics of high performance turbomachines
[AD-A192073] 19 p2664 N88-25840
Experimental and theoretical study of the dynamic operational behavior of a three stage radial compressor
[ETN-88-92129] 20 p2811 N88-26676
JTDE 1 XTE34 materials research and development report
[AD-A194268] 22 p3044 N88-28063
Erosion of metals exposed to hot, dense gases
[AD-A193708] 22 p3056 N88-28131
AGARD (Advisory Group for Aerospace Research and Development) engine disc material cooperative test (supplementary program)
[AD-A193678] 23 p3179 N88-28925
E3 10C compressor test analysis of high-speed post-stall data
[NASA-CR-179521] 23 p3179 N88-28929
A mapping of the viscous flow behavior in a controlled diffusion compressor cascade using laser Doppler velocimetry and preliminary evaluation of codes for the prediction of stall
[AD-A194490] 23 p3211 N88-29112
Reduction in mill air compressor power requirements through installation of a variable frequency speed control
[DE88-008493] 23 p3221 N88-29171
Development of the Simplified Compressor Model (SCM) for performance analysis of gaseous diffusion compressors
[DE88-009066] 23 p3221 N88-29173

COMPTON EFFECT

The development of diagnostic fuses
[SAND-86-0395] 03 p0311 N88-11963
Relativistic corrections for one- and two-photon matrix elements of weakly-bound systems
[NOTA-INTERNA-884] 07 p0929 N88-15645
A search for medium energy gamma ray pulsars
11 p1568 N88-19385
Experimental set-up for measurements of Compton scattering cross section on light nuclei
[DE88-700161] 12 p1688 N88-20097
Three-wave parametric resonance in plasma of relativistic electron flux 14 p1972 N88-21772
Waves and instabilities in an electron-positron plasma in an ultra-strong magnetic field
23 p3283 N88-29551

COMPUTATION

NT COMPUTATIONAL GEOMETRY
NT ORBIT CALCULATION
A parallel model of the kinetic depth effect using local computations
[AD-A181945] 01 p0083 N88-10536
Computational methods and software for differential equations and their applications
[DE87-014601] 02 p0226 N88-11424
Deviatoric constitutive relationship for anisotropic materials
[AD-A184332] 03 p0295 N88-11854
Combined calculation of deformation and stress for the body and sabot of an APFSDS
03 p0302 N88-11899
Institute for Computational Mechanics in Propulsion (ICOMP) first year summary
[NASA-TM-100225] 03 p0370 N88-12330
Aircraft dynamic response calculation based on discrete-continual model 04 p0424 N88-12624
Calculation of three-dimensional stationary turbulent boundary layer on root section of wing ignoring compressibility 04 p0424 N88-12630
Back-of-the-envelope problems
[AD-A184105] 04 p0484 N88-12980
Calculation of helicopter rotor blade/vortex interaction by Navier-Stokes procedures
[NASA-CR-177441] 05 p0540 N88-13291
Efficient computation of periodic Green's functions with application to grating structures
[AD-A184853] 05 p0640 N88-13912
Computer calculations of PIN diode limiter characteristics
[AD-A185563] 06 p0697 N88-14277
Methods for reducing computational costs of typical finite element unsteady hydrodynamic models
[AD-A185499] 06 p0702 N88-14312
Fast algorithms for structural optimization and least squares
[AD-A185766] 06 p0724 N88-14452
Optimal pre-scheduling of problem remappings
[NASA-CR-178378] 06 p0756 N88-14633
Development of symbolic computation methods for nonlinear dynamics
[AD-A185562] 06 p0758 N88-14653
Computing block-angular Karmarker projections with applications to stochastic programming, revision
[AD-A185647] 06 p0759 N88-14656
Diffusion first passage times: Approximations and related differential equations
[AD-A185592] 06 p0765 N88-14700
An efficient algorithm for computing the crossovers in satellite altimetry
[NASA-CR-182389] 07 p0871 N88-15286
Stability analysis of finite difference schemes for hyperbolic systems, and problems in applied and computational linear algebra
[AD-A185824] 07 p0908 N88-15499
The classification problem of finite rings by computable means
[AD-A185869] 07 p0908 N88-15500
Explicit construction and analysis of some efficient empirical production functions in data envelopment analysis
[AD-A185907] 07 p0908 N88-15502
Recent developments in the numerical solution of differential/algebraic systems
[DE88-001885] 07 p0912 N88-15535
Computers in theoretical physics
[DE88-700516] 07 p0941 N88-15720
Acta Aerodynamica Sinica (selected articles)
[AD-A185723] 08 p0949 N88-15757
Calculation evaluation of the boundary conditions of autoinflammation of propulsive charges
[PB87-139044] 08 p0974 N88-15890
Computational prediction of propellant reorientation
08 p0982 N88-15940
New directions for multivariate statistical computation and data analysis
[AD-A186523] 08 p1074 N88-16480
A rapid method for the computation of equilibrium chemical composition of air to 15000 K
[NASA-TP-2792] 09 p1140 N88-16830
Computational analysis of propagation properties of integrated-optical waveguides using a domain integral equation
[PB87-163358] 09 p1154 N88-16917
An efficient method for computing leading Eigenvalues and Eigenvectors of large asymmetric matrices
09 p1159 N88-16949

Design of a neural network simulator on a transputer array
09 p1205 N88-17221
A fast bottom-up algorithm for computing the cut sets of noncoherent fault trees
[DE88-003741] 09 p1220 N88-17320
A multithreaded processor architecture for parallel symbolic computation
[AD-A187034] 09 p1222 N88-17327
A note on computing robust regression estimates via iteratively reweighted least squares
[AD-A185709] 09 p1227 N88-17352
Advances in reliable numerical computation: A summary --- conference
[NPL-DITC-102/87] 09 p1229 N88-17367
On exact solutions of multidimensional Schroedinger equation with polynomial potentials
[DE88-700460] 09 p1230 N88-17373
Calculating measurement imprecision and uncertainty
[DE88-003981] 09 p1233 N88-17391
A computational study of thrust augmenting ejectors based on a viscous-inviscid approach
10 p1326 N88-17929
Annotated computer output for split plot design: GENSTAT ANOVA
[AD-A187120] 10 p1385 N88-18271
Machine models and simulations
[PB88-118690] 10 p1388 N88-18280
The effects of data structure on total time on test plots
[AD-A187628] 10 p1389 N88-18296
Recent progress in the p and h-p version on the finite element method
[AD-A187254] 10 p1400 N88-18347
International Conference on Industrial and Applied Mathematics
[AD-A188251] 11 p1483 N88-18651
A semianalytical technique for sensitivity analysis of unsteady aerodynamic computations
[NASA-TM-100810] 11 p1503 N88-18976
Institute for Computational Mechanics in Propulsion (ICOMP)
[NASA-TM-100790] 11 p1540 N88-19202
Theory and practice of fault tolerance in distributed systems
[AD-A187559] 11 p1540 N88-19204
Core-core and core-valence correlation
[NASA-CR-182552] 11 p1544 N88-19226
Theoretical studies of the potential surface for the F - H2 greater than HF + H reaction
[NASA-CR-182551] 11 p1557 N88-19319
Spire based speaker-independent continuous speech recognition using mixed feature sets
[AD-A188834] 12 p1620 N88-19688
Support for concurrent computing environments
[AD-A188498] 12 p1680 N88-20043
Uncertain knowledge in distributed systems
[AD-A189017] 12 p1685 N88-20076
Computation of LMS (Least-Mean-Square) and matched digital filters for optical clutter suppression
[AD-A186885] 12 p1687 N88-20093
Pion absorption in nuclei: The pion(+ or -),proton reactions
[LA-10997-T] 12 p1688 N88-20098
A cost analysis for the implementation of commonality in the family of commuter airplanes, revised
[NASA-CR-182569] 12 p1706 N88-20221
Application of a flux vector splitting methodology towards the solution of unsteady transonic flows, with future emphasis on the blade flutter problem
[AD-A189500] 13 p1716 N88-20260
Implementation of a 3-D nonlinear MHD (magnetohydrodynamics) calculation on the Intel hypercube
[DE88-000625] 13 p1816 N88-20848
Computing with structured connections networks
[AD-A189244] 13 p1821 N88-20886
Numerical solution of ill posed problems in partial differential equations
[AD-A189383] 13 p1825 N88-20909
Algebraic specifications for parameterized data types: The case of minimal computable algebras and parameters with equality
[CWI-CS-R8714] 13 p1826 N88-20916
Computation and graphics in mathematical research
[DE88-005796] 13 p1831 N88-20953
A low-frequency measurement of the spectrum of the cosmic microwave background radiation
13 p1858 N88-21112
Comparison of methods for the calculation of thermal contact resistance of the first Brazilian satellite
[NASA-TT-20180] 14 p1880 N88-21239
On the theory of the conversion of metallic mixed phases. 5: Fluctuations and nucleation in sub-cooled phases
[NASA-TT-20249] 14 p1890 N88-21296
Computational aspects of sensitivity calculations in transient structural analysis
[NASA-TM-100589] 14 p1924 N88-21467
Measurements of optical nonlinearities in MOCVD-grown GaAs/GaAlAs multiple quantum wells
14 p1975 N88-21787
Calibration and processing of AVHRR data for temperature estimation
[INPE-4493-PRE/1257] 15 p2095 N88-22485
Optical Conceptual Computing and Associative Memory (OCCAM)
[AD-A190030] 15 p2107 N88-22550
Rapid feature extraction via the radon transform
[AD-A190032] 15 p2110 N88-22573
Microvax networked computer system
[AD-A190308] 15 p2114 N88-22596
High speed transcendental elementary function architecture in support of the Vector Wave Equation (VWE)
[AD-A189746] 15 p2119 N88-22627
Numerical methods for linear and nonlinear optimization
[AD-A190029] 15 p2120 N88-22631
Research on algebraic manipulation
[AD-A190149] 15 p2120 N88-22634
A physically consistent model for artificial dissipation in transonic potential flow computations
[NASA-TM-100846] 15 p2122 N88-22652
Interface formation and precursory dynamics
[AD-A190741] 15 p2144 N88-22794
INPE position paper on the CCSDS standardized method of link budget computation
[INPE-4533-NTE/279] 15 p2148 N88-22820
KOMPOT Program complex for the calculation of spatial magnetostatic fields of electromagnetic systems
[DE88-701691] 16 p2192 N88-23072
Coherent structure
16 p2199 N88-23117
Coherent structures: Comments on mechanisms
16 p2199 N88-23118
Multigrid for structures analysis
16 p2218 N88-23232
A computational procedure for automated flutter analysis
16 p2220 N88-23250
Approximate agreement
[AD-A191030] 16 p2251 N88-23455
Generalizing the structure of explanations in explanation-based learning
[AD-A191327] 16 p2256 N88-23481
Computation of a complete elliptic integral of the first kind using q-expansion
16 p2257 N88-23490
BRYNTRN: A baryon transport computer code, computation procedures and data base
[NASA-TM-4037] 16 p2290 N88-23714
Scientific computing environments
[AD-A191239] 17 p2385 N88-24175
The exact calculation of quadrupole sources for some incompressible flows
[NASA-TM-100623] 17 p2395 N88-24240
Quench detection by fluid dynamic means in cable-in-conduit superconductors
[DE88-007269] 18 p2585 N88-25359
Comment on non-renormalization theorem in the four dimensional superstrings
[DE88-752551] 18 p2586 N88-25367
Two-dimensional viscous flow computations of hypersonic scramjet nozzle flowfields at design and off-design conditions
[NASA-CR-182150] 19 p2603 N88-25459
Material void opening computation using particle method
[DE88-010950] 19 p2680 N88-25936
High speed inlet calculations with real gas effects
[NASA-CR-182167] 20 p2752 N88-26336
Off-boundary approach to the boundary element method
[AD-A192931] 20 p2815 N88-26701
Numerical model for the computation of radiance distributions in natural waters with wind-roughened surfaces
[PB88-192703] 20 p2826 N88-26765
Fully implicit splitting method for accurate tidal computations
[PB88-183637] 20 p2828 N88-26781
The role of working memory in language comprehension
[AD-A192721] 20 p2833 N88-26805
A computational analysis of under-expanded jets in the hypersonic regime
[NASA-TM-101319] 21 p2893 N88-27174
Numerical simulation of fuel droplet interactions and breakup
[AD-A192431] 21 p2941 N88-27470
Numerical experiments on turbulent mixing
[AD-A192572] 21 p2942 N88-27473
Computational boundary conditions for the incompressible Navier-Stokes equations in channels and pipes
[AD-A193356] 21 p2944 N88-27487
Numerical treatment of the pressure singularity at a re-entrant corner
[AD-A193357] 21 p2944 N88-27488
Neural network research: A personal perspective
[AD-A192717] 21 p3003 N88-27808
Parallel solutions to geometric problems on the scan model of computation
[AD-A192321] 21 p3004 N88-27819
Computing partial correlations from the data matrix
[AD-A193904] 22 p3138 N88-28659
On the computation of finite invariant sets of mappings
[AD-A193670] 22 p3143 N88-28690
Computation of the eigenvalues for perturbations of Poiseuille flow using a two-point boundary value method
[AD-A193479] 23 p3210 N88-29104
Solving the symmetric tridiagonal eigenvalue problem on the hypercube
[AD-A193905] 23 p3250 N88-29344
The history of Martian volcanism determined from a revised relative chronology 23 p3301 N88-29657
Calculation of non-stationary aerodynamic forces in the near sonic range
[NASA-TT-20310] 24 p3322 N88-29782
A new computational capability for ramjet projectiles
[AD-A196061] 24 p3327 N88-29812
Multilevel computational theory of stereoscopic visual image processing
[AD-A195331] 24 p3408 N88-30288
A model for architectural comparison
[AD-A195993] 24 p3411 N88-30302
Nonequilibrium flow computations. 1: An analysis of numerical formulations of conservation laws
[NASA-CR-177489] 24 p3425 N88-30384
Regularity and numerical solution of eigenvalue problems with piecewise analytic data
[AD-A194993] 24 p3425 N88-30387
Instrumentation for computational statistical research
[AD-A195887] 24 p3426 N88-30390

COMPUTATIONAL CHEMISTRY

A quantum theoretical study of polyimides
[NASA-CR-181495] 03 p0292 N88-11831

COMPUTATIONAL FLUID DYNAMICS

Rayleigh-Benard convection in a Hele-Shaw cell: A numerical study
[KFK-4212] 01 p0044 N88-10280
Generation of body-fitted grids for two dimensional interior domains by the solution of a system of Poisson equations using multigrid techniques
[GMD-246] 01 p0044 N88-10281
Mean flow structure of a turbulent junction vortex
[PB87-206231] 01 p0047 N88-10301
Numerical calculation of the turbulent flow about a cubic body
[ETN-87-90418] 01 p0047 N88-10302
Application of new conformal solution of theories
[PB87-214557] 01 p0105 N88-10684
Numerical computation of transonic potential flow about 3-dimensional inlets
[NAL-TR-924] 02 p0122 N88-10770
Calculation of aerodynamic heat transfer for blunt-nosed thin wings at different angles of attack at supersonic speeds
[NASA-TT-20127] 02 p0123 N88-10776
FDM-FEM zonal method for viscous flow computations over multiple-bodies
[NAL-TR-925T] 02 p0170 N88-11069
Computational fluid dynamics in the United Kingdom
[RAE-TM-AERO-2098] 02 p0171 N88-11073
Numerical simulation of transient two-phase flow
[CFDU/87/4] 02 p0171 N88-11077
Comparison between numerical solutions and measurements for a high speed turbine blade
[PNR90402] 02 p0172 N88-11082
Coolant passage heat transfer with rotation
02 p0186 N88-11160
The spatially nonuniform convergence of the numerical solution of flows
[NASA-TM-100037] 02 p0226 N88-11429
A supersonic potential gradient method for the calculation of unsteady aerodynamic pressures on harmonically oscillating wings
[ESA-TT-930] 03 p0259 N88-11631
Efficient numerical approaches for predicting supersonic flows with viscous/inviscid interaction
03 p0260 N88-11637
Analytic investigation of helicopter rotor blade appended aeroelastic devices
[NASA-CR-166525] 03 p0266 N88-11676
Analysis of compressible flow on high-velocity jet penetration 03 p0302 N88-11898

Turbulence modelling through one point closures-applications-enlightening by large eddy simulation 03 p0312 N88-11972
Numerical calculation of two dimensional fluid flow with strong shocks
[KFK-4191] 03 p0314 N88-11986
The Proceedings of the Symposium on Mechanics for Space Flight
[ISAS-SP-5] 03 p0317 N88-12006
On the scheme dependency of the three-dimensional Euler solutions 03 p0318 N88-12010
Numerical study of the entrance flow and its transition in a circular pipe (2) 03 p0318 N88-12011
Solution of the two-dimensional Euler equations on unstructured triangular meshes 04 p0396 N88-12469
Experimental aerothermodynamic research of hypersonic aircraft
[NASA-CR-181533] 04 p0399 N88-12483
USSR report: Engineering and equipment
[JPRS-UEQ-87-008] 04 p0423 N88-12621
Some asymptotic modes of transonic vortex flow 04 p0425 N88-12632
Numerical study of supersonic flow around blunt bodies with extended needle nose 04 p0425 N88-12635
Studies of pressure-velocity coupling schemes for analysis of incompressible and compressible flows
[NASA-CR-181526] 04 p0443 N88-12748
Optimization of explicit time-stepping algorithms and Stream-Function-Coordinate (SFC) concept for fluid dynamics problems 04 p0445 N88-12762
Cauchy problem for linearized system of Navier-Stokes equations considering compressibility 04 p0459 N88-12837
Asymptotic form of stationary solutions of the Navier-Stokes equations for large Reynolds numbers 04 p0459 N88-12838
Aerodynamics of Hypersonic Lifting Vehicles
[AGARD-CP-428] 05 p0529 N88-13219
Numerical simulation of the hypersonic flow around lifting vehicles 05 p0532 N88-13234
On the numerical simulation of three-dimensional hypersonic flow 05 p0532 N88-13237
Aerothermodynamics research at NASA Ames 05 p0533 N88-13242
The RAE experimental data-base for missiles at high Mach number and its use in assessing CFD methods 05 p0534 N88-13250
Proceedings of the 4th NAL Symposium on Aircraft Computational Aerodynamics
[NAL-SP-7] 05 p0535 N88-13253
An analysis of the compressible-viscous flow field around a 3D-oscillating wing 05 p0535 N88-13254
Computation of dynamic stall of NACA0012 airfoil by block pentadiagonal matrix scheme 05 p0535 N88-13255
Numerica calculation in the Laplace domain for subsonic unsteady aerodynamic forces acting on a finite wing 05 p0535 N88-13256
Practical application of two-dimensional viscous flow computation 05 p0535 N88-13257
A numerical investigation on wing/nacelle interferences 05 p0535 N88-13258
The role of computation fluid dynamics in aeronautical engineering (4). The development and applications of implicit TVD finite volume code 05 p0536 N88-13259
Practical and modern simulation by systematic connection of the LU-ADI code and the solution adaptive grid program 05 p0536 N88-13260
Numerical calculations of the flowfield around propellers 05 p0536 N88-13261
Numerical analysis of cascade flow solving Navier-Stokes equations 05 p0536 N88-13262
Inverse design method for two-dimensional transonic cascades 05 p0536 N88-13263
Development of the computer program for turbulent boundary layers 05 p0536 N88-13264
Numerical prediction of turbulent flows in dump diffusers 05 p0537 N88-13265
Numerical analysis of supersonic flows using panel method 05 p0537 N88-13266
Computation of nacelle interference using boundary element method 05 p0537 N88-13267
Application of discrete vortex method to analysis of separated flow around aerofoils 05 p0537 N88-13268
Programming techniques for high-speed processing of large scale numerical simulation on supercomputers 05 p0537 N88-13269
Vectorizing the FFTs on supercomputer SX system 05 p0537 N88-13270
Tridiagonal approximate factorization method: A preconditioning technique for solving nonsymmetric linear systems suitable to supercomputers 05 p0537 N88-13271
Numerical analysis of axisymmetric flow with H2-O2 reactions 05 p0538 N88-13272
Rarefied gas numerical wind tunnel. 2: Two-dimensional and axially symmetric bodies 05 p0538 N88-13273
Numerical analysis of flow characteristics of supersonic free-jets 05 p0538 N88-13274
Numerical simulation of splash of droplet at unit gravity 05 p0538 N88-13275
Computer graphics for computational aerodynamics 05 p0538 N88-13276
Flow visualization in computational fluid dynamics 05 p0538 N88-13277
Visualization of an aircraft accident based on digital flight data recorder information 05 p0538 N88-13278
A perspective of computational fluid dynamics 05 p0538 N88-13279
Three-dimensional flow past a two-dimensional body 05 p0539 N88-13280
Computational study of three-dimensional wake structures
[REPT-2] 05 p0539 N88-13281
Computations of compressible viscous flows over multiple-bodies 05 p0539 N88-13282
Relaxation method for the compressible Navier-Stokes equations using upwind schemes 05 p0539 N88-13283
Computation of flow around 2-D circular cylinder 05 p0539 N88-13284
Time-marching finite-difference methods for the three-dimensional Euler equations of contravariant velocity components 05 p0539 N88-13285
Navier-Stokes analysis of laminar flow control of a two-dimensional airfoil 05 p0540 N88-13286
Analytical method for generating computational grids about complete aircraft configurations 05 p0540 N88-13287
Navier-Stokes simulation of transonic transportation aircraft configurations. 1: Flow-field simulation over wing-fuselage combinations 05 p0540 N88-13288
Numerical simulation of transonic aircraft in comparison to wind tunnel test 05 p0540 N88-13289
Validation elements of the computation methods and measurement techniques for high lift aerodynamic systems
[SNIAS-872-111-101] 05 p0541 N88-13299
Compressible Euler solution on a multiblock grid around a wing-fuselage configuration
[FFA-TN-1987-46] 05 p0542 N88-13303
The role of experimental investigation and computational fluid dynamics during fighter aircraft design 05 p0546 N88-13326
A numerical study of the effects of curvature and convergence on dilution jet mixing
[NASA-TM-89878] 05 p0549 N88-13347
A note on the use of symmetric line Gauss-Seidel for the steady upwind differenced Euler equations
[AD-A185223] 05 p0580 N88-13540
Utilization of a high rate vector computer in computational fluid mechanics for aeronautics
[ETN-88-91171] 05 p0581 N88-13547
Physical analysis and numerical simulation of coherent turbulent structures in mixed layers, jets, and wakes
[ETN-88-91183] 05 p0581 N88-13548
Vortical Flows Research Program of the Fluid Dynamics Research Branch
[NASA-TM-88332] 05 p0582 N88-13549
Numerical analysis, computing and fundamental studies in fluid mechanics
[DE88-001912] 05 p0582 N88-13550
Low thrust viscous nozzle flow fields prediction
[NASA-CR-182334] 05 p0582 N88-13551
SHARP simulation of discontinuities in highly convective steady flow
[NASA-TM-100240] 05 p0642 N88-13931
Transonic Navier-Stokes computations of strake-generated vortex interactions for a fighter-like configuration 06 p0664 N88-14073
Numerical study of chemically reacting flows using an LU scheme
[NASA-CR-180862] 06 p0668 N88-14094
Analysis of internal flows relative to the space shuttle main engine
[NASA-CR-179240] 06 p0674 N88-14125
Computation of turbulent flow of air through smooth and rough pipes using a two-equation turbulence model 06 p0700 N88-14298
Introduction to Computational Fluid Dynamics
[VKI-LS-1987-02] 06 p0701 N88-14300
Introduction 06 p0701 N88-14301
Boundary layer equations and methods of solution 06 p0701 N88-14302
Finite element techniques 06 p0701 N88-14303
Implicit time dependent methods for inviscid and viscous compressible flows 06 p0701 N88-14304
Computational methods for complex flowfields
[AD-A185793] 06 p0703 N88-14317
Small High Pressure Ratio Turbines --- conference
[VKI-LS-1987-07] 06 p0712 N88-14364
Computation of free boundaries
[PB87-226023] 06 p0763 N88-14680
Method of calculations for flow of ideal gas through plane and axisymmetric nozzles with broken-line contour 06 p0771 N88-14737
Langley Symposium on Aerodynamics, volume 1
[NASA-CP-2397] 07 p0809 N88-14926
Computational fluid dynamics overview 07 p0809 N88-14927
Finite-volume scheme for transonic potential flow about airfoils and bodies in an arbitrarily shaped channel 07 p0809 N88-14928
Breakdown of the conservative potential equation 07 p0809 N88-14929
Application of a full potential method for analysis of complex aircraft geometries 07 p0809 N88-14930
A multistage time-stepping scheme for the thin-layer Navier-Stokes equations 07 p0810 N88-14932
Numerical simulation of a controlled boundary layer 07 p0810 N88-14933
Viscous vortex flows 07 p0810 N88-14934
A theory for the core flow of leading-edge vortices 07 p0810 N88-14935
Analysis and performance prediction of scramjet inlets utilizing a three-dimensional Navier-Stokes code 07 p0811 N88-14936
Wind tunnel wall interference 07 p0811 N88-14938
Separated flow 07 p0812 N88-14944
Modern wing flutter analysis by computational fluid dynamics methods
[NASA-TM-100531] 07 p0816 N88-14965
Numerical methods for fluid flow problems
[DE88-000156] 07 p0854 N88-15190
Unsteady transonic algorithm improvements for realistic aircraft applications
[NASA-TM-100516] 08 p0949 N88-15760
Consistent boundary conditions for Reduced Navier-Stokes (RNS) scheme applied to 3-dimensional internal viscous flows
[NASA-CR-180874] 08 p0950 N88-15782
Chemical reacting flows 08 p0955 N88-15793
High-speed inlet research program and supporting analyses 08 p0958 N88-15811
Numerical simulation of heat transfer turbulence, volume 2
[AD-A185130] 08 p0983 N88-15947
A computationally efficient modelling of laminar separation bubbles
[NASA-CR-182417] 08 p0984 N88-15949
Computational Fluid Dynamics
[VKI-LS-1987-04] 08 p0984 N88-15951
Characteristic flux averaging approach to the solution of Euler's equations 08 p0984 N88-15955
Finite element methods for compressible flows 08 p0984 N88-15956
Adaptive finite difference methods in fluid dynamics 08 p0985 N88-15958
Finite element fundamentals, part 1 08 p0985 N88-15961
Finite element method computer implementation 08 p0985 N88-15963
Finite Element Calculation Methods and Their Application to Turbomachinery, volume 2
[VKI-LS-1987-05-VOL-2] 08 p0985 N88-15965
Inviscid flows, part 2 08 p0985 N88-15966
Mesh generation 08 p0986 N88-15971
Introduction to the Modeling of Turbulence
[VKI-LS-81-06] 08 p0986 N88-15972
Turbulence models for practical applications 08 p0986 N88-15974
Modeling the unsteady flow found in axial turbomachinery
[ECL-87-07] 08 p0987 N88-15980
Comparative performance of the conjugate gradient and SOR (Successive Over Relaxation) methods for computational thermal hydraulics
[DE88-002553] 08 p0988 N88-15986
Spectral analysis of an orographically structured area in the forefield of mesoscale flow simulations 08 p1016 N88-16160
NASA/Army Rotorcraft Technology. Volume 1: Aerodynamics, and Dynamics and Aeroelasticity
[NASA-CP-2495-VOL-1] 09 p1105 N88-16625
The development of CFD methods for rotor applications 09 p1105 N88-16627
A summary of recent NASA/Army contributions to rotorcraft vibrations and structural dynamics technology 09 p1105 N88-16628
A review of research in rotor loads 09 p1106 N88-16629
Comprehensive rotorcraft analysis methods 09 p1106 N88-16630

Rotorcraft aeroelastic stability
09 p1106 N88-16631
A decade of aeroacoustic research at NASA Ames Research Center 09 p1109 N88-16648
Aeroacoustic research programs at the Army Aviation Research and Technology Activity
09 p1109 N88-16649
An initial investigation into methods of computing transonic aerodynamics sensitivity coefficients
[NASA-CR-182444] 09 p1112 N88-16663
New techniques in computational aerodynamics
[AD-A186719] 09 p1112 N88-16664
Computational unsteady aerodynamics for aeroelastic analysis
[NASA-TM-100523] 09 p1112 N88-16668
CFD validation experiments for internal flows
[NASA-TM-100797] 09 p1114 N88-16679
Solid fuel combustion chamber
[VTH-LR-515] 09 p1141 N88-16842
The viscous flow on surfaces with streamwise riblets
[DFVLR-FB-87-21] 09 p1162 N88-16961
Calculation on film preparation and film motion of a swirl atomizer
[DFVLR-FB-87-25] 09 p1162 N88-16962
Numerical and physical aspects of large eddy simulation of turbulent flows
[ETN-88-91611] 09 p1162 N88-16965
Calculation of the flow through a single-sided sudden expansion with the Computer Program for Parabolic and Elliptic Flows (COPPEF) computer program
[VTH-LR-523] 09 p1163 N88-16973
The dynamics of heat transfer at a turbulent pipe flow
[OEFZS-4400] 09 p1164 N88-16975
A guide to the transient three phase porous flow model implemented in the two-dimensional CRAY-TENSOR code: Physics, numerics, and code description
[DE88-003709] 09 p1165 N88-16983
Computational fluid dynamics and aerothermodynamics
[NASA-CR-182490] 09 p1166 N88-16989
Scientific Colloquium in Honor of Prof. Dr. Rer. Nat. Hermann L. Jordan
[DFVLR-MITT-87-11] 09 p1240 N88-17432
Numerical fluid mechanics 09 p1240 N88-17434
Solution of the three-dimensional Navier-Stokes equations for transonic flow using a multigrid method
10 p1267 N88-17579
Application of empirical and linear methods to VSTOL powered-lift aerodynamics
[NASA-TM-100048] 10 p1267 N88-17581
Wall jet analysis for circulation control aerodynamics. Part 1: Fundamental CFD and turbulence modeling concepts 10 p1269 N88-17588
Transonic blade design on rotational stream surfaces
10 p1282 N88-17671
Computation of secondary flows in an axial multistage compressor 10 p1284 N88-17681
Shuttle rocket booster computational fluid dynamics
[NASA-CR-182518] 10 p1293 N88-17733
Boundary layer calculation using digital computers
[REPT-MM-4] 10 p1309 N88-17821
Zonal solutions for viscous flow problems. Finite approximations in fluid mechanics
[MBB/LKE-122/S/PUB/226] 10 p1313 N88-17846
The use of multigrid techniques in the solution of the Elrod algorithm for a dynamically loaded journal bearing
[NASA-CR-180873] 10 p1331 N88-17954
A visual programming environment for the Navier-Stokes computer
[NASA-CR-181615] 10 p1390 N88-18299
Hypersonic blunt body computations including real gas effects
[NASA-TM-100074] 10 p1400 N88-18344
A code development system for computational fluid dynamics
[AD-A188050] 11 p1482 N88-18848
Specialized instrumentation for computational fluid dynamics research
[AD-A188160] 11 p1482 N88-18849
Finite element methods of analysis for high speed viscous flows
[NASA-CR-182529] 11 p1483 N88-18852
Chaos, mappings and spatial complexity in fluids
11 p1484 N88-18860
Theoretical and experimental analysis of pressure pulse transmission in non-Newtonian pipe flow
11 p1485 N88-18863
A posteriori error estimates in computational fluid mechanics 11 p1486 N88-18869
Topology and grid adaption for high-speed flow computations
[NASA-CR-182586] 11 p1487 N88-18875
Turbulence modeling in non-inertial frames of reference
[NASA-CR-181646] 11 p1488 N88-18880
Application of advanced computational technology to propulsion CFD
[NASA-TM-100843] 11 p1525 N88-19102
Generation of surface grids through elliptic partial differential equations for aircraft and missile configurations
[AD-A186631] 11 p1535 N88-19169
A numerical procedure for conformal mapping of the exterior of a circle onto the exterior of a wing profile with a spoiler
[ISL-R-110/86] 11 p1536 N88-19180
Multigrid methods: Special topics and applications — conference
[GMD-120] 11 p1537 N88-19187
A generalisation of Hall's scheme for solving the Euler equations for two-dimensional flows
11 p1537 N88-19188
A multigrid solver for two-dimensional transonic full potential flow calculations 11 p1538 N88-19189
Implementation of multigrid in SOLA algorithm — fluid flow 11 p1538 N88-19191
Solution of the Euler equations: Explicit schemes acceleration by a multigrid method
11 p1538 N88-19192
Unstructured multigrid methods
11 p1538 N88-19193
Solution of a rotating Navier-Stokes problem by a nonlinear multigrid algorithm 11 p1538 N88-19194
Application of the multigrid technique to the pressure-correction equation for the SIMPLE algorithm — Semi-Implicit Method for Pressure Linked Equations (SIMPLE) 11 p1539 N88-19196
Calculation of flow about posts and powerhead model
[NASA-CR-179305] 12 p1625 N88-19722
Accelerating the computation of steady state solutions for non-equilibrium, chemically reacting flow fields
12 p1625 N88-19724
Time-accurate simulations of a shear layer forced at a single frequency
[NASA-TM-100836] 12 p1628 N88-19740
Reynold stress closure in jet flows using wave models
[NASA-CR-182662] 12 p1628 N88-19741
Application of a nonisentropic full potential method to AGARD standard airfoils
[NASA-TM-100560] 13 p1716 N88-20263
Computational technique for compressible vortex flows using the integral equation solution
[NASA-CR-182695] 13 p1718 N88-20271
Mixing of viscous fluids: Behavior of microstructures and chaos
[DE88-006287] 13 p1766 N88-20566
Three-dimensional shear layer experiments and their use as test cases for calculation methods
[NLR-MP-86036-U] 13 p1767 N88-20570
Solution of two-dimensional Euler equations: Experience with a finite volume code
[DFVLR-FB-87-41] 13 p1767 N88-20572
Graphics and flow visualization of computer generated flow fields
[NASA-CR-182679] 13 p1767 N88-20573
Pseudo-stationary oblique-shock-wave reflections in low gamma gases: Isobutane and sulphur hexafluoride
[UTIAS-TN-267] 13 p1768 N88-20576
Calculations of viscous flows with a multigrid method
13 p1769 N88-20580
General fuselage coordinates for the calculation of three-dimensional boundary layers
[MBB/LKE-122/S/PUB/244] 13 p1771 N88-20596
Activities report of the Lille Institute of Fluid Mechanics
[ETN-88-91983] 13 p1771 N88-20597
Comparison between computed and measured swirl and turbulence in reciprocating engines
[PDR/CFDU/IC/32] 13 p1779 N88-20647
Activities report of the Aerodynamics Department
[ETN-88-91979] 14 p1862 N88-21123
Utilization of parallel processing in solving the inviscid form of the average-passage equation system for multistage turbomachinery
[NASA-TM-89845] 14 p1868 N88-21160
Discrete vortex analysis of unsteady flow about two-dimensional cambered plates
[DE88-006597] 14 p1909 N88-21407
An experimental-computational investigation of transonic shock wave-turbulent boundary layer interaction in a curved test section
[CWI-NM-R8716] 14 p1909 N88-21408
Solutions for direct and indirect problems in free surface flows
[REPT-87-35] 14 p1909 N88-21409
Problems in fluid dynamics
[NASA-CR-182678] 14 p1909 N88-21410
An explicit method for the solution of the Euler equations applied to unsteady two-dimensional flows
[MBB/LKE-121/S/PUB/257] 14 p1910 N88-21411
High-speed flow calculations past 3-D configurations based on the Reynolds averaged Navier-Stokes equations
[NASA-TM-100082] 14 p1911 N88-21421
Potential applications of computational fluid dynamics to biofluid analysis
[NASA-TM-100089] 14 p1911 N88-21422
Accuracy requirements and benchmark experiments for CFD validation
[NASA-TM-100087] 14 p1911 N88-21423
One dimensional calculation model for laser produced plasmas expanding in vacuum
[ISL-R-128/86] 14 p1984 N88-21836
Computational fluid dynamics drag prediction: Results from the Viscous Transonic Airfoil Workshop
[NASA-TM-100095] 15 p2014 N88-22009
Trends in Computational Fluid Dynamics (CFD) for aeronautical 3D steady applications: The Dutch situation
[NLR-MP-86074-U] 15 p2015 N88-22017
Split-coefficient matrix solution and experimental study of axisymmetric underexpanded exhaust plumes
15 p2054 N88-22242
Theoretical model and numerical solution for compressible viscous vortex cores
15 p2054 N88-22243
Mixed direct-inverse problem of transonic cascade
15 p2054 N88-22244
Zero-lift drag predictions in supersonic flow for complex configurations 15 p2054 N88-22246
A panel method based on velocity potential to compute harmonically oscillating lift surface systems
[ETN-88-91886] 15 p2061 N88-22290
Duct flow nonuniformities: Effect of struts in SSME HGM II(+)
[NASA-CR-179285] 15 p2062 N88-22296
Theoretical investigation of secondary instability of three-dimensional boundary-layer flows with application to the DFVLR-F5 model wing
[DFVLR-FB-87-44] 15 p2068 N88-22330
Numerical study of unsteady viscous hypersonic blunt body flows with an impinging shock
[NASA-TM-100096] 15 p2122 N88-22650
High-resolution shock-capturing schemes for inviscid and viscous hypersonic flows
[NASA-TM-100097] 15 p2122 N88-22651
A multilifting line method and its application in design and analysis of nonplanar wing configurations
[DFVLR-FB-87-51] 16 p2155 N88-22860
Numerical analysis of critical penetration velocity for jet perpendicular penetration 16 p2186 N88-23037
Ejection mechanisms in the sublayer of a turbulent channel 16 p2195 N88-23090
EDQNM closure: A homogeneous simulation to support it. A quasi-homogeneous simulation to disprove it
16 p2195 N88-23091
Validation of EDQNM for subgrid and supergrid models 16 p2195 N88-23092
Angular distribution of turbulence in wave space
16 p2195 N88-23093
Premixed turbulent flame calculation
16 p2196 N88-23098
Analysis of non-premixed turbulent reacting flows
16 p2196 N88-23100
A statistical investigation of the single-point pdf of velocity and vorticity based on direct numerical simulations 16 p2196 N88-23101
On local approximations of the pressure-strain term in turbulence models 16 p2197 N88-23102
Local structure of intercomponent energy transfer in homogeneous turbulent shear flow
16 p2197 N88-23103
A general form for the dissipation length scale in turbulent shear flows 16 p2197 N88-23104
Test code for the assessment and improvement of Reynolds stress models 16 p2197 N88-23105
Evaluation of a theory for pressure-strain rate
16 p2198 N88-23108
Relations between two-point correlations and pressure strain terms 16 p2198 N88-23109
The simulation of coherent structures in a laminar boundary layer 16 p2198 N88-23111
Conditionally-averaged structures in wall-bounded turbulent flows 16 p2198 N88-23112
Coherent structures — in turbulent flows
16 p2199 N88-23121
La Recherche Aerospatiale, bimonthly bulletin, number 1987-3, 238/May-June
[ESA-TT-1075] 16 p2206 N88-23161
Numerical treatment of Navier-Stokes equations
[REPT-87-22] 16 p2206 N88-23162
On the use of nonstaggered pressure-velocity arrangement for the numerical solution of incompressible flows
[KU-SFB-210/T/35] 16 p2206 N88-23165

A small concentration expansion for the effective heat conductivity of a random disperse two-component material; an assessment of Batchelor's renormalization method
[REPT-87-71] 16 p2207 N88-23168
Investigation of subgrid models in homogeneous incompressible turbulence
[ONERA-RSF-13/3419-AY-106-A] 16 p2209 N88-23183
Two-equation low-Reynolds-number turbulence modeling of transitional boundary layer flows characteristic of gas turbine blades
[NASA-CR-4145] 16 p2209 N88-23185
Aeroelastic forced response analysis of turbomachinery 16 p2220 N88-23247
Methodology for matching experimental and computational aerodynamic data
[NASA-TM-100592] 17 p2295 N88-23728
Numerical simulation of scramjet inlet flow fields
[NASA-TP-2517] 17 p2296 N88-23735
An efficient parallel algorithm for the simulation of three-dimensional compressible transition on a 20 processor Flex/32 multicomputer
[NASA-CR-178340] 17 p2337 N88-23943
Numerical method for unsteady viscous-inviscid interaction to calculate buffeting
[ONERA-RSF-02/3617-AY-008-A] 17 p2338 N88-23949
Development and improvement of a code to calculate small, three dimensional, unsteady transonic perturbations
[ONERA-RTS-31/3064-RY-062-R] 17 p2338 N88-23951
Accounting for the effects of unsteady, separated boundary layers in transonic two dimensional calculations
[ONERA-RT-30/3064-RY-063-R] 17 p2338 N88-23952
Surface curvature and pressure gradient effects on turbulent flow: An assessment based on numerical solution of the Reynolds equations 17 p2338 N88-23954
Numerical modelling of flows using phoenics 17 p2339 N88-23955
Progress and future directions in computational fluid dynamics
[NASA-TM-100091] 18 p2456 N88-24579
Prediction of laminar and turbulent flows past single and twin airfoils 18 p2457 N88-24589
A transonic small disturbance wing design methodology 18 p2457 N88-24590
A formulation for the boundary-layer equations in general coordinates
[NASA-TM-100079] 18 p2459 N88-24600
Some rotorcraft applications of computational fluid dynamics
[NASA-TM-100066] 18 p2459 N88-24601
Applications of the Navier-Stokes equations to wings and complex configurations using a zonal approach
[NASA-TM-100080] 18 p2459 N88-24602
A decade of computer simulations for space shuttle aerodynamics
[NASA-TM-100990] 18 p2459 N88-24603
Simulations of a missile with liquid payload under launch conditions
[AD-A191479] 18 p2463 N88-24625
Internal fluid dynamics within a nonspinning partially liquid-filled shell due to burster rupture
[AD-A191055] 18 p2507 N88-24874
Adaptive local grid refinement in computational fluid mechanics
[AD-A192215] 18 p2510 N88-24890
Computational fluid dynamics applied to the prediction of the heat-transfer, mechanical and thermal-stress behavior of heat exchangers
[CFDU/87/7] 18 p2510 N88-24893
CFD benefits, goals, stepping-stones and techniques. Proposals for the scientific programme of the European Reserch Centre on flow, turbulence and combustion --- computational fluid dynamics
[CFDU/88/1] 18 p2510 N88-24894
Three dimensional spectral energy measurement on turbulence subjected to a high degree of plane deformation
[ETN-88-92537] 18 p2511 N88-24896
Two dimensional hyperbolic grid generation
[VKI-TN-162] 18 p2511 N88-24897
Duct flow nonuniformities for Space Shuttle Main Engine (SSME)
[NASA-CR-179338] 18 p2511 N88-24899
Improving the performance of a finite element method using vector analysis on CRAY 1
[ETN-88-92153] 18 p2513 N88-24907
Theoretical analysis of laminar incompressible flow in slender channels
[VTH-LR-517] 18 p2513 N88-24909
Review of numerical methods for radionuclide transport in three-dimensional porous media, at high Peclet numbers
[CFDU/87/10] 18 p2538 N88-25061
NAS: The first year
[NASA-TM-101006] 18 p2560 N88-25196
The 24th JANNAF Combustion Meeting, volume 2
[AD-A190164] 19 p2622 N88-25554
Dual Stokes cars measurements in supersonic combusting flow 19 p2625 N88-25569
Numerical grid generation and flow simulation in SSME thrust chamber 19 p2626 N88-25577
A computer program for performance prediction of tripropellant rocket engines with tangential slot injection 19 p2627 N88-25581
Proceedings of the 5th NAL Symposium on Aircraft Computational Aerodynamics
[NAL-SP-8] 19 p2635 N88-25630
On the NAL numerical simulator system 19 p2635 N88-25631
Numerical simulations of flow around shuttle orbiter 19 p2635 N88-25633
Finite element analysis of incompressible viscous flow around multi-element aerofoils 19 p2635 N88-25634
Numerical simulations of astrophysical jets 19 p2636 N88-25635
Numerical calculation of supersonic flow by the PNS equations 19 p2636 N88-25636
Computation of flow around NACA0012 airfoil at high angle of attack 19 p2636 N88-25640
Aerodynamic simulation for complete ASKA aircraft configuration 19 p2637 N88-25641
Numerical simulation of viscous flows over transonic aircraft configurations 19 p2637 N88-25642
Calculations of unsteady aerodynamics for a full aircraft configuration using boundary element method 19 p2637 N88-25643
Rarefied gas numerical wind tunnel 3. Universal code for three dimensional bodies 19 p2637 N88-25644
A numerical analysis of flow characteristics in laser propulsion system 19 p2637 N88-25645
Numerical simulation of the shock tube flows by TVD scheme 19 p2638 N88-25648
Numerical calculation of three dimensional flow by TVD scheme 19 p2638 N88-25649
Numerical analysis of three dimensional cascade flow by solving Navier-Stokes equations 19 p2638 N88-25650
Simulation of axisymmetric flow with H2O2 reactions 19 p2638 N88-25651
The role of computational fluid dynamics in aeronautical engineering (5). Improvements and applications of implicit TVD finite volume code 19 p2638 N88-25653
Extensive verification of blade-to-blade flow code based on Denton scheme 19 p2638 N88-25654
Application of computational fluid dynamics to design of compressor cascade 19 p2639 N88-25655
On the accuracy of upwind biased finite volume method 19 p2639 N88-25656
On symmetric TVD schemes 19 p2639 N88-25659
Numerical simulation of transition to turbulence in plane Poiseuille flow by a spectral method 19 p2640 N88-25661
Numerical simulation of turbulent flow using the exponential expression of k-Epsilon equation 19 p2640 N88-25662
Relaxation scheme for compressible flows 19 p2640 N88-25663
The modified-fluid-in-cell method to which adaptive mesh and multigrid were applied 19 p2640 N88-25664
Grid generation of a helicopter rotary-wing 19 p2640 N88-25665
The development of an intelligent interface to a computational fluid dynamics flow-solver code
[NASA-TM-100908] 19 p2716 N88-26127
Acoustic wave dispersion in a viscous, compressible, liquid-filled cylindrical elastic tube 19 p2722 N88-26164
An initial investigation into methods of computing transonic aerodynamic sensitivity coefficients
[NASA-CR-183061] 20 p2752 N88-26332
The Proceedings of the Symposium on Mechanics for Space Flight 1987
[ISAS-SP-6] 20 p2782 N88-26499
Use of direct solvers for multidimensional fluid flow computations
[DE88-010063] 20 p2799 N88-26611
Three-dimensional viscous flow computations of a circular jet in subsonic and supersonic cross flow
[NASA-CR-182153] 20 p2800 N88-26616
A study of flow separation in transonic flow using inviscid and viscous computational fluid dynamics (CFD) schemes
[NASA-CR-183119] 20 p2801 N88-26618
Improved 3-D turbomachinery CFD algorithm
[NASA-CR-179364] 20 p2801 N88-26619
Study of a water-steam two phase flow in a T-branch
[ETN-88-92306] 20 p2801 N88-26624
Preliminary design and analysis of procedures for the numerical generation of 3D block-structured grids
[NLR-TR-86102-U] 20 p2802 N88-26628
Parallelization on a multiprocessor system of a solution method for the unsteady Navier-Stokes equations at high Reynolds numbers
[ONERA-NT-1987-8] 20 p2803 N88-26632
Hybrid procedure for dynamic measurements in transonic wind tunnels: Demonstrated by pitch oscillation
[DFVLR-FB-88-19] 21 p2900 N88-27211
Computational fluid dynamics on parallel processors
[AD-A192397] 21 p2941 N88-27469
Aerodynamics of Hypersonic Lifting Vehicles: Fluid Dynamics Panel AGARD Symposium
[AGARD-AR-246] 21 p2943 N88-27480
A Navier-Stokes study of cascade flow fields including inlet distortion and rotating stall
[AD-A193109] 21 p2943 N88-27483
Numerical computation of three-dimensional turbulent flow in tightly curved ducts and spiral turbine casings
[ETN-88-92362] 21 p2948 N88-27511
Method to predict external store carriage characteristics at transonic speeds
[NASA-CR-4170] 22 p3037 N88-28034
Transonic blade-vortex interactions 22 p3037 N88-28035
An improved version of NCOREL: A computer program for 3-D nonlinear supersonic potential flow computations
[NASA-CR-4165] 22 p3038 N88-28039
Field methods for computing high Reynolds number viscous flow
[FFA-TN-1988-01] 22 p3039 N88-28046
Advanced computational methods for turbomachinery blade design
[PNR90438] 22 p3044 N88-28065
The calculation of the flow through a two-dimensional faired diffuser
[PNR90433] 22 p3076 N88-28259
Application of rectangular co-ordinates to the problem of laminar combined convection in a straight horizontal tube whose circumference is heated nonuniformly
[PDR/CFDU/IC/33] 22 p3076 N88-28263
A new method of calculating the boundary layer characteristics downstream of manipulators. Part 1: Boundary layer integral parameters
[PNR90455] 22 p3078 N88-28279
A new method of calculating the boundary layer characteristics downstream of manipulators. Part 2: Skin friction and net drag reduction
[PNR90456] 22 p3078 N88-28280
Numerical predictions for the flow induced by an enclosed rotating disc
[PNR90463] 22 p3078 N88-28281
Non-reflecting boundary conditions for computations of unsteady flows in turbomachines
[PNR90469] 22 p3079 N88-28284
Boundary layer simulation and control in wind tunnels
[AGARD-AR-224] 23 p3167 N88-28857
Complex configurations 23 p3167 N88-28861
Computational tools for simulation methodologies 23 p3168 N88-28865
Empirical tools for simulation methodologies 23 p3168 N88-28866
Transport-type configurations 23 p3169 N88-28867
Combat aircraft 23 p3169 N88-28868
Missiles, fuselages and similar bodies 23 p3169 N88-28869
Introduction and critical flow phenomena 23 p3169 N88-28870
Boundary layer manipulation 23 p3170 N88-28877
An unsteady helicopter rotor: Fuselage interaction analysis
[NASA-CR-4178] 23 p3171 N88-28880
Accurate solutions, parameter studies and comparisons for the Euler and potential flow equations
[NASA-TM-100664] 23 p3173 N88-28892
Variable Sweep Transition Flight Experiment (VSTFE)-parametric pressure distribution boundary layer stability study and wing glove design task
[NASA-CR-3992] 23 p3173 N88-28894
Steady and unsteady internal flow computations via the solution of the compressible Navier Stokes equations for low Mach numbers 23 p3209 N88-29100
Three-dimensional laser Doppler velocimeter studies of flow in a 90 deg curved duct having a square cross-section 23 p3209 N88-29101
Numerical investigations in three-dimensional internal flows
[NASA-CR-183108] 23 p3210 N88-29106

Navier-Stokes calculations of transonic flows past cavities
[NASA-CR-180484] 23 p3212 N88-29116
Computational fluid dynamics methods for low Reynolds number precessing/spinning incompressible flows
[AD-A193891] 23 p3212 N88-29119
A calculation of the turbulent boundary layer on a slender ellipsoid at low incidence
[FFA-TN-1988-02] 23 p3213 N88-29126
European research program on viscous flows
[DFVLR-AVA-IB-227-87-A-15] 23 p3214 N88-29129
Three dimensional grid generation for complex configurations: Recent progress
[AGARD-AG-309] 23 p3245 N88-29313
Experience with three dimensional composite grids
23 p3247 N88-29324
Overview of computational vibro acoustics. State of the art and future development
[FFA-TN-1988-17] 23 p3279 N88-29521
The computation of flow past an oblique wing using the thin-layer Navier-Stokes equations
[NASA-TM-88317] 24 p3320 N88-29774
Computational methods for the problems of the tip vortex
[NASA-CR-181438] 24 p3320 N88-29775
Recent advances in transonic computational aeroelasticity
[NASA-TM-100663] 24 p3321 N88-29778
Gas turbine combustion modeling
24 p3349 N88-29936
Numerical modeling of combustion processes in gas turbines 24 p3350 N88-29939
Numerical simulation of nozzle flows
[AD-A195144] 24 p3369 N88-30064
The viscous flow on surfaces with streamline riblets
[ESA-TT-1091] 24 p3370 N88-30067
Knowledge-based flow field zoning
[NASA-TM-101023] 24 p3412 N88-30314
Convergence acceleration for vector sequences and applications to computational fluid dynamics
[NASA-TM-101327] 24 p3424 N88-30377

COMPUTATIONAL GEOMETRY

Scanline algorithms on a grid
[PB88-103379] 06 p0766 N88-14710
Computer aided geometric design
[AD-A187324] 10 p1389 N88-18293
Steps into a geometer's workbench
[CWI-CS-R8726] 13 p1819 N88-20870
Geometry and graphics applied to robotics
[CWI-CS-R8727] 13 p1824 N88-20903

COMPUTATIONAL GRIDS

Problem and solution formulations for the generation of 3D block-structured grids --- aircraft design
[NLR-MP-86020-U] 01 p0005 N88-10028
Generation of body-fitted grids for two dimensional interior domains by the solution of a system of Poisson equations using multigrid techniques
[GMD-246] 01 p0044 N88-10281
Computational fluid dynamics in the United Kingdom
[RAE-TM-AERO-2098] 02 p0171 N88-11073
Development and testing of a vertically-nested regional prediction system --- weather forecasting
02 p0210 N88-11322
Differencing the diffusion equation on a mesh of triangles and quadrilaterals
[DE87-011550] 02 p0224 N88-11408
Finite elements for 2D elliptic equations with moving nodes
[DE87-013501] 02 p0224 N88-11410
FLIP (Fluid-Implicit-Particle): A low-dissipation, particle-in-cell method for fluid flow
[DE87-014745] 03 p0313 N88-11981
Numerical solution of partial differential equations on irregular grids
[DE87-014760] 03 p0369 N88-12324
Theoretical and practical aspects of multigrid methods in boundary element calculations
[NLR-MP-85021-U] 03 p0370 N88-12328
Solution of the two-dimensional Euler equations on unstructured triangular meshes
04 p0396 N88-12469
Generating meshes for finite-difference analysis using a solid modeler
[DE88-001458] 04 p0439 N88-12729
Parallel superconvergent multigrid
[DE87-013153] 04 p0480 N88-12960
High resolution finite volume methods on arbitrary grids via wave propagation
[NASA-CR-178397] 04 p0484 N88-12979
The finite element method for electronic structure
[DE88-001708] 04 p0485 N88-12989
Numerical simulation of the hypersonic flow around lifting vehicles 05 p0532 N88-13234
Computation of dynamic stall of NACA0012 airfoil by block pentadiagonal matrix scheme
05 p0535 N88-13255
Practical and modern simulation by systematic connection of the LU-ADI code and the solution adaptive grid program 05 p0536 N88-13260
A perspective of computational fluid dynamics
05 p0538 N88-13279
Computation of flow around 2-D circular cylinder
05 p0539 N88-13284
Analytical method for generating computational grids about complete aircraft configurations
05 p0540 N88-13287
Compressible Euler solution on a multiblock grid around a wing-fuselage configuration
[FFA-TN-1987-46] 05 p0542 N88-13303
A Cartesian finite-volume method for the Euler equations 05 p0579 N88-13532
Finite-element grid improvement by minimization of stiffness matrix trace
[NASA-TM-100255] 05 p0591 N88-13604
Free Lagrange reconnection algorithms for hydrocodes using a quadrilateral mesh
[DE88-001580] 05 p0611 N88-13752
Vectorization of a multigrid method for the compressible Navier-Stokes equations
[PB87-230496] 06 p0698 N88-14284
Finite element techniques 06 p0701 N88-14303
A zonal approach for the solution of coupled Euler and potential solutions of flows with complex geometries
[AD-A185465] 06 p0702 N88-14310
Computational methods for complex flowfields
[AD-A185793] 06 p0703 N88-14317
Adaptive grid for polyhedral visibility in object space: An implementation
[PB88-100938] 06 p0760 N88-14663
Scanline algorithms on a grid
[PB88-103379] 06 p0766 N88-14710
Shuttle computational grid generation
06 p0794 N88-14863
Multitasked embedded multigrid for three-dimensional flow simulation
[NASA-CR-182398] 07 p0852 N88-15173
Local uniform mesh refinement for partial differential equations
[AD-A186312] 07 p0910 N88-15519
The k-grid Fourier analysis of multigrid-type iterative methods
[AD-A186315] 07 p0910 N88-15520
Nacelle-wing interactions (studies 1986) development of a finite element code in a multi-domain version
[ONERA-RTS-10/3417-AY-308A]
08 p0950 N88-15764
A multistage mesh generator for solving the average-passage equation system
[NASA-CR-179539] 08 p0951 N88-15769
Finite element methods for compressible flows
08 p0984 N88-15956
Finite element method computer implementation
08 p0985 N88-15963
Finite Element Calculation Methods and Their Application to Turbomachinery, volume 2
[VKI-LS-1987-05-VOL-2] 08 p0985 N88-15965
Mesh generation 08 p0986 N88-15971
Adaptive finite element methods for parabolic systems in one- and two-space dimensions
[AD-A186534] 08 p1073 N88-16475
Review of fatigue and fracture research at NASA Langley Research Center 09 p1106 N88-16633
An automatic finite element mesh generator
[AD-A186939] 09 p1216 N88-17291
Finite element mesh generation and isoparametric elements
[NPL-DITC-97/87] 09 p1229 N88-17365
Modification of a successive corrections objective analysis for improved higher order calculations
[NASA-CR-182467] 09 p1230 N88-17370
Implicit solution of the incompressible Navier-Stokes equations in primitive variables on non-staggered grids
10 p1326 N88-17930
The use of multigrid techniques in the solution of the Elrod algorithm for a dynamically loaded journal bearing
[NASA-CR-180873] 10 p1331 N88-17954
Schwarz splitting and template operators
[AD-A187956] 10 p1404 N88-18370
A new computational technique for generating algorithms, with application to the solution of the time-dependent incompressible Navier-Stokes equations
11 p1485 N88-18864
Topology and grid adaption for high-speed flow computations
[NASA-CR-182586] 11 p1487 N88-18875
Numerical fracture mechanics using finite element method 11 p1501 N88-18966
Computer-aided modeling and prediction of performance of the modified Lundell class of alternators in space station solar dynamic power systems
[NASA-CR-182538] 11 p1507 N88-19000
Workshop on the Integration of Finite Element Modeling with Geometric Modeling
[NASA-CR-182515] 11 p1526 N88-19111
Approaches to the automatic generation and control of finite element meshes 11 p1526 N88-19113
Integration of geometric modeling and advanced finite element preprocessing 11 p1526 N88-19114
Finite element meshing of ANSYS (trademark) solid models 11 p1526 N88-19115
Solid/FEM integration at SNLA
[SAND-87-0882A] 11 p1526 N88-19116
Octree based automatic meshing from CSG models
11 p1527 N88-19117
Geometrical and topological issues in octree based automatic meshing 11 p1527 N88-19118
A hierarchical structure for automatic meshing and adaptive FEM analysis 11 p1527 N88-19119
Toward automatic finite element analysis
11 p1527 N88-19120
Finite octree meshing through topologically driven geometric operators 11 p1527 N88-19121
Multigrid methods: Special topics and applications --- conference
[GMD-120] 11 p1537 N88-19187
A generalisation of Hall's scheme for solving the Euler equations for two-dimensional flows
11 p1537 N88-19188
A multigrid solver for two-dimensional transonic full potential flow calculations 11 p1538 N88-19189
Multigrid methods in convex optimization
11 p1538 N88-19190
Implementation of multigrid in SOLA algorithm --- fluid flow 11 p1538 N88-19191
Solution of the Euler equations: Explicit schemes acceleration by a multigrid method
11 p1538 N88-19192
Unstructured multigrid methods
11 p1538 N88-19193
Solution of a rotating Navier-Stokes problem by a nonlinear multigrid algorithm 11 p1538 N88-19194
A multigrid full potential transonic code for arbitrary configurations --- aircraft 11 p1539 N88-19195
Application of the multigrid technique to the pressure-correction equation for the SIMPLE algorithm --- Semi-Implicit Method for Pressure Linked Equations (SIMPLE) 11 p1539 N88-19196
A signal processing approach to the numerical solution of parabolic differential equations
11 p1539 N88-19197
Discretizations for multigrid methods
11 p1539 N88-19198
Incorporation of multigrid in accelerator software --- particle accelerators 11 p1539 N88-19199
Applications of a multigrid finite volume method with Runge-Kutta time integrations for solving the Euler and Navier-Stokes equations 11 p1539 N88-19201
An L-U implicit multigrid algorithm to solve the Euler equations for transonic flow in rotating turbomachinery passages 13 p1718 N88-20270
The construction of a three-dimensional finite volume grid generator for a wing in a wind tunnel with application to Navier-Stokes flow solvers
[FFA-TN-1987-58] 13 p1719 N88-20277
An adaptive grid technique for solution of the Euler equations 13 p1768 N88-20579
Calculations of viscous flows with a multigrid method
13 p1769 N88-20580
Multigrid solution of the Euler equations
13 p1769 N88-20582
Data traffic reduction schemes for sparse Cholesky factorizations
[NASA-CR-181626] 13 p1813 N88-20831
A knowledge system for automatic finite element mesh generation: AMEKS
[DE87-014894] 13 p1826 N88-20914
A Lagrangian moving grid scheme for one-dimensional evolutionary partial differential equations
[CWI-NM-R8713] 13 p1827 N88-20922
Conservative finite volume solutions of a linear hyperbolic transport equation in two and three dimensions using multiple grids
[NASA-CR-182715] 13 p1828 N88-20934
Three-dimensional mesh-generation and plotting routines for use with a boundary element program (BIE3D)
[AD-A188079] 14 p1958 N88-21675
COMESH: A corner mesh finite difference code to solve multigroup diffusion equations in multidimensions
[DE88-701248] 15 p2108 N88-22555
Efficient, high resolution computations of projectile and missile flow fields
[AD-A191086] 16 p2158 N88-22873
Validation of EDQNM for subgrid and supergrid models 16 p2195 N88-23092

Application of a multigrid method for solving the Navier-Stokes equation in two-dimensional flow problems
[KU-SFB-210/T/32] 16 p2206 N88-23164
Fast algorithms for Euler and Navier-Stokes simulations
[AD-A190897] 16 p2208 N88-23175
Mixed finite element formulation applied to shape optimization 16 p2221 N88-23252
Development of adaptive grid schemes based on Poisson grid generators
[AD-A190953] 16 p2262 N88-23528
Incompressible Euler solution on a multiblock grid around a car configuration
[FFA-TN-1987-65] 18 p2457 N88-24586
Accurate multigrid solution of the Euler equations on unstructured and adaptive meshes
[NASA-CR-181679] 18 p2460 N88-24608
Adaptive local grid refinement in computational fluid mechanics
[AD-A192215] 18 p2510 N88-24890
Two dimensional hyperbolic grid generation
[VKI-TN-162] 18 p2511 N88-24897
Application of advanced grid generation techniques for flow field computations about complex configurations
[NASA-CR-183049] 18 p2515 N88-24922
DOD 1985 world magnetic model: Charts and grid values
[AD-A191484] 18 p2541 N88-25080
Adaptive grid refinement for numerical weather prediction
[AD-A192172] 18 p2544 N88-25101
Multigrid methods for elliptic Partial Differential Equations (PDEs)
[CWI-NM-R8722] 18 p2566 N88-25242
Aerodynamic simulation for complete ASKA aircraft configuration 19 p2637 N88-25641
The role of computational fluid dynamics in aeronautical engineering (5). Improvements and applications of implicit TVD finite volume code 19 p2638 N88-25653
On the accuracy of upwind biased finite volume method 19 p2639 N88-25656
The modified-fluid-in-cell method to which adaptive mesh and multigrid were applied 19 p2640 N88-25664
The solution of the Elrod algorithm for a dynamically loaded journal bearing using multigrid techniques
[NASA-TM-100941] 19 p2666 N88-25854
Automatic routing in symbolic IC design environment 19 p2714 N88-26112
A diagonally inverted LU implicit multigrid scheme
[NASA-TM-100911] 20 p2753 N88-26340
Numerical solution of weak forms of conservation laws on optimal unstructured triangular grids 20 p2797 N88-26597
Multigrid computation of practical fluid flows and heat transfer
[DE88-010064] 20 p2799 N88-26609
Preliminary design and analysis of procedures for the numerical generation of 3D block-structured grids
[NLR-TR-86102-U] 20 p2802 N88-26628
The construction of composite grids for general three-dimensional regions 20 p2843 N88-26872
Prolongation, restriction and coarse grid approximation in a three-dimensional cell-centered multigrid method
[REPT-88-02] 20 p2846 N88-26889
Creating aspect graphs for use in object recognition 21 p2928 N88-27379
Three-dimensional zonal grids about arbitrary shapes by Poisson's equation
[NASA-TM-101018] 22 p3039 N88-28042
High performance solutions of the Stokes problem using mini-elements, self-adaptive grids, and multigrid methods: Applications
[ECL-87-15] 22 p3077 N88-28266
Partitioning of regular computation on multiprocessor systems
[NASA-CR-183176] 22 p3141 N88-28678
An efficient patched grid Navier-Stokes solution for multiple bodies, phase 1
[AD-A194166] 23 p3211 N88-29110
Adaptive computational methods for aerothermal heating analysis
[NASA-CR-181636] 23 p3212 N88-29115
Three dimensional grid generation for complex configurations: Recent progress
[AGARD-AG-309] 23 p3245 N88-29313
Lessons learned in the mesh generation for PN/S calculations 23 p3245 N88-29314
Three-dimensional elliptic grid generation for an F-16 23 p3246 N88-29315
Component adaptive grid generation for aircraft configurations 23 p3246 N88-29316
Generation of multiple block grids for arbitrary 3D geometries 23 p3246 N88-29317
Grid generation on and about a cranked-wing fighter aircraft configuration 23 p3246 N88-29318
Grid generation for an advanced fighter aircraft 23 p3246 N88-29319
Algebraic grid generation for fighter type aircraft 23 p3246 N88-29320
Composite grid generation for aircraft configurations with the EAGLE code 23 p3246 N88-29321
Analytical surfaces and grids 23 p3247 N88-29322
Experience with three dimensional composite grids 23 p3247 N88-29324
Grid generation around transport aircraft configurations using a multi-block structured computational domain 23 p3247 N88-29325
An adaptive overlapping local grid refinement method for two-dimensional parabolic systems
[AD-A193560] 23 p3271 N88-29464
The computation of flow past an oblique wing using the thin-layer Navier-Stokes equations
[NASA-TM-88317] 24 p3320 N88-29774
Knowledge-based flow field zoning
[NASA-TM-101023] 24 p3412 N88-30314
Generation of surface grids through elliptic partial differential equations for aircraft and missile configurations
[AD-A195639] 24 p3424 N88-30378

COMPUTER AIDED DESIGN

Problem and solution formulations for the generation of 3D block-structured grids --- aircraft design
[NLR-MP-86020-U] 01 p0005 N88-10028
Shape optimization of linear antennas
[ETN-87-90413] 01 p0036 N88-10233
An interactive optimization procedure for the computer aided dimensioning of integrated circuits
[ETN-87-90414] 01 p0082 N88-10531
A reference guide for IGVIEW: An IGES-compatible geometry system
[DE87-013441] 01 p0083 N88-10534
A preliminary investigation into the feasibility of implementing a direct sideforce control system on the Astra Hawk by means of an active control surface --- aircraft control
[ETN-87-90924] 02 p0126 N88-10795
Heat transfer in a real engine environment 02 p0186 N88-11155
Contribution to the development of smart design techniques for VLSI integrated circuits --- CMOS
[LAAS-87-181] 02 p0221 N88-11395
Computer aided engineering/manufacturing at Rolls-Royce
[PNR90395] 02 p0222 N88-11397
Development of standard cells in NMOS technology for the design of digital integrated circuits
[FI-62-TB-6] 03 p0310 N88-11953
Double-effect absorption heat pump, phase 3
[PB87-232195] 03 p0317 N88-12005
The structure-mapping engine: Algorithm and examples
[AD-A184042] 03 p0368 N88-12315
The impact of information technology on research in science and engineering
[DE88-000342] 03 p0385 N88-12417
Digital-flight-control-system software written in automated-engineering-design language: A user's guide of verification and validation tools
[NASA-TM-88313] 04 p0401 N88-12494
Numerical simulation system 04 p0404 N88-12511
New feedback design methodologies for large space structures: A multi-criterion optimization approach 04 p0408 N88-12535
Interactions between science and precision engineering
[DE87-010873] 04 p0426 N88-12643
A procedural method for the efficient implementation of full-custom VLSI designs 04 p0436 N88-12701
A new state space model for the NASA/JPL 70-meter antenna servo controls 04 p0436 N88-12702
Large change-of-curvature effects in quadratic finite elements for CAD of membrane structures 04 p0480 N88-12958
Computer-aided X-ray image system design and evaluation
[DE88-000997] 04 p0481 N88-12965
Numerical simulation applied to the development of a pyrotechnical system
[SNIAS-872-430-115] 05 p0571 N88-13479
Applications of fatigue analyses: Transportation 05 p0608 N88-13733
An extension to the multilevel logic simulator for microcomputers
[AD-A185032] 05 p0634 N88-13879
Overall description of the computer aided design and manufacturing systems associated with the A320 program at Aerospatiale and its partners
[SNIAS-872-111-104] 05 p0635 N88-13883
Presentation of SIGMA (Interactive Assisted Geometry System). A computer assisted shape design program developed at the Aerospatiale Aircraft Division
[SNIAS-872-111-110] 05 p0635 N88-13884
Structural optimization in the design process --- aircraft
[SNIAS-872-111-115] 05 p0635 N88-13885
XCUT: A rule-based expert system for the automated process planning of machined parts
[DE87-011638] 05 p0639 N88-13905
Using hierarchically structured problem-solving knowledge in a rule-based process planning system
[DE87-011639] 05 p0639 N88-13906
Computer modeling of complete IC fabrication process
[AD-A184807] 05 p0654 N88-14012
Benchmarking and evaluation of hardware description languages for design of VLSI systems
[PB87-134557] 06 p0758 N88-14848
Scanline algorithms on a grid
[PB88-103379] 06 p0766 N88-14710
Computational design of natural laminar flow wings for transonic transport application 07 p0813 N88-14948
Fault tree reliability analysis of the Naval Postgraduate School mini-satellite (ORION)
[AD-A186283] 07 p0866 N88-15250
Computer aided design for Petri Nets
[AD-A186109] 07 p0902 N88-15465
Extraction of MOS VLSI (Very-Large-Scale-Integrated) circuit models including critical interconnect parasitics
[AD-A185847] 08 p0979 N88-15914
Pulse width modulator controller design for a brushless DC motor position servo
[AD-A186618] 08 p0980 N88-15921
HSTDEK: Developing a methodology for construction of large-scale, multi-use knowledge bases 08 p1057 N88-16377
FMEAssist: A knowledge-based approach to Failure Modes and Effects Analysis 08 p1060 N88-16395
Automatic mathematical modeling for space application 08 p1060 N88-16402
A learning apprentice for software parts composition 08 p1065 N88-16436
Automatic program generation from specifications using Prolog 08 p1065 N88-16437
On acquisition of programming knowledge 08 p1065 N88-16438
System analysis in rotorcraft design: The past decade 09 p1110 N88-16852
Kinematic optimization of mechanisms, a finite element approach
[ISBN-90-370-0012-6] 09 p1175 N88-17039
Optimized structure design using reanalysis techniques 09 p1180 N88-17067
First Annual Workshop on Space Operations Automation and Robotics (SOAR 87)
[NASA-CP-2491] 09 p1203 N88-17206
The use of computer graphic simulation in the development of robotic systems 09 p1214 N88-17275
Interfacing slave designs to Fastbus: Practical experience
[DE88-002807] 09 p1215 N88-17286
Methodological and structural principles for flexible geometric modeling in computer aided design
[MA-48] 09 p1218 N88-17306
A raster scan algorithm for generating visible parametric surfaces
[DE88-003222] 09 p1220 N88-17321
A generalized method for automatic downhand and wirefeed control of a welding robot and positioner
[NASA-TP-2807] 10 p1316 N88-17869
Optimal design and parameter identification of flexible rotor-bearing systems 10 p1339 N88-18002
Directions in computer graphics architecture 10 p1379 N88-18233
Computer aided geometric design
[AD-A187324] 10 p1389 N88-18293
Development of tokamak reactor system analysis code NEW-TORSAC
[DE88-751067] 10 p1411 N88-18417
Computer-Aided Design Information System (CADIS): User's manual
[DE88-004365] 10 p1424 N88-18509
Computer program for conceptual tandem rotor helicopter design
[AD-A187832] 11 p1439 N88-18584
Probabilistic and reliability design procedures for flexible airfield pavements: Elastic layered method
[AD-A187533] 11 p1442 N88-18600
Chinese 7760 CAD/CAMM software system introduced 11 p1468 N88-18756

Computer-aided design analysis of 57-mm, angular-contact, cryogenic turbopump bearings
[NASA-TP-2816] 11 p1496 N88-18933
Computer-aided modeling and prediction of performance of the modified Lundell class of alternators in space station solar dynamic power systems
[NASA-CR-182538] 11 p1507 N88-19000
Computer Applications in Geotechnical Engineering (CAGE) and Geotechnical aspects of the Computer-Aided Structural Engineering (G-CASE) projects. User's guide. UTEXAS2 slope-stability package. Volume 1: User's manual
[AD-A187674] 11 p1511 N88-19025
A multigrid full potential transonic code for arbitrary configurations — aircraft 11 p1539 N88-19195
Incorporation of multigrid in accelerator software --- particle accelerators 11 p1539 N88-19199
Columbus Simulation Facility (CSF)
12 p1590 N88-19522
An EHF telecommunication system engineering model
12 p1618 N88-19674
Parts-R-Us
[AD-A188621] 12 p1622 N88-19705
Hercules: A power analyzer for MOS VLSI circuits
[AD-A188702] 12 p1623 N88-19706
A digital circuit design environment
[AD-A188831] 12 p1623 N88-19709
An automatic system for extraction of information from a Computer Aided Design (CAD), selection, sequencing, and execution of turning processes
[INPE-4350-TDL/294] 12 p1676 N88-20020
Twenty-fourth Industrial Associates Review
12 p1679 N88-20039
Development cost reduction using integrated CAE-CAD-CAM techniques 12 p1701 N88-20162
Time and cost reduction through computer integrated manufacture 12 p1703 N88-20191
Development of a dependency theory toolbox for database design
[AD-A188872] 12 p1707 N88-20216
Australian aerodynamic design codes for aerial tow bodies
[AD-A189048] 13 p1715 N88-20258
Computer-aided transformation of descriptive mode of mathematical models of a control system
13 p1756 N88-20503
Gridless routing for generalized cell assemblies: Report and user manual
[EUT-87-E-180] 13 p1764 N88-20549
On the sensitivity of complex, internally coupled systems
[NASA-TM-100537] 13 p1813 N88-20829
MacCAD (Macintosh Computer Aided Design), computer aided design tool for system analysis
[AD-A189241] 13 p1815 N88-20843
Computer aided surface representation
[DE88-005408] 13 p1817 N88-20854
The concept of intelligent integrated interactive CAD systems
[CWI-CS-R8717] 13 p1818 N88-20865
Organization of design knowledge in an intelligent CAD environment
[CWI-CS-R8720] 13 p1819 N88-20868
An integrated data description language for coding design knowledge
[CWI-CS-R8731] 13 p1819 N88-20871
GM: A gate matrix layout generator
[EUT-87-E-179] 13 p1820 N88-20875
Finite State Tables for general computer programming applications
[DE88-006254] 13 p1820 N88-20881
Computer aided design of aircraft structures
[ETN-88-91353] 14 p1867 N88-21154
A sequentially deployable structure for space applications 14 p1875 N88-21202
GADL: A gate array description language
[EUT-87-E-165] 14 p1907 N88-21396
Higher levels of a silicon compiler
[EUT-86-E-163] 14 p1955 N88-21650
Generating layouts for random logic: Cell generation schemes
[EUT-86-E-164] 14 p1956 N88-21658
ESKISS: A program for optimal state assignment
[EUT-87-E-167] 14 p1956 N88-21659
Supercomputer-aided generalized mixer analysis and optimization
[FUB-15-1986] 14 p1957 N88-21668
Activities report of the Computer Science Department
[ETN-88-91980] 14 p1958 N88-21672
Representing knowledge in two distinct descriptions: Extensional vs. intensional
[CWI-CS-R8728] 14 p1961 N88-21699
Technology mapping from Boolean expressions to standard cells
[EUT-87-E-174] 14 p1963 N88-21709
An optimal CMOS structure for the design of a cell library
[EUT-87-E-166] 14 p1985 N88-21841
Characteristics of LSI-wiring expert system discussed
15 p2052 N88-22226
Reliability analysis within a Computer Aided Engineering (CAE) infrastructure
[NLR-MP-86059-U] 15 p2074 N88-22369
Investigation into the development of computer aided design software for space based sensors
[NASA-CR-180772] 15 p2107 N88-22552
Software structuring principles for VLSI CAD
[AD-A190386] 15 p2112 N88-22579
A graphics editor for structured analysis with a data dictionary
[AD-A190618] 15 p2112 N88-22584
High speed transcendental elementary function architecture in support of the Vector Wave Equation (VWE)
[AD-A189746] 15 p2119 N88-22627
Rapid prototyping of complex avionics system architectures
[ETN-88-92275] 16 p2162 N88-22898
Status of CAD/CAM in medium-sized industries described 16 p2184 N88-23022
Automatic layout generation of data processing sections of VLSI microprocessor-like circuits
[ETN-88-92185] 16 p2245 N88-23411
Computer aided design tools for integrated silicon system structures
[ETN-88-92186] 16 p2247 N88-23424
Silicon compilers: Application to the compilation of the control area
[ETN-88-92188] 16 p2247 N88-23425
Contribution to the automatic generation of floor plan placing — integrated circuit design
[ETN-88-92193] 16 p2247 N88-23426
Design as a formal, knowledge engineered activity
[CWI-CS-R8744] 16 p2248 N88-23431
Knowledge engineering in design
[CWI-CS-R8745] 16 p2248 N88-23432
Correctness proofs for systolic algorithms: A palindrome recognizer
[CWI-CS-R8747] 16 p2248 N88-23434
Piecewise linear approach for timing simulation of VLSI (Very-Large-Scale-Integrated) circuits on serial and parallel computers
[AD-A191328] 16 p2252 N88-23462
Data base management in CAD/CAM systems: Requirements for CAD/CAM data bases, actual market offer, advice for an efficient data base management, development tendencies
[MBB/LWD-11/S/PUB/254] 16 p2285 N88-23683
It's time to reinvent the general aviation airplane
17 p2294 N88-23726
Computational wing design studies relating to natural laminar flow 17 p2297 N88-23740
The Design, Development and Testing of Complex Avionics Systems
[AGARD-CP-417] 17 p2302 N88-23767
Rapid prototyping of complex avionic system architectures 17 p2302 N88-23771
The avionics software architecture impact on system architecture 17 p2303 N88-23778
Managing advanced avionic system design
17 p2304 N88-23783
Advanced development of a cockpit automation design support system 17 p2304 N88-23785
Design and development of an avionics system adapted to helicopter missions 17 p2305 N88-23786
Developing systems using state-of-the-art CAD/CAM technology 17 p2306 N88-23795
Interfacing and integrating hardware and software design systems 17 p2306 N88-23796
Avionics systems: Development method and computer tools 17 p2306 N88-23799
A software life cycle support environment
17 p2306 N88-23800
Coherent functional development: Key to successful future system integration 17 p2307 N88-23803
A software design tool for the analysis of robot dynamics properties
[NLR-MP-86064-U] 17 p2385 N88-24171
Simulation and computer aided engineering (the necessity of an integrated approach)
[NLR-MP-86050-U] 17 p2386 N88-24178
Expert systems approach to modeling systems with the ATHENA thermal-hydraulics code
17 p2416 N88-24365
An OOD (Object-Oriented Design) paradigm for flight simulators
[AD-A191097] 18 p2467 N88-24647
Computer aided design of monolithic microwave and millimeter wave integrated circuits and subsystems
[AD-A191593] 18 p2503 N88-24852
Calculation of root-mean-square loads
[BLL-M-37776-(5828.4)] 18 p2531 N88-25015
The Environment for Application Software Integration and Execution (EASIE), version 1.0. Volume 3: Program execution guide
[NASA-TM-100575] 18 p2558 N88-25184
The Sizing and Optimization Language, (SOL): Computer language for design problems
[NASA-TM-100565] 18 p2559 N88-25190
Extensive verification of blade-to-blade flow code based on Denton scheme 19 p2638 N88-25654
Semi-Markov adjunction to the Computer-Aided Markov Evaluator (CAME)
[NASA-CR-181645] 19 p2678 N88-25924
Improved method for stress and compatibility analysis of multicomponent rotating systems
[NASA-TM-100884] 19 p2680 N88-25935
Fault diagnosis in distributed computer networks
[AD-A192406] 19 p2718 N88-26140
Research in VLSI computer systems
[AD-A192915] 20 p2835 N88-26816
The knowledge based automatic extraction of the machinable surfaces for automatic CAD-CAM system
[INPE-4542-PRE/1288] 20 p2838 N88-26824
Enumeration, comments and discussion concerning papers presented during the Conference on Computer Applications in Production and Engineering (CAPE) 87
[NLR-MP-87015-U] 20 p2839 N88-26844
A survey of freeform solid modeling methods
[REPT-87-81] 20 p2839 N88-26847
Interaction management in CAD systems with a history mechanism
[CWI-CS-R8756] 20 p2840 N88-26851
NEXT: An expert system development tool to support engineering design
[NLR-MP-86070-U] 20 p2843 N88-26871
Programs for preliminary design of composite materials which were developed by the design group of Aerospatiale Aquitaine
[REPT-881-430-112] 21 p2907 N88-27251
Investigation of expert system design approaches for electronic design environments
21 p2926 N88-27365
The integration of decision support problems into feature modeling based design 21 p2927 N88-27372
Mitsubishi Electric Advance (R and D Edition), Volume 41
[PB88-194162] 21 p2929 N88-27388
Computer-Aided Engineering (CAE) for engineering design 21 p2929 N88-27390
STAR: Sandia Timing Analyzer Routine
[DE88-012412] 21 p2940 N88-27463
Optimization of planetary gears
[ETN-88-92375] 21 p2958 N88-27573
Computer aided design for linear control State Variable System (SVS)
[AD-A193282] 21 p2997 N88-27775
Research into the architecture of CAD based robot vision systems
[AD-A193330] 21 p2997 N88-27776
Benefits of an object approach in a computer aided design environment
[SNIAS-881-440-102] 21 p3000 N88-27791
A PRELUDE (analysis and design of control systems-preliminary utilities depository). A data-based interactive system of control software, user's guid e
[DFVLR-MITT-88-12] 21 p3000 N88-27795
Large-signal modeling of gallium arsenide field-effect transistors 22 p3073 N88-28242
Advanced manufacturing management current and forthcoming technologies
[PNR90445] 22 p3159 N88-28802
Structural dynamics of maneuvering aircraft
[AD-A192376] 23 p3176 N88-28908
Computer aided filter design
[AD-A193959] 23 p3208 N88-29093
Interactive plotting of NASTRAN aerodynamic models using NPLOT and DISSPLA
[AD-A194115] 23 p3226 N88-29204
Second Conference on Artificial intelligence for Space Applications
[NASA-CP-3007] 23 p3251 N88-29351
Hologram representation of design data in an expert system knowledge base 23 p3251 N88-29354
The use of computer graphic simulation in the development of robotic systems
23 p3257 N88-29388
Computer-Aided-Control Engineering (CACE) primitives for robust and adaptive control systems, phase 1
[AD-A192446] 23 p3265 N88-29439
Plasma torch design codes package
[SNIAS-881-430-115] 23 p3286 N88-29569
Special Course on Missile Aerodynamics
[AGARD-R-754] 24 p3317 N88-29755
Semiempirical methods for airbreathing missiles
24 p3318 N88-29763

Study on conceptual design of spacecraft using Computer Aided Engineering (CAE)
[SNIAS-920-CA/TS] 24 p3333 N88-29841
MANIP — spacecraft modeling program
[MANIP-217A] 24 p3335 N88-29855
Development of a general software package for the analysis and synthesis of planar antenna arrays for space applications
[S-247-02] 24 p3359 N88-30000
Computer-Aided Structural Engineering (CASE) project. Development of design formulas for ribbed mat foundations on expansive soils
[AD-A194807] 24 p3412 N88-30307
Computer-Aided Structural Engineering (CASE) project. Computer program for analysis of planar grid structures (CGRID), user's guide
[AD-A195977] 24 p3413 N88-30317
Geometric modeling for computer aided design
[NASA-CR-183161] 24 p3413 N88-30320
The triangle: A multiprocessor architecture for fast curve and surface generation
[AD-A195882] 24 p3414 N88-30324
The P-3 Scheduling Support System (P-3 S3)
[AD-A194824] 24 p3436 N88-30450

COMPUTER AIDED ENGINEERING
U COMPUTER AIDED DESIGN

COMPUTER AIDED MANUFACTURING
Automatic seam welding with infrared sensor feedback
[DE87-013556] 01 p0055 N88-10352
A CAMAC system controlled by an IBM AT computer for time-resolved spectroscopy
[DE87-010111] 01 p0080 N88-10514
A reference guide for IGVIEW: An IGES-compatible geometry system
[DE87-013441] 01 p0083 N88-10534
Computer aided engineering/manufacturing at Rolls-Royce
[PNR90395] 02 p0222 N88-11397
Interactions between science and precision engineering
[DE87-010873] 04 p0426 N88-12643
Overall description of the computer aided design and manufacturing systems associated with the A320 program at Aerospatiale and its partners
[SNIAS-872-111-104] 05 p0635 N88-13883
XCUT: A rule-based expert system for the automated process planning of machined parts
[DE87-011638] 05 p0639 N88-13905
Using hierarchically structured problem-solving knowledge in a rule-based process planning system
[DE87-011639] 05 p0639 N88-13906
Computer modeling of complete IC fabrication process
[AD-A184807] 05 p0654 N88-14012
Selected aspects of microelectronics technology and applications: Numerically controlled machine tools. Technology trends series no. 2
[PB87-132973] 06 p0696 N88-14268
Robot accuracy improvement through kinematic parameter identification 06 p0712 N88-14363
LISP based simulation generators for modeling complex space processes 08 p1061 N88-16403
Information handling architecture and software for CIM (Computer Integrated Manufacturing)
[PB88-105820] 08 p1067 N88-16453
The use of computer graphic simulation in the development of robotic systems
09 p1214 N88-17275
A generalized method for automatic downhand and wirefeed control of a welding robot and positioner
[NASA-TP-2807] 10 p1316 N88-17869
Chinese 7760 CAD/CAMM software system introduced 11 p1468 N88-18756
An automatic system for extraction of information from a Computer Aided Design (CAD), selection, sequencing, and execution of turning processes
[INPE-4350-TDL/294] 12 p1676 N88-20020
Development cost reduction using integrated CAE-CAD-CAM techniques 12 p1701 N88-20182
Prototype manufacturing techniques for reducing cost, schedule, and technical risk 12 p1702 N88-20189
Time and cost reduction through computer integrated manufacture 12 p1703 N88-20191
Status of CAD/CAM in medium-sized industries described 16 p2184 N88-23022
Recognizing and locating partially occluded planar objects for assembly routines
[LAAS-87-360] 16 p2247 N88-23422
Automatic control of an industrial process and computer aided process control by means of an expert system
[LAAS-88-004] 16 p2255 N88-23476
Data base management in CAD/CAM systems: Requirements for CAD/CAM data bases, actual market offer, advice for an efficient data base management, development tendencies
[MBB/LWD-11/S/PUB/254] 16 p2285 N88-23683
Developing systems using state-of-the-art CAD/CAM technology 17 p2306 N88-23795
Simulation and computer aided engineering (the necessity of an integrated approach)
[NLR-MP-86050-U] 17 p2386 N88-24178
The knowledge based automatic extraction of the machinable surfaces for automatic CAD-CAM system
[INPE-4542-PRE/1288] 20 p2836 N88-26824
Enumeration, comments and discussion concerning papers presented during the Conference on Computer Applications in Production and Engineering (CAPE) 87
[NLR-MP-87015-U] 20 p2839 N88-26844
A survey of freeform solid modeling methods
[REPT-87-81] 20 p2839 N88-26847
Advanced manufacturing management current and forthcoming technologies
[PNR90445] 22 p3159 N88-28802
The use of computer graphic simulation in the development of robotic systems
23 p3257 N88-29388
The concurrent common Lisp development environment 23 p3263 N88-29422
Utilizing dynamic stability of orient parts
[AD-A195730] 24 p3427 N88-30397

COMPUTER AIDED MAPPING
The program DSMME: Digital Situation Model, Measurement — mapping 01 p0065 N88-10418
Detection of critical points: The first step to automatic line generalization 05 p0619 N88-13803
Matching segments from a map and an aerial image using relaxation techniques
[SNIAS-872-422-103] 05 p0620 N88-13809
The use of color in electronic maps. Part 1: Generation and analysis of color on the Gould/DeAnza image processing system
[IZF-1986-32] 05 p0635 N88-13882
The digital landmass simulation production overview
[AD-A187978] 11 p1503 N88-18978
Three-dimensional computer graphics brain-mapping project
[AD-A187202] 11 p1528 N88-19126
The US Army Electronic Map Data (EMD) initiative
[AD-A188209] 11 p1565 N88-19372
Development of a digital terrain modeling system for microcomputers
[INPE-4406-TDL/303] 12 p1639 N88-19816
Computer aided cartographic representation of traffic data: The traffic intensity maps of Baden-Wuerttemberg (Federal Republic of Germany)
16 p2225 N88-23282
Computer-assisted symbolization by raster data processing — mapping 16 p2225 N88-23284
Computer based modeling of thematic mapping
16 p2225 N88-23285
Extraction of texts and symbols from unstructured vector data — mapping 16 p2225 N88-23287
Mass digitization of topographic-cartographic information 16 p2226 N88-23288
Computer-assisted cartography research and development report of the Federal Republic of Germany 1984 - 1986 16 p2226 N88-23289
The representation of the sea-bottom in deep sea areas by the Digital Terrain Model (DTM) program TASH
16 p2226 N88-23293
Computer assisted generalization of buildings for digital landscape models by classification methods
16 p2226 N88-23294
Thailand in maps. Application of the mapping system THEMAK2 for specific purpose atlas preparation
16 p2226 N88-23295
Presentation of map information on a color display
[FOA-C-20687-2.7] 17 p2368 N88-24103
Coupling of satellite remote sensing to digitized topographic map to detect changes in land use
[B8735129] 17 p2369 N88-24104
Digital monoplotting, part 1
[B8735122-PT-1] 17 p2369 N88-24106
Digital monoplotting, part 2
[B8735122-PT-2] 17 p2369 N88-24107
Reports on cartography and geodesy. Series 1, no. 99
[ETN-88-92387] 18 p2533 N88-25025
West German Geodetic Working Group: Official topographic-cartographic information system (ATKIS), content description 18 p2533 N88-25026
West German Geodetic Working Group: Official topographic-cartographic information system (ATKIS), technical conception 18 p2533 N88-25027
Vector graphics and raster data processing for spatial information systems 18 p2533 N88-25028
Digitizing the traffic network of JOG 250 by scanning — JOG 250 map 18 p2533 N88-25029
Tests for the automatic pattern recognition of building surfaces by the TK 50 18 p2533 N88-25030
Creation of digital topographic models with the ALK-GIAP. The DLM 25 as an example
18 p2534 N88-25031
Topographic data processing for environmental planning 18 p2534 N88-25032
Digital maps for an electronic traffic guide
18 p2534 N88-25033
Development in data structures in PHOCUS for digital mapping 18 p2534 N88-25034
State of development of ALK (October 1986)
18 p2534 N88-25035
Vectorization of raster algorithms for elevation data processing 18 p2534 N88-25036
Geometric rectangular data file (GERD): An aid to the rapid access to position data 18 p2534 N88-25037
Recent developments in software and hardware by Scitex Co. — computer aided mapping
18 p2535 N88-25038
Personal computer as a workstation in a cartographic automation system? 18 p2535 N88-25039
Use of modern scanner techniques in cartography
18 p2535 N88-25040
The transition from traditional to modern map reproduction
[B8735128] 20 p2818 N88-26718
Graphical communication and symbolism in a computerized cartography and map compilation system
[PB88-124672] 20 p2818 N88-26720
Development of automatic names placement software
[AD-A192786] 21 p2996 N88-27770

COMPUTER AIDED TOMOGRAPHY
X-ray tomography and nuclear magnetic resonance imaging applications for advanced ceramic materials
[DE87-011534] 01 p0027 N88-10171
Fast dynamic studies with PC384-7B; system improvements and development of an automated blood sampling system — tomography
[USIP-87-05] 01 p0075 N88-10481
Study of the distribution of a multi-electrode circular system sensitivity for the reconstruction of bioelectrical impedance images
[ISAL-IDI1-87-01] 02 p0217 N88-11368
Projection-space iterative interpolation for limited-angle tomography in parallel- and fan-beam geometry, part 1
[DE87-013965] 02 p0221 N88-11391
Computed neutron tomography and coded aperture holography from real time neutron images
04 p0427 N88-12645
A comparison of film-based tomography and computed tomography for advanced ceramic materials
[DE88-003114] 07 p0837 N88-15079
The development of emission tomography for the nuclear industry
[AERE-R-12319] 10 p1341 N88-18014
Application of X-ray computed tomography to ceramic/ceramic composites
[DE88-002903] 11 p1464 N88-18728
South African Association of Physicists in Medicine and Biology: 26th Annual Congress
[DE88-700824] 11 p1521 N88-19082
Nondestructive testings of HTGR graphites
13 p1747 N88-20448
Recent developments in nondestructive evaluation for structural ceramics
[DE88-005889] 13 p1751 N88-20473
X-ray computed tomography for structural ceramic applications: Beam hardening corrections
[DE88-005891] 13 p1752 N88-20474
A hardware/software system for implementing geophysical diffraction tomography
[DE88-006411] 15 p2094 N88-22480
Computer tomography and hybrid optical/digital methods for aerodynamic measurements
[AD-A190909] 16 p2157 N88-22872
Model-based computed tomography for nondestructive evaluation: An overview and proposal
[DE88-010600] 19 p2679 N88-25926
Turbulent flow field visualization with integral interferometric imaging and computed tomography
21 p2950 N88-27521
Direct visualization of surfaces from computed tomography data
[AD-A193646] 22 p3153 N88-28758

COMPUTER ANIMATION
Visualization of an aircraft accident based on digital flight data recorder information 05 p0538 N88-13278
Dynamics of high-speed mechanisms with elastic members 13 p1779 N88-20643
Investigation into the use of texturing for real-time computer animation
[AD-A191008] 16 p2251 N88-23454

COMPUTER ARCHITECTURE
U ARCHITECTURE (COMPUTERS)

COMPUTER ASSISTED INSTRUCTION
An object-oriented architecture for intelligent tutoring systems
[AD-A184790] 03 p0368 N88-12314

LISP as a rapid prototyping environment: The chinese tutor
[AD-A184328] 03 p0369 N88-12319
The pros and cons of using a CAI package on a central computer as opposed to a microprocessor: What's your CAI MO, mainframe or micro
[DE87-011123] 04 p0475 N88-12929
Stress effects and the optimum format of a scrolling seven-line VDT text window
[AD-A185559] 06 p0758 N88-14651
Field evaluation of interactive simulation for maintenance training: SH-3 helicopter electro-mechanical bladefold system
[AD-A185923] 07 p0821 N88-14991
Finite element method computer implementation 08 p0985 N88-15963
A prototype of pilot knowledge evaluation by an intelligent CAI (Computer-Aided Instruction) system using a Bayesian diagnostic model
[AD-A186080] 08 p1054 N88-16358
The use and generation of illustrative examples in computer-based instructional systems 08 p1060 N88-16400
Training in satellite ground system operations 09 p1129 N88-16775
IMIS: Integrated Maintenance Information System. A maintenance information delivery concept 09 p1203 N88-17207
An intelligent training system for payload-assist module deploys 09 p1204 N88-17214
Tutoring electronic troubleshooting in a simulated maintenance work environment 09 p1204 N88-17215
An intelligent tutor for the space domain 09 p1204 N88-17217
The desktop interface in intelligent tutoring systems 09 p1205 N88-17225
Computer assisted instruction: Two decades in perspective
[AD-A186813] 09 p1216 N88-17289
Computer aided design of aircraft structures
[ETN-88-91353] 14 p1867 N88-21154
Tutorial on GAMS (Generalized Algebraic Modeling System): A modeling language for optimization
[AD-A189867] 15 p2109 N88-22568
Development of training implying man-machine interface: From the aircraft to the spacecraft 19 p2700 N88-26052
Computer-aided writing
[AD-A192516] 20 p2838 N88-26837
Script editor: An editor for the specification phase in the development of computer based learning
[REPT-87-68] 20 p2839 N88-26846
The sine and cosine function for class 4-VWO. Exploration of possible bottlenecks
[REPT-87-72] 20 p2881 N88-27105
Design and development of courseware for goniometry
[REPT-87-73] 20 p2881 N88-27106

COMPUTER CODES
U COMPUTER PROGRAMS

COMPUTER COMPONENTS
Chips: A tool for developing software interfaces interactively
[AD-A187499] 10 p1389 N88-18295
Real time pipelined system for forming the sum of products in the processing of video data
[NASA-CASE-NPO-16462-1-CU] 17 p2384 N88-24169

COMPUTER DESIGN
Multi-processor architectures for artificial intelligence processing
[OUEL-1671/87] 02 p0219 N88-11380
A taxonomy of analytical computer performance models for computer design
[AD-A185561] 06 p0755 N88-14632
Annotated computer output for split plot design: GENSTAT ANOVA
[AD-A187120] 10 p1385 N88-18271
Design and implementation of a parallel computer for expert system applications
[DE88-005288] 15 p2115 N88-22601
Coding for write-unidirectional memories and conflict resolution
[ENST-87C005] 16 p2245 N88-23408
Locality, communication and interconnect length in multicomputers
[CWI-CS-R8743] 16 p2254 N88-23466
Optical computer and optical methods for data processing 18 p2518 N88-24939
Design of high performance microcomputers for numerical data processing
[ETN-88-92371] 20 p2835 N88-26818

COMPUTER GRAPHICS
NT COMPUTER ANIMATION
Recording multiple signals on a single waveform recorder
[DE87-011632] 01 p0049 N88-10313
Input devices for tasks using interactive video
[NPL-DITC-87/87] 01 p0080 N88-10510
A graphical tool for observing the behavior of parallel logic programs
[DE87-011467] 01 p0080 N88-10516
TIPS-1 user's manual: Cray-1 version
[DE87-013297] 01 p0081 N88-10522
Boundary integral technique for performing analysis of two-dimensional volumes of revolution
[DE87-013053] 01 p0082 N88-10524
DETOUR: A deformed mesh/contour plot program
[DE87-013119] 01 p0082 N88-10525
A reference guide for IGVIEW: An IGES-compatible geometry system
[DE87-013441] 01 p0083 N88-10534
An interactive computer program for materials analysis by means of ion scattering
[MRL-R-1040] 01 p0091 N88-10596
Nowcasting microbursts using Doppler radar in a forecaster-computer environment 02 p0200 N88-11246
The impact of new computer technology on accelerator control
[DE87-014021] 02 p0219 N88-11376
Illustrations of a density-equalizing map projection technique
[DE87-013992] 03 p0339 N88-12130
A scientific workstation operator-interface for accelerator control
[DE87-014689] 03 p0362 N88-12278
A simulation study of a speed control system for autonomous on-road operation of automotive vehicles
[AD-A184030] 03 p0362 N88-12279
The Macintosh computer as a tool for rapid data analysis and for producing camera ready viewgraphs/publications
[DE87-014350] 03 p0362 N88-12280
Technology applications branch graphics projects
[AD-A184821] 03 p0364 N88-12291
Issues in image processing software development for a multi-user, multi-programming environment
[DE88-000358] 03 p0365 N88-12298
End of year report for parallel vision algorithm design and implementation
[AD-A184327] 03 p0366 N88-12301
Layering central authentication on the interactive services of an existing homogeneous distributed system
[DE87-011544] 03 p0366 N88-12304
Low-level vision on warp and the apply programming model
[AD-A184330] 03 p0369 N88-12320
An inexpensive real-time interactive three-dimensional flight simulation system
[AD-A184340] 04 p0402 N88-12499
NACHOS 2: A finite element computer program for incompressible flow problems. Part 2: User's manual
[DE88-001451] 04 p0443 N88-12750
CGI delay compensation
[NASA-TM-86703] 04 p0476 N88-12932
An interactive computer graphics network monitor for a tactical communications network
[AD-A184131] 04 p0477 N88-12938
The ISI (Information Sciences Institute) grapher: A portable tool for displaying graphs pictorially
[AD-A184354] 04 p0478 N88-12944
Implementation and performance of a complex vision system on a systolic array machine
[AD-A184331] 04 p0482 N88-12971
GOLD: Integration of model-based control systems with artificial intelligence and workstations
[DE88-000506] 04 p0483 N88-12976
GOLD: Integration of model-based control systems with artificial intelligence and workstations
[DE88-000706] 04 p0483 N88-12977
Computer graphics for computational aerodynamics 05 p0538 N88-13276
Flow visualization in computational fluid dynamics 05 p0538 N88-13277
Visualization of an aircraft accident based on digital flight data recorder information 05 p0538 N88-13278
Implementation of an FIR band pass filter using a bit-slice processor
[AD-A184895] 05 p0634 N88-13875
The use of color in electronic maps. Part 1: Generation and analysis of color on the Gould/DeAnza image processing system
[IZF-1986-32] 05 p0635 N88-13882
Digitization functions in computer graphics
[ETN-88-91363] 05 p0635 N88-13887
An Ada graphical tool to support software development
[DE87-014854] 05 p0636 N88-13891
A general solution to the silhouette problem
[NASA-TP-2695] 06 p0755 N88-14629
Window system: A toolbox for interactive computer graphics
[PB87-234282] 06 p0756 N88-14637
The Wilson-Fowler spline in a global IGES (Initial Graphics Exchange Specification) coordinate frame
[DE88-001942] 06 p0757 N88-14640
Nonconformity testing for the Graphical Kernel System (GKS)
[GMD/VAL-86-104] 06 p0757 N88-14644
Virtual image processor: A prototype implementation
[AD-A185560] 06 p0758 N88-14652
Interaction of different modules in depth perception: Stereo and shading
[AD-A185607] 06 p0759 N88-14655
Adaptive grid for polyhedral visibility in object space: An implementation
[PB88-100938] 06 p0760 N88-14663
Development of a graphical display on the DMS test bed 06 p0794 N88-14864
An inexpensive real-time interactive three dimensional flight simulation system
[AD-A184868] 07 p0821 N88-14989
TRACKER: A 3-D radio ray tracing code
[DE88-003267] 07 p0847 N88-15137
Creating title blocks for vehicle animations
[AD-A185620] 07 p0904 N88-15473
After ten years of metafiles: Where does the Computer Graphics Metafile fit
[DE88-001840] 07 p0904 N88-15474
GENLPLOT: An interactive program for display and analysis of data, user's manual
[DE88-002292] 07 p0905 N88-15485
Methodology for testing and validating knowledge bases 08 p1055 N88-16364
Development of a task-level robot programming and simulation system 08 p1058 N88-16387
FMEAssist: A knowledge-based approach to Failure Modes and Effects Analysis 08 p1060 N88-16395
TOPP: A post-processor for TOPAZ, the one dimensional pipe flow analysis code
[DE88-003711] 09 p1164 N88-16981
An interactive-graphics method for dynamic system modelling, applying consistency rules 09 p1181 N88-17072
Vision algorithms and psychophysics
[AD-A186773] 09 p1200 N88-17193
The use of computer graphic simulation in the development of robotic systems 09 p1214 N88-17275
Fractal images: Procedure and theory
[AD-A187014] 09 p1217 N88-17293
Mathematical structures for speech recognition
[AD-A187063] 09 p1217 N88-17295
Interactive generation of fractal objects
[CWI-CS-R8706] 09 p1218 N88-17302
Solid modelling with faceted primitives
[ETN-88-91593] 09 p1218 N88-17305
Methodological and structural principles for flexible geometric modeling in computer aided design
[MA-48] 09 p1218 N88-17306
A raster scan algorithm for generating visible parametric surfaces
[DE88-003222] 09 p1220 N88-17321
Directions in computer graphics architecture 10 p1379 N88-18233
Personal computers and All-In-1: Document transfer and translation
[DE88-003760] 10 p1384 N88-18264
Graph transformation algorithms for array memory optimization in applicative languages
[DE88-004727] 10 p1387 N88-18283
CUEMAP: A tool for generating hierarchical charts and dataflow diagrams
[DE88-004778] 10 p1387 N88-18284
Chips: A tool for developing software interfaces interactively
[AD-A187499] 10 p1389 N88-18295
Development of tokamak reactor system analysis code NEW-TORSAC
[DE88-751067] 10 p1411 N88-18417
A computer simulation study of an expert system for walking machine motion planning
[AD-A187907] 11 p1438 N88-18577
Motion planning and control of robot manipulators via application of a computer graphics animated display 11 p1496 N88-18932
Brightness contrast and character height of five flat panel computer displays
[AD-A187743] 11 p1524 N88-19096
Workshop on the Integration of Finite Element Modeling with Geometric Modeling
[NASA-CR-182515] 11 p1526 N88-19111
Integration of finite element modeling with solid modeling through a dynamic interface 11 p1526 N88-19112
Approaches to the automatic generation and control of finite element meshes 11 p1526 N88-19113

Finite element meshing of ANSYS (trademark) solid models 11 p1526 N88-19115
Octree based automatic meshing from CSG models 11 p1527 N88-19117
Geometrical and topological issues in octree based automatic meshing 11 p1527 N88-19118
Toward automatic finite element analysis 11 p1527 N88-19120
Design modeling for shape optimization 11 p1527 N88-19122
Shape optimization of three-dimensional stamped and solid automotive components [GMR-5168] 11 p1528 N88-19123
Postprocessing techniques for 3D non-linear structures 11 p1528 N88-19124
Geometric versus finite element modeling current and future trends at Northrop 11 p1528 N88-19125
Three-dimensional computer graphics brain-mapping project [AD-A187202] 11 p1528 N88-19126
Distributed computation of graphics primitives on a transputer network [NASA-TM-100814] 11 p1531 N88-19147
A computer graphics simulation of the endgame in aircraft combat survivability [AD-A187826] 11 p1541 N88-19214
Visual recognition training: Effectiveness of computer graphics [AD-A188302] 12 p1669 N88-19997
Twenty-fourth Industrial Associates Review 12 p1679 N88-20039
An interactive user-friendly approach to surface-fitting three-dimensional geometries [NASA-CR-4126] 12 p1682 N88-20058
CODAC (Cockpit Oriented Display of Aircraft Configurations) version 1.4 user's guide [NASA-CR-181650] 13 p1718 N88-20273
Western aeronautical test range real-time graphics software package MAGIC [NASA-TM-100425] 13 p1757 N88-20506
Graphics and flow visualization of computer generated flow fields [NASA-CR-182679] 13 p1767 N88-20573
Analysis for architecture for image processing [INPE-4294-PRE/1165] 13 p1791 N88-20715
Logical input devices and interaction --- computer graphics [CWI-CS-R8738] 13 p1814 N88-20836
MASPLT: A one-dimensional graphics post processor for wave propagation codes [DE88-005506] 13 p1817 N88-20856
HISPLT: A history graphics post processor for wave propagation codes [DE88-005507] 13 p1817 N88-20857
CSQPLT: A graphics post processor for multidimensional wave propagation codes [DE88-005508] 13 p1817 N88-20858
A model for graphical interaction --- computer graphics [CWI-CS-R8718] 13 p1818 N88-20866
Parallel graphical output from dialogue cells [CWI-CS-R8719] 13 p1818 N88-20867
Steps into a geometer's workbench [CWI-CS-R8726] 13 p1819 N88-20870
Dynamic run-time graphics [DE87-008997] 13 p1820 N88-20879
Geometry and graphics applied to robotics [CWI-CS-R8727] 13 p1824 N88-20903
Computation and graphics in mathematical research [DE88-005796] 13 p1831 N88-20953
Definition and display of profiled sweep-objects --- computer graphics [REPT-87-45] 14 p1957 N88-21665
Error reduction in two-dimensional pulse-area modulation, with application to computer-generated transparencies --- optical field synthesis [EUT-87-E-172] 14 p1982 N88-21825
DataViews: A personalizable, interactive, data display system for the decisionmaker [AD-A188509] 14 p1991 N88-21868
Effects of update and refresh rates on flight simulation visual displays [NASA-TM-100415] 15 p2018 N88-22033
Geometric modeling of flight information for graphical cockpit display [AD-A190484] 15 p2021 N88-22043
Investigation into the development of computer aided design software for space based sensors [NASA-CR-180772] 15 p2107 N88-22552
The visit problem: Visibility graph-based solution [DE88-000343] 15 p2108 N88-22556
Computer graphics tools for the study of minimal surfaces [DE88-006421] 15 p2108 N88-22557
PLOT3D (version-5): A computer code for drawing three dimensional graphs, maps and histograms, in single or multiple colours, for mono or stereoscopic viewing [DE88-701410] 15 p2108 N88-22558
A graphics editor for structured analysis with a data dictionary [AD-A190618] 15 p2112 N88-22584
The elliptic Sinh-Gordon equation and the construction of toroidal soap bubbles [DE88-006426] 15 p2113 N88-22585
Two-dimensional graphics tools for a transputer based display board [NASA-TM-100820] 15 p2113 N88-22591
Rapid prototyping of simulations in artificial intelligence environments [DE88-004295] 15 p2117 N88-22612
Discrete event simulation in the artificial intelligence environment [DE88-004296] 15 p2117 N88-22613
Higher order crossings [AD-A190489] 15 p2121 N88-22641
The program Kennedy Approach as an experimental design of a dynamic computerized air traffic control test [DFVLR-FB-87-50] 16 p2159 N88-22881
Multiprocessor graphics computation and display using transputers 16 p2218 N88-23236
The integration of digital maps in vehicle navigation systems 16 p2225 N88-23286
Resource management in dialog cell specification (DICE) method [CWI-CS-R8746] 16 p2248 N88-23433
C-GKS, a C implementation of GKS, the graphical kennel system [CWI-CS-R8753] 16 p2249 N88-23438
PLOT300: A Tektronics PLOT10 emulator for HP 9000 series 200/300 computers [NASA-TM-100606] 16 p2250 N88-23447
Editfont an interactive font editing system [AD-A191007] 16 p2251 N88-23453
Investigation into the use of texturing for real-time computer animation [AD-A191008] 16 p2251 N88-23454
The geometric workstation, a new approach for geometric corrections of remotely sensed data 17 p2352 N88-24017
The Systeme d'Analyse Geographique (SAGE) geographic analysis system 17 p2353 N88-24019
Evolution of a family of image processing systems at INPE 17 p2361 N88-24065
Automatic registration of satellite imagery 17 p2364 N88-24080
Visualization of digital terrain models 17 p2364 N88-24081
Presentation of map information on a color display [FOA-C-20687-2.7] 17 p2368 N88-24103
Graphics software tool for VT terminals (VTGRAPH) [NASA-TM-100331] 17 p2389 N88-24201
Description of graphics translation software between Intergraph and Tektronix systems [NASA-TM-100335] 17 p2389 N88-24202
An analytic model for aerodynamic shapes [AD-A191573] 18 p2456 N88-24583
Airplane runway performance monitoring system [NASA-CASE-LAR-13854-1-CU] 18 p2462 N88-24621
The coordination of multiple robotic manipulators [AD-A190869] 18 p2522 N88-24963
Vector graphics and raster data processing for spatial information systems 18 p2533 N88-25028
Personal computer as a workstation in a cartographic automation system? 18 p2535 N88-25039
Knowledge acquisition tool implementation [AD-A190415] 18 p2555 N88-25164
IGUANA: Interactive graphics utility for automated NEC analysis [AD-A191760] 18 p2556 N88-25174
A graphical, intelligent interface for discrete-event simulations [DE88-000522] 18 p2557 N88-25181
Considerations involved in the display of finite element results using animation [DE88-007581] 18 p2559 N88-25189
The ISI (Information Sciences Institute) grapher manual [AD-A192198] 18 p2561 N88-25200
Engineering drawings and changes: Storing and controlling by the tens of terrabytes [DE88-007605] 18 p2589 N88-25387
Cellular Array Processor (CAP) and its application to computer graphics 19 p2641 N88-25667
Application of interactive graphic system (CAD/CAM) in the determination of process evolution in land use in the Ribeirao Preto municipality 19 p2684 N88-25956
Graphical Multiprocessing Analysis Tool (GMAT) [DE88-008019] 19 p2715 N88-26116
Checkout system software for INPE satellites [INPE-4554-PRE/1297] 19 p2715 N88-26120
RAGS (Realtime Acquisition and Graphics System): An off-the-shelf hardware and system software small data acquisition computer [DE88-008399] 19 p2716 N88-26128
Logic and fault simulation on the Mach1000 hardware accelerator [DE88-009794] 19 p2717 N88-26130
GRAPHICS MANAGER (GFXMGR): An interactive graphics software program for the Advanced Electronics Design (AED) graphics controller, Model 767 [DE88-010370] 19 p2717 N88-26131
The transition from traditional to modern map reproduction [B8735128] 20 p2818 N88-26718
Graphical communication and symbolism in a computerized cartography and map compilation system [PB88-124672] 20 p2818 N88-26720
XDATAP [DE88-007161] 20 p2837 N88-26827
Interactive computer programme for the analysis of a two-way Wilkinson divider/combiner [PB88-105424] 20 p2837 N88-26831
Editfont: An interactive font editing system [AD-A192373] 20 p2838 N88-26836
A survey of freeform solid modeling methods [REPT-87-81] 20 p2839 N88-26847
An expeditious technique for keyboard input of information to FORTRAN computer programs [DE88-009617] 20 p2840 N88-26855
Three-dimensional scene analysis using stero based imaging [AD-A193120] 21 p2894 N88-27178
An aspect graph-based control strategy for 3-D object recognition 21 p2927 N88-27377
Creating aspect graphs for use in object recognition 21 p2928 N88-27379
The effect of input device on user performance with a menu-based natural language interface [AD-A193095] 21 p2996 N88-27772
A menu-driven menu editor and associated menu system [DE88-008026] 21 p2998 N88-27781
TRANSL: A PATRAN translator subroutine library [DE88-010976] 21 p2998 N88-27784
Contribution to almost realistic picture processing by a computer graphics procedure [ETN-88-92372] 21 p2999 N88-27789
A hidden-surface removal algorithm for structures defined by triangular and rectangular surface patches [DFVLR-MITT-88-03] 21 p3000 N88-27792
User's manual for the two-dimensional transputer graphics toolkit [NASA-TM-100974] 21 p3001 N88-27799
LO-CO-GRAF (low cost graphics): Generating maps to support command and control/crisis management using small computers [AD-A193964] 22 p3139 N88-28661
Rendering of surfaces from volume data [AD-A193649] 22 p3143 N88-28689
Interactive, networked moving platform simulators [AD-A192374] 23 p3182 N88-28940
Interactive plotting of NASTRAN aerodynamic models using NPLOT and DISSPLA [AD-A194115] 23 p3226 N88-29204
The use of computer graphic simulation in the development of robotic systems 23 p3257 N88-29388
Numerical simulation of nozzle flows [AD-A195144] 24 p3369 N88-30064
Implementation of the NCAR (National Centre for Atmospheric Research) graphics package at ARL (Aeronautical Research Laboratory) [AD-A195163] 24 p3391 N88-30193
Geometric modeling for computer aided design [NASA-CR-183161] 24 p3413 N88-30320

COMPUTER INFORMATION SECURITY

New technologies and intellectual property: An economic analysis [N-2601-NSF] 01 p0107 N88-10695
Confidentiality of data --- Columbus Polar Platforms 03 p0339 N88-12136
A classified bibliography on publications relevant to data security in LANs --- local area networks (LANS) [NPL-DITC-99/87] 09 p1223 N88-17331
A framework for evaluating computer architectures to support systems with security requirements, with applications [AD-A187082] 10 p1392 N88-18303
Defending secrets, sharing data: New locks and keys for electronic information [PB88-143185] 12 p1706 N88-20210
The TEMPIS project: Current status [AD-A188963] 12 p1707 N88-20220

Monitoring the usage of a computer system
[DE88-004310] 15 p2106 N88-22542
Protection and security mechanisms in the SMITE capability computer
[RSRE-MEMO-4117] 17 p2384 N88-24167
Development environment for secure software
[RSRE-87015] 17 p2386 N88-24179
Separability and security models — software
[RSRE-87020] 17 p2386 N88-24180
Computer resource management technology program (PE 64740F). Task no. 9: Advanced user authentication
[PB88-183066] 18 p2555 N88-25163
A mixed-modem solution for sensitive data segregation on a broadband network
[DE88-001765] 19 p2718 N88-26139
An evaluation methodology for dependable multiprocessors
[AD-A192799] 20 p2842 N88-26863
A state-of-the-art survey of low-cost security in local area networks
[NPL-DITC-113/88] 22 p3141 N88-28678
The SMITE modular compilation system
[RSRE-MEMO-4145] 23 p3244 N88-29307

COMPUTER METHODS
U COMPUTER PROGRAMS

COMPUTER NETWORKS
NT LOCAL AREA NETWORKS
HF (High Frequency) broadcasting planning model: A comparison of two versions
[PB87-210282] 01 p0036 N88-10230
EAGLES: An interactive environment for scientific computing
[DE87-013564] 01 p0084 N88-10541
Semantic network processing systems — artificial intelligence
[OUEL-1677/87] 02 p0223 N88-11401
An examination of the Advanced Communications Technology Satellite (ACTS) and its application to the Defense Data Network (DDN)
[AD-A184003] 03 p0276 N88-11742
The network queueing system
[NASA-CR-177433] 03 p0365 N88-12297
Center for Supercomputing Research and Development (CEDAR)
[DE88-000807] 04 p0475 N88-12930
A data analysis environment for HP (Hewlett-Packard) 1000 computers
[DE87-010511] 04 p0477 N88-12936
A survey of object oriented languages in programming environments
[AD-A184127] 04 p0477 N88-12937
A network definition and solution of simulation problems
[DE88-000675] 04 p0481 N88-12962
Managing distributed derived data: A preliminary proposal
[DE88-000714] 04 p0481 N88-12966
An approach to implementing state space searches on heterogeneous systems of multiprocessors
[DE88-001321] 04 p0482 N88-12967
Relational data handling system for scientists
[PB87-223426] 05 p0658 N88-14038
Connecting RPC (Remote Procedure Call)-based distributed systems using wide-area networks
[PB87-234423] 05 p0658 N88-14041
Distribution of records on a ring of processors
[PB87-235784] 06 p0758 N88-14649
Wide-area communication under Amoeba
[PB87-234431] 06 p0760 N88-14665
USSR report: Cybernetics, computers and automation technology
[JPRS-UCC-86-014] 06 p0761 N88-14669
Distributed infimum approximation
[PB87-234969] 06 p0764 N88-14695
Image understanding by Image-Seeking Adaptive Networks (ISAN)
[AD-A186214] 07 p0906 N88-15492
Compilation and development of K-6 aerospace materials for implementation in NASA spacelink electronic information system 07 p0922 N88-15605
Enhancement of computer system for applications software branch 07 p0923 N88-15610
Short pseudorandom test sequences
[AD-A185883] 08 p1054 N88-16357
Integration of symbolic and algorithmic hardware and software for the automation of space station subsystems 08 p1056 N88-16373
Foundation: Transforming data bases into knowledge bases 08 p1063 N88-16423
The European space physics analysis network 08 p1099 N88-16613
NASA JSC neural network survey results 09 p1205 N88-17220
Description of a limited VAX-Ada program support environment developed within UDP division version 1.0
[ARE-TM(UDP)-87103] 09 p1219 N88-17308
Interdisciplinary research in applied mathematics
[AD-A186793] 09 p1226 N88-17344
Multiple-bus interconnection for future multiprocessor systems 10 p1375 N88-18203
An anlysis of the reliability of tree-structured interconnection networks 10 p1378 N88-18228
A strategy for failure prediction 10 p1380 N88-18243
Future directions in computer architecture and software workshop 10 p1383 N88-18258
Personal computers and All-In-1: Document transfer and translation
[DE88-003760] 10 p1384 N88-18264
An Ethernet local area network controller with supporting operating system software
[DE88-003534] 10 p1392 N88-18304
The Lambda network: A new permutation network
[DE88-003568] 10 p1392 N88-18305
Shared workspaces for real-time collaboration in distributed networks: Concepts, techniques, problems
[AD-A188150] 10 p1394 N88-18315
Guidelines for exchanging computerized information
[DE88-004736] 10 p1425 N88-18510
Networking requirements and future alternatives
[NASA-TM-89711] 10 p1426 N88-18517
Optical symbolic processor for expert system execution
[AD-A187882] 11 p1525 N88-19103
Distributed computation of graphics primitives on a transputer network
[NASA-TM-100814] 11 p1531 N88-19147
District information system of National Information Centre
[PB88-134739] 11 p1565 N88-19373
MOBICALC: An integrated and interactive system for development of administrative models
[INPE-4335-TDL/291] 12 p1679 N88-20038
A prototype for remotely shared textual workspaces
[AD-A188352] 12 p1679 N88-20040
Experience with Berkeley UNIX interprocess communications
[AD-A188353] 12 p1680 N88-20041
National Informatics Centre: Profile of services
[PB88-134135] 12 p1706 N88-20211
Computing with structured connections networks
[AD-A189244] 13 p1821 N88-20886
A fully abstract semantics for data flow nets
[CWI-CS-R8724] 13 p1822 N88-20893
Two queues with alternating service and switching times
[CWI-OS-R8712] 13 p1831 N88-20949
A menu-driven knowledge retrieval system accessing ASCII data
[DE88-001742] 13 p1851 N88-21079
Activities and operations of the Advanced Computing Research Facility, October 1986-October 1987
[DE88-006223] 14 p1955 N88-21653
Deadlock-free message routing in processor networks
[CS-8706] 14 p1960 N88-21691
Sigma system: Overview, prospects 15 p2052 N88-22230
Project Monitoring Package (PMP): A package for project activity monitoring
[DE88-701234] 15 p2107 N88-22554
Logarithmically connected, repetitive computer networks and numerical applications
[DE88-006632] 15 p2114 N88-22592
Multiprocessor graphics computation and display using transputers 16 p2218 N88-23236
A queueing network model for analyzing a class of branch and bound algorithms on a master-slave architecture
[CWI-OS-R8717] 16 p2249 N88-23441
Reference nuclear data for space applications
[DE88-007041] 16 p2270 N88-23583
Network architecture for OPS5
[DE88-002802] 18 p2560 N88-25194
A mixed-modem solution for sensitive data segregation on a broadband network
[DE88-001765] 19 p2718 N88-26139
Fault diagnosis in distributed computer networks
[AD-A192406] 19 p2718 N88-26140
Computer science research, 1987: Computation Directorate
[DE88-008637] 20 p2834 N88-26812
A linear-programming method inspired by the neural networks framework
[DE88-008688] 20 p2842 N88-26862
Optical interconnections for digital image coding 21 p2928 N88-27381
Implementing direct, spatially isolated problems on transputer networks
[NASA-TM-101297] 21 p3000 N88-27796
A modular proof of correctness for a network synchronizer
[AD-A192726] 21 p3002 N88-27802
Improving the performance of AI algorithms
[AD-A192848] 21 p3003 N88-27809
Finding minimum-cost circulations by canceling negative cycles
[AD-A192727] 21 p3005 N88-27825
Survey of neural net paradigms for specification of discrete networks
[AD-A192682] 22 p3141 N88-28674
Queueing network models for parallel processing of task systems: An operational approach
[NASA-CR-183174] 22 p3141 N88-28677
Process migration in UNIX environments
[NASA-CR-182951] 23 p3245 N88-29311
Issues on the use of meta-knowledge in expert systems 23 p3252 N88-29357
Intelligent test integration system 23 p3254 N88-29371
Knowledge based programming environments: A perspective 23 p3258 N88-29393
Two implementations of the Expert System for the Flight Analysis System (ESFAS) project 23 p3259 N88-29400
Mathematical algorithms for approximate reasoning 23 p3262 N88-29418
The concurrent common Lisp development environment 23 p3263 N88-29422
Networking and AI systems: Requirements and benefits 23 p3263 N88-29425
Radial basis functions, multi-variable functional interpolation and adaptive networks
[RSRE-MEMO-4148] 23 p3265 N88-29436
Improved time bounds for the maximum flow problem
[AD-A194034] 23 p3272 N88-29471
Signals and systems 24 p3363 N88-30026
Telescience testbed pilot program
[NASA-CR-183207] 24 p3412 N88-30309
Performance analysis of FDDI
[NASA-CR-183206] 24 p3413 N88-30321
The LTPP communication processor — Columbus and Hermes
[CL/CP/SES/FR/004] 24 p3415 N88-30328
Knowledge-based integrated information systems engineering: Highlights and bibliography. Knowledge-Based Integrated Information Systems Engineering (KBIISE) Project, volume 1
[AD-A195850] 24 p3435 N88-30449
Integrating images, applications, and communications networks, volume 5
[AD-A195854] 24 p3436 N88-30452
Knowledge-Based Integrated Information Systems Development Methodologies Plan. Knowledge-Based Integrated Information Systems Engineering (KBIISE) report, volume 2
[AD-A195851] 24 p3436 N88-30455

COMPUTER PROGRAM INTEGRITY
Computing systems dependability and fault tolerance: Basic concepts and terminology 02 p0127 N88-10797
Some approaches to the design of high integrity software 02 p0127 N88-10799
ISAURE: Integration of security and fault tolerance in the REALITE 2000 system 02 p0127 N88-10802
ADAMEASURE: An implementation of the Halstead and Henry metrics
[AD-A184005] 03 p0365 N88-12299
Approaches to the verification of rule-based expert systems 09 p1206 N88-17232
Evaluating software testing methods to reduce testing duplication in US Army communications equipment acquisition
[AD-A186961] 09 p1216 N88-17292
Methodology for software reliability prediction, volume 1
[AD-A190018] 15 p2110 N88-22571
Methodology for software reliability prediction, volume 3
[AD-A190019] 15 p2110 N88-22572
Introduction to logic programming
[CWI-CS-R8741] 16 p2248 N88-23430
Development environment for secure software
[RSRE-87015] 17 p2386 N88-24179
Separability and security models — software
[RSRE-87020] 17 p2386 N88-24180
Nebula support software
[AD-A192281] 20 p2837 N88-26833

COMPUTER PROGRAMMING
NT LANGUAGE PROGRAMMING
NT LOGIC PROGRAMMING
NT MICROPROGRAMMING
NT PARALLEL PROGRAMMING
NT SYMBOLIC PROGRAMMING
Space Station Mission Planning System (MPS) development study. Volume 2
[NASA-CR-179200] 01 p0009 N88-10048

Space Station Mission Planning Study (MPS) development study. Volume 3: Software development plan
[NASA-CR-179203] 01 p0009 N88-10049
Report outline of a programming variable and application through example
[INPE-4211-PRE/1092] 01 p0081 N88-10521
On perfect hash functions
[ENST-86D008] 01 p0087 N88-10565
File management using balanced trees
[ENST-87D001] 01 p0106 N88-10693
Knowledge Based Concepts and Artificial Intelligence: Applications to Guidance and Control
[AGARD-LS-155] 02 p0128 N88-10806
How to use PROLOG for expert system programming
02 p0129 N88-10816
Knowledge acquisition issues encountered during the development of an estimating expert system
[DE87-013320] 02 p0248 N88-11568
Hardware-assisted multiprocessor performance measurements
[PB87-226908] 03 p0363 N88-12282
Integrating syntax, semantics, and discourse DARPA (Defense Advanced Research Projects Agency) Natural Language Understanding Program
[AD-A184505] 03 p0364 N88-12289
A survey of object oriented languages in programming environments
[AD-A184127] 04 p0477 N88-12937
Guidelines for preparing software user documentation
[NASA-CR-181550] 04 p0480 N88-12959
COLA2: A computer program for the structural synthesis of two components using general modal coordinates
[DE88-001457] 04 p0481 N88-12963
Programming techniques for high-speed processing of large scale numerical simulation on supercomputers
05 p0537 N88-13269
Vectorizing the FFTs on supercomputer SX system
05 p0537 N88-13270
An APL workspace for conducting nonparametric statistical inference
[AD-A184971] 05 p0634 N88-13877
Digitization functions in computer graphics
[ETN-88-91363] 05 p0635 N88-13887
Some distance problems in coding theory
[B8711398] 05 p0635 N88-13888
A requirements specification for a software design support system
[NASA-CR-182333] 05 p0637 N88-13896
Presentation of a computer program permitting the exploitation of tests designed to determine the sensitivity of one shot devices to a parameter. Application to a degenerate one shot sequence
[SNIAS-872-430-117] 05 p0644 N88-13945
Objects architecture: A comprehensive design approach for real-time, distributed, fault-tolerant, reactive operating systems
[AD-A185476] 06 p0755 N88-14631
Set of multi-process primitives for stack based machines
[PB87-234381] 06 p0756 N88-14636
Learning to program methodically. 3: The newly designed course of the elementary programming
[PB87-119871] 06 p0757 N88-14643
Data processing of the JPA instrument. Part 1: Data management
[IFSI-86-15-PT-1] 06 p0757 N88-14645
Development of symbolic computation methods for nonlinear dynamics
[AD-A185562] 06 p0758 N88-14653
Research study for materials/properties test results database
[NASA-CR-178923] 07 p0861 N88-15222
Formalizing reusable software components in the programmer's apprentice
[AD-A185843] 07 p0901 N88-15457
Documentation in a software maintenance environment
[AD-A185892] 07 p0901 N88-15459
FORTRAN 77 programming guidelines
[DFVLR-MITT-87-10] 07 p0905 N88-15487
AFL-1: A programming language for massively concurrent computers
[AD-A186422] 07 p0906 N88-15489
Nacelle-wing interactions (studies 1986) development of a finite element code in a multi-domain version
[ONERA-RTS-10/3417-AY-308A]
08 p0950 N88-15764
Adaptive finite difference methods in fluid dynamics
08 p0985 N88-15958
Finite element method computer implementation
08 p0985 N88-15963
Solution in vibration problems of rectangular plates with spline function
[PB87-143459] 08 p0996 N88-16029
Changing the layers of mind
[AD-A186648] 08 p1052 N88-16350
An easy-to-use diagnostic system development shell
08 p1055 N88-16366
Development of a task-level robot programming and simulation system 08 p1058 N88-16387
Rapid prototyping and AI programming environments applied to payload modeling 08 p1061 N88-16405
On acquisition of programming knowledge
08 p1065 N88-16438
Standardization of software development
[INPE-4330-NTE/272] 08 p1068 N88-16455
Replication and reconfiguration in a distributed mail repository
[AD-A186967] 09 p1151 N88-16897
Application of satellite data in variational analysis for global cyclonic systems
[NASA-CR-182468] 09 p1193 N88-17152
Simplifying the construction of domain-specific automatic programming systems: The NASA automated software development workstation project
09 p1204 N88-17212
The knowledge-based software assistant
09 p1204 N88-17213
Task-level robot programming: Integral part of evolution from teleoperation to autonomy
09 p1214 N88-17279
Types and effects towards the integration of functional and imperative programming
[AD-A186930] 09 p1216 N88-17290
FORTRAN 77 guidelines for the software projects RASP and ANDECS
[DFVLR-MITT-87-09] 09 p1218 N88-17301
Methodological and structural principles for flexible geometric modeling in computer aided design
[MA-48] 09 p1218 N88-17306
Concept of a programmable maintenance processor applicable to multiprocessing systems
[NASA-TM-100406] 09 p1223 N88-17333
Development of an engineering model atmosphere for Mars
[NASA-CR-182462] 09 p1263 N88-17568
Data reduction and analysis of HELIOS plasma wave data
[NASA-CR-182466] 09 p1264 N88-17572
Image texture classification with an optical crossbar interconnected processor 10 p1375 N88-18202
Predicate analysis for parallel program generation
10 p1377 N88-18222
Software support for heterogeneous machines
10 p1378 N88-18224
Semi-applicative programming
10 p1380 N88-18239
An applicative programmer's approach to matrix algebra, lessons for hardware and software
10 p1382 N88-18251
Implementing logical variables on a graph reduction architecture 10 p1382 N88-18252
Experience with Omega: Implementation of a prototype programming environment, part 6
[AD-A187080] 10 p1385 N88-18270
Using program structure to achieve prefetching for cache memories
[DE88-003599] 10 p1387 N88-18282
Programming methodology and performance issues for advanced computer architectures
[DE88-003098] 10 p1387 N88-18287
Development of a graphics based two-attribute utility assessment program with application to mission planning
[AD-A187276] 10 p1388 N88-18292
Deriving abstractions from a software object network
[AD-A187472] 10 p1389 N88-18294
Performance studies of a parallel processor for large linear programming problems
[PB88-121611] 10 p1393 N88-18310
SETI data controllers 11 p1474 N88-18795
KR: An efficient knowledge representation system
[AD-A187705] 11 p1529 N88-19129
Compact high order schemes for the Euler equations
[NASA-CR-181625] 11 p1530 N88-19138
An IBM PC version of ASENT
[DE88-004244] 11 p1532 N88-19150
Evaluating expert system tools: A framework and methodology-workshops
[AD-A187190] 11 p1533 N88-19159
The SAS (Statistical Analysis System) by forms: Putting statistical power into the hands of an end-user
[DE88-002217] 11 p1541 N88-19212
Progress toward a cosmic dust collection facility on space station
[NASA-CR-182427] 12 p1598 N88-19566
BLITZ: Blitzen's micron-code assembly language design document, version 1.0
[TR88-14] 12 p1676 N88-20019
EqL's user's guide
[AD-A188351] 12 p1677 N88-20025
Research on automatic verification of finite-state concurrent systems
[AD-A188618] 12 p1677 N88-20029
Building software systems economically with mechanized logic: Initial design proposal
[AD-A188791] 12 p1678 N88-20031
A knowledge acquisition tool for the intelligent processing of materials
[AD-A188982] 12 p1679 N88-20036
ARCTIC: Programmer's manual and tutorial
[AD-A188619] 12 p1680 N88-20047
OPS83: Style guide for high performance
[AD-A188505] 12 p1681 N88-20051
KREME (Knowledge Representation, Editing and Modeling Environment): A user's introduction, phase 1
[AD-A188906] 12 p1681 N88-20052
Object-oriented design in numerical linear algebra
[AD-A189427] 12 p1685 N88-20073
Towards a solution to the proper integration of a logic programming system and a large knowledge based management system
[AD-A188949] 12 p1705 N88-20207
Intergrated circuit design, phase 2
[AD-A189060] 13 p1760 N88-20530
Laser programming integrated circuits
[AD-A189590] 13 p1762 N88-20537
Finite State Tables for general computer programming applications
[DE88-006254] 13 p1820 N88-20881
Expert system techniques and decision support system: A case study (Dec. 1985 - Jun. 1986)
[ETN-88-91347] 13 p1821 N88-20884
Research in applied mathematics ralated to identification of noisy systems
[AD-A189355] 13 p1825 N88-20908
Oceanographic export system development, year 1
[AD-A189134] 14 p1950 N88-21623
Description of ground motion data processing codes, volume 2
[DE88-007137] 15 p2095 N88-22481
Tutorial on GAMS (Generalized Algebraic Modeling System): A modeling language for optimization
[AD-A189867] 15 p2109 N88-22568
Contour interactive extraction using image numerical treatment
[ISL-R-114/86] 15 p2113 N88-22587
Inference engine for expert systems
[INPE-4465-TDL/321] 15 p2113 N88-22590
Numerical methods for linear and nonlinear optimization
[AD-A190029] 15 p2120 N88-22631
PLASMOR: A laser-plasma simulation code, part 2
[DE88-701289] 15 p2135 N88-22736
New generation knowledge processing, volume 1
[AD-A190165] 15 p2149 N88-22826
Adapting high-level language programs for parallel processing using data flow 16 p2218 N88-23234
Principles of lazy and incremental program generation
[CWI-CS-R8749] 16 p2249 N88-23435
COBOL Analysis System (CAS) users manual
[PB88-171442] 16 p2250 N88-23445
Program profiling in Cedar
[AD-A190883] 16 p2250 N88-23449
Concurrency efficiency user's manual
[AD-A190884] 16 p2251 N88-23450
Supercomputer programming environments
[AD-A190887] 16 p2251 N88-23452
Unique normal forms for lambda calculus with surjective pairing
[PB88-173539] 16 p2260 N88-23508
New generation knowledge processing, volume 2
[AD-A190166] 16 p2285 N88-23681
New generation knowledge processing, volume 3
[AD-A190167] 16 p2285 N88-23682
Mapping from LANDSAT and SPOT satellite imagery
17 p2352 N88-24018
The SAGE geographic analysis system
17 p2361 N88-24063
The Environment for Application Software Integration and Execution (EASIE) version 1.0. Volume 4: System installation and maintenance guide
[NASA-TM-100576] 17 p2386 N88-24185
An OOD (Object-Oriented Design) paradigm for flight simulators
[AD-A191097] 18 p2467 N88-24647
Calculation of assemblies bonded with quasi-elastic adhesives
[REPT-47-632/F] 18 p2493 N88-24793
Automated cartographic generalization for linear map features 18 p2532 N88-25021
LispSEI: The programmer's manual
[AD-A191632] 18 p2556 N88-25172

CIMAG2: The computer program to generate color images
[AD-A191847] 18 p2557 N88-25175
Beyond Ada: Generating Ada code from equational specifications
[AD-A191866] 18 p2557 N88-25176
System overview: Teragon 4000, an image processing equipment at FOA 3
[FOA-C-30465-3.3] 18 p2557 N88-25179
KA-PROLOG. KAP-computer: Computer model and instructions set
[ETN-88-91948] 18 p2558 N88-25186
The Sizing and Optimization Language, (SOL): Computer language for design problems
[NASA-TM-100585] 18 p2559 N88-25190
Introduction to compliance in programming of robots
[ETN-88-92189] 18 p2561 N88-25201
Modeling of geometric reasoning for robot programming
[ETN-88-92290] 18 p2561 N88-25202
Design of partially replicated distributed database systems: An integrated methodology
18 p2589 N88-25383
The scaling of the threshold conditions for solid propellant erosive burning 19 p2630 N88-25601
Theory of numerical information environment and its applications 19 p2640 N88-25666
The new MININEC (version 3): A mini-numerical electromagnetic code
[AD-A191778] 19 p2642 N88-25675
Accurate, productive aerodynamic simulation on patched mesh systems
[AD-A192040] 19 p2714 N88-26110
A comparative study of project estimating tools
[DE88-009059] 19 p2740 N88-26266
Research in computer science 1985/6
[PB88-113840] 20 p2835 N88-26815
Nebula support software
[AD-A192281] 20 p2837 N88-26833
Why is it difficult to program in von Neumann languages
[AD-A192830] 20 p2838 N88-26839
Directions for programming in FORTRAN 77
[NASA-TT-20317] 20 p2839 N88-26842
Diagnosing faults in autonomous robot plan execution
[NASA-CR-182480] 20 p2841 N88-26859
Definition of an auxiliary processor dedicated to real-time operating system kernels
[NASA-CR-183070] 20 p2841 N88-26860
PAX ECONOPACK economic analysis package users manual
[AD-A192949] 20 p2883 N88-27117
Linear programming for Air Force decision aiding
21 p2928 N88-27378
A programmable systolic array for factorial analysis. Part 2: The symmetric eigenvalue problem
[AD-A192396] 21 p2995 N88-27762
Inspection methods in programming: Cliches and plans
[AD-A192782] 21 p2996 N88-27767
Synchronizable series expressions. Part 2: Overview of the theory and implementation
[AD-A192783] 21 p2996 N88-27768
The programmer's apprentice project: A research overview
[AD-A192784] 21 p2996 N88-27769
Contribution to almost realistic picture processing by a computer graphics procedure
[ETN-88-92372] 21 p2999 N88-27789
FORTRAN 77 implementation of abstract datatype models
[DFVLR-MITT-88-08] 21 p3000 N88-27794
Improving the performance of AI algorithms
[AD-A192848] 21 p3003 N88-27809
Literal dynamic modeling
[REPT-881-440-114] 22 p3048 N88-28083
Loading and linking in a modular language, an exercise in verification by unification
[INF-87-30] 22 p3136 N88-28642
Optimization techniques for relational database systems 22 p3137 N88-28650
Loglisp programming system users manual
[AD-A193933] 22 p3142 N88-28682
Uncertainty analysis in automatic robot programming
[RR-695-I-IMAG-58-LIFIA] 22 p3142 N88-28685
ADP (Automated Data Processing) requirements definition and documentation through user-developed prototypes
[AD-A194407] 23 p3248 N88-29332
Level 1 Ada/SQL (Structured Query Language) database language interface user's guide
[AD-A194480] 23 p3249 N88-29335
Analyst-centered models for systems design, analysis, and development 23 p3253 N88-29364
Archetyping: A software generation and management methodology 23 p3256 N88-29382
Programming model for distributed intelligent systems
23 p3257 N88-29390
Knowledge based programming environments: A perspective 23 p3258 N88-29393
A standard library for modeling satellite orbits on a microcomputer
[AD-A195759] 24 p3331 N88-29830
Syntactic closures
[AD-A195921] 24 p3412 N88-30311

COMPUTER PROGRAMS

NT APPLICATIONS PROGRAMS (COMPUTERS)
NT COMPILERS
NT COMPUTER SYSTEMS PROGRAMS
NT EDITING ROUTINES (COMPUTERS)
NT INPUT/OUTPUT ROUTINES
NT MERGING ROUTINES
NT NASTRAN
NT OBJECT PROGRAMS
NT OPERATING SYSTEMS (COMPUTERS)
NT SUBROUTINE LIBRARIES (COMPUTERS)
NT SUBROUTINES
Transonic analysis and design of axisymmetric bodies in nonuniform flow
[NASA-CR-4101] 01 p0003 N88-10013
Satellite orbits: Plot routines
[UIO-SR-87-02] 01 p0011 N88-10060
NASA-VOF3D: A three-dimensional computer program for incompressible flows with free surfaces
[DE87-011849] 01 p0045 N88-10288
A brief discussion of formally based approaches to rapid prototyping
[BAE-WAA-RP-RES-SWE-440]
01 p0079 N88-10508
A graphical tool for observing the behavior of parallel logic programs
[DE87-011467] 01 p0080 N88-10516
A look at the evolution of mathematical software for dense matrix problems over the past fifteen years
[DE87-011485] 01 p0081 N88-10517
Boundary integral technique for performing analysis of two-dimensional volumes of revolution
[DE87-013053] 01 p0082 N88-10524
Blade loss transient dynamics analysis, volume 1. Task 2: TETRA 2 theoretical development
[NASA-CR-179632] 02 p0125 N88-10791
Computer modeling of two-phase flow
[CFDU/87/5] 02 p0171 N88-11078
Computation of transonic separated wing flows using an Euler/Navier-Stokes zonal approach
[NASA-TM-88311] 02 p0173 N88-11089
Combustor-diffuser interaction program
02 p0185 N88-11152
Heat transfer in a real engine environment
02 p0186 N88-11155
Hanford Meteorological Station computer codes. Volume 2: The PROD computer code
[DE87-014807] 02 p0215 N88-11355
Software reliability models for fault-tolerant avionics computers and related topics
[NASA-CR-181440] 02 p0220 N88-11382
Tutorial and hands-on demonstration of a fluent interpreter for CARE 3
[NASA-TM-4011] 02 p0220 N88-11383
Implementation and evaluation of several continuously imbedded methods of Sarafyan
[DE88-000025] 02 p0221 N88-11393
IMPSOR: A fully vectorized FORTRAN code for three dimensional moving boundary problems with Dirichlet or Neumann boundary conditions
[DE87-014964] 02 p0226 N88-11427
BIMOND3: Monotone piecewise bicubic Hermite interpolation code
[DE87-014612] 02 p0229 N88-11442
Interactive Design of Accelerators (IDA)
[DE87-013298] 02 p0234 N88-11476
A relativistic Monte Carlo binary collision model for use in plasma particle simulation codes
[DE87-013287] 02 p0237 N88-11494
QUICKSILVER: A 3D, electromagnetic, PIC code
[DE87-013013] 02 p0245 N88-11547
Dynamic image interpretation for autonomous vehicle navigation
[AD-A184043] 03 p0262 N88-11647
Combined calculation of deformation and stress for the body and sabot of an APFSDS
03 p0302 N88-11899
Application of an upwind algorithm to the parabolized Navier-Stokes equations 03 p0316 N88-12000
NBS (National Bureau of Standards) wideband sampling wattmeter
[PB87-210324] 03 p0323 N88-12041
A microwave FEL (Free Electron Laser) code using waveguide modes
[DE88-000225] 03 p0330 N88-12084
Optical laser technology, specifically CD-ROM (Compact Disc - Read Only Memory) and its application to the storage and retrieval of information
[AD-A184111] 03 p0330 N88-12086
Reliability-based optimal structural and mechanical design 03 p0335 N88-12109
Balloon track data analysis
[AD-A184750] 03 p0350 N88-12213
Documentation of NCAR (National Center for Atmospheric Research) CCM1 program modules
[PB87-213567] 03 p0352 N88-12220
FORTRAN compiler performance benchmarks for the IBM personal computer
[LA-10883-MS] 03 p0363 N88-12284
A FORTRAN code for the calculation of probe volume geometry changes in a laser anemometry system caused by window refraction
[NASA-TM-100210] 03 p0364 N88-12288
Technology applications branch graphics projects
[AD-A184621] 03 p0364 N88-12291
Annotated computer output for illustrative examples of clustering using the mixture method and two comparable methods from SAS
[AD-A184687] 03 p0364 N88-12292
The circular serial autocorrelation computer program
[AD-A184795] 03 p0365 N88-12295
The network queueing system
[NASA-CR-177433] 03 p0365 N88-12297
UNIX benchmark system
[AD-A184492] 03 p0367 N88-12308
A prototype expert system for separation science
[DE87-013542] 03 p0371 N88-12333
NAVSIM 2: A computer program for simulating aided-inertial navigation for aircraft
[NASA-CR-177438] 04 p0398 N88-12478
Aircraft dynamic response calculation based on discrete-continual model 04 p0424 N88-12624
Automated microwave dielectric constant measurement
[AD-A184182] 04 p0431 N88-12667
A simplified procedure for correcting both errors and erasures of a Reed-Solomon code using the Euclidean algorithm 04 p0435 N88-12698
Departmental report on program EMTP-machine windings surge transients: Travelling wave method
[PB87-123733] 04 p0438 N88-12719
TOPAZ: The transient one-dimensional pipe flow analyzer: An update on code improvements and increased capabilities
[DE88-001781] 04 p0443 N88-12751
NCSU code: Validation and extension on NAL's UNIVAC 1100/60 system
[PD-FM-8716] 04 p0476 N88-12931
A data analysis environment for HP (Hewlett-Packard) 1000 computers
[DE87-010511] 04 p0477 N88-12936
Software reliability perspectives
[NASA-CR-181523] 04 p0479 N88-12952
INS3D: An incompressible Navier-Stokes code in generalized three-dimensional coordinates
[NASA-TM-100012] 04 p0485 N88-12991
The development of a computer code (U2DIIF) for the numerical solution of unsteady, inviscid and incompressible flow over an airfoil
[AD-A185033] 05 p0541 N88-13293
Development of an interface for an ultrareliable fault-tolerant control system and an electronic servo-control unit
[NASA-TM-88236] 05 p0553 N88-13367
A computer code to process and plot laser altimetry data interactively on a microcomputer
[NASA-TM-100687] 05 p0554 N88-13371
A computer code to calculate line by line atmospheric transmission spectra on a microcomputer
[NASA-TM-100686] 05 p0554 N88-13372
Stress intensity factors for cracking metal structures under rapid thermal loading, phase 1
[AD-A184112] 05 p0591 N88-13606
BASIC desk-top computer program for the three-dimensional static configuration of an extensible flexible cable in a uniform stream
[AD-A184852] 05 p0609 N88-13737
RADSPHERE: A computer program for calculating the steady-state, axially symmetric, forced response and radiation field of a submerged spherical shell
[AD-A185025] 05 p0609 N88-13738
Development of a data analysis system for the detection of lower level atmospheric turbulence with an acoustic sounder
[AD-A184972] 05 p0624 N88-13821
Media calibrations of the Doppler signal for a gravitational wave experiment — interplanetary medium
[IFSI-86-13] 05 p0625 N88-13825
ZEUS: A knowledge-based expert system that assists in predicting visibility at airbases
[AD-A184197] 05 p0626 N88-13829

Hanford Meteorological Station computer codes. Volume 5: The TOWER computer code
[DE88-001610] 05 p0628 N88-13843
Usage analysis of user files in UNIX
[NASA-CR-181561] 05 p0633 N88-13868
Performability modeling based on real data: A casestudy
[NASA-CR-181563] 05 p0633 N88-13870
A prototype ray tracer
[AD-A184863] 05 p0634 N88-13874
Implementation of an FIR band pass filter using a bit-slice processor
[AD-A184895] 05 p0634 N88-13875
Software design for an airborne gravity measurement system
[AD-A185000] 05 p0634 N88-13878
Illustrative examples of principal component analysis using BMDP/4M
[AD-A185179] 05 p0635 N88-13881
Sandia software guidelines: Software quality planning
[DE88-001931] 05 p0636 N88-13894
Illustrative examples of principal component analysis using GENSTAT/PCP
[AD-A185085] 05 p0644 N88-13941
Modeling and generating input processes
[DE87-013162] 05 p0645 N88-13948
Technology upgrade of a silicon compiler
[AD-A184873] 05 p0655 N88-14016
Approaches and possible improvements in the area of multibody dynamics modeling
[NASA-CR-179227] 06 p0663 N88-14067
Program description of FIBRAM: A radiation attenuation model for optical fibers
[PB87-230686] 06 p0690 N88-14229
An investigation of fatigue crack growth in a ductile material at high growth rates 06 p0715 N88-14383
Fast, colour displays of digital terrain elevation data
[AD-A185596] 06 p0729 N88-14485
Integrated systems with applications to the multi-phases of the ephemerides, physics and methematics of the upper atmosphere
[AD-A185748] 06 p0743 N88-14570
Atmospheric electricity
[NASA-CR-179239] 06 p0744 N88-14575
How to estimate the total number of errors in a software system
[PB87-132130] 06 p0756 N88-14647
Stress effects and the optimum format of a scrolling seven-line VDT text window
[AD-A185559] 06 p0758 N88-14651
Interaction of different modules in depth perception: Stereo and shading
[AD-A185607] 06 p0759 N88-14655
Estimating the distribution of fault latency in a digital processor
[NASA-TM-100521] 06 p0760 N88-14666
Genie inference engine rule writer's guide
[AD-A185709] 06 p0762 N88-14675
Solution of non-symmetric linear systems by biconjugate gradients or conjugate gradients squared
[PB87-226387] 06 p0763 N88-14679
Plasma parameters for alternate operating modes of TIBER-2
[DE88-001890] 06 p0783 N88-14802
Geographic application of the relational data base system Cantor
[PB87-120945] 06 p0791 N88-14851
Shuttle computational grid generation
06 p0794 N88-14863
Development of a graphical display on the DMS test bed 06 p0794 N88-14864
Modern wing flutter analysis by computational fluid dynamics methods
[NASA-TM-100531] 07 p0816 N88-14965
Microwave Landing System (MLS) mathematical model installation manual
[AD-A185612] 07 p0819 N88-14978
An autopilot design for the United States Marine Corps' airborne remotely operated device
[AD-A186379] 07 p0820 N88-14983
A space transportation system operations model
[NASA-TM-100481] 07 p0823 N88-14999
Some performance comparisons for a fluid dynamics code
[PB88-113709] 07 p0852 N88-15175
Internal fluid mechanics research on supercomputers for aerospace propulsion systems
[NASA-TM-100289] 07 p0854 N88-15188
The KIVA-2 computer program for transient multidimensional chemically reactive flows with sprays
[DE88-000502] 07 p0854 N88-15191
An interactive visual interface for Fastbus diagnostics
[DE88-002569] 07 p0900 N88-15453
Formalizing reusable software components in the programmer's apprentice
[AD-A185843] 07 p0901 N88-15457
Program translation via abstraction and reimplementation
[AD-A185845] 07 p0901 N88-15458
A plan for collecting ada software development cost, schedule and environment data
[AD-A185905] 07 p0902 N88-15460
Investigation and implementation of an algorithm for computing optimal search paths
[AD-A185927] 07 p0902 N88-15461
A software planning and development methodology with resource allocation capability
[AD-A186088] 07 p0902 N88-15462
Parallel logic programming and ZMOB and parallel systems software and hardware
[AD-A186300] 07 p0903 N88-15470
Automated program recognition
[AD-A186421] 07 p0903 N88-15472
Creating title blocks for vehicle animations
[AD-A185620] 07 p0904 N88-15473
Modelling of clustering effects in point processes: An application to failures in SPC-systems (stored program control-systems)
[PB87-149241] 07 p0904 N88-15480
Algorithm and program for recognition of compactly positioned vertices of events for the HPD minimum guidance system
[DE88-700542] 07 p0905 N88-15482
A multiple node software development environment
[DE87-010995] 07 p0905 N88-15484
Sublinear upper bounds for stochastic programs with recourse, revision
[AD-A186436] 07 p0916 N88-15564
Feasibility of software built-in test for SDI (Strategic Defense Initiative) applications
[AD-A185750] 07 p0917 N88-15572
TeXting the FORMULARY: A collection of examples of the use of TeX to produce ruled tables and displayed equations
[AD-A185920] 07 p0921 N88-15598
Investigation of candidate data structures and search algorithms to support a knowledge based fault diagnosis system 07 p0923 N88-15606
Verification of FANTASTIC integrated code
07 p0924 N88-15613
The feasibility of using TAE as the UIL for the space station and for other internal NASA tasks and projects
07 p0925 N88-15618
The determination of equivalent bearing loading for the BSMT that simulate SSME high pressure oxidizer turbopump conditions using the SHABERTH/SINDA computer programs 07 p0925 N88-15623
Analysis of relativistic nucleus-nucleus interactions in emulsion chambers 07 p0926 N88-15624
Thermodynamic values from computer summation of group additivity data
[AD-A186131] 07 p0940 N88-15711
Self-adaptive data bases
[AD-A186414] 07 p0942 N88-15729
Rotorcraft transmission 08 p0956 N88-15802
Attitude determination of artificial satellites through joint application of static and dynamic optimal estimation techniques
[INPE-4415-TDL/306] 08 p0963 N88-15832
Scanning finite element calculation method
[PB87-143442] 08 p0995 N88-16017
Investigation of vibration problems with heterodyne holographic interferometer 08 p1000 N88-16058
Vertical atmospheric sounding
[INPE-4370-PRE/1195] 08 p1036 N88-16283
Preliminary evaluation of a micro-based repeated measures testing system
[NASA-CR-172038] 08 p1048 N88-16331
Deriving descriptions of the mind
[AD-A186647] 08 p1052 N88-16349
Third Conference on Artificial Intelligence for Space Applications, part 1
[NASA-CP-2492-Pt-1] 08 p1055 N88-16360
Verification issues for rule-based expert systems
08 p1055 N88-16361
Temporal and contextual knowledge in model-based expert systems 08 p1055 N88-16363
KBS V and V as related to automation of space station subsystems: Rationale for a KBS lifecycle
08 p1057 N88-16375
Automatic mathematical modeling for space application 08 p1060 N88-16402
Similarity networks as a knowledge representation for space applications 08 p1062 N88-16411
Qualitative models for planning: A gentle introduction
08 p1062 N88-16414
Intelligent man/machine interfaces on the space station 08 p1063 N88-16418
A data structure and algorithm for fault diagnosis
08 p1065 N88-16432
A learning apprentice for software parts composition
08 p1065 N88-16436
Automatic program generation from specifications using Prolog 08 p1065 N88-16437
Application of artificial intelligence to impulsive orbital transfers 08 p1066 N88-16439
TES: A modular systems approach to expert system development for real time space applications
08 p1066 N88-16441
Digital image processing: A summary of main techniques
[INPE-4404-PRE/1220] 08 p1068 N88-16454
Replication and reconfiguration in a distributed mail repository
[AD-A186967] 09 p1151 N88-16897
Symbolic, algebraic, and numeric solutions to heat conduction problems using Green's functions
09 p1165 N88-16987
Sea surface current estimates off central California as derived from enhanced AVHRR (Advanced Very High Resolution Radiometer) infrared images
[AD-A186867] 09 p1194 N88-17155
Simplifying the construction of domain-specific automatic programming systems: The NASA automated software development workstation project
09 p1204 N88-17212
The knowledge-based software assistant
09 p1204 N88-17213
User interface devices for mission control
09 p1205 N88-17224
The IDEAL (Integrated Design and Engineering Analysis Languages) modeling methodology: Capabilities and Applications 09 p1206 N88-17227
Expert system verification concerns in an operations environment 09 p1207 N88-17234
Robotic air vehicle. Blending artificial intelligence with conventional software 09 p1210 N88-17252
The KATE shell: An implementation of model-based control, monitor and diagnosis 09 p1210 N88-17255
An automatic finite element mesh generator
[AD-A186939] 09 p1216 N88-17291
Recovery using virtual memory
[AD-A187098] 09 p1217 N88-17296
FORTRAN 77 guidelines for the software projects RASP and ANDECS
[DFVLR-MITT-87-09] 09 p1218 N88-17301
Methods for evaluating the quality and reliability of aerodynamic software programs
[PB87-169793] 09 p1219 N88-17314
Software program validity: A survey
[PB87-170593] 09 p1219 N88-17315
A methodology for the synthesis of robust feedback systems
[NASA-CR-182455] 09 p1225 N88-17342
Examples of nonconservatism in the CARE 3 program
[NASA-TM-100524] 09 p1233 N88-17390
Overview of heat transfer and fluid flow problem areas encountered in Stirling engine modeling
[NASA-TM-100131] 09 p1262 N88-17561
Investigation of dynamic stall using LDV (Laser Doppler Velocimetry): Mean flow studies
[AD-A187629] 10 p1272 N88-17611
A transonic-small-disturbance wing design methodology
[NASA-TP-2806] 10 p1273 N88-17614
Transport delay compensation for computer-generated imagery systems
[NASA-TM-100084] 10 p1277 N88-17645
Shuttle rocket booster computational fluid dynamics
[NASA-CR-182518] 10 p1293 N88-17733
Satellite interference analysis and simulation using personal computers
[NASA-CR-182522] 10 p1319 N88-17890
A ring model of the lasertron
[DE88-004656] 10 p1323 N88-17908
Signal processing studies program VLSI designs for unary functions
[AD-A188053] 10 p1325 N88-17922
NF85: A three-dimensional, air-dynamics computer code for analyzing explosions in structures
[DE88-005085] 10 p1331 N88-17953
AEV local verification for aviation, precipitation and temperature programs: AV, REL, TEM (September 1987 revision)
[PB88-115662] 10 p1355 N88-18101
Proceedings of the Workshop on Future Directions in Computer Architecture and Software
[AD-A184949] 10 p1373 N88-18191
Why reusable software isn't 10 p1376 N88-18212
Future directions in computer architecture and software: The year 2000 10 p1377 N88-18218
Systolic array adaptive beamforming
[AD-A187496] 10 p1385 N88-18269
Annotated computer output for split plot design: GENSTAT ANOVA
[AD-A187120] 10 p1385 N88-18271

CUEMAP: A tool for generating hierarchical charts and dataflow diagrams
[DE88-004778] 10 p1387 N88-18284
Semantics of EqL
[AD-A188151] 10 p1389 N88-18297
The Lambda network: A new permutation network
[DE88-003568] 10 p1392 N88-18305
Development of tokamak reactor system analysis code NEW-TORSAC
[DE88-751067] 10 p1411 N88-18417
A performance index approach to aerodynamic design with the use of analysis codes only
[NASA-TP-2805] 11 p1433 N88-18552
Computer program for conceptual tandem rotor helicopter design
[AD-A187832] 11 p1439 N88-18584
Procedures for quantitative sensitivity and performance validation studies of a deterministic fire safety model
[NBS/GCR-88/544] 11 p1469 N88-18762
An evaluation of the impact of variable temporal and spatial data resolution upon IREPS (Integrated Refractive Effects Prediction System)
[AD-A187764] 11 p1470 N88-18769
GERA computer code for calculation of two-dimensional electromagnetic fields in resonators and electron-optical systems by the finite element method
[DE88-700678] 11 p1480 N88-18831
Digital control of the Czochralski growth of Gallium arsenide-controller software reference manual
[AD-A187210] 11 p1528 N88-19127
Report on desktop publishing
[AD-A187698] 11 p1528 N88-19128
Dynamic analysis of plane frames by microcomputer
11 p1531 N88-19143
A theory of program correctness, and algorithms for proofs
[ANL-87-4] 11 p1531 N88-19146
A maximum likelihood parameter estimation program for general non-linear systems
[ARL-AERO-TM-392] 11 p1532 N88-19154
Accurate efficient evaluation of Bessel transform: Programs and error analysis
[AD-A187718] 11 p1536 N88-19174
ICF special studies
[DE88-004057] 11 p1551 N88-19281
Structural design requirements for aircraft incorporating active control technology 12 p1580 N88-19453
Computer aided deflection measurement of an aircraft wing
[AD-A187778] 12 p1581 N88-19461
Relative motion of two satellites in close-elliptical orbits
[AD-A188851] 12 p1594 N88-19543
Calculation of eclipses for elliptical orbits
[INPE-4412-NTE/277] 12 p1594 N88-19545
HELIOS modelling of point-focusing solar concentrators
[DE88-004933] 12 p1640 N88-19820
Enhancements to the atmospheric transmittance/radiance program FASCODE
[AD-A188863] 12 p1643 N88-19839
Aircrew training devices: Utility and utilization of advanced instructional features, phase 4
[AD-A188418] 12 p1670 N88-20000
A computer code for the solution of large scale network reliability analysis problems
[AD-A188455] 12 p1680 N88-20042
A laboratory facility for research in parallel computation
[AD-A188499] 12 p1680 N88-20044
HP-41CX programs for HgCdTe detectors and IR systems
[AD-A188935] 12 p1692 N88-20120
Fully-coupled analysis of jet mixing problems. Three-dimensional PNS model, SCIP3D
[NASA-CR-4139] 13 p1715 N88-20256
Australian aerodynamic design codes for aerial tow bodies
[AD-A189048] 13 p1715 N88-20258
CODAC (Cockpit Oriented Display of Aircraft Configurations) version 1.4 user's guide
[NASA-CR-181650] 13 p1718 N88-20273
Documentation and installation of the hypersonic arbitrary-body computer program (Mark 3 version) of A.E. Gentry on the IBM computer system
[MBB/LKE-127/S/PUB/256] 13 p1719 N88-20276
Architecture specification for PAVE PILLAR avionics
[AD-A188722] 13 p1723 N88-20303
Trajectory code studies, 1987
[DE88-006218] 13 p1728 N88-20335
MOPAC manual: A general molecular orbital package, fourth edition
[AD-A188623] 13 p1733 N88-20362
A simplified computer code for reduction to burning rates of closed bomb pressure-time data (MINICB)
[AD-A189112] 13 p1736 N88-20380
Interactive automated system for testing analog units of digital seismic stations 13 p1789 N88-20702
MacCAD (Macintosh Computer Aided Design), computer aided design tool for system analysis
[AD-A189241] 13 p1815 N88-20843
Preconditioned conjugate gradient algorithms and software for solving large sparse linear systems
[DE88-002180] 13 p1816 N88-20849
A report on the study of algorithms to enhance vector computer performance for the discretized one-dimensional time-dependent heat conduction equation: EPIC research, phase 1
[DE88-005642] 13 p1820 N88-20880
Distributed transaction processing and the Camelot system
[AD-A188614] 13 p1821 N88-20885
Local refinement of stress field by finite element method
[INPE-4321-TDL/288] 13 p1828 N88-20930
A novel method for sputter-deposition of high T(sub c) superconductor films via a computer-controlled mass analyzed ion beam
[DE88-006001] 13 p1848 N88-21064
NNEPEQ: Chemical equilibrium version of the Navy/NASA Engine Program
[NASA-TM-100851] 14 p1868 N88-21161
The quasi-static contact problem with friction for three dimensional elastic bodies
[REPT-87-51] 14 p1918 N88-21447
CARE 3 User's Workshop
[NASA-CP-10011] 14 p1954 N88-21646
Applicability of nonlinear programming in decision support systems: Realization of user-friendly software
[REPT-87-42] 14 p1957 N88-21663
Monte Carlo modified method for Green function. Algorithm and computer code for calculations in equal mass many-body system
[DE88-701114] 14 p1957 N88-21667
Examination of the effects of using Ada (trade name) in flight control software
[AD-A189679] 14 p1959 N88-21683
User's manual for LINEAR, a FORTRAN program to derive linear aircraft models
[NASA-TP-2768] 14 p1967 N88-21740
Basic research on flame radiation
[PB88-168372] 15 p2032 N88-22105
Computer program in BASIC language for computation of spectrochemical analytical data
[DE88-701229] 15 p2032 N88-22106
Status of electric vehicle simulation programs at the INEL: Summer 1987
[DE88-006745] 15 p2058 N88-22271
An improved method for calculating power density in the Fresnel region of circular parabolic reflector antennas
[AD-A190569] 15 p2060 N88-22284
Traction model development
[AD-A188450] 15 p2073 N88-22359
Development of a computer code CRACK for elastic and elastoplastic fracture mechanics analysis of 2-D structures by finite element technique
[DE88-701231] 15 p2075 N88-22370
The composite blade structural analyzer (COBSTRAN)
15 p2078 N88-22390
Three-dimensional inelastic approximate analysis code (MOMM) 15 p2079 N88-22392
Specialty three-dimensional finite element analysis codes 15 p2079 N88-22393
MHOST: An efficient finite element program for inelastic analysis of solids and structures
15 p2079 N88-22394
METCAN: The metal matrix composite analyzer
15 p2079 N88-22395
Computational simulation methods for composite fracture mechanics 15 p2079 N88-22396
Probabilistic structural analysis computer code (NESSUS) 15 p2079 N88-22397
Structural tailoring of high-speed turbine blades (SSME/STAEBL) 15 p2080 N88-22398
Computational structural mechanics for engine structures 15 p2080 N88-22399
Structural tailoring of advanced turboprops
15 p2080 N88-22400
Geometric restoration of satellite image data
[AD-A190462] 15 p2089 N88-22450
Satellite UV image processing
[AD-A190466] 15 p2089 N88-22451
Updating of the municipal official register of real estate through a geographical information system
[INPE-4459-PRE/1238] 15 p2090 N88-22453
A survey of denser-than-air atmospheric dispersion models
[DE88-006626] 15 p2092 N88-22467
A hardware/software system for implementing geophysical diffraction tomography
[DE88-006411] 15 p2094 N88-22480
Motion sickness: Quantitative, algorithmic malaise indication in real time
[AD-A189674] 15 p2101 N88-22518
Analysis of head response to torso acceleration. Volume 2: Description of data retrieval, analysis and display software
[PB88-156765] 15 p2104 N88-22536
Project Monitoring Package (PMP): A package for project activity monitoring
[DE88-701234] 15 p2107 N88-22554
COMESH: A corner mesh finite difference code to solve multigroup diffusion equations in multidimensions
[DE88-701248] 15 p2108 N88-22555
PLOT3D (version-5): A computer code for drawing three dimensional graphs, maps and histograms, in single or multiple colours, for mono or stereoscopic viewing
[DE88-701410] 15 p2108 N88-22558
Computer grading of extensometers (BS 3846)
[NPL-DMA(A)-152] 15 p2108 N88-22560
Methodology for software reliability prediction, volume 1
[AD-A190018] 15 p2110 N88-22571
Methodology for software reliability prediction, volume 3
[AD-A190019] 15 p2110 N88-22572
Transformations of concurrent algorithms for highly parallel systems: A one year project summary report
[AD-A190236] 15 p2111 N88-22576
CK-LOG system conversion (user's manual and user interface)
[AD-A190273] 15 p2111 N88-22577
Software verification using partition analysis
[AD-A190570] 15 p2112 N88-22582
Memory-based expert systems
[AD-A190203] 15 p2116 N88-22606
ONTIC: A knowledge representation system for mathematics
[AD-A190553] 15 p2121 N88-22643
An approximation technique for solving a system of Fredholm integral equations for asymmetric detector response functions
[AD-A190577] 15 p2121 N88-22645
Analysis and testing of the SURE program
[NASA-TP-2817] 15 p2123 N88-22653
A chemical method for achieving acceleration of macroparticles to ultrahigh velocities
[DE88-006377] 15 p2128 N88-22695
Sources of digital spatial data for geographic information systems
[AD-A189788] 15 p2148 N88-22824
KOMPOT Program complex for the calculation of spatial magnetostatic fields of electromagnetic systems
[DE88-701691] 16 p2192 N88-23072
Computerized life and reliability modelling for turboprop transmissions
[NASA-TM-100918] 16 p2215 N88-23220
Multiprocessor graphics computation and display using transputers 16 p2218 N88-23236
Vibration and flutter analysis of the SR-7L large-scale propfan 16 p2221 N88-23254
Supersonic axial-flow fan flutter
16 p2221 N88-23255
Integrated multidisciplinary analysis tool IMAT users' guide
[NASA-TM-100605] 16 p2223 N88-23273
Extending problem solver capabilities through case-based inference
[AD-A191332] 16 p2243 N88-23401
Alpha structure based B-HIVE multicomputer
[AD-A188708] 16 p2244 N88-23405
The good, the bad and the ugly: Comparing high-speed computer systems
[DE88-007498] 16 p2245 N88-23412
Digital filter unit for selection of spectrometric information
[DE87-702990] 16 p2246 N88-23415
Portability of software. The use of software in the hardware mixture
[MBB/LWD-11/S/PUB/253] 16 p2246 N88-23416
Investigation into the use of texturing for real-time computer animation
[AD-A191008] 16 p2251 N88-23454
The PAWS and STEM reliability analysis programs
[NASA-TM-100572] 16 p2262 N88-23526
Computer program for parameterization of nucleus-nucleus electromagnetic dissociation cross sections
[NASA-TM-4038] 16 p2270 N88-23584
BRYNTRN: A baryon transport computer code, computation procedures and data base
[NASA-TM-4037] 16 p2290 N88-23714
PAN AIR analysis of the NASA/MCAIR 279-3: An advanced supersonic V/STOL fighter/attack aircraft
[NASA-TM-86838] 17 p2298 N88-23750

Modeling of functional specifications for onboard software: Experience with the Rafale avionics system
17 p2303 N88-23777
The avionics software architecture impact on system architecture 17 p2303 N88-23778
Workshops for the design of avionics systems and the development of onboard software
17 p2307 N88-23802
EnviroNET: An interactive space-environment information resource
[NASA-TM-101137] 17 p2309 N88-23812
Preventing aircraft corrosion by predictive corrosion modeling 17 p2321 N88-23863
Preliminary 2-D shell analysis of the space shuttle solid rocket boosters
[NASA-TM-100515] 17 p2348 N88-23989
The multi-disciplinary design study: A life cycle cost algorithm
[NASA-CR-4156] 17 p2385 N88-24172
A timing evaluator for C programs generated by the model system
[AD-A191204] 17 p2385 N88-24174
MIPS: The good, the bad and the useful
[NASA-CR-182893] 17 p2386 N88-24184
A robotic language for cooperative multi-robots
17 p2387 N88-24186
Third Conference on Artificial Intelligence for Space Applications, part 2
[NASA-CP-2492-PT-2] 17 p2387 N88-24188
Automatic program generation from specifications using PROLOG 17 p2388 N88-24196
TES: A modular systems approach to expert system development for real-time space applications
17 p2388 N88-24197
Mentat: An object-oriented macro data flow system
[NASA-TM-101165] 17 p2388 N88-24199
Description of graphics translation software between Intergraph and Tektronix systems
[NASA-TM-100335] 17 p2389 N88-24202
Cermet fuel thermal conductivity
17 p2410 N88-24329
ATHENA simulation of the 300 kW SP-100
17 p2414 N88-24357
Expert systems approach to modeling systems with the ATHENA thermal-hydraulics code
17 p2416 N88-24365
SP-100 system modeling: SNPSAM update
17 p2417 N88-24372
The Lewis heat pipe code with application to SP-100 GES heat pipes 17 p2421 N88-24395
HTPIPE: A steady state heat pipe analysis program
17 p2421 N88-24396
The THROHPUT code: Thermohydraulic heat pipe modeling 17 p2421 N88-24399
MACRAD: A mass analysis code for radiators
17 p2424 N88-24418
Energy storage evaluation for burst power applications
17 p2426 N88-24430
Space Power Reference Source (SPRS): A user's guide to SDI Space Power Technology Programs
17 p2427 N88-24440
Transient analyses of multimegawatt space reactors
17 p2430 N88-24456
A system status monitor for the National Aerospace Plane
[AD-A190681] 18 p2463 N88-24624
An OOD (Object-Oriented Design) paradigm for flight simulators
[AD-A191097] 18 p2467 N88-24647
Automated test device for FASR (Fixed Array Surveillance Radar) beam steering componentry
[AD-A191650] 18 p2500 N88-24829
Practical VLF/LF radio test system
[AD-A191768] 18 p2500 N88-24831
Transient particle deposition in a boundary layer of impulsive flow over a flat plate
[AD-A191537] 18 p2508 N88-24880
SOLA-DM: A numerical solution algorithm for transient three-dimensional flows
[DE88-007159] 18 p2514 N88-24913
The development of KENO and the calculation of differential parameters with KENO
[DE88-006176] 18 p2555 N88-25166
Annotated computer output for split plot design: SAS GLM
[AD-A190800] 18 p2555 N88-25167
A general approach for automating source code verification
[AD-A191461] 18 p2556 N88-25170
Research in enumeration and graph theory with applications to computer science
[AD-A191567] 18 p2556 N88-25171
IGUANA: Interactive graphics utility for automated NEC analysis
[AD-A191760] 18 p2556 N88-25174
CIMAG2: The computer program to generate color images
[AD-A191847] 18 p2557 N88-25175
An electrostatic potential comparator
[AD-A192051] 18 p2557 N88-25177
Design of catalytic monoliths for closed-cycle carbon dioxide lasers
[NASA-CR-182983] 18 p2558 N88-25185
KA-PROLOG. KAP-computer: Computer model and instructions set
[ETN-88-91948] 18 p2558 N88-25186
The ISI (Information Sciences Institute) grapher manual
[AD-A192198] 18 p2561 N88-25200
State of tuning
[NASA-TT-20195] 18 p2561 N88-25205
PAFEC level 6.2 application program
[AD-A191037] 18 p2562 N88-25209
NFEARS: A nonlinear adaptive finite element solver, part 1
[AD-A191823] 18 p2563 N88-25215
A perspective of PC-based probabilistic risk assessment
[DE88-006715] 18 p2568 N88-25251
QN3D: A 3-dimensional quasi-neutral hybrid particle-in-cell code with applications to the tilt mode instability in field reversed configurations
18 p2580 N88-25325
Department of Defense statement on the X-ray Lithography Program to the Research and Development Subcommittee of the House Armed Services Committee of 100th Congress, second session
[AD-A191854] 18 p2582 N88-25341
Defense Technical Information Center cataloging guidelines
[AD-A192200] 18 p2589 N88-25382
Submunitions simulations, volume 2
[TR-CR-RD-SS-87-7-VOL-2] 19 p2641 N88-25669
Codes for QPSK modulation with invariance under 90 degrees rotation 19 p2648 N88-25720
Navier-Stokes code NS3D for blunt bodies. Part 1: Analysis, results and verification
[DE88-010105] 19 p2666 N88-25855
Hydrogen turbines for space power systems: A simplified axial flow gas turbine model
[DE88-009585] 19 p2677 N88-25920
The development of an intelligent interface to a computational fluid dynamics flow-solver code
[NASA-TM-100908] 19 p2716 N88-26127
The MAFIA approach to solving Maxwell's equations in three dimensions
[DE88-007826] 19 p2720 N88-26155
Digital control of the czochralski growth of gallium arsenide. System reference manual. Valid for Czochralski growth controller software version 2.4
[AD-A191997] 19 p2732 N88-26227
Real time data base management
[AD-A191758] 19 p2739 N88-26265
High speed inlet calculations with real gas effects
[NASA-CR-182167] 20 p2752 N88-26336
An interactive computer code for preliminary design of solid propellant rocket motors
[AD-A192869] 20 p2766 N88-26399
Experimental and theoretical analysis of the radiative transfer within a sooty pool fire
[DE88-007099] 20 p2769 N88-26419
A numerical study of Rayleigh-Taylor instability in aluminum and steel plates
[DE88-010475] 20 p2774 N88-26449
Vertical ship motions and sea loads considering nonlinear effects
[TAE-592] 20 p2784 N88-26515
Parameter identification of the passenger simulation model MADYMO: Methods and experience
20 p2788 N88-26536
MAXWELL3: A 3D finite element electromagnetic modeling code
[DE88-010602] 20 p2790 N88-26551
The Oak Ridge Heat Pump Design Model: Mark 3 version program documentationon
[DE88-007863] 20 p2799 N88-26607
A study of flow separation in transonic flow using inviscid and viscous computational fluid dynamics (CFD) schemes
[NASA-CR-183119] 20 p2801 N88-26618
Improved 3-D turbomachinery CFD algorithm
[NASA-CR-179364] 20 p2801 N88-26619
A general-purpose approach to computer-aided dynamic analysis of a flexible helicopter
[NASA-TM-101002] 20 p2816 N88-26709
A control program for global radiation measurements
[KNMI-TR-100] 20 p2824 N88-26757
Computer controlled data acquisition system for the NASA 1986 Rocket Triggered Lightning Program
[DE88-008335] 20 p2826 N88-26766
Managing microcomputer applications: A primer and guide to good practice
[AD-A192992] 20 p2835 N88-26817
Common Data Format (CDF) to store images
[NASA-CR-179366] 20 p2836 N88-26825
XDATAP
[DE88-007161] 20 p2837 N88-26827
Interactive computer programme for the analysis of a two-way Wilkinson divider/combiner
[PB88-105424] 20 p2837 N88-26831
SIMS: Single Interface to Multiple Systems
[AD-A192264] 20 p2837 N88-26832
Nebula support software
[AD-A192281] 20 p2837 N88-26833
Computer programs for high-current beam transport in accelerators
[AD-A192356] 20 p2838 N88-26835
Computer-aided writing
[AD-A192516] 20 p2838 N88-26837
Colored stochastic Petri nets. Application to real time distributed systems
[ENST-87E017] 20 p2839 N88-26843
An expeditious technique for keyboard input of information to FORTRAN computer programs
[DE88-009617] 20 p2840 N88-26855
An evaluation methodology for dependable multiprocessors
[AD-A192799] 20 p2842 N88-26863
The construction of composite grids for general three-dimensional regions 20 p2843 N88-26872
Qualitative reasoning for physicists
[PB88-116298] 20 p2848 N88-26906
Recent applications of Monte Carlo methods for semiconductor microdevice simulation
20 p2871 N88-27046
Knowledge-based cost estimating vs traditional software cost models
[DE88-009707] 20 p2883 N88-27116
A comparison of the various helicopter mathematical models used in the methodology assessment
21 p2889 N88-27149
Aeromechanical stability analysis of COPTER
21 p2891 N88-27161
FORTRAN programs for computation of time dependent sea levels and trajectory errors from satellite altimeter data
[BONN-MITT-73] 21 p2901 N88-27216
Evaluation and improvement of liquid propellant rocket chugging analysis techniques. Part 1: A one-dimensional analysis of low frequency combustion instability in the fuel preburner of the space shuttle main engine
[NASA-CR-183106] 21 p2903 N88-27224
Evaluation and improvement of liquid propellant rocket chugging analysis techniques. Part 2: A study of low frequency combustion instability in rocket engine preburners using a heterogeneous stirred tank reactor model
[NASA-CR-182724] 21 p2903 N88-27225
Programs for preliminary design of composite materials which were developed by the design group of Aerospatiale Aquitaine
[REPT-881-430-112] 21 p2907 N88-27251
Hole diameters in plates impacted by projectiles
21 p2929 N88-27386
Control of free-flying space robot manipulator systems
[NASA-CR-183017] 21 p2956 N88-27562
Development of a biaxial test system for thin-walled metal tubes using tensile-compressive axial load and internal-external pressure
[DE88-011279] 21 p2962 N88-27592
IEMIS (Integrated Emergency Management Information System) floodplain mapping based on a LIDAR derived data set
[AD-A193071] 21 p2966 N88-27616
Validate algorithms for the determination of rainfall rates from SSM/I microwave satellite imagery
[AD-A192299] 21 p2974 N88-27664
Vision research. A national plan: 1983-1987, 1987 evaluation and update
[PB88-192604] 21 p2985 N88-27726
A cockpit natural language study: Vocabulary and grammar analyses
[AD-A193289] 21 p2993 N88-27753
Full analysis of a powerful window random access algorithm
[AD-A192437] 21 p2995 N88-27763
Using IMSL mathematical and statistical computer subroutines in physiological and biomechanical research
[AD-A192594] 21 p2995 N88-27765
Development of automatic names placement software
[AD-A192786] 21 p2996 N88-27770
The effect of input device on user performance with a menu-based natural language interface
[AD-A193095] 21 p2996 N88-27772

Computer aided design for linear control State Variable System (SVS)
[AD-A193262] 21 p2997 N88-27775
Synopsis of a computer program designed to interface a personal computer with the fast data acquisition system of a time-of-flight mass spectrometer
[NASA-CR-177474] 21 p3001 N88-27798
The SAS System by forms: Putting statistical power into the hands of an end-user
[DE88-010512] 21 p3010 N88-27857
Comparison of results based on a deterministic versus a statistical uncertainty analysis
[DE88-010751] 21 p3010 N88-27858
Development of direct-inverse 3-D methods for applied transonic aerodynamic wing design and analysis
[NASA-CR-183127] 22 p3037 N88-28033
VSAERO analysis of tip planforms for the free-tip rotor
[NASA-CR-177487] 22 p3038 N88-28036
An improved version of NCOREL: A computer program for 3-D nonlinear supersonic potential flow computations
[NASA-CR-4165] 22 p3038 N88-28039
Numerical computation of space shuttle orbiter flow field
[NASA-CR-183193] 22 p3040 N88-28048
Large-signal modeling of gallium arsenide field-effect transistors 22 p3073 N88-28242
Surface tension and viscosity with Lagrangian hydrodynamics on a triangular mesh
[AD-A194120] 22 p3075 N88-28258
What's on the menu? Friendlier computers
[AD-A194393] 22 p3135 N88-28637
Walter user's manual (Version 1.0)
[AD-A192542] 22 p3136 N88-28644
Software quality measurement demonstration project (1)
[AD-A193429] 22 p3136 N88-28646
VAXGAP: A code for the routine analysis of gamma-ray pulse-height spectra on a VAX computer
[DE88-011702] 22 p3137 N88-28648
Air Force Systems Command software independent verification and validation implementation analysis and guidance
[AD-A194309] 22 p3137 N88-28653
Computers in weapons systems: A look at the F-15
[AD-A194498] 23 p3178 N88-28920
Hot-wire measurements of compressor blade wakes in a cascade wind tunnel
[AD-A194737] 23 p3181 N88-28936
Evaluation of atmospheric effects for operational tactical decision aid
[AD-A194205] 23 p3232 N88-29236
Atmospheric angular momentum and length of day
[AD-A194505] 23 p3233 N88-29238
Electrochemical and optical studies of model photosynthetic systems
[DE88-009291] 23 p3237 N88-29264
Process migration in UNIX environments
[NASA-CR-182951] 23 p3245 N88-29311
Composite grid generation for aircraft configurations with the EAGLE code 23 p3246 N88-29321
Waveform analysis on the IBM PC
[AD-A194249] 23 p3248 N88-29330
OMV docking simulator 23 p3255 N88-29379
Archetyping: A software generation and management methodology 23 p3256 N88-29382
Generic supervisor: A knowledge-based tool for control of space station on-board systems
23 p3257 N88-29389
Software development without languages
23 p3257 N88-29392
Automated software development workstation
23 p3263 N88-29423
Programming language concepts for multiprocessors
[AD-A193465] 23 p3264 N88-29430
MACSYMA program for the painleve test of nonlinear ordinary and partial differential equations
[AD-A194293] 23 p3270 N88-29458
Space marching Euler solvers
24 p3318 N88-29759
Prediction of dynamic derivatives
24 p3318 N88-29761
Prediction of base-flows 24 p3319 N88-29765
Computer programs for generation of NASTRAN and VIBRA-6 aircraft models
[AD-A195467] 24 p3323 N88-29792
A new computational capability for ramjet projectiles
[AD-A196061] 24 p3327 N88-29812
N-version software demonstration for digital flight controls
[NASA-CR-181483] 24 p3328 N88-29815
Computer programs for calculation of sting pitch and roll angles required to obtain angles of attack and sideslip on wind tunnel models
[NASA-TM-100659] 24 p3329 N88-29820
Development of computer-controlled thermogravimetric instrumentation for measurement of environmental and high temperature volatilization and desorption of contaminants from polymeric materials
[AD-A195934] 24 p3343 N88-29900
Scattering impulse response synthesis using random noise illumination: Initial concept evaluation
[AD-A195086] 24 p3364 N88-30034
DATATRAN: Datum transformation software
[AD-A195723] 24 p3387 N88-30175
Computer-Aided Structural Engineering (CASE) project. Computer program for analysis of planar grid structures (CGRID), user's guide
[AD-A195977] 24 p3413 N88-30317
The eivaN: A forward-looking interactive orbital trajectory plotting tool for use with proximity operations (PROX OPS) and other maneuvers: Description and user's manual
[NASA-CR-177490] 24 p3414 N88-30327
Automatic qualitative analysis of ordinary differential equations using piecewise linear approximations
[AD-A196310] 24 p3424 N88-30379
Linguistic-technical aspects of machine translation
24 p3438 N88-30461

COMPUTER SECURITY
U COMPUTER INFORMATION SECURITY
COMPUTER SIMULATION
U COMPUTERIZED SIMULATION
COMPUTER STORAGE DEVICES
NT BUBBLE MEMORY DEVICES
NT BUFFER STORAGE
NT MAGNETIC DISKS
NT MAGNETIC TAPES
NT OPTICAL DISKS
NT RANDOM ACCESS MEMORY
NT READ-ONLY MEMORY DEVICES
NT REGISTERS (COMPUTERS)
Amorphous or microcrystalline semiconductor memory device
[EP-PATENT-0-162-529-A1] 01 p0026 N88-10167
The associative memory ME7
[ESA-TT-1033] 01 p0079 N88-10506
Estimation of the position and orientation of objects using associative memories
[ESA-TT-1034] 01 p0079 N88-10507
Implementation of preconditioned s-step conjugate gradient methods on a multiprocessor system with memory hierarchy
[DE87-014401] 02 p0222 N88-11400
QUICKSILVER: A 3D, electromagnetic, PIC code
[DE87-013013] 02 p0245 N88-11547
Documentation of NCAR (National Center for Atmospheric Research) CCM1 program modules
[PB87-213567] 03 p0352 N88-12220
Electronic Records Administration at the Savannah River Plant
[DE87-014842] 03 p0384 N88-12415
Storing photomicrographs on optical laser disks
[DE87-013747] 04 p0449 N88-12785
Center for Supercomputing Research and Development (CEDAR)
[DE88-000807] 04 p0475 N88-12930
Some distance problems in coding theory
[B8711398] 05 p0635 N88-13888
Distribution of records on a ring of processors
[PB87-235784] 06 p0758 N88-14649
Online monitoring of laserpulses using the GPIB-interface of a Tektronix 2430 Digital Storage Oscilloscope
[DE88-002636] 07 p0856 N88-15201
UNITY: A framework for study of parallel programming problem-solving
[AD-A185616] 07 p0906 N88-15490
Communications patterns in a symbolic multiprocessor
[AD-A186896] 09 p1215 N88-17282
Recovery using virtual memory
[AD-A187098] 09 p1217 N88-17296
An efficient sparse matrix multiplication scheme for the CYBER 205 computer
[NASA-TM-4028] 10 p1390 N88-18302
Performance and evaluation at the Center for Supercomputing Research and Development
[DE88-003563] 10 p1417 N88-18456
Optical memory cards: A comparison with other current technologies and potential military applications
[AD-A187287] 10 p1425 N88-18512
Modular CAMAC system, 2
[DE88-700237] 11 p1525 N88-19106
OPS83: Style guide for high performance
[AD-A188505] 12 p1681 N88-20051
An interface between object-oriented systems
[AD-A189245] 13 p1815 N88-20644
Application of static memory for data acquisition and transmission into a computer
[DE88-701491] 15 p2106 N88-22544
Parallel memory addressing using coincident optical pulses
[AD-A189767] 15 p2106 N88-22547
Memory efficient evaluations of nonlinear stochastic equations and C3 applications
[AD-A189872] 15 p2110 N88-22569
Design of an algorithm to translate nested relational algebra queries to GENESIS trace manager commands
[AD-A190502] 15 p2112 N88-22581
Microvax networked computer system
[AD-A190308] 15 p2114 N88-22596
The modeling, simulation and comparison of interconnection networks for parallel processing
[AD-A190571] 15 p2115 N88-22599
The algebraic structure of convolutional codes
[AD-A190280] 15 p2120 N88-22635
Coding for write-unidirectional memories and conflict resolution
[ENST-87C005] 16 p2245 N88-23408
IPC for modular software requires a third party connect
[AD-A189199] 16 p2246 N88-23414
A computational model of motor behavior
[AD-A191179] 18 p2553 N88-25152
The role of working memory in language comprehension
[AD-A192721] 20 p2833 N88-26805
Common Data Format (CDF) to store images
[NASA-CR-179366] 20 p2836 N88-26825
Implementation of an OPS5 derivative on the Novix RISC processor
[DE88-011392] 21 p2994 N88-27758
Content-addressable memory storage by neural networks: A general model and global Liapunov method
[AD-A192716] 21 p3002 N88-27807
Research on wide area workstations
[AD-A192529] 22 p3136 N88-28643
Programming language concepts for multiprocessors
[AD-A193465] 23 p3264 N88-29430
Laser sensing for identification and control of distributed parameter systems
[AD-A195886] 24 p3379 N88-30124

COMPUTER SYSTEMS DESIGN
The program DSMME: Digital Situation Model, Measurement --- mapping 01 p0065 N88-10418
System adaptivity and the modelling of stereotypes --- human-computer interaction
[NPL-DITC-91/87] 01 p0077 N88-10494
Digital bus unit engineering model: Design, manufacture and test
[MRM/TREP/1003/SAAB] 01 p0083 N88-10537
Study and design of a communication processor unit
[RIDU/TREP/1002/SAAB] 01 p0083 N88-10538
The application of emulation techniques in the analysis of highly reliable, guidance and control computer systems 02 p0127 N88-10798
ISAURE: Integration of security and fault tolerance in the REALITE 2000 system 02 p0127 N88-10802
A mini system for nowcasting
02 p0204 N88-11278
FRONTIERS: An operational system for nowcasting precipitation 02 p0204 N88-11279
The impact of new computer technology on accelerator control
[DE87-014021] 02 p0219 N88-11376
Memory systems for single bus multiprocessor architecture. Application to the SCQM system
[ENST-86E022] 02 p0219 N88-11379
A design methodology for the utilization of metrics within various phases of software lifecycle models
[DE87-010519] 02 p0220 N88-11385
Praxis: The programming language: An advanced overview
[DE87-014319] 02 p0220 N88-11388
Design and development of a database for spectral data and analysis results
[DE87-011323] 02 p0247 N88-11564
Delft parallel processor 84/16
[PB87-226254] 03 p0366 N88-12305
Methods for design and evaluation of integrated hardware/software systems for concurrent computation
[NASA-CR-181522] 04 p0479 N88-12953
User interface for a partially incompatible system software environment with non-ADP users
[DE88-001518] 04 p0482 N88-12968
Study of fault tolerant techniques for satellite data handling
[FTT/REP/0001/SAAB] 05 p0632 N88-13860
Introduction to local area network design on Ariane 5 and future launchers
[SNIAS-872-422-102] 05 p0635 N88-13886
Conceptual issues in measuring the behavior of a distributed real-time process-control computer system
[DE87-009748] 05 p0638 N88-13898

Connecting RPC (Remote Procedure Call)-based distributed systems using wide-area networks
[PB87-234423] 05 p0658 N88-14041
Study of synthetic aperture radar data compression and encoding, Part 4: Algorithm implementation aspects
[NLR-TR-85085-L-PT-4] 06 p0692 N88-14249
Diagnostic emulation: Implementation and user's guide
[NASA-CR-178391] 06 p0756 N88-14638
Software-implemented fault insertion: An FTMP example
[NASA-CR-178423] 06 p0761 N88-14668
A Multipurpose Adaptive Controller (MAC) for real time digital regulation
[REPT-87-028] 06 p0762 N88-14673
Life sciences flight experiments microcomputer 06 p0792 N88-14857
Expert system study for spacecraft management
[TL-2699-ISS-1] 07 p0824 N88-15004
Packet telecommand. System performance assessment study --- onboard data handling
[PTC/TNOT/0015/SAAB] 07 p0843 N88-15113
Annotated bibliography on reliable system design
[PB88-109848] 07 p0866 N88-15254
DOE data exchange format specification, mechanical products/drafting: Version 1.2.2: CADCAM-045
[DE88-001923] 07 p0904 N88-15477
Facility design validation of the information systems laboratory
[AD-A186309] 07 p0906 N88-15488
AFL-1: A programming language for massively concurrent computers
[AD-A186422] 07 p0906 N88-15489
Enhancement of computer system for applications software branch 07 p0923 N88-15610
Can space station software be specified through Ada? 07 p0925 N88-15622
Reliability issues in distributed operating systems
[PB88-100870] 08 p0993 N88-16009
Interactive knowledge acquisition tools 08 p1060 N88-16401
Proposal of a methodology for the conceptual design of the Distributed Data Base
[INPE-4315-TDL/282] 08 p1093 N88-16576
Experiment control and data system for an infrared detector array with maximum sensitivity
[ETN-88-91497] 09 p1136 N88-16813
User engineering: A new look at system engineering 09 p1206 N88-17231
The implementation and use of Ada on distributed systems with high reliability requirements
[NASA-CR-182481] 09 p1221 N88-17326
A type-oriented approach to knowledged-based systems
[MA-47] 09 p1222 N88-17329
A proposal for a feasibility study on the design of software interfaces in large systems
[NPL-DITC-89/87] 09 p1222 N88-17330
An advanced microcomputer design for processing of semiconductor materials 10 p1288 N88-17703
Inexpensive solution for the mass distribution of satellite images
[PB88-114038] 10 p1317 N88-17873
Proceedings of the Workshop on Future Directions in Computer Architecture and Software
[AD-A184949] 10 p1373 N88-18191
Some further observations about reduced instruction set computers 10 p1373 N88-18192
An empirical analysis of the Lilith instruction set 10 p1373 N88-18193
High-performance CPU implementation of the nebula instruction set architecture 10 p1373 N88-18194
The design of ultra high-speed numeric intensive systems (having fault tolerant and load balancing capabilities) 10 p1374 N88-18196
Research and development trends for memory hierarchies --- cache memories 10 p1374 N88-18198
On parallelism in software/hardware design tools 10 p1374 N88-18200
A large-grain dataflow architecture 10 p1375 N88-18207
Towards reusable software designs and implementations 10 p1376 N88-18213
The case for a shared address space 10 p1378 N88-18225
Design for a TPL complier system: A system for retargeting high level language programs 10 p1381 N88-18248
Cumulative reports and publications through December 31, 1987
[NASA-CR-181624] 11 p1524 N88-19099
Application of knowledge based systems to the maintenance of inertial system electronics 12 p1578 N88-19441
The RVD mission: The on-board data processing requirements 12 p1586 N88-19495
EUROSIM: A design concept for an in-orbit operations simulator 12 p1589 N88-19517
Definition of the EUROSIM simulation subsystem 12 p1592 N88-19532
The concept of intelligent integrated interactive CAD systems
[CWI-CS-R8717] 13 p1818 N88-20865
Organization of design knowledge in an intelligent CAD environment
[CWI-CS-R8720] 13 p1819 N88-20868
The German processing and archiving facility for ERS-1
[ESA-CR(P)-2531] 13 p1851 N88-21082
Software quality assurance workstation
[P-1124/RT-14791] 14 p1957 N88-21670
Distributed operating systems: An overview
[INF-87-29] 14 p1960 N88-21688
Conception of a knowledge-based system for designing distributed systems
[DFVLR-MITT-87-16] 14 p1961 N88-21694
Passive coupler, network adapter, and network acquisition procedure for optical local networks
[ETN-88-92130] 14 p1961 N88-21695
Sigma system: Overview, prospects 15 p2052 N88-22230
An intelligent simulation model generator
[REPT-87-053] 15 p2109 N88-22562
Transformations of concurrent algorithms for highly parallel systems: A one year project summary report
[AD-A190236] 15 p2111 N88-22576
Strategies for concurrent processing of complex algorithms in data driven architectures
[NASA-CR-181657] 16 p2193 N88-23083
Fundamentals of microprocessor-based design: A tutorial, second edition
[DE88-006761] 16 p2244 N88-23406
The PAWS and STEM reliability analysis programs
[NASA-TM-100572] 16 p2262 N88-23526
Automated database design technology and tools
[NASA-CR-182875] 16 p2286 N88-23687
Activities of the Institute for Computer Applications in Science and Engineering (ICASE)
[NASA-CR-181666] 17 p2384 N88-24166
Protection and security mechanisms in the SMITE capability computer
[RSRE-MEMO-4117] 17 p2384 N88-24167
Simulation and computer aided engineering (the necessity of an integrated approach)
[NLR-MP-86050-U] 17 p2386 N88-24178
MIPS: The good, the bad and the useful
[NASA-CR-182893] 17 p2386 N88-24184
Interconnection of high-speed local area networks 17 p2390 N88-24205
A multiprocess operating system for 16 bit microcomputers or porting Unix (trademark) to a NS32016 with enhancements 20 p2836 N88-26822
Computer science and technology: Knowledge-based system for physical database design
[PB88-193289] 20 p2882 N88-27109
An integrated, multi-vendor distributed data acquisition system
[DE88-008900] 20 p2882 N88-27113
Computer system for the primary fly-by-wire control of civil transport aircraft (experimental system)
[FBW-TB-2086/88] 21 p2898 N88-27204
MINIAC: A small embedded computer
[DE88-008142] 21 p2994 N88-27757
A menu-driven menu editor and associated menu system
[DE88-008026] 21 p2998 N88-27781
Notes on operating system requirements for the next millennium
[DE88-010712] 21 p3002 N88-27805
Event monitoring functions introduced by the Onboard Life Monitoring System (OLMOS) into a German aircraft 22 p3034 N88-28008
Proposal for the on-board part of a future aircraft integrated monitoring system 22 p3035 N88-28016
Faultfinder: A diagnostic expert system with graceful degradation for onboard aircraft applications 22 p3035 N88-28018
The Sundstrand B747-400 data management unit 22 p3035 N88-28021
Interface techniques and systems for standard aircraft data buses 22 p3036 N88-28028
Microsupercomputers: Design and implementation
[AD-A194712] 22 p3135 N88-28638
Reliable onboard computing for critical space systems
[RR-670-I] 22 p3135 N88-28641
V2500 Condition Monitoring and Performance Analysis Software System (COMPASS): Overview of system --- aircraft engine
[PNR90418] 22 p3139 N88-28666
On eclecticism in specifications: A case study centered around Petri nets --- software engineering
[REPT-87-008] 22 p3140 N88-28671
Use of Markov probability and reliability model generation methods in the analysis of reliability of a fault tolerant hardware and software based system with flexible repair policies
[PNR90467] 22 p3145 N88-28706
The SMITE modular compilation system
[RSRE-MEMO-4145] 23 p3244 N88-29307
The SMITE object oriented backing store
[RSRE-MEMO-4147] 23 p3244 N88-29308
Formal specification of a secure document control system for SMITE
[RSRE-88002] 23 p3245 N88-29309
Computer systems for the representation and manipulation of mathematical knowledge
[AD-A193547] 23 p3249 N88-29340
A software engineering approach to expert system design and verification 23 p3252 N88-29356
Issues on the use of meta-knowledge in expert systems 23 p3252 N88-29357
An approach to combining heuristic and qualitative reasoning in an expert system 23 p3253 N88-29362
Expertise and reasoning with possibility: An explanation of modal logic and expert systems 23 p3253 N88-29363
DAISY-DAMP: A distributed AI system for the dynamic allocation and management of power 23 p3254 N88-29373
Requirements for a tool to aid in the development of expert systems for space station applications 23 p3258 N88-29398
Life-span knowledge engineering for space operations 23 p3259 N88-29401
Intelligent interface design and evaluation 23 p3260 N88-29405
Design consideration in constructing high performance embedded Knowledge-Based Systems (KBS) 23 p3261 N88-29415
A nonlinear filtering process diagnostic system for the Space Station 23 p3262 N88-29417
A flexible search strategy for production systems 23 p3262 N88-29420
Central user and browse service --- ERS-1 ground segment
[CU-PG-MDA-SY-0005] 23 p3297 N88-29637
Telescience testbed pilot program
[NASA-CR-183207] 24 p3412 N88-30309
Scheme86: A system for interpreting SCHEME
[AD-A195931] 24 p3413 N88-30319
The LTPP communication processor --- Columbus and Hermes
[CL/CP/SES/FR/004] 24 p3415 N88-30328
The P-3 Scheduling Support System (P-3 S3)
[AD-A194824] 24 p3436 N88-30450

COMPUTER SYSTEMS PERFORMANCE

High performance clause indexing
[DE87-011399] 01 p0106 N88-10688
Short range forecast of the daily maximum temperature 02 p0209 N88-11313
Evaluating computers and their performance: Perspectives, pitfalls, and paths
[DE87-014264] 02 p0218 N88-11375
Layering central authentication on the interactive services of an existing homogeneous distributed system
[DE87-011544] 03 p0366 N88-12304
Applications of the hybrid automated reliability predictor
[NASA-TP-2760] 04 p0475 N88-12928
Parallelization of hydrocodes on the Intel Hypercube, part 2
[DE88-001591] 04 p0480 N88-12957
Towards automated consulting: Design feedback from the performance of online documentation
[DE87-012243] 04 p0501 N88-13082
An empirical investigation of load indices for load balancing applications
[AD-A185763] 06 p0724 N88-14451
A taxonomy of analytical computer performance models for computer design
[AD-A185561] 06 p0755 N88-14632
Nonconformity testing for the Graphical Kernel System (GKS)
[GMD/VAL-86-104] 06 p0757 N88-14644
Image understanding by Image-Seeking Adaptive Networks (ISAN)
[AD-A186214] 07 p0906 N88-15492
Computer control of a microgravity mammalian cell bioreactor 09 p1197 N88-17172
Expert system applications in spacecraft subsystem controllers 09 p1210 N88-17254
Beyond rules: The next generation of expert systems 09 p1210 N88-17256
Communication and control in an integrated manufacturing system 09 p1212 N88-17263
A comparison of the Cray-2 performance before and after the installation of memory pseudo-banking
[NASA-CR-177462] 09 p1215 N88-17287

Implementation of elementary functions in Ada
[CWI-NM-R8709] 09 p1218 N88-17303
Proceedings of the Workshop on Future Directions in Computer Architecture and Software
[AD-A184949] 10 p1373 N88-18191
Hardware implementation for special functions. An application for combat simulation
10 p1374 N88-18197
A comparative study of heurstic algorithms for task assignment in distributed computing systems
10 p1376 N88-18211
A paradigm for concurrency control performance evaluation 10 p1377 N88-18220
A strategy for failure prediction
10 p1380 N88-18243
Parallelism at the microlevel: Cooperative microcontrollers with real time considerations
10 p1381 N88-18246
Design for a TPL complier system: A system for retargeting high level language programs
10 p1381 N88-18248
A measurement-based study of concurrency in a multiprocessor
[DE88-003536] 10 p1383 N88-18260
Measurement and effects of transport delays in a state-of-the-art F-16C flight simulator
[AD-A187367] 11 p1441 N88-18599
Modules of nanosecond logic electronics system with computer control
[DE88-700190] 11 p1479 N88-18828
KR: An efficient knowledge representation system
[AD-A187705] 11 p1529 N88-19129
Efficient instruction level simulation of computers
[AD-A187821] 11 p1529 N88-19130
Performance measurements of distributed simulation strategies
[AD-A187824] 11 p1529 N88-19133
The Livermore FORTRAN Kernels: A computer test of the numerical performance range --- benchmark tests
[UCRL-53745] 11 p1531 N88-19144
NFEARS (Nonlinear Finite Element Adaptive Research Solver): A nonlinear adaptive finite element solver. Part 2: User's manual
[AD-A189009] 12 p1684 N88-20070
A report on the study of algorithms to enhance vector computer performance for the discretized one-dimensional time-dependent heat conduction equation: EPIC research, phase 1
[DE88-005642] 13 p1820 N88-20880
Performance analysis of slotted ring protocols in High Speed Local Area Networks (HSLANS)
[INF-87-31] 14 p1955 N88-21652
Parallel processes in the knowledge based system HYDRA
[REPT-87-38] 14 p1960 N88-21689
Methodology for software reliability prediction, volume 1
[AD-A190018] 15 p2110 N88-22571
Methodology for software reliability prediction, volume 3
[AD-A190019] 15 p2110 N88-22572
CK-LOG system conversion (user's manual and user interface)
[AD-A190273] 15 p2111 N88-22577
The Colored Stochastic Petri Net (CS-PN) software: Application to the validation and the performance evaluation of distributed systems
[ENST-87D005] 15 p2113 N88-22589
Implementation and performance analysis of parallel assignment algorithms on a hypercube computer
[AD-A190678] 15 p2115 N88-22600
Toward a mathematical formalism of performance, task difficulty, and activation 16 p2239 N88-23372
Fundamentals of microprocessor-based design: A tutorial, second edition
[DE88-006761] 16 p2244 N88-23406
Beyond Ada: Generating Ada code from equational specifications
[AD-A191865] 18 p2557 N88-25176
Solving bidiagonal systems of linear equations on the CDC CYBER 205
[CWI-NM-R8725] 18 p2558 N88-25187
Gaussian techniques on shared-memory multiprocessors
[DE88-010594] 19 p2716 N88-26126
GRAPHICS MANAGER (GFXMGR): An interactive graphics software program for the Advanced Electronics Design (AED) graphics controller, Model 767
[DE88-010370] 19 p2717 N88-26131
A multiprocess operating system for 16 bit microcomputers or porting Unix (trademark) to a NS32016 with enhancements 20 p2836 N88-26822
Aircraft refueling demonstrator using a microbot alpha 2 robot 21 p2926 N88-27367
Constructing a highly-available location service for a distributed environment
[AD-A192723] 21 p3001 N88-27801
Modeling and approximate performance analysis of multiuser computer systems
[ETN-88-92137] 21 p3002 N88-27806
The SAS System by forms: Putting statistical power into the hands of an end-user
[DE88-010512] 21 p3010 N88-27857
DAISY-DAMP: A distributed AI system for the dynamic allocation and management of power
23 p3254 N88-29373
SCARES: A Spacecraft Control Anomaly Resolution Expert System 23 p3256 N88-29381
Archetyping: A software generation and management methodology 23 p3256 N88-29382
Benchmarking expert system tools
23 p3259 N88-29399
A space station onboard scheduling assistant
23 p3259 N88-29402
Intelligent interface design and evaluation
23 p3260 N88-29405
Design consideration in constructing high performance embedded Knowledge-Based Systems (KBS)
23 p3261 N88-29415
A flexible search strategy for production systems
23 p3262 N88-29420
A new computational capability for ramjet projectiles
[AD-A196061] 24 p3327 N88-29812
Telescience testbed pilot program
[NASA-CR-183207] 24 p3412 N88-30309

COMPUTER SYSTEMS PROGRAMS
NT INPUT/OUTPUT ROUTINES
NT OPERATING SYSTEMS (COMPUTERS)
NT SUBROUTINE LIBRARIES (COMPUTERS)
PRMIXn: A computer program for thermophysical properties of real gases and gas mixtures
[GKSS-86/E/59] 01 p0020 N88-10125
The associative memory ME7
[ESA-TT-1033] 01 p0079 N88-10506
An evaluation of WPS-Plus word processing software for the IBM PC and compatibles
[DE87-011972] 01 p0081 N88-10518
Maximum likelihood estimates of parameters in linear systems with process and measurement noise
[DFVLR-FB-87-20] 01 p0083 N88-10532
A data analysis package for RDF-determination fromEXELFS-spectra
[USIP-87-07] 01 p0104 N88-10681
A severe weather forecast software package
02 p0206 N88-11294
The VAXONLINE software system at Fermilab
[DE87-013565] 02 p0220 N88-11387
Computational methods and software for differential equations and their applications
[DE87-014601] 02 p0226 N88-11424
A requirements specification for a software design support system
[NASA-CR-182333] 05 p0637 N88-13896
Software enhancements and modifications to Program FDTD executable on the Cray X-MP computer
[DE88-001877] 07 p0904 N88-15476
Feasibility of software built-in test for SDI (Strategic Defense Initiative) applications
[AD-A185750] 07 p0917 N88-15572
Thermal structural control modelling techniques --- spacecraft
[FOK-TR-R-86-030] 08 p0962 N88-15828
Computerized evaluation of interferograms of the Michelson Interferometer for Passive Atmospheric Sounding (MIPAS) Laboratory Model (LM)
08 p1019 N88-16177
Calculation of the flow through a single-sided sudden expansion with the Computer Program for Parabolic and Elliptic Flows (COPPEF) computer program
[VTH-LR-523] 09 p1163 N88-16973
FABSTRAN: A computer program for frame and beam static and transient response analysis (nonlinear)
[ARE-TR-86205] 09 p1182 N88-17079
Development of a comprehensive software engineering environment 09 p1203 N88-17211
Software for integrated manufacturing systems, part 1
09 p1211 N88-17261
Software for integrated manufacturing systems, part 2
09 p1211 N88-17262
Evaluating software testing methods to reduce testing duplication in US Army communications equipment acquisition
[AD-A186961] 09 p1216 N88-17292
FORTRAN 77 guidelines for the software projects RASP and ANDECS
[DFVLR-MITT-87-09] 09 p1218 N88-17301
Transient sound radiation from infinite thin plate
[ARE-TM(UHA)-87508] 09 p1243 N88-17449
An empirical analysis of the Lilith instruction set
10 p1373 N88-18193
Experimenting with parallel programing in logic
10 p1380 N88-18240
Real time artificial intelligence architecture
10 p1380 N88-18242
Experience with Omega: Implementation of a prototype programming environment, part 6
[AD-A187080] 10 p1385 N88-18270
Factors causing unexpected variations in Ada benchmarks
[AD-A187231] 10 p1388 N88-18291
Deriving abstractions from a software object network
[AD-A187472] 10 p1389 N88-18294
An Ethernet local area network controller with supporting operating system software
[DE88-003534] 10 p1392 N88-18304
Feasibility study of generating plans and strategies for software testing by knowledge based system
[AD-A187834] 11 p1529 N88-19134
SIMSAT: Simulation package for flexible systems. Beams in space
[TW-278] 13 p1730 N88-20348
Probabilistic analysis of crack containing structures with the PARIS code
[KFK-4286] 14 p1924 N88-21465
DASM: A tool for Decomposition and Analysis of Sequential Machines
[EUT-87-E-170] 14 p1956 N88-21660
Activities report of the Computer Science Department
[ETN-88-91980] 14 p1958 N88-21672
Three-dimensional mesh-generation and plotting routines for use with a boundary element program (BIE3D)
[AD-A188079] 14 p1958 N88-21675
Software structuring principles for VLSI CAD
[AD-A190386] 15 p2112 N88-22579
Parafrase restructuring of FORTRAN code for parallel processing 16 p2221 N88-23258
The radiometric processing of SLAR measuring values using the PARES program
[BCRS-86-04] 16 p2227 N88-23301
Results of the testing of the segmentation program on RESEDA
[BCRS-87-01] 16 p2228 N88-23304
Introduction to the VMS (DEC) operating system
[ENST-87D006] 16 p2245 N88-23409
IPC for modular software requires a third party connect
[AD-A189199] 16 p2246 N88-23414
Portability of software. The use of software in the hardware mixture
[MBB/LWD-11/S/PUB/253] 16 p2246 N88-23416
Digital monoplotting, part 1
[B8735122-PT-1] 17 p2369 N88-24106
Digital monoplotting, part 2
[B8735122-PT-2] 17 p2369 N88-24107
Automated analysis of crack growth rate for obtaining da/dN versus delta K relation
[FFA-TN-1987-70] 18 p2527 N88-24996
Nebula support software
[AD-A192281] 20 p2837 N88-26833
Capitalizing on experience with intelligence gateway software
[AD-A193362] 21 p3028 N88-27971
COMPASS ground based engine monitoring program for general application --- Condition Monitoring and Performance Analysis Software System (COMPASS)
[PNR90420] 22 p3044 N88-28064
Software modifications to total data reporting accessory for metabolic measurement cart
[AD-A193641] 22 p3132 N88-28623
An evaluation of Interactive Laboratory System software, ILS-PC/DOS: A digital signal processing software package
[AD-A193838] 22 p3138 N88-28657
Artificial intelligence software acquisition program, volume 2
[AD-A194239] 22 p3141 N88-28680
Project management software
22 p3161 N88-28821
Plasma torch design codes package
[SNIAS-881-430-115] 23 p3286 N88-29569
N-version software demonstration for digital flight controls
[NASA-CR-181483] 24 p3328 N88-29815
Development of a general software package for the analysis and synthesis of planar antenna arrays for space applications
[S-247-02] 24 p3359 N88-30000
Improvements of DCAP 1, phase 2-3/A
[D2-RP-AI-106] 24 p3414 N88-30325

COMPUTER SYSTEMS SIMULATION
The roll back chip: Hardware support for distributed simulation using time warp
[AD-A187823] 11 p1529 N88-19132

Development of training implying man-machine interface: From the aircraft to the spacecraft
19 p2700 N88-26052

COMPUTER TECHNIQUES
NT COMPUTER AIDED DESIGN
NT COMPUTER AIDED MANUFACTURING
NT COMPUTER AIDED MAPPING
NT COMPUTER AIDED TOMOGRAPHY
NT COMPUTER ANIMATION
NT COMPUTER ASSISTED INSTRUCTION
A parallel model of the kinetic depth effect using local computations
[AD-A181945] 01 p0083 N88-10536
Transactions of the 4th Army Conference on Applied Mathematics and Computing
[AD-A183544] 01 p0085 N88-10547
Problems in integrating geographic data
[DE87-012880] 01 p0106 N88-10689
Space lab system analysis
[NASA-CR-179207] 02 p0138 N88-10869
Proceedings of Conference on Vibrodiagnostics discussed 02 p0158 N88-10990
REDUCE-aided study of a problem in Hermitian matrix theory
[DE87-014331] 02 p0229 N88-11445
A review of computer-assisted photo interpretation research at USAETL (US Army Engineer Topographic Laboratories)
[AD-A184034] 03 p0346 N88-12186
Computer-controlled testing of visual-spatial ability
[AD-A183971] 03 p0357 N88-12249
JPRS report: Science and technology. China
[JPRS-CST-87-032] 03 p0376 N88-12365
Band 2 VHF antenna for home construction
[BBC-RD-1987/13] 04 p0432 N88-12677
Statistical inference: Computer oriented algorithmic approach
[DE87-013874] 04 p0478 N88-12948
Automatic telescope operations
04 p0519 N88-13190
Stress intensity factors for cracking metal structures under rapid thermal loading, phase 1
[AD-A184112] 05 p0591 N88-13606
Computer aided modeling and fatigue failure forecast under stochastic loading 05 p0607 N88-13720
Development of a data analysis system for the detection of lower level atmospheric turbulence with an acoustic sounder
[AD-A184972] 05 p0624 N88-13821
Efficient computation of periodic Green's functions with application to grating structures
[AD-A184853] 05 p0640 N88-13912
Computer-aided study of a class of Riemannian space-times
[DE87-703367] 05 p0645 N88-13950
Relational data handling system for scientists
[PB87-223426] 05 p0658 N88-14038
An automated supernova search and the design strategy
[DE88-001827] 05 p0660 N88-14051
Computer calculations of PIN diode limiter characteristics
[AD-A185563] 06 p0697 N88-14277
Stress effects and the optimum format of a scrolling seven-line VDT text window
[AD-A185559] 06 p0758 N88-14651
Virtual image processor: A prototype implementation
[AD-A185560] 06 p0758 N88-14652
Interaction of different modules in depth perception: Stereo and shading
[AD-A185607] 06 p0759 N88-14655
USSR report: Cybernetics, computers and automation technology
[JPRS-UCC-86-014] 06 p0761 N88-14669
Genie inference engine rule writer's guide
[AD-A185709] 06 p0762 N88-14675
An inexpensive real-time interactive three dimensional flight simulation system
[AD-A184868] 07 p0821 N88-14989
Inadequacy of conventional dynamic recovery mechanisms in the presence of temporary failures
[AD-A186311] 07 p0866 N88-15251
Data acquisition, reduction and analysis of shock and vibration testing using a super microcomputer
[AD-A186123] 07 p0867 N88-15260
Model-based building verification in aerial photographs
[AD-A186010] 07 p0870 N88-15278
Reliability modelling for fault-tolerant parallel processor
[AD-A185867] 07 p0900 N88-15451
Computer-aided analysis for the Mechanics of Granular Materials (MGM) experiment, part 2
07 p0926 N88-15626
Flow field measurements using hotwire anemometry
[AD-A187029] 09 p1160 N88-16951
Ultrasonic inspection of advanced CFRP structures by computer-controlled, pulse-echo technique
[ETN-88-91665] 09 p1177 N88-17051
Mathematical structures for speech recognition
[AD-A187063] 09 p1217 N88-17295
Application of ac-impedance method on determination of corrosion rate of metals
[DE88-750307] 10 p1300 N88-17771
Methods of eliciting information from experts
[AD-A187468] 10 p1372 N88-18189
Deriving abstractions from a software object network
[AD-A187472] 10 p1389 N88-18294
Contour-to-grid interpolation with nonlinear finite elements: A feasibility study
[AD-A188108] 11 p1503 N88-18980
Terrain Analyst Work Station (TAWS) demonstrations
[AD-A188139] 11 p1504 N88-18981
A spectral method for computing complete synthetic seismograms
[AD-A187663] 11 p1510 N88-19024
Computer Applications in Geotechnical Engineering (CAGE) and Geotechnical aspects of the Computer-Aided Structural Engineering (G-CASE) projects. User's guide. UTEXAS2 slope-stability package. Volume 1: User's manual
[AD-A187674] 11 p1511 N88-19025
Theory and practice of fault tolerance in distributed systems
[AD-A187559] 11 p1540 N88-19204
The optimum solution to instrument quantization effects 12 p1577 N88-19434
Automatic knowledge acquisition for aerial image interpretation
[AD-A188616] 12 p1638 N88-19810
The formal specification of computer systems
[AD-A188947] 12 p1675 N88-20013
Automatic restructuring of FORTRAN programs for parallel execution
[DE88-003585] 12 p1676 N88-20018
Modification, implementation, and evaluation of a remote terminal emulator as a software validation and stress testing tool
[AD-A188833] 12 p1678 N88-20034
Development of a dependency theory toolbox for database design
[AD-A188872] 12 p1707 N88-20216
A simplified computer code for reduction to burning rates of closed bomb pressure-time data (MINICB)
[AD-A189112] 13 p1736 N88-20380
A study of satellite emission computed tomography
[AD-A189567] 13 p1797 N88-20745
Advanced human factors engineering tool technologies
[AD-A189390] 13 p1812 N88-20825
Computer aided surface representation
[DE88-005408] 13 p1817 N88-20854
Quality enhancement with machine intelligence
[DE88-005639] 13 p1824 N88-20901
Exhaustive and pseudo-exhaustive testing
[AD-A190140] 15 p2111 N88-22574
Argus reference manual
[AD-A190382] 15 p2111 N88-22578
Simulation of fault tolerance in a hypercube arrangement of discrete processors
[AD-A189682] 15 p2114 N88-22594
A zonal approach for the solution of coupled Euler and potential solutions of flows with complex geometries
[AD-A189752] 15 p2114 N88-22595
MultiScheme: A parallel processing system based on MIT (Massachusetts Institute of Technology) scheme
[AD-A190383] 15 p2114 N88-22597
Data base design and implementation
[AD-A190414] 15 p2149 N88-22827
Computer tomography and hybrid optical/digital methods for aerodynamic measurements
[AD-A190909] 16 p2157 N88-22872
A computer model investigation of a half square log-periodic array
[AD-A190955] 16 p2190 N88-23062
Lewis Structures Technology, 1988. Volume 1: Structural Dynamics
[NASA-CP-3003-VOL-1] 16 p2217 N88-23226
Parallel computer methods for eigenvalue extraction
16 p2218 N88-23233
Parafrase restructuring of FORTRAN code for parallel processing 16 p2221 N88-23258
Extending problem solver capabilities through case-based inference
[AD-A191332] 16 p2243 N88-23401
Axiomatic specificatin of database domain statics
[PB88-176284] 16 p2250 N88-23444
Approximate agreement
[AD-A191030] 16 p2251 N88-23455
Fast Algorithm Simulation and Test (FAST) facility
[AD-A191183] 16 p2252 N88-23457
Sensitivity analysis and multidisciplinary optimization for aircraft design: Recent advances and results
[NASA-TM-100630] 17 p2302 N88-23766
Effectiveness evaluation of fault-tolerant multiprocessor systems
[AD-A191688] 18 p2554 N88-25158
A multiprocessor data flow accelerator module
[DE88-007587] 18 p2554 N88-25161
Feature extraction using the Hough transform
[AD-A190679] 18 p2555 N88-25165
Optical symbolic processor for expert system execution
[AD-A192005] 18 p2575 N88-25296
Computer aided remote control: A general concept for intervention in the nuclear, underwater, and space domains 19 p2699 N88-26046
Computer-aided research
[DE88-007771] 19 p2714 N88-26114
Fault diagnosis in distributed computer networks
[AD-A192406] 19 p2718 N88-26140
Application of Moment Iteration Method (MIM) to electromagnetic field computation
[PB88-194139] 20 p2789 N88-26546
Graphical communication and symbolism in a computerized cartography and map compilation system
[PB88-124672] 20 p2818 N88-26720
Inference and discovery in an exploratory laboratory
[AD-A192231] 20 p2832 N88-26801
Managing microcomputer applications: A primer and guide to good practice
[AD-A192992] 20 p2835 N88-26817
Computer-aided writing
[AD-A192516] 20 p2836 N88-26837
United States Air Force Graduate Student Summer Support Program, volume 2
[AD-A191122] 21 p2924 N88-27355
CEEG dynamic brain mapping: A new method to evaluate brain function in different psychological and drug conditions 21 p2977 N88-27685
Fourth generation neurocognitive pattern analysis system 21 p2977 N88-27686
A statistical procedure for the evaluation of presence/non-presence of stimulus-related EEG activity
21 p2978 N88-27689
Assessing and enhancing human performance: Utility of a workstation network
[AD-A192840] 21 p2991 N88-27743
Issues in computer-assisted interpretation of graphs and quantitative information
[PB88-116280] 21 p2998 N88-27783
A review of parallel methods for solving sets of linear equations and their application within optimisation algorithms
[AD-A193137] 21 p3006 N88-27830
Research for reducing the labor intensive nature of high-resolution terrain analysis feature extraction
[AD-A192661] 22 p3089 N88-28345
Computer-aided decision making
[AD-A194210] 22 p3137 N88-28651
An evaluation of Interactive Laboratory System software, ILS-PC/DOS: A digital signal processing software package
[AD-A193838] 22 p3138 N88-28657
A virtual statistical mechanical neural computer
[AD-A193962] 22 p3139 N88-28660
LO-CO-GRAF (low cost graphics): Generating maps to support command and control/crisis management using small computers
[AD-A193964] 22 p3139 N88-28661
Natural object categorization
[AD-A194103] 22 p3139 N88-28662
A computer-aided approach to nonlinear control systhesis
[NASA-CR-179391] 22 p3140 N88-28673
Rendering of surfaces from volume data
[AD-A193649] 22 p3143 N88-28689
Computer-controlled measurements of nonlinear standing waves
[AD-A193840] 22 p3147 N88-28717
Direct visualization of surfaces from computed tomography data
[AD-A193646] 22 p3153 N88-28758
Automatic landing by computer vision
[ETN-88-92991] 23 p3175 N88-28905
LRS-2: A specialized knowledge system for launch resource scheduling
[AD-A194625] 23 p3182 N88-28941
Analysis of edge detection techniques for radiographic image measurement
[AD-A193650] 23 p3186 N88-28961
Approximate evaluation of semi-Markov chain reliability models
[AD-A194669] 23 p3223 N88-29185
Analysis of the effect of faulty spares on the performance of diagnostic algorithms in reliable systems
[AD-A193526] 23 p3223 N88-29186

Alterations in upper extremity motor function in soldiers during acute high altitude exposure
[AD-A192676] 23 p3238 N88-29272
Failure modes and effects analysis automation 23 p3254 N88-29370
A static scheduler for the computer aided prototyping system: An implementation guide
[AD-A194340] 24 p3414 N88-30322

COMPUTER VISION
Evaluation of vision systems for teleoperated land vehicles
[DE87-013066] 03 p0333 N88-12100
End of year report for parallel vision algorithm design and implementation
[AD-A184327] 03 p0366 N88-12301
Low-level vision on warp and the apply programming model
[AD-A184330] 03 p0369 N88-12320
On the recognition of curved objects
[AD-A184441] 04 p0478 N88-12945
Implementation and performance of a complex vision system on a systolic array machine
[AD-A184331] 04 p0482 N88-12971
Dealing with unanticipated events in autonomous navigation
[DE88-000590] 05 p0590 N88-13602
Some vision algorithms 06 p0795 N88-14871
Time-domain robotic vision application 06 p0798 N88-14886
A demonstration of autonomous navigation and machine vision using the HERMIES-2B robot
[DE88-002298] 07 p0862 N88-15228
Parallel algorithms for computer vision on the connection machine
[AD-A185842] 07 p0901 N88-15456
Proceedings of Image Understanding Workshop, volume 1
[AD-A186103] 07 p0902 N88-15463
Proceedings of Image Understanding Workshop, volume 2
[AD-A186104] 07 p0902 N88-15464
Image understanding by Image-Seeking Adaptive Networks (ISAN)
[AD-A186214] 07 p0906 N88-15492
Vision algorithms and psychophysics
[AD-A186773] 09 p1200 N88-17193
Development of Moire machine vision 09 p1212 N88-17264
Implementation of a robotic flexible assembly system 09 p1212 N88-17265
Vision technology/algorithms for space robotics applications 09 p1212 N88-17267
Telerobotic truss assembly 09 p1213 N88-17272
Multiple-object motion estimation by maximal matching of 3-D point and line features 09 p1220 N88-17322
An overview of vision-based navigation for autonomous land vehicles 1986
[AD-A188186] 10 p1276 N88-17640
Visual integration and detection of discontinuities: The key role of intensity edges
[AD-A188012] 11 p1520 N88-19076
Object recognition on a systolic array
[AD-A187726] 11 p1534 N88-19164
Three-dimensional information from stereovision process 12 p1593 N88-19540
A texture analysis approach to computer vision for identification of roads in aerial photographs
[AD-A189340] 12 p1639 N88-19815
Retinotopic mapping of the human visual system with magnetoencephalography
[AD-A189557] 13 p1810 N88-20811
On relaxation algorithms based on Markov random fields
[AD-A189043] 13 p1814 N88-20840
Mathematic modeling of visual perception problems
[INPE-4355-PRE/1186] 13 p1823 N88-20897
Aspects and applications of primary processing of visual information
[INPE-4290-PRE/1161] 13 p1841 N88-21015
On the geometric interpretation of image contours
[RR-647-I-IMAG-57-LIFIA] 15 p2109 N88-22563
Concurrent algorithms for a mobile robot vision system
[DE88-005850] 15 p2117 N88-22614
Recognizing and locating partially occluded planar objects for assembly routines
[LAAS-87-360] 16 p2247 N88-23422
Conversational Analysis of Color Images (CAICOU): An interactive development system for the analysis of color images
[RR-641-I-IMAG-39-LIFIA] 17 p2342 N88-23964
Linguistic definition of generic models in computer vision
[RSRE-MEMO-4110] 17 p2386 N88-24182
Orbital navigation, docking and obstacle avoidance as a form of three dimensional model-based image understanding 17 p2388 N88-24194
A concurrent on-board vision system for a mobile robot
[DE88-007475] 19 p2676 N88-25914
Intermediate level computer vision processing algorithm development for the content addressable array parallel processor
[AD-A192066] 19 p2714 N88-26111
Sensor fusion for robot navigation
[DE88-008383] 20 p2809 N88-26663
Research into the architecture of CAD based robot vision systems
[AD-A193330] 21 p2997 N88-27776
Neural network research: A personal perspective
[AD-A192717] 21 p3003 N88-27808
Automatic landing by computer vision
[ETN-88-92991] 23 p3175 N88-28905
Optimization-driven machine-oriented motion measurement 23 p3245 N88-29312
Second Conference on Artificial Intelligence for Space Applications
[NASA-CP-3007] 23 p3251 N88-29351
Machine vision for real time orbital operations 23 p3253 N88-29367
Two dimensional convolute integers for machine vision and image recognition 23 p3254 N88-29369
A generic expert system for materials processing in space 23 p3255 N88-29376
Using primal sketch primitives as the basis for the Hough transform
[INPE-4564-PRE/1305] 24 p3412 N88-30310
An automated computerized vision technique for determination of three-dimensional object geometry 24 p3419 N88-30348

COMPUTERIZED CONTROL
U NUMERICAL CONTROL

COMPUTERIZED DESIGN
U COMPUTER AIDED DESIGN

COMPUTERIZED SIMULATION
NT ANALOG SIMULATION
NT DIGITAL SIMULATION
Current experimental and theoretical understanding of detonation waves in heterogeneous solid explosives
[DE87-012177] 01 p0032 N88-10201
Simulations using the pseudo-current algorithm
[DE87-012403] 01 p0040 N88-10255
Cloud climatology derived from the AFGWC (Air Force Global Weather Central) 3D-nephanalysis for January and July 1979
[AD-A183686] 01 p0070 N88-10446
Adaptive line of sight algorithms
[DE87-014275] 01 p0081 N88-10523
DETOUR: A deformed mesh/contour plot program
[DE87-013119] 01 p0082 N88-10525
Workshop on AI (Artificial Intelligence) and Simulation (2nd) held in Seattle, Washington on 14 July 1987
[AD-A183736] 01 p0084 N88-10542
Dynamical simulation of structural multiplicity in grain boundaries
[DE87-012746] 01 p0103 N88-10676
Application of new conformal solution of theories
[PB87-214557] 01 p0105 N88-10684
RE-1000 free-piston Stirling engine hydraulic output system description
[NASA-TM-100185] 01 p0108 N88-10700
Computer modeling of metal forming
[DE87-013804] 02 p0157 N88-10984
On adaptive signal processing of RF signals
[DE87-014192] 02 p0161 N88-11007
Computer simulation of thermal modeling of primary lithium cells 02 p0163 N88-11022
Results of a wind turbine/sealed lead-acid battery experiment
[DE87-012720] 02 p0166 N88-11044
Computations of hypervelocity impact using the CTH shock wave physics code
[DE87-013067] 02 p0169 N88-11062
Modeling shockwave deformation via molecular dynamics
[DE87-013157] 02 p0169 N88-11063
Computer modeling of two-phase flow
[CFDU/87/5] 02 p0171 N88-11078
Numerical simulation of Tollmien-Schlichting waves by use of a modified vortex particle-in-cell method
[IC-AERO-85-02] 02 p0171 N88-11079
Time-resolved absorption measurements on OMEGA
[DE87-014465] 02 p0179 N88-11112
Numerical simulation of laser filamentation experiments
[ETN-87-90959] 02 p0179 N88-11118
Production of NO by galactic cosmic rays and lightning
[DE87-014613] 02 p0197 N88-11230
Numerical simulation of Tokamaks: Ideal MHD equilibrium and stability
[DE87-013452] 02 p0218 N88-11373
Study into a data relay satellite mission analysis tool
[ESA-CR(P)-2422] 02 p0220 N88-11384
Projection-space iterative interpolation for limited-angle tomography in parallel- and fan-beam geometry, part 1
[DE87-013965] 02 p0221 N88-11391
On the relational modeling of discrete PDE problems
[DE87-013336] 02 p0224 N88-11409
Computer models for kinetic equations of magnetically confined plasmas
[DE87-011571] 02 p0236 N88-11492
A relativistic Monte Carlo binary collision model for use in plasma particle simulation codes
[DE87-013287] 02 p0237 N88-11494
Thin film microstructures: Simulation and theory
[DE87-014732] 02 p0246 N88-11553
Computer simulations of knock-on processes in bcc Ta crystal
[DE87-752980] 02 p0246 N88-11554
Improvements to the adaptive maneuvering logic program
[NASA-CR-3985] 03 p0262 N88-11648
Fin gaps and body slots of guided projectiles: Effects, data correlation and modeling
[AD-A184440] 03 p0270 N88-11698
Modeling of environmentally-induced effects within satellites. Part 1: NASCAP modeling of satellites 03 p0273 N88-11721
Charging calculations for the HIPPARCOS satellite 03 p0274 N88-11728
Electrodynamic tether system study
[NASA-CR-172024] 03 p0275 N88-11737
The structure and reactivity of heterogeneous surfaces and study of the geometry of surface complexes
[DE88-000158] 03 p0279 N88-11754
Numerical simulation of turbulent premixed combustion and decay of turbulent swirling flow
[DE87-014253] 03 p0284 N88-11787
An antenna array processing system for multiple source bearing estimation 03 p0305 N88-11927
Numerical simulation of the interaction of vortex rings in viscous fluid 03 p0318 N88-12008
Numerical study of the entrance flow and its transition in a circular pipe (2) 03 p0318 N88-12011
Numerical simulation of internal combustion engine flows: Development and users guide for MAGIC radial-azimuthal version
[DE87-014453] 03 p0332 N88-12091
On the control of a compliant robot arm 03 p0332 N88-12095
Teleoperator and robotics system analysis
[NASA-CR-179220] 03 p0334 N88-12105
A quasi-physical model for converting hourly global horizontal to direct normal insolation
[DE87-012273] 03 p0349 N88-12204
Radar measurement methods for the observation of convective clouds, and comparison of measurements and numerical simulation
[ESA-TT-1049] 03 p0352 N88-12223
The development of low level coastal flow fields when solar radiation is blocked by smoke
[DE87-014348] 03 p0354 N88-12230
Mass balances for a biological life support system simulation model 03 p0361 N88-12272
A simulation study of a speed control system for autonomous on-road operation of automotive vehicles
[AD-A184030] 03 p0362 N88-12279
Mapping a battlefield simulation onto message-passing parallel architectures
[NASA-CR-178396] 03 p0363 N88-12287
ERIC: An object-oriented simulation language
[AD-A184757] 03 p0364 N88-12293
Token execution strategies for distributed algorithms: Simulation studies
[AD-A184792] 03 p0365 N88-12294
The structure-mapping engine: ' Algorithm and examples
[AD-A184042] 03 p0368 N88-12315
Microcomputer control of a hydraulically actuated piston
[AD-A184130] 03 p0368 N88-12317
Monte Carlo simulation of modulated phases
[NASA-TM-89654] 03 p0369 N88-12323
Computer simulations of fragmentation
[DE87-900985] 03 p0375 N88-12358
Dynamics of atoms in low-symmetry systems
[AD-A184318] 03 p0375 N88-12361
Mathematical models of plasma discharge control in a tokamak
[DE87-702891] 03 p0378 N88-12377
Simulation of the layer-growth dynamics in silver films: Dynamics of adatom clusters and vacancy clusters on Ag(100)
[DE87-014764] 03 p0380 N88-12390

Competition Analysis Model (CAM). Volume 2: Computer manual
[AD-A184017] 03 p0384 N88-12411
NAVSIM 2: A computer program for simulating aided-inertial navigation for aircraft
[NASA-CR-177438] 04 p0398 N88-12478
Simulation of an enhanced TCAS 2 system in operation
[NASA-CR-181545] 04 p0398 N88-12479
An inexpensive real-time interactive three-dimensional flight simulation system
[AD-A184340] 04 p0402 N88-12499
Numerical simulation system 04 p0404 N88-12511
Analytical investigation of the dynamics of tethered constellations in Earth orbit (phase 2)
[NASA-CR-179218] 04 p0408 N88-12533
Simulation studies for surfaces and materials strength
[NASA-CR-181535] 04 p0412 N88-12557
The Pierce diode with an external circuit. Part 1: Simulations in the linear regime
[DE88-000413] 04 p0440 N88-12731
PRAAGE: An interactive IBM-PC code for unreliability/aging analysis
[DE87-012124] 04 p0453 N88-12803
A portable hypercube simulator
[DE87-013369] 04 p0478 N88-12947
A network definition and solution of simulation problems
[DE88-000675] 04 p0481 N88-12962
Development of the non-equilibrium reactive chemical transport code CHMTRNS
[DE88-000682] 04 p0481 N88-12964
Computer-aided X-ray image system design and evaluation
[DE88-000997] 04 p0481 N88-12965
GOLD: Integration of model-based control systems with artificial intelligence and workstations
[DE88-000506] 04 p0483 N88-12976
GOLD: Integration of model-based control systems with artificial intelligence and workstations
[DE88-000706] 04 p0483 N88-12977
Monocrystal sputtering by the computer simulation code ACOCT
[IPPJ-848] 04 p0493 N88-13035
Theory and simulations of Zone 2 microstructures in thin films
[DE87-014752] 04 p0499 N88-13071
Subjective probability, combination of expert opinion and probabilistic approaches to information retrieval 04 p0501 N88-13085
Practical and modern simulation by systematic connection of the LU-ADI code and the solution adaptive grid program 05 p0536 N88-13260
Programming techniques for high-speed processing of large scale numerical simulation on supercomputers 05 p0537 N88-13269
Rarefied gas numerical wind tunnel. 2: Two-dimensional and axially symmetric bodies 05 p0538 N88-13273
Numerical simulation of splash of droplet at unit gravity 05 p0538 N88-13275
A perspective of computational fluid dynamics 05 p0538 N88-13279
Navier-Stokes simulation of transonic transportation aircraft configurations. 1: Flow-field simulation over wing-fuselage combinations 05 p0540 N88-13288
Numerical simulation of transonic aircraft in comparison to wind tunnel test 05 p0540 N88-13289
Computation of transonic flows with nacelle simulation
[SNIAS-872-111-117] 05 p0542 N88-13300
Correction of inertial navigation system drift errors for an autonomous land vehicle using optical radar terrain data
[AD-A184973] 05 p0544 N88-13311
The role of experimental investigation and computational fluid dynamics during fighter aircraft design 05 p0546 N88-13326
A numerical study of the effects of curvature and convergence on dilution jet mixing
[NASA-TM-89878] 05 p0549 N88-13347
Computer code simulations of explosions in flow networks and comparison with experiments
[DE88-001946] 05 p0573 N88-13491
Noise modelling in the time domain with the aid of Spice
[PB87-221941] 05 p0573 N88-13492
Numerical and analytical study of the equivalent permittivity or permeability of nonhomogeneous materials. Application to the experimental electromagnetic characterization of composites
[SNIAS-872-430-104] 05 p0575 N88-13509
Dynamics of propellant feedline systems
[AD-A184865] 05 p0580 N88-13537
Physical analysis and numerical simulation of coherent turbulent structures in mixed layers, jets, and wakes
[ETN-88-91183] 05 p0581 N88-13548
Low thrust viscous nozzle flow fields prediction
[NASA-CR-182334] 05 p0582 N88-13551
Development of response models for the Earth Radiation Budget Experiment (ERBE) sensors. Part 1: Dynamic models and computer simulations for the ERBE nonscanner, scanner and solar monitor sensors
[NASA-CR-178292] 05 p0584 N88-13557
Collision-free motion of two robot arms in a common workspace
[CSE-87-00002] 05 p0589 N88-13596
Trajectory control of robot manipulators with closed-kinematic chain mechanism
[NASA-TM-89305] 05 p0591 N88-13605
Applications of fatigue analyses: Transportation 05 p0608 N88-13733
Free Lagrange reconnection algorithms for hydrocodes using a quadrilateral mesh
[DE88-001580] 05 p0611 N88-13752
An adaptive lattice algorithm for spectral line estimation
[AD-A184970] 05 p0634 N88-13876
SUSIE reference manual
[DE88-001462] 05 p0636 N88-13893
Optimal control of large space structures via generalized inverse matrix
[NASA-CR-182336] 05 p0639 N88-13907
Modeling and generating input processes
[DE87-013162] 05 p0645 N88-13948
Molecular dynamics studies of aromatic hydrocarbon liquids
[DE88-001473] 05 p0648 N88-13973
Computer modeling of complete IC fabrication process
[AD-A184807] 05 p0654 N88-14012
Range imagery algorithms for the detection of obstacles by autonomous vehicles
[AD-A185421] 05 p0659 N88-14045
Advanced simulation and analysis of a geopotential research mission
[NASA-CR-182355] 06 p0670 N88-14108
JPRS report: Science and technology. Japan
[JPRS-JST-87-028] 06 p0675 N88-14130
Numerical simulation of flight body circumference flow 06 p0676 N88-14137
Development of transonic speed cascade design method using Euler code and inverse solution 06 p0676 N88-14139
Surface gouging by hypervelocity sliding contact between metallic materials
[DE88-001937] 06 p0682 N88-14178
Advanced numerical modeling of microwave penetration and coupling for complex structures
[DE88-001873] 06 p0690 N88-14231
Documentation of computer programs for optimization and simulation of multicarrier SAW-based demodulator
[PB87-134532] 06 p0693 N88-14252
Model development for induction heating
[DE88-002376] 06 p0699 N88-14289
Computer simulation of the L/sub 3/-edge densitometer
[DE88-001944] 06 p0705 N88-14324
Numerical simulation of flows in axial and radial turbomachines using Euler solvers 06 p0713 N88-14372
Some investigations of molecular beam epitaxial growth of 3-5 semiconductor films via Monte-Carlo computer simulations, carrier tunnelling and spectroscopic ellipsometry
[AD-A185520] 06 p0789 N88-14839
Atmospheric entry heating of cosmic dust 06 p0794 N88-14865
Dynamics formulations for the real-time simulation of constrained motion 06 p0795 N88-14872
Viscous vortex flows 07 p0810 N88-14934
An orbit simulation study of a geopotential research mission including satellite-to-satellite tracking and disturbance compensation systems
[NASA-CR-182353] 07 p0823 N88-14997
Impact of solids on composite materials
[NASA-CR-182395] 07 p0827 N88-15015
Computer simulation of impurities and interfaces in body centered cubic metals
[PB88-108162] 07 p0832 N88-15047
Computer simulation of pencil glide in B.C.C. metals
[DE88-001802] 07 p0834 N88-15062
Channel access protocols for multihop packet radio networks
[AD-A186074] 07 p0842 N88-15105
An additional study and implementation of tone calibrated technique of modulation
[NASA-CR-182377] 07 p0844 N88-15117
High resolution simulation of turbulent flow in a channel
[AD-A186022] 07 p0848 N88-15150
Numerical calculation of appendage, flat plate junction flow
[AD-A186371] 07 p0850 N88-15158
Multitasked embedded multigrid for three-dimensional flow simulation
[NASA-CR-182398] 07 p0852 N88-15173
Numerical methods for fluid flow problems
[DE88-000156] 07 p0854 N88-15190
Computer simulations of ballistic experiments
[DE87-005835] 07 p0862 N88-15226
Analysis of the mass formula dependence of spallation product distribution
[DE88-750297] 07 p0864 N88-15243
Discrete reliability growth models using failure discounting
[AD-A186380] 07 p0866 N88-15252
Computing support for basic research in perception and cognition
[AD-A186192] 07 p0897 N88-15437
Massively parallel implementations of theories for apparent motion
[AD-A185841] 07 p0901 N88-15455
Computer aided design for Petri Nets
[AD-A186109] 07 p0902 N88-15465
Problems of organization of mass processes of simulation, acquisition and processing of experimental data at computers
[DE88-700547] 07 p0905 N88-15483
Improved input representation for enhancement of neural network performance
[DE88-001830] 07 p0907 N88-15496
Monte Carlo simulation of triangulated random surfaces in grand canonical ensemble
[DE88-700378] 07 p0941 N88-15718
Computers in theoretical physics
[DE88-700516] 07 p0941 N88-15720
A dynamic simulation and feedback control scheme for the U.S. Marine Corps' Airborne Remotely Operated Device (AROD)
[AD-A186597] 08 p0953 N88-15784
The NASA aircraft icing research program 08 p0957 N88-15803
Non-steady group combustion of a cloud of char particles
[DE87-010773] 08 p0966 N88-15849
Use of a general control simulation program to evaluate HVAC control stability
[DE88-000476] 08 p0975 N88-15896
A simultaneous M-ary channel hypothesis test with least-mean-square signal amplitude estimation
[AD-A186526] 08 p0978 N88-15913
Integration of Navier-Stokes equations in finite volume formulation 08 p0984 N88-15954
Finite Element Calculation Methods and Their Application to Turbomachinery Flows, volume 1
[VKI-LS-1987-05-VOL-1] 08 p0985 N88-15960
Introduction to the Modeling of Turbulence
[VKI-LS-81-06] 08 p0986 N88-15972
Examples of turbulence-model applications 08 p0987 N88-15975
Direct and large eddy simulation of turbulence. Summary of the state of art 1987 08 p0987 N88-15977
Turbulence modeling for compressible flows 08 p0987 N88-15978
Computer program for the calculation of the profile-vortices interactions (two dimensional inviscid incompressible flow with point singularities)
[ISL-R-124/86] 08 p0987 N88-15982
Qualitative and temporal reasoning in engine behavior analysis 08 p1058 N88-16383
Development of a task-level robot programming and simulation system 08 p1058 N88-16387
Automatic mathematical modeling for space application 08 p1060 N88-16402
LISP based simulation generators for modeling complex space processes 08 p1061 N88-16403
Knowledge-based simulation 08 p1061 N88-16404
Case-based reasoning for space applications: Utilization of prior experience in knowledge-based systems 08 p1065 N88-16433
Development of a computer model for missile simulation, or simulation of a kinetic coverage area for a target detection missile
[FOA-C-20666-2.5] 08 p1067 N88-16449
Development of a computer model for missile simulation, or simulation of a kinetic coverage area for a collimation guided missile
[FOA-C-20667-2.5] 08 p1067 N88-16450
User's guide to DIANE: A microcomputer program for modeling battery performance in electric vehicles
[DE88-003713] 08 p1068 N88-16456
FOR3D: A computer model for solving the LSS (Lee-Saad-Schultz) three-dimensional, wide angle wave equation
[AD-A186649] 08 p1080 N88-16511
Depth of origin of sputtered atoms: Experimental and theoretical study of Cu/Ru(0001)
[DE88-002848] 08 p1082 N88-16520

An integrated approach to rotorcraft human factors research 09 p1110 N88-16653
Contribution to the design of flexible manufacturing systems: Modeling, simulation, and evaluation of parameters
[ISAL-IDI1-87-04] 09 p1151 N88-16894
Optimizing HF antenna systems on the Dolphin and Sea Hawk helicopters
[AD-A186552] 09 p1152 N88-16901
Mode media interactions in an FEL (Free Electron Laser)
[DE88-003155] 09 p1172 N88-17029
Control system simulation for a single-link flexible arm
[AD-A187037] 09 p1174 N88-17035
An interactive-graphics method for dynamic system modelling, applying consistency rules 09 p1181 N88-17072
A comparison of different module configurations for multibandgap solar cells
[DE88-002718] 09 p1187 N88-17113
SWAN: An expert system with natural language interface for tactical air capability assessment 09 p1210 N88-17253
Development of a facility using robotics for testing automation of inertial instruments 09 p1213 N88-17271
The use of computer graphic simulation in the development of robotic systems 09 p1214 N88-17275
Acceleration techniques for decoupling algorithms in semiconductor simulation
[DE88-003593] 09 p1221 N88-17323
Plasma theory and simulation
[AD-A187100] 09 p1249 N88-17486
An evaluation of project scheduling techniques in a dynamic environment
[AD-A187057] 09 p1260 N88-17554
Radar returns from ground clutter in vicinity of airports 10 p1274 N88-17624
Wind shear radar simulation 10 p1274 N88-17625
Simulator investigation of wind shear recovery techniques 10 p1275 N88-17630
Numerical simulation of diffuser/combustor dome interaction 10 p1281 N88-17663
Simulation test beds for the space station electrical power system
[NASA-TM-100786] 10 p1290 N88-17715
ESL batteries and multi-segment applications --- ESA Simulation Language (ESL)
[CS-1029/00-QFIN4] 10 p1322 N88-17901
Multidimensional modeling of convective heat transfer with application to IC engines
[DE88-003398] 10 p1330 N88-17948
Emittance studies at the Los Alamos National Laboratory Free-Electron Laser (FEL)
[DE88-003146] 10 p1334 N88-17975
Instrumentation and quantitative methods of evaluation
[DE87-013639] 10 p1342 N88-18017
Simulation and modeling of whistler mode wave growth through cyclotron resonance with energetic electrons in the magnetosphere 10 p1353 N88-18089
Numerical simulations of the California current: Filament formation as related to baroclinic instability
[AD-A187573] 10 p1358 N88-18115
Hardware implementation for special functions. An application for combat simulation 10 p1374 N88-18197
Parallel discrete event simulation: A shared memory approach
[NASA-CR-182521] 10 p1393 N88-18312
Microscopic modeling of sound waves in granular material
[DE88-000348] 10 p1405 N88-18375
The numerical simulation of accelerator components
[DE87-011597] 10 p1412 N88-18423
Benchmarks of neutral beam injection codes for stellarators
[DE88-003786] 10 p1412 N88-18428
Plasma theory and simulation
[DE88-003620] 10 p1414 N88-18437
Simulation and processing of high resolution images of defects and interfaces in superconducting YBa2Cu3O7
[DE88-003856] 10 p1420 N88-18480
Cosmic strings: A problem or a solution
[DE88-003410] 10 p1429 N88-18535
La Recherche Aerospatiale, bimonthly bulletin, number 1987-2, 237/March-April
[ESA-TT-1074] 11 p1433 N88-18550
A computer simulation study of an expert system for walking machine motion planning
[AD-A187907] 11 p1438 N88-18577
Simulation of infrared spectra
[AD-A187881] 11 p1453 N88-18658
The coaxial colinear antenna: Theoretical and experimental models 11 p1475 N88-18803
The Pierce diode with an external circuit. 2: Non-uniform equilibria
[AD-A188027] 11 p1478 N88-18818
Computational studies of wave-shaping in a blast simulator by perforated plates in the driver
[AD-A188200] 11 p1483 N88-18850
Experimental results of a high-gain microwave FEL operating at 140 GHz
[DE88-004358] 11 p1492 N88-18907
Further development of a finite element model of orthogonal metal cutting
[DE88-004048] 11 p1494 N88-18921
The digital landmass simulation production overview
[AD-A187978] 11 p1503 N88-18978
Test results of a 40-kW Stirling engine and comparison with the NASA Lewis computer code predictions
[NASA-TM-87050] 11 p1508 N88-19013
A worked example of an application of the SAINT simulation program
[AD-A188198] 11 p1524 N88-19097
Mathematical modeling of two-state classification technology transfer summary and user's guide
[DE88-003849] 11 p1526 N88-19110
Efficient instruction level simulation of computers
[AD-A187821] 11 p1529 N88-19130
Optimal performance of distributed simulation programs
[AD-A187822] 11 p1529 N88-19131
Performance measurements of distributed simulation strategies
[AD-A187824] 11 p1529 N88-19133
Algorithmic alternatives
[DE88-003905] 11 p1531 N88-19149
Concepts and nomenclature in the world modeling system (a lesson in applied metaphysics)
[AD-A188246] 11 p1534 N88-19166
A computer graphics simulation of the endgame in aircraft combat survivability
[AD-A187826] 11 p1541 N88-19214
Computer modeling for optical waveguide sensors
[AD-A187702] 11 p1549 N88-19263
Design of an aeroelastic composite wing wind tunnel model
[AD-A188855] 12 p1582 N88-19466
Columbus Simulation Facility (CSF) 12 p1590 N88-19522
Orbital analysis of a STS (Space Transportation System) external tank in low earth orbit
[AD-A188829] 12 p1593 N88-19542
The use of hardware-in-the-loop-techniques in the development of a modern air-to-surface missile system 12 p1597 N88-19562
Computer aided fast turnaround laboratory for research in VLSI (Very Large Scale Integration)
[AD-A189451] 12 p1624 N88-19715
Compressible friction coefficients in a simulated heat pipe
[AD-A188818] 12 p1627 N88-19735
A simulation of void lining during ductile fracture
[AD-A188404] 12 p1635 N88-19792
HELIOS modelling of point-focusing solar concentrators
[DE88-004933] 12 p1640 N88-19820
Comparison of simulation modeling and satellite techniques for monitoring ecological processes
[NASA-CR-182592] 12 p1641 N88-19825
Modification, implementation, and evaluation of a remote terminal emulator as a software validation and stress testing tool
[AD-A188833] 12 p1678 N88-20034
A numerical analysis of the dynamics of PRIZ operation
[AD-A188853] 12 p1678 N88-20035
Primal-dual parallel solution of very large sparse linear programs
[AD-A188500] 12 p1680 N88-20045
The automated symbolic derivation of state equations for dynamic systems
[DE88-005222] 12 p1683 N88-20060
ADAM (Acquisition Deployment and Maneuvering): The space game
[AD-A189512] 12 p1685 N88-20078
Simulation of nuclear collisions at high energies in the frames of quark-gluon string model
[DE88-700914] 12 p1690 N88-20113
Improved zero dimensional model of a reversed field pinch fusion device
[DE88-005212] 12 p1693 N88-20127
X-ray source model for Z-pinch aluminum plasmas
[AD-A189509] 12 p1695 N88-20148
Systems analysis and simulation techniques: Essential tools for balanced complex weapon system designs in terms of performance and cost 12 p1702 N88-20187
Mars Lander/Rover vehicle development: An advanced space design project for USRA and NASA/OAST
[NASA-CR-182562] 12 p1709 N88-20226
AVSCOM'S modifications to Teledyne Systems Company's air-to-air fire control system simulation model
[AD-A189136] 13 p1722 N88-20294
Trajectory code studies, 1987
[DE88-006218] 13 p1728 N88-20335
SIMSAT: Simulation package for flexible systems. Beams in space
[TW-278] 13 p1730 N88-20348
Bipropellant combustion in a liquid rocket combustion chamber 13 p1733 N88-20359
Mixing of viscous fluids: Behavior of microstructures and chaos
[DE88-006287] 13 p1766 N88-20566
Multigrid solution of the Euler equations 13 p1769 N88-20582
Particle-dynamics calculations of gravity flow of inelastic, frictional spheres
[DE88-005224] 13 p1770 N88-20586
Dynamics of high-speed mechanisms with elastic members 13 p1779 N88-20643
Human problem solving in dynamic environments. Understanding and supporting operators in large-scale, complex systems
[AD-A189539] 13 p1812 N88-20826
Simulation of measuring points for three dimensional measurements
[WPB-0115] 13 p1821 N88-20883
A fault injection experiment using the AIRLAB Diagnostic Emulation Facility
[NASA-CR-178390] 13 p1823 N88-20895
SEAT: A strategic engagement analysis tool
[DE88-000498] 13 p1830 N88-20944
Physics at large transverse momenta
[DE88-005758] 13 p1836 N88-20986
Numerical simulations of multiphoton processes in many electron atoms
[DE88-003293] 13 p1837 N88-20990
Activities report of the Toulouse Research Center
[ETN-88-91988] 13 p1850 N88-21077
Resonant Alfven wave instabilities driven by streaming fast particles 13 p1855 N88-21104
Determination of canopy loads for a light aircraft by wind tunnel testing and computer modelling
[BU-353] 14 p1869 N88-21167
Hygrothermomechanical fiber composite fatigue: Computational simulation
[NASA-TM-100840] 14 p1884 N88-21257
Activities report of the Energetics Department
[ETN-88-91981] 14 p1888 N88-21281
Numerical simulation of turbulent premixed combustion and decay of turbulent swirling flow
[DE88-006588] 14 p1888 N88-21284
Millimeter-wave pulse distortion by a single adsorption line simulating the terrestrial atmosphere
[PB88-161237] 14 p1906 N88-21388
Materials dependence of deformation texture development in various deformation modes
[DE88-004312] 14 p1922 N88-21457
Oceanographic export system development, year 1
[AD-A189134] 14 p1950 N88-21623
Activities report of the Computer Science Department
[ETN-88-91980] 14 p1958 N88-21672
Comprehensive model for laser instability in a CO2 laser with gaseous saturable absorber 14 p1979 N88-21808
Velocity and concentration fields over a crystal growing in a water solution. Experimental study and numerical simulation 14 p1987 N88-21856
Development and evaluation of an airplane fuel tank ullage composition model. Volume 2: Experimental determination of airplane fuel tank ullage compositions
[AD-A190408] 15 p2017 N88-22025
Linear state space modeling of a turbofan engine
[AD-A190110] 15 p2019 N88-22035
Moving-bank multiple model adaptive estimation applied to flexible spacestructure control
[AD-A190761] 15 p2026 N88-22071
Status of electric vehicle simulation programs at the INEL: Summer 1987
[DE88-006745] 15 p2058 N88-22271
Basic characteristics of heat-exchanger-type steam reformer heated by high-temperature helium gas (2). Analysis by simulation model (2)
[DE87-702962] 15 p2061 N88-22291
Finite element simulation of perforation of aluminum plates
[DE88-002092] 15 p2073 N88-22362
Computational simulation methods for composite fracture mechanics 15 p2079 N88-22396
Performance evaluation of molten salt thermal storage systems
[DE87-014645] 15 p2091 N88-22461

Advanced geothermal technologies
[DE88-004307] 15 p2091 N88-22463
Anthropomorphic phantom radiation dosimetry at the NATO standard reference point at Aberdeen Proving Ground
[AD-A190508] 15 p2103 N88-22528
An intelligent simulation model generator
[REPT-87-053] 15 p2109 N88-22562
A UNIX-based interactive VHDL (hardware description language) simulator
[AD-A189749] 15 p2109 N88-22565
Memory efficient evaluations of nonlinear stochastic equations and C3 applications
[AD-A189872] 15 p2110 N88-22569
SEARCH: An interactive computer program for optimizing two-variable, unconstrained experiments or simulation
[AD-A190593] 15 p2112 N88-22583
The modeling, simulation and comparison of interconnection networks for parallel processing
[AD-A190571] 15 p2115 N88-22599
Rapid prototyping of simulations in artificial intelligence environments
[DE88-004295] 15 p2117 N88-22612
Discrete event simulation in the artificial intelligence environment
[DE88-004296] 15 p2117 N88-22613
Properties of some Bayesian scoring procedures for computerized adaptive tests
[AD-A189925] 15 p2124 N88-22660
PLASMOR: A laser-plasma simulation code, part 2
[DE88-701289] 15 p2135 N88-22736
Transport simulations of ohmic ignition experiment: IGNITEX
[DE88-006055] 15 p2138 N88-22757
Interface formation and precursory dynamics
[AD-A190741] 15 p2144 N88-22794
Infrared simulation model Sensor Atmosphere Target (SENSAT)-2A
[DFVLR-FB-88-01] 16 p2165 N88-22910
Railgun rail gouging by hypervelocity sliding contact
[DE88-006866] 16 p2166 N88-22916
An integrated and modular digital modeling approach for the space station electrical power system development
[NASA-TM-100904] 16 p2170 N88-22935
A computer model investigation of a half square log-periodic array
[AD-A190955] 16 p2190 N88-23062
WAVFLD: A program to compute ionospheric height gain functions and field strengths at VLF
[AD-A191159] 16 p2191 N88-23066
Analysis of non-premixed turbulent reacting flows
16 p2196 N88-23100
Test code for the assessment and improvement of Reynolds stress models 16 p2197 N88-23105
Reynolds stress models of homogeneous turbulence
16 p2197 N88-23106
Evaluation of a theory for pressure-strain rate
16 p2198 N88-23108
Shear-layer structures in near-wall turbulence
16 p2198 N88-23110
The simulation of coherent structures in a laminar boundary layer 16 p2198 N88-23111
Fast algorithms for Euler and Navier-Stokes simulations
[AD-A190897] 16 p2208 N88-23175
Path following robot
[AD-A190960] 16 p2215 N88-23217
Automatic control of robot motion
[AD-A191012] 16 p2215 N88-23218
Computer simulation of a motor pump unit to aid in interpreting vibration data
[DE88-004481] 16 p2223 N88-23270
Algorithms and intuition
[NASA-CR-182900] 16 p2252 N88-23459
Piecewise linear approach for timing simulation of VLSI (Very-Large-Scale-Integrated) circuits on serial and parallel computers
[AD-A191328] 16 p2252 N88-23462
Simulation of FELIN logics. Polynomials roots simultaneous computation algorithms
[ETN-88-92182] 16 p2253 N88-23464
Domain decomposition in parallel reservoir simulation
[REPT-87-63] 16 p2254 N88-23469
Advanced turboprop aircraft flyover noise: Annoyance to counter-rotating-propeller configurations with an equal number of blades on each rotor, preliminary results
[NASA-TM-100612] 16 p2265 N88-23547
Numerical simulation for particle acceleration and trapping by an electromagnetic wave
16 p2277 N88-23626
Simulation code for ICF including radiative energy transfer 16 p2277 N88-23627
Some aspects of the unified model of non-ideal high-parameter plasmas: Electron EOS and conduction coefficients 16 p2277 N88-23632
Stability requirement FOT ignition and high gain implosion = 2-D simulation for high neutron yield experiment = 16 p2278 N88-23633
Two-dimensional focusing of self-magnetically insulated plasma focus diode 16 p2278 N88-23639
Coherent functional development: Key to successful future system integration 17 p2307 N88-23803
Numerical method for unsteady viscous-inviscid interaction to calculate buffeting
[ONERA-RSF-02/3617-AY-008-A]
17 p2338 N88-23949
Simulation: A simulation system in Ada
[FOA-A-20043-2.7] 17 p2385 N88-24176
Dialog design: General requirements and analysis of an Ada system --- user interface design
[FOA-C-20691-2.7] 17 p2385 N88-24177
A generic multibody simulation
[NASA-CR-182949] 17 p2388 N88-24198
Parallel discrete-event simulation of FCFS stochastic queueing networks
[NASA-CR-181669] 17 p2389 N88-24203
Parametric analysis of power requirements for space-based radar 17 p2399 N88-24260
ATHENA heat pipe transient model
17 p2412 N88-24344
Detailed transient model of a liquid-metal heat pipe
17 p2412 N88-24345
SP-100 control system modeling
17 p2414 N88-24356
ATHENA simulation of the 300 kW SP-100
17 p2414 N88-24357
EETAP (End-to-End Transient Analysis Program) for space nuclear power system simulation
17 p2418 N88-24381
A decade of computer simulations for space shuttle aerodynamics
[NASA-TM-100990] 18 p2459 N88-24603
Simulations of a missile with liquid payload under launch conditions
[AD-A191479] 18 p2463 N88-24625
Computational design of low aspect ratio wing-winglet configurations for transonic wind-tunnel tests
[NASA-CR-183021] 18 p2464 N88-24630
Analytic and numerical modeling of heat and material transport in electrical hypervelocity guns
[AD-A192178] 18 p2469 N88-24655
Use of a two-stage light-gas gun as an injector for electromagnetic railguns
[DE88-007200] 18 p2469 N88-24657
Simulations of the electrostatic charging of ESA communications satellites
[ESA-STM-239] 18 p2472 N88-24670
Computer simulation of turbulent combustion in reciprocating engines
[CFDU/87/11] 18 p2482 N88-24725
Calculation of assemblies bonded with quasi-elastic adhesives
[REPT-47-632/F] 18 p2493 N88-24793
Numerical simulations of the flat-plate laminar boundary layer in subsonic and supersonic flow
[PDR/CFDU/IC/36] 18 p2511 N88-24895
Numerical simulation of nonlinear structural dynamics of large scale unsteady flow
[ETN-88-92156] 18 p2513 N88-24908
An investigation of a distributed clock for local area networks with ring topology 18 p2516 N88-24924
Finite element analysis of an underground structure
[AD-A191747] 18 p2527 N88-24991
Yaw dynamics of horizontal axis wind turbines
[DE88-001137] 18 p2537 N88-25055
Report on project WIND: Preliminary experiments w ith the UK Meteorological Office mesoscale model, September 1987
[AD-A191621] 18 p2544 N88-25099
Analysis of lightning field changes during active thunderstorms in Florida 18 p2545 N88-25103
LispSEI: The programmer's manual
[AD-A191632] 18 p2556 N88-25172
A graphical, intelligent interface for discrete-event simulations
[DE88-000522] 18 p2557 N88-25181
Computer simulation of uphill diffusion in ternary ionic system
[NASA-TT-20194] 18 p2573 N88-25285
Accelerator research studies
[DE88-007124] 18 p2574 N88-25290
Determination of doping profiles in silicon from resistivity measurements via the four-point probe in combination with layer strippings via anodic oxidation
18 p2583 N88-25347
Numerical simulation of compressible homogeneous turbulence: Effects of fluid compressibility
[PB88-127154] 19 p2597 N88-25433
An assessment of the state of the art in predicting the failure of ceramics
[DE88-008996] 19 p2621 N88-25551
Numerical grid generation and flow simulation in SSME thrust chamber 19 p2626 N88-25577
Proceedings of the 5th NAL Symposium on Aircraft Computational Aerodynamics
[NAL-SP-8] 19 p2635 N88-25630
On the NAL numerical simulator system
19 p2635 N88-25631
Numerical simulations of aerodynamic contribution of flows about a space-plane-type configuration
19 p2635 N88-25632
Aerodynamic simulation for complete ASKA aircraft configuration 19 p2637 N88-25641
Numerical simulation of viscous flows over transonic aircraft configurations 19 p2637 N88-25642
A numerical analysis of flow characteristics in laser propulsion system 19 p2637 N88-25645
Numerical simulation of the shock tube flows by TVD scheme 19 p2638 N88-25648
Trellis-coded MPSK modulation techniques for MSAT-X(sup)1 19 p2648 N88-25721
Performance of the ICAO standard core service modulation and coding techniques
19 p2648 N88-25723
Picosecond measurements of gain-switching in a semiconductor laser driven by ultrashort electrical pulses
19 p2658 N88-25800
Non-stationary transport in MODFET's and heterojunction devices 19 p2659 N88-25804
Investigation of Rossby-number similarity in the neutral boundary layer using large-eddy simulation
[DE88-008910] 19 p2666 N88-25851
Thin-membrane Lamb-mode acoustic oscillators for chemical detection 19 p2673 N88-25895
An intelligent processing environment for real-time simulation
[NASA-CR-183056] 19 p2715 N88-26119
Hybrid simulations
[DE88-009125] 19 p2715 N88-26123
Logic and fault simulation on the Mach1000 hardware accelerator
[DE88-009794] 19 p2717 N88-26130
Adaptive residual mode filter control of distributed parameter systems for large space structure applications
19 p2719 N88-26143
Computer modeling of time dependent SBS (Stimulated Brillouin Scattering) in two and three dimensions
[DE88-008922] 19 p2720 N88-26150
Gone with the solar wind: A study of protons accelerated by interplanetary shocks 19 p2743 N88-26283
The role of aviation technology in the Caribbean Basin
[NASA-CR-183069] 20 p2745 N88-26289
Computer simulation of a single pilot flying a modern high-performance helicopter
[NASA-TM-100182] 20 p2761 N88-26376
Computer simulation of multiple pilots flying a modern high performance helicopter
[NASA-TM-100183] 20 p2761 N88-26377
A simulation of post boost vehicle deployment of multiple reentry vehicles
[DE88-009537] 20 p2764 N88-26391
Computation equipment for damage simulation in laminated composites
[AD-A193013] 20 p2768 N88-26412
Rare Gas Halide (RGH) kinetics
[AD-A192352] 20 p2770 N88-26425
Grain boundaries
[DE88-009889] 20 p2773 N88-26446
Fundamental studies of elastomers
[DE88-009679] 20 p2778 N88-26471
Statistical mechanics of polymer systems
[DE88-011172] 20 p2778 N88-26477
Vortex filament simulation for the crosslinking rings
20 p2782 N88-26501
MAXWELL3: A 3D finite element electromagnetic modeling code
[DE88-010602] 20 p2790 N88-26551
Freely expanding detonation products: Scaling of rate processes
[DE88-007827] 20 p2799 N88-26606
Axisymmetric liquid sloshing under low-g conditions: Numerical simulation method (reference manual)
[NLR-TR-86057-U] 20 p2802 N88-26627
Fluid flow modeling in casting processes and its implications
[DE88-010009] 20 p2810 N88-26671
Analytical and experimental investigation of ringless piston concept
[AD-A192835] 20 p2810 N88-26673
Microstructural effects in static and dynamic numerical experiments
[DE88-004289] 20 p2813 N88-26690

Circulation statistics from seasonal and perpetual January and July simulations with the NCAR (National Center for Atmospheric Research) Community Climate Model (CCM1):R15
[PB88-192620] 20 p2823 N88-26748

Synoptic patterns related to tropical cyclone recurvature
[AD-A192338] 20 p2827 N88-26771

Automated system for mathematical processing of the data from a hybrid spectrometer
[DE87-702995] 20 p2836 N88-26820

Proceedings of the 2nd US-Japan Workshop on Advanced Plasma Modeling, volume 3
[IPPJ-867] 20 p2855 N88-26957

A Vlasov ion zero mass electron model for plasma simulations 20 p2855 N88-26958

Modeling of subtle kinetic processes in plasma simulation 20 p2856 N88-26959

Drift wave vortices and anomalous transport
[DE88-009562] 20 p2859 N88-26982

MACH2: A two-dimensional magnetohydrodynamic simulation code for complex experimental configurations
[AD-A192285] 20 p2860 N88-26988

Cosmological helium production simplified
[DE88-009578] 20 p2885 N88-27130

A feasibility study in path planning using optimization techniques
[AD-A193030] 21 p2894 N88-27177

Simulation of moisture diffusion of fiber reinforced components of aircraft for general air transportation
[IFL-IB-87-05] 21 p2907 N88-27253

Computer simulation of elastic properties of grain boundary materials
[DE88-011965] 21 p2916 N88-27305

SARLAC: A relativistic electron beam code
[AD-A193134] 21 p2932 N88-27411

Calculations of high-frequency parameters of disc-loaded waveguides
[DE88-702178] 21 p2933 N88-27417

STAR: Sandia Timing Analyzer Routine
[DE88-012412] 21 p2940 N88-27463

Implicit finite-difference simulation of an internal flow on a hypercube
[AD-A192474] 21 p2942 N88-27471

Simulation and analysis of wave propagation through random media 21 p2947 N88-27503

Numerical simulation and stability analysis of the absolutely and convectively unstable wake
[DFVLR-FB-88-09] 21 p2949 N88-27518

Initial electron distributions for free-electron lasers generated by injector and accelerator simulations
[DE88-007022] 21 p2953 N88-27540

Development of a hybrid simulator for robotic manipulators
[AD-A193119] 21 p2956 N88-27557

Control of free-flying space robot manipulator systems
[NASA-CR-183017] 21 p2956 N88-27562

Experimental validation of a zero-dimensional computer model for spark-ignition engines
[DE88-009034] 21 p2957 N88-27565

Solar cell modeling and simulation
[AD-A193249] 21 p2966 N88-27620

Approximate analytical formulae for electron density and collision frequency in the natural and nuclear-disturbed ionosphere and inner magnetosphere
[AD-A193129] 21 p2972 N88-27654

Large-eddy simulations of concentration fluctuations
[DE88-009480] 21 p2973 N88-27660

Update on the meso-microscale meteorological hierarchy
[DE88-009133] 21 p2975 N88-27670

Three-dimensional wind simulation
[DE88-009793] 21 p2975 N88-27671

Computer simulation procedure for designing airborne aerometric monitoring programs
[DE88-011896] 21 p2975 N88-27674

The VITE model: A neutral command circuit for a generating arm and articulator trajectories
[AD-A192715] 21 p2987 N88-27734

Demodulation processes in auditory perception
[AD-A193421] 21 p2988 N88-27740

Assessing and enhancing human performance: Utility of a workstation network
[AD-A192840] 21 p2991 N88-27743

Block Oriented Simulation System (BOSS)
[NASA-CR-182947] 21 p2995 N88-27760

Simulation methodology
[AD-A192548] 21 p2995 N88-27764

Bisimulation can't be traced
[AD-A192725] 21 p2996 N88-27766

Simulation of real time problem solving
[AD-A193436] 21 p2997 N88-27778

Verification of flight software written in C using ACSL
[DE88-006100] 21 p2998 N88-27779

Dose-enhancement effects in TaSi/Al- and Al-gate MOS devices
[DE88-005483] 21 p3020 N88-27926

Dynamical evolution of cosmic strings
[DE88-011724] 21 p3030 N88-27989

A computer model for the flow of a molten polymer in a narrow cavity
[NPL-DMA(A)-157] 22 p3058 N88-28146

Two-dimensional flow through a turbine cascade
[PDR/CFDU/IC/34] 22 p3076 N88-28264

High performance solutions of the Stokes problem using mini-elements, self-adaptive grids, and multigrid methods: Applications
[ECL-87-15] 22 p3077 N88-28266

Development and application of a finite element method to compute strongly heated turbulent flows
[ECL-88-02] 22 p3077 N88-28267

Variable-compression-ratio pistons for high power output diesel engines 22 p3084 N88-28316

Aspects of the 30-60 day oscillation in a GCM simulation 22 p3121 N88-28545

Simulation studies of the influence of sea-surface temperature anomalies on the Sahelian circulation and rainfall 22 p3122 N88-28553

Estimating reliability with discrete growth models
[AD-A193845] 22 p3143 N88-28692

Customizing Space Nuclear Power System Analysis Model (SNPSAM): Introducing a secondary coolant loop
[AD-A194620] 22 p3151 N88-28750

A new model for the simulation of interfaces at high temperature
[DE88-009926] 22 p3155 N88-28772

Computer simulation of electromigration in thin films
[AD-A194526] 22 p3157 N88-28782

The influence of numerical boundary conditions on transonic flow
[DFVLR-FB-88-06] 23 p3172 N88-28890

Automatic classification of digitally modulated signals
[AD-A194623] 23 p3203 N88-29064

Vortex dynamics of coherent and chaotic structures (including algorithms for computer simulations and diagnosis)
[AD-A193580] 23 p3212 N88-29117

Free electron lasers with small period wigglers
[DE88-011627] 23 p3218 N88-29156

Analysis of the hopfield neural networks and their application to pattern recognition
[AD-A193827] 23 p3239 N88-29279

Three-dimensional elliptic grid generation for an F-16 23 p3246 N88-29315

Feasibility study of a microprocessor controlled actuator test mechanism
[AD-A194654] 23 p3249 N88-29337

An algorithm for determining the location of points in computer simulations
[AD-A193713] 23 p3250 N88-29343

OMV docking simulator 23 p3255 N88-29379

The use of computer graphic simulation in the development of robotic systems 23 p3257 N88-29388

AI and simulation: What can they learn from each other 23 p3257 N88-29391

Acoustic pressure distribution on the bottom of a wedge-shaped ocean
[AD-A193961] 23 p3278 N88-29518

Stability experimental results of cable-in-conduit superconductor for fusion
[DE88-753424] 23 p3290 N88-29589

The interaction of Io with the plasma torus 23 p3308 N88-29704

Numerical methods: Euler time dependent solver 24 p3318 N88-29760

A fiber optic collective flight control system for helicopters
[AD-A195406] 24 p3328 N88-29818

Minimum-complexity helicopter simulation math model
[NASA-CR-177476] 24 p3328 N88-29819

Experiments and modeling of multi-component fuel behavior in combustion
[AD-A195011] 24 p3343 N88-29896

Numerical field model simulation of full scale fire tests in a closed spherical/cylindrical vessel
[AD-A195067] 24 p3359 N88-29998

Track performance considerations for monopulse radars
[AD-A196232] 24 p3360 N88-30007

The focal plane reception pattern calculation for a paraboloidal antenna with a nearby fence
[NASA-TM-100691] 24 p3365 N88-30039

The 1988 Goddard Conference on Space Applications of Artificial Intelligence
[NASA-CP-3009] 24 p3415 N88-30330

Automatic mathematical modeling for real time simulation system 24 p3420 N88-30356

A simulation engine: Combining an expert system with a simulation language 24 p3421 N88-30358

Adaptive control in positioning a rigid-flexible robot arm
[AD-A195194] 24 p3422 N88-30367

Knowledge based simulation: An artificial intelligence approach to system modeling and automating the simulation life cycle
[AD-A195838] 24 p3423 N88-30372

Design and performance analysis of a relational replicated database system
[AD-A196290] 24 p3437 N88-30456

The origin of the moon: Further studies of the giant impact 24 p3440 N88-30474

COMPUTERS

NT AIRBORNE/SPACEBORNE COMPUTERS
NT ANALOG COMPUTERS
NT CDC CYBER 205 COMPUTER
NT CRAY COMPUTERS
NT DIGITAL COMPUTERS
NT EMBEDDED COMPUTER SYSTEMS
NT HEWLETT-PACKARD COMPUTERS
NT HYBRID COMPUTERS
NT HYPERCUBE MULTIPROCESSORS
NT IBM COMPUTERS
NT MICROCOMPUTERS
NT MIMD (COMPUTERS)
NT MINICOMPUTERS
NT OPTICAL COMPUTERS
NT PARALLEL COMPUTERS
NT PERSONAL COMPUTERS
NT SEQUENTIAL COMPUTERS
NT SIMD (COMPUTERS)
NT SUPERCOMPUTERS
NT VAX COMPUTERS

Gender and cognitive style differences at the human-computer interface
[NPL-DITC-90/87] 01 p0077 N88-10493

Evaluating computers and their performance: Perspectives, pitfalls, and paths
[DE87-014264] 02 p0218 N88-11375

Los Alamos National Laboratory computer benchmarking 1986
[LA-10898-MS] 03 p0363 N88-12285

The development of ODE methods: A symbiosis between hardware and numerical analysis
[DE87-014925] 03 p0370 N88-12325

On computing environments in data analysis
[DE88-000078] 04 p0480 N88-12961

Prospectus for the development of a linear algebra library for high-performance computers
[DE88-003715] 08 p1068 N88-16457

Development and experimentation of an eye/brain/task testbed 09 p1205 N88-17219

A visual programming environment for the Navier-Stokes computer
[NASA-CR-181615] 10 p1390 N88-18299

Relaxing the brightness constancy assumption in computing optical flow
[AD-A187437] 10 p1410 N88-18410

Specialized instrumentation for computational fluid dynamics research
[AD-A188160] 11 p1482 N88-18849

JPRS report. Science and technology: Europe and Latin America
[JPRS-ELS-87-054] 12 p1573 N88-19406

Some questions of using coding theory and analytical calculation methods on computers
[DE88-700905] 12 p1676 N88-20021

JPRS report. Science and technology: Europe and Latin America
[JPRS-ELS-87-055] 12 p1686 N88-20086

Online aiding for human-computer interfaces
[AD-A189239] 13 p1815 N88-20842

JPRS report: Science and technology. Japan
[JPRS-JST-88-001] 15 p2051 N88-22218

JPRS report: Science and technology. Japan
[JPRS-JST-87-029] 15 p2052 N88-22228

Complex sound processing: An interdisciplinary approach
[AD-A189782] 15 p2102 N88-22523

Extension of computer based algorithms by operator analysts
[NASA-CR-182798] 15 p2111 N88-22575

Design of the Detector 2: A CMOS gate array for the study of concurrent error detection techniques
[AD-A191247] 16 p2193 N88-23079

A new block solver for large, full, unsymmetric, complex systems of linear algebraic equations
[AD-A190590] 16 p2256 N88-23483

Computer and model changes at National Meteorological Center (NWC) 18 p2547 N88-25116

Technical communication in the computer industry: An information-development process to track, measure and ensure quality 23 p3297 N88-29635

Heavy ion and proton tests for subsystem upset
[AD-A195267] 24 p3434 N88-30442

CONCATENATED CODES
The design plan of a VLSI single chip (255, 223) Reed-Solomon decoder 04 p0435 N88-12697
Error control techniques for satellite and space communications
[NASA-CR-181581] 05 p0576 N88-13516
A concatenated coded modulation scheme for error control
[NASA-CR-182639] 12 p1621 N88-19697
CONCAVITY
Analytical investigation of reflection of a regular or mach reflection over a secondary wedge
[AD-A185690] 06 p0703 N88-14316
The heat transfer and fluid dynamics of concave surface curvature
[AD-A193064] 21 p2943 N88-27479
CONCENTRATION (COMPOSITION)
NT ATMOSPHERIC MOISTURE
NT CARBON DIOXIDE CONCENTRATION
NT METEOROID CONCENTRATION
NT MOISTURE CONTENT
High ionic conductivity in PEO.PPG block polymer and salt solutions
[AD-A183502] 01 p0026 N88-10168
Inerting and atmospheres 04 p0406 N88-12524
Investigation of the nature and concentration of vapor and mist during the cleaning of aircraft
[PML-1985-29] 05 p0623 N88-13817
Hydrochemical structure of Gulf Stream frontal zone waters 06 p0727 N88-14476
Realization of an instrument to measure temperature and concentration gradients in fluids — microgravity
[CISE-3128] 09 p1168 N88-17003
An infra-red investigation of HAN (Hydroxylammonium Nitrate)-based liquid propellants
[AD-A187226] 10 p1307 N88-17815
Determination of the equilibrium concentration of characteristic defects by the measurement of thermal expansion using neutron scattering and laser interferometry
[ETN-88-91489] 11 p1490 N88-18890
Hydrogen embrittlement of gun steel
[AD-A188972] 13 p1740 N88-20407
An experimental method for species concentration measurements in a welding arc using laser-induced fluorescence
[DE88-005638] 13 p1778 N88-20636
Research on influence of individual sea water components on spectral brightness coefficient of outgoing radiation 13 p1785 N88-20682
The effect of H2S concentration and pH on the cracking resistance of AISI 410 stainless steel in 5 percent brine
[NPL-DMA(A)-149] 14 p1890 N88-21294
Ultrasonic oxygen sensor
[AD-A189723] 15 p2105 N88-22537
Selective detection in gas chromatography
[AD-A191499] 18 p2481 N88-24718
Preferential surface adsorption in miscible blends of polystyrene and poly(vinyl methyl ether)
[AD-A191451] 18 p2490 N88-24769
Workshop on Atmospheric OH
[BPT-7/87] 18 p2538 N88-25063
Measurement of atmospheric OH with laser differential optical absorption spectroscopy (LDOAS)
18 p2539 N88-25068
Tropospheric OH measurements by long path absorption with rapid spectral concordance
18 p2539 N88-25069
Determination of tropospheric H concentrations by a double-pulsed UV laser method
18 p2539 N88-25070
Development of continuous wave laser frequency modulation of OH in tropospheric concentrations range
18 p2540 N88-25073
Evaluation of the toxicity of products from the thermal degradation of materials
[ETN-88-91995] 18 p2549 N88-25130
Characterization of yttrium aluminum garnet/YAG/using 14 MeV neutron activation
[AD-A191925] 18 p2582 N88-25342
Pyrolyzed organic polymer nitrogen dioxide sensor
19 p2669 N88-25868
Retrieval of temperature and concentration profiles from a limited number of absorption measurements
21 p2947 N88-27501
National ambient Volatile Organic Compounds (VOCs) data base update, documentation
[PB88-195631] 21 p2971 N88-27646
Nonseismic, surface geophysical and geochemical prospecting technology
[PB88-196613] 23 p3227 N88-29207
CONCENTRATORS
Focusing solar energy collector
02 p0159 N88-10996
Fundamentals and techniques of nonimaging optics research
[DE87-014544] 02 p0236 N88-11488
Mechanically stacked multijunction solar cells: An update on Sandia programs
[DE87-014641] 03 p0347 N88-12190
Crystalline cell research status and direction
[DE87-014214] 03 p0382 N88-12402
Solar converging method 04 p0403 N88-12504
Radiation performance of AlGaAs concentrator cells and expected performance of cascade structures
[NASA-TM-100145] 04 p0465 N88-12878
Development of mechanically stacked tandem concentrator cells
[DE88-001926] 06 p0730 N88-14490
Performance of highly concentrating mirror collectors and collector systems
[DFVLR-FB-87-29] 09 p1186 N88-17107
Solar concentrator advanced development program, task 1
[NASA-CR-179489] 10 p1350 N88-18068
Side-by-side comparisons of evacuated compound parabolic concentrator and flat plate solar collector systems at temperatures of 90 to 100°C
[DE88-004717] 10 p1351 N88-18073
Performance and cost benefits associated with nonimaging secondary concentrators used in point-focus dish solar thermal applications
[DE88-001104] 13 p1792 N88-20718
Point-focus concentrator reflector assembly, phase 1
[DE88-003616] 13 p1792 N88-20720
Space station solar concentrator materials research
[NASA-TM-100862] 14 p1882 N88-21250
Recent advances in photovoltaic concentrator technology
[DE88-003948] 15 p2091 N88-22462
Thermal distortion analysis of the space station solar dynamic concentrator
[NASA-TM-100868] 19 p2606 N88-25475
Influence of refractive index and solar concentration on optical power absorption in slabs
[NASA-TM-4056] 19 p2726 N88-26190
Photovoltaic concentrator technology: Recent results
[DE88-009588] 20 p2819 N88-26726
Performance sensitivities for point-focus dish systems with secondary concentrators
[DE88-001152] 21 p2968 N88-27629
Photovoltaic Energy. Electricity from Sunlight: A current awareness bulletin
[DE88-008289] 21 p2969 N88-27634
CONCENTRIC CYLINDERS
Study of temperature and stress fields of two sliding cylinders
[ETN-88-92134] 20 p2815 N88-26704
CONCENTRIC SPHERES
Finitely many delta-interactions with supports on concentric spheres
[DE88-701834] 20 p2880 N88-27101
Radiative heat transfer to chemically reacting flow between concentric rotating spheres
[DE88-702538] 22 p3118 N88-28525
CONCENTRICITY
Fitting a circle to radially suppressed data
[NPL-DITC-103/87] 17 p2392 N88-24223
CONCORDE AIRCRAFT
Supersonic transport/hypersonic transport (SST/HST) development
[REPT-881-111-101] 21 p2896 N88-27192
CONCRETE STRUCTURES
The Shock and Vibration Bulletin. Part 4: Structural Dynamics and Modal Test and Analysis
[AD-A186751] 09 p1179 N88-17062
Analysis of reinforced concrete structures under the effects of localized detonations
09 p1179 N88-17064
Reinforced concrete arches under blast and shock environments 09 p1180 N88-17065
Reliability of structures with stiffness and strength degradation 09 p1180 N88-17068
CONCRETES
Reinforced flexural elements for TEMP-STRESS Program
[DE87-012961] 01 p0061 N88-10391
The ability of modified pavement quality concrete to resist ground erosion caused by VTOL aircraft
[BAE-ARG-238] 03 p0267 N88-11683
Open-graded bases for airfield pavements
[AD-A184461] 04 p0402 N88-12500
A laboratory study of asphalt concrete mix designs for high-contact pressure aircraft traffic
[AD-A185753] 06 p0670 N88-14106
Comparative study of nondestructive pavement testing, MacDill Air Force Base, Florida
[AD-A186082] 07 p0822 N88-14993
Investigation of the inter-relationship between base pavement stiffness and asphalt overlay compaction
[DOT/FAA/ES-88/1] 14 p1869 N88-21170
Design of overlays for rigid airport pavements
[DOT/FAA/PM-87/19] 18 p2468 N88-24652
A simple unified method for predicting the deflections of reinforced concrete structures
19 p2679 N88-25930
An assessment of modelling techniques for the finite element analysis of reinforced concrete plate and shell structures
[AD-A192263] 20 p2814 N88-26697
CONCURRENT PROCESSING
Strategies for concurrent processing of complex algorithms in data driven architectures
[NASA-CR-181435] 01 p0082 N88-10527
Petri nets as a support to symbolic execution of concurrent Ada programs
[REPT-87-007] 01 p0082 N88-10529
Local concurrent error detection and correction in data structures using virtual backpointers
[NASA-CR-181432] 01 p0106 N88-10692
Delft parallel processor 84/16
[PB87-226254] 03 p0366 N88-12305
Comparing barrier algorithms
[NASA-CR-178377] 04 p0476 N88-12934
Methods for design and evaluation of integrated hardware/software systems for concurrent computation
[NASA-CR-181522] 04 p0479 N88-12953
Indirect solution of static problems using concurrent vector processing computers
[DE87-012105] 05 p0636 N88-13889
Structuring data for concurrent vectorized processing in a transient dynamics finite element program
[DE87-013082] 05 p0636 N88-13890
Fault-tolerant computer architecture based on INMOS transputer processor 06 p0797 N88-14880
AFL-1: A programming language for massively concurrent computers
[AD-A186422] 07 p0906 N88-15489
SISAL: Initial MIMD performance results
10 p1375 N88-18208
A paradigm for concurrency control performance evaluation 10 p1377 N88-18220
Concurrency control and reliability in replicated database systems 10 p1377 N88-18221
Strategies for concurrent processing of complex algorithms 10 p1379 N88-18236
Resilient procedures: A structured replication approach 10 p1381 N88-18245
A digital logic simulator with concurrent programming considerations
[AD-A188823] 12 p1678 N88-20032
Support for concurrent computing environments
[AD-A188498] 12 p1680 N88-20043
The effects of two Carlucci initiatives concurrency and streamlining, on the test and evaluation phase of system acquisitions 12 p1704 N88-20198
The physical structure of concurrent problems and concurrent computers
[DE88-005812] 13 p1814 N88-20835
On proving register atomicity
[CWI-CS-R8707] 13 p1818 N88-20862
A proof rule process creation
[CWI-CS-R8710] 13 p1822 N88-20891
Merge and termination in process algebra
[CWI-CS-R8716] 13 p1826 N88-20918
Abstraction and empty process in process algebra
[CWI-CS-R8721] 13 p1826 N88-20919
Atomic multireader register — computer storage
[CWI-CS-R8722] 14 p1954 N88-21648
Verification of an algorithm for log-time sorting by square comparison
[CWI-CS-R8729] 14 p1958 N88-21656
On the design of some systolic algorithms
[CS-8705] 14 p1957 N88-21666
The software repeater (an exercise in Z specification)
[RSRE-MEMO-4090] 14 p1958 N88-21677
Strategies for concurrent processing of complex algorithms in data driven architectures
[NASA-CR-181657] 16 p2193 N88-23083
Correctness proofs for systolic algorithms: A palindrome recognizer
[CWI-CS-R8747] 16 p2248 N88-23434
A very simple construction for atomic multiwriter register
[CWI-CS-R8751] 16 p2249 N88-23436
Concurrency efficiency user's manual
[AD-A190884] 16 p2251 N88-23450
Systolic algorithm for matrix-vector multiplication
[PB88-165394] 16 p2256 N88-23484
Readiness and failures in the algebra of communicating processes
[CWI-CS-R8748] 16 p2258 N88-23499

Design, implementation and evaluation of an operating system for a network of transputers
[AD-A186593] 18 p2559 N88-25193
Modeling and optimum time performance for concurrent processing
[NASA-CR-4167] 20 p2797 N88-26595
Contractions in comparing concurrency semantics
[CWI-CS-R8755] 20 p2840 N88-26850
Markov chain computations to a solution of the mutual-exclusion problem in concurrency
[REPT-87-89] 20 p2847 N88-26896
Computer system for the primary fly-by-wire control of civil transport aircraft (experimental system)
[FBW-TB-2086/88] 21 p2898 N88-27204
Model for dynamically structured communicating systems
[PB88-105283] 21 p2931 N88-27402
Bisimulation can't be traced
[AD-A192725] 21 p2996 N88-27766
Image processing using a parallel architecture
[AD-A192633] 21 p3002 N88-27803
Queueing network models for parallel processing of task systems: An operational approach
[NASA-CR-183174] 22 p3141 N88-28677
Using Petri nets for real-time development environments
[REPT-88-005] 22 p3141 N88-28679
The concurrent common Lisp development environment 23 p3263 N88-29422
Performance analysis of k-ary n-cube interconnection networks
[AD-A195542] 24 p3361 N88-30010
Performance prediction of concurrent systems
[NASA-CR-183175] 24 p3412 N88-30312

CONDENSATES
Rayleigh scattering measurements of a freejet with homogeneous condensation 03 p0319 N88-12020
An investigation of the infrared emission spectra of carbon condensates 14 p1886 N88-21272
Method of evaporation
[NASA-CASE-NPO-15609-2] 17 p2318 N88-23846

CONDENSATION
Experimental and theoretical study of condensation in multicomponent mixtures
[DE88-002715] 07 p0830 N88-15033
Vapor condensation on a turbulent liquid interface 08 p0982 N88-15939

CONDENSED MATTER PHYSICS
Shock-induced cooling in dense fluids
[DE87-014343] 02 p0170 N88-11067
Physics of condensed matter at extreme conditions
[DE88-006232] 13 p1832 N88-20958
Research in the theory of condensed matter and elementary particles
[DE88-010180] 22 p3151 N88-28749
Nonlinear optical processes in molecular systems
[AD-A193871] 23 p3282 N88-29546

CONDENSER RADIATORS
U CONDENSERS (LIQUEFIERS)
U HEAT RADIATORS

CONDENSERS
Dynamic isotope power system critical component verification 17 p2425 N88-24421
Vapor Compression Distillation Subsystem (VCDS) component enhancement, testing and expert fault diagnostics development, volume 1
[NASA-CR-172072] 22 p3134 N88-28634
Study of toluene rotary fluid management device and shear flow condenser performance for a space-based organic Rankine power system
[NASA-CR-180885] 24 p3338 N88-29872

CONDENSERS (LIQUEFIERS)
Design of a condenser-boiler for a binary mercury-organic Rankine cycle solar dynamic space power system
[AD-A184188] 03 p0348 N88-12198
Proceedings of the 1987 International Symposium on Condensing Heat Exchangers
[DE88-005230] 13 p1766 N88-20564
Experimental demonstrations of organic Rankine cycle waste heat rejection systems 17 p2432 N88-24469
Tower evaporator
[NASA-CASE-NPO-15609-2] 18 p2497 N88-24815

CONDENSING
NT FILM CONDENSATION
Statistical mechanical theory of condensed explosives
[DE87-009137] 01 p0031 N88-10197
An investigation of the behavior of outgassed molecules in thermal vacuums 02 p0133 N88-10836
Experimental and theoretical study of condensation in multicomponent vapors
[DE87-013663] 02 p0145 N88-10907
Turbine airfoil deposition models and their hot corrosion implications 02 p0189 N88-11178
Mesoscale very short-range numerical prediction with dynamical initialization including condensation heating 02 p0213 N88-11341
Experimental and theoretical study of condensation in multicomponent mixtures
[DE88-000897] 04 p0413 N88-12563
Inertial confinement fusion reactor cavity analysis
[DE88-000788] 04 p0492 N88-13028
Advanced condensing heat exchangers
[DE88-001485] 06 p0699 N88-14288
Equation of state of condensed materials physical principles and applications
[NASA-TT-20007] 08 p0968 N88-15855
Some problems of the theory of bubble growth and condensation in bubble chambers
[NASA-TT-20232] 13 p1771 N88-20593
Dependence of structure of stabilized ZrO2 coatings on condensation rate 16 p2180 N88-22990
Static dielectric breakdown strength of condensed heterogeneous high explosives
[AD-A191035] 16 p2183 N88-23014
Proceedings of the Cooling, Condensation, and Storage of Hydrogen Cluster Ions Workshop
[AD-A189857] 16 p2266 N88-23555
Associative two-body condensation in laser-cooled sodium and hydrogen 16 p2267 N88-23559
Key problems and hydrogen atom formation 16 p2269 N88-23573
The cluster ion approach to the condensation and storage of antihydrogen 16 p2269 N88-23575
Analysis of containerless condensation of polyatomic hydrogen ions, with emphasis on H3(+,-) association channels and a future workshop to study related topics 16 p2269 N88-23576
Small molecule and small cluster ion formation in a low-density containerless mixture of electrons, protons and hydrogen atoms 16 p2269 N88-23577
Transient analysis of heat pipe vapor dynamics 17 p2412 N88-24341
Analysis and interpretation of low gravity boiling experiments in the KC-135 17 p2432 N88-24466
Storage of thermal energy by means of an absorption cycle
[PB88-190814] 21 p2966 N88-27619
Finite-rate water condensation in combustion-heated wind tunnels
[NASA-TP-2833] 22 p3046 N88-28075
Electronic states of the Xe(sub n)HCl systems in gas and condensed phases
[AD-A193881] 23 p3192 N88-28997

CONDITIONED RESPONSES
U CONDITIONING (LEARNING)

CONDITIONING (LEARNING)
Short- and long-term effects of nonlethal levels of fast high-energy helium ions on retention of developed and formation of new behavioral patterns in rats 10 p1362 N88-18140
Two attentional models of classical conditioning: Variations in CS effectiveness revisited
[AD-A187697] 11 p1522 N88-19088
A neuronal model of classical conditioning
[AD-A188378] 12 p1670 N88-19999
Learning by experimentation
[AD-A188912] 12 p1681 N88-20053
Behavior, physiology and energy deposition in rats chronically exposed to 2450 MHz radiation
[PB88-171418] 16 p2237 N88-23363

CONDITIONS
NT ADIABATIC CONDITIONS
NT FLIGHT CONDITIONS
NT KUTTA-JOUKOWSKI CONDITION
NT LIPSCHITZ CONDITION
NT NONEQUILIBRIUM CONDITIONS
NT RUNWAY CONDITIONS

CONDUCTANCE
U RESISTANCE

CONDUCTING MEDIA
U CONDUCTORS

CONDUCTION BANDS
Silicon-germanium heterostructures 13 p1844 N88-21034
Recent data on Si:As impurity band conduction multiplexed arrays
[AD-A191752] 18 p2582 N88-25340
Investigation of electronic band structure of semiconductors by photoemission
[ETN-88-92370] 21 p3025 N88-27957

CONDUCTION ELECTRONS
Gaining control over rare earth valence fluctuations
[DE87-010116] 01 p0103 N88-10671
Point defect structure of Cr2O3
[AD-A187620] 11 p1556 N88-19317

CONDUCTIVE HEAT TRANSFER
Analytical treatment of the melting and solidification of latent heat store materials in finned tube geometries
[IKE-5-223] 03 p0314 N88-11985
Microgravity nucleation and particle coagulation experiments support
[NASA-CR-181540] 04 p0423 N88-12618
Microgravity nucleation and particle coagulation experiments support
[NASA-CR-181541] 04 p0423 N88-12619
The unsteady ground heat flow at the contact surface between a glacier run and the subsoil 08 p1014 N88-16147
A semianalytical solution of the heat conduction equation for several boundary conditions 08 p1014 N88-16148
Determination of the heat conduction coefficient of the soil from the advance of the diurnal temperature wave 08 p1015 N88-16151
Symbolic, algebraic, and numeric solutions to heat conduction problems using Green's functions 09 p1165 N88-16987
Numerical solutions of two moving boundary problems by both finite difference and finite element methods with applications
[DE88-002867] 09 p1230 N88-17374
Approximate solutions of heat conduction in a medium with variable properties
[AD-A186933] 10 p1326 N88-17925
Electron heat transport in TFR with Electron Cyclotron Resonance Heating (ECRH) 12 p1694 N88-20135
A report on the study of algorithms to enhance vector computer performance for the discretized one-dimensional time-dependent heat conduction equation: EPIC research, phase 1
[DE88-005642] 13 p1820 N88-20880
Efficiency of fusion during periodic-pulse laser-beam welding 14 p1897 N88-21324
A small concentration expansion for the effective heat conductivity of a random disperse two-component material; an assessment of Batchelor's renormalization method
[REPT-87-71] 16 p2207 N88-23168
Three-dimensional curved shell and solid-shell transition finite elements with temperature and temperature gradients as primary variables for steady state heat conduction 17 p2349 N88-23997
Mathematical modelling of the heat and water vapour transport in the human respiratory tract 17 p2382 N88-24160
Microgravity thaw experiment (MITEX) 17 p2427 N88-24439
Ammonia boiling in long tubes. Heat transfer and charge loss in vertical and horizontal tubes
[NASA-TT-20313] 19 p2667 N88-25858
Moment approach to neoclassical flows, currents and transport in auxiliary heated tokamaks
[DE88-008024] 21 p3016 N88-27901
Steady conduction of heat in prolate spheroidal systems
[LRT-WE-9-FB-16(1987)] 22 p3077 N88-28272
Heat transport in a parabolic tube of circular cross-section
[LRT-WE-9-FB-2(1988)] 22 p3078 N88-28274
Applications of an exponential finite difference technique
[NASA-TM-100939] 22 p3084 N88-28312
An analysis of heat transfer after loss of primary coolant in the SP-100 reactor system
[AD-A194619] 23 p3281 N88-29539

CONDUCTIVITY
Electronic conduction in molten sodium chloride
[DE87-010083] 02 p0144 N88-10901
DC conductivity studies in Li5AlO4 at intermediate temperatures and its possible application for the electrolysis of water
[AD-A185489] 06 p0697 N88-14276
Electromagnetic scattering from and natural resonances of the circular strip 13 p1759 N88-20523
The protonic Beta double prime aluminas: Preparation, stability, conductivity and structure
[DE88-008442] 20 p2768 N88-26415
Theoretical aspects of electron transport in modulated structures 20 p2865 N88-27016
Hydrogen concentration cells as converters of heat into electricity
[DE88-009662] 23 p3229 N88-29216

CONDUCTIVITY METERS
NT ELECTRICAL CONDUCTIVITY METERS

CONDUCTORS
NT BUS CONDUCTORS
NT ELECTRIC CONDUCTORS
NT ELECTRIC WIRE
NT ELECTROLYTES
NT HIGH TEMPERATURE SUPERCONDUCTORS
NT ION EXCHANGE MEMBRANE ELECTROLYTES
NT MOLTEN SALT ELECTROLYTES
NT NONAQUEOUS ELECTROLYTES
NT PHOTOCONDUCTORS
NT SOLID ELECTROLYTES
NT SUPERCONDUCTORS

Novel conductive polymers
[EP-PATENT-0-182-548-A2] 01 p0026 N88-10163
Experiments: Test range facilities, part 2
03 p0305 N88-11921
Electromagnetic scattering by a thick strip on a half-space
[PB87-227096] 03 p0306 N88-11928
The dc conductivity studies of an hydroxide ion conductor at intermediate temperatures
[AD-A186044] 07 p0847 N88-15142
Processing, fabrication, applications and limitations of inherently conducting polymers
[DE88-003210] 08 p0973 N88-15883
Lithium fast-ion conductors: Polymer based materials
[AD-A187879] 11 p1461 N88-18712
The effects of various conductor components on Nb3Sn filament prestrain in cable-in-conduit conductors
[DE88-003956] 11 p1479 N88-18824
Measurement of the properties of lossy materials inside a finite conducting cylinder
[NASA-CR-182664] 13 p1832 N88-20962
Characterization of proton conducting polymer blends
19 p2669 N88-25867
Conductor loss in superconducting power transmission cables
[DE88-011414] 23 p3290 N88-29586

CONES
NT ABLATIVE NOSE CONES
NT CONICAL BODIES
NT NOSE CONES
NT ROCKET NOSE CONES
NT SLENDER CONES
Hydroburst test of a carbon-carbon involute exit cone
[NASA-TP-2556] 06 p0671 N88-14112
Calculation of symmetric and asymmetric vortex seperation on cones and tangent ogives based on discrete vortex models
[NASA-CR-4122] 08 p0950 N88-15768

CONFERENCES
International Conference on the Aerodynamics at Low Reynolds Numbers between 10(4) and 10(6)
[ONRL-7-023-C] 01 p0002 N88-10010
Spacecraft 2000
[NASA-CP-2473] 01 p0015 N88-10084
Ceramic-Ceramic Composites Meeting in Belgium
[ONRL-7-020-R] 01 p0019 N88-10118
Remote Sensing-Arid Lands Workshop, Page, Arizona, June 10-12, 1986
[DE87-012368] 01 p0064 N88-10412
Remote sensing of environmental pollution
[DFVLR-MITT-87-04] 01 p0067 N88-10428
Transactions of the 4th Army Conference on Applied Mathematics and Computing
[AD-A183544] 01 p0085 N88-10547
ESA Workshop on Optical Interferometry in Space
[ESA-SP-273] 01 p0094 N88-10613
STIP Symposium on Physical Interpretation of Solar/Interplanetary and Cometary Intervals
[NASA-CR-181201] 01 p0110 N88-10709
Overview of STIP intervals 15-19
01 p0110 N88-10710
Solar events and their influence on the interplanetary medium 01 p0115 N88-10734
Knowledge Based Concepts and Artificial Intelligence: Applications to Guidance and Control
[AGARD-LS-155] 02 p0128 N88-10806
Fourteenth Space Simulation Conference: Testing for a Permanent Presence in Space
[NASA-CP-2446] 02 p0132 N88-10829
Space Construction
[NASA-CP-2490] 02 p0138 N88-10870
The 1986 Goddard Space Flight Center Battery Workshop
[NASA-CP-2486] 02 p0163 N88-11021
Turbine Engine Hot Section Technology, 1985
[NASA-CP-2405] 02 p0184 N88-11140
Proceedings of the Solar Thermal Technology Conference
[DE87-014441] 02 p0195 N88-11220
Siting and Geotechnical Program Focus and Directions. Report upon the deliberations of a workshop held at the Illinois Institute of Technology, Chicago, Illinois on August 4-5, 1986
[PB87-206272] 02 p0198 N88-11238
Mesoscale Analysis and Forecasting: Incorporating Nowcasting
[ESA-SP-282] 02 p0199 N88-11239
Tutorial and hands-on demonstration of a fluent interpreter for CARE 3
[NASA-TM-4011] 02 p0220 N88-11383
Proceedings of the Workshop on Opportunities for Atomic Physics Using Slow, Highly-Charged Ions
[DE87-013991] 02 p0231 N88-11457
Rotorcraft Design for Operations
[AGARD-CP-423] 03 p0262 N88-11649
Space Environment Technology --- conference
[ISBN-2-85428-170-5] 03 p0271 N88-11702
International Conference on Microstructology held in Gainesville, Florida on 7-9 May 1986
[AD-A184604] 03 p0290 N88-11822
Technical evaluation report on the Fluid Dynamics Panel Symposium on aerodynamic and related hydrodynamic studies using water facilities
[AGARD-AR-225] 03 p0312 N88-11968
Commercial Opportunities for Remote Sensing with Polar Platforms
[ESA-SP-269] 03 p0339 N88-12131
SPOT 1: First In-Flight Results --- conferences
[ISBN-2-85428-177-2] 03 p0340 N88-12143
The Conference on the Dynamics of Molecular Collisions held in Oglebay Park, Wheeling, West Virginia on 12-17 July 1987
[AD-A184690] 03 p0374 N88-12354
Spacecraft Fire Safety
[NASA-CP-2476] 04 p0406 N88-12520
Proceedings of the Fifth Symposium on Energy Engineering Sciences: Instrumentation, Diagnostics, and Material Behavior
[DE88-001479] 04 p0429 N88-12660
Proceedings: SDIO/DARPA Workshop on Laser Propulsion. Volume 3: Viewgraphs
[DE88-000964] 04 p0450 N88-12790
Proceedings of the Eleventh DOE Solar Photochemistry Research Conference
[DE88-000678] 04 p0466 N88-12883
Research papers and publications (1981-1987): Workload research program
[NASA-TM-100016] 04 p0474 N88-12924
Proceedings of the Japan-US Workshop P-92 on Plasma Material Interaction/High Heat Flux Data Needs for the Next Step Ignition and Steady State Devices
[DE87-013568] 04 p0494 N88-13042
Fifth Cambridge Workshop on Cool Stars, Stellar Systems and the Sun 04 p0502 N88-13092
Aerodynamics of Hypersonic Lifting Vehicles
[AGARD-CP-428] 05 p0529 N88-13219
Proceedings of the 4th NAL Symposium on Aircraft Computational Aerodynamics
[NAL-SP-7] 05 p0535 N88-13253
Special Course on Fundamentals of Fighter Aircraft Design
[AGARD-R-740] 05 p0544 N88-13315
Workshop on Avionics Corrosion Control
[AGARD-R-733] 05 p0547 N88-13331
Static Aeroelastic Effects on High Performance Aircraft
[AGARD-CP-403] 05 p0550 N88-13348
The 58th Shock and Vibration Symposium, volume 1
[NASA-CP-2488-VOL-1] 05 p0592 N88-13609
Fatigue 87, volume 1
[AD-A184045] 05 p0597 N88-13645
Scientific and Operational Requirements for TOMS Data
[NASA-CP-2497] 05 p0615 N88-13774
Proceedings of the 17th International Conference on Phenomena in Ionized Gases held in Budapest, Hungary, July 8-12, 1985: Invited papers
[DE87-703562] 05 p0651 N88-13987
Calendar of selected aeronautical and space meetings
[AGARD-CAL-87/1] 05 p0657 N88-14033
Calendar of selected aeronautical and space meetings
[AGARD-CAL-88/1] 05 p0658 N88-14037
Guidance for conference rapporteurs
[NASA-CR-182338] 05 p0659 N88-14042
Summary of discussions at the Ninth Meeting of the Sandia Cooperative Group on the Aerothermochemistry of Turbulent Combustion
[DE88-002281] 06 p0680 N88-14165
Proceedings of the 2nd Regional Electromagnetic Workshop at Argonne National Laboratory
[DE87-004633] 06 p0690 N88-14230
Report of the 3rd Finnish EISCAT Workshop --- European Incoherent Scatter Radar (EISCAT)
[REPT-111] 06 p0691 N88-14233
Eddy Current Seminar, 24-26 March 1986
[PB87-124988] 06 p0696 N88-14269
International workshop on two-phase flow fundamentals
[DE88-001478] 06 p0699 N88-14287
Introduction to Computational Fluid Dynamics
[VKI-LS-1987-02] 06 p0701 N88-14300
Airborne Visible/Infrared Imaging Spectrometer (AVIRIS). A description of the sensor, ground data processing facility, laboratory calibration, and first results
[NASA-CR-182365] 06 p0705 N88-14325
Small High Pressure Ratio Turbines --- conference
[VKI-LS-1987-07] 06 p0712 N88-14364
Fatigue 87, volume 2
[AD-A184046] 06 p0715 N88-14381
Strategic Defense Initiative Organization/DARPA (Defense Advanced Research Projects Agency) workshop on laser propulsion. Volume 1: Executive summary
[DE87-003254] 06 p0768 N88-14722
Research in elementary particle physics
[DE88-002130] 06 p0777 N88-14771
Langley Symposium on Aerodynamics, volume 1
[NASA-CP-2397] 07 p0809 N88-14926
Wind shear detection. Forward-looking sensor technology
[NASA-CP-10004] 07 p0817 N88-14970
Round table on the future of satellite communications and broadcasting in Europe
[ESA-STR-221] 07 p0843 N88-15112
Flow in Centrifugal Compressors --- conference
[VKI-LS-1987-01] 07 p0850 N88-15160
The results of the 1984/1985 Round-Robin Calibration of Reference Solar Cells for the Summit Working Group on Technology, Growth and Employment
[DE88-900215] 07 p0874 N88-15303
Highlights of the 70th Flight Mechanics Panel Symposium on Flight Vehicle Development Time and Cost Reduction
[AD-A185831] 07 p0901 N88-15454
Proceedings of Image Understanding Workshop, volume 1
[AD-A186103] 07 p0902 N88-15463
Proceedings of Image Understanding Workshop, volume 2
[AD-A186104] 07 p0902 N88-15464
Proceedings of the Second International Symposium on Methodologies for Intelligent Systems: Colloquia program
[DE88-001490] 07 p0907 N88-15498
Recent developments in the numerical solution of differential/algebraic systems
[DE88-001885] 07 p0912 N88-15535
Finnish-Soviet Symposium on Radio Astronomy (1st) held at Otaniemi on August 26-27, 1985
[PB87-140661] 07 p0944 N88-15736
Influence of Environmental Factors on Aircraft Wing Performance
[VKI-LS-1987-03] 08 p0951 N88-15771
Aeropropulsion '87. Session 4: Instrumentation and Controls Research
[NASA-CP-10003-SESS-4] 08 p0955 N88-15794
Aeropropulsion '87. Session 5: Subsonic Propulsion Technology
[NASA-CP-10003-SESS-5] 08 p0956 N88-15800
Aeropropulsion '87. Session 6: High-Speed Propulsion Technology
[NASA-CP-10003-SESS-6] 08 p0957 N88-15807
Cryogenic Fluid Management Technology Workshop. Volume 1: Presentation material and discussion
[NASA-CP-10001] 08 p0980 N88-15924
Computational Fluid Dynamics
[VKI-LS-1987-04] 08 p0984 N88-15951
Finite Element Calculation Methods and Their Application to Turbomachinery Flows, volume 1
[VKI-LS-1987-05-VOL-1] 08 p0985 N88-15960
Introduction to the Modeling of Turbulence
[VKI-LS-81-06] 08 p0986 N88-15972
Solid mechanics research for quantitative non-destructive evaluation
[AD-A186599] 08 p0993 N88-16010
The Shock and Vibration Bulletin. Part 3: Isolation and damping, vibration test criteria, and vibration analysis and test
[AD-A186750] 08 p0997 N88-16040
Proceedings of the 8th ESA Symposium on European Rocket and Balloon Programs and Related Research
[ESA-SP-270] 08 p1024 N88-16201
Ocean Colour Workshop --- conference
[ESA-SP-1083] 08 p1042 N88-16292
USSR Space Life Sciences Digest, issue 14
[NASA-CR-3922(16)] 08 p1045 N88-16317
Proceedings of the DOD Workload Assessment Workshop on Workload Assessment Techniques and Tools held in Dayton, Ohio on 27-28 September 1986
[AD-A185850] 08 p1052 N88-16352
Third Conference on Artificial Intelligence for Space Applications, part 1
[NASA-CP-2492-Pt-1] 08 p1055 N88-16360
Proceedings of the 21st ESLAB Symposium on Small Scale Processes in the Chromosphere/Corona, Interplanetary Medium and Planetary Magnetospheres
[ESA-SP-275] 08 p1094 N88-16582
NASA/Army Rotorcraft Technology. Volume 1: Aerodynamics, and Dynamics and Aeroelasticity
[NASA-CP-2495-VOL-1] 09 p1105 N88-16625
NASA/Army Rotorcraft Technology. Volume 2: Materials and Structures, Propulsion and Drive Systems, Flight Dynamics and Control, and Acoustics
[NASA-CP-2495-VOL-2] 09 p1106 N88-16632
Unispace 82 09 p1128 N88-16766

Proceedings of the ESA Workshop on Co-Orbiting Platform Elements (COPE)
[ESA-SP-1093] 09 p1129 N88-16777
The Shock and Vibration Bulletin. Part 2: Instrumentation, shock analysis, and shock testing
[AD-A186749] 09 p1178 N88-17053
The Shock and Vibration Bulletin. Part 4: Structural Dynamics and Modal Test and Analysis
[AD-A186751] 09 p1179 N88-17062
Space Bioreactor Science Workshop
[NASA-CP-2485] 09 p1196 N88-17168
First Annual Workshop on Space Operations Automation and Robotics (SOAR 87)
[NASA-CP-2491] 09 p1203 N88-17206
Scientific Colloquium in Honor of Prof. Dr. Rer. Nat. Hermann L. Jordan
[DFVLR-MITT-87-11] 09 p1240 N88-17432
Proceedings of the International Workshop on Engineering Design of Next Step Reversed Field Pinch Devices
[DE88-001915] 09 p1251 N88-17494
Airborne Wind Shear Detection and Warning Systems: First Combined Manufacturers' and Technologists' Conference
[NASA-CP-10006] 10 p1273 N88-17616
Advanced Technology for Aero Gas Turbine Components
[AGARD-CP-421] 10 p1279 N88-17647
High resolution electron and ion microscopy
[AERE-R-12502] 10 p1297 N88-17754
Second All-Union Conference on Physiology of Extreme States and Individual Protection of Man
10 p1363 N88-18147
Minutes of the meeting of the Indo-US Subcommission on Science and Technology (8th) held at Washington, D.C. on September 22-24, 1986
[PB88-130158] 10 p1423 N88-18503
International Conference on Industrial and Applied Mathematics
[AD-A188251] 11 p1483 N88-18851
The 58th Shock and Vibration Symposium, volume 2
[NASA-CP-2488-VOL-2] 11 p1499 N88-18948
8th Wind Energy Symposium
[DE88-770028] 11 p1507 N88-19004
Proceedings of the 12th Symposium of Japan Solar Energy Society
[DE88-770029] 11 p1507 N88-19005
Proceedings of the 1987 High-Efficiency Photovoltaic Subcontractors' Review Meeting
[DE88-003354] 11 p1508 N88-19011
Alternative Energy in the Midwest: Research and Applications. Conference Proceedings, Rosemont, Illinois, March 19-20, 1987
[PB88-142278] 11 p1509 N88-19015
Proceedings of the 19th DOE/NRC Airborne Waste Management and Air Cleaning Conference
[NUREG/CP-0086-VOL-1] 11 p1509 N88-19018
Proceedings of the 19th DOE/NRC Airborne Waste Management and Air Cleaning Conference
[NUREG/CP-0086-VOL-2] 11 p1509 N88-19019
Cumulative reports and publications through December 31, 1987
[NASA-CR-181624] 11 p1524 N88-19099
Multigrid methods: Special topics and applications --- conference
[GMD-120] 11 p1537 N88-19187
Sixteenth AINSE Plasma Physics Conference. Conference handbook
[DE88-700825] 11 p1552 N88-19290
Proceedings of US-Japan Heliotron-Stellarator Workshop, volume 3
[DE88-004788] 11 p1554 N88-19299
Proceedings of US-Japan Heliotron-Stellarator Workshop, volume 2
[DE88-004789] 11 p1554 N88-19300
Proceedings of the Polycrystalline Thin Film Program Meeting
[DE87-001169] 11 p1557 N88-19321
Proceedings of the First International Symposium on Physical and Technical Problems of Superconductivity Application in Power Generation
[DE88-700818] 11 p1559 N88-19332
Whither many-body theory. A summary of the Oulu Conference
[DE88-003095] 11 p1563 N88-19358
Thirteenth Biennial Guidance Test Symposium, volume 1
[AD-A185782] 12 p1576 N88-19427
Workshop on Design Loads for Advanced Fighters
[AGARD-R-746] 12 p1579 N88-19449
Proceedings of the 1st European In-Orbit Operations Technology Symposium
[ESA-SP-272] 12 p1585 N88-19484
Advances in Air-Launched Weapon Guidance and Control
[AGARD-CP-431] 12 p1596 N88-19553
Progress toward a cosmic dust collection facility on space station
[NASA-CR-182427] 12 p1598 N88-19566
Terrestrial Propagation Characteristics in Modern Systems of Communications, Surveillance, Guidance and Control
[AGARD-CP-407] 12 p1614 N88-19653
Proceedings of the Forest-Atmosphere Interaction Workshop
[CONF-8510250] 12 p1641 N88-19824
Proceedings of an ESA-NASA Workshop on a Joint Solid Earth Program
[NASA-CR-182642] 12 p1644 N88-19844
Proceedings of the 3rd European Symposium on Life Sciences Research in Space
[ESA-SP-271] 12 p1652 N88-19893
FOM contributions to the 14th European Conference on Controlled Fusion and Plasma Physics
[REPT-87-174] 12 p1693 N88-20129
Martian geomorphology and its relation to subsurface volatiles
[NASA-CR-182428] 12 p1711 N88-20237
Gordon Conference on Intermetallic Compounds held at Tilton, New Hampshire on 20-24 July 1987
[AD-A188502] 13 p1745 N88-20435
IAEA Specialists' Meeting on Graphite Component Structural Design
[DE88-780006] 13 p1746 N88-20439
Proceedings of the 1987 International Symposium on Condensing Heat Exchangers
[DE88-005230] 13 p1766 N88-20564
Cryogenic Fluid Management Technology Workshop. Volume 2: Roundtable Discussion of Technology Requirements
[NASA-CP-10009] 13 p1772 N88-20599
Sixteenth NASTRAN (trademark) Users' Colloquium
[NASA-CP-2505] 13 p1780 N88-20652
Dynamics of the Oceanic Surface Mixed Layer
[AD-A188348] 13 p1804 N88-20785
Regional Conference on the Analysis of the Unbalanced Mixed Model
[AD-A188747] 13 p1830 N88-20943
ONR Far East Scientific Bulletin, volume 12, number 3, July-September 1987
[AD-A188554] 13 p1851 N88-21081
Proceedings of the 3rd European Space Mechanisms and Tribology Symposium
[ESA-SP-279] 14 p1874 N88-21191
Towards a tribology information system: The results of a Planning Workshop held at the National Bureau of Standards, July-August 1985
[PB88-168604] 14 p1918 N88-21448
Climatology and space observations
[ISBN-2-85-428179-9] 14 p1935 N88-21536
CARE 3 User's Workshop
[NASA-CP-10011] 14 p1954 N88-21646
United States - Japan Seminar on Quantum Mechanical Aspects of Quantum Electronics
[AD-A186938] 14 p1974 N88-21781
Proceedings of the Seminar on Hydrodynamics and Crystal Growth
[ETN-88-92025] 14 p1987 N88-21853
Proceedings of the International Symposium on the Diversity and Similarity of Comets
[ESA-SP-278] 14 p1994 N88-21884
Summary of the 1987 Gordon Research Conference on Corrosion
[AD-A189737] 15 p2041 N88-22161
Lewis Structures Technology, 1988. Volume 3: Structural Integrity Fatigue and Fracture Wind Turbines HOST
[NASA-CP-3003-VOL-3] 15 p2081 N88-22408
Proceedings of the Lightning Threat Warning Workshop
[DE88-006607] 15 p2098 N88-22499
Ocean general circulation models: Report on proceedings of a meeting of ocean and climate modelers
[DE88-005530] 15 p2099 N88-22504
NASA scientific and technical publications: A catalog of Special Publications, Reference Publications, Conference Publications, and Technical Papers, 1987
[NASA-SP-7063(02)] 15 p2149 N88-22830
Studying Turbulence Using Numerical Simulation Databases. Proceedings of the 1987 Summer Program
[NASA-CR-182692] 16 p2194 N88-23086
A review of the NATO special group of experts on Naval hydromechanics and related problems
16 p2205 N88-23157
Lewis Structures Technology, 1988. Volume 1: Structural Dynamics
[NASA-CP-3003-VOL-1] 16 p2217 N88-23226
Contributions to geodesy, photogrammetry and cartography. Series 1, number 46 --- conference
[ISSN-0469-4244] 16 p2225 N88-23279
Proceedings of Symposium on Physics of Target Implosion and Pulsed Power Techniques
[IPPJ-859] 16 p2276 N88-23619
DOE (Department of Energy) national laboratories and the semiconductor industry: Continuing the joint planning
[PB88-170295] 16 p2281 N88-23657
Laminar Flow Aircraft Certification
[NASA-CP-2413] 17 p2296 N88-23737
The Design, Development and Testing of Complex Avionics Systems
[AGARD-CP-417] 17 p2302 N88-23767
Structural Ceramics
[NASA-CP-2427] 17 p2323 N88-23872
Noncontact Temperature Measurement
[NASA-CP-2503] 17 p2327 N88-23895
Latin American Symposium on Remote Sensing. 4th Brazilian Remote Sensing Symposium and 6th SELPER Plenary Meeting, volume 1 17 p2352 N88-24013
Space Station Human Factors Research Review. Volume 1: EVA Research and Development
[NASA-CP-2426-VOL-1] 17 p2379 N88-24145
Third Conference on Artificial Intelligence for Space Applications, part 2
[NASA-CP-2492-PT-2] 17 p2387 N88-24188
Transactions of the Fifth Symposium on Space Nuclear Power Systems
[DE88-006165] 17 p2417 N88-24374
Summary report on the Japan-US Workshop on the Assessment of Spectroscopic Data for Temperature and Density Measurements --- plasma diagnostics
[IPPJ-861] 17 p2439 N88-24512
Proceedings of the American Society for Composites
[AD-A189861] 18 p2477 N88-24693
High resolution radar techniques: Five contributions to MILINF 86
[PB88-172721] 18 p2498 N88-24821
Optics: Perspectives for Measurement Techniques and Signal Processing for Flight Guidance --- conference
[DFVLR-MITT-87-21] 18 p2516 N88-24928
Proceedings of the 1987 Biomass Thermochemical Conversion Contractors' Review Meeting
[DE88-006730] 18 p2535 N88-25041
Workshop on Atmospheric OH
[BPT-7/87] 18 p2538 N88-25063
The Effect of the Ionosphere on Communication, Navigation and Surveillance Systems Based on Ionospheric Effects Symposium held on 5-7 May 1987 in Springfield, Virginia
[AD-A191855] 18 p2541 N88-25081
Dynamics Explorer-2 measurements during an isolated auroral substorm
[AD-A191202] 18 p2543 N88-25091
Infinite dimensional dynamical systems and their finite dimensional analogues
[AD-A192041] 18 p2563 N88-25216
A Study of Space Station Contamination Effects --- conference
[NASA-CP-3002] 18 p2590 N88-25390
Zero/zero rotorcraft certification issues. Volume 1: Executive summary
[NASA-CR-177483-VOL-1] 19 p2602 N88-25453
Zero/zero rotorcraft certification issues. Volume 2: Plenary session presentations
[NASA-CR-177483-VOL-2] 19 p2602 N88-25454
Zero/zero rotorcraft certification issues. Volume 3: Working group results
[NASA-CR-177483-VOL-3] 19 p2602 N88-25455
The 24th JANNAF Combustion Meeting, volume 2
[AD-A190164] 19 p2622 N88-25554
The 24th JANNAF Combustion Meeting, volume 1
[AD-A190163] 19 p2627 N88-25585
Solid rocket motor performance: A workshop report
19 p2631 N88-25607
Proceedings of the 5th NAL Symposium on Aircraft Computational Aerodynamics
[NAL-SP-8] 19 p2635 N88-25630
Proceedings of the Mobile Satellite Conference
[NASA-CR-182964] 19 p2643 N88-25680
Organization of a Topical Meeting on Picosecond Electronics and Optoelectronics
[AD-A187136] 19 p2655 N88-25765
National Meeting on Remote Sensing Applied to Municipal Planning 19 p2681 N88-25939
Proceedings of the Colloquium on Space and Sea
[ESA-SP-280] 19 p2695 N88-26016
Electromechanical Research Symposium, August 20-21, 1987
[PB88-148457] 19 p2713 N88-26109
Report on the Second Catalog Interoperability Workshop
[NASA-TM-100701] 19 p2718 N88-26135
Workshop report and presentations from the Semiconductor Research Corporation-DOE Semiconductor Task Force Workshop
[DE88-007690] 19 p2733 N88-26232

Flight Mechanics Panel Symposium on Rotorcraft Design for Operations: Technical evaluation report
[AGARD-AR-243] 20 p2758 N88-26362
System identification in vehicle dynamics
[DFVLR-MITT-87-22] 20 p2785 N88-26518
Proceedings of the Array Signal Processing Symposium: Treaty Verification Program
[DE88-006346] 20 p2790 N88-26548
Proceedings of the 2nd US-Japan Workshop on Advanced Plasma Modeling, volume 3
[IPPJ-867] 20 p2855 N88-26957
Third International Conference on Superlattices, Microstructures and Microdevices
[AD-A191416] 20 p2861 N88-26995
Integrated Technology Rotor Methodology Assessment Workshop
[NASA-CP-10007] 21 p2889 N88-27148
Very High Speed Integrated Circuits (VHSIC)
[AD-A193225] 21 p2937 N88-27442
Aerodynamics of Hypersonic Lifting Vehicles: Fluid Dynamics Panel AGARD Symposium
[AGARD-AR-246] 21 p2943 N88-27480
Finite element methodology for integrated flow-thermal-structural analysis
[NASA-CR-183144] 21 p2964 N88-27606
Photovoltaic Energy. Electricity from Sunlight: A current awareness bulletin
[DE88-008289] 21 p2969 N88-27634
Electric and Magnetic Activity of the Central Nervous System: Research and Clinical Applications in Aerospace Medicine
[AGARD-CP-432] 21 p2977 N88-27683
Proceedings of the 14th Symposium on Aircraft Integrated Monitoring Systems
[DFVLR-MITT-88-04] 22 p3033 N88-28001
SPOT 1 Image Utilization, Assessment, Results
[ISBN-2-85-428188-8] 22 p3089 N88-28346
Proceedings of the Twelfth Annual Climate Diagnostics Workshop
[PB88-191747] 22 p3119 N88-28534
Management of large space projects --- conference
[ISBN-2-85-428192-6] 22 p3159 N88-28803
Visual Effects in the High Performance Aircraft Cockpit
[AGARD-LS-156] 23 p3241 N88-29291
MEVTV Workshop on Nature and Composition of Surface Units on Mars
[NASA-CR-183075] 23 p3300 N88-29654
The NASA Electric Propulsion Program
[NASA-TM-101324] 24 p3336 N88-29859
Performance Prediction for Coatings. Proceedings of a Workshop
[AD-A188973] 24 p3354 N88-29966
The 1988 Goddard Conference on Space Applications of Artificial Intelligence
[NASA-CP-3009] 24 p3415 N88-30330
Barriers to Information Transfer and Approaches Toward Their Reduction
[AGARD-CP-430] 24 p3437 N88-30458
Information technology to facilitate group interaction
24 p3438 N88-30463
NASA MEVTV Program Working Group Meeting: Volcanism on Mars
[NASA-CR-183074] 24 p3442 N88-30487
Workshop on the Origins of Solar Systems
[NASA-CR-183025] 24 p3451 N88-30536

CONFIDENCE
Error modeling and confidence interval estimation for inductively coupled plasma calibration curves
[AD-A186711] 09 p1250 N88-17488
A method to adjust climatological time series for discontinuous inhomogeneities
22 p3124 N88-28570

CONFIDENCE LIMITS
An APL workspace for conducting nonparametric statistical inference
[AD-A184971] 05 p0634 N88-13877
Determining differences in rates corresponding to a given significance level
[AD-A185004] 05 p0644 N88-13940
Robust prediction and interpolation for vector stationary processes, 2d enriched version
[AD-A185875] 07 p0865 N88-15247
A comparison of the effects of group dynamics on individuals assigned to integral and non-integral aircrews
[AD-A186467] 08 p1051 N88-16345
Measuring the dependence between two point processes through confidence intervals for the second order distribution
[AD-A186735] 08 p1074 N88-16481
Regional Conference on the Analysis of the Unbalanced Mixed Model
[AD-A188747] 13 p1830 N88-20943
Large quantile estimation under extreme-value conditions
[CWI-MS-R8711] 14 p1966 N88-21730
Mathematics clinic probabilistic position-fixing
[NASA-CR-182753] 15 p2125 N88-22672
Burn-in with mixed populations
[AD-A194651] 22 p3085 N88-28321
Exact lower confidence limits for the reliability of k of n systems for zero failures and nonconservativeness of the maximus method
[AD-A194299] 23 p3274 N88-29485

CONFIGURATION INTERACTION
Applications and limitations of deuterium labeling methods to neutron scattering studies of polymers
[DE87-012936] 02 p0151 N88-10945
The H5(+) potential energy hypersurface: Characterization of ten distinct energetically low-lying stationary points 16 p2267 N88-23561
Quantum Monte Carlo study of the MIES associated with H2(X 1 sigma g +) and H2(B 1 sigma u +)
16 p2268 N88-23564
On the bond distance in methane
[NASA-CR-181436] 22 p3150 N88-28741
An unsteady helicopter rotor: Fuselage interaction analysis
[NASA-CR-4178] 23 p3171 N88-28880

CONFIGURATION MANAGEMENT
AGARD standard aeroelastic configurations for dynamic response. Candidate configuration I.-wing 445.6
[NASA-TM-100492] 02 p0192 N88-11202
A study of the Department of Defense configuration management policies and procedures as applied to the FA-18 Strike/Fighter program
[AD-A184872] 05 p0657 N88-14034
Chicago's O'Hare Runway Configuration Management System (RCMS). Volume 1: Description of the operational software
[AD-A185886] 07 p0821 N88-14990
Chicago's O'Hare Runway Configuration Management System (RCMS). Volume 2: Users guide
[AD-A186222] 08 p0953 N88-15783
Configuration management issues and objectives for a real-time research flight test support facility
[NASA-TM-100437] 13 p1813 N88-20832
Vibration isolation system for the Stratospheric Observatory For Infrared Astronomy (SOFIA)
14 p1926 N88-21483
Reconfigurable work station for a video display unit and keyboard
[NASA-CASE-MFS-26009-1-SB]
17 p2382 N88-24163
Configuration control in compiler construction
[AD-A193916] 22 p3135 N88-28639
System configuration management --- space systems
22 p3160 N88-28813
Management of large space projects. Case study: The Hermes program 22 p3162 N88-28830
Intelligent resource management for local area networks: Approach and evolution
23 p3256 N88-29385
Dynamically reconfigurable distributed database systems
[AD-A194716] 23 p3297 N88-29636

CONFIGURATIONS
Automatically reconfigurable computer architecture
10 p1375 N88-18204

CONFINEMENT
Relative merits of size, field, and current on ignited Tokamak performance: A comparison of CITs and Super-JETs
[DE88-000038] 02 p0241 N88-11521
Feasibility of alpha particle measurement in a magnetically confined plasma by CO2 laser Thomson scattering
[DE88-000039] 02 p0241 N88-11522
Human adaptation to isolated and confined environments
[NASA-CR-181502] 03 p0357 N88-12248
Confinement of energy in tokamak-10 plasma during electron-cyclotron-resonance heating
06 p0773 N88-14750
Long duration confinement of aquatic organisms in weightlessness (aquaspace) 07 p0887 N88-15380
Proceedings of the Energy Independence Conference: Fusion Energy and Plasma Physics
[DE88-700657] 09 p1253 N88-17507
Experimental investigation of two-dimensional confined jet thrust vector control
[AD-A189845] 15 p2027 N88-22077
Heating and confinement studies of electron cyclotron resonance heated plasmas in Heliotron E
[DE88-752312] 15 p2136 N88-22746
A study of runaway electron confinement in the ASDEX tokamak
[DE88-007327] 18 p2579 N88-25319
Physiological effects on man of long duration confinement in a carbon dioxide enriched environment
19 p2695 N88-26017

CONFIRMATION
U PROVING

CONFLUENCE
U CONVERGENCE

CONFORMAL MAPPING
The geometry of the Karnaugh map --- Boolean expressions
[ETN-87-90961] 02 p0227 N88-11432
Application of new conformal solution theories
[PB87-211934] 02 p0247 N88-11558
Superconformal invariance and superstring in background fields
[DE87-703097] 02 p0247 N88-11561
Shuttle computational grid generation
06 p0794 N88-14863
Centerplane source distribution for slender bodies
10 p1328 N88-17940
A numerical procedure for conformal mapping of the exterior of a circle onto the exterior of a wing profile with a spoiler
[ISL-R-110/86] 11 p1536 N88-19180
Conformal geometry, Hotine's conjecture, and differential geodesy
[AD-A189265] 13 p1790 N88-20709
What do multistep methods approximate
[PB88-148838] 13 p1828 N88-20932
Action-angle maps and scattering theory for some finite-dimensional integrable systems. The pure solution case
[CWI-PM-R8704] 13 p1831 N88-20955
Linear programming along the trajectory of the problem
[REPT-87-41] 14 p1956 N88-21662
Hyperbolicity and invariant measures for general C sq interval maps satisfying the Misiurewicz condition
[REPT-87-46] 14 p1966 N88-21733
Absolutely continuous invariant measures for C sq unimodal maps satisfying the Collet-Eckmann conditions
[REPT-87-55] 14 p1966 N88-21735
Nonlinear conformal transformations and Clifford algebras
[PB87-225942] 19 p2719 N88-26147
Image force expression for the dislocation near a crack
[DE88-701894] 20 p2814 N88-26692
Geometry of superconformal manifolds, part 1
[DE88-702405] 21 p3011 N88-27863
Geometry of superconformal manifolds, part 2
[DE88-702406] 21 p3011 N88-27864
A fast algorithm for the numerical evaluation of conformal mappings
[AD-A193903] 22 p3138 N88-28658
Distortion estimates for negative Schwarzian maps
[AD-A193172] 23 p3228 N88-29209

CONFORMAL TRANSFORMATIONS
U CONFORMAL MAPPING

CONFUSION
Resources, confusions and compatibility in dual axis tracking: Displays, controls and dynamics
[AD-A185871] 07 p0898 N88-15440

CONGESTION
Communications using channels formed by meteor bursts
[AD-A192088] 18 p2501 N88-24834

CONGRESSIONAL REPORTS
Budget reimbursements: The National Aeronautics and Space Administration's reimbursable work
[PB87-207296] 01 p0107 N88-10696
Results of the development motor 8 test firing
[GPO-78-692] 03 p0278 N88-11751
Global environmental change research
[S-HRG-100-301] 03 p0348 N88-12199
National Aeronautics and Space Administration Authorization Act, 1988
[PUB-LAW-100-147] 03 p0385 N88-12422
Department of Housing and Urban Development, and Certain Independent Agencies Appropriations, 1988, Part 2
[S-HRG-100-106-PT-2] 03 p0385 N88-12423
Department of Housing and Urban Development-Independent Agencies Appropriations for fiscal year 1988, Thursday, 9 April 1987: National Aeronautics and Space Administration
03 p0386 N88-12424
Department of Housing and Urban Development-Independent Agencies Appropriations for fiscal year 1988, Friday, 10 April 1987: National Aeronautics and Space Administration
03 p0386 N88-12425
National Aeronautics and Space Administration space station proposal, fiscal year 1988
[S-HRG-100-328] 05 p0659 N88-14043
The 1988 NASA (National Aeronautics and Space Administration) authorization
[GPO-80-245] 05 p0659 N88-14044

The 1988 National Aeronautics and Space Administration (NASA) authorization
[GPO-76-600] 06 p0792 N88-14854
Report to Congress on the Automotive Technology Development Program
[DE88-003742] 07 p0864 N88-15242
Advancing automation and robotics technology for the space station and for the US economy: Submitted to the United States Congress May 15, 1987
[NASA-TM-89811] 08 p0959 N88-15817
Advancing automation and robotics technology for the space station and for the US economy: Submitted to the United States Congress October 1, 1986
[NASA-TM-89190] 08 p0960 N88-15818
Department of Housing and Urban Development independent agencies appropriations for 1989. Part 7: National Aeronautics and Space Administration
[GPO-85-166] 16 p2286 N88-23689
Department of Defense Statement on the Technology Base to the Subcommittee on Defense Industry and Technology of the Committee on Armed Services, United States Senate, 100th Congress, second session
[AD-A191839] 18 p2588 N88-25376
Department of Defense statement on defense agency research and development to the Subcommittee on Defense of the Committee on Appropriations, United States House of Representatives, 100th Congress, second session
[AD-A191840] 18 p2588 N88-25377
Department of Defense Statement on the Balanced Technology Initiative to the Committee on Armed Services, United States Senate, 100th Congress, second session
[AD-A191841] 18 p2588 N88-25378
The FY 1989 Department of Defense statement on the Science and Technology Program to 100th Congress, second session
[AD-A191843] 18 p2588 N88-25380
Report to Congress on the effectiveness of the Civil Aviation Security Program
[AD-A195282] 24 p3322 N88-29784

CONICAL BODIES
NT SLENDER CONES
Conical wing with maximum lift-to-drag ratio in supersonic gas flow 04 p0425 N88-12633
Dynamic stability of hypersonic conical lifting vehicles according to Newton-Busemann theory 05 p0534 N88-13247
Interferometric data for a shock-wave/boundary-layer interaction
[NASA-TM-88227] 05 p0543 N88-13306
Development, construction and testing of a novel internal combustion engine with conical rotating slide valve
[DE88-900071] 05 p0589 N88-13593
Control of vortical separation on conical bodies 10 p1267 N88-17580
Fluid motion in a spinning, coning cylinder via spatial eigenfunction expansion
[AD-A190758] 15 p2066 N88-22319
Almond test body --- for microwave anechoic chambers
[NASA-CASE-LAR-13747-1] 18 p2502 N88-24845
Numerical calculations of the response of a spinning spheroidal payload to coning motion
[AD-A195890] 24 p3368 N88-30059

CONICAL FLARE
U CONES

CONICAL FLOW
Numerical calculations of the response of a spinning spheroidal payload to coning motion
[AD-A195890] 24 p3368 N88-30059

CONICAL SCANNING
Realization of a conical four-part antenna for the scanning of interference fields
[REPT-13-86] 01 p0034 N88-10216

CONICAL SHELLS
Effective treatment of membrane and shear locking phenomena in curved shear-deformable axisymmetric shell element 04 p0428 N88-12652
Analysis and testing of predamaged shell structures 04 p0428 N88-12653
Coupled FE and HIE method for exterior acoustics of axisymmetric shells --- finite element (FE) Helmholtz integral equation (HIE)
[ARE-TM(UHA)-87506] 09 p1243 N88-17448
Numerical and experimental research on propagation of elastic stress waves in conical shell under axial impulsive loading 15 p2053 N88-22238
Nonlinear liquid motion in conical containers
[LRT-WE-9-FB-10(1987)] 22 p3077 N88-28270

CONICS
NT ELLIPSES
NT PARABOLAS
On line search termination criteria for and convergence of conic algorithms for minimization
[DE88-002844] 09 p1227 N88-17351
Conic algorithms for unconstrained minimization with special consideration of problems with large sparse Hessians: A summary of research performed
[DE88-002549] 13 p1816 N88-20850
Algorithms with conic termination for nonlinear optimization
[DE88-005893] 13 p1816 N88-20851

CONIFERS
The use of airborne imaging spectrometer data to determine experimentally induced variation in coniferous canopy chemistry 05 p0612 N88-13761
Measuring near infrared spectral reflectance changes from water stressed conifer stands with AIS-2 05 p0613 N88-13765
Variations in spectral reflectance signature in healthy stands of pine and spruce
[FOA-C-30468-3.1] 22 p3116 N88-28512

CONJUGATE GRADIENT METHOD
S-step iterative methods for symmetric linear systems
[DE87-010819] 01 p0086 N88-10559
Implementation of preconditioned s-step conjugate gradient methods on a multiprocessor system with memory hierarchy
[DE87-014401] 02 p0222 N88-11400
Iterative solution of a nonlinear system arising in phase change problems
[DE87-014672] 02 p0226 N88-11426
Solution of geometrically nonlinear problem for reinforced shell of revolution having arbitrary shape 04 p0426 N88-12637
Indirect solution of static problems using concurrent vector processing computers
[DE87-012105] 05 p0636 N88-13889
Solution of non-symmetric linear systems by biconjugate gradients or conjugate gradients squared
[PB87-226387] 06 p0763 N88-14679
Upper bounds on the expected value of a convex function using gradient and conjugate function information
[AD-A186246] 07 p0910 N88-15517
Numerical experiments with a parallel conjugate gradient method
[DE88-002178] 08 p1066 N88-16445
Conjugate gradient spectral iterative technique
[PB88-126917] 10 p1398 N88-18337
Polynomial preconditioning for conjugate gradient methods
[DE88-005214] 10 p1399 N88-18342
Preconditioned conjugate gradient algorithms and software for solving large sparse linear systems
[DE88-002180] 13 p1816 N88-20849
Iterative finite element solver on transputer networks 16 p2218 N88-23235
A practical termination criterion for the conjugate gradient method
[REPT-87-62] 16 p2259 N88-23506
A taxonomy for conjugate gradient methods
[DE88-008574] 21 p3004 N88-27817

CONJUGATION
NT PHASE CONJUGATION
Optical bistable behavior of a planar quasi-waveguide interferometer made with a conjugated organic polymer film
[AD-A194349] 22 p3152 N88-28756

CONNECTICUT
The Windsor Locks, Connecticut tornado of 3 October 1979: An analysis of an intermittant severe weather event 02 p0208 N88-11305

CONNECTIONS
U JOINTS (JUNCTIONS)

CONNECTIVE TISSUE
NT BONE MARROW
NT COLLAGENS

CONNECTORS
NT ELECTRIC CONNECTORS
Development of an intermodule connector for serviceable spacecraft 14 p1877 N88-21212
Fabrication and electrical characterization of multilevel aluminum interconnects used to achieve silicon-hybrid wafer-scale integration
[AD-A190519] 15 p2060 N88-22282
Toggle release
[NASA-CASE-MSC-21354-1] 18 p2523 N88-24969
Developing a connector selection DBMS (database management system) using NIAM (Nijssen's Information Analysis Methodology)
[DE88-008110] 21 p3028 N88-27972
Connectionist models and artificial intelligence
[RR-684-I-IMAG-66-LIFIA] 22 p3142 N88-28684
Collet lock joint for space station truss
[NASA-CASE-MSC-21207-1] 23 p3222 N88-29180

CONNECTORS (ELECTRIC)
U ELECTRIC CONNECTORS

CONOIDS
U CONICAL BODIES

CONSCIOUSNESS
F-16 control stick response during +Gz-induced loss of consciousness
[AD-A184107] 04 p0400 N88-12491
Fighter design for human load limits 12 p1580 N88-19451
Physiological monitoring methodology in the USAFSAM centrifuge 21 p2924 N88-27356

CONSERVATION
NT ENERGY CONSERVATION
Conservatism implications of shock test tailoring for multiple design environments 05 p0592 N88-13611
Effects of fire on composition, biomass, and nutrients in oak scrub vegetation on John F. Kennedy Space Center, Florida
[NASA-TM-100305] 08 p1020 N88-16182
Period-doubling universality in multidimensional dissipative and conservative systems
[PB88-148812] 13 p1832 N88-20961
Application of remote sensing in the conservation of natural areas: Ribeira Valley 19 p2683 N88-25949

CONSERVATION EQUATIONS
Conservation and transport properties of turbulence with large density variations
[LA-10911-MS] 03 p0321 N88-12032
Breakdown of the conservative potential equation 07 p0809 N88-14929
A new boundary integral equation formulation for elastodynamic and elastostatic crack analysis
[AD-A192967] 20 p2815 N88-26702
Adaptive finite element methods for shells
[AD-A193221] 21 p2960 N88-27585
Shock waves in unsteady flows
[NASA-TT-20329] 23 p3214 N88-29134
Experimental and analytical study of two-phase flow in zero gravity
[AD-A195223] 24 p3358 N88-29993

CONSERVATION LAWS
Some aspects of high resolution numerical methods for hyperbolic systems of conservation laws, with applications to gas dynamics
[DMS-86-7] 03 p0321 N88-12031
New notions about space-time and gravitation
[DE87-703259] 03 p0383 N88-12408
High resolution finite volume methods on arbitrary grids via wave propagation
[NASA-CR-178397] 04 p0484 N88-12979
Nonlinear hyperbolic conservation laws
[AD-A184963] 05 p0580 N88-13538
A multistage time-stepping scheme for the thin-layer Navier-Stokes equations 07 p0810 N88-14932
Analysis of the spectral vanishing viscosity method for periodic conservation laws
[NASA-CR-181613] 09 p1231 N88-17378
A study of numerical methods for hyperbolic conservation laws with stiff source terms
[NASA-TM-100075] 10 p1399 N88-18343
Total Variation Diminishing (TVD) schemes of uniform accuracy
[NASA-TM-100552] 11 p1436 N88-18566
Plasma rotation in a tokamak
[DE88-700855] 12 p1693 N88-20128
Lie groups in prolongation theory
[B8721781] 14 p1967 N88-21743
Super Virasoro algebra and solvable supersymmetric quantum field theories
[DE88-752299] 15 p2127 N88-22681
Simulation of axisymmetric flow with H2O2 reactions 19 p2638 N88-25651
On the propagating speed in difference approximations for conservation laws 19 p2639 N88-25658
Semi-discrete approximations to nonlinear systems of conservation laws; consistency and L(infinity)-stability imply convergence
[NASA-CR-181683] 19 p2721 N88-26157
Numerical solution of weak forms of conservation laws on optimal unstructured triangular grids 20 p2797 N88-26597
Piecewise-parabolic methods for systems of hyperbolic conservation laws in multiprocessing environments
[DE88-010202] 23 p3248 N88-29329
An analysis of finite-difference and finite-volume formulations of conservation laws
[NASA-CR-177416] 24 p3370 N88-30071
Nonequilibrium flow computations. 1: An analysis of numerical formulations of conservation laws
[NASA-CR-177489] 24 p3425 N88-30384

CONSISTENCY
Consistency question in the renormalization group analysis of deep inelastic scattering
[DE87-703372] 04 p0487 N88-12999
Strong consistency of M-estimates for the linear model
[AD-A185487] 06 p0764 N88-14696

Strong consistency of estimation of number of regression variables when the errors are independent and their expectations are not equal to each other
[AD-A186025] 07 p0909 N88-15507
Strong consistency of maximum likelihood parameter estimation of superimposed exponential signals in noise
[AD-A186384] 07 p0911 N88-15526
On the direction of arrival estimation
[AD-A186031] 07 p0914 N88-15546
Consistent linearization of the element-independent corotational formulation for the structural analysis of general shells
[NASA-CR-178418] 09 p1181 N88-17078
Consistency of rule-based expert systems
[CWI-CS-R8736] 13 p1831 N88-20950
On a consistent estimate of the index of an extreme value distribution
[CWI-MS-R8710] 14 p1966 N88-21729
Derivation of consistent surface fixed fields for use in a global NWP model
[AD-A190131] 15 p2093 N88-22475
Constant amplitude fatigue life data for notched and unnotched annealed Ti-6Al-4V sheet
[AD-A193420] 21 p2913 N88-27287

CONSOLES
NT REMOTE CONSOLES
Western aeronautical test range real-time graphics software package MAGIC
[NASA-TM-100425] 13 p1757 N88-20506

CONSOLIDATION
Effects of combining vertical and horizontal information into a primary flight display
[NASA-TP-2783] 04 p0399 N88-12487
Characterization of an explosively consolidated rapidly solidified Fe-16Ni-9Cr-5Mo-2Cu alloy powder
[DE88-006733] 15 p2041 N88-22162
Superconductor consolidation
[DE88-010938] 21 p3024 N88-27949

CONSTANT SPEED PROPELLERS
U VARIABLE PITCH PROPELLERS

CONSTANTS
NT GRAVITATIONAL CONSTANT
NT HUBBLE CONSTANT
NT SOLAR CONSTANT
NT TIME CONSTANT
Evaluation and prediction of Henry's law constants and aqueous solubilities for solvents and hydrocarbon fuel components. Volume 1: Technical discussion
[AD-A188571] 12 p1613 N88-19643
Measurement of rate constants of elementary gas reactions of importance to upper atmosphere and combustion systems
[AD-A189432] 13 p1737 N88-20386
Involution-dependent constants and the cancellation of divergences in the 1-loop open string amplitude
[DE88-006537] 15 p2146 N88-22811
A simulation analysis of errors in the measurement of standard electrochemical rate constants from phase-selective impedance data
[AD-A192739] 20 p2770 N88-26426
Parameter identification of material constants in a composite shell structure
[DE88-008115] 22 p3086 N88-28326
Can we calculate the fundamental dimensionless constants of physics
[DE88-702641] 23 p3295 N88-29625

CONSTELLATIONS
NT AURIGA CONSTELLATION
NT CORONA BOREALIS CONSTELLATION
NT CYGNUS CONSTELLATION
NT LYRA CONSTELLATION
NT SCORPIUS CONSTELLATION

CONSTITUTION
Science, technology and the Constitution: Background paper
[PB88-142534] 12 p1708 N88-20222

CONSTITUTIONAL DIAGRAMS
U PHASE DIAGRAMS

CONSTITUTIVE EQUATIONS
Constitutive modeling of superalloy single crystals with verification testing 02 p0188 N88-11169
Deviatoric constitutive relationship for anisotropic materials
[AD-A184332] 03 p0295 N88-11854
Nonlinear thermoviscoelastic analysis of metallic plane curved beams 03 p0336 N88-12119
Application of viscoplastic constitutive equations in finite element programs
[KFK-4254] 03 p0370 N88-12329
A direct method to obtain constitutive model constants from cylinder impact test results
04 p0427 N88-12647
On a numerical method to solve contact problems — forming processes
[B8711403] 05 p0642 N88-13930
A critical review of the development of several viscoplastic constitutive theories
[AD-A185652] 07 p0867 N88-15262
The paradoxical asymptotic status of massless springs
[AD-A185625] 07 p0928 N88-15637
Structure of a viscoplastic theory
[NASA-TM-100794] 11 p1501 N88-18968
Nonlinear Constitutive Relations for High Temperature Applications, 1986
[NASA-CP-10010] 14 p1928 N88-21498
A viscoplastic constitutive theory for metal matrix composites at high temperature
14 p1929 N88-21500
Development of a unified constitutive model for an isotropic nickel base superalloy Rene 80
14 p1929 N88-21501
An internal variable constitutive model for the large deformation of metals at high temperatures
14 p1929 N88-21503
Constitutive modeling and thermoviscoplasticity
14 p1930 N88-21506
A theory of viscoplasticity accounting for internal damage 14 p1930 N88-21508
A constitutive model with damage for high temperature superalloys 14 p1930 N88-21510
Evaluation of structural analysis methods for life prediction 14 p1930 N88-21511
Data requirements to model creep in 9Cr-1Mo-V steel
14 p1931 N88-21512
Controlled-strain rate tests at very low strain rates of 2618 aluminum at 200 C 14 p1931 N88-21513
An experimental comparison of several current viscoplastic constitutive models at elevated temperature
14 p1931 N88-21516
An automated procedure for material parameter evaluation for viscoplastic constitutive models
14 p1932 N88-21520
A constitutive material model for nonlinear finite element structural analysis using an iterative matrix approach
14 p1932 N88-21521
Unified constitutive models for high-temperature structural applications 14 p1932 N88-21523
Constitutive response of Rene 80 under thermal mechanical loads 14 p1932 N88-21524
A constitutive model for an overlay coating
14 p1933 N88-21525
Life assessment of combustor liner using unified constitutive models 15 p2077 N88-22384
Biaxial experiments supporting the development of constitutive theories for advanced high-temperature materials 15 p2078 N88-22386
Unified constitutive model development for metal matrix composites at high temperature
15 p2078 N88-22387
Unified constitutive model for single crystal deformation behavior with applications 15 p2078 N88-22388
Finite element (MARC) solution technologies for viscoplastic analyses 15 p2078 N88-22389
Models in nonlinear thermomechanics. Finite element models and constitutive models for large deformation elastoplasticity
[ETN-88-92240] 16 p2222 N88-23262
An endochronic rate-sensitive constitutive equation for metals, application to generalized creep and large deformations
[AD-A194167] 22 p3055 N88-28125
Constitutive modeling for isotropic materials
[NASA-CR-182132] 24 p3327 N88-29811
Anisotropic constitutive modeling for nickel-base single crystal superalloys
[NASA-CR-182157] 24 p3353 N88-29961
Stability of stick-slip phenomenon by using constitutive friction laws of Dietrich and Ruina
[ILR-MITT-197] 24 p3379 N88-30127

CONSTRAINTS
NT METEOROLOGICAL PARAMETERS
Integration of dynamic, aerodynamic and structural optimization of helicopter rotor blades
[NASA-CR-181441] 01 p0002 N88-10012
Attitude Control Working Group report
01 p0016 N88-10099
Study of closed loop control singularity in dynamic systems with a constraint on the final state
[LAAS-87-180] 02 p0223 N88-11405
Numerical solution of bound constrained problems
[DE88-000653] 03 p0371 N88-12334
An exact penalization viewpoint of constrained optimization
[DE88-001477] 04 p0486 N88-12995
Performance-limiting factors in MPD thrusters
[AD-A185605] 06 p0674 N88-14128
High pressure ratio turbine design constraints
[TRR-0279] 06 p0712 N88-14365
Parallel algorithms for unconstrained and constrained nonlinear optimization
[PB87-230454] 06 p0756 N88-14634
Collider constraints in the choices for wavelength and gradient scaling
[PB87-123691] 06 p0779 N88-14783
Dynamics formulations for the real-time simulation of constrained motion 06 p0795 N88-14872
Feasibility studies of optical processing of image bandwidth compression schemes
[AD-A186073] 07 p0932 N88-15660
Processing, fabrication, applications and limitations of inherently conducting polymers
[DE88-003210] 08 p0973 N88-15883
Computation of the tensile and bending restraint intensities of welded specimens by finite element method
[PB87-143798] 08 p0995 N88-16024
Limitation of spacecraft orbit near colinear libration center of limited elliptical three body problem
08 p1003 N88-16075
Resolution limitations and optimization of the ITT F4157 streak tube focus for fast (10 ps) operation
[DE88-003727] 09 p1169 N88-17007
Trimodal interpretation of constraints for planning
09 p1209 N88-17248
A posteriori error estimates in computational fluid mechanics 11 p1486 N88-18869
A tool for the analysis of quasi-Newton methods with application to unconstrained minimization
[DE88-005783] 11 p1532 N88-19153
Minimum weight design of rectangular and tapered helicopter rotor blades with frequency constraints
[NASA-TM-100561] 12 p1582 N88-19465
A representation for serial robotic tasks
12 p1681 N88-20048
Describing constraints on a digital circuit's behavior
[AD-A189200] 13 p1761 N88-20531
Practical constraints on sources for pulsed beam lithographies
[DE88-006594] 13 p1776 N88-20623
Active cooling design for scramjet engines using optimization methods
[NASA-TM-100581] 13 p1783 N88-20669
Constrained nonlinear programming
[DE88-005695] 13 p1817 N88-20860
Measurement of the elastic-plastic surface flaw back surface topology and its relation to constraint
[DE88-006765] 15 p2087 N88-22437
Minimum weight design of rotorcraft blades with multiple frequency and stress constraints
[NASA-TM-100569] 16 p2161 N88-22892
Discrete generalized networks: Application to integer constrained flow problems
[AD-A190823] 16 p2190 N88-23060
A constraint algorithm for maintaining rigid bonds in molecular dynamics simulations of large molecules
[AD-A191663] 18 p2572 N88-25277
Mechanisms for particle acceleration: Possibilities and constraints
[PB88-102538] 19 p2725 N88-26184
N=2 supergravity in superspace: Solution to the constraints
[DE88-702135] 19 p2741 N88-26272
Range of a constrained random walk
[PB88-126867] 20 p2847 N88-26897
Cooperating knowledge-based systems
[NASA-CR-183109] 23 p3247 N88-29327
On recognizing ignorance 23 p3254 N88-29372
Constraints on the origin of fractured terrane, Northern Martian plains 23 p3304 N88-29684
Origin of northern lowland plains: Constraints from boundary morphology 23 p3305 N88-29687
The bounded rationality constraint: Experimental and analytical results
[AD-A195897] 24 p3413 N88-30318

CONSTRICTIONS
Design of a sound neck in connection with the model-support system of a transonic wind tunnel test section
[ILR-MITT-186(1987)] 14 p1869 N88-21171

CONSTRUCTION
Construction and characterization of amorphous-silicon test structures
[DE87-013595] 01 p0029 N88-10182
Mission Peculiar Equipment Support Structure: A platform for space construction
02 p0139 N88-10874
Marshall Space Flight Center's role in EASE/ACCESS mission management 02 p0139 N88-10875
Results of the ACCESS experiment
02 p0140 N88-10880
Development, construction and testing of a novel internal combustion engine with conical rotating slide valve
[DE88-900071] 05 p0589 N88-13593
Controlled ecological life support systems: Development of a plant growth module 05 p0630 N88-13854

Investigation of design concepts for large space structures to support military applications
[AD-A186098] 07 p0824 N88-15000
Fabrication techniques used in the construction of a high resolution X-ray framing camera
[DE88-002653] 07 p0856 N88-15200
Mechanical design and construction of a 200 mA, 100 keV, dc, negative ion accelerator
[DE88-003855] 11 p1548 N88-19257
State-of-the-art technologies for construction in space: A review
[AD-A188412] 12 p1585 N88-19483
The space station assembly phase: Flight telerobotic servicer feasibility, volume 1
[NASA-CR-182689] 13 p1731 N88-20351
Campaign graphs
[DE88-005336] 13 p1831 N88-20952
Materials qualification in oceanology and the offshore industry 19 p2700 N88-26050
Construction of gallium arsenide solar concentrator for space use
[AD-A194658] 23 p3230 N88-29222
Structure and dynamics of solutions of lithium salts relevant to battery construction
[AD-A195399] 24 p3366 N88-30044

CONSTRUCTION IN SPACE
U ORBITAL ASSEMBLY

CONSTRUCTION MATERIALS
Development of highly porous calcium silicate hydrate materials with extremely low thermal conductivity
[BMFT-FB-T-86-164] 02 p0150 N88-10941
Investigations on the crack growth retardation behavior and fatigue life prediction in structural materials
[PB87-143756] 07 p0827 N88-15016
Characterization of current steels. The 35 NCD 16 alloy in 30 mm diam laminated bars made by Aubert and Duval
[CEAT-41/N/76] 07 p0832 N88-15046
Space environmental effects on polymeric materials
[NASA-CR-182418] 07 p0838 N88-15082
Metals and Ceramics Division
[DE88-008955] 19 p2618 N88-25530

CONSULTING
Towards automated consulting: Design feedback from the performance of online documentation
[DE87-012243] 04 p0501 N88-13082

CONSUMABLES (SPACECREW SUPPLIES)
NT SPACE RATIONS
Orbital Spacecraft Consumables Resupply System (OSCRS): Monopropellant application to space station and OMV automatic refueling impacts of an ELV launch, volume 4
[NASA-CR-172029] 03 p0276 N88-11741
The determination of nutritional requirements for Safe Haven Food Supply System (emergency/survival foods) 06 p0792 N88-14856
Space and sea: Is there a place for ionization? 19 p2699 N88-26043

CONSUMERS
Spinoff, 1987
[NASA-TM-89652] 02 p0250 N88-11577

CONSUMPTION
NT ENERGY CONSUMPTION
NT FUEL CONSUMPTION
NT OXYGEN CONSUMPTION

CONTACT LENSES
A field study on soft contact lens wear in USAF military transport aircraft
[AD-A195962] 24 p3407 N88-30285

CONTACT LOADS
NT ROLLING CONTACT LOADS
On a numerical method to solve contact problems — forming processes
[B8711403] 05 p0642 N88-13930
Analysis of load-bearing capacity of nitrided layer
[PB87-144176] 08 p0968 N88-15857
Reliability based analysis of contact problems
[NASA-CR-182117] 11 p1503 N88-18975
Spur gears: Optimal geometry, methods for generation and Tooth Contact Analysis (TCA) program
[NASA-CR-4135] 16 p2215 N88-23216
Design and evaluation of high contact ratio gearing
[NASA-CR-174958] 22 p3085 N88-28319

CONTACT RESISTANCE
Comparison of methods for the calculation of thermal contact resistance of the first Brazilian satellite
[NASA-TT-20180] 14 p1880 N88-21239
Friction, wear and electrical contact resistance of precious metal alloys
[DE88-011244] 21 p2938 N88-27450

CONTACTORS
Hollow cathode plasma coupling study, 1986
[NASA-CR-171985] 03 p0309 N88-11949
Advanced electric propulsion and space plasma contactor research
[NASA-CR-180662] 06 p0674 N88-14126
Plasma contactors for use with electodynamic tethers for power generation
[NASA-CR-182424] 08 p1087 N88-16547
Space plasma contactor research, 1987
[NASA-CR-182148] 16 p2280 N88-23649

CONTACTS (ELECTRIC)
U ELECTRIC CONTACTS

CONTACTS (GEOLOGY)
The unsteady ground heat flow at the contact surface between a glacier run and the subsoil 08 p1014 N88-16147

CONTAINERLESS MELTS
Preliminary study of a containerless processing facility for Columbus, executive summary
[ESA-ITT/AO/1-1834/85F] 01 p0032 N88-10203
Center for the Space Processing of Engineering Materials 07 p0838 N88-15083
Non-proprietary research projects of the Center for the Space Processing of Engineering Materials
[AR-2] 10 p1426 N88-18516
Containerless glass melting 15 p2051 N88-22222
Prospects for antiproton production and propulsion 16 p2267 N88-23556
Large hydrogen cluster ions 16 p2267 N88-23558
Infrared spectroscopy of H3(+) 16 p2268 N88-23565
Key problems and hydrogen atom formation 16 p2269 N88-23573
The cluster ion approach to the condensation and storage of antihydrogen 16 p2269 N88-23575
Analysis of containerless condensation of polyatomic hydrogen ions, with emphasis on H3(+,-) association channels and a future workshop to study related topics 16 p2269 N88-23576
Small molecule and small cluster ion formation in a low-density containerless mixture of electrons, protons and hydrogen atoms 16 p2269 N88-23577
Program for the feasibility of developing a high pressure acoustic levitator
[NASA-CR-182154] 20 p2782 N88-26498

CONTAINERS
Buckling and breakdown problems in structural mechanics. Failure of prestressed double-walled containers or rings
[MBB-UR-E-956/87] 13 p1783 N88-20671
Durability of compound cylinder under static internal-pressure repeat load of long duration 16 p2180 N88-22991
Sample decomposition in sealed teflon vessels
[NASA-TT-20189] 18 p2494 N88-24798

CONTAINMENT
Completely magnetically contained electrothermal thrusters
[AD-A185674] 06 p0674 N88-14129
The application of high-rate biaxial testing to the design of containment vessels for radioisotope heat sources 17 p2426 N88-24428

CONTAMINANTS
NT RADIOACTIVE CONTAMINANTS
NT TRACE CONTAMINANTS
Contamination control of the space shuttle Orbiter crew compartment 02 p0133 N88-10834
Influence of surfactants on damping of gravity-capillary waves. 1: Frequency dependence 04 p0459 N88-12843
Photoacoustic infrared laser spectroscopy for analyzing gaseous contaminants
[ETN-88-90805] 07 p0831 N88-15041
Pollution from motor vehicles and aircraft at Stapleton International Airport (abbreviated report), revision 2
[AD-A185916] 07 p0875 N88-15307
Estimation of aerial deposition and foliar uptake of xenobiotics: Assessment of current models
[DE88-000993] 09 p1188 N88-17117
Sampling intervals
[AD-A189445] 12 p1573 N88-19408
Reverse osmosis treatment to remove inorganic contaminants from drinking water
[PB88-147780] 12 p1605 N88-19598
Chemical cleaning of metal surfaces in vacuum systems by exposure to reactive gases
[AD-A188588] 12 p1608 N88-19616
Production and turnover of suspended organic detritus in the coastal water of the southeastern continental shelf
[DE88-005118] 14 p1951 N88-21631
A Study of Space Station Contamination Effects — conference
[NASA-CP-3002] 18 p2590 N88-25390
Neutral environment for space station 18 p2590 N88-25391
Space station neutral external environment 18 p2590 N88-25392
Contaminant ions and waves in the space station environment 18 p2590 N88-25393
Space station particulate contamination environment 18 p2591 N88-25397
The particulate environment surrounding the space station: Estimates from the PACS data 18 p2591 N88-25398
Effects of meteoroids and space debris on the particulate environment for space station 18 p2591 N88-25399
Contamination of optical surfaces — Space Station 18 p2592 N88-25400
Surface interactions relevant to space station contamination problems 18 p2592 N88-25401
Contamination of the space station environment by vented chemicals 18 p2592 N88-25403
Composite, meso-gamma scale diagnostic modeling
[DE88-008189] 19 p2689 N88-25983
Pollutant formation in heterogeneous mixtures of fuel drops and air
[DOE/CE-50052/H1] 19 p2689 N88-25986
Overview of the PRECP (processing of emissions by clouds and precipitation) Program
[DE88-008205] 20 p2822 N88-26741
Analysis of debris from accelerated life test of the Hughes five-year Vuilleumier cryocooler
[AD-A193101] 21 p2931 N88-27400
Blue-green laser diode research program
[AD-A191980] 23 p3218 N88-29153
Development of computer-controlled thermogravimetric instrumentation for measurement of environmental and high temperature volatilization and desorption of contaminants from polymeric materials
[AD-A195934] 24 p3343 N88-29900

CONTAMINATION
NT FUEL CONTAMINATION
NT SPACECRAFT CONTAMINATION
Use of a 35mm camera for remote surface cleanliness verification 02 p0133 N88-10835
An investigation of the behavior of outgassed molecules in thermal vacuums 02 p0133 N88-10836
Redistribution of particulates in shuttle bay during launch 02 p0133 N88-10837
Shear stress cleaning for surface departiculation 02 p0134 N88-10838
Space station contamination considerations 02 p0137 N88-10859
A life test of a 22-Newton (5-lbf) hydrazine rocket
[NASA-TM-100232] 03 p0278 N88-11750
Insect contamination protection for laminar flow surfaces 07 p0814 N88-14954
On copper peroxide
[NASA-TT-20263] 15 p2037 N88-22135
Reclamation of water contaminated with fuel system icing inhibitor. Phase 1: Literature review and information compilation
[DE88-006575] 16 p2183 N88-23013
A zoomable and adaptable hidden fine-mesh approach to solving advection-dispersion equations
[DE88-006174] 21 p3004 N88-27816
Experimental evaluation of resistojet thruster plume shields
[NASA-TM-101363] 24 p3338 N88-29868
Contamination and distortion of steady flow field induced by discrete frequency disturbances in aircraft gas engines
[AD-A195440] 24 p3370 N88-30069

CONTENT
NT BONE MINERAL CONTENT

CONTEXT
A review of hypertext in a NASA project management context 06 p0793 N88-14859

CONTEXT FREE LANGUAGES
Formal grammars and Markov models
[RSRE-MEMO-4051] 09 p1219 N88-17311

CONTINENTAL DRIFT
Crustal dynamics project data analysis, 1987. Volume 2: Mobile VLBI geodetic results, 1982-1986
[NASA-TM-100689-VOL-2] 08 p1035 N88-16280
Constraints on continental accretion from sedimentation 24 p3392 N88-30202
Metamorphic P-T paths and Precambrian crustal growth in East Antarctica 24 p3395 N88-30218

CONTINENTAL MARGINS
U CONTINENTAL SHELVES

CONTINENTAL SHELVES
Marine minerals: Exploring our new ocean frontier
[PB87-217725] 02 p0216 N88-11364
RRS DISCOVERY Cruise 161, 15 August (227)-19 September (262) 1986. Portuguese Ocean-continent boundary, plate boundaries west of Iberia and seismic structure of sediments off Madeira
[PB87-222006] 06 p0747 N88-14596
Sea resonance vibrational source of seismic waves 08 p1010 N88-16126
Continental shelf processes affecting the oceanography of the South Atlantic Bight
[DE88-004102] 09 p1196 N88-17166

Trace element geochemistry of the South Atlantic Bight
[DE88-003515] 10 p1356 N88-18108
Coordination: Southeast continental shelf studies
[DE88-003680] 10 p1357 N88-18110
Mesoscale coastal ocean dynamics
11 p1517 N88-19060
Synthesis of finite displacements and displacements in continental margins
[NASA-CR-182616] 12 p1642 N88-19832
Research on the physical oceanography of the Gulf Stream
[AD-A188512] 12 p1649 N88-19877
Circulation and exchange processes on the South Atlantic Bight Continental Shelf
[DE88-003330] 13 p1804 N88-20781
Production and turnover of suspended organic detritus in the coastal water of the southeastern continental shelf
[DE88-005118] 14 p1951 N88-21631
Simulation analysis of moored fluorometer time series from the Mid-Atlantic Bight
[DE88-006066] 15 p2099 N88-22505
A computerized investigation using the method of images to predict the sound field in a fluid wedge overlying a slow fluid half-space
[AD-A190013] 15 p2130 N88-22704
Influence of the Yukon River on the Bering Sea
[NASA-CR-182802] 17 p2376 N88-24126
Effects of a temperature-dependent rheology on large scale continental extension
[NASA-CR-183117] 20 p2825 N88-26759
Prediction of continental shelf sediment transport using a theoretical model of the wave-current boundary layer
[AD-A192272] 20 p2829 N88-26783
Stability of a coastal upwelling front over topography
[AD-A192354] 20 p2829 N88-26784
Mid to late proterozoic magmatism within Northeastern North America and its iplications for the growth of the continental crust 24 p3397 N88-30229

CONTINENTS
NT AFRICA
NT ASIA
NT AUSTRALIA
NT EUROPE
NT NORTH AMERICA
NT SOUTH AMERICA
New method of estimating continentality of climate on global scale 06 p0725 N88-14460
Geomechanical model of seismofocal zone of active continental margin 08 p1011 N88-16128
Numerical studies of propagation of Lg waves across ocean continent boundaries using the Representation Theorem (RT) 10 p1353 N88-18085
Geophysical study of the structure and processes of the continental convergence zones: Alpine-Himalayan Belt
[NASA-CR-182647] 12 p1644 N88-19842
Continental surface processes and water cycle
14 p1937 N88-21555
Workshop on the Growth of Continental Crust
[NASA-CR-183073] 24 p3392 N88-30201
Constraints on continental accretion from sedimentation 24 p3392 N88-30202
Recycling of lower continental crust through foundering of cumulates from contaminated mafic intrusions
24 p3393 N88-30204
Growth of continental crust: Clues from Nd isotopes and Nb-Th relationships in mantle-derived magmas
24 p3393 N88-30205
An illustration of the complexity of continent formation
24 p3393 N88-30207
The Kerala Khondalite Belt (KKB) of Southern India: An ensialic mobile belt 24 p3393 N88-30208
Genesis of archean granitoids in the Pilbara block and implications for crustal growth 24 p3394 N88-30210
Does subduction zone magmatism produce average continental crust 24 p3394 N88-30214
Decoupled Rb-Sr and Sm-Nd isotopic evolution of the continental crust 24 p3395 N88-30216
The growth of continents and some consequences since 1.5 Ga 24 p3395 N88-30220
Thermal models pertaining to continental growth
24 p3397 N88-30230
Growth of the lower continental crust
24 p3398 N88-30236
Continental crustal formation and recycling: Evidence from oceanic basalts 24 p3398 N88-30238
Physical processes in the growth of the continental crust 24 p3398 N88-30240
Continental growth through time by underplating of subducted oceanic crust: Evidence from kimberlites in South Africa and SW Pacific 24 p3399 N88-30244
The growth of the continental crust: Constraints from radiogenic isotope geochemistry
24 p3399 N88-30245
Mineralization through geologic time: Evolution of continental crust 24 p3400 N88-30250
Growth of the continental crust: A planetary-mantle perspective 24 p3400 N88-30251
The effect of thicker oceanic crust in the Archaean on the growth of continental crust through time
24 p3401 N88-30254

CONTINUITY
On the relations between increasing functions associated with two-parameter continuous martingales
[AD-A185572] 06 p0765 N88-14699
Finite element method with continuous mass elements
[PB87-143384] 08 p0995 N88-16019
Continuity of symmetric stable processes
[AD-A190324] 15 p2125 N88-22667

CONTINUITY (MATHEMATICS)
The periodic Lyapunov equations
[REPT-86-007] 01 p0087 N88-10567
Estimation of gravity vector components from Bell gravity gradiometer and auxiliary data under consideration of topography and associated analytical upward continuation aspects
[AD-A188146] 10 p1355 N88-18099
Computation and characteristics of pulsatile multi-bifurcation flow 18 p2483 N88-24729

CONTINUITY EQUATION
Efficient numerical techniques for complex fluid flows
02 p0185 N88-11151
The p-version of the finite element method for elliptic equations of order 2l
[AD-A186334] 07 p0911 N88-15523
Experimental and analytical studies of compressible vortices 19 p2665 N88-25848

CONTINUOUS FLOW ELECTROPHORESIS
U ELECTROPHORESIS

CONTINUOUS RADIATION
NT MODULATED CONTINUOUS RADIATION
Application of lattice filtering techniques to CW measured time domain data
[AD-A184351] 04 p0431 N88-12671
Phenomena at a focus in a laser system
[AD-A185442] 05 p0588 N88-13585
Performance of a small, graphite electrode, multistage depressed collector with a 500-W, continuous wave, 4.8- to 9.6-GHz traveling wave tube
[NASA-TP-2788] 07 p0848 N88-15146
Evaluation of CWMS (Continuous-Wave Measurement System) single-wire dipole antenna
[DE88-003979] 09 p1155 N88-16920
CEBAF design overview and project status
[CEBAF-PR-88-001] 09 p1246 N88-17470
A technique for low level, wide range CW microwave power meter calibrations
[DE88-004147] 10 p1333 N88-17966
Nucleon resonances and nuclei: Experimental aspects
[CEBAF-PR-87-025] 11 p1545 N88-19233
The injector for the CEBAF CW superconducting linac
[CEBAF-PR-87-011] 11 p1546 N88-19241
Perturbation effects in the CEBAF beam transport system
[CEBAF-PR-87-010] 11 p1546 N88-19242
Investigation of multiple particle final states at CEBAF (Continuous Electron Beam Accelerator Facility)
[CEBAF-PR-87-026] 11 p1547 N88-19250
RF steering in the CEBAF CW superconducting linac
[CEBAF-PR-87-013] 11 p1547 N88-19251
The CEBAF project and its few-body research program
[CEBAF-PR-87-014] 11 p1547 N88-19253
Application of radio frequency superconductivity to recirculating linacs
[CEBAF-PR-88-002] 12 p1690 N88-20107
The continuous electron beam accelerator facility
[CEBAF-PR-87-017] 13 p1838 N88-20996
Discussion of two-mode two-photon CW laser oscillation 16 p2187 N88-23042
Effects of translational and rotational nonequilibrium on CW (Continuous Wave) chemical laser performance
[AD-A191425] 16 p2214 N88-23210
The loss parameters for very short bunches
[CEBAF-PR-88-005] 18 p2574 N88-25291
Effects of pulsed and CW (Continuous Wave) 2450 MHz radiation on transformation and chromosomes of human lymphocytes in vitro
[AD-A193104] 21 p2987 N88-27736
Analysis of free electron laser performance utilizing the National Bureau of Standards CW microtron
[AD-A194217] 23 p3219 N88-29160
Static and dynamic behavior of a quasi one-dimensional Heisenberg antiferromagnet in the long-range ordered state. A nuclear magnetic resonance study performed with a He3-He4 dilution refrigerator
[B8705564] 23 p3281 N88-29533
Aeronomic problems of the molecular oxygen photodissociation. Part 3: Solar spectral irradiances in the region of the O2 Herzberg continuum, Schumann-Runge bands and continuum
[AERONOMICA-ACTA-A-332-1988]
24 p3343 N88-29897
Aeronomic problems of molecular oxygen photodissociation. Part 4: The various parameters for the Herzberg continuum
[AERONOMICA-ACTA-A-333-1988]
24 p3352 N88-29955

CONTINUOUS WAVE LASERS
High intensity 5 eV O-atom exposure facility for material degradation studies 02 p0135 N88-10847
Silicon oxidation photoassisted with a continuous wave CO2 laser beam and contribution to the study of silica layers obtained
[LAAS-87-158] 02 p0179 N88-11115
Computer simulation of cw HF chemical laser unstable resonator performance
[AD-A185059] 05 p0587 N88-13581
An experimental study of CW HF chemical laser amplifier performance and zero power gain
[AD-A185241] 05 p0588 N88-13584
USSR report: Physics and mathematics
[JPRS-UPM-87-006] 06 p0708 N88-14344
Repetitively pulsed and continuous wave CO2 lasers pumped by a pulsed self-sustained discharge for thermal processing 06 p0709 N88-14346
Production-process CO2 laser with amplified pulse-repetition operation 06 p0771 N88-14739
Frequency locking of two lasers
[FOA-C-30456-3.1] 08 p0992 N88-16000
Remote measurement of aerosol stream velocity with continuous-wave CO2-laser 08 p1079 N88-16506
Mirrors for high-power continuous-wave Ar-lasers
09 p1235 N88-17404
Instabilities and chaos in a multimode, standing-wave, CW dye laser
[DE88-005028] 10 p1337 N88-17993
Studies of fluorine combustion
[AD-A187646] 11 p1452 N88-18656
Characteristics of welds joining parts of high-strength pipe steels and produced by beam of continuous-wave CO2-laser 14 p1897 N88-21325
Laser-heterodyne interferometry with streak camera detection
[DE88-003292] 14 p1914 N88-21437
Effects of translational and rotational nonequilibrium on CW (Continuous Wave) chemical laser performance
[AD-A191425] 16 p2214 N88-23210
Distributed feedback lasers
[NASA-CR-4154] 18 p2520 N88-24948
Strained layer and lattice matched transverse junction stripe quantum well lasers for continuous room temperature operation 20 p2863 N88-27004

CONTINUOUS WAVE RADAR
Method and apparatus for measuring distance
[NASA-CASE-MSC-20912-1] 20 p2793 N88-26568

CONTINUOUS WAVES
U CONTINUOUS RADIATION

CONTINUUM FLOW
Energy efficient continuous flow ash lockhopper
[NASA-CASE-NPO-16985-1-CU]
18 p2497 N88-24814
Studies of error in temperature measurement with thermistors in the range between continual and free-molecule flows
[NASA-TT-20302] 19 p2674 N88-25900

CONTINUUM MECHANICS
Relativistic stochastic mechanics
[PREPRINT-543] 06 p0790 N88-14842
A critical review of the development of several viscoplastic constitutive theories
[AD-A185652] 07 p0867 N88-15262
Conference on Maximum Principles and Eigenvalue Problems in Partial Differential Equations
[AD-A187870] 11 p1536 N88-19175
A continuum damage model for viscoelastic materials
[AD-A189426] 12 p1637 N88-19800
Stability and uniqueness in nonlinear continuum mechanics
[AD-A189616] 12 p1699 N88-20172
Problems in nonlinear continuum dynamics
[AD-A190538] 15 p2128 N88-22691
Small-scale cleavage test of polymer products
[PB88-165360] 16 p2181 N88-23001
On microphysical principles of thermofluid dynamics
[ETN-88-92095] 20 p2801 N88-26620
An anisotropic continuum damage model for creep-dominated, multiaxial loading histories
21 p2964 N88-27608
Some stability criteria in fluid and solid mechanics
21 p3027 N88-27966
A transversely isotropic thermoelastic theory
[NASA-TM-101302] 22 p3087 N88-28332

The construction of the thermoelasticity equations on the basis of contemporary notions of nonlinear continua mechanics
[NASA-TT-20307] 23 p3296 N88-29631
Theory of filtering and control with application to control of large space structures
[AD-A195500] 24 p3335 N88-29851
Damage initiation in the short beam shear test of composite materials using stiffness reduction
[AD-A194880] 24 p3340 N88-29883

CONTINUUM MODELING
Continuum modeling of large lattice structures: Status and projections
[NASA-TP-2787] 06 p0672 N88-14115
A continuum damage model for viscoelastic materials
[AD-A189426] 12 p1637 N88-19800
Continuum modeling and dynamic analysis of large truss structures 17 p2349 N88-23995
An anisotropic continuum damage model for creep-dominated, multiaxial loading histories 21 p2964 N88-27608

CONTINUUMS
Radio continuum emission from the ionized stellar winds of the cool supergiants in zeta Aurigae-like systems 04 p0514 N88-13160
Automatic continuum analysis of reflectance spectra 05 p0614 N88-13770
Continuum theories for fluid-particle flows: Some aspects of lift forces and turbulence
[DE88-007038] 18 p2511 N88-24898
Investigation of the higher-order elements in the SAMSON2 code
[AD-A193638] 23 p3271 N88-29465

CONTOUR SENSORS
Contour interactive extraction using image numerical treatment
[ISL-R-114/86] 15 p2113 N88-22587

CONTOURS
Detection of critical points: The first step to automatic line generalization 05 p0619 N88-13803
The aerodynamic design of hypersonic contoured axisymmetric nozzles including real gas effects
[VKI-TM-43] 06 p0665 N88-14076
Fast, colour displays of digital terrain elevation data
[AD-A185596] 06 p0729 N88-14485
The information metric for univariate linear elliptic models
[AD-A186385] 07 p0911 N88-15527
Contour-to-grid interpolation with nonlinear finite elements: A feasibility study
[AD-A188108] 11 p1503 N88-18980
On the geometric interpretation of image contours
[RR-647-I-IMAG-57-LIFIA] 15 p2109 N88-22563
Test results at transonic speeds on a contoured over-the-wing propfan model
[NASA-TM-88206] 23 p3177 N88-28918
Implementation of the NCAR (National Centre for Atmospheric Research) graphics package at ARL (Aeronautical Research Laboratory)
[AD-A195163] 24 p3391 N88-30193
A digital terrain model system for a microcomputer
[INPE-4610-PRE/1333] 24 p3413 N88-30316

CONTRACT MANAGEMENT
A comparison of the basket method and the stratified random sampling for contract change order negotiations
[AD-A184170] 04 p0500 N88-13080
The appropriate use of contract types in development contracts (a systems approach with emphasis on the European space sector)
[ESA-STR-222] 08 p1092 N88-16573
Streamlining invitation for bids
[AD-A188941] 12 p1705 N88-20206
Human organization --- space projects 22 p3160 N88-28808
Contracts 22 p3160 N88-28810

CONTRACT NEGOTIATION
A comparison of the basket method and the stratified random sampling for contract change order negotiations
[AD-A184170] 04 p0500 N88-13080
NASA (National Aeronautics and Space Administration) procurement: The 1973 space shuttle solid rocket motor contractor selection
[PB88-135264] 11 p1447 N88-18623
The impact of independent research and development regulations on companies not required to negotiate advanced independent research and development agreements
[AD-A190007] 15 p2147 N88-22818

CONTRACTION
On the relations between cyclic contraction ratio, flow stress, and deformation mechanisms in bainitic CrMoV steels
[VTT-36] 01 p0025 N88-10158
Cardiac contractility in weightlessness according to spatial ballistocardiography 07 p0890 N88-15393
On hypercontractivity of alpha-stable random variables, 0 less than alpha less than 2
[AD-A186425] 07 p0915 N88-15559
Contraction design for small low-speed wind tunnels
[NASA-CR-182747] 15 p2021 N88-22045

CONTRACTORS
A method for assessing the software engineering capability of contractors: Preliminary version
[AD-A187230] 10 p1388 N88-18290
A comparison of projection methods in the forecasting of overhead costs for seven government aerospace contractors
[AD-A187572] 10 p1425 N88-18514

CONTRACTS
NT INSURANCE (CONTRACTS)
A comparison of the basket method and the stratified random sampling for contract change order negotiations
[AD-A184170] 04 p0500 N88-13080
The appropriate use of contract types in development contracts (a systems approach with emphasis on the European space sector)
[ESA-STR-222] 08 p1092 N88-16573
Selling to NASA
[NASA-TM-89724] 12 p1705 N88-20208
Defense Small Business Innovation Research Program (SBIR). Volume 3: Air Force abstracts of phase 1 awards, 1987 17 p2448 N88-24548
Contracts 22 p3160 N88-28810

CONTRAROTATING PROPELLERS
Noise of a model high speed counterrotation propeller at simulated takeoff/approach conditions (F7/A7)
[NASA-TM-100206] 01 p0091 N88-10592
Summary of low-speed wind tunnel results of several high-speed counterrotation propeller configurations
[NASA-TM-100945] 18 p2458 N88-24597

CONTRAST
NT IMAGE CONTRAST
Contrast between the chemical, structural and electronic properties of thin films of Cu and Ni on the Ru(0001) surface
[DE88-002360] 07 p0938 N88-15698
Visual contrast sensitivity functions obtained from untrained observers using tracking and staircase procedures
[AD-A187715] 11 p1522 N88-19089
Brightness contrast and character height of five flat panel computer displays
[AD-A187743] 11 p1524 N88-19096
Auger electron spectroscopy of contrast-forming layers on metals
[NASA-TT-20182] 16 p2178 N88-22980

CONTROL
Conceptual issues in measuring the behavior of a distributed real-time process-control computer system
[DE87-009748] 05 p0638 N88-13898
Conceptual issues in measuring the behavior of a distributed real-time process-control computer system
[DE87-014251] 05 p0638 N88-13899
Controlling XeCl-laser by means of external signal with less than 2 W/cm (sup)2 intensity 14 p1972 N88-21768
Pulse duration control of XeCl*-laser by means of plasma shutter 14 p1973 N88-21774

CONTROL BOARDS
Quantifying some information processing aspects of the pilot's instrument crosscheck
[AD-A186114] 07 p0898 N88-15443
Design of a velocity and position control laboratory servo system
[AD-A186596] 08 p0990 N88-15997

CONTROL DEVICES
U CONTROL EQUIPMENT

CONTROL EQUIPMENT
NT CONTROL STICKS
NT CRYOSTATS
NT PRESSURE REGULATORS
NT SPEED REGULATORS
NT TELEOPERATORS
Optimal control of windpowered plants
[FOA-C-20610-2.7] 08 p1022 N88-16188
Ergonomics of car controls for disabled people, phase 1. Part 1: Chapters 1-7. Part 2: Appendices. Part 3: References
[ISBN-0-947767-82-7] 09 p1202 N88-17204
The KATE shell: An implementation of model-based control, monitor and diagnosis 09 p1210 N88-17255
A fiber-optic link for pressure control of ion sources
[DE88-001782] 09 p1248 N88-17484
Symmetries in nonlinear control systems and their applications 11 p1496 N88-18929
Western aeronautical test range real-time graphics software package MAGIC
[NASA-TM-100425] 13 p1757 N88-20506
Full electronic control system for diesel engine 16 p2185 N88-23025
An integrated on-chip pressure sensor for accurate control applications 19 p2671 N88-25880

CONTROL MOMENT GYROSCOPES
Equal-modulus vector programmed frequency control of minimally redundant structure of powered, single-degree-of-freedom gyroscopes for spacecraft attitude control system 02 p0159 N88-10994
Gyrostabilizer system of Kvant module 08 p1006 N88-16099
SIRTF nod maneuvers
[NASA-TM-101007] 22 p3048 N88-28085
An approach to CMG steering using feedback linearization
[NASA-CR-183172] 24 p3422 N88-30369

CONTROL PANELS
U CONTROL BOARDS

CONTROL RODS
SP-100 system modeling: SNPSAM update 17 p2417 N88-24372

CONTROL SIMULATION
A simulation study of a speed control system for autonomous on-road operation of automotive vehicles
[AD-A184030] 03 p0362 N88-12279
Thermal structural control modelling techniques --- spacecraft
[FOK-TR-R-86-030] 08 p0962 N88-15828
Use of a general control simulation program to evaluate HVAC control stability
[DE88-000476] 08 p0975 N88-15896
Control variate selection for multiresponse simulation
[AD-A186637] 08 p1069 N88-16463
Flight test technique, illustrated by Advanced Technologies Testing Aircraft System (ATTAS) 09 p1240 N88-17433
Preliminary design of the ORION attitude control system
[AD-A187179] 10 p1292 N88-17729
Perception and control of simulated self motion
[AD-A187444] 10 p1372 N88-18188
A comparative survey of mathematical models for dynamic simulation of in-orbit manipulation operations 12 p1592 N88-19533
Dynamics modeling, simulation, and control of a spacecraft/manipulator system 12 p1592 N88-19534
Design of a spherical air bearing simulator for tests of the attitude control system of artificial satellites
[INPE-4284-PRE/1155] 12 p1595 N88-19551
Active vibration control of a cantilevered beam with three elastic coordinates
[AD-A188824] 12 p1636 N88-19797
Integrated autopilot/autothrottle based on a total energy control concept: Design and evaluation of additional autopilot modes
[NASA-CR-4131] 13 p1724 N88-20308
F-16 simulator for man-in-the-loop testing of aircraft control systems (SIMTACS)
[AD-A189675] 14 p1870 N88-21178
A packet-switched wide-area communication network simulator
[FUB-3-1986] 14 p1905 N88-21381
Multiple model parameter adaptive control for in-flight simulation
[AD-A190568] 15 p2021 N88-22044
Models describing muscle behavior and control
[LR-522] 16 p2238 N88-23368
The biomorphic model of the human operator controlling a single or a double integrator
[LR-505] 16 p2243 N88-23402
A queueing network model for analyzing a class of branch and bound algorithms on a master-slave architecture
[CWI-OS-R8717] 16 p2249 N88-23441
A software design tool for the analysis of robot dynamics properties
[NLR-MP-86064-U] 17 p2385 N88-24171
Four-axis side-arm flight control simulator investigation
[AD-A196026] 24 p3409 N88-30294

CONTROL STABILITY
Extensions of the small mu test for robust stability
[OUEL-1666/87-REV] 02 p0223 N88-11406
Survey on large scale system control methods
[NASA-CR-181556] 05 p0554 N88-13374
Equivalence of input-output stability and exponential stability for infinite dimensional systems
[TW-276] 05 p0638 N88-13903
Use of a general control simulation program to evaluate HVAC control stability
[DE88-000476] 08 p0975 N88-15896
A direct approach to almost disturbance and almost input-output decoupling
[MEMO-641] 08 p1072 N88-16471
Microscopic control of metallization stability
[AD-A187553] 10 p1421 N88-18487
Control test and validation for a large diameter high stability centrifuge 12 p1577 N88-19437

Modelling and control of an annular momentum control device
[NASA-CR-4138] 13 p1754 N88-20491
Mode priming in an overmoded gyrotron oscillator
[AD-A189151] 13 p1772 N88-20602
Systolic determination of absolute stability in feedback control systems
[OUEL-1704/87] 14 p1962 N88-21705
Boundary stabilization of the reaction-diffusion equation with unilateral conditions
[RR-315] 14 p1964 N88-21720
Servo-actuator control for sampled-data feedback disturbance rejection --- helicopters
[ESA-TT-1002] 16 p2163 N88-22903
Feedback decoupling and stabilization for linear systems with multiple exogenous variables
[ETN-88-92245] 16 p2255 N88-23474
Control law parameterization for an aeroelastic wind-tunnel model equipped with an active roll control system and comparison with experiment
[NASA-TM-100593] 17 p2308 N88-23807

CONTROL STICKS
Steering mechanism --- vehicles
[EP-PATENT-0-181-700-A1] 01 p0053 N88-10338
F-16 control stick response during +Gz-induced loss of consciousness
[AD-A184107] 04 p0400 N88-12491

CONTROL SURFACES
NT AILERONS
NT FLAPS (CONTROL SURFACES)
NT GUIDE VANES
NT JET FLAPS
NT JET VANES
NT LEADING EDGE FLAPS
NT RUDDERS
NT SPOILERS
NT TABS (CONTROL SURFACES)
NT TRAILING EDGE FLAPS
NT UPPER SURFACE BLOWN FLAPS
NT VORTEX FLAPS
NT WING FLAPS
Experimental aerothermodynamic research of hypersonic aircraft
[NASA-CR-181533] 04 p0399 N88-12483
Effectiveness of various control surfaces in quasi-steady and unsteady conditions
[AGARD-R-735] 10 p1284 N88-17682
Design of an aeroelastic composite wing wind tunnel model
[AD-A188855] 12 p1582 N88-19466
Multivariable control law design for the AFTI/F-16 with a failed control surface using a parameter-adaptive controller
[AD-A189848] 15 p2020 N88-22040
Stability and control methodology for conceptual aircraft design. Volume 1: Methodology manual
[AD-A191314] 16 p2164 N88-22906
Steady and unsteady transonic pressure measurements on a clipped delta wing for pitching and control-surface oscillations
[NASA-TP-2594] 23 p3173 N88-28895

CONTROL SYSTEMS
U CONTROL

CONTROL SYSTEMS DESIGN
The method of rigid armature flux orientation for the field-oriented control of highly dynamic drives with synchronous machines
[ETN-87-90405] 01 p0042 N88-10269
The design of a turboshaft speed governor using modern control techniques
[NASA-CR-175046] 01 p0053 N88-10339
Augmenting the control of a flexible manipulator with passive mechanical damping 01 p0055 N88-10350
Improvements to the precision pan and tilt head
[RSRE-MEMO-3996] 01 p0057 N88-10365
Adaptive control of hydraulic devices
[FB-1/85] 01 p0084 N88-10543
Digital algorithms for the control and dynamic decoupling of industrial robot axes
[ETN-87-90441] 01 p0084 N88-10546
Fiber optic engineering sensor system. Preliminary program management plan, phase 3 revision
[AD-A183663] 01 p0093 N88-10608
A survey of aircraft integrated control technology
[AR-004-561] 02 p0126 N88-10794
A preliminary investigation into the feasibility of implementing a direct sideforce control system on the Astra Hawk by means of an active control surface --- aircraft control
[ETN-87-90924] 02 p0126 N88-10795
Fault tolerant considerations and methods for guidance and control systems
[AGARD-AG-289] 02 p0126 N88-10796
Flight test of a resident backup software system
02 p0128 N88-10805
Investigation of control law for active flutter suppression
[NASA-TT-20126] 02 p0130 N88-10818
A treatment of jw-axis model-matching transformation zeros in the optimal H squared and H infinity control designs
[OUEL-1673/87] 02 p0223 N88-11407
Control and stabilization mechanisms of submunitions
[DFVLR-IB-111-86/9] 03 p0259 N88-11630
Theoretical and experimental study of flow-control devices for inlets of indraft wind tunnels
03 p0268 N88-11684
Control design challenges of large space systems and spacecraft control laboratory experiment (SCOLE)
[NASA-CR-178392] 03 p0275 N88-11735
Wavefront error sensing
[NASA-CR-181504] 03 p0321 N88-12030
A scientific workstation operator-interface for accelerator control
[DE87-014689] 03 p0362 N88-12278
Space station resistojet system requirements and interface definition study
[NASA-CR-180832] 04 p0409 N88-12541
US Naval Air Force avionic and electrical system corrosion prevention and control maintenance
05 p0547 N88-13334
Development of an interface for an ultrareliable fault-tolerant control system and an electronic servo-control unit
[NASA-TM-88236] 05 p0553 N88-13367
Survey on large scale system control methods
[NASA-CR-181556] 05 p0554 N88-13374
Design of low order controllers for robust disturbance rejection in large space structures
[AD-A185202] 05 p0555 N88-13376
Plant Growth Module (PGM) conceptual design
05 p0631 N88-13855
Behavioral Architecture Robot Control System (BARCS): A new way of building robots
[REPT-87-036] 05 p0638 N88-13902
Balanced realizations: Canonical form, parametrization, model reduction
[PB87-123360] 06 p0757 N88-14642
Knowledge acquisition for a simple expert controller
[NASA-TT-20118] 06 p0761 N88-14672
An autopilot design for the United States Marine Corps' airborne remotely operated device
[AD-A186379] 07 p0820 N88-14983
Advanced helicopter cockpit and control configurations for helicopter combat missions
[NASA-TM-100017] 07 p0821 N88-14988
Faraday cup characterization of electron beam welding parameters
[DE88-001896] 07 p0864 N88-15241
Scientific research in the field of measurement and control technology
[SMBT-322] 07 p0907 N88-15493
A weighting sequence approach to the analysis and design of multivariable control systems
[AD-A186086] 07 p0917 N88-15570
Aeropropulsion '87. Session 2: Aeropropulsion Structures Research
[NASA-CP-10003-SESS-2] 08 p0954 N88-15785
Aeropropulsion '87. Session 4: Instrumentation and Controls Research
[NASA-CP-10003-SESS-4] 08 p0955 N88-15794
Directions in propulsion control
08 p0956 N88-15799
Supersonic STOVL propulsion technology program: An overview
08 p0957 N88-15808
Design of a velocity and position control laboratory servo system
[AD-A186596] 08 p0990 N88-15997
Clips as a knowledge based language
08 p1055 N88-16365
An innovative workstation 08 p1063 N88-16421
Neural networks as a possible architecture for the distributed control of space systems
08 p1064 N88-16431
Aircraft flight test trajectory control
[NASA-CR-179428] 09 p1120 N88-16707
Multisurface control mechanism for a deployable antenna: Far Infrared and Submillimeter Space Telescope (FIRST) technology study
[RP-FA-D003] 09 p1135 N88-16807
Design of a gas mass flow control system for the gas inlet installation of a solid fuel combustion chamber
[VTH-LR-471] 09 p1141 N88-16839
A control system for maintaining high stability in gas pressure
[DE88-003712] 09 p1175 N88-17042
Adaptive proximate time-optimal servomechanisms
09 p1175 N88-17043
A formal approach to validation and verification for knowledge-based control systems
09 p1207 N88-17233
Crew interface with a telerobotic control station
09 p1213 N88-17273
A method for designing robust multivariable feedback systems
[NASA-CR-182459] 09 p1225 N88-17341
Navigation planning using quadtrees
[DE88-003706] 09 p1225 N88-17343
Applications of nonlinear systems theory to control design
[NASA-CR-182485] 09 p1231 N88-17377
The impact of circulation control on rotary aircraft controls systems 10 p1271 N88-17601
Sensitivity of active vibration control to structural changes and model reduction 10 p1284 N88-17683
An application of eigenspace methods to symmetric flutter suppression
[NASA-CR-181618] 10 p1284 N88-17684
Light Electronic Control System (LECOS): A proposal for a interconnected error-tolerant, optoelectronic control system
[MBB-UT-004/87] 10 p1311 N88-17836
Active control technology with adaptive control concept in the aircraft construction
[MBB/LKE-294/S/PUB/295] 10 p1313 N88-17845
Local bifurcation control
[AD-A187435] 10 p1324 N88-17915
Joint services electronics program
[AD-A187587] 10 p1325 N88-17920
NASA/NBS (National Aeronautics and Space Administration/National Bureau of Standards) standard reference model for Telerobot Control System Architecture (NASREM)
[PB88-124773] 10 p1338 N88-17999
Study on a rotor speed control system for a horizontal axis windmill
[NAL-TR-931] 10 p1349 N88-18062
Parallels between control PDE's (Partial Differential Equations) and systems of ODE's (Ordinary Differential Equations)
[NASA-CR-182487] 10 p1398 N88-18331
On observer problems for systems governed by partial differential equations
[AD-A187430] 10 p1400 N88-18351
Further developments in exact state reconstruction in deterministic digital control systems
[NASA-TP-2812] 11 p1468 N88-18751
Optical links in the angle-data assembly of the 70-meter antennas 11 p1474 N88-18792
Optically controlled phased-array antenna technology for space communication systems
[NASA-TM-100852] 11 p1476 N88-18809
Construction of control systems with diversified redundancy for electrical machines
[BIA-5/86] 11 p1481 N88-18842
Time varying controller design for robot manipulator control
[AD-A188094] 11 p1494 N88-18919
Motion planning and control of robot manipulators via application of a computer graphics animated display
11 p1496 N88-18932
Design for performance enhancement in feedback control systems with multiple saturating nonlinearities
[NASA-CR-182614] 11 p1535 N88-19168
Control test and validation for a large diameter high stability centrifuge 12 p1577 N88-19437
Interaction between structural considerations and system design in advanced flight controls
12 p1580 N88-19458
Presentation of flight control design and handling quality commonality by separate surface stability augmentation for the family of commuter airplanes
[NASA-CR-182567] 12 p1583 N88-19471
Output aiming control
[AD-A188463] 12 p1583 N88-19473
On a knowledge based assisted system for highly autonomous control of experiment-manipulators in the Man-Tended Free Flyer 12 p1588 N88-19505
A knowledge-based approach for sensory-controlled assembly operations 12 p1588 N88-19506
Intelligent on board control for field emission electric propulsion system 12 p1589 N88-19513
Promising concepts for ground-to-orbit experiment teleoperation --- Columbus 12 p1590 N88-19518
Ground based supervisory and programming system for automatic experiment execution in orbit
12 p1590 N88-19519
Design of a spherical air bearing simulator for tests of the attitude control system of artificial satellites
[INPE-4284-PRE/1155] 12 p1595 N88-19551
Table with aerostatic bearings for simulation in one degree of freedom attitude control systems of artificial satellites
[INPE-4272-PRE/1144] 12 p1595 N88-19552
Advances in Air-Launched Weapon Guidance and Control
[AGARD-CP-431] 12 p1598 N88-19553

Automatic flight control system for modern helicopters 12 p1597 N88-19556
Speed control of a missile with throttleable ducted rocket propulsion 12 p1597 N88-19561
The use of hardware-in-the-loop-techniques in the development of a modern air-to-surface missile system 12 p1597 N88-19562
Reaction wheel control through digital technique using reference models
[INPE-4220-PRE/1100] 12 p1599 N88-19570
Analysis of the sensitivity of the attitude control system of an artificial satellite
[INPE-4285-PRE/1157] 12 p1599 N88-19573
Cold gas jet system for satellite attitude control-modeling and simulation
[INPE-4279-PRE/1150] 12 p1601 N88-19583
An analysis of DREO's (Defence Research Establishment Ottawa) analog rebalance loops for the CSG-2 (Canadian Strapdown Gyroscope) tuned-rotor gyroscope
[AD-A188577] 12 p1629 N88-19749
Low cost mobile robot
[AD-A188507] 12 p1633 N88-19778
Design of feedback control systems for stable plants with saturating actuators
[NASA-CR-182613] 12 p1681 N88-20050
Control augmented structural synthesis
[NASA-CR-4132] 13 p1721 N88-20290
Integrated autopilot/autothrottle based on a total energy control concept: Design and evaluation of additional autopilot modes
[NASA-CR-4131] 13 p1724 N88-20308
Computer-aided transformation of descriptive mode of mathematical models of a control system 13 p1756 N88-20503
Numerical methods in the resolution of control electrovalve model
[INPE-4154-RPE/540] 13 p1764 N88-20554
Control of structure in turbulent flows: Bifurcating and blooming jets
[AD-A189607] 13 p1766 N88-20562
Feasibility demonstration of a sensor for high-quality two-phase flow — Space Station
[NLR-TR-87009-U] 13 p1767 N88-20569
Control strategies and hardware used in solar thermal applications
[DE88-004631] 13 p1794 N88-20731
Robust decentralized control of large flexible structures
[DE88-005416] 13 p1824 N88-20902
Using trace theory to model discrete events
[CS-8708] 13 p1824 N88-20904
Performance improvements of an F-15 airplane with an integrated engine-flight control system
[NASA-TM-100431] 14 p1867 N88-21159
Towards a practical microgravity environment — isolation mount 14 p1878 N88-21223
Development and qualification of the OLYMPUS antenna pointing mechanism 14 p1879 N88-21227
A joint actuator design for a robotic manipulator 14 p1879 N88-21232
Modeling of a hydraulic motor and servo-valve to produce a desired system response using analogue and digital compensation techniques
[ETN-88-92079] 14 p1899 N88-21337
Development of a total electric vehicle drive system
[DE88-900367] 14 p1917 N88-21446
Development of a magnetically suspended, tetrahedron-shaped antenna pointing system 14 p1926 N88-21478
Practical considerations for structural control: System uncertainty, system time delay and truncation of small control forces
[PB88-163738] 14 p1933 N88-21528
Improving the man-machine interface to robotic systems
[NPL-DITC-100/87] 14 p1953 N88-21641
A new approach to almost decoupling problems for linear and nonlinear systems
[MEMO-660] 14 p1962 N88-21700
A polynomial approach to the H sub infinity control design method
[MEMO-662] 14 p1962 N88-21701
A state-space approach to super-optimal H sup infinity control problems
[OUEL-1690/87] 14 p1962 N88-21702
Systolic determination of absolute stability in feedback control systems
[OUEL-1704/87] 14 p1962 N88-21705
Linear state space modeling of a turbofan engine
[AD-A190110] 15 p2019 N88-22035
Design of an integrated control system for flutter margin augmentation and gust load alleviation, tested on a dynamic windtunnel model
[PB88-149885] 15 p2020 N88-22038
Application of eigenstructure assignment techniques in the design of a longitudinal flight control system
[AD-A189644] 15 p2020 N88-22039
Telerobotic operation of conventional robot manipulators
[DE88-005718] 15 p2073 N88-22363
Representation, analysis and design of multirate discrete-time control systems
[AD-A190499] 15 p2116 N88-22608
Optical switching and control techniques using nonlinear optical wave mixing
[AD-A190467] 15 p2134 N88-22730
Development of a mobile research flight test support capability
[NASA-TM-100428] 16 p2159 N88-22883
Basic design of a flight director system for NAL STOL research aircraft
[DE88-751806] 16 p2162 N88-22897
Analysis and design of gain scheduled control systems
[NASA-CR-182667] 16 p2163 N88-22904
An investigation of the ability to recover from transients following failures for single-pilot rotorcraft
[NASA-TM-100078] 16 p2164 N88-22905
Microgravity robotics technology program
[NASA-TM-100898] 16 p2215 N88-23219
Integrated multidisciplinary analysis tool IMAT users' guide
[NASA-TM-100605] 16 p2223 N88-23273
Distributed matchmaking
[CWI-CS-R8750] 16 p2254 N88-23467
Contribution to the adaptive dynamic control of a robot manipulator
[LAAS-87-350] 16 p2255 N88-23475
Identification of control structures — expert systems
[REPT-87-66] 16 p2255 N88-23479
Investigation of air transportation technology at Princeton University, 1986 17 p2294 N88-23724
Control law parameterization for an aeroelastic wind-tunnel model equipped with an active roll control system and comparison with experiment
[NASA-TM-100593] 17 p2308 N88-23807
Soviet spacecraft engineering research
[FASAC-TAR-3090] 17 p2311 N88-23823
Impact of control errors on the volume/weight demand of the Ventilation and Dryer (VAD) concept — EURECA Botany Facility
[TN-RB524-006/87] 17 p2377 N88-24132
An algorithm for super-optimal H sup inf design: The 2-block case
[OUEL-1711/87] 17 p2391 N88-24210
A state-space approach to discrete-time super-optimal H sup inf control problems
[OUEL-1712/87] 17 p2391 N88-24211
Precise computer controlled positioning of robot end effectors using force sensors
[NASA-CR-182887] 17 p2391 N88-24213
The calculation of casually constrained optima in the active control of sound
[ISVR-TR-147] 17 p2395 N88-24237
Safety constraints and considerations in the development of nuclear powered propulsion 17 p2401 N88-24276
Two-phase fluid management for a Rankine cycle isotope power system 17 p2405 N88-24303
Interaction of the control system with core nuclear design for fast spectrum space power reactors 17 p2405 N88-24304
Reactor instrumentation and control design and performance simulation for SP-100 17 p2406 N88-24306
An adaptive load-following control system for a space nuclear power system 17 p2406 N88-24307
SP-100 control system modeling 17 p2414 N88-24356
Automatic reactor control system for transient operation 17 p2436 N88-24493
An optimal disturbance rejection control system for multimegawatt space nuclear power systems 17 p2436 N88-24495
SP-100 ground engineering systems test facility control systems 17 p2436 N88-24496
Analysis and design of detection filters within closed-loop systems 18 p2525 N88-24980
Vibration protection of inelastic structures by means of active and passive control 18 p2528 N88-25001
The efficacy of using human myoelectric signals to control the limbs of robots in space
[NASA-CR-182901] 18 p2553 N88-25155
Electronic controller for reciprocating rotary crystallizer
[NASA-TM-101140] 18 p2584 N88-25354
Sensors for process control requirements for design and test 19 p2671 N88-25877
Analysis of the electrical harmonic characteristics of a slip recovery variable speed generating system for wind turbine applications
[DE88-001140] 19 p2687 N88-25972
ELIT: An autonomous underwater observation robot 19 p2699 N88-26048
Automation tools for demonstration of goal directed and self-repairing flight control systems
[NASA-CR-179433] 19 p2715 N88-26121
Stable discrete-time adaptive control 19 p2719 N88-26142
Adaptive residual mode filter control of distributed parameter systems for large space structure applications 19 p2719 N88-26143
Model reduction methods for control design
[NASA-CR-179434] 19 p2719 N88-26144
Computer simulation of multiple pilots flying a modern high performance helicopter
[NASA-TM-100183] 20 p2761 N88-26377
A reusable rocket engine intelligen control
[NASA-TM-100963] 20 p2766 N88-26401
Nonlinear identification of an aircraft for the direct calculation of an anticipatory control 20 p2787 N88-26535
Design of a controller to reduce residual vibration in the positioning control of flexible robotic manipulators 20 p2808 N88-26658
An introduction to robot joint control methods
[NLR-TR-86080-U] 20 p2811 N88-26677
Expert system application education project
[NASA-CR-183089] 20 p2843 N88-26867
Numerical optimization, system theoretic and software tools for the integrated design of flexible structures and their control systems
[AD-A192927] 21 p2895 N88-27183
Thermal-sensation control: A new method of controlling cooled/heated environments 21 p2930 N88-27394
A conceptual design study of a hovering system controller for an autonomous underwater vehicle
[AD-A193423] 21 p2930 N88-27399
The robust tracking control of nonlinear systems with uncertain dynamics 21 p2999 N88-27788
A PRELUDE (analysis and design of control systems-preliminary utilities depository). A data-based interactive system of control software, user's guid e
[DFVLR-MITT-88-12] 21 p3000 N88-27795
More on exact state reconstruction in deterministic digital control systems
[NASA-TP-2847] 22 p3063 N88-28177
Strawman Optical Reception Development Antenna (SORDA) 22 p3065 N88-28187
DSS 13 microprocessor antenna controller 22 p3066 N88-28192
A computer-aided approach to nonlinear control systhesis
[NASA-CR-179391] 22 p3140 N88-28673
Design of multirate control systems via parameter optimization
[REPT-87-013] 22 p3142 N88-28686
Robust design of cascade control
[REPT-88-006] 22 p3142 N88-28687
Study of standard generic approach for spacecraft (S/C) autonomy and automation (phase 3). Book A: Autonomy concept description
[ESA-CR(P)-2555-VOL-1] 23 p3185 N88-28955
Study of standard generic approach for spacecraft (S/C) autonomy and automation (phase 3). Book B: Autonomy concept application example
[ESA-CR(P)-2555-VOL-2] 23 p3185 N88-28956
Study of standard generic approach for spacecraft (S/C) autonomy and automation (phase 3). Book C: Autonomy concept summary
[ESA-CR(P)-2555-VOL-3] 23 p3185 N88-28957
Study on design and control of torque-controlled manipulators
[NASA-TT-20197] 23 p3223 N88-29183
Distributed cooperating processes in a mobile robot control system 23 p3256 N88-29386
Concepts for robot motion primitives required for space station teleoperations 23 p3257 N88-29387
Generic supervisor: A knowledge-based tool for control of space station on-board systems 23 p3257 N88-29389
Programming model for distributed intelligent systems 23 p3257 N88-29390
Blackboard architectures and their relationship to autonomous space systems 23 p3261 N88-29414
Real-time space system control with expert systems 23 p3262 N88-29419
Computer-Aided-Control Engineering (CACE) primitives for robust and adaptive control systems, phase 1
[AD-A192446] 23 p3265 N88-29439
Space structure (dynamics and control) theme development
[NASA-TM-100597] 24 p3335 N88-29850

Aircraft battery state of charge and charge control system
[AD-A194979] 24 p3367 N88-30052
ARC length control for plasma welding
[NASA-CASE-MSC-20900-1] 24 p3380 N88-30131
Robust design of distributed controllers for large flexible space structures
[NASA-CR-183202] 24 p3380 N88-30134
The design of an intelligent multidisk control module for VME bus based systems
[AD-A195587] 24 p3411 N88-30303
A shared-world conceptual model for integrating space station life sciences telescience operations
24 p3416 N88-30333
Artificial intelligence in a mission operations and satellite test environment 24 p3416 N88-30334
Automated space vehicle control for rendezvous proximity operations 24 p3416 N88-30335
Automated satellite control in Ada
24 p3416 N88-30336
Low level image processing techniques using the pipeline image processing engine in the flight telerobotic servicer 24 p3418 N88-30346

CONTROL THEORY

The associative memory ME7
[ESA-TT-1033] 01 p0079 N88-10506
A survey of aircraft integrated control technology
[AR-004-561] 02 p0126 N88-10794
A treatment of jw-axis model-matching transformation zeros in the optimal H squared and H infinity control designs
[OUEL-1673/87] 02 p0223 N88-11407
On the control of a compliant robot arm
03 p0332 N88-12095
Identification of linear structural models
03 p0337 N88-12121
Analytical investigation of the dynamics of tethered constellations in Earth orbit (phase 2)
[NASA-CR-179218] 04 p0408 N88-12533
Natural control of flexible space structures
04 p0408 N88-12534
A modern control theory based algorithm for control of the NASA/JPL 70-meter antenna axis servos
04 p0436 N88-12706
Survey on large scale system control methods
[NASA-CR-181556] 05 p0554 N88-13374
Error control techniques for satellite and space communications
[NASA-CR-181581] 05 p0576 N88-13516
Trajectory control of robot manipulators with closed-kinematic chain mechanism
[NASA-TM-89305] 05 p0591 N88-13605
Control of an unstable launcher in atmospheric flight using minimax optimal control laws
[SNIAS-872-422-107] 05 p0638 N88-13901
Equivalence of input-output stability and exponential stability for infinite dimensional systems
[TW-276] 05 p0638 N88-13903
On linear periodic controllers
[DE87-011174] 05 p0639 N88-13904
Balanced realizations: Canonical form, parametrization, model reduction
[PB87-123360] 06 p0757 N88-14642
Heuristic control of the Utah/MIT dextrous robot hand
06 p0793 N88-14858
Scientific research in the field of measurement and control technology
[SMBT-322] 07 p0907 N88-15493
Simplified self-tuning control algorithms
[OUEL-1657/86] 07 p0907 N88-15494
Optimal observers for ARMA models
[OUEL-1659/86] 07 p0907 N88-15495
Characterization of all controlled invariant sub-spaces for spectral systems
[PB88-106638] 07 p0912 N88-15532
Directions in propulsion control
08 p0956 N88-15799
Design of a velocity and position control laboratory servo system
[AD-A186596] 08 p0990 N88-15997
A modal control based limiting performance formulation for shock excited systems 08 p0998 N88-16046
A direct approach to almost disturbance and almost input-output decoupling
[MEMO-641] 08 p1072 N88-16471
Some aspects of control for semilinear distributed parameter systems
[INPE-4147-PRE/1054] 08 p1075 N88-16484
Helicopter mathematical models and control law development for handling qualities research
09 p1108 N88-16642
Analytical interactive approach for phenomena involving structures, thermal and control aspects. Volume 1: Theory — spacecraft structures
[ESA-CR(P)-2503-VOL-1] 09 p1134 N88-16803
Analytical interactive approach for phenomena involving structures, thermal, and control aspects. Volume 2: Toward the solution — spacecraft structures
[ESA-CR(P)-2503-VOL-2] 09 p1134 N88-16804
Analytical interactive approach for phenomena involving structures, thermal, and control aspects. Volume 3: Executive summary — spacecraft structures
[ESA-CR(P)-2503-VOL-3] 09 p1134 N88-16805
Adaptive proximate time-optimal servomechanisms
09 p1175 N88-17043
Feedback stabilization of distributed systems
[AD-A187111] 09 p1222 N88-17328
Regulation of nonlinear and generalized linear systems
[AD-A186706] 09 p1224 N88-17338
Boundary stabilization of thin elastic plates
[AD-A187123] 10 p1343 N88-18025
Nonlinear filtering and large deviations: A PDE-Control theoretic approach
[AD-A187436] 10 p1396 N88-18321
Boundary value problems for differential and functional differential equations
[AD-A187378] 10 p1400 N88-18349
Viscosity methods in optimal control of distributed systems
[AD-A188086] 10 p1401 N88-18357
Time varying controller design for robot manipulator control
[AD-A188094] 11 p1494 N88-18919
Kinematic and dynamic analyses of the Stanford/JPL robot hand
[DE88-004637] 11 p1495 N88-18923
Analysis and synthesis of two degrees of freedom control systems 11 p1495 N88-18928
Optimal control theory of load-following and parameter-tracking of nonlinear systems: An application of Pontryagin Maximum Principle to reactor dynamics
[DE88-004770] 11 p1532 N88-19152
Nonlinear input-output systems
[NASA-CR-182484] 11 p1535 N88-19171
Output aiming control
[AD-A188463] 12 p1583 N88-19473
Safe and fuel minimum reference trajectories for closed loop controlled approaches — space stations
12 p1585 N88-19488
Computational aspects of robotic experiment manipulation in a microgravity environment
12 p1589 N88-19512
Dynamics modeling, simulation, and control of a spacecraft/manipulator system
12 p1592 N88-19534
Attitude control of an artificial satellite through the extension of the linear quadratic regulator theory
[INPE-4407-TDL/304] 12 p1600 N88-19577
Integrated autopilot/autothrottle based on a total energy control concept: Design and evaluation of additional autopilot modes
[NASA-CR-4131] 13 p1724 N88-20308
Using trace theory to model discrete events
[CS-8708] 13 p1824 N88-20904
An efficient gradient projection optimization scheme for a seven-degree-of-freedom redundant robot with spherical wrist
[DE88-005440] 14 p1919 N88-21453
A new approach to almost decoupling problems for linear and nonlinear systems
[MEMO-660] 14 p1962 N88-21700
A polynomial approach to the H sub infinity control design method
[MEMO-662] 14 p1962 N88-21701
A complexity transform for NP-complete problems
[OUEL-1708/87] 14 p1962 N88-21703
Bilinear systems in the frequency domain and an application to optimal control
[RR-320] 14 p1962 N88-21704
Parametric methods of analysing linear and nonlinear systems
[RR-318] 14 p1967 N88-21741
Model selection for the multiple model adaptive algorithm for in-flight simulation
[AD-A189715] 15 p2016 N88-22022
Multivariable control law design for the AFTI/F-16 with a failed control surface using a parameter-adaptive controller
[AD-A189848] 15 p2020 N88-22040
Wave propagation and dynamics of lattice structures
[AD-A190037] 15 p2025 N88-22066
Telerobotic operation of conventional robot manipulators
[DE88-005718] 15 p2073 N88-22363
Instrumentation for scientific computing in neural networks, information science, artificial intelligence and applied mathematics
[AD-A189981] 15 p2106 N88-22549
Insertions using geometric analysis and hybrid force-position control: Method and analysis
[DE87-013652] 15 p2117 N88-22611
Information capacity of Gaussian channels
[AD-A190316] 15 p2127 N88-22686
Feedback decoupling and stabilization for linear systems with multiple exogenous variables
[ETN-88-92245] 16 p2255 N88-23474
Identification of control structures — expert systems
[REPT-87-66] 16 p2255 N88-23479
Derivative arrays, geometric control theory and realizations of linear descriptor systems
[AD-A190882] 16 p2260 N88-23513
Error control techniques for satellite and space communications
[NASA-CR-182886] 17 p2332 N88-23922
Generalized predictive control of multivariable systems
[OUEL-1640/86] 17 p2391 N88-24209
Experimental evaluation of the MIT-SNL period-generated minimum time control laws for the rapid adjustment of reactor power 17 p2436 N88-24494
Attitude control laws for gas-jet spacecraft
18 p2467 N88-24643
Estimation and control of distributed models for certain elastic systems arising in large space structures
[AD-A192120] 18 p2472 N88-24866
A feedback linearization approach to spacecraft control using momentum exchange devices
[NASA-CR-172057] 18 p2472 N88-24868
Dynamics of a flexible orbiting platform with MRMS
[ISSN-0285-6808] 18 p2473 N88-24873
Automatic feedback control of a rigid body for finite displacements 18 p2473 N88-24874
The coordination of multiple robotic manipulators
[AD-A190869] 18 p2522 N88-24963
Real-time implementation of a kinematic optimization scheme for seven-degree-of-freedom redundant robots with spherical wrists
[DE88-006785] 18 p2524 N88-24974
Mixed min-max optimization problem with restrictions
18 p2565 N88-25232
Structural properties of multivariable linear systems
[PB88-181375] 19 p2717 N88-26134
Stable discrete-time adaptive control
19 p2719 N88-26142
An introduction to robot joint control methods
[NLR-TR-86080-U] 20 p2811 N88-26677
The analysis and control of robotic manipulators operating at or near kinematically singular configurations
22 p3084 N88-28315
On the pseudo-linearization problem for nonlinear systems
[AD-A194021] 22 p3142 N88-28683
Gravitation control 22 p3158 N88-28795
Convex duality approach to the optimal control or diffusions
[AD-A194535] 23 p3266 N88-29442
Canonical forms in the control of DPS
[AD-A194571] 23 p3270 N88-29461
Minimizing escape probabilities: A large deviations approach
[AD-A194534] 23 p3275 N88-29496
Feedback stabilization of du/dt=Au + bf in Hilbert space when the normalization function is less than or equal to r
[AD-A193510] 23 p3277 N88-29506
Theory of filtering and control with application to control of large space structures
[AD-A195500] 24 p3335 N88-29851
K(sup th)-order extended linearization
[AD-A194786] 24 p3421 N88-30363
Analytical methods in stochastic control and nonlinear filtering
[AD-A194272] 24 p3426 N88-30388

CONTROL UNITS (COMPUTERS)

A timing evaluator for C programs generated by the model system
[AD-A191204] 17 p2385 N88-24174
Design and testing of a luminance and chrominance stabilization system for a computer-controlled color display
[AD-A191922] 18 p2554 N88-25159
An investigation of performance improvement in knowledge-based control systems
21 p2928 N88-27382

CONTROL VALVES

Dynamic modelling of an electromechanical valve using frequency response data
[AD-A187908] 11 p1494 N88-18918
Electromagnetic modeling of a control valve
[INPE-4140-PRE/1048] 12 p1622 N88-19700
Development of a motorized cryovalve for the control of superfluid liquid helium 14 p1925 N88-21477
A pyrotechnical opening valve
[SNIAS-MU/TYS-NT-2-06(0)] 16 p2167 N88-22922

Characterization of accelerating pipe flow
[AD-A193065] 21 p2943 N88-27481

CONTROLLABILITY
Investigation of pilot behavior in a training program for assessing handling qualities using a ground simulator
[ESA-TT-999] 03 p0357 N88-12247
Control of a flexible one-link manipulator
[AD-A185035] 05 p0590 N88-13598
Impact of flying qualities on mission effectiveness for helicopter air combat, volume 1
[NASA-CR-166568] 06 p0669 N88-14100
NASA/Army Rotorcraft Technology. Volume 2: Materials and Structures, Propulsion and Drive Systems, Flight Dynamics and Control, and Acoustics
[NASA-CP-2495-VOL-2] 09 p1106 N88-16632
Helicopter mathematical models and control law development for handling qualities research
09 p1108 N88-16642
Rotorcraft handling-qualities design criteria development 09 p1109 N88-16645
The impact of vertical axis characteristics on helicopter handling qualities
[AD-A188964] 12 p1583 N88-19474
Electron beam sensitive devices for controllability
[RR-658-I] 14 p1908 N88-21403
The effects of torque response and time delay on rotorcraft vertical axis handling qualities
[AD-A189873] 15 p2017 N88-22023
Preliminary airworthiness evaluation of the UH-60A with Advanced Digital Optical Control System (ADOCS)
[AD-A190674] 15 p2018 N88-22030
An investigation of the ability to recover from transients following failures for single-pilot rotorcraft
[NASA-TM-100078] 16 p2164 N88-22905
Advances in Flying Qualities
[AGARD-LS-157] 24 p3314 N88-29735
Advances in flying qualities: Concepts and criteria for a mission oriented flying qualities specification
24 p3314 N88-29739
A second look at MIL prime flying qualities requirements 24 p3314 N88-29740
The optimal control pilot model and applications
24 p3315 N88-29741
The role of simulation in flying qualities and flight control system related development 24 p3315 N88-29742
An analysis of lateral-directional handling qualities and Eigenstructure of high performance aircraft
[AD-A194874] 24 p3328 N88-29814
Minimum-complexity helicopter simulation math model
[NASA-CR-177476] 24 p3328 N88-29819

CONTROLLED ATMOSPHERES
NT CABIN ATMOSPHERES
NT HELIUM-OXYGEN ATMOSPHERES
NT INERT ATMOSPHERE
NT SPACECRAFT CABIN ATMOSPHERES
Fire-related medical science 04 p0406 N88-12525
Performance characteristics of magnesium-sodium nitrate flares in oxygen-nitrogen atmospheres
[AD-A185274] 05 p0570 N88-13476
Fibrous glass aerosols: A literature review
[AD-A188420] 12 p1672 N88-20008
Advancements in oxygen generation and humidity control by water vapor electrolysis
[NASA-CR-172073] 22 p3134 N88-28633

CONTROLLED FUSION
Massachusetts Institute of Technology Plasma Fusion Center: 1986-1987 Report to the President
[DE87-013518] 01 p0101 N88-10661
New directions in Vlasov plasma turbulence and anomalous transport
[DE87-014425] 02 p0238 N88-11500
Applications of neutral beam and rf technologies
[DE87-014936] 03 p0379 N88-12382
Advanced fusion power: A preliminary assessment
[AD-A185903] 07 p0933 N88-15664
Studies on parametric instabilities in high-frequency wave heating of fusion plasmas
[PH-156] 07 p0933 N88-15667
SOAR: Space orbiting advanced fusion power reactor
[AD-A189234] 13 p1732 N88-20356
Helium-3 fusion fuel resources for space power
17 p2410 N88-24330

CONTROLLED STABILITY
U CONTROL

CONTROLLERS
NT SERVOMECHANISMS
NT SERVOMOTORS
Space station propulsion technology: Space station propulsion system test bed test plan
[NASA-CR-179201] 01 p0017 N88-10104
Test of the Hipparcos payload in the Liege vacuum facility focal 02 p0135 N88-10850
A digital control system for high level acoustic noise generation 02 p0138 N88-10865
Minimisation of helicopter vibration through active control of structural response 03 p0264 N88-11662
On the control of a compliant robot arm
03 p0332 N88-12095
Local-optimal control in systems with delay
04 p0424 N88-12627
A modern control theory based algorithm for control of the NASA/JPL 70-meter antenna axis servos
04 p0436 N88-12706
On linear periodic controllers
[DE87-011174] 05 p0639 N88-13904
Intelligent controllers
[DE88-001862] 07 p0904 N88-15475
Evaluation of high-voltage, high-power, solid-state remote power controllers for amps
07 p0924 N88-15612
Space station propulsion technology
[NASA-CR-179260] 08 p0964 N88-15835
Pulse width modulator controller design for a brushless DC motor position servo
[AD-A186618] 08 p0980 N88-15921
Telerobotic controller development
08 p1056 N88-16370
Software simulation of time delay in teleoperation
08 p1056 N88-16371
Task path planning, scheduling and learning for free-ranging robot systems 08 p1058 N88-16386
A framework for real-time distributed expert systems: On-orbit spacecraft fault diagnosis, monitoring and control 08 p1066 N88-16440
Prototype space station automation system delivered and demonstrated at NASA 08 p1066 N88-16442
A control system for maintaining high stability in gas pressure
[DE88-003712] 09 p1175 N88-17042
Computer control of a microgravity mammalian cell bioreactor 09 p1197 N88-17172
Development and experimentation of an eye/brain/task testbed 09 p1205 N88-17219
Expert system applications in spacecraft subsystem controllers 09 p1210 N88-17254
TDAS: The Thermal Expert System (TEXSYS) data acquisition system 09 p1211 N88-17258
A method for designing robust multivariable feedback systems
[NASA-CR-182459] 09 p1225 N88-17341
Pumping systems and flow interfaces for rapid response electronic reheat controls 10 p1282 N88-17665
Possibilities for on-line surge suppression by fast guide vane adjustment in axial compressors
10 p1283 N88-17674
Optically controlled devices and ultrafast laser sources for signal processing
[AD-A187417] 10 p1338 N88-17995
An Ethernet local area network controller with supporting operating system software
[DE88-003534] 10 p1392 N88-18304
The implementation of artificial intelligence in control systems
[DE88-003497] 10 p1396 N88-18318
The representation of knowledge within model-based control systems
[DE88-004863] 10 p1396 N88-18319
The Telecommunications and Data Acquisition Report
[NASA-CR-182545] 11 p1471 N88-18774
New mode switching algorithm for the JPL 70-meter antenna servo controller 11 p1474 N88-18791
The design and implementation of the Technical Facilities Controller (TFC) for the Goldstone deep space communications complex 11 p1474 N88-18794
SETI data controllers 11 p1474 N88-18795
Research on output feedback control
[NASA-CR-182543] 11 p1534 N88-19167
Multi-axis control of telemanipulators
12 p1593 N88-19539
Advances in Air-Launched Weapon Guidance and Control
[AGARD-CP-431] 12 p1596 N88-19553
Speed control of a missile with throttleable ducted rocket propulsion 12 p1597 N88-19561
Practical system for the use of alcohol in diesel engines
[PB88-147863] 12 p1612 N88-19638
NAVLAB: An autonomous navigation testbed
[AD-A189049] 13 p1720 N88-20283
Control of structure in turbulent flows: Bifurcating and blooming jets
[AD-A189607] 13 p1766 N88-20562
Force distribution and trajectory control for closed kinematic chains with applications to walking machines
13 p1779 N88-20642
Industrial electric motors and controllers
[PB88-139589] 14 p1907 N88-21394
Multivariable control law design for the AFTI/F-16 with a failed control surface using a parameter-adaptive controller
[AD-A189848] 15 p2020 N88-22040
Microgravity mechanisms and robotics program
16 p2219 N88-23237
The TMS32010 evaluation module controller --- signal processor
[EUT-86-E-162] 16 p2245 N88-23407
Reconfigurable work station for a video display unit and keyboard
[NASA-CASE-MFS-26009-1-SB]
17 p2382 N88-24163
Connecting remote systems for demonstration of automation technologies 17 p2387 N88-24191
Genetic algorithms for adaptive real-time control in space systems 17 p2388 N88-24195
A universal computer control system for motors
[NASA-CASE-NPO-17134-1-CU]
18 p2506 N88-24864
Electronic controller for reciprocating rotary crystallizer
[NASA-TM-101140] 18 p2584 N88-25354
Adaptive residual mode filter control of distributed parameter systems for large space structure applications
19 p2719 N88-26143
L(sub infinity symbol)-approximations of complex functions and robust controllers for large flexible space structures
[PB88-186226] 20 p2764 N88-26390
COSPAS/SARSAT 406-MHz emergency beacon digital controller
[NASA-TM-100859] 20 p2792 N88-26566
Design of a controller to reduce residual vibration in the positioning control of flexible robotic manipulators
20 p2808 N88-26658
SP-100 Ground Engineering Systems: Test facility control systems
[DE88-009195] 21 p3015 N88-27895
The feasibility of the disturbance accommodating controller for precision antenna pointing
22 p3064 N88-28182
DSS 13 microprocessor antenna controller
22 p3066 N88-28192
Motion planning with obstacles and dynamic constraints 23 p3222 N88-29175
Nanosequencer digital logic controller
[NASA-CASE-NPO-16116-2] 23 p3245 N88-29310
Artificial intelligence applied to process signal analysis
23 p3252 N88-29359
Identification and control of time-varying flexible structures: An artificial intelligence approach
23 p3265 N88-29437
Robust design of distributed controllers for large flexible space structures
[NASA-CR-183202] 24 p3380 N88-30134
An intelligent training system for space shuttle flight controllers 24 p3415 N88-30331

CONVAIR MILITARY AIRCRAFT
U MILITARY AIRCRAFT

CONVECTION
NT FORCED CONVECTION
NT FREE CONVECTION
NT MARANGONI CONVECTION
NT RAYLEIGH-BENARD CONVECTION
Phase dynamics: A review and a perspective
[DE87-013173] 01 p0048 N88-10306
Statistical relationships between the mesoscale organization of convection and the large-scale wind profiles during GATE --- GARP Atlantic Tropical Experiment (GATE) 02 p0208 N88-11302
Convective cross section analysis
[PB87-204566] 02 p0216 N88-11361
Thermally driven convective cells and tokamak edge turbulence
[DE87-014424] 02 p0238 N88-11499
The duskside plasmapause/ring current interface: Convection and plasma wave observations
[MPE-PREPRINT-93] 02 p0243 N88-11533
A heat transfer model for a heated helium airship
[AD-A183786] 03 p0259 N88-11629
The diffusion-convection vortex method for solving two-dimensional incompressible Navier-Stokes equation
03 p0317 N88-12001
Banded ion morphology 04 p0468 N88-12892
Relations between chromospheric and coronal structure, flux-flux correlations and convective zone properties
04 p0510 N88-13138
Global convection patterns in the high latitude
[AD-A185794] 06 p0743 N88-14571
Stabilized Galerkin method for convection-diffusion problems
[PB87-234985] 06 p0764 N88-14694
Comments on the theory of absolute and convective instabilities
[PB87-124624] 06 p0783 N88-14808
Solar Dynamics and G-modes
[NASA-CR-180737] 06 p0805 N88-14911
The use of the direct measurement of solar radiation for the determination of Pasquill Stability Parameter
[AD-A186084] 07 p0946 N88-15750

Influence of the friction coefficients, the power and the flowrate on the two-phase flow instabilities in natural circulation
[DE88-700036] 08 p0983 N88-15946
Some stability results for the hopscotch difference method when applied to convection-diffusion equations
[CWI-NM-R8711] 08 p1072 N88-16465
Interaction of the cold conveyor belt with polar jet streaks
[AD-A186774] 09 p1192 N88-17145
Convective wind fields as investigated with doppler lidar
[PB88-115472] 09 p1193 N88-17151
Influence of convection on microstructure
[NASA-CR-182489] 10 p1302 N88-17784
Periodic natural convection in a rectangular enclosure of low aspect ratio 10 p1329 N88-17941
A multigrid preconditioner applied to a two-dimensional convection-diffusion problem
[DE88-004765] 10 p1397 N88-18329
Radial mixing in turbomachines
[AD-A188028] 11 p1482 N88-18847
Travelling waves and chaos in double-diffusive convection 11 p1484 N88-18857
The Hamiltonian structure of nonlinear elasticity: The convective representation of solids, rods, and plates
[AD-A187200] 11 p1498 N88-18943
MCT crystal growth
[NASA-CR-179297] 11 p1557 N88-19318
Dynamical modeling of marine boundary layer convection 13 p1797 N88-20750
Fingering flow patterns of thermosolutal convection in rectangular enclosures
[NASA-TM-100854] 14 p1911 N88-21417
Taiwan area mesoscale experiment: P-3 aircraft operations summary
[PB88-169073] 18 p2544 N88-25098
Dendritic growth in the presence of convection 18 p2580 N88-25328
Dynamics explorer data analysis
[NASA-CR-181428] 19 p2691 N88-25996
Satellite observed Mesoscale Convective System (MCS) propagation characteristics and a 3-12 hour heavy precipitation forecast index
[PB88-180161] 19 p2692 N88-26004
Cosmions and stars
[DE88-010886] 20 p2887 N88-27145
Time-dependent thermal convection of Earth mantle and double diffusive convection in magma chambers
[MITT-52] 21 p2974 N88-27663
Application of rectangular co-ordinates to the problem of laminar combined convection in a straight horizontal tube whose circumference is heated nonuniformly
[PDR/CFDU/IC/33] 22 p3076 N88-28263
The influence of conductivities consistent with field-aligned currents on high-latitude convection patterns
[TRITA-EPP-88-02] 22 p3119 N88-28533
The patterns of tropical convection during the 1986-87 ENSO 22 p3120 N88-28537
The dynamics and thermodynamics of a 30-60 day oscillation 22 p3121 N88-28543
Aspects of the 30-60 day oscillation in a GCM simulation 22 p3121 N88-28545
An observational study of interaction between large scale tropical cumulus convection and the equatorial circulation anomalies 22 p3124 N88-28564
Natural convection immersion cooling of an array of simulated chips in an enclosure filled with dielectric liquid
[AD-A193594] 23 p3207 N88-29088
Ionospheric convection and structure using ground-based digital ionosondes
[AD-A194246] 23 p3233 N88-29237
Influence of the convection on evaporation and combustion of a fuel droplet 24 p3351 N88-29948

CONVECTION CLOUDS
NT ARC CLOUDS
NT CUMULUS CLOUDS
Forecasting and nowcasting cumulus convection with soundings released from a storm-intercept vehicle 02 p0202 N88-11262
Detailed analysis of a mesoscale convective complex situation in the Carpathian Basin (Europe) 02 p0207 N88-11296
Effects of the large scale motion and horizontal inhomogeneity of the moist static instability on development of the mesoscale convective systems in the midlatitudes 02 p0207 N88-11297
Radar measurement methods for the observation of convective clouds, and comparison of measurements and numerical simulation
[ESA-TT-1049] 03 p0352 N88-12223
Study of isolated convective clouds in the lower Alps in summer 1984, using radar and a simple Weinstein numerical model
[ESA-TT-1061] 03 p0353 N88-12224
Cloud physics studies in SCPP (Sierra Cooperative Pilot Project) from 1977-87
[PB88-136924] 11 p1516 N88-19054
Stratospheric electric field and conductivity measurements over electrified convective clouds in the South American region, revised
[INPE-4046-PRE/1012-REV-3] 15 p2095 N88-22483
A study on electric fields and conductivity associated with electrified clouds in the region of South America
[INPE-4487-TDL/325] 15 p2096 N88-22486
Ice formation on aircraft
[ETN-88-92154] 18 p2545 N88-25104
Parametric methodologies of cloud vertical transport for acid deposition models
[PB88-191374] 20 p2825 N88-26762
Dynamic interaction of convective cumulus with large-scale environment
[MITT-55] 20 p2827 N88-26773

CONVECTION CURRENTS
Convective scale interaction: Arc cloud lines and the development and evolution of deep convection
[NASA-CR-181469] 02 p0215 N88-11357
Environmental and convective influence on tropical cyclone development versus non-development
[AD-A185231] 05 p0627 N88-13835
Analysis of quasi-geostrophic forcing during the AIMCS (Airborne Investigations of Mesoscale Convective System) Project. Volume 1: Discussion
[PB88-133095] 12 p1645 N88-19860
Numerical simulation of generation of mesoscale convective systems in large-scale environment 14 p1900 N88-21344
Open cell associated with warm advection 17 p2351 N88-24010

CONVECTIVE FLOW
NT RAYLEIGH-BENARD CONVECTION
Magnetic field twist driven by remote convective motions: Characteristics and twist rates 01 p0113 N88-10724
Preparative electrophoresis for space
[NASA-TP-2777] 02 p0156 N88-10977
Continuous flow electrophoresis system experiments on shuttle flights STS-6 and STS-7
[NASA-TP-2778] 02 p0156 N88-10978
On the role of convective motion during dendrite growth: Experiments under variable gravity, revised
[NASA-CR-179213] 02 p0156 N88-10979
Detailed analysis of a mesoscale convective complex situation in the Carpathian Basin (Europe) 02 p0207 N88-11296
Effects of the large scale motion and horizontal inhomogeneity of the moist static instability on development of the mesoscale convective systems in the midlatitudes 02 p0207 N88-11297
Convective scale interaction: Arc cloud lines and the development and evolution of deep convection
[NASA-CR-181469] 02 p0215 N88-11357
Conjugated heat transfer from a radiating fluid in a rectangular channel 03 p0317 N88-12003
High latitude F-region drift studies
[AD-A184466] 04 p0467 N88-12889
SHARP simulation of discontinuities in highly convective steady flow
[NASA-TM-100240] 05 p0642 N88-13931
Observations of a midlatitude squall line boundary layer wake
[AD-A185609] 06 p0746 N88-14589
The numerical and analytical study of bifurcation and multicellular flow instability due to natural convection between narrow horizontal isothermal cylindrical annuli at high Rayleigh numbers
[AD-A186113] 07 p0849 N88-15151
Assessment of VAS-derived products created by a simultaneous algorithm on a convectively active day
[AD-A186158] 08 p1054 N88-16359
A payload for investigating the influence of convection on GaAs crystal growth 10 p1288 N88-17702
Disk pumping test
[AD-A187199] 11 p1440 N88-18591
Suspension of small metallic plates: A versatile sensor
[PB88-130901] 11 p1487 N88-18874
High Rayleigh number convection in rectangular enclosures with differentially heated vertical walls and aspect ratios between zero and unity
[NASA-TM-100277] 12 p1628 N88-19739
Velocity and concentration fields over a crystal growing in a water solution. Experimental study and numerical simulation 14 p1987 N88-21856
Transport processes during directional solidification and crystal growth: Scaling and experimental study 14 p1988 N88-21857
Convection effects on stability at the solidification front 14 p1988 N88-21860
Acoustic convective system
[NASA-CASE-NPO-17278-1-CU] 18 p2498 N88-24818
Dendritic growth in the presence of convection 18 p2580 N88-25328
Experimental and analytical studies of compressible vortices 19 p2665 N88-25848
Stationary, wave type, and chaos type convection in spherical symmetry geometries
[ETN-88-92358] 20 p2801 N88-26625

CONVECTIVE HEAT TRANSFER
Multidimensional modeling of convective heat transfer with application to IC engines
[DE87-011046] 01 p0055 N88-10353
Recent progress in magma energy extraction
[DE87-013083] 01 p0066 N88-10424
Radiative and free-convective heat transfer from a finite horizontal plate inside an enclosure 02 p0133 N88-10833
An approximate solution to the problem of heating massive bodies by both radiation and convection
[BLL-M-37315-(5828.4)] 02 p0170 N88-11068
The effect of heat transfer on the dispersion of cold dense gases
[OUEL-1688/87] 02 p0171 N88-11076
Heat transfer in the tip region of a rotor blade simulator 02 p0186 N88-11159
Finite element analysis of three-dimensional steady and unsteady temperature fields (computation of temperature distribution of turbine blade with composite cooling) 03 p0300 N88-11887
Multidimensional modeling of convective heat transfer with application to I.C. engines
[DE87-014983] 03 p0322 N88-12036
Measurement of local convective heat transfer coefficients from a smooth and roughened NACA-0012 airfoil: Flight test data
[NASA-TM-100284] 05 p0582 N88-13552
Cooling electronic equipment at simulated high altitude in hypobaric chambers
[AD-A185196] 05 p0584 N88-13560
Thin film and gradient-driven instability mechanisms
[PB88-101522] 07 p0853 N88-15182
Rational considerations for modelling human thermoregulation during cold water immersion
[AD-A186226] 08 p1048 N88-16329
Determination of the effect of walking on the forced convective heat transfer coefficient using an articulated mannikin
[AD-A186452] 08 p1049 N88-16335
Experimental study of local natural convection heat transfer in inclined and rotating enclosures 09 p1165 N88-16986
Interferometric study of natural convection heat transfer from a vertical flat plate with transverse roughness elements 10 p1327 N88-17935
Multidimensional modeling of convective heat transfer with application to IC engines
[DE88-003398] 10 p1330 N88-17948
Mixed turbulent convective heat transfer in vertical ducts 11 p1485 N88-18865
Convective heat transfer and its effect on inertial measurement units 12 p1578 N88-19442
Characteristics of the thermal environment
[AD-A188359] 12 p1641 N88-19827
Structures and fluxes in a deep convecting mixed layer 13 p1804 N88-20786
The mixed layer of the western equatorial Pacific Ocean
[HIG-1861] 13 p1805 N88-20789
Similarity theories and microturbulence in the atmospheric mixed layer 13 p1806 N88-20802
Heat transfer modeling of jet vane Thrust Vector Control (TVC) systems
[AD-A190106] 15 p2019 N88-22034
Heat transfer from a negatively buoyant wall jet
[NBS/GCR-88/541] 15 p2050 N88-22208
Thermal instability and heat transfer characteristics in water/ice systems
[AD-A189627] 15 p2062 N88-22297
Experimental measurements of heat transfer from an iced surface during artificial and natural cloud icing conditions
[AIAA-PAPER-88-1352] 17 p2293 N88-23718
Review of convectively cooled structures for hypersonic flight
[NASA-TM-87740] 17 p2310 N88-23817
Single phase liquid immersion cooling of discrete heat sources in a vertical channel
[AD-A191224] 17 p2337 N88-23944
Acoustic convective system
[NASA-CASE-NPO-17278-1-CU] 18 p2498 N88-24818

Thermal management of integrated microsensors
19 p2670 N88-25875
Multidimensional modeling of convective heat transfer with application to I.C. engines
[DE88-007446] 19 p2738 N88-26257
An arranging method on L/D of two-phase closed thermosyphons 20 p2783 N88-26508
Forced-convective boiling in small diameter tube
20 p2783 N88-26510
The heat transfer and fluid dynamics of concave surface curvature
[AD-A193064] 21 p2943 N88-27479
Application of rectangular co-ordinates to the problem of laminar combined convection in a straight horizontal tube whose circumference is heated nonuniformly
[PDR/CFDU/IC/33] 22 p3076 N88-28263
Estimation of transient heat transfer coefficients in multidimensional problems by using inverse heat transfer methods 23 p3210 N88-29108
Impact of ETO propellants on the aerothermodynamic analyses of propulsion components
[NASA-TM-101303] 24 p3374 N88-30094

CONVERGENCE
An exponential example for Terlaky's pivoting rule for the criss-cross simplex method
[REPT-87-18] 01 p0080 N88-10512
Semidiscrete Galerkin method for semilinear evolution equations with a differential operator of third order
[BONNER-MATHE-SCHR-181]
01 p0087 N88-10570
The use of advanced data sets in the short-range forecasting of the development of a tornadic thunderstorm along a mesoscale convergence zone
02 p0200 N88-11250
The spatially nonuniform convergence of the numerical solution of flows
[NASA-TM-100037] 02 p0226 N88-11429
Compactness of quasi-conforming element spaces, convergence of quasi-conforming element method
03 p0301 N88-11896
Concepts for radically increasing the numerical convergence rate of the Euler equations
[NASA-CR-177456] 04 p0395 N88-12463
Parallel superconvergent multigrid
[DE87-013153] 04 p0480 N88-12960
A numerical study of the effects of curvature and convergence on dilution jet mixing
[NASA-TM-89878] 05 p0549 N88-13347
A note on the use of symmetric line Gauss-Seidel for the steady upwind differenced Euler equations
[AD-A185223] 05 p0580 N88-13540
Characteristics of a separating confluent boundary layer and the downstream wake
[NASA-TM-100046] 06 p0704 N88-14323
Stochastic approximation and large deviations: General results for w.p.l. Convergence
[AD-A185818] 06 p0768 N88-14721
On the convergence of the p-version of the boundary element Galerkin method
[AD-A186198] 07 p0910 N88-15514
Weak convergence of sums of moving averages in the alpha-stable domain of attraction
[AD-A186430] 07 p0912 N88-15529
On rate of convergence of equivariation linear prediction estimates of the number of signals and frequencies of multiple sinusoids
[AD-A186034] 07 p0914 N88-15549
On the characterization of certain point processes
[AD-A186427] 07 p0916 N88-15560
Strong representation of weak convergence
[AD-A186433] 07 p0916 N88-15563
Target size and luminance effects on accommodation and vergence
[AD-A185861] 08 p1051 N88-16343
Strong convergence and convergence rates of approximating solutions for algebraic Riccati equations in Hilbert spaces
[AD-A186190] 08 p1072 N88-16464
Method of iterative coupling between periodic aerodynamic and dynamic fields
[PB87-169934] 09 p1113 N88-16669
On line search termination criteria for and convergence of conic algorithms for minimization
[DE88-002844] 09 p1227 N88-17351
A multigrid preconditioner applied to a two-dimensional convection-diffusion problem
[DE88-004765] 10 p1397 N88-18329
The convergence rate for the strong law of large numbers: General lattice distributions
[AD-A187560] 10 p1402 N88-18362
Probability bounds for M-Skorohod oscillations
[AD-A187961] 10 p1404 N88-18371
Geophysical study of the structure and processes of the continental convergence zones: Alpine-Himalayan Belt
[NASA-CR-182647] 12 p1644 N88-19842
Convolution metrics and rates of convergence in the CLT (Central Limit Theorem)
[AD-A189341] 12 p1686 N88-20084
A convergence theorem in process algebra
[CWI-CS-R8733] 13 p1827 N88-20920
Convergence of Runge-Kutta methods on classes of stiff initial value problems
[CWI-NM-R8717] 13 p1827 N88-20924
Some maximum norm estimates for the finite element method applied to nonlinear two dimensional boundary value problems
[ETN-88-91505] 14 p1964 N88-21715
The global convergence of partitioned BFGS on problems with convex decompositions and Lipschitzian gradients
[DE88-006249] 14 p1968 N88-21744
Development and application of the p-version of the finite element method
[AD-A190036] 15 p2120 N88-22633
Trust regions and projected gradients
[DE88-005829] 15 p2122 N88-22646
Detection of the number, locations and magnitudes of jumps
[AD-A190328] 15 p2125 N88-22671
Convergence qualification of partition algorithms in global optimization
[REPT-87-61] 16 p2259 N88-23505
Unique normal forms for lambda calculus with surjective pairing
[PB88-173539] 16 p2260 N88-23508
Accuracy versus convergence rates for a three dimensional multistage Euler code
[NASA-CR-181665] 16 p2261 N88-23519
Inference for a nonlinear semimartingale regression model
[AD-A190657] 16 p2262 N88-23527
Almost sure L(gamma)-norm convergence for data-based histogram density estimates
[AD-A189944] 17 p2393 N88-24228
Study of the convergence of a finite difference scheme for acoustic propagation in the atmosphere in a parabolic approximation. Statistical calculation of the sound field in the presence of kinematic turbulence
[ONERA-RS-8/3641-PY-160-P]
17 p2394 N88-24235
An empirical model of the effects of curvature and convergence on dilution jet mixing
[NASA-TM-100896] 18 p2466 N88-24640
Gram-Schmidt implementation of a linearly constrained adaptive array
[AD-A191651] 18 p2560 N88-25198
A concurrent neural network algorithm for the traveling salesman problem
[DE88-006981] 18 p2562 N88-25208
Stability and convergence of the Peaceman-Rachford ADI method for initial-boundary value problems
[CWI-NM-R8724] 18 p2566 N88-25243
Optimal discrete-time LQR problems for parabolic systems with unbounded input: Approximation and convergence
[NASA-CR-181673] 18 p2567 N88-25247
On the use of convergent beam electron diffraction for identification of antiphase boundaries in GaAs grown on Si
[DE88-008220] 18 p2585 N88-25362
Some supraconvergent schemes for hyperbolic equations on irregular grids
[DE88-009113] 19 p2720 N88-26151
Semi-discrete approximations to nonlinear systems of conservation laws; consistency and L(infinity)-stability imply convergence
[NASA-CR-181683] 19 p2721 N88-26157
Application of Moment Iteration Method (MIM) to electromagnetic field computation
[PB88-194139] 20 p2789 N88-26546
Conditions for finite convergence of algorithms for nonlinear programs and variational inequalities
[AD-A192355] 20 p2838 N88-26834
Stability and convergence in the numerical solution of stiff initial value problems
[B8681480] 23 p3272 N88-29474
Convergence acceleration for vector sequences and applications to computational fluid dynamics
[NASA-TM-101327] 24 p3424 N88-30377
Convergence of Galerkin approximations for operator Riccati equations: A nonlinear evolution equation approach
[NASA-CR-181706] 24 p3425 N88-30386

CONVERGENT NOZZLES
Static performance of nonaxisymmetric nozzles with yaw thrust-vectoring vanes
[NASA-TP-2813] 14 p1861 N88-21118
Effect of flow convergence on turbulence level in stream 14 p1973 N88-21773
Application of laser diffraction techniques to particle sizing in solid propellant rocket motors
[AD-A193841] 22 p3049 N88-28089

CONVERGENT-DIVERGENT NOZZLES
Static performance of an axisymmetric nozzle with post-exit vanes for multiaxis thrust vectoring
[NASA-TP-2800] 13 p1719 N88-20280
Static performance of nonaxisymmetric nozzles with yaw thrust-vectoring vanes
[NASA-TP-2813] 14 p1861 N88-21118
Nozzle fabrication technique
[NASA-CASE-MSC-21299-1] 18 p2475 N88-24684
Techniques utilized in the simulated altitude testing of a 2D-CD vectoring and reversing nozzle
[NASA-TM-100872] 19 p2604 N88-25464
Implicit finite-difference simulation of an internal flow in a nozzle: An example of a physical application on a hypercube
[AD-A192475] 21 p2942 N88-27472

CONVERSION
Ethanol as a fuel of a lorry. Use experience from a diesel engine modified to an otto engine
[DE88-752870] 21 p2958 N88-27569
Software engineering for the EBR-2 data acquisition system conversion
[DE88-009950] 22 p3136 N88-28647

CONVERTAPLANES
U V/STOL AIRCRAFT

CONVERTERS
Rust converters
[AD-A188767] 14 p1891 N88-21299

CONVERTIBLE FAN-SHAFT ENGINES
Test stand performance of a convertible engine for advanced V/STOL and rotorcraft propulsion
[NASA-TM-100211] 03 p0266 N88-11679
The convertible engine: A dual-mode propulsion system 09 p1108 N88-16639

CONVEXITY
Analytical investigation of reflection of a regular or mach reflection over a secondary wedge
[AD-A185690] 06 p0703 N88-14316
An O(n3L) interior point algorithm for convex quadratic programming
[AD-A186001] 07 p0909 N88-15504
Bounding the expectation of convex functions with limited distribution information
[AD-A186147] 07 p0910 N88-15512
Upper bounds on the expected value of a convex function using gradient and conjugate function information
[AD-A186246] 07 p0910 N88-15517
Sublinear upper bounds for stochastic programs with recourse, revision
[AD-A186436] 07 p0916 N88-15564
Multigrid methods in convex optimization
11 p1538 N88-19190
A primal-dual algorithm for the computation of the minimum of a convex function on the intersection of convex functions, and its application in data analysis
[RR-638-M] 18 p2563 N88-25217
Linear programming in R sup 3 and the skeleton and largest incircle of a convex polygon
[PB88-124664] 20 p2846 N88-26892

CONVOLUTION INTEGRALS
On the concept of resolution ellipse in aperture synthesis matched deconvolution with error analysis — astronomical interferometry 01 p0095 N88-10621
Optimal application of Morrison's iterative noise removal for deconvolution. Appendices
[NASA-CR-182477] 09 p1231 N88-17376
Small degree solutions for the polynomial Bezout equation
[AD-A187630] 10 p1401 N88-18355
Convolution metrics and rates of convergence in the CLT (Central Limit Theorem)
[AD-A189341] 12 p1686 N88-20084
The algebraic structure of convolutional codes
[AD-A190280] 15 p2120 N88-22635
Near optimal blind deconvolution
[REPT-87-016] 15 p2123 N88-22655
Real time pipelined system for forming the sum of products in the processing of video data
[NASA-CASE-NPO-16462-1-CU]
17 p2384 N88-24169
A deconvolution technique using least-squares model-fitting and its application to optical pulse measurement
[NPL-DES-87] 22 p3144 N88-28694
Two dimensional convolute integers for machine vision and image recognition 23 p3254 N88-29369

CONVOLUTIONS (MATHEMATICS)
U CONVOLUTION INTEGRALS

COOL STARS
NT CARBON STARS
NT FLARE STARS
NT K STARS

NT M STARS
NT MIRA VARIABLES
NT S STARS
The M-type stars
[NASA-SP-492] 02 p0252 N88-11592
Basic properties and variability
02 p0252 N88-11593
Spectroscopy and nonthermal processes
02 p0252 N88-11594
Circumstellar shells, the formation of grains, and radiation transfer 02 p0252 N88-11596
Mass loss 02 p0253 N88-11597
Circumstellar chemistry 02 p0253 N88-11598
Fifth Cambridge Workshop on Cool Stars, Stellar Systems and the Sun 04 p0502 N88-13092
The photospheric magnetic fields of cool stars: Recent results of survey and time-variability programs
04 p0503 N88-13094
Flux tube dynamics and solar/stellar redshift measurements 04 p0503 N88-13095
Nonthermal phenomena in stellar coronae: Evidence from radio observations 04 p0503 N88-13096
Observational constraints and evidence for saturation
04 p0503 N88-13097
Heating of stellar chromospheres and coronae: Evidence for non-magnetic basal heating
04 p0503 N88-13098
Automatic photometric monitoring of cool stars
04 p0504 N88-13103
Evidence for expanding magnetic loops in coronae of cool stars 04 p0510 N88-13134
Empirical relations between photospheric magnetic fields and atmospheric radiative losses for cool dwarf stars 04 p0511 N88-13145
Radio continuum emission from the ionized stellar winds of the cool supergiants in zeta Aurigae-like systems
04 p0514 N88-13160
IRAS and cool stellar mass loss
04 p0515 N88-13166
The Wilson-Bappu relationship: A barometric effect
04 p0516 N88-13170
IUE observations of the hybrid K3 II star Iota Aurigae and constraints on the outer atmospheric structure
04 p0516 N88-13171
Synthetic spectra for the N-type carbon star TX Psc
04 p0516 N88-13173

COOLANT LOSS
U LOSS OF COOLANT

COOLANTS
Quantitative determination of a hydrogen impurity in a sodium coolant by hydride thermal dissociation
[NASA-TT-20239] 13 p1740 N88-20402
Thermal-hydraulic considerations for particle bed reactors 17 p2400 N88-24266
The effect of operating temperature on open, multimegawatt space power systems
17 p2414 N88-24352
Fabrication of a niobium 1 percent zirconium containment for SP-100 primary lithium system materials mass transfer studies 17 p2417 N88-24373
Reactor core coolability with reduced power levels
17 p2425 N88-24425
Customizing Space Nuclear Power System Analysis Model (SNPSAM): Introducing a secondary coolant loop
[AD-A194620] 22 p3151 N88-28750

COOLERS
Cryogenics program overview
08 p0981 N88-15926
Ames Research Center cryogenics program
08 p0981 N88-15927
The Goddard Space Flight Center mechanical cooler program 08 p0983 N88-15944

COOLING
NT ABSORPTION COOLING
NT AIR COOLING
NT CRYOGENIC COOLING
NT EVAPORATIVE COOLING
NT FILM COOLING
NT GAS COOLING
NT LIQUID COOLING
NT MAGNETIC COOLING
NT PLASMA COOLING
NT QUENCHING (COOLING)
NT RADIANT COOLING
NT REGENERATIVE COOLING
NT SPACE COOLING (BUILDINGS)
NT SUPERCOOLING
NT SURFACE COOLING
NT SWEAT COOLING
NT THERMOELECTRIC COOLING
The dissociation of dense liquid nitrogen and shock cooling
[DE87-013490] 01 p0022 N88-10136
Applications of heat pipes to cool PWBS and hybrid microcircuits 02 p0136 N88-10858
Operating experiences and test results of six cold helium compressors
[DE87-012115] 02 p0157 N88-10982
Shock-induced cooling in dense fluids
[DE87-014343] 02 p0170 N88-11067
Heat transfer in the tip region of a rotor blade simulator 02 p0186 N88-11159
Coolant passage heat transfer with rotation
02 p0186 N88-11160
Heat transfer with very high free stream turbulence
02 p0186 N88-11161
Local heat/mass transfer and pressure drop in a two-pass rib-roughened channel for turbine airfoil cooling
[NASA-CR-179635] 03 p0322 N88-12039
Completely magnetically contained electrothermal thrusters
[AD-A185674] 06 p0674 N88-14129
Undercooling and nucleation in iron nickel alloys
[AD-A185500] 06 p0683 N88-14184
Investigation of the auto-tempering of low-carbon martensite
[PB87-143970] 07 p0833 N88-15053
Thermal stress analysis of a cooled monochromator crystal
[DE88-002116] 07 p0937 N88-15696
Rapid hypothermia subsequent to oral nicotinic acid and immersion in warm (30C) water
[AD-A186458] 08 p1050 N88-16339
Description of tests run in the T2 cryogenic wind tunnel
[PB87-170296] 09 p1113 N88-16672
Mesospheric dynamics and chemistry from SME data
[NASA-CR-182465] 09 p1191 N88-17139
The role of hydration on peripheral response to cold
[AD-A186448] 09 p1199 N88-17186
Mechanistic model for void distribution in flashing flow
[DE88-002948] 10 p1326 N88-17928
Disk pumping test
[AD-A187199] 11 p1440 N88-18591
Microstructural characterization of HSLA-100 GMA-weldments
[AD-A187782] 11 p1457 N88-18683
Microstructural characterization of the heat affected zone of HSLA (High Strength Low Alloy)-100 steel GMA (Gas Metal Arc)-weldment
[AD-A187825] 11 p1457 N88-18686
Theory of laser cooling and spectroscopy of harmonically trapped single atoms
[AD-A189576] 13 p1775 N88-20617
The cooling of electronic equipment in fighter aircraft
[MBB/LKE-312/S/PUB/258] 14 p1866 N88-21147
On the theory of the conversion of metallic mixed phases. 5: Fluctuations and nucleation in sub-cooled phases
[NASA-TT-20249] 14 p1890 N88-21296
Laser cooling of neon metastable states
14 p1975 N88-21785
Structural analyses of engine wall cooling concepts and materials 15 p2081 N88-22405
Status, trends in research on internal combustion engines 16 p2185 N88-23027
Long duration coherent Lyman-alpha sources
16 p2268 N88-23571
Hydrogen turbines for space power systems: A simplified axial flow gas turbine model 17 p2419 N88-24385
Possible creep studies of lithium with a compact device 17 p2422 N88-24404
Reactor core coolability with reduced power levels
17 p2425 N88-24425
The effect of operating temperature and turbine blade cooling on Brayton cycle space power systems
17 p2435 N88-24489
Space power radiation cooled dc transmission line analysis 17 p2438 N88-24506
Fraction eutectic measurements in slowly cooled Pb - 15 wt percent Sn alloys
[NASA-CR-180830] 19 p2618 N88-25531
Heat pump augmented radiator for low-temperature space applications
[DE88-008369] 20 p2765 N88-26393
Thermal-sensation control: A new method of controlling cooled/heated environments 21 p2930 N88-27394
Some evidence for a Northern Hemispheric extratropic trigger mechanism of ENSO events
22 p3123 N88-28558
High temperature electric arc furnace
[NASA-CASE-MFS-28281-1] 23 p3181 N88-28938
Surface Tension Confined Liquid Cryogen Cooler (STCLCC)
[NASA-CASE-GSC-13112-1] 23 p3201 N88-29050
Thermocouple for heating and cooling of memory metal actuators
[NASA-CASE-NPO-17068-1-CU]
23 p3217 N88-29151
Spontaneous force optical traps
[AD-A196103] 24 p3377 N88-30114

COOLING FINS
Advanced radiator concepts utilizing honeycomb panel heat pipes
[NASA-CR-172017] 04 p0443 N88-12747

COOLING FLOWS (ASTROPHYSICS)
Finnish-Soviet Symposium on Radio Astronomy (1st) held at Otaniemi on August 26-27, 1985
[PB87-140661] 07 p0944 N88-15736

COOLING SYSTEMS
Understanding passive cooling systems
[PB87-210464] 02 p0194 N88-11211
The effect of maximum-allowable payload temperature on the mass of a multimegawatt space-based platform
[DE88-001921] 05 p0555 N88-13381
Self operating absorption cooling system using solar energy: Small power experimental plant
[DE88-900194] 07 p0874 N88-15299
An adiabatic demagnetization cooled bolometer system for millimeter continuum astronomy
07 p0943 N88-15735
Aircraft engine hot section technology: An overview of the HOST Project 08 p0957 N88-15804
Comparison of a thermoelectric cooling system and a groundwater heat pump
[DE88-001753] 08 p0984 N88-15950
Experimental study of secondary flow in the presence of two jet arrays on the wall of a turbine blade
[ECL-87-11] 08 p0987 N88-15981
Advanced techniques employed in blade cooling research 10 p1281 N88-17659
Active cooling design for scramjet engines using optimization methods
[NASA-TM-100581] 13 p1783 N88-20669
Development of an engineering model dynamic cooler --- spacecraft payloads
[F+W-TF-B-1885] 14 p1895 N88-21311
Superconducting magnet technique for ASTROMAG on the space station
[DE88-004560] 15 p2025 N88-22063
Liquid droplet radiator development
17 p2424 N88-24415
The effect of maximum allowable payload temperature on the mass of a multimegawatt space based platform
17 p2424 N88-24416
MACRAD: A mass analysis code for radiators
17 p2424 N88-24418
Heat pump-augmented systems for spacecraft thermal management 17 p2424 N88-24419
Dynamic isotope power system critical component verification 17 p2425 N88-24421
An experimental setup for the study of polarized He3 and dilute He3-He4 mixtures
[B8705589] 23 p3193 N88-29001
An analysis of heat transfer after loss of primary coolant in the SP-100 reactor system
[AD-A194619] 23 p3281 N88-29539

COOPERATION
Technology transfer from US Federal laboratories: Report of a roundtable
[PB88-144803] 12 p1709 N88-20228

COORDINATE SYSTEMS
U COORDINATES

COORDINATE TRANSFORMATIONS
Analytical treatment of the spatial trilateration problem (4, 6, 0, 0)
[SER-A-104] 01 p0085 N88-10548
A study on local level inertial surveying systems. Error model for the stationary system
[B8736714] 16 p2229 N88-23312
A description of the reference frames and the coordinate transformations used in AMEER (Aero-Mechanical Equations Evaluations Routines)
[DE88-007960] 19 p2720 N88-26153

COORDINATES
NT CARTESIAN COORDINATES
NT COMPUTATIONAL GRIDS
NT GEODETIC COORDINATES
NT HYPERBOLIC COORDINATES
NT LAGRANGE COORDINATES
NT SPHERICAL COORDINATES
Asymptotics of the effective potentials and wave functions of a three-body problem in suitable coordinates
[DE87-703323] 03 p0370 N88-12326
Separable orthogonal coordinates and particle creation for an accelerating observer
[DE87-703358] 05 p0657 N88-14029
Example of correlation between space and spin coordinates
[DE87-703366] 05 p0657 N88-14030
The Wilson-Fowler spline in a global IGES (Initial Graphics Exchange Specification) coordinate frame
[DE88-001942] 06 p0757 N88-14640
Evaluation of magnetic coordinates in finite-beta, asymmetric plasmas
[DE88-003665] 10 p1412 N88-18424

Reference position vector 12 p1577 N88-19432
Coordinate-momentum probability operator for point particles in a stationary electromagnetic field
[DE88-701165] 16 p2188 N88-23044
Full-wave calculations in flux coordinates for toroidal geometry
[DE88-010131] 20 p2860 N88-26985
Three-dimensional adaptive grid generation for body-fitted coordinate system
[NASA-CR-182192] 21 p2950 N88-27520
DATATRAN: Datum transformation software
[AD-A195723] 24 p3387 N88-30175

COORDINATION
Hydrogen Energy Coordinating Committee: Summary of DOE hydrogen programs for FY 1987
[DE88-003960] 10 p1306 N88-17811
The coordination cluster theory for metallic solutions
[DE88-005934] 13 p1738 N88-20389
Coordination in decision-making organizations
[AD-A191952] 19 p2739 N88-26261
Soluble metal chelate polymers of coordination numbers six, seven and eight
[AD-A192485] 21 p2917 N88-27314
Cockpit and cabin crew coordination
[AD-A192445] 21 p2993 N88-27752

COORDINATION POLYMERS
Soluble metal chelate polymers of coordination numbers six, seven and eight
[AD-A185094] 05 p0568 N88-13459

COPILOTS
U AIRCRAFT PILOTS

COPLANARITY
Modeling of some coplanar waveguide discontinuities
[NASA-TM-100808] 10 p1318 N88-17880
Confirmation of slow-waves in a crosstie overlay coplanar waveguide and its application to band-reject gratings and reflectors
[AD-A194981] 24 p3361 N88-30011

COPOLYMERIZATION
Conducting hybrid polymeric systems
[DE88-000527] 04 p0421 N88-12611
Polyether-polyester graft copolymer
[NASA-CASE-LAR-13447-1] 11 p1463 N88-18725
NMR analysis of a fluorocarbon copolymer
[DE88-002364] 15 p2043 N88-22170
Interactions in miscible polymer blends
[AD-A193824] 22 p3058 N88-28144

COPOLYMERS
NT VINYL COPOLYMERS
Novel polymers and copolymers and production of poly(acetylene)
[EP-PATENT-0-173-473-A2] 01 p0026 N88-10161
High ionic conductivity in PEO.PPG block polymer and salt solutions
[AD-A183502] 01 p0026 N88-10168
Polymer chain segment orientation during stress relaxation
[DE87-013392] 01 p0027 N88-10174
Applications and limitations of deuterium labeling methods to neutron scattering studies of polymers
[DE87-012936] 02 p0151 N88-10945
Urea-polyurethane and polydimethylsiloxane mixtures. Morphology control using a block copolymer
[ISAL-IDI1-87-05] 02 p0153 N88-10959
Synthesis and characterization of block copolymers
[AD-A184405] 03 p0295 N88-11855
Synthesis and characterization of block copolymers
[AD-A184406] 03 p0296 N88-11856
Polymer composition --- cable insulation
[EP-PATENT-0-199-444-A1] 04 p0418 N88-12594
Synthesis, NMR characterization and electrical properties of siloxane-based polymer electrolytes
[AD-A184184] 04 p0418 N88-12596
Conductive polymers via reactive oligomer
[AD-A184270] 04 p0419 N88-12597
Advances in inherently conducting polymers
[DE88-000501] 04 p0421 N88-12610
Conducting hybrid polymeric systems
[DE88-000527] 04 p0421 N88-12611
Effect of sidechain length and crosslinking on ionic conductivity in polyphosphazene solid electrolytes
[AD-A184419] 04 p0497 N88-13058
Flexibilized copolyimide adhesives
[NASA-TM-89303] 05 p0570 N88-13474
Group contribution analysis of the damping behavior of homopolymers, statistical copolymers and interpenetrating polymer networks based on acrylic, vinyl and styrenic mers
[AD-A185904] 07 p0836 N88-15070
The morphology of emulsion polymerized latex particles
[DE86-002672] 08 p0972 N88-15879
Synthesis of high molecular weight peptide polymers and copolymers containing L-dope residues
[AD-A186462] 08 p0973 N88-15887
Lithium/polymer electrolyte interfacial instability
[AD-A187164] 09 p1147 N88-16874
Study of molecular mobility of noncrystaline polymer alloys of different compatibility using mechanical spectrometry
[ISAL-87-0032] 09 p1149 N88-16883
Synthesis and structure property studies of toughened epoxy resins via functionalized polysiloxanes
[AD-A187984] 11 p1462 N88-18715
Synthesis and structure property studies of toughened epoxy resins via functionalized polysiloxanes. Friction and wear studies
[AD-A188258] 11 p1462 N88-18718
Polyether-polyester graft copolymer
[NASA-CASE-LAR-13447-1] 11 p1463 N88-18725
Statistical-mechanical study of polyvinylidene fluoride
[AD-A188310] 12 p1609 N88-19624
A new polymer-based hydrogen getter
[DE88-004538] 13 p1751 N88-20467
Ceramic materials from preceramic organometallic copolymers
[DE88-006067] 14 p1892 N88-21301
NMR analysis of a fluorocarbon copolymer
[DE88-002364] 15 p2043 N88-22170
Singlet oxygen behavior in solid polymer matrices
[DE88-005171] 15 p2043 N88-22171
Donor acceptor polymerization chemistry as a vehicle to low energy cure matrix resins
[AD-A190119] 15 p2044 N88-22179
Distribution of chain ends inside the polybutadiene microspheres of SB diblock copolymers
[AD-A191257] 16 p2182 N88-23007
High strength/sigh modulus aromatic heterocyclic ABA block copolymers
[AD-A191666] 18 p2491 N88-24774
Diffusion of homopolymers into nonequilibrum diblock copolymer structures
[DE88-005306] 18 p2494 N88-24794
Improved structural polymer alloys and composites
[AD-A192092] 19 p2619 N88-25536
Interaction of vinylidene fluoride: Tetrafluoroethylene copolymer with ammonia
[NASA-TT-20292] 19 p2620 N88-25542
Synthesis of model polymers and related structures in support of vinyl monomer grafting studies
[DE88-010245] 20 p2778 N88-26476
Initial adhesive screening of novel polyamide-imides and their copolymers
[NASA-TM-100641] 20 p2779 N88-26481
Ionic conductive polymers based on crosslinked elastic siloxane-ethylene oxide copolymers
[DE88-011243] 21 p2917 N88-27311
Spatial organization of homopolymer chains inside spherical polybutadiene domains of SB diblock copolymers
[AD-A193390] 21 p2918 N88-27321
Interactions in miscible polymer blends
[AD-A193824] 22 p3058 N88-28144
Dissolution rates of polymers and copolymers based on methyl, ethyl and butyl methacrylate
[AD-A194713] 23 p3197 N88-29027
Transport of organic vapors in multiphase polymer system
[AD-A194097] 23 p3198 N88-29033
Polyazidoesters as energetic polymers and copolymer components with fluoro derivatives
[AD-A194236] 23 p3199 N88-29039

COPPER
Relation between shock strength and strain-rate plasticity at maximum deviatoric stress
[DE87-011736] 01 p0061 N88-10390
Elastic moduli of copper under compression
[DE87-013137] 02 p0147 N88-10922
The water permeability of multi-layer coatings
[BLL-M-37252-(5828.4)] 02 p0148 N88-10927
Bond character at a silicon/copper surface
[AD-A184167] 03 p0295 N88-11851
Diffusion bonding depleted uranium to copper
[RFP-3783-REV] 03 p0333 N88-12098
The effect of organic inhibitors on the atmospheric corrosion and solderability of copper
[DE86-000261] 04 p0414 N88-12565
Studies on high-speed electroforming
[DE88-001395] 04 p0429 N88-12656
Data base on the high heat flux behaviour of metals and carbon materials for plasma facing components: Experiments at the 10 MW neutral beam injection test stand of the IPP Nagoya
[IPPJ-AM-53] 04 p0492 N88-13031
Jet initiation of PBX 9502
[DE88-000493] 05 p0571 N88-13481
The initiation and growth of small fatigue cracks in copper at room and cryogenic temperatures 05 p0600 N88-13668
Fatigue crack growth and fracture of copper-bismuth bicrystals 06 p0715 N88-14385
Orientation effects in copper single crystals fatigued at elevated temperatures 06 p0720 N88-14423
The influence of phosphorus on the solid state reaction between copper and silicon or germanium
[ETN-88-91361] 06 p0789 N88-14838
Model Cu/ZnO catalysts for methanol synthesis: The role of surface structure
[DE88-002354] 07 p0830 N88-15037
Microstructural observations of the Sn-Pb solder/Cu system and thermal fatigue of the solder joint
[DE88-001392] 07 p0832 N88-15048
Contrast between the chemical, structural and electronic properties of thin films of Cu and Ni on the Ru(0001) surface
[DE88-002360] 07 p0938 N88-15698
Localization of Cu 3d levels in the high Tc superconductor YBa2Cu3O approximately 7 by Cu2p X-ray photoelectron spectroscopy
[NOTA-INTERNA-887] 07 p0939 N88-15710
Electroformation: Principle electrochemical process of electrodeposition and electroformation of copper
[INPE-4374-NTE/274] 08 p0969 N88-15863
Copper electroforming from acid sulfate baths: Preliminary studies
[INPE-4375-RPE/554] 08 p0969 N88-15864
Investigation on diffusion reaction brazing of aluminium
[PB87-143368] 08 p0992 N88-16001
Magnetic investigations of superconductive, polycrystalline (RE)1Ba2Cu3O(7-x) compounds (RE = Y, Gd, Ho, Dy)
[DE88-002537] 08 p1090 N88-16558
Coulomb interactions and effective strong coupling Hamiltonians in Cu-O superconductors
[DE88-002942] 08 p1090 N88-16561
Development of methods for low temperature diffusion bonding
[AD-A186875] 09 p1174 N88-17033
Free energy calculation via MD (molecular dynamics): Methodology and application to bicrystals
[DE88-002902] 09 p1256 N88-17532
Growth and electronic properties of strained metal overlayers
[DE87-010956] 10 p1417 N88-18463
The effects of various conductor components on Nb3Sn filament prestrain in cable-in-conduit conductors
[DE88-003956] 11 p1479 N88-18824
Atom probe microanalysis of superconducting YBa2Cu3O(sub 7-x)
[DE88-003203] 11 p1557 N88-19322
A direct correlation of strength with impact velocity
[AD-A189251] 13 p1741 N88-20409
A viscoplastic theory applied to copper
[NASA-TM-100831] 14 p1928 N88-21497
Thermal expansion behavior of randomly oriented short carbon fiber reinforced copper composites
[NASA-TT-20175] 15 p2031 N88-22099
Reciprocating sliding wear characteristics of copper-carbon fiber composites
[NASA-TT-20176] 15 p2031 N88-22100
Application of copper-carbon fiber composites to power semiconductor devices
[NASA-TT-20171] 15 p2031 N88-22101
Use of long-distance pair potentials in calculations of defect characteristics in metals
[DE88-701039] 15 p2037 N88-22138
Laser enhanced adhesion of copper films to sapphire substrates
[DE88-006802] 15 p2038 N88-22144
Vapor phase deposition and growth of polyimide films on copper
[AD-A189969] 15 p2044 N88-22178
RF properties of superconducting Pb electroplated onto Cu
[DE88-005918] 15 p2139 N88-22765
Magnetic anomalies in the rare earth oxide superconductors GdBa2Cu3O(7-x) and YbBa2Cu3O(7-x)
[AD-A190713] 15 p2144 N88-22793
Thermal conductivity, electrical conductivity and specific heat of copper-carbon fiber composite
[NASA-TT-20172] 16 p2172 N88-22948
High temperature superconductivity
[AD-A190259] 16 p2281 N88-23655
Effects of 67.5 MeV electron irradiation on Y-Ba-Cu-O and Gd-Ba-Cu-O high-temperature superconductors
[AD-A191271] 16 p2283 N88-23669
On quench sensitivity of Cu-Cr alloys
[NASA-TT-20174] 18 p2489 N88-24765
Fabrication of a flexible conductor by vapor deposition
[DE88-007500] 19 p2661 N88-25826
Anomalous RF magnetoresistance in copper at 4 K
[DE88-010232] 19 p2722 N88-26162
The T-T-T curve in Cu-Cr alloy
[NASA-TT-20167] 20 p2774 N88-26453

Oxygen vacancy ordering and superconductivity in YBa2Cu3O(sub 7-x)
[DE88-010005] 20 p2877 N88-27083
Pure metallic bridge and point-contact tunneling into single- and polycrystal YBa2Cu3O(sub 7-y)
[DE88-010030] 20 p2878 N88-27084
Electron irradiation effects in YBa2Cu3O7-Delta single crystals
[DE88-010050] 20 p2878 N88-27085
Growth and characterization of CuGaS2, CuAlS2 and CuGa0.9Al0.1S2 single crystals
[AD-A192963] 21 p3021 N88-27930
Relation between strength, creep and relaxation behavior in Cu and Al at room temperature
[ETN-88-92982] 23 p3195 N88-29015
Magnetic phase transitions in 90-K superconductors Ho1Ba2Cu3O(7-delta) and Gd1Ba2Cu3O(7-delta) observed by ZF-muon(+)SR
[DE88-752611] 23 p3290 N88-29588
Theoretical investigation of image states of the hydrogen covered Cu (100)
[DE88-702662] 23 p3292 N88-29604
An electrochemical impedance spectroscopy study of reactions at the metal/coating interface
24 p3355 N88-29975

COPPER ALLOYS
NT BRASSES
NT BRONZES
High velocity erosion of metal interfaces
[DE87-013937] 01 p0025 N88-10155
Effects of state recovery on creep buckling induced by thermomechanical loading 03 p0336 N88-12116
A comparison of high damping shape memory alloys with Cu-Mn-based and Fe-Cr-based alloys
[AD-A184110] 04 p0414 N88-12566
Phase diagram and thermochemical properties of the Al-Cu system
[ETN-88-91015] 05 p0566 N88-13447
Effectiveness of electrodeposited coatings in reducing atmospheric corrosion of copper substrates
[DE87-013651] 05 p0566 N88-13448
Fatigue crack growth behavior in hydrogen gas environment 06 p0716 N88-14391
The effects of low doses of 14 MeV neutrons on the tensile properties of three binary copper alloys
[DE88-003400] 11 p1458 N88-18691
Joining of dissimilar materials with the pulsed Nd-YAG laser
[DE88-003757] 11 p1458 N88-18693
Crystallization and glass formation in electron and laser beam irradiated Cu-Zr alloys
[DE88-003390] 11 p1464 N88-18729
Preparation and characterization of Cu2Zn1-xMnxGeS4
[AD-A188113] 11 p1556 N88-19315
Superconducting transition temperature of Cu-Nb microcomposites 14 p1973 N88-21775
Characterization of an explosively consolidated rapidly solidified Fe-16Ni-9Cr-5Mo-2Cu alloy powder
[DE88-006733] 15 p2041 N88-22162
Effects of cold working on precipitation in age hardenable alloys: On the copper alloys
[NASA-TT-20164] 16 p2177 N88-22973
Interface characterization of Cu-Cu and Cu-Ag-Cu low temperature solid state bonds
[AD-A191015] 16 p2283 N88-23667
Strain hardening at large strains in aluminum alloys
[DE88-007415] 18 p2484 N88-24737
Characterization of the 2219 Cegedur alloy. Data acquisition of the fracture mechanics --- aircraft construction materials
[REPT-48-442/F] 18 p2487 N88-24751
Aluminum alloy
[NASA-CASE-LAR-13924-1-CU] 18 p2487 N88-24753
The precipitation processes of Cu-Zr-Cr alloys
[NASA-TT-20168] 18 p2488 N88-24758
High temperature embrittleness of Cu-Cr alloy
[NASA-TT-20184] 18 p2488 N88-24759
Critical cooling rates on solution treatment of Cu-Cr and Cu-Be alloys
[NASA-TT-20163] 18 p2488 N88-24760
On the reversion phenomena of Cu-3 percent Ti alloys
[NASA-TT-20170] 18 p2488 N88-24762
On the abnormal phenomena observed in the electrical resistivity measurement during the decomposition process of saturated Cu-Fe alloys
[NASA-TT-20183] 18 p2507 N88-24869
Inelastic ion-surface collisions
[AFGL-TR-87-0206] 19 p2724 N88-26174
Formation of metastable structures and amorphous phases in Cu-W alloys using the triod sputtering technique
[DE88-009051] 21 p2915 N88-27298
Structural relationship between icosahedral and Frank-Kasper phases of Al-Li-Cu
[AD-A193768] 23 p3195 N88-29011

COPPER CHLORIDES
Efficient narrow linewidth waveguide dye laser pumped by CuCl laser 16 p2187 N88-23038

COPPER COMPOUNDS
NT COPPER CHLORIDES
NT COPPER OXIDES
NT COPPER SELENIDES
NT COPPER SULFIDES
Structural relationships in high temperature superconductors
[DE88-002924] 09 p1257 N88-17534
An investigation of metal complexes of some 2-substituted and 2,6-disubstituted pyridine N-oxides
11 p1460 N88-18701
Decomposition of hypochlorite in the presence of copper in a homogeneous medium
[NASA-TT-20199] 13 p1740 N88-20403
Copper peroxide
[NASA-TT-20245] 14 p1888 N88-21282
Improvements to Raney copper zinc methanol synthesis catalysts 17 p2318 N88-23844
The catalytic reactivity of thin film crystal surfaces
[DE88-006387] 19 p2732 N88-26228
Compilation of NRL publications on high temperature superconductivity
[AD-A189137] 21 p3019 N88-27921

COPPER OXIDES
Atomic-level studies of superconducting YBa2Cu3O sub 7-x
[DE88-002522] 06 p0788 N88-14831
Fabrication of YBa2Cu3O7 superconducting ceramics
[DE88-003012] 07 p0938 N88-15701
Theory of the tetragonal-to-orthorhombic structural phase transition in La2CuO4
[AD-A187141] 09 p1254 N88-17514
Bulk superconductivity in La2CuO4
[DE88-002509] 09 p1254 N88-17516
Superconductivity in La/sub 1.85-x/Nd/sub x/Sr/sub .15/CuO
[DE88-003014] 09 p1258 N88-17540
High temperature superconductivity research at Argonne National Laboratory
[DE88-003055] 09 p1258 N88-17541
Copper oxidation states, vacancy ordering and their effect on high temperature superconductivity
[DE88-003079] 09 p1258 N88-17542
Single-crystal structural study of La2Cu/sub 0.95/Li/sub 0.05/O4
[DE88-003482] 11 p1554 N88-19302
Potassium cuprate (3)
[NASA-TT-20246] 13 p1739 N88-20401
Characterization and fundamental studies on CuO sorbent materials to determine attrition mechanisms on substrate gamma alumina
[DE88-003674] 13 p1749 N88-20456
Large momentum pairing in one-dimensional systems
[AD-A189228] 13 p1835 N88-20981
The relationship of the chemical bonding topology of high critical temperature copper oxide superconductors to that of the chevrel phases and the ternary lanthanide rhodium borides
[AD-A189255] 13 p1845 N88-21042
On copper peroxide
[NASA-TT-20263] 15 p2037 N88-22135
Superconductivity and the tailoring of lattice parameters of the compound YBa2Cu3O(sub x)
[DE88-005904] 15 p2140 N88-22769
Thermochemistry and high temperature thermodynamic properties of rare earth-alkaline earth-copper oxide superconductors
[DE88-005976] 15 p2140 N88-22770
High temperature superconductors in the La(sub 1+x)Ba(sub 2-x)Cu O(sub y system
[DE88-006367] 15 p2145 N88-22802
Synthesis and characterization of high-T(sub c) screen-printed Y-Ba-Cu-O films on alumina
[NASA-TM-100860] 15 p2146 N88-22805
Comparison between muon spin rotation and neutron scattering studies on the 3-dimensional magnetic ordering of La2CuO(4-y) 17 p2396 N88-24244
Vacancy ordering in the basal plane of YBa2Cu3O(sub)z
[DE88-004572] 18 p2583 N88-25348
Paramagnetic spins in oxygen-loaded ceramic La2CuO4/sub 4+delta/
[DE88-007114] 19 p2619 N88-25539
Search for new high-temperature superconducting copper oxides
[DE88-009922] 19 p2735 N88-26245
All-electron local density theory of electronic structure and superconductivity in YBa2Cu3O7 and YBa2Cu3O6
[DE88-009944] 19 p2735 N88-26246
Phase transformations and thermodynamic behavior of the YBa2Cu3O(sub)x system via EMF measurements
[DE88-010054] 20 p2878 N88-27086
Superconducting properties of LaBa2Cu3O(sub x) and YBa2Cu3O(sub y)
[DE88-012038] 21 p3024 N88-27952
Preparation and characterization of isotopic oxygen-enriched yttrium barium copper oxide
[DE88-010939] 22 p3154 N88-28766
Possible mechanism for high-temperature superconductivity in the BaSr-La(Y)-CuO systems
[DE88-702060] 23 p3288 N88-29578
La2CuO(sub 4 + delta): A superconducting superoxide
[DE88-010325] 23 p3288 N88-29578
Theory of superconductivity in oxides
[AD-A195647] 24 p3433 N88-30432

COPPER SELENIDES
Device physics related to the granular nature of CuInSe2 solar cells
[DE88-001159] 21 p2967 N88-27622

COPPER SULFIDES
Physico-chemical studies on copper sulfide behavior in the CdS-Cu2S solar cell
[ETN-88-91068] 09 p1187 N88-17109
Electrically conducting polymer-copper sulphide composite films, preparation by treatment of polymer-copper (2) acetate composites with hydrogen sulfide
[NASA-TT-20204] 10 p1305 N88-17803
Investigation of the subsequent treatment and the stability of CuxS-CdS thin-film solar cells
[ETN-88-91488] 11 p1507 N88-19006
Activities of As, Sb, Bi and Pb in copper mattes and their effects on impurity elimination
[TKK-V-A10(1988)] 15 p2041 N88-22165

CORAL HEADS
U CORAL REEFS

CORAL REEFS
Mesoscale coastal ocean dynamics
11 p1517 N88-19060

CORDITE
U DOUBLE BASE PROPELLANTS

CORE FLOW
Flame driving of longitudinal instabilities in liquid fueled dump combustors
[AD-A183536] 01 p0006 N88-10033
High Rayleigh number convection in rectangular enclosures with differentially heated vertical walls and aspect ratios between zero and unity
[NASA-TM-100277] 12 p1628 N88-19739
Theoretical model and numerical solution for compressible viscous vortex cores
15 p2054 N88-22243
Physiological responses to acute exercise-heat stress
[AD-A192606] 21 p2986 N88-27732

CORE SAMPLING
Recommendations for a US ice coring program
[PB88-115043] 09 p1185 N88-17102
Data-base of Antarctic pre-Pleistocene sediment cores
[PB88-124151] 10 p1354 N88-18094
The comet rendezvous asteroid flyby mission
14 p2005 N88-21956
Retrieving samples from comet nuclei
14 p2006 N88-21959

CORES
NT EARTH CORE
NT HONEYCOMB CORES
NT REACTOR CORES
NT STELLAR CORES
Properties of Nb3Sn superconductor wires with composite cores
[KFK-4263] 02 p0246 N88-11557
Composite ceramic superconducting filaments for superconducting cable
[AD-A187833] 11 p1556 N88-19312
Low power consumption current transducer
[NASA-CASE-NPO-16888-1-CU] 17 p2335 N88-23937
High resolution detection of solute segregation to the cores of dislocations in grain boundaries
[DE88-009168] 20 p2877 N88-27078

CORIOLIS EFFECT
Effects of Coriolis acceleration on the vibrations of spinning structures 18 p2522 N88-24966
Activity-rotation relations for lower main sequence stars 23 p3298 N88-29640

CORN
Estimating scattered and absorbed radiation in plant canopies by remote sensing
[NASA-CR-181390] 02 p0193 N88-11205
Cytomorphology and ultrastructure of corn root meristem in weightlessness 12 p1651 N88-19891
Remote sensing techniques in the estimation of the area cultivated with beans, corn, and castor beans in the Irece County (Bahia State) 17 p2358 N88-24045

Spectral behavior of crops through analysis of LANDSAT-TM data 17 p2358 N88-24047
Evaluation of TM false color composites for crop discrimination 17 p2367 N88-24096

CORNEA
A field study on soft contact lens wear in USAF military transport aircraft
[AD-A195962] 24 p3407 N88-30285

CORNER FLOW
Experimental evaluation of turning vane designs for high-speed and coupled fan-drive corners of 0.1-scale model of NASA Lewis Research Center's proposed altitude wind tunnel
[NASA-TP-2681] 10 p1285 N88-17686
Laser velocimeter measurements in a wing-fuselage type juncture
[NASA-TM-100586] 15 p2014 N88-22012

CORNERS
Corner compensation structures for (110) oriented silicon
[DE88-003300] 10 p1417 N88-18455
Semilinear elliptic problems on domains with corners
[REPT-87-83] 20 p2846 N88-26888
Numerical treatment of the pressure singularity at a re-entrant corner
[AD-A193357] 21 p2944 N88-27488

CORONA BOREALIS CONSTELLATION
A large X-ray flare on Sigma 2 coronae borealis observed with exosat 04 p0508 N88-13121

CORONA DISCHARGES
U ELECTRIC CORONA

CORONAGRAPHS
Development of high stability fiber optic spectrophotometric systems for study of solar/stellar magnetic activity
[AD-A189327] 13 p1852 N88-21088

CORONAL HOLES
STIP Symposium on Physical Interpretation of Solar/Interplanetary and Cometary Intervals
[NASA-CR-181201] 01 p0110 N88-10709
Meterwave observations of a coronal hole 01 p0114 N88-10730
Study of the mechanism for solar wind formation 01 p0118 N88-10756

CORONAL LOOPS
Diagnostics of solar coronal loops at interferometric angular resolution 01 p0098 N88-10642
Active region flows 02 p0255 N88-11611
Pressure structure of solar coronal loops 02 p0256 N88-11618
A numerical study of the thermal stability of solar loops 02 p0256 N88-11619
Solar transition region and coronal response to heating rate perturbations 02 p0256 N88-11620
Loop interaction in the visible emission corona: Morphological details 02 p0256 N88-11622
Evidence for expanding magnetic loops in coronae of cool stars 04 p0510 N88-13134
Magnetic reconnection and solar flare loops 08 p1094 N88-16583
Flux tubes and loops in the solar chromosphere and corona 08 p1095 N88-16591
The effects of viscosity on resistive ballooning modes in line-tied coronal magnetic fields 08 p1097 N88-16599

CORONARY ARTERY DISEASE
Relationships between coronary heart disease risk factors and serum ionized calcium in Kennedy Space Center Cohort
[NASA-TM-100979] 10 p1368 N88-18177

CORONARY CIRCULATION
Response of coronary blood flow to step changes in plasma protein concentration in the isolated rat heart 12 p1651 N88-19892
Cardiac and peripheral circulation assessment by ultrasound on 3 astronauts during two 7-day space flights (1982 Salyut-7 - 1985 STS 51G) 12 p1656 N88-19921

CORONAS
NT CORONAL HOLES
NT CORONAL LOOPS
NT ELECTRIC CORONA
NT SOLAR CORONA
NT STELLAR CORONAS
LLE review
[DE87-014468] 02 p0178 N88-11110
Study of ionization equilibrium of high temperature and low density plasma
[DE87-703070] 02 p0238 N88-11502
Coronal magnetic fields produced by photospheric shear
[NASA-CR-181514] 03 p0390 N88-12447
Chromospheric and coronal heating in a bias-free sample of K dwarfs 04 p0518 N88-13184
Transverse flow deflections associated with fast coronal mass ejecta in interplanetary space
[DE88-003180] 09 p1263 N88-17566
Extended atmospheres of outer planet satellites and comets
[NASA-CR-181449] 10 p1430 N88-18540
The properties of solar coronal active regions deduced from X-ray line spectra
[AD-A193026] 20 p2886 N88-27141

COROTATION
Consistent linearization of the element-independent corotational formulation for the structural analysis of general shells
[NASA-CR-178418] 09 p1181 N88-17078
Prediction of the pressure distribution for radial inflow between co-rotating discs
[PNR90464] 22 p3076 N88-28261

CORPUSCLES (BLOOD)
U BLOOD CELLS

CORPUSCULAR RADIATION
NT BETA PARTICLES
NT ELECTRON BEAMS
NT ELECTRON PRECIPITATION
NT ENERGETIC PARTICLES
NT PRIMARY COSMIC RAYS
NT RADIATION BELTS
NT RELATIVISTIC ELECTRON BEAMS
NT SOLAR COSMIC RAYS
NT SOLAR ELECTRONS
NT SOLAR NEUTRONS
NT SOLAR PROTONS
Corpuscular plasma diagnostics complex on a tokamak with a strong field
[DE88-701576] 16 p2279 N88-23646

CORRECTION
NT ATMOSPHERIC CORRECTION
NT OPTICAL CORRECTION PROCEDURE
Wall interference tests of a CAST 10-2/DOA 2 airfoil in an adaptive-wall test section
[NASA-TM-4015] 02 p0122 N88-10772
Correction of inertial navigation system drift errors for an autonomous land vehicle using optical radar terrain data
[AD-A184973] 05 p0544 N88-13311
Photochemical ozone overburden correction 05 p0615 N88-13778
Correction method for Barker-coded modulation 06 p0691 N88-14240
Improved understanding of the loss-of-symmetry phenomenon in the conventional Kalman filter
[NASA-TM-100041] 06 p0766 N88-14709
Realization of active high pass filters for group velocity correction
[MPE-IN-REPT-47] 08 p0979 N88-15918
Intrinsic corrections to optical guiding in a free-electron laser: Beam Research Program
[DE88-002667] 09 p1172 N88-17026
Optimal correction problem of a multidimensional stochastic system
[AD-A186727] 09 p1228 N88-17353
Application of the multigrid technique to the pressure-correction equation for the SIMPLE algorithm --- Semi-Implicit Method for Pressure Linked Equations (SIMPLE) 11 p1539 N88-19196
Orbit correction requirements for a natural resources satellite
[INPE-4286-PRE/1158] 12 p1594 N88-19548
Holographically correcting synthetic aperture aberrations
[AD-A189510] 12 p1692 N88-20123
Orbit correction strategy for an Earth observation satellite
[INPE-4287-PRE/1159] 13 p1727 N88-20331
A numerical simulation of side force effects by aerodynamic flight trajectory correction
[ISL-CO-211/87] 21 p2896 N88-27191

CORRELATION
NT ANGULAR CORRELATION
NT AUTOCORRELATION
NT CORRELATION COEFFICIENTS
NT CORRELATION DETECTION
NT CROSS CORRELATION
NT DATA CORRELATION
NT SPECTRAL CORRELATION
NT STATISTICAL CORRELATION
Correlation of velocity and velocity-density turbulence in the exhaust of an atmospheric burner 02 p0185 N88-11147
The correlation between microstructure and thermomechanical properties of two-phase materials and porous sintered materials
[KFK-4205] 03 p0292 N88-11835
Interfacing distributed operating systems
[AD-A184489] 03 p0366 N88-12306
Using a new characterization of turbulent wind for accurate correlation of wind turbine response with wind speed
[DE88-001453] 04 p0466 N88-12881
Illustrative examples of principal component analysis using SYSTAT/FACTOR
[AD-A184920] 05 p0644 N88-13939
Example of correlation between space and spin coordinates
[DE87-703366] 05 p0657 N88-14030
Thermoelectric power in disordered electronic systems near the Anderson transition
[PREPRINT-547] 06 p0731 N88-14494
Correlation effects on double electron capture in highly-charged, low-energy ion-atom collisions
[DE87-013179] 07 p0930 N88-15651
High T/sub c/ superconductor as a strongly correlated state
[DE88-003194] 08 p1091 N88-16569
Strong consistency of certain information theoretic criteria for model selection in calibration, discriminant analysis and canonical correlation analysis
[AD-A186584] 09 p1232 N88-17385
Correlated processes in atomic collisions
[DE88-003508] 10 p1406 N88-18383
The correlation between methodological and low-level angle-of-arrival measurements 12 p1617 N88-19668
Correlations between photons in resonance fluorescence emitted by an atom near a metal surface
[AD-A188385] 12 p1689 N88-20102
A direct correlation of strength with impact velocity
[AD-A189251] 13 p1741 N88-20409
Estimation-correlation, modeling, and identification in adaptive array processors
[AD-A189130] 13 p1757 N88-20512
Periodically correlated processes and their stationary dilations
[NASA-CR-182904] 16 p2263 N88-23530
Sub-Saharan rainfall anomalies and global sea-surface temperature relationships for the recent fifteen year (1970-1984) period 22 p3122 N88-28552
Interannual variability of 850 mb temperatures during the Northern Hemisphere winter 22 p3123 N88-28562
The relationship between polar sea ice and the position of the near equatorial convergence zone 22 p3123 N88-28563
Computing partial correlations from the data matrix
[AD-A193904] 22 p3138 N88-28659
Extremal two-correlations of two-valued stationary one-dependent processes
[REPT-88-01] 22 p3145 N88-28704
Correlations between wettability and structure in monolayers of alkanethiols adsorbed on gold
[AD-A194348] 23 p3191 N88-28991
Application of optical correlation techniques to particle imaging velocimetry
[NASA-TM-101306] 23 p3218 N88-29152
Mathematical correlation between variations in solar radiation parameters. Part 1: Daily sums of global radiation and midday global radiation
[DE88-702742] 23 p3236 N88-29253
Performance of DS/SSMA communications in impulsive channels. Part 1: Correlation receivers
[AD-A195712] 24 p3362 N88-30021

CORRELATION COEFFICIENTS
Variances and higher order correlation coefficients: Continued
[RR-655-M] 18 p2563 N88-25219
Variations in the atmosphere associated with the 11-year solar cycle 22 p3122 N88-28557
Correlation method and sensors adapted to the environment 22 p3149 N88-28732

CORRELATION DETECTION
Corrections for the pseudorapidity gap correlation method --- particle correlations
[USIP-87-12] 09 p1245 N88-17463
Broadband correlation analysis
[AD-A188732] 13 p1814 N88-20839

CORRELATION FUNCTIONS
U CORRELATION

CORRELATORS
NT IMAGE CORRELATORS
Reception of pseudo noise-modulated signals using digital correlators for satellite navigation tasks
[ETN-87-90426] 01 p0037 N88-10234
A simplified, general-purpose deep-space ranging correlator design 11 p1473 N88-18786
Digital correlator for the portable channel prober measurement instrument
[AD-A189065] 14 p1904 N88-21377
Optical correlation using the magneto-optic device
[AD-A192342] 20 p2854 N88-26950
An optical 2-dimensional correlator for pattern recognition in embedded computing
[DE88-007198] 21 p2998 N88-27780

A fiber optic synchronous detector using sample-and-hold circuits
[DE88-010973] 21 p3016 N88-27899
Evaluation of multi-focus holographic lenses
[AD-A196167] 24 p3377 N88-30110

CORROSION
NT CAVITATION CORROSION
NT ELECTROCHEMICAL CORROSION
NT FRETTING CORROSION
NT FUEL CORROSION
NT HOT CORROSION
NT INTERGRANULAR CORROSION
NT RUSTING
NT SCALE (CORROSION)
NT STRESS CORROSION
NT STRESS CORROSION CRACKING
The corrosion of iron rotating hemispheres in 1 M sulfuric acid: An electrochemical impedance study
[DE87-014679] 02 p0148 N88-10925
Computer simulation of thermal modeling of primary lithium cells 02 p0163 N88-11022
Wear of iron and nickel in corrosive liquid environments
[NASA-TM-100246] 03 p0289 N88-11817
The effect of organic inhibitors on the atmospheric corrosion and solderability of copper
[DE88-000261] 04 p0414 N88-12565
Corrosion strength of niobium and its alloys
[DE87-703693] 04 p0416 N88-12578
Corrosion of ferritic steels by molten lithium: Influence of competing thermal gradient mass transfer and surface product reactions
[DE88-000334] 04 p0417 N88-12585
Ceramic technology for advanced heat engines project
[DE88-001520] 04 p0420 N88-12605
The role of inclusions in corrosion fatigue crack initiation in Q1N 05 p0604 N88-13699
Modeling the effect of sulfur on the threshold environmental cracking rate of steels in high temperature water 05 p0604 N88-13703
Monitoring corrosion and process physical-chemical parameters in electric power plants
[CISE-3708] 06 p0682 N88-14182
The factors which govern the acceleration of corrosion fatigue crack growth rate of a ferritic stainless steel 06 p0717 N88-14402
Fatigue thresholds of C.Mn steels in saline environments 06 p0717 N88-14403
Study of the vapor-liquid equilibria used in the fabrication process of hydrogen by thermochemistry
[DE88-900239] 07 p0830 N88-15035
Low frequency eddy current detection and evaluation of corrosion in aircraft skins
[ETN-88-91664] 09 p1144 N88-16859
Materials processing in space: An introduction to the G-480 payload 10 p1287 N88-17695
Application of ac-impedance method on determination of corrosion rate of metals
[DE88-750307] 10 p1300 N88-17771
Environment assisted degradation mechanisms in aluminum-lithium alloys
[NASA-CR-182482] 10 p1301 N88-17782
A review of pitting corrosion in high temperature aqueous solutions
[DE88-003547] 10 p1302 N88-17787
Corrosion behavior of sputter-deposited aluminum-based alloys exposed to chloride solutions
[AD-A187262] 10 p1303 N88-17794
Investigation of materials for inert electrodes in aluminum electrodeposition cells
[DE88-003380] 10 p1323 N88-17906
Fundamental studies of corrosion of nonoxide structural ceramics
[PB88-141536] 11 p1461 N88-18709
Corrosion, passivity and breakdown of alloys used in high energy density batteries
[DE88-004891] 13 p1743 N88-20422
Improve the lifetime of the hollow fiber sodium sulfur cell
[DE88-004881] 13 p1751 N88-20469
A five year weathering experiment with solar collectors
[DE88-900369] 13 p1796 N88-20740
JPRS report: Science and technology. USSR: Materials science
[JPRS-UMS-87-009] 14 p1884 N88-21261
Rust converters
[AD-A188767] 14 p1891 N88-21299
Durability testing of an iridium-plated storable rocket engine injector
[AD-A190707] 15 p2027 N88-22078
Galvanic corrosion initiatives
[AD-A190658] 15 p2040 N88-22155
Effect of P implantation on the corrosion behavior of Fe-Cr alloys
[DE88-005732] 15 p2040 N88-22158
Summary of the 1987 Gordon Research Conference on Corrosion
[AD-A189737] 15 p2041 N88-22161
User's manual for EULER3DS
[AD-A191048] 16 p2208 N88-23177
Microscopic control of semiconductor interface reactivity
[AD-A191193] 16 p2283 N88-23668
Corrosion and fatigue properties of FeCrB/Si metallic glass wires in aqueous environments 17 p2320 N88-23855
Structural Ceramics
[NASA-CP-2427] 17 p2323 N88-23872
Review of alkali metal and refractory alloy compatibility for Rankine cycle applications 17 p2428 N88-24447
Predictive corrosion modeling, volume 1
[AD-A191229] 18 p2485 N88-24739
Environmental integrity of coating/metal interface
[AD-A192184] 18 p2492 N88-24786
Corrosion in aircraft structures. Part 1: Text
[LR-527-PT-1] 20 p2775 N88-26458
Corrosion in aircraft structures. Part 2: Figures
[LR-527-PT-2] 20 p2775 N88-26459
Determination of Tafel constants in nonlinear polarization curves
[AD-A192335] 21 p2912 N88-27282
A critical review of IR drops and electrode potentials within pits, crevices and cracks
[AD-A192481] 21 p2935 N88-27431
Significance of the local electrode potential within pits, crevices and cracks
[AD-A192482] 21 p2935 N88-27432
Corrosion fatigue of small cracks: Mechanics and chemistry
[DE88-012121] 21 p2964 N88-27605
Proceedings of the 1987 Tri-Service Conference on Corrosion, volume 1
[AD-A191295] 22 p3053 N88-28114
Corrosion problems associated with computer disk packs 22 p3054 N88-28121
Electronic failure analysis-corrosion of avionics 22 p3054 N88-28122
Low cost corrosion sensors 22 p3054 N88-28123
A review of solid particle erosion of engineering materials
[DE88-010065] 22 p3054 N88-28124
Study of the erosion corrosion of alloys and coatings
[AD-A194337] 22 p3055 N88-28128
Erosion of metals exposed to hot, dense gases
[AD-A193706] 22 p3056 N88-28131
Some effects of nitrates on the tensile properties of Al 7075-T7351
[AD-A195118] 24 p3354 N88-29965
Performance Prediction for Coatings. Proceedings of a Workshop
[AD-A188973] 24 p3354 N88-29966
Degradation of protective coatings on steel in corrosive environments 24 p3354 N88-29969
Evaluation of organic coating deterioration and substrate corrosion in seawater using electrochemical impedance measurements 24 p3355 N88-29976
Alternative immersion accelerated testing of coating systems for Naval shoreline facilities 24 p3355 N88-29977
Zinc filled coatings 24 p3355 N88-29978

CORROSION PREVENTION
Workshop on Avionics Corrosion Control
[AGARD-R-733] 05 p0547 N88-13331
Avionic corrosion 05 p0547 N88-13332
Corrosion of electronic components 05 p0547 N88-13333
US Naval Air Force avionic and electrical system corrosion prevention and control maintenance 05 p0547 N88-13334
Corrosion in avionics and associated equipment; cause, effect and prevention 05 p0547 N88-13335
Avionics and corrosion 05 p0547 N88-13336
Simulated service test behavior of various internal and external coatings applied on CF6-50 first stage turbine blades
[NLR-MP-86018-U] 05 p0549 N88-13343
Ion plating for corrosion control
[AD-A185061] 05 p0565 N88-13442
Paints required for aeronautical construction
[SNIAS-872-551-102] 05 p0569 N88-13470
Multipurpose corrosion inhibitors for aerospace materials in Naval environments
[AD-A186728] 09 p1143 N88-16853
Corrosion-wear process under rolling-sliding motion
[AD-A189603] 13 p1778 N88-20635
Controlling stress corrosion cracking in mechanism components of ground support equipment 14 p1926 N88-21480
Development of a high-temperature resistant (700 F), corrosion-preventive organic coating
[AD-A191407] 16 p2182 N88-23009
Proceedings of the 1987 Tri-Service Conference on Corrosion, Volume 2
[AD-A189660] 17 p2319 N88-23847
Corrosion and corrosion inhibition of metals/alloys in methyphosphonic difluoride 17 p2319 N88-23850
Development of microencapsulated DNBM quaternary ammonium inhibitors for paints 17 p2319 N88-23851
Inadequacies of EMI-seal material: A corrosion study 17 p2319 N88-23852
Surface conditioning products as tools for corrosion removal and corrosion prevention 17 p2320 N88-23856
The effect of titanium reinforcement on the life of positive grids in lead-acid batteries 17 p2320 N88-23857
Recent advances in metallic/ceramic coatings for corrosion control in military applications 17 p2320 N88-23858
Carboxylate formation at the interface between a polyimide coating and cobalt 17 p2320 N88-23859
Agenda for advancing electrochemical science and technology 17 p2321 N88-23861
Vanadic hot corrosion of gas turbine blade coating materials 17 p2321 N88-23864
AC impedance analysis of corrosion fatigue in naval aircraft alloys
[AD-A190822] 17 p2322 N88-23865
The influence of cathodic protection on erosion-corrosion of metals and model alloys
[AD-A191613] 18 p2485 N88-24742
An investigation of ceramic coatings for protection of SiC from high-temperature corrosion
[DE88-007873] 18 p2493 N88-24790
Polyacrylic acid electrolyte-modified zinc phosphate conversion coatings for corrosion protection of steel
[DE88-004878] 19 p2617 N88-25527
Guide to the control of high temperature corrosion and protection of gas turbine materials
[PB88-107412] 20 p2760 N88-26370
Corrosion prevention in gas turbines
[NLR-MP-87029-U] 20 p2760 N88-26373
Development of protective coatings for ceramic tubular components
[PB88-197165] 20 p2776 N88-26463
Unified methods of accelerated laboratory tests of the preparations for temporary protection of cars
[NASA-TT-20298] 21 p2921 N88-27336
Proceedings of the 1987 Tri-Service Conference on Corrosion, volume 1
[AD-A191295] 22 p3053 N88-28114
Corrosion and stress corrosion of metals in decontamination solutions 22 p3054 N88-28118
Avionic and electrical system corrosion prevention and control maintenance 22 p3054 N88-28119
Shielding effectiveness of metallic joints versus corrosion prevention 22 p3054 N88-28120
Design guidelines for prevention of corrosion in combat and tactical vehicles
[AD-A194172] 22 p3055 N88-28126
Corrosion control through a better understanding of the metallic substrate/organic coating/interface
[AD-A193981] 22 p3056 N88-28132
Degradation of protective coatings on steel in corrosive environments 24 p3354 N88-29969
Reduced time frame for predicting coating performance 24 p3356 N88-29979

CORROSION RESISTANCE
NT OXIDATION RESISTANCE
Optimizing the application of high temperature corrosion resistant aluminium-silicon-base coatings
[BLL-M-37222-(5828.4)] 01 p0018 N88-10112
Polyitaconic acid macromolecule primer for adhesive bonding and corrosion control of aluminum
[DE87-013306] 01 p0027 N88-10173
Determination of the fatigue strength of mechanically, thermally and corrosively loaded multilayer materials
[ETN-87-90375] 01 p0058 N88-10372
JPRS report: Science and technology. USSR: Materials science
[JPRS-UMS-87-006] 03 p0285 N88-11791
Corrosion resistance of silver-plated carbon-aluminum composite 03 p0285 N88-11793
Corrosion-electrochemical and mechanical properties of composite graphite-carbide metal materials based on titanium and its alloys 03 p0285 N88-11794
Corrosion-resistant amorphous metallic coatings: Engineering development
[NASA-CR-181487] 03 p0287 N88-11802
Ion plating: Fundamental processing studies and synthesis of high performance coatings
[AD-A184766] 03 p0303 N88-11908
Double-effect absorption heat pump, phase 3
[PB87-232195] 03 p0317 N88-12005
Corrosion behavior of P/M mechanically alloyed IN-9052.1: An electro-chemical investigation
[AD-A184191] 04 p0414 N88-12567

Work-in-progress presented at the Army Symposium on Solid Mechanics, 1986: Lightening of the Force
[AD-A184791] 04 p0427 N88-12644
Composite materials applications program at the US Army Ballistic Research Laboratory: Work in progress
04 p0428 N88-12651
Corrosion control by composite material substitution with application to the M-939 5-ton truck
04 p0428 N88-12654
Corrosion susceptibility study of candidate pin materials for ALTC (Active Lithium/Thionyl Chloride) batteries
[DE88-001449] 04 p0440 N88-12734
Reliability of Li/SO2 cells for long-life applications
[DE88-001360] 04 p0440 N88-12735
An examination of coating failure on wing pivot fittings of f111 aircraft
[AD-A185028] 05 p0546 N88-13328
Corrosion resistance of sintered alloy steels
[BLL-M-37363-(5828.4)] 05 p0564 N88-13438
Effectiveness of electrodeposited coatings in reducing atmospheric corrosion of copper substrates
[DE87-013651] 05 p0566 N88-13448
Resistance of canopy materials against chemicals
[PML-1985-22] 05 p0569 N88-13466
Coupling effects between the ferrite and austenite phases during corrosion fatigue of a ferrite/austenite duplex stainless steel 05 p0605 N88-13706
The effect of ion implantation on the corrosion behavior of a high-density sintered tungsten alloy
[AD-A185713] 06 p0683 N88-14185
Study on characteristics of SCC propagation da/dt for welded joint
[PB87-143640] 07 p0869 N88-15270
Modification of properties of metals by high-power ion beams 08 p1079 N88-16507
Corrosion behavior of high density tungsten alloys
[AD-A187106] 09 p1143 N88-16852
Effect of low-temperature aging on the mechanical properties of cast stainless steels
[DE88-002872] 10 p1300 N88-17774
Studies of the initiation of pitting corrosion on stainless steels
[AERE-M-3615] 10 p1301 N88-17778
Corrosion performance of high damping alloys in 3.5 percent sodium chloride environment
[AD-A188048] 11 p1457 N88-18687
Corrosion resistance of electrodeposited amorphous Ni-Cr-P alloys
[DE88-005116] 11 p1459 N88-18695
Protecting old oil tanks made of steel against internal corrosion using organic coatings
[DE88-751089] 11 p1459 N88-18698
Institute for Materials Science and Engineering, Metallurgy: Technical activities 1987
[PB88-157722] 11 p1460 N88-18702
The intergranular segregation of boron in substoichiometric Ni3Al
[DE88-004783] 11 p1462 N88-18720
Anodic behavior of Ni-P and Ni-Cr-P metallic glasses
[DE88-005334] 11 p1463 N88-18722
Characteristics and use of lubricating greases
[DE88-751103] 11 p1463 N88-18723
The effects of thin polymeric surface films in reducing fretting corrosion and wear
[AD-A188633] 12 p1611 N88-19634
Hydrogen embrittlement of gun steel
[AD-A188972] 13 p1740 N88-20407
A fundamental understanding of the effect of alloying elements on the corrosion resistance of rapidly solidified Mg alloys
[AD-A189385] 13 p1741 N88-20413
Optimization of binary pigment coatings
[AD-A189103] 13 p1748 N88-20450
Controlling stress corrosion cracking in mechanism components of ground support equipment
14 p1926 N88-21480
Corrosion and electrochemical behavior of binary magnesium alloys
[AD-A190624] 15 p2040 N88-22154
The corrosion resistance of an aluminum alloy coated with polysilazane derived ceramics
[AD-A190703] 15 p2046 N88-22189
Corrosion of electroless nickel-coated steel
[AD-A191045] 16 p2179 N88-22985
Proceedings of the 1987 Tri-Service Conference on Corrosion, Volume 2
[AD-A189660] 17 p2319 N88-23847
Polyitaconic acid macromolecule primer for adhesive bonding and corrosion control of aluminum
17 p2319 N88-23849
Stress corrosion cracking properties of Al-Li alloys
17 p2320 N88-23853
Corrosion of tungsten alloys in marine environments
17 p2320 N88-23854
Ion beam alloying of aluminum for corrosion resistance 17 p2321 N88-23860
Improving knowledge of the corrosion behavior of aluminum alloys of the 7XXX series
[REPT-48-451/F] 18 p2486 N88-24750
Characterization of 7090 and 7091 profiles made with Cegedur powder — powder metallurgy, aircraft construction materials
[REPT-48-441/F] 18 p2487 N88-24752
Optimization of mechanical/corrosion properties of TI-CODE 12 plate and sheet. Part 2: Thermomechanical processing effects
[DE88-007493] 19 p2616 N88-25517
Electrodeposition of amorphous Ni-Cr-P alloys
[DE88-006868] 19 p2616 N88-25521
Guide to the control of high temperature corrosion and protection of gas turbine materials
[PB88-107412] 20 p2760 N88-26370
Nickel aluminides: A new family of nickel + aluminum alloys featuring simple composition, low density, excellent oxidation resistance and high yield strength that increases with temperature
[DE88-010692] 20 p2776 N88-26461
Performance Prediction for Coatings. Proceedings of a Workshop
[AD-A188973] 24 p3354 N88-29966
Electrochemical evaluation of the long term corrosion resistance of polymer coated steel
24 p3355 N88-29974
Zinc filled coatings 24 p3355 N88-29978
Reduced time frame for predicting coating performance 24 p3356 N88-29979

CORROSION TESTS
NT SALT SPRAY TESTS
Crevice corrosion of stainless steels and related alloys. Part 2: Summary of experimental test data for input to mathematical model
[BR99871-PT-2] 03 p0289 N88-11816
Corrosion and deterioration testing in humid tropic environments
[AD-A186917] 10 p1302 N88-17783
Improving knowledge of the corrosion behavior of aluminum alloys of the 7XXX series
[REPT-48-451/F] 18 p2486 N88-24750
Reduced time frame for predicting coating performance 24 p3356 N88-29979

CORRUGATED PLATES
Stiffened titanium panels
[NASA-CASE-LAR-13814-1] 18 p2497 N88-24816

CORRUGATING
Characteristics of long size thermosyphons made of corrugated tube 20 p2784 N88-26511
Variational analysis of dielectrically loaded multidepth corrugated waveguides
[PB88-193602] 20 p2793 N88-26573

CORTICOSTEROIDS
NT ALDOSTERONE
Influence of general vertical vibration on relationships between mediators in various segments of brain
06 p0751 N88-14613
Evaluation of the endogenous glucocorticoid hypothesis of denervation atrophy
[NASA-CR-182848] 17 p2381 N88-24157

CORUNDUM
U ALUMINUM OXIDES

COS-B SATELLITE
COS-B in-orbit study
[ESA-CR(P)-2420] 01 p0017 N88-10102

COSINE SERIES
Method of assessing changes in biorhythmological structure of human physiological functions
19 p2706 N88-26088

COSMIC BACKGROUND EXPLORER SATELLITE
Surface scattering characteristics and the measurement of particulate contamination 02 p0137 N88-10862
Space Infrared Telescope Facility (SIRTF) design and thermal analysis 08 p0982 N88-15934
DIRBE External Calibrator (DEC)
[NASA-CR-180761] 12 p1631 N88-19760

COSMIC DUST
NT INTERPLANETARY DUST
NT ZODIACAL DUST
Composition, structure and chemistry of interstellar dust
[NASA-TM-88350] 02 p0253 N88-11603
Monte Carlo modeling and meteor showers
06 p0740 N88-14549
Atmospheric entry heating of cosmic dust
06 p0794 N88-14865
Exobiology and life science 07 p0883 N88-15358
Progress toward a cosmic dust collection facility on space station
[NASA-CR-182427] 12 p1598 N88-19566
A mass spectrometer evolved gas analysis experiment for in-situ analysis of cometary dust volatiles
13 p1854 N88-21097
CCD-observations of gas and dust jets in the coma of Comet Halley 14 p1998 N88-21912
Profiles of the major gas emissions and distribution of dust particles in the inner coma (0 to 10,000 km) of Comet Halley 14 p1999 N88-21919
Dust coma morphology of Comet Halley during the Giotto encounter 14 p2000 N88-21921
New properties of cometary dust
14 p2001 N88-21926
Anisotropic emission from comets: Fans versus jets. 1: Concept and modeling 14 p2001 N88-21927
Anisotropic emission from comets: Fans versus jets. 2: Periodic Comet Tempel 2 14 p2001 N88-21928
Comet P/Halley's near-nucleus jet activity
14 p2001 N88-21929
Dust photometry in the near nucleus region of Comet Halley from VEGA-2 observations
14 p2001 N88-21930
Dynamics of charged submicron grains in Halley's coma 14 p2001 N88-21931
Composition of cometary dust particles — Halley
14 p2001 N88-21932
Isotopic composition of Halley dust
14 p2002 N88-21933
P/Halley dust coma: Grains or rocks?
14 p2002 N88-21936
The origin of low mass particles within and beyond the dust coma envelopes of Comet Halley
14 p2002 N88-21938
Optical and hydrodynamic implications of Comet Halley dust size distribution 14 p2003 N88-21939
Similarity and diversity of the polarization of comets
14 p2003 N88-21940
The dust around the nucleus of Comet Halley
14 p2003 N88-21942
Variation of grain properties at the dust outbursts — Halley's comet 14 p2003 N88-21943
The evolution of the mass distribution of cometary particles 14 p2004 N88-21946
The dust tail of Comet Halley
14 p2008 N88-21974
Dust tail streamers and Halley's nucleus rotation
14 p2008 N88-21979
A spectroscopic study of absorption and emission features of interstellar dust components
[B8681462] 16 p2289 N88-23706
Stars, gas and dust in the Andromeda galaxy
[B8679680] 16 p2289 N88-23708
Optical and infrared observations of high latitude dust clouds — interstellar matter
[B8621135] 16 p2289 N88-23709
Modeling of a cometary dust coma
[ETN-88-92980] 23 p3300 N88-29651

COSMIC GAMMA RAY BURSTS
U GAMMA RAY BURSTS

COSMIC GASES
NT INTERPLANETARY GAS
NT INTERSTELLAR GAS
NT NEUTRAL GASES

COSMIC PLASMA
Cosmology in the plasma universe
[TRITA-EPP-87-07] 05 p0660 N88-14053
Cosmic electric currents and the generalized Bennett pinch
[TRITA-EPP-87-14] 22 p3154 N88-28764

COSMIC RADIATION
U COSMIC RAYS

COSMIC RADIO WAVES
U EXTRATERRESTRIAL RADIO WAVES

COSMIC RAY SHOWERS
Cosmic-ray nuclear event with an anomalously strong concentration of energy and particles in the central region
[DE87-703376] 04 p0526 N88-13213
A combined cosmic ray muon spectrometer and high energy air shower array
[DE88-003057] 09 p1264 N88-17574

COSMIC RAYS
NT COSMIC RAY SHOWERS
NT GALACTIC COSMIC RAYS
NT GAMMA RAY BURSTS
NT PRIMARY COSMIC RAYS
NT SOLAR COSMIC RAYS
Summary and conclusions of the 6th Moriond workshop — standard electroweak model
[USIP-87-11] 01 p0092 N88-10602
Solar modulation of the cosmic radiation in the heliosphere 01 p0112 N88-10720
Solar-geophysical data number 513, May 1987. Part 1: (Prompt reports). Data for April, March 1987 and late data
[PB87-204939] 01 p0119 N88-10760
Research in particles and fields
[NASA-CR-180412] 01 p0119 N88-10763
Particle injection and cosmic ray acceleration at collisionless parallel shocks
[DE88-000507] 04 p0430 N88-12665

Activities report in interplanetary space physics
[IFSI-86-5] 05 p0659 N88-14047
Budget and programs for 1986 research
[IFSI-86-16] 05 p0660 N88-14048
Cosmic ray NM-64 neutron monitor data 14, Rome, Italy, January - December 1985
[IFSI-87-8] 05 p0661 N88-14060
Astromag: A particle spectrometer for the Space Station
[PREPRINT-557] 06 p0707 N88-14336
Solar-geophysical activity reports for STIP (Study of Travelling Interplanetary Phenomena) interval 15, 12-21 February 1984 ground level event and STIP interval 16, 20 April-4 May 1984 Forbush decrease
[PB88-101274] 06 p0802 N88-14906
Rome Neutron Monitor (NM) - 64 data for 5 solar particle ground-level events
[IFSI-86-7] 06 p0806 N88-14918
A compilation of Sudden Storm Commencements (SSCs), associated interplanetary disturbances, and cosmic ray variations
[IFSI-86-11] 06 p0807 N88-14923
Xiphophorus: A system to recognize radiation-induced mutations and to study the effects of zero-gravity environment on embryo development
07 p0885 N88-15372
Application of correlation method of reception of direct and reflected cosmic radiation to study of plasmaspheres of planet and distribution of radiation brightness
08 p1004 N88-16085
Life sciences experiments on stratospheric balloons and sounding rockets 08 p1033 N88-16262
A research program in neutrino physics, cosmic rays and elementary particles
[DE88-003507] 09 p1264 N88-17575
Radiation problems in manned space flight with a view to the Space Station 12 p1658 N88-19934
Effects of cosmic heavy ion radiation and space microgravity on plant systems 12 p1658 N88-19936
HNC: A detector to study ultraheavy cosmic rays
12 p1713 N88-20252
A low-frequency measurement of the spectrum of the cosmic microwave background radiation
13 p1858 N88-21112
High energy cosmic muons and the calibration of the L3 electromagnetic calorimeter
[NOTA-INTERNA-895] 14 p2011 N88-21999
Hydrodynamical models of supernova SN 1987 A in the LMC
[DE88-701123] 15 p2151 N88-22837
A map of the cosmic background radiaton at 3 millimeters
[INPE-4529-PRE/1279] 15 p2152 N88-22850
Solar-geophysical data number 520, December 1987. Part 1: (Prompt reports). Data for November 1987, October 1987 and late data
[PB88-164199] 16 p2290 N88-23712
Observations of cosmic rays in the outer heliosphere
[NASA-CR-182942] 18 p2596 N88-25425
Products from cosmic-ray interactions in extraterrestrial matter: What they tell us about radiation backgrounds in space
[DE88-009143] 19 p2743 N88-26288
Effects of cosmic rays on single event upsets
[NASA-CR-183053] 20 p2793 N88-26569
Observation of a point source in Cygnus constellation with the underground detector at Frejus (France)
[PITHA-87/02] 20 p2884 N88-27122
Time-dependent mass loss from hot stars with and without radiative driving
[DE88-008899] 20 p2884 N88-27128
Studies of HZE particle interactions and transport for space radiation protection purposes
[NASA-TM-101159] 20 p2886 N88-27142
Research in particle and gamma-ray astrophysics
[NASA-CR-183111] 20 p2887 N88-27146
Are Centauros diffractive
[DE88-008767] 21 p3032 N88-27996
Embryogenesis and organogenesis of Carausius morosus under spaceflight conditions
22 p3061 N88-28167
On the nucleonics component of cosmic radiation, in the atmosphere
[DE88-702493] 22 p3166 N88-28854
Research in particle and gamma-ray astrophysics
[NASA-CR-183126] 24 p3455 N88-30566
The Single Event Upset (SEU) test facility on the Hardwell tandem generator for cosmic ray simulation
[AERE-R-12896] 24 p3459 N88-30580

COSMIC X RAYS
Center for X-Ray Optics, 1986
[DE88-000715] 04 p0449 N88-12783

COSMOCHEMISTRY
Reports and contributions of the Max-Planck Institute of Chemistry (Otto Hahn Institute)
[REPT-1/87] 11 p1570 N88-19398
Advances in geochemistry and cosmochemistry: Trace element microdistributions with the synchrotron X-ray fluorescence microprobe
[DE88-006355] 15 p2032 N88-22108
,Workshop on the Origins of Solar Systems
[NASA-CR-183025] 24 p3451 N88-30536
Nebular processes recorded in chondritic meteorites
24 p3451 N88-30541
Cosmochemical trends of volatile elements in the solar system 24 p3451 N88-30542

COSMOGONY
U COSMOLOGY

COSMOLOGY
NT BIG BANG COSMOLOGY
NT MISSING MASS (ASTROPHYSICS)
Spontaneous symmetry breaking in N=3 supergravity
[DE87-702753] 01 p0109 N88-10705
New class of spherically symmetric interior solution with cosmological constant
[DE87-703095] 02 p0226 N88-11422
On the cosmological constant in the heterotic string theory
[DE87-703099] 02 p0247 N88-11562
On the degree of generality of inflationary solutions in cosmological models with a scalar field
[DE87-703079] 02 p0251 N88-11586
Crucial cosmological observations
[DE87-703081] 02 p0251 N88-11587
Geometrization of Planck length in composite gravity and supergravity
[DE87-703085] 02 p0251 N88-11588
Magnitude-redshift relation in a perturbed Friedmann universe
[DE87-753020] 02 p0252 N88-11590
Torsion as a source of expansion in a Bianchi type I universe in the self-consistent Einstein-Cartan theory of a perfect fluid with spin density
[AD-A184200] 03 p0322 N88-12037
Number count-redshift relation in universe models with nonzero cosmological constant
[DE87-703043] 03 p0388 N88-12435
Cosmology with decaying vacuum energy
[DE88-000698] 03 p0389 N88-12443
Homogeneous space-time of Goedel type in higher-derivate gravity
[DE87-703690] 04 p0500 N88-13077
Cosmological applications of singular hypersurfaces in general relativity 04 p0521 N88-13202
Galaxy formation by gravitational collapse in a universe dominated by cold dark matter 04 p0521 N88-13205
Model of earlier stage of universe's evolution
06 p0775 N88-14758
Evolution of perturbations in expanding universe
06 p0775 N88-14759
Gravitational interaction of massless fields with higher spins (s greater than 2) 06 p0775 N88-14760
Number count-redshift relation in a perturbed Friedmann universe
[DE88-750302] 07 p0945 N88-15743
Evolution from pure states into mixed states in de Sitter space
[DE88-750316] 07 p0945 N88-15745
Qualitative methods in nonhomogeneous cosmology
[DE88-700620] 10 p1417 N88-18458
Quark matter in astrophysics and cosmology
[DE88-003406] 10 p1429 N88-18534
Cosmic strings: A problem or a solution
[DE88-003410] 10 p1429 N88-18535
Velocity reversal and the arrows of time
[DE88-004237] 10 p1429 N88-18536
Notes on a class of homogeneous space-times
[DE88-700138] 11 p1562 N88-19353
Experimental analysis of absolute space-time Lorentz theories
[DE88-700140] 11 p1563 N88-19355
Seventy years of the general theory of relativity
[DE88-700784] 11 p1563 N88-19356
Can the causal pathologies of Goedel-type universes be avoided in higher-derivative gravity
[DE88-700185] 11 p1568 N88-19387
Reports and contributions of the Max-Planck Institute of Chemistry (Otto Hahn Institute)
[REPT-1/87] 11 p1570 N88-19398
Modified theory of gravity
[DE88-700835] 12 p1642 N88-19830
On (p,n) systematics and the cosmological connection
[DE88-005031] 12 p1712 N88-20245
Rotation of universe --- metagalaxies
14 p1974 N88-21780
Finite width corrections to the Nambu action for the Nielsen-Olesen string
[DE88-006996] 15 p2147 N88-22812
Density perturbations in a rotating universe
[DE87-703036] 15 p2151 N88-22840
String driven inflation
[DE88-006994] 15 p2151 N88-22841
Cosmology for high energy physicists
[DE88-005705] 15 p2151 N88-22842
Particle cosmology comes of age
[DE88-006998] 15 p2151 N88-22844
Stable, heavy, neutral particles in the sun and in toponium decay 17 p2452 N88-24568
Light propagation through gravitationally perturbed Friedmann universes 18 p2577 N88-25307
Inevitable inflation in Einstein-Cartan theory with improved energy-momentum tensor with spin
[NASA-TM-101146] 18 p2586 N88-25365
The geometry of the Virasoro group for physicists
[DE88-007374] 18 p2586 N88-25366
Cosmic wavefunction with induced gravity
[DE88-701873] 20 p2884 N88-27129
Cosmological helium production simplified
[DE88-009578] 20 p2885 N88-27130
Cosmions and stars
[DE88-010886] 20 p2887 N88-27145
Cosmological parameters and evolution of the galaxy luminosity function
[NASA-CR-183081] 21 p3030 N88-27986
Dynamical evolution of cosmic strings
[DE88-011724] 21 p3030 N88-27989
Newtonian and Einsteinian gravitation
22 p3158 N88-28791
Cosmological applications 22 p3158 N88-28794
Evolution of heavy-element abundances in the galactic halo and disk
[DE88-011736] 22 p3164 N88-28845
Cosmology in an N-dimensional vector space
[DE88-702550] 23 p3277 N88-29507
Clustering of galaxies and clusters of galaxies in a decaying-particle cosmological model with a massive decay product
[DE88-753434] 23 p3298 N88-29642
Systematic properties of clusters of galaxies in different cosmological scenarios 23 p3299 N88-29646
Activities in astrophysics
[INPE-4582-PRE/1316] 24 p3456 N88-30570

COSMONAUTS
Present stage of space medicine
10 p1364 N88-18151
Results of long-term electrocardiographic monitoring of cosmonauts 10 p1364 N88-18152
Hypnosis: Possible applications for cosmonauts
12 p1665 N88-19984
History of manned spaceflight
[CNES-NT-121] 21 p3032 N88-28000

COSMOS SATELLITES
NT INTERCOSMOS SATELLITES
Analysis of the orbit of Cosmos 1335 (1982-07A) at 3:12 resonance
[RAE-TR-87041] 14 p1872 N88-21185
Determining near-water wind speed using radar data from Cosmos-1500 artificial earth satellite
24 p3449 N88-30524

COSPAS
COSPAS/SARSAT 406-MHz emergency beacon digital controller
[NASA-TM-100859] 20 p2792 N88-26566
KOSPAS-SARSAT satellites used for ocean current study 24 p3450 N88-30534

COST ANALYSIS
Comparison of costs and benefits for dc and ac transmission
[DE87-008774] 02 p0167 N88-11052
Models for conducting economic analysis of alternative fuel vehicles
[AD-A184028] 03 p0334 N88-12103
Competition Analysis Model (CAM). Volume 2: Computer manual
[AD-A184017] 03 p0384 N88-12411
CNET (Chief of Naval Education and Training) Program Automated Tracking System (CPATS): A comprehensive study
[AD-A184694] 03 p0385 N88-12418
Hypersonic aerodynamics: Applications for HOTOL
05 p0535 N88-13252
A study of the Department of Defense configuration management policies and procedures as applied to the FA-18 Strike/Fighter program
[AD-A184872] 05 p0657 N88-14034
The 1988 NASA (National Aeronautics and Space Administration) authorization
[GPO-80-245] 05 p0659 N88-14044
Ceramic technology for advanced heat engines
[PB87-232997] 06 p0683 N88-14188
Life-cycle cost analysis of residential heat pumps and alternative HVAC (Heating, Ventilating and Air-Conditioning) systems
[DE88-003701] 07 p0839 N88-15090
The Shock and Vibration Bulletin. Part 1: Welcome, Keynote Address, Invited Papers, Nondevelopment Items Workshop and Pyrotechnic Shock Workshop
[AD-A186748] 08 p0997 N88-16034

Guidelines for qualifying non-development equipment to shock and vibration 08 p0997 N88-16036
Commonality analysis as a knowledge acquisition problem 08 p1062 N88-16413
A problem of machine repair with a variable number of heterogeneous servers
[INPE-4245-PRE/1118] 08 p1074 N88-16482
A model for estimating depot maintenance costs for Air Force fighter and attack aircraft
[AD-A187097] 09 p1105 N88-16624
A cost and benefit analysis of hydraulic fluid systems for the next generation of tactical aircraft
[AD-A186911] 09 p1116 N88-16690
Turbine engine monitoring systems: Can they benefit component improvement program management?
[AD-A186992] 09 p1120 N88-16706
Communications satellite systems operations with the space station. Volume 3: Supplementary technical report
[NASA-CR-180875] 09 p1133 N88-16794
Cape Blanco wind farm feasibility study
[DE88-003748] 10 p1348 N88-18059
Cape Blanco wind farm feasibility study
[DE88-003749] 10 p1349 N88-18060
Robustness in cost performance models
[AD-A187183] 11 p1566 N88-19374
Flight Vehicle Development Time and Cost Reduction
[AGARD-CP-424] 12 p1700 N88-20173
Picking winners: Parametric cost estimating and project management 12 p1700 N88-20176
Parametric study of the total cost of aircraft modernization in terms of development and equipment series costs 12 p1700 N88-20177
The increased time and cost of development: Causes and (some) remedies 12 p1701 N88-20178
Reasons for increasing development cost of rotary wing aircraft and ideas to reverse the trend
12 p1701 N88-20179
What can be done to face growing development costs
12 p1701 N88-20181
Schedule and cost control of development
12 p1704 N88-20196
Task allocation for efficient performance of a decentralized organization
[AD-A188699] 12 p1705 N88-20204
A cost analysis for the implementation of commonality in the family of commuter airplanes, revised
[NASA-CR-182569] 12 p1708 N88-20221
Expected value analysis for an unmanned expendable launch vehicle payload escape system
[AD-A189494] 13 p1728 N88-20337
Turnaround operations analysis for OTV. Volume 3: Technology development plan
[NASA-CR-179318] 13 p1729 N88-20342
Performance and cost benefits associated with nonimaging secondary concentrators used in point-focus dish solar thermal applications
[DE88-001104] 13 p1792 N88-20718
Advanced avionics system analysis. Modular avionics cost benefit study formulation
[AD-A189019] 14 p1887 N88-21158
Requirements and cost considerations for a Combined Space Nuclear Reactor Test Facility
[DE88-006763] 15 p2132 N88-22719
A method for estimating and controlling the cost of extending technology
[AD-A190717] 15 p2150 N88-22831
Status of CAD/CAM in medium-sized industries described 16 p2184 N88-23022
The multi-disciplinary design study: A life cycle cost algorithm
[NASA-CR-4156] 17 p2385 N88-24172
Requirements and cost considerations for a combined space nuclear reactor test facility
17 p2401 N88-24277
System capacity and economic modeling computer tool for satellite mobile communications systems
19 p2644 N88-25686
Engine component retirement for cause. Volume 1: Executive summary
[AD-A192730] 20 p2760 N88-26371
Finding minimum-cost circulations by successive approximation
[AD-A192724] 21 p3005 N88-27824
Approximations and optimal control for the pathwise average cost per unit time and discounted problems for wideband noise driven systems
[AD-A192712] 21 p3008 N88-27847
Sources and nature of cost analysis data base reference manual
[AD-A193099] 21 p3028 N88-27976
Price estimates and analysis
22 p3161 N88-28818
Aircraft avionics and missile system installation cost study. Volume 1: Technical report and appendices A through E
[AD-A194605] 23 p3178 N88-28923
A plan for time-phased incorporation of automation and robotics on the US space station
23 p3255 N88-29377
Finding minimum-cost circulations by canceling negative cycles
[AD-A194027] 23 p3271 N88-29468
Finding minimum-cost circulations by successive approximation
[AD-A194028] 23 p3272 N88-29469
New developments in capital cost estimating
[DE88-005392] 23 p3297 N88-29638
Aircraft airframe cost estimating relationships: Study approach and conclusions
[R-3255-AF] 24 p3324 N88-29795
The cost and performance implications of reliability improvements in the F-16A/B
[AD-A195096] 24 p3324 N88-29796
Aircraft avionics and missile system installation cost study. Volume 2: Appendices F and G
[AD-A195372] 24 p3325 N88-29801
Centaur operations at the space station: Cost and transportation analysis
[NASA-CR-182128] 24 p3332 N88-29835
Space systems cost study
[AD-A196024] 24 p3439 N88-30469

COST EFFECTIVENESS

Gallium arsenide and multibandgap solar cell research
[DE87-012260] 02 p0194 N88-11215
Nowcasting for the national economy needs
02 p0199 N88-11241
Automotive Stirling engine: Mod 2 design report
[NASA-CR-175106] 02 p0250 N88-11578
Experiments in fault tolerant software reliability
[NASA-CR-181554] 05 p0632 N88-13863
Concept definition study for recovery of tumbling satellites. Volume 2: Supporting research and technology report
[NASA-CR-179229] 06 p0672 N88-14117
Ceramic technology for advanced heat engines
[PB87-232997] 06 p0683 N88-14188
Methods for reducing computational costs of typical finite element unsteady hydrodynamic models
[AD-A185499] 06 p0702 N88-14312
Strategic Defense Initiative Organization/DARPA (Defense Advanced Research Projects Agency) workshop on laser propulsion. Volume 1: Executive summary
[DE87-003254] 06 p0768 N88-14722
Collider constraints in the choices for wavelength and gradient scaling
[PB87-123691] 06 p0779 N88-14783
Risk analysis methodology survey
07 p0922 N88-15604
A cost and benefit analysis of hydraulic fluid systems for the next generation of tactical aircraft
[AD-A186911] 09 p1116 N88-16690
Evaluation of bituminous materials used in pavement recycling projects at Tyndall, MacDill, and Hurlburt Air Force Bases
[AD-A188068] 10 p1317 N88-17871
Analysis of the performance of an air-water heat pump: Regulation of intrinsic performances
[DE88-900241] 10 p1349 N88-18061
Applications of lower cost computers to dimensional gaging
[BDX-613-3606] 11 p1525 N88-19108
Cost-effective orbit transfer modes for satellite retrieval and servicing --- Space Station
12 p1586 N88-19489
Cost effective development of a national test bed
[NASA-TM-100321] 12 p1601 N88-19585
High shear rate rheometry of low-viscosity liquids
[AD-A188447] 12 p1627 N88-19733
Reducing rotary wing aircraft development time/cost through the use of simulation 12 p1702 N88-20186
Systems analysis and simulation techniques: Essential tools for balanced complex weapon system designs in terms of performance and cost
12 p1702 N88-20187
Minimizing development flight test time and cost in the US Air Force 12 p1703 N88-20192
EDF's studies and first choices regarding the design of electrical equipment
[NASA-TT-20222] 13 p1764 N88-20553
Advances in personal computers for scientific applications
[DE88-009824] 19 p2713 N88-26107
The intelligent QAR and its cost effective role in new generation AIMS --- quick access recorder (QAR); aircraft integrated monitoring systems (AIMS)
22 p3035 N88-28020
Report to congress on the strategic defense system architecture
[AD-A195476] 24 p3426 N88-30393

COST ESTIMATES

Cost savings possible with Air Force conversion to JP-8 as its primary fuel
[AD-A183784] 01 p0030 N88-10192
Space station: National Aeronautics and Space Administration's 1987 cost estimate
[PB87-220760] 02 p0140 N88-10883
Determination of life cycle costs in astronautics
[MBB-UR-E-910/86-PUB] 02 p0249 N88-11572
Carbon Dioxide observational platform system (CO-OPS) Feasibility Study
[NASA-CR-179225] 06 p0671 N88-14113
Feasibility study of a carbon dioxide observational platform system. Volume 2: Programmatics
[NASA-CR-180404] 06 p0672 N88-14114
Highlights of the 70th Flight Mechanics Panel Symposium on Flight Vehicle Development Time and Cost Reduction
[AD-A185831] 07 p0901 N88-15454
Iterative-deepening heuristic search for optimal and semi-optimal resource allocation
08 p1062 N88-16410
A model for estimating depot maintenance costs for Air Force fighter and attack aircraft
[AD-A187097] 09 p1105 N88-16624
A comparison of projection methods in the forecasting of overhead costs for seven government aerospace contractors
[AD-A187572] 10 p1425 N88-18514
Analysis of learning curve fitting techniques
[AD-A187680] 11 p1535 N88-19173
Robustness in cost performance models
[AD-A187183] 11 p1566 N88-19374
Turnaround operations analysis for OTV. Volume 2: Detailed technical report
[NASA-CR-179317] 13 p1729 N88-20341
Turnaround operations analysis for OTV. Volume 4: WBS and dictionary and cost methodology
[NASA-CR-179319] 13 p1729 N88-20343
A method for estimating and controlling the cost of extending technology
[AD-A190717] 15 p2150 N88-22831
A comparative study of project estimating tools
[DE88-009059] 19 p2740 N88-26266
Knowledge-based cost estimating vs traditional software cost models
[DE88-009707] 20 p2883 N88-27116
Price estimates and analysis
22 p3161 N88-28818
Aircraft avionics and missile system installation cost study. Volume 1: Technical report and appendices A through E
[AD-A194605] 23 p3178 N88-28923
New developments in capital cost estimating
[DE88-005392] 23 p3297 N88-29638
Aircraft avionics and missile system installation cost study. Volume 2: Appendices F and G
[AD-A195372] 24 p3325 N88-29801

COST REDUCTION

Cost savings possible with Air Force conversion to JP-8 as its primary fuel
[AD-A183784] 01 p0030 N88-10192
Development of an innovative, low-cost solar collector
[PB87-206819] 02 p0194 N88-11210
Making space nickel/hydrogen batteries lighter and less expensive
[DE88-000168] 05 p0578 N88-13530
Methods for reducing computational costs of typical finite element unsteady hydrodynamic models
[AD-A185499] 06 p0702 N88-14312
Highlights of the 70th Flight Mechanics Panel Symposium on Flight Vehicle Development Time and Cost Reduction
[AD-A185831] 07 p0901 N88-15454
Guidelines for qualifying non-development equipment to shock and vibration 08 p0997 N88-16036
The ILV: A new commercial expendable launch vehicle --- Industrial Launch Vehicle (ILV)
08 p1035 N88-16275
Commonality analysis as a knowledge acquisition problem 08 p1062 N88-16413
Small gas turbine engine technology
09 p1107 N88-16638
Software for integrated manufacturing systems, part 1
09 p1211 N88-17261
Software for integrated manufacturing systems, part 2
09 p1211 N88-17262
Apollo Lightcraft project
[NASA-CR-182575] 11 p1445 N88-18615
Commonality in the design and production of the H-423 (F3) and H-770 (F-15) RLG inertial navigation systems
12 p1577 N88-19431
Changes in USAF structural loads requirements
12 p1580 N88-19452

Concentrating photovoltaic collectors: Fabrication design
[PB88-148051] 12 p1640 N88-19821
The formal specification of computer systems
[AD-A188947] 12 p1675 N88-20013
Flight Vehicle Development Time and Cost Reduction
[AGARD-CP-424] 12 p1700 N88-20173
Risk reduction cost avoidance for full scale development begins with concept formulation
12 p1700 N88-20174
Development savings through parametric modeling of program costs 12 p1700 N88-20175
What can be done to face growing development costs
12 p1701 N88-20181
Development cost reduction using integrated CAE-CAD-CAM techniques 12 p1701 N88-20182
Organization of helicopter development activities with a view toward reduction of costs and cycles
12 p1704 N88-20200
Direct nuclear propulsion for Earth-to-orbit vehicles
17 p2400 N88-24271
Space systems cost study
[AD-A196024] 24 p3439 N88-30469

COSTS
NT AIRCRAFT PRODUCTION COSTS
NT LIFE CYCLE COSTS
NT LOW COST
NT OPERATING COSTS
Design study for asteroidal exploitation
03 p0389 N88-12445
A comparison of the basket method and the stratified random sampling for contract change order negotiations
[AD-A184170] 04 p0500 N88-13080
A plan for collecting ada software development cost, schedule and environment data
[AD-A185905] 07 p0902 N88-15480
A comparison of fitting techniques for the cumulative average learning curves with historical lot cost data
[AD-A187127] 09 p1227 N88-17349
Sigma system: Overview, prospects
15 p2052 N88-22230
Microvax networked computer system
[AD-A190308] 15 p2114 N88-22596
A method for estimating and controlling the cost of extending technology
[AD-A190717] 15 p2150 N88-22831
Timing regulations to prevent stratospheric-ozone depletion
[R-3495-JMO/RC] 19 p2690 N88-25987
Costs --- space projects 22 p3160 N88-28816
Artificial intelligence costs, benefits, risks for selected spacecraft ground system automation scenarios
24 p3416 N88-30332
Information technology to facilitate group interaction
24 p3438 N88-30463

COTTON
Research on cotton plants grown in space
08 p1006 N88-16098
Identification of farming systems in the cotton area of West Burkina Faso from SPOT-1 data
22 p3097 N88-28389

COUCHES
Ergonomy and interior furnishing of the cabins of deep diving manned submarines: The Nautile example --- couch 19 p2697 N88-26032

COUETTE FLOW
The aspect ratio dependence of the attractor dimension in Taylor-Couette flow
[AD-A196297] 24 p3369 N88-30065

COULOMB COLLISIONS
Effect of collisional broadening on the polarizability of a two-dimensional electron gas
[DE87-013928] 02 p0237 N88-11497
Application of a two fluid theoretical plasma transport model on current Tokamak reactor designs
[DE87-013511] 03 p0377 N88-12373
Coulomb interactions and effective strong coupling Hamiltonians in Cu-O superconductors
[DE88-002942] 08 p1090 N88-16561
Determination of molecular-ion structures through the use of accelerated beams
[DE88-002960] 09 p1246 N88-17467
QED description of relativistic Coulomb excitation in heavy ion collisions
[DE88-700834] 12 p1689 N88-20100

COULOMB POTENTIAL
Effect of collisional broadening on the polarizability of a two-dimensional electron gas
[DE87-013928] 02 p0237 N88-11497
Superfluidity of a two dimensional Boson Coulomb gas
[DE88-009827] 19 p2735 N88-26244

COUNTER ROTATION
Noise of a model high speed counterrotation propeller at simulated takeoff/approach conditions (F7/A7)
[NASA-TM-100206] 01 p0091 N88-10592
Turbines with counterrotating runners for aircraft power plants 02 p0158 N88-10992
Noise of a model counterrotation propeller with reduced aft rotor diameter at simulated takeoff/approach conditions (F7/A3)
[NASA-TM-100254] 05 p0647 N88-13961
Secondary flow measurements with L2F-technique in centrifugal compressors 10 p1283 N88-17676
Porous wind tunnel corrections for counterrotation propeller testing
[NASA-TM-100873] 15 p2015 N88-22019
The 2-D and 3-D time marching transonic potential flow method for propfans 16 p2220 N88-23245
Numerical solutions of the Euler equations for the flow field around counter-rotating propellers
19 p2636 N88-25638

COUNTERFLOW
Innovative, counterflow gas/fine solids, direct contact heat exchanger
[DE88-004744] 13 p1770 N88-20585
Superfluid turbulence in counterflowing helium II
19 p2665 N88-25849

COUNTERMEASURES
NT ANTIRADAR COATINGS
NT ELECTRONIC COUNTERMEASURES
NT JAMMING
NT OPTICAL COUNTERMEASURES
Application of the analysis phase of the instructional system development to the MK-105 magnetic minesweeping mission of the MH-53E helicopter
[AD-A186282] 07 p0822 N88-14994
Laser countermeasure impacts and penalties
[DE88-006871] 18 p2520 N88-24947
MIDIR (Mid-Infrared) laser, phase 1
[AD-A193935] 23 p3220 N88-29166

COUNTERS
NT CERENKOV COUNTERS
NT ELECTRON COUNTERS
NT NEUTRON COUNTERS
NT NEUTRON SPECTROMETERS
NT PARTICLE TELESCOPES
NT PROPORTIONAL COUNTERS
NT RADIATION COUNTERS
NT SCINTILLATION COUNTERS
NT SPARK CHAMBERS
Design, fabricate, calibrate, test and deliver two satellite electron flux detectors
[AD-A190799] 16 p2169 N88-22930
The design and performance of a real-time self excited vocoder 19 p2653 N88-25753
Robust vector quantization for noisy channels
19 p2653 N88-25754
Analysis and improvement of the vector quantization in SELP (Stochastically Excited Linear Prediction)
19 p2653 N88-25756

COUNTING
A Prohorov bound for a Poisson process and a Bernoulli process
[CWI-MS-R8701] 09 p1232 N88-17388
Random truncation models and Markov processes
[CWI-MS-R8702] 09 p1232 N88-17389
Performance of a photon counting microchannel plate intensifier with wedge and strip image readout
[DE88-003831] 10 p1334 N88-17970
Product-integrals and counting processes
[CWI-MS-R8707] 14 p1985 N88-21727
Inference for a nonlinear semimartingale regression model
[AD-A190857] 16 p2262 N88-23527
Coincidence counting corrections under conditions used by A. DeVolpi
[NPL-RS(EXT)-90] 17 p2393 N88-24224

COUNTING CIRCUITS
NT SCALERS

COUPLED MODES
The Coupled Cluster Single and Double excitation (CCSD) method in quantum chemistry: An efficient formulation of the theory and application to closed shell molecular systems
[DE88-000475] 07 p0930 N88-15650
Hydromagnetic cavity eigenmodes in a non-uniform plasma 08 p1098 N88-16610
Studies of spectral line ratio fluctuations using Inductively Coupled Plasma (ICP) light
[IRF-PREPRINT-100] 18 p2578 N88-25311
Coupled even-parity superconducting states: Square lattice
[AD-A193432] 21 p3022 N88-27938
Modal synthesis by use of substructures with fixed or free coupling points
[ILR-MITT-191] 22 p3089 N88-28341
Band pass with cavity resonators by use of three oscillation types
[ETN-88-92984] 23 p3209 N88-29096
Role of ordinary to extraordinary mode wave coupling in ionospheric heating experiments
[AD-A195335] 24 p3362 N88-30017

COUPLERS
NT COUPLING CIRCUITS
NT DIPLEXERS
Integrated fiber-optic coupler
[AD-A184494] 03 p0377 N88-12369
Eigenmode analysis of parallel waveguide couplers
[PB87-132122] 06 p0693 N88-14254
Coupled high power waveguide laser research
[AD-A189800] 15 p2071 N88-22345
Current-drive on the Versator-2 tokamak with a slotted-waveguide fast-wave coupler
[DE88-006261] 15 p2136 N88-22743
Study and implementation of ultrahigh frequency coupling devices using the fin line technology --- millimeter waves
[ETN-88-92307] 20 p2796 N88-26588
Theoretical and experimental study of a mode-converting coupler for application to a harmonic gyrotron amplifier
[AD-A193760] 22 p3081 N88-28294

COUPLES
A substructure method for dynamic simulation of flexible mechanical systems with geometric nonlinearities
09 p1176 N88-17044

COUPLING
NT ELECTROMAGNETIC COUPLING
NT MAGNETOSPHERE-IONOSPHERE COUPLING
NT MICROWAVE COUPLING
NT OPTICAL COUPLING
NT SPIN-SPIN COUPLING
NT THERMODYNAMIC COUPLING
Optimum size of staged flux compression generators
[DE87-011741] 01 p0038 N88-10244
Modeling of environmentally-induced transients within satellites. Part 2: Discharge coupling transients
03 p0273 N88-11722
Ion-matrix coupling in polymer electrolytes from relaxation time studies
[AD-A184632] 03 p0293 N88-11841
Bonding and coupling of C sub 1 fragments on metal surfaces
[AD-A184186] 03 p0295 N88-11852
Modeling of proximity coupling between superconducting filaments in superconducting dipole magnets
[DE87-014684] 03 p0382 N88-12403
Coupled elastic rotor/body vibrations with inplane degrees of freedom 05 p0596 N88-13643
Non-minimal interaction of gravity with other physical fields: An overview
[DE87-703362] 05 p0624 N88-13819
Determination of the neutral current chiral coupling constants u sublsq, u subrsq, d sublsq and d subrsq from an (anti)neutrino-deuterium experiment
[B8715857] 06 p0779 N88-14780
Coulomb interactions and effective strong coupling Hamiltonians in Cu-O superconductors
[DE88-002942] 08 p1090 N88-16561
Coupling of microscopic and macroscopic processes in the Earth's magnetotail 08 p1095 N88-16588
Method of iterative coupling between periodic aerodynamic and dynamic fields
[PB87-169934] 09 p1113 N88-16669
Development of a coupled expert system for the spacecraft attitude control problem
09 p1205 N88-17223
Coupling finite element and spectral methods: First results
[NASA-CR-181606] 09 p1231 N88-17379
Renormalization group analysis of the temperature dependent coupling constant in massless theory
[DE88-751059] 09 p1259 N88-17552
Experimental evaluation of turning vane designs for high-speed and coupled fan-drive corners of 0.1-scale model of NASA Lewis Research Center's proposed altitude wind tunnel
[NASA-TP-2681] 10 p1285 N88-17686
Dynamics of coupled electron-nucleon motion in a laser field
[DE88-005063] 10 p1337 N88-17994
The dynamics of two coupled rigid bodies
[AD-A187592] 10 p1341 N88-18012
Piezoelectric laminates for torsional and bending model control: Theory and experiment
10 p1343 N88-18029
The dynamics of coupled planar rigid bodies. Part 1: Reduction, equilibria and stability
[AD-A187467] 10 p1345 N88-18042
Application of a multigrid method to a buoyancy-induced flow problem
[DE88-003961] 10 p1397 N88-18326
A superelement component dynamic synthesis method 11 p1500 N88-18958

Efficient parallel architecture for highly coupled real-time linear system applications
[NASA-CR-182649] 12 p1675 N88-20015
Interaction of particulate and transformation toughening
[AD-A189321] 13 p1741 N88-20412
Comparison of methods for the calculation of thermal contact resistance of the first Brazilian satellite
[NASA-TT-20180] 14 p1880 N88-21239
Inductive spurious coupling of a dc-SQUID to resonant input circuit
[NOTA-INTERNA-894] 14 p1908 N88-21401
Equatorial dynamics and ocean-atmosphere coupling 14 p1938 N88-21565
Stabilization and control problems in structural dynamics
[AD-A190197] 15 p2073 N88-22361
Coupled bending-torsion steady-state response of pretwisted, nonuniform rotating beams using a transfer-matrix method
[NASA-TM-100596] 15 p2086 N88-22435
Control of combustion and acoustically coupled fluid dynamic instabilities 17 p2318 N88-23843
Magnetic drive coupling
[NASA-CASE-MSC-21171-1] 17 p2344 N88-23973
Optical pressure sealing couping (light joint)
[NASA-CASE-MFS-29348-1] 18 p2576 N88-25303
Velocity coupling 19 p2629 N88-25596
Analysis of plasma coupling with the prototype DIII-D ICRF antenna
[DE88-008085] 19 p2729 N88-26204
N=2 supergravity in superspace: different versions and matter couplings
[DE88-702137] 19 p2741 N88-26274
Coupling of a spark source mass spectrograph and a ND-YAG laser
[DE88-012116] 21 p2951 N88-27530
HPM (High-Power Microwave) coupling into realistic targets
[DE88-011788] 23 p3207 N88-29084

COUPLING CIRCUITS
Low frequency IF transformer designs having variable coupling
[RAE-TM-RAD-NAV-291] 01 p0043 N88-10272
Research relative to an advanced rod control system for quadrupole mass spectrometry applications
[NASA-CR-181458] 02 p0167 N88-11050

COUPLING COEFFICIENTS
A microwave FEL (Free Electron Laser) code using waveguide modes
[DE88-000225] 03 p0330 N88-12084

COUPLINGS
Ammonia transfer across rotating joints in space 14 p1927 N88-21492
Development of a rotary fluid transfer coupling and support mechanism for space station 14 p1928 N88-21493
Multi-metallic galvanic corrosion
[AD-A195995] 24 p3353 N88-29963

COURSES
U PATHS

COVARIANCE
Breakdown points of affine equivariant estimators of multivariate location and covariance matrices
[REPT-87-14] 01 p0088 N88-10574
Identification of multivariate outliers and leverage points by means of robust covariance matrices
[REPT-87-15] 01 p0088 N88-10575
Covariant Lorentz anomalies in higher dimensional space
[DE87-753021] 02 p0230 N88-11448
A heteroscedastic hierarchical model
[AD-A184256] 03 p0372 N88-12340
Illustrative examples of principal component analysis using BMDP/4M
[AD-A185179] 05 p0635 N88-13881
Illustrative examples of principal component analysis using SYSTAT/FACTOR
[AD-A184920] 05 p0644 N88-13939
Development of a technique for estimating noise covariances using multiple observers
[NASA-TM-4020] 06 p0669 N88-14098
On the asymptotic joint distributions of the eigenvalues of random matrices which arise under components of covariance model
[AD-A186387] 07 p0915 N88-15558
Operator foundation of functional integral in non-Abelian gauge theory
[DE88-700508] 07 p0941 N88-15719
Control variate selection for multiresponse simulation
[AD-A186637] 08 p1069 N88-16463
The linear dependency structure of covariance nonstationary time series
[AD-A186548] 09 p1232 N88-17383
Five-diagonal weighting scheme for geoidal profiles
[AD-A188033] 10 p1347 N88-18054
Covariance analysis and post-processing of gravity compensation effects for aided multi-state navigation systems
[PAPER-87-13] 12 p1577 N88-19430
Computer programs for calculating group cross-section covariances from uncertainty parameters in the ENDF/B-V format. UNC 32/33 --- neutron physics
[ECN-202] 13 p1837 N88-20995
Mathematics clinic probabilistic position-fixing
[NASA-CR-182753] 15 p2125 N88-22672
State covariance assignment of discrete systems: Development and applications 17 p2393 N88-24225
Annotated computer output for split plot design: SAS GLM
[AD-A190800] 18 p2555 N88-25167
Optimal a priori covariance selection for the solution of ill-conditioned nonlinear inverse problems 18 p2564 N88-25222
Computing partial correlations from the data matrix
[AD-A193904] 22 p3138 N88-28659
The covariance of scalar fields scattered by pressure-release randomly rough surfaces
[AD-A192489] 22 p3146 N88-28714

COVERINGS
An experimental investigation of rocket ramjet nozzle assembly base pressures
[AD-A189714] 15 p2027 N88-22076
Solar cell cover glasses for satellites 15 p2052 N88-22225
Hatch cover
[NASA-CASE-MSC-21356-1] 18 p2472 N88-24671

COVES
U BAYS (TOPOGRAPHIC FEATURES)

COWELL METHOD
U NUMERICAL INTEGRATION

COWLINGS
Thermostructural analysis of simulated cowl lips 15 p2080 N88-22403

CRAB NEBULA
Gamma-ray imaging observations of the Crab and Cygnus regions 10 p1427 N88-18522
The application of imaging to the atmospheric Cerenkov technique: Observations of the Crab nebula 20 p2884 N88-27126
Application of two-dimensional imaging to very high energy gamma ray astronomy
[DE88-010120] 21 p3030 N88-27983

CRACK ARREST
Summary of HSST wide-plate crack-arrest tests and analyses
[DE88-002601] 08 p1000 N88-16061
Crack arrest fracture toughness of armor steels
[AD-A187711] 11 p1456 N88-18681
Applications of elastic-viscoplastic constitutive models in dynamic analyses of crack run-arrest events 14 p1930 N88-21507
Analysis of crack arrest toughness
[AD-A193340] 21 p2913 N88-27286

CRACK CLOSURE
Fatigue 87, volume 1
[AD-A184045] 05 p0597 N88-13645
Closure behavior under constant effective stress intensity loading conditions 05 p0598 N88-13656
The influence of the topography of fracture surfaces on crack closure 05 p0598 N88-13657
Significance of fatigue crack closure under spectrum loading 05 p0599 N88-13662
Fatigue crack propagation of short and long cracks: Phys. basis, prediction methods and engineering significance 05 p0599 N88-13664
The growth behavior of small fatigue cracks; the effect of microstructure and crack closure 05 p0600 N88-13673
An experimental study of closure behavior of naturally initiated small cracks 05 p0601 N88-13676
Behavior of long and short fatigue cracks in a powder metallurgy superalloy at room and at high temperature 05 p0601 N88-13677
Closure and propagation behavior of short fatigue cracks at different R-ratios 05 p0601 N88-13679
A unified model for fatigue crack initiation, short crack growth, long crack propagation, and closure effects 05 p0601 N88-13680
Observations on the effect of overloads on fatigue crack growth 05 p0602 N88-13684
Crack growth in contrasting titanium alloys under the conjoint action of high and low cycle fatigue 05 p0602 N88-13686
Near-threshold growth of defects in engineering materials 05 p0603 N88-13691
Effects of MN dispersoids on near threshold fatigue crack growth in 2134 type alloys 05 p0603 N88-13692
Fatigue 87, volume 3
[AD-A184047] 05 p0604 N88-13700
Occurance and growth of fatigue cracks in corrosion environment 05 p0604 N88-13704
Fracture kinetics of corrosion fatigue 05 p0605 N88-13708
Constraint effects in fatigue crack growth 05 p0606 N88-13719
An optical interferometry technique to evaluate closure along a crack front 05 p0607 N88-13726
Fatigue 87, volume 2
[AD-A184046] 06 p0715 N88-14381
Notch-geometry effect on propagation threshold of short fatigue cracks in notched components 06 p0716 N88-14393
Influence of crack closure on fatigue crack propagation and threshold 06 p0716 N88-14394
The relationship between microstructural size and fatigue threshold in iron and steel 06 p0716 N88-14396
Effect of compressive portion of loading cycles on the near threshold fatigue closure behavior 06 p0717 N88-14398
Absolute fatigue thresholds in metallic materials 06 p0717 N88-14399
A model for ultra-low fatigue crack growth 06 p0717 N88-14404
Influence of stress ratio R on fatigue threshold delta K(th) for 40Cr steel 06 p0718 N88-14405
The effects of loading history on fatigue crack growth threshold 06 p0718 N88-14406
Threshold and crack-growth tests on pre-cracked specimens produced in cyclic compression 06 p0718 N88-14412
The effect of prestraining on fatigue crack growth in nickel-base alloys 06 p0719 N88-14415
Crack closure phenomena in modes 1 and 2 interactions 06 p0719 N88-14417
Effect of temperature exposure on fatigue crack propagation 06 p0720 N88-14421
Analysis of crack closure under plane strain conditions
[NASA-CR-182369] 06 p0722 N88-14439
Random loading fatigue crack growth: Crack closure considerations 06 p0797 N88-14881
Investigations on the crack growth retardation behavior and fatigue life prediction in structural materials
[PB87-143756] 07 p0827 N88-15016
Comparative investigations of indirect crack length measurement under fatigue loading in a corrosive environment
[GKSS-86/E/64] 11 p1502 N88-18972
The fatigue behavior of ferritic and austenitic steels at elevated temperatures
[DE88-006304] 13 p1744 N88-20431
Cyclic crack growth emanating at a round notch considering viscoplasticity
[AD-A189577] 13 p1781 N88-20655
Bimodular behavior and crack closure in compression in a brittle material
[AD-A191267] 16 p2224 N88-23275
Three-dimensional aspects of fatigue crack closure
[AD-A192296] 21 p2960 N88-27581

CRACK FORMATION
U CRACK INITIATION

CRACK GEOMETRY
Fatigue crack growth 05 p0608 N88-13734
Development and calibration of Direct Current Potential Difference (DCPD) crack length measurement equipment
[VTT-RR-480] 09 p1182 N88-17083
Scattering of impulsive acoustic waves by a semi-infinite crack in the plane interface of a half-space and a layer
[PB88-126396] 10 p1405 N88-18377
Comparative investigations of indirect crack length measurement under fatigue loading in a corrosive environment
[GKSS-86/E/64] 11 p1502 N88-18972
Sensitivity to crack initiation in thick assemblies. Test report 48-444
[REPT-48-444] 20 p2758 N88-26365
Wide range stress intensity factor expression for an edge-cracked round bar bend specimen
[AD-A196285] 24 p3382 N88-30147

CRACK INITIATION
Evaluation of cracking in aluminum cylinders
[PB87-201398] 01 p0024 N88-10149
A quantitative statistical model for cleavage fracture initiation in carbide strengthened steels
[ETN-87-90735] 01 p0025 N88-10157
Crack initiation life estimations for notched specimens with residual stresses based on local strains
[FF-17/1986] 01 p0060 N88-10385
Fracture mechanical analysis of the initiation and propagation of matrix and surface cracks in thermally loaded fiber composite models
[ETN-87-90439] 01 p0082 N88-10400
The effect of temperature on fatigue crack initiation from aluminosilicate inclusions
[PNR90377] 02 p0154 N88-10962

Crack behavior in ceramic materials under static, slowly increasing, and cyclic loading conditions
[KFK-4209] 02 p0154 N88-10964
An acoustic emission digital data acquisition workstation
[DE87-012425] 02 p0191 N88-11191
Some new fatigue tests in high temperature water and liquid sodium environment
[DE87-753019] 02 p0192 N88-11197
Fracture mechanism of fine grain graphite under high heat fluxes
[IPPJ-842] 02 p0242 N88-11527
Resistance of welded joints in high temperature Hastelloy N-type nickel alloy to hot crack formation 03 p0286 N88-11798
Flaw imaging and ultrasonic techniques for characterizing sintered silicon carbide
[NASA-TM-100177] 03 p0334 N88-12106
Application of fracture mechanics theory in the reliability analysis of structural ceramics in multiaxial loading 03 p0335 N88-12113
Crack initiation and propagation due to cyclic thermal gradients --- aircraft turbine blades
[ESA-TT-1023] 03 p0336 N88-12114
Spread of plastic deformation in notched and cracked plates 03 p0337 N88-12122
Computational methods and results for dynamic fracture 03 p0337 N88-12123
A probabilistic model of brittle crack formation
[AD-A184423] 03 p0338 N88-12129
Creep life prediction based on stochastic model of microstructurally short crack growth
[NASA-TM-100245] 04 p0456 N88-12825
Data base on the high heat flux behaviour of metals and carbon materials for plasma facing components: Experiments at the 10 MW neutral beam injection test stand of the IPP Nagoya
[IPPJ-AM-53] 04 p0492 N88-13031
Fatigue 87, volume 1
[AD-A184045] 05 p0597 N88-13645
Cyclic deformation and crack initiation 05 p0597 N88-13646
Effect of grain orientation on the origination and the initial growth of fatigue cracks in pure iron 05 p0597 N88-13647
The mechanics of fatigue-crack nucleation in a low-alloy steel under fretting conditions 05 p0597 N88-13649
Surface deformation and fatigue crack initiation of alpha-iron 05 p0598 N88-13651
The effect of ion beam mixed Ni-Al surface layers on PSB extrusion morphology in fatigued nickel 05 p0598 N88-13652
The orientations of dipolar walls produced by cyclic deformation 05 p0598 N88-13655
Growth of short fatigue cracks in a squeeze formed aluminum alloy 05 p0598 N88-13658
The effect of alpha platelet morphology and beta-grain size on the initiation and growth of short fatigue cracks in Ti65S 05 p0600 N88-13667
The initiation and growth of small fatigue cracks in copper at room and cryogenic temperatures 05 p0600 N88-13668
Behavior of short cracks in a 2024 aluminum alloy sheet tested at several stress ratios 05 p0600 N88-13669
The influence of microstructure and residual stresses on the initiation and propagation of short surface cracks on AlMgSi1 05 p0601 N88-13674
Threshold stress for fatigue crack initiation from a small crack 05 p0601 N88-13675
A unified model for fatigue crack initiation, short crack growth, long crack propagation, and closure effects 05 p0601 N88-13680
Fatigue of 30CrMnSiNi2A notched specimens under spectrum loading 05 p0602 N88-13689
The initiation and growth of fatigue cracks in carburised 9Cr1Mo steel 05 p0603 N88-13696
The role of inclusions in corrosion fatigue crack initiation in Q1N 05 p0604 N88-13699
Fatigue 87, volume 3
[AD-A184047] 05 p0604 N88-13700
A study of corrosion fatigue crack initiation, growth and the threshold condition under variable amplitude loading 05 p0604 N88-13701
The effect of environment on low cycle fatigue properties in HSLA steel 05 p0605 N88-13705
Coupling effects between the ferrite and austenite phases during corrosion fatigue of a ferrite/austenite duplex stainless steel 05 p0605 N88-13706
Fatigue crack propagation in Al-Zn-Mg bicrystals and its dependence on the environment 05 p0605 N88-13707
Crack initiation studies in hydrogen embrittled spring steel strip 05 p0605 N88-13710
Telemetric laser extensometry technique for monitoring deflections in small cracks 05 p0607 N88-13724
An overview of fatigue 05 p0608 N88-13729
Deformation mechanisms and crack initiation in fatigue 05 p0608 N88-13730
Fatigue 87, volume 2
[AD-A184046] 06 p0715 N88-14381
Threshold behaviour of semi-elliptic hydrogen-induced and fatigue-induced cracks 06 p0717 N88-14397
Threshold stress intensity for stable crack growth in high strength steel at ambient temperature and below 06 p0718 N88-14407
Role of interstitials and precipitates in initiation and propagation of L.C.F. cracks in austenitic stainless steels 06 p0718 N88-14411
Micromechanics of fatigue crack initiation under axial and torsional loadings 06 p0719 N88-14413
Study of the characteristic curve of hardening and softening during low-cycle fatigue process 06 p0719 N88-14414
Fatigue oxidation interaction in low cycle fatigue 06 p0719 N88-14420
The effect of temperature on fatigue crack initiation from aluminosilicate inclusions 06 p0720 N88-14427
Summary of comparison between experimental and analytical (including empirical) results for initiation of crack growth for surface cracks
[DE88-001604] 06 p0721 N88-14433
Fatigue life prediction modeling for turbine hot section materials
[NASA-TM-100291] 06 p0724 N88-14453
Determination of the critical crack length a (sub IC) in turbine discs
[PB87-144812] 07 p0820 N88-14986
Propagation of fatigue crack in the medium-carbon steel contaiing both martensite and ferrite
[PB87-143962] 07 p0869 N88-15273
Methods of improving compacting quality of intricately shaped powder components
[BLL-M-37412-(5828.4)] 08 p0968 N88-15859
Fracture-resistant characteristics of medium-strength plates with regard to the initiation, stable and unstable propagation of surface cracks
[PB87-144804] 08 p0996 N88-16025
To determine the stress distribution in the vicinity of GRP end pads where the specimen is held and loaded (CFC coupon specimens) --- glass reinforced plastic (GRP) carbon fiber composite (CFC)
[BAE-WST-R-RES-CFC-12023] 09 p1182 N88-17080
Further tests to determine the stress distribution in the vicinity of GRP end pads where the specimen is held and loaded (CFC coupon specimens) --- glass reinforced plastic (GRP) carbon fiber composite (CFC)
[BAE-WST-R-RES-CFC-12023-ADD-1] 09 p1182 N88-17081
La Recherche Aerospatiale, bimonthly bulletin, number 1987-2, 237/March-April
[ESA-TT-1074] 11 p1433 N88-18550
Influence of hydrogen on crack formation tendency in heat-affected zone with stress concentrator 14 p1887 N88-21276
The effect of H2S concentration and pH on the cracking resistance of AISI 410 stainless steel in 5 percent brine
[NPL-DMA(A)-149] 14 p1890 N88-21294
Evaluation of structural analysis methods for life prediction 14 p1930 N88-21511
Computational simulation methods for composite fracture mechanics 15 p2079 N88-22396
In situ fatigue loading stage inside scanning electron microscope 15 p2083 N88-22419
Grain boundary oxidation and low-cycle fatigue at elevated temperatures 15 p2083 N88-22420
Fatigue damage mapping 15 p2084 N88-22423
Life prediction modeling based on strainrange partitioning 15 p2084 N88-22425
Life prediction modeling based on cyclic damage accumulation 15 p2085 N88-22426
Fatigue damage modeling for coated single crystal superalloys 15 p2085 N88-22427
The analysis of fatigue crack growth mechanism and oxidation and fatigue life at elevated temperatures
[NASA-CR-182129] 16 p2179 N88-22987
Investigation of the effect of minimum loads and compression of load spectra on the prediction capacities of the ONERA crack model --- wings
[ONERA-RTS-33/7169-RY-064-R] 18 p2527 N88-24994
Cyclic fatigue damage characteristics observed for simple loadings extended to multiaxial life prediction
[NASA-CR-182126] 18 p2531 N88-25016
Dimensional analysis and experimental observation of the coupling phenomena between combustion and fracture of damaged propellant samples 19 p2630 N88-25603
Characterization of fatigue crack initiation and propagation in Ti-6Al-4V with electrical potential drop technique
[NASA-TM-100877] 19 p2681 N88-25937
Failure analysis of Chloride Silent Power, Ltd. PB cells
[DE88-010567] 21 p2938 N88-27448
AGARD engine disc cooperative test programme
[AGARD-R-766] 23 p3179 N88-28926
Development of creep fracture modelling in ceramics
[PB88-202825] 23 p3196 N88-29021
The use of a surface acoustic wave technique to study the growth behavior of small cracks in a high strength steel alloy 23 p3225 N88-29193
Thermal stress analysis in PMR-15 carbon fibre laminates
[ETN-88-93123] 24 p3341 N88-29886

CRACK OPENING DISPLACEMENT

Experimental investigation of ductile fracture by white light moire interferometry 22 p3087 N88-28329
Ultrasonic method and apparatus for determining crack opening load
[NASA-CASE-LAR-13889-1] 24 p3385 N88-30160

CRACK PROPAGATION

Evaluation of cracking in aluminum cylinders
[PB87-201398] 01 p0024 N88-10149
Behavior of graphites under intense heat loads
[DE87-012128] 01 p0028 N88-10179
Crack propagation behavior of the materials StE 460 and AlMg 4.5Mn
[FD-1/1986] 01 p0058 N88-10373
Modelling of crack-tip deformation and transient electrochemical processes in relation to corrosion fatigue of steels cathodically protected in marine environments
[NPL-DMA(A)-145] 01 p0059 N88-10379
Criteria for determination of significant load cycles in variable amplitude load sequences
[NLR-MP-86013-U] 01 p0060 N88-10386
Fatigue crack propagation of low-alloy steel in a vacuum environment
[DE87-013770] 01 p0061 N88-10393
Fracture mechanical analysis of the initiation and propagation of matrix and surface cracks in thermally loaded fiber composite models
[ETN-87-90439] 01 p0062 N88-10400
Mechanism of mechanical fatigue of fused silica
[DE87-014199] 02 p0152 N88-10950
Crack behavior in ceramic materials under static, slowly increasing, and cyclic loading conditions
[KFK-4209] 02 p0154 N88-10964
Elevated temperature crack growth 02 p0188 N88-11174
Applications of dislocation theory to crack growth problems 02 p0190 N88-11188
A numerical method for the treatment of kinked cracks in finite bodies 02 p0190 N88-11189
An acoustic emission digital data acquisition workstation
[DE87-012425] 02 p0191 N88-11191
Investigation on ductile fracture behavior of 3-inch diameter Type 304 stainless steel pipe with a circumferential through-wall crack
[DE87-753016] 02 p0191 N88-11196
Some new fatigue tests in high temperature water and liquid sodium environment
[DE87-753019] 02 p0192 N88-11197
Fracture mechanism of fine grain graphite under high heat fluxes
[IPPJ-842] 02 p0242 N88-11527
Resistance of welded joints in high temperature Hastelloy N-type nickel alloy to hot crack formation 03 p0286 N88-11798
Microstructural effects on the fatigue behavior of Fe-C-X alloys
[DE88-000155] 03 p0288 N88-11809
Investigation of creep crack growth in heat resistant tube steels
[ETN-87-90606] 03 p0288 N88-11813
Indentation damage in ceramics
[AD-A184686] 03 p0294 N88-11844
Crack initiation and propagation due to cyclic thermal gradients --- aircraft turbine blades
[ESA-TT-1023] 03 p0336 N88-12114
Kinetics of crack growth: Thermal/mechanical interaction 03 p0337 N88-12124
A probabilistic model of brittle crack formation
[AD-A184423] 03 p0338 N88-12129
Mechanical behavior of a controlled rolled high-strength low alloy steeel plate, microalloyed with Nb and V
[DE87-703507] 04 p0415 N88-12571
Effects of stress-relieving on the mechanical properties and the structure of specimens of high-temperature fine-grained structural steels heat-treated to simulate welding
[BLL-CE-TRANS-8258-(9022.09)] 04 p0417 N88-12586
Development of advanced fiber reinforced ceramics
[DE88-000779] 04 p0420 N88-12604
Plastic strain localization between voids in shear deformation fields 04 p0427 N88-12648

Method for the ultrasonic inspection of the soundness of the metal in weld joints in two-ply pipes
[BLL-CE-TRANS-8265-(9022.09)] 04 p0453 N88-12805

Creep life prediction based on stochastic model of microstructurally short crack growth
[NASA-TM-100245] 04 p0456 N88-12825

Micromechanisms of fatigue crack growth and fracture toughness in metal matrix composites
[AD-A185200] 05 p0558 N88-13392

Environmentally assisted cracking: Overview of evidence for an adsorption-induced localised-slip process
[AD-A185175] 05 p0565 N88-13443

Stress intensity factors for cracking metal structures under rapid thermal loading, phase 1
[AD-A184112] 05 p0591 N88-13606

Fatigue 87, volume 1
[AD-A184045] 05 p0597 N88-13645

Effect of grain orientation on the origination and the initial growth of fatigue cracks in pure iron 05 p0597 N88-13647

The growth of persistent slip bands 05 p0597 N88-13648

Closure behavior under constant effective stress intensity loading conditions 05 p0598 N88-13656

Growth of short fatigue cracks in a squeeze formed aluminum alloy 05 p0598 N88-13658

Influence of microstructure and aging condition on the fatigue crack propagation in age hardened aluminium alloys 05 p0599 N88-13659

Fatigue crack growth behavior of A356-T6 cast aluminum alloy 05 p0599 N88-13660

Striations and the fatigue growth mechanism in a micro-alloyed steel 05 p0599 N88-13661

Near-threshold short crack growth behavior in Nimonic 105 05 p0599 N88-13663

Fatigue crack propagation of short and long cracks: Phys. basis, prediction methods and engineering significance 05 p0599 N88-13664

Low cycle fatigue life predictions of a 1CrMoV steel in terms of a J-controlled short crack growth model 05 p0599 N88-13665

The statistics of the shape of small fatigue cracks 05 p0599 N88-13666

The effect of alpha platelet morphology and beta-grain size on the initiation and growth of short fatigue cracks in Ti65S 05 p0600 N88-13667

Behavior of short cracks in a 2024 aluminum alloy sheet tested at several stress ratios 05 p0600 N88-13669

On the role of crack tip shielding in influencing the behavior of long and small fatigue cracks in aluminum-lithium alloy 2090 05 p0600 N88-13671

The influence of slip mechanism on fatigue of Mg and Mg-2.3Li 05 p0600 N88-13672

The growth behavior of small fatigue cracks; the effect of microstructure and crack closure 05 p0600 N88-13673

The influence of microstructure and residual stresses on the initiation and propagation of short surface cracks on AlMgSi1 05 p0601 N88-13674

Threshold stress for fatigue crack initiation from a small crack 05 p0601 N88-13675

Behavior of long and short fatigue cracks in a powder metallurgy superalloy at room and at high temperature 05 p0601 N88-13677

Propagation of small fatigue cracks in 2024-T3 aluminum alloy 05 p0601 N88-13678

Closure and propagation behavior of short fatigue cracks at different R-ratios 05 p0601 N88-13679

A unified model for fatigue crack initiation, short crack growth, long crack propagation, and closure effects 05 p0601 N88-13680

Fatigue crack retardation in aluminium alloys 05 p0602 N88-13681

Fatigue crack growth under random overloads 05 p0602 N88-13682

A dislocation model for fatigue crack propagation under variable amplitude loading 05 p0602 N88-13683

Observations on the effect of overloads on fatigue crack growth 05 p0602 N88-13684

A study of fatigue crack growth life under random stresses 05 p0602 N88-13685

Crack growth in contrasting titanium alloys under the conjoint action of high and low cycle fatigue 05 p0602 N88-13686

Variable amplitude fatigue crack growth in aluminum alloys 2090-T8E41 and 7075-T651 05 p0602 N88-13687

Crack growth prediction in 3D structures under aeronautical-type spectrum loadings 05 p0602 N88-13688

Near-threshold growth of defects in engineering materials 05 p0603 N88-13691

Effects of MN dispersoids on near threshold fatigue crack growth in 2134 type alloys 05 p0603 N88-13692

Crack propagation properties of sintered steel 05 p0604 N88-13698

The role of inclusions in corrosion fatigue crack initiation in Q1N 05 p0604 N88-13699

Fatigue 87, volume 3
[AD-A184047] 05 p0604 N88-13700

A study of corrosion fatigue crack initiation, growth and the threshold condition under variable amplitude loading 05 p0604 N88-13701

The influence of crack conditions on hydrogen uptake by steels 05 p0604 N88-13702

Modeling the effect of sulfur on the threshold environmental cracking rate of steels in high temperature water 05 p0604 N88-13703

Occurance and growth of fatigue cracks in corrosion environment 05 p0604 N88-13704

Coupling effects between the ferrite and austenite phases during corrosion fatigue of a ferrite/austenite duplex stainless steel 05 p0605 N88-13706

Fatigue crack propagation in Al-Zn-Mg bicrystals and its dependence on the environment 05 p0605 N88-13707

the influence of temper embrittlement on fatigue crack growth in hydrogen 05 p0605 N88-13709

Crack initiation studies in hydrogen embrittled spring steel strip 05 p0605 N88-13710

Fatigue mechanisms in ARALL, a fatigue resistant hybrid aluminum aramid composite material 05 p0605 N88-13711

The effect of heat treatment on fatigue crack growth in polycarbonate 05 p0606 N88-13714

Effect of test temperature and frequency on fatigue crack propagation in PVC 05 p0606 N88-13715

Environmental fracture toughness and static fatigue crack propagation of silica glass 05 p0606 N88-13716

Fatigue crack growth: Statistical considerations 05 p0606 N88-13718

Constraint effects in fatigue crack growth 05 p0606 N88-13719

A comparison of plastic work energy and external input for fatigue crack propagation 05 p0607 N88-13722

On the geometrical description of fatigue crack surfaces 05 p0607 N88-13727

An overview of fatigue 05 p0608 N88-13729

Environmentally assisted fatigue crack growth 05 p0608 N88-13731

Fatigue crack growth 05 p0608 N88-13734

The Shock and Vibration Digest, Volume 19, No. 12 05 p0610 N88-13746

Experimental studies on acoustic emission monitoring of crack propagation in offshore structures: A literature survey 05 p0610 N88-13748

Acoustic emissions at an open crack
[DE88-001504] 05 p0611 N88-13751

Fractographic study of fiber composites 06 p0677 N88-14146

The effect of texture on the crack growth resistance of alumina
[NASA-TM-100250] 06 p0686 N88-14206

Fatigue 87, volume 2
[AD-A184046] 06 p0715 N88-14381

Fatigue damage maps 06 p0715 N88-14382

An investigation of fatigue crack growth in a ductile material at high growth rates 06 p0715 N88-14383

Fatigue crack growth and fracture of copper-bismuth bicrystals 06 p0715 N88-14385

Influence of cleavage on fatigue propagation rates in a low carbon steel 06 p0716 N88-14389

Effect of metal surface properties on the fatigue crack growth behavior 06 p0716 N88-14390

Fatigue crack growth behavior in hydrogen gas environment 06 p0716 N88-14391

Near-threshold fatigue 06 p0716 N88-14392

Notch-geometry effect on propagation threshold of short fatigue cracks in notched components 06 p0716 N88-14393

Influence of crack closure on fatigue crack propagation and threshold 06 p0716 N88-14394

An explanation of the fractography of near-threshold fatigue in FCC metals 06 p0716 N88-14395

Threshold behaviour of semi-elliptic hydrogen-induced and fatigue-induced cracks 06 p0717 N88-14397

Effect of compressive portion of loading cycles on the near threshold fatigue closure behavior 06 p0717 N88-14398

Absolute fatigue thresholds in metallic materials 06 p0717 N88-14399

Thermometrical investigations on the near threshold fatigue crack propagation behavior 06 p0717 N88-14400

A re-evaluation of fatigue threshold test methods 06 p0717 N88-14401

The factors which govern the acceleration of corrosion fatigue crack growth rate of a ferritic stainless steel 06 p0717 N88-14402

Fatigue thresholds of C.Mn steels in saline environments 06 p0717 N88-14403

A model for ultra-low fatigue crack growth 06 p0717 N88-14404

The effects of loading history on fatigue crack growth threshold 06 p0718 N88-14406

Threshold stress intensity for stable crack growth in high strength steel at ambient temperature and below 06 p0718 N88-14407

The effect of shear lips on fatigue crack growth in Al-2024 sheet material 06 p0718 N88-14408

Near-threshold fatigue crack growth behavior at cryogenic temperature 06 p0718 N88-14409

The effect of non-metallic inclusions on fatigue and fatigue thresholds of 25Mn-5Cr-1Ni steel 06 p0718 N88-14410

Role of interstitials and precipitates in initiation and propagation of L.C.F. cracks in austenitic stainless steels 06 p0718 N88-14411

Threshold and crack-growth tests on pre-cracked specimens produced in cyclic compression 06 p0718 N88-14412

The effect of prestraining on fatigue crack growth in nickel-base alloys 06 p0719 N88-14415

Mixed mode fatigue crack growth using the Brasilian disc 06 p0719 N88-14416

Crack closure phenomena in modes 1 and 2 interactions 06 p0719 N88-14417

Effect of temperature exposure on fatigue crack propagation 06 p0720 N88-14421

Elevated temperature fatigue crack propagation 06 p0720 N88-14424

The effect of temperature on fatigue crack initiation from aluminosilicate inclusions 06 p0720 N88-14427

An analysis of temperature effect on LCF crack growth rates in superalloy GH36 06 p0721 N88-14431

Summary of comparison between experimental and analytical (including empirical) results for initiation of crack growth for surface cracks
[DE88-001604] 06 p0721 N88-14433

Analysis of crack closure under plane strain conditions
[NASA-CR-182369] 06 p0722 N88-14439

Study of the evolution of short cracks in fatigue analysis --- aircraft construction materials
[DCQ/L-46-555] 06 p0722 N88-14442

Fatigue life prediction modeling for turbine hot section materials
[NASA-TM-100291] 06 p0724 N88-14453

Transients in elevated temperature crack growth
[DE87-013189] 06 p0724 N88-14454

Development of crack under periodically pulsed laser radiation 06 p0774 N88-14754

Random loading fatigue crack growth: Crack closure considerations 06 p0797 N88-14881

Fracture study of windshield glass panes 06 p0799 N88-14891

Investigations on the crack growth retardation behavior and fatigue life prediction in structural materials
[PB87-143756] 07 p0827 N88-15016

Performance of low upper-shelf material under pressurized-thermal-shock loading (PTSE-2)
[DE88-002297] 07 p0832 N88-15049

Effect of overload ratios on fatigue crack growth behavior in Ti-6Al-4V alloy
[PB87-147062] 07 p0833 N88-15055

J-estimation procedure based on moire interferometry data
[AD-A185965] 07 p0867 N88-15258

Analysis of stable crack growth with isotropic and kinematic hardening
[PB87-144911] 07 p0868 N88-15266

Study on fracture behaviour of a joint with a crack in transverse hard layer: Effect of hard layer width on COD
[PB87-143855] 07 p0868 N88-15267

Study on characteristics of SCC propagation da/dt for welded joint
[PB87-143640] 07 p0869 N88-15270

Propagation of fatigue crack in the medium-carbon steel contaiing both martensite and ferrite
[PB87-143962] 07 p0869 N88-15273

Elastic-plastic fracture investigation on stable crack growth for plane stress
[PB87-144820] 08 p0995 N88-16022

Fracture-resistant characteristics of medium-strength plates with regard to the initiation, stable and unstable propagation of surface cracks
[PB87-144804] 08 p0996 N88-16025

Summary of HSST wide-plate crack-arrest tests and analyses
[DE88-002601] 08 p1000 N88-16061

Micromechanisms of fatigue crack growth and fracture toughness in metal matrix composites
[AD-A186941] 09 p1137 N88-16816

Finite element analysis of damaged cross-ply composite laminates
[CCMS-87-10] 09 p1139 N88-16829
Multipurpose corrosion inhibitors for aerospace materials in Naval environments
[AD-A186728] 09 p1143 N88-16853
Reliability of structures with stiffness and strength degradation 09 p1180 N88-17068
Experimental determination of crack growth rates in cyclic stress applications, for improving the forecasted computed durability in operation
[FF-14/1986] 09 p1182 N88-17085
Finite element analysis for the calculation of calibration curves of fracture mechanics specimen for semicircular surface cracks with several starting depths, for the crack depth measurement following the dc potential method
[GKSS-87/E/19] 09 p1183 N88-17086
Fracture mechanics characterization of crack growth under creep and fatigue conditions
[W-2/87] 09 p1183 N88-17087
Detection of hydrogen-assisted-cracking in U-0.8Ti alloy weldments by acoustic emission monitoring
[DE88-003221] 09 p1184 N88-17093
Analytical and experimental characterization of damage processes in composite laminates
[AD-A187221] 10 p1296 N88-17746
Mechanisms of intergranular attack and stress corrosion cracking of alloy 600 by high-temperature caustic solutions containing impurities
[DE87-012820] 10 p1300 N88-17773
Some aspects of the mechanics and mechanisms of dynamic brittle fracture 10 p1343 N88-18028
Theoretical analysis of adhesive fracture and crack-damage interactions 10 p1343 N88-18030
Fatigue crack growth due to random loading
[DE88-004641] 10 p1345 N88-18038
Brittle to ductile transition to cleavage fracture
[DE88-004074] 10 p1420 N88-18481
Effects of sulfur content on the plain strain fracture toughness of inertia welds in 4340 steel
[AD-A188192] 11 p1458 N88-18689
Effects of thermal and thermo-mechanical treatments on the mechanical properties of centrifugally cast alloy 718
[AD-A188195] 11 p1458 N88-18690
Fracture mechanisms and strengthening of slab lasers
[DE88-004002] 11 p1493 N88-18914
The stress field surrounding the tip of a crack propagating in a finite body 11 p1500 N88-18962
Numerical fracture mechanics using finite element method 11 p1501 N88-18966
Comparative investigations of indirect crack length measurement under fatigue loading in a corrosive environment
[GKSS-86/E/64] 11 p1502 N88-18972
Determination of the elastic-plastic fracture toughness parameters under special consideration of the activities of the European Group on Fracture (EGF)
[GKSS-87/E/30] 11 p1502 N88-18973
Study of the effects of metallurgical factors on the growth of fatigue microcracks
[AD-A188475] 12 p1608 N88-19615
Elevated temperature crack growth studies of advanced titanium aluminides
[AD-A189025] 12 p1608 N88-19618
Thermal-mechanical fatigue testing of a titanium-aluminide alloy
[AD-A189555] 12 p1609 N88-19620
Advanced durability analysis. Volume 1: Analytical methods
[AD-A188341] 12 p1635 N88-19789
On the energy release rate for dynamic transient anti-plane shear crack propagation in a general linear viscoelastic body
[AD-A188385] 12 p1635 N88-19791
Crack distribution and growth rates for critical fastener holes in Mirage wing RH79
[AD-A189080] 13 p1722 N88-20293
Composites strengthening
[AD-A189258] 13 p1734 N88-20364
High-temperature metal matrix composites
[AD-A189516] 13 p1734 N88-20367
Fracture characteristics of carbon and aramid unidirectional composites in interlaminar shear and open hole tensile tests
[NLR-TR-86063-U] 13 p1735 N88-20371
Materials Research Laboratory at Brown University
[AD-A188006] 13 p1739 N88-20396
Hydrogen induced cracks in armor steel weldments fabricated with austenitic filler alloys
[AD-A188733] 13 p1740 N88-20406
The effect of microstructure on the fatigue crack growth resistance of nickel base superalloys
[AD-A189526] 13 p1741 N88-20414
Threshold fatigue crack growth in Ti-6Al-2Sn-4Zr-6Mo
[AD-A189560] 13 p1741 N88-20415
Stress corrosion cracking and metal-induced embrittlement: Comparative studies of local chemistries
[DE88-003235] 13 p1742 N88-20419
Non-destructive evaluation techniques applied to the study of fatigue microcrack growth in steel alloys
[DE88-004090] 13 p1742 N88-20420
Fracture mechanics and creep crack growth of 1 percent Cr 1/2 percent Mo steel with and without prior exposure to creep conditions
[NLR-TR-86051-U] 13 p1743 N88-20426
PNL-1 improved ceramic composites through controlled fiber matrix interaction
[DE88-005680] 13 p1750 N88-20462
Laser ignition of nitramine composite propellants and crack propagation and branching in burning solid propellants
[AD-A189260] 13 p1753 N88-20483
A study of the dynamics of high temperature brittle intergranular fracture by acoustic emission
[AERE-R-12479] 13 p1780 N88-20650
Cyclic crack growth emanating at a round notch considering viscoplasticity
[AD-A189577] 13 p1781 N88-20655
Theory and experiments of fracture in cyclic compression: Single phase ceramics, transforming ceramics and ceramic composites
[DE88-005792] 13 p1781 N88-20659
Fracture criteria for discontinuously reinforced metal matrix composites
[NASA-CR-182665] 13 p1782 N88-20662
Crack resistance of multilayer ceramic-based composite material 14 p1885 N88-21265
Monolithic nature of transversely reinforced composites 14 p1885 N88-21267
JPRS report: Science and technology. USSR: Materials science
[JPRS-UMS-87-007] 14 p1895 N88-21312
Some structural aspects of crack propagation in heat-resistant steels under cyclic thermal and mechanical load 14 p1896 N88-21317
Growth of fatigue cracks in nickel alloys at high temperatures 14 p1896 N88-21318
Investigation of the behavior of fast propagating cracks using numerical simulation calculations
[W-6/87] 14 p1934 N88-21532
Fracture toughness testing of a ceramic matrix composite
[AD-A189846] 15 p2029 N88-22089
Fractography of composite delamination
[NASA-CR-182757] 15 p2030 N88-22096
The effective fracture toughness of aluminum at rapid heating rates
[AD-A189745] 15 p2038 N88-22146
Stress corrosion of ceramic materials
[AD-A190501] 15 p2045 N88-22187
Crack opening and extension in inert solid propellant. An experimental study
[AD-A189808] 15 p2048 N88-22201
Environmentally assisted crack growth in structural alloys: Perspectives and new directions
[AD-A190137] 15 p2076 N88-22377
The growth of corner cracks under the conjoint action of high and low cycle fatigue
[AD-A190510] 15 p2076 N88-22379
Mode 2 fracture mechanics 15 p2083 N88-22418
In situ fatigue loading stage inside scanning electron microscope 15 p2083 N88-22419
Grain boundary oxidation and low-cycle fatigue at elevated temperatures 15 p2083 N88-22420
Elevated temperature crack growth 15 p2084 N88-22421
Fatigue damage mapping 15 p2084 N88-22423
A simplified key-curve approach for J-R-curve testing of CT specimens
[VTT-RR-503] 15 p2088 N88-22444
Ultrasonic Time-Of-Flight Diffraction (TOFD) measurements of crack depths in an acceleration reservoir of a high velocity research gun
[DE88-006644] 16 p2164 N88-22907
Fatigue crack growth behavior of a single crystal alloy as observed through an in situ fatigue loading stage
[NASA-TM-100863] 16 p2179 N88-22986
The analysis of fatigue crack growth mechanism and oxidation and fatigue life at elevated temperatures
[NASA-CR-182129] 16 p2179 N88-22987
Fatigue crack growth under full-scale cyclic plasticity
[DFVLR-FB-87-48] 16 p2222 N88-23263
Crack retardation under load spectra. Experimental study and numerical simulation using the simplified K constant model --- light alloys, aircraft construction materials
[ONERA-RT-30/7169-RY-054-R] 16 p2222 N88-23266
Environment effects on crack propagation with tensile stress
[GKSS-87/E/46] 16 p2223 N88-23267
Study of mechanisms of time-dependent crack growth at elevated temperature
[DE88-006918] 16 p2223 N88-23271
On governing equations for crack layer propagation
[NASA-CR-182120] 16 p2223 N88-23272
Heating at a propagating crack tip in a viscoplastic material
[AD-A190952] 16 p2224 N88-23274
AC impedance analysis of corrosion fatigue in naval aircraft alloys
[AD-A190822] 17 p2322 N88-23865
Fracture mechanics 17 p2324 N88-23877
Effect of test sample geometry on the fatigue crack growth of X10NiCrAlTi 32 20 and NiCr22 Co 12Mo
[JUEL-SPEZ-399] 17 p2348 N88-23990
Analysis of crack-tip fields in a viscoplastic material 17 p2349 N88-23996
Composite repair of cracked aluminum alloy aircraft structure
[AD-A190514] 18 p2455 N88-24573
Mixed-mode fracture of uniaxial fiber reinforced composites
[AD-A191629] 18 p2478 N88-24700
Predictive corrosion modeling, volume 1
[AD-A191229] 18 p2485 N88-24739
Role of cracks in the creep of structural polycrystalline ceramics
[AD-A191485] 18 p2490 N88-24770
Environmental effects on slow crack growth in silicon nitride
[DE88-007206] 18 p2494 N88-24795
Fracture mechanics analysis for short cracks
[AD-A192002] 18 p2527 N88-24992
Some stress intensity factor equations
[FFA-TN-1987-07] 18 p2527 N88-24995
Automated analysis of crack growth rate for obtaining da/dN versus delta K relation
[FFA-TN-1987-70] 18 p2527 N88-24996
Resolved shear stress intensity coefficient and fatigue crack growth in large crystals
[NASA-CR-182137] 18 p2528 N88-24997
Self-consistent model for the brittle response of solids 18 p2528 N88-24999
Fatigue crack growth due to random loading 18 p2531 N88-25017
An assessment of the state of the art in predicting the failure of ceramics
[DE88-008998] 19 p2621 N88-25551
Dimensional analysis and experimental observation of the coupling phenomena between combustion and fracture of damaged propellant samples 19 p2630 N88-25603
Study of probabilistic fatigue crack growth and associated scatter under constant-and-variable amplitude loading spectrum
[AD-A192027] 19 p2679 N88-25929
Material void opening computation using particle method
[DE88-010950] 19 p2680 N88-25936
Characterization of fatigue crack initiation and propagation in Ti-6Al-4V with electrical potential drop technique
[NASA-TM-100877] 19 p2681 N88-25937
Accelerated fatigue crack growth behavior of PWA 1480 single crystal alloy and its dependence on the deformation mode
[NASA-TM-100943] 20 p2772 N88-26436
Study of the influence of metallurgical factors on fatigue and fracture of aerospace structural materials
[AD-A192909] 20 p2774 N88-26452
Irreversible deformations during fracture in polymers
[W-7/86] 20 p2780 N88-26485
Fatigue crack growth under far-field cyclic compression
[DE88-011215] 20 p2813 N88-26689
Automated measurement of crack length and load line displacement at elevated temperature
[AGARD-R-751] 20 p2814 N88-26695
A new boundary integral equation formulation for elastodynamic and elastostatic crack analysis
[AD-A192967] 20 p2815 N88-26702
Prediction of fatigue growth
[NLR-MP-87052-U] 20 p2816 N88-26707
Analysis of crack arrest toughness
[AD-A193340] 21 p2913 N88-27286
Three-dimensional aspects of fatigue crack closure
[AD-A192296] 21 p2960 N88-27581
Diffusion models of crack growth due to random overloads
[DE88-008811] 21 p2962 N88-27595
Corrosion fatigue of small cracks: Mechanics and chemistry
[DE88-012121] 21 p2964 N88-27605
Computation of failure probability of fatigue loaded cracked structures
[ETN-88-92360] 21 p2964 N88-27607

Analyses and correlations of environment assisted fatigue crack propagation for attachment lugs
22 p3053 N88-28116
Study of fatigue cracks in aluminum alloys. Influence of microstructure
[REPT-48-553] 22 p3056 N88-28134
Experimental investigation of ductile fracture by white light moire interferometry 22 p3087 N88-28329
Empirical fatigue crack growth data for a tension loaded threaded fastener
[AD-A194112] 22 p3088 N88-28334
Load interaction effects on compression fatigue crack growth in ductile solids
[FFA-TN-1988-12] 22 p3089 N88-28342
AGARD engine disc cooperative test programme
[AGARD-R-766] 23 p3179 N88-28926
Stress intensity factors for cracked metallic structures under rapid thermal loading
[AD-A191219] 23 p3193 N88-29004
Stress corrosion of ceramic materials
[AD-A191979] 23 p3195 N88-29016
Development of creep fracture modelling in ceramics
[PB88-202825] 23 p3196 N88-29021
The use of a surface acoustic wave technique to study the growth behavior of small cracks in a high strength steel alloy 23 p3225 N88-29193
Results on the influence of crack tip plasticity during dynamic crack growth
[AD-A193460] 23 p3225 N88-29194
Elastic-plastic analysis of part-through crack propagation in piping and pressure vessels
[DE88-701619] 23 p3225 N88-29198
Critical conditions for failure in materials subjected to high rates of loading
[AD-A194697] 23 p3226 N88-29201
J-integral measurement using moire interferometry
[AD-A193751] 23 p3226 N88-29202
Fatigue crack growth characteristics of ARALL (trademark)-1
[AD-A196185] 24 p3341 N88-29889
Stress intensity factors for cracked metallic structures under rapid thermal loading
[AES-8609709F-1] 24 p3353 N88-29962
Modeling of micromechanisms of fatigue and fracture in hybrid materials
[AD-A195604] 24 p3382 N88-30142
Automated early fatigue damage sensing system
[AD-A195717] 24 p3382 N88-30143
Fatigue crack propagation: Probabilistic modeling and statistical analysis
[AD-A195885] 24 p3384 N88-30155
The development of acoustic emission for structural integrity monitoring of aircraft
[AD-A196264] 24 p3427 N88-30398

CRACK TIPS
Modelling of crack-tip deformation and transient electrochemical processes in relation to corrosion fatigue of steels cathodically protected in marine environments
[NPL-DMA(A)-145] 01 p0059 N88-10379
Computational methods and results for dynamic fracture 03 p0337 N88-12123
A study of the crack tip parameters that govern environmentally assisted cracking by use of the rising displacement test 04 p0427 N88-12649
On the role of crack tip shielding in influencing the behavior of long and small fatigue cracks in aluminum-lithium alloy 2090 05 p0600 N88-13671
A unified model for fatigue crack initiation, short crack growth, long crack propagation, and closure effects
05 p0601 N88-13680
A dislocation model for fatigue crack propagation under variable amplitude loading 05 p0602 N88-13683
Observations on the effect of overloads on fatigue crack growth 05 p0602 N88-13684
Modeling the effect of sulfur on the threshold environmental cracking rate of steels in high temperature water 05 p0604 N88-13703
Effect of test temperature and frequency on fatigue crack propagation in PVC 05 p0606 N88-13715
Constraint effects in fatigue crack growth
05 p0606 N88-13719
Embrittling effect of the plastic zone
05 p0607 N88-13721
Telemetric laser extensometry technique for monitoring deflections in small cracks 05 p0607 N88-13724
An optical interferometry technique to evaluate closure along a crack front 05 p0607 N88-13726
Thermometrical investigations on the near threshold fatigue crack propagation behavior
06 p0717 N88-14400
Threshold stress intensity for stable crack growth in high strength steel at ambient temperature and below
06 p0718 N88-14407
Analysis of stable crack growth with isotropic and kinematic hardening
[PB87-144911] 07 p0868 N88-15266
Study on fracture behaviour of a joint with a crack in transverse hard layer: Effect of hard layer width on COD
[PB87-143855] 07 p0868 N88-15267
Stress strain fields at crack tip and stress intensity factors in Reissner's plate
[PB87-144945] 08 p0994 N88-16014
Numerical-experimental investigation of singularity at a crack in nonlinear rubber elasticity
11 p1500 N88-18961
Investigation of the components of the energy-momentum tensor in the neighborhood of crack tips under special materials and loading conditions
[W-4/87] 14 p1934 N88-21531
Heating at a propagating crack tip in a viscoplastic material
[AD-A190952] 16 p2224 N88-23274
Analysis of crack-tip fields in a viscoplastic material
17 p2349 N88-23996
Determination of the toughness of a brittle material using strain gages
[ETN-88-92540] 18 p2527 N88-24993
Plastic yielding at crack tips
[AD-A192549] 21 p2960 N88-27582
Results on the influence of crack tip plasticity during dynamic crack growth
[AD-A193460] 23 p3225 N88-29194

CRACKING (CHEMICAL ENGINEERING)
NT HYDROCRACKING
NT PYROLYSIS
A review of methanol vehicles and air quality impacts
[DE88-002846] 08 p1023 N88-16194
Thermal cracking and variable properties effects on free boundary layer diffusion flames
[NBS/GCR-88/542] 12 p1614 N88-19852
Turbine fuels from tar sands bitumen and heavy oil. Volume 2, phase 3: Process design specifications for a turbine fuel refinery charging San Ardo heavy crude oil
[AD-A190120] 16 p2183 N88-23011

CRACKING (FRACTURING)
NT STRESS CORROSION CRACKING
A study of the crack tip parameters that govern environmentally assisted cracking by use of the rising displacement test 04 p0427 N88-12649
Fracture kinetics of corrosion fatigue
05 p0605 N88-13708
On the geometrical description of fatigue crack surfaces 05 p0607 N88-13727
Effect of rare earth elements on the hydrogen-induced cracking in high strength low alloy steel
[PB87-143806] 07 p0833 N88-15052
Nonlinear line-spring model for surface crack analysis with particular reference to work hardening materials
[PB87-144838] 08 p0994 N88-16016
Analysis of composite laminates with matrix cracks
[CCMS-88-03] 11 p1451 N88-18645
Metallurgical analysis of fractured F-27 aircraft landing gear
[DE88-005885] 11 p1460 N88-18705
Reliability based analysis of contact problems
[NASA-CR-182117] 11 p1503 N88-18975
Advanced durability analysis. Volume 1: Analytical methods
[AD-A188341] 12 p1635 N88-19789
Fracture toughness testing of a ceramic matrix composite
[AD-A189846] 15 p2029 N88-22089
An investigation of the failure response of laminates under biaxial stress
[AD-A190039] 15 p2029 N88-22090
Stress-intensity factors for small surface and corner cracks in plates
[NASA-TM-100599] 15 p2088 N88-22445
A finite-element alternating method for two-dimensional Mode-1 crack configurations
[NASA-TM-100616] 16 p2224 N88-23276
Analysis and developments of failure concepts in fracture mechanics based on research results in the field of component safety topics: J-integral concept; crack resistance curves; dynamic criterion
[V-19/86] 18 p2530 N88-25009
Higher frequency ambient noise in the arctic ocean
[AD-A192203] 18 p2547 N88-25122
Automated measurement of crack length and load line displacement at elevated temperature
[AGARD-R-751] 20 p2814 N88-26695
Influence of microstructure and microdamage processes on fracture at high loading rates
[AD-A192957] 21 p2960 N88-27583
Environmental cracking of a superferritic stainless steel under slow strain rate conditions
22 p3053 N88-28117
AGARD (Advisory Group for Aerospace Research and Development) engine disc material cooperative test (supplementary program)
[AD-A193678] 23 p3179 N88-28925
AGARD engine disc cooperative test programme
[AGARD-R-766] 23 p3179 N88-28926
Stress intensity factors for cracked metallic structures under rapid thermal loading
[AD-A191219] 23 p3193 N88-29004
Critical conditions for failure in materials subjected to high rates of loading
[AD-A194697] 23 p3226 N88-29201
An improved boundary force method for analyzing cracked anisotropic materials
[NASA-TM-101495] 24 p3340 N88-29879

CRACKS
NT CRACK TIPS
NT MICROCRACKS
NT SHORT CRACKS
NT SURFACE CRACKS
The application of group radiators for the determination of tension crack corrosion
[BAM-06264] 01 p0022 N88-10141
Fatigue and thermal fatigue of Pb-Sn solder joints
[DE87-012881] 01 p0024 N88-10150
Stationary reconstruction method. Development, test and comparison in ultrasonic testing
[REPT-860125-TW] 01 p0057 N88-10368
Mechanism of mechanical fatigue of fused silica
[DE87-014199] 02 p0152 N88-10950
Crevice corrosion of stainless steels and related alloys. Part 2: Summary of experimental test data for input to mathematical model
[BR99871-PT-2] 03 p0289 N88-11816
Welding and weldability of ductile intermetallic alloys
[DE87-014061] 04 p0416 N88-12582
Development of an acoustic emission monitor and monitoring techniques for long-term monitoring of U-0.8Ti electron-beam weldments for postweld cracking
[DE88-000819] 04 p0453 N88-12804
An adaptive subdivision method with crack prevention for rendering beta-spline objects
[AD-A184249] 04 p0477 N88-12940
Fatigue 87, volume 1
[AD-A184045] 05 p0597 N88-13645
Cyclic deformation and crack initiation
05 p0597 N88-13646
Effect of grain orientation on the origination and the initial growth of fatigue cracks in pure iron
05 p0597 N88-13647
The mechanics of fatigue-crack nucleation in a low-alloy steel under fretting conditions 05 p0597 N88-13649
Growth of short fatigue cracks in a squeeze formed aluminum alloy 05 p0598 N88-13658
Fatigue crack growth behavior of A356-T6 cast aluminum alloy 05 p0599 N88-13660
Near-threshold short crack growth behavior in Nimonic 105 05 p0599 N88-13663
Fatigue crack propagation of short and long cracks: Phys. basis, prediction methods and engineering significance 05 p0599 N88-13664
Low cycle fatigue life predictions of a 1CrMoV steel in terms of a J-controlled short crack growth model
05 p0599 N88-13665
The statistics of the shape of small fatigue cracks
05 p0599 N88-13666
The effect of alpha platelet morphology and beta-grain size on the initiation and growth of short fatigue cracks in Ti65S 05 p0600 N88-13667
The initiation and growth of small fatigue cracks in copper at room and cryogenic temperatures
05 p0600 N88-13668
Behavior of short cracks in a 2024 aluminum alloy sheet tested at several stress ratios 05 p0600 N88-13669
On the role of crack tip shielding in influencing the behavior of long and small fatigue cracks in aluminum-lithium alloy 2090 05 p0600 N88-13671
The influence of slip mechanism on fatigue of Mg and Mg-2.3Li 05 p0600 N88-13672
Threshold stress for fatigue crack initiation from a small crack 05 p0601 N88-13675
An experimental study of closure behavior of naturally initiated small cracks 05 p0601 N88-13676
Behavior of long and short fatigue cracks in a powder metallurgy superalloy at room and at high temperature
05 p0601 N88-13677
Closure and propagation behavior of short fatigue cracks at different R-ratios 05 p0601 N88-13679
A unified model for fatigue crack initiation, short crack growth, long crack propagation, and closure effects
05 p0601 N88-13680
Fatigue crack retardation in aluminium alloys
05 p0602 N88-13681
Fatigue crack growth under random overloads
05 p0602 N88-13682
A dislocation model for fatigue crack propagation under variable amplitude loading 05 p0602 N88-13683
Variable amplitude fatigue crack growth in aluminum alloys 2090-T8E41 and 7075-T651
05 p0602 N88-13687

Near-threshold growth of defects in engineering materials 05 p0603 N88-13691
Effects of MN dispersoids on near threshold fatigue crack growth in 2134 type alloys 05 p0603 N88-13692
The initiation and growth of fatigue cracks in carburised 9Cr1Mo steel 05 p0603 N88-13696
The role of inclusions in corrosion fatigue crack initiation in Q1N 05 p0604 N88-13699
Acoustic emissions at an open crack [DE88-001504] 05 p0611 N88-13751
Fractographic study of fiber composites 06 p0677 N88-14146
Electron microscopy studies of tensile cyclic fatigue-tested silicon nitride ceramics [DE88-001438] 06 p0685 N88-14196
Fatigue 87, volume 2 [AD-A184046] 06 p0715 N88-14381
Fatigue damage maps 06 p0715 N88-14382
An investigation of fatigue crack growth in a ductile material at high growth rates 06 p0715 N88-14383
On cleavage in fatigue for rail steels 06 p0716 N88-14388
Fatigue crack growth behavior in hydrogen gas environment 06 p0716 N88-14391
Notch-geometry effect on propagation threshold of short fatigue cracks in notched components 06 p0716 N88-14393
Influence of crack closure on fatigue crack propagation and threshold 06 p0716 N88-14394
An explanation of the fractography of near-threshold fatigue in FCC metals 06 p0716 N88-14395
Threshold behaviour of semi-elliptic hydrogen-induced and fatigue-induced cracks 06 p0717 N88-14397
Effect of compressive portion of loading cycles on the near threshold fatigue closure behavior 06 p0717 N88-14398
Influence of stress ratio R on fatigue threshold delta K(th) for 40Cr steel 06 p0718 N88-14405
Threshold stress intensity for stable crack growth in high strength steel at ambient temperature and below 06 p0718 N88-14407
Near-threshold fatigue crack growth behavior at cryogenic temperature 06 p0718 N88-14409
Role of interstitials and precipitates in initiation and propagation of L.C.F. cracks in austenitic stainless steels 06 p0718 N88-14411
Micromechanics of fatigue crack initiation under axial and torsional loadings 06 p0719 N88-14413
Study of the characteristic curve of hardening and softening during low-cycle fatigue process 06 p0719 N88-14414
The effect of prestraining on fatigue crack growth in nickel-base alloys 06 p0719 N88-14415
Mixed mode fatigue crack growth using the Brasilian disc 06 p0719 N88-14416
Elevated temperature fatigue crack propagation 06 p0720 N88-14424
Creep-fatigue cracking in high temperature turbine rotors 06 p0720 N88-14426
The effect of temperature on fatigue crack initiation from aluminosilicate inclusions 06 p0720 N88-14427
Sulfur-induced ductility-dip cracking in weld metal of low-carbon steel [PB87-143814] 07 p0833 N88-15051
On the convergence of the p-version of the boundary element Galerkin method [AD-A186198] 07 p0910 N88-15514
Fully plastic analysis of mixed mode plane-strain crack problems [PB87-144929] 08 p0994 N88-16015
Crack opening displacement test in tension [PB87-143848] 08 p0996 N88-16026
Mode 3 problems of doubly-periodic rhombic and rectangular array of equal cracks in an infinite plate [PB87-144846] 08 p0996 N88-16031
Boundary elements combined with singular fields for three-dimensional cracked solids [RAE-TR-87038] 09 p1183 N88-17088
Stress intensity and crack displacement for small edge cracks [NASA-TP-2801] 09 p1184 N88-17095
Analytical and experimental characterization of damage processes in composite laminates [AD-A187221] 10 p1296 N88-17746
A detailed microstructural examination of the cause of HAZ cracking in type 316 steel [AERE-R-12428] 10 p1301 N88-17777
Durability and damage tolerance of aluminum castings [AD-A186444] 10 p1341 N88-18013
Theoretical analysis of adhesive fracture and crack-damage interactions 10 p1343 N88-18030
Fatigue crack growth due to random loading [DE88-004641] 10 p1345 N88-18038
Brittle to ductile transition to cleavage fracture [DE88-004074] 10 p1420 N88-18481
On delamination of (+ or - theta sub m/90 sub n/2) sub s laminates subject to tensile loading [AD-A188095] 11 p1447 N88-18626
Backscatter from flaws in fiber-reinforced composites 11 p1450 N88-18639
Joining of dissimilar materials with the pulsed Nd-YAG laser [DE88-003757] 11 p1458 N88-18693
Thermal fatigue of stainless steel [DE88-004146] 11 p1458 N88-18694
Reference standards for nondestructive tests [AD-A187766] 11 p1497 N88-18936
Three-dimensional scattering of impulsive acoustic waves by a semi-infinite crack in the plane interface of a half space and a layer [PB88-146998] 12 p1687 N88-20089
Crack distribution and growth rates for critical fastener holes in Mirage wing RH79 [AD-A189080] 13 p1722 N88-20293
Material instabilities in solids [AD-A189525] 13 p1738 N88-20388
Hydrogen induced cracks in armor steel weldments fabricated with austenitic filler alloys [AD-A188733] 13 p1740 N88-20406
Threshold fatigue crack growth in Ti-6Al-2Sn-4Zr-6Mo [AD-A189560] 13 p1741 N88-20415
Nondestructive evaluation of carbon-carbon coatings [AD-A189524] 13 p1748 N88-20453
Ductile failure [AD-A189429] 13 p1781 N88-20654
Influence of hydrogen on crack formation tendency in heat-affected zone with stress concentrator 14 p1887 N88-21276
Cracking tendencies of restrained welds in high strength low alloy steels under hyperbaric conditions [AD-A190255] 15 p2039 N88-22150
Ultrasonic characterization of ceramic joints [DE88-005844] 15 p2043 N88-22173
An evaluation of nondestructive methods for ceramic heat exchanger applications [DE88-006731] 15 p2068 N88-22328
Detection sensitivity in thick assemblies --- eddy currents, light alloys, aircraft construction materials [REPT-48-912/F] 16 p2216 N88-23221
Nondestructive Evaluation (NDE) of structural ceramics by photoacoustic microscopy 17 p2325 N88-23884
SiC fiber reinforced reaction-bonded Si3N4 composites 17 p2326 N88-23892
Weldability of general purpose heat source iridium capsules 17 p2426 N88-24429
A method for the numerical solution of random Cauchy singular integral equation 18 p2565 N88-25234
Fracture physics of delamination of composite materials [AD-A192021] 19 p2609 N88-25482
Study of probabilistic fatigue crack growth and associated scatter under constant-and-variable amplitude loading spectrum [AD-A192027] 19 p2679 N88-25929
A simple unified method for predicting the deflections of reinforced concrete structures 19 p2679 N88-25930
Helium induced degradation in the weldability of an austenitic stainless steel [DE88-009062] 20 p2773 N88-26443
Image force expression for the dislocation near a crack [DE88-701894] 20 p2814 N88-26692
Time-domain boundary element analysis of dynamic near-tip fields for impact-loaded collinear cracks [AD-A192930] 20 p2815 N88-26700
A new boundary integral equation formulation for elastodynamic and elastostatic crack analysis [AD-A192967] 20 p2815 N88-26702
Application of controlled interfacial pore structures to kinetic studies in alumina [DE88-010884] 21 p2919 N88-27326
Significance of the local electrode potential within pits, crevices and cracks [AD-A192482] 21 p2935 N88-27432
Plastic yielding at crack tips [AD-A192549] 21 p2960 N88-27582
Thermo-mechanical cracking in coated media with a cavity by a moving asperity friction [AD-A193311] 21 p2961 N88-27586
Analysis of stiffness reduction, failure and stress concentration in fiber composite laminates [AD-A193519] 22 p3050 N88-28096
The mechanical behavior of surface modified ceramics [DE88-010564] 23 p3196 N88-29022
Obtaining stress intensity factors on cracks, by means of fitting techniques on numerical results calculated with the finite element method 24 p3384 N88-30153

CRAFT
U VEHICLES

CRANES
NT GANTRY CRANES
Renewed interest in airships for industry use discussed 04 p0424 N88-12628
Design and implementation of the ESL compact range underhung bridge crane [NASA-CR-182396] 07 p0862 N88-15231
Oscillation damped movement of suspended objects [DE88-005715] 15 p2086 N88-22433
Space spider crane [NASA-CASE-LAR-13411-1-SB] 17 p2312 N88-23828
Required operational capacity for a 7-1/2 ton capacity, Air Mobile Crane (AMC) [AD-A192023] 19 p2601 N88-25451

CRANKED WINGS
U SWEPT WINGS

CRANKS
U ECCENTRICS

CRASH LANDING
NT DITCHING (LANDING)
An analytical method for ditching analysis of an airborne vehicle [NASA-CR-4120] 07 p0816 N88-14968
Aircraft accident report: Northwest Airlines, Inc., McDonnell Douglas DC-9-82, N312RC, Detroit Metropolitan Wayne County Airport, Romulus, Michigan, August 16, 1987 [PB88-910406] 19 p2601 N88-25449

CRASHES
NT CRASH LANDING
NT DITCHING (LANDING)
Full-scale transport controlled impact demonstration program [NASA-TM-89642] 01 p0004 N88-10021
KRASH parametric sensitivity study: Transport category airplanes [AD-A189962] 15 p2017 N88-22024
Improved procedure for impact probability computation of aircraft crash based on Balfanz model [JUEL-SPEZ-425] 21 p2894 N88-27176
Crash simulation calculations and component idealization for an airframe. Computer code KRASH 79 [ETN-88-92971] 23 p3174 N88-28899
Centralized class A flight mishap investigation [AD-A194397] 24 p3322 N88-29786

CRASHWORTHINESS
Steering mechanism --- vehicles [EP-PATENT-0-181-700-A1] 01 p0053 N88-10338
Helicopter crashworthiness research program 09 p1107 N88-16635
Peak Acceleration Device (PAD) [AD-A191639] 18 p2461 N88-24611
Fuel containment concepts: Transport category airplanes [AD-A189818] 18 p2494 N88-24799
Crash simulation calculations and component idealization for an airframe. Computer code KRASH 79 [ETN-88-92971] 23 p3174 N88-28899

CRATERING
NT PROJECTILE CRATERING
A new look at the use of linear methods to predict aircraft dynamic response to taxi over bomb damaged and repaired airfields 09 p1180 N88-17069
Analysis of impact crater arrangement on the Venutian surface (from photographic materials of the Venera-15 and -16 spacecraft) [NASA-TT-20211] 11 p1571 N88-19401
Martian geomorphology and its relation to subsurface volatiles [NASA-CR-182428] 12 p1711 N88-20237
Early cratering rates and the nature of the Martian cratered uplands 23 p3306 N88-29694
Early intense cratering: Effects on growth of earth's crust 24 p3395 N88-30219

CRATERS
NT LUNAR CRATERS
NT METEORITE CRATERS
Bilateral symmetry elements of the Zhamanshin impact crater [NASA-TT-20288] 15 p2096 N88-22490
Sub-kilometer rampart craters in the equatorial region of Mars: Possible implications for the state and distribution of regolith H2O 23 p3302 N88-29666
Topography of large craters on Mars: Implications for the highlands resurfacing history 23 p3306 N88-29691
Variation in the thickness of ejecta cover on Mars with increasing crater density 23 p3307 N88-29701

CRATONS
Archean crustal evolution of the northern North China Craton 24 p3398 N88-30235
Evolution of the Dharwar Craton: A terrain of early Archean crustal stability, long term orogenic cycles and large scale palaeobiological activity 24 p3399 N88-30241

Crustal underplating in the North American Craton: Evidence from the Petrogenesis of anorthositic rocks in the Middle Proterozoic Midcontinent Rift System
24 p3400 N88-30252

CRAY COMPUTERS
Software enhancements and modifications to Program FDTD executable on the Cray X-MP computer
[DE88-001877] 07 p0904 N88-15476
A comparison of the Cray-2 performance before and after the installation of memory pseudo-banking
[NASA-CR-177462] 09 p1215 N88-17287
A performance comparison of the Cray-2 and the Cray X-MP
[NASA-CR-177461] 09 p1216 N88-17288
Multitasking and microtasking experience on the NA S Cray-2 and ACF Cray X-MP
[NASA-CR-177464] 09 p1221 N88-17325
Vector performance of register-to-register vector computers
[DE88-004013] 10 p1384 N88-18265
Dynamic run-time graphics
[DE87-008997] 13 p1820 N88-20879
Vectorization of the odd-even hopscotch scheme and the alternating direction implicit scheme for the two-dimensional Burgers' equations
[CWI-NM-R8720] 16 p2249 N88-23440
The performance of the NEC SX-2 and Cray X-MP supercomputers
[DE88-009177] 20 p2835 N88-26813
Supermap for Cray FORTRAN: A user's guide
[NASA-CR-177410] 24 p3412 N88-30306

CRAZING
U SURFACE CRACKS

CREATION
U CREATIVITY

CREATIVITY
Separable orthogonal coordinates and particle creation for an accelerating observer
[DE87-703358] 05 p0657 N88-14029
Innovation and creativity: A critical linkage
[DE88-003309] 10 p1426 N88-18515
Computer aided fast turnaround laboratory for research in VLSI (Very Large Scale Integration)
[AD-A189451] 12 p1624 N88-19715
Idea processing for creativity and management
[DE88-006110] 19 p2714 N88-26113

CREEP ANALYSIS
A creep measurement of unidirectional epoxy-fiberglass rod
[DE87-014812] 04 p0411 N88-12553
Propagation of creep waves around rough cylindrical surface 09 p1234 N88-17400
Verification of the ADINA finite element code for creep analysis: Problems from the open literature
[DE88-011826] 21 p2962 N88-27594

CREEP BUCKLING
Effects of state recovery on creep buckling induced by thermomechanical loading 03 p0336 N88-12116
Effects of state recovery on creep buckling under variable loading 14 p1933 N88-21527
Interaction of creep and fatigue damage in gas turbine blade material
[PNR90440] 22 p3088 N88-28335

CREEP DIAGRAMS
Investigations of creep cavitation in Type 304 stainless steel
[DE87-014198] 03 p0287 N88-11803

CREEP PROPERTIES
NT SHEAR CREEP
Creep fatigue life prediction for engine hot section materials (isotropic): Third year progress review
02 p0186 N88-11173
Investigations of creep cavitation in Type 304 stainless steel
[DE87-014198] 03 p0287 N88-11803
Investigation of creep crack growth in heat resistant tube steels
[ETN-87-90606] 03 p0288 N88-11813
Effect of helium on irradiation creep in an austenitic stainless steel
[DE87-013754] 03 p0290 N88-11824
Modified 14Cr-16Ni stainless steels with improved creep resistance at 700 C due to tailored precipitate microstructures
[DE87-014788] 03 p0290 N88-11825
Computerized system for studies on creep of irradiated materials in the BR-10 reactor. Control system for electric motor
[DE87-702888] 03 p0310 N88-11952
Comparison of measured temperatures, thermal stresses and creep residues with predictions on a built-up titanium structure
[NASA-TM-86814] 03 p0337 N88-12125
Some stochastic aspects of intergranular creep cavitation
[DE88-000065] 04 p0416 N88-12581
Influence of creep on the precipitate structure under conditions of long-term creep. 4: Experiments on 10 CrMo 9 10 steel
[BLL-CE-TRANS-8256-(9022.09)] 04 p0417 N88-12589
Creep life prediction based on stochastic model of microstructurally short crack growth
[NASA-TM-100245] 04 p0456 N88-12825
Study of the influence of mechanical - thermal treatments on the creep behavior of a niobium stainless steel
[DE87-703506] 05 p0583 N88-13431
Cu-2 mechanical properties and microstructural stability of advanced steam cycle materials
[DE88-001519] 05 p0566 N88-13452
Thermo-mechanical behavior of high temperature fiber composites 06 p0678 N88-14149
Creep-fatigue cracking in high temperature turbine rotors 06 p0720 N88-14426
Dependence of strainrange partitioned fatigue life at elevated temperature on monotonic stress-strain properties 06 p0721 N88-14428
Axial creep-fatigue damage assessment in type 316 SS material 06 p0721 N88-14430
Transients in elevated temperature crack growth
[DE87-013189] 06 p0724 N88-14454
Creep test of Hastelloy X for use as the components of OGL-1 in helium environment
[DE88-750289] 07 p0834 N88-15059
Aeropropulsion '87. Session 1: Aeropropulsion Materials Research
[NASA-CP-10003-SESS-1] 09 p1118 N88-16697
Creep and fatigue research efforts on advanced materials 09 p1119 N88-16701
Effects of a regenerating heat treatment on the creep behavior and the lifetime during creep test loading
[ETN-88-91063] 09 p1144 N88-16855
The role of composition and microstructure gradients on weld metal properties and behavior
[DE88-004956] 10 p1303 N88-17791
Relationship between fatigue life in the creep-fatigue region and stress-strain response
[NASA-TM-100796] 10 p1345 N88-18040
Effects of thermal and thermo-mechanical treatments on the mechanical properties of centrifugally cast alloy 718
[AD-A188195] 11 p1458 N88-18690
Creep behavior of tungsten/niobium and tungsten/niobium-1 percent zirconium composites
[NASA-TM-100804] 11 p1460 N88-18707
Structure of a viscoplastic theory
[NASA-TM-100794] 11 p1501 N88-18968
Elevated temperature crack growth studies of advanced titanium aluminides
[AD-A189025] 12 p1608 N88-19618
High-temperature metal matrix composites
[AD-A189516] 13 p1734 N88-20367
Creep behavior of consolidated rapidly solidified Type 304 stainless steel powder containing helium
[DE88-005536] 13 p1743 N88-20424
Fracture mechanics and creep crack growth of 1 percent Cr 1/2 percent Mo steel with and without prior exposure to creep conditions
[NLR-TR-86051-U] 13 p1743 N88-20426
The fatigue behavior of ferritic and austenitic steels at elevated temperatures
[DE88-006304] 13 p1744 N88-20431
Processing, physical metallurgy and creep of NiAl + Ta and NiAl + Nb alloys
[NASA-CR-182113] 14 p1890 N88-21295
Some implications for cyclic plastic and viscoplastic equations based on nonproportional loading experiments
14 p1931 N88-21515
A unified creep-plasticity model suitable for thermo-mechanical loading 14 p1932 N88-21518
Effect of strain rate on high-temperature low-cycle fatigue behavior of Hastelloy X and Hastelloy XR
[DE88-752302] 15 p2037 N88-22140
Study of mechanisms of time-dependent crack growth at elevated temperature
[DE88-006918] 16 p2223 N88-23271
Creep behavior of tungsten/niobium and tungsten/niobium-1 percent zirconium composites
17 p2425 N88-24427
Role of cracks in the creep of structural polycrystalline ceramics
[AD-A191485] 18 p2490 N88-24770
Damage by creep fatigue: Influence of the visco-elasticity of the matrix
[PB88-124706] 18 p2528 N88-24998
Compression creep of filamentary composites
[NASA-CR-182550] 20 p2798 N88-26601
Effect of the matrix on the creep-behavior of carbon-carbon composite
[AD-A193211] 21 p2905 N88-27235
Controlling phase formation and stability to improve the high temperature creep resistance of austenitic stainless steels
[DE88-011401] 21 p2914 N88-27293
Creep behavior for Hastelloy-XR
[DE88-753428] 21 p2914 N88-27295
Verification of the ADINA finite element code for creep analysis: Problems from the open literature
[DE88-011826] 21 p2962 N88-27594
An anisotropic continuum damage model for creep-dominated, multiaxial loading histories
21 p2964 N88-27608
An endochronic rate-sensitive constitutive equation for metals, application to generalized creep and large deformations
[AD-A194167] 22 p3055 N88-28125
The high temperature creep deformation of Si3N4-6Y2O3-2Al2O3
[NASA-CR-183204] 23 p3190 N88-28981
Development of creep fracture modelling in ceramics
[PB88-202825] 23 p3196 N88-29021

CREEP RESISTANCE
U CREEP STRENGTH

CREEP RUPTURE STRENGTH
Comparative tests of high temperature creep-rupture behavior of the austenitic CrNi steel DIN W.NR.1.4970 in argon and steam
[KFK-4261] 01 p0063 N88-10402
Stress rupture behavior of silicon carbide coated, low modulus carbon/carbon composites
[NASA-CR-180863] 06 p0678 N88-14150
Long-term aging of cast stainless steels: Mechanisms and resulting properties
[DE88-002888] 09 p1145 N88-16864
Aging degradation of cast stainless steels: Effects on mechanical properties
[DE88-003053] 09 p1145 N88-16866
Fracture mechanics characterization of crack growth under creep and fatigue conditions
[W-2/87] 09 p1183 N88-17087
Creep rupture analysis of a beam resting on high temperature foundation 14 p1930 N88-21509

CREEP STRENGTH
Development of creep resistant austenitic stainless steels for advanced steam cycle superheater application
[DE87-012929] 01 p0023 N88-10147
Modified 14Cr-16Ni stainless steels with improved creep resistance at 700 C due to tailored precipitate microstructures
[DE87-014788] 03 p0290 N88-11825
Effect of the matrix on the creep-behavior of carbon-carbon composite
[AD-A193211] 21 p2905 N88-27235

CREEP TESTS
Creep-fatigue behavior of NiCoCrAlY coated PWA 1480 02 p0189 N88-11176
A loading system for creep testing under constant compressive stress
[NASA-TT-20119] 06 p0722 N88-14441
Creep test of Hastelloy X for use as the components of OGL-1 in helium environment
[DE88-750289] 07 p0834 N88-15059
Effects of a regenerating heat treatment on the creep behavior and the lifetime during creep test loading
[ETN-88-91063] 09 p1144 N88-16855
Creep rupture analysis of a beam resting on high temperature foundation 14 p1930 N88-21509
Data requirements to model creep in 9Cr-1Mo-V steel
14 p1931 N88-21512
Controlled-strain rate tests at very low strain rates of 2618 aluminum at 200 C 14 p1931 N88-21513
Automated measurement of crack length and load line displacement at elevated temperature
[AGARD-R-751] 20 p2814 N88-26595
Automated measurement of crack length and load line displacement at elevated temperature
[NLR-MP-87049-U] 20 p2816 N88-26706
Prediction of long-term creep in polypropylene from short-term tests
[NPL-DMA(A)-156] 22 p3088 N88-28337

CRESTATRONS
U TRAVELING WAVE TUBES

CRESTS
U WAVES

CREVASSES
NT GLACIERS

CREVICES
U CRACKS

CREW PROCEDURES (INFLIGHT)
Parameter-adaptive model-following for in-flight simulation
[AD-A190567] 18 p2487 N88-24645

CREW PROCEDURES (PREFLIGHT)
Checklist interruption and resumption: A linguistic study
[NASA-CR-177460] 20 p2758 N88-26348

CREW STATIONS
U CREW WORKSTATIONS
CREW WORKSTATIONS
Personnel occupied woven envelope robot power
[NASA-CR-182367] 07 p0856 N88-15196
Development of a C3 generic workstation: System overview 16 p2242 N88-23396
C3 generic workstation: Performance metrics and applications 16 p2242 N88-23397
Crewstation Information and Development System (CIDS) 17 p2304 N88-23781
Space station architectural elements model study
[NASA-CR-4027] 18 p2464 N88-24632
CREWS
NT FLIGHT CREWS
NT SPACECREWS
Man rating the b-1B molecular sieve oxygen generation system
[AD-A186275] 07 p0899 N88-15447
Portable, ambient air microclimate cooling in simulated desert and tropic conditions
[AD-A186457] 08 p1050 N88-16338
Team problem solving: Effects of communication and function overlap
[AD-A187010] 09 p1152 N88-16898
Checklist interruption and resumption: A linguistic study
[NASA-CR-177460] 20 p2756 N88-26348
Human factors report on information management requirements for next-generation manned bombers
[AD-A195870] 24 p3409 N88-30296
CRIMPING
U FOLDING
CRITERIA
NT STRUCTURAL DESIGN CRITERIA
Multiaxial fatigue failure criterion: A new approach 06 p0719 N88-14418
TECOM's research efforts in the dynamic environments 08 p0999 N88-16048
Strong consistency of certain information theoretic criteria for model selection in calibration, discriminant analysis and canonical correlation analysis
[AD-A186584] 09 p1232 N88-17385
A practical termination criterion for the conjugate gradient method
[REPT-87-62] 16 p2259 N88-23506
Systems for the 21st century 17 p2302 N88-23769
Accuracy criteria for evaluating supersonic aerodynamic coefficient predictions 24 p3317 N88-29756
CRITICAL EXPERIMENTS
Fast critical experiment data for space reactors
[DE87-007005] 01 p0093 N88-10605
CRITICAL FLOW
Development of an equation of state for computation of supercompressibility factors, critical flow factors and other properties for wet, sour natural gases, synthetic gases and admixtures
[PB88-202676] 20 p2798 N88-26602
Introduction and critical flow phenomena 23 p3169 N88-28870
Boundary layer development and transition 23 p3169 N88-28871
CRITICAL LOADING
Determination of the critical crack length a (sub IC) in turbine discs
[PB87-144812] 07 p0820 N88-14986
CRITICAL MACH NUMBER
U CRITICAL VELOCITY
U MACH NUMBER
CRITICAL MASS
Particle bed reactor scaling relationships 17 p2400 N88-24267
CRITICAL POINT
Detection of critical points: The first step to automatic line generalization 05 p0619 N88-13803
Phase equilibria and density calculations in the critical region: A phenomenological correction for a classical equation of state
[PB88-185335] 19 p2723 N88-26167
Critical point wetting drop tower experiment
[NASA-CR-183062] 20 p2798 N88-26603
Investigation on refrigerant R12 critical boiling point in narrow flow pipes considered as model fluid
[ETN-88-92374] 20 p2802 N88-26626
Nontrivial critical points for asymptotically quadratic function
[DE88-101851] 20 p2845 N88-26881
Thermal conductivity of pure fluids in a large region around the critical point
[ETN-88-92135] 20 p2881 N88-27103
Fluid physics double rack — Spacelab
[SD-TN-AI-012] 24 p3358 N88-29992
CRITICAL REYNOLDS NUMBER
U CRITICAL VELOCITY
U REYNOLDS NUMBER
CRITICAL SPEED
U CRITICAL VELOCITY
CRITICAL STRESS
U CRITICAL LOADING
CRITICAL TEMPERATURE
Welding and weldability of ductile intermetallic alloys
[DE87-014061] 04 p0416 N88-12582
Magnetic field dependence of the specific heat of some high-T/sub c/ superconductors
[DE87-014078] 04 p0497 N88-13063
Investigation of critical heating in narrow flow channels with R12 refrigerant as model fluid
[GKSS-87/E/25] 09 p1163 N88-16972
Stability limits in the monoclinic-tetragonal transformations of zirconia
[DE88-005924] 14 p1986 N88-21849
Dependence of high critical temperature of ceramic superconductors on the nominal Cu(sup 3+)Cu(sup 2+) ratio
[DE88-702734] 23 p3293 N88-29611
CRITICAL VELOCITY
Critical Ionization Velocity (CIV) interaction: Some unsolved questions
[TRITA-EPP-87-12] 09 p1250 N88-17491
On the role of the ionization frequency to gyrofrequency ratio in the critical ionization velocity interaction
[TRITA-EPP-86-10] 10 p1410 N88-18414
Open channel flow near the resonance speed 18 p2514 N88-24918
A critical speed study for aircraft bias ply tires
[AD-A193616] 22 p3084 N88-28313
CROP GROWTH
Estimating scattered and absorbed radiation in plant canopies by remote sensing
[NASA-CR-181390] 02 p0193 N88-11205
Wheat production in controlled environments
[UAES-PAPER-3324] 03 p0361 N88-12270
Controlled Ecological Life Support System. Design, Development, and Use of a Ground-Based Plant Growth Module
[NASA-CP-2479] 05 p0630 N88-13852
CELSS Program Meeting 05 p0630 N88-13853
Controlled ecological life support systems: Development of a plant growth module 05 p0630 N88-13854
Plant Growth Module (PGM) conceptual design 05 p0631 N88-13855
Modeling the growth dynamics of four candidate crops for Controlled Ecological Life Support Systems (CELSS) 06 p0799 N88-14889
Report on phase 1 of the project estimate development of a model for yield estimation of sugar cane based on LANDSAT and agromet data
[INPE-4466-RPE/560] 12 p1638 N88-19807
Assessment of crop loss from air pollutants: Meteorology-atmospheric chemistry and long range transport
[PB88-146857] 15 p2089 N88-22448
Estimation of an area cultivated with wheat from LANDSAT data through a two-phase sampling method 17 p2357 N88-24041
Remote sensing techniques in the estimation of the area cultivated with beans, corn, and castor beans in the Irece County (Bahia State) 17 p2358 N88-24045
CANASATE: Sugar cane mapping by satellite 17 p2358 N88-24046
Identification of areas cultivated with soybeans in the cerrados regions, through digital processingof satellite images: A methodological approach 17 p2358 N88-24048
Comparative variations of spectral signatures in a cultivated area of the Paris Basin (27 May, 26 June, 1 July 1986) 22 p3095 N88-28382
LANDSAT TM and agrometeorological data for wheat yield estimation at the farm level
[INPE-4591-PRE/1321] 24 p3388 N88-30180
CROP IDENTIFICATION
SPOT data for crop discrimination in southern Brazil 03 p0343 N88-12169
A procedure for automatic classification of crop areas
[INPE-4467-PRE/1240] 13 p1790 N88-20708
A comparison of supervised maximum likelihood and decision tree classification for crop cover estimation from multitemporal LANDSAT MSS data 17 p2352 N88-24014
Spectral behavior of crops through analysis of LANDSAT-TM data 17 p2358 N88-24047
Identification of areas cultivated with soybeans in the cerrados regions, through digital processingof satellite images: A methodological approach 17 p2358 N88-24048
Separability of cultivation through digital analysis of SPOT and TM data
[INPE-4541-PRE/1287] 19 p2685 N88-25963
Comparative study of crop and soil mapping using multitemporal and multispectral SPOT and LANDSAT data 22 p3091 N88-28354
Changes in species composition of heathland, monitored by means of remote sensing and field mapping: The results of the HEISPOT project 22 p3092 N88-28360
Evaluation of automatic texture analysis for increased crop identification accuracy with SPOT data 22 p3094 N88-28373
Digital and visual analysis of SPOT and TM data for crop discrimination in southern Brazil 22 p3096 N88-28385
Identification of farming systems in the cotton area of West Burkina Faso from SPOT-1 data 22 p3097 N88-28389
Using SPOT HRV data to update the distribution of the paddy field in Taiwan 22 p3097 N88-28393
CROP INVENTORIES
Crop forecasting in Brazil: A short history of productivity models
[INPE-4150-PRE/1056] 12 p1637 N88-19801
A procedure for automatic classification of crop areas
[INPE-4467-PRE/1240] 13 p1790 N88-20708
Methodological developments on crop inventories using SPOT and ground surveys 22 p3094 N88-28371
Evaluation of annual crop surfaces and territorial inventory in the Paris basin by combining classic statistical inquiries and SPOT data (Preliminary Evaluation Program for SPOT 127) 22 p3094 N88-28372
Attempt to inventory vines using oblique SPOT images 22 p3095 N88-28380
Evaluation of SPOT data for crop inventory and monitoring in Sudanian Africa. Example of Bane area (Burkina Faso) 22 p3096 N88-28388
Monitoring Tunisia's steppes with SPOT 22 p3097 N88-28390
CROP INVENTORIES BY REMOTE SENSING
U AGRISTARS PROJECT
CROP VIGOR
Estimating scattered and absorbed radiation in plant canopies by remote sensing
[NASA-CR-181390] 02 p0193 N88-11205
Application of multitemporal SPOT data for crop monitoring: Effects of frost and drought 03 p0344 N88-12171
Species biology and potential for controlling four exotic plants (Ammophila arenaria, Carpobrotus edulis, Cortaderia jubata and Gasoul crystallinum) on Vandenberg Air Force Base, California
[NASA-TM-100980] 10 p1363 N88-18148
Crop forecasting in Brazil: A short history of productivity models
[INPE-4150-PRE/1056] 12 p1637 N88-19801
Changes in species composition of heathland, monitored by means of remote sensing and field mapping: The results of the HEISPOT project 22 p3092 N88-28360
CROPLANDS
U FARMLANDS
CROPS
Application of remote sensing to agricultural field trials
[ISBN-90-6754-089-7] 06 p0729 N88-14483
CROSS CORRELATION
Cross-correlation of uniform cyclic difference set sequences
[AD-A184879] 05 p0640 N88-13913
Stability, reliability and cross-mode correlations of tests in a recommended 8-minute performance assessment battery
[NASA-CR-172039] 08 p1052 N88-16351
Detecting squeezed states by cross-correlation 14 p1978 N88-21806
A diagnostic technique used to obtain cross range radiation centers from antenna patterns
[NASA-CR-182903] 16 p2192 N88-23071
Self similarity of two point correlations in wall bounded turbulent flows 16 p2195 N88-23089
The display of multivariate information: The effects of auto- and cross-correlation, reliability and heterogeneity
[AD-A191070] 16 p2243 N88-23398
Development of advanced flow simulation system by water flow model. New method of velocity measurement using cross-correlation
[DE88-753120] 20 p2799 N88-26608
Dependence of medium range forecast errors upon the large-scale initial state 22 p3126 N88-28585
CROSS FAULTS
U GEOLOGICAL FAULTS
CROSS FLOW
Comparison of different kinds of compact cross flow heat exchangers
[DFVLR-FB-86-63] 01 p0048 N88-10305
A 15 cm aperture LED scintillometer for C(n) squared and crosswind measurements
[KNMI-WR-87-3] 01 p0070 N88-10448
Laminar flow over a spinning projectile at an angle of attack 02 p0121 N88-10766
Aerothermal modeling program, phase 2 02 p0185 N88-11149

Dilution jet mixing program, phase 3
02 p0185 N88-11153
On the mixing of a row of jets with a confined crossflow
02 p0185 N88-11154
Theoretical analysis of primary instabilities in three dimensional boundary layer flows
[ESA-TT-1063] 03 p0315 N88-11992
Theory of one and two-pass cross-flow heat exchanger
[PB87-225157] 04 p0441 N88-12736
Comparative studies in the near-field of turbulent transports of heated and unheated jets normal to a cross stream
04 p0444 N88-12756
Computational design of natural laminar flow wings for transonic transport application 07 p0813 N88-14948
Numerical calculation of appendage, flat plate junction flow
[AD-A186371] 07 p0850 N88-15158
Cross flow in the Alps and flat foehn during the experiment MERKUR --- mesoscale experiment
08 p1013 N88-16142
A jet in a crossflow
[NASA-CR-182469] 09 p1113 N88-16674
Simulations of thermally induced winds and cross flow situations
[MITT-57] 09 p1193 N88-17148
Control of vortical separation on conical bodies
10 p1267 N88-17580
Leeside crossflow modeling in Euler space-marching computations
[NASA-TM-89710] 10 p1325 N88-17924
Investigation of non-symmetric jets in cross flow
10 p1327 N88-17932
Time-resolved heat transfer measurements and analysis in the wage region of a cylinder in crossflow
10 p1328 N88-17939
Experimental research on center of pressure of slender body with two pointed ends 14 p1864 N88-21137
Comparison of different kinds of compact crossflow heat exchangers
[ESA-TT-1076] 16 p2207 N88-23169
Crossflow vorticity sensor
[NASA-CASE-LAR-13436-1-CU]
17 p2300 N88-23759
The calculation of transonic flow over the shuttle orbiter using slender body theory 18 p2460 N88-24606
Cross stream differencing for integral boundary layer equations
[AD-A191744] 18 p2509 N88-24886
Measurement of burning rates of NOSOL-363 propellants under cross-flow and strand burner conditions using real-time X-ray radiography
19 p2623 N88-25560
Three-dimensional viscous flow computations of a circular jet in subsonic and supersonic cross flow
[NASA-CR-182153] 20 p2800 N88-26616
Cross flow induced vibrations in tube bundle by displaced and misaligned tube configurations
[ETN-88-92132] 20 p2801 N88-26621
A numerical study of turbulent plane jets in still and flowing environments employing two-equation k-epsilon model 23 p3211 N88-29109

CROSS SECTIONS
Convective cross section analysis
[PB87-204566] 02 p0216 N88-11361
Use of boundary-layer method for problem of sound propagation through channel with variable cross-section containing stream of fluid 09 p1233 N88-17396
Computer program for parameterization of nucleus-nucleus electromagnetic dissociation cross sections
[NASA-TM-4038] 16 p2270 N88-23584
Total photoionization cross sections of atomic oxygen from threshold to 44.3A
[NASA-CR-182992] 17 p2397 N88-24252
The role of integral experiments and nuclear cross section evaluations in space nuclear reactor design
17 p2404 N88-24293
Density diagnostics by hydrogen line intensity ratios: Excitation cross section between excited states
17 p2441 N88-24522
Distorted-wave-method calculation of electron-impact excitation of atomic ions 17 p2443 N88-24532
Nonlinear interaction between overall and local buckling of stiffened panels with symmetric cross-sections
[PB88-104054] 21 p2960 N88-27580

CROSSED FIELDS
Vortex dynamics and transport to the wall in a crossed-field plasma sheath
[DE87-013286] 01 p0100 N88-10857
Crossed molecular beam studies of substitution and exchange reactions
[DE88-006322] 14 p1980 N88-21814
Vortex formation and particle transport in a cross-field plasma sheath
[DE88-008931] 23 p3284 N88-29553
Vortex formation and particle transport in a cross-field plasma sheath
[AD-A194838] 24 p3432 N88-30425

CROSSINGS
HOC spectral analysis of an almost periodic random sequence in noise
[AD-A185528] 06 p0765 N88-14697
Higher order crossings
[AD-A190489] 15 p2121 N88-22641

CROSSLINKING
NT VULCANIZING
Effect of sidechain length and crosslinking on ionic conductivity in polyphosphazene solid electrolytes
[AD-A184419] 04 p0497 N88-13058
Development of microencapsulation techniques
[AD-A185019] 05 p0567 N88-13457
Interface effects on the mechanical properties of ceramic composites
[AD-A185899] 07 p0825 N88-15009
Polyether-polyester graft copolymer
[NASA-CASE-LAR-13447-1] 11 p1463 N88-18725
Study of crosslinking and nonelastic mechanical properties of epoxy and PSP networks --- epoxy resins; polystyrylpyridine resins (psp)
[ETN-88-92740] 21 p2921 N88-27337
The radiation sensitivity of select metal chelate polymers: Mechanistic changes at higher energies
[AD-A193467] 23 p3196 N88-29019

CROSSOVERS
Geosat crossover analysis in the tropical Pacific. Part 1: Constrained sinusoidal crossover adjustment
[NASA-CR-182391] 07 p0871 N88-15285
An efficient algorithm for computing the crossovers in satellite altimetry
[NASA-CR-182389] 07 p0871 N88-15286

CROSSTALK
Crosstalk in braided shield coaxial cables
01 p0035 N88-10224
The design and testing of an analog optical communication link capable of the simultaneous transmission of four frequency division multiplexed audio signals
[AD-A184695] 03 p0307 N88-11936
Crosstalk analysis of a broadband data communications system
[DE88-003652] 09 p1156 N88-16927

CRUCIBLES
Model development for induction heating
[DE88-002376] 06 p0699 N88-14269
A study of surface tension driven segregation in monotectic alloy systems
[NASA-CR-182894] 16 p2178 N88-22983

CRUCIFORM WINGS
Wind tunnel investigation of wing and control panel loads at transonic and supersonic speeds on some schematic cruciform missile configurations
[FFA-TN-1986-43-SUPPL-1] 22 p3039 N88-28044

CRUDE OIL
Aviation turbine fuels from tar sands bitumen and heavy oils. Part 2: Laboratory sample production
[AD-A185744] 06 p0687 N88-14211
Aviation turbine fuels from tar sands bitumen and heavy oils. Part 3: Laboratory sample production
[AD-A189278] 13 p1753 N88-20484
Turbine fuels from tar sands bitumen and heavy oil. Volume 2, phase 3: Process design specifications for a turbine fuel refinery charging San Ardo heavy crude oil
[AD-A190120] 16 p2183 N88-23011

CRUISE MISSILES
NT TOMAHAWK MISSILES
Performance optimization of a cruise missile using dynamic-stall induced lift augmentation
[AD-A190497] 15 p2017 N88-22027

CRUISING FLIGHT
Techniques for performance optimisation in cruise and manoeuverability 05 p0545 N88-13321
Propulsion challenges and opportunities for high-speed transport aircraft 08 p0958 N88-15809
The initial calculation of range and mission fuel during conceptual design --- aircraft design
[LR-525] 16 p2161 N88-22889
Inflow measurement made with a laser velocimeter on a helicopter model in forward flight. Volume 5: Tapered planform blades at an advance ratio of 0.23
[NASA-TM-100545] 17 p2299 N88-23755
Inflow measurements made with a laser velocimeter on a helicopter model in forward flight. Volume 1: Rectangular planform blades at an advance ration of 0.15
[NASA-TM-100541] 18 p2460 N88-24607
Periodic solutions in aircraft cruise-dash optimization
18 p2464 N88-24631

CRUSTAL DYNAMICS
U EARTH CRUST
U GEODYNAMICS

CRUSTAL FRACTURES
An algorithmic approach to crustal deformation analysis
[NASA-CR-181497] 03 p0349 N88-12203
An algorithmic approach to crustal deformation analysis 04 p0468 N88-12891
The analysis of recent crustal movements in static and kinematic models
[SER-B-279] 09 p1191 N88-17136
Study of fractures as subsidiary research of ground water in the Sergipe state: An approach through remote sensing data
[INPE-4319-TDL/286] 12 p1639 N88-19813
Correlation of data on strain accumulation adjacent to the San Andreas Fault with available models
[NASA-CR-180757] 13 p1796 N88-20742
Drilling investigation of a young magmatic intrusion beneath the Inyo Domes, Long Valley, California: Structural and textural studies
[DE88-006613] 18 p2541 N88-25078

CRUSTS
NT EARTH CRUST
NT LUNAR CRUST
NT PLANETARY CRUSTS
Crustal models of the evolving comet nucleus
14 p2005 N88-21953

CRYOGENIC COOLING
Measurement and analysis of cryogenic sapphire dielectric resonators and DROs
04 p0433 N88-12686
Low-noise cryogenic transmission line
04 p0434 N88-12688
A 2.3-GHz cryogenically cooled HEMT amplifier for DSS 13
04 p0434 N88-12689
Evaluation of a cryogenic refrigerator for cooling focal plane instrumentation --- satellite instruments
[BAE-TP-8095-VOL-1] 05 p0572 N88-13485
Evaluation of a cryogenic refrigerator for cooling focal plane instrumentation. Appendix B: Accommodation study --- satellite instruments
[BAE-TP-8095-VOL-2] 05 p0572 N88-13486
Oxygen chemisorption cryogenic refrigerator
[NASA-CASE-NPO-16734-1-CU]
06 p0689 N88-14223
Advanced fabrication techniques for hydrogen-cooled engine structures
[NASA-CR-3949] 06 p0723 N88-14447
Photoinduced low-temperature changes in optical losses in fiber optics based on chalcogenide glasses
06 p0770 N88-14731
Tests of cold helium compressors at Fermilab
[DE88-002837] 07 p0862 N88-15230
Cryogenic Fluid Management Technology Workshop. Volume 1: Presentation material and discussion
[NASA-CP-10001] 08 p0980 N88-15924
Cryogenics program overview
08 p0981 N88-15926
Ames Research Center cryogenics program
08 p0981 N88-15927
The Goddard Space Flight Center mechanical cooler program 08 p0983 N88-15944
Air Force cryocooler development for spacecraft
08 p0983 N88-15945
An infrared grating spectrometer for GIRL
[ETN-88-91071] 09 p1167 N88-16997
Study of helium transfer technology for STICCR: Fluid management
[NASA-CR-177463] 10 p1291 N88-17720
Low-noise cryogenically cooled broad-band microwave preamplifiers
[DE88-004561] 10 p1324 N88-17912
Cryocooler systems demonstration
[AD-A188025] 11 p1467 N88-18745
Development of an electronically-scanned pressure module for operation at cryogenic temperatures
[NASA-CR-181610] 12 p1629 N88-19746
Cyropreservation of isolated rat hepathocytes for future use in Spacelab experiments: Preliminary results
12 p1680 N88-19950
Workshop on Technology Development Issues for the Large Deployable Reflector (LDR)
[NASA-CP-2407] 12 p1710 N88-20235
Development of a motorized cryovalve for the control of superfluid liquid helium 14 p1925 N88-21477
Review of convectively cooled structures for hypersonic flight
[NASA-TM-87740] 17 p2310 N88-23817
Krypton based adsorption type cryogenic refrigerator
[NASA-CASE-NPO-17334-1-CU]
17 p2331 N88-23917
Cryogenic regenerator including saran-carbon heat conduction matrix
[NASA-CASE-NPO-17291-1-CU]
17 p2337 N88-23946

Analysis of debris from accelerated life test of the Hughes five-year Vuilleumier cryocooler
[AD-A193101] 21 p2931 N88-27400
CryoSQUID: A SQUID-based magnetic field sensor
[AD-A194237] 23 p3239 N88-29275
Static and dynamic behavior of a quasi one-dimensional Heisenberg antiferromagnet in the long-range ordered state. A nuclear magnetic resonance study performed with a He3-He4 dilution refrigerator
[B8705564] 23 p3281 N88-29533
Development of a unit cell for a Ge:Ga detector array
[NASA-CR-177445] 24 p3375 N88-30100

CRYOGENIC EQUIPMENT
Cryogenic cell --- neutron borehole logging
[GB-PATENT-2-139-745-A] 01 p0048 N88-10308
Operating experiences and test results of six cold helium compressors
[DE87-012115] 02 p0157 N88-10982
Materials studies for magnetic fusion energy applications at low temperatures-X
[PB87-232575] 03 p0381 N88-12395
A cold ejector for closed-cycle helium refrigerators 04 p0434 N88-12690
Evaluation of a cryogenic refrigerator for cooling focal plane instrumentation --- satellite instruments
[BAE-TP-8095-VOL-1] 05 p0572 N88-13485
Evaluation of a cryogenic refrigerator for cooling focal plane instrumentation. Appendix B: Accommodation study --- satellite instruments
[BAE-TP-8095-VOL-2] 05 p0572 N88-13486
Capacitive resonant transducer for the Frascati gravitational antenna
[IFSI-86-9] 05 p0578 N88-13528
AF cryogenic and fluid management spacecraft technology program 08 p0981 N88-15925
Cryogenics program overview 08 p0981 N88-15926
Ames Research Center cryogenics program 08 p0981 N88-15927
Orbital transfer vehicle studies overview 08 p0981 N88-15931
Large capacity cryopropellant orbital storage facility 08 p0981 N88-15932
Space Infrared Telescope Facility (SIRTF) design and thermal analysis 08 p0982 N88-15934
The Goddard Space Flight Center mechanical cooler program 08 p0983 N88-15944
Air Force cryocooler development for spacecraft 08 p0983 N88-15945
Development of a multiplexer module for use in a spaceborne cryogenic environment based on GaAs MESFET technology
[RPT/CRY/62463/BOP] 11 p1559 N88-19335
Development of a cryogenic stepping drive for ISO/LWS 14 p1878 N88-21220
Cryogenic mechanism for ISO camera 14 p1878 N88-21221
Materials testing at cryogenic temperatures
[BU-359] 14 p1923 N88-21462
Electromagnetic dampers for cryogenic applications 16 p2218 N88-23231
Extension of the vegetation mission to thermal infrared spectral bands
[CNES-T-86/224-CT/DRT/TIT/IO] 16 p2227 N88-23299
Low temperature storage container for transporting perishables to space station
[NASA-CASE-MFS-28248-1] 18 p2498 N88-24817
Study of a magnetic refrigerator for space applications for temperatures under 20 K
[NASA-TT-20283] 19 p2641 N88-25668
Cyrogenic test facilities for an optical cryomechanism qualification
[REPT-881-440-116] 21 p2901 N88-27219
Analysis of debris from accelerated life test of the Hughes five-year Vuilleumier cryocooler
[AD-A193101] 21 p2931 N88-27400
Surface Tension Confined Liquid Cryogen Cooler (STCLCC)
[NASA-CASE-GSC-13112-1] 23 p3201 N88-29050

CRYOGENIC FLUID STORAGE
Cryogenic Fluid Management Technology Workshop. Volume 1: Presentation material and discussion
[NASA-CP-10001] 08 p0980 N88-15924
AF cryogenic and fluid management spacecraft technology program 08 p0981 N88-15925
Cryogenics program overview 08 p0981 N88-15926
LeRC cryogenic fluid management program overview 08 p0981 N88-15928
Large capacity cryopropellant orbital storage facility 08 p0981 N88-15932
Space environmental considerations for a long-term cryogenic storage vessel 08 p0981 N88-15933
Thermal analysis for the Cryogenic Fluid Management Flight Experiment (CFMFE) 08 p0982 N88-15935
Development of on-orbit fluid gaging techniques 08 p0982 N88-15936
Technology requirements for an orbiting fuel depot: A necessary element of a space infrastructure
[NASA-TM-101370] 24 p3334 N88-29845

CRYOGENIC FLUIDS
NT FERMI LIQUIDS
NT LIQUID HELIUM
NT LIQUID HELIUM 2
NT LIQUID HYDROGEN
NT LIQUID NITROGEN
NT LIQUID OXYGEN
Cryogenic Fluid Management Technology Workshop. Volume 1: Presentation material and discussion
[NASA-CP-10001] 08 p0980 N88-15924
AF cryogenic and fluid management spacecraft technology program 08 p0981 N88-15925
Cryogenics program overview 08 p0981 N88-15926
Ames Research Center cryogenics program 08 p0981 N88-15927
Cryogenic fluid management program flight concept definition 08 p0981 N88-15929
SAMSS: An in-progress review of the Spacecraft Assembly, Maintenance, and Servicing Study 08 p0981 N88-15930
Orbital transfer vehicle studies overview 08 p0981 N88-15931
Space Infrared Telescope Facility (SIRTF) design and thermal analysis 08 p0982 N88-15934
Thermal analysis for the Cryogenic Fluid Management Flight Experiment (CFMFE) 08 p0982 N88-15935
Vapor condensation on a turbulent liquid interface 08 p0982 N88-15939
Computer-aided design analysis of 57-mm, angular-contact, cryogenic turbopump bearings
[NASA-TP-2816] 11 p1496 N88-18933
Cryogenic Fluid Management Technology Workshop. Volume 2: Roundtable Discussion of Technology Requirements
[NASA-CP-10009] 13 p1772 N88-20599
Nucleate pool boiling: High gravity to reduced gravity; liquid metals to cryogens 17 p2431 N88-24464

CRYOGENIC ROCKET PROPELLANTS
Cryogenic Fluid Management Technology Workshop. Volume 1: Presentation material and discussion
[NASA-CP-10001] 08 p0980 N88-15924
The HM-7 engine of Ariane's third stage 09 p1126 N88-16753
STS propellant scavenging systems study. Part 2, volume 1: Executive summary and study results
[NASA-CR-179275] 10 p1290 N88-17716
STS propellant scavenging systems study. Part 2, volume 2: Cost and WBS/dictionary
[NASA-CR-179276] 10 p1290 N88-17717
Noncryogenic propellants for a nuclear orbit transfer vehicle 17 p2428 N88-24444
Breadboard RL10-2B low-thrust operating mode (second iteration) test report
[NASA-CR-182160] 24 p3338 N88-29867

CRYOGENIC TEMPERATURE
Study on the cryogenic toughness of stainless steel weld metals
[PB87-143830] 07 p0834 N88-15057
Long-time tunneling in amorphous metals at helium temperatures
[DE88-701150] 16 p2281 N88-23654
Hot carrier effects in CMOS field effect transistors at cryogenic temperatures 19 p2662 N88-25829
Low noise cryogenic dielectric resonator oscillator
[NASA-CASE-NPO-17157-1-CU] 20 p2797 N88-26596
Cryogenic free jets
[DFVLR-FB-88-16] 21 p2900 N88-27210

CRYOGENIC WIND TUNNELS
Wall interference tests of a CAST 10-2/DOA 2 airfoil in an adaptive-wall test section
[NASA-TM-4015] 02 p0122 N88-10772
Description of tests run in the T2 cryogenic wind tunnel
[PB87-170296] 09 p1113 N88-16672
Pressure distributions from high Reynolds number transonic tests of an NACA 0012 airfoil in the Langley 0.3-meter transonic cryogenic tunnel
[NASA-TM-100526] 11 p1435 N88-18565
High Reynolds number transonic tests on a NACA 0012 airfoil in the Langley 0.3-meter transonic cryogenic tunnel
[NASA-TM-100527] 11 p1436 N88-18571
Preliminary experiments on surface flow visualization in the cryogenic wind tunnel by use of condensing or freezing gases
[NASA-CR-181634] 11 p1442 N88-18602
Aerodynamic performance and pressure distributions for a NASA SC(2)-0714 airfoil tested in the Langley 0.3-meter transonic cryogenic tunnel
[NASA-TM-4044] 18 p2456 N88-24580
Design study. Manipulator systems for model handling in European transonic wind tunnels
[ETN-88-91944] 18 p2468 N88-24651
Method of forming a multiple layer dielectric and a hot film sensor therewith
[NASA-CASE-LAR-13678-1] 18 p2584 N88-25355
Wall interference assessment/correction of data from tests of a CAST 10-2/DOA 2 airfoil in the Langley 0.3-m transonic cryogenic tunnel 20 p2751 N88-26331
Technology for pressure-instrumented thin airfoil models
[NASA-CR-4173] 23 p3180 N88-28933

CRYOGENICS
Thermal Control Working Group report 01 p0016 N88-10094
Characteristics and performance of the ESTEC large space simulator cryogenic system 02 p0135 N88-10849
Tensile behavior of superplastic Al-Cu-Li-Zr alloy 2090 at cryogenic temperatures
[DE87-014084] 02 p0147 N88-10923
Spectroscopic and retrieval studies in support of SCRIBE (Stratospheric Cryogenic Interferometer Balloon Experiment)
[AD-A184037] 03 p0351 N88-12216
Dramatically improved radiation hardness for CMOS silicon gate integrated circuits even down to cryogenic temperatures
[AD-A184672] 03 p0381 N88-12398
Design concepts for the ASTROMAG cryogenic system
[NASA-CR-181505] 04 p0497 N88-13060
Fatigue strength of alloy A286 at cryogenic temperature 05 p0603 N88-13695
Near-threshold fatigue crack growth behavior at cryogenic temperature 06 p0718 N88-14409
Cryogenic Fluid Management Technology Workshop. Volume 1: Presentation material and discussion
[NASA-CP-10001] 08 p0980 N88-15924
AF cryogenic and fluid management spacecraft technology program 08 p0981 N88-15925
Cryogenics program overview 08 p0981 N88-15926
Ames Research Center cryogenics program 08 p0981 N88-15927
LeRC cryogenic fluid management program overview 08 p0981 N88-15928
Cryogenic fluid management program flight concept definition 08 p0981 N88-15929
Large capacity cryopropellant orbital storage facility 08 p0981 N88-15932
Thermal analysis for the Cryogenic Fluid Management Flight Experiment (CFMFE) 08 p0982 N88-15935
Cryogenic acoustic microscopy
[AD-A187274] 10 p1299 N88-17767
Study on the dynamics of executive electromechanism with thyristor commutator for cryogenic systems
[DE87-703209] 12 p1622 N88-19702
A method of calculating nonstationary heat flow in hydrogasodynamic processes in closed cryogenic systems
[DE88-700884] 12 p1626 N88-19727
Development of a constitutive equation for HSLA (High-Strength Low-Alloy)-100 at cryogenic temperatures
[AD-A189243] 13 p1740 N88-20408
Advanced components for spaceborne infrared astronomy
[NASA-CR-177470] 13 p1772 N88-20601
Materials testing at cryogenic temperatures
[BU-359] 14 p1923 N88-21462
Thin superconducting film characterization by surface acoustic waves
[AD-A190417] 15 p2143 N88-22791
Gigawatt, closed cycle, vapor core-MHD space power system conceptual design study 17 p2433 N88-24473
Thermodynamic modeling of the no-vent fill methodology for transferring cryogens in low gravity
[NASA-TM-100932] 18 p2476 N88-24686
Electrodynamic driver for the space thermoacoustic refrigerator (STAR)
[AD-A192337] 20 p2785 N88-26517
Development of external cooling cryo-resistive cable systems. Part 2: Insulation characteristics on 66 kV rated cryo-resistive testing cable
[DE88-770191] 20 p2793 N88-26571
A 2.3-GHz low-noise cryo-FET amplifier 22 p3066 N88-28195
LLE (Laboratory for Laser Energetics) review
[DE88-008065] 23 p3219 N88-29158

CRYOPUMPING
The Jeffcott equations in nonlinear rotordynamics
07 p0928 N88-15636
CRYOSORPTION
U SORPTION
CRYOSTATS
Components for cryostat --- spaceborne
[MBB/ISO-TN-CD00.003-REV-A]
01 p0032 N88-10207
Development activities for a 21-T superconducting magnet and cryostat
[DE88-004370] 11 p1558 N88-19327
Development of a motorized cryovalve for the control of superfluid liquid helium 14 p1925 N88-21477
CRYPTOGRAPHY
Components and cycles of a random function
[DE87-014155] 02 p0228 N88-11437
Minimum disclosure proofs of knowledge
[CWI-PM-R8710] 20 p2840 N88-26854
CRYSTAL DEFECTS
NT CRYSTAL DISLOCATIONS
NT EDGE DISLOCATIONS
NT POINT DEFECTS
NT SCREW DISLOCATIONS
NT VACANCIES (CRYSTAL DEFECTS)
Theory of defects in non-metallic solids
[DE87-014068] 02 p0152 N88-10949
Hydrogen annealing of P(sub) b and E prime defect centers in oxidized silicon wafers
[DE87-014293] 02 p0152 N88-10951
Defect characterization in quartz and related materials
[AD-A184754] 03 p0294 N88-11846
Impedance of passive lithium anodes in SOCl2 solutions under low-field polarization
[DE88-000922] 04 p0439 N88-12728
Structural characterization of ion implanted beta-SiC thin films
[DE87-014567] 05 p0656 N88-14027
Effect of optical inhomogeneities on space coherence of radiation emitted by laser with unstable resonator
06 p0771 N88-14738
The role of hydrogen in radiation-induced defect formation in polysilicon gate MOS devices
[DE87-012374] 06 p0785 N88-14814
X-ray measurements of phason distortion in ion-implanted Al-Mn
[DE87-014566] 07 p0937 N88-15694
Formation and passivation of new paramagnetic defects associated with thermal oxides on silicon
[DE88-002720] 07 p0938 N88-15699
Density of states of electrons bound to impurities in quantum wells of GaAlAs/GaAs
[INPE-4257-PRE/1130] 08 p1089 N88-16557
High-temperature charge-density studies of CeO/sub 2-x/ using X-ray and neutron diffraction techniques
[DE88-002998] 09 p1257 N88-17536
Control of solid-excitation-based photochemical dry etching of semiconductors by ion-bombardment-induced damage
[DE88-003214] 09 p1257 N88-17537
Models for ionic transport in glass
[DE88-002860] 10 p1304 N88-17799
Positron-annihilation 2D-ACAR studies of disordered and defected alloys
[DE88-003118] 10 p1416 N88-18454
Solving complex and disordered surface structures with electron diffraction
[DE88-003863] 10 p1418 N88-18457
Grazing incidence X-ray scattering study of defect structures in MBE GaAs/Si using synchrotron radiation
[DE88-004556] 10 p1420 N88-18483
Determination of the equilibrium concentration of characteristic defects by the measurement of thermal expansion using neutron scattering and laser interferometry
[ETN-88-91489] 11 p1490 N88-18890
Atomistic studies of the structure and properties of grain boundaries with substitutional impurities
[DE88-004161] 11 p1545 N88-19237
Structural characterization of undoped and doped GaAs: A comparative study of four techniques
[DE88-004552] 11 p1555 N88-19304
Spatial distribution of carbon and native defects in large-diameter bulk grown GaAs
[DE88-003870] 11 p1562 N88-19348
Hydrodynamic simulation of forced convection in the Czochralski process
[INPE-4471-TDL/323] 12 p1697 N88-20158
Experimental and theoretical methods for investigating helium effects in rapidly solidified metals
[DE88-005542] 13 p1743 N88-20425
A calorimetric determination of the enthalpy of formation and a description of the defect structure of the ordered beta-phase /Ni, Cu/ /1-x/ Al/x/
[NASA-TT-20157] 13 p1745 N88-20434
Fingering flow patterns of thermosolutal convection in rectangular enclosures
[NASA-TM-100854] 14 p1911 N88-21417
Materials dependence of deformation texture development in various deformation modes
[DE88-004312] 14 p1922 N88-21457
Experimental studies of elastic properties of crystals by Brillouin scattering
[DE88-005923] 14 p1986 N88-21848
Absolute pressure derivatives of deep level defects in 3-5 semiconductors
[DE88-006318] 15 p2140 N88-22772
The structure of the boron-hydrogen complex in silicon
[DE88-005433] 15 p2144 N88-22795
Annihilation momentum density of positrons trapped at vacancy-type defects in metals and alloys
[DE88-005936] 15 p2144 N88-22797
Development program for 1.93-micron lasers
[NASA-CR-4148] 16 p2212 N88-23198
Improved silicon carbide for advanced heat engines
17 p2324 N88-23879
Strength optimization of alpha-SiC by improved processing 17 p2324 N88-23880
Improved processing of Si3N4
17 p2325 N88-23882
Defects in cubic silicon carbide on silicon
17 p2408 N88-24317
On the use of convergent beam electron diffraction for identification of antiphase boundaries in GaAs grown on Si
[DE88-008220] 18 p2585 N88-25362
Defects in high-mobility semiconductor systems
[AD-A191618] 19 p2732 N88-26224
Aharonov-Bohm effects in disordered metals
20 p2864 N88-27008
EXAFS studies of the microstructure of semiconductor alloys, defects and semiconductor-metal interfaces
20 p2868 N88-27031
Aperiodic superlattices: Structured randomness
20 p2873 N88-27055
Fermi level dependent native defect formation: Consequences for metal-semiconductor and semiconductor-semiconductor interfaces
[DE88-008247] 20 p2875 N88-27066
Electron irradiation effects in YBa2Cu3O7-Delta single crystals
[DE88-010050] 20 p2878 N88-27085
Defect characterization of the redox behavior and stability of conducting oxides
[DE88-010799] 20 p2878 N88-27088
Migration and stability of HgCdTe lattice defects
[AD-A193293] 21 p3021 N88-27935
Probing the electronic and defect structure of perovskite superconductors
[DE88-006349] 21 p3022 N88-27939
Deep level defects in semiconductors: Stress and pressure studies
[DE88-010855] 21 p3024 N88-27948
Local environment approach for deep-level defects in semiconductors: Application to the vacancy in silicon
[DE88-702017] 23 p3287 N88-29573
An HVEM study of displacement cascade damage in Nb3Sn at 13 K
[DE88-009997] 23 p3289 N88-29584
Rapid thermal annealing of silicon layers amorphized by ion implantation
[DE88-702307] 23 p3290 N88-29591
Chemical kinetics of hydrogen and P(sub b) centers
[DE88-010528] 23 p3291 N88-29594
Localized excitations in one-dimensional molecular crystal with structural defect
[DE88-702691] 23 p3293 N88-29607
Streaking images that appear only in the plane of diffraction in undoped GaAs single crystals: Diffraction imaging (topography) by monochromatic synchrotron radiation
[NASA-CR-183267] 24 p3433 N88-30437
CRYSTAL DISLOCATIONS
NT EDGE DISLOCATIONS
NT SCREW DISLOCATIONS
Study of the microscopic mechanisms of cyclic deformation. Development of a new approach: The case of aluminum
[ISAL-87-0003] 02 p0149 N88-10936
Need for composites, new materials discussed
02 p0160 N88-11001
Raman scattering spectrum along a bevel etched GaAs on Si, TEM (Transmission Electron Microscope) study and GaAs P-I-N photodetector on Si
[DE88-000210] 04 p0498 N88-13066
Orientation effects in copper single crystals fatigued at elevated temperatures 06 p0720 N88-14423
Computer simulation of impurities and interfaces in body centered cubic metals
[PB88-108162] 07 p0832 N88-15047
Evolution of radiation-induced voids and dislocations at low temperature
[DE88-700350] 07 p0939 N88-15704
Some present limitations on the lattice imaging of grain boundaries
[DE87-014665] 09 p1256 N88-17530
Silicon and indium doping of GaAs: Measurements of the effect of doping on mechanical behavior and relation with dislocation formation
[DE88-003862] 11 p1554 N88-19303
Image force expression for the dislocation near a crack
[DE88-701894] 20 p2814 N88-26692
On the possibility of the soliton description of acoustic emission during plastic deformation of crystals
[DE88-701878] 20 p2876 N88-27075
Diffusion and solubility of some interstitial impurities in deformed metals
[DE88-701859] 21 p2914 N88-27296
The influence of solute segregation on the dislocation structure of small and large angle (001) twist boundaries in Fe-Sb alloys
[DE88-009166] 22 p3155 N88-28770
CRYSTAL GROWTH
NT CZOCHRALSKI METHOD
NT DIRECTIONAL SOLIDIFICATION (CRYSTALS)
NT EPITAXY
NT LIQUID PHASE EPITAXY
NT MOLECULAR BEAM EPITAXY
NT VAPOR PHASE EPITAXY
Prephase A study of a crystallization laboratory for Columbus, executive summary
[ESA-ITT/AO/1-1866/85F] 01 p0032 N88-10206
Direct formation of thin films and epitaxial overlayers at low temperatures using a low-energy (10-500 eV) ion beam deposition system
[DE87-012291] 01 p0103 N88-10675
Grain boundary phase equilibria in metallic systems
[DE87-014123] 01 p0104 N88-10679
Experimental and theoretical study of condensation in multicomponent vapors
[DE87-013663] 02 p0145 N88-10907
On the role of convective motion during dendrite growth: Experiments under variable gravity, revised
[NASA-CR-179213] 02 p0156 N88-10979
A finite element model for induction heating of a metal crucible
[DE87-014246] 02 p0246 N88-11551
The structure and reactivity of heterogeneous surfaces and study of the geometry of surface complexes
[DE88-000158] 03 p0279 N88-11754
International Conference on Microstructology held in Gainesville, Florida on 7-9 May 1986
[AD-A184604] 03 p0290 N88-11822
Consortium for Materials Development in Space. Technical section
[NASA-CR-181508] 03 p0296 N88-11859
Physical vapor transport crystal growth
03 p0296 N88-11860
Mass spectroscopic facility 03 p0296 N88-11861
Highly Non-Linear Optical (NLO) organic crystals
03 p0297 N88-11865
Highly Non-Linear Optical (NLO) organic crystals and films. Electrooptical organic materials
03 p0297 N88-11866
Numerical analysis of Marangoni convection in Bridgman method 03 p0319 N88-12014
Deformation mechanisms of thermostructural materials
[AD-A184070] 03 p0338 N88-12128
Simulation of the layer-growth dynamics in silver films: Dynamics of adatom clusters and vacancy clusters on Ag(100)
[DE87-014764] 03 p0380 N88-12390
Phase equilibrium and crystal growth studies on AgGaSe2 and related nonlinear optical materials
[AD-A184768] 03 p0382 N88-12400
Investigation of hexagonal ferrite film growth techniques for millimeter-wave systems applications
[AD-A184335] 03 p0383 N88-12406
Evaluation of the Mellen EDG furnace for growth of large diameter GaAs single crystals in a horizontal configuration
[DE88-000463] 04 p0498 N88-13068
United States - Japan Workshop on Dielectric and Piezoelectric Ceramics (3rd) held in Toyama, Japan on November 9-12, 1986
[AD-A185113] 05 p0568 N88-13460
MBE growth of InAsSb strained-layer superlattices
[DE88-000365] 05 p0654 N88-14011
Molecular beam epitaxial growth and characterization of 3-5 compound semiconductor single and multiple interface structures
[AD-A185400] 05 p0656 N88-14021
Novel heterojunction devices
[DE87-013716] 05 p0656 N88-14026

Growth of solid solution single crystals
[NASA-TP-2787] 06 p0688 N88-14212
Heteroepitaxial growth of 3-5 semiconductor compounds by metal-organic chemical vapor deposition for device applications
[NASA-CR-182346] 06 p0788 N88-14832
Method for investigating the formation of crystals in a transparent material
[NASA-CASE-MFS-26008-1-CU] 06 p0788 N88-14835
Some investigations of molecular beam epitaxial growth of 3-5 semiconductor films via Monte-Carlo computer simulations, carrier tunnelling and spectroscopic ellipsometry
[AD-A185520] 06 p0789 N88-14839
Cellular solidification in a monotectic system
[NASA-TM-100317] 07 p0829 N88-15027
Allowable gravity-levels for Spacelab, Columbus and EURECA --- materials science
[BF-R-66.525-2] 07 p0838 N88-15084
Resolution of holograms produced by the fluid experiment system and the holography ground system 07 p0923 N88-15609
A numerical study of transient heat and mass transfer in crystal growth 07 p0925 N88-15619
High-temperature electronics 08 p0956 N88-15797
A laboratory study of tin whisker growth
[ESA-STR-223] 08 p1089 N88-16553
Visible InGaAsP/GaAsP lasers produced by epitaxial growth from liquid phase 09 p1237 N88-17416
Superlattice photodetectors
[AD-A186956] 09 p1253 N88-17511
Molecular beam epitaxy for research on quantum well structures
[AD-A186791] 09 p1255 N88-17522
Electrochemical growth of linear conducting crystals in microgravity 10 p1287 N88-17698
Protein-crystal growth experiment (planned) 10 p1287 N88-17700
A payload for investigating the influence of convection on GaAs crystal growth 10 p1288 N88-17702
An advanced microcomputer design for processing of semiconductor materials 10 p1288 N88-17703
Application of Hoffman modulation contrast microscopy coupled with three-wavelength two-beam interferometry to the in situ direct observation of the growth process of a crystal in microgravity 10 p1288 N88-17704
Project Explorer takes its second step: GAS-608 in engineering development 10 p1288 N88-17707
Formation of optical waveguides by ion implantation
[DE88-003894] 10 p1409 N88-18407
High temperature processing of superconducting Y1Ba2Cu3O6.9
[DE88-003002] 10 p1416 N88-18449
Growth and electronic properties of strained metal overlayers
[DE87-010956] 10 p1417 N88-18463
Stability diagrams for epitaxial strained layers
[DE88-003935] 10 p1418 N88-18470
Nucleation and growth of calcium carbonate crystals on surface-modified polyethylene and polystyrene
[DE88-005126] 11 p1465 N88-18733
Development of a planar heterojunction bipolar transistor for very high speed logic
[AD-A188137] 11 p1478 N88-18820
Growth and characteristics of materials for tunable lasers in the near infrared spectral region
[NASA-CR-182501] 11 p1491 N88-18901
Proceedings of the 1987 High-Efficiency Photovoltaic Subcontractors' Review Meeting
[DE88-003354] 11 p1508 N88-19011
Optical waveguide formation by ion implantation of Ti or Ag
[DE88-004595] 11 p1551 N88-19278
MCT crystal growth
[NASA-CR-179297] 11 p1557 N88-19318
Growth of Cr,Nd:Gd3Sc2Al3O12 (Cr,Nd:GSAG) crystals by the Heat Exchanger Method (HEM)(trademark)
[DE88-004041] 11 p1558 N88-19326
Feasibility studies of the growth of 3-5 compounds of boron by MOCVD
[NASA-CR-181622] 11 p1561 N88-19343
Analysis of low gravity tolerance of model experiments for space station: Preliminary results for directional solidification
[NASA-CR-182657] 12 p1614 N88-19648
High Rayleigh number convection in rectangular enclosures with differentially heated vertical walls and aspect ratios between zero and unity
[NASA-TM-100277] 12 p1628 N88-19739
Mass transport and chemical demixing of Y-Ba-Cu-O compounds during sintering in temperature gradients
[DE88-004887] 12 p1696 N88-20151
Stability and uniqueness in nonlinear continuum mechanics
[AD-A189616] 12 p1699 N88-20172
Research on mercury cadmium telluride
[AD-A189155] 13 p1845 N88-21039
Initial stages of silicon growth on the (100) surface of silicon by localized laser CVD
[DE88-005420] 13 p1848 N88-21059
Proceedings of the Seminar on Hydrodynamics and Crystal Growth
[ETN-88-92025] 14 p1987 N88-21853
Numerical simulations of buoyancy driven flows in cylinders and cavities for vapor crystal growth 14 p1987 N88-21854
Velocity and concentration fields over a crystal growing in a water solution. Experimental study and numerical simulation 14 p1987 N88-21856
Transport processes during directional solidification and crystal growth: Scaling and experimental study 14 p1988 N88-21857
Selective growth velocity in needle crystals 14 p1988 N88-21858
Convection effects on stability at the solidification front 14 p1988 N88-21860
Grain growth behavior of extrusion consolidated centrifugally atomized Type 304 stainless steel powder
[DE88-006788] 15 p2038 N88-22142
Fundamental studies on high temperature deformation recrystallization, and grain growth of two-phase materials
[AD-A189725] 15 p2038 N88-22145
JPRS report: Science and technology. Japan
[JPRS-JST-88-002] 15 p2050 N88-22210
Single crystal growth by laser CVD 15 p2050 N88-22213
Pb(1-x)Sn(x)Te crystal growth in space 15 p2051 N88-22223
Atomic beam study of crystalline order and precipitation in nickel based alloys
[ETN-88-91994] 16 p2177 N88-22975
JPRS report: Science and technology. USSR: Materials science
[JPRS-UMS-88-006] 16 p2179 N88-22988
New method of grafting crystals 16 p2180 N88-22992
Tunable optical sources/growth and characterization of nonlinear optical materials
[AD-A190874] 16 p2274 N88-23608
Non-contact temperature measurement requirements for electronic materials processing 17 p2328 N88-23898
Method and apparatus for growing crystals
[NASA-CASE-MFS-28137-1] 17 p2446 N88-24544
Liquid encapsulated float zone process and apparatus
[NASA-CASE-MFS-28144-1] 17 p2446 N88-24545
Optical monitoring of protein crystal growth
[NASA-CR-182869] 18 p2484 N88-24738
Preparation for microgravity: The role of the microgravity materials science laboratory
[NASA-TM-100906] 18 p2497 N88-24811
Joint services electronics program research in electronics
[AD-A192206] 18 p2504 N88-24857
Dendritic growth in the presence of convection 18 p2580 N88-25328
Two puzzling aspects of protein crystal growth 18 p2580 N88-25329
The morphological stability of continuous intergranular phases: Thermodynamic considerations
[DE88-006328] 18 p2584 N88-25350
Electronic controller for reciprocating rotary crystallizer
[NASA-TM-101140] 18 p2584 N88-25354
Hanging drop crystal growth apparatus and method
[NASA-CASE-MFS-28206-1-SB] 18 p2585 N88-25356
Crystal growth apparatus
[NASA-CASE-MFS-28182-1] 18 p2585 N88-25357
Epitaxial iron films
[AD-A191815] 19 p2732 N88-26225
The structure and properties of grain boundaries in B2 ordered alloys
[DE88-009890] 20 p2773 N88-26447
Preparation of oxide superconductors
[DE88-009136] 20 p2875 N88-27063
Analysis of grain refinement and superplasticity in aluminum-magnesium alloys
[AD-A193029] 21 p2912 N88-27283
Processing and additive effects of ZrO2 on microstructure and dielectric porperties of BaTiO3 ceramics
[AD-A193126] 21 p2917 N88-27316
Growth and characterization of CuGaS2, CuAlS2 and CuGa0.9Al0.1S2 single crystals
[AD-A192963] 21 p3021 N88-27930
Phase equilibrium and crystal growth studies on AgGaSe2 and related nonlinear optical materials
[AD-A193763] 22 p3157 N88-28783
High temperature electric arc furnace
[NASA-CASE-MFS-28281-1] 23 p3181 N88-28938
New method for preparation of (Cd, Hg)Te thin films
[DE88-702727] 23 p3293 N88-29608
Growth and characterization of materials for tunable lasers in the near infrared spectral region
[NASA-CR-183132] 24 p3377 N88-30113
Growth of GaAs crystals by the Heat Exchanger Method for microwave device applications
[AD-A196028] 24 p3433 N88-30435

CRYSTAL LATTICES
NT BODY CENTERED CUBIC LATTICES
NT CUBIC LATTICES
NT FACE CENTERED CUBIC LATTICES
NT SUPERLATTICES
LLE review
[DE87-014468] 02 p0178 N88-11110
Surface chemistry of transition metal carbides: A theoretical analysis
[AD-A184237] 03 p0291 N88-11829
Modeling of irradiation-induced amorphization in a titanate ceramic
[DE87-014751] 03 p0292 N88-11833
New theory for competing interactions and microstructures in partially-ordered (liquid-crystalline) phases
[DE87-014739] 03 p0380 N88-12389
A study of mechanisms of hydrogen diffusion in separation devices
[DE88-000328] 04 p0416 N88-12584
Radiation induced collapse of the crystalline structure
[DE87-014407] 04 p0498 N88-13064
Raman scattering spectrum along a bevel etched GaAs on Si, TEM (Transmission Electron Microscope) study and GaAs P-I-N photodetector on Si
[DE88-000210] 04 p0498 N88-13066
MBE growth of InAsSb strained-layer superlattices
[DE88-000365] 05 p0654 N88-14011
The pseudopotential density functional method applied to semiconducting crystals
[ETN-88-91362] 05 p0656 N88-14024
Novel heterojunction devices
[DE87-013716] 05 p0656 N88-14026
Basic energy sciences research in the Metals and Ceramics Division of Oak Ridge National Laboratory
[DE87-013538] 06 p0681 N88-14171
Structural investigations of some metallic glasses
[ECN-198] 06 p0686 N88-14203
X-ray structure analyses and molecular mechanics analyses of dense energetic materials
[AD-A185462] 06 p0779 N88-14781
Silicon microscale mechanisms from (110) oriented wafers
[DE88-002096] 06 p0787 N88-14825
Structural relaxation in strained-layer heterostructures
[DE88-002326] 07 p0868 N88-15264
Phonon dispersion for several surfaces with ordered overlayers: A lattice dynamical study 07 p0876 N88-15315
Embedded cluster models for electronic structure and energetics of complex oxides
[DE88-003097] 07 p0938 N88-15702
Structural properties of high-T/sub c/ oxide super conductors
[DE88-002974] 08 p1090 N88-16563
Thermodynamic and conductivity studies of nonstoichiometric cerium dioxide by Coulometric titration: A simultaneous measurement
[DE88-003054] 08 p1091 N88-16566
Heavy Fermions and coherence in Kondo lattices: Specific heat of low energy excitation in Cer systems
[ETN-88-91080] 09 p1255 N88-17525
High-temperature charge-density studies of CeO/sub 2-x/ using X-ray and neutron diffraction techniques
[DE88-002988] 09 p1257 N88-17536
Molecular dynamics study of high-temperature grain-boundary stability in a (100) sigma = 29 bicrystal model
[DE88-002955] 09 p1258 N88-17546
Crystalline sulfur dioxide: Crystal field splittings, absolute band intensities and complex refractive indices derived from infrared spectra
[NASA-CR-182502] 09 p1258 N88-17547
Fabrication, phase transformation studies and characterization of SiC-AlN-Al2OC ceramics
[DE88-004053] 10 p1306 N88-17807
Study of quantum mechanical effects in deep submicron, grating-gate field effect transistors
[AD-A188283] 10 p1325 N88-17923
Optical characterization of GaAs/sub 1-x/Sb/sub x/ and GaAs/sub 1-x/Sb/sub x/GaAs strained layer superlattices
[DE88-003393] 10 p1418 N88-18464
Simple renormalization group method for calculating thermal equations of states
[DE88-700143] 11 p1454 N88-18668

National Center for Small-Angle Scattering Research: Reports on measurements carried out by users of the facilities of the NCSASR, December 1, 1985-September 30, 1987
[DE88-003754] 11 p1462 N88-18719
Algorithmic alternatives
[DE88-003905] 11 p1531 N88-19149
Atomistic simulation of low-energy beam deposition
[DE88-004344] 11 p1544 N88-19228
Single-crystal structural study of La2Cu/sub 0.95/Li/sub 0.05/O4
[DE88-003482] 11 p1554 N88-19302
Scanning tunneling microscopy of silver, gold, and aluminium monomers and small clusters on graphite
[DE88-003871] 11 p1562 N88-19349
Temperature dependence of Kr precipitation in Ni
[DE88-005953] 13 p1744 N88-20429
Lattice relaxation of the DX centers in Ga/sub 1-x/Al/sub x/As and of the pressure-induced deep donors in GaAs
[DE88-005452] 13 p1848 N88-21061
Effect of Mg impurity on local vibrations of U-centers in LiF lattice 14 p1969 N88-21753
Breathing mode lattice relaxation associated with carrier emission and capture by deep electronic levels in silicon
[DE88-003844] 14 p1985 N88-21842
Grain boundaries
[DE88-006628] 14 p1987 N88-21852
High energy cosmic muons and the calibration of the L3 electromagnetic calorimeter
[NOTA-INTERNA-895] 14 p2011 N88-21999
Absolute pressure derivatives of deep level defects in 3-5 semiconductors
[DE88-006318] 15 p2140 N88-22772
First-principles calculations of quasiparticle energies at surfaces and interfaces: Semiconductor surface-state spectra and band offsets
[DE88-006340] 15 p2141 N88-22773
Fundamental properties and devices applications of Ge(x)Si(1-x)/Si superlattices
[AD-A190129] 15 p2143 N88-22787
The structure of the boron-hydrogen complex in silicon
[DE88-005433] 15 p2144 N88-22795
MBE of HgCdTe
[AD-A191423] 16 p2283 N88-23671
Structural studies on La/sub 2/CuO/sub 4+delta/
[DE88-006826] 16 p2581 N88-25330
Abnormal diffusion of vacancies in metals
[DE88-701880] 20 p2773 N88-26441
Lattice strain in heteroepitaxial films
20 p2868 N88-27032
Lattice theory of fracture of solids with layered structure
[DE88-701867] 20 p2876 N88-27073
Derivation of space groups in mm2, 222 and mmm crystal classes
[DE88-701881] 20 p2876 N88-27076
Contribution to the study of order effects in the Ising model framework: Ground states and phase diagrams
[ONERA-NT-1987] 20 p2880 N88-27095
Picosecond transient reflectivity of unpinned gallium arsenide (100) surfaces
[AD-A193242] 21 p3021 N88-27933
Topics in quasicrystallography
21 p3023 N88-27947
Deep level defects in semiconductors: Stress and pressure studies
[DE88-010855] 21 p3024 N88-27948
Theory of surface melting and non-melting
[DE88-702652] 22 p3157 N88-28785
Soliton and polaron dynamics in conducting polymers
[DE88-702539] 23 p3198 N88-29035

CRYSTAL OPTICS
Gamma-ray optics of multi-beam Borrmann modes with possible applications to nuclear lasing
04 p0449 N88-12784
Use of lasers with F sub A(II)-color center KCl:Li crystals in the intraresonator laser spectroscopy method
06 p0769 N88-14729
Observation of instabilities in time during dynamic self-diffraction of light in anisotropic nonhomogeneous medium 06 p0769 N88-14730
High-efficiency GaAs semiconductor laser with longitudinal excitation by scanning electron beam
09 p1238 N88-17421
Note on the double crystal method of measuring heat transfer coefficient
[OUEL-1710/87] 17 p2338 N88-23950
Liquid crystal optics for laser systems
[DE88-008475] 20 p2854 N88-26948

CRYSTAL OSCILLATORS
NT PIEZOELECTRIC CRYSTALS
Surface wave accelerometer
[ETN-88-92000] 16 p2210 N88-23192
Quartz crystal resonators and oscillators for frequency control and timing applications
[AD-A193310] 21 p2937 N88-27443
Specifications and performance of ultrastable oscillators in the DORIS orbitography and positioning system
[ETN-88-92761] 24 p3331 N88-29831

CRYSTAL RECTIFIERS
Pierce diode with external circuit. Part 3: Chaotic behavior
[AD-A194837] 24 p3365 N88-30041

CRYSTAL STRUCTURE
Electronic structure of crystalline NaSn
[DE87-702583] 01 p0102 N88-10669
Structure of rapidly solidified Ni-Ti
[DE87-012252] 02 p0147 N88-10921
Field ion microscope studies of surface reconstructions
[DE87-014644] 02 p0147 N88-10924
Theory of defects in non-metallic solids
[DE87-014068] 02 p0152 N88-10949
Need for composites, new materials discussed
02 p0160 N88-11001
Production of metallic monocrystals described
03 p0286 N88-11796
Modelling and theories of alloy phase behavior
[DE87-014399] 03 p0287 N88-11804
International Conference on Microstructology held in Gainesville, Florida on 7-9 May 1986
[AD-A184604] 03 p0290 N88-11822
Surface chemistry of transition metal carbides: A theoretical analysis
[AD-A184237] 03 p0291 N88-11829
Indentation damage in ceramics
[AD-A184686] 03 p0294 N88-11844
Monte Carlo simulation of modulated phases
[NASA-TM-89654] 03 p0369 N88-12323
Shock-induced chemical synthesis of phases similar to the high temperature superconductor oxides
[DE87-013725] 03 p0380 N88-12387
Equilibria, lattices and chaotic dynamics of point vortices 04 p0444 N88-12758
Properties of refractory metals processed by enhanced sintering treatments
[AD-A184944] 05 p0565 N88-13440
Study of boundary structures
[AD-A184808] 05 p0655 N88-14013
Diffraction by glasses with a layer structure
[DE88-003059] 07 p0837 N88-15078
Change of europium crystallographic symmetry at helicoidal magnetic ordering
[DE88-700559] 07 p0939 N88-15707
Wave functions for bound states of relativistic electrons in a crystal at electron movement along crystallographic planes
[DE88-700563] 07 p0939 N88-15708
Interface characteristics and the mechanical properties of metal matrix composites
[AD-A186441] 08 p0966 N88-15845
JPRS report: Science and technology. USSR: Physics and mathematics
[JPRS-UPM-87-010] 08 p1075 N88-16485
Metal-oxide superconductor BaPbsub1-xBisubxO3: Unusual properties and new applications
08 p1077 N88-16494
New branch of solid-state physics
08 p1079 N88-16508
Experimental aspects of high-T/sub c/ superconductors
[DE88-003019] 08 p1090 N88-16564
Neutron- and X-ray-small angle scattering with Fe-base metallic glasses
[DE88-002538] 09 p1147 N88-16876
Physical properties of summer sea ice in the Fram Strait, June-July 1984
[AD-A186937] 09 p1194 N88-17156
Superconductivity and crystal structure of high-pressure phases in V-Ru-H system 09 p1239 N88-17426
Some present limitations on the lattice imaging of grain boundaries
[DE87-014665] 09 p1256 N88-17530
Corner compensation structures for (110) oriented silicon
[DE88-003300] 10 p1417 N88-18455
Growth and electronic properties of strained metal overlayers
[DE87-010956] 10 p1417 N88-18463
Solving complex and disordered surface structures with electron diffraction
[DE88-003863] 10 p1418 N88-18467
Order-disorder transition of Au and Pt (110) surfaces: The significance of relaxations and vibrations
[DE88-004651] 10 p1419 N88-18473
Perturbed angular correlations in zirconia ceramics
[DE88-004117] 11 p1464 N88-18731
The first gallium-arsenic compound containing a single Ga3As unit: Isolation and crystal structure of ((thf)Br2Ga)3As (thf = tetrahydrofuran)
[AD-A187457] 11 p1555 N88-19309
A procedure for estimating the crystal densities of organic explosives
[AD-A189023] 12 p1613 N88-19646
Fast protonic conducting solid electrolytes
[AD-A188524] 12 p1698 N88-20160
CdZnTe as a wide-band-gap absorber for a tandem, thin-film solar cell
[DE88-001114] 13 p1793 N88-20724
Modeling growth of interdendritic silicon ribbons
14 p1897 N88-21322
Ordered structures in YBa2Cu3O/sub 7-y/, La2Cu3O/sub 7-y/, La/sub 2-x/Sr/sub x/CuO/sub 4-par. delta/ and related perovskites
[DE88-006461] 14 p1987 N88-21851
Grain boundaries
[DE88-006628] 14 p1987 N88-21852
Investigation and synthesis of high temperature and increased stiffness RSP aluminum alloys
[AD-A190407] 15 p2039 N88-22151
Superconductivity and the tailoring of lattice parameters of the compound YBa2Cu3O(sub x)
[DE88-005904] 15 p2140 N88-22769
Atomic beam study of crystalline order and precipitation in nickel based alloys
[ETN-88-91994] 16 p2177 N88-22975
New method of grafting crystals
16 p2180 N88-22992
High-strength ceramic based on tetragonal ZrO2 with Al2O3 admixture 16 p2180 N88-22996
Initial stages of molecular beam heteroepitaxial growth in GaAs-(Ca,Sr)F2 and GaAs/Si systems
[LAAS-87-355] 16 p2281 N88-23658
Disclination structures in carbon and graphite
[AD-A191056] 17 p2322 N88-23868
The structural analysis of some crystalline and semi-crystalline substances using X-ray and neutron diffraction 17 p2445 N88-24540
Fundamental studies of beta phase decomposition modes in titanium alloys
[AD-A191495] 18 p2485 N88-24740
Superplasticity: A fundamental investigation on deformation mechanism and cavitation phenomena
[AD-A191548] 18 p2485 N88-24741
Liquid carbon
[AD-A191707] 18 p2491 N88-24776
Raman characterization of AsF5-intercalated vapor grown graphite fibers
[AD-A191709] 18 p2491 N88-24778
Structural studies on La/sub 2/CuO/sub 4+delta/
[DE88-006828] 18 p2581 N88-25330
Magnetic superlattices
[AD-A191450] 18 p2581 N88-25334
Phase stability and alloy design of ordered intermetallics
[DE88-007479] 20 p2772 N88-26435
Strained layer and lattice matched transverse junction stripe quantum well lasers for continuous room temperature operation 20 p2863 N88-27004
Metallic superlattices 20 p2864 N88-27012
Growth of high quality CoSi2/Si superstructures on Si(111) 20 p2869 N88-27034
Characterization of structural and magnetic order of Er/Y superlattices 20 p2873 N88-27056
Raman and absorption spectrophotometric studies of selected lanthanide, californium-doped lanthanide, and actinide trihalides in the solid state
[DE88-008234] 20 p2874 N88-27061
Lattice theory of fracture of solids with layered structure
[DE88-701867] 20 p2876 N88-27073
Derivation of space groups in mm2, 222 and mmm crystal classes
[DE88-701881] 20 p2876 N88-27076
Electronic and geometric structure of silver and palladium on aluminum (111) in monoatomic surface layers
[ETN-88-92120] 20 p2879 N88-27093
Epitaxy and properties of two dimensional GaInAs semiconductor structures
[ETN-88-92357] 20 p2879 N88-27094
Contribution to the study of order effects in the Ising model framework: Ground states and phase diagrams
[ONERA-NT-1987] 20 p2880 N88-27095
Thermomechanical processing of Al alloy 2090 for grain refinement and superplasticity
[AD-A192333] 21 p2912 N88-27281
Analysis of grain refinement and superplasticity in aluminum-magnesium alloys
[AD-A193029] 21 p2912 N88-27283
Polarization selective Raman microspectroscopy
21 p2930 N88-27397

Meaning of energy diagrams used to describe hetero-structures
[DE88-702219] 21 p3023 N88-27943
Prediction of deep levels and equilibrium concentrations of defects in semiconductors 21 p3023 N88-27945
X-ray studies of strain, interface and impurities in semiconductors
[DE88-012460] 21 p3025 N88-27954
Characterization of crystalline silicon by electrochemical and Raman spectroscopy at the frontier semiconductor/electrolyte
[ETN-88-92354] 21 p3025 N88-27956
Raman spectroscopy on simple molecular systems at very high density
[DE88-010947] 23 p3191 N88-28987
Structural relationship between icosahedral and Frank-Kasper phases of Al-Li-Cu
[AD-A193768] 23 p3195 N88-29011
Influence of local volume forces on surface relaxation of pure metals and alloys: Applications to Ni, Al, Ni3Al
[DE88-702718] 23 p3195 N88-29014
Band electronic structures and crystal packing forces
[DE88-010247] 23 p3289 N88-29585
Preparation and testing of Nb-Zr and Nb-ZrO2 single crystals for deformation studies
[DE88-702798] 23 p3293 N88-29613
Crystal structures of ordered carbon metal alloys
[AD-A195597] 24 p3353 N88-29959
Discovery of a low temperature form of TAGN (Triaminoguanidinium Nitrate)
[AD-A196059] 24 p3357 N88-29989
Crystal structure and density of helium to 232 kbar
24 p3441 N88-30481

CRYSTAL SURFACES
The effect of additives on the reactivity of palladium surfaces for the chemisorption and hydrogenation of carbon monoxide: A surface science and catalytic study
[DE87-014685] 02 p0145 N88-10909
Materials preparation and longevity in hyperthermal atomic oxygen 03 p0297 N88-11862
The structure of adsorbed sulfur and carbon on molybdenum and rhenium single crystal surfaces, and their influence on carbon monoxide and hydrocarbon chemisorption
[DE88-001393] 04 p0499 N88-13073
Surface deformation and fatigue crack initiation of alpha-iron 05 p0598 N88-13651
Laser pulse width dependent surface ripples on silicon
[PB88-127311] 10 p1336 N88-17982
A scientific basis for an alternate cathode architecture
[AD-A191498] 18 p2481 N88-24717
The catalytic reactivity of thin film crystal surfaces
[DE88-006387] 19 p2732 N88-26228
Theory of surface melting and non-melting
[DE88-702652] 22 p3157 N88-28785
Attenuated total reflectance FT-IR spectroscopy to measure interfacial reaction kinetics at silica surfaces
[AD-A196330] 24 p3344 N88-29908

CRYSTALLINITY
EXELFS (Extended Electron Energy Loss Fine Structure) of amorphous and crystalline SiC
[DE87-013551] 02 p0151 N88-10948
Modeling of irradiation-induced amorphization in a titanate ceramic
[DE87-014751] 03 p0292 N88-11833
Gamma-ray optics of multi-beam Borrmann modes with possible applications to nuclear lasing
04 p0449 N88-12784
Radiation induced collapse of the crystalline structure
[DE87-014407] 04 p0498 N88-13064
Microstructure of amorphous and crystalline zirconium alloys rapidly solidified
[DE87-703700] 05 p0564 N88-13432
Helium atom surface scattering apparatus for studies of crystalline surface dynamics
[DE88-002104] 06 p0787 N88-14826
Crystalline sulfur dioxide: Crystal field splittings, absolute band intensities and complex refractive indices derived from infrared spectra
[NASA-CR-182502] 09 p1258 N88-17547
Crystalline photovoltaic cell technology: Present and future
[DE88-004684] 13 p1795 N88-20734
Analysis of explosives. 1: Computer programs for processing of X-ray powder deffraction data
[PB88-156898] 14 p1894 N88-21309
Blends of crystallizable polybutadienes
[AD-A194536] 23 p3197 N88-29026
Preliminary analysis of recent 2.2-4.2 micrometers telescopic observations of Elysium, Mars: Implications for crystallinity and hydration state of surface materials
23 p3306 N88-29692
A method for the quantitative determination of crystalline phases by X-ray
[NASA-TT-20324] 24 p3434 N88-30444

CRYSTALLITES
Characterization of catalysts with metal-support effects and of the species adsorbed on their surfaces
[DE87-014636] 04 p0414 N88-12564
Gigantic optical nonlinearity in low dimensional systems 14 p1975 N88-21786
Enhanced excitonic optical nonlinearity and exciton dynamics in semiconductor microstructures
14 p1977 N88-21795
The crystallization of tough thermoplastic resins in the presence of carbon fibers
[NASA-CR-182984] 20 p2776 N88-26464

CRYSTALLIZATION
NT DIRECTIONAL SOLIDIFICATION (CRYSTALS)
NT MELT SPINNING
NT RECRYSTALLIZATION
Stability relationship for water droplet crystallization with the NASA Lewis icing spray
[NASA-TM-100220] 02 p0125 N88-10790
Study of the micromechanical behavior of a SiO2-Al2O3-Li2O glass ceramic and its relation to the microstructure
[ISAL-ITC1-87-01] 02 p0153 N88-10960
Ultra-fine grained alloy material
[AD-A184500] 03 p0290 N88-11820
Joining of silicon carbide reinforced ceramics
[DE87-014881] 03 p0294 N88-11847
Continued research on direct contact heat exchangers: Effects of crystallization
[DE87-014931] 03 p0322 N88-12035
Investigations of crystallization velocity and boron diffusion in glassy iron-boron alloys and of activity coefficients of boron in crystalline iron-boron alloys
[ETN-87-90613] 03 p0381 N88-12393
Studies on some Ge-Se-Te glasses
[PD-MT-8721] 04 p0420 N88-12607
T.E.M. study of boehmite gels and of their transformation into alpha-alumina
[SNIAS-872-430-121] 05 p0656 N88-14023
Undercooling and nucleation in iron nickel alloys
[AD-A185500] 06 p0683 N88-14184
Processing and interfacial analysis of glass-ceramic to metal seals
[DE88-002999] 08 p0971 N88-15873
Protein-crystal growth experiment (planned)
10 p1287 N88-17700
Crystallization and glass formation in electron and laser beam irradiated Cu-Zr alloys
[DE88-003390] 11 p1464 N88-18729
In situ ultrahigh vacuum friction measurement and wear track analysis of ion implanted 304 stainless steel
[DE88-004537] 11 p1494 N88-18922
Formation of buried nitride layers in (110) silicon
[DE88-003255] 11 p1557 N88-19323
Zone crystallization experiments in mirror heating facilities
[BMFT-FB-W-86-023] 16 p2184 N88-23016
Effect of size of precipitates on recrystallization temperatures in Cu-Cr, Cu-Zr, and Cu-Zr-Cr alloys
[NASA-TT-20166] 18 p2489 N88-24763
NASA research Program: The roles of fluid motion and other transport phenomena in the morphology of materials
[NASA-CR-182801] 18 p2580 N88-25327
Electronic controller for reciprocating rotary crystallizer
[NASA-TM-101140] 18 p2584 N88-25354
The crystallization of tough thermoplastic resins in the presence of carbon fibers
[NASA-CR-182984] 20 p2776 N88-26464
Crystallization of aluminum hydroxide in the aluminum-air battery: Literature review, crystallizer design and results of integrated system tests
[DE88-010510] 20 p2797 N88-26594
Microchemical analysis of polycrystalline Ni3Al and other ordered alloys using the field-ion microscope atom probe
[DE88-011519] 2. p2914 N88-27294
Formation of metastable structures and amorphous phases in Cu-W alloys using the triod sputtering technique
[DE88-009051] 21 p2915 N88-27298
Homogeneity of glasses: Experiment WL-IHF-05 in D1 mission --- Spacelab
[ETN-88-92339] 21 p2924 N88-27353
Experiments in microgravity environment: Protein crystallization
[REPT-881-430-101] 21 p2924 N88-27354
Laser crystallized silicon films on alumina ceramic substrates and application to thin film c-Si solar cells
[PB88-131966] 22 p3116 N88-28515
Influence of the interface on the crystallization of amorphous Ge in Pb/Ge multilayers
[DE88-010072] 22 p3156 N88-28776
Origin of SNC kaersutitic amphibole: Experimental data 23 p3306 N88-29693

CRYSTALLOGRAPHY
Constitutive modeling for single crystal superalloys
02 p0187 N88-11168
International Conference on Microstructology held in Gainesville, Florida on 7-9 May 1986
[AD-A184604] 03 p0290 N88-11822
Effect of grain orientation on the origination and the initial growth of fatigue cracks in pure iron
05 p0597 N88-13647
The growth of persistent slip bands
05 p0597 N88-13648
The orientations of dipolar walls produced by cyclic deformation 05 p0598 N88-13655
The influence of slip mechanism on fatigue of Mg and Mg-2.3Li 05 p0600 N88-13672
An explanation of the fractography of near-threshold fatigue in FCC metals 06 p0716 N88-14395
Orientation effects in copper single crystals fatigued at elevated temperatures 06 p0720 N88-14423
A continuous oxidizer regression model for the combustion of composite solid propellants
[AD-A186742] 08 p0974 N88-15894
NBS/Sandia/ICDD electron diffraction database
[DE88-004635] 11 p1454 N88-18665
Stress corrosion cracking and metal-induced embrittlement: Comparative studies of local chemistries
[DE88-003235] 13 p1742 N88-20419
Recent progress in structure determination by LEED (Low-Energy Electron Diffraction) measure the properties of the deep donors (DX-cent)
[DE88-003851] 13 p1846 N88-21048
Interface characterization of Cu-Cu and Cu-Ag-Cu low temperature solid state bonds
[AD-A191015] 16 p2283 N88-23667
Influence of carbon fiber surface treatment
[ETN-88-92536] 18 p2492 N88-24787
Dendritic growth in the presence of convection
18 p2580 N88-25328
Topics in quasicrystallography
21 p3023 N88-27947
Characterization of crystalline silicon by electrochemical and Raman spectroscopy at the frontier semiconductor/electrolyte
[ETN-88-92354] 21 p3025 N88-27956
Muon-spin rotation experiment (micro + SR) on aluminum and indium after low temperature electron irradiation
[ETN-88-92985] 23 p3294 N88-29617
Crystal fractionation in the SNC meteorites: Implications for surface units on Mars 23 p3307 N88-29698

CRYSTALS
NT BICRYSTALS
NT BRAVAIS CRYSTALS
NT CRYSTAL OSCILLATORS
NT CRYSTALLITES
NT DENDRITIC CRYSTALS
NT DOPED CRYSTALS
NT LIQUID CRYSTALS
NT METAL CRYSTALS
NT MICROCRYSTALS
NT MIXED CRYSTALS
NT PIEZOELECTRIC CRYSTALS
NT POLYCRYSTALS
NT QUARTZ CRYSTALS
NT SINGLE CRYSTALS
NT WHISKERS (CRYSTALS)
Interaction between defects and the formation of dissipative structures in irradiated impure crystals
[DE87-703125] 02 p0246 N88-11552
Highly Non-Linear Optical (NLO) organic crystals
03 p0297 N88-11865
Highly Non-Linear Optical (NLO) organic crystals and films. Electrooptical organic materials
03 p0297 N88-11866
Theory of atomic additivity in molecular hyperpolizabilities 03 p0297 N88-11867
Large-aperture high-efficiency frequency doubling using tandem KDP crystals 03 p0301 N88-11894
Evaluation system for crystal streak cameras
[DE88-000238] 03 p0324 N88-12048
Interatomic Auger rates for the sodium fluoride crystal
[DE87-013012] 03 p0382 N88-12401
Crystalline cell research status and direction
[DE87-014214] 03 p0382 N88-12402
Research and development on high strength ceramic heaters discussed 04 p0404 N88-12508
Far infrared Fourier transform spectroscopy of semiconductors
[DE88-000188] 04 p0499 N88-13072
Cyclic deformation of an extruded AlMgSi alloy
05 p0598 N88-13654
Structure of layered crystals studied by high energy ion beams
[DE88-001675] 06 p0786 N88-14822
Diamond turning of silicon for optics applications
[DE88-002501] 07 p0840 N88-15095

Intracavity spectrum analyzer with NaF:F2(+):F3(-) crystal laser for long-wave IR wave band
07 p0919 N88-15584
Thermal stress analysis of a cooled monochromator crystal
[DE88-002116] 07 p0937 N88-15696
Gamma radiation at the 970 MeV plane positron channeling in diamond crystals
[DE88-700557] 07 p0939 N88-15705
Effect of irradiation on the diffusion evolution of void ensemble in crystals
[DE88-700558] 07 p0939 N88-15706
Wave functions for bound states of relativistic electrons in a crystal at electron movement along crystallographic planes
[DE88-700563] 07 p0939 N88-15708
Tunable Al2O3:Ti3+-laser with optical pumping
09 p1237 N88-17415
Recent progress in the dynamic applications of piezoelectric crystals 10 p1417 N88-18460
The structure and properties of twin boundaries in superconducting YBa2Cu3O7
[DE88-003864] 10 p1418 N88-18468
UHV (Ultra-High Vacuum) double crystal monochromator design
[DE88-003904] 11 p1456 N88-18676
Nucleation and growth of calcium carbonate crystals on surface-modified polyethylene and polystyrene
[DE88-005126] 11 p1465 N88-18733
Growth and characteristics of materials for tunable lasers in the near infrared spectral region
[NASA-CR-182501] 11 p1491 N88-18901
Investigation of defect and electronic interactions associated with GaAs device processing
[AD-A188021] 11 p1556 N88-19313
Raman scattering in mixed crystal semiconductors
12 p1696 N88-20149
Parametric study of acceleration-induced stresses and frequency changes in doubly-rotated crystal resonators
[AD-A189261] 13 p1761 N88-20532
Thermionic Technology Program. A: Insulator test and evaluation
[DE88-004707] 13 p1795 N88-20735
Multiple scattering of polarized light in cirrus clouds
13 p1801 N88-20768
Nonlinear refractive index measurements of glasses and crystals
[DE88-005673] 13 p1840 N88-21009
Effect of Mg impurity on local vibrations of U-centers in LiF lattice 14 p1969 N88-21753
Nucleation in super-saturated products
[NASA-TT-20275] 15 p2037 N88-22134
On rotating sphere-on-a-plate experiments and the questions of whether high angle grain boundaries melt below bulk melting temperatures
[DE88-006627] 15 p2038 N88-22142
High-performance polymeric materials
[AD-A190708] 15 p2048 N88-22190
Does the pipe diffusion of self-interstitials in crystals under stresses exist
[DE88-701027] 15 p2139 N88-22762
Optical characterization of microcrystals
[DE88-006622] 15 p2141 N88-22775
Tunable optical sources/growth and characterization of nonlinear optical materials
[AD-A190874] 16 p2274 N88-23608
Investigation of non-linear optical behavior of semiconductors for optical switching, volume 1
[AD-A191297] 16 p2274 N88-23611
Effects of irradiation on thermal coalescence of pores in real crystals
[DE88-701683] 16 p2282 N88-23663
Dynamic range compression/expansion of light beams by photorefractive crystals
[NASA-CASE-NPO-17140-1-CU]
17 p2438 N88-24508
Joint services electronics program
[AD-A190239] 18 p2503 N88-24848
NASA research Program: The roles of fluid motion and other transport phenomena in the morphology of materials
[NASA-CR-182801] 18 p2580 N88-25327
Structure and refinement of ordered aromatic heterocyclic polymers by diffraction methods: Application of results to electro-optic phenomena
[AD-A191859] 19 p2619 N88-25537
Time-resolved doubly bent crystal X-ray spectrometer
[DE88-007899] 20 p2805 N88-26637
Phase equilibrium and crystal growth studies on AgGaSe2 and related nonlinear optical materials
[AD-A193763] 22 p3157 N88-28783
Theory of surface melting and non-melting
[DE88-702652] 22 p3157 N88-28785
Short pulse X-ray diffraction studies of shocked and annealed crystals using the JANUS research laser
[DE88-011329] 23 p3288 N88-29579
Research on crystal and film ferroelectric materials for optoelectronic applications
[AD-A193512] 23 p3291 N88-29597
Absorption spectra and energy levels of Gd(3+), Nd(3+) and Cr(3+) in the garnet Gd3Sc2Ga3O12
[AD-A193634] 23 p3292 N88-29599
General equations for the motions of ice crystals and water drops in gravitational and electric fields
[NASA-CR-183229] 24 p3370 N88-30070

CTD
U CHARGE TRANSFER DEVICES

CUBANE
Theoretical investigations of nitrocubane decomposition
[AD-A194556] 23 p3200 N88-29047

CUBES (MATHEMATICS)
Twisted cube
[PB87-162814] 09 p1220 N88-17316
Procedure for converting a Wilson-Fowler spline to a cubic B-spline with double knots
[DE88-008971] 20 p2844 N88-26878

CUBIC EQUATIONS
Evaluation of closed cubic failure criterion for graphite/epoxy laminates
[NASA-CR-182375] 06 p0679 N88-14158

CUBIC LATTICES
NT BODY CENTERED CUBIC LATTICES
NT FACE CENTERED CUBIC LATTICES
Compilation of temperature factors of cubic elements
[PB88-108170] 21 p2908 N88-27260
Theoretical predictions of precipitate shapes in cubic alloys
[DE88-010856] 21 p2914 N88-27291

CUES
Handling qualities criterion for very low visibility rotorcraft 03 p0263 N88-11654
Effect of motion cues during complex curved approach and landing tasks: A piloted simulation study
[NASA-TP-2773] 04 p0398 N88-12480
The role of adaptive supplemental visual cuing in flight simulation
[AD-A185932] 07 p0822 N88-14992
Visual attention effects on discrimination of line orientation and line arrangement
[AD-A187013] 09 p1200 N88-17190
Visual integration and detection of discontinuities: The key role of intensity edges
[AD-A188012] 11 p1520 N88-19076
Analysis procedures and subjective flight results of a simulator validation and cue fidelity experiment
[NASA-TM-88270] 18 p2465 N88-24634
Eye and head response to an attention cue in a dual task paradigm
[AD-A191052] 18 p2551 N88-25143

CUESTAS
U RIDGES

CULTIVATION
Biomass recycle as a means to improve the energy efficiency of CELSS algal culture systems
03 p0358 N88-12254
Trickle water and feeding system in plant culture and light-dark cycle effects on plant growth
03 p0361 N88-12273
Controlled ecological life support systems: Development of a plant growth module 05 p0630 N88-13854

CULTURE (SOCIAL SCIENCES)
Maps for tourists. A systematic approach to tourist cartography 16 p2227 N88-23296
Linguistic and cultural barriers to the transfer of information 24 p3437 N88-30459

CULTURE TECHNIQUES
Superoxide dismutase assays
[AD-A183972] 03 p0356 N88-12242
Space Bioreactor Science Workshop
[NASA-CP-2485] 09 p1196 N88-17168
Suspension cell culture in microgravity and development of a space bioreactor 09 p1196 N88-17169
Space bioreactor: Design/process flow
09 p1197 N88-17170
Bioreactor design concepts 09 p1197 N88-17171
Shear and mixing effects on cells in agitated microcarrier tissue culture reactors 09 p1197 N88-17173
Fed-batch control based upon the measurement of intracellular NADH 09 p1197 N88-17175
Nutrient requirements and other factors involved in the culture of human kidney cells on microcarrier beads
09 p1197 N88-17176
Plant cell technologies in space: Background, strategies and prospects 09 p1198 N88-17177
Design concepts for bioreactors in space
09 p1198 N88-17179
Cell culture experiments planned for the space bioreactor 09 p1198 N88-17180
Research on a solar biotechnology based on the culture of photosynthetic cells
[DE88-900129] 10 p1359 N88-18120
Growth and differentiation of cells in organotypical rat embryo cerebellar culture developing in weightlessness
19 p2703 N88-26076
Effects of pulsed and CW (Continuous Wave) 2450 MHz radiation on transformation and chromosomes of human lymphocytes in vitro
[AD-A193104] 21 p2987 N88-27736

CUMULATIVE DAMAGE
Cumulative fatigue and life prediction of fibre composites. Part 1: Literature reviews
[BR101013] 02 p0142 N88-10893
Cumulative fatigue and life prediction of fibre composites. Part 2: Experimental techniques and results
[BR101014] 02 p0142 N88-10894
Ensuring the service life of designs (experience in aircraft construction) 02 p0157 N88-10986
Damage considerations in sizing aircraft cells. Life predictions
[SNIAS-872-111-116] 05 p0546 N88-13330
Colloquium on damage mechanics of graphite/expoxy laminates during fatigue
[DFVLR-MITT-87-08] 11 p1448 N88-18630
Damage mechanics of fiber reinforced plastics: A general view 11 p1448 N88-18631
Influence of different parameters on damage development --- carbon fiber reinforced plastics
11 p1448 N88-18632
Initiation and propagation of damage in notched unidirectional and multidirectional CFRE resin laminates
11 p1449 N88-18633
Damage initiation and growth in sateen laminates under static and cyclic loading 11 p1449 N88-18634
Damage mechanisms of CFRP riveted joints
11 p1449 N88-18636
Damage mechanisms and fatigue life prediction of graphite/epoxy laminates 11 p1449 N88-18637
Fatigue damage development of various CFRP-laminates
[NASA-TT-20247] 16 p2172 N88-22945
Study of mechanisms of time-dependent crack growth at elevated temperature
[DE88-006918] 16 p2223 N88-23271
Interaction of creep and fatigue damage in gas turbine blade material
[PNR90440] 22 p3088 N88-28335

CUMULUS CLOUDS
Cumulus and thunderstorm initiation by mountains
02 p0207 N88-11301
Study of isolated convective clouds in the lower Alps in summer 1984, using radar and a simple Weinstein numerical model
[ESA-TT-1061] 03 p0353 N88-12224
Dynamic interaction of convective cumulus with large-scale environment
[MITT-55] 20 p2827 N88-26773
An observational study of interaction between large scale tropical cumulus convection and the equatorial circulation anomalies 22 p3124 N88-28564

CURIE TEMPERATURE
Spin disorder resistivity and bare Curie temperature in the ferromagnetic superconductor ErRh4B4
[DE88-003016] 10 p1415 N88-18445

CURING
The water absorption of model epoxy resin networks cured with aromatic diamines
[BR100722] 01 p0027 N88-10169
Addition polyimide composition
[EP-PATENT-0-167-304-A1] 01 p0053 N88-10337
Cure and properties of thermosetting polymers
[AD-A184669] 03 p0293 N88-11843
Effects of cure pressure on resin flow, voids, and mechanical properties
[AD-A184267] 03 p0295 N88-11853
Radiation curing: Comparison of heat, UV, and radiation curing
[OEFZS-4393] 06 p0689 N88-14224
Effect of post-cure heat-treatment on static and fatigue behaviour of XAS-914C carbon fibre composite
[AD-A186943] 10 p1294 N88-17735
High-temperature thermosets derived from the Diels-Alder polymerization of bisbenzocyclobutenes and bimaleimides
[AD-A188800] 13 p1747 N88-20449
Effect of moisture level in PBXW-109(E) (plastic-bonded explosive) mixes on the aging of the cured explosive
[AD-A190200] 15 p2048 N88-22202
Correlation between dielectric and structural properties during epoxy cure
[AD-A190696] 16 p2181 N88-22997
Cellular thermosetting fluoropolymers and process for making them
[NASA-CASE-GSC-13008-1] 17 p2326 N88-23894
Current and future molecular structures of aerospace organic matrix resins 18 p2477 N88-24695

The 700 F properties of autoclave cured PMR-2 composites
[NASA-TM-100923] 18 p2480 N88-24712
A compatible encapsulant for explosives
[DE88-007212] 18 p2495 N88-24806
Determination of the glass transition temperature of cured composite materials
[DT-87/62-R] 21 p2906 N88-27246
Determination of lumped-mass thermal properties associated with autoclave curing of graphite/epoxy composites 21 p2925 N88-27364
A fundamental study of P/M processed elevated temperature aluminum alloys
[AD-A192958] 23 p3194 N88-29005

CURL (VECTORS)
NT VORTICITY

CURRENT AMPLIFIERS
NT PHOTOMULTIPLIER TUBES

CURRENT CONVERTERS (AC TO DC)
Mathematical model for the dc-ac inverter for the Space Shuttle 06 p0793 N88-14860

CURRENT DENSITY
Simulations using the pseudo-current algorithm
[DE87-012403] 01 p0040 N88-10255
Abrikosov vortex motion and elementary pinning force in a SNS Josephson junction
[DE87-013607] 01 p0105 N88-10683
Use of polarimetry to measure the current profile in MTX
[DE87-013835] 02 p0237 N88-11495
Short-pulse high-current-density photoemission in high electric fields
[DE87-014909] 03 p0310 N88-11951
Magnetic fluctuation behaviour of current termination in reversed field pinch
[IPPJ-849] 04 p0492 N88-13034
Reversed field pinch plasmas with various boundary conditions
[DE88-000832] 05 p0653 N88-14004
Study of vibration relaxation in active medium of CO2-laser using phase-absorption method 07 p0919 N88-15582
Possibility of calculation of magnetic surface function gradient and related quantities
[DE88-700561] 07 p0936 N88-15686
Shape of the plasma boundary in TBR
[INPE-4388-PRE/1208] 08 p1086 N88-16540
Application of high temperature ceramic superconductors (CSC) to commercial tokamak reactors
[DE88-003973] 09 p1257 N88-17538
Application of ac-impedance method on determination of corrosion rate of metals
[DE88-750307] 10 p1300 N88-17771
Investigation of materials for inert electrodes in aluminum electrodeposition cells
[DE88-003380] 10 p1323 N88-17906
High-current density, high-brightness electron beams from large-area lanthanum hexaboride cathodes
[AD-A187700] 11 p1477 N88-18813
A novel class of positive electrodes for rechargeable batteries
[DE88-004559] 13 p1763 N88-20545
Simplified physical approach of the control by eddy current
[DE88-701076] 13 p1764 N88-20552
Stratospheric electric field and conductivity measurements over electrified convective clouds in the South American region, revised
[INPE-4046-PRE/1012-REV-3] 15 p2095 N88-22483
High-T(sub c) superconducting wire fabrication and testing
[DE88-005989] 15 p2144 N88-22798
High temperature superconductors in the La(sub 1+x)Ba(sub 2-x)Cu O(sub y system
[DE88-006367] 15 p2145 N88-22802
Electron current effect on stability of plasma channel 16 p2276 N88-23625
Carrier transport in semiconductor magnetic sensors under nonuniform fields 19 p2672 N88-25888
Poloidal field measurements using laser enhanced attenuation of an energetic lithium beam
[DE88-008360] 20 p2856 N88-26963
Linear thyratron
[AD-A194111] 23 p3208 N88-29094
Currents induced in a human being for electromagnetic fields to 10 kHz-50 MHz
[AD-A191977] 23 p3238 N88-29268

CURRENT DISTRIBUTION
Efficiency aspects of short, low velocity railguns
[AR-004-847] 04 p0405 N88-12517
Mathematical model for the dc-ac inverter for the Space Shuttle 06 p0793 N88-14860
The coaxial colinear antenna: Theoretical and experimental models 11 p1475 N88-18803

CURRENT SHEETS
Equilibrium and tearing stability of thin current layers in magnetic arcades 01 p0118 N88-10754
Observations of small scale structures using data from the wave experiment on the AMPTE-UKS spacecraft 08 p1099 N88-16612
On the potential role of concentrated field-aligned currents in solar physics 08 p1099 N88-16614
Observation of enhanced electric field in an RF-plugged sheet plasma in the RFC-XX-M open-ended machine
[IPPJ-857] 09 p1252 N88-17503
A study of the magnetic field annihilation process in the magnetosphere and some geotechnical applications
[DE88-004165] 10 p1355 N88-18096

CURRENTS (OCEANOGRAPHY)
U WATER CURRENTS

CURTAINS
Gain evaluation for an idealized curtain array antenna
[PB87-210290] 02 p0161 N88-11006

CURTISS-WRIGHT MILITARY AIRCRAFT
U MILITARY AIRCRAFT

CURVATURE
Fronts propagating with curvature dependent speed: Algorithms based on Hamilton-Jacobi formulations
[NASA-CR-178382] 01 p0077 N88-10495
A numerical study of the effects of curvature and convergence on dilution jet mixing
[NASA-TM-89878] 05 p0549 N88-13347
Vision algorithms and psychophysics
[AD-A186773] 09 p1200 N88-17193
The deposition rate dependence of plasma polymerization on the radius of curvature of the substrate
[DE88-003811] 10 p1412 N88-18429
Terrain classification from digital elevation data using slope and curvature information
[AD-A188940] 12 p1639 N88-19812
Complete minimal surfaces in R^3 of low total curvature
[DE88-006425] 15 p2118 N88-22619
Surface curvature and pressure gradient effects on turbulent flow: An assessment based on numerical solution of the Reynolds equations 17 p2338 N88-23954
Cylindrical surface profile and diameter measuring tool and method
[NASA-CASE-MFS-28287-1] 17 p2341 N88-23959
An empirical model of the effects of curvature and convergence on dilution jet mixing
[NASA-TM-100896] 18 p2466 N88-24640
Aerodynamics of lifting bodies with combined transverse and longitudinal curvature 19 p2598 N88-25436
Synoptic patterns related to tropical cyclone recurvature
[AD-A192338] 20 p2827 N88-26771
Applications of differential geometry to the shape analysis of gray-value images 21 p2924 N88-27358
A novel method to correct radiation pattern distortion of conformal antennas
[AD-A193675] 23 p3204 N88-29066
A technique for measuring area under a curve
[AD-A193559] 23 p3271 N88-29463

CURVE FITTING
A comparison of fitting techniques for the cumulative average learning curves with historical lot cost data
[AD-A187127] 09 p1227 N88-17349
Fitting a generalized parabola to data
[NPL-DITC-96/87] 09 p1229 N88-17364
Strategies for knot placement in least squares data fitting by splines
[NPL-DITC-101/87] 09 p1229 N88-17366
Using frequency-domain methods to identify XV-15 aeroelastic modes
[NASA-TM-100033] 10 p1277 N88-17646
Analysis of learning curve fitting techniques
[AD-A187680] 11 p1535 N88-19173
Position finding and tolerances
[AD-A187685] 11 p1540 N88-19205
Motion sickness: Quantitative, algorithmic malaise indication in real time
[AD-A189674] 15 p2101 N88-22518
Fitting a circle to radially suppressed data
[NPL-DITC-103/87] 17 p2392 N88-24223
Simplified curve fits for the transport properties of equilibrium air
[NASA-CR-178411] 18 p2513 N88-24911
Fitting an ellipse to data
[NPL-DITC-95/87] 22 p3143 N88-28693

CURVED BEAMS
Nonlinear thermoviscoelastic analysis of metallic plane curved beams 03 p0336 N88-12119
Delamination stresses in semicircular laminated composite bars
[NASA-TM-4026] 13 p1735 N88-20375
Non-isothermal elastoviscoplastic analysis of planar curved beams 14 p1933 N88-21526

CURVED PANELS
Vibration and buckling of geometrically imperfect laminated cylindrical shells 04 p0456 N88-12822
A study of damage tolerance in curved composite panels
[AD-A190617] 15 p2029 N88-22092

CURVED SURFACES
U CONTOURS
U SHAPES
U SURFACES

CURVES
Innovative design of composite structures: Further studies in the use of a curvilinear fiber format to improve structural efficiency
[NASA-CR-182576] 11 p1450 N88-18641
Method and models for R-curve instability calculations
[NASA-TM-100935] 16 p2224 N88-23278
Peturbational analysis of the curved anisotropic optical fiber for the birefringence due to the geometry
[PB88-171848] 19 p2726 N88-26189
The T-T-T curve in Cu-Cr alloy
[NASA-TT-20167] 20 p2774 N88-26453
The triangle: A multiprocessor architecture for fast curve and surface generation
[AD-A195882] 24 p3414 N88-30324

CURVES (GEOMETRY)
NT CATENARIES
NT S CURVES
Response of helical structures to high speed pulses or when can a helix be called an inductor
[DE87-014347] 01 p0090 N88-10587
Transversely anisotropic curved optical fibres: Variational analysis of a nonstandard Eigenproblem
[PB88-112966] 08 p1083 N88-16528
Numerical arc segmentation algorithm for a radio conference-NASARC, version 2.0: User's manual
[NASA-TM-100161] 09 p1156 N88-16928
Computation of the zeta-function of an algebraic curve with the differentials of the first kind
[PB88-127527] 10 p1399 N88-18339
Open or closed curves by regularized B-splines
[RR-652-M] 18 p2563 N88-25218
Calculating the self-intersections of Bezier curves
[AD-A192371] 19 p2721 N88-26156

CURVILINEAR COORDINATES
U SPHERICAL COORDINATES

CUT-OUTS
U OPENINGS

CUTANEOUS PERCEPTION
U TOUCH

CUTTERS
NT DRILLS
XCUT: A rule-based expert system for the automated process planning of machined parts
[DE87-011638] 05 p0639 N88-13905
Tribological studies on high speed steel cutting tools
[DE88-002550] 07 p0864 N88-15246
Characterization of coating wear phenomena in nitride and carbide coated tool inserts
[DE88-011196] 20 p2779 N88-26478

CUTTING
NT LASER CUTTING
NT METAL CUTTING
NT MILLING (MACHINING)
NT SHEARING
NT SPARK MACHINING
Diamond turning of silicon for optics applications
[DE88-002501] 07 p0840 N88-15095
A fast bottom-up algorithm for computing the cut sets of noncoherent fault trees
[DE88-003741] 09 p1220 N88-17320
Drilling metal matrix composites
[AD-A190480] 15 p2029 N88-22091
Contribution to the study of modern materials for cutting tools
[ISAL-IDI1-87-17] 16 p2185 N88-23029
High power axial flow CO2 laser
[ETN-88-91951] 18 p2521 N88-24959
Characterization of coating wear phenomena in nitride and carbide coated tool inserts
[DE88-011196] 20 p2779 N88-26478
Ductile-brittle transition of cutting behavior in diamond turning of single crystal Si
[DE88-008890] 20 p2809 N88-26664
Microcircuit trace cutting with focused ion beams
[AD-A196030] 24 p3367 N88-30050

CW RADAR
U CONTINUOUS WAVE RADAR

CYANIDE EMISSION
U CN EMISSION

CYANIDES
NT ACETONITRILE
NT CYANOGEN

CYANO COMPOUNDS
NT ISOCYANATES

Application of photosynthetic N(2)-fixing cyanobacteria to the CELSS program 03 p0358 N88-12257
The photochemistry of some possible cometary CN parent species 14 p1997 N88-21905
The evolution of CN emission in Halley's comet with heliocentric distance 14 p2006 N88-21961
First detection of HCN J = 9 to 8 (797 GHz) line emission: Very high densities in the Orion core
[MPE-PREPRINT-110] 22 p3165 N88-28847

CYANOGEN
Simultaneous, cospatial imaging of the Sun in cyanogen and singly-ionized calcium 04 p0507 N88-13114
Laser studies of the dynamics of free radical reactions
[DE88-004431] 10 p1337 N88-17989

CYANOPHYTA
U BLUE GREEN ALGAE

CYBERNETICS
USSR report: Cybernetics, computers and automation technology
[JPRS-UCC-86-014] 06 p0761 N88-14669
Spire based speaker-independent continuous speech recognition using mixed feature sets
[AD-A188834] 12 p1620 N88-19668
Novel nonlinear signal processing principles
[AD-A191644] 19 p2707 N88-26097

CYCLES
NT ACTIVITY CYCLES (BIOLOGY)
NT BRAYTON CYCLE
NT CARBON CYCLE
NT HYDROLOGICAL CYCLE
NT RANKINE CYCLE
NT SOLAR CYCLES
NT STIRLING CYCLE
NT STRESS CYCLES
NT SUNSPOT CYCLE
NT THERMODYNAMIC CYCLES
NT WORK-REST CYCLE
The impact of varves on solar physics
[NASA-CR-181519] 03 p0390 N88-12448
Cross-correlation of uniform cyclic difference set sequences
[AD-A184879] 05 p0640 N88-13913
Thermal mechanical low cycle fatigue of 25CDV4-10 steel 06 p0721 N88-14429
The 35-day cycle of Hercules X-1
[MPE-204] 11 p1571 N88-19405
Global mixed-layer natural and anthropogenic fluxes 13 p1807 N88-20803
The influence of uncompensated solution resistance on the determination and standard electrochemical rate constants using cyclic voltammetry and some comparisons with AC voltammetry
[AD-A192825] 20 p2770 N88-26427
Two families of graphs satisfying the cycle basis interpolation property
[PB88-127808] 20 p2846 N88-26890
Algorithm for generating the minimal cycle basis of a graph
[PB88-126610] 20 p2846 N88-26891
Modeling discrete bathtub and upside down bathtub mean residual life functions
[AD-A192000] 22 p3085 N88-28320
Time periodic control of a multi-blade helicopter
[AD-A194435] 23 p3180 N88-28931
Finding minimum-cost circulations by canceling negative cycles
[AD-A194027] 23 p3271 N88-29468
The OFP (Operational Flight Program) update cycle needs you
[AD-A194910] 24 p3325 N88-29798

CYCLIC ACCELERATORS
NT BETATRONS
NT STORAGE RINGS (PARTICLE ACCELERATORS)
NT SYNCHROTRONS
Bevalac external beamline optics
[LBL-23240] 19 p2727 N88-26194
Rf cavity primer for cyclic proton accelerators
[DE88-010655] 20 p2853 N88-26938

CYCLIC COMPOUNDS
NT ADENOSINE TRIPHOSPHATE
NT ADENOSINES
NT ANTHRACENE
NT ATROPINE
NT AZOLES
NT AZULENE
NT BENZENE
NT CAFFEINE
NT CARBAZOLES
NT CYCLIC HYDROCARBONS
NT CYCLOBUTANE
NT CYCLOHEXANE
NT ERGOTAMINE
NT FURANS
NT HETEROCYCLIC COMPOUNDS
NT HMX
NT MORPHINE
NT NAPHTHALENE
NT NAPHTHENES
NT NICOTINIC ACID
NT PHTHALOCYANIN
NT PYRIDINES
NT PYRROLES
NT RDX
NT THYMINE
NT URACIL
NT XANTHINES
Thermoplastic elastomers as LOVA (Low Vulnerability Ammunition) binders
[AD-A184350] 04 p0419 N88-12599
Synthesis of energetic materials
[AD-A189115] 13 p1753 N88-20482
Aromatic cyclotriphosphazenes
[NASA-CASE-ARC-11428-3] 18 p2477 N88-24692
Structural study of the TGMDA-DDS system --- epoxy system
[ONERA-RT-4/3346-M] 18 p2493 N88-24792

CYCLIC HYDROCARBONS
NT ANTHRACENE
NT BENZENE
NT CYCLOBUTANE
NT CYCLOHEXANE
NT NAPHTHALENE
NT NAPHTHENES
High-temperature thermosets derived from the Diels-Alder polymerization of bisbenzocyclobutenes and bimaleimides
[AD-A188800] 13 p1747 N88-20449

CYCLIC LOADS
The effect of fretting corrosion on the fatigue strength of steel and cast iron under sinusoidal and random loading
[LBF-FB-177] 01 p0023 N88-10142
The fatigue properties of aerospace steels under constant amplitude and flight-by-flight simulated loading
[BAE-MSM-R-GEN-0566] 01 p0059 N88-10377
Criteria for determination of significant load cycles in variable amplitude load sequences
[NLR-MP-86013-U] 01 p0060 N88-10386
Influence of thermocyclic treatment on mobility of grain boundaries
[BLL-M-37329-(5828.4)] 02 p0149 N88-10933
Constitutive modeling for isotropic materials 02 p0188 N88-11171
The influence of load cycle reconstitution on fatigue behaviour
[ARL-STRUC-R-424] 02 p0192 N88-11198
A low-power arcjet cyclic lifetest
[NASA-TM-100233] 03 p0278 N88-11748
Crack initiation and propagation due to cyclic thermal gradients --- aircraft turbine blades
[ESA-TT-1023] 03 p0336 N88-12114
Composite materials applications program at the US Army Ballistic Research Laboratory: Work in progress 04 p0428 N88-12651
X-ray analysis of polycrystalline aluminium subjected to fatigue cycling
[NAL-TM-MT-8706] 05 p0564 N88-13434
Application of finite element methods with cyclic elasto-plastic strain analysis to low cycle fatigue analysis of engine components
[AR-004-512] 05 p0596 N88-13642
Fatigue 87, volume 3
[AD-A184047] 05 p0604 N88-13700
A study of corrosion fatigue crack initiation, growth and the threshold condition under variable amplitude loading 05 p0604 N88-13701
The effect of environment on low cycle fatigue properties in HSLA steel 05 p0605 N88-13705
Fatigue crack propagation in Al-Zn-Mg bicrystals and its dependence on the environment 05 p0605 N88-13707
Low cycle fatigue behaviour of notched specimens of nickel based superalloy single crystal 05 p0605 N88-13712
Computer aided modeling and fatigue failure forecast under stochastic loading 05 p0607 N88-13720
Embrittling effect of the plastic zone 05 p0607 N88-13721
X-ray fatigue failure prediction based on plasticity response to microcracks 05 p0607 N88-13725
Electron microscopy studies of tensile cyclic fatigue-tested silicon nitride ceramics
[DE88-001438] 06 p0685 N88-14196
Investigation of instability, dynamic forces, and effect of dynamic loading on strength of cages for the bearings in the high pressure oxygen turbopumps for the space shuttle main engine
[NASA-CR-178970] 06 p0714 N88-14378
On the relations between cyclic contraction ratio flowstress and deformation mechanisms in bainitic CrMoV steels
[DE87-753043] 08 p0968 N88-15856
Experimental determination of crack growth rates in cyclic stress applications, for improving the forecasted computed durability in operation
[FF-14/1986] 09 p1182 N88-17085
Elastoplastic response of unidirectional graphite/aluminum under combined tension-compression cyclic loading
[CCMS-88-01] 11 p1451 N88-18647
Lead-acid load-leveling battery testing at Argonne National Laboratory
[DE88-002853] 11 p1480 N88-18837
Evaluation of advanced lead-acid batteries developed for load-leveling applications
[DE88-002871] 11 p1481 N88-18838
The cyclic stress-strain behavior of a single crystal nickel-base superalloy
[NASA-TM-100269] 12 p1607 N88-19610
Cyclic crack growth emanating at a round notch considering viscoplasticity
[AD-A189577] 13 p1781 N88-20655
Cyclic uniaxial and biaxial hardening of type 304 stainless steel modeled by the viscoplasticity theory based on overstress 14 p1931 N88-21514
Some implications for cyclic plastic and viscoplastic equations based on nonproportional loading experiments 14 p1931 N88-21515
The growth of corner cracks under the conjoint action of high and low cycle fatigue
[AD-A190510] 15 p2076 N88-22379
High-temperature combustor liner tests in structural component response test facility 15 p2077 N88-22383
Life assessment of combustor liner using unified constitutive models 15 p2077 N88-22384
Development of a flexible and economic helicopter engine monitoring system
[PB88-165147] 16 p2160 N88-22887
Fatigue crack growth under full-scale cyclic plasticity
[DFVLR-FB-87-48] 16 p2222 N88-23263
A cyclic ground test of an ion auxiliary propulsion system: Description and operational considerations
[NASA-TM-100870] 17 p2313 N88-23829
Investigation of the long term effects of aging on carbon epoxy composites exposed naturally to the weather under cyclic loads. (Results of sampling after 2.5 years). Test report M1-641300
[CEAT-39/M/79-C-M1-641300] 17 p2316 N88-23834
An extended life and performance test of a low-power arcjet
[NASA-TM-100942] 18 p2476 N88-24687
Cyclic fatigue damage characteristics observed for simple loadings extended to multiaxial life prediction
[NASA-CR-182126] 18 p2531 N88-25016
Energy dissipation in a rolling aircraft tire
[NASA-CR-182978] 19 p2676 N88-25913
Fatigue crack growth under far-field cyclic compression
[DE88-011215] 20 p2813 N88-26689
Damage in a perforated graphite-epoxy plate under monotonic, cyclic biaxial loading
[ONERA-NT-1987-5] 20 p2816 N88-26708
Load interaction effects on compression fatigue crack growth in ductile solids
[FFA-TN-1988-12] 22 p3089 N88-28342
An investigation of constitutive models for predicting viscoplastic response during cyclic loading
[AD-A194875] 24 p3385 N88-30163

CYCLING
U CYCLES

CYCLOBUTANE
Research in energetic compounds
[AD-A192953] 20 p2781 N88-26494

CYCLOGENESIS
Australian East Coast cyclones 3: Case study of the storm of August 1986 02 p0204 N88-11276
Cumulus and thunderstorm initiation by mountains 02 p0207 N88-11301
The Windsor Locks, Connecticut tornado of 3 October 1979: An analysis of an intermittant severe weather event 02 p0208 N88-11305
Magnetospheric storms 03 p0272 N88-11711
Environmental and convective influence on tropical cyclone development versus non-development
[AD-A185231] 05 p0627 N88-13835
Simulation of a lee cyclogenesis using a numerical model 08 p1016 N88-16162
Interplanetary Magnetic Field (IMF) influence on the magnetic configuration and particle fluxes at geostationary orbit and on the substorm onset 08 p1031 N88-16247
A possible role for ionospheric ions in triggering a geomagnetic substorm onset 08 p1096 N88-16594
The structure and dynamics of monsoon depressions 10 p1355 N88-18102

Analysis of quasi-geostrophic forcing during the AIMCS (Airborne Investigations of Mesoscale Convective System) Project. Volume 1: Discussion
[PB88-133095] 12 p1646 N88-19860
A paper on horizontal deformation in the frontogenesis in south Brazil
[INPE-4469-TDL/322] 12 p1647 N88-19867
Tropical cyclones, 1987: Central North Pacific
[PB88-188081] 18 p2547 N88-25119

CYCLOHEXANE
Cross section of resonant Raman scattering of light by polyenes 07 p0920 N88-15591

CYCLONES
NT HURRICANES
NT TYPHOONS
Tropical cyclone center locations from enhanced infrared satellite imagery
[PB87-213450] 01 p0071 N88-10455
Summary of 1987 Atlantic tropical cyclone activity and verification of author's seasonal forecast 02 p0215 N88-11356
Tropical cyclone intensity prediction based on empirical orthogonal function representation of wind and shear fields
[AD-A184699] 03 p0353 N88-12229
Annual tropical cyclone report, 1986
[AD-A184082] 04 p0470 N88-12903
Lower-stratospheric/upper-tropospheric exchange processes associated with tropical cyclones as observed by TOMS 05 p0616 N88-13782
Opportunities for tropical cyclone motion research in the Northwest Pacific region
[AD-A185068] 05 p0627 N88-13834
Estimation of rainfall rates in tropical cyclones by passive microwave radiometry 06 p0744 N88-14577
The effect of latitude on the development of tropical cyclones
[AD-A185670] 06 p0746 N88-14590
Interim review of the possibilities and opportunities for the ONR tropical cyclone motion research initiative
[AD-A185679] 06 p0746 N88-14592
Thunderstorms with snow: A comprehensive, empirical study of their occurrence, development and structure
[AD-A185929] 07 p0879 N88-15329
Recent Colorado State University tropical cyclone research of interest to forecasters
[AD-A185996] 07 p0879 N88-15332
Typhoon structural evolution
[AD-A186090] 07 p0879 N88-15333
Numerical investigation of orographically enhanced instability
[AD-A186841] 09 p1189 N88-17125
The role of vortex structure in tropical cyclone motion
[AD-A190961] 16 p2235 N88-23351
Mariners weather log, volume 32, number 1, Winter 1988
[PB88-173869] 18 p2544 N88-25097
Suggested hurricane operational scenario for GOES I-M
[NASA-TM-89729] 19 p2692 N88-26002
Tropical cyclone report
[AD-A191883] 19 p2693 N88-26009
Passive microwave measurements of water vapor fields and rain for locating fronts in cyclonic storms
[AD-A195632] 24 p3404 N88-30267

CYCLONES (EQUIPMENT)
U CENTRIFUGES

CYCLOTETRAMETHYLENE TETRANITRAMINE
U HMX

CYCLOTRIMETHYLENE TRINITRAMINE
U RDX

CYCLOTRON FREQUENCY
Elements of plasma physics 03 p0271 N88-11703
Fundamental cyclotron frequency generation from a cusptron oscillator
[AD-A188187] 10 p1321 N88-17898
Microwave generation from a cusptron oscillator with a six-vane circuit
[AD-A188377] 12 p1619 N88-19680
The effects of a dc electric field on the current driven ion cyclotron instability
[AD-A188877] 12 p1695 N88-20142
Observations of electron cyclotron harmonic emissions associated with field-aligned electron beams
[SD-TR-87-33] 19 p2724 N88-26173

CYCLOTRON RADIATION
NT ION CYCLOTRON RADIATION
Nonthermal phenomena in stellar coronae: Evidence from radio observations 04 p0503 N88-13096
Higher harmonic generation in the induced resonance electron cyclotron maser
[AD-A186236] 07 p0858 N88-15210
Experimental evaluation for efficiency of excitation slow plasma and cyclotron waves in collective accelerators
[DE88-700566] 07 p0936 N88-15687
Absorption of cyclotron radiation in skin layer in Araks experiment 08 p1003 N88-16076
Conceptual design of a radio-frequency driven compact tokamak
[INPE-4364-PRE/1190] 08 p1085 N88-16535
Absorption of electron cyclotron radiation in tokamak plasmas with a superthermal tail in the electron velocity distribution
[INPE-4391-PRE/1211] 08 p1086 N88-16541
Advanced studies of integrable systems
[AD-A186792] 09 p1151 N88-16895
Microwave generation from a cusptron oscillator with a six-vane circuit
[AD-A188377] 12 p1619 N88-19680
Measurements of optically thin electron cyclotron emission from relativistic electrons
[DE88-004713] 12 p1688 N88-20096
Heating and confinement studies of electron cyclotron resonance heated plasmas in Heliotron E
[DE88-752312] 15 p2136 N88-22746
Kinetic modulational instability of electron cyclotron waves in plasmas
[DE88-701893] 20 p2859 N88-26978
EXO033319-2554.2: A 55-MG eclipsing AM Herculis binary
[MPE-PREPRINT-114] 22 p3163 N88-28838

CYCLOTRON RESONANCE
Nonthermal phenomena in stellar coronae: Evidence from radio observations 04 p0503 N88-13096
Anomalies in electromagnetic absorption of circularly polarized ultrasonic waves by tungsten within Doppler-shifted cyclotron resonance range 06 p0775 N88-14756
Development of FTMS methods for the detection of trace chemical species and development of FTMS methods for the analysis of various chemical species
[AD-A185857] 07 p0828 N88-15023
Current generation and induced conductivity of a plasma under common action of constant electric field and lower-hybrid or ECR waves
[DE88-700345] 07 p0935 N88-15680
The effect of asymmetric current-supporting electron velocity distributions on second harmonic electron cyclotron resonance heating: A ray-tracing treatment for the compass tokamak
[INPE-4389-PRE/1209] 08 p1087 N88-16549
Simulation and modeling of whistler mode wave growth through cyclotron resonance with energetic electrons in the magnetosphere 10 p1353 N88-18089
Application of ECR ion source beams in atomic physics
[DE88-003767] 10 p1406 N88-18384
ATF experimental plans
[DE88-004177] 10 p1414 N88-18439
Mode priming in an overmoded gyrotron oscillator
[AD-A189151] 13 p1772 N88-20602
Heating and confinement studies of electron cyclotron resonance heated plasmas in Heliotron E
[DE88-752312] 15 p2136 N88-22746
Status of RF superconductivity at Argonne National Laboratory
[DE88-005913] 15 p2144 N88-22796
Parallel gradient effects on ICRH (Ion Cyclotron Resonance Heating) in tokamaks
[DE88-009038] 19 p2730 N88-26216
Kinetic modulational instability of electron cyclotron waves in plasmas
[DE88-701893] 20 p2859 N88-26978
Ion kinetics in silane plasmas
[AD-A196202] 24 p3431 N88-30423

CYCLOTRON RESONANCE DEVICES
Optimization of mode converters for generating the fundamental TE(06) gyrotron output at 140 GHz
[IPF-87-1] 01 p0043 N88-10273
Mode purity measurements on gyrotrons for plasma heating at the stellarator W 7-AS
[IPF-87-3] 01 p0101 N88-10660
High peak power ka-band gyrotron oscillator experiment
[AD-A185424] 05 p0585 N88-13563
Theoretical and experimental investigation of electron beam acceleration and sub-millimeter wave generation in cyclotron resonant cavities
[AD-A184806] 05 p0649 N88-13975
Initial operation of a high-power whispering-gallery-mode gyrotron
[DE88-002500] 07 p0857 N88-15207
Higher harmonic generation in the induced resonance electron cyclotron maser
[AD-A186236] 07 p0858 N88-15210
Gyrotron development at the Instituto de Pesquisas Espaciais
[INPE-4240-PRE/1115] 08 p0990 N88-15992
Recent results of plasma research activities at the Instituto de Pesquisas Espaciais
[INPE-4383-PRE/1203] 08 p1085 N88-16538
First and second harmonic ECRH experience at gyrotron frequencies at LLNL
[DE88-003998] 10 p1413 N88-18430
High peak power Ka-band gyrotron oscillator experiments with slotted and unslotted cavities
[AD-A188109] 11 p1478 N88-18819
Trip electrical circuit of the gyrotron
[INPE-4336-NTE/273] 12 p1622 N88-19701
Time-dependent Slow-Time-Scale theory of free-running and phase-locked gyrotron oscillators
[AD-A188910] 12 p1629 N88-19752
Measurement technique for characterization of the gyrotron
[INPE-4322-RPE/550] 12 p1630 N88-19758
Mode priming in an overmoded gyrotron oscillator
[AD-A189151] 13 p1772 N88-20602
Synthesis method applied to the design of an electron gun for a gyrotron
[INPE-4357-TDL/298] 13 p1773 N88-20607
Calculation of the efficiency of a resonant cyclotronic electron maser (gyrotrons)
[INPE-4387-PRE/1207] 14 p1915 N88-21444
Theoretical and experimental study of a mode-converting coupler for application to a harmonic gyrotron amplifier
[AD-A193760] 22 p3081 N88-28294
Wide band gyrotron traveling wave amplifier analysis
[AD-A194269] 23 p3216 N88-29139
The study of hydromagnetic waves and RF heating using the TORTUS tokamak, the development of diagnostic techniques based on submillimeter lasers and the gyrotron, and gas discharge 24 p3431 N88-30419

CYCLOTRONS
NT MICROTRONS

CYGNUS CONSTELLATION
Gamma-ray imaging observations of the Crab and Cygnus regions 10 p1427 N88-18522
Colliding stellar winds in the eclipsing Wolf-Rayet binary V444 Cygni
[NASA-CR-182937] 17 p2451 N88-24563
Gamma rays from Cygnus X-1: Modeling and nonthermal pair production
[DE88-006830] 18 p2596 N88-25426
Observation of a point source in Cygnus constellation with the underground detector at Frejus (France)
[PITHA-87/02] 20 p2884 N88-27122

CYLINDERS
Hot piston ring/cylinder liner materials: Selection and evaluation
[NASA-TM-100276] 08 p0971 N88-15872
Cast iron-base alloy for cylinder/regenerator housing
[NASA-CR-182116] 12 p1608 N88-19613
An interferometric investigation of the diffraction of planar shock waves over a half-diamond cylinder in air
[UTIAS-322] 13 p1768 N88-20575
Measurement of the properties of lossy materials inside a finite conducting cylinder
[NASA-CR-182664] 13 p1832 N88-20962

CYLINDRICAL AFTERBODIES
U AFTERBODIES
U CYLINDRICAL BODIES

CYLINDRICAL BODIES
NT ROTATING CYLINDERS
Possibilities for the modeling of dynamically loaded cylindrical structural parts in the wind tunnel
[KU-SFB-210/T/24] 01 p0001 N88-10005
Evaluation of cracking in aluminum cylinders
[PB87-201398] 01 p0024 N88-10149
Design and analysis of a broadband TM(sub 01) mode generator in cylindrical waveguide
[DE87-011308] 01 p0038 N88-10243
Cooling effect of a single evaporating droplet on a hot semi-infinite metal body
[PB87-201802] 01 p0046 N88-10294
The wear process during the RUNNING-IN of steel in lubricated sliding
[NAL-TR-922T] 02 p0181 N88-11130
Flow visualization on an ogive-nosed circular cylinder body at high incidence using the laser light sheet method
[ESA-TT-1066] 03 p0315 N88-11993
Scaling of size/time/temperature associated with dilatation and distortion in uniaxial specimens 03 p0336 N88-12117
Breaking wave forces on vertical cylinders
[RR-CE71] 03 p0338 N88-12126
Analytic model of an imploding Z-pinch plasma colliding inelastically with a thin-shelled cylindrical target
[DE88-000051] 03 p0378 N88-12379
Driving mechanism of unsteady separation shock motion in hypersonic interactive flow 05 p0530 N88-13226
Three-dimensional flow past a two-dimensional body 05 p0539 N88-13280
Computational study of three-dimensional wake structures
[REPT-2] 05 p0539 N88-13281

Computation of flow around 2-D circular cylinder
05 p0539 N88-13284
Interferometric data for a shock-wave/boundary-layer interaction
[NASA-TM-88227] 05 p0543 N88-13306
An analytical study of the effects of transverse shear deformation and anisotropy on buckling loads of laminated cylinders
[NASA-TM-100508] 05 p0557 N88-13387
The simulation of the viscous flow around a cylinder by the random vortex method 05 p0579 N88-13534
Fiber-optic accelerometer investigation
[AD-A185359] 05 p0584 N88-13561
Alignment and assembly tool for very large diameter cylinders
[NASA-CASE-MFS-28001-2] 06 p0711 N88-14360
The numerical and analytical study of bifurcation and multicellular flow instability due to natural convection between narrow horizontal isothermal cylindrical annuli at high Rayleigh numbers
[AD-A186113] 07 p0849 N88-15151
A project to experimentally and theoretically examine fluid interfacial wave phenomena in a rotating cylindrical geometry: Current results and future plans
[DE88-003738] 09 p1165 N88-16984
Propagation of creep waves around rough cylindrical surface 09 p1234 N88-17400
An analytical study of the effects of transverse shear deformation and anisotropy on natural vibration frequencies of laminated cylinders
[NASA-TM-100554] 10 p1295 N88-17739
The numerical and analytical study of bifurcation and multicellular flow instability due to natural convection between narrow horizontal isothermal cylindrical annuli at high Rayleigh numbers 10 p1328 N88-17937
Fluctuations and massive separation in three-dimensional shock-wave/boundary-layer interactions
[NASA-TM-89224] 11 p1434 N88-18559
A study of damage tolerance in curved composite panels
[AD-A190617] 15 p2029 N88-22092
Bodies in unsteady flow
[AD-A190416] 15 p2064 N88-22308
Experimental determination of the coefficients of the hydraulic resistance of apertures in the rotary disks
[AD-A190627] 15 p2066 N88-22317
Buckling of blast loaded cylinder
[AD-A190124] 15 p2076 N88-22376
Thermal stress in high temperature cylindrical fasteners
[NASA-TM-100611] 15 p2087 N88-22438
Multiple scattering from nonspherical targets
[AD-A189939] 15 p2133 N88-22723
Experimental investigation of the hypersonic flow over a six finned configuration
[AD-A190670] 16 p2157 N88-22871
Electromagnetic scattering from nonlinear anisotropic cylinders 17 p2333 N88-23930
Cylindrical surface profile and diameter measuring tool and method
[NASA-CASE-MFS-28287-1] 17 p2341 N88-23959
Experimental investigation of simplest inhomogeneities in cylindrical slit line
[DE88-702388] 21 p2933 N88-27418
Determination of the local heat-transfer characteristics on glaze ice accretions on a cylinder and a NACA 0012 airfoil 21 p2946 N88-27500
The three-dimensional stress field around a cylindrical inclusion in a plate of arbitrary thickness
21 p2963 N88-27602
Marangoni convection in finite cylindrical liquid bridges
[LRT-WE-9-FB-5(1988)] 22 p3078 N88-28277
AGARD (Advisory Group for Aerospace Research and Development) engine disc material cooperative test (supplementary program)
[AD-A193678] 23 p3179 N88-28925
Additional fracture and strength test results for A723 steel and 38644 titanium
[AD-A196329] 24 p3353 N88-29960
The aspect ratio dependence of the attractor dimension in Taylor-Couette flow
[AD-A196297] 24 p3369 N88-30065

CYLINDRICAL CHAMBERS
Overview of free-piston Stirling engine technology for space power application
[NASA-TM-88886] 03 p0386 N88-12427

CYLINDRICAL PLASMAS
Effect of plasma rotation in tokamak on stabilizing action of electrically conducting wall 06 p0773 N88-14748
Experimental study of scattered waves and cylindrical antenna sheaths in a microwave driven plasma
11 p1553 N88-19293
Numerical research of dispersion properties of plasma cylindrical waveguides located in magnetic field
[DE87-703009] 16 p2275 N88-23615

CYLINDRICAL SHELLS
Rational reinforcement of cylindrical shells with variable stiffness frames subjected to external pressure
04 p0426 N88-12638
A direct method to obtain constitutive model constants from cylinder impact test results
04 p0427 N88-12647
Analysis and testing of predamaged shell structures
04 p0428 N88-12653
Vibration and buckling of geometrically imperfect laminated cylindrical shells 04 p0456 N88-12822
Experimental studies on the tripping behavior of narrow T-stiffened flat plates subjected to hydrostatic pressure and underwater shock 05 p0592 N88-13613
Experimental investigation of damping characteristics of bolted structural connections for plates and shells
[AD-A186075] 07 p0867 N88-15259
Influence of radiation and thermal conduction on temperature distribution in the thin wall of a hollow cylinder
[INPE-4428-TDL/308] 12 p1626 N88-19730
Monolithic nature of transversely reinforced composites 14 p1885 N88-21267
Forced motion of initially stressed shells and plates
18 p2529 N88-25005
A study of fluid-structure problems
21 p2941 N88-27468
Nonlinear oscillations of a nonviscous cylindrical liquid system in weightlessness condition
[LRT-WE-9-FB-14(1987)] 22 p3063 N88-28175
Nonlinear vibrations of imperfect thin walled cylindrical shells
[ETN-88-92904] 23 p3227 N88-29205
Stresses in cylindrical shells with tangential nozzles submitted to external loads and internal pressure
[CRIF-MT-172] 24 p3382 N88-30146
Large displacement and rotational formulation for laminated cylindrical shells including parabolic transverse shear
[AD-A194871] 24 p3384 N88-30158
Behaviour and hysteresis losses of irreversible type-2 superconducting cylindrical shell
[DE88-702708] 24 p3433 N88-30434

CYLINDROIDS
U CYLINDRICAL BODIES

CYTOCHROMES
Cytochrome electron transfer and biomolecular electronics
[AD-A195482] 24 p3406 N88-30277

CYTOGENESIS
NT CELL DIVISION
NT DIFFERENTIATION (BIOLOGY)
NT HEMATOPOIESIS
NT MITOSIS
Review of cytoskeleton research in cell differentiation and development
[AD-A185832] 07 p0882 N88-15353
Investigation of genetic structures of rat germ cells following flight aboard Cosmos-1514 biosatellite during their prenatal development 10 p1364 N88-18155

CYTOLOGY
Electron cytochemical detection of Ca(2)+-ATPase in protonema of moss funaria hygrometrica (H e d w.) under hypogravitation 06 p0749 N88-14602
Third Soviet-French Symposium on Space Cytology
07 p0893 N88-15411
Changes in hemostasis system of animals under conditions of granulocytopoiesis inhibition under effect of decreased barometric pressure
12 p1651 N88-19890
Cytomorphology and ultrastructure of corn root meristem in weightlessness 12 p1651 N88-19891
Electrical and chemical sensors for biological cell research 19 p2669 N88-25866
The effect of microgravity on mammalian cell polarization at the ultrastructural level --- Spacelab D1 mission
22 p3061 N88-28164

CYTOPLASM
Review of cytoskeleton research in cell differentiation and development
[AD-A185832] 07 p0882 N88-15353

CZECHOSLOVAKIA
Proceedings of the First International Symposium on Physical and Technical Problems of Superconductivity Application in Power Generation
[DE88-700818] 11 p1559 N88-19332

CZOCHRALSKI METHOD
Digital control of the Czochralski growth of Gallium arsenide-controller software reference manual
[AD-A187210] 11 p1528 N88-19127
Autonomous Liquid Encapsulated Czochralski (LEC) growth of single crystal GaAs by intelligent digital control
[AD-A187211] 11 p1555 N88-19305
Hydrodynamic simulation of forced convection in the Czochralski process
[INPE-4471-TDL/323] 12 p1697 N88-20158
Modeling growth of interdendritic silicon ribbons
14 p1897 N88-21322
Stress corrosion of ceramic materials
[AD-A190501] 15 p2045 N88-22187
Autonomous control system for Czochralski growth of LEC GaAs
[AD-A189726] 15 p2141 N88-22779
Real time thermal imaging of high temperature semiconductor melts 17 p2330 N88-23914
Digital control of the czochralski growth of gallium arsenide. System reference manual. Valid for Czochralski growth controller software version 2.4
[AD-A191997] 19 p2732 N88-26227

D

D LAYER
U D REGION

D REGION
Future developments of auroral D-region research using the EISCAT VHF incoherent scatter radar
08 p1035 N88-16278
On formulating a simple D-region model
[AD-A195841] 24 p3392 N88-30197
Photochemistry of ionospheric D-region with injection of nitrogen oxides 24 p3444 N88-30499

DAEMO (DATA ANALYSIS)
U DATA PROCESSING
U DATA REDUCTION
U DATA TRANSMISSION

DAMA
U DEMAND ASSIGNMENT MULTIPLE ACCESS

DAMAGE
NT CUMULATIVE DAMAGE
NT EARTHQUAKE DAMAGE
NT FIRE DAMAGE
NT FROST DAMAGE
NT IMPACT DAMAGE
NT LASER DAMAGE
NT METEORITIC DAMAGE
NT RADIATION DAMAGE
NT RAIN IMPACT DAMAGE
NT STORM DAMAGE
Space station integrated wall design and penetration damage control
[NASA-CR-179169] 01 p0013 N88-10070
Structural reliability and damage tolerance of ceramic composites for high-temperature applications
[PB87-208310] 01 p0019 N88-10119
Contribution to the study of composite materials and their damage
[NASA-TT-20107] 02 p0143 N88-10897
Airworthiness of long-life jet transport structures
03 p0285 N88-11674
Indentation damage in ceramics
[AD-A184686] 03 p0294 N88-11844
Analysis and testing of predamaged shell structures
04 p0428 N88-12653
Data base on the high heat flux behaviour of metals and carbon materials for plasma facing components: Experiments at the 10 MW neutral beam injection test stand of the IPP Nagoya
[IPPJ-AM-53] 04 p0492 N88-13031
Fiber composite structural durability and damage tolerance: Simplified predictive methods
[NASA-TM-100179] 05 p0560 N88-13409
Raman microprobe characterization of dielectric films following high-energy pulsed laser irradiation
[DE88-000559] 05 p0588 N88-13587
Fretting wear and fretting fatigue damage
05 p0603 N88-13697
Study of damage in carbon fiber-epoxy composite materials. Utilization to assess broken specimens
[DCQ/L-45-650/F] 06 p0678 N88-14152
Characterization of mechanical damage mechanisms in ceramic composite materials
[AD-A185549] 06 p0686 N88-14205
Fatigue damage maps 06 p0715 N88-14382
Transients in elevated temperature crack growth
[DE87-013189] 06 p0724 N88-14454
Ion mixing and surface modification in metal-semiconductor systems
[DE88-001702] 06 p0786 N88-14823
Natural frequencies and structural integrity assessment of large space structures
[AD-A186139] 07 p0824 N88-15001
Finite element analysis of damaged cross-ply composite laminates
[CCMS-87-10] 09 p1139 N88-16829
Reliability of structures with stiffness and strength degradation 09 p1180 N88-17068
Analytical and experimental characterization of damage processes in composite laminates
[AD-A187221] 10 p1296 N88-17746

Relationship between fatigue life in the creep-fatigue region and stress-strain response
[NASA-TM-100796] 10 p1345 N88-18040
Modeling of the non-auditory response to blast overpressure
[AD-A187397] 10 p1369 N88-18184
Atomistic simulation of low-energy beam deposition
[DE88-004344] 11 p1544 N88-19228
A continuum damage model for viscoelastic materials
[AD-A189426] 12 p1637 N88-19800
Abrasion resistant porous silica antireflective coatings
[DE88-006230] 14 p1894 N88-21308
Structural consequences of railgun augmentation
[DE88-007036] 15 p2023 N88-22058
A study of damage tolerance in curved composite panels
[AD-A190617] 15 p2029 N88-22092
Buckling of blast loaded cylinder
[AD-A190124] 15 p2076 N88-22376
Evolution of hardening and damage during viscoplastic deformation
[AD-A190714] 15 p2077 N88-22381
Rainfall rates and drop-size distributions for environmental testing
[AD-A191342] 16 p2236 N88-23354
Damage by creep fatigue: Influence of the visco-elasticity of the matrix
[PB88-124706] 18 p2528 N88-24998
Optical damage in epoxy polymers by millisecond light pulses
[DE88-008675] 19 p2620 N88-25547
Modulation efficiency limited high frequency performance of the MODFET 19 p2657 N88-25786
Laser induced surface emission of neutral species and its relationship to optical surface damage processes
[DE88-008035] 19 p2726 N88-26192
Stiffness degradation of composite laminates
20 p2767 N88-26405
Computation equipment for damage simulation in laminated composites
[AD-A193013] 20 p2768 N88-26412
The influence of foreign particles on bearing metals
[NASA-TT-20155] 20 p2775 N88-26454
Irreversible deformations during fracture in polymers
[W-7/86] 20 p2780 N88-26485
Mobile robot survival
[DE88-009108] 20 p2809 N88-26665
Damage in a perforated graphite-epoxy plate under monotonic, cyclic biaxial loading
[ONERA-NT-1987-5] 20 p2816 N88-26708
Vibrational impacts of hush house operation
[DE88-006983] 21 p2899 N88-27207
Fiber-optics used to record high-speed photographs inside a pressurized tank during lethality testing
[DE88-011283] 21 p2951 N88-27529
Critical issues and directions for fracture mechanics and structural integrity
[AD-A193050] 21 p2960 N88-27584
The relationship between observed fatigue damage and life estimation models
[NASA-CR-182191] 21 p2965 N88-27611
Analysis of stiffness reduction, failure and stress concentration in fiber composite laminates
[AD-A193519] 22 p3050 N88-28096
Procedures for identification and handling of Printed Circuit Boards (PCBs)
[AD-A191177] 23 p3206 N88-29078
Photorefractive damage mechanism in electro-optic materials
[AD-A194560] 23 p3282 N88-29543
Damage initiation in the short beam shear test of composite materials using stiffness reduction
[AD-A194880] 24 p3340 N88-29883
Automated early fatigue damage sensing system
[AD-A195717] 24 p3382 N88-30143
An investigation of constitutive models for predicting viscoplastic response during cyclic loading
[AD-A194875] 24 p3385 N88-30163

DAMAGE ASSESSMENT

Calculation of the damage of highly loaded gas turbine disks under real flight conditions
[ETN-87-90416] 01 p0007 N88-10036
New fatigue damage analysis of complex engineering components based on Finite Element Methods (FEM)
[DFVLR-FB-87-15] 01 p0062 N88-10401
Investigation of large scale impact of air pollution components on forest ecosystems in Bavaria, West Germany
[DFVLR-FB-87-17] 01 p0068 N88-10434
Development of a method for forest damage inventory using multispectral scanner data
[KFK-PEF-25] 03 p0345 N88-12182
Failure control techniques for the SSME
[NASA-CR-179224] 04 p0409 N88-12537
Low-cost teleoperator-controlled vehicle for damage assessment and dose measurement
[DE88-000713] 04 p0451 N88-12794
Contribution of acoustic analysis to assess damage in fluid storage tanks under high pressure --- composite materials, filament winding
[SNIAS-872-430-119] 05 p0559 N88-13407
Overview of Austrian Airborne Imaging Spectrometer (AIS) programme and first results
05 p0612 N88-13762
Review of fatigue and fracture research at NASA Langley Research Center 09 p1106 N88-16633
Optimized approach to damage tolerance --- spacecraft
[FOK-FSS-R-87-024] 09 p1134 N88-16806
Sublaminate damage mechanisms in composite structures
[AD-A186807] 09 p1137 N88-16815
Mechanical properties of carbon fiber reinforced thermoplastic matrix composites
[NAL-TR-934] 09 p1139 N88-16827
A chemical precursor to optical damage. Studies by laser ionization mass spectrometry
[DE88-004321] 10 p1409 N88-18408
Profilometer for bomb-damage-repaired airfield pavements and measurement of pavement upheaval. Report 1: Technology evaluation
[AD-A187985] 11 p1442 N88-18601
Sub-scaling of projectile/target system damaged by hypervelocity
[AD-A188683] 12 p1634 N88-19779
Activities report of the Structures Department
[ETN-88-91986] 13 p1783 N88-20672
A theory of viscoplasticity accounting for internal damage 14 p1930 N88-21508
Creep rupture analysis of a beam resting on high temperature foundation 14 p1930 N88-21509
A constitutive model with damage for high temperature superalloys 14 p1930 N88-21510
Damage models for delamination and transverse fracture
[AD-A189652] 15 p2029 N88-22088
Oxide optical coatings prepared by metal-organic vapor deposition
[DE88-006809] 15 p2043 N88-22175
Impact damage in composite laminates
15 p2080 N88-22402
Life prediction modeling based on cyclic damage accumulation 15 p2085 N88-22426
Towards a damage tolerance philosophy for composite materials and structures
[NASA-TM-100548] 16 p2173 N88-22949
Tornado tracks in Southwestern Brazil, Eastern Paraguay, and Northwestern Argentina
17 p2362 N88-24071
Dimensional analysis and experimental observation of the coupling phenomena between combustion and fracture of damaged propellant samples
19 p2630 N88-25803
Characterization of fatigue crack initiation and propagation in Ti-6Al-4V with electrical potential drop technique
[NASA-TM-100877] 19 p2681 N88-25937
Principles of a nondestructive evaluation process for damage location, damage profile, and damage extension in welded joints by radiometric measurements
[MPA-86-02] 20 p2812 N88-26683
T55-L-714 engine development and qualification. Engine M11 low cycle fatigue test report. (0213-005-87)
[AD-A192765] 21 p2897 N88-27197
T55-l-714 engine development and qualification. Engine M11 low cycle fatigue test report. (0213-005-87), volume 2, part 1
[AD-A192766] 21 p2897 N88-27198
Techniques for characterizing damage zones in composite materials 21 p2905 N88-27240
Design and implementation of contact ultrasonic sensors to assess internal damage
[I-177/87] 21 p2906 N88-27247
An anisotropic continuum damage model for creep-dominated, multiaxial loading histories
21 p2964 N88-27608
Assessment of cochlear damage after microwave irradiation
[AD-A193237] 21 p2987 N88-27737
Study of the forests on the banks of the Gambia and criteria for detecting mortality 22 p3091 N88-28356
Contribution to the mapping of forests in an intensively divided area, with the help of SPOT image data
22 p3107 N88-28453
Evaluation of the contribution of SPOT in the framework of the mineral exploration program of the Aitutaki Atoll (Cook Islands). Preliminary study of the impact of the passage of Hurricane Sally 22 p3109 N88-28463
A comprehensive study on damage tolerance properties of notched composite laminates
[AD-A192952] 23 p3188 N88-28968

DAMAGE THRESHOLD

U YIELD POINT

DAMPERS

Rotational evolution of dynamically symmetric gyrostat with internal friction 24 p3448 N88-30509

DAMPING

NT ELASTIC DAMPING
NT LANDAU DAMPING
NT VIBRATION DAMPING
NT VISCOELASTIC DAMPING
NT VISCOUS DAMPING
Investigation of control law for active flutter suppression
[NASA-TT-20126] 02 p0130 N88-10818
Damping characteristics of a composite-reinforced stainless-steel tube
[DE87-012455] 02 p0191 N88-11192
A comparison of high damping shape memory alloys with Cu-Mn-based and Fe-Cr-based alloys
[AD-A184110] 04 p0414 N88-12566
Damping characteristics of a composite-reinforced stainless-steel plate
[DE88-000303] 04 p0457 N88-12828
Influence of surfactants on damping of gravity-capillary waves. 1: Frequency dependence
04 p0459 N88-12843
An analysis of sound absorbing linings for the interior of the NASA Ames 80 x 120-foot wind tunnel
[NASA-CR-177396] 04 p0488 N88-13006
Non-linear shipboard shock analysis of the Tomahawk missile shock isolation system 05 p0592 N88-13614
Improvement of modal scaling factors using mass additive technique 05 p0593 N88-13620
Group contribution analysis of the damping behavior of homopolymers, statistical copolymers and interpenetrating polymer networks based on acrylic, vinyl and styrenic mers
[AD-A185904] 07 p0836 N88-15070
Coherent states for the damped harmonic oscillator
[AD-A186111] 07 p0922 N88-15599
On free decay damping tests
08 p0997 N88-16041
A modal control based limiting performance formulation for shock excited systems 08 p0998 N88-16046
Active control technology with adaptive control concept in the aircraft construction
[MBB/LKE-294/S/PUB/295] 10 p1313 N88-17845
Characterization of damped structural connections for multi-component systems
[NASA-TM-100801] 11 p1502 N88-18974
The impact of vertical axis characteristics on helicopter handling qualities
[AD-A188964] 12 p1583 N88-19474
Practical considerations for structural control: System uncertainty, system time delay and truncation of small control forces
[PB88-163738] 14 p1933 N88-21528
Oscillation damped movement of suspended objects
[DE88-005715] 15 p2086 N88-22433
Electromagnetic dampers for cryogenic applications
16 p2218 N88-23231
Characterization of structural connections for multicomponent systems 16 p2220 N88-23251
Driving of axial acoustic fields by side-wall stabilized premixed flames 19 p2629 N88-25592
Statistical evaluation of light water reactor piping damping data for use in PRA (Probabilistic Risk Assessment) analyses
[DE88-007708] 19 p2661 N88-25828
The importance of steady and dynamic inflow on the stability of rotor-body systems 21 p2890 N88-27156
Comparison of experimental rotor damping data-reduction techniques 21 p2891 N88-27159
Experimental determination of aerodynamic damping in a three-stage transonic axial-flow compressor
[NASA-TM-100953] 21 p2897 N88-27200
Damping characteristics of metal matrix composites
[AD-A193144] 21 p2904 N88-27233
Development of a nitrile rubber for dynamic damping
[AD-A194060] 22 p3058 N88-28145
Power flow analysis of two coupled plates with arbitrary characteristics
[NASA-CR-183165] 22 p3075 N88-28251
Waves and instabilities in an electron-positron plasma in an ultra-strong magnetic field
23 p3283 N88-29551
Analytical and experimental studies of beam waveguide absorbers for structural damping
[AD-A195085] 24 p3382 N88-30144

DAMPING FACTOR

U DAMPING

DAMPING IN PITCH
U DAMPING
U PITCH (INCLINATION)
DAMPING IN ROLL
U DAMPING
U ROLL
DAMPING IN YAW
U DAMPING
U YAW
DAMPING TESTS
Analytical and experimental studies of beam waveguide absorbers for structural damping
[AD-A195085] 24 p3382 N88-30144
DAMPNESS
U MOISTURE CONTENT
DANGER
U HAZARDS
DARK ADAPTATION
Effect of intermittent hypercapnia on visual analyzer function 07 p0896 N88-15431
Night Vision: Current Research and Future Directions, symposium proceedings
[PB88-132006] 11 p1550 N88-19274
Mechanisms of early light and dark adaptations 12 p1663 N88-19972
DARK MATTER
Might dark matter not be concentric with luminous matter
[DE87-703094] 02 p0252 N88-11589
Galaxy formation by gravitational collapse in a universe dominated by cold dark matter 04 p0521 N88-13205
Infrared constraints on the nature of dark matter 13 p1855 N88-21102
The comet flux and the 15 Myr galactic cycle 14 p1995 N88-21889
Stable, heavy, neutral particles in the sun and in toponium decay 17 p2452 N88-24568
Non-linear scale invariance in a cold-dark-matter universe
[DE88-011725] 23 p3299 N88-29644
Gravitational redshift of self-gravitating systems of dark matter in the universe
[DE88-702688] 23 p3300 N88-29650
DARKENING
NT LIMB DARKENING
DARKNESS
Trickle water and feeding system in plant culture and light-dark cycle effects on plant growth 03 p0361 N88-12273
The accommodative status in the dark of US Navy fighter pilots
[AD-A188188] 10 p1370 N88-18186
DART TURBOPROP ENGINES
U TURBOPROP ENGINES
DASSAULT AIRCRAFT
NT MIRAGE AIRCRAFT
Acceleration of prototype development and reduction of cost by multidisciplinary integration 12 p1704 N88-20199
DATA ACQUISITION
Space station propulsion technology: Space station propulsion system test bed test plan
[NASA-CR-179201] 01 p0017 N88-10104
Outgassing data for selecting spacecraft materials
[NASA-RP-1124] 01 p0019 N88-10117
Estimation from satellite imagery of summertime rainfall over varied space and time scales
[PB87-203246] 01 p0071 N88-10454
Input devices for tasks using interactive video
[NPL-DITC-87/87] 01 p0080 N88-10510
A CAMAC system controlled by an IBM AT computer for time-resolved spectroscopy
[DE87-010111] 01 p0080 N88-10514
EAGLES: An interactive environment for scientific computing
[DE87-013564] 01 p0084 N88-10541
Direct detection of optical radiation through a sampling orifice for inductively coupled plasma atomic emission spectroscopy
[DE87-013609] 01 p0101 N88-10662
The status of the international Halley watch 01 p0116 N88-10744
Nickel hydrogen low Earth orbit test program update and status 02 p0164 N88-11028
Further development of the dynamic gas temperature measurement system 02 p0184 N88-11141
An acoustic emission digital data acquisition workstation
[DE87-012425] 02 p0191 N88-11191
An isentropic coordinate model used in a mesoscale data assimilation system 02 p0212 N88-11333
The future of data in mesoscale numerical models 02 p0214 N88-11344
The challenge of using mesoscale data in mesoscale numerical models 02 p0214 N88-11346
Implementing and managing change: A guide for assessing information technology
[DE88-000035] 02 p0249 N88-11571
GEOSAT altimeter geophysical data record user handbook
[PB87-213336] 03 p0276 N88-11743
SPOT: A tool for agricultural statistics 03 p0344 N88-12170
A Workshop on Desert Processes, September 24-28, 1984: Report on the conference
[AD-A184599] 03 p0345 N88-12184
Calendar year 1985 solar and weather data for Austin, Texas
[PB87-220174] 03 p0352 N88-12219
The MicroVAX-based data acquisition system for D0
[DE87-014475] 03 p0366 N88-12303
Automated microwave dielectric constant measurement
[AD-A184182] 04 p0431 N88-12667
The Telecommunications and Data Acquisition Report
[NASA-CR-181546] 04 p0432 N88-12679
Traveling-wave maser closed-cycle refrigerator data acquisition and display system 04 p0437 N88-12708
Tau ranging revisited 04 p0437 N88-12710
Computerized certification of digital ultrasonic instrumentation
[DE88-000820] 04 p0488 N88-13008
Automatic photometric monitoring of cool stars 04 p0504 N88-13103
High frequency data acquisition system for space shuttle main engine testing 05 p0595 N88-13630
The Portable Instant Display and Analysis Spectrometer (PIDAS) 05 p0611 N88-13756
Plant Growth Module (PGM) conceptual design 05 p0631 N88-13855
Software design for an airborne gravity measurement system
[AD-A185000] 05 p0634 N88-13878
Boeing 727 MLS (Microwave Landing System) terminal instrument procedures (TERPS) approach data collection and processing, data report
[AD-A185523] 06 p0667 N88-14090
Area detectors for X-ray spectroscopy
[DE88-001429] 06 p0679 N88-14163
Description of data handling system installed December 11, 1986 --- EISCAT 06 p0692 N88-14242
AVIRIS onboard data handling and control 06 p0706 N88-14332
Application of remote sensing to agricultural field trials
[ISBN-90-6754-089-7] 06 p0729 N88-14483
The archiving of meteor research information 06 p0732 N88-14505
Tropical hydrology
[WMO-655] 06 p0745 N88-14584
Acquisition of gust statistics from Aircraft Integrated Data Systems (AIDS) recorded data
[NLR-MP-86048-U-ISS-2] 06 p0745 N88-14586
Facilities for research and weather observations on the 213 m tower at Cabauw (Netherlands) and at remote locations
[KNMI-WR-87-5] 06 p0746 N88-14587
Wave and wind data sources, environmental conditions committee report, International Ship and Offshore Structures Congress
[PB87-234902] 06 p0746 N88-14588
Data acquisition, reduction and analysis of shock and vibration testing using a super microcomputer
[AD-A186123] 07 p0867 N88-15260
Data on existing wind energy converters in Denmark
[DE88-900199] 07 p0874 N88-15300
Collecting of new data on existing wind energy converters
[DE88-900221] 07 p0875 N88-15305
Biotechnology in western Europe
[PB88-105887] 07 p0883 N88-15360
A learning model as a basis for investigations of the effects of gravity on the learning processes and memory formulation 07 p0886 N88-15374
Problems of organization of mass processes of simulation, acquisition and processing of experimental data at computers
[DE88-700547] 07 p0905 N88-15483
SSME environment database development
[NASA-CR-179245] 08 p0964 N88-15836
Laboratory vibration test schedules development beyond MIL-STD-810D 08 p0999 N88-16050
Alouette-ISIS program summary
[NASA-CR-180747] 08 p1023 N88-16195
High-speed assembly language (80386/80387) programming for laser spectra scan control and data acquisition providing improved resolution water vapor spectroscopy
[NASA-CR-4117] 08 p1053 N88-16355
Interactive knowledge acquisition tools 08 p1060 N88-16401
Flow field measurements using hotwire anemometry
[AD-A187029] 09 p1160 N88-16951
Data acquisition and analysis system for the Sandia 34-meter Vertical Axis Wind Turbine
[DE88-002417] 09 p1187 N88-17112
Design knowledge capture for the space station 09 p1208 N88-17239
TDAS: The Thermal Expert System (TEXSYS) data acquisition system 09 p1211 N88-17258
Management Information and Downloader Interface System (MIDIS)
[AD-A186978] 09 p1261 N88-17557
A reliable data collection/control system 10 p1289 N88-17708
Speech recognition: Acoustic-phonetic knowledge acquisition and representation
[AD-A187293] 10 p1320 N88-17893
Evaluation of surface energy and radiation balance systems on the Konza Prairie
[NASA-CR-182534] 10 p1355 N88-18097
Developments in National Weather Service meteorological data collection programs as related to EPA (Environmetal Protection Agency) air pollution models
[PB88-130240] 10 p1356 N88-18104
Minimum Energy Routing through Interactive Techniques (MERIT) modeling
[NASA-CR-182535] 10 p1356 N88-18105
Methods of eliciting information from experts
[AD-A187468] 10 p1372 N88-18189
MICRO system for control, acquisition and processing of experimental data
[DE88-700724] 10 p1386 N88-18278
SETI data controllers 11 p1474 N88-18795
Overview of multi-input frequency domain modal testing methods with an emphasis on sine testing 11 p1499 N88-18949
Data acquisition and processing for surface plate calibration
[AD-A187264] 11 p1564 N88-19366
The global positioning system as an aid to the testing of inertial navigation units (volume 1, addendum 1)
[AD-A185783] 12 p1578 N88-19443
Automatic data acquisition system utilizing microcomputers: Automatic Meteorological Stations (AMS)
[INPE-4215-PRE/1096] 12 p1646 N88-19859
Homogenizing surface and satellite observations of cloud. Aspects of bias in surface data
[AD-A188523] 12 p1648 N88-19869
A knowledge acquisition tool for the intelligent processing of materials
[AD-A188982] 12 p1679 N88-20036
Pion absorption in nuclei: The pion(+ or -),proton reactions
[LA-10997-T] 12 p1688 N88-20098
RIAR automated research and management systems
[DE88-700934] 12 p1706 N88-20209
An analysis of physiological data related to motion sickness for use in a real-time motion sickness indicator
[AD-A189589] 13 p1810 N88-20812
Solar cell experiment on the first satellite of the Brazilian complete space mission
[INPE-4248-PRE/1121] 14 p1880 N88-21238
A data acquisition system for atmospheric tracer studies
[DE88-006211] 14 p1991 N88-21869
Enhancement of data acquisition and numerical computation capabilities for unsteady fluid dynamics
[AD-A190115] 15 p2063 N88-22302
Calibration and processing of AVHRR data for temperature estimation
[INPE-4493-PRE/1257] 15 p2095 N88-22485
A multivariate variational objective analysis-assimilation method. Part 2: Case study results with and without satellite data
[NASA-CR-182653] 15 p2097 N88-22492
Real-time environmental Arctic monitoring (R-TEAM)
[AD-A189948] 15 p2099 N88-22508
Complex sound processing: An interdisciplinary approach
[AD-A189782] 15 p2102 N88-22523
Fast analog-to-digital converter
[DE88-701488] 15 p2106 N88-22543
Application of static memory for data acquisition and transmission into a computer
[DE88-701491] 15 p2106 N88-22544
A compact high resolution piezoresistive digital tactile sensor
[DE88-000430] 16 p2210 N88-23188
Low-cost optical data acquisition system for blade vibration measurement 16 p2219 N88-23240
Accurate positioning of long, flexible ARM's (Articulated Robotic Manipulator) 16 p2219 N88-23243
Seasonal variation for structural strength value
[PB88-169248] 16 p2222 N88-23260

Overground Excess Sound Attenuation (ESA). Volume 1: Experimental study for flat grassy terrains
[AD-A191289] 16 p2265 N88-23549
The Engineer Studies Center guide to research and data collection
[AD-A189971] 16 p2285 N88-23680
Investigation of air transportation technology at Ohio University, 1986 17 p2293 N88-23719
Modeling of functional specifications for onboard software: Experience with the Rafale avionics system 17 p2303 N88-23777
Presentation of the METEOSAT system and the roles of EUMETSAT within the meteorological community 17 p2357 N88-24039
ERS-1 data products and services and their value for tropical countries 17 p2357 N88-24040
Processing of HRPT data from the NOAA series satellites 17 p2359 N88-24053
Cessna 172 MLS (Microwave Landing System) terminal instrument procedures (TERPS) approach data collection and processing data report
[AD-A191241] 18 p2461 N88-24613
Adaptive data acquisition multiplexing system and method
[NASA-CASE-MSC-21170-1] 18 p2471 N88-24662
Taiwan area mesoscale experiment: P-3 aircraft operations summary
[PB88-169073] 18 p2544 N88-25098
Knowledge acquisition tool implementation
[AD-A190415] 18 p2555 N88-25164
SAMS: The synchronization and monitoring system for ATF (Advanced Toroidal Facility) data acquisition provides unified data access for ATF data acquisition
[DE88-007268] 18 p2589 N88-25386
The JPL MSAT mobile laboratory and the pilot field experiments 19 p2646 N88-25708
Ultrasonic and video computerized data acquisition for automated welding
[DE88-006741] 19 p2677 N88-25918
Monitoring of divers/astronauts during missions 19 p2698 N88-26036
RAGS (Realtime Acquisition and Graphics System): An off-the-shelf hardware and system software small data acquisition computer
[DE88-008399] 19 p2716 N88-26128
Meteorological satellite product support and research for project GALE
[NASA-CR-180989] 19 p2727 N88-26193
Measurement of HO2 and other trace gases in the stratosphere using a high resolution far-infrared spectrometer at 28 KM
[NASA-CR-180400] 20 p2821 N88-26737
Computer controlled data acquisition system for the NASA 1986 Rocket Triggered Lightning Program
[DE88-008335] 20 p2826 N88-26766
An expeditious technique for keyboard input of information to FORTRAN computer programs
[DE88-009617] 20 p2840 N88-26855
An overview of the development of a linear broadband analog fiber-optic link
[DE88-008668] 20 p2854 N88-26945
An integrated, multi-vendor distributed data acquisition system
[DE88-008900] 20 p2882 N88-27113
FTMP data acquisition environment
[NASA-TM-100636] 21 p2938 N88-27447
Army space systems for terrestrial applications
[AD-A192735] 21 p2965 N88-27613
The Hanford meteorological data collection system and data base
[DE88-008632] 21 p2975 N88-27672
Synopsis of a computer program designed to interface a personal computer with the fast data acquisition system of a time-of-flight mass spectrometer
[NASA-CR-177474] 21 p3001 N88-27798
SERI standard broadband format: A solar and meteorological data archival format
[DE88-001145] 21 p3028 N88-27975
Test and calibration system for monitoring the Advanced Technologies Testing Aircraft System (ATTAS) data acquisition system 22 p3037 N88-28029
Mark IV-85 mission support planning and future mission set 22 p3067 N88-28202
Research for reducing the labor intensive nature of high-resolution terrain analysis feature extraction
[AD-A192661] 22 p3089 N88-28345
SPOT data acquisition and distribution 22 p3115 N88-28505
Software engineering for the EBR-2 data acquisition system conversion
[DE88-009950] 22 p3136 N88-28647
Computer-controlled measurements of nonlinear standing waves
[AD-A193840] 22 p3147 N88-28717
Space shuttle phase B wind tunnel model and test information. Volume 2: Orbiter configuration
[NASA-CR-178415-VOL-2-PT-1] 23 p3171 N88-28881
Knowledge acquisition and rapid protyping of an expert system: Dealing with real world problems 23 p3258 N88-29394
Acquisition of gust statistics from AIDS-recorded data 24 p3313 N88-29733
MIZEX (marginal ice zone experiment) 1987 SAR (Synthetic Aperture Radar) data summary
[AD-A195560] 24 p3364 N88-30035
Laser sensing for identification and control of distributed parameter systems
[AD-A195886] 24 p3379 N88-30124
Microwave remote sensing at INPE (Institute for Space Research) Brazil: Concepts and future prospects of soil moisture studies
[INPE-4569-PRE/1310] 24 p3388 N88-30178
China's acquisition and use of foreign aviation technology
[AD-A194827] 24 p3440 N88-30471

DATA ADAPTIVE EVALUATOR/MONITOR

U DATA PROCESSING
U DATA REDUCTION
U DATA TRANSMISSION

DATA ANALYSIS

U DATA PROCESSING
U DATA REDUCTION

DATA BASE MANAGEMENT SYSTEMS

Object-oriented data base management for robot programming
[ETN-87-90367] 01 p0105 N88-10687
High performance clause indexing
[DE87-011399] 01 p0106 N88-10688
A new compression method with fast searching on large databases
[DE87-010986] 01 p0106 N88-10691
File management using balanced trees
[ENST-87D001] 01 p0106 N88-10693
The microcomputer as an engineering management tool
[DE87-014882] 02 p0219 N88-11378
Summaries of the FY 1987 applied mathematical sciences research program
[DE87-014447] 02 p0225 N88-11416
Design and development of a database for spectral data and analysis results
[DE87-011323] 02 p0247 N88-11564
Definitions as database records
[DE87-014057] 02 p0248 N88-11570
Comparison of pascal and the dBASE 3 PLUS language in programming an inventory management system
[AD-A184027] 03 p0365 N88-12300
Electronic Records Administration at the Savannah River Plant
[DE87-014842] 03 p0384 N88-12415
IDMS application documentation made easy
[DE88-000199] 03 p0384 N88-12416
User's guide to NCAR (National Center for Atmospheric Research) CCM1
[PB87-224366] 04 p0469 N88-12899
Managing distributed derived data: A preliminary proposal
[DE88-000714] 04 p0481 N88-12966
A data translation method for heterogeneous database systems 04 p0501 N88-13081
Towards automated consulting: Design feedback from the performance of online documentation
[DE87-012243] 04 p0501 N88-13082
Relational data handling system for scientists
[PB87-223426] 05 p0658 N88-14038
Scientific data manipulation in a relational database system
[PB87-124400] 06 p0791 N88-14850
Computer aided design for Petri Nets
[AD-A186109] 07 p0902 N88-15465
GENLPLOT: An interactive program for display and analysis of data, user's manual
[DE88-002292] 07 p0905 N88-15485
Enhancement of computer system for applications software branch 07 p0923 N88-15610
Expert system development for commonality analysis in space programs 07 p0928 N88-15635
Interface between astrophysical datasets and distributed database management systems (DAVID)
[NASA-CR-182394] 07 p0942 N88-15731
SSME environment database development
[NASA-CR-179245] 08 p0964 N88-15836
Third Conference on Artificial Intelligence for Space Applications, part 1
[NASA-CP-2492-Pt-1] 08 p1055 N88-16360
Conceptual information processing: A robust approach to KBS-DBMS integration 08 p1063 N88-16422
Foundation: Transforming data bases into knowledge bases 08 p1063 N88-16423
Proposal of a methodology for the conceptual design of the Distributed Data Base
[INPE-4315-TDL/282] 08 p1093 N88-16576
Critical issues in NASA information systems
[NASA-CR-182380] 08 p1093 N88-16577
Design and implementation of a data base system for Digital Land Mass System (DLMS) data
[FEL-IR-1987-19] 09 p1185 N88-17101
Nested transactions, conflict-based locking, and dynamic atomicity
[AD-A187033] 09 p1217 N88-17294
Management of complex information in support of evolving autonomous expert systems
[AD-A186680] 09 p1224 N88-17337
Application of a database system for inventory management of classified material
[AD-A186986] 09 p1261 N88-17558
KBGIS-II: A knowledge-based geographic information system
[NASA-CR-182492] 09 p1261 N88-17559
Computer-Aided Design Information System (CADIS): User's manual
[DE88-004365] 10 p1424 N88-18509
Cockpit data management
[NASA-CR-178407] 11 p1438 N88-18579
Cockpit data management
[NASA-CR-178407-SUPPL] 11 p1438 N88-18580
Ceramic technology for advanced heat engines program data base
[DE88-003922] 11 p1464 N88-18730
The design and implementation of pedagogical software for the multi-backend/multi-lingual database system
[AD-A188106] 11 p1530 N88-19135
The design of the POSTGRES storage system
[AD-A187244] 11 p1564 N88-19365
UNIVERS product, phase 1
[AD-A187405] 11 p1564 N88-19367
Supporting valid time: An historical algebra
[AD-A187740] 11 p1565 N88-19368
Accessing hierarchical databases via SQL transactions in a multi-model database system
[AD-A187878] 11 p1565 N88-19369
Regenerative life support system research
[NASA-CR-182606] 12 p1671 N88-20006
Towards a solution to the proper integration of a logic programming system and a large knowledge based management system
[AD-A188949] 12 p1705 N88-20207
The TempIS Project: Performance analysis of temporal queries
[AD-A188354] 12 p1706 N88-20213
The TEMPIS project: Current status
[AD-A188963] 12 p1707 N88-20220
Martian Clouds Data Workshop
[NASA-CR-182431] 12 p1711 N88-20238
HISPLT: A history graphics post processor for wave propagation codes
[DE88-005507] 13 p1817 N88-20857
CSQPLT: A graphics post processor for multidimensional wave propagation codes
[DE88-005508] 13 p1817 N88-20858
Using design axioms and topology to model database semantics
[CWI-CS-R8711] 13 p1818 N88-20863
Distributed transaction processing and the Camelot system
[AD-A188614] 13 p1821 N88-20885
Reference model for DBMS (database management system) user facility
[PB88-169446] 13 p1851 N88-21080
Laboratory Information Management System (LIMS): A case study
[NASA-TM-100835] 14 p1961 N88-21697
Common database interface for heterogeneous software engineering tools
[AD-A189628] 14 p1991 N88-21870
Design of an algorithm to translate nested relational algebra queries to GENESIS trace manager commands
[AD-A190502] 15 p2112 N88-22581
A graphics editor for structured analysis with a data dictionary
[AD-A190618] 15 p2112 N88-22584
Modeling a parallel architecture for image processing
[RR-646-I] 15 p2114 N88-22593
Application of new technologies to DTIC document processing
[AD-A189778] 15 p2148 N88-22823
Data base design and implementation
[AD-A190414] 15 p2149 N88-22827
Georelational data model
[INPE-4490-PRE/1254] 15 p2149 N88-22829
Axiomatic specificatin of database domain statics
[PB88-176284] 16 p2250 N88-23444

Data management and language enhancement for generalized set theory computer language for operation of large relational databases
[NASA-CR-182868] 16 p2250 N88-23446
PPDS compas-primer
[DE88-701589] 16 p2266 N88-23554
Reference nuclear data for space applications
[DE88-007041] 16 p2270 N88-23583
Data base management in CAD/CAM systems: Requirements for CAD/CAM data bases, actual market offer, advice for an efficient data base management, development tendencies
[MBB/LWD-11/S/PUB/254] 16 p2285 N88-23683
Automated database design technology and tools
[NASA-CR-182875] 16 p2286 N88-23687
Crewstation Information and Development System (CIDS) 17 p2304 N88-23781
EnviroNET: An interactive space-environment information resource
[NASA-TM-101137] 17 p2309 N88-23812
Reports on cartography and geodesy. Series 1, no. 99
[ETN-88-92367] 18 p2533 N88-25025
West German Geodetic Working Group: Official topographic-cartographic information system (ATKIS), content description 18 p2533 N88-25026
West German Geodetic Working Group: Official topographic-cartographic information system (ATKIS), technical conception 18 p2533 N88-25027
Creation of digital topographic models with the ALK-GIAP. The DLM 25 as an example 18 p2534 N88-25031
Topographic data processing for environmental planning 18 p2534 N88-25032
State of development of ALK (October 1986) 18 p2534 N88-25035
Geometric rectangular data file (GERD): An aid to the rapid access to position data 18 p2534 N88-25037
Photovoltaic Advanced Research and Development Project, solar radiation research
[DE88-001143] 18 p2537 N88-25056
The human genome: Computational challenges
[DE88-006465] 18 p2549 N88-25131
The ATF (Advanced Toroidal Facility) Data M Management System
[DE88-007265] 18 p2589 N88-25385
Computer-aided research
[DE88-007771] 19 p2714 N88-26114
Report on the Second Catalog Interoperability Workshop
[NASA-TM-100701] 19 p2718 N88-26135
MVS (Multiple Virtual Storage) batch computing and data management at ANL
[DE88-007342] 19 p2718 N88-26137
Real time data base management
[AD-A191758] 19 p2739 N88-26265
Issues and recommendations associated with distributed computation and data management systems for the space sciences
[NASA-CR-183026] 20 p2881 N88-27108
Computer science and technology: Knowledge-based system for physical database design
[PB88-193289] 20 p2882 N88-27109
Towards knowledge bases-semantics, rules and object-oriented programming
[PB88-108154] 20 p2882 N88-27110
Space shuttle phase B wind tunnel model and test information. Volume 2: Orbiter configuration
[NASA-CR-178415-VOL-2-PT-2] 21 p2893 N88-27172
Database design and management in engineering optimization
[AD-A193325] 21 p3003 N88-27813
Developing a connector selection DBMS (database management system) using NIAM (Nijssen's Information Analysis Methodology)
[DE88-008110] 21 p3028 N88-27972
Pattern information processing and multimedia database system: Current research on multimedia information system
[PB88-131917] 21 p3028 N88-27973
Sources and nature of cost analysis data base reference manual
[AD-A193099] 21 p3028 N88-27976
Space shuttle phase B wind tunnel model and test information. Volume 2: Orbiter configuration
[NASA-CR-178415-VOL-2-PT-1] 23 p3171 N88-28881
Regional environmental studies using national data bases and GIS (Geographic Information System)
[DE88-008368] 23 p3230 N88-29225
A relational data-knowledge base system and its potential in developing a distributed data-knowledge system 23 p3251 N88-29353
Analyst-centered models for systems design, analysis, and development 23 p3253 N88-29364
Avionic expert systems 23 p3253 N88-29365
Intelligent resource management for local area networks: Approach and evolution 23 p3256 N88-29385
The emergence of multi-user expert systems 23 p3260 N88-29406
Central user and browse service --- ERS-1 ground segment
[CU-PG-MDA-SY-0005] 23 p3297 N88-29637
Catalog of open clusters and associated interstellar matter
[NASA-RP-1202] 23 p3300 N88-29652
Space shuttle phase B wind tunnel model and test information. Volume 3: Launch configuration
[NASA-CR-178416-VOL-3-PT-2] 24 p3315 N88-29744
Space shuttle phase B wind tunnel model and test information. Volume 1: Booster configuration
[NASA-CR-178414-VOL-1-PT-1] 24 p3315 N88-29745
Space shuttle phase B wind tunnel model and test information. Volume 1: Booster configuration
[NASA-CR-178414-VOL-1-PT-2] 24 p3320 N88-29770
An operations manual for the digital data system
[NASA-CR-181688] 24 p3415 N88-30329
The second generation intelligent user interface for the crustal dynamics data information system 24 p3419 N88-30352
The P-3 Scheduling Support System (P-3 S3)
[AD-A194824] 24 p3436 N88-30450
Integrating images, applications, and communications networks, volume 5
[AD-A195854] 24 p3436 N88-30452

DATA BASES

Standard reference data publications, 1985-1986
[PB87-210241] 01 p0021 N88-10128
Digital Name Data Base Antarctic as a component of a landscape data base of the Antarctic 01 p0065 N88-10419
Nickel hydrogen low Earth orbit test program update and status 02 p0164 N88-11028
Using bibliographic databases in technology transfer
[NASA-CR-181403] 02 p0222 N88-11399
Design and development of a database for spectral data and analysis results
[DE87-011323] 02 p0247 N88-11564
Maintaining state constraints in relational databases: A proof theoretic basis
[DE87-014329] 02 p0248 N88-11569
Energy Data Base: Subject Thesaurus
[DE87-008007] 03 p0384 N88-12414
Advanced techniques for the storage and use of very large, heterogeneous spatial databases. The representation of geographic knowledge: Toward a universal framework --- relations (mathematics)
[NASA-CR-181517] 03 p0385 N88-12421
Statistical distribution of solar radiation (hourly sums): Cumulative frequency curves preparation of a European data set and direction for use
[PB87-107454] 04 p0467 N88-12886
Cloud cover determination in polar regions from satellite imagery
[NASA-CR-181544] 04 p0471 N88-12908
A tight upper bound for the speed-up of parallel best-first branch-and-bound algorithms
[AD-A184246] 04 p0477 N88-12939
Data base on the high heat flux behaviour of metals and carbon materials for plasma facing components: Experiments at the 10 MW neutral beam injection test stand of the IPP Nagoya
[IPPJ-AM-53] 04 p0492 N88-13031
The RAE experimental data-base for missiles at high Mach number and its use in assessing CFD methods 05 p0534 N88-13250
A rudimentary database for three-dimensional objects using structural representation
[CSE-87-00004] 05 p0590 N88-13597
Improvement of modal scaling factors using mass additive technique 05 p0593 N88-13620
Space shuttle main engine vibration data base 05 p0595 N88-13631
Role of technical information in innovation
[PB87-235388] 05 p0658 N88-14039
Boeing 727 MLS (Microwave Landing System) terminal instrument procedures (TERPS) approach data collection and processing, data report
[AD-A185523] 06 p0667 N88-14090
Octree data structures and creation by stacking
[PB87-234795] 06 p0758 N88-14650
Using user models and automatic expertise acquisition in data base interactions
[PB87-234357] 06 p0791 N88-14848
Geographic application of the relational data base system Cantor
[PB87-120945] 06 p0791 N88-14851
Communications for the DTroll distributed database system
[AD-A185579] 06 p0791 N88-14853
A review of hypertext in a NASA project management context 06 p0793 N88-14859
Overview of the Langley viscous drag reduction program 07 p0812 N88-14946
FAA air traffic control operations concepts. Volume 2: ACF/ACCC (Area Control Facility/Area Control Computer Complex) terminal and en route controll ers
[AD-A185980] 07 p0818 N88-14974
FAA air traffic control operations concepts. Volume 3: ISSS (Initial Sector Suite System) en route controllers
[AD-A185981] 07 p0818 N88-14975
FAA air traffic control operations concepts. Volume 4: TAAS (Terminal Advanced Automation System) terminal controllers
[AD-A185982] 07 p0818 N88-14976
FAA air traffic control operations concepts. Volume 5: ATCT/TCCC (Airport Traffic Control Tower/Tower Control Computer Complex) tower controllers
[AD-A185983] 07 p0818 N88-14977
An approach to validation and verification of the communications load model with supporting user's guide
[AD-A185926] 07 p0840 N88-15098
Research study for materials/properties test results database
[NASA-CR-178923] 07 p0861 N88-15222
Determination of network attributes from a high resolution terrain data base
[AD-A186078] 07 p0870 N88-15279
Explicit construction and analysis of some efficient empirical production functions in data envelopment analysis
[AD-A185907] 07 p0908 N88-15502
Thermodynamic values from computer summation of group additivity data
[AD-A186131] 07 p0940 N88-15711
DoD Gateway Information System (DGIS): Common command language mapping
[AD-A185951] 07 p0942 N88-15726
Self-adaptive data bases
[AD-A186414] 07 p0942 N88-15729
Catalog of infrared observations. Part 1: Data
[NASA-RP-1196-PT-1-ED-2] 07 p0944 N88-15738
SSME environment database development
[NASA-CR-179245] 08 p0964 N88-15836
TECOM's research efforts in the dynamic environments 08 p0999 N88-16048
Methodology for testing and validating knowledge bases 08 p1055 N88-16364
HSTDEK: Developing a methodology for construction of large-scale, multi-use knowledge bases 08 p1057 N88-16377
Space shuttle main engine anomaly data and inductive knowledge based systems: Automated corporate expertise 08 p1060 N88-16398
Conceptual information processing: A robust approach to KBS-DBMS integration 08 p1063 N88-16422
Foundation: Transforming data bases into knowledge bases 08 p1063 N88-16423
A data structure and algorithm for fault diagnosis 08 p1065 N88-16432
The crustal dynamics intelligent user interface anthology
[NASA-TM-100693] 08 p1067 N88-16448
Rotorcraft handling-qualities design criteria development 09 p1109 N88-16645
Global digital data sets of soil type, soil texture, surface slope and other properties: Documentation of archived data tape
[NASA-TM-100685] 09 p1185 N88-17097
User's guide to a data base of current environmental monitoring projects in the US-Canadian transboundary region
[DE88-002476] 09 p1188 N88-17119
An efficient representation of spatial information for expert reasoning in robotic vehicles 09 p1214 N88-17278
Metal hydrides
[DE88-005083] 10 p1299 N88-17766
Extension of nuclear structure data base searches for gamma-ray laser candidates
[DE88-004288] 10 p1336 N88-17985
Data-base of Antarctic pre-Pleistocene sediment cores
[PB88-124151] 10 p1354 N88-18094
A paradigm for concurrency control performance evaluation 10 p1377 N88-18220
Concurrency control and reliability in replicated database systems 10 p1377 N88-18221
Utilization of the JANAF (Joint Army Navy Air Force) database for chemical thermodynamic calculations
[DE88-004571] 10 p1423 N88-18501
Space shuttle phase B wind tunnel test database
[NASA-CR-4121] 11 p1444 N88-18611

NBS/Sandia/ICDD electron diffraction database
[DE88-004635] 11 p1454 N88-18665
The metallurgical database of Aladin: An alloy de sign system
[AD-A187724] 11 p1457 N88-18682
Overview of multi-input frequency domain modal testing methods with an emphasis on sine testing
11 p1499 N88-18949
The design and implementation of pedagogical software for the multi-backend/multi-lingual database system
[AD-A188106] 11 p1530 N88-19135
TYPICAL: A knowledge representation system for automated discovery and inference
[AD-A187483] 11 p1533 N88-19160
The design of the POSTGRES storage system
[AD-A187244] 11 p1564 N88-19365
Allocation of database files across parallel stores for efficient processing of partial-match queries
[AD-A188196] 11 p1565 N88-19371
Mono- and bistatic radar coverage diagrams including diffractive wave propagation 12 p1616 N88-19660
Historical electromagnetic propagation condition database description
[AD-A189157] 12 p1621 N88-19695
Department of Defense World Geodetic System 1984: Its definition and relationships with local geodetic systems
[AD-A188815] 12 p1639 N88-19811
Terrain classification from digital elevation data using slope and curvature information
[AD-A188940] 12 p1639 N88-19812
Worldwide distributions of shipboard surface meteorological observations for EM propagation analysis
[AD-A188771] 12 p1648 N88-19871
Application of ARIADNE: A data bank-based information system for human physiology research --- Spacelab Anthrorack 12 p1662 N88-19962
An evaluation of historical algebras
[AD-A188350] 12 p1684 N88-20067
A directory of databases available through SearchMAESTRO
[AD-A188813] 12 p1706 N88-20214
Design methodology for allocating data in a distributed database
[AD-A188826] 12 p1706 N88-20215
Development of a dependency theory toolbox for database design
[AD-A188872] 12 p1707 N88-20216
Database of average-power damage thresholds at 1064 nm
[DE88-004352] 13 p1776 N88-20626
An analysis of physiological data related to motion sickness for use in a real-time motion sickness indicator
[AD-A189589] 13 p1810 N88-20812
Knowledge retrieval as specialized inference
[AD-A189042] 13 p1823 N88-20899
Towards a tribology information system: The results of a Planning Workshop held at the National Bureau of Standards, July-August 1985
[PB88-168604] 14 p1918 N88-21448
Perfect knowledge and beyond --- chess endgames
[REPT-87-37] 14 p1967 N88-21738
Common database interface for heterogeneous software engineering tools
[AD-A189628] 14 p1991 N88-21870
LGM-30B stage 2 disected motor test report
[AD-A190771] 15 p2027 N88-22079
An expert system for discrete component digital circuit design
[AD-A189680] 15 p2059 N88-22274
Analysis of head response to torso acceleration. Volume 2: Description of data retrieval, analysis and display software
[PB88-156765] 15 p2104 N88-22536
A UNIX-based interactive VHDL (hardware description language) simulator
[AD-A189749] 15 p2109 N88-22565
ONTIC: A knowledge representation system for mathematics
[AD-A190553] 15 p2121 N88-22643
Sources of digital spatial data for geographic information systems
[AD-A189788] 15 p2148 N88-22824
Space communication link propagation data for selected cities within the multiple beam and steerable antenna coverage areas of the advanced communications technology satellite
[NASA-TM-100861] 16 p2191 N88-23070
Axiomatic specificatin of database domain statics
[PB88-176284] 16 p2250 N88-23444
Editfont an interactive font editing system
[AD-A191007] 16 p2251 N88-23453
A description of an automated database comparison program
[NASA-TM-100609] 16 p2253 N88-23463
Leave-K-Out diagnostics for time series
[AD-A191343] 16 p2261 N88-23518
Overground Excess Sound Attenuation (ESA). Volume 1: Experimental study for flat grassy terrains
[AD-A191289] 16 p2265 N88-23549
Reference nuclear data for space applications
[DE88-007041] 16 p2270 N88-23583
Data base management in CAD/CAM systems: Requirements for CAD/CAM data bases, actual market offer, advice for an efficient data base management, development tendencies
[MBB/LWD-11/S/PUB/254] 16 p2285 N88-23683
A likelihood based grouping method for multidimensional observations. An interactive method used on large transportation data bases
[REPT-87-74] 16 p2286 N88-23685
BRYNTRN: A baryon transport computer code, computation procedures and data base
[NASA-TM-4037] 16 p2290 N88-23714
Operation and performance of an integrated helicopter communication system 17 p2305 N88-23787
The SAGE geographic analysis system
17 p2361 N88-24063
Implantation of a geo-cartographical information system through microcomputers 17 p2361 N88-24064
An irradiation performance data base for nitride fuels
17 p2427 N88-24438
Cessna 172 MLS (Microwave Landing System) terminal instrument procedures (TERPS) approach data collection and processing data report
[AD-A191241] 18 p2461 N88-24613
Evaluation of NMC (National Meteorological Center) global analyses: 1979-1987
[PB88-178157] 18 p2544 N88-25096
Identification and acoustic characterization of seamounts
[AD-A192204] 18 p2548 N88-25123
EPL (Equational Programing Language) system design: Intermediate processing steps
[AD-A191203] 18 p2556 N88-25169
Phase diagrams in materials science and the use of the computer in their calculation
[PB88-155262] 18 p2586 N88-25364
Defense Technical Information Center cataloging guidelines
[AD-A192200] 18 p2589 N88-25382
Design of partially replicated distributed database systems: An integrated methodology
18 p2589 N88-25383
ECMWF (European Centre for Medium Range Weather Forecasts) global analyses 1979-1986: Circulation statistics and data evaluation
[PB88-178165] 19 p2692 N88-26001
The CERSAT archiving and processing center --- ERS-1 19 p2701 N88-26059
Accurate, productive aerodynamic simulation on patched mesh systems
[AD-A192040] 19 p2714 N88-26110
Meteorological satellite product support and research for project GALE
[NASA-CR-180989] 19 p2727 N88-26193
Analysis and synthesis of decision-making organizations
[AD-A191948] 19 p2738 N88-26258
SIMS: Single Interface to Multiple Systems
[AD-A192264] 20 p2837 N88-26832
Nucleon-nucleus interaction data base: Total nuclear and absorption cross sections
[NASA-TM-4053] 20 p2852 N88-26935
Automatic line network extraction from aerial imagery of urban areas through knowledge based image analysis
[AD-A193067] 21 p2965 N88-27615
National air toxics information clearinghouse: NATICH data base users guide for data viewing, February 1988
[PB88-197470] 21 p2970 N88-27645
Space shuttle natural environment analysis
[NASA-CR-179337] 21 p2976 N88-27676
A PRELUDE (analysis and design of control systems-preliminary utilities depository). A data-based interactive system of control software, user's guid e
[DFVLR-MITT-88-12] 21 p3000 N88-27795
Basic database operations on the butterfly parallel processor: Experiment results
[AD-A193199] 21 p3002 N88-27804
Capitalizing on experience with intelligence gateway software
[AD-A193362] 21 p3028 N88-27971
SPOT: A data capture and data updating tool for the French National Geographic Institute's (IGN's) cartographic data base 22 p3114 N88-28497
On the modes of growing-season precipitation over central North America 22 p3124 N88-28567
The effects of changes in observation and data assimilation systems on CAC climate data sets
22 p3124 N88-28568
Evaluation of global data sets for climate studies
22 p3124 N88-28569
A method to adjust climatological time series for discontinuous inhomogeneities
22 p3124 N88-28570
Global-scale temperature changes to August 1987 and a comparison of satellite and conventional data
22 p3125 N88-28572
Optimization techniques for relational database systems 22 p3137 N88-28650
Computing partial correlations from the data matrix
[AD-A193904] 22 p3138 N88-28659
ALGRES: A system for the specification and prototyping of complex databases
[REPT-87-018] 22 p3140 N88-28668
A comparison of typical meteorological year solar radiation information with the SOLMET data base
[DE88-009242] 23 p3234 N88-29247
Level 1 Ada/SQL (Structured Query Language) database language interface user's guide
[AD-A194480] 23 p3249 N88-29335
A fast parametric maximum flow algorithm, revision
[AD-A194026] 23 p3250 N88-29345
A relational data-knowledge base system and its potential in developing a distributed data-knowledge system 23 p3251 N88-29353
Hologram representation of design data in an expert system knowledge base 23 p3251. N88-29354
An expert system for reliability modeling
23 p3252 N88-29355
A knowledge-based decision support system for payload scheduling 23 p3252 N88-29358
An approach to combining heuristic and qualitative reasoning in an expert system 23 p3253 N88-29362
Avionic expert systems 23 p3253 N88-29365
Knowledge elicitation for an operator assistant system in process control tasks 23 p3253 N88-29366
Failure modes and effects analysis automation
23 p3254 N88-29370
Knowledge based programming environments: A perspective 23 p3258 N88-29393
A methodology for multiple rule system integration and resolution within a singular knowledge base
23 p3261 N88-29413
A survey of the current experimental database for lower hybrid current-drive and heating
[DE88-009830] 23 p3283 N88-29552
Central user and browse service --- ERS-1 ground segment
[CU-PG-MDA-SY-0005] 23 p3297 N88-29637
More than a solar cycle of synoptic solar and coronal data: A video presentation
[NASA-CR-181459] 23 p3308 N88-29708
The advice taker/inquirer: A system for high-level acquisition of expert knowledge
24 p3421 N88-30359
Partitioned storage for temporal databases
[AD-A195093] 24 p3436 N88-30451
Technical opinions regarding knowledge-based integrated information systems engineering, volume 8
[AD-A195857] 24 p3436 N88-30454
Design and performance analysis of a relational replicated database system
[AD-A196290] 24 p3437 N88-30456

DATA BUSSES

U CHANNELS (DATA TRANSMISSION)

DATA COMPACTION

U DATA COMPRESSION

DATA COMPRESSION

Study, design, and evaluation of data reduction by encoding or information extraction. Part 1: Data generation analysis --- multispectral satellite imagery
[NLR-TR-85094-L-PT-1] 01 p0078 N88-10501
Study, design and evaluation of data reduction by encoding or information extraction. Part 2: Operational considerations --- multispectral satellite imagery
[NLR-TR-85094-L-PT-2] 01 p0079 N88-10502
Study, design and evaluation of data reduction by encoding or information extraction. Part 3: Algorithm design --- multispectral satellite imagery
[NLR-TR-85094-L-PT-3] 01 p0079 N88-10503
Study, design and evaluation of data reduction by encoding or information extraction. Part 4: Performance demonstration --- multispectral satellite imagery
[NLR-TR-85094-L-PT-4] 01 p0079 N88-10504
Study, design and evaluation of data reduction by encoding or information extraction. Part 5: Algorithm implementation aspects --- multispectral satellite imagery
[NLR-TR-85094-L-PT-5] 01 p0079 N88-10505
Study on data compression systems for operational remote sensing --- meteosat imagery
[NLR-TR-86029-L] 05 p0620 N88-13808
Study of synthetic aperture radar data compression and encoding. Part 3: Performance evaluation of speckle suppression and data compression algorithms
[NLR-TR-85085-L-PT-3] 06 p0692 N88-14248

Study of synthetic aperture radar data compression and encoding. Part 4: Algorithm implementation aspects
[NLR-TR-85085-L-PT-4] 06 p0692 N88-14249
Study of synthetic aperture radar data compression and encoding. Part 1: SAR image data analysis
[NLR-TR-85085-L-PT-1] 07 p0843 N88-15115
Study of synthetic aperture radar data compression and encoding. Part 2: SAR image speckle suppression and data compression algorithms
[NLR-TR-85085-L-PT-2] 07 p0843 N88-15116
Feasibility studies of optical processing of image bandwidth compression schemes
[AD-A186073] 07 p0932 N88-15660
A hybrid transform/DPCM encoder for data compression
[DE88-003725] 09 p1154 N88-16919
A hybrid transform/DPCM encoder for data compression
[DE87-014852] 13 p1758 N88-20518
A study of data compactation using numerical methods
[INPE-4317-TDL/284] 13 p1828 N88-20929
Performance of data compression codes in channels with errors
[AD-A189667] 15 p2055 N88-22253
Efficient and fast data compression codes for discrete sources with memory
[ETN-88-92233] 16 p2246 N88-23420
Narrative compression coding for a channel with errors
[AD-A191577] 19 p2642 N88-25673
Optical interconnections for digital image coding
21 p2928 N88-27381
Compression and decompression of imaging sensor signals (CADISS): A multiprocessor system for image compression/decompression on board scientific satellites
[NLR-TR-87076-L] 24 p3414 N88-30323

DATA CONVERSION ROUTINES
NT SUBROUTINES
Design and implementation of a data base system for Digital Land Mass System (DLMS) data
[FEL-IR-1987-19] 09 p1185 N88-17101

DATA CONVERTERS
NT ANALOG TO DIGITAL CONVERTERS
NT DIGITAL TO ANALOG CONVERTERS
Data on existing wind energy converters in Denmark
[DE88-900199] 07 p0874 N88-15300
Collecting of new data on existing wind energy converters
[DE88-900221] 07 p0875 N88-15305

DATA CORRELATION
High temperature low cycle fatigue behavior and creep-fatigue interation of MA 6000 ODS alloy
06 p0720 N88-14425
Method for joint adjustment of satellite and surface geodetic networks 08 p1007 N88-16105
Unidimensional Rasch model and multidimensional data: An analytic approach
[PB88-105861] 10 p1372 N88-18187
Loran-C monitor correlation over a 92-mile baseline in Ohio 17 p2293 N88-23720
Study of data distributions and functions for the development of thermodynamic equations of state
[PB88-196365] 18 p2587 N88-25370

DATA FLOW ANALYSIS
Advanced Information Processing System (AIPS) proof-of-concept system functional design I/O network system services
[NASA-CR-181488] 03 p0384 N88-12413
Massive fine-grain parallelism in array computation: A data flow solution 10 p1382 N88-18254
Automated data flow diagram verification
10 p1382 N88-18255
Data flow graph optimization in IF1
[DE88-004396] 11 p1532 N88-19151
Verification of a systolic algorithm for string comparison
[CWI-CS-R8734] 13 p1819 N88-20873
A fully abstract semantics for data flow nets
[CWI-CS-R8724] 13 p1822 N88-20893
An extension of the MS pivoting rule to capacitated network flow problems
[REPT-87-33] 14 p1963 N88-21711
Strategies for concurrent processing of complex algorithms in data driven architectures
[NASA-CR-181657] 16 p2193 N88-23083
Adapting high-level language programs for parallel processing using data flow 16 p2216 N88-23234
Mental: An object-oriented macro data flow system
[NASA-TM-101165] 17 p2388 N88-24199
Statistical properties of real time events in an ATC (Air Traffic Control) system
[PB88-116781] 20 p2756 N88-26353
Finding minimum-cost circulations by canceling negative cycles
[AD-A192727] 21 p3005 N88-27825
Modularity in the PASCAL model compiler
[NPL-DITC-111/88] 22 p3139 N88-28664
Faster algorithms for the shortest path problem
[AD-A194031] 23 p3250 N88-29347
Improved time bounds for the maximum flow problem
[AD-A194034] 23 p3272 N88-29471

DATA HANDLING SYSTEMS
U DATA SYSTEMS

DATA INTEGRATION
Adaptive segmentation evaluation
[AD-A190965] 16 p2274 N88-23609
Remote sensing and data integration: Practical solutions for resource managers 17 p2356 N88-24034

DATA LINKS
Coherent infrared detection, volume B --- CO2 laser intersatellite data link
[ESA-CR(P)-2392-VOL-1] 01 p0034 N88-10218
Coherent infrared detection, volume D --- CO2 laser intersatellite data link
[ESA-CR(P)-2392-VOL-2] 01 p0034 N88-10219
Interoperability and integration of data relay satellite systems 03 p0339 N88-12134
The atmosphere of Mars and optical communications
04 p0434 N88-12692
Test and evaluation of the transputer in a multi-transputer system
[AD-A184969] 05 p0631 N88-13859
Land mobile satellite transmission measurements at 869 MHz. A comparison of error probabilities for various message block durations and fade margins as a function of vegetation shadowing
[NASA-CR-179929] 06 p0693 N88-14255
Media independent interface
[NASA-CR-172033] 08 p1066 N88-16446
Media independent interface. Interface control document
[NASA-CR-172032] 08 p1067 N88-16447
The European space physics analysis network
08 p1099 N88-16613
Horizontal estimation and information fusion in multitarget and multisensor environments
[AD-A186935] 09 p1224 N88-17336
Code division multiple access applied to fiber optic data transmission
[AD-A186873] 09 p1247 N88-17477
Information transfer in the National Airspace System
10 p1275 N88-17634
Design and implementation of a fiber optic RS232 link
[AD-A187319] 10 p1409 N88-18409
Cockpit data management
[NASA-CR-178407-SUPPL] 11 p1438 N88-18580
Development of VLSI optical data link
[AD-A187883] 11 p1549 N88-19265
Development of VLSI optical data link
[AD-A187884] 11 p1549 N88-19266
A pointing mechanism for intersatellite link system
14 p1874 N88-21194
Spatial distribution of traffic in a cellular mobile data network
[EUT-87-E-168] 14 p1904 N88-21378
Degradation of downlink distance measurement indexes by the addition of a third tone --- tone ranging
[CNES-CT/DRT/TIT/TR-122-T]
15 p2058 N88-22268
Connecting remote systems for demonstration of automation technologies 17 p2387 N88-24191
Development and validation of transmission measurements techniques of image contrast, utilizing existing IR imagers
[AD-A191471] 18 p2541 N88-25079
NASA's mobile satellite development program
19 p2643 N88-25682
Mobile satellite service for Canada
19 p2643 N88-25683
Development of the network architecture of the Canadian MSAT system 19 p2646 N88-25702
An operational open-end file transfer protocol for mobile satellite communications 19 p2651 N88-25738
Model for dynamically structured communicating systems
[PB88-105283] 21 p2931 N88-27402
Long haul underwater fiber optic link
[AD-A194487] 23 p3282 N88-29542
Optical multiple access intersatellite links
[BAE-TP-8502] 24 p3361 N88-30013
The LTPP communication processor --- Columbus and Hermes
[CL/CP/SES/FR/004] 24 p3415 N88-30328

DATA MANAGEMENT
Personal computers: A powerful tool for project management
[DE87-013381] 02 p0219 N88-11377
Confidentiality of data --- Columbus Polar Platforms
03 p0339 N88-12136
Performance evaluation of artificial intelligence systems
[AD-A184054] 03 p0368 N88-12316
Relational data handling system for scientists
[PB87-223426] 05 p0658 N88-14038
Report of the first session of the International Working Group on Data Management for the Global Precipitation Climatology project
[WCP-132] 06 p0745 N88-14582
Data processing of the JPA instrument. Part 1: Data management
[IFSI-86-15-PT-1] 06 p0757 N88-14645
Self-adaptive data bases
[AD-A186414] 07 p0942 N88-15729
Knowledge-based monitoring of the pointing control system on the Hubble space telescope
08 p1057 N88-16378
A multiprocessing architecture for real-time monitoring
08 p1059 N88-16390
Commonality analysis as a knowledge acquisition problem 08 p1062 N88-16413
Media independent interface
[NASA-CR-172033] 08 p1066 N88-16446
The crustal dynamics intelligent user interface anthology
[NASA-TM-100693] 08 p1067 N88-16448
Telemetry applications handbook
[AD-A186825] 09 p1132 N88-16789
MPAD MCC workstation system: ADDAM and EEVE
09 p1203 N88-17209
Beyond rules: The next generation of expert systems
09 p1210 N88-17256
Nested transactions, conflict-based locking, and dynamic atomicity
[AD-A187033] 09 p1217 N88-17294
Using SIR (Scientific Information Retrival) system for data management during a field program
[DE88-001555] 10 p1424 N88-18508
Rocketdyne automated dynamics data analysis and management system 11 p1499 N88-18954
National Severe Storms Laboratory, fiscal year 1987
[PB88-140108] 12 p1647 N88-19863
JEDA (Joint Environmental Data Analysis) Center report on tropical Pacific subsurface thermal data management, 1986
[PB88-140090] 12 p1649 N88-19875
Editing master oceanographic observation data set 4
[AD-A188405] 12 p1649 N88-19876
National Informatics Centre: Profile of services
[PB88-134135] 12 p1706 N88-20211
GADL: A gate array description language
[EUT-87-E-165] 14 p1907 N88-21396
Higher levels of a silicon compiler
[EUT-86-E-163] 14 p1955 N88-21650
Generating layouts for random logic: Cell generation schemes
[EUT-86-E-164] 14 p1956 N88-21658
Technology mapping from Boolean expressions to standard cells
[EUT-87-E-174] 14 p1963 N88-21709
An optimal CMOS structure for the design of a cell library
[EUT-87-E-166] 14 p1985 N88-21841
Sigma system: Overview, prospects
15 p2052 N88-22230
Synthetic-aperture radars viewed as interferometers with matched filter processing of the collected data
[AD-A190608] 15 p2057 N88-22262
Proposals for the pre-operational use of data from the European Remote Sensing Satellite ERS-1
[BCRS-86-02] 16 p2227 N88-23300
WMO Region 2/Region 5 Training Seminar on Climate Data Management and User Services
[WCP-133] 16 p2234 N88-23344
A timestamp ordering mechanism with dynamic selection of rollback objects 16 p2257 N88-23489
Adaptive segmentation evaluation
[AD-A190965] 16 p2274 N88-23609
Data management strategies in the industrial environment
[NLR-MP-87002-U] 16 p2286 N88-23684
Test philosophy of the EH101 integrated avionic
17 p2303 N88-23775
Implantation of a geo-cartographical information system through microcomputers 17 p2361 N88-24064
Image management research
17 p2380 N88-24150
The ATF (Advanced Toroidal Facility) Data M Management System
[DE88-007265] 18 p2589 N88-25385
The CERSAT archiving and processing center --- ERS-1 19 p2701 N88-26059
Real time data base management
[AD-A191758] 19 p2739 N88-26265

The role of working memory in language comprehension
[AD-A192721] 20 p2833 N88-26805
A PRELUDE (analysis and design of control systems-preliminary utilities depository). A data-based interactive system of control software, user's guid e
[DFVLR-MITT-88-12] 21 p3000 N88-27795
The Sundstrand B747-400 data management unit 22 p3035 N88-28021
Investigation of the use of High Order Languages (HOLs) for on-board software
[CRI/FR/HOL-C/1/87] 23 p3251 N88-29349
Automated cataloging and characterization of space-derived data 24 p3420 N88-30354
A design for a ground-based data management system 24 p3420 N88-30355
Knowledge-Based Integrated Information Systems Development Methodologies Plan. Knowledge-Based Integrated Information Systems Engineering (KBIISE) report, volume 2
[AD-A195851] 24 p3436 N88-30455

DATA PROCESSING
NT ASSOCIATIVE PROCESSING (COMPUTERS)
NT BATCH PROCESSING
NT CENSORED DATA (MATHEMATICS)
NT CEPSTRAL ANALYSIS
NT CONCURRENT PROCESSING
NT DATA CORRELATION
NT DATA REDUCTION
NT DATA RETRIEVAL
NT DATA SMOOTHING
NT DATA STORAGE
NT DATA TRANSFER (COMPUTERS)
NT DISTRIBUTED PROCESSING
NT MULTIPROCESSING (COMPUTERS)
NT ONBOARD DATA PROCESSING
NT OPTICAL DATA PROCESSING
NT PARALLEL PROCESSING (COMPUTERS)
NT PIPELINING (COMPUTERS)
NT SCENE ANALYSIS
NT SIGNAL ANALYSIS
NT SIGNAL PROCESSING
NT VOICE DATA PROCESSING

TIROS-N/NOAA A-J space environment monitor subsystem
[PB87-203998] 01 p0015 N88-10083
Manual for GetData version 3.1: A FORTRAN utility program for time history data
[NASA-TM-88288] 01 p0081 N88-10520
EAGLES: An interactive environment for scientific computing
[DE87-013564] 01 p0084 N88-10541
Horizontal shape matching applied to VAS data --- Visible and Infrared Spin Scan Radiometer Atmospheric Sounder (VAS)
02 p0201 N88-11254
A mini system for nowcasting 02 p0204 N88-11278
The Pacific Weather Center Satellite Facility: An overview 02 p0205 N88-11286
Comments on the challenge of using mesoscale data in mesoscale numerical models
02 p0214 N88-11348
Personal computers: A powerful tool for project management
[DE87-013381] 02 p0219 N88-11377
Knowledge acquisition issues encountered during the development of an estimating expert system
[DE87-013320] 02 p0248 N88-11568
An algorithmic approach to crustal deformation analysis
[NASA-CR-181497] 03 p0349 N88-12203
Antithesis: A study in clause combining and discourse structure
[AD-A184789] 03 p0368 N88-12313
Experimental and theoretical study of condensation in multicomponent mixtures
[DE88-000897] 04 p0413 N88-12563
Interferometry theory for the block 2 processor
[NASA-CR-181551] 04 p0440 N88-12730
Complex for ocean study from space and hydroacoustic stations 04 p0458 N88-12836
A data analysis environment for HP (Hewlett-Packard) 1000 computers
[DE87-010511] 04 p0477 N88-12936
On computing environments in data analysis
[DE88-000078] 04 p0480 N88-12961
A computer code to process and plot laser altimetry data interactively on a microcomputer
[NASA-TM-100687] 05 p0554 N88-13371
The analysis of nonstationary vibration data
05 p0592 N88-13610
A new method to real-normalize measured complex modes 05 p0593 N88-13618
TOMS: The Antarctic ozone hole and ozone trends
05 p0615 N88-13775
Application of TOMS data to weather analysis models
05 p0617 N88-13787
TOMS ozone data compared at mesoscale resolution to tropopause heights from the AVE radiosonde network and to VAS radiances over the south-central United States 05 p0617 N88-13790
Development of a data analysis system for the detection of lower level atmospheric turbulence with an acoustic sounder
[AD-A184972] 05 p0624 N88-13821
Hanford Meteorological Station computer codes. Volume 5: The TOWER computer code
[DE88-001610] 05 p0628 N88-13843
File usage analysis and resource usage prediction: A measurement-based study
[NASA-CR-181553] 05 p0633 N88-13867
Predictability of process resource usage: A measurement-based study of UNIX
[NASA-CR-181562] 05 p0633 N88-13869
Performability modeling based on real data: A casestudy
[NASA-CR-181563] 05 p0633 N88-13870
Conceptual issues in measuring the behavior of a distributed real-time process-control computer system
[DE87-014251] 05 p0638 N88-13899
Status, outlook of optical technology in information equipment field 06 p0689 N88-14222
EISCAT research in Finland in 1986
06 p0691 N88-14234
Data analysis at the Oulu (Finland) EISCAT laboratory
06 p0691 N88-14241
Computer simulation of the L/sub 3/-edge densitometer
[DE88-001944] 06 p0705 N88-14324
AVIRIS onboard data handling and control
06 p0706 N88-14332
AVIRIS ground data-processing system
06 p0707 N88-14333
Regional weather satellite data processing center opens in Tashkent 06 p0725 N88-14457
Effective methods of gravimetric and magnetometric data processing 06 p0728 N88-14479
Geographic application of the relational data base system Cantor
[PB87-120945] 06 p0791 N88-14851
Digital processing of flight test data without using anti-aliasing filters, using a helicopter as an example
[DFVLR-MITT-87-12] 07 p0819 N88-14981
Data acquisition, reduction and analysis of shock and vibration testing using a super microcomputer
[AD-A186123] 07 p0867 N88-15260
SEQUAL (seasonal Equatorial Atlantic) meteorological data from Moorings S2, S5 and S6 (March 1983 - March 1985)
[PB88-108048] 07 p0880 N88-15337
Moored current meter data from the Canary Basin near 32 deg N, 24 W (84-1986), volume 40
[PB88-108105] 07 p0882 N88-15351
Quantifying some information processing aspects of the pilot's instrument crosscheck
[AD-A186114] 07 p0898 N88-15443
Multichannel scaling analyzer
[DE88-700541] 07 p0905 N88-15481
Algorithm and program for recognition of compactly positioned vertices of events for the HPD minimum guidance system
[DE88-700542] 07 p0905 N88-15482
Problems of organization of mass processes of simulation, acquisition and processing of experimental data at computers
[DE88-700547] 07 p0905 N88-15483
Strategies of data analysis
[AD-A186033] 07 p0914 N88-15548
NASA (National Aeronautics and Space Administration) ADP (Automated Data Processing) system: Information on the automated mission and the payload tracking system
[PB88-104989] 07 p0942 N88-15730
High Resolution Picture Transmission (HRPT) data processing from NOAA series satellites
[INPE-4372-PRE/1195] 08 p0963 N88-15831
SSME environment database development
[NASA-CR-179245] 08 p0964 N88-15836
Summary record of presentations to the Federal Telecommunication Standards Committee/Fiber optics task group
[PB88-110853] 08 p0978 N88-15911
Laboratory vibration test schedules development beyond MIL-STD-810D 08 p0999 N88-16050
Method for joint adjustment of satellite and surface geodetic networks 08 p1007 N88-16105
Processes in the quiet and disturbed equatorial-low latitude ionosphere: Sundial campaign, 1984
[INPE-4152-PRE/1057] 08 p1036 N88-16282
A knowledge-based system for monitoring the electrical power system of the Hubble Space Telescope
08 p1058 N88-16380
Spacelab Data Processing Facility (SLDPF) quality assurance expert systems development
08 p1059 N88-16394
Media independent interface
[NASA-CR-172033] 08 p1066 N88-16446
New directions for multivariate statistical computation and data analysis
[AD-A186523] 08 p1074 N88-16480
TOPP: A post-processor for TOPAZ, the one dimensional pipe flow analysis code
[DE88-003711] 09 p1164 N88-16981
Application of satellite data in variational analysis for global cyclonic systems
[NASA-CR-182468] 09 p1193 N88-17152
Comparison of alphanumeric data entry methods for advanced helicopter cockpits
[AD-A186934] 09 p1201 N88-17201
The effectiveness of caches and data prefetch buffers in large-scale shared memory multiprocessors
[DE88-003594] 09 p1223 N88-17334
Code division multiple access applied to fiber optic data transmission
[AD-A186873] 09 p1247 N88-17477
Data reduction and analysis of HELIOS plasma wave data
[NASA-CR-182466] 09 p1264 N88-17572
Wide band data transmission system using optical fibers
[DE88-004555] 10 p1319 N88-17889
Minimum Energy Routing through Interactive Techniques (MERIT) modeling
[NASA-CR-182535] 10 p1356 N88-18105
A VLSI implementable block oriented data driven multiprocessor 10 p1381 N88-18249
Data prefetching in shared memory multiprocessors
[DE88-003576] 10 p1394 N88-18314
Fixed and adaptive interframe image prediction for remote piloting application
[AD-A187987] 11 p1471 N88-18771
Effect of experimental variables on flash thermal diffusivity data analysis
[DE88-003631] 11 p1487 N88-18877
Rocketdyne automated dynamics data analysis and management system 11 p1499 N88-18954
Multisource context classification methods in remote sensing 11 p1504 N88-18985
Interfacing of a microcomputer with a simultaneous atomic-emission spectrometer
[PB88-139571] 11 p1526 N88-19109
Spaceborne gravity gradiometry characterizing the data type 12 p1644 N88-19847
Quality control of upper air conventional data (TEMP and PILOT)
[INPE-4223-RPE/546] 12 p1647 N88-19862
Design of the primary pre-TRMM and TRMM ground truth site
[NASA-CR-182609] 12 p1647 N88-19865
Some questions of using coding theory and analytical calculation methods on computers
[DE88-700905] 12 p1676 N88-20021
Procedure for initial data input and checkup in the system for film data mathematical processing
[DE88-700926] 12 p1676 N88-20022
Experimental analysis of algorithms
[AD-A188528] 12 p1677 N88-20028
Experience with Berkeley UNIX interprocess communications
[AD-A188353] 12 p1680 N88-20041
The use of least squares in undetermined problems
[DE88-004473] 12 p1682 N88-20059
Pion absorption in nuclei: The pion(+ or -),proton reactions
[LA-10997-T] 12 p1688 N88-20098
Investigation of low energy space plasma
[NASA-CR-182611] 12 p1694 N88-20138
RIAR automated research and management systems
[DE88-700934] 12 p1706 N88-20209
The Joint NASA/Goddard-University of Maryland Research Program in Charged Particle and High Energy Photon Detector Technology
[NASA-CR-182612] 12 p1712 N88-20247
A comparison of two chord keyboard coding systems for alphanumeric data entry
[AD-A189230] 13 p1813 N88-20834
Distributed transaction processing and the Camelot system
[AD-A186614] 13 p1821 N88-20885
Optimal and conventional space-time processing in flow noise
[AD-A189104] 13 p1833 N88-20965
Aspects and applications of primary processing of visual information
[INPE-4290-PRE/1161] 13 p1841 N88-21015
The German processing and archiving facility for ERS-1
[ESA-CR(P)-2531] 13 p1851 N88-21082

Data processing method for high angle of attack testing with rolling angle 14 p1864 N88-21134
Lasers: Invention to application [PB88-161583] 14 p1914 N88-21436
From satellite altimetry to ocean topography, a survey of data processing techniques [ETN-88-91841] 14 p1939 N88-21575
DASM: A tool for Decomposition and Analysis of Sequential Machines [EUT-87-E-170] 14 p1956 N88-21660
Data analysis of an observation of the quasar 3C 273 in the high-energy X-ray range, and the significance for astrophysical models [ETN-88-91493] 14 p1993 N88-21878
Real-time flight test data distribution and display [NASA-TM-100424] 15 p2022 N88-22050
Baseline observing system experiments using the AFGL global data assimilation system [AD-A188861] 15 p2024 N88-22062
Basic research on flame radiation [PB88-168372] 15 p2032 N88-22105
Fast analog-to-digital converter [DE88-701488] 15 p2106 N88-22543
Digital processing of flight data of a helicopter without using anti-aliasing filters [ESA-TT-1094] 16 p2161 N88-22890
Multiple address facility for packet radio: An investigation of performance/complexity trade off [AD-A191043] 16 p2190 N88-23064
Computer-assisted symbolization by raster data processing --- mapping 16 p2225 N88-23284
Near-real-time TOMS, telecommunications and meteorological support for the 1987 Airborne Antarctic Ozone Experiment [NASA-CR-4133] 16 p2233 N88-23338
Axiomatic specificatin of database domain statics [PB88-176284] 16 p2250 N88-23444
Parallelism in a Prolog knowledge base machine [ETN-88-92187] 16 p2255 N88-23477
New generation knowledge processing, volume 3' [AD-A190167] 16 p2285 N88-23682
VISSR line number monitoring system 17 p2351 N88-24008
Some problems with regard to the TOVS processing detected by using NOAA-HRPT data check program 17 p2351 N88-24009
Latin American Symposium on Remote Sensing. 4th Brazilian Remote Sensing Symposium and 6th SELPER Plenary Meeting, volume 1 17 p2352 N88-24013
Presentation of the METEOSAT system and the roles of EUMETSAT within the meteorological community 17 p2357 N88-24039
Identification of areas cultivated with soybeans in the cerrados regions, through digital processingof satellite images: A methodological approach 17 p2358 N88-24048
Digital processing of infrared and visible images from the GOES satellite and its integration with meteorological radar data 17 p2360 N88-24057
Thematic mapping utilizing data from the Thematic Mapper sensor of the LANDSAT satellite 17 p2361 N88-24060
Parallel binary and parallel coded decimal time code formats [AD-A190126] 17 p2384 N88-24170
Unified interchange format for computer data (standard file format) [ESA-STR-225] 17 p2386 N88-24183
Western Pacific Omega validation: Project description [AD-A191753] 18 p2462 N88-24617
Automated test device for FASR (Fixed Array Surveillance Radar) beam steering componentry [AD-A191650] 18 p2500 N88-24829
Information and stochastic systems [AD-A192167] 18 p2501 N88-24838
Optical computer and optical methods for data processing 18 p2518 N88-24939
Vectorization of raster algorithms for elevation data processing 18 p2534 N88-25036
Development and validation of transmission measurements techniques of image contrast, utilizing existing IR imagers [AD-A191471] 18 p2541 N88-25079
Evaluation of NMC (National Meteorological Center) global analyses: 1979-1987 [PB88-178157] 18 p2544 N88-25096
Visual information processing in the perception of features and objects [AD-A192026] 18 p2552 N88-25148
LispSEI: The programmer's manual [AD-A191632] 18 p2556 N88-25172
IGUANA: Interactive graphics utility for automated NEC analysis [AD-A191760] 18 p2556 N88-25174
PAFEC level 6.2 application program [AD-A191037] 18 p2562 N88-25209
Phase diagrams in materials science and the use of the computer in their calculation [PB88-155262] 18 p2586 N88-25364
Defense Technical Information Center cataloging guidelines [AD-A192200] 18 p2589 N88-25382
The ATF (Advanced Toroidal Facility) Data M Management System [DE88-007265] 18 p2589 N88-25385
SAMS: The synchronization and monitoring system for ATF (Advanced Toroidal Facility) data acquisition provides unified data access for ATF data acquisition [DE88-007268] 18 p2589 N88-25386
Diagnostic studies of the HxOy-NzOy-O3 photochemical system using data from NASA GTE field expeditions [NASA-CR-183038] 19 p2689 N88-25984
ECMWF (European Centre for Medium Range Weather Forecasts) global analyses 1979-1986: Circulation statistics and data evaluation [PB88-178165] 19 p2692 N88-26001
The CERSAT archiving and processing center --- ERS-1 19 p2701 N88-26059
Idea processing for creativity and management [DE88-006110] 19 p2714 N88-26113
An intelligent processing environment for real-time simulation [NASA-CR-183056] 19 p2715 N88-26119
Checkout system software for INPE satellites [INPE-4554-PRE/1297] 19 p2715 N88-26120
Meteorological satellite product support and research for project GALE [NASA-CR-180989] 19 p2727 N88-26193
Treatment of systematic errors in the processing of wide angle sonar sensor data for robotic navigation [DE88-008961] 20 p2756 N88-26352
Statistical properties of real time events in an ATC (Air Traffic Control) system [PB88-116781] 20 p2756 N88-26353
Laser ranging data analysis [NASA-CR-183115] 20 p2792 N88-26567
Automated system for mathematical processing of the data from a hybrid spectrometer [DE87-702995] 20 p2836 N88-26820
Narrative domain implementation [AD-A192265] 20 p2843 N88-26868
Knowledge-based cost estimating vs traditional software cost models [DE88-009707] 20 p2883 N88-27116
Supercomputer for parallel data analysis [DE88-702148] 21 p2995 N88-27759
A programmable systolic array for factorial analysis. Part 2: The symmetric eigenvalue problem [AD-A192396] 21 p2995 N88-27762
Issues in computer-assisted interpretation of graphs and quantitative information [PB88-116280] 21 p2998 N88-27783
Basic database operations on the butterfly parallel processor: Experiment results [AD-A193199] 21 p3002 N88-27804
Analysis of lower hybrid current drive and rampup experiments on the JT-60 tokamak [DE88-753136] 21 p3018 N88-27915
Pattern information processing and multimedia database system: Current research on multimedia information system [PB88-131917] 21 p3028 N88-27973
Non-Gaussian models for surface clutter 22 p3068 N88-28212
Atlantic SST variability and high latitude climate fluctuations 22 p3122 N88-28551
The effects of changes in observation and data assimilation systems on CAC climate data sets 22 p3124 N88-28568
Evaluation of global data sets for climate studies 22 p3124 N88-28569
Software modifications to total data reporting accessory for metabolic measurement cart [AD-A193641] 22 p3132 N88-28623
Research on wide area workstations [AD-A192529] 22 p3136 N88-28643
Proof-of-principle high speed electronic imaging system, phase 2 [AD-A193798] 23 p3181 N88-28937
Hierarchical organization for large, dynamic radio networks [AD-A193942] 23 p3204 N88-29067
Distortions in processed signals and their application in electronic design. Part 3: An automated generator of communication jamming signals [DE88-702733] 23 p3205 N88-29072
Waveform analysis on the IBM PC [AD-A194249] 23 p3248 N88-29330
ADP (Automated Data Processing) requirements definition and documentation through user-developed prototypes [AD-A194407] 23 p3248 N88-29332
Expert system technology as a data processing tool 23 p3263 N88-29427
Advanced information processing system: Input/output network management software [NASA-CR-181678] 23 p3264 N88-29431
On the design and optimization of distributed signal detection and parameter estimation systems [AD-A193934] 23 p3266 N88-29446
Automatic prober for the dc characterisation of gallium arsenide devices. Part 2: The data sorting and display facility [AD-A195408] 24 p3377 N88-30111
Method for combined image interpolation-restoration through a fir filter design technique [INPE-4561-PRE/1302] 24 p3413 N88-30315
Spacelab data processing facility (SLDPF) Quality Assurance (QA)/Data Accounting (DA) expert systems: Transition from prototypes to operational systems 24 p3420 N88-30353
Automated cataloging and characterization of space-derived data 24 p3420 N88-30354

DATA PROCESSING EQUIPMENT
NT AIRBORNE/SPACEBORNE COMPUTERS
NT ANALOG COMPUTERS
NT CDC CYBER 205 COMPUTER
NT COMPUTERS
NT CRAY COMPUTERS
NT DATA PROCESSING TERMINALS
NT DIGITAL COMPUTERS
NT EMBEDDED COMPUTER SYSTEMS
NT HEWLETT-PACKARD COMPUTERS
NT HYBRID COMPUTERS
NT HYPERCUBE MULTIPROCESSORS
NT IBM COMPUTERS
NT MICROCOMPUTERS
NT MICROPROCESSORS
NT MIMD (COMPUTERS)
NT MINICOMPUTERS
NT OPTICAL COMPUTERS
NT PARALLEL COMPUTERS
NT PERIPHERAL EQUIPMENT (COMPUTERS)
NT PERSONAL COMPUTERS
NT PRINTERS (DATA PROCESSING)
NT REMOTE CONSOLES
NT SEQUENTIAL COMPUTERS
NT SIMD (COMPUTERS)
NT SUPERCOMPUTERS
NT VAX COMPUTERS
Concepts and techniques for support of real time distributed operating systems [AD-A184491] 03 p0367 N88-12307
A comparison of two chord keyboard coding systems for alphanumeric data entry [AD-A189230] 13 p1813 N88-20834
A methodolgy, based on analytical modeling, for the design of parallel and distributed architectures for relational database query processors [AD-A189844] 15 p2149 N88-22825
Measurement data processing system based on personal computer: For scramjet combustion test [DE88-751807] 16 p2174 N88-22959
Real time pipelined system for forming the sum of products in the processing of video data [NASA-CASE-NPO-16462-1-CU] 17 p2384 N88-24169

DATA PROCESSING TERMINALS
Health hazards of video display terminals. A comprehensive, annotated bibliography on a critical issue of workplace health and safety with sources for obtaining items and list of terminal suppliers [RSI-IAS-4] 03 p0355 N88-12240
Performance and preference with various VDT (Video Display Terminal) phosphors [AD-A184085] 04 p0475 N88-12925
Presentation of map information on a color display [FOA-C-20687-2.7] 17 p2368 N88-24103
Adaptive data acquisition multiplexing system and method [NASA-CASE-MSC-21170-1] 18 p2471 N88-24662
Frequency addressable beams for land mobile communications 19 p2652 N88-25744

DATA PROCESSORS
U DATA PROCESSING EQUIPMENT

DATA READOUT SYSTEMS
U DATA SYSTEMS
U DISPLAY DEVICES

DATA RECORDERS
Maintenance support for military aircraft by intelligent on-board maintenance data panel 22 p3034 N88-28012
The intelligent QAR and its cost effective role in new generation AIMS --- quick access recorder (QAR); aircraft integrated monitoring systems (AIMS) 22 p3035 N88-28020
Development of a maintenance data bus monitor and recorder 22 p3036 N88-28022

DATA RECORDING
Detective quantum efficiency and design of a parallel data recording system for EXELFS-measurements --- electron microscopy
[USIP-87-06] 01 p0050 N88-10318
The management of software in airborne recording systems 22 p3035 N88-28019
DATA REDUCTION
NT DATA SMOOTHING
Study, design, and evaluation of data reduction by encoding or information extraction. Part 1: Data generation analysis --- multispectral satellite imagery
[NLR-TR-85094-L-PT-1] 01 p0078 N88-10501
Study, design and evaluation of data reduction by encoding or information extraction. Part 2: Operational considerations --- multispectral satellite imagery
[NLR-TR-85094-L-PT-2] 01 p0079 N88-10502
Study, design and evaluation of data reduction by encoding or information extraction. Part 3: Algorithm design --- multispectral satellite imagery
[NLR-TR-85094-L-PT-3] 01 p0079 N88-10503
Study, design and evaluation of data reduction by encoding or information extraction. Part 4: Performance demonstration --- multispectral satellite imagery
[NLR-TR-85094-L-PT-4] 01 p0079 N88-10504
Study, design and evaluation of data reduction by encoding or information extraction. Part 5: Algorithm implementation aspects --- multispectral satellite imagery
[NLR-TR-85094-L-PT-5] 01 p0079 N88-10505
Short reference year
[PB87-107470] 03 p0352 N88-12221
The Macintosh computer as a tool for rapid data analysis and for producing camera ready viewgraphs/publications
[DE87-014350] 03 p0362 N88-12280
A digital low pass filter for the reduction of large quantities of data
[ESA-TT-1058] 03 p0363 N88-12281
Analysis of photopole data reduction models 05 p0593 N88-13616
The Portable Instant Display and Analysis Spectrometer (PIDAS) 05 p0611 N88-13756
AIS-2 radiometry and a comparison of methods for the recovery of ground reflectance 05 p0611 N88-13757
Software design for an airborne gravity measurement system
[AD-A185000] 05 p0634 N88-13878
Data analysis at the Oulu (Finland) EISCAT laboratory 06 p0691 N88-14241
The archiving of meteor research information 06 p0732 N88-14505
A computer decision-making process for the elimination of noise from data
[AD-A185746] 06 p0759 N88-14659
Data acquisition and analysis system for the Sandia 34-meter Vertical Axis Wind Turbine
[DE88-002417] 09 p1187 N88-17112
Data reduction and analysis of HELIOS plasma wave data
[NASA-CR-182466] 09 p1264 N88-17572
Multi-processor reduction machines 10 p1382 N88-18253
An improved data reduction procedure for accelerometer centrifuge data 12 p1577 N88-19436
A view of unconstrained optimization
[AD-A188327] 12 p1684 N88-20066
Data traffic reduction schemes for sparse Cholesky factorizations
[NASA-CR-181626] 13 p1813 N88-20831
Data analysis of an observation of the quasar 3C 273 in the high-energy X-ray range, and the significance for astrophysical models
[ETN-88-91493] 14 p1993 N88-21878
A multivariate variational objective analysis-assimilation method. Part 2: Case study results with and without satellite data
[NASA-CR-182653] 15 p2097 N88-22492
Data volume reduction for imaging radar polarimetry
[NASA-CASE-NPO-17184-1-CU] 20 p2788 N88-26541
Comparison of experimental rotor damping data-reduction techniques 21 p2891 N88-27159
Calibration and data reduction techniques for the AFGL infrared array spectrometer 21 p2927 N88-27374
Development of a hot-wire measurement technique for moderate intensity three-dimensional flows 22 p3080 N88-28289
Autonomous image data reduction by analysis and interpretation 24 p3418 N88-30347
DATA RETRIEVAL
The microcomputer as an engineering management tool
[DE87-014882] 02 p0219 N88-11378
Using bibliographic databases in technology transfer
[NASA-CR-181403] 02 p0222 N88-11399
Description of data handling system installed December 11, 1986 --- EISCAT 06 p0692 N88-14242
SSME environment database development
[NASA-CR-179245] 08 p0964 N88-15836
Retrieval of three-dimensional wind and temperature fields from single-Doppler radar data 12 p1646 N88-19858
Basic research on flame radiation
[PB88-168372] 15 p2032 N88-22105
Analysis of head response to torso acceleration. Volume 2: Description of data retrieval, analysis and display software
[PB88-156765] 15 p2104 N88-22536
Retrieval of temperature and concentration profiles from a limited number of absorption measurements 21 p2947 N88-27501
DATA SAMPLING
Using a parallel computer system for statistical resampling methods
[REPT-87-47] 14 p1960 N88-21690
Digital processing of flight data of a helicopter without using anti-aliasing filters
[ESA-TT-1094] 16 p2161 N88-22890
Servo-actuator control for sampled-data feedback disturbance rejection --- helicopters
[ESA-TT-1002] 16 p2163 N88-22903
Application of sampling techniques to near-field far-field transformation
[ESA-CR(P)-2546] 24 p3359 N88-30002
DATA SIMULATION
Use of simulated satellite radiances from a mesoscale numerical model to understand kinematic and dynamic processes 02 p0202 N88-11261
Simulation of mesoscale satellite sounder data from a mesoscale numerical model 02 p0214 N88-11345
Windfield simulations from a hierarchy of nested meso- and micrometeorological models 02 p0215 N88-11351
High resolution satellite imagery simulation --- treaty verification
[FOA-C-30462-3.3,9.3] 05 p0620 N88-13810
Inversion of simulated satellite signals 08 p1017 N88-16168
Improved resolution atmospheric density measurements based on simulations 08 p1027 N88-16221
Simulation of measuring points for three dimensional measurements
[WPB-0115] 13 p1821 N88-20883
Simulation: A simulation system in Ada
[FOA-A-20043-2.7] 17 p2385 N88-24176
DATA SMOOTHING
Algorithms and hardware for efficient image smoothing
[TR-149] 03 p0365 N88-12296
Improvements in profiler wind estimates using smoothed data in the spectrum finder algorithm
[PB88-102181] 07 p0881 N88-15342
Multigrid methods in convex optimization 11 p1538 N88-19190
Stabilization of explicit difference schemes by smoothing techniques
[CWI-NM-R8714] 13 p1827 N88-20923
Weighted averaging method for image smoothing reported 14 p1901 N88-21352
Smoothing technique to resolve X-ray spectra in laser nuclear fusion 15 p2053 N88-22235
Residual smoothing for accelerating the Alternating Direction Implicit (ADI) iteration method for elliptic difference equations
[CWI-NM-R8721] 16 p2259 N88-23500
A fast and efficient procedure for generalized cross-validation with large data sets. Application to image reconstruction
[RR-669-M] 18 p2563 N88-25220
DATA STORAGE
Measurements in the functional mock up test of the NAL QSTOL aircraft control system
[NAL-TR-928] 02 p0126 N88-10793
Design and implementation of a debugger for an abstract machine
[AD-A184691] 03 p0363 N88-12283
UNIX benchmark system
[AD-A184492] 03 p0367 N88-12308
Competition Analysis Model (CAM). Volume 2: Computer manual
[AD-A184017] 03 p0384 N88-12411
Advanced techniques for the storage and use of very large, heterogeneous spatial databases. The representation of geographic knowledge: Toward a universal framework --- relations (mathematics)
[NASA-CR-181517] 03 p0385 N88-12421
Complex for ocean study from space and hydroacoustic stations 04 p0458 N88-12836
A rudimentary database for three-dimensional objects using structural representation
[CSE-87-00004] 05 p0590 N88-13597
Storing and retrieving data in a parallel distributed memory system
[AD-A185177] 05 p0637 N88-13897
Status, outlook of optical technology in information equipment field 06 p0689 N88-14222
The archiving of meteor research information 06 p0732 N88-14505
Octree data structures and creation by stacking
[PB87-234795] 06 p0758 N88-14650
A review of hypertext in a NASA project management context 06 p0793 N88-14859
SSME environment database development
[NASA-CR-179245] 08 p0964 N88-15836
Similarity networks as a knowledge representation for space applications 08 p1062 N88-16411
Data prefetching in shared memory multiprocessors
[DE88-003576] 10 p1394 N88-18314
The design of the POSTGRES storage system
[AD-A187244] 11 p1564 N88-19365
Allocation of database files across parallel stores for efficient processing of partial-match queries
[AD-A188196] 11 p1565 N88-19371
RIAR automated research and management systems
[DE88-700934] 12 p1706 N88-20209
Holographic disk for data storage 14 p1972 N88-21771
A data acquisition system for atmospheric tracer studies
[DE88-006211] 14 p1991 N88-21869
Method and device for the detection and identification of a helicopter
[NASA-TT-20251] 15 p2129 N88-22698
The flying characteristics of the membrane slider bearing 18 p2522 N88-24965
The CERSAT archiving and processing center --- ERS-1 19 p2701 N88-26059
Use of optical disk technology at the Air Command and Staff College
[AD-A192424] 21 p3027 N88-27969
Space shuttle phase B wind tunnel model and test information. Volume 2: Orbiter configuration
[NASA-CR-178415-VOL-2-PT-1] 23 p3171 N88-28881
Laser sensing for identification and control of distributed parameter systems
[AD-A195886] 24 p3379 N88-30124
Partitioned storage for temporal databases
[AD-A195093] 24 p3436 N88-30451
DATA STRUCTURES
Local concurrent error detection and correction in data structures using virtual backpointers
[NASA-CR-181432] 01 p0106 N88-10692
Advanced techniques for the storage and use of very large, heterogeneous spatial databases. The representation of geographic knowledge: Toward a universal framework --- relations (mathematics)
[NASA-CR-181517] 03 p0385 N88-12421
Octree data structures and creation by stacking
[PB87-234795] 06 p0758 N88-14650
A data structure and algorithm for fault diagnosis 08 p1065 N88-16432
Unidimensional Rasch model and multidimensional data: An analytic approach
[PB88-105861] 10 p1372 N88-18187
Portable (and disposable) interpreters 10 p1380 N88-18237
The effects of data structure on total time on test plots
[AD-A187628] 10 p1389 N88-18296
Dynamic processor self-scheduling for general parallel nested loops
[DE88-003572] 10 p1393 N88-18311
TYPICAL: A knowledge representation system for automated discovery and inference
[AD-A187483] 11 p1533 N88-19160
Development in data structures in PHOCUS for digital mapping 18 p2534 N88-25034
EPL (Equational Programing Language) system design: Intermediate processing steps
[AD-A191203] 18 p2556 N88-25169
Algorithms and data structures for an expanded family of matroid intersection problems
[AD-A191482] 18 p2562 N88-25213
Design of high performance microcomputers for numerical data processing
[ETN-88-92371] 20 p2835 N88-26818
An introduction to the nested sequence of tuples data model and algebra
[REPT-87-049] 22 p3145 N88-28702
Lisp Object State Saver (LOSS): A facility used to save partial schedules of the Hubble Space Telescope 24 p3421 N88-30360
DATA SYSTEMS
NT AIR DATA SYSTEMS
Interfacing distributed operating systems
[AD-A184489] 03 p0366 N88-12306

Description of data handling system installed December 11, 1986 --- EISCAT
06 p0692 N88-14242

The crustal dynamics intelligent user interface anthology
[NASA-TM-100693] 08 p1067 N88-16448

MPAD MCC workstation system: ADDAM and EEVE
09 p1203 N88-17209

Modular CAMAC system, 2
[DE88-700237] 11 p1525 N88-19106

Baseline observing system experiments using the AFGL global data assimilation system
[AD-A188861] 15 p2024 N88-22062

Proposals for the pre-operational use of data from the European Remote Sensing Satellite ERS-1
[BCRS-86-02] 16 p2227 N88-23300

DATA TRANSFER (COMPUTERS)

Measurement of fault-tolerant parallel processors
[PB87-208328] 01 p0084 N88-10539

Analysis of counting errors in the phase/Doppler particle analyzer
[NASA-TM-100231] 03 p0323 N88-12043

Guidelines for exchanging computerized information
[DE88-004736] 10 p1425 N88-18510

Interconnection of high-speed local area networks
17 p2390 N88-24205

Theory of numerical information environment and its applications
19 p2640 N88-25666

An operational open-end file transfer protocol for mobile satellite communications
19 p2651 N88-25738

The high speed local area network
19 p2717 N88-26133

DATA TRANSMISSION

NT ALOHA SYSTEM
NT AUTOMATIC PICTURE TRANSMISSION
NT CODE DIVISION MULTIPLE ACCESS
NT FREQUENCY DIVISION MULTIPLE ACCESS
NT MULTIPLE ACCESS
NT PACKET TRANSMISSION
NT SINGLE CHANNEL PER CARRIER TRANSMISSION

Telemetry, Tracking, and Control Working Group report
01 p0016 N88-10096

Data Management Working Group report
01 p0016 N88-10097

Digital receiver structures and methods for the determination of the scanning frequency in modems for fast data transmission via telephone channels
[ETN-87-90429] 01 p0037 N88-10235

Study on the suitability of a European data relay satellite to support a system of remote sensing satellites
[ESA-CR(P)-2400] 01 p0063 N88-10406

Rapid toxicity detection in water quality control utilizing automated multispecies biomonitoring for permanent space stations
02 p0135 N88-10848

An examination of the Advanced Communications Technology Satellite (ACTS) and its application to the Defense Data Network (DDN)
[AD-A184003] 03 p0276 N88-11742

Lewis Information Network (LINK): Background and overview
[NASA-TM-100162] 03 p0305 N88-11925

Design of source coders and joint source/channel coders for noisy channels
[NASA-CR-181547] 04 p0432 N88-12678

An exact analysis and performance of framed ALOHA with capture
[AD-A185006] 05 p0574 N88-13500

Test and evaluation of the transputer in a multi-transputer system
[AD-A184969] 05 p0631 N88-13859

Soliton mode of propagation of light pulses through single-mode optical fibers and problems of its experimental realization
07 p0920 N88-15592

Development and study of fibre-optic link lines on the basis of the KEM-8-4PD, KEM-8-4PR quantum-electronic modules
[DE88-700372] 07 p0932 N88-15663

Requirements and options for communications services in support of the Systems Autonomy Demonstration Project
08 p1057 N88-16374

A hybrid transform/DPCM encoder for data compression
[DE88-003725] 09 p1154 N88-16919

Experimental Radio Data System (RDS): A survey of reception reliability in the UK
[BBC-RD-1987/17] 09 p1155 N88-16922

Crosstalk analysis of a broadband data communications system
[DE88-003652] 09 p1156 N88-16927

Code division multiple access applied to fiber optic data transmission
[AD-A186673] 09 p1247 N88-17477

Information transfer in the National Airspace System
10 p1275 N88-17634

Signal processing for an optical wide band data transmission system
[DE88-003854] 10 p1319 N88-17888

Wide band data transmission system using optical fibers
[DE88-004555] 10 p1319 N88-17889

Personal computers and All-In-1: Document transfer and translation
[DE88-003760] 10 p1384 N88-18264

Failure-resistant Fibre-Optical Communication Line (FOCL)
[DE88-700470] 10 p1408 N88-18400

Guidelines for exchanging computerized information
[DE88-004736] 10 p1425 N88-18510

AITI Test Report 87-002: Pratt and Whitney technical order transfer tests
[DE88-004045] 11 p1564 N88-19363

AITI Report 87-003: Honeywell technical order transfer tests
[DE88-004046] 11 p1564 N88-19364

Terrestrial Propagation Characteristics in Modern Systems of Communications, Surveillance, Guidance and Control
[AGARD-CP-407] 12 p1614 N88-19653

Envelope and phase statistics for non-Gaussian noise and resulting error probabilities for digital communications systems
12 p1617 N88-19672

A concatenated coded modulation scheme for error control
[NASA-CR-182639] 12 p1621 N88-19697

A hybrid transform/DPCM encoder for data compression
[DE87-014852] 13 p1758 N88-20518

Datacast: The transmission system
[BBC-RD-1988/1] 14 p1905 N88-21385

Application of static memory for data acquisition and transmission into a computer
[DE88-701491] 15 p2106 N88-22544

Multiple address facility for packet radio: An investigation of performance/complexity trade off
[AD-A191043] 16 p2190 N88-23064

A PC-based receiver-decoder for remote sensor monitoring
[DE88-004733] 16 p2192 N88-23075

Investigation of air transportation technology at Ohio University, 1986
17 p2293 N88-23719

Connecting remote systems for demonstration of automation technologies
17 p2387 N88-24191

Automated test device for FASR (Fixed Array Surveillance Radar) beam steering componentry
[AD-A191650] 18 p2500 N88-24829

Land mobile satellite demonstration system
19 p2646 N88-25706

A framework for implementing data services in multi-service mobile satellite systems
19 p2650 N88-25733

Robust vector quantization for noisy channels
19 p2653 N88-25754

The performance of Eurocom error correction schemes for data communications
[FEL-1987-56] 20 p2792 N88-26563

An integrated circuit for error protection in modern data communication systems conforming to Eurocom specifications
[FEL-1987-48] 20 p2796 N88-26593

A high speed serial link interface for SANDAC-V
[DE88-007694] 20 p2842 N88-26861

Use of fiber optic equipment for security
[DE88-007898] 20 p2853 N88-26943

A VLSI single-chip (225,223) Reed-Solomon encoder with interleaver
[NASA-CASE-NPO-17280-1-CU] 21 p2902 N88-27220

Multichannel data transmission through a fiber optic cable
[AD-A193842] 22 p3070 N88-28221

Use of a coherent square wave reference to demodulate BPSK (Binary Phase Shift Keying) carriers and a visual indicator of the quality of received QPSK (Quadrature Phase Shift Keying) carriers
[AD-A193528] 23 p3204 N88-29065

Hierarchical organization for large, dynamic radio networks
[AD-A193942] 23 p3204 N88-29067

Distortions in processed signals and their application in electronic design. Part 1: Basic and general formulations
[DE88-702731] 23 p3204 N88-29070

An OKQPSK modem incorporating numerically controlled carrier synthesis
[DE88-009536] 23 p3244 N88-29304

Design of a self-timed VLSI multicomputer communication controller
[AD-A194567] 24 p3361 N88-30014

Integrating images, applications, and communications networks, volume 5
[AD-A195854] 24 p3436 N88-30452

DATING

U CHRONOLOGY
U TIME MEASUREMENT

DAYGLOW

Theoretical and observational problems with Holes in the far UV dayglow
[AD-A188190] 10 p1355 N88-18100

DAYTIME

The lengthening and shortening of the day
[KNMI-TR-91] 05 p0628 N88-13839

Peculiarities of daytime ionosphere of Venus during years of low and high solar activity
08 p1005 N88-16091

Task listing: Visually assisted and visually dependent tasks for fighter aircraft
[AD-A191041] 16 p2244 N88-23404

Atmospheric angular momentum and length of day
[AD-A194505] 23 p3233 N88-29238

DBS (SATELLITES)

U DIRECT BROADCAST SATELLITES

DC (CURRENT)

U DIRECT CURRENT

DC 9 AIRCRAFT

Aircraft accident report: Northwest Airlines, Inc., McDonnell Douglas DC-9-82, N312RC, Detroit Metropolitan Wayne County Airport, Romulus, Michigan, August 16, 1987
[PB88-910406] 19 p2601 N88-25449

DE LAVAL NOZZLES

U CONVERGENT-DIVERGENT NOZZLES

DEACCLIMATIZATION

U ACCLIMATIZATION

DEACTIVATION

Deactivation of alumina based catalysts
11 p1455 N88-18673

DEAD RECKONING

Advanced dead reckoning navigation for mobile robots
03 p0262 N88-11646

Simple 2-D navigation for wheeled vehicles
[DE88-007115] 20 p2756 N88-26351

DEADWEIGHT

U STATIC LOADS

DEBRIS

NT SPACE DEBRIS

Far infrared circumstellar debris shells of red supergiant stars
04 p0515 N88-13165

Fretting wear and fretting fatigue damage
05 p0603 N88-13697

Analysis of debris from accelerated life test of the Hughes five-year Vuilleumier cryocooler
[AD-A193101] 21 p2931 N88-27400

DEBUGGING

U CHECKOUT

DEBYE TEMPERATURE

U SPECIFIC HEAT

DECAMETRIC WAVES

A Jupiter Data Analysis Program (JDAP) research grant on wave accessibility and attributes
[NASA-CR-182348] 06 p0804 N88-14908

Ray tracing of Jovian low frequency radiation
[NASA-CR-179262] 08 p1101 N88-16620

DECAY

NT ALPHA DECAY
NT NEUTRON DECAY
NT NEUTRON EMISSION
NT PLASMA DECAY
NT RADIOACTIVE DECAY
NT SPACECRAFT GLOW
NT WEAK ENERGY INTERACTIONS
NT WEAK INTERACTIONS (FIELD THEORY)

Numerical simulation of turbulent premixed combustion and decay of turbulent swirling flow
[DE87-014253] 03 p0284 N88-11787

On charm decays: Present status and future goals
[DE87-013586] 03 p0375 N88-12356

Dynamical analysis of molecular decay at spherical surfaces
[AD-A184908] 05 p0647 N88-13964

Surface and interface electronic structure
[DE88-003363] 09 p1258 N88-17545

An experimental measurement of metal multilayer X-ray reflectivity degradation due to intense X-ray flux
[LA-10989-T] 11 p1547 N88-19255

Orbital analysis of a STS (Space Transportation System) external tank in low earth orbit
[AD-A188829] 12 p1593 N88-19542

Numerical simulation of turbulent premixed combustion and decay of turbulent swirling flow
[DE88-006588] 14 p1888 N88-21284

Study of energy levels and decay mechanisms for singlet Rydberg states of molecular nitrogen
[AD-A192505] 21 p3014 N88-27886

An exponential decay estimate for the stationary perturbation of Poiseuille flow
[AD-A193480] 23 p3210 N88-29105
The influence of delay effects on the decay of liquid jets
[MPIS-14/1987] 23 p3214 N88-29130

DECAY RATES
Influences of the astrophysical environment on nuclear decay rates
[DE88-001461] 04 p0522 N88-13208
On free decay damping tests
08 p0997 N88-16041
Note on boundary stabilization of wave equations
[AD-A187113] 09 p1227 N88-17348
An exponential decay estimate for the stationary perturbation of Poiseuille flow
[AD-A193480] 23 p3210 N88-29105

DECELERATION
NT SPIN REDUCTION
Control and stabilization mechanisms of submunitions
[DFVLR-IB-111-86/9] 03 p0259 N88-11630
X-ray pulsars: Accretion flow deceleration
03 p0390 N88-12451
Atmospheric entry heating of cosmic dust
06 p0794 N88-14865
Liquid ventilation: New data and possible use in space medicine 12 p1654 N88-19908
An experimental investigation of decelerating flow about two-dimensional cambered plates
[DE88-006598] 13 p1766 N88-20567
Soft-ground aircraft arresting systems
[AD-A190838] 16 p2165 N88-22912
New concepts for atmospheric braking deceleration in planetary atmosphere entry
[SNIAS-CAS-DECE-P003-DPAA]
16 p2168 N88-22923

DECELERATORS
U BRAKES (FOR ARRESTING MOTION)

DECEPTION
The Soviet Stealth fighter: Check or checkmate
[AD-A195200] 24 p3323 N88-29791

DECIMETER WAVES
Observations of the brightness temperature distribution of the quiet solar corona at decametric wavelengths
01 p0114 N88-10729

DECISION ELEMENTS
U LOGICAL ELEMENTS

DECISION MAKING
Optimization of a controlled two-server maintenance system
[INPE-4202-PRE/1083] 01 p0107 N88-10694
Application of knowledge-based techniques to aircraft trajectory generation and control
02 p0129 N88-10811
Knowledge acquisition issues encountered during the development of an estimating expert system
[DE87-013320] 02 p0248 N88-11568
Interfacing distributed operating systems
[AD-A184489] 03 p0366 N88-12306
Performance evaluation of artificial intelligence systems
[AD-A184054] 03 p0368 N88-12316
The pros and cons of using a CAI package on a central computer as opposed to a microprocessor: What's your CAI MO, mainframe or micro
[DE87-011123] 04 p0475 N88-12929
Material design of high-purpose glass discussed
06 p0675 N88-14133
An empirical investigation of load indices for load balancing applications
[AD-A185763] 06 p0724 N88-14451
A computer decision-making process for the elimination of noise from data
[AD-A185746] 06 p0759 N88-14659
Artificial intelligence systems
06 p0761 N88-14670
Using concept mapping to define problems and identify key kernels during the development of a decision support system
[AD-A185636] 06 p0762 N88-14674
Tools and technologies for expert systems: A human factors perspective 06 p0797 N88-14882
Human performance data needed for training device design decisions
[AD-A185988] 07 p0898 N88-15441
A software planning and development methodology with resource allocation capability
[AD-A186088] 07 p0902 N88-15462
Computer aided design for Petri Nets
[AD-A186109] 07 p0902 N88-15465
Proceedings of the Second International Symposium on Methodologies for Intelligent Systems: Colloquia program
[DE88-001490] 07 p0907 N88-15498
Contributions to selection and ranking theory with special reference to logistic populations
[AD-A185629] 07 p0917 N88-15568
Air Force Human Resources Laboratory technical reports and technical papers
[AD-A186830] 09 p1201 N88-17200
A situation-response model for intelligent pilot aiding
09 p1208 N88-17241
A human performance modelling approach to intelligent decision support systems 09 p1208 N88-17242
Autonomous control procedures for shuttle rendezvous proximity operations 09 p1208 N88-17244
Artificial Intelligence (AI), Operations Research (OR), and Decision Support Systems (DSS): A conceptual framework 09 p1209 N88-17245
Advanced decision aiding techniques applicable to space 09 p1209 N88-17250
Real-time artificial intelligence issues in the development of the adaptive tactical navigator
09 p1211 N88-17260
Management of complex information in support of evolving autonomous expert systems
[AD-A186680] 09 p1224 N88-17337
Critical issues for establishment of a permanently-occupied lunar base
[AD-A187128] 09 p1263 N88-17567
Windshear training aid. Volume 1: Overview, pilot guide, training program
[PB88-127196] 10 p1276 N88-17637
Real time artificial intelligence architecture
10 p1380 N88-18242
Development of a graphics based two-attribute utility assessment program with application to mission planning
[AD-A187276] 10 p1388 N88-18292
A two-stage isolated-word recognition system using discriminant analysis
[AD-A187425] 10 p1402 N88-18360
Modeling incorrect responses to multiple-choice items with multilinear formula score theory
[AD-A187887] 11 p1522 N88-19090
Effects of stress on judgement and decision making in dynamic tasks
[AD-A188203] 11 p1523 N88-19092
When decision aids fail
[AD-A187531] 11 p1523 N88-19095
Evaluating expert system tools: A framework and methodology-workshops
[AD-A187190] 11 p1533 N88-19159
De Finetti's approach to group decision making
[AD-A188074] 11 p1536 N88-19177
Computer aided tactics for air combat
12 p1597 N88-19559
Brain activity during tactical decision-making. Part 2: Probe-evoked potentials and workload
[AD-A188688] 12 p1667 N88-19994
Physics for robots
[AD-A189056] 12 p1682 N88-20054
Design methodology for allocating data in a distributed database
[AD-A188826] 12 p1706 N88-20215
The design of aircraft using the decision support problem technique
[NASA-CR-4134] 13 p1721 N88-20291
Expected value analysis for an unmanned expendable launch vehicle payload escape system
[AD-A189494] 13 p1728 N88-20337
A personalized and prescriptive decision aid for choice from a database of options
[AD-A188726] 13 p1811 N88-20820
SEAT: A strategic engagement analysis tool
[DE88-000498] 13 p1830 N88-20944
Expert systems for decision support in military aircraft mission preparation
[NLR-MP-87013-U] 13 p1830 N88-20946
Application of expert systems in project management decision aiding
[NASA-CR-180762] 13 p1850 N88-21074
Applicability of nonlinear programming in decision support systems: Realization of user-friendly software
[REPT-87-42] 14 p1957 N88-21663
Selective mechanisms in auditory and bimodal signal processing
[AD-A190529] 15 p2103 N88-22530
Conflict resolution in cooperative systems
[AD-A190351] 15 p2104 N88-22535
C3 generic workstation: Performance metrics and applications 16 p2242 N88-23397
Bayesian solutions to a 2 x 2 decision matrix using interval scaled payoffs with an application to foreign policy decisions
[AD-A190863] 16 p2260 N88-23511
A change in system design emphasis: From machine to man 17 p2304 N88-23782
A proposal of adaptation of a knowledge-based scene analysis model to some remote sensing problems
17 p2354 N88-24026
Remote sensing and data integration: Practical solutions for resource managers 17 p2356 N88-24034
A proposal of adaptation of a knowledge-based scene analysis model to some remote sensing problems
17 p2362 N88-24068
Timesharing performance as an indicator of pilot mental workload
[NASA-CR-182807] 18 p2552 N88-25150
Representation and decision mechanisms in artificial intelligence
[AD-A191083] 18 p2560 N88-25197
A perspective of PC-based probabilistic risk assessment
[DE88-006715] 18 p2568 N88-25251
Selection and effects of channels in distributed communication and decision making tasks: A theoretical review and a proposed research paradigm
[AD-A191807] 18 p2587 N88-25375
Modeling and evaluation of variable structure organizations
[AD-A191947] 18 p2588 N88-25381
High-speed optical logic using GaAs
19 p2656 N88-25773
Algorithmic generation of feasible system architectures
[AD-A191722] 19 p2713 N88-26106
Analysis and synthesis of decision-making organizations
[AD-A191948] 19 p2738 N88-26258
Decision aiding and coordination in decision-making organizations
[AD-A191950] 19 p2738 N88-26259
Modeling and evaluation of expert systems in decisionmaking organizations
[AD-A191951] 19 p2739 N88-26260
Coordination in decision-making organizations
[AD-A191952] 19 p2739 N88-26261
A semantic approach to fairness
[CWI-CS-R8759] 20 p2840 N88-26853
Expert system application education project
[NASA-CR-183089] 20 p2843 N88-26867
The integration of decision support problems into feature modeling based design 21 p2927 N88-27372
Linear programming for Air Force decision aiding
21 p2928 N88-27378
Future SDI (Strategic Defense Initiative) decision making
[AD-A192794] 21 p3010 N88-27860
Rules, schema and decision making
[AD-A193389] 21 p3027 N88-27967
Computer-aided decision making
[AD-A194210] 22 p3137 N88-28651
Linear goal programming as a military decision aid
[AD-A194276] 22 p3137 N88-28652
A virtual statistical mechanical neural computer
[AD-A193962] 22 p3139 N88-28660
LO-CO-GRAF (low cost graphics): Generating maps to support command and control/crisis management using small computers
[AD-A193964] 22 p3139 N88-28661
Decision making aids: Methods and risks
22 p3161 N88-28820
Project management software
22 p3161 N88-28821
LRS-2: A specialized knowledge system for launch resource scheduling
[AD-A194625] 23 p3182 N88-28941
Method for Veterbi decoding of large constraint length convolutional codes
[NASA-CASE-NPO-17310-1-CU]
23 p3183 N88-28946
Motion planning for legged locomotion systems on uneven terrain 23 p3221 N88-29170
Evaluation of atmospheric effects for operational tactical decision aid
[AD-A194205] 23 p3232 N88-29236
A knowledge-based decision support system for payload scheduling 23 p3252 N88-29358
An approach to combining heuristic and qualitative reasoning in an expert system 23 p3253 N88-29362
On the design and optimization of distributed signal detection and parameter estimation systems
[AD-A193934] 23 p3266 N88-29446
SDI (Strategic Defense Initiative): A policy analysis
[AD-A194240] 23 p3275 N88-29493
Distributed knowledge base systems for diagnosis and information retrieval
[AD-A193107] 23 p3296 N88-29633
Reduced flexibility in processing Titan 4 space launch vehicles at Cape Canaveral Air Force Station
[AD-A194908] 24 p3332 N88-29834

A detection theory analysis of visual display performance
[AD-A196291] 24 p3409 N88-30292
The bounded rationality constraint: Experimental and analytical results
[AD-A195897] 24 p3413 N88-30318
The advice taker/inquirer: A system for high-level acquisition of expert knowledge
24 p3421 N88-30359
Verification and validation of rulebased systems for Hubble Space Telescope ground support
24 p3421 N88-30361
Venture theory: A model of decision weights
[AD-A194809] 24 p3426 N88-30391
Looking beyond the strategic defense initiative
[AD-A195079] 24 p3427 N88-30394
Strategic, organizational and standardization aspects of integrated information systems, volume 6
[AD-A195855] 24 p3437 N88-30457
Technical change needs organizational change
24 p3438 N88-30466

DECISION THEORY
NT STATISTICAL DECISION THEORY
Modeling of human judgement in multicriteria analysis using pairwise comparison
[REPT-87-01] 01 p0076 N88-10484
Using concept mapping to define problems and identify key kernels during the development of a decision support system
[AD-A185636] 06 p0762 N88-14674
Deriving descriptions of the mind
[AD-A186647] 08 p1052 N88-16349
Modeling incorrect responses to multiple-choice items with multilinear formula score theory
[AD-A187887] 11 p1522 N88-19090
Task allocation for efficient performance of a decentralized organization
[AD-A188699] 12 p1705 N88-20204
Expert system techniques and decision support system: A case study (Dec. 1985 - Jun. 1986)
[ETN-88-91347] 13 p1821 N88-20884
Problem solving in a natural task as a function of experience
[AD-A191180] 16 p2243 N88-23399
A comparison of supervised maximum likelihood and decision tree classification for crop cover estimation from multitemporal LANDSAT MSS data
17 p2352 N88-24014
An extension of the Hopfield-Tank model for solution of the multiple traveling salesmen problem
[DE88-008377] 19 p2715 N88-26122
Combining expert opinions: An optimization framework
[REPT-87-84] 20 p2846 N88-26895
Uncertainty analysis in automatic robot programming
[RR-695-I-IMAG-88-LIFIA] 22 p3142 N88-28685

DECODERS
NT VITERBI DECODERS
NOSTRADAMUS programmable translator user's manual and programmer's manual
[DE87-013414] 01 p0083 N88-10533
More on the decoder error probability for Reed-Solomon codes 04 p0435 N88-12699
On the VLSI design of a pipeline Reed-Solomon decoder using systolic arrays 04 p0436 N88-12700
Packet telecommand. System performance assessment study -- onboard data handling
[PTC/TNOT/0015/SAAB] 07 p0843 N88-15113
Further results on finite-state codes
11 p1472 N88-18782
Speech coding at 4800 bps for mobile satellite communications 19 p2652 N88-25749
Development of an 8000 bps voice codec for AvSat
19 p2653 N88-25755

DECODING
A method resolving an ambiguity of measured distances by means of NAVSTAR GPS signals
01 p0065 N88-10417
Weighted decoding of block codes and some topics on decoding complexity
[ENST-87E005] 02 p0221 N88-11394
A lower bound for the decoder error probability of the linear MDS code 11 p1472 N88-18780
A concatenated coded modulation scheme for error control
[NASA-CR-182639] 12 p1621 N88-19697
Performance of single and multiple system AM stereo decoder receivers
[PB88-168307] 15 p2057 N88-22265
Soft decoding of recorded HF data
[FOA-C-30473-3.3] 15 p2058 N88-22269
Parallel memory addressing using coincident optical pulses
[AD-A189767] 15 p2106 N88-22547
A PC-based receiver-decoder for remote sensor monitoring
[DE88-004733] 16 p2192 N88-23075
Method for Veterbi decoding of large constraint length convolutional codes
[NASA-CASE-NPO-17310-1-CU] 23 p3183 N88-28946

DECOMPOSITION
NT AMMONOLYSIS
NT CRACKING (CHEMICAL ENGINEERING)
NT HYDROCRACKING
NT PHOTODECOMPOSITION
NT PHOTODISSOCIATION
NT PHOTOLYSIS
NT PROPELLANT DECOMPOSITION
NT PYROLYSIS
NT RADIOLYSIS
NT THERMAL DECOMPOSITION
Prediction and spectral decomposition of wide sense stationary processes on Z squared
[ENST-87C001] 01 p0087 N88-10564
A surface science investigation of potential intermediates, catalysts, and promoters in the synthesis of higher alcohols by metals
[DE87-014188] 02 p0144 N88-10906
Using MINOS (Modular In-core Nonlinear Optimization System) as a subroutine for decomposition
[DE87-013086] 02 p0221 N88-11390
Free radical detection and reactions in the decomposition of energetic materials
[AD-A184677] 03 p0296 N88-11858
Performance analysis of advanced spacecraft TPS
[NASA-CR-181532] 04 p0399 N88-12484
Application of Vandermonde decomposition to directional and modal analysis of broadband transients
[AD-A185007] 05 p0646 N88-13956
DC conductivity studies in Li5AlO4 at intermediate temperatures and its possible application for the electrolysis of water
[AD-A185489] 06 p0697 N88-14276
Hydroxide ion conductors as possible electrolytes in intermediate temperature fuel cells
[AD-A185508] 06 p0731 N88-14495
High temperature solar electrothermal processing-3. Zinc from zinc oxide at 1200-1675K using a non-consumable anode
[AD-A186600] 09 p1141 N88-16836
Determination of the melting and decomposition points of different materials in an oxygen stream
[INFORME-I-158/86] 09 p1142 N88-16844
Analysis of the decomposition of transparent polymer materials (blocks) under the action of laser beams in free generation mode
[AD-A187090] 09 p1147 N88-16873
DSC (Differential Scanning Calorimeter) stability test for liquid propellants: A preliminary report
[AD-A187115] 09 p1150 N88-16888
A three-dimensional dual potential procedure for rotational flows 10 p1329 N88-17942
A multiprocessor scheme for the singular value decomposition
[DE88-003591] 10 p1388 N88-18288
Fast Poisson solver on irregular regions by boundary integral-based domain decomposition methods
[DE88-003583] 10 p1399 N88-18340
Domain decomposition preconditioners for the spectral collocation method
[NASA-CR-181620] 10 p1400 N88-18345
High temperature processing of superconducting Y1Ba2Cu3O6.9
[DE88-003002] 10 p1416 N88-18449
Ceramic decomposition under irradiation
[DE88-004327] 11 p1464 N88-18732
Parallel pseudospectral domain decomposition techniques
[NASA-CR-181629] 11 p1524 N88-19101
Decomposition of hypochlorite in the presence of copper in a homogeneous medium
[NASA-TT-20199] 13 p1740 N88-20403
Molecular dynamics of laser ablation of a polymer coating
[DE88-004337] 13 p1750 N88-20466
DASM: A tool for Decomposition and Analysis of Sequential Machines
[EUT-87-E-170] 14 p1956 N88-21660
Structural decomposition of multiple time scale Markov processes
[AD-A189739] 15 p2123 N88-22657
Surface enhanced Raman scattering applied to surface chemical kinetics
[AD-A191275] 16 p2178 N88-22969
A low dimensional dynamical system for the wall layer
16 p2194 N88-23088
Fundamental studies of beta phase decomposition modes in titanium alloys
[AD-A191495] 18 p2485 N88-24740
Sample decomposition in sealed teflon vessels
[NASA-TT-20189] 18 p2494 N88-24798
Liquid phase decomposition in slurry fuels
19 p2624 N88-25564
Chemical kinetics modeling of HMX combustion
19 p2633 N88-25617
A domain decomposition method for boundary layer problems
[DE88-008917] 19 p2666 N88-25852
Two domain decomposition techniques for Stokes problems
[DE88-008724] 19 p2720 N88-26149
Manufacturing of a barium titanate with high dielectric coefficient by decomposition of precipitates of double oxalates
[ISAL-IDI1-88-02] 21 p2911 N88-27278
Coherent structures in the axisymmetric turbulent jet mixing layer 21 p2947 N88-27504
A study on Lebesgue decomposition of measures induced by stable processes
[AD-A192893] 21 p3009 N88-27850
Decomposition of energetic materials on the drop-weight impact machine
[DE88-009154] 22 p3059 N88-28152
Experiments and modeling of multi-component fuel behavior in combustion
[AD-A195011] 24 p3343 N88-29896
Decomposition of hydrazine by high frequency glow electrical discharges
[NASA-TT-20240] 24 p3344 N88-29906

DECOMPRESSION
U PRESSURE REDUCTION

DECOMPRESSION SICKNESS
Contribution of ultrasonic Doppler detection of circulating bubbles to human interventions under the sea and in space 19 p2697 N88-26029
Decompression procedures and accidents in space and sea 19 p2698 N88-26035
Reducing risks inherent in operating underwater craft: The contribution of classification, the example of the SAGA highly autonomous support submarine
19 p2699 N88-26042
Analysis of clinical symptoms of human decompression sickness during altitude chamber studies
19 p2703 N88-26074

DECONTAMINATION
Corrosion and stress corrosion of metals in decontamination solutions 22 p3054 N88-28118

DECOUPLING
Digital algorithms for the control and dynamic decoupling of industrial robot axes
[ETN-87-90441] 01 p0084 N88-10546
Decoupling and stabilization of speed and height in F4 Phantom aircraft using output feedback
[ETN-87-90926] 02 p0125 N88-10787
Ion-matrix coupling in polymer electrolytes from relaxation time studies
[AD-A184632] 03 p0293 N88-11841
The consequences of intergrain Josephson coupling in ceramic high-temperature superconductors
[DE87-013713] 06 p0785 N88-14816
Decoupling identities and predictable transformations in exchangeability
[AD-A186013] 07 p0913 N88-15540
A direct approach to almost disturbance and almost input-output decoupling
[MEMO-641] 08 p1072 N88-16471
Acceleration techniques for decoupling algorithms in semiconductor simulation
[DE88-003593] 09 p1221 N88-17323
A new approach to almost decoupling problems for linear and nonlinear systems
[MEMO-660] 14 p1962 N88-21700
Feedback decoupling and stabilization for linear systems with multiple exogenous variables
[ETN-88-92245] 16 p2255 N88-23474
Continuous decoupling transformations for linear boundary value problems
[ETN-88-92248] 16 p2258 N88-23493

DECREMENTING
U REDUCTION

DEEP SPACE
NT INTERPLANETARY SPACE
NT INTERSTELLAR SPACE

DEEP SPACE NETWORK
The Telecommunications and Data Acquisition Report
[NASA-CR-181546] 04 p0432 N88-12679
Low-noise cryogenic transmission line
04 p0434 N88-12688
A 2.3-GHz cryogenically cooled HEMT amplifier for DSS 13
04 p0434 N88-12689
Frequency doubling conversion efficiencies for deep space optical communications 04 p0434 N88-12691
The 8.4-GHz low-noise maser pump source assembly
04 p0436 N88-12705
A modern control theory based algorithm for control of the NASA/JPL 70-meter antenna axis servos
04 p0436 N88-12706

Power density measurements in the near field of the DSS 13 26-meter antenna 04 p0437 N88-12711
Deep space target location with Hubble Space Telescope (HST) and Hipparcos data
[NASA-CR-182520] 10 p1427 N88-18524
The Telecommunications and Data Acquisition Report
[NASA-CR-182545] 11 p1471 N88-18774
The JPL trapped mercury ion frequency standard 11 p1471 N88-18776
An optimal structure for a 34-meter millimeter-wave center-fed BWG antenna: The Cross-Box concept 11 p1472 N88-18778
A 2.3-GHz maser at Usuda, Japan, for TDRSS-orbiting VLBI experiment 11 p1472 N88-18779
A simplified, general-purpose deep-space ranging correlator design 11 p1473 N88-18786
A noise-adding radiometer for the Parkes antenna 11 p1473 N88-18788
X-band system performance of the very large array 11 p1473 N88-18789
DSS 14 64-meter antenna S- and X-band efficiency and system noise temperature calibrations, September 1987 11 p1473 N88-18790
Optical links in the angle-data assembly of the 70-meter antennas 11 p1474 N88-18792
The design and implementation of the Technical Facilities Controller (TFC) for the Goldstone deep space communications complex 11 p1474 N88-18794
Simulated performance of an order statistic threshold strategy for detection of narrowband signals 11 p1474 N88-18796
The Deep Space Network
[NASA-CR-182700] 13 p1759 N88-20524
The Telecommunications and Data Acquisition Report
[NASA-CR-183131] 22 p3063 N88-28178
The limits of direct satellite tracking with the Global Positioning System (GPS) 22 p3064 N88-28179
X-band resonant ring operation at 450 kW 22 p3064 N88-28181
Digital carrier demodulation for the DSN Advanced Receiver 22 p3064 N88-28183
Telemetry SNR improvement using the DSN Advanced Receiver with results for Pioneer 10 22 p3064 N88-28184
Advanced Receiver tracking of Voyager 2 near solar conjunction 22 p3065 N88-28185
Strawman Optical Reception Development Antenna (SORDA) 22 p3065 N88-28187
DSN very long baseline interferometry system Mark IV-88 22 p3067 N88-28199
Mark IV-85 mission support planning and future mission set 22 p3067 N88-28202
Determination of the Venus flyby orbits of the Soviet Vega probes using VLBI techniques 22 p3067 N88-28203
Mars earth-based radar: 1986 results and 1988-1990 opportunities 23 p3306 N88-29697
The Deep Space Network: An instrument for radio astronomy research
[NASA-CR-183219] 24 p3453 N88-30554

DEEP WATER
Deep water mass circulation in the Alboran Basin. Measurements - January to April 1982: ALBORAN 2
[AD-A189205] 13 p1803 N88-20777

DEFECTS
NT CRYSTAL DEFECTS
NT CRYSTAL DISLOCATIONS
NT EDGE DISLOCATIONS
NT INCLUSIONS
NT POINT DEFECTS
NT SCREW DISLOCATIONS
NT SPEECH DEFECTS
NT SURFACE DEFECTS
NT VACANCIES (CRYSTAL DEFECTS)
Theory of defects in non-metallic solids
[DE87-014068] 02 p0152 N88-10949
Detection of defects on structures
[EP-PATENT-0-210-794-A2] 04 p0453 N88-12807
Vibration and buckling of geometrically imperfect laminated cylindrical shells 04 p0456 N88-12822
Flaw effects: Behavior in operation of delamination in a crossed multilayer composite specimen
[DCQ/L-47-363/F] 06 p0678 N88-14153
Study on automatic detection and identification of defects in weld by microcomputer
[PB87-143897] 07 p0863 N88-15237
Methods of improving compacting quality of intricately shaped powder components
[BLL-M-37412-(5828.4)] 08 p0968 N88-15859
Nondestructive control: Modeling of electromagnetic phenomena, defect characterization, and sensor optimization
[ECL-86-14] 08 p0993 N88-16008
Acoustic emission measurements of PWR weld materials with inserted defects
[AERE-R-12386] 10 p1341 N88-18016
Flaw identification from forced vibration testing
[DE88-002641] 10 p1342 N88-18018
The influence of small defects on tensile specimen ductility and symmetry of deformation
[AD-A187983] 10 p1346 N88-18044
Grain boundaries, planar defects and superconducting properties of YBa2Cu3O7
[DE88-003477] 10 p1419 N88-18475
Simulation and processing of high resolution images of defects and interfaces in superconducting YBa2Cu3O7
[DE88-003856] 10 p1420 N88-18480
Fracture toughness of steel weldments containing lack of penetration defects 11 p1501 N88-18965
Investigation of defect and electronic interactions associated with GaAs device processing
[AD-A188021] 11 p1556 N88-19313
Study of defects in metals by positron annihilation
[DE88-701042] 13 p1745 N88-20432
Gordon Conference on Intermetallic Compounds held at Tilton, New Hampshire on 20-24 July 1987
[AD-A188502] 13 p1745 N88-20435
A defect investigation of Thunderflash MK N5 (Navy)
[MRL-TN-522] 13 p1754 N88-20488
Implementation and evaluation of a combined test-error correction procedure for memories with defects
[EUT-87-E-169] 14 p1955 N88-21651
Use of long-distance pair potentials in calculations of defect characteristics in metals
[DE88-701039] 15 p2037 N88-22138
Nondestructive evaluation of sintered ceramics 15 p2083 N88-22416
Processing defects and strength of alumina substrates
[W-10/87] 15 p2087 N88-22441
The use of rule induction to assist in the diagnosis of avionic circuit board defects
[ETN-88-92077] 16 p2162 N88-22899
Nondestructive evaluation of large scale composite components
[AD-A190998] 16 p2173 N88-22954
Micro-Raman analysis of dielectric optical thin films
[AD-A191228] 17 p2445 N88-24537
Harmfulness of defects: Behaviour in service of a delamination in a composite containing many differently oriented layers
[PB88-124714] 18 p2479 N88-24705
Application of magnification xeroradiography to advanced ceramics
[DE88-009965] 20 p2778 N88-26473
Microfocus X-ray techniques for flaw location
[DE88-008636] 20 p2812 N88-26680
Defects and disorder in amorphous and damaged silicon
[AD-A192277] 20 p2879 N88-27089
Defects in high-mobility semiconductor systems
[AD-A192298] 20 p2879 N88-27090
NDE performance in predicting failure strength of spherical composite specimens with implanted flaws
[DE88-008223] 21 p2959 N88-27575
Critical issues and directions for fracture mechanics and structural integrity
[AD-A193050] 21 p2960 N88-27584
Probing the electronic and defect structure of perovskite superconductors
[DE88-008349] 21 p3022 N88-27939
Direct and inverse diffraction problems for QNDE (Quantitative Non-Destructive Evaluation) applications
[AD-A194721] 22 p3085 N88-28322
Phase equilibrium and crystal growth studies on AgGaSe2 and related nonlinear optical materials
[AD-A193763] 22 p3157 N88-28783
The effect of oriented defects on long-range ordering of hydrocarbon films: Azulene on Pt(111)
[AD-A196089] 24 p3344 N88-29904
Predicting the durability of adhesives and coatings by remote detection of hidden defects and coating-thickness irregularities: A theoretical and numerical study 24 p3355 N88-29972

DEFENSE COMMUNICATIONS SATELLITE SYSTEM
NT FLEET SATELLITE COMMUNICATION SYSTEM

DEFENSE INDUSTRY
The military techniques of tomorrow. A contribution to active peace assurance
[MBB-UA-1049/87] 10 p1315 N88-17860
The effects of two Carlucci initiatives concurrency and streamlining, on the test and evaluation phase of system acquisitions 12 p1704 N88-20198
JPRS report: Science and technology. Japan
[JPRS-JST-88-001] 15 p2051 N88-22218
JPRS report: Science and technology. Japan
[JPRS-JST-87-029] 15 p2052 N88-22228
Department of Defense Statement on the Technology Base to the Subcommittee on Defense Industry and Technology of the Committee on Armed Services, United States Senate, 100th Congress, second session
[AD-A191839] 18 p2588 N88-25376

DEFENSE METEOROLOGICAL SATELLITE PROGRAM
U DMSP SATELLITES

DEFENSE PROGRAM
Source header list. Volume 2: L through Z
[AD-A184001] 03 p0385 N88-12419
Information analysis centers in the department of defense, revision
[AD-A184002] 03 p0385 N88-12420
Source header list. Volume 1: A through K
[AD-A184000] 04 p0501 N88-13086
University research initiative research program summaries
[AD-A184876] 05 p0658 N88-14035
Source hierarchy list. Volume 3: P through Z
[AD-A185902] 07 p0942 N88-15724
Concurrency control and reliability in replicated database systems 10 p1377 N88-18221
Streamlining invitation for bids
[AD-A188941] 12 p1705 N88-20206
A directory of databases available through SearchMAESTRO
[AD-A188813] 12 p1706 N88-20214
Free electron lasers in strategic defense
[DE88-007024] 17 p2394 N88-24231
Department of Defense statement on the X-ray Lithography Program to the Research and Development Subcommittee of the House Armed Services Committee of 100th Congress, second session
[AD-A191854] 18 p2582 N88-25341
Department of Defense Statement on the Technology Base to the Subcommittee on Defense Industry and Technology of the Committee on Armed Services, United States Senate, 100th Congress, second session
[AD-A191839] 18 p2588 N88-25376
Department of Defense statement on defense agency research and development to the Subcommittee on Defense of the Committee on Appropriations, United States House of Representatives, 100th Congress, second session
[AD-A191840] 18 p2588 N88-25377
Department of Defense Statement on the Balanced Technology Initiative to the Committee on Armed Services, United States Senate, 100th Congress, second session
[AD-A191841] 18 p2588 N88-25378
The Department of Defense report on the merit review process for competitive selection of university research projects and an analysis of the potential for expanding the geographic distribution of research for the Committees on Appropriations, United States Congress
[AD-A191842] 18 p2588 N88-25379
The FY 1989 Department of Defense statement on the Science and Technology Program to 100th Congress, second session
[AD-A191843] 18 p2588 N88-25380
The Army's role in space: Support for the battlefield commander
[RAND-P-7396] 19 p2721 N88-26159
The Oak Ridge National Laboratory strategic defense initiative shield optimization program
[DE88-008946] 19 p2721 N88-26160
An agenda for the strategic defense initiative
[RAND-P-7404] 20 p2847 N88-26898
The Oak Ridge National Laboratory strategic defense initiative shield optimization program: Executive summary
[DE88-008016] 20 p2847 N88-26899
Monitoring space weaponry: Detection and verification issues
[DE88-008726] 20 p2847 N88-26900
SDI: Myth or reality
[DE88-009121] 20 p2847 N88-26901
SDI and/or arms control
[RAND-P-7357] 20 p2848 N88-26903
Overview of the SDI (Strategic Defense Initiative) Program in short wavelength chemical lasers
[DE88-007912] 21 p3010 N88-27861
Stress/fatigue and the ARNG (Army National Guard) aviator
[AD-A194184] 22 p3132 N88-28621
SDI (Strategic Defense Initiative): A policy analysis
[AD-A194240] 23 p3275 N88-29493
SDI (Strategic Defense Initiative). Where do we go from here
[AD-A194544] 23 p3275 N88-29497
SSTS (Space Surveillance and Tracking System): The importance of early test and evaluation organizational participation
[AD-A193745] 23 p3276 N88-29499

DEFLAGRATION
Flame acceleration and transition to detonation in channels
[DE87-014193] 03 p0284 N88-11786
Steady tonation and flagration waves in reactive continua
[RARDE-2/73] 03 p0315 N88-11989

On the possibility of high velocity deflagration front propagation by radiative energy transfer
[AD-A189022] 12 p1613 N88-19645
Deformation, fracture and explosive properties of reactive materials
[AD-A193080] 21 p2923 N88-27348

DEFLATING
U INFLATABLE STRUCTURES
U PRESSURE REDUCTION

DEFLECTION
Telemetric laser extensometry technique for monitoring deflections in small cracks 05 p0607 N88-13724
Mechanisms in thermal mechanical forming of plates
[AD-A187797] 11 p1466 N88-18744
Computer aided deflection measurement of an aircraft wing
[AD-A187778] 12 p1581 N88-19461
Data processing method for high angle of attack testing with rolling angle 14 p1864 N88-21134
Further study of relation of von Karman equation for elastic large deflection problem and Schrodinger equation for quantum eigenvalues problem
14 p1899 N88-21341
Cubic spline solution of symmetric buckling problems of clamped shallow spherical shells
15 p2053 N88-22239
Deflection of a circular liquid jet on a flat plate perpendicular to the flow direction
[NASA-TT-20279] 16 p2207 N88-23173
Fast acting optical beam detection and deflection system
[AD-A192161] 18 p2521 N88-24954
Plate response analysis using shock tube
[AD-A190828] 18 p2526 N88-24987
Simulation of diaphragm-type IC pressure sensors
19 p2672 N88-25887
A simple unified method for predicting the deflections of reinforced concrete structures
19 p2679 N88-25930
Optical measurement of propeller blade deflections
[NASA-TP-2841] 22 p3079 N88-28286
Optical measurement of unducted fan blade deflections
[NASA-TM-100966] 23 p3216 N88-29142
Free vibration of rectangular plates with a small initial curvature
[NASA-CR-179370] 24 p3383 N88-30148

DEFLECTORS
The Shock and Vibration Bulletin. Part 4: Structural Dynamics and Modal Test and Analysis
[AD-A186751] 09 p1179 N88-17062
Qualification by analysis of IUS plume deflectors
09 p1179 N88-17063
Multimode-waveguide laser beam deflector
[DE88-006222] 13 p1776 N88-20622

DEFORESTATION
Monitoring Moneragala (Sri Lanka) with SPOT imagery
22 p3099 N88-28405
Study of deforestation in the Vosges (France) by remote sensing 22 p3107 N88-28452

DEFORMATION
NT AXIAL STRAIN
NT ELASTIC BENDING
NT ELASTIC BUCKLING
NT ELASTIC DEFORMATION
NT PLASTIC DEFORMATION
NT STATIC DEFORMATION
NT TENSILE DEFORMATION
NT WAVE FRONT DEFORMATION
On the association of erupting magnetic fields with eruptive prominences and coronal mass ejections
01 p0113 N88-10727
Modeling shockwave deformation via molecular dynamics
[DE87-013157] 02 p0169 N88-11063
Buckling of viscoelastic columns
02 p0190 N88-11187
Investigation of the deformation behavior of ferritic two-phase Fe-Ni-Al alloys with high concentrations of the intermetallic (Fe, Ni)Al phase at high temperatures
[ETN-87-90605] 03 p0288 N88-11812
Deformation mechanisms of thermostructural materials
[AD-A184070] 03 p0338 N88-12128
An algorithmic approach to crustal deformation analysis
[NASA-CR-181497] 03 p0349 N88-12203
Finite deformations of shell with rigid inclusion
04 p0426 N88-12639
Fatigue failure of thin porous strips
04 p0426 N88-12640
Explicit and implicit soil modelling for dynamic soil-structure interaction problems
04 p0428 N88-12650
Effective treatment of membrane and shear locking phenomena in curved shear-deformable axisymmetric shell element 04 p0428 N88-12652
A refined nonlinear analysis of laminated composite plates and shells
[AD-A184436] 04 p0454 N88-12811
An algorithmic approach to crustal deformation analysis 04 p0468 N88-12891
Measurement of model deformation in wind tunnels
05 p0551 N88-13358
An analytical study of the effects of transverse shear deformation and anisotropy on buckling loads of laminated cylinders
[NASA-TM-100508] 05 p0557 N88-13387
Cyclic deformation and crack initiation
05 p0597 N88-13646
The orientations of dipolar walls produced by cyclic deformation 05 p0598 N88-13655
Striations and the fatigue growth mechanism in a micro-alloyed steel 05 p0599 N88-13661
The influence of slip mechanism on fatigue of Mg and Mg-2.3Li 05 p0600 N88-13672
Fatigue 87, volume 3
[AD-A184047] 05 p0604 N88-13700
Deformation mechanisms and crack initiation in fatigue 05 p0608 N88-13730
Deformation, fatigue and fracture behavior of two cast anisotropic superalloys 05 p0608 N88-13732
Viscoelastic properties of EA951 adhesive: A source of creep deformations of a strongback
[DE88-001581] 06 p0685 N88-14197
The evaluation of a deformable diffraction grating for a stigmatic EUV spectroheliometer
[NASA-CR-182371] 06 p0707 N88-14337
Fatigue 87, volume 2
[AD-A184046] 06 p0715 N88-14381
Cyclic deformation behaviour of cast irons with various graphite shapes in the temperature range 20 C less than or = T less than or = 500 C 06 p0715 N88-14384
Transients in elevated temperature crack growth
[DE87-013189] 06 p0724 N88-14454
Composite reliability enhancement via preloading
[AD-A185938] 07 p0826 N88-15010
Deformation effects on microwave reflectivity
[AD-A185684] 07 p0844 N88-15120
Deformation induced cracking in steel girder bridges and retrofit guidelines
[PB88-102710] 07 p0868 N88-15265
The aerophotogrammetric determination of Earth surface deformations
[SER-C-321] 07 p0872 N88-15288
Assessment of anomalous gravitational field of elastic Earth 07 p0921 N88-15594
Study on the mechanical stresses in the elements of the model of a toroidal magnet of a tokamak with strong field
[DE88-700343] 07 p0935 N88-15679
Steady-state deformation of some lithium ceramics
[DE88-003116] 08 p0972 N88-15882
A review of research in rotor loads
09 p1106 N88-16629
Investigation of the deformation behavior of the intermetallic phase (Fe,Ni)Al at high temperatures
[ETN-88-91062] 09 p1143 N88-16854
Successful mixed formulation for axisymmetric shell analysis employing discontinuous stress fields of the same order as the displacement field
[DE88-700021] 09 p1178 N88-17052
An analytical study of the effects of transverse shear deformation and anisotropy on natural vibration frequencies of laminated cylinders
[NASA-TM-100554] 10 p1295 N88-17739
Micro-mechanisms of deformation in SiC/Al composites
[AD-A188282] 10 p1296 N88-17749
Boundary integral analysis of flow and deformation of long bubbles in capillaries
[DE88-002110] 10 p1326 N88-17927
Acoustic emission-microstructural relations in ferritic steels. Part 3: The effect of inclusion content
[AERE-R-12041] 10 p1341 N88-18015
The analysis of deformations and strains in composites by moire interferometry
[AD-A187482] 10 p1345 N88-18043
Continuous deformation algorithm on the product space of unit simplices, revised version
[PB88-114210] 10 p1387 N88-18281
Stability diagrams for epitaxial strained layers
[DE88-003935] 10 p1418 N88-18470
Approximate method for predicting the permanent set in a beam in vacuo and in water subject to a shock wave 11 p1500 N88-18957
Deformations in VLBI antennas
[NASA-TM-100696] 11 p1502 N88-18970
Vibrations of shells containing fluid
12 p1635 N88-19787
Geophysical study of the structure and processes of the continental convergence zones: Alpine-Himalayan Belt
[NASA-CR-182647] 12 p1644 N88-19842
A paper on horizontal deformation in the frontogenesis in south Brazil
[INPE-4489-TDL/322] 12 p1647 N88-19867
Processing, structure and properties of heavily deformed in situ composites
[AD-A189611] 13 p1742 N88-20416
Use of the LLNL 40 kV electric gun to study the shock response of 21-6-9 stainless steel
[DE87-014550] 13 p1742 N88-20418
Grain refinement during primary breakdown of alloy 718
[DE88-005193] 13 p1743 N88-20423
Gordon Conference on Intermetallic Compounds held at Tilton, New Hampshire on 20-24 July 1987
[AD-A188502] 13 p1745 N88-20435
Geodetic measurement of deformation east of the San Andreas fault in Central California
[NASA-CR-182709] 13 p1798 N88-20754
Mechanical properties of sea ice and sea ice deformation in the near-shore zone
[PB88-147889] 13 p1804 N88-20782
Materials dependence of deformation texture development in various deformation modes
[DE88-004312] 14 p1922 N88-21457
Pressure induced ageing of polymers
14 p1929 N88-21504
A unified creep-plasticity model suitable for thermo-mechanical loading 14 p1932 N88-21518
Fundamental studies on high temperature deformation recrystallization, and grain growth of two-phase materials
[AD-A189725] 15 p2038 N88-22145
The buckling and vibration of composite plates using the Levy method considering shear deformation and rotary inertia
[AD-A189743] 15 p2076 N88-22374
Evolution of hardening and damage during viscoplastic deformation
[AD-A190714] 15 p2077 N88-22381
Unified constitutive model for single crystal deformation behavior with applications 15 p2078 N88-22388
Fundamental properties and devices applications of Ge(x)Si(1-x)/Si superlattices
[AD-A190129] 15 p2143 N88-22787
Deformation of rapidly solidified dispersion strengthened titanium alloys
[AD-A190793] 16 p2179 N88-22984
Disclination structures in carbon and graphite
[AD-A191056] 17 p2322 N88-23868
Superplasticity: A fundamental investigation on deformation mechanism and cavitation phenomena
[AD-A191548] 18 p2485 N88-24741
Role of cracks in the creep of structural polycrystalline ceramics
[AD-A191485] 18 p2490 N88-24770
Influence of strain rate on the substructure evolution and yield behavior of Ti-6Al-4V
[DE88-006457] 19 p2616 N88-25520
Accelerated fatigue crack growth behavior of PWA 1480 single crystal alloy and its dependence on the deformation mode
[NASA-TM-100943] 20 p2772 N88-26436
Irreversible deformations during fracture in polymers
[W-7/86] 20 p2780 N88-26485
Spatial dynamics of deformable multibody systems with variable kinematic structure 20 p2813 N88-26687
Diffusion and solubility of some interstitial impurities in deformed metals
[DE88-701859] 21 p2914 N88-27296
Slew-induced deformations in a space-based electromagnetic rail gun 21 p2929 N88-27385
Development of a biaxial test system for thin-walled metal tubes using tensile-compressive axial load and internal-external pressure
[DE88-011279] 21 p2962 N88-27592
DYNA3D (Nonlinear Dynamic Analysis of Structures in Three Dimensions) user's manual
[DE88-012242] 21 p2963 N88-27604
Theory of acoustoplasticity and ultrasonic measurements of residual stresses
22 p3087 N88-28328
The high temperature creep deformation of Si3N4-6Y2O3-2Al2O3
[NASA-CR-183204] 23 p3190 N88-28981
Static and dynamic metal-metal friction at plastic stress levels
[DE88-011281] 23 p3222 N88-29176
Intraplate deformation, stress in the lithosphere and the driving mechanism for plate motions
[NASA-CR-183121] 23 p3231 N88-29231
Preparation and testing of Nb-Zr and Nb-ZrO2 single crystals for deformation studies
[DE88-702798] 23 p3293 N88-29613

DEGENERATION
Regularity properties of a doubly degenerate equation in hydrology
[REPT-87-07] 01 p0064 N88-10409
Squeezed state in degenerate parametric amplification discussed by H. Takahasi in 1963
14 p1976 N88-21790
Squeezed states of light 14 p1976 N88-21791
Quantum statistics of parametric oscillators above threshold 14 p1979 N88-21811
Signal processing with degenerate four-wave mixing
[AD-A191496] 18 p2499 N88-24825
Regularity of solutions for nonlinear degenerate elliptic boundary value problems
[DE88-702646] 22 p3146 N88-28710
DEGRADATION
NT BIODEGRADATION
NT THERMAL DEGRADATION
NT WAVE DEGRADATION
Mechanisms of polymer degradation using an oxygen plasma generator
[NASA-TM-100681] 01 p0018 N88-10110
Mathematical modelling of solar ultraviolet radiation induced optical degradation in anodized aluminum
02 p0135 N88-10846
High intensity 5 eV O-atom exposure facility for material degradation studies 02 p0135 N88-10847
Models of degradation of stratified composite structures
[ONERA-RT-13/3542-RY-061-R]
02 p0142 N88-10892
Degradation mechanisms of materials for large space systems in low Earth orbit
[NASA-CR-181472] 02 p0143 N88-10896
Prevention of radiation induced degradations and of electrostatic perturbations on the Arabsat spacecraft in flight results 03 p0275 N88-11734
Surface catalytic degradation study of two linear perfluoropolyalkylethers at 345 C
[NASA-TP-2774] 04 p0410 N88-12543
Micromechanics of the degradation of composite materials
[SNIAS-872-430-113] 05 p0559 N88-13405
Development of a data analysis system for the detection of lower level atmospheric turbulence with an acoustic sounder
[AD-A184972] 05 p0624 N88-13821
Mechanistic studies of polymeric samples exposed aboard STS 8
[NASA-CR-182364] 06 p0686 N88-14202
Feasibility studies of optical processing of image bandwidth compression schemes
[AD-A186073] 07 p0932 N88-15660
Improved perfluoroalkylether fluid development
[NASA-CR-180872] 08 p0967 N88-15851
Space environmental effects on polymeric materials
[NASA-CR-182454] 09 p1148 N88-16879
Radiant power degradation of silicon-doped gallium arsenide and gallium aluminum arsenide infrared light-emitting diodes
[AD-A186726] 09 p1157 N88-16935
Time dependent degradation of energetic electrons in gaseous and condensed media
[DE88-002912] 09 p1246 N88-17465
Operation of gas turbine engines in dust-laden environments 10 p1280 N88-17654
Environment assisted degradation mechanisms in aluminum-lithium alloys
[NASA-CR-182482] 10 p1301 N88-17782
An experimental measurement of metal multilayer X-ray reflectivity degradation due to intense X-ray flux
[LA-10989-T] 11 p1547 N88-19255
Carbon residue studies of polyphenyl ethers and ester-based lubricants using a microcarbon residue tester
[AD-A188585] 12 p1611 N88-19632
MOSFET performance degradation due to hot carriers
13 p1848 N88-21063
The performance of perfluoropolyalkylether oils under boundary lubrication conditions
[AD-A191057] 17 p2323 N88-23869
Shape stability in composites
18 p2479 N88-24706
Predictive corrosion modeling, volume 1
[AD-A191229] 18 p2485 N88-24739
Environment assisted degradation mechanisms in advanced light metals
[NASA-CR-182907] 18 p2486 N88-24746
Evaluation of the toxicity of products from the thermal degradation of materials
[ETN-88-91995] 18 p2549 N88-25130
Molecular characterization of structure and bonding in thin film materials
[DE88-006811] 18 p2584 N88-25351
Temperature-dependent tensile and shear response of graphite/aluminum
[NASA-CR-182914] 19 p2609 N88-25484
Modeling and experimental measurements of solid propellant flame structure 19 p2631 N88-25605
Predicting optical degradation of a laser beam through a turbulent shear layer 21 p2927 N88-27376
Degradation of fiber composites during storage
[FOA-C-20702-2.6] 22 p3051 N88-28102
The behavior of a Costas loop in the presence of space telemetry signals 22 p3067 N88-28198
Long-term behavior of energy production systems with the example of HELIOS and SYMPHONIE
[ETN-88-92988] 23 p3230 N88-29223
Photoacoustic Fourier transform infrared spectroscopy. An early detection technique for coatings degradation
24 p3354 N88-29968
Degradation of protective coatings on steel in corrosive environments 24 p3354 N88-29969
Prediction of degradation of polymeric coating materials 24 p3354 N88-29970
A reliability-based program for predicting the service life of organic coating systems 24 p3355 N88-29971
DEGREES OF FREEDOM
Traction-drive seven degrees-of-freedom telerobot arm: A concept for manipulation in space
[DE87-010895] 01 p0054 N88-10346
Coupled elastic rotor/body vibrations with inplane degrees of freedom 05 p0596 N88-13643
Analysis and synthesis of two degrees of freedom control systems 11 p1495 N88-18928
An efficient gradient projection optimization scheme for a seven-degree-of-freedom redundant robot with spherical wrist
[DE88-005440] 14 p1919 N88-21453
Distributions of quadratic forms
[AD-A190224] 15 p2124 N88-22663
The VITE model: A neutral command circuit for a generating arm and articulator trajectories
[AD-A192715] 21 p2987 N88-27734
Bifurcations of periodic solutions of non-integrable Hamiltonians with two degrees of freedom: Numerical and analytical results
[DE88-702747] 23 p3272 N88-29473
DEHUMIDIFICATION
Experimental studies of heat and mass exchange in parallel-passage rotary desiccant dehumidifiers for solar cooling applications
[DE88-001119] 10 p1350 N88-18069
DEHYDRATION
Evidence for human adaptive response to dehydration: Increase of circulating protein mass
[AD-A186225] 08 p1048 N88-16328
The role of hydration on peripheral response to cold
[AD-A186448] 09 p1199 N88-17186
Medical problems related to altitude in: Human performance physiology and environmental medicine at terrestrial extremes, chapter 14
[AD-A188340] 12 p1666 N88-19989
Variability in intake and dehydration in young men during a simulated desert walk
[AD-A192654] 22 p3131 N88-28613
DEICERS
Calibration of the ARL (Aeronautical Research Laboratories) rain and icing facility
[AD-A186776] 09 p1121 N88-16710
JUH-1H redesigned pneumatic boot deicing system flight test evaluation
[AD-A194918] 24 p3322 N88-29785
DEICING
Theoretical analysis of the electrical aspects of the basic electro-impulse problem in aircraft de-icing applications
[NASA-CR-180845] 05 p0543 N88-13310
Effects of aircraft deicing/antiicing fluids on airfoil characteristics 08 p0952 N88-15776
The NASA aircraft icing research program
08 p0957 N88-15803
DEICING SYSTEMS
U DEICERS
DEIMOS
Power requirements for mining and microwave processing of extraterrestrial resources
17 p2420 N88-24389
DEKATRONS
U COUNTERS
DELAMINATING
A stochastic delamination growth model for fatigue loaded laminated composite materials
02 p0141 N88-10888
Free-edge delamination: Laminate width and loading conditions effects
[NASA-TM-100238] 04 p0411 N88-12551
Higher order theory analysis of a modified free-edge delamination specimen 04 p0455 N88-12820
Strain-energy-release rate analysis of the end-notched flexure specimen using the finite-element method
[NASA-TM-100494] 05 p0608 N88-13735
Flaw effects: Behavior in operation of delamination in a crossed multilayer composite specimen
[DCQ/L-47-363/F] 06 p0678 N88-14153
Measurement of mechanical parameters to define damage criteria in delamination of crossed stratified layers
[DCQ/L-47-361/F] 06 p0678 N88-14154
Delamination durability of composite materials for rotorcraft 09 p1107 N88-16634
A fiber-resin micromechanics analysis of the delamination front in a DCB specimen
[NASA-TM-100540] 10 p1294 N88-17737
Cost 501 Project UK10 part 3: Thermal fatigue damage of Fecralloy steel-sprayed and co-extruded tubing
[AERE-R-12230] 10 p1343 N88-18026
On delamination of (+ or - theta sub m/90 sub n/2) sub s laminates subject to tensile loading
[AD-A188095] 11 p1447 N88-18626
Damage mechanics of fiber reinforced plastics: A general view 11 p1448 N88-18631
Ply-level failure analysis of a graphite/epoxy laminate under bearing-bypass loading
[NASA-TM-100578] 13 p1735 N88-20372
Delamination stresses in semicircular laminated composite bars
[NASA-TM-4026] 13 p1735 N88-20375
Detection of bondline delaminations in multilayer structures with lossy components
[NASA-CR-182716] 14 p1883 N88-21256
Damage models for delamination and transverse fracture
[AD-A189652] 15 p2029 N88-22088
Fractography of composite delamination
[NASA-CR-182757] 15 p2030 N88-22096
Postbuckling delamination of a stiffened composite panel using finite element methods
[NASA-CR-182803] 15 p2030 N88-22098
Delamination analysis in crossed layer composites
[REPT-48-447/F] 16 p2171 N88-22942
Characterization of Mode 1 and Mode 2 delamination growth and thresholds in graphite/peek composites
[NASA-TM-100577] 16 p2172 N88-22947
Mechanics of instability-related delimination growth
[NASA-TM-100622] 17 p2349 N88-23998
Thermographic detection of buried debonds
[AD-A192115] 18 p2475 N88-24680
Detecting delaminations in CFRP specimens using X-ray techniques
[FFA-TN-1988-04] 18 p2479 N88-24704
Harmfulness of defects: Behaviour in service of a delamination in a composite containing many differently oriented layers
[PB88-124714] 18 p2479 N88-24705
Local delamination buckling in layered structures
18 p2480 N88-24711
Fracture physics of delamination of composite materials
[AD-A192021] 19 p2609 N88-25482
Instability-related delamination growth of embedded and edge delaminations 20 p2767 N88-26406
Three-dimensional analysis of a postbuckled embedded delamination
[NASA-TP-2823] 20 p2812 N88-26684
Failure analysis of laminated composite angles
21 p2959 N88-27578
Fracture behavior in multidimensional fiber-reinforced composites 22 p3051 N88-28099
DELAWARE
Seasonal cycling of sulfur and iron in porewaters of a Delaware salt marsh
[NASA-CR-182385] 07 p0876 N88-15311
DELAWARE BAY (US)
YABLED cruises part 2: Data from YABLED-17 through YABLED-26, January-October 1985
[PB88-163597] 14 p1950 N88-21627
DELAWARE RIVER BASIN (US)
YABLED cruises part 2: Data from YABLED-17 through YABLED-26, January-October 1985
[PB88-163597] 14 p1950 N88-21627
DELAY
On oscillation of a kind of integro-differential equation with delay
[DE87-703059] 02 p0225 N88-11417
Design of efficient FIR filters with minimal delay
[PB87-100434] 04 p0438 N88-12717
A finite element analysis of adhesively bonded composite joints including geometric nonlinearity, nonlinear viscoelasticity moisture diffusion and delayed failure
[AD-A187455] 10 p1296 N88-17747
A pyrotechnic delay ignition system for a submarine launched marine signal
[MRL-R-1079] 13 p1754 N88-20487

Time characteristics of ultrashort light pulses from dye lasers with distributed feedback
14 p1970 N88-21759
Investigation of combustion in large vortices
[AD-A190406] 15 p2035 N88-22121
Estimation of time- and state-dependent delays and other parameters in functional differential equations
[NASA-CR-181663] 17 p2383 N88-24164
The influence of delay effects on the decay of liquid jets
[MPIS-14/1987] 23 p3214 N88-29130

DELAY CIRCUITS
On adaptive signal processing of RF signals
[DE87-014192] 02 p0161 N88-11007
Measured noise performance of a direct-sequence spread-spectrum system and a comparison of single vice dual-channel delay-lock loops
[AD-A186286] 07 p0843 N88-15110
Modules of nanosecond logic electronics system with computer control
[DE88-700190] 11 p1479 N88-18828

DELIVERY
NT PAYLOAD DELIVERY (STS)
NT WEAPONS DELIVERY
Developmental airdrop testing techniques and devices
[AGARD-AG-300-VOL-6] 04 p0398 N88-12481

DELPHI METHOD (FORECASTING)
Critical issues for establishment of a permanently-occupied lunar base
[AD-A187128] 09 p1263 N88-17567

DELTA DART AIRCRAFT
U F-106 AIRCRAFT

DELTA FUNCTION
Finitely many delta-interactions with supports on concentric spheres
[DE88-701834] 20 p2880 N88-27101

DELTA MODULATION
Method for set-up for researching signal curve development
[NASA-TT-20235] 13 p1760 N88-20526

DELTA WINGS
An experimental investigation of dynamic ground effect
[NASA-CR-4105] 04 p0394 N88-12458
Computation of flow past conical hypersonic wings using a second order Godunov method
05 p0533 N88-13241
Vortex formation over delta, double-delta and wave rider configurations at supersonic speeds
05 p0533 N88-13243
Study of the effect of mass transfer on a transonic boundary layer. Application to flow relaminarization
[ETN-88-91169] 05 p0541 N88-13296
Delta wing in incompressible flow. Experimental study in F2
[ONERA-RT-36/1147-AN-249-G]
05 p0541 N88-13298
Examples of static aeroelastic effects on present combat aircraft projects 05 p0550 N88-13349
Supersonic aerodynamics of delta wings
[NASA-TP-2771] 10 p1273 N88-17615
Design loads for Swedish military aircraft in a twenty years' perspective 12 p1580 N88-19456
Research on flow control
[AD-A189014] 12 p1627 N88-19736
Tests on the AFWAL 65 deg delta wing at NLR: A study of vortex flow development between Mach = 0.4 and 4
[NLR-MP-86058-U] 13 p1717 N88-20266
The international vortex flow experiment: A test case for compressible Euler codes
[NLR-MP-86076-U] 13 p1717 N88-20267
Computational technique for compressible vortex flows using the integral equation solution
[NASA-CR-182695] 13 p1718 N88-20271
Vortex flow over a delta wing with apex flaps using laser flow visualisation
[BU-356] 14 p1862 N88-21121
Experimental investigation of the transonic flow at the leeward side of a delta wing at high incidence
[LR-518] 16 p2156 N88-22861
Investigation on the movement of vortex burst position with dynamically changing angle of attack for a schematic deltawing in a watertunnel with correlation to similar studies in windtunnel 16 p2204 N88-23152
Numerical study of delta wing leading edge blowing
[NASA-CR-183101] 20 p2752 N88-26335
Flow around a delta wing with or without a canard control surface (phi BA = 60 deg). Part 1: Hydrodynamic visualization in permanent regime
[ONERA-RT-10/2891-AN-101-A-PT-1]
21 p2892 N88-27170
An experimental study of the effect of pitch rate on delta wing aerodynamics and stability
[NASA-CR-183159] 21 p2893 N88-27173
Optimal control of the wing rock phenomenon
21 p2927 N88-27373
Delta wing configurations 23 p3167 N88-28860
Steady and unsteady transonic pressure measurements on a clipped delta wing for pitching and control-surface oscillations
[NASA-TP-2594] 23 p3173 N88-28895

DELTAS
SDVS (State Delta Verification System): Program verification system development fiscal year 1986
[AD-A184338] 03 p0366 N88-12302
Expectations for water level deviations at the delta works: Zierikzee (Netherlands), November 1981-February 1986
[KNMI-TR-93] 05 p0628 N88-13840
Turbidity patterns in the delta waters of southwest Netherlands on Thematic Mapper (TM) and multispectral scanner (MSS) satellite images
[BCRS-86-06] 16 p2227 N88-23303
Study of the Arachon (France) underwater delta using Thematic Mapper data 19 p2702 N88-26064

DEMAGNETIZATION
An adiabatic demagnetization cooled bolometer system for millimeter continuum astronomy
07 p0943 N88-15735
Statistical analysis of feasibility of non-destructive inspection of mechanical properties of hot worked pipes of alloy steels
[BLL-M-37596-(5828.4)] 14 p1922 N88-21455

DEMAND ASSIGNMENT MULTIPLE ACCESS
L-band and SHF multiple access schemes for the MSAT system 19 p2650 N88-25734
Integrated voice/data protocols for satellite channels
19 p2651 N88-25739

DEMINERALIZING
NT BONE DEMINERALIZATION

DEMODULATION
An additional study and implementation of tone calibrated technique of modulation
[NASA-CR-182377] 07 p0844 N88-15117
The ratio detector: A method of amplitude insensitive frequency demodulation
[RAE-TR-87008] 09 p1153 N88-16910
Trellis-coded MPSK modulation techniques for MSAT-X(sup)1 19 p2648 N88-25721
Demodulation processes in auditory perception
[AD-A193421] 21 p2988 N88-27740
Observational/numerical study of the upper ocean response to hurricanes
[AD-A193592] 22 p3128 N88-28598

DEMODULATORS
NT MODEMS
NT PHASE DEMODULATORS
Documentation of computer programs for optimization and simulation of multicarrier SAW-based demodulator
[PB87-134532] 06 p0693 N88-14252
Multicarrier demodulator design, volume 1 --- communication satellites
[ESA-CR(P)-2468-VOL-1] 09 p1158 N88-16941
Multicarrier demodulator design. Volume 2: Executive summary --- communication satellites
[ESA-CR(P)-2468-VOL-2] 09 p1158 N88-16942
A Differential Phase Shift Keying (DPSK) modulator for a frequency hopping short wave system
[FOA-C-30460-3.3] 18 p2501 N88-24840
Digital carrier demodulation for the DSN Advanced Receiver 22 p3064 N88-28183

DEMOGRAPHY
Problems in integrating geographic data
[DE87-012880] 01 p0106 N88-10689
Contributions to selection and ranking theory with special reference to logistic populations
[AD-A185629] 07 p0917 N88-15566
Ion content and infrared absorption of moist atmospheric air
[AD-A188839] 12 p1643 N88-19838
Survival analysis using additive risk models
[AD-A189053] 13 p1825 N88-20906
Behavioral, psychological and demographic predictors of physical fitness
[AD-A192697] 21 p2986 N88-27733
Utilization of remote sensing for the observation of urban populations. Ongoing research in Quito (Ecuador)
22 p3098 N88-28399

DEMONSTRATION
U PROVING

DENATURATION (BIOPOLYMERS)
U BIOPOLYMER DENATURATION

DENDRITIC CRYSTALS
On the role of convective motion during dendrite growth: Experiments under variable gravity, revised
[NASA-CR-179213] 02 p0156 N88-10979
Modeling growth of interdendritic silicon ribbons
14 p1897 N88-21322
Dendritic growth in the presence of convection
16 p2580 N88-25328
Survey of the literature on fractals with possible applications to phase change processes
[DE88-012240] 21 p2911 N88-27277

DENDRITIC DRAINAGE
U DRAINAGE PATTERNS

DENSE PLASMAS
NT PLASMA FOCUS
NT STRONGLY COUPLED PLASMAS
Variable collision frequency effects on hose and sausage instabilities in relativistic electron beams
[AD-A184206] 04 p0490 N88-13021
Photoionization of atoms and ions: Application of time-dependent response method within the density functional theory
[AD-A185686] 07 p0930 N88-15649
Absorption of electron cyclotron waves by superthermal electron velocity distributions in tokamak plasmas
[INPE-4385-PRE/1205] 08 p1086 N88-16539
New mode conversion process and overdense plasma heating in the electron cyclotron range of frequencies
[IPPJ-854] 10 p1411 N88-18420
Consistency between current ramp-up/recharging scenario by non-inductive current drive and dense and cold divertor plasma. Conceptual design study of FY86 FER
[DE88-751438] 14 p1984 N88-21833
Application of particle simulations to the NRL laser experiment
[AD-A191641] 18 p2520 N88-24953
The influence of ionization within a plasma opening switch
[AD-A193147] 21 p3017 N88-27906

DENSIFICATION
Cast iron freezing mechanisms
03 p0298 N88-11870
Sintering and densification of particulate composites: Inclusion size and clustering
[DE88-002230] 06 p0685 N88-14199

DENSIMETERS
Gamma-ray densitometry: Nondestructive analysis of density evolution during ceramic powder processing
[DE88-006671] 15 p2047 N88-22198

DENSITOMETERS
NT MICRODENSITOMETERS
Computer simulation of the L/sub 3/-edge densitometer
[DE88-001944] 06 p0705 N88-14324

DENSITY (MASS/VOLUME)
NT ATMOSPHERIC DENSITY
NT SPACE DENSITY
Relationships governing change in density in liquid ferrous alloys
[BLL-M-37305-(5828.4)] 02 p0149 N88-10935
Correlation of velocity and velocity-density turbulence in the exhaust of an atmospheric burner
02 p0185 N88-11147
Conservation and transport properties of turbulence with large density variations
[LA-10911-MS] 03 p0321 N88-12032
Studies on some Ge-Se-Te glasses
[PD-MT-8721] 04 p0420 N88-12607
Hydrogen and deuterium in the local interstellar medium 04 p0521 N88-13204
Evolution of spectral densities in weakly inhomogeneous plasmas
[PB87-137402] 06 p0784 N88-14811
Experimental and theoretical studies of dense fluid mixtures
[DE88-002710] 07 p0831 N88-15039
Assessment of anomalous gravitational field of elastic Earth 07 p0921 N88-15594
Void formation in solidification
[DE88-003895] 11 p1452 N88-18650
Injection compression for short fiber reinforced plastics
[SNIAS-881-430-118] 21 p2922 N88-27344
A theoretical determination of the density at a traveling source that emitts particles
[ISAS-RN-351] 21 p3013 N88-27883
Diamond like carbon coatings: Categorization by atomic number density
[NASA-CR-174895] 22 p3059 N88-28151

DENSITY (NUMBER/VOLUME)
NT CARRIER DENSITY (SOLID STATE)
NT ELECTRON DENSITY (CONCENTRATION)
NT ELECTRON DENSITY PROFILES
NT ELECTRON DISTRIBUTION
NT ION DENSITY (CONCENTRATION)
NT IONOSPHERIC ELECTRON DENSITY
NT IONOSPHERIC ION DENSITY
NT MAGNETOSPHERIC ELECTRON DENSITY
NT MAGNETOSPHERIC ION DENSITY
NT METEOROID CONCENTRATION
NT PARTICLE DENSITY (CONCENTRATION)

NT PLASMA DENSITY
NT PROTON DENSITY (CONCENTRATION)
NT SPACE DENSITY
Simulations using the pseudo-current algorithm
[DE87-012403] 01 p0040 N88-10255
Rayleigh scattering measurements of a freejet with homogeneous condensation 03 p0319 N88-12020
Refueling and density control in the ZT-40M reversed field pinch
[DE88-000504] 04 p0493 N88-13040
X-rays, color, and the Vaughan-Preston gap 04 p0510 N88-13135
Sliding charge density waves and related problems
[AD-A186720] 09 p1157 N88-16934
Large ionic species in sooting acetylene and benzene flames 24 p3348 N88-29932

DENSITY (RATE/AREA)
U FLUX DENSITY

DENSITY DISTRIBUTION
The pseudopotential density functional method applied to semiconducting crystals
[ETN-88-91362] 05 p0656 N88-14024
Maximum likelihood principle and model selection when the true model is unspecified
[AD-A186027] 07 p0914 N88-15544
Effects of uniform target density on random search
[AD-A186468] 08 p1073 N88-16473
To relate measurements of gravity and geoid anomalies over the oceans to near surface density distributions
[AD-A192168] 18 p2547 N88-25120
Experimental and analytical studies of compressible vortices 19 p2665 N88-25848
Turbulence modelling of flows with non-uniform density 22 p3075 N88-28256

DENSITY MEASUREMENT
Time-resolved temperature and density measurements in ionizing, uniformly irradiated UV-laser-produced plasmas
[DE87-014649] 02 p0238 N88-11504
A composite grating for moire interferometry
[AD-A186330] 07 p0832 N88-15044
Velocity and density measurements in a turbulent nonpremixed flame with comparison to numerical model predictions
[DE87-014695] 08 p0967 N88-15854
Improved resolution atmospheric density measurements based on simulations 08 p1027 N88-16221
Small scale plasma density structures observed by the Viking double probe instrument --- Swedish satellite 08 p1098 N88-16604
Development of an engineering model atmosphere for Mars
[NASA-CR-182462] 09 p1263 N88-17568
Assessment of intercompartment fluid shifts by blood densitometry in astronauts 12 p1661 N88-19958
Study of photochromic materials for use in optical signal processing
[AD-A189068] 13 p1839 N88-21006
Investigation of the inter-relationship between base pavement stiffness and asphalt overlay compaction
[DOT/FAA/ES-88/1] 14 p1869 N88-21170
Estimates of masses, volumes and densities of short-period comet nuclei 14 p2004 N88-21950
Density measurements on solids and liquids
[PB88-164934] 15 p2036 N88-22129
Gamma-ray densitometry: Nondestructive analysis of density evolution during ceramic powder processing
[DE88-006671] 15 p2047 N88-22198
A method of atmospheric density measurements during space shuttle entry using ultraviolet-laser Rayleigh scattering
[NASA-TM-100056] 15 p2069 N88-22337
Annihilation momentum density of positrons trapped at vacancy-type defects in metals and alloys
[DE88-005936] 15 p2144 N88-22797
Summary report on the Japan-US Workshop on the Assessment of Spectroscopic Data for Temperature and Density Measurements --- plasma diagnostics
[IPPJ-861] 17 p2439 N88-24512
Measurements of Z(sub eff) profile with a visible bremsstrahlung continuum detector array 17 p2443 N88-24529
A rapid electrochemical technique for determining the current efficiency for cadmium plating
[AD-A193679] 22 p3056 N88-28130
Wave structures in thermospheric density from satellite electrostatic triaxial accelerometer measurements
[AD-A194134] 23 p3233 N88-29240

DENSITY WAVE MODEL
Dynamical and photometric studies of Saturn's rings 12 p1711 N88-20241
Electrostatic whistler mode conversion at plasma resonance
[AD-A192951] 20 p2860 N88-26989

DEOXYRIBONUCLEIC ACID
DNA damage and repair in human skin in situ
[DE87-014288] 03 p0356 N88-12241
Biopolymers: Protein and nucleic acids
[AD-A185837] 07 p0835 N88-15066
Spleen lymphocyte nucleic acids in pregnant rats flown in space and their offspring 07 p0892 N88-15403
Optimization of the southern electrophoretic transfer method
[DE88-004527] 10 p1299 N88-17765
Effect of weightlessness on replicative function of rat hepatocyte DNA 10 p1360 N88-18129
Ultraviolet (180 to 300 nm) action spectra for inactivation and DNA photoproduct formation of Bacillus subtilis spores under ultrahigh vacuum 12 p1657 N88-19931
Calculation of far infrared absorption in B poly(dA).poly(dT)
[AD-A193128] 21 p2918 N88-27318
Storing bits on a DNA polymer chain
[AD-A195701] 24 p3356 N88-29981

DEPENDENCE
NT SPATIAL DEPENDENCIES
NT TEMPERATURE DEPENDENCE
NT TIME DEPENDENCE
Dependence effects in unique signal transmission
[DE88-010331] 21 p2933 N88-27419

DEPENDENCY
U DEPENDENCE

DEPLETION
NT OZONE DEPLETION
Diffusion bonding depleted uranium to copper
[RFP-3783-REV] 03 p0333 N88-12098
Research studies on extreme ultraviolet and soft X-ray lasers
[AD-A189163] 12 p1633 N88-19773
The timing and mechanism of depletion in Lewisian granulites 24 p3394 N88-30209

DEPLOYMENT
Automation strategy and results for an airbase command and control information system
[NLR-MP-86031-U] 01 p0035 N88-10223
Why mechanisms are critical to spacecraft performance 09 p1125 N88-16737
Space station structures development
[NASA-CR-179261] 09 p1133 N88-16792
The impact of deployment rates on the effectiveness of strategic defenses
[AD-A186907] 09 p1233 N88-17393
Automatic in-orbit payload deployment mechanisms, logistic operations and transport vehicle design compatibilities 12 p1586 N88-19493
Workshop on Technology Development Issues for the Large Deployable Reflector (LDR)
[NASA-CP-2407] 12 p1710 N88-20235
The evaluation and selection of a 5th ground antenna site for the global positioning system
[AD-A189495] 13 p1720 N88-20286
A 60-meter erectable assembly concept for a control of flexible structures flight experiment
[NASA-TM-100497] 14 p1873 N88-21190
Payload deployment system --- STS 14 p1875 N88-21199
The development status of the strongback array --- spacecraft structure 14 p1875 N88-21201
DARM: A new deployment and retraction mechanism which does not need electric power 14 p1876 N88-21206
Deployment, hold down and release mechanisms for Wind Scatterometer Antenna (WSA) --- ERS-1 wind scatterometer antenna (WSA) 14 p1876 N88-21207
Design of a linear actuator and breadboard test result --- far IR telescope 14 p1877 N88-21217
The EURECA antenna deployment and retraction mechanisms 14 p1878 N88-21225
Thermally stable deployable structure 14 p1925 N88-21472
Motion synchronization of a mechanism to deploy and restow a truss beam 14 p1925 N88-21474
A spin and deployment mechanism 14 p1926 N88-21479
Real-time environmental Arctic monitoring (R-TEAM)
[AD-A189948] 15 p2099 N88-22508
Tethered diagnostic package for use from the space station
[DE88-006264] 16 p2167 N88-22921
Payload deployment method and system
[NASA-CASE-MSC-21330-1] 18 p2470 N88-24660
A simulation of post boost vehicle deployment of multiple reentry vehicles
[DE88-009537] 20 p2764 N88-26391
Remotely Operated Vehicle (ROV) reliability study, phase 1
[AD-A194367] 23 p3222 N88-29177
Antisatellite weapons and satellite deployment strategies
[AD-A195014] 24 p3427 N88-30396

DEPOLARIZATION
Investigation of lidar backscatter including depolarization and higher scattering orders
[ETN-87-90431] 01 p0052 N88-10334
Airborne lidar studies of Arctic polar stratospheric clouds 01 p0069 N88-10443
Scattering and depolarization by random rough terrain and vegetation covered terrain-unified full wave approach 12 p1615 N88-19657
Theory of Muon method for study of solid and liquid hydrogen 14 p1972 N88-21770

DEPOLARIZERS
U DEPOLARIZATION

DEPOSITION
NT ANODIZING
NT ELECTRODEPOSITION
NT ELECTROLESS DEPOSITION
NT ELECTROPLATING
NT VACUUM DEPOSITION
NT VAPOR DEPOSITION
Low temperature deposition by laser induced breakdown in the vapor phase
[DE87-007509] 01 p0024 N88-10151
Use of sol-gels in the application of ceramic oxide thin films
[DE87-013610] 01 p0028 N88-10176
The dependence of the normalized ice accretion thickness on cloud-physical parameters
[DFVLR-FB-87-08] 01 p0072 N88-10464
Direct formation of thin films and epitaxial overlayers at low temperatures using a low-energy (10-500 eV) ion beam deposition system
[DE87-012291] 01 p0103 N88-10675
Multilayer monochromators for neutron spectrometers
[DE87-014291] 02 p0175 N88-11093
Turbine airfoil deposition models and their hot corrosion implications 02 p0189 N88-11178
CuInSe2 solar cell research by sputter deposition
[DE87-001184] 02 p0195 N88-11219
Compilation and analysis of air quality data in support of acid deposition research
[DE87-014428] 02 p0196 N88-11226
Thin film microstructures: Simulation and theory
[DE87-014732] 02 p0246 N88-11553
Tribological properties of rf-sputtered MoS2 coatings
[DE88-000266] 04 p0452 N88-12802
A review of parameterizations of microphysical processes in clouds for application in models of regional atmospheric deposition
[DE88-000451] 04 p0471 N88-12909
Far-infrared spectra of lithium deposited on a gold electrode: Interpretation using a cluster model
[AD-A184231] 04 p0495 N88-13050
Computation of rime ice accretion on airfoils
[FFA-TN-1987-08] 05 p0542 N88-13301
Effects of hydrolysis on metallo-organic solution deposition of PZT films
[ATR-86(8443)-1] 06 p0679 N88-14160
The tribological properties of MoS2 coatings in vacuum, low relative humidity and high relative humidity environments
[DE88-001611] 06 p0711 N88-14356
On 1064 nm and 350 nm laser damage thresholds of high index oxide films deposited from organic solutions and sols
[DE88-001636] 07 p0859 N88-15217
Astrophysics and the solar nebula 07 p0883 N88-15355
Nb3Al formation in sputter-deposited Nb/Al multi-layer samples
[DE88-003192] 08 p0970 N88-15868
Spray deposition: A fundamental study of droplet impingement, spreading and consolidation
[AD-A186627] 08 p0970 N88-15869
Submerged arc flux welding with CaF2-CaO-SiO2 fluxes: Possible electrochemical effects on weld metal
[DE88-003107] 08 p0992 N88-16004
Simulation of global wet and dry deposition of nitric acid in a three-dimensional chemistry-transport model
[DE87-009847] 09 p1188 N88-17116
Estimation of aerial deposition and foliar uptake of xenobiotics: Assessment of current models
[DE88-000993] 09 p1188 N88-17117
Surface acoustic wave deposition sensor
[DE87-006527] 09 p1243 N88-17452
Corrosion behavior of sputter-deposited aluminum-based alloys exposed to chloride solutions
[AD-A187262] 10 p1303 N88-17794
Adhesion of vapour phase deposited ultra-thin polyimide films on polycrystalline silver
[AD-A187930] 10 p1306 N88-17810
The soft/hard wet anodization of aluminum oxide and its use in a thin film multilayered capacitor
[AD-A187575] 10 p1325 N88-17919

Apparatus for the study of silicon film deposition and silicon etching
[AD-A187616] 10 p1334 N88-17972
The deposition rate dependence of plasma polymerization on the radius of curvature of the substrate
[DE88-003811] 10 p1412 N88-18429
Growth and electronic properties of strained metal overlayers
[DE87-010956] 10 p1417 N88-18463
Atomistic simulation of low-energy beam deposition
[DE88-004344] 11 p1544 N88-19228
The influence of processing variables on physical properties of sol-gel derived TiO2 films
[DE88-005155] 11 p1559 N88-19331
Scanning tunneling microscopy of silver, gold, and aluminium monomers and small clusters on graphite
[DE88-003871] 11 p1562 N88-19349
Polymeric materials for electro-optic testing
[AD-A188382] 12 p1610 N88-19627
Thin-film diffusion barriers for metal-semiconductor contacts
[AD-A188712] 13 p1844 N88-21035
Photon-controlled growth of multilayered structures
[DE88-005061] 13 p1847 N88-21054
A novel method for sputter-deposition of high T(sub c) superconductor films via a computer-controlled mass analyzed ion beam
[DE88-006001] 13 p1848 N88-21064
An experimental and theoretical study of the ice accretion process during artificial and natural icing conditions
[NASA-CR-182119] 14 p1865 N88-21143
Spatial and temporal distribution of precipitation chemistry across Maryland in 1984, volume 1
[PB88-148929] 14 p1943 N88-21595
Laser photodeposition and etching study
[AD-A190535] 15 p2040 N88-22153
Thin film research diagnostics instrumentation
[AD-A191240] 16 p2213 N88-23207
Standardized ice accretion thickness as a function of cloud physics parameters
[ESA-TT-1080] 16 p2234 N88-23346
Electrophoretic coatings. Part 1: Sandia applications
[DE88-008666] 20 p2776 N88-26465
The effects of Hertzian stress and test ambient on the friction coefficient of MoS2 coatings
[DE88-008118] 20 p2777 N88-26467
Overview of the PRECP (processing of emissions by clouds and precipitation) Program
[DE88-008205] 20 p2822 N88-26741
Carbon deposition model for oxygen-hydrocarbon combustion, volume 1
[NASA-CR-179375] 21 p2908 N88-27254
Carbon deposition model for oxygen-hydrocarbon combustion, volume 2
[NASA-CR-179376] 21 p2908 N88-27255
Amorphous silicon solar cells using a metal substrate
[PB88-131941] 21 p2958 N88-27628
Foliar nitrate reductase: A marker for assimilation of atmospheric nitrogen oxides
[DE88-010453] 21 p2971 N88-27648
Atomic layer epitaxy of ZnS and ZnSe
[AD-A192307] 21 p3020 N88-27928
Erosion/redeposition modeling and calculations for carbon
[DE88-010382] 22 p3057 N88-28139
Atmospheric deposition of nitrate to the ocean surface 23 p3231 N88-29227
New method for preparation of (Cd, Hg)Te thin films
[DE88-702727] 23 p3293 N88-29608
Cluster beam studies
[AD-A195182] 24 p3434 N88-30443

DEPOSITS
Raman scattering as a diagnostic technique for cathode characterization
[AD-A184434] 04 p0439 N88-12726
Development of a laboratory test for multiport injector deposits: Approaches 1 and 2
[AD-A190697] 15 p2048 N88-22203
Development of a laboratory test for multiport fuel injector deposits - evaluation of the Jet Fuel Thermal Oxidation Test apparatus (JFTOT)
[AD-A191313] 16 p2183 N88-23015
Constraints on the origin of fractured terrane, Northern Martian plains 23 p3304 N88-29684
Early cratering rates and the nature of the Martian cratered uplands 23 p3306 N88-29694
Ridged and gullied terrains in the Martian uplands 23 p3307 N88-29700

DEPRESSIONS (TOPOGRAPHY)
U STRUCTURAL BASINS

DEPRESSURIZATION
U PRESSURE REDUCTION

DEPRIVATION
NT SLEEP DEPRIVATION

DEPTH
Transform fault earthquakes in the North Atlantic: Source mechanisms and depth of faulting 03 p0350 N88-12208
Master plots for predicting the case-depth in laser surface treatments
[PB87-221875] 05 p0586 N88-13574
The effect of microstructure on the surface crack length: Crack depth relationship for short cracks 05 p0600 N88-13670
CTD observations in the coastal transition zone off northern California, 16-25 February 1987
[AD-A187283] 10 p1357 N88-18111
Airborne electromagnetic sounding of sea ice thickness and sub-ice bathymetry
[AD-A188939] 12 p1649 N88-19879
Physical, chemical and CTD (Conductivity/Temperature/Depth) data from the Marathon 2 expedition
[AD-A189930] 15 p2099 N88-22507
Television monitor field shifter and an opto-electronic method for obtaining a stereo image of optimal depth resolution and reduced depth distrotion on a single screen
[NASA-CASE-NPO-17249-1-CU] 17 p2332 N88-23924
Construction of approximations to acoustic Green's functions for nonhomogeneous oceans using transmutation
[PB88-185384] 18 p2548 N88-25126
Variational analysis of dielectrically loaded multidepth corrugated waveguides
[PB88-193602] 20 p2793 N88-26573
MIZPAC (marginal ice zone Pacific) 84-86 CTD (Conductivity, Temperature, Depth) data report
[AD-A192478] 21 p2976 N88-27679
Signal processing software for ground penetrating radar, user's manual
[AD-A194286] 23 p3203 N88-29059
Improvements in techniques of microwave thermography
[AD-A193620] 23 p3239 N88-29276
Kalman filter-based algorithms for estimating depth from image sequences
[AD-A195818] 24 p3424 N88-30380

DEPTH MEASUREMENT
Estimation of marine boundary layer depth and relative humidity with multispectral satellite measurements
[AD-A184881] 05 p0620 N88-13804
Penetration depth measurements of YBa2Cu3O/sub 7-delta/ at 4 MHz
[DE88-003493] 10 p1420 N88-18478
Improvements in end point detection — semiconductor fabrication
[RSRE-MEMO-4035/A] 14 p1899 N88-21336
In-flight measurement of ice growth on an airfoil using an array of ultrasonic transducers
[AIAA-PAPER-87-0178] 17 p2293 N88-23717
Mining volume measurement system
[NASA-CASE-LAR-13519-1] 17 p2342 N88-23963
Contribution of spaceborne high resolution radiometers to mapping of precoastal depths 19 p2701 N88-26063

DEPTH PERCEPTION
U SPACE PERCEPTION

DERIVATION
Studies on syntheses of amine-carboxyboranes (boron analogues of amino acids) and derivatives
[AD-A184838] 05 p0557 N88-13386
Deriving descriptions of the mind
[AD-A186647] 08 p1052 N88-16349
Norm inequalities for derivatives and differences
[DE88-002920] 09 p1230 N88-17371
Derivation of consistent surface fixed fields for use in a global NWP model
[AD-A190131] 15 p2093 N88-22475
Absolute pressure derivatives of deep level defects in 3-5 semiconductors
[DE88-006318] 15 p2140 N88-22772
Microstructure of thin intercalated benezene derived graphite fibers
[AD-A191724] 19 p2618 N88-25534

DESCENT
NT PARACHUTE DESCENT
Study of descent of probes with high lift-drag ratio into the atmosphere of Jupiter 08 p1006 N88-16101

DESCENT TRAJECTORIES
NT REENTRY TRAJECTORIES
The Valec fireball and predicted meteorite fall 06 p0739 N88-14547
Investigation of the validity of the non-rotating planet assumption for three-dimensional earth atmospheric entry
[AD-A194877] 24 p3331 N88-29829

DESCRIPTIONS
Linguistic definition of generic models in computer vision
[RSRE-MEMO-4110] 17 p2386 N88-24182

DESCRIPTIVE GEOMETRY
Workshop on the Integration of Finite Element Modeling with Geometric Modeling
[NASA-CR-182515] 11 p1526 N88-19111
Finite element meshing of ANSYS (trademark) solid models 11 p1526 N88-19115
Solid/FEM integration at SNLA
[SAND-87-0882A] 11 p1526 N88-19116
Octree based automatic meshing from CSG models 11 p1527 N88-19117
Geometrical and topological issues in octree based automatic meshing 11 p1527 N88-19118
A hierarchical structure for automatic meshing and adaptive FEM analysis 11 p1527 N88-19119
Geometric versus finite element modeling current and future trends at Northrop 11 p1528 N88-19125
Definition and display of profiled sweep-objects --- computer graphics
[REPT-87-45] 14 p1957 N88-21665

DESERTIFICATION
Desertification in the Sahelian and Sudanian Zones of West Africa
[PB87-217063] 03 p0345 N88-12183
Environmental processes and spectral reflectance characteristics associated with soil erosion in desert fringe regions
[NASA-CR-182332] 05 p0620 N88-13811
Sensitivity of general circulation models to surface processes 14 p1937 N88-21556
Evaluation of the grassy biomass in the Sahelian zone in the South Tamesna region (Niger): Prospects and limits of use of SPOT data 22 p3092 N88-28359
Preliminary comparative analysis of LANDSAT and SPOT data for the study of the sanding phenomenon: Zaafrane region (Algeria) 22 p3099 N88-28402

DESERTS
NT SAHARA DESERT (AFRICA)
Enhancement of surface-atmosphere fluxes by desert-fringe vegetation through reduction of surface albedo and of soil heat flux
[NASA-CR-181442] 02 p0197 N88-11231
Desertification in the Sahelian and Sudanian Zones of West Africa
[PB87-217063] 03 p0345 N88-12183
A Workshop on Desert Processes, September 24-28, 1984: Report on the conference
[AD-A184599] 03 p0345 N88-12184
Environmental processes and spectral reflectance characteristics associated with soil erosion in desert fringe regions
[NASA-CR-182332] 05 p0620 N88-13811
Daily dynamics of some physiological indicators of man under desert condition 06 p0750 N88-14605
Summary of along-track data from the Earth radiation budget satellite for several major desert regions
[NASA-RP-1197] 13 p1802 N88-20772

DESICCANTS
Mass transfer mechanisms for water adsorbed on silica gel
[DE88-005993] 15 p2032 N88-22107

DESICCATION
U DRYING

DESIGN ANALYSIS
A feasibility study of a hypersonic real-gas facility
[NASA-CR-180423] 01 p0008 N88-10043
Space station integrated wall design and penetration damage control
[NASA-CR-179169] 01 p0013 N88-10070
Redesign of solid rocket booster/external tank attachment ring for the space transportation system
[NASA-TM-100476] 01 p0017 N88-10101
Design and analysis of a broadband TM(sub 01) mode generator in cylindrical waveguide
[DE87-011308] 01 p0038 N88-10243
V-band IMPATT power amplifier
[NASA-CR-180711] 01 p0042 N88-10267
Assessment of the COFSI/MAST I project
[NASA-CR-181366] 01 p0053 N88-10340
Study of free-piston Stirling engine driven linear alternators
[NASA-CR-181425] 01 p0055 N88-10355
Monitored background radiometer 02 p0133 N88-10831
Vacuum pumps and systems: A review of current practice 02 p0134 N88-10839
Contribution to the development of smart design techniques for VLSI integrated circuits --- CMOS
[LAAS-87-181] 02 p0221 N88-11395
A neutron detector based on microchannel plates
[DE87-014703] 02 p0232 N88-11466
Saturn: A large area X-ray simulation accelerator
[DE87-012021] 02 p0233 N88-11472

A conceptual design of Final Focus Systems for linear colliders
[DE87-012840] 02 p0234 N88-11475
Rotorcraft Design for Operations
[AGARD-CP-423] 03 p0262 N88-11649
The influence of operational requirements on LHX concept formulation 03 p0262 N88-11650
Design requirements for future commercial operations 03 p0262 N88-11651
Combined calculation of deformation and stress for the body and sabot of an APFSDS 03 p0302 N88-11899
Physical design of parameters of Nd:YAG disk laser 03 p0302 N88-11904
Conceptual design of a high-resolution pion (0) spectrometer
[DE87-014757] 03 p0324 N88-12047
Conservatism implications of shock test tailoring for multiple design environments
[DE87-013927] 03 p0338 N88-12127
The design and preliminary calibration of a boundary-layer flow channel
[NASA-CR-178399] 04 p0394 N88-12457
Structural analysis of a bolted joint concept for the space shuttle's solid rocket motor casing
[NASA-TM-89092] 04 p0407 N88-12531
Optimization techniques applied to passive measures for in-orbit spacecraft survivability
[NASA-CR-179216] 04 p0408 N88-12532
New feedback design methodologies for large space structures: A multi-criterion optimization approach 04 p0408 N88-12535
Multicast gateway design considerations
[PB87-219960] 04 p0430 N88-12663
On the VLSI design of a pipeline Reed-Solomon decoder using systolic arrays 04 p0436 N88-12700
A procedural method for the efficient implementation of full-custom VLSI designs 04 p0436 N88-12701
On dynamic loads in parallel shaft transmissions. 1: Modelling and analysis
[NASA-TM-100180] 04 p0451 N88-12797
On dynamic loads in parallel shaft transmissions. 2: Parameter study
[NASA-TM-100181] 04 p0452 N88-12798
Nonlinear axial stiffness characteristics of axisymmetric bolted joints 04 p0452 N88-12799
Design and development of absorption heat pumps
[DE88-900082] 04 p0466 N88-12885
An expert system for materials design
[DE88-000191] 04 p0483 N88-12974
Design concepts for the ASTROMAG cryogenic system
[NASA-CR-181505] 04 p0497 N88-13060
Thermodynamic properties for natural gas binaries
[PB87-226833] 04 p0500 N88-13074
Aerodynamics of Hypersonic Lifting Vehicles
[AGARD-CP-428] 05 p0529 N88-13219
Lifting bodies: An attractive aerodynamic configuration choice for hypervelocity vehicles 05 p0534 N88-13248
Design of wings and wing/body configurations for transonic and supersonic speeds 05 p0545 N88-13318
Aeroelastic analysis of modern transport aircraft --- European Airbus
[SNIAS-872-111-102] 05 p0546 N88-13329
Design and assembly sequence analysis of option 3 for CETF reference space station
[NASA-TM-100503] 05 p0553 N88-13369
Evaluation of device figure of merit in microwave switching circuit design
[AD-A184896] 05 p0577 N88-13520
A complete linearized theory for the analysis and design of two-dimensional hydrofoils near a free surface
[UTIAS-TN-264] 05 p0579 N88-13531
Conservatism implications of shock test tailoring for multiple design environments 05 p0592 N88-13611
Near-threshold growth of defects in engineering materials 05 p0603 N88-13691
Utilization of dynamic characteristics of materials to optimize military explosive charges. Application to antiship devices
[SNIAS-872-320-101] 05 p0610 N88-13743
STAEBL/general composites with hygrothermal effects (STAEBL/GENCOM)
[NASA-TM-100266] 05 p0611 N88-13754
High speed propeller performance and noise predictions at takeoff/landing conditions
[NASA-TM-100267] 05 p0646 N88-13960
Photon counting image sensor development for astronomical applications
[NASA-CR-181507] 05 p0660 N88-14049
Ducted propeller design and analysis
[DE88-001925] 06 p0664 N88-14069
Nonlinear aerodynamic wing design
[NASA-CR-3950] 06 p0665 N88-14079
Large-Scale Advanced Prop-Fan (LAP) blade design
[NASA-CR-174790] 06 p0668 N88-14097
Design verification and fabrication of active control systems for the DAST ARW-2 high aspect ratio wing, part 1
[NASA-CR-177959-PT-1] 06 p0669 N88-14101
Design verification and fabrication of active control systems for the DAST ARW-2 high aspect ratio wing. Part 2: Appendices
[NASA-CR-177959-PT-2] 06 p0669 N88-14102
Small High Pressure Ratio Turbines --- conference
[VKI-LS-1987-07] 06 p0712 N88-14364
High pressure ratio turbine design constraints
[TRR-0279] 06 p0712 N88-14365
Mainline performance prediction for radial inflow turbines 06 p0712 N88-14366
Conclusions from a research program on mixed flow gas generator turbines 06 p0713 N88-14368
Highlights from a research program on a very highly loaded axial gas generator turbine 06 p0713 N88-14369
Aerodynamic design of first stage turbines for small aero engines 06 p0713 N88-14370
Design, fabrication and delivery of a miniature Cassegrainian concentrator solar array system
[NASA-CR-179237] 06 p0730 N88-14493
Controlled Ecological Life Support Systems (CELSS) conceptual design option study
[NASA-CR-177421] 06 p0754 N88-14625
Using concept mapping to define problems and identify key kernels during the development of a decision support system
[AD-A185636] 06 p0762 N88-14674
Overview of the TIBER 2 (Thermal Ignition/Burn Experimental Reactor) design
[DE88-001892] 06 p0783 N88-14804
Maximum entropy/optimal projection design synthesis for decentralized control of large space structures
[AD-A186359] 07 p0824 N88-15003
Space station onboard propulsion system: Technology study
[NASA-CR-179233] 07 p0825 N88-15006
Simplified procedures for designing composite bolted joints
[NASA-TM-100281] 07 p0828 N88-15020
Flow in Centrifugal Compressors --- conference
[VKI-LS-1987-01] 07 p0850 N88-15160
Centrifugal compressors 07 p0850 N88-15162
The technology of centrifugal compressors: A design approach and new goals for research 07 p0850 N88-15163
Identification and avoidance of instabilities in high performance turbomachinery 07 p0850 N88-15164
Flow in labyrinth seals and its influence on rotor stability of turbocompressors 07 p0851 N88-15168
Human performance data needed for training device design decisions
[AD-A185988] 07 p0898 N88-15441
On two methods of identifying influential sets of observations
[AD-A186270] 07 p0910 N88-15518
The development of test methodology for testing glassy materials 07 p0927 N88-15633
Development of direct-inverse 3-D methods for applied aerodynamic design and analysis
[NASA-CR-182436] 08 p0950 N88-15767
Aeropropulsion '87. Session 2: Aeropropulsion Structures Research
[NASA-CP-10003-SESS-2] 08 p0954 N88-15785
Aeropropulsion structures 08 p0954 N88-15786
Determining structural performance 08 p0954 N88-15787
Life prediction technologies for aeronautical propulsion systems 08 p0954 N88-15788
Integrated analysis and applications 08 p0954 N88-15789
Aircraft engine hot section technology: An overview of the HOST Project 08 p0957 N88-15804
Analysis, design, construction and testing of a reaction wheel model for space applications
[INPE-4358-TDL/299] 08 p0963 N88-15834
Servicer system demonstration plan and capability development
[NASA-CR-179246] 08 p0975 N88-15895
Liquid spring design methodology for shock isolation system applications 08 p0998 N88-16043
Design and test of a spacecraft instrument shock isolator 08 p0998 N88-16044
Review of fatigue and fracture research at NASA Langley Research Center 09 p1106 N88-16633
A note on the aerodynamic design of thin parallel-sided aerofoil sections
[ARL-AERO-TM-388] 09 p1114 N88-16677
Columbus feasibility studies. Volume 1: Requirements and system concept
[ETN-88-91073] 09 p1134 N88-16799
Design procedures for fiber composite box beams
[NASA-TM-100296] 09 p1139 N88-16828
Study on a double reflector compact range --- satellite antennas
[S-201-05] 09 p1153 N88-16908
The WAFTER: A versatile wear and friction tester
[MRL-TN-519] 09 p1169 N88-17012
Design feasibility report on investigation of magnetic bearings for the ocean colour monitor radiometer scanner
[BAE-TP-7849] 09 p1174 N88-17036
An integration test for accelerometer evaluation 09 p1178 N88-17054
Study of large solar arrays (SOLA), phase 2A
[BAE-SS/1109] 09 p1186 N88-17106
A comparison of different module configurations for multibandgap solar cells
[DE88-002718] 09 p1187 N88-17113
Bioreactor design concepts 09 p1197 N88-17171
Design of a neural network simulator on a transputer array 09 p1205 N88-17221
Interchange of electronic design through VHDL and EIS 09 p1205 N88-17222
The IDEAL (Integrated Design and Engineering Analysis Languages) modeling methodology: Capabilities and Applications 09 p1206 N88-17227
Interfacing slave designs to Fastbus: Practical experience
[DE88-002807] 09 p1215 N88-17286
CEBAF design overview and project status
[CEBAF-PR-88-001] 09 p1246 N88-17470
Two-phase reduced gravity experiments for a space reactor design
[DE86-015530] 09 p1247 N88-17475
Study of Large Solar Arrays (SOLA). Phase 2A: Amplifying information to final report (SS/1109)
[BAE-SS/1110] 09 p1248 N88-17480
The TITAN Reversed-Field Pinch Reactor: Design-point determination and parametric studies
[DE88-001824] 09 p1251 N88-17498
A transonic-small-disturbance wing design methodology
[NASA-TP-2806] 10 p1273 N88-17614
An integrated aero/mechanical performance approach to high technology turbine design 10 p1280 N88-17657
Design and test of a high blade speed, high work capacity transonic turbine 10 p1281 N88-17658
Design and development of an advanced F100 compressor 10 p1283 N88-17678
Design and testing of a front stage for an advanced high pressure compressor 10 p1283 N88-17679
The design of trellis codes for fading channels
[NASA-CR-182523] 10 p1320 N88-17891
Solid-state voltage standard performance and design guidelines
[PB88-123757] 10 p1322 N88-17905
A computational study of thrust augmenting ejectors based on a viscous-inviscid approach 10 p1326 N88-17929
Three-dimensional incompressible flowfield analysis for establishing rotor designs which optimize power extraction 10 p1329 N88-17943
Optimal design and parameter identification of flexible rotor-bearing systems 10 p1339 N88-18002
Design sensitivity analysis of nonlinear structural systems and numerical implementation with established finite element codes 10 p1344 N88-18032
Optimum design of geodesically stiffened composite plates
[NASA-CR-182499] 10 p1344 N88-18035
Design and implementation of a fiber optic RS232 link
[AD-A187319] 10 p1409 N88-18409
A collaborative program of research in engineering sciences
[DE88-003383] 10 p1423 N88-18504
A performance index approach to aerodynamic design with the use of analysis codes only
[NASA-TP-2805] 11 p1433 N88-18552
The aerodynamic design optimisation of a forward swept wing fighter aircraft
[CAR-87-18] 11 p1433 N88-18553
Modification of integrated partial payload lifting assembly
[NASA-CR-182573] 11 p1443 N88-18607
Orbiter transfer vehicle concept definition and system analysis study. Volume 4: Space station accommodations. Revision 1
[NASA-CR-179293] 11 p1444 N88-18609
Orbital transfer vehicle concept definition and system analysis study. Volume 4, Appendix A: Space station accommodations. Revision 1
[NASA-CR-179294] 11 p1444 N88-18610
An optimal structure for a 34-meter millimeter-wave center-fed BWG antenna: The Cross-Box concept 11 p1472 N88-18778

STA-2A NDT testing
[NASA-CR-179301] 11 p1497 N88-18637
Application of advanced computational technology to propulsion CFD
[NASA-TM-100843] 11 p1525 N88-19102
Aerodynamic characteristics of wings designed with a combined-theory method to cruise at a Mach number of 4.5
[NASA-TP-2799] 12 p1575 N88-19420
Evaluation of a miniature horizontal pendulum tilt transducer 12 p1577 N88-19435
Presentation of structural component designs for the family of commuter airplanes
[NASA-CR-182568] 12 p1581 N88-19463
A class 2 weight assessment for the implementation of commonality and preliminary structural designs for the family of commuter airplanes
[NASA-CR-182565] 12 p1581 N88-19464
Rotorcraft flight-propulsion control integration: An eclectic design concept
[NASA-TP-2815] 12 p1584 N88-19475
Conceptualization and design of a variable-gravity research facility
[NASA-CR-182574] 12 p1595 N88-19550
Structural shape optimization in multidisciplinary system synthesis
[NASA-TM-100538] 12 p1614 N88-19650
VSLI design generators
[AD-A188706] 12 p1623 N88-19707
Concentrating photovoltaic collectors: Fabrication design
[PB88-148051] 12 p1640 N88-19821
Regenerative life support system research
[NASA-CR-182606] 12 p1671 N88-20006
Development savings through parametric modeling of program costs 12 p1700 N88-20175
The Joint NASA/Goddard-University of Maryland Research Program in Charged Particle and High Energy Photon Detector Technology
[NASA-CR-182612] 12 p1712 N88-20247
The design and use of a temperature-compensated hot-film anemometer system for boundary-layer flow transition detection on supersonic aircraft
[NASA-TM-100421] 13 p1723 N88-20304
Turnaround operations analysis for OTV. Volume 1: Executive summary
[NASA-CR-179316] 13 p1729 N88-20340
Turnaround operations analysis for OTV. Volume 2: Detailed technical report
[NASA-CR-179317] 13 p1729 N88-20341
Synthesis method applied to the design of an electron gun for a gyrotron
[INPE-4357-TDL/298] 13 p1773 N88-20607
On the sensitivity of complex, internally coupled systems
[NASA-TM-100537] 13 p1813 N88-20829
A new algorithm for general multiobjective optimization
[NASA-TM-100536] 13 p1813 N88-20830
Potential off-normal events and associated radiological source terms for the compact ignition tokamak: Fusion Safety Program
[DE88-004112] 13 p1842 N88-21024
Optimal filament shells loaded with internal pressure in a centrifugal force field 14 p1885 N88-21266
Design, optimization and construction of a dc-SQUID with complete flux transformer circuits
[PB88-160742] 14 p1907 N88-21399
Performance of elastomeric bearings
[PB88-159470] 14 p1918 N88-21450
Advanced transmission studies
[NASA-TM-100867] 14 p1919 N88-21454
Computational aspects of sensitivity calculations in transient structural analysis
[NASA-TM-100589] 14 p1924 N88-21467
Aero/structural tailoring of engine blades (AERO/STAEBL)
[NASA-CR-180805] 14 p1959 N88-21682
Comparison of entropy generation and conventional design methods for heat exchangers
[AD-A190256] 15 p2064 N88-22306
FLOSIN: A fluid loop analyzer for SINDA 15 p2066 N88-22321
Constellation sizing for modest directed energy platforms
[DE88-007033] 15 p2070 N88-22343
Improvements to tilt rotor performance through passive blade twist control
[NASA-TM-100583] 15 p2086 N88-22434
Water facilities in retrospect and prospect: An illuminating tool for vehicle design 16 p2200 N88-23126
Aerodynamic and thermal modeling of electromagnetic brakes. Evaluation of convective exchange coefficients and friction losses in the rough wall channels
[ISAE-ITC1-87-02] 16 p2215 N88-23214
Mixed finite element formulation applied to shape optimization 16 p2221 N88-23252
Design of high yield microprocessors
[ETN-88-92184] 16 p2245 N88-23410
Silicon compilers: Application to the compilation of the control area
[ETN-88-92188] 16 p2247 N88-23425
Full potential methods for analysis/design of complex aerospace configurations
[NASA-CR-3982] 17 p2296 N88-23736
Sensitivity analysis and multidisciplinary optimization for aircraft design: Recent advances and results
[NASA-TM-100630] 17 p2302 N88-23766
A structured approach to weapon system design 17 p2303 N88-23773
A change in system design emphasis: From machine to man 17 p2304 N88-23782
Interfacing and integrating hardware and software design systems 17 p2306 N88-23796
A design analysis for an automated robotic workpiece manipulator 17 p2344 N88-23975
Assessment of nuclear reactor concepts for low power space applications 17 p2423 N88-24409
The Curie point radiator 17 p2424 N88-24420
Computational design of low aspect ratio wing-winglet configurations for transonic wind-tunnel tests
[NASA-CR-183021] 18 p2464 N88-24630
Design study. Manipulator systems for model handling in European transonic wind tunnels
[ETN-88-91944] 18 p2468 N88-24651
A design study of onboard navigation and guidance during aerocapture at Mars
[NASA-CR-172053] 18 p2469 N88-24654
Designing to safe power limits in hybrid circuits
[DE88-005533] 18 p2506 N88-24865
Optimization of reserve lithium thionyl chloride battery electrochemical design parameters
[DE88-007109] 18 p2506 N88-24868
Aurora status and plans
[DE88-006476] 18 p2521 N88-24955
Applications of fault tree analysis to the design process
[DE88-007048] 18 p2525 N88-24982
Limits of design feasibility of multiwing wind turbines with individual articulated wing structure
[ILR-MITT-180] 18 p2537 N88-25052
Systems analysis of INTOR-like designs
[DE88-004422] 18 p2578 N88-25316
Design studies of low aspect-ratio torsatrons
[DE88-007562] 18 p2579 N88-25320
Space station architectural elements and issues definition study
[NASA-CR-3941] 18 p2587 N88-25371
Two-dimensional viscous flow computations of hypersonic scramjet nozzle flowfields at design and off-design conditions
[NASA-CR-182150] 19 p2603 N88-25459
Advanced heat receiver conceptual design study
[NASA-CR-180901] 19 p2688 N88-25977
Mechanisms for particle acceleration: Possibilities and constraints
[PB88-102538] 19 p2725 N88-26184
Some operational aspects of a rotating advanced-technology space station for the year 2025
[NASA-CR-181617] 20 p2765 N88-26397
Radar cross section studies/compact range research
[NASA-CR-183124] 20 p2792 N88-26565
The Oak Ridge Heat Pump Design Model: Mark 3 version program documentationón
[DE88-007863] 20 p2799 N88-26607
Improvement of head-up display standards. Volume 1: Head-up display design guide, appendix
[AD-A192973] 20 p2834 N88-26809
Programs for preliminary design of composite materials which were developed by the design group of Aerospatiale Aquitaine
[REPT-881-430-112] 21 p2907 N88-27251
Estimation of power-energy plots for secondary batteries
[DE88-011922] 21 p2940 N88-27460
Optimization of planetary gears
[ETN-88-92375] 21 p2958 N88-27573
Modal testing in the design evaluation of wind turbines
[DE88-010374] 21 p2968 N88-27632
Magnetic heat pumps
[DE88-012058] 21 p2969 N88-27639
Computer simulation procedure for designing airborne aerometric monitoring programs
[DE88-011896] 21 p2975 N88-27674
Development of direct-inverse 3-D methods for applied transonic aerodynamic wing design and analysis
[NASA-CR-183127] 22 p3037 N88-28033
Dual adaptive control: Design principles and applications
[NASA-CR-177485] 22 p3038 N88-28038
Advanced computational methods for turbomachinery blade design
[PNR90438] 22 p3044 N88-28065
Holographic interferometry for flow visualization studies in high speed fans
[PNR90459] 22 p3045 N88-28072
Structural Tailoring of Advanced Turboprops (STAT)
[NASA-CR-180861] 22 p3045 N88-28074
Design analysis in polymeric materials
[NPL-DMA(A)-159] 22 p3058 N88-28147
Coupled inviscid - boundary layer methods for turbomachinery blading design
[PNR90437] 22 p3076 N88-28260
Modeling, designing and simulating a pointing control system for balloon-borne solar experiments
[NASA-TM-100337] 22 p3082 N88-28300
Design and evaluation of high contact ratio gearing
[NASA-CR-174958] 22 p3085 N88-28319
Reliable onboard computing for critical space systems
[RR-670-I] 22 p3135 N88-28641
A contribution to the quantitative analysis of the influence of design parameters on the optimal design of passenger aircraft
[ETN-88-92979] 23 p3176 N88-28912
SRB/SLEEC (Solid Rocket Booster/Shingle Lap Extendible Exit Cone) feasibility study, volume 1
[NASA-CR-178973] 23 p3187 N88-28964
LLE (Laboratory for Laser Energetics) review
[DE88-008065] 23 p3219 N88-29158
Leaf spring
[GB-PATENT-2-192-689-A] 23 p3222 N88-29179
Digital filter design techniques
[AD-A194484] 23 p3274 N88-29486
Euler analysis of a swirl recovery vane design for use with an advanced single-rotation propfan
[NASA-TM-101357] 24 p3320 N88-29771
Spacecraft mass estimation, relationships and engine data: Task 1.1 of the lunar base systems study
[NASA-CR-172061] 24 p3332 N88-29836
Design criteria for extraction with chemical reaction and liquid membrane permeation
[NASA-TT-20352] 24 p3343 N88-29899
Circuit design criteria for stable lateral inhibition neural networks
[AD-A195066] 24 p3366 N88-30046
Advanced planar array development for space station
[NASA-CR-179373] 24 p3389 N88-30181
Design and performance analysis of a relational replicated database system
[AD-A196290] 24 p3437 N88-30456

DESIGN OF EXPERIMENTS
U EXPERIMENT DESIGN

DESIGN TO COST
Operational groups at the Aerospatiale Aircraft Division
[SNIAS-872-111-107] 05 p0658 N88-14036
The space station assembly phase: Flight telerobotic servicer feasibility, volume 1
[NASA-CR-182689] 13 p1731 N88-20351

DESORPTION
Study of field adsorption using pulsed-laser field ion microscopy
[DE88-000310] 03 p0330 N88-12085
Ro-vibrational laser spectroscopy of ESD neutrals from chemisorbed species
[DE87-013011] 04 p0447 N88-12770
Photon stimulated desorption from oxidized Al(110)
[DE88-002209] 06 p0787 N88-14828
Particle desorption from nonconducting surfaces by high energy heavy ions
[ETN-88-91088] 09 p1245 N88-17461
Laser-induced desorption determinations of surface diffusion on Rh(111)
[DE88-005159] 11 p1454 N88-18667
Laser measurements of state-resolved Ga and in atom sticking and desorption on metal and semiconductor surfaces
[AD-A187644] 11 p1555 N88-19310
Electron stimulated desorption and coherent electron scattering
[AD-A189091] 13 p1835 N88-20978
Image charge, coherent scattering, and symmetry effects in electron stimulated desorption: O(-) from O sub 2 condensed on metals
[AD-A189093] 13 p1835 N88-20979
The magnitude of secondary electron contributions in photon stimulated desorption
[AD-A189094] 13 p1835 N88-20980
Hydrogen pumping and release by graphite under high flux plasma bombardment
[DE88-005880] 13 p1842 N88-21021
Implications of the trapping-desorption and direct inelastic scattering channels on Dicke-narrowed lineshapes
[AD-A191410] 16 p2270 N88-23581

A mass spectrometer for the analysis of thermally labile compounds 19 p2668 N88-25859
Isothermal measurement and thermal desorption using SAW devices 19 p2671 N88-25881
Development of computer-controlled thermogravimetric instrumentation for measurement of environmental and high temperature volatilization and desorption of contaminants from polymeric materials
[AD-A195934] 24 p3343 N88-29900

DESPINNING
U SPIN REDUCTION

DESTRUCTION
Destruction test of small scaled solid propellant motors
[ISAS-R-620] 03 p0278 N88-11752
Formation and destruction of nitrous oxide in lean, premixed combustion
[DE88-001390] 05 p0562 N88-13423

DESTRUCTIVE TESTS
NT BURST TESTS

DESULFURIZING
Compact regenerable sulfur scrubber for phosphoric acid fuel cells
[AD-A191356] 16 p2230 N88-23318

DESYNCHRONIZATION (BIOLOGY)
Desynchronization of heart rate and breathing frequency after transmeridional flight across three time zones 12 p1663 N88-19968
Risk of hypertension and functional cerebral laterality in oil expedition works in far north 12 p1665 N88-19980
Biological rhythms, sleep, and wakefulness in prolonged confinement 19 p2696 N88-26022

DESYNCHRONIZED SLEEP
U RAPID EYE MOVEMENT STATE

DETECTION
NT AIRCRAFT DETECTION
NT CHANGE DETECTION
NT CORRELATION DETECTION
NT MISSILE DETECTION
NT RADAR DETECTION
NT REMOTE SENSING
NT SIGNAL DETECTION
NT TARGET RECOGNITION
NT ULTRASONIC FLAW DETECTION
Detection of CO2-induced climate change
[DE87-013127] 01 p0071 N88-10457
Optimal detection of sensor failures in flight control systems using deterministic observers 02 p0128 N88-10803
Incipient fault detection study for advanced spacecraft systems
[NASA-CR-172014] 02 p0183 N88-11138
Detection of vapors of flammable liquids in air by atmospheric sampling mass spectrometry/mass spectrometry
[DE88-000030] 02 p0196 N88-11227
Evaluation of one-sided nuclear magnetic resonance for remote detection of explosives
[AD-A184490] 03 p0296 N88-11857
Free radical detection and reactions in the decomposition of energetic materials
[AD-A184677] 03 p0296 N88-11858
Techniques for fire detection 04 p0406 N88-12521
Incipient failure detection of space shuttle main engine turbopump bearings using vibration envelope detection 05 p0595 N88-13629
Development of FTMS methods for the detection of trace chemical species and development of FTMS methods for the analysis of various chemical species
[AD-A185857] 07 p0828 N88-15023
A comparison of film-based tomography and computed tomography for advanced ceramic materials
[DE88-003114] 07 p0837 N88-15079
Study on automatic detection and identification of defects in weld by microcomputer
[PB87-143897] 07 p0863 N88-15237
Inadequacy of conventional dynamic recovery mechanisms in the presence of temporary failures
[AD-A186311] 07 p0866 N88-15251
Model-based building verification in aerial photographs
[AD-A186010] 07 p0870 N88-15278
NORSAR detection processing system
[AD-A185968] 07 p0877 N88-15318
Object detection in images from outdoor scenes using evidential reasoning
[FOA-C-30461-3.3] 08 p1020 N88-16183
A data structure and algorithm for fault diagnosis 08 p1065 N88-16432
Effects of uniform target density on random search
[AD-A186468] 08 p1073 N88-16473
Low frequency eddy current detection and evaluation of corrosion in aircraft skins
[ETN-88-91664] 09 p1144 N88-16859
Fundamental aspects of the physics of remote sensing
[ESA-TT-1045] 09 p1185 N88-17100
Pattern-recognition software detecting the onset of failures in complex systems
[DE88-002861] 09 p1220 N88-17318
Strong consistency of certain information theoretic criteria for model selection in calibration, discriminant analysis and canonical correlation analysis
[AD-A186584] 09 p1232 N88-17385
Airborne Wind Shear Detection and Warning Systems: First Combined Manufacturers' and Technologists' Conference
[NASA-CP-10006] 10 p1273 N88-17616
Windshear detection effect of static air temperature bias 10 p1274 N88-17621
Lidar windshear detection and avoidance: Performance and technical assessment 10 p1274 N88-17626
The advanced low-level windshear alert system operational demonstration results, Summer, 1987, Denver Stapleton International Airport 10 p1275 N88-17633
NMR (Nuclear Magnetic Resonance) imaging for detecting binder/plasticizers in green-state structural ceramics
[DE88-003111] 10 p1304 N88-17800
Detection of signals in non-Gaussian correlated noise derived from Cauchy processes
[AD-A187488] 10 p1320 N88-17894
Trace analysis by MS/MS on a double focussing mass spectrometer
[AD-A187954] 10 p1334 N88-17973
Tactile sensing and inverse problems
[AD-A187464] 10 p1340 N88-18011
Piezoelectric laminates for torsional and bending model control: Theory and experiment 10 p1343 N88-18029
Rapid underway sediment classification by electrical methods
[AD-A187477] 10 p1357 N88-18114
CARS measurements of combustion. 2: Gas species concentration measurements
[NAL-TR-940] 11 p1453 N88-18663
Diagnostics for research in atomization and turbulent two-phase flows
[AD-A187338] 11 p1482 N88-18843
Visual integration and detection of discontinuities: The key role of intensity edges
[AD-A188012] 11 p1520 N88-19076
Simultaneous estimation and detection of bias shifts for inertial navigation systems 12 p1576 N88-19429
Homogenizing surface and satellite observations of cloud. Aspects of bias in surface data
[AD-A188523] 12 p1648 N88-19869
Analysis, estimation, and control for perturbed and singular systems and for systems subject to discrete events
[AD-A188496] 12 p1677 N88-20026
Detecting serial correlation in the error structure of a cross-lagged panel model
[AD-A189070] 12 p1685 N88-20077
Specification for an infrared satellite surveillance system for the detection of aircraft
[AD-A189592] 13 p1797 N88-20746
Reduced tolerance imaging 2, volume 2
[AD-A189604] 13 p1829 N88-20939
Searches for forces weaker than gravity
[DE88-003579] 13 p1832 N88-20959
Optimal and conventional space-time processing in flow noise
[AD-A189104] 13 p1833 N88-20965
Physics at large transverse momenta
[DE88-005758] 13 p1836 N88-20986
Enzyme-based fiber optic sensors
[DE88-005674] 13 p1840 N88-21013
Detection of bondline delaminations in multilayer structures with lossy components
[NASA-CR-182716] 14 p1883 N88-21256
Laser pulse detection with infrared range semiconductor detectors
[DE88-700857] 14 p1914 N88-21432
Spectrographic detection of nitrogen impurity in helium
[DE88-752301] 15 p2033 N88-22111
Optimum signal processing in distributed sensor systems
[AD-A189443] 15 p2055 N88-22250
A multiple model adaptive tracking algorithm against airborne targets
[AD-A190619] 15 p2057 N88-22263
Detecting the gas bubbles in a liquid metal coolant by means of magnetic flowmeters
[DE88-701427] 15 p2062 N88-22294
Infrared differential absorption lidar for vapor detection
[AD-A190600] 15 p2098 N88-22497
Proceedings of the Lightning Threat Warning Workshop
[DE88-006607] 15 p2098 N88-22499
An evaluation of the effects of high visual taskload on the separate behaviors involved in complex monitoring performance
[AD-A190641] 15 p2105 N88-22538
Finding texture boundaries in images
[AD-A190554] 15 p2117 N88-22609
Mechanisms mediating the perception of complex acoustic patterns
[AD-A190112] 15 p2130 N88-22705
Expanded envelope concepts for aircraft control-element failure detection and identification
[NASA-CR-181664] 16 p2160 N88-22886
Universal detection of ions by replacement-ion chromatography employing an anion-replacement method and an ultraviolet-visible spectrophotometric detector
[AD-A191326] 16 p2176 N88-22971
Thomson scattering for determining electron concentrations and temperatures in an inductively coupled plasma. 2: Description and evaluation of a multichannel instrument
[AD-A191324] 16 p2280 N88-23652
Shape detection in remote sensing through graph isomorphism 17 p2354 N88-24028
TES: A modular systems approach to expert system development for real-time space applications 17 p2388 N88-24197
Dynamic range compression/expansion of light beams by photorefractive crystals
[NASA-CASE-NPO-17140-1-CU] 17 p2438 N88-24508
User's guide to the Fault Inferring Nonlinear Detection System (FINDS) computer program
[NASA-CR-178410] 18 p2482 N88-24619
Fast acting optical beam detection and deflection system
[AD-A192161] 18 p2521 N88-24954
Analysis and design of detection filters within closed-loop systems 18 p2525 N88-24980
Lightning detection and locating systems 18 p2546 N88-25112
Effectiveness evaluation of fault-tolerant multiprocessor systems
[AD-A191688] 18 p2554 N88-25158
Quench detection by fluid dynamic means in cable-in-conduit superconductors
[DE88-007269] 18 p2585 N88-25359
Trellis-coded CPM for satellite-based mobile communications 19 p2648 N88-25718
Interleaver design for trellis-coded differential 8-PSK modulation with non-coherent detection 19 p2648 N88-25719
Evaluation of engineering leak before break assessment methods by piping tests
[PB88-126982] 20 p2788 N88-26538
Laser spectoscopy of plasmas
[AD-A193009] 20 p2861 N88-26991
High resolution detection of solute segregation to the cores of dislocations in grain boundaries
[DE88-009168] 20 p2877 N88-27078
Detection of absorption lines in the spectra of X-ray bursts from X1608-52
[ISAS-RN-360] 20 p2887 N88-27143
The P delta V fundamental gas leak calibration system qualification report
[DE88-008964] 21 p2951 N88-27526
The detection and interpretation of long-term changes in ozone from space
[NASA-TM-101135] 21 p2971 N88-27650
Array detectors for plasma spectrochemistry
[AD-A194220] 22 p3052 N88-28105
Low cost corrosion sensors 22 p3054 N88-28123
Recent advances in optical spectroscopy using high performance array detectors
[AD-A194219] 22 p3152 N88-28753
Analysis of edge detection techniques for radiographic image measurement
[AD-A193650] 23 p3186 N88-28961
Infrared detection using Rydberg atoms
[AD-A194308] 23 p3191 N88-28990
Basic research in electronics (JSEP) Joint Services Electronics Program
[AD-A193072] 23 p3206 N88-29079
Airborne radar technology for windshear detection
[NASA-CR-183203] 23 p3236 N88-29257
An investigation of acoustic cavitation produced by pulsed ultrasound
[AD-A193523] 23 p3278 N88-29516
Neutrino detection primer
[AD-A193805] 23 p3280 N88-29529
Noncontact photo-thermal sensing
[AD-A195450] 24 p3344 N88-29905
Performance Prediction for Coatings. Proceedings of a Workshop
[AD-A188973] 24 p3354 N88-29966
Ultrasonic detection of diffusion and adhesion loss 24 p3354 N88-29967

Photoacoustic Fourier transform infrared spectroscopy. An early detection technique for coatings degradation
24 p3354 N88-29968
Predicting the durability of adhesives and coatings by remote detection of hidden defects and coating-thickness irregularities: A theoretical and numerical study
24 p3355 N88-29972
Electrical detection of coating deterioration
24 p3355 N88-29973
Experimental aspects of using time-averaged holographic interferometry to detect barely visible impact damage in a graphite/epoxy composite plate
[AD-A194418] 24 p3375 N88-30097
Laser sensing for identification and control of distributed parameter systems
[AD-A195886] 24 p3379 N88-30124
In situ fault detection by the hybrid ray mode method
[AD-A195226] 24 p3381 N88-30137
Automated early fatigue damage sensing system
[AD-A195717] 24 p3382 N88-30143

DETECTORS
Spectrometric test of a linear array sensor
[NASA-TM-100676] 01 p0064 N88-10414
An account of a flare related shock event recorded by the energetic particle detector EPONA of the Giotto spacecraft during September 1985 (STIP interval 18)
01 p0118 N88-10757
Semiconductor detector performance for low-energy X-rays
[DE87-014132] 02 p0244 N88-11542
Detecting squeezed states by cross-correlation
14 p1978 N88-21806
Miniature respiratory sensor
[AD-A193430] 23 p3243 N88-29300

DETERIORATION
Space environmental effects on polymeric materials
[NASA-CR-182454] 09 p1148 N88-16879
Corrosion and deterioration testing in humid tropic environments
[AD-A186917] 10 p1302 N88-17783
Electrical detection of coating deterioration
24 p3355 N88-29973
Evaluation of organic coating deterioration and substrate corrosion in seawater using electrochemical impedance measurements 24 p3355 N88-29976

DETERMINANTS
Optimal detection of sensor failures in flight control systems using deterministic observers
02 p0128 N88-10803
Deterministic uncertainty analysis
[DE88-006139] 13 p1829 N88-20942

DETERMINATION
U MEASUREMENT

DETONABLE GAS MIXTURES
Photochemical ignition studies. 3: Ignition by efficient and resonant multiphoton photochemical formation of microplasmas
[AD-A184644] 03 p0283 N88-11780
Measurement of detonation temperature of hydrogen-oxygen mixture by CARS (Coherent Anti-Stokes Raman Spectroscopy)
[NASA-TT-20227] 13 p1739 N88-20398

DETONATION
A study of diverging detonation in high-explosive systems
[DE87-006070] 01 p0031 N88-10194
Real time analysis of detonation products
[DE87-007453] 01 p0031 N88-10195
Shock measurements on explosives in the supra compressive region
[DE87-008423] 01 p0031 N88-10196
Statistical mechanical theory of condensed explosives
[DE87-009137] 01 p0031 N88-10197
Optically time-resolved detonation break out
[DE87-010340] 01 p0031 N88-10199
Experimental measurements and numerical simulations of metal spallation by detonating solid explosives
[DE87-013227] 01 p0054 N88-10347
The use of fiber optics in the determination of temperature and extent of reaction in detonating explosives
[DE87-012632] 01 p0094 N88-10612
Visible emission from granular explosives during shock initiation
[DE87-012361] 02 p0155 N88-10970
The equation of state of PETN detonation products
[DE87-013796] 02 p0155 N88-10971
Spectroscopic studies of shocked and detonating explosives
[DE87-014216] 02 p0155 N88-10972
Flame acceleration and transition to detonation in channels
[DE87-014193] 03 p0284 N88-11786
A transient model for thermal detonation
[IKE-2-75] 03 p0314 N88-11984
Steady tonation and flagration waves in reactive continua
[RARDE-2/73] 03 p0315 N88-11989
Particle transport in microdetonations --- inertial confinement fusion pellets
[OEFZS-4402] 09 p1164 N88-16976
Blast waves generated by planar detonations
[DE88-002219] 09 p1164 N88-16979
Analysis of reinforced concrete structures under the effects of localized detonations
09 p1179 N88-17064
A lecture on detonation-shock dynamics
[DE88-004313] 11 p1487 N88-18879
Measurement of detonation temperature of hydrogen-oxygen mixture by CARS (Coherent Anti-Stokes Raman Spectroscopy)
[NASA-TT-20227] 13 p1739 N88-20398
Theoretical investigation of the wave shaping process in a section of ladder fracture tape
[MRL-R-1081] 13 p1771 N88-20595
Timing control system
[NASA-CASE-NPO-16882-1-CU]
18 p2506 N88-24863
A concept for an electro-optic explosive device
[DE88-009696] 21 p2923 N88-27349
Semiconductor bridge (SCB) igniter studies. 1: Comparison of SCB and hot-wire pyrotechnic actuators
[DE88-008802] 23 p3200 N88-29046

DETONATION WAVES
Current experimental and theoretical understanding of detonation waves in heterogeneous solid explosives
[DE87-012177] 01 p0032 N88-10201
Effect of dissipation on propagation of spherical detonation shock wave 02 p0159 N88-10998
Thrust and specific impulse of repetitively-pulsed-laser propulsion rocket 03 p0318 N88-12012
Blast waves generated by planar detonations
[DE88-002219] 09 p1164 N88-16979
Flame propagation in the approximation of straight-line trajectories of burning products
[DE88-700675] 10 p1297 N88-17756
Diffusion description of flame propagation due to the translational motion of burning reaction products
[DE88-700676] 10 p1297 N88-17757
Combustion theory and related questions
[AD-A189160] 13 p1737 N88-20382
Detonation velocity of the hydrazinum nitrate-hydrazine water system
[NASA-TT-20213] 13 p1770 N88-20590
Numerical modeling of divergent detonation wave
14 p1903 N88-21373
Shock initiation studies on heterogeneous explosives
[DE88-008681] 21 p2923 N88-27351

DETONATORS
Langlie Test Method Program for use with the HP-41CV/X calculator
[DE88-001935] 06 p0687 N88-14210
An electro-optic explosive igniter
[DE88-004726] 11 p1466 N88-18738
A concept for an electro-optic explosive device
[DE88-009696] 21 p2923 N88-27349

DEUTERIUM
Applications and limitations of deuterium labeling methods to neutron scattering studies of polymers
[DE87-012936] 02 p0151 N88-10945
Refueling and density control in the ZT-40M reversed field pinch
[DE88-000504] 04 p0493 N88-13040
Hydrogen and deuterium in the local interstellar medium 04 p0521 N88-13204
Magneto-Inertia Confinement Approach (MICA) to fusion in dynamic Z-pinch formed from a frozen deuterium-tritium tube
[IPPJ-856] 09 p1252 N88-17504
Helium-3 fusion fuel resources for space power
17 p2410 N88-24330
Effect of hydrogen, deuterium and oxygen on the anelastic properties of refractory alloys
[DE88-007349] 18 p2484 N88-24736
Deuterium isotope effects in the combustion of formulated nitramine propellants
19 p2632 N88-25611
Factors which affect operation of a plasma focus in various gases
[DE88-701882] 20 p2858 N88-26975

DEUTERIUM COMPOUNDS
Energy transfer studies with lasers
[DE88-004864] 10 p1337 N88-17991

DEUTERIUM PLASMA
SOAR: Space orbiting advanced fusion power reactor
[AD-A189234] 13 p1732 N88-20356

DEUTERON IRRADIATION
Experimental set-up for measurements of Compton scattering cross section on light nuclei
[DE88-700161] 12 p1688 N88-20097
Study of defects in metals by positron annihilation
[DE88-701042] 13 p1745 N88-20432

DEUTERONS
Experimental studies of electromagnetic properties of few body systems
[DE87-014610] 02 p0161 N88-11008
Ion energy diagnostics for voltage determinations in plasma-erosion-opening-switch experiments
[DE88-004822] 11 p1479 N88-18827

DEVELOPERS (PHOTOGRAPHY)
U PHOTOGRAPHIC DEVELOPERS

DEVELOPING NATIONS
Unispace 82 09 p1128 N88-16766
Centre for International Co-Operation and Approriate Technology (CICAT)
[PB88-165501] 18 p2590 N88-25389
Use of SPOT data in preliminary steps of road project studies especially suited for developing countries
22 p3098 N88-28396

DEVIATION
The deviation of light rays passing through a curved windscreen --- aircraft
[BAE-MSC.115] 01 p0093 N88-10610
Stochastic approximation and large deviations: General results for w.p.l. Convergence
[AD-A185818] 06 p0768 N88-14721
Nonlinear filtering and large deviations: A PDE-Control theoretic approach
[AD-A187436] 10 p1396 N88-18321
Asymptotic expansions for large deviation probabilities in the strong law of large numbers
[AD-A187432] 10 p1402 N88-18361
Deviation equation as an equation of motion
[DE88-702134] 19 p2722 N88-26161

DEVITRIFICATION
U CRYSTALLIZATION

DEW POINT
Use of time changes of surface data parameters in short range forecasting 02 p0206 N88-11291

DEWAR SYSTEMS
U CRYOGENIC EQUIPMENT

DEWETTING
U DRYING

DIABETES MELLITUS
Design considerations for the development of an implantable sensor for the continuous measurement of glucose in the diabetic patient 17 p2382 N88-24159

DIAGNOSIS
Proceedings of Conference on Vibrodiagnostics discussed 02 p0158 N88-10990
Programmable 10 MHz optical fiducial system for hydrodiagnostic cameras
[DE87-013223] 02 p0175 N88-11091
In-flight diagnosis: Analysis of spurious events --- spacecraft 03 p0274 N88-11724
The development of diagnostic fuses
[SAND-86-0395] 03 p0311 N88-11963
Diagnostics aid for mass spectrometer trouble-shooting
[DE88-000350] 03 p0324 N88-12049
Computer-controlled testing of visual-spatial ability
[AD-A183971] 03 p0357 N88-12249
The characterization of diagnostic tasks for engineering systems
[DE88-000093] 04 p0483 N88-12973
Diagnostic reasoning in digital systems
[NASA-CR-181564] 05 p0633 N88-13871
Human physical fields 06 p0750 N88-14609
Diagnostic emulation: Implementation and user's guide
[NASA-CR-178391] 06 p0756 N88-14638
A solid phase enzyme-linked immunosorbent assay for the antigenic detection of Legionella pneumophila (serogroup 1): A compliment for the space station diagnostic capability 06 p0795 N88-14868
Development of a prototype H-46 helicopter diagnostic expert system
[AD-A186077] 07 p0809 N88-14924
Modal analyses of the Kermville diagnostic canister
[DE88-003268] 07 p0870 N88-15277
Development of methods for the study of space motion sickness 07 p0892 N88-15408
Diagnostic value of some load tests in evaluation of nonspecific electrocardiographic changes
07 p0895 N88-15426
An interactive visual interface for Fastbus diagnostics
[DE88-002569] 07 p0900 N88-15453
Innovating systems and techniques for the diagnosis of materials and industrial plants
[CISE-3856] 08 p0976 N88-15901
• On line instrument systems for monitoring steam turbogenerators
[CISE-3860] 08 p0990 N88-15995
Prognosis using spectral embedding --- weather forecasting 08 p1016 N88-16157
An easy-to-use diagnostic system development shell
08 p1055 N88-16366

An inference engine for embedded diagnostic systems
08 p1056 N88-16367
Qualitative and temporal reasoning in engine behavior analysis
08 p1058 N88-16383
EUREX D: An expert system for failure diagnosis and recovery in the TCS of the European retrievable carrier EURECA
08 p1058 N88-16385
A data structure and algorithm for fault diagnosis
08 p1065 N88-16432
Integrated diagnostics
09 p1111 N88-16655
Knowledge based jet engine diagnostics
09 p1203 N88-17210
Diagnosis: Reasoning from first principles and experiential knowledge
09 p1207 N88-17236
Diagnostics for research in atomization and turbulent two-phase flows
[AD-A187338]
11 p1482 N88-18843
Three-dimensional computer graphics brain-mapping project
[AD-A187202]
11 p1528 N88-19126
Expert systems: Their impact on performance and cognitive strategies in diagnostic inference
[AD-A188518]
12 p1677 N88-20027
Progress in diagnostic techniques for SC cavities
[CEBAF-PR-88-003]
13 p1772 N88-20600
Clinical measurements using fiber optic sensors
[DE88-005624]
15 p2134 N88-22731
Thin film research diagnostics instrumentation
[AD-A191240]
16 p2213 N88-23207
Leave-K-Out diagnostics for time series
[AD-A191343]
16 p2261 N88-23518
Optical diagnostics for a high power, rf-inductively coupled plasma
[DE88-007822]
18 p2579 N88-25322
Fracture physics of delamination of composite materials
[AD-A192021]
19 p2609 N88-25482
Asynchronous optical sampling for laser-based combustion diagnostics in high pressure flames
[AD-A192920]
20 p2770 N88-26428
Laser diagnostics applied to advanced combustion systems
[DE88-753119]
20 p2806 N88-26649
Laser probes and numerical modeling as process diagnostics in chemical vapor deposition
[DE88-011622]
21 p2911 N88-27275
Vortex dynamics of coherent and chaotic structures (including algorithms for computer simulations and diagnosis)
[AD-A193580]
23 p3212 N88-29117
Improvements in techniques of microwave thermography
[AD-A193620]
23 p3239 N88-29276
Distributed knowledge base systems for diagnosis and information retrieval
[AD-A193107]
23 p3296 N88-29633
Optical measurements of soot and temperature profiles in premixed propane-oxygen flames
[NASA-TM-101343]
24 p3358 N88-29997
Stress related failures causing open metallization
[AD-A195061]
24 p3383 N88-30150

DIAGRAMS
NT BENDING DIAGRAMS
NT BLOCK DIAGRAMS
NT CIRCUIT DIAGRAMS
NT COLOR-MAGNITUDE DIAGRAM
NT CREEP DIAGRAMS
NT FEYNMAN DIAGRAMS
NT HERTZSPRUNG-RUSSELL DIAGRAM
NT PHASE DIAGRAMS
NT S-N DIAGRAMS
NT STRESS-STRAIN DIAGRAMS

Integrated 3-parameter diagram for determining thermodynamic properties of fluids
03 p0298 N88-11874
CUEMAP: A tool for generating hierarchical charts and dataflow diagrams
[DE88-004778]
10 p1387 N88-18284
PLOT3D (version-5): A computer code for drawing three dimensional graphs, maps and histograms, in single or multiple colours, for mono or stereoscopic viewing
[DE88-701410]
15 p2108 N88-22558
Characterization of lubricants in terms of transition diagram data
[AD-A194264]
23 p3197 N88-29025

DIAMAGNETISM
The thermal conductivity of dirty type 2 superconductors
[B8681488]
23 p3294 N88-29615

DIAMETERS
The angular diameter of alpha Scorpii in the near-infrared Ca II triplet
04 p0514 N88-13162
Explosive absorption of laser beam of finite diameter
07 p0921 N88-15597
Cylindrical surface profile and diameter measuring tool and method
[NASA-CASE-MFS-28287-1]
17 p2341 N88-23959
Hole diameters in plates impacted by projectiles
21 p2929 N88-27386
Effect of fiber diameter on the reliability of composites - automated laser diffraction implementation
[AD-A193524]
23 p3188 N88-28972

DIAMINES
NT GUANIDINES
The water absorption of model epoxy resin networks cured with aromatic diamines
[BR100722]
01 p0027 N88-10169

DIAMOND WINGS
U LOW ASPECT RATIO WINGS
U SWEPT WINGS

DIAMONDS
Theory of the carbon phase diagram at high pressures and temperatures
[DE87-012245]
01 p0028 N88-10180
Diamond turning of silicon for optics applications
[DE88-002501]
07 p0840 N88-15095
Gamma radiation at the 970 MeV plane positron channeling in diamond crystals
[DE88-700557]
07 p0939 N88-15705
Drilling metal matrix composites
[AD-A190480]
15 p2029 N88-22091
Diamond like carbon coatings: Categorization by atomic number density
[NASA-CR-174895]
22 p3059 N88-28151
The diamond as a new electronic material
[NASA-TT-20354]
23 p3209 N88-29098
Diamond film by hot filament CVD method
[NASA-TT-20335]
23 p3294 N88-29618

DIAPHRAGMS (MECHANICS)
Diffraction effects during materials treatment with laser beams
[ETN-87-90614]
03 p0328 N88-12075
Low gravity liquid motions in spacecraft
08 p0982 N88-15941
Test of a prototype gate with fast opening equipping the shock tube 0 2.40 m at CEG
[PB87-227864]
19 p2604 N88-25465
Simulation of diaphragm-type IC pressure sensors
19 p2672 N88-25887

DIATOMIC GASES
Evaluation and compilation of thermodynamic properties of high temperature chemical species
[AD-A187509]
11 p1452 N88-18654

DIATOMIC MOLECULES
On the signal strength dependency on pressure in laser sub-Doppler saturation spectroscopy with special attention to gaseous diatonic molecules
[USIP-87-13]
09 p1171 N88-17023
Theory of the dissociation dynamics of small molecules on metal surfaces: Finite temperature studies
[DE88-006495]
15 p2132 N88-22716
A constraint algorithm for maintaining rigid bonds in molecular dynamics simulations of large molecules
[AD-A191663]
18 p2572 N88-25277
Nuclear magnetic ordering and paramagnetic relaxation of diatomic molecules in Ca (OH)2
[B8681469]
23 p3281 N88-29532

DIATOMS (UNICELLULAR PLANTS)
U ALGAE

DICARBOXYLIC ACIDS
Synthesis and characterization of 1,2-cyclobutenedicarboxamides: Thermally generated polymers and Diels-Alder adducts
[AD-A188591]
12 p1611 N88-19633

DICHLORIDES
A theoretical model of the washout of trace gases by raindrops in the atmosphere
17 p2375 N88-24125

DICHROISM
Near-infrared dichroism of a mesogenic transition metal complex and its solubility in nematic hosts
[DE87-014471]
03 p0287 N88-11805

DICHROMATES
U CHROMATES

DICKE RADIOMETERS
Implications of the trapping-desorption and direct inelastic scattering channels on Dicke-narrowed lineshapes
[AD-A191410]
16 p2270 N88-23581

DICKE TYPE RADIOMETERS
U DICKE RADIOMETERS

DICTIONARIES
Energy Data Base: Subject Thesaurus
[DE87-008007]
03 p0384 N88-12414
IDMS application documentation made easy
[DE88-000199]
03 p0384 N88-12416
A graphics editor for structured analysis with a data dictionary
[AD-A190618]
15 p2112 N88-22584
NASA combined file postings statistics based on NASA thesaurus, Jan. 1988 - July 1988
[NASA-CR-182985]
18 p2589 N88-25384
A glossary for carbon dioxide and climate
[DE88-007885]
19 p2689 N88-25982

DIELECTRIC CONSTANT
U PERMITTIVITY

DIELECTRIC MATERIALS
U DIELECTRICS

DIELECTRIC POLARIZATION
Effect of collisional broadening on the polarizability of a two-dimensional electron gas
[DE87-013928]
02 p0237 N88-11497
Spontaneous decay and atomic fluorescence near a metal surface of an absorbing dielectric
[AD-A187508]
13 p1835 N88-20975
Field-aligned structure of the storm time Pc 5 wave of November 14-15, 1979
[AD-A193022]
21 p2972 N88-27653

DIELECTRIC PROPERTIES
NT PERMITTIVITY
Voltammetric investigation of porous silicon for integrated circuit applications
[DE87-009287]
02 p0166 N88-11042
Dielectric response of ionic conductors
[DE87-013552]
02 p0166 N88-11045
Coupling and absorption phenomena in semiconductor-clad dielectric optical waveguides
[DE87-013446]
03 p0307 N88-11939
United States - Japan Workshop on Dielectric and Piezoelectric Ceramics (3rd) held in Toyama, Japan on November 9-12, 1986
[AD-A185113]
05 p0568 N88-13460
Numerical and analytical study of the equivalent permittivity or permeability of nonhomogeneous materials. Application to the experimental electromagnetic characterization of composites
[SNIAS-872-430-104]
05 p0575 N88-13509
Ionic transport and electrical relaxation in glass
[DE88-000887]
05 p0657 N88-14028
Vibrational properties of disordered solids. Far infrared studies: Performance report
[DE88-001474]
06 p0786 N88-14821
Power and charge dissipation from an electrodynamic tether
06 p0795 N88-14869
Dielectric behavior of electromagnetic (EM) windows materials irradiated by a CW CO2 high-power laser --- hypersonic/reentry vehicles
[ISL-CO-239/86]
09 p1154 N88-16913
RELIC: A reliability simulator for integrated circuits
[AD-A187493]
11 p1477 N88-18811
Microwave dielectric spectrum of rocks
[NASA-TM-89719]
12 p1642 N88-19831
Microwave and structural properties of saline ice
[AD-A189307]
13 p1803 N88-20779
Increasing the rate at which ceramic castings undergo preliminary heat-treatment in an ultra-high frequency magnetic field
14 p1886 N88-21275
Microwave dispersion and absorption in tissues: Molecular mechanisms
[AD-A190118]
15 p2100 N88-22512
Correlation between dielectric and structural properties during epoxy cure
[AD-A190596]
16 p2181 N88-22997
Static dielectric breakdown strength of condensed heterogeneous high explosives
[AD-A191035]
16 p2183 N88-23014
Deep dielectric charging effects due to high energy electrons in earth's outer magnetosphere
[AD-A192154]
18 p2541 N88-25083
Theoretical basis for an experimental test with regard to the origin of VHF (Very High Frequency) radiation from natural lightning
[DE88-007535]
18 p2544 N88-25102
Development of external cooling cryo-resistive cable systems. Part 2: Insulation characteristics on 66 kV rated cryo-resistive testing cable
[DE88-770191]
20 p2793 N88-26571
Variational analysis of dielectrically loaded multidepth corrugated waveguides
[PB88-193602]
20 p2793 N88-26573
Low noise cryogenic dielectric resonator oscillator
[NASA-CASE-NPO-17157-1-CU]
20 p2797 N88-26596
Modeling of subtle kinetic processes in plasma simulation
20 p2856 N88-26959
Manufacturing of a barium titanate with high dielectric coefficient by decomposition of precipitates of double oxalates
[ISAL-IDI1-88-02]
21 p2911 N88-27278
Processing and additive effects of ZrO2 on microstructure and dielectric porperties of BaTiO3 ceramics
[AD-A193126]
21 p2917 N88-27316
Surface-wave model uncertainty assessment
[AD-A193094]
21 p2932 N88-27408

Effects on the resonant frequencies caused by loading a spherical cavity with a dielectric sphere
[AD-A193864] 23 p3277 N88-29511

DIELECTRICS
NT RADOME MATERIALS
Energy transformation in molecular electronic systems
[DE87-013916] 03 p0282 N88-11771
Automated microwave dielectric constant measurement
[AD-A184182] 04 p0431 N88-12667
Measurement and analysis of cryogenic sapphire dielectric resonators and DROs 04 p0433 N88-12686
Raman microprobe characterization of dielectric films following high-energy pulsed laser irradiation
[DE88-000559] 05 p0588 N88-13587
Extinction by dielectric particles at optical and infrared wavelength
[AD-A184818] 05 p0650 N88-13981
Dependence of acoustical characteristics of laser-induced breakdown in dielectric materials on shape of inelastic region 06 p0774 N88-14753
Assessment of electroceramics research in Europe and the Middle East
[AD-A186377] 07 p0836 N88-15074
Deformation effects on microwave reflectivity
[AD-A185684] 07 p0844 N88-15120
Materials for acceleration by surface electromagnetic waves
[DE88-700312] 07 p0846 N88-15133
Failure modes of laminate structures
[DE88-002579] 08 p0996 N88-16033
Plane wave diffraction by a thin dielectric wedge
[RSRE-MEMO-4045] 09 p1153 N88-16912
Guided-wave approaches to spectrally selective energy absorption
[NASA-CR-182532] 10 p1320 N88-17892
Voltammetric investigation of porous silicon for integrated circuit applications
[DE88-004024] 11 p1456 N88-18677
Research on high-specific-heat dielectrics
[AD-A187248] 11 p1461 N88-18710
Layered-capacitor method for dielectric bridge measurements. Algorithms for inversion and parameter fitting: Documentation, verification, data analysis
[PB88-131479] 11 p1505 N88-18989
Transport properties of conductive polymers
[AD-A188411] 12 p1610 N88-19628
Transformation coefficient in wave-field acceleration scheme
[DE88-700158] 13 p1757 N88-20507
Vapor-mist for lightweight high voltage space insulation systems
[DE87-011704] 13 p1762 N88-20538
Causes of damage in multilayer dielectric coatings exposed to high average power visible laser radiation
[DE88-005363] 13 p1775 N88-20619
Spontaneous decay and atomic fluorescence near a metal surface of an absorbing dielectric
[AD-A187508] 13 p1835 N88-20975
Spacecraft dielectric surface charging property determination
[NASA-CR-180879] 14 p1881 N88-21243
Method for characterizing end-plate surface resistance of dielectric resonator 14 p1903 N88-21371
On the theory of electromagnetic scattering from a raindrop splash
[AD-A188720] 14 p1906 N88-21393
Infrared reflection-absorption spectroscopy of hyperfine layers on surfaces of semiconductors and dielectrics 14 p1969 N88-21755
Exact image theory for the problem of dielectric/magnetic slab
[NASA-CR-182865] 16 p2189 N88-23055
Optimization of metal-dielectric laser mirrors of TiO2/SiO2 and silver
[ESA-TT-1068] 16 p2212 N88-23199
Low gravity thermal management using dielectrophoretic forces 17 p2432 N88-24470
Micro-Raman analysis of dielectric optical thin films
[AD-A191228] 17 p2445 N88-24537
Arcing and rf signal generation during target irradiation by a high-energy, pulsed neutral particle beam
[DE88-007169] 18 p2471 N88-24664
Born-type reconstruction of material parameters of an inhomogeneous, lossy dielectric slab from reflected-field data
[PB88-188958] 18 p2569 N88-25261
Molecular characterization of structure and bonding in thin film materials
[DE88-006811] 18 p2584 N88-25351
Method of forming a multiple layer dielectric and a hot film sensor therewith
[NASA-CASE-LAR-13678-1] 18 p2584 N88-25355
Research and development programs on advanced structural ceramics in Korea 19 p2633 N88-25620
Characteristics of shielded microstrip lines on GaAs-Si at millimeter-wave frequencies 19 p2657 N88-25787
Dielectric compound parabolic concentrating solar collector with frustrated total internal reflection absorber
[DE88-009986] 19 p2688 N88-25976
Visible tunable source
[DE88-006442] 20 p2854 N88-26944
Processing and additive effects of ZrO2 on microstructure and dielectric properties of BaTiO3 ceramics
[AD-A193126] 21 p2917 N88-27316
Preparation and properties of high Q microwave dielectrics in the (CA, SR, BA) zirconate system
[AD-A193127] 21 p2918 N88-27317
Effects of surface tension and contact angle on sensible heating and boiling incipience in dielectric falling films
[DE88-007057] 21 p2945 N88-27492
Measurement of the thermal conductivity of dielectric thin solid films with a thermal comparator
[DE88-008468] 21 p3016 N88-27898
On the self-consistent equation for the microscopic local electric field in dielectric systems
[PREPRINT-589] 22 p3074 N88-28247
Stress corrosion of ceramic materials
[AD-A191979] 23 p3195 N88-29016
Basic research in electronics (JSEP) Joint Services Electronics Program
[AD-A193072] 23 p3206 N88-29079
Natural convection immersion cooling of an array of simulated chips in an enclosure filled with dielectric liquid
[AD-A193594] 23 p3207 N88-29088
Effects on the resonant frequencies caused by loading a spherical cavity with a dielectric sphere
[AD-A193864] 23 p3277 N88-29511
Research on crystal and film ferroelectric materials for optoelectronic applications
[AD-A193512] 23 p3291 N88-29597
Polymer-ceramic composites
[AD-A195789] 24 p3356 N88-29983
Transient interaction of electromagnetic pulses in dielectrics and microwave biophysics
[AD-A195687] 24 p3360 N88-30008
Dielectric millimeter waveguides: A feasibility study for a novel dielectric millimeter waveguide
[AD-A195104] 24 p3366 N88-30042

DIELECTRONIC SATELLITE LINES
U RESONANCE LINES

DIELS-ALDER REACTIONS
Study of improved methods for predicting chemical equilibria
[DE87-014647] 02 p0145 N88-10908
High-temperature thermosets derived from the Diels-Alder polymerization of bisbenzocyclobutenes and bimaleimides
[AD-A188800] 13 p1747 N88-20449

DIENCEPHALON
NT HYPOTHALAMUS
NT THALAMUS

DIENES
NT BUTADIENE
NT POLYBUTADIENE

DIES
Studies on estimation of nickel in zinc base die casting by D.C. polarography
[PD-MT-8729] 04 p0417 N88-12588

DIESEL ENGINES
Piston ring friction and vehicle fuel economy
[DE87-014536] 02 p0181 N88-11127
Use of natural gas diesel engines in mechanical pulp production: A preliminary study
[DE87-753065] 02 p0181 N88-11129
Adiabatic diesel engine component development: Reference engine for on-highway applications
[NASA-CR-179531] 03 p0386 N88-12428
Ceramic technology for advanced heat engines project
[DE88-001520] 04 p0420 N88-12605
Report to Congress on the Automotive Technology Development Program
[DE88-003742] 07 p0864 N88-15242
The effects of fuel composition on ignition delay in homogeneous charge and direct injection compression ignition engines
[DE88-003691] 09 p1143 N88-16849
Effect of translucence of engineering ceramics on heat transfer in diesel engines
[DE88-003732] 10 p1305 N88-17804
Experimental study of thermal loading at the wall of an industrial Diesel motor
[ISAL-IDI1-87-10] 10 p1339 N88-18000
Liquid sprays and flow studies in the direct-injection diesel engine under motored conditions
[NASA-TM-100135] 11 p1440 N88-18594
Prototype thin-film thermocouple/heat-flux sensor for a ceramic-insulated diesel engine
[NASA-TM-100798] 11 p1490 N88-18892
Concept and analysis of a direct-injection alcohol layer charge motor
[ETN-88-91482] 11 p1495 N88-18925
Practical system for the use of alcohol in diesel engines
[PB88-147863] 12 p1612 N88-19638
Engine testing for synfuel operation
[DE88-006044] 13 p1779 N88-20645
Cetane scale evaluation and possible modification
[AD-A189730] 15 p2048 N88-22200
JPRS report: Science and technology, Japan
[JPRS-JST-87-026] 16 p2184 N88-23018
Full electronic control system for diesel engine 16 p2185 N88-23025
Status, trends in research on internal combustion engines 16 p2185 N88-23027
Servojet retrofit
[AD-A191075] 18 p2522 N88-24964
Direct gas injection with glow plug ignition
[PB88-187323] 19 p2676 N88-25911
An investigation of high pressure/late cycle injection of CNG (Compressed Natural Gas) as a fuel for rail applications
[DE88-009000] 19 p2677 N88-25917
Pulsed spray structure and atomisation techniques
[AD-A192280] 20 p2800 N88-26614
Documentation of the Benson Diesel Engine Simulation Program
[NASA-TM-100940] 21 p2898 N88-27201
Ceramic technology for advanced heat engines project
[DE88-008945] 21 p2919 N88-27323
The 210-HP diesel engine endurance and performance testing with fire resistant diesel fuel
[AD-A193153] 21 p2956 N88-27558
Basic mechanisms of diesel lubrication correlation of bench and engine tests
[AD-A193360] 21 p2956 N88-27561
Ethanol as a fuel of a lorry. Use experience from a diesel engine modified to an otto engine
[DE88-752870] 21 p2958 N88-27569
Diesel combustion fundamentals, phase 1, volume 1
[AD-A193831] 22 p3052 N88-28107
Modeling of spray combustion in direct injection diesel engine
[AD-A193787] 22 p3084 N88-28314
Variable-compression-ratio pistons for high power output diesel engines 22 p3084 N88-28316

DIESEL FUELS
Formation of sediments in fuels containing added sulphonic acids --- marine diesel fuels
[RAE-TM-NAV-ENG-1163] 09 p1150 N88-16891
Concept and analysis of a direct-injection alcohol layer charge motor
[ETN-88-91482] 11 p1495 N88-18925
Analysis of model fuels and their compatibility with selected elastomers, part 1
[AD-A188361] 12 p1612 N88-19639
Flammability characteristics of distillate fuels
[AD-A188497] 12 p1612 N88-19642
Engine testing for synfuel operation
[DE88-006044] 13 p1779 N88-20645
Cetane scale evaluation and possible modification
[AD-A189730] 15 p2048 N88-22200
An investigation of high pressure/late cycle injection of CNG (Compressed Natural Gas) as a fuel for rail applications
[DE88-009000] 19 p2677 N88-25917
Effects of ceramic surfaces on autoignition in a constant volume combustion apparatus
[AD-A193055] 21 p2909 N88-27266
A study relating to the fog oil replacement program
[AD-A192536] 21 p2923 N88-27347
The 210-HP diesel engine endurance and performance testing with fire resistant diesel fuel
[AD-A193153] 21 p2956 N88-27558
Diesel combustion fundamentals, phase 1, volume 1
[AD-A193831] 22 p3052 N88-28107

DIETS
Operation Everest 2: Nutrition and body composition
[AD-A186449] 08 p1049 N88-16333
Manipulation of muscle glycogen concentrations using high and low carbohydrate diets and exercise
[AD-A187732] 11 p1519 N88-19089
Dietary factors related to physical fitness
[AD-A190272] 15 p2103 N88-22527

DIFFERENCE EQUATIONS
Cross-correlation of uniform cyclic difference set sequences
[AD-A184879] 05 p0640 N88-13913

A fully redundant double difference algorithm for obtaining minimum variance estimates from GPS observations
[NASA-CR-182363] 06 p0667 N88-14089
Analysis of smoothing matrices for the preconditioning of elliptic difference equations
[CWI-NM-R8705] 09 p1228 N88-17357
Predicting oscillatory finite difference solutions to the heat equation: A comparative study of the coefficient and matrix methods
[AD-A189591] 13 p1825 N88-20911
Accuracy versus convergence rates for a three dimensional multistage Euler code
[NASA-CR-181665] 16 p2261 N88-23519
Numerical solutions to stochastic difference equations 18 p2564 N88-25229
A comparative study of Chebyshev acceleration and residue smoothing in the solution of nonlinear elliptic difference equations
[CWI-NM-R8723] 18 p2569 N88-25259
Effects of numerical dissipation on finite-volume solutions of compressible flow problems
[AD-A193173] 21 p2944 N88-27485
Interferometric tomography of continuous fields with incomplete projections
[NASA-CR-183181] 22 p3081 N88-28295

DIFFERENCES
GPS vertical axis performance enhancement for helicopter precision landing approach
[NASA-CR-177443] 04 p0397 N88-12477
On the norm equivalence of singularly perturbed elliptic difference operators
[DE88-006353] 13 p1826 N88-20913

DIFFERENTIAL ALGEBRA
U MATRICES (MATHEMATICS)

DIFFERENTIAL ANALYZERS
Digital method for correction of the phase error in the discrete generation of periodic signals in real time
[INPE-4327-RPE/552] 12 p1618 N88-19676

DIFFERENTIAL EQUATIONS
NT BIHARMONIC EQUATIONS
NT BURGER EQUATION
NT CAUCHY-RIEMANN EQUATIONS
NT COSINE SERIES
NT ELLIPTIC DIFFERENTIAL EQUATIONS
NT EULER-CAUCHY EQUATIONS
NT FOKKER-PLANCK EQUATION
NT GAUSS EQUATION
NT HELMHOLTZ VORTICITY EQUATION
NT HYPERBOLIC DIFFERENTIAL EQUATIONS
NT PARABOLIC DIFFERENTIAL EQUATIONS
NT PARTIAL DIFFERENTIAL EQUATIONS
NT POISSON EQUATION
NT RICCATI EQUATION
NT VLASOV EQUATIONS
NT VORTICITY EQUATIONS
The reliability of numerical solutions of ordinary differential equations, obtained by implicit calculation schemes
[PTB-W-30] 01 p0085 N88-10549
Parallel computation of a domain decomposition method
[DE87-011444] 01 p0086 N88-10560
Implementation and evaluation of several continuously imbedded methods of Sarafyan
[DE88-000025] 02 p0221 N88-11393
On oscillation of a kind of integro-differential equation with delay
[DE87-703059] 02 p0225 N88-11417
Oscillatory and nonoscillatory properties of first order differential equations with piecewise constant deviating arguments
[DE87-703061] 02 p0225 N88-11418
Finite-dimensional matrix representation of the differential operator, determinental form and zeros of special functions
[DE87-703091] 02 p0225 N88-11421
The method of lines for time dependent free boundary problems
[DE87-013929] 02 p0226 N88-11423
Computational methods and software for differential equations and their applications
[DE87-014601] 02 p0226 N88-11424
Parallel methods for ordinary differential equations
[DE87-014667] 02 p0226 N88-11425
A collection of test problems for ordinary differential equation solvers which have provisions for rootfinding
[DE88-000045] 02 p0226 N88-11428
Numerical modeling: Finite methods 03 p0304 N88-11918
Operator multiple-tasking study for remotely operated platforms
[AD-A184487] 03 p0362 N88-12276
The development of ODE methods: A symbiosis between hardware and numerical analysis
[DE87-014925] 03 p0370 N88-12325
Implementation of the Runge-Kutta-Fehlberg method for solution of ordinary differential equations on a parallel processor
[AD-A184660] 03 p0370 N88-12331
Applications of a theory of ferromagnetic hysteresis
[DE87-014725] 03 p0373 N88-12348
Oscillation theory for linear second-order differential systems
[DE87-011393] 04 p0484 N88-12983
The shifted Adams method for ordinary differential equations
[DE88-000810] 04 p0486 N88-12994
A note on the use of symmetric line Gauss-Seidel for the steady upwind differenced Euler equations
[AD-A185223] 05 p0580 N88-13540
The numerical and analytic of implicit differential equations and their application to control and circuit problems
[AD-A185404] 05 p0641 N88-13922
Development of an unsteady wake theory appropriate for aeroelastic analyses of rotors in hover and forward flight
[NASA-CR-182357] 06 p0664 N88-14075
Steady waves in a nonlinear theory of viscoelasticity
[AD-A185548] 06 p0723 N88-14448
Development of symbolic computation methods for nonlinear dynamics
[AD-A185562] 06 p0758 N88-14653
Pseudodifferential operators on the circle and finite differences
[PB87-222352] 06 p0763 N88-14681
Local and global techniques for the tracking of periodic solutions of parameter-dependent functional differential equations
[AD-A185756] 06 p0766 N88-14704
Characteristic trajectories of generalized Lanchester equations
[AD-A185762] 06 p0766 N88-14705
Shadow systems and attractors in reaction-diffusion equations
[AD-A185804] 06 p0766 N88-14706
There exists a C sup infinity symbol Kupka-Smale diffeomorphism of S sup 2 with neither sinks nor sources
[PB87-225967] 06 p0769 N88-14725
Modeling the growth dynamics of four candidate crops for Controlled Ecological Life Support Systems (CELSS) 06 p0799 N88-14889
Theoretical investigations of chaotic dynamics
[AD-A186404] 07 p0867 N88-15261
Recent developments in the numerical solution of differential/algebraic systems
[DE88-001885] 07 p0912 N88-15535
Boundary value problems for ordinary differential equations with multiple turning points
[CWI-AM-R8701] 09 p1228 N88-17354
Diagonally implicit Runge-Kutta-Nystrom methods for oscillatory problems
[CWI-NM-R8704] 09 p1228 N88-17356
A note on a diagonally implicit Runge-Kutta-Nystrom method
[CWI-NM-R8706] 09 p1228 N88-17358
Stability results for theta methods applied to a class of stiff differential-algebraic equations
[CWI-NM-R8708] 09 p1228 N88-17360
Perturbation theory for dual semigroups 2. Time-dependent perturbations in the sun-reflexive case
[PB88-113097] 09 p1230 N88-17369
Core spline method for solution of quantum-mechanical systems of differential equations for bound states
[DE88-700492] 09 p1259 N88-17551
Parallels between control PDE's (Partial Differential Equations) and systems of ODE's (Ordinary Differential Equations)
[NASA-CR-182487] 10 p1398 N88-18331
Straightening and the Stanley decomposition for the (2;n)-nilpotent vectorfield
[PB88-126685] 10 p1398 N88-18336
Boundary value problems for differential and functional differential equations
[AD-A187378] 10 p1400 N88-18349
Generalized equations for emittance and field energy of high-current beams in periodic focusing
[DE88-004448] 10 p1404 N88-18372
Performance and optimization of direct implicit time integration schemes for use in electrostatic particle simulation codes
[DE88-003254] 10 p1406 N88-18381
A cause of divergence in the Kalman gain equation 12 p1578 N88-19438
What do multistep methods approximate
[PB88-148839] 13 p1828 N88-20932
Analytic solutions to dynamic equations of plasma armature railguns
[DE88-006842] 15 p2023 N88-22057
Fluid motion in a spinning, coning cylinder via spatial eigenfunction expansion
[AD-A190758] 15 p2066 N88-22319
Evolution of hardening and damage during viscoplastic deformation
[AD-A190714] 15 p2077 N88-22381
Logarithmically connected, repetitive computer networks and numerical applications
[DE88-006632] 15 p2114 N88-22592
A zonal approach for the solution of coupled Euler and potential solutions of flows with complex geometries
[AD-A189752] 15 p2114 N88-22595
Numerical solution of nonlinear algebraic equations in stiff ODE solving
[DE88-006634] 15 p2118 N88-22622
Numerical methods for singularly perturbed differential equations with applications
[AD-A189786] 15 p2119 N88-22628
Normed Bellman equation with degenerate diffusion coefficients and its application to differential equations
[AD-A190319] 15 p2120 N88-22637
Formal solution of differential linear systems in the proximity of a singularity
[ETN-88-92190] 16 p2258 N88-23495
Estimation of time- and state-dependent delays and other parameters in functional differential equations
[NASA-CR-181663] 17 p2383 N88-24164
Minimal parameter solution of the orthogonal matrix differential equation
[NASA-TM-4043] 17 p2383 N88-24165
Existence of periodic solutions in n-dimensional retarded functional differential equations
[RR-325] 17 p2392 N88-24221
Computational sciences
[AD-A190826] 18 p2564 N88-25226
Approximate solution of random differential equation 18 p2565 N88-25233
Solution of Faddeev-Yakubovsky differential equations by the finite-dimensional approximation method for four spinless particles in the 1+3 scattering problem
[DE87-702983] 19 p2719 N88-26145
Propagation of inernio-acoustic gravity waves in a rotating and radiating opaque atmosphere
[DE88-701866] 20 p2823 N88-26750
A practical shifted Adams algorithm
[DE88-008573] 20 p2837 N88-26830
Canonical construction of differential operators intertwining representations of real semisimple Lie groups
[DE88-701852] 20 p2845 N88-26882
Theory of pseudo-differential operators over C*-algebras
[DE88-701860] 20 p2845 N88-26883
A full but elementary treatment of systems of homogeneous ordinary linear differential equations with constant coefficients
[REPT-87-82] 20 p2845 N88-26887
A Wong-Zakai type theorem for certain discontinuous semimartingales
[AD-A192713] 21 p3005 N88-27822
KRYSI, an ODE solver combining a semi-implicit Runge-Kutta method and a preconditioned Krylov method
[DE88-012245] 21 p3008 N88-27841
Rational Newton algorithms to compute formal solutions of linear differential equations in an irregular singular point
[RR-704-M] 22 p3140 N88-28670
Second order differential equations in the complex domain
[RR-674-M] 22 p3144 N88-28695
Convex duality approach to the optimal control or diffusions
[AD-A194535] 23 p3266 N88-29442
On the distribution equations
[DE88-702217] 23 p3270 N88-29454
Minimizing escape probabilities: A large deviations approach
[AD-A194534] 23 p3275 N88-29496
Mathematical theory and calculations of magnetic hysteresis curves
[DE88-011055] 23 p3277 N88-29510
Resonance excitation of linear and non-linear spiral density waves in a gaseous disk 23 p3299 N88-29643
Automatic qualitative analysis of ordinary differential equations using piecewise linear approximations
[AD-A196310] 24 p3424 N88-30379

DIFFERENTIAL GEOMETRY
NT LIE GROUPS
NT RIEMANN MANIFOLD
NT TENSOR ANALYSIS
On Hotelling's approach to testing for a nonlinear parameter in regression
[AD-A191189] 17 p2393 N88-24229

Applications of differential geometry to the shape analysis of gray-value images 21 p2924 N88-27358
Critical values of functionals on Banach surfaces
[DE88-702735] 23 p3272 N88-29472

DIFFERENTIAL INTERFEROMETRY
A review of some flow visualization experiments carried out at the Institut Franco-Allemand de Recherches (ISL) shock tubes
[ISL-CO-243/86] 09 p1163 N88-16974

DIFFERENTIAL OPERATORS
U DIFFERENTIAL EQUATIONS
U OPERATORS (MATHEMATICS)

DIFFERENTIAL PULSE CODE MODULATION
A hybrid transform/DPCM encoder for data compression
[DE88-003725] 09 p1154 N88-16919

DIFFERENTIAL THERMAL ANALYSIS
U THERMAL ANALYSIS

DIFFERENTIATION (BIOLOGY)
Xiphophorus: A system to recognize radiation-induced mutations and to study the effects of zero-gravity environment on embryo development
07 p0885 N88-15372
Questions on the evolution of the development program of the vertebrate inner ear under long term zero-g conditions 07 p0886 N88-15379
Differentiation of hemopoietic stem cells during adaptation to high altitude 07 p0893 N88-15410
Embryonic development of guppy in weightlessness
10 p1360 N88-18127
Growth and differentiation of cells in organotypical rat embryo cerebellar culture developing in weightlessness
19 p2703 N88-26076
Growth and differentiation of Bacillus subtilis under microgravity conditions 22 p3060 N88-28158

DIFFRACTION
NT ELECTRON DIFFRACTION
NT FRESNEL DIFFRACTION
NT NEUTRON DIFFRACTION
NT PULSE DIFFRACTION
NT WAVE DIFFRACTION
NT X RAY DIFFRACTION
The deviation of light rays passing through a curved windscreen --- aircraft
[BAE-MSC.115] 01 p0093 N88-10610
Use of a 35mm camera for remote surface cleanliness verification 02 p0133 N88-10835
Uniform geometrical theory of diffraction
03 p0303 N88-11911
A theoretical study of enhanced Smith-Purcell radiation from a bigrating
[AD-A184530] 03 p0329 N88-12080
Interior impedance wedge diffraction with surface waves
[NASA-CR-182405] 07 p0854 N88-15186
Nonlinear and diffraction effects in sound beams with random transverse structure 09 p1235 N88-17402
Geophysical diffraction tomography for imaging isolated subsurface inclusions
[DE88-003918] 11 p1505 N88-18990
Three-dimensional scattering of impulsive acoustic waves by a semi-infinite crack in the plane interface of a half space and a layer
[PB88-146998] 12 p1687 N88-20089
An interferometric investigation of the diffraction of planar shock waves over a half-diamond cylinder in air
[UTIAS-322] 13 p1768 N88-20575
Space infrared telescope facility wide field and diffraction limited array camera (IRAC)
[NASA-CR-182704] 13 p1853 N88-21092
Research on certain aspects of laser diffraction particle sizing relevant to autonomous self-diagnosing instrumentation
[AD-A190220] 15 p2071 N88-22348
A hardware/software system for implementing geophysical diffraction tomography
[DE88-006411] 15 p2094 N88-22480
Ultrasonic Time-Of-Flight Diffraction (TOFD) measurements of crack depths in an acceleration reservoir of a high velocity research gun
[DE88-006644] 16 p2164 N88-22907
Joint services electronics program
[AD-A191749] 18 p2504 N88-24853
Structure and refinement of ordered aromatic heterocyclic polymers by diffraction methods: Application of results to electro-optic phenomena
[AD-A191859] 19 p2619 N88-25537
Scattering patterns of dihedral corner reflectors with impedance surface impedances
[NASA-CR-183078] 20 p2789 N88-26545
Acoustic diffraction by an absorbing finite strip in a moving fluid
[PB88-191382] 20 p2849 N88-26912
The evaluation of a deformable diffraction grating for a stigmatic EUV spectrohelioimeter
[NASA-CR-183064] 20 p2853 N88-26941
Are Centauros diffractive
[DE88-008767] 21 p3032 N88-27996
Application of laser diffraction techniques to particle sizing in solid propellant rocket motors
[AD-A193841] 22 p3049 N88-28089
Comparison of edge diffraction theories
[AD-A193880] 22 p3070 N88-28223
Direct and inverse diffraction problems for QNDE (Quantitative Non-Destructive Evaluation) applications
[AD-A194721] 22 p3085 N88-28322
Approximate and numerical methods in acousto-optics. Part 1: Normal incidence of the light
[AD-A194294] 22 p3152 N88-28755
Effect of fiber diameter on the reliability of composites - automated laser diffraction implementation
[AD-A193524] 23 p3188 N88-28972
Qualitative characteristics of open waveguide resonator spectra
[DE88-702387] 23 p3202 N88-29056
Evaluation of multi-focus holographic lenses
[AD-A196167] 24 p3377 N88-30110
Diffraction imaging (topography) with monochromatic synchrotron radiation
[NASA-CR-183264] 24 p3433 N88-30431
Streaking images that appear only in the plane of diffraction in undoped GaAs single crystals: Diffraction imaging (topography) by monochromatic synchrotron radiation
[NASA-CR-183267] 24 p3433 N88-30437

DIFFRACTION GRATINGS
U GRATINGS (SPECTRA)

DIFFRACTION LIMITED CAMERAS
Inverse scattering analysis of diffraction limited SAR
[FOA-C-30459-3.2] 05 p0576 N88-13512

DIFFRACTION PATHS
Sound propagation over uneven ground and irregular topography
[NASA-CR-182956] 20 p2849 N88-26911

DIFFRACTION PATTERNS
Photodiode matrix for the analysis of two-beam interferences
[PTB-OPT-23] 01 p0048 N88-10310
Performances of an Actively Stabilized Stellar Interferometer (ASSI): Faint magnitudes, low fringe contrast measurements and operationality
01 p0097 N88-10641
Phase-locked semiconductor quantum well laser arrays
[AD-A185155] 05 p0588 N88-13583
New description of Lau effect based on theory of raster image forming process 06 p0772 N88-14744
Research on acoustical scattering, diffraction catastrophes, optics of bubbles, photoacoustics, and acoustical phase conjugation
[AD-A185785] 06 p0776 N88-14761
Diffraction by glasses with a layer structure
[DE88-003059] 07 p0837 N88-15078
The magic of carrier patterns in moire interferometry
[AD-A187582] 10 p1296 N88-17748
Measuring accuracy of 3-dimensional bodies by the GOMER-1 device
[DE87-703230] 12 p1628 N88-19744
Nonlinear optical principles and the photorefractive effect applied to optical phase conjugation
[AD-A188856] 12 p1691 N88-20119
A review on holography, its principles and applications
[ISL-CO-242/86] 15 p2069 N88-22338
Complex space monofilar approximation of diffraction currents on a conducting half plane
[NASA-CR-182883] 16 p2273 N88-23605
Multiple scattering effects in drop sizing of dense fuel sprays by laser diffraction 24 p3346 N88-29917

DIFFRACTION PROPAGATION
An improved spherical earth diffraction algorithm for SEKE
[AD-A195847] 24 p3360 N88-30005

DIFFRACTION RADIATION
Diffraction transition radiation from periodic electron bunches
[AD-A193593] 23 p3280 N88-29528

DIFFRACTION TELESCOPES
U SPECTROSCOPIC TELESCOPES

DIFFRACTOMETERS
Realization of an instrument to measure temperature and concentration gradients in fluids --- microgravity
[CISE-3128] 09 p1168 N88-17003

DIFFUSE RADIATION
Optical spectroscopy of IRAS sources with infrared emission bands. 1: IRAS 21282+5050 and the diffuse interstellar bands
[NASA-CR-181387] 01 p0094 N88-10611
Magnetic diffuse scattering
[DE87-013539] 04 p0489 N88-13014
Calibration of the EGRET gamma ray telescope with a back-scattered laser beam 06 p0800 N88-14895
DIRBE External Calibrator (DEC)
[NASA-CR-180761] 12 p1631 N88-19760
Investigation of the diffuse ultraviolet background with DE data
[NASA-CR-182863] 19 p2741 N88-26271

DIFFUSERS
Combustor-diffuser interaction program
02 p0185 N88-11152
Numerical prediction of turbulent flows in dump diffusers 05 p0537 N88-13265
Numerical simulation of axisymmetric turbulent flow in combustors and diffusors
[NASA-CR-4115] 10 p1268 N88-17582
The advantage of variable geometry for turbine engines at low power 10 p1280 N88-17653
Numerical simulation of diffuser/combustor dome interaction 10 p1281 N88-17663

DIFFUSION
NT AMBIPOLAR DIFFUSION
NT ATMOSPHERIC DIFFUSION
NT GASEOUS DIFFUSION
NT IONIC DIFFUSION
NT MAGNETIC DIFFUSION
NT MOLECULAR DIFFUSION
NT PARTICLE DIFFUSION
NT PLASMA DIFFUSION
NT SELF DIFFUSION (SOLID STATE)
NT SPECIES DIFFUSION
NT SURFACE DIFFUSION
NT THERMAL DIFFUSION
NT TURBULENT DIFFUSION
New concepts for high current self-sustained diffuse discharge closing switches
[DE87-011678] 01 p0040 N88-10252
A microstructural lattice model for strain oriented problems: A combined Monte Carlo finite element technique
[NASA-TM-100215] 02 p0150 N88-10939
Thermophysical Properties Measurement Facility (TPMF) --- Columbus space station
[ESA-CR(P)-2417] 02 p0157 N88-10981
Differencing the diffusion equation on a mesh of triangles and quadrilaterals
[DE87-011550] 02 p0224 N88-11408
An adaptive pseudo-spectral method for reaction diffusion problems
[NASA-CR-178394] 02 p0224 N88-11414
Review of diffusion barrier technology for application in SP-100 fuel pins
[DE88-000021] 02 p0234 N88-11480
The diffusion-convection vortex method for solving two-dimensional incompressible Navier-Stokes equation
03 p0317 N88-12001
Thermal analysis of electromagnetic launcher rails
[DE88-000166] 04 p0405 N88-12514
A study of mechanisms of hydrogen diffusion in separation devices
[DE88-000328] 04 p0416 N88-12584
Thermophoresis of spherical aerosol particle at arbitrary Knudsen numbers 04 p0461 N88-12850
Automated design of controlled diffusion blades
[NASA-TM-100251] 05 p0542 N88-13304
Numerical methods for reaction-diffusion problems with non-differentiable kinetics
[AD-A185405] 05 p0641 N88-13923
Freidlin-Wentzell type estimates and the law of the iterated logarithm for a class of stochastic processes related to symmetric statistics
[AD-A185366] 05 p0644 N88-13944
On the correlation free forms for nonlinear stochastic systems
[DE87-011169] 05 p0645 N88-13947
An evaluation of a translator for finite element data to resistor/capacitor data for the heat diffusion equation
[DE87-013926] 06 p0698 N88-14285
Stabilized Galerkin method for convection-diffusion problems
[PB87-234985] 06 p0764 N88-14694
Diffusion first passage times: Approximations and related differential equations
[AD-A185592] 06 p0765 N88-14700
Shadow systems and attractors in reaction-diffusion equations
[AD-A185804] 06 p0766 N88-14706
A new method of boundary parameter estimation for a two-dimensional diffusion system under noisy observations
[NASA-CR-178405] 06 p0767 N88-14714
Sound pressure distribution in front of a serrated boundary: Standing wave suppression and diffusion
07 p0928 N88-15639
Some stability results for the hopscotch difference method when applied to convection-diffusion equations
[CWI-NM-R8711] 08 p1072 N88-16465
Oxygen diffusion in high T/sub c/-superconductors
[DE88-002965] 08 p1090 N88-16562

Oscillations of solar models with internal element diffusion
[DE88-003156] 09 p1264 N88-17573
Ytterbium monolayer diffusion barriers at Hg(1-x)Cd(x)Te/Al junctions
[AD-A188013] 10 p1299 N88-17768
Diffusion studies in amorphous NiZr alloys
[DE88-003009] 10 p1301 N88-17781
A multigrid preconditioner applied to a two-dimensional convection-diffusion problem
[DE88-004765] 10 p1397 N88-18329
High temperature processing of superconducting Y1Ba2Cu3O6.9
[DE88-003002] 10 p1416 N88-18449
Improved magnetization for YBa2Cu3O/sub 7-delta annealed in oxygen above 1000 C
[DE88-003934] 10 p1418 N88-18469
Fundamental studies of corrosion of nonoxide structural ceramics
[PB88-141536] 11 p1461 N88-18709
The intergranular segregation of boron in substoichiometric Ni3Al
[DE88-004783] 11 p1462 N88-18720
Subroutines for solving the equation of diffusion in media with anisotropic properties
[DE88-700743] 11 p1536 N88-19179
Path integration on the upper half-plane
[DE88-751050] 12 p1682 N88-20057
Vertical turbulent transfer of matter in thin ocean surface layer during daytime heating 13 p1787 N88-20693
Thin-film diffusion barriers for metal-semiconductor contacts
[AD-A188712] 13 p1844 N88-21035
Modeling scalar flux and the energy and dissipation equations 16 p2196 N88-23096
Analysis of non-premixed turbulent reacting flows 16 p2196 N88-23100
Research in nonlinear partial differential equations and bifurcation theory
[AD-A190986] 16 p2260 N88-23514
Nonlinear wave and diffusion equations
[AD-A191421] 16 p2265 N88-23544
Microscopic control of semiconductor interface reactivity
[AD-A191193] 16 p2283 N88-23668
Theory of neutron moisture probes and interpretation of measurements in complex soil and water systems 17 p2342 N88-23965
A review of diffusion barrier technology for application in SP-100 fuel pins 17 p2410 N88-24328
Chemical compatibility between silicon carbide and a nickel aluminide
[DE88-006188] 18 p2479 N88-24708
Diffusion of homopolymers into nonequilibrum diblock copolymer structures
[DE88-005306] 18 p2494 N88-24794
Application of computational fluid dynamics to design of compressor cascade 19 p2639 N88-25655
Five-point form of the nodal diffusion method and comparison with finite-difference
[DE88-004141] 19 p2720 N88-26154
Theory of oxygen content, atomic ordering and oxygen diffusion in 1,2,3 superconducting oxides as a function of temperature and oxygen pressure
[DE88-007961] 19 p2735 N88-26248
Abnormal diffusion of vacancies in metals
[DE88-701880] 20 p2773 N88-26441
Comparison theorems and their use in the analysis of some nonlinear diffusion problems
[DE88-010032] 20 p2845 N88-26884
Neoclassical diffusion due to trapping/detrapping orbits in stellarators
[DE88-008566] 20 p2857 N88-26968
Simulation of moisture diffusion of fiber reinforced components of aircraft for general air transportation
[IFL-IB-87-05] 21 p2907 N88-27253
Diffusion and solubility of some interstitial impurities in deformed metals
[DE88-701859] 21 p2914 N88-27296
The diffusion of vorticity from a plane boundary
[AD-A192706] 21 p2942 N88-27474
Diffusion models of crack growth due to random overloads
[DE88-008811] 21 p2962 N88-27595
Large-eddy simulations of concentration fluctuations
[DE88-009480] 21 p2973 N88-27660
Project wind, phase 4 (smoke test), Meadow Brook Valley, Red Bluff, California
[AD-A194742] 22 p3128 N88-28596
On the nucleonics component of cosmic radiation, in the atmosphere
[DE88-702493] 22 p3166 N88-28854
Evaluation of a diffusion/trapping model for hydrogen ingress in high-strength alloys
[AD-A194301] 23 p3194 N88-29008
Transport of organic vapors in multiphase polymer system
[AD-A194097] 23 p3198 N88-29033
Convex duality approach to the optimal control or diffusions
[AD-A194535] 23 p3266 N88-29442
Polynomial definition of discrete field points of map of diffusion equation, part 1
[AD-A193697] 23 p3271 N88-29467
Minimizing escape probabilities: A large deviations approach
[AD-A194534] 23 p3275 N88-29496
Ultrasonic detection of diffusion and adhesion loss 24 p3354 N88-29967
Analytical methods in stochastic control and nonlinear filtering
[AD-A194272] 24 p3426 N88-30388

DIFFUSION BONDING
U DIFFUSION WELDING

DIFFUSION COEFFICIENT
Influence of a magnetic field on the diffusion of small particles in a turbulent flow
[DE87-702877] 01 p0046 N88-10291
Mass transport by diffusion 03 p0297 N88-11864
Optimal correction problem of a multidimensional stochastic system
[AD-A186727] 09 p1228 N88-17353
A finite element analysis of adhesively bonded composite joints including geometric nonlinearity, nonlinear viscoelasticity moisture diffusion and delayed failure
[AD-A187455] 10 p1296 N88-17747
Normed Bellman equation with degenerate diffusion coefficients and its application to differential equations
[AD-A190319] 15 p2120 N88-22637
Development of a model procedure for the determination of volume diffusion lengths by transient measurements on monocrystal silicon solar cells
[ETN-88-92119] 20 p2821 N88-26733

DIFFUSION EFFECT
U DIFFUSION

DIFFUSION ELECTRODES
Advanced materials for solid oxide fuel cells
[DE88-002338] 10 p1350 N88-18071
The kinetics of contact noise in NaBeta alumina
[AD-A190651] 15 p2130 N88-22707

DIFFUSION FLAMES
Combustion in turbulent jets and buoyant flames
[PB87-232674] 03 p0283 N88-11779
Extinguishing diffusion flames with dry powder and halon at low Froude numbers
[PB87-111365] 06 p0679 N88-14159
Mixing and combustion of pulsed gas jets
[PB88-112834] 06 p0680 N88-14169
Mixing and combustion of pulsed gas jets
[PB88-108014] 06 p0680 N88-14170
Carbon monoxide and turbulence-chemistry interactions: Blowoff and extinction of turbulent diffusion flames
[AD-A186276] 07 p0828 N88-15025
Diffusion description of flame propagation due to the translational motion of burning reaction products
[DE88-700676] 10 p1297 N88-17757
Fuels combustion research
[AD-A187688] 11 p1453 N88-18657
Studies on homogeneous and heterogeneous reactive flows 11 p1484 N88-18861
Thermal cracking and variable properties effects on free boundary layer diffusion flames
[NBS/GCR-88/542] 12 p1614 N88-19652
Turbulence and flame propagation
[PB87-228912] 19 p2612 N88-25499
Combustion rate limits of hydrogen plus hydrocarbon fuel: Air diffusion flames from an opposed jet burner technique 19 p2624 N88-25567
Heterogeneous diffusion flame stabilization
[AD-A193014] 20 p2771 N88-26429
The structure and stability of nonpremixed gas jet flames 21 p2908 N88-27257
A study of the interaction of diffusion flames with a vortex pair flowfield 21 p2908 N88-27258
Experimental research of combustion systems 21 p2927 N88-27371
Radiation from soot-containing flames 24 p3347 N88-29927
Flamelet chemistry modelling of soot formation for radiation 24 p3348 N88-29928
The influence of pressure on soot formation 24 p3349 N88-29934
Three-dimensional combustor predictors: A comparison of equilibrium and laminar flamelet chemistry models 24 p3350 N88-29940

DIFFUSION LENGTH
Multigroup flux-limited asymptotic diffusion Fokker-Planck equation
[DE88-700958] 15 p2118 N88-22615

DIFFUSION THEORY
Dynamical friction
[DE88-002194] 06 p0711 N88-14358
Effect of irradiation on the diffusion evolution of void ensemble in crystals
[DE88-700558] 07 p0939 N88-15706
COMESH: A corner mesh finite difference code to solve multigroup diffusion equations in multidimensions
[DE88-701248] 15 p2108 N88-22555
Multigroup flux-limited asymptotic diffusion Fokker-Planck equation
[DE88-700958] 15 p2118 N88-22615

DIFFUSION WELDING
Stress state of welded joints of dissimilar materials obtained by diffusion welding 03 p0286 N88-11799
The mechanical properties of solid state diffusion bonds between Ti-6Al-4V and 304L stainless steel
[BAJ-TR-113-1987] 03 p0332 N88-12093
Diffusion bonding depleted uranium to copper
[RFP-3783-REV] 03 p0333 N88-12098
Investigation on diffusion reaction brazing of aluminium
[PB87-143368] 08 p0992 N88-16001
Development of methods for low temperature diffusion bonding
[AD-A186875] 09 p1174 N88-17033
Diffusion welding of aluminomagnesium alloys to ceramics 14 p1898 N88-21333
Joints in fiber-reinforced aluminum alloys
[NASA-TT-20160] 15 p2031 N88-22104
Interface characterization of Cu-Cu and Cu-Ag-Cu low temperature solid state bonds
[AD-A191015] 16 p2283 N88-23667
An investigation into the metallurgical aspects of joining rapidly-solidified aluminum alloys
[AD-A194677] 23 p3194 N88-29009

DIFFUSIVITY
IR laser excitation in molecules: Chaos and diffusive energy growth
[DE87-013147] 02 p0178 N88-11105
Investigation of structure-permeability relationships of silicone polymer membranes
[PB87-230181] 03 p0293 N88-11839
Mass transport phenomena between bubbles and dissolved gases in liquids under reduced gravity conditions
[NASA-TM-100273] 11 p1455 N88-18672
Modeling of turbulent transport as a volume process 16 p2196 N88-23099
UV-Laser reactions of molecular adsorbates
[AD-A190796] 16 p2212 N88-23201
Calculation of oxidation rates for iron in CO-CO2
[DE88-007313] 18 p2487 N88-24757

DIFLUORIDES
NT CALCIUM FLUORIDES

DIFLUORO COMPOUNDS
NT POLYTETRAFLUOROETHYLENE
NT TEFLON (TRADEMARK)
Corrosion and corrosion inhibition of metals/alloys in methyphosphonic difluoride 17 p2319 N88-23850

DIGESTIVE SYSTEM
NT GASTROINTESTINAL SYSTEM
NT INTESTINES
NT STOMACH

DIGITAL CIRCUITS
U DIGITAL ELECTRONICS
U LOGIC CIRCUITS

DIGITAL COMMAND SYSTEMS
Low cost telemetry and telecommand system for remote measurement of magnitude character
[INPE-4273-PRE/1145] 12 p1598 N88-19564

DIGITAL COMMUNICATION
U PULSE COMMUNICATION

DIGITAL COMPUTERS
NT CDC CYBER 205 COMPUTER
NT HEWLETT-PACKARD COMPUTERS
NT MICROCOMPUTERS
NT MIMD (COMPUTERS)
NT MINICOMPUTERS
NT PARALLEL COMPUTERS
NT PERSONAL COMPUTERS
NT SEQUENTIAL COMPUTERS
NT SIMD (COMPUTERS)
NT VAX COMPUTERS
Reliability modeling of fault-tolerant computer based systems 02 p0127 N88-10801
Technology upgrade of a silicon compiler
[AD-A184873] 05 p0655 N88-14016
Microprocessor emulating the intermediate code for FORTRAN compiler
[DE88-700540] 07 p0900 N88-15452
The formal specification of computer systems
[AD-A188947] 12 p1675 N88-20013
Evaluation of chemical and atmospheric sciences research
[AD-A188468] 12 p1687 N88-20091

Interfacing and integrating hardware and software design systems 17 p2306 N88-23796
Specification for IBM/IBM compatible 3480 tape cartridge
[NASA-TM-100702] 17 p2384 N88-24168
Architecture for optical digital computers
[AD-A195477] 24 p3430 N88-30416

DIGITAL DATA
An acoustic emission digital data acquisition workstation
[DE87-012425] 02 p0191 N88-11191
Directory of geomagnetic observatories with high-resolution digital results, 1987
[PB87-221156] 03 p0348 N88-12201
High frequency data acquisition system for space shuttle main engine testing 05 p0595 N88-13630
Space shuttle main engine vibration data base 05 p0595 N88-13631
Fast, colour displays of digital terrain elevation data
[AD-A185596] 06 p0729 N88-14485
Digital signal processing algorithms for automatic voice recognition 06 p0793 N88-14862
Digital processing of flight test data without using anti-aliasing filters, using a helicopter as an example
[DFVLR-MITT-87-12] 07 p0819 N88-14981
Determination of network attributes from a high resolution terrain data base
[AD-A186078] 07 p0870 N88-15279
Textural features for image classification in remote sensing
[INPE-4169-PRE/1066] 08 p1020 N88-16181
Critical issues in NASA information systems
[NASA-CR-182380] 08 p1093 N88-16577
Information transfer in the National Airspace System 10 p1275 N88-17634
Space shuttle phase B wind tunnel test database
[NASA-CR-4121] 11 p1444 N88-18611
Fixed and adaptive interframe image prediction for remote piloting application
[AD-A187987] 11 p1471 N88-18771
The digital landmass simulation production overview
[AD-A187978] 11 p1503 N88-18978
Digital data dubbing capability
[AD-A188252] 11 p1525 N88-19105
The US Army Electronic Map Data (EMD) initiative
[AD-A188209] 11 p1585 N88-19372
Envelope and phase statistics for non-Gaussian noise and resulting error probabilities for digital communications systems 12 p1617 N88-19672
Digital method for correction of the phase error in the discrete generation of periodic signals in real time
[INPE-4327-RPE/552] 12 p1618 N88-19676
An application of digital cartography updating middle and small scale thematic maps using orbital data
[INPE-4460-TDL/317] 12 p1637 N88-19805
Report on phase 1 of the project estimate development of a model for yield estimation of sugar cane based on LANDSAT and agromet data
[INPE-4466-RPE/560] 12 p1638 N88-19807
Digital Topographic Support System (DTSS)
[AD-A188304] 12 p1638 N88-19808
Terrain classification from digital elevation data using slope and curvature information
[AD-A188940] 12 p1639 N88-19812
Development of a digital terrain modeling system for microcomputers
[INPE-4406-TDL/303] 12 p1639 N88-19816
Some questions of using coding theory and analytical calculation methods on computers
[DE88-700905] 12 p1676 N88-20021
Interpolation algorithms for digital terrain models
[INPE-4373-PRE/1196] 13 p1820 N88-20877
Proposal for a parallel system with image processing applications
[INPE-4293-PRE/1164] 14 p1961 N88-21696
Direct bit detection receiver noise performance analysis for 32-PSK and 64-PSK modulated signals
[AD-A190009] 15 p2056 N88-22256
Calibration and processing of AVHRR data for temperature estimation
[INPE-4493-PRE/1257] 15 p2095 N88-22485
NASA and the challenge of ISDN: The role of satellites in an ISDN world
[NASA-CR-182749] 15 p2126 N88-22676
Textural features for image classification in remote sensing 17 p2354 N88-24027
Thematic mapping utilizing data from the Thematic Mapper sensor of the LANDSAT satellite 17 p2361 N88-24060
Geometric image correction: An approach for the registration of LANDSAT-TM digital images supported by topographical maps of medium and great scales 17 p2361 N88-24061
Visualization of digital terrain models 17 p2364 N88-24081
Application of its transformation in color enhancement of LANDSAT imagery 17 p2365 N88-24082
Preliminary study on the application of digital processing of TM-LANDSAT data in the mapping of apple orchards in Fraiburgo (SC) 17 p2367 N88-24093
Reports on cartography and geodesy. Series 1, no. 99
[ETN-88-92387] 18 p2533 N88-25025
Digital maps for an electronic traffic guide 18 p2534 N88-25033
Development in data structures in PHOCUS for digital mapping 18 p2534 N88-25034
Space shuttle phase B wind tunnel model and test information. Volume 2: Orbiter configuration
[NASA-CR-178415-VOL-2-PT-2] 21 p2893 N88-27172
Optical interconnections for digital image coding 21 p2928 N88-27381
Analysis of remotely sensed imagery using digital morphology
[AD-A192738] 21 p2965 N88-27614
Relief effect correction on LANDSAT imagery for forest applications using digital terrain models
[INPE-4611-PRE/1334] 24 p3388 N88-30179
Method for combined image interpolation-restoration through a fir filter design technique
[INPE-4561-PRE/1302] 24 p3413 N88-30315
An operations manual for the digital data system
[NASA-CR-181688] 24 p3415 N88-30329

DIGITAL ELECTRONICS
NT LOGIC CIRCUITS
Establishment of complete minimum test sets for digital circuits with safety engineering significance
[ETN-88-90599] 05 p0578 N88-13526
Avionics systems integration technology 09 p1110 N88-16654
Describing constraints on a digital circuit's behavior
[AD-A189200] 13 p1761 N88-20531
Analytical sensor redundancy assessment
[NASA-CR-182892] 16 p2163 N88-22901

DIGITAL FILTERS
NT FIR FILTERS
Ultra-low power digital filter
[AD-A184485] 03 p0310 N88-11959
Integrated circuit design
[AD-A184486] 03 p0311 N88-11960
A digital low pass filter for the reduction of large quantities of data
[ESA-TT-1058] 03 p0363 N88-12281
Design of digital filters for electronic instrumentation
[PB87-100418] 04 p0438 N88-12716
Implementation of an FIR band pass filter using a bit-slice processor
[AD-A184895] 05 p0634 N88-13875
Digital processing of flight test data without using anti-aliasing filters, using a helicopter as an example
[DFVLR-MITT-87-12] 07 p0819 N88-14981
Description, analysis and simulation of a new realization of digital filters
[AD-A187763] 11 p1477 N88-18814
Computation of LMS (Least-Mean-Square) and matched digital filters for optical clutter suppression
[AD-A188885] 12 p1687 N88-20093
Intergrated circuit design, phase 2
[AD-A189060] 13 p1760 N88-20530
Utilization of space color transformation, linear contrast and filtration for enhancement of colored digital images
[INPE-4310-PRE/1176] 14 p1983 N88-21831
Digital processing of flight data of a helicopter without using anti-aliasing filters
[ESA-TT-1094] 16 p2161 N88-22890
Digital filter unit for selection of spectrometric information
[DE87-702990] 16 p2246 N88-23415
Modeling, filtering and control of stochastic processes --- communication networks
[ENST-87E021] 17 p2333 N88-23925
Spatial filtering on digital images 17 p2354 N88-24025
A numerically efficient digital matched filter for periodic and windowed periodic radar waveforms
[AD-A193132] 21 p2932 N88-27410
A method of improving remote reproduction of a sound field by one-third-octave analysis and digital filtering
[RAE-TM-FS(F)-679] 22 p3147 N88-28722
Computer aided filter design
[AD-A193959] 23 p3208 N88-29093
Digital filter design techniques
[AD-A194484] 23 p3274 N88-29486

DIGITAL NAVIGATION
Digital fiber optic displacement sensors 18 p2518 N88-24937
Accuracy of satellite data navigation
[AD-A195877] 24 p3322 N88-29787

DIGITAL RADAR SYSTEMS
The Newcastle meteor radar 06 p0741 N88-14556
Moving Target Indicator (MTI) interface for simple radar
[FOA-C-30463-3.2] 09 p1154 N88-16914

DIGITAL SIMULATION
The importance sampling and its application to radar simulation 01 p0012 N88-10085
Model adaptation and imbalance compensation in rotors with active magnetic bearings
[ETN-87-90440] 01 p0056 N88-10361
Monte Carlo calculations for the simulation of channeling experiments on irradiated aluminum alloys. Calculation of angle-dependent efficiency curves
[HMI-B-433] 01 p0092 N88-10597
Numerical simulation of unsteady separated flows
[AD-A184132] 04 p0442 N88-12741
Computer modeling aids studies of precipitation formation 04 p0458 N88-12832
Numerical simulation of the Reversed Field Pinch
[AD-A184353] 04 p0491 N88-13023
Numerical simulation of the hypersonic flow around lifting vehicles 05 p0532 N88-13234
The polar ionosphere and interplanetary field
[AD-A185386] 05 p0624 N88-13822
An extension to the multilevel logic simulator for microcomputers
[AD-A185032] 05 p0634 N88-13879
Analysis, design, construction and testing of a reaction wheel model for space applications
[INPE-4358-TDL/299] 08 p0963 N88-15834
Simulation of a typical flow in a broad valley 08 p1015 N88-16154
Simulation of a lee cyclogenesis using a numerical model 08 p1016 N88-16162
Numerical simulation of the flow about New Zealand 08 p1017 N88-16163
Numerical modeling of radiation fog 08 p1017 N88-16166
Inversion of simulated satellite signals 08 p1017 N88-16168
Numerical simulation of the interaction of pressure waves with laminar and turbulent boundary layers
[DFVLR-FB-87-18] 09 p1161 N88-16960
Numerical simulation of thermally generated mountain-foreland circulation
[DFVLR-FB-87-30] 09 p1190 N88-17132
Simulations of thermally induced winds and cross flow situations
[MITT-57] 09 p1193 N88-17148
Coronal heating by means of helical magnetohydrodynamic turbulence
[AD-A187084] 10 p1410 N88-18413
A digital logic simulator with concurrent programming considerations
[AD-A188823] 12 p1678 N88-20032
Simulation of electron cyclotron heating in TFR 12 p1693 N88-20130
Modelling of a hydraulic motor and servo-valve to produce a desired system response using analogue and digital compensation techniques
[ETN-88-92079] 14 p1899 N88-21337
Numerical simulation of medium scale disturbance on meiyu front 14 p1900 N88-21346
Investigation of the behavior of fast propagating cracks using numerical simulation calculations
[W-6/87] 14 p1934 N88-21532
Numerical treatment of Navier-Stokes equations
[REPT-87-22] 16 p2206 N88-23162
Simulation and computer aided engineering (the necessity of an integrated approach)
[NLR-MP-86050-U] 17 p2386 N88-24178
CFD benefits, goals, stepping-stones and techniques. Proposals for the scientific programme of the European Reserch Centre on flow, turbulence and combustion --- computational fluid dynamics
[CFDU/88/1] 18 p2510 N88-24894
Direct numerical simulations of the PDF's (Probability Density Functions) of a passive scalar in a forced mixing layer
[AD-A192134] 18 p2568 N88-25256
Direct simulations of chemically reacting turbulent mixing layers, part 2
[NASA-CR-180853] 19 p2667 N88-25857
Noise and chaos in driven Josephson junctions 19 p2734 N88-26238
A high fidelity real-time simulation of a small turboshaft engine
[NASA-TM-100991] 20 p2761 N88-26378
A simulation analysis of errors in the measurement of standard electrochemical rate constants from phase-selective impedance data
[AD-A192739] 20 p2770 N88-26426
The influence of uncompensated solution resistance on the determination and standard electrochemical rate constants using cyclic voltammetry and some comparisons with AC voltammetry
[AD-A192825] 20 p2770 N88-26427

Simulation models for the dynamics of tracked vehicle systems: State-of-the-art and open problems
20 p2785 N88-26522
Parameter identification of the passenger simulation model MADYMO: Methods and experience
20 p2788 N88-26536
Robust digital model following controller for helicopters
[DFVLR-FB-88-07] 21 p2898 N88-27203
Simulation of attitude and maneuvers for the Brazilian spin-stabilized satellite
[INPE-4271-PRE/1143] 22 p3046 N88-28079
Digital terrain modelling with SPOT data and geological applications 22 p3110 N88-28474
Automatic production of orthophoto using SPOT images 22 p3112 N88-28487
Automatic creation of digital terrain models from SPOT image pairs 22 p3113 N88-28490
A method for determining absolute velocities from hydrographic data: The numerical code
[AD-A193997] 22 p3129 N88-28603
Description of a tool for the simulation of imagery systems 22 p3147 N88-28724
Acoustic-seismic helicopter detection
22 p3149 N88-28734
Crash simulation calculations and component idealization for an airframe. Computer code KRASH 79
[ETN-88-92971] 23 p3174 N88-28899
Coupling expert systems and simulation
23 p3252 N88-29360
Modeling of a cometary dust coma
[ETN-88-92980] 23 p3300 N88-29651
Numerical simulation of unsteady incompressible flow in a partially-filled rotating cylinder
[AD-A196001] 24 p3371 N88-30073
Numerical simulation of the interaction of pressure waves with laminar and turbulent boundary layers
[ESA-TT-1089] 24 p3371 N88-30075
Numerical simulation of unsteady incompressible viscous flows in generalized coordinate systems
[NASA-TM-101016] 24 p3373 N88-30085
A digital simulation technique for the Dryden atmospheric model
[NASA-TT-20342] 24 p3404 N88-30266

DIGITAL SYSTEMS

NT DIGITAL NAVIGATION
NT DIGITAL RADAR SYSTEMS
Digital system bus integrity
[NASA-CR-181446] 01 p0006 N88-10030
ELF/VLF/LF propagation and system design
[AD-A183261] 01 p0033 N88-10212
A compact digital communications system. Part 3: Generalising the phase locked loop
[RSRE-MEMO-4027-PT-3] 01 p0035 N88-10222
Implementation of a digital optical matrix-vector multiplier using a holographic look-up table and residue arithmetic
[NASA-CR-180431] 01 p0078 N88-10496
Reliability modeling of fault-tolerant computer based systems 02 p0127 N88-10801
A digital control system for high level acoustic noise generation 02 p0138 N88-10865
A digital audio link to the Channel Islands in the UHF television band: Preliminary experimental results
[BBC-RD-1987/9] 02 p0161 N88-11011
A review of computer-assisted photo interpretation research at USAETL (US Army Engineer Topographic Laboratories)
[AD-A184034] 03 p0346 N88-12186
SBNR (Signed Binary Number Representations) digital signal processor architecture
[AD-A184603] 03 p0364 N88-12290
Microcomputer control of a hydraulically actuated piston
[AD-A184130] 03 p0368 N88-12317
Digital-flight-control-system software written in automated-engineering-design language: A user's guide of verification and validation tools
[NASA-TM-88313] 04 p0401 N88-12494
Diagnostic reasoning in digital systems
[NASA-CR-181564] 05 p0633 N88-13871
Error propagation in a digital avionic mini processor
[NASA-CR-181565] 05 p0633 N88-13872
Two digital X-ray imaging systems for applications in X-ray diffraction
[PB87-123683] 06 p0669 N88-14103
An analysis of simplified feed architectures for MMIC (Monolithic Microwave Integrated Circuit) T/R (Transmit/Receive) module arrays
[AD-A185474] 06 p0697 N88-14275
Diagnostic emulation: Implementation and user's guide
[NASA-CR-178391] 06 p0756 N88-14638
Estimating the distribution of fault latency in a digital processor
[NASA-TM-100521] 06 p0760 N88-14666
A Multipurpose Adaptive Controller (MAC) for real time digital regulation
[REPT-87-028] 06 p0762 N88-14673
Online monitoring of laserpulses using the GPIB-interface of a Tektronix 2430 Digital Storage Oscilloscope
[DE88-002836] 07 p0856 N88-15201
Proceedings of Image Understanding Workshop, volume 1
[AD-A186103] 07 p0902 N88-15463
Advanced gyros in spacecraft control. Digital capture loops for dry tuned gyros
[LITEF-120046] 08 p0962 N88-15827
Digital control of high frequency pulse-width modulated inverters
[ETN-87-90711] 09 p1157 N88-16936
Spectral density estimates of coarsely quantized random vibration data 09 p1178 N88-17055
Regulation of nonlinear and generalized linear systems
[AD-A186706] 09 p1224 N88-17338
Transport delay compensation for computer-generated imagery systems
[NASA-TM-100084] 10 p1277 N88-17645
Formal multilevel hierarchical verification of synchronous MOS VLSI circuits
[AD-A187532] 10 p1324 N88-17918
Orthogonal patterns in binary neural networks
[NASA-TM-100060] 10 p1396 N88-18320
Subpicosecond optical digital computation using phase conjugate parametric generators
[AD-A188279] 10 p1410 N88-18411
Further developments in exact state reconstruction in deterministic digital control systems
[NASA-TP-2812] 11 p1468 N88-18751
Terrain Analyst Work Station (TAWS) demonstrations
[AD-A188139] 11 p1504 N88-18981
The Quick Response Multicolor Printer (QRMP) system
[AD-A188140] 11 p1504 N88-18982
Digital data dubbing capability
[AD-A188252] 11 p1525 N88-19105
Autonomous Liquid Encapsulated Czochralski (LEC) growth of single crystal GaAs by intelligent digital control
[AD-A187211] 11 p1555 N88-19305
Digital bit error rate estimator for telemetry links
[INPE-4351-TDL/295] 12 p1598 N88-19563
Radio and radar holes and multipath zones: The global and local influences on atmospheric refractive structure and resulting adverse radio and radar performance
12 p1617 N88-19667
Space-diversity effects on line-of-sight propagation paths 12 p1617 N88-19670
The 6 GHz propagation measurements over a 51 km path in the UK 12 p1617 N88-19673
Evaluating the performance of the LPC (Linear Predictive Coding) 2.4 kbps (kilobits per second) processor with bit errors using a sentence verification task
[AD-A188573] 12 p1620 N88-19686
A methodology for hardware verification based on logic simulation
[AD-A188553] 12 p1622 N88-19704
A digital circuit design environment
[AD-A188831] 12 p1623 N88-19709
VLSI implementations for digital signal processing
[AD-A189612] 12 p1624 N88-19719
Soft maps for US Army electronic map background applications
[AD-A188427] 12 p1638 N88-19809
Architecture specification for PAVE PILLAR avionics
[AD-A188722] 13 p1723 N88-20303
Operational viewpoint of the X-29A digital flight control system
[NASA-TM-100434] 14 p1866 N88-21152
Digital correlator for the portable channel prober measurement instrument
[AD-A189065] 14 p1904 N88-21377
DataViews: A personalizable, interactive, data display system for the decisionmaker
[AD-A188509] 14 p1991 N88-21868
Preliminary airworthiness evaluation of the UH-60A with Advanced Digital Optical Control System (ADOCS)
[AD-A190674] 15 p2018 N88-22030
Subharmonic aliasing and its effects on the AFTI/F-16 digital flight control system
[AD-A190614] 15 p2020 N88-22042
A fully abstract semantics for event-based simulation
[AD-A190560] 15 p2060 N88-22283
Exhaustive and pseudo-exhaustive testing
[AD-A190140] 15 p2111 N88-22574
Design and implementation of VLSI prime factor algorithm processor
[AD-A190483] 15 p2112 N88-22580
Representation, analysis and design of multirate discrete-time control systems
[AD-A190499] 15 p2116 N88-22608
Two papers on a symbolic analyzer for MOS (Metal-Oxide Semiconductors) circuits
[AD-A188617] 15 p2139 N88-22761
Sources of digital spatial data for geographic information systems
[AD-A189788] 15 p2148 N88-22824
Computer tomography and hybrid optical/digital methods for aerodynamic measurements
[AD-A190909] 16 p2157 N88-22872
Automated test device for FASR (Fixed Array Surveillance Radar) beam steering componentry
[AD-A191650] 18 p2500 N88-24829
Some unsolved problems in modelling self-timed circuits using Petri Nets, series B, number 2
[PB88-181466] 18 p2507 N88-24872
Digital television routing systems: A survey of optical and electrical techniques
[BBC-RD-1988/3] 19 p2654 N88-25763
Digital control of the czochralski growth of gallium arsenide. System reference manual. Valid for Czochralski growth controller software version 2.4
[AD-A191997] 19 p2732 N88-26227
Digital communication transmitter and receiver test procedures
[AD-A191218] 20 p2788 N88-26540
COSPAS/SARSAT 406-MHz emergency beacon digital controller
[NASA-TM-100859] 20 p2792 N88-26566
Development of a hybrid simulator for robotic manipulators
[AD-A193119] 21 p2956 N88-27557
More on exact state reconstruction in deterministic digital control systems
[NASA-TP-2847] 22 p3063 N88-28177
Use of a coherent square wave reference to demodulate BPSK (Binary Phase Shift Keying) carriers and a visual indicator of the quality of received QPSK (Quadrature Phase Shift Keying) carriers
[AD-A193528] 23 p3204 N88-29065
Distortions in processed signals and their application in electronic design. Part 1: Basic and general formulations
[DE88-702731] 23 p3204 N88-29070
Digital phase-lock loop having an estimator and predictor of error
[NASA-CASE-NPO-17196-1-CU] 23 p3205 N88-29076
Ionospheric convection and structure using ground-based digital ionosondes
[AD-A194246] 23 p3233 N88-29237
Object discrimination via bulk temperature/velocity filtering, phase 1
[AD-A194533] 23 p3274 N88-29487
N-version software demonstration for digital flight controls
[NASA-CR-181483] 24 p3328 N88-29815
Performance of DS/SSMA communications in impulsive channels. Part 1: Correlation receivers
[AD-A195712] 24 p3362 N88-30021
Estimation of short-wavelength gravity on a dense grid using digital terrain elevation data
[AD-A196325] 24 p3391 N88-30196
Binary star measurements using digital speckle interferometer of 6-m telescope
24 p3448 N88-30521

DIGITAL TECHNIQUES

Digital receiver structures and methods for the determination of the scanning frequency in modems for fast data transmission via telephone channels
[ETN-87-90429] 01 p0037 N88-10235
A digital audio link to the Channel Islands in the UHF television band: Protection of television signals from digitally modulated interference
[BBC-RD-1987/7] 02 p0161 N88-11010
Development of standard cells in NMOS technology for the design of digital integrated circuits
[FI-62-TB-6] 03 p0310 N88-11953
Input/output technologies: An overview of image scanning, storage, and display
[DE87-014837] 04 p0476 N88-12933
Measured characteristics of 800/900 MHz mobile radio channels with high-angle propagation through moderately dense foliage
[CRC-1398] 05 p0573 N88-13493
Modem for digital phase modulation: Results and summary
[PB87-149233] 07 p0845 N88-15129
Evaluation of the flooding areas of the Sao Goncalo Canal through LANDSAT 5 thematic mapper images
[INPE-4118-PRE/1039] 08 p1020 N88-16185
Digital image processing: A summary of main techniques
[INPE-4404-PRE/1220] 08 p1068 N88-16454
Digital image processing
[INPE-4131-TDL/264] 08 p1083 N88-16527

Techniques of flow visualization
[AGARD-AG-302] 09 p1164 N88-16977
Digital imaging techniques for single- and multi-phase reacting flowfields 10 p1327 N88-17933
A microspectrofluorometer system based on real time digital techniques
[REPT-86-014] 11 p1490 N88-18891
Reaction wheel control through digital technique using reference models
[INPE-4220-PRE/1100] 12 p1599 N88-19570
Digital enhancement of flow field images
[NASA-TP-2770] 13 p1813 N88-20833
On-board processing for mobile satellite communications
[ESA-CR(P)-2519] 14 p1905 N88-21382
Classification of small image areas by digital correlation for the connection of different images in photogrammetry and long-range reconnaissance
[ETN-88-91506] 14 p1940 N88-21578
Comparative utilization of analog and digital processes in the treatment of MSS-LANDSAT data for studying the national parks of Brazil
[INPE-4011-TDL/240] 15 p2090 N88-22456
Development of a digital sun sensor for a spin-stabilized satellite
[INPE-4508-TDL/327] 16 p2169 N88-22929
Computer assisted generalization of buildings for digital landscape models by classification methods
16 p2226 N88-23294
Digital avionics design and reliability analyzer
[NASA-CR-181641] 16 p2254 N88-23472
Visual enhancement of digital color imagery utilizing transformation in color coordinates (IHS transformation)
[INPE-4482-PRE/1248] 16 p2273 N88-23606
Method of digital surface photometry of galaxies and its application to the edge-on galaxy NGC 5907
16 p2287 N88-23695
Clinical applications of computerized thermography
17 p2330 N88-23915
Digital processing of infrared and visible images from the GOES satellite and its integration with meteorological radar data 17 p2360 N88-24057
Temporal analysis of the changes in Parque Estadual de Jacupiranga vegetation through digital treatment of LANDSAT imagery 17 p2367 N88-24094
Evaluation of TM false color composites for crop discrimination 17 p2367 N88-24096
A digitally implemented phase-locked loop detection scheme for analysis of the phase and power stability of a calibration tone 22 p3066 N88-28196
Avionics system design for high energy fields: A guide for the designer and airworthiness specialist
[NASA-CR-181590] 23 p3178 N88-28919
Nanosequencer digital logic controller
[NASA-CASE-NPO-16116-2] 23 p3245 N88-29310
Evaluation of LANDSAT-TM data for geomorphological mapping
[INPE-4593-PRE/1324] 24 p3386 N88-30168
Use of digital images as a mineral prospecting tool in the tin province of Goias, Brazil
[INPE-4537-PRE/1284] 24 p3387 N88-30173
LANDSAT-TM data to map flooded areas
[INPE-4594-PRE/1324] 24 p3387 N88-30177

DIGITAL TELEVISION
Accommodating the residue of processed or computed digital video signals within the 8 bit CCIR recommendation 601
[BBC-RD-1987/12] 04 p0432 N88-12676
Digital video bit-rate reduction: DPCM for sub-Nyquist PAL
[BBC-RD-1987/16] 05 p0573 N88-13494
Television motion measurement for DATV and other applications
[BBC-RD-1987/11] 05 p0573 N88-13496
Limiting of YUV digital video signals
[BBC-RD-1987/22] 09 p1155 N88-16924

DIGITAL TO ANALOG CONVERTERS
Digital to analog and analog to digital conversion using pulse duration modulation
[ETN-87-90415] 01 p0078 N88-10499
Life sciences flight experiments microcomputer
06 p0792 N88-14857
Description, analysis and simulation of a new realization of digital filters
[AD-A187763] 11 p1477 N88-18814

DIGITAL TRANSDUCERS
Vital signs rate meter
[AD-A187015] 09 p1198 N88-17183
Photo-optical converter of angular displacements in digital servomechanisms
[DE87-703208] 14 p1961 N88-21698

DIGITIZERS
U ANALOG TO DIGITAL CONVERTERS

DIGITS
NT BINARY DIGITS
Experiments in isolated digit recognition using the multilayer perceptron
[RSRE-MEMO-4073] 17 p2333 N88-23927

DIHEDRAL ANGLE
Scattering patterns of dihedral corner reflectors with impedance surface impedances
[NASA-CR-183078] 20 p2789 N88-26545

DIHEDRAL EFFECT
U LATERAL STABILITY

DIKES (GEOLOGY)
U ROCK INTRUSIONS

DILATATION
U STRETCHING

DILATOMETERS
U EXTENSOMETERS

DILUTION
NT GEOMETRIC DILUTION OF PRECISION
Dilution jet mixing program, phase 3
02 p0185 N88-11153
Influence of bond dilution on the free surface and interface Potts ferromagnetism
[DE87-703360] 04 p0497 N88-13061
A numerical study of the effects of curvature and convergence on dilution jet mixing
[NASA-TM-89878] 05 p0549 N88-13347
An empirical model of the effects of curvature and convergence on dilution jet mixing
[NASA-TM-100896] 18 p2466 N88-24640
DARPA-URI consortium meetings on submicron heterostructures of diluted magnetic semiconductors
[AD-A193499] 23 p3206 N88-29081

DIMENSIONAL ANALYSIS
Dimensional analysis of nonlinear oscillations in brain, heart and muscle
[DE87-014749] 06 p0751 N88-14614
Display and processing of multidimensional signals with the aid of fractal image sequences
[ETN-88-92131] 20 p2806 N88-26642

DIMENSIONAL MEASUREMENT
The determination of exhaust cloud dimensions from films of space shuttle launches
[NASA-CR-4103] 06 p0732 N88-14500
Development and calibration of Direct Current Potential Difference (DCPD) crack length measurement equipment
[VTT-RR-480] 09 p1182 N88-17083
Effect of fiber diameter on the reliability of composites - automated laser diffraction implementation
[AD-A193524] 23 p3188 N88-28972

DIMENSIONAL STABILITY
NT SHELL STABILITY
NT STRUCTURAL STABILITY
Carbon-fiber reinforced plastics
04 p0403 N88-12506
New equilibrium forms of free surface of confined magnetic fluid 06 p0770 N88-14734
Cost 501 Project UK10 part 3: Thermal fatigue damage of Fecralloy steel-sprayed and co-extruded tubing
[AERE-R-12230] 10 p1343 N88-18026
Contribution to the study of materials behavior in space environment
[SNIAS-881-430-104] 23 p3189 N88-28977

DIMENSIONLESS NUMBERS
NT FROUDE NUMBER
NT HIGH REYNOLDS NUMBER
NT LOW REYNOLDS NUMBER
NT MACH NUMBER
NT NUSSELT NUMBER
NT PECLET NUMBER
NT PRANDTL NUMBER
NT RAYLEIGH NUMBER
NT REYNOLDS NUMBER
NT RICHARDSON NUMBER
Can we calculate the fundamental dimensionless constants of physics
[DE88-702641] 23 p3295 N88-29625

DIMENSIONS
NT DEPTH
NT DIAMETERS
NT DIFFUSION LENGTH
NT FILM THICKNESS
NT FRACTALS
NT HEIGHT
NT LENGTH
NT RADII
NT SCALE HEIGHT
NT TARGET THICKNESS
Multidimensional modeling of convective heat transfer with application to IC engines
[DE87-011046] 01 p0055 N88-10353
EVA reference manual
[DE87-014073] 01 p0082 N88-10526
An interactive optimization procedure for the computer aided dimensioning of integrated circuits
[ETN-87-90414] 01 p0082 N88-10531
Two dimensional imaging observations of meter-decameter bursts associated with the February 1986 flare activity 01 p0113 N88-10723
Theory of the one- and two-dimensional electron gas
[DE87-012864] 02 p0244 N88-11540
A two-dimensional finite difference program for thermal analysis of rocket thrust chambers
[NASA-TM-100191] 04 p0409 N88-12539
INS3D: An incompressible Navier-Stokes code in generalized three-dimensional coordinates
[NASA-TM-100012] 04 p0485 N88-12991
BASIC desk-top computer program for the three-dimensional static configuration of an extensible flexible cable in a uniform stream
[AD-A184852] 05 p0609 N88-13737
Evolution of mean square magnetic vector potential in compressible, two-dimensional, magnetofluid turbulence
[AD-A184985] 05 p0651 N88-13990
Comparison of 2D memory SEU transport simulation with experiments
[ATR-86(8139)-2-REV-A] 05 p0656 N88-14025
The inverse back scattering problem for the Schroedinger equation in two space dimensions
[AD-A185603] 06 p0765 N88-14701
A new method of boundary parameter estimation for a two-dimensional diffusion system under noisy observations
[NASA-CR-178405] 06 p0767 N88-14714
An inexpensive real-time interactive three dimensional flight simulation system
[AD-A184868] 07 p0821 N88-14989
The KIVA-2 computer program for transient multidimensional chemically reactive flows with sprays
[DE88-000502] 07 p0854 N88-15191
Three dimensional display of meteorological scientific data
[DE88-000776] 07 p0880 N88-15339
Dimensions of ignition zones in blow-outs of combustible gases from rectangular and circular ports
07 p0918 N88-15577
Adaptive finite element methods for parabolic systems in one- and two-space dimensions
[AD-A186534] 08 p1073 N88-16475
Zero-dimensional model of a reversed field pinch fusion reactor
[DE88-005213] 10 p1414 N88-18442
GERA computer code for calculation of two-dimensional electromagnetic fields in resonators and electron-optical systems by the finite element method
[DE88-700678] 11 p1480 N88-18831
Applications of lower cost computers to dimensional gaging
[BDX-613-3606] 11 p1525 N88-19108
Motion in a random gyrotropic environment in D dimensions
[PB87-170650] 12 p1685 N88-20079
Strings in four dimensions
[DE88-006435] 14 p1990 N88-21864
Finite dimensionality in the complex Ginzburg-Landau equation
[DE88-006480] 16 p2263 N88-23534
The two-dimensional one component plasma in a doubly periodic background: Exact results
[AD-A191260] 16 p2280 N88-23650
Three-dimensional models of conventional and vertical junction laser-photovoltaic energy converters
[NASA-TM-4039] 17 p2370 N88-24111
Solving time-dependent two-dimensional eddy current problems
[NASA-TM-100875] 18 p2566 N88-25239
Computer modeling of time dependent SBS (Stimulated Brillouin Scattering) in two and three dimensions
[DE88-008922] 19 p2720 N88-26150
The MAFIA approach to solving Maxwell's equations in three dimensions
[DE88-007826] 19 p2720 N88-26155
Analysis of gas turbine test cell number 1, Lemoore Naval Air Station, California
[AD-A192870] 20 p2762 N88-26380
Vertical viewing ECE diagnostic for the D3-D tokamak
[DE88-010586] 20 p2860 N88-26987
Global gauge anomaly of classical groups in even dimension
[DE88-008572] 22 p3158 N88-28797
Comparison of 2-D Fourier and spatial techniques for removing noise in real-time X-ray radiography
[AD-A193700] 23 p3187 N88-28962
Bifurcations of periodic solutions of non-integrable Hamiltonians with two degrees of freedom: Numerical and analytical results
[DE88-702747] 23 p3272 N88-29473
Cosmology in an N-dimensional vector space
[DE88-702550] 23 p3277 N88-29507

Robust finite-dimensional LQG (Linear Quadric Gaussian)-based controllers for a class of distributed parameter systems
[AD-A194872] 24 p3425 N88-30362

DIMERIZATION
Synthesis and characterization of 1,2-cyclobutenedicarboxamides: Thermally generated polymers and Diels-Alder adducts
[AD-A188591] 12 p1611 N88-19633

DIMERS
Van der Waals clusters of aromatic molecules studied using supersonic molecular jet spectroscopy
[AD-A186087] 07 p0929 N88-15644
Energy-related atomic and molecular structure and scattering studies
[DE88-004246] 10 p1406 N88-18386
Chemical activation of molecules by metals: Experimental studies of electron distributions and bonding
[DE88-004465] 10 p1407 N88-18393
Comparison of low temperature photoluminescence of bulk MBE (Molecular Beam Epitaxy) grown AlGaAs and GaAs using a graphite generated dimer versus a standard tetramer arsenic group-V source
[DE88-004939] 11 p1558 N88-19329
Scanning tunneling microscopy of silver, gold, and aluminium monomers and small clusters on graphite
[DE88-003871] 11 p1562 N88-19349
Electrochemistry in near-critical and supercritical fluids. 5: The dimerization of quinoline and acridine radical anions and dianions in ammonia from -70 C to 150 C
[AD-A190858] 16 p2175 N88-22967

DIMINUTION
U REDUCTION

DINING PHILOSOPHERS PROBLEM
A nonmythical generalization of Dekker's algorithm and its ramifications --- mutually exclusive processes
[CS-8702] 01 p0080 N88-10513

DIODES
NT AVALANCHE DIODES
NT CRYSTAL RECTIFIERS
NT GERMANIUM DIODES
NT GUNN DIODES
NT JUNCTION DIODES
NT LIGHT EMITTING DIODES
NT MIM DIODES
NT PHOTODIODES
NT PLASMA DIODES
NT SCHOTTKY DIODES
NT SEMICONDUCTOR DIODES
NT THERMIONIC DIODES
NT TUNNEL DIODES
Diode pumped solid-state laser oscillators for spectroscopic applications
[NASA-CR-180576] 01 p0052 N88-10331
High energy efficient solid state laser sources
[NASA-CR-181362] 01 p0052 N88-10332
Generating soft X-ray spectra using the SPEED pentaxial diode
[DE87-013591] 01 p0098 N88-10647
Trajectory versus PIC methods in diode design
[DE87-012135] 02 p0166 N88-11043
Quantum well laser diodes: Modeling and realization of GaAs/GaAlAs
[LAAS-87-165] 02 p0179 N88-11116
Ultrafast photoconductor detector-laser-diode transmitter
[DE87-013803] 03 p0329 N88-12082
Fast autotuning of a hydrogen maser by cavity Q modulation 04 p0436 N88-12707
The Pierce diode with an external circuit. Part 1: Simulations in the linear regime
[DE88-000413] 04 p0440 N88-12731
Computer calculations of PIN diode limiter characteristics
[AD-A185563] 06 p0697 N88-14277
Evaluation of a satellite laser ranging technique using pseudonoise code modulated laser diodes
[NASA-CR-182347] 06 p0708 N88-14343
Magnetically insulated ion diode with a gas-breakdown plasma anode
[INPE-4382-PRE/1202] 08 p1085 N88-16537
Radiant power degradation of silicon-doped gallium arsenide and gallium aluminum arsenide infrared light-emitting diodes
[AD-A186726] 09 p1157 N88-16935
Solid state research
[AD-A185987] 09 p1253 N88-17508
Evaluation of a temperature remote sensing technique
[AD-A187885] 10 p1347 N88-18053
The Pierce diode with an external circuit. 2: Non-uniform equilibria
[AD-A188027] 11 p1478 N88-18818
Diode pumped fiber laser
[AD-A187694] 11 p1491 N88-18902
The qualitative determination of high injection effects in flux-loaded P-I-N diodes using the recombination radiation measuring method
[ETN-88-91475] 11 p1560 N88-19336
Study of the vibrational modes of subsurface oxygen on Al (111) using diode laser infrared reflection-absorption spectroscopy
[AD-A188322] 12 p1632 N88-19769
High power, high efficiency, 2D laser diode arrays for pumping solid state lasers
[DE88-004042] 13 p1777 N88-20632
Surface-emitting two-dimensional laser diode arrays constructed on zig-zag heat sink surface
[DE88-005215] 14 p1915 N88-21439
Development of Electromagnetic PIC code for LIB diode 16 p2276 N88-23622
Two-dimensional focusing of self-magnetically insulated plasma focus diode 16 p2278 N88-23639
Research on anode plasma behavior of flashover pulsed ion sources 16 p2279 N88-23640
Study on the flashover ion diode with cryogenic anode 16 p2279 N88-23642
High pressure operation of beam diodes for generating relativistic electron beams 16 p2279 N88-23643
MSAT-X electronically steered phased array antenna system 19 p2647 N88-25712
Energy variations in optical pulses from gain-switched AlGaAs diode lasers 19 p2658 N88-25796
Microwave and millimeter-wave resonant tunneling diodes 19 p2659 N88-25809
Quantum transport calculation of resonant-tunneling response time 19 p2659 N88-25810
Silicon pulse sharpening diodes-switching kilovolts in 10's of picoseconds 19 p2661 N88-25824
Electrical study of metal/group 3-5 semiconductor interfaces: Comparison with the atomic-level studies 20 p2874 N88-27059
Silicon-on-insulator pin diodes
[AD-A193359] 21 p2937 N88-27445
Techniques and instrumentation for transient characterization of metal-insulator-semiconductor diodes. Applications to metal-insulator InP system
[ECL-87-17] 21 p3025 N88-27959
The 1985-86 measurements with the tunable diode laser absorption spectrometer
[PB88-214002] 23 p3231 N88-29226
On 3-5 heterojunction structures and high speed devices
[AD-A195464] 24 p3433 N88-30438

DIOXIDES
NT CARBON DIOXIDE
NT HYDROGEN PEROXIDE
NT QUARTZ
NT SILICON DIOXIDE
NT SULFUR DIOXIDES
Hydrogen retention and release from uranium dioxide
[DE88-002042] 07 p0829 N88-15030
A dense and strong ceramic material made from zirconium dioxide 14 p1886 N88-21274
Low temperature film growth of the oxides of zinc, aluminum and vanadium (and related systems, oxides of gold and germanium, nitrides of aluminum and tungsten) by reactive sputter deposition
[AD-A193497] 23 p3191 N88-28986

DIPHOSPHATES
Use of diphosphonates to correct disorders in calcium metabolism and mineral composition of bone tissue with 60-day hypokinesia in rats
[NASA-TT-20220] 13 p1809 N88-20807

DIPLEXERS
A polarization diversity meteorological radar system
[AD-A189291] 13 p1758 N88-20515

DIPOLE ANTENNAS
NBS (National Bureau of Standards) calibration procedures for horizontal dipole antennas (25 to 1000 MHz)
[PB87-210233] 03 p0305 N88-11922
The use of coaxial transmission line elements in log-periodic dipole arrays
[AD-A184864] 05 p0574 N88-13499
Evaluation of CWMS (Continuous-Wave Measurement System) single-wire dipole antenna
[DE88-003979] 09 p1155 N88-16920
Improved backfire antenna using circular dipole 11 p1468 N88-18757
An improved method for calculating power density in the Fresnel region of circular parabolic reflector antennas
[AD-A190569] 15 p2060 N88-22284

DIPOLE MOMENTS
NT ELECTRIC MOMENTS
NT MAGNETIC MOMENTS
The polarization field for pulsed Raman transitions
[DE87-013118] 01 p0035 N88-10227
Theoretical atomic and molecular photophysics
[DE87-014249] 02 p0231 N88-11458
Core-core and core-valence correlation
[NASA-CR-182552] 11 p1544 N88-19226
Cooperative effects and intrinsic optical bistability in collections of atoms
[AD-A193993] 23 p3280 N88-29530
Passage of relativistic magnetic dipole moments through magnetic fields
[DE88-702640] 23 p3295 N88-29624

DIPOLES
Dipole component of relict radiation determined from Relikt experiment data 08 p1002 N88-16070
Mushroom-shaped currents (eddy dipoles) under rotation and stratification conditions 13 p1784 N88-20678

DIPPING
The effect on initial bond strength and durability of a Phosphoric Acid Dip (PAD) following chromic acid anodising of aluminum
[ARE-TM(UMM)-87402] 10 p1300 N88-17772
Studies on hot-dip zinc-aluminum coated sheet steels
[ETN-88-92217] 15 p2042 N88-22166

DIRAC EQUATION
Polarization of electrons in an electromagnetic wave field in the presence of magnetic field
[DE88-700169] 13 p1757 N88-20509

DIRECT BROADCAST SATELLITES
Study of reconfigurable payloads for direct broadcast satellites, summary
[DBS87-0004] 09 p1135 N88-16808
An outdoor unit for Direct Broadcast Satellite (DBS) digital sound reception
[BMFT-FB-W-86-016] 16 p2189 N88-23050
Organization of the TDF1/TDF2 program 22 p3161 N88-28827

DIRECT CURRENT
Comparison of costs and benefits for dc and ac transmission
[DE87-008774] 02 p0167 N88-11052
Analysis of nickel sulphamate bath using charging current compensated D.C. polarography
[NAL-TM-MT-8705] 05 p0564 N88-13433
Digital control of a direct current converter for a hybrid vehicle
[LAAS-87-266] 05 p0578 N88-13527
DC conductivity studies in Li5AlO4 at intermediate temperatures and its possible application for the electrolysis of water
[AD-A185489] 06 p0697 N88-14276
The dc conductivity studies of an hydroxide ion conductor at intermediate temperatures
[AD-A186044] 07 p0847 N88-15142
The effect of propane on atomic spectrometric signals in the direct current plasma
[DE88-002457] 07 p0934 N88-15676
Pulse width modulator controller design for a brushless DC motor position servo
[AD-A186618] 08 p0980 N88-15921
Sliding charge density waves and related problems
[AD-A186720] 09 p1157 N88-16934
Development and calibration of Direct Current Potential Difference (DCPD) crack length measurement equipment
[VTT-RR-480] 09 p1182 N88-17083
Rapid underway sediment classification by electrical methods
[AD-A187477] 10 p1357 N88-18114
Photoconductor switch and circuit analysis
[AD-A188168] 11 p1478 N88-18821
Automatic prober for the dc characterization of gallium arsenide devices. Part 1: The measurement facility
[AD-A187583] 11 p1560 N88-19337
Inductive spurious coupling of a dc-SQUID to resonant input circuit
[NOTA-INTERNA-894] 14 p1908 N88-21401
Electrical dc conductivity of pitch
[AD-A191266] 16 p2182 N88-23008
The LDCM actuator for vibration suppression
[NASA-CR-182898] 17 p2335 N88-23940
Arcjet power supply and start circuit
[NASA-CASE-LEW-14374-1] 23 p3181 N88-28939
The dc power control for a liquid-fed resistojet
[NASA-TM-101326] 24 p3338 N88-29869
Numerical simulation of the function of scientific instrumentation for measuring the speed of electron devices
[AD-A194969] 24 p3376 N88-30103
Automatic prober for the dc characterisation of gallium arsenide devices. Part 2: The data sorting and display facility
[AD-A195408] 24 p3377 N88-30111

DIRECT POWER GENERATORS
NT ALKALINE BATTERIES
NT ELECTROSTATIC GENERATORS
NT FUEL CELLS
NT HYDROGEN OXYGEN FUEL CELLS
NT MAGNETOHYDRODYNAMIC GENERATORS
NT METAL AIR BATTERIES

NT NICKEL ZINC BATTERIES
NT PHOSPHORIC ACID FUEL CELLS
NT PHOTOELECTRIC GENERATORS
NT PHOTOVOLTAIC CELLS
NT PRIMARY BATTERIES
NT RADIOISOTOPE BATTERIES
NT REGENERATIVE FUEL CELLS
NT SNAP 19
NT SODIUM SULFUR BATTERIES
NT SOLAR CELLS
NT THERMAL BATTERIES
NT THERMIONIC CONVERTERS
NT THERMOELECTRIC GENERATORS
NT VERTICAL JUNCTION SOLAR CELLS
NT ZINC-OXYGEN BATTERIES

Data on existing wind energy converters in Denmark
[DE88-900199] 07 p0874 N88-15300

Collecting of new data on existing wind energy converters
[DE88-900221] 07 p0875 N88-15305

Direct nuclear propulsion for Earth-to-orbit vehicles
17 p2400 N88-24271

Ultra high temperature direct propulsion
17 p2401 N88-24275

Safety constraints and considerations in the development of nuclear powered propulsion
17 p2401 N88-24276

Nuclear propulsion: Past, present and future
17 p2427 N88-24441

Gas core reactors for direct nuclear propulsion
17 p2428 N88-24442

Long-term behavior of energy production systems with the example of HELIOS and SYMPHONIE
[ETN-88-92988] 23 p3230 N88-29223

DIRECTION FINDING

Monitoring of harmful interference to the HF (High Frequency) broadcasting service. 3: Results of the June 1986 coordinated monitoring period
[PB87-210274] 01 p0036 N88-10229

Bearing detection in the presence of two sources of varying coherence using the complex cepstrum
[NASA-CR-181605] 09 p1243 N88-17451

Method for determining artillery position
[NASA-TT-20238] 13 p1834 N88-20973

Method for determining artillery position
[NASA-TT-20237] 13 p1834 N88-20974

Method for determining artillery position
[NASA-TT-20236] 14 p1979 N88-21813

Acoustic direction finding of flying helicopters
22 p3148 N88-28728

Examples of the application of acoustics for the detection and classification of targets 22 p3148 N88-28729

A fiber optic beamforming processor for wideband direction finding
[AD-A194862] 24 p3428 N88-30404

Ultra-wideband direction finding using a fiber optic beamforming processor
[AD-A194861] 24 p3430 N88-30413

DIRECTIONAL ANTENNAS

NT DIPOLE ANTENNAS
NT HELICAL ANTENNAS
NT LOG PERIODIC ANTENNAS
NT LOOP ANTENNAS
NT PARABOLIC ANTENNAS
NT REFLECTOR ANTENNAS
NT SLOT ANTENNAS
NT STEERABLE ANTENNAS
NT TWO REFLECTOR ANTENNAS

Study of advanced satellite concept using a multifeed reconfigurable antenna
[ESA-CR(P)-2406-VOL-1] 01 p0013 N88-10073

Study of advanced satellite concept using a multifeed reconfigurable antenna. Detailed report on mission definition, coverage analysis and performance requirements, antenna geometry
[ITS-TR-014.C/85] 01 p0013 N88-10074

Study of advanced satellite concept using a multifeed reconfigurable antenna. Detailed report on Polarization Sensitive Reflector (PSR) and offset parabolic antennas, Appendix 1
[ESA-CR(P)-2406-VOL-3] 01 p0013 N88-10075

Study of advanced satellite concept using a multifeed reconfigurable antenna. Appendix 3 : Feeding network, final performance analysis, study of reconfiguration possibilities
[ITS-TR-032/85] 01 p0014 N88-10076

Shape optimization of linear antennas
[ETN-87-90413] 01 p0036 N88-10233

Adaptive detection in non-stationary interference, part 3
[AD-A185622] 07 p0844 N88-15118

Performance of linear vertical antenna in refractive multimode waveguide 08 p1076 N88-16489

Investigation of design considerations for Telemetry, Tracking and Command (TT and C) antenna system on Naval Postgraduate School Orion mini-satellite
[AD-A187130] 10 p1291 N88-17718

The characteristics of two broadband (2 MHz to 10 MHz) switched vee antennas
[AD-A187874] 11 p1471 N88-18770

Sidelobe level of an adaptive array using the SMI (Sampled Matrix Inversion) algorithm
[AD-A193131] 21 p2932 N88-27409

DIRECTIONAL CONTROL

NT THRUST VECTOR CONTROL

Effect of rotation on the lateral stability of a free-flying column subjected to an axial thrust with directional control
[AD-A188690] 13 p1728 N88-20338

Compliant robotic structures, part 3
[AD-A192426] 21 p2955 N88-27556

DIRECTIONAL SOLIDIFICATION (CRYSTALS)

Contributions to the investigation of mechanical behavior of gamma/gamma NbC Cotac composites at medium and at high temperature
[ESA-TT-1031] 03 p0280 N88-11760

Development of a shell system for DS moulds at RR precision casting facility — directional solidification (DS)
[PNR90400] 09 p1151 N88-16893

Influence of convection on microstructure
[NASA-CR-182489] 10 p1302 N88-17784

Study of the production of some superconducting and magnetic materials by solidification in the drop tube and drop tower
[NASA-CR-182494] 11 p1461 N88-18708

MCT crystal growth
[NASA-CR-179297] 11 p1557 N88-19318

Analysis of low gravity tolerance of model experiments for space station: Preliminary results for directional solidification
[NASA-CR-182657] 12 p1614 N88-19648

Transport processes during directional solidification and crystal growth: Scaling and experimental study
14 p1988 N88-21857

Convection effects on stability at the solidification front 14 p1988 N88-21860

SSME single-crystal turbine blade dynamics
16 p2221 N88-23257

DIRECTIONAL STABILITY

NT GYROSCOPIC STABILITY

Effects of the installation and operation of jet-exhaust yaw vanes on the longitudinal and lateral-directional characteristics of the F-14 airplane
[NASA-TP-2769] 04 p0393 N88-12455

A comparison between theory and experiment for the yaw moment induced by a loose internal part
[AD-A187053] 09 p1131 N88-16787

Calculation of aerodynamic characteristics of airplane configurations at high angles of attack
[NASA-CR-4182] 23 p3172 N88-28891

DIRECTIVITY

The wavenumber: An alternative to the directional coupler for multimode analysis in oversized waveguides
[IPF-87-2] 01 p0037 N88-10237

Study on a unidirectional ring laser gyro. Part 1: Proposition of the principle and studies on the components
[NAL-TR-933] 09 p1169 N88-17010

Special relativity theory (one-dimensional case) without the postulate on the equality of directions
[DE88-701368] 16 p2284 N88-23674

An analysis of the efficiency and directivity of the sound generated by a moving laser source
[AD-A192220] 20 p2849 N88-26914

DIRECTORIES

Middle Atmosphere Program: Handbook for MAP, volume 24
[NASA-CR-181451] 01 p0069 N88-10444

Directory of geomagnetic observatories with high-resolution digital results, 1987
[PB87-221156] 03 p0348 N88-12201

Director of R and D institutions (Government of India)
[PB88-127162] 10 p1285 N88-17685

A directory of databases available through SearchMAESTRO
[AD-A188813] 12 p1706 N88-20214

Federal Council on Science, Engineering and Technology: Committee on Computer Research and Applications, Subcommittee on Science and Engineering Computing: The US Supercomputer Industry
[DE88-011262] 21 p2994 N88-27756

Design and performance analysis of a relational replicated database system
[AD-A196290] 24 p3437 N88-30456

DIRICHLET PROBLEM

IMPSOR: A fully vectorized FORTRAN code for three dimensional moving boundary problems with Dirichlet or Neumann boundary conditions
[DE87-014964] 02 p0226 N88-11427

Parameter estimation for the Dirichlet-Multinomial Distribution (DMD) using supplementary beta-binomial data
[AD-A186335] 07 p0911 N88-15524

Nontrivial critical points for asymptotically quadratic function
[DE88-101851] 20 p2845 N88-26881

Semilinear elliptic problems on domains with corners
[REPT-87-83] 20 p2846 N88-26886

Dirichlet prior in Bayesian estimation of item response curves
[AD-A195311] 24 p3426 N88-30392

DIRIGIBLES

U AIRSHIPS

DISCHARGE COEFFICIENT

Measurement of the electron density and the attachment rate coefficient in silane/helium discharges
[AD-A184268] 04 p0496 N88-13051

DISCHARGE TUBES

U GAS DISCHARGE TUBES

DISCHARGERS

NT STATIC DISCHARGERS

DISCONNECT DEVICES

Toggle release
[NASA-CASE-MSC-21354-1] 18 p2523 N88-24969

DISCONNECTORS

U DISCONNECT DEVICES

DISCONTINUITY

Interactions of oblique interplanetary discontinuities and their manifestations during STIP intervals 15-19
01 p0119 N88-10758

A numerical method for the treatment of kinked cracks in finite bodies 02 p0190 N88-11189

SHARP simulation of discontinuities in highly convective steady flow
[NASA-TM-100240] 05 p0642 N88-13931

Modeling of some coplanar waveguide discontinuities
[NASA-TM-100808] 10 p1318 N88-17880

The relation of solar wind structure to hydromagnetic discontinuities
[DE88-004304] 10 p1431 N88-18546

Visual integration and detection of discontinuities: The key role of intensity edges
[AD-A188012] 11 p1520 N88-19076

Detection of the number, locations and magnitudes of jumps
[AD-A190328] 15 p2125 N88-22671

Discontinuous inverse Sturm-Liouville problems with symmetric potentials
[DE88-009803] 19 p2720 N88-26152

A Wong-Zakai type theorem for certain discontinuous semimartingales
[AD-A192713] 21 p3005 N88-27822

DISCOVERING

U EXPLORATION

DISCOVERY (ORBITER)

Lateral and longitudinal stability and control parameters for the space shuttle discovery as determined from flight test data
[NASA-TM-100555] 13 p1724 N88-20309

DISCRETE FUNCTIONS

Analytical treatment of the spatial trilateration problem (4, 6, 0, 0)
[SER-A-104] 01 p0085 N88-10548

The periodic Lyapunov equations
[REPT-86-007] 01 p0087 N88-10567

Nonlinear techniques for detection and filtering of discrete-time signals 02 p0160 N88-11004

Stability of semidiscrete approximations for hyperbolic initial-boundary-value problems: An eigenvalue analysis
[NASA-TM-88328] 02 p0227 N88-11434

Solution of the two-dimensional Euler equations on unstructured triangular meshes
04 p0396 N88-12469

Tactile sensing and inverse problems
[AD-A187464] 10 p1340 N88-18011

Ideal shrinking and expansion of discrete sequences
[NASA-TM-88202] 11 p1524 N88-19100

Boltzmann-Fokker-Planck calculations using standard discrete-ordinates codes
[DE88-005393] 11 p1537 N88-19185

Using trace theory to model discrete events
[CS-8708] 13 p1824 N88-20904

Representation, analysis and design of multirate discrete-time control systems
[AD-A190499] 15 p2116 N88-22608

Parallel discrete-event simulation of FCFS stochastic queueing networks
[NASA-CR-181669] 17 p2389 N88-24203

Optimal discrete-time LQR problems for parabolic systems with unbounded input: Approximation and convergence
[NASA-CR-181673] 18 p2567 N88-25247

Modeling discrete bathtub and upside down bathtub mean residual life functions
[AD-A192000] 22 p3085 N88-28320

Stability of semidiscrete approximations for hyperbolic initial-boundary-value problems: Stationary modes
[NASA-TM-100994] 23 p3270 N88-29455
Polynomial definition of discrete field points of map of diffusion equation, part 1
[AD-A193697] 23 p3271 N88-29467

DISCRIMINANT ANALYSIS (STATISTICS)
Feature selection applied to radar target identification
[AD-A183880] 01 p0034 N88-10215
The importance of the lower level windshear profile in tornado/non-tornado discrimination
02 p0208 N88-11304
Strong consistency of certain information theoretic criteria for model selection in calibration, discriminant analysis and canonical correlation analysis
[AD-A186584] 09 p1232 N88-17385
Nonparametric discriminant analysis applied to the extraction and selection of radar target signature features
[AD-A191849] 18 p2501 N88-24833

DISCRIMINANT FUNCTIONS
U DISCRIMINANT ANALYSIS (STATISTICS)

DISCRIMINATION
NT BRIGHTNESS DISCRIMINATION
NT TACTILE DISCRIMINATION
NT VISUAL DISCRIMINATION
Automated satellite cloud analysis: A multispectral approach to the problem of snow/cloud discrimination
[AD-A185672] 06 p0746 N88-14591
Environmental gradient analysis, ordination, and classification in environmental impact assessments
[AD-A187294] 11 p1509 N88-19016
Auditory pattern memory: Mechanisms of tonal sequence discrimination by human observers
[AD-A190337] 15 p2104 N88-22534
A method for discrimination of radar targets using complex natural resonances
[AD-A191848] 18 p2500 N88-24832
Object discrimination via bulk temperature/velocity filtering, phase 1
[AD-A194533] 23 p3274 N88-29487
Discrimination studies using short-period P waves at upper mantle distances
[AD-A195468] 24 p3401 N88-30257

DISCRIMINATORS
NT FREQUENCY DISCRIMINATORS
A two-stage isolated-word recognition system using discriminant analysis
[AD-A187425] 10 p1402 N88-18360
Rules, schema and decision making
[AD-A193389] 21 p3027 N88-27967

DISEASES
NT ANEMIAS
NT ASTHMA
NT BACTERIAL DISEASES
NT BONE DEMINERALIZATION
NT CANCER
NT CORONARY ARTERY DISEASE
NT DIABETES MELLITUS
NT EPILEPSY
NT FIBROSIS
NT FUNGAL DISEASES
NT HEART DISEASES
NT INFECTIOUS DISEASES
NT MYOCARDIAL INFARCTION
NT NEOPLASMS
NT OCCUPATIONAL DISEASES
NT OSTEOPOROSIS
NT PARASITIC DISEASES
NT RADIATION SICKNESS
NT TACHYCARDIA
Physiological and immunological aspects of human adaptation to temperature elevation in a closed environment 07 p0895 N88-15424
Forecasting complications of cardiovascular disease in flight personnel 10 p1361 N88-18136
Central serous chorioretinopathy in USAF aviators: A review
[AD-A195697] 24 p3407 N88-30280

DISHES
U PARABOLIC REFLECTORS

DISILICIDES
Study on iron disilicide thermoelectric generator
[AD-A193082] 22 p3116 N88-28517

DISK GALAXIES
Infrared constraints on the nature of dark matter
13 p1855 N88-21102
The stability of disk galaxies and constraints on their mass-luminosity ratio
[SER-C-PREPUBL-FASC-27] 24 p3455 N88-30565

DISKS
Kinetic theory for plane flows of rough, inelastic, circular disks 21 p2946 N88-27499

DISKS (SHAPES)
NT ACTUATOR DISKS
NT INTERVERTEBRAL DISKS
NT ROTATING DISKS
Physical design of parameters of Nd:YAG disk laser
03 p0302 N88-11904
Mixed mode fatigue crack growth using the Brasilian disc 06 p0719 N88-14416
Development of composite polymer-glass edge claddings for Nova laser disks
[DE88-002389] 07 p0860 N88-15220
Disk pumping test
[AD-A187199] 11 p1440 N88-18591
AGARD (Advisory Group for Aerospace Research and Development) engine disc material cooperative test (supplementary program)
[AD-A193678] 23 p3179 N88-28925

DISLOCATIONS (MATERIALS)
NT CRYSTAL DISLOCATIONS
NT EDGE DISLOCATIONS
NT SCREW DISLOCATIONS
Applications of dislocation theory to crack growth problems 02 p0190 N88-11188
A dislocation model for fatigue crack propagation under variable amplitude loading 05 p0602 N88-13683
Dislocation free zone model of fracture under reverse loading
[DE88-002676] 07 p0869 N88-15276
An investigation of the influence of dislocation substructures on the deformation behavior of AK, DQ steel sheets
[DE88-006337] 14 p1889 N88-21289

DISORDERS
Instanton in supersymmetric theory with static disorder
[DE88-700357] 07 p0940 N88-15716
Raman scattering in mixed crystal semiconductors
12 p1696 N88-20149
Defects and disorder in amorphous and damaged silicon
[AD-A192277] 20 p2879 N88-27089
Normative developmental equations for the EEG and their sensitivity to neurological and psychiatric disorders
21 p2977 N88-27687

DISORIENTATION
NT DESYNCHRONIZATION (BIOLOGY)
NT DISORDERS
NT JET LAG

DISPENSERS
Aerodynamic aspects of the configurational systems layout of a dispenser
[MBB-UA-1047/87] 10 p1315 N88-17863
Deployable booms and antennas on AMPTE-IRM
14 p1874 N88-21196
Preliminary airworthiness evaluation of the UH-60A equipped with the XM-139 VOLCANO mine dispensing system
[AD-A190604] 15 p2018 N88-22029
A scientific basis for an alternate cathode architecture
[AD-A191498] 18 p2481 N88-24717
Method of dispensing reagent chemicals in space
[NASA-CASE-LAR-13607-1-CU] 23 p3200 N88-29048

DISPERSING
The effect of heat transfer on the dispersion of cold dense gases
[OUEL-1688/87] 02 p0171 N88-11076
Aircraft engine exhaust plume dynamics
[AD-A184238] 04 p0400 N88-12488
Activities at government research laboratories reported 04 p0403 N88-12503
Compatability of dispersion-strengthened platinum with resistojet propellants
[NASA-TP-2765] 04 p0409 N88-12538
Full scale and wind tunnel surface pressure measurements on the T.R.R.L. spray dispersion programme vehicles
[REPT-8623] 09 p1114 N88-16676
Design and characteristics of a liquid aerosol generator
[AD-A186942] 09 p1174 N88-17034
Dispersive hole transport in SiO2
[AD-A187077] 09 p1254 N88-17513
Soft X-ray beamsplitters and highly dispersive multilayer mirrors for use as soft X-ray laser cavity components
[DE88-004003] 11 p1549 N88-19270
Dense-spray structure and phenomena. Part 1. Turbulence/dispersed-phase interactions
[AD-A190606] 15 p2065 N88-22315
Microwave dispersion and absorption in tissues: Molecular mechanisms
[AD-A190118] 15 p2100 N88-22512
The optical properties of aerosols
[AD-A191420] 16 p2176 N88-22972
Examination of methods for pollen storage and dispersal
[TN-RB524-097/86] 17 p2378 N88-24134

Acoustic wave dispersion in a viscous, compressible, liquid-filled cylindrical elastic tube
19 p2722 N88-26164
Prediction of regional pollutant dispersion using a nested-grid, three-dimensional numerical model
21 p2971 N88-27649
Measuring dispersion effects of factors in factorial experiments
[AD-A193216] 21 p3006 N88-27831
Project wind, phase 4 (smoke test), Meadow Brook Valley, Red Bluff, California
[AD-A194742] 22 p3128 N88-28596
Particle size measurements in sooting combustion systems 24 p3348 N88-29931

DISPERSION
Development on thin wall tubes of dispersion type
[DE87-703384] 05 p0571 N88-13483
Dynamical properties of aluminium from experimental dispersion relations
[DE88-700240] 11 p1459 N88-18697
NOAA (National Oceanic and Atmospheric Administration) Meteorology Division support to the Environmental Protection Agency
[PB88-179866] 19 p2689 N88-25980
A zoomable and adaptable hidden fine-mesh approach to solving advection-dispersion equations
[DE88-006174] 21 p3004 N88-27816

DISPERSION PRECIPITATION HARDENING
U PRECIPITATION HARDENING

DISPERSIONS
NT AEROSOLS
NT COLLOIDS
NT EMULSIONS
NT FOG
NT LIQUID-GAS MIXTURES
NT SMOKE
High explosive moulding powders from RDX and aqueous polyurethane dispersions
[AD-A185026] 05 p0568 N88-13458
High temperature low cycle fatigue of oxide dispersion strengthened and single crystal nickel base superalloys
06 p0720 N88-14422
High temperature low cycle fatigue behavior and creep-fatigue interation of MA 6000 ODS alloy
06 p0720 N88-14425
A survey of denser-than-air atmospheric dispersion models
[DE88-006626] 15 p2092 N88-22467
Preparation and characterization of ceramic materials based on Al2O3 reinforced with a ZrO2 dispersion
[ISAL-87-0041] 21 p2922 N88-27340
Theoretical and experimental investigations on the structure of stationary shock waves in gas particle dispersions
[ETN-88-92983] 23 p3213 N88-29122

DISPLACEMENT
NT CRACK OPENING DISPLACEMENT
A numerical method for the treatment of kinked cracks in finite bodies 02 p0190 N88-11189
A study of the crack tip parameters that govern environmentally assisted cracking by use of the rising displacement test 04 p0427 N88-12649
The dynamics of solar magnetic flux tubes subjected to resonant foot point shaking 04 p0507 N88-13118
Hypersonic laminar boundary layer: Parametric study for the representation of real gas effects
05 p0532 N88-13236
Telemetric laser extensometry technique for monitoring deflections in small cracks 05 p0607 N88-13724
Stresses and displacements in two, three and four layered structures submitted to flexible or rigid loads
[AD-A185707] 06 p0723 N88-14450
Generalized displacement method in the finite element analysis of incompressible material
[PB87-143434] 08 p0995 N88-16018
Calculated sputtering and atomic displacement cross-sections for applications to medium voltage analytical electron microscopy
[DE88-002904] 09 p1168 N88-17006
A summary of experimental results on square plates and stiffened panels subjected to air-blast loading
09 p1178 N88-17057
Stress intensity and crack displacement for small edge cracks
[NASA-TP-2801] 09 p1184 N88-17095
Dynamic analysis of plane frames by microcomputer
11 p1531 N88-19143
Synthesis of finite displacements and displacements in continental margins
[NASA-CR-182616] 12 p1642 N88-19832
The effects of humidity on the profile of photographic plates
[NPL-DMOM-88] 14 p1913 N88-21429
Photo-optical converter of angular displacements in digital servomechanisms
[DE87-703208] 14 p1961 N88-21698

An efficient Mindlin finite strip plate element based on assumed strain distribution 15 p2081 N88-22407
Automatic feedback control of a rigid body for finite displacements 18 p2473 N88-24674
Large displacement and rotational formulation for laminated cylindrical shells including parabolic transverse shear
[AD-A194871] 24 p3384 N88-30158

DISPLACEMENT MEASUREMENT
Device for measuring hole elongation in a bolted joint
[NASA-CASE-LAR-13453-1] 06 p0712 N88-14361
A composite grating for moire interferometry
[AD-A186330] 07 p0832 N88-15044
A quantitative method for evaluating sensor layouts 09 p1178 N88-17056
Experimental and analytical investigation on a proposed embedded fiber optic displacement sensor
[AD-A189030] 12 p1630 N88-19756
Digital fiber optic displacement sensors 18 p2518 N88-24937
A review of non-contacting displacement measurement techniques used to monitor the movement of rotor blades in gas turbine aero engines
[PNR90457] 22 p3045 N88-28071
Optical measurement of propeller blade deflections
[NASA-TP-2841] 22 p3079 N88-28286
J-integral measurement using moire interferometry
[AD-A193751] 23 p3226 N88-29202
A technique for measuring area under a curve
[AD-A193559] 23 p3271 N88-29463

DISPLAY DEVICES
NT HEAD-UP DISPLAYS
NT HELMET MOUNTED DISPLAYS
NT PLASMA DISPLAY DEVICES
NT POSITION INDICATORS
NT TACHOMETERS
Color display programming for aviation
[DFVLR-MITT-87-03] 01 p0006 N88-10031
Input devices for tasks using interactive video
[NPL-DITC-87/87] 01 p0080 N88-10510
Fiber optic engineering sensor system. Preliminary program management plan, phase 3 revision
[AD-A183663] 01 p0093 N88-10608
The impact of new computer technology on accelerator control
[DE87-014021] 02 p0219 N88-11376
MBB simulation facilities applied for rotorcraft research 03 p0263 N88-11655
The flight evaluation of an advanced engine display and monitoring system 03 p0264 N88-11659
Helicopter (performance) management 03 p0264 N88-11666
Integrated voice and visual systems research topics
[NASA-CR-177417] 03 p0356 N88-12246
Computer-controlled testing of visual-spatial ability
[AD-A183971] 03 p0357 N88-12249
A scientific workstation operator-interface for accelerator control
[DE87-014689] 03 p0362 N88-12278
Effects of combining vertical and horizontal information into a primary flight display
[NASA-TP-2783] 04 p0399 N88-12487
Traveling-wave maser closed-cycle refrigerator data acquisition and display system 04 p0437 N88-12708
Input/output technologies: An overview of image scanning, storage, and display
[DE87-014837] 04 p0476 N88-12933
An interactive computer graphics network monitor for a tactical communications network
[AD-A184131] 04 p0477 N88-12938
Displaying three-dimensional data
[AD-A185347] 05 p0580 N88-13541
The Portable Instant Display and Analysis Spectrometer (PIDAS) 05 p0611 N88-13756
The use of color in electronic maps. Part 1: Generation and analysis of color on the Gould/DeAnza image processing system
[IZF-1986-32] 05 p0635 N88-13882
Fast, colour displays of digital terrain elevation data
[AD-A185596] 06 p0729 N88-14485
Use of colour on electronic data displays (second study)
[PB87-126744] 06 p0754 N88-14627
A general solution to the silhouette problem
[NASA-TP-2695] 06 p0755 N88-14629
Stress effects and the optimum format of a scrolling seven-line VDT text window
[AD-A185559] 06 p0758 N88-14651
FAA air traffic control operations concepts. Volume 1: ATC background and analysis methodology
[AD-A185979] 07 p0818 N88-14973
An inexpensive real-time interactive three dimensional flight simulation system
[AD-A184868] 07 p0821 N88-14989
The role of adaptive supplemental visual cuing in flight simulation
[AD-A185932] 07 p0822 N88-14992
Three dimensional display of meteorological scientific data
[DE88-000776] 07 p0880 N88-15339
Creating title blocks for vehicle animations
[AD-A185620] 07 p0904 N88-15473
Through-transmission/pulse-echo ultrasonic equipment evaluation
[AD-A186340] 07 p0929 N88-15641
Electro-optical studies of semiconductor compounds for electroluminescent and laser devices
[PH-155] 07 p0937 N88-15693
Comparison of alphanumeric data entry methods for advanced helicopter cockpits
[AD-A186934] 09 p1201 N88-17201
An intelligent tutor for the space domain 09 p1204 N88-17217
The advanced low-level windshear alert system operational demonstration results, Summer, 1987, Denver Stapleton International Airport 10 p1275 N88-17633
Information transfer in the National Airspace System 10 p1275 N88-17634
Helicopter external vision requirements and visual display characteristics: A report/bibliography, revision A
[AD-A187075] 10 p1276 N88-17641
Electrochromic cells with lutetium diphthalocyanine and semisolid polymer electrolytes
[AD-A188031] 10 p1352 N88-18078
Generation of specific chromaticities on CRT monitors
[AD-A187739] 11 p1440 N88-18590
Report on desktop publishing
[AD-A187698] 11 p1528 N88-19128
A comparison of keyboard designs for cockpit applications
[AD-A187775] 12 p1581 N88-19460
Soft maps for US Army electronic map background applications
[AD-A188427] 12 p1638 N88-19809
Brain activity during tactical decision-making. Part 2: Probe-evoked potentials and workload
[AD-A188688] 12 p1667 N88-19994
Human efficiency for visual detection of targets on CRT displays using a two-level multiple channel time history format
[AD-A188419] 12 p1670 N88-20001
OMV man/system simulation integration: A preliminary analysis and recommendation
[NASA-CR-182602] 12 p1671 N88-20005
Visual display representation of multidimensional systems: The effect of information correlation and display integrality
[AD-A188655] 12 p1672 N88-20010
CODAC (Cockpit Oriented Display of Aircraft Configurations) version 1.4 user's guide
[NASA-CR-181650] 13 p1718 N88-20273
Development of an interactive real-time graphics system for the display of vehicle space positioning
[NASA-TM-100429] 13 p1730 N88-20344
Restoration techniques for redisplay of LANDSAT-5 satellite imagery
[INPE-4189-PRE/1076] 13 p1791 N88-20712
Multi-crew pictorial format display evaluation
[AD-A189349] 13 p1812 N88-20824
Solid-state electrochemical processes in dye films
[AD-A188756] 13 p1844 N88-21036
The PC/AT compatible computer as a mission control center display processor at Ames-Dryden Flight Research Facility
[NASA-TM-100426] 14 p1955 N88-21654
DataViews: A personalizable, interactive, data display system for the decisionmaker
[AD-A188509] 14 p1991 N88-21868
Effects of update and refresh rates on flight simulation visual displays
[NASA-TM-100415] 15 p2018 N88-22033
Geometric modeling of flight information for graphical cockpit display
[AD-A190484] 15 p2021 N88-22043
Real-time flight test data distribution and display
[NASA-TM-100424] 15 p2022 N88-22050
Basic research on flame radiation
[PB88-168372] 15 p2032 N88-22105
A 3-D solid rendering of NDT data
[DE88-006199] 15 p2076 N88-22373
Auditory pattern memory: Mechanisms of tonal sequence discrimination by human observers
[AD-A190337] 15 p2104 N88-22534
A graphics editor for structured analysis with a data dictionary
[AD-A190618] 15 p2112 N88-22584
Two-dimensional graphics tools for a transputer based display board
[NASA-TM-100620] 15 p2113 N88-22591
Basic design studies for the realization of liquid crystal display systems in aircraft
[VA-87-001] 16 p2163 N88-22900
Crewstation Information and Development System (CIDS) 17 p2304 N88-23781
Presentation of map information on a color display
[FOA-C-20687-2.7] 17 p2368 N88-24103
Virtual interface environment 17 p2381 N88-24153
Denver ARTCC evaluation of PROFS (Prototype Regional Observations and Forecast System) mesoscale weather products 18 p2547 N88-25117
Eye and head response to an attention cue in a dual task paradigm
[AD-A191052] 18 p2551 N88-25143
Design and testing of a luminance and chrominance stabilization system for a computer-controlled color display
[AD-A191922] 18 p2554 N88-25159
IGUANA: Interactive graphics utility for automated NEC analysis
[AD-A191760] 18 p2556 N88-25174
Considerations involved in the display of finite element results using animation
[DE88-007581] 18 p2559 N88-25189
On-line measurement of heat of combustion
[NASA-CR-183076] 19 p2738 N88-26255
XDATAP
[DE88-007161] 20 p2837 N88-26827
Editfont: An interactive font editing system
[AD-A192373] 20 p2838 N88-26836
An evaluation of flight path formats head-up and head-down
[NASA-CR-4176] 21 p2897 N88-27196
The effect of input device on user performance with a menu-based natural language interface
[AD-A193095] 21 p2996 N88-27772
Improvement of head-up display standards. Volume 4: Head-up display dynamics flight tests
[AD-A193617] 22 p3042 N88-28060
System status display evaluation
[NASA-CR-4181] 22 p3042 N88-28061
Stereo and eye movement
[AD-A193588] 22 p3142 N88-28681
Rendering of surfaces from volume data
[AD-A193649] 22 p3143 N88-28689
Future visual environment and concerns 23 p3242 N88-29299
Use of color CRTs (Cathode Ray Tubes) in aircraft cockpit: A literature search, revision B
[AD-A195062] 24 p3324 N88-29797
A detection theory analysis of visual display performance
[AD-A196291] 24 p3409 N88-30292

DISPLAY SYSTEMS
U DISPLAY DEVICES

DISPOSAL
NT HAZARDOUS MATERIAL DISPOSAL (IN SPACE)
NT WASTE DISPOSAL
Real time AI expert system for robotic applications 08 p1061 N88-16408
Nuclear-powered space debris sweeper 17 p2418 N88-24380

DISRUPTING
Modeling of thermal effects on TIBER 2 (Thermal Ignition/Burn Experimental Reactor) divertor during plasma disruptions
[DE88-001893] 06 p0783 N88-14805
Vaporization studies of plasma interactive materials in simulated plasma disruption events
[DE88-010100] 19 p2731 N88-26222

DISSIPATION
NT ENERGY DISSIPATION
NT OHMIC DISSIPATION
FLIP (Fluid-Implicit-Particle): A low-dissipation, particle-in-cell method for fluid flow
[DE87-014745] 03 p0313 N88-11981
A dissipation principle and its consequences for structured shock waves in thermoelastic materials
[DE87-013723] 04 p0454 N88-12813
Canonical transformations and exact invariants for dissipative systems
[DE87-703663] 04 p0485 N88-12985
Reynolds-stress and dissipation rate budgets in a turbulent channel flow
[NASA-TM-89451] 07 p0852 N88-15174
Period-doubling universality in multidimensional dissipative and conservative systems
[PB88-148812] 13 p1832 N88-20961
A physically consistent model for artificial dissipation in transonic potential flow computations
[NASA-TM-100846] 15 p2122 N88-22652
On 3-5 transistors for MM-wave applications
[AD-A191580] 19 p2661 N88-25825

Determination of multiaxial flow surfaces at elevated temperatures using the concept of dissipation potential
[ORNL/TM-10787] 24 p3383 N88-30149

DISSIPATORS
U DISSIPATION

DISSOCIATION
NT AUTOIONIZATION
NT GAS DISSOCIATION
NT PHOTODISSOCIATION
NT RADIOLYSIS
NT THERMAL DISSOCIATION
Nitrogen at high pressure
[DE87-013797] 01 p0021 N88-10130
Nitrogen at very high pressure
[DE87-013800] 01 p0021 N88-10131
Chemical equilibrium calculations for the high pressure and temperature dissociation of liquid nitrogen
[DE87-013788] 01 p0021 N88-10135
The dissociation of dense liquid nitrogen and shock cooling
[DE87-013490] 01 p0022 N88-10136
Computational fluid dynamics and aerothermodynamics
[NASA-CR-182490] 09 p1166 N88-16989
Atomic data for hydrogens in collisions with electrons: Addenda
[IPPJ-AM-55-ADD] 09 p1252 N88-17502
Excimer laser photolysis studies of T-V (Translation-to-Vibration) energy transfer
[AD-A189613] 13 p1837 N88-20989
NNEPEQ: Chemical equilibrium version of the Navy/NASA Engine Program
[NASA-TM-100851] 14 p1868 N88-21161
Theory of the dissociation dynamics of small molecules on metal surfaces: Finite temperature studies
[DE88-006495] 15 p2132 N88-22716
The H5(+) potential energy hypersurface: Characterization of ten distinct energetically low-lying stationary points 16 p2267 N88-23561
Theoretical calculations of XeF ground state kinetics
[AD-A191398] 16 p2270 N88-23580
Computer program for parameterization of nucleus-nucleus electromagnetic dissociation cross sections
[NASA-TM-4038] 16 p2270 N88-23584
Molecular sources of ionospheric holes
[AD-A191857] 18 p2541 N88-25082
Half collision studies of inelastic energy transfer processes
[DE88-008096] 19 p2724 N88-26178
High resolution spectroscopy of dissociating molecules
[DE88-007959] 20 p2851 N88-26924
Theory of the dissociation dynamics of small molecules on metal surfaces: Finite temperature studies
[DE88-007763] 21 p3013 N88-27882
Modification of YBa2Cu3O(7-x) ceramics by adsorbed water and other gases
[DE88-011518] 22 p3057 N88-28140
Measurements of XeF (Xenon Fluoride) ground state dissociation and vibrational equilibration
[AD-A194611] 23 p3280 N88-29527
Nonequilibrium flow of a dissociating gas in a horizontal channel with axial temperature variation
[DE88-702536] 24 p3373 N88-30089
Ion kinetics in silane plasmas
[AD-A196202] 24 p3431 N88-30423

DISSOLUTION
U DISSOLVING

DISSOLVED GASES
Mass transport phenomena between bubbles and dissolved gases in liquids under reduced gravity conditions
[NASA-TM-100273] 11 p1455 N88-18672

DISSOLVING
De-alloying
[DE87-012488] 01 p0022 N88-10139
Irreversible dissolution of solid solutions: A kinetic and stoichiometric model
[DE88-009194] 19 p2614 N88-25513
Dissolution rates of polymers and copolymers based on methyl, ethyl and butyl methacrylate
[AD-A194713] 23 p3197 N88-29027

DISSYMMETRY
U ASYMMETRY

DISTANCE
NT DIFFUSION LENGTH
NT RADAR RANGE
NT RADIO RANGE
NT RANGE AND RANGE RATE TRACKING
Research in geodesy based upon radio interferometric observations of GPS (Global Positioning System) satellites
[AD-A184040] 03 p0346 N88-12187
A computational examination of orthogonal distance regression
[AD-A184374] 03 p0371 N88-12337
Results of one way transit time measuring in navigation experiment NAVEX
[DFVLR-MITT-87-17] 14 p1865 N88-21145
The Monte Generoso-Zimmerwald (Switzerland) baseline from satellite laser ranging data using various analysis techniques
[LR-533] 14 p1940 N88-21576
The distance to the center of the galaxy: H2O maser proper motions in Sgr B2(N)
[MPE-PREPRINT-104] 16 p2288 N88-23702
Modeling the primary events of photosynthesis using chlorophyll containing fixed distance donor-acceptor molecules
[DE88-010033] 20 p2831 N88-26793

DISTANCE MEASURING EQUIPMENT
NT ALTIMETERS
NT LASER ALTIMETERS
NT LASER RANGE FINDERS
NT RADIO ALTIMETERS
NT RANGE FINDERS
Contributions to geodesy, photogrammetry, and cartography. Series 2, number 45
[ISSN-0469-4244] 01 p0065 N88-10416
A method resolving an ambiguity of measured distance by means of NAVSTAR GPS signals
01 p0065 N88-10417
Degradation of downlink distance measurement indexes by the addition of a third tone --- tone ranging
[CNES-CT/DRT/TIT/TR-122-T] 15 p2058 N88-22268
Method and apparatus for measuring distance
[NASA-CASE-MSC-20912-1] 20 p2793 N88-26568

DISTANCE PERCEPTION
U SPACE PERCEPTION

DISTILLATION
Flammability characteristics of distillate fuels
[AD-A188497] 12 p1612 N88-19642
Feasibility of producing jet fuel from GPGP (Great Plains Gasification Plant) by-products
[DE88-010233] 20 p2781 N88-26492
Vapor Compression Distillation Subsystem (VCDS) component enhancement, testing and expert fault diagnostics development, volume 2
[NASA-CR-172076] 21 p2994 N88-27755
Vapor Compression Distillation Subsystem (VCDS) component enhancement, testing and expert fault diagnostics development, volume 1
[NASA-CR-172072] 22 p3134 N88-28634

DISTILLATION EQUIPMENT
Vapor compression distiller and membrane technology for water revitalization 03 p0359 N88-12262

DISTORTION
NT FLOW DISTORTION
NT SIGNAL DISTORTION
NT SURFACE DISTORTION
USSR report: Physics and mathematics
[JPRS-UPM-87-006] 06 p0708 N88-14344
Compensation of small-scale phase distortions by means of a Fourier phase corrector
06 p0708 N88-14345
Distortional buckling formulae for thin-walled channel columns
[PB87-124012] 06 p0722 N88-14437
X-ray measurements of phason distortion in ion-implanted Al-Mn
[DE87-014566] 07 p0937 N88-15694
Flat-field response and geometric distortion measurements of optical streak cameras
[DE88-002394] 09 p1168 N88-17005
Reduction of residual stresses and distortion in girth welded pipes
[AD-A187728] 11 p1494 N88-18920
Effect of spatial inlet temperature and pressure distortion on turbofan engine stability
[NASA-TM-100850] 14 p1868 N88-21162
Millimeter-wave pulse distortion by a single absorption line simulating the terrestrial atmosphere
[PB88-161237] 14 p1906 N88-21388
Ultrasonic beam distortion in transversely isotropic media
[DE88-005937] 15 p2129 N88-22699
Analytical approximation of a distorted reflector surface defined by a discrete set of points
[NASA-TM-101323] 21 p2934 N88-27424
A Navier-Stokes study of cascade flow fields including inlet distortion and rotating stall
[AD-A193109] 21 p2943 N88-27483
Effects of pulsed and CW (Continuous Wave) 2450 MHz radiation on transformation and chromosomes of human lymphocytes in vitro
[AD-A193104] 21 p2987 N88-27736
Distortion functions
[DE88-752634] 21 p3015 N88-27896
Distortion effects in isoparametric elements, an analytic approach
[PNR90454] 22 p3145 N88-28703
Aerodynamics of seeing on large transport aircraft
[NASA-CR-183122] 23 p3174 N88-28896
A novel method to correct radiation pattern distortion of conformal antennas
[AD-A193675] 23 p3204 N88-29066
Distortions in processed signals and their application in electronic design. Part 1: Basic and general formulations
[DE88-702731] 23 p3204 N88-29070
Distortions in processed signals and their application in electronic design. Part 2: A new variable signal generator
[DE88-702732] 23 p3205 N88-29071
Distortion estimates for negative Schwarzian maps
[AD-A193172] 23 p3228 N88-29209
Theory of filtering and control with application to control of large space structures
[AD-A195500] 24 p3335 N88-29851
Contamination and distortion of steady flow field induced by discrete frequency disturbances in aircraft gas engines
[AD-A195440] 24 p3370 N88-30069

DISTRIBUTED AMPLIFIERS
Enhanced performance ultrabroadband distributed amplifiers 19 p2656 N88-25775

DISTRIBUTED FEEDBACK LASERS
Distributed feedback effects in lasers and high gain laser instabilities in optically pumped CH3F
03 p0329 N88-12079
Time characteristics of ultrashort light pulses from dye lasers with distributed feedback
14 p1970 N88-21759
Characteristics of distributed feedback lasers discussed 16 p2185 N88-23028
Distributed feedback lasers
[NASA-CR-4154] 18 p2520 N88-24948

DISTRIBUTED PARAMETER SYSTEMS
Structural frequency functions for an impulsive, distributed forcing function
[DE87-013811] 03 p0333 N88-12101
A new method of boundary parameter estimation for a two-dimensional diffusion system under noisy observations
[NASA-CR-178405] 06 p0767 N88-14714
A unified framework for approximation in inverse problems for distributed parameter systems
[NASA-CR-181621] 10 p1400 N88-18346
Calculation of the distributed loads on the blades of individual multiblade propellers in axial flow using linear and nonlinear lifting surface theories
[NASA-TT-20173] 13 p1719 N88-20278
Feedback control of distributed parameter systems with applications to large space structures
[AD-A190536] 15 p2025 N88-22068
Instrumentation to provide an active control capability for distributed parameter systems
[AD-A190043] 15 p2076 N88-22375
Boundary shape identification problems in two-dimensional domains related to thermal testing of materials
[NASA-CR-181654] 15 p2105 N88-22541
The Colored Stochastic Petri Net (CS-PN) software: Application to the validation and the performance evaluation of distributed systems
[ENST-87D005] 15 p2113 N88-22589
Approximation methods for the identification and control of distributed parameter systems
[AD-A190201] 15 p2124 N88-22662
An approximation theory for the identification of nonlinear distributed parameter systems
[NASA-CR-181658] 16 p2260 N88-23510
Galerkin approximation for inverse problems for nonautonomous nonlinear distributed systems
[NASA-CR-181676] 18 p2567 N88-25246
Finite-dimensional approximation for optimal fixed-order compensation of distributed parameter systems
[NASA-CR-181674] 20 p2843 N88-26873
Connectionist models and artificial intelligence
[RR-684-I-IMAG-66-LIFIA] 22 p3142 N88-28684
Laser sensing for identification and control of distributed parameter systems
[AD-A195886] 24 p3379 N88-30124
Robust finite-dimensional LQG (Linear Quadric Gaussian)-based controllers for a class of distributed parameter systems
[AD-A194872] 24 p3425 N88-30382

DISTRIBUTED PROCESSING
A nonmythical generalization of Dekker's algorithm and its ramifications --- mutually exclusive processes
[CS-8702] 01 p0080 N88-10513
Methodology of performance evaluation of real time distributed systems
[ENST-87D003] 02 p0228 N88-11440

Token execution strategies for distributed algorithms: Simulation studies
[AD-A184792] 03 p0365 N88-12294
Layering central authentication on the interactive services of an existing homogeneous distributed system
[DE87-011544] 03 p0366 N88-12304
Interfacing distributed operating systems
[AD-A184489] 03 p0366 N88-12306
Concepts and techniques for support of real time distributed operating systems
[AD-A184491] 03 p0367 N88-12307
Managing distributed derived data: A preliminary proposal
[DE88-000714] 04 p0481 N88-12966
Storing and retrieving data in a parallel distributed memory system
[AD-A185177] 05 p0637 N88-13897
Conceptual issues in measuring the behavior of a distributed real-time process-control computer system
[DE87-009748] 05 p0638 N88-13898
Conceptual issues in measuring the behavior of a distributed real-time process-control computer system
[DE87-014251] 05 p0638 N88-13899
Connecting RPC (Remote Procedure Call)-based distributed systems using wide-area networks
[PB87-234423] 05 p0658 N88-14041
An empirical investigation of load indices for load balancing applications
[AD-A185763] 06 p0724 N88-14451
Objects architecture: A comprehensive design approach for real-time, distributed, fault-tolerant, reactive operating systems
[AD-A185476] 06 p0755 N88-14631
Distribution of records on a ring of processors
[PB87-235784] 06 p0758 N88-14649
Distributed infimum approximation
[PB87-234969] 06 p0764 N88-14695
Communications for the DTroll distributed database system
[AD-A185579] 06 p0791 N88-14853
Study of communication options in a distributed data handling system and survey of advanced man machine communications schemes. Work package 1: Interprocess communication
[ESA-CR(P)-2447] 07 p0843 N88-15114
Annotated bibliography on reliable system design
[PB88-109848] 07 p0866 N88-15254
UNITY: A framework for study of parallel programming problem-solving
[AD-A185616] 07 p0906 N88-15490
Interface between astrophysical datasets and distributed database management systems (DAVID)
[NASA-CR-182394] 07 p0942 N88-15731
Reliability issues in distributed operating systems
[PB88-100870] 08 p0993 N88-16009
A distributed architecture for intelligent monitoring and anomaly diagnosis of the Hubble Space Telescope
08 p1057 N88-16379
A knowledge-based system for monitoring the electrical power system of the Hubble Space Telescope
08 p1058 N88-16380
Problem solving as intelligent retrieval from distributed knowledge sources 08 p1059 N88-16392
Application of parallel distributed processing to space based systems 08 p1059 N88-16393
Neural network based speech synthesizer: A preliminary report 08 p1064 N88-16429
A framework for real-time distributed expert systems: On-orbit spacecraft fault diagnosis, monitoring and control 08 p1066 N88-16440
Prototype space station automation system delivered and demonstrated at NASA 08 p1066 N88-16442
Proposal of a methodology for the conceptual design of the Distributed Data Base
[INPE-4315-TDL/282] 08 p1093 N88-16576
Analysis of tasks for dynamic man/machine load balancing in advanced helicopters
[DE88-003735] 09 p1117 N88-16696
Replication and reconfiguration in a distributed mail repository
[AD-A186967] 09 p1151 N88-16897
First Annual Workshop on Space Operations Automation and Robotics (SOAR 87)
[NASA-CP-2491] 09 p1203 N88-17206
Development of a comprehensive software engineering environment 09 p1203 N88-17211
Task allocation in a distributed computing system
09 p1206 N88-17230
Software for integrated manufacturing systems, part 1
09 p1211 N88-17261
Software for integrated manufacturing systems, part 2
09 p1211 N88-17262
The implementation and use of Ada on distributed systems with high reliability requirements
[NASA-CR-182481] 09 p1221 N88-17326
Clouds: A support architecture for fault tolerant, distributed systems 10 p1375 N88-18206
A distributed system architecture based on macro dataflow model 10 p1376 N88-18210
A comparative study of heurstic algorithms for task assignment in distributed computing systems
10 p1376 N88-18211
Distributed control of large parallel computers
10 p1376 N88-18215
The design of load balancing strategies for distributed systems 10 p1376 N88-18216
Experiments with parallel program execution on a network of workstations 10 p1377 N88-18217
Distributed query processing: Present status and future direction 10 p1377 N88-18219
Concurrency control and reliability in replicated database systems 10 p1377 N88-18221
An anlysis of the reliability of tree-structured interconnection networks 10 p1378 N88-18228
On the number of task assignments in distributed computing systems 10 p1378 N88-18230
Reuse: A Reliable Unified Service Environment for distributed systems 10 p1379 N88-18231
Resilient procedures: A structured replication approach 10 p1381 N88-18245
Features of a TeraFlop supercomputer
[DE88-003540] 10 p1384 N88-18263
Optimal performance of distributed simulation programs
[AD-A187822] 11 p1529 N88-19131
The roll back chip: Hardware support for distributed simulation using time warp
[AD-A187823] 11 p1529 N88-19132
Performance measurements of distributed simulation strategies
[AD-A187824] 11 p1529 N88-19133
Distributed computation of graphics primitives on a transputer network
[NASA-TM-100814] 11 p1531 N88-19147
A shared memory algorithm and proof for the alternative construct in CSP (Communicating Sequential Processes)
[AD-A187820] 11 p1533 N88-19156
Implementing dynamic arrays: A challenge for high-performance machines
[AD-A188142] 11 p1533 N88-19157
Theory and practice of fault tolerance in distributed systems
[AD-A187559] 11 p1540 N88-19204
Uncertain knowledge in distributed systems
[AD-A189017] 12 p1685 N88-20076
Design methodology for allocating data in a distributed database
[AD-A188826] 12 p1706 N88-20215
Two normal form theorems for Communicating Sequential Processes (CSP) program
[CWI-CS-R8735] 13 p1819 N88-20874
Distributed transaction processing and the Camelot system
[AD-A188614] 13 p1821 N88-20885
On the design of parallel numerical methods in message passing and shared memory environments
[DE88-003566] 13 p1822 N88-20888
An amoeba replicated service organisation --- Amoeba operating system
[CWI-CS-R8723] 13 p1822 N88-20892
GADL: A gate array description language
[EUT-87-E-165] 14 p1907 N88-21396
Higher levels of a silicon compiler
[EUT-86-E-163] 14 p1955 N88-21650
Generating layouts for random logic: Cell generation schemes
[EUT-86-E-164] 14 p1956 N88-21658
ESKISS: A program for optimal state assignment
[EUT-87-E-167] 14 p1956 N88-21659
Distributed operating systems: An overview
[INF-87-29] 14 p1960 N88-21688
Conception of a knowledge-based system for designing distributed systems
[DFVLR-MITT-87-16] 14 p1961 N88-21694
Technology mapping from Boolean expressions to standard cells
[EUT-87-E-174] 14 p1963 N88-21709
An optimal CMOS structure for the design of a cell library
[EUT-87-E-166] 14 p1985 N88-21841
Argus reference manual
[AD-A190382] 15 p2111 N88-22578
The Colored Stochastic Petri Net (CS-PN) software: Application to the validation and the performance evaluation of distributed systems
[ENST-87D005] 15 p2113 N88-22589
A methodolgy, based on analytical modeling, for the design of parallel and distributed architectures for relational database query processors
[AD-A189844] 15 p2149 N88-22825
Distributed matchmaking
[CWI-CS-R8750] 16 p2254 N88-23467
A timestamp ordering mechanism with dynamic selection of rollback objects 16 p2257 N88-23489
TALOS: A distributed architecture for intelligent monitoring and anomaly diagnosis of the Hubble Space Telescope 17 p2388 N88-24193
Low authority control of large space structures using a constrained threshold control formulation
18 p2472 N88-24667
Design, implementation and evaluation of an operating system for a network of transputers
[AD-A186593] 18 p2559 N88-25193
Design of partially replicated distributed database systems: An integrated methodology
18 p2589 N88-25383
Distributed mathematics in a heterogeneous environment
[DE88-009128] 19 p2716 N88-26124
The high speed local area network
19 p2717 N88-26133
Fault diagnosis in distributed computer networks
[AD-A192406] 19 p2718 N88-26140
Research in computer science 1985/6
[PB88-113840] 20 p2835 N88-26815
Correctness criteria for process migration
[NASA-CR-182939] 20 p2836 N88-26823
Distributed fault tolerant embeddings of binary trees in hypercubes
[AD-A192929] 20 p2839 N88-26840
Issues and recommendations associated with distributed computation and data management systems for the space sciences
[NASA-CR-183026] 20 p2881 N88-27108
An integrated, multi-vendor distributed data acquisition system
[DE88-008900] 20 p2882 N88-27113
Computational fluid dynamics on parallel processors
[AD-A192397] 21 p2941 N88-27469
Distributed algorithms for probabilistic solution of computational vision problems
[AD-A193150] 21 p2997 N88-27773
A menu-driven menu editor and associated menu system
[DE88-008026] 21 p2998 N88-27781
Constructing a highly-available location service for a distributed environment
[AD-A192723] 21 p3001 N88-27801
Intelligent test integration system
23 p3254 N88-29371
Distributed cooperating processes in a mobile robot control system 23 p3256 N88-29386
AI and simulation: What can they learn from each other 23 p3257 N88-29391
An expert system for a distributed real-time trainer
23 p3261 N88-29411
Large-grain pipelining on distributed-memory multiprocessors
[DE88-009974] 23 p3264 N88-29432
On the design and optimization of distributed signal detection and parameter estimation systems
[AD-A193934] 23 p3266 N88-29446
Dynamically reconfigurable distributed database systems
[AD-A194716] 23 p3297 N88-29636
Performance analysis of FDDI
[NASA-CR-183206] 24 p3413 N88-30321
Parallel and distributed computation for fault-tolerant object recognition 24 p3419 N88-30350
Knowledge-based integrated information systems engineering: Highlights and bibliography. Knowledge-Based Integrated Information Systems Engineering (KBIISE) Project, volume 1
[AD-A195850] 24 p3435 N88-30449

DISTRIBUTION (PROPERTY)

- NT ANGULAR DISTRIBUTION
- NT ANTENNA RADIATION PATTERNS
- NT BOLTZMANN DISTRIBUTION
- NT BRIGHTNESS DISTRIBUTION
- NT CHARGE DISTRIBUTION
- NT CURRENT DISTRIBUTION
- NT DIFFRACTION PATTERNS
- NT ELECTRON DENSITY PROFILES
- NT ELECTRON DISTRIBUTION
- NT ENERGY DISTRIBUTION
- NT FLOW DISTRIBUTION
- NT FORCE DISTRIBUTION
- NT FREQUENCY DISTRIBUTION
- NT HOLE DISTRIBUTION (ELECTRONICS)
- NT HOLE DISTRIBUTION (MECHANICS)
- NT INTERFERENCE LIFT
- NT ION DISTRIBUTION
- NT LOAD DISTRIBUTION (FORCES)
- NT MASS DISTRIBUTION
- NT MOMENT DISTRIBUTION
- NT PRESSURE DISTRIBUTION

NT RADIAL DISTRIBUTION
NT RADIATION DISTRIBUTION
NT SIDELOBES
NT SPATIAL DISTRIBUTION
NT SPECTRAL ENERGY DISTRIBUTION
NT STAR DISTRIBUTION
NT STRAIN DISTRIBUTION
NT STRESS CONCENTRATION
NT STRESS DISTRIBUTION
NT TEMPERATURE DISTRIBUTION
NT VELOCITY DISTRIBUTION
NT VERTICAL DISTRIBUTION
Measurement of agglomerate strength distributions in agglomerated powders
[DE87-013605] 01 p0090 N88-10591
A 10 W transverse flow excimer laser 03 p0302 N88-11901
Macroscopic distribution of fiber finish
[DCQ/L-48-283/F] 07 p0827 N88-15013
Advanced communication systems: A report on fiber optic technology and its possible applications in the gas industry
[PB88-112792] 07 p0845 N88-15125
On the extreme points of the set of all 2xn bivariate positive quadrant dependent distributions with fixed marginals and some applications
[AD-A186316] 07 p0911 N88-15521
Some new approaches to multivariate probability distributions
[AD-A186038] 07 p0914 N88-15551
An analytic model for ionization distributions produced in nanometer sites by protons
[DE88-003943] 10 p1406 N88-18385
Stratospheric trace gas distributions from fair infrared thermal emission spectroscopy 13 p1797 N88-20749
The Earth radiation budget and its spatial and temporal variations 14 p1936 N88-21548
Assessment of crop loss from air pollutants: Meteorology-atmospheric chemistry and long range transport
[PB88-146857] 15 p2089 N88-22448
Rocket-borne low energy ion measurements in space 18 p2593 N88-25412
Measurements of vacuum arc ion charge state distributions
[DE88-008249] 23 p3284 N88-29558

DISTRIBUTION FUNCTIONS
Measures of diversity based on fuzzy multinomial distributions
[DE87-010617] 02 p0228 N88-11439
Enhanced noise and Raman scattering in plasma
[DE87-014466] 02 p0238 N88-11501
Monte Carlo analysis of neoclassical transport for a compact helical system
[IPPJ-850] 04 p0492 N88-13033
Extrema of skewed stable processes
[AD-A185422] 05 p0642 N88-13925
Further studies in estimation of life distribution characteristics from censored data
[AD-A184862] 05 p0643 N88-13937
Restoration of particle pitch angle distribution functions by a maximum entropy algorithm
[ATR-86(7098)-3] 05 p0648 N88-13969
Slowing down tail enhanced, neoclassical and classical alpha particle fluxes in tokamak reactors
[DE88-001930] 06 p0783 N88-14806
Electron acceleration by wave processes in the earth's ionosphere
[AD-A186110] 07 p0877 N88-15320
Bounding the expectation of convex functions with limited distribution information
[AD-A186147] 07 p0910 N88-15512
A smooth nonparametric quantile estimator from right-censored data
[AD-A186180] 07 p0915 N88-15552
Electron temperature measurements in an argon/cesium plasma diode
[AD-A188835] 12 p1695 N88-20141
Peetre's Theorem and generalized functions
[MEMO-661] 14 p1967 N88-21742
Distributions of quadratic forms
[AD-A190224] 15 p2124 N88-22663
Estimation of convolution tails
[AD-A190323] 15 p2125 N88-22666
A model of intrazonal trip distribution considering centrality index 16 p2257 N88-23486
Symmetrized nearest neighbor regression estimates
[AD-A191998] 18 p2568 N88-25254
Ion thermal conductivity and ion distribution function in the banana regime
[IPPJ-865] 19 p2729 N88-26208
A modal approach to Arctic noise modelling with implied vertical coherence
[AD-A192966] 20 p2850 N88-26916
Moment approach to neoclassical flows, currents and transport in auxiliary heated tokamaks
[DE88-008024] 21 p3016 N88-27901
Analysis of lower hybrid current drive and rampup experiments on the JT-60 tokamak
[DE88-753136] 21 p3018 N88-27915
Equilibrium distribution functions for limited plasma-molecular systems
[DE88-702412] 21 p3018 N88-27916
Comparison of the bidirectional reflectance distribution function of various surfaces
[NASA-TM-101317] 22 p3153 N88-28760
On the nucleonics component of cosmic radiation, in the atmosphere
[DE88-702493] 22 p3166 N88-28854
Wigner distribution function: Relation to short-term spectral estimation, smoothing and performance in noise
[AD-A193865] 23 p3275 N88-29492
Sequential approach to Colombeau's theory of generalized functions
[DE88-701869] 23 p3276 N88-29503
Moment invariants for particle beams
[DE88-011052] 23 p3281 N88-29537

DISTRIBUTION MOMENTS
NT MEAN
NT ORTHOGONALITY
NT STANDARD DEVIATION
Variances and higher order correlation coefficients: Continued
[RR-655-M] 18 p2563 N88-25219

DISTRIBUTORS
Harmonic considerations for electrical distribution feeders
[DE88-007849] 18 p2505 N88-24860

DISTURBANCE THEORY
U PERTURBATION THEORY

DISTURBANCES
A finite-amplitude analysis of the buoyant instability of a highly viscous film over a less viscous half-space 13 p1769 N88-20581

DISULFIDES
Lithium/disulfide battery R and D
[DE88-003032] 11 p1481 N88-18839

DITCHING (LANDING)
An analytical method for ditching analysis of an airborne vehicle
[NASA-CR-4120] 07 p0816 N88-14968

DITHIOLS
U THIOLS

DIURNAL RHYTHMS
U CIRCADIAN RHYTHMS

DIURNAL VARIATIONS
Asymmetry and variations of solar limb darkening along the diameter defined by diurnal motion in April 1981 04 p0506 N88-13111
An analytical soil thermodynamic model for the diurnal variation of ground surface temperature
[AD-A185388] 05 p0625 N88-13823
The lengthening and shortening of the day
[KNMI-TR-91] 05 p0628 N88-13839
Variations of the semi-diurnal tidal wind in the meteor region with periods of about 27 and 13.5 days 06 p0734 N88-14516
Tidal activity in the meteor zone over Budrio, Italy 06 p0734 N88-14517
Density variations of meteor flux along the Earth's orbit 06 p0739 N88-14545
Area of reduced electron concentration in terrestrial plasmasphere 08 p1003 N88-16078
Determination of the heat conduction coefficient of the soil from the advance of the diurnal temperature wave 08 p1015 N88-16151
Solar tides in the upper equatorial thermosphere: A comparison between AE-E data and the NCAR thermospheric general circulation model
[AD-A186160] 08 p1023 N88-16196
The influence of atmospheric thermal tides on diurnal variations in chemical constituents in the mesosphere 11 p1512 N88-19035
Radiation balance components above the tropical evergreen Amazon forests (3rd campaign of data collection)
[INPE-4195-PRE/1079] 11 p1513 N88-19039
Computer simulation of tropospheric chemistry
[JUEL-2144] 13 p1798 N88-20756
Diurnal variations in optical depth at Mars: Observations and interpretations
[NASA-TM-100057] 18 p2595 N88-25420
Interpretation of the northward B sub z (NBZ) Birkeland current system and polar cap convection patterns in terms of the impulsive penetration model
[AERONOMICA-ACTA-A-321-1987] 18 p2595 N88-25422
Urbanization: Its detection and effect in the United States climate record 22 p3125 N88-28571
Comparison of morning with afternoon nitrogen elimination in resting subjects breathing 100 percent oxygen
[AD-A196191] 24 p3407 N88-30282

DIVERGENCE
A study of diverging detonation in high-explosive systems
[DE87-006070] 01 p0031 N88-10194
The application of divergence equation in the analysis of heavy rainfall 02 p0207 N88-11299
Particle velocity and stress gage measurements in spherical diverging flow
[DE87-007333] 03 p0321 N88-12033
Wing divergence of trimmed aircraft 05 p0550 N88-13354
Periodically pulsed excimer master oscillator-regenerative amplifier laser set 06 p0772 N88-14741
Particle-gas temperature differentials resulting from time-dependent radiative-conductive heat flux divergences in the tenuous dust-laden atmosphere of mars
[AD-A185888] 07 p0945 N88-15747
A cause of divergence in the Kalman gain equation 12 p1578 N88-19438
Effect of electron beam divergence on the gain of free electron lasers 14 p1902 N88-21358
Involution-dependent constants and the cancellation of divergences in the 1-loop open string amplitude
[DE88-006537] 15 p2146 N88-22811
Current flight test experience related to structural divergence of forward-swept wings
[NASA-TM-100445] 18 p2464 N88-24633
Utilization of a single clear-air Doppler radar beam to measure vertical divergence
[AD-A195543] 24 p3405 N88-30271

DIVERTERS
Simulation an experiment on plasma instability investigation in a tokamak with a divertor
[DE88-700352] 07 p0935 N88-15683
Two-dimensional analysis for a scrapeoff and divertor regions with an MHD model. Conceptual design study of FY86 FER
[DE88-751069] 09 p1251 N88-17497
Design of divertor plate and measurements of double-null open divertor plasma in the JFT-2M tokamak
[DE88-753130] 21 p3018 N88-27914

DIVIDING (MATHEMATICS)
Spectral representation of infinitely divisible processes
[AD-A186210] 07 p0910 N88-15515

DIVING (UNDERWATER)
Challenges of physiological monitoring in a Navy operational setting 16 p2239 N88-23374
Subsea approach to work systems development 17 p2379 N88-24146
Proceedings of the Colloquium on Space and Sea
[ESA-SP-280] 19 p2695 N88-26016
Experience in occupational medicine, derived from 16 operational deep saturation trimix 5 dives in GUSI from 150 to 600 m 19 p2695 N88-26018
Life in a hyperbaric environment. A new O2-H2 breathing mixture for industrial diving 19 p2695 N88-26019
Technical challenges in the development of a European space suit system and comparison with underwater suits 19 p2696 N88-26024
The relationship between preflight underwater training and space motion sickness 19 p2696 N88-26025
Similarities between diving operations and space missions 19 p2697 N88-26027
Contribution of ultrasonic Doppler detection of circulating bubbles to human interventions under the sea and in space 19 p2697 N88-26029
Different techniques for intervening under the sea: Possible links with space applications 19 p2697 N88-26030
The SAGA highly autonomous assistance submarine 19 p2698 N88-26034
Decompression procedures and accidents in space and sea 19 p2698 N88-26035
Monitoring of divers/astronauts during missions 19 p2698 N88-26036
Safety aspects in design and operation practice of GKSS underwater simulation plant GUSI 19 p2698 N88-26037
Reducing risks inherent in operating underwater craft: The contribution of classification, the example of the SAGA highly autonomous support submarine 19 p2699 N88-26042
Space and sea: Is there a place for ionization? 19 p2699 N88-26043
ELIT: An autonomous underwater observation robot 19 p2699 N88-26048
Study of human factors engineering criteria for Extra Vehicular Activity (EVA) systems, volume 2
[STF23-F87025-VOL-2] 24 p3409 N88-30293

DIVISION
Theory of dividing vortons 03 p0318 N88-12009

DMSP SATELLITES
Instantaneous pictures of the high-latitude electrodynamics using Viking and DMSP/F7 observations --- Swedish satellite
08 p1025 N88-16209
An assessment of the application of in situ ion-density data from DMSP to modeling of transionospheric scintillation
[AD-A188919] 12 p1643 N88-19840
DMSP-SSM/1 NASA algorithm validation using primarily LANDSAT and secondarily DMSP and/or AVHRR visible and thermal infrared satellite imagery
[NASA-CR-182979] 18 p2532 N88-25024
Investigations of magnetosphere-ionosphere coupling relevant to operational systems
[AD-A195972] 24 p3391 N88-30195
Passive microwave measurements of water vapor fields and rain for locating fronts in cyclonic storms
[AD-A195632] 24 p3404 N88-30267
DNA
U DEOXYRIBONUCLEIC ACID
DO-28 AIRCRAFT
Flight test preparation and measuring data validation for parameter identification 20 p2786 N88-26529
DOCKING
U SPACECRAFT DOCKING
DOCUMENT STORAGE
After ten years of metafiles: Where does the Computer Graphics Metafile fit
[DE88-001840] 07 p0904 N88-15474
Common database interface for heterogeneous software engineering tools
[AD-A189628] 14 p1991 N88-21870
Narrative compression coding for a channel with errors
[AD-A191577] 19 p2642 N88-25673
DOCUMENTATION
Documentation as a management strategy for reaching goals in high-risk research-oriented projects
[DE87-012394] 01 p0105 N88-10685
Guidance for conference rapporteurs
[NASA-CR-182338] 05 p0659 N88-14042
Alouette-ISIS program summary
[NASA-CR-180747] 08 p1023 N88-16195
A hypertext writing environment and its cognitive basis
[AD-A188179] 10 p1389 N88-18298
Documentation for computer code NACL
[LBL-21859] 11 p1531 N88-19145
NASA scientific and technical publications: A catalog of Special Publications, Reference Publications, Conference Publications, and Technical Papers, 1987
[NASA-SP-7063(02)] 15 p2149 N88-22830
The -mdoc macro package: A software tool to support computer documentation standards
[DE88-000500] 18 p2559 N88-25188
Documentation of the Benson Diesel Engine Simulation Program
[NASA-TM-100940] 21 p2898 N88-27201
Engineering data compendium. Human perception and performance. User's guide
[LC-87-19560] 21 p2993 N88-27749
Engineering data compendium. Human perception and performance, volume 1
[LC-87-19560] 22 p3134 N88-28630
Engineering data compendium. Human perception and performance, volume 2
[LC-87-19560] 22 p3134 N88-28631
Engineering data compendium. Human perception and performance, volume 3
[LC-87-19560] 22 p3134 N88-28632
Bibliography of Lewis Research Center technical publications announced in 1987
[NASA-TM-100910] 22 p3162 N88-28832
Technical communication in the computer industry: An information-development process to track, measure and ensure quality 23 p3297 N88-29635
DOCUMENTS
NT ABSTRACTS
NT ASTRONOMICAL CATALOGS
NT BIBLIOGRAPHIES
NT CATALOGS (PUBLICATIONS)
NT ENGINEERING DRAWINGS
NT HANDBOOKS
NT MANUALS
NT PAPERS
NT PERIODICALS
NT PRESIDENTIAL REPORTS
NT RECORDS
NT SUPPLEMENTS
NT TEXTBOOKS
NT TEXTS
NT THESES
NT USER MANUALS (COMPUTER PROGRAMS)
A summary of the Naval Postgraduate School research program
[AD-A186362] 07 p0942 N88-15727
Index of USA-CERL publications for October 1984 - June 1987
[AD-A186375] 07 p0942 N88-15728
FY87 scientific and technical reports, articles, papers, and presentations
[NASA-TM-100318] 08 p1093 N88-16578
Preliminary analysis of an integrated logistics system for OSSA payloads. Volume 3: OSSA integrated logistics support planning document 12 p1584 N88-19480
Streamlining invitation for bids
[AD-A188941] 12 p1705 N88-20206
Application of new technologies to DTIC document processing
[AD-A189778] 15 p2148 N88-22823
Publications on acoustics research at the Langley Research Center during 1980-1986
[NASA-TM-100590] 21 p3013 N88-27881
Development of graded reference radiographs for aluminum welds, phase 1
[AD-A195594] 24 p3381 N88-30140
DOGS
Combined effect of ionizing radiation and altered gas atmosphere on central nervous system
10 p1367 N88-18168
DOMAINS
Modeling XV-15 tilt-rotor aircraft dynamics by frequency and time-domain identification techniques
03 p0263 N88-11657
Weak convergence of sums of moving averages in the alpha-stable domain of attraction
[AD-A186430] 07 p0912 N88-15529
Computational analysis of propagation properties of integrated-optical waveguides using a domain integral equation
[PB87-163358] 09 p1154 N88-16917
Time domain wave propagation in multilayered integrated circuits
[AD-A187462] 10 p1324 N88-17916
Fast Poisson solver on irregular regions by boundary integral-based domain decomposition methods
[DE88-003583] 10 p1399 N88-18340
Domain decomposition preconditioners for the spectral collocation method
[NASA-CR-181620] 10 p1400 N88-18345
Parallel pseudospectral domain decomposition techniques
[NASA-CR-181629] 11 p1524 N88-19101
Boundary shape identification problems in two-dimensional domains related to thermal testing of materials
[NASA-CR-181654] 15 p2105 N88-22541
A domain decomposition method for boundary layer problems
[DE88-006917] 19 p2666 N88-25852
Two domain decomposition techniques for Stokes problems
[DE88-006724] 19 p2720 N88-26149
A microcomputer based frequency-domain processor for laser Doppler anemometry
[NASA-TM-100998] 20 p2803 N88-26634
Spatial organization of homopolymer chains inside spherical polybutadiene domains of SB diblock copolymers
[AD-A193390] 21 p2918 N88-27321
Multiple solutions and bifurcation for a class of nonlinear Sturm-Liouville eigenvalue problems on an unbounded domain
[AD-A195954] 24 p3426 N88-30389
DOMES (GEOLOGY)
Diapirs of the Mediterranean ridge: The tectonic regime of an incipient accreted terrane
24 p3396 N88-30224
DOMES (STRUCTURAL FORMS)
Airborne tracking sunphotometer apparatus and system
[NASA-CASE-ARC-11622-1] 06 p0730 N88-14492
DONOR MATERIALS
Excimer laser-assisted deposition of GaAs, AlAs and (Al,Ga)As from Lewis acid-base adducts
[AD-A184588] 03 p0329 N88-12081
Modeling the primary events of photosynthesis using chlorophyll containing fixed distance donor-acceptor molecules
[DE88-010033] 20 p2831 N88-26793
DOORS
Some highlights on ROSAT mechanisms
14 p1874 N88-21195
DOPED CRYSTALS
Structural characterization of ion implanted beta-SiC thin films
[DE87-014567] 05 p0656 N88-14027
Investigation of silicon surface passivation by silicon nitride film deposition
[NASA-CR-182350] 06 p0729 N88-14487
Use of lasers with F sub A(II)-color center KCl:Li crystals in the intraresonator laser spectroscopy method
06 p0769 N88-14729
Structural characterization of undoped and doped GaAs: A comparative study of four techniques
[DE88-004552] 11 p1555 N88-19304
Growth of Cr,Nd:Gd3Sc2Al3O12 (Cr,Nd:GSAG) crystals by the Heat Exchanger Method (HEM)(trademark)
[DE88-004041] 11 p1558 N88-19326
Optical absorption in doped CdxHg1-xTe
[AD-A187434] 11 p1560 N88-19338
Pressure-dependent DLTS (Deep Level Transient Spectroscopy) experiments on Si-doped AlGaAs
[DE88-003842] 13 p1846 N88-21047
Singlet oxygen behavior in solid polymer matrices
[DE88-005171] 15 p2043 N88-22171
Superconductivity and the tailoring of lattice parameters of the compound YBa2Cu3O(sub x)
[DE88-005904] 15 p2140 N88-22769
Electrical and optical properties of Hg/sub 1-x/Cd/sub x/Te doped layers grown by Liquid Phase Epitaxy (LPE)
[DE88-701023] 16 p2281 N88-23653
Improved GaP doped SiGe thermoelectric material
17 p2437 N88-24503
Determination of doping profiles in silicon from resistivity measurements via the four-point probe in combination with layer strippings via anodic oxidation
18 p2583 N88-25347
Electron tunneling in junctions doped with semiconductors and metals 19 p2734 N88-26236
Superlattice doping interfaces
20 p2866 N88-27019
Blue-green laser diode research program
[AD-A191980] 23 p3218 N88-29153
Solid-state laser research report: Energy transfer in non-uniform codoped crystals
[AD-A194358] 23 p3219 N88-29161
Development of a unit cell for a Ge:Ga detector array
[NASA-CR-177445] 24 p3375 N88-30100
Growth and characterization of materials for tunable lasers in the near infrared spectral region
[NASA-CR-183132] 24 p3377 N88-30113
DOPES
Blue-green laser diode research program
[AD-A183517] 01 p0051 N88-10323
Investigation of two laser beam coupling and amplification in Ce-doped SBN single crystals
03 p0327 N88-12069
Numerical calculations of dopent diffusion involving flashlamp heating of silicon 21 p2929 N88-27384
DOPING (ADDITIVES)
U ADDITIVES
DOPPLER EFFECT
The sequential evaluation of Doppler satellite observations
[REPT-141] 01 p0010 N88-10057
Analysis of counting errors in the phase/Doppler particle analyzer
[NASA-TM-100231] 03 p0323 N88-12043
Flux tube dynamics and solar/stellar redshift measurements 04 p0503 N88-13095
Doppler snapshots 04 p0508 N88-13125
Anomalies in electromagnetic absorption of circularly polarized ultrasonic waves by tungsten within Doppler-shifted cyclotron resonance range
06 p0775 N88-14756
Experimental research of electron beam instability on the Doppler anomalous effect
[DE88-700565] 07 p0932 N88-15658
A generalized description of the anomalous Doppler resonance and the stabilizing role of ion dynamics
[INPE-4384-PRE/1204] 08 p1081 N88-16513
Comparison of UNL laser imaging and sizing system and a phase/Doppler system for analyzing sprays from a NASA nozzle
[NASA-CR-182437] 09 p1161 N88-16956
Product kinetic and internal energy distributions via velocity-aligned Doppler spectroscopy
[DE88-003510] 10 p1298 N88-17764
Position, scale, and rotation invariant target recognition using range imagery
[AD-A188828] 12 p1633 N88-19772
Observations of the upper ocean using a multi-beam Doppler sonar
[AD-A188896] 12 p1649 N88-19878
A polarization diversity meteorological radar system
[AD-A189291] 13 p1758 N88-20515
Observations of waves and Langmuir circulation with Doppler sonars 13 p1805 N88-20790
Determination of beam orientation of optical diagnostics of excited 200-MeV hydrogen atoms resulting from photodetachment of H(-)ions
[AD-A189976] 14 p1981 N88-21823
Laser Doppler anemometry
[NASA-TM-100072] 16 p2210 N88-23187

Considerations pertinent to the Doppler effect for space reactors 17 p2399 N88-24264
Delay-doppler radar imaging
[AD-A191509] 18 p2499 N88-24826
Feature extraction using the Hough transform
[AD-A190679] 18 p2555 N88-25165
Doppler distortion of solar Fraunhofer lines in zodiacal light by reflection from interplanetary dust 19 p2740 N88-26270
Developing diagnostic methods for plasma-particle interaction
[DE88-007726] 20 p2858 N88-26973
Laser spectoscopy of plasmas
[AD-A193009] 20 p2861 N88-26991
Radar information from the partial derivatives of the echo signal phase from a point scatterer
[AD-A193402] 21 p2933 N88-27415
Is the 3C273 quasar Mach nearer
[DE88-702235] 21 p3030 N88-27988
The behavior of a Costas loop in the presence of space telemetry signals 22 p3067 N88-28198
Particle sizing in combustion systems, using scattered laser light
[AD-A196231] 24 p3352 N88-29953
Doppler-corrected differential detection system
[NASA-CASE-NPO-16987-1-CU] 24 p3359 N88-30001

DOPPLER RADAR
NT MULTISTATIC RADAR
New nowcasting opportunities using modern meteorological radar 02 p0199 N88-11245
Nowcasting microbursts using Doppler radar in a forecaster-computer environment 02 p0200 N88-11246
Use of a 5 cm Doppler radar to detect and forecast severe thunderstorms in a real time forecast operation 02 p0200 N88-11247
Thunderstorm nowcasting using Doppler radar and soundings 02 p0200 N88-11248
A real-time system for automatic single-Doppler wind field analysis 02 p0200 N88-11249
Diagnosing short term changes in temperature and moisture profiles from single Doppler radar 02 p0200 N88-11251
Delay-Doppler radar imaging
[AD-A184165] 03 p0308 N88-11943
Study of an airborne Doppler radar: Project Asterix
[BLL-MO-TRANS-1667-(9022.552)] 04 p0432 N88-12675
Media calibrations of the Doppler signal for a gravitational wave experiment --- interplanetary medium
[IFSI-86-13] 05 p0625 N88-13825
Meteor observation by the Kyoto meteor radar 06 p0733 N88-14507
Meteor detection on ST (MST) radars 06 p0740 N88-14554
The Cyclone meteor radar system for routine wind measurements in the lower thermosphere 06 p0741 N88-14555
Radar observations of changes in precipitation size spectra associated with lightning 06 p0744 N88-14576
Wind shear detection. Forward-looking sensor technology
[NASA-CP-10004] 07 p0817 N88-14970
Waveform for short-dwell-time meteorological Doppler radars
[PB88-102199] 07 p0845 N88-15126
Problems and possible solutions involved in hard target calibration of coherent Doppler lidar 07 p0922 N88-15602
Development of a Doppler wind lidar system for atmospheric wind measurements 08 p1027 N88-16217
Remote measurement of aerosol stream velocity with continuous-wave CO2-laser 08 p1079 N88-16506
Meteorological radar and its usage in the Navy
[AD-A186650] 09 p1152 N88-16902
Backscattering signal analysis concerning a three-dimensional object configuration on the basis of object motion
[ESA-TT-1044] 09 p1154 N88-16915
Airborne Wind Shear Detection and Warning Systems: First Combined Manufacturers' and Technologists' Conference
[NASA-CP-10006] 10 p1273 N88-17616
Airborne Doppler radar technology for wind shear detection 10 p1274 N88-17622
Crew interface with windshear systems 10 p1275 N88-17631
Status of FAA terminal Doppler weather radar programs 10 p1275 N88-17632
The advanced low-level windshear alert system operational demonstration results, Summer, 1987, Denver Stapleton International Airport 10 p1275 N88-17633
New monostatic balanced Doppler velocimeter using a polarization preserving fiber
[PB88-130869] 11 p1490 N88-18895
Ground clutter processing for wind measurements with airport surveillance radars
[AD-A187708] 11 p1514 N88-19044
Retrieval of three-dimensional wind and temperature fields from single-Doppler radar data 12 p1646 N88-19858
Remote sensing of meteorological parameters with the aid of a clear-air Doppler radar
[PB88-142518] 12 p1647 N88-19864
Development and testing of the gust front algorithm
[AD-A189722] 14 p1949 N88-21622
A very wide frequency band pulsed/IF radar system
[NASA-CR-182889] 16 p2190 N88-23059
TDWR (Terminal Doppler Weather Radar) clutter residue map generation and usage
[AD-A191148] 16 p2235 N88-23352
Doppler radar with multiphase modulation of transmitted and reflected signal
[NASA-CASE-MSC-18808-1] 17 p2332 N88-23923
Observation of stratiform rain with 94 GHz and s-b and Doppler radar
[AD-A192013] 18 p2544 N88-25100
Aircraft/lidar turbulence comparison 18 p2546 N88-25111
The Federal Aviation Administration/Massachusetts Institute of Technology (FAA/MIT) Lincoln Laboratory Doppler weather radar program 18 p2547 N88-25118
TDWR (Terminal Doppler Weather Radar) PRF (Pulse Repetition Frequency) selection criteria
[AD-A193089] 21 p2932 N88-27407
Definition of long ocean wave slope for radar applications
[AD-A193198] 21 p2933 N88-27412
Application of acoustic-Doppler current profiler and expendable bathythermograph measurements to the study of the velocity structure and transport of the Gulf Stream
[NASA-CR-183188] 22 p3129 N88-28605
Application of the Hilbert transform to Doppler radar signals from a hypervelocity gun
[AD-A193690] 22 p3146 N88-28716
Airborne radar technology for windshear detection
[NASA-CR-183203] 23 p3236 N88-29257
The NAE atmospheric research aircraft 24 p3313 N88-29730
Doppler radar analysis of coastal marine atmospheric boundary layer structure during a cold air outbreak
[AD-A196023] 24 p3403 N88-30261
Utilization of a single clear-air Doppler radar beam to measure vertical divergence
[AD-A195543] 24 p3405 N88-30271

DORNIER AIRCRAFT
NT DO-28 AIRCRAFT

DORNIER DO-28 AIRCRAFT
U DO-28 AIRCRAFT

DOSAGE
NT RADIATION DOSAGE
Dexamethasone as prophylaxis for acute mountain sickness: Effect of dose level
[AD-A185848] 08 p1047 N88-16325
Low doses of atropine sulfate impair retention of a well-learned spatial task
[AD-A194065] 23 p3237 N88-29266
Heavy ion and proton tests for subsystem upset
[AD-A195267] 24 p3434 N88-30442

DOSE
U DOSAGE

DOSIMETERS
NT THRESHOLD DETECTORS (DOSIMETERS)
Low altitude flux and dose measurements during two solar flare events 01 p0111 N88-10713
Fabricate, calibrate and test a dosimeter for integration into the CRRES (Combined Release and Radiation Effects Satellite) satellite
[AD-A185439] 05 p0585 N88-13564
NBS (National Bureau of Standards) measurement services: Fricke dosimetry in high-energy electron beams
[PB88-110374] 06 p0781 N88-14795
An analytic model for ionization distributions produced in nanometer sites by protons
[DE88-003943] 10 p1406 N88-18385
Characterization of space radiation environment in terms of the energy deposition in functionally important volumes
[DE88-005627] 15 p2100 N88-22513
Anthropomorphic phantom radiation dosimetry at the NATO standard reference point at Aberdeen Proving Ground
[AD-A190508] 15 p2103 N88-22528
Dosimetric mapping inside Biorack --- Spacelab D1 mission 22 p3062 N88-28169
A study of the National Physics Laboratory microdosimetry research programme in collaboration with the University of Leeds (United Kingdom)
[NPL-RS(EXT)-93] 23 p3217 N88-29148

DOSIMETRY
U DOSIMETERS

DOUBLE BASE PROPELLANTS
NT DOUBLE BASE ROCKET PROPELLANTS
Nonlinear mechanisms of solid propellant combustion instability 19 p2628 N88-25588

DOUBLE BASE ROCKET PROPELLANTS
Ignition studies in a two-stage closed vessel using various igniter materials
[ISL-CO-231/86] 09 p1142 N88-16843
Combusion of a double base fuel in the presence of inert gases
[INPE-4516-RPE/564] 16 p2170 N88-22936

DOUBLE STARS
NT BINARY STARS
NT CATACLYSMIC VARIABLES
NT DWARF NOVAE
NT ECLIPSING BINARY STARS
NT NEMESIS (STAR)
Observation of a point source in Cygnus constellation with the underground detector at Frejus (France)
[PITHA-87/02] 20 p2884 N88-27122

DOUGLAS AIRCRAFT
NT DC 9 AIRCRAFT

DOUGLAS DC-9 AIRCRAFT
U DC 9 AIRCRAFT

DOUGLAS MILITARY AIRCRAFT
U MILITARY AIRCRAFT

DOVAP
U DOPPLER EFFECT

DOWNLINKING
Rapid toxicity detection in water quality control utilizing automated multispecies biomonitoring for permanent space stations 02 p0135 N88-10848
Analysis of the ICE combiner for multiple antenna arraying 04 p0436 N88-12704
MARCE data evaluation 10 p1286 N88-17693
X-band system performance of the very large array 11 p1473 N88-18789
Project SKYLITE: A design exploration
[AD-A187906] 11 p1511 N88-19030
INPE position paper on the CCSDS standardized method of link budget computation
[INPE-4533-NTE/279] 15 p2148 N88-22820
Satellite communications experiment for the Ontario air ambulance service 19 p2646 N88-25705
A VLSI single-chip (225,223) Reed-Solomon encoder with interleaver
[NASA-CASE-NPO-17280-1-CU] 21 p2902 N88-27220
A statistical rain attenuation prediction model with application to the advanced communication technology satellite project. 1: Theoretical development and application to yearly predictions for selected cities in the United States
[NASA-CR-179498] 23 p3205 N88-29077

DOWNWASH
Reduction of tilt rotor download using circulation control 10 p1271 N88-17605
A simple, analytic 3-dimensional downburst model based on boundary layer stagnation flow
[NASA-TM-100632] 22 p3042 N88-28058

DPCM (MODULATION)
U DIFFERENTIAL PULSE CODE MODULATION

DRAFTING (DRAWING)
Development of a line-drawing algorithm
[CS-8701] 01 p0082 N88-10530

DRAG
NT AERODYNAMIC DRAG
NT FRICTION DRAG
NT INTERFERENCE DRAG
NT PRESSURE DRAG
NT SATELLITE DRAG
NT SUPERSONIC DRAG
NT VISCOUS DRAG
Boundary effects on the drag of an oscillating sphere: Applications to the magnetic sphere rheometer. Attenuation and dispersion of acoustic waves in nematic liquid crystals 04 p0488 N88-13007
The drag of slender axisymmetric cones in rarefied hypersonic flow 05 p0531 N88-13229
Aerodynamic and propeller performance characteristics of a propfan-powered, semispan model
[NASA-TM-86705] 06 p0667 N88-14092
Propulsion challenges and opportunities for high-speed transport aircraft 08 p0958 N88-15809
Influence of base modifications on in-flight base drag in the presence of jet exhaust for Mach numbers from 0.7 to 1.5
[NASA-TP-2802] 11 p1488 N88-18881

Experimental investigation of hypersonic aerodynamics
[NASA-CR-182973] 18 p2458 N88-24591
Continuum theories for fluid-particle flows: Some aspects of lift forces and turbulence
[DE88-007038] 18 p2511 N88-24898
Drag measurements on a laminar flow body of revolution in Langley's 13 inch magnetic suspension and balance system
[NASA-CR-182909] 19 p2597 N88-25432
Ludwig Prandtl collected treatises on applied mechanics, hydro- and aerodynamics, part 2, IV interfaces and resistance
[NASA-TT-20315] 20 p2752 N88-26338
Why plasma armature railguns don't work (and what can be done about it)
[DE88-007900] 20 p2763 N88-26384
Experimental investigation of turbulent flow in smooth and longitudinal grooved tubes
[NASA-TM-77480] 20 p2800 N88-26615
Infrared detectors based on the photon drag effect and intersubband absorption by a two-dimensional electron gas 20 p2867 N88-27024

DRAG BALANCE
U AERODYNAMIC BALANCE
U LIFT DRAG RATIO

DRAG CHUTES
Discrete vortex analysis of unsteady flow about two-dimensional cambered plates
[DE88-006597] 14 p1909 N88-21407
Unsteady flow about cambered plates
[AD-A191226] 17 p2337 N88-23945

DRAG COEFFICIENTS
An experimental evaluation of advanced rotorcraft airfoils in the NASA Ames eleven-foot transonic wind tunnel
[NASA-CR-166587] 03 p0261 N88-11640
The effect of sting interference at low speeds on the drag coefficient of an ellipsoidal body using a magnetic suspension and balance system
[NASA-CR-181611] 13 p1718 N88-20274

DRAG DEVICES
NT DRAG CHUTES
NT LEADING EDGE FLAPS
NT SPOILERS
NT TRAILING EDGE FLAPS
NT VORTEX FLAPS
NT WING FLAPS

DRAG EFFECT
U DRAG

DRAG MEASUREMENT
Flow field measurements using hotwire anemometry
[AD-A187029] 09 p1160 N88-16951
Precision measurement of the Fresnel drag coefficient using a ring laser
[AD-A196025] 24 p3366 N88-30043
Experimental determination of drag modifications due to elastic compliant surfaces using quantitative visual techniques
[AD-A194785] 24 p3372 N88-30082

DRAG REDUCTION
Transonic analysis and design of axisymmetric bodies in nonuniform flow
[NASA-CR-4101] 01 p0003 N88-10013
Investigations on a transonic airfoil with a 30 mm wide perforation/cavity arrangement
[ESA-TT-1072] 03 p0260 N88-11634
Navier-Stokes analysis of laminar flow control of a two-dimensional airfoil 05 p0540 N88-13286
Wakes of two dimensional bluff bodies in subsonic flow. Influence of a separating plate and of a pulsed injection of momentum
[IMFL-4200-86/75] 05 p0541 N88-13297
Combined riblet and lebu drag reduction system
[NASA-CASE-LAR-13286-1] 06 p0664 N88-14071
Turbulence, turbulence control, and drag reduction
[AD-A185643] 06 p0665 N88-14080
Flight and wind-tunnel measurements showing base drag reduction provided by a trailing disk for high Reynolds number turbulent flow for subsonic and transonic Mach numbers
[NASA-TP-2638] 06 p0701 N88-14299
Wall turbulence control 07 p0812 N88-14943
Overview of the Langley viscous drag reduction program 07 p0812 N88-14946
Natural laminar flow nacelle for transport aircraft 07 p0813 N88-14949
Flight research on natural laminar flow 07 p0813 N88-14950
Design and experimental evaluation of a swept supercritical Laminar Flow Control (LFC) airfoil 07 p0813 N88-14951
Riblets for aircraft skin-friction reduction 07 p0814 N88-14955
Airfoil large eddy breakup devices for turbulent drag reduction 07 p0814 N88-14956
Viscous drag reduction of horizontal plates
[VKI-TN-159] 07 p0851 N88-15171
Full scale and wind tunnel surface pressure measurements on the T.R.R.L. spray dispersion programme vehicles
[REPT-8623] 09 p1114 N88-16676
An application of active surface heating for augmenting lift and reducing drag of an airfoil
[NASA-TM-100563] 11 p1436 N88-18570
Structure of shear flow turbulence and its control
[AD-A187909] 11 p1482 N88-18846
Changes in the turbulent boundary layer structure associated with net drag reduction by outer layer manipulators
[NASA-CR-178152] 11 p1483 N88-18853
Flight tests of external modifications used to reduce blunt base drag
[NASA-TM-100433] 13 p1719 N88-20279
Investigation into the effects of flap end modifications on the performance of a wing with a single slotted flap
[BU-357] 14 p1866 N88-21148
Control of laminar flow around of the wing in free-air conditions
[AD-A187479] 15 p2013 N88-22004
Enhanced viscous flow drag reduction using acoustic excitation
[NASA-CR-182734] 15 p2062 N88-22295
Study of a system for reducing base drag by controlling vortices
[REPT-87/43] 17 p2295 N88-23730
An assessment of the drag reduction properties of riblets and the penalties of off-design conditions
[RAE-TM-AERO-2113] 17 p2295 N88-23731
High-flaps for natural laminar flow airfoils 17 p2296 N88-23739
Wind tunnel testing of low-drag airfoils 17 p2297 N88-23741
Flight experiences with laminar flow 17 p2297 N88-23744
Operational considerations for laminar flow aircraft 17 p2298 N88-23748
Injection of drag reducing additives into turbulent water flows
[AD-A192072] 18 p2509 N88-24888
Manipulation of the structure of a turbulent boundary layer 18 p2512 N88-24901
Aerodynamic analysis of natural laminar flow airfoil 19 p2634 N88-25624
Drag reduction of turbulent boundary layers by means of grooved surfaces
[ETN-88-92618] 20 p2802 N88-26630
Investigations on drag reduction in turbulent pipe flows by addition of ionic and nonionic high polymers
[ETN-88-92380] 21 p2949 N88-27515
VSAERO analysis of tip planforms for the free-tip rotor
[NASA-CR-177487] 22 p3038 N88-28036
A new method of calculating the boundary layer characteristics downstream of manipulators. Part 1: Boundary layer integral parameters
[PNR90455] 22 p3078 N88-28279
A new method of calculating the boundary layer characteristics downstream of manipulators. Part 2: Skin friction and net drag reduction
[PNR90456] 22 p3078 N88-28280
A preliminary investigation of drag reduction and mechanism for a blunt body of revolution with slanted base
[NASA-TT-20349] 24 p3317 N88-29753
Compression pylon
[NASA-CASE-LAR-13777-1] 24 p3323 N88-29789
Development and design of windtunnel and test facility for RPV (Remote Piloted Vehicle) enhancement devices
[AD-A194842] 24 p3329 N88-29822
The viscous flow on surfaces with streamline riblets
[ESA-TT-1091] 24 p3370 N88-30067

DRAGULATORS
U BRAKES (FOR ARRESTING MOTION)

DRAINAGE
Open-graded bases for airfield pavements
[AD-A184461] 04 p0402 N88-12500
Partial likelihood analysis of time series models with application to rainfall-runoff data
[AD-A191157] 16 p2261 N88-23516
Characteristics of drainage determinations in aerial photographs and relief determination on different scales planialtimetric charts for three soils in the state of Sao Paulo 17 p2367 N88-24095
Criteria for planimetric and altimetric correction of maps restituted from aerial photographs in 1:100,000 scale 17 p2367 N88-24097
Use of remote sensing in the study of superficial formation certifying the development of integrated economy-case example: Rio Claro (SP) region 19 p2683 N88-25950

DRAINAGE PATTERNS
Hydrologic models for land-atmosphere retrospective studies of the use of LANDSAT and AVHRR data
[NASA-CR-182862] 20 p2818 N88-26716

DRAINING
U DRAINAGE

DRAWINGS
NT ENGINEERING DRAWINGS
PLOT3D (version-5): A computer code for drawing three dimensional graphs, maps and histograms, in single or multiple colours, for mono or stereoscopic viewing
[DE88-701410] 15 p2108 N88-22558

DREDGING
Use of SPOT HRV data in the US Army Corps of Engineers dredging program 22 p3109 N88-26466

DRIFT
Theoretical investigations of drift waves in a magnetic quadrupole 18 p2578 N88-25312

DRIFT (INSTRUMENTATION)
Testing of a gravimeter LCR G 785
[B8735061] 20 p2806 N88-26643

DRIFT RATE
Sea ice kinematics: Space and time scales
[AD-A191162] 17 p2376 N88-24128

DRILLING
Design and test of high performance composite tubes for use in deep water drilling and production systems
[SNIAS-872-430-107] 05 p0572 N88-13487
High performance composite tubes for offshore applications
[SNIAS-872-430-116] 05 p0572 N88-13488
Geological evolution and analysis of confirmed or suspected gas hydrate localities. Volume 9: Formation and stability of gas hydrates of the Middle America Trench
[DE88-001007] 10 p1347 N88-18050
Drilling metal matrix composites
[AD-A190480] 15 p2029 N88-22091

DRILLS
Investigation into the operation of the new special drills for drilling holes in thin components made of composite materials --- aircraft components
[LR-519] 16 p2215 N88-23215
Frequency Analysis of Acoustic Emission - Application to machining and welding
[DE88-701478] 18 p2570 N88-25262

DRINKING
Reverse osmosis treatment to remove inorganic contaminants from drinking water
[PB88-147780] 12 p1605 N88-19598
Variability in intake and dehydration in young men during a simulated desert walk
[AD-A192654] 22 p3131 N88-28613

DROGUE PARACHUTES
U DRAG CHUTES

DROGUES
U TOWED BODIES

DRONE AIRCRAFT
Towards the unmanned cockpit 02 p0129 N88-10812

DRONE HELICOPTERS
U DRONE AIRCRAFT
U HELICOPTERS

DRONE VEHICLES
NT DRONE AIRCRAFT
An efficient representation of spatial information for expert reasoning in robotic vehicles 09 p1214 N88-17278

DROP SIZE
Stability relationship for water droplet crystallization with the NASA Lewis icing spray
[NASA-TM-100220] 02 p0125 N88-10790
Drop formation from an orifice in an electric field
[DE87-014405] 03 p0322 N88-12034
Analysis of counting errors in the phase/Doppler particle analyzer
[NASA-TM-100231] 03 p0323 N88-12043
Anthropogenic effects on the droplet formation process, and ion concentrations in droplets --- clouds 08 p1018 N88-16175
Digital imaging techniques for single- and multi-phase reacting flowfields 10 p1327 N88-17933
Three-dimensional trajectory analyses of two drop sizing instruments: PMS OAP and PMS FSSP
[NASA-CR-4113] 11 p1437 N88-18574
Diagnostics for research in atomization and turbulent two-phase flows
[AD-A187338] 11 p1482 N88-18843
A propagation campaign in a marine environment utilizing a digital system at 36 GHz 12 p1618 N88-19675
Droplet size characteristics and energy input requirements of emulsions formed using high-intensity-pulsed electric fields
[DE88-005912] 15 p2128 N88-22692
Rainfall rates and drop-size distributions for environmental testing
[AD-A191342] 16 p2236 N88-23354

A theoretical model of the washout of trace gases by raindrops in the atmosphere 17 p2375 N88-24125
Small-droplet spray measurements with a scattered-light scanner
[NASA-TM-100973] 20 p2806 N88-26645
Experimental research of combustion systems 21 p2927 N88-27371
Cloud simulation warm cloud experiments: Droplet growth and aerosol scavenging
[AD-A192944] 21 p2974 N88-27666
Holographic determination of droplet size distributions
[DFVLR-MITT-88-05] 22 p3074 N88-28250
Alternative fuel spray behavior 24 p3345 N88-29912
Simulation study of spraying, streaming and vaporization phenomena associated with fuel injection 24 p3345 N88-29914
Multiple scattering effects in drop sizing of dense fuel sprays by laser diffraction 24 p3346 N88-29917
Influence of operating conditions on the atomization and distribution of fuel by air blast atomizers 24 p3346 N88-29918

DROP TESTS
Study of aeropropulsion laboratory pressure drop rig and recommended test procedure
[AD-A184333] 03 p0322 N88-12038
Decomposition of energetic materials on the drop-weight impact machine
[DE88-009154] 22 p3059 N88-28152
Calibration of quartz load cells: An in-situ procedure for instrumented falling weight impact machines
[NPL-DMA(A)-155] 22 p3081 N88-28297

DROP TOWERS
Study of the production of some superconducting and magnetic materials by solidification in the drop tube and drop tower
[NASA-CR-182494] 11 p1461 N88-18708
Critical point wetting drop tower experiment
[NASA-CR-183062] 20 p2798 N88-26603

DROP TUBES
U DROP TOWERS

DROP WEIGHT TESTS
U DROP TESTS

DROPS (LIQUIDS)
NT RAINDROPS
Cooling effect of a single evaporating droplet on a hot semi-infinite metal body
[PB87-201802] 01 p0046 N88-10294
Stability relationship for water droplet crystallization with the NASA Lewis icing spray
[NASA-TM-100220] 02 p0125 N88-10790
Ignition and flame propagation in sprays
[AD-A184679] 03 p0283 N88-11781
A method for remote sensing of precipitable water vapor and liquid in the atmosphere using a 22-ghz radiometer
[AD-A184204] 03 p0354 N88-12232
Experimental evidence for modifying the current physical model for ice accretion on aircraft surfaces
[NASA-TM-87184] 04 p0397 N88-12473
The TAB method for numerical calculation of spray droplet breakup
[DE87-011756] 04 p0442 N88-12743
Energy balance in laser-irradiated vaporizing droplets
[DE88-000525] 04 p0449 N88-12782
Numerical simulation of splash of droplet at unit gravity 05 p0538 N88-13275
Operating envelopes of particle sizing instrumentation used for icing research
[NASA-CR-180870] 05 p0586 N88-13573
A study of the interaction of laser light with liquid propellant drops
[AD-A185117] 05 p0587 N88-13582
Extinction by dielectric particles at optical and infrared wavelength
[AD-A184818] 05 p0650 N88-13981
Undercooling and nucleation in iron nickel alloys
[AD-A185500] 06 p0683 N88-14184
Atmospheric science 07 p0883 N88-15357
Spray deposition: A fundamental study of droplet impingement, spreading and consolidation
[AD-A186627] 08 p0970 N88-15869
Investigation of real-time two-dimensional visualization of fuel spray liquid/vapor distribution via exciplex fluorescence
[AD-A188268] 10 p1307 N88-17816
Transient cooling of a hot surface by droplets evaporation, March 1986 - March 1987
[PB88-153341] 10 p1330 N88-17950
Droplet formation for liquid monopropellant jets
[AD-A187172] 10 p1331 N88-17956
Turbulence interactions in single- and multi-phase turbulent mixing and combustion processes
[AD-A187505] 10 p1332 N88-17960
Three-dimensional trajectory analyses of two drop sizing instruments: PMS OAP and PMS FSSP
[NASA-CR-4113] 11 p1437 N88-18574
Electrohydrodynamic migration of charged droplets in an insulating fluid
[NASA-TM-100849] 14 p1912 N88-21424
Laser induced ignition of propellants
[AD-A191100] 16 p2168 N88-22927
Rainfall rates and drop-size distributions for environmental testing
[AD-A191342] 16 p2236 N88-23354
Method of evaporation
[NASA-CASE-NPO-15609-2] 17 p2318 N88-23846
Liquid droplet radiator development 17 p2424 N88-24415
The liquid droplet radiator in space: A parametric approach 17 p2427 N88-24437
Tower evaporator
[NASA-CASE-NPO-15609-2] 18 p2497 N88-24815
The behavior of drop-containing turbulent eddies
[AD-A191669] 18 p2509 N88-24883
Simple high speed camera with CCD-sensor
[MPIS-8/1987] 18 p2518 N88-24940
Hanging drop crystal growth apparatus and method
[NASA-CASE-MFS-28206-1-SB] 18 p2585 N88-25356
Crystal growth apparatus
[NASA-CASE-MFS-28182-1] 18 p2585 N88-25357
Droplet formation for liquid monopropellant jets 19 p2623 N88-25557
Fuel droplet vaporization and temperature distributions of axisymmetric unsteady sprays 19 p2626 N88-25579
Small-droplet spray measurements with a scattered-light scanner
[NASA-TM-100973] 20 p2806 N88-26645
Numerical simulation of fuel droplet interactions and breakup
[AD-A192431] 21 p2941 N88-27470
Combustion studies of acoustically suspended liquid droplets
[AD-A193892] 23 p3192 N88-28998
High energy and high intensity laser effects on aerosols: Changes in droplet morphology, surrounding temperature and vapor concentration
[AD-A193825] 23 p3220 N88-29164
Influence of the convection on evaporation and combustion of a fuel droplet 24 p3351 N88-29948
General equations for the motions of ice crystals and water drops in gravitational and electric fields
[NASA-CR-183229] 24 p3370 N88-30070

DROSOPHILA
Drosophila geotaxis as a tool for the study of aging 10 p1288 N88-17706
Effects of short spaceflights on Drosophila melanogaster embryogenesis and life span 22 p3061 N88-28166

DROUGHT
Enhancement of surface-atmosphere fluxes by desert-fringe vegetation through reduction of surface albedo and of soil heat flux
[NASA-CR-181442] 02 p0197 N88-11231
Application of multitemporal SPOT data for crop monitoring: Effects of frost and drought 03 p0344 N88-12171
Drought, solar activity link established by Leningrad geophysicists 04 p0458 N88-12835
A drought watch system
[WCP-134] 16 p2234 N88-23345
Using space photography of the Earth in the classroom: Drought in Africa
[NASA-CR-182948] 19 p2685 N88-25960

DROUGHT CONDITIONS
U DROUGHT

DROWSINESS
U SLEEP

DRUG THERAPY
U CHEMOTHERAPY

DRUGS
NT ADRENERGICS
NT ANTIBIOTICS
NT ANTICONVULSANTS
NT ATROPINE
NT CAFFEINE
NT EPINEPHRINE
NT ERGOTAMINE
NT HEMOSTATICS
NT MORPHINE
NT NOREPINEPHRINE
NT PSYCHOTROPIC DRUGS
NT SEDATIVES
NT SEROTONIN
NT STIMULANTS
NT TRANQUILIZERS
Effect of pyrocetam on mouse resistance to hypoxic hypoxia 2-3 months after exposure to X-radiation 07 p0895 N88-15425
Dexamethasone as prophylaxis for acute mountain sickness: Effect of dose level
[AD-A185848] 08 p1047 N88-16325
Efficiency of human workers and means to increase it 12 p1666 N88-19986
A cardiostimulant protein from the Australian Red Waratah Sea anemone, Actinia tenebrosa 18 p2550 N88-25138
Measurement and classification of the mode of action of antidepressant drugs 21 p2983 N88-27714
Measurement of electrical activity in the CNS with cortical evoked potentials and EEG: Efficacy profiles of drugs using factor analysis 21 p2983 N88-27715
An approach to studying the effects of psychostimulants on cerebral electrical activity in the non-human primate 21 p2983 N88-27716
Emetic mechanism in acute radiation sickness
[AD-A194102] 23 p3238 N88-29267

DRUMLINS
U GLACIAL DRIFT

DRUMS (CONTAINERS)
Containment of a silicone fluid free surface in reduced gravity using barrier coatings
[NASA-TM-101314] 24 p3371 N88-30072

DRY CELLS
NT NICKEL ZINC BATTERIES

DRY FRICTION
Dry adhesive friction of elastomers: A study of the fundamental mechanical aspects
[ETN-88-92903] 23 p3198 N88-29036

DRY HEAT
Geothermal energy technology: Issues, R and D (Research and Development) and cooperative arrangements
[PB88-193107] 21 p2967 N88-27626

DRYING
NT DEHUMIDIFICATION
NT DEHYDRATION
Effect of the band-gap characteristics on laser-induced dry etching of semiconductors
[DE88-001853] 07 p0937 N88-15695
The mechanical behavior of particle filled thermoplastics
[ETN-88-92234] 16 p2181 N88-22999
Impact of control errors on the volume/weight demand of the Ventilation and Dryer (VAD) concept — EURECA Botany Facility
[TN-RB524-006/87] 17 p2377 N88-24132
Prospects for hot dry rock in the future
[DE88-010909] 20 p2820 N88-26730
Ellipsometric imaging of drying sol-gel films
[DE88-011785] 21 p2921 N88-27335

DTA (ANALYSIS)
U THERMAL ANALYSIS

DTMB-111 GROUND EFFECT MACHINE
U GROUND EFFECT MACHINES

DTMB-430 GROUND EFFECT MACHINE
U GROUND EFFECT MACHINES

DUAL MODE PROPULSION
U HYBRID PROPULSION

DUALITY PRINCIPLE
An extension of the MS pivoting rule to capacitated network flow problems
[REPT-87-33] 14 p1963 N88-21711

DUALITY THEOREM
Position finding and tolerances
[AD-A187685] 11 p1540 N88-19205
Action-angle maps and scattering theory for some finite-dimensional integrable systems. The pure solution case
[CWI-PM-R8704] 13 p1831 N88-20955
Lagrangian of the self-duality equation and d = 10, N = 2b supergravity
[DE88-701554] 24 p3455 N88-30563

DUCTED FANS
Velocity scaled aeroelastic testing of an unducted fan
[GTL-191] 05 p0548 N88-13337
A dynamic simulation and feedback control scheme for the U.S. Marine Corps' Airborne Remotely Operated Device (AROD)
[AD-A186597] 08 p0953 N88-15784
Aerodynamic performance of a scale-model, counter-rotating unducted fan 10 p1282 N88-17666
Airborne remote operated device
[DE88-010324] 21 p2895 N88-27188

DUCTED FLOW
Flow field measurements in a 90 degree turning duct 02 p0186 N88-11157
Mixed turbulent convective heat transfer in vertical ducts 11 p1485 N88-18865
A survey of oscillating flow in Stirling engine heat exchangers
[NASA-CR-182108] 15 p2067 N88-22322
An investigation of ducted propellers in axisymmetric shear flow 16 p2202 N88-23136
Surface curvature and pressure gradient effects on turbulent flow: An assessment based on numerical solution of the Reynolds equations 17 p2338 N88-23954

Antenna heights for the optimum utilization of the oceanic evaporation duct. Part 3: Results from the Mediterranean measurements, volume 2
[AD-A192311] 20 p2791 N88-26554
Antenna heights for the optimum utilization of the oceanic evaporation duct. Part 1: Results from the Pacific measurements. Part 2: Results from the Key West measurements, volume 1
[AD-A192358] 20 p2791 N88-26555

DUCTED PROPELLERS
U SHROUDED PROPELLERS

DUCTED ROCKET ENGINES
Speed control of a missile with throttleable ducted rocket propulsion 12 p1597 N88-19561
An experimental investigation of rocket ramjet nozzle assembly base pressures
[AD-A189714] 15 p2027 N88-22076

DUCTILITY
Investigation on ductile fracture behavior of 3-inch diameter Type 304 stainless steel pipe with a circumferential through-wall crack
[DE87-753016] 02 p0191 N88-11196
Ultra-fine grained alloy material
[AD-A184500] 03 p0290 N88-11820
Modified 14Cr-16Ni stainless steels with improved creep resistance at 700 C due to tailored precipitate microstructures
[DE87-014788] 03 p0290 N88-11825
Welding and weldability of ductile intermetallic alloys
[DE87-014061] 04 p0416 N88-12582
Investigation by differential scanning calorimetry of microstructure in a superplastic Al-Mg-Zr alloy
[AD-A184902] 05 p0564 N88-13439
An investigation of fatigue crack growth in a ductile material at high growth rates 06 p0715 N88-14383
Sulfur-induced ductility-dip cracking in weld metal of low-carbon steel
[PB87-143814] 07 p0833 N88-15051
J-estimation procedure based on moire interferometry data
[AD-A185965] 07 p0867 N88-15258
The relationship of tensile specimen size and geometry effects to unique constitutive parameters for ductile materials
[AD-A186020] 08 p0994 N88-16012
The influence of small defects on tensile specimen ductility and symmetry of deformation
[AD-A187983] 10 p1346 N88-18044
Brittle to ductile transition to cleavage fracture
[DE88-004074] 10 p1420 N88-18481
Effects of sulfur content on the plain strain fracture toughness of inertia welds in 4340 steel
[AD-A188192] 11 p1458 N88-18689
A simulation of void lining during ductile fracture
[AD-A188404] 12 p1635 N88-19792
Material instabilities in solids
[AD-A189525] 13 p1738 N88-20388
Development of a constitutive equation for HSLA (High-Strength Low-Alloy)-100 at cryogenic temperatures
[AD-A189243] 13 p1740 N88-20408
Ductile failure
[AD-A189429] 13 p1781 N88-20654
The effect of strain rate on the strength and ductility of SiCw/2124 Al composite
[OUEL-1692/87] 14 p1924 N88-21466
The effective fracture toughness of aluminum at rapid heating rates
[AD-A189745] 15 p2038 N88-22146
The variation of torsional ductility of high-purity aluminum with temperature and strain rate
[DE88-005618] 18 p2487 N88-24755
Theoretical and experimental damping values of piping systems at high ductilities
[DE88-006717] 18 p2526 N88-24986
Extended ductility of Al and alpha-Fe alloys through dynamic recovery mechanisms
[DE88-008679] 19 p2616 N88-25522
Optimizing superplastic response in lithium containing aluminum-magnesium alloys
[AD-A192217] 20 p2774 N88-26451
Ductile-brittle transition of cutting behavior in diamond turning of single crystal Si
[DE88-008890] 20 p2809 N88-26664
Microchemical analysis of polycrystalline Ni3Al and other ordered alloys using the field-ion microscope atom probe
[DE88-011519] 21 p2914 N88-27294
Plastic yielding at crack tips
[AD-A192549] 21 p2960 N88-27582
Experimental investigation of ductile fracture by white light moire interferometry 22 p3087 N88-28329
Load interaction effects on compression fatigue crack growth in ductile solids
[FFA-TN-1988-12] 22 p3089 N88-28342
Modeling of micromechanisms of fatigue and fracture in hybrid materials
[AD-A195604] 24 p3382 N88-30142

DUCTS
NT ACOUSTIC DUCTS
NT AIR DUCTS
NT ANNULAR DUCTS
Ducted propeller design and analysis
[DE88-001925] 06 p0664 N88-14069
Aeropropulsion '87. Session 3: Internal Fluid Mechanics Research
[NASA-CP-10003-SESS-3] 08 p0954 N88-15790
Inlets, ducts and nozzles 08 p0955 N88-15791
An estimate of the noise shielding on the fuselage resulting from installing a short duct around an advanced propeller
[NASA-TM-100262] 10 p1405 N88-18379
Unsteady heat transfer in turbine blade ducts: Focus on combustor sources
[NASA-TM-100815] 11 p1486 N88-18870
Electromagnetic propagation in PEC and absorbing curved S-ducts
[NASA-TM-100833] 12 p1621 N88-19698
Flow/acoustic interaction in duct inflow
[AD-A189264] 13 p1833 N88-20967
Numerical and experimental investigation of multiple shock wave/turbulent boundary layer interactions in a rectangular duct
[AD-A190772] 15 p2066 N88-22320
ALEX results: A comparison of measurements from a round and a rectangular duct with 3-D code predictions
[DE88-005947] 15 p2135 N88-22741
Numerical analysis of duct flow using three-dimensional parabolized Navier-Stokes equation
19 p2638 N88-25652
MHD (magnetohydrodynamic) thermal hydraulic analysis of three-dimensional liquid metal flows in fusion blanket ducts
[DE88-009929] 19 p2731 N88-26219
Steady and unsteady internal flow computations via the solution of the compressible Navier Stokes equations for low Mach numbers 23 p3209 N88-29100
Optical measurement of unducted fan blade deflections
[NASA-TM-100966] 23 p3216 N88-29142

DUMMIES
Determination of the effect of walking on the forced convective heat transfer coefficient using an articulated mannikin
[AD-A186452] 08 p1049 N88-16335
User's guide: Lower neck transducer for the Hybrid 3 dummy
[PB88-133319] 12 p1628 N88-19743
Evaluation tests of lower neck transducer for the Hybrid 3 Dummy
[PB88-133327] 12 p1628 N88-19745
Anthropomorphic phantom radiation dosimetry at the NATO standard reference point at Aberdeen Proving Ground
[AD-A190508] 15 p2103 N88-22528

DUMMY LOADS
U IMPEDANCE
U OUTPUT

DUMP COMBUSTORS
Flame driving of longitudinal instabilities in liquid fueled dump combustors
[AD-A183536] 01 p0006 N88-10033

DUNES
Environmental processes and spectral reflectance characteristics associated with soil erosion in desert fringe regions
[NASA-CR-182332] 05 p0620 N88-13811
Dune fields in central Western Argentina
17 p2366 N88-24088
A bibliography of dunes: Earth, Mars, and Venus
[NASA-CR-4149] 20 p2885 N88-27134
Discrimination of sand transport rates and environmental consequences in central Egypt from SPOT data
22 p3093 N88-28366
Preliminary comparative analysis of LANDSAT and SPOT data for the study of the sanding phenomenon: Zaafrane region (Algeria) 22 p3099 N88-28402

DUNGEYS WIND SHEAR MECHANISM
U WIND SHEAR

DUPLICATING
U REPRODUCTION (COPYING)

DURABILITY
Durability (lifetime) predictions adhesively bonded structures
[AD-A184069] 03 p0335 N88-12110
Work-in-progress presented at the Army Symposium on Solid Mechanics, 1986: Lightening of the Force
[AD-A184791] 04 p0427 N88-12644
Durability of powdered aluminum structures
04 p0429 N88-12655
High polymer sensor materials discussed
06 p0676 N88-14140
Experimental determination of crack growth rates in cyclic stress applications, for improving the forecasted computed durability in operation
[FF-14/1986] 09 p1182 N88-17085
The effect on initial bond strength and durability of a Phosphoric Acid Dip (PAD) following chromic acid anodising of aluminum
[ARE-TM(UMM)-87402] 10 p1300 N88-17772
Advanced durability analysis. Volume 1: Analytical methods
[AD-A188341] 12 p1635 N88-19789
Durability testing of an iridium-plated storable rocket engine injector
[AD-A190707] 15 p2027 N88-22078
Computational structural mechanics for engine structures 15 p2080 N88-22399
Durability of continuous fiber reinforced metal matrix composites
[AD-A193868] 22 p3050 N88-28097
Predicting the durability of adhesives and coatings by remote detection of hidden defects and coating-thickness irregularities: A theoretical and numerical study
24 p3355 N88-29972

DURATION
U TIME

DUST
NT COSMIC DUST
NT INTERPLANETARY DUST
NT TERRESTRIAL DUST BELT
NT ZODIACAL DUST
Stratospheric particles: Synchrotron X-ray fluorescence determination of trace element contents
[DE87-012482] 02 p0198 N88-11234
Circumstellar shells, the formation of grains, and radiation transfer 02 p0252 N88-11596
Physics and chemistry 07 p0883 N88-15359
Particle-gas temperature differentials resulting from time-dependent radiative-conductive heat flux divergences in the tenuous dust-laden atmosphere of mars
[AD-A185888] 07 p0945 N88-15747
Aerosols in Martian Atmosphere and Natural Dust Observation (AMANDO). Proposal for the Mars orbiter balloon and rover to study the Martian atmosphere, its thermal content, and its interaction with the soil
[IFSI-87-9] 08 p1100 N88-16619
Christiansen effect in infrared spectra of soil-derived atmospheric dusts
[AD-A187071] 09 p1248 N88-17479
Operation of gas turbine engines in dust-laden environments 10 p1280 N88-17654
Simulation of the plasma interaction with thin dust clouds 11 p1552 N88-19291
How dirty is Mars' North Polar cap, and why isn't it black 23 p3303 N88-29677
The surface composition of Mars from earthbased observations 23 p3306 N88-29696
AGN (OIII) emission line profiles: Dependencies on galaxy inclination and Balmer decrement
[INPE-4596-PRE/1324] 24 p3459 N88-30577

DUST COLLECTORS
Characteristics of pressure loss during filtration using a porous ceramic filter
[DE88-752547] 20 p2798 N88-26604

DWARF NOVAE
SW UMa and V426 Oph: EXOSAT surprises
19 p2740 N88-26269
Regular orbital variations in the ultraviolet resonance lines of YZ Cnc
[MPE-PREPRINT-117] 22 p3165 N88-28850
The ultrashort period dwarf nova SW Ursae Majoris
24 p3453 N88-30553

DWARF STARS
NT DWARF NOVAE
NT FLARE STARS
NT RED DWARF STARS
The atmospheres of M dwarfs: Observations
02 p0253 N88-11601
M dwarfs: Theoretical work 02 p0253 N88-11602
The photospheric magnetic fields of cool stars: Recent results of survey and time-variability programs
04 p0503 N88-13094
Angular momentum evolution of young stars
04 p0504 N88-13099
Post-zero-age main sequence rotation
04 p0504 N88-13100
Atmospheres of stars in the limits of thin and thick convection zones: The M dwarfs
04 p0505 N88-13104
Differential B and V light curves of the bright BY Draconis star HD80715 04 p0509 N88-13130
Broadband linear polarization and chromospheric CaII H and K line emission in late-type main sequence stars
04 p0511 N88-13140
The onset of chromospheric activity among the A- and F- type stars 04 p0511 N88-13144

Empirical relations between photospheric magnetic fields and atmospheric radiative losses for cool dwarf stars
04 p0511 N88-13145
VLA observations of the X-ray bright Hyades M-dwarfs
04 p0512 N88-13147
MHD energy fluxes for late type dwarfs
04 p0512 N88-13148
A search for very low mass (brown dwarf) stars as wide binaries using a seven element infrared camera-photometer
04 p0512 N88-13150
Chromospheric and coronal heating in a bias-free sample of K dwarfs
04 p0518 N88-13184
Measurements of stellar magnetic fields: Empirical constraints on dynamo and rotational evolution theories
04 p0518 N88-13185
M dwarfs from the Einstein medium sensitivity survey
04 p0519 N88-13188
Duplicity in the solar neighborhood. Part 3: New spectroscopic elements for nine solar-type binary stars [SER-C-PREPUBL-FASC-18-PT-3]
18 p2592 N88-25405
Molecular hydrogen in galaxies
23 p3299 N88-29645
Duplicity in the solar neighborhood: Part 4: Spectroscopic orbits for four dwarf M stars [SER-C-PREPUBL-FASC-21]
24 p3454 N88-30561

DYADICS

Statistical analysis of dyadic stationary processes [AD-A193057]
21 p3009 N88-27853

DYE LASERS

Status, development of laser devices in China
03 p0303 N88-11907
Laser induced fluorescent study of relativistic electron beams [AD-A184456]
04 p0447 N88-12774
All-optical beam control by forced Rayleigh scattering [AD-A184315]
04 p0490 N88-13018
Laser action from syn-(methyl,methyl) bimane [AD-A186314]
07 p0858 N88-15211
Time characteristics of travelling wave lasing with two-photon picosecond optical pumping
07 p0918 N88-15578
Study of kinetics of intracavity absorption in pulsed dye lasers
07 p0919 N88-15585
Characteristics of LKI-501 tunable dye laser with dyes in solid matrix
07 p0920 N88-15587
Dye laser for holographic interferometry
07 p0920 N88-15588
Energy disposal in ion-molecule reactions [AD-A186772]
09 p1171 N88-17019
Dye lasers pumped by radiation from high-power semiconductor lasers
09 p1237 N88-17417
Photoionization dynamics of excited molecular states [DE88-002982]
09 p1246 N88-17468
Product kinetic and internal energy distributions via velocity-aligned Doppler spectroscopy [DE88-003510]
10 p1298 N88-17764
Modern pulsed wavemeters [DE88-003875]
10 p1335 N88-17978
Nonlinear optics with broad-band lasers [DE88-005026]
10 p1337 N88-17992
Instabilities and chaos in a multimode, standing-wave, CW dye laser [DE88-005028]
10 p1337 N88-17993
Studies of fluorine combustion [AD-A187646]
11 p1452 N88-18656
Diode pumped fiber laser [AD-A187694]
11 p1491 N88-18902
Quenched-laser operation of a Littman dye oscillator [DE88-004020]
11 p1493 N88-18915
Resonantly-enhanced, four-photon ionization of krypton at laser intensities exceeding 10(12) W/sq cm [DE88-005038]
11 p1544 N88-19229
Discharge excitation of dye vapors [AD-A188428]
12 p1632 N88-19770
Resonance energy transfer between carbon monoxide and oxygen molecules using dye laser intracavity absorption spectroscopy [AD-A188488]
12 p1689 N88-20104
Instrumentation for collisional energy transfer studies [AD-A188495]
12 p1689 N88-20105
Doubly periodic output from a dye laser pumped by a free-running argon laser [DE88-005027]
13 p1778 N88-20633
XeCl laser-pumped nanosecond dye lasers
14 p1902 N88-21359
A picosecond tunable ultrashort cavity dye laser
14 p1902 N88-21361
Theoretical study of colliding pulse mode-locking in dye lasers
14 p1903 N88-21366
Time characteristics of ultrashort light pulses from dye lasers with distributed feedback
14 p1970 N88-21759
Solid hosts for dye laser rods. Part 1: Criteria for choosing a host material [DE88-006478]
15 p2072 N88-22355
Efficient narrow linewidth waveguide dye laser pumped by CuCl laser
16 p2187 N88-23038
XUV source for ultra-high resolution photoionization spectroscopy [DE88-007531]
19 p2614 N88-25510
A plasma ultraviolet source for short wavelength lasers [AD-A192844]
21 p2952 N88-27537

DYES

Saturable absorbers for colliding pulse-locked Nd:YAG lasers
03 p0302 N88-11902
Characteristics of LKI-501 tunable dye laser with dyes in solid matrix
07 p0920 N88-15587
Nonlinear optical waveguides containing a transition metal-based dye molecule [DE88-003257]
11 p1550 N88-19275
Evidence for laser emission from the TICT exciplex of coumarin dyes [DE88-702544]
23 p3220 N88-29167

DYNAMIC CHARACTERISTICS

NT AERODYNAMIC DRAG
NT AERODYNAMIC STABILITY
NT AIRCRAFT STABILITY
NT BOUNDARY LAYER STABILITY
NT COMBUSTION STABILITY
NT CONTROL STABILITY
NT DIRECTIONAL STABILITY
NT DRAG
NT DYNAMIC PRESSURE
NT DYNAMIC STABILITY
NT FLAME STABILITY
NT FLOW CHARACTERISTICS
NT FLOW DISTRIBUTION
NT FLOW STABILITY
NT FLOW VELOCITY
NT FREQUENCY STABILITY
NT FRICTION DRAG
NT GYROSCOPIC STABILITY
NT INTERFERENCE DRAG
NT INTERFERENCE LIFT
NT JET LIFT
NT LATERAL STABILITY
NT LIFT
NT LONGITUDINAL STABILITY
NT LOW SPEED STABILITY
NT MAGNETOHYDRODYNAMIC STABILITY
NT MOTION STABILITY
NT PRESSURE DRAG
NT ROTARY STABILITY
NT SATELLITE DRAG
NT SOLAR WIND VELOCITY
NT SPACECRAFT STABILITY
NT SUPERSONIC DRAG
NT TRANSIENT RESPONSE
NT VISCOUS DRAG
NT ZERO LIFT

Determination of the dynamic parameters of annular clearances with turbulent flow and incompressible media [ETN-87-90434]
01 p0047 N88-10303
Contribution to the dynamical analysis of rheolinear nonconservative, gyroscopic systems using finite element methods [ETN-87-90410]
01 p0050 N88-10320
Exact solution of the inverse problem for a six-link manipulator with a mechanical offset [DE87-702646]
01 p0054 N88-10349
Structure-dependent matrix representation of manipulator kinematics and its inverse solution [DE87-752966]
02 p0229 N88-11447
Dynamic image interpretation for autonomous vehicle navigation [AD-A184043]
03 p0262 N88-11647
The structure and reactivity of heterogeneous surfaces and study of the geometry of surface complexes [DE88-000158]
03 p0279 N88-11754
Hovering helicopter flight dynamics: A study of vertical motion [AR-004-526]
04 p0399 N88-12485
Dynamics of cables and chains
05 p0610 N88-13747
Molecular dynamics studies of aromatic hydrocarbon liquids [DE88-001473]
05 p0648 N88-13973
Dynamic processes in field-reversed-configuration compact toroids [DE87-014756]
05 p0652 N88-13998
Studies of the structural dynamic behavior of satellite antenna system [AD-A185526]
06 p0673 N88-14121
Gas diffusion studies in steady and nonsteady cavities [AD-A185795]
06 p0704 N88-14318
On the pairing process in an excited, plane, turbulent mixing layer [AD-A186355]
07 p0850 N88-15157
Blade vibration due to different flow excitation
07 p0851 N88-15166
Data acquisition, reduction and analysis of shock and vibration testing using a super microcomputer [AD-A186123]
07 p0867 N88-15260
State-of-the-art for assessing earthquake hazards in the United States. Report 26: Parameters for specifying magnitude-related earthquake ground motions [AD-A185997]
07 p0877 N88-15319
Global bifurcation of periodic solutions with symmetry [AD-A185881]
07 p0908 N88-15501
Critical analysis of the dynamic behavior laws for metallic materials --- ballistics [ISL-NB-401/86]
08 p0969 N88-15862
Method of iterative coupling between periodic aerodynamic and dynamic fields [PB87-169934]
09 p1113 N88-16669
Predicting dynamic separation characteristics of general configurations [AD-A186689]
09 p1116 N88-16691
Experimental and theoretical study on cavitation inception and bubbly flow dynamics. Part 1: Design, development and operation of a cavitation susceptibility meter. Part 2: Linearized dynamics of bubbly and cavitating flows with bubble dynamics effects [AD-A187133]
09 p1160 N88-16952
Dynamic analysis of multimesh-gear helicopter transmissions [NASA-TP-2789]
09 p1176 N88-17045
Frequency response functions of a nonlinear system
09 p1180 N88-17070
Optimal correction problem of a multidimensional stochastic system [AD-A186727]
09 p1228 N88-17353
An evaluation of project scheduling techniques in a dynamic environment [AD-A187057]
09 p1260 N88-17554
Mechanisms of wear in single- and two-phase materials [DE88-003846]
10 p1305 N88-17806
The dynamics of two coupled rigid bodies [AD-A187592]
10 p1341 N88-18012
The dynamics of coupled planar rigid bodies. Part 1: Reduction, equilibria and stability [AD-A187467]
10 p1345 N88-18042
Collaborative studies of polar cap ionospheric dynamics [AD-A187888]
10 p1355 N88-18098
Energy transfers for multilayer hydrodynamic ocean models: General formulation and specific examples [AD-A187604]
10 p1358 N88-18116
Dynamic observers as asymptotic limits of recursive filters: Special cases [AD-A187578]
10 p1397 N88-18324
Growth and electronic properties of strained metal overlayers [DE87-010956]
10 p1417 N88-18463
State-of-the-art for assessing earthquake hazards in the US. Parameters for specifying intensity-related earthquake ground motions [AD-A188230]
11 p1512 N88-19032
Implementing dynamic arrays: A challenge for high-performance machines [AD-A188142]
11 p1533 N88-19157
Picosecond laser studies of excited state processes [AD-A189606]
12 p1607 N88-19607
Dynamics of small and large scale irregularities at sub-auroral latitudes [AD-A189052]
12 p1645 N88-19853
A numerical analysis of the dynamics of PRIZ operation [AD-A188853]
12 p1678 N88-20035
A study of methods to predict and measure the transmission of sound through the walls of light aircraft [NASA-CR-182656]
12 p1687 N88-20090
Dynamics of high-speed mechanisms with elastic members
13 p1779 N88-20643
Large-scale ocean dynamics
14 p1938 N88-21562
The effects of torque response and time delay on rotorcraft vertical axis handling qualities [AD-A189873]
15 p2017 N88-22023
KRASH parametric sensitivity study: Transport category airplanes [AD-A189962]
15 p2017 N88-22024
Nonlinear analysis and optimal design of dynamic mechanical systems for spacecraft application [AD-A190644]
15 p2026 N88-22070
Molecular dynamics of materials possessing high energy content [AD-A190034]
15 p2034 N88-22118
Unsteady flow field measurements using LDV (Laser Doppler Velocimetry) [AD-A189907]
15 p2063 N88-22298
The CRREL (Cold Regions Research and Engineering Laboratory) Hopkinson bar apparatus [AD-A190599]
15 p2077 N88-22380

Railgun rail gouging by hypervelocity sliding contact
[DE88-006866] 16 p2166 N88-22916
The nonlinear dynamics of a spacecraft coupled to the vibration of a contained fluid
[DE88-007035] 16 p2168 N88-22925
North Carolina Biomolecular Engineering and Materials Applications Center (NC-BEMAC)
[AD-A190923] 16 p2237 N88-23364
Dynamic characteristics of a vibrating beam with periodic variation in bending stiffness
[NASA-TP-2697] 17 p2348 N88-23988
Time-frequency representations for speech signals
[AD-A188661] 18 p2495 N88-24819
A dynamic analysis of piezoelectric strained elements
[AD-A191478] 18 p2503 N88-24851
Infinite dimensional dynamical systems and their finite dimensional analogues
[AD-A192041] 18 p2563 N88-25216
A constraint algorithm for maintaining rigid bonds in molecular dynamics simulations of large molecules
[AD-A191663] 18 p2572 N88-25277
Theoretical studies of dynamics combustion
[DE88-007565] 19 p2611 N88-25495
The MUF (Maximum Usable Frequency) (3000) as an indicator for F-region variations
[AD-A191655] 19 p2690 N88-25991
Half collision studies of inelastic energy transfer processes
[DE88-008096] 19 p2724 N88-26178
Decision aiding and coordination in decision-making organizations
[AD-A191950] 19 p2738 N88-26259
On the dynamic behavior of balloon during its launch; application of panel method and extension to unsteady problem
[ISAS-RN-622] 20 p2751 N88-26330
Numerical simulation of fuel droplet interactions and breakup
[AD-A192431] 21 p2941 N88-27470
Coupled experimental and theoretical investigations of instability, chaos and turbulence in an axisymmetric jet flow
[AD-A192943] 21 p2942 N88-27476
An analysis of horizontal temperature gradients and heat content in the mixed layer and the surface forcing during PATCHEX
[AD-A192330] 21 p2976 N88-27678
Research in applied mathematics
[AD-A192385] 21 p3004 N88-27820
Literal dynamic modeling
[REPT-881-440-114] 22 p3048 N88-28083
The dynamic behavior of a turbulent boundary layer subjected to a shock-induced separation
[AD-A194164] 22 p3075 N88-28252
Reaction dynamics on semiconductor surfaces
[AD-A194305] 22 p3156 N88-28781
Spallation and dynamic fracture as an effect of laser induced shock waves
[AD-A193513] 23 p3188 N88-28971
A multiple-scales partial solution of the pulse-forced Rayleigh-Plesset equation of cavitation bubble dynamics
[AD-A193733] 23 p3212 N88-29118
Interactions between synoptic and planetary scales of motion
[AD-A192328] 23 p3234 N88-29246
Transformations of short-term visual memory
[AD-A193873] 23 p3241 N88-29290
The acoustic field scattered from some approximate pressure release materials
[AD-A194768] 23 p3278 N88-29515
A dynamic analysis of piezoelectric strained elements
[AD-A196079] 24 p3432 N88-30430

DYNAMIC CONTROL

The method of rigid armature flux orientation for the field-oriented control of highly dynamic drives with synchronous machines
[ETN-87-90405] 01 p0042 N88-10269
Photochemical ozone overburden correction
05 p0615 N88-13778
Investigation, development, and application of optimal output feedback theory. Volume 3: The relationship between dynamic compensators and observers and Kalman filters
[NASA-CR-4107] 05 p0638 N88-13900
Turbulence, turbulence control, and drag reduction
[AD-A185643] 06 p0665 N88-14080
Development of symbolic computation methods for nonlinear dynamics
[AD-A185562] 06 p0758 N88-14653
An autopilot design for the United States Marine Corps' airborne remotely operated device
[AD-A186379] 07 p0820 N88-14983
Roles of knowledge in motor learning
[AD-A186420] 07 p0897 N88-15438
Resources, confusions and compatibility in dual axis tracking: Displays, controls and dynamics
[AD-A185871] 07 p0898 N88-15440
A dynamic simulation and feedback control scheme for the U.S. Marine Corps' Airborne Remotely Operated Device (AROD)
[AD-A186597] 08 p0953 N88-15784
Control system simulation for a single-link flexible arm
[AD-A187037] 09 p1174 N88-17035
Viscosity methods in optimal control of distributed systems
[AD-A188086] 10 p1401 N88-18357
A wind tunnel model with dynamic control
[BU-352] 13 p1724 N88-20310
Modelling and control of an annular momentum control device
[NASA-CR-4138] 13 p1754 N88-20491
The dynamic control of robotic manipulators in space
[NASA-CR-182710] 13 p1779 N88-20646
Linear state space modeling of a turbofan engine
[AD-A190110] 15 p2019 N88-22035
Feedback control of distributed parameter systems with applications to large space structures
[AD-A190536] 15 p2025 N88-22068
Effect of friction and control parameters on the tracking accuracy of a target seeker
[AD-A190010] 15 p2056 N88-22257
Problems in nonlinear continuum dynamics
[AD-A190538] 15 p2128 N88-22691
Vibration control of large structures
[AD-A191358] 16 p2168 N88-22928
Automatic control of robot motion
[AD-A191012] 16 p2215 N88-23218
Contribution to the adaptive dynamic control of a robot manipulator
[LAAS-87-350] 16 p2255 N88-23475
Dynamics and control of turbulent shear flows
[AD-A191527] 18 p2508 N88-24879
A method for reducing the coning of a spinning vehicle
[DE88-010971] 21 p2896 N88-27189
Development of a hybrid simulator for robotic manipulators
[AD-A193119] 21 p2956 N88-27557
Vibration control of large structures
[AD-A193317] 21 p2961 N88-27587
Hierarchical organization for large, dynamic radio networks
[AD-A193942] 23 p3204 N88-29067
Anti-aliasing filters for dynamics and control experiments
[AD-A193758] 23 p3226 N88-29203
Topics in adaptive control and inference
[AD-A194718] 23 p3266 N88-29443
Dynamics of articulated aerospace structures
[AD-A195685] 24 p3324 N88-29794

DYNAMIC LOADS

NT AERODYNAMIC LOADS
NT BLAST LOADS
NT CONTACT LOADS
NT CYCLIC LOADS
NT GUST LOADS
NT IMPACT LOADS
NT LANDING LOADS
NT ROLLING CONTACT LOADS
NT SHOCK LOADS
NT TRANSIENT LOADS
NT VIBRATORY LOADS
NT WING LOADING
Possibilities for the modeling of dynamically loaded cylindrical structural parts in the wind tunnel
[KU-SFB-210/T/24] 01 p0001 N88-10005
Determination of the fatigue strength of mechanically, thermally and corrosively loaded multilayer materials
[ETN-87-90375] 01 p0058 N88-10372
Effect of viscosity on a vertical cylinder due to surface waves
[ETN-87-90960] 02 p0171 N88-11075
Diffraction moire: The dynamic regime
[DE87-014883] 03 p0335 N88-12111
Breaking wave forces on vertical cylinders
[RR-CE71] 03 p0338 N88-12126
Dynamic response of a 330 KW horizontal axis wind turbine generator
[DE87-014867] 03 p0347 N88-12195
Free-edge delamination: Laminate width and loading conditions effects
[NASA-TM-100238] 04 p0411 N88-12551
Static standing and dynamic walking of a practical biped robot
[DE88-001367] 04 p0451 N88-12795
On dynamic loads in parallel shaft transmissions. 1: Modelling and analysis
[NASA-TM-100180] 04 p0451 N88-12797
On dynamic loads in parallel shaft transmissions. 2: Parameter study
[NASA-TM-100181] 04 p0452 N88-12798
Input turbulence features at a megawatt-size wind turbine, Medicine Bow, Wyoming
[DE88-000098] 04 p0464 N88-12873
Measurements and calculations of aerodynamic torques for a vertical-axis wind turbine
[DE88-001783] 04 p0465 N88-12876
Experimental studies on the tripping behavior of narrow T-stiffened flat plates subjected to hydrostatic pressure and underwater shock 05 p0592 N88-13613
BASIC desk-top computer program for the three-dimensional static configuration of an extensible flexible cable in a uniform stream
[AD-A184852] 05 p0609 N88-13737
RADSPHERE: A computer program for calculating the steady-state, axially symmetric, forced response and radiation field of a submerged spherical shell
[AD-A185025] 05 p0609 N88-13738
Accurate rotor loads prediction using the FLAP (Force and Loads Analysis Program) dynamics code
[DE88-001109] 05 p0623 N88-13815
Structuring data for concurrent vectorized processing in a transient dynamics finite element program
[DE87-013082] 05 p0636 N88-13890
Mean and peak wind load reduction on heliostats
[DE87-012281] 07 p0873 N88-15296
Pressure and mass velocity measurements in solids subjected to dynamic loadings 07 p0921 N88-15595
Study on the mechanical stresses in the elements of the model of a toroidal magnet of a tokamak with strong field
[DE88-700343] 07 p0935 N88-15679
SAHAYOG: A testbed for load sharing under failure
[AD-A186515] 08 p1069 N88-16460
Analysis of tasks for dynamic man/machine load balancing in advanced helicopters
[DE88-003735] 09 p1117 N88-16696
Strength and toughness of a brittle material
[VTT-RR-479] 09 p1183 N88-17089
VAWT (Vertical-Axis Wind Turbine) stochastic loads produced by atmospheric turbulence
[DE88-001355] 09 p1187 N88-17110
The use of multigrid techniques in the solution of the Elrod algorithm for a dynamically loaded journal bearing
[NASA-CR-180873] 10 p1331 N88-17954
Preliminary results from the dynamic response testing of the Westinghouse 600-kW wind turbine
[DE88-001123] 10 p1350 N88-18070
Analysis of wind turbines on offshore support structures excited by random wind and random waves
[DE88-004772] 10 p1351 N88-18074
Determination of the ultimate loads for corrugated-steel, barrel-type shell structures
[AD-A187716] 11 p1498 N88-18944
Computer aided deflection measurement of an aircraft wing
[AD-A187778] 12 p1581 N88-19461
Changes in the status of the human tibia during antiorthostatic hypokinesia
[NASA-TT-20221] 13 p1810 N88-20813
Pressure measurements of impinging jet with asymmetric nozzle
[NASA-CR-182759] 15 p2014 N88-22011
Development of a computer code CRACK for elastic and elastoplastic fracture mechanics analysis of 2-D structures by finite element technique
[DE88-701231] 15 p2075 N88-22370
FLAP (Force and Loads Analysis Program) code development and validation
[DE88-001131] 15 p2075 N88-22371
The CRREL (Cold Regions Research and Engineering Laboratory) Hopkinson bar apparatus
[AD-A190599] 15 p2077 N88-22380
Behaviour of fibre-reinforced composites under dynamic loading
[AD-A191310] 16 p2174 N88-22955
Dynamic shear band development in plane strain
[AD-A190915] 18 p2526 N88-24988
Finite element analysis of an underground structure
[AD-A191747] 18 p2527 N88-24991
Dynamic response of plates to moving loads: Structural impedance and finite element methods
18 p2528 N88-25000
The solution of the Elrod algorithm for a dynamically loaded journal bearing using multigrid techniques
[NASA-TM-100941] 19 p2668 N88-25854
Diffusion models of crack growth due to random overloads
[DE88-008811] 21 p2962 N88-27595
Modal testing in the design evaluation of wind turbines
[DE88-010374] 21 p2968 N88-27632
Static and dynamic metal-metal friction at plastic stress levels
[DE88-011281] 23 p3222 N88-29176

Influence of peak pressure on the substructure evolution and shock wave profiles of Ti-6Al-4V
[DE88-006458] 23 p3225 N88-29197
An investigation of acoustic cavitation produced by pulsed ultrasound
[AD-A193523] 23 p3278 N88-29516
Ultrasonic method and apparatus for determining crack opening load
[NASA-CASE-LAR-13889-1] 24 p3385 N88-30160

DYNAMIC MODELS

Use of simulated satellite radiances from a mesoscale numerical model to understand kinematic and dynamic processes 02 p0202 N88-11261
Mesoscale very short-range numerical prediction with dynamical initialization including condensation heating 02 p0213 N88-11341
A simplified approach to the dynamics of charged particles in the magnetosphere 03 p0273 N88-11718
A statistical rain attenuation prediction model with application to the advanced communication technology satellite project. Part 2: Theoretical development of a dynamic model and application to rain fade durations and tolerable control delays for fade countermeasures
[NASA-TM-100242] 03 p0308 N88-11945
Development of response models for the Earth Radiation Budget Experiment (ERBE) sensors. Part 1: Dynamic models and computer simulations for the ERBE nonscanner, scanner and solar monitor sensors
[NASA-CR-178292] 05 p0584 N88-13557
The tail lobe ion spectrometer: Theory and observations
[IFSI-86-12] 05 p0585 N88-13569
The kinetics and dynamics of iodine monofluoride formation in gas-phase collisions
[AD-A185715] 06 p0709 N88-14352
Characteristic trajectories of generalized Lanchester equations
[AD-A185762] 06 p0766 N88-14705
The global balance of dynamic vorticity in relation to heat sources and sinks 07 p0876 N88-15316
Roles of knowledge in motor learning
[AD-A186420] 07 p0897 N88-15438
Three-dimensional unsteady flow elicited by finite wings and complex configurations
[AD-A186464] 08 p0951 N88-15770
Attitude dynamics for satellites stabilized through spin
[INPE-4403-NTE/275] 08 p0963 N88-15833
Dynamic modeling of the middle atmosphere 08 p1028 N88-16227
A unified model for the WTS and the generation on Pi 2 pulsations --- Westward Traveling Surge (WTS) 08 p1096 N88-16593
A possible role for ionospheric ions in triggering a geomagnetic substorm onset 08 p1096 N88-16594
Dynamic tests of the Ariane launch vehicle 09 p1126 N88-16749
Dynamical characteristics of weak turbulence
[AD-A186724] 09 p1161 N88-16957
Dynamic modelling by finite element method of an elasto-acoustic beam with due consideration of flow and viscosity
[PB87-178166] 09 p1164 N88-16978
Control system simulation for a single-link flexible arm
[AD-A187037] 09 p1174 N88-17035
An interactive-graphics method for dynamic system modelling, applying consistency rules 09 p1181 N88-17072
The analysis of recent crustal movements in static and kinematic models
[SER-B-279] 09 p1191 N88-17136
A model for stationary and dynamic impression of undercooled boiling in coupled thermohydraulic and neutron physics calculations of nuclear reactors
[IKE-6-171] 09 p1247 N88-17472
Strength and structure of Ga sub 1-xIn sub xAs alloys
[AD-A188092] 10 p1303 N88-17795
Microwave semiconductor research-materials, devices and circuits
[AD-A187121] 10 p1415 N88-18444
A superelement component dynamic synthesis method 11 p1500 N88-18956
Center for nonlinear dynamics of the brain
[AD-A187245] 11 p1518 N88-19068
Realtime pilot model parameter identification
[AD-A188873] 12 p1584 N88-19476
A comparative survey of mathematical models for dynamic simulation of in-orbit manipulation operations 12 p1592 N88-19533
Dynamics modeling, simulation, and control of a spacecraft/manipulator system 12 p1592 N88-19534
Visualization of the air flowing through a dynamic model of the vocal folds
[ISVR-TR-154] 14 p1952 N88-21634
Procedures for updating dynamic mathematical models
[EMSB-23/86] 14 p1964 N88-21716
Laser photodeposition and etching study
[AD-A190535] 15 p2040 N88-22153
The role of vortex structure in tropical cyclone motion
[AD-A190961] 16 p2235 N88-23351
The representational code of the internal model of dynamic systems: An individual differences and dual task approach
[AD-A190876] 16 p2244 N88-23403
Behavior of a two-layered beam under impact loading
[OUEL-1716/87] 17 p2349 N88-23993
Nonlinear flying quality parameters based on dynamic inversion
[AD-A192146] 18 p2464 N88-24627
A dynamic model of liquid propellant combustion 19 p2622 N88-25556
Modeling and evaluation of expert systems in decisionmaking organizations
[AD-A191951] 19 p2739 N88-26260
Coordination in decision-making organizations
[AD-A191952] 19 p2739 N88-26261
Dynamic modelling and estimation of the error due to asynchronism in a redundant asynchronous multiprocessor system
[NASA-CR-177427] 21 p2898 N88-27205
Control of free-flying space robot manipulator systems
[NASA-CR-183017] 21 p2956 N88-27562
On the dynamics of the metagalaxy
[TRITA-EPP-88-05] 22 p3166 N88-28852
Performance of GPS-aided INS during high-dynamic maneuvers
[AD-A194624] 23 p3175 N88-28903
Vortex dynamics of coherent and chaotic structures (including algorithms for computer simulations and diagnosis)
[AD-A193580] 23 p3212 N88-29117
Dynamics of interacting galaxies 23 p3299 N88-29647
Procedures for updating dynamic mathematical models, test phase --- spacecraft hardware
[MEBS-38/87] 24 p3335 N88-29852
MANIP --- spacecraft modeling program
[MANIP-217A] 24 p3335 N88-29855
Nonlinear dynamics of coupled oscillator arrays
[AD-A194888] 24 p3367 N88-30053
Modeling robot flexibility for endpoint force control
[AD-A195923] 24 p3380 N88-30132
Continental growth through time by underplating of subducted oceanic crust: Evidence from kimberlites in South Africa and SW Pacific 24 p3399 N88-30244
Dynamical systems and motion vision
[AD-A195932] 24 p3422 N88-30366

DYNAMIC PRESSURE

A 150,000 pounds per square inch dynamic pressure calibrator
[AD-A190659] 15 p2069 N88-22335
Synthesis of metastable superconductors by high dynamic pressure
[DE88-005620] 15 p2139 N88-22764

DYNAMIC PROGRAMMING

Investigation and implementation of an algorithm for computing optimal search paths
[AD-A185927] 07 p0902 N88-15461
On stochastic optimality of policies in first passage problems
[AD-A186293] 07 p0915 N88-15554
Optimal correction problem of a multidimensional stochastic system
[AD-A186727] 09 p1228 N88-17353
Spire based speaker-independent continuous speech recognition using mixed feature sets
[AD-A188834] 12 p1620 N88-19688
Application of dynamic programming to image registration
[ENST-87E022] 18 p2557 N88-25180
SIMS: Single Interface to Multiple Systems
[AD-A192264] 20 p2837 N88-26832

DYNAMIC PROPERTIES

U DYNAMIC CHARACTERISTICS

DYNAMIC RESPONSE

NT TRANSIENT RESPONSE
Investigation of interactions between limb-manipulator dynamics and effective vehicle roll control characteristics
[NASA-CR-3983] 01 p0007 N88-10039
Blade loss transient dynamics analysis, volume 1. Task 2: TETRA 2 theoretical development
[NASA-CR-179632] 02 p0125 N88-10791
Blade loss transient dynamics analysis, volume 2. Task 2: TETRA 2 user's manual
[NASA-CR-179633] 02 p0126 N88-10792
Effect of adhesive layers on impact damage and dynamic response in composite laminates 02 p0141 N88-10887
AGARD standard aeroelastic configurations for dynamic response. Candidate configuration I.-wing 445.6
[NASA-TM-100492] 02 p0192 N88-11202
Dynamic response of a 330 KW horizontal axis wind turbine generator
[DE87-014867] 03 p0347 N88-12195
An experimental investigation of dynamic ground effect
[NASA-CR-4105] 04 p0394 N88-12458
A method for the efficient calculation of elastic rotor blade dynamic response in forward flight 04 p0394 N88-12460
Aircraft dynamic response calculation based on discrete-continual model 04 p0424 N88-12624
A comparison of structural frequency response functions measured with forces from 500 to 250,000 lb
[DE88-000668] 04 p0457 N88-12829
Using a new characterization of turbulent wind for accurate correlation of wind turbine response with wind speed
[DE88-001453] 04 p0466 N88-12881
Aircraft dynamics: Aerodynamic aspects and wind tunnel techniques 05 p0545 N88-13320
Modal survey of the space shuttle solid rocket motor using multiple input methods 05 p0593 N88-13617
Dynamical analysis of molecular decay at spherical surfaces
[AD-A184908] 05 p0647 N88-13964
Analysis and test evaluation of the dynamic response and stability of three advanced turboprop models at low forward speed
[NASA-CR-175026] 06 p0668 N88-14096
Studies of the structural dynamic behavior of satellite antenna system
[AD-A185526] 06 p0673 N88-14121
Acquisition of gust statistics from Aircraft Integrated Data Systems (AIDS) recorded data
[NLR-MP-86048-U-ISS-2] 06 p0745 N88-14586
Rotor dynamic behavior of centrifugal pumps 08 p0975 N88-15898
Modal analysis using frequency response measurement data 08 p0976 N88-15899
Kinetic isolation tether experiment
[NASA-CR-182458] 09 p1135 N88-16810
The Shock and Vibration Bulletin. Part 2: Instrumentation, shock analysis, and shock testing
[AD-A186749] 09 p1178 N88-17053
Retarded potential technique applied for shock wave loading of doubly symmetric submerged structures 09 p1179 N88-17058
Mechanical impact: Theoretical simulation and correlation 09 p1179 N88-17060
Measurement, data analysis and prediction of pyrotechnic shock from pin-pullers and separation joints 09 p1179 N88-17061
A new look at the use of linear methods to predict aircraft dynamic response to taxi over bomb damaged and repaired airfields 09 p1180 N88-17069
Dynamic response of a geared train of rotors subjected to random support excitations 09 p1181 N88-17073
Monitoring interfacial dynamics by pulsed laser techniques
[DE88-003362] 10 p1335 N88-17976
Dynamic response of some structural elements fabricated from a non-linear elastic material 10 p1344 N88-18031
Qualification of frequency response functions using the rigid-body response
[DE88-000745] 10 p1344 N88-18033
Frequency response function estimation at level
[DE88-002644] 10 p1344 N88-18034
Vibration and flutter characteristics of the SR7L large-scale propfan
[NASA-TM-100272] 10 p1344 N88-18036
On the dynamic estimation of relative weights for observation and forecast in numerical weather prediction
[NASA-CR-182531] 10 p1356 N88-18106
Elastoplastic response of unidirectional graphite/aluminum under combined tension-compression cyclic loading
[CCMS-88-01] 11 p1451 N88-18647
Microwave response of an HEMT photoconductor
[NASA-TM-100819] 11 p1480 N88-18835
Prediction of the response and optimal control of stochastic parametrically and externally excited nonlinear systems 11 p1496 N88-18930
Dynamic substructuring for shock spectrum analysis using component mode synthesis 11 p1499 N88-18950
Dynamic analysis of plane frames by microcomputer 11 p1531 N88-19143
Response of coronary blood flow to step changes in plasma protein concentration in the isolated rat heart 12 p1651 N88-19892
Dynamics of high-speed mechanisms with elastic members 13 p1779 N88-20643

Application of the NARMAX method to nonlinear frequency response estimation
[RR-319] 14 p1964 N88-21721
Shape sensitivity analysis of wing static aeroelastic characteristics
[NASA-TP-2808] 15 p2018 N88-22031
Feedback control of distributed parameter systems with applications to large space structures
[AD-A190536] 15 p2025 N88-22068
Galvanic corrosion initiatives
[AD-A190658] 15 p2040 N88-22155
Influence of unsteady aerodynamic forces on dynamic response of variable sweep aircraft 15 p2054 N88-22245
The concept of an impact resonance diagram for characterizing the nonlinear response of impact vibration
[DE88-005475] 15 p2086 N88-22432
Coupled bending-torsion steady-state response of pretwisted, nonuniform rotating beams using a transfer-matrix method
[NASA-TM-100596] 15 p2086 N88-22435
The analysis of non-linear dynamic behavior (including snap-through) of postbuckled plates by simple analytical solution
[NASA-TM-89165] 15 p2087 N88-22439
Vibration control of large structures
[AD-A191358] 16 p2168 N88-22928
Dynamic fracture toughness evaluation by measurement of CTOD
[WNS/ASD-88-02] 16 p2178 N88-22982
Investigation on the movement of vortex burst position with dynamically changing angle of attack for a schematic deltawing in a watertunnel with correlation to similar studies in windtunnel 16 p2204 N88-23152
Revised Impact Dynamic Design-Analysis Method (RIDDAM)
[AD-A190479] 16 p2217 N88-23225
Stall flutter analysis of propfans 16 p2221 N88-23256
An adaptive load-following control system for a space nuclear power system 17 p2406 N88-24307
Research on aero-thermodynamic distortion induced structural dynamic response of multi-stage compressor blading
[AD-A192169] 18 p2456 N88-24584
The flying characteristics of the membrane slider bearing 18 p2522 N88-24965
Theoretical and experimental damping values of piping systems at high ductilities
[DE88-006717] 18 p2526 N88-24986
Dynamic response of plates to moving loads: Structural impedance and finite element methods 18 p2528 N88-25000
Vehicle dynamics: Identification in the frequency domain 20 p2785 N88-26523
Frequency domain identification of the dynamics of a scaled remotely-piloted helicopter 20 p2786 N88-26524
Multivariable identification of a flexible transport aircraft 20 p2786 N88-26525
Identification methods for transport dynamical investigations 20 p2787 N88-26531
Instrumentation for the measurement of penetrator dynamic response to permit force estimation
[DE88-010608] 20 p2809 N88-26666
Experimental and theoretical study of the dynamic operational behavior of a three stage radial compressor
[ETN-88-92129] 20 p2811 N88-26676
Contact force history and dynamic response due to the impact of a soft projectile
[NASA-TM-100961] 20 p2811 N88-26679
AGARD standard aeroelastic configurations for dynamic response. 1: Wing 445.6
[AGARD-R-765] 21 p2896 N88-27193
The robust tracking control of nonlinear systems with uncertain dynamics 21 p2999 N88-27788
Self-energies and the interactions of particles with surfaces
[DE88-010451] 21 p3014 N88-27885
Maximum dynamic responses using matched filter theory and random process theory
[NASA-TM-100653] 22 p3042 N88-28059
The dynamic behavior of a turbulent boundary layer subjected to a shock-induced separation
[AD-A194164] 22 p3075 N88-28252
Modal synthesis by use of substructures with fixed or free coupling points
[ILR-MITT-191] 22 p3089 N88-28341
Experimental investigation of propfan aeroelastic response in off-axis flow with mistuning
[NASA-TM-101320] 22 p3089 N88-28344
Structural dynamics of maneuvering aircraft
[AD-A192376] 23 p3176 N88-28908
Nonlinear dynamic analysis and optimal control of shallow shells 23 p3224 N88-29191
Dynamic response of a 330-kW horizontal axis wind turbine generator
[DE88-001136] 23 p3228 N88-29212
Dynamic analysis of computer and communications sytems: Semi-Markov approach 23 p3244 N88-29305
The Flight of Flexible Aircraft in Turbulence: State-of-the-Art in the Description and Modelling of Atmospheric Turbulence
[AGARD-R-734] 24 p3312 N88-29725
Status review of atmosphere turbulence and aircraft response 24 p3312 N88-29726
Aircraft dynamics: Aerodynamic aspects and wind tunnel techniques 24 p3313 N88-29731
Acquisition of gust statistics from AIDS-recorded data 24 p3313 N88-29733
Analytical study of graphite-epoxy tube response to thermal loads
[NASA-CR-183215] 24 p3341 N88-29884
Rotational evolution of dynamically symmetric gyrostat with internal friction 24 p3446 N88-30509

DYNAMIC STABILITY
NT AERODYNAMIC STABILITY
NT AIRCRAFT STABILITY
NT BOUNDARY LAYER STABILITY
NT COMBUSTION STABILITY
NT CONTROL STABILITY
NT DIRECTIONAL STABILITY
NT FLAME STABILITY
NT FLOW STABILITY
NT FREQUENCY STABILITY
NT GYROSCOPIC STABILITY
NT LATERAL STABILITY
NT LONGITUDINAL STABILITY
NT LOW SPEED STABILITY
NT MAGNETOHYDRODYNAMIC STABILITY
NT MOTION STABILITY
NT ROTARY STABILITY
NT SPACECRAFT STABILITY
Hypersonic static and dynamic stability of axisymmetric shapes: A comparison of prediction methods and experiment 05 p0534 N88-13246
Dynamic stability of hypersonic conical lifting vehicles according to Newton-Busemann theory 05 p0534 N88-13247
Dynamic behavior of dissymmetric rotor bearings modelled with a periodic coefficient large system 05 p0596 N88-13640
Analysis and test evaluation of the dynamic stability of three advanced turboprop models at zero forward speed
[NASA-CR-175025] 06 p0668 N88-14095
Investigation of instability, dynamic forces, and effect of dynamic loading on strength of cages for the bearings in the high pressure oxygen turbopumps for the space shuttle main engine
[NASA-CR-178970] 06 p0714 N88-14378
Effect of plasma rotation in tokamak on stabilizing action of electrically conducting wall 06 p0773 N88-14748
Parametric dependence in the equilibrium dynamics of rotating structures
[AD-A187817] 11 p1498 N88-18945
On relaxation algorithms based on Markov random fields
[AD-A189043] 13 p1814 N88-20840
Vibrations of structures with parametric uncertainties
[AD-A190400] 15 p2076 N88-22378
An experimental study to determine the flow and the subsonic static and dynamic stability characteristics of aircraft operating at high angles-of-attack 16 p2201 N88-23129
Unstable behavior of lasers and other optical systems
[AD-A190875] 16 p2213 N88-23204
Optimal rheological characteristics in dynamic stability of polymer flow through porous media
[DE88-001225] 21 p2918 N88-27322
Application of the Single-Axis rate Table (SAT) of the DFVLR for the evaluation of stationary and dynamic gyro properties
[DFVLR-MITT-88-09] 21 p2952 N88-27533
Dynamic stability of elastic rotor-bearing systems via Liapunov's direct method 21 p2958 N88-27571
Utilizing dynamic stability of orient parts
[AD-A195730] 24 p3427 N88-30397

DYNAMIC STRUCTURAL ANALYSIS
Efficient placement of structural dynamics sensors on the space station
[NASA-CR-172015] 01 p0017 N88-10103
A DMAP for updating dynamic mathematical models with measured data
[NLR-MP-86027-U] 01 p0060 N88-10387
Recent advances in structural dynamics of large space structures
[NASA-TM-100513] 02 p0138 N88-10867
Structural Assembly Demonstration Experiment (SADE)
[NASA-CR-179205] 02 p0138 N88-10868
Concurrent algorithms for transient nonlinear FE analysis
[NASA-CR-181455] 02 p0221 N88-11389
Frequency domain identification of structural dynamic systems with general damping matrices 03 p0337 N88-12120
Linearized aeroelastic analysis of a wind turbine with a two-bladed rotor
[ETN-87-90600] 03 p0347 N88-12192
A comparison of structural frequency response functions measured with forces from 500 to 250,000 lb
[DE88-000668] 04 p0457 N88-12829
Aircraft interior noise reduction by alternate resonance tuning
[NASA-CR-181530] 04 p0488 N88-13005
Predictions of F-111 TACT aircraft buffet response and correlations of fluctuating pressures measured on aluminum and steel models and the aircraft
[NASA-CR-4069] 05 p0529 N88-13218
The 58th Shock and Vibration Symposium, volume 1
[NASA-CP-2488-VOL-1] 05 p0592 N88-13609
Improvement of modal scaling factors using mass additive technique 05 p0593 N88-13620
Initial dynamic load estimates during configuration design 05 p0593 N88-13621
Viscous damped space structure for reduced jitter 05 p0594 N88-13623
A system identification technique based on the random decrement signatures. Part 1: Theory and simulation 05 p0594 N88-13625
A system identification technique based on the random decrement signatures. Part 2: Experimental results 05 p0594 N88-13626
An efficient frequency response solution for nonproportionally damped systems 05 p0595 N88-13634
Shape optimization of damping layers 05 p0595 N88-13635
Dynamic response of laminated composite plates using a three-dimensional hybrid-stress finite-element formulation 05 p0596 N88-13639
Dynamic behavior of dissymmetric rotor bearings modelled with a periodic coefficient large system 05 p0596 N88-13640
Utilization of dynamic characteristics of materials to optimize military explosive charges. Application to antiship devices
[SNIAS-872-320-101] 05 p0610 N88-13743
Accurate rotor loads prediction using the FLAP (Force and Loads Analysis Program) dynamics code
[DE88-001109] 05 p0623 N88-13815
Analysis and test evaluation of the dynamic response and stability of three advanced turboprop models at low forward speed
[NASA-CR-175026] 06 p0668 N88-14096
Studies of the structural dynamic behavior of satellite antenna system
[AD-A185526] 06 p0673 N88-14121
Studies on fluid-structural vibration using boundary element method
[PB87-129508] 06 p0699 N88-14291
Distortional buckling formulae for thin-walled channel columns
[PB87-124012] 06 p0722 N88-14437
Boundary element analysis for dynamic loading of a circular plate on an elastic medium
[CI-86] 06 p0722 N88-14443
Fast algorithms for structural optimization and least squares
[AD-A185766] 06 p0724 N88-14452
Determining structural performance 08 p0954 N88-15787
Modal analysis using frequency response measurement data 08 p0976 N88-15899
The nonlinear dynamic response of an elastic-plastic thin plate under impulse loading
[AD-A182147] 08 p0994 N88-16013
Dynamic analysis of a structure with sliding base 08 p0998 N88-16045
A summary of recent NASA/Army contributions to rotorcraft vibrations and structural dynamics technology 09 p1105 N88-16628
Rotorcraft aeroelastic stability 09 p1106 N88-16631
Parametric and experimental analysis using a power flow approach
[NASA-CR-182460] 09 p1116 N88-16693
A substructure method for dynamic simulation of flexible mechanical systems with geometric nonlinearities 09 p1176 N88-17044
The Shock and Vibration Bulletin. Part 2: Instrumentation, shock analysis, and shock testing
[AD-A186749] 09 p1178 N88-17053
Retarded potential technique applied for shock wave loading of doubly symmetric submerged structures 09 p1179 N88-17058

Mechanical impact: Theoretical simulation and correlation 09 p1179 N88-17060
Dynamic stress at critical locations of a structure as a criterion for mathematical model modification 09 p1180 N88-17066
Reliability of structures with stiffness and strength degradation 09 p1180 N88-17068
Experimental identification of nonlinear structural models [DE88-001795] 09 p1184 N88-17094
Dynamic response of some structural elements fabricated from a non-linear elastic material 10 p1344 N88-18031
Frequency response function estimation at level [DE88-002644] 10 p1344 N88-18034
A component synthesis method using Lanczos vectors [DE88-002263] 10 p1403 N88-18368
The 58th Shock and Vibration Symposium, volume 2 [NASA-CP-2488-VOL-2] 11 p1499 N88-18948
A superelement component dynamic synthesis method 11 p1500 N88-18956
Numerical fracture mechanics using finite element method 11 p1501 N88-18966
Characterization of damped structural connections for multi-component systems [NASA-TM-100801] 11 p1502 N88-18974
Computer aided deflection measurement of an aircraft wing [AD-A187778] 12 p1581 N88-19461
Preliminary investigation of stability of a fin-stiffened slender strut [NASA-TM-4034] 12 p1599 N88-19568
A numerical study of automated dynamic relaxation for nonlinear static tensioned structures [AD-A188372] 12 p1635 N88-19790
Control augmented structural synthesis [NASA-CR-4132] 13 p1721 N88-20290
The Euler-Bernoulli beam equation with boundary energy dissipation [AD-A189517] 13 p1765 N88-20560
A flight test investigation into flow separation and structural response for a transport aircraft at buffet onset [RAE-TR-87006] 14 p1867 N88-21156
Some structural aspects of crack propagation in heat-resistant steels under cyclic thermal and mechanical load 14 p1896 N88-21317
Stress-strain behaviour of a bolt hole in carbon fibre composite plates [BU-354] 14 p1923 N88-21460
The effect of strain rate on the strength and ductility of SiCw/2124 Al composite [OUEL-1692/87] 14 p1924 N88-21466
Computational aspects of sensitivity calculations in transient structural analysis [NASA-TM-100589] 14 p1924 N88-21467
Test facilities of the structural dynamics branch of NASA Lewis Research Center [NASA-TM-100800] 14 p1934 N88-21534
Wave propagation and dynamics of lattice structures [AD-A190037] 15 p2025 N88-22066
Wave propagation and dynamics of lattice structures [AD-A190611] 15 p2025 N88-22069
Nonlinear analysis and optimal design of dynamic mechanical systems for spacecraft application [AD-A190644] 15 p2026 N88-22070
Stabilization and control problems in structural dynamics [AD-A190197] 15 p2073 N88-22361
FLAP (Force and Loads Analysis Program) code development and validation [DE88-001131] 15 p2075 N88-22371
Lewis Structures Technology, 1988. Volume 2: Structural Mechanics [NASA-CP-3003-VOL-2] 15 p2077 N88-22382
Lewis Structures Technology, 1988. Volume 3: Structural Integrity Fatigue and Fracture Wind Turbines HOST [NASA-CP-3003-VOL-3] 15 p2081 N88-22408
Structural dynamics branch research and accomplishments for fiscal year 1987 [NASA-TM-100279] 15 p2088 N88-22446
On the computation of stationary deterministic behavior of nonlinear dynamic systems with applications to rotor-bearing structures [ETN-88-92241] 16 p2214 N88-23213
Lewis Structures Technology, 1988. Volume 1: Structural Dynamics [NASA-CP-3003-VOL-1] 16 p2217 N88-23226
Periodic response of nonlinear systems 16 p2217 N88-23228
Characterization of structural connections for multicomponent systems 16 p2220 N88-23251
Integrated multidisciplinary analysis tool IMAT users' guide [NASA-TM-100605] 16 p2223 N88-23273
Unsteady pressure and structural response measurements of an elastic supercritical wing [NASA-TM-100591] 17 p2299 N88-23756
Preliminary 2-D shell analysis of the space shuttle solid rocket boosters [NASA-TM-100515] 17 p2348 N88-23989
Parameter identification methods for improving structural dynamic models [NASA-TM-100812] 17 p2349 N88-23994
Continuum modeling and dynamic analysis of large truss structures 17 p2349 N88-23995
Application of integrated fluid-thermal-structural analysis methods [NASA-TM-100625] 17 p2350 N88-24001
Parallel processors and nonlinear structural dynamics algorithms and software [NASA-CR-182925] 17 p2387 N88-24187
Aircraft aeroelasticity and structural dynamics research at the NASA Langley Research Center: Some illustrative results [NASA-TM-100627] 18 p2459 N88-24598
Current flight test experience related to structural divergence of forward-swept wings [NASA-TM-100445] 18 p2464 N88-24633
Experimental study of active vibration control [AD-A191454] 18 p2526 N88-24989
Dynamic response of plates to moving loads: Structural impedance and finite element methods 18 p2528 N88-25000
Reduced order modelling and analytical model modification for structural dynamics and control 18 p2529 N88-25006
Analysis and developments of failure concepts in fracture mechanics based on research results in the field of component safety topics: J-integral concept; crack resistance curves; dynamic criterion [V-19/86] 18 p2530 N88-25009
Multishaker modal testing [NASA-CR-179355] 18 p2530 N88-25010
SRM propellant and polymer materials structural test program [NASA-TP-2821] 18 p2530 N88-25013
Single-mode projection filters for modal parameter identification for flexible structures [NASA-CR-182680] 18 p2566 N88-25244
Design of a controller to reduce residual vibration in the positioning control of flexible robotic manipulators 20 p2808 N88-26658
Contact force history and dynamic response due to the impact of a soft projectile [NASA-TM-100961] 20 p2811 N88-26679
A general-purpose approach to computer-aided dynamic analysis of a flexible helicopter [NASA-TM-101002] 20 p2816 N88-26709
Vibration control of large structures [AD-A193317] 21 p2961 N88-27587
DYNA3D (Nonlinear Dynamic Analysis of Structures in Three Dimensions) user's manual [DE88-012242] 21 p2963 N88-27604
Power flow analysis of two coupled plates with arbitrary characteristics [NASA-CR-183165] 22 p3075 N88-28251
A critical speed study for aircraft bias ply tires [AD-A193616] 22 p3084 N88-28313
Structural dynamics of maneuvering aircraft [AD-A192376] 23 p3176 N88-28908
Recursive mass matrix factorization and inversion: An operator approach to open- and closed-chain multibody dynamics [NASA-CR-182516] 23 p3247 N88-29328
ASKA-acoustics: Theory and applications --- vibro acoustics [FFA-TN-1988-13] 23 p3279 N88-29519
Space structure (dynamics and control) theme development [NASA-TM-100597] 24 p3335 N88-29850
Geometric and material nonlinear analysis of structures comprising rectangular hollow sections [CE-79] 24 p3382 N88-30141

DYNAMIC TESTS

Computer-controlled testing of visual-spatial ability [AD-A183971] 03 p0357 N88-12249
Modal analyses of the Kernville diagnostic canister [DE88-003268] 07 p0870 N88-15277
Dynamic testing: Seven years later 08 p0997 N88-16035
Dynamic tests of the Ariane launch vehicle 09 p1126 N88-16749
Comprehensive analysis of helicopters with bearingless rotors [NASA-CR-182537] 10 p1390 N88-18300
Cost effective development of a national test bed [NASA-TM-100321] 12 p1601 N88-19585
KRASH parametric sensitivity study: Transport category airplanes [AD-A189962] 15 p2017 N88-22024
Hybrid procedure for dynamic measurements in transonic wind tunnels: Demonstrated by pitch oscillation [DFVLR-FB-88-19] 21 p2900 N88-27211
Soviet dynamic fracture mechanics research [FASAC-TAR-3140] 21 p2962 N88-27597

DYNAMICAL SYSTEMS

Dynamics of spacecraft control laboratory experiment (SCOLE) slew maneuvers [NASA-CR-4098] 01 p0014 N88-10082
Vortex dynamics and transport to the wall in a crossed-field plasma sheath [DE87-013286] 01 p0100 N88-10657
Dynamical simulation of structural multiplicity in grain boundaries [DE87-012746] 01 p0103 N88-10676
Hot spots: Subnanometer femtosecond energy localization [DE87-010276] 02 p0155 N88-10968
Modeling shockwave deformation via molecular dynamics [DE87-013157] 02 p0169 N88-11063
Dimension densities for turbulent systems with spatially decaying correlation functions [DE87-010119] 02 p0169 N88-11066
IR laser excitation in molecules: Chaos and diffusive energy growth [DE87-013147] 02 p0178 N88-11105
Possible dynamical mechanisms for the Martian polar warming phenomenon [NASA-CR-181454] 02 p0254 N88-11605
A deterministic approach to turbulence: Chaos in Rayleigh-Benard convection 03 p0313 N88-11975
Transition to turbulence via spatio-temporal intermittency 03 p0313 N88-11976
Point vortex dynamics: Recent results and open problems [DE87-014759] 03 p0314 N88-11982
Dynamics and stability of bipedal locomotion robots 03 p0333 N88-12096
Measurements of vapor flux, liquid water contents, precipitation rates and riming in a Utah mountain cloud system [PB87-224945] 04 p0469 N88-12900
Propagation of random initial conditions in time 04 p0486 N88-12993
Novel dynamical investigations of excitons and their structure in semiconductors [DE87-014868] 04 p0499 N88-13070
Non-minimal interaction of gravity with other physical fields: An overview [DE87-703362] 05 p0624 N88-13819
Approaches and possible improvements in the area of multibody dynamics modeling [NASA-CR-179227] 06 p0663 N88-14067
Dynamical friction [DE88-002194] 06 p0711 N88-14358
Darboux transformation and special solutions for the two-dimensional Toda-lattice [PREPRINT-562] 06 p0764 N88-14692
Group quantization of constrained systems [PREPRINT-564] 06 p0790 N88-14844
Anomalous scaling laws in multifractal objects [NOTA-INTERNA-883] 07 p0916 N88-15565
The Jeffcott equations in nonlinear rotordynamics 07 p0928 N88-15636
Attitude determination of artificial satellites through joint application of static and dynamic optimal estimation techniques [INPE-4415-TDL/306] 08 p0963 N88-15832
Dynamic finite element with diagonalized consistent mass matrix and elastic-plastic impact calculation [PB87-143376] 08 p0995 N88-16020
The entropy of the Lorentz model 08 p1015 N88-16153
Lie algebraic method in filtering and identification [CWI-PM-R8606] 08 p1072 N88-16467
An interactive-graphics method for dynamic system modelling, applying consistency rules 09 p1181 N88-17072
Magneto-Inertia Confinement Approach (MICA) to fusion in dynamic Z-pinch formed from a frozen deuterium-tritium tube [IPPJ-856] 09 p1252 N88-17504
An analysis of the motion and effects of hairpin vortices [AD-A187261] 10 p1331 N88-17958
Dynamical properties of aluminium from experimental dispersion relations [DE88-700240] 11 p1459 N88-18697
Optimal control theory of load-following and parameter-tracking of nonlinear systems: An application of Pontryagin Maximum Principle to reactor dynamics [DE88-004770] 11 p1532 N88-19152
Photohydrodynamical processes near compact objects 11 p1569 N88-19390

Motion simulation for in-orbit operations
12 p1589 N88-19514
Analysis of a rotating advanced-technology space station for the year 2025
[NASA-CR-178345] 12 p1600 N88-19580
The automated symbolic derivation of state equations for dynamic systems
[DE88-005222] 12 p1683 N88-20060
Transient dynamics of fibre reinforced composite plates
[IIT-B/CE/RR/87-1] 13 p1734 N88-20370
Unfoldings of quasi-periodic tori
[ZW-8706] 13 p1828 N88-20926
Period-doubling universality in multidimensional dissipative and conservative systems
[PB88-148812] 13 p1832 N88-20961
Optical studies of dynamical processes in disordered system
[DE88-005965] 13 p1837 N88-20993
Laser spectroscopy and dynamics of combustion intermediates
[DE88-006541] 15 p2033 N88-22110
On new solvable many-body dynamical systems with velocity dependent forces
[PREPRINT-581] 15 p2127 N88-22683
A low dimensional dynamical system for the wall layer
16 p2194 N88-23088
Coherent structures and dynamical systems
16 p2199 N88-23119
On the computation of stationary deterministic behavior of nonlinear dynamic systems with applications to rotor-bearing structures
[ETN-88-92241] 16 p2214 N88-23213
Dynamic range compression/expansion of light beams by photorefractive crystals
[NASA-CASE-NPO-17140-1-CU]
17 p2438 N88-24508
Reliability of stochastically forced systems (extended version)
[CWI-AM-R8801] 18 p2526 N88-24985
Infinite dimensional dynamical systems and their finite dimensional analogues
[AD-A192041] 18 p2563 N88-25216
Dynamical properties of a collapsing spherical cavity
19 p2623 N88-25562
Stability of dynamical systems supported by rubber springs 19 p2680 N88-25932
System identification in vehicle dynamics
[DFVLR-MITT-87-22] 20 p2785 N88-26518
Parameter estimation of dynamical systems
20 p2785 N88-26519
Simulation models for the dynamics of tracked vehicle systems: State-of-the-art and open problems
20 p2785 N88-26522
Dynamical evolution of cosmic strings
[DE88-011724] 21 p3030 N88-27989
An analytical investigation of geared system dynamics containing spur and helical gears
22 p3085 N88-28317
General analytic solution of certain functional equations of addition type
[PREPRINT-583] 22 p3144 N88-28699
Analytical investigation of the dynamics of tethered constellations in earth orbit
[NASA-CR-179371] 23 p3184 N88-28950
Method of forming dynamic membrane on stainless steel support
[NASA-CASE-MSC-18172-3] 23 p3201 N88-29052
Coupling expert systems and simulation
23 p3252 N88-29360
Unfoldings of quasi-periodic tori
[B8811116] 23 p3278 N88-29513
Can we calculate the fundamental dimensionless constants of physics
[DE88-702641] 23 p3295 N88-29625
Studies on pressure response of gas bubbles contributions of condensed droplets in bubbles generated by a uniform nucleation
[NASA-TT-20343] 24 p3370 N88-30068
Prediction and measurement of human pilot dynamic characteristics in a manned rotorcraft simulation
[NASA-CR-183246] 24 p3410 N88-30297
Dynamical systems and motion vision
[AD-A195932] 24 p3422 N88-30366
Intramolecular dynamics: A study of molecules at high levels of vibrational excitation
[AD-A195285] 24 p3428 N88-30400
Ring current role in dynamics of fluctuating electron and ion fluxes in low-latitude magnetosphere
24 p3447 N88-30514

DYNAMICS
Dynamics of propellant feedline systems
[AD-A184865] 05 p0580 N88-13537
Recursive forward dynamics for multiple robot arms moving a common task object
[NASA-CR-182526] 10 p1340 N88-18008
Improved description of base dynamics in the modeling of bipolar transistors
[PB88-181516] 19 p2732 N88-26229
Structural dynamics of high-latitude magnetosphere determined from solar electron data
24 p3444 N88-30500

DYNAMICS EXPLORER SATELLITES
NT DYNAMICS EXPLORER 1 SATELLITE

DYNAMICS EXPLORER 1 SATELLITE
Dynamics explorer data analysis
[NASA-CR-181428] 19 p2691 N88-25996
Investigation of the diffuse ultraviolet background with DE data
[NASA-CR-182863] 19 p2741 N88-26271

DYNAMO THEORY
Atmospheres of stars in the limits of thin and thick convection zones: The M dwarfs
04 p0505 N88-13104

DYNAMOMETERS
Design verification tests for an axial gap permanent magnet compressor motor
[DE87-014360] 02 p0167 N88-11049

DYNAMOS
U ROTATING GENERATORS

DYSPROSIUM
Epitaxial growth and new phase of single crystal Dy by molecular beam epitaxy
[DE88-002850] 09 p1256 N88-17531

E

E GLASS
NT S GLASS
Cumulative fatigue and life prediction of fibre composites. Part 2: Experimental techniques and results
[BR101014] 02 p0142 N88-10894
Effects of processing variables on the behavior of E-glass/913 and XAS carbon fibre/913 laminates subjected to hot/wet environmental conditions
[BR101940] 09 p1138 N88-16820

E LAYERS
U E REGION

E REGION
NT SPORADIC E LAYER
The new CP3 06 p0691 N88-14237
Meteor matter interaction with the Earth's atmosphere and the ionospheric E-region structure
06 p0738 N88-14537
The rocket and scatter experiment ROSE: Presentation of the scientific payload 08 p1034 N88-16269
Spectrophotometric remote sensing of the diffuse aurora
[AD-A188599] 12 p1643 N88-19837
Rocket measurements of ionospheric electron temperature over Natal
[INPE-4485-PRE/1250] 15 p2096 N88-22489
Studies of ionosphere/magnetosphere dynamics using SABRE and HILAT
[AD-A190947] 16 p2232 N88-23333
Low frequency electrostatic turbulence in the polar cap E-region
[DRI-3-88] 18 p2540 N88-25077

EAR
NT COCHLEA
NT MIDDLE EAR
NT OTOLITH ORGANS
NT SEMICIRCULAR CANALS
NT VESTIBULES
Questions on the evolution of the development program of the vertebrate inner ear under long term zero-g conditions 07 p0886 N88-15379
Assessment of cochlear damage after microwave irradiation
[AD-A193237] 21 p2987 N88-27737

EARLY STARS
NT A STARS
NT B STARS
NT HOT STARS
NT O STARS
NT WHITE DWARF STARS
NT WOLF-RAYET STARS
Magnetic fields on K and M stars
04 p0510 N88-13137
The Einstein survey of the young stars in the Orion Nebula 04 p0518 N88-13182
Galactic interstellar abundance surveys with IUE and IRAS 04 p0522 N88-13206

EARLY WARNING SYSTEMS
Icing detector with early warning capability
[AOA-4.1.0055] 03 p0325 N88-12050
Radio and radar holes and multipath zones: The global and local influences on atmospheric refractive structure and resulting adverse radio and radar performance
12 p1617 N88-19667
SPOT imagery for landslide cartography in mountainous areas. Example of the French Maritime Alps
22 p3105 N88-28440

EARTH (PLANET)
Steady distortion of shape of geoid and normal gravity field under influence of tidal potential
04 p0459 N88-12839
A Jupiter Data Analysis Program (JDAP) research grant on wave accessibility and attributes
[NASA-CR-182348] 06 p0804 N88-14908
Assessment of anomalous gravitational field of elastic Earth 07 p0921 N88-15594
Planet X probe: A fresh new look at an old familiar place 10 p1287 N88-17699
A program for the calculation of radio-wave transmission loss over the spherical earth and over obstacles
12 p1616 N88-19662
Evaluation of a model of the Earth's gravity field
[EPSHOM-003/87] 17 p2373 N88-24116
Research in particle and gamma-ray astrophysics
[NASA-CR-183111] 20 p2887 N88-27146
Spectral analysis of the Elatina varve series
[NASA-CR-183085] 24 p3402 N88-30260
Exotic minerals in 3,500 million year old rocks: Evidence for large meteorite impacts 24 p3440 N88-30475
LSU scientists discover evidence of large meteorite impacts on the early earth 24 p3441 N88-30480

EARTH ALBEDO
The role of anisotropy in the long range reconnaissance of the albedo of land surfaces 08 p1017 N88-16169
Nimbus 7 Solar Backscatter Ultraviolet (SBUV) spectral scan solar irradiance and Earth radiance product user's guide
[NASA-RP-1199] 09 p1184 N88-17096

EARTH ATMOSPHERE
NT D REGION
NT E REGION
NT EARTH IONOSPHERE
NT F REGION
NT F 2 REGION
NT FREE ATMOSPHERE
NT LOWER ATMOSPHERE
NT LOWER IONOSPHERE
NT MESOPAUSE
NT MESOSPHERE
NT MIDDLE ATMOSPHERE
NT MIDLATITUDE ATMOSPHERE
NT OZONOSPHERE
NT PRIMITIVE EARTH ATMOSPHERE
NT SPORADIC E LAYER
NT STRATOPAUSE
NT STRATOSPHERE
NT THERMOSPHERE
NT TROPOPAUSE
NT TROPOSPHERE
NT UPPER ATMOSPHERE
NT UPPER IONOSPHERE
A study of carbon monoxide distribution determinations for a global transport model
[NASA-CR-181423] 01 p0057 N88-10432
The effects of minor trace gases on the transfer of thermal infrared radiation through the Earth's atmosphere 04 p0468 N88-12893
National Center for Atmospheric Research
[PB87-228391] 04 p0470 N88-12901
A review of parameterizations of microphysical processes in clouds for application in models of regional atmospheric deposition
[DE88-000451] 04 p0471 N88-12909
Anti-Stokes generation of 226 nm light
[DE88-001612] 05 p0589 N88-13590
Ozone formation due to interaction of meteoroids with Earth's atmosphere 06 p0738 N88-14536
The global climate system: Autumn 1984 to spring 1986
[CSM-R84/86] 06 p0745 N88-14583
Nonuniformity of electromagnetic field at Lambda = 10.6 micron wavelength inside atmospheric aerosol particles
06 p0772 N88-14743
A long term radiological risk model for plutonium-fueled and fission reactor space nuclear system
[DE87-010466] 06 p0779 N88-14782
Microsecond beam propagation in air
[DE88-002221] 07 p0845 N88-15127
Chapter 2: Threshold for Raman conversion of FEL laser pulses in the atmosphere
[DE88-002470] 07 p0859 N88-15215
MAXIE 1 (Magnetospheric Atmospheric X-ray Imaging Experiment) Program
[AD-A185878] 07 p0877 N88-15317
Atmospheric heating from optical absorption by aerosols
[DE88-002654] 07 p0878 N88-15327
Estimation of broadband planetary albedo from operational narrowband satellite measurements
[PB88-107644] 07 p0945 N88-15748

A raytrace method for a laterally heterogeneous environment
[AD-A186525] 08 p0978 N88-15912
Vertical atmospheric sounding
[INPE-4370-PRE/1195] 08 p1036 N88-16283
Induced turbulence in aerosol-loaded atmospheres, Jun. 1987
[DE87-014724] 09 p1192 N88-17141
Parameterization of radiative transfer in the Earth's atmosphere with specific applications to clouds
10 p1353 N88-18087
Theoretical and observational problems with Holes in the far UV dayglow
[AD-A188190] 10 p1355 N88-18100
Remote sensing of atmospheric optical thickness and sea-water attenuation when submerged: Wavelength selection and anticipated errors
[AD-A187609] 11 p1548 N88-19262
Review of recent developments in evaporation ducting assessment 12 p1616 N88-19664
High resolution infrared absorption spectra of various trace gases present in the upper atmosphere of the Earth
[NASA-CR-182590] 12 p1642 N88-19829
The effects of atmospheric and thermohaline variability on the validation of the GEOSAT altimeter oceanographic signal between Scotland and Iceland
[AD-A189324] 12 p1650 N88-19882
Investigations of high resolution imaging through the Earth's atmosphere using speckle interferometry
[AD-A189295] 12 p1692 N88-20121
An automated ozone photometer
[NASA-TM-100064] 14 p1908 N88-21404
Introduction to the dynamics of the ocean and the atmosphere 14 p1935 N88-21537
Observational and theoretical studies of greenhouse climate effects
[DE88-006237] 14 p1948 N88-21621
Ozone in the atmosphere 18 p2539 N88-25064
Brunt-Doppler ducting of buoyancy waves in a temperature- and wind-stratified atmosphere
18 p2542 N88-25086
Linear and nonlinear acoustic wave propagation in the atmosphere
[NASA-CR-4157] 18 p2571 N88-25268
High spatial frequency thermal blooming instability: A linear stability analysis
[DE88-010711] 20 p2807 N88-26655
The seasonal exchange of carbon dioxide between the atmosphere and the terrestrial biosphere: Extrapolation from site-specific models to regional models
[DE88-007870] 20 p2822 N88-26740
Our climate in danger
[DE88-701824] 20 p2822 N88-26743
The NASA Marshall engineering thermosphere model
[NASA-CR-179359] 20 p2825 N88-26760
The application of imaging to the atmospheric Cerenkov technique: Observations of the Crab nebula
20 p2884 N88-27126
Multifilter spectrometer (FEB) for microwave atmospheric sounder
[AD-A192312] 21 p2935 N88-27426
Activities report of the Institute for Extraterrestrial Physics
[MPE-206] 21 p3029 N88-27981
On the nucleonics component of cosmic radiation, in the atmosphere
[DE88-702493] 22 p3166 N88-28854
Atmospheric angular momentum and length of day
[AD-A194505] 23 p3233 N88-29238
Basic causes of amplitude modulation in climatic/weather parameters
[DE88-702743] 23 p3236 N88-29254
Hadrons produced in atmospheric interactions
[DE88-702492] 23 p3309 N88-29712
Implementation of the NCAR (National Centre for Atmospheric Research) graphics package at ARL (Aeronautical Research Laboratory)
[AD-A195163] 24 p3391 N88-30193
Did the greenhouse effect kill the dinosaurs
24 p3442 N88-30484

EARTH AXIS

Axial anisotropy of the intensity of the cosmic ray nuclear component
[IFSI-87-7] 05 p0662 N88-14061

EARTH CORE

Seismic body waves and the earth's inner core
[DE88-007395] 19 p2691 N88-25994
An illustration of the complexity of continent formation
24 p3393 N88-30207

EARTH CRUST

A new approach to modeling and interpreting electromagnetic sounding data
[DE88-000460] 04 p0438 N88-12715
An algorithmic approach to crustal deformation analysis 04 p0468 N88-12891
Effective methods of gravimetric and magnetometric data processing 06 p0728 N88-14479
New data on structure of earth's crust and seismicity of basins in Atlantic and Indian Oceans
08 p1010 N88-16123
Crustal dynamics project data analysis, 1987. Volume 1: Fixed station VLBI geodetic results, 1979-1986
[NASA-TM-100682] 08 p1035 N88-16279
Crustal dynamics project data analysis, 1987. Volume 2: Mobile VLBI geodetic results, 1982-1986
[NASA-TM-100689-VOL-2] 08 p1035 N88-16280
The analysis of recent crustal movements in static and kinematic models
[SER-B-279] 09 p1191 N88-17136
Materials of the World Data Center B. Deep Seismic Sounding (DSS): Pacific data 09 p1196 N88-17167
Numerical studies of propagation of Lg waves across ocean continent boundaries using the Representation Theorem (RT) 10 p1353 N88-18085
Analysis of gases in the earth's crust
[PB88-141619] 10 p1354 N88-18093
Crustal Dynamics Project: Catalogue of site information
[NASA-RP-1198] 11 p1513 N88-19037
Isotopic and chemical studies of early crustal metasedimentary rocks
[NASA-CR-182711] 14 p1944 N88-21601
The interpretation of crustal dynamics data in terms of plate interactions and active tectonics of the Anatolian Plate and surrounding regions in the Middle East
[NASA-CR-183024] 18 p2543 N88-25092
Influence of scattering on seismic waves: Physical mechanisms contributing to attenuation in the crust
[AD-A191699] 19 p2690 N88-25992
Seismic reflection experiments imaging the physical nature of crustal structures in southern California
23 p3232 N88-29235
Relationships among earth's gravity field, magnetic field, crustal structure and the magnetic character of crustal rocks
[AD-A195539] 24 p3392 N88-30198
Workshop on the Growth of Continental Crust
[NASA-CR-183073] 24 p3392 N88-30201
Constraints on continental accretion from sedimentation 24 p3392 N88-30202
Nd isotopes and crustal growth rate
24 p3392 N88-30203
Recycling of lower continental crust through foundering of cumulates from contaminated mafic intrusions
24 p3393 N88-30204
Growth of continental crust: Clues from Nd isotopes and Nb-Th relationships in mantle-derived magmas
24 p3393 N88-30205
Pluton emplacement and magmatic arc construction: A model from the Patagonian batholith
24 p3393 N88-30206
The Kerala Khondalite Belt (KKB) of Southern India: An ensialic mobile belt 24 p3393 N88-30208
Genesis of archean granitoids in the Pilbara block and implications for crustal growth 24 p3394 N88-30210
Role of zircon in tracing crustal growth and recycling
24 p3394 N88-30211
Construction of mass-age curves for the continental crust: An empirical model and an example from the western US 24 p3394 N88-30213
Does subduction zone magmatism produce average continental crust 24 p3394 N88-30214
Pb isotope constaints on the extent of crustal recycling into a steady state mantle 24 p3394 N88-30215
Decoupled Rb-Sr and Sm-Nd isotopic evolution of the continental crust 24 p3395 N88-30216
Metamorphic P-T paths and Precambrian crustal growth in East Antarctica 24 p3395 N88-30218
Early intense cratering: Effects on growth of earth's crust 24 p3395 N88-30219
The growth of continents and some consequences since 1.5 Ga 24 p3395 N88-30220
The early archaean crustal history of West Greenland as recorded by detrital zircons 24 p3395 N88-30221
Deep seismic reflection profiling and continental growth curves 24 p3396 N88-30222
Growth of early archaean crust in the ancient Gneiss complex of Swaziland and adjacent Barberton Greenstone Belt, Southern Africa 24 p3396 N88-30223
Evidence for crustal recycling during the Archean: The parental magmas of the stillwater complex
24 p3396 N88-30226
Changing styles of crustal growth in Southern Africa: Constraints from geochemical and Sr-Nd isotope studies in Archaean to Pan African terrains
24 p3396 N88-30227
Structure of Southwestern Michipicoten Greenstone Belt, Ontario: Evidence for Archean accretion
24 p3397 N88-30228
Mid to late proterozoic magmatism within Northeastern North America and its iplications for the growth of the continental crust 24 p3397 N88-30229
Thermal models pertaining to continental growth
24 p3397 N88-30230
Ridge-trench collision in Archean and Post-Archean crustal growth: Evidence from southern Chile
24 p3397 N88-30233
Reappraisal of the geology of Kangimut Sammisoq, Ameralik Fjord, Southern West Greenland: Crustal structure and interpretation of isotopic data
24 p3398 N88-30234
Archean crustal evolution of the northern North China Craton 24 p3398 N88-30235
Growth of the lower continental crust
24 p3398 N88-30236
The complexity, depth, and rapidity of processes that formed the lunar crust 24 p3398 N88-30237
Continental crustal formation and recycling: Evidence from oceanic basalts 24 p3398 N88-30238
Geochronological and lead-isotope evidences for rapid crust formation in middle-proterozoic time: The Labrador example 24 p3398 N88-30239
Physical processes in the growth of the continental crust 24 p3398 N88-30240
Trace element differences between Archean, Proterozoic and Phanerozoic crustal components: Implications for crustal growth processes
24 p3399 N88-30243
The growth of the continental crust: Constraints from radiogenic isotope geochemistry
24 p3399 N88-30245
Crustal growth in the Archean: The geochemical evidence 24 p3400 N88-30246
Solid earth as a recycling systems and the lateral growth of Precambrian North America 24 p3400 N88-30249
Mineralization through geologic time: Evolution of continental crust 24 p3400 N88-30250
Growth of the continental crust: A planetary-mantle perspective 24 p3400 N88-30251
Crustal underplating in the North American Craton: Evidence from the Petrogenesis of anorthositic rocks in the Middle Proterozoic Midcontinent Rift System
24 p3400 N88-30252
Late-Archaean crustal growth in the Lewisian Complex of Northwest Scotland: Diachroneity in magmatic accretion and implications for models of crustal growth
24 p3401 N88-30253
The effect of thicker oceanic crust in the Archaean on the growth of continental crust through time
24 p3401 N88-30254
Volcanic contribution to crustal growth in the Central Andes: A new estimate and a discussion of uncertainties
24 p3401 N88-30255
The second generation intelligent user interface for the crustal dynamics data information system
24 p3419 N88-30352
Non-atmospheric noble gases from CO(sub 2) well ga
24 p3441 N88-30476
Lava thicknesses: Implications for rheological and crustal development 24 p3443 N88-30490

EARTH ENVIRONMENT

Global environmental change research
[S-HRG-100-301] 03 p0348 N88-12199

EARTH FIGURE

U GEODESY

EARTH GRAVITATION

Estimability of potential coefficients from orbit perturbations --- satellite geodesy
[REPT-86.1] 01 p0064 N88-10408
On the theory of the Michelson-Morley experiment in the Earth's gravitational field
[DE87-703077] 02 p0198 N88-11233
Study of a satellite-to-satellite tracking gravity mission
[ESA-CR(P)-2419] 02 p0198 N88-11237
Steady distortion of shape of geoid and normal gravity field under influence of tidal potential
04 p0459 N88-12839
Analysis and synthesis of the Earth's gravity field variable in space and time using vector surface spherical functions
[SER-C-325] 07 p0878 N88-15328
Assessment of anomalous gravitational field of elastic Earth 07 p0921 N88-15594
Department of Defense World Geodetic System 1984: Its definition and relationships with local geodetic systems
[AD-A188815] 12 p1639 N88-19811
Terrestrial gravity data and comparisons with satellite data 12 p1644 N88-19848
Gradiometer accommodation on board a drag-free satellite 12 p1645 N88-19850
Gradiometer mission spectral analysis and simulation studies: Past and future 12 p1645 N88-19851

Comparisons of global topographic/isostatic models to the Earth's observed gravity field
[NASA-CR-182696] 13 p1798 N88-20752
Program for the feasibility of developing a high pressure acoustic levitator
[NASA-CR-182154] 20 p2782 N88-26498

EARTH IONOSPHERE
NT D REGION
NT E REGION
NT F REGION
NT F 2 REGION
NT LOWER IONOSPHERE
NT SPORADIC E LAYER
NT UPPER IONOSPHERE
The combined release and radiation effects satellite, a joint NASA/DOD program 02 p0135 N88-10851
Ionospheric total electron content estimation for single-frequency global positioning system receivers 02 p0161 N88-11005
Ionosphere and plasmasphere 03 p0272 N88-11709
Satellite environment: Polar orbits 03 p0272 N88-11713
JPRS report: Science and technology. China
[JPRS-CST-87-031] 03 p0299 N88-11880
Height profile inversion of ionospheric movement from observed parameters of HF radio echoes 03 p0299 N88-11884
Method estimating integral mean value of enhancement factor and path latitude for whistlers below magnetic latitude 10 deg 03 p0300 N88-11885
Activities report of the Ionospheric Observatory
[UIO-SR-87-01] 05 p0625 N88-13827
Polar Geophysical Institute's studies of magnetosphere, ionosphere 06 p0728 N88-14480
Global convection patterns in the high latitude
[AD-A185794] 06 p0743 N88-14571
Solar-geophysical activity reports for STIP (Study of Travelling Interplanetary Phenomena) interval 15, 12-21 February 1984 ground level event and STIP interval 16, 20 April-4 May 1984 Forbush decrease
[PB88-101274] 06 p0802 N88-14906
EISCAT (European incoherent scatter radar) electron density studies
[AD-A185998] 07 p0841 N88-15099
TRACKER: A 3-D radio ray tracing code
[DE88-003267] 07 p0847 N88-15137
Holography of the ionosphere at HIPAS
[AD-A186237] 07 p0877 N88-15322
Satellite monitoring of earthquake precursor effects in magnetosphere 08 p1007 N88-16103
Diagnostic concept of the resonance cone technique and its application in ground and space experiments 08 p1027 N88-16222
Developments in instrumental techniques for observations of magnetospheric and ionospheric shaped charge releases 08 p1031 N88-16248
CAESAR investigations — Coordinated Auroral Experiment using Scatter And Rockets (CAESAR) 08 p1031 N88-16249
Collaborative studies of polar cap ionospheric dynamics
[AD-A187888] 10 p1355 N88-18098
Temporal evolution of ionospheric electric field driven by field-aligned current 11 p1469 N88-18761
USU (Utah State University) Center of Excellence in Theory and Analysis of the Geo-Plasma Environment
[AD-A187687] 11 p1511 N88-19026
Propagation in longitudinally varying ducts, with emphasis on guiding to antiguiding transitions 12 p1615 N88-19658
An assessment of the application of in situ ion-density data from DMSP to modeling of transionospheric scintillation
[AD-A188919] 12 p1643 N88-19840
Dynamics of small and large scale irregularities at sub-auroral latitudes
[AD-A189052] 12 p1645 N88-19853
WAVFLD: A program to compute ionospheric height gain functions and field strengths at VLF
[AD-A191159] 16 p2191 N88-23066
Ionospheric research in Antarctica
[INPE-4521-PRE/1273] 16 p2232 N88-23331
Centrifugal acceleration of ions in the polar magnetosphere
[NASA-TM-101148] 17 p2374 N88-24120
The Effect of the Ionosphere on Communication, Navigation and Surveillance Systems Based on Ionosph eric Effects Symposium held on 5-7 May 1987 in Springfield, Virginia
[AD-A191855] 18 p2541 N88-25081
Rocket-borne low energy ion measurements in space 18 p2593 N88-25412
Dynamics explorer data analysis
[NASA-CR-181428] 19 p2691 N88-25996
High latitude ionospheric radio studies
[AD-A192270] 20 p2824 N88-26753
Rocket measurements within a polar cap arc: Ionospheric modelling
[AD-A192381] 20 p2824 N88-26754
On the dynamics of the auroral ionosphere during the breakup of a substorm
[AD-A193368] 21 p2972 N88-27657
Optimized observation periods required to achieve geodetic accuracies using the global positioning system
[AD-A193844] 22 p3041 N88-28052
A model of the ionosphere in the altitude interval 50 to 4000 km. Part 1: Atomic ions (H(+), He(+), N(+), O(+))
[DFVLR-FB-88-11-PT-1] 23 p3233 N88-29241
A model of the ionosphere in the altitude interval 50 to 4000 km. Part 2: Molecular ions (N2(+), NO(+), O2(+)) and electron density
[DFVLR-FB-88-12-PT-2] 23 p3234 N88-29242
The effect of equatorial ionospheric irregularities on the performance of a south-looking OTH-B (Over-The-Horizon-Backscatter) radar
[AD-A195090] 24 p3362 N88-30018
On formulating a simple D-region model
[AD-A195841] 24 p3392 N88-30197
Model representation of electron concentration distribution in outer middle-latitude ionosphere using data from Intercosmos-19 artificial earth satellite 24 p3447 N88-30513

EARTH LIMB
Description of data on the Nimbus 7 LIMS map archive tape: Water vapor and nitrogen dioxide
[NASA-TP-2761] 06 p0744 N88-14572

EARTH MAGNETOSPHERE
NT GEOMAGNETIC TAIL
NT MAGNETOPAUSE
Current-driven lower hybrid waves at the inner edge of the ring current — magnetosphere
[MPE-PREPRINT-94] 02 p0243 N88-11534
Morphology of the Earth's environment 03 p0272 N88-11706
Hot plasmas in the Earth's magnetosphere 03 p0272 N88-11710
A simplified approach to the dynamics of charged particles in the magnetosphere 03 p0273 N88-11718
Slow-mode shocks in the earth's magnetosphere
[DE88-000483] 04 p0468 N88-12895
Conditions for geomagnetically trapping sub-micron lunar ejecta between L = 1.2 and L = 3.1 04 p0521 N88-13203
Activities report of the Ionospheric Observatory
[UIO-SR-87-01] 05 p0625 N88-13827
Laboratory and near-earth space plasma as a key to the plasma universe
[TRITA-EPP-87-09] 05 p0652 N88-13996
Polar Geophysical Institute's studies of magnetosphere, ionosphere 06 p0728 N88-14480
Curvature driven drift mirror instability in the magnetosphere
[IFSI-86-14] 06 p0742 N88-14568
MAXIE 1 (Magnetospheric Atmospheric X-ray Imaging Experiment) Program
[AD-A185878] 07 p0877 N88-15317
Satellite monitoring of earthquake precursor effects in magnetosphere 08 p1007 N88-16103
Developments in instrumental techniques for observations of magnetospheric and ionospheric shaped charge releases 08 p1031 N88-16248
CAESAR investigations — Coordinated Auroral Experiment using Scatter And Rockets (CAESAR) 08 p1031 N88-16249
Proceedings of the 21st ESLAB Symposium on Small Scale Processes in the Chromosphere/Corona, Interplanetary Medium and Planetary Magnetospheres
[ESA-SP-275] 08 p1094 N88-16582
Microphysics of the auroral acceleration region of other regions of the magnetosphere 08 p1096 N88-16592
Numerical simulation of solar wind and magnetospheric phenomena 08 p1097 N88-16600
Ion flows in magnetospheric flux transfer events 08 p1098 N88-16607
Simulation and modeling of whistler mode wave growth through cyclotron resonance with energetic electrons in the magnetosphere 10 p1353 N88-18089
A study of the magnetic field annihilation process in the magnetosphere and some geotechnical applications
[DE88-004165] 10 p1355 N88-18096
USU (Utah State University) Center of Excellence in Theory and Analysis of the Geo-Plasma Environment
[AD-A187687] 11 p1511 N88-19026
Energetic particle drift motions in the outer dayside magnetosphere
[DE88-005097] 11 p1512 N88-19034
Electric fields in Earth orbital space. Magnetospheric structural dynamic response to external variables
[AD-A188592] 12 p1643 N88-19836
Observation of a hydromagnetic wave in the earth's magnetosphere
[AD-A188942] 12 p1644 N88-19841
Studies of ionosphere/magnetosphere dynamics using SABRE and HILAT
[AD-A190947] 16 p2232 N88-23333
A plasma wave instrument on the AMPTE/IRM (Active Magnetospheric Particle Tracing Explorers/Ion Release Module) spacecraft
[AD-A191216] 16 p2233 N88-23336
Centrifugal acceleration of ions in the polar magnetosphere
[NASA-TM-101148] 17 p2374 N88-24120
Spacecraft requirements for predictions of geomagnetic activity (a tutorial)
[AD-A191943] 19 p2685 N88-25959
Outer zone electron precipitation produced by a VLF transmitter
[AD-A191944] 19 p2691 N88-25993
MAXIE-1 (Magnetospheric Atmospheric X-ray Imaging Experiment)
[AD-A192846] 21 p2902 N88-27221
Field-aligned structure of the storm time Pc 5 wave of November 14-15, 1979
[AD-A193022] 21 p2972 N88-27653
The low-latitude auroral boundary: Steady-state and time-dependent representations
[AD-A193200] 21 p2972 N88-27656
Solar flares and magnetospheric particles: Investigations based upon the ONR-602 and ONR-604 experiments
[AD-A193396] 21 p3031 N88-27994
Structural dynamics of high-latitude magnetosphere determined from solar electron data 24 p3444 N88-30500
Ring current role in dynamics of fluctuating electron and ion fluxes in low-latitude magnetosphere 24 p3447 N88-30514
Plasma of earth's magnetosphere ring currents. Model compared with results of AMPTE/CCE experiment 24 p3447 N88-30515

EARTH MANTLE
Upper mantle heterogeneity and composition of primary ocean island magmas 08 p1009 N88-16120
Ocean floor magmatism and problems of lithosphere formation 08 p1009 N88-16121
Study of asthenosphere: Project ELAS 08 p1013 N88-16138
The determination of gravity and topography from seismic velocities, accounting for dynamic behavior of the Earth's mantle
[ETN-88-92420] 17 p2374 N88-24117
Carbon analysis in natural olivine crystals of deep origin
[NASA-TT-20311] 19 p2734 N88-26239
Time-dependent thermal convection of Earth mantle and double diffusive convection in magma chambers
[MITT-52] 21 p2974 N88-27663
Workshop on the Growth of Continental Crust
[NASA-CR-183073] 24 p3392 N88-30201
Recycling of lower continental crust through foundering of cumulates from contaminated mafic intrusions 24 p3393 N88-30204
An illustration of the complexity of continent formation 24 p3393 N88-30207
Pb isotope constaints on the extent of crustal recycling into a steady state mantle 24 p3394 N88-30215
The petrogenesis of oceanic kimberlites and included mantle megacrysts: The Malaitan alnoite 24 p3397 N88-30232
Growth of the continental crust: A planetary-mantle perspective 24 p3400 N88-30251
Discrimination studies using short-period P waves at upper mantle distances
[AD-A195468] 24 p3401 N88-30257
Non-atmospheric noble gases from CO(sub 2) well ga 24 p3441 N88-30476

EARTH MOVEMENTS
NT EARTHQUAKES
NT LANDSLIDES
The analysis of recent crustal movements in static and kinematic models
[SER-B-279] 09 p1191 N88-17136
State-of-the-art for assessing earthquake hazards in the US. Parameters for specifying intensity-related earthquake ground motions
[AD-A188230] 11 p1512 N88-19032
Description of ground motion data processing codes, volume 2
[DE88-007137] 15 p2095 N88-22481
Influence of scattering on seismic waves: Physical mechanisms contributing to attenuation in the crust
[AD-A191699] 19 p2690 N88-25992

Stochastic geologic effects on near-field ground motions in alluvium
[AD-A192315] 21 p2972 N88-27652

EARTH OBSERVATIONS (FROM SPACE)
NT SATELLITE OBSERVATION
NT SPOT (FRENCH SATELLITE)
Study of a payload for Columbus Polar Platform Earth observation demonstration mission, executive summary
[ESA-CR(P)-2412] 01 p0014 N88-10079
Payload configurations and serviceability --- Columbus Polar Platforms 03 p0339 N88-12133
Legal protection of the Polar Platform's users 03 p0339 N88-12135
Market potential for commercial remote sensing 03 p0339 N88-12137
MBB-ERNO view of remote sensing commercialization 03 p0340 N88-12140
Latitude coverage of observations of the middle atmosphere by solar absorption spectrometry from a heliosynchronous orbit
[AERONOMICA-ACTA-A-316-1987] 06 p0742 N88-14566
From pattern to process: The strategy of the Earth Observing System: Volume 2: EOS Science Steering Committee report
[NASA-TM-89702] 07 p0871 N88-15283
Academic course Space Methods for Studying Modern Landscapes of Continents 08 p1012 N88-16133
The Cryogenic Infrared Spectrometer and Telescope for the Atmosphere (CRISTA) experiment on Astro-SPAS 08 p1034 N88-16270
Status and prospects of the Joint Research Commitee (JRC) work on the application of ocean colour monitoring from space 08 p1043 N88-16299
Canadian activities and goals in remote sensing of ocean colour and fluorescence from space 08 p1043 N88-16300
Federal Republic of Germany's interests, activities and goals in remote sensing of ocean colour/fluorescence from space 08 p1043 N88-16302
French activities in ocean colour observations 08 p1043 N88-16303
The use of chlorophyll fluorescence measurements from space for separating constituents of sea water 08 p1043 N88-16307
Unispace 82 09 p1128 N88-16766
Proceedings of the ESA Workshop on Co-Orbiting Platform Elements (COPE)
[ESA-SP-1093] 09 p1129 N88-16777
An overview of the current Earth observation programs (Europe, USA, and Japan) 09 p1129 N88-16778
Polar platform element of Space Station: Mission objectives, European priorities, candidate instrumentation and selection procedure 09 p1129 N88-16779
Tethers: An outline of a new concept for Earth observation 09 p1129 N88-16781
Microgravity payloads and missions for Space Station: Some issues affecting compatibility with other payloads 09 p1129 N88-16783
Report of the Workshop on Space Systems Possibilities for a Global Energy and Water Cycle Experiment
[WCP-137] 09 p1193 N88-17147
Planet X probe: A fresh new look at an old familiar place 10 p1287 N88-17699
Space-based remote sensing of the Earth: A report to the Congress
[NASA-TM-89709] 10 p1346 N88-18046
NASA's geodynamics program 12 p1644 N88-19845
Space projects for the 90's relevant to climatology 14 p1935 N88-21539
The International Satellite Land-Surface Climatology Project (ISLSCP) 14 p1937 N88-21558
Measurement of the water content of soil from space and application to the regional water balance 14 p1938 N88-21561
Study of the dynamic topography of oceans by means of satellite altimetry 14 p1938 N88-21567
International cooperation in remote sensing: The ESA experience 17 p2356 N88-24038
The role of space borne imaging radars in environmental monitoring: Some shuttle imaging radar results in Asia
[NASA-TM-101178] 18 p2502 N88-24844
Overview of space missions and techniques for ocean monitoring 19 p2700 N88-26053
The Army's role in space: Support for the battlefield commander
[RAND-P-7396] 19 p2721 N88-26159
The detection and interpretation of long-term changes in ozone from space
[NASA-TM-101135] 21 p2971 N88-27650
Determining earth's rotation from laser observations of Lageos artificial earth satellite (during period of main merit campaign) 24 p3449 N88-30528
Obligue metallogenic zones recognized by interpreting space photographs of southern Tien Shan 24 p3450 N88-30529

EARTH OBSERVING SYSTEM (EOS)
Radiometric calibration of the Earth observing system's imaging sensors
[NASA-CR-181542] 04 p0463 N88-12865
HIRIS (High-Resolution Imaging Spectrometer: Science opportunities for the 1990s. Earth observing system. Volume 2C: Instrument panel report
[NASA-TM-89703] 07 p0871 N88-15282
From pattern to process: The strategy of the Earth Observing System: Volume 2: EOS Science Steering Committee report
[NASA-TM-89702] 07 p0871 N88-15283
SAR (Synthetic Aperture Radar). Earth observing system. Volume 2F: Instrument panel report
[NASA-TM-89701] 07 p0871 N88-15284

EARTH ORBITAL ENVIRONMENTS
Effect of NASA advanced designs on thermal behavior of Ni-H2 cells
[NASA-TM-100197] 01 p0021 N88-10132
Partial analysis of experiment LDEF A-0114
[NASA-CR-179236] 06 p0780 N88-14787
Investigation of the feasibility of an analytical method of accounting for the effects of atmospheric drag on satellite motion 07 p0923 N88-15608
A Study of Space Station Contamination Effects --- conference
[NASA-CP-3002] 18 p2590 N88-25390
Neutral environment for space station 18 p2590 N88-25391
Space station neutral external environment 18 p2590 N88-25392
Contaminant ions and waves in the space station environment 18 p2590 N88-25393
Space station induced electromagnetic effects 18 p2591 N88-25394
Space station contamination study: Assessment of contaminant spectral brightness 18 p2591 N88-25395
Calculation of space station infrared irradiance from atmosphere-induced emissions 18 p2591 N88-25396
Space station particulate contamination environment 18 p2591 N88-25397
The particulate environment surrounding the space station: Estimates from the PACS data 18 p2591 N88-25398
Effects of meteoroids and space debris on the particulate environment for space station 18 p2591 N88-25399
Contamination of optical surfaces --- Space Station 18 p2592 N88-25400
Surface interactions relevant to space station contamination problems 18 p2592 N88-25401
Laboratory experiments of relevance to the space station environment 18 p2592 N88-25402
Contamination of the space station environment by vented chemicals 18 p2592 N88-25403
Application of superconducting technology to earth-to-orbit electromagnetic launch systems
[DE88-010022] 20 p2763 N88-26386
Relationship between characteristics of low-energy electrons and geomagnetic disturbance in geostationary orbit 24 p3444 N88-30501

EARTH ORBITING SPACE STATIONS
U SPACE STATIONS

EARTH ORBITS
NT GEOSYNCHRONOUS ORBITS
The combined release and radiation effects satellite, a joint NASA/DOD program 02 p0135 N88-10851
Nickel hydrogen low Earth orbit test program update and status 02 p0164 N88-11028
Spacecraft surface exposure to atomic oxygen in low Earth orbit 03 p0273 N88-11715
Low Earth orbit environmental effects on the space station photovoltaic power generation systems
[NASA-TM-100230] 03 p0387 N88-12429
Precise near-earth navigation with GPS: A survey of techniques 04 p0433 N88-12682
Simulation and analysis of a geopotential research mission
[NASA-CR-182354] 06 p0670 N88-14109
Investigation of design concepts for large space structures to support military applications
[AD-A186098] 07 p0824 N88-15000
Single-burn transfer to nominally periodic orbit in the vicinity of point L2 of Earth-Sun system and related problems 08 p1006 N88-16100
Verification of a micro-thrusting model to maintain satellites in low orbit
[AD-A186874] 09 p1133 N88-16793
A lunar transportation system
[NASA-CR-182561] 11 p1567 N88-19379
State-of-the-art technologies for construction in space: A review
[AD-A188412] 12 p1585 N88-19483
Orbital analysis of a STS (Space Transportation System) external tank in low earth orbit
[AD-A188829] 12 p1593 N88-19542
NAVARES: A prototype expert system for NAVSTAR anomaly resolution
[AD-A189491] 12 p1600 N88-19579
Survey of the Air Force P78-2 (SCATHA) satellite plasma wave data during electron gun operations
[AD-A191014] 16 p2168 N88-22926
The prediction of satellite lifetimes
[RAE-TR-87030] 17 p2310 N88-23818
Advanced nuclear rocket engine mission analysis
[DE88-006797] 18 p2475 N88-24681
A standard library for modeling satellite orbits on a microcomputer
[AD-A195759] 24 p3331 N88-29830
Particle trajectories and potentials in a plane sheath moving in a magnetoplasma
[AD-A196228] 24 p3390 N88-30190

EARTH PLANETARY STRUCTURE
Department of Defense World Geodetic System 1984: Its definition and relationships with local geodetic systems
[AD-A188815] 12 p1639 N88-19811
Ultrasonic physical modeling of seismic wave propagation from graben-like structures
[AD-A189066] 13 p1796 N88-20744
DOD 1985 world magnetic model: Charts and grid values
[AD-A191484] 18 p2541 N88-25080
Deep seismic reflection profiling and continental growth curves 24 p3396 N88-30222

EARTH RADIATION
U TERRESTRIAL RADIATION

EARTH RADIATION BUDGET
Atlas of wide-field-of-view outgoing longwave radiation derived from Nimbus 7 Earth radiation budget data set - November 1978 to October 1985
[NASA-RP-1186] 01 p0070 N88-10451
Earth Radiation Budget Satellite (ERBS) orbiting profiles and Ni-Cd use 02 p0165 N88-11034
An Earth radiation budget climate model
[NASA-CR-182368] 06 p0744 N88-14578
High-spatial-resolution TOVS observations for the FIRE/SRB Wisconsin experiment region from October 14 through November 2, 1986
[NASA-TM-100522] 06 p0747 N88-14593

EARTH RADIATION BUDGET EXPERIMENT
Development of response models for the Earth Radiation Budget Experiment (ERBE) sensors. Part 2: Analysis of the ERBE integrating sphere ground calibration
[NASA-CR-178293] 01 p0049 N88-10316
Development of response models for the Earth Radiation Budget Experiment (ERBE) sensors. Part 4: Preliminary nonscanner models and count conversion algorithms
[NASA-CR-178295] 01 p0050 N88-10317
Atlas of wide-field-of-view outgoing longwave radiation derived from Nimbus 7 Earth radiation budget data set - November 1978 to October 1985
[NASA-RP-1186] 01 p0070 N88-10451
Development of response models for the Earth Radiation Budget Experiment (ERBE) sensors. Part 3: ERBE scanner measurement accuracy analysis due to reduced housekeeping data
[NASA-CR-178294] 05 p0583 N88-13553
Development of response models for the Earth Radiation Budget Experiment (ERBE) sensors. Part 1: Dynamic models and computer simulations for the ERBE nonscanner, scanner and solar monitor sensors
[NASA-CR-178292] 05 p0584 N88-13557
Report of the Joint Scientific Commitee Ad Hoc Working Group on Radiative Flux Measurements --- Earth radiation budget
[WCP-136] 06 p0742 N88-14567
Operational aspects of a spacecraft planning/scheduling expert system 08 p1062 N88-16415
Summary of along-track data from the Earth radiation budget satellite for several major desert regions
[NASA-RP-1197] 13 p1802 N88-20772
The Earth radiation budget and its spatial and temporal variations 14 p1936 N88-21548

EARTH RESOURCES
NT AQUIFERS
NT COAL
NT CRUDE OIL
NT FORESTS
NT FOSSIL FUELS
NT GEOTHERMAL RESOURCES
NT GLACIERS
NT ICEBERGS
NT LAND ICE
NT MARINE RESOURCES

NT NATURAL GAS
NT OIL FIELDS
NT RAIN FORESTS
NT TAR SANDS
NT UNDERWATER RESOURCES
NT WATER RESOURCES
Study of Earth from space and strengthening of economy 01 p0010 N88-10055
Space photographs of the Onega-Ladoga isthmus and prediction of useful minerals 08 p1008 N88-16108
Use of space photographs for geomorphological studies in southwestern Tajikistan 08 p1008 N88-16109
Critical issues in NASA information systems [NASA-CR-182380] 08 p1093 N88-16577
Fine attitude measurement system study. Volume 1: Executive summary [BAE-TP-7831-VOL-1] 09 p1133 N88-16795
Fine attitude measurement system study, volume 2 [BAE-TP-7831-VOL-2] 09 p1133 N88-16796
Fine attitude measurement system study. Volume 3: Appendices [BAE-TP-7831-VOL-3] 09 p1133 N88-16797
System-wide medium-term environment programme for the period 1990-1995: Strategies of the United Nations system for the environment [UNEP/GCSS.I/2] 12 p1641 N88-19826
The use of four-photon Raman spectroscopy for the remote sensing of natural objects [NASA-TT-20257] 13 p1791 N88-20716
Earth resources: A continuing bibliography with indexes (issue 57) [NASA-SP-7041(57)] 16 p2229 N88-23314
A proposal for a project entitled assessment of forest resources in Uruguay submitted to the United Nations Industrial Development Organization (UNIDO) 17 p2352 N88-24016
The application of satellites in connection with the environment [ETN-88-92474] 18 p2532 N88-25020
Survey for least bell's vireo in riparian habitat on Vandenberg Air Force Base, Santa Barbara County, California [NASA-TM-100984] 20 p2822 N88-26744

EARTH RESOURCES EXPERIMENT PACKAGE
U EREP

EARTH RESOURCES PROGRAM
Earth resources: A continuing bibliography with indexes (issue 55) [NASA-SP-7041(55)] 01 p0065 N88-10415
Earth resources: A continuing bibliography with indexes (supplement 56) [NASA-SP-7041(56)] 10 p1347 N88-18051

EARTH RESOURCES TECHNOLOGY SATELLITES
U LANDSAT SATELLITES

EARTH ROTATION
Crustal dynamics project data analysis, 1987. Volume 1: Fixed station VLBI geodetic results, 1979-1986 [NASA-TM-100682] 08 p1035 N88-16279
On error equations for determining Earth rotation parameters with VLBI network 13 p1756 N88-20500
Determination of Earth rotation by the combination of data from different space geodetic systems [NASA-CR-181388] 13 p1791 N88-20713
Basic research for the geodynamics program [NASA-CR-183149] 21 p2973 N88-27662
Intraseasonal variability in atmospheric surface pressure and relationship to polar motion 22 p3120 N88-28540
Investigation of the validity of the non-rotating planet assumption for three-dimensional earth atmospheric entry [AD-A194877] 24 p3331 N88-29829
Determining earth's rotation from laser observations of Lageos artificial earth satellite (during period of main merit campaign) 24 p3449 N88-30528

EARTH SHAPE
U GEODESY

EARTH SURFACE
Unified Sun and sky illumination for shadows under trees [DE87-014232] 01 p0083 N88-10535
The aerophotogrammetric determination of Earth surface deformations [SER-C-321] 07 p0872 N88-15288
Space applications in geography 08 p1007 N88-16104
Multistep component analysis of correlations 08 p1009 N88-16115
Electromagnetic induction in spherical earth containing oceans and continents in electrical contact with underlying section: Theory, method, example 08 p1011 N88-16127
Vertical atmospheric sounding [INPE-4370-PRE/1195] 08 p1036 N88-16283
Earth penetrator strain gage applications [DE88-002260] 09 p1166 N88-16993
General determination of Earth surface type and cloud amount using multispectral AVHRR data [NOAA-TR-NESDIS-39] 11 p1508 N88-18997
Terrestrial Propagation Characteristics in Modern Systems of Communications, Surveillance, Guidance and Control [AGARD-CP-407] 12 p1614 N88-19853
Estimating the solar irradiance of an intermountain region using GOES (Geostationary Operational Environmental Satellite) satellite data: A test of two statistical models [AD-A188414] 12 p1642 N88-19834
Resolution of the magnetotelluric method for determining local inhomogeneities in the sedimentary cover 13 p1789 N88-20701
Remote sensing of earth terrain [NASA-CR-182677] 13 p1790 N88-20711
Measurement from satellites of land surface parameters and fluxes in the thermal infrared bands: Problems and methods 14 p1937 N88-21557
The International Satellite Land-Surface Climatology Project (ISLSCP) 14 p1937 N88-21558
A low cost automatic Earth observation satellite tracking ground receiving station 17 p2309 N88-23815
The Shuttle Imaging Radar B (SIR-B) experiment report [NASA-CR-182923] 17 p2334 N88-23932
Comparison of the solar radiation estimation method by satellites 17 p2360 N88-24055
A bibliography of dunes: Earth, Mars, and Venus [NASA-CR-4149] 20 p2885 N88-27134
Metric applications of SPOT's lateral stereoscopy 22 p3111 N88-28480
Interactions between air and ground sound at the Earth surface 22 p3149 N88-28733
Estimation of short-wavelength gravity on a dense grid using digital terrain elevation data [AD-A196325] 24 p3391 N88-30196

EARTH TIDES
Steady distortion of shape of geoid and normal gravity field under influence of tidal potential 04 p0459 N88-12839
Observations of Earth tides by the German Geodetic Research Institute, division 1, in the period 1979-1985 at the Berchtesgaden and Wettzell stations [SER-B-280] 07 p0872 N88-15291
Effectiveness of oceanographic method in earthquake prediction 08 p1010 N88-16124

EARTH-MOON SYSTEM
Relative motion near the triangular libration points in the Earth-Moon system 01 p0097 N88-10636
The dust ring of the Earth [RAE-TRANS-2163] 22 p3119 N88-28530

EARTHNET
National Point Of Contact (NPOC)-SPOT inquiry 1986 [NLR-MP-86055-U] 05 p0620 N88-13807
International cooperation in remote sensing: The ESA experience 17 p2356 N88-24038

EARTHQUAKE DAMAGE
SPOT for earthquake hazard zoning in southern Italy, a provisional report 03 p0342 N88-12161
State-of-the-art for assessing earthquake hazards in the US. Parameters for specifying intensity-related earthquake ground motions [AD-A188230] 11 p1512 N88-19032

EARTHQUAKE RESISTANT STRUCTURES
Practical considerations for structural control: System uncertainty, system time delay and truncation of small control forces [PB88-163738] 14 p1933 N88-21528

EARTHQUAKES
Historical catalog of Southern Great Basin earthquakes, 1868-1978 [DE87-014340] 02 p0198 N88-11232
Siting and Geotechnical Program Focus and Directions. Report upon the deliberations of a workshop held at the Illinois Institute of Technology, Chicago, Illinois on August 4-5, 1986 [PB87-206272] 02 p0198 N88-11238
SPOT for earthquake hazard zoning in southern Italy, a provisional report 03 p0342 N88-12161
Earthquake source mechanisms and transform fault tectonics in the Gulf of California 03 p0349 N88-12206
Interseismic deformation for normal fault earthquakes 03 p0349 N88-12207
Transform fault earthquakes in the North Atlantic: Source mechanisms and depth of faulting 03 p0350 N88-12208
Hypocenters (1977-1984) around the Richton Dome and the Melvin, Alabama, 1978 earthquake [DE87-014336] 03 p0351 N88-12214
RRS DISCOVERY Cruise 161, 15 August (227)-19 September (262) 1986. Portuguese Ocean-continent boundary, plate boundaries west of Iberia and seismic structure of sediments off Madeira [PB87-222006] 06 p0747 N88-14596
State-of-the-art for assessing earthquake hazards in the United States. Report 26: Parameters for specifying magnitude-related earthquake ground motions [AD-A185997] 07 p0877 N88-15319
Satellite monitoring of earthquake precursor effects in magnetosphere 08 p1007 N88-16103
Effectiveness of oceanographic method in earthquake prediction 08 p1010 N88-16124
Comprehensive method for defining seismogenic zones 08 p1011 N88-16129
Correlation between seismic activity and variations of microseismic oscillations 08 p1011 N88-16131
Naval weapons center active fault map series [AD-A188425] 12 p1643 N88-19835
Correlation of data on strain accumulation adjacent to the San Andreas Fault with available models [NASA-CR-180757] 13 p1796 N88-20742
Tectonics and three-dimensional structure of spreading centers: Microearthquake studies and tomographic inversions [PB88-163290] 14 p1945 N88-21602
Earthquakes from peninsular India: Data from the Gauribidanur seismic array [DE88-701232] 15 p2093 N88-22471
Characteristics of seismic sources of some Asian earthquakes and Soviet underground explosions from Gauribidanur array records [DE88-701233] 15 p2093 N88-22472
Specific features of emanation, temperature and hydrodynamic fields in the epicentral zone of tectonic earthquake [DE88-701140] 17 p2373 N88-24114
SPOT for earthquake hazard zoning in southern Italy 22 p3093 N88-28365

EBERT SPECTROMETERS
An infrared grating spectrometer for GIRL [ETN-88-91071] 09 p1167 N88-16997

EBR-2 REACTOR
U EXPERIMENTAL BREEDER REACTOR 2

EBULLITION
U BOILING

ECCENTRIC ORBITS
An evaluation of semianalytical satellite theory against long arcs of real data for highly eccentric orbits [AD-A185825] 08 p0960 N88-15819

ECCENTRICITY
Relative motion of two satellites in close-elliptical orbits [AD-A188851] 12 p1594 N88-19543
Orbit determination of 1965-09A for analysis of the eccentricity at 15th-order resonance [RAE-TR-87059] 22 p3047 N88-28081

ECCENTRICS
Pin joints, gears, springs, cranks and other novel micromechanical structures [DE88-002504] 07 p0864 N88-15245

ECHELON FAULTS
U GEOLOGICAL FAULTS

ECHO SOUNDING
Detection of targets in the presence of clutter using target echo modulations caused by rotating structures [REPT-12-86] 01 p0036 N88-10231
Utilization of dense packed planar acoustic echosounders to identify turbulence structure in the lowest levels of the atmosphere [AD-A191006] 16 p2233 N88-23335

ECHOCARDIOGRAPHY
Cardiovascular adaptation to zero-g during a long term flight (237 days) on board the Salyut 7 Soviet space station (1984) * 12 p1655 N88-19920
Variation of carotid flow under load, studied by the Doppler echo method --- acceleration tolerance [REPT-1149] 23 p3240 N88-29282

ECHOES
NT CLUTTER
NT RADAR ECHOES
NT RADIO ECHOES
NT SIGNAL REFLECTION
NT VENUS RADAR ECHOES
Radar information from the partial derivatives of the echo signal phase from a point scatterer [AD-A193402] 21 p2933 N88-27415

ECLIPSES
NT SOLAR ECLIPSES
Was the eclipse comet of 1893 a disconnected coronal transient? 01 p0115 N88-10733
Calculation of eclipses for elliptical orbits [INPE-4412-NTE/277] 12 p1594 N88-19545
Colliding stellar winds in the eclipsing Wolf-Rayet binary V444 Cygni [NASA-CR-182937] 17 p2451 N88-24563

ECLIPSING BINARY STARS
NT DWARF NOVAE
The hard X-ray eclipse in the intermediate polar EX Hydrae [MPE-PREPRINT-95] 02 p0251 N88-11582

Contemporaneous B,V,R,I photometry and H alpha spectroscopy of YY Gem 04 p0513 N88-13155
Light curve behaviour in the near IR of the CG Cyg system 04 p0513 N88-13156
A flash spectrum of Cl I, C I, N I, and Ni II absorption in 31 Cygni: A direct observation of the reversing layer 04 p0513 N88-13158
New results from high angular resolution observations of alpha Ori 04 p0514 N88-13161
Stromgren photometry of RSCVn and HD108102 04 p0519 N88-13187
BE Ursae Majoris: A detached binary with a unique reprocessing spectrum
[NASA-CR-182419] 08 p1083 N88-16526
EXO033319-2554.2: A 55-MG eclipsing AM Herculis binary
[MPE-PREPRINT-114] 22 p3163 N88-28838

ECLOGITE
Crustal evolution and the eclogite to granulite phase transition in xenoliths from the West African Craton 24 p3395 N88-30217

ECOLOGICAL SYSTEMS
U ECOLOGY

ECOLOGY
NT COASTAL ECOLOGY
China report: Science and technology
[JPRS-CST-87-015] 03 p0298 N88-11873
Compilation of 1986 annual reports of the Navy ELF (Extremely Low Frequency) communications system ecological monitoring program, volume 1
[AD-A184561] 03 p0306 N88-11930
Compilation of 1986 annual reports of the Navy ELF (Extremely Low Frequency) communications system ecological monitoring program, volume 2
[AD-A184562] 03 p0306 N88-11931
New book on space ecology reviewed 07 p0897 N88-15434
Detection of soil erosion with Thematic Mapper (TM) satellite data within Pinyon-Juniper woodlands
[NASA-CR-182476] 09 p1185 N88-17103
Comparison of simulation modeling and satellite techniques for monitoring ecological processes
[NASA-CR-182592] 12 p1641 N88-19825
Characteristics of the thermal environment
[AD-A188359] 12 p1641 N88-19827
Changes in the Antarctic atmosphere due to the reduction of stratospheric ozone
[ETN-88-92565] 18 p2540 N88-25074
Ecological risk factors related to environmental uses of genetically engineered organisms
[DE88-006674] 18 p2549 N88-25132
Extremely Low Frequency (ELF) communications system ecological monitoring program: Summary of 1986 progress
[AD-A192014] 19 p2642 N88-25676

ECONOMETRICS
Explicit construction and analysis of some efficient empirical production functions in data envelopment analysis
[AD-A185907] 07 p0908 N88-15502
Estimation and testing in truncated and nontruncated linear median-regression models
[AD-A186317] 07 p0911 N88-15522

ECONOMIC ANALYSIS
New technologies and intellectual property: An economic analysis
[N-2601-NSF] 01 p0107 N88-10695
Models for conducting economic analysis of alternative fuel vehicles
[AD-A184028] 03 p0334 N88-12103
Application of Organic Rankine Cycles (ORCs) to decentralized power generation, preliminary study
[DE87-753331] 03 p0347 N88-12197
A large-scale perspective on ecosystems 03 p0360 N88-12265
Economics of fusion reactors
[DE88-000580] 05 p0653 N88-14002
Mathematical-cartographic modeling of economic utilization of Atlantic Ocean 06 p0726 N88-14469
Summary of the report of the Senior Committee on Environmental, Safety and Economic Aspects of Magnetic Fusion Energy
[DE88-003270] 07 p0937 N88-15692
An extended Cobb-Douglas form for use in production economics
[AD-A186372] 07 p0943 N88-15733
Definition and economic evaluation of Space Solar Power Systems (SSPS), part 1
[ILR-MITT-184-1(1987)] 08 p1022 N88-16189
Definition and economic evaluation of Space Solar Power Systems (SSPS), part 2
[ILR-MITT-184-2(1987)] 08 p1022 N88-16190
Exponential lower bounds for finding Brouwer fixed points
[DE88-002864] 10 p1425 N88-18513
An economic analysis of a multi-commodity fruit and vegetable irradiator
[DE88-003425] 11 p1524 N88-19098
Status of emerging technologies: An economic/technological assessment to the year 2000
[PB88-155775] 11 p1567 N88-19381
Robotics applications in the testing of inertial sensors 12 p1577 N88-19433
An assessment methodology for thermal energy storage evaluation
[DE88-004642] 13 p1794 N88-20732
European Progress on Space (EPOS): Participation in the creation of long term European space programs
[ILR-MITT-189] 14 p1871 N88-21180
Northern lights: The economic and practical potential of imported power from Canada
[DE88-006026] 15 p2093 N88-22473
Production costs of hydrocarbon fuels from biomass
[DE88-006667] 18 p2495 N88-24804
Technical and economic evaluation of emerging biomass pyrolysis processes for gasoline production 18 p2536 N88-25048
System capacity and economic modeling computer tool for satellite mobile communications systems 19 p2644 N88-25686
Mutually exclusive alternatives by clustering
[DE88-007707] 20 p2882 N88-27115
PAX ECONOPACK economic analysis package users manual
[AD-A192949] 20 p2883 N88-27117
A comparative economic evaluation of industrial heat pumps. Part 2: Addendum
[DE88-011701] 22 p3117 N88-28519
Absorption heat pumps
[DE88-752820] 23 p3229 N88-29218
Possibilities of economical improvements for Moon based rocket propulsion using lunar propellants
[ILR-MITT-196] 24 p3338 N88-29871

ECONOMIC DEVELOPMENT
Messerschmitt-Boelkow-Blohm: A company with a tradition 10 p1316 N88-17866
Spin off businesses as mechanisms for transferring technologies
[DE88-005640] 13 p1852 N88-21085

ECONOMIC FACTORS
Problems in integrating geographic data
[DE87-012880] 01 p0106 N88-10689
Nowcasting for the national economy needs 02 p0199 N88-11241
GSSR powder metallurgy research, production expanding 03 p0286 N88-11797
Commercial perspective of an imaging spectrometer development program 03 p0340 N88-12138
Summary of the report of the Senior Committee on Environmental, Safety and Economic Aspects of Magnetic Fusion Energy
[DE88-003270] 07 p0937 N88-15692
Technical-economical evaluation of a novel propfan concept in comparison with the turbofan for the nineties
[ETN-88-91022] 11 p1441 N88-18596
Review of commercial spacecraft: Recovery and repair experiences. Implications for future spacecraft designs and operations 12 p1591 N88-19528
Activities report of Lufthansa
[ISSN-0176-5086] 16 p2155 N88-22855
Corrosion in aircraft structures. Part 1: Text
[LR-527-PT-1] 20 p2775 N88-26458
Corrosion in aircraft structures. Part 2: Figures
[LR-527-PT-2] 20 p2775 N88-26459
Trends in civil aircraft propulsion
[PNR90441] 22 p3044 N88-28067
Real-time space system control with expert systems 23 p3262 N88-29419

ECONOMIC IMPACT
Understanding and accepting fusion as an alternative energy source
[DE88-004356] 10 p1413 N88-18432
Understanding CO2 and climate
[PB88-167655] 16 p2234 N88-23341
Evaluation of a flood period (June, 1984) in the southern region of Laguna dos Patos, through remote sensing data, meteorological and oceanographic 17 p2365 N88-24083
Acid rain: Delays and management changes in the Federal research program
[GAO/RCED-87-89] 19 p2690 N88-25988
Economic impact of space flight activities in West Germany. Influence of allocations of Bundesministerium fuer Forschung und Technologie
[ETN-88-92106] 21 p2901 N88-27215

ECONOMICS
Study of Earth from space and strengthening of economy 01 p0010 N88-10055
A role for national laboratories in enhancing economic competitiveness. The example of high-temperature superconductors: CNSS papers, No. 1
[DE87-013633] 03 p0379 N88-12386
Technology transfer to China
[PB87-223418] 04 p0502 N88-13087
The role of basic research in society
[DE88-000459] 04 p0502 N88-13090
Economics of fusion reactors
[DE88-000580] 05 p0653 N88-14002
Impressions, observations and comments on science and technology in Japan
[PB87-235743] 06 p0799 N88-14893
On the role of complete reducibility in general competitive equilibrium models
[DE88-005693] 13 p1851 N88-21083
Advances in applied superconductivity: A preliminary evaluation of goals and impacts
[DE88-006441] 14 p1986 N88-21844
Technology transfer to China. Volume 2: Working papers, part 1
[PB88-158704] 14 p1992 N88-21872
Review of power requirements for satellite remote sensing systems 17 p2419 N88-24387
Remote sensing applied to the monitoring of mineral extraction in the proximity of urban areas: Pros and cons 19 p2684 N88-25954
A basis of settlement: Economic foundations of permanent pioneer communities
[DE88-010907] 20 p2762 N88-26382
Political and economic barriers to information transfer 24 p3437 N88-30460
Formulation and solution of economic equilibrium problems
[AD-A196034] 24 p3439 N88-30470

ECONOMY
Japanese industrial research on lean combustion: A case study: International Research Monitoring Program
[DE87-013839] 02 p0144 N88-10904
Advancing automation and robotics technology for the space station and for the US economy: Submitted to the United States Congress October 1, 1987
[NASA-TM-100777] 08 p0959 N88-15816
Advancing automation and robotics technology for the space station and for the US economy: Submitted to the United States Congress October 1, 1986
[NASA-TM-89190] 08 p0960 N88-15818
The impact of hemp production on the development of the municipalities of Araras, Leme, Santa Cruz da Conceicao and Pirassununga 19 p2683 N88-25948
Use of remote sensing in the study of superficial formation certifying the development of integrated economy-case example: Rio Claro (SP) region 19 p2683 N88-25950

ECOSYSTEMS
Spatial characterization of acid rain stress in Canadian Shield Lakes
[NASA-CR-181136] 01 p0067 N88-10430
Spatial characterization of acid rain stress in Canadian Shield Lakes
[NASA-CR-180577] 01 p0067 N88-10431
Investigation of large scale impact of air pollution components on forest ecosystems in Bavaria, West Germany
[DFVLR-FB-87-17] 01 p0068 N88-10434
Compilation of 1986 annual reports of the Navy ELF (Extremely Low Frequency) communications system ecological monitoring program, volume 2
[AD-A184562] 03 p0306 N88-11931
Compilation of 1986 annual reports of the Navy ELF (Extremely Low Frequency) communications system ecological monitoring program, volume 3
[AD-A184563] 03 p0306 N88-11932
A modular BLSS simulation model 03 p0359 N88-12260
A large-scale perspective on ecosystems 03 p0360 N88-12265
Disturbance and recovery of Arctic Alaskan tundra terrain. A review of recent investigations
[AD-A184442] 04 p0467 N88-12887
Semi-arid ecosystem development as a function of resource processing and allocation
[DE88-000890] 07 p0875 N88-15308
ELF (Extremely Low Frequency) communications system ecological monitoring program: Electromagnetic field measurements and engineering support, 1986
[AD-A188057] 11 p1509 N88-19017
Comparison of simulation modeling and satellite techniques for monitoring ecological processes
[NASA-CR-182592] 12 p1641 N88-19825
The use of SLAR and SIRA imagenes for the classification of forest typen in tropical rain forests 17 p2356 N88-24036
Structure and dynamics of vegetation in the middle semi-arid tropics. Quixaba's Caatinga (PE): Terrain analysis of MSS/LANDSAT data 17 p2358 N88-24049

Interpretation of MSS/LANDSAT data for evaluation of physical distribution of mangroves in Cananeia-Iguape (SP) 17 p2363 N88-24072
Application of remote sensing in the conservation of natural areas: Ribeira Valley 19 p2683 N88-25949
Spatial and spectral registration of Javanese landscape units with SPOT 22 p3092 N88-28362
Investigation of the large-scale impact of air pollution components on forest ecosystems in Bavaria [ESA-TT-1087] 24 p3390 N88-30187

ECS
U EUROPEAN COMMUNICATIONS SATELLITE

EDDIES
U VORTICES

EDDY CURRENTS
Eddy current density in wedge-shaped conducting cylinders with inhomogeneous conductivity [ETN-87-90404] 01 p0042 N88-10268
Pulsed eddy-current inspection of thin-walled stainless steel tubing [DE88-001492] 04 p0457 N88-12830
Proceedings of the 2nd Regional Electromagnetic Workshop at Argonne National Laboratory [DE87-004633] 06 p0690 N88-14230
Eddy Current Seminar, 24-26 March 1986 [PB87-124988] 06 p0696 N88-14269
A pulsed eddy current method for examining thin-walled stainless steel tubing [DE88-002294] 07 p0866 N88-15255
Nondestructive control: Modeling of electromagnetic phenomena, defect characterization, and sensor optimization [ECL-86-14] 08 p0993 N88-16008
Low frequency eddy current detection and evaluation of corrosion in aircraft skins [ETN-88-91664] 09 p1144 N88-16859
Simplified physical approach of the control by eddy current [DE88-701076] 13 p1764 N88-20552
Eddy current losses induced by rotation of magnetisation [BLL-M-37634-(5828.4)] 14 p1890 N88-21298
Eddy current nondestructive inspection of graphite epoxy using ferrite cup core probes [AD-A189823] 15 p2074 N88-22365
Aerodynamic and thermal modeling of electromagnetic brakes. Evaluation of convective exchange coefficients and friction losses in the rough wall channels [ISAL-ITC1-87-02] 16 p2215 N88-23214
Detection sensitivity in thick assemblies — eddy currents, light alloys, aircraft construction materials [REPT-48-912/F] 16 p2216 N88-23221
Solving time-dependent two-dimensional eddy current problems [NASA-TM-100875] 18 p2566 N88-25239
Investigation of Rossby-number similarity in the neutral boundary layer using large-eddy simulation [DE88-008910] 19 p2666 N88-25851
Sensitivity to crack initiation in thick assemblies. Test report 48-444 [REPT-48-444] 20 p2758 N88-26365
The calculation of time dependent eddy currents in tokamaks [REPT-206] 23 p3286 N88-29568

EDDY DIFFUSION
U TURBULENT DIFFUSION

EDDY VISCOSITY
Evaluation of a research circulation control airfoil using Navier-Stokes methods 10 p1269 N88-17591
Determining Langmuir circulation parameters on basis of similarity theory 13 p1785 N88-20680
On the zonal momentum balance at the equator 13 p1805 N88-20788
Interaction of a strong vortex with decaying turbulence [DE88-007102] 14 p1911 N88-21420

EDGE DISLOCATIONS
The growth of persistent slip bands 05 p0597 N88-13648
The effects of thin anodic films on the cyclic microstrain/macrostrain behavior of tungsten 05 p0597 N88-13650
Cyclic deformation of an extruded AlMgSi alloy 05 p0598 N88-13654
The orientations of dipolar walls produced by cyclic deformation 05 p0598 N88-13655

EDGE LOADING
An integral equation analysis of inelastic shells 03 p0336 N88-12118
FEB (Multifilter Electronics Box) lifting device analysis, revision A [AD-A192313] 21 p2935 N88-27427
Failure analysis of quasi-isotropic composite laminates with free edges under off-axis loading 22 p3049 N88-28092

EDGES
NT LEADING EDGES
NT SHARP LEADING EDGES
NT TRAILING EDGES
Heavy-particle collisions in the plasma edge [DE87-012928] 02 p0237 N88-11493
Recognizing rigid objects by aligning them with an image [AD-A184253] 03 p0368 N88-12318
Helicity dissipation in the plasma edge [DE87-014762] 03 p0378 N88-12376
Free-edge delamination: Laminate width and loading conditions effects [NASA-TM-100238] 04 p0411 N88-12551
Local likelihood method in the problems related to change points [AD-A185604] 06 p0768 N88-14718
Statistical investigations of the behavior of a product correlator and an edge detector in critical situations [MBB-UA-1034/87] 06 p0781 N88-14793
Edge plasmas and plasma/wall interactions in an ignition-class reversed field pinch [DE88-001825] 06 p0782 N88-14799
L2,3 XANES of the high T sub c superconductor YBa2Cu3O7 with variable oxygen content [NOTA-INTERNA-888] 06 p0788 N88-14837
A composite grating for moire interferometry [AD-A186330] 07 p0832 N88-15044
Development of composite polymer-glass edge claddings for Nova laser disks [DE88-002389] 07 p0860 N88-15220
Proceedings of Image Understanding Workshop, volume 1 [AD-A186103] 07 p0902 N88-15463
Stress intensity and crack displacement for small edge cracks [NASA-TP-2801] 09 p1184 N88-17095
Visual integration and detection of discontinuities: The key role of intensity edges [AD-A188012] 11 p1520 N88-19076
Generalised threshold selection for edge detection [RAE-TR-87035] 14 p1941 N88-21581
Finding texture boundaries in images [AD-A190554] 15 p2117 N88-22609
The theory of flotation [NASA-TT-20278] 16 p2207 N88-23172
Measurements of edge turbulence with Langmuir probes in currentless Heliotron E plasmas [DE88-752313] 16 p2275 N88-23617
Curvature of blended rolled edge reflectors at the shadow boundary contour [NASA-CR-182974] 18 p2576 N88-25300
Instability-related delamination growth of embedded and edge delaminations 20 p2767 N88-26406
Comparison of edge diffraction theories [AD-A193880] 22 p3070 N88-28223
Analysis of edge detection techniques for radiographic image measurement [AD-A193650] 23 p3186 N88-28961
A linear-time algorithm for finding a minimum spanning pseudoforest [AD-A194029] 23 p3250 N88-29346
Improved time bounds for the maximum flow problem [AD-A194034] 23 p3272 N88-29471

EDITING
Personal computers and All-In-1: Document transfer and translation [DE88-003760] 10 p1384 N88-18264
Editing master oceanographic observation data set 4 [AD-A188405] 12 p1649 N88-19876
Editfont an interactive font editing system [AD-A191007] 16 p2251 N88-23453
Editfont: An interactive font editing system [AD-A192373] 20 p2838 N88-26836
Script editor: An editor for the specification phase in the development of computer based learning [REPT-87-68] 20 p2839 N88-26846

EDITING ROUTINES (COMPUTERS)
A hypertext writing environment and its cognitive basis [AD-A188179] 10 p1389 N88-18298
Editfont an interactive font editing system [AD-A191007] 16 p2251 N88-23453
Editfont: An interactive font editing system [AD-A192373] 20 p2838 N88-26836

EDUCATION
NT ASTRONAUT TRAINING
NT FLIGHT TRAINING
NT MAINTENANCE TRAINING
NT PILOT TRAINING
NT SPACE FLIGHT TRAINING
An object-oriented architecture for intelligent tutoring systems [AD-A184790] 03 p0368 N88-12314
CNET (Chief of Naval Education and Training) Program Automated Tracking System (CPATS): A comprehensive study [AD-A184694] 03 p0385 N88-12418
The pros and cons of using a CAI package on a central computer as opposed to a microprocessor: What's your CAI MO, mainframe or micro [DE87-011123] 04 p0475 N88-12929
Special Course on Fundamentals of Fighter Aircraft Design [AGARD-R-740] 05 p0544 N88-13315
Calendar of selected aeronautical and space meetings [AGARD-CAL-87/1] 05 p0657 N88-14033
Learning to program methodically. 3: The newly designed course of the elementary programming [PB87-119871] 06 p0757 N88-14643
A study of the minority college programs at the NASA Johnson Space Center 06 p0798 N88-14887
Activities report of the Technical University of Twente [ETN-88-90620] 06 p0799 N88-14892
Field evaluation of interactive simulation for maintenance training: SH-3 helicopter electro-mechanical bladefold system [AD-A185923] 07 p0821 N88-14991
Application of the analysis phase of the instructional system development to the MK-105 magnetic minesweeping mission of the MH-53E helicopter [AD-A186282] 07 p0822 N88-14994
Compilation and development of K-6 aerospace materials for implementation in NASA spacelink electronic information system 07 p0922 N88-15605
A summary of the Naval Postgraduate School research program [AD-A186362] 07 p0942 N88-15727
Academic course Space Methods for Studying Modern Landscapes of Continents 08 p1012 N88-16133
Overlearning and positive thinking alleviate negative effects of stress on performance [FOA-C-50051-5.3] 08 p1051 N88-16344
The use and generation of illustrative examples in computer-based instructional systems 08 p1060 N88-16400
ESA Bulletin No. 25 [ISSN-0376-4265] 09 p1128 N88-16767
Training in satellite ground system operations 09 p1129 N88-16775
The desktop interface in intelligent tutoring systems 09 p1205 N88-17225
Computer assisted instruction: Two decades in perspective [AD-A186813] 09 p1216 N88-17289
Training guidelines in non-destructive testing techniques [DE88-700613] 10 p1342 N88-18019
Interdisciplinary research in mathematics, science and technology education [PB88-131446] 10 p1398 N88-18333
The design and implementation of pedagogical software for the multi-backend/multi-lingual database system [AD-A188106] 11 p1530 N88-19135
Report of the participation in the International Training Course: Remote Sensing in Village Forestry [INPE-4476-NTE/278] 12 p1637 N88-19802
Aircrew training devices: Utility and utilization of advanced instructional features, phase 4 [AD-A188418] 12 p1670 N88-20000
Field dependence-independence and its relationship to flight training performance [AD-A188886] 12 p1670 N88-20003
Northeast Artificial Intelligence Consortium (NAIC) administrative matters and ancillary functions, volume 1 [AD-A189466] 12 p1682 N88-20055
Text organization and comprehensibility in technical writing [AD-A188913] 12 p1707 N88-20217
Down-to-Earth approach for final projects in Karlsruhe (Federal Republic of Germany) 16 p2226 N88-23292
Elementary and middle school science improvement project [NASA-CR-179328] 16 p2285 N88-23679
Technique to obtain the agricultural ownership limits by satellite imagery, to approve control, and to accompany agricultural activity 19 p2682 N88-25943
Using space photography of the Earth in the classroom: Drought in Africa [NASA-CR-182948] 19 p2685 N88-25960
Selection and training of subjects to live and work in hostile and unusual environments 19 p2696 N88-26026
Communication training for aircrews: A review of theoretical and pragmatic aspects of training program design [NASA-CR-177459] 20 p2756 N88-26349
Inference and discovery in an exploratory laboratory [AD-A192231] 20 p2832 N88-26801

United States Air Force Graduate Student Summer Support Program, volume 2
[AD-A191122] 21 p2924 N88-27355
Can CNV amplitude predict ability to accomplish a demanding task? 21 p2980 N88-27700
Space imagery as a teaching aid in secondary education 22 p3114 N88-28500
Training of the Group for the Development of Aerospace Remote sensing 22 p3114 N88-28501
Effects of psychophysical lifting training on maximal repetitive lifting capacity
[AD-A192605] 23 p3238 N88-29271
Future air-to-air training for the RF-4
[AD-A194363] 23 p3240 N88-29284
Proposed improvements to the USAF flight screening program
[AD-A194506] 23 p3240 N88-29285
Commentary on Harold Hotelling's articles on the teaching of statistics
[AD-A194215] 23 p3273 N88-29484
Integration of LANTIRN (Low Altitude Navigation and Targeting Infrared for Night) into operational fighter training
[AD-A194906] 24 p3325 N88-29799

EEG (ELECTROENCEPHALOGRAMS)
U ELECTROENCEPHALOGRAPHY

EFFECTIVENESS
NT COST EFFECTIVENESS
NT SYSTEM EFFECTIVENESS
Effectiveness of electrodeposited coatings in reducing atmospheric corrosion of copper substrates
[DE87-013651] 05 p0566 N88-13448
Impact of flying qualities on mission effectiveness for helicopter air combat, volume 1
[NASA-CR-166568] 06 p0669 N88-14100
The effectiveness of caches and data prefetch buffers in large-scale shared memory multiprocessors
[DE88-003594] 09 p1223 N88-17334
Ion beam modification of film stress and the effectiveness of thin film encapsulants on GaAs
[DE88-004458] 11 p1558 N88-19328
Film cooling effectiveness on a flat plate in high free-stream turbulence using a single row of 30 deg slant-hole injectors
[AD-A190500] 15 p2147 N88-22816
Effectiveness evaluation of fault-tolerant multiprocessor systems
[AD-A191688] 18 p2554 N88-25158
Report to Congress on the effectiveness of the Civil Aviation Security Program
[AD-A195282] 24 p3322 N88-29784

EFFECTORS
U CONTROL EQUIPMENT

EFFERENT NERVOUS SYSTEMS
A survey of artificial neural systems
[AD-A184759] 03 p0368 N88-12312
Motor control in man and monkey 11 p1518 N88-19065

EFFICIENCY
NT CHARGE EFFICIENCY
NT COMBUSTION EFFICIENCY
NT COMPRESSOR EFFICIENCY
NT ENERGY CONVERSION EFFICIENCY
NT NOZZLE EFFICIENCY
NT POWER EFFICIENCY
NT PROPELLER EFFICIENCY
NT PROPULSIVE EFFICIENCY
NT THERMODYNAMIC EFFICIENCY
NT TRANSMISSION EFFICIENCY
High energy efficient solid state laser sources
[NASA-CR-181362] 01 p0052 N88-10332
Impact of turbulence modeling on numerical accuracy and efficiency of compressible flow simulations
[NASA-TM-88333] 02 p0173 N88-11088
Semiconductor detector performance for low-energy X-rays
[DE87-014132] 02 p0244 N88-11542
Efficiency analysis of airborne Electronic CounterMeasures (ECM) systems
[AD-A184606] 03 p0306 N88-11934
High power ion thruster performance
[NASA-TM-100127] 04 p0409 N88-12542
MHD energy fluxes for late type dwarfs 04 p0512 N88-13148
An empirical investigation of load indices for load balancing applications
[AD-A185763] 06 p0724 N88-14451
An efficient algorithm for computing the crossovers in satellite altimetry
[NASA-CR-182389] 07 p0871 N88-15286
Advanced propeller research 08 p0957 N88-15806
Knowledge representation by connection matrices: A method for the on-board implementation of large expert systems 08 p1065 N88-16434
Frequency-sampling design of two-dimensional FIR digital filters with nonuniform samples
[AD-A187773] 11 p1477 N88-18815
Limiting efficiency of a thermionic diode
[DE88-700598] 11 p1479 N88-18830
Growth of Cr,Nd:Gd3Sc2Al3O12 (Cr,Nd:GSAG) crystals by the Heat Exchanger Method (HEM)(trademark)
[DE88-004041] 11 p1558 N88-19326
Efficiency of human workers and means to increase it 12 p1666 N88-19986
Minimizing development flight test time and cost in the US Air Force 12 p1703 N88-20192
Engineering management for validation prototype phase 12 p1703 N88-20195
High power, high efficiency, 2D laser diode arrays for pumping solid state lasers
[DE88-004042] 13 p1777 N88-20632
Demonstration of efficient full aperture Type 1/Type 2 third harmonic conversion on Nova
[DE88-003834] 14 p1914 N88-21438
Polysilicon-contacted p+ emitters for silicon solar cell applications
[DE88-005106] 14 p1942 N88-21586
Supercomputer programming environments
[AD-A190887] 16 p2251 N88-23452
Study of light transmission methods from scintillators to optical fiber with wave length shifter
[DE88-701587] 18 p2574 N88-25292
Advanced energy system program
[PB88-183025] 19 p2686 N88-25965
An efficient computational tool for ramjet combustor research
[DE88-010034] 20 p2760 N88-26369
Heat pump augmented radiators for spacecraft thermal management
[DE88-007890] 20 p2764 N88-26392
A matroid algorithm and its application to the efficient solution of two optimization problems on graphs, revision
[AD-A192709] 20 p2838 N88-26838
Efficiency optimization for FEL oscillators
[AD-A192541] 21 p2952 N88-27536
A rapid electrochemical technique for determining the current efficiency for cadmium plating
[AD-A193679] 22 p3056 N88-28130
Solar energy absorption efficiency of an ellipsoidal receiver-reactor with specularly reflecting walls
[AD-A193726] 22 p3117 N88-28520
Recent advances in high-power microwave amplifiers
[DE88-007820] 23 p3206 N88-29083
An efficient patched grid Navier-Stokes solution for multiple bodies, phase 1
[AD-A194166] 23 p3211 N88-29110
Experimental and analytical study of two-phase flow in zero gravity
[AD-A195223] 24 p3358 N88-29993
A standard architecture for controlling robots
[AD-A195929] 24 p3423 N88-30371

EFFLUENTS
Real-time evaluation and prediction of coastal dispersion near the SW tip of Africa --- effluents 02 p0210 N88-11318
Comparison of open and closed multimegawatt space power systems 17 p2414 N88-24353

EFFORT
Attention, effort, and fatigue: Neuropsychological perspectives 16 p2241 N88-23387

EFFUSIVES
NT LAVA
Low pressure gas flow analysis through an effusive inlet using mass spectrometry
[NASA-CR-182712] 14 p1910 N88-21413
Progress in determining the thickness and distribution of volcanic materials on Mars 23 p3302 N88-29670
Volcano evolution on Mars 23 p3305 N88-29686

EGGS
Effects of heavy ions on egg-developing systems 12 p1658 N88-19935

EGYPT
Discrimination of sand transport rates and environmental consequences in central Egypt from SPOT data 22 p3093 N88-28366
Evaluation of SPOT imagery contribution to petroleum exploration: The Suez Rift (Egypt) 22 p3102 N88-28425

EIGENFUNCTIONS
U EIGENVECTORS

EIGENSTATES
U EIGENVECTORS

EIGENVALUES
The polarization field for pulsed Raman transitions
[DE87-013118] 01 p0035 N88-10227
On the maximum of solutions for a semilinear elliptic problem
[REPT-87-08] 01 p0086 N88-10554
Stability of semidiscrete approximations for hyperbolic initial-boundary-value problems: An eigenvalue analysis
[NASA-TM-88328] 02 p0227 N88-11434
Stability of spheroidal spheromak plasma by use of force-free approximation
[IPPJ-846] 02 p0241 N88-11523
Investigation, development and application of optimal output feedback theory. Vol. 4: Measures of eigenvalue/eigenvector sensitivity to system parameters and unmodeled dynamics
[NASA-CR-4108] 04 p0482 N88-12969
Ballooning modes or Fourier modes in a toroidal plasma?
[AD-A184299] 04 p0491 N88-13022
Eigenvalue projection theory for linear operator equations of electromagnetics
[AD-A185434] 05 p0575 N88-13504
Simultaneous structural and control optimization via linear quadratic regulator eigenstructure assignment 05 p0594 N88-13622
Eigenvalues and eigenvectors of field tensors and associated energy tensors
[DE88-001951] 06 p0763 N88-14682
Diffusion first passage times: Approximations and related differential equations
[AD-A185592] 06 p0765 N88-14700
The effect of response scaling on the detection of singularities in multiresponse estimation
[AD-A185964] 07 p0908 N88-15503
On the asymptotic joint distributions of the eigenvalues of random matrices which arise under components of covariance model
[AD-A186387] 07 p0915 N88-15558
Transversely anisotropic curved optical fibres: Variational analysis of a nonstandard Eigenproblem
[PB88-112966] 08 p1083 N88-16528
An efficient method for computing leading Eigenvalues and Eigenvectors of large asymmetric matrices 09 p1159 N88-16949
Developments related to scattering eigen elements in Schroedinger operators for particles with spin
[ETN-88-91077] 09 p1229 N88-17361
On an overdetermined Neumann problem
[AD-A187451] 10 p1401 N88-18352
Eigenvalue problems
[AD-A188069] 10 p1401 N88-18356
An O(N squared) method for computing the eigensystem of N by N symmetric tridiagonal matrices by the divide and conquer approach
[NASA-CR-181647] 11 p1537 N88-19184
An application of dimensionless Eigenvalues to underwater acoustic ducts
[AD-A188167] 11 p1542 N88-19219
Design graphs for the first two bending Eigenvibration forms of rotating beams consisting of two beam points
[IW-86006R] 13 p1783 N88-20670
Numerical solution of ill posed problems in partial differential equations
[AD-A189383] 13 p1825 N88-20909
Further study of relation of von Karman equation for elastic large deflection problem and Schrodinger equation for quantum eigenvalues problem 14 p1899 N88-21341
A parallel algorithm for computing the singular value decomposition of a matrix
[DE88-007059] 14 p1958 N88-21673
Application of eigenstructure assignment techniques in the design of a longitudinal flight control system
[AD-A189644] 15 p2020 N88-22039
Fluid motion in a spinning, coning cylinder via spatial eigenfunction expansion
[AD-A190758] 15 p2066 N88-22319
Parallel computer methods for eigenvalue extraction 16 p2218 N88-23233
Reduced order models for nonlinear aerodynamics 16 p2220 N88-23248
Theoretical investigations of drift waves in a magnetic quadrupole 18 p2578 N88-25312
Eigenmatrix representations of radiance distributions in layered natural waters with wind-roughened surfaces
[PB88-188701] 20 p2828 N88-26780
Computing small singular values of bidiagonal matrices with guaranteed high relative accuracy: LAPACK working note number 3
[DE88-008465] 20 p2837 N88-26629
Eigenmodes of a random walk on a 2-D lattice torus with one trap
[DE88-007830] 20 p2844 N88-26874
Superconducting rf and beam-cavity interactions
[DE88-008598] 20 p2852 N88-26936
Computation of the eigenvalues for perturbations of Poiseuille flow using a two-point boundary value method
[AD-A193479] 23 p3210 N88-29104
Solving the symmetric tridiagonal eigenvalue problem on the hypercube
[AD-A193905] 23 p3250 N88-29344

Numerical calculations of the response of a spinning spheroidal payload to coning motion
[AD-A195890] 24 p3368 N88-30059
Regularity and numerical solution of eigenvalue problems with piecewise analytic data
[AD-A194993] 24 p3425 N88-30387
Multiple solutions and bifurcation for a class of nonlinear Sturm-Liouville eigenvalue problems on an unbounded domain
[AD-A195954] 24 p3426 N88-30389

EIGENVECTORS
Graph partitioning by eigenvectors
[AD-A184430] 03 p0372 N88-12338
New feedback design methodologies for large space structures: A multi-criterion optimization approach
04 p0408 N88-12535
Investigation, development and application of optimal output feedback theory. Vol. 4: Measures of eigenvalue/eigenvector sensitivity to system parameters and unmodeled dynamics
[NASA-CR-4108] 04 p0482 N88-12969
Eigenvectors of distance-regular graphs
[AD-A185375] 05 p0641 N88-13919
Eigenmode analysis of parallel waveguide couplers
[PB87-132122] 06 p0693 N88-14254
Eigenvalues and eigenvectors of field tensors and associated energy tensors
[DE88-001951] 06 p0763 N88-14682
Eigenvectors of graphs
[AD-A185538] 06 p0765 N88-14698
An efficient method for computing leading Eigenvalues and Eigenvectors of large asymmetric matrices
09 p1159 N88-16949
An application of eigenspace methods to symmetric flutter suppression
[NASA-CR-181618] 10 p1284 N88-17684
Eigenvalue problems
[AD-A188069] 10 p1401 N88-18356
A component synthesis method using Lanczos vectors
[DE88-002263] 10 p1403 N88-18368
An O(N squared) method for computing the eigensystem of N by N symmetric tridiagonal matrices by the divide and conquer approach
[NASA-CR-181647] 11 p1537 N88-19184
Application of eigenstructure assignment techniques in the design of a longitudinal flight control system
[AD-A189644] 15 p2020 N88-22039
Fluid motion in a spinning, coning cylinder via spatial eigenfunction expansion
[AD-A190758] 15 p2066 N88-22319
Reduced order models for nonlinear aerodynamics
16 p2220 N88-23248
Discontinuous inverse Sturm-Liouville problems with symmetric potentials
[DE88-009803] 19 p2720 N88-26152
Observational/numerical study of the upper ocean response to hurricanes
[AD-A193592] 22 p3128 N88-28598

EIKONAL EQUATION
Eikonal solutions to optical model coupled-channel equations
[NASA-TP-2830] 24 p3426 N88-30402

EINSTEIN EQUATIONS
Torsion as a source of expansion in a Bianchi type I universe in the self-consistent Einstein-Cartan theory of a perfect fluid with spin density
[AD-A184200] 03 p0322 N88-12037
Cosmological applications of singular hypersurfaces in general relativity 04 p0521 N88-13202
Ambiguity in determining the effective action for string-corrected Einstein gravity
[PB87-166153] 09 p1259 N88-17550
Raychaudhuri equation in the self-consistent Einstein-Cartan theory with spin-density
[NASA-TM-101145] 17 p2447 N88-24546
Inflation in Einstein-Cartan theory with energy-momentum tensor with spin
[NASA-TM-101164] 17 p2447 N88-24547
Inevitable inflation in Einstein-Cartan theory with improved energy-momentum tensor with spin
[NASA-TM-101146] 18 p2586 N88-25365
N=2 supergravity in superspace: different versions and matter couplings
[DE88-702137] 19 p2741 N88-26274
Towards a finite quantum gravity
[DE88-701497] 23 p3294 N88-29619

EINSTEIN OBSERVATORY
U HEAO 2

EISCAT RADAR SYSTEM (EUROPE)
Report of the 3rd Finnish EISCAT Workshop --- European Incoherent Scatter Radar (EISCAT)
[REPT-111] 06 p0691 N88-14233
EISCAT research in Finland in 1986
06 p0691 N88-14234
Finnish contributions to EISCAT science in 1986
06 p0691 N88-14235
CP-1-H analysis tests 06 p0691 N88-14236
The new CP3 06 p0691 N88-14237
The solution of large linear inverse problems
06 p0691 N88-14238
Incoherent radar spectra 06 p0691 N88-14239
Correction method for Barker-coded modulation
06 p0691 N88-14240
Data analysis at the Oulu (Finland) EISCAT laboratory
06 p0691 N88-14241
Description of data handling system installed December 11, 1986 --- EISCAT 06 p0692 N88-14242
EISCAT research programs for 1987
06 p0692 N88-14244
EISCAT (European incoherent scatter radar) electron density studies
[AD-A185998] 07 p0841 N88-15099
First results from the Viking associated Aureid-VIP rocket and EISCAT campaign --- auroras; Swedish satellite
08 p1026 N88-16211
CAESAR investigations --- Coordinated Auroral Experiment using Scatter And Rockets (CAESAR)
08 p1031 N88-16249
EISCAT measurements of ion velocities during Coordinated Auroral Experiment using Scatter And Rockets (CAESAR) campaign 08 p1031 N88-16251
Future developments of auroral D-region research using the EISCAT VHF incoherent scatter radar
08 p1035 N88-16278
Coordinated Auroral Experiments using Scatter And Rocket investigations (CAESAR investigations)
[MPAE-W-47-87-13] 15 p2096 N88-22487

EJECTA
Conditions for geomagnetically trapping sub-micron lunar ejecta between L = 1.2 and L = 3.1
04 p0521 N88-13203
Magnetic field draping about coronal mass ejecta
[DE88-001805] 05 p0661 N88-14057
Dynamics of meteor streams
06 p0732 N88-14503
Bilateral symmetry elements of the Zhamanshin impact crater
[NASA-TT-20288] 15 p2096 N88-22490
Effects of meteoroids and space debris on the particulate environment for space station 18 p2591 N88-25399
Variation in the thickness of ejecta cover on Mars with increasing crater density 23 p3307 N88-29701

EJECTION
NT STELLAR MASS EJECTION
Design of a gas mass flow control system for the gas inlet installation of a solid fuel combustion chamber
[VTH-LR-471] 09 p1141 N88-16839
Ejection mechanisms in the sublayer of a turbulent channel 16 p2195 N88-23090
Ejection situations in the U-2/TR-1: An analysis of emotions and events
[AD-A192872] 21 p2893 N88-27175

EJECTORS
A cold ejector for closed-cycle helium refrigerators
04 p0434 N88-12690
A computational study of thrust augmenting ejectors based on a viscous-inviscid approach
10 p1326 N88-17929
CRRES chemical release mechanisms
14 p1874 N88-21192
A spin and deployment mechanism
14 p1926 N88-21479
Numerical and experimental investigation of multiple shock wave/turbulent boundary layer interactions in a rectangular duct
[AD-A190772] 15 p2066 N88-22320

EL NINO
On the interannual variability of South American climate and the Southern Oscillation 04 p0470 N88-12905
Equatorial dynamics and ocean-atmosphere coupling
14 p1938 N88-21565
The patterns of tropical convection during the 1986-87 ENSO 22 p3120 N88-28537
Prolonged periods of above-normal temperatures in Canada, 1986/87 22 p3120 N88-28538
Zonal wind observations at Christmas Island (2 deg N, 157 deg W) during the 1986-1987 El-Nino
22 p3120 N88-28539
Climatology of various synoptic systems over the tropical North Pacific 22 p3121 N88-28542
Modes of interannual climate variability and Sahel rainfall anomalies 22 p3121 N88-28547
Tropospheric biennial variability and its relationship to the southern oscillation 22 p3121 N88-28549
ENSO, sea-surface temperatures and African rainfall
22 p3122 N88-28550
Sub-Saharan rainfall anomalies and global sea-surface temperature relationships for the recent fifteen year (1970-1984) period 22 p3122 N88-28552
Simulation studies of the influence of sea-surface temperature anomalies on the Sahelian circulation and rainfall 22 p3122 N88-28553
On the energy source of 1982-83 ENSO episode simulated by the NCAR community climate model
22 p3122 N88-28556
Some evidence for a Northern Hemispheric extratropic trigger mechanism of ENSO events
22 p3123 N88-28558
The impact of the El Nino event on the ECMWF model performance 22 p3125 N88-28576

ELASTIC ANISOTROPY
Wave propagation in laminated composite plates
[AD-A188999] 12 p1804 N88-19594
A hybrid-stress finite element approach for stress and vibration analysis in linear anisotropic elasticity
[NASA-CR-179311] 12 p1634 N88-19784

ELASTIC BARS
Unstable elastic materials and the visco-elastic response of bars in tension
[AD-A187969] 11 p1498 N88-18946

ELASTIC BENDING
The Hamiltonian structure of nonlinear elasticity: The convective representation of solids, rods, and plates
[AD-A187200] 11 p1498 N88-18943
The surface crack problem in an orthotropic plate under bending and tension
[NASA-CR-178281] 18 p2531 N88-25014
Compliant robotic structures, part 3
[AD-A192426] 21 p2955 N88-27556

ELASTIC BODIES
Scattering of longitudinal wave normally incident on discal cavity in elastic body 08 p1077 N88-16492
The Hamiltonian structure of nonlinear elasticity: The convective representation of solids, rods, and plates
[AD-A187200] 11 p1498 N88-18943
The quasi-static contact problem with friction for three dimensional elastic bodies
[REPT-87-51] 14 p1918 N88-21447
Dynamic stability of elastic rotor-bearing systems via Liapunov's direct method 21 p2958 N88-27571
Dynamics of articulated aerospace structures
[AD-A195685] 24 p3324 N88-29794

ELASTIC BUCKLING
Vibration and buckling of geometrically imperfect laminated cylindrical shells 04 p0456 N88-12822
Local delamination buckling in layered structures
18 p2480 N88-24711

ELASTIC COLLISIONS
U ELASTIC SCATTERING

ELASTIC CONSTANTS
U ELASTIC PROPERTIES

ELASTIC CYLINDERS
Study of temperature and stress fields of two sliding cylinders
[ETN-88-92134] 20 p2615 N88-26704
The acoustic field scattered from some approximate pressure release materials
[AD-A194768] 23 p3278 N88-29515

ELASTIC DAMPING
NT VISCOELASTIC DAMPING
Theoretical and experimental damping values of piping systems at high ductilities
[DE88-006717] 18 p2526 N88-24986

ELASTIC DEFORMATION
NT ELASTIC BENDING
NT ELASTIC BUCKLING
An integral equation analysis of inelastic shells
03 p0336 N88-12118
A critical review of the development of several viscoplastic constitutive theories
[AD-A185652] 07 p0867 N88-15262
On the relations between cyclic contraction ratio flowstress and deformation mechanisms in bainitic CrMoV steels
[DE87-753043] 08 p0968 N88-15856
The relationship of tensile specimen size and geometry effects to unique constitutive parameters for ductile materials
[AD-A186020] 08 p0994 N88-16012
A substructure method for dynamic simulation of flexible mechanical systems with geometric nonlinearities
09 p1176 N88-17044
Stress intensity and crack displacement for small edge cracks
[NASA-TP-2801] 09 p1184 N88-17095
A large strain thermomechanical forming model for elastic-viscoplastic behavior in metals
10 p1301 N88-17780
Institute for Materials Science and Engineering, Fracture and Deformation Division: Technical activities, 1987
[PB88-153622] 10 p1345 N88-18039
Unstable elastic materials and the visco-elastic response of bars in tension
[AD-A187969] 11 p1498 N88-18946
On the dissipative response due to discontinuous strains in bars of unstable elastic material
[AD-A188114] 11 p1498 N88-18947

Equilibrium shocks in plane deformations of incompressible elastic materials
[AD-A188696] 12 p1636 N88-19796
Body tensor formalism in finite deformation elasticity and application to the torsion of a circular cylinder
13 p1780 N88-20651
An analysis of large deformation axisymmetric inelastic problems by finite element and boundary element methods 13 p1782 N88-20664
Unified constitutive models for high-temperature structural applications 14 p1932 N88-21523
A constitutive model for an overlay coating
14 p1933 N88-21525
Non-isothermal elastoviscoplastic analysis of planar curved beams 14 p1933 N88-21526
Phenomenological modelling of rate-dependent plasticity for high strain rate problems
[DE88-006647] 15 p2087 N88-22440
Critical issues and directions for fracture mechanics and structural integrity
[AD-A193050] 21 p2960 N88-27584
An endochronic rate-sensitive constitutive equation for metals, application to generalized creep and large deformations
[AD-A194167] 22 p3055 N88-28125
Dynamics of articulated aerospace structures
[AD-A195685] 24 p3324 N88-29794

ELASTIC MEDIA

Refraction of shear wave into nonlinearly elastic or elastoplastic half-space 02 p0159 N88-10999
Boundary element analysis for dynamic loading of a circular plate on an elastic medium
[CI-86] 06 p0722 N88-14443
Functional and mechanical analysis of continuous media-application to the study of elastic composites with periodic structure: Homogenization
[NASA-TT-20188] 18 p2480 N88-24710
A numerical treatment of the fluid/elastic interface under range-dependent environments
[AD-A192476] 21 p3005 N88-27821

ELASTIC MODULUS

U MODULUS OF ELASTICITY

ELASTIC PLATES

An exact theory of elastic plates
[ETN-87-90675] 01 p0062 N88-10396
Correction to a single higher order theory of elastic plates
[ETN-87-90676] 01 p0062 N88-10397
Boundary stabilization of thin elastic plates
[AD-A187123] 10 p1343 N88-18025
Acoustic radiation from line- and point-loaded plates: Uniformly asymptotic solutions
[AD-A189367] 13 p1834 N88-20969
Kinematic support using elastic elements
14 p1926 N88-21481
Estimation and control of distributed models for certain elastic systems arising in large space structures
[AD-A192120] 18 p2472 N88-24666
Tripping of stiffened plates using a refined beam theory
[AD-A193989] 22 p3087 N88-28333
Elastic wave dispersion in laminated composite plate
[AD-A192289] 23 p3188 N88-28967

ELASTIC PROPERTIES

NT AEROELASTICITY
NT ANELASTICITY
NT ELASTOPLASTICITY
NT HYDROELASTICITY
NT MAGNETOSTRICTION
NT MODULUS OF ELASTICITY
NT PHOTOELASTICITY
NT PROPORTIONAL LIMIT
NT THERMOELASTICITY
NT THERMOVISCOELASTICITY
NT VISCOELASTICITY

Contribution to the numerical calculation of fracture-mechanical quantities for elastic and elastic-plastic material behavior, especially for mixed loads
[ETN-87-90435] 01 p0062 N88-10399
Perfine: Personal finite elements on a microcomputer
[ETN-87-90678] 01 p0082 N88-10528
Energy changes in transforming solids
[DE87-011257] 02 p0191 N88-11194
Ultrasonic characterization of the nonlinear elastic properties of unidirectional graphite/epoxy composites
[NASA-CR-4100] 03 p0281 N88-11767
A method for the efficient calculation of elastic rotor blade dynamic response in forward flight
04 p0394 N88-12460
Carbon-fiber reinforced plastics
04 p0403 N88-12506
Natural control of flexible space structures
04 p0408 N88-12534
Model for ultrasonic attenuation and elastic constant in chromium and its alloys
[DE87-703478] 04 p0415 N88-12570
Nonlinear acoustics
[AD-A184271] 04 p0488 N88-13004
Soliton twin boundaries of the cubic-tetragonal martensitic transformations in ferroelastic materials
[DE87-014741] 04 p0495 N88-13047
Coupled elastic rotor/body vibrations with inplane degrees of freedom 05 p0596 N88-13643
Two low-order mixed methods for the elasticity problem
[PB87-225272] 05 p0610 N88-13749
A simulation study of the flight dynamics of elastic aircraft. Volume 1: Experiment, results and analysis
[NASA-CR-4102] 06 p0669 N88-14099
The effective elastic properties of low-density foams
[DE87-014629] 06 p0684 N88-14194
Thermometrical investigations on the near threshold fatigue crack propagation behavior
06 p0717 N88-14400
Fastening high resistance bolts in real assemblies
[CRIF-MT-171] 07 p0861 N88-15221
Assessment of anomalous gravitational field of elastic Earth 07 p0921 N88-15594
Interrelation and measurement of formability, strengthening, and thermomechanical processing under metalworking conditions
[DE88-002485] 08 p0967 N88-15850
Ultrasonic characterization of layered composite systems 10 p1404 N88-18374
Probabilistic and reliability design procedures for flexible airfield pavements: Elastic layered method
[AD-A187533] 11 p1442 N88-18600
Mechanical response of unidirectional boron/aluminum under combined loading
[NASA-CR-182595] 12 p1604 N88-19591
High shear rate rheometry of low-viscosity liquids
[AD-A188447] 12 p1627 N88-19733
The elastic analysis of a thin toroidal shell
[AD-A187801] 12 p1635 N88-19785
Wave curves for simple isotropic elastic solids
[AD-A188865] 12 p1636 N88-19798
Stress analysis in elastic solids with many cracks
[AD-A189015] 12 p1636 N88-19799
The Euler-Bernoulli beam equation with boundary energy dissipation
[AD-A189517] 13 p1765 N88-20560
Dynamics of high-speed mechanisms with elastic members 13 p1779 N88-20643
Mathematical models of sound waves in fluids
[AD-A189270] 13 p1834 N88-20968
Guidelines for estimation and characterization of the thermo-mechanical properties of new optical materials
[DE88-004359] 13 p1840 N88-21010
Woven frameworks for three-dimensional reinforcement 14 p1884 N88-21262
Further study of relation of von Karman equation for elastic large deflection problem and Schrodinger equation for quantum eigenvalues problem
14 p1899 N88-21341
Investigation of the components of the energy-momentum tensor in the neighborhood of crack tips under special materials and loading conditions
[W-4/87] 14 p1934 N88-21531
The elastic properties of monoclinic ZrO2
[DE88-005920] 14 p1986 N88-21847
Experimental studies of elastic properties of crystals by Brillouin scattering
[DE88-005923] 14 p1986 N88-21848
Brillouin scattering and transmission electron microscopy studies of radiation-induced elastic softening, disordering and amorphization of intermetallic compounds
[DE88-005927] 14 p1987 N88-21850
High-performance polymeric materials
[AD-A190708] 15 p2046 N88-22190
A three-dimensional model for the elastic properties of a foam
[DE88-006197] 15 p2046 N88-22192
A new method of measuring multigrade oil shear elasticity and viscosity at high shear rates
[AD-A190145] 15 p2064 N88-22304
The CRREL (Cold Regions Research and Engineering Laboratory) Hopkinson bar apparatus
[AD-A190599] 15 p2077 N88-22380
Measurement of the elastic-plastic surface flaw back surface topology and its relation to constraint
[DE88-006765] 15 p2087 N88-22437
Parallel computer methods for eigenvalue extraction
16 p2218 N88-23233
Energy transfer processes in free radicals: A collaborative experimental and theoretical investigation
[AD-A191264] 16 p2269 N88-23578
Mixed-mode fracture of uniaxial fiber reinforced composites
[AD-A191629] 18 p2478 N88-24700
Vibration protection of inelastic structures by means of active and passive control 18 p2528 N88-25001
Vibrations of rotating thick or thin rings
18 p2529 N88-25003
Time-domain boundary element analysis of dynamic near-tip fields for impact-loaded collinear cracks
[AD-A192930] 20 p2815 N88-26700
Off-boundary approach to the boundary element method
[AD-A192931] 20 p2815 N88-26701
Characterization of elastic-plastic properties of AS4/APC-2 thermoplastic composite
[NASA-CR-183145] 21 p2906 N88-27242
An IETS (Inelastic Electron Tunneling Spectroscopy) study of surface reactions applicable to adhesion
[AD-A192274] 21 p2909 N88-27261
Computer simulation of elastic properties of grain boundary materials
[DE88-011965] 21 p2916 N88-27305
Ionic conductive polymers based on crosslinked elastic siloxane-ethylene oxide copolymers
[DE88-011243] 21 p2917 N88-27311
Three-dimensional aspects of fatigue crack closure
[AD-A192296] 21 p2960 N88-27581
Effects of applied stress and temperature on the nonlinear elastic properties of graphite fibers
[AD-A194469] 22 p3050 N88-28093
A critical speed study for aircraft bias ply tires
[AD-A193616] 22 p3084 N88-28313
Elastic behavior of a rubber layer bonded between two rigid spheres
[AD-A193698] 23 p3198 N88-29030
Metal halide optical glasses
[AD-A193794] 23 p3198 N88-29032
Experimental determination of drag modifications due to elastic compliant surfaces using quantitative visual techniques
[AD-A194785] 24 p3372 N88-30082
A dynamic analysis of piezoelectric strained elements
[AD-A196079] 24 p3432 N88-30430

ELASTIC SCATTERING

The elastic scattering of intermediate energy protons from (40)Ca and (208)Pb 01 p0092 N88-10599
Experimental studies of electromagnetic properties of few body systems
[DE87-014610] 02 p0161 N88-11008
On the spin structure of the elastic ppbar scattering amplitude
[NOTA-INTERNA-892] 06 p0778 N88-14772
A research program in neutrino physics, cosmic rays and elementary particles
[DE88-003507] 09 p1264 N88-17575
Pion elastic and inelastic scattering near N = 28
[LA-10968-T] 11 p1544 N88-19232
Medium high energy physics at Syracuse University
[DE88-003670] 11 p1545 N88-19235
Nuclear structure studies by the scattering of medium-energy electrons
[DE88-003803] 11 p1545 N88-19236
Intermediate energy neutrino physics
[DE88-005378] 13 p1836 N88-20984
Nuclear structure studies at intermediate energies
[DE88-006683] 18 p2571 N88-25271
Theoretical atomic and molecular physics
[DE88-007122] 19 p2724 N88-26175
Comparison of exclusive reactions at large momentum transfer
[DE88-007544] 20 p2851 N88-26922
Are Centauros diffractive
[DE88-008767] 21 p3032 N88-27996
Dispersion effects in elastic electron scattering from C12
[B8805297] 23 p3281 N88-29536
Eikonal solutions to optical model coupled-channel equations
[NASA-TP-2830] 24 p3428 N88-30402

ELASTIC SHELLS

RADSPHERE: A computer program for calculating the steady-state, axially symmetric, forced response and radiation field of a submerged spherical shell
[AD-A185025] 05 p0609 N88-13738
The elastic analysis of a thin toroidal shell
[AD-A187801] 12 p1635 N88-19785
The acoustic field scattered from some approximate pressure release materials
[AD-A194768] 23 p3278 N88-29515

ELASTIC STABILITY

U DAMPING

ELASTIC STRENGTH

U PROPORTIONAL LIMIT

ELASTIC WAVES
NT AERODYNAMIC NOISE
NT AIRCRAFT NOISE
NT BAROCLINIC WAVES
NT BLADE SLAP NOISE
NT CAPILLARY WAVES
NT COMPRESSION WAVES
NT DETONATION WAVES
NT ELECTROSTATIC WAVES
NT ENGINE NOISE
NT GRAVITY WAVES
NT ION ACOUSTIC WAVES
NT IONIC WAVES
NT JET AIRCRAFT NOISE
NT LAMB WAVES
NT MAGNETOACOUSTIC WAVES
NT MAGNETOHYDRODYNAMIC WAVES
NT NOISE (SOUND)
NT OBLIQUE SHOCK WAVES
NT P WAVES
NT PHONON BEAMS
NT PHONONS
NT PLASMA WAVES
NT POLARIZED ELASTIC WAVES
NT RAYLEIGH WAVES
NT RIPPLES
NT S WAVES
NT SEISMIC WAVES
NT SHOCK WAVES
NT SONIC BOOMS
NT SOUND WAVES
NT STRESS WAVES
NT THERMAL NOISE
NT TOLLMEIN-SCHLICHTING WAVES
NT ULTRASONIC RADIATION

Density flows at the mountain edge
08 p1016 N88-16156

Scattering of longitudinal wave normally incident on discal cavity in elastic body
08 p1077 N88-16492

Numerical simulation of the interaction of pressure waves with laminar and turbulent boundary layers
[DFVLR-FB-87-18] 09 p1161 N88-16960

A spectral method for computing complete synthetic seismograms
[AD-A187663] 11 p1510 N88-19024

Three-dimensional scattering of impulsive acoustic waves by a semi-infinite crack in the plane interface of a half space and a layer
[PB88-146998] 12 p1687 N88-20089

Phase velocity and attenuation of plane elastic waves in a particle-reinforced composite medium
[AD-A189414] 13 p1734 N88-20366

Initial condition effect on pressure waves in an axisymmetric jet
[NASA-TM-100915] 16 p2209 N88-23184

Remote sensing of acoustic properties of shallow water sediments: A review
[AD-A192107] 18 p2570 N88-25267

Numerical simulation of the interaction of pressure waves with laminar and turbulent boundary layers
[ESA-TT-1089] 24 p3371 N88-30075

Determination of the specific area of liquid gas and the velocity of weak pressure waves in aqueous foams
[NASA-TT-20347] 24 p3373 N88-30087

ELASTICITY
U ELASTIC PROPERTIES

ELASTICIZERS
U PLASTICIZERS

ELASTODYNAMICS
NT ELASTIC DAMPING
NT ELASTOHYDRODYNAMICS
NT VISCOELASTIC DAMPING

Elastodynamic ray theory and asymptotic methods for direct and inverse scattering problems
03 p0335 N88-12108

The acoustic-electric field analysis of multilayered surface acoustic wave devices
[ETN-88-91592] 09 p1242 N88-17446

Transient analysis of a plate on an elastic foundation under a moving load
19 p2680 N88-25933

Determination of the residual stresses in welded structures using the elastoplastodynamic method
[ETN-88-92745] 22 p3087 N88-28330

ELASTOHYDRODYNAMICS

Film thicknesses in circular elastohydrodynamic contacts
[PB87-123725] 06 p0710 N88-14354

The numerical solution of the elastohydrodynamically lubricated line and point contact problem, using multigrid techniques
[ISBN-90-9001583-3] 06 p0714 N88-14377

ELASTOMERS
NT VULCANIZED ELASTOMERS

Rheological behaviors of an elastomeric membrane
[DE87-013105] 01 p0061 N88-10392

Rheological and aging characterization of elastomers
[DE87-009598] 02 p0151 N88-10944

Urea-polyurethane and polydimethylsiloxane mixtures. Morphology control using a block copolymer
[ISAL-IDI1-87-05] 02 p0153 N88-10959

Buckling of viscoelastic columns
02 p0190 N88-11187

Thermoplastic elastomer compositions --- cable jackets
[EP-PATENT-0-204-453-A1] 04 p0418 N88-12593

Thermoplastic elastomers as LOVA (Low Vulnerability Ammunition) binders
[AD-A184350] 04 p0419 N88-12599

Process for the production of a thermoplastic elastomer composition
[EP-PATENT-0-202-782-A2] 05 p0569 N88-13465

Coaxial cable connector
[NASA-CASE-NPO-16764-1-CU]
06 p0696 N88-14270

Thermoplastic elastomers as LOVA binders
[AD-A185864] 07 p0835 N88-15067

Thermoplastic elastomers as LOVA binders
[AD-A185865] 07 p0835 N88-15068

Structure-property relationships in thermoplastic elastomers 4. Dynamic mechanical relaxations in poly(dioxolane), poly(butyltrioxocane) and poly(propylene oxide) polyurethanes
[AD-A186278] 07 p0836 N88-15073

Factors affecting the sticking of insects on modified aircraft wings
[NASA-CR-182451] 09 p1148 N88-16878

Morphology control and reinforcing mechanisms using an elastomer in an epoxy network based on diamine menthane
[ISAL-IDI1-87-09] 09 p1148 N88-16881

Thermoplastic elastomers as LOVA binders
[AD-A186563] 10 p1304 N88-17797

Cavitation in model elastomeric composites
[AD-A187401] 11 p1447 N88-18625

The effects of thin polymeric surface films in reducing fretting corrosion and wear
[AD-A188633] 12 p1611 N88-19634

Analysis of model fuels and their compatibility with selected elastomers, part 1
[AD-A188361] 12 p1612 N88-19639

Investigation of constrained-layer technique using exact elasticity theory
[AD-A188664] 12 p1636 N88-19795

Performance of elastomeric bearings
[PB88-159470] 14 p1918 N88-21450

High-performance polymeric materials
[AD-A190708] 15 p2046 N88-22190

Armoured vehicle track elastomers: Research and development at MRL
[MRL-GD-0012] 19 p2620 N88-25541

Fundamental studies of elastomers
[DE88-009679] 20 p2778 N88-26471

Development of a nitrile rubber for dynamic damping
[AD-A194060] 22 p3058 N88-28145

Dry adhesive friction of elastomers: A study of the fundamental mechanical aspects
[ETN-88-92903] 23 p3198 N88-29036

ELASTOPLASTICITY

Estimation multiaxial elastic-plastic notch stresses and strains in combined loading
[FB-2/1986] 01 p0060 N88-10382

The use of Hencky's equations for the estimation of multiaxial elastic-plastic notch stresses and strains
[FB-3/1986] 01 p0060 N88-10383

Contribution to the numerical calculation of fracture-mechanical quantities for elastic and elastic-plastic material behavior, especially for mixed loads
[ETN-87-90435] 01 p0062 N88-10399

A numerical and analytical investigation of Rayleigh-Taylor instability in a solid tungsten plate
[DE87-013593] 01 p0087 N88-10562

Refraction of shear wave into nonlinearly elastic or elastoplastic half-space
02 p0159 N88-10999

Spread of plastic deformation in notched and cracked plates
03 p0337 N88-12122

Computation of bonded assemblies. Elastoplastic adhesives, first part
[SNIAS-NT-16926/AQET] 05 p0569 N88-13467

Application of finite element methods with cyclic elasto-plastic strain analysis to low cycle fatigue analysis of engine components
[AR-004-512] 05 p0596 N88-13642

Behavior of a steel cylinder under the influence of a local load in the elastic and elasto-plastic area
[PB87-154787] 07 p0869 N88-15272

The nonlinear dynamic response of an elastic-plastic thin plate under impulse loading
[AD-A182147] 08 p0994 N88-16013

Dynamic finite element with diagonalized consistent mass matrix and elastic-plastic impact calculation
[PB87-143376] 08 p0995 N88-16020

Elastic-plastic fracture investigation on stable crack growth for plane stress
[PB87-144820] 08 p0995 N88-16022

The J-integral concept for elastic-plastic material behavior
[W-5/87] 08 p1000 N88-16059

Matrix-fiber stress transfer in composite materials: Elasto-plastic model with an interphase layer
[PB88-136635] 11 p1450 N88-18643

Elastoplastic response of unidirectional graphite/aluminum under combined tension-compression cyclic loading
[CCMS-88-01] 11 p1451 N88-18647

An analysis of large deformation axisymmetric inelastic problems by finite element and boundary element methods
13 p1782 N88-20664

Non-isothermal elastoviscoplastic analysis of planar curved beams
14 p1933 N88-21526

Development of a computer code CRACK for elastic and elastoplastic fracture mechanics analysis of 2-D structures by finite element technique
[DE88-701231] 15 p2075 N88-22370

Numerical analysis of critical penetration velocity for jet perpendicular penetration
16 p2186 N88-23037

Models in nonlinear thermomechanics. Finite element models and constitutive models for large deformation elastoplasticity
[ETN-88-92240] 16 p2222 N88-23262

Crack retardation under load spectra. Experimental study and numerical simulation using the simplified K constant model --- light alloys, aircraft construction materials
[ONERA-RT-30/7169-RY-054-R]
16 p2222 N88-23266

Theoretical and experimental damping values of piping systems at high ductilities
[DE88-006717] 18 p2526 N88-24986

A comparison of analytical techniques for modeling the Rayleigh-Taylor response of elastic-plastic solids
[DE88-010372] 21 p2962 N88-27596

Determination of the residual stresses in welded structures using the elastoplastodynamic method
[ETN-88-92745] 22 p3087 N88-28330

Results on the influence of crack tip plasticity during dynamic crack growth
[AD-A193460] 23 p3225 N88-29194

ELASTOSTATICS

The quasi-static contact problem with friction for three dimensional elastic bodies
[REPT-87-51] 14 p1918 N88-21447

A new boundary integral equation formulation for elastodynamic and elastostatic crack analysis
[AD-A192967] 20 p2815 N88-26702

ELECTRETS

Thin film electret boundary layer transition detector: A feasibility study
[AD-A185675] 07 p0856 N88-15199

Observations on electrostatic effects in a filter test system
[AD-A188797] 13 p1736 N88-20378

ELECTRIC AIRCRAFT
U FLY BY WIRE CONTROL

ELECTRIC APPLIANCES
U ELECTRIC EQUIPMENT

ELECTRIC ARCS

Recovery of vacuum gaps after arcing
[DE87-013852] 01 p0039 N88-10250

Experimental study and modeling of the physical mechanisms of the gliding spark
[ESA-TT-1029] 01 p0070 N88-10447

Current-filamentation instability in railgun arcs
[AD-A184618] 03 p0269 N88-11693

An investigation of unipolar arcing at atmospheric pressure in aluminum 2024 and aluminum coated glass slides
[AD-A184903] 05 p0577 N88-13521

Theoretical model of the cathode spot on a unipolar arc
[AD-A190109] 15 p2059 N88-22277

Welding torch gas cup extension
[NASA-CASE-MFS-29252-1] 17 p2345 N88-23980

Arc-textured metal surfaces for high thermal emittance space radiators
[NASA-TM-100894] 18 p2487 N88-24754

Extinction behavior of low voltage switching arc under consideration of cathodic coatings and dynamic arc column
[ETN-88-92384] 20 p2796 N88-26591

Physical-chemical reactions at welding arc/molten pool interfaces
[DE88-007717] 20 p2808 N88-26662

Measurements of vacuum arc ion charge state distributions
[DE88-008249] 23 p3284 N88-29558

ELECTRIC AUTOMOBILES
Metal-air battery assessment
[DE88-011361] 21 p2940 N88-27459

ELECTRIC BATTERIES
NT ALKALINE BATTERIES
NT LEAD ACID BATTERIES
NT LITHIUM SULFUR BATTERIES
NT METAL AIR BATTERIES
NT NICKEL CADMIUM BATTERIES
NT NICKEL HYDROGEN BATTERIES
NT NICKEL IRON BATTERIES
NT NICKEL ZINC BATTERIES
NT PRIMARY BATTERIES
NT REDOX CELLS
NT SODIUM SULFUR BATTERIES
NT STORAGE BATTERIES
NT THERMAL BATTERIES
NT ZINC-BROMIDE BATTERIES
NT ZINC-OXYGEN BATTERIES
Ionically conductive polymers: Application to solid state batteries
[AD-A183733] 01 p0037 N88-10239
Zinc-redox battery: A technology update
[DE87-010737] 01 p0040 N88-10256
Evaluation of LiCl- LiBr- KBr electrolyte for Li- alloy/metal disulfide cells
[DE87-011356] 01 p0041 N88-10258
Overcharge protection in Li-alloy/metal disulfide cells
[DE87-011364] 01 p0041 N88-10260
Lithium/iron sulfide batteries: Development and demonstration
[DE87-014222] 01 p0042 N88-10265
Highlights of the Chemical Technology Division's research activities
[DE88-000233] 03 p0282 N88-11773
Applications of multivalent ionic conductors to polymeric electrolyte batteries
[AD-A184252] 04 p0439 N88-12722
Corrosion susceptibility study of candidate pin materials for ALTC (Active Lithium/Thionyl Chloride) batteries
[DE88-001449] 04 p0440 N88-12734
Reliability of Li/SO2 cells for long-life applications
[DE88-001360] 04 p0440 N88-12735
A hydrogen/nickel oxide battery for remote applications
[DE87-009048] 04 p0464 N88-12872
High energy density rechargeable batteries for aerospace power requirements
[AD-A184883] 05 p0577 N88-13519
An investigation of the rechargability of certain modified forms of MnO2
[AD-A185919] 07 p0847 N88-15140
User's guide to DIANE: A microcomputer program for modeling battery performance in electric vehicles
[DE88-003713] 08 p1068 N88-16456
The European space battery test center
09 p1125 N88-16738
The railgun and its power source
[MRL-R-1058] 09 p1130 N88-16786
Laboratory evaluation and analysis of advanced lead-acid load-leveling batteries
[DE88-002851] 10 p1349 N88-18064
Fuel cell/battery hybrid vehicle assessment
[DE88-005087] 10 p1427 N88-18520
Lithium/disulfide battery R and D
[DE88-003032] 11 p1481 N88-18839
Improving battery reliability by using regression trees
[DE88-004539] 11 p1481 N88-18841
Performance test results for the Eaton dc development power train in an electric test bed vehicle
[DE88-005458] 12 p1622 N88-19699
An electrochemical and spectroscopic study of electrode systems
[AD-A189274] 13 p1737 N88-20384
Corrosion, passivity and breakdown of alloys used in high energy density batteries
[DE88-004891] 13 p1743 N88-20422
Polymeric electrolytes for ambient temperature lithium batteries
[DE88-004896] 13 p1763 N88-20547
Mission directed goals for electric vehicle battery research and development: The Task Force on electric vehicle battery goals
[DE88-005601] 13 p1763 N88-20548
Testing and development of electric vehicle batteries for EPRI Electric Transportation Program
[DE88-005894] 13 p1764 N88-20551
GTE battery management system: State of charge indicator evaluation
[DE88-006800] 15 p2058 N88-22272
Nickel hydroxide active material densities
[AD-A191411] 16 p2230 N88-23319
Energy storage for nuclear burst power systems
17 p2426 N88-24431
An overview of advanced battery development at Sandia National Laboratories
[DE88-006823] 18 p2506 N88-24867
Optimization of reserve lithium thionyl chloride battery electrochemical design parameters
[DE88-007109] 18 p2506 N88-24868
All inorganic ambient temperature rechargeable lithium battery
[DE88-008425] 19 p2662 N88-25834
Advanced photovoltaic power system technology for lunar base applications
[NASA-TM-100965] 20 p2766 N88-26402
Loss evaluation of self-commutated power conditioner for battery energy storage system
[DE88-752075] 20 p2794 N88-26575
Exploratory battery technology development and testing report for 1986
[DE88-009870] 20 p2794 N88-26578
Modeling and thermal management of advanced batteries
[DE88-010023] 20 p2794 N88-26580
Molten salt electrolytes for high-temperature lithium cells
[DE88-010058] 20 p2794 N88-26581
Computer controlled procedures for traction battery power performance tests
[ETN-88-92352] 20 p2796 N88-26589
High power pulse energy system concept
[AD-A192440] 21 p2935 N88-27429
Preparation and development of advanced battery catalysts
[AD-A193208] 21 p2937 N88-27441
Estimation of power-energy plots for secondary batteries
[DE88-011922] 21 p2940 N88-27460
Advanced calcium-thionyl chloride high-power battery
[AD-A194401] 22 p3072 N88-28238
Optimization and scale-up performance of polymer electrolyte batteries
[AD-A193987] 22 p3073 N88-28243
The overcharge behavior of polymer electrolyte cells
[AD-A193984] 22 p3117 N88-28522
Structure and dynamics of solutions of lithium salts relevant to battery construction
[AD-A195399] 24 p3366 N88-30044
Aircraft battery state of charge and charge control system
[AD-A194979] 24 p3367 N88-30052

ELECTRIC BRIDGES
Balancing strain gauge bridges
[GB-PATENT-2-129-567-A] 01 p0048 N88-10307
Comparative evaluation of resistive and inductive techniques for measuring temperature of superconducting transition
[DE88-700603] 10 p1417 N88-18457
Layered-capacitor method for dielectric bridge measurements. Algorithms for inversion and parameter fitting: Documentation, verification, data analysis
[PB88-131479] 11 p1505 N88-18989
Development of an optical feedback based high accuracy beam transmissometer
[AD-A189396] 12 p1692 N88-20122
Giant Josephson signal in wide superconducting films
14 p1973 N88-21777
Pure metallic bridge and point-contact tunneling into single- and polycrystal YBa2Cu3O(sub 7-y)
[DE88-010030] 20 p2878 N88-27084

ELECTRIC CHARGE
NT ELECTRIC DIPOLES
NT ELECTROSTATIC CHARGE
NT ION CHARGE
NT SPACE CHARGE
Simulations using the pseudo-current algorithm
[DE87-012403] 01 p0040 N88-10255
Theory of the one- and two-dimensional electron gas
[DE87-012864] 01 p0244 N88-11540
A theoretical analysis of the deactivation of metal surfaces upon carburization
[AD-A184556] 03 p0290 N88-11821
Analysis of nickel sulphamate bath using charging current compensated D.C. polarography
[NAL-TM-MT-8705] 05 p0564 N88-13433
An investigation of the rechargability of certain modified forms of MnO2
[AD-A185919] 07 p0847 N88-15140
Sliding charge density waves and related problems
[AD-A186720] 09 p1157 N88-16934
High-temperature charge-density studies of CeO/sub 2-x/ using X-ray and neutron diffraction techniques
[DE88-002988] 09 p1257 N88-17536
Survey of the Air Force P78-2 (SCATHA) satellite plasma wave data during electron gun operations
[AD-A191014] 16 p2168 N88-22926
Finite element simulation of the atmosphere's electromagnetic response to charge perturbations associated with lightning 17 p2375 N88-24124
The theory of random alloys
[DE88-006408] 18 p2487 N88-24756
Development of test methods for the electrostatic properties of nonhomogeneous fabrics, phase 2
[AD-A190853] 18 p2489 N88-24767
Electronic and ionic transport in polymers
[AD-A191642] 18 p2490 N88-24772
A severe spacecraft-charging event on SCATHA in September 1982
[AD-A193007] 20 p2765 N88-26396
Results from life test in progress on eagle-picher nickel cadmium cells
[AD-A192816] 21 p2936 N88-27434
Discrete variational methods and their application to electronic structures
[DE88-702215] 21 p3014 N88-27888
Model for bimetallic interfaces, part 2
[DE88-702672] 22 p3157 N88-28787

ELECTRIC CHOPPERS
Low-current behavior and current chopping of vacuum arcs
[ISBN-90-9001649-X] 05 p0578 N88-13529

ELECTRIC CIRCUITS
U CIRCUITS

ELECTRIC COILS
NT MAGNET COILS
NT MAGNETIC COILS
Departmental report on program EMTP-machine windings surge transients: Travelling wave method
[PB87-123733] 04 p0438 N88-12719

ELECTRIC CONDUCTORS
Eddy current density in wedge-shaped conducting cylinders with inhomogeneous conductivity
[ETN-87-90404] 01 p0042 N88-10268
Dielectric response of ionic conductors
[DE87-013552] 02 p0166 N88-11045
Advances in inherently conducting polymers
[DE88-000501] 04 p0421 N88-12610
Departmental report on program EMTP-machine windings surge transients: Travelling wave method
[PB87-123733] 04 p0438 N88-12719
Molecular and supramolecular orientation in conducting polymers
[DE88-000533] 05 p0569 N88-13472
Hydroxide ion conductors as possible electrolytes in intermediate temperature fuel cells
[AD-A185508] 06 p0731 N88-14495
Failure modes of laminate structures
[DE88-002579] 08 p0996 N88-16033
Electronic and ionic transport in polymers
[AD-A187253] 11 p1452 N88-18651
The effects of various conductor components on Nb3Sn filament prestrain in cable-in-conduit conductors
[DE88-003956] 11 p1479 N88-18824
Contrasting conductance/viscosity relations in liquid states of vitreous and polymer solid electrolytes
[AD-A189378] 13 p1748 N88-20452
Electron emission from conductors subjected to intense, short-pulse electric fields
[DE88-005412] 13 p1836 N88-20985
Strategies in the topological approach to electromagnetic interference control
[AD-A189874] 15 p2056 N88-22255
Fast ion conducting glasses
[AD-A191412] 16 p2183 N88-23010
Fabrication of a flexible conductor by vapor deposition
[DE88-007500] 19 p2661 N88-25826
Determination of quantum corrections for electrical conductivity mechanism of three dimensional, perturbed copper coatings. Weak localization and electron-electron interaction
[ETN-88-92378] 21 p2941 N88-27466

ELECTRIC CONNECTORS
Design principles and practices for implementation of MIL-STD-1760 in aircraft and stores
[AD-A183724] 01 p0005 N88-10027
Coaxial cable connector
[NASA-CASE-NPO-16764-1-CU]
06 p0696 N88-14270
Measurement of shielding effectiveness of different cable and shielding configurations by mode-stirred techniques
[PB88-155791] 10 p1319 N88-17685
Separable electrical connectors for space: A tribological and electrical assessment 14 p1879 N88-21231
Development of a slip-ring system for energy transfer in space conditions. Space flight qualification and extended life tests
[BMFT-FB-W-86-019] 16 p2169 N88-22932
Investigation of non-linear optical behavior of semiconductors for optical switching, volume 1
[AD-A191297] 16 p2274 N88-23611

Studies of optical matrix multiplication and reconfigurable optical interconnect concepts
[AD-A191635] 18 p2575 N88-25295
Circuit design criteria for stable lateral inhibition neural networks
[AD-A195066] 24 p3366 N88-30046

ELECTRIC CONTACTS
Toward pulsed power uses for photoconductive semiconductor switches: Closing switches
[DE87-012020] 01 p0041 N88-10262
Ohmic contacting schemes to gallium arsenide devices
[DE87-014627] 02 p0244 N88-11544
Influence of arsenic superficial enrichment on the ohmicity of the n-GaAs:In/Au contact
[ECL-87-09] 08 p1089 N88-16554
Development of a planar heterojunction bipolar transistor for very high speed logic
[AD-A188137] 11 p1478 N88-18820
The physics of very small structures
[AD-A187672] 11 p1556 N88-19311
Corrosion-wear process under rolling-sliding motion
[AD-A189603] 13 p1778 N88-20635
Stable, high-efficiency, CuInSe2-based, polycrystalline, thin-film tandem solar cells
[DE88-001116] 13 p1793 N88-20726
Thin-film diffusion barriers for metal-semiconductor contacts
[AD-A188712] 13 p1844 N88-21035
Polysilicon-contacted p+ emitters for silicon solar cell applications
[DE88-005106] 14 p1942 N88-21586
The kinetics of contact noise in NaBeta alumina
[AD-A190651] 15 p2130 N88-22707
The influence of current stressing on the structure of Ag contacts to GaAs
[DE88-005988] 15 p2140 N88-22771
Effects of 67.5 MeV electron irradiation on Y-Ba-Cu-O and Gd-Ba-Cu-O high-temperature superconductors
[AD-A191271] 16 p2283 N88-23669
Friction, wear and electrical contact resistance of precious metal alloys
[DE88-011244] 21 p2938 N88-27450

ELECTRIC CONTROL
Electrical flight commands in transport aircraft
[SNIAS-872-111-108] 05 p0551 N88-13361

ELECTRIC CORONA
The effects of corona on current surges induced on conducting lines by EMP: A comparison of experiment data with results of analytic corona models
[DE87-014970] 03 p0305 N88-11924
Personal overview of solar wind 6
[DE88-003147] 10 p1430 N88-18543
Molecular collision processes in gases and at surfaces
[AD-A189519] 13 p1836 N88-20962
The growth potential of corona discharges from aircraft flying in precipitation
[AD-A190507] 15 p2094 N88-22478
Theoretical basis for an experimental test with regard to the origin of VHF (Very High Frequency) radiation from natural lightning
[DE88-007535] 18 p2544 N88-25102

ELECTRIC CURRENT
NT ALTERNATING CURRENT
NT ARC DISCHARGES
NT AURORAL ELECTROJETS
NT BEAM CURRENTS
NT DIRECT CURRENT
NT EDDY CURRENTS
NT ELECTRIC ARCS
NT ELECTRIC CORONA
NT ELECTRIC DISCHARGES
NT ELECTRIC SPARKS
NT EQUATORIAL ELECTROJET
NT EXTERNAL SURFACE CURRENTS
NT FLASHOVER
NT GAS DISCHARGES
NT GLOW DISCHARGES
NT HIGH CURRENT
NT IONOSPHERIC CURRENTS
NT LIGHTNING
NT LINE CURRENT
NT LOW CURRENTS
NT PLASMA CURRENTS
NT RING CURRENTS
NT THRESHOLD CURRENTS
A tutorial on Rogowski coil theory and operation
[DE88-000006] 02 p0230 N88-11449
MHD (magnetohydrodynamics) channel development
[DE87-014126] 02 p0237 N88-11498
Rotation of magnetized particle in electrically conducting viscous medium 06 p0770 N88-14733
Mathematical model for the dc-ac inverter for the Space Shuttle 06 p0793 N88-14860
Simulation an experiment on plasma instability investigation in a tokamak with a divertor
[DE88-700352] 07 p0935 N88-15683
The effects of a geomagnetic storm on thermospheric circulation
[AD-A186638] 09 p1190 N88-17128
Temporal evolution of ionospheric electric field driven by field-aligned current 11 p1469 N88-18761
Bloch oscillations in small Josephson junctions: Their manifestation in switching effects 14 p1969 N88-21756
Optical sensors for the measurement of electric current and voltage
[PB88-172945] 16 p2193 N88-23077
Monte Carlo analysis of lateral collection diode arrays
[RSRE-MEMO-4080] 17 p2335 N88-23938
Photocurrent modeling of modern microcircuit PN junctions
[DE88-007037] 19 p2662 N88-25832
Fast parametrization procedure for solar cells
[PB88-186416] 19 p2686 N88-25966
Computer programs for high-current beam transport in accelerators
[AD-A192356] 20 p2838 N88-26835
A rapid electrochemical technique for determining the current efficiency for cadmium plating
[AD-A193679] 22 p3056 N88-28130
Current induced by high-altitude electromagnetic pulse (HEMP) on wire above ground
[FOA-C-30485-4.2] 22 p3072 N88-28235

ELECTRIC DIPOLES
Power flow in terms of Poynting vector for Extremely Low Frequency (ELF) dipole sources in seawater
[ARE-TM(UTM)-87102] 01 p0035 N88-10221
Electromagnetic interaction between an electric discharge and cabling inside a satellite 03 p0274 N88-11725
Theory of atomic additivity in molecular hyperpolizabilities 03 p0297 N88-11867
Electromagnetic scattering from and natural resonances of the circular strip 13 p1759 N88-20523
On the self-consistent equation for the microscopic local electric field in dielectric systems
[PREPRINT-589] 22 p3074 N88-28247

ELECTRIC DISCHARGES
NT ARC DISCHARGES
NT ELECTRIC ARCS
NT ELECTRIC CORONA
NT ELECTRIC SPARKS
NT FLASHOVER
NT GAS DISCHARGES
NT GLOW DISCHARGES
NT LIGHTNING
Characterization of surface discharge switches and high performance applications
[DE87-011763] 01 p0041 N88-10261
Segmented hollow cathode discharges for copper ion lasers
[ETN-87-90403] 01 p0052 N88-10333
International Ultraviolet Explorer (IUE) spacecraft battery performance update 02 p0164 N88-11033
Discharge phenomena --- spacecraft 03 p0274 N88-11723
Electromagnetic interaction between an electric discharge and cabling inside a satellite 03 p0274 N88-11725
Electromagnetic effects of a discharge on circuitry --- spacecraft 03 p0274 N88-11726
Irradiation testing 03 p0274 N88-11727
MARECS-A case 03 p0274 N88-11729
Electromagnetic compatibility (EMC) phenomena and prevention of the effects --- spacecraft 03 p0274 N88-11731
Discharge prevention of geosynchronous orbit conductive thermal control materials and grounding systems 03 p0274 N88-11732
Electrostatic discharges in geostationary orbit: The case of Telecom 1 03 p0275 N88-11733
Prevention of radiation induced degradations and of electrostatic perturbations on the Arabsat spacecraft in flight results 03 p0275 N88-11734
Mathematical models of plasma discharge control in a tokamak
[DE87-702891] 03 p0378 N88-12377
Nitrogen energy transfer study
[AD-A184457] 04 p0464 N88-12869
Electromagnetics and electrothermal approach to evaluate failures in microelectronic devices caused by electrostatic discharges: Stochastical aspects of the device reliability
[AD-A184906] 05 p0577 N88-13522
Atmospheric electricity
[NASA-CR-179239] 06 p0744 N88-14575
State parameters of pulse-discharge plasma in xenon-filled closed tube 06 p0773 N88-14747
Power and charge dissipation from an electrodynamic tether 06 p0795 N88-14869
A numerical thermal model of the rapid solidification parameters in the capacitor discharge welding process
[DE88-002206] 07 p0864 N88-15244
Atmospheric science 07 p0883 N88-15357
Investigation of self-discharge characteristics of spacecraft nickel-cadmium cells at elevated temperatures
[AD-A186497] 08 p0979 N88-15919
Wire-cut electrical discharge machinability of ceramics
[AD-A186989] 09 p1146 N88-16870
Air gap testing using Trailing Wire Antenna (TWA) waveform
[AD-A187639] 11 p1477 N88-18812
Partial discharges and the electrical aging of cross linked polyethene (XLPE) cable insulation
[EUT-86-E-160] 14 p1892 N88-21300
The growth potential of corona discharges from aircraft flying in precipitation
[AD-A190507] 15 p2094 N88-22478
Kinetics of electrons and molecules at plasma-beam discharge in molecular gases
[DE88-701196] 16 p2275 N88-23616
Electrostatic discharge test apparatus
[NASA-CASE-MSC-21094-1] 18 p2518 N88-24941
Deep dielectric charging effects due to high energy electrons in earth's outer magnetosphere
[AD-A192154] 18 p2541 N88-25083
Theoretical basis for an experimental test with regard to the origin of VHF (Very High Frequency) radiation from natural lightning
[DE88-007535] 18 p2544 N88-25102
Plasma neutralizer work at BNL (Brookhaven National Laboratory)
[DE88-007046] 18 p2579 N88-25317
Spacecraft requirements for predictions of geomagnetic activity (a tutorial)
[AD-A191943] 19 p2685 N88-25959
A severe spacecraft-charging event on SCATHA in September 1982
[AD-A193007] 20 p2765 N88-26396
Electron-impact-ionization and electron-attachment cross sections of radicals important in transient gaseous discharges
[AD-A192248] 20 p2770 N88-26424
A bibliography and author index for electrical discharges in vacuum (1897-1986)
[DE88-008744] 20 p2794 N88-26579
Failure analysis of Chloride Silent Power, Ltd. PB cells
[DE88-010567] 21 p2938 N88-27448
Production of intensive electron beam impulsions by setup of pseudoglare discharges
[ISL-CO-210/87] 21 p3019 N88-27920
Surface properties in electric discharge machining
[NASA-TT-20243] 23 p3223 N88-29182
In-house capacitor technology program
[AD-A194804] 24 p3367 N88-30049
Transverse CO2 laser two-dimensional gain distributions
[AD-A196240] 24 p3378 N88-30119

ELECTRIC ENERGY STORAGE
Technology Base Research Project for electrochemical energy storage
[DE88-000649] 04 p0464 N88-12868
On the potential role of concentrated field-aligned currents in solar physics 08 p1099 N88-16614
Assessment of energy storage concepts for use in sprint power 17 p2407 N88-24312
Development of inductive storage pulsed power generators
[AD-A193878] 22 p3117 N88-28521

ELECTRIC EQUIPMENT
US Naval Air Force avionic and electrical system corrosion prevention and control maintenance 05 p0547 N88-13334
Avionic and electrical system corrosion prevention and control maintenance 22 p3054 N88-28119

ELECTRIC EQUIPMENT TESTS
The European space battery test center 09 p1125 N88-16738
EDF's studies and first choices regarding the design of electrical equipment
[NASA-TT-20222] 13 p1764 N88-20553

ELECTRIC FIELD STRENGTH
Electrodynamics of midnight sector of auroral oval in period of slight disturbance 08 p1003 N88-16077
Magnetic control of low pressure discharges
[AD-A186794] 10 p1322 N88-17900
Development of a ground-conductivity map for the area of the Federal Republic of Germany from measured field-strength contours 12 p1615 N88-19656
Mono- and bistatic radar coverage diagrams including diffractive wave propagation 12 p1616 N88-19660

Measurement technique for characterization of the gyrotron
[INPE-4322-RPE/550] 12 p1630 N88-19758

ELECTRIC FIELDS

The polarization field for pulsed Raman transitions
[DE87-013118] 01 p0035 N88-10227
Studies on temporal field emission from stainless steel surfaces
[DE87-014237] 02 p0147 N88-10919
Progress in stellarator/heliotron research, 1981-1986: Executive summary
[DE88-000017] 02 p0241 N88-11519
Short-pulse high-current-density photoemission in high electric fields
[DE87-014909] 03 p0310 N88-11951
Drop formation from an orifice in an electric field
[DE87-014405] 03 p0322 N88-12034
Effect of electrostatic field on behaviour of peripheric plasma at high-frequency heating
[DE87-703328] 03 p0378 N88-12378
The effect of object potentials on the wake of a flowing plasma
[AD-A184038] 03 p0379 N88-12385
Thermal analysis of electromagnetic launcher rails
[DE88-000166] 04 p0405 N88-12514
An electric field meter based upon a new principle: A dummy displacement electrode. Application to aerospace vehicles
[SNIAS-872-422-106] 05 p0585 N88-13567
Electric field measurements on Viking: First results
[TRITA-EPP-87-04] 05 p0625 N88-13826
Research for electric energy systems
[DE88-001733] 06 p0695 N88-14265
Finite-element method for three-dimensional electric and electromagnetic field problems
[PB87-138731] 06 p0696 N88-14274
Materials for acceleration by surface electromagnetic waves
[DE88-700312] 07 p0846 N88-15133
Dynamics Explorer guest investigator
[NASA-CR-181494] 07 p0878 N88-15325
Lightning spectra in the near infrared
[DE88-002218] 07 p0880 N88-15341
Current generation and induced conductivity of a plasma under common action of constant electric field and lower-hybrid or ECR waves
[DE88-700345] 07 p0935 N88-15680
Embedded cluster models for electronic structure and energetics of complex oxides
[DE88-003097] 07 p0938 N88-15702
First results of balloon-borne X-ray and electric field observations near the footprint of the Viking satellite
08 p1026 N88-16215
Acceleration of auroral particles by magnetic field-aligned electric fields 08 p1031 N88-16246
Low frequency electrostatic waves observed on board the Coordinated Auroral Experiment using Scatter And Rockets (CAESAR) 2 payload 08 p1032 N88-16253
Processes in the quiet and disturbed equatorial-low latitude ionosphere: Sundial campaign, 1984
[INPE-4152-PRE/1057] 08 p1036 N88-16282
Nonlinear diffusion in the presence of a time-dependent external electric field
[INPE-4378-PRE/1198] 08 p1085 N88-16533
Preliminary results from the dc electric field experiment on Viking --- Swedish satellite
[TRITA-EPP-87-03] 09 p1190 N88-17130
Acceleration of auroral particles by magnetic field-aligned electric fields
[TRITA-EPP-87-08] 09 p1190 N88-17131
The acoustic-electric field analysis of multilayered surface acoustic wave devices
[ETN-88-91592] 09 p1242 N88-17446
Observation of enhanced electric field in an RF-plugged sheet plasma in the RFC-XX-M open-ended machine
[IPPJ-857] 09 p1252 N88-17503
Effect of external electrostatic field on catecholamine secretion by rat adrenals 10 p1366 N88-18166
Light absorption by an atom moving inside a spherical box
[AD-A167241] 10 p1407 N88-18395
Temporal evolution of ionospheric electric field driven by field-aligned current 11 p1469 N88-18761
Return stroke velocities and currents using a solid state silicon detector system 11 p1515 N88-19050
Electric fields in Earth orbital space. Magnetospheric structural dynamic response to external variables
[AD-A188592] 12 p1643 N88-19836
Waves and static electric fields in the auroral acceleration region 12 p1646 N88-19856
The effects of a dc electric field on the current driven ion cyclotron instability
[AD-A188877] 12 p1695 N88-20142
Atmospheric electrical modeling in support of the NASA F-106 storm hazards project
[NASA-CR-181639] 13 p1799 N88-20758
Upward propagating electric fields from thunderstorms and VLF transmitters 13 p1801 N88-20767
Double layer polarization of nonconducting spheroidal particles and its application to Kerr effect
[ISSN-0208-5658] 13 p1832 N88-20960
Comparison of analytic and full guiding center behavior at a trapped-passing interface in stellarators
[DE88-004174] 13 p1842 N88-21025
Arcs in cesium seeded noble gases resulting from a magnetically induced electric field
[EUT-87-E-177] 13 p1843 N88-21028
Competing interactions in metallic superlattices
[DE88-005344] 13 p1847 N88-21057
Particle simulation research by plasma parametric heating caused by strong laser
14 p1903 N88-21368
Statistical analysis of feasibility of non-destructive inspection of mechanical properties of hot worked pipes of alloy steels
[BLL-M-37598-(5828.4)] 14 p1922 N88-21455
Optical properties of quantum well structures with electric field: Life time free switching of luminescence intensity and virtual charge-induced ultrafast optical nonlinearity 14 p1976 N88-21794
Physical processes in the vicinity of the cometopause interpreted on the basis of plasma, magnetic field and plasma wave data measured on board VEGA-2 spacecraft --- Halley's comet 14 p1996 N88-21894
Correlation between magnetic and electric field fluctuations observed during flyby near Halley's comet
14 p1996 N88-21897
Stratospheric electric field and conductivity measurements over electrified convective clouds in the South American region, revised
[INPE-4046-PRE/1012-REV-3]
15 p2095 N88-22483
A study on electric fields and conductivity associated with electrified clouds in the region of South America
[INPE-4487-TDL/325] 15 p2096 N88-22486
On the acceleration of electrons and positive ions in the same direction along magnetic field lines by parallel electric fields
[IRF-PREPRINT-103] 15 p2096 N88-22488
Experimental comparison of lightning simulation techniques to CV-580 airborne lightning strike measurements
[AD-A190576] 15 p2098 N88-22496
Droplet size characteristics and energy input requirements of emulsions formed using high-intensity-pulsed electric fields
[DE88-005912] 15 p2128 N88-22692
Parametric instabilities of inhomogeneous plasma near the lower-hybrid resonance
[DE88-701201] 15 p2137 N88-22748
High power, high frequency radiation from beam-plasma interactions
[AD-A190207] 15 p2137 N88-22752
Classical non-Abelian solutions for nonstandard Lagrangians
[DE88-701305] 16 p2263 N88-23532
Low gravity thermal management using dielectrophoretic forces 17 p2432 N88-24470
Cascade fluorescences from laser-excited lithium atom for plasma diagnostics 17 p2442 N88-24526
Electromagnetic penetration into a conducting circular cylinder through a narrow slot, TE case
[AD-A191602] 18 p2500 N88-24828
Electric field measurement by S-520-9 sounding rocket using the time of flight technique of lithium ion beam
[ISAS-RN-367] 18 p2543 N88-25095
Space station induced electromagnetic effects
18 p2591 N88-25394
Dynamics explorer data analysis
[NASA-CR-181428] 19 p2691 N88-25996
Calculation of the line shapes of radiators immersed in plasma 19 p2729 N88-26210
Degradation of beam brightness by field emission from a cathode shroud
[DE88-008345] 20 p2794 N88-26576
High spatial frequency thermal blooming instability: A linear stability analysis
[DE88-010711] 20 p2807 N88-26655
Interaction of biological systems with static and ELF electric and magnetic fields
[DE88-007951] 20 p2831 N88-26792
Sources of polarized ions and atoms
[DE88-010910] 20 p2852 N88-26931
Field-enhanced lithium ion sources for PBFA 2
[DE88-007195] 20 p2856 N88-26960
Ultrafast optical nonlinearity in quantum well structures with electric field 20 p2863 N88-27003
Electric and Magnetic Activity of the Central Nervous System: Research and Clinical Applications in Aerospace Medicine
[AGARD-CP-432] 21 p2977 N88-27683
Electric and magnetic brain activity related to cognitive performance 21 p2979 N88-27692
Staggered-grid finite element solution technique for the Maxwell's equations in the time domain
[DE88-011731] 21 p3007 N88-27838
On plasma stability under anisotropic random electric field influence
[DE88-702422] 21 p3019 N88-27918
Measurement of macroscopic electric fields in solar plasma structures
[AD-A193291] 21 p3031 N88-27993
TE/TM (Transverse Electric/Transverse Magnetic) height profile measurements of transpolar VLF (Very Low Frequency) signals
[AD-A194503] 22 p3069 N88-28216
The far field from a hybrid electromagnetic pulse (HPD) simulator
[FOA-C-30480-4.2] 22 p3071 N88-28231
On the self-consistent equation for the microscopic local electric field in dielectric systems
[PREPRINT-589] 22 p3074 N88-28247
Physiological effects of extremely low frequency electric and magnetic fields
[DE88-752814] 22 p3132 N88-28620
A study of electronic transport and breakdown in SiO2
[AD-A194258] 22 p3156 N88-28780
Kinetic theory for electrostatic waves due to transverse velocity shears
[AD-A193404] 23 p3284 N88-29557
Ion gun generated electromagnetic interference on the SCATHA satellite
[AD-A195179] 24 p3335 N88-29853
Wave propagation and remote sensing
24 p3364 N88-30029
General equations for the motions of ice crystals and water drops in gravitational and electric fields
[NASA-CR-183229] 24 p3370 N88-30070

ELECTRIC FILTERS

NT BANDSTOP FILTERS
NT DIGITAL FILTERS
NT FIR FILTERS
NT MICROWAVE FILTERS
NT RADAR FILTERS
NT RADIO FILTERS
NT TRACKING FILTERS
NT WAVEGUIDE FILTERS
On adaptive signal processing of RF signals
[DE87-014192] 02 p0161 N88-11007
Documentation of computer programs for optimization and simulation of multicarrier SAW-based demodulator
[PB87-134532] 06 p0693 N88-14252
A contribution to the realization of active filters for high frequency applications
[ETN-88-90811] 06 p0696 N88-14272

ELECTRIC FUSES

Experimental and mathematical investigation of response characteristics and aging phenomena in safety fuse elements
[ETN-88-91478] 11 p1480 N88-18832

ELECTRIC GENERATORS

NT AC GENERATORS
NT ALKALINE BATTERIES
NT DIRECT POWER GENERATORS
NT DYNAMOMETERS
NT ELECTROSTATIC GENERATORS
NT FUEL CELLS
NT HYDROGEN OXYGEN FUEL CELLS
NT MAGNETOHYDRODYNAMIC GENERATORS
NT METAL AIR BATTERIES
NT NICKEL ZINC BATTERIES
NT PHOSPHORIC ACID FUEL CELLS
NT PHOTOELECTRIC GENERATORS
NT PHOTOVOLTAIC CELLS
NT PRIMARY BATTERIES
NT RADIOISOTOPE BATTERIES
NT REGENERATIVE FUEL CELLS
NT ROTATING GENERATORS
NT SNAP 19
NT SODIUM SULFUR BATTERIES
NT SOLAR CELLS
NT SOLAR DYNAMIC POWER SYSTEMS
NT SOLAR GENERATORS
NT THERMAL BATTERIES
NT THERMIONIC CONVERTERS
NT THERMOELECTRIC GENERATORS
NT TURBOGENERATORS
NT VERTICAL JUNCTION SOLAR CELLS
NT ZINC-OXYGEN BATTERIES
Evaluation of stand-alone inverters for remote applications
[DE87-010957] 01 p0040 N88-10257
Solar energy: European research and development
[PB87-107645] 04 p0463 N88-12866
Design description report for a photovoltaic power system for a remote satellite earth terminal
[NASA-CR-179586] 04 p0465 N88-12875

Laser production and heating of plasma for MHD application
[NASA-TP-2798] 10 p1415 N88-18443
Advances in applied superconductivity: A preliminary evaluation of goals and impacts
[DE88-006441] 14 p1986 N88-21844
Superconductivity in power engineering
[DE88-701414] 15 p2141 N88-22776
Analysis of the electrical harmonic characteristics of a slip recovery variable speed generating system for wind turbine applications
[DE88-001140] 19 p2687 N88-25972
Analysis of the electrical characteristics of a Westinghouse variable speed generating system for wind turbine applications
[DE88-001139] 20 p2818 N88-26721
Comparative analysis of the space power architecture studies
[NASA-TM-100977] 22 p3049 N88-28090

ELECTRIC IGNITION
Measuring technical and mathematical investigation of multiple reignitions at the switching of a motor using vacuum circuit breakers
[ETN-87-90406] 01 p0042 N88-10270
Electrical ignition of HAN-based liquid propellants
[AD-A191349] 18 p2495 N88-24801

ELECTRIC IMPULSES
U ELECTRIC PULSES

ELECTRIC MOMENTS
Neutrino electrodynamics and possible effects for solar neutrinos
[DE88-701647] 23 p3308 N88-29705

ELECTRIC MOTOR VEHICLES
DOT fuel-cell-powered bus feasibility study
[DE87-012705] 01 p0107 N88-10699
Performance monitoring and analysis of electric van fleet vehicles
[DE88-900066] 04 p0502 N88-13091
Digital control of a direct current converter for a hybrid vehicle
[LAAS-87-266] 05 p0578 N88-13527
Research and development of advanced lead-acid batteries for electric vehicle propulsion
[DE87-014661] 07 p0873 N88-15297
User's guide to DIANE: A microcomputer program for modeling battery performance in electric vehicles
[DE88-003713] 08 p1068 N88-16456
Fuel cell/battery hybrid vehicle assessment
[DE88-005087] 10 p1427 N88-18520
Electric vehicle demonstration project
[DE88-004076] 11 p1566 N88-19376
Performance test results for the Eaton dc development power train in an electric test bed vehicle
[DE88-005458] 12 p1622 N88-19699
Mission directed goals for electric vehicle battery research and development: The Task Force on electric vehicle battery goals
[DE88-005601] 13 p1763 N88-20548
Testing and development of electric vehicle batteries for EPRI Electric Transportation Program
[DE88-005894] 13 p1764 N88-20551
Development of a total electric vehicle drive system
[DE88-900367] 14 p1917 N88-21446
Status of electric vehicle simulation programs at the INEL: Summer 1987
[DE88-006745] 15 p2058 N88-22271
A microcomputer-based control and simulation of an advanced IPM (Interior Permanent Magnet) synchronous machine drive system for electric vehicle propulsion
[DE88-006735] 18 p2505 N88-24859
Test results of the Electric Vehicle Field-Laboratory Correspondence Program, phase 1 report
[DE88-007706] 19 p2661 N88-25827
Computer controlled procedures for traction battery power performance tests
[ETN-88-92352] 20 p2796 N88-26589
Voltage directive drive with claw pole motor and control without rotor position indicator
[ETN-88-93120] 24 p3366 N88-30047

ELECTRIC MOTORS
NT ASYNCHRONOUS MOTORS
NT INDUCTION MOTORS
NT STEPPING MOTORS
NT SYNCHRONOUS MOTORS
NT TORQUE MOTORS
Computerized system for studies on creep of irradiated materials in the BR-10 reactor. Control system for electric motor
[DE87-702888] 03 p0310 N88-11952
The use of alloy 117 as a liquid metal current collector
[AD-A185740] 06 p0698 N88-14281
Pulse width modulator controller design for a brushless DC motor position servo
[AD-A186618] 08 p0980 N88-15921
Electro-mechanical vibratory system 11 p1500 N88-18958
Performance test results for the Eaton dc development power train in an electric test bed vehicle
[DE88-005458] 12 p1622 N88-19699
Development of a total electric vehicle drive system
[DE88-900367] 14 p1917 N88-21446
High output paraffin actuators: Utilization in aerospace mechanisms 14 p1924 N88-21470
Computer simulation of a motor pump unit to aid in interpreting vibration data
[DE88-004481] 16 p2223 N88-23270
The LDCM actuator for vibration suppression
[NASA-CR-182898] 17 p2335 N88-23940
A microcomputer-based control and simulation of an advanced IPM (Interior Permanent Magnet) synchronous machine drive system for electric vehicle propulsion
[DE88-006735] 18 p2505 N88-24859
Contribution to speed regulation of small motors with phase-locked loops
[ETN-88-92373] 20 p2796 N88-26590
Voltage directive drive with claw pole motor and control without rotor position indicator
[ETN-88-93120] 24 p3366 N88-30047

ELECTRIC NETWORKS
Design principles and practices for implementation of MIL-STD-1760 in aircraft and stores
[AD-A183724] 01 p0005 N88-10027
Development of methods for the analysis of the frequency and voltage statics of electricity users and electrical networks
[ETN-87-90412] 01 p0043 N88-10271
Performance optimization of electronic networks in the frequency domain
[PB87-123873] 04 p0438 N88-12720
Photoconductor switch and circuit analysis
[AD-A188168] 11 p1478 N88-18821
ECP (Electrical Circuitry Program): A proposed program for electrical circuitry analysis
[AD-A190494] 15 p2060 N88-22280
Some equivalent circuit models for AC impedance analysis of pyrite/solution interface
[DE88-010574] 21 p2939 N88-27452
On broadband matching of multiport electrical networks with applications
[AD-A194224] 23 p3207 N88-29086

ELECTRIC POTENTIAL
NT BIOELECTRIC POTENTIAL
NT COULOMB POTENTIAL
NT LOW VOLTAGE
NT QUANTUM WELLS
NT THRESHOLD VOLTAGE
On the interaction of a planar metal surface with a charge and with a molecule
[DE87-703083] 02 p0147 N88-10920
Departmental report on program EMTP-machine windings surge transients: Travelling wave method
[PB87-123733] 04 p0438 N88-12719
Conditions for geomagnetically trapping sub-micron lunar ejecta between L = 1.2 and L = 3.1 04 p0521 N88-13203
High energy density rechargeable batteries for aerospace power requirements
[AD-A184883] 05 p0577 N88-13519
Rotation of magnetized particle in electrically conducting viscous medium 06 p0770 N88-14733
Calculated sputtering and atomic displacement cross-sections for applications to medium voltage analytical electron microscopy
[DE88-002904] 09 p1168 N88-17006
Development and calibration of Direct Current Potential Difference (DCPD) crack length measurement equipment
[VTT-RR-480] 09 p1182 N88-17083
Nonlinear dynamic maximum power theorem
[AD-A187491] 11 p1477 N88-18810
Hercules: A power analyzer for MOS VLSI circuits
[AD-A188702] 12 p1623 N88-19706
Analysis of pre-flight modulator voltage calibration data for the Voyager plasma science experiment
[NASA-CR-182577] 12 p1710 N88-20236
Bloch oscillations in small Josephson junctions: Their manifestation in switching effects 14 p1969 N88-21756
Modeling the effects of heavy charged particles on MOSFETs (Metal-Oxide-Semiconductor Field Effect Transistors)
[AD-A190575] 15 p2143 N88-22792
Optical sensors for the measurement of electric current and voltage
[PB88-172945] 16 p2193 N88-23077
An electrostatic potential comparator
[AD-A192051] 18 p2557 N88-25177
Generation, and forming of ultrashort high voltage pulses 19 p2657 N88-25782
Carrier transport in semiconductor magnetic sensors under nonuniform fields 19 p2672 N88-25888
Characterization of fatigue crack initiation and propagation in Ti-6Al-4V with electrical potential drop technique
[NASA-TM-100877] 19 p2681 N88-25937
Fast parametrization procedure for solar cells
[PB88-186416] 19 p2686 N88-25966
Voltages induced by lightning on electric power distribution lines: Field data and analysis results for the period July 1984-1986
[DE88-007841] 19 p2693 N88-26006
Discontinuous inverse Sturm-Liouville problems with symmetric potentials
[DE88-009803] 19 p2720 N88-26152
Transport study on Si/Si(1-x)Ge(x) superlattices selectively doped by secondary implantation of Sb 20 p2867 N88-27027
A planar IC-compatible transferred electron device for millimeter-wave operation
[AD-A192692] 21 p2936 N88-27433
Results from life test in progress on eagle-picher nickel cadmium cells
[AD-A192816] 21 p2936 N88-27434
Studies of the intact human brain: Implications for performance 21 p2977 N88-27684
Dissecting the visual and auditory pathways by means of the two-input technique 21 p2978 N88-27690
Event-related brain potentials as indices of mental workload and attentional allocation 21 p2979 N88-27696
Using ERPS to study human information processing 21 p2980 N88-27698
Withstand voltage of slightly polluted insulator chains in humid weather conditions
[DE88-752818] 22 p3072 N88-28237
Development of inductive storage pulsed power generators
[AD-A193878] 22 p3117 N88-28521

ELECTRIC POWER CONVERSION
U ELECTRIC GENERATORS

ELECTRIC POWER PLANTS
NT FUEL CELL POWER PLANTS
NT NUCLEAR POWER PLANTS
NT SOLAR THERMAL ELECTRIC POWER PLANTS
USSR report: Engineering and equipment
[JPRS-UEQ-87-008] 04 p0423 N88-12621
Solar energy: European research and development
[PB87-107645] 04 p0463 N88-12866
Cu-2 mechanical properties and microstructural stability of advanced steam cycle materials
[DE88-001519] 05 p0566 N88-13452
Monitoring corrosion and process physical-chemical parameters in electric power plants
[CISE-3708] 06 p0682 N88-14182
Innovating systems and techniques for the diagnosis of materials and industrial plants
[CISE-3856] 08 p0976 N88-15901
On line instrument systems for monitoring steam turbogenerators
[CISE-3860] 08 p0990 N88-15995
The role of repowering in America's power generation future
[DOE/FE-0096] 10 p1351 N88-18076
An analysis of gas-steam total power recovery energy system 20 p2784 N88-26512

ELECTRIC POWER SUPPLIES
NT AIRCRAFT POWER SUPPLIES
NT SOLAR DYNAMIC POWER SYSTEMS
NT SPACE STATION POWER SUPPLIES
NT SPACECRAFT POWER SUPPLIES
Evaluation of stand-alone inverters for remote applications
[DE87-010957] 01 p0040 N88-10257
The fundamentals of photovoltaic system electrical design
[DE87-009061] 02 p0194 N88-11214
Operation of multistage power supplies for electron beam welding installations 03 p0286 N88-11800
Recent progress in space photovoltaic systems
[NASA-TM-100208] 03 p0311 N88-11966
A 40-kW fuel cell field test summary utilities activities report
[PB88-112800] 06 p0731 N88-14496
Evaluation of high-voltage, high-power, solid-state remote power controllers for amps 07 p0924 N88-15612
Microprocessor control and networking for the amps breadboard 07 p0924 N88-15615
Plasma contactors for use with electodynamic tethers for power generation
[NASA-CR-182424] 08 p1087 N88-16547
Test results on dual resonant power supply with flat top and flat bottom current
[DE87-007506] 09 p1157 N88-16933
Project Explorer takes its second step: GAS-608 in engineering development 10 p1288 N88-17707

A methodology to assess the effects of high altitude electromagnetic pulse (HEMP) on electric power systems
[DE88-000338] 11 p1476 N88-18808
High frequency power distribution system
[NASA-CR-175071] 17 p2335 N88-23939
Arc lamp power supply using a voltage multiplier
[NASA-CASE-LAR-13202-1] 17 p2335 N88-23942
Magnet shielding analysis for SOAR: A space fusion reactor 17 p2400 N88-24269
Magnetically switched power supply system for lasers
[NASA-CASE-NPO-16402-2] 18 p2505 N88-24862
Photovoltaic energy systems
[DE88-007504] 19 p2687 N88-25968
Advanced photovoltaic power system technology for lunar base applications
[NASA-TM-100965] 20 p2766 N88-26402

ELECTRIC POWER TRANSMISSION
Comparison of costs and benefits for dc and ac transmission
[DE87-008774] 02 p0167 N88-11052
The ac power system testbed
[NASA-CR-175068] 03 p0309 N88-11948
Safety research of insulating materials of cable for nuclear power generating station
[NASA-TT-20202] 13 p1752 N88-20477
Power transmission studies for tethered SP-100
[NASA-TM-100864] 14 p1883 N88-21251
Northern lights: The economic and practical potential of imported power from Canada
[DE88-006026] 15 p2093 N88-22473
Optical sensors for the measurement of electric current and voltage
[PB88-172945] 16 p2193 N88-23077
Harmonic considerations for electrical distribution feeders
[DE88-007849] 18 p2505 N88-24860
Technologies applicable to space tethers
[NASA-CR-183055] 19 p2606 N88-25471
Voltages induced by lightning on electric power distribution lines: Field data and analysis results for the period July 1984-1986
[DE88-007841] 19 p2693 N88-26006

ELECTRIC PROPULSION
NT ELECTROMAGNETIC PROPULSION
NT ELECTROSTATIC PROPULSION
NT ION PROPULSION
NT LASER PROPULSION
NT PLASMA PROPULSION
Auxiliary propulsion system flight package
[NASA-CR-180828] 02 p0141 N88-10886
A low-power arcjet cyclic lifetest
[NASA-TM-100233] 03 p0278 N88-11748
Post-test analyses of aqueous batteries developed for electric propulsion
[DE88-000655] 03 p0311 N88-11965
High power ion thruster performance
[NASA-TM-100127] 04 p0409 N88-12542
Advanced electric propulsion and space plasma contactor research
[NASA-CR-180862] 06 p0674 N88-14126
Performance-limiting factors in MPD thrusters
[AD-A185605] 06 p0674 N88-14128
Completely magnetically contained electrothermal thrusters
[AD-A185674] 06 p0674 N88-14129
ESA Bulletin No. 10
[ETN-87-90514] 09 p1123 N88-16728
Electric propulsion: A controversial must for long-lived applications satellites 09 p1124 N88-16735
A comparative study of various electric propulsion systems and their impact on a nominal ship design
[AD-A187800] 11 p1477 N88-18816
Physical fluid mechanics in MPD thrusters
[AD-A190309] 15 p2138 N88-22754
Megawatt level electric propulsion perspectives 17 p2404 N88-24294
High power ion thruster performance 17 p2404 N88-24295
Electric propulsion options for the SP-100 reference mission 17 p2404 N88-24296
Status of high power electric propulsion technology 17 p2428 N88-24443
Performance and long duration test of a 30 kw thermal arcjet engine
[AD-A190962] 18 p2474 N88-24677
Performance of a hydrogen pulsed electrothermal thruster. Strategic defense initiative organization innovative science and technology. SBIR, phase 1
[AD-A191999] 18 p2475 N88-24679
The NASA Electric Propulsion Program
[NASA-TM-101324] 24 p3336 N88-29859
Performance and lifetime assessment of MPD arc thruster technology
[NASA-TM-101293] 24 p3336 N88-29860
The dc power control for a liquid-fed resistojet
[NASA-TM-101326] 24 p3338 N88-29869
Successful completion of a cyclic ground test of a mercury ion auxiliary propulsion system
[NASA-TM-101351] 24 p3339 N88-29873

ELECTRIC PULSES
NBS (National Bureau of Standards) wideband sampling wattmeter
[PB87-210324] 03 p0323 N88-12041
On M-ARY sequential hypotheses testing for the classification of radar signals
[AD-A184094] 04 p0430 N88-12666
State parameters of pulse-discharge plasma in xenon-filled closed tube 06 p0773 N88-14747
Pulsed power sources based on MHD generators (a state-of-art review)
[DE88-700296] 07 p0935 N88-15677
Optimum transformer design for a pulsed power system
[DE88-006054] 13 p1760 N88-20525
Harmonic and rectangular pulse reproduction through current transformers
[EUT-88-E-159] 14 p1907 N88-21395

ELECTRIC REACTORS
NT SATURABLE REACTORS

ELECTRIC ROCKET ENGINES
NT ARC JET ENGINES
NT ELECTROSTATIC ENGINES
NT ELECTROTHERMAL ENGINES
NT ION ENGINES
NT MERCURY ION ENGINES
NT PLASMA ENGINES
NT RESISTOJET ENGINES
Nuclear electric power for multimegawatt orbit transfer vehicles 17 p2399 N88-24261

ELECTRIC SPARKS
Experimental study and modeling of the physical mechanisms of the gliding spark
[ESA-TT-1029] 01 p0070 N88-10447

ELECTRIC STIMULI
Facilitory effects of voluntary movements on vestibulomotor reaction 12 p1664 N88-19976

ELECTRIC SWITCHES
NT VACUUM ARC SWITCHES
Characterization of PEOS (Plasma Erosion Opening Switch) plasma parameters and conduction phase properties
[AD-A189024] 12 p1624 N88-19714

ELECTRIC WELDING
NT ARC WELDING
NT ELECTRON BEAM WELDING
NT GAS TUNGSTEN ARC WELDING
NT PLASMA ARC WELDING

ELECTRIC WIRE
Properties of Nb3Sn superconductor wires with composite cores
[KFK-4263] 02 p0246 N88-11557
Electromagnetic interaction between an electric discharge and cabling inside a satellite 03 p0274 N88-11725
A design-philosophy for grounding and inter-unit wiring
[EMCR-20/85] 03 p0310 N88-11954
Discussions in support of the design-philosophy for grounding and inter-unit wiring
[EMCR-21/85] 03 p0310 N88-11955
Assessment of existing specifications against the design-philosophy for grounding and inter-unit wiring (EMCR 20/85)
[EMCR-22/85] 03 p0310 N88-11956
Alternatives to the techniques implicit in the design philosophy, and the penalties in performance associated with them --- grounding and wiring
[EMCR-31/85] 03 p0310 N88-11957
Powder metallurgical preparation of A15 superconductors
[ETN-88-91072] 09 p1144 N88-16858
Nature of gigantic resistance fluctuations in metal-oxide-semiconductor wires
[DE88-002905] 09 p1256 N88-17533
Evaluation of flammability for cable-like polymers
[NASA-TT-20225] 13 p1752 N88-20476
On the use of thermal degradation data to predict cable ignition performance
[DE88-002276] 19 p2621 N88-25549

ELECTRIC WIRING
U ELECTRIC WIRE
U WIRING

ELECTRICAL BREAKDOWN
U ELECTRICAL FAULTS

ELECTRICAL CONDUCTIVITY
U ELECTRICAL RESISTIVITY

ELECTRICAL CONDUCTIVITY METERS
Definition and use of sensors for measuring electrical conductivity in thunderclouds
[ESA-TT-1047] 03 p0352 N88-12222

ELECTRICAL ENGINEERING
Electrical heating method --- pipelines, metal tanks
[GB-PATENT-2-137-059-A] 01 p0043 N88-10274
Center for Electronics and Electrical Engineering Technical Progress Bulletin covering center programs, October to December 1986 with 1987 CEEE events calendar
[PB87-226890] 02 p0168 N88-11058
Center for Electronics and Electrical Engineering technical publication announcements covering center programs, July to September 1986 with 1987 CEEE events calendar
[PB87-223442] 02 p0168 N88-11059
Center for Electronics and Electrical Engineering Technical Progress Bulletin covering center programs, January to March 1987 with 1987 CEEE events calendar
[PB87-224648] 03 p0309 N88-11946
Electronics engineering thrust area report, FY86
[DE87-014616] 03 p0309 N88-11950
A design-philosophy for grounding and inter-unit wiring
[EMCR-20/85] 03 p0310 N88-11954
National Science Foundation
[PB87-228375] 03 p0384 N88-12410
Bulletin of the Yamagata University (Engineering), Volume 20, No. 1, January 1988
[ISSN-0085-834X] 07 p0839 N88-15091
Helsinki University of Technology Communications Laboratory
[PB88-112974] 10 p1318 N88-17881
Construction of control systems with diversified redundancy for electrical machines
[BIA-5/86] 11 p1481 N88-18842
MacCAD (Macintosh Computer Aided Design), computer aided design tool for system analysis
[AD-A189241] 13 p1815 N88-20843
Center for Electronics and Electrical Engineering technical publication announcements covering Center programs, July to September 1987
[PB88-196530] 20 p2793 N88-26572
Analytical determination of critical crack size in solar cells
[NASA-CR-183128] 20 p2821 N88-26736
Statistical analysis of the LMS (Last Mean Squares) and modified stochastic gradient
[AD-A195497] 24 p3424 N88-30376

ELECTRICAL FAULTS
NT SHORT CIRCUITS
In-flight diagnosis: Analysis of spurious events --- spacecraft 03 p0274 N88-11724
Low-current behavior and current chopping of vacuum arcs
[ISBN-90-9001649-X] 05 p0578 N88-13529
RELIC: A reliability simulator for integrated circuits
[AD-A187493] 11 p1477 N88-18811
Air gap testing using Trailing Wire Antenna (TWA) waveform
[AD-A187639] 11 p1477 N88-18812
Application of knowledge based systems to the maintenance of inertial system electronics 12 p1578 N88-19441

ELECTRICAL GROUNDING
A design-philosophy for grounding and inter-unit wiring
[EMCR-20/85] 03 p0310 N88-11954
Discussions in support of the design-philosophy for grounding and inter-unit wiring
[EMCR-21/85] 03 p0310 N88-11955
Assessment of existing specifications against the design-philosophy for grounding and inter-unit wiring (EMCR 20/85)
[EMCR-22/85] 03 p0310 N88-11956
Alternatives to the techniques implicit in the design philosophy, and the penalties in performance associated with them --- grounding and wiring
[EMCR-31/85] 03 p0310 N88-11957
Human engineering laboratory grounding analysis (HELGA)-2
[AD-A185367] 05 p0578 N88-13524

ELECTRICAL IMPEDANCE
NT CONTACT RESISTANCE
NT ELECTRICAL RESISTANCE
NT SKIN RESISTANCE
NT TRANSCONDUCTANCE
Surface topography and electrical response of metal-electrolyte interface
[DE87-013553] 02 p0166 N88-11046
Study of the distribution of a multi-electrode circular system sensitivity for the reconstruction of bioelectrical impedance images
[ISAL-IDI1-87-01] 02 p0217 N88-11368
Time domain electromagnetic waves in multilayered media
[AD-A185055] 05 p0574 N88-13502
Analytical solution of the equations for a coaxial plasma gun operating in the snowplow mode. 1. Weak coupling limit
[AD-A185370] 05 p0652 N88-13994

Application of ac-impedance method on determination of corrosion rate of metals
[DE88-750307] 10 p1300 N88-17771
Operators manual for a computer controlled impedance measurement system
[AD-A187513] 10 p1324 N88-17917
Characterization of proton conducting polymer blends 19 p2669 N88-25867
Electrical detection of coating deterioration 24 p3355 N88-29973
Electrochemical evaluation of the long term corrosion resistance of polymer coated steel 24 p3355 N88-29974
An electrochemical impedance spectroscopy study of reactions at the metal/coating interface 24 p3355 N88-29975
Evaluation of organic coating deterioration and substrate corrosion in seawater using electrochemical impedance measurements 24 p3355 N88-29976
Review of Radio Science, 1984-1986 24 p3383 N88-30023
Electromagnetic metrology 24 p3383 N88-30024

ELECTRICAL INSULATION
The influence of microvoids on the electrical strength of glass fiber reinforced epoxy resins
[ETN-87-90443] 01 p0030 N88-10189
Design and testing of electrical insulation for superconducting coils
[DE87-012256] 01 p0039 N88-10246
Discharge prevention of geosynchronous orbit conductive thermal control materials and grounding systems 03 p0274 N88-11732
Polymer composition --- cable insulation
[EP-PATENT-0-199-444-A1] 04 p0418 N88-12594
Coaxial cable connector
[NASA-CASE-NPO-16764-1-CU] 06 p0696 N88-14270
Particle desorption from nonconducting surfaces by high energy heavy ions
[ETN-88-91088] 09 p1245 N88-17461
Application of high temperature ceramic superconductors (CSC) to commercial tokamak reactors
[DE88-003973] 09 p1257 N88-17538
Measurement of shielding effectiveness of different cable and shielding configurations by mode-stirred techniques
[PB88-155791] 10 p1319 N88-17885
Evaluation of flammability for cable-like polymers
[NASA-TT-20225] 13 p1752 N88-20476
Vapor-mist for lightweight high voltage space insulation systems
[DE87-011704] 13 p1762 N88-20538
Power transmission studies for tethered SP-100
[NASA-TM-100864] 14 p1883 N88-21251
Partial discharges and the electrical aging of cross linked polyethene (XLPE) cable insulation
[EUT-88-E-160] 14 p1892 N88-21300
Irradiation test results on thermionic fuel element sheath insulators 17 p2402 N88-24280
Research and development of electrical insulators for thermionic applications 17 p2429 N88-24449
Ceramic electrical insulator development for thermoelectric SACE power system 17 p2430 N88-24459
Development of external cooling cryo-resistive cable systems. Part 2: Insulation characteristics on 66 kV rated cryo-resistive testing cable
[DE88-770191] 20 p2793 N88-26571
A model for insulated wires in the method of moments code NEC (Numerical Electromagnetics Code)
[DE88-008920] 20 p2794 N88-26577
Withstand voltage of slightly polluted insulator chains in humid weather conditions
[DE88-752818] 22 p3072 N88-28237
System suitable for observing surface plasmon in a semi-infinite semiconductor superlattice
[DE88-702686] 23 p3293 N88-29606

ELECTRICAL LEADS
U ELECTRIC CONDUCTORS

ELECTRICAL MEASUREMENT
NT POLAROGRAPHY
Optical power line voltage and current measurement systems. Volume 1: Limits to the precision of electro-optic and magneto-optic sensors
[DE87-014558] 02 p0175 N88-11092
Analysis of free cutting brass by A.C. polarography
[PD-MT-8728] 04 p0417 N88-12587
Electromagnetic tests
[SNIAS-872-430-103] 05 p0575 N88-13508
An electric field meter based upon a new principle: A dummy displacement electrode. Application to aerospace vehicles
[SNIAS-872-422-106] 05 p0585 N88-13567
Electric field measurements on Viking: First results
[TRITA-EPP-87-04] 05 p0625 N88-13826
High frequency periodic time domain waveform measurement system
[PB87-225256] 06 p0695 N88-14264
Development and calibration of Direct Current Potential Difference (DCPD) crack length measurement equipment
[VTT-RR-480] 09 p1182 N88-17083
Preliminary results from the dc electric field experiment on Viking --- Swedish satellite
[TRITA-EPP-87-03] 09 p1190 N88-17130
Automatic prober for the dc characterization of gallium arsenide devices. Part 1: The measurement facility
[AD-A187583] 11 p1560 N88-19337
Planning, construction, and commissioning of a vacuum apparatus with a cold surface for the measurement of transistor functions at 20 K
[JUEL-SPEZ-397] 12 p1622 N88-19703
Separable electrical connectors for space: A tribological and electrical assessment 14 p1879 N88-21231
Calculating depletion region carrier concentrations with capacitance-voltage measurements and etching
[AD-A189630] 15 p2141 N88-22777
Electrochemistry in near-critical and supercritical fluids. 5: The dimerization of quinoline and acridine radical anions and dianions in ammonia from -70 C to 150 C
[AD-A190858] 16 p2175 N88-22967
Optical sensors for the measurement of electric current and voltage
[PB88-172945] 16 p2193 N88-23077
Electrochemistry in near-critical and supercritical fluids. 6: The electrochemistry of ferrocene and phenazine in acetonitrile between 25C and 300C
[AD-A192171] 18 p2482 N88-24723
Recent advances in capacitance type of blade tip clearance measurements
[NASA-TM-101291] 19 p2603 N88-25460
Voltages induced by lightning on electric power distribution lines: Field data and analysis results for the period July 1984-1986
[DE88-007841] 19 p2693 N88-26006
The influence of uncompensated solution resistance on the determination and standard electrochemical rate constants using cyclic voltammetry and some comparisons with AC voltammetry
[AD-A192825] 20 p2770 N88-26427
A rapid electrochemical technique for determining the current efficiency for cadmium plating
[AD-A193679] 22 p3056 N88-28130
Results of the use of an automated electrical measuring instrument calibration system
[SNIAS-881-430-107] 23 p3217 N88-29146
Electrical detection of coating deterioration 24 p3355 N88-29973
Electrochemical evaluation of the long term corrosion resistance of polymer coated steel 24 p3355 N88-29974
Evaluation of organic coating deterioration and substrate corrosion in seawater using electrochemical impedance measurements 24 p3355 N88-29976

ELECTRICAL PROPERTIES
NT CAPACITANCE
NT CAPACITANCE-VOLTAGE CHARACTERISTICS
NT CARRIER MOBILITY
NT CHARGE DISTRIBUTION
NT CONTACT RESISTANCE
NT DIELECTRIC PROPERTIES
NT ELECTRIC MOMENTS
NT ELECTRICAL IMPEDANCE
NT ELECTRICAL RESISTANCE
NT ELECTRICAL RESISTIVITY
NT ELECTRON MOBILITY
NT ELECTROSTRICTION
NT FERROELECTRICITY
NT HOLE MOBILITY
NT INDUCTANCE
NT KONDO EFFECT
NT MAGNETORESISTIVITY
NT PERMITTIVITY
NT PHOTOCONDUCTIVITY
NT PHOTOVOLTAIC EFFECT
NT PIEZOELECTRICITY
NT PLASMA CONDUCTIVITY
NT PROXIMITY EFFECT (ELECTRICITY)
NT PYROELECTRICITY
NT SKIN RESISTANCE
NT SUPERCONDUCTIVITY
NT TRANSCONDUCTANCE
Electrical behavior of layers implanted with low energy pions in Si
[INPE-4199-PRE/1051] 01 p0102 N88-10670
The preparation of thin films for photovoltaic conversion by novel MOCVD techniques
[DE87-001185] 02 p0194 N88-11212
Electrical properties of high T/sub c/ superconductors under high pressures
[DE87-012818] 02 p0245 N88-11546
Vacuum ultraviolet electronic properties of liquids
[DE88-000165] 03 p0282 N88-11772
Research and development on high strength ceramic heaters discussed 04 p0404 N88-12508
Synthesis, NMR characterization and electrical properties of siloxane-based polymer electrolytes
[AD-A184184] 04 p0418 N88-12596
A study of charged particles/radiation damage to VLSI device materials
[NASA-CR-172036] 05 p0577 N88-13518
Material design of high performance glasses discussed 06 p0688 N88-14216
Picosecond cable calibrator: Beam Research Program
[DE88-002375] 06 p0695 N88-14266
Investigation of silicon surface passivation by silicon nitride film deposition
[NASA-CR-182350] 06 p0729 N88-14487
Contrast between the chemical, structural and electronic properties of thin films of Cu and Ni on the Ru(0001) surface
[DE88-002360] 07 p0938 N88-15698
Rapid underway sediment classification by electrical methods
[AD-A187477] 10 p1357 N88-18114
Electrical properties of medium field, chem-prep varistors
[DE88-006147] 13 p1762 N88-20540
Scale-up of a batch-type chemical powder preparation process for high field varistor fabrication
[DE88-006601] 13 p1762 N88-20541
Measurement of the properties of lossy materials inside a finite conducting cylinder
[NASA-CR-182664] 13 p1832 N88-20962
A general 2D electrical model for diagonally connected MHD generators
[DE88-004283] 14 p1984 N88-21835
Electrical circuit modeling of reversed field pinches
[DE88-006942] 15 p2136 N88-22745
Preparation of large area NbN/AlN/NbN Josephson junctions
[DE88-006074] 15 p2145 N88-22799
Laser induced ignition of propellants
[AD-A191100] 16 p2168 N88-22927
Electrical dc conductivity of pitch
[AD-A191266] 16 p2182 N88-23008
The inspection of electronic metallurgical bonds
[AD-A192197] 18 p2486 N88-24745
Progress and challenges in HEMT LSI technology 19 p2656 N88-25779
The structure and properties of RF reactive sputtered IrO2 films 19 p2672 N88-25884
Electrodynamic driver for the space thermoacoustic refrigerator (STAR)
[AD-A192337] 20 p2785 N88-26517
Analysis of the electrical characteristics of a Westinghouse variable speed generating system for wind turbine applications
[DE88-001139] 20 p2818 N88-26721
Pressure-dependent measurement on n + GaAs (Si, Sn): The effect of deep donor (DX) states on the electrical properties and presistent photoconductivity effects 20 p2866 N88-27020
Electrical properties of p-type and n-type ZnSe-ZnTe strained-layer superlattices 20 p2868 N88-27029
MBE growth of HgTe/CdTe superlattices on Si(100) substrates 20 p2869 N88-27033
On a-Si:H/a-SiN(x):H superlattices: Confinement or contamination 20 p2870 N88-27040
Influence of interfaces on electronic and magnetic properties of MnSe/ZnSe superlattices near monolayer limit 20 p2872 N88-27050
Electrical study of metal/group 3-5 semiconductor interfaces: Comparison with the atomic-level studies 20 p2874 N88-27059
Investigations on the MBE (Molecular Beam Epitaxy) growth and properties of Al(sub y)Ga(sub y)In(sub 1-x-y)AsInP and InGaAs-InAlAs superlattices
[DE88-009105] 21 p3022 N88-27941
Electrical properties of metal-oxide-silicon structures with sol-gel oxides
[DE88-011791] 22 p3156 N88-28779
Cytochrome electron transfer and biomolecular electronics
[AD-A195482] 24 p3406 N88-30277
A dynamic analysis of piezoelectric strained elements
[AD-A196079] 24 p3432 N88-30430

ELECTRICAL RESISTANCE
NT CONTACT RESISTANCE
NT SKIN RESISTANCE
NT TRANSCONDUCTANCE
The development of a high temperature static strain gage system 02 p0184 N88-11142
On the stressing of annealed NITINOL: The electrical resistance and calorimetric effects
[AD-A184465] 04 p0414 N88-12569

Studies of alumina additions in zirconia - magnesia
[DE87-703500] 04 p0419 N88-12602
Extraction of MOS VLSI (Very-Large-Scale-Integrated) circuit models including critical interconnect parasitics
[AD-A185847] 08 p0979 N88-15914
Comparative evaluation of resistive and inductive techniques for measuring temperature of superconducting transition
[DE88-700603] 10 p1417 N88-18457
Method for characterizing end-plate surface resistance of dielectric resonator 14 p1903 N88-21371
Effects of cold working on precipitation in age hardenable alloys: On the copper alloys
[NASA-TT-20164] 16 p2177 N88-22973
Liquid carbon
[AD-A191707] 18 p2491 N88-24776
Observation of metallic conductivity in liquid carbon
[AD-A191723] 19 p2618 N88-25533
The influence of uncompensated solution resistance on the determination and standard electrochemical rate constants using cyclic voltammetry and some comparisons with AC voltammetry
[AD-A192825] 20 p2770 N88-26427
A critical review of IR drops and electrode potentials within pits, crevices and cracks
[AD-A192481] 21 p2935 N88-27431
Friction, wear and electrical contact resistance of precious metal alloys
[DE88-011244] 21 p2938 N88-27450
Conductivity mechanism and operating behavior of electrically conductive adhesives on the example of a power transistor
[ETN-88-92355] 21 p2940 N88-27464
Shielding effectiveness of metallic joints versus corrosion prevention 22 p3054 N88-28120
Superconducting properties of oxygen deficient YBa2Cu3O(sub 7-delta)
[DE88-009969] 22 p3155 N88-28774
Electrical properties of materials for elevated temperature resistance strain gage application
[NASA-CR-182214] 24 p3376 N88-30106

ELECTRICAL RESISTIVITY

NT KONDO EFFECT
NT MAGNETORESISTIVITY
NT PHOTOCONDUCTIVITY
NT PLASMA CONDUCTIVITY
NT SUPERCONDUCTIVITY
Eddy current density in wedge-shaped conducting cylinders with inhomogeneous conductivity
[ETN-87-90404] 01 p0042 N88-10268
Electrical behavior of layers implanted with low energy pions in Si
[INPE-4199-PRE/1051] 01 p0102 N88-10670
Electrical conductivity and equation of state measurements on planetary fluids at high pressures and temperatures
[DE87-013787] 01 p0110 N88-10708
Continuous flow electrophoresis system experiments on shuttle flights STS-6 and STS-7
[NASA-TP-2778] 02 p0156 N88-10978
Frozen-field, rigid-beam, uniform-conductivity-channel tracking force calculation
[DE87-012510] 02 p0190 N88-11190
Transport analysis of OH and NBI heated discharges in JT-60
[DE87-752985] 02 p0239 N88-11511
External surface charging mechanisms — spacecraft 03 p0273 N88-11719
A quantum theoretical study of polyimides
[NASA-CR-181495] 03 p0292 N88-11831
Wittig synthesis of conductive segmented block polymer compositions
[AD-A184018] 03 p0295 N88-11850
Research and development on high strength ceramic heaters discussed 04 p0404 N88-12508
Ultimate velocities for induction launchers
[DE87-012360] 04 p0404 N88-12513
Studies on some Ge-Se-Te glasses
[PD-MT-8721] 04 p0420 N88-12607
Proton abstraction as a route to conductive polymers
[AD-A184019] 04 p0421 N88-12612
Resistivity of EuBa2(Cu/sub 1-y/Zn/sub y/)3O/sub x/ as a ffunction of temperature, magnetic field, pressure and Zn concentration
[DE87-014740] 04 p0499 N88-13069
Human engineering laboratory grounding analysis (HELGA)-2
[AD-A185367] 05 p0578 N88-13524
Superconducting material development 06 p0688 N88-14217
Conductivity studies on hydroxide ion conductors in the Li-Al-O-H system at intermediate temperatures
[AD-A185714] 06 p0697 N88-14279
Phase behavior in the Li-Al-O-H system at intermediate temperatures
[AD-A185732] 06 p0697 N88-14280
Rotation of magnetized particle in electrically conducting viscous medium 06 p0770 N88-14733
Effect of plasma rotation in tokamak on stabilizing action of electrically conducting wall 06 p0773 N88-14748
Interface characteristics and the mechanical properties of metal matrix composites
[AD-A186441] 08 p0966 N88-15845
Study of asthenosphere: Project ELAS 08 p1013 N88-16138
Influence of arsenic superficial enrichment on the ohmicity of the n-GaAs:In/Au contact
[ECL-87-09] 08 p1089 N88-16554
Interpretation of the temperature dependence of conductivity in superconducting oxides
[DE88-003028] 08 p1091 N88-16565
Thermodynamic and conductivity studies of nonstoichiometric cerium dioxide by Coulometric titration: A simultaneous measurement
[DE88-003054] 08 p1091 N88-16566
High temperature solar electrothermal processing-3. Zinc from zinc oxide at 1200-1675K using a non-consumable anode
[AD-A186600] 09 p1141 N88-16836
Evaluation of the magnetic induction conductivity method for detecting frazil ice deposits
[AD-A186940] 09 p1194 N88-17157
Structural relationships in high temperature superconductors
[DE88-002924] 09 p1257 N88-17534
Effect of the subgap conductance on the metastable states in a Josephson tunnel junction
[DE88-003102] 09 p1258 N88-17543
Electrically conducting polymer-copper sulphide composite films, preparation by treatment of polymer-copper (2) acetate composites with hydrogen sulfide
[NASA-TT-20204] 10 p1305 N88-17803
Design of a charge sensitive preamplifier on high resistivity silicon
[DE88-003491] 10 p1323 N88-17907
Rapid underway sediment classification by electrical methods
[AD-A187477] 10 p1357 N88-18114
Realistic conductivity geometry model of the human head for interpretation of neuromagnetic data
[PB88-112230] 10 p1369 N88-18179
The physics of metallic superlattices: An experimental point of view
[DE88-003080] 10 p1416 N88-18452
Determination of distributed resistance of base of bipolar transistors measuring noise spectral densities
[DE88-700197] 11 p1479 N88-18829
Limiting efficiency of a thermionic diode
[DE88-700598] 11 p1479 N88-18830
Morphological studies of conductive polymers
[AD-A188456] 12 p1610 N88-19629
Development of a ground-conductivity map for the area of the Federal Republic of Germany from measured field-strength contours 12 p1615 N88-19656
Characterization of PEOS (Plasma Erosion Opening Switch) plasma parameters and conduction phase properties
[AD-A189024] 12 p1624 N88-19714
Changes in blood conductivity during immersion 12 p1663 N88-19969
Fast protonic conducting solid electrolytes
[AD-A188524] 12 p1698 N88-20160
Simplified physical approach of the control by eddy current
[DE88-701076] 13 p1764 N88-20552
New method of examining microнonhomogeneity of local centers in high-resistivity semiconductor materials under scanning electron microscope 14 p1969 N88-21754
Electrical resistivities of some compound forming liquid metal alloys
[PB88-145172] 15 p2037 N88-22137
Research on stable processible conducting polymers for electronic applications
[AD-A190246] 15 p2044 N88-22180
Temperature-dependent conductivity of oxygen-depleted YBCO ceramics
[AD-A190340] 15 p2044 N88-22182
Analysis of anomalous resistivity during the conduction phase of the plasma erosion opening switch
[DE88-006382] 15 p2061 N88-22286
Stratospheric electric field and conductivity measurements over electrified convective clouds in the South American region, revised
[INPE-4046-PRE/1012-REV-3] 15 p2095 N88-22483
A study on electric fields and conductivity associated with electrified clouds in the region of South America
[INPE-4487-TDL/325] 15 p2096 N88-22486
Physical, chemical and CTD (Conductivity/Temperature/Depth) data from the Marathon 2 expedition
[AD-A189930] 15 p2099 N88-22507
Thermal conductivity, electrical conductivity and specific heat of copper-carbon fiber composite
[NASA-TT-20172] 16 p2172 N88-22948
Electrical dc conductivity of pitch
[AD-A191266] 16 p2182 N88-23008
Electrical anisotropy of layered semiconductor ZrSe2 16 p2257 N88-23488
Some aspects of the unified model of non-ideal high-parameter plasmas: Electron EOS and conduction coefficients 16 p2277 N88-23632
Optimisation of the thermoelectric figure of merit of modified silicon germanium alloys
[AD-A191347] 16 p2283 N88-23670
Electrical resistivity as quantum chaos
[DE88-007026] 16 p2284 N88-23675
Apparatus for the measurement of resistivity of glasses and ceramics 17 p2431 N88-24460
The precipitation processes of Cu-Zr-Cr alloys
[NASA-TT-20168] 18 p2488 N88-24758
On the reversion phenomena of Cu-3 percent Ti alloys
[NASA-TT-20170] 18 p2488 N88-24762
Size effects in the electrical resistivity of benzene-derived carbon fibers
[AD-A191708] 18 p2491 N88-24777
Raman characterization of AsF5-intercalated vapor grown graphite fibers
[AD-A191709] 18 p2491 N88-24778
Electrical conduction in thin film carbons
[AD-A191726] 18 p2491 N88-24780
On the abnormal phenomena observed in the electrical resistivity measurement during the decomposition process of saturated Cu-Fe alloys
[NASA-TT-20183] 18 p2507 N88-24869
Sulfur-tolerant anode materials
[DE88-001034] 18 p2537 N88-25054
Determination of doping profiles in silicon from resistivity measurements via the four-point probe in combination with layer strippings via anodic oxidation 18 p2583 N88-25347
Stress modeling of microdiaphragm pressure sensors 19 p2670 N88-25873
Surface acoustic wave gas sensor based on film conductivity changes 19 p2673 N88-25894
Theory on conductivity measurement technique for Langmuir probes in the stratosphere
[INPE-4514-PRE/1268] 19 p2692 N88-25999
Search for new high-temperature superconducting copper oxides
[DE88-009922] 19 p2735 N88-26245
Electrical resistivity of carbon-carbon composites
[AD-A193006] 20 p2768 N88-26410
Precipitation study by electrical resistivity measurement in Ni-Al alloys
[DE88-701877] 20 p2773 N88-26440
Visible tunable source
[DE88-006442] 20 p2854 N88-26944
Defect characterization of the redox behavior and stability of conducting oxides
[DE88-010799] 20 p2878 N88-27088
On the electrical properties of carbon/carbon composites densified by chemical deposit in vapor phase
[SNIAS-881-430-117] 21 p2907 N88-27252
Thermal cycling tests on surface-mount assemblies
[DE88-007695] 21 p2939 N88-27453
Conductivity mechanism and operating behavior of electrically conductive adhesives on the example of a power transistor
[ETN-88-92355] 21 p2940 N88-27464
Determination of quantum corrections for electrical conductivity mechanism of three dimensional, perturbed copper coatings. Weak localization and electron-electron interaction
[ETN-88-92378] 21 p2941 N88-27466
MIZPAC (marginal ice zone Pacific) 84-86 CTD (Conductivity, Temperature, Depth) data report
[AD-A192478] 21 p2976 N88-27679
A resistive-film based force transducer for the study of exercise
[AD-A192601] 21 p2986 N88-27730
High temperature electric arc furnace
[NASA-CASE-MFS-28281-1] 23 p3181 N88-28938
Polymeric electrolytes
[AD-A193766] 23 p3198 N88-29031
Soliton and polaron dynamics in conducting polymers
[DE88-702539] 23 p3198 N88-29035
The 1983 direct strike lightning data, part 1
[NASA-TM-86426-PT-1] 23 p3237 N88-29259
The 1983 direct strike lightning data, part 2
[NASA-TM-86426-PT-2] 23 p3237 N88-29260
The 1983 direct strike lightning data, part 3
[NASA-TM-86426-PT-3] 23 p3237 N88-29261

Thermostimulated conductivity in amorphous semiconductors with non-exponential density of localized states
[DE86-702737] 23 p3293 N88-29612
Electrical conductivity of GaAs layers implanted on semi-insulator nondoped substrates
[CERT-422000/RF] 23 p3294 N88-29614
Temperature dependence of conductivity and of Hall coefficients for noble metal films
[ETN-88-92981] 23 p3294 N88-29616

ELECTRICITY
NT ALTERNATING CURRENT
NT ATMOSPHERIC ELECTRICITY
NT AURORAL ELECTROJETS
NT EQUATORIAL ELECTROJET
NT GEOELECTRICITY
NT IONOSPHERIC CURRENTS
NT STATIC ELECTRICITY

Use of natural gas diesel engines in mechanical pulp production: A preliminary study
[DE87-753065] 02 p0181 N88-11129
Northern lights: The economic and practical potential of imported power from Canada
[DE86-006026] 15 p2093 N88-22473
A qualitative approach to electricity
[AD-A189854] 15 p2128 N88-22693
Inference and discovery in an exploratory laboratory
[AD-A192231] 20 p2832 N88-26801
Plasma technology: Preliminary studies 2
[DE88-752815] 22 p3154 N88-28763

ELECTRIFICATION
Utilization of LANDSAT-TM imagery in the hydroenergetic inventory of the Paraiba do Sul River Basin 17 p2364 N88-24077

ELECTRO-OPTICAL EFFECT
X-ray diffraction imaging (topography) of electrooptic crystals by synchrotron radiation
[NASA-CR-183266] 24 p3432 N88-30427

ELECTRO-OPTICAL PHOTOGRAPHY
Progress toward a crystal streak camera using tungsten bronze crystals for the electrooptic material
[DE87-013110] 03 p0323 N88-12044
PLZT (Lead-Lathanium-Zirconium-Titanium) electro-optic photographic system
[AD-A193473] 23 p3215 N88-29137

ELECTRO-OPTICAL SWITCHING
U OPTICAL SWITCHING

ELECTRO-OPTICS
Masking effects of fine and coarse grain pictorial noise
[IZF-1985-21] 01 p0076 N88-10485
An optoelectronic alignment telescope for straightness measurements
[ETN-87-90383] 01 p0093 N88-10609
Programmable 10 MHz optical fiducial system for hydrodiagnostic cameras
[DE87-013223] 02 p0175 N88-11091
Consortium for Materials Development in Space. Technical section
[NASA-CR-181508] 03 p0296 N88-11859
Highly Non-Linear Optical (NLO) organic crystals and films. Electrooptical organic materials 03 p0297 N88-11866
Limits to the precision of electro-optic and magneto-optic sensors
[PB87-212536] 03 p0323 N88-12040
A high-speed, eight-frame image intensified electro-optic camera with 200-800mm zoom objective capability
[DE88-000229] 03 p0326 N88-12059
Development of optical modulators for measurements of solar magnetic fields
[NASA-TM-100315] 04 p0490 N88-13016
Optoelectronic measurement methods for ballistic experiments
[PB87-110706] 05 p0583 N88-13554
Status, outlook of optical technology in information equipment field 06 p0689 N88-14222
Multilayer holographic functional element in analog-digital converter 07 p0921 N88-15593
Electro-optical studies of semiconductor compounds for electroluminescent and laser devices
[PH-155] 07 p0937 N88-15693
Fiber optics for controls 08 p0956 N88-15798
Gyrotron development at the Instituto de Pesquisas Espaciais
[INPE-4240-PRE/1115] 08 p0990 N88-15992
Management Information and Downloader Interface System (MIDIS)
[AD-A186978] 09 p1261 N88-17557
Optically controlled devices and ultrafast laser sources for signal processing
[AD-A187417] 10 p1338 N88-17995
Multidimensional system analysis of electro-optic sensors with sampled deterministic output
[AD-A187083] 10 p1408 N88-18399
An electro-optic explosive igniter
[DE88-004726] 11 p1466 N88-18738
Automated radar target recognition based on models of neural nets 11 p1476 N88-18804
AFGL (Air Force Geophysics Laboratory) fiscal year 1988 Air Force technical objectives document
[AD-A187701] 11 p1503 N88-18977
Polymeric materials for electro-optic testing
[AD-A188382] 12 p1610 N88-19627
A numerical analysis of the dynamics of PRIZ operation
[AD-A188853] 12 p1678 N88-20035
Nonlinear optical principles and the photorefractive effect applied to optical phase conjugation
[AD-A188856] 12 p1691 N88-20119
Summary and conclusions on electrooptical streak camera project
[DE88-006616] 15 p2069 N88-22334
Collective rotation of molecules driven by the angular momentum of light in a nematic film
[FUB-6-1986] 15 p2131 N88-22714
Gas source MBE (Molecular Beam Epitaxy)
[AD-A189783] 15 p2142 N88-22782
Research on materials and components for opto-electronic signal processing and computing
[AD-A190130] 15 p2143 N88-22788
Applications research studies of microtubules
[AD-A190855] 16 p2182 N88-23005
High-speed electron beam lithography devices discussed 16 p2185 N88-23023
Instrumentation for ultrafast electronics
[AD-A191379] 16 p2193 N88-23080
Fast Algorithm Simulation and Test (FAST) facility
[AD-A191183] 16 p2252 N88-23457
Fiber waveguide sensors for intelligent materials
[NASA-CR-183028] 17 p2343 N88-23968
Topological stereochemistry
[AD-A191867] 18 p2477 N88-24691
Silicon-sapphire waveguides
[AD-A191754] 18 p2504 N88-24854
Investigations in electro-optical multistability for signal processing 18 p2518 N88-24938
Structure and refinement of ordered aromatic heterocyclic polymers by diffraction methods: Application of results to electro-optic phenomena
[AD-A191859] 19 p2619 N88-25537
Organization of a Topical Meeting on Picosecond Electronics and Optoelectronics
[AD-A187136] 19 p2655 N88-25765
A non-contact picosecond prober for integrated circuit testing 19 p2655 N88-25766
Picosecond sampling of integrated circuits 19 p2655 N88-25767
Electro-optic sampling of high-speed, InP-based integrated circuits 19 p2655 N88-25769
Photoconductive generation of sub-picosecond electrical pulses and their measurement applications 19 p2656 N88-25778
Picosecond switching in Josephson tunnel junctions 19 p2657 N88-25780
Fast GaAs photoconductive detectors with high sensitivity integrated in coplanar systems onto GaAs substrates 19 p2658 N88-25790
Picosecond optoelectronic switches using composite electronic materials 19 p2658 N88-25792
A technique for wing suppressed IR sampling 19 p2658 N88-25794
Energy variations in optical pulses from gain-switched AlGaAs diode lasers 19 p2658 N88-25796
Picosecond optical autocorrelation experiments on fast photodetectors 19 p2659 N88-25802
High-speed phenomena in GaAs multiple-quantum-wells 19 p2660 N88-25812
Characteristics and application of wideband guided-wave devices 19 p2660 N88-25817
A new optoelectronic CW microwave source 19 p2660 N88-25818
Optical modulation above 20 GHz using a waveguide electrooptic switch 19 p2660 N88-25819
Picosecond response of an optically controlled millimeter wave phase shifter 19 p2660 N88-25820
Electron device probing in the femtosecond time scale 19 p2660 N88-25821
Picosecond optoelectronic study of a thin film transmission line structure 19 p2661 N88-25823
Integrated optoelectronic circuits utilizing InGaAsP grown by molecular beam epitaxy (erbium doping of MBE GaAs)
[AD-A192269] 20 p2795 N88-26584
The evaluation of a deformable diffraction grating for a stigmatic EUV spectroheliometer
[NASA-CR-183064] 20 p2853 N88-26941
Electro-optical studies of Al(x)Ga(1-x)As/GaAs coupled quantum wells 20 p2862 N88-26999
Novel quantum well optical devices 20 p2868 N88-27028
A concept for an electro-optic explosive device
[DE88-009696] 21 p2923 N88-27349
Picosecond optoelectronic sampling of electrical waveforms produced by an optically excited field effect transistor
[AD-A192384] 21 p2935 N88-27428
Solar cell modeling and simulation
[AD-A193249] 21 p2966 N88-27620
Molecular beam epitaxy of GaP films on Si substrates
[PB88-131974] 21 p3020 N88-27923
Strawman Optical Reception Development Antenna (SORDA) 22 p3065 N88-28187
A high frequency GaAlAs travelling wave electro-optic modulator at 0.82 micrometers
[NASA-TM-100970] 22 p3073 N88-28240
Recent advances in optical spectroscopy using high performance array detectors
[AD-A194219] 22 p3152 N88-28753
MIDIR (Mid-Infrared) laser, phase 1
[AD-A193935] 23 p3220 N88-29166
Photorefractive damage mechanism in electro-optic materials
[AD-A194560] 23 p3282 N88-29543
Quasi-liquid crystalline materials with special electro-optic properties
[AD-A194579] 23 p3282 N88-29544
Center for opto-electronic systems research instrumentation grant
[AD-A193711] 23 p3282 N88-29545
Studies on strained (In,Ga)As/GaAs semiconductors and optical devices 23 p3287 N88-29575
Research on crystal and film ferroelectric materials for optoelectronic applications
[AD-A193512] 23 p3291 N88-29597
Electronic and optical devices and applications 24 p3363 N88-30027
Mode locking of semiconductor laser with external cavity
[AD-A196018] 24 p3378 N88-30117
Report on an overseas visit to USA relating to the thermoelastic measurement of stresses, 16-21 August 1987
[AD-A195313] 24 p3385 N88-30161
A fiber optic beamforming processor for wideband direction finding
[AD-A194862] 24 p3428 N88-30404
Center for opto-electronic systems research
[AD-A195159] 24 p3429 N88-30411
Ultra-wideband direction finding using a fiber optic beamforming processor
[AD-A194861] 24 p3430 N88-30413
Common modules: A success story
[AD-A195937] 24 p3430 N88-30415
Power MISFETs on OnP
[AD-A195242] 24 p3433 N88-30436

ELECTROACOUSTIC TRANSDUCERS
NT HYDROPHONES
NT MICROPHONES

Noncontact temperature measurements of hot steel bodies using an electromagnetic acoustic transducer (EMAT)
[DE88-000560] 04 p0446 N88-12765

ELECTROCARDIOGRAMS
U ELECTROCARDIOGRAPHY

ELECTROCARDIOGRAPHY
Vital signs rate meter
[AD-A187015] 09 p1198 N88-17183
Results of long-term electrocardiographic monitoring of cosmonauts 10 p1364 N88-18152

ELECTROCATALYSTS
Metal containing polymers as fuel cell catalysts
[AD-A184605] 03 p0347 N88-12194
Internal reforming development for solid oxide fuel cells
[DE87-006518] 04 p0464 N88-12871
Electrochemical hydrogen concentrator for phosphoric acid fuel cells
[AD-A191355] 16 p2229 N88-23317
Compact regenerable sulfur scrubber for phosphoric acid fuel cells
[AD-A191356] 16 p2230 N88-23318
In situ spectroscopic studies of transition metal macrocycles as catalysts for the electrochemical reduction of oxygen
[PB88-203195] 20 p2769 N88-26416
Electrocatalysts for oxygen electrodes
[DE88-008397] 20 p2819 N88-26724
Electrocatalytic reduction of oxygen on modified oxide surfaces
[NASA-TM-101333] 24 p3352 N88-29952

ELECTROCHEMICAL CELLS
NT ALKALINE BATTERIES
NT ELECTRIC BATTERIES
NT FUEL CELLS
NT HYDROGEN OXYGEN FUEL CELLS
NT LEAD ACID BATTERIES

NT LITHIUM SULFUR BATTERIES
NT METAL AIR BATTERIES
NT NICKEL CADMIUM BATTERIES
NT NICKEL HYDROGEN BATTERIES
NT NICKEL IRON BATTERIES
NT NICKEL ZINC BATTERIES
NT PHOSPHORIC ACID FUEL CELLS
NT PRIMARY BATTERIES
NT REDOX CELLS
NT REGENERATIVE FUEL CELLS
NT SODIUM SULFUR BATTERIES
NT STORAGE BATTERIES
NT THERMAL BATTERIES
NT ZINC-BROMIDE BATTERIES
NT ZINC-OXYGEN BATTERIES
Effect of NASA advanced designs on thermal behavior of Ni-H2 cells
[NASA-TM-100197] 01 p0021 N88-10132
New materials for electrochemical cells
[AD-A183659] 01 p0037 N88-10238
Zinc-redox battery: A technology update
[DE87-010737] 01 p0040 N88-10256
The 250AH/90A active lithium-thionyl chloride cell for Centaur-G application 02 p0163 N88-11023
ECC (Electrochemical Concentration Cell) ozonesonde observations at South Pole, Antarctica during 1986
[PB87-207502] 02 p0197 N88-11228
Reliability of Li/SO2 cells for long-life applications
[DE88-001360] 04 p0440 N88-12735
Technology Base Research Project for electrochemical energy storage
[DE88-000649] 04 p0464 N88-12868
Re-usable thin-layer spectroelectrochemical cell for non-aqueous solvent systems
[AD-A186951] 09 p1248 N88-17478
Electrochemical hydrogen concentrator for phosphoric acid fuel cells
[AD-A191355] 16 p2229 N88-23317
Thermal and power availability transient responses for the Argonne monolithic solid oxide fuel cell 17 p2419 N88-24384
Optimization of reserve lithium thionyl chloride battery electrochemical design parameters
[DE88-007109] 18 p2506 N88-24868
Photovoltaic cells with n-silicon and conductive polymers
[ETN-88-92133] 20 p2821 N88-26734
Preparation and development of advanced battery catalysts
[AD-A193208] 21 p2937 N88-27441
The overcharge behavior of polymer electrolyte cells
[AD-A193984] 22 p3117 N88-28522

ELECTROCHEMICAL CORROSION
Modelling of crack-tip deformation and transient electrochemical processes in relation to corrosion fatigue of steels cathodically protected in marine environments
[NPL-DMA(A)-145] 01 p0059 N88-10379
Crevice corrosion of stainless steels and related alloys. Part 2: Summary of experimental test data for input to mathematical model
[BR99871-PT-2] 03 p0289 N88-11816
Corrosion behavior of P/M mechanically alloyed IN-9052.1: An electro-chemical investigation
[AD-A184191] 04 p0414 N88-12567
Corrosion behavior of high density tungsten alloys
[AD-A187108] 09 p1143 N88-16852
Corrosion performance of high damping alloys in 3.5 percent sodium chloride environment
[AD-A188048] 11 p1457 N88-18687
Corrosion-wear process under rolling-sliding motion
[AD-A189603] 13 p1778 N88-20635
Corrosion and electrochemical behavior of binary magnesium alloys
[AD-A190624] 15 p2040 N88-22154
Galvanic corrosion initiatives
[AD-A190658] 15 p2040 N88-22155
High temperature oxidation and electrochemical studies related to hot corrosion
[AD-A190699] 15 p2040 N88-22156
Corrosion Research Center, University of Minnesota
[DE88-006681] 15 p2041 N88-22160
Corrosion and corrosion inhibition of metals/alloys in methyphosphonic difluoride 17 p2319 N88-23850
Preventing aircraft corrosion by predictive corrosion modeling 17 p2321 N88-23863
AC impedance analysis of corrosion fatigue in naval aircraft alloys
[AD-A190822] 17 p2322 N88-23865
The influence of cathodic protection on erosion-corrosion of metals and model alloys
[AD-A191613] 18 p2485 N88-24742
Effect of double layer structure on the determination of corrosion rates from polarization measurements
[DE88-010097] 20 p2774 N88-26448
Corrosion of aluminium alloys by IRFNA
[AD-A194319] 22 p3055 N88-28127
Laser and electrochemical studies of metallizations in electronic devices
[AD-A193786] 23 p3208 N88-29090
Multi-metallic galvanic corrosion
[AD-A195995] 24 p3353 N88-29963

ELECTROCHEMICAL OXIDATION
The photophysics and chemistry of PAH (Polycyclic Aromatic Hydrocarbons) compounds
[DE87-014455] 02 p0153 N88-10954
Reduction of CO2 to methanol and methane by photo and dark reactions on semiconductor and metal electrodes
[PB87-226825] 02 p0156 N88-10975
Voltammetric investigation of porous silicon for integrated circuit applications
[DE87-009287] 02 p0166 N88-11042
Submerged arc flux welding with CaF2-CaO-SiO2 fluxes: Possible electrochemical effects on weld metal
[DE88-003107] 08 p0992 N88-16004
Electrosorptive detection based on double-layer capacitance for selective anion monitoring in ion chromatography. Part 1: Mercury electrodes
[AD-A188780] 12 p1606 N88-19603
Characterization of redox states of nickel hydroxide film electrodes by in-situ Raman spectroscopy
[AD-A189288] 13 p1741 N88-20411
High temperature oxidation and electrochemical studies related to hot corrosion
[AD-A190699] 15 p2040 N88-22156
Electrochemical hydrogen concentrator for phosphoric acid fuel cells
[AD-A191355] 16 p2229 N88-23317
AC impedance analysis of corrosion fatigue in naval aircraft alloys
[AD-A190822] 17 p2322 N88-23865
Electrochemistry in near-critical and supercritical fluids. 6: The electrochemistry of ferrocene and phenazine in acetonitrile between 25C and 300C
[AD-A192171] 18 p2482 N88-24723
Studies in support of oxidation-resistant composite materials
[AD-A193320] 21 p2905 N88-27238

ELECTROCHEMISTRY
NT ELECTROLYSIS
NT PHOTOELECTROCHEMISTRY
De-alloying
[DE87-012488] 01 p0022 N88-10139
Evaluation of LiCl- LiBr- KBr electrolyte for Li- alloy/metal disulfide cells
[DE87-011356] 01 p0041 N88-10258
Overcharge protection in Li-alloy/metal disulfide cells
[DE87-011364] 01 p0041 N88-10260
The corrosion of iron rotating hemispheres in 1 M sulfuric acid: An electrochemical impedance study
[DE87-014679] 02 p0148 N88-10925
The 1986 Goddard Space Flight Center Battery Workshop
[NASA-CP-2486] 02 p0163 N88-11021
Computer simulation of thermal modeling of primary lithium cells 02 p0163 N88-11022
Fault tree safety analysis of a large Li/SOCl(sub)2 spacecraft battery 02 p0163 N88-11025
Chemical analysis of charged Li/SO(sub)2 cells 02 p0163 N88-11026
Advances in nickel hydrogen technology at Yardney Battery Division 02 p0164 N88-11029
Photocatalytic electrochemistry at a biological-membrane metal-colloid interface
[DE87-009122] 02 p0166 N88-11041
Stress corrosion cracking of high-strength steels in aqueous environments 03 p0289 N88-11818
Thin films for geothermal sensing
[DE88-000154] 03 p0326 N88-12061
Metal containing polymers as fuel cell catalysts
[AD-A184605] 03 p0347 N88-12194
Metal intercalation characteristics of n-HfS2 photoelectrodes in non-aqueous electrolytes
[AD-A184381] 03 p0383 N88-12407
Advances in inherently conducting polymers
[DE88-000501] 04 p0421 N88-12610
Chemically modified microelectrode arrays. New kinds of electronic devices
[AD-A184389] 04 p0439 N88-12724
The effect of ion implantation on the corrosion behavior of a high-density sintered tungsten alloy
[AD-A185713] 06 p0683 N88-14185
Conductivity studies on hydroxide ion conductors in the Li-Al-O-H system at intermediate temperatures
[AD-A185714] 06 p0697 N88-14279
Phase behavior in the Li-Al-O-H system at intermediate temperatures
[AD-A185732] 06 p0697 N88-14280
Electrochemical characteristics of acid electrolytes for fuel cells
[PB88-104641] 06 p0731 N88-14497
Fundamental studies of surfaces processes and trace analysis using solid electrodes
[AD-A186156] 07 p0828 N88-15024
Surface chemistry of chemically sensitive field effect transistors
[AD-A185917] 07 p0847 N88-15139
The dc conductivity studies of an hydroxide ion conductor at intermediate temperatures
[AD-A186044] 07 p0847 N88-15142
Electrochemical processing of solid waste
[NASA-CR-182413] 08 p0967 N88-15852
Electroformation: Principle electrochemical process of electrodeposition and electroformation of copper
[INPE-4374-NTE/274] 08 p0969 N88-15863
Electrochemical carbon dioxide concentrator subsystem development
[NASA-CR-177411] 08 p1053 N88-16353
Factors governing light driven electron and proton translocation in proteins across membranes
[DE88-002716] 08 p1082 N88-16519
Re-usable thin-layer spectroelectrochemical cell for non-aqueous solvent systems
[AD-A186951] 09 p1248 N88-17478
Electrochemical growth of linear conducting crystals in microgravity 10 p1287 N88-17698
Studies in finite time thermodynamics
[DE88-004531] 10 p1423 N88-18500
Electronic and ionic transport in polymers
[AD-A187253] 11 p1452 N88-18651
Electrochemical and optical investigations on ion-implanted TiO2 samples
[ETN-88-91485] 11 p1455 N88-18670
Voltammetric investigation of porous silicon for integrated circuit applications
[DE88-004024] 11 p1456 N88-18677
Solar-assisted hydrogen generation by photoelectrocatalysis
[PB88-160932] 12 p1605 N88-19597
Some applications of surface Raman and infrared spectroscopies to mechanistic electrochemistry involved adsorbed species
[AD-A188777] 12 p1606 N88-19602
An electrochemical and spectroscopic study of electrode systems
[AD-A189274] 13 p1737 N88-20384
A fundamental understanding of the effect of alloying elements on the corrosion resistance of rapidly solidified Mg alloys
[AD-A189385] 13 p1741 N88-20413
Thermionic Technology Program. A: Insulator test and evaluation
[DE88-004707] 13 p1795 N88-20735
Solid-state electrochemical processes in dye films
[AD-A188756] 13 p1844 N88-21036
Electronic and ionic transport in polymers
[AD-A190434] 15 p2045 N88-22185
Electrochemistry in near-critical and supercritical fluids. 5: The dimerization of quinoline and acridine radical anions and dianions in ammonia from -70 C to 150 C
[AD-A190858] 16 p2175 N88-22967
Water tunnel measurements by an electrochemical method 16 p2203 N88-23146
North Carolina Biomolecular Engineering and Materials Applications Center (NC-BEMAC)
[AD-A190923] 16 p2237 N88-23364
Agenda for advancing electrochemical science and technology 17 p2321 N88-23861
Electrochemistry in liquid crystals
[AD-A191554] 18 p2481 N88-24719
Electrochemistry in near-critical and supercritical fluids. 6: The electrochemistry of ferrocene and phenazine in acetonitrile between 25C and 300C
[AD-A192171] 18 p2482 N88-24723
In situ spectroscopic studies of transition metal macrocycles as catalysts for the electrochemical reduction of oxygen
[PB88-203195] 20 p2769 N88-26416
A simulation analysis of errors in the measurement of standard electrochemical rate constants from phase-selective impedance data
[AD-A192739] 20 p2770 N88-26426
The influence of uncompensated solution resistance on the determination and standard electrochemical rate constants using cyclic voltammetry and some comparisons with AC voltammetry
[AD-A192825] 20 p2770 N88-26427
High power pulse energy system concept
[AD-A192440] 21 p2935 N88-27429
Corrosion fatigue of small cracks: Mechanics and chemistry
[DE88-012121] 21 p2964 N88-27605
Advanced EMU electrochemically regenerable CO2 and moisture absorber module breadboard
[NASA-CR-172054] 21 p2993 N88-27754

A rapid electrochemical technique for determining the current efficiency for cadmium plating
[AD-A193679] 22 p3056 N88-28130
Advanced calcium-thionyl chloride high-power battery
[AD-A194401] 22 p3072 N88-28238
Studies of photochemically and electrochemically driven electron transport in zeolites
[DE88-008644] 22 p3155 N88-28769
Phenomena of the ionic transport in the stress corrosion of metals
[DE88-702502] 23 p3195 N88-29013
Polymeric electrolytes
[AD-A193766] 23 p3198 N88-29031
Electrochemical and optical studies of model photosynthetic systems
[DE88-009291] 23 p3237 N88-29264
Potential induced structural transformations of the Au(100) and Au(111) surfaces
[DE88-005446] 23 p3287 N88-29571
An electrochemical impedance spectroscopy study of reactions at the metal/coating interface
24 p3355 N88-29975
Evaluation of organic coating deterioration and substrate corrosion in seawater using electrochemical impedance measurements 24 p3355 N88-29976
Cytochrome electron transfer and biomolecular electronics
[AD-A195482] 24 p3406 N88-30277

ELECTROCHROMISM
Electrochromic thin films
[DE88-751099] 11 p1550 N88-19334
The structure and properties of RF reactive sputtered IrO2 films 19 p2672 N88-25884

ELECTROCONDUCTIVITY
U ELECTRICAL RESISTIVITY

ELECTRODE MATERIALS
Interfacial effects in thin Li/PEO cells at room temperature
[AD-A186974] 09 p1157 N88-16931
Re-usable thin-layer spectroelectrochemical cell for non-aqueous solvent systems
[AD-A186951] 09 p1248 N88-17478

ELECTRODEPOSITION
NT ELECTROPLATING
Surface coatings and catalyst production by electrodeposition 03 p0297 N88-11863
Mass transport by diffusion 03 p0297 N88-11864
Studies on high-speed electroforming
[DE88-001395] 04 p0429 N88-12656
Effectiveness of electrodeposited coatings in reducing atmospheric corrosion of copper substrates
[DE87-013651] 05 p0566 N88-13448
Electroformation: Principle electrochemical process of electrodeposition and electroformation of copper
[INPE-4374-NTE/274] 08 p0969 N88-15863
Materials processing in space: An introduction to the G-480 payload 10 p1287 N88-17695
Ion chromatography in the manufacture of multilayer circuit boards
[DE88-002428] 10 p1322 N88-17902
Investigation of materials for inert electrodes in aluminum electrodeposition cells
[DE88-003380] 10 p1323 N88-17906
Corrosion resistance of electrodeposited amorphous Ni-Cr-P alloys
[DE88-005116] 11 p1459 N88-18695
Institute for Materials Science and Engineering, Metallurgy: Technical activities 1987
[PB88-157722] 11 p1460 N88-18702
Technology base research on zinc/air battery systems
[DE88-004893] 13 p1763 N88-20546
Electrodeposition of amorphous Ni-Cr-P alloys
[DE88-006866] 19 p2616 N88-25521

ELECTRODES
NT ANODES
NT CATHODES
NT CELL ANODES
NT CELL CATHODES
NT DIFFUSION ELECTRODES
NT HOLLOW CATHODES
NT ION SELECTIVE ELECTRODES
NT PHOTOCATHODES
NT PLASMA ELECTRODES
NT SOLID ELECTRODES
NT THERMIONIC CATHODES
NT TUBE CATHODES
Overcharge protection in Li-alloy/metal disulfide cells
[DE87-011364] 01 p0041 N88-10260
The corrosion of iron rotating hemispheres in 1 M sulfuric acid: An electrochemical impedance study
[DE87-014679] 02 p0148 N88-10925
Reduction of CO2 to methanol and methane by photo and dark reactions on semiconductor and metal electrodes
[PB87-226825] 02 p0156 N88-10975
Surface topography and electrical response of metal-electrolyte interface
[DE87-013553] 02 p0166 N88-11046
Performance of high power S-band klystrons focused with permanent magnet
[DE87-753024] 02 p0167 N88-11053
DSA RuO2/TiO2 electrode modeled by ion implantation: An in situ characterization by photoacoustic and photocurrent spectroscopy
[DE87-009129] 02 p0245 N88-11545
Post-test analyses of aqueous batteries developed for electric propulsion
[DE88-000655] 03 p0311 N88-11965
Effects of pressure fluctuations on nickel electrodes
[AD-A184293] 03 p0311 N88-11967
Metal intercalation characteristics of n-HfS2 photoelectrodes in non-aqueous electrolytes
[AD-A184381] 03 p0383 N88-12407
Chemically modified microelectrode arrays. New kinds of electronic devices
[AD-A184389] 04 p0439 N88-12724
Far-infrared spectra of lithium deposited on a gold electrode: Interpretation using a cluster model
[AD-A184231] 04 p0495 N88-13050
An electric field meter based upon a new principle: A dummy displacement electrode. Application to aerospace vehicles
[SNIAS-872-422-106] 05 p0585 N88-13567
Behavior and structure of metal vapor arc plasma between molten electrodes
[DE88-001854] 06 p0782 N88-14801
Performance of a small, graphite electrode, multistage depressed collector with a 500-W, continuous wave, 4.8- to 9.6-GHz traveling wave tube
[NASA-TP-2788] 07 p0848 N88-15146
Research and development of advanced lead-acid batteries for electric vehicle propulsion
[DE87-014661] 07 p0873 N88-15297
High temperature solar electrothermal processing-3. Zinc from zinc oxide at 1200-1675K using a non-consumable anode
[AD-A186600] 09 p1141 N88-16836
The 5-GHz operation of the ITT and RCA streak tubes with a 7.5-ns time window
[DE88-003342] 09 p1169 N88-17008
Materials development for JPL oxygen plant
[DE88-003067] 10 p1297 N88-17752
Magnetic control of low pressure discharges
[AD-A186794] 10 p1322 N88-17900
Investigation of materials for inert electrodes in aluminum electrodeposition cells
[DE88-003380] 10 p1323 N88-17906
Determination of optimum electrolyte composition for molten carbonate fuel cells literature review
[DE88-001015] 10 p1348 N88-18058
Reactions of some thiol collectors at noble-metal and pyrite electrodes
[PB88-138318] 11 p1455 N88-18674
Photochemical energy storage: Studies of inorganic photoassistance agents
[DE88-002596] 11 p1508 N88-19010
In-situ vibrational spectroscopy of specifically adsorbed azide on silver electrodes
[AD-A188511] 12 p1605 N88-19600
Electrosorptive detection based on double-layer capacitance for selective anion monitoring in ion chromatography. Part 1: Mercury electrodes
[AD-A188780] 12 p1606 N88-19603
An electrochemical and spectroscopic study of electrode systems
[AD-A189274] 13 p1737 N88-20384
Aluminum-air battery development
[DE88-006618] 13 p1762 N88-20543
Electron emission from conductors subjected to intense, short-pulse electric fields
[DE88-005412] 13 p1836 N88-20985
Application of copper-carbon fiber composites to power semiconductor devices
[NASA-TT-20171] 15 p2031 N88-22101
Growth and deformation mechanisms of refractory alloy hybrid materials
[AD-A190492] 15 p2039 N88-22152
Evaporation characteristics of elements during vacuum arc remelting of alloy A-286 15 p2055 N88-22248
Laser induced ignition of propellants
[AD-A191100] 16 p2168 N88-22927
Effects of cadmium electrode properties on nickel-cadmium cell performance
[AD-A191394] 16 p2193 N88-23081
Nickel hydroxide active material densities
[AD-A191411] 16 p2230 N88-23319
AMTEC electrode development
17 p2409 N88-24324
High power density electrodes for AMTEC
17 p2437 N88-24501
Electrochemistry in liquid crystals
[AD-A191554] 18 p2481 N88-24719
Optical investigations of the thermal boundary layer in arc plasmas 18 p2578 N88-25313
Electrode films of porous agarose: The effects of physical structure on electron transport processes
[DE88-007366] 19 p2611 N88-25493
Employment of porous polytetrafluoroethylene Membrane with a hydrophilic and hydrophobic stratal structure for construction of an enzyme electrode
[NASA-TT-20296] 19 p2620 N88-25543
Performance of lightweight nickel electrodes
[NASA-TM-100958] 20 p2771 N88-26430
Nickel hydrogen cell positive-electrode studies: Cobalt segregation in reducing environments
[AD-A193025] 20 p2796 N88-26587
Electrocatalysts for oxygen electrodes
[DE88-008397] 20 p2819 N88-26724
A critical review of IR drops and electrode potentials within pits, crevices and cracks
[AD-A192481] 21 p2935 N88-27431
The kinetics of charge-transfer reactions on passive lithium electrodes
[DE88-009256] 21 p2939 N88-27454
Metal-air battery assessment
[DE88-011361] 21 p2940 N88-27459
Post-test observations on CSPL (Chloride Silent Power Limited) cells
[DE88-011975] 21 p2940 N88-27461
Monolithic fuel cells
[DE88-012004] 21 p2969 N88-27638
Corrosion of aluminium alloys by IRFNA
[AD-A194319] 22 p3055 N88-28127
Liquid metal thermal-electric converter electrode development
[DE88-009252] 23 p3230 N88-29221
An electrochemical impedance spectroscopy study of reactions at the metal/coating interface
24 p3355 N88-29975

ELECTRODYNAMICS
NT ELECTROHYDRODYNAMICS
NT ELECTROMECHANICS
NT QUANTUM ELECTRODYNAMICS
Continuous flow electrophoresis system experiments on shuttle flights STS-6 and STS-7
[NASA-TP-2778] 02 p0156 N88-10978
Electrodynamic tether system study
[NASA-CR-172024] 03 p0275 N88-11737
Hollow cathode plasma coupling study, 1986
[NASA-CR-171985] 03 p0309 N88-11949
Theoretical analysis of the electrical aspects of the basic electro-impulse problem in aircraft de-icing applications
[NASA-CR-180845] 05 p0543 N88-13310
Colloidal stability of oxidized silicon particles in ethanolic and aqueous media
[DE87-014783] 05 p0562 N88-13421
Tethers in space handbook
[NASA-CR-181371] 06 p0673 N88-14123
Performance-limiting factors in MPD thrusters
[AD-A185605] 06 p0674 N88-14126
Power and charge dissipation from an electrodynamic tether 06 p0795 N88-14869
New techniques for rocket and balloon-borne instrumentation for investigations of the structure, dynamics and electrodynamics of the middle atmosphere 08 p1027 N88-16220
Electrodynamics of the high latitude middle atmosphere 08 p1028 N88-16225
Polar cusp electrodynamics 08 p1030 N88-16242
Processes in the quiet and disturbed equatorial-low latitude ionosphere: Sundial campaign, 1984
[INPE-4152-PRE/1057] 08 p1036 N88-16282
Plasma contactors for use with electodynamic tethers for power generation
[NASA-CR-182424] 08 p1087 N88-16547
Comparative evaluation of resistive and inductive techniques for measuring temperature of superconducting transition
[DE88-700603] 10 p1417 N88-18457
Phase transitions in two-dimensional superconducting arrays in a transverse magnetic field
[INPE-4457-RPE/559] 12 p1697 N88-20157
Theoretical investigation of EM wave generation and radiation in the ULF, ELF and VLF bands by the electrodynamic orbiting tether
[NASA-CR-182720] 13 p1760 N88-20529
Chronometrically invariant formulation of electrodynamics equation
[DE88-701030] 13 p1849 N88-21071
Galilei relativity principle in classical electrodynamics
[DE87-703203] 14 p1904 N88-21376
A general 2D electrical model for diagonally connected MHD generators
[DE88-004283] 14 p1984 N88-21835
Dynamics of charged submicron grains in Halley's coma 14 p2001 N88-21931

Space plasma contactor research, 1987
[NASA-CR-182148] 16 p2280 N88-23649
Electrodynamic driver for the space thermoacoustic refrigerator (STAR)
[AD-A192337] 20 p2785 N88-26517
Snapshots of high-latitude electrodynamics using Viking and DMSP/F7 observations
[TRITA-EPP-88-01] 23 p3234 N88-29244
Neutrino electrodynamics and possible effects for solar neutrinos
[DE88-701647] 23 p3308 N88-29705

ELECTRODYNAMOMETERS
U DYNAMOMETERS

ELECTROENCEPHALOGRAM
U ELECTROENCEPHALOGRAPHY

ELECTROENCEPHALOGRAPHY
Change in functional activity of cortical brain structures and their blood supply in alert rabbits in response to rocking 04 p0473 N88-12916
Dimensional analysis of nonlinear oscillations in brain, heart and muscle
[DE87-014749] 06 p0751 N88-14614
Measurement and modification of sensorimotor system function during visual-motor performance
[AD-A186351] 07 p0889 N88-15387
An innovative workstation 08 p1063 N88-16421
Development and experimentation of an eye/brain/task testbed 09 p1205 N88-17219
The linear dependency structure of covariance nonstationary time series
[AD-A186548] 09 p1232 N88-17383
Realistic conductivity geometry model of the human head for interpretation of neuromagnetic data
[PB88-112230] 10 p1369 N88-18179
Electromagnetic metrics of mental workload
[AD-A188205] 11 p1523 N88-19093
Brain activity during tactical decision-making. Part 2: Probe-evoked potentials and workload
[AD-A188688] 12 p1667 N88-19994
Neurocognitive predictions of performance
[AD-A186323] 12 p1669 N88-19998
Retinotopic mapping of the human visual system with magnetoencephalography
[AD-A189557] 13 p1810 N88-20811
Identification of visual evoked response parameters sensitive to pilot mental state
[NASA-CR-4140] 13 p1811 N88-20822
Steady-state evoked potentials possibilities for mental-state estimation 16 p2240 N88-23380
Electroencephalographic changes during equilibrium test in the presence of rhythmic photic interference 19 p2703 N88-26075
Effect of different modes of voluntary control of breathing on human electroencephalogram with exposure to acute hypoxic hypoxia 19 p2707 N88-26093
Physiological monitoring methodology in the USAFSAM centrifuge 21 p2924 N88-27356
Normative developmental equations for the EEG and their sensitivity to neurological and psychiatric disorders 21 p2977 N88-27687
The application of non-stationary data analysis techniques in the identification of changes in the electroencephalogram associated with the onset of drowsiness 21 p2978 N88-27688
A statistical procedure for the evaluation of presence/non-presence of stimulus-related EEG activity 21 p2978 N88-27689
The effect of endogenous alpha on hemispheric asymmetries and the relationship of frontal theta to sustained attention 21 p2980 N88-27701
Evoked potential analysis of impact acceleration experiments 21 p2981 N88-27708
EEG indices of G-induced Loss Of Consciousness (G-LOC) 21 p2982 N88-27709
Electroencephalographic correlates of pilot performance: Simulation and in-flight studies 21 p2982 N88-27711
Measurement of electrical activity in the CNS with cortical evoked potentials and EEG: Efficacy profiles of drugs using factor analysis 21 p2983 N88-27715
An approach to studying the effects of psychostimulants on cerebral electrical activity in the non-human primate 21 p2983 N88-27716
Correlation between EEG abnormal activity and aircraft accidents: A long term observation 21 p2984 N88-27719
Detection of latent epilepsy in aircrew candidates 21 p2984 N88-27720
New method for the study of spontaneous brain activity
[AD-A193813] 22 p3132 N88-28624
Methods and instrumentation for biomagnetism
[AD-A193811] 23 p3239 N88-29278

ELECTROEROSION
U SPARK MACHINING

ELECTROEXPLOSIVE DEVICES
U INITIATORS (EXPLOSIVES)

ELECTROFORMING
Studies on high-speed electroforming
[DE88-001395] 04 p0429 N88-12656
Electroformation: Principle electrochemical process of electrodeposition and electroformation of copper
[INPE-4374-NTE/274] 08 p0969 N88-15863
Copper electroforming from acid sulfate baths: Preliminary studies
[INPE-4375-RPE/554] 08 p0969 N88-15864

ELECTROGENERATORS
U ELECTRIC GENERATORS

ELECTROHYDRAULIC CONTROL
U ELECTRIC CONTROL
U HYDRAULIC CONTROL

ELECTROHYDRODYNAMICS
Preparative electrophoresis for space
[NASA-TP-2777] 02 p0156 N88-10977
Instantaneous pictures of the high-latitude electrodynamics using Viking and DMSP/F7 observations --- Swedish satellite 08 p1025 N88-16209
Electrohydrodynamic migration of charged droplets in an insulating fluid
[NASA-TM-100849] 14 p1912 N88-21424

ELECTROJETS
NT AURORAL ELECTROJETS
NT EQUATORIAL ELECTROJET

ELECTROKINETICS
Preparative electrophoresis for space
[NASA-TP-2777] 02 p0156 N88-10977
Mathematical models of continuous flow electrophoresis: Electrophoresis technology
[NASA-CR-179241] 07 p0828 N88-15021
The electrokinetic behavior of calcium oxalate monohydrate in macromolecular solutions
[NASA-TM-101144] 18 p2493 N88-24791

ELECTROLESS DEPOSITION
Acoustic wave electroless deposition monitor
[DE88-004023] 11 p1489 N88-18887
Corrosion of electroless nickel-coated steel
[AD-A191045] 16 p2179 N88-22985

ELECTROLUMINESCENCE
Electro-optical studies of semiconductor compounds for electroluminescent and laser devices
[PH-155] 07 p0937 N88-15693
Study for the determination of general and specific properties of wide energy-band gap HgCdTe in the 1 to 2 micrometer wavelength range
[AD-A191091] 17 p2334 N88-23934

ELECTROLUMINESCENT LAMPS
U ELECTROLUMINESCENCE
U LUMINAIRES

ELECTROLYSIS
Phase purity of NiCo2O4, a catalyst candidate for electrolysis of water
[NASA-TM-100239] 05 p0556 N88-13385
DC conductivity studies in Li5AlO4 at intermediate temperatures and its possible application for the electrolysis of water
[AD-A185489] 06 p0697 N88-14276
Electrochemical processing of solid waste
[NASA-CR-182413] 08 p0967 N88-15852
Cavitation inception
[AD-A189220] 13 p1765 N88-20557

ELECTROLYTE METABOLISM
Biorhythmic aspects of intercontinental Antarctic adaptation 08 p1046 N88-16321
Fluid volume changes in astronauts: How they fit our understanding of physiology 12 p1655 N88-19919
The influence of space flight on water-salt homeostasis in man and animals 12 p1659 N88-19943
Physiology of prolonged bed rest
[NASA-TM-101010] 22 p3130 N88-28607

ELECTROLYTES
NT ION EXCHANGE MEMBRANE ELECTROLYTES
NT MOLTEN SALT ELECTROLYTES
NT NONAQUEOUS ELECTROLYTES
NT SOLID ELECTROLYTES
Adhesion properties of polyelectrolyte-chemisorbed zinc phosphate conversion coatings
[DE87-012489] 01 p0029 N88-10186
Evaluation of LiCl- LiBr- KBr electrolyte for Li- alloy/metal disulfide cells
[DE87-011356] 01 p0041 N88-10258
Overcharge protection in Li-alloy/metal disulfide cells
[DE87-011364] 01 p0041 N88-10260
Synthesis of novel acid electrolytes for phosphoric acid fuel cells
[PB87-221305] 01 p0066 N88-10426
Surface topography and electrical response of metal-electrolyte interface
[DE87-013553] 02 p0166 N88-11046
Ion-matrix coupling in polymer electrolytes from relaxation time studies
[AD-A184632] 03 p0293 N88-11841
Metal intercalation characteristics of n-HfS2 photoelectrodes in non-aqueous electrolytes
[AD-A184381] 03 p0383 N88-12407
Applications of multivalent ionic conductors to polymeric electrolyte batteries
[AD-A184252] 04 p0439 N88-12722
Colloidal stability of oxidized silicon particles in ethanolic and aqueous media
[DE87-014783] 05 p0562 N88-13421
Analysis of nickel sulphamate bath using charging current compensated D.C. polarography
[NAL-TM-MT-8705] 05 p0564 N88-13433
Ionic transport and electrical relaxation in glass
[DE88-000887] 05 p0657 N88-14028
Geochemistry of freezing brines, low-temperature properties of sodium chloride
[AD-A185751] 06 p0680 N88-14168
Conductivity studies on hydroxide ion conductors in the Li-Al-O-H system at intermediate temperatures
[AD-A185714] 06 p0697 N88-14279
Hydroxide ion conductors as possible electrolytes in intermediate temperature fuel cells
[AD-A185508] 06 p0731 N88-14495
Electrochemical characteristics of acid electrolytes for fuel cells
[PB88-104641] 06 p0731 N88-14497
The dc conductivity studies of an hydroxide ion conductor at intermediate temperatures
[AD-A186044] 07 p0847 N88-15142
Excess thermodynamic properties of aqueous electrolytes to high temperatures and pressures
[DE88-001768] 07 p0940 N88-15712
High temperature solar electrothermal processing-3. Zinc from zinc oxide at 1200-1675K using a non-consumable anode
[AD-A186600] 09 p1141 N88-16836
Some investigations of electrical discharges at the surfaces of solid cathodes immersed in aqueous electrolyte solutions
[PB87-168209] 09 p1159 N88-16946
Materials development for JPL oxygen plant
[DE88-003067] 10 p1297 N88-17752
Models for ionic transport in glass
[DE88-002860] 10 p1304 N88-17799
Electrochromic cells with lutetium diphthalocyanine and semisolid polymer electrolytes
[AD-A188031] 10 p1352 N88-18078
In-situ vibrational spectroscopy of specifically adsorbed azide on silver electrodes
[AD-A188511] 12 p1605 N88-19600
Human adaptation to various hypercapnic conditions in relation to salivary electrolyte dynamics and renal function 12 p1664 N88-19977
Contrasting conductance/viscosity relations in liquid states of vitreous and polymer solid electrolytes
[AD-A189378] 13 p1748 N88-20452
Polymeric electrolytes for ambient temperature lithium batteries
[DE88-004896] 13 p1763 N88-20547
Double layer polarization of nonconducting spheroidal particles and its application to Kerr effect
[ISSN-0208-5658] 13 p1832 N88-20960
Prediction of high-temperature thermodynamic properties of mixed electrolyte solutions including solubility equilibria, vapor pressure depression and boiling point elevation
[DE88-006344] 13 p1849 N88-21069
Prediction of thermodynamic properties, including solubility equilibria and vapor pressures, for mixed aqueous electrolytes to high temperatures
[DE88-006317] 14 p1990 N88-21863
Fast ion conducting glasses
[AD-A191412] 16 p2183 N88-23010
Characterization of crystalline silicon by electrochemical and Raman spectroscopy at the frontier semiconductor/electrolyte
[ETN-88-92354] 21 p3025 N88-27956
Advanced calcium-thionyl chloride high-power battery
[AD-A194401] 22 p3072 N88-28238
Optimization and scale-up performance of polymer electrolyte batteries
[AD-A193987] 22 p3073 N88-28243
Performance of polymer electrolyte cells at +25 to +100 C
[AD-A193988] 22 p3073 N88-28244
Hormonal regulation of fluid and electrolytes: Effects of heat exposure and exercise in the heat
[AD-A192655] 22 p3131 N88-28614
Potential induced structural transformations of the Au(100) and Au(111) surfaces
[DE88-005446] 23 p3287 N88-29571

High power storage system based on thin film solid ionics
[AD-A193623] 23 p3291 N88-29598
Multi-metallic galvanic corrosion
[AD-A195995] 24 p3353 N88-29963
Structure and dynamics of solutions of lithium salts relevant to battery construction
[AD-A195399] 24 p3366 N88-30044

ELECTROLYTIC CELLS
New materials for electrochemical cells
[AD-A183659] 01 p0037 N88-10238
Ionically conductive polymers: Application to solid state batteries
[AD-A183733] 01 p0037 N88-10239
Evaluation of LiCl- LiBr- KBr electrolyte for Li- alloy/metal disulfide cells
[DE87-011356] 01 p0041 N88-10258
The corrosion of iron rotating hemispheres in 1 M sulfuric acid: An electrochemical impedance study
[DE87-014679] 02 p0148 N88-10925
Effects of pressure fluctuations on nickel electrodes
[AD-A184293] 03 p0311 N88-11987
Survey state of the art: Electrical load management techniques and equipment
[AD-A184083] 05 p0577 N88-13517
An investigation of the rechargability of certain modified forms of MnO2
[AD-A185919] 07 p0847 N88-15140
Investigation of self-discharge characteristics of spacecraft nickel-cadmium cells at elevated temperatures
[AD-A186497] 08 p0979 N88-15919
Investigation of materials for inert electrodes in aluminum electrodeposition cells
[DE88-003380] 10 p1323 N88-17906
Determination of optimum electrolyte composition for molten carbonate fuel cells literature review
[DE88-001015] 10 p1348 N88-18058
Recent advances in solid polymer electrolyte fuel cell technology
[DE88-005380] 15 p2092 N88-22464
Oxygen reduction in fuel cell electrolytes
[DE88-008240] 20 p2819 N88-26723
Preparation and development of advanced battery catalysts
[AD-A193208] 21 p2937 N88-27441
Estimation of power-energy plots for secondary batteries
[DE88-011922] 21 p2940 N88-27460
Optimization and scale-up performance of polymer electrolyte batteries
[AD-A193987] 22 p3073 N88-28243
Performance of polymer electrolyte cells at +25 to +100 C
[AD-A193988] 22 p3073 N88-28244
The overcharge behavior of polymer electrolyte cells
[AD-A193984] 22 p3117 N88-28522
Morphological changes in polymer electrolyte cells
[AD-A195821] 24 p3368 N88-30054

ELECTROMAGNETIC ABSORPTION
NT GAMMA RAY ABSORPTION
NT INFRARED ABSORPTION
NT MULTIPHOTON ABSORPTION
NT PHOTOABSORPTION
NT ULTRAVIOLET ABSORPTION
NT X RAY ABSORPTION
Pure dephasing of a vibrational adbond
[AD-A185222] 05 p0609 N88-13740
Anomalies in electromagnetic absorption of circularly polarized ultrasonic waves by tungsten within Doppler-shifted cyclotron resonance range
06 p0775 N88-14756
Characteristics of thermooptical sound excitation in metals 08 p1076 N88-16486
Absorption of electron cyclotron radiation in tokamak plasmas with a superthermal tail in the electron velocity distribution
[INPE-4391-PRE/1211] 08 p1086 N88-16541
Linear theory of generation of longitudinal sound waves in semiconductors upon interband absorption of optical radiation 09 p1234 N88-17397
Numerical simulation of the propagation and absorption due to air breakdown of long microwave pulses
[DE88-005227] 11 p1475 N88-18798
Photochemistry at structured surfaces: A classical electromagnetic approach
[AD-A189519] 13 p1737 N88-20387
Anisotropy of light absorption by color centers in waveguides produced on photochromic glasses by diffusion 14 p1896 N88-21320
Microwave dispersion and absorption in tissues: Molecular mechanisms
[AD-A190118] 15 p2100 N88-22512
Research on materials and components for opto-electronic signal processing and computing
[AD-A190130] 15 p2143 N88-22788
Light scattering of intracellular gas vacuoles: Anomalous behavior of forward and perpendicular light scattering of a cyanobacterium due to intracellular gas vacuoles
[BCRS-87-08] 16 p2228 N88-23308
Research investigation directed toward extending the useful range of the electromagnetic spectrum, appendix
[AD-A190199] 17 p2332 N88-23921
Influence of refractive index and solar concentration on optical power absorption in slabs
[NASA-TM-4056] 19 p2726 N88-26190
Diode laser ignition of high explosives and pyrotechnics
[DE88-008771] 21 p2923 N88-27352
Bioeffects of electromagnetic waves
24 p3364 N88-30032

ELECTROMAGNETIC ACCELERATION
Multi-stage plasma thruster
[AD-A183635] 01 p0017 N88-10105

ELECTROMAGNETIC COMPATIBILITY
Electromagnetic compatibility (EMC) phenomena and prevention of the effects --- spacecraft
03 p0274 N88-11731
A design-philosophy for grounding and inter-unit wiring
[EMCR-20/85] 03 p0310 N88-11954
Discussions in support of the design-philosophy for grounding and inter-unit wiring
[EMCR-21/85] 03 p0310 N88-11955
Measurements in an electromagnetic test laboratory
[SNIAS-872-430-102] 05 p0575 N88-13507
Model of space platform electromagnetic (EMC) configuration
[ESA-CR(P)-2500] 09 p1135 N88-16809
Recommended test specification for the electromagnetic compatibility of aircraft equipment
[RAE-TM-FS(F)-510] 14 p1867 N88-21155
Radio frequency compatibility between IRS and SPOT 3: Preliminary study
[CNES-86/CT/DRT/TIT/TR/011]
14 p1905 N88-21383
Strategies in the topological approach to electromagnetic interference control
[AD-A189874] 15 p2056 N88-22255
Electromagnetic compatability: An introduction to the theory of interference and shielding, 3rd revised edition
[PB88-165410] 15 p2057 N88-22264
The electromagnetic threat to future avionic systems
17 p2305 N88-23790
Aircraft field degradation and electromagnetic compatibility
[PB88-183975] 19 p2602 N88-25456
Study and temporal simulation of the electromagnetic susceptibility of interconnected systems
[ECL-87-19] 22 p3071 N88-28228
Electromagnetic compatibility. View of the near future
[SNIAS-881-422-104] 22 p3071 N88-28229

ELECTROMAGNETIC CONTROL
U ELECTROMAGNETS
U REMOTE CONTROL

ELECTROMAGNETIC COUPLING
NT MICROWAVE COUPLING
NT OPTICAL COUPLING
An excitation-term modification for a certain class of electromagnetic aperture-coupling problems
[DE88-000260] 04 p0437 N88-12713
Advanced numerical modeling of microwave penetration and coupling for complex structures
[DE88-001873] 06 p0690 N88-14231

ELECTROMAGNETIC DEDUCTION
U MAGNETIC INDUCTION

ELECTROMAGNETIC FIELDS
NT FAR FIELDS
NT NEAR FIELDS
Numerical predictions of EML system performance
[DE87-011727] 01 p0011 N88-10061
Theory of atoms in strong, pulsed electromagnetic fields. 2: A free electron and a harmonically bound electron
[DE87-012571] 01 p0035 N88-10225
Anechoic Chamber test of the Electromagnetic Measurement System ground test unit
[DE87-012998] 01 p0035 N88-10226
Simulations using the pseudo-current algorithm
[DE87-012403] 01 p0040 N88-10255
Different ways of looking at the electromagnetic vacuum
[DE87-013150] 01 p0089 N88-10584
Research in particles and fields
[NASA-CR-180412] 01 p0119 N88-10763
Quantum-mechanical aspects of classically chaotic driven systems
[DE87-013152] 02 p0178 N88-11106
Electromagnetic effects of a discharge on circuitry --- spacecraft 03 p0274 N88-11726
Numerical modeling: Integral equation method
03 p0304 N88-11919
A microwave FEL (Free Electron Laser) code using waveguide modes
[DE88-000225] 03 p0330 N88-12084
A new approach to modeling and interpreting electromagnetic sounding data
[DE88-000460] 04 p0438 N88-12715
Proceedings of the 2nd Regional Electromagnetic Workshop at Argonne National Laboratory
[DE87-004633] 06 p0690 N88-14230
Advanced numerical modeling of microwave penetration and coupling for complex structures
[DE88-001873] 06 p0690 N88-14231
Spectral- and spatial-domain filtering and sampling approach to the numerical solution of electromagnetic scattering problems
[PB88-106711] 06 p0694 N88-14261
Finite-element method for three-dimensional electric and electromagnetic field problems
[PB87-138731] 06 p0696 N88-14274
Human physical fields 06 p0750 N88-14609
Eigenvalues and eigenvectors of field tensors and associated energy tensors
[DE88-001951] 06 p0763 N88-14682
Nonuniformity of electromagnetic field at Lambda = 10.6 micron wavelength inside atmospheric aerosol particles
06 p0772 N88-14743
Electromagnetic fields backscattered from an s-shaped inlet cavity with an absorber coating on its inner walls
[NASA-CR-182401] 07 p0845 N88-15130
Interaction of intense electromagnetic fields with SF/sub 6/ molecules and clusters in supersonic expansion
[DE88-700310] 07 p0846 N88-15132
Treatment of small wire loops in the method of moments code NEC (Numerical Electromagnetics Code)
[DE88-002995] 07 p0846 N88-15136
Experimental investigation of a three-stage railgun incorporating puff-switching
[MRL-R-1056] 09 p1130 N88-16785
Exact image principle in electromagnetic field computation
[EL-57] 09 p1153 N88-16907
Evaluation of CWMS (Continuous-Wave Measurement System) single-wire dipole antenna
[DE88-003979] 09 p1155 N88-16920
A qualitative study of wake fields for very short bunches
[DE88-002565] 09 p1164 N88-16980
Space-time processing of field produced by moving source 09 p1234 N88-17399
Properties of superconducting tunnel structures in microwave radiation field 09 p1239 N88-17424
Time-domain reciprocity theorems for electromagnetic fields in dispersive media
[PB88-126925] 10 p1319 N88-17886
Forces on neutral atoms due to electromagnetic fields
[AD-A187461] 10 p1408 N88-18396
The stability of free-electron lasers against filamentation
[DE88-004712] 10 p1414 N88-18435
A dynamic analysis of the parallel-plate EMP (electromagnetic pulse) simulator using a wire mesh approximation and the numerical electromagnetics code
[AD-A187535] 11 p1470 N88-18767
GERA computer code for calculation of two-dimensional electromagnetic fields in resonators and electron-optical systems by the finite element method
[DE88-700678] 11 p1480 N88-18831
ELF (Extremely Low Frequency) communications system ecological monitoring program: Electromagnetic field measurements and engineering support, 1986
[AD-A188057] 11 p1509 N88-19017
Critical phenomena and electromagnetic effects in biological membranes
[AD-A188156] 11 p1518 N88-19064
Validation of GEMACS (General Electromagnetic Model for the Analysis of Complex Systems) for modeling lightning-induced electromagnetic fields
[AD-A188822] 12 p1620 N88-19687
Observation of a hydromagnetic wave in the earth's magnetosphere
[AD-A188942] 12 p1644 N88-19841
Negative-energy quanta
[DE88-700904] 12 p1689 N88-20101
Structural integrity of metallic armature rail guns
[AD-A188735] 13 p1728 N88-20333
Photochemistry at structured surfaces: A classical electromagnetic approach
[AD-A189519] 13 p1737 N88-20387
Transformation coefficient in wave-field acceleration scheme
[DE88-700158] 13 p1757 N88-20507
Optimum transformer design for a pulsed power system
[DE88-006054] 13 p1760 N88-20525

Resolution of the magnetotelluric method for determining local inhomogeneities in the sedimentary cover 13 p1789 N88-20701
Reduced tolerance imaging 2, volume 2
[AD-A189604] 13 p1829 N88-20939
Numerical simulations of multiphoton processes in many electron atoms
[DE88-003293] 13 p1837 N88-20990
Topics in curved and flat space electromagnetism 13 p1854 N88-21100
Exact image method for Gaussian beam problems involving a planar interface
[NASA-CR-182702] 14 p1905 N88-21380
A qualitative approach to electricity
[AD-A189854] 15 p2128 N88-22693
Coordinate-momentum probability operator for point particles in a stationary electromagnetic field
[DE88-701165] 16 p2188 N88-23044
Exact image theory for the problem of dielectric/magnetic slab
[NASA-CR-182865] 16 p2189 N88-23055
Finite elements for the computation of three-dimensional electromagnetic fields in inhomogeneous media (revised)
[PB88-173471] 16 p2190 N88-23057
A computer model investigation of a half square log-periodic array
[AD-A190955] 16 p2190 N88-23062
Pulsed power simulation problems in magic
[AD-A191110] 16 p2191 N88-23065
KOMPOT Program complex for the calculation of spatial magnetostatic fields of electromagnetic systems
[DE88-701691] 16 p2192 N88-23072
Development of Electromagnetic PIC code for LIB diode 16 p2276 N88-23622
Finite element simulation of the atmosphere's electromagnetic response to charge perturbations associated with lightning 17 p2375 N88-24124
Electromagnetic penetration into a conducting circular cylinder through a narrow slot, TE case
[AD-A191602] 18 p2500 N88-24828
Electromagnetic field penetration into structures
[AD-A192127] 18 p2501 N88-24836
Space station induced electromagnetic effects 18 p2591 N88-25394
Gravitation and polarization properties of electromagnetic field
[DE88-702166] 19 p2654 N88-25761
Application of Moment Iteration Method (MIM) to electromagnetic field computation
[PB88-194139] 20 p2789 N88-26546
A maximum entropy solution for the underdetermined electromagnetic field within a volume
[DE88-007020] 20 p2790 N88-26550
MAXWELL3: A 3D finite element electromagnetic modeling code
[DE88-010602] 20 p2790 N88-26551
Research in electromagnetic shielding theory. Part11. Shielding by rectangular enclosures
[AD-A192881] 20 p2791 N88-26557
Computer programs for high-current beam transport in accelerators
[AD-A192356] 20 p2838 N88-26835
Research in particle and gamma-ray astrophysics
[NASA-CR-183111] 20 p2887 N88-27146
SSVCO feed characteristics
[DE88-011322] 22 p3068 N88-28208
Activities report of the Electromagnetic Environment Division
[FOA-C-30484-3.2/3.3/4.1/4.2]
22 p3071 N88-28233
Open bosonic string in background electromagnetic field
[DE88-702140] 23 p3201 N88-29053
Development of a multiport-hybrid-mode exciter for use in antennas for polarimetric field measurements
[REPT-12-87] 23 p3205 N88-29075
The 1983 direct strike lightning data, part 1
[NASA-TM-86426-PT-1] 23 p3237 N88-29259
The 1983 direct strike lightning data, part 2
[NASA-TM-86426-PT-2] 23 p3237 N88-29260
The 1983 direct strike lightning data, part 3
[NASA-TM-86426-PT-3] 23 p3237 N88-29261
Currents induced in a human being for electromagnetic fields to 10 kHz-50 MHz
[AD-A191977] 23 p3238 N88-29268
Passage of relativistic magnetic dipole moments through magnetic fields
[DE88-702640] 23 p3295 N88-29624
Neutrino electrodynamics and possible effects for solar neutrinos
[DE88-701647] 23 p3308 N88-29705
Electromagnetic metrology 24 p3363 N88-30024
Bioeffects of electromagnetic waves
24 p3364 N88-30032
Research in particle and gamma-ray astrophysics
[NASA-CR-183126] 24 p3455 N88-30566

ELECTROMAGNETIC INTERACTIONS

NT LASER PLASMA INTERACTIONS
NT PLASMA-ELECTROMAGNETIC INTERACTION
Electromagnetic interaction between an electric discharge and cabling inside a satellite
03 p0274 N88-11725
Numerical modeling: Finite methods
03 p0304 N88-11918
Rotation of magnetized particle in electrically conducting viscous medium 06 p0770 N88-14733
Parametric and resonance interaction of ultrashort light pulses in nonlinear multilevel medium
06 p0773 N88-14746
Statistical model of interaction of electromagnetic waves with natural objects being sensed
08 p1008 N88-16112
Particle acceleration to high energies and amplification of coherent radiation by electromagnetic interactions in plasmas
[DE88-701020] 15 p2135 N88-22737
Space-charge-wave solid state microwave amplifier
[AD-A193792] 23 p3208 N88-29091

ELECTROMAGNETIC INTERFERENCE

NT CHIRP
NT CROSSTALK
NT ELECTROMAGNETIC NOISE
NT IONOSPHERIC NOISE
NT JAMMING
NT RADIO FREQUENCY INTERFERENCE
NT SHOT NOISE
NT THERMAL NOISE
NT WHISTLERS
NT WHITE NOISE
Crosstalk in braided shield coaxial cables
01 p0035 N88-10224
Ionospheric total electron content estimation for single-frequency global positioning system receivers
02 p0161 N88-11005
Electromagnetic effects of a discharge on circuitry --- spacecraft 03 p0274 N88-11726
Irradiation testing 03 p0274 N88-11727
MARECS-A case 03 p0274 N88-11729
Experimental and analytic studies of the triggered lightning environment of the F106B
[NASA-CR-4104] 04 p0469 N88-12897
Two-signal cross modulation effects, half-IF effects and interference criteria in land mobile sharing with UHF (Ultra High Frequency) television
[PB87-228037] 05 p0576 N88-13514
Receiver susceptibility measurements relating to interference between UHF (Ultra High Frequency) television and land mobile radio services
[PB87-228029] 06 p0690 N88-14228
Radio frequency electromagnetic interference fields. A study in Swedish industry
[FOA-E-30007-3.3] 06 p0692 N88-14247
New description of Lau effect based on theory of raster image forming process 06 p0772 N88-14744
Shielding effectiveness against electromagnetic interference
[DE88-003664] 07 p0846 N88-15131
Space-time processing of field produced by moving source 09 p1234 N88-17399
Measurement of shielding effectiveness of different cable and shielding configurations by mode-stirred techniques
[PB88-155791] 10 p1319 N88-17885
Satellite interference analysis and simulation using personal computers
[NASA-CR-182522] 10 p1319 N88-17890
A dynamic analysis of the parallel-plate EMP (electromagnetic pulse) simulator using a wire mesh approximation and the numerical electromagnetics code
[AD-A187535] 11 p1470 N88-18767
Envelope and phase statistics for non-Gaussian noise and resulting error probabilities for digital communications systems 12 p1617 N88-19672
Influence of hydrometeorological factors on visibility of objects detected by radar 13 p1790 N88-20707
Strategies in the topological approach to electromagnetic interference control
[AD-A189874] 15 p2056 N88-22255
Electromagnetic compatability: An introduction to the theory of interference and shielding, 3rd revised edition
[PB88-165410] 15 p2057 N88-22264
The electromagnetic threat to future avionic systems
17 p2305 N88-23790
Inadequacies of EMI-seal material: A corrosion study
17 p2319 N88-23852
Adaptive interference techniques for mobile antennas
19 p2647 N88-25714
Modulation and coding for fast fading mobile satellite communication channels 19 p2648 N88-25722
Random quantum interference in microdevices
20 p2866 N88-27021
Quantum interference and transport in microstructures
20 p2866 N88-27022
Study and temporal simulation of the electromagnetic susceptibility of interconnected systems
[ECL-87-19] 22 p3071 N88-28228
Electromagnetic compatibility. View of the near future
[SNIAS-881-422-104] 22 p3071 N88-28229
Electromagnetic interference to radar and radio link systems caused by large scale wind turbines
[FOA-C-30486-3.2] 22 p3071 N88-28234
Ion gun generated electromagnetic interference on the SCATHA satellite
[AD-A195179] 24 p3335 N88-29853

ELECTROMAGNETIC MEASUREMENT

Anechoic Chamber test of the Electromagnetic Measurement System ground test unit
[DE87-012998] 01 p0035 N88-10226
Measurements in an electromagnetic test laboratory
[SNIAS-872-430-102] 05 p0575 N88-13507
Electromagnetic tests
[SNIAS-872-430-103] 05 p0575 N88-13508
Numerical and analytical study of the equivalent permittivity or permeability of nonhomogeneous materials. Application to the experimental electromagnetic characterization of composites
[SNIAS-872-430-104] 05 p0575 N88-13509
Microwave and structural properties of saline ice
[AD-A189307] 13 p1803 N88-20779
Wind measurements by electromagnetic probes
[NASA-TM-4066] 23 p3236 N88-29256
The 1983 direct strike lightning data, part 1
[NASA-TM-86426-PT-1] 23 p3237 N88-29259
The 1983 direct strike lightning data, part 2
[NASA-TM-86426-PT-2] 23 p3237 N88-29260
The 1983 direct strike lightning data, part 3
[NASA-TM-86426-PT-3] 23 p3237 N88-29261

ELECTROMAGNETIC NOISE

NT IONOSPHERIC NOISE
NT SHOT NOISE
NT THERMAL NOISE
NT WHISTLERS
NT WHITE NOISE
Surface effects and low frequency noises in GaAs field effect transistors
[LAAS-87-179] 02 p0168 N88-11055
Signal to noise ratios --- SPOT images
03 p0341 N88-12150
On a circular correlation technique for filtering randomly noisy data
[AD-A184317] 04 p0431 N88-12669
Area of reduced electron concentration in terrestrial plasmasphere 08 p1003 N88-16078
Calculation of noise in spatial speckle-field holograms under conditions of saturated photoresponse
09 p1235 N88-17403
Studies of nonlinear and chaotic phenomena in solid state systems
[DE88-002330] 09 p1254 N88-17515
Contact and current noise in beta alumina and Nasicon ceramics
[AD-A189168] 12 p1611 N88-19635
Envelope and phase statistics for non-Gaussian noise and resulting error probabilities for digital communications systems 12 p1617 N88-19672
Evaluation of chemical and atmospheric sciences research
[AD-A188468] 12 p1687 N88-20091
Fluxons and order in long Josephson junctions
[AD-A190879] 16 p2282 N88-23665
Research investigation directed toward extending the useful range of the electromagnetic spectrum
[AD-A190198] 17 p2332 N88-23920
Research investigation directed toward extending the useful range of the electromagnetic spectrum, appendix
[AD-A190199] 17 p2332 N88-23921
A Differential Phase Shift Keying (DPSK) modulator for a frequency hopping short wave system
[FOA-C-30460-3.3] 18 p2501 N88-24840
Extending the impulse response in order to reduce errors due to impulse noise and signal fading
19 p2649 N88-25730
Noise in piezoresistive and capacitive sensors
19 p2670 N88-25874
Analytical description of noise in phase-conjugate resonators
[PB88-171947] 19 p2726 N88-26188
Study and temporal simulation of the electromagnetic susceptibility of interconnected systems
[ECL-87-19] 22 p3071 N88-28228
SQUID (superconducting quantum interference device) arrays for simultaneous magnetic measurements: Calibration and source localization performance
[AD-A193815] 23 p3216 N88-29143
Electromagnetic noise and interference
24 p3363 N88-30028

ELECTROMAGNETIC PROPAGATION
U ELECTROMAGNETIC WAVE TRANSMISSION

ELECTROMAGNETIC PROPERTIES
NT ABSORPTIVITY
NT BIDIRECTIONAL REFLECTANCE
NT BIREFRINGENCE
NT BRIGHTNESS
NT BRIGHTNESS DISTRIBUTION
NT COLOR
NT DICHROISM
NT FARADAY EFFECT
NT INDUCTANCE
NT KERR ELECTROOPTICAL EFFECT
NT KERR MAGNETOOPTICAL EFFECT
NT LUMINOSITY
NT MAGNETORESISTIVITY
NT OPACITY
NT OPTICAL BISTABILITY
NT OPTICAL PROPERTIES
NT OPTICAL REFLECTION
NT PHOSPHORESCENCE
NT PHOTOCONDUCTIVITY
NT PHOTOELASTICITY
NT PROXIMITY EFFECT (ELECTRICITY)
NT RADIANCE
NT REFLECTANCE
NT REFRACTIVITY
NT SKY BRIGHTNESS
NT SPECTRAL REFLECTANCE
NT STELLAR LUMINOSITY
NT STIGMATISM
NT TRANSLUCENCE
NT TRANSMISSIVITY
NT TRANSMITTANCE
NT TRANSPARENCE
NT TURBIDITY
NT WATER COLOR

Analysis of the electromagnetic performance characteristics of stripline transformers
[DE87-012515] 01 p0042 N88-10264
Experimental studies of electromagnetic properties of few body systems
[DE87-014610] 02 p0161 N88-11008
Modulation of an intense beam by an external microwave source: Theory and simulation
[AD-A185683] 07 p0848 N88-15145
Electron paramagnetic resonance studies of Mn(2+) in 2-6 semiconductor alloys 11 p1560 N88-19340
Electromagnetic modeling of a control valve
[INPE-4140-PRE/1048] 12 p1622 N88-19700
Research in remote sensing of vegetation
[NASA-CR-182663] 12 p1639 N88-19817
Joint services electronics program
[AD-A189262] 13 p1761 N88-20533
Topics in curved and flat space electromagnetism 13 p1854 N88-21100
Properties of superconductors with strong electron-phonon interaction 14 p1974 N88-21779
Preparation and properties of high Q microwave dielectrics in the (CA, SR, BA) zirconate system
[AD-A193127] 21 p2918 N88-27317

ELECTROMAGNETIC PROPULSION
NT MASS DRIVERS (PAYLOAD DELIVERY)

Analysis of a series of electromagnetic launcher firings
[AR-005-131] 04 p0405 N88-12516
Electromagnetic powered vehicles (EMPV) for Mars exploration 17 p2419 N88-24388
Power and energy requirements for electromagnetic launchers 17 p2420 N88-24391
Fabrication issues and technology development for HELEOS (Hypervelocity Electromagnetic Launcher for Equation Of State)
[DE88-007419] 18 p2470 N88-24658
Application of superconducting technology to earth-to-orbit electromagnetic launch systems
[NASA-TM-101134] 20 p2763 N88-26385

ELECTROMAGNETIC PULSES
Theory of atoms in strong, pulsed electromagnetic fields. 2: A free electron and a harmonically bound electron
[DE87-012571] 01 p0035 N88-10225
Optical damage in polymers by millisecond light pulses
[DE87-013106] 02 p0151 N88-10943
Method for single-shot measurement of picosecond laser pulse-lengths without electronic time dispersion
[DE87-013171] 02 p0178 N88-11107
Singularity expansion method: Target Resonances 03 p0303 N88-11912
The effects of corona on current surges induced on conducting lines by EMP: A comparison of experiment data with results of analytic corona models
[DE87-014970] 03 p0305 N88-11924
The development of diagnostic fuses
[SAND-86-0395] 03 p0311 N88-11963
Ultimate velocities for induction launchers
[DE87-012360] 04 p0404 N88-12513
Nitrogen energy transfer study
[AD-A184457] 04 p0464 N88-12869
All-optical beam control by forced Rayleigh scattering
[AD-A184315] 04 p0490 N88-13018
Theoretical analysis of the electrical aspects of the basic electro-impulse problem in aircraft de-icing applications
[NASA-CR-180845] 05 p0543 N88-13310
Solitons in stimulated Raman scattering: Generation and control of ultrashort optical pulses
[AD-A185141] 05 p0650 N88-13983
A paper about electromagnetic pulse and principles of EMP protection
[FOA-C-30455-4.2] 06 p0692 N88-14246
Ferromagnetic mitigation of electromagnetic pulse effects
[AD-A185685] 06 p0694 N88-14258
Parametric and resonance interaction of ultrashort light pulses in nonlinear multilevel medium 06 p0773 N88-14746
High repetition rate electron beam RF-acceleration and sub-millimeter wave generation via a free electron laser
[AD-A186066] 07 p0858 N88-15209
A dynamic analysis of the parallel-plate EMP (electromagnetic pulse) simulator using a wire mesh approximation and the numerical electromagnetics code
[AD-A187535] 11 p1470 N88-18767
Numerical simulation of the propagation and absorption due to air breakdown of long microwave pulses
[DE88-005227] 11 p1475 N88-18798
A methodology to assess the effects of high altitude electromagnetic pulse (HEMP) on electric power systems
[DE88-000338] 11 p1476 N88-18808
Photoconductor switch and circuit analysis
[AD-A188168] 11 p1478 N88-18821
Electrophoretically deposited styrene-acrylate coatings for suppression of internal electromagnetic pulse effects
[DE88-003820] 12 p1609 N88-19621
Two-dimensional electron fluid computer calculations of nanosecond pulse, low pressure microwave air breakdown in a rectangular waveguide and their verification by experimental measurement
[DE88-004407] 12 p1618 N88-19678
Electron emission from conductors subjected to intense, short-pulse electric fields
[DE88-005412] 13 p1836 N88-20985
Equipment test methods for externally produced electromagnetic transients
[RAE-TM-FS(F)-457] 14 p1865 N88-21140
Space-time structure of ultrashort light pulses formed during stimulated backscattering of laser beam 14 p1972 N88-21767
EMR (Electromagnetic Radiation) test facilities evaluation of reverberating chamber located at RADC (Rome Air Development Center), Griffiss AFB (Air Force Base), Rome, New York
[PB88-178827] 15 p2022 N88-22048
Investigations of test methodology for the stress loading facility
[PB88-166095] 15 p2022 N88-22049
Parallel memory addressing using coincident optical pulses
[AD-A189767] 15 p2106 N88-22547
Investigation of ultrashort traveling-wave amplified spontaneous emission 16 p2187 N88-23040
The electromagnetic threat to future avionic systems 17 p2305 N88-23790
Arcing and rf signal generation during target irradiation by a high-energy, pulsed neutral particle beam
[DE88-007169] 18 p2471 N88-24664
Optical damage in epoxy polymers by millisecond light pulses
[DE88-008675] 19 p2620 N88-25547
High bandwidth optoelectronic signal link for use in an EMP (electromagnetic pulse) plus radiation environment
[DE88-009254] 20 p2795 N88-26549
The use of commercial off-the-shelf equipment and its impact on C3 (Command, Control and Communications EMP (electromagnetic pulse), survivability
[AD-A192614] 20 p2791 N88-26556
Research in electromagnetic shielding theory. Part 2: EMP (electromagnetic pulse) simulation using small loops
[AD-A192882] 20 p2791 N88-26558
Picosecond optoelectronic sampling of electrical waveforms produced by an optically excited field effect transistor
[AD-A192384] 21 p2935 N88-27428
A GaAs solid state device model for high power applications
[DE88-011320] 21 p2939 N88-27457
Direct measurement of solids: High temperature sensing. Experimental development and testing of high temperature pulsed EMATs
[DE88-009859] 21 p2954 N88-27546
Wave equations for pulse propagation
[DE88-011760] 21 p2954 N88-27548
Electromagnetic characterization and acceptance test of the electromagnetic pulse (EMP) simulator SPERANS
[FOA-C-30476-4.2] 22 p3071 N88-28230
The far field from a hybrid electromagnetic pulse (HPD) simulator
[FOA-C-30480-4.2] 22 p3071 N88-28231
Current induced by high-altitude electromagnetic pulse (HEMP) on wire above ground
[FOA-C-30485-4.2] 22 p3072 N88-28235
An interface for the connection of the SCP2160A pulse analyser to a Hewlett-Packard desk-top computer
[RSRE-MEMO-4030] 22 p3073 N88-28245
Effects of charge distribution within a particle beam on the sub-Cerenkov radiation
[AD-A193992] 22 p3150 N88-28742
Waveform analysis on the IBM PC
[AD-A194249] 23 p3248 N88-29330
EMPTAC (Electromagnetic Pulse Test Aircraft) user's guide
[AD-A195072] 24 p3360 N88-30006
Transient interaction of electromagnetic pulses in dielectrics and microwave biophysics
[AD-A195687] 24 p3360 N88-30008
Electromagnetic noise and interference 24 p3363 N88-30028

ELECTROMAGNETIC PUMPS
Optimization of SP-100 thermoelectric electromagnetic pump 17 p2418 N88-24382

ELECTROMAGNETIC RADIATION
NT AIRGLOW
NT BLACK BODY RADIATION
NT BREMSSTRAHLUNG
NT CENTIMETER WAVES
NT CERENKOV RADIATION
NT CN EMISSION
NT COHERENT ELECTROMAGNETIC RADIATION
NT COHERENT LIGHT
NT COSMIC X RAYS
NT CYCLOTRON RADIATION
NT DAYGLOW
NT DECAMETRIC WAVES
NT DECIMETER WAVES
NT DIFFRACTION RADIATION
NT ELECTROMAGNETIC PULSES
NT ELECTROMAGNETIC SURFACE WAVES
NT EXTRATERRESTRIAL RADIO WAVES
NT EXTREME ULTRAVIOLET RADIATION
NT FAR INFRARED RADIATION
NT FAR ULTRAVIOLET RADIATION
NT GALACTIC RADIO WAVES
NT GAMMA RAY BURSTS
NT GAMMA RAYS
NT GEOCORONAL EMISSIONS
NT H WAVES
NT HYDROXYL EMISSION
NT INFRARED RADIATION
NT ION CYCLOTRON RADIATION
NT KILOMETRIC WAVES
NT LASER BEAMS
NT LIGHT (VISIBLE RADIATION)
NT LIGHT BEAMS
NT LONG WAVE RADIATION
NT LYMAN ALPHA RADIATION
NT MICROWAVE EMISSION
NT MICROWAVES
NT MILLIMETER WAVES
NT MODULATED CONTINUOUS RADIATION
NT MONOCHROMATIC RADIATION
NT NEAR INFRARED RADIATION
NT NEAR ULTRAVIOLET RADIATION
NT NIGHTGLOW
NT NONEQUILIBRIUM RADIATION
NT NONTHERMAL RADIATION
NT PHONON BEAMS
NT PHOTON BEAMS
NT PLANETARY RADIATION
NT PLASMONS
NT POLARIZED ELECTROMAGNETIC RADIATION
NT POLARIZED LIGHT
NT RADIO BURSTS
NT RADIO EMISSION
NT RADIO WAVES
NT SHORT WAVE RADIATION
NT SKY RADIATION
NT SOLAR RADIO BURSTS
NT SOLAR RADIO EMISSION
NT SOLAR X-RAYS
NT SUBMILLIMETER WAVES
NT SUNLIGHT
NT SYNCHROTRON RADIATION
NT TERRESTRIAL RADIATION
NT THERMAL RADIATION
NT TROPOSPHERIC RADIATION
NT TYPE 3 BURSTS

NT ULTRAVIOLET RADIATION
NT WHISTLERS
NT X RAYS
NT ZODIACAL LIGHT
Compilation of 1986 annual reports of the Navy ELF (Extremely Low Frequency) communications system ecological monitoring program, volume 1
[AD-A184561] 03 p0306 N88-11930
Compilation of 1986 annual reports of the Navy ELF (Extremely Low Frequency) communications system ecological monitoring program, volume 2
[AD-A184562] 03 p0306 N88-11931
Compilation of 1986 annual reports of the Navy ELF (Extremely Low Frequency) communications system ecological monitoring program, volume 3
[AD-A184563] 03 p0306 N88-11932
Scaling the electromagnetically driven explosive shock simulator 05 p0592 N88-13612
Cerenkov radiation field analysis due to a passing electron beam
[AD-A184870] 05 p0649 N88-13976
On the wave excitation in the turbulent meteor trace 06 p0737 N88-14530
Power and charge dissipation from an electrodynamic tether 06 p0795 N88-14869
Interaction of intense electromagnetic fields with SF/sub 6/ molecules and clusters in supersonic expansion
[DE88-700310] 07 p0846 N88-15132
Materials for acceleration by surface electromagnetic waves
[DE88-700312] 07 p0846 N88-15133
Plane longitudinal waves in solutions of Maxwell equations
[DE88-700347] 07 p0846 N88-15135
Propagation of radiation along a constricting optical waveguide 07 p0920 N88-15590
Satellite monitoring of earthquake precursor effects in magnetosphere 08 p1007 N88-16103
Statistical model of interaction of electromagnetic waves with natural objects being sensed 08 p1008 N88-16112
Instability of strong-absorption domain in semiconductor 08 p1077 N88-16495
Interaction of acoustic and electromagnetic waves involved in anomalous skin effect 08 p1079 N88-16503
Advanced studies of integrable systems
[AD-A186792] 09 p1151 N88-16895
Transient electromagnetic scattering from heterogeneous lossy spheres
[AD-A186669] 09 p1152 N88-16903
Plane wave diffraction by a thin dielectric wedge
[RSRE-MEMO-4045] 09 p1153 N88-16912
Direct scattering of electromagnetic waves by one- and two-dimensional objects and its use for inverse profiling
[PB88-126909] 10 p1319 N88-17887
Velocity reversal and the arrows of time
[DE88-004237] 10 p1429 N88-18536
Backscattering from three dimensional conducting bodies
[AD-A187570] 11 p1470 N88-18768
ELF (Extremely Low Frequency) communications system ecological monitoring program: Electromagnetic field measurements and engineering support, 1986
[AD-A188057] 11 p1509 N88-19017
Experimental aspects of hypernuclear physics at CEBAF
[CEBAF-R-86-013] 11 p1546 N88-19245
Electromagnetic propagation in PEC and absorbing curved S-ducts
[NASA-TM-100833] 12 p1621 N88-19698
Airborne electromagnetic sounding of sea ice thickness and sub-ice bathymetry
[AD-A188939] 12 p1649 N88-19879
Time-domain system for identification of the natural resonant frequencies of aircraft relevant to electromagnetic compatibility testing
[PB88-164520] 13 p1759 N88-20519
Theoretical investigation of EM wave generation and radiation in the ULF, ELF and VLF bands by the electrodynamic orbiting tether
[NASA-CR-182720] 13 p1760 N88-20529
Three-wave parametric resonance in plasma of relativistic electron flux 14 p1972 N88-21772
AGARD Highlights 88/1 14 p2012 N88-22001
Strategies in the topological approach to electromagnetic interference control
[AD-A189874] 15 p2056 N88-22255
Electromagnetic sensor arrays for nondestructive evaluation and robot control
[AD-A190210] 15 p2056 N88-22260
Theoretical studies of the heating of toroidal plasmas with radiofrequency electromagnetic radiation
[DE88-006913] 15 p2137 N88-22749
IREPS (Integrated Refractive Effects Prediction System) 3.0, user's manual
[AD-A190398] 16 p2188 N88-23045
Theoretical and numerical solution of the forward-scattering problem in a circularly cylindrical configuration
[PB88-173489] 16 p2189 N88-23056
Numerical simulation for particle acceleration and trapping by an electromagnetic wave 16 p2277 N88-23626
Electromagnetic penetration into a conducting circular cylinder through a narrow slot, TE case
[AD-A191602] 18 p2500 N88-24828
Electromagnetic field penetration into structures
[AD-A192127] 18 p2501 N88-24836
Joint services electronics program
[AD-A191749] 18 p2504 N88-24853
Theoretical basis for an experimental test with regard to the origin of VHF (Very High Frequency) radiation from natural lightning
[DE88-007535] 18 p2544 N88-25102
Extremely Low Frequency (ELF) communications program: Non-ionizing electromagnetic radiation literature evaluation and assessment, 1986-1987 literature review
[AD-A192024] 19 p2642 N88-25677
Method and apparatus for measuring distance
[NASA-CASE-MSC-20912-1] 20 p2793 N88-26568
Comparative analysis of passive communications satellites employing the SHF and HF spectrum for use in a strategic role
[AD-A194682] 24 p3362 N88-30019
Review of Radio Science, 1984-1986 24 p3363 N88-30023
Bioeffects of electromagnetic waves 24 p3364 N88-30032
Time-domain far-field scattering of plane electromagnetic waves by a penetrable object in the Born approximation
[PB87-176129] 24 p3365 N88-30040
Vanderbilt free electron laser project in biomedical and materials research
[AD-A195961] 24 p3378 N88-30121

ELECTROMAGNETIC SCATTERING
NT HALOS
NT LIGHT SCATTERING
NT MICROWAVE SCATTERING
NT MIE SCATTERING
NT RAMAN SPECTRA
NT RAYLEIGH SCATTERING
NT THOMSON SCATTERING
NT X RAY SCATTERING
Input signal shaping: K-pulse 03 p0304 N88-11917
Experiments: Test range facilities, part 1 03 p0304 N88-11920
Electromagnetic scattering by a thick strip on a half-space
[PB87-227096] 03 p0306 N88-11928
A comparative analysis of equatorial and auroral-zone phase scintillation data
[AD-A184509] 03 p0350 N88-12212
New main reflector, subreflector and dual chamber concepts for compact range applications
[NASA-CR-181506] 04 p0402 N88-12498
A study of scattering from E-plane circuit elements
[AD-A184473] 04 p0431 N88-12673
Efficient computation of periodic Green's functions with application to grating structures
[AD-A184853] 05 p0640 N88-13912
Spectral- and spatial-domain filtering and sampling approach to the numerical solution of electromagnetic scattering problems
[PB88-106711] 06 p0694 N88-14261
Study of extended least-square iterative techniques in electromagnetic scattering by penetrable objects
[PB88-105879] 06 p0694 N88-14262
Electromagnetic scattering problem in the wave-vector-time domain
[PB88-106083] 06 p0694 N88-14263
EISCAT (European incoherent scatter radar) electron density studies
[AD-A185998] 07 p0841 N88-15099
Absorption, scattering, and thermal radiation by conductive fibers
[AD-A186105] 07 p0842 N88-15106
Interior impedance wedge diffraction with surface waves
[NASA-CR-182405] 07 p0854 N88-15186
The application of vector diffraction to the scalar anomalous diffraction approximation of Van de Hulst
[AD-A185930] 07 p0929 N88-15643
Transient electromagnetic scattering from heterogeneous lossy spheres
[AD-A186669] 09 p1152 N88-16903
Calculation of the spatial-temporal deformation of laser pulses in multiple scattering
[MBB-Z-111/87] 10 p1311 N88-17837
Direct scattering of electromagnetic waves by one- and two-dimensional objects and its use for inverse profiling
[PB88-126909] 10 p1319 N88-17887
Three-dimensional transient electromagnetic modeling for exploration geophysics 10 p1346 N88-18047
A dynamic analysis of the parallel-plate EMP (electromagnetic pulse) simulator using a wire mesh approximation and the numerical electromagnetics code
[AD-A187535] 11 p1470 N88-18767
The application of the hybrid iterative method to scattering by perfectly conducting bodies of revolution 11 p1475 N88-18802
Experimental study of scattered waves and cylindrical antenna sheaths in a microwave driven plasma 11 p1553 N88-19293
An efficient numerical algorithm for solving scattering and inverse scattering problems of electromagnetic waves
[AD-A188479] 12 p1619 N88-19684
Electromagnetic scattering from and natural resonances of the circular strip 13 p1759 N88-20523
Electromagnetic shadowing by an exponentially distributed rough surface
[AD-A189677] 14 p1906 N88-21391
Electromagnetic scattering by an exponentially distributed rough surface with the introduction of a rough surface generation technique
[AD-A189678] 14 p1906 N88-21392
On the theory of electromagnetic scattering from a raindrop splash
[AD-A188720] 14 p1906 N88-21393
Polarimetric ISAR imaging using either measured or calculated transient signatures
[AD-A190077] 15 p2056 N88-22259
Models for electromagnetic scattering from the sea at extremely low grazing angles
[AD-A190472] 15 p2057 N88-22261
Efficiency of some computational techniques for electromagnetic scattering problems
[PB88-148895] 16 p2187 N88-23043
Computer program for parameterization of nucleus-nucleus electromagnetic dissociation cross sections
[NASA-TM-4038] 16 p2270 N88-23584
Electromagnetic scattering from nonlinear anisotropic cylinders 17 p2333 N88-23930
Born-type reconstruction of material parameters of an inhomogeneous, lossy dielectric slab from reflected-field data
[PB88-188958] 18 p2569 N88-25261
Curvature of blended rolled edge reflectors at the shadow boundary contour
[NASA-CR-182974] 18 p2576 N88-25300
New hybrid method for solving time-domain integral equations (one-dimensional scattering problems)
[PB88-186192] 20 p2789 N88-26547
Stochastic modeling of EM scattering from foliage
[AD-A192258] 20 p2790 N88-26553
Comparison of edge diffraction theories
[AD-A193880] 22 p3070 N88-28223
Diffraction by a simple deep phase object --- integrated circuit measurement
[RSRE-MEMO-4039] 22 p3070 N88-28224
Review of Radio Science, 1984-1986 24 p3363 N88-30023
Fields and waves 24 p3363 N88-30025
Time-domain far-field scattering of plane electromagnetic waves by a penetrable object in the Born approximation
[PB87-176129] 24 p3365 N88-30040

ELECTROMAGNETIC SHIELDING
Crosstalk in braided shield coaxial cables 01 p0035 N88-10224
Shielding effectiveness against electromagnetic interference
[DE88-003864] 07 p0846 N88-15131
Measurement of shielding effectiveness of different cable and shielding configurations by mode-stirred techniques
[PB88-155791] 10 p1319 N88-17885
Strategies in the topological approach to electromagnetic interference control
[AD-A189874] 15 p2056 N88-22255
Electromagnetic compatability: An introduction to the theory of interference and shielding, 3rd revised edition
[PB88-165410] 15 p2057 N88-22264
Electromagnetic field penetration into structures
[AD-A192127] 18 p2501 N88-24836
Research in electromagnetic shielding theory. Part1. Shielding by rectangular enclosures
[AD-A192881] 20 p2791 N88-26557

Research in electromagnetic shielding theory. Part 2: EMP (electromagnetic pulse) simulation using small loops
[AD-A192882] 20 p2791 N88-26558
Shielding effectiveness of metallic joints versus corrosion prevention 22 p3054 N88-28120
Electromagnetic noise and interference 24 p3363 N88-30028

ELECTROMAGNETIC SPECTRA
NT BALMER SERIES
NT ELECTRONIC SPECTRA
NT FRAUNHOFER LINES
NT GAMMA RAY SPECTRA
NT H ALPHA LINE
NT H BETA LINE
NT H LINES
NT INFRARED SPECTRA
NT K LINES
NT LINE SPECTRA
NT LYMAN SPECTRA
NT MICROWAVE SPECTRA
NT RADIO SPECTRA
NT RAMAN SPECTRA
NT RYDBERG SERIES
NT SOLAR SPECTRA
NT STELLAR SPECTRA
NT ULTRAVIOLET SPECTRA
NT VIBRATIONAL SPECTRA
NT VISIBLE SPECTRUM
NT X RAY SPECTRA
Extreme ultraviolet beam-foil spectroscopy of highly ionized neon and argon
[AD-A185197] 05 p0561 N88-13418
Research investigation directed toward extending the useful range of the electromagnetic spectrum
[AD-A190198] 17 p2332 N88-23920
Research investigation directed toward extending the useful range of the electromagnetic spectrum, appendix
[AD-A190199] 17 p2332 N88-23921
The electromagnetic spectrum: The information mine
[AD-A194316] 22 p3069 N88-28215

ELECTROMAGNETIC SURFACE WAVES
Interior impedance wedge diffraction with surface waves
[NASA-CR-182405] 07 p0854 N88-15186

ELECTROMAGNETIC WAVE FILTERS
NT BANDPASS FILTERS
NT BANDSTOP FILTERS
NT DIGITAL FILTERS
NT ELECTRIC FILTERS
NT FIR FILTERS
NT MATCHED FILTERS
NT MICROWAVE FILTERS
NT OPTICAL FILTERS
NT RADAR FILTERS
NT RADIO FILTERS
NT TRACKING FILTERS
NT WAVEGUIDE FILTERS
A notch filter instrument for measuring ELF (Extremely Low Frequency) MSK (Minimum Shift Keying) signals
[AD-A193324] 21 p2933 N88-27414

ELECTROMAGNETIC WAVE TRANSMISSION
NT HALOS
NT IONOSPHERIC PROPAGATION
NT LIGHT SCATTERING
NT LIGHT TRANSMISSION
NT MICROWAVE ATTENUATION
NT MICROWAVE TRANSMISSION
NT MULTIPATH TRANSMISSION
NT RADAR TRANSMISSION
NT RADIO TRANSMISSION
NT SCATTER PROPAGATION
NT SHORT WAVE RADIO TRANSMISSION
NT SPREAD SPECTRUM TRANSMISSION
NT TELEVISION TRANSMISSION
NT TRANSEQUATORIAL PROPAGATION
ELF/VLF/LF propagation and system design
[AD-A183261] 01 p0033 N88-10212
Open accelerating structures
[DE87-010540] 01 p0092 N88-10603
A computer code to calculate line by line atmospheric transmission spectra on a microcomputer
[NASA-TM-100686] 05 p0554 N88-13372
An investigation of millimeter wave propagation in the atmosphere: Measurement program
[AD-A184837] 05 p0574 N88-13498
Time domain electromagnetic waves in multilayered media
[AD-A185055] 05 p0574 N88-13502
Analysis of electromagnetic wave propagation in slightly inhomogeneous hollow waveguides
[DFVLR-FB-87-23] 09 p1152 N88-16904
Studies on nonlinear mechanisms of excimer laser propagation in fused silica fibers
[AD-A186822] 09 p1156 N88-16929
Active and passive remote sensing of ice
[AD-A186685] 09 p1195 N88-17162
An evaluation of the impact of variable temporal and spatial data resolution upon IREPS (Integrated Refractive Effects Prediction System)
[AD-A187764] 11 p1470 N88-18769
Integral equations with modified fundamental solutions for exterior boundary value problems from electromagnetic wave theory
[ETN-88-91483] 11 p1475 N88-18800
USU (Utah State University) Center of Excellence in Theory and Analysis of the Geo-Plasma Environment
[AD-A187687] 11 p1511 N88-19026
Historical electromagnetic propagation condition database description
[AD-A189157] 12 p1621 N88-19695
Electric fields in Earth orbital space. Magnetospheric structural dynamic response to external variables
[AD-A188592] 12 p1643 N88-19836
Worldwide distributions of shipboard surface meteorological observations for EM propagation analysis
[AD-A188771] 12 p1648 N88-19871
High speed transcendental elementary function architecture in support of the Vector Wave Equation (VWE)
[AD-A189746] 15 p2119 N88-22627
Parametric instabilities of inhomogeneous plasma near the lower-hybrid resonance
[DE88-701201] 15 p2137 N88-22748
Beam waves in random inhomogeneous media
[DE88-701631] 16 p2190 N88-23058
Pulsed power simulation problems in magic
[AD-A191110] 16 p2191 N88-23065
WAVFLD: A program to compute ionospheric height gain functions and field strengths at VLF
[AD-A191159] 16 p2191 N88-23066
Validate algorithms for the determination of rainfall rates from SSM/I microwave satellite imagery
[AD-A191337] 16 p2236 N88-23353
Development of 20 GHz monolithic transmit modules
[NASA-CR-182134] 17 p2445 N88-24539
Propagation of neutralized ion beams
[AD-A191599] 18 p2574 N88-25289
Theoretical plasma physics research of active space experiments
[AD-A192075] 18 p2577 N88-25309
New hybrid method for solving time-domain integral equations (one-dimensional scattering problems)
[PB88-186192] 20 p2789 N88-26547
On the self-trapping of an electromagnetic wave in magnetized plasma
[DE88-701872] 20 p2858 N88-26974
Airborne measurement of low frequency atmospheric noise ALFAN 1
[AD-A193056] 21 p2931 N88-27405
SARLAC: A relativistic electron beam code
[AD-A193134] 21 p2932 N88-27411
Staggered-grid finite element solution technique for the Maxwell's equations in the time domain
[DE88-011731] 21 p3007 N88-27838
Propagation of charged particle beams in the atmosphere
[AD-A193185] 21 p3014 N88-27887
Electromagnetic wave incoherent reflection by a half-space of weakly-ionized plasma with an absorbing boundary
[DE88-702413] 21 p3019 N88-27917
The spatial and temporal variability of the arctic atmospheric boundary layer and its effect on electromagnetic (EM) propagation
[AD-A193958] 23 p3204 N88-29068
Currents induced in a human being for electromagnetic fields to 10 kHz-50 MHz
[AD-A191977] 23 p3238 N88-29268
Nonlinear optical phase conjugation techniques to reduce the physical size of lasers
[AD-A196170] 24 p3379 N88-30122
Consideration of plasma opening switches from a wave propagation perspective
[AD-A195681] 24 p3431 N88-30421

ELECTROMAGNETIC WAVES
U ELECTROMAGNETIC RADIATION

ELECTROMAGNETICS
U ELECTROMAGNETISM

ELECTROMAGNETISM
NT MAGNETOSTATICS
Response of helical structures to high speed pulses or when can a helix be called an inductor
[DE87-014347] 01 p0090 N88-10587
Process support compressor motor electromagnetic design summary
[DE87-014359] 02 p0167 N88-11048
Eigenvalue projection theory for linear operator equations of electromagnetics
[AD-A185434] 05 p0575 N88-13504
Nature and the nonlinear evolution of electrostatic waves associated with the AMPTE (Active Magnetosphere Particle Tracer Explorers) solar wind releases
[AD-A185471] 06 p0806 N88-14920
Properties of a magnetic dipole
[AD-A186128] 07 p0922 N88-15600
Primordial nucleosynthesis during the keV era
[DE88-002233] 08 p1104 N88-16623
Exact image principle in electromagnetic field computation
[EL-57] 09 p1153 N88-16907
Investigation of iterative and spectral Galerkin techniques for solving electromagnetic boundary value problems 09 p1155 N88-16925
Cold gas jet system for satellite attitude control-modeling and simulation
[INPE-4279-PRE/1150] 12 p1601 N88-19583
Influence of magnetic material on the transient of a controle electrovalve
[INPE-4418-PRE/1223] 12 p1624 N88-19713
Electric fields in Earth orbital space. Magnetospheric structural dynamic response to external variables
[AD-A188592] 12 p1643 N88-19836
Topics in curved and flat space electromagnetism 13 p1854 N88-21100
Electromagnetic shadowing by an exponentially distributed rough surface
[AD-A189677] 14 p1906 N88-21391
Launchability of base-driven electromagnetic projectiles
[AD-A189635] 15 p2023 N88-22055
Electromagnetic dampers for cryogenic applications 16 p2218 N88-23231
Electromagnetic manipulation of atomic hydrogen 16 p2268 N88-23568
Electromagnetic damping and vibration isolation of space structures
[AD-A191492] 18 p2471 N88-24665
A model for insulated wires in the method of moments code NEC (Numerical Electromagnetics Code)
[DE88-008920] 20 p2794 N88-26577
Gravitation electromagnetic theory 22 p3158 N88-28790
Gravitation and electromagnetism 22 p3158 N88-28792
Electromagnetic theory of the gravitation 22 p3158 N88-28793
Cosmological applications 22 p3158 N88-28794
Electromagnetic metrology 24 p3363 N88-30024
X- and gamma-ray background observations in Antarctic
[INPE-4583-PRE/1317] 24 p3459 N88-30578

ELECTROMAGNETS
NT SUPERCONDUCTING MAGNETS
Exact solutions to the governing dynamic equations of plasma armature electromagnetic railguns
[DE87-014442] 01 p0011 N88-10063
Different ways of looking at the electromagnetic vacuum
[DE87-013150] 01 p0089 N88-10584
Process support compressor motor electromagnetic design summary
[DE87-014359] 02 p0167 N88-11048
Performance evaluation of a half-wave resonant slot antenna over perfect ground using NEC (Numerical Electromagnetic Code)
[AD-A184004] 03 p0308 N88-11942
An excitation-term modification for a certain class of electromagnetic aperture-coupling problems
[DE88-000260] 04 p0437 N88-12713
A long electromagnetic wiggler for the paladin free-electron laser experiments
[DE88-000970] 05 p0586 N88-13589
Development of a strong electromagnet wiggler
[DE88-000971] 05 p0645 N88-13952
Development of a laced electromagnetic wiggler
[DE88-000972] 05 p0646 N88-13953
Proceedings of the 2nd Regional Electromagnetic Workshop at Argonne National Laboratory
[DE87-004633] 06 p0690 N88-14230
Test results on dual resonant power supply with flat top and flat bottom current
[DE87-007506] 09 p1157 N88-16933

ELECTROMECHANICAL DEVICES
Operator multiple-tasking study for remotely operated platforms
[AD-A184487] 03 p0362 N88-12276
Corrosion behavior of high density tungsten alloys
[AD-A187108] 09 p1143 N88-16852
Dynamic modelling of an electromechanical valve using frequency response data
[AD-A187908] 11 p1494 N88-18918
Dynamics of high-speed mechanisms with elastic members 13 p1779 N88-20643
The 15-meter diameter hoop/column antenna surface control actuator system 14 p1924 N88-21469

Aerodynamic and thermal modeling of electromagnetic brakes. Evaluation of convective exchange coefficients and friction losses in the rough wall channels
[ISAL-ITC1-87-02] 16 p2215 N88-23214
Nickel hydroxide active material densities
[AD-A191411] 16 p2230 N88-23319

ELECTROMECHANICS

A feasibility study of a hypersonic real-gas facility
[NASA-CR-180423] 01 p0008 N88-10043
On the glitches in the force transmitted by an electrodynamic exciter to a structure
05 p0594 N88-13624
Electromechanical timing measurement technique
[DE88-005098] 11 p1489 N88-18889
Dynamic modelling of an electromechanical valve using frequency response data
[AD-A187908] 11 p1494 N88-18918
Electromechanical Research Symposium, August 20-21, 1987
[PB88-148457] 19 p2713 N88-26109

ELECTROMIGRATION

Computer simulation of electromigration in thin films
[AD-A194526] 22 p3157 N88-28782

ELECTROMOTIVE FORCES

NT PONDEROMOTIVE FORCES
Effects of cold working on precipitation in age hardenable alloys: On the copper alloys
[NASA-TT-20164] 16 p2177 N88-22973

ELECTRON ACCELERATION

Simulation of tokamak runaway-electron events. Study of the response of materials by use of an electron linear accelerator
[IPPJ-841] 02 p0242 N88-11528
Nonthermal phenomena in stellar coronae: Evidence from radio observations 04 p0503 N88-13096
Electron acceleration by wave processes in the earth's ionosphere
[AD-A186110] 07 p0877 N88-15320
Wave acceleration of auroral electrons
08 p1031 N88-16245
Electron acceleration by laser fields in a gas
[DE88-003337] 08 p1082 N88-16523
Collective acceleration of electrons and ions in a high relativistic electron beam
[DE88-005261] 13 p1838 N88-20998
Relationship between characteristics of low-energy electrons and geomagnetic disturbance in geostationary orbit 24 p3444 N88-30501

ELECTRON ACCELERATORS

NT BETATRONS
Phase control of the microwave radiation in free electron laser two-beam accelerator
[DE88-001460] 07 p0859 N88-15219
Energy distribution of Cerenkov radiation for finite frequency intervals
[AD-A186901] 09 p1244 N88-17454
A ring model of the lasertron
[DE88-004656] 10 p1323 N88-17908
Nucleon resonances and nuclei: Experimental aspects
[CEBAF-PR-87-025] 11 p1545 N88-19233
RF steering in the CEBAF CW superconducting linac
[CEBAF-PR-87-013] 11 p1547 N88-19251
The CEBAF project and its few-body research program
[CEBAF-PR-87-014] 11 p1547 N88-19253
Two dimensional simulations of multipass beam breakup
[CEBAF-PR-87-008] 11 p1547 N88-19254
Application of radio frequency superconductivity to recirculating linacs
[CEBAF-PR-88-002] 12 p1690 N88-20107
On (e,e'N) reactions
[CEBAF-PR-87-028] 12 p1690 N88-20109
Trajectory code studies, 1987
[DE88-006218] 13 p1728 N88-20335
The continuous electron beam accelerator facility
[CEBAF-PR-87-017] 13 p1838 N88-20996
Design of electron beam accelerator for microwave application
[DE88-005252] 13 p1838 N88-20999
The loss parameters for very short bunches
[CEBAF-PR-88-005] 18 p2574 N88-25291

ELECTRON AFFINITY

K-CO on transition metals: A local ionic interaction
[AD-A184342] 04 p0496 N88-13056

ELECTRON ATTACHMENT

Ion and electron interactions of atmospheric importance
[AD-A192255] 20 p2824 N88-26751

ELECTRON BEAM WELDING

Operation of multistage power supplies for electron beam welding installations 03 p0286 N88-11800
Development of an acoustic emission monitor and monitoring techniques for long-term monitoring of U-0.8Ti electron-beam weldments for postweld cracking
[DE88-000819] 04 p0453 N88-12804
Faraday cup characterization of electron beam welding parameters
[DE88-001896] 07 p0864 N88-15241
Detection of hydrogen-assisted-cracking in U-0.8Ti alloy weldments by acoustic emission monitoring
[DE88-003221] 09 p1184 N88-17093
Microstructural characterization and properties of 3Cr-1.5Mo-O.1V thick section electron beam welds
[DE88-004330] 18 p2486 N88-24747
An investigation into the metallurgical aspects of joining rapidly-solidified aluminum alloys
[AD-A194677] 23 p3194 N88-29009

ELECTRON BEAMS

NT RELATIVISTIC ELECTRON BEAMS
Effects of electron and proton irradiations on n/p and p/n GaAs cells grown by MOCVD
[NASA-TM-100199] 01 p0042 N88-10266
Electron beam requirements for soft X-ray/XUV free-electron lasers
[DE87-011750] 01 p0051 N88-10325
Linear emittance damper with megagauss fields
[DE87-013562] 01 p0093 N88-10606
Electron beam irradiation effects on carbon fiber reinforced PEEK composite
[DE87-753001] 02 p0142 N88-10890
Studies on temporal field emission from stainless steel surfaces
[DE87-014237] 02 p0147 N88-10919
Hydrogen annealing of P(sub) b and E prime defect centers in oxidized silicon wafers
[DE87-014293] 02 p0152 N88-10951
Trajectory versus PIC methods in diode design
[DE87-012135] 02 p0166 N88-11043
On the collective variables description of a high gain free electron laser
[DE87-013315] 02 p0178 N88-11108
Enhanced noise and Raman scattering in plasma
[DE87-014466] 02 p0238 N88-11501
Fusion reactivity enhancement due to ion tail formation by beam and ion cyclotron heating
[DE87-753018] 02 p0240 N88-11518
Effects of injection of free electron lasers on axial velocity spread of beams 03 p0299 N88-11878
Excimer laser cell with longitudinal electron-beam excitation 03 p0302 N88-11903
A theoretical study of enhanced Smith-Purcell radiation from a bigrating
[AD-A184530] 03 p0329 N88-12080
The lasertron RF generator for FEL (Free-Electron Laser) applications
[DE88-000515] 04 p0448 N88-12776
Development of an acoustic emission monitor and monitoring techniques for long-term monitoring of U-0.8Ti electron-beam weldments for postweld cracking
[DE88-000819] 04 p0453 N88-12804
Use of electron beam instruments to determine fluctuations in vertical refraction partial angle
04 p0461 N88-12853
Narrow linewidth gain measurements in a KrF excimer amplifier pumped longitudinally by a high-power electron beam
[DE88-001365] 05 p0586 N88-13575
Theoretical and experimental investigation of electron beam acceleration and sub-millimeter wave generation in cyclotron resonant cavities
[AD-A184806] 05 p0649 N88-13975
Cerenkov radiation field analysis due to a passing electron beam
[AD-A184870] 05 p0649 N88-13976
Optimization of field emission electron beam sources for high-power lasers
[PB87-218814] 06 p0708 N88-14341
NBS (National Bureau of Standards) measurement services: Fricke dosimetry in high-energy electron beams
[PB88-110374] 06 p0781 N88-14795
Stabilized X-ray generator power supply
[DE88-700297] 07 p0830 N88-15034
Cage mode propagation experiments
[AD-A186019] 07 p0841 N88-15100
Microsecond beam propagation in air
[DE88-002221] 07 p0845 N88-15127
High repetition rate electron beam RF-acceleration and sub-millimeter wave generation via a free electron laser
[AD-A186066] 07 p0858 N88-15209
Generation of light pulses in semiconductor laser upon excitation by several electron beams
07 p0920 N88-15589
Experimental research of electron beam instability on the Doppler anomalous effect
[DE88-700565] 07 p0932 N88-15658
Experimental evaluation for efficiency of excitation slow plasma and cyclotron waves in collective accelerators
[DE88-700566] 07 p0936 N88-15687
Gyrotron development at the Instituto de Pesquisas Espaciais
[INPE-4240-PRE/1115] 08 p0990 N88-15992
MAIMIK: A high current electron beam experiment on a sounding rocket from Andoya rocket range (Norway)
08 p1030 N88-16243
Electron acceleration by laser fields in a gas
[DE88-003337] 08 p1082 N88-16523
Resolution limitations and optimization of the ITT F4157 streak tube focus for fast (10 ps) operation
[DE88-003727] 09 p1169 N88-17007
Intrinsic corrections to optical guiding in a free-electron laser: Beam Research Program
[DE88-002667] 09 p1172 N88-17026
Mode media interactions in an FEL (Free Electron Laser)
[DE88-003155] 09 p1172 N88-17029
High-efficiency GaAs semiconductor laser with longitudinal excitation by scanning electron beam
09 p1238 N88-17421
Periodic-pulse semiconductor laser with electron-beam pumping 09 p1238 N88-17422
CEBAF design overview and project status
[CEBAF-PR-88-001] 09 p1246 N88-17470
Intense electron beams
[DE88-002456] 09 p1247 N88-17474
A ring model of the lasertron
[DE88-004656] 10 p1323 N88-17908
Preliminary injector, accelerator, and beamline design for rf-linac-driven XUV free-electron lasers
[DE88-003185] 10 p1336 N88-17983
Betatron oscillations in a free electron laser
[DE88-004859] 10 p1337 N88-17990
Tapered wiggler analysis of high gain free electron laser oscillators
[AD-A187997] 10 p1338 N88-17997
The stability of free-electron lasers against filamentation
[DE88-004712] 10 p1414 N88-18435
Effects of X irradiation and high field electron injection on the electrical properties of rapid thermal oxides
[DE88-002642] 10 p1417 N88-18461
Operation of electron-beam controlled CO2 laser at 6 atmospheres 11 p1468 N88-18758
Microwave radiation from rotating, annular electron beams 11 p1475 N88-18801
High-current density, high-brightness electron beams from large-area lanthanum hexaboride cathodes
[AD-A187700] 11 p1477 N88-18813
The injector for the CEBAF CW superconducting linac
[CEBAF-PR-87-011] 11 p1546 N88-19241
Perturbation effects in the CEBAF beam transport system
[CEBAF-PR-87-010] 11 p1546 N88-19242
High energy polarized electron beams
[CEBAF-R-87-002] 11 p1546 N88-19244
Investigation of multiple particle final states at CEBAF (Continuous Electron Beam Accelerator Facility)
[CEBAF-PR-87-026] 11 p1547 N88-19250
Two dimensional simulations of multipass beam breakup
[CEBAF-PR-87-008] 11 p1547 N88-19254
An analysis of whistler-mode radiation from the Spacelab-2 electron beam, revision
[AD-A188228] 11 p1552 N88-19287
Generalised scattering model for the quantum modulation of electrons 11 p1563 N88-19357
Application of radio frequency superconductivity to recirculating linacs
[CEBAF-PR-86-002] 12 p1690 N88-20107
Optics of the CEBAF CW superconducting accelerator
[CEBAF-PR-87-012] 12 p1690 N88-20110
Electronic properties of semiconductor inversion layers in sub-micron structures
[AD-A188635] 12 p1698 N88-20161
Mode priming in an overmoded gyrotron oscillator
[AD-A189151] 13 p1772 N88-20602
Development of electrostatic-accelerator free-electron lasers
[AD-A189507] 13 p1774 N88-20614
The continuous electron beam accelerator facility
[CEBAF-PR-87-017] 13 p1838 N88-20996
Rapid e-beam heating for measuring thermodynamics of metastable materials
[DE88-003565] 13 p1849 N88-21066
Effect of electron beam divergence on the gain of free electron lasers 14 p1902 N88-21358
Electron beam sensitive devices for controllability
[RR-658-I] 14 p1908 N88-21403
New method of examining microononhomogeneity of local centers in high-resistivity semiconductor materials under scanning electron microscope 14 p1969 N88-21754
Kinetics of slow electrons in excimer laser with electron-beam pumping 14 p1970 N88-21760
Emission characteristics of XeCl-laser excited by electron beam of microsecond duration
14 p1970 N88-21762

Growth and deformation mechanisms of refractory alloy hybrid materials
[AD-A190492] 15 p2039 N88-22152
Directed-energy electron-beam processing of a hypoeutectic Cr90Ta10 alloy
[DE88-005621] 15 p2040 N88-22157
Discharge excitation of the XeF C to A transition
[DE88-006448] 15 p2070 N88-22339
Numerical modelling specific energy charcteristics of excimer KrF lasers with electron beam excitation
[DE88-701525] 15 p2070 N88-22344
Nonlinear effects in plasma wake field acceleration
[DE88-700972] 15 p2134 N88-22734
High power, high frequency radiation from beam-plasma interactions
[AD-A190207] 15 p2137 N88-22752
Survey of the Air Force P78-2 (SCATHA) satellite plasma wave data during electron gun operations
[AD-A191014] 16 p2168 N88-22926
JPRS report: Science and technology. USSR: Materials science
[JPRS-UMS-88-006] 16 p2179 N88-22988
High-speed electron beam lithography devices discussed 16 p2185 N88-23023
Beam waves in random inhomogeneous media
[DE88-701631] 16 p2190 N88-23056
Kinetics of electrons and molecules at plasma-beam discharge in molecular gases
[DE88-701196] 16 p2275 N88-23616
Isotope separation using tuned laser and electron beam
[NASA-CASE-NPO-16907-1-CU] 18 p2483 N88-24732
Microstructural characterization and properties of 3Cr-1.5Mo-O.1V thick section electron beam welds
[DE88-004330] 18 p2486 N88-24747
Integral equation for the laser field: Multimode description of a free-electron laser oscillator
[DE88-007050] 18 p2521 N88-24956
Null steering applications of polynomials with unimodular coefficients
[AD-A191087] 18 p2562 N88-25211
Trochoidal analysis of scattered electrons in a merged electron-ion beam
[NASA-CASE-NPO-16789-1-CU] 18 p2573 N88-25281
Accelerator research studies
[DE88-007124] 18 p2574 N88-25290
The loss parameters for very short bunches
[CEBAF-PR-88-005] 18 p2574 N88-25291
Observations of electron cyclotron harmonic emissions associated with field-aligned electron beams
[SD-TR-87-33] 19 p2724 N88-26173
REFLEX: An energy deposition code that models the effects of electron reflection during electron beam heating tests
[DE88-009789] 19 p2726 N88-26186
Accelerator research studies
[DE88-008236] 19 p2726 N88-26187
Vaporization studies of plasma interactive materials in simulated plasma disruption events
[DE88-010100] 19 p2731 N88-26222
Electron-impact-ionization and electron-attachment cross sections of radicals important in transient gaseous discharges
[AD-A192248] 20 p2770 N88-26424
The free-electron laser: Theoretical innovations and gas-loaded experiment 20 p2806 N88-26646
Results from the SLAC lasertron
[DE88-007816] 20 p2806 N88-26647
Inelastic mean free paths of electrons and positrons in matter
[DE88-008086] 20 p2851 N88-26929
Visible tunable source
[DE88-006442] 20 p2854 N88-26944
Excitonic properties of GaAs-AlGaAs nanostructures 20 p2867 N88-27023
High-speed, precision processing using an electron beam 21 p2929 N88-27391
Equipment for an advanced electron beam lithography system
[AD-A192956] 21 p2936 N88-27435
Optical guiding in the separable beam limit
[AD-A192452] 21 p2952 N88-27534
Production of intensive electron beam impulsions by setup of pseudoglare discharges
[ISL-CO-210/87] 21 p3019 N88-27920
Guided radiation beams in free electron lasers
[AD-A194525] 22 p3082 N88-28305
Development of inductive storage pulsed power generators
[AD-A193878] 22 p3117 N88-28521
Effects of charge distribution within a particle beam on the sub-Cerenkov radiation
[AD-A193992] 22 p3150 N88-28742
The NBS/NRL (National Bureau of Standards/Naval Research Laboratory) free electron laser facility
[AD-A194214] 23 p3219 N88-29159
Diffraction transition radiation from periodic electron bunches
[AD-A193593] 23 p3280 N88-29528
Plasmoid propagation
[AD-A192378] 23 p3284 N88-29555
Microcircuit trace cutting with focused ion beams
[AD-A196030] 24 p3367 N88-30050
Reactive plasticizers in negative E-beam resists
[AD-A195161] 24 p3368 N88-30056
Influence of plasma parameters on VLF radiation in near-rocket region 24 p3448 N88-30518

ELECTRON BOMBARDMENT
The design and development of mercury vaporisers for use with electron-bombardment ion engines
[RAE-TR-70042] 01 p0018 N88-10108
The effect of oriented defects on long-range ordering of hydrocarbon films: Azulene on Pt(111)
[AD-A196089] 24 p3344 N88-29904

ELECTRON BUNCHING
A crude scaling law for lasertrons
[DE88-003880] 09 p1173 N88-17032
Multipass beam breakup in recirculating linacs
[CEBAF-PR-87-007] 12 p1690 N88-20111
Calculation of the efficiency of a resonant cyclotronic electron maser (gyrotrons)
[INPE-4387-PRE/1207] 14 p1915 N88-21444
Results from the SLAC lasertron
[DE88-007816] 20 p2806 N88-26647
Diffraction transition radiation from periodic electron bunches
[AD-A193593] 23 p3280 N88-29528

ELECTRON CAPTURE
Electron capture from solids by positrons
[DE87-014355] 02 p0232 N88-11463
Final (n,l) state-resolved electron capture by multiply charged ions from neutral atoms
[IPPJ-AM-54] 04 p0492 N88-13030
Correlation effects on double electron capture in highly-charged, low-energy ion-atom collisions
[DE87-013179] 07 p0930 N88-15651
Correlation effects on double electron capture in highly-charged, low-energy ion-atom collisions
[DE87-013179] 07 p0930 N88-15651
Total and partial cross sections for electron capture for C(q+) (q=6-2) and O(q+) (q=8-2) ions in collisions with H, H2 and He atoms
[IPPJ-AM-56] 09 p1252 N88-17501
Application of ECR ion source beams in atomic physics
[DE88-003767] 10 p1406 N88-18384
A neutral-beam diagnostic for fast confined alpha particles in a burning plasma: Applicatoin on CIT (Compact Ignition Tokamak)
[DE88-004890] 11 p1554 N88-19301
Breathing mode lattice relaxation associated with carrier emission and capture by deep electronic levels in silicon
[DE88-003844] 14 p1985 N88-21842
Selective detection in gas chromatography
[AD-A191499] 18 p2481 N88-24718

ELECTRON COLLISIONS
U ELECTRON SCATTERING

ELECTRON COMPOUNDS
U INTERMETALLICS

ELECTRON COUNTERS
Multichannel electron counter with high space resolution
[DE88-700564] 07 p0857 N88-15204
Design, fabricate, calibrate, test and deliver two satellite electron flux detectors
[AD-A190799] 16 p2169 N88-22930

ELECTRON CYCLOTRON HEATING
ATF (Advanced Toroidal Facility) ECH (Electron Cyclotron Heating) waveguide component development and testing
[DE88-001432] 06 p0782 N88-14797
Activities report of the Institute of Plasma Physics
[ETN-88-91020] 07 p0933 N88-15668
A ray-tracing study of electron cyclotron resonance heating in tokamak plasmas with a superthermal electron tail
[INPE-4381-PRE/1201] 08 p1085 N88-16536
Absorption of electron cyclotron waves by superthermal electron velocity distributions in tokamak plasmas
[INPE-4385-PRE/1205] 08 p1086 N88-16539
Absorption of electron cyclotron radiation in tokamak plasmas with a superthermal tail in the electron velocity distribution
[INPE-4391-PRE/1211] 08 p1086 N88-16541
The effect of asymmetric current-supporting electron velocity distributions on second harmonic electron cyclotron resonance heating: A ray-tracing treatment for the compass tokamak
[INPE-4389-PRE/1209] 08 p1087 N88-16549
New mode conversion process and overdense plasma heating in the electron cyclotron range of frequencies
[IPPJ-854] 10 p1411 N88-18420
First and second harmonic ECRH experience at gyrotron frequencies at LLNL
[DE88-003998] 10 p1413 N88-18430
Trip electrical circuit of the gyrotron
[INPE-4336-NTE/273] 12 p1622 N88-19701
Measurements of optically thin electron cyclotron emission from relativistic electrons
[DE88-004713] 12 p1688 N88-20096
Simulation of electron cyclotron heating in TFR 12 p1693 N88-20130
Electron heat transport in TFR with Electron Cyclotron Resonance Heating (ECRH) 12 p1694 N88-20135
A high field launch for electron cyclotron heating using an external window
[DE88-005350] 13 p1838 N88-21000
Preparing the Alcator C bolometer system for use on MTX (Microwave Tokamak Experiment)
[DE88-006724] 15 p2134 N88-22733
ECRH current drive in tokamak plasmas
[IPPJ-864] 19 p2729 N88-26209
A mode-transforming polarization-rotatable launcher for the ATF (Advanced Toroidal Facility) fusion experiment
[DE88-005070] 19 p2730 N88-26213
A survey of the current experimental database for lower hybrid current-drive and heating
[DE88-009830] 23 p3283 N88-29552
Initial operation and edge plasma studies in ATF (Advanced Toroidal Facility)
[DE88-011400] 23 p3285 N88-29562

ELECTRON DENSITY (CONCENTRATION)
NT CARRIER DENSITY (SOLID STATE)
NT ELECTRON DENSITY PROFILES
NT IONOSPHERIC ELECTRON DENSITY
NT MAGNETOSPHERIC ELECTRON DENSITY
Fast wave injection into high temperature tokamak plasmas in the lower-hybrid-density regime of JIPP T-IIU
[ISSN-0469-4732] 01 p0099 N88-10649
Electron capture from solids by positrons
[DE87-014355] 02 p0232 N88-11463
Enhanced noise and Raman scattering in plasma
[DE87-014466] 02 p0238 N88-11501
Enhanced Thomson scattering from laser plasmas
[DE87-014463] 02 p0238 N88-11503
Loop interaction in the visible emission corona: Morphological details 02 p0256 N88-11622
The effect of object potentials on the wake of a flowing plasma
[AD-A184038] 03 p0379 N88-12385
Equilibrium calculations of ionization in tracer flames
[PB87-104154] 04 p0412 N88-12555
J = O Task Force
[DE88-001326] 04 p0450 N88-12788
Measurement of the electron density and the attachment rate coefficient in silane/helium discharges
[AD-A184268] 04 p0496 N88-13051
EISCAT (European incoherent scatter radar) electron density studies
[AD-A185998] 07 p0841 N88-15099
Interaction between a module cluster and a plasma in a magnetic field
[PB87-148276] 07 p0934 N88-15675
The effect of propane on atomic spectrometric signals in the direct current plasma
[DE88-002457] 07 p0934 N88-15676
Relativistic plasma concentration measuring by Bremsstrahlung
[DE88-700560] 07 p0936 N88-15685
Embedded cluster models for electronic structure and energetics of complex oxides
[DE88-003097] 07 p0938 N88-15702
Absorption of electron cyclotron waves by superthermal electron velocity distributions in tokamak plasmas
[INPE-4385-PRE/1205] 08 p1086 N88-16539
Double layer formed by beam driven ion-acoustic turbulence
[INPE-4292-PRE/1163] 08 p1086 N88-16543
Experimental investigation of double layers formed by ion-acoustic turbulence
[INPE-4296-PRE/1167] 08 p1086 N88-16544
Diagonal and off-diagonal disorder in doped quantum wells
[INPE-4255-PRE/1128] 08 p1089 N88-16556
Minimum necessary intensity of source of preionization for stabilization of a self-sustaining laser discharge with mean power raised by electron beam or X-rays
[PB87-178158] 09 p1171 N88-17024
F-layer polar cap arcs
[AD-A186592] 09 p1190 N88-17127
Chemical activation of molecules by metals: Experimental studies of electron distributions and bonding
[DE88-004465] 10 p1407 N88-18393

Specific heat of novel thin-film material systems
10 p1415 N88-18446
Positron-annihilation 2D-ACAR studies of disordered and defected alloys
[DE88-003118] 10 p1416 N88-18454
Penetration depth measurements of YBa2Cu3O/sub 7-delta/ at 4 MHz
[DE88-003493] 10 p1420 N88-18478
Two-dimensional electron fluid computer calculations of nanosecond pulse, low pressure microwave air breakdown in a rectangular waveguide and their verification by experimental measurement
[DE88-004407] 12 p1618 N88-19678
Measurements of optically thin electron cyclotron emission from relativistic electrons
[DE88-004713] 12 p1688 N88-20096
Large scale plasma irregularities observed in the nighttime ionosphere over Natal using a rocket-borne Langmuir probe
[INPE-4422-PRE/1226] 12 p1694 N88-20139
Upward propagating electric fields from thunderstorms and VLF transmitters 13 p1801 N88-20767
Thomson scattering for determining electron concentrations and temperatures in an inductively coupled plasma. 1: Assessment of the technique for a low-flow, low-power plasma
[AD-A191323] 16 p2280 N88-23651
Thomson scattering for determining electron concentrations and temperatures in an inductively coupled plasma. 2: Description and evaluation of a multichannel instrument
[AD-A191324] 16 p2280 N88-23652
Narrow-band photographic observations of the HII Region S296 in Canis Major 16 p2288 N88-23696
Density diagnostics by hydrogen line intensity ratios: Excitation cross section between excited states
17 p2441 N88-24522
Spectral diagnostics for temperature and density measurements on ATF 17 p2442 N88-24525
Cascade fluorescences from laser-excited lithium atom for plasma diagnostics 17 p2442 N88-24526
The theory of random alloys
[DE88-006408] 18 p2487 N88-24756
A two-wavelength infrared interferometer/polarimeter system for CIT (Compact Ignition Tokamak)
[DE88-007681] 18 p2579 N88-25321
Superthermal electron processes in the upper atmosphere of Uranus: Aurora and electroglow
[NASA-TM-101150] 18 p2594 N88-25417
Simultaneously time- and space-resolved spectroscopic characterization of laser-produced plasmas
[DE88-008038] 19 p2728 N88-26202
All-electron local density theory of electronic structure and superconductivity in YBa2Cu3O7 and YBa2Cu3O6
[DE88-009944] 19 p2735 N88-26246
Megagauss field variation along axis of wire target in laser produced plasma
[DE88-701895] 20 p2859 N88-26979
Ultraviolet-visible spectroscopy of laser-produced aluminum plasmas
[AD-A193004] 20 p2860 N88-26990
Far-infrared studies of doped AlGaAs/GaAs multiple-quantum-well structures
20 p2862 N88-26998
Optical guiding in the separable beam limit
[AD-A192452] 21 p2952 N88-27534
Approximate analytical formulae for electron density and collision frequency in the natural and nuclear-disturbed ionosphere and inner magnetosphere
[AD-A193129] 21 p2972 N88-27654
A study of tunneling phenomena in gallium arsenide-aluminum gallium arsenide heterostructures
21 p3023 N88-27946
Linear thyratron
[AD-A194111] 23 p3208 N88-29094
On formulating a simple D-region model
[AD-A195841] 24 p3392 N88-30197
Model representation of electron concentration distribution in outer middle-latitude ionosphere using data from Intercosmos-19 artificial earth satellite
24 p3447 N88-30513

ELECTRON DENSITY PROFILES
Height profile inversion of ionospheric movement from observed parameters of HF radio echoes
03 p0299 N88-11884
Investigations on an RF plasma related to plasma etching
[ETN-88-91366] 06 p0784 N88-14809
Electron acceleration by wave processes in the earth's ionosphere
[AD-A186110] 07 p0877 N88-15320
Comparison of simultaneous MST radar and electron density probe measurements in the polar mesosphere --- Mesospheric, Stratospheric, Tropospheric (MST)
08 p1028 N88-16226
Electron density profile reconstruction by maximum entropy method with multichannel HCN laser interferometer system on SPAC 7
[IPPJ-858] 11 p1553 N88-19295
Arcs in cesium seeded noble gases resulting from a magnetically induced electric field
[EUT-87-E-177] 13 p1843 N88-21028
Support for FY87 midlatitude electron-density calibration campaign
[AD-A190174] 15 p2094 N88-22476

ELECTRON DETECTORS
U ELECTRON COUNTERS

ELECTRON DIFFRACTION
Surface modification by metal deposition and laser irradiation 01 p0023 N88-10148
Energy-selected electron diffraction experiments using the rocking-crystal method in the raster microscope for the investigation of localization effects in single crystals
[ETN-87-90409] 01 p0104 N88-10682
Extending the range of Low Energy Electron Diffraction (LEED) surface structure determination: Co-adsorbed molecules, incommensurate overlayers and alloy surface order studied by new video and electron counting LEED techniques
[DE88-001401] 06 p0786 N88-14820
Solving complex and disordered surface structures with electron diffraction
[DE88-003863] 10 p1418 N88-18467
NBS/Sandia/ICDD electron diffraction database
[DE88-004635] 11 p1454 N88-18665
Recent progress in structure determination by LEED (Low-Energy Electron Diffraction) measure the properties of the deep donors (DX-cent)
[DE88-003851] 13 p1846 N88-21048
Electron diffraction evidence for the ordering of excess nickel atoms by relation to stoichiometry in nickel-rich beta'-NiAl formation of a nickel-aluminum (Ni2Al) superlattices
[NASA-TT-20177] 14 p1890 N88-21297
Fundamental properties and devices applications of Ge(x)Si(1-x)/Si superlattices
[AD-A190129] 15 p2143 N88-22787
On the use of convergent beam electron diffraction for identification of antiphase boundaries in GaAs grown on Si
[DE88-008220] 18 p2585 N88-25362
Diffraction transition radiation from periodic electron bunches
[AD-A193593] 23 p3280 N88-29528
The effect of oriented defects on long-range ordering of hydrocarbon films: Azulene on Pt(111)
[AD-A196089] 24 p3344 N88-29904

ELECTRON DISTRIBUTION
NT ELECTRON DENSITY PROFILES
Self-consistent modification of a fast tail distribution by resonant fields in nonuniform plasmas
[AD-A183790] 01 p0099 N88-10650
The single particle and collective descriptions of the anomalous Doppler resonance and the role of ion dynamics
[INPE-4390-PRE/1210] 08 p0976 N88-15904
Interaction of acoustic and electromagnetic waves involved in anomalous skin effect
08 p1079 N88-16503
The structure of the sideband spectrum in free electron lasers
[AD-A186952] 09 p1170 N88-17015
A moment approach to modeling negative ion sources
[AD-A188858] 12 p1691 N88-20114
Electron temperature measurements in an argon/cesium plasma diode
[AD-A188835] 12 p1695 N88-20141
Hot electron diagnostics using X-ray imaging on GAMMA10 17 p2443 N88-24530
Application of particle simulations to the NRL laser experiment
[AD-A191641] 18 p2520 N88-24953
Observations of electron cyclotron harmonic emissions associated with field-aligned electron beams
[SD-TR-87-33] 19 p2724 N88-26173
On the conjugacy of the aurora: High and low latitudes
[AD-A193008] 20 p2824 N88-26755
Initial electron distributions for free-electron lasers generated by injector and accelerator simulations
[DE88-007022] 21 p2953 N88-27540

ELECTRON EMISSION
NT FIELD EMISSION
NT PHOTOELECTRIC EMISSION
NT SECONDARY EMISSION
Electron emission from conductors subjected to intense, short-pulse electric fields
[DE88-005412] 13 p1836 N88-20985
JPRS report: Science and technology. China
[JPRS-CST-87-041] 14 p1902 N88-21365
Breathing mode lattice relaxation associated with carrier emission and capture by deep electronic levels in silicon
[DE88-003844] 14 p1985 N88-21842
Theoretical model of the cathode spot on a unipolar arc
[AD-A190109] 15 p2059 N88-22277
Question on the measurement of the metal work function in an electron spectrometer by the secondary-electron emission threshold method
[NASA-TT-20190] 16 p2178 N88-22979
Degradation of beam brightness by field emission from a cathode shroud
[DE88-008345] 20 p2794 N88-26576
Effects of secondary electron emission on the collector and source sheaths of a finite ion temperature plasma
[DE88-008930] 20 p2858 N88-26971
Hot electron emission in semiconductors
[AD-A194101] 23 p3292 N88-29601

ELECTRON ENERGY
NT ELECTRON STATES
The optimum illumination conditions for EXELFS studies in a CTEM
[USIP-87-08] 01 p0092 N88-10600
A data analysis package for RDF-determination fromEXELFS-spectra
[USIP-87-07] 01 p0104 N88-10681
EXELFS (Extended Electron Energy Loss Fine Structure) of amorphous and crystalline SiC
[DE87-013551] 02 p0151 N88-10948
Analysis of energy confinement of slideaway discharges
[DE87-753008] 02 p0240 N88-11515
Application of a two fluid theoretical plasma transport model on current Tokamak reactor designs
[DE87-013511] 03 p0377 N88-12373
The effect of object potentials on the wake of a flowing plasma
[AD-A184038] 03 p0379 N88-12385
Methods and first results of plasma non-isothermal parameters measurements in meteor trails
06 p0737 N88-14531
Absorption of cyclotron radiation in skin layer in Araks experiment 08 p1003 N88-16076
Geometric structure, pseudoband gaps, and surface vibrational resonances on metal surfaces
[AD-A187001] 09 p1143 N88-16851
Magnetic control of low pressure discharges
[AD-A186794] 10 p1322 N88-17900
Kinetic studies following state-selective laser excitation
[DE88-004094] 10 p1335 N88-17981
Limiting efficiency of a thermionic diode
[DE88-700598] 11 p1479 N88-18830
Measurements of optically thin electron cyclotron emission from relativistic electrons
[DE88-004713] 12 p1688 N88-20096
Electron temperature measurements in an argon/cesium plasma diode
[AD-A188835] 12 p1695 N88-20141
To what extent is mass loading responsible for the Venus bowshock precursor?
[NASA-TM-89307] 12 p1711 N88-20239
Experimental studies of plasma heating due to the parametric decay of a large amplitude pump into lower hybrid waves 13 p1841 N88-21017
Arcs in cesium seeded noble gases resulting from a magnetically induced electric field
[EUT-87-E-177] 13 p1843 N88-21028
Calculation of the efficiency of a resonant cyclotronic electron maser (gyrotrons)
[INPE-4387-PRE/1207] 14 p1915 N88-21444
Rocket measurements of ionospheric electron temperature over Natal
[INPE-4485-PRE/1250] 15 p2096 N88-22489
Time-resolved spectroscopic measurement of anode plasma in magnetically-insulated diode
16 p2279 N88-23641
Thomson scattering for determining electron concentrations and temperatures in an inductively coupled plasma. 1: Assessment of the technique for a low-flow, low-power plasma
[AD-A191323] 16 p2280 N88-23651
Thomson scattering for determining electron concentrations and temperatures in an inductively coupled plasma. 2: Description and evaluation of a multichannel instrument
[AD-A191324] 16 p2280 N88-23652
Spectral diagnostics for temperature and density measurements on ATF 17 p2442 N88-24525
Hot electron diagnostics using X-ray imaging on GAMMA10 17 p2443 N88 24530
The Io sulfur torus in 1981
[NASA-TM-101139] 18 p2595 N88-25419
Outer zone electron precipitation produced by a VLF transmitter
[AD-A191944] 19 p2691 N88-25993

Properties of hydrogen/helium accretion plasmas
[DE88-006831] 19 p2728 N88-26197
Thermal inhibition by megagauss field due to variation of electron temperature in laser plasma
[DE88-701887] 20 p2859 N88-26977
Studying the physics and operation of multi-terminal near-micron and sub-micron length, hot electron semiconductor devices
[AD-A193380] 21 p2938 N88-27446
A study of tunneling phenomena in gallium arsenide-aluminum gallium arsenide heterostructures
21 p3023 N88-27946

ELECTRON FLUX
U ELECTRONS
U FLUX (RATE)

ELECTRON FLUX DENSITY
Field-aligned fluxes of energetic electrons related to the onset of magnetospheric substorms
08 p1096 N88-16595
Observations and analyses of summer whistlers at the Great Wall Station of Antarctica
11 p1469 N88-18759

ELECTRON GAS
Effect of collisional broadening on the polarizability of a two-dimensional electron gas
[DE87-013928] 02 p0237 N88-11497
Theory of the one- and two-dimensional electron gas
[DE87-012864] 02 p0244 N88-11540
Self-similar solutions of MHD equations of plasma filament in the case of complete degenerated ultrarelativistic electron gas
[DE86-700684] 10 p1412 N88-18426
Electrical resistivity as quantum chaos
[DE88-007026] 16 p2284 N88-23675

ELECTRON GUNS
Gyrotron development at the Instituto de Pesquisas Espaciais
[INPE-4240-PRE/1115] 08 p0990 N88-15992
Synthesis method applied to the design of an electron gun for a gyrotron
[INPE-4357-TDL/298] 13 p1773 N88-20807
Development of electrostatic-accelerator free-electron lasers
[AD-A189507] 13 p1774 N88-20614
Modulatable thin film field emission space gun
[AD-A189279] 13 p1845 N88-21043
Survey of the Air Force P78-2 (SCATHA) satellite plasma wave data during electron gun operations
[AD-A191014] 16 p2168 N88-22926

ELECTRON IMPACT
Simulation of tokamak runaway-electron events. Study of the response of materials by use of an electron linear accelerator
[IPPJ-841] 02 p0242 N88-11528
Atomic data for hydrogens in collisions with electrons: Addenda
[IPPJ-AM-55-ADD] 09 p1252 N88-17502
Contributions of autoionizing resonances to the electron collisional excitation rates for Be-like ions
[AD-A190924] 18 p2572 N88-25275
Development of the field-induced electron injection and impact ionization (F4I) technique for radiation hardness testing of MOS (Metal-Oxide-Semiconductor) gate insulators
[AD-A192114] 18 p2583 N88-25345
Electron impact ionization cross-section of some organic compounds
[DE88-702044] 23 p3280 N88-29525
Ion kinetics in silane plasmas
[AD-A196202] 24 p3431 N88-30423

ELECTRON INTENSITY
U ELECTRON FLUX DENSITY

ELECTRON INTERACTIONS
U ELECTRON SCATTERING

ELECTRON IONIZATION
U IONIZATION

ELECTRON IRRADIATION
Effects of 67.5 MeV electron irradiation on Y-Ba-Cu-O and Gd-Ba-Cu-O high-temperature superconductors
[AD-A191271] 16 p2283 N88-23669
Electron irradiation effects in YBa2Cu3O7-Delta single crystals
[DE88-010050] 20 p2878 N88-27085
Muon-spin rotation experiment (micro + SR) on aluminum and indium after low temperature electron irradiation
[ETN-88-92985] 23 p3294 N88-29617

ELECTRON MICROSCOPES
Electron sputtering in the analytical electron microscope: Calculations and experimental data
[DE87-011457] 01 p0049 N88-10312
Development of methods for low temperature diffusion bonding
[AD-A186875] 09 p1174 N88-17033
The measurement of chemical compositon with high spatial resolution using a dedicated scanning transmission electron microscope
[AERE-R-12317] 10 p1297 N88-17753
The contribution of electron microscopy of materials science to society
[DE88-006341] 15 p2028 N88-22082
In situ fatigue loading stage inside scanning electron microscope 15 p2083 N88-22419
Equipment for an advanced electron beam lithography system
[AD-A192956] 21 p2936 N88-27435

ELECTRON MICROSCOPY
Contribution to the study of the Ti-Al phase diagram by conventional and high resolution electron microscopy
[ESA-TT-1021] 01 p0023 N88-10143
Si - SiO2 interfaces: A High Resolution Transmission Electron Microscopy (HRTEM) study
[DE87-012255] 01 p0028 N88-10181
Detective quantum efficiency and design of a parallel data recording system for EXELFS-measurements --- electron microscopy
[USIP-87-06] 01 p0050 N88-10318
The optimum illumination conditions for EXELFS studies in a CTEM
[USIP-87-08] 01 p0092 N88-10600
Instrumental and operational aspects of an EXELFS system connected to JEOL 100C STEM
[USIP-87-09] 01 p0092 N88-10601
Energy-selected electron diffraction experiments using the rocking-crystal method in the raster microscope for the investigation of localization effects in single crystals
[ETN-87-90409] 01 p0104 N88-10682
Analytical electron microscopy characterization of boron in sintered alpha-SiC
[DE87-012532] 02 p0142 N88-10889
Study of the morphology of thermosetting matrices
[ONERA-RT-5/3346-M] 02 p0153 N88-10961
Solute segregation to phase interfaces and grain boundaries: Studies by analytical electron microscopy and profile deconvolution
[DE87-012129] 02 p0243 N88-11537
Modified 14Cr-16Ni stainless steels with improved creep resistance at 700 C due to tailored precipitate microstructures
[DE87-014788] 03 p0290 N88-11825
Fractographic study of fiber composites
06 p0677 N88-14146
Effect of temperature exposure on fatigue crack propagation 06 p0720 N88-14421
Atomic-level studies of superconducting YBa2Cu3O sub 7-x
[DE88-002522] 06 p0788 N88-14831
Study on the correlation of polystyrene (PS) film craze to its fracture behaviour by TEM (Transmission Electron Microscopy)
[PB87-143343] 08 p0970 N88-15870
Characterization of duplex stainless steel by TEM (Transmission Electron Microscopy), SANS (Small-Angle Neutron Scattering) and APFIM (Atom-Probe Field Ion Microscopy) techniques
[DE88-002916] 09 p1145 N88-16865
Calculated sputtering and atomic displacement cross-sections for applications to medium voltage analytical electron microscopy
[DE88-002904] 09 p1166 N88-17006
Optimization of imaging energy filters for analytical electron microscopy
[ETN-88-91079] 09 p1248 N88-17483
High resolution electron and ion microscopy
[AERE-R-12502] 10 p1297 N88-17754
Transmission electron microscopy studies of titanium-containing braze/alumina seals
[DE88-005243] 10 p1303 N88-17792
Application of nondestructive testing techniques to materials testing
[AD-A187645] 10 p1342 N88-18021
Simulation and processing of high resolution images of defects and interfaces in superconducting YBa2Cu3O7
[DE88-003856] 10 p1420 N88-18480
Electron tunneling microscopy
[AD-A187426] 11 p1452 N88-18652
Structural characterization of undoped and doped GaAs: A comparative study of four techniques
[DE88-004552] 11 p1555 N88-19304
Electron microscopy study of morphology and composition of a ferrisilicate catalyst
[DE88-005754] 11 p1562 N88-19352
Examination of polysulfide sealants by scanning electron microscopy
[MRL-R-1096] 13 p1752 N88-20478
Improved methods for high resolution electron microscopy
[DE88-005731] 13 p1774 N88-20609
Electron beam sensitive devices for controliability
[RR-658-I] 14 p1908 N88-21403
New method of examining micronon homogeneity of local centers in high-resistivity semiconductor materials under scanning electron microscope 14 p1969 N88-21754
Brillouin scattering and transmission electron microscopy studies of radiation-induced elastic softening, disordering and amorphization of intermetallic compounds
[DE88-005927] 14 p1987 N88-21850
Grain boundaries
[DE88-006628] 14 p1987 N88-21852
The contribution of electron microscopy of materials science to society
[DE88-006341] 15 p2028 N88-22082
An investigation of the crystalchemistry and thermochemistry of selected mineral systems
[AD-A189758] 15 p2142 N88-22781
Interface characterization of Cu-Cu and Cu-Ag-Cu low temperature solid state bonds
[AD-A191015] 16 p2283 N88-23667
SHaRE: Collaborative materials science research
[DE88-007175] 18 p2467 N88-24646
Electron microscopy of ceramic superconductors
[DE88-006446] 23 p3288 N88-29580
Degradation of protective coatings on steel in corrosive environments 24 p3354 N88-29969
Scanning electron microscopy study of adhesion in sea urchin blastulae
[NASA-CR-183136] 24 p3406 N88-30275

ELECTRON MOBILITY
Effect of collisional broadening on the polarizability of a two-dimensional electron gas
[DE87-013928] 02 p0237 N88-11497
Transport coefficients close to the mobility edge and nonlinear sigma model composite operators --- electron transport
[PREPRINT-541] 06 p0777 N88-14767
Thermodynamic and conductivity studies of nonstoichiometric cerium dioxide by Coulometric titration: A simultaneous measurement
[DE88-003054] 08 p1091 N88-16566
Defects in high-mobility semiconductor systems
[AD-A191618] 19 p2732 N88-26224
Transport study on Si/Si(1-x)Ge(x) superlattices selectively doped by secondary implantation of Sb
20 p2867 N88-27027
A GaAs solid state device model for high power applications
[DE88-011320] 21 p2939 N88-27457

ELECTRON MULTIPLIERS
U PHOTOMULTIPLIER TUBES

ELECTRON OPTICS
Optimization of imaging energy filters for analytical electron microscopy
[ETN-88-91079] 09 p1248 N88-17483
GERA computer code for calculation of two-dimensional electromagnetic fields in resonators and electron-optical systems by the finite element method
[DE88-700678] 11 p1480 N88-18831
Advanced electron optics for vibrational spectroscopy
[AD-A188469] 12 p1629 N88-19747
The new UCSB (University of California, Santa Barbara) compact far-infrared FEL
[AD-A190864] 16 p2212 N88-23203

ELECTRON ORBITALS
Core-core and core-valence correlation
[NASA-CR-182552] 11 p1544 N88-19226
Theoretical studies of the potential surface for the F - H2 greater than HF + H reaction
[NASA-CR-182551] 11 p1557 N88-19319
Numerical simulations of multiphoton processes in many electron atoms
[DE88-003293] 13 p1837 N88-20990

ELECTRON OSCILLATIONS
Tapered wiggler analysis of high gain free electron laser oscillators
[AD-A187997] 10 p1338 N88-17997
Research on a two-stage free electron laser oscillator
[AD-A195991] 24 p3377 N88-30115

ELECTRON PARAMAGNETIC RESONANCE
Formation and passivation of new paramagnetic defects associated with thermal oxides on silicon
[DE88-002720] 07 p0938 N88-15699
Electron Spin Resonance (ESR) measurements on intermediate-valence Cer compounds doped with paramagnetic ions: CeOs2:Gd ion and CePd3:Mn-ion
[ETN-88-91081] 09 p1256 N88-17526
Electron paramagnetic resonance studies of Mn(2+) in 2-6 semiconductor alloys 11 p1560 N88-19340
Excitations in magnetic low-dimensional systems: A spectroscopic study
[ETN-88-92230] 15 p2129 N88-22697
Structure and function of the manganese complex involved in photosynthetic oxygen evolution determined by X-ray adsorption spectroscopy and electron paramagnetic resonance spectroscopy
[DE88-010360] 21 p2985 N88-27725

Paramagnetic point defects in boron-implanted HgO.7CdO.3Te
[AD-A193276] 21 p3021 N88-27934
Photorefractive damage mechanism in electro-optic materials
[AD-A194560] 23 p3282 N88-29543
Chemical kinetics of hydrogen and P(sub b) centers
[DE88-010528] 23 p3291 N88-29594

ELECTRON PATHS
U ELECTRON TRAJECTORIES

ELECTRON PHONON INTERACTIONS
Properties of superconductors with strong electron-phonon interaction 14 p1974 N88-21779
Electron-Rayleigh wave interaction in thin film carbons
[AD-A191727] 18 p2492 N88-24781
Electron-phonon interactions in In(0.53)Ga(0.47)As and in In(0.53)Ga(0.47)As/InP quantum wells 20 p2869 N88-27037
Hot electrons in silicon dioxide: Ballistic to steady-state transport 20 p2871 N88-27042
The theory of electron-polar phonon scattering rates in semiconductor micro-structures 20 p2871 N88-27043
Anharmonic model for high-Tc superconductors
[DE88-702196] 21 p3020 N88-27924

ELECTRON PHOTON CASCADES
Energy cascading in the beat-wave accelerator
[DE87-014727] 03 p0377 N88-12374
Model-independent requirements to the source of positrons in the galactic centre
[DE88-700968] 14 p1992 N88-21874
Cascade fluorescences from laser-excited lithium atom for plasma diagnostics 17 p2442 N88-24526

ELECTRON PLASMA
Nonlinear, relativistic Langmuir waves in astrophysical magnetospheres
[NASA-CR-182422] 08 p1024 N88-16197
Self-similar solutions of MHD equations of plasma filament in the case of complete degenerated ultrarelativistic electron gas
[DE88-700684] 10 p1412 N88-18426
Electron heat transport in TFR with Electron Cyclotron Resonance Heating (ECRH) 12 p1694 N88-20135
Arcs in cesium seeded noble gases resulting from a magnetically induced electric field
[EUT-87-E-177] 13 p1843 N88-21028
The foreshock region upstream from the Comet Halley bow shock 14 p1995 N88-21893
Measurement of time evolution of plasma electron component parameters on the Ogra-4 device by the Thomson scattering method
[DE88-701575] 16 p2282 N88-23662
Nonlinear optical properties and subpicosecond dynamics of excitons and electron-hole plasmas in multiple quantum well structures
[AD-A191926] 19 p2727 N88-26196
Alternative analysis of CO2-laser-produced plasma waves
[DE88-008434] 19 p2730 N88-26215

ELECTRON PRECIPITATION
Configurations of the quiet polar cap and its response to a sudden increase of the energy input rate epsilon
[DMI-GEOPHYS-PAPERS-R-74] 03 p0350 N88-12210
Relativistic electron precipitations in a pulsating aurora 04 p0468 N88-12894
First results from the Viking associated Aureld-VIP rocket and EISCAT campaign --- auroras; Swedish satellite 08 p1026 N88-16211
Spectrophotometric remote sensing of the diffuse aurora
[AD-A188599] 12 p1643 N88-19837
Stimulated Emission of Energetic Particles (SEEP)
[AD-A188724] 13 p1853 N88-21094
The Jovian aurora: Electron or ion precipitation
[NASA-TM-101153] 17 p2452 N88-24566
Outer zone electron precipitation produced by a VLF transmitter
[AD-A191944] 19 p2691 N88-25993
Rocket measurements within a polar cap arc: Ionospheric modelling
[AD-A192381] 20 p2824 N88-26754
On the conjugacy of the aurora: High and low latitudes
[AD-A193008] 20 p2824 N88-26755
Investigation of the potential impact of new photonic materials on optical processing systems 21 p2924 N88-27359
The low-latitude auroral boundary: Steady-state and time-dependent representations
[AD-A193200] 21 p2972 N88-27656

ELECTRON PROBES
Quantitative electron probe microanalysis investigation of the oxidation of high temperature alloys at low oxygen partial pressures
[JUEL-2120] 03 p0288 N88-11811

ELECTRON PUMPING
Electron acceleration by wave processes in the earth's ionosphere
[AD-A186110] 07 p0877 N88-15320
Generation of light pulses in semiconductor laser upon excitation by several electron beams 07 p0920 N88-15589
Nuclear excitation via the motion of electrons in a strong laser field
[AD-A187166] 09 p1171 N88-17017
Semiconductor laser with electron-beam pumping and fiber-optic output waveguide 09 p1235 N88-17405
High-efficiency GaAs semiconductor laser with longitudinal excitation by scanning electron beam 09 p1238 N88-17421
Periodic-pulse semiconductor laser with electron-beam pumping 09 p1238 N88-17422
X-ray lasers: State of art and prospect
[ETN-88-92003] 14 p1914 N88-21434
Blue-green laser diode research program
[AD-A191980] 23 p3218 N88-29153
Proof of the feasibility of coherent and incoherent schemes for pumping a gamma-ray laser
[AD-A193856] 23 p3220 N88-29165

ELECTRON RADIATION
NT BETA PARTICLES
NT ELECTRON BEAMS
NT RELATIVISTIC ELECTRON BEAMS

ELECTRON RECOMBINATION
NT RADIATIVE RECOMBINATION

ELECTRON RING ACCELERATORS
U STORAGE RINGS (PARTICLE ACCELERATORS)

ELECTRON SCATTERING
Ab initio methods for electron-molecule collisions
[DE87-011728] 01 p0092 N88-10598
Electron interactions with nuclei
[DE87-014587] 02 p0232 N88-11460
Complex scattering dynamics and the integer quantum Hall effect
[DE87-011790] 02 p0243 N88-11536
Extending the range of Low Energy Electron Diffraction (LEED) surface structure determination: Co-adsorbed molecules, incommensurate overlayers and alloy surface order studied by new video and electron counting LEED techniques
[DE88-001401] 06 p0786 N88-14820
Electron scattering off palladium isotopes. An investigation of the equivalence of the anharmonic vibrator model and the interacting boson model
[B8671274] 07 p0931 N88-15654
Hyperspherical coordinate theory of two-electron processes: Future plans
[DE87-010653] 08 p1081 N88-16516
Group 2A metastable collision complexes: Spectroscopy and behavior in intense radiation fields
[AD-A186737] 08 p1082 N88-16524
Semiclassical theory of the nuclear response function. Quasielastic electron scattering
[ETN-88-91082] 09 p1245 N88-17459
Investigation of a new magnetic dipole mode in the heavy, deformed nuclei 154 Sm, 156 Gd, 158 Gd, 164 Dy, 168 Er, and 174 Yb with high resolution electron scattering
[ETN-88-91084] 09 p1245 N88-17460
A research program in neutrino physics, cosmic rays and elementary particles
[DE88-003507] 09 p1264 N88-17575
Correlated processes in atomic collisions
[DE88-003508] 10 p1406 N88-18383
Generalised scattering model for the quantum modulation of electrons 11 p1563 N88-19357
Photohydrodynamical processes near compact objects 11 p1569 N88-19390
Advanced electron optics for vibrational spectroscopy
[AD-A188469] 12 p1629 N88-19747
Experimental set-up for measurements of Compton scattering cross section on light nuclei
[DE88-700161] 12 p1688 N88-20097
Models of recombination lines in radio H2 regions
[INPE-4302-TDL/277] 12 p1710 N88-20232
Electron stimulated desorption and coherent electron scattering
[AD-A189091] 13 p1835 N88-20978
Renormalized Fermi liquid theory for disordered electron systems and the metal-insulator transition
[NOTA-INTERNA-900] 14 p1988 N88-21862
Effective electron interactions due to virtual charge and spin excitations in an extended Hubbard model for Cu-O superconductors
[DE88-005971] 15 p2139 N88-22766
An electron-scattering study of N-15
[ETN-88-92479] 16 p2266 N88-23552
Measurement of time evolution of plasma electron component parameters on the Ogra-4 device by the Thomson scattering method
[DE88-701575] 16 p2282 N88-23662
Distorted-wave-method calculation of electron-impact excitation of atomic ions 17 p2443 N88-24532
Trochoidal analysis of scattered electrons in a merged electron-ion beam
[NASA-CASE-NPO-16789-1-CU] 18 p2573 N88-25281
Ion and electron interactions of atmospheric importance
[AD-A192255] 20 p2824 N88-26751
Inelastic electron scattering and electron-hole excitations in iron and nickel
[DE88-011843] 21 p2915 N88-27303
Nonlinear dynamics of the electron self-field interaction
[DE88-010597] 21 p2934 N88-27420
Self energy corrections to the ab initio band structures: Chromium
[DE88-701825] 21 p3020 N88-27927
Effect of a laser field in the electron inelastic scattering into plasma fields
[DE88-702295] 23 p3218 N88-29157
On selection rules and inelastic electron scattering at intermediate energies
[DE88-701833] 23 p3280 N88-29526
Dispersion effects in elastic electron scattering from C12
[B8805297] 23 p3281 N88-29536

ELECTRON SOURCES
Higher harmonic generation in the induced resonance electron cyclotron maser
[AD-A186236] 07 p0858 N88-15210
The measurement of chemical compositon with high spatial resolution using a dedicated scanning transmission electron microscope
[AERE-R-12317] 10 p1297 N88-17753
X-ray source model for Z-pinch aluminum plasmas
[AD-A189509] 12 p1696 N88-20148
Program to research laser-driven thermionic electron sources for free electron lasers
[AD-A190473] 15 p2072 N88-22353
Optical guiding in the separable beam limit
[AD-A192452] 21 p2952 N88-27534

ELECTRON SPECTROSCOPY
Application of spin-sensitive electron spectroscopies to investigations of electronic and magnetic properties of solid surfaces and epitaxial systems
[DE87-014235] 02 p0245 N88-11550
Multichannel electron counter with high space resolution
[DE88-700564] 07 p0857 N88-15204
Near threshold behavior of photoelectron satellite intensities
[DE88-002231] 08 p1081 N88-16512
Studies of the electron spectrum with reference to the clean surfaces of iron, cobalt and nickel and their subsequent exposure to oxygen 11 p1459 N88-18700
An electron spectroscopic investigation of high-temperature superconducting oxides
[DE88-003807] 11 p1558 N88-19325
An interpretation of the ethylenic, carbidic, and graphite auger lineshapes of chemisorbed carbon species
[AD-A189092] 13 p1736 N88-20379
Question on the measurement of the metal work function in an electron spectrometer by the secondary-electron emission threshold method
[NASA-TT-20190] 16 p2178 N88-22979
Interface characterization of Cu-Cu and Cu-Ag-Cu low temperature solid state bonds
[AD-A191015] 16 p2283 N88-23667
Ballistic transport and hot electron spectroscopy in Tunneling Hot Electron Transfer Amplifier (THETA) 19 p2659 N88-25808
Resonant tunneling electron spectroscopy 19 p2660 N88-25811
An IETS (Inelastic Electron Tunneling Spectroscopy) study of surface reactions applicable to adhesion
[AD-A192274] 21 p2909 N88-27261
Application of Auger electron spectroscopy to the study of trace element effects on weldability
[DE88-010457] 21 p2915 N88-27301

ELECTRON SPIN RESONANCE
U ELECTRON PARAMAGNETIC RESONANCE

ELECTRON STATES
Nitrogen energy transfer study
[AD-A184457] 04 p0464 N88-12869
Effect of rapid solidification on short-range order: A magnetic study
[AD-A185216] 05 p0565 N88-13444
Density of states of electrons bound to impurities in quantum wells of GaAlAs/GaAs
[INPE-4257-PRE/1130] 08 p1089 N88-16557
Energy disposal in ion-molecule reactions
[AD-A186772] 09 p1171 N88-17019

Electronic and chemical structure of 3-5/metal and Si/metal interfaces
[AD-A186579] 09 p1254 N88-17518
Clusters: Link between molecules and solids
[AD-A188170] 11 p1543 N88-19224
Investigation of multiple particle final states at CEBAF (Continuous Electron Beam Accelerator Facility)
[CEBAF-PR-87-026] 11 p1547 N88-19250
Photoenhanced attachment for optical control of diffuse discharges
[AD-A188989] 12 p1696 N88-20147
Overview of hydrogen clusters
16 p2267 N88-23557
Direct subpicosecond measurement of carrier mobility of photoexcited electrons in GaAs
19 p2659 N88-25803
Monte Carlo investigation of hot photoexcited electron relaxation in GaAs 19 p2659 N88-25805
Charge storage and switching phenomena in metal complexes
[AD-A193778] 23 p3192 N88-28996
Electronic states of the Xe(sub n)HCl systems in gas and condensed phases
[AD-A193881] 23 p3192 N88-28997
Theoretical investigation of image states of the hydrogen covered Cu (100)
[DE88-702662] 23 p3292 N88-29604

ELECTRON SWEEPING
U SWEEP FREQUENCY

ELECTRON TELESCOPES
U PARTICLE TELESCOPES

ELECTRON TEMPERATURE
U ELECTRON ENERGY

ELECTRON TRAJECTORIES
Trajectory versus PIC methods in diode design
[DE87-012135] 02 p0166 N88-11043

ELECTRON TRANSFER
Monte Carlo simulation of primitive atom-transfer reactions in solution
[AD-A183977] 03 p0375 N88-12360
Vectorial electron transfer on designed surfaces
[PB87-232229] 03 p0381 N88-12394
A strategy to determine the transition state of an electron transfer reaction
[AD-A183976] 03 p0382 N88-12404
K-CO on transition metals: A local ionic interaction
[AD-A184342] 04 p0496 N88-13056
The role of electronic structure calculation in mechanistic analysis of electron transfer reactions in the liquid phase
[DE87-014395] 05 p0647 N88-13963
Photoinduced charge separation by polymer-bound chromophores
[DE88-002101] 06 p0685 N88-14198
Artificial photosynthesis using chlorophyll based carotenoid-quinone triads
[DE88-001660] 07 p0884 N88-15362
Effects of energy, distance and orientation on electron transfer rates studied by pulse radiolysis in organic media
[DE88-002906] 08 p1082 N88-16521
Insights into the mechanisms of chemical reactions: Reaction paths for chemical reactions
[DE88-003041] 10 p1297 N88-17755
Energy transfer and photochemistry in biomimetic solar conversion
[PB88-130026] 10 p1348 N88-18057
Correlated processes in atomic collisions
[DE88-003508] 10 p1406 N88-18383
Electron transfer to iron(3) oxide colloids
[DE88-002885] 10 p1416 N88-18448
Mechanisms of photoinduced electron transfer
[DE88-004917] 13 p1836 N88-20983
Electrochemistry in near-critical and supercritical fluids. 5: The dimerization of quinoline and acridine radical anions and dianions in ammonia from -70 C to 150 C
[AD-A190658] 16 p2175 N88-22967
Spectroscopic data relevant to alpha particle diagnostics 17 p2442 N88-24527
Electrode films of porous agarose: The effects of physical structure on electron transport processes
[DE88-007366] 19 p2611 N88-25493
Ballistic transport and hot electron spectroscopy in Tunneling Hot Electron Transfer Amplifier (THETA)
19 p2659 N88-25808
Mechanisms of photochemical energy conversion by chlorophyll
[DE88-008763] 20 p2819 N88-26725
Ferromagnetic/semiconductor hybrid structures
20 p2865 N88-27013
Hot electrons in silicon dioxide: Ballistic to steady-state transport 20 p2871 N88-27042
Vertical electronic transport in novel semiconductor heterojunction structures 20 p2871 N88-27045
Factors governing light driven electron and proton translocation in proteins across membranes
[DE88-011120] 21 p2984 N88-27724
Studies of photochemically and electrochemically driven electron transport in zeolites
[DE88-008644] 22 p3155 N88-28769
Electrochemical and optical studies of model photosynthetic systems
[DE88-009291] 23 p3237 N88-29264
Cytochrome electron transfer and biomolecular electronics
[AD-A195482] 24 p3406 N88-30277

ELECTRON TRANSITIONS
Gaining control over rare earth valence fluctuations
[DE87-010116] 01 p0103 N88-10671
A strategy to determine the transition state of an electron transfer reaction
[AD-A183976] 03 p0382 N88-12404
XUV emission features from the Livermore soft X-ray laser experiments
[DE88-000420] 04 p0448 N88-12779
J = O Task Force
[DE88-001326] 04 p0450 N88-12788
Wavelengths of the 3p-3d transitions of the Co- and Fe-like ions: The effects of electron correlation
[DE88-000219] 04 p0498 N88-13067
Nitrogen scale-up
[AD-A185702] 06 p0709 N88-14351
Thermoelectric power in disordered electronic systems near the Anderson transition
[PREPRINT-547] 06 p0731 N88-14494
Experimental observation of photoresonance of electrons localized above surface of solid hydrogen
06 p0774 N88-14755
Electronic band structure and photoemission: A review and projection
[DE88-002236] 06 p0787 N88-14829
Electron scattering off palladium isotopes. An investigation of the equivalence of the anharmonic vibrator model and the interacting boson model
[B8671274] 07 p0931 N88-15654
Theoretical studies of atomic transitions
[DE88-004719] 10 p1407 N88-18389
Nuclear transitions induced by atomic excitations
[DE88-004311] 11 p1545 N88-19239
Correlations between photons in resonance fluorescence emitted by an atom near a metal surface
[AD-A188365] 12 p1689 N88-20102
Macroscopic quantum jumps in a single atom
14 p1975 N88-21784
Laser cooling of neon metastable states
14 p1975 N88-21785
Theoretical studies of solar-pumped lasers
[NASA-CR-182929] 17 p2344 N88-23971
Transition probabilities in OH A 2 sigma + - X 2 pi i: Bands with v prime = 0 and 1, v double prime = 0 to 4
[NASA-CR-182946] 18 p2584 N88-25353
Inner-shell X-ray line spectra of highly ionized titanium, chromium, iron and nickel and their appliation to laboratory plasmas
[PB87-225181] 19 p2730 N88-26212

ELECTRON TUBES
NT CATHODE RAY TUBES
NT COLD CATHODE TUBES
NT CYCLOTRON RESONANCE DEVICES
NT GAS DISCHARGE TUBES
NT IMAGE DISSECTOR TUBES
NT IMAGE TUBES
NT KLYSTRONS
NT MAGNETRONS
NT MICROWAVE TUBES
NT PHOTOMULTIPLIER TUBES
NT THERMIONIC DIODES
NT THYRATRONS
NT TRAVELING WAVE TUBES
NT VIDICONS

ELECTRON TUNNELING
Superconducting properties of metallic superlattices
[DE87-012725] 01 p0023 N88-10146
Vacuum ultraviolet electronic properties of liquids
[DE88-000165] 03 p0282 N88-11772
Monte Carlo simulation of primitive atom-transfer reactions in solution
[AD-A183977] 03 p0375 N88-12360
Studies of tunneling in metals under high pressure
06 p0775 N88-14757
Macroscopic quantum effects in a Josephson tunnel junction
[DE88-002239] 06 p0787 N88-14830
Some investigations of molecular beam epitaxial growth of 3-5 semiconductor films via Monte-Carlo computer simulations, carrier tunnelling and spectroscopic ellipsometry
[AD-A185520] 06 p0789 N88-14839
Experimental aspects of high-T/sub c/ superconductors
[DE88-003019] 08 p1090 N88-16564
Properties of superconducting tunnel structures in microwave radiation field 09 p1239 N88-17424
Electron tunneling microscopy
[AD-A187426] 11 p1452 N88-18652
Joint services electronics program
[AD-A188173] 11 p1478 N88-18822
The physics of very small structures
[AD-A187672] 11 p1556 N88-19311
Microelectronic applications of the conductor-thin insulator-semiconductor (CIS) structure
11 p1560 N88-19341
Dynamical aspects of carrier tunneling in semiconductor superlattices 14 p1977 N88-21799
Long-time tunneling in amorphous metals at helium temperatures
[DE88-701150] 16 p2281 N88-23654
Local density of states in double-barrier resonant tunneling structures
[AD-A190673] 16 p2281 N88-23656
A proposed Quantum Well Injection Transit Time device (QWITT) 19 p2657 N88-25785
Ballistic transport and hot electron spectroscopy in Tunneling Hot Electron Transfer Amplifier (THETA)
19 p2659 N88-25808
Microwave and millimeter-wave resonant tunneling diodes 19 p2659 N88-25809
Resonant tunneling electron spectroscopy
19 p2660 N88-25811
Electron device probing in the femtosecond time scale
19 p2660 N88-25821
Electron tunneling in junctions doped with semiconductors and metals 19 p2734 N88-26236
Third International Conference on Superlattices, Microstructures and Microdevices
[AD-A191416] 20 p2861 N88-26995
Theoretical aspects of electron transport in modulated structures 20 p2865 N88-27016
Resonant tunneling transistors and resonant tunneling hot electron spectroscopy 20 p2866 N88-27018
Pressure-dependent measurement on n + GaAs (Si, Sn): The effect of deep donor (DX) states on the electrical properties and presistent photoconductivity effects
20 p2866 N88-27020
Resonant tunneling in InGaAs-InP double-barrier structures and superlattices 20 p2871 N88-27047
Excellent negative differential resistance of InGaAs/InAlAs resonant tunneling barrier structures and applications to a new functional device, RHET
20 p2872 N88-27048
Pure metallic bridge and point-contact tunneling into single- and polycrystal YBa2Cu3O(sub 7-y)
[DE88-010030] 20 p2878 N88-27084
An IETS (Inelastic Electron Tunneling Spectroscopy) study of surface reactions applicable to adhesion
[AD-A192274] 21 p2909 N88-27261
Solar energy conversion through the interaction of plasmons with tunnel junctions. Part A: Solar cell analysis. Part B: Photoconductor analysis
[NASA-CR-183044] 21 p2967 N88-27621
A study of tunneling phenomena in gallium arsenide-aluminum gallium arsenide heterostructures
21 p3023 N88-27946
Tunnelling currents in reverse biased CMT photodiodes
[HSRE-MEMO-4137] 23 p3209 N88-29097

ELECTRON-HOLE DROPS
Free carrier nonlinear optics 14 p1977 N88-21796

ELECTRON-ION RECOMBINATION
NT RADIATIVE RECOMBINATION
Molecular sources of ionospheric holes
[AD-A191857] 18 p2541 N88-25082

ELECTRON-POSITRON ANNIHILATION
U POSITRON ANNIHILATION

ELECTRON-POSITRON PAIRS
Vector boson pair production in e(+)e(-) collisions
[PREPRINT-549] 06 p0778 N88-14774
Electronic factors for K-shell-electron conversion probability and electron-positron pair formation probability in electric monopole transitions
[DE87-753040] 08 p1089 N88-16551

ELECTRONIC AIRCRAFT
Testing of the engine compartment fire extinguishing system in the F/EF-111 aircraft
[AD-A188801] 12 p1576 N88-19423

ELECTRONIC AMPLIFIERS
U AMPLIFIERS

ELECTRONIC CONTROL
Engine/airframe response evaluation of the HH-60A helicopter equipped with the T700-GE-701 transient droop improvement electronic control unit
[AD-A184443] 04 p0401 N88-12492
Radio frequency electromagnetic interference fields. A study in Swedish industry
[FOA-E-30007-3.3] 06 p0692 N88-14247
Faraday cup characterization of electron beam welding parameters
[DE88-001896] 07 p0864 N88-15241

Pumping systems and flow interfaces for rapid response electronic reheat controls 10 p1282 N88-17665
Photo-optical converter of angular displacements in digital servomechanisms
[DE87-703208] 14 p1961 N88-21698
The design of an intelligent multidisk control module for VME bus based systems
[AD-A195587] 24 p3411 N88-30303

ELECTRONIC COUNTERMEASURES
NT ANTIRADAR COATINGS
A study of infrared missile seekers and the countermeasure techniques employed to defeat them
[ETN-87-90927] 02 p0131 N88-10822
Airborne bistatic radar applications
[ETN-87-90930] 02 p0163 N88-11020
JPRS report: Science and technology. China
[JPRS-CST-87-031] 03 p0299 N88-11880
Efficiency analysis of airborne Electronic CounterMeasures (ECM) systems
[AD-A184606] 03 p0306 N88-11934
A Gram-Schmidt space-time adaptive canceller using adaptive lattice filters
[AD-A189684] 14 p1959 N88-21684
High speed transcendental elementary function architecture in support of the Vector Wave Equation (VWE)
[AD-A189746] 15 p2119 N88-22627
Acta aeronautica et astronautica sinica (selected articles)
[AD-A191552] 18 p2455 N88-24575
Computation of ECM (Electronic Counter-Measures) war reserve materiel spare requirements
[AD-A193301] 21 p2897 N88-27195
Sidelobe level of an adaptive array using the SMI (Sampled Matrix Inversion) algorithm
[AD-A193131] 21 p2932 N88-27409
Distortions in processed signals and their application in electronic design. Part 3: An automated generator of communication jamming signals
[DE88-702733] 23 p3205 N88-29072
The surface evaporative duct height product: An evaluation
[AD-A195918] 24 p3392 N88-30199

ELECTRONIC EQUIPMENT
NT AVALANCHE DIODES
NT BIPOLAR TRANSISTORS
NT CHARGE COUPLED DEVICES
NT CHARGE TRANSFER DEVICES
NT CMOS
NT CRYSTAL RECTIFIERS
NT DIODES
NT ELECTRONIC FILTERS
NT ELECTRONIC MODULES
NT ELECTRONIC PACKAGING
NT ELECTRONIC TRANSDUCERS
NT FIELD EFFECT TRANSISTORS
NT GALLIUM ARSENIDE LASERS
NT GERMANIUM DIODES
NT GUNN DIODES
NT HETEROJUNCTION DEVICES
NT HIGH ELECTRON MOBILITY TRANSISTORS
NT JFET
NT JUNCTION DIODES
NT JUNCTION TRANSISTORS
NT LIGHT EMITTING DIODES
NT METAL OXIDE SEMICONDUCTORS
NT MIM (SEMICONDUCTORS)
NT MIM DIODES
NT MINIATURE ELECTRONIC EQUIPMENT
NT MIS (SEMICONDUCTORS)
NT MODFETS
NT MSM (SEMICONDUCTORS)
NT PHOTODIODES
NT PHOTOVOLTAIC CELLS
NT PLASMA DIODES
NT RUBY LASERS
NT SCHOTTKY DIODES
NT SEMICONDUCTOR DEVICES
NT SEMICONDUCTOR DIODES
NT SEMICONDUCTOR LASERS
NT SILICON TRANSISTORS
NT SIS (SEMICONDUCTORS)
NT SOI (SEMICONDUCTORS)
NT SOLAR CELLS
NT SOLID STATE DEVICES
NT SOLID STATE LASERS
NT SOS (SEMICONDUCTORS)
NT SPACECRAFT ELECTRONIC EQUIPMENT
NT THERMIONIC DIODES
NT THERMISTORS
NT THYRISTORS
NT TRANSFERRED ELECTRON DEVICES
NT TRANSISTOR AMPLIFIERS
NT TRANSISTORS
NT TUNNEL DIODES
NT VARISTORS
NT VERTICAL JUNCTION SOLAR CELLS
NT YAG LASERS
Center for Electronics and Electrical Engineering Technical Progress Bulletin covering center programs, October to December 1986 with 1987 CEEE events calendar
[PB87-226890] 02 p0168 N88-11058
Center for Electronics and Electrical Engineering technical publication announcements covering center programs, July to September 1986 with 1987 CEEE events calendar
[PB87-223442] 02 p0168 N88-11059
Application of electronic fuel injection to the optimum engine for methanol utilization
[PB87-201950] 02 p0180 N88-11120
A tutorial on Rogowski coil theory and operation
[DE86-000006] 02 p0230 N88-11449
Identifying areas of leading edge Japanese science and technology: Patent activity and citation analysis using US POC (Patent Office Classification) classification
[PB87-204095] 02 p0249 N88-11575
Estimating payload internal temperatures and radiator size for multimegawatt space platforms
[DE88-000244] 03 p0275 N88-11738
Center for Electronics and Electrical Engineering Technical Progress Bulletin covering center programs, January to March 1987 with 1987 CEEE events calendar
[PB87-224648] 03 p0309 N88-11946
Electronic system reliability and effectiveness
[AD-A184522] 03 p0311 N88-11961
Dramatically improved radiation hardness for CMOS silicon gate integrated circuits even down to cryogenic temperatures
[AD-A184672] 03 p0381 N88-12398
Design of digital filters for electronic instrumentation
[PB87-100418] 04 p0438 N88-12716
Alternating current circuit theory and pulsed NMR (Nuclear Magnetic Resonance)
[DE88-000641] 04 p0440 N88-12732
Corrosion of electronic components
05 p0547 N88-13333
Development of an interface for an ultrareliable fault-tolerant control system and an electronic servo-control unit
[NASA-TM-88236] 05 p0553 N88-13367
Electromagnetics and electrothermal approach to evaluate failures in microelectronic devices caused by electrostatic discharges: Stochastical aspects of the device reliability
[AD-A184906] 05 p0577 N88-13522
Fabricate, calibrate and test a dosimeter for integration into the CRRES (Combined Release and Radiation Effects Satellite) satellite
[AD-A185439] 05 p0585 N88-13564
Developments in electronics ceramics reported
06 p0684 N88-14192
Use of colour on electronic data displays (second study)
[PB87-126744] 06 p0754 N88-14627
Survey of electronic measurement needs below 10 MHz
[PB88-110366] 07 p0844 N88-15121
Supportability in aircraft systems through technology and acquisition strategy applications
[AD-A186465] 08 p0949 N88-15759
Validation of a stochastic model to determine failure rates for communication-electronic systems
[AD-A186536] 08 p0980 N88-15920
A study of the TCAS 2 collision avoidance system mounted on a Boeing 737 aircraft
[NASA-CR-182457] 09 p1116 N88-16687
Interchange of electronic design through VHDL and EIS 09 p1205 N88-17222
Joint services electronics program
[AD-A187587] 10 p1325 N88-17920
MBE growth, characterization and electronic device processing of HgCdTe, HgZnTe related heterojunctions and HgCdTe-CdTe superlattices
[AD-A187456] 10 p1421 N88-18486
A new fire protection concept for electronic equipment
[AD-A188884] 12 p1614 N88-19651
Development of an electronically-scanned pressure module for operation at cryogenic temperatures
[NASA-CR-181610] 12 p1629 N88-19746
Joint services electronics program
[AD-A189262] 13 p1761 N88-20533
The cooling of electronic equipment in fighter aircraft
[MBB/LKE-312/S/PUB/258] 14 p1866 N88-21147
A data acquisition system for atmospheric tracer studies
[DE88-006211] 14 p1991 N88-21869
Investigations of test methodology for the stress loading facility
[PB88-166095] 15 p2022 N88-22049
Experimental studies on electronic properties of HgTe/CdTe and Hg sub 1-z Cd sub x Te/CdTe heterostructures and superlattices
[AD-A189826] 15 p2142 N88-22783
Nondestructive evaluation of large scale composite components
[AD-A190998] 16 p2173 N88-22954
A PC-based receiver-decoder for remote sensor monitoring
[DE88-004733] 16 p2192 N88-23075
X-ray production in low energy proton stopping
[NASA-TM-100619] 16 p2270 N88-23582
Developing systems using state-of-the-art CAD/CAM technology 17 p2306 N88-23795
Single phase liquid immersion cooling of discrete heat sources in a vertical channel
[AD-A191224] 17 p2337 N88-23944
Joint services electronics program
[AD-A192076] 18 p2504 N88-24856
The inspection of metallurgical bounds in electronic systems
[AD-A192064] 18 p2582 N88-25343
Electronic controller for reciprocating rotary crystallizer
[NASA-TM-101140] 18 p2584 N88-25354
Aircraft field degradation and electromagnetic compatibility
[PB88-183975] 19 p2602 N88-25456
Research and development programs on advanced structural ceramics in Korea 19 p2633 N88-25620
Failure rate prediction of electronic components
[PB87-228953] 19 p2678 N88-25925
The Oak Ridge National Laboratory strategic defense initiative shield optimization program
[DE88-008946] 19 p2721 N88-26160
Decision aiding and coordination in decision-making organizations
[AD-A191950] 19 p2738 N88-26259
High bandwidth optoelectronic signal link for use in an EMP (electromagnetic pulse) plus radiation environment
[DE88-009254] 20 p2790 N88-26549
The Oak Ridge National Laboratory strategic defense initiative shield optimization program: Executive summary
[DE88-008016] 20 p2847 N88-26899
Superconducting electronic film structures
[AD-A192907] 20 p2879 N88-27091
Investigation of expert system design approaches for electronic design environments
21 p2926 N88-27365
A method for estimating the susceptibility of electronic systems to HPM (High Power Microwave)
[DE88-012246] 21 p2934 N88-27422
FEB (Multifilter Electronics Box) lifting device analysis, revision A
[AD-A192313] 21 p2935 N88-27427
Equipment for an advanced electron beam lithography system
[AD-A192956] 21 p2936 N88-27435
Electronic failure analysis-corrosion of avionics
22 p3054 N88-28122
Burn-in with mixed populations
[AD-A194651] 22 p3085 N88-28321
Avionics system design for high energy fields: A guide for the designer and airworthiness specialist
[NASA-CR-181590] 23 p3178 N88-28919
Laser and electrochemical studies of metallizations in electronic devices
[AD-A193786] 23 p3208 N88-29090
Center for opto-electronic systems research instrumentation grant
[AD-A193711] 23 p3282 N88-29545
Numerical simulation of the function of scientific instrumentation for measuring the speed of electron devices
[AD-A194969] 24 p3376 N88-30103
Electronic materials and devices prepared by molecular beam epitaxy
[AD-A195694] 24 p3433 N88-30433

ELECTRONIC EQUIPMENT TESTS
Instrument for radiation testing/screening electronic devices over an extended temperature range
[AD-A184245] 03 p0326 N88-12060
The Shock and Vibration Bulletin. Part 1: Welcome, Keynote Address, Invited Papers, Nondevelopment Items Workshop and Pyrotechnic Shock Workshop
[AD-A186748] 08 p0997 N88-16034
Designing electronics for pyrotechnic shock
08 p0997 N88-16038
The ESA centralized management system for satellite electronic test and checkout instrumentation
09 p1124 N88-16731
The response of a power MOSFET (N-channel) and a dielectric isolated operational amplifier to the combined environmental effects of high temperature and total dose gamma radiation 17 p2406 N88-24309

Aircraft field degradation and electromagnetic compatibility
[PB88-183975] 19 p2602 N88-25456
A non-contact picosecond prober for integrated circuit testing 19 p2655 N88-25766
Development of an airborne facility for advanced avionics research
[NLR-MP-87012-U] 20 p2760 N88-26368
RLE progress report, January 1 to December 31, 1987
[RLE-PR-130] 21 p3011 N88-27869

ELECTRONIC FILTERS
Advanced capacitor development
[AD-A189985] 15 p2059 N88-22276

ELECTRONIC LEVELS
U ELECTRON ENERGY
U ENERGY LEVELS

ELECTRONIC MAIL
Replication and reconfiguration in a distributed mail repository
[AD-A186967] 09 p1151 N88-16897

ELECTRONIC MODULES
New approach to telemetry development will significantly increase productivity of Joint Test Assembly (JTA) teams
[DE88-001676] 05 p0554 N88-13373
Application of knowledge based systems to the maintenance of inertial system electronics 12 p1578 N88-19441

ELECTRONIC PACKAGING
Applications of heat pipes to cool PWBS and hybrid microcircuits 02 p0136 N88-10858
Plasma and ion etching for failure analysis. Part 2. The etching of plastic encapsulant and other semiconductor device materials, using the Technics Giga Etch 100-E plasma etch system
[AERE-R-12212] 09 p1177 N88-17050
Advanced packaging for VLSI/VHSIC (Very Large Scale Integrated Circuits/Very High Speed Integrated Circuits) applications: Electrical, thermal and mechanical considerations, an IR and D report
[AD-A189666] 14 p1965 N88-21724
Hermetically sealable package for hybrid solid-state electronic devices and the like
[NASA-CASE-MSC-20181-1] 17 p2335 N88-23941
Application-specific packaging for custom micromechanical structures 19 p2671 N88-25879

ELECTRONIC PHOTOGRAPHY
U ELECTRO-OPTICAL PHOTOGRAPHY

ELECTRONIC SIGNAL MEASUREMENT
U SIGNAL MEASUREMENT

ELECTRONIC SPECTRA
Multichannel electron counter with high space resolution
[DE88-700564] 07 p0857 N88-15204
Contributions of autoionizing resonances to the electron collisional excitation rates for Be-like ions
[AD-A190924] 18 p2572 N88-25275
Basic research in electronics (JSEP) Joint Services Electronics Program
[AD-A193072] 23 p3206 N88-29079

ELECTRONIC STRUCTURE
U ATOMIC STRUCTURE

ELECTRONIC SWITCHES
U SWITCHING CIRCUITS

ELECTRONIC TRANSDUCERS
Definition and use of sensors for measuring electrical conductivity in thunderclouds
[ESA-TT-1047] 03 p0352 N88-12222

ELECTRONIC WARFARE
Radar ECCM's new area: Anti-STEALTH and anti-ARM 03 p0299 N88-11681
Brain activity during tactical decision-making. Part 2: Probe-evoked potentials and workload
[AD-A188688] 12 p1667 N88-19994
The integration of artificial intelligence techniques to improve the effectiveness of electronic countermeasure strategies in a tactical environment
[AD-A189483] 12 p1682 N88-20056
Bragg-cell receiver study
[NASA-CR-182684] 13 p1761 N88-20535
The electromagnetic threat to future avionic systems 17 p2305 N88-23790

ELECTRONICS
Detective quantum efficiency and design of a parallel data recording system for EXELFS-measurements --- electron microscopy
[USIP-87-06] 01 p0050 N88-10318
Center for Electronics and Electrical Engineering technical publication announcements covering Center programs, July to September 1987
[PB88-196530] 20 p2793 N88-26572

ELECTRONS
NT CONDUCTION ELECTRONS
NT FREE ELECTRONS
NT HIGH ENERGY ELECTRONS
NT HOT ELECTRONS
NT PHOTOELECTRONS
NT POLARONS
NT RELATIVISTIC ELECTRON BEAMS
NT SOLAR ELECTRONS
Theory of atoms in strong, pulsed electromagnetic fields. 2: A free electron and a harmonically bound electron
[DE87-012571] 01 p0035 N88-10225
Ab initio methods for electron-molecule collisions
[DE87-011726] 01 p0092 N88-10598
Low altitude flux and dose measurements during two solar flare events 01 p0111 N88-10713
Electronic conduction in molten sodium chloride
[DE87-010063] 02 p0144 N88-10901
Confinement time of electrons and H(-)/D(-) ions in the Uramoto type sheet plasma
[IPPJ-852] 04 p0492 N88-13032
Prompt simultaneous acceleration of protons and electrons to relativistic energies by shock waves in solar flares
[IPPJ-851] 04 p0493 N88-13037
Tetrahedral carbon and interstitial electrons in Li cluster: CLi4 and (LiCH3)4
[AD-A184277] 04 p0496 N88-13055
Experimental observation of photoresonance of electrons localized above surface of solid hydrogen 06 p0774 N88-14755
Improving the method of calculating electronic properties of narrow bandgap semiconductors 07 p0926 N88-15627
Study of tau pairs and search for new particles
[B8680488] 07 p0931 N88-15655
Field-aligned fluxes of energetic electrons related to the onset of magnetospheric substorms 08 p1096 N88-16595
Introductory review: Physics of electron slowing-down processes
[DE88-002918] 09 p1246 N88-17486
Dynamics of coupled electron-nucleon motion in a laser field
[DE88-005063] 10 p1337 N88-17994
Suppression of X-rays generated by runaway electrons in ATF
[DE88-004179] 10 p1414 N88-18440
Electron transfer to iron(3) oxide colloids
[DE88-002885] 10 p1416 N88-18448
The electronic structure of YBa2Cu3O/sub 7-delta/ above and below T/sub c/
[DE88-003495] 10 p1420 N88-18479
Calculations of rate constants for the three-body recombination of H2 in the presence of H2
[NASA-CR-182548] 11 p1454 N88-18664
Nuclear structure studies by the scattering of medium-energy electrons
[DE88-003803] 11 p1545 N88-19236
High pressure electronic transport in semiconductors
[AD-A187428] 11 p1555 N88-19308
Gas phase reactions of electrons, negative ions and free-radicals with transition metal complexes 11 p1560 N88-19339
Measurements of optically thin electron cyclotron emission from relativistic electrons
[DE88-004713] 12 p1688 N88-20096
Polarization of electrons in an electromagnetic wave field in the presence of magnetic field
[DE88-700169] 13 p1757 N88-20509
Image charge, coherent scattering, and symmetry effects in electron stimulated desorption: O(-) from O sub 2 condensed on metals
[AD-A189093] 13 p1835 N88-20979
The magnitude of secondary electron contributions in photon stimulated desorption
[AD-A189094] 13 p1835 N88-20980
Topics in curved and flat space electromagnetism 13 p1854 N88-21100
Kinetics of slow electrons in excimer laser with electron-beam pumping 14 p1970 N88-21760
Three-wave parametric resonance in plasma of relativistic electron flux 14 p1972 N88-21772
Ground-state correlations in C12 and the mechanism of the (e,e'p) reaction
[B8729349] 14 p1980 N88-21816
Developments in ceramic superconducting materials 15 p2052 N88-22229
On the acceleration of electrons and positive ions in the same direction along magnetic field lines by parallel electric fields
[IRF-PREPRINT-103] 15 p2096 N88-22488
Improvement of plasma confinement due to electron Landau damping in tokamaks
[DE88-752339] 15 p2136 N88-22747
Effective electron interactions due to virtual charge and spin excitations in an extended Hubbard model for Cu-O superconductors
[DE88-005971] 15 p2139 N88-22766
Survey of the Air Force P78-2 (SCATHA) satellite plasma wave data during electron gun operations
[AD-A191014] 16 p2168 N88-22926
Small molecule and small cluster ion formation in a low-density containerless mixture of electrons, protons and hydrogen atoms 16 p2269 N88-23577
Electron current effect on stability of plasma channel 16 p2276 N88-23625
Ion generator and ion application system
[NASA-CASE-MFS-28122-1] 17 p2397 N88-24253
Contributions of autoionizing resonances to the electron collisional excitation rates for Be-like ions
[AD-A190924] 18 p2572 N88-25275
A study of runaway electron confinement in the ASDEX tokamak
[DE88-007327] 18 p2579 N88-25319
Physical properties of f electron systems
[DE88-006886] 18 p2581 N88-25331
Contaminant ions and waves in the space station environment 18 p2590 N88-25393
Electronic structure of Zintl phase compounds by nonlinear optimization
[DE88-009998] 19 p2613 N88-25508
Modulation efficiency limited high frequency performance of the MODFET 19 p2657 N88-25786
Primer on coupling collective electronic oscillations to nuclei
[LA-10878] 19 p2723 N88-26170
Experiments on insulation of relativistic electron flows in oblique and tapered magnetic fields
[DE88-007199] 19 p2724 N88-26176
Electron-positron physics at 1 TeV
[DE88-009019] 19 p2725 N88-26180
Electron-acoustic waves in a beam-plasma system
[DE88-702053] 19 p2729 N88-26207
Infrared detectors based on the photon drag effect and intersubband absorption by a two-dimensional electron gas 20 p2867 N88-27024
A 10 microns photoexcited avalanche gain due to electron impact ionization from GaAs quantum well superlattices 20 p2867 N88-27026
Monte Carlo simulations of femtosecond relaxation of photoexcited electrons in AlGaAs/GaAs quantum wells 20 p2869 N88-27036
Direct measurement of ultrafast electron-hole plasma expansion at high density at an asymmetric GaAs quantum well 20 p2871 N88-27044
Superconductivity of heavy-electron uranium compounds
[DE88-007901] 20 p2875 N88-27065
Nonlinear dynamics of the electron self-field interaction
[DE88-010597] 21 p2934 N88-27420
Theory and simulation of relaxed plasmoids
[AD-A192884] 21 p3032 N88-27997
Large area nuclear particle detectors using ET materials
[NASA-CR-180777] 23 p3215 N88-29136
Particle trajectories and potentials in a plane sheath moving in a magnetoplasma
[AD-A196228] 24 p3390 N88-30190
Ring current role in dynamics of fluctuating electron and ion fluxes in low-latitude magnetosphere 24 p3447 N88-30514

ELECTROPHORESIS
Preparative electrophoresis for space
[NASA-TP-2777] 02 p0156 N88-10977
Continuous flow electrophoresis system experiments on shuttle flights STS-6 and STS-7
[NASA-TP-2778] 02 p0156 N88-10978
Mathematical models of continuous flow electrophoresis: Electrophoresis technology
[NASA-CR-179241] 07 p0828 N88-15021
Use of hydrophilic polymer coatings for control of electroosmosis and protein adsorption 07 p0925 N88-15620
A comparison of algorithms for the analysis of images generated by two-dimensional electrophoresis
[DE88-003730] 09 p1220 N88-17319
GAS 450: A space payload for the People Central Coast Student Experimenters 10 p1289 N88-17709
Optimization of the southern electrophoretic transfer method
[DE88-004527] 10 p1299 N88-17765
Electrophoretically deposited styrene-acrylate coatings for suppression of internal electromagnetic pulse effects
[DE88-003820] 12 p1609 N88-19621
Moving wall, continuous flow electronphoresis apparatus
[NASA-CASE-MFS-28142-1] 17 p2318 N88-23845
Electrophoretic coatings. Part 1: Sandia applications
[DE88-008666] 20 p2776 N88-26465

ELECTROPHOTOMETERS
A new technique for rocket and space-borne investigations of time-dependant auroral morphology 08 p1030 N88-16241

Five channel auroral photometer
[REPT-112] 24 p3375 N88-30101

ELECTROPHOTOMETRY
Surface photometric investigations for spiral galaxies of large dimension structures in edge-on gemetry
[ETN-88-92126] 21 p3030 N88-27985

ELECTROPHYSICS
NT ELECTRO-OPTICS
NT MOLECULAR ELECTRONICS
Air Force ultrafast optical electronics center
[AD-A191491] 17 p2438 N88-24507
Joint services electronics program
[AD-A190239] 18 p2503 N88-24848
Joint services electronics program
[AD-A192076] 18 p2504 N88-24856

ELECTROPHYSIOLOGY
Biophysical and biochemical mechanisms in synaptic transmitter release
[AD-A187059] 09 p1199 N88-17184
Brain potentials and personality: A new look at stress susceptibility
[AD-A186931] 09 p1199 N88-17189
Center for nonlinear dynamics of the brain
[AD-A187245] 11 p1518 N88-19068
Studies of model ion channels in defect-free multibilayers of phospholipids
[AD-A188740] 16 p2238 N88-23365
Challenges of physiological monitoring in a Navy operational setting 16 p2239 N88-23374
Electric and Magnetic Activity of the Central Nervous System: Research and Clinical Applications in Aerospace Medicine
[AGARD-CP-432] 21 p2977 N88-27683
Normative developmental equations for the EEG and their sensitivity to neurological and psychiatric disorders 21 p2977 N88-27687
The application of non-stationary data analysis techniques in the identification of changes in the electroencephalogram associated with the onset of drowsiness 21 p2978 N88-27688
A statistical procedure for the evaluation of presence/non-presence of stimulus-related EEG activity 21 p2978 N88-27689
Electric and magnetic brain activity related to cognitive performance 21 p2979 N88-27692
Cognitive task demands as reflected in physiological measures 21 p2980 N88-27699
The effect of endogenous alpha on hemispheric asymmetries and the relationship of frontal theta to sustained attention 21 p2980 N88-27701
Psychophysiological measures of drowsiness as estimators of mental fatigue and performance degradation during sleep deprivation 21 p2980 N88-27702
Fighter pilot performance during airborne and simulator missions: Physiological comparisons 21 p2981 N88-27704
Event-related and steady potential changes in the brain related to workload during tracking 21 p2981 N88-27705
The neuroelectric selection of Naval aviation personnel: An evaluation 21 p2981 N88-27707
An approach to studying the effects of psychostimulants on cerebral electrical activity in the non-human primate 21 p2983 N88-27716
Relation between VEP and visual function in lesions of the optic nerve and visual pathway 21 p2983 N88-27718
The auditory evoked response in military pilots 21 p2984 N88-27721

ELECTROPLATING
Synergism of electroplating and vacuum processes
[DE87-013496] 01 p0033 N88-10211
Composite ceramic superconducting filaments for superconducting cable
[AD-A187833] 11 p1556 N88-19312
RF properties of superconducting Pb electroplated onto Cu
[DE88-005918] 15 p2139 N88-22765

ELECTRORETINOGRAPHY
Microesotropia patients performa well as military jet pilots 21 p2925 N88-27363

ELECTROSEISMIC EFFECT
U ELECTRIC CURRENT
U SEISMIC WAVES

ELECTROSTATIC CHARGE
The physics of charge separation preceding lightning strokes in thunderclouds
[NASA-CR-178371] 01 p0071 N88-10452
Introduction to the problem of environmentally induced discharges 03 p0273 N88-11717
Charging calculations for the HIPPARCOS satellite 03 p0274 N88-11728
Effect of electrostatic field on behaviour of peripheric plasma at high-frequency heating
[DE87-703328] 03 p0378 N88-12378
Conditions for geomagnetically trapping sub-micron lunar ejecta between L = 1.2 and L = 3.1 04 p0521 N88-13203
Study of electrostatic modulation of fuel sprays to enhance combustion performance in an aviation gas turbine
[AD-A184967] 05 p0548 N88-13341
Electromagnetics and electrothermal approach to evaluate failures in microelectronic devices caused by electrostatic discharges: Stochastical aspects of the device reliability
[AD-A184906] 05 p0577 N88-13522
Lightning discharge protection rod
[NASA-CASE-LAR-13470-1] 06 p0666 N88-14083
Simulations of the electrostatic charging of ESA communications satellites
[ESA-STM-239] 18 p2472 N88-24670
Reference filters for electrostatic charging tendency measurements of fuels
[AD-A191717] 18 p2495 N88-24803
An electrostatic potential comparator
[AD-A192051] 18 p2557 N88-25177
Procedures for identification and handling of Printed Circuit Boards (PCBs)
[AD-A191177] 23 p3206 N88-29078

ELECTROSTATIC ENGINES
Advanced electric propulsion research
[NASA-CR-182130] 16 p2170 N88-22937

ELECTROSTATIC EROSION
U SPARK MACHINING

ELECTROSTATIC FIELDS
U ELECTRIC FIELDS

ELECTROSTATIC GENERATORS
Proposal for construction of an Energetic Particle Injector (EPI)
[INPE-4242-RPE/548] 12 p1690 N88-20112

ELECTROSTATIC PLASMA
U PLASMAS (PHYSICS)

ELECTROSTATIC PROBES
Comparison of simultaneous MST radar and electron density probe measurements in the polar mesosphere — Mesospheric, Stratospheric, Tropospheric (MST) 08 p1028 N88-16226
Asymmetric double Langmuir probe for fast and automatic measurements of plasma temperature
[DE88-004773] 10 p1414 N88-18436
An experimental investigation of an arcjet thruster exhaust using Langmuir probes
[NASA-TM-100258] 14 p1883 N88-21253
Measurements of edge turbulence with Langmuir probes in currentless Heliotron E plasmas
[DE88-752313] 16 p2275 N88-23617
Rocket-borne low energy ion measurements in space 18 p2593 N88-25412
Theory on conductivity measurement technique for Langmuir probes in the stratosphere
[INPE-4514-PRE/1268] 19 p2692 N88-25999
Calibration technique and study on metrological characteristics of a high-voltage inverse square-law function generator
[DE88-702101] 22 p3072 N88-28236

ELECTROSTATIC PROPULSION
NT ION PROPULSION
Advanced electric propulsion and space plasma contactor research
[NASA-CR-180862] 06 p0674 N88-14126

ELECTROSTATIC WAVES
Nature and the nonlinear evolution of electrostatic waves associated with the AMPTE (Active Magnetosphere Particle Tracer Explorers) solar wind releases
[AD-A185471] 06 p0806 N88-14920
Electrostatic VLF emission determined from rocket and satellite experiments 08 p1002 N88-16068
Low frequency electrostatic waves observed on board the Coordinated Auroral Experiment using Scatter And Rockets (CAESAR) 2 payload 08 p1032 N88-16253
Theoretical investigations of drift waves in a magnetic quadrupole 18 p2578 N88-25312
Electrostatic whistler mode conversion at plasma resonance
[AD-A192951] 20 p2860 N88-26989
Kinetic theory for electrostatic waves due to transverse velocity shears
[AD-A193404] 23 p3284 N88-29557

ELECTROSTATICS
Physics and device design of vacuum integrated circuits 01 p0039 N88-10251
Electromagnetic compatibility (EMC) phenomena and prevention of the effects — spacecraft 03 p0274 N88-11731
Electrostatic discharges in geostationary orbit: The case of Telecom 1 03 p0275 N88-11733
Prevention of radiation induced degradations and of electrostatic perturbations on the Arabsat spacecraft in flight results 03 p0275 N88-11734
Some new ideas in liquid detectors
[DE88-000732] 04 p0446 N88-12768
Analysis of geophysical data bases and models for spacecraft interactions
[AD-A184809] 05 p0555 N88-13375
Plasma theory and simulation
[AD-A187100] 09 p1249 N88-17486
Dynamical aspects of electrostatic double layers
[TRITA-EPP-87-13] 09 p1250 N88-17492
Mechanical design and construction of a 200 mA, 100 keV, dc, negative ion accelerator
[DE88-003855] 11 p1548 N88-19257
GRADIO three-axis electrostatic accelerometers 12 p1645 N88-19849
Waves and static electric fields in the auroral acceleration region 12 p1646 N88-19856
Nonlinear optical principles and the photorefractive effect applied to optical phase conjugation
[AD-A188856] 12 p1691 N88-20119
The effects of a dc electric field on the current driven ion cyclotron instability
[AD-A188877] 12 p1695 N88-20142
Observations on electrostatic effects in a filter test system
[AD-A188797] 13 p1736 N88-20378
Development of electrostatic-accelerator free-electron lasers
[AD-A189507] 13 p1774 N88-20614
Chaotic diffusion across magnetic field in a model of electrostatic turbulent plasma
[PREPRINT-566] 14 p1985 N88-21839
A qualitative approach to electricity
[AD-A189854] 15 p2128 N88-22693
The new UCSB (University of California, Santa Barbara) compact far-infrared FEL
[AD-A190864] 16 p2212 N88-23203
A new fiber-optic-based ion sensor
[AD-A191322] 16 p2274 N88-23612
Development of test methods for the electrostatic properties of nonhomogeneous fabrics, phase 2
[AD-A190853] 18 p2489 N88-24767
Demixing of aqueous polymer two-phase systems in low gravity
[NASA-TM-101141] 18 p2496 N88-24809
Electrostatic discharge test apparatus
[NASA-CASE-MSC-21094-1] 18 p2518 N88-24941
Low frequency electrostatic turbulence in the polar cap E-region
[DRI-3-88] 18 p2540 N88-25077
A severe spacecraft-charging event on SCATHA in September 1982
[AD-A193007] 20 p2765 N88-26396
Meaning of energy diagrams used to describe hetero-structures
[DE88-702219] 21 p3023 N88-27943
Wave structures in thermospheric density from satellite electrostatic triaxial accelerometer measurements
[AD-A194134] 23 p3233 N88-29240

ELECTROSTRICTION
Piezoelectric and electrostrictive materials for transducer applications, volume 1
[AD-A194957] 24 p3374 N88-30096
Piezoelectric and electrostrictive materials for transducer applications, volume 2
[AD-A194956] 24 p3376 N88-30104
Piezoelectric and electrostrictive materials for transducer applications, volume 3
[AD-A194949] 24 p3377 N88-30112

ELECTROTHERMAL ENGINES
NT ARC JET ENGINES
NT PLASMA ENGINES
NT RESISTOJET ENGINES
Characterization of the arc/spark excitation sources used in the spectrometric oil analysis program
[AD-A187131] 10 p1297 N88-17758
Development and qualification of an Augmented Electro-Thermal Hydrazine-Thruster (AEHT) with 0.1 to 0.2 N vacuum thrust
[BMFT-FB-W-86-012] 16 p2169 N88-22931
Performance of a hydrogen pulsed electrothermal thruster. Strategic defense initiative organization innovative science and technology. SBIR, phase 1
[AD-A191999] 18 p2475 N88-24679

ELEMENT ABUNDANCE
U ABUNDANCE

ELEMENTARY EXCITATIONS
NT EXCITONS
NT MAGNONS
NT PHONON BEAMS
NT PHONONS
NT PLASMONS
NT POLARONS
First-principles calculations of quasiparticle energies at surfaces and interfaces: Semiconductor surface-state spectra and band offsets
[DE88-006340] 15 p2141 N88-22773

Electronic structure, elementary excitations, optical and transport properties of semiconductor superlattices
[AD-A190795] 18 p2581 N88-25333

ELEMENTARY PARTICLE INTERACTIONS
NT ELECTRON CAPTURE
NT HIGH ENERGY INTERACTIONS
NT NUCLEAR CAPTURE
NT NUCLEON-NUCLEON INTERACTIONS
NT STRONG INTERACTIONS (FIELD THEORY)
NT WEAK ENERGY INTERACTIONS
NT WEAK INTERACTIONS (FIELD THEORY)
Experimental studies of elementary particle interactions at high energies
[DE88-000804] 05 p0648 N88-13971
Corrections for the pseudorapidity gap correlation method --- particle correlations
[USIP-87-12] 09 p1245 N88-17463
Topics in gauge theories and the unification of elementary particle interactions
[DE88-008112] 19 p2738 N88-26256
Nucleon-nucleus interaction data base: Total nuclear and absorption cross sections
[NASA-TM-4053] 20 p2852 N88-26935
Activities report of the Werner-Heisenberg Institute of Physics
[ETN-88-92946] 21 p3015 N88-27893
Production of pi(0) mesons and charged hadrons in nu bar neon and nu neon charges current interactions
[MPI-PAE/EXP.EL.188] 22 p3150 N88-28743

ELEMENTARY PARTICLES
NT ALPHA PARTICLES
NT ANTINEUTRINOS
NT ANTINUCLEONS
NT ANTIPARTICLES
NT ANTIPROTONS
NT BARYONS
NT BETA PARTICLES
NT BOSONS
NT CONDUCTION ELECTRONS
NT DEUTERONS
NT ELECTRON-POSITRON PAIRS
NT ELECTRONS
NT FAST NEUTRONS
NT FERMIONS
NT FREE ELECTRONS
NT GLUONS
NT GRAVITONS
NT HADRONS
NT HIGH ENERGY ELECTRONS
NT HOT ELECTRONS
NT KAONS
NT LEPTONS
NT MESON RESONANCE
NT MESONS
NT MUONS
NT NEUTRINOS
NT NEUTRONS
NT NUCLEONS
NT PARTONS
NT PHOTOELECTRONS
NT PHOTONS
NT PIONS
NT POLARONS
NT POSITRONS
NT PROTONS
NT QUARKS
NT SOLAR ELECTRONS
NT SOLAR NEUTRINOS
NT SOLAR NEUTRONS
NT SOLAR PROTONS
NT THERMAL NEUTRONS
Current experiments in elementary particle physics
[DE87-013961] 02 p0231 N88-11456
Research program in elementary particle theory
[DE88-000159] 02 p0233 N88-11468
Research in elementary particle physics
[DE88-002130] 06 p0777 N88-14771
A simplified model of elementary particles
[NOTA-INTERNA-890] 07 p0930 N88-15647
Experimental elementary particle physics at the University of Pittsburgh
[DE88-003542] 11 p1545 N88-19234
Theory of elementary particle studies in weak iteration and grand unification and studies in accelerator design
[DE88-004261] 11 p1545 N88-19238
Research in high energy elementary particle physics
[DE88-006065] 13 p1837 N88-20994
Research in the theory of condensed matter and elementary particles
[DE88-010180] 22 p3151 N88-28749

ELEVATION
Terrain classification from digital elevation data using slope and curvature information
[AD-A188940] 12 p1639 N88-19812
Interpolation algorithms for digital terrain models
[INPE-4373-PRE/1196] 13 p1820 N88-20877
Prediction of high-temperature thermodynamic properties of mixed electrolyte solutions including solubility equilibria, vapor pressure depression and boiling point elevation
[DE88-006344] 13 p1849 N88-21069
Mapping from LANDSAT and SPOT satellite imagery
17 p2352 N88-24018
Vectorization of raster algorithms for elevation data processing 18 p2534 N88-25036
The use of SPOT data for mapping and DEM production --- digital elevation model (DEM)
22 p3110 N88-28475
Automatic extraction of high resolution elevation data from SPOT stereo images 22 p3113 N88-28489
Estimation of short-wavelength gravity on a dense grid using digital terrain elevation data
[AD-A196325] 24 p3391 N88-30196

ELEVATION ANGLE
Results on the low elevation angle propagation experiment, part 1
[TUD-R-328] 06 p0693 N88-14250

ELEVATIONS (DRAWINGS)
U DRAWINGS

ELEVATORS (LIFTS)
Analytical investigation of the dynamics of tethered constellations in Earth orbit (phase 2)
[NASA-CR-179218] 04 p0408 N88-12533
A device and methodology for measuring repetitive lifting VO2max (oxygen consumption rate)
[AD-A185195] 05 p0630 N88-13850
Tether Elevator Crawler Systems (TECS)
07 p0927 N88-15631
Orbiter processing facility service platform failure and redesign 14 p1928 N88-21494

ELIMINATION
Elimination of subboundaries in 0.5-micron-thick Si-on-insulation films produced by ZMR
[AD-A184590] 03 p0381 N88-12396
Eliminating columns in the simplex method for linear programming
[DE88-004191] 10 p1386 N88-18277
Elimination of quantifiers of linear variables and corresponding transfer principles
[DE88-005692] 13 p1826 N88-20912
Comparison of morning with afternoon nitrogen elimination in resting subjects breathing 100 percent oxygen
[AD-A196191] 24 p3407 N88-30282

ELLIPSES
Spectral methods: Analysis and applications to flow problems
[AD-A186265] 07 p0850 N88-15156
The information metric for univariate linear elliptic models
[AD-A186385] 07 p0911 N88-15527
Wind tunnel tests of elliptical missile body configurations at Mach numbers 0.4 to 5.0
[AD-A193525] 22 p3038 N88-28040
Fitting an ellipse to data
[NPL-DITC-95/87] 22 p3143 N88-28693

ELLIPSOIDS
The effect of sting interference at low speeds on the drag coefficient of an ellipsoidal body using a magnetic suspension and balance system
[NASA-CR-181611] 13 p1718 N88-20274
Periodic orbits around a satellite modelled as a triaxial ellipsoid
[AD-A190592] 15 p2022 N88-22051
Solar energy absorption efficiency of an ellipsoidal receiver-reactor with specularly reflecting walls
[AD-A193726] 22 p3117 N88-28520
A calculation of the turbulent boundary layer on a slender ellipsoid at low incidence
[FFA-TN-1988-02] 23 p3213 N88-29126

ELLIPSOMETERS
Some investigations of molecular beam epitaxial growth of 3-5 semiconductor films via Monte-Carlo computer simulations, carrier tunnelling and spectroscopic ellipsometry
[AD-A185520] 06 p0789 N88-14839
Thin film research diagnostics instrumentation
[AD-A191240] 16 p2213 N88-23207
Ellipsometric imaging of drying sol-gel films
[DE88-011785] 21 p2921 N88-27335

ELLIPTIC DIFFERENTIAL EQUATIONS
Finite elements for 2D elliptic equations with moving nodes
[DE87-013501] 02 p0224 N88-11410
Research and development of finite elements and iterative algorithms for elliptic partial differential equations
[DE88-001381] 05 p0643 N88-13934
The p-version of the finite element method for elliptic equations of order 2l
[AD-A186334] 07 p0911 N88-15523
A parallel block cyclic reduction algorithm for the fast solution of elliptic equations
[DE88-003595] 09 p1221 N88-17324
Analysis of smoothing matrices for the preconditioning of elliptic difference equations
[CWI-NM-R8705] 09 p1228 N88-17357
Recent progress in the p and h-p version on the finite element method
[AD-A187254] 10 p1400 N88-18347
The h-p version of the finite element method for problems with nonhomogeneous essential boundary condition
[AD-A187356] 10 p1400 N88-18348
Generation of surface grids through elliptic partial differential equations for aircraft and missile configurations
[AD-A188631] 11 p1535 N88-19169
The inverse power method for semilinear elliptic equations
[DE88-006427] 15 p2118 N88-22620
Residual smoothing for accelerating the Alternating Direction Implicit (ADI) iteration method for elliptic difference equations
[CWI-NM-R8721] 16 p2259 N88-23500
Multigrid methods for elliptic Partial Differential Equations (PDEs)
[CWI-NM-R8722] 18 p2566 N88-25242
A comparative study of Chebyshev acceleration and residue smoothing in the solution of nonlinear elliptic difference equations
[CWI-NM-R8723] 18 p2569 N88-25259
Unified multilevel adaptive finite element methods for elliptic problems
[DE88-011938] 21 p3007 N88-27840
Composite grid generation for aircraft configurations with the EAGLE code 23 p3246 N88-29321
Nonlinear elliptic problems with critical exponent in shrinking annuli
[W-02/87] 23 p3273 N88-29477
Elliptic equations with nearly critical growth
[W-16-87] 23 p3273 N88-29478
Generation of surface grids through elliptic partial differential equations for aircraft and missile configurations
[AD-A195639] 24 p3424 N88-30378

ELLIPTIC FUNCTIONS
On the maximum of solutions for a semilinear elliptic problem
[REPT-87-08] 01 p0086 N88-10554
A comparison of adaptive refinement techniques for elliptic problems
[DE88-000805] 04 p0485 N88-12987
General solution of certain functional equations
[PREPRINT-554] 06 p0764 N88-14689
Mode 3 problems of doubly-periodic rhombic and rectangular array of equal cracks in an infinite plate
[PB87-144846] 08 p0996 N88-16031
On the norm equivalence of singularly perturbed elliptic difference operators
[DE88-006353] 13 p1826 N88-20913
Computation of a complete elliptic integral of the first kind using q-expansion 16 p2257 N88-23490
Semilinear elliptic problems on domains with corners
[REPT-87-83] 20 p2846 N88-26888
Three-dimensional elliptic grid generation technique with application to turbomachinery cascades
[NASA-TM-101330] 24 p3372 N88-30078

ELLIPTIC INTEGRALS
U ELLIPTIC FUNCTIONS

ELLIPTICAL CYLINDERS
An experimental investigation of appendage-flat plate junction flow. Volume 2. Elliptical nose appendage data base
[AD-A184974] 05 p0580 N88-13539
Numerical simulation of the shock tube flows by TVD scheme 19 p2638 N88-25648

ELLIPTICAL GALAXIES
Stochasticity in elliptical galaxies
[SER-C-PREPUBL-FASC-20] 17 p2450 N88-24556

ELLIPTICAL ORBITS
NT TRANSFER ORBITS
Limitation of spacecraft orbit near colinear libration center of limited elliptical three body problem
08 p1003 N88-16075
Periodic orbits of limited elliptical three body problem
08 p1004 N88-16081
Relative motion of two satellites in close-elliptical orbits
[AD-A188851] 12 p1594 N88-19543
Calculation of eclipses for elliptical orbits
[INPE-4412-NTE/277] 12 p1594 N88-19545

ELLIPTICAL POLARIZATION
Observation of instabilities in time during dynamic self-diffraction of light in anisotropic nonhomogeneous medium 06 p0769 N88-14730

ELLIPTICITY
Dependence of acoustical characteristics of laser-induced breakdown in dielectric materials on shape of inelastic region
06 p0774 N88-14753
Wind tunnel studies of circulation control elliptical airfoils
10 p1270 N88-17598

ELONGATION
Development of a polyimide matrix for filament winding with improved extensibility and fracture toughness for permanent use at 200 C
[BMFT-FB-T-86-118] 01 p0030 N88-10190
The effect of strain rate on the yield behavior of iron-base LRO alloys at elevated temperatures
[DE87-014893] 03 p0288 N88-11808
BASIC desk-top computer program for the three-dimensional static configuration of an extensible flexible cable in a uniform stream
[AD-A184852] 05 p0609 N88-13737
Effects of sulfur content on the plain strain fracture toughness of inertia welds in 4340 steel
[AD-A188192] 11 p1458 N88-18689
Determination of the modulus of elasticity of structural silicone sealants
[PB88-157458] 14 p1893 N88-21307
Superplasticity: A fundamental investigation on deformation mechanism and cavitation phenomena
[AD-A191548] 18 p2485 N88-24741
Phenomena of the ionic transport in the stress corrosion of metals
[DE88-702502] 23 p3195 N88-29013

EMANATION
U EMISSION

EMBEDDED COMPUTER SYSTEMS
NT AIRBORNE/SPACEBORNE COMPUTERS
An embedded multiprocessor computer for proof-of-principle testing of exploratory systems concepts
[DE87-012735] 02 p0218 N88-11372
Praxis: The programming language: An advanced overview
[DE87-014319] 02 p0220 N88-11388
The implementation and use of Ada on distributed systems with high reliability requirements
[NASA-CR-182481] 09 p1221 N88-17326
Factors causing unexpected variations in Ada benchmarks
[AD-A187231] 10 p1388 N88-18291
Implementing embedded artificial intelligence rules within algorithmic programming languages
[NASA-CR-178393] 14 p1959 N88-21686
A high speed serial link interface for SANDAC-V
[DE88-007694] 20 p2842 N88-26861
MINIAC: A small embedded computer
[DE88-008142] 21 p2994 N88-27757
An optical 2-dimensional correlator for pattern recognition in embedded computing
[DE88-007198] 21 p2998 N88-27780
Design consideration in constructing high performance embedded Knowledge-Based Systems (KBS)
23 p3261 N88-29415

EMBEDDING
Embedding topological median algebras in products of dendrons
[PB88-100888] 06 p0767 N88-14713
Study of the embedded atom method of atomistic calculations for metals and alloys
[DE88-002798] 07 p0835 N88-15065
Embedded cluster models for electronic structure and energetics of complex oxides
[DE88-003097] 07 p0938 N88-15702
Prognosis using spectral embedding --- weather forecasting
08 p1016 N88-16157
Experimental and analytical investigation on a proposed embedded fiber optic displacement sensor
[AD-A189030] 12 p1630 N88-19756
Effects of toroidal forces in current loops embedded in a background plasma
[AD-A188878] 12 p1695 N88-20143
Graph labelings
[AD-A189649] 14 p1964 N88-21722
Embedded minimal sufaces with an infinite number of ends
[DE88-006429] 15 p2126 N88-22680
Instability-related delamination growth of embedded and edge delaminations
20 p2767 N88-26406
Distributed fault tolerant embeddings of binary trees in hypercubes
[AD-A192929] 20 p2839 N88-26840
Laboratory feasibility study of a composite embedded fiber optic sensor for measurement of structural vibrations
[AD-A194270] 22 p3152 N88-28754
Archetyping: A software generation and management methodology
23 p3256 N88-29382
A parametric study of embedded cantilever retaining walls: The results of a finite element study
[RR-CE83] 24 p3383 N88-30152

EMBOLISMS
NT AEROEMBOLISM

EMBRITTLEMENT
Tensile properties of extrusion consolidated Type 304 SS rapidly solidified powders
[DE87-014875] 05 p0566 N88-13450
Experimental method for investigating helium effects in irradiated vanadium
[DE88-002891] 08 p0969 N88-15865
Kinetics and mechanism of thermal aging embrittlement of duplex stainless steels
[DE88-002987] 08 p0969 N88-15866
Long-term-aging embrittlement of cast duplex stainless steels: Mechanism and kinetics
[DE88-002929] 09 p1145 N88-16861
Influence of post-anneal cooling treatments on suppression of cryogenic intergranular fracture in experimental Ni-free high-Mn austenitic steels
[DE88-002766] 09 p1145 N88-16863
Long-term aging of cast stainless steels: Mechanisms and resulting properties
[DE88-002888] 09 p1145 N88-16864
Aging degradation of cast stainless steels: Effects on mechanical properties
[DE88-003053] 09 p1145 N88-16866
Neutron- and X-ray-small angle scattering with Fe-base metallic glasses
[DE88-002538] 09 p1147 N88-16876
Effect of low-temperature aging on the mechanical properties of cast stainless steels
[DE88-002872] 10 p1300 N88-17774
Weldability of tritium-charged 304L stainless steel
[DP-1740] 12 p1607 N88-19611
Stress corrosion cracking and metal-induced embrittlement: Comparative studies of local chemistries
[DE88-003235] 13 p1742 N88-20419
Creep behavior of consolidated rapidly solidified Type 304 stainless steel powder containing helium
[DE88-005536] 13 p1743 N88-20424
A study of the dynamics of high temperature brittle intergranular fracture by acoustic emission
[AERE-R-12479] 13 p1780 N88-20650
The role of oxygen on the mechanical behavior of molybdenum alloys
17 p2401 N88-24278
High temperature embrittleness of Cu-Cr alloy
[NASA-TT-20184] 18 p2488 N88-24759
Method and apparatus for non-destructive testing of temper embrittlement in steels
[NASA-CASE-LAR-13817-1] 23 p3195 N88-29012

EMBRYOLOGY
Embryonic development of guppy in weightlessness
10 p1360 N88-18127
Effects of heavy ions on egg-developing systems
12 p1658 N88-19935
Embryonic development of the newt Cynops pyrrhogaster in very weak magnetic fields
[ISAS-RN-357] 19 p2702 N88-26068
Effects of short spaceflights on Drosophila melanogaster embryogenesis and life span
22 p3061 N88-28166
Embryogenesis and organogenesis of Carausius morosus under spaceflight conditions
22 p3061 N88-28167
The role of gravity in the establishment of the dorso/ventral axis in the amphibian embryo --- Spacelab D1 mission
22 p3062 N88-28168

EMBRYOS
Changes in the morphological and molecular biological processes during early embryo development in amphibians under micro-g conditions
07 p0885 N88-15371
Xiphophorus: A system to recognize radiation-induced mutations and to study the effects of zero-gravity environment on embryo development
07 p0885 N88-15372
Semi-microdroplet assay for cell adhesion molecules
[NASA-CR-183139] 24 p3406 N88-30274
Immunofluorescence localization of dissociation supernatant and extracellular matrix components in Lytechinus pictus sectioned embryos
[NASA-CR-183137] 24 p3406 N88-30276

EMERGENCIES
The determination of nutritional requirements for Safe Haven Food Supply System (emergency/survival foods)
06 p0792 N88-14856
Sudden in-flight incapacitation in general aviation
[AD-A187044] 09 p1115 N88-16682
Safety study: Commercial emergency medical service helicopter operation
[PB88-917001] 12 p1575 N88-19422
IEMIS (Integrated Emergency Management Information System) floodplain mapping based on a LIDAR derived data set
[AD-A193071] 21 p2966 N88-27616
Cockpit and cabin crew coordination
[AD-A192445] 21 p2993 N88-27752
Application of SPOT imagery for oil spill contingency planning
22 p3108 N88-28460

EMERGENCY LOCATOR TRANSMITTERS
COSPAS/SARSAT 406-MHz emergency beacon digital controller
[NASA-TM-100859] 20 p2792 N88-26566

EMISSION
NT ACOUSTIC EMISSION
NT BIOLUMINESCENCE
NT CHEMILUMINESCENCE
NT CN EMISSION
NT ELECTROLUMINESCENCE
NT ELECTRON EMISSION
NT EXHAUST EMISSION
NT FIELD EMISSION
NT FLUORESCENCE
NT HYDROXYL EMISSION
NT ION EMISSION
NT LASER INDUCED FLUORESCENCE
NT LIGHT EMISSION
NT LUMINESCENCE
NT MICROWAVE EMISSION
NT NEUTRON EMISSION
NT OPTICAL RESONANCE
NT PARTICLE EMISSION
NT PHOSPHORESCENCE
NT PHOTOELECTRIC EMISSION
NT PHOTOIONIZATION
NT PHOTOLUMINESCENCE
NT RADIO BURSTS
NT RADIO EMISSION
NT RESONANCE FLUORESCENCE
NT SECONDARY EMISSION
NT SOLAR RADIO BURSTS
NT SOLAR RADIO EMISSION
NT SPACECRAFT GLOW
NT SPECTRAL EMISSION
NT SPONTANEOUS EMISSION
NT STIMULATED EMISSION
NT THERMAL EMISSION
NT THERMIONIC EMISSION
NT TYPE 3 BURSTS
NT WATER MASERS
NT X RAY FLUORESCENCE
Quantum electrodynamics based on self-energy: Spontaneous emission in cavities
[DE87-703071] 02 p0232 N88-11461
Studies of the processing of single words using positron tomographic measures of cerebral blood flow change
[AD-A184058] 03 p0356 N88-12244
Emerging environmental constraints on the use of gasoline and diesel fuel and tradeoffs associated with the use of alternative fuels
[DE87-011504] 04 p0422 N88-12614
Impacts of world development on selected characteristics of the atmosphere: An integrative approach. Volume 1: Main report
[DE88-001495] 07 p0875 N88-15309
Impacts of world development on selected characteristics of the atmosphere: An integrative approach. Volume 2: Appendices
[DE88-001496] 07 p0875 N88-15310
Emission angles for soft X-ray coherent transition radiation
[AD-A186851] 09 p1151 N88-16896
Emission of gamma rays from various materials pulsed with 14-MeV neutrons
[DE88-003837] 11 p1544 N88-19227
A study of satellite emission computed tomography
[AD-A189567] 13 p1797 N88-20745
Effects of translational and rotational nonequilibrium on CW (Continuous Wave) chemical laser performance
[AD-A191425] 16 p2214 N88-23210
Timing regulations to prevent stratospheric-ozone depletion
[R-3495-JMO/RC] 19 p2690 N88-25987
Laser induced surface emission of neutral species and its relationship to optical surface damage processes
[DE88-008035] 19 p2726 N88-26192
Review of methods for remote sensing of atmospheric emissions from stationary sources
[PB88-190483] 20 p2821 N88-26739
Radiative heat transfer and selective emission in planar slab coatings on hot emissive substrates
[AD-A193133] 21 p2918 N88-27319
Filling of the atmospheric transmission window due to emission from very high rotational levels of NO and O3
[AD-A194670] 23 p3233 N88-29239

EMISSION SPECTRA
Optical spectroscopy of IRAS sources with infrared emission bands. 1: IRAS 21282+5050 and the diffuse interstellar bands
[NASA-CR-181387] 01 p0094 N88-10611

Photolytic processes for measurement of combustion heats of formation and reaction rates
[DE87-014047] 02 p0144 N88-10905
Visible emission from granular explosives during shock initiation
[DE87-012361] 02 p0155 N88-10970
Design study for measurement of neutral hydrogen atom density by laser induced fluorescence method
[DE87-752964] 02 p0179 N88-11114
X-ray emission from high-Z spherical laser plasmas: Implications for plasma dynamics
[DE87-014722] 02 p0239 N88-11506
Design and development of a database for spectral data and analysis results
[DE87-011323] 02 p0247 N88-11564
Spectroscopy and nonthermal processes
02 p0252 N88-11594
Spectroscopic and retrieval studies in support of SCRIBE (Stratospheric Cryogenic Interferometer Balloon Experiment)
[AD-A184037] 03 p0351 N88-12216
Investigations of extragalactic hydroxyl
03 p0389 N88-12441
Excess emission in the wings of the Hydrogen Balmer lines during a flare on the late-type dMe star YZ CMi
04 p0511 N88-13146
Emission features in IRAS LRS spectra of MS, S and CS stars 04 p0514 N88-13163
The Wilson-Bappu relationship: A barometric effect
04 p0516 N88-13170
JHK photometry of CN-rich field giants
04 p0516 N88-13175
Water masers associated with 2 carbon stars: EU Andromedae and V778 Cygni 04 p0517 N88-13176
Chromospheric variability mechanisms affecting pre-main sequence stars 04 p0517 N88-13180
The Einstein survey of the young stars in the Orion Nebula 04 p0518 N88-13182
M dwarfs from the Einstein medium sensitivity survey
04 p0519 N88-13188
A helium flare on the active G5 dwarf Kappa Ceti
04 p0519 N88-13189
Atomic beam studies of the interaction of hydrogen with transition metal surfaces
[DE88-000208] 05 p0648 N88-13970
Satellite observations of extreme ultraviolet radiation
[AD-A185043] 05 p0661 N88-14059
Characterization of Er,Cr:YSGG
[AD-A185885] 07 p0932 N88-15659
Gamma radiation at the 970 MeV plane positron channeling in diamond crystals
[DE88-700557] 07 p0939 N88-15705
Low-power photolytically pumped lasers
[DE88-002448] 08 p0991 N88-15998
VLBI research on OH-maser IN W33
08 p1001 N88-16064
Holes in OI 130 nm emission fields of upper atmosphere during day 08 p1004 N88-16082
Long range reconnaissance of trace gases: A special aspect of emission spectroscopy
08 p1018 N88-16172
Stimulated Raman scattering of picosecond light pulses in long dispersive medium 08 p1078 N88-16498
Soft X-ray absorption and emission spectra and the electronic structure of the Ba2YCu3O/sub 7-x/ superconductor
[DE88-002609] 08 p1090 N88-16559
Theoretical studies of mass loss and shock phenomena in cool star envelopes
[NASA-CR-182433] 08 p1099 N88-16616
The structure of the sideband spectrum in free electron lasers
[AD-A186952] 09 p1170 N88-17015
Excimer plasma displays
[AD-A186731] 09 p1250 N88-17489
The development of emission tomography for the nuclear industry
[AERE-R-12319] 10 p1341 N88-18014
Simulation of infrared spectra
[AD-A187881] 11 p1453 N88-18658
Theory of two-photon emission from atomic inner shells
[AD-A187742] 11 p1543 N88-19223
Presentations to the SuperHILAC Program Advisory Committee
[DE88-003853] 11 p1547 N88-19256
Spectroscopic stuoies of a laser-produced carbon plasma in the near and extreme ultraviolet
11 p1553 N88-19292
Stratospheric trace gas distributions from fair infrared thermal emission spectroscopy
13 p1797 N88-20749
IUE program SUGSD: Varability time scale of H Ly-alpha from Uranus
[NASA-CR-182706] 13 p1856 N88-21107
The astrophysics of nebulae and active galactic nuclear emission-line regions: New methods and applications
13 p1858 N88-21111
An investigation of the infrared emission spectra of carbon condensates 14 p1886 N88-21272
Techniques for studying fast reactions in liquids
[DE88-005917] 14 p1888 N88-21285
Spatial distribution of O(supra 1D) from Comet Halley
14 p1999 N88-21913
Objective-prism spectra of the Comets Honda (1968 e), Hartley-Good (1985 l) and Halley
14 p2000 N88-21924
The evolution of CN emisaion in Halley's comet with heliocentric distance 14 p2006 N88-21961
On the interpretation of the CH cometary spectrum
14 p2007 N88-21969
Alkali metal diffuse band lasers
[AD-A190244] 15 p2071 N88-22350
Sequential excitation preparation of molecular energy levels with special structural and chemical properties
[AD-A190041] 15 p2132 N88-22718
Tokamak studies of density sensitive line ratios
17 p2441 N88-24521
IUE evidence on the nature of the innermost broad-line region in Seyfert 1 galaxies 17 p2450 N88-24552
Molecular sources of ionospheric holes
[AD-A191857] 18 p2541 N88-25082
Optical diagnostics for a high power, rf-inductively coupled plasma
[DE88-007822] 18 p2579 N88-25322
Ultraviolet-visible spectroscopy of laser-produced aluminum plasmas
[AD-A193004] 20 p2860 N88-26990
Analysis of emission features in IRAS LRS spectra
21 p2928 N88-27380
Spectral line shapes from highly ionized sodium plasmas
[AD-A193401] 21 p3017 N88-27907
Array detectors for plasma spectrochemistry
[AD-A194220] 22 p3052 N88-28105
Modification of YBa2Cu3O(7-x) ceramics by adsorbed water and other gases
[DE88-011518] 22 p3057 N88-28140
The electromagnetic spectrum: The information mine
[AD-A194316] 22 p3069 N88-28215
High spatial resolution dbservations of neutral atomic carbon in the molecular clouds M17 and W51
[MPE-PREPRINT-109] 22 p3164 N88-28846
First detection of HCN J = 9 to 8 (797 GHz) line emission: Very high densities in the Orion core
[MPE-PREPRINT-110] 22 p3165 N88-28847

EMISSIVITY
Lidar-radiometric method for determining liquid-water content of cirrus clouds 04 p0461 N88-12854
Determination of cloud base height and emissivity from downwelling angular radiances
[AD-A185985] 07 p0879 N88-15331
An analysis of whistler-mode radiation from the Spacelab-2 electron beam, revision
[AD-A188228] 11 p1552 N88-19287
Multilayer thermal insulation tests
[INPE-4475-PRE/1243] 12 p1626 N88-19729
Measurement of emissivity of industrial surfaces using a simple method
[NASA-TT-20165] 15 p2036 N88-22130
The thermal radiative properties of metals at high temperature
[DE88-006625] 15 p2038 N88-22141
Direct emissivity measurements on liquids and corrections to multi-color pyrometers
17 p2329 N88-23906
Laser pyrometry 17 p2330 N88-23910
Anomalous emissivity from periodic micro-machined silicon surfaces 19 p2670 N88-25872
A probabilistic model of the apparent radiance of a rough sea
[AD-A193867] 22 p3129 N88-28602
Soot and radiation in a gas turbine combustor
[AD-A191991] 23 p3179 N88-28924

EMISSOGRAPHS
U RECORDING INSTRUMENTS

EMITTANCE
Linear emittance damper with megagauss fields
[DE87-013562] 01 p0093 N88-10606
Emittance studies at the Los Alamos National Laboratory Free-Electron Laser (FEL)
[DE88-003146] 10 p1334 N88-17975
Generalized equations for emittance and field energy of high-current beams in periodic focusing
[DE88-004448] 10 p1404 N88-18372
The new UCSB (University of California, Santa Barbara) compact far-infrared FEL
[AD-A190864] 16 p2212 N88-23203
Enhanced emittance of oxidized 304 stainless steel
17 p2423 N88-24408

EMITTERS
NT THERMIONIC CATHODES
NT THERMIONIC EMITTERS
New application of transition metal carbides detailed
06 p0675 N88-14132
Optimal selection of global positioning system set to minimize emitter location errors
[AD-A189559] 12 p1579 N88-19447
Large-aperture sparse array antenna systems of moderate bandwidth for multiple emitter location
[AD-A188409] 12 p1619 N88-19683
Bragg-cell receiver study
[NASA-CR-182684] 13 p1761 N88-20535
Passive DF: A tutorial, part 1
[NASA-CR-182669] 13 p1815 N88-20846
Modulatable thin film field emission space gun
[AD-A189279] 13 p1845 N88-21043
Polysilicon-contacted p+ emitters for silicon solar cell applications
[DE88-005106] 14 p1942 N88-21586
Mathematics clinic probabilistic position-fixing
[NASA-CR-182753] 15 p2125 N88-22672

EMOTIONAL FACTORS
Ejection situations in the U-2/TR-1: An analysis of emotions and events
[AD-A192872] 21 p2893 N88-27175

EMPENNAGE
U TAIL ASSEMBLIES

EMPTYING
Gastric emptying during walking and running: Effects of varied exercise intensity
[AD-A194025] 23 p3240 N88-29281

EMULSIONS
Reactions of porphyrins in surfactant assemblies, microemulsions and in solutions
[AD-A184797] 05 p0560 N88-13412
Analysis of relativistic nucleus-nucleus interactions in emulsion chambers 07 p0926 N88-15624
The morphology of emulsion polymerized latex particles
[DE88-002672] 08 p0972 N88-15879
National Center for Small-Angle Scattering Research: Reports on measurements carried out by users of the facilities of the NCSASR, December 1, 1985-September 30, 1987
[DE88-003754] 11 p1462 N88-18719
Droplet size characteristics and energy input requirements of emulsions formed using high-intensity-pulsed electric fields
[DE88-005912] 15 p2128 N88-22692

ENAMELS
Contribution to the development of coated fiber ceramic insolation material
[ETN-88-92361] 21 p2906 N88-27243

ENCAPSULATED MICROCIRCUITS
Chemical multisensors with selective encapsulation of ion-selective membranes 19 p2670 N88-25869

ENCAPSULATING
Development of microencapsulation techniques
[AD-A185019] 05 p0567 N88-13457
Development of encapsulated lithium hydride thermal energy storage for space power systems
[DE88-004762] 11 p1507 N88-19001
Ion beam modification of film stress and the effectiveness of thin film encapsulants on GaAs
[DE88-004458] 11 p1558 N88-19328
Development of microencapsulated DNBM quaternary ammonium inhibitors for paints
17 p2319 N88-23851
The application of high-rate biaxial testing to the design of containment vessels for radioisotope heat sources
17 p2426 N88-24428
Liquid encapsulated float zone process and apparatus
[NASA-CASE-MFS-28144-1] 17 p2446 N88-24545
A compatible encapsulant for explosives
[DE88-007212] 18 p2495 N88-24806
Primerless RTV silicones
[BDX-613-3807] 24 p3356 N88-29980

ENCKE COMET
On orbits and association of meteor streams with Comets P/Halley and P/Encke
14 p2003 N88-21945
A model of the nongravitational motion of Comet P/Encke 14 p2010 N88-21993

ENCLOSURES
The use of Kevlar on aero-engine fan containment casings
[PNR90410] 02 p0182 N88-11134
Plant Growth Module (PGM) conceptual design
05 p0631 N88-13855
Some performance comparisons for a fluid dynamics code
[PB88-113709] 07 p0852 N88-15175
Thermosolutal convection in high-aspect-ratio enclosures
[NASA-TM-100803] 11 p1486 N88-18871

Fingering flow patterns of thermosolutal convection in rectangular enclosures
[NASA-TM-100854] 14 p1911 N88-21417
Research in electromagnetic shielding theory. Part1. Shielding by rectangular enclosures
[AD-A192881] 20 p2791 N88-26557

ENCODERS
U CODERS

ENCODING
U CODING

END EFFECTORS
The ESA/Fokker service end-effector subsystem. A robotic/man-compatible servicing approach
12 p1587 N88-19502
System and concept design of the SSRMS latching end effector --- Space Station 14 p1875 N88-21204
Precise computer controlled positioning of robot end effectors using force sensors
[NASA-CR-182887] 17 p2391 N88-24213

END MORAINES
U GLACIAL DRIFT

END PLATES
Method for characterizing end-plate surface resistance of dielectric resonator 14 p1903 N88-21371

END-TO-END DATA SYSTEMS
Solid Earth mission end-to-end data system study
[C04825.08/FR] 17 p2309 N88-23811

ENDANGERED SPECIES
Survey for least bell's vireo in riparian habitat on Vandenberg Air Force Base, Santa Barbara County, California
[NASA-TM-100984] 20 p2822 N88-26744

ENDOCRINE GLANDS
NT ADRENAL GLAND
NT HYPOTHALAMUS
NT PITUITARY GLAND
NT TESTES

ENDOCRINE SECRETIONS
NT ALDOSTERONE
NT CORTICOSTEROIDS
NT HORMONES
NT PITUITARY HORMONES

ENDOCRINE SYSTEMS
Interplanetary travel: Is gravity needed to close the loop
[NASA-TM-101013] 22 p3132 N88-28622

ENDOCRINOLOGY
Investigations of the reproductive physiology of the rainbow trout (Salmo gairdneri Richardson)
07 p0885 N88-15370
Endocrine responses to resistance exercise
[AD-A188681] 12 p1667 N88-19993
Hormonal regulation of fluid and electrolytes: Effects of heat exposure and exercise in the heat
[AD-A192655] 22 p3131 N88-28614

ENDOSCOPES
Ultrafast holography using optical fibers
[ISL-R-101/86] 02 p0176 N88-11096

ENDOTHELIUM
Interactions of cultured human endothelial cells with polymeric surfaces
[PB88-112255] 10 p1369 N88-18178

ENDOTHERMIC REACTIONS
Investigation by differential scanning calorimetry of microstructure in a superplastic Al-Mg-Zr alloy
[AD-A184902] 05 p0564 N88-13439

ENERGETIC PARTICLES
NT ARGON PLASMA
NT BETA PARTICLES
NT BOUNDARY LAYER PLASMAS
NT CESIUM PLASMA
NT COLD PLASMAS
NT COLLISIONAL PLASMAS
NT COLLISIONLESS PLASMAS
NT CONDUCTION ELECTRONS
NT COSMIC PLASMA
NT CYLINDRICAL PLASMAS
NT DENSE PLASMAS
NT DEUTERIUM PLASMA
NT ELECTRON PLASMA
NT ELECTRONS
NT EVEN-EVEN NUCLEI
NT HEAVY NUCLEI
NT HELIUM PLASMA
NT HIGH ENERGY ELECTRONS
NT HIGH TEMPERATURE PLASMAS
NT HOT ELECTRONS
NT HYDROGEN PLASMA
NT HYPERNUCLEI
NT LASER PLASMAS
NT METALLIC PLASMAS
NT NITROGEN PLASMA
NT NONEQUILIBRIUM PLASMAS
NT NONUNIFORM PLASMAS
NT NUCLEI (NUCLEAR PHYSICS)
NT ODD-ODD NUCLEI
NT OXYGEN PLASMA
NT PLASMA FOCUS
NT PLASMAS (PHYSICS)
NT RELATIVISTIC PLASMAS
NT ROTATING PLASMAS
NT SEMICONDUCTOR PLASMAS
NT SOLAR WIND
NT SPACE PLASMAS
NT SPHERICAL PLASMAS
NT STELLAR WINDS
NT STRONGLY COUPLED PLASMAS
NT THERMAL PLASMAS
NT TOROIDAL PLASMAS
The elastic scattering of intermediate energy protons from (40)Ca and (208)Pb 01 p0092 N88-10599
Solar energetic particles events observed by Prognoz-10 Intercosmos (May-October 1985)
01 p0111 N88-10716
An account of a flare related shock event recorded by the energetic particle detector EPONA of the Giotto spacecraft during September 1985 (STIP interval 18)
01 p0118 N88-10757
Particle desorption from nonconducting surfaces by high energy heavy ions
[ETN-88-91088] 09 p1245 N88-17461
Time dependent degradation of energetic electrons in gaseous and condensed media
[DE88-002912] 09 p1246 N88-17465
Research in experimental nuclear physics
[DE88-004100] 10 p1408 N88-18397
Energetic particle drift motions in the outer dayside magnetosphere
[DE88-005097] 11 p1512 N88-19034
Proposal for construction of an Energetic Particle Injector (EPI)
[INPE-4242-RPE/548] 12 p1690 N88-20112
Stimulated Emission of Energetic Particles (SEEP)
[AD-A188724] 13 p1853 N88-21094
Observation of energetic particles (E greater than 30 keV) by the Giotto experiment EPA in the magnetic cavity of Comet Halley 14 p1997 N88-21903
Nuclear and ionic charge distribution experiment on ISEE-1 and ISEE-3
[NASA-CR-180776] 23 p3183 N88-28947

ENERGY
Inflation in Einstein-Cartan theory with energy-momentum tensor with spin
[NASA-TM-101164] 17 p2447 N88-24547
Difficulties with interpretation of underground muons from Cygnus X-3
[DE88-701645] 23 p3309 N88-29710

ENERGY ABSORPTION
NT ELECTROMAGNETIC ABSORPTION
NT GAMMA RAY ABSORPTION
NT INFRARED ABSORPTION
NT MODERATION (ENERGY ABSORPTION)
NT MOLECULAR ABSORPTION
NT MULTIPHOTON ABSORPTION
NT PHOTOABSORPTION
NT RADIATION ABSORPTION
NT THERMAL ABSORPTION
NT THERMALIZATION (ENERGY ABSORPTION)
NT ULTRAVIOLET ABSORPTION
NT X RAY ABSORPTION
Vibration-absorbing characteristics of metal-polymer shells 02 p0158 N88-10991
Time-resolved absorption measurements on OMEGA
[DE87-014465] 02 p0179 N88-11112
Toward detecting California shrubland canopy chemistry with AIS data 05 p0613 N88-13764
Fractographic study of fiber composites
06 p0677 N88-14146
Helicopter crashworthiness research program
09 p1107 N88-16635
Thermal energy storage by means of an absorption cycle
[ETN-88-91614] 09 p1186 N88-17108
Note on boundary stabilization of wave equations
[AD-A187113] 09 p1227 N88-17348
Guided-wave approaches to spectrally selective energy absorption
[NASA-CR-182532] 10 p1320 N88-17892
Transmitting boundary for finite-difference calculations with finite modeling of an infinite medium
[AD-A191441] 18 p2570 N88-25264
REFLEX: An energy deposition code that models the effects of electron reflection during electron beam heating tests
[DE88-009789] 19 p2726 N88-26186

ENERGY ABSORPTION FILMS
Investigation of the subsequent treatment and the stability of CuxS-CdS thin-film solar cells
[ETN-88-91488] 11 p1507 N88-19006

ENERGY BANDS
NT BLOCH BAND
NT CONDUCTION BANDS
Banded ion morphology 04 p0468 N88-12892
Population inversion in gapless semiconductors as result of interband pumping 06 p0770 N88-14732
Tailorable infrared sensing device with strain layer superlattice structure
[NASA-CASE-NPO-16607-1-CU]
06 p0788 N88-14836
Self energy corrections to the ab initio band structures: Chromium
[DE88-701825] 21 p3020 N88-27927
Investigation of electronic band structure of semiconductors by photoemission
[ETN-88-92370] 21 p3025 N88-27957
Multiphoton transitions in semiconductors in the non-perturbative approach
[DE88-702664] 22 p3157 N88-28786

ENERGY BUDGETS
NT ATMOSPHERIC HEAT BUDGET
NT EARTH RADIATION BUDGET
NT HEAT BUDGET
Energy balance in laser-irradiated vaporizing droplets
[DE88-000525] 04 p0449 N88-12782
Reynolds-stress and dissipation rate budgets in a turbulent channel flow
[NASA-TM-89451] 07 p0852 N88-15174
Use of the thermodynamic evaporation formula of Hoffmann in energy balance models for flowing water
08 p1013 N88-16143
Energy balance and discharge of an Alpine glacier, illustrated by Mount Vernagtferner in the Oetzal Alps, Tyrol 08 p1014 N88-16145
Low authority control of large space structures using a constrained threshold control formulation
18 p2472 N88-24667

ENERGY CONSERVATION
Cost savings possible with Air Force conversion to JP-8 as its primary fuel
[AD-A183784] 01 p0030 N88-10192
Automotive Stirling engine: Mod 2 design report
[NASA-CR-175106] 02 p0250 N88-11578
Oxygen enriched combustion system performance study
[DE88-001500] 05 p0562 N88-13424
Riblets for aircraft skin-friction reduction
07 p0814 N88-14955
Feedback stabilization of distributed systems
[AD-A187111] 09 p1222 N88-17328
Mathematical modeling of two-state classification technology transfer summary and user's guide
[DE88-003849] 11 p1526 N88-19110
Systems approach to energy quality and efficiency
[PB88-139506] 12 p1640 N88-19823
Large-Scale Advanced Prop-Fan (LAP)
[NASA-CR-182112] 13 p1723 N88-20306
Overview of the DOE-ECUT Tribology Program
[DE88-002878] 13 p1778 N88-20637
Applicability of aerospace thermal insulation technologies to the civilian sector
[DE88-003717] 13 p1852 N88-21086
Overview of 1987 moonlight project
15 p2052 N88-22231
Wave energy flow conservation for propagation in inhomogeneous Vlasov-Maxwell equilibria
[DE88-006705] 15 p2055 N88-22251
NASA advanced turboprop research and concept validation program
[NASA-TM-100891] 16 p2163 N88-22902
Three axis attitude control system
[NASA-CASE-GSC-12970-1] 17 p2308 N88-23808
NASA/industry advanced turboprop technology program
[NASA-TM-100929] 18 p2466 N88-24641
Reduction in mill air compressor power requirements through installation of a variable frequency speed control
[DE88-008493] 23 p3221 N88-29171

ENERGY CONSUMPTION
Use of natural gas diesel engines in mechanical pulp production: A preliminary study
[DE87-753065] 02 p0181 N88-11129
Optimized ground coupled heat pump mechanical package
[DE87-014899] 04 p0441 N88-12738
Life-cycle cost analysis of residential heat pumps and alternative HVAC (Heating, Ventilating and Air-Conditioning) systems
[DE88-003701] 07 p0839 N88-15090
Short Reference Years: Short weather data sets for faster simulations of solar energy systems and energy consumption in buildings
[DE88-900198] 07 p0881 N88-15343
Regulation of energy metabolism during parachute jumps 07 p0896 N88-15428
Hercules: A power analyzer for MOS VLSI circuits
[AD-A189702] 12 p1623 N88-19706

Droplet size characteristics and energy input requirements of emulsions formed using high-intensity-pulsed electric fields
[DE88-005912] 15 p2128 N88-22692
Sunshine project for FY 1987 outlined 16 p2184 N88-23021
Tactical Rubidium Frequency Standard (TRFS)
[AD-A191049] 16 p2193 N88-23078
Costs and benefits of AC propulsion
[PB88-173380] 16 p2287 N88-23691

ENERGY CONVERSION
NT BIOMASS ENERGY PRODUCTION
NT GEOTHERMAL ENERGY CONVERSION
NT OCEAN THERMAL ENERGY CONVERSION
NT PHOTOTHERMAL CONVERSION
NT PHOTOVOLTAIC CONVERSION
NT SOLAR ENERGY CONVERSION
NT WATERWAVE ENERGY CONVERSION
Fifty years in synthetic fuels information: Have we lost a strategic national resource
[DE87-010902] 02 p0155 N88-10973
Satellite techniques of solar resource assessment for focusing and non-focusing solar collector systems
[DE88-001657] 07 p0874 N88-15298
Advanced energy conversion concept for beamed-energy propulsion
[AD-A187336] 10 p1324 N88-17914
Point-focus concentrator reflector assembly, phase 1
[DE88-003616] 13 p1792 N88-20720
Multi-hundred kilowatt roll ring assembly evaluation results
[NASA-TM-100865] 14 p1904 N88-21375
Rotating-hoop, pulsed-energy converter 17 p2426 N88-24433
A multimegawatt space power source radiator design 17 p2427 N88-24436
Energy conversion system optimization study for multimegawatt space nuclear power application 17 p2436 N88-24492
Mechanisms of photochemical energy conversion by chlorophyll
[DE88-008763] 20 p2819 N88-26725
Comparative analysis of the space power architecture studies
[NASA-TM-100977] 22 p3049 N88-28090
Hydrogen concentration cells as converters of heat into electricity
[DE88-009662] 23 p3229 N88-29216

ENERGY CONVERSION EFFICIENCY
High-efficiency silicon solar cells: Numerical modeling, transient measurements, efficiency goals, and v-shaped grooves
[DE87-012842] 01 p0066 N88-10423
Recent progress in magma energy extraction
[DE87-013083] 01 p0066 N88-10424
Focusing solar energy collector 02 p0159 N88-10996
The fundamentals of photovoltaic system electrical design
[DE87-009061] 02 p0194 N88-11214
Gallium arsenide and multibandgap solar cell research
[DE87-012260] 02 p0194 N88-11215
Tapping the earth's geothermal resources: Hydrothermal today, magma tomorrow
[DE87-014718] 02 p0196 N88-11223
Electricity from photovoltaic solar cells. Flat-Plate Solar Array Project of the US Department of Energy's National Photovoltaics Program: 10 years of progress
[NASA-TM-89653] 03 p0346 N88-12188
Performance analysis of solar thermal power systems
[DE88-000563] 04 p0465 N88-12874
International Energy Agency (IEA) Small Solar Power Systems (SSPS) sodium cavity and external receiver performance comparison
[DE88-001310] 04 p0465 N88-12879
An overview of the DOE/SANDIA/USDA vertical axis wind turbine Test Bed Project
[DE88-000604] 05 p0622 N88-13812
The high performance solar array GSR3
[SNIAS-872-422-108] 05 p0622 N88-13814
Development of mechanically stacked tandem concentrator cells
[DE88-001926] 06 p0730 N88-14490
Actual performance and economic feasibility of residential solar water heaters
[INPE-4399-RPE/555] 08 p1023 N88-16191
Variable band gap materials for thermophotovoltaic generators
[AD-A186858] 09 p1186 N88-17104
A comparison of different module configurations for multibandgap solar cells
[DE88-002718] 09 p1187 N88-17113
The application of liquid-metal MHD (magnetohydrodynamics) to renewable energy sources
[DE88-003083] 09 p1251 N88-17495
A ring model of the lasertron
[DE88-004656] 10 p1323 N88-17908
Laser production and heating of plasma for MHD application
[NASA-TP-2798] 10 p1415 N88-18443
Coherent VUV source at 130 nm: Theory and modeling
[DE88-003874] 11 p1549 N88-19269
Wind energy resource survey of New Zealand: National resource assessment
[PB88-139365] 12 p1640 N88-19822
Research on multibandgap solar cells
[DE87-012261] 13 p1792 N88-20721
Stable, high-efficiency, CuInSe2-based, polycrystalline, thin-film tandem solar cells
[DE88-001116] 13 p1793 N88-20726
Crystalline photovoltaic cell technology: Present and future
[DE88-004684] 13 p1795 N88-20734
Overview of recent activities in the Heat Cycle Research Program
[DE88-005544] 13 p1795 N88-20738
Thin-film cadmium telluride solar cells
[DE88-001107] 13 p1846 N88-21050
Recent advances in photovoltaic concentrator technology
[DE88-003948] 15 p2091 N88-22462
Comparison of electrically driven lasers for space power transmission
[NASA-TM-4045] 16 p2212 N88-23197
Three-dimensional models of conventional and vertical junction laser-photovoltaic energy converters
[NASA-TM-4039] 17 p2370 N88-24111
Overview of NASA Lewis Research Center free-piston Stirling engine technology activities applicable to space power systems 17 p2398 N88-24255
Benefits of 20 kHz PMAD in a nuclear space station 17 p2398 N88-24256
Acoustical gas core reactor with MHD power generation for burst power in a bimodal system 17 p2403 N88-24290
A liquid metal MHD concept for multimegawatt space power application 17 p2413 N88-24348
Parametric analyses of the TE SP-100 system performance 17 p2415 N88-24358
The closed Brayton cycle: An energy conversion system for near-term military space missions 17 p2435 N88-24488
Progress in InP solar cell research
[NASA-TM-100914] 18 p2507 N88-24870
An investigation of high pressure/late cycle injection of CNG (Compressed Natural Gas) as a fuel for rail applications
[DE88-009000] 19 p2677 N88-25917
Integrated solar reforming for thermochemical energy transport
[DE88-005010] 19 p2686 N88-25967
Study of Staebler-Wronsky degradation effect in a Si:H based P-I-N solar cells
[NASA-CR-182564] 19 p2687 N88-25970
Dielectric compound parabolic concentrating solar collector with frustrated total internal reflection absorber
[DE88-009986] 19 p2688 N88-25976
Photovoltaic concentrator technology: Recent results
[DE88-009588] 20 p2819 N88-26726
Estimation of power-energy plots for secondary batteries
[DE88-011922] 21 p2940 N88-27460
Solar energy conversion through the interaction of plasmons with tunnel junctions. Part A: Solar cell analysis. Part B: Photoconductor analysis
[NASA-CR-183044] 21 p2967 N88-27621
Experimental fabrication of thin film single crystalline solar cells
[PB88-131958] 22 p3116 N88-28516
An examination of wake effects and power production for a group of large wind turbines
[DE88-009906] 22 p3117 N88-28518
Energy conversion measurements in laser-sustained argon plasmas for application to rocket propulsion
[AD-A194931] 24 p3337 N88-29861

ENERGY CONVERTERS
U DIRECT POWER GENERATORS

ENERGY DENSITY
U FLUX DENSITY

ENERGY DISSIPATION
A data analysis package for RDF-determination fromEXELFS-spectra
[USIP-87-07] 01 p0104 N88-10681
Navier-Stokes cascade analysis with a stiff Kappa-Epsilon turbulence solver
[NASA-TM-100218] 02 p0123 N88-10778
EXELFS (Extended Electron Energy Loss Fine Structure) of amorphous and crystalline SiC
[DE87-013551] 02 p0151 N88-10948
Focusing solar energy collector 02 p0159 N88-10996
Potential formation in the plasma confinement region of a radio-frequency plugged linear device
[IPPJ-843] 02 p0242 N88-11526
XeCl excimer laser with magnetic compressor 03 p0299 N88-11879
Physical design of parameters of Nd:YAG disk laser 03 p0302 N88-11904
On helicity fluctuations and the energy cascade in turbulence
[NASA-CR-178403] 03 p0321 N88-12028
Resistor cooling in a vacuum
[DE88-000696] 04 p0440 N88-12733
Heating of stellar chromospheres and coronae: Evidence for non-magnetic basal heating 04 p0503 N88-13098
Chromospheric and coronal heating in a bias-free sample of K dwarfs 04 p0518 N88-13184
Power and charge dissipation from an electrodynamic tether 06 p0795 N88-14869
Ionization losses in BGO
[NOTA-INTERNA-889] 07 p0856 N88-15198
Study of vibration relaxation in active medium of CO2-laser using phase-absorption method 07 p0919 N88-15582
Effect of peel angle on peel force
[AD-A188117] 08 p0972 N88-15878
Stellar energy loss and anomalous contributions to the (photon photon) (neutrino antineutrino) interaction
[DE88-700618] 10 p1428 N88-18529
Experimental study of scattered waves and cylindrical antenna sheaths in a microwave driven plasma 11 p1553 N88-19293
The Euler-Bernoulli beam equation with boundary energy dissipation
[AD-A189517] 13 p1765 N88-20560
On the zonal momentum balance at the equator 13 p1805 N88-20788
Thermal modeling of solar central receiver cavities
[DE88-004940] 14 p1943 N88-21594
Modeling scalar flux and the energy and dissipation equations 16 p2196 N88-23096
A general form for the dissipation length scale in turbulent shear flows 16 p2197 N88-23104
On the magnetic structure and energy balance of EUV-emitting plasma in the quiet Sun 17 p2452 N88-24567
Electromagnetic damping and vibration isolation of space structures
[AD-A191492] 18 p2471 N88-24665
Extrema principles of entrophy production and energy dissipation in fluid mechanics
[NASA-TM-100992] 18 p2519 N88-24945
Energy dissipation in a rolling aircraft tire
[NASA-CR-182978] 19 p2676 N88-25913
Propagation of charged particle beams in the atmosphere
[AD-A193185] 21 p3014 N88-27887
Customizing Space Nuclear Power System Analysis Model (SNPSAM): Introducing a secondary coolant loop
[AD-A194620] 22 p3151 N88-28750
Mathematical theory and calculations of magnetic hysteresis curves
[DE88-011055] 23 p3277 N88-29510

ENERGY DISTRIBUTION
NT SPECTRAL ENERGY DISTRIBUTION
Measurement of parallel ion energy distribution function in PISCES plasma
[DE88-000108] 03 p0378 N88-12380
The closest solar analogs in the bright star catalogue 04 p0506 N88-13110
Statistical properties of small high-velocity events in the solar transition region 04 p0506 N88-13112
Lagrangian procedures for higher order field equations
[DE87-703365] 05 p0840 N88-13911
Calibration of the EGRET gamma ray telescope with a back-scattered laser beam 06 p0800 N88-14895
A survey study of energy distribution in component stars of Algol-type binary systems 06 p0801 N88-14901
Energy distribution of Cerenkov radiation for finite frequency intervals
[AD-A186901] 09 p1244 N88-17454
Product kinetic and internal energy distributions via velocity-aligned Doppler spectroscopy
[DE88-003510] 10 p1298 N88-17764
Procedure for detection and identification of a helicopter
[NASA-TT-20234] 13 p1722 N88-20297
Kinetics of slow electrons in excimer laser with electron-beam pumping 14 p1970 N88-21760
Femtosecond studies in hot carrier relaxation in GaAs and AlGaAs 14 p1977 N88-21801
Angular resolved energy analysis of (69)Ga+ ions from a gallium liquid metal ion source
[AERE-R-12649] 15 p2139 N88-22760

An evaluation of energy-independent heavy ion transport coefficient approximations
[NASA-TM-101158] 17 p2397 N88-24251
Evaluation of surface energy and radiation balance systems for FIFE
[NASA-CR-183118] 20 p2828 N88-26778
Energy distribution and transfer in flowing hydrogen microwave plasmas 21 p3019 N88-27919

ENERGY EFFICIENCY TRANSPORT PROGRAM
U ACEE PROGRAM

ENERGY EXCHANGE
U ENERGY TRANSFER

ENERGY GAPS (SOLID STATE)
Wide bandgap passivation layers on silicon
[DE87-014307] 02 p0244 N88-11543
Improving the method of calculating electronic properties of narrow bandgap semiconductors 07 p0926 N88-15627
Effect of the band-gap characteristics on laser-induced dry etching of semiconductors
[DE88-001853] 07 p0937 N88-15695
Experimental aspects of high-T/sub c/ superconductors
[DE88-003019] 08 p1090 N88-16564
Interpretation of the temperature dependence of conductivity in superconducting oxides
[DE88-003028] 08 p1091 N88-16565
Variable band gap materials for thermophotovoltaic generators
[AD-A186858] 09 p1186 N88-17104
Raman scattering in mixed crystal semiconductors 12 p1696 N88-20149
Research on multibandgap solar cells
[DE87-012261] 13 p1792 N88-20721
Study for the determination of general and specific properties of wide energy-band gap HgHdTe in the 1-2 micrometer wavelength range
[AD-A189177] 13 p1845 N88-21041
Developments in ceramic superconducting materials 15 p2052 N88-22229
Meaning of energy diagrams used to describe hetero-structures
[DE88-702219] 21 p3023 N88-27943
Techniques and instrumentation for transient characterization of metal-insulator-semiconductor diodes. Applications to metal-insulator InP system
[ECL-87-17] 21 p3025 N88-27959
Theoretical investigation of image states of the hydrogen covered Cu (100)
[DE88-702662] 23 p3292 N88-29604

ENERGY LEVELS
NT ATOMIC ENERGY LEVELS
NT ELECTRON STATES
NT GROUND STATE
NT MOLECULAR ENERGY LEVELS
Accurate ab initio calculations which demonstrate a 3 Pi u ground state for Al2
[NASA-TM-89302] 01 p0102 N88-10666
Electronic structure of crystalline NaSn
[DE87-702583] 01 p0102 N88-10669
Studies on surface chemical states of some metals and ceramics bombarded with energetic light-ions
[DE87-752975] 02 p0145 N88-10910
J = O Task Force
[DE88-001326] 04 p0450 N88-12788
Characterization of Er,Cr:YSGG
[AD-A185885] 07 p0932 N88-15659
Wave functions for bound states of relativistic electrons in a crystal at electron movement along crystallographic planes
[DE88-700563] 07 p0939 N88-15708
Low-power photolytically pumped lasers
[DE88-002448] 08 p0991 N88-15998
New branch of solid-state physics 08 p1079 N88-16508
Near threshold behavior of photoelectron satellite intensities
[DE88-002231] 08 p1081 N88-16512
Design, construction and operation of a small RFP for turbulent plasma studies
[INPE-4241-PRE/1116] 08 p1087 N88-16545
Properties of nuclei and elementary particles at low and intermediate energies
[DE88-001913] 09 p1244 N88-17456
Frequency response function estimation at level
[DE88-002644] 10 p1344 N88-18034
Charge exchange in low energy (keV) and hyperthermal energy (10-100 eV) ion scattering
[AD-A187643] 11 p1543 N88-19222
Spectral line-broadening codes for hydrogen-, helium- and lithium-like ions in plasmas
[DE88-005238] 11 p1552 N88-19289
A neutral-beam diagnostic for fast confined alpha particles in a burning plasma: Applicatoin on CIT (Compact Ignition Tokamak)
[DE88-004890] 11 p1554 N88-19301
A moment approach to modeling negative ion sources
[AD-A188858] 12 p1691 N88-20114
An experimental method for species concentration measurements in a welding arc using laser-induced fluorescence
[DE88-005638] 13 p1778 N88-20636
Quantum Monte Carlo study of the MIES associated with H2 (X 1 sigma sub g (+)) and H2 (B 1 sigma sub u (+))
[AD-A189063] 13 p1835 N88-20977
Image charge, coherent scattering, and symmetry effects in electron stimulated desorption: O(-) from O sub 2 condensed on metals
[AD-A189093] 13 p1835 N88-20979
Discharge excitation of the XeF C to A transition
[DE88-006448] 15 p2070 N88-22339
Fermi level stabilization in semiconductors: Implications for implant activation efficiency
[DE88-006332] 15 p2145 N88-22801
On 1/n-expansion and wave functions
[DE88-701639] 16 p2260 N88-23509
Optical properties of heterostructures and superlattices
[AD-A191542] 18 p2581 N88-25335
Accuracy of analytic energy level formulas applied to hadronic spectroscopy of heavy mesons
[NASA-TM-4042] 19 p2725 N88-26185
Energy levels and magneto-electric effects in some quasi uni-dimensional semiconductor heterostructures 20 p2864 N88-27009
Superconducting electronic film structures
[AD-A192907] 20 p2879 N88-27091
Filling of the atmospheric transmission window due to emission from very high rotational levels of NO and O3
[AD-A194670] 23 p3233 N88-29239
Electronic states in tunneling semiconductor superlattices
[DE88-011571] 23 p3290 N88-29587
Absorption spectra and energy levels of Gd(3+), Nd(3+) and Cr(3+) in the garnet Gd3Sc2Ga3O12
[AD-A193634] 23 p3292 N88-29599
Relativistic theory of the Lamb shift based on self energy
[DE88-702658] 23 p3295 N88-29626

ENERGY LOSSES
U ENERGY DISSIPATION

ENERGY METHODS
NT BERNSTEIN ENERGY PRINCIPLE
NT STRAIN ENERGY METHODS
A work station for EXELFS data acquisition and analysis
[USIP-87-10] 01 p0078 N88-10498
The optimum illumination conditions for EXELFS studies in a CTEM
[USIP-87-08] 01 p0092 N88-10600
Instrumental and operational aspects of an EXELFS system connected to JEOL 100C STEM
[USIP-87-09] 01 p0092 N88-10601
A data analysis package for RDF-determination fromEXELFS-spectra
[USIP-87-07] 01 p0104 N88-10681
Fully plastic analysis of mixed mode plane-strain crack problems
[PB87-144929] 08 p0994 N88-16015

ENERGY OF FORMATION
Use of long-distance pair potentials in calculations of defect characteristics in metals
[DE88-701039] 15 p2037 N88-22138

ENERGY POLICY
Fifty years in synthetic fuels information: Have we lost a strategic national resource
[DE87-010902] 02 p0155 N88-10973
Numerical and experimental investigation of the unsteady temperature distribution in solar central receivers
[ESA-TT-1050] 03 p0347 N88-12193
Energy Data Base: Subject Thesaurus
[DE87-008007] 03 p0384 N88-12414
Emerging environmental constraints on the use of gasoline and diesel fuel and tradeoffs associated with the use of alternative fuels
[DE87-011504] 04 p0422 N88-12614
Fuel cells --- military applications
[PML-1986-43] 05 p0622 N88-13813
Satellite power systems under consideration by the United Nations 09 p1128 N88-16773
The role of repowering in America's power generation future
[DOE/FE-0096] 10 p1351 N88-18076
Understanding and accepting fusion as an alternative energy source
[DE88-004356] 10 p1413 N88-18432
Technical highlights of the Alternative Fuels Utilization Program
[DE88-005064] 15 p2049 N88-22205
Solar dynamic power systems
[ETN-88-92969] 23 p3230 N88-29224

ENERGY REQUIREMENTS
A large X-ray flare on Sigma 2 coronae borealis observed with exosat 04 p0508 N88-13121
Power systems for production, construction, life support and operations in space
[NASA-TM-100838] 14 p1883 N88-21254
Droplet size characteristics and energy input requirements of emulsions formed using high-intensity-pulsed electric fields
[DE88-005912] 15 p2128 N88-22692

ENERGY SOURCES
A proposal for a project entitled assessment of forest resources in Uruguay submitted to the United Nations Industrial Development Organization (UNIDO) 17 p2352 N88-24016

ENERGY SPECTRA
NT ELECTRONIC SPECTRA
NT NEUTRON SPECTRA
Relativisitic heavy ion collisions
[DE87-014292] 02 p0232 N88-11462
Heavy element compositions and energy spectra of galactic and solar cosmic rays 03 p0272 N88-11714
A multiple-time-scale turbulence model based on variable partitioning of turbulent kinetic energy spectrum
[NASA-CR-179222] 04 p0444 N88-12754
Spectral evolution equation for the sideband instability in a free-electron laser oscillator
[DE88-000510] 04 p0447 N88-12771
Simultaneous, cospatial imaging of the Sun in cyanogen and singly-ionized calcium 04 p0507 N88-13114
Multiply charged particles in primary cosmic rays with energy less than or equal to 2 TeV 07 p0921 N88-15596
Fully turbulent internal flow excitation of pipe systems 08 p1000 N88-16056
Observations of gamma bursts from GBS 0526-66 08 p1001 N88-16065
Interpretation of equatorial current meter data as internal waves
[PB88-108113] 08 p1044 N88-16309
New branch of solid-state physics 08 p1079 N88-16508
Near threshold behavior of photoelectron satellite intensities
[DE88-002231] 08 p1081 N88-16512
Investigation of the quantitative determination of two dimensional sea surface wave spectra from shipborne radar measurements
[GKSS-87/E/10] 09 p1195 N88-17163
Properties of nuclei and elementary particles at low and intermediate energies
[DE88-001913] 09 p1244 N88-17456
Vibration spectra of oxygen and vanadium atoms in vanadium-oxygen disordered interstitial alloys
[DE87-703166] 13 p1740 N88-20404
Study of spectra of sea waves on horizontally nonuniform current in rip zone 13 p1788 N88-20699
Energy spectra of pick-up ions recorded during the encounter of Giotto with Comet Halley 14 p1997 N88-21901
Spectral measurements in a disturbed boundary layer over snow
[AD-A190217] 15 p2097 N88-22494
Computing X-ray effects in optics
[DE88-006722] 15 p2134 N88-22732
Time-frequency representations for speech signals
[AD-A188661] 18 p2498 N88-24819
Accuracy of analytic energy level formulas applied to hadronic spectroscopy of heavy mesons
[NASA-TM-4042] 19 p2725 N88-26185
Meaning of energy diagrams used to describe hetero-structures
[DE88-702219] 21 p3023 N88-27943
Cascade model of gamma-ray bursts: Power-law and annihilation-line components
[NASA-TM-101176] 21 p3032 N88-27998
Nuclear and ionic charge distribution experiment on ISEE-1 and ISEE-3
[NASA-CR-180776] 23 p3183 N88-28947

ENERGY STORAGE
NT ELECTRIC ENERGY STORAGE
NT HEAT STORAGE
Electrical Power Working Group report 01 p0016 N88-10095
Ionically conductive polymers: Application to solid state batteries
[AD-A183733] 01 p0037 N88-10239
Apparatus for storing kinetic energy
[EP-PATENT-0-181-736-A1] 01 p0066 N88-10422
Results of a wind turbine/sealed lead-acid battery experiment
[DE87-012720] 02 p0166 N88-11044
Electrodynamic tether system study
[NASA-CR-172024] 03 p0275 N88-11737

Heats of mixing for thermal energy storage systems. Phase 1: Selection of suitable liquid-liquid mixtures
[DE87-014971] 03 p0347 N88-12196
A study of the optimal transition temperatue of PCM (Phase Change Material) wallboard for solar energy storage
[DE88-001522] 04 p0466 N88-12882
Extended abstracts: Eighth Battery and Electrochemical Contractors' Conference
[DE88-000960] 06 p0730 N88-14489
Solar assisted absorption or motor driven heat pump with earth seasonal storage, part 1
[DE88-900191] 09 p1187 N88-17114
Value-assessment of energy storage concepts in burst power systems
[DE87-013756] 09 p1187 N88-17115
Development of encapsulated lithium hydride thermal energy storage for space power systems
[DE88-004762] 11 p1507 N88-19001
Photochemical energy storage: Studies of inorganic photoassistance agents
[DE88-002596] 11 p1508 N88-19010
Proof of the feasibility of coherent and incoherent schemes for pumping a gamma-ray laser
[AD-A189236] 13 p1774 N88-20613
Power systems for production, construction, life support and operations in space
[NASA-TM-100838] 14 p1883 N88-21254
Energy storage and transport by reversible chemical reactions
[DE88-900370] 14 p1942 N88-21587
Overview of 1987 moonlight project
15 p2052 N88-22231
Performance evaluation of molten salt thermal storage systems
[DE87-014645] 15 p2091 N88-22461
Value of energy storage in pulsed space power systems
[AD-A191311] 16 p2170 N88-22938
Nickel hydroxide active material densities
[AD-A191411] 16 p2230 N88-23319
The cluster ion approach to the condensation and storage of antihydrogen 16 p2269 N88-23575
Aerospace energy systems laboratory: Requirements and design approach
[NASA-TM-100423] 17 p2390 N88-24206
Energy storage evaluation for burst power applications
17 p2426 N88-24430
Energy storage for nuclear burst power systems
17 p2426 N88-24431
Value assessment of energy storage concepts in burst power systems 17 p2426 N88-24432
Rotating-hoop, pulsed-energy converter
17 p2426 N88-24433
Candidate advanced energy storage concepts for multimegawatt burst power systems
17 p2426 N88-24434
High power density alkaline fuel cell technology for MMW space burst power 17 p2429 N88-24451
Polymer fuel cell as an energy storage component for space power applications 17 p2429 N88-24452
Solar assisted absorption or motor driven heat pump with earth seasonal storage. Part 2: Tables and figures
[DE88-900226] 19 p2686 N88-25964
Effect of LEO cycling at shallow depths of discharge on MANTECH IPV nickel-hydrogen cells
[NASA-TM-101300] 19 p2688 N88-25978
Loss evaluation of self-commutated power conditioner for battery energy storage system
[DE88-752075] 20 p2794 N88-26575
Recent developments in nickel hydrogen technology
[DE88-011248] 21 p2939 N88-27456
Storage of thermal energy by means of an absorption cycle
[PB88-190814] 21 p2966 N88-27619
Thermal energy storage
[DE88-010753] 21 p2967 N88-27625
Energy storage considerations for a robotic Mars surface sampler
[NASA-TM-100969] 22 p3156 N88-28853
Transient thermal analysis of three fast-charging latent heat storage configurations for a space-based power system
[DE88-009714] 23 p3186 N88-28960
Charge storage and switching phenomena in metal complexes
[AD-A193778] 23 p3192 N88-28996
Proof of the feasibility of coherent and incoherent schemes for pumping a gamma-ray laser
[AD-A193856] 23 p3220 N88-29165
High power storage system based on thin film solid ionics
[AD-A193623] 23 p3291 N88-29598
Regenerative fuel cell energy storage system for a low earth orbit space station
[NASA-CR-174802] 24 p3389 N88-30184

ENERGY STORAGE DEVICES
U ENERGY STORAGE
ENERGY TECHNOLOGY
NT GEOTHERMAL TECHNOLOGY
Solar thermal technology
[DE87-001171] 02 p0195 N88-11218
Spinoff, 1987
[NASA-TM-89652] 02 p0250 N88-11577
JPRS report: Science and technology. China
[JPRS-CST-87-031] 03 p0299 N88-11880
The Black College satellite telecommunications network planning in support of energy-related collaborative research
[DE88-000182] 03 p0307 N88-11940
Proceedings of the Fifth Symposium on Energy Engineering Sciences: Instrumentation, Diagnostics, and Material Behavior
[DE88-001479] 04 p0429 N88-12660
Basic energy sciences research in the Metals and Ceramics Division of Oak Ridge National Laboratory
[DE87-013538] 06 p0681 N88-14171
Research needs for hydrocarbon fuels
[DE87-014555] 06 p0687 N88-14209
Satellite power systems under consideration by the United Nations 09 p1128 N88-16773
Thermal energy storage by means of an absorption cycle
[ETN-88-91614] 09 p1186 N88-17108
Side-by-side comparisons of evacuated compound parabolic concentrator and flat plate solar collector systems at temperatures of 90 to 100°C
[DE88-004717] 10 p1351 N88-18073
Understanding and accepting fusion as an alternative energy source
[DE88-004356] 10 p1413 N88-18432
Minutes of the meeting of the Indo-US Subcommission on Science and Technology (8th) held at Washington, D.C. on September 22-24, 1986
[PB88-130158] 10 p1423 N88-18503
Proceedings of the 12th Symposium of Japan Solar Energy Society
[DE88-770029] 11 p1507 N88-19005
Alternative Energy in the Midwest: Research and Applications. Conference Proceedings, Rosemont, Illinois, March 19-20, 1987
[PB88-142278] 11 p1509 N88-19015
Starpower: The US and the international quest for fusion energy
[PB88-128731] 11 p1551 N88-19283
Systems approach to energy quality and efficiency
[PB88-139506] 12 p1640 N88-19823
Federal Ocean Energy Technology
[DE87-012279] 13 p1792 N88-20722
Power from the sun: Principles of high temperature solar thermal technology
[DE87-001104] 13 p1795 N88-20736
Technology '87: Research and Development Laboratory Technology Transfer Program
[DE88-003142] 13 p1852 N88-21084
JPRS report: Science and technology. Japan
[JPRS-JST-87-029] 15 p2052 N88-22228
Overview of 1987 moonlight project
15 p2052 N88-22231
JPRS report: Science and technology. Japan
[JPRS-JST-87-026] 16 p2184 N88-23018
Sunshine project for FY 1987 outlined
16 p2184 N88-23021
Advanced energy system program
[PB88-183025] 19 p2686 N88-25965
Fuel cell systems program plan: Fiscal year 1988
[DE88-011080] 20 p2820 N88-26731
ENERGY TRANSFER
Laser probes of natural gas ignition chemistry
[PB87-209599] 01 p0021 N88-10129
Acceleration to hypervelocities using minimum energy concepts
[DE87-011796] 01 p0089 N88-10583
An interactive computer program for materials analysis by means of ion scattering
[MRL-R-1040] 01 p0091 N88-10596
A microstructural lattice model for strain oriented problems: A combined Monte Carlo finite element technique
[NASA-TM-100215] 02 p0150 N88-10939
Migration and transfer of triplet energy in selected polymer systems
[DE87-014432] 02 p0152 N88-10953
Hot spots: Subnanometer femtosecond energy localization
[DE87-010276] 02 p0155 N88-10968
Energy transformation in molecular electronic systems
[DE87-013916] 03 p0282 N88-11771
Kinetics of crack growth: Thermal/mechanical interaction 03 p0337 N88-12124
Application of solar technology to fuel production chemical processing, and thermochemical energy transport: Status and future
[DE87-014172] 03 p0346 N88-12189
Configurations of the quiet polar cap and its response to a sudden increase of the energy input rate epsilon
[DMI-GEOPHYS-PAPERS-R-74]
03 p0350 N88-12210
The Conference on the Dynamics of Molecular Collisions held in Oglebay Park, Wheeling, West Virginia on 12-17 July 1987
[AD-A184690] 03 p0374 N88-12354
Theory of heat and moisture exchange between finely disperse storm-generated spray and turbulent air flow
04 p0461 N88-12851
Nitrogen energy transfer study
[AD-A184457] 04 p0464 N88-12869
Variable collision frequency effects on hose and sausage instabilities in relativistic electron beams
[AD-A184206] 04 p0490 N88-13021
Intramolecular energy transfer reactions as a method for metal complex assisted production of hydrogen
[DE88-001621] 05 p0562 N88-13425
Energy dependence of ion-induced sputtering yields of monatomic solids in the low energy region
[IPPJ-AM-52] 05 p0651 N88-13988
Photoinduced charge separation by polymer-bound chromophores
[DE88-002101] 06 p0685 N88-14198
Nitrogen scale-up
[AD-A185702] 06 p0709 N88-14351
Solar cosmic ray propagation in high-velocity solar wind stream 08 p1002 N88-16073
The role of anabatic winds in the heating of valleys
08 p1014 N88-16144
FTE like variations in the geomagnetic field at ground based conjugate stations in the cusp regions
[INPE-4345-PRE/1182] 08 p1024 N88-16199
Effects of energy, distance and orientation on electron transfer rates studied by pulse radiolysis in organic media
[DE88-002906] 08 p1082 N88-16521
Group 2A metastable collision complexes: Spectroscopy and behavior in intense radiation fields
[AD-A186737] 08 p1082 N88-16524
Energy transmission using coherent, quasimonochromatic light beams
09 p1241 N88-17436
Energy distribution of Cerenkov radiation for finite frequency intervals
[AD-A186901] 09 p1244 N88-17454
A dynamical system/coherent structure approach to the fully developed turbulent wall layer
10 p1267 N88-17578
Kinetic studies following state-selective laser excitation
[DE88-004094] 10 p1335 N88-17981
Energy transfer studies with lasers
[DE88-004864] 10 p1337 N88-17991
Research on fluid dynamic energy separation
[DE88-002776] 10 p1339 N88-18001
Energy transfer and photochemistry in biomimetic solar conversion
[PB88-130026] 10 p1348 N88-18057
Energy transfers for multilayer hydrodynamic ocean models: General formulation and specific examples
[AD-A187604] 10 p1358 N88-18116
Spectroscopic studies of energy transfer in photosynthetic reaction centers of higher plants
[DE88-003850] 10 p1359 N88-18121
State-to-state dynamics of molecular energy transfer
[DE88-003282] 10 p1406 N88-18382
Coronal heating by means of helical magnetohydrodynamic turbulence
[AD-A187084] 10 p1410 N88-18413
Photophysics and photochemistry of poly(di-n-hexylsilane) in room temperature solution
[AD-A187890] 11 p1462 N88-18714
Nonlinear dynamic maximum power theorem
[AD-A187491] 11 p1477 N88-18810
Transient radiative energy transfer in incompressible laminar flows
[NASA-CR-182605] 11 p1488 N88-18883
On the possibility of high velocity deflagration front propagation by radiative energy transfer
[AD-A189022] 12 p1613 N88-19645
Millimeter and submillimeter wave research: Spectroscopy, energy transfer, and techniques
[AD-A188952] 12 p1620 N88-19691
On the energy release rate for dynamic transient anti-plane shear crack propagation in a general linear viscoelastic body
[AD-A188385] 12 p1635 N88-19791

Resonance energy transfer between carbon monoxide and oxygen molecules using dye laser intracavity absorption spectroscopy
[AD-A188488] 12 p1689 N88-20104
Instrumentation for collisional energy transfer studies
[AD-A188495] 12 p1689 N88-20105
To what extent is mass loading responsible for the Venus bowshock precursor?
[NASA-TM-89307] 12 p1711 N88-20239
Solar flares and magnetic topology
[AD-A188692] 12 p1712 N88-20244
Molecular dynamics of laser ablation of a polymer coating
[DE88-004337] 13 p1750 N88-20466
Turbulent transfer of momentum and heat in boundary layer of fluid beyond an obstacle. 1: Hydrodynamic characteristics 13 p1787 N88-20690
Power spectral density analysis of wind-shear turbulence for related flight simulations
[NASA-CR-182721] 13 p1802 N88-20773
Energy and momentum fluxes through the sea surface 13 p1806 N88-20798
Excimer laser photolysis studies of T-V (Translation-to-Vibration) energy transfer
[AD-A189613] 13 p1837 N88-20989
Observations on energy transport in tokamaks: A new formula for turbulent transport
[DE88-005309] 13 p1841 N88-21019
Physical process for maintenance of mean meridional and zonal circulation of atmosphere in middle latitudes, volume 2 14 p1900 N88-21345
Calculation of the efficiency of a resonant cyclotronic electron maser (gyrotrons)
[INPE-4387-PRE/1207] 14 p1915 N88-21444
Energy storage and transport by reversible chemical reactions
[DE88-900370] 14 p1942 N88-21587
Electronic energy transfer processes in the alkali/alkaline earth metal vapors
[AD-A190035] 15 p2034 N88-22119
Molecular reaction and energy transfer rate estimation for chemical-laser analysis
[AD-A190664] 15 p2035 N88-22126
Reactions of N2(A sup 3 sigma sup + sub u) candidates for short wavelength lasers
[DE88-007018] 15 p2070 N88-22342
Characterization of space radiation environment in terms of the energy deposition in functionally important volumes
[DE88-005627] 15 p2100 N88-22513
The adhesive bonding of thermoplastic composites
[AD-A190994] 16 p2173 N88-22953
Study of one-dimensional spectral dynamic equations of the Reynolds stresses in homogeneous anisotropic turbulence: Application to split-spectrum modeling 16 p2196 N88-23095
Local structure of intercomponent energy transfer in homogeneous turbulent shear flow 16 p2197 N88-23103
The decay of isotropic turbulence in a rapidly rotating frame 16 p2197 N88-23107
Energy transfer processes in free radicals: A collaborative experimental and theoretical investigation
[AD-A191264] 16 p2269 N88-23578
Proceedings of Symposium on Physics of Target Implosion and Pulsed Power Techniques
[IPPJ-859] 16 p2276 N88-23619
Simulation code for ICF including radiative energy transfer 16 p2277 N88-23627
Bimolecular reactions and energy-transfer processes of highly vibrationally excited molecules related to energetic materials
[AD-A189013] 18 p2571 N88-25270
Energy-transfer properties and mechanisms
[DE88-007107] 18 p2571 N88-25272
Spectroscopy and energy transfer kinetics of the interhalogens
[AD-A192103] 18 p2583 N88-25344
Transition probabilities in OH A 2 sigma + - X 2 pi i: Bands with v prime = 0 and 1, v double prime = 0 to 4
[NASA-CR-182946] 18 p2584 N88-25353
Numerical investigation of acoustic energy exchange through flow turning 19 p2629 N88-25593
Numerical simulation studies of laminar-turbulent transition in the plan channel 19 p2665 N88-25850
Pressure drop and heat transfer in turbulent non-Newtonian pipe flow of advanced energy transmission fluids
[DE88-010021] 19 p2666 N88-25853
Integrated solar reforming for thermochemical energy transport
[DE88-005010] 19 p2686 N88-25967
Half collision studies of inelastic energy transfer processes
[DE88-008096] 19 p2724 N88-26178
Electrodynamic driver for the space thermoacoustic refrigerator (STAR)
[AD-A192337] 20 p2785 N88-26517
Effects of cosmic rays on single event upsets
[NASA-CR-183053] 20 p2793 N88-26569
Energy migration, motion and order in synthetic polymers
[AD-A193334] 21 p2918 N88-27320
Energy distribution and transfer in flowing hydrogen microwave plasmas 21 p3019 N88-27919
Chemically-produced N2(A) to NO(X) energy transfer in a supersonic flow
[AD-A192501] 22 p3082 N88-28302
On the energy source of 1982-83 ENSO episode simulated by the NCAR community climate model 22 p3122 N88-28556
The active layer of the upper Atlantic Ocean 22 p3124 N88-28566
Solid-state laser research report: Energy transfer in non-uniform codoped crystals
[AD-A194358] 23 p3219 N88-29161
Preliminary studies of NF3+H2 production of N2(A3 sigma(+)u) in a supersonic flow
[AD-A194479] 23 p3219 N88-29162
N2(A3epsilon u+) by reaction of N2F4+H2 in a supersonic flow
[AD-A194493] 23 p3219 N88-29163
Vanderbilt free electron laser project in biomedical and materials research
[AD-A195961] 24 p3378 N88-30121
Energy budget and ground temperatures in hot regions
[AD-A196298] 24 p3404 N88-30268

ENGINE AIRFRAME INTEGRATION
Transonic analysis and design of axisymmetric bodies in nonuniform flow
[NASA-CR-4101] 01 p0003 N88-10013

ENGINE ANALYZERS
Proceedings of the 14th Symposium on Aircraft Integrated Monitoring Systems
[DFVLR-MITT-88-04] 22 p3033 N88-28001
Use of penetrating radiations for the dynamic examination of aero gas turbines
[PNR90470] 22 p3045 N88-28073

ENGINE CONTROL
NT ROCKET ENGINE CONTROL
NT TURBOJET ENGINE CONTROL
A heat transfer model for a heated helium airship
[AD-A183786] 03 p0259 N88-11629
The flight evaluation of an advanced engine display and monitoring system 03 p0264 N88-11659
Engine/airframe response evaluation of the HH-60A helicopter equipped with the T700-GE-701 transient droop improvement electronic control unit
[AD-A184443] 04 p0401 N88-12492
Pumping systems and flow interfaces for rapid response electronic reheat controls 10 p1282 N88-17665
Possibilities for on-line surge suppression by fast guide vane adjustment in axial compressors 10 p1283 N88-17674

ENGINE DESIGN
NT ROCKET ENGINE DESIGN
The design and development of mercury vaporisers for use with electron-bombardment ion engines
[RAE-TR-70042] 01 p0018 N88-10108
First article test noise survey of the A/F32T-9 large turbo fan engine enclosed noise suppressor system, Sky Harbor IAP (International Airport), Phoenix, Arizona
[AD-A183799] 01 p0090 N88-10588
The wide chord fan blade: A Rolls Royce first
[PNR90416] 02 p0125 N88-10789
Turbines with counterrotating runners for aircraft power plants 02 p0158 N88-10992
Transmission efficiency in advanced aerospace powerplant
[PNR90391] 02 p0182 N88-11133
Computer aided engineering/manufacturing at Rolls-Royce
[PNR90395] 02 p0222 N88-11397
Advanced natural gas fueled engine development. Part 1: Design and analyses
[PB87-224804] 03 p0331 N88-12087
Advanced natural gas fueled engine development. Part 2: Materials investigation
[PB87-223160] 03 p0331 N88-12088
The structure-mapping engine: Algorithm and examples
[AD-A184042] 03 p0368 N88-12315
Adiabatic diesel engine component development: Reference engine for on-highway applications
[NASA-CR-179531] 03 p0386 N88-12428
Automated design of controlled diffusion blades
[NASA-TM-100251] 05 p0542 N88-13304
Development of an integrated BEM approach for hot fluid structure interaction
[NASA-CR-181577] 05 p0556 N88-13384
Ceramic technology for advanced heat engines
[PB87-232997] 06 p0683 N88-14188
Development, features of roller rocker arm reported 06 p0689 N88-14219
Small High Pressure Ratio Turbines --- conference
[VKI-LS-1987-07] 06 p0712 N88-14364
Hot piston ring tests
[NASA-TM-100256] 06 p0729 N88-14486
Aeropropulsion '87. Session 5: Subsonic Propulsion Technology
[NASA-CP-10003-SESS-5] 08 p0956 N88-15800
Small engine technology programs 08 p0956 N88-15801
Aircraft engine hot section technology: An overview of the HOST Project 08 p0957 N88-15804
Advanced propeller research 08 p0957 N88-15806
Propulsion challenges and opportunities for high-speed transport aircraft 08 p0958 N88-15809
NASA/Army Rotorcraft Technology. Volume 2: Materials and Structures, Propulsion and Drive Systems, Flight Dynamics and Control, and Acoustics
[NASA-CP-2495-VOL-2] 09 p1106 N88-16632
Technology developments for a compound cycle engine 09 p1107 N88-16637
Small gas turbine engine technology 09 p1107 N88-16638
The convertible engine: A dual-mode propulsion system 09 p1108 N88-16639
Aeropropulsion '87. Session 1: Aeropropulsion Materials Research
[NASA-CP-10003-SESS-1] 09 p1118 N88-16697
Impact and promise of NASA aeropropulsion technology 09 p1118 N88-16698
High temperature polymer matrix composites 09 p1119 N88-16700
Ceramics for engines 09 p1119 N88-16704
An investigation into the feasibility of using a dual-combustion mode ramjet in a high Mach number tactical missile
[AD-A186906] 09 p1119 N88-16705
Advanced Technology for Aero Gas Turbine Components
[AGARD-CP-421] 10 p1279 N88-17647
The coming revolution in turbine engine technology 10 p1279 N88-17648
An examination of the impact of potential advances in component technology for future military engines 10 p1279 N88-17650
Specification of an engine and its components starting from a consideration of aircraft missions 10 p1279 N88-17651
Experimental evaluation of a translating nozzle sidewall radial turbine 10 p1280 N88-17656
An integrated aero/mechanical performance approach to high technology turbine design 10 p1280 N88-17657
Design and testing of a small radial turbine for auxiliary power units 10 p1281 N88-17661
Design and aerodynamic performance of a small mixed-flow gas generator turbine 10 p1281 N88-17662
Development of a plenum chamber burner system for an advanced VTOL engine 10 p1281 N88-17664
Analysis of possible transmission arrangements applicable for driving single or twin counterrotating fans on propfan engines 10 p1282 N88-17670
Advanced propfan analysis for the family of commuter airplanes
[NASA-CR-182566] 12 p1582 N88-19468
Optimizing powerplant design and development cycles 12 p1701 N88-20183
Activities report of the Energetics Department
[ETN-88-91981] 14 p1888 N88-21281
Visualisation of the flow at the tip of a high speed axial flow turbine rotor: An assessment of flow visualisation techniques and the requirement of the experimental turbine
[AD-A189929] 15 p2063 N88-22301
Continuous fiber ceramic matrix composites for heat engine components 15 p2082 N88-22411
Full electronic control system for diesel engine 16 p2185 N88-23025
Status, trends in research on internal combustion engines 16 p2185 N88-23027
Status and prognosis for alternative engine materials
[NASA-TM-100903] 18 p2486 N88-24749
Design, manufacture and spin test of high contact ratio helicopter transmission utilizing Self-Aligning Bearingless Planetary (SABP)
[NASA-CR-4155] 18 p2524 N88-24975
Development of a generic combustion stability code for liquid propellant rocket engines 19 p2626 N88-25576
Numerical grid generation and flow simulation in SSME thrust chamber 19 p2626 N88-25577

Boundary layer simulator (BLIMPJ) improvement
19 p2627 N88-25582
Motor test data comparisons with laboratory data and stability predictions
19 p2629 N88-25594
A multiple chamber volume-filling model for prediction of transient solid rocket motor ballistic performance
19 p2633 N88-25618
Analysis of flow through pump of large rocket engine
19 p2637 N88-25646
Extensive verification of blade-to-blade flow code based on Denton scheme
19 p2638 N88-25654
Application of computational fluid dynamics to design of compressor cascade
19 p2639 N88-25655
Permanent magnet excitation of axial flow synchronous machines with high rotation moment
[ETN-88-92385] 20 p2796 N88-26592
Analytical and experimental investigation of ringless piston concept
[AD-A192835] 20 p2810 N88-26673
The design and fabrication of a Stirling engine heat exchanger module with an integral heat pipe
[NASA-TM-101296] 20 p2820 N88-26732
Documentation of the Benson Diesel Engine Simulation Program
[NASA-TM-100940] 21 p2898 N88-27201
Analytical and experimental investigation of ringless piston concept
[AD-A193213] 21 p2956 N88-27559
The design and testing of aero engines to minimise hazard from birds
[PNR90436] 22 p3040 N88-28049
Trends in civil aircraft propulsion
[PNR90441] 22 p3044 N88-28067
Variable-compression-ratio pistons for high power output diesel engines
22 p3084 N88-28316
V2500 engine collaboration
[PNR90423] 24 p3326 N88-29803
Developing the Rolls-Royce Tay
[PNR90447] 24 p3327 N88-29809
Combustion and fuels in gas turbine engines
[AGARD-CP-422] 24 p3345 N88-29910
Voltage directive drive with claw pole motor and control without rotor position indicator
[ETN-88-93120] 24 p3356 N88-30047
Impact of ETO propellants on the aerothermodynamic analyses of propulsion components
[NASA-TM-101303] 24 p3374 N88-30094

ENGINE FAILURE

A natural low frequency oscillation in the wake of an airfoil near stalling conditions
[NASA-TM-100213] 02 p0123 N88-10779
Blade excitation criteria developed for aero derived engines in Arctic Alaska
[PNR90368] 02 p0182 N88-11131
Incipient failure detection of space shuttle main engine turbopump bearings using vibration envelope detection
05 p0595 N88-13629
Preliminary airworthiness evaluation of a UH-1 equipped with a terrain mapping receiver antenna
[AD-A186274] 07 p0819 N88-14980
RB-ARD: A proof of concept rule-based abort
08 p1065 N88-16435
Verification of obstacle accountability areas using a simple mathematical model. Part 1: Description of general model and application for a specific case --- engine failure at takeoff
[NLR-TR-85069-U] 09 p1115 N88-16683
Army maintenance: Actions to reduce the likelihood of helicopter gear failures
[PB88-135256] 11 p1433 N88-18551
Flight simulator experiments concerning take-off visibility minima
[NLR-TR-86050-U] 13 p1719 N88-20281

ENGINE INLETS

Boundary layer profile investigations downstream of an aero-engine intake anti-icing air exhaust slot
[PNR90378] 02 p0171 N88-11080
Numerical and experimental investigation of multiple shock wave/turbulent boundary layer interactions in a rectangular duct
[AD-A190772] 15 p2066 N88-22320
The calculation of the flow through a two-dimensional faired diffuser
[PNR90433] 22 p3076 N88-28259
Experimental and analytical evaluation of the effects of simulated engine inlets on the blade vibratory stresses of the SR-3 model prop-fan
[NASA-CR-174959] 23 p3179 N88-28927

ENGINE MONITORING INSTRUMENTS

Engine condition monitoring civil requirements: A British Airways view
22 p3033 N88-28002
From turboprop aircraft to multi-engined jet aircraft Aircraft Integrated Monitoring Systems (AIMS)
22 p3033 N88-28003
German Air Force requirements for the on-board life monitoring system (OLMOS) on Tornado
22 p3033 N88-28007
Onboard Life Monitoring System (OLMOS), hardware equipment onboard and on ground
22 p3034 N88-28009
Onboard Life Monitoring System (OLMOS): Engine life cycle calculation and trending
22 p3034 N88-28010
V2500 Condition Monitoring and Performance Analysis Software System (COMPASS): Overview of system --- aircraft engine
[PNR90418] 22 p3139 N88-28666
Development and installation of an instrumentation package for GE F404 investigative testing
[AD-A196265] 24 p3376 N88-30107

ENGINE NOISE

Advanced turboprop wing installation effects measured by unsteady blade pressure and noise
[NASA-TM-100200] 01 p0002 N88-10008
First article test noise survey of the A/F32T-9 large turbo fan engine enclosed noise suppressor system, Sky Harbor IAP (International Airport), Phoenix, Arizona
[AD-A183799] 01 p0090 N88-10588
Noise emission of civil and military aero-engines. Sources of generation and measures for attenuation
[ETN-87-91021] 01 p0091 N88-10595
Measured and calculated acoustic attenuation rates of tuned resonator arrays for two surface impedance distribution models with flow
[NASA-TP-2766] 09 p1241 N88-17440
Annoyance caused by advanced turboprop aircraft flyover noise: Single-rotating propeller configuration
[NASA-TP-2782] 09 p1242 N88-17441
Noise assessment of unsuppressed TF-34-GE-100A engine at Warfield ANG, Baltimore, Maryland
[AD-A189966] 15 p2129 N88-22702
First article noise survey of the A/F32T-9 large turbo fan engine enclosed noise suppressor system, far-field noise, Ellsworth AFB, South Dakota
[AD-A191938] 19 p2602 N88-25457

ENGINE PARTS

Development of a statistically proven injection molding method for reaction bonded silicon nitride, sintering reaction bonded silicon nitride, and sintered silicon nitride
[ETN-87-90575] 02 p0160 N88-11002
Investment foundry melting stock. Rolls Royce requirements and demands in terms of quality and the relationship to end product performance
[PNR90397] 02 p0160 N88-11003
Stirling engine research at national and university laboratories in Japan
[DE87-014622] 02 p0180 N88-11123
High temperature stress-strain analysis
02 p0188 N88-11170
Adiabatic diesel engine component development: Reference engine for on-highway applications
[NASA-CR-179531] 03 p0386 N88-12428
Composite mechanics for engine structures
[NASA-TM-100176] 04 p0411 N88-12552
Application of finite element methods with cyclic elasto-plastic strain analysis to low cycle fatigue analysis of engine components
[AR-004-512] 05 p0596 N88-13642
An analysis of temperature effect on LCF crack growth rates in superalloy GH36
06 p0721 N88-14431
Aeropropulsion '87. Session 1: Aeropropulsion Materials Research
[NASA-CP-10003-SESS-1] 09 p1118 N88-16697
Ceramics for engines
09 p1119 N88-16704
Turbine engine monitoring systems: Can they benefit component improvement program management?
[AD-A186992] 09 p1120 N88-16706
Development of a shell system for DS moulds at RR precision casting facility --- directional solidification (DS)
[PNR90400] 09 p1151 N88-16893
A comparison of measurements from the A/E35U-3 and PWMA (Portable Wear Metal Analyzer) spectrometers
[AD-A186855] 09 p1177 N88-17047
An examination of the impact of potential advances in component technology for future military engines
10 p1279 N88-17650
Specification of an engine and its components starting from a consideration of aircraft missions
10 p1279 N88-17651
Free-piston Stirling engine diaphragm-coupled heat-actuated heat pump component technology program, phase 1C
[DE88-003654] 10 p1330 N88-17949
Ceramic bearings for use in gas turbine engines
[NASA-TM-100288] 10 p1340 N88-18007
An evaluation of effectiveness of PTFE (polytetrafluoroethylene) type friction reducers on reducing friction and wear
[AD-A187440] 10 p1340 N88-18010
Effects of thermal and thermo-mechanical treatments on the mechanical properties of centrifugally cast alloy 718
[AD-A188195] 11 p1458 N88-18690
Structural analysis methods development for turbine hot section components
[NASA-TM-100298] 11 p1501 N88-18967
Sampling intervals
[AD-A189445] 12 p1573 N88-19408
Advanced Gas Turbine (AGT) Technology Development Project, ceramic component developments
[NASA-CR-180871] 12 p1709 N88-20229
Aircraft corrosion problems and research in the Netherlands
[NLR-MP-86066-U] 13 p1744 N88-20427
Small engine components test facility turbine testing cell
[NASA-TM-100887] 15 p2019 N88-22037
Specialty three-dimensional finite element analysis codes
15 p2079 N88-22393
Computational structural mechanics for engine structures
15 p2080 N88-22399
Thermal-structural analyses of Space Shuttle Main Engine (SSME) hot section components
15 p2081 N88-22404
Evaluation of ceramic thermal barrier coatings for gas turbine engine components
[ETN-88-91947] 16 p2181 N88-22998
Molten salt corrosion of SiC and Si3N4
17 p2325 N88-23885
Thermal cyclic durability testing of ceramic materials for turbine engines
17 p2325 N88-23886
Fractographic and microstructural evaluation of 3500-hour durability specimens
17 p2325 N88-23887
Thermal stress minimized, two component, turbine shroud seal
[NASA-CASE-LEW-14212-1] 17 p2345 N88-23978
Composite piston
[NASA-CASE-LAR-13435-1] 17 p2346 N88-23981
Status and prognosis for alternative engine materials
[NASA-TM-100903] 18 p2486 N88-24749
Component improvement of free-piston Stirling engine key technology for space power
[NASA-TM-100950] 19 p2607 N88-25476
Guide to the control of high temperature corrosion and protection of gas turbine materials
[PB88-107412] 20 p2760 N88-26370
Engine component retirement for cause. Volume 1: Executive summary
[AD-A192730] 20 p2760 N88-26371
The outlook for ceramics in heat engines, 1990-2010: Results of a worldwide Delphi survey
[DE88-010075] 20 p2778 N88-26475
Ceramic Technology for Advanced Heat Engines Program data base
[DE88-008954] 20 p2780 N88-26489
T55-l-714 engine development and qualification. Engine M11 low cycle fatigue test report. (0213-005-87), volume 2, part 1
[AD-A192766] 21 p2897 N88-27198
Ceramic technology for advanced heat engines project
[DE88-008945] 21 p2919 N88-27323
Studies of dynamic contact of ceramics and alloys for advanced heat engines
[DE88-008996] 21 p2919 N88-27324
JTDE 1 XTE34 materials research and development report
[AD-A194268] 22 p3044 N88-28063
V2500 engine collaboration
[PNR90423] 24 p3326 N88-29803
Determination of the hydroperoxide potential of jet fuels
[AD-A195975] 24 p3357 N88-29991
An investigation of constitutive models for predicting viscoplastic response during cyclic loading
[AD-A194875] 24 p3385 N88-30163

ENGINE TESTS

NT COLD FLOW TESTS
NT STATIC FIRING
Diagnosis of flow channel in aircraft gas-turbine engines on basis of vibration spectrum characteristics
02 p0159 N88-10993
The use of holographic interferometry for turbomachinery fan evaluation during rotating tests
[PNR90390] 02 p0176 N88-11098
Marine gas turbines - engine health monitoring, new approaches
[PNR90369] 02 p0182 N88-11132
Test stand performance of a convertible engine for advanced V/STOL and rotorcraft propulsion
[NASA-TM-100211] 03 p0266 N88-11679
SPRE 1 free-piston Stirling engine testing at NASA Lewis Research Center
[NASA-TM-100241] 03 p0277 N88-11747

A life test of a 22-Newton (5-lbf) hydrazine rocket
[NASA-TM-100232] 03 p0278 N88-11750
Performance and combustion characteristics of direct-injection stratified-charge rotary engines
[NASA-TM-100134] 04 p0400 N88-12490
Incipient failure detection of space shuttle main engine turbopump bearings using vibration envelope detection 05 p0595 N88-13629
High frequency data acquisition system for space shuttle main engine testing 05 p0595 N88-13630
Hot piston ring tests
[NASA-TM-100256] 06 p0729 N88-14486
Efficiency testing of a helicopter transmission planetary reduction stage
[NASA-TP-2795] 07 p0861 N88-15224
Pattern recognition techniques for failure trend detection in SSME ground tests 07 p0924 N88-15614
Propulsion estimation techniques 07 p0927 N88-15632
Space station propulsion technology
[NASA-CR-179260] 08 p0964 N88-15835
SSME environment database development
[NASA-CR-179245] 08 p0964 N88-15836
Hot piston ring/cylinder liner materials: Selection and evaluation
[NASA-TM-100276] 08 p0971 N88-15872
Space shuttle main engine anomaly data and inductive knowledge based systems: Automated corporate expertise 08 p1060 N88-16398
ESA Bulletin No. 15: Ariane, the European launcher for the 1980's
[ESA-BULLETIN-NO-15] 09 p1125 N88-16741
Design and testing of a small radial turbine for auxiliary power units 10 p1281 N88-17661
Design and development of an advanced F100 compressor 10 p1283 N88-17678
Rocketdyne automated dynamics data analysis and management system 11 p1499 N88-18954
Test results of a 40-kW Stirling engine and comparison with the NASA Lewis computer code predictions
[NASA-TM-87050] 11 p1508 N88-19013
Engine testing for synfuel operation
[DE88-006044] 13 p1779 N88-20645
Performance improvements of an F-15 airplane with an integrated engine-flight control system
[NASA-TM-100431] 14 p1867 N88-21159
NNEPEQ: Chemical equilibrium version of the Navy/NASA Engine Program
[NASA-TM-100851] 14 p1868 N88-21161
China constructing high-altitude test cell 14 p1901 N88-21351
Small engine components test facility turbine testing cell
[NASA-TM-100887] 15 p2019 N88-22037
LGM-30B stage 2 disected motor test report
[AD-A190771] 15 p2027 N88-22079
High-temperature combustor liner tests in structural component response test facility 15 p2077 N88-22383
Description of an oscillating flow pressure drop test rig
[NASA-TM-100905] 16 p2170 N88-22933
The 1988 overview of free-piston Stirling technology for space power at the NASA Lewis Research Center
[NASA-TM-100795] 16 p2170 N88-22934
SSME technology test bed fast shutdown assessment
[NASA-CR-179354] 17 p2314 N88-23831
Liquid metal testing at ETEC for the SP-100 program 17 p2428 N88-24446
Aircraft emissions characterization: TF41-A2, TF30-P103 and TF30-P109 engines
[AD-A192053] 18 p2466 N88-24638
Aircraft accident report: Air New Orleans, DBA continental express flight 962 British Aerospace 3101 (Jetstream 31), N331CY, New Orleans International Airport, Kenner, Louisiana, May 26, 1987
[PB88-910408] 19 p2601 N88-25450
Techniques utilized in the simulated altitude testing of a 2D-CD vectoring and reversing nozzle
[NASA-TM-100872] 19 p2604 N88-25464
An investigation of high pressure/late cycle injection of CNG (Compressed Natural Gas) as a fuel for rail applications
[DE88-009000] 19 p2677 N88-25917
Environmental monitoring of a titan 34D 5 1/2 segment solid rocket motor static firing
[AD-A192975] 20 p2766 N88-26400
Ceramic Technology for Advanced Heat Engines Program data base
[DE88-008954] 20 p2780 N88-26489
T55-L-714 engine development and qualification. Engine M11 low cycle fatigue test report. (0213-005-87)
[AD-A192765] 21 p2897 N88-27197
T55-I-714 engine development and qualification. Engine M11 low cycle fatigue test report. (0213-005-87), volume 2, part 1
[AD-A192766] 21 p2897 N88-27198
Documentation of the Benson Diesel Engine Simulation Program
[NASA-TM-100940] 21 p2898 N88-27201
Ceramic technology for advanced heat engines project
[DE88-008945] 21 p2919 N88-27323
The 210-HP diesel engine endurance and performance testing with fire resistant diesel fuel
[AD-A193153] 21 p2956 N88-27558
Analytical and experimental investigation of ringless piston concept
[AD-A193213] 21 p2956 N88-27559
Basic mechanisms of diesel lubrication correlation of bench and engine tests
[AD-A193360] 21 p2956 N88-27561
Phase 1 results from the Stirling-powered vehicle project
[NASA-TM-100978] 21 p3029 N88-27980
JTDE 1 XTE34 materials research and development report
[AD-A194268] 22 p3044 N88-28063
Orbital transfer vehicle 3000 LBF thrust chamber assembly hot fire test program
[NASA-CR-182145] 24 p3336 N88-29858
Fuel property effects on the US Navy's TF30 engine 24 p3345 N88-29911
Comparison of the performance of a reverse flow annular combustion chamber under low and high pressure conditions 24 p3347 N88-29923
Fuel effects on flame radiation and hot-section durability 24 p3347 N88-29925
Testing of a variable-stroke Stirling engine
[NASA-TM-100899] 24 p3440 N88-30472

ENGINEERING
A review of the knowledge engineering process 02 p0129 N88-10814

ENGINEERING DEVELOPMENT
U PRODUCT DEVELOPMENT

ENGINEERING DRAWINGS
Build, install and demonstrate a variable stroke pump control and windmill system
[DE87-014656] 03 p0347 N88-12191
DOE data exchange format specification, mechanical products/drafting: Version 1.2.2: CADCAM-045
[DE88-001923] 07 p0904 N88-15477
Free-piston Stirling engine diaphragm-coupled heat-actuated heat pump component technology program, phase 1C
[DE88-003654] 10 p1330 N88-17949
Engineering drawings and changes: Storing and controlling by the tens of terrabytes
[DE88-007605] 18 p2589 N88-25387

ENGINEERING MANAGEMENT
The microcomputer as an engineering management tool
[DE87-014882] 02 p0219 N88-11378
Image processing for optical engineering applications
[PB87-210035] 03 p0376 N88-12364
Proceedings of the Fifth Symposium on Energy Engineering Sciences: Instrumentation, Diagnostics, and Material Behavior
[DE88-001479] 04 p0429 N88-12660
The characterization of diagnostic tasks for engineering systems
[DE88-000093] 04 p0483 N88-12973
Summaries of FY 1987 engineering research
[DE88-002572] 07 p0840 N88-15096
Physics rationale for the engineering specifications for ZTH
[DE88-000938] 07 p0936 N88-15690
Research in progress at the Institute for Computer Applications in Science and Engineering
[NASA-CR-181607] 08 p1053 N88-16354
Interchange of electronic design through VHDL and EIS 09 p1205 N88-17222
The IDEAL (Integrated Design and Engineering Analysis Languages) modeling methodology: Capabilities and Applications 09 p1206 N88-17227
Non-proprietary research projects of the Center for the Space Processing of Engineering Materials
[AR-2] 10 p1426 N88-18516
Engineering thrust areas, 1988
[DE88-005103] 11 p1468 N88-18753
Description of MSFC engineering photographic analysis
[NASA-TM-4035] 11 p1491 N88-18900
Picking winners: Parametric cost estimating and project management 12 p1700 N88-20176
Reasons for increasing development cost of rotary wing aircraft and ideas to reverse the trend 12 p1701 N88-20179
Engineering management for validation prototype phase 12 p1703 N88-20195
Schedule and cost control of development 12 p1704 N88-20196
A perspective of PC-based probabilistic risk assessment
[DE88-006715] 18 p2568 N88-25251
Pyrotechnic system failures: Causes and prevention
[NASA-TM-100633] 20 p2765 N88-26394
The NASA Marshall engineering thermosphere model
[NASA-CR-179359] 20 p2825 N88-26760
Numerical methods for incompressible viscous flows with engineering applications
[NASA-CR-183143] 21 p2948 N88-27508
Engineering data compendium. Human perception and performance. User's guide
[LC-87-19560] 21 p2993 N88-27749
TRANSL: A PATRAN translator subroutine library
[DE88-010976] 21 p2998 N88-27784
Engineering data compendium. Human perception and performance, volume 1
[LC-87-19560] 22 p3134 N88-28630
Engineering data compendium. Human perception and performance, volume 2
[LC-87-19560] 22 p3134 N88-28631
Engineering data compendium. Human perception and performance, volume 3
[LC-87-19560] 22 p3134 N88-28632
An improvement in the numerical integration procedure used in the NASA Marshall engineering thermosphere model
[NASA-CR-179389] 24 p3392 N88-30200

ENGINES
NT AIR BREATHING ENGINES
NT APOGEE BOOST MOTORS
NT ARC JET ENGINES
NT BOOSTER ROCKET ENGINES
NT CONVERTIBLE FAN-SHAFT ENGINES
NT DIESEL ENGINES
NT DUCTED ROCKET ENGINES
NT ELECTRIC ROCKET ENGINES
NT ELECTROSTATIC ENGINES
NT ELECTROTHERMAL ENGINES
NT FREE-PISTON ENGINES
NT GAS TURBINE ENGINES
NT HELICOPTER ENGINES
NT HYDRAZINE ENGINES
NT HYDROGEN ENGINES
NT HYDROGEN OXYGEN ENGINES
NT INTERNAL COMBUSTION ENGINES
NT ION ENGINES
NT J-57 ENGINE
NT JET ENGINES
NT LIQUID AIR CYCLE ENGINES
NT LIQUID PROPELLANT ROCKET ENGINES
NT MERCURY ION ENGINES
NT NOZZLELESS ROCKET ENGINES
NT NUCLEAR ENGINE FOR ROCKET VEHICLES
NT NUCLEAR ROCKET ENGINES
NT PISTON ENGINES
NT PLASMA ENGINES
NT RAMJET ENGINES
NT RESISTOJET ENGINES
NT REUSABLE ROCKET ENGINES
NT ROCKET ENGINES
NT ROTARY ENGINES
NT SOLID PROPELLANT ROCKET ENGINES
NT SPACE SHUTTLE BOOSTERS
NT SPACE SHUTTLE MAIN ENGINE
NT STIRLING ENGINES
NT SUPERSONIC COMBUSTION RAMJET ENGINES
NT TF-30 ENGINE
NT TF-34 ENGINE
NT TURBINE ENGINES
NT TURBOFAN ENGINES
NT TURBOJET ENGINES
NT TURBOPROP ENGINES
NT UPPER STAGE ROCKET ENGINES
NT WANKEL ENGINES
Structural reliability and damage tolerance of ceramic composites for high-temperature applications
[PB87-208310] 01 p0019 N88-10119
Heat engine regenerators: Research status and needs
[DE87-013581] 01 p0054 N88-10348
Analysis of wear metals in engine oils using the atomic absorption spectrophotometric method
[NAL-TM-MT-8704] 05 p0564 N88-13435
Fuel nitrogen conversion in a supercharged spark ignition engine
[DE88-003739] 08 p0974 N88-15893
Ceramic technology for advanced heat engines program data base
[DE88-003922] 11 p1464 N88-18730
Design features of small Brayton cycles for autonomous underwater vehicles
[AD-A187799] 11 p1506 N88-18999
Advanced components for spaceborne infrared astronomy
[NASA-CR-177470] 13 p1772 N88-20601

Some design considerations for ceramic components in heat engine applications 17 p2323 N88-23875
Nondestructive evaluation of structural ceramics 17 p2324 N88-23876
Improved silicon carbide for advanced heat engines 17 p2324 N88-23879
Improved silicon nitride for advanced heat engines 17 p2324 N88-23881
Experimental validation of a zero-dimensional computer model for spark-ignition engines [DE88-009034] 21 p2957 N88-27565
A lubrication study of engine bearings 21 p2958 N88-27574
Empirical flutter prediction method [AD-A195699] 24 p3327 N88-29810

ENGLAND
Experimental Radio Data System (RDS): A survey of reception reliability in the UK [BBC-RD-1987/17] 09 p1155 N88-16922

ENGLISH LANGUAGE
Language modelling for automatic speech recognition: A review [RSRE-MEMO-4038] 01 p0084 N88-10544
Conversion of productions in OPS5 to their equivalent English [ORNL/TM-10246] 24 p3411 N88-30306

ENHANCEMENT
U AUGMENTATION

ENLARGING
U EXPANSION

ENRICHMENT
NT ISOTOPIC ENRICHMENT

ENSTROPHY
U VORTICITY

ENTHALPY
NT GIBBS FREE ENERGY
NT HEAT OF FORMATION
NT HEAT OF FUSION
NT LATENT HEAT
Theory of interstitial solutions [BLL-M-37314-(5828.4)] 02 p0233 N88-11469
An automated flow calorimeter for heat capacity and enthalpy measurements at elevated temperatures and pressures [DE88-002357] 07 p0857 N88-15206
Thermodynamic values from computer summation of group additivity data [AD-A186131] 07 p0940 N88-15711
Cohesive energies of transition metal silicides and phosphides --- Knudsen effusion [AD-A186691] 09 p1254 N88-17519
A calorimetric determination of the enthalpy of formation and a description of the defect structure of the ordered beta-phase /Ni, Cu/ /1-x/ Al/x/ [NASA-TT-20157] 13 p1745 N88-20434
Radiative processes affecting ocean mixed-layer heat content and their monitoring from satellite 13 p1806 N88-20800
The thermodynamic properties of organic oxygen compounds [DE88-001208] 13 p1849 N88-21065
Evaluation of direct methane conversion to higher hydrocarbons and oxygenates [DE88-003812] 15 p2049 N88-22204
Research in nonlinear partial differential equations and bifurcation theory [AD-A190986] 16 p2260 N88-23514
The thermodynamic properties of quinoline and isoquinoline [DE88-001218] 18 p2484 N88-24735
Calculation of the specific and volumetric enthalpies of Ge-Si alloys [DE88-006949] 21 p3026 N88-27965

ENTIRE FUNCTIONS
Lax representation and complete integrability for the periodic relativistic Toda lattice [PREPRINT-594] 22 p3146 N88-28711

ENTRAINMENT
A study of chaos and mixing in Rayleigh-Taylor and Richtmyer-Meshkov unstable interfaces [AD-A184751] 03 p0320 N88-12026
Turbulent mixing in a rotating, stratified fluid 04 p0445 N88-12759
Wall turbulence control 07 p0812 N88-14943
Foam generation and air entrainment near a free surface [AD-A185986] 07 p0848 N88-15149
An experimental investigation of straight and curved annular wall jets [NASA-CR-182546] 11 p1434 N88-18557
Structures and fluxes in a deep convecting mixed layer 13 p1804 N88-20786
Subduction 13 p1806 N88-20796
Gravity currents with heat transfer effects [PB88-180047] 16 p2205 N88-23158
Gas diffusion studies in steady and nonsteady cavities 18 p2512 N88-24902
Direct numerical simulations of the PDF's (Probability Density Functions) of a passive scalar in a forced mixing layer [AD-A192134] 18 p2568 N88-25256

ENTROPY
Cosmology with decaying vacuum energy [DE88-000698] 03 p0389 N88-12443
A dissipation principle and its consequences for structured shock waves in thermoelastic materials [DE87-013723] 04 p0454 N88-12813
Maximum entropy/optimal projection design synthesis for decentralized control of large space structures [AD-A186359] 07 p0824 N88-15003
Thermodynamic values from computer summation of group additivity data [AD-A186131] 07 p0940 N88-15711
The entropy of the Lorentz model 08 p1015 N88-16153
A study of the free energy of the Lenz-Ising model using the cluster variation method of Morita [AD-A186023] 08 p1073 N88-16476
Outlier resistant predictive source encoding for a Gaussian stationary nominal source [AD-A186725] 09 p1232 N88-17387
The approach to equilibrium in a quark-gluon plasma [DE88-002117] 09 p1251 N88-17499
Studies in finite time thermodynamics [DE88-004531] 10 p1423 N88-18500
Unsteady transonic small-disturbance theory including entropy and vorticity effects [NASA-TM-100568] 12 p1575 N88-19418
Linear and nonlinear acoustics with nonuniform entropy in combustion chambers 12 p1607 N88-19609
The thermodynamic properties of organic oxygen compounds [DE88-001208] 13 p1849 N88-21065
Research in nonlinear partial differential equations and bifurcation theory [AD-A190986] 16 p2260 N88-23514
Extrema principles of entrophy production and energy dissipation in fluid mechanics [NASA-TM-100992] 18 p2519 N88-24946
Improved potential flow computational methods with Euler corrections for airfoil and wing/body design [AD-A192303] 20 p2752 N88-26334
Investigations on the entropy of cloudy air [ESA-TT-1060] 23 p3234 N88-29245
Monotone recurrence relations, their Birkhoff orbits and topological entropy [AD-A193481] 23 p3276 N88-29504

ENTROPY (STATISTICS)
NT MAXIMUM ENTROPY METHOD
Adaptive time series analysis using predictive inference and entropy [AD-A191858] 18 p2560 N88-25199

ENVIRONMENT EFFECTS
Investigation of large scale impact of air pollution components on forest ecosystems in Bavaria, West Germany [DFVLR-FB-87-17] 01 p0068 N88-10434
Testimony to the US Senate on the greenhouse effect [DE87-013995] 01 p0071 N88-10458
Global environmental change research [S-HRG-100-301] 03 p0348 N88-12199
Emerging environmental constraints on the use of gasoline and diesel fuel and tradeoffs associated with the use of alternative fuels [DE87-011504] 04 p0422 N88-12614
Disturbance and recovery of Arctic Alaskan tundra terrain. A review of recent investigations [AD-A184442] 04 p0467 N88-12887
Impacts of world development on selected characteristics of the atmosphere: An integrative approach. Volume 1: Main report [DE88-001495] 07 p0875 N88-15309
Impacts of world development on selected characteristics of the atmosphere: An integrative approach. Volume 2: Appendices [DE88-001496] 07 p0875 N88-15310
Summary of the report of the Senior Committee on Environmental, Safety and Economic Aspects of Magnetic Fusion Energy [DE88-003270] 07 p0937 N88-15692
Effects of fire on composition, biomass, and nutrients in oak scrub vegetation on John F. Kennedy Space Center, Florida [NASA-TM-100305] 08 p1020 N88-16182
Trends in research and development in the Netherlands. The influence of national science policy between 1973 and 1986 [B8701588] 08 p1094 N88-16580
Cape Blanco wind farm feasibility study [DE88-003748] 10 p1348 N88-18059
Cape Blanco wind farm feasibility study [DE88-003749] 10 p1349 N88-18060
Review of selenium thermodynamic data [DE88-006194] 13 p1849 N88-21068
Assessment of crop loss from air pollutants: Meteorology-atmospheric chemistry and long range transport [PB88-146857] 15 p2089 N88-22448
Detection, monitoring and analysis of some environmental effects of fires in the Amazon region through utilization of NOAA and LANDSAT satellite imagery and aircraft data [INPE-4503-TDL/326] 16 p2230 N88-23322
Environmental projects. Volume 6: Environmental assessment. New 34-meter antenna at Venus site [NASA-CR-182922] 17 p2332 N88-23919
Detection of biomass burning and smoke plumes in the Amazon region through NOAA satellite imagery 17 p2365 N88-24085
Environmental effects on slow crack growth in silicon nitride [DE88-007206] 18 p2494 N88-24795
Changes in the Antarctic atmosphere due to the reduction of stratospheric ozone [ETN-88-92565] 18 p2540 N88-25074
Monitoring biological impacts of space shuttle launches from Vandenberg Air Force Base: Establishment of baseline conditions [NASA-TM-100982] 18 p2549 N88-25133
Photointerpretation with instrumentation for evaluation of environmental impact: Mata Atlantica in Cubatao 19 p2683 N88-25946
Study of evolution of vegetal cover and slide scars in the Cubatao municipality-Sao Paulo 19 p2683 N88-25947
Application of remote sensing in the conservation of natural areas: Ribeira Valley 19 p2683 N88-25949
Remote sensing applied to the monitoring of mineral extraction in the proximity of urban areas: Pros and cons 19 p2684 N88-25954
Health and environmental consequences of the Chernobyl nuclear power plant accident [DOE/ER-0332] 19 p2689 N88-25985
Acid rain: Delays and management changes in the Federal research program [GAO/RCED-87-89] 19 p2690 N88-25988
Discrimination of sand transport rates and environmental consequences in central Egypt from SPOT data 22 p3093 N88-28366
Regional environmental studies using national data bases and GIS (Geographic Information System) [DE88-008368] 23 p3230 N88-29225
Investigation of the large-scale impact of air pollution components on forest ecosystems in Bavaria [ESA-TT-1087] 24 p3390 N88-30187

ENVIRONMENT MANAGEMENT
Activities report in aeronautics and astronautics [ETN-88-91332] 13 p1859 N88-21115
The suitability of SPOT imagery for monitoring landscape patterns 22 p3094 N88-28376

ENVIRONMENT MODELS
Conception and discussion of a model describing ice formation on various obstacles [ONERA-NT-1986-6] 01 p0072 N88-10460
Effects of enviromentally imposed roughness on airfoil performance 08 p0952 N88-15778
Evaluation of regional-scale air quality models: Chairmen reports from four workshops [DE88-001397] 10 p1352 N88-18080
Tactical Rubidium Frequency Standard (TRFS) [AD-A191049] 16 p2193 N88-23078
Coordination in decision-making organizations [AD-A191952] 19 p2739 N88-26261
Weathering of sulfides on Mars 23 p3301 N88-29662

ENVIRONMENT POLLUTION
NT AIR POLLUTION
NT GLOBAL AIR POLLUTION
NT INDOOR AIR POLLUTION
NT OIL POLLUTION
NT WATER POLLUTION
Remote sensing of environmental pollution [DFVLR-MITT-87-04] 01 p0067 N88-10428
Space station contamination considerations 02 p0137 N88-10859
First flight of the ATMOS instrument during the Spacelab 3 Mission, April 29 through May 6, 1985 [NASA-CR-182360] 06 p0728 N88-14482
Environmental projects. Volume 4: Asbestos survey [NASA-CR-182527] 10 p1353 N88-18083
System-wide medium-term environment programme for the period 1990-1995: Strategies of the United Nations system for the environment [UNEP/GCSS.I/2] 12 p1641 N88-19826
Evaluation of existing total human exposure models [PB88-146840] 15 p2101 N88-22517

JPRS report. Science and technology. China
[JPRS-CST-88-001] 16 p2186 N88-23036
Acid Precipitation: A current awareness bulletin
[DE88-007987] 20 p2821 N88-26738

ENVIRONMENT PROTECTION

System-wide medium-term environment programme for the period 1990-1995: Strategies of the United Nations system for the environment
[UNEP/GCSS.I/2] 12 p1641 N88-19826
Perspectives in microclimate cooling involving protective clothing in hot environments
[AD-A188370] 12 p1671 N88-20007
Environmental projects. Volume 5, part 1: Study of subsurface contamination. Part 2: Guide to implement environmental compliance programs
[NASA-CR-182691] 13 p1796 N88-20741
NOAA (National Oceanic and Atmospheric Administration) Meteorology Division support to the Environmental Protection Agency
[PB88-179866] 19 p2689 N88-25980
Vegetation studies on Vandenberg Air Force Base, California
[NASA-TM-100985] 20 p2831 N88-26795

ENVIRONMENT SIMULATION

NT ALTITUDE SIMULATION
NT NEUTRAL BUOYANCY SIMULATION
NT SPACE ENVIRONMENT SIMULATION
NT WEIGHTLESSNESS SIMULATION
Portable, ambient air microclimate cooling in simulated desert and tropic conditions
[AD-A186457] 08 p1050 N88-16338

ENVIRONMENT SIMULATORS

NT SOLAR SIMULATORS
NT SPACE SIMULATORS

ENVIRONMENTAL CHAMBERS

U TEST CHAMBERS

ENVIRONMENTAL CHEMISTRY

NT AEROTHERMOCHEMISTRY
NT ATMOSPHERIC CHEMISTRY
NT BIOGEOCHEMISTRY
NT GEOCHEMISTRY
NT MARINE CHEMISTRY
Environment assisted degradation mechanisms in aluminum-lithium alloys
[NASA-CR-182482] 10 p1301 N88-17782
Workshop on Atmospheric OH
[BPT-7/87] 18 p2538 N88-25063

ENVIRONMENTAL CONTROL

Development of a graphical display on the DMS test bed 06 p0794 N88-14864
Man rating the b-1B molecular sieve oxygen generation system
[AD-A186275] 07 p0899 N88-15447
Space station accommodations for life sciences research facilities. Phase 1: Conceptual design and programmatics studies for Missions SAAX0307, SAAX0302 and the transition from SAAX0307 to SAAX0302. Volume 2: Study results
[NASA-CR-179244] 08 p0962 N88-15829
Prototype space station automation system delivered and demonstrated at NASA 08 p1066 N88-16442
Computer control of a microgravity mammalian cell bioreactor 09 p1197 N88-17172
Fed-batch control based upon the measurement of intracellular NADH 09 p1197 N88-17175
ARGES: An expert system for fault diagnosis within space-based ECLS systems 23 p3255 N88-29380
Development of computer-controlled thermogravimetric instrumentation for measurement of environmental and high temperature volatilization and desorption of contaminants from polymeric materials
[AD-A195934] 24 p3343 N88-29900

ENVIRONMENTAL LABORATORIES

MBA payload testing by Compact Antenna Test Range (CATR)
[ESA-CR(P)-2473] 08 p0977 N88-15906
A test facility for the in-vacuo assessment of dry lubricants and small mechanisms at cryogenic temperatures 14 p1878 N88-21224

ENVIRONMENTAL MONITORING

TIROS-N/NOAA A-J space environment monitor subsystem
[PB87-203998] 01 p0015 N88-10083
Remote sensing of environmental pollution
[DFVLR-MITT-87-04] 01 p0067 N88-10428
Airborne lidar experiments at the Savannah River Plant
[NASA-TM-4007] 02 p0194 N88-11209
NOAA's (National Oceanic and Atmospheric Administration's) Northeast Monitoring Program (NEMP): A report on progress of the first five years (1979-84) and a plan for the future
[PB87-210100] 02 p0196 N88-11225
Applicability of SPOT for forest inventory, mapping and change monitoring 03 p0344 N88-12174
Contribution of SPOT data to the physiographic study of coastal environment: La Pointe d'Arcay and l'Anse de l'Aiguillon (France) 03 p0344 N88-12176
Global environmental change research
[S-HRG-100-301] 03 p0348 N88-12199
Evaluation of the sensidyne toxic gas sensor for HF (Hydrogen Fluoride) vapor
[DE88-000647] 04 p0446 N88-12767
On-site meteorological program guidance for regulatory modeling applications
[PB87-227542] 06 p0731 N88-14498
Integrated Global Background Monitoring Network
[DE88-001503] 06 p0731 N88-14499
Current issues in atmospheric change
[NASA-CR-182406] 08 p1039 N88-16287
Fatigue and damage tolerance design data for carbon fibre composites
[BAE-MSM-R-GEN-0454] 09 p1138 N88-16818
User's guide to a data base of current environmental monitoring projects in the US-Canadian transboundary region
[DE88-002476] 09 p1188 N88-17119
Computer control of a microgravity mammalian cell bioreactor 09 p1197 N88-17172
Fed-batch control based upon the measurement of intracellular NADH 09 p1197 N88-17175
Meteorological and aerosol measurements from the NOAA WP-3D aircraft during WATOX-86, January 4-9, 1986
[PB88-120860] 10 p1352 N88-18079
Environmental projects. Volume 4: Asbestos survey
[NASA-CR-182527] 10 p1353 N88-18083
ELF (Extremely Low Frequency) communications system ecological monitoring program: Electromagnetic field measurements and engineering support, 1986
[AD-A188057] 11 p1509 N88-19017
System-wide medium-term environment programme for the period 1990-1995: Strategies of the United Nations system for the environment
[UNEP/GCSS.I/2] 12 p1641 N88-19826
Aerosol lidar for environment protection and meteorology
[DFVLR-FB-87-43] 14 p1982 N88-21828
Real-time environmental Arctic monitoring (R-TEAM)
[AD-A189948] 15 p2099 N88-22508
Geochemistry of the middle and lower atmosphere: Environmental impact through the deterioration of the ozone layer
[INPE-4477-PRE/1241] 16 p2230 N88-23321
Study of reservoir water quality utilizing remote sensing techniques: Methodological concepts 17 p2364 N88-24076
The role of space borne imaging radars in environmental monitoring: Some shuttle imaging radar results in Asia
[NASA-TM-101178] 18 p2502 N88-24844
The application of satellites in connection with the environment
[ETN-88-92474] 18 p2532 N88-25020
Monitoring biological impacts of space shuttle launches from Vandenberg Air Force Base: Establishment of baseline conditions
[NASA-TM-100982] 18 p2549 N88-25133
Evaluation of the ion trap mass spectrometer for potential application in the space station
[DE88-008940] 19 p2674 N88-25902
Environmental monitoring of a titan 34D 5 1/2 segment solid rocket motor static firing
[AD-A192975] 20 p2766 N88-26400
The role of space borne imaging radars in environmental monitoring: Some shuttle imaging radar results in Asia
[NASA-TM-101175] 20 p2789 N88-26544
Advanced life support control/monitor instrumentation concepts for flight application
[NASA-CR-177378] 20 p2833 N88-26807
Initial testing of the tunable diode laser absorption spectrometer for measuring HNO3 in diesel engine exhaust, stage 2
[PB88-193073] 21 p2970 N88-27641
Computer simulation procedure for designing airborne aerometric monitoring programs
[DE88-011896] 21 p2975 N88-27674
An evaluation of SPOT imagery for wetland monitoring 22 p3091 N88-28353
Review of the studies of geography and environment and studies on spectral characteristics of SPOT HRV data 22 p3091 N88-28358
Spatial and spectral registration of Javanese landscape units with SPOT 22 p3092 N88-28362
Following the seasonal evolution of a natural environment in a humid tropical region. Preliminary Evaluation of SPOT (PEPS) number 186: Bangui, Central Africa 22 p3093 N88-28368
An evaluation of the applicability of SPOT stereoscopic imagery to the Canada Land Use Monitoring Program (CLUMP) 22 p3099 N88-28403
Monitoring Moneragala (Sri Lanka) with SPOT imagery 22 p3099 N88-28405
Assessment of SPOT satellite based system in humid tropical vegetation identification, classification and monitoring 22 p3100 N88-28408

ENVIRONMENTAL QUALITY

NT AIR QUALITY
NT WATER QUALITY
User's guide to a data base of current environmental monitoring projects in the US-Canadian transboundary region
[DE88-002476] 09 p1188 N88-17119

ENVIRONMENTAL SURVEYS

Compilation of 1986 annual reports of the Navy ELF (Extremely Low Frequency) communications system ecological monitoring program, volume 1
[AD-A184561] 03 p0306 N88-11930
Compilation of 1986 annual reports of the Navy ELF (Extremely Low Frequency) communications system ecological monitoring program, volume 2
[AD-A184562] 03 p0306 N88-11931
Compilation of 1986 annual reports of the Navy ELF (Extremely Low Frequency) communications system ecological monitoring program, volume 3
[AD-A184563] 03 p0306 N88-11932
Environmental gradient analysis, ordination, and classification in environmental impact assessments
[AD-A187294] 11 p1509 N88-19016
Toxic effects of man-made mineral fibers with particular reference to ceramic fibers
[AD-A187949] 11 p1519 N88-19072
Environmental projects. Volume 6: Environmental assessment. New 34-meter antenna at Venus site
[NASA-CR-182922] 17 p2332 N88-23919
Extremely Low Frequency (ELF) communications system ecological monitoring program: Summary of 1986 progress
[AD-A192014] 19 p2642 N88-25676

ENVIRONMENTAL TEMPERATURE

U AMBIENT TEMPERATURE

ENVIRONMENTAL TESTS

NT COLD WEATHER TESTS
NT CORROSION TESTS
NT HIGH TEMPERATURE TESTS
NT LOW TEMPERATURE TESTS
NT NEUTRAL BUOYANCY SIMULATION
NT SALT SPRAY TESTS
NT UNDERWATER TESTS
Partial analysis of experiment LDEF A-0114
[NASA-CR-179236] 06 p0780 N88-14787
Major spacecraft hardware testing in Europe 09 p1125 N88-16740
Effects of processing variables on the behavior of E-glass/913 and XAS carbon fibre/913 laminates subjected to hot/wet environmental conditions
[BR101940] 09 p1138 N88-16820
Cavitation inception
[AD-A189220] 13 p1765 N88-20557
Environment test laboratory
[ETN-88-91885] 14 p1869 N88-21166
Effect of loading conditions on environment-sensitive fracture
[BR102697] 14 p1934 N88-21533
Hybrid PV HgCdTe IR detectors technology reliability and failure program: Environmental stress testing plan
[AD-A191165] 16 p2211 N88-23195
Laser cladding of Ni, Nb and Mg alloys for improved environmental resistance at high temperature
[AD-A191274] 16 p2213 N88-23208
Materials qualification in oceanology and the offshore industry 19 p2700 N88-26050
Flight testing under extreme environmental conditions
[AGARD-AG-300-VOL-8] 21 p2951 N88-27525
Qualification test levels for units to be derived from mechanical test data analysis --- ESA
[REPT-87-158-EI/ET/AG] 24 p3381 N88-30139

ENVIRONMENTS

NT AEROSPACE ENVIRONMENTS
NT CHROMOSPHERE
NT EARTH ENVIRONMENT
NT EARTH MAGNETOSPHERE
NT EARTH ORBITAL ENVIRONMENTS
NT FRICTIONLESS ENVIRONMENTS
NT GEOMAGNETIC TAIL
NT HIGH ALTITUDE ENVIRONMENTS
NT HIGH GRAVITY ENVIRONMENTS
NT HIGH TEMPERATURE ENVIRONMENTS
NT ICE ENVIRONMENTS
NT INNER RADIATION BELT
NT INTERPLANETARY SPACE
NT INTERSTELLAR SPACE
NT JUPITER ATMOSPHERE
NT LOW TEMPERATURE ENVIRONMENTS
NT MAGNETOPAUSE
NT MARINE ENVIRONMENTS
NT MARS ATMOSPHERE

NT MARS ENVIRONMENT
NT MIDLATITUDE ATMOSPHERE
NT NEPTUNE ATMOSPHERE
NT PLANETARY ATMOSPHERES
NT PLANETARY ENVIRONMENTS
NT PLANETARY IONOSPHERES
NT ROTATING ENVIRONMENTS
NT SATELLITE ATMOSPHERES
NT SATURN ATMOSPHERE
NT SOLAR ATMOSPHERE
NT SPACECRAFT ENVIRONMENTS
NT STELLAR ATMOSPHERES
NT THERMAL ENVIRONMENTS
NT URANUS ATMOSPHERE
NT VENUS ATMOSPHERE
NT VENUS CLOUDS

The impact of environmental factors on the performance of millimeter wave seekers in smart munitions
[DE87-014277] 03 p0270 N88-11697

Wear of iron and nickel in corrosive liquid environments
[NASA-TM-100246] 03 p0289 N88-11817

On computing environments in data analysis
[DE88-000079] 04 p0480 N88-12961

User interface for a partially incompatible system software environment with non-ADP users
[DE88-001518] 04 p0482 N88-12968

Avionics and corrosion 05 p0547 N88-13336

Interim review of the possibilities and opportunities for the ONR tropical cyclone motion research initiative
[AD-A185679] 06 p0746 N88-14592

A hypertext writing environment and its cognitive basis
[AD-A188179] 10 p1389 N88-18298

Motion in a random gyrotropic environment in D dimensions
[PB87-170650] 12 p1685 N88-20079

Effects of natural environment on first generation solid rocket booster thermal protection system materials
[NASA-TM-100329] 17 p2373 N88-24113

The Environment for Application Software Integration and Execution (EASIE) version 1.0. Volume 4: System installation and maintenance guide
[NASA-TM-100576] 17 p2386 N88-24185

Relating design and environmental variables to reliability 17 p2418 N88-24383

An intelligent processing environment for real-time simulation
[NASA-CR-183056] 19 p2715 N88-26119

Distributed mathematics in a heterogeneous environment
[DE88-009128] 19 p2716 N88-26124

Thermal conductivity of selected foams and systems from 100 to 300 K
[PB88-201553] 20 p2777 N88-26466

Nutrient requirements for high stress environments
[AD-A194595] 23 p3243 N88-29301

Multi-metallic galvanic corrosion
[AD-A195995] 24 p3353 N88-29963

Analysis of environmental parameters from the Panama City tower radar experiment
[AD-A194994] 24 p3404 N88-30264

ENZYME ACTIVITY
NT FERMENTATION

A solid phase enzyme-linked immunosorbent assay for the antigenic detection of Legionella pneumophila (serogroup 1): A compliment for the space station diagnostic capability 06 p0795 N88-14866

Myosin Ca sup (2+), Mg sup (2+)-adenosine triphosphatase activity in ray myocardium following 30-day expose to 1.1 and 2.0 G 10 p1362 N88-18141

Oxidative enzyme activity in healthy subjects and individuals with neurocirculatory dystonia during graded exercise 10 p1367 N88-18170

Dexamethasone regulates glutamine synthetase expression in rat skeletal muscles
[NASA-CR-182935] 18 p2549 N88-25129

Methods of quantifying and enhancing reactive oxygen species production 21 p2924 N88-27357

ENZYMES
NT CARBONIC ANHYDRASE
NT CATALASE
NT CHOLINESTERASE
NT CYTOCHROMES

Electron cytochemical detection of Ca(2)+-ATPase in protonema of moss funaria hygrometrica (H e d w.) under hypogravitation 06 p0749 N88-14602

Spectroscopic studies of energy transfer in photosynthetic reaction centers of higher plants
[DE88-003850] 10 p1359 N88-18121

Enzyme-based fiber optic sensors
[DE88-005674] 13 p1840 N88-21013

North Carolina Biomolecular Engineering and Materials Applications Center (NC-BEMAC)
[AD-A190923] 16 p2237 N88-23364

Employment of porous polytetrafluoroethylene Membrane with a hydrophilic and hydrophobic stratal structure for construction of an enzyme electrode
[NASA-TT-20296] 19 p2620 N88-25543

The design of methane activation catalysts
[DE88-002265] 23 p3199 N88-29043

ENZYMOLOGY
Superoxide dismutase assays
[AD-A183972] 03 p0356 N88-12242

EOS
U LANDSAT SATELLITES

EPHEMERIDES
Dynamic positioning at sea using the global positioning system
[AD-A184453] 04 p0397 N88-12476

Integrated systems with applications to the multi-phases of the ephemerides, physics and methematics of the upper atmosphere
[AD-A185748] 06 p0743 N88-14570

Optimized observation periods required to achieve geodetic accuracies using the global positioning system
[AD-A193844] 22 p3041 N88-28052

EPHEMERIS TIME
IMP 7 (Explorer 47) trajectory, September 26, 1972 to September 25, 1978
[NASA-CR-182697] 14 p1871 N88-21183

EPIDEMIOLOGY
Illustrations of a density-equalizing map projection technique
[DE87-013992] 03 p0339 N88-12130

JPRS report: Science and technology. USSR: Life sciences
[JPRS-ULS-87-012] 03 p0355 N88-12238

JPRS report: Science and technology. USSR: Life sciences
[JPRS-ULS-87-009] 04 p0473 N88-12915

Toxic effects of man-made mineral fibers with particular reference to ceramic fibers
[AD-A187949] 11 p1519 N88-19072

USSR report: Life sciences. Biomedical and behavioral sciences
[JPRS-UBB-87-010] 12 p1651 N88-19889

EPILEPSY
Detection of latent epilepsy in aircrew candidates 21 p2984 N88-27720

EPINEPHRINE
NT NOREPINEPHRINE

Individual functional typology of sympathoadrenal system as indicator of physiological status in adverse environments 12 p1665 N88-19979

A program for the study of skeletal muscle catabolism following physical trauma
[AD-A189771] 15 p2102 N88-22521

Distinctive features in blood clotting and fibrinolytic properties under effect of epinephrine in presence of hypoxia and hypercapnia 19 p2705 N88-26082

EPITAXY
NT LIQUID PHASE EPITAXY
NT MOLECULAR BEAM EPITAXY
NT VAPOR PHASE EPITAXY

Structure of rapidly solidified Ni-Ti
[DE87-012252] 02 p0147 N88-10921

Novel heterojunction devices
[DE87-013716] 05 p0656 N88-14026

Heteroepitaxial growth of 3-5 semiconductor compounds by metal-organic chemical vapor deposition for device applications
[NASA-CR-182346] 06 p0788 N88-14832

The role of thermodynamic phase diagrams and lattice matching in superlattice growth
[DE88-003113] 08 p1091 N88-16568

Visible InGaAsP/GaAsP lasers produced by epitaxial growth from liquid phase 09 p1237 N88-17416

Formation of optical waveguides by ion implantation
[DE88-003894] 10 p1409 N88-18407

Deposition of device quality epitaxial layers of gallium nitride and indium nitride for electronic applications
[AD-A188001] 11 p1453 N88-18661

Development of VLSI optical data link
[AD-A187883] 11 p1549 N88-19265

Development of VLSI optical data link
[AD-A187884] 11 p1549 N88-19266

Laser evaporation studies
[AD-A189815] 15 p2071 N88-22346

Fundamental properties and devices applications of Ge(x)Si(1-x)/Si superlattices
[AD-A190129] 15 p2143 N88-22787

Equilibrium stability of strained epitaxial layers on a rigid substrate
[INPE-4254-PRE/1127] 15 p2145 N88-22804

Limited reaction processing for semiconductor device fabrication
[AD-A190913] 16 p2283 N88-23666

Growth of high quality CoSi2/Si superstructures on Si(111) 20 p2869 N88-27034

Epitaxy and properties of two dimensional GaInAs semiconductor structures
[ETN-88-92357] 20 p2879 N88-27094

Superconducting thin films, composites and junctions
[AD-A193123] 21 p2937 N88-27440

Atomic layer epitaxy of ZnS and ZnSe
[AD-A192307] 21 p3020 N88-27928

Blue-green laser diode research program
[AD-A191980] 23 p3218 N88-29153

Laser induced chemical vapor epitaxial growth of gallium arsenide films
[AD-A194254] 23 p3291 N88-29595

EPOCHS
U TIME MEASUREMENT

EPOXIDES
U EPOXY COMPOUNDS

EPOXY COMPOUNDS
NT PROPYLENE OXIDE

An interdisciplinary approach to predictive modeling of structural adhesive bonding: Factors affecting the durability of titanium/epoxy bonds
[AD-A189503] 12 p1611 N88-19636

Thermoviscoelastic characterization and predictions of Kevlar/epoxy composite laminates
[NASA-CR-182878] 16 p2172 N88-22946

Structural study of impregnating resins of TGMDA/DDS type
[ETN-88-92167] 20 p2780 N88-26488

Degradation of fiber composites during storage
[FOA-C-20702-2.6] 22 p3051 N88-28102

Electrical detection of coating deterioration 24 p3355 N88-29973

EPOXY MATRIX COMPOSITES
NT BORON-EPOXY COMPOSITES

Study of the morphology of thermosetting matrices
[ONERA-RT-5/3346-M] 02 p0153 N88-10961

Cure and properties of thermosetting polymers
[AD-A184669] 03 p0293 N88-11843

A creep measurement of unidirectional epoxy-fiberglass rod
[DE87-014812] 04 p0411 N88-12553

In-situ characterization of the interface of glass reinforced composites
[AD-A185136] 05 p0557 N88-13391

Utilization of microwave measuring systems for nondestructive control of composite materials
[SNIAS-872-430-109] 05 p0559 N88-13402

Study of damage in carbon fiber-epoxy composite materials. Utilization to assess broken specimens
[DCQ/L-45-650/F] 06 p0678 N88-14152

Flaw effects: Behavior in operation of delamination in a crossed multilayer composite specimen
[DCQ/L-47-363/F] 06 p0678 N88-14153

Measurement of mechanical parameters to define damage criteria in delamination of crossed stratified layers
[DCQ/L-47-361/F] 06 p0678 N88-14154

Experimental and theoretical investigation of mechanically fastened composites
[AD-A185896] 07 p0826 N88-15008

Interfacial shear strength of pitch and high strain pan fibers in an epoxy matrix
[AD-A185966] 07 p0826 N88-15011

Improving the interlaminar shear strength of carbon fiber-epoxy composites through carbon fiber bromination
[NASA-TM-100248] 07 p0827 N88-15018

Study of selection criteria for adhesives used in aircraft structure bonding
[ETN-88-91619] 08 p0971 N88-15875

Fatigue and damage tolerance design data for carbon fibre composites
[BAE-MSM-R-GEN-0454] 09 p1138 N88-16818

Effect of post-cure heat-treatment on static and fatigue behaviour of XAS-914C carbon fibre composite
[AD-A186943] 10 p1294 N88-17735

Damage mechanisms of CFRP riveted joints 11 p1449 N88-18636

Matrix-fiber stress transfer in composite materials: Elasto-plastic model with an interphase layer
[PB88-136635] 11 p1450 N88-18643

An experimental and numerical study of notch sensitivity of ARALL laminates
[CCMS-88-04] 11 p1450 N88-18644

Oxidation and protection of fiberglass-epoxy composite masts for photovoltaic arrays in the low Earth orbital environment
[NASA-TM-100839] 11 p1465 N88-18734

The place for thermoplastic composites in structural components
[AD-A189149] 12 p1604 N88-19596

Fracture characteristics of carbon and aramid unidirectional composites in interlaminar shear and open hole tensile tests
[NLR-TR-86083-U] 13 p1735 N88-20371

Environmental effects on the post-impact compressive strength of CFC
[RAE-TM-MAT-STR-1088] 14 p1884 N88-21258
An investigation of the mechanical properties of improved carbon fibre composite materials
[RAE-TR-86021] 14 p1884 N88-21259
The percolation approach as a basis for experimental research on the mechanical properties of composite materials 14 p1886 N88-21271
Elementary characterization of Fibredux 913 CTS 5 34 percent preimpregnated carbon-epoxy from Ciba Geigy
[M-484300] 16 p2171 N88-22941
Investigation of the long term effects of aging on carbon epoxy composites exposed naturally to the weather under cyclic loads. (Results of sampling after 2.5 years). Test report M1-641300
[CEAT-39/M/79-C-M1-641300] 17 p2316 N88-23834
Elementary characterization of preimpregnated carbon epoxy T400H/DA0506 from STRUCTIL. Test report M6-577100
[CEAT-047426] 18 p2478 N88-24703
Determination of the glass transition temperature of cured composite materials
[DT-87/62-R] 21 p2906 N88-27246

EPOXY RESINS

The water absorption of model epoxy resin networks cured with aromatic diamines
[BR100722] 01 p0027 N88-10169
The influence of microvoids on the electrical strength of glass fiber reinforced epoxy resins
[ETN-87-90443] 01 p0030 N88-10189
Shear strength of the ASDEX upgrade Toroidal Field (TF) coil insulation: Rupture, fatigue and creep behavior --- tokamak
[IPP-1/230] 01 p0059 N88-10376
Optical damage in polymers by millisecond light pulses
[DE87-013106] 02 p0151 N88-10943
The effect of thermal shock on carbon fiber epoxy composites
[FOA-C-20675-2.6] 08 p0965 N88-15841
Structural study of the impregnating resins of the type TGMDA/DDS --- expoxy resins
[ETN-88-91616] 08 p0965 N88-15842
Morphology control and reinforcing mechanisms using an elastomer in an epoxy network based on diamine menthane
[ISAL-IDI1-87-09] 09 p1148 N88-16881
Analytical and experimental characterization of damage processes in composite laminates
[AD-A187221] 10 p1296 N88-17746
Initiation and propagation of damage in notched unidirectional and multidirectional CFRE resin laminates 11 p1449 N88-18633
Synthesis and structure property studies of toughened epoxy resins via functionalized polysiloxanes
[AD-A187984] 11 p1462 N88-18715
Synthesis and structure property studies of toughened epoxy resins via functionalized polysiloxanes. Friction and wear studies
[AD-A188258] 11 p1462 N88-18718
Environmental effects on the post-impact compressive strength of CFC
[RAE-TM-MAT-STR-1088] 14 p1884 N88-21258
Eddy current nondestructive inspection of graphite epoxy using ferrite cup core probes
[AD-A189823] 15 p2074 N88-22365
The adhesive bonding of thermoplastic composites
[AD-A190994] 16 p2173 N88-22953
Behaviour of fibre-reinforced composites under dynamic loading
[AD-A191310] 16 p2174 N88-22955
Correlation between dielectric and structural properties during epoxy cure
[AD-A190696] 16 p2181 N88-22997
Interfacial shear phenomena in graphite epoxy composites under impact loading using dynamic moire interferometry
[DE88-006773] 18 p2479 N88-24709
High strength/sigh modulus aromatic heterocyclic ABA block copolymers
[AD-A191666] 18 p2491 N88-24774
The influence of the chemical nature of resins on their reticulation kinetics and the consequences for their nonelastic mechanical properties
[ETN-88-92539] 18 p2493 N88-24788
Structural study of the TGMDA-DDS system --- epoxy system
[ONERA-RT-4/3346-M] 18 p2493 N88-24792
Research work completed at the Naval Surface Warfare Center Solid State Group of the Radiation Division
[AD-A191627] 18 p2582 N88-25339
Properties of two composite materials made of toughened epoxy resin and high-strain graphite fiber
[NASA-TP-2826] 19 p2609 N88-25480
Optical damage in epoxy polymers by millisecond light pulses
[DE88-008675] 19 p2620 N88-25547
High temperature resins for injection. High temperature pre-impregnated
[RC-648676] 20 p2780 N88-26486
Polymerization of epoxy matrix composites using pulsed microwaves
[CERT-3/1324-MO] 20 p2780 N88-26487
Structural study of impregnating resins of TGMDA/DDS type
[ETN-88-92167] 20 p2780 N88-26488
Relation between the mechanical characteristics of carbon-resin composites and their impact strength
[REPT-48-284/F] 21 p2907 N88-27249
Simulation of moisture diffusion of fiber reinforced components of aircraft for general air transportation
[IFL-IB-87-05] 21 p2907 N88-27253
Rubber-modified epoxies: Interfacial tension and morphology
[AD-A192464] 21 p2917 N88-27313
Study of crosslinking and nonelastic mechanical properties of epoxy and PSP networks --- epoxy resins; polystyrylpyridine resins (psp)
[ETN-88-92740] 21 p2921 N88-27337
Optical emission behavior and radiation resistance of epoxy resins
[DE88-752629] 23 p3196 N88-29023
Alternative immersion accelerated testing of coating systems for Naval shoreline facilities 24 p3355 N88-29977
Experimental aspects of using time-averaged holographic interferometry to detect barely visible impact damage in a graphite/epoxy composite plate
[AD-A194418] 24 p3375 N88-30097

EQUATIONS

On error equations for determining Earth rotation parameters with VLBI network 13 p1756 N88-20500

EQUATIONS OF MOTION

NT EULER EQUATIONS OF MOTION
NT HELMHOLTZ VORTICITY EQUATION
NT HYDRODYNAMIC EQUATIONS
NT KINEMATIC EQUATIONS
NT KINETIC EQUATIONS
NT NAVIER-STOKES EQUATION
NT REYNOLDS EQUATION

Research on one-dimensional two-phase flow. Theory on hydrodynamic balance in two fluid model and its application
[DE87-702615] 01 p0045 N88-10290
Nonlinear fluid equations for a low collisionality toroidal plasma
[DE87-013006] 01 p0100 N88-10655
Decoupling and stabilization of speed and height in F4 Phantom aircraft using output feedback
[ETN-87-90926] 02 p0125 N88-10787
Modeling shockwave deformation via molecular dynamics
[DE87-013157] 02 p0169 N88-11063
On the collective variables description of a high gain free electron laser
[DE87-013315] 02 p0178 N88-11108
Improvements to the adaptive maneuvering logic program
[NASA-CR-3985] 03 p0262 N88-11648
The evolution of HOBO
[DE87-014742] 03 p0313 N88-11980
Theory of dividing vortons 03 p0318 N88-12009
Effect of void gas lying between fluid slugs in nutation dampers 03 p0319 N88-12015
Linearized aeroelastic analysis of a wind turbine with a two-bladed rotor
[ETN-87-90600] 03 p0347 N88-12192
A method for the efficient calculation of elastic rotor blade dynamic response in forward flight 04 p0394 N88-12460
Natural control of flexible space structures 04 p0408 N88-12534
Aircraft dynamic response calculation based on discrete-continual model 04 p0424 N88-12624
Local-optimal control in systems with delay 04 p0424 N88-12627
Analytical studies of axially symmetric motion of an incompressible viscous fluid between two concentric rotating spheres 04 p0444 N88-12757
Non-linear maximum likelihood estimation of stability derivatives from range data
[NAL-TM-SE-8608] 05 p0552 N88-13365
Dynamics of propellant feedline systems
[AD-A184865] 05 p0580 N88-13537
Tutorial on elementary bifurcation theory
[DE87-014849] 05 p0642 N88-13932
Analytical solution of the equations for a coaxial plasma gun operating in the snowplow mode. 1. Weak coupling limit
[AD-A185370] 05 p0652 N88-13994
Dynamics formulations for the real-time simulation of constrained motion 06 p0795 N88-14872
Post-Newtonian equations of motion in an expanding universe
[DE88-750303] 07 p0945 N88-15744
Viscous flows, part 2 08 p0986 N88-15968
Gyrotron development at the Instituto de Pesquisas Espaciais
[INPE-4240-PRE/1115] 08 p0990 N88-15992
A modal control based limiting performance formulation for shock excited systems 08 p0998 N88-16046
The effects of rotor unbalance on the vertical response of a soft-mounted block 08 p1000 N88-16057
Relativistic electromagnetic waves in an electron-ion plasma
[NASA-CR-182421] 08 p1085 N88-16532
Mechanical impact: Theoretical simulation and correlation 09 p1179 N88-17060
Maneuverable reentry vehicle trajectory footprints: Calculation and properties
[DE88-004726] 10 p1292 N88-17726
Generalized equations for emittance and field energy of high-current beams in periodic focusing
[DE88-004448] 10 p1404 N88-18372
Experimental set-up and mathematical modeling of H-shaped beam type structure
[AD-A187196] 11 p1466 N88-18743
On exterior variational calculus
[DE88-700861] 12 p1683 N88-20062
Quantization of quadratic friction revisited
[DE88-700839] 12 p1686 N88-20081
Contribution to theory of quasigeostrophic motions of finite amplitude in viscous stratified ocean 13 p1788 N88-20695
Experimental and theoretical studies of coherent and nonthermal processes in semiconductors probed by femtosecond laser techniques 14 p1977 N88-21800
A model of the nongravitational motion of Comet P/Encke 14 p2010 N88-21993
A three dimensional non-singular modelling of rigid manipulators
[AD-A189707] 15 p2116 N88-22604
Singular Lagrangians. Classical dynamics and quantization. Lectures for young scientists
[DE88-701158] 15 p2146 N88-22806
A numerical model of unsteady, subsonic aeroelastic behavior
[NASA-TM-101126] 16 p2156 N88-22862
The nonlinear dynamics of a spacecraft coupled to the vibration of a contained fluid
[DE88-007035] 16 p2168 N88-22925
Coherent structures --- in turbulent flows 16 p2199 N88-23121
Solution of the compressible Navier-Stokes equations of motion by Chebyshev polynomials for laminar shock-boundary layer flow
[AD-A191033] 16 p2208 N88-23176
Application of Navier-Stokes analysis to stall flutter 16 p2220 N88-23249
Classical non-Abelian solutions for nonstandard Lagrangians
[DE88-701305] 16 p2263 N88-23532
Analysis for fuel implosion in ICF target and pellet gain 16 p2276 N88-23620
Integrability of fermionic string in superfluid Hamiltonian approach
[DE88-701662] 16 p2284 N88-23678
Nonlinear programming extensions to rational function approximation methods for unsteady aerodynamic forces
[NASA-TP-2776] 18 p2463 N88-24623
Particle-laden weakly swirling free jets: Measurements and predictions
[NASA-TM-100920] 18 p2466 N88-24639
Effects of Coriolis acceleration on the vibrations of spinning structures 18 p2522 N88-24966
Vibrations of rotating thick or thin rings 18 p2529 N88-25003
Forced motion of initially stressed shells and plates 18 p2529 N88-25005
A constraint algorithm for maintaining rigid bonds in molecular dynamics simulations of large molecules
[AD-A191663] 18 p2572 N88-25277
Color charge motion in non-Abelian fields
[DE88-701306] 19 p2642 N88-25672
LLNL Granular Solids Flow Project
[DE88-008023] 19 p2664 N88-25844
Stability of dynamical systems supported by rubber springs 19 p2680 N88-25932
A description of the reference frames and the coordinate transformations used in AMEER (Aero-Mechanical Equations Evaluations Routines)
[DE88-007960] 19 p2720 N88-26153
Deviation equation as an equation of motion
[DE88-702134] 19 p2722 N88-26161
Random vibration analysis of rattling structures
[DE88-007196] 20 p2813 N88-26691

Neoclassical diffusion due to trapping/detrapping orbits in stellarators
[DE88-008566] 20 p2857 N88-26968
Effects of static equilibrium and higher-order nonlinearities on rotor blade stability in hover
21 p2890 N88-27157
In-flight motor torque estimates for the second-stage Strypi 9 launch vehicle
[DE88-010833] 21 p2902 N88-27222
Lax representation and complete integrability for the periodic relativistic Toda lattice
[PREPRINT-594] 22 p3146 N88-28711
Open bosonic string in background electromagnetic field
[DE88-702140] 23 p3201 N88-29053
The acoustic field scattered from some approximate pressure release materials
[AD-A194768] 23 p3278 N88-29515
General equations for the motions of ice crystals and water drops in gravitational and electric fields
[NASA-CR-183229] 24 p3370 N88-30070
Nonlinear stress-strain and inelastic rebound with exponential stiffness
[AD-A195667] 24 p3384 N88-30159
Canonical variables and canonical integrals for motion in near-circular orbits 24 p3446 N88-30512
Lagrangian of the self-duality equation and d = 10, N = 2b supergravity
[DE88-701554] 24 p3455 N88-30563

EQUATIONS OF STATE
Nitrogen at high pressure
[DE87-013797] 01 p0021 N88-10130
Application of new conformal solution of theories
[PB87-214557] 01 p0105 N88-10684
Electrical conductivity and equation of state measurements on planetary fluids at high pressures and temperatures
[DE87-013787] 01 p0110 N88-10708
The equation of state of PETN detonation products
[DE87-013796] 02 p0155 N88-10971
Material behaviour at high rates of strain
[OUEL-1684/87] 02 p0192 N88-11200
The LLNL 150-mm equation-of-state gun system
[DE88-000423] 04 p0405 N88-12519
Studies of pressure-velocity coupling schemes for analysis of incompressible and compressible flows
[NASA-CR-181526] 04 p0443 N88-12748
Core bounce supernovae
[DE87-014910] 04 p0520 N88-13197
Utilization of FEP energetics
[NASA-CR-182373] 06 p0714 N88-14379
Experimental and theoretical studies of dense fluid mixtures
[DE88-002710] 07 p0831 N88-15039
Equation of state of condensed materials physical principles and applications
[NASA-TT-20007] 08 p0968 N88-15855
Zero temperature quark matter equation of state
[DE88-003408] 10 p1422 N88-18496
Simple renormalization group method for calculating thermal equations of states
[DE88-700143] 11 p1454 N88-18668
Further developments in exact state reconstruction in deterministic digital control systems
[NASA-TP-2812] 11 p1466 N88-18751
The automated symbolic derivation of state equations for dynamic systems
[DE88-005222] 12 p1683 N88-20060
The automated symbolic derivation of state equations for dynamic systems
[DE88-000968] 13 p1830 N88-20945
Quark core stars, quark stars and strange stars
[DE88-006991] 17 p2450 N88-24555
Use of a two-stage light-gas gun as an injector for electromagnetic railguns
[DE88-007200] 18 p2469 N88-24657
Fabrication issues and technology development for HELEOS (Hypervelocity Electromagnetic Launcher for Equation Of State)
[DE88-007419] 18 p2470 N88-24658
The high pressure sound velocity and equation of state of aqueous solutions of hydroxylammonium nitrate and triethanolammonium nitrate
[AD-A191740] 18 p2570 N88-25266
Nuclear and astrophysical evidence on the equation of state
[DE88-007397] 18 p2572 N88-25279
Study of data distributions and functions for the development of thermodynamic equations of state
[PB88-196365] 18 p2587 N88-25370
Phase equilibria and density calculations in the critical region: A phenomenological correction for a classical equation of state
[PB88-185335] 19 p2723 N88-26167
Equation of state of solid neon from X-ray diffraction measurements to 110 GPa
[DE88-008723] 19 p2734 N88-26241
Development of an equation of state for computation of supercompressibility factors, critical flow factors and other properties for wet, sour natural gases, synthetic gases and admixtures
[PB88-202676] 20 p2798 N88-26602
Freely expanding detonation products: Scaling of rate processes
[DE88-007827] 20 p2799 N88-26606
Nonlinear equation of state effects and the momentum-dilution trade-off in a turbulent buoyant jet
[DE88-701839] 20 p2799 N88-26610
An analysis of the efficiency and directivity of the sound generated by a moving laser source
[AD-A192220] 20 p2849 N88-26914
Shock wave compression and metallization of simple molecules
[DE88-008031] 20 p2851 N88-26925
On linear relationship between shock velocity and particle velocity
[DE88-701827] 20 p2880 N88-27099
State variable approach to deformation phenomena in Face Centered Cubic (FCC) metals
[VTT-44] 24 p3354 N88-29964

EQUATORIAL ATMOSPHERE
Atmosphere dynamics in the equatorial meteor zone
06 p0733 N88-14508
Characteristics of atmospheric disturbances with a quasi-two day period 06 p0734 N88-14515
Longitudinal variations of equatorial ionosphere determined from Intercosmos-19 artificial Earth satellite data 08 p1003 N88-16074
Solar tides in the upper equatorial thermosphere: A comparison between AE-E data and the NCAR thermospheric general circulation model
[AD-A186160] 08 p1023 N88-16196
Study of passages of cross-equatorial current during southern monsoon 14 p1900 N88-21347
In-situ plasma bubble observations associated with equatorial spread-F over Natal
[INPE-4488-PRE/1252] 15 p2095 N88-22482
One equatorial anomaly in nighttime ionospheric F region 24 p3447 N88-30517

EQUATORIAL ELECTROJET
Project CONDOR: Middle atmosphere wind structure obtained with lightweight inflatable spheres near the equatorial electrojet 08 p1028 N88-16230

EQUATORIAL ORBITS
NT STATIONARY ORBITS

EQUATORIAL REGIONS
CTD/02 measurements during 1984 and 1985 as part of the Equatorial Pacific Ocean Climate Studies (EPOCS)
[PB88-102082] 06 p0748 N88-14600
Processes in the quiet and disturbed equatorial-low latitude ionosphere: Sundial campaign, 1984
[INPE-4152-PRE/1057] 08 p1036 N88-16282
Interpretation of equatorial current meter data as internal waves
[PB88-108113] 08 p1044 N88-16309
An analysis of longitude variations in the equatorial spectrum of Saturn 10 p1430 N88-18539
Equatorial turbulence: Mixed layer and thermocline
13 p1804 N88-20787
On the zonal momentum balance at the equator
13 p1805 N88-20788
Mixed-layer shear related to wind stress in the central equatorial Pacific 13 p1805 N88-20793
Equatorial dynamics and ocean-atmosphere coupling
14 p1938 N88-21565
CTD/O2 data collected in 1985 and 1986 for EPOCS (Equatorial Pacific Ocean Climate Studies)
[PB88-160775] 14 p1951 N88-21629
A study of the dynamics of the Intertropical Convergence Zone (ITCZ) in a symmetric atmosphere-ocean model
[NASA-TM-86220] 19 p2693 N88-26005
The relationship between polar sea ice and the position of the near equatorial convergence zone
22 p3123 N88-28563

EQUATORS
Tropic heat MR (Meteorological Recorder) meteorological data (April 1984 - June 1985)
[PB88-161286] 14 p1948 N88-21620

EQUILIBRIUM
Grain boundary phase equilibria in metallic systems
[DE87-014123] 01 p0104 N88-10679
Equilibrium and tearing stability of thin current layers in magnetic arcades 01 p0118 N88-10754
Study of ionization equilibrium of high temperature and low density plasma
[DE87-703070] 02 p0238 N88-11502
Application of prediction of equilibrium to servo-controlled calorimetry measurements
[DE87-013745] 03 p0324 N88-12046
Phase equilibrium and crystal growth studies on AgGaSe2 and related nonlinear optical materials
[AD-A184768] 03 p0382 N88-12400
Theoretical studies of multicomponent mixtures: Phase equilibrium and transport
[DE88-002717] 07 p0831 N88-15040
Equilibrium retention in the nozzle of oxygen hydrogen propulsion systems 07 p0924 N88-15616
Free-boundary equilibrium problem for helically symmetric plasmas
[DE88-700101] 07 p0934 N88-15674
General equilibrium characteristics of a dual-lift helicopter system
[NASA-TP-2615] 12 p1573 N88-19407
Domain perturbation method in the static equilibrium of masses in rotation
[INPE-4217-PRE/1098] 12 p1686 N88-20085
Wave energy flow conservation for propagation in inhomogeneous Vlasov-Maxwell equilibria
[DE88-006705] 15 p2055 N88-22251
Equilibrium stability of strained epitaxial layers on a rigid substrate
[INPE-4254-PRE/1127] 15 p2145 N88-22804
On the prediction of equilibrium states in homogeneous turbulence
[NASA-CR-181659] 16 p2207 N88-23174
The two-dimensional one component plasma in a doubly periodic background: Exact results
[AD-A191260] 16 p2280 N88-23650
Equilibrium distribution functions for limited plasma-molecular systems
[DE88-702412] 21 p3018 N88-27916
The VPE-hydride technique with alloy source: Equilibrium analysis
[AD-A194036] 22 p3157 N88-28784

EQUILIBRIUM DIAGRAMS
U PHASE DIAGRAMS

EQUILIBRIUM EQUATIONS
Flap-lag-torsion aeroelastic stability of a circulation control rotor in forward flight 10 p1271 N88-17600
The dynamics of coupled planar rigid bodies. Part 1: Reduction, equilibria and stability
[AD-A187467] 10 p1345 N88-18042
Error questions in the computation of solution manifolds of parametrized equations
[AD-A188648] 12 p1684 N88-20068
Effects of translational and rotational nonequilibrium on CW (Continuous Wave) chemical laser performance
[AD-A191425] 16 p2214 N88-23210
A thermal equilibrium model for multi-megawatt space platforms 17 p2410 N88-24332
On the Nash point equilibria in the calculus of variations
[AD-A194959] 24 p3424 N88-30381
Formulation and solution of economic equilibrium problems
[AD-A196034] 24 p3439 N88-30470

EQUILIBRIUM FLOW
Continuation finite element analysis of viscoelastic fluids 04 p0445 N88-12761
Simplified curve fits for the transport properties of equilibrium air
[NASA-CR-178411] 18 p2513 N88-24911

EQUILIBRIUM METHODS
A parametric study of embedded cantilever retaining walls: The results of a finite element study
[RR-CE83] 24 p3383 N88-30152

EQUIPMENT SPECIFICATIONS
A program to study antiprotons in the cosmic rays: Arizona collaboration
[NASA-CR-180702] 01 p0120 N88-10764
Photon counting image sensor development for astronomical applications
[NASA-CR-181507] 05 p0660 N88-14049
Servicer system demonstration plan and capability development
[NASA-CR-179246] 08 p0975 N88-15895
Electric design rules related to latch-up and radiation --- simulation
[FOA-E-30006-3.1] 08 p0979 N88-15917
Supercritical fluid extraction-gas chromatography of Volatile Organic Compounds (VOC) from tenax devices
[PB88-124300] 10 p1298 N88-17759
An attempt to measure the diffuse brightness of the sky at submillimeter wavelengths
12 p1710 N88-20233
The Joint NASA/Goddard-University of Maryland Research Program in Charged Particle and High Energy Photon Detector Technology
[NASA-CR-182612] 12 p1712 N88-20247
Considerations in GaAs standard cell design
[DE88-003310] 14 p1985 N88-21840
UARS spacecraft recorder
[NASA-CR-180768] 15 p2068 N88-22331
In situ fatigue loading stage inside scanning electron microscope 15 p2093 N88-22419

Research sensors 15 p2085 N88-22430
Preliminary study of a coherent radar [BCRS-86-03] 16 p2189 N88-23051
Processing of HRPT data from the NOAA series satellites 17 p2359 N88-24053
High power density electrodes for AMTEC 17 p2437 N88-24501
Tower evaporator [NASA-CASE-NPO-15609-2] 18 p2497 N88-24815
Electrostatic discharge test apparatus [NASA-CASE-MSC-21094-1] 18 p2518 N88-24941
Mars rover/sample return mission requirements affecting space station [NASA-CR-172048] 18 p2594 N88-25414
An 8.4-GHz dual maser front end for Parkes reimplementation 22 p3066 N88-28197
Baseband assembly analog-to-digital converter board 22 p3067 N88-28201
An electronically tuned, stable 8415-MHz dielectric resonator FET oscillator for space applications 22 p3068 N88-28205
Description of a tool for the simulation of imagery systems 22 p3147 N88-28724
Elemental composition of the Martian surface 23 p3302 N88-29665
Gamma-ray/neutron spectroscopy from the Mars observer 23 p3302 N88-29671
Very high energy cosmic gamma rays from radio and X-ray pulsars 23 p3309 N88-29711

EQUIVALENCE
Topological equivalence of certain function spaces 2 [PB88-100904] 06 p0767 N88-14712
Symmetry and equivalence restrictions in electronic structure calculations [NASA-TM-89252] 11 p1557 N88-19320
On the norm equivalence of singularly perturbed elliptic difference operators [DE88-006353] 13 p1826 N88-20913
Constructive version of the approximation induction principle [PB88-165477] 15 p2122 N88-22647
On matrix pencil equivalents of a general polynomial matrix [MATH-REPT-207] 23 p3273 N88-29479

EQUIVALENT CIRCUITS
A study of scattering from E-plane circuit elements [AD-A184473] 04 p0431 N88-12673
Equivalent circuit consideration on the rotation of resonant modes of double resonant vibrators 07 p0839 N88-15092
Analyses by equivalent mechanical circuits of bending vibration bars with load-impedance at one end 07 p0840 N88-15093
An investigation of the equivalent circuit and carrier lifetimes of Si/SiGe heterostructure p-n diodes for frequencies between 0.5 and 18.5 MHz [FOA-C-30469-3.2] 09 p1256 N88-17529
On the choice of a element low-noise preamplifier on bipolar transistors [DE88-700639] 10 p1322 N88-17904
Some equivalent circuit models for AC impedance analysis of pyrite/solution interface [DE88-010574] 21 p2939 N88-27452

ERBE
U EARTH RADIATION BUDGET EXPERIMENT

ERBIUM
Characterization of Er,Cr:YSGG [AD-A185885] 07 p0932 N88-15659
The YAlO(sub 3):Er laser [PB88-130877] 11 p1493 N88-18911
Integrated optoelectronic circuits utilizing InGaAsP grown by molecular beam epitaxy (erbium doping of MBE GaAs) [AD-A192269] 20 p2795 N88-26584
Characterization of structural and magnetic order of Er/Y superlattices 20 p2873 N88-27056

ERECTION
U CONSTRUCTION

EREP
Earth resources: A continuing bibliography with indexes (issue 55) [NASA-SP-7041(55)] 01 p0065 N88-10415

ERGODIC PROCESS
Nonlinear relaxation and ergodicity breakdown in random anisotropy spin glasses [PREPRINT-565] 06 p0764 N88-14693

ERGOMETERS
A new isodynamically-braked arm ergometer including the demonstration of a prototype 12 p1661 N88-19957

ERGONOMICS
U HUMAN FACTORS ENGINEERING

ERGOTAMINE
Does dihydroergotamine used in therapeutical doses influence the physical and psychomotor performance of young pilots or other traffic drivers subjected to hypotonia? [ETN-88-92136] 20 p2632 N88-26799

EROSION
NT SOIL EROSION
High velocity erosion of metal interfaces [DE87-013937] 01 p0025 N88-10155
The ability of modified pavement quality concrete to resist ground erosion caused by VTOL aircraft [BAE-ARG-238] 03 p0267 N88-11683
Spacecraft surface exposure to atomic oxygen in low Earth orbit 03 p0273 N88-11715
Materials preparation and longevity in hyperthermal atomic oxygen 03 p0297 N88-11862
Pipe and bend erosion by pneumatic transport of solids at high temperature [DE88-001345] 04 p0429 N88-12658
Data base on the high heat flux behaviour of metals and carbon materials for plasma facing components: Experiments at the 10 MW neutral beam injection test stand of the IPP Nagoya [IPPJ-AM-53] 04 p0492 N88-13031
PISCES: Plasma-surface interactions and materials research [DE88-001323] 04 p0494 N88-13044
Studies in Aeolian geology [NASA-CR-182328] 05 p0625 N88-13828
Modern concept concerning transport of bottom sediments in abyssal regions of world ocean 06 p0728 N88-14478
Gas erosion of impeller housing in the operation of a high-temperature, high-pressure helium circulator [DE88-002607] 09 p1175 N88-17041
Detection of soil erosion with Thematic Mapper (TM) satellite data within Pinyon-Juniper woodlands [NASA-CR-182476] 09 p1185 N88-17103
Operation of gas turbine engines in dust-laden environments 10 p1280 N88-17654
Effects of ion implantation on cavitation erosion of a cobalt based metal/carbide alloy [AD-A187239] 10 p1303 N88-17793
Mechanisms of wear in single- and two-phase materials [DE88-003846] 10 p1305 N88-17806
High performance Solid Rocket Motor (SRM) submerged nozzle/combustion cavity flowfield assessment [NASA-CR-179307] 11 p1446 N88-18622
Characterization of PEOS (Plasma Erosion Opening Switch) plasma parameters and conduction phase properties [AD-A189024] 12 p1624 N88-19714
Erosion in dual-phase microstructures [DE88-004507] 13 p1743 N88-20421
Reduction of erosion in elbows due to flow modifications, phase 1 [DE88-001028] 13 p1769 N88-20584
Hydrogen pumping and release by graphite under high flux plasma bombardment [DE88-005880] 13 p1842 N88-21021
Durability testing of an iridium-plated storable rocket engine injector [AD-A190707] 15 p2027 N88-22078
Investigation of laser diagnostics of PACVD processes for depositing hard face coatings [DE88-007083] 15 p2043 N88-22176
Analysis of anomalous resistivity during the conduction phase of the plasma erosion opening switch [DE88-006382] 15 p2061 N88-22286
Analytic and numerical modeling of heat and material transport in electrical hypervelocity guns [AD-A192178] 18 p2469 N88-24655
Internal erosion rates of a 10-kW xenon ion thruster [NASA-TM-100954] 18 p2476 N88-24688
The influence of cathodic protection on erosion-corrosion of metals and model alloys [AD-A191613] 18 p2485 N88-24742
A 3 MW wood fired gas turbine at Red Boiling Springs, Tennessee 18 p2536 N88-25051
Solid rocket motor performance: A workshop report 19 p2631 N88-25607
Study of evolution of vegetal cover and slide scars in the Cubatao municipality-Sao Paulo 19 p2683 N88-25947
Oxidation-erosion of metals and alloys: Models, verification, and prediction [DE88-010016] 21 p2915 N88-27300
A review of solid particle erosion of engineering materials [DE88-010065] 22 p3054 N88-28124
Study of the erosion corrosion of alloys and coatings [AD-A194337] 22 p3055 N88-28128
Erosion of metals exposed to hot, dense gases [AD-A193708] 22 p3056 N88-28131
Erosion/redeposition modeling and calculations for carbon [DE88-010382] 22 p3057 N88-28139
Analysis of edge detection techniques for radiographic image measurement [AD-A193650] 23 p3186 N88-28961
Spectral characteristics and the extent of paleosols of the Palouse formation [NASA-CR-180947] 23 p3228 N88-29210
Distribution and timing of thick transient air-fall deposits in Electris: Implications for the nature of the upland plains 23 p3303 N88-29674

EROSIVE BURNING
A study of flame spreading and combustion phenomena of stick propellants [AD-A193598] 22 p3052 N88-28106

ERROR ANALYSIS
Error estimates for finite element approximations of parabolic variational equations [BONNER-MATHE-SCHR-179] 01 p0087 N88-10569
Semidiscrete Galerkin method for semilinear evolution equations with a differential operator of third order [BONNER-MATHE-SCHR-181] 01 p0087 N88-10570
On the concept of resolution ellipse in aperture synthesis matched deconvolution with error analysis --- astronomical interferometry 01 p0095 N88-10621
Some approaches to the design of high integrity software 02 p0127 N88-10799
A general approach to error propagation [DE87-014287] 02 p0224 N88-11412
A critical assessment of wind tunnel results for the NACA 0012 airfoil [NASA-TM-100019] 03 p0260 N88-11636
Analysis of undulator field errors for XUV FELs (Extreme Ultraviolet Free Electron Laser) [DE87-014734] 03 p0328 N88-12073
Detector normalization --- SPOT remote sensors 03 p0341 N88-12151
Kinds of bootstraps and kinds of jackknives, discussed in terms of a year of weather-related data [AD-A184495] 03 p0353 N88-12227
Accommodating the residue of processed or computed digital video signals within the 8 bit CCIR recommendation 601 [BBC-RD-1987/12] 04 p0432 N88-12676
More on the decoder error probability for Reed-Solomon codes 04 p0435 N88-12699
Kinematic formulation of finite elements for plate bending 04 p0455 N88-12821
Correction of inertial navigation system drift errors for an autonomous land vehicle using optical radar terrain data [AD-A184973] 05 p0544 N88-13311
Error control techniques for satellite and space communications [NASA-CR-181581] 05 p0576 N88-13516
Assessment of the reliability of a correction procedure for WGT (Wet Globe Thermometer) (Botsball) measurements of heat stress [AD-A185193] 05 p0584 N88-13559
Operating envelopes of particle sizing instrumentation used for icing research [NASA-CR-180870] 05 p0586 N88-13573
Experiments in fault tolerant software reliability [NASA-CR-181554] 05 p0632 N88-13863
Reliability of voting in fault-tolerant software systems for small output spaces [TR-87-16] 05 p0632 N88-13864
Effectiveness of back-to-back testing [TR-87-08] 05 p0632 N88-13865
Diagnostic reasoning in digital systems [NASA-CR-181564] 05 p0633 N88-13871
Error propagation in a digital avionic mini processor [NASA-CR-181565] 05 p0633 N88-13872
Flightpath reconstruction and systematic radar error estimation from multiradar range-azimuth measurements [NLR-MP-85064-U] 06 p0693 N88-14251
How to estimate the total number of errors in a software system [PB87-132130] 06 p0758 N88-14647
Estimating the distribution of fault latency in a digital processor [NASA-TM-100521] 06 p0760 N88-14666
Round-off error propagation in four generally applicable, recursive, least-squares-estimation schemes [NASA-TM-100055] 06 p0766 N88-14708
Improved understanding of the loss-of-symmetry phenomenon in the conventional Kalman filter [NASA-TM-100041] 06 p0766 N88-14709
Error assessments of widely-used orbit error approximations in satellite altimetry [NASA-CR-182390] 07 p0823 N88-14998

Estimating system reliability: Monte Carlo methods, sensitivity and errors in input parameters
[AD-A186182] 07 p0865 N88-15248
How errors in component reliability affect system reliability
[AD-A186264] 07 p0865 N88-15249
Geosat crossover analysis in the tropical Pacific. Part 1: Constrained sinusoidal crossover adjustment
[NASA-CR-182391] 07 p0871 N88-15285
Determination of cloud base height and emissivity from downwelling angular radiances
[AD-A185985] 07 p0879 N88-15331
Tracking procedure for non-normally distributed measurement errors
[AD-A186287] 07 p0903 N88-15468
Necessary and sufficient conditions for the convergence of integrated and mean-integrated r-th order error of histogram density estimates
[AD-A186037] 07 p0914 N88-15550
Investigation of candidate data structures and search algorithms to support a knowledge based fault diagnosis system 07 p0923 N88-15606
Zeroshift of piezoelectric accelerometers in pyroshock measurements 08 p0997 N88-16039
Limiting accuracy of scatterometer determination of wind speed over ocean from satellite 08 p1007 N88-16107
Assessment of VAS-derived products created by a simultaneous algorithm on a convectively active day
[AD-A186158] 08 p1054 N88-16359
Error analysis for geotechnical engineering
[AD-A186795] 09 p1189 N88-17124
Advances in reliable numerical computation: A summary --- conference
[NPL-DITC-102/87] 09 p1229 N88-17367
Designing variable-length codes with good error-recovery properties
[BBC-RD-1987/19] 10 p1317 N88-17876
Seventy-meter antenna performance predictions: GTD analysis compared with traditional ray-tracing methods 11 p1474 N88-18793
Improvement in robot positioning accuracy by a kinematic identification model 11 p1496 N88-18931
Error detection and recovery for robot motion planning with uncertainty
[AD-A187746] 11 p1534 N88-19165
Accurate efficient evaluation of Bessel transform: Programs and error analysis
[AD-A187718] 11 p1536 N88-19174
Position finding and tolerances
[AD-A187685] 11 p1540 N88-19205
Digital bit error rate estimator for telemetry links
[INPE-4351-TDL/295] 12 p1598 N88-19563
Design of the primary pre-TRMM and TRMM ground truth site
[NASA-CR-182609] 12 p1647 N88-19865
The effects of atmospheric and thermohaline variability on the validation of the GEOSAT altimeter oceanographic signal between Scotland and Iceland
[AD-A189324] 12 p1650 N88-19882
An experiment in software reliability: Additional analyses using data from automated replications
[NASA-CR-178395] 12 p1676 N88-20017
Procedure for initial data input and checkup in the system for film data mathematical processing
[DE88-700926] 12 p1676 N88-20022
Error questions in the computation of solution manifolds of parametrized equations
[AD-A188648] 12 p1684 N88-20068
Detecting serial correlation in the error structure of a cross-lagged panel model
[AD-A189070] 12 p1685 N88-20077
Formulation of a general technique for predicting pneumatic attenuation errors in airborne pressure sensing devices
[NASA-TM-100430] 13 p1723 N88-20302
Generalized expression for radio navigation parameter error 13 p1787 N88-20691
On a bound of the modeling errors of black-box transfer function estimates
[EUT-87-E-173] 14 p1963 N88-21708
Aircraft accident report: North Star Aviation, Inc., PA-32 RT-300, N39614 and Alameda Aero Club Cessna 172, N75584, Oakland, California, March 31, 1987
[PB87-910412] 15 p2016 N88-22021
Methodology for software reliability prediction, volume 1
[AD-A190018] 15 p2110 N88-22571
Methodology for software reliability prediction, volume 3
[AD-A190019] 15 p2110 N88-22572
A posterior error estimation in a finite element method for parabolic partial differential equations
[AD-A190296] 15 p2120 N88-22636
Analysis and testing of the SURE program
[NASA-TP-2817] 15 p2123 N88-22653
A study on local level inertial surveying systems. Error model for the stationary system
[B8736714] 16 p2229 N88-23312
Note on the double crystal method of measuring heat transfer coefficient
[OUEL-1710/87] 17 p2338 N88-23950
Adjusting a finite element model using vibration type experimental data. Concept and error detection
[ONERA-RT-7/3313-RY-060-R] 17 p2392 N88-24220
A recursive prediction error parameter estimator for nonlinear models
[RR-326] 17 p2392 N88-24222
Determination of doping profiles in silicon from resistivity measurements via the four-point probe in combination with layer strippings via anodic oxidation 18 p2583 N88-25347
Studies of error in temperature measurement with thermistors in the range between continual and free-molecule flows
[NASA-TT-20302] 19 p2674 N88-25900
A simulation analysis of errors in the measurement of standard electrochemical rate constants from phase-selective impedance data
[AD-A192739] 20 p2770 N88-26426
Coherent RF error statistics
[AD-A193002] 20 p2792 N88-26560
A control program for global radiation measurements
[KNMI-TR-100] 20 p2824 N88-26757
Dynamic modelling and estimation of the error due to asynchronism in a redundant asynchronous multiprocessor system
[NASA-CR-177427] 21 p2898 N88-27205
Studies on system performance of SPOT (space and ground segments) 22 p3112 N88-28485
A bulk model for the unstable planetary boundary layer over the sea. A sensitivity investigation
[DM-51] 22 p3129 N88-28600
Stereo and eye movement
[AD-A193588] 22 p3142 N88-28681
Fine resolution errors in secondary surveillance radar altitude reporting
[RSRE-87019] 23 p3175 N88-28906
Digital phase-lock loop having an estimator and predictor of error
[NASA-CASE-NPO-17196-1-CU] 23 p3205 N88-29076
NBS (National Bureau of Standards) measurement services: The NBS photodetector spectral response calibration transfer program
[PB88-201595] 24 p3376 N88-30109
Performance prediction of concurrent systems
[NASA-CR-183175] 24 p3412 N88-30312
Achieving real-time performance in FIESTA 24 p3418 N88-30344

ERROR BAND
U ACCURACY

ERROR CORRECTING CODES
Local concurrent error detection and correction in data structures using virtual backpointers
[NASA-CR-181432] 01 p0106 N88-10692
A simplified procedure for correcting both errors and erasures of a Reed-Solomon code using the Euclidean algorithm 04 p0435 N88-12698
More on the decoder error probability for Reed-Solomon codes 04 p0435 N88-12699
Further results on finite-state codes 11 p1472 N88-18782
Implementation and evaluation of a combined test-error correction procedure for memories with defects
[EUT-87-E-169] 14 p1955 N88-21651
FORTRAN 77 error handling of the RASP library
[DFVLR-MITT-87-14] 14 p1957 N88-21669
Error reduction in two-dimensional pulse-area modulation, with application to computer-generated transparencies --- optical field synthesis
[EUT-87-E-172] 14 p1982 N88-21825
A general approach for automating source code verification
[AD-A191461] 18 p2556 N88-25170
Long haul communications in the HF spectrum utilizing high speed modems
[AD-A194683] 24 p3360 N88-30003

ERROR CORRECTING DEVICES
Multimedia sensory systems for the solution of the error recovery problem --- robots
[REPT-87-010] 01 p0084 N88-10545
Design of source coders and joint source/channel coders for noisy channels
[NASA-CR-181547] 04 p0432 N88-12678
Implementation of encoders and decoders for Reed-Solomon codes
[PB88-126628] 10 p1387 N88-18286
A control technique for improved robot performance 17 p2391 N88-24212
The performance of Eurocom error correction schemes for data communications
[FEL-1987-56] 20 p2792 N88-26563
An integrated circuit for error protection in modern data communication systems conforming to Eurocom specifications
[FEL-1987-48] 20 p2796 N88-26593

ERROR DETECTION CODES
Local concurrent error detection and correction in data structures using virtual backpointers
[NASA-CR-181432] 01 p0106 N88-10692
A lower bound for the decoder error probability of the linear MDS code 11 p1472 N88-18780
Frame synchronization performance and analysis 11 p1473 N88-18787
Error detection and recovery for robot motion planning with uncertainty
[AD-A187746] 11 p1534 N88-19165
Shorts in self-checking circuits
[RR-657-I] 14 p1908 N88-21402
Random access memory testing: Theory and practice. The gains of fault modeling
[EUT-86-E-161] 14 p1955 N88-21649
Implementation and evaluation of a combined test-error correction procedure for memories with defects
[EUT-87-E-169] 14 p1955 N88-21651
Self-checking logic arrays
[RR-656-I] 15 p2106 N88-22545
Design of the Detector 2: A CMOS gate array for the study of concurrent error detection techniques
[AD-A191247] 16 p2193 N88-23079
Automatically generated acceptance test: A software reliability experiment
[NASA-CR-181667] 17 p2347 N88-23984
Knowledge-based fault diagnosis on future space vehicles 23 p3254 N88-29374

ERROR FUNCTIONS
A prediction-error estimation algorithm for nonlinear output-affine systems
[RR-314] 14 p1959 N88-21679

ERROR SIGNALS
Solution of the Lloyd-Max quantizer parameters by the method of successive substitution
[AD-A187829] 11 p1540 N88-19207
Long haul communications in the HF spectrum utilizing high speed modems
[AD-A194683] 24 p3360 N88-30003

ERRORS
NT INSTRUMENT ERRORS
NT PHASE ERROR
NT PILOT ERROR
NT POSITION ERRORS
NT ROOT-MEAN-SQUARE ERRORS
NT TRUNCATION ERRORS
Measurement of fault-tolerant parallel processors
[PB87-208328] 01 p0084 N88-10539
Optical alignment of Centaur's inertial guidance system
[NASA-TM-88844] 04 p0405 N88-12515
Calibration of a laser-pumped, thermographic phosphor remote thermometry system
[DE88-000452] 04 p0449 N88-12781
Radial orbit error reduction and sea surface topography determination using satellite altimetry 04 p0462 N88-12861
GOLD: Integration of model-based control systems with artificial intelligence and workstations
[DE88-000706] 04 p0483 N88-12977
Determination of total ozone from HIRS2/MSU sounding data 05 p0619 N88-13799
AVHRR/HIRS (Advanced Very High Resolution Radiometer/High Resolution Infra-Red Sounder) operational method for satellite based sea surface temperature determination
[PB88-107594] 06 p0708 N88-14340
Space station software reliability analysis based on failures observed during testing at the multisystem integration facility 06 p0798 N88-14884
Packet error probabilities in frequency-hopped spread spectrum packet radio networks. Markov frequency hopping patterns considered
[AD-A186071] 07 p0841 N88-15104
Inadequacy of conventional dynamic recovery mechanisms in the presence of temporary failures
[AD-A186311] 07 p0866 N88-15251
Annotated bibliography on reliable system design
[PB88-109848] 07 p0866 N88-15254
Roles of knowledge in motor learning
[AD-A186420] 07 p0897 N88-15438
Strong consistency of estimation of number of regression variables when the errors are independent and their expectations are not equal to each other
[AD-A186025] 07 p0909 N88-15507
Statistical measures of clipped random signals 08 p1000 N88-16055

Investigation of vibration problems with heterodyne holographic interferometer 08 p1000 N88-16058
Exploring hypotheses in attitude control fault diagnosis 08 p1058 N88-16384
Comparison of direct and heterodyne detection optical intersatellite communication links 09 p1169 N88-17013
Calculating measurement imprecision and uncertainty [DE88-003981] 09 p1233 N88-17391
Error modeling and confidence interval estimation for inductively coupled plasma calibration curves [AD-A186711] 09 p1250 N88-17488
Emittance studies at the Los Alamos National Laboratory Free-Electron Laser (FEL) [DE88-003146] 10 p1334 N88-17975
Systematic errors of the FSU global spectral model 10 p1356 N88-18103
Source and event selection for radio-planetary frame-tie measurements using the Phobos Landers 11 p1471 N88-18775
Using ridge regression in systematic pointing error corrections 11 p1472 N88-18777
A lower bound for the decoder error probability of the linear MDS code 11 p1472 N88-18780
A comparison of VLSI architectures for time and transform domain decoding of Reed-Solomon codes 11 p1472 N88-18783
A posteriori error estimates in computational fluid mechanics 11 p1486 N88-18869
Core-core and core-valence correlation [NASA-CR-182552] 11 p1544 N88-19226
Covariance analysis and post-processing of gravity compensation effects for aided multi-state navigation systems [PAPER-87-13] 12 p1577 N88-19430
On error equations for determining Earth rotation parameters with VLBI network 13 p1756 N88-20500
Two dimensional uncorrelated bias in fix algorithms [NASA-CR-182683] 13 p1815 N88-20847
A low-frequency measurement of the spectrum of the cosmic microwave background radiation 13 p1858 N88-21112
Investigation of the misfueling of reciprocating piston aircraft engines [NASA-TP-2803] 14 p1865 N88-21144
The Spring 1985 high precision baseline test of the JPL GPS-based geodetic system [NASA-CR-182686] 14 p1940 N88-21577
Merit of Hadamard transform active absorption spectrometer described 15 p2053 N88-22232
An expert system for discrete component digital circuit design [AD-A189680] 15 p2059 N88-22274
COBOL Analysis System (CAS) users manual [PB88-171442] 16 p2250 N88-23445
Error control techniques for satellite and space communications [NASA-CR-182886] 17 p2332 N88-23922
Theory of neutron moisture probes and interpretation of measurements in complex soil and water systems 17 p2342 N88-23965
The modeling of error budget analysis and tolerance specifications for BRESEX multiband linear array CCD camera 17 p2355 N88-24029
Digital processing of infrared and visible images from the GOES satellite and its integration with meteorological radar data 17 p2360 N88-24057
Geometric image correction: An approach for the registration of LANDSAT-TM digital images supported by topographical maps of medium and great scales 17 p2361 N88-24061
Study of methods of post-processing applied to a problem of standard classification 17 p2362 N88-24067
Fault diagnosis in orbital refueling operations 17 p2381 N88-24154
Coincidence counting corrections under conditions used by A. DeVolpi [NPL-RS(EXT)-90] 17 p2393 N88-24224
Angular position measurements at high temperatures and high radiation environments 17 p2434 N88-24479
Reducing sensitivity to errors in free electron laser amplifiers [DE88-007017] 18 p2522 N88-24960
Effectiveness evaluation of fault-tolerant multiprocessor systems [AD-A191688] 18 p2554 N88-25158
Robust vector quantization for noisy channels 19 p2653 N88-25754
Some supraconvergent schemes for hyperbolic equations on irregular grids [DE88-009113] 19 p2720 N88-26151
A VLSI single-chip (225,223) Reed-Solomon encoder with interleaver [NASA-CASE-NPO-17280-1-CU] 21 p2902 N88-27220
A unified approach to estimation in linear models with fixed and mixed effects [AD-A193060] 21 p3006 N88-27829
The feasibility of the disturbance accommodating controller for precision antenna pointing 22 p3064 N88-28182
The effects of changes in observation and data assimilation systems on CAC climate data sets 22 p3124 N88-28568
Analysis of the dynamic extended range forecast experiment 22 p3126 N88-28581
Correction of systematic errors in NMC medium range forecasts 22 p3126 N88-28584
Dependence of medium range forecast errors upon the large-scale initial state 22 p3126 N88-28585
Theoretical and practical limits of predictability of the NMC medium-range model 22 p3127 N88-28586
The predictability of low frequency patterns in the NMC MRF 22 p3127 N88-28587
On Wiener-Masani's algorithm for finding the generating function of multivariate stochastic processes [NASA-CR-182905] 23 p3273 N88-29481
In situ fault detection by the hybrid ray mode method [AD-A195226] 24 p3381 N88-30137

ERS-1 (ESA SATELLITE)
The German processing and archiving facility for ERS-1 [ESA-CR(P)-2531] 13 p1851 N88-21082
Seasat orbit determination experiments in preparation for the ERS-1 altimetry mission [ETN-88-91842] 14 p1871 N88-21182
Deployment, hold down and release mechanisms for Wind Scatterometer Antenna (WSA) --- ERS-1 wind scatterometer antenna (WSA) 14 p1876 N88-21207
Proposals for the pre-operational use of data from the European Remote Sensing Satellite ERS-1 [BCRS-86-02] 16 p2227 N88-23300
Preparation of the operational phase of the European Remote Sensing Satellite ERS-1 [BCRS-87-06] 16 p2228 N88-23307
Study of the plan for a national data center for the European Remote Sensing Satellite ERS-1 [BCRS-87-11] 16 p2228 N88-23309
ERS-1 data products and services and their value for tropical countries 17 p2357 N88-24040
The CERSAT archiving and processing center --- ERS-1 19 p2701 N88-26059
Ocean satellite data and the needs of designers and operators of marine units 19 p2701 N88-26061
Central user and browse service --- ERS-1 ground segment [CU-PG-MDA-SY-0005] 23 p3297 N88-29637
ERS-1: A satellite with an oceanographic mission [NLR-MP-86072-U] 24 p3333 N88-29838
Development of procedures for performing end-to-end tests on the ERS-1 radar altimeter and AMI using a compact antenna test range --- Active Microwave Instrument (AMI) [ESA-CR(P)-2558] 24 p3363 N88-30022
A study of the feasibility of using sea and wind information from the ERS-1 satellite. Part 1: Wind scatterometer data [NASA-CR-182833] 24 p3386 N88-30167
A study of the feasibility of using sea and wind information from the ERS-1 satellite. Part 2: Use of scatterometer and altimeter data in wave modeling and assimilation [ESA-CR(P)-2604-PT-2] 24 p3387 N88-30176

ERTS
U LANDSAT SATELLITES

ERYTHROCYTES
Hypoxic hypoxia as a stimulus of erythropoiesis in vivo and in vitro 07 p0885 N88-15373
Polycythemia and hydration status: Effects on blood volume and thermoregulation during exercise-heat stress [AD-A185946] 07 p0888 N88-15383
Differentiation of hemopoietic stem cells during adaptation to high altitude 07 p0893 N88-15410
Life sciences experiments on stratospheric balloons and sounding rockets 08 p1033 N88-16262
Hemolysis in runners as evidenced by low serum haptoglobin: Implications for preflight monitoring of astronauts [NASA-TM-100304] 11 p1518 N88-19067
Human erykthrocyte metabolism in the presence of hyperoxygenation during antiorthostatic hypokinesia 19 p2706 N88-26092

ESA
U EUROPEAN SPACE AGENCY

ESA SATELLITES
NT COS-B SATELLITE
NT ERS-1 (ESA SATELLITE)
NT EUROPEAN COMMUNICATIONS SATELLITE
NT EXOSAT SATELLITE
NT GEOS SATELLITES (ESA)
NT HIPPARCOS SATELLITE
NT INFRARED SPACE OBSERVATORY (ISO)
NT L-SAT
NT MARECS MARITIME SATELLITES
NT METEOSAT SATELLITE
Report on the scientific satellites of the European Space Agency [ESA-SP-1090] 01 p0014 N88-10081
The TV-SAT/TDF/TELE-X pyrotechnical system [CNES-87/CT/DRT/TVE/IL/358] 08 p0974 N88-15891
Coordinated use of European test facilities 09 p1123 N88-16726
Control and stabilization of ESA satellites 09 p1124 N88-16734
Projects under development 09 p1126 N88-16750
ESA Bulletin No. 24 [ISSN-0376-4265] 09 p1127 N88-16755
Report presented by the European Space Agency to the 22nd COSPAR meeting [ESA-SP-1014] 09 p1129 N88-16776
Assessment of optical communications systems for Data Relay Satellite. Volume 1: Executive summary [ESA-CR(P)-2488-VOL-1] 18 p2502 N88-24841
Assessment of optical communications systems for the Data Relay Satellite [ESA-CR(P)-2488-VOL-2] 18 p2502 N88-24842
Study of a safe attitude for the Infrared Space Observatory (ISO) during perigee pass [SNIAS-881-440-113] 23 p3185 N88-28954
PSDE/SAT 2: Preliminary spacecraft configuration study, executive summary [ESA-CR(P)-2618] 24 p3333 N88-29840
The high-throughput X-ray spectroscopy mission: The mission-science report [ESA-SP-1097] 24 p3453 N88-30557

ESA SPACECRAFT
NT COLUMBUS SPACE STATION
NT COS-B SATELLITE
NT ERS-1 (ESA SATELLITE)
NT ESA SATELLITES
NT EUROPEAN COMMUNICATIONS SATELLITE
NT EXOSAT SATELLITE
NT GEOS SATELLITES (ESA)
NT GIOTTO MISSION
NT HIPPARCOS SATELLITE
NT INFRARED SPACE OBSERVATORY (ISO)
NT L-SAT
NT MARECS MARITIME SATELLITES
NT METEOSAT SATELLITE
Study on conceptual design of spacecraft using Computer Aided Engineering (CAE) [SNIAS-920-CA/TS] 24 p3333 N88-29841

ESAKI DIODES
U TUNNEL DIODES

ESCAPE CAPSULES
Hypervelocity Technology (HVT) crew escape 09 p1214 N88-17280

ESCAPE SYSTEMS
Hypervelocity Technology (HVT) crew escape 09 p1214 N88-17280
Expected value analysis for an unmanned expendable launch vehicle payload escape system [AD-A189494] 13 p1728 N88-20337

ESCHERICHIA
Study of certain biological characteristics of bacteria during the French-Soviet CYTOS-2 space experiment 04 p0473 N88-12917
The effects of microgravity on genetic recombination in Escherichia coli --- Spacelab D1 mission 22 p3060 N88-28157

ESKERS
U GLACIAL DRIFT

ESRO
U EUROPEAN SPACE AGENCY

ESRO SATELLITES
U ESA SATELLITES

ESTERS
NT ACRYLATES
NT CARBAMATES (TRADENAME)
NT CARBOXYLATES
NT ISOCYANATES
NT LACTATES
NT PETN
NT POLYCARBONATES
NT POLYESTERS
NT SULFONATES
NT URETHANES
Polyvinyl esters of omega-H-perfluoroacids and polyvinyl alcohol obtained from them [AD-A184633] 03 p0279 N88-11755

Carbon residue studies of polyphenyl ethers and ester-based lubricants using a microcarbon residue tester
[AD-A188585] 12 p1611 N88-19632

Dual mechanism bifunctional polymers: Design, synthesis and application of a new category of metal ion complexing agents
[DE88-008233] 20 p2777 N88-26468

Polyazidoesters as energetic polymers and copolymer components with fluoro derivatives
[AD-A194236] 23 p3199 N88-29039

ESTIMATES
NT COST ESTIMATES

Estimates of satellite EHF communication outages due to attenuation by rain
[AD-A183969] 03 p0307 N88-11941

Exploiting auxiliary information about items in the estimation of Rasch item difficulty parameters
[AD-A184383] 03 p0372 N88-12341

Studies on estimation of nickel in zinc base die casting by D.C. polarography
[PD-MT-8729] 04 p0417 N88-12588

Model-based motion estimation and its application to restoration and interpolation of motion pictures
[AD-A185054] 05 p0584 N88-13558

Estimation of marine boundary layer depth and relative humidity with multispectral satellite measurements
[AD-A184881] 05 p0620 N88-13804

An adaptive lattice algorithm for spectral line estimation
[AD-A184970] 05 p0634 N88-13876

Further studies in estimation of life distribution characteristics from censored data
[AD-A184862] 05 p0643 N88-13937

Freidlin-Wentzell type estimates and the law of the iterated logarithm for a class of stochastic processes related to symmetric statistics
[AD-A185366] 05 p0644 N88-13944

New method of estimating continentality of climate on global scale 06 p0725 N88-14460

Round-off error propagation in four generally applicable, recursive, least-squares-estimation schemes
[NASA-TM-100055] 06 p0766 N88-14708

A new method of boundary parameter estimation for a two-dimensional diffusion system under noisy observations
[NASA-CR-178405] 06 p0767 N88-14714

Testing and interval estimation in a change-point model allowing at most one change
[AD-A185525] 06 p0767 N88-14716

On estimating the basin-scale ocean circulation from satellite altimetry. Part 1: Straightforward spherical harmonic expansion
[NASA-CR-182387] 07 p0862 N88-15352

Strong consistency of estimation of number of regression variables when the errors are independent and their expectations are not equal to each other
[AD-A186025] 07 p0909 N88-15507

Detecting and interval estimation about a slope change point
[AD-A186030] 07 p0909 N88-15509

A new method of estimation in a moving average model of order one
[AD-A186039] 07 p0909 N88-15510

Estimation and testing in truncated and nontruncated linear median-regression models
[AD-A186317] 07 p0911 N88-15522

Parameter estimation for the Dirichlet-Multinomial Distribution (DMD) using supplementary beta-binomial data
[AD-A186335] 07 p0911 N88-15524

On simultaneous estimation of the number of signals and frequencies under a model with multiple sinusoids
[AD-A186026] 07 p0913 N88-15543

Nonparametric estimation of the generalized variance
[AD-A186029] 07 p0914 N88-15545

On the direction of arrival estimation
[AD-A186031] 07 p0914 N88-15546

On rate of convergence of equivariation linear prediction estimates of the number of signals and frequencies of multiple sinusoids
[AD-A186034] 07 p0914 N88-15549

Necessary and sufficient conditions for the convergence of integrated and mean-integrated r-th order error of histogram density estimates
[AD-A186037] 07 p0914 N88-15550

Attitude determination of artificial satellites through joint application of static and dynamic optimal estimation techniques
[INPE-4415-TDL/306] 08 p0963 N88-15832

Estimation and comparison of changes in the presence of information right censoring by modeling the censoring process
[AD-A186320] 08 p1074 N88-16478

New model to estimate the perforation power of kinetic energy projectiles
[PB87-166757] 09 p1175 N88-17040

Sea surface current estimates off central California as derived from enhanced AVHRR (Advanced Very High Resolution Radiometer) infrared images
[AD-A186867] 09 p1194 N88-17155

Horizontal estimation and information fusion in multitarget and multisensor environments
[AD-A186935] 09 p1224 N88-17336

A note on computing robust regression estimates via iteratively reweighted least squares
[AD-A186709] 09 p1227 N88-17352

Frequency response function estimation at level
[DE88-002644] 10 p1344 N88-18034

On the dynamic estimation of relative weights for observation and forecast in numerical weather prediction
[NASA-CR-182531] 10 p1356 N88-18106

Well-posedness and spectral estimation for infinite dimensional systems
[AD-A187621] 10 p1401 N88-18354

Spacecraft telecommunications system mass estimates 11 p1473 N88-18784

A posteriori error estimates in computational fluid mechanics 11 p1486 N88-18869

Optimal recursive maximum likelihood estimation
[AD-A187980] 11 p1536 N88-19176

Simultaneous estimation and detection of bias shifts for inertial navigation systems 12 p1576 N88-19429

Preliminary analysis of an integrated logistics system for OSSA payloads. Volume 1: Executive summary 12 p1584 N88-19478

Digital bit error rate estimator for telemetry links
[INPE-4351-TDL/295] 12 p1598 N88-19563

Lower bounds on acceleration estimation accuracy
[AD-A188383] 12 p1619 N88-19681

Cramer-Rao bounds on the accuracy of location and velocity estimations using CCD optical sensors
[AD-A188481] 12 p1629 N88-19748

Estimation of the probability of a long time to the first entrance to a state in a semi-Markov model
[AD-A188960] 12 p1685 N88-20074

Picking winners: Parametric cost estimating and project management 12 p1700 N88-20176

Estimation-correlation, modeling, and identification in adaptive array processors
[AD-A189130] 13 p1757 N88-20512

Detection and angle estimation of coherent plane waves 13 p1759 N88-20522

Energy and momentum fluxes through the sea surface 13 p1806 N88-20798

Bias reduction when there is no unbiased estimate
[AD-A189407] 13 p1829 N88-20937

Regional Conference on the Analysis of the Unbalanced Mixed Model
[AD-A188747] 13 p1830 N88-20943

Temperature estimates for a free flowing railgun plasma
[MRL-R-1054] 13 p1843 N88-21032

Moving-bank multiple model adaptive estimation applied to flexible spacestructure control
[AD-A190761] 15 p2026 N88-22071

Boundary shape identification problems in two-dimensional domains related to thermal testing of materials
[NASA-CR-181654] 15 p2105 N88-22541

Consistent estimates of autoregressive parameters for autoregressive moving average models
[RR-663-I] 15 p2109 N88-22564

Estimation of convolution tails
[AD-A190323] 15 p2125 N88-22666

Analysis of a range estimator which uses MLS angle measurements
[NASA-CR-182896] 16 p2160 N88-22884

Multichannel 2-D power spectral estimation and applications
[AD-A191273] 16 p2191 N88-23068

Stochastic estimation of conditional eddies in turbulent channel flow 16 p2194 N88-23087

Studies in reliability and inference
[AD-A191389] 16 p2217 N88-23223

Parameter estimation for boundary value problems by integral equations of the second kind
[NASA-CR-181660] 17 p2332 N88-23918

Comparison of the solar radiation estimation method by satellites 17 p2360 N88-24055

Digital processing of infrared and visible images from the GOES satellite and its integration with meteorological radar data 17 p2360 N88-24057

Improved estimators in simultaneous estimation of scale parameters
[AD-A191108] 17 p2392 N88-24216

Performance estimates for operations conducted while wearing individual protective equipment: User manual
[AD-A191871] 18 p2553 N88-25154

Symmetrized nearest neighbor regression estimates
[AD-A191998] 18 p2568 N88-25254

Preliminary estimates of radiation exposures for manned interplanetary missions from anomalously large solar flare events
[NASA-TM-100620] 18 p2596 N88-25427

Estimation of balloon position from wind data
[DE88-008968] 19 p2597 N88-25434

Instrumentation for the measurement of penetrator dynamic response to permit force estimation
[DE88-010608] 20 p2809 N88-26666

Hydrologic models for land-atmosphere retrospective studies of the use of LANDSAT and AVHRR data
[NASA-CR-182861] 20 p2817 N88-26712

Dynamic modelling and estimation of the error due to asynchronism in a redundant asynchronous multiprocessor system
[NASA-CR-177427] 21 p2898 N88-27205

Estimation of power-energy plots for secondary batteries
[DE88-011922] 21 p2940 N88-27460

A unified approach to estimation in linear models with fixed and mixed effects
[AD-A193060] 21 p3006 N88-27829

On the estimation of a variance ratio
[AD-A193190] 21 p3009 N88-27854

Use of LANDSAT images of vegetation cover to estimate effective hydraulic properties of soils
[NASA-CR-183185] 22 p3116 N88-28514

Estimation forces acting on an underwater vehicle with G.P.S. (Global Positioning System) and Kalman filtering
[AD-A194339] 23 p3175 N88-28901

Progress in determining the thickness and distribution of volcanic materials on Mars 23 p3302 N88-29670

Spacecraft mass estimation, relationships and engine data: Task 1.1 of the lunar base systems study
[NASA-CR-172061] 24 p3332 N88-29836

Monte-Carlo estimation of the influence of plant architecture parameters on spectral brightness 24 p3450 N88-30533

ESTIMATING
NT ORBITAL POSITION ESTIMATION
NT PARAMETER IDENTIFICATION
NT SYSTEM IDENTIFICATION

Estimating scattered and absorbed radiation in plant canopies by remote sensing
[NASA-CR-181390] 02 p0193 N88-11205

The maximum likelihood estimator method of image reconstruction: Its fundamental characteristics and their origin
[DE88-000462] 05 p0636 N88-13892

Development of a technique for estimating noise covariances using multiple observers
[NASA-TM-4020] 06 p0669 N88-14098

Estimating the distribution of fault latency in a digital processor
[NASA-TM-100521] 06 p0760 N88-14666

Recursive m-estimators of location and scale for dependent sequences
[AD-A186292] 07 p0903 N88-15469

A modified kernel quantile estimator under censoring
[AD-A186364] 07 p0911 N88-15525

Estimation of multivariate binary density using orthonormal functions
[AD-A186386] 07 p0912 N88-15528

A smooth nonparametric quantile estimator from right-censored data
[AD-A186180] 07 p0915 N88-15552

Short data length effects in an asymptotically efficient ARMA (AutoRegressive Moving Average) spectral estimator
[AD-A186561] 08 p1068 N88-16458

A model for estimating depot maintenance costs for Air Force fighter and attack aircraft
[AD-A187097] 09 p1105 N88-16624

A generalized quantile estimator under censoring
[AD-A188280] 10 p1402 N88-18364

Fixed and adaptive interframe image prediction for remote piloting application
[AD-A187987] 11 p1471 N88-18771

Calibration of the solar radiation estimation method by satellites
[INPE-4349-PRE/1185] 12 p1646 N88-19861

Tidal estimation in the Pacific with application to SEASAT altimetry
[NASA-TM-100694] 13 p1803 N88-20780

Empirical and hierarchical Bayes competitors of preliminary test estimators in two sample problems
[AD-A190327] 15 p2125 N88-22670

Mental-State Estimation, 1987
[NASA-CP-2504] 16 p2239 N88-23370

Improved estimators in simultaneous estimation of scale parameters
[AD-A191108] 17 p2392 N88-24216

RSMASS: A simple model for estimating reactor/shield masses 17 p2414 N88-24355

Asymptotic theory for weighted least squares estimators in Aalen's additive risk model
[AD-A191085] 18 p2562 N88-25210
Estimating reliability with discrete growth models
[AD-A193845] 22 p3143 N88-28692
Digital phase-lock loop having an estimator and predictor of error
[NASA-CASE-NPO-17196-1-CU] 23 p3205 N88-29076
Estimation of transient heat transfer coefficients in multidimensional problems by using inverse heat transfer methods 23 p3210 N88-29108
A minitab macro for the Kaplan-Meier product limit estimator and the Tarone-Ware class of tests
[AD-A194298] 23 p3248 N88-29331
On the design and optimization of distributed signal detection and parameter estimation systems
[AD-A193934] 23 p3266 N88-29446
Two biased estimation techniques in linear regression: Application to aircraft
[NASA-TM-100649] 23 p3274 N88-29489

ESTUARIES
The effect of wind and currents on gas exchange in an estuarine system
[NASA-CR-181424] 01 p0073 N88-10468
YABLED cruises part 2: Data from YABLED-17 through YABLED-26, January-October 1985
[PB88-163597] 14 p1950 N88-21627
SPOT investigations of estuaries and coastal zones: An overview 22 p3107 N88-28455
The monitoring of sediment transport, water circulation and mixing in estuaries and coastal waters 22 p3108 N88-28457
Evaluation of SPOT data for remote sensing of physical and biological properties of estuaries and coastal zones 22 p3108 N88-28458
Contributions of SPOT imagery to the study of the littoral environments of Saloum (Senegal) 22 p3109 N88-28467

ETALONS
Fabry-Perot etalons as prefilters for astronomical far infrared Fourier transform spectroscopy
[MPE-205] 16 p2273 N88-23603
High-speed optical logic using GaAs 19 p2656 N88-25773

ETCHING
Metallography of maraging 350 steel
[DE87-013746] 04 p0418 N88-12591
Partial analysis of experiment LDEF A-0114
[NASA-CR-179236] 06 p0780 N88-14787
Investigations on an RF plasma related to plasma etching
[ETN-88-91366] 06 p0784 N88-14809
Effect of the band-gap characteristics on laser-induced dry etching of semiconductors
[DE88-001853] 07 p0937 N88-15695
Plasma and ion etching for failure analysis. Part 2. The etching of plastic encapsulant and other semiconductor device materials, using the Technics Giga Etch 100-E plasma etch system
[AERE-R-12212] 09 p1177 N88-17050
Control of solid-excitation-based photochemical dry etching of semiconductors by ion-bombardment-induced damage
[DE88-003214] 09 p1257 N88-17537
The mechanism of anisotropic silicon etching and its relevance for micromachinings
[MBB-UA-1013/86] 10 p1311 N88-17838
Apparatus for the study of silicon film deposition and silicon etching
[AD-A187616] 10 p1334 N88-17972
SiO2 film stress distribution during thermal oxidation of Si
[AD-A189552] 12 p1612 N88-19637
Metal contacts to cadmium telluride (CdTe)
[AD-A188306] 12 p1698 N88-20159
Laser photodeposition and etching study
[AD-A190535] 15 p2040 N88-22153
Calculating depletion region carrier concentrations with capacitance-voltage measurements and etching
[AD-A189630] 15 p2141 N88-22777
Microelectronics the next fifteen years 17 p2305 N88-23792
Excitonic properties of GaAs-AlGaAs nanostructures 20 p2867 N88-27023
Equipment for building and testing superconductive flux flow electronic devices
[AD-A192959] 21 p2936 N88-27436

ETHANE
Optical determination of the virial coefficients of the gases C2H4, C2H6 and SF6
[ETN-87-90610] 03 p0282 N88-11776
Catalytic combustion of methane
[PB88-123112] 07 p0829 N88-15028
Gas hydrate model development and validation
[DE88-001004] 10 p1298 N88-17762
Temperature dependence of ultraviolet absorption cross sections of chlorofluoroethanes
[AERONOMICA-ACTA-A-325-1987] 18 p2482 N88-24726

ETHANE NITRILE
U ACETONITRILE

ETHANOL
U ETHYL ALCOHOL

ETHERS
Surface catalytic degradation study of two linear perfluoropolyalkylethers at 345 C
[NASA-TP-2774] 04 p0410 N88-12543
Improved perfluoroalkylether fluid development
[NASA-CR-180872] 08 p0967 N88-15851
Space environmental effects on polymeric materials
[NASA-CR-182454] 09 p1148 N88-16879
Carbon residue studies of polyphenyl ethers and ester-based lubricants using a microcarbon residue tester
[AD-A188585] 12 p1611 N88-19632
The performance of perfluoropolyalkylether oils under boundary lubrication conditions
[AD-A191057] 17 p2323 N88-23869
Preferential surface adsorption in miscible blends of polystyrene and poly(vinyl methyl ether)
[AD-A191451] 18 p2490 N88-24769

ETHYL ALCOHOL
Practical system for the use of alcohol in diesel engines
[PB88-147863] 12 p1612 N88-19638
Ethanol as a fuel of a lorry. Use experience from a diesel engine modified to an otto engine
[DE88-752870] 21 p2958 N88-27569

ETHYL COMPOUNDS
Dissolution rates of polymers and copolymers based on methyl, ethyl and butyl methacrylate
[AD-A194713] 23 p3197 N88-29027

ETHYLENE
NT VINYLIDENE
Ionic conductive polymers based on crosslinked elastic siloxane-ethylene oxide copolymers
[DE88-011243] 21 p2917 N88-27311

ETHYLENE COMPOUNDS
NT CHLOROETHYLENE
Organic metal (ET)4Hg3Br8A quasi-two-dimensional superconductor 14 p1974 N88-21778

ETIOLOGY
Trace-element metabolism in man and animals in the presence of hypoxic states of diverse etiology 07 p0889 N88-15390

ETTINGSHAUSEN COOLERS
U THERMOELECTRIC COOLING

EUCLIDEAN GEOMETRY
NT ANALYTIC GEOMETRY
NT ANGLE OF ATTACK
NT ANGLES (GEOMETRY)
NT BRAGG ANGLE
NT CARTESIAN COORDINATES
NT CATENARIES
NT CIRCLES (GEOMETRY)
NT CIRCUMFERENCES
NT CONICS
NT CUBES (MATHEMATICS)
NT DESCRIPTIVE GEOMETRY
NT DIHEDRAL ANGLE
NT ELEVATION ANGLE
NT ELLIPSES
NT FIXED POINTS (MATHEMATICS)
NT GEODESIC LINES
NT ICOSAHEDRONS
NT INFLECTION POINTS
NT LEADING EDGE SWEEP
NT LINES (GEOMETRY)
NT OBLATE SPHEROIDS
NT PARABOLAS
NT POINTS (MATHEMATICS)
NT POLYGONS
NT POLYHEDRONS
NT PROJECTIVE GEOMETRY
NT PROLATE SPHEROIDS
NT PYRAMIDS
NT QUADRANTS
NT RADII
NT RECTANGLES
NT RHOMBOIDS
NT S CURVES
NT SWEEP ANGLE
NT SWEEPBACK
NT TANGENTS
NT TORUSES
NT TRIANGLES
Complete minimal surfaces in R^3 of low total curvature
[DE88-006425] 15 p2118 N88-22619
Mathematical morphology for structures without translation symmetry
[CWI-AM-R8803] 18 p2566 N88-25241

EUCLIDEAN SPACE
U EUCLIDEAN GEOMETRY

EUKARYOTES
Biorack experiments in Spacelab D-1 and TML-1: Further developments in gravitational biology 12 p1661 N88-19953
The evolution of glutathione metabolism in phototrophic microorganisms
[NASA-CR-182902] 19 p2695 N88-26015

EULER EQUATIONS OF MOTION
Numerical solution of Euler equations for compressible fluids by the finite element method, volume 3
[ETN-87-90650] 02 p0170 N88-11070
Computation of transonic separated wing flows using an Euler/Navier-Stokes zonal approach
[NASA-TM-88311] 02 p0173 N88-11089
Numerical calculation of two dimensional fluid flow with strong shocks
[KFK-4191] 03 p0314 N88-11986
Application of Runge Kutta time marching scheme for the computation of transonic flows in turbomachines
[NASA-TM-86997] 04 p0394 N88-12461
Concepts for radically increasing the numerical convergence rate of the Euler equations
[NASA-CR-177456] 04 p0395 N88-12463
Solution of the two-dimensional Euler equations on unstructured triangular meshes 04 p0396 N88-12469
A free-Lagrange method for 2-D compressible flows
[DE88-000216] 04 p0442 N88-12745
Numerical analysis of flow through scramjet engine inlets 05 p0532 N88-13233
A 3-D Euler solution for hypersonic Mach numbers 05 p0533 N88-13240
The off-design performance of hypersonic waveriders 05 p0533 N88-13244
Time-marching finite-difference methods for the three-dimensional Euler equations of contravariant velocity components 05 p0539 N88-13285
A Cartesian finite-volume method for the Euler equations 05 p0579 N88-13532
Solution procedure for the Navier-Stokes equations applied to rotors 05 p0579 N88-13533
A note on the use of symmetric line Gauss-Seidel for the steady upwind differenced Euler equations
[AD-A185223] 05 p0580 N88-13540
SHARP simulation of discontinuities in highly convective steady flow
[NASA-TM-100240] 05 p0642 N88-13931
Development of transonic speed cascade design method using Euler code and inverse solution 06 p0676 N88-14139
Euler solution of multiblade rotor flow
[NASA-TM-100014] 06 p0704 N88-14322
Numerical simulation of flows in axial and radial turbomachines using Euler solvers 06 p0713 N88-14372
Computational fluid dynamics overview 07 p0809 N88-14927
Upwind relaxation algorithms for Euler/Navier-Stokes equations 07 p0810 N88-14931
Viscous vortex flows 07 p0810 N88-14934
Multitasked embedded multigrid for three-dimensional flow simulation
[NASA-CR-182398] 07 p0852 N88-15173
An explicit method for the solution of the Euler equations, applied to unsteady two dimensional flows
[ETN-88-90807] 07 p0855 N88-15194
Advanced propeller research 08 p0957 N88-15806
Upwind formulations for the Euler equations 08 p0984 N88-15952
A survey of upwind principles for the multidimensional Euler equations 08 p0984 N88-15953
Characteristic flux averaging approach to the solution of Euler's equations 08 p0984 N88-15955
Inviscid flows, part 2 08 p0985 N88-15966
Viscous flows, part 1 08 p0986 N88-15967
Radial compressor design using an Euler solver 10 p1283 N88-17675
Three-dimensional Euler solutions for hypersonic Mach numbers
[MBB-UR-944/87] 10 p1315 N88-17859
Finite element methods of analysis for high speed viscous flows
[NASA-CR-182529] 11 p1483 N88-18852
Compact high order schemes for the Euler equations
[NASA-CR-181625] 11 p1530 N88-19138
A generalisation of Hall's scheme for solving the Euler equations for two-dimensional flows 11 p1537 N88-19168
Solution of the Euler equations: Explicit schemes acceleration by a multigrid method 11 p1538 N88-19192
Unstructured multigrid methods 11 p1538 N88-19193

Applications of a multigrid finite volume method with Runge-Kutta time integrations for solving the Euler and Navier-Stokes equations 11 p1539 N88-19201
An L-U implicit multigrid algorithm to solve the Euler equations for transonic flow in rotating turbomachinery passages 13 p1718 N88-20270
Solution of two-dimensional Euler equations: Experience with a finite volume code
[DFVLR-FB-87-41] 13 p1767 N88-20572
Multigrid solution of the Euler equations 13 p1769 N88-20582
A symmetric set of Euler angles and oblique orientation space sections
[DE88-005317] 13 p1847 N88-21056
An explicit method for the solution of the Euler equations applied to unsteady two-dimensional flows
[MBB/LKE-121/S/PUB/257] 14 p1910 N88-21411
Choice of implicit and explicit operators for the upwind differencing method
[NASA-TM-100857] 14 p1964 N88-21718
On the prediction of highly vortical flows using an Euler equation model, part 2
[AD-A190245] 15 p2064 N88-22305
High-resolution shock-capturing schemes for inviscid and viscous hypersonic flows
[NASA-TM-100097] 15 p2122 N88-22651
Accuracy versus convergence rates for a three dimensional multistage Euler code
[NASA-CR-181665] 16 p2261 N88-23519
Incompressible Euler solution on a multiblock grid around a car configuration
[FFA-TN-1987-65] 18 p2457 N88-24586
Applications of the Navier-Stokes equations to wings and complex configurations using a zonal approach
[NASA-TM-100080] 18 p2459 N88-24602
Accurate multigrid solution of the Euler equations on unstructured and adaptive meshes
[NASA-CR-181679] 18 p2460 N88-24608
Composite reduced Navier-Stokes procedures for flow problems with strong pressure interactions
[AD-A191127] 18 p2508 N88-24875
Numerical simulations of flow around shuttle orbiter 19 p2635 N88-25633
Numerical solutions of the Euler equations for the flow field around counter-rotating propellers 19 p2636 N88-25638
Numerical simulation of supersonic free-jets 19 p2636 N88-25639
Numerical calculation of three dimensional flow by TVD scheme 19 p2638 N88-25649
An implicit, high order accurate, upwind scheme for unsteady Euler equations 19 p2639 N88-25657
On the stationary solutions of three-dimensional Euler equations by the TVD difference schemes 19 p2639 N88-25660
Improved potential flow computational methods with Euler corrections for airfoil and wing/body design
[AD-A192303] 20 p2752 N88-26334
A diagonally inverted LU implicit multigrid scheme
[NASA-TM-100911] 20 p2753 N88-26340
Vortex methods for separated flows
[NASA-TM-100068] 20 p2753 N88-26342
Euler equation computations for the flow over a hovering helicopter rotor
[NASA-CR-177493] 22 p3038 N88-28037
The influence of numerical boundary conditions on transonic flow
[DFVLR-FB-88-06] 23 p3172 N88-28890
Accurate solutions, parameter studies and comparisons for the Euler and potential flow equations
[NASA-TM-100664] 23 p3173 N88-28892
Generation of multiple block grids for arbitrary 3D geometries 23 p3246 N88-29317
Mesh generation for industrial application of Euler and Navier Stokes solvers 23 p3247 N88-29323
A streamwise upwind algorithm for the Euler and Navier-Stokes equations applied to transonic flows
[NASA-TM-101019] 24 p3316 N88-29751
Space marching Euler solvers 24 p3318 N88-29759
Numerical methods: Euler time dependent solver 24 p3318 N88-29760
Euler analysis of a swirl recovery vane design for use with an advanced single-rotation propfan
[NASA-TM-101357] 24 p3320 N88-29771

EULER-CAUCHY EQUATIONS
On the distribution equations
[DE88-702217] 23 p3270 N88-29454

EULER-LAGRANGE EQUATION
A free-Lagrange method for 2-D compressible flows
[DE88-000216] 04 p0442 N88-12745
Three-dimensional, free-Lagrange hydrodynamics
[DE88-000494] 04 p0443 N88-12749
Free Lagrange reconnection algorithms for hydrocodes using a quadrilateral mesh
[DE88-001580] 05 p0611 N88-13752
Perturbative coherence in field theory
[DE88-700386] 07 p0941 N88-15717
The dynamics of an oscillating four-bar linkage 09 p1181 N88-17074
A Lagrangian model of dry thermals
[DM-50] 09 p1193 N88-17150
An adaptive grid technique for solution of the Euler equations 13 p1768 N88-20579
Introduction to classical mechanics of systems with constraints, part 1
[DE88-701055] 13 p1832 N88-20957
Introduction to classical mechanics of systems with constraints, part 2
[DE88-701056] 13 p1849 N88-21072
A semigroup for Lagrangian 1D isentropic flow
[DE88-006464] 18 p2513 N88-24912
Fuel droplet vaporization and temperature distributions of axisymmetric unsteady sprays 19 p2626 N88-25579

EURECA (ESA)
Allowable gravity-levels for Spacelab, Columbus and EURECA --- materials science
[BF-R-66.525-2] 07 p0838 N88-15084
External payload servicing: Operational requirements and technology 12 p1593 N88-19541
Exobiology and botany facilities for EURECA 12 p1652 N88-19898
Microgravity User Support Center (MUSC) for EURECA, Spacelab and Columbus missions 12 p1660 N88-19947
Latching mechanisms for IOC --- EURECA 14 p1875 N88-21205
The EURECA antenna deployment and retraction mechanisms 14 p1878 N88-21225
Botany Facility pre-phase C/D. Core payload for EURECA, volume 2
[BF-RP-ER-015-VOL-2] 17 p2377 N88-24130
Life Support Subsystem (LSS). Concept for the Botany Facility --- EURECA
[TN-RB524-107/86] 17 p2377 N88-24131
Impact of control errors on the volume/weight demand of the Ventilation and Dryer (VAD) concept --- EURECA Botany Facility
[TN-RB524-006/87] 17 p2377 N88-24132
Summary of the activities performed during the Botany Facility (BF) predevelopment phase for the Life Support S/S (LSS)
[TB-RB524-002/87] 17 p2378 N88-24133
Examination of methods for pollen storage and dispersal
[TN-RB524-097/86] 17 p2378 N88-24134
Botany Facility. Thermal Control (TC) subsystem test report on experiment container of laboratory model and breadboard centrifuge
[BF-TN-ER-061/86] 17 p2378 N88-24135
Botany Facility: Test report on breadboard tests for the determination of the heat transfer at the glass disk and of the temperature distribution in the fluorescent tube
[BF-TN-ER-053] 17 p2378 N88-24136
Botany Facility: Breadboarding results of the illumination system
[SIRA-A/7373/WP110/MAC003] 17 p2378 N88-24137
Botany Facility: Magnetic fluid seal considerations for the centrifuge
[SIRA-A/7373/WP110/MAC004] 17 p2378 N88-24138
Botany Facility: Considerations and analyses of the balancing system philosophy proposed for the BF centrifuge
[SIRA-A/7373/WP110/PWF001] 17 p2378 N88-24139
Botany Facility: The problems of plant fixation
[SIRA-A/7373/WP220/RJS/001] 17 p2379 N88-24140
Botany Facility: Problems of water supply, plant nutrients and soil in the Botany Facility
[SIRA-A/7373/WP220/RJS/003] 17 p2379 N88-24141
Supply and distribution of plant nutrients in the Botany Facility
[SIRA-A/7373/WP220/RJS/004] 17 p2379 N88-24142
EURECA Botany Facility. Technical note: Removal of phytotoxins
[SIRA-A/7373/WP220/RJS/005] 17 p2379 N88-24143
Botany Facility pre-phase C/D. Core payload for EURECA, volume 1
[BF-RP-ER-015-VOL-1] 17 p2379 N88-24144
Operational facilities of EURECA A1 mission
[ETN-88-91939] 18 p2496 N88-24810
Study of standard generic approach for spacecraft (S/C) autonomy and automation (phase 3). Book B: Autonomy concept application example
[ESA-CR(P)-2555-VOL-2] 23 p3185 N88-28956

EUROPE
COST-73 and its application in very short range forecasting 02 p0199 N88-11242
Foreign language identification: First step in the translation process
[DE87-011065] 02 p0248 N88-11565
Composite materials in western Europe
[PB87-102943] 03 p0279 N88-11759
Short reference year
[PB87-107470] 03 p0352 N88-12221
Solar energy: European research and development
[PB87-107645] 04 p0463 N88-12866
European industrial consortia, for space projects: Their origins, development and possible evolution 09 p1128 N88-16765
An investigation of terrain related variables for predicting the multipath fade depth distribution on terrestrial microwave lines 12 p1615 N88-19654
Ozone sonde and Dobson spectrometer data obtained during the MAP/GLOBUS 1983 campaign over Western Europe
[BPT-5/87] 13 p1802 N88-20771
European transonic wind tunnel project: Assistance to the design group
[ONERA-RSF-11/0694-GY-010-G] 21 p2900 N88-27208
Studies concerning the European transonic wind tunnel
[ONERA-RSF-10/0694-GY-010-G] 21 p2900 N88-27209
Application of SPOT to agricultural information systems in temperate regions 22 p3093 N88-28369

EUROPEAN AIRBUS
NT A-300 AIRCRAFT
NT A-320 AIRCRAFT
Assessment of software quality for the AIRBUS A310 automatic pilot 02 p0128 N88-10804
Aeroelastic analysis of modern transport aircraft --- European Airbus
[SNIAS-872-111-102] 05 p0546 N88-13329
Testing of a schematic transport plane model in several European windtunnels
[PB87-170270] 09 p1113 N88-16671
Airbus, the successful European cooperation
[MBB-UT-005/87] 10 p1313 N88-17847
Automatic riveting machine for spherically-formed airframe structures
[ETN-88-91024] 11 p1495 N88-18924
Airbus 1987: Success in Europe
[ETN-88-92099] 20 p2758 N88-26364
Variable wing camber control systems for the future Airbus program
[MBB-UT-104/88] 23 p3180 N88-28932

EUROPEAN COMMUNICATIONS SATELLITE
Alternative force structuring strategies for military satellite communication systems
[AD-A189492] 13 p1758 N88-20516
Study of the assembly, integration and verification programs of telecommunication satellites applicable to other satellite programs
[MATRA-100/CC/MLG/031/87] 24 p3334 N88-29847

EUROPEAN INCOHERENT SCATTER RADAR
U EISCAT RADAR SYSTEM (EUROPE)

EUROPEAN LARGE TELECOMM SATELLITE
U L-SAT

EUROPEAN RETRIEVABLE CARRIER
U EURECA (ESA)

EUROPEAN SPACE AGENCY
Battery development and testing at ESA 02 p0164 N88-11027
Generic specifications for hybrid microcircuits
[ESA-PSS-01-608-ISSUE-2] 06 p0696 N88-14273
Overview of ESA's activities in ocean colour remote sensing 08 p1042 N88-16294
The appropriate use of contract types in development contracts (a systems approach with emphasis on the European space sector)
[ESA-STR-222] 08 p1092 N88-16573
Studies for future scientific projects 09 p1123 N88-16720
A policy for international relations 09 p1123 N88-16724
ESA Bulletin No. 10
[ETN-87-90514] 09 p1123 N88-16726
Specialist support for projects: Activities, methods and infrastructure 09 p1124 N88-16729
The objectives and methods of the technological research program 09 p1124 N88-16730
The ESA centralized management system for satellite electronic test and checkout instrumentation 09 p1124 N88-16731
ESTEC's product assurance activities 09 p1125 N88-16739
Projects under development 09 p1126 N88-16750

ESA Bulletin No. 24
|ISSN-0376-4265| 09 p1127 N88-16755
Programs under development and operations
09 p1127 N88-16762
The new approach to the definition of the ESA technological research program
09 p1127 N88-16763
Promotion of European components for ESA projects
09 p1128 N88-16764
ESA Bulletin No. 25
|ISSN-0376-4265| 09 p1128 N88-16767
Entry into force of the ESA convention
09 p1128 N88-16768
Parallel-processing computer systems and their possible applications in the agency 09 p1128 N88-16774
Report presented by the European Space Agency to the 22nd COSPAR meeting
|ESA-SP-1014| 09 p1129 N88-16776
PCM telemetry standard
|ESA-PSS-46(TTC.A.02)ISSUE-1|
09 p1132 N88-16790
Study for history of technology developments in European space projects
|REPT-8518-1| 10 p1286 N88-17690
Spacelab: An international success story
|NASA-SP-487| 11 p1566 N88-19375
The European Space Agency's role in life sciences and research in space 12 p1652 N88-19894
Life sciences in the framework of the ESA microgravity program and future flight opportunities
12 p1652 N88-19895
The preparation, assembly and mounting of RF coaxial cables
|ESA-PSS-01-718-ISSUE-1| 13 p1756 N88-20504
Design method for Ada programs
|ESA-CR(P)-2528| 14 p1958 N88-21671
Preparing for the new programs. The ESA technological research and development program 1988-1990
|ESA-SP-1095| 17 p2309 N88-23814
International cooperation in remote sensing: The ESA experience 17 p2356 N88-24038
The technical reporting and approval procedure for materials and processes
|ESA-PSS-01-700-ISSUE-1| 22 p3162 N88-28833
Material and process selection and quality control for ESA space systems and associated equipment
|ESA-PSS-01-70-ISSUE-3| 23 p3224 N88-29190
Focus 86: A summary of the 1986 annual report of the activities of the European Space Agency
|ESA-BR-34| 23 p3309 N88-29713
Candidate functions for advanced technology implementation in the Columbus mission planning environment 24 p3417 N88-30340
With an eye to the future: ESA general studies program 1988
|ESA-SP-1100| 24 p3435 N88-30447
ESA report to the 27th COSPAR meeting
|ESA-SP-1098| 24 p3453 N88-30556

EUROPEAN SPACE PROGRAMS
Columbus preparatory program. Payload element study on a technology demonstration mission, executive summary
|CS-RP-AI-016| 01 p0014 N88-10080
Report on the scientific satellites of the European Space Agency
|ESA-SP-1090| 01 p0014 N88-10081
Preliminary study of a biotechnology research facility for microgravity, executive summary
|MATRA-EPT/AS/VT209/246/NT|
01 p0032 N88-10204
Preliminary study of a gravitational biology facility for Columbus, executive summary
|MATRA-EPT/AS/VT209/255/NT|
01 p0032 N88-10205
Components for cryostat --- spaceborne
|MBB/ISO-TN-CD00.003-REV-A|
01 p0032 N88-10207
Robotic sensors and actuators for a service manipulator system. Volume 1: Executive summary
|MATRA-EPT/DT/VT187/120|
01 p0053 N88-10341
Robotic sensors and actuators for a service manipulator system. Volume 2: Service Manipulator System (SMS) handbook
|MATRA-EPT/DT/VT187/227|
01 p0053 N88-10342
Robotic sensors and actuators for a service manipulator system. Volume 3, phase A report and program plan
|MATRA-EPT/DT/VT187/228|
01 p0054 N88-10343
Study on the suitability of a European data relay satellite to support a system of remote sensing satellites
|ESA-CR(P)-2400| 01 p0063 N88-10406
Aquarack: Aims and Possible Research Projects
|DFVLR-MITT-87-01| 01 p0073 N88-10469
Life support systems for biological experiments under weightlessness in the German and European space programs 01 p0074 N88-10477
ESA Workshop on Optical Interferometry in Space
|ESA-SP-273| 01 p0094 N88-10613
Space station based interferometry
01 p0096 N88-10628
ESA technological research activities on lightweight mirrors --- spaceborne interferometry
01 p0096 N88-10629
Aerospace research at the National Aerospace Laboratory (NLR)
|ETN-87-90821| 01 p0107 N88-10697
Mechanical design of the ac bracket package for the RETE experiment
|IFSI-87-4| 05 p0555 N88-13379
Budget and programs for 1986 research
|IFSI-86-16| 05 p0660 N88-14048
Generic specifications for hybrid microcircuits
|ESA-PSS-01-608-ISSUE-2| 06 p0696 N88-14273
Activities report in aircraft design and astronautics
|ETN-88-90618| 07 p0809 N88-14925
Round table on the future of satellite communications and broadcasting in Europe
|ESA-STR-221| 07 p0843 N88-15112
Study of a Radio Relay Link (RRL). Cassini mission. Data package for final presentation
|ESA-CR(P)-2472| 07 p0847 N88-15138
The role of the DFVLR project management life sciences in the space program of the Federal Republic of Germany 07 p0884 N88-15364
German space policy on the threshold of the century. Analysis and proposals for the future
|ETN-88-90573| 07 p0943 N88-15734
The TV-SAT/TDF/TELE-X pyrotechnical system
|CNES-87/CT/DRT/TVE/IL/358|
08 p0974 N88-15891
The German scientific balloon and sounding rocket program 08 p1024 N88-16202
The Norwegian scientific balloon and sounding rocket program 1987-1990 08 p1025 N88-16204
Swiss scientific balloon and sounding rocket experiments 1985-1987 08 p1025 N88-16206
Flight results of the ESA experiment modules in Materials Science Experiment Rocket (MASER) 1
08 p1033 N88-16261
Europe's position concerning ocean colour activities
08 p1042 N88-16293
Overview of ESA's activities in ocean colour remote sensing 08 p1042 N88-16294
Federal Republic of Germany's interests, activities and goals in remote sensing of ocean colour/fluorescence from space 08 p1043 N88-16302
The European space physics analysis network
08 p1099 N88-16613
ESA Bulletin No. 8
|ETN-87-90513| 09 p1122 N88-16718
Studies for future scientific projects
09 p1123 N88-16720
The 2.4 m Space Telescope and ESA participation in the program 09 p1123 N88-16721
European developments in antenna technology
09 p1123 N88-16725
Coordinated use of European test facilities
09 p1123 N88-16726
ESA Bulletin No. 10
|ETN-87-90514| 09 p1123 N88-16728
Specialist support for projects: Activities, methods and infrastructure 09 p1124 N88-16729
The objectives and methods of the technological research program 09 p1124 N88-16730
Heat pipes for space use 09 p1124 N88-16736
The European space battery test center
09 p1125 N88-16738
ESTEC's product assurance activities
09 p1125 N88-16739
Major spacecraft hardware testing in Europe
09 p1125 N88-16740
ESA Bulletin No. 15: Ariane, the European launcher for the 1980's
|ESA-BULLETIN-NO-15| 09 p1125 N88-16741
Projects under development 09 p1126 N88-16750
ESA Bulletin No. 24
|ISSN-0376-4265| 09 p1127 N88-16755
The Meteosat operational program
09 p1127 N88-16759
Programs under development and operations
09 p1127 N88-16762
The new approach to the definition of the ESA technological research program
09 p1127 N88-16763
European industrial consortia, for space projects: Their origins, development and possible evolution
09 p1128 N88-16765
ESA Bulletin No. 25
|ISSN-0376-4265| 09 p1128 N88-16767
Parallel-processing computer systems and their possible applications in the agency 09 p1128 N88-16774
Report presented by the European Space Agency to the 22nd COSPAR meeting
|ESA-SP-1014| 09 p1129 N88-16776
Proceedings of the ESA Workshop on Co-Orbiting Platform Elements (COPE)
|ESA-SP-1093| 09 p1129 N88-16777
An overview of the current Earth observation programs (Europe, USA, and Japan) 09 p1129 N88-16778
The Columbus program, an overview
09 p1130 N88-16784
Coorbiting Platform Utilization Study (CPLUS), executive summary --- Columbus
|SN-WP-4000-DOC-6609/85/F|
09 p1133 N88-16798
Study on long term evolution towards European manned space flight. Volume 1: Executive summary
|MBB-RA3-004/87-VOL-1| 10 p1286 N88-17689
Study for history of technology developments in European space projects
|REPT-8518-1| 10 p1286 N88-17690
AZUR, the first German research satellite 625-A, 1964-1969 10 p1310 N88-17827
Trends in the development of space transportation systems
|MBB-UR-911/86| 10 p1315 N88-17857
JPRS report: Science and Technology. Europe and Latin America
|JPRS-ELS-88-002| 10 p1316 N88-17870
Columbus feasibility studies. Volume 4: Integration, test, and operations
|ETN-88-90576| 11 p1445 N88-18614
Assembly and servicing of a European Space Station
12 p1586 N88-19492
Utilization of SMS and EVA for the servicing of European Space Station 12 p1587 N88-19500
The ESA/Fokker service end-effector subsystem. A robotic/man-compatible servicing approach
12 p1587 N88-19502
Robotic intelligence issues for space manipulator monitoring, control programming
12 p1588 N88-19504
Robotics servicing experiment --- European space programs 12 p1591 N88-19529
Definition of the EUROSIM simulation subsystem
12 p1592 N88-19532
Man-tended options for European space robotics
12 p1593 N88-19538
The European Space Agency's role in life sciences and research in space 12 p1652 N88-19894
Life sciences in the framework of the ESA microgravity program and future flight opportunities
12 p1652 N88-19895
Life science techonology --- space applications
12 p1653 N88-19900
European activities in exobiological research in space
12 p1657 N88-19929
European Progress on Space (EPOS): Participation in the creation of long term European space programs
|ILR-MITT-189| 14 p1871 N88-21180
Investigation of European remote sensing user needs in accessing MOS-1 payload
|ESA-CR(P)-2535| 14 p1940 N88-21580
Securing the timescale of the NAVEX-reference clock and rate determinations by time comparisons with the help of the Global Positioning System (GPS) --- Spacelab D1 mission
|DFVLR-MITT-87-20| 16 p2159 N88-22879
Navigation experiment NAVEX. The reading differences between all ground station measuring clocks during each Spacelab pass of the D1 mission
|DFVLR-MITT-87-23| 16 p2159 N88-22880
New concepts for atmospheric braking deceleration in planetary atmosphere entry
|SNIAS-CAS-DECE-P003-DPAA|
16 p2168 N88-22923
Preparation of the operational phase of the European Remote Sensing Satellite ERS-1
|BCRS-87-06| 16 p2228 N88-23307
Study of the plan for a national data center for the European Remote Sensing Satellite ERS-1
|BCRS-87-11| 16 p2228 N88-23309
Preparing for the new programs. The ESA technological research and development program 1988-1990
|ESA-SP-1095| 17 p2309 N88-23814
Columbus feasibility studies, executive summary
|ETN-88-92334| 17 p2311 N88-23820
Insert design handbook
|ESA-PSS-03-1202-ISSUE-1| 17 p2311 N88-23822
International cooperation in remote sensing: The ESA experience 17 p2356 N88-24038
The high-throughput X-ray spectroscopy mission E6889478 MN513835 --- ESA program
|ESA-SP-1092| 17 p2450 N88-24554

Economic impact of space flight activities in West Germany. Influence of allocations of Bundesministerium fuer Forschung und Technologie
[ETN-88-92106] 21 p2901 N88-27215
Cyrogenic test facilities for an optical cryomechanism qualification
[REPT-881-440-116] 21 p2901 N88-27219
Study on NAVSAT system evaluation, phase 2. Part 1: Study results
[NLR-TR-87061-L-PT-1] 22 p3041 N88-28054
Reaching for the skies: The Ariane family story and beyond. An introduction to Europe's successful series of space transportation systems
[ESA-BR-42] 22 p3046 N88-28078
Study of biological effects and radiation protection to future European manned space flights
[DGT-33061] 23 p3281 N88-29535
Focus 86: A summary of the 1986 annual report of the activities of the European Space Agency
[ESA-BR-34] 23 p3309 N88-29713
Study on long-term evolution towards European manned spaceflight. Volume 1: Executive summary
[ERNO-OX1-002/88-VOL-1] 24 p3330 N88-29827
ERS-1: A satellite with an oceanographic mission
[NLR-MP-86072-U] 24 p3333 N88-29838
Study of the assembly, integration and verification programs of telecommunication satellites applicable to other satellite programs
[MATRA-100/CC/MLG/031/87] 24 p3334 N88-29847
Interim Flight Opportunity (IFO). Volume 1: Executive summary --- space platform
[SE/LS/AP-36-818/CN-VOL-1] 24 p3334 N88-29849
Qualification test levels for units to be derived from mechanical test data analysis --- ESA
[REPT-87-158-EI/ET/AG] 24 p3381 N88-30139
Study on industrial organization for European Ground Support Equipment (EGSE) to support European space programs. Volume 1: Technical reports
[SD-RP-AI-009-VOL-1] 24 p3435 N88-30446
With an eye to the future: ESA general studies program 1988
[ESA-SP-1100] 24 p3435 N88-30447
Study on industrial organization for European Ground Support Equipment (EGSE) to support European space programs. Volume 2: Technical reports
[SD-RP-AI-009-VOL-2] 24 p3435 N88-30448
ESA report to the 27th COSPAR meeting
[ESA-SP-1098] 24 p3453 N88-30556
The high-throughput X-ray spectroscopy mission: The mission-science report
[ESA-SP-1097] 24 p3453 N88-30557

EUROPEAN SPACE RESEARCH ORGANIZATION
U EUROPEAN SPACE AGENCY

EUROPEAN SPACE RESEARCH ORGANIZATION SAT
U ESA SATELLITES

EUROPIUM
Change of europium crystallographic symmetry at helicoidal magnetic ordering
[DE88-700559] 07 p0939 N88-15707

EUROPIUM COMPOUNDS
Resistivity of EuBa2(Cu/sub 1-y/Zn/sub y/)3O/sub x/ as a ffunction of temperature, magnetic field, pressure and Zn concentration
[DE87-014740] 04 p0499 N88-13069
Growth of Pb/sub 1-x/Eu/sub x/Te epitaxial layers by the liquid phase epitaxy technique
[DE88-701022] 15 p2139 N88-22763

EUTECTIC ALLOYS
Directed-energy electron-beam processing of a hypoeutectic Cr90Ta10 alloy
[DE88-005621] 15 p2040 N88-22157
Fraction eutectic measurements in slowly cooled Pb - 15 wt percent Sn alloys
[NASA-CR-180830] 19 p2618 N88-25531

EUTECTIC COMPOSITES
Influence of convection on microstructure
[NASA-CR-182489] 10 p1302 N88-17784

EUTECTIC DIAGRAMS
U PHASE DIAGRAMS

EUTECTICS
NT EUTECTIC ALLOYS
Low-pressure eutectic bonding of depleted uranium to copper
[DE87-014625] 02 p0181 N88-11128
Ultra-fine grained alloy material
[AD-A184500] 03 p0290 N88-11820
Laser cladding of Ni, Nb and Mg alloys for improved environmental resistance at high temperature
[AD-A191274] 16 p2213 N88-23208

EVACUATING (TRANSPORTATION)
Smoke hoods: Net safety benefit analysis --- aircraft accidents
[CAA-PAPER-87017] 23 p3174 N88-28898

EVALUATION
NT TRAINING EVALUATION
Hardware fault insertion and instrumentation system: Mechanization and validation
[NASA-CR-181445] 01 p0078 N88-10497
An evaluation of WPS-Plus word processing software for the IBM PC and compatibles
[DE87-011972] 01 p0081 N88-10518
Assessment of software quality for the AIRBUS A310 automatic pilot 02 p0128 N88-10804
Experiments of the selection of a method evaluating the fire resistance of some materials based on macromolecular compounds
[NASA-TT-20129] 02 p0154 N88-10966
An evaluation of the LEC-460 solar collector
[DE88-000052] 02 p0196 N88-11224
Evaluating computers and their performance: Perspectives, pitfalls, and paths
[DE87-014264] 02 p0218 N88-11375
Hypocenters (1977-1984) around the Richton Dome and the Melvin, Alabama, 1978 earthquake
[DE87-014336] 03 p0351 N88-12214
Los Alamos National Laboratory computer benchmarking 1986
[LA-10898-MS] 03 p0363 N88-12285
An evaluation plan of bus architectures and protocols using the NASA Ames intelligent redundant actuation system
[NASA-CR-177458] 04 p0398 N88-12482
Non-linearity in measurement systems: Evaluation method and application to microwave radiometers 04 p0433 N88-12684
Standard fatigue test specimens for fastener evaluation
[AGARD-AG-304] 04 p0455 N88-12818
Methods for design and evaluation of integrated hardware/software systems for concurrent computation
[NASA-CR-181522] 04 p0479 N88-12953
Evaluation of device figure of merit in microwave switching circuit design
[AD-A184896] 05 p0577 N88-13520
Test and evaluation of the transputer in a multi-transputer system
[AD-A184969] 05 p0631 N88-13859
Analysis and test evaluation of the dynamic stability of three advanced turboprop models at zero forward speed
[NASA-CR-175025] 06 p0668 N88-14095
Analysis and test evaluation of the dynamic response and stability of three advanced turboprop models at low forward speed
[NASA-CR-175026] 06 p0668 N88-14096
The evaluation of a deformable diffraction grating for a stigmatic EUV spectroheliometer
[NASA-CR-182371] 06 p0707 N88-14337
Experiences in teleoperation of land vehicles
[DE88-001695] 06 p0711 N88-14357
Evaluation method of the brittle fracture strength in structurally stress-concentrated regions
[PB87-129490] 06 p0721 N88-14435
Controlled Ecological Life Support Systems (CELSS) physiochemical waste management systems evaluation
[NASA-CR-177422] 06 p0754 N88-14626
Software-implemented fault insertion: An FTMP example
[NASA-CR-178423] 06 p0761 N88-14668
Evaluation of high-voltage, high-power, solid-state remote power controllers for amps 07 p0924 N88-15612
A study to evaluate STS heads-up ascent trajectory performance employing a minimum-Hamiltonian optimization strategy
[NASA-TP-2793] 08 p0960 N88-15820
Calculation evaluation of the boundary conditions of autoinflammation of propulsive charges
[PB87-139044] 08 p0974 N88-15890
Actual performance and economic feasibility of residential solar water heaters
[INPE-4399-RPE/555] 08 p1023 N88-16191
Using output to evaluate and refine rules in rule-based expert systems 08 p1055 N88-16362
Evaluating software testing methods to reduce testing duplication in US Army communications equipment acquisition
[AD-A186961] 09 p1216 N88-17292
Corrosion and deterioration testing in humid tropic environments
[AD-A186917] 10 p1302 N88-17783
Evaluation of bituminous materials used in pavement recycling projects at Tyndall, MacDill, and Hurlburt Air Force Bases
[AD-A188068] 10 p1317 N88-17871
Laboratory evaluation and analysis of advanced lead-acid load-leveling batteries
[DE88-002851] 10 p1349 N88-18064
Supercomputer performance: The theory, practice, and results
[DE88-004697] 10 p1384 N88-18266
A method for assessing the software engineering capability of contractors: Preliminary version
[AD-A187230] 10 p1388 N88-18290
Quantitative non-destructive evaluation of porous composite materials based on ultrasonic wave propagation
[NASA-CR-182544] 11 p1447 N88-18627
Lead-acid load-leveling battery testing at Argonne National Laboratory
[DE88-002853] 11 p1480 N88-18837
Evaluation of advanced lead-acid batteries developed for load-leveling applications
[DE88-002871] 11 p1481 N88-18838
The judgement and evaluation of long-term investments demonstrated by means of a civil aircraft program 12 p1701 N88-20180
The effects of two Carlucci initiatives concurrency and streamlining, on the test and evaluation phase of system acquisitions 12 p1704 N88-20198
Combustion theory and related questions
[AD-A189160] 13 p1737 N88-20382
Method to evaluate image-recovery algorithms based on task performance
[DE88-005382] 13 p1816 N88-20853
Development and evaluation of instrumentation and methods for multi-element analysis
[AD-A189345] 13 p1841 N88-21018
Multi-hundred kilowatt roll ring assembly evaluation results
[NASA-TM-100865] 14 p1904 N88-21375
A graph separator theorem and its application to Gaussian elimination to optimize Boolean expressions for parallel evaluation
[AD-A188527] 14 p1962 N88-21706
EMR (Electromagnetic Radiation) test facilities evaluation of reverberating chamber located at RADC (Rome Air Development Center), Griffiss AFB (Air Force Base), Rome, New York
[PB88-178827] 15 p2022 N88-22048
Today's photovoltaic systems: An evaluation of their performance
[DE88-006926] 15 p2090 N88-22457
Prediction of physical fitness: Estimated percent body fat using body circumferences versus weight-height measures
[AD-A190233] 15 p2103 N88-22526
Instrumentation for ultrafast electronics
[AD-A191379] 16 p2193 N88-23080
Evaluation of the endogenous glucocorticoid hypothesis of denervation atrophy
[NASA-CR-182848] 17 p2381 N88-24157
Evaluation of the communications impact of a low power arcjet thruster
[NASA-TM-100926] 18 p2475 N88-24682
Evaluating evaporation with satellite thermal data
[AD-A192042] 18 p2531 N88-25019
Effectiveness evaluation of fault-tolerant multiprocessor systems
[AD-A191688] 18 p2554 N88-25158
Multi-sensor integration on the NCUBE hypercube computer
[DE88-007472] 18 p2554 N88-25162
Evaluation of vertical monopole antennas with elevated radials
[DE88-008339] 19 p2654 N88-25760
Performance evaluation for multiprocessors programmed using monitors
[DE88-010056] 19 p2718 N88-26138
Engineering research centers and their evaluation
[PB88-180054] 19 p2739 N88-26262
Procedures for peer review assessments
[DE88-007749] 19 p2739 N88-26263
Evaluation of engineering leak before break assessment methods by piping tests
[PB88-126982] 20 p2788 N88-26538
Loss evaluation of self-commutated power conditioner for battery energy storage system
[DE88-752075] 20 p2794 N88-26575
Australian structures response evaluation: Ground shock and air blast measurements for site investigation survey
[MRL-TN-526] 20 p2813 N88-26685
An evaluation of flight path formats head-up and head-down
[NASA-CR-4176] 21 p2897 N88-27196
Evaluation of fracture models through pressurized-thermal-shock testing
[DE88-011834] 21 p2963 N88-27603
Performance evaluation of large-area glass-mirror heliostats
[DE88-011883] 21 p2969 N88-27636
System status display evaluation
[NASA-CR-4181] 22 p3042 N88-28061

Development of sensors for ceramic components in advanced propulsion systems: Survey and evaluation of measurement techniques for temperature, strain and heat flux for ceramic components in advanced propulsion systems
| NASA-CR-182111 | 22 p3081 N88-28299
Design and evaluation of high contact ratio gearing
| NASA-CR-174958 | 22 p3085 N88-28319
Reliability assessment of Surface Mount Technology (SMT)
| AD-A193759 | 23 p3208 N88-29089
Present state of knowledge of the upper atmosphere 1988: An assessment report
| NASA-RP-1208 | 23 p3232 N88-29233
SSTS (Space Surveillance and Tracking System): The importance of early test and evaluation organizational participation
| AD-A193745 | 23 p3276 N88-29499
Quality measures and assurance for AI (Artificial Intelligence) software
| NASA-CR-4187 | 24 p3411 N88-30304

EVANESCENCE
Monolithic integration on a GaAs substrate of a quarter ring laser and an optical guide coupled by an evanescent wave
| ETN-88-92308 | 17 p2344 N88-23969

EVAPORATION
NT EVAPOTRANSPIRATION
NT TRANSPIRATION
Preparation and properties of evaporated CdTe films
| DE87-012270 | 02 p0195 N88-11216
Production of atom flows at materials evaporation by laser radiation
| DE87-703327 | 03 p0328 N88-12074
Ceramics thin film 04 p0403 N88-12505
Effects of rainfall on the seasonal thermocline
| AD-A184432 | 04 p0472 N88-12912
Use of the thermodynamic evaporation formula of Hoffmann in energy balance models for flowing water 08 p1013 N88-16143
Laval nozzle flow of a binary, retrograde mixture
| MPIS-1/1987 | 11 p1488 N88-18882
Review of recent developments in evaporation ducting assessment 12 p1616 N88-19664
Model catalyst studies of SMSI (Strong Metal/Support Interactions) and the role of D-electrons in chemisorption and catalysis
| DE88-004518 | 13 p1738 N88-20393
The thermodynamic properties of organic oxygen compounds
| DE88-001208 | 13 p1849 N88-21065
Superfine grain development by laser 15 p2050 N88-22215
Hard ceramic film by laser PVD 15 p2051 N88-22216
Evaporation characteristics of elements during vacuum arc remelting of alloy A-286 15 p2055 N88-22248
Laser evaporation studies
| AD-A189815 | 15 p2071 N88-22346
Method of evaporation
| NASA-CASE-NPO-15609-2 | 17 p2318 N88-23846
Transient analysis of heat pipe vapor dynamics 17 p2412 N88-24341
Heating and evaporation of turbulent liquid films: Measurement of film thickness and the onset of nucleate boiling
| DE88-006388 | 18 p2512 N88-24905
Evaluating evaporation with satellite thermal data
| AD-A192042 | 18 p2531 N88-25019
Report on project WIND: Preliminary experiments w ith the UK Meteorological Office mesoscale model, September 1987
| AD-A191621 | 18 p2544 N88-25099
Liquid phase decomposition in slurry fuels 19 p2624 N88-25564
Antenna heights for the optimum utilization of the oceanic evaporation duct. Part 3: Results from the Mediterranean measurements, volume 2
| AD-A192311 | 20 p2791 N88-26554
Antenna heights for the optimum utilization of the oceanic evaporation duct. Part 1: Results from the Pacific measurements. Part 2: Results from the Key West measurements, volume 1
| AD-A192358 | 20 p2791 N88-26555
Schottky-barrier formation on a covalent semiconductor without Fermi-level pinning: The Metal-MoS2(0001) interface
| AD-A193044 | 21 p3021 N88-27931
Influence of the convection on evaporation and combustion of a fuel droplet 24 p3351 N88-29948

EVAPORATION RATE
Development of computer-controlled thermogravimetric instrumentation for measurement of environmental and high temperature volatilization and desorption of contaminants from polymeric materials
| AD-A195934 | 24 p3343 N88-29900

EVAPORATIVE COOLING
NT FILM COOLING
NT SWEAT COOLING
Cooling effect of a single evaporating droplet on a hot semi-infinite metal body
| PB87-201802 | 01 p0046 N88-10294
The role of low-level cooling in a conceptual model of the Australian summertime cool change: Implications for very-short-range forecasting 02 p0204 N88-11275
Advanced radiator concepts utilizing honeycomb panel heat pipes
| NASA-CR-172017 | 04 p0443 N88-12747
Transient cooling of a hot surface by droplets evaporation, March 1986 - March 1987
| PB88-153341 | 10 p1330 N88-17950

EVAPORATORS
Tower evaporator
| NASA-CASE-NPO-15609-2 | 18 p2497 N88-24815
An experimental investigation of transient characteristics in a gravity-assisted heat pipe 20 p2783 N88-26506
Forced-convective boiling in small diameter tube 20 p2783 N88-26510

EVAPOTRANSPIRATION
Estimating regional evapotranspiration from remotely sensed data by surface energy balance models
| NASA-CR-181400 | 01 p0064 N88-10411
Remote Sensing-Arid Lands Workshop, Page, Arizona, June 10-12, 1986
| DE87-012368 | 01 p0064 N88-10412

EVASIVE ACTIONS
The isotropic rocket: A surveillance evasion game
| REPT-87-21 | 05 p0645 N88-13949

EVECTION
U ORBIT PERTURBATION

EVEN-EVEN NUCLEI
Influence of pairing correlations on the probability and dynamics of tunneling through the barrier in fission and fusion of complex nuclei
| DE88-701500 | 23 p3286 N88-29570

EVOKED RESPONSE (PSYCHOPHYSIOLOGY)
Visual evoked responses to sinusoidal gratings presented in central and right visual fields: 1
| DE87-014731 | 04 p0473 N88-12919
Brain activity during tactical decision-making. Part 2: Probe-evoked potentials and workload
| AD-A188688 | 12 p1667 N88-19994
Identification of visual evoked response parameters sensitive to pilot mental state
| NASA-CR-4140 | 13 p1811 N88-20822
Pupil measures of alertness and mental load 16 p2239 N88-23378
Probe-evoked event-related potential techniques for evaluating aspects of attention and information processing 16 p2240 N88-23379
Steady-state evoked potentials possibilities for mental-state estimation 16 p2240 N88-23380
Primary task event-related potentials related to different aspects of information processing 16 p2240 N88-23382
The N2-P3 complex of the evoked potential and human performance 16 p2241 N88-23388
Eye and head response to an attention cue in a dual task paradigm
| AD-A191052 | 18 p2551 N88-25143
Contra- and ipsilateral auditory stimuli produce different activation patterns at the human auditory cortex: A neuromagnetic study
| PB88-181490 | 19 p2708 N88-26098
Auditory evoked magnetic fields in man
| PB88-193446 | 20 p2831 N88-26796
A statistical procedure for the evaluation of presence/non-presence of stimulus-related EEG activity 21 p2978 N88-27689
Dissecting the visual and auditory pathways by means of the two-input technique 21 p2978 N88-27690
Squid instrumentation for neuromagnetic study of complex brain activity 21 p2978 N88-27691
Neuromagnetic evidence of place mechanisms for frequency and intensity coding in the human auditory cortex 21 p2979 N88-27693
Neurophysiological precursors of accurate visuomotor performance 21 p2981 N88-27706
The effect of mild hypoxia on the vestibular evoked response 21 p2982 N88-27713
Measurement of electrical activity in the CNS with cortical evoked potentials and EEG: Efficacy profiles of drugs using factor analysis 21 p2983 N88-27715
The auditory evoked response in military pilots 21 p2984 N88-27721
Human auditory and visual continuous evoked potentials 23 p3238 N88-29269

EVOLUTION
Rotational evolution of dynamically symmetric gyrostat with internal friction 24 p3446 N88-30509
Evolution of thermal structure of Benguela upswelling system according to satellite and shipboard data 24 p3449 N88-30525

EVOLUTION (DEVELOPMENT)
NT BIOLOGICAL EVOLUTION
NT CHEMICAL EVOLUTION
NT GALACTIC EVOLUTION
NT LUNAR EVOLUTION
NT PLANETARY EVOLUTION
NT STAR FORMATION
NT STELLAR EVOLUTION
NT STELLAR MASS ACCRETION
Semidiscrete Galerkin method for semilinear evolution equations with a differential operator of third order
| BONNER-MATHE-SCHR-181 | 01 p0087 N88-10570
High explosive simulations of supernovae and the supernova shell fragmentation model of solar system formation
| DE87-014708 | 02 p0251 N88-11584
Cosmological applications of singular hypersurfaces in general relativity 04 p0521 N88-13202
The evolution of local mechanical properties of Al 2219-T851 during fatigue 05 p0598 N88-13653
Model of earlier stage of universe's evolution 06 p0775 N88-14758
Evolution of perturbations in expanding universe 06 p0775 N88-14759
The origin of the spicule skeleton of fresh water sponges (Spongillides) 07 p0885 N88-15368
Limb regeneration in amphibians, a suitable model for investigations of the effects of weightlessness as regards evolution and modifications 07 p0885 N88-15369
Evolution from pure states into mixed states in de Sitter space
| DE88-750316 | 07 p0945 N88-15745
Morphological manifestations of primate adaptation to orthograde statics and walking erect 10 p1366 N88-18162
Five New South Wales barrier lagoons: Their macrobenthic fauna and seagrass communities 11 p1517 N88-19059
Cometary evolution: Clues from chondritic interplanetary dust particles 14 p2002 N88-21934
Crustal models of the evolving comet nucleus 14 p2005 N88-21953
Diversity of comets, synergic temperature effects and the stability of organic compounds in icy nuclei 14 p2005 N88-21955
The structure of the Halley meteor stream and the orbital history of the comet 14 p2008 N88-21975
The mass loss rates of periodic comets 14 p2010 N88-21991
Aerial photography as an instrument of municipal and regional planning: Metropolitan area of Sao Paulo (SP) 19 p2684 N88-25957
Embryonic development of the newt Cynops pyrrhogaster in very weak magnetic fields
| ISAS-RN-357 | 19 p2702 N88-26068
Cometary nucleus as aggregate of planetesimals
| ISAS-RN-364 | 19 p2741 N88-26275
Evolution of hairpin vortices in a shear flow
| NASA-TM-100858 | 20 p2845 N88-26885
Dynamical evolution of cosmic strings
| DE88-011724 | 21 p3030 N88-27989
Intercrater plains deposits and the origin of Martian valleys 23 p3301 N88-29661
Volcano evolution on Mars 23 p3305 N88-29686
Mid to late proterozoic magmatism within Northeastern North America and its iplications for the growth of the continental crust 24 p3397 N88-30229
Thermal models pertaining to continental growth 24 p3397 N88-30230
Ridge-trench collision in Archean and Post-Archean crustal growth: Evidence from southern Chile 24 p3397 N88-30233
Archean crustal evolution of the northern North China Craton 24 p3398 N88-30235
Growth of the lower continental crust 24 p3398 N88-30236
The complexity, depth, and rapidity of processes that formed the lunar crust 24 p3398 N88-30237
Geochronological and lead-isotope evidences for rapid crust formation in middle-proterozoic time: The Labrador example 24 p3398 N88-30239
Physical processes in the growth of the continental crust 24 p3398 N88-30240
Evolution of the Dharwar Craton: A terrain of early Archean crustal stability, long term orogenic cycles and large scale palaeobiological activity 24 p3399 N88-30241
Lithospheric evolution of the Northern Arabian Shield: Chemical and isotopic evidence from basalts, xenoliths and granites 24 p3399 N88-30242

Trace element differences between Archean, Proterozoic and Phanerozoic crustal components: implications for crustal growth processes
24 p3399 N88-30243

Continental growth through time by underplating of subducted oceanic crust: Evidence from kimberlites in South Africa and SW Pacific 24 p3399 N88-30244

Growth of planetary crusts 24 p3400 N88-30247

Mineralization through geologic time: Evolution of continental crust 24 p3400 N88-30250

Volcanic contribution to crustal growth in the Central Andes: A new estimate and a discussion of uncertainties
24 p3401 N88-30255

A compilation of information and data on the Manson impact structure
|NASA-CR-183169| 24 p3401 N88-30258

Noble gases, C,N, and Si isotopes in interstellar SiC form the Murchison carbonaceous chondrite
24 p3442 N88-30483

Observations of star formation
24 p3451 N88-30538

Nebular processes recorded in chondritic meteorites
24 p3451 N88-30541

EVOLUTION (LIBERATION)
NT GAS EVOLUTION

EXACTNESS
U PRECISION

EXCHANGING
NT CHARGE EXCHANGE
NT GAS EXCHANGE
NT ION EXCHANGING
NT RESONANCE CHARGE EXCHANGE

Lower-stratospheric/upper-tropospheric exchange processes associated with tropical cyclones as observed by TOMS 05 p0616 N88-13782

EXCIMER LASERS

XeCl excimer laser with magnetic compressor
03 p0299 N88-11879

JPRS report: Science and technology. China
|JPRS-CST-87-031| 03 p0299 N88-11880

JPRS report: Science and technology. China
|JPRS-CST-87-034| 03 p0301 N88-11897

A 10 W transverse flow excimer laser
03 p0302 N88-11901

Excimer laser cell with longitudinal electron-beam excitation 03 p0302 N88-11903

JPRS Report: Science and Technology. China
|JPRS-CST-87-033| 03 p0326 N88-12062

Operational performance of repetitive KrF, XeCl excimer lasers 03 p0327 N88-12068

Gas flow effects in pulse avalanche discharge XeCl excimer lasers 03 p0328 N88-12070

Narrow linewidth gain measurements in a KrF excimer amplifier pumped longitudinally by a high-power electron beam
|DE88-001365| 05 p0586 N88-13575

Photocurrent generation from basic metals, utilizing a short pulsed ArF excimer laser
|AD-A184928| 05 p0587 N88-13579

Anti-Stokes generation of 226 nm light
|DE88-001612| 05 p0589 N88-13590

Chemical analysis for excimer laser systems
|DE88-001941| 05 p0589 N88-13591

Laser development, evolution of applied technologies described 06 p0689 N88-14221

Periodically pulsed excimer master oscillator-regenerative amplifier laser set
06 p0772 N88-14741

Studies on nonlinear mechanisms of excimer laser propagation in fused silica fibers
|AD-A186822| 09 p1156 N88-16929

Where directed energy stands in strategic defense
|DE88-005092| 10 p1403 N88-18365

Practical constraints on sources for pulsed beam lithographies
|DE88-006594| 13 p1776 N88-20823

XeF excimer laser pumped by high-intensity relativistic electron beam 14 p1901 N88-21355

Folded long-pulse XeCl excimer laser described
14 p1901 N88-21357

Kinetics of slow electrons in excimer laser with electron-beam pumping 14 p1970 N88-21760

Effects of emission energy transient in periodic-pulse XeCl excimer laser of approximately 400 W average power 14 p1971 N88-21763

Laser processing-status, perspectives
15 p2050 N88-22211

Numerical modelling specific energy charcteristics of excimer KrF lasers with electron beam excitation
|DE88-701525| 15 p2070 N88-22344

Alkali metal diffuse band lasers
|AD-A190244| 15 p2071 N88-22350

Thin film research diagnostics instrumentation
|AD-A191240| 16 p2213 N88-23207

Theoretical calculations of XeF ground state kinetics
|AD-A191398| 16 p2270 N88-23580

Realization of an XeCl laser producing 100W on average
|ETN-88-92541| 17 p2344 N88-23970

Aurora status and plans
|DE88-006476| 18 p2521 N88-24955

Use of magnetic materials in excimer laser circuits
|DE88-006449| 19 p2674 N88-25903

Systematics of excimer laser ablation: Thin film preparation of high T(sub c) material
|DE88-010569| 19 p2675 N88-25909

Laser and electrochemical studies of metallizations in electronic devices
|AD-A193786| 23 p3208 N88-29090

EXCIMERS

Excimer laser-assisted deposition of GaAs, AlAs and (Al,Ga)As from Lewis acid-base adducts
|AD-A184588| 03 p0329 N88-12081

Energy disposal in ion-molecule reactions
|AD-A186772| 09 p1171 N88-17019

Excimer plasma displays
|AD-A186731| 09 p1250 N88-17489

EXCITATION
NT ACOUSTIC EXCITATION
NT ATOMIC EXCITATIONS
NT HARMONIC EXCITATION
NT MOLECULAR EXCITATION
NT SELF EXCITATION
NT WAVE EXCITATION

KR+ laser excitation of NH2 in atmospheric pressure flames
|AD-A183421| 01 p0050 N88-10322

IR laser excitation in molecules: Chaos and diffusive energy growth
|DE87-013147| 02 p0178 N88-11105

Excimer laser cell with longitudinal electron-beam excitation 03 p0302 N88-11903

Excitation of natural oscillations of a boundary layer by an external acoustic field 04 p0425 N88-12634

An excitation-term modification for a certain class of electromagnetic aperture-coupling problems
|DE88-000260| 04 p0437 N88-12713

Alternating current circuit theory and pulsed NMR (Nuclear Magnetic Resonance)
|DE88-000641| 04 p0440 N88-12732

J = O Task Force
|DE88-001326| 04 p0450 N88-12788

Thermomechanical cracking in coated media due to high speed asperity excitation
|AD-A184176| 04 p0454 N88-12809

Mechanical shock test specification using nonstationary random excitation models
|DE87-013650| 04 p0454 N88-12812

Vibration and parametric excitation in rotating asymmetric circular plates 04 p0456 N88-12823

Implementation of a new shock testing procedure using nonstationary random excitation
|DE87-014643| 04 p0456 N88-12827

Nitrogen energy transfer study
|AD-A184457| 04 p0464 N88-12869

On the glitches in the force transmitted by an electrodynamic exciter to a structure
05 p0594 N88-13624

Blade excitation due to unsteady flow phenomena
07 p0851 N88-15167

The Coupled Cluster Single and Double excitation (CCSD) method in quantum chemistry: An efficient formulation of the theory and application to closed shell molecular systems
|DE88-000475| 07 p0930 N88-15650

The effect of propane on atomic spectrometric signals in the direct current plasma
|DE88-002457| 07 p0934 N88-15676

Fully turbulent internal flow excitation of pipe systems
08 p1000 N88-16056

Nuclear excitation via the motion of electrons in a strong laser field
|AD-A187166| 09 p1171 N88-17017

Photoionization dynamics of excited molecular states
|DE88-002982| 09 p1246 N88-17468

Atomic data for hydrogens in collisions with electrons: Addenda
|IPPJ-AM-55-ADD| 09 p1252 N88-17502

Memory effects on infrared adsorbate spectra
|AD-A186976| 09 p1253 N88-17512

Frequency response function estimation at level
|DE88-002644| 10 p1344 N88-18034

Correlated processes in atomic collisions
|DE88-003508| 10 p1406 N88-18383

Electronic structure, charge transfer excitations and high temperature superconductivity
|DE88-003096| 10 p1416 N88-18453

Experimental aspects of hypernuclear physics at CEBAF
|CEBAF-R-86-013| 11 p1546 N88-19245

Presentations to the SuperHILAC Program Advisory Committee
|DE88-003853| 11 p1547 N88-19256

Picosecond laser studies of excited state processes
|AD-A189606| 12 p1607 N88-19607

Reactions of N2(A(3)(SIGMA)/sub u/(+)) and candidates for short wavelength lasers
|DE88-005366| 12 p1632 N88-19767

Discharge excitation of dye vapors
|AD-A188428| 12 p1632 N88-19770

QED description of relativistic Coulomb excitation in heavy ion collisions
|DE88-700834| 12 p1689 N88-20100

Seasonal variations and excitation mechanisms of the equatorially trapped waves 13 p1798 N88-20751

Image charge, coherent scattering, and symmetry effects in electron stimulated desorption: O(-) from O sub 2 condensed on metals
|AD-A189093| 13 p1835 N88-20979

The magnitude of secondary electron contributions in photon stimulated desorption
|AD-A189094| 13 p1835 N88-20980

Electronic energy transfer processes in the alkali/alkaline earth metal vapors
|AD-A190035| 15 p2034 N88-22119

Discharge excitation of the XeF C to A transition
|DE88-006448| 15 p2070 N88-22339

Numerical modelling specific energy charcteristics of excimer KrF lasers with electron beam excitation
|DE88-701525| 15 p2070 N88-22344

Effect of vibrational excitation on rate parameters of atmospheric reactions
|AD-A190454| 15 p2094 N88-22477

Sequential excitation preparation of molecular energy levels with special structural and chemical properties
|AD-A190041| 15 p2132 N88-22718

Effective electron interactions due to virtual charge and spin excitations in an extended Hubbard model for Cu-O superconductors
|DE88-005971| 15 p2139 N88-22766

First-principles calculations of quasiparticle energies at surfaces and interfaces: Semiconductor surface-state spectra and band offsets
|DE88-006340| 15 p2141 N88-22773

The effect of internal relaxation on optoacoustic conversion in liquids
|AD-A191307| 16 p2176 N88-22970

Saturation and the limit of jet mixing enhancement by single frequency plane wave excitation: Experiment and theory
|NASA-TM-100882| 17 p2295 N88-23732

Search for bound states of the eta-meson in light nuclei 17 p2397 N88-24248

Robust adaptive regulation without persistent excitation
|NASA-TM-100571| 18 p2561 N88-25204

Trochoidal analysis of scattered electrons in a merged electron-ion beam
|NASA-CASE-NPO-16789-1-CU|
18 p2573 N88-25281

Optical properties of heterostructures and superlattices
|AD-A191542| 18 p2581 N88-25335

Direct subpicosecond measurement of carrier mobility of photoexcited electrons in GaAs
19 p2659 N88-25803

Longitudinally localized optical carrier injection for femtosecond transport studies 19 p2659 N88-25806

Dynamics of below-gap photoexcitation in GaAs quantum wells 19 p2660 N88-25815

Enhancement of volume H(-) production by vibrationally pre-exciting the hydrogen molecules
|DE88-010783| 20 p2853 N88-26937

Magnetic excitations in transition metal systems
|DE88-011022| 21 p2912 N88-27279

Inelastic electron scattering and electron-hole excitations in iron and nickel
|DE88-011843| 21 p2915 N88-27303

Picosecond optoelectronic sampling of electrical waveforms produced by an optically excited field effect transistor
|AD-A192384| 21 p2935 N88-27428

Nonlinear stochastic interaction in aeroelastic structures
|AD-A193427| 21 p2961 N88-27589

Evidence for laser emission from the TICT exciplex of coumarin dyes
|DE88-702544| 23 p3220 N88-29167

Investigation of non-classical effects in two-photon interference processes 23 p3282 N88-29541

Localized excitations in one-dimensional molecular crystal with structural defect
|DE88-702691| 23 p3293 N88-29607

Localized excitations in one-dimensional molecular crystal with structural defect
|DE88-702691| 23 p3293 N88-29607

EXCITED STATES
U EXCITATION
EXCITONS
A physico-chemical study of some areas of fundamental significance to biophysics
|DE87-013457| 02 p0217 N88-11365
Novel dynamical investigations of excitons and their structure in semiconductors
|DE87-014868| 04 p0499 N88-13070
Enhanced excitonic optical nonlinearity and exciton dynamics in semiconductor microstructures
14 p1977 N88-21795
Dynamical aspects of carrier tunneling in semiconductor superlattices 14 p1977 N88-21799
Experimental and theoretical studies of coherent and nonthermal processes in semiconductors probed by femtosecond laser techniques 14 p1977 N88-21800
Exciton relaxation phenomena in a disordered system
14 p1978 N88-21802
Nonlinear optical properties and subpicosecond dynamics of excitons and electron-hole plasmas in multiple quantum well structures
|AD-A191926| 19 p2727 N88-26196
Excitonic properties of GaAs-AlGaAs nanostructures
20 p2867 N88-27023
Laser spectroscopy of quantum well and superlattice structures
|AD-A193336| 21 p3022 N88-27937
EXCLUSION
Markov chain computations to a solution of the mutual-exclusion problem in concurrency
|REPT-87-89| 20 p2847 N88-26896
EXCRETION
Biorhythmic aspects of intercontinental Antarctic adaptation 08 p1046 N88-16321
EXECUTIVE AIRCRAFT
U GENERAL AVIATION AIRCRAFT
U PASSENGER AIRCRAFT
EXECUTIVE SYSTEMS (COMPUTERS)
U OPERATING SYSTEMS (COMPUTERS)
EXERCISE
U PHYSICAL EXERCISE
EXERCISE PHYSIOLOGY
Oxygen transport during exercise at extreme simulated altitude: Operation Everest 2
|AD-A185720| 06 p0752 N88-14620
Influence of a 6 hr head-out water immersion on different tests of endurance performance capacity
12 p1653 N88-19903
P-31 Magnetic Resonance Spectroscopy (MRS) of limb muscles during bedrest with exercise countermeasures
12 p1656 N88-19925
Effects of anti-g suit inflation on renin and aldosterone response physical exercise 12 p1659 N88-19944
A new isodynamically-braked arm ergometer including the demonstration of a prototype
12 p1661 N88-19957
Fish as a tool for testing fitness in space
12 p1662 N88-19963
Endocrine responses to resistance exercise
|AD-A188681| 12 p1667 N88-19993
Hormonal regulation of fluid and electrolytes: Effects of heat exposure and exercise in the heat
|AD-A192655| 22 p3131 N88-28614
Effects of air polution on human exercise performance
|AD-A192660| 22 p3131 N88-28617
Gastric emptying during walking and running: Effects of varied exercise intensity
|AD-A194025| 23 p3240 N88-29281
EXERTION
U PHYSICAL WORK
EXHAUST EMISSION
Adiabatic diesel engine component development: Reference engine for on-highway applications
|NASA-CR-179531| 03 p0386 N88-12428
Summary and analysis of comments on the recommended practice for the measurement of refueling emissions
|PB88-101530| 07 p0876 N88-15313
Aircraft emissions characterization: TF41-A2, TF30-P103 and TF30-P109 engines
|AD-A192053| 18 p2466 N88-24638
A 3 MW wood fired gas turbine at Red Boiling Springs, Tennessee 18 p2536 N88-25051
Motor vehicles as sources of compounds important to tropospheric and stratospheric ozone
|PB88-195219| 18 p2540 N88-25076
Initial testing of the tunable diode laser absorption spectrometer for measuring HNO3 in diesel engine exhaust, stage 2
|PB88-193073| 21 p2970 N88-27641
EXHAUST FLOW SIMULATION
Investigation of the effect of laterally ejected gas jets on flows
|ISL-R-107/86| 05 p0581 N88-13545
Split-coefficient matrix solution and experimental study of axisymmetric underexpanded exhaust plumes
15 p2054 N88-22242
EXHAUST GASES
Boundary layer profile investigations downstream of an aero-engine intake anti-icing air exhaust slot
|PNR90378| 02 p0171 N88-11080
The determination of exhaust cloud dimensions from films of space shuttle launches
|NASA-CR-4103| 06 p0732 N88-14500
Hydrogen chloride measurements in launch-vehicle exhaust clouds
|DE87-011552| 08 p0964 N88-15837
Exhaust-gas pressure and temperature survey of F404-GE-400 turbofan engine
|NASA-TM-88273| 13 p1724 N88-20307
An experimental investigation of an arcjet thruster exhaust using Langmuir probes
|NASA-TM-100258| 14 p1883 N88-21253
Investigation of aeroacoustic mechanisms by remote thermal imaging
|DE88-002612| 15 p2021 N88-22046
An experimental investigation of rocket ramjet nozzle assembly base pressures
|AD-A189714| 15 p2027 N88-22076
Split-coefficient matrix solution and experimental study of axisymmetric underexpanded exhaust plumes
15 p2054 N88-22242
Aircraft emissions characterization: TF41-A2, TF30-P103 and TF30-P109 engines
|AD-A192053| 18 p2466 N88-24638
Techniques utilized in the simulated altitude testing of a 2D-CD vectoring and reversing nozzle
|NASA-TM-100872| 19 p2604 N88-25464
EXHAUST JETS
U EXHAUST GASES
EXHAUST NOZZLES
NT CONVERGENT-DIVERGENT NOZZLES
Hydroburst test of a carbon-carbon involute exit cone
|NASA-TP-2556| 06 p0671 N88-14112
An experimental and numerical investigation of swirling flows in a rectangular nozzle 06 p0700 N88-14295
Advanced Technology for Aero Gas Turbine Components
|AGARD-CP-421| 10 p1279 N88-17647
Experimental evaluation of a translating nozzle sidewall radial turbine 10 p1280 N88-17656
A computational study of thrust augmenting ejectors based on a viscous-inviscid approach
10 p1326 N88-17929
Exhaust-gas pressure and temperature survey of F404-GE-400 turbofan engine
|NASA-TM-88273| 13 p1724 N88-20307
Variable Mach number wall jets for control/propulsion on hypervelocity projectiles/interceptors: Tests with an existing model
|AD-A192845| 21 p2892 N88-27167
Application of laser diffraction techniques to particle sizing in solid propellant rocket motors
|AD-A193841| 22 p3049 N88-28089
Numerical simulation of nozzle flows
|AD-A195144| 24 p3369 N88-30064
EXHAUST SYSTEMS
Adiabatic diesel engine component development: Reference engine for on-highway applications
|NASA-CR-179531| 03 p0386 N88-12428
EXHAUSTION
Metabolic and cardiorespiratory parameters during three consecutive days of exhaustive running
|AD-A192598| 21 p2985 N88-27728
EXISTENCE THEOREMS
Existence and stability of transition layers
|AD-A185806| 06 p0766 N88-14707
On a class of similarity solutions of the equation u sub t (absolute value of u sup m-1 u sub x) sub x with m greater than -1
|REPT-87-54| 14 p1963 N88-21713
EXITS (DOORS)
U DOORS
EXOBIOLOGY
Preliminary study of a gravitational biology facility for Columbus, executive summary
|MATRA-EPT/AS/VT209/255/NT|
01 p0032 N88-10205
Aquarack: Aims and Possible Research Projects
|DFVLR-MITT-87-01| 01 p0073 N88-10469
The Aquarack as a potential instrument for basic research work in space biology: Inventory and scientific dispositions 01 p0073 N88-10470
Life support systems for biological experiments under weightlessness in the German and European space programs 01 p0074 N88-10477
Aerospace medicine and biology: A continuing bibliography with indexes
|NASA-SP-7011(303)| 02 p0217 N88-11367
Environmental life support system technology study --- space flight
|ESA-CR(P)-2432| 02 p0218 N88-11371
Aerospace medicine and biology: A continuing bibliography with indexes
|NASA-SP-7011(304)| 04 p0474 N88-12922
Aerospace medicine and biology: A continuing bibliography with indexes (supplement 305)
|NASA-SP-7011(305)| 06 p0752 N88-14616
Exobiology and life science 07 p0883 N88-15358
Proceedings and program draft in Gravitational Biology in the Federal Republic of Germany --- Effects of Weightlessness on the Human Organism
|ESA-TT-988| 07 p0884 N88-15363
Some remarks on gravitational biology
07 p0884 N88-15366
JPRS report: Science and technology. USSR: Space Biology and Aerospace Medicine, volume 21, no. 3, May - June 1987
|JPRS-USB-88-001| 07 p0889 N88-15389
JPRS report: Science and technology. USSR: Space Biology and Aerospace Medicine, volume 21, no. 4, July - August 1987
|JPRS-USB-88-002| 07 p0893 N88-15412
Bibliography of space biology and medicine
07 p0897 N88-15435
JPRS report: Science and technology. USSR: Space
|JPRS-USP-87-006| 08 p1001 N88-16063
Space biology and medicine 08 p1006 N88-16096
Life sciences experiments on stratospheric balloons and sounding rockets 08 p1033 N88-16262
The D-1 Biorack results: A base for further space biological investigations 08 p1033 N88-16263
Contribution of stratospheric balloon flights in space biology 08 p1033 N88-16266
USSR Space Life Sciences Digest, issue 14
|NASA-CR-3922(16)| 08 p1045 N88-16317
Aerospace medicine and biology: A continuing bibliography with indexes (supplement 307)
|NASA-SP-7011(307)| 08 p1049 N88-16332
Publications of the exobiology program for 1986: A special bibliography
|NASA-TM-4029| 09 p1203 N88-17205
Present stage of space medicine
10 p1364 N88-18151
NASA Workshop on Biological Adaptation
|NASA-TM-89468| 10 p1368 N88-18174
USSR Space Life Sciences Digest, issue 15
|NASA-CR-3922(18)| 10 p1368 N88-18175
Aerospace medicine and biology: A cumulative index to a continuing bibliography (supplement 306)
|NASA-SP-7011(306)| 10 p1369 N88-18180
Aerospace medicine and biology: A continuing bibliography with indexes (supplement 308)
|NASA-SP-7011(308)| 10 p1369 N88-18183
Genetic research in space
|NASA-TT-20216| 11 p1518 N88-19066
The ESA facility Biorack 12 p1652 N88-19897
Exobiology and botany facilities for EURECA
12 p1652 N88-19898
BIOTEX, a project for biotechnological basic experiments under microgravity --- Spacelab
12 p1652 N88-19899
Life science techonology --- space applications
12 p1653 N88-19900
Plant biology in space 12 p1654 N88-19910
Plant cell cultures in space biology studies
12 p1654 N88-19913
The use of plant protoplasts in biotechnological space research 12 p1655 N88-19914
Ecological algal system in microgravity conditions: Preliminary results 12 p1655 N88-19915
Closed system physiology: Role of oxygen in the development of wheat 12 p1655 N88-19916
Aspects of bioregenerative life support systems
12 p1655 N88-19917
European activities in exobiological research in space
12 p1657 N88-19929
Survival under space vacuum: Biochemical aspects
12 p1657 N88-19930
Ultraviolet (180 to 300 nm) action spectra for inactivation and DNA photoproduct formation of Bacillus subtilis spores under ultrahigh vacuum 12 p1657 N88-19931
Survival and mutation induction of dehydrated yeast cells after UV exposure 12 p1657 N88-19932
Cellular effects of heavy ions: Experimental results and theoretical approaches --- space radiation
12 p1658 N88-19933
Effects of heavy ions on egg-developing systems
12 p1658 N88-19935
Medilab: A project of a medical laboratory in space
12 p1660 N88-19946
Cell cultures in space: From basic research to biotechnology 2 12 p1660 N88-19948

Cyropreservation of isolated rat hepathocytes for future use in Spacelab experiments: Preliminary results
12 p1660 N88-19950
Organs and tissues regeneration in amphibia under the space flight conditions 12 p1660 N88-19951
Antibiotic activity in space, results and hypothesis
12 p1660 N88-19952
Biorack experiments in Spacelab D-1 and TML-1: Further developments in gravitational biology
12 p1661 N88-19953
Why life science in space? The next step to go beyond 12 p1661 N88-19954
Aerospace medicine and biology: A continuing bibliography with indexes (supplement 309)
|NASA-SP-7011(309)| 13 p1810 N88-20814
USSR Space Life Sciences Digest, issue 16
|NASA-CR-3922(19)| 15 p2101 N88-22515
Aerospace medicine and biology: A continuing bibliography with indexes (supplement 310)
|NASA-SP-7011(310)| 16 p2238 N88-23369
Botany Facility pre-phase C/D. Core payload for EURECA, volume 1
|BF-RP-ER-015-VOL-1| 17 p2379 N88-24144
USSR Space Life Sciences Digest, issue 17
|NASA-CR-3922(20)| 17 p2381 N88-24155
Aerospace medicine and biology: A continuing bibliography with indexes (supplement 311)
|NASA-SP-7011(311)| 17 p2382 N88-24161
Aerospace medicine and biology: A continuing bibliography with indexes (supplement 312)
|NASA-SP-7011(312)| 18 p2551 N88-25141
JPRS report: Science and technology. USSR: Space Biology and Aerospace Medicine, volume 22, no. 1, January - February 1988
|JPRS-USB-88-005| 19 p2702 N88-26069
Macaca rhesus tolerance to +Gz accelerations
19 p2704 N88-26080
USSR space life sciences digest, issue 18
|NASA-CR-3922(21)| 19 p2707 N88-26096
Aerospace medicine and biology: A continuing bibliography with indexes (supplement 313)
|NASA-SP-7011(313)| 20 p2832 N88-26800
Aerospace Medicine and Biology: A continuing bibliography with indexes (supplement 314)
|NASA-SP-7011(314)| 21 p2988 N88-27742
Biorack on Spacelab D1: An overview of the first flight of Biorack, an ESA facility for life sciences research in microgravity
|ESA-SP-1091| 22 p3059 N88-28154
A brief overview of the results of the experiments using the ESA Biorack Facility on the German Spacelab D1 mission 22 p3060 N88-28155
The Biorack facility and its performance during the D1 Spacelab mission 22 p3060 N88-28156
The effects of microgravity on genetic recombination in Escherichia coli --- Spacelab D1 mission
22 p3060 N88-28157
Growth and differentiation of Bacillus subtilis under microgravity conditions 22 p3060 N88-28158
The Antibio experiment --- Spacelab D1 mission
22 p3060 N88-28159
Contraction behavior and protoplasmic streaming in the slime mold Physarum polycephalum (Physarum kinetics) --- Spacelab D1 mission 22 p3060 N88-28160
The Paramecium experiment --- Spacelab D1 mission
22 p3060 N88-28161
The biological clock of Chlamydomonas reinhardii in space 22 p3061 N88-28162
Effect of microgravity on lymphocyte activation --- Spacelab D1 mission 22 p3061 N88-28163
The effect of microgravity on mammalian cell polarization at the ultrastructural level --- Spacelab D1 mission
22 p3061 N88-28164
Graviperception of lentil seedling roots grown in space
22 p3061 N88-28165
Effects of short spaceflights on Drosophila melanogaster embryogenesis and life span 22 p3061 N88-28166
Embryogenesis and organogenesis of Carausius morosus under spaceflight conditions
22 p3061 N88-28167
The role of gravity in the establishment of the dorso/ventral axis in the amphibian embryo --- Spacelab D1 mission 22 p3062 N88-28168
Dosimetric mapping inside Biorack --- Spacelab D1 mission 22 p3062 N88-28169
Biorack thermal performance during the D1 mission --- Spacelab 22 p3062 N88-28170
Biosample: Preservation, handling and observation system synthesis and breadboarding --- Spacelab
|ESA-CR(P)-2609| 24 p3336 N88-29857
Aerospace medicine and biology: A continuing bibliography with indexes (supplement 315)
|NASA-SP-7011(315)| 24 p3407 N88-30281

EXOSAT SATELLITE
The X-ray orbital lightcurves of AR Lac and TY Pyx
04 p0509 N88-13129
Evidence for expanding magnetic loops in coronae of cool stars 04 p0510 N88-13134
Exosat results on the dMe flare Star Wolf 630AB and on VB 8 04 p0512 N88-13151
Investigation of nuclei of active galaxies as well as sources in the Large Magellanic Cloud using the X-ray astronomy satellite EXOSAT
|ETN-88-91494| 11 p1570 N88-19399
The 35-day cycle of Hercules X-1
|MPE-204| 11 p1571 N88-19405
EXOSAT observations of active galaxies in the medium-energy X-ray domain
|ETN-88-91499| 14 p1993 N88-21879
SW UMa and V426 Oph: EXOSAT surprises
19 p2740 N88-26269
EXOSAT observations of Hercules X-1
|MPE-PREPRINT-119| 22 p3164 N88-28841

EXOTHERMIC REACTIONS
Hot-spot reaction in unsustained shocks
|DE87-011781| 01 p0044 N88-10277
The carbon dioxide chaperon efficiency for the reaction H + O2 + M yields HO2 + M from ignition delay times behind reflected shock waves
|NASA-TM-100125| 07 p0830 N88-15036

EXPANDABLE STRUCTURES
NT BALLOONS
NT GAS BAGS
NT HIGH ALTITUDE BALLOONS
NT INFLATABLE STRUCTURES
NT JIMSPHERE BALLOONS
Assessment of the COFSI/MAST I project
|NASA-CR-181366| 01 p0053 N88-10340

EXPANSION
NT GAS EXPANSION
NT SERIES EXPANSION
NT THERMAL EXPANSION
The expansion of magnetic clouds
01 p0115 N88-10737
Singularity expansion method: Target Resonances
03 p0303 N88-11912
Cosmology with decaying vacuum energy
|DE88-000698| 03 p0389 N88-12443
Pulse-mode expansions and refractive indices in plane-wave propagation
|DE88-001328| 04 p0437 N88-12714
Qualification of expansion and joint welding procedures of tube-to-tubesheet joints for heat exchangers in nuclear power plants
|DE87-703526| 05 p0589 N88-13592
Bubble expansion and collapse studies
|DE88-002377| 06 p0699 N88-14290
A directed method for locating the focus of expansion
|AD-A185840| 07 p0906 N88-15491
Harmonic expansion for the magnetic field of the helical solenoid
|DE88-700100| 07 p0928 N88-15638
Post-Newtonian equations of motion in an expanding universe
|DE88-750303| 07 p0945 N88-15744
Evolution from pure states into mixed states in de Sitter space
|DE88-750316| 07 p0945 N88-15745
Calculation of the flow through a single-sided sudden expansion with the Computer Program for Parabolic and Elliptic Flows (COPPEF) computer program
|VTH-LR-523| 09 p1163 N88-16973
Asymptotic expansions for large deviation probabilities in the strong law of large numbers
|AD-A187432| 10 p1402 N88-18361
Piston-driven, unsteady separation at a sudden expansion in a tube: Flow visualization and Laser Doppler Anemometer (LDA) measurements
|ETN-88-92104| 15 p2068 N88-22329
String driven inflation
|DE88-006994| 15 p2151 N88-22841
Cosmology for high energy physicists
|DE88-005705| 15 p2151 N88-22842
Self-similar expansions in ion beam fusion
16 p2278 N88-23635
Dynamic range compression/expansion of light beams by photorefractive crystals
|NASA-CASE-NPO-17140-1-CU|
17 p2438 N88-24508
Turbulent heat transfer and fluid flow measurements downstream of abrupt expansions and in a cavity of a circular tube at a uniform wall temperature
18 p2515 N88-24920
The Department of Defense report on the merit review process for competitive selection of university research projects and an analysis of the potential for expanding the geographic distribution of research for the Committees on Appropriations, United States Congress
|AD-A191842| 18 p2588 N88-25379
Non equilibrium expansion of a radiating gas in a channel of varying section
|DE88-702063| 19 p2665 N88-25845
An interferometric measurement technique for railgun structures
|AD-A192851| 21 p2901 N88-27217
Perturbation expansions generated by an approximate propagator
|DE88-702435| 21 p3011 N88-27866
Velocity measurements downstream of a sudden expansion using the Laser Doppler Velocimeters (LDV) technique. Part 1: Method of measurement and experimental facility
|FOA-C-20700-2.1-PT-1| 22 p3076 N88-28262
Performance of the Los Alamos expanding telescope
|DE88-010924| 22 p3151 N88-28751
Qualification of expansion and welding procedures of tube-to-tubesheet joints for heat exchangers in nuclear power plants
|DE88-701621| 23 p3221 N88-29174
Cosmology in an N-dimensional vector space
|DE88-702550| 23 p3277 N88-29507

EXPANSION WAVES
U ELASTIC WAVES

EXPECTANCY HYPOTHESIS
Object detection in images from outdoor scenes using evidential reasoning
|FOA-C-30461-3.3| 08 p1020 N88-16183

EXPECTATION
Expectations for water level deviations at the delta works: Zierikzee (Netherlands), November 1981-February 1986
|KNMI-TR-93| 05 p0628 N88-13840
Strong consistency of estimation of number of regression variables when the errors are independent and their expectations are not equal to each other
|AD-A186025| 07 p0909 N88-15507
On the expectation of the product of four matrix-valued Gaussian random variables
|EUT-87-E-178| 13 p1828 N88-20927

EXPEDITIONS
Huurre expedition to the North Pole in 1984
|PB87-220935| 04 p0462 N88-12858
Varifront 3 expedition data report (USNS DE STEIGUER CRUISE 1202-82). Bioluminescence, hydrographic, nutrient, and satellite data from the Gulf of California (November-December 1981)
|AD-A185011| 05 p0620 N88-13805
Risk of hypertension and functional cerebral laterality in oil expedition works in far north
12 p1665 N88-19980
Physical, chemical and CTD (Conductivity/Temperature/Depth) data from the Marathon 2 expedition
|AD-A189930| 15 p2099 N88-22507

EXPENDABLE STAGES (SPACECRAFT)
Communications satellite systems operations with the space station. Volume 3: Supplementary technical report
|NASA-CR-180875| 09 p1133 N88-16794
Assessment of mixed fleet potential for space station launch and assembly
|NASA-TM-100550| 11 p1443 N88-18608

EXPERIENCE
Diagnosis: Reasoning from first principles and experiential knowledge 09 p1207 N88-17236

EXPERIMENT DESIGN
NT FACTORIAL DESIGN
Preliminary study of a containerless processing facility for Columbus, executive summary
|ESA-ITT/AO/1-1834/85F| 01 p0032 N88-10203
Investigations of the survey of the reproductive biology of Xiphophorus in an Aquarack
01 p0074 N88-10471
Control design challenges of large space systems and spacecraft control laboratory experiment (SCOLE)
|NASA-CR-178392| 03 p0275 N88-11735
Access to microgravity: A technical description of the NAE T-33 microgravity facility
|NAE-AN-47| 04 p0405 N88-12518
Experimental use of artificial intelligence for (future) ATC systems
|PB87-106449| 04 p0482 N88-12970
Controlled Ecological Life Support System. Design, Development, and Use of a Ground-Based Plant Growth Module
|NASA-CP-2479| 05 p0630 N88-13852
CELSS Program Meeting 05 p0630 N88-13853
Controlled ecological life support systems: Development of a plant growth module 05 p0630 N88-13854
CP-1-H analysis tests 06 p0691 N88-14236
The standard theory group: Summary and conclusions
|PREPRINT-551| 06 p0778 N88-14776
A possible accelerator experiment to solve the solar neutrino puzzle
|PREPRINT-556| 06 p0778 N88-14778
Overview of the TIBER 2 (Thermal Ignition/Burn Experimental Reactor) design
|DE88-001892| 06 p0783 N88-14804

Allowable gravity-levels for Spacelab, Columbus and EURECA --- materials science
| BF-R-66.525-2 | 07 p0838 N88-15084
Optimal repeated measurements designs for comparing test treatments with a control
| AD-A185999 | 07 p0917 N88-15569
Tether Elevator Crawler Systems (TECS)
07 p0927 N88-15631
The ESA Anthrorack project: Integrated research in human physiology 08 p1033 N88-16265
Basic physics program for a low energy antiproton source in North America
| DE88-003148 | 08 p1082 N88-16522
Microphysics of the auroral acceleration region of other regions of the magnetosphere 08 p1096 N88-16592
Microgravity payloads and missions for Space Station: Some issues affecting compatibility with other payloads
09 p1129 N88-16783
The challenge of G-376 10 p1288 N88-17705
The NORSTAR Program: Space shuttle to space station 10 p1289 N88-17710
Annotated computer output for split plot design: GENSTAT ANOVA
| AD-A187120 | 10 p1385 N88-18271
Experimental aspects of hypernuclear physics at CEBAF
| CEBAF-R-86-013 | 11 p1546 N88-19245
Promising concepts for ground-to-orbit experiment teleoperation --- Columbus 12 p1590 N88-19518
Ground based supervisory and programming system for automatic experiment execution in orbit
12 p1590 N88-19519
Life sciences research in space: The requirement for animal models 12 p1654 N88-19909
Implications of shiftwork in space for human physiology experiments 12 p1659 N88-19942
Some reflections on the standardization of bed-rest procedures for weightlessness simulation (cardiovascular and endocrine apsects) 12 p1662 N88-19961
Animal research on the Space Station
12 p1662 N88-19964
Interfacial adhesion: Theory and experiment
| NASA-TM-100830 | 13 p1742 N88-20417
Three-dimensional shear layer experiments and their use as test cases for calculation methods
| NLR-MP-86036-U | 13 p1767 N88-20570
Experimental verification of a finite-difference time-domain thin slot algorithm
| DE88-005572 | 13 p1817 N88-20859
Equipment test methods for externally produced electromagnetic transients
| RAE-TM-FS(F)-457 | 14 p1865 N88-21140
Recommended test specification for the electromagnetic compatibility of aircraft equipment
| RAE-TM-FS(F)-510 | 14 p1867 N88-21155
Efficient monotone sequential design
| CWI-MS-R8705 | 14 p1962 N88-21707
Simulation of cometary nuclei
14 p2005 N88-21954
Short experiment study of four-wire helical antennas (half turn half wave)
| CNES-CT/DRT/TIT/AN-249-T |
15 p2058 N88-22266
Experimental design and structural optimization
| PB88-169255 | 15 p2087 N88-22436
Experimental study on the influence of wind on acoustic pressure sensors
| ISL-R-121/86 | 15 p2131 N88-22712
The German Front Experiment 1987: Experimental design
| DFVLR-MITT-87-24 | 16 p2234 N88-23343
The WOCE Core Project Planning Meeting on the Gyre Dynamics Experiment --- ocean dynamics
| WCP-139 | 16 p2236 N88-23358
Experimental design and structural optimization
| ETN-88-92232 | 16 p2257 N88-23492
Analysis of means in some nonstandard situations
| ETN-88-92247 | 16 p2262 N88-23522
Operational facilities of EURECA A1 mission
| ETN-88-91939 | 18 p2496 N88-24810
Study of flow tracer behavior models and experimental validation with multiple exposure holographic velocimetry
| IMFL-87/30 | 20 p2801 N88-26622
Simulation of the neutronic characteristics of large fast neutron reactors
| ETN-88-92305 | 20 p2853 N88-26940
Fluid physics double rack --- Spacelab
| SD-TN-AI-012 | 24 p3358 N88-29992
Accommodation concept for fluid physics facilities, volume 2 --- Spacelab
| SG-TN-AI-027-VOL-2 | 24 p3358 N88-29994

EXPERIMENTAL AIRCRAFT
U RESEARCH AIRCRAFT

EXPERIMENTAL BREEDER REACTOR 2
Pattern-recognition software detecting the onset of failures in complex systems
| DE88-002861 | 09 p1220 N88-17318

EXPERIMENTATION
NT PHYSICS AND CHEMISTRY EXPERIMENT IN SPACE
Dynamics of spacecraft control laboratory experiment (SCOLE) slew maneuvers
| NASA-CR-4098 | 01 p0014 N88-10082
A plethysmograph for measuring pulmonary ventilation in small animals
| AD-A184978 | 05 p0629 N88-13846
Experimental Radio Data System (RDS): A survey of reception reliability in the UK
| BBC-RD-1987/17 | 09 p1155 N88-16922
On-orbit technology experiment facility definition
| NASA-TM-100614 | 17 p2311 N88-23824
Modeling, designing and simulating a pointing control system for balloon-borne solar experiments
| NASA-TM-100337 | 22 p3082 N88-28300

EXPERT SYSTEMS
Data Model of Objects and Relations (DAMOR): A data model for knowledge representation
| REPT-87-05 | 01 p0085 N88-10553
Knowledge Based Concepts and Artificial Intelligence: Applications to Guidance and Control
| AGARD-LS-155 | 02 p0128 N88-10806
Overview of AGARD Lecture Series No. 155: Knowledge-based concepts and artificial intelligence applications to guidance and control
02 p0128 N88-10807
AI expert system technology issues for guidance and control applications 02 p0128 N88-10808
DEDALE: An expert system for analog circuit maintenance 02 p0128 N88-10809
An expert system for aircraft conflict resolution in dense airspaces 02 p0129 N88-10810
Towards the unmanned cockpit
02 p0129 N88-10812
Generating diagnostic knowledge from a structural and functional description 02 p0129 N88-10813
A review of the knowledge engineering process
02 p0129 N88-10814
A rule-based system for arrival sequencing and scheduling in air traffic control 02 p0129 N88-10815
How to use PROLOG for expert system programming
02 p0129 N88-10816
Real-time expert systems: A status report
02 p0129 N88-10817
Mesoscale thunderstorm forecasting using RAOB data, surface mesonet observations, and an expert system
02 p0206 N88-11293
Contribution to the development of smart design techniques for VLSI integrated circuits --- CMOS
| LAAS-87-181 | 02 p0221 N88-11395
Semantic network processing systems --- artificial intelligence
| OUEL-1677/87 | 02 p0223 N88-11401
Synthesizing controllers for uncertain systems by a quantitative pole-placement
| PB87-195590 | 02 p0223 N88-11403
On the relational modeling of discrete PDE problems
| DE87-013336 | 02 p0224 N88-11409
RANDOM NUMBER: A syntax-directed package to produce random numbers in user-specified, univariate distributions. User's guide
| DE87-014278 | 02 p0228 N88-11436
Knowledge acquisition issues encountered during the development of an estimating expert system
| DE87-013320 | 02 p0248 N88-11568
JPRS report: Science and technology. China
| JPRS-CST-87-026 | 03 p0269 N88-11688
Diagnostics aid for mass spectrometer trouble-shooting
| DE88-000350 | 03 p0324 N88-12049
The user's guide to the BACK system --- knowledge representation
| KIT-42 | 03 p0367 N88-12310
A prototype expert system for separation science
| DE87-013542 | 03 p0371 N88-12333
Potential applications of expert systems and operations research to space station logistics functions
| NASA-CR-180473 | 03 p0372 N88-12342
An evaluation plan of bus architectures and protocols using the NASA Ames intelligent redundant actuation system
| NASA-CR-177458 | 04 p0398 N88-12482
Expert robots in nuclear plants
| DE87-014839 | 04 p0452 N88-12800
Experimental use of artificial intelligence for (future) ATC systems
| PB87-106449 | 04 p0482 N88-12970
The characterization of diagnostic tasks for engineering systems
| DE88-000093 | 04 p0483 N88-12973
An expert system for materials design
| DE88-000191 | 04 p0483 N88-12974
GOLD: Integration of model-based control systems with artificial intelligence and workstations
| DE88-000506 | 04 p0483 N88-12976
GOLD: Integration of model-based control systems with artificial intelligence and workstations
| DE88-000706 | 04 p0483 N88-12977
Intelligent signal analysis and recognition
| NASA-CR-181531 | 04 p0501 N88-13084
ZEUS: A knowledge-based expert system that assists in predicting visibility at airbases
| AD-A184197 | 05 p0626 N88-13829
A single-station weather forecasting expert system
| AD-A184889 | 05 p0627 N88-13832
XCUT. A rule-based expert system for the automated process planning of machined parts
| DE87-011638 | 05 p0639 N88-13905
Using hierarchically structured problem-solving knowledge in a rule-based process planning system
| DE87-011639 | p0639 N88-13906
Computer architectures for ar[illegible]l intelligence
| PB87-123824 | p0761 N88-14671
Knowledge acquisition for a simple expert controller
| NASA-TT-20118 | 06 p0761 N88-14672
Using user models and automatic expertise acquisition in data base interactions
| PB87-234357 | 06 p0791 N88-14848
National Aeronautics and Space Administration (NASA)/American Society for Engineering Education (ASEE) Summer Faculty Fellowship Program, 1987. Volume 2
| NASA-CR-172009-VOL-2 | 06 p0796 N88-14874
A general architecture for intelligent training systems
06 p0796 N88-14875
Dynamics, control and sensor issues pertinent to robotic hands for the EVA retriever system
06 p0796 N88-14876
Tools and technologies for expert systems: A human factors perspective 06 p0797 N88-14882
Development of a prototype H-46 helicopter diagnostic expert system
| AD-A186077 | 07 p0809 N88-14924
Expert system study for spacecraft management
| TL-2699-ISS-1 | 07 p0824 N88-15004
Intelligent controllers
| DE88-001862 | 07 p0904 N88-15475
Integration of symbolic and algorithmic hardware and software for the automation of space station subsystems
| NASA-TM-89705 | 07 p0907 N88-15497
Proceedings of the Second International Symposium on Methodologies for Intelligent Systems: Colloquia program
| DE88-001490 | 07 p0907 N88-15498
Investigation of candidate data structures and search algorithms to support a knowledge based fault diagnosis system 07 p0923 N88-15606
Microprocessor control and networking for the amps breadboard 07 p0924 N88-15615
Expert system technology 07 p0926 N88-15628
Expert system development for commonality analysis in space programs 07 p0928 N88-15635
A knowledge-based object recognition system for applications in the space station
| NASA-CR-182411 | 08 p0989 N88-15991
Cirrus: An automated protocol analysis tool
| AD-A186646 | 08 p1052 N88-16348
Third Conference on Artificial Intelligence for Space Applications, part 1
| NASA-CP-2492-Pt-1 | 08 p1055 N88-16360
Verification issues for rule-based expert systems
08 p1055 N88-16361
Using output to evaluate and refine rules in rule-based expert systems 08 p1055 N88-16362
Temporal and contextual knowledge in model-based expert systems 08 p1055 N88-16363
An easy-to-use diagnostic system development shell
08 p1055 N88-16366
An inference engine for embedded diagnostic systems
08 p1056 N88-16367
CLIPS: An expert system tool for delivery and training
08 p1056 N88-16368
Integration of symbolic and algorithmic hardware and software for the automation of space station subsystems
08 p1056 N88-16373
HSTDEK: Developing a methodology for construction of large-scale, multi-use knowledge bases
08 p1057 N88-16377
Knowledge-based monitoring of the pointing control system on the Hubble space telescope
08 p1057 N88-16378
A distributed architecture for intelligent monitoring and anomaly diagnosis of the Hubble Space Telescope
08 p1057 N88-16379

A knowledge-based system for monitoring the electrical power system of the Hubble Space Telescope
08 p1058 N88-16380
Artificial intelligence and space power systems automation 08 p1058 N88-16381
Embedded expert system for space shuttle main engine maintenance 08 p1058 N88-16382
Exploring hypotheses in attitude control fault diagnosis 08 p1058 N88-16384
EUREX D: An expert system for failure diagnosis and recovery in the TCS of the European retrievable carrier EURECA 08 p1058 N88-16385
Expert systems relations in space applications
08 p1059 N88-16391
Problem solving as intelligent retrieval from distributed knowledge sources 08 p1059 N88-16392
Application of parallel distributed processing to space based systems 08 p1059 N88-16393
Spacelab Data Processing Facilty (SLDPF) quality assurance expert systems development
08 p1059 N88-16394
ESSAA: Embedded system safety analysis assistant
08 p1060 N88-16396
Intelligent process development of foam molding for the Thermal Protection System (TPS) of the space shuttle external tank 08 p1060 N88-16397
Space shuttle main engine anomaly data and inductive knowledge based systems: Automated corporate expertise 08 p1060 N88-16398
An expert system to analyze high frequency dependent data for the space shuttle main engine turbopumps
08 p1060 N88-16399
Interactive knowledge acquisition tools
08 p1060 N88-16401
Real time AI expert system for robotic applications
08 p1061 N88-16408
Commonality analysis as a knowledge acquisition problem 08 p1062 N88-16413
Qualitative models for planning: A gentle introduction
08 p1062 N88-16414
Operational aspects of a spacecraft planning/scheduling expert system
08 p1062 N88-16415
Planning activities in space 08 p1063 N88-16417
Interfacing the expert: Characteristics and requirements for the user interface in expert systems
08 p1063 N88-16419
Conceptual information processing: A robust approach to KBS-DBMS integration 08 p1063 N88-16422
The intelligent user interface for NASA's advanced information management systems
08 p1063 N88-16424
Scheduling spacecraft operations
08 p1064 N88-16426
The resource envelope as a basis for space station management system scheduling
08 p1064 N88-16427
Prototype resupply scheduler
08 p1064 N88-16428
Case-based reasoning for space applications: Utilization of prior experience in knowledge-based systems
08 p1065 N88-16433
Knowledge representation by connection matrices: A method for the on-board implementation of large expert systems 08 p1065 N88-16434
RB-ARD: A proof of concept rule-based abort
08 p1065 N88-16435
A learning apprentice for software parts composition
08 p1065 N88-16436
Automatic program generation from specifications using Prolog 08 p1065 N88-16437
On acquisition of programming knowledge
08 p1065 N88-16438
A framework for real-time distributed expert systems: On-orbit spacecraft fault diagnosis, monitoring and control 08 p1066 N88-16440
TES: A modular systems approach to expert system development for real time space applications
08 p1066 N88-16441
Prototype space station automation system delivered and demonstrated at NASA 08 p1066 N88-16442
Applications of expert systems for satellite autonomy
08 p1066 N88-16443
The crustal dynamics intelligent user interface anthology
[NASA-TM-100693] 08 p1067 N88-16448
Dynamic function allocation in fighter cockpits
[AD-A185397] 09 p1201 N88-17199
First Annual Workshop on Space Operations Automation and Robotics (SOAR 87)
[NASA-CP-2491] 09 p1203 N88-17206
Space shuttle onboard navigation console expert/trainer system 09 p1203 N88-17208
MPAD MCC workstation system: ADDAM and EEVE
09 p1203 N88-17209
Knowledge based jet engine diagnostics
09 p1203 N88-17210
Simplifying the construction of domain-specific automatic programming systems: The NASA automated software development workstation project
09 p1204 N88-17212
The knowledge-based software assistant
09 p1204 N88-17213
An intelligent training system for payload-assist module deploys 09 p1204 N88-17214
Development of a coupled expert system for the spacecraft attitude control problem
09 p1205 N88-17223
The desktop interface in intelligent tutoring systems
09 p1205 N88-17225
Approaches to the verification of rule-based expert systems 09 p1206 N88-17232
A formal approach to validation and verification for knowledge-based control systems
09 p1207 N88-17233
Expert system verification concerns in an operations environment 09 p1207 N88-17234
Building validation tools for knowledge-based systems
09 p1207 N88-17235
Diagnosis: Reasoning from first principles and experiential knowledge 09 p1207 N88-17236
Verifying shuttle onboard software using expert systems 09 p1207 N88-17237
Design knowledge capture for the space station
09 p1208 N88-17239
CONFIG: Qualitative simulation tool for analyzing behavior of engineering devices
09 p1208 N88-17240
The empirical accuracy of uncertain inference models
09 p1208 N88-17243
Robotic planner expert system (RPLANES)
09 p1209 N88-17246
Expert mission planning and replanning scheduling system for NASA KSC payload operations
09 p1209 N88-17247
Trimodal interpretation of constraints for planning
09 p1209 N88-17248
Advanced decision aiding techniques applicable to space 09 p1209 N88-17250
Automatic routing module 09 p1210 N88-17251
SWAN: An expert system with natural language interface for tactical air capability assessment
09 p1210 N88-17253
Expert system applications in spacecraft subsystem controllers 09 p1210 N88-17254
The KATE shell: An implementation of model-based control, monitor and diagnosis 09 p1210 N88-17255
Beyond rules: The next generation of expert systems
09 p1210 N88-17256
TDAS: The Thermal Expert System (TEXSYS) data acquisition system 09 p1211 N88-17258
Implementing clips on a parallel computer
09 p1211 N88-17259
An efficient representation of spatial information for expert reasoning in robotic vehicles
09 p1214 N88-17278
A type-oriented approach to knowledged-based systems
[MA-47] 09 p1222 N88-17329
Management of complex information in support of evolving autonomous expert systems
[AD-A186680] 09 p1224 N88-17337
An expert system to support the verification/validation of flight-critical software
[MBB-UT-102/87] 10 p1314 N88-17852
Methods of eliciting information from experts
[AD-A187468] 10 p1372 N88-18189
Archetyping: A knowledge-based reuse paradigm
10 p1376 N88-18214
Optical symbolic processor for expert system execution
[AD-A187494] 10 p1385 N88-18268
A computer simulation study of an expert system for walking machine motion planning
[AD-A187907] 11 p1438 N88-18577
The metallurgical database of Aladin: An alloy de sign system
[AD-A187724] 11 p1457 N88-18682
Rocketdyne automated dynamics data analysis and management system 11 p1499 N88-18954
Optical symbolic processor for expert system execution
[AD-A187882] 11 p1525 N88-19103
Feasibility study of generating plans and strategies for software testing by knowledge based system
[AD-A187834] 11 p1529 N88-19134
Evaluating expert system tools: A framework and methodology-workshops
[AD-A187190] 11 p1533 N88-19159
Application of knowledge based systems to the maintenance of inertial system electronics
12 p1578 N88-19441
Robotic intelligence issues for space manipulator monitoring, control programming
12 p1588 N88-19504
On a knowledge based assisted system for highly autonomous control of experiment-manipulators in the Man-Tended Free Flyer 12 p1588 N88-19505
A knowledge-based approach for sensory-controlled assembly operations 12 p1588 N88-19506
Treatment of unforeseen situations by online knowledge-based diagnostic systems --- spacecraft maintenance 12 p1589 N88-19511
NAVARES: A prototype expert system for NAVSTAR anomaly resolution
[AD-A189491] 12 p1600 N88-19579
Regenerative life support system research
[NASA-CR-182606] 12 p1671 N88-20006
Expert systems: Their impact on performance and cognitive strategies in diagnostic inference
[AD-A188518] 12 p1677 N88-20027
Knowledge-based system analysis and control
[AD-A188163] 12 p1681 N88-20049
Physics for robots
[AD-A189056] 12 p1682 N88-20054
Northeast Artificial Intelligence Consortium (NAIC) administrative matters and ancillary functions, volume 1
[AD-A189466] 12 p1682 N88-20055
The concept of intelligent integrated interactive CAD systems
[CWI-CS-R8717] 13 p1818 N88-20865
Organization of design knowledge in an intelligent CAD environment
[CWI-CS-R8720] 13 p1819 N88-20868
An integrated data description language for coding design knowledge
[CWI-CS-R8731] 13 p1819 N88-20871
An implementation of the OPS5 language for computers compatible with IBM-PC
[INPE-4291-PRE/1162] 13 p1821 N88-20882
Expert system techniques and decision support system: A case study (Dec. 1985 - Jun. 1986)
[ETN-88-91347] 13 p1821 N88-20884
The use of an automated flight test management system in the development of a rapid-prototyping flight research facility
[NASA-TM-100435] 13 p1823 N88-20896
SEAT: A strategic engagement analysis tool
[DE88-000498] 13 p1830 N88-20944
Expert systems for decision support in military aircraft mission preparation
[NLR-MP-87013-U] 13 p1830 N88-20946
Consistency of rule-based expert systems
[CWI-CS-R8736] 13 p1831 N88-20950
Application of expert systems in project management decision aiding
[NASA-CR-180762] 13 p1850 N88-21074
A menu-driven knowledge retrieval system accessing ASCII data
[DE88-001742] 13 p1851 N88-21079
Oceanographic export system development, year 1
[AD-A189134] 14 p1950 N88-21623
Implementing embedded artificial intelligence rules within algorithmic programming languages
[NASA-CR-178393] 14 p1959 N88-21686
Parallel processes in the knowledge based system HYDRA
[REPT-87-38] 14 p1960 N88-21689
Conception of a knowledge-based system for designing distributed systems
[DFVLR-MITT-87-16] 14 p1961 N88-21694
Representing knowledge in two distinct descriptions: Extensional vs. intensional
[CWI-CS-R8728] 14 p1961 N88-21699
Kalman filter residual expert system
[AD-A190520] 15 p2020 N88-22041
Characteristics of LSI-wiring expert system discussed
15 p2052 N88-22226
An expert system for discrete component digital circuit design
[AD-A189680] 15 p2059 N88-22274
Inference engine for expert systems
[INPE-4465-TDL/321] 15 p2113 N88-22590
Design and implementation of a parallel computer for expert system applications
[DE88-005288] 15 p2115 N88-22601
Memory-based expert systems
[AD-A190203] 15 p2116 N88-22606
Rapid prototyping of simulations in artificial intelligence environments
[DE88-004295] 15 p2117 N88-22612
Rapid prototyping of complex avionics system architectures
[ETN-88-92275] 16 p2162 N88-22898

The use of rule induction to assist in the diagnosis of avionic circuit board defects
[ETN-88-92077] 16 p2162 N88-22899
Design as a formal, knowledge engineered activity
[CWI-CS-R8744] 16 p2248 N88-23431
Knowledge engineering in design
[CWI-CS-R8745] 16 p2248 N88-23432
STRUTEX: A prototype knowledge-based system for initially configuring a structure to support point loads in two dimensions
[NASA-TM-100613] 16 p2250 N88-23448
Intelligent systems interconnection: What should come after open systems interconnection?
[CWI-CS-R8742] 16 p2253 N88-23465
Automatic control of an industrial process and computer aided process control by means of an expert system
[LAAS-88-004] 16 p2255 N88-23476
Identification of control structures --- expert systems
[REPT-87-66] 16 p2255 N88-23479
Architecture and role of the Sensor Subsystem in future aircraft weapon systems 17 p2302 N88-23770
Rapid prototyping of complex avionic system architectures 17 p2302 N88-23771
Psychosensory cockpit ergonomics, advantages of intelligent information systems 17 p2304 N88-23784
A proposal of adaptation of a knowledge-based scene analysis model to some remote sensing problems
17 p2354 N88-24026
A proposal of adaptation of a knowledge-based scene analysis model to some remote sensing problems
17 p2362 N88-24068
Fault diagnosis in orbital refueling operations
17 p2381 N88-24154
Third Conference on Artificial Intelligence for Space Applications, part 2
[NASA-CP-2492-PT-2] 17 p2387 N88-24188
Integration of symbolic and algorithmic hardware and software for the automation of space station subsystems
17 p2387 N88-24190
Connecting remote systems for demonstration of automation technologies 17 p2387 N88-24191
Knowledge based system verification and validation as related to automation of space station subsystems: Rationale for a knowledge based system lifecycle
17 p2387 N88-24192
TALOS: A distributed architecture for intelligent monitoring and anomaly diagnosis of the Hubble Space Telescope 17 p2388 N88-24193
Genetic algorithms for adaptive real-time control in space systems 17 p2388 N88-24195
TES: A modular systems approach to expert system development for real-time space applications
17 p2388 N88-24197
Expert systems approach to modeling systems with the ATHENA thermal-hydraulics code
17 p2416 N88-24365
Knowledge based systems in nondestructive evaluation
[DE88-006653] 18 p2525 N88-24981
Timesharing performance as an indicator of pilot mental workload
[NASA-CR-182807] 18 p2552 N88-25150
Application of flight systems methodologies to the validation of knowledge-based systems
[NASA-TM-100442] 18 p2561 N88-25207
Optical symbolic processor for expert system execution
[AD-A192005] 18 p2575 N88-25296
Ultrasonic and video computerized data acquisition for automated welding
[DE88-006741] 19 p2677 N88-25918
BOLETIM: An expert system for weather forecasting
[INPE-4538-TDL/329] 19 p2693 N88-26011
Automation tools for demonstration of goal directed and self-repairing flight control systems
[NASA-CR-179433] 19 p2715 N88-26121
An expert system model using predicate transition nets
[AD-A191953] 19 p2718 N88-26141
Modeling and evaluation of expert systems in decisionmaking organizations
[AD-A191951] 19 p2739 N88-26260
A comparative study of project estimating tools
[DE88-009059] 19 p2740 N88-26266
Intelligent guidance and control for wind shear encounter
[NASA-CR-183060] 20 p2755 N88-26347
A reusable rocket engine intelligen control
[NASA-TM-100963] 20 p2766 N88-26401
Preliminary study within a project for the development of intelligent assistance to piloting: Formal description of combat pilot expertise and implementation of an interactive system to represent operations
[CERMA-87-31] 20 p2833 N88-26806
Delfi-3 as a development environment for expert systems
[REPT-8767] 20 p2839 N88-26845
A network approach to the certainty factor model --- expert systems
[CWI-CS-R8757] 20 p2840 N88-26852
Expert system application education project
[NASA-CR-183089] 20 p2843 N88-26867
NEXT: An expert system development tool to support engineering design
[NLR-MP-86070-U] 20 p2843 N88-26871
Combining expert opinions: An optimization framework
[REPT-87-84] 20 p2846 N88-26895
Computer science and technology: Knowledge-based system for physical database design
[PB88-193289] 20 p2882 N88-27109
Knowledge representation in geographic information systems
[ETN-88-92470] 20 p2882 N88-27112
EXSAT: Expert system to configure telecommunication satellites
[SNIAS-881-440-101] 21 p2902 N88-27223
United States Air Force Graduate Student Summer Support Program, volume 2
[AD-A191122] 21 p2924 N88-27355
Investigation of expert system design approaches for electronic design environments
21 p2926 N88-27365
An investigation of performance improvement in knowledge-based control systems
21 p2928 N88-27382
Computer-Aided Engineering (CAE) for engineering design 21 p2929 N88-27390
The MELCOM PSI 2 AI workstation
21 p2930 N88-27395
Motor-response learning at a process control panel by an autonomous robot
[DE88-005055] 21 p2955 N88-27554
Vapor Compression Distillation Subsystem (VCDS) component enhancement, testing and expert fault diagnostics development, volume 2
[NASA-CR-172076] 21 p2994 N88-27755
Implementation of an OPS5 derivative on the Novix RISC processor
[DE88-011392] 21 p2994 N88-27758
Block Oriented Simulation System (BOSS)
[NASA-CR-182947] 21 p2995 N88-27760
Benefits of an object approach in a computer aided design environment
[SNIAS-881-440-102] 21 p3000 N88-27791
Intelligent Mobile Autonomous System (IMAS)
[AD-A193181] 21 p3003 N88-27811
Introduction to artificial intelligence and expert systems
[SNIAS-881-320-101] 21 p3004 N88-27814
Expert system contribution to logistics improvement
[SNIAS-881-320-102] 21 p3004 N88-27815
Faultfinder: A diagnostic expert system with graceful degradation for onboard aircraft applications
22 p3035 N88-28018
Heat exchanger demonstration expert system
22 p3066 N88-28193
From the extraction of linear networks towards following of them on SPOT images with the help of a knowledge-based interpretation system
22 p3113 N88-28494
Rule-based circuit optimization for CMOS VLSI
22 p3137 N88-28649
Cooperating knowledge-based systems
[NASA-CR-183109] 23 p3247 N88-29327
Second Conference on Artificial Intelligence for Space Applications
[NASA-CP-3007] 23 p3251 N88-29351
Space station as a vital focus for advancing the technologies of automation and robotics
[IAF-86-62] 23 p3251 N88-29352
A relational data-knowledge base system and its potential in developing a distributed data-knowledge system 23 p3251 N88-29353
Hologram representation of design data in an expert system knowledge base 23 p3251 N88-29354
An expert system for reliability modeling
23 p3252 N88-29355
A software engineering approach to expert system design and verification 23 p3252 N88-29356
Issues on the use of meta-knowledge in expert systems 23 p3252 N88-29357
A knowledge-based decision support system for payload scheduling 23 p3252 N88-29358
Coupling expert systems and simulation
23 p3252 N88-29360
Optimization of low gravity materials processing experiments using expert systems
23 p3252 N88-29361
An approach to combining heuristic and qualitative reasoning in an expert system 23 p3253 N88-29362
Expertise and reasoning with possibility: An explanation of modal logic and expert systems
23 p3253 N88-29363
Analyst-centered models for systems design, analysis, and development 23 p3253 N88-29364
Avionic expert systems 23 p3253 N88-29365
Knowledge elicitation for an operator assistant system in process control tasks 23 p3253 N88-29366
Machine vision for real time orbital operations
23 p3253 N88-29367
Automatic object recognition
23 p3254 N88-29368
Two dimensional convolute integers for machine vision and image recognition 23 p3254 N88-29369
On recognizing ignorance 23 p3254 N88-29372
Expert systems for MSFC power systems
23 p3255 N88-29375
A generic expert system for materials processing in space 23 p3255 N88-29376
ARGES: An expert system for fault diagnosis within space-based ECLS systems 23 p3255 N88-29380
SCARES: A Spacecraft Control Anomaly Resolution Expert System 23 p3256 N88-29381
A scheduling and resource management system for space applications 23 p3256 N88-29383
An expert systems application to space base data processing 23 p3256 N88-29384
Generic supervisor: A knowledge-based tool for control of space station on-board systems
23 p3257 N88-29389
Knowledge based programming environments: A perspective 23 p3258 N88-29393
Knowledge acquisition and rapid protyping of an expert system: Dealing with real world problems
23 p3258 N88-29394
Automated generation of spacecraft activity plans
23 p3258 N88-29396
Intelligent interfaces for expert systems
23 p3258 N88-29397
Requirements for a tool to aid in the development of expert systems for space station applications
23 p3258 N88-29398
Benchmarking expert system tools
23 p3259 N88-29399
Two implementations of the Expert System for the Flight Analysis System (ESFAS) project
23 p3259 N88-29400
Life-span knowledge engineering for space operations
23 p3259 N88-29401
NOA: A Network Operator Assistant for scheduling Tracking and Data Relay Satellite System (TDRSS)
23 p3259 N88-29403
Experiment scheduling for Spacelab missions
23 p3259 N88-29404
The emergence of multi-user expert systems
23 p3260 N88-29406
An expert system for a distributed real-time trainer
23 p3261 N88-29411
Utilization of artificial intelligence techniques for the Space Station power system 23 p3261 N88-29412
A methodology for multiple rule system integration and resolution within a singular knowledge base
23 p3261 N88-29413
Design consideration in constructing high performance embedded Knowledge-Based Systems (KBS)
23 p3261 N88-29415
Validation of expert systems 23 p3262 N88-29416
Mathematical algorithms for approximate reasoning
23 p3262 N88-29418
Real-time space system control with expert systems
23 p3262 N88-29419
A flexible search strategy for production systems
23 p3262 N88-29420
Semantic based man-machine interface for real-time communication 23 p3262 N88-29421
Automated software development workstation
23 p3263 N88-29423
An expert system for natural language processing
23 p3263 N88-29426
Expert system technology as a data processing tool
23 p3263 N88-29427
Next-generation space manipulator
23 p3263 N88-29428
Parallel real-time expert systems
[AD-A193673] 23 p3264 N88-29434
Contribution of expert systems to avionics advance. Application on AS30 laser weapon system
[SNIAS-881-320-103] 23 p3267 N88-29449
Active explanation reduction: An approach to the multiple explanations problem
[AD-A194127] 23 p3276 N88-29501
Threat expert system technology advisor
[NASA-CR-177479] 24 p3328 N88-29816
The 1988 Goddard Conference on Space Applications of Artificial Intelligence
[NASA-CP-3009] 24 p3415 N88-30330

An intelligent training system for space shuttle flight controllers 24 p3415 N88-30331
Artificial intelligence costs, benefits, risks for selected spacecraft ground system automation scenarios 24 p3416 N88-30332
Artificial intelligence in a mission operations and satellite test environment 24 p3416 N88-30334
Automated space vehicle control for rendezvous proximity operations 24 p3416 N88-30335
Automated satellite control in Ada 24 p3416 N88-30336
Knowledge based tools for Hubble Space Telescope planning and scheduling: Constraints and strategies 24 p3417 N88-30338
The proposal entry processor: Telescience applications for Hubble Space Telescope science operations 24 p3417 N88-30339
Candidate functions for advanced technology implementation in the Columbus mission planning environment 24 p3417 N88-30340
A rule-based systems approach to spacecraft communications configuration optimization 24 p3417 N88-30341
MOORE: A prototype expert system for diagnosing spacecraft problems 24 p3418 N88-30343
Achieving real-time performance in FIESTA 24 p3418 N88-30344
Mission telemetry system monitor: A real-time knowledge-based system 24 p3418 N88-30345
Low level image processing techniques using the pipeline image processing engine in the flight telerobotic servicer 24 p3418 N88-30346
An interactive testbed for development of expert tools for pattern recognition 24 p3419 N88-30349
The second generation intelligent user interface for the crustal dynamics data information system 24 p3419 N88-30352
Spacelab data processing facility (SLDPF) Quality Assurance (QA)/Data Accounting (DA) expert systems: Transition from prototypes to operational systems 24 p3420 N88-30353
Automated cataloging and characterization of space-derived data 24 p3420 N88-30354
A design for a ground-based data management system 24 p3420 N88-30355
Automatic mathematical modeling for real time simulation system 24 p3420 N88-30356
A simulation engine: Combining an expert system with a simulation language 24 p3421 N88-30358
The advice taker/inquirer: A system for high-level acquisition of expert knowledge 24 p3421 N88-30359
Verification and validation of rulebased systems for Hubble Space Telescope ground support 24 p3421 N88-30361
The need for a comprehensive expert system development methodology 24 p3421 N88-30362
Knowledge-based integrated information systems engineering: Highlights and bibliography. Knowledge-Based Integrated Information Systems Engineering (KBIISE) Project, volume 1 [AD-A195850] 24 p3435 N88-30449
Technical opinions regarding knowledge-based integrated information systems engineering, volume 8 [AD-A195857] 24 p3436 N88-30454
Knowledge-Based Integrated Information Systems Development Methodologies Plan. Knowledge-Based Integrated Information Systems Engineering (KBIISE) report, volume 2 [AD-A195851] 24 p3436 N88-30455
Information retrieval systems evolve-advances for easier and more successful use 24 p3438 N88-30462

EXPLODING CONDUCTOR CIRCUITS
U CIRCUITS

EXPLORATION
NT MINERAL EXPLORATION
NT OIL EXPLORATION
NT SPACE EXPLORATION
Remote acoustic sounding of ferromanganese nodules 06 p0727 N88-14471
Research on visual information processing with special reference to oculomotor behavior in the areas of exploration, recognition and search [AD-A186598] 08 p1051 N88-16346
Analysis of gases in the earth's crust [PB88-141619] 10 p1354 N88-18093

EXPLORER SATELLITES
NT COSMIC BACKGROUND EXPLORER SATELLITE
NT DYNAMICS EXPLORER 1 SATELLITE
NT EXPLORER 47 SATELLITE
NT EXPLORER 51 SATELLITE
NT EXPLORER 54 SATELLITE
NT EXPLORER 55 SATELLITE
NT INTERNATIONAL SUN EARTH EXPLORER 3
NT INTERNATIONAL SUN EARTH EXPLORERS
NT SOLAR MESOSPHERE EXPLORER
Alouette-ISIS program summary [NASA-CR-180747] 08 p1023 N88-16195
Into the thermosphere: The atmosphere explorers [NASA-SP-490] 10 p1353 N88-18084

EXPLORER 47 SATELLITE
IMP 7 (Explorer 47) trajectory, September 26, 1972 to September 25, 1978 [NASA-CR-182697] 14 p1871 N88-21183

EXPLORER 51 SATELLITE
Into the thermosphere: The atmosphere explorers [NASA-SP-490] 10 p1353 N88-18084

EXPLORER 54 SATELLITE
Into the thermosphere: The atmosphere explorers [NASA-SP-490] 10 p1353 N88-18084

EXPLORER 55 SATELLITE
Into the thermosphere: The atmosphere explorers [NASA-SP-490] 10 p1353 N88-18084

EXPLOSION SUPPRESSION
Correlation of air pressure drop and flame arrestor characteristics for explosion suppression materials [AD-A184960] 05 p0548 N88-13340

EXPLOSIONS
NT AERIAL EXPLOSIONS
NT CHEMICAL EXPLOSIONS
NT GAS EXPLOSIONS
NT NUCLEAR EXPLOSIONS
NT UNDERGROUND EXPLOSIONS
NT UNDERWATER EXPLOSIONS
Chemical analysis of charged Li/SO(sub)2 cells 02 p0163 N88-11026
High explosive simulations of supernovae and the supernova shell fragmentation model of solar system formation [DE87-014708] 02 p0251 N88-11584
General-Purpose Heat Source Safety Verification Test Program: Edge-on flyer plate tests [DE87-006309] 03 p0376 N88-12362
Aircraft fire safety research 04 p0406 N88-12526
Scaling the electromagnetically driven explosive shock simulator 05 p0592 N88-13612
On the simulation of ballistic shock loads 05 p0593 N88-13615
Langlie Test Method Program for use with the HP-41CV/X calculator [DE88-001935] 06 p0687 N88-14210
Analysis and interpretation of satellite fragmentation data 06 p0798 N88-14885
Explosive absorption of laser beam of finite diameter 07 p0921 N88-15597
Blast waves generated by planar detonations [DE88-002219] 09 p1164 N88-16979
Reinforced concrete arches under blast and shock environments 09 p1180 N88-17065
NF85: A three-dimensional, air-dynamics computer code for analyzing explosions in structures [DE88-005085] 10 p1331 N88-17953
Modeling of the non-auditory response to blast overpressure [AD-A187397] 10 p1369 N88-18184
Supernova mechanisms: Before and after SN1987a [DE88-003489] 10 p1429 N88-18533
Theoretical investigation of the wave shaping process in a section of ladder fracture tape [MRL-R-1081] 13 p1771 N88-20595
Nuclear and astrophysical evidence on the equation of state [DE88-007397] 18 p2572 N88-25279
Development of an experimental system for studying fast transient ignition phenomena [DE88-011917] 21 p2911 N88-27276
Stochastic geologic effects on near-field ground motions in alluvium [AD-A192315] 21 p2972 N88-27652
Initiation of explosive molten aluminum-water interactions at wet or underwater surfaces [DE88-004686] 23 p3194 N88-29006

EXPLOSIVE DEVICES
NT BOMBS (ORDNANCE)
NT BOOSTERS (EXPLOSIVES)
NT DETONATORS
NT INITIATORS (EXPLOSIVES)
NT PRIMERS (EXPLOSIVES)
NT SHAPED CHARGES
NT TORPEDOES
Influence of shock wave and gas pressure on the behavior of a pyrotechnical device [SNIAS-872-430-111] 05 p0570 N88-13477
Measurement, data analysis and prediction of pyrotechnic shock from pin-pullers and separation joints 09 p1179 N88-17061
Investigation of Super*Zip separation joint [NASA-TM-4031] 15 p2026 N88-22072
Toggle release [NASA-CASE-MSC-21354-1] 18 p2523 N88-24969

EXPLOSIVE FORMING
Characterization of an explosively consolidated rapidly solidified Fe-16Ni-9Cr-5Mo-2Cu alloy powder [DE88-006733] 15 p2041 N88-22162
Superconductor consolidation [DE88-010936] 21 p3024 N88-27949

EXPLOSIVE WELDING
Tool and process for miniature explosive joining of tubes [NASA-CASE-LAR-13662-1] 06 p0711 N88-14359
Evaluation of explosive bonding for patching aluminum with aluminum [AD-A193303] 21 p2913 N88-27285

EXPLOSIVES
NT HMX
NT RDX
NT TETRYL
NT TRINITROTOLUENE
A study of diverging detonation in high-explosive systems [DE87-006070] 01 p0031 N88-10194
Shock measurements on explosives in the supra compressive region [DE87-008423] 01 p0031 N88-10196
Statistical mechanical theory of condensed explosives [DE87-009137] 01 p0031 N88-10197
Optically time-resolved detonation break out [DE87-010340] 01 p0031 N88-10199
Microstructural effects in shock initiation of granular explosives [DE87-011282] 01 p0031 N88-10200
Current experimental and theoretical understanding of detonation waves in heterogeneous solid explosives [DE87-012177] 01 p0032 N88-10201
The use of fiber optics in the determination of temperature and extent of reaction in detonating explosives [DE87-012632] 01 p0094 N88-10612
Pyrotechnic component development at Sandia National Laboratory [DE87-006899] 02 p0154 N88-10967
Hot spots: Subnanometer femtosecond energy localization [DE87-010276] 02 p0155 N88-10968
Visible emission from granular explosives during shock initiation [DE87-012361] 02 p0155 N88-10970
Spectroscopic studies of shocked and detonating explosives [DE87-014216] 02 p0155 N88-10972
High explosive simulations of supernovae and the supernova shell fragmentation model of solar system formation [DE87-014708] 02 p0251 N88-11584
Evaluation of one-sided nuclear magnetic resonance for remote detection of explosives [AD-A184490] 03 p0296 N88-11857
The LLNL 150-mm equation-of-state gun system [DE88-000423] 04 p0405 N88-12519
DOE explosives safety manual [DE88-000831] 04 p0422 N88-12616
High explosive moulding powders from RDX and aqueous polyurethane dispersions [AD-A185026] 05 p0568 N88-13458
Compatibility of explosives: A data base system [PB87-234464] 06 p0687 N88-14208
Calculation evaluation of the boundary conditions of autoinflammation of propulsive charges [PB87-139044] 08 p0974 N88-15890
Organic coatings to improve the storageability and safety of pyrotechnic compositions [AD-A187158] 09 p1150 N88-16889
Mechanism of and particle size effects on shock sensitivity of heterogeneous pressed explosives: Preliminary assessment of binderless RDX in fuze trains [MRL-R-1077] 09 p1150 N88-16892
EXPLO: Explosives thermal analysis computer code [DE88-001938] 10 p1307 N88-17814
An electro-optic explosive igniter [DE88-004728] 11 p1466 N88-18738
Novel analytical X-ray Non-Destructive Evaluation (NDE) tool for quality control of energetic materials [AD-A187737] 11 p1497 N88-18935
A procedure for estimating the crystal densities of organic explosives [AD-A189023] 12 p1613 N88-19646
Ignition and high speed photography of energetic materials with a copper vapor laser [DE88-004831] 12 p1631 N88-19765
Anomalous shock sensitivity/density relationship for RDX-polyethylene wax and related formulations from MRL Small Scale Gap Test (SSGT) measurements [MRL-R-1099] 13 p1739 N88-20399
A comparative assessment of US and UK explosives qualified as replacements for tetryl [MRL-R-1094] 13 p1754 N88-20486

Some properties of Australian produced explosive composition H-6
[MRL-TN-525] 13 p1754 N88-20490
Analysis of explosives. 1: Computer programs for processing of X-ray powder deffraction data
[PB88-156898] 14 p1894 N88-21309
Effect of moisture level in PBXW-109(E) (plastic-bonded explosive) mixes on the aging of the cured explosive
[AD-A190200] 15 p2048 N88-22202
Static dielectric breakdown strength of condensed heterogeneous high explosives
[AD-A191035] 16 p2183 N88-23014
Thermal decomposition studies of explosives for component applications
[DE88-007201] 18 p2495 N88-24805
A compatible encapsulant for explosives
[DE88-007212] 18 p2495 N88-24806
An extinguisher to quench propellant fires
[AD-A190785] 18 p2497 N88-24813
The viscosity of molten TNT
[MRL-R-1100] 19 p2622 N88-25553
Research in energetic compounds
[AD-A192953] 20 p2781 N88-26494
Deformation, fracture and explosive properties of reactive materials
[AD-A193060] 21 p2923 N88-27348
A concept for an electro-optic explosive device
[DE88-009696] 21 p2923 N88-27349
Relative flow rates of explosive powders
[DE88-010767] 21 p2923 N88-27350
Stochastic geologic effects on near-field ground motions in alluvium
[AD-A192315] 21 p2972 N88-27652
Decomposition of energetic materials on the drop-weight impact machine
[DE88-009154] 22 p3059 N88-28152
Response of SMA (Shielded Metal Arc) and narrow gap HY80 weldments to explosive shock loading
[AD-A195994] 24 p3385 N88-30162

EXPONENTIAL FUNCTIONS
NT LOGARITHMS
The matrix exponential in transient structural analysis
05 p0593 N88-13619
Strong consistency of maximum likelihood parameter estimation of superimposed exponential signals in noise
[AD-A186384] 07 p0911 N88-15526
Exponential lower bounds for finding Brouwer fixed points
[DE88-002864] 10 p1425 N88-18513
Electromagnetic shadowing by an exponentially distributed rough surface
[AD-A189677] 14 p1906 N88-21391
High speed transcendental elementary function architecture in support of the Vector Wave Equation (VWE)
[AD-A189746] 15 p2119 N88-22627
A note on phase-type, almost phase-type, generalized hyperexponential and Coxian distribution, revision
[AD-A191236] 16 p2261 N88-23517
Portable implementation of a generic exponential function in Ada
[DE88-007699] 19 p2715 N88-26117
Applications of an exponential finite difference technique
[NASA-TM-100939] 22 p3084 N88-28312

EXPONENTS
Nonlinear elliptic problems with critical exponent in shrinking annuli
[W-02/87] 23 p3273 N88-29477

EXPORTS
U INTERNATIONAL TRADE

EXPOSURE
High intensity 5 eV O-atom exposure facility for material degradation studies 02 p0135 N88-10847
Effects of solvent exposures on poly(etheretherketone) (PEEK) and PEEK-fiberglass composites
[MLM-3405] 03 p0281 N88-11766
Materials preparation and longevity in hyperthermal atomic oxygen 03 p0297 N88-11862
Investigation of the exposure to harmful compounds in the workshop of nondestructive materials testing at Gilze-Rijen (Netherlands)
[PML-1985-42] 05 p0623 N88-13816
Effects of aviation fluids on fiber composite material
[FOA-C-20674-2.6] 08 p0965 N88-15840
Corrosion and deterioration testing in humid tropic environments
[AD-A186917] 10 p1302 N88-17783
Los Alamos optical materials reliability, maintainability, and exposure testing program
[DE88-001953] 10 p1409 N88-18404
Chemical cleaning of metal surfaces in vacuum systems by exposure to reactive gases
[AD-A186588] 12 p1608 N88-19616
Medical problems related to altitude in: Human performance physiology and environmental medicine at terrestrial extremes, chapter 14
[AD-A188340] 12 p1666 N88-19989
Evaluation of existing total human exposure models
[PB88-146840] 15 p2101 N88-22517
Assessment of cochlear damage after microwave irradiation
[AD-A193237] 21 p2987 N88-27737
Alternative immersion accelerated testing of coating systems for Naval shoreline facilities
24 p3355 N88-29977
Reduced time frame for predicting coating performance 24 p3356 N88-29979

EXPRESSIONS (MATHEMATICS)
U FORMULAS (MATHEMATICS)

EXTARS
U X RAY STARS

EXTENDED DURATION SPACE FLIGHT
U LONG DURATION SPACE FLIGHT

EXTENSIONS
Personnel occupied woven envelope robot power
[NASA-CR-182367] 07 p0856 N88-15196
A note on extended quasi-likelihood
[AD-A186318] 07 p0915 N88-15555

EXTENSOMETERS
Strain gages in engineering geodesy
[SER-C-320] 01 p0048 N88-10309
Optimization of dilatometer test procedures
[DE87-014998] 04 p0447 N88-12769
Small-diameter wire tensile testing
[DE88-000835] 04 p0455 N88-12815
Computer grading of extensometers (BS 3846)
[NPL-DMA(A)-152] 15 p2108 N88-22560

EXTERNAL COMBUSTION ENGINES
NT STIRLING ENGINES

EXTERNAL STORE SEPARATION
Store separation of nuclear weapons
[DE87-010778] 02 p0124 N88-10785
Airframe/store compatibility 05 p0545 N88-13323
Airplane load drop and missile firing: Experimental methods for predicting trajectories
[PB87-170494] 09 p1117 N88-16695
Store separation and missile firing from aircraft: Experimental methods for trajectory projection
[NASA-TT-20214] 11 p1439 N88-18589
The present status and the future of missile aerodynamics
[NASA-TM-100063] 24 p3320 N88-29773

EXTERNAL STORES
Design principles and practices for implementation of MIL-STD-1760 in aircraft and stores
[AD-A183724] 01 p0005 N88-10027
Method to predict external store carriage characteristics at transonic speeds
[NASA-CR-4170] 22 p3037 N88-28034
Preliminary airworthiness evaluation of the UH-60A/ESSS (External Stores Support System) with HELLFIRE launcher installed
[AD-A196187] 24 p3323 N88-29793

EXTERNAL SURFACE CURRENTS
Complex space monofilar approximation of diffraction currents on a conducting half plane
[NASA-CR-182883] 16 p2273 N88-23605

EXTERNAL TANKS
Redesign of solid rocket booster/external tank attachment ring for the space transportation system
[NASA-TM-100476] 01 p0017 N88-10101
Structural analysis of the space shuttle solid rocket booster/external tank attach ring
[NASA-TM-100510] 11 p1446 N88-18618
Orbital analysis of a STS (Space Transportation System) external tank in low earth orbit
[AD-A188829] 12 p1593 N88-19542
Modification and development of the external tank hydrogen vent umbilical system for the space shuttle vehicle 14 p1928 N88-21496
External tank gamma ray imaging telescope study. Final review, phase 2
[NASA-CR-179320] 15 p2150 N88-22834
The effects of RCS jet firing on the isolated Orbiter and mated coast phases of the glide return to launch site maneuver at Mach number 6 (IA302B)
[NASA-CR-180223] 20 p2766 N88-26403

EXTERNALLY BLOWN FLAPS
NT UPPER SURFACE BLOWN FLAPS

EXTINCTION
NT INTERSTELLAR EXTINCTION
Measurements of iridium and the meteoric impact hypothesis at cretaceous end
[DE87-703765] 04 p0521 N88-13200
Carbon monoxide and turbulence-chemistry interactions: Blowoff and extinction of turbulent diffusion flames
[AD-A186276] 07 p0828 N88-15025
Optical characterization of tropospheric aerosols
[AD-A187839] 11 p1511 N88-19029
SAGE 1 and SAM 2 measurements of 1 micron aerosol extinction in the free troposphere
[NASA-CR-182945] 17 p2374 N88-24121
Dynamics of propellant ignition
19 p2628 N88-25590
Extinction behavior of low voltage switching arc under consideration of cathodic coatings and dynamic arc column
[ETN-88-92384] 20 p2796 N88-26591
Evaluation of atmospheric effects for operational tactical decision aid
[AD-A194205] 23 p3232 N88-29236
Optical measurements of soot in premixed flames
[NASA-TM-101305] 24 p3373 N88-30090
A compilation of information and data on the Manson impact structure
[NASA-CR-183169] 24 p3401 N88-30258
Intermediate polars observed in Brazil in the last eight years
[INPE-4567-PRE/1308] 24 p3454 N88-30559

EXTINGUISHERS
U FIRE EXTINGUISHERS

EXTINGUISHING
Spacecraft fire detection and extinguishment: A bibliography
[NASA-CR-180880] 11 p1444 N88-18612
An extinguisher to quench propellant fires
[AD-A190785] 18 p2497 N88-24813
Extinguishing agent for magnesium fire, phases 5 and 6
[AD-A192436] 21 p2930 N88-27398
Ignition and extinguishing of a Solid Fuel Ramjet (SOFRAM)
[FOA-C-20713-2.1] 24 p3337 N88-29865

EXTRACTION
NT GEOTHERMAL ENERGY EXTRACTION
NT ION EXTRACTION
Low extractable wipers for cleaning space flight hardware 02 p0137 N88-10863
Increasing the rate at which ceramic castings undergo preliminary heat-treatment in an ultra-high frequency magnetic field 14 p1886 N88-21275
Automatic line network extraction from aerial imagery of urban areas through knowledge based image analysis
[AD-A193067] 21 p2965 N88-27615
Uses of lunar sulfur
[DE88-009119] 21 p3031 N88-27990
Design criteria for extraction with chemical reaction and liquid membrane permeation
[NASA-TT-20352] 24 p3343 N88-29899

EXTRAGALACTIC LIGHT
U EXTRATERRESTRIAL RADIATION
U LIGHT (VISIBLE RADIATION)

EXTRAGALACTIC MEDIA
U INTERGALACTIC MEDIA

EXTRAGALACTIC RADIO SOURCES
NT RADIO GALAXIES
NT RADIO JETS (ASTRONOMY)
Neutron stars observations as astrophysical probes
06 p0800 N88-14896
VLBI research on OH-maser IN W33
08 p1001 N88-16064
Relativistic jet models for the BL Lacertae object Mrk 421 during three epochs of observation
[NASA-TM-89727] 13 p1853 N88-21090

EXTRAPOLATION
Operational experiment in very short range forecast of precipitation 02 p0204 N88-11280
Extrapolation of extremum values of the wind velocity
08 p1015 N88-16150
Report of Atmospheric-Canopy Exchange Panel
[DE88-004478] 14 p1944 N88-21597
Comparison of results based on a deterministic versus a statistical uncertainty analysis
[DE88-010751] 21 p3010 N88-27858
Application of sampling techniques to near-field far-field transformation
[ESA-CR(P)-2546] 24 p3359 N88-30002
Convergence acceleration for vector sequences and applications to computational fluid dynamics
[NASA-TM-101327] 24 p3424 N88-30377

EXTRATERRESTRIAL ENVIRONMENTS
NT CHROMOSPHERE
NT EARTH ORBITAL ENVIRONMENTS
NT INTERPLANETARY SPACE
NT INTERSTELLAR SPACE
NT JUPITER ATMOSPHERE
NT MARS ATMOSPHERE
NT MARS ENVIRONMENT
NT NEPTUNE ATMOSPHERE
NT PLANETARY ATMOSPHERES
NT PLANETARY ENVIRONMENTS
NT PLANETARY IONOSPHERES
NT SATELLITE ATMOSPHERES

NT SATURN ATMOSPHERE
NT SOLAR ATMOSPHERE
NT STELLAR ATMOSPHERES
NT URANUS ATMOSPHERE
NT VENUS ATMOSPHERE
NT VENUS CLOUDS

EXTRATERRESTRIAL INTELLIGENCE
The Telecommunications and Data Acquisition Report
[NASA-CR-181546] 04 p0432 N88-12679
Intelligent signal analysis and recognition
[NASA-CR-181531] 04 p0501 N88-13084

EXTRATERRESTRIAL LIFE
Publications of the exobiology program for 1986: A special bibliography
[NASA-TM-4029] 09 p1203 N88-17205
European activities in exobiological research in space 12 p1657 N88-19929

EXTRATERRESTRIAL MATTER
NT COSMIC PLASMA
NT DARK MATTER
NT INTERPLANETARY GAS
NT INTERSTELLAR GAS
NT INTERSTELLAR MATTER
NT NEUTRAL GASES
Products from cosmic-ray interactions in extraterrestrial matter: What they tell us about radiation backgrounds in space
[DE88-009143] 19 p2743 N88-26288

EXTRATERRESTRIAL RADIATION
NT EXTRATERRESTRIAL RADIO WAVES
NT GALACTIC COSMIC RAYS
NT GALACTIC RADIATION
NT GALACTIC RADIO WAVES
NT GAMMA RAY BURSTS
NT INTERSTELLAR RADIATION
NT PLANETARY RADIATION
NT PRIMARY COSMIC RAYS
NT RADIO BURSTS
NT SOLAR COSMIC RAYS
NT SOLAR ELECTRONS
NT SOLAR NEUTRINOS
NT SOLAR NEUTRONS
NT SOLAR PROTONS
NT SOLAR RADIATION
NT SOLAR RADIO BURSTS
NT SOLAR RADIO EMISSION
NT SOLAR WIND
NT SOLAR X-RAYS
NT STELLAR RADIATION
NT STELLAR WINDS
NT SUNLIGHT
NT TYPE 3 BURSTS
NT ZODIACAL LIGHT
Irradiations. Accumulated doses. Heavy ions --- space environment 03 p0272 N88-11708
Fabricate, calibrate and test a dosimeter for integration into the CRRES (Combined Release and Radiation Effects Satellite) satellite
[AD-A185439] 05 p0585 N88-13564
Characterization of space radiation environment in terms of the energy deposition in functionally important volumes
[DE88-005627] 15 p2100 N88-22513
Space nuclear reactor shielding optimization studies 17 p2408 N88-24320
From general relativity to the theory of superstrings 18 p2587 N88-25369

EXTRATERRESTRIAL RADIO WAVES
NT GALACTIC RADIO WAVES
NT RADIO BURSTS
NT SOLAR RADIO BURSTS
NT SOLAR RADIO EMISSION
NT TYPE 3 BURSTS
Analysis of deep sky sources found by the infrared astronomy satellite
[AD-A189605] 13 p1853 N88-21089
New CCIR report on SETI 22 p3067 N88-28204

EXTRATERRESTRIAL ROVING VEHICLES
U ROVING VEHICLES

EXTRAVEHICULAR ACTIVITY
Structural Assembly Demonstration Experiment (SADE)
[NASA-CR-179205] 02 p0138 N88-10868
Space Construction
[NASA-CP-2490] 02 p0138 N88-10870
Experimental assembly of structures in EVA: Hardware morphology and development issues 02 p0139 N88-10872
Access flight hardware design and development 02 p0139 N88-10873
Mission Peculiar Equipment Support Structure: A platform for space construction 02 p0139 N88-10874
Marshall Space Flight Center's role in EASE/ACCESS mission management 02 p0139 N88-10875
A monograph of the National Space Transportation System Office (NSTSO) integration activities conducted at the NASA Lyndon B. Johnson Space Center for the EASE/ACCESS payload flown on STS 61-B 02 p0139 N88-10876
Research and development at the Marshall Space Flight Center Neutral Buoyancy Simulator 02 p0139 N88-10878
A synopsis of the EVA training conducted on EASE/ACCESS for STS-61-B 02 p0140 N88-10879
Results of the ACCESS experiment 02 p0140 N88-10880
EASE (Experimental Assembly of Structures in EVA) overview of selected results 02 p0140 N88-10881
Space suit extravehicular hazards protection development
[NASA-TM-100458] 04 p0475 N88-12927
Automatic antenna switching design for Extra Vehicular Activity (EVA) communication system 06 p0797 N88-14883
Goal driven kinematic simulation of flexible arm robot for space station missions 08 p1059 N88-16388
NASA Office of Space Flight (OSF) in-orbit servicing program 12 p1587 N88-19498
In-orbit and laboratory exchange of ORUs designed/not designed for servicing 12 p1587 N88-19499
Utilization of SMS and EVA for the servicing of European Space Station 12 p1587 N88-19500
EVA, the technological challenge 12 p1592 N88-19535
The space station assembly phase: Flight telerobotic servicer feasibility. Volume 2: Methodology and case study
[NASA-CR-182690] 13 p1731 N88-20352
An evaluation of the methods for rescuing EVA (Extravehicular Activities) crewmembers and recovering equipment detached and adrift from the space station
[AD-A189683] 14 p1871 N88-21181
Design, development and evaluation of Stanford/Ames EVA prehensors
[NASA-CR-182688] 15 p2105 N88-22540
An investigation of conformable antennas for the astronaut backpack communication system
[NASA-CR-182908] 17 p2333 N88-23929
Space Station Human Factors Research Review. Volume 1: EVA Research and Development
[NASA-CP-2426-VOL-1] 17 p2379 N88-24145
Advanced EVA system design requirements study 17 p2380 N88-24147
Nuclear electric power for multimegawatt orbit transfer vehicles 17 p2399 N88-24261
Space cabin atmosphere and extracurricular sortie --- embolisms 19 p2696 N88-26023
The US space programme spacewalk/extravehicular activity experience: Past, present and future 19 p2697 N88-26031
Decompression procedures and accidents in space and sea 19 p2698 N88-26035
Safety of extravehicular space activities 19 p2698 N88-26038
Marintek's ocean basin, a training facility for extravehicular activity? 19 p2698 N88-26041
Man versus machine: The role of astronauts in extravehicular activity 19 p2699 N88-26045
Maintenance and supply options
[NASA-CR-172062] 24 p3332 N88-29837
Study of human factors engineering criteria for extravehicular activity (EVA) systems, volume 1
[STF23-F87025-VOL-1] 24 p3410 N88-30298

EXTRAVEHICULAR MOBILITY UNITS
Advanced EMU electrochemically regenerable CO2 and moisture absorber module breadboard
[NASA-CR-172054] 21 p2993 N88-27754

EXTREMA
U RANGE (EXTREMES)

EXTREME ULTRAVIOLET RADIATION
Electron beam requirements for soft X-ray/XUV free-electron lasers
[DE87-011750] 01 p0051 N88-10325
What's needed in the UV and EUV 02 p0255 N88-11612
Analysis of undulator field errors for XUV FELs (Extreme Ultraviolet Free Electron Laser)
[DE87-014734] 03 p0328 N88-12073
XUV emission features from the Livermore soft X-ray laser experiments
[DE88-000420] 04 p0448 N88-12779
Extreme ultraviolet beam-foil spectroscopy of highly ionized neon and argon
[AD-A185197] 05 p0561 N88-13418
Satellite observations of extreme ultraviolet radiation
[AD-A185043] 05 p0661 N88-14059
The evaluation of a deformable diffraction grating for a stigmatic EUV spectroheliometer
[NASA-CR-182371] 06 p0707 N88-14337
The EUV line flux variations and activity in Alpha Orionis 08 p1032 N88-16256
Preliminary injector, accelerator, and beamline design for rf-linac-driven XUV free-electron lasers
[DE88-003185] 10 p1336 N88-17983
Spectroscopic studies of a laser-produced carbon plasma in the near and extreme ultraviolet 11 p1553 N88-19202
Projected performance of RF-linac-driven free-electron lasers in the VUV and soft X-ray regions
[DE88-004294] 13 p1776 N88-20625
XUV source for ultra-high resolution photoionization spectroscopy
[DE88-007531] 19 p2614 N88-25510
Progress toward a soft X-ray FEL
[DE88-007669] 19 p2675 N88-25905
Development of a free-electron laser user facility for the extreme ultraviolet
[DE88-007892] 21 p2953 N88-27541

EXTREMELY HIGH FREQUENCIES
An investigation on Faraday rotators and quarter-wave plates of a 35 GHz radar signature system
[DFVLR-FB-87-14] 01 p0037 N88-10236
V-band IMPATT power amplifier
[NASA-CR-180711] 01 p0042 N88-10267
Optimization of mode converters for generating the fundamental TE(06) gyrotron output at 140 GHz
[IPF-87-1] 01 p0043 N88-10273
Estimates of satellite EHF communication outages due to attenuation by rain
[AD-A183969] 03 p0307 N88-11941
High peak power ka-band gyrotron oscillator experiment
[AD-A185424] 05 p0585 N88-13563
Technology developments to meet tomorrow's need for higher satellite frequencies 09 p1124 N88-16732
High peak power Ka-band gyrotron oscillator experiments with slotted and unslotted cavities
[AD-A188109] 11 p1478 N88-18819
An EHF telecommunication system engineering model 12 p1618 N88-19674
Research on Faraday rotators and quarter-wave plates of a 35-GHz radar signature system
[ESA-TT-1081] 16 p2189 N88-23052
Experimental radio frequency link for Ka-band communications applications
[NASA-TM-100824] 18 p2470 N88-24659
An evaluation of two millimeter wave propagation models for horizontal atmospheric attenuation at 70-115 GHZ
[AD-A192699] 21 p2931 N88-27403
The 44/20 GHz ground terminal
[AD-A194002] 23 p3204 N88-29069

EXTREMELY LOW FREQUENCIES
ELF/VLF/LF propagation and system design
[AD-A183261] 01 p0033 N88-10212
Power flow in terms of Poynting vector for Extremely Low Frequency (ELF) dipole sources in seawater
[ARE-TM(UTM)-87102] 01 p0035 N88-10221
Compilation of 1986 annual reports of the Navy ELF (Extremely Low Frequency) communications system ecological monitoring program, volume 1
[AD-A184561] 03 p0306 N88-11930
Compilation of 1986 annual reports of the Navy ELF (Extremely Low Frequency) communications system ecological monitoring program, volume 2
[AD-A184562] 03 p0306 N88-11931
Compilation of 1986 annual reports of the Navy ELF (Extremely Low Frequency) communications system ecological monitoring program, volume 3
[AD-A184563] 03 p0306 N88-11932
Applicability of extremely low frequency global resonances for study of Venusian storm activity 08 p1005 N88-16093
ELF (Extremely Low Frequency) communications system ecological monitoring program: Electromagnetic field measurements and engineering support, 1986
[AD-A188057] 11 p1509 N88-19017
WAVFLD: A program to compute ionospheric height gain functions and field strengths at VLF
[AD-A191159] 16 p2191 N88-23066
Extremely Low Frequency (ELF) communications system ecological monitoring program: Summary of 1986 progress
[AD-A192014] 19 p2642 N88-25676
Extremely Low Frequency (ELF) communications program: Non-ionizing electromagnetic radiation literature evaluation and assessment, 1986-1987 literature review
[AD-A192024] 19 p2642 N88-25677
Interaction of biological systems with static and ELF electric and magnetic fields
[DE88-007951] 20 p2831 N88-26792
Experimental proof of quasilongitudinal propagation of low-frequency waves in middle latitudes in upper ionosphere 24 p3447 N88-30516

EXTREMELY LOW RADIO FREQUENCIES
Ultra-low frequency vibration data acquisition concerns in operating flight simulators
[DE88-004795] 10 p1285 N88-17687
EXTREMUM VALUES
NT LIMITS (MATHEMATICS)
NT MAXIMA
NT MINIMA
Extrapolation of extremum values of the wind velocity 08 p1015 N88-16150
On a consistent estimate of the index of an extreme value distribution
[CWI-MS-R8710] 14 p1966 N88-21729
Approximations in extreme value theory
[AD-A189817] 15 p2124 N88-22659
Extreme value for dependent sequences via the Stein-Chen method of poisson approximation
[AD-A190325] 15 p2125 N88-22668
EXTRUDING
NT PULTRUSION
Slip casting and extruding shapes of rhenium with metal oxide additives. Part 2: Development of grain stabilized rhenium parts for resistojets
[NASA-CR-180851] 03 p0278 N88-11749
Activities at government research laboratories reported 04 p0403 N88-12503
Continuation finite element analysis of viscoelastic fluids 04 p0445 N88-12761
Tensile properties of extrusion consolidated Type 304 SS rapidly solidified powders
[DE87-014875] 05 p0566 N88-13450
Development on thin wall tubes of dispersion type
[DE87-703384] 05 p0571 N88-13483
Cyclic deformation of an extruded AlMgSi alloy 05 p0598 N88-13654
Fabrication of YBa2Cu3O7 superconducting ceramics
[DE88-003012] 07 p0938 N88-15701
Cost 501 Project UK10 part 3: Thermal fatigue damage of Fecralloy steel-sprayed and co-extruded tubing
[AERE-R-12230] 10 p1343 N88-18026
Processing, physical metallurgy and creep of NiAl + Ta and NiAl + Nb alloys
[NASA-CR-182113] 14 p1890 N88-21295
Grain growth behavior of extrusion consolidated centrifugally atomized Type 304 stainless steel powder
[DE88-006788] 15 p2038 N88-22143
Mechanical testing and microscopic analysis of structure of extruded powder aluminum
[DE88-007193] 19 p2617 N88-25528
Volcanic contribution to crustal growth in the Central Andes: A new estimate and a discussion of uncertainties 24 p3401 N88-30255
EYE (ANATOMY)
NT CORNEA
NT FOVEA
NT OCULOMOTOR NERVES
NT PUPILS
NT RETINA
Motion and space sickness 04 p0404 N88-12510
Vision of details in space and time
[B8711402] 06 p0753 N88-14624
Effect of intermittent hypercapnia on visual analyzer function 07 p0896 N88-15431
Considerations concerning the basic bandwidth reduction of high definition television systems (HDTV) component signals, based on psychophysiological properties of the eye
[IRT-B-83/87] 09 p1153 N88-16909
A-scan ultrasound measurement of ocular changes during accommodation
[AD-A186818] 09 p1198 N88-17181
Development and experimentation of an eye/brain/task testbed 09 p1205 N88-17219
Multiaperture optical system research
[AD-A188211] 11 p1549 N88-19267
Protection against laser damage to human body reviewed 15 p2053 N88-22237
Laboratory equipment update
[AD-A189781] 15 p2102 N88-22522
Future visual environment and concerns 23 p3242 N88-29299
Central serous chorioretinopathy in USAF aviators: A review
[AD-A195697] 24 p3407 N88-30280
EYE MOVEMENTS
NT NYSTAGMUS
NT SACCADIC EYE MOVEMENTS
NT VESTIBULAR NYSTAGMUS
Quantifying some information processing aspects of the pilot's instrument crosscheck
[AD-A186114] 07 p0898 N88-15443
Research on visual information processing with special reference to oculomotor behavior in the areas of exploration, recognition and search
[AD-A186598] 08 p1051 N88-16346
An innovative workstation 08 p1063 N88-16421
Refinement of eye-point-of-regard measurement with helicopter pilots in a flight experiment
[ESA-TT-1073] 09 p1200 N88-17195
Development and experimentation of an eye/brain/task testbed 09 p1205 N88-17219
Neck receptor stimulation in 0 and 1 g 12 p1658 N88-19938
Studies of the vestibulo-ocular reflex on STS 4, 5 and 6
[NASA-TM-100461] 12 p1666 N88-19987
Eye and head response to an attention cue in a dual task paradigm
[AD-A191052] 18 p2551 N88-25143
A human factors evaluation of the Advanced Visual Technology System (AVTS) eye tracking oculometer 21 p2925 N88-27361
Fighter pilot performance during airborne and simulator missions: Physiological comparisons 21 p2981 N88-27704
Stereo and eye movement
[AD-A193588] 22 p3142 N88-28681
Eye movements and spatial pattern vision
[AD-A195496] 24 p3408 N88-30290
EYE PROTECTION
Aerosol lidar for environment protection and meteorology
[DFVLR-FB-87-43] 14 p1982 N88-21828

F

F CENTERS
U COLOR CENTERS
F DISPLAYS
U F REGION
F LAYER
U F REGION
F REGION
NT F 2 REGION
A comparative analysis of equatorial and auroral-zone phase scintillation data
[AD-A184509] 03 p0350 N88-12212
High latitude F-region drift studies
[AD-A184466] 04 p0467 N88-12889
The polar ionosphere and interplanetary field
[AD-A185386] 05 p0624 N88-13822
CP-1-H analysis tests 06 p0691 N88-14236
EISCAT (European incoherent scatter radar) electron density studies
[AD-A185998] 07 p0841 N88-15099
Dynamics Explorer guest investigator
[NASA-CR-181494] 07 p0878 N88-15325
Multispectral optical observations of ionospheric F-region storm effects at low latitude
[INPE-4231-PRE/1105] 08 p1024 N88-16198
MAIMIK: A high current electron beam experiment on a sounding rocket from Andoya rocket range (Norway) 08 p1030 N88-16243
Effect of neutral wind on the latitudinal variation of nighttime F-layer vertical movements 08 p1030 N88-16244
F-layer polar cap arcs
[AD-A186592] 09 p1190 N88-17127
High altitude chemical release systems for project BIME (Brazilian Ionospheric Modification Experiments) project IMS (Ionospheric Modification Studies) project PIIE (Polar Ionospheric Irregularities Experiment) project polar arcs
[AD-A188299] 12 p1642 N88-19833
Dynamics of small and large scale irregularities at sub-auroral latitudes
[AD-A189052] 12 p1645 N88-19853
Model of Jovian F region ionosphere
[NASA-CR-182587] 13 p1855 N88-21105
In-situ plasma bubble observations associated with equatorial spread-F over Natal
[INPE-4488-PRE/1252] 15 p2095 N88-22482
Rocket measurements of ionospheric electron temperature over Natal
[INPE-4485-PRE/1250] 15 p2096 N88-22489
The MUF (Maximum Usable Frequency) (3000) as an indicator for F-region variations
[AD-A191655] 19 p2690 N88-25991
Investigation of the Sun-aligned F-region walls and related phenomena in the auroral latitude range
[AFGL-TR-87-0248] 19 p2692 N88-26000
Design, development, fabrication and launch support for a high altitude release of neodymium vapor
[AD-A194196] 22 p3118 N88-28527
Ionospheric convection and structure using ground-based digital ionosondes
[AD-A194246] 23 p3233 N88-29237
One equatorial anomaly in nighttime ionospheric F region 24 p3447 N88-30517
F STARS
The onset of chromospheric activity among the A- and F- type stars 04 p0511 N88-13144
An analysis of the photospheric line profiles in F, G, and K supergiants 04 p0513 N88-13157
F 2 REGION
Longitudinal variations of equatorial ionosphere determined from Intercosmos-19 artificial Earth satellite data 08 p1003 N88-16074
F-80 AIRCRAFT
U T-33 AIRCRAFT
F-4 AIRCRAFT
Robust control system design 02 p0127 N88-10800
F-110 AIRCRAFT
U F-4 AIRCRAFT
F-14 AIRCRAFT
Effects of the installation and operation of jet-exhaust yaw vanes on the longitudinal and lateral-directional characteristics of the F-14 airplane
[NASA-TP-2769] 04 p0393 N88-12455
Computational design of natural laminar flow wings for transonic transport application 07 p0813 N88-14948
Techniques used in the F-14 variable-sweep transition flight experiment
[NASA-TM-100444] 24 p3374 N88-30093
F-15 AIRCRAFT
Fighter design for human load limits 12 p1580 N88-19451
Performance improvements of an F-15 airplane with an integrated engine-flight control system
[NASA-TM-100431] 14 p1867 N88-21159
Augmentor performance of an F100 engine model derivative engine in an F-15 airplane
[NASA-TM-86745] 17 p2307 N88-23805
F-16 AIRCRAFT
Fighter design for human load limits 12 p1580 N88-19451
The integration of artificial intelligence techniques to improve the effectiveness of electronic countermeasure strategies in a tactical environment
[AD-A189483] 12 p1682 N88-20056
F-16 simulator for man-in-the-loop testing of aircraft control systems (SIMTACS)
[AD-A189675] 14 p1870 N88-21178
Multivariable control law design for the AFTI/F-16 with a failed control surface using a parameter-adaptive controller
[AD-A189848] 15 p2020 N88-22040
Subharmonic aliasing and its effects on the AFTI/F-16 digital flight control system
[AD-A190614] 15 p2020 N88-22042
Three-dimensional elliptic grid generation for an F-16 23 p3246 N88-29315
The cost and performance implications of reliability improvements in the F-16A/B
[AD-A195096] 24 p3324 N88-29796
LANTIRN simulator training in the F-16C
[AD-A195201] 24 p3330 N88-29826
F-18 AIRCRAFT
A study of the Department of Defense configuration management policies and procedures as applied to the FA-18 Strike/Fighter program
[AD-A184872] 05 p0657 N88-14034
Surface flow visualization of separated flows on the forebody of an F-18 aircraft and wind-tunnel model
[NASA-TM-100436] 14 p1863 N88-21127
F-27 AIRCRAFT
Metallurgical analysis of fractured F-27 aircraft landing gear
[DE88-005885] 11 p1460 N88-18705
F-106 AIRCRAFT
An experimental investigation of dynamic ground effect
[NASA-CR-4105] 04 p0394 N88-12458
Experimental and analytic studies of the triggered lightning environment of the F106B
[NASA-CR-4104] 04 p0469 N88-12887
Vortex dynamics 07 p0812 N88-14945
Atmospheric electrical modeling in support of the NASA F-106 storm hazards project
[NASA-CR-181639] 13 p1799 N88-20758
Sensitivity of F-106B leading-edge-vortex images to flight and vapor-screen parameters
[NASA-TP-2818] 17 p2300 N88-23760
Investigations into the triggered lightning response of the F106B thunderstorm research aircraft
[NASA-CR-3902] 23 p3236 N88-29258
F-111 AIRCRAFT
Predictions of F-111 TACT aircraft buffet response and correlations of fluctuating pressures measured on aluminum and steel models and the aircraft
[NASA-CR-4089] 05 p0529 N88-13218
FAB (PROGRAMMING LANGUAGE)
U FORTRAN
FABRICATION
NT SPACE MANUFACTURING

Fabrication of standardized piezoelectric polymer shock gauges by the Bauer method
[DE87-012738] 01 p0049 N88-10315
Optimization of SIS mixer elements
[NASA-CR-180710] 01 p0104 N88-10680
Multilayer monochromators for neutron spectrometers
[DE87-014291] 02 p0175 N88-11093
Preparation and properties of evaporated CdTe films
[DE87-012270] 02 p0195 N88-11216
Review of diffusion barrier technology for application in SP-100 fuel pins
[DE88-000021] 02 p0234 N88-11480
Investigation of the fabrication parameters of laser mirrors with hard oxide interference coatings
[ESA-TT-1064] 03 p0329 N88-12077
Mechanically stacked multijunction solar cells: An update on Sandia programs
[DE87-014641] 03 p0347 N88-12190
Development of advanced fiber reinforced ceramics
[DE88-000779] 04 p0420 N88-12604
Raman scattering spectrum along a bevel etched GaAs on Si, TEM (Transmission Electron Microscope) study and GaAs P-I-N photodetector on Si
[DE88-000210] 04 p0498 N88-13066
Performance monitoring and analysis of electric van fleet vehicles
[DE88-900066] 04 p0502 N88-13091
Fabrication of composites by chemical vapor deposition
[DE87-014565] 05 p0559 N88-13408
The production of ultrasmall and superfine holographic diffraction gratings using synchrotron radiation and lithographic techniques
[AD-A185395] 05 p0585 N88-13562
Fabricate, calibrate and test a dosimeter for integration into the CRRES (Combined Release and Radiation Effects Satellite) satellite
[AD-A185439] 05 p0585 N88-13564
Computer modeling of complete IC fabrication process
[AD-A184807] 05 p0654 N88-14012
Design verification and fabrication of active control systems for the DAST ARW-2 high aspect ratio wing, part 1
[NASA-CR-177959-PT-1] 06 p0669 N88-14101
Design verification and fabrication of active control systems for the DAST ARW-2 high aspect ratio wing. Part 2: Appendices
[NASA-CR-177959-PT-2] 06 p0669 N88-14102
Investigation of silicon surface passivation by silicon nitride film deposition
[NASA-CR-182350] 06 p0729 N88-14487
Development of mechanically stacked tandem concentrator cells
[DE88-001926] 06 p0730 N88-14490
Study of the vapor-liquid equilibria used in the fabrication process of hydrogen by thermochemistry
[DE88-900239] 07 p0830 N88-15035
Development of a low noise 10 K J-T refrigeration system
[AD-A186004] 07 p0838 N88-15085
Fabrication techniques used in the construction of a high resolution X-ray framing camera
[DE88-002653] 07 p0856 N88-15200
Pin joints, gears, springs, cranks and other novel micromechanical structures
[DE88-002504] 07 p0864 N88-15245
Fabrication of YBa2Cu3O7 superconducting ceramics
[DE88-003012] 07 p0938 N88-15701
High-temperature electronics
08 p0956 N88-15797
Processing, fabrication, applications and limitations of inherently conducting polymers
[DE88-003210] 08 p0973 N88-15883
Effects of fabrication on the fatigue capacity of welded steel structures
[PB87-144226] 08 p0995 N88-16021
Fabrication and packaging of discontinuous MIM (Metal-Insulator-Metal) film arrays for efficient MM wave and IR detection and mixing
[AD-A186809] 09 p1146 N88-16869
Nanoelectronics
[AD-A186969] 09 p1156 N88-16930
GaAs varactor diode MMIC fabrication technology --- monolithic microwave integrated circuit (MMIC)
[RSRE-MEMO-4022] 09 p1158 N88-16943
Interdisciplinary research in applied mathematics
[AD-A186793] 09 p1226 N88-17344
CEBAF design overview and project status
[CEBAF-PR-88-001] 09 p1246 N88-17470
Fabrication, phase transformation studies and characterization of SiC-AlN-Al2OC ceramics
[DE88-004053] 10 p1306 N88-17807
An integrated pressure sensor for in-vivo use
10 p1333 N88-17965
On systolic architectures for interpolation and integration
10 p1382 N88-18250
Fabrication and evaluation of transmissive multilayer optics for 8 keV X-rays
[DE88-003999] 10 p1409 N88-18402
The effect of magnetic impurities and barriers on the magnetization and critical current of fine filament NbTi composites
[DE88-004443] 10 p1419 N88-18472
Design and fabrication of advanced hybrid circuits for high energy physics
[DE88-004392] 11 p1479 N88-18825
Measurements as a process
[DE88-005275] 11 p1497 N88-18938
Radiation effects on gallium arsenide integrated optical devices
[DE88-004107] 11 p1551 N88-19277
Atomic monolayer metallic superlattices
[DE88-005348] 12 p1607 N88-19612
Development of a CCD characterization system
[INPE-4361-TDL/301] 12 p1623 N88-19712
Concentrating photovoltaic collectors: Fabrication design
[PB88-148051] 12 p1640 N88-19821
Use of reinforced inorganic cement materials for spark wire and drift chamber wire frames
[NASA-CR-180759] 13 p1746 N88-20438
A new process for synthesis of silicon nitride powders for advanced ceramics
[AD-A189354] 13 p1748 N88-20451
Scale-up of a batch-type chemical powder preparation process for high field varistor fabrication
[DE88-006601] 13 p1762 N88-20541
Low threshold ridge waveguide single quantum well lasers 13 p1777 N88-20631
Research on high-efficiency, stacked, multijunction, amorphous silicon alloy thin-film solar cells
[DE88-001108] 13 p1793 N88-20723
Research on single-crystal CdTe solar cells
[DE88-001115] 13 p1793 N88-20725
Stable, high-efficiency, CuInSe2-based, polycrystalline, thin-film tandem solar cells
[DE88-001116] 13 p1793 N88-20726
Design of the Sandia-Israel 20-kW reflux heat-pipe solar receiver/reactor
[DE88-001312] 13 p1794 N88-20729
Molybdenum-base cermet fuel development
[DE88-005529] 13 p1839 N88-21003
Focused ion beam fabrication of graded channel FET's in GaAs and Si
[AD-A189166] 13 p1845 N88-21040
Thin-film cadmium telluride solar cells
[DE88-001107] 13 p1846 N88-21050
Solar cell experiment on the first satellite of the Brazilian complete space mission
[INPE-4248-PRE/1121] 14 p1880 N88-21238
Surface-emitting two-dimensional laser diode arrays constructed on zig-zag heat sink surface
[DE88-005215] 14 p1915 N88-21439
Polysilicon-contacted p+ emitters for silicon solar cell applications
[DE88-005106] 14 p1942 N88-21586
Fabrication and characterization of semiconductor lasers of Pb(1-x)Sn(x)Te
[INPE-4253-PRE/1126] 15 p2072 N88-22357
Synthesis of metastable superconductors by high dynamic pressure
[DE88-005620] 15 p2139 N88-22764
Beam assisted fabrication of 3-5/Si monolithic devices
[AD-A189979] 15 p2142 N88-22785
High-T(sub c) superconducting wire fabrication and testing
[DE88-005989] 15 p2144 N88-22798
Preparation of large area NbN/AlN/NbN Josephson junctions
[DE88-006074] 15 p2145 N88-22799
Design, fabricate, calibrate, test and deliver two satellite electron flux detectors
[AD-A190799] 16 p2169 N88-22930
Limited reaction processing for semiconductor device fabrication
[AD-A190913] 16 p2283 N88-23666
Study for the determination of general and specific properties of wide energy-band gap HgCdTe in the 1 to 2 micrometer wavelength range
[AD-A191091] 17 p2334 N88-23934
Miniature traveling wave tube and method of making
[NASA-CASE-LEW-14520-1] 17 p2335 N88-23936
Fabrication of SP-100 fuel barrier structures by chemical vapor deposition 17 p2416 N88-24371
Molybdenum-base cermet fuel development
17 p2434 N88-24481
Nozzle fabrication technique
[NASA-CASE-MSC-21299-1] 18 p2475 N88-24684
Sol/gel processing techniques for glass matrix composites
[AD-A191748] 18 p2478 N88-24701
Strong fibers
[DE88-007798] 19 p2610 N88-25486
Fabrication of a flexible conductor by vapor deposition
[DE88-007500] 19 p2661 N88-25826
Thermionic integrated circuit program
[DE88-010119] 19 p2662 N88-25833
Interface modification in Nicalon (trademark)/SiC composites
[DE88-009708] 20 p2767 N88-26409
Fabrication technology
[DE88-010598] 20 p2855 N88-26955
Epitaxy and properties of two dimensional GaInAs semiconductor structures
[ETN-88-92357] 20 p2879 N88-27094
Focused ion beam fabrication of graded channel FETs in GaAs and Si
[AD-A193098] 21 p2936 N88-27439
Experimental fabrication of thin film single crystalline solar cells
[PB88-131958] 21 p2967 N88-27627
Amorphous silicon solar cells using a metal substrate
[PB88-131941] 21 p2968 N88-27628
Optical evaluation of prototype stretched-membrane mirror modules for solar central receivers
[DE88-011884] 21 p2969 N88-27637
Ceramic fabrication technology for high-T(sub)c materials
[DE88-012060] 21 p3024 N88-27953
Development of 30 micrometers extrinsic silicon multiplexed infrared detector array
[NASA-CR-177446] 22 p3082 N88-28301
Experimental fabrication of thin film single crystalline solar cells
[PB88-131958] 22 p3116 N88-28516
Fabrication of bulk superconducting ceramics
[DE88-009956] 22 p3155 N88-28773
Method for Veterbi decoding of large constraint length convolutional codes
[NASA-CASE-NPO-17310-1-CU] 23 p3183 N88-28946
A fundamental study of P/M processed elevated temperature aluminum alloys
[AD-A192958] 23 p3194 N88-29005
Advanced processing and properties of high performance alloys
[AD-A193767] 23 p3194 N88-29010
Preparation of superconducting YBa2Cu3O(sub 7-x) films by magnetron sputtering
[DE88-009977] 23 p3289 N88-29583
Tolerances for phase locking of semiconductor laser arrays
[AD-A195974] 24 p3378 N88-30120
Ion exchange processes for fabrication of integrated optical waveguide structures into glass substrates
[VTT-46] 24 p3429 N88-30405
Cluster beam studies
[AD-A195182] 24 p3434 N88-30443

FABRICS
NT PARACHUTE FABRICS
Low extractable wipers for cleaning space flight hardware 02 p0137 N88-10863
A hybrid fibreglass-CFRP cloth for new furnishings --- aircraft cabins
[SNIAS-872-111-109] 05 p0558 N88-13396
Flammability test on aircraft seats equipped with fire barrier fabrics for the Porcher company
[CEAT-M5-525200] 06 p0666 N88-14084
Method of obtaining of fire resistant polyacrylonitrile fiber or cloth from it
[AD-A185941] 07 p0836 N88-15071
Composite materials for rail transit systems
[NASA-CR-178401] 10 p1294 N88-17738
Tribological properties of alumina-boria-silicate fabric from 25 to 850 C
[NASA-TM-100806] 11 p1464 N88-18726
Fabric space radiators
[DE88-005569] 14 p1880 N88-21237
A reflux tube fabric radiator 17 p2421 N88-24394
Fabric radiators 17 p2427 N88-24435
Development of materials for fabric radiators
17 p2429 N88-24448
Investigation of leaks in fiberglass-reinforced pressure vessels by direct observation of hollow fibers in glass cloth
[DE88-006936] 19 p2609 N88-25485
Stressed fabric abrasion test procedure for urethane coated fabric fuel tanks
[AD-A196327] 24 p3356 N88-29982

FABRY-PEROT INTERFEROMETERS
Experimental measurements and numerical simulations of metal spallation by detonating solid explosives
[DE87-013227] 01 p0054 N88-10347
Program to development an optical transistor and switch
[AD-A185666] 06 p0697 N88-14278

Modern pulsed wavemeters
[DE88-003875] 10 p1335 N88-17978
Study of the ionic and neutral species in the coma of Comet Halley with an image intensifier camera
14 p2006 N88-21962

FABRY-PEROT LASERS
U LASERS

FABRY-PEROT SPECTROMETERS
A new liquid helium-cooled Fabry-Perot spectrometer used in a far infrared astronomical balloon experiment
08 p1028 N88-16224
Velocity resolved far-infrared spectroscopy of galactic sources 13 p1854 N88-21099
Fabry-Perot etalons as prefilters for astronomical far infrared Fourier transform spectroscopy
[MPE-205] 16 p2273 N88-23603

FACE CENTERED CUBIC LATTICES
State variable approach to deformation phenomena in Face Centered Cubic (FCC) metals
[VTT-44] 24 p3354 N88-29964

FACETS
U FLAT SURFACES

FACILITIES
Lewis materials research and technology: An overview
09 p1119 N88-16699

FACSIMILE COMMUNICATION
NT AUTOMATIC PICTURE TRANSMISSION
Document transfer by a digital satellite link
[NLR-MP-86071-U] 20 p2792 N88-26564

FACSIMILE TRANSMISSION
U FACSIMILE COMMUNICATION

FACTOR ANALYSIS
Assessment of fatigue in aviation crews
[AD-A184129] 03 p0356 N88-12245
Application of Vandermonde decomposition to directional and modal analysis of broadband transients
[AD-A185007] 05 p0646 N88-13956
On the work needed to factor a symmetric positive definite matrix
[AD-A185781] 06 p0759 N88-14660
Use of principal component method for analysis of multidimensional quantitative data in biomedical investigations 19 p2706 N88-26089
A programmable systolic array for factorial analysis. Part 2: The symmetric eigenvalue problem
[AD-A192396] 21 p2995 N88-27762
Recursive mass matrix factorization and inversion: An operator approach to open- and closed-chain multibody dynamics
[NASA-CR-182516] 23 p3247 N88-29328
Advancement of latent trait theory
[AD-A194302] 24 p3408 N88-30299

FACTORIAL DESIGN
Statistical selection procedures
[AD-A185868] 07 p0913 N88-15538
SEARCH: An interactive computer program for optimizing two-variable, unconstrained experiments or simulation
[AD-A190593] 15 p2112 N88-22583
Contribution to the automatic generation of floor plan placing --- integrated circuit design
[ETN-88-92193] 16 p2247 N88-23426
A programmable systolic array for factorial analysis. Part 2: The symmetric eigenvalue problem
[AD-A192396] 21 p2995 N88-27762
Measuring dispersion effects of factors in factorial experiments
[AD-A193216] 21 p3006 N88-27831

FACTORIES
U INDUSTRIAL PLANTS

FACTORIZATION
Numerical computation of transonic potential flow about 3-dimensional inlets
[NAL-TR-924] 02 p0122 N88-10770
Concurrent algorithms for transient nonlinear FE analysis
[NASA-CR-181455] 02 p0221 N88-11389
QR factorization of a dense matrix on a shared-memory multiprocessor
[DE88-001506] 04 p0480 N88-12956
Two classes of preconditioners computed using block matrix factorization techniques
[DE88-001313] 04 p0485 N88-12988
Analysis of a parallel solution method for tridiagonal systems
[PB87-230538] 06 p0762 N88-14678
Parallel LU-factorization algorithms for dense matrices
[DE88-002179] 07 p0904 N88-15478
A Schur-complement method for sparse quadratic programming
[DE88-002520] 07 p0904 N88-15479
A parallel algorithm for the general LU-factorization
[DE88-002177] 08 p1066 N88-16444
Navier-Stokes simulation of wind-tunnel flow using LU-ADI factorization algorithm
[NASA-TM-100042] 10 p1268 N88-17584
A multiprocessor scheme for the singular value decomposition
[DE88-003591] 10 p1388 N88-18288
Compact high order schemes for the Euler equations
[NASA-CR-181625] 11 p1530 N88-19138
QR factorization of a dense matrix on a hypercube multiprocessor
[DE88-009187] 19 p2716 N88-26129
Factorization of large integers on a massively parallel computer
[DE88-011625] 21 p2999 N88-27786
Second order differential equations in the complex domain
[RR-674-M] 22 p3144 N88-28695

FACULAE
Solar-geophysical data number 513, May 1987. Part 2: (Comprehensive reports). Data for November 1986 and miscellanea
[PB87-204974] 01 p0119 N88-10761
Spectral images and multi-component models of the chromospheres of AR Lacertae
11 p1568 N88-19384

FADDEEV EQUATIONS
Solution of Faddeev-Yakubovsky differential equations by the finite-dimensional approximation method for four spinless particles in the 1+3 scattering problem
[DE87-702983] 19 p2719 N88-26145
A systolic array for efficient execution of the Faddeev algorithm
[DE88-011330] 22 p3135 N88-28635

FADING
NT SIGNAL FADING
A statistical rain attenuation prediction model with application to the advanced communication technology satellite project. Part 2: Theoretical development of a dynamic model and application to rain fade durations and tolerable control delays for fade countermeasures
[NASA-TM-100242] 03 p0308 N88-11945
Spread spectrum mobile radio communications
[AD-A187487] 11 p1470 N88-18765
Identification of microwave line-of-sight multipath components 12 p1616 N88-19665
Refractive index, meteorology and fading in line-of-sight transmission paths 12 p1616 N88-19666
Radio and radar holes and multipath zones: The global and local influences on atmospheric refractive structure and resulting adverse radio and radar performance
12 p1617 N88-19667
MM-wave propagation and application in military communication systems 12 p1617 N88-19669
Space-diversity effects on line-of-sight propagation paths 12 p1617 N88-19670
The 6 GHz propagation measurements over a 51 km path in the UK 12 p1617 N88-19673

FAHRENHEIT TEMPERATURE SCALE
U TEMPERATURE SCALES

FAIL-SAFE SYSTEMS
Towards a damage tolerance philosophy for composite materials and structures
[NASA-TM-100548] 16 p2173 N88-22949

FAILURE
NT ENGINE FAILURE
NT STRUCTURAL FAILURE
NT SYSTEM FAILURES
Fatigue failure of thin porous strips
04 p0426 N88-12640
Programmable Logic Arrays (PLA's) design for testability
[PB87-102935] 04 p0438 N88-12718
An examination of coating failure on wing pivot fittings of f111 aircraft
[AD-A185028] 05 p0546 N88-13328
Electromagnetics and electrothermal approach to evaluate failures in microelectronic devices caused by electrostatic discharges: Stochastical aspects of the device reliability
[AD-A184906] 05 p0577 N88-13522
Computer aided modeling and fatigue failure forecast under stochastic loading 05 p0607 N88-13720
Deformation mechanisms and crack initiation in fatigue 05 p0608 N88-13730
A data structure and algorithm for fault diagnosis
08 p1065 N88-16432
Maximum likelihood estimates for the discrete application of the AMSAA growth model
[AD-A186921] 09 p1177 N88-17048
A finite element analysis of adhesively bonded composite joints including geometric nonlinearity, nonlinear viscoelasticity moisture diffusion and delayed failure
[AD-A187455] 10 p1296 N88-17747
Latent failures and coverage in fault-tolerant systems. A VLSI CMOS circuit design technique to aid test generation
[AD-A187615] 10 p1325 N88-17921
Estimating system and component reliabilities under partial information on cause of failure
[AD-A189107] 13 p1780 N88-20653
Multivariable control law design for the AFTI/F-16 with a failed control surface using a parameter-adaptive controller
[AD-A189848] 15 p2020 N88-22040
An investigation of the failure response of laminates under biaxial stress
[AD-A190039] 15 p2029 N88-22090
Galvanic corrosion initiatives
[AD-A190658] 15 p2040 N88-22155
Hybrid PV HgCdTe IR detectors technology reliability and failure program: Environmental stress testing plan
[AD-A191165] 16 p2211 N88-23195
Aircraft accident report: Midair collision of SkyWest Airlines Swearingen METRO 2, N163SW, and Mooney M20, N6485U, Kearns, Utah, January 15, 1987
[PB88-910404] 20 p2755 N88-26346
Probabilistic anisotropic failure criteria for composite materials
[AD-A193046] 21 p2904 N88-27232
NDE performance in predicting failure strength of spherical composite specimens with implanted flaws
[DE88-008223] 21 p2959 N88-27575
Influence of microstructure and microdamage processes on fracture at high loading rates
[AD-A192957] 21 p2960 N88-27583
Analysis of stiffness reduction, failure and stress concentration in fiber composite laminates
[AD-A193519] 22 p3050 N88-28096
Approximate evaluation of semi-Markov chain reliability models
[AD-A194669] 23 p3223 N88-29185
Plastic flow and failure modeling under high strain rate loading
[AD-A194223] 23 p3226 N88-29199
Critical conditions for failure in materials subjected to high rates of loading
[AD-A194697] 23 p3226 N88-29201
Systolic array fault tolerance performance analysis
[AD-A193521] 23 p3244 N88-29306
Exact lower confidence limits for the reliability of k of n systems for zero failures and nonconservativeness of the maximus method
[AD-A194299] 23 p3274 N88-29485
Criteria for matrix dominated failure
[AD-A196263] 24 p3341 N88-29887
Multi-metallic galvanic corrosion
[AD-A195995] 24 p3353 N88-29963
Electrochemical evaluation of the long term corrosion resistance of polymer coated steel
24 p3355 N88-29974
Automated early fatigue damage sensing system
[AD-A195717] 24 p3382 N88-30143
Stress related failures causing open metallization
[AD-A195061] 24 p3383 N88-30150
Heavy ion and proton tests for subsystem upset
[AD-A195267] 24 p3434 N88-30442

FAILURE ANALYSIS
Compendium of post-failure analysis techniques for composite materials
[AD-A183783] 01 p0018 N88-10113
Endurance testing of a natural gas-fueled rotary engine
[PB87-215703] 01 p0055 N88-10356
Optimal detection of sensor failures in flight control systems using deterministic observers
02 p0128 N88-10803
The 1986 Goddard Space Flight Center Battery Workshop
[NASA-CP-2486] 02 p0163 N88-11021
Fault tree safety analysis of a large Li/SOCl(sub)2 spacecraft battery 02 p0163 N88-11025
Failure analysis of a 3.5 inch, 50 ampere-hour nickel-hydrogen cell 02 p0164 N88-11030
Blade excitation criteria developed for aero derived engines in Arctic Alaska
[PNR90368] 02 p0182 N88-11131
Joining of silicon carbide reinforced ceramics
[DE87-014881] 03 p0294 N88-11847
Scaling of size/time/temperature associated with dilatation and distortion in uniaxial specimens
03 p0336 N88-12117
Kinetics of crack growth: Thermal/mechanical interaction 03 p0337 N88-12124
Electricity from photovoltaic solar cells. Flat-Plate Solar Array Project of the US Department of Energy's National Photovoltaics Program: 10 years of progress
[NASA-TM-89653] 03 p0346 N88-12188
Analysis of 7- X 10-foot high speed wind tunnel shaft loads in support of fan blade failure investigation
[NASA-TM-100504] 04 p0402 N88-12496
Failure analysis of composite structure materials
[AD-A184468] 04 p0410 N88-12548

Corrosion of electronic components
05 p0547 N88-13333
Applications of fatigue analyses: Transportation
05 p0608 N88-13733
Evaluation of closed cubic failure criterion for graphite/epoxy laminates
[NASA-CR-182375] 06 p0679 N88-14158
On the influence of false plots on tracking reliability: Simulations and preliminary analyses
[FOA-C-30443-3.2] 06 p0692 N88-14245
A software reliability model with variable fault exposure coefficient
[REPT-87-029] 06 p0757 N88-14646
Estimating the distribution of fault latency in a digital processor
[NASA-TM-100521] 06 p0760 N88-14666
Space station software reliability analysis based on failures observed during testing at the multisystem integration facility 06 p0798 N88-14884
Impact of solids on composite materials
[NASA-CR-182395] 07 p0827 N88-15015
Verification of FANTASTIC integrated code
07 p0924 N88-15613
Pattern recognition techniques for failure trend detection in SSME ground tests 07 p0924 N88-15614
Delamination durability of composite materials for rotorcraft 09 p1107 N88-16634
Mechanical properties of carbon fiber reinforced thermoplastic matrix composites
[NAL-TR-934] 09 p1139 N88-16827
Residual stiffness and strength of Kevlar/epoxy laminated impulsively loaded to 7.9 ktaps
[DE88-003724] 09 p1149 N88-16886
Plasma and ion etching for failure analysis. Part 2. The etching of plastic encapsulant and other semiconductor device materials, using the Technics Giga Etch 100-E plasma etch system
[AERE-R-12212] 09 p1177 N88-17050
The failure and fracture analysis of adhesive bonds
[ETN-87-90713] 09 p1181 N88-17077
CONFIG: Qualitative simulation tool for analyzing behavior of engineering devices
09 p1208 N88-17240
The implementation and use of Ada on distributed systems with high reliability requirements
[NASA-CR-182481] 09 p1221 N88-17326
Studies of the initiation of pitting corrosion on stainless steels
[AERE-M-3615] 10 p1301 N88-17778
Institute for Materials Science and Engineering, Fracture and Deformation Division: Technical activities, 1987
[PB88-153622] 10 p1345 N88-18039
A strategy for failure prediction
10 p1360 N88-18243
Finite element analysis of adhesively bonded composite joints including geometric nonlinearity, nonlinear viscoelasticity, moisture diffusion and delayed failure
[PB88-147822] 11 p1451 N88-18648
Study of the mechanical behavior of a 2-D carbon-carbon composite
[NASA-CR-182594] 11 p1451 N88-18649
A nonlinear computational model for the strength and failure of composite plates and shells
11 p1501 N88-18964
Treatment of unforeseen situations by online knowledge-based diagnostic systems --- spacecraft maintenance 12 p1589 N88-19511
Mechanical response of unidirectional boron/aluminum under combined loading
[NASA-CR-182595] 12 p1604 N88-19591
On the energy release rate for dynamic transient anti-plane shear crack propagation in a general linear viscoelastic body
[AD-A186385] 12 p1635 N88-19791
Ply-level failure analysis of a graphite/epoxy laminate under bearing-bypass loading
[NASA-TM-100578] 13 p1735 N88-20372
Improve the lifetime of the hollow fiber sodium sulfur cell
[DE88-004881] 13 p1751 N88-20469
Fracture criteria for discontinuously reinforced metal matrix composites
[NASA-CR-182665] 13 p1782 N88-20662
Strength and failure analysis of composite laminate containing a circular hole with reinforcement
[AD-A189629] 14 p1884 N88-21260
Failure mechanism of He-Ne lasers
14 p1902 N88-21362
Shorts in self-checking circuits
[RR-657-I] 14 p1908 N88-21402
Probabilistic analysis of crack containing structures with the PARIS code
[KFK-4286] 14 p1924 N88-21465
On the danger of redundancies in some aerospace mechanisms 14 p1925 N88-21475
Orbiter processing facility service platform failure and redesign 14 p1928 N88-21494
Random access memory testing: Theory and practice. The gains of fault modeling
[EUT-86-E-161] 14 p1955 N88-21649
The 1988 failure rate screening data for fusion reliability and risk analysis
[DE88-006798] 14 p1984 N88-21837
Investigation of Super*Zip separation joint
[NASA-TM-4031] 15 p2026 N88-22072
Modeling failures of intermittently used machines
[AD-A190298] 15 p2074 N88-22367
Buckling of blast loaded cylinder
[AD-A190124] 15 p2076 N88-22376
Experiments investigating advanced materials under thermomechanical loading 15 p2077 N88-22385
Monolithic ceramic analysis using the SCARE program
15 p2081 N88-22409
Fracture technology for brittle materials
15 p2083 N88-22417
The use of rule induction to assist in the diagnosis of avionic circuit board defects
[ETN-88-92077] 16 p2162 N88-22899
An investigation of the ability to recover from transients following failures for single-pilot rotorcraft
[NASA-TM-100078] 16 p2164 N88-22905
Characterization of Mode 1 and Mode 2 delamination growth and thresholds in graphite/peek composites
[NASA-TM-100577] 16 p2172 N88-22947
Readiness and failures in the algebra of communicating processes
[CWI-CS-R8748] 16 p2258 N88-23499
Fault tree analysis and synthesis
[ETN-88-92236] 16 p2261 N88-23521
Local buckling and crippling of composite stiffener sections
[NASA-TM-101133] 17 p2317 N88-23840
User's guide to the Fault Inferring Nonlinear Detection System (FINDS) computer program
[NASA-CR-178410] 18 p2462 N88-24619
Internal erosion rates of a 10-kW xenon ion thruster
[NASA-TM-100954] 18 p2476 N88-24688
Environment assisted degradation mechanisms in advanced light metals
[NASA-CR-182907] 18 p2486 N88-24746
Analysis and design of detection filters within closed-loop systems 18 p2525 N88-24980
An assessment of the state of the art in predicting the failure of ceramics
[DE88-008998] 19 p2621 N88-25551
Dimensional analysis and experimental observation of the coupling phenomena between combustion and fracture of damaged propellant samples
19 p2630 N88-25603
Failure rate prediction of electronic components
[PB87-228953] 19 p2678 N88-25925
Determining system maintainability as a probability
[DE88-007722] 19 p2679 N88-25927
Pyrotechnic system failures: Causes and prevention
[NASA-TM-100633] 20 p2765 N88-26394
Diagnosing faults in autonomous robot plan execution
[NASA-CR-182480] 20 p2841 N88-26859
Failure analysis of Chloride Silent Power, Ltd. PB cells
[DE88-010567] 21 p2938 N88-27448
Sodium/sulfur cell evaluation results
[DE88-011488] 21 p2938 N88-27451
Failure analysis of laminated composite angles
21 p2959 N88-27578
Computation of failure probability of fatigue loaded cracked structures
[ETN-88-92360] 21 p2964 N88-27607
Vapor Compression Distillation Subsystem (VCDS) component enhancement, testing and expert fault diagnostics development, volume 2
[NASA-CR-172076] 21 p2994 N88-27755
Failure analysis of quasi-isotropic composite laminates with free edges under off-axis loading
22 p3049 N88-28092
Fracture behavior in multidimensional fiber-reinforced composites 22 p3051 N88-28099
Proceedings of the 1987 Tri-Service Conference on Corrosion, volume 1
[AD-A191295] 22 p3053 N88-28114
An expert system for reliability modeling
23 p3252 N88-29355
Failure modes and effects analysis automation
23 p3254 N88-29370
ARGES: An expert system for fault diagnosis within space-based ECLS systems 23 p3255 N88-29380
Utilization of artificial intelligence techniques for the Space Station power system 23 p3261 N88-29412
A nonlinear filtering process diagnostic system for the Space Station 23 p3262 N88-29417
Intelligent fault diagnosis and failure management of flight control actuation systems
[NASA-CR-177481] 24 p3323 N88-29790
Failure analysis for gas turbines
[NLR-MP-87037-U] 24 p3326 N88-29808
Rupture of carbon fiber reinforced plastics (T300-914) composite materials: Influence of initial first ply failures on the fatigue behavior
[SNIAS-881-422-103] 24 p3342 N88-29892

FAILURE MODES

Joints in carbon fibre reinforced composites
[BR99969] 01 p0019 N88-10114
Fracture mode research of boron aluminum composite materials by Acoustic Emission (AE)
[NAL-TR-927] 02 p0142 N88-10891
Behavior of bolted joints in composite laminates
06 p0677 N88-14148
Causes and distribution of failures in semiconductor lasers (a review) 07 p0919 N88-15581
FMEAssist: A knowledge-based approach to Failure Modes and Effects Analysis 08 p1060 N88-16395
ESSAA: Embedded system safety analysis assistant
08 p1060 N88-16396
Mode 2 fracture mechanics 15 p2083 N88-22418
Some design considerations for ceramic components in heat engine applications 17 p2323 N88-23875
Evaluation of UN fuel pin failure modes and motion of fuel during severe accidents for reactors in space
17 p2425 N88-24424
Fatigue failure of regenerator screens in a high frequency Stirling engine 17 p2436 N88-24491
Analysis of notched metal matrix composites under tension loading
[NASA-TM-100629] 18 p2480 N88-24713
Applications of fault tree analysis to the design process
[DE88-007048] 18 p2525 N88-24982
Loading rate sensitivity of open hole composites in compression
[NASA-TM-100634] 19 p2610 N88-25490
Failure analysis of laminated composite angles
21 p2959 N88-27578
Micromechanics of composite laminate compression failures
[NASA-CR-183179] 22 p3050 N88-28098
Thin film-residual stress assessment
[AD-A193205] 23 p3196 N88-29018
A study of the floating roller peel test for adhesives
[AD-A194114] 23 p3198 N88-29034
Visual related accidents/incidents
23 p3242 N88-29293
Failure modes and effects analysis automation
23 p3254 N88-29370

FAINT OBJECT CAMERA

A search for very low mass (brown dwarf) stars as wide binaries using a seven element infrared camera-photometer 04 p0512 N88-13150

FAINT OBJECTS

Survival analysis, or what to do with upper limits in astronomical surveys
[NASA-CR-182936] 17 p2449 N88-24551
Ultraviolet spectra of two magnetic white dwarfs and ultraviolet spectra of subluminous objects found in the Kiso Schmidt survey
[NASA-CR-183051] 18 p2593 N88-25408
Observations of faint field galaxies
[NASA-CR-183251] 24 p3453 N88-30555

FAIRCHILD MILITARY AIRCRAFT

U MILITARY AIRCRAFT

FAIRINGS

Effect of a model support strut on measurement of aerodynamic longitudinal and lateral coefficients
[PB87-170288] 09 p1113 N88-16670
Ariane 4, long version: Pressure distribution measurements on two models of different scale of the Ariane 4 nose fairings in the transonic tunnel of F+W Emmen (Switzerland) with varying tunnel configurations. Comparison with measurements taken at Modane (France) and with calculations after the Euler method
[F+W-TF-1878] 09 p1122 N88-16716
The Ariane fairing and its separation systems
09 p1126 N88-16754

FALLING SPHERES

Improved resolution atmospheric density measurements based on simulations 08 p1027 N88-16221
Project CONDOR: Middle atmosphere wind structure obtained with lightweight inflatable spheres near the equatorial electrojet 08 p1028 N88-16230

FALLOUT

Health and environmental consequences of the Chernobyl nuclear power plant accident
[DOE/ER-0332] 19 p2689 N88-25985
Acute radiation syndromes and their management
[DE88-009839] 20 p2831 N88-26797

FALSE ALARMS

Response of wind shear warning systems to turbulence with implication of nuisance alerts
10 p1274 N88-17618

Windshear warning aerospatiale approach
10 p1274 N88-17620
Airworthiness considerations
10 p1276 N88-17636
On adaptive cell-averaging CFAR (Constant False-Alarm Rate) radar signal detection
[AD-A196286] 24 p3360 N88-30009
Evaluation of LISBON TAR SSR radar
[EEC/NOTE-5/87] 24 p3362 N88-30015

FAN BLADES
First article test noise survey of the A/F32T-9 large turbo fan engine enclosed noise suppressor system, Sky Harbor IAP (International Airport), Phoenix, Arizona
[AD-A183799] 01 p0090 N88-10586
The wide chord fan blade: A Rolls Royce first
[PNR90416] 02 p0125 N88-10789
The use of holographic interferometry for turbomachinery fan evaluation during rotating tests
[PNR90390] 02 p0176 N88-11098
The use of Kevlar on aero-engine fan containment casings
[PNR90410] 02 p0182 N88-11134
Analysis of 7- X 10-foot high speed wind tunnel shaft loads in support of fan blade failure investigation
[NASA-TM-100504] 04 p0402 N88-12496
Aerodynamic performance of a scale-model, counter-rotating unducted fan 10 p1282 N88-17666
The composite blade structural analyzer (COBSTRAN)
15 p2078 N88-22390
Structural tailoring of advanced turboprops
15 p2080 N88-22400
Detailed on-blade measurements on a transonic fan in unstalled supersonic flutter
[PNR90424] 22 p3039 N88-28043
An experimental investigation of two 15 percent-scale wind tunnel fan-blade designs
[NASA-TM-88256] 22 p3046 N88-28076
Optical measurement of unducted fan blade deflections
[NASA-TM-100966] 23 p3216 N88-29142

FANLIFT DEVICES
U LIFT FANS

FANS
Supersonic throughflow fans for high-speed aircraft
08 p0958 N88-15810

FAR FIELDS
Helicopter main-rotor speed effects on far-field acoustic levels
[NASA-TM-100512] 02 p0230 N88-11451
High power phased array and tailored gain semiconductor lasers 03 p0329 N88-12078
Far field of steady waves produced by local perturbation sources in stream of stratified fluid
06 p0771 N88-14736
Overestimation of on-axis power density by the Fraunhofer (far-field) approximation
[AD-A186399] 07 p0843 N88-15111
Study on a double reflector compact range --- satellite antennas
[S-201-05] 09 p1153 N88-16908
State-of-the-art for assessing earthquake hazards in the US. Parameters for specifying intensity-related earthquake ground motions
[AD-A188230] 11 p1512 N88-19032
Determination of characteristic radiation properties of a torus antenna: Integral equation method
[DFVLR-FB-87-46] 16 p2188 N88-23049
Transmitting boundary for finite-difference calculations with finite modeling of an infinite medium
[AD-A191441] 18 p2570 N88-25264
First article noise survey of the A/F32T-9 large turbo fan engine enclosed noise suppressor system, far-field noise, Ellsworth AFB, South Dakota
[AD-A191938] 19 p2602 N88-25457
Fatigue crack growth under far-field cyclic compression
[DE88-011215] 20 p2813 N88-26689
The far field from a hybrid electromagnetic pulse (HPD) simulator
[FOA-C-30480-4.2] 22 p3071 N88-28231
Development and demonstration of an on-board mission planner for helicopters
[NASA-CR-177482] 24 p3328 N88-29817
Application of sampling techniques to near-field far-field transformation
[ESA-CR(P)-2546] 24 p3359 N88-30002

FAR INFRARED RADIATION
Precise measurement of refractive index and absorption coefficient of near millimeter wave and far infrared materials
[AD-A184538] 03 p0293 N88-11840
Absorption of far IR-radiation by H2O-N2 complexes under atmospheric conditions 04 p0462 N88-12855
Far-infrared spectra of lithium deposited on a gold electrode: Interpretation using a cluster model
[AD-A184231] 04 p0495 N88-13050
Far infrared Fourier transform spectroscopy of semiconductors
[DE88-000188] 04 p0499 N88-13072
Far infrared circumstellar debris shells of red supergiant stars 04 p0515 N88-13165
Justification and prospects of observations of interstellar, far-infrared emission lines, using a small-sized balloon-borne telescope 08 p1032 N88-16254
Fast switching of far infrared radiation by refractive index change in semiconductors using photoionization
[ETN-88-91490] 11 p1551 N88-19279
Development of electrostatic-accelerator free-electron lasers
[AD-A189507] 13 p1774 N88-20614
Stratospheric trace gas distributions from fair infrared thermal emission spectroscopy
13 p1797 N88-20749
Velocity resolved far-infrared spectroscopy of galactic sources 13 p1854 N88-21099
Far-infrared (120-300 micron) observations of the Carina Nebula 14 p1993 N88-21876
Theoretical studies of Resonance Enhanced Stimulated Raman Scattering (RESRS) of frequency-doubled Alexandrite laser wavelength in cesium vapor
[NASA-CR-182870] 15 p2036 N88-22133
Experimental studies on electronic properties of HgTe/CdTe and Hg sub 1-z Cd sub x Te/CdTe heterostructures and superlattices
[AD-A189826] 15 p2142 N88-22783
Fabry-Perot etalons as prefilters for astronomical far infrared Fourier transform spectroscopy
[MPE-205] 16 p2273 N88-23603
Balloon-borne three-meter telescope for far-infrared and submillimeter astronomy
[NASA-CR-182924] 17 p2449 N88-24550
Infrared and far-infrared laser development for plasma diagnostics at Oak Ridge National Laboratory
[DE88-007262] 19 p2674 N88-25904
Far- and mid-infrared properties of metal-insulator composite materials
[AD-A193227] 21 p2905 N88-27236
Calculation of far infrared absorption in B poly(dA).poly(dT)
[AD-A193128] 21 p2918 N88-27318
IR (infrared) sky radiance distributions in the marine boundary layer
[AD-A193683] 22 p3119 N88-28531
Far infrared supplement: Catalog of infrared observations, second edition
[NASA-RP-1205] 24 p3452 N88-30545

FAR ULTRAVIOLET RADIATION
NT LYMAN ALPHA RADIATION
Vacuum ultraviolet electronic properties of liquids
[DE88-000165] 03 p0282 N88-11772
A comprehensive exploration of late-type stars in the far-ultraviolet 04 p0520 N88-13194
Theoretical and observational problems with Holes in the far UV dayglow
[AD-A188190] 10 p1355 N88-18100
Survival and mutation induction of dehydrated yeast cells after UV exposure 12 p1657 N88-19932
Wavelength scaling of lithium-like recombination scheme for X-UV gain production --- X-ray lasers
[ETN-88-92002] 13 p1778 N88-20634

FARADAY EFFECT
An investigation on Faraday rotators and quarter-wave plates of a 35 GHz radar signature system
[DFVLR-FB-87-14] 01 p0037 N88-10236
Laser induced fluorescent study of relativistic electron beams
[AD-A184456] 04 p0447 N88-12774
Research on Faraday rotators and quarter-wave plates of a 35-GHz radar signature system
[ESA-TT-1081] 16 p2189 N88-23052
Studies for the definition of a Faraday converter for space nuclear systems 17 p2411 N88-24339
Thermal and mechanical analysis of the Faraday shield for the compact ignition tokamak
[DE88-007855] 20 p2856 N88-26962

FARADAY ROTATION
U FARADAY EFFECT

FARM CROPS
NT COFFEE
NT CORN
NT COTTON
NT FRUITS
NT GRAINS (FOOD)
NT LEGUMINOUS PLANTS
NT POTATOES
NT RICE
NT SOYBEANS
NT SUGAR CANE
NT WHEAT
Low-temperature thermochemical conversion of high moisture biomass feedstocks 18 p2536 N88-25047

FARMLANDS
Evaluation of SPOT imagery for monitoring irrigated lands 22 p3090 N88-28352

FAST FOURIER TRANSFORMATIONS
Synthetic-aperture radars viewed as interferometers with matched filter processing of the collected data
[AD-A190608] 15 p2057 N88-22262
Design and implementation of VLSI prime factor algorithm processor
[AD-A190483] 15 p2112 N88-22580
Spatial filtering on digital images
17 p2354 N88-24025
Simulation and analysis of wave propagation through random media 21 p2947 N88-27503
Detection of acceleration (+Gz) induced blackout by matched-filtering of visual evoked potentials
21 p2982 N88-27710
Waveform analysis on the IBM PC
[AD-A194249] 23 p3248 N88-29330

FAST NEUTRONS
Superconductivity of pseudobinary compounds A15 (V-Cr)3Si, (V-MO)3Si, Mo3(Si-Re), bombarded with fast neutrons 03 p0285 N88-11792
Neutron radiation tolerance of Au-activated silicon
17 p2408 N88-24316
Simulation of the neutronic characteristics of large fast neutron reactors
[ETN-88-92305] 20 p2853 N88-26940

FAST NUCLEAR REACTORS
NT EXPERIMENTAL BREEDER REACTOR 2
NT LIQUID METAL FAST BREEDER REACTORS
The results of application studies for space nuclear power 17 p2398 N88-24259
BIFOLD: A dual-mode nuclear space power system
17 p2404 N88-24292
Interaction of the control system with core nuclear design for fast spectrum space power reactors
17 p2405 N88-24304
A dynamic model for the aft accumulator in the TE SP-100 system 17 p2414 N88-24354
Parametric analyses of the TE SP-100 system performance 17 p2415 N88-24358
Simulation of the neutronic characteristics of large fast neutron reactors
[ETN-88-92305] 20 p2853 N88-26940
Heat and mass transfer in a transport channel
[DE88-701968] 21 p2945 N88-27493

FASTENERS
NT BOLTS
NT LOCKS (FASTENERS)
NT PINS
NT RIVETS
NT SCREWS
Standard fatigue test specimens for fastener evaluation
[AGARD-AG-304] 04 p0455 N88-12818
Experimental and theoretical investigation of mechanically fastened composites
[AD-A185896] 07 p0826 N88-15008
Fastening high resistance bolts in real assemblies
[CRIF-MT-171] 07 p0861 N88-15221
The Shock and Vibration Digest, volume 20, no. 3
12 p1635 N88-19786
Crack distribution and growth rates for critical fastener holes in Mirage wing RH79
[AD-A189080] 13 p1722 N88-20293
Thermal stress in high temperature cylindrical fasteners
[NASA-TM-100611] 15 p2087 N88-22438
Toggle release
[NASA-CASE-MSC-21354-1] 18 p2523 N88-24969
Standard fatigue specimens for fastener evaluation --- aircraft components
[FFA-TN-1987-68] 24 p3384 N88-30157

FATIGUE (BIOLOGY)
NT FLIGHT FATIGUE
NT MUSCULAR FATIGUE
Assessment of fatigue in aviation crews
[AD-A184129] 03 p0356 N88-12245
Assessment of physical activity intensity by heart rate during sleep limited military operations
[AD-A185913] 07 p0688 N88-15382
Computer response time measurements of mood, fatigue and symptom scale items: Implications for scale response time uses
[AD-A186093] 07 p0888 N88-15384
The use of heart rate in the prescription and evaluation of exercise programs
[AD-A186454] 08 p1049 N88-16336
Carbamates, atropine, and diazepam: Effects on performance in the running rat
[AD-A188009] 11 p1517 N88-19062
Causes and prevention of occupational Repetition Strain Injuries (RSI) 11 p1521 N88-19083

Individual functional typology of sympathoadrenal system as indicator of physiological status in adverse environments 12 p1665 N88-19979
Challenges of physiological monitoring in a Navy operational setting 16 p2239 N88-23374
Attention, effort, and fatigue: Neuropsychological perspectives 16 p2241 N88-23387
Neurophysiological predictors of quality of performance 16 p2242 N88-23391
Method for observing changes in functional state of human operator 20 p2830 N88-26789
Psychophysiological measures of drowsiness as estimators of mental fatigue and performance degradation during sleep deprivation 21 p2980 N88-27702
Neurophysiological patterns of operational fatigue: Preliminary results 21 p2981 N88-27703
Plasma volume expansion in rats: Effects on thermoregulation and exercise
[AD-A192656] 22 p3130 N88-28606
The impact of hyperthermia and hypohydration on circulation, strength, endurance and health
[AD-A192657] 22 p3131 N88-28615
Stress/fatigue and the ARNG (Army National Guard) aviator
[AD-A194184] 22 p3132 N88-28621

FATIGUE (MATERIALS)
NT ACOUSTIC FATIGUE
NT BENDING FATIGUE
NT METAL FATIGUE
NT STRUCTURAL STRAIN
NT THERMAL FATIGUE

Low cycle fatigue on isotropic fine-grained graphite
[DE87-702627] 01 p0028 N88-10177
Determination of the fatigue strength of mechanically, thermally and corrosively loaded multilayer materials
[ETN-87-90375] 01 p0058 N88-10372
New fatigue damage analysis of complex engineering components based on Finite Element Methods (FEM)
[DFVLR-FB-87-15] 01 p0062 N88-10401
Mechanism of mechanical fatigue of fused silica
[DE87-014199] 02 p0152 N88-10950
Creep-fatigue behavior of NiCoCrAlY coated PWA 1480 02 p0189 N88-11176
Lewis' enhanced laboratory for research into the fatigue and constitutive behavior of high temperature materials 02 p0189 N88-11177
The influence of load cycle reconstitution on fatigue behaviour
[ARL-STRUC-R-424] 02 p0192 N88-11198
Prediction of fatigue cracking and rupture of large structures
[ONERA-RT-31/7169-RY-055-R] 02 p0192 N88-11199
Review of investigations of aeronautical fatigue in the Federal Republic of Germany
[LBF-S-178] 02 p0192 N88-11201
Operational load measurements on service helicopters 03 p0263 N88-11658
Laminated ferrous composites based on ultrahigh carbon (UHC) steels
[AD-A184617] 03 p0280 N88-11764
Deformation mechanisms of thermostructural materials
[AD-A184070] 03 p0338 N88-12128
Mechanical behavior of a controlled rolled high-strength low alloy steeel plate, microalloyed with Nb and V
[DE87-703507] 04 p0415 N88-12571
Work-in-progress presented at the Army Symposium on Solid Mechanics, 1986: Lightening of the Force
[AD-A184791] 04 p0427 N88-12644
Micromechanisms of fatigue crack growth and fracture toughness in metal matrix composites
[AD-A185200] 05 p0558 N88-13392
X-ray analysis of polycrystalline aluminium subjected to fatigue cycling
[NAL-TM-MT-8706] 05 p0564 N88-13434
Fatigue 87, volume 3
[AD-A184047] 05 p0604 N88-13700
Fracture kinetics of corrosion fatigue 05 p0605 N88-13708
Fatigue crack growth: Statistical considerations 05 p0606 N88-13718
Telemetric laser extensometry technique for monitoring deflections in small cracks 05 p0607 N88-13724
An optical interferometry technique to evaluate closure along a crack front 05 p0607 N88-13726
On the geometrical description of fatigue crack surfaces 05 p0607 N88-13727
An overview of fatigue 05 p0608 N88-13729
Deformation mechanisms and crack initiation in fatigue 05 p0608 N88-13730
Experimental studies on acoustic emission monitoring of crack propagation in offshore structures: A literature survey 05 p0610 N88-13748
Study of the evolution of short cracks in fatigue analysis --- aircraft construction materials
[DCQ/L-46-555] 06 p0722 N88-14442
Random loading fatigue crack growth: Crack closure considerations 06 p0797 N88-14881
Contribution to modeling flexion fatigue damage in unidirectional composite materials
[ECL-87-12] 08 p0965 N88-15843
The Shock and Vibration Bulletin. Part 3: Isolation and damping, vibration test criteria, and vibration analysis and test
[AD-A186750] 08 p0997 N88-16040
The development of laboratory vibration test schedules: Philosophies and techniques 08 p0999 N88-16049
Fatigue effects of a swept sine test 08 p0999 N88-16054
Aeropropulsion '87. Session 1: Aeropropulsion Materials Research
[NASA-CP-10003-SESS-1] 09 p1118 N88-16697
Micromechanisms of fatigue crack growth and fracture toughness in metal matrix composites
[AD-A186941] 09 p1137 N88-16816
Fatigue behaviour of hybrid composites
[BR102236] 09 p1138 N88-16819
Mechanical properties of carbon fiber reinforced thermoplastic matrix composites
[NAL-TR-934] 09 p1139 N88-16827
Multipurpose corrosion inhibitors for aerospace materials in Naval environments
[AD-A186728] 09 p1143 N88-16853
Development of methods for low temperature diffusion bonding
[AD-A186875] 09 p1174 N88-17033
Fracture mechanics characterization of crack growth under creep and fatigue conditions
[W-2/87] 09 p1183 N88-17087
Effect of post-cure heat-treatment on static and fatigue behaviour of XAS-914C carbon fibre composite
[AD-A186943] 10 p1294 N88-17735
Influence of different parameters on damage development --- carbon fiber reinforced plastics 11 p1448 N88-18632
Effects of thermal and thermo-mechanical treatments on the mechanical properties of centrifugally cast alloy 718
[AD-A188195] 11 p1458 N88-18690
Status of the special-purpose airfoil families
[DE88-001124] 11 p1506 N88-18998
Elevated temperature crack growth studies of advanced titanium aluminides
[AD-A189025] 12 p1608 N88-19618
The Shock and Vibration Digest, volume 20, no. 3 12 p1635 N88-19786
Crack distribution and growth rates for critical fastener holes in Mirage wing RH79
[AD-A189080] 13 p1722 N88-20293
High-temperature metal matrix composites
[AD-A189516] 13 p1734 N88-20367
The effect of microstructure on the fatigue crack growth resistance of nickel base superalloys
[AD-A189526] 13 p1741 N88-20414
Threshold fatigue crack growth in Ti-6Al-2Sn-4Zr-6Mo
[AD-A189560] 13 p1741 N88-20415
Environmentally assisted crack growth in structural alloys: Perspectives and new directions
[AD-A190137] 15 p2076 N88-22377
Lewis Structures Technology, 1988. Volume 2: Structural Mechanics
[NASA-CP-3003-VOL-2] 15 p2077 N88-22382
Mode 2 fracture mechanics 15 p2083 N88-22418
In situ fatigue loading stage inside scanning electron microscope 15 p2083 N88-22419
Grain boundary oxidation and low-cycle fatigue at elevated temperatures 15 p2083 N88-22420
Cumulative fatigue damage models 15 p2084 N88-22422
Fatigue damage mapping 15 p2084 N88-22423
Spectrum fatigue testing for materials characterization
[VTT-RR-502] 15 p2088 N88-22443
Fatigue crack growth behavior of a single crystal alloy as observed through an in situ fatigue loading stage
[NASA-TM-100863] 16 p2179 N88-22986
Proceedings of the 1987 Tri-Service Conference on Corrosion, Volume 2
[AD-A189660] 17 p2319 N88-23847
Corrosion and fatigue properties of FeCrB/Si metallic glass wires in aqueous environments 17 p2320 N88-23855
Effect of test sample geometry on the fatigue crack growth of X10NiCrAlTi 32 20 and NiCr22 Co 12Mo
[JUEL-SPEZ-399] 17 p2348 N88-23990
Fatigue failure of regenerator screens in a high frequency Stirling engine 17 p2436 N88-24491
Design of overlays for rigid airport pavements
[DOT/FAA/PM-87/19] 18 p2468 N88-24652
Predictive corrosion modeling, volume 1
[AD-A191229] 18 p2485 N88-24739
Resolved shear stress intensity coefficient and fatigue crack growth in large crystals
[NASA-CR-182137] 18 p2528 N88-24997
Fatigue crack growth due to random loading 18 p2531 N88-25017
Fatigue testing and damage development in continuous fiber reinforced metal matrix composites
[NASA-TM-100628] 19 p2610 N88-25489
Research on fractography of heat-resistant alloys 19 p2634 N88-25625
Study of probabilistic fatigue crack growth and associated scatter under constant-and-variable amplitude loading spectrum
[AD-A192027] 19 p2679 N88-25929
Study of the influence of metallurgical factors on fatigue and fracture of aerospace structural materials
[AD-A192909] 20 p2774 N88-26452
Fatigue of lithium-aluminum alloys: An example of localization of the plastic deformation
[ETN-88-92309] 20 p2775 N88-26456
Significance of the local electrode potential within pits, crevices and cracks
[AD-A192482] 21 p2935 N88-27432
Three-dimensional aspects of fatigue crack closure
[AD-A192296] 21 p2960 N88-27581
Applications of fatigue analyses: Aircraft engines
[PNR90439] 22 p3044 N88-28066
Empirical fatigue crack growth data for a tension loaded threaded fastener
[AD-A194112] 22 p3088 N88-28334
Interaction of creep and fatigue damage in gas turbine blade material
[PNR90440] 22 p3088 N88-28335
The use of a surface acoustic wave technique to study the growth behavior of small cracks in a high strength steel alloy 23 p3225 N88-29193
Fatigue crack growth characteristics of ARALL (trademark)-1
[AD-A196185] 24 p3341 N88-29889
Modeling of micromechanisms of fatigue and fracture in hybrid materials
[AD-A195604] 24 p3382 N88-30142
Automated early fatigue damage sensing system
[AD-A195717] 24 p3382 N88-30143
Fatigue crack propagation: Probabilistic modeling and statistical analysis
[AD-A195885] 24 p3384 N88-30155
An investigation of constitutive models for predicting viscoplastic response during cyclic loading
[AD-A194875] 24 p3385 N88-30163
The development of acoustic emission for structural integrity monitoring of aircraft
[AD-A196264] 24 p3427 N88-30398

FATIGUE DIAGRAMS
U S-N DIAGRAMS

FATIGUE LIFE
The effect of fretting corrosion on the fatigue strength of steel and cast iron under sinusoidal and random loading
[LBF-FB-177] 01 p0023 N88-10142
Determination of the fatigue strength of mechanically, thermally and corrosively loaded multilayer materials
[ETN-87-90375] 01 p0058 N88-10372
The effect of size and surface on the lifetime prediction of StE 460 notched bars
[FD-6/1986] 01 p0058 N88-10374
The fatigue properties of aerospace steels under constant amplitude and flight-by-flight simulated loading
[BAE-MSM-R-GEN-0566] 01 p0059 N88-10377
Fatigue life evaluation according to local strain concept
[FF-14/1985] 01 p0059 N88-10381
Estimation multiaxial elastic-plastic notch stresses and strains in combined loading
[FB-2/1986] 01 p0060 N88-10382
Stress-strain analysis and life predictions of a notched shaft under multiaxial loading
[FB-5/1986] 01 p0060 N88-10384
Crack initiation life estimations for notched specimens with residual stresses based on local strains
[FF-17/1986] 01 p0060 N88-10385
Criteria for determination of significant load cycles in variable amplitude load sequences
[NLR-MP-86013-U] 01 p0060 N88-10386
Cumulative fatigue and life prediction of fibre composites. Part 1: Literature reviews
[BR101013] 02 p0142 N88-10893
Cumulative fatigue and life prediction of fibre composites. Part 2: Experimental techniques and results
[BR101014] 02 p0142 N88-10894
Blade excitation criteria developed for aero derived engines in Arctic Alaska
[PNR90368] 02 p0182 N88-11131
Marine gas turbines - engine health monitoring, new approaches
[PNR90369] 02 p0182 N88-11132

Creep fatigue life prediction for engine hot section materials (isotropic): Third year progress review
02 p0188 N88-11173
The influence of load cycle reconstitution on fatigue behaviour
[ARL-STRUC-R-424] 02 p0192 N88-11198
Review of investigations of aeronautical fatigue in the Federal Republic of Germany
[LBF-S-178] 02 p0192 N88-11201
Operational load measurements on service helicopters
03 p0263 N88-11658
Durability of powdered aluminum structures
04 p0429 N88-12655
Input turbulence features at a megawatt-size wind turbine, Medicine Bow, Wyoming
[DE88-000098] 04 p0464 N88-12873
Damage considerations in sizing aircraft cells. Life predictions
[SNIAS-872-111-116] 05 p0546 N88-13330
Welded joint fatigue of a AISI 304 L type stainless steel
[DE87-703530] 05 p0592 N88-13607
A study of fatigue crack growth life under random stresses 05 p0602 N88-13685
The how and why of variable amplitude testing
05 p0603 N88-13690
Tensile mean stress effects on uniaxial fatigue behavior of 1045 HR steel 05 p0603 N88-13694
Fretting wear and fretting fatigue damage
05 p0603 N88-13697
A study of corrosion fatigue crack initiation, growth and the threshold condition under variable amplitude loading
05 p0604 N88-13701
Low cycle fatigue behaviour of notched specimens of nickel based superalloy single crystal
05 p0605 N88-13712
Fatigue characteristics of ion treated surfaces
05 p0606 N88-13713
The effect of heat treatment on fatigue crack growth in polycarbonate 05 p0606 N88-13714
Effect of test temperature and frequency on fatigue crack propagation in PVC 05 p0606 N88-13715
Environmental fracture toughness and static fatigue crack propagation of silica glass
05 p0606 N88-13716
Effect of interface on mechanical properties of graphite/201 aluminum composites
05 p0606 N88-13717
Constraint effects in fatigue crack growth
05 p0606 N88-13719
Computer aided modeling and fatigue failure forecast under stochastic loading 05 p0607 N88-13720
A comparison of plastic work energy and external input for fatigue crack propagation 05 p0607 N88-13722
Fatigue under nonnormal random stresses using Monte Carlo method 05 p0607 N88-13723
X-ray fatigue failure prediction based on plasticity response to microcracks 05 p0607 N88-13725
Development of research on fatigue of spot-weld in automobile structures in Japan
05 p0608 N88-13728
Accurate rotor loads prediction using the FLAP (Force and Loads Analysis Program) dynamics code
[DE88-001109] 05 p0623 N88-13815
Temperature dependent mechanical properties of an alumina fiber reinforced aluminum composite
06 p0677 N88-14147
Fatigue 87, volume 2
[AD-A184046] 06 p0715 N88-14381
Effect of hold time on fatigue of lead rich PbSn solder
06 p0715 N88-14387
Near-threshold fatigue 06 p0716 N88-14392
Fatigue oxidation interaction in low cycle fatigue
06 p0719 N88-14420
High temperature low cycle fatigue of oxide dispersion strengthened and single crystal nickel base superalloys
06 p0720 N88-14422
High temperature low cycle fatigue behavior and creep-fatigue interation of MA 6000 ODS alloy
06 p0720 N88-14425
Creep-fatigue cracking in high temperature turbine rotors 06 p0720 N88-14426
Dependence of strainrange partitioned fatigue life at elevated temperature on monotonic stress-strain properties 06 p0721 N88-14428
Fatigue life prediction modeling for turbine hot section materials
[NASA-TM-100291] 06 p0724 N88-14453
Investigations on the crack growth retardation behavior and fatigue life prediction in structural materials
[PB87-143756] 07 p0827 N88-15016
Developing an accelerated endurance test for greases: A status report
[AD-A185963] 07 p0836 N88-15072
Life prediction of thermomechanical fatigue using total strain version of strainrange partitioning (SRP): A proposal
[NASA-TP-2779] 07 p0867 N88-15263
Life prediction technologies for aeronautical propulsion systems 08 p0954 N88-15788
Analysis of load-bearing capacity of nitrided layer
[PB87-144176] 08 p0968 N88-15857
Experimental investigation on the bending fatigue performance of gas carbonitrided and carburized gears
[PB87-147997] 08 p0992 N88-16003
Effects of fabrication on the fatigue capacity of welded steel structures
[PB87-144226] 08 p0995 N88-16021
Effects of a regenerating heat treatment on the creep behavior and the lifetime during creep test loading
[ETN-88-91063] 09 p1144 N88-16855
VAWT (Vertical-Axis Wind Turbine) stochastic loads produced by atmospheric turbulence
[DE88-001355] 09 p1187 N88-17110
Relationship between fatigue life in the creep-fatigue region and stress-strain response
[NASA-TM-100796] 10 p1345 N88-18040
Statistical evaluation of experimental results from fatigue strength tests on CFRP composite materials
11 p1449 N88-18635
Damage mechanisms and fatigue life prediction of graphite/epoxy laminates 11 p1449 N88-18637
Advanced durability analysis. Volume 1: Analytical methods
[AD-A188341] 12 p1635 N88-19789
Dynamic tensile cyclic fatigue of Si3N4
[DE88-003919] 13 p1781 N88-20658
Fatigue load measurements and evaluation of the 25m Horizontal Axis Wind Turbine (HAWT) at Petten, The Netherlands
[NLR-MP-86054-U] 13 p1782 N88-20660
European approaches in standard spectrum development --- aircraft load spectra
[NLR-MP-87007-U] 13 p1782 N88-20661
Hygrothermomechanical fiber composite fatigue: Computational simulation
[NASA-TM-100840] 14 p1884 N88-21257
Effect of protective coatings on high-temperature fatigue of heat-resistant alloys 14 p1895 N88-21314
A constitutive model for an overlay coating
14 p1933 N88-21525
Life assessment of combustor liner using unified constitutive models 15 p2077 N88-22384
Computational structural mechanics for engine structures 15 p2080 N88-22399
Large-scale wind turbine structures
15 p2085 N88-22429
Random Process Simulation for stochastic fatigue analysis
[NASA-TM-100464] 15 p2123 N88-22654
Fatigue damage development of various CFRP-laminates
[NASA-TT-20247] 16 p2172 N88-22945
The analysis of fatigue crack growth mechanism and oxidation and fatigue life at elevated temperatures
[NASA-CR-182129] 16 p2179 N88-22987
Durability of compound cylinder under static internal-pressure repeat load of long duration
16 p2180 N88-22991
Computerized life and reliability modelling for turboprop transmissions
[NASA-TM-100918] 16 p2215 N88-23220
Application of the ONERA model to the life estimation under fatigue cracking of a Al-Li alloy. Parameter identification and test-experiment comparison under FALSTAFF loading
[ONERA-RT-32/7169-RY-063-R]
16 p2222 N88-23264
Damage by creep fatigue: Influence of the visco-elasticity of the matrix
[PB88-124706] 16 p2528 N88-24998
Cyclic fatigue damage characteristics observed for simple loadings extended to multiaxial life prediction
[NASA-CR-182126] 18 p2531 N88-25016
Surface fatigue life of CBN and vitreous ground carburized and hardened AISI 9310 spur gears
[NASA-TM-100960] 19 p2677 N88-25916
Investigation of rolling contact fatigue of ball bearings
[NASA-TT-20196] 19 p2678 N88-25922
Prediction of fatigue life of notched specimens under aircraft loading and importance of the relative method in the case of local strain approach, part 2
[TAE-595-PT-2] 19 p2680 N88-25934
Engine component retirement for cause. Volume 1: Executive summary
[AD-A192730] 20 p2760 N88-26371
Stiffness degradation of composite laminates
20 p2767 N88-26405
Accelerated fatigue crack growth behavior of PWA 1480 single crystal alloy and its dependence on the deformation mode
[NASA-TM-100943] 20 p2772 N88-26436
Fatigue crack growth under far-field cyclic compression
[DE88-011215] 20 p2813 N88-26689
Prediction of fatigue growth
[NLR-MP-87052-U] 20 p2816 N88-26707
Constant amplitude fatigue life data for notched and unnotched annealed Ti-6Al-4V sheet
[AD-A193420] 21 p2913 N88-27287
Optimal design of viscoelastic structures
21 p2959 N88-27579
The relationship between observed fatigue damage and life estimation models
[NASA-CR-182191] 21 p2965 N88-27611
Onboard Life Monitoring System (OLMOS): Engine life cycle calculation and trending 22 p3034 N88-28010
Tornado: Airframe fatigue life monitoring
22 p3034 N88-28011
Applications of fatigue analyses: Aircraft engines
[PNR90439] 22 p3044 N88-28066
Analyses and correlations of environment assisted fatigue crack propagation for attachment lugs
22 p3053 N88-28116
The effect of coatings on fatigue in aerospace materials --- gas turbine engines
[PNR90460] 22 p3059 N88-28150
Human acclimatization and physical performance at high altitude
[AD-A192651] 22 p3130 N88-28611
AGARD (Advisory Group for Aerospace Research and Development) engine disc material cooperative test (supplementary program)
[AD-A193678] 23 p3179 N88-28925
Spray automated balancing of rotors: Methods and materials
[NASA-CR-182151] 24 p3330 N88-29825
Rupture of carbon fiber reinforced plastics (T300-914) composite materials: Influence of initial first ply failures on the fatigue behavior
[SNIAS-881-422-103] 24 p3342 N88-29892

FATIGUE TESTS

Study of the microscopic mechanisms of cyclic deformation. Development of a new approach: The case of aluminum
[ISAL-87-0003] 02 p0149 N88-10936
Creep fatigue life prediction for engine hot section materials (isotropic): Third year progress review
02 p0188 N88-11173
Creep-fatigue behavior of NiCoCrAlY coated PWA 1480 02 p0189 N88-11176
Some new fatigue tests in high temperature water and liquid sodium environment
[DE87-753019] 02 p0192 N88-11197
Review of investigations of aeronautical fatigue in the Federal Republic of Germany
[LBF-S-178] 02 p0192 N88-11201
JPRS report: Science and technology. China
[JPRS-CST-87-025] 03 p0300 N88-11888
Standard fatigue test specimens for fastener evaluation
[AGARD-AG-304] 04 p0455 N88-12818
Application of finite element methods with cyclic elasto-plastic strain analysis to low cycle fatigue analysis of engine components
[AR-004-512] 05 p0596 N88-13642
Fatigue 87, volume 1
[AD-A184045] 05 p0597 N88-13645
The mechanics of fatigue-crack nucleation in a low-alloy steel under fretting conditions 05 p0597 N88-13649
Fatigue crack growth behavior of A356-T6 cast aluminum alloy 05 p0599 N88-13660
Variable amplitude fatigue crack growth in aluminum alloys 2090-T8E41 and 7075-T651
05 p0602 N88-13687
Fatigue of 30CrMnSiNi2A notched specimens under spectrum loading 05 p0602 N88-13689
The how and why of variable amplitude testing
05 p0603 N88-13690
Fatigue strength of alloy A286 at cryogenic temperature 05 p0603 N88-13695
The role of inclusions in corrosion fatigue crack initiation in Q1N 05 p0604 N88-13699
Crack initiation studies in hydrogen embrittled spring steel strip 05 p0605 N88-13710
Applications of fatigue analyses: Transportation
05 p0608 N88-13733
Fatigue crack growth 05 p0608 N88-13734
Cyclic fatigue of ceramics at high temperatures
[PB87-127700] 06 p0685 N88-14200
Fatigue 87, volume 2
[AD-A184046] 06 p0715 N88-14381
An investigation of fatigue crack growth in a ductile material at high growth rates 06 p0715 N88-14383

Cyclic deformation behaviour of cast irons with various graphite shapes in the temperature range 20 C less than or = T less than or = 500 C 06 p0715 N88-14384
Effect of hold time on fatigue of lead rich PbSn solder 06 p0715 N88-14387
Absolute fatigue thresholds in metallic materials 06 p0717 N88-14399
A re-evaluation of fatigue threshold test methods 06 p0717 N88-14401
Fatigue thresholds of C.Mn steels in saline environments 06 p0717 N88-14403
Mixed mode fatigue crack growth using the Brasilian disc 06 p0719 N88-14416
Crack closure phenomena in modes 1 and 2 interactions 06 p0719 N88-14417
Study of the evolution of short cracks in fatigue analysis --- aircraft construction materials
[DCQ/L-46-555] 06 p0722 N88-14442
Characterization of current steels. The 35 NCD 16 alloy in 30 mm diam laminated bars made by Aubert and Duval
[CEAT-41/N/76] 07 p0832 N88-15046
Static and dynamic determination of aluminum oxide toughness
[PB87-146999] 07 p0869 N88-15275
Fatigue and damage tolerance design data for carbon fibre composites
[BAE-MSM-R-GEN-0454] 09 p1138 N88-16818
Colloquium on damage mechanics of graphite/expoxy laminates during fatigue
[DFVLR-MITT-87-08] 11 p1448 N88-18630
Statistical evaluation of experimental results from fatigue strength tests on CFRP composite materials 11 p1449 N88-18635
Comparative investigations of indirect crack length messurement under fatigue loading in a corroeive environment
[GKSS-86/E/64] 11 p1502 N88-18972
Determination of the elastic-plastic fracture toughness parameters under special consideration of the activities of the European Group on Fracture (EGF)
[GKSS-87/E/30] 11 p1502 N88-18973
Effects of moisture, elevated temperature, and fatigue loading on the behavior of graphite/epoxy buffer strip panels with center cracks
[NASA-TM-100558] 12 p1603 N88-19590
The cyclic stress-strain behavior of a single crystal nickel-base superalloy
[NASA-TM-100269] 12 p1607 N88-19610
Thermal-mechanical fatigue testing of a titanium-aluminide alloy
[AD-A189555] 12 p1609 N88-19620
Thermal-mechanical fatigue testing of a titanium-aluminide alloy
[AD-A189555] 12 p1609 N88-19620
Crack distribution and growth rates for critical fastener holes in Mirage wing RH79
[AD-A189080] 13 p1722 N88-20293
Dynamic tensile cyclic fatigue of Si3N4
[DE88-003919] 13 p1781 N88-20658
An investigation of the mechanical properties of improved carbon fibre composite materials
[RAE-TR-86021] 14 p1884 N88-21259
Effect of protective coatings on high-temperature fatigue of heat-resistant alloys 14 p1895 N88-21314
Growth of fatigue cracks in nickel alloys at high temperatures 14 p1896 N88-21318
Bithermal fatigue of a nickel-base superalloy single crystal
[NASA-TM-100885] 15 p2042 N88-22168
Spectrum fatigue testing for materials characterization
[VTT-RR-502] 15 p2088 N88-22443
Test procedures and standards for mechanical property measurements on metal matrix composites
[NPL-DMA(A)-153] 16 p2172 N88-22944
Application of the ONERA model to the life estimation under fatigue cracking of a Al-Li alloy. Parameter identification and test-experiment comparison under FALSTAFF loading
[ONERA-RT-32/7169-RY-063-R] 16 p2222 N88-23264
Detecting delaminations in CFRP specimens using X-ray techniques
[FFA-TN-1988-04] 18 p2479 N88-24704
Predictive corrosion modeling, volume 1
[AD-A191229] 18 p2485 N88-24739
Fatigue testing and damage development in continuous fiber reinforced metal matrix composites
[NASA-TM-100628] 19 p2610 N88-25489
Apparatus for pressure welding of titanium structures with a controlled rate of deformation
[RAE-TRANS-2161] 19 p2677 N88-25915
Automated measurement of crack length and load line displacement at elevated temperature
[AGARD-R-751] 20 p2814 N88-26695
T55-L-714 engine development and qualification. Engine M11 low cycle fatigue test report. (0213-005-87)
[AD-A192765] 21 p2897 N88-27197
T55-L-714 engine development and qualification. Engine M11 low cycle fatigue test report. (0213-005-87), volume 2, part 1
[AD-A192766] 21 p2897 N88-27198
Study of fatigue cracks in aluminum alloys. Influence of microstructure
[REPT-48-553] 22 p3056 N88-28134
AGARD engine disc cooperative test programme
[AGARD-R-766] 23 p3179 N88-28926
Damage initiation in the short beam shear test of composite materials using stiffness reduction
[AD-A194880] 24 p3340 N88-29883
Standard fatigue specimens for fastener evaluation --- aircraft components
[FFA-TN-1987-68] 24 p3384 N88-30157
The development of acoustic emission for structural integrity monitoring of aircraft
[AD-A196264] 24 p3427 N88-30398

FATTY ACIDS
NT ACETIC ACID

FAULT MECHANICS
U FRACTURE MECHANICS

FAULT TOLERANCE
Hardware fault insertion and instrumentation system: Mechanization and validation
[NASA-CR-181445] 01 p0078 N88-10497
Measurement of fault-tolerant parallel processors
[PB87-208328] 01 p0084 N88-10539
Fault tolerant considerations and methods for guidance and control systems
[AGARD-AG-289] 02 p0126 N88-10796
Computing systems dependability and fault tolerance: Basic concepts and terminology 02 p0127 N88-10797
Some approaches to the design of high integrity software 02 p0127 N88-10799
Robust control system design 02 p0127 N88-10800
Reliability modeling of fault-tolerant computer based systems 02 p0127 N88-10801
ISAURE: Integration of security and fault tolerance in the REALITE 2000 system 02 p0127 N88-10802
Flight test of a resident backup software system 02 p0128 N88-10805
Software reliability models for fault-tolerant avionics computers and related topics
[NASA-CR-181440] 02 p0220 N88-11382
Development of an interface for an ultrareliable fault-tolerant control system and an electronic servo-control unit
[NASA-TM-88236] 05 p0553 N88-13367
Study of fault tolerant techniques for satellite data handling
[FTT/REP/0001/SAAB] 05 p0632 N88-13860
Experiments in fault tolerant software reliability
[NASA-CR-181554] 05 p0632 N88-13863
Reliability of voting in fault-tolerant software systems for small output spaces
[TR-87-16] 05 p0632 N88-13864
Effectiveness of back-to-back testing
[TR-87-08] 05 p0632 N88-13865
RSDIMU acceptance testing system: Overview of acceptance software and procedures 05 p0632 N88-13866
Objects architecture: A comprehensive design approach for real-time, distributed, fault-tolerant, reactive operating systems
[AD-A185476] 06 p0755 N88-14631
Diagnostic emulation: Implementation and user's guide
[NASA-CR-178391] 06 p0756 N88-14636
Estimating the distribution of fault latency in a digital processor
[NASA-TM-100521] 06 p0760 N88-14666
Software-implemented fault insertion: An FTMP example
[NASA-CR-178423] 06 p0761 N88-14668
National Aeronautics and Space Administration (NASA)/American Society for Engineering Education (ASEE) Summer Faculty Fellowship Program, 1987. Volume 2
[NASA-CR-172009-VOL-2] 06 p0796 N88-14874
Fault-tolerant computer architecture based on INMOS transputer processor 06 p0797 N88-14880
Inadequacy of conventional dynamic recovery mechanisms in the presence of temporary failures
[AD-A186311] 07 p0866 N88-15251
Annotated bibliography on reliable system design
[PB88-109848] 07 p0866 N88-15254
Reliability modelling for fault-tolerant parallel processor
[AD-A185867] 07 p0900 N88-15451
Investigation of candidate data structures and search algorithms to support a knowledge based fault diagnosis system 07 p0923 N88-15606
EUREX D: An expert system for failure diagnosis and recovery in the TCS of the European retrievable carrier EURECA 08 p1058 N88-16385
Integrated diagnostics 09 p1111 N88-16655
SURE reliability analysis: Program and mathematics
[NASA-TP-2764] 09 p1231 N88-17380
Examples of nonconservatism in the CARE 3 program
[NASA-TM-100524] 09 p1233 N88-17390
Latent failures and coverage in fault-tolerant systems. A VLSI CMOS circuit design technique to aid test generation
[AD-A187615] 10 p1325 N88-17921
Navigation recovery block design description
[NASA-CR-182473] 10 p1342 N88-18022
Clouds: A support architecture for fault tolerant, distributed systems 10 p1375 N88-18206
Resilient procedures: A structured replication approach 10 p1381 N88-18245
Automated radar target recognition based on models of neural nets 11 p1476 N88-18804
Theory and practice of fault tolerance in distributed systems
[AD-A187559] 11 p1540 N88-19204
Evaluation of network communication multiprocessor fault tolerance
[INPE-4305-PRE/1171] 12 p1674 N88-20011
An experiment in software reliability: Additional analyses using data from automated replications
[NASA-CR-178395] 12 p1676 N88-20017
A survey of provably correct fault-tolerant clock synchronization techniques
[NASA-TM-100553] 13 p1823 N88-20894
A fault injection experiment using the AIRLAB Diagnostic Emulation Facility
[NASA-CR-178390] 13 p1823 N88-20895
CARE 3 User's Workshop
[NASA-CP-10011] 14 p1954 N88-21646
Methodology for software reliability prediction, volume 1
[AD-A190018] 15 p2110 N88-22571
Methodology for software reliability prediction, volume 3
[AD-A190019] 15 p2110 N88-22572
Exhaustive and pseudo-exhaustive testing
[AD-A190140] 15 p2111 N88-22574
Argus reference manual
[AD-A190382] 15 p2111 N88-22578
Simulation of fault tolerance in a hypercube arrangement of discrete processors
[AD-A189682] 15 p2114 N88-22594
Analysis and testing of the SURE program
[NASA-TP-2817] 15 p2123 N88-22653
A fault tolerant supervision system
[INPE-4419-TDL/307] 15 p2148 N88-22819
Approximate agreement
[AD-A191030] 16 p2251 N88-23455
The PAWS and STEM reliability analysis programs
[NASA-TM-100572] 16 p2262 N88-23526
Rule-based fault-tolerant flight control 17 p2294 N88-23725
Development of a generic architecture 17 p2303 N88-23774
Toggle release
[NASA-CASE-MSC-21354-1] 18 p2523 N88-24969
Analysis and design of detection filters within closed-loop systems 18 p2525 N88-24980
Effectiveness evaluation of fault-tolerant multiprocessor systems
[AD-A191688] 18 p2554 N88-25158
Semi-Markov adjunction to the Computer-Aided Markov Evaluator (CAME)
[NASA-CR-181645] 19 p2678 N88-25924
Distributed fault tolerant embeddings of binary trees in hypercubes
[AD-A192929] 20 p2839 N88-26840
Diagnosing faults in autonomous robot plan execution
[NASA-CR-182480] 20 p2841 N88-26859
An evaluation methodology for dependable multiprocessors
[AD-A192799] 20 p2842 N88-26863
FTMP data acquisition environment
[NASA-TM-100636] 21 p2938 N88-27447
Faultfinder: A diagnostic expert system with graceful degradation for onboard aircraft applications 22 p3035 N88-28018
Reliable onboard computing for critical space systems
[RR-670-1] 22 p3135 N88-28641
Approximate evaluation of semi-Markov chain reliability models
[AD-A194669] 23 p3223 N88-29185
Analysis of the effect of faulty spares on the performance of diagnostic algorithms in reliable systems
[AD-A193526] 23 p3223 N88-29186

Systolic array fault tolerance performance analysis
[AD-A193521] 23 p3244 N88-29306
Knowledge-based fault diagnosis on future space vehicles 23 p3254 N88-29374
ARGES: An expert system for fault diagnosis within space-based ECLS systems 23 p3255 N88-29380
SCARES: A Spacecraft Control Anomaly Resolution Expert System 23 p3256 N88-29381
Knowledge acquisition and rapid protyping of an expert system: Dealing with real world problems 23 p3258 N88-29394
Reasoning about fault diagnosis for the space station common module thermal control system 23 p3258 N88-29395
A methodology for multiple rule system integration and resolution within a singular knowledge base 23 p3261 N88-29413
Semantic based man-machine interface for real-time communication 23 p3262 N88-29421
MOORE: A prototype expert system for diagnosing spacecraft problems 24 p3418 N88-30343
Achieving real-time performance in FIESTA 24 p3418 N88-30344
Parallel and distributed computation for fault-tolerant object recognition 24 p3419 N88-30350

FAULT TREES
Fault tree safety analysis of a large Li/SOCl(sub)2 spacecraft battery 02 p0163 N88-11025
Diagnostic reasoning in digital systems
[NASA-CR-181564] 05 p0633 N88-13871
Conceptual issues in measuring the behavior of a distributed real-time process-control computer system
[DE87-009748] 05 p0638 N88-13898
Fault tree reliability analysis of the Naval Postgraduate School mini-satellite (ORION)
[AD-A186283] 07 p0866 N88-15250
A fast bottom-up algorithm for computing the cut sets of noncoherent fault trees
[DE88-003741] 09 p1220 N88-17320
Fault tree analysis and synthesis
[ETN-88-92236] 16 p2261 N88-23521
Applications of fault tree analysis to the design process
[DE88-007048] 18 p2525 N88-24982
Logic and fault simulation on the Mach1000 hardware accelerator
[DE88-009794] 19 p2717 N88-26130

FAUNA
U ANIMALS

FCC LATTICES
U FACE CENTERED CUBIC LATTICES

FDMA
U FREQUENCY DIVISION MULTIPLE ACCESS

FEASIBILITY
Laser gyro attitude control system feasibility
[AD-A189368] 13 p1720 N88-20285
Feasibility report: Operation of light air cushion vehicle at McMurdo Sound, Antarctica
[AD-A189057] 13 p1755 N88-20494

FEASIBILITY ANALYSIS
Preliminary study of a containerless processing facility for Columbus, executive summary
[ESA-ITT/AO/1-1834/85F] 01 p0032 N88-10203
The 250AH/90A active lithium-thionyl chloride cell for Centaur-G application 02 p0163 N88-11023
Evaluation of a scale-model experiment to investigate long-range acoustic propagation
[NASA-TP-2748] 02 p0230 N88-11450
Feasibility of alpha particle measurement in a magnetically confined plasma by CO2 laser Thomson scattering
[DE88-000039] 02 p0241 N88-11522
The Black College satellite telecommunications network planning in support of energy-related collaborative research
[DE88-000182] 03 p0307 N88-11940
Repulsive force support system feasibility study
[NASA-CR-178400] 04 p0402 N88-12497
Light funnel concentrator panel for solar power
[NASA-CR-179223] 04 p0464 N88-12870
The VISTA spacecraft: Advantages of ICF (Inertial Confinement Fusion) for interplanetary fusions propulsion applications
[NASA-CR-181549] 04 p0491 N88-13024
Ground vehicle convoying
[DE88-000360] 04 p0502 N88-13088
Performance monitoring and analysis of electric van fleet vehicles
[DE88-900066] 04 p0502 N88-13091
Study of the feasiblity of a satellite communication system for road transportation home office to vehicle communication. Volume 1: Conceptual analysis
[SC/87-E/6-VOL-1] 05 p0575 N88-13505
Study of the feasibility of a satellite communication system for road transportation home office to vehicle communication. Volume 2: Market study
[SC/87-E/6-VOL-2] 05 p0575 N88-13506
The gamma-ray laser project
[AD-A184824] 05 p0587 N88-13578
Stress intensity factors for cracking metal structures under rapid thermal loading, phase 1
[AD-A184112] 05 p0591 N88-13606
Feasibility study for gas-grain simulation facility
[NASA-CR-177468] 05 p0646 N88-13954
Feasibility study of a carbon dioxide observational platform system. Volume 2: Programmatics
[NASA-CR-180404] 06 p0672 N88-14114
Diamond turning of silicon for optics applications
[DE88-002501] 07 p0840 N88-15095
Holography of the ionosphere at HIPAS
[AD-A186237] 07 p0877 N88-15322
Measurement and modification of sensorimotor system function during visual-motor performance
[AD-A186351] 07 p0889 N88-15387
The feasibility of using TAE as the UIL for the space station and for other internal NASA tasks and projects 07 p0925 N88-15618
Columbus feasibility studies. Volume 1: Requirements and system concept
[ETN-88-91073] 09 p1134 N88-16799
Study of large solar arrays (SOLA), phase 2A
[BAE-SS/1109] 09 p1186 N88-17106
A proposal for a feasibility study on the design of software interfaces in large systems
[NPL-DITC-89/87] 09 p1222 N88-17330
Feasibility of chemical lasers based on chain reaction involving hydrogen fluorination with thermal branching mechanism 09 p1238 N88-17420
Study of Large Solar Arrays (SOLA). Phase 2A: Amplifying information to final report (SS/1109)
[BAE-SS/1110] 09 p1248 N88-17480
Rendezvous and docking verification and demonstration in orbit, executive summary
[MBB-303-16/86] 10 p1291 N88-17719
Cape Blanco wind farm feasibility study
[DE88-003748] 10 p1348 N88-18059
Cape Blanco wind farm feasibility study
[DE88-003749] 10 p1349 N88-18060
Rapid underway sediment classification by electrical methods
[AD-A187477] 10 p1357 N88-18114
Computer architecture for research in meteorology and atmospheric chemistry
[PB88-145313] 11 p1510 N88-19020
An economic analysis of a multi-commodity fruit and vegetable irradiator
[DE88-003425] 11 p1524 N88-19098
Feasibility study of generating plans and strategies for software testing by knowledge based system
[AD-A187834] 11 p1529 N88-19134
Feasibility studies of the growth of 3-5 compounds of boron by MOCVD
[NASA-CR-181622] 11 p1561 N88-19343
The status of R and D for superconducting power transmission systems
[DE88-003499] 11 p1561 N88-19346
Mars Lander/Rover vehicle development: An advanced space design project for USRA and NASA/OAST
[NASA-CR-182570] 11 p1567 N88-19380
A technique for capture analysis of low thrust missions in a planetary system
[AD-A188934] 12 p1594 N88-19544
A new fire protection concept for electronic equipment
[AD-A188884] 12 p1614 N88-19651
An investigation of classical dynamic scaling techniques applied to an oleo-pneumatic landing gear strut
[AD-A187664] 13 p1721 N88-20292
Proof of the feasibility of coherent and incoherent schemes for pumping a gamma-ray laser
[AD-A189238] 13 p1774 N88-20613
Federal Ocean Energy Technology
[DE87-012279] 13 p1792 N88-20722
An assessment methodology for thermal energy storage evaluation
[DE88-004642] 13 p1794 N88-20732
Conservative finite volume solutions of a linear hyperbolic transport equation in two and three dimensions using multiple grids
[NASA-CR-182715] 13 p1828 N88-20934
Molybdenum-base cermet fuel development
[DE88-005529] 13 p1839 N88-21003
Modulatable thin film field emission space gun
[AD-A189279] 13 p1845 N88-21043
Statistical analysis of feasibility of non-destructive inspection of mechanical properties of hot worked pipes of alloy steels
[BLL-M-37598-(5828.4)] 14 p1922 N88-21455
Preliminary market analysis for large zeolite crystals
[NASA-CR-182882] 15 p2049 N88-22207
Superconductivity in power engineering
[DE88-701414] 15 p2141 N88-22776
Time-domain frequency-selective optical memories: A study of the basic mechanisms and potential systems
[AD-A190854] 16 p2274 N88-23607
MBE of HgCdTe
[AD-A191423] 16 p2283 N88-23671
Colombus feasibility studies, executive summary
[ETN-88-92334] 17 p2311 N88-23820
Automatically generated acceptance test: A software reliability experiment
[NASA-CR-181667] 17 p2347 N88-23984
Assessment of nuclear reactor concepts for low power space applications 17 p2423 N88-24409
Heat pump-augmented systems for spacecraft thermal management 17 p2424 N88-24419
Molybdenum-base cermet fuel development 17 p2434 N88-24481
TRICE design, evaluation and feasibility tests 17 p2437 N88-24498
Search and rescue satellite system (SERES), phase A0
[ETN-88-92335] 18 p2472 N88-24669
The efficacy of using human myoelectric signals to control the limbs of robots in space
[NASA-CR-182901] 18 p2553 N88-25155
Technical feasibility study of applying auto-control methods to plating process solutions
[DE88-008014] 19 p2641 N88-25670
Inertial fusion in the nineties
[DE88-007913] 19 p2730 N88-26214
Feasibility of producing jet fuel from GPGP (Great Plains Gasification Plant) by-products
[DE88-010233] 20 p2781 N88-26492
Program for the feasibility of developing a high pressure acoustic levitator
[NASA-CR-182154] 20 p2782 N88-26498
SDI: Myth or reality
[DE88-009121] 20 p2847 N88-26901
Study of comet nucleus gamma-ray spectrometer penetration system
[NASA-CR-177393] 20 p2883 N88-27120
Theoretical-numerical study of feasibility of use of winglets on low aspect ration wings at subsonic and transonic Mach numbers at reduce drag
[NASA-CR-4174] 21 p2892 N88-27168
Supersonic transport/hypersonic transport (SST/HST) development
[REPT-881-111-101] 21 p2896 N88-27192
Experimental investigation of simplest inhomogeneities in cylindrical slit line
[DE88-702388] 21 p2933 N88-27418
Application of Dynamic Extended Range Forecasting (DERF) to the monthly forecast problem 22 p3125 N88-28578
Laboratory feasibility study of a composite embedded fiber optic sensor for measurement of structural vibrations
[AD-A194270] 22 p3152 N88-28754
Performance and technical tolerance — space projects 22 p3160 N88-28812
SRB/SLEEC (Solid Rocket Booster/Shingle Lap Extendible Exit Cone) feasibility study, volume 1
[NASA-CR-178973] 23 p3187 N88-28964
Space-charge-wave solid state microwave amplifier
[AD-A193792] 23 p3208 N88-29091
Large area nuclear particle detectors using ET materials
[NASA-CR-180777] 23 p3215 N88-29136
Advanced development waste processing unit for combat vehicles, phase 2
[AD-A193793] 23 p3243 N88-29302
Feasibility study of a microprocessor controlled actuator test mechanism
[AD-A194654] 23 p3249 N88-29337
Lattice-matched HgZnTe epitaxy development
[AD-A193677] 23 p3292 N88-29600
New developments in capital cost estimating
[DE88-005392] 23 p3297 N88-29638
JUH-1H redesigned pneumatic boot deicing system flight test evaluation
[AD-A194918] 24 p3322 N88-29785
Dielectric millimeter waveguides: A feasibility study for a novel dielectric millimeter waveguide
[AD-A195104] 24 p3366 N88-30042

FEATURE EXTRACTION
U PATTERN RECOGNITION

FEDERAL BUDGETS
National Aeronautics and Space Administration Authorization Act, 1988
[PUB-LAW-100-147] 03 p0385 N88-12422
Department of Housing and Urban Development, and Certain Independent Agencies Appropriations, 1988, Part 2
[S-HRG-100-106-PT-2] 03 p0385 N88-12423

Department of Housing and Urban Development-Independent Agencies Appropriations for fiscal year 1988. Thursday, 9 April 1987: National Aeronautics and Space Administration
03 p0386 N88-12424
Department of Housing and Urban Development-Independent Agencies Appropriations for fiscal year 1988. Friday, 10 April 1987: National Aeronautics and Space Administration
03 p0386 N88-12425
The 1988 NASA (National Aeronautics and Space Administration) authorization
[GPO-80-245] 05 p0659 N88-14044
The 1988 National Aeronautics and Space Administration (NASA) authorization
[GPO-76-600] 06 p0792 N88-14854
Department of Housing and Urban Development independent agencies appropriations for 1989. Part 7: National Aeronautics and Space Administration
[GPO-85-166] 16 p2286 N88-23889
The Department of Defense report on the merit review process for competitive selection of university research projects and an analysis of the potential for expanding the geographic distribution of research for the Committees on Appropriations, United States Congress
[AD-A191842] 18 p2588 N88-25379
Competition: Issued on establishing and using Federally funded research and development centers
[PB88-178884] 23 p3296 N88-29632

FEDERAL REPUBLIC OF GERMANY
U WEST GERMANY

FEED SYSTEMS
Trickle water and feeding system in plant culture and light-dark cycle effects on plant growth
03 p0361 N88-12273
Dynamics of propellant feedline systems
[AD-A184865] 05 p0580 N88-13537
Gas feed system for the T-15 tokamak discharge chamber
[DE88-700351] 07 p0935 N88-15682
An advanced extruder-feeder biomass liquefaction reactor system 18 p2535 N88-25042

FEEDBACK
NT BIOFEEDBACK
NT NONLINEAR FEEDBACK
NT SENSORY FEEDBACK
New feedback design methodologies for large space structures: A multi-criterion optimization approach
04 p0408 N88-12535
Investigation, development and application of optimal output feedback theory. Vol. 4: Measures of eigenvalue/eigenvector sensitivity to system parameters and unmodeled dynamics
[NASA-CR-4108] 04 p0482 N88-12969
Sojourn times in the M/G/1 queue with deterministic feedback
[CWI-OS-R8708] 08 p1074 N88-16479
The linear dependency structure of covariance nonstationary time series
[AD-A186548] 09 p1232 N88-17383
Local bifurcation control
[AD-A187435] 10 p1324 N88-17915
Summary of Payload Integration Plan (PIP) for Starlab-1 flight experiment, enclosure 3
[NASA-TM-89713] 11 p1522 N88-19086
A comparison of keyboard designs for cockpit applications
[AD-A187775] 12 p1581 N88-19460
Development of an optical feedback based high accuracy beam transmissometer
[AD-A189396] 12 p1692 N88-20122
Robust decentralized control of large flexible structures
[DE88-005416] 13 p1824 N88-20902
Ultrahigh coherent semiconductor lasers and their applications to Rb atomic clock
14 p1976 N88-21789
Generation of number-phase minimum uncertainty states 14 p1978 N88-21803
Conditions for information capacity of the discrete-time Gaussian channel to be increased by feedback
[AD-A190317] 15 p2127 N88-22687
Optimizing feedback utilization in motor skill training
[AD-A191559] 18 p2552 N88-25146
A random access algorithm for environments with capture and limited feedback capabilities
[AD-A192233] 20 p2790 N88-26552
Force servo control of a commercial gantry robot
[DE88-006649] 20 p2805 N88-26660
Mode locking of semiconductor laser with external cavity
[AD-A196018] 24 p3378 N88-30117

FEEDBACK CONTROL
NT CASCADE CONTROL
The design of a turboshaft speed governor using modern control techniques
[NASA-CR-175046] 01 p0053 N88-10339
Study of closed loop control singularity in dynamic systems with a constraint on the final state
[LAAS-87-180] 02 p0223 N88-11405
Extensions of the small mu test for robust stability
[OUEL-1666/87-REV] 02 p0223 N88-11406
An autonomous, closed-loop pointing system for use with satellite optics
[DE87-012011] 02 p0235 N88-11483
Active control of helicopter vibration using multiloop self-adaptive control 03 p0264 N88-11660
A modern control theory based algorithm for control of the NASA/JPL 70-meter antenna axis servos
04 p0436 N88-12706
Fast autotuning of a hydrogen maser by cavity Q modulation 04 p0436 N88-12707
Design of low order controllers for robust disturbance rejection in large space structures
[AD-A185202] 05 p0555 N88-13376
Simultaneous structural and control optimization via linear quadratic regulator eigenstructure assignment
05 p0594 N88-13622
On linear periodic controllers
[DE87-011174] 05 p0639 N88-13904
Super-short yttrium aluminate pulse generator with controlled resonator Q-factor 06 p0772 N88-14740
Active control of flexural vibrations in beams
06 p0794 N88-14865
An autopilot design for the United States Marine Corps' airborne remotely operated device
[AD-A186379] 07 p0820 N88-14983
MIG welding with pulsed wire feed
[PB87-143582] 07 p0863 N88-15234
Pulsed plasma arc welding process with double closed-loop adaptive penetration control system
[PB87-143780] 07 p0863 N88-15236
A weighting sequence approach to the analysis and design of multivariable control systems
[AD-A186086] 07 p0917 N88-15570
A dynamic simulation and feedback control scheme for the U.S. Marine Corps' Airborne Remotely Operated Device (AROD)
[AD-A186597] 08 p0953 N88-15784
Identification and feedback control of machine tool vibrations
[PB88-109715] 08 p0976 N88-15902
Design of a velocity and position control laboratory servo system
[AD-A186596] 08 p0990 N88-15997
Large-angle slewing maneuvers for flexible spacecraft
[NASA-CR-4123] 08 p1000 N88-16060
A direct approach to almost disturbance and almost input-output decoupling
[MEMO-641] 08 p1072 N88-16471
A method for designing robust multivariable feedback systems
[NASA-CR-182459] 09 p1225 N88-17341
A methodology for the synthesis of robust feedback systems
[NASA-CR-182455] 09 p1225 N88-17342
A fiber-optic link for pressure control of ion sources
[DE88-001782] 09 p1248 N88-17484
Robust controller design for flexible structures
[AD-A187217] 10 p1340 N88-18009
Piezoelectric laminates for torsional and bending model control: Theory and experiment
10 p1343 N88-18029
Time delays and boundary feedback stabilization in one-dimensional viscoelasticity, appendices A through H
[AD-A187534] 10 p1401 N88-18353
Research on output feedback control
[NASA-CR-182543] 11 p1534 N88-19167
Design for performance enhancement in feedback control systems with multiple saturating nonlinearities
[NASA-CR-182614] 11 p1535 N88-19168
Active feedback interaction with a shear layer
[AD-A188525] 12 p1573 N88-19410
Speed control of a missile with throttleable ducted rocket propulsion 12 p1597 N88-19561
The use of hardware-in-the-loop-techniques in the development of a modern air-to-surface missile system
12 p1597 N88-19562
An analysis of DREO's (Defence Research Establishment Ottawa) analog rebalance loops for the CSG-2 (Canadian Strapdown Gyroscope) tuned-rotor gyroscope
[AD-A188577] 12 p1629 N88-19749
Active vibration control of a cantilevered beam with three elastic coordinates
[AD-A188824] 12 p1636 N88-19797
Design of feedback control systems for stable plants with saturating actuators
[NASA-CR-182613] 12 p1681 N88-20050
Gas consumption estimation of an attitude control system of an artificial satellite (utilizing DRF) in limit cycle phase
[INPE-4338-RPE/553] 13 p1731 N88-20350
Sojourn times in feedback queues
[CWI-OS-R8710] 13 p1830 N88-20947
A feedback double path compensating control structure for the attitude control of a flexible spacecraft
[INPE-4464-PRE/1239] 14 p1880 N88-21240
Implementation of a visual servoing system for evaluation of robotic refueling applications
[AD-A189676] 14 p1954 N88-21645
A new approach to almost decoupling problems for linear and nonlinear systems
[MEMO-660] 14 p1962 N88-21700
A complexity transform for NP-complete problems
[OUEL-1708/87] 14 p1962 N88-21703
Systolic determination of absolute stability in feedback control systems
[OUEL-1704/87] 14 p1962 N88-21705
Open questions in closed-loop photodetection
14 p1979 N88-21812
Application of eigenstructure assignment techniques in the design of a longitudinal flight control system
[AD-A189644] 15 p2020 N88-22039
Multivariable control law design for the AFTI/F-16 with a failed control surface using a parameter-adaptive controller
[AD-A189848] 15 p2020 N88-22040
Feedback control of distributed parameter systems with applications to large space structures
[AD-A190536] 15 p2025 N88-22068
Approximation methods for the identification and control of distributed parameter systems
[AD-A190201] 15 p2124 N88-22662
Servo-actuator control for sampled-data feedback disturbance rejection --- helicopters
[ESA-TT-1002] 16 p2163 N88-22903
Analysis and design of gain scheduled control systems
[NASA-CR-182867] 16 p2163 N88-22904
Models describing muscle behavior and control
[LR-522] 16 p2238 N88-23368
Feedback decoupling and stabilization for linear systems with multiple exogenous variables
[ETN-88-92245] 16 p2255 N88-23474
Investigation of air transportation technology at Princeton University, 1986 17 p2294 N88-23724
Control of combustion and acoustically coupled fluid dynamic instabilities 17 p2318 N88-23843
Precise computer controlled positioning of robot end effectors using force sensors
[NASA-CR-182887] 17 p2391 N88-24213
Experimental evaluation of the MIT-SNL period-generated minimum time control laws for the rapid adjustment of reactor power 17 p2436 N88-24494
An optimal disturbance rejection control system for multimegawatt space nuclear power systems
17 p2436 N88-24495
Automatic feedback control of a rigid body for finite displacements 18 p2473 N88-24674
Analysis and design of detection filters within closed-loop systems 18 p2525 N88-24980
Multishaker modal testing
[NASA-CR-179355] 18 p2530 N88-25010
Design and testing of a luminance and chrominance stabilization system for a computer-controlled color display
[AD-A191922] 18 p2554 N88-25159
Frequency Analysis of Acoustic Emission - Application to machining and welding
[DE88-701478] 18 p2570 N88-25262
F-14 modeling study
[NASA-CR-4164] 19 p2603 N88-25462
Control of combustion instabilities in ramjet motors
19 p2625 N88-25574
Joint angle sensors for closed-loop control
19 p2673 N88-25891
Automatic calibration of space based manipulators and mechanisms
[NASA-CR-182804] 19 p2676 N88-25912
RRSAS (Robotic Radiation Survey and Analysis System) Project: A real time sensor driven robotic system
[DE88-006825] 20 p2808 N88-26661
Vibration control of large structures
[AD-A193317] 21 p2961 N88-27587
Feedback control of a hyperbolic partial-differential equation with viscoelastic damping
[AD-A192896] 21 p3003 N88-27810
Time periodic control of a multi-blade helicopter
[AD-A194435] 23 p3180 N88-28931
Robust control of multivariable and large scale systems
[AD-A194250] 23 p3266 N88-29441
Pilot modeling 24 p3314 N88-29736
Pilot modeling applications 24 p3314 N88-29737

An analysis of lateral-directional handling qualities and Eigenstructure of high performance aircraft
[AD-A194874] 24 p3328 N88-29814
Track performance considerations for monopulse radars
[AD-A196232] 24 p3360 N88-30007
K(sup th)-order extended linearization
[AD-A194786] 24 p3421 N88-30363
An approach to CMG steering using feedback linearization
[NASA-CR-183172] 24 p3422 N88-30369

FEEDERS
Harmonic considerations for electrical distribution feeders
[DE88-007849] 18 p2505 N88-24860

FEEDFORWARD CONTROL
A linear quadratic Gaussian with loop transfer recovery proximity operations autopilot for spacecraft
[NASA-CR-172028] 02 p0227 N88-11433
Investigation, development, and application of optimal output feedback theory. Volume 3: The relationship between dynamic compensators and observers and Kalman filters
[NASA-CR-4107] 05 p0638 N88-13900

FEEDING (SUPPLYING)
Utilizing dynamic stability of orient parts
[AD-A195730] 24 p3427 N88-30397

FEELINGS
U SENSORY FEEDBACK

FEMALES
Temperature regulation at rest and exercise during the human menstrual cycle
[AD-A186461] 08 p1050 N88-16341
Meta-analysis of leadership differences between males and females and the effect on performance
[AD-A187769] 11 p1564 N88-19361
Human factor in engineering work
12 p1663 N88-19970
Fit evaluation of female body armor
[AD-A188721] 14 p1953 N88-21638

FERMENTATION
Fed-batch control based upon the measurement of intracellular NADH 09 p1197 N88-17175
Design concepts for bioreactors in space
09 p1198 N88-17179

FERMI LIQUIDS
Renormalized Fermi liquid theory for disordered electron systems and the metal-insulator transition
[NOTA-INTERNA-900] 14 p1988 N88-21862

FERMI SURFACES
High T/sub c/ superconductor as a strongly correlated state
[DE88-003194] 08 p1091 N88-16569
Fermi level stabilization in semiconductors: Implications for implant activation efficiency
[DE88-006332] 15 p2145 N88-22801
Fermi level dependent native defect formation: Consequences for metal-semiconductor and semiconductor-semiconductor interfaces
[DE88-008247] 20 p2875 N88-27066

FERMIONS
NT ANTINEUTRINOS
NT BARYONS
NT CONDUCTION ELECTRONS
NT FAST NEUTRONS
NT LEPTONS
NT MESON RESONANCE
NT MUONS
NT NEUTRINOS
NT NEUTRONS
NT PROTONS
NT SOLAR NEUTRINOS
NT SOLAR NEUTRONS
NT SOLAR PROTONS
NT THERMAL NEUTRONS
Scalar densities and baryon mass differences in lattice QCD with Wilson fermions
[PREPRINT-544] 06 p0778 N88-14773
Phenomenological model of superconductivity of heavy fermions in U(sub 1-x)ThsubxBesub13
09 p1238 N88-17423
Magnetic properties of heavy fermion superconductors
[ETN-88-91078] 09 p1255 N88-17524
Heavy Fermions and coherence in Kondo lattices: Specific heat of low energy excitation in Cer systems
[ETN-88-91080] 09 p1255 N88-17525
Symmetry problems in particle physics
[DE88-004927] 12 p1688 N88-20099
Chiral symmetry breaking in finite quantum electrodynamics
[DE88-700860] 12 p1699 N88-20169
Mixing coefficients of the lattice weak Hamiltonian with dimension five operators
[PREPRINT-576] 14 p1968 N88-21749
Integrability of fermionic string in superfluid Hamiltonian approach
[DE88-701662] 16 p2284 N88-23678
Introduction to covariant formulation of superstring (field) theory
[DE87-703038] 18 p2586 N88-25363
Geometry of superconformal manifolds, part 1
[DE88-702405] 21 p3011 N88-27863
An overview of lattice QCD
[DE88-010867] 21 p3026 N88-27963
Gravitational redshift of self-gravitating systems of dark matter in the universe
[DE88-702688] 23 p3300 N88-29650

FERRIC IONS
Determination of aquo-complexes of chromium and iron in chromium plating and polishing solutions by ion chromatography
[AD-A190168] 15 p2039 N88-22148

FERRIMAGNETS
Theoretical and experimental investigations on a linear, permanently excited stepping motor
[ETN-88-91061] 09 p1158 N88-16939
The operational behavior of microprocessor-controlled and pulsed inverter-fed synchronous machines with permanent magnet excitation
[ETN-88-91479] 11 p1480 N88-18833

FERRITES
Static magnetization and microwave loss in shock-modified ferrites
[DE87-012362] 02 p0146 N88-10916
Loss measurement of 3-port ferrite switches in the 90 GHz range
[ESA-TT-1054] 03 p0310 N88-11958
Investigation of hexagonal ferrite film growth techniques for millimeter-wave systems applications
[AD-A184335] 03 p0383 N88-12406
The initiation and growth of fatigue cracks in carburised 9Cr1Mo steel 05 p0603 N88-13696
Propagation of fatigue crack in the medium-carbon steel contaiing both martensite and ferrite
[PB87-143962] 07 p0869 N88-15273
New technique for enhancing helium production in ferritic materials
[DE88-003048] 09 p1142 N88-16847
Eddy current nondestructive inspection of graphite epoxy using ferrite cup core probes
[AD-A189823] 15 p2074 N88-22365

FERRITIC STAINLESS STEELS
Laminated ferrous composites based on ultrahigh carbon (UHC) steels
[AD-A184617] 03 p0280 N88-11764
Reduced-activation ferritic steels: A comparison with Cr-Mo steels
[DE88-000332] 03 p0290 N88-11826
Impact behavior of 9-Cr and 12-Cr ferritic steels after low-temperature irradiation
[DE88-000333] 03 p0291 N88-11827
Mechanical properties of an acicular ferrite steel microalloyed to niobium and vanadium
[DE87-703547] 04 p0415 N88-12574
Swelling behavior of ferritic/martensitic steels
[DE88-001757] 06 p0682 N88-14177
Fracture-mechanical, statistics and fractographic investigations on the steel 20 MnMoNi 55 in the ductile-brittle transition domain
[ETN-88-91064] 09 p1144 N88-16856
Cost 501 Project U.K.10. Part 4: The oxidation of fecralloy steel co-extruded onto strong steel substrates
[AERE-R-12432-PT-4] 11 p1456 N88-18679
The fatigue behavior of ferritic and austenitic steels at elevated temperatures
[DE88-006304] 13 p1744 N88-20431
Low-chromium reduced-activation ferritic steels
[DE88-009060] 19 p2617 N88-25524
Environmental cracking of a superferritic stainless steel under slow strain rate conditions
22 p3053 N88-28117

FERROALLOYS
U IRON ALLOYS

FERROCENES
Investigation of fuel additive effects on sooting flames
[AD-A186403] 07 p0829 N88-15026

FERROELECTRICITY
Improper ferroelectricity: A theoretical and experimental study
[AD-A184614] 03 p0381 N88-12397
Assessment of electroceramics research in Europe and the Middle East
[AD-A186377] 07 p0836 N88-15074
Radiation hardness evaluation of thin film ferroelectric capacitors
[DE88-001357] 07 p0848 N88-15147
Physics and chemistry 07 p0883 N88-15359
Ferroelectric properties and impact behavior of the PVF2 polymer and the VF2/C2F3H polarized copolymers --- vinylidene polyfluorides
[ISL-CO-245/86] 08 p0971 N88-15876
Piezoelectric laminates for torsional and bending model control: Theory and experiment
10 p1343 N88-18029
Statistical-mechanical study of polyvinylidene fluoride
[AD-A188310] 12 p1609 N88-19624
Effect of uniaxial compression on physical and mechanical properties of ferroelectric ceramic material
16 p2180 N88-22993
Topological stereochemistry
[AD-A191867] 18 p2477 N88-24691
Research on crystal and film ferroelectric materials for optoelectronic applications
[AD-A193512] 23 p3291 N88-29597

FERROMAGNETIC MATERIALS
Applications of a theory of ferromagnetic hysteresis
[DE87-014725] 03 p0373 N88-12348
Influence of bond dilution on the free surface and interface Potts ferromagnetism
[DE87-703360] 04 p0497 N88-13061
Spin disorder resistivity and bare Curie temperature in the ferromagnetic superconductor ErRh4B4
[DE88-003016] 10 p1415 N88-18445
Excitations in magnetic low-dimensional systems: A spectroscopic study
[ETN-88-92230] 15 p2129 N88-22697
The Curie point radiator 17 p2424 N88-24420

FERROMAGNETISM
Influence of bond dilution on the free surface and interface Potts ferromagnetism
[DE87-703360] 04 p0497 N88-13061
Magnetic rare earth superlattices
[DE88-003483] 10 p1418 N88-18465
Simplified physical approach of the control by eddy current
[DE88-701076] 13 p1764 N88-20552
Algorithm for accounting the conditions in infinity for two-dimensional magnetostatics problems
[DE88-701673] 16 p2264 N88-23541
The Potts model in a random field
19 p2721 N88-26158
Ferromagnetic/semiconductor hybrid structures
20 p2865 N88-27013
Properties of synthetic magnetic superlattices
20 p2865 N88-27014
Observation of ferromagnetism in ultrathin f.c.c. films by spin polarised neutron reflection
20 p2865 N88-27015
Contribution to the study of order effects in the Ising model framework: Ground states and phase diagrams
[ONERA-NT-1987] 20 p2880 N88-27095

FERROUS METALS
JPRS report: Science and technology. USSR: Materials science
[JPRS-UMS-87-006] 03 p0285 N88-11791
GSSR powder metallurgy research, production expanding 03 p0286 N88-11797
Concentration coefficients of elements in ferromanganese nodules relative to ocean sediments
06 p0726 N88-14464
Remote acoustic sounding of ferromanganese nodules
06 p0727 N88-14471
Ferromanganese nodules of Antarctic sector in Pacific Ocean 06 p0727 N88-14472

FET (TRANSISTORS)
U FIELD EFFECT TRANSISTORS

FETUSES
Mother-fetus system as object for investigation of mechanisms of physiological effect of weightlessness
07 p0891 N88-15402
Spleen lymphocyte nucleic acids in pregnant rats flown in space and their offspring 07 p0892 N88-15403
Brain morphogenesis in rats developing in weightlessness 07 p0894 N88-15415

FEYNMAN DIAGRAMS
Chiral symmetry in the path-integral approach
[DE88-700833] 12 p1699 N88-20168
Calculations in perturbative string field theory
[DE88-011616] 22 p3158 N88-28798

FFT
U FAST FOURIER TRANSFORMATIONS

FIBER COMPOSITES
NT CARBON FIBER REINFORCED PLASTICS
NT GLASS FIBER REINFORCED PLASTICS
Ceramic-Ceramic Composites Meeting in Belgium
[ONRL-7-020-R] 01 p0019 N88-10118
Pressure effects on the thermal stability of SiC fibers
[NASA-TM-100146] 01 p0019 N88-10120
Behavior of graphites under intense heat loads
[DE87-012128] 01 p0028 N88-10179
Fiber-reinforced composite hot-gas filters
[DE87-012257] 01 p0033 N88-10208

Fracture mechanical analysis of the initiation and propagation of matrix and surface cracks in thermally loaded fiber composite models
[ETN-87-90439] 01 p0062 N88-10400
Electron beam irradiation effects on carbon fiber reinforced PEEK composite
[DE87-753001] 02 p0142 N88-10890
Cumulative fatigue and life prediction of fibre composites. Part 1: Literature reviews
[BR101013] 02 p0142 N88-10893
Cumulative fatigue and life prediction of fibre composites. Part 2: Experimental techniques and results
[BR101014] 02 p0142 N88-10894
Need for composites, new materials discussed 02 p0160 N88-11001
The ability of modified pavement quality concrete to resist ground erosion caused by VTOL aircraft
[BAE-ARG-238] 03 p0267 N88-11683
Processing and properties of SiC/Nicalon composites
[DE87-013685] 03 p0279 N88-11757
Transply crack density detection by acousto-ultrasonics
[NASA-TM-100224] 03 p0279 N88-11758
Contributions to the investigation of mechanical behavior of gamma/gamma NbC Cotac composites at medium and at high temperature
[ESA-TT-1031] 03 p0280 N88-11760
Plasticity of fibrous composites
[AD-A184637] 03 p0280 N88-11765
Ultrasonic characterization of the nonlinear elastic properties of unidirectional graphite/epoxy composites
[NASA-CR-4100] 03 p0281 N88-11767
Development and application of composites 03 p0286 N88-11795
Carbon fiber reinforced glass matrix composites for space based applications
[AD-A184355] 04 p0410 N88-12546
Molecular composites: Processing, post-treatment and mechanics
[AD-A184458] 04 p0410 N88-12547
Interfacial strength development in thermoplastic resins and fiber-reinforced thermoplastic composites
[NASA-CR-181525] 04 p0411 N88-12549
Development of advanced fiber reinforced ceramics
[DE88-000779] 04 p0420 N88-12604
Optimal ribbing of long plate made of composite material 04 p0426 N88-12641
In-situ characterization of the interface of glass reinforced composites
[AD-A185136] 05 p0557 N88-13391
Fiber composite structural durability and damage tolerance: Simplified predictive methods
[NASA-TM-100179] 05 p0560 N88-13409
Study of ceramic-fiber/ceramic sol-gel based matrix composites
[SNIAS-872-430-120] 05 p0569 N88-13469
Design and test of high performance composite tubes for use in deep water drilling and production systems
[SNIAS-872-430-107] 05 p0572 N88-13487
Fatigue mechanisms in ARALL, a fatigue resistant hybrid aluminum aramid composite material 05 p0605 N88-13711
Temperature dependent mechanical properties of an alumina fiber reinforced aluminum composite 06 p0677 N88-14147
Thermo-mechanical behavior of high temperature fiber composites 06 p0678 N88-14149
Advanced organic composite materials for aircraft structures: Future program
[NASA-CR-181467] 06 p0678 N88-14155
Bending properties of aluminum base composite with CVD-fiber
[PB87-130878] 06 p0678 N88-14156
Characterization of mechanical damage mechanisms in ceramic composite materials
[AD-A185549] 06 p0686 N88-14205
Interface effects on the mechanical properties of ceramic composites
[AD-A185899] 07 p0826 N88-15009
Bibliography of textbooks on fibre reinforced plastics (212 books)
[PB87-146080] 07 p0827 N88-15017
Numerical solution methods for viscoelastic orthotropic materials
[NASA-CR-182381] 08 p0971 N88-15874
Effect of an optimized fiber orientation on transonic flutter characteristics of a high-aspect-ratio composite wing
[NAL-TR-930] 09 p1120 N88-16709
Fatigue behaviour of hybrid composites
[BR102236] 09 p1138 N88-16819
Design procedures for fiber composite box beams
[NASA-TM-100296] 09 p1139 N88-16828
Effect of post-cure heat-treatment on static and fatigue behaviour of XAS-914C carbon fibre composite
[AD-A186943] 10 p1294 N88-17735
Fabrication and materials evaluation of high performance aligned ceramic fibre reinforced glass matrix composite
[AERE-R-12517] 10 p1294 N88-17736
A fiber-resin micromechanics analysis of the delamination front in a DCB specimen
[NASA-TM-100540] 10 p1294 N88-17737
Mechanics of composite materials: Past, present and future
[NASA-TM-100793] 10 p1295 N88-17744
Finite element substructuring methods for composite mechanics
[NASA-TM-100297] 10 p1296 N88-17745
Friction and wear of monolithic and fiber reinforced silicon-ceramics sliding against IN-718 alloy at 25 to 800 C in atmospheric air at ambient pressure
[NASA-TM-100294] 10 p1304 N88-17796
Testing of a tail rotor system in a fiber composite type of construction
[MBB-UD-472/86] 10 p1314 N88-17854
Cavitation in model elastomeric composites
[AD-A187401] 11 p1447 N88-18625
Damage mechanics of fiber reinforced plastics: A general view 11 p1448 N88-18631
Backscatter from flaws in fiber-reinforced composites 11 p1450 N88-18639
Innovative design of composite structures: Further studies in the use of a curvilinear fiber format to improve structural efficiency
[NASA-CR-182576] 11 p1450 N88-18641
Matrix-fiber stress transfer in composite materials: Elasto-plastic model with an interphase layer
[PB88-136635] 11 p1450 N88-18643
Radiation and temperature effects on the time-dependent response of T300/934 graphite/epoxy
[NASA-CR-182603] 11 p1451 N88-18646
Oxidation and protection of fiberglass-epoxy composite masts for photovoltaic arrays in the low Earth orbital environment
[NASA-TM-100839] 11 p1465 N88-18734
Ultrasonic-velocity studies of composite and heterogeneous materials
[AD-A189000] 12 p1604 N88-19595
The place for thermoplastic composites in structural components
[AD-A189149] 12 p1604 N88-19596
Structural materials: The changing scene 12 p1703 N88-20190
Viscoelastic behavior of a polyetheretherketone (PEEK) composite
[AD-A189545] 13 p1734 N88-20368
Transient dynamics of fibre reinforced composite plates
[IIT-B/CE/RR/87-1] 13 p1734 N88-20370
Interfacial chemistry-structure and fracture of ceramic composites
[DE88-005516] 13 p1750 N88-20461
Hygrothermomechanical fiber composite fatigue: Computational simulation
[NASA-TM-100840] 14 p1884 N88-21257
Monolithic nature of transversely reinforced composites 14 p1885 N88-21267
Interface structure and properties of alumina/glass ceramic composites
[DE88-006219] 14 p1892 N88-21302
Superconducting transition temperature of Cu-Nb microcomposites 14 p1973 N88-21775
Structure and surface characterizations of high strength carbon fibers
[AD-A189642] 15 p2029 N88-22087
Damage models for delamination and transverse fracture
[AD-A189652] 15 p2029 N88-22088
Fracture toughness testing of a ceramic matrix composite
[AD-A189846] 15 p2029 N88-22089
An investigation of the failure response of laminates under biaxial stress
[AD-A190039] 15 p2029 N88-22090
Interfacial structure-property relationships at the fiber-matrix interphase in advanced composites
[AD-A190649] 15 p2030 N88-22093
Thermal expansion behavior of randomly oriented short carbon fiber reinforced copper composites
[NASA-TT-20175] 15 p2031 N88-22099
Reciprocating sliding wear characteristics of copper-carbon fiber composites
[NASA-TT-20176] 15 p2031 N88-22100
Fiber-reinforced plastic composites. Possibilities and limitations of applications as machine-construction materials
[NASA-TT-20159] 15 p2031 N88-22102
Processing, microstructure, and mechanical properties of silicon carbide particulate reinforced aluminum alloys
[AD-A188981] 15 p2037 N88-22136
The composite blade structural analyzer (COBSTRAN) 15 p2078 N88-22390
Whisker-reinforced ceramic composites for heat engine components 15 p2082 N88-22410
Nondestructive evaluation by acousto-ultrasonics 15 p2082 N88-22412
Design studies of primary aircraft structures in ARALL laminates
[LR-520] 16 p2160 N88-22888
A study of failure characteristics in thermoplastic composite material
[AD-A190613] 16 p2171 N88-22940
Behaviour of fibre-reinforced composites under dynamic loading
[AD-A191310] 16 p2174 N88-22955
Acousto-ultrasonic input-output characterization of unidirectional fiber composite plate by SV waves
[NASA-CR-4152] 16 p2217 N88-23224
Ceramics for turbine engines 17 p2323 N88-23873
Ceramic matrix composites 17 p2325 N88-23888
Polymer precursors for ceramic composites 17 p2326 N88-23890
SiC fiber reinforced reaction-bonded Si3N4 composites 17 p2326 N88-23892
Input-output characterization of fiber composites by SH waves
[NASA-CR-4153] 17 p2347 N88-23986
Creep behavior of tungsten/niobium and tungsten/niobium-1 percent zirconium composites 17 p2425 N88-24427
Carbon matrix composites prospective roles for biotechnology 18 p2477 N88-24694
Mixed-mode fracture of uniaxial fiber reinforced composites
[AD-A191629] 18 p2478 N88-24700
Sol/gel processing techniques for glass matrix composites
[AD-A191748] 18 p2478 N88-24701
Interaction of ultrasonic waves with composite plates
[AD-A191879] 18 p2478 N88-24702
Analysis of notched metal matrix composites under tension loading
[NASA-TM-100629] 18 p2480 N88-24713
Multiple scattering of waves in discrete random media
[AD-A191068] 18 p2499 N88-24823
Fatigue testing and damage development in continuous fiber reinforced metal matrix composites
[NASA-TM-100628] 19 p2610 N88-25489
Loading rate sensitivity of open hole composites in compression
[NASA-TM-100634] 19 p2610 N88-25490
Acousto-ultrasonic input-output characterization of unidirectional fiber composite plate by P waves
[NASA-CR-4162] 19 p2678 N88-25923
Structural optimization of fiber composite turbomachine blades
[ETN-88-92351] 20 p2760 N88-26372
The two isotropic asymptotes of fiber composites
[AD-A192305] 21 p2904 N88-27231
Effects of electron beam irradiation on mechanical properties at low and high temperature of fiber reinforced composites using PEEK as matrix material
[DE88-753134] 21 p2905 N88-27239
Fabrication of SiC fiber reinforced glass matrix by extrusion process and investigation of its mechanical properties
[ETN-88-92367] 21 p2906 N88-27244
Programs for preliminary design of composite materials which were developed by the design group of Aerospatiale Aquitaine
[REPT-881-430-112] 21 p2907 N88-27251
Simulation of moisture diffusion of fiber reinforced components of aircraft for general air transportation
[IFL-IB-87-05] 21 p2907 N88-27253
As-received microstructure of a SiC/Ti-15-3 composite
[NASA-TM-100938] 22 p3050 N88-28095
Analysis of stiffness reduction, failure and stress concentration in fiber composite laminates
[AD-A193519] 22 p3050 N88-28096
Durability of continuous fiber reinforced metal matrix composites
[AD-A193868] 22 p3050 N88-28097
Fracture behavior in multidimensional fiber-reinforced composites 22 p3051 N88-28099
Wave propagation and vibration of fibre reinforced laminates
[AD-A194144] 22 p3051 N88-28101
Elastic wave dispersion in laminated composite plate
[AD-A192289] 23 p3188 N88-28967
The effects of moisture loss and elevated temperature upon the material damping of fibre reinforced polymer matrix composites
[UTIAS-324] 23 p3188 N88-28970

Effect of fiber diameter on the reliability of composites - automated laser diffraction implementation
[AD-A193524] 23 p3188 N88-28972
An investigation of some basic properties of hybrid composite materials
[AD-A194136] 23 p3189 N88-28975
Investigation of a SiC/Ti-24Al-11Nb composite
[NASA-TM-100956] 23 p3190 N88-28980
A test for interfacial effects and stress transfer in ceramic matrix composites
[NASA-CR-182873] 24 p3340 N88-29880
A study of the critical factors controlling the synthesis of ceramic matrix composites from preceramic polymers
[AD-A195405] 24 p3340 N88-29881

FIBER OPTICS

Test equipment with fiber optic data bus and laser gyro strapdown system LTN-90 for the helicopter BO-105
[ESA-TT-1038] 01 p0005 N88-10025
Data Management Working Group report 01 p0016 N88-10097
Mid infrared LHS system packaging using flexible waveguides
[NASA-CR-181192] 01 p0093 N88-10607
Fiber optic engineering sensor system. Preliminary program management plan, phase 3 revision
[AD-A183663] 01 p0093 N88-10608
The use of fiber optics in the determination of temperature and extent of reaction in detonating explosives
[DE87-012632] 01 p0094 N88-10612
Fiber-linked telescope arrays on the ground and in space 01 p0095 N88-10626
Optical fiber interferometric sensor to measure temperature in gas flow
[ENST-87E006] 02 p0170 N88-11071
Ultrafast holography using optical fibers
[ISL-R-101/86] 02 p0176 N88-11096
Effects of radiation damage in optical fibers: A tutorial
[PB87-210308] 02 p0235 N88-11482
Radiation-induced transient attenuation of optical fibers at 800 and 1300 nm
[DE87-013165] 02 p0235 N88-11485
The design and construction of a thermally controlled single mode fiber switch
[ETN-87-90929] 02 p0236 N88-11491
The design and testing of an analog optical communication link capable of the simultaneous transmission of four frequency division multiplexed audio signals
[AD-A184695] 03 p0307 N88-11936
Integrated fiber-optic coupler
[AD-A184494] 03 p0377 N88-12369
An inexpensive real-time interactive three-dimensional flight simulation system
[AD-A184340] 04 p0402 N88-12499
Spectroscopic monitoring of RS CVn stars at Kitt Peak using the Penn State fiber optic echelle 04 p0509 N88-13127
In-situ characterization of the interface of glass reinforced composites
[AD-A185136] 05 p0557 N88-13391
Fiber-optic accelerometer investigation
[AD-A185359] 05 p0584 N88-13561
Streak camera dynamic range optimization
[DE88-001632] 05 p0586 N88-13571
Optical probe
[EP-PATENT-0-210-869-A1] 05 p0650 N88-13984
JPRS report: Science and technology. Japan
[JPRS-JST-87-027] 06 p0688 N88-14213
Developments in optical sensor technologies described 06 p0689 N88-14220
Program description of FIBRAM: A radiation attenuation model for optical fibers
[PB87-230686] 06 p0690 N88-14229
AVIRIS foreoptics, fiber optics and on-board calibrator 06 p0706 N88-14328
Photoinduced low-temperature changes in optical losses in fiber optics based on chalcogenide glasses 06 p0770 N88-14731
Fiber optic video link
[FOA-C-30444-3.1] 06 p0780 N88-14789
Fiber optic single mode sensors
[FOA-C-30453-3.1] 06 p0780 N88-14790
An inexpensive real-time interactive three dimensional flight simulation system
[AD-A184868] 07 p0821 N88-14989
Advanced communication systems: A report on fiber optic technology and its possible applications in the gas industry
[PB88-112792] 07 p0845 N88-15125
Soliton mode of propagation of light pulses through single-mode optical fibers and problems of its experimental realization 07 p0920 N88-15592
Fiber optics refractometer for absorption machines
[DE88-002296] 07 p0932 N88-15662
Development and study of fibre-optic link lines on the basis of the KEM-8-4PD, KEM-8-4PR quantum-electronic modules
[DE88-700372] 07 p0932 N88-15663
Aeropropulsion '87. Session 4: Instrumentation and Controls Research
[NASA-CP-10003-SESS-4] 08 p0955 N88-15794
Optical measurement systems 08 p0955 N88-15796
Fiber optics for controls 08 p0956 N88-15798
Summary record of presentations to the Federal Telecommunication Standards Committee/Fiber optics task group
[PB88-110853] 08 p0978 N88-15911
Stimulated Raman scattering of picosecond light pulses in long dispersive medium 08 p1078 N88-16498
Pressure and tension dependence of phase shift of polarization modes in birefringent single-mode fiber-optic waveguide 08 p1078 N88-16501
Parametric interaction of optical modes in fiber-optic light guide 09 p1235 N88-17406
Multichannel anisotropic single-mode fiber optics for transducers 09 p1240 N88-17429
Code division multiple access applied to fiber optic data transmission
[AD-A186873] 09 p1247 N88-17477
Failure-resistant Fibre-Optical Communication Line (FOCL)
[DE88-700470] 10 p1408 N88-18400
Design and implementation of a fiber optic RS232 link
[AD-A187319] 10 p1409 N88-18409
A conceptual design of an inertial navigation system for an autonomous submersible testbed vehicle
[AD-A188038] 11 p1438 N88-18578
Joint services electronics program
[AD-A188173] 11 p1478 N88-18822
Optically coupled tactile sensor array for robotics 11 p1550 N88-19273
A prototype fibre optic gyroscope for missile guidance applications 12 p1596 N88-19554
A fiber optic gyro strapdown reference system for guided weapons 12 p1597 N88-19560
Development of a high speed InGaAs/InP Schottky barrier photodetector for millimeter-wave fiber optical links
[AD-A188594] 12 p1629 N88-19750
Experimental and analytical investigation on a proposed embedded fiber optic displacement sensor
[AD-A189030] 12 p1630 N88-19756
Development of fiber optic systems for recording and transmitting holographic information
[AD-A189406] 13 p1773 N88-20603
Remote fiber fluorimetry techniques for pressure measurements
[DE88-004486] 13 p1773 N88-20604
Enzyme-based fiber optic sensors
[DE88-005674] 13 p1840 N88-21013
Development of high stability fiber optic spectrophotometric systems for study of solar/stellar magnetic activity
[AD-A189327] 13 p1852 N88-21088
Berry's phase in fiber optics 14 p1977 N88-21797
Amplification of signals in fiber optics using the stimulated Raman effect
[AD-A190281] 15 p2133 N88-22727
A 104-km unrepeatered bidirectional fiber optic demonstration link
[AD-A190282] 15 p2134 N88-22728
Clinical measurements using fiber optic sensors
[DE88-005624] 15 p2134 N88-22731
Tethered diagnostic package for use from the space station
[DE88-006264] 16 p2167 N88-22921
A new fiber-optic-based ion sensor
[AD-A191322] 16 p2274 N88-23612
A new fiber-optic-based phase-resolved phosphorescence spectrometer
[AD-A191325] 16 p2275 N88-23613
The role of fiberoptics in remote temperature measurement 17 p2329 N88-23909
Fiber waveguide sensors for intelligent materials
[NASA-CR-183028] 17 p2343 N88-23968
Optics: Perspectives for Measurement Techniques and Signal Processing for Flight Guidance --- conference
[DFVLR-MITT-87-21] 18 p2516 N88-24928
Navigation using the Teldix fiber-optic gyroscope 18 p2517 N88-24933
Digital fiber optic displacement sensors 18 p2518 N88-24937
Activities report of the Division of Optical Technology
[FOA-C-30477-3] 18 p2576 N88-25299
Optical pressure sealing couping (light joint)
[NASA-CASE-MFS-29348-1] 18 p2576 N88-25303
Low-loss, high-isolation, fiber-optic isolator
[NASA-CASE-NPO-17207-1-CU] 18 p2576 N88-25304
Overview of NASA research in fiber optics for aircraft controls
[NASA-TM-100919] 19 p2603 N88-25458
High speed opto-isolator for radar applications 19 p2658 N88-25795
MESFET compatible IMSM detectors 19 p2659 N88-25801
Radar and EW applications of multi-gigahertz optical components and systems 19 p2660 N88-25816
Characteristics and application of wideband guided-wave devices 19 p2660 N88-25817
Fiber optic sensors 19 p2670 N88-25870
Active phase compensation system for fiber optic holography
[NASA-TM-101295] 20 p2805 N88-26641
Fiber optic sensors with internal referencing
[NASA-TM-100893] 20 p2806 N88-26644
Use of fiber optic equipment for security
[DE88-007898] 20 p2853 N88-26943
An overview of the development of a linear broadband analog fiber-optic link
[DE88-008668] 20 p2854 N88-26945
A concept for an electro-optic explosive device
[DE88-009696] 21 p2923 N88-27349
Fiber-optics used to record high-speed photographs inside a pressurized tank during lethality testing
[DE88-011283] 21 p2951 N88-27529
A fiber optic synchronous detector using sample-and-hold circuits
[DE88-010973] 21 p3016 N88-27899
Modulated-splitting-ratio fiber-optic temperature sensor
[NASA-TM-101332] 22 p3042 N88-28062
Multichannel data transmission through a fiber optic cable
[AD-A193842] 22 p3070 N88-28221
Fiber optic sensing systems using high frequency resonant sensing heads with intensity sensors
[NASA-TM-101318] 22 p3080 N88-28293
Laboratory feasibility study of a composite embedded fiber optic sensor for measurement of structural vibrations
[AD-A194270] 22 p3152 N88-28754
Long haul underwater fiber optic link
[AD-A194487] 23 p3262 N88-29542
A fiber optic collective flight control system for helicopters
[AD-A195406] 24 p3328 N88-29818
Performance analysis of FDDI
[NASA-CR-183206] 24 p3413 N88-30321
A fiber optic beamforming processor for wideband direction finding
[AD-A194862] 24 p3428 N88-30404
Ultra-wideband direction finding using a fiber optic beamforming processor
[AD-A194861] 24 p3430 N88-30413

FIBER ORIENTATION

Ultrasonic characterization of the nonlinear elastic properties of unidirectional graphite/epoxy composites
[NASA-CR-4100] 03 p0281 N88-11767
Generalized coupled-mode equations, applications to fiber couplers 03 p0298 N88-11875
Determination of the fiber ratio in carbon fiber/resin composites by means of image analysis
[SNIAS-872-422-101] 05 p0558 N88-13398
Advanced organic composite materials for aircraft structures: Future program
[NASA-CR-181467] 06 p0678 N88-14155
Contribution to modeling flexion fatigue damage in unidirectional composite materials
[ECL-87-12] 08 p0965 N88-15843
Experimental study on the effect of fiber orientation on flutter characteristics of high-aspect-ratio transport wing
[NAL-TR-936] 09 p1120 N88-16708
Effect of an optimized fiber orientation on transonic flutter characteristics of a high-aspect-ratio composite wing
[NAL-TR-930] 09 p1120 N88-16709
A study of the mechanical behavior of a 2-D carbon-carbon composite 11 p1449 N88-18638
Innovative design of composite structures: Further studies in the use of a curvilinear fiber format to improve structural efficiency
[NASA-CR-182576] 11 p1450 N88-18641
Reinforcing of thermoplastic polycarbonate and polysulfone with carbon fibers: Production and characteristics of UD-compound objects
[NASA-TT-20158] 13 p1735 N88-20374
A viscoplastic constitutive theory for metal matrix composites at high temperature 14 p1929 N88-21500
Thermal expansinn behavior of randomly oriented short carbon fiber reinforced copper composites
[NASA-TT-20175] 15 p2031 N88-22099
Reciprocating sliding wear characteristics of copper-carbon fiber composites
[NASA-TT-20176] 15 p2031 N88-22100

Fatigue damage development of various CFRP-laminates
[NASA-TT-20247] 16 p2172 N88-22945
Rupture of carbon fiber reinforced plastics (T300-914) composite materials: Influence of initial first ply failures on the fatigue behavior
[SNIAS-881-422-103] 24 p3342 N88-29892

FIBER REINFORCED COMPOSITES
Fiber-reinforced composite hot-gas filters
[DE87-012257] 01 p0033 N88-10208
Carbon fiber reinforced glass matrix composites for space based applications
[AD-A184355] 04 p0410 N88-12546
Molecular composites: Processing, post-treatment and mechanics
[AD-A184458] 04 p0410 N88-12547

FIBER STRENGTH
Pressure effects on the thermal stability of SiC fibers
[NASA-TM-100146] 01 p0019 N88-10120
Carbon-fiber reinforced aluminum
04 p0403 N88-12507
Lifetime of pristine optical fibers
[ETN-88-92246] 16 p2273 N88-23602
Strong fibers
[DE88-007798] 19 p2610 N88-25486
Relation between the mechanical characteristics of carbon-resin composites and their impact strength
[REPT-48-284/F] 21 p2907 N88-27249
A test for interfacial effects and stress transfer in ceramic matrix composites
[NASA-CR-182873] 24 p3340 N88-29880
Rupture of carbon fiber reinforced plastics (T300-914) composite materials: Influence of initial first ply failures on the fatigue behavior
[SNIAS-881-422-103] 24 p3342 N88-29892

FIBERGLASS
U GLASS FIBERS

FIBERS
NT BORON FIBERS
NT CARBON FIBERS
NT CERAMIC FIBERS
NT GLASS FIBERS
NT HAIR
NT METAL FIBERS
NT NYLON (TRADEMARK)
NT OPTICAL FIBERS
NT REINFORCING FIBERS
NT SYNTHETIC FIBERS
Ceramic composites by chemical vapor infiltration
[DE87-009128] 01 p0029 N88-10185
The friction and wear of TPS fibers
[NASA-CR-181496] 03 p0291 N88-11830
Method of obtaining of fire resistant polyacrylonitrile fiber or cloth from it
[AD-A185941] 07 p0836 N88-15071
Absorption, scattering, and thermal radiation by conductive fibers
[AD-A186105] 07 p0842 N88-15106
Comparison of ultrasonic flaw detection analysis for spherical composite test specimens using two data acquisition techniques
[DE88-005002] 12 p1634 N88-19782
The influence of the fiber-matrix bond on the mechanical behavior of NICALON/SiC composites
[DE88-006155] 13 p1734 N88-20369
Recommendations on developing polycrystalline alumina fiber
13 p1756 N88-20502
Polymer precursors for SiC ceramic materials
17 p2326 N88-23889
Raman characterization of AsF5-intercalated vapor grown graphite fibers
[AD-A191709] 18 p2491 N88-24778
Stress measurements in graphite fibers by laser raman spectroscopy
[AD-A191710] 18 p2491 N88-24779
Interface modification in Nicalon (trademark)/SiC composites
[DE88-009708] 20 p2767 N88-26409
A micromechanics model of the stiffness and strength of laminates with fiber waviness
[NASA-CR-181670] 20 p2768 N88-26413
Laboratory feasibility study of a composite embedded fiber optic sensor for measurement of structural vibrations
[AD-A194270] 22 p3152 N88-28754

FIBERS (MATHEMATICS)
Division algebras and sphere fibrations
[ETN-87-90677] 01 p0087 N88-10566

FIBONACCI NUMBERS
On color polynomials of Fibonacci graphs
[AD-A184133] 04 p0486 N88-12996
Relaxed heaps: An alternative to fibonacci heaps
[AD-A194030] 23 p3272 N88-29470

FIBRINOGEN
Distinctive features in blood clotting and fibrinolytic properties under effect of epinephrine in presence of hypoxia and hypercapnia 19 p2705 N88-26082

FIBROSIS
Toxic effects of man-made mineral fibers with particular reference to ceramic fibers
[AD-A187949] 11 p1519 N88-19072
Hierarchical structure in polymeric solids and its influence on properties
[AD-A194720] 23 p3197 N88-29029

FIBROUS MATERIALS
U FIBERS

FIDELITY
U ACCURACY

FIDUCIARIES
Programmable 10 MHz optical fiducial system for hydrodiagnostic cameras
[DE87-013223] 02 p0175 N88-11091

FIELD EFFECT TRANSISTORS
NT JFET
NT MODFETS
Phase 2 development of a 12 GHz MMIC FET amplifier
[IM-I86-1010] 01 p0038 N88-10240
Surface effects and low frequency noises in GaAs field effect transistors
[LAAS-87-179] 02 p0168 N88-11055
A study of charged particles/radiation damage to VLSI device materials
[NASA-CR-172036] 05 p0577 N88-13518
A GaAs MESFET balanced mixer with very low intermodulation
[AD-A184848] 05 p0655 N88-14015
Surface chemistry of chemically sensitive field effect transistors
[AD-A185917] 07 p0847 N88-15139
A report on the effects of neutron irradiation of GaAs semiconductors
[AD-A186816] 09 p1253 N88-17510
Nature of gigantic resistance fluctuations in metal-oxide-semiconductor wires
[DE88-002905] 09 p1256 N88-17533
Design of a charge sensitive preamplifier on high resistivity silicon
[DE88-003491] 10 p1323 N88-17907
Study of quantum mechanical effects in deep submicron, grating-gate field effect transistors
[AD-A188283] 10 p1325 N88-17923
Development of a multiplexer module for use in a spaceborne cryogenic environment based on GaAs MESFET technology
[RPT/CRY/62463/BOP] 11 p1559 N88-19335
Microelectronic applications of the conductor-thin insulator-semiconductor (CIS) structure
11 p1560 N88-19341
Radiation response of thin oxides grown by rapid thermal oxidation and rapid thermal annealing techniques
[DE88-003632] 11 p1561 N88-19347
Planning, construction, and commissioning of a vacuum apparatus with a cold surface for the measurement of transistor functions at 20 K
[JUEL-SPEZ-397] 12 p1622 N88-19703
Response characteristics of dual MOSFET gamma-ray sensors produced by Mitel Corporation
[AD-A189026] 12 p1630 N88-19755
Characterization of enhanced Schottky-barrier InGaAs/Al(1-x)As strained channel modulation-doped field-effect transistors
[AD-A188820] 12 p1698 N88-20162
Fundamental studies and device development in beta silicon carbide
[AD-A189540] 12 p1699 N88-20165
Focused ion beam fabrication of graded channel FET's in GaAs and Si
[AD-A189166] 13 p1845 N88-21040
Energy loss rates for light holes in InGaAs/GaAs strained layer single quantum wells
[DE88-005744] 13 p1848 N88-21062
MOSFET performance degradation due to hot carriers
13 p1848 N88-21063
Examination of temperature effects on gate-to-drain avalanche breakdown in GaAs MESFETs (Metal-Semiconductor Field Effect Transistors) by measuring light emission under RF drive
[AD-A189634] 15 p2141 N88-22778
Modeling the effects of heavy charged particles on MOSFETs (Metal-Oxide-Semiconductor Field Effect Transistors)
[AD-A190575] 15 p2143 N88-22792
The response of a power MOSFET (N-channel) and a dielectric isolated operational amplifier to the combined environmental effects of high temperature and total dose gamma radiation 17 p2406 N88-24309
Modeling of radiation dose dependence of MOSFETs
17 p2416 N88-24370
The response of selected semiconductor technologies to the combined environmental effects of high temperature and total dose gamma radiation
17 p2431 N88-24462
Development of 20 GHz monolithic transmit modules
[NASA-CR-182134] 17 p2445 N88-24539
A monolithic reduced-size Ku-Band SPOT (Single-Pole Double Throw) FET switch
[DE88-006273] 18 p2505 N88-24858
Planar fully ion-implanted high power InP MISFETs
[AD-A191589] 18 p2582 N88-25338
Multigigahertz logic based on InP-MISFET's exhibiting extremely high transconductance
19 p2656 N88-25771
An optically strobed sample and hold circuit
19 p2656 N88-25772
Enhanced performance ultrabroadband distributed amplifiers 19 p2656 N88-25775
MESFET compatible IMSM detectors
19 p2659 N88-25801
Hot carrier effects in CMOS field effect transistors at cryogenic temperatures 19 p2662 N88-25829
Electrical and chemical sensors for biological cell research 19 p2669 N88-25866
Chemical multisensors with selective encapsulation of ion-selective membranes 19 p2670 N88-25869
Miniature radiation dosimeter for in vivo radiation measurements 19 p2672 N88-25889
Effect of process conditions on aluminum oxide thin film used in pH ISFET 19 p2673 N88-25892
Microwave amplifiers
[AD-A192974] 20 p2795 N88-26585
Transport in GaAs heterojunction ring structures
20 p2864 N88-27011
Resonant tunneling transistors and resonant tunneling hot electron spectroscopy 20 p2866 N88-27018
Random quantum interference in microdevices
20 p2866 N88-27021
Picosecond optoelectronic sampling of electrical waveforms produced by an optically excited field effect transistor
[AD-A192384] 21 p2935 N88-27428
Focused ion beam fabrication of graded channel FETs in GaAs and Si
[AD-A193098] 21 p2936 N88-27439
Techniques and instrumentation for transient characterization of metal-insulator-semiconductor diodes. Applications to metal-insulator InP system
[ECL-87-17] 21 p3025 N88-27959
A 2.3-GHz low-noise cryo-FET amplifier
22 p3066 N88-28195
An electronically tuned, stable 8415-MHz dielectric resonator FET oscillator for space applications
22 p3068 N88-28205
Large-signal modeling of gallium arsenide field-effect transistors 22 p3073 N88-28242
Functional study of the Si/SiO2 structures. Application to the implementation of an integrated ion sensor
[ECL-87-16] 22 p3073 N88-28246
Development and experimental verification of a two-dimensional numerical model of piezoelectrically induced threshold voltage shifts in GaAs MESFETs
[AD-A193462] 23 p3206 N88-29080
Optoelectronic gain control of a microwave single stage GaAs MESFET amplifier
[NASA-CR-182201] 24 p3368 N88-30055
Power MISFETs on OnP
[AD-A195242] 24 p3433 N88-30436
Joint services electronics program
[AD-A195731] 24 p3434 N88-30439

FIELD EMISSION
Different ways of looking at the electromagnetic vacuum
[DE87-013150] 01 p0089 N88-10584
Studies on temporal field emission from stainless steel surfaces
[DE87-014237] 02 p0147 N88-10919
Conditions for geomagnetically trapping sub-micron lunar ejecta between L = 1.2 and L = 3.1
04 p0521 N88-13203
New application of transition metal carbides detailed
06 p0675 N88-14132
Optimization of field emission electron beam sources for high-power lasers
[PB87-218814] 06 p0708 N88-14341
The acoustic-electric field analysis of multilayered surface acoustic wave devices
[ETN-88-91592] 09 p1242 N88-17446
Intelligent on board control for field emission electric propulsion system 12 p1589 N88-19513
A study of the interaction of light with sub-micron metallic surfaces
[DE88-003138] 13 p1776 N88-20624
Modulatable thin film field emission space gun
[AD-A189279] 13 p1845 N88-21043

Degradation of beam brightness by field emission from a cathode shroud
[DE88-008345] 20 p2794 N88-26576
Development of liquid metal field-emission sources for use in fast repetitive opening switches
[AD-A192230] 20 p2795 N88-26583
Progress in diagnostic techniques for SC (superconducting) cavities
[DE88-008600] 20 p2876 N88-27077

FIELD OF VIEW

Two dimensional path planning with obstacles and shadows
[AD-A184075] 04 p0397 N88-12474
A system overview of the Airborne Visible/Infrared Imaging Spectrometer (AVIRIS)
06 p0705 N88-14326
Space infrared telescope facility wide field and diffraction limited array camera (IRAC)
[NASA-CR-182704] 13 p1853 N88-21092
Flight simulator: Field of view utilized in performing tactical maneuvers
[AD-A192412] 20 p2762 N88-26379
Assessments of maneuverability with the TeleOperated Vehicle (TOV)
[AD-A191584] 21 p2993 N88-27751
Visual sensitivities under reduced oxygen
[AD-A195628] 24 p3406 N88-30279

FIELD STRENGTH

NT ELECTRIC FIELD STRENGTH
NT MAGNETIC FLUX
Monocrystalline silicon gradiometer for gravity experiments in space
[NASA-CR-181452] 01 p0050 N88-10321
Magnetic flux tubes as sources of wave generation
04 p0505 N88-13108
Measurements of stellar magnetic fields: Empirical constraints on dynamo and rotational evolution theories
04 p0518 N88-13185
Observations and analysis of the photospheric magnetic fields on dwarf G, K and M stars
04 p0520 N88-13196
Nonuniformity of electromagnetic field at Lambda = 10.6 micron wavelength inside atmospheric aerosol particles
06 p0772 N88-14743
Local properties of index-alpha stable fields
[AD-A186432] 07 p0912 N88-15530
Evaluation of CWMS (Continuous-Wave Measurement System) single-wire dipole antenna
[DE88-003979] 09 p1155 N88-16920
Some measurements of height gain at V.H.F.
12 p1617 N88-19671
Magnet strength fluctuations in the SSC (Superconducting Super Collider) lattice. Part 2: Frequency modulation
[DE88-006491] 15 p2141 N88-22774
Classical non-Abelian solutions for nonstandard Lagrangians
[DE88-701305] 16 p2263 N88-23532
Optical sensing of magnetic fields
19 p2670 N88-25871
Measurement of macroscopic electric fields in solar plasma structures
[AD-A193291] 21 p3031 N88-27993

FIELD THEORY (ALGEBRA)

NT CUBIC EQUATIONS
NT QUADRATIC EQUATIONS
Prediction and spectral decomposition of wide sense stationary processes on Z squared
[ENST-87C001] 01 p0087 N88-10564
Integrable quantum systems and classical Lie algebras
[DE88-700872] 12 p1683 N88-20063
On the equivalence of four-dimensional self-duality equations to continual analog of the main chiral field problem
[DE88-700871] 12 p1686 N88-20083
String theory and algebraic geometry of moduli spaces
[CWI-PM-R8705] 13 p1849 N88-21070
Exact image theory for the problem of dielectric/magnetic slab
[NASA-CR-182865] 16 p2189 N88-23055
An introduction to poloidal and toroidal fields
[MITT-54] 17 p2394 N88-24232
General relativity invariance and string field theory
[DE88-702045] 19 p2737 N88-26252
Algebraic and arithmetic geometry in string theory
[CWI-PM-R8708] 20 p2848 N88-26904
Theory of Laplacian fractals: Diffusion limited aggregation and dielectric breakdown model
[PREPRINT-590] 22 p3144 N88-28701

FIELD THEORY (PHYSICS)

NT GRAND UNIFIED THEORY
NT INSTANTONS
NT QUANTUM CHROMODYNAMICS
NT STRONG INTERACTIONS (FIELD THEORY)
NT UNIFIED FIELD THEORY
NT WEAK INTERACTIONS (FIELD THEORY)
Anomalies in gauge theories
[DE87-014087] 02 p0229 N88-11444
Regular effective action of gauge field theory and quantum gravity
[DE87-703076] 02 p0247 N88-11560
On the degree of generality of inflationary solutions in cosmological models with a scalar field
[DE87-703079] 02 p0251 N88-11586
New notions about space-time and gravitation
[DE87-703259] 03 p0383 N88-12408
Gravity from symmetry breakdown of a gauge affine theory
[DE88-001671] 04 p0500 N88-13079
Non-minimal interaction of gravity with other physical fields: An overview
[DE87-703362] 05 p0624 N88-13819
Lagrangian procedures for higher order field equations
[DE87-703365] 05 p0640 N88-13911
Introduction to string field theory
[DE87-014583] 05 p0657 N88-14032
Gravitational interaction of massless fields with higher spins (s greater than 2) 06 p0775 N88-14760
Nonsymmetric metrics in nonlinear field theory
[DE88-700509] 07 p0913 N88-15537
Existence of absolutely closed universe
08 p1080 N88-16509
Activities report in nuclear physics
[ETN-88-91609] 09 p1245 N88-17458
Research in theoretical physics
[DE88-003201] 09 p1259 N88-17548
Single nucleon coincidence cross sections in a relativistic mean field theory
[CEBAF-PR-87-016] 11 p1546 N88-19243
On exterior variational calculus
[DE88-700861] 12 p1683 N88-20062
Topics in string theory: Task D
[DE88-004532] 12 p1699 N88-20167
Super Virasoro algebra and solvable supersymmetric quantum field theories
[DE88-752299] 15 p2127 N88-22681
To the field theory with a fundamental mass
[DE88-701159] 15 p2146 N88-22807
Secondary gauge conditions in field theory
[DE88-701499] 15 p2147 N88-22814
On a generalization of renormalization group equations to quantum field theories of an arbitrary type
[DE88-701143] 16 p2263 N88-23531
Computational quantum field theory
[DE88-700918] 16 p2284 N88-23672
Introduction to covariant formulation of superstring (field) theory
[DE87-703038] 18 p2586 N88-25363
Combining relativity and quantum mechanics: Schroedinger's interpretation of psi
[DE88-701899] 20 p2880 N88-27102
Superalgebras with Grassmann algebra-valued structure constants from superfields
[DE88-702239] 21 p3011 N88-27862
Closed string fields as parameters of extra gauge symmetry of open string field theory
[DE88-702046] 21 p3026 N88-27960
The Hilbert space of the closed bosonic string
[USIP-88-04] 22 p3151 N88-28747
Research in the theory of condensed matter and elementary particles
[DE88-010180] 22 p3151 N88-28749
Calculations in perturbative string field theory
[DE88-011616] 22 p3158 N88-28798
On the quantization of constrained generalized dynamics
[DE88-702223] 23 p3277 N88-29505
On neutrino fields in Einstein-Cartan theory
[MATH-REPT-208] 23 p3295 N88-29629
Introduction to string theory
[DE88-702706] 24 p3435 N88-30445

FIGHTER AIRCRAFT

NT F-4 AIRCRAFT
NT F-14 AIRCRAFT
NT F-15 AIRCRAFT
NT F-16 AIRCRAFT
NT F-18 AIRCRAFT
NT F-27 AIRCRAFT
NT F-106 AIRCRAFT
NT F-111 AIRCRAFT
NT HARRIER AIRCRAFT
NT MIG AIRCRAFT
NT MIRAGE AIRCRAFT
HiMAT flight program: Test results and program assessment overview
[NASA-TM-86725] 01 p0005 N88-10026
Comparison of wind tunnel and flight test afterbody and nozzle pressures for a twin-jet fighter aircraft at transonic speeds
[NASA-TP-2588] 02 p0121 N88-10765
Application of knowledge-based techniques to aircraft trajectory generation and control
02 p0129 N88-10811
The influence of load cycle reconstitution on fatigue behaviour
[ARL-STRUC-R-424] 02 p0192 N88-11198
Soviet aviation technology's state of the art SU-27 fighter
[AD-A184121] 03 p0259 N88-11628
Improvements to the adaptive maneuvering logic program
[NASA-CR-3985] 03 p0262 N88-11648
Flight propulsion control integration for V/STOL aircraft
[NASA-TM-100226] 03 p0267 N88-11680
Special Course on Fundamentals of Fighter Aircraft Design
[AGARD-R-740] 05 p0544 N88-13315
Fundamentals of fighter aircraft design
05 p0544 N88-13316
Mission requirements and aircraft sizing
05 p0545 N88-13317
Design of wings and wing/body configurations for transonic and supersonic speeds
05 p0545 N88-13318
Aircraft dynamics: Aerodynamic aspects and wind tunnel techniques 05 p0545 N88-13320
Techniques for performance optimisation in cruise and manoeuverability 05 p0545 N88-13321
Fundamentals of fighter aircraft design: Engine intake and afterbody 05 p0545 N88-13322
Airframe/store compatibility 05 p0545 N88-13323
Aeroelasticity and optimization in fighter aircraft design
05 p0546 N88-13324
Materials for fighter aircraft 05 p0546 N88-13325
Requirements and recommendations for the development of theoretical codes and experimental facilities in the near future 05 p0546 N88-13327
Examples of static aeroelastic effects on present combat aircraft projects 05 p0550 N88-13349
Trends in aeroelastic analysis of combat aircraft
05 p0550 N88-13350
A study of the Department of Defense configuration management policies and procedures as applied to the FA-18 Strike/Fighter program
[AD-A184872] 05 p0657 N88-14034
NASA supersonic STOVL propulsion technology program
[NASA-TM-100227] 06 p0668 N88-14093
Highlights of the 70th Flight Mechanics Panel Symposium on Flight Vehicle Development Time and Cost Reduction
[AD-A185831] 07 p0901 N88-15454
A model for estimating depot maintenance costs for Air Force fighter and attack aircraft
[AD-A187097] 09 p1105 N88-16624
A cost and benefit analysis of hydraulic fluid systems for the next generation of tactical aircraft
[AD-A186911] 09 p1116 N88-16690
Dynamic function allocation in fighter cockpits
[AD-A185397] 09 p1201 N88-17199
Neural network based architectures for aerospace applications 09 p1204 N88-17218
An examination of the impact of potential advances in component technology for future military engines
10 p1279 N88-17650
Research and development. Technical-scientific publications (1956-1987): Retrospective view and prospects. Jubilee edition on the occasion of the 75th birthday of Dipl.-Engr. Dr.-Engr. E. H. Ludwig Boelkow
[ISSN-0931-9751] 10 p1309 N88-17819
Future fighter maneuverability for air combat
[MBB/LKE-1/S/PUB/120] 10 p1312 N88-17843
Flight testing of fighter aircraft
[MBB/LKE-62/S/PUB/292] 10 p1312 N88-17844
The aerodynamic design optimisation of a forward swept wing fighter aircraft
[CAR-87-18] 11 p1433 N88-18553
Testing of the engine compartment fire extinguishing system in the F/EF-111 aircraft
[AD-A188801] 12 p1576 N88-19423
Workshop on Design Loads for Advanced Fighters
[AGARD-R-746] 12 p1579 N88-19449
Changes in USAF structural loads requirements
12 p1580 N88-19452
The relationship between operational flight manoeuvre parameters and design parameters
12 p1580 N88-19454
Design loads for Swedish military aircraft in a twenty years' perspective 12 p1580 N88-19456
Determination of design loads for modern combat aircraft 12 p1580 N88-19457
Manned simulation: Helpful means to determine and improve structural load criteria 12 p1581 N88-19459
Computer aided tactics for air combat
12 p1597 N88-19559

Avionics acquisition, trends and future approaches
12 p1702 N88-20184
Use of demonstration/validation prototypes: Impact on total development costs and times
12 p1703 N88-20194
Crack distribution and growth rates for critical fastener holes in Mirage wing RH79
[AD-A189080] 13 p1722 N88-20293
Viscoelastic behavior of a polyetheretherketone (PEEK) composite
[AD-A189545] 13 p1734 N88-20368
The cooling of electronic equipment in fighter aircraft
[MBB/LKE-312/S/PUB/258] 14 p1866 N88-21147
Model selection for the multiple model adaptive algorithm for in-flight simulation
[AD-A189715] 15 p2016 N88-22022
Multivariable control law design for the AFTI/F-16 with a failed control surface using a parameter-adaptive controller
[AD-A189848] 15 p2020 N88-22040
Kalman filter residual expert system
[AD-A190520] 15 p2020 N88-22041
Flow visualization study of vortex manipulation on fighter configurations at high angles of attack
16 p2201 N88-23130
Task listing: Visually assisted and visually dependent tasks for fighter aircraft
[AD-A191041] 16 p2244 N88-23404
PAN AIR analysis of the NASA/MCAIR 279-3: An advanced supersonic V/STOL fighter/attack aircraft
[NASA-TM-88838] 17 p2298 N88-23750
Pilot report: AFTI (Advanced Fighter Technology Integration) F-111
[AD-A192937] 21 p2895 N88-27184
A cockpit natural language study: Vocabulary and grammar analyses
[AD-A193289] 21 p2993 N88-27753
The impact of increased aircraft reliability on maintenance facility design
[AD-A194395] 22 p3042 N88-28057
Combat aircraft
23 p3169 N88-28868
Inflight rearming
[AD-A193564] 23 p3176 N88-28909
Multiple-Purpose Subsonic Naval Aircraft (MPSNA): Multiple Application Propfan Study (MAPS)
[NASA-CR-175104] 23 p3177 N88-28917
Computers in weapons systems: A look at the F-15
[AD-A194498] 23 p3178 N88-28920
General operational and training visual concerns
23 p3242 N88-29295
Grid generation on and about a cranked-wing fighter aircraft configuration
23 p3246 N88-29318
Grid generation for an advanced fighter aircraft
23 p3246 N88-29319
Algebraic grid generation for fighter type aircraft
23 p3246 N88-29320
Aircraft dynamics: Aerodynamic aspects and wind tunnel techniques
24 p3313 N88-29731
The Soviet Stealth fighter: Check or checkmate
[AD-A195200] 24 p3323 N88-29791
The cost and performance implications of reliability improvements in the F-16A/B
[AD-A195096] 24 p3324 N88-29796
Integration of LANTIRN (Low Altitude Navigation and Targeting Infrared for Night) into operational fighter training
[AD-A194906] 24 p3325 N88-29799

FIGURE OF MERIT
Evaluation of device figure of merit in microwave switching circuit design
[AD-A184896] 05 p0577 N88-13520
High-resolution Real-Time Radiography (RTR) system design
[AD-A187107] 09 p1166 N88-16992
Optimisation of the thermoelectric figure of merit of modified silicon germanium alloys
[AD-A191347] 16 p2283 N88-23670
Preparation of improved PbSnTe thermoelectric alloys and evaluation of their figure of merit
[AD-A191346] 17 p2445 N88-24538

FILAMENT WINDING
Development of a polyimide matrix for filament winding with improved extensibility and fracture toughness for permanent use at 200 C
[BMFT-FB-T-86-118] 01 p0030 N88-10190
Composite bearing materials containing solid lubricant in filamentary form, stages 3 and 4
[IRD-87/2] 01 p0054 N88-10344
Core material --- honeycombs
[EP-PATENT-0-196-926-A2] 05 p0558 N88-13393
The structures of large wound propulsion shells --- carbon fiber composites filament winding
[SNIAS-872-430-118] 05 p0559 N88-13406
Comparison of ultrasonic flaw detection analysis for spherical composite test specimens using two data acquisition techniques
[DE88-005002] 12 p1634 N88-19782
Woven frameworks for three-dimensional reinforcement 14 p1884 N88-21262
Optimal filament shells loaded with internal pressure in a centrifugal force field 14 p1885 N88-21266
Design of booster wound structures --- spacecraft structures
[SNIAS-881-430-102] 21 p2903 N88-27228
Reinforced plastics: Winding and weaving technologies for space products
[SNIAS-881-430-103] 21 p2922 N88-27341
NDE performance in predicting failure strength of spherical composite specimens with implanted flaws
[DE88-008223] 21 p2959 N88-27575

FILAMENT WOUND CONSTRUCTION
U FILAMENT WINDING

FILAMENTS
Modeling of proximity coupling between superconducting filaments in superconducting dipole magnets
[DE87-014684] 03 p0382 N88-12403
Solar-geophysical data number 514, June 1987. Part 2: (Comprehensive reports). Data for December 1986
[PB87-217279] 03 p0390 N88-12450
Mechanism of change of vortex structure orientation in type-2 superconductors 09 p1239 N88-17425
Solar-geophysical data number 519, November 1987. Part 2: (Comprehensive reports). Data for May 1987 and miscellanea
[PB88-158910] 14 p2011 N88-21997
Diamond film by hot filament CVD method
[NASA-TT-20335] 23 p3294 N88-29618

FILAMENTS (SOLAR PHYSICS)
U SOLAR PROMINENCES

FILE MAINTENANCE (COMPUTERS)
File usage analysis and resource usage prediction: A measurement-based study
[NASA-CR-181553] 05 p0633 N88-13867
Usage analysis of user files in UNIX
[NASA-CR-181561] 05 p0633 N88-13868
Relational data handling system for scientists
[PB87-223426] 05 p0658 N88-14038
Ada user library
[FOA-C-20657-2.7] 16 p2246 N88-23418
Unified interchange format for computer data (standard file format)
[ESA-STR-225] 17 p2386 N88-24183
The SMITE object oriented backing store
[RSRE-MEMO-4147] 23 p3244 N88-29308

FILLERS
Microstructural characterization of HSLA-100 GMA-weldments
[AD-A187782] 11 p1457 N88-18683
Plasma joining of metal matrix composites
[AD-A188559] 12 p1604 N88-19593
Hydrogen induced cracks in armor steel weldments fabricated with austenitic filler alloys
[AD-A188733] 13 p1740 N88-20406
Ultrasonic characterization of ceramic joints
[DE88-005844] 15 p2043 N88-22173
The mechanical behavior of particle filled thermoplastics
[ETN-88-92234] 16 p2181 N88-22999

FILLETS
Methods of improving compacting quality of intricately shaped powder components
[BLL-M-37412-(5828.4)] 08 p0968 N88-15859

FILM BOILING
Effects of surface tension and contact angle on sensible heating and boiling incipience in dielectric falling films
[DE88-007057] 21 p2945 N88-27492

FILM CONDENSATION
Dilution refrigerator with non-valve adsorption system of sup 3/He circulation
[DE88-700974] 15 p2050 N88-22209

FILM COOLING
Film cooling heat transfer on a turbine airfoil
02 p0186 N88-11156
Finite element analysis of three-dimensional steady and unsteady temperature fields (computation of temperature distribution of turbine blade with composite cooling)
03 p0300 N88-11887
National Aerospace Laboratory experiment
04 p0404 N88-12509
Film cooling effectiveness on a flat plate in high free-stream turbulence using a single row of 30 deg slant-hole injectors
[AD-A190500] 15 p2147 N88-22816
Investigation of annular flow at high evaporation rates in view of liquid film cooling
[DFVLR-FB-88-08] 21 p2949 N88-27517
Studies of gas turbine heat transfer airfoil surface and end-wall cooling effects
[AD-A195165] 24 p3326 N88-29805
The thermal behavior of film cooled turbulent boundary layers as affected by longitudinal vortices
[AD-A195155] 24 p3374 N88-30095

FILM THICKNESS
Characterization of the dimensions of colloidal calcium carbonate dispersions in toluene with neutron small-angle scattering
[ECN-197] 06 p0680 N88-14167
Film thicknesses in circular elastohydrodynamic contacts
[PB87-123725] 06 p0710 N88-14354
Effect of the gate oxide thickness on the speed of MOS integrated circuits
[PB88-155783] 10 p1323 N88-17910
Specific heat of novel thin-film material systems
10 p1415 N88-18446
Basic mechanisms of diesel lubrication correlation of bench and engine tests
[AD-A193360] 21 p2956 N88-27561

FILTERING
U FILTRATION

FILTERS
Least squares linear lags and limited memory filters
[NASA-CR-178381] 03 p0372 N88-12339
Single-mode projection filters for modal parameter identification for flexible structures
[NASA-CR-182680] 18 p2566 N88-25244

FILTRATION
NT SPATIAL FILTERING
Fiber-reinforced composite hot-gas filters
[DE87-012257] 01 p0033 N88-10208
Reduction of temperature rise in high-speed photography
[NASA-TM-100222] 02 p0176 N88-11100
Vapor compression distiller and membrane technology for water revitalization 03 p0359 N88-12262
Plume mechanics and aerosol growth processes
[AD-A184467] 04 p0442 N88-12742
Proceedings of the 19th DOE/NRC Airborne Waste Management and Air Cleaning Conference
[NUREG/CP-0086-VOL-1] 11 p1509 N88-19018
Proceedings of the 19th DOE/NRC Airborne Waste Management and Air Cleaning Conference
[NUREG/CP-0086-VOL-2] 11 p1509 N88-19019
WKBJ method and strained coordinates for high frequency inertial wave filtering
[INPE-4214-PRE/1095] 11 p1537 N88-19186
Observations on electrostatic effects in a filter test system
[AD-A188797] 13 p1736 N88-20378
Reference filters for electrostatic charging tendency measurements of fuels
[AD-A191717] 18 p2495 N88-24803
Characteristics of pressure loss during filtration using a porous ceramic filter
[DE88-752547] 20 p2798 N88-26604

FINANCE
National Aeronautics and Space Administration Authorization Act, 1988
[PUB-LAW-100-147] 03 p0385 N88-12422
Department of Housing and Urban Development, and Certain Independent Agencies Appropriations, 1988, Part 2
[S-HRG-100-106-PT-2] 03 p0385 N88-12423
Means of financing --- space projects
22 p3161 N88-28823

FINANCIAL MANAGEMENT
Financial reporting: NASA (National Aeronautics and Space Administration) can improve compliance with GAO (General Accounting Office) standards and treasury requirements
[PB88-172523] 18 p2587 N88-25373
Costs --- space projects 22 p3160 N88-28816
Value engineering --- space projects
22 p3160 N88-28817
Price estimates and analysis
22 p3161 N88-28818
Value analysis 22 p3161 N88-28819
Management of large space projects. Financial means. Part 1: Financing of constructors
22 p3161 N88-28822
Means of financing --- space projects
22 p3161 N88-28823
The role and the place of insurance of large space projects 22 p3161 N88-28826

FINE STRUCTURE
A work station for EXELFS data acquisition and analysis
[USIP-87-10] 01 p0078 N88-10498
The optimum illumination conditions for EXELFS studies in a CTEM
[USIP-87-08] 01 p0092 N88-10600

Instrumental and operational aspects of an EXELFS system connected to JEOL 100C STEM
[USIP-87-09] 01 p0092 N88-10601
Solar interferometry with a 4-aperture nonredundant and stabilized network 01 p0097 N88-10639
A data analysis package for RDF-determination fromEXELFS-spectra
[USIP-87-07] 01 p0104 N88-10681
EXELFS (Extended Electron Energy Loss Fine Structure) of amorphous and crystalline SiC
[DE87-013551] 02 p0151 N88-10948
Theoretical modelling of the fine structures in sunspots 02 p0256 N88-11617
Main results of atmospheric fine structure parameter observation in the lower thermosphere 06 p0735 N88-14518
Statistical fine structure in inhomogeneously broadened absorption lines in solids
[AD-A190341] 16 p2174 N88-22957
Statistical fine structure in the inhomogeneously broadened electronic origin of pentacene in p-terphenyl
[AD-A191211] 16 p2176 N88-22968
Functional and mechanical analysis of continuous media-application to the study of elastic composites with periodic structure: Homogenization
[NASA-TT-20188] 18 p2480 N88-24710
EXAFS studies of the microstructure of semiconductor alloys, defects and semiconductor-metal interfaces 20 p2868 N88-27031
Structural studies of (Ga,In)(As,P) alloys and (InAs) sub m (GaAs) sub n strained-layer superlattices by fluorescence-detected EXAFS 20 p2872 N88-27051
Can we calculate the fundamental dimensionless constants of physics
[DE88-702641] 23 p3295 N88-29625

FINENESS RATIO

Planform effects on the supersonic aerodynamics of multibody configurations
[NASA-TP-2762] 04 p0393 N88-12454

FINES

Study of mean free path effects on growth of ultrafine metallic aerosols
[AD-A190206] 15 p2039 N88-22149
Fine grain development by laser CVD 15 p2050 N88-22214
Superfine grain development by laser 15 p2050 N88-22215

FINGERS

Tactile sensing and inverse problems
[AD-A187464] 10 p1340 N88-18011

FINISHES

NT ENAMELS
NT GLAZES
Macroscopic distribution of fiber finish
[DCQ/L-48-283/F] 07 p0827 N88-15013

FINITE DIFFERENCE THEORY

Description of NCAR (National Center for Atmospheric Research) Community Climate Model (CCM1)
[PB87-203782] 01 p0072 N88-10462
A numerical and analytical investigation of Rayleigh-Taylor instability in a solid tungsten plate
[DE87-013593] 01 p0087 N88-10562
Finite difference solution of a generic differential equation
[PB87-205878] 01 p0087 N88-10568
FDM-FEM zonal method for viscous flow computations over multiple-bodies
[NAL-TR-925T] 02 p0170 N88-11069
Comparison between numerical solutions and measurements for a high speed turbine blade
[PNR90402] 02 p0172 N88-11082
Improved numerical methods for turbulent viscous recirculating flows 02 p0185 N88-11148
Differencing the diffusion equation on a mesh of triangles and quadrilaterals
[DE87-011550] 02 p0224 N88-11408
QUICKSILVER: A 3D, electromagnetic, PIC code
[DE87-013013] 02 p0245 N88-11547
Efficient numerical approaches for predicting supersonic flows with viscous/inviscid interaction 03 p0260 N88-11637
Numerical modeling: Finite methods 03 p0304 N88-11918
Numerical and experimental investigation of the unsteady temperature distribution in solar central receivers
[ESA-TT-1050] 03 p0347 N88-12193
Application of the finite difference method to the solution of mixed partial differential equations for the case of transonic flow
[ETN-87-90760] 03 p0370 N88-12327
A two-dimensional finite difference program for thermal analysis of rocket thrust chambers
[NASA-TM-100191] 04 p0409 N88-12539
Calculation of three-dimensional stationary turbulent boundary layer on root section of wing ignoring compressibility 04 p0424 N88-12630
Generating meshes for finite-difference analysis using a solid modeler
[DE88-001458] 04 p0439 N88-12729
Time-marching finite-difference methods for the three-dimensional Euler equations of contravariant velocity components 05 p0539 N88-13285
Steady waves in a nonlinear theory of viscoelasticity
[AD-A185548] 06 p0723 N88-14448
Numerical simulation of a controlled boundary layer 07 p0810 N88-14933
The numerical and analytical study of bifurcation and multicellular flow instability due to natural convection between narrow horizontal isothermal cylindrical annuli at high Rayleigh numbers
[AD-A186113] 07 p0849 N88-15151
Stability analysis of finite difference schemes for hyperbolic systems, and problems in applied and computational linear algebra
[AD-A185824] 07 p0908 N88-15499
Unsteady transonic algorithm improvements for realistic aircraft applications
[NASA-TM-100516] 08 p0949 N88-15760
The simulation of three-dimensional viscous supersonic flow past blunt bodies with a hybrid implicit/explicit finite difference method
[DFVLR-FB-87-32] 08 p0950 N88-15765
Computational Fluid Dynamics
[VKI-LS-1987-04] 08 p0984 N88-15951
A survey of upwind principles for the multidimensional Euler equations 08 p0984 N88-15953
Integration of Navier-Stokes equations in finite volume formulation 08 p0984 N88-15954
Adaptive finite difference methods in fluid dynamics 08 p0985 N88-15958
A study of finite difference and finite element vertical discretization schemes for baroclinic prediction equations
[AD-A186617] 08 p1040 N88-16291
FOR3D: A computer model for solving the LSS (Lee-Saad-Schultz) three-dimensional, wide angle wave equation
[AD-A186649] 08 p1080 N88-16511
Numerical calculation of turbulent recirculating flows
[TUM-LSM-84/29] 09 p1161 N88-16959
A quasi-three-dimensional calculation procedure for the prediction of flow and heat transfer in heat exchanger passages 09 p1165 N88-16985
Numerical solutions of two moving boundary problems by both finite difference and finite element methods with applications
[DE88-002867] 09 p1230 N88-17374
Navier-Stokes computations for circulation control airfoils 10 p1269 N88-17592
EXPLO: Explosives thermal analysis computer code
[DE88-001938] 10 p1307 N88-17814
A three-dimensional dual potential procedure for rotational flows 10 p1329 N88-17942
Application of a multigrid method to a buoyancy-induced flow problem
[DE88-003961] 10 p1397 N88-18326
Total Variation Diminishing (TVD) schemes of uniform accuracy
[NASA-TM-100552] 11 p1436 N88-18566
Accurate boundary conditions for exterior problems in gas dynamics
[NASA-TM-100807] 11 p1537 N88-19182
An adaptive grid finite difference method for time-dependent Magnetohydrodynamic (MHD) flows and its astrogeophysical applications 11 p1553 N88-19294
Experimental verification of a finite-difference time-domain thin slot algorithm
[DE88-005572] 13 p1817 N88-20859
Predicting oscillatory finite difference solutions to the heat equation: A comparative study of the coefficient and matrix methods
[AD-A189591] 13 p1825 N88-20911
A Lagrangian moving grid scheme for one-dimensional evolutionary partial differential equations
[CWI-NM-R8713] 13 p1827 N88-20922
Monolithic nature of transversely reinforced composites 14 p1885 N88-21267
Investigation of the behavior of fast propagating cracks using numerical simulation calculations
[W-6/87] 14 p1934 N88-21532
COMESH: A corner mesh finite difference code to solve multigroup diffusion equations in multidimensions
[DE88-701248] 15 p2108 N88-22555
Efficient, high resolution computations of projectile and missile flow fields
[AD-A191086] 16 p2158 N88-22873
Reduced order models for nonlinear aerodynamics 16 p2220 N88-23248
The good, the bad and the ugly: Comparing high-speed computer systems
[DE88-007498] 16 p2245 N88-23412
Study of the convergence of a finite difference scheme for acoustic propagation in the atmosphere in a parabolic approximation. Statistical calculation of the sound field in the presence of kinematic turbulence
[ONERA-RS-8/3641-PY-160-P] 17 p2394 N88-24235
Fundamental limits to the velocity of solid armatures in railguns 18 p2469 N88-24656
Cross stream differencing for integral boundary layer equations
[AD-A191744] 18 p2509 N88-24886
Adaptive local grid refinement in computational fluid mechanics
[AD-A192215] 18 p2510 N88-24890
Adaptive grid refinement for numerical weather prediction
[AD-A192172] 18 p2544 N88-25101
Transmitting boundary for finite-difference calculations with finite modeling of an infinite medium
[AD-A191441] 18 p2570 N88-25264
Modelling of thermal plasma systems 18 p2578 N88-25314
A multiple chamber volume-filling model for prediction of transient solid rocket motor ballistic performance 19 p2633 N88-25618
An implicit, high order accurate, upwind scheme for unsteady Euler equations 19 p2639 N88-25657
On the propagating speed in difference approximations for conservation laws 19 p2639 N88-25658
Some supraconvergent schemes for hyperbolic equations on irregular grids
[DE88-009113] 19 p2720 N88-26151
Five-point form of the nodal diffusion method and comparison with finite-difference
[DE88-004141] 19 p2720 N88-26154
Semi-discrete approximations to nonlinear systems of conservation laws; consistency and L(infinity)-stability imply convergence
[NASA-CR-181683] 19 p2721 N88-26157
Axisymmetric liquid sloshing under low-g conditions: Numerical simulation method (reference manual)
[NLR-TR-86057-U] 20 p2802 N88-26627
Implicit finite-difference simulation of an internal flow on a hypercube
[AD-A192474] 21 p2942 N88-27471
Implicit finite-difference simulation of an internal flow in a nozzle: An example of a physical application on a hypercube
[AD-A192475] 21 p2942 N88-27472
User's manual for C-HEMP: A two-dimensional wave propagation code. Volume 1: Description and derivations of the code
[AD-A193197] 21 p2944 N88-27486
Numerical predictions for the flow induced by an enclosed rotating disc
[PNR90463] 22 p3078 N88-28281
Applications of an exponential finite difference technique
[NASA-TM-100939] 22 p3084 N88-28312
Transient thermal analysis of three fast-charging latent heat storage configurations for a space-based power system
[DE88-009714] 23 p3186 N88-28960
Space marching Euler solvers 24 p3318 N88-29759
Three-dimensional gas turbine combustor modelling 24 p3349 N88-29937
On the application of finite-difference techniques for the computation of the flow field in gas turbine combustors with complex geometries 24 p3349 N88-29938
Numerical field model simulation of full scale fire tests in a closed spherical/cylindrical vessel
[AD-A195067] 24 p3359 N88-29998
An analysis of finite-difference and finite-volume formulations of conservation laws
[NASA-CR-177416] 24 p3370 N88-30071
Finite-difference simulations of Rayleigh-wave scattering by shallow heterogeneity
[AD-A194961] 24 p3402 N88-30259

FINITE ELEMENT METHOD

Contribution to the dynamical analysis of rheolinear nonconservative, gyroscopic systems using finite element methods
[ETN-87-90410] 01 p0050 N88-10320
Stress-strain behavior of components subject to residual stresses taking the example of an orifice plate
[FF-10/1986] 01 p0059 N88-10375
A DMAP for updating dynamic mathematical models with measured data
[NLR-MP-86027-U] 01 p0060 N88-10387
Thermal stress analysis of space shuttle orbiter subjected to reentry aerodynamic heating
[NASA-TM-88286] 01 p0061 N88-10389

Reinforced flexural elements for TEMP-STRESS Program
[DE87-012961] 01 p0061 N88-10391
A mixed finite element method for the computation of stress in a composite with loaded holes
[ONERA-RT-34/4242-RY-054-R] 01 p0062 N88-10395
Correction to a single higher order theory of elastic plates
[ETN-87-90676] 01 p0062 N88-10397
Contribution to the numerical calculation of fracture-mechanical quantities for elastic and elastic-plastic material behavior, especially for mixed fmads
[ETN-87-90435] 01 p0062 N88-10399
New fatigue damage analysis of complex engineering components based on Finite Element Methods (FEM)
[DFVLR-FB-87-15] 01 p0062 N88-10401
DETOUR: A deformed mesh/contour plot program
[DE87-013119] 01 p0082 N88-10525
Perfine: Personal finite elements on a microcomputer
[ETN-87-90678] 01 p0082 N88-10528
Error estimates for finite element approximations of parabolic variational equations
[BONNER-MATHE-SCHR-179] 01 p0087 N88-10569
A microstructural lattice model for strain oriented problems: A combined Monte Carlo finite element technique
[NASA-TM-100215] 02 p0150 N88-10939
FDM-FEM zonal method for viscous flow computations over multiple-bodies
[NAL-TR-925T] 02 p0170 N88-11069
Numerical solution of Euler equations for compressible fluids by the finite element method, volume 3
[ETN-87-90650] 02 p0170 N88-11070
Implementation of finite element quality assurance in a commercial industrial organisation
[PNR90393] 02 p0183 N88-11137
Reliability of finite element methods in North America
[AGARD-R-748] 02 p0184 N88-11139
Component specific modeling 02 p0187 N88-11166
Constitutive modeling for single crystal superalloys 02 p0187 N88-11168
Constitutive modeling for isotropic materials 02 p0188 N88-11171
Constitutive modeling for isotropic materials 02 p0188 N88-11172
Thermal expansion mismatch and oxidation in thermal barrier coatings 02 p0189 N88-11182
A numerical method for the treatment of kinked cracks in finite bodies 02 p0190 N88-11189
Concurrent algorithms for transient nonlinear FE analysis
[NASA-CR-181455] 02 p0221 N88-11389
Finite elements for 2D elliptic equations with moving nodes
[DE87-013501] 02 p0224 N88-11410
A finite element model for induction heating of a metal crucible
[DE87-014246] 02 p0246 N88-11551
Stability of mechanical joints in launching vehicles: Local and global stationary values of energy density 03 p0270 N88-11696
Theoretical investigation of stress concentrations in damaged carbon fibre reinforced plastic plate structures. Volume 1: Main text
[BR99872-VOL-1] 03 p0280 N88-11761
Theoretical investigation of stress concentrations in damaged carbon fibre reinforced plastic plate structures. Volume 2: Tables, figures and plates
[BR99873-VOL-2] 03 p0280 N88-11762
Three-dimensional finite element based, interative approach for analysis of laminated composites 03 p0280 N88-11763
Finite element analysis of three-dimensional steady and unsteady temperature fields (computation of temperature distribution of turbine blade with composite cooling) 03 p0300 N88-11887
Generalized hybrid variational principle, corresponding finite element model 03 p0301 N88-11895
Compactness of quasi-conforming element spaces, convergence of quasi-conforming element method 03 p0301 N88-11896
Numerical modeling: Finite methods 03 p0304 N88-11918
Calculation of the three dimensional flow in the impeller of hydraulic turbomachines using a finite element method
[ETN-87-90612] 03 p0315 N88-11988
Application of viscoplastic constitutive equations in finite element programs
[KFK-4254] 03 p0370 N88-12329
Total linearisation method for solving viscous free boundary flow problems by the finite element method
[PB87-222337] 04 p0441 N88-12737
NACHOS 2: A finite element computer program for incompressible flow problems. Part 2: User's manual
[DE88-001451] 04 p0443 N88-12750
TOPAZ: The transient one-dimensional pipe flow analyzer: An update on code improvements and increased capabilities
[DE88-001781] 04 p0443 N88-12751
Continuation finite element analysis of viscoelastic fluids 04 p0445 N88-12761
Nonlinear axial stiffness characteristics of axisymmetric bolted joints 04 p0452 N88-12799
A refined nonlinear analysis of laminated composite plates and shells
[AD-A184436] 04 p0454 N88-12811
Kinematic formulation of finite elements for plate bending 04 p0455 N88-12821
Large change-of-curvature effects in quadratic finite elements for CAD of membrane structures 04 p0480 N88-12958
A comparison of adaptive refinement techniques for elliptic problems
[DE88-000805] 04 p0485 N88-12987
The finite element method for electronic structure
[DE88-001708] 04 p0485 N88-12989
A finite element procedure for interference-fit and cold-working problems with limited yielding
[AR-004-517] 04 p0485 N88-12992
Trends in aeroelastic analysis of combat aircraft 05 p0550 N88-13350
Finite-element grid improvement by minimization of stiffness matrix trace
[NASA-TM-100255] 05 p0591 N88-13604
Finite element model for the stress and flexibility analysis of curved pipes
[DE87-703632] 05 p0592 N88-13608
Non-linear shipboard shock analysis of the Tomahawk missile shock isolation system 05 p0592 N88-13614
Modal survey of the space shuttle solid rocket motor using multiple input methods 05 p0593 N88-13617
Initial dynamic load estimates during configuration design 05 p0593 N88-13621
Exact finite element method analysis of viscoelastic tapered structures to transient loads 05 p0595 N88-13632
An efficient frequency response solution for nonproportionally damped systems 05 p0595 N88-13634
Shape optimization of damping layers 05 p0595 N88-13635
Dynamic response of laminated composite plates using a three-dimensional hybrid-stress finite-element formulation 05 p0596 N88-13639
Significance of foundation-soil separation in dynamic soil-structure interaction 05 p0596 N88-13641
Application of finite element methods with cyclic elasto-plastic strain analysis to low cycle fatigue analysis of engine components
[AR-004-512] 05 p0596 N88-13642
Strain-energy-release rate analysis of the end-notched flexure specimen using the finite-element method
[NASA-TM-100494] 05 p0608 N88-13735
An element of a multilayer shell for the computation of composite structures
[ONERA-RT-14/3542-RY-051-R] 05 p0610 N88-13742
Thermal finite-element analysis of space shuttle main engine turbine blade
[NASA-TM-100117] 05 p0610 N88-13745
Two low-order mixed methods for the elasticity problem
[PB87-225272] 05 p0610 N88-13749
Structuring data for concurrent vectorized processing in a transient dynamics finite element program
[DE87-013082] 05 p0636 N88-13890
Research and development of finite elements and iterative algorithms for elliptic partial differential equations
[DE88-001381] 05 p0643 N88-13934
Finite-element method for three-dimensional electric and electromagnetic field problems
[PB87-138731] 06 p0696 N88-14274
An evaluation of a translator for finite element data to resistor/capacitor data for the heat diffusion equation
[DE87-013926] 06 p0698 N88-14285
Extensions of the control volume based finite element method for fluid flow problems 06 p0700 N88-14296
Introduction to Computational Fluid Dynamics
[VKI-LS-1987-02] 06 p0701 N88-14300
Introduction 06 p0701 N88-14301
Finite element techniques 06 p0701 N88-14303
A zonal approach for the solution of coupled Euler and potential solutions of flows with complex geometries
[AD-A185465] 06 p0702 N88-14310
Methods for reducing computational costs of typical finite element unsteady hydrodynamic models
[AD-A185499] 06 p0702 N88-14312
Calculations of the turbulent wake behind a slender self-propelled double-body and comparisons with experiment
[AD-A185661] 06 p0703 N88-14314
Geometrically nonlinear analysis of stiffened panels 06 p0722 N88-14440
A periodic small-cluster approach to many-body problems
[DE88-002235] 06 p0763 N88-14683
Stabilized Galerkin method for convection-diffusion problems
[PB87-234985] 06 p0764 N88-14694
Impact of solids on composite materials
[NASA-CR-182395] 07 p0827 N88-15015
SRB combustion dynamics analysis computer program (CDA-1)
[NASA-CR-182404] 07 p0830 N88-15032
User manual for ATILA, a finite-element code for modeling piezoelectric transducers
[AD-A185948] 07 p0847 N88-15141
Hybrid FEM (Finite Element Method) approach to stress distribution in the vicinity of a notch in non-homogeneous materials
[PB87-143392] 07 p0868 N88-15268
The p-version of the finite element method for elliptic equations of order 2l
[AD-A186334] 07 p0911 N88-15523
Nacelle-wing interactions (studies 1986) development of a finite element code in a multi-domain version
[ONERA-RTS-10/3417-AY-308A] 08 p0950 N88-15764
Finite element methods for compressible flows 08 p0984 N88-15956
Finite Element Calculation Methods and Their Application to Turbomachinery Flows, volume 1
[VKI-LS-1987-05-VOL-1] 08 p0985 N88-15960
Finite element fundamentals, part 1 08 p0985 N88-15961
Finite element fundamentals, part 2 08 p0985 N88-15962
Finite element method computer implementation 08 p0985 N88-15963
Inviscid flows, part 1: Formulation of inviscid rotational flow problems by velocity potential and stream function methods. Applications to turbomachines 08 p0985 N88-15964
Finite Element Calculation Methods and Their Application to Turbomachinery, volume 2
[VKI-LS-1987-05-VOL-2] 08 p0985 N88-15965
Inviscid flows, part 2 08 p0985 N88-15966
Viscous flows, part 1 08 p0986 N88-15967
Viscous flows, part 2 08 p0986 N88-15968
Viscous flows. Part 3: Formulation of the Navier-Stokes equations by stream function vorticity methods 08 p0986 N88-15969
Mesh generation 08 p0986 N88-15971
Scanning finite element calculation method
[PB87-143442] 08 p0995 N88-16017
Generalized displacement method in the finite element analysis of incompressible material
[PB87-143434] 08 p0995 N88-16018
Finite element method with continuous mass elements
[PB87-143384] 08 p0995 N88-16019
Dynamic finite element with diagonalized consistent mass matrix and elastic-plastic impact calculation
[PB87-143376] 08 p0995 N88-16020
Computation of the tensile and bending restraint intensities of welded specimens by finite element method
[PB87-143798] 08 p0995 N88-16024
Mixed method of finite strip and finite element
[PB87-143467] 08 p0996 N88-16027
A study of finite difference and finite element vertical discretization schemes for baroclinic prediction equations
[AD-A186617] 08 p1040 N88-16291
Adaptive finite element methods for parabolic systems in one- and two-space dimensions
[AD-A186534] 08 p1073 N88-16475
Finite element analysis of damaged cross-ply composite laminates
[CCMS-87-10] 09 p1139 N88-16829
Dynamic modelling by finite element method of an elasto-acoustic beam with due consideration of flow and viscosity
[PB87-178166] 09 p1164 N88-16978
Qualification by analysis of IUS plume deflectors 09 p1179 N88-17063
Optimized structure design using reanalysis techniques 09 p1180 N88-17067
Dynamic response of a geared train of rotors subjected to random support excitations 09 p1181 N88-17073

Self-adaptive analysis of three-dimensional structures using a p-version of finite element method
[FFA-TN-1987-31] 09 p1182 N88-17084
Finite element analysis for the calculation of calibration curves of fracture mechanics specimen for semicircular surface cracks with several starting depths, for the crack depth measurement following the dc potential method
[GKSS-87/E/19] 09 p1183 N88-17086
A comparison of the predicted and measured gravitational stresses in VAWT (Vertical Axis Wind Turbine) blades
[DE88-002113] 09 p1187 N88-17111
An automatic finite element mesh generator
[AD-A186939] 09 p1216 N88-17291
A raster scan algorithm for generating visible parametric surfaces
[DE88-003222] 09 p1220 N88-17321
Finite element mesh generation and isoparametric elements
[NPL-DITC-97/87] 09 p1229 N88-17365
Numerical solutions of two moving boundary problems by both finite difference and finite element methods with applications
[DE88-002867] 09 p1230 N88-17374
Coupling finite element and spectral methods: First results
[NASA-CR-181606] 09 p1231 N88-17379
Measured and calculated acoustic attenuation rates of tuned resonator arrays for two surface impedance distribution models with flow
[NASA-TP-2766] 09 p1241 N88-17440
Coupled FE and HIE method for exterior acoustics of axisymmetric shells --- finite element (FE) Helmholtz integral equation (HIE)
[ARE-TM(UHA)-87506] 09 p1243 N88-17448
Finite element substructuring methods for composite mechanics
[NASA-TM-100297] 10 p1296 N88-17745
A finite element analysis of adhesively bonded composite joints including geometric nonlinearity, nonlinear viscoelasticity moisture diffusion and delayed failure
[AD-A187455] 10 p1296 N88-17747
A large strain thermomechanical forming model for elastic-viscoplastic behavior in metals
10 p1301 N88-17780
Zonal solutions for viscous flow problems. Finite approximations in fluid mechanics
[MBB/LKE-122/S/PUB/226] 10 p1313 N88-17846
Boundary integral analysis of flow and deformation of long bubbles in capillaries
[DE88-002110] 10 p1326 N88-17927
Design sensitivity analysis of nonlinear structural systems and numerical implementation with established finite element codes 10 p1344 N88-18032
Vibration and flutter characteristics of the SR7L large-scale propfan
[NASA-TM-100272] 10 p1344 N88-18036
Benchmark computation and finite element performance evaluation for a rhombic plate bending problem
[AD-A187402] 10 p1345 N88-18041
Recent progress in the p and h-p version on the finite element method
[AD-A187254] 10 p1400 N88-18347
The h-p version of the finite element method for problems with nonhomogeneous essential boundary condition
[AD-A187356] 10 p1400 N88-18348
Eigenvalue problems
[AD-A188069] 10 p1401 N88-18356
On delamination of (+ or - theta sub m/90 sub n/2) sub s laminates subject to tensile loading
[AD-A188095] 11 p1447 N88-18626
Finite element analysis of adhesively bonded composite joints including geometric nonlinearity, nonlinear viscoelasticity, moisture diffusion and delayed failure
[PB88-147822] 11 p1451 N88-18648
Study of the mechanical behavior of a 2-D carbon-carbon composite
[NASA-CR-182594] 11 p1451 N88-18649
Experimental set-up and mathematical modeling of H-shaped beam type structure
[AD-A187196] 11 p1466 N88-18743
GERA computer code for calculation of two-dimensional electromagnetic fields in resonators and electron-optical systems by the finite element method
[DE88-700678] 11 p1480 N88-18831
Finite element methods of analysis for high speed viscous flows
[NASA-CR-182529] 11 p1483 N88-18852
A velocity-pressure integrated, mixed interpolation, Galerkin finite element method for high Reynolds number laminar flows
[NASA-CR-179264] 11 p1486 N88-18868
Further development of a finite element model of orthogonal metal cutting
[DE88-004048] 11 p1494 N88-18921
The 58th Shock and Vibration Symposium, volume 2
[NASA-CP-2488-VOL-2] 11 p1499 N88-18948
Dynamic substructuring for shock spectrum analysis using component mode synthesis
11 p1499 N88-18950
Approximate method for predicting the permanent set in a beam in vacuo and in water subject to a shock wave 11 p1500 N88-18957
Numerical fracture mechanics using finite element method 11 p1501 N88-18966
Effect of element size on the solution accuracies of finite-element heat transfer and thermal stress analyses of space shuttle orbiter
[NASA-TM-88292] 11 p1502 N88-18971
Contour-to-grid interpolation with nonlinear finite elements: A feasibility study
[AD-A188108] 11 p1503 N88-18980
Workshop on the Integration of Finite Element Modeling with Geometric Modeling
[NASA-CR-182515] 11 p1526 N88-19111
Integration of finite element modeling with solid modeling through a dynamic interface 11 p1526 N88-19112
Approaches to the automatic generation and control of finite element meshes 11 p1526 N88-19113
Integration of geometric modeling and advanced finite element preprocessing 11 p1526 N88-19114
Finite element meshing of ANSYS (trademark) solid models 11 p1526 N88-19115
Solid/FEM integration at SNLA
[SAND-87-0882A] 11 p1526 N88-19116
Octree based automatic meshing from CSG models
11 p1527 N88-19117
Geometrical and topological issues in octree based automatic meshing 11 p1527 N88-19118
A hierarchical structure for automatic meshing and adaptive FEM analysis 11 p1527 N88-19119
Toward automatic finite element analysis
11 p1527 N88-19120
Finite octree meshing through topologically driven geometric operators 11 p1527 N88-19121
Design modeling for shape optimization
11 p1527 N88-19122
Shape optimization of three-dimensional stamped and solid automotive components
[GMR-5168] 11 p1528 N88-19123
Postprocessing techniques for 3D non-linear structures 11 p1528 N88-19124
Geometric versus finite element modeling current and future trends at Northrop 11 p1528 N88-19125
Multigrid methods: Special topics and applications --- conference
[GMD-120] 11 p1537 N88-19187
A generalisation of Hall's scheme for solving the Euler equations for two-dimensional flows
11 p1537 N88-19188
A multigrid solver for two-dimensional transonic full potential flow calculations 11 p1538 N88-19189
Multigrid methods in convex optimization
11 p1538 N88-19190
Implementation of multigrid in SOLA algorithm --- fluid flow 11 p1538 N88-19191
Solution of the Euler equations: Explicit schemes acceleration by a multigrid method
11 p1538 N88-19192
Unstructured multigrid methods
11 p1538 N88-19193
Discretizations for multigrid methods
11 p1539 N88-19198
Reliability analyses of a surface mounted package using finite element simulation
[AD-A189488] 12 p1624 N88-19717
Sub-scaling of projectile/target system damaged by hypervelocity
[AD-A188683] 12 p1634 N88-19779
A hybrid-stress finite element approach for stress and vibration analysis in linear anisotropic elasticity
[NASA-CR-179311] 12 p1634 N88-19784
Vibrations of shells containing fluid
12 p1635 N88-19787
On analysis of viscoelastic structures
[AD-A188445] 12 p1636 N88-19793
A technique for local refinement of the stress field by finite element method
[INPE-4219-PRE/1099] 12 p1683 N88-20061
Further refinement and applications of the mixed computational algorithm for plane elastic contact problems
[AD-A188308] 12 p1683 N88-20065
NFEARS (Nonlinear Finite Element Adaptive Research Solver): A nonlinear adaptive finite element solver. Part 2: User's manual
[AD-A189009] 12 p1684 N88-20070
Study of inhomogeneously filled cylindrical resonant cavities by the finite integration technique
[PB88-133707] 12 p1697 N88-20156
Finite element calculations for aerodynamic coefficients of a 3-dimensional body in subsonic flow using Green's function method
[NASA-TT-20208] 13 p1718 N88-20272
Effect of rotation on the lateral stability of a free-flying column subjected to an axial thrust with directional control
[AD-A188690] 13 p1728 N88-20338
Nondestructive evaluation of carbon-carbon coatings
[AD-A189524] 13 p1748 N88-20453
Dynamics of high-speed mechanisms with elastic members 13 p1779 N88-20643
Finite element methods for quasi-prismatic bodies with application to gears 13 p1779 N88-20644
A preliminary investigation of finite-element modeling for composite rotor blades
[NASA-TM-100559] 13 p1781 N88-20656
Theory and experiments of fracture in cyclic compression: Single phase ceramics, transforming ceramics and ceramic composites
[DE88-005792] 13 p1781 N88-20659
Finite element methodology for nonlinear free and harmonic forced vibrations of beam and plate structures
13 p1782 N88-20663
An analysis of large deformation axisymmetric inelastic problems by finite element and boundary element methods 13 p1782 N88-20664
Correlation of data on strain accumulation adjacent to the San Andreas Fault with available models
[NASA-CR-180757] 13 p1796 N88-20742
The use of a barotropic finite element model for the study of circulation on the continental shelf of the southeast coast of Brazil
[INPE-4401-PRE/1218] 13 p1802 N88-20774
Finite State Tables for general computer programming applications
[DE88-006254] 13 p1820 N88-20881
A knowledge system for automatic finite element mesh generation: AMEKS
[DE87-014894] 13 p1826 N88-20914
Local refinement of stress field by finite element method
[INPE-4321-TDL/288] 13 p1828 N88-20930
Modeling of laser ultrasound generation in a weld pool
[DE88-005546] 13 p1834 N88-20971
JPRS report: Science and technology. China
[JPRS-CST-87-042] 14 p1899 N88-21338
Finite element explicit algorithm for solving temporal temperature fields 14 p1899 N88-21339
Analysis of induction motors based on the numerical solution of the magnetic field and circuit equations
[EL-59] 14 p1907 N88-21398
Evaluation of structural analysis methods for life prediction 14 p1930 N88-21511
On the global/local time incrementing for viscoplastic analysis 14 p1932 N88-21519
A constitutive material model for nonlinear finite element structural analysis using an iterative matrix approach
14 p1932 N88-21521
Nonlinear structural analysis of a turbine airfoil using the Walker viscoplastic material model for B1900 + Hf
14 p1932 N88-21522
On 3-D inelastic analysis methods for hot section components. Volume 1: Special finite element models
[NASA-CR-180893] 14 p1934 N88-21535
Some maximum norm estimates for the finite element method applied to nonlinear two dimensional boundary value problems
[ETN-88-91505] 14 p1964 N88-21715
A general 2D electrical model for diagonally connected MHD generators
[DE88-004283] 14 p1984 N88-21835
Moving-bank multiple model adaptive estimation applied to flexible spacestructure control
[AD-A190761] 15 p2026 N88-22071
Postbuckling delamination of a stiffened composite panel using finite element methods
[NASA-CR-182803] 15 p2030 N88-22098
Finite element simulation of perforation of aluminum plates
[DE88-002092] 15 p2073 N88-22362
Development of a computer code CRACK for elastic and elastoplastic fracture mechanics analysis of 2-D structures by finite element technique
[DE88-701231] 15 p2075 N88-22370
Elasto-plastic analysis using a stress-based finite element method and an endochronic theory of plasticity
[DE88-003001] 15 p2075 N88-22372
Finite element (MARC) solution technologies for viscoplastic analyses 15 p2078 N88-22389
Three-dimensional inelastic approximate analysis code (MOMM) 15 p2079 N88-22392
Specialty three-dimensional finite element analysis codes 15 p2079 N88-22393

MHOST: An efficient finite element program for inelastic analysis of solids and structures
15 p2079 N88-22394
Fatigue damage modeling for coated single crystal superalloys 15 p2085 N88-22427
Development and application of the p-version of the finite element method
[AD-A190036] 15 p2120 N88-22633
A posterior error estimation in a finite element method for parabolic partial differential equations
[AD-A190296] 15 p2120 N88-22636
Homogenization study of matrix behavior in a composite material
[ONERA-RT-1/7256-RY-060-R]
16 p2172 N88-22943
Dynamic fracture toughness evaluation by measurement of CTOD
[WNS/ASD-88-02] 16 p2178 N88-22982
Finite elements for the computation of three-dimensional electromagnetic fields in inhomogeneous media (revised)
[PB88-173471] 16 p2190 N88-23057
Parallel computer methods for eigenvalue extraction
16 p2218 N88-23233
Iterative finite element solver on transputer networks
16 p2218 N88-23235
Mixed finite element formulation applied to shape optimization 16 p2221 N88-23252
Models in nonlinear thermomechanics. Finite element models and constitutive models for large deformation elastoplasticity
[ETN-88-92240] 16 p2222 N88-23262
A nonlinear computation for composite structures
[ONERA-RT-15/3542-RY-062-R]
16 p2222 N88-23265
A finite-element alternating method for two-dimensional Mode-1 crack configurations
[NASA-TM-100616] 16 p2224 N88-23276
Experimental design and structural optimization
[ETN-88-92232] 16 p2257 N88-23492
Three-dimensional curved shell and solid-shell transition finite elements with temperature and temperature gradients as primary variables for steady state heat conduction
17 p2349 N88-23997
The Shock and Vibration Digest, volume 20, no. 4
17 p2391 N88-24214
State-of-the-art in true space-time finite element method 17 p2391 N88-24215
Adjusting a finite element model using vibration type experimental data. Concept and error detection
[ONERA-RT-7/3313-RY-060-R]
17 p2392 N88-24220
Simulations of a missile with liquid payload under launch conditions
[AD-A191479] 18 p2463 N88-24625
Fundamental limits to the velocity of solid armatures in railguns 18 p2469 N88-24656
Mixed-mode fracture of uniaxial fiber reinforced composites
[AD-A191629] 18 p2478 N88-24700
Adaptive local grid refinement in computational fluid mechanics
[AD-A192215] 18 p2510 N88-24890
A variational finite element method for three-dimensional, steady, compressible, viscous flows
18 p2512 N88-24904
Improving the performance of a finite element method using vector analysis on CRAY 1
[ETN-88-92153] 18 p2513 N88-24907
Finite element solution of 3-D turbulent Navier-Stokes equations for propeller-driven slender bodies
18 p2515 N88-24919
Finite element analysis of an underground structure
[AD-A191747] 18 p2527 N88-24991
Fracture mechanics analysis for short cracks
[AD-A192002] 18 p2527 N88-24992
Dynamic response of plates to moving loads: Structural impedance and finite element methods
18 p2528 N88-25000
The stress analysis of ceramic, polymeric, and metallic composite systems by the finite element method
18 p2529 N88-25004
Reduced order modelling and analytical model modification for structural dynamics and control
18 p2529 N88-25006
Considerations involved in the display of finite element results using animation
[DE88-007581] 18 p2559 N88-25189
Algorithms and software for solving finite element equations on serial and parallel architectures
[NASA-CR-183027] 18 p2559 N88-25191
PAFEC level 6.2 application program
[AD-A191037] 18 p2562 N88-25209
NFEARS: A nonlinear adaptive finite element solver, part 1
[AD-A191823] 18 p2563 N88-25215
Probabilistic finite element methods
18 p2564 N88-25223
New mixed finite element methods
18 p2567 N88-25248
Fuel droplet vaporization and temperature distributions of axisymmetric unsteady sprays
19 p2626 N88-25579
Finite element analysis of incompressible viscous flow around multi-element aerofoils 19 p2635 N88-25634
Improved method for stress and compatibility analysis of multicomponent rotating systems
[NASA-TM-100884] 19 p2680 N88-25935
Semi-discrete approximations to nonlinear systems of conservation laws; consistency and L(infinity)-stability imply convergence
[NASA-CR-181683] 19 p2721 N88-26157
Stability of spheromak against current driven modes: Effects of flux hole on stability
[IPPJ-868] 19 p2730 N88-26211
Finite element approximation to a model problem of transonic flow
[DE88-701835] 20 p2752 N88-26333
A finite element analysis for the hydroforming of aluminum
[DE88-008050] 20 p2784 N88-26516
MAXWELL3: A 3D finite element electromagnetic modeling code
[DE88-010602] 20 p2790 N88-26551
Velocity-pressure integrated versus penalty finite element methods for high Reynolds number flows
[NASA-CR-179357] 20 p2803 N88-26635
Finite element welding computations using general purpose nonlinear analysis codes
[DE88-005398] 20 p2808 N88-26659
Three-dimensional analysis of a postbuckled embedded delamination
[NASA-TP-2823] 20 p2812 N88-26684
An assessment of modelling techniques for the finite element analysis of reinforced concrete plate and shell structures
[AD-A192263] 20 p2814 N88-26697
Thermo-viscoelastic analysis of composite materials, volume 1
[NASA-CR-183048-VOL-1] 21 p2904 N88-27230
An h-p adaptive finite element method for steady compressible flow 21 p2941 N88-27467
A study of fluid-structure problems
21 p2941 N88-27468
Stream function-vorticity finite elements and the resolution of the Navier-Stokes equations
[DE88-702318] 21 p2945 N88-27494
Optimal design of viscoelastic structures
21 p2959 N88-27579
Adaptive finite element methods for shells
[AD-A193221] 21 p2960 N88-27585
Verification of the ADINA finite element code for creep analysis: Problems from the open literature
[DE88-011826] 21 p2962 N88-27594
DYNA3D (Nonlinear Dynamic Analysis of Structures in Three Dimensions) user's manual
[DE88-012242] 21 p2963 N88-27604
Finite element methodology for integrated flow-thermal-structural analysis
[NASA-CR-183144] 21 p2964 N88-27606
Staggered-grid finite element solution technique for the Maxwell's equations in the time domain
[DE88-011731] 21 p3007 N88-27838
Unified multilevel adaptive finite element methods for elliptic problems
[DE88-011938] 21 p3007 N88-27840
Finite element method for plate structures with inclined angles
[ILR-MITT-182] 21 p3008 N88-27842
Coupled inviscid - boundary layer methods for turbomachinery blading design
[PNR90437] 22 p3076 N88-28260
High performance solutions of the Stokes problem using mini-elements, self-adaptive grids, and multigrid methods: Applications
[ECL-87-15] 22 p3077 N88-28266
Development and application of a finite element method to compute strongly heated turbulent flows
[ECL-88-02] 22 p3077 N88-28267
Two-dimensional sequential and concurrent finite element analysis of unstiffened and stiffened aluminum and composite panels with hole
[NASA-CR-183083] 22 p3086 N88-28325
Mixed finite element methods to compute stress in a load composite specimen with holes: Numerical results
[ONERA-RT-37/4242-RY-062-R]
22 p3088 N88-28336
Parametric identification of mechanical structures
[ETN-88-92881] 22 p3088 N88-28339
Refining finite element models. Numerical application to a lattice structure. Study of a macroelement of Timoshenko beam type
[ONERA-RT-8/3313-RY-070-R]
22 p3144 N88-28696
Distortion effects in isoparametric elements, an analytic approach
[PNR90454] 22 p3145 N88-28703
Finite Element Composite Analysis Program (FECAP) for a microcomputer
[NASA-TM-100670] 23 p3190 N88-28982
Development and experimental verification of a two-dimensional numerical model of piezoelectrically induced threshold voltage shifts in GaAs MESFETs
[AD-A193462] 23 p3206 N88-29080
Static and dynamic metal-metal friction at plastic stress levels
[DE88-011281] 23 p3222 N88-29176
Elastic-plastic analysis of part-through crack propagation in piping and pressure vessels
[DE88-701619] 23 p3225 N88-29198
An adaptive overlapping local grid refinement method for two-dimensional parabolic systems
[AD-A193560] 23 p3271 N88-29464
Investigation of the higher-order elements in the SAMSON2 code
[AD-A193638] 23 p3271 N88-29465
Finite element analysis of steady and transiently moving/rolling nonlinear viscoelastic structure. Part 1: Theory
[NASA-CR-179886] 23 p3273 N88-29480
Analysis of the transmission of sound into the passenger compartment of a propeller aircraft using the finite element method
[FFA-TN-1988-15] 23 p3279 N88-29520
Damage initiation in the short beam shear test of composite materials using stiffness reduction
[AD-A194880] 24 p3340 N88-29883
Numerical modelling of premixed flames in gaseous media 24 p3350 N88-29944
Geometric and material nonlinear analysis of structures comprising rectangular hollow sections
[CE-79] 24 p3382 N88-30141
A parametric study of embedded cantilever retaining walls: The results of a finite element study
[RR-CE83] 24 p3383 N88-30152
Obtaining stress intensity factors on cracks, by means of fitting techniques on numerical results calculated with the finite element method 24 p3384 N88-30153

FINITE IMPULSE RESPONSE FILTERS

U FIR FILTERS

FINITE VOLUME METHOD

Computational fluid dynamics in the United Kingdom
[RAE-TM-AERO-2098] 02 p0171 N88-11073
High resolution finite volume methods on arbitrary grids via wave propagation
[NASA-CR-178397] 04 p0484 N88-12979
Solution of some 3-D viscous and inviscid supersonic flow problems by finite-volume space-marching schemes
05 p0532 N88-13235
The role of computation fluid dynamics in aeronautical engineering (4). The development and applications of implicit TVD finite volume code
05 p0536 N88-13259
Compressible Euler solution on a multiblock grid around a wing-fuselage configuration
[FFA-TN-1987-46] 05 p0542 N88-13303
A Cartesian finite-volume method for the Euler equations 05 p0579 N88-13532
Euler solution of multiblade rotor flow
[NASA-TM-100014] 06 p0704 N88-14322
Finite-volume scheme for transonic potential flow about airfoils and bodies in an arbitrarily shaped channel
07 p0809 N88-14928
A multistage time-stepping scheme for the thin-layer Navier-Stokes equations 07 p0810 N88-14932
Computational Fluid Dynamics
[VKI-LS-1987-04] 08 p0984 N88-15951
Integration of Navier-Stokes equations in finite volume formulation 08 p0984 N88-15954
Numerical implementation and performance of Reynolds stress closures in finite volume computations of recirculating and strongly swirling flows
08 p0987 N88-15976
Solution of the three-dimensional Navier-Stokes equations for transonic flow using a multigrid method
10 p1267 N88-17579
Radial compressor design using an Euler solver
10 p1283 N88-17675
Applications of a multigrid finite volume method with Runge-Kutta time integrations for solving the Euler and Navier-Stokes equations 11 p1539 N88-19201
The construction of a three-dimensional finite volume grid generator for a wing in a wind tunnel with application to Navier-Stokes flow solvers
[FFA-TN-1987-58] 13 p1719 N88-20277

Solution of two-dimensional Euler equations: Experience with a finite volume code
[DFVLR-FB-87-41] 13 p1767 N88-20572
Conservative finite volume solutions of a linear hyperbolic transport equation in two and three dimensions using multiple grids
[NASA-CR-182715] 13 p1828 N88-20934
Mixed direct-inverse problem of transonic cascade 15 p2054 N88-22244
Zero-lift drag predictions in supersonic flow for complex configurations 15 p2054 N88-22246
The 2-D and 3-D time marching transonic potential flow method for propfans 16 p2220 N88-23245
The role of computational fluid dynamics in aeronautical engineering (5). Improvements and applications of implicit TVD finite volume code 19 p2638 N88-25653
On the accuracy of upwind biased finite volume method 19 p2639 N88-25656
Navier-Stokes simulation of shock-tube flows over a wedge-type step by finite volume method
[ISAS-RN-628] 20 p2797 N88-26599
Preliminary design and analysis of procedures for the numerical generation of 3D block-structured grids
[NLR-TR-86102-U] 20 p2802 N88-26628
Effects of numerical dissipation on finite-volume solutions of compressible flow problems
[AD-A193173] 21 p2944 N88-27485
Investigation of viscous/inviscid interaction in transonic flow over airfoils with suction
[NASA-CR-183112] 21 p2945 N88-27490
Runge-Kutta finite-volume simulation of laminar transonic flow over the ONERA M6 wing using the Navier-Stokes equations
[FFA-TN-1987-06] 22 p3039 N88-28045
On the application of finite-difference techniques for the computation of the flow field in gas turbine combustors with complex geometries 24 p3349 N88-29938
An analysis of finite-difference and finite-volume formulations of conservation laws
[NASA-CR-177416] 24 p3370 N88-30071
Numerical simulation of unsteady incompressible viscous flows in generalized coordinate systems
[NASA-TM-101016] 24 p3373 N88-30085

FINITE-STATE MACHINES
U TURING MACHINES

FINLAND
Huurre expedition to the North Pole in 1984
[PB87-220935] 04 p0462 N88-12858
Report of the 3rd Finnish EISCAT Workshop --- European Incoherent Scatter Radar (EISCAT)
[REPT-111] 06 p0691 N88-14233
EISCAT research in Finland in 1986 06 p0691 N88-14234
EISCAT research programs for 1987 06 p0692 N88-14244
Helsinki University of Technology Communications Laboratory
[PB88-112974] 10 p1318 N88-17881
Research field of fire technology in Finland
[DE88-751094] 11 p1467 N88-18747
Last spring frosts and first autumn frosts in Finland
[FMI-6] 19 p2693 N88-26008
On the global radiation incident variously orientated surfaces on the South Coast of Finland
[FMI-5] 20 p2823 N88-26746

FINNED BODIES
Analytical treatment of the melting and solidification of latent heat store materials in finned tube geometries
[IKE-5-223] 03 p0314 N88-11985
Performance evaluation of plate-fin heat exchangers
[AD-A187798] 11 p1482 N88-18845

FINS
NT COOLING FINS
Fin gaps and body slots of guided projectiles: Effects, data correlation and modeling
[AD-A184440] 03 p0270 N88-11698
The effects of sweep and bluntness on a glancing shock wave turbulent boundary layer interaction 05 p0531 N88-13227
The use of aeroelastic wind tunnel models to prove structural design 05 p0551 N88-13355
Indirect measurement of local condensing heat-transfer coefficient around horizontal finned tubes
[AD-A186929] 09 p1160 N88-16950
Measurement of forces and moments on, and velocity about a body of revolution with an attached fin at angles of attack
[AD-A187796] 11 p1433 N88-18554
Preliminary investigation of stability of a fin-stiffened slender strut
[NASA-TM-4034] 12 p1599 N88-19568
Fish as a tool for testing fitness in space 12 p1662 N88-19963
Experimental investigation of the hypersonic flow over a six finned configuration
[AD-A190870] 16 p2157 N88-22871
Study and implementation of ultrahigh frequency coupling devices using the fin line technology --- millimeter waves
[ETN-88-92307] 20 p2796 N88-26588
The use of fins to reduce the pressure drop in a rotating cavity with a radial flow
[PNR90465] 22 p3079 N88-28282
Feasibility study of a microprocessor controlled actuator test mechanism
[AD-A194654] 23 p3249 N88-29337

FIR FILTERS
Design of efficient FIR filters with minimal delay
[PB87-100434] 04 p0438 N88-12717
Implementation of an FIR band pass filter using a bit-slice processor
[AD-A184895] 05 p0634 N88-13875
Frequency-sampling design of two-dimensional FIR digital filters with nonuniform samples
[AD-A187773] 11 p1477 N88-18815
Digital filter design techniques
[AD-A194484] 23 p3274 N88-29486

FIRE CONTROL
Helicopter fire control: Advantages of an automatic target tracker 03 p0264 N88-11667
AVSCOM'S modifications to Teledyne Systems Company's air-to-air fire control system simulation model
[AD-A189136] 13 p1722 N88-20294
Method and device for the detection and identification of a helicopter
[NASA-TT-20251] 15 p2129 N88-22698

FIRE DAMAGE
Effects of fire on composition, biomass, and nutrients in oak scrub vegetation on John F. Kennedy Space Center, Florida
[NASA-TM-100305] 08 p1020 N88-16182
Evaluation of a burned area and the vegetation regeneration affected by the burning in the Parque Nacional de Brazilia through TM/LANDSAT data 17 p2363 N88-24073

FIRE EXTINGUISHERS
Spacecraft Fire Safety
[NASA-CP-2476] 04 p0406 N88-12520
Fire extinguishment and inhibition in spacecraft environments 04 p0406 N88-12523
Inerting and atmospheres 04 p0406 N88-12524
Aircraft fire safety research 04 p0406 N88-12526
Space station internal environmental and safety concerns 04 p0407 N88-12527
Extinguishing diffusion flames with dry powder and halon at low Froude numbers
[PB87-111365] 06 p0679 N88-14159
Testing of the engine compartment fire extinguishing system in the F/EF-111 aircraft
[AD-A188801] 12 p1576 N88-19423
An extinguisher to quench propellant fires
[AD-A190785] 18 p2497 N88-24813
Next-generation fire extinguishing agent. Phase 1: Suppression concepts
[AD-A192279] 19 p2614 N88-25514
Extinguishing agent for magnesium fire, phases 5 and 6
[AD-A192436] 21 p2930 N88-27398

FIRE FIGHTING
Test results and predictions for the response of near-ceiling sprinkler links in a full-scale compartment fire
[NBSIR-87/3633] 01 p0033 N88-10209
Research field of fire technology in Finland
[DE88-751094] 11 p1467 N88-18747

FIRE PREVENTION
Comparison of fire resistance of metallic and nonmetallic structures
[SNIAS-872-551-101] 05 p0572 N88-13489
Spacecraft fire detection and extinguishment: A bibliography
[NASA-CR-180880] 11 p1444 N88-18612
Procedures for quantitative sensitivity and performance validation studies of a deterministic fire safety model
[NBS/GCR-88/544] 11 p1469 N88-18762
A new fire protection concept for electronic equipment
[AD-A188884] 12 p1614 N88-19651
Spacecraft fire-safety experiments for space station: Technology development mission
[NASA-CR-182114] 13 p1731 N88-20353
Flame retardants
[NASA-TT-20250] 13 p1739 N88-20400
A systems analysis of fire suppression alternatives for the US space station
[AD-A189847] 15 p2025 N88-22064
Study of benefits of passenger protective breathing equipment from analysis of past accidents
[DOT/FAA/CT-88/03] 18 p2461 N88-24610
Aircraft accident report: Air New Orleans, DBA continental express flight 962 British Aerospace 3101 (Jetstream 31), N331CY, New Orleans International Airport, Kenner, Louisiana, May 26, 1987
[PB88-910408] 19 p2601 N88-25450
Fire retardant coatings for military equipment: A review
[MRL-R-1104] 19 p2619 N88-25540
Flame retardation treatment of synthetic rubbers and synthetic resins
[NASA-TT-20285] 19 p2620 N88-25544

FIRE RESISTANCE
U FLAMMABILITY

FIRE RETARDANTS
U FLAME RETARDANTS

FIREPROOFING
Comparison of fire resistance of metallic and nonmetallic structures
[SNIAS-872-551-101] 05 p0572 N88-13489

FIRES
NT FOREST FIRES
Measurements of gas velocities and temperatures in a large open pool fire
[DE87-005853] 03 p0261 N88-11641
Measurements in large JP-4 pool fires
[DE87-013445] 03 p0284 N88-11783
Spacecraft Fire Safety
[NASA-CP-2476] 04 p0406 N88-12520
Techniques for fire detection 04 p0406 N88-12521
Fire-related standards and testing 04 p0406 N88-12522
Fire extinguishment and inhibition in spacecraft environments 04 p0406 N88-12523
Inerting and atmospheres 04 p0406 N88-12524
Fire-related medical science 04 p0406 N88-12525
Aircraft fire safety research 04 p0406 N88-12526
Space station internal environmental and safety concerns 04 p0407 N88-12527
Microgravity combustion fundamentals 04 p0407 N88-12528
Spacecraft material flammability testing and configurations 04 p0407 N88-12529
Catalog of compartment fire model algorithms and associated computer subroutines
[PB88-110861] 07 p0839 N88-15087
Effects of additives on fire properties of polyethylene
[AD-A187064] 09 p1146 N88-16871
Testing of the engine compartment fire extinguishing system in the F/EF-111 aircraft
[AD-A188801] 12 p1576 N88-19423
Flammability characteristics of distillate fuels
[AD-A188497] 12 p1612 N88-19642
A new fire protection concept for electronic equipment
[AD-A188884] 12 p1614 N88-19651
Numerical simulation of near-surface environments and particulate clouds generated by large-area fires
[AD-A188375] 12 p1641 N88-19828
Heat transfer from a negatively buoyant wall jet
[NBS/GCR-88/541] 15 p2050 N88-22208
Detection, monitoring and analysis of some environmental effects of fires in the Amazon region through utilization of NOAA and LANDSAT satellite imagery and aircraft data
[INPE-4503-TDL/326] 16 p2230 N88-23322
Detection of biomass burning and smoke plumes in the Amazon region through NOAA satellite imagery 17 p2365 N88-24085
An extinguisher to quench propellant fires
[AD-A190785] 18 p2497 N88-24813
Current fire safety design aspects of commuter aircraft
[DOT/FAA/CT-87/32] 19 p2600 N88-25448
Experimental and theoretical analysis of the radiative transfer within a sooty pool fire
[DE88-007099] 20 p2769 N88-26419
Extinguishing agent for magnesium fire, phases 5 and 6
[AD-A192436] 21 p2930 N88-27398
The 210-HP diesel engine endurance and performance testing with fire resistant diesel fuel
[AD-A193153] 21 p2956 N88-27558
Numerical field model simulation of full scale fire tests in a closed spherical/cylindrical vessel
[AD-A195067] 24 p3359 N88-29998

FIREWORKS
U PYROTECHNICS

FIRING (IGNITING)
NT ROCKET FIRING
NT STATIC FIRING
NT TEST FIRING
A nondissipative Pyrotechnic Arming and Firing Unit (PAFU)
[CRA/REPO/8019] 02 p0155 N88-10974

FIRMWARE
High bit rate serial input multipliers
[REPT-87-012] 11 p1530 N88-19140

A serial input pipelined multiplier
[REPT-87-030] 11 p1530 N88-19141
On serial-input multipliers for two-complement numbers
[REPT-86-035] 11 p1536 N88-19181

FISH
U FISHES

FISHERIES
Two decades of achievement in the ocean, 1968-1988
[PB88-167077] 16 p2236 N88-23356
Contribution of space to marine activities 19 p2700 N88-26057

FISHES
Investigations of the survey of the reproductive biology of Xiphophorus in an Aquarack 01 p0074 N88-10471
Xiphophorus as an experimental system for genetic and biological development studies under microgravity conditions 01 p0074 N88-10472
Long term investigations of the growth, metabolism, and reproduction of fish under conditions close to weightlessness 01 p0074 N88-10473
Compilation of 1986 annual reports of the Navy ELF (Extremely Low Frequency) communications system ecological monitoring program, volume 3
[AD-A184563] 03 p0306 N88-11932
Irradiation preservation of seafood: Literature review
[DE88-001691] 05 p0631 N88-13858
Investigations of the reproductive physiology of the rainbow trout (Salmo gairdneri Richardson) 07 p0885 N88-15370
Function-dependent plasticity in the nervous system 07 p0886 N88-15377
Embryonic development of guppy in weightlessness 10 p1360 N88-18127
Fish as a tool for testing fitness in space 12 p1662 N88-19963

FISHTAILING
U YAW

FISSION
New nuclear structure calculations and the astrophysical r-process
[DE88-000979] 08 p1082 N88-16518

FISSION ELECTRIC CELLS
Noncryogenic propellants for a nuclear orbit transfer vehicle 17 p2428 N88-24444

FISSION PRODUCTS
Analysis of a nuclear orbital transfer vehicle reentry accident 17 p2425 N88-24426

FISSURES (GEOLOGY)
The aerophotogrammetric determination of Earth surface deformations
[SER-C-321] 07 p0872 N88-15288
Experimental and theoretical constraints on the origin of mid-ocean ridge geothermal fluids 13 p1804 N88-20784

FITNESS
NT PHYSICAL FITNESS
Three-dimensional adaptive grid generation for body-fitted coordinate system
[NASA-CR-182192] 21 p2950 N88-27520

FITTING
Evaluation of the US Army fitting program for the integrated helmet unit of the integrated helmet and display sighting system
[AD-A191616] 18 p2465 N88-24635

FITTINGS
An examination of coating failure on wing pivot fittings of f111 aircraft
[AD-A185028] 05 p0546 N88-13328
User's manual for EULER3DS
[AD-A191048] 16 p2208 N88-23177
Expandable pallet for space station interface attachments
[NASA-CASE-MSC-21117-1] 23 p3185 N88-28958

FITZGERALD-LORENTZ CONTRACTION
U LORENTZ CONTRACTION

FIX
U FIXING

FIXED POINTS (MATHEMATICS)
Numerical resolution of the equations of three-dimensional stable compressible transonic flows
[PB87-168415] 09 p1113 N88-16673
Exponential lower bounds for finding Brouwer fixed points
[DE88-002864] 10 p1425 N88-18513
Solving reflexive domain equations in a category of complete metric spaces
[CWI-CS-R8709] 13 p1832 N88-20956

FIXED WINGS
Boeing 727 MLS (Microwave Landing System) terminal instrument procedures (TERPS) approach data collection and processing, data report
[AD-A185523] 06 p0667 N88-14090
Analysis of a fixed-pitch X-wing rotor employing lower surface blowing 10 p1271 N88-17602
Fixed wing CCW aerodynamics with and without supplementary thrust deflection 10 p1272 N88-17607
Aircraft aeroelasticity and structural dynamics research at the NASA Langley Research Center: Some illustrative results
[NASA-TM-100627] 18 p2459 N88-24598
Analysis of a fixed-pitch X-wing rotor employing lower surface blowing
[AD-A187379] 24 p3321 N88-29779

FIXED-WING AIRCRAFT
U AIRCRAFT CONFIGURATIONS
U FIXED WINGS

FIXING
Botany Facility: The problems of plant fixation
[SIRA-A/7373/WP220/RJS/001] 17 p2379 N88-24140

FLAME FRONTS
U FLAME PROPAGATION

FLAME HOLDERS
Ignition and flameholding in supersonic flow by injection of dissociated hydrogen 05 p0560 N88-13410
Flame stabilization in a reheat combustor 24 p3346 N88-29921

FLAME INTERACTION
U CHEMICAL REACTIONS
U FLAME PROPAGATION

FLAME IONIZATION
Combustion of hydrogen and hydrocarbons in fluorine
[AD-A188018] 11 p1453 N88-18662
Kinetic mechanisms for ionization and afterburning suppression
[AD-A189219] 13 p1737 N88-20383
Selective detection in gas chromatography
[AD-A191499] 18 p2481 N88-24718

FLAME PROBES
Studies of fluorine combustion
[AD-A187646] 11 p1452 N88-18656

FLAME PROPAGATION
Turbulent Bunsen burner flames
[ETN-87-90433] 01 p0021 N88-10134
Fronts propagating with curvature dependent speed: Algorithms based on Hamilton-Jacobi formulations
[NASA-CR-178382] 01 p0077 N88-10495
Measurement of solid propellant combustion velocity by means of microwaves
[CERT-1/1316-MO] 03 p0283 N88-11778
Ignition and flame propagation in sprays
[AD-A184679] 03 p0283 N88-11781
Fire-related standards and testing 04 p0406 N88-12522
Space station internal environmental and safety concerns 04 p0407 N88-12527
Microgravity combustion fundamentals 04 p0407 N88-12528
The effect of microgravity on flame spread over a thin fuel
[NASA-TM-100195] 08 p0967 N88-15853
Heat transfer from impinging flame jets
[ETN-88-91610] 09 p1162 N88-16964
Flame propagation in the approximation of straight-line trajectories of burning products
[DE88-700675] 10 p1297 N88-17756
Diffusion description of flame propagation due to the translational motion of burning reaction products
[DE88-700676] 10 p1297 N88-17757
Studies on homogeneous and heterogeneous reactive flows 11 p1484 N88-18861
Linear and nonlinear acoustics with nonuniform entropy in combustion chambers 12 p1607 N88-19609
Flammability characteristics of distillate fuels
[AD-A188497] 12 p1612 N88-19642
Evaluation of flammability for cable-like polymers
[NASA-TT-20225] 13 p1752 N88-20476
Problems appearing at interface balances — flames 14 p1987 N88-21855
On the structure, propagation, extinction and stability of laminar premixed flames in dissociation equilibrium 18 p2483 N88-24728
Turbulence and flame propagation
[PB87-228912] 19 p2612 N88-25499
Flame spread mechanisms over PMMA surfaces
[NASA-TT-20284] 19 p2612 N88-25500
Effect of thickness on downward flame spread over paper
[NASA-TT-20282] 19 p2612 N88-25501
Combustion rate limits of hydrogen plus hydrocarbon fuel: Air diffusion flames from an opposed jet burner technique 19 p2624 N88-25567
Mach 2 combustion characteristics of hydrogen/hydrocarbon fuel mixtures 19 p2625 N88-25568
Recent advances in photochemical techniques for ignition and combustion enhancement 19 p2625 N88-25570
Minimum ignition energy measurements using laser induced spark initiation 19 p2632 N88-25610
Ignition and flame spread of PMMA
[NASA-TT-20290] 20 p2771 N88-26431
Premixed turbulent flame propagation
[AD-A192955] 21 p2909 N88-27265
Summary of discussions at the Tenth Meeting of the Sandia Cooperative Group on the Aerothermochemistry of Turbulent Combustion
[DE88-008467] 21 p2910 N88-27269
Theoretical study and numerical simulation of flame fronts
[PB88-122932] 22 p3051 N88-28104
A study of flame spreading and combustion phenomena of stick propellants
[AD-A193598] 22 p3052 N88-28106
Interactions between coherent structures and premixed flame fronts
[ETN-88-92885] 22 p3053 N88-28111
Combustion dynamics and thermal structure of a planar spray flame 23 p3190 N88-28985
Numerical modelling of premixed flames in gaseous media 24 p3350 N88-29944
Gaseous premixed flames in non-uniform flows 24 p3351 N88-29945
Flamespreading processes in obliquely loaded stick propellant beds
[AD-A195081] 24 p3352 N88-29956

FLAME QUENCHING
U EXTINGUISHING
U QUENCHING (COOLING)

FLAME RETARDANTS
Thermoplastic elastomer compositions — cable jackets
[EP-PATENT-0-204-453-A1] 04 p0418 N88-12593
Flame retardant phenolic foams
[EP-PATENT-0-223-489-A2] 05 p0568 N88-13464
Method of obtaining of fire resistant polyacrylonitrile fiber or cloth from it
[AD-A185941] 07 p0836 N88-15071
Effects of additives on fire properties of polyethylene
[AD-A187064] 09 p1146 N88-16871
Fire tests on loose-fill insulation materials
[DE88-751182] 11 p1467 N88-18748
Kinetic mechanisms for ionization and afterburning suppression
[AD-A189219] 13 p1737 N88-20383
Flame retardants
[NASA-TT-20250] 13 p1739 N88-20400
Differential technology in plastics industries differentiation in combination technology nonflammability technology
[NASA-TT-20256] 18 p2494 N88-24797
Fire retardant coatings for military equipment: A review
[MRL-R-1104] 19 p2619 N88-25540
Flame retardation treatment of synthetic rubbers and synthetic resins
[NASA-TT-20285] 19 p2620 N88-25544
The 210-HP diesel engine endurance and performance testing with fire resistant diesel fuel
[AD-A193153] 21 p2956 N88-27558

FLAME SPECTROSCOPY
Single-laboratory evaluation of SW-846 methods 7090/7091 determination of beryllium by flame and furnace atomic absorption spectrophotometry
[PB88-171434] 16 p2175 N88-22963
La Recherche Aerospatiale, bimonthly bulletin, number 1987-3, 238/May-June
[ESA-TT-1075] 16 p2206 N88-23161

FLAME SPRAYING
Combustion dynamics and thermal structure of a planar spray flame 23 p3190 N88-28985

FLAME STABILITY
Flame driving of longitudinal instabilities in liquid fueled dump combustors
[AD-A183536] 01 p0006 N88-10033
Combustion related shear-flow dynamics in elliptic supersonic jets 05 p0531 N88-13232
Mixing and combustion of pulsed gas jets
[PB88-112834] 06 p0680 N88-14169
Bistable cellular flames
[DE88-003074] 09 p1142 N88-16848
Basic instability mechanisms in chemically reacting subsonic and supersonic flows
[AD-A190101] 15 p2034 N88-22120
The structure and stability of spherically expanding flames 17 p2318 N88-23842
On the structure, propagation, extinction and stability of laminar premixed flames in dissociation equilibrium 18 p2483 N88-24728
Development of a computerized analysis for solid propellant combustion instability with turbulence
[NASA-CR-182351] 19 p2611 N88-25497
Flame stabilization in a reheat combustor 24 p3346 N88-29921

Modeling the stability of a turbulent premixed flame, downstream from a step by a Lagrangian method
24 p3350 N88-29943

FLAME TEMPERATURE
The development of a user friendly thermodynamic code for the personal computer
19 p2623 N88-25559
Soot and radiation in a gas turbine combustor
[AD-A191991] 23 p3179 N88-28924

FLAMEOUT
On the structure, propagation, extinction and stability of laminar premixed flames in dissociation equilibrium
18 p2483 N88-24728

FLAMES
NT DIFFUSION FLAMES
NT PREMIXED FLAMES
KR+ laser excitation of NH2 in atmospheric pressure flames
[AD-A183421] 01 p0050 N88-10322
Flame acceleration and transition to detonation in channels
[DE87-014193] 03 p0284 N88-11786
Development of many-body methods for flame chemistry and large molecule applications
[AD-A184451] 03 p0284 N88-11789
Equilibrium calculations of ionization in tracer flames
[PB87-104154] 04 p0412 N88-12555
Correlation of air pressure drop and flame arrestor characteristics for explosion suppression materials
[AD-A184960] 05 p0548 N88-13340
Formation and destruction of nitrous oxide in lean, premixed combustion
[DE88-001390] 05 p0562 N88-13423
Summary of discussions at the Ninth Meeting of the Sandia Cooperative Group on the Aerothermochemistry of Turbulent Combustion
[DE88-002281] 06 p0680 N88-14165
Velocity and density measurements in a turbulent nonpremixed flame with comparison to numerical model predictions
[DE87-014695] 08 p0967 N88-15854
Removal of out-of-plane distortion in mild steel panels using flame heating, volume 1
[AD-A187802] 11 p1457 N88-18684
Removal of out-of-plane distortion in mild steel panels using flame heating, volume 2
[AD-A187803] 11 p1457 N88-18685
On the possibility of high velocity deflagration front propagation by radiative energy transfer
[AD-A189022] 12 p1613 N88-19645
Laser ignition of nitramine composite propellants and crack propagation and branching in burning solid propellants
[AD-A189260] 13 p1753 N88-20483
Measurement of species concentrations in flames by laser-induced fluorescence
[DE88-007096] 14 p1889 N88-21286
Application of laser-induced fluorescence in an atmospheric-pressure boron-seeded flame
[AD-A189631] 14 p1889 N88-21287
Problems appearing at interface balances --- flames
14 p1987 N88-21855
Numerical simulation of turbulent flames using vortex methods
[AD-A189813] 15 p2034 N88-22116
Application of Rayleigh scattering to turbulent flow with heat transfer and combustion
[AD-A191565] 18 p2481 N88-24720
Measurement of the radiative properties of gas and oil flames
[NASA-TT-20299] 19 p2612 N88-25502
Modeling and experimental measurements of solid propellant flame structure
19 p2631 N88-25605
Ultraviolet imaging of hydrogen flames
[DE88-009152] 20 p2769 N88-26422
Asynchronous optical sampling for laser-based combustion diagnostics in high pressure flames
[AD-A192920] 20 p2770 N88-26428
Study of the local behavior of a flame
[ETN-88-92300] 20 p2771 N88-26433
Reducing adhesion and agglomeration within a cloud of combustible particles
[NASA-TM-100902] 20 p2788 N88-26539
Summary of discussions at the Tenth Meeting of the Sandia Cooperative Group on the Aerothermochemistry of Turbulent Combustion
[DE88-008467] 21 p2910 N88-27269
A study of flame spreading and combustion phenomena of stick propellants
[AD-A193598] 22 p3052 N88-28106
Interactions between coherent structures and premixed flame fronts
[ETN-88-92885] 22 p3053 N88-28111

FLAMMABILITY
Experiments of the selection of a method evaluating the fire resistance of some materials based on macromolecular compounds
[NASA-TT-20129] 02 p0154 N88-10966
Detection of vapors of flammable liquids in air by atmospheric sampling mass spectrometry/mass spectrometry
[DE88-000030] 02 p0196 N88-11227
Flammability limits in cocurrent smoldering combustion
[DE87-014102] 03 p0284 N88-11785
Fabrication and testing of fire resistant graphite composite panels
[NASA-CR-177397] 04 p0397 N88-12472
Spacecraft Fire Safety
[NASA-CP-2476] 04 p0406 N88-12520
Fire-related standards and testing
04 p0406 N88-12522
Spacecraft material flammability testing and configurations
04 p0407 N88-12529
An experimental investigation of the ignition and flammability limits of various hydrocarbon fuels in a two-dimensional solid fuel ramjet
[AD-A184968] 05 p0549 N88-13342
Flammability test on aircraft seats equipped with fire barrier fabrics for the Porcher company
[CEAT-M5-525200] 06 p0666 N88-14084
Flammability, smoke and toxicity test on fire barrier fabric from the Porcher company --- Airbus aircraft
[ETN-88-91168] 06 p0666 N88-14085
Correlation between flammability and heat of combustion of polymers
[NASA-TT-20116] 08 p0973 N88-15884
Review of thermal properties of graphite composite materials
[NASA-TM-100049] 09 p1139 N88-16825
Flammability characteristics of distillate fuels
[AD-A188497] 12 p1612 N88-19642
Evaluation of flammability for cable-like polymers
[NASA-TT-20225] 13 p1752 N88-20476
Burning characteristics and flammability of PVC cables in groups
[NASA-TT-20226] 14 p1893 N88-21303
Ignition and flammability characteristics of solid fuel ramjets
19 p2626 N88-25575
Reducing adhesion and agglomeration within a cloud of combustible particles
[NASA-TM-100902] 20 p2788 N88-26539
Determination of relative flammability of materials by pyrolysis and gas-chromatographic light hydrocarbon analysis
[DE88-012449] 24 p3343 N88-29898

FLAMMABLE GASES
NT GASEOUS FUELS
NT LIQUEFIED NATURAL GAS

FLANGES
Crack distribution and growth rates for critical fastener holes in Mirage wing RH79
[AD-A189080] 13 p1722 N88-20293
GTAW characterization for weld penetration on 304L stainless steel
[DE88-010611] 20 p2810 N88-26672
FEB structural analysis, revision H
[AD-A192302] 20 p2814 N88-26698

FLAP CONTROL
U AIRCRAFT CONTROL
U FLAPS (CONTROL SURFACES)

FLAPPING
Propulsive performance of a lifting flapping wing
17 p2295 N88-23733

FLAPPING HINGES
Impacts of rotor hub design criteria on the operational capabilities of rotorcraft systems
03 p0264 N88-11663
Flap-lag equations of motion of rigid, articulated rotor blades with three hinge sequences
[NASA-TM-100023] 04 p0401 N88-12495

FLAPS (CONTROL SURFACES)
NT JET FLAPS
NT LEADING EDGE FLAPS
NT TRAILING EDGE FLAPS
NT UPPER SURFACE BLOWN FLAPS
NT VORTEX FLAPS
NT WING FLAPS
Flap-lag equations of motion of rigid, articulated rotor blades with three hinge sequences
[NASA-TM-100023] 04 p0401 N88-12495
Design and control of repairs of carbon fiber lift augmentation flaps in the ATR42 aircraft
[SNIAS-872-111-112] 05 p0529 N88-13217
Validation elements of the computation methods and measurement techniques for high lift aerodynamic systems
[SNIAS-872-111-101] 05 p0541 N88-13299
An experimental investigation of the aerodynamics of a NACA 64A010 airfoil-flap combination with and without flap oscillations. Part 1: Steady-state characteristics
[NASA-TM-88217] 05 p0542 N88-13305
Flaps-up takoff performance of the OV-1D aircraft with YT53-L-704 engine installed
[AD-A185960] 07 p0819 N88-14979
An experimental investigation of the flap-lag-torsion aeroelastic stability of a small-scale hingeless helicopter rotor in hover
[NASA-TP-2546] 13 p1715 N88-20257
Operational considerations for laminar flow aircraft
17 p2298 N88-23748
Characteristics of merging shear layers and turbulent wakes of a multi-element airfoil
[NASA-TM-100053] 18 p2511 N88-24900
The identification of the direct lift control flap system of the research aircraft ATTAS
20 p2786 N88-26527
Variable wing camber control systems for the future Airbus program
[MBB-UT-104/88] 23 p3180 N88-28932

FLARE STARS
A spectral survey of 26 G9-M6 flare stars in the solar neighborhood
04 p0512 N88-13149
Exosat results on the dMe flare Star Wolf 630AB and on VB 8
04 p0512 N88-13151
IUE/Optical/VLA flares on AD Leo
04 p0512 N88-13152
Microwave observations of red dwarf flare stars
04 p0513 N88-13153
A VLA survey of dMe flare stars
04 p0513 N88-13154
Flares: Solar and stellar
[PB87-124962] 06 p0806 N88-14917

FLASH BLINDNESS
A comparison of visual evoked potential and behavioral measures of flashblindness in humans
[AD-A189757] 15 p2101 N88-22519

FLASH LAMPS
Laser induced ignition of propellants
[AD-A191099] 16 p2213 N88-23206

FLASH POINT
Flash threshold of shocked aluminum silicofluoride
[DE88-003978] 10 p1339 N88-18005

FLASH TUBES
U FLASH LAMPS

FLASHING (VAPORIZING)
Mechanistic model for void distribution in flashing flow
[DE88-002948] 10 p1326 N88-17928

FLASHOVER
Gases released by surface flashover of insulators
[DE87-013851] 01 p0039 N88-10249
Withstand voltage of slightly polluted insulator chains in humid weather conditions
[DE88-752818] 22 p3072 N88-28237

FLAT COAXIAL TRANSMISSION LINES
U MICROSTRIP TRANSMISSION LINES

FLAT PLATES
A note on the instability of a vortex sheet leaving a semi-infinite plate
[DFVLR-FB-87-16] 01 p0004 N88-10019
Radiative and free-convective heat transfer from a finite horizontal plate inside an enclosure
02 p0133 N88-10833
Heat transfer with very high free stream turbulence
02 p0186 N88-11161
Kinematic formulation of finite elements for plate bending
04 p0455 N88-12821
A Cartesian finite-volume method for the Euler equations
05 p0579 N88-13532
An experimental investigation of appendage-flat plate junction flow. Volume 2. Elliptical nose appendage data base
[AD-A184974] 05 p0580 N88-13539
Experimental studies on the tripping behavior of narrow T-stiffened flat plates subjected to hydrostatic pressure and underwater shock
05 p0592 N88-13613
Analysis of photopole data reduction models
05 p0593 N88-13616
Dynamic response of laminated composite plates using a three-dimensional hybrid-stress finite-element formulation
05 p0596 N88-13639
Dual cylindrical wave Laser-Doppler method for measurement of skin friction in fluid flow
06 p0700 N88-14297
Numerical calculation of appendage, flat plate junction flow
[AD-A186371] 07 p0850 N88-15158
Investigation of large-scale structures in the near wake of a parallel flat plate
[DFVLR-FB-87-31] 09 p1162 N88-16967
Interferometric study of natural convection heat transfer from a vertical flat plate with transverse roughness elements
10 p1327 N88-17935

Side-by-side comparisons of evacuated compound parabolic concentrator and flat plate solar collector systems at temperatures of 90 to 100°C
[DE88-004717] 10 p1351 N88-18073
Effects of waves on the boundary layer of a surface-piercing flat plate: Experiment and theory
[AD-A188356] 12 p1626 N88-19731
Modification of parabolic dish antenna pattern using two symmetrically placed circular flat plates
[AD-A189543] 13 p1758 N88-20517
Investigation of heat transfer to a flat plate in a shock tube
[AD-A189538] 13 p1766 N88-20561
Film cooling effectiveness on a flat plate in high free-stream turbulence using a single row of 30 deg slant-hole injectors
[AD-A190500] 15 p2147 N88-22816
Test code for the assessment and improvement of Reynolds stress models 16 p2197 N88-23105
Deflection of a circular liquid jet on a flat plate perpendicular to the flow direction
[NASA-TT-20279] 16 p2207 N88-23173
Two-equation low-Reynolds-number turbulence modeling of transitional boundary layer flows characteristic of gas turbine blades
[NASA-CR-4145] 16 p2209 N88-23185
Numerical simulations of the flat-plate laminar boundary layer in subsonic and supersonic flow
[PDR/CFDU/IC/38] 18 p2511 N88-24895
Forced motion of initially stressed shells and plates 18 p2529 N88-25005
Active control of 2-D instability waves on an axisymmetric body
[AD-A191578] 19 p2663 N88-25835
Drag reduction of turbulent boundary layers by means of grooved surfaces
[ETN-88-92618] 20 p2802 N88-26630
Comparison of edge diffraction theories
[AD-A193880] 22 p3070 N88-28223
Modal synthesis by use of substructures with fixed or free coupling points
[ILR-MITT-191] 22 p3089 N88-28341
Stability and drag reduction in a boundary layer with microbubbles
[AD-A191975] 23 p3209 N88-29099
Studies of gas turbine heat transfer airfoil surface and end-wall cooling effects
[AD-A195165] 24 p3326 N88-29805
Investigation of large-scale structures in the near wake of a parallel flat plate
[ESA-TT-1100] 24 p3372 N88-30080

FLAT SURFACES
Film thicknesses in circular elastohydrodynamic contacts
[PB87-123725] 06 p0710 N88-14354
Solid modelling with faceted primitives
[ETN-88-91593] 09 p1218 N88-17305

FLAVOR (PARTICLE PHYSICS)
Quark core stars, quark stars and strange stars
[DE88-006991] 17 p2450 N88-24555
Experimental elementary particle physics
[DE88-007510] 18 p2572 N88-25274
A method for the analysis of heavy flavor decays
[NOTA-INTERNA-909] 22 p3150 N88-28744

FLAW DETECTION
U NONDESTRUCTIVE TESTS

FLAWS
U DEFECTS

FLEET SATELLITE COMMUNICATION SYSTEM
Thermal testing by internal IR heating of the FEP module 02 p0136 N88-10854

FLEETSATCOM
U FLEET SATELLITE COMMUNICATION SYSTEM

FLEXIBILITY
Processing and properties of SiC/Nicalon composites
[DE87-013885] 03 p0279 N88-11757
On the control of a compliant robot arm 03 p0332 N88-12095
A swept wing panel in a low speed flexible walled test section
[NASA-CR-4106] 05 p0540 N88-13292
Flexibilized copolyimide adhesives
[NASA-TM-89303] 05 p0570 N88-13474
Control of a flexible one-link manipulator
[AD-A185035] 05 p0590 N88-13598
Finite element model for the stress and flexibility analysis of curved pipes
[DE87-703632] 05 p0592 N88-13606
Stability analysis of a rigid body with a flexible attachment using the energy-casimir method
[AD-A185646] 06 p0723 N88-14449
Solid modelling for the manipulative robot arm (power) and adaptive vision control for space station missions 08 p1061 N88-16409
Implementation of a robotic flexible assembly system 09 p1212 N88-17265
Probabilistic and reliability design procedures for flexible airfield pavements: Elastic layered method
[AD-A187533] 11 p1442 N88-18600
Adaptive control of a manipulator with a flexible link
[NASA-CR-181637] 11 p1476 N88-18807
Free boundary problems arising in the control of a flexible robot arm
[AD-A189124] 12 p1634 N88-19781
PNL-1 improved ceramic composites through controlled fiber matrix interaction
[DE88-005680] 13 p1750 N88-20462
A 60-meter erectable assembly concept for a control of flexible structures flight experiment
[NASA-TM-100497] 14 p1873 N88-21190
Ultrasonic characterization of ceramic joints
[DE88-005844] 15 p2043 N88-22173
Vibration and control of flexible rotor supported by magnetic bearings
[NASA-TM-100688] 17 p2345 N88-23977
Single-mode projection filters for modal parameter identification for flexible structures
[NASA-CR-182680] 18 p2566 N88-25244
Empty test section streamlining of the transonic self-streamlining wind tunnel fitted with new walls
[NASA-CR-181680] 19 p2598 N88-25442
Reduced flexibility in processing Titan 4 space launch vehicles at Cape Canaveral Air Force Station
[AD-A194908] 24 p3332 N88-29834
Modeling robot flexibility for endpoint force control
[AD-A195923] 24 p3380 N88-30132

FLEXIBLE BODIES
NT FLEXIBLE SPACECRAFT
Wall interference tests of a CAST 10-2/DOA 2 airfoil in an adaptive-wall test section
[NASA-TM-4015] 02 p0122 N88-10772
Recent advances in structural dynamics of large space structures
[NASA-TM-100513] 02 p0138 N88-10867
Identification of linear structural models 03 p0337 N88-12121
Finite deformations of shell with rigid inclusion 04 p0426 N88-12639
A simulation study of the flight dynamics of elastic aircraft. Volume 1: Experiment, results and analysis
[NASA-CR-4102] 06 p0669 N88-14099
Studies of the structural dynamic behavior of satellite antenna system
[AD-A185526] 06 p0673 N88-14121
A simulation study of the flight dynamics of elastic aircraft. Volume 2: Data
[NASA-CR-4102-VOL-2] 08 p0959 N88-15813
Control system simulation for a single-link flexible arm
[AD-A187037] 09 p1174 N88-17035
A substructure method for dynamic simulation of flexible mechanical systems with geometric nonlinearities 09 p1176 N88-17044
Robust controller design for flexible structures
[AD-A187217] 10 p1340 N88-18009
Experimental set-up and mathematical modeling of H-shaped beam type structure
[AD-A187196] 11 p1466 N88-18743
Structure of shear flow turbulence and its control
[AD-A187909] 11 p1482 N88-18846
A superelement component dynamic synthesis method 11 p1500 N88-18956
Predictive wall adjustment strategy for two-dimensional flexible walled adaptive wind tunnel: A detailed description of the first one-step method
[NASA-CR-181635] 12 p1573 N88-19409
Moveable thermal joints for deployable or steerable spacecraft radiator systems
[NLR-MP-87016-U] 13 p1730 N88-20347
Dynamic modelling of flexible rotor shafts mounted on hydrodynamic bearings 13 p1779 N88-20641
Optimal control and identification of space structures
[AD-A190033] 15 p2025 N88-22065
Approximation methods for the identification and control of distributed parameter systems
[AD-A190201] 15 p2124 N88-22662
Analysis of rotating flexible blades using MSC/NASTRAN 16 p2222 N88-23259
Nonlinear programming extensions to rational function approximation methods for unsteady aerodynamic forces
[NASA-TP-2776] 18 p2483 N88-24623
Experimental study of active vibration control
[AD-A191454] 18 p2526 N88-24989
Large planar maneuvers for articulated flexible manipulators
[NASA-CR-183079] 19 p2711 N88-26104
Experiments in adaptive control of a very flexible one link manipulator 20 p2842 N88-26865
Identification and control of time-varying flexible structures: An artificial intelligence approach 23 p3265 N88-29437
Current and proposed gust criteria and analysis methods: An FAA overview 24 p3311 N88-29718
Measured and predicted responses of the Nord 260 aircraft to the low altitude atmospheric turbulence 24 p3312 N88-29723
Dynamics of articulated aerospace structures
[AD-A195685] 24 p3324 N88-29794
Robust design of distributed controllers for large flexible space structures
[NASA-CR-183202] 24 p3380 N88-30134

FLEXIBLE SPACECRAFT
Structures and Materials Working Group report 01 p0016 N88-10093
Attitude Control Working Group report 01 p0016 N88-10099
Pinhole occulter experiment
[NASA-CR-179206] 02 p0235 N88-11481
Control design challenges of large space systems and spacecraft control laboratory experiment (SCOLE)
[NASA-CR-178392] 03 p0275 N88-11735
Natural control of flexible space structures 04 p0408 N88-12534
Simultaneous structural and control optimization via linear quadratic regulator eigenstructure assignment 05 p0594 N88-13622
Personnel occupied woven envelope robot power
[NASA-CR-182367] 07 p0856 N88-15196
Large-angle slewing maneuvers for flexible spacecraft
[NASA-CR-4123] 08 p1000 N88-16060
Emulating a flexible space structure: Modeling
[NASA-TM-100320] 09 p1135 N88-16812
SIMSAT: Simulation package for flexible systems. Beams in space
[TW-278] 13 p1730 N88-20348
Robust decentralized control of large flexible structures
[DE88-005416] 13 p1824 N88-20902
A feedback double path compensating control structure for the attitude control of a flexible spacecraft
[INPE-4464-PRE/1239] 14 p1880 N88-21240
Maximum likelihood parameter identification of flexible spacecraft
[LR-508] 16 p2168 N88-22924
L(sub infinity symbol)-approximations of complex functions and robust controllers for large flexible space structures
[PB88-186226] 20 p2764 N88-26390
Numerical optimization, system theoretic and software tools for the integrated design of flexible structures and their control systems
[AD-A192927] 21 p2895 N88-27183

FLEXING
Strain-energy-release rate analysis of the end-notched flexure specimen using the finite-element method
[NASA-TM-100494] 05 p0608 N88-13735
Cyclic fatigue of ceramics at high temperatures
[PB87-127700] 06 p0685 N88-14200
Active control of flexural vibrations in beams 06 p0794 N88-14866
An engineering study of hybrid adaptation of wind tunnel walls for three-dimensional testing
[NASA-CR-178374] 07 p0814 N88-14957
Contribution to modeling flexion fatigue damage in unidirectional composite materials
[ECL-87-12] 08 p0965 N88-15843
Mechanical properties of carbon fiber reinforced thermoplastic matrix composites
[NAL-TR-934] 09 p1139 N88-16827

FLEXURE
U FLEXING

FLICKER
Universal power spectra for wave turbulence: Applications to wind waves, flicker noise, solar wind spectrum and classical second sound 10 p1318 N88-17879

FLIGHT ALTITUDE
Decoupling and stabilization of speed and height in F4 Phantom aircraft using output feedback
[ETN-87-90926] 02 p0125 N88-10787

FLIGHT CHARACTERISTICS
NT FLIGHT ENVELOPES
Rotorcraft Design for Operations
[AGARD-CP-423] 03 p0262 N88-11649
Mission-oriented flying qualities criteria for helicopter design via in-flight simulation 03 p0263 N88-11652
Investigation of vertical axis handling qualities for helicopter hover and NOE flight 03 p0263 N88-11653
Handling qualities criterion for very low visibility rotorcraft 03 p0263 N88-11654
MBB simulation facilities applied for rotorcraft research 03 p0263 N88-11655
Impacts of rotor hub design criteria on the operational capabilities of rotorcraft systems 03 p0264 N88-11663
Development and application of computational aerothermodynamics flowfield computer codes
[NASA-CR-181534] 04 p0395 N88-12465

Hovering helicopter flight dynamics: A study of vertical motion
[AR-004-526] 04 p0399 N88-12485
Model helicopter rotor rig and associated strain gauge balance for performance studies
[NAL-TM-AE-8704] 05 p0552 N88-13364
A simulation study of the flight dynamics of elastic aircraft. Volume 1: Experiment, results and analysis
[NASA-CR-4102] 06 p0669 N88-14099
Impact of flying qualities on mission effectiveness for helicopter air combat, volume 1
[NASA-CR-166568] 06 p0669 N88-14100
Handling qualities of a wide-body transport airplane utilizing Pitch Active Control Systems (PACS) for relaxed static stability application
[NASA-TP-2482] 07 p0821 N88-14987
A simulation study of the flight dynamics of elastic aircraft. Volume 2: Data
[NASA-CR-4102-VOL-2] 08 p0959 N88-15813
Lateral stability and control derivatives extracted from space shuttle Challenger flight data
[NASA-TM-100520] 09 p1132 N88-16788
Workshop on Design Loads for Advanced Fighters
[AGARD-R-746] 12 p1579 N88-19449
Manned simulation: Helpful means to determine and improve structural load criteria 12 p1581 N88-19459
Bifurcations in unsteady aerodynamics-implications for testing
[NASA-TM-100083] 15 p2015 N88-22014
Airworthiness and flight characteristics test of a ski assembly for the UH-60A Black Hawk helicopter
[AD-A191414] 16 p2162 N88-22895
Certification aspects of airplanes which may operate with significant natural laminar flow 17 p2298 N88-23749
Airbus 1987: Success in Europe
[ETN-88-92099] 20 p2758 N88-26364
Contribution to the numerical solution of airplane spin motion
[ETN-88-92368] 21 p2896 N88-27190
A numerical simulation of side force effects by aerodynamic flight trajectory correction
[ISL-CO-211/87] 21 p2896 N88-27191
Japan Air Line's Aircraft Integrated Monitoring System (AIMS) activities 22 p3034 N88-28014
Advances in Flying Qualities
[AGARD-LS-157] 24 p3314 N88-29735
Advances in flying qualities: Concepts and criteria for a mission oriented flying qualities specification 24 p3314 N88-29739
A second look at MIL prime flying qualities requirements 24 p3314 N88-29740
The role of simulation in flying qualities and flight control system related development 24 p3315 N88-29742

FLIGHT CLOTHING
Validation of mathematical model predictions of immersion survival times
[IAM-652] 14 p1952 N88-21635
Further development of a mathematical model for the specification of immersion clothing insulation
[IAM-653] 14 p1954 N88-21644

FLIGHT COMPUTERS
U AIRBORNE/SPACEBORNE COMPUTERS

FLIGHT CONDITIONS
Calculation of the damage of highly loaded gas turbine disks under real flight conditions
[ETN-87-90416] 01 p0007 N88-10036

FLIGHT CONTROL
NT ANNULAR SUSPENSION AND POINTING SYSTEM
NT AUTOMATIC FLIGHT CONTROL
NT AUTOMATIC LANDING CONTROL
NT FLY BY WIRE CONTROL
NT POINTING CONTROL SYSTEMS
NT THRUST VECTOR CONTROL
Digital system bus integrity
[NASA-CR-181446] 01 p0006 N88-10030
A survey of aircraft integrated control technology
[AR-004-561] 02 p0126 N88-10794
Robust control system design 02 p0127 N88-10800
Optimal detection of sensor failures in flight control systems using deterministic observers 02 p0128 N88-10803
Flight test of a resident backup software system 02 p0128 N88-10805
The flight evaluation of an advanced engine display and monitoring system 03 p0264 N88-11659
Flight propulsion control integration for V/STOL aircraft
[NASA-TM-100226] 03 p0267 N88-11680
An evaluation plan of bus architectures and protocols using the NASA Ames intelligent redundant actuation system
[NASA-CR-177458] 04 p0398 N88-12482
Digital-flight-control-system software written in automated-engineering-design language: A user's guide of verification and validation tools
[NASA-TM-88313] 04 p0401 N88-12494
Applications of the hybrid automated reliability predictor
[NASA-TP-2760] 04 p0475 N88-12928
Nonlinear lift control at high speed and high angle of attack using vortex flow technology 05 p0545 N88-13319
Integrated control and display research for transition and vertical flight on the NASA V/STOL Research Aircraft (VSRA)
[NASA-TM-100029] 05 p0551 N88-13359
Electrical flight commands in transport aircraft
[SNIAS-872-111-108] 05 p0551 N88-13361
Reduced order optimal command applied to longitudinal automatic pilots
[SNIAS-872-111-114] 05 p0552 N88-13362
Control of an unstable launcher in atmospheric flight using minimax optimal control laws
[SNIAS-872-422-107] 05 p0638 N88-13901
Advanced helicopter cockpit and control configurations for helicopter combat missions
[NASA-TM-100017] 07 p0821 N88-14988
Guidance of high-altitude sounding rockets using the S19 and Spinning Rocket Altitude Control (SPINRAC) systems 08 p1034 N88-16273
NASA/Army Rotorcraft Technology. Volume 1: Aerodynamics, and Dynamics and Aeroelasticity
[NASA-CP-2495-VOL-1] 09 p1105 N88-16625
Helicopter mathematical models and control law development for handling qualities research 09 p1108 N88-16642
Rotorcraft flight-propulsion control integration 09 p1108 N88-16643
Rotorcraft technology at Boeing Vertol: Recent advances 09 p1111 N88-16658
A piloted simulation investigating handling qualities and performance requirements of a single-pilot helicopter in air combat employing a helmet-driven turreted gun
[AD-A186878] 09 p1116 N88-16689
Lateral stability and control derivatives extracted from space shuttle Challenger flight data
[NASA-TM-100520] 09 p1132 N88-16788
MPAD MCC workstation system: ADDAM and EEVE 09 p1203 N88-17209
User interface devices for mission control 09 p1205 N88-17224
Flight test technique, illustrated by Advanced Technologies Testing Aircraft System (ATTAS) 09 p1240 N88-17433
Light Electronic Control System (LECOS): A proposal for a interconnected error-tolerant, optoelectronic control system
[MBB-UT-004/87] 10 p1311 N88-17836
Trends in the distribution of tasks between commercial pilots and flight control systems
[MBB-UT-008/87] 10 p1314 N88-17851
The development of manoeuvre load criteria for agile aircraft 12 p1579 N88-19450
Interaction between structural considerations and system design in advanced flight controls 12 p1580 N88-19458
Manned simulation: Helpful means to determine and improve structural load criteria 12 p1581 N88-19459
Presentation of flight control design and handling quality commonality by separate surface stability augmentation for the family of commuter airplanes
[NASA-CR-182567] 12 p1583 N88-19471
The impact of vertical axis characteristics on helicopter handling qualities
[AD-A188964] 12 p1583 N88-19474
User perceptions of side-arm flight control in rotary-wing aircraft
[AD-A188519] 12 p1672 N88-20009
A fault injection experiment using the AIRLAB Diagnostic Emulation Facility
[NASA-CR-178390] 13 p1823 N88-20895
Operational viewpoint of the X-29A digital flight control system
[NASA-TM-100434] 14 p1866 N88-21152
Performance improvements of an F-15 airplane with an integrated engine-flight control system
[NASA-TM-100431] 14 p1867 N88-21159
F-16 simulator for man-in-the-loop testing of aircraft control systems (SIMTACS)
[AD-A189675] 14 p1870 N88-21178
The PC/AT compatible computer as a mission control center display processor at Ames-Dryden Flight Research Facility
[NASA-TM-100426] 14 p1955 N88-21654
Examination of the effects of using Ada (trade name) in flight control software
[AD-A189679] 14 p1959 N88-21683
Application of eigenstructure assignment techniques in the design of a longitudinal flight control system
[AD-A189644] 15 p2020 N88-22039
Multivariable control law design for the AFTI/F-16 with a failed control surface using a parameter-adaptive controller
[AD-A189848] 15 p2020 N88-22040
Kalman filter residual expert system
[AD-A190520] 15 p2020 N88-22041
Subharmonic aliasing and its effects on the AFTI/F-16 digital flight control system
[AD-A190614] 15 p2020 N88-22042
Multiple model parameter adaptive control for in-flight simulation
[AD-A190568] 15 p2021 N88-22044
Basic design of a flight director system for NAL STOL research aircraft
[DE88-751806] 16 p2162 N88-22897
Analytical sensor redundancy assessment
[NASA-CR-182892] 16 p2163 N88-22901
Stability and control methodology for conceptual aircraft design. Volume 1: Methodology manual
[AD-A191314] 16 p2164 N88-22906
Integrated avionics reliability 17 p2294 N88-23723
Investigation of air transportation technology at Princeton University, 1986 17 p2294 N88-23724
Rule-based fault-tolerant flight control 17 p2294 N88-23725
A comparison of integrated and separate systems for flight control and navigation 17 p2303 N88-23779
Software engineering for the British Aerospace Experimental Aircraft Programme (EAP) 17 p2306 N88-23798
Development of an airborne facility for advanced avionics research 17 p2307 N88-23801
Parameter-adaptive model-following for in-flight simulation
[AD-A190567] 18 p2467 N88-24645
Simultaneous multiple control force exertion capabilities of males and females versus helicopter control force design limits
[AD-A191653] 18 p2553 N88-25153
Model reduction methods for control design
[NASA-CR-179434] 19 p2719 N88-26144
Control of flight through microburst wind shear using deterministic trajectory optimization 20 p2761 N88-26375
Computer simulation of a single pilot flying a modern high-performance helicopter
[NASA-TM-100182] 20 p2761 N88-26376
Theoretical and experimental investigations of a vortex drag behind a wing profile with spoiler
[ISL-PU-309/87] 21 p2892 N88-27169
Investigations of aircraft control with jet spoilers
[ISL-R-112/87] 21 p2898 N88-27202
Robust digital model following controller for helicopters
[DFVLR-FB-88-07] 21 p2898 N88-27203
Improvement of head-up display standards. Volume 4: Head-up display dynamics flight tests
[AD-A193617] 22 p3042 N88-28060
System status display evaluation
[NASA-CR-4181] 22 p3042 N88-28061
Improvement of head-up display standards. Volume 2: Evaluation of head-up displays to enhance unusual attitude recovery
[AD-A194601] 23 p3178 N88-28921
Improvement of head-up display standards. Volume 5: Head up display ILS (Instrument Landing System) accuracy flight tests
[AD-A194602] 23 p3178 N88-28922
Time periodic control of a multi-blade helicopter
[AD-A194435] 23 p3180 N88-28931
Avionic expert systems 23 p3253 N88-29365
Motion planning for a free-flying robot 23 p3255 N88-29378
Advances in Flying Qualities
[AGARD-LS-157] 24 p3314 N88-29735
Low-speed longitudinal flying qualities of modern transport aircraft 24 p3314 N88-29738
Advances in flying qualities: Concepts and criteria for a mission oriented flying qualities specification 24 p3314 N88-29739
The role of simulation in flying qualities and flight control system related development 24 p3315 N88-29742
Intelligent fault diagnosis and failure management of flight control actuation systems
[NASA-CR-177481] 24 p3323 N88-29790
A multiprocessor avionics system for an unmanned research vehicle
[AD-A194806] 24 p3325 N88-29800
An analysis of lateral-directional handling qualities and Eigenstructure of high performance aircraft
[AD-A194874] 24 p3328 N88-29814

N-version software demonstration for digital flight controls
[NASA-CR-181483] 24 p3328 N88-29815
A fiber optic collective flight control system for helicopters
[AD-A195406] 24 p3328 N88-29818
Controlled degradation of resolution of high-quality flight simulator images for training effectiveness evaluation
[AD-A196189] 24 p3330 N88-29823
Four-axis side-arm flight control simulator investigation
[AD-A196026] 24 p3409 N88-30294
Improvement of head-up display standards. Volume 3: An evaluation of head-up display safety
[AD-A195787] 24 p3410 N88-30300
Space station proximity operations windows: Human factors design guidelines
[NASA-TM-88233] 24 p3410 N88-30301
An intelligent training system for space shuttle flight controllers 24 p3415 N88-30331

FLIGHT CREWS
NT SPACECREWS
An aerodynamic performance evaluation of the NASA/Ames Research Center advanced concepts flight simulator
[NASA-TM-89659] 03 p0268 N88-11685
Assessment of fatigue in aviation crews
[AD-A184129] 03 p0356 N88-12245
A comparison of the effects of group dynamics on individuals assigned to integral and non-integral aircrews
[AD-A186467] 08 p1051 N88-16345
Ultra-low frequency vibration data acquisition concerns in operating flight simulators
[DE88-004795] 10 p1285 N88-17687
Forecasting complications of cardiovascular disease in flight personnel 10 p1361 N88-18136
Cockpit data management
[NASA-CR-178407] 11 p1438 N88-18579
First encounters of the close kind: The formation process of airline flight crews
[AD-A187977] 11 p1523 N88-19091
Field dependence-independence and its relationship to flight training performance
[AD-A188888] 12 p1670 N88-20003
Multi-crew pictorial format display evaluation
[AD-A189349] 13 p1812 N88-20824
Proceedings of the Workshop on the Assessment of Crew Workload Measurements Methods, Techniques and Procedures. Volume 1: Preliminary Selection of Measures
[AD-A189004] 13 p1812 N88-20827
Development of a C3 generic workstation: System overview 16 p2242 N88-23396
Communication training for aircrews: A review of theoretical and pragmatic aspects of training program design
[NASA-CR-177459] 20 p2756 N88-26349
Detection of latent epilepsy in aircrew candidates 21 p2984 N88-27720
Cockpit and cabin crew coordination
[AD-A192445] 21 p2993 N88-27752
Future air-to-air training for the RF-4
[AD-A194363] 23 p3240 N88-29284
A field study on soft contact lens wear in USAF military transport aircraft
[AD-A195962] 24 p3407 N88-30285

FLIGHT ENVELOPES
Full-envelope aerodynamic modeling of the Harrier aircraft
[NASA-TM-88376] 05 p0552 N88-13363
Australian aerodynamic design codes for aerial tow bodies
[AD-A189048] 13 p1715 N88-20258
Multiple model parameter adaptive control for in-flight simulation
[AD-A190568] 15 p2021 N88-22044
Flight testing a V/STOL aircraft to identify a full-envelope aerodynamic model
[NASA-TM-100996] 17 p2301 N88-23762
Current flight test experience related to structural divergence of forward-swept wings
[NASA-TM-100445] 18 p2464 N88-24633

FLIGHT FATIGUE
Measurement and modification of sensorimotor system function during visual-motor performance
[AD-A186351] 07 p0889 N88-15387

FLIGHT HAZARDS
NT METEOROID HAZARDS
Aircraft accidents
[JB-84] 01 p0004 N88-10020
Contributions to the modeling of wind shear for danger studies
[ETN-87-90442] 01 p0072 N88-10463
The dependence of the normalized ice accretion thickness on cloud-physical parameters
[DFVLR-FB-87-08] 01 p0072 N88-10464
Meteorological systems support to critical shuttle requirements on the Eastern Test Range --- STS
02 p0205 N88-11281
Influence of Environmental Factors on Aircraft Wing Performance
[VKI-LS-1987-03] 08 p0951 N88-15771
Characterization of meteorological phenomena influencing aircraft operations 08 p0951 N88-15772
The influence of wind shear, downdraft, and turbulence in aircraft performance 08 p0952 N88-15773
The potential influence of rain on airfoil performance
08 p0952 N88-15774
Effects of wing simulated ground frost on aircraft performance 08 p0952 N88-15775
Low altitude windshear threat to commercial aircraft
08 p0952 N88-15777
Analysis of bird strikes to UK registered aircraft 1985 (civil aircraft over 5700 kg maximum weight
[CAA-PAPER-87012] 09 p1115 N88-16684
Lapwings and birdstrikes. The biology of the lapwing Vanellus vanellus in relation to the birdstrike hazard it presents
[CAA-PAPER-87015] 14 p1865 N88-21142
Bibliography of icing on aircraft (status 1987)
[DFVLR-MITT-87-18] 16 p2158 N88-22876
Standardized ice accretion thickness as a function of cloud physics parameters
[ESA-TT-1080] 16 p2234 N88-23346
Ice formation on aircraft
[ETN-88-92154] 18 p2545 N88-25104
Flight-management strategies for escape from microburst encounters
[NASA-TM-4057] 19 p2803 N88-25461
New ice detection system 22 p3037 N88-28030
Contributions to the modeling of wind shear for danger studies
[NASA-TT-20293] 23 p3174 N88-28900

FLIGHT INSTRUMENTS
NT ATTITUDE INDICATORS
NT AUTOMATIC PILOTS
NT FLIGHT TEST INSTRUMENTS
NT HORIZON SCANNERS
NT RADIO ALTIMETERS
Geometric modeling of flight information for graphical cockpit display
[AD-A190484] 15 p2021 N88-22043
Basic design studies for the realization of liquid crystal display systems in aircraft
[VA-87-001] 16 p2163 N88-22900
The pneumatic wind shear sensor: A tool for meteorological investigations and flight management
22 p3036 N88-28024
New ice detection system 22 p3037 N88-28030
The NAE atmospheric research aircraft
24 p3313 N88-29730
Improvement of head-up display standards. Volume 3: An evaluation of head-up display safety
[AD-A195787] 24 p3410 N88-30300

FLIGHT MANAGEMENT SYSTEMS
Optimal detection of sensor failures in flight control systems using deterministic observers
02 p0128 N88-10803
Application of flight systems methodologies to the validation of knowledge-based systems
[NASA-TM-100442] 18 p2561 N88-25207
Development of an airborne facility for advanced avionics research
[NLR-MP-87012-U] 20 p2760 N88-26368

FLIGHT MECHANICS
Maximum likelihood estimates of parameters in linear systems with process and measurement noise
[DFVLR-FB-87-20] 01 p0083 N88-10532
Revision of the information standards for flight mechanics
[DFVLR-MITT-87-06] 03 p0265 N88-11675
The Proceedings of the Symposium on Mechanics for Space Flight
[ISAS-SP-5] 03 p0317 N88-12006
Aerodynamics of Hypersonic Lifting Vehicles
[AGARD-CP-428] 05 p0529 N88-13219
Calendar of selected aeronautical and space meetings
[AGARD-CAL-87/1] 05 p0657 N88-14033
Highlights of the 70th Flight Mechanics Panel Symposium on Flight Vehicle Development Time and Cost Reduction
[AD-A185831] 07 p0901 N88-15454
An overview of key technology thrusts at Bell Helicopter Textron 09 p1111 N88-16657
Special flight mechanical features of the bearingless helicopter rotor
[MBB-FM-315/O] 10 p1309 N88-17825
Intelligent interfaces for expert systems
23 p3258 N88-29397

FLIGHT OPERATIONS
NT CREW PROCEDURES (INFLIGHT)
Report of safety survey: Human integration of approach charts
[DOT/FAA/PM-87/15] 01 p0076 N88-10488
A linear quadratic Gaussian with loop transfer recovery proximity operations autopilot for spacecraft
[NASA-CR-172028] 02 p0227 N88-11433
Eighth Session of the Commission for Aeronautical Meteorology (abridged)
[WMO-673] 06 p0745 N88-14585
Moisture plotting of carbon fiber composite in flight operations
[MBB-UT-119/87] 09 p1138 N88-16823
Selected aspects of triazolam in relation to aviator performance in naval flight operations
[AD-A189322] 12 p1667 N88-19996

FLIGHT OPTIMIZATION
Optimal thrust vector control of coplanar orbital evasive maneuvers
[AD-A189544] 13 p1730 N88-20346
Periodic solutions in aircraft cruise-dash optimization
18 p2464 N88-24631
The OFP (Operational Flight Program) update cycle needs you
[AD-A194910] 24 p3325 N88-29798

FLIGHT PATHS
Approach trajectory planning system for maximum concealment
[NASA-TM-88258] 02 p0227 N88-11435
The Avionics Flight Evaluation System (AFES) of the DFVLR
[ESA-TT-1037] 03 p0266 N88-11677
Flightpath reconstruction and systematic radar error estimation from multiradar range-azimuth measurements
[NLR-MP-85064-U] 06 p0693 N88-14251
Verification of obstacle accountability areas using a simple mathematical model. Part 1: Description of general model and application for a specific case --- engine failure at takeoff
[NLR-TR-85069-U] 09 p1115 N88-16683
Automatic routing module 09 p1210 N88-17251
The estimation of target trajectory parameters from Closest Point of Approach (CPA) time measurements in a field of acoustic sensors
[FB-3-87] 11 p1439 N88-18586
Development of an interactive real-time graphics system for the display of vehicle space positioning
[NASA-TM-100429] 13 p1730 N88-20344
Method for determining artillery position
[NASA-TT-20237] 13 p1834 N88-20974
Modification of the BLUEMAX 2 terrain following model to incorporate radar detection
[AD-A190594] 15 p2017 N88-22028
Geometric modeling of flight information for graphical cockpit display
[AD-A190484] 15 p2021 N88-22043
Flight penetration of wind shear: Control strategies
17 p2294 N88-23727
Method for prediction and determination of takeoff performance for vectored thrust vehicles
[AD-A191809] 18 p2463 N88-24626
Periodic solutions in aircraft cruise-dash optimization
18 p2464 N88-24631
Geographical information for design purposes
[NLR-MP-87014-U] 20 p2818 N88-26719
An evaluation of flight path formats head-up and head-down
[NASA-CR-4176] 21 p2897 N88-27196

FLIGHT PERFORMANCE
U FLIGHT CHARACTERISTICS

FLIGHT RECORDERS
Development of a multipurpose smart recorder for general aviation aircraft
[NASA-CR-168353] 18 p2465 N88-24637
Maintenance support for military aircraft by intelligent on-board maintenance data panel
22 p3034 N88-28012
The management of software in airborne recording systems 22 p3035 N88-28019
The intelligent QAR and its cost effective role in new generation AIMS --- quick access recorder (QAR); aircraft integrated monitoring systems (AIMS)
22 p3035 N88-28020
Development of a maintenance data bus monitor and recorder 22 p3036 N88-28022
The role played by FDRs in understanding the windshear phenomenon 22 p3036 N88-28023

FLIGHT RULES
NT INSTRUMENT FLIGHT RULES
NT VISUAL FLIGHT RULES
Air traffic control
[FAA-ORDER-7110.65E] 12 p1576 N88-19426

FLIGHT SAFETY
Report of safety survey: Human integration of approach charts
[DOT/FAA/PM-87/15] 01 p0076 N88-10488

UK airmiss statistics
[CAP-530] 03 p0261 N88-11642
Report of the helicopter human factors working group --- accident prevention
[CAA-PAPER-87007] 03 p0361 N88-12274
Airline safety: A comparative analysis
[AD-A185358] 05 p0543 N88-13308
The influence of wind shear, downdraft, and turbulence in aircraft performance 08 p0952 N88-15773
Instrumentation utilisation for risk control in safety operations --- balloons and rockets 08 p1030 N88-16240
Annual review of aircraft accident data: US air carrier operations calendar year 1985
[PB88-135843] 10 p1276 N88-17638
AEV local verification for aviation, precipitation and temperature programs: AV, REL, TEM (September 1987 revision)
[PB88-115662] 10 p1355 N88-18101
Medical and psychological problems of assuring flight safety under present conditions 10 p1359 N88-18123
Proceedings of a Workshop on Innovative Solutions for Safety in Air Transportation
[ILR-MITT-178(1987)] 11 p1437 N88-18573
Activities report in air traffic control
[ETN-88-91092] 11 p1438 N88-18581
Safe rendezvous approach to a space station by impulsive transfers and continuous thrust arcs 12 p1585 N88-19486
Proceedings of the Workshop on the Assessment of Crew Workload Measurements Methods, Techniques and Procedures. Volume 1: Preliminary Selection of Measures
[AD-A189004] 13 p1812 N88-20827
UK airmiss statistics
[REPT-3/87] 14 p1865 N88-21141
UK airmiss statistics
[CAA-1/87] 17 p2300 N88-23761
Meteorological and Environmental Inputs to Aviation Systems
[NASA-CP-2498] 18 p2545 N88-25105
General-aviation's view of progress in the aviation weather system 18 p2546 N88-25110
Aircraft field degradation and electromagnetic compatibility
[PB88-183975] 19 p2602 N88-25456
Flight-management strategies for escape from microburst encounters
[NASA-TM-4057] 19 p2603 N88-25461
System identification in vehicle dynamics
[DFVLR-MITT-87-22] 20 p2785 N88-26518
The exploitation of Aircraft Integrated Monitoring System (AIMS) data in height-keeping studies for aircraft operating above FL 290 22 p3036 N88-28026
UK airmisses involving commercial air transport
[CAA-1/88] 23 p3176 N88-28907

FLIGHT SIMULATION

The fatigue properties of aerospace steels under constant amplitude and flight-by-flight simulated loading
[BAE-MSM-R-GEN-0566] 01 p0059 N88-10377
Contributions to the modeling of wind shear for danger studies
[ETN-87-90442] 01 p0072 N88-10463
Global positioning satellite-based automatic landing system and wind estimated feedback for the AH-64 helicopter 02 p0124 N88-10784
Improvements to the adaptive maneuvering logic program
[NASA-CR-3985] 03 p0262 N88-11648
Rotorcraft Design for Operations
[AGARD-CP-423] 03 p0262 N88-11649
Investigation of vertical axis handling qualities for helicopter hover and NOE flight 03 p0263 N88-11653
An inexpensive real-time interactive three-dimensional flight simulation system
[AD-A184340] 04 p0402 N88-12499
CGI delay compensation
[NASA-TM-86703] 04 p0476 N88-12932
Shock tunnels for real gas hypersonics 05 p0530 N88-13223
Overlooked potential of systems with Markovian coefficients
[NLR-MP-86049-U] 05 p0552 N88-13366
Noise of a model counterrotation propeller with reduced aft rotor diameter at simulated takeoff/approach conditions (F7/A3)
[NASA-TM-100254] 05 p0647 N88-13961
Experimental design of a piloted helicopter off-axis-tracking simulation using a helmet mounted display
[AD-A186228] 07 p0820 N88-14982
Handling qualities of a wide-body transport airplane utilizing Pitch Active Control Systems (PACS) for relaxed static stability application
[NASA-TP-2482] 07 p0821 N88-14987
An inexpensive real-time interactive three dimensional flight simulation system
[AD-A184868] 07 p0821 N88-14989
The role of adaptive supplemental visual cuing in flight simulation
[AD-A185932] 07 p0822 N88-14992
A simulation study of the flight dynamics of elastic aircraft. Volume 2: Data
[NASA-CR-4102-VOL-2] 08 p0959 N88-15813
Numerical analysis of motion of solid bodies in atmosphere 08 p1079 N88-16505
Rotorcraft handling-qualities design criteria development 09 p1109 N88-16645
Status of NASA/Army rotorcraft research and development piloted flight simulation 09 p1110 N88-16651
Helicopters as test carriers for avionics systems (HETAS)
[DFVLR-IB-112-85/18] 09 p1116 N88-16692
Upgrading of NASA-Ames high-energy hypersonic facilities: A Study
[NASA-CR-182475] 09 p1122 N88-16717
Frequency-response identification of XV-15 tilt-rotor aircraft dynamics 10 p1277 N88-17643
Transport delay compensation for computer-generated imagery systems
[NASA-TM-100084] 10 p1277 N88-17645
Realtime pilot model parameter identification
[AD-A188873] 12 p1584 N88-19476
Standardized environmental fatigue sequence for the evaluation of composite components in combat aircraft (ENSTAFF = ENvironmental faiSTAFF)
[LBF-FB-179] 13 p1722 N88-20300
Power spectral density analysis of wind-shear turbulence for related flight simulations
[NASA-CR-182721] 13 p1802 N88-20773
Determination of canopy loads for a light aircraft by wind tunnel testing and computer modelling
[BU-353] 14 p1869 N88-21167
China constructing high-altitude test cell 14 p1901 N88-21351
Masking of motion cues by random motion: Comparison of human performance with a signal detection model
[UTIAS-313] 14 p1953 N88-21639
Model selection for the multiple model adaptive algorithm for in-flight simulation
[AD-A189715] 15 p2016 N88-22022
Effects of update and refresh rates on flight simulation visual displays
[NASA-TM-100415] 15 p2018 N88-22033
Application of eigenstructure assignment techniques in the design of a longitudinal flight control system
[AD-A189644] 15 p2020 N88-22039
Multiple model parameter adaptive control for in-flight simulation
[AD-A190568] 15 p2021 N88-22044
Probe-evoked event-related potential techniques for evaluating aspects of attention and information processing 16 p2240 N88-23379
Wind tunnel investigation of wing and control panel loads at transonic and supersonic speeds on some schematic cruciform missile configurations
[FFA-TN-1986-43] 18 p2457 N88-24585
Parameter-adaptive model-following for in-flight simulation
[AD-A190567] 18 p2467 N88-24645
Simulator evaluation of lineup visual landing aids for night carrier landing
[AD-A191212] 18 p2468 N88-24648
F-14 modeling study
[NASA-CR-4164] 19 p2603 N88-25462
Research on piloting under conditions of breakdown in flight
[PB87-217980] 19 p2710 N88-26102
On the dynamic behavior of balloon during its launch; application of panel method and extension to unsteady problem
[ISAS-RN-622] 20 p2751 N88-26330
A high fidelity real-time simulation of a small turboshaft engine
[NASA-TM-100991] 20 p2761 N88-26378
Robust digital model following controller for helicopters
[DFVLR-FB-88-07] 21 p2898 N88-27203
System status display evaluation
[NASA-CR-4181] 22 p3042 N88-28061
Complex configurations 23 p3167 N88-28861
Contributions to the modeling of wind shear for danger studies
[NASA-TT-20293] 23 p3174 N88-28900
The role of simulation in flying qualities and flight control system related development 24 p3315 N88-29742
Minimum-complexity helicopter simulation math model
[NASA-CR-177476] 24 p3328 N88-29819
A digital simulation technique for the Dryden atmospheric model
[NASA-TT-20342] 24 p3404 N88-30266
Prediction and measurement of human pilot dynamic characteristics in a manned rotorcraft simulation
[NASA-CR-183246] 24 p3410 N88-30297

FLIGHT SIMULATORS

NT COCKPIT SIMULATORS

A research on pilot performance in the case of aircraft malfunction
[ETN-87-90652] 02 p0217 N88-11369
A research on pilot performance in a flight incident situation
[ETN-87-90653] 02 p0217 N88-11370
Mission-oriented flying qualities criteria for helicopter design via in-flight simulation 03 p0263 N88-11652
MBB simulation facilities applied for rotorcraft research 03 p0263 N88-11655
Research simulators for helicopters 03 p0263 N88-11656
An aerodynamic performance evaluation of the NASA/Ames Research Center advanced concepts flight simulator
[NASA-TM-89659] 03 p0268 N88-11685
An inexpensive real-time interactive three-dimensional flight simulation system
[AD-A184340] 04 p0402 N88-12499
The role of adaptive supplemental visual cuing in flight simulation
[AD-A185932] 07 p0822 N88-14992
Application of the analysis phase of the instructional system development to the MK-105 magnetic minesweeping mission of the MH-53E helicopter
[AD-A186282] 07 p0822 N88-14994
Scientific Colloquium in Honor of Prof. Dr. Rer. Nat. Hermann L. Jordan
[DFVLR-MITT-87-11] 09 p1240 N88-17432
Flight test technique, illustrated by Advanced Technologies Testing Aircraft System (ATTAS) 09 p1240 N88-17433
Investigation of the influence of wind shear on the aerodynamic characteristics of aircraft using a vortex-lattice method 10 p1274 N88-17619
Ultra-low frequency vibration data acquisition concerns in operating flight simulators
[DE88-004795] 10 p1285 N88-17687
Measurement and effects of transport delays in a state-of-the-art F-16C flight simulator
[AD-A187367] 11 p1441 N88-18599
Aircrew training devices: Utility and utilization of advanced instructional features, phase 4
[AD-A188418] 12 p1670 N88-20000
F-16 simulator for man-in-the-loop testing of aircraft control systems (SIMTACS)
[AD-A189675] 14 p1870 N88-21178
First flight simulator test of the head-up display for NAL QSTOL experimental aircraft (ASUKA)
[DE88-751804] 16 p2162 N88-22896
A look toward the future of complex avionics systems development using the USAF Test Pilot School's avionics systems test training aircraft 17 p2306 N88-23797
Digital monoplotting, part 1
[B8735122-PT-1] 17 p2369 N88-24106
Digital monoplotting, part 2
[B8735122-PT-2] 17 p2369 N88-24107
Analysis procedures and subjective flight results of a simulator validation and cue fidelity experiment
[NASA-TM-88270] 18 p2465 N88-24634
An OOD (Object-Oriented Design) paradigm for flight simulators
[AD-A191097] 18 p2467 N88-24647
F-14 modeling study
[NASA-CR-4164] 19 p2603 N88-25462
Flight simulator: Field of view utilized in performing tactical maneuvers
[AD-A192412] 20 p2762 N88-26379
An evaluation of flight path formats head-up and head-down
[NASA-CR-4176] 21 p2897 N88-27196
Simulator sickness in the AH-64 Apache combat mission simulator
[AD-A193419] 21 p2988 N88-27739
System status display evaluation
[NASA-CR-4181] 22 p3042 N88-28061
OMV docking simulator 23 p3255 N88-29379
Controlled degradation of resolution of high-quality flight simulator images for training effectiveness evaluation
[AD-A196189] 24 p3330 N88-29823
LANTIRN simulator training in the F-16C
[AD-A195201] 24 p3330 N88-29826

FLIGHT STABILITY TESTS
Preliminary airworthiness evaluation of the UH-60A equipped with the XM-139 VOLCANO mine dispensing system
[AD-A190604] 15 p2018 N88-22029
FLIGHT STRESS (BIOLOGY)
NT SPACE FLIGHT STRESS
Brain activity during tactical decision-making. Part 2: Probe-evoked potentials and workload
[AD-A188688] 12 p1667 N88-19994
FLIGHT TECHNICAL ERROR
U PILOT ERROR
FLIGHT TEST INSTRUMENTS
Test equipment with fiber optic data bus and laser gyro strapdown system LTN-90 for the helicopter BO-105
[ESA-TT-1038] 01 p0005 N88-10025
Effect of installation and calibration errors of sensors on system identification results of an aircraft
[ESA-TT-1059] 03 p0266 N88-11678
Boeing 727 MLS (Microwave Landing System) terminal instrument procedures (TERPS) approach data collection and processing, data report
[AD-A185523] 06 p0667 N88-14090
Refinement of eye-point-of-regard measurement with helicopter pilots in a flight experiment
[ESA-TT-1073] 09 p1200 N88-17195
Flight test technique, illustrated by Advanced Technologies Testing Aircraft System (ATTAS)
09 p1240 N88-17433
Trajectory measurement of the Fokker 100 aircraft during autoland testing
[NLR-MP-86010-U] 20 p2758 N88-26366
Development of an airborne facility for advanced avionics research
[NLR-MP-87012-U] 20 p2760 N88-26368
Interface techniques and systems for standard aircraft data buses 22 p3036 N88-28028
Test and calibration system for monitoring the Advanced Technologies Testing Aircraft System (ATTAS) data acquisition system 22 p3037 N88-28029
FLIGHT TESTS
NT FLIGHT STABILITY TESTS
NT SPACE TRANSPORTATION SYSTEM 4 FLIGHT
HiMAT flight program: Test results and program assessment overview
[NASA-TM-86725] 01 p0005 N88-10026
Comparison of wind tunnel and flight test afterbody and nozzle pressures for a twin-jet fighter aircraft at transonic speeds
[NASA-TP-2588] 02 p0121 N88-10765
Flight research at NASA Ames Research Center: A test pilot's perspective
[NASA-TM-100025] 02 p0125 N88-10788
Flight test of a resident backup software system
02 p0128 N88-10805
Auxiliary propulsion system flight package
[NASA-CR-180828] 02 p0141 N88-10886
The 1986 Goddard Space Flight Center Battery Workshop
[NASA-CP-2486] 02 p0163 N88-11021
BRASILSAT A2: Ground and in-orbit anomalies
02 p0164 N88-11032
Handling qualities criterion for very low visibility rotorcraft 03 p0263 N88-11654
The Avionics Flight Evaluation System (AFES) of the DFVLR
[ESA-TT-1037] 03 p0266 N88-11677
Comparison of flight-measured and calculated temperatures on the space shuttle orbiter
[NASA-TM-88278] 03 p0321 N88-12029
Developmental airdrop testing techniques and devices
[AGARD-AG-300-VOL-6] 04 p0398 N88-12481
Human respiratory responses during high performance flight
[AGARD-AG-312] 04 p0474 N88-12923
Full-envelope aerodynamic modeling of the Harrier aircraft
[NASA-TM-88376] 05 p0552 N88-13363
Visible boundary layer transition points through flight tests 06 p0675 N88-14136
An investigation of the effects of the propeller slipstream on a wing boundary layer 06 p0700 N88-14293
Flight and wind-tunnel measurements showing base drag reduction provided by a trailing disk for high Reynolds number turbulent flow for subsonic and transonic Mach numbers
[NASA-TP-2638] 06 p0701 N88-14299
First results from the Airborne Visible/Infrared Imaging Spectrometer (AVIRIS) 06 p0707 N88-14335
Laminar flow integration: Flight tests status and plans
07 p0813 N88-14952
Digital processing of flight test data without using anti-aliasing filters, using a helicopter as an example
[DFVLR-MITT-87-12] 07 p0819 N88-14981
Overview of NASA PTA propfan flight test program
08 p0957 N88-15805
Analysis of shock and vibration environments for cargo on C9B transport aircraft 08 p0999 N88-16051
Comprehensive inflight vibration and acoustic testing
08 p0999 N88-16052
NASA/Army Rotorcraft Technology. Volume 3: Systems Integration, Research Aircraft, and Industry
[NASA-CP-2495-VOL-3] 09 p1110 N88-16650
Rotorcraft flight research with emphasis on rotor systems 09 p1111 N88-16656
McDonnell Douglas Helicopter Company independent research and development: Preparing for the future
09 p1111 N88-16660
A flight-test methodology for identification of an aerodynamic model for a V/STOL aircraft
[NASA-TM-100067] 09 p1117 N88-16694
Aircraft flight test trajectory control
[NASA-CR-179426] 09 p1120 N88-16707
ASSESS-2: An aircraft simulation of Spacelab
09 p1123 N88-16723
Flight test technique, illustrated by Advanced Technologies Testing Aircraft System (ATTAS)
09 p1240 N88-17433
Recommendations for ground effects research for V/STOL and STOL aircraft and associated equipment for large scale testing
[NASA-CR-177429] 10 p1268 N88-17585
A potential flight evaluation of an upper-surface-blowing/circulation-control-wing concept
10 p1272 N88-17609
X-29A forward-swept-wing flight research program status
[NASA-TM-100413] 10 p1277 N88-17644
Flight testing of fighter aircraft
[MBB/LKE-62/S/PUB/292] 10 p1312 N88-17844
Effect of transition aerodynamics on aeroassist flight experiment trajectories
[NASA-TM-100546] 11 p1446 N88-18620
Influence of base modifications on in-flight base drag in the presence of jet exhaust for Mach numbers from 0.7 to 1.5
[NASA-TP-2802] 11 p1488 N88-18881
Analysis of in-flight acoustic data for a twin-engined turboprop airplane
[NASA-CR-178389] 11 p1543 N88-19220
Calculated unsteady aerodynamics of wings
[AD-A189608] 12 p1574 N88-19415
A perspective on 15 years of proof-of-concept aircraft development and flight research at Ames-Moffett by the Rotorcraft and Powered-Lift Flight Projects Division, 1970-1985
[NASA-RP-1187] 12 p1582 N88-19467
Minimizing development flight test time and cost in the US Air Force 12 p1703 N88-20192
Improved flight test productivity using advanced on line data systems 12 p1703 N88-20193
A review of technologies applicable to low-speed flight of high-performance aircraft investigated in the Langley 14- x 22-foot subsonic tunnel
[NASA-TP-2796] 13 p1717 N88-20264
Flight tests of external modifications used to reduce blunt base drag
[NASA-TM-100433] 13 p1719 N88-20279
A correlation study of X-29A aircraft and associated analytical development
[NASA-CR-183103] 13 p1722 N88-20296
Aircraft flight flutter testing at the NASA Ames-Dryden Flight Research Facility
[NASA-TM-100417] 13 p1723 N88-20301
The design and use of a temperature-compensated hot-film anemometer system for boundary-layer flow transition detection on supersonic aircraft
[NASA-TM-100421] 13 p1723 N88-20304
Lateral and longitudinal stability and control parameters for the space shuttle discovery as determined from flight test data
[NASA-TM-100555] 13 p1724 N88-20309
Western aeronautical test range real-time graphics software package MAGIC
[NASA-TM-100425] 13 p1757 N88-20506
Preliminary in-flight boundary layer transition measurements on a 45 deg swept wing at Mach Numbers between 0.9 and 1.8
[NASA-TM-100412] 13 p1772 N88-20598
Atmospheric electrical modeling in support of the NASA F-106 storm hazards project
[NASA-CR-181639] 13 p1799 N88-20758
Configuration management issues and objectives for a real-time research flight test support facility
[NASA-TM-100437] 13 p1813 N88-20832
The use of an automated flight test management system in the development of a rapid-prototyping flight research facility
[NASA-TM-100435] 13 p1823 N88-20896
Predictive monitoring research: Summary of the PREMON system
[NASA-CR-182667] 13 p1824 N88-20905
An experimental and theoretical study of the ice accretion process during artificial and natural icing conditions
[NASA-CR-182119] 14 p1865 N88-21143
Development and flight test of an experimental maneuver autopilot for a highly maneuverable aircraft
[NASA-TP-2618] 14 p1867 N88-21153
A flight test investigation into flow separation and structural response for a transport aircraft at buffet onset
[RAE-TR-87006] 14 p1867 N88-21156
Development of an integrated set of research facilities for the support of research flight test
[NASA-TM-100427] 14 p1869 N88-21169
The NASA integrated test facility and its impact on flight research
[NASA-TM-100418] 14 p1870 N88-21177
Psychophysical load of glider pilots on long-duration flights
[DFVLR-FB-87-38] 14 p1953 N88-21642
The PC/AT compatible computer as a mission control center display processor at Ames-Dryden Flight Research Facility
[NASA-TM-100426] 14 p1955 N88-21654
Bifurcations in unsteady aerodynamics-implications for testing
[NASA-TM-100083] 15 p2015 N88-22014
Real-time flight test data distribution and display
[NASA-TM-100424] 15 p2022 N88-22050
The growth potential of corona discharges from aircraft flying in precipitation
[AD-A190507] 15 p2094 N88-22478
Oil flow patterns on a series of capsule-type re-entry vehicles at hypersonic speeds
[DE88-751805] 16 p2155 N88-22858
Development of a mobile research flight test support capability
[NASA-TM-100428] 16 p2159 N88-22883
Digital processing of flight data of a helicopter without using anti-aliasing filters
[ESA-TT-1094] 16 p2161 N88-22890
Airworthiness and flight characteristics test of a ski assembly for the UH-60A Black Hawk helicopter
[AD-A191414] 16 p2162 N88-22895
Experimental investigation of Hover flowfields in water at the McDonnell Douglas Research Laboratories
16 p2202 N88-23135
Boundary layer flow visualization for flight testing
17 p2297 N88-23742
Flight experiences with laminar flow
17 p2297 N88-23744
Operational considerations for laminar flow aircraft
17 p2298 N88-23748
Flight testing a V/STOL aircraft to identify a full-envelope aerodynamic model
[NASA-TM-100996] 17 p2301 N88-23762
The integration, characterisation and trialling of a modern complex airborne radar 17 p2305 N88-23791
Rotorcraft TCAS (traffic alert and collision avoidance system) evaluation: Group 3 results
[AD-A191719] 18 p2461 N88-24614
Western Pacific Omega validation: Project description
[AD-A191753] 18 p2462 N88-24617
Method for prediction and determination of takeoff performance for vectored thrust vehicles
[AD-A191809] 18 p2463 N88-24626
Current flight test experience related to structural divergence of forward-swept wings
[NASA-TM-100445] 18 p2464 N88-24633
Analysis procedures and subjective flight results of a simulator validation and cue fidelity experiment
[NASA-TM-88270] 18 p2465 N88-24634
Flight research and testing
[NASA-TM-100439] 20 p2758 N88-26361
Flight test preparation and measuring data validation for parameter identification 20 p2786 N88-26529
Utilization of identification methods in the time and frequency domain for the determination of the XV-15 (tilt-rotor) dynamics for lateral motion in hover flight
20 p2787 N88-26532
Application of complementary parameter identification techniques to flight test data of a transport aircraft
20 p2787 N88-26533
A comparison of theory and flight test of the BO 105/BMR in hover and forward flight
21 p2890 N88-27155
Pilot report: AFTI (Advanced Fighter Technology Integration) F-111
[AD-A192937] 21 p2895 N88-27184
Air-to-air radar flight testing
[AGARD-AG-300-VOL-7] 21 p2932 N88-27406
Flight testing under extreme environmental conditions
[AGARD-AG-300-VOL-8] 21 p2951 N88-27525
Hypersonic flight testing
[DE88-001655] 21 p3015 N88-27894

Improvement of head-up display standards. Volume 4: Head-up display dynamics flight tests
[AD-A193617] 22 p3042 N88-28060
Proof-of-principle high speed electronic imaging system, phase 2
[AD-A193798] 23 p3181 N88-28937
Two biased estimation techniques in linear regression: Application to aircraft
[NASA-TM-100649] 23 p3274 N88-29489
Flight test equipment for the on-board measurement of wind turbulence 24 p3311 N88-29719
Angle of attack and sideslip estimation using an inertial reference platform
[AD-A194876] 24 p3319 N88-29769
Preliminary airworthiness evaluation of the UH-60A/ESSS (External Stores Support System) with HELLFIRE launcher installed
[AD-A196187] 24 p3323 N88-29793
A multiprocessor avionics system for an unmanned research vehicle
[AD-A194806] 24 p3325 N88-29800
An analysis of lateral-directional handling qualities and Eigenstructure of high performance aircraft
[AD-A194874] 24 p3328 N88-29814
Space structure (dynamics and control) theme development
[NASA-TM-100597] 24 p3335 N88-29850
Techniques used in the F-14 variable-sweep transition flight experiment
[NASA-TM-100444] 24 p3374 N88-30093

FLIGHT TIME
General aviation activity and avionics survey: 1986 data
[AD-A189986] 15 p2013 N88-22003

FLIGHT TRAINING
NT SPACE FLIGHT TRAINING
An aerodynamic performance evaluation of the NASA/Ames Research Center advanced concepts flight simulator
[NASA-TM-89659] 03 p0268 N88-11685
The role of adaptive supplemental visual cuing in flight simulation
[AD-A185932] 07 p0822 N88-14992
Field dependence-independence and its relationship to flight training performance
[AD-A188888] 12 p1670 N88-20003
An enumeration of research to determine the optimal design and use of Army flight training simulators
[AD-A191242] 18 p2468 N88-24649
Flight simulator: Field of view utilized in performing tactical maneuvers
[AD-A192412] 20 p2762 N88-26379
Proposal for a new aggressor aircraft
[AD-A194311] 22 p3041 N88-28056
Future air-to-air training for the RF-4
[AD-A194363] 23 p3240 N88-29284
Proposed improvements to the USAF flight screening program
[AD-A194506] 23 p3240 N88-29285
Integration of LANTIRN (Low Altitude Navigation and Targeting Infrared for Night) into operational fighter training
[AD-A194906] 24 p3325 N88-29799

FLIGHT VEHICLES
Flight vehicle system identification: Status and prospects 20 p2785 N88-26520

FLIR DETECTORS
Wind shear detection. Forward-looking sensor technology
[NASA-CP-10004] 07 p0817 N88-14970
Passive autonomous infrared sensor technology
[AD-A188698] 13 p1839 N88-21005
A multiple model adaptive tracking algorithm against airborne targets
[AD-A190619] 15 p2057 N88-22263
IR (infrared) sky radiance distributions in the marine boundary layer
[AD-A193683] 22 p3119 N88-28531

FLOAT ZONES
Liquid encapsulated float zone process and apparatus
[NASA-CASE-MFS-28144-1] 17 p2446 N88-24545
Marangoni convection in finite cylindrical liquid bridges
[LRT-WE-9-FB-5(1988)] 22 p3078 N88-28277

FLOATING
Flotation processes
[PB88-180302] 18 p2540 N88-25075

FLOATING POINT ARITHMETIC
The warp computer: Architecture, implementation, and performance
[AD-A184329] 03 p0363 N88-12286
Implementation and performance of a complex vision system on a systolic array machine
[AD-A184331] 04 p0482 N88-12971
A comparison of the Cray-2 performance before and after the installation of memory pseudo-banking
[NASA-CR-177462] 09 p1215 N88-17287
The Livermore FORTRAN Kernels: A computer test of the numerical performance range --- benchmark tests
[UCRL-53745] 11 p1531 N88-19144
Scientific computing environments
[AD-A191239] 17 p2385 N88-24175
MIPS: The good, the bad and the useful
[NASA-CR-182893] 17 p2386 N88-24184

FLOATS
Moored current meter data from the Canary Basin near 32 deg N, 24 W (84-1986), volume 40
[PB88-108105] 07 p0882 N88-15351

FLOOD CONTROL
Flood monitoring using SPOT
03 p0342 N88-12162
Review of the potential of satellite remote sensing for marine flood protection
[IOS-237] 07 p0870 N88-15280

FLOOD PLAINS
Flood monitoring using SPOT
03 p0342 N88-12162
A comparative thematic mapping analysis of SPOT data: The Vientiane Plain (Laos) 03 p0343 N88-12168
Geomorphologic sector maps of Niquizanga-Mayares, province of San Juan, Argentina
17 p2368 N88-24098
Oxidation and reduction rates for organic carbon in the Amazon mainstream tributary and floodplain, inferred from distributions of dissolved gases
[NASA-CR-182943] 18 p2538 N88-25062
IEMIS (Integrated Emergency Management Information System) floodplain mapping based on a LIDAR derived data set
[AD-A193071] 21 p2966 N88-27616
A comparative thematic mapping analysis of SPOT data: The Vientiane Plain (Lao PDR)
22 p3096 N88-28386

FLOOD PREDICTIONS
Flood monitoring using SPOT
03 p0342 N88-12162
NWS (National Weather Service) watch/warning verification flash flood, winter storm and high wind, January 1980 - June 1986
[PB87-223053] 04 p0469 N88-12898
Review of the potential of satellite remote sensing for marine flood protection
[IOS-237] 07 p0870 N88-15280
Large quantile estimation under extreme-value conditions
[CWI-MS-R8711] 14 p1966 N88-21730

FLOODS
Flood monitoring using SPOT
03 p0342 N88-12162
Hurricane Elena storm surge data
[AD-A184573] 03 p0353 N88-12228
Evaluation of the flooding areas of the Sao Goncalo Canal through LANDSAT 5 thematic mapper images
[INPE-4118-PRE/1039] 08 p1020 N88-16185
Project CODEAMA/FUNCATE (test-area of Barreirinha-AM): Field report
[INPE-4500-RPE/563] 15 p2090 N88-22455
Taiwan area mesoscale experiment: Daily operations summary
[PB88-169081] 16 p2235 N88-23348
Evaluation of the floodable area of the canal of Sao Goncalo through TM-LANDSAT 5 imagery
17 p2364 N88-24078
Evaluation of a flood period (June, 1984) in the southern region of Laguna dos Patos, through remote sensing data, meteorological and oceanographic
17 p2365 N88-24083
Mapping of plant associations and the variation of surface water in the Pantanal Mato-Grossense National Park, through remote sensing techniques
17 p2366 N88-24092
The impact of disorganized occupation of urban sub-basins: Sub-basin of the Cabucu River, metropolitan area of Sao Paulo (SP) 19 p2682 N88-25945
IEMIS (Integrated Emergency Management Information System) floodplain mapping based on a LIDAR derived data set
[AD-A193071] 21 p2966 N88-27616
LANDSAT-TM data to map flooded areas
[INPE-4594-PRE/1324] 24 p3387 N88-30177
Constraints on continental accretion from sedimentation 24 p3392 N88-30202

FLORA
U PLANTS (BOTANY)

FLORIDA
Nearshore wave transformation study of sites near Port Canaveral Inlet, Florida
[AD-A188965] 09 p1195 N88-17159
Design of the primary pre-TRMM and TRMM ground truth site
[NASA-CR-182609] 12 p1647 N88-19865
Pre-convective environmental conditions indicative of non-tornadic severe thunderstorm winds over Southeast Florida
[AD-A188679] 12 p1648 N88-19870
Distribution of summertime lightning as a function of low-level wind flow in central Florida
[PB88-160759] 14 p1948 N88-21619
Current velocity and hydrographic observations in the Straits of Florida, the Caribbean Sea and offshore of the Antillean Archipelago: Subtropical Atlantic Climate Studies (STACS) 1986
[PB88-160767] 14 p1951 N88-21628
Critical nuclear launch issues: A perspective from the State of Florida 17 p2423 N88-24412

FLOTATION
The theory of flotation
[NASA-TT-20278] 16 p2207 N88-23172
Flotation processes
[PB88-180302] 18 p2540 N88-25075

FLOTATION SYSTEMS
U FLOATS

FLOW CHAMBERS
Moving wall, continuous flow electronphoresis apparatus
[NASA-CASE-MFS-28142-1] 17 p2318 N88-23845

FLOW CHARACTERISTICS
NT BOUNDARY LAYER STABILITY
NT FLAME STABILITY
NT FLOW DISTRIBUTION
NT FLOW STABILITY
NT FLOW VELOCITY
NT MAGNETOHYDRODYNAMIC STABILITY
Direct Absorption Receiver flow experiments
[DE87-014655] 02 p0196 N88-11221
Experimental investigation of the subsonic high-altitude operation of the NASA Lewis 10- by 10-foot supersonic wind tunnel
[NASA-TM-100214] 08 p0959 N88-15814
The bimodality of large scale averaged flow parameters --- statistical weather forecasting
08 p1016 N88-16159
Numerical simulation of diffuser/combustor dome interaction 10 p1281 N88-17663
Problems in fluid dynamics
[NASA-CR-182678] 14 p1909 N88-21410
Flow quality of NAL two-dimensional transonic wind tunnel. Part 1: Mach number distributions, flow angularities and preliminary study of side wall boundary layer suction
[NASA-TT-20209] 16 p2165 N88-22911
Forced response unsteady aerodynamics in a multistage compressor 18 p2512 N88-24903
A numerical analysis of flow characteristics in laser propulsion system 19 p2637 N88-25645
Flow characteristics of a model annular combustor
24 p3347 N88-29924

FLOW CHARTS
The circular serial autocorrelation computer program
[AD-A184795] 03 p0365 N88-12295
Formalizing reusable software components in the programmer's apprentice
[AD-A185843] 07 p0901 N88-15457

FLOW COEFFICIENTS
NT DISCHARGE COEFFICIENT
Measurement of rate constants of elementary gas reactions of importance to upper atmosphere and combustion systems
[AD-A189432] 13 p1737 N88-20386

FLOW DEFLECTION
Transverse flow deflections associated with fast coronal mass ejecta in interplanetary space
[DE88-003180] 09 p1263 N88-17566
Computation of flow around NACA0012 airfoil at high angle of attack 19 p2636 N88-25640

FLOW DISTORTION
Moving wall, continuous flow electronphoresis apparatus
[NASA-CASE-MFS-28142-1] 17 p2318 N88-23845
Cross flow induced vibrations in tube bundle by displaced and misaligned tube configurations
[ETN-88-92132] 20 p2801 N88-26621
Numerical simulation of fuel droplet interactions and breakup
[AD-A192431] 21 p2941 N88-27470

FLOW DISTRIBUTION
Rayleigh-Benard convection in a Hele-Shaw cell: A numerical study
[KFK-4212] 01 p0044 N88-10280
Numerical computation of transonic potential flow about 3-dimensional inlets
[NAL-TR-924] 02 p0122 N88-10770
Wall interference tests of a CAST 10-2/DOA 2 airfoil in an adaptive-wall test section
[NASA-TM-4015] 02 p0122 N88-10772
The phenomenology of Karman vortex streets via sound in oscillatory flow
[MPIS-MITT-84-1987] 02 p0122 N88-10775

Navier-Stokes cascade analysis with a stiff Kappa-Epsilon turbulence solver
[NASA-TM-100218] 02 p0123 N88-10778
A natural low frequency oscillation in the wake of an airfoil near stalling conditions
[NASA-TM-100213] 02 p0123 N88-10779
FDM-FEM zonal method for viscous flow computations over multiple-bodies
[NAL-TR-925T] 02 p0170 N88-11069
Computer modeling of two-phase flow
[CFDU/87/5] 02 p0171 N88-11078
Large scale structures in turbulent pipe flow
[MPIS-MITT-83-1987] 02 p0172 N88-11085
The four spot time-of-flight laser anemometer
02 p0184 N88-11145
Fuel-injector/air-swirl characterization
02 p0185 N88-11150
Combustor-diffuser interaction program
02 p0185 N88-11152
Heat transfer in a real engine environment
02 p0186 N88-11155
Flow field measurements in a 90 degree turning duct
02 p0186 N88-11157
Heat transfer with very high free stream turbulence
02 p0186 N88-11161
Flow in a model turbine stator
02 p0187 N88-11163
A preliminary demonstration of the use of boundary-layer models of flow in complex terrain for high resolution surface wind forecasting 02 p0212 N88-11330
The spatially nonuniform convergence of the numerical solution of flows
[NASA-TM-100037] 02 p0226 N88-11429
Active region flows 02 p0255 N88-11611
The physics and mathematical description of the Achilles heel of stationary wind turbine aerodynamics: The tip flow
[R-812-D] 03 p0260 N88-11635
Efficient numerical approaches for predicting supersonic flows with viscous/inviscid interaction
03 p0260 N88-11637
Theoretical and experimental study of flow-control devices for inlets of indraft wind tunnels
03 p0268 N88-11684
Wake shield 03 p0298 N88-11871
Homogeneous turbulence two-point closures and applications to one-point closures
03 p0312 N88-11973
Calculation of the three dimensional flow in the impeller of hydraulic turbomachines using a finite element method
[ETN-87-90612] 03 p0315 N88-11986
Measurement of gas flow velocities near obstacles: Analysis and optimization of an optical barrier velocimeter. Associated signal processing
[ESA-TT-1056] 03 p0315 N88-11991
Laser Doppler measurements in a turbulent free jet
[ESA-TT-1067] 03 p0315 N88-11994
Mechanical and flow excited vibrations of elastic plates and cylindrical shells in dense fluids
03 p0316 N88-11996
Application of an upwind algorithm to the parabolized Navier-Stokes equations 03 p0316 N88-12000
An experimental investigation of quasi-conical shock wave/turbulent boundary layer interactions
03 p0317 N88-12004
Thrust and specific impulse of repetitively-pulsed-laser propulsion rocket 03 p0318 N88-12012
Numerical simulation and visualization of a flowfield by interaction of two parallel two-dimensional freejets
03 p0320 N88-12021
Visualization of the flow field around a generic destroyer model in a simulated turbulent atmospheric boundary layer
[AD-A184658] 03 p0320 N88-12023
Calibration of a five hole probe and testing of an evaluation method for flow field measurements
[ESA-TT-1051] 03 p0325 N88-12051
Properties of the atmospheric boundary layer above a subtropical oceanic front
[AD-A184006] 03 p0351 N88-12215
The development of low level coastal flow fields when solar radiation is blocked by smoke
[DE87-014348] 03 p0354 N88-12230
Application of the finite difference method to the solution of mixed partial differential equations for the case of transonic flow
[ETN-87-90760] 03 p0370 N88-12327
An experimental investigation of noise generation and noise reduction in a pipe flow downstream of a discontinuous area enlargement
[ESA-TT-1027] 03 p0374 N88-12351
Development and application of computational aerothermodynamics flowfield computer codes
[NASA-CR-181534] 04 p0395 N88-12465
Three-dimensional unsteady flow elicited by finite wings and complex configurations 04 p0395 N88-12468
A study of two-phase flow in a reduced gravity environment
[NASA-CR-172035] 04 p0422 N88-12617
Ideal-viscoplastic extrusion model with application to deforming pistons in light-gas guns
[UTIAS-TN-266] 04 p0429 N88-12657
Equilibria, lattices and chaotic dynamics of point vortices 04 p0444 N88-12758
Optimization of explicit time-stepping algorithms and Stream-Function-Coordinate (SFC) concept for fluid dynamics problems 04 p0445 N88-12762
Experimental investigations on blunt bodies and corner configurations in hypersonic flow
05 p0530 N88-13225
Driving mechanism of unsteady separation shock motion in hypersonic interactive flow 05 p0530 N88-13226
Numerical simulation of the hypersonic flow around lifting vehicles 05 p0532 N88-13234
Solution of some 3-D viscous and inviscid supersonic flow problems by finite-volume space-marching schemes
05 p0532 N88-13235
Numerical experiments with hypersonic flows beneath a cone-delta-wing combination 05 p0532 N88-13238
A 3-D Euler solution for hypersonic Mach numbers
05 p0533 N88-13240
Computation of flow past conical hypersonic wings using a second order Godunov method
05 p0533 N88-13241
Aerothermodynamics research at NASA Ames
05 p0533 N88-13242
Vortex formation over delta, double-delta and wave rider configurations at supersonic speeds
05 p0533 N88-13243
Numerical optimization of conical flow waveriders including detailed viscous effects
05 p0533 N88-13245
An analysis of the compressible-viscous flow field around a 3D-oscillating wing 05 p0535 N88-13254
Computation of dynamic stall of NACA0012 airfoil by block pentadiagonal matrix scheme
05 p0535 N88-13255
Numerical calculations of the flowfield around propellers 05 p0536 N88-13261
Navier-Stokes simulation of transonic transportation aircraft configurations. 1: Flow-field simulation over wing-fuselage combinations 05 p0540 N88-13288
Computation of transonic flows with nacelle simulation
[SNIAS-872-111-117] 05 p0542 N88-13300
Compressible Euler solution on a multiblock grid around a wing-fuselage configuration
[FFA-TN-1987-46] 05 p0542 N88-13303
Vortex interaction with a leading-edge of finite thickness
[NASA-CR-182341] 05 p0543 N88-13307
Unsteady aerodynamics of an oscillating cascade in a compressible flow field
[NASA-TM-100219] 05 p0549 N88-13346
A numerical study of the effects of curvature and convergence on dilution jet mixing
[NASA-TM-89878] 05 p0549 N88-13347
The simulation of the viscous flow around a cylinder by the random vortex method 05 p0579 N88-13534
An experimental investigation of appendage-flat plate junction flow. Volume 2. Elliptical nose appendage data base
[AD-A184974] 05 p0580 N88-13539
Conditional second order closure for turbulent shear flows
[AD-A185369] 05 p0581 N88-13542
Low thrust viscous nozzle flow fields prediction
[NASA-CR-182334] 05 p0582 N88-13551
Transonic Navier-Stokes computations of strake-generated vortex interactions for a fighter-like configuration 06 p0664 N88-14073
Numerical study of chemically reacting flows using an LU scheme
[NASA-CR-180882] 06 p0668 N88-14094
Numerical simulation of flight body circumference flow
06 p0676 N88-14137
Research on internal fluid mechanism between turbine blades 06 p0676 N88-14138
Computation of turbulent flow of air through smooth and rough pipes using a two-equation turbulence model
06 p0700 N88-14298
A zonal approach for the solution of coupled Euler and potential solutions of flows with complex geometries
[AD-A185465] 06 p0702 N88-14310
Computational methods for complex flowfields
[AD-A185793] 06 p0703 N88-14317
Gasdynamic effects in linear MHD generators
[ETN-88-91372] 06 p0784 N88-14810
A theory for the core flow of leading-edge vortices
07 p0810 N88-14935
Wind tunnel wall interference
07 p0811 N88-14938
Preliminary calibration and test results from the National Transonic Facility 07 p0811 N88-14941
Separated flow 07 p0812 N88-14944
Computational design of natural laminar flow wings for transonic transport application 07 p0813 N88-14948
Turbulence in hypersonic flow
[AD-A185624] 07 p0815 N88-14961
Mathematical models of continuous flow electrophoresis: Electrophoresis technology
[NASA-CR-179241] 07 p0828 N88-15021
On the pairing process in an excited, plane, turbulent mixing layer
[AD-A186355] 07 p0850 N88-15157
Flow in volutes and the influence on the flow in centrifugal compressors 07 p0851 N88-15169
An investigation into flow regimes for two-phase helium flow
[DE88-002834] 07 p0853 N88-15181
Blood redistribution in man with lower body negative pressure 07* p0891 N88-15397
Laser thermal propulsion
[AD-A186407] 07 p0933 N88-15666
An experimental mapping of the flow field behind a glaze ice shape on a NACA 0012 airfoil
[NASA-CR-180847] 08 p0950 N88-15766
Theoretical and experimental studies of the transonic flow field and associated boundary conditions near a longitudinally-slotted wind-tunnel wall
[NASA-CR-181169] 08 p0959 N88-15815
Mean velocities and Reynolds stresses in the juncture flow and in the shear layer downstream of an appendage
[AD-A185819] 08 p0980 N88-15923
Numerical simulation of turbulent spots in channel and boundary layer flows 08 p0983 N88-15948
Active control of jet flowfields
[AD-A186736] 08 p0989 N88-15989
Experimental investigation of shock-induced disturbances on transonic airfoils
[DFVLR-FB-87-28] 09 p1112 N88-16666
Full scale and wind tunnel surface pressure measurements on the T.R.R.L. spray dispersion programme vehicles
[REPT-8623] 09 p1114 N88-16676
CFD validation experiments for internal flows
[NASA-TM-100797] 09 p1114 N88-16679
Flow field measurements using hotwire anemometry
[AD-A187029] 09 p1160 N88-16951
Investigation of large-scale structures in the near wake of a parallel flat plate
[DFVLR-FB-87-31] 09 p1162 N88-16967
Two-phase flow forms and pressure drop in horizontal T tube joints with vertical branch
[GKSS-87/E/12] 09 p1163 N88-16969
Techniques of flow visualization
[AGARD-AG-302] 09 p1164 N88-16977
Investigations of a circulation control airfoil flowfield using an advanced laser velocimeter
10 p1269 N88-17589
Evaluation of a research circulation control airfoil using Navier-Stokes methods 10 p1269 N88-17591
On the effect of leading edge blowing on circulation control airfoil aerodynamics 10 p1270 N88-17595
Pressure distributions and oil-flow patterns for a swept circulation-control wing 10 p1270 N88-17596
The impact of circulation control on rotary aircraft controls systems 10 p1271 N88-17601
Investigation of dynamic stall using LDV (Laser Doppler Velocimetry): Mean flow studies
[AD-A187629] 10 p1272 N88-17611
Numerical methods for propeller aerodynamics and acoustics at DFVLR 10 p1282 N88-17668
Investigation of dihedral effects in compressor cascades 10 p1282 N88-17672
Parametric study of choke flutter with a linear theory
10 p1283 N88-17673
Secondary flow measurements with L2F-technique in centrifugal compressors 10 p1283 N88-17676
Zonal solutions for viscous flow problems. Finite approximations in fluid mechanics
[MBB/LKE-122/S/PUB/226] 10 p1313 N88-17846
Mechanistic model for void distribution in flashing flow
[DE88-002948] 10 p1326 N88-17928
A computational study of thrust augmenting ejectors based on a viscous-inviscid approach
10 p1326 N88-17929
Investigation of non-symmetric jets in cross flow
10 p1327 N88-17932
The numerical and analytical study of bifurcation and multicellular flow instability due to natural convection between narrow horizontal isothermal cylindrical annuli at high Rayleigh numbers 10 p1328 N88-17937

Three-dimensional incompressible flowfield analysis for establishing rotor designs which optimize power extraction 10 p1329 N88-17943
Experimental research on swept shock wave/boundary layer interactions
[AD-A187250] 10 p1331 N88-17957
Flow patterns induced by vortices
[NAL-TR-932] 10 p1332 N88-17963
Relaxing the brightness constancy assumption in computing optical flow
[AD-A187437] 10 p1410 N88-18410
Liquid sprays and flow studies in the direct-injection diesel engine under motored conditions
[NASA-TM-100135] 11 p1440 N88-18594
High performance Solid Rocket Motor (SRM) submerged nozzle/combustion cavity flowfield assessment
[NASA-CR-179307] 11 p1446 N88-18622
A code development system for computational fluid dynamics
[AD-A186050] 11 p1482 N88-18848
Three-dimensional flow fields past reentry vehicles 11 p1484 N88-18858
Mixed turbulent convective heat transfer in vertical ducts 11 p1485 N88-18865
Two and three dimensional elliptic flows 11 p1485 N88-18866
A discretization of the integral equation for the time dependent linearized subsonic potential flow over a wing
[AD-A188534] 12 p1574 N88-19411
Three-dimensional incompressible Navier-Stokes computations of internal flows
[NASA-TM-100076] 12 p1576 N88-19425
A new parabolized Navier-Stokes code for chemically reacting flow fields 12 p1625 N88-19721
Calculation of flow about posts and powerhead model
[NASA-CR-179305] 12 p1625 N88-19722
Accelerating the computation of steady state solutions for non-equilibrium, chemically reacting flow fields 12 p1625 N88-19724
On the Kutta condition for flows around lifting airfoils and wings
[DFVLR-FB-87-40] 13 p1717 N88-20268
Air-jet spoiler
[BU-364] 13 p1722 N88-20299
Numerical model of the time independent mean flow in a rotating rocket motor 13 p1733 N88-20360
Coherent structure-reflective turbulent viscous flow modeling
[AD-A188339] 13 p1765 N88-20556
Graphics and flow visualization of computer generated flow fields
[NASA-CR-182679] 13 p1767 N88-20573
Reduction of erosion in elbows due to flow modifications, phase 1
[DE88-001028] 13 p1769 N88-20584
Measurement and analysis of the noise radiated by low Mach numbers centrifugal blowers
[AD-A189226] 13 p1833 N88-20966
Data processing method for high angle of attack testing with rolling angle 14 p1864 N88-21134
Research on flow around bluff bodies, flow induced vibrations 14 p1864 N88-21135
The 30 x 30 inch wind tunnel
[IC-AERO-87-01] 14 p1869 N88-21168
Experimental and numerical study of liquid distribution in dispersive-annular flow
[DE88-700844] 14 p1909 N88-21406
Solutions for direct and indirect problems in free surface flows
[REPT-87-35] 14 p1909 N88-21409
Mean flow structure in the near wake of a turbulent junction vortex
[PB88-150115] 14 p1910 N88-21416
High Reynolds number, low Mach number, steady flow field calculations over a NACA 0012 airfoil using Navier-Stokes and interactive boundary layer theory
[AD-A189871] 15 p2013 N88-22005
Transonic Navier-Stokes computations of strake-generated vortex interactions for a fighter-like configuration
[NASA-TM-100009] 15 p2014 N88-22010
Contraction design for small low-speed wind tunnels
[NASA-CR-182747] 15 p2021 N88-22045
Turbulent reacting flows and supersonic combustion
[AD-A189690] 15 p2034 N88-22115
An investigation of flow structure, mixing and chemical reaction in combusting turbulent flows
[AD-A189980] 15 p2034 N88-22117
Unsteady flow field measurements using LDV (Laser Doppler Velocimetry)
[AD-A189807] 15 p2063 N88-22298
On the prediction of highly vortical flows using an Euler equation model, part 2
[AD-A190245] 15 p2064 N88-22305
Interaction of a two-dimensional bluff body and incompressible jet and annulus flows
[AD-A190503] 15 p2064 N88-22310
Cavitation inception in rectangular two-dimensional slots
[AD-A190677] 15 p2066 N88-22318
Changes in the California current system observed off northern California during July-August 1986
[AD-A190027] 15 p2100 N88-22510
MPD (magnetoplasmadynamic) thrust chamber flow dynamics
[AD-A189940] 15 p2137 N88-22751
Oil flow patterns on a series of capsule-type re-entry vehicles at hypersonic speeds
[DE88-751805] 16 p2155 N88-22858
Experimental investigation of the transonic flow at the leeward side of a delta wing at high incidence
[LR-518] 16 p2156 N88-22861
Propulsion and airframe aerodynamic interactions of supersonic V/STOL configurations. Volume 1: Wind tunnel test pressure data report
[NASA-CR-177343-VOL-1] 16 p2157 N88-22866
Propulsion and airframe aerodynamic interactions of supersonic V/STOL configurations. Volume 2: Wind tunnel test force and moment data report
[NASA-CR-177343-VOL-2] 16 p2157 N88-22867
Propulsion and airframe aerodynamic interactions of supersonic V/STOL configurations. Volume 4: Summary
[NASA-CR-177343-VOL-4] 16 p2157 N88-22868
Experimental investigation of the hypersonic flow over a six finned configuration
[AD-A190870] 16 p2157 N88-22871
Computer tomography and hybrid optical/digital methods for aerodynamic measurements
[AD-A190909] 16 p2157 N88-22872
Efficient, high resolution computations of projectile and missile flow fields
[AD-A191086] 16 p2158 N88-22873
Description of an oscillating flow pressure drop test rig
[NASA-TM-100905] 16 p2170 N88-22933
Vortex breakdown and control experiments in the Ames-Dryden water tunnel 16 p2200 N88-23127
Short duration flow establishment on a profile in a Water-Ludwieg-Tunnel 16 p2201 N88-23134
Experimental investigation of Hover flowfields in water at the McDonnell Douglas Research Laboratories 16 p2202 N88-23135
Matched index laser anemometry systems for flow studies in complex geometries 16 p2203 N88-23145
A comparative study of vortex flows in wind and water tunnels 16 p2204 N88-23151
The role of vortex structure in tropical cyclone motion
[AD-A190961] 16 p2235 N88-23351
A numerical study of the hot gas environment around a STOVL aircraft in ground proximity
[NASA-TM-100895] 17 p2295 N88-23729
Unsteady flow about cambered plates
[AD-A191226] 17 p2337 N88-23945
Indentification of shallow groundwater regions in semi-arid Brazil by remote sensing methods 17 p2355 N88-24030
Theoretical and experimental investigation of swirl flow phase separators for microgravity applications 17 p2411 N88-24335
A compressible vapor flux model for transient heat pipe analysis 17 p2412 N88-24343
ATHENA simulation of the 300 kW SP-100 17 p2414 N88-24357
Theoretical prediction of single phase turbulent flow distribution in particulate bed reactors 17 p2419 N88-24386
Microgravity two-phase fluid flow pattern modeling 17 p2432 N88-24467
Experiment investigation on longitudinal characteristics of the forward swept wing
[AD-A191553] 18 p2456 N88-24582
Supplements to the study of the wake of a Mirage G8 model at F2 --- wind tunnel
[CERT-RT-OA-20/5025-AYD] 18 p2458 N88-24596
A decade of computer simulations for space shuttle aerodynamics
[NASA-TM-100990] 18 p2459 N88-24603
Solid rocket motor aft field joint flow field analysis
[NASA-CR-179288] 18 p2474 N88-24675
Research study: Space shuttle main engine plume flowfield model
[NASA-CR-179336] 18 p2474 N88-24676
Analysis of molecular mixing and chemical reaction in mixing layer
[AD-A191600] 18 p2482 N88-24721
Computation and characteristics of pulsatile multi-bifurcation flow 18 p2483 N88-24729
Joint services electronics program
[AD-A191749] 18 p2504 N88-24853
Transient particle deposition in a boundary layer of impulsive flow over a flat plate
[AD-A191537] 18 p2508 N88-24880
Theoretical investigation of 3-D shock wave-turbulent boundary layer interactions, part 6
[AD-A191546] 18 p2509 N88-24882
Axisymmetric viscid-inviscid interaction by a frozen vorticity approximation
[AD-A191743] 18 p2509 N88-24885
Fast algorithm development for large-eddy simulation of circular-jet turbulence
[AD-A192044] 18 p2509 N88-24887
Two dimensional hyperbolic grid generation
[VKI-TN-162] 18 p2511 N88-24897
Characteristics of merging shear layers and turbulent wakes of a multi-element airfoil
[NASA-TM-100053] 18 p2511 N88-24900
A single streamwise vortical structure and its instability in shear flows 18 p2515 N88-24921
Application of advanced grid generation techniques for flow field computations about complex configurations
[NASA-CR-183049] 18 p2515 N88-24922
Two-dimensional viscous flow computations of hypersonic scramjet nozzle flowfields at design and off-design conditions
[NASA-CR-182150] 19 p2603 N88-25459
The viscosity of molten TNT
[MRL-R-1100] 19 p2622 N88-25553
Numerical investigation of acoustic energy exchange through flow turning 19 p2629 N88-25593
Proceedings of the 5th NAL Symposium on Aircraft Computational Aerodynamics
[NAL-SP-8] 19 p2635 N88-25630
Navier-Stokes analysis of transonic transport aircraft empennage 19 p2636 N88-25637
Numerical calculation of three dimensional flow by TVD scheme 19 p2638 N88-25649
The modified-fluid-in-cell method to which adaptive mesh and multigrid were applied 19 p2640 N88-25664
Study of the structure of turbulence in accelerating transitional boundary layers
[AD-A191698] 19 p2663 N88-25837
Analysis and synthesis of decision-making organizations
[AD-A191948] 19 p2738 N88-26258
Decision aiding and coordination in decision-making organizations
[AD-A191950] 19 p2738 N88-26259
Heterogeneous diffusion flame stabilization
[AD-A193014] 20 p2771 N88-26429
The Proceedings of the Symposium on Mechanics for Space Flight 1987
[ISAS-SP-6] 20 p2782 N88-26499
Numerical analysis of reconnection of vortex rings 20 p2782 N88-26500
Vortex filament simulation for the crosslinking rings 20 p2782 N88-26501
Crosslinking of two vortex rings side by side 20 p2782 N88-26502
Forced-convective boiling in small diameter tube 20 p2783 N88-26510
Wind tunnel study of atmospheric diffusion in unstable stratified boundary layer. Part 2: Characteristic scale and diffusion
[DE88-753109] 20 p2823 N88-26749
Flow around a delta wing with or without a canard control surface (phi BA = 60 deg). Part 1: Hydrodynamic visualization in permanent regime
[ONERA-RT-10/2891-AN-101-A-PT-1] 21 p2892 N88-27170
Prediction of the aeroelastic behavior of tuned blades. Application to aircraft engines
[ISAL-87-0046] 21 p2897 N88-27199
Gaseous tracer techniques for pore structure characterization of granular materials
[DE88-011542] 21 p2911 N88-27274
Design of a mechanism to control wind tunnel turbulence 21 p2926 N88-27370
A Navier-Stokes study of cascade flow fields including inlet distortion and rotating stall
[AD-A193109] 21 p2943 N88-27483
Cavitation inception in a turbulent shear flow
[DE88-011486] 21 p2946 N88-27497
Turbulent flow field visualization with integral interferometric imaging and computed tomography 21 p2950 N88-27521
Study of three-dimensional transonic flow separations
[AD-A193018] 22 p3037 N88-28032
Euler equation computations for the flow over a hovering helicopter rotor
[NASA-CR-177493] 22 p3038 N88-28037
Mass transport in flow of sources
[LRT-WE-9-FB-4(1987)] 22 p3077 N88-28268
Mass transport in a parabolic conduit
[LRT-WE-9-FB-1(1988)] 22 p3077 N88-28273

Experimental tools: The tunnel and the model
23 p3168 N88-28864
Computational tools for simulation methodologies
23 p3168 N88-28865
Transport-type configurations
23 p3169 N88-28867
Combat aircraft 23 p3169 N88-28868
Missiles, fuselages and similar bodies
23 p3169 N88-28869
Introduction and critical flow phenomena
23 p3169 N88-28870
Vortex flows 23 p3170 N88-28875
Noise generation and boundary layer effects in vortex-airfoil interaction and methods of digital hologram analysis for these flow fields
[AD-A194191] 23 p3171 N88-28883
Unsteady flow past an NACA 0012 airfoil at high angles of attack
[AD-A194650] 23 p3172 N88-28886
Aerodynamics of seeing on large transport aircraft
[NASA-CR-183122] 23 p3174 N88-28896
Flow visualization by laser sheet
[AD-A194481] 23 p3211 N88-29111
Coupling between radiation and gas dynamics
[AD-A194593] 23 p3211 N88-29113
Navier-Stokes calculations of transonic flows past cavities
[NASA-CR-180484] 23 p3212 N88-29116
High effectiveness contour matching contact heat exchanger
[NASA-CASE-MSC-20840-1] 23 p3214 N88-29132
Study of experimental technique of oil flow with emphasis on quantitative determination of the flow position parameters on the surface
[NASA-TT-20341] 23 p3215 N88-29135
Application of optical correlation techniques to particle imaging velocimetry
[NASA-TM-101306] 23 p3218 N88-29152
Preliminary studies of NF3+H2 production of N2(A3 sigma(+)u) in a supersonic flow
[AD-A194479] 23 p3219 N88-29162
Three-dimensional elliptic grid generation for an F-16
23 p3246 N88-29315
Component adaptive grid generation for aircraft configurations 23 p3246 N88-29316
Generation of multiple block grids for arbitrary 3D geometries 23 p3246 N88-29317
Grid generation for an advanced fighter aircraft
23 p3246 N88-29319
Algebraic grid generation for fighter type aircraft
23 p3246 N88-29320
Analytical surfaces and grids
23 p3247 N88-29322
Grid generation around transport aircraft configurations using a multi-block structured computational domain
23 p3247 N88-29325
Lava flow-field morphology: A case study from Mount Etna, Sicily 23 p3303 N88-29676
Numerical solutions of unsteady inviscid transonic turbine cascade flows
[AD-A196111] 24 p3316 N88-29748
A streamwise upwind algorithm for the Euler and Navier-Stokes equations applied to transonic flows
[NASA-TM-101019] 24 p3316 N88-29751
Space marching Euler solvers
24 p3318 N88-29759
Prediction of base-flows 24 p3319 N88-29765
The computation of flow past an oblique wing using the thin-layer Navier-Stokes equations
[NASA-TM-88317] 24 p3320 N88-29774
Computational methods for the problems of the tip vortex
[NASA-CR-181438] 24 p3320 N88-29775
A new computational capability for ramjet projectiles
[AD-A196061] 24 p3327 N88-29812
An experimental study of an adaptive-wall wind tunnel
[NASA-CR-183152] 24 p3329 N88-29821
Alternative fuel spray behavior
24 p3345 N88-29912
Flow characteristics of a model annular combustor
24 p3347 N88-29924
Flamelet chemistry modelling of soot formation for radiation 24 p3348 N88-29928
On the application of finite-difference techniques for the computation of the flow field in gas turbine combustors with complex geometries 24 p3349 N88-29938
Analysis of the flow through double swirl airblast atomizers 24 p3351 N88-29949
Volumetric measurement of vorticity vectors by optical probe
[AD-A195997] 24 p3369 N88-30061
User's manual for three dimensional boundary layer (BL3-D) code
[NASA-CR-174899] 24 p3369 N88-30063
Assessment of a 3-D boundary layer analysis to predict heat transfer and flow field in a turbine passage
[NASA-CR-174894] 24 p3370 N88-30066
Contamination and distortion of steady flow field induced by discrete frequency disturbances in aircraft gas engines
[AD-A195440] 24 p3370 N88-30069
Numerical simulation of unsteady incompressible flow in a partially-filled rotating cylinder
[AD-A196001] 24 p3371 N88-30073
Investigation of large-scale structures in the near wake of a parallel flat plate
[ESA-TT-1100] 24 p3372 N88-30080
Experimental and numerical investigation of the effect of distributed suction on oblique shock wave/turbulent boundary layer interaction
[NASA-TM-101334] 24 p3372 N88-30084
Studies of unsteady axial-compressor functioning
24 p3380 N88-30129
Determination of multiaxial flow surfaces at elevated temperatures using the concept of dissipation potential
[ORNL/TM-10787] 24 p3383 N88-30149
Vibrational power flow analysis of rods and beams
[NASA-CR-183166] 24 p3383 N88-30151
Knowledge-based flow field zoning
[NASA-TM-101023] 24 p3412 N88-30314

FLOW EQUATIONS
NT BOUNDARY LAYER EQUATIONS
NT HELMHOLTZ VORTICITY EQUATION
NT NAVIER-STOKES EQUATION
NT REYNOLDS EQUATION
NT VON KARMAN EQUATION
NT VORTICITY EQUATIONS
An inviscid model of planar, separated flows of finite extent
[RAE-TR-86070] 01 p0044 N88-10279
Use of a thermodynamic analog for pneumatic transport in horizontal pipes
[AD-A184076] 04 p0441 N88-12740
Computation of transonic flows with nacelle simulation
[SNIAS-872-111-117] 05 p0542 N88-13300
Research on internal fluid mechanism between turbine blades 06 p0676 N88-14138
Introduction to Computational Fluid Dynamics
[VKI-LS-1987-02] 06 p0701 N88-14300
Wind tunnel wall interference
07 p0811 N88-14938
Centrifugal compressors 07 p0850 N88-15162
Flow in volutes and the influence on the flow in centrifugal compressors 07 p0851 N88-15169
Upwind formulations for the Euler equations
08 p0984 N88-15952
Integration of Navier-Stokes equations in finite volume formulation 08 p0984 N88-15954
Characteristic flux averaging approach to the solution of Euler's equations 08 p0984 N88-15955
Time accurate techniques using characteristic flux averaging with application to unsteady aerodynamics
08 p0985 N88-15957
Finite element fundamentals, part 1
08 p0985 N88-15961
Finite element fundamentals, part 2
08 p0985 N88-15962
Inviscid flows, part 2 08 p0985 N88-15966
Viscous flows, part 2 08 p0986 N88-15968
Review of the equations of fluid mechanics and heat transfer 08 p0986 N88-15970
Numerical resolution of the equations of three-dimensional stable compressible transonic flows
[PB87-168415] 09 p1113 N88-16673
Implementation of multigrid in SOLA algorithm --- fluid flow 11 p1538 N88-19191
Solution of the Euler equations: Explicit schemes acceleration by a multigrid method
11 p1538 N88-19192
Unstructured multigrid methods
11 p1538 N88-19193
On the Kutta condition for flows around lifting airfoils and wings
[DFVLR-FB-87-40] 13 p1717 N88-20268
Transonic flow field analysis for real fuselage configurations 14 p1864 N88-21133
Coherent structures --- in turbulent flows
16 p2199 N88-23121
Modeling of cavitation phenomena in homogeneous flow in transitory regimes in pipes
[ISAL-IDI1-87-15] 17 p2337 N88-23948
Analysis of molecular mixing and chemical reaction in mixing layer
[AD-A191600] 18 p2482 N88-24721
Transient particle deposition in a boundary layer of impulsive flow over a flat plate
[AD-A191537] 18 p2508 N88-24880
Numerical simulation of nonlinear structural dynamics of large scale unsteady flow
[ETN-88-92156] 18 p2513 N88-24908
Accurate solutions, parameter studies and comparisons for the Euler and potential flow equations
[NASA-TM-100664] 23 p3173 N88-28892
European research program on viscous flows
[DFVLR-AVA-IB-227-87-A-15] 23 p3214 N88-29129
Mathematical problems of nonlinear wave propagation and of waves in heterogeneous media
[AD-A195970] 24 p3368 N88-30057

FLOW FIELDS
U FLOW DISTRIBUTION

FLOW GEOMETRY
Instability of steady flow with constant vorticity in vessels with elliptical cross-section 02 p0159 N88-10997
Laser thermal propulsion
[AD-A188407] 07 p0933 N88-15666
Transonic flow field analysis for real fuselage configurations 14 p1864 N88-21133
Three dimensional spectral energy measurement on turbulence subjected to a high degree of plane deformation
[ETN-88-92537] 18 p2511 N88-24896
Active control of 2-D instability waves on an axisymmetric body
[AD-A191578] 19 p2663 N88-25835
Direct-solution techniques for viscous flows and their control
[AD-A194775] 23 p3211 N88-29114

FLOW MEASUREMENT
Experimental investigation in a wind tunnel of the stability and vorticity of the vortex breakdown phenomenon above delta wings, using the ultrasonic laser method
[DFVLR-FB-87-06] 01 p0003 N88-10017
Turbulent Bunsen burner flames
[ETN-87-90433] 01 p0021 N88-10134
Measurement techniques in low-speed turbulent flows: A report on EUROMECH 202
[NLR-MP-86038-U] 01 p0045 N88-10283
Nonintrusive ultrasonic flow measurement techniques and their applications to BTU metering
[DE87-011390] 01 p0045 N88-10286
Optical flow diagnostic measurements in turbomachinery
[PNR90396] 02 p0172 N88-11081
Comparison between numerical solutions and measurements for a high speed turbine blade
[PNR90402] 02 p0172 N88-11082
Large scale structures in turbulent pipe flow
[MPIS-MITT-83-1987] 02 p0172 N88-11085
The four spot time-of-flight laser anemometer
02 p0184 N88-11145
Observations of wind waves on a reservoir
[IOS-234] 02 p0193 N88-11206
The air flow on hills from models and experiments
[BMFT-FB-T-86-175] 02 p0198 N88-11236
A calculation method for the propulsive jet and its aerodynamic interaction with an afterbody
[ESA-TT-1039] 03 p0259 N88-11632
Investigations on a transonic airfoil with a 30 mm wide perforation/cavity arrangement
[ESA-TT-1072] 03 p0260 N88-11634
Laser Doppler measurements in a turbulent free jet
[ESA-TT-1067] 03 p0315 N88-11994
Calibration of a five hole probe and testing of an evaluation method for flow field measurements
[ESA-TT-1051] 03 p0325 N88-12051
Interferometric data for a shock-wave/boundary-layer interaction
[NASA-TM-88227] 05 p0543 N88-13306
Determination of a flow velocity field using four-exposure laser holography
[IMFL-3114-85/32] 05 p0585 N88-13565
Dual mode laser velocimeter
[NASA-CASE-ARC-11634-1] 06 p0709 N88-14350
Measurements in centrifugal compressors
07 p0850 N88-15161
An automated flow calorimeter for heat capacity and enthalpy measurements at elevated temperatures and pressures
[DE88-002357] 07 p0857 N88-15206
Moored current meter data from the Canary Basin near 32 deg N, 24 W (84-1986), volume 40
[PB88-108105] 07 p0882 N88-15351
Transonic wind tunnel calibration 1986: Force measurements on three ONERA-C5 models and three half sphere cylinder calibration bodies in the F+W transonic test section
[F+W-FO-1854] 09 p1122 N88-16714
Influence of the wall boundary layer on force measurements on half models in the transonic wind tunnel
[F+W-TF-1876] 09 p1122 N88-16715
Investigation of large-scale structures in the near wake of a parallel flat plate
[DFVLR-FB-87-31] 09 p1162 N88-16967
Turbine flow meter with optical fiber pick-up
[NAL-TR-923] 09 p1169 N88-17009

Boundary-layer and wake measurements on a swept, circulation-control wing 10 p1270 N88-17597
Turbulence interactions in single- and multi-phase turbulent mixing and combustion processes
[AD-A187505] 10 p1332 N88-17960
Laser Doppler velocimetry primer
[NASA-CR-177386] 12 p1631 N88-19761
Tests on the AFWAL 65 deg delta wing at NLR: A study of vortex flow development between Mach = 0.4 and 4
[NLR-MP-86058-U] 13 p1717 N88-20266
Verification of the momemtum theory for rotors using measurements on a model helicopter
[R-840-S] 13 p1718 N88-20275
Comparison between computed and measured swirl and turbulence in reciprocating engines
[PDR/CFDU/IC/32] 13 p1779 N88-20647
Deep water mass circulation in the Alboran Basin. Measurements - January to April 1982: ALBORAN 2
[AD-A189205] 13 p1803 N88-20777
Measurements on a helicopter rotor
[R-764-S] 14 p1861 N88-21119
Correlation and spectral density measurements by LDA --- flow measurement
[ISL-CO-244/86] 14 p1910 N88-21412
Low pressure gas flow analysis through an effusive inlet using mass spectrometry
[NASA-CR-182712] 14 p1910 N88-21413
Boundary-layer and wake measurements on a swept, circulation-control wing
[NASA-TM-89426] 15 p2014 N88-22013
Inflow measurement made with a laser velocimeter on a helicopter model in forward flight. Volume 3: Rectangular planform blades at an advance ratio of 0.30
[NASA-TM-100543] 15 p2015 N88-22015
Piston-driven, unsteady separation at a sudden expansion in a tube: Flow visualization and Laser Doppler Anemometer (LDA) measurements
[ETN-88-92104] 15 p2068 N88-22329
Computer tomography and hybrid optical/digital methods for aerodynamic measurements
[AD-A190909] 16 p2157 N88-22872
Flow measurements in a water tunnel using a holocinematographic velocimeter
16 p2203 N88-23141
Matched index laser anemometry systems for flow studies in complex geometries 16 p2203 N88-23145
Flow velocity measurements by image processing of optically modulated traces 16 p2203 N88-23147
A non-invasive experimental technique for the measurement of unsteady velocity and vorticity fields
16 p2204 N88-23148
The development of a microanemometer. New possibilities for measuring very low air velocities
[ETN-88-92244] 16 p2210 N88-23191
Crossflow vorticity sensor
[NASA-CASE-LAR-13436-1-CU]
17 p2300 N88-23759
Supplements to the study of the wake of a Mirage G8 model at F2 --- wind tunnel
[CERT-RT-OA-20/5025-AYD] 18 p2458 N88-24596
Inflow measurements made with a laser velocimeter on a helicopter model in forward flight. Volume 1: Rectangular planform blades at an advance ration of 0.15
[NASA-TM-100541] 18 p2460 N88-24607
Method of forming a multiple layer dielectric and a hot film sensor therewith
[NASA-CASE-LAR-13678-1] 18 p2584 N88-25355
Study of flow tracer behavior models and experimental validation with multiple exposure holographic velocimetry
[IMFL-87/30] 20 p2801 N88-26622
Velocity measurements and flow visualization in turbulent three-dimensional supersonic flows using oxygen flow tagging
[AD-A192551] 21 p2892 N88-27165
Investigation of the quasi-steady approach used in transient two-phase flow analysis
[DE88-004303] 21 p2944 N88-27489
Laser-Doppler measurements of turbulence structures in free streams behind flat and rotation symmetrical profiles
[ETN-88-92336] 21 p2948 N88-27510
Use of penetrating radiations for the dynamic examination of aero gas turbines
[PNR90470] 22 p3045 N88-28073
Velocity measurements downstream of a sudden expansion using the Laser Doppler Velocimeters (LDV) technique. Part 1: Method of measurement and experimental facility
[FOA-C-20700-2.1-PT-1] 22 p3076 N88-28262
Calibration of a triple wire probe for turbulence measurements
[AD-A193956] 22 p3081 N88-28296
Project wind, phase 4 (smoke test), Meadow Brook Valley, Red Bluff, California
[AD-A194742] 22 p3128 N88-28596
Reynolds number effects and the wind tunnel environment 23 p3168 N88-28862
Construction of a laser Doppler anemometer and its use for the testing of a novel probe for the measurement of the variations of the lateral component of the vortex vector
[MPIS-13/1987] 23 p3217 N88-29147
Volumetric measurement of vorticity vectors by optical probe
[AD-A195997] 24 p3369 N88-30061
Investigation of large-scale structures in the near wake of a parallel flat plate
[ESA-TT-1100] 24 p3372 N88-30080
Laser Doppler Velocimeter (LDV) and pressure measurements of gas particle flows in bends
[VKI-TN-163] 24 p3372 N88-30083
Positron emission tomography: A new technique for observing fluid behavior in engineering systems
[PNR90471] 24 p3374 N88-30091

FLOW PATTERNS
U FLOW DISTRIBUTION

FLOW RATE
U FLOW VELOCITY

FLOW REGULATORS
Combined riblet and lebu drag reduction system
[NASA-CASE-LAR-13286-1] 06 p0664 N88-14071
Moving wall, continuous flow electronphoresis apparatus
[NASA-CASE-MFS-28142-1] 17 p2318 N88-23845
Energy efficient continuous flow ash lockhopper
[NASA-CASE-NPO-16985-1-CU]
18 p2497 N88-24814
The use of fins to reduce the pressure drop in a rotating cavity with a radial flow
[PNR90465] 22 p3079 N88-28282

FLOW RESISTANCE
NT AERODYNAMIC DRAG
NT FRICTION DRAG
NT SUPERSONIC DRAG
NT VISCOUS DRAG
The axisymmetric sealing gap with variable viscosity. A variable hydraulic resistance
[ETN-87-90604] 03 p0314 N88-11987

FLOW SEPARATION
U BOUNDARY LAYER SEPARATION
U SEPARATED FLOW

FLOW STABILITY
NT BOUNDARY LAYER STABILITY
NT FLAME STABILITY
NT MAGNETOHYDRODYNAMIC STABILITY
Experimental investigation in a wind tunnel of the stability and vorticity of the vortex breakdown phenomenon above delta wings, using the ultrasonic laser method
[DFVLR-FB-87-06] 01 p0003 N88-10017
A note on the instability of a vortex sheet leaving a semi-infinite plate
[DFVLR-FB-87-16] 01 p0004 N88-10019
Instability of steady flow with constant vorticity in vessels with elliptical cross-section 02 p0159 N88-10997
Computer modeling of two-phase flow
[CFDU/87/5] 02 p0171 N88-11078
Nonequilibrium fluctuations and transport in sheared fluids 03 p0316 N88-11999
Numerical study of the entrance flow and its transition in a circular pipe (2) 03 p0318 N88-12011
A study of chaos and mixing in Rayleigh-Taylor and Richtmyer-Meshkov unstable interfaces
[AD-A184751] 03 p0320 N88-12026
On the instability of thin circular shear layers
04 p0395 N88-12467
The use of alloy 117 as a liquid metal current collector
[AD-A185740] 06 p0698 N88-14281
Numerical simulation of a controlled boundary layer
07 p0810 N88-14933
Mathematical models of continuous flow electrophoresis: Electrophoresis technology
[NASA-CR-179241] 07 p0828 N88-15021
The numerical and analytical study of bifurcation and multicellular flow instability due to natural convection between narrow horizontal isothermal cylindrical annuli at high Rayleigh numbers
[AD-A186113] 07 p0849 N88-15151
On the parabolized Navier-Stokes equations without sublayer assumptions
[AD-A186127] 07 p0849 N88-15152
Chemical reactions in turbulent mixing flows
[AD-A186141] 07 p0849 N88-15153
Effects of turbulence on stationary and non-stationary processes in C-systems
[AD-A186215] 07 p0849 N88-15154
Identification and avoidance of instabilities in high performance turbomachinery 07 p0850 N88-15164
Thin film and gradient-driven instability mechanisms
[PB88-101522] 07 p0853 N88-15182
The effect of asymmetric heating on flow stability and heat transfer for flow in a vertical tube
[DE88-003242] 07 p0855 N88-15193
Influence of the friction coefficients, the power and the flowrate on the two-phase flow instabilities in natural circulation
[DE88-700036] 08 p0983 N88-15946
Flight results of the ESA experiment modules in Materials Science Experiment Rocket (MASER) 1
08 p1033 N88-16261
Numerical resolution of the equations of three-dimensional stable compressible transonic flows
[PB87-168415] 09 p1113 N88-16673
Control of vortical separation on conical bodies
10 p1267 N88-17580
Possibilities for on-line surge suppression by fast guide vane adjustment in axial compressors
10 p1283 N88-17674
Instability and transition in curved channel flow
10 p1328 N88-17938
Droplet formation for liquid monopropellant jets
[AD-A187172] 10 p1331 N88-17956
On the stability of the supersonic boundary layer
11 p1435 N88-18561
Measurement of rate constants of elementary gas reactions of importance to upper atmosphere and combustion systems
[AD-A189432] 13 p1737 N88-20386
Development of disturbances in swept wing flows
[NASA-CR-182675] 13 p1768 N88-20574
Effect of spatial inlet temperature and pressure distortion on turbofan engine stability
[NASA-TM-100850] 14 p1868 N88-21162
Problems in fluid dynamics
[NASA-CR-182678] 14 p1909 N88-21410
Hydrodynamical regimes in molten metals under a horizontal temperature gradient
14 p1988 N88-21859
The sensitivity of boundary layer instability growth rates to compliant wall properties
[AD-A190433] 15 p2064 N88-22309
Generation and coalescence of bubbles and stability of foams under microgravity conditions
[BMFT-FB-W-86-020] 16 p2184 N88-23017
Self similarity of two point correlations in wall bounded turbulent flows 16 p2195 N88-23089
Inflectional instabilities in the wall region of bounded turbulent shear flows 16 p2199 N88-23114
Coherent structures and modeling: Some background comments 16 p2199 N88-23120
Control of combustion and acoustically coupled fluid dynamic instabilities 17 p2318 N88-23843
Numerical simulation of nonlinear structural dynamics of large scale unsteady flow
[ETN-88-92156] 18 p2513 N88-24908
A single streamwise vortical structure and its instability in shear flows 18 p2515 N88-24921
Low frequency pressure oscillations in a model ramjet combustor 19 p2625 N88-25571
Numerical simulation of transition to turbulence in plane Poiseuille flow by a spectral method
19 p2640 N88-25661
Fluid dynamics of high performance turbomachines
[AD-A192073] 19 p2664 N88-25840
Analysis and modeling of complex non-stationary flows
[PB88-127188] 19 p2664 N88-25842
Cross flow induced vibrations in tube bundle by displaced and misaligned tube configurations
[ETN-88-92132] 20 p2801 N88-26621
Stationary, wave type, and chaos type convection in spherical symmetry geometries
[ETN-88-92358] 20 p2801 N88-26625
Numerical simulation and stability analysis of the absolutely and convectively unstable wake
[DFVLR-FB-88-09] 21 p2949 N88-27518
The Kelvin-Helmholtz instability in a stratified shear flow
[CFD/88/2] 22 p3076 N88-28265
Stability of parallel inviscid shear flow with mean spanwise variation
[FFA-TN-1987-57] 22 p3079 N88-28285
Boundary layer development and transition
23 p3169 N88-28871
Transition at hypersonic speeds
[NASA-CR-178315] 24 p3368 N88-30058

FLOW THEORY
NT MIXING LENGTH FLOW THEORY
Research on one-dimensional two-phase flow. Theory on hydrodynamic balance in two fluid model and its application
[DE87-702615] 01 p0045 N88-10290
Numerical calculation of the turbulent flow about a cubic body
[ETN-87-90418] 01 p0047 N88-10302

A flow function method for the axisymmetric calculation of the transonic turbomachine flow taking into account the flow differences in circumferential direction
[ETN-87-90428] 01 p0056 N88-10359
Theoretical investigations of three turbine cascades using a two dimensional time marching procedure
[DFVLR-FB-87-02] 01 p0057 N88-10362
Calculation of stationary and low frequency unsteady flows in a steam turbine end stage
[MITT-23] 01 p0057 N88-10364
Shearing flow over Stokes wave. Part one: General theory
[ETN-87-90957] 02 p0171 N88-11074
The physics and mathematical description of the Achilles heel of stationary wind turbine aerodynamics: The tip flow
[R-812-D] 03 p0260 N88-11635
Linear and nonlinear theories of flow through an actuator disk --- windpowered pumps
[R-803-A] 03 p0316 N88-11995
Steady shearing in a viscoplastic solid
[AD-A184341] 04 p0454 N88-12810
Implicit time dependent methods for inviscid and viscous compressible flows 06 p0701 N88-14304
Viscous drag reduction of horizontal plates
[VKI-TN-159] 07 p0851 N88-15171
An efficient method for computing leading Eigenvalues and Eigenvectors of large asymmetric matrices
09 p1159 N88-16949
Numerical calculation of turbulent recirculating flows
[TUM-LSM-84/29] 09 p1161 N88-16959
Numerical and physical aspects of large eddy simulation of turbulent flows
[ETN-88-91611] 09 p1162 N88-16965
Activities report of the Aerodynamics Department
[ETN-88-91979] 14 p1862 N88-21123
Theoretical investigations of three turbine cascades using a 2-D time marching procedure
[ESA-TT-1077] 16 p2207 N88-23170

FLOW VELOCITY
NT SOLAR WIND VELOCITY
The four spot time-of-flight laser anemometer
02 p0184 N88-11145
Correlation of velocity and velocity-density turbulence in the exhaust of an atmospheric burner
02 p0185 N88-11147
Measurements of gas velocities and temperatures in a large open pool fire
[DE87-005853] 03 p0261 N88-11641
A 10 W transverse flow excimer laser
03 p0302 N88-11901
Numerical study of the entrance flow and its transition in a circular pipe (2) 03 p0318 N88-12011
Geometric analysis of ensemble of solutions in two-phase flow and complete resolution of problem of choking
[DE88-001687] 04 p0445 N88-12764
Variations of the vertical and horizontal velocities of the small-scale structures and the physical problems related to overshoot layers 04 p0507 N88-13115
Ducted propeller design and analysis
[DE88-001925] 08 p0664 N88-14069
Review of nucleation and incipient boiling under pool and forced convection conditions
08 p0982 N88-15938
Investigation of vibration problems with heterodyne holographic interferometer 08 p1000 N88-16058
Experimental and theoretical study on cavitation inception and bubbly flow dynamics. Part 1: Design, development and operation of a cavitation susceptibility meter. Part 2: Linearized dynamics of bubbly and cavitating flows with bubble dynamics effects
[AD-A187133] 09 p1160 N88-16952
An analysis of the closure conditions for two-fluid models of two-phase flow
[DE88-003355] 09 p1164 N88-16982
Turbine flow meter with optical fiber pick-up
[NAL-TR-923] 09 p1169 N88-17009
O2-I laser (Oxygen-iodine) mixing studies using LIF (Laser Induced Fluorescence)
[AD-A186667] 09 p1171 N88-17018
Parametric study of choke flutter with a linear theory
10 p1283 N88-17673
Possibilities for on-line surge suppression by fast guide vane adjustment in axial compressors
10 p1283 N88-17674
Development and application of oxygen flow tagging for velocity measurements and flow visualization in turbulent three-dimensional supersonic flows
[AD-A187982] 10 p1289 N88-17714
Laser velocimeter measurements of solids in multiphase flow
[DE88-000196] 11 p1487 N88-18876
Laser fluorescence velocimeter
[AD-A189010] 12 p1630 N88-19753
Laser Doppler velocimetry primer
[NASA-CR-177396] 12 p1631 N88-19761
Perspectives in microclimate cooling involving protective clothing in hot environments
[AD-A188370] 12 p1671 N88-20007
Boundary effects on the drag of a cylinder in axial motion at low Reynolds number 13 p1768 N88-20578
Turbulent transfer of momentum and heat in boundary layer of fluid beyond an obstacle. 1: Hydrodynamic characteristics 13 p1787 N88-20690
Contribution to theory of quasigeostrophic motions of finite amplitude in viscous stratified ocean
13 p1788 N88-20695
Correlation and spectral density measurements by LDA --- flow measurement
[ISL-CO-244/86] 14 p1910 N88-21412
An investigation of flow structure, mixing and chemical reaction in combusting turbulent flows
[AD-A189980] 15 p2034 N88-22117
Calorimetric technique for measuring liquid helium flow rate
[DE88-701308] 16 p2200 N88-23123
Flow velocity measurements by image processing of optically modulated traces 16 p2203 N88-23147
The development of a microanemometer. New possibilities for measuring very low air velocities
[ETN-88-92244] 16 p2210 N88-23191
Evaluation of a flood period (June, 1984) in the southern region of Laguna dos Patos, through remote sensing data, meteorological and oceanographic
17 p2365 N88-24083
Reference filters for electrostatic charging tendency measurements of fuels
[AD-A191717] 18 p2495 N88-24803
Correlations of velocity and temperature fluctuations in the stagnation-point flow of circular cylinder in turbulent flow
[NASA-TM-100930] 19 p2597 N88-25435
Velocity coupling 19 p2629 N88-25596
The propagation of pressure perturbations in bubbly air/water flows 19 p2664 N88-25843
Development of advanced flow simulation system by water flow model. New method of velocity measurement using cross-correlation
[DE88-753120] 20 p2799 N88-26608
Cryogenic free jets
[DFVLR-FB-88-16] 21 p2900 N88-27210
Optimal rheological characteristics in dynamic stability of polymer flow through porous media
[DE88-001225] 21 p2918 N88-27322
Relative flow rates of explosive powders
[DE88-010767] 21 p2923 N88-27350
Heat and mass transfer in a transport channel
[DE88-701958] 21 p2945 N88-27493
Energy distribution and transfer in flowing hydrogen microwave plasmas 21 p3019 N88-27919
Velocity measurements downstream of a sudden expansion using the Laser Doppler Velocimeters (LDV) technique. Part 1: Method of measurement and experimental facility
[FOA-C-20700-2.1-PT-1] 22 p3076 N88-28262
NF (a 1 delta) production in a supersonic flow using N2F4 + H2 in a BCL-16 nozzle
[AD-A194478] 22 p3082 N88-28304
Delta wing configurations 23 p3167 N88-28860
Unsteady water channel
[AD-A194231] 23 p3171 N88-28884
A study of the effect of random input motion on low Reynolds number flows
[AD-A195559] 24 p3316 N88-29747
Flow characteristics of a model annular combustor
24 p3347 N88-29924

FLOW VISUALIZATION
NT NUMERICAL FLOW VISUALIZATION
Dispersion in the wake of aircraft: An investigation of the effects of a ground plane on trailing vortices. Literature survey
[IC-AERO-REP-86-04] 01 p0003 N88-10014
Optical flow diagnostic measurements in turbomachinery
[PNR90396] 02 p0172 N88-11081
Improving coherent visualization by means of film optical filtering --- projectile visualization
[ISL-R-116/86] 02 p0176 N88-11097
Flow visualization on an ogive-nosed circular cylinder body at high incidence using the laser light sheet method
[ESA-TT-1066] 03 p0315 N88-11993
The diffusion-convection vortex method for solving two-dimensional incompressible Navier-Stokes equation
03 p0317 N88-12001
An experimental investigation of quasi-conical shock wave/turbulent boundary layer interactions
03 p0317 N88-12004
Numerical simulation and visualization of a flowfield by interaction of two parallel two-dimensional freejets
03 p0320 N88-12021
Visualization of the flow field around a generic destroyer model in a simulated turbulent atmospheric boundary layer
[AD-A184658] 03 p0320 N88-12023
Structural characteristics of dean vortices in a curved channel
[AD-A184724] 03 p0320 N88-12024
Development of flow visualization techniques for use in the Hot Gas Laboratory
[BAE-ARG-233] 03 p0325 N88-12052
Experimental aerothermodynamic research of hypersonic aircraft
[NASA-CR-181533] 04 p0399 N88-12483
Observations on the hydrodynamic flow visualization at ONERA
[PD-FM-8718] 04 p0444 N88-12753
Experimental investigations on blunt bodies and corner configurations in hypersonic flow
05 p0530 N88-13225
An ultra-high-speed cinematographic method for the study of wakes in hypersonic ballistic ranges
05 p0531 N88-13228
Flow visualization in computational fluid dynamics
05 p0538 N88-13277
Visualization of an aircraft accident based on digital flight data recorder information 05 p0538 N88-13278
Transient development of stratification in a partially divided enclosure
[DE87-011742] 05 p0572 N88-13490
Vortical Flows Research Program of the Fluid Dynamics Research Branch
[NASA-TM-88332] 05 p0582 N88-13549
Flow diagnostics and visualization in wind tunnels and flight 07 p0811 N88-14940
A flow visualization study of the leading edge separation bubble on a NACA 0012 airfoil with simulated glaze ice
[NASA-CR-180846] 07 p0816 N88-14966
An experimental investigation of the chopping of helicopter main rotor tip vortices by the tail rotor. Part 2: High speed photographic study
[NASA-CR-177457] 09 p1114 N88-16678
Velocity interferometry in shock tubes and shock tunnels
[ISL-CO-203/87] 09 p1122 N88-16713
Unsteady behavior of three-dimensional vortices relevant to turbulent boundary layers
[AD-A186767] 09 p1161 N88-16958
A review of some flow visualization experiments carried out at the Institut Franco-Allemand de Recherches (ISL) shock tubes
[ISL-CO-243/86] 09 p1163 N88-16974
Techniques of flow visualization
[AGARD-AG-302] 09 p1164 N88-16977
Development and application of oxygen flow tagging for velocity measurements and flow visualization in turbulent three-dimensional supersonic flows
[AD-A187982] 10 p1289 N88-17714
Experimental research on swept shock wave/boundary layer interactions
[AD-A187250] 10 p1331 N88-17957
Preliminary experiments on surface flow visualization in the cryogenic wind tunnel by use of condensing or freezing gases
[NASA-CR-181634] 11 p1442 N88-18602
Production by pyrolysis of diffusion particles for velocimetry in shock tubes
[ISL-R-119/86] 11 p1455 N88-18671
Hydrodynamic simulation of forced convection in the Czochralski process
[INPE-4471-TDL/323] 12 p1697 N88-20158
An experimental investigation of decelerating flow about two-dimensional cambered plates
[DE88-006598] 13 p1766 N88-20567
Graphics and flow visualization of computer generated flow fields
[NASA-CR-182679] 13 p1767 N88-20573
Digital enhancement of flow field images
[NASA-TP-2770] 13 p1813 N88-20833
Vortex flow over a delta wing with apex flaps using laser flow visualisation
[BU-356] 14 p1862 N88-21121
Surface flow visualization of separated flows on the forebody of an F-18 aircraft and wind-tunnel model
[NASA-TM-100436] 14 p1863 N88-21127
Investigation into the effects of flap end modifications on the performance of a wing with a single slotted flap
[BU-357] 14 p1866 N88-21148
Main features of the 0.43m x 0.43m wind tunnel
[AXM-132] 14 p1870 N88-21175
Visualization of the air flowing through a dynamic model of the vocal folds
[ISVR-TR-154] 14 p1952 N88-21634

Unsteady flow field measurements using LDV (Laser Doppler Velocimetry)
[AD-A189907] 15 p2063 N88-22298
Visualization of flows in turbomachinery
[AD-A189927] 15 p2063 N88-22299
Visualisation of the flow at the tip of a high speed axial flow turbine rotor
[AD-A189928] 15 p2063 N88-22300
Visualisation of the flow at the tip of a high speed axial flow turbine rotor: An assessment of flow visualisation techniques and the requirement of the experimental turbine
[AD-A189929] 15 p2063 N88-22301
Dense-spray structure and phenomena. Part 2: Pressure-atomized sprays
[AD-A190312] 15 p2064 N88-22307
Interaction of a two-dimensional bluff body and incompressible jet and annulus flows
[AD-A190503] 15 p2064 N88-22310
Chemically reacting turbulent flow
[AD-A190522] 15 p2065 N88-22311
Numerical and experimental investigation of multiple shock wave/turbulent boundary layer interactions in a rectangular duct
[AD-A190772] 15 p2066 N88-22320
Piston-driven, unsteady separation at a sudden expansion in a tube: Flow visualization and Laser Doppler Anemometer (LDA) measurements
[ETN-88-92104] 15 p2068 N88-22329
Oil flow patterns on a series of capsule-type re-entry vehicles at hypersonic speeds
[DE88-751805] 16 p2155 N88-22858
Structure of turbulent shear flows
16 p2198 N88-23113
Water facilities in retrospect and prospect: An illuminating tool for vehicle design
16 p2200 N88-23126
Qualification of a water tunnel for force measurements on aeronautical models 16 p2200 N88-23128
Flow visualization study of vortex manipulation on fighter configurations at high angles of attack
16 p2201 N88-23130
Description of a water tank facility: Study of a missile at high incidence 16 p2201 N88-23133
Experimental investigation of Hover flowfields in water at the McDonnell Douglas Research Laboratories
16 p2202 N88-23135
Water flow visualisation of a ramrocket combustion chamber 16 p2202 N88-23138
The ONERA water tunnels test possibilities for flow visualization in aeronautical and Naval domains
16 p2202 N88-23139
The use of a water towing tank for aerodynamic testing and methods for quantitative evaluation of photographs
16 p2202 N88-23140
Flow measurements in a water tunnel using a holocinematographic velocimeter
16 p2203 N88-23141
Three-dimensional flow visualization using laser-sheet scanning 16 p2203 N88-23143
Flow velocity measurements by image processing of optically modulated traces 16 p2203 N88-23147
A non-invasive experimental technique for the measurement of unsteady velocity and vorticity fields
16 p2204 N88-23148
Some visualization studies on turbulent boundary layers using multiwire hydrogen bubble generation
16 p2204 N88-23153
Structure of unsteady flows at leading- and trailing-edges: Flow visualization and its interpretation
16 p2205 N88-23154
La Recherche Aerospatiale, bimonthly bulletin, number 1987-3, 238/May-June
[ESA-TT-1075] 16 p2206 N88-23161
Study of a system for reducing base drag by controlling vortices
[REPT-87/43] 17 p2295 N88-23730
Boundary layer flow visualization for flight testing
17 p2297 N88-23742
Acoustically excited heated jets. 1: Internal excitation
[NASA-CR-4129-PT-1] 17 p2298 N88-23751
Acoustically excited heated jets. 2: In search of a better understanding
[NASA-CR-4129-PT-2] 17 p2299 N88-23752
Acoustically excited heated jets. 3: Mean flow data
[NASA-CR-4129-PT-3] 17 p2299 N88-23753
Single phase liquid immersion cooling of discrete heat sources in a vertical channel
[AD-A191224] 17 p2337 N88-23944
Dual wavelength holographic interferometry system
[NASA-CASE-MFS-28242-1] 17 p2341 N88-23960
Unsteady flow around a profile subjected to pulsed motions
[ETN-88-92151] 18 p2458 N88-24594
Quantitative use of exciplex-based vapor/liquid visualization systems, users' manual
[AD-A191649] 19 p2610 N88-25491
A review of particle sizing methods in rocket propulsion 19 p2630 N88-25597
Solid rocket motor performance: A workshop report
19 p2631 N88-25607
A twin-mirrored galvanometer laser light sheet generator
[NASA-TM-100587] 19 p2674 N88-25901
The determination of the topological structure of skin friction lines on a rectangular wing-body combination
[NASA-CR-4168] 20 p2753 N88-26343
Development of advanced flow simulation system by water flow model. New method of velocity measurement using cross-correlation
[DE88-753120] 20 p2799 N88-26608
Study of flow tracer behavior models and experimental validation with multiple exposure holographic velocimetry
[IMFL-87/30] 20 p2801 N88-26622
Velocity measurements and flow visualization in turbulent three-dimensional supersonic flows using oxygen flow tagging
[AD-A192551] 21 p2892 N88-27165
Flow around a delta wing with or without a canard control surface (phi BA = 60 deg). Part 1: Hydrodynamic visualization in permanent regime
[ONERA-RT-10/2891-AN-101-A-PT-1]
21 p2892 N88-27170
The structure and stability of nonpremixed gas jet flames 21 p2908 N88-27257
Experimental research of combustion systems
21 p2927 N88-27371
Liquid crystals for unsteady surface shear stress visualization
[DE88-010570] 21 p2951 N88-27527
Holographic interferometry for flow visualization studies in high speed fans
[PNR90459] 22 p3045 N88-28072
Use of penetrating radiations for the dynamic examination of aero gas turbines
[PNR90470] 22 p3045 N88-28073
Holographic flow visualization
[PNR90466] 22 p3079 N88-28283
Calibration of a triple wire probe for turbulence measurements
[AD-A193956] 22 p3081 N88-28296
Noise generation and boundary layer effects in vortex-airfoil interaction and methods of digital hologram analysis for these flow fields
[AD-A194191] 23 p3171 N88-28883
Three-dimensional vortex interactions
[AD-A194066] 23 p3172 N88-28889
Flow visualization on a small scale
[AD-A194728] 23 p3181 N88-28935
Flow visualization by laser sheet
[AD-A194481] 23 p3211 N88-29111
Application of Particle Image Displacement Velocimetry (PIDV) to complex flows: Velocity field measurements in front of a heavy gas cloud
[VKI-TN-166] 23 p3213 N88-29125
Study of experimental technique of oil flow with emphasis on quantitative determination of the flow position parameters on the surface
[NASA-TT-20341] 23 p3215 N88-29135
A study of the effect of random input motion on low Reynolds number flows
[AD-A195559] 24 p3316 N88-29747
Positron emission tomography: A new technique for observing fluid behavior in engineering systems
[PNR90471] 24 p3374 N88-30091
Use of holography in vibration and flutter study of fans
[PNR90458] 24 p3375 N88-30098

FLOWMETERS
NT HOT-WIRE FLOWMETERS
Nonintrusive ultrasonic flow measurement techniques and their applications to BTU metering
[DE87-011390] 01 p0045 N88-10286
An automated flow calorimeter for heat capacity and enthalpy measurements at elevated temperatures and pressures
[DE88-002357] 07 p0857 N88-15206
Low-g propellant gaging 08 p0982 N88-15937
Detecting the gas bubbles in a liquid metal coolant by means of magnetic flowmeters
[DE88-701427] 15 p2062 N88-22294
Calorimetric technique for measuring liquid helium flow rate
[DE88-701308] 16 p2200 N88-23123
Crossflow vorticity sensor
[NASA-CASE-LAR-13436-1-CU]
17 p2300 N88-23759
A monolithic gas flow sensor with polyimide as thermal insulator 19 p2669 N88-25864

FLTSATCOM
U FLEET SATELLITE COMMUNICATION SYSTEM

FLUCTUATION
U VARIATIONS

FLUCTUATION THEORY
Measurements of the free stream fluctuations above a turbulent boundary layer
[NASA-TM-100036] 06 p0704 N88-14321

FLUENCE
Microstructural change of Al on H implantation
[IPPJ-847] 04 p0493 N88-13036
Experimental method for investigating helium effects in irradiated vanadium
[DE88-002891] 08 p0969 N88-15865

FLUID AMPLIFICATION
U FLUID AMPLIFIERS

FLUID AMPLIFIERS
Microminiature fluidic amplifier
19 p2669 N88-25865

FLUID BOUNDARIES
NT LIQUID-LIQUID INTERFACES
NT LIQUID-SOLID INTERFACES
NT LIQUID-VAPOR INTERFACES
Fluid motion in a spinning, coning cylinder via spatial eigenfunction expansion
[AD-A190758] 15 p2066 N88-22319
A numerical treatment of the fluid/elastic interface under range-dependent environments
[AD-A192476] 21 p3005 N88-27821

FLUID DYNAMICS
NT AERODYNAMICS
NT AEROTHERMODYNAMICS
NT COMPUTATIONAL FLUID DYNAMICS
NT ELASTOHYDRODYNAMICS
NT ELECTROHYDRODYNAMICS
NT GAS DYNAMICS
NT HYDRODYNAMICS
NT INTERACTIONAL AERODYNAMICS
NT MAGNETOHYDRODYNAMICS
NT RAREFIED GAS DYNAMICS
NT ROTOR AERODYNAMICS
NT SUPERSONICS
NT UNSTEADY AERODYNAMICS
NT VORTEX SHEDDING
The structure of separated flow regions occurring near the leading edge of airfoils including transition
[NASA-CR-181434] 01 p0002 N88-10011
Plasma properties
[DE87-013662] 01 p0101 N88-10663
Aerospace research at the National Aerospace Laboratory (NLR)
[ETN-87-90821] 01 p0107 N88-10697
Vortex/boundary-layer interactions: Data report, volume 2
[NASA-CR-181463] 02 p0122 N88-10769
Efficient numerical techniques for complex fluid flows
02 p0185 N88-11151
Technical evaluation report on the Fluid Dynamics Panel Symposium on aerodynamic and related hydrodynamic studies using water facilities
[AGARD-AR-225] 03 p0312 N88-11968
Special Course on Modern Theoretical and Experimental Approaches to Turbulent Flow Structure and its Modelling
[AGARD-R-755] 03 p0312 N88-11970
Homogeneous turbulence two-point closures and applications to one-point closures
03 p0312 N88-11973
Dynamics and routes to chaos from quasiperiodicity
03 p0312 N88-11974
A deterministic approach to turbulence: Chaos in Rayleigh-Benard convection 03 p0313 N88-11975
Transition to turbulence via spatio-temporal intermittency 03 p0313 N88-11976
Determination of fractal dimension, connection of space and temporal chaos and application to experimental results 03 p0313 N88-11977
A study of chaos and mixing in Rayleigh-Taylor and Richtmyer-Meshkov unstable interfaces
[AD-A184751] 03 p0320 N88-12026
Dynamics of reverse flows at pump inlet
04 p0425 N88-12636
European hypersonic wind tunnels
05 p0530 N88-13221
Combustion related shear-flow dynamics in elliptic supersonic jets 05 p0531 N88-13232
Application of modified loss and deviation correlations to transonic axial compressors
[AGARD-R-745] 05 p0549 N88-13344
Static aeroelastic effects on the flutter of a supercritical wing 05 p0550 N88-13353
Displaying three-dimensional data
[AD-A185347] 05 p0580 N88-13541
A system of three-dimensional complex variables
[NASA-TM-88318] 05 p0645 N88-13951
Calendar of selected aeronautical and space meetings
[AGARD-CAL-87/1] 05 p0657 N88-14033

Studies of supersonic turbulence and hot-wire response using Laser-Induced Fluorescence (LIF)
06 p0664 N88-14072
Post stall behavior in axial-flow compressors
[AD-A185712] 06 p0665 N88-14081
Utilization of FEP energetics
[NASA-CR-182373] 06 p0714 N88-14379
JPRS report: Science and technology. USSR: Physics and mathematics
[JPRS-UPM-87-008] 06 p0769 N88-14727
Some performance comparisons for a fluid dynamics code
[PB88-113709] 07 p0852 N88-15175
Rayleigh-Taylor instability in compressible fluids
[DE88-002473] 07 p0852 N88-15179
USSR report: Physics and mathematics
[JPRS-UPM-87-002] 07 p0918 N88-15575
Resolution of holograms produced by the fluid experiment system and the holography ground system
07 p0923 N88-15609
Acta Aerodynamica Sinica (selected articles)
[AD-A185723] 08 p0949 N88-15757
Computational prediction of propellant reorientation
08 p0962 N88-15940
Experimental and theoretical study on cavitation inception and bubbly flow dynamics. Part 1: Design, development and operation of a cavitation susceptibility meter. Part 2: Linearized dynamics of bubbly and cavitating flows with bubble dynamics effects
[AD-A187133] 09 p1160 N88-16952
O2-I laser (Oxygen-iodine) mixing studies using LIF (Laser Induced Fluorescence)
[AD-A186667] 09 p1171 N88-17018
Experimental research on swept shock wave/boundary layer interactions
[AD-A187250] 10 p1331 N88-17957
Research on fluid dynamic energy separation
[DE88-002776] 10 p1339 N88-18001
On the start up of supersonic underexpanded jets --- Mach disks
11 p1435 N88-18563
Suspension of small metallic plates: A versatile sensor
[PB88-130901] 11 p1487 N88-18874
Structures and fluxes in a deep convecting mixed layer
13 p1804 N88-20786
Hamiltonian description of the interaction of surface waves with mixed-layer currents
13 p1806 N88-20799
Development of an optical diagnostic instrument. Part 2: Instrument development --- space laboratories
[NLR-TR-87079-L-PT-2] 13 p1841 N88-21016
Enhancement of data acquisition and numerical computation capabilities for unsteady fluid dynamics
[AD-A190115] 15 p2063 N88-22302
Effect of freestream turbulence on a two dimensional cascade, with different surface roughness, at high Reynolds number
[AD-A190615] 15 p2065 N88-22316
Review and assessment of the HOST turbine heat transfer program
15 p2086 N88-22431
A physically consistent model for artificial dissipation in transonic potential flow computations
[NASA-TM-100846] 15 p2122 N88-22652
MPD (magnetoplasmadynamic) thrust chamber flow dynamics
[AD-A189940] 15 p2137 N88-22751
Tip vortices of isolated wings and helicopter rotor blades
[AD-A191336] 16 p2158 N88-22874
Aerodynamic and Related Hydrodynamic Studies Using Water Facilities
[AGARD-CP-413] 16 p2200 N88-23125
Qualification of a water tunnel for force measurements on aeronautical models
16 p2200 N88-23128
The use of a water towing tank for aerodynamic testing and methods for quantitative evaluation of photographs
16 p2202 N88-23140
Coronal fluid-dynamics in laser fusion
16 p2278 N88-23634
Control of combustion and acoustically coupled fluid dynamic instabilities
17 p2318 N88-23843
Noncontact temperature measurements in the microgravity fluids and transport phenomena discipline
17 p2328 N88-23901
Fluid dynamics of spherical cavity reactors
17 p2403 N88-24291
Dynamics and control of turbulent shear flows
[AD-A191527] 18 p2508 N88-24879
Nonlinear waves
[AD-A192148] 18 p2510 N88-24889
Gas diffusion studies in steady and nonsteady cavities
18 p2512 N88-24902
Correlations of velocity and temperature fluctuations in the stagnation-point flow of circular cylinder in turbulent flow
[NASA-TM-100930] 19 p2597 N88-25435
Fluid dynamics of high performance turbomachines
[AD-A192073] 19 p2664 N88-25840
Boundary layer development as a function of chamber pressure in the NASA Lewis 1030:1 area ratio rocket nozzle
[NASA-TM-100917] 19 p2664 N88-25841
Scaling laws for homogeneous turbulent shear flows in a rotating frame
[NASA-CR-181672] 19 p2665 N88-25847
Stationary, wave type, and chaos type convection in spherical symmetry geometries
[ETN-88-92358] 20 p2801 N88-26625
Computer science research, 1987: Computation Directorate
[DE88-008637] 20 p2834 N88-26812
Fluid dynamical model of ultrarelativistic heavy ion collisions
[DE88-007905] 20 p2850 N88-26921
The heat transfer and fluid dynamics of concave surface curvature
[AD-A193064] 21 p2943 N88-27479
Flow dynamics stimulated by hairpin-like vortices in initially laminar boundary layers
[AD-A194253] 22 p3075 N88-28254
Accommodation concept for fluid physics facilities, volume 2 --- Spacelab
[SG-TN-AI-027-VOL-2] 24 p3358 N88-29994
Assessment of a 3-D boundary layer analysis to predict heat transfer and flow field in a turbine passage
[NASA-CR-174894] 24 p3370 N88-30066

FLUID FILLED SHELLS
NT LIQUID FILLED SHELLS
Calculation of the eigenvibrations of axisymmetric fluid configurations with a singularity method, taking into account surface tension effects under reduced gravity
[ETN-87-90438] 01 p0048 N88-10304
Coupled FE and HIE method for exterior acoustics of axisymmetric shells --- finite element (FE) Helmholtz integral equation (HIE)
[ARE-TM(UHA)-87506] 09 p1243 N88-17448
The Shock and Vibration Digest, volume 20, no. 3
12 p1635 N88-19786
Vibrations of shells containing fluid
12 p1635 N88-19787
The nonlinear dynamics of a spacecraft coupled to the vibration of a contained fluid
[DE88-007035] 16 p2168 N88-22925
Quantitative particle characterization by scattered ultrasound
20 p2848 N88-26908

FLUID FILMS
NT SQUEEZE FILMS
Studies of thin surface films aim at seeing deep ocean processes
04 p0460 N88-12847
Literature review of solid lubrication mechanisms
[AD-A185010] 05 p0567 N88-13456
Research on acoustical scattering, diffraction catastrophes, optics of bubbles, photoacoustics, and acoustical phase conjugation
[AD-A185785] 06 p0776 N88-14761
Calculation on film preparation and film motion of a swirl atomizer
[DFVLR-FB-87-25] 09 p1162 N88-16962
Standardization of lubricity test
[AD-A187776] 11 p1465 N88-18736
Lubricating properties of molybdenum disulfide. Part 3: Performance of molybdenum disulfide-containing oils in fluid lubrication
[NASA-TT-20156] 13 p1752 N88-20480
Heating and evaporation of turbulent liquid films: Measurement of film thickness and the onset of nucleate boiling
[DE88-006388] 18 p2512 N88-24905
The use of liquid films for spacecraft survivability to laser radiation
[AD-A192954] 20 p2765 N88-26395

FLUID FILTERS
NT AIR FILTERS
Fiber-reinforced composite hot-gas filters
[DE87-012257] 01 p0033 N88-10208
Reference filters for electrostatic charging tendency measurements of fuels
[AD-A191717] 18 p2495 N88-24803

FLUID FLOW
NT AIR CURRENTS
NT AIR FLOW
NT AIR JETS
NT ANNULAR FLOW
NT AXIAL FLOW
NT AXISYMMETRIC FLOW
NT BAROTROPIC FLOW
NT BASE FLOW
NT BELTRAMI FLOW
NT BLASIUS FLOW
NT BLOOD FLOW
NT BOUNDARY LAYER FLOW
NT BOUNDARY LAYER SEPARATION
NT CAPILLARY FLOW
NT * CASCADE FLOW
NT CAVITATION FLOW
NT CHANNEL FLOW
NT COAXIAL FLOW
NT COMBUSTIBLE FLOW
NT COMPRESSIBLE FLOW
NT CONICAL FLOW
NT CONTINUUM FLOW
NT CONVECTIVE FLOW
NT COOLING FLOWS (ASTROPHYSICS)
NT CORE FLOW
NT CORNER FLOW
NT COUETTE FLOW
NT COUNTERFLOW
NT CRITICAL FLOW
NT CROSS FLOW
NT DUCTED FLOW
NT EQUILIBRIUM FLOW
NT FREE FLOW
NT FREE MOLECULAR FLOW
NT FUEL FLOW
NT GAS FLOW
NT HELICAL FLOW
NT HYPERSONIC FLOW
NT HYPERVELOCITY FLOW
NT INCOMPRESSIBLE FLOW
NT INLET FLOW
NT INVISCID FLOW
NT ISOTHERMAL FLOW
NT JET FLOW
NT JET MIXING FLOW
NT JET STREAMS (METEOROLOGY)
NT LAMINAR FLOW
NT LIQUID FLOW
NT MAGNETOHYDRODYNAMIC FLOW
NT MASS FLOW
NT MERIDIONAL FLOW
NT MOLECULAR FLOW
NT MULTIPHASE FLOW
NT NONEQUILIBRIUM FLOW
NT NONNEWTONIAN FLOW
NT NONUNIFORM FLOW
NT NOZZLE FLOW
NT ONE DIMENSIONAL FLOW
NT OPEN CHANNEL FLOW
NT OSCILLATING FLOW
NT PARALLEL FLOW
NT PIPE FLOW
NT PLASTIC FLOW
NT POTENTIAL FLOW
NT PROPELLANT TRANSFER
NT RADIAL FLOW
NT RAYLEIGH-BENARD CONVECTION
NT REATTACHED FLOW
NT RECIRCULATIVE FLUID FLOW
NT REVERSED FLOW
NT SECONDARY FLOW
NT SEPARATED FLOW
NT SHEAR FLOW
NT SINGLE-PHASE FLOW
NT SLIP FLOW
NT SMALL PERTURBATION FLOW
NT SOLIDS FLOW
NT STAGNATION FLOW
NT STEADY FLOW
NT STEAM FLOW
NT STOKES FLOW
NT STRATIFIED FLOW
NT SUBSONIC FLOW
NT SUPERCRITICAL FLOW
NT SUPERSONIC FLOW
NT SUPERSONIC JET FLOW
NT THREE DIMENSIONAL FLOW
NT TRANSITION FLOW
NT TRANSONIC FLOW
NT TURBULENT FLOW
NT TWO DIMENSIONAL FLOW
NT TWO PHASE FLOW
NT UNIFORM FLOW
NT UNSTEADY FLOW
NT VERTICAL AIR CURRENTS
NT VISCOUS FLOW
NT WALL FLOW
NT WATER FLOW
NT WEDGE FLOW
Performance of rotary regenerative heat exchanger: A numerical simulation
01 p0046 N88-10292
Experimental and theoretical studies of vertical annular liquid jets
[DE87-013907] 01 p0047 N88-10299
Nonlinear fluid equations for a low collisionality toroidal plasma
[DE87-013006] 01 p0100 N88-10655

Analytical modeling of helicopter static and dynamic induced velocity in GRASP
[NASA-TM-100026] 02 p0123 N88-10777
Heat transfer in the tip region of a rotor blade simulator 02 p0186 N88-11159
Direct Absorption Receiver flow experiments
[DE87-014655] 02 p0196 N88-11221
Fundamentals of turbulence for turbulence modeling and simulation 03 p0312 N88-11971
The evolution of HOBO
[DE87-014742] 03 p0313 N88-11980
FLIP (Fluid-Implicit-Particle): A low-dissipation, particle-in-cell method for fluid flow
[DE87-014745] 03 p0313 N88-11981
Structural characteristics of dean vortices in a curved channel
[AD-A184724] 03 p0320 N88-12024
Theory of one and two-pass cross-flow heat exchanger
[PB87-225157] 04 p0441 N88-12736
Studies of pressure-velocity coupling schemes for analysis of incompressible and compressible flows
[NASA-CR-181526] 04 p0443 N88-12748
Three-dimensional, free-Lagrange hydrodynamics
[DE88-000494] 04 p0443 N88-12749
The modelling of orientation in planar polymer welding flows
[AD-A184404] 04 p0451 N88-12793
A spatial marching technique for the inviscid blunt body problem 05 p0533 N88-13239
A perspective of computational fluid dynamics 05 p0538 N88-13279
Development of an integrated BEM approach for hot fluid structure interaction
[NASA-CR-181577] 05 p0556 N88-13384
Three-dimensional dynamic labyrinth seal analysis
[AD-A185353] 05 p0590 N88-13599
Fluid mass and thermal loading effects on the modal characteristics of space shuttle main engine liquid oxygen inlet splitter vanes 05 p0594 N88-13628
Turbulence, turbulence control, and drag reduction
[AD-A185643] 06 p0665 N88-14080
Description and analysis of a cascade control of fluid flow
[PB87-112686] 06 p0698 N88-14282
Model development for induction heating
[DE88-002376] 06 p0699 N88-14289
Extensions of the control volume based finite element method for fluid flow problems 06 p0700 N88-14296
Dual cylindrical wave Laser-Doppler method for measurement of skin friction in fluid flow 06 p0700 N88-14297
A study of rotor broadband noise mechanisms and helicopter tail rotor noise 06 p0777 N88-14766
The numerical and analytical study of bifurcation and multicellular flow instability due to natural convection between narrow horizontal isothermal cylindrical annuli at high Rayleigh numbers
[AD-A186113] 07 p0849 N88-15151
Numerical methods for fluid flow problems
[DE88-000156] 07 p0854 N88-15190
An automated flow calorimeter for heat capacity and enthalpy measurements at elevated temperatures and pressures
[DE88-002357] 07 p0857 N88-15206
Turbomachinery 08 p0955 N88-15792
Chemical reacting flows 08 p0955 N88-15793
Fluid mechanical issues in polymer processing
[DE88-002767] 08 p0972 N88-15880
Zero-G thermodynamic vent system for shuttle/Centaur 08 p0983 N88-15943
Comparative performance of the conjugate gradient and SOR (Successive Over Relaxation) methods for computational thermal hydraulics
[DE88-002553] 08 p0988 N88-15986
Response of a sequential damper to shock inputs 08 p0998 N88-16042
Study of pattern formation at liquid interfaces
[DE88-001399] 09 p1160 N88-16954
Techniques of flow visualization
[AGARD-AG-302] 09 p1164 N88-16977
TOPP: A post-processor for TOPAZ, the one dimensional pipe flow analysis code
[DE88-003711] 09 p1164 N88-16981
A project to experimentally and theoretically examine fluid interfacial wave phenomena in a rotating cylindrical geometry: Current results and future plans
[DE88-003738] 09 p1165 N88-16984
Use of boundary-layer method for problem of sound propagation through channel with variable cross-section containing stream of fluid 09 p1233 N88-17396
Two-dimensional analysis for a scrapeoff and divertor regions with an MHD model. Conceptual design study of FY86 FER
[DE88-751069] 09 p1251 N88-17497
Overview of heat transfer and fluid flow problem areas encountered in Stirling engine modeling
[NASA-TM-100131] 09 p1262 N88-17561
Pumping systems and flow interfaces for rapid response electronic reheat controls 10 p1282 N88-17665
One-dimensional leakage-flow vibration instabilities
[DE88-002875] 10 p1330 N88-17947
Application of a multigrid method to a buoyancy-induced flow problem
[DE88-003961] 10 p1397 N88-18326
Experimental investigation of low gravity two-phase flow behavior
[DE88-003779] 11 p1466 N88-18741
Experiments on the flow of viscoelastic fluids between eccentric rotating cylinders 12 p1625 N88-19723
Rotational flow of rarefied gas between two coaxial cylinders with slip conditions
[INPE-4277-PRE/1149] 12 p1627 N88-19738
Fluidization mechanisms in slurry flows
[DE88-005191] 13 p1766 N88-20563
Velocity and concentration measurements in flowing suspensions by nuclear magnetic resonance
[DE88-006225] 13 p1770 N88-20589
Subduction 13 p1806 N88-20796
Hamiltonian description of the interaction of surface waves with mixed-layer currents 13 p1806 N88-20799
Development of a rotary fluid transfer coupling and support mechanism for space station 14 p1928 N88-21493
Mixing: Stretching, breakup and chaos
[DE88-006899] 15 p2067 N88-22327
Deflection of a circular liquid jet on a flat plate perpendicular to the flow direction
[NASA-TT-20279] 16 p2207 N88-23173
Modal forced response of propfans in yawed flow 16 p2221 N88-23253
Numerical modelling of flows using phoenics 17 p2339 N88-23955
Dual wavelength holographic interferometry system
[NASA-CASE-MFS-28242-1] 17 p2341 N88-23960
Pressure measuring probe
[NASA-CASE-LAR-13853-1] 17 p2341 N88-23961
Simulations of a missile with liquid payload under launch conditions
[AD-A191479] 18 p2463 N88-24625
Adaptive local grid refinement in computational fluid mechanics
[AD-A192215] 18 p2510 N88-24890
A semigroup for Lagrangian 1D isentropic flow
[DE88-006464] 18 p2513 N88-24912
NASA research Program: The roles of fluid motion and other transport phenomena in the morphology of materials
[NASA-CR-182801] 18 p2580 N88-25327
Applications of some new ideas on irreversible processes to particular fluids
[AD-A191610] 19 p2663 N88-25836
The propagation of pressure perturbations in bubbly air/water flows 19 p2664 N88-25843
Multigrid computation of practical fluid flows and heat transfer
[DE88-010064] 20 p2799 N88-26609
Use of direct solvers for multidimensional fluid flow computations
[DE88-010063] 20 p2799 N88-26611
Fluid flow modeling in casting processes and its implications
[DE88-010009] 20 p2810 N88-26671
Acoustic diffraction by an absorbing finite strip in a moving fluid
[PB88-191382] 20 p2849 N88-26912
Optimal rheological characteristics in dynamic stability of polymer flow through porous media
[DE88-001225] 21 p2918 N88-27322
Characterization of accelerating pipe flow
[AD-A193065] 21 p2943 N88-27481
Effects of numerical dissipation on finite-volume solutions of compressible flow problems
[AD-A193173] 21 p2944 N88-27485
Numerical treatment of the pressure singularity at a re-entrant corner
[AD-A193357] 21 p2944 N88-27488
Stream function-vorticity finite elements and the resolution of the Navier-Stokes equations
[DE88-702318] 21 p2945 N88-27494
Superfluid Helium On-Orbit Transfer (SHOOT) operatons
[NASA-TM-101009] 22 p3048 N88-28084
Solidification with natural circulation
[DE88-011197] 22 p3074 N88-28248
Study of experimental technique of oil flow with emphasis on quantitative determination of the flow position parameters on the surface
[NASA-TT-20341] 23 p3215 N88-29135
Mapping of volcanic units at Alba Patera, Mars 23 p3301 N88-29663
Lava flow-field morphology: A case study from Mount Etna, Sicily 23 p3303 N88-29676
Preliminary investigation of flow modeling during solid propellant processing
[AD-A196168] 24 p3357 N88-29987
Experimental and analytical study of two-phase flow in zero gravity
[AD-A195223] 24 p3358 N88-29993
The use of upwind schemes at high Reynolds number: A cautionary note
[AD-A196227] 24 p3371 N88-30074
Approximation of viscoelastic stresses from Newtonian turbulent kinematics
[AD-A194317] 24 p3371 N88-30077
Simulations of lava flows on Mars 24 p3443 N88-30495
Small-scale volcanic landforms indicative of distributary tube systems 24 p3444 N88-30496
Volcanic styles at Alba Patera, Mars: Implications of lava flow morphology to the volcanic history 24 p3444 N88-30497

FLUID INJECTION
NT GAS INJECTION
NT WATER INJECTION
Insect contamination protection for laminar flow surfaces 07 p0814 N88-14954
Numerical simulation of ignition of hydrogen jet in hot air 19 p2637 N88-25647

FLUID JET AMPLIFIERS
U FLUID AMPLIFIERS

FLUID JETS
NT AIR JETS
NT FREE JETS
NT GAS JETS
NT HYDRAULIC JETS
JPRS report: Science and technology. China
[JPRS-CST-87-034] 03 p0301 N88-11897
Analysis of compressible flow on high-velocity jet penetration 03 p0302 N88-11898
Droplet formation for liquid monopropellant jets
[AD-A187172] 10 p1331 N88-17956
Effect of mass-velocity on liquid jet atomization in Mach 1 gasflow
[NASA-TM-100813] 16 p2211 N88-23194
Supercritical fluid chromatography/supersonic jet spectroscopy
[DE88-007935] 19 p2614 N88-25511
Droplet formation for liquid monopropellant jets 19 p2623 N88-25557
Liquid Engine Jet Atomization Workshop report 19 p2627 N88-25584
Small-droplet spray measurements with a scattered-light scanner
[NASA-TM-100973] 20 p2806 N88-26645
The influence of delay effects on the decay of liquid jets
[MPIS-14/1987] 23 p3214 N88-29130

FLUID MANAGEMENT
Components for cryostat --- spaceborne
[MBB/ISO-TN-CD00.003-REV-A] 01 p0032 N88-10207
Space station integrated propulsion and fluid system study: Fluid systems configuration databook
[NASA-CR-179215] 03 p0278 N88-11753
Space station resistojet system requirements and interface definition study
[NASA-CR-180832] 04 p0409 N88-12541
AF cryogenic and fluid management spacecraft technology program 08 p0981 N88-15925
Cryogenics program overview 08 p0981 N88-15926
Ames Research Center cryogenics program 08 p0981 N88-15927
LeRC cryogenic fluid management program overview 08 p0981 N88-15928
Cryogenic fluid management program flight concept definition 08 p0981 N88-15929
Orbital transfer vehicle studies overview 08 p0981 N88-15931
Large capacity cryopropellant orbital storage facility 08 p0981 N88-15932
Thermal analysis for the Cryogenic Fluid Management Flight Experiment (CFMFE) 08 p0982 N88-15935
Zero-G thermodynamic vent system for shuttle/Centaur 08 p0983 N88-15943
Study of helium transfer technology for STICCR: Fluid management
[NASA-CR-177463] 10 p1291 N88-17720
Cryogenic Fluid Management Technology Workshop. Volume 2: Roundtable Discussion of Technology Requirements
[NASA-CP-10009] 13 p1772 N88-20599

Vibration characteristics of pumped fluid systems (VCPFS) --- microgravity payloads
[ESA-CR(P)-2499] 14 p1895 N88-21310
Development of a motorized cryovalve for the control of superfluid liquid helium 14 p1925 N88-21477
FLOSIN: A fluid loop analyzer for SINDA 15 p2066 N88-22321
Two-phase fluid management for a Rankine cycle isotope power system 17 p2405 N88-24303
Turbomachinery in space 17 p2408 N88-24321
Superfluid Helium On-Orbit Transfer (SHOOT) operations
[NASA-TM-101009] 22 p3048 N88-28084
Study of toluene rotary fluid management device and shear flow condenser performance for a space-based organic Rankine power system
[NASA-CR-180885] 24 p3338 N88-29872

FLUID MECHANICS
NT AERODYNAMICS
NT AEROTHERMODYNAMICS
NT COMPUTATIONAL FLUID DYNAMICS
NT ELASTOHYDRODYNAMICS
NT ELECTROHYDRODYNAMICS
NT FLUID DYNAMICS
NT GAS DYNAMICS
NT HYDRODYNAMICS
NT HYDROMECHANICS
NT HYDROSTATICS
NT INTERACTIONAL AERODYNAMICS
NT MAGNETOHYDRODYNAMICS
NT PNEUMATICS
NT RAREFIED GAS DYNAMICS
NT ROTOR AERODYNAMICS
NT SUPERSONICS
NT UNSTEADY AERODYNAMICS
NT VORTEX SHEDDING
Rayleigh-Taylor instability in compressible fluids
[DE87-013494] 01 p0047 N88-10297
Mean flow structure of a turbulent junction vortex
[PB87-206231] 01 p0047 N88-10301
Steady state theta pinch concept for slow formation of FRC
[ISSN-0469-4732] 01 p0098 N88-10648
USSR Report: Engineering and Equipment
[JPRS-UEQ-87-007] 02 p0157 N88-10985
A preliminary study of a fluid science laboratory for space station (Columbus). Part 4: Executive summary
[NLR-TR-87023-L-PT-4] 02 p0170 N88-11072
Personal Computer (PC) based image processing applied to fluid mechanics
[NASA-TM-100024] 02 p0172 N88-11087
Point vortex dynamics: Recent results and open problems
[DE87-014759] 03 p0314 N88-11982
The Proceedings of the Symposium on Mechanics for Space Flight
[ISAS-SP-5] 03 p0317 N88-12006
Some experiences with the viscous-inviscid interaction approach
[NASA-TM-100015] 04 p0395 N88-12466
Low gravity fluid-thermal experiments
[DE88-000553] 04 p0423 N88-12620
Proceedings of the Fifth Symposium on Energy Engineering Sciences: Instrumentation, Diagnostics, and Material Behavior
[DE88-001479] 04 p0429 N88-12660
NACHOS 2: A finite element computer program for incompressible flow problems. Part 2: User's manual
[DE88-001451] 04 p0443 N88-12750
A spatial marching technique for the inviscid blunt body problem 05 p0533 N88-13239
Experimental study of the fluid mechanics of unsteady turbulent boundary layers
[AD-A184856] 05 p0580 N88-13536
Numerical analysis, computing and fundamental studies in fluid mechanics
[DE88-001912] 05 p0582 N88-13550
Damping analysis of flexural waves in fluid-loaded single and constrained plates
[AD-A185116] 05 p0609 N88-13739
Research on internal fluid mechanism between turbine blades 06 p0676 N88-14138
Internal fluid mechanics research on supercomputers for aerospace propulsion systems
[NASA-TM-100289] 07 p0854 N88-15188
Aeropropulsion '87. Session 3: Internal Fluid Mechanics Research
[NASA-CP-10003-SESS-3] 08 p0954 N88-15790
Inlets, ducts and nozzles 08 p0955 N88-15791
Chemical reacting flows 08 p0955 N88-15793
Aeropropulsion '87. Session 4: Instrumentation and Controls Research
[NASA-CP-10003-SESS-4] 08 p0955 N88-15794
Aeropropulsion '87. Session 5: Subsonic Propulsion Technology
[NASA-CP-10003-SESS-5] 08 p0956 N88-15800
Aeropropulsion '87. Session 6: High-Speed Propulsion Technology
[NASA-CP-10003-SESS-6] 08 p0957 N88-15807
Fluid mechanical issues in polymer processing
[DE88-002767] 08 p0972 N88-15880
Review of the equations of fluid mechanics and heat transfer 08 p0986 N88-15970
Active control of jet flowfields
[AD-A186736] 08 p0989 N88-15989
An efficient method for computing leading Eigenvalues and Eigenvectors of large asymmetric matrices 09 p1159 N88-16949
Techniques of flow visualization
[AGARD-AG-302] 09 p1164 N88-16977
Investigation of surface tension driven convection as a feasibility study for a micro-gravity experiment
[NASA-CR-182504] 11 p1466 N88-18739
International Conference on Industrial and Applied Mathematics
[AD-A188251] 11 p1483 N88-18851
Studies on homogeneous and heterogeneous reactive flows 11 p1484 N88-18861
Numerical analysis, computing and fundamental studies in fluid mechanics
[DE88-005343] 12 p1625 N88-19725
A review of approaches to the study of turbulence modification by means of non-Newtonian additives
[AD-A188799] 12 p1627 N88-19734
Research on flow control
[AD-A189014] 12 p1627 N88-19736
Fluidization mechanisms in slurry flows
[DE88-005191] 13 p1766 N88-20563
Fluid-thermal-structural study of aerodynamically heated leading edges
[NASA-TM-100579] 13 p1783 N88-20666
On the structure of pulsed plasma jets 13 p1843 N88-21030
Mixing: Stretching, breakup and chaos
[DE88-006699] 15 p2067 N88-22327
Physical fluid mechanics in MPD thrusters
[AD-A190309] 15 p2138 N88-22754
Research and technology
[NASA-TM-100172] 15 p2153 N88-22851
The nonlinear dynamics of a spacecraft coupled to the vibration of a contained fluid
[DE88-007035] 16 p2168 N88-22925
Fundamental aspects of the structure of supersonic turbulent boundary layers
[AD-A191494] 18 p2456 N88-24581
Internal fluid dynamics within a nonspinning partially liquid-filled shell due to burster rupture
[AD-A191055] 18 p2507 N88-24874
Heating and evaporation of turbulent liquid films: Measurement of film thickness and the onset of nucleate boiling
[DE88-006388] 18 p2512 N88-24905
Extrema principles of entrophy production and energy dissipation in fluid mechanics
[NASA-TM-100992] 18 p2519 N88-24946
A Navier-Stokes solver for cascade flows
[NASA-CR-181682] 19 p2666 N88-25856
Laser probes and numerical modeling as process diagnostics in chemical vapor deposition
[DE88-011622] 21 p2911 N88-27275
Some stability criteria in fluid and solid mechanics 21 p3027 N88-27966
A study of the vortex sheet method for solving the Prandtl boundary layer equations
[DE88-011346] 22 p3074 N88-28249
Three-dimensional vortex interactions
[AD-A194066] 23 p3172 N88-28889
A limiting viscosity approach to the Riemann problem for materials exhibiting change of phase
[AD-A193477] 23 p3210 N88-29103
Development of the Simplified Compressor Model (SCM) for performance analysis of gaseous diffusion compressors
[DE88-009066] 23 p3221 N88-29173
Fluid physics double rack --- Spacelab
[SD-TN-AI-012] 24 p3358 N88-29992

FLUID POWER
Microcomputer control of a hydraulically actuated piston
[AD-A184130] 03 p0368 N88-12317
Laser thermal propulsion
[AD-A186407] 07 p0933 N88-15666
Advanced energy conversion concept for beamed-energy propulsion
[AD-A187336] 10 p1324 N88-17914

FLUID PRESSURE
Physics of immiscible flow in porous media
[PB88-131008] 11 p1487 N88-18873

FLUID TRANSMISSION LINES
Ammonia transfer across rotating joints in space 14 p1927 N88-21492

FLUID TRANSPIRATION
U TRANSPIRATION

FLUID-SOLID INTERACTIONS
NT GAS-SOLID INTERACTIONS
Experimental study of three-dimensional turbulent jet-solid boundary interaction 01 p0046 N88-10293
Time-dependent hypersonic viscous interactions
[AD-A185764] 06 p0665 N88-14082
Studies on fluid-structural vibration using boundary element method
[PB87-129508] 06 p0699 N88-14291
Validation of the Underwater Shock Analysis (USA) program. Part 1: Theoretical considerations --- ship design
[REPT-5073713-86-01] 06 p0702 N88-14308
Abrasion and impact resistant coatings
[DE88-003562] 13 p1750 N88-20464

FLUIDIC CIRCUITS
Microminiature fluidic amplifier 19 p2669 N88-25865

FLUIDICS
Dynamics and control of turbulent shear flows
[AD-A191527] 18 p2508 N88-24879
Pulsatile fluidic pump performance at elevated temperatures
[DE88-008046] 19 p2677 N88-25919

FLUIDS
China report: Science and technology
[JPRS-CST-87-015] 03 p0298 N88-11873
Integrated 3-parameter diagram for determining thermodynamic properties of fluids 03 p0298 N88-11874
Theory of neutron scattering experiments on momen tum distributions in quantum fluids
[DE87-01369] 05 p0648 N88-13968
New equilibrium forms of free surface of confined magnetic fluid 06 p0770 N88-14734
Experimental and theoretical constraints on the origin of mid-ocean ridge geothermal fluids 13 p1804 N88-20784
Fluids, gels and glasses under extreme conditions of pressure and temperature
[AD-A190655] 15 p2035 N88-22125

FLUORESCENCE
NT LASER INDUCED FLUORESCENCE
NT PHOSPHORESCENCE
NT RESONANCE FLUORESCENCE
NT X RAY FLUORESCENCE
KR+ laser excitation of NH2 in atmospheric pressure flames
[AD-A183421] 01 p0050 N88-10322
Photolytic processes for measurement of combustion heats of formation and reaction rates
[DE87-014047] 02 p0144 N88-10905
Theoretical atomic and molecular photophysics
[DE87-014249] 02 p0231 N88-11458
OH(A-X) fluorescence from photodissociative excitation of HO2 at 157.5 nm
[NASA-CR-181580] 05 p0563 N88-13429
Artificial photosynthesis using chlorophyll based carotenoid-quinone triads
[DE88-001660] 07 p0884 N88-15362
The use of chlorophyll fluorescence measurements from space for separating constituents of sea water 08 p1043 N88-16307
Fed-batch control based upon the measurement of intracellular NADH 09 p1197 N88-17175
Excimer plasma displays
[AD-A186731] 09 p1250 N88-17489
Investigation of real-time two-dimensional visualization of fuel spray liquid/vapor distribution via exciplex fluorescence
[AD-A188268] 10 p1307 N88-17816
Multicomponent analysis using synchronous-excitation phase-resolved fluorescence spectroscopy
[AD-A188883] 12 p1606 N88-19604
Discharge excitation of dye vapors
[AD-A188428] 12 p1632 N88-19770
Nondestructive evaluation of carbon-carbon coatings
[AD-A189524] 13 p1748 N88-20453
Remote fiber fluorimetry techniques for pressure measurements
[DE88-004486] 13 p1773 N88-20604
Laser fluorescence spectroscopy of zinc neutrals originating from laser-irradiated and ion-bombarded zinc sulfide and zinc surfaces
[DE88-006033] 13 p1776 N88-20620
Noncontact thermometry via laser pumped, thermographic phosphors: Characterization of systematic errors and industrial applications
[DE88-005599] 13 p1777 N88-20628
Spontaneous decay and atomic fluorescence near a metal surface of an absorbing dielectric
[AD-A187508] 13 p1835 N88-20975
What has been done and what will be done by subnatural linewidth spectroscopy 14 p1978 N88-21807

Polarization of molecular fluorescence bands in comets: Recent observations and interpretation
14 p1998 N88-21907
Light scattering of intracellular gas vacuoles: Anomalous behavior of forward and perpendicular light scattering of a cyanobacterium due to intracellular gas vacuoles
[BCRS-87-08] 16 p2228 N88-23308
A new fiber-optic-based ion sensor
[AD-A191322] 16 p2274 N88-23612
Cascade fluorescences from laser-excited lithium atom for plasma diagnostics 17 p2442 N88-24526
Flux density measurements of neutral iron in TEXTOR with laser induced fluorescence
17 p2442 N88-24528
Optical diagnostics for a high power, rf-inductively coupled plasma
[DE88-007822] 18 p2579 N88-25322
Determination of low molecular weight thiols using monobromobimane fluorescent labeling and high-performance liquid chromatography
[NASA-CR-182932] 19 p2608 N88-25478
Laser fluorescence spectroscopy of zinc neutrals originating from laser-irradiated and ion-bombarded zinc sulfide and zinc surfaces
[DE88-008037] 20 p2769 N88-26418
Physical-chemical reactions at welding arc/molten pool interfaces
[DE88-007717] 20 p2808 N88-26662
Molecular fluorescence measurements with a charge-coupled device detector
[AD-A194221] 22 p3080 N88-28291
Program to increase the measurement capabilities of the AFGL (Air Force Geophysics Laboratory) fixed and mobile high altitude lidar systems
[AD-A194614] 23 p3203 N88-29063
Molecular fluorescence measurements with a charge-coupled device detector
[AD-A194437] 23 p3216 N88-29141
Autoionization for lower level detrapping in X-ray lasers
[AD-A195845] 24 p3379 N88-30123
Immunofluorescence localization of dissociation supernatant and extracellular matrix components in Lytechinus pictus sectioned embryos
[NASA-CR-183137] 24 p3406 N88-30276

FLUORESCENT EMISSION
U FLUORESCENCE

FLUORIDES
NT ALUMINUM FLUORIDES
NT CALCIUM FLUORIDES
NT CHLORINE FLUORIDES
NT HYDROFLUORIC ACID
NT LITHIUM FLUORIDES
NT NITROGEN FLUORIDES
NT POLYVINYL FLUORIDE
NT SODIUM FLUORIDES
NT SULFUR FLUORIDES
NT URANIUM FLUORIDES
The kinetics and dynamics of iodine monofluoride formation in gas-phase collisions
[AD-A185715] 06 p0709 N88-14352
SBIR-Long fluoride fiber
[AD-A188595] 13 p1754 N88-20492
NMR analysis of a fluorocarbon copolymer
[DE88-002364] 15 p2043 N88-22170
Interaction of vinylidene fluoride: Tetrafluoroethylene copolymer with ammonia
[NASA-TT-20292] 19 p2620 N88-25542
NF (a 1 delta) production in a supersonic flow using N2F4+H2 in a BCL-16 nozzle
[AD-A194478] 22 p3082 N88-28304

FLUORINATION
Elementary fluorination of polymers
[ETN-88-90812] 07 p0836 N88-15075
Feasibility of chemical lasers based on chain reaction involving hydrogen fluorination with thermal branching mechanism 09 p1238 N88-17420
Polymerization of fluorinated diacetylenes
[AD-A188051] 11 p1462 N88-18716
A new approach to highly fluorinated lubricants
[AD-A190523] 15 p2045 N88-22188

FLUORINE
Studies of fluorine combustion
[AD-A187646] 11 p1452 N88-18656
Combustion of hydrogen and hydrocarbons in fluorine
[AD-A188018] 11 p1453 N88-18662
Numerical modelling specific energy charcteristics of excimer KrF lasers with electron beam excitation
[DE88-701525] 15 p2070 N88-22344

FLUORINE COMPOUNDS
NT ALUMINUM FLUORIDES
NT CALCIUM FLUORIDES
NT CHLORINE FLUORIDES
NT DIFLUORO COMPOUNDS
NT FLUORIDES
NT FLUORINE ORGANIC COMPOUNDS
NT FLUORO COMPOUNDS
NT FLUOROCARBONS
NT FLUOROHYDROCARBONS
NT FLUOROPOLYMERS
NT HYDROFLUORIC ACID
NT LITHIUM FLUORIDES
NT NITROGEN FLUORIDES
NT POLYTETRAFLUOROETHYLENE
NT POLYVINYL FLUORIDE
NT SODIUM FLUORIDES
NT SULFUR FLUORIDES
NT TEFLON (TRADEMARK)
NT URANIUM FLUORIDES
Photocurrent generation from basic metals, utilizing a short pulsed ArF excimer laser
[AD-A184928] 05 p0587 N88-13579
Study of the micromechanical properties of fluor glasses based on ZrF4
[ISAL-ITC1-87-03] 09 p1148 N88-16882
Theoretical calculations of XeF ground state kinetics
[AD-A191398] 16 p2270 N88-23580

FLUORINE ORGANIC COMPOUNDS
NT FLUOROCARBONS
NT FLUOROHYDROCARBONS
NT FLUOROPOLYMERS
NT POLYVINYL FLUORIDE
NT TEFLON (TRADEMARK)
Supersonic turbines for organic fluid Rankine cycles from 3 to 1300 kW 06 p0713 N88-14375
Improved perfluoroalkylether fluid development
[NASA-CR-180872] 08 p0967 N88-15851

FLUORO COMPOUNDS
NT DIFLUORO COMPOUNDS
NT FLUORINE ORGANIC COMPOUNDS
NT FLUOROCARBONS
NT FLUOROHYDROCARBONS
NT FLUOROPOLYMERS
NT POLYTETRAFLUOROETHYLENE
NT TEFLON (TRADEMARK)
Organic Rankine-cycle power systems working fluids study. Topical report No. 1: Fluorinol 85
[DE87-014604] 02 p0195 N88-11217
Flash threshold of shocked aluminum silicofluoride
[DE88-003978] 10 p1339 N88-18005
Polyazidoesters as energetic polymers and copolymer components with fluoro derivatives
[AD-A194236] 23 p3199 N88-29039

FLUOROCARBONS
Impact on ozone attainment of CFC (chlorofluorocarbon) controls used to prevent future depletion of stratospheric ozone
[PB88-195177] 19 p2690 N88-25989
Substituted 1,1,1-Triaryl-2,2,2-Trifluoroethanes and processes for their synthesis
[NASA-CASE-LEW-14345-1] 20 p2767 N88-26404

FLUOROHYDROCARBONS
NT POLYTETRAFLUOROETHYLENE
NT TEFLON (TRADEMARK)
Distributed feedback effects in lasers and high gain laser instabilities in optically pumped CH3F
03 p0329 N88-12079
Polymerization of fluorinated diacetylenes
[AD-A188051] 11 p1462 N88-18716
Thermal oxide growth on silicon: Intrinsic stress and silicon cleaning effects
[AD-A188790] 13 p1736 N88-20377
Natural convection immersion cooling of an array of simulated chips in an enclosure filled with dielectric liquid
[AD-A193594] 23 p3207 N88-29088

FLUOROPLASTICS
U FLUOROPOLYMERS

FLUOROPOLYMERS
NT POLYTETRAFLUOROETHYLENE
NT POLYVINYL FLUORIDE
NT TEFLON (TRADEMARK)
Ferroelectric properties and impact behavior of the PVF2 polymer and the VF2/C2F3H polarized copolymers --- vinylidene polyfluorides
[ISL-CO-245/86] 08 p0971 N88-15876
Cellular thermosetting fluoropolymers and process for making them
[NASA-CASE-GSC-13008-1] 17 p2326 N88-23894
Substituted 1,1,1-Triaryl-2,2,2-Trifluoroethanes and processes for their synthesis
[NASA-CASE-LEW-14345-1] 20 p2767 N88-26404
Polymer-ceramic composites
[AD-A193244] 21 p2905 N88-27237
Plasma treatment of polymers for improved adhesion
[DE88-011623] 21 p2921 N88-27334

FLUOROSCOPY
A microspectrofluorometer system based on real time digital techniques
[REPT-86-014] 11 p1490 N88-18891

FLUTING
U GROOVING

FLUTTER
NT SUPERSONIC FLUTTER
NT TRANSONIC FLUTTER
Flutter suppression and gust load alleviation. Part 1: Results of phase 1 to 3. Part 2: Description of the Garteur model
[MBB/LKE-292/S/PUB/191] 01 p0007 N88-10038
A natural low frequency oscillation in the wake of an airfoil near stalling conditions
[NASA-TM-100213] 02 p0123 N88-10779
Static aeroelastic effects on the flutter of a supercritical wing 05 p0550 N88-13353
Integration of a supersonic unsteady aerodynamic code into the NASA FASTEX system
[NASA-CR-182329] 06 p0663 N88-14068
Parametric study of choke flutter with a linear theory
10 p1283 N88-17673
The application of modern aeroelastic developments for future projects
[MBB-UT-007/87] 10 p1313 N88-17850
The effects of rotational flow, viscosity, thickness, and shape on transonic flutter dip phenomena
[NASA-TM-100811] 11 p1502 N88-18969
A semianalytical technique for sensitivity analysis of unsteady aerodynamic computations
[NASA-TM-100810] 11 p1503 N88-18976
Application of a flux vector splitting methodology towards the solution of unsteady transonic flows, with future emphasis on the blade flutter problem
[AD-A189500] 13 p1716 N88-20260
Design of an integrated control system for flutter margin augmentation and gust load alleviation, tested on a dynamic windtunnel model
[PB88-149885] 15 p2020 N88-22038
Development of aeroelastic analysis methods for turborotors and propfans, including mistuning
16 p2219 N88-23244
Application of Navier-Stokes analysis to stall flutter
16 p2220 N88-23249
Empirical flutter prediction method
[AD-A195699] 24 p3327 N88-29810

FLUTTER ANALYSIS
Investigation of control law for active flutter suppression
[NASA-TT-20126] 02 p0130 N88-10818
The Green's function method for fully unsteady aerodynamics around three-dimensional bodies and its application to flutter analysis
[UTIAS-298] 03 p0260 N88-11639
Velocity scaled aeroelastic testing of an unducted fan
[GTL-191] 05 p0548 N88-13337
Influence of the static deformation on a wing in the unsteady aerodynamic 05 p0551 N88-13357
Modern wing flutter analysis by computational fluid dynamics methods
[NASA-TM-100531] 07 p0816 N88-14965
Unsteady transonic algorithm improvements for realistic aircraft applications
[NASA-TM-100516] 08 p0949 N88-15760
Experimental study on the effect of fiber orientation on flutter characteristics of high-aspect-ratio transport wing
[NAL-TR-936] 09 p1120 N88-16708
Effect of an optimized fiber orientation on transonic flutter characteristics of a high-aspect-ratio composite wing
[NAL-TR-930] 09 p1120 N88-16709
An application of eigenspace methods to symmetric flutter suppression
[NASA-CR-181618] 10 p1284 N88-17684
La Recherche Aerospatiale, bimonthly bulletin, number 1987-2, 237/March-April
[ESA-TT-1074] 11 p1433 N88-18550
Modeling of limit cycle stall flutter oscillations
12 p1583 N88-19472
Aircraft flight flutter testing at the NASA Ames-Dryden Flight Research Facility
[NASA-TM-100417] 13 p1723 N88-20301
A computational procedure for automated flutter analysis 16 p2220 N88-23250
Vibration and flutter analysis of the SR-7L large-scale propfan 16 p2221 N88-23254
Supersonic axial-flow fan flutter
16 p2221 N88-23255
A characteristic method for calculating the generalized flat flutter aerodynamic forces
[NASA-TT-20300] 19 p2598 N88-25438
Parametric flutter studies of an arrow-wing configuration: Some early results
[NASA-TM-100608] 19 p2599 N88-25444
Detailed on-blade measurements on a transonic fan in unstalled supersonic flutter
[PNR90424] 22 p3039 N88-28043
A streamwise upwind algorithm for the Euler and Navier-Stokes equations applied to transonic flows
[NASA-TM-101019] 24 p3316 N88-29751

Application of unsteady aerodynamic methods for transonic aeroelastic analysis
[NASA-TM-100665] 24 p3317 N88-29754
Recent advances in transonic computational aeroelasticity
[NASA-TM-100663] 24 p3321 N88-29778
Use of holography in vibration and flutter study of fans
[PNR90458] 24 p3375 N88-30098

FLUX (RATE PER UNIT AREA)
U FLUX DENSITY

FLUX (RATE)
NT HEAT FLUX
NT MAGNETIC FLUX
NT SOLAR FLUX
Change in interplanetary shock acceleration preceding STIP Interval 17 01 p0112 N88-10719
Coronal mass ejections: The long-term variation of their occurrence rate and the solar wind mass flux 01 p0114 N88-10732
VLA observations of rapid 6 cm flux variations in alpha Ori 04 p0515 N88-13169
A comprehensive exploration of late-type stars in the far-ultraviolet 04 p0520 N88-13194
Gamma ray lines from novae 04 p0526 N88-13214
FTE like variations in the geomagnetic field at ground based conjugate stations in the cusp regions
[INPE-4345-PRE/1182] 08 p1024 N88-16199
Interplanetary Magnetic Field (IMF) influence on the magnetic configuration and particle fluxes at geostationary orbit and on the substorm onset 08 p1031 N88-16247
Johnson noise thermometer for high radiation and high temperature environments
[DE88-003770] 10 p1323 N88-17911
Turbulence interactions in single- and multi-phase turbulent mixing and combustion processes
[AD-A187505] 10 p1332 N88-17960
Energy and momentum fluxes through the sea surface 13 p1806 N88-20798
Radiative processes affecting ocean mixed-layer heat content and their monitoring from satellite 13 p1806 N88-20800
Three-wave parametric resonance in plasma of relativistic electron flux 14 p1972 N88-21772
Design, fabricate, calibrate, test and deliver two satellite electron flux detectors
[AD-A190799] 16 p2169 N88-22930
Johnson noise thermometer for high-radiation and high-temperature environments 17 p2434 N88-24480
Ring current role in dynamics of fluctuating electron and ion fluxes in low-latitude magnetosphere 24 p3447 N88-30514

FLUX DENSITY
NT CURRENT DENSITY
NT ELECTRON FLUX DENSITY
NT ILLUMINANCE
NT IRRADIANCE
NT LUMINANCE
NT LUMINOUS INTENSITY
NT NEUTRON FLUX DENSITY
NT PARTICLE FLUX DENSITY
NT RADIANCE
NT RADIANT FLUX DENSITY
NT SOLAR CONSTANT
NT SOLAR FLUX DENSITY
NT SOUND INTENSITY
An evaluation of the LEC-460 solar collector
[DE88-000052] 02 p0196 N88-11224
Kinetics of crack growth: Thermal/mechanical interaction 03 p0337 N88-12124
Power density measurements in the near field of the DSS 13 26-meter antenna 04 p0437 N88-12711
Measurements of vapor flux, liquid water contents, precipitation rates and riming in a Utah mountain cloud system
[PB87-224945] 04 p0469 N88-12900
Calibration of the Ca II K line-core density and the magnetic flux density in stars using solar data 04 p0507 N88-13116
VLA observations of the X-ray bright Hyades M-dwarfs 04 p0512 N88-13147
MHD energy fluxes for late type dwarfs 04 p0512 N88-13148
Density variations of meteor flux along the Earth's orbit 06 p0739 N88-14545
Some models of the Geminids meteor stream formation 06 p0740 N88-14551
Experimental study of thermal loading at the wall of an industrial Diesel motor
[ISAL-IDI1-87-10] 10 p1339 N88-18000
Applications of energy density theory in cyclic plasticity
[AD-A186947] 10 p1342 N88-18023
An experimental measurement of metal multilayer X-ray reflectivity degradation due to intense X-ray flux
[LA-10989-T] 11 p1547 N88-19255
Corrosion, passivity and breakdown of alloys used in high energy density batteries
[DE88-004891] 13 p1743 N88-20422
Study on the burnout with variations of flow twisting over tube length
[DE87-703170] 14 p1909 N88-21405
The turbulent heat flux in low Mach number flows with large density variations
[DE88-006445] 14 p1911 N88-21419
Correlation between magnetic and electric field fluctuations observed during flyby near Halley's comet 14 p1996 N88-21897
Magnetic fusion energy plasma interactive and high heat flux components. Volume 5: Technical assessment of critical issues in the steady state operation of fusion confinement devices
[DE88-006920] 15 p2136 N88-22744
Local density of states in double-barrier resonant tunneling structures
[AD-A190673] 16 p2281 N88-23656
Flux density measurements of neutral iron in TEXTOR with laser induced fluorescence 17 p2442 N88-24528
Difficulties with interpretation of underground muons from Cygnus X-3
[DE88-701645] 23 p3309 N88-29710
Matching P.S.D.: Design loads 24 p3312 N88-29720
In-house capacitor technology program
[AD-A194804] 24 p3367 N88-30049
Vibrational power flow analysis of rods and beams
[NASA-CR-183166] 24 p3383 N88-30151

FLUX MAPPING
U FLUX DENSITY
U MAPPING

FLUX PINNING
Generation of flux tube waves in stellar convection zones. 1: Longitudinal tube waves
[NASA-TM-101152] 17 p2451 N88-24561

FLUX VECTOR SPLITTING
Numerical simulation of the hypersonic flow around lifting vehicles 05 p0532 N88-13234
A Cartesian finite-volume method for the Euler equations 05 p0579 N88-13532
Vectorization of a multigrid method for the compressible Navier-Stokes equations
[PB87-230496] 06 p0698 N88-14284
Application of a flux vector splitting methodology towards the solution of unsteady transonic flows, with future emphasis on the blade flutter problem
[AD-A189500] 13 p1716 N88-20260
Splitting of inviscid fluxes for real gases
[NASA-TM-100856] 14 p1964 N88-21717
Choice of implicit and explicit operators for the upwind differencing method
[NASA-TM-100857] 14 p1964 N88-21718

FLUXES
Optimum size of staged flux compression generators
[DE87-011741] 01 p0038 N88-10244
Investigation of the structure of coatings of self fluxing alloys fused by laser energy
[BLL-M-37301-(5828.4)] 02 p0148 N88-10930
Slowing down tail enhanced, neoclassical and classical alpha particle fluxes in tokamak reactors
[DE88-001930] 06 p0783 N88-14806
Submerged arc flux welding with CaF2-CaO-SiO2 fluxes: Possible electrochemical effects on weld metal
[DE88-003107] 08 p0992 N88-16004
Cleanliness tests with the Omega Meter: A comparative study for solder flux removal
[DE88-004634] 11 p1460 N88-18704
Evaluation of solder flux solvents in a vapor-degreasing application for hybrid microcircuits
[BDX-613-3638] 11 p1468 N88-18752

FLUXMETERS
U MAGNETIC MEASUREMENT
U MEASURING INSTRUMENTS

FLY BY WIRE CONTROL
Flight test of a resident backup software system 02 p0128 N88-10805
Recent Sikorsky R and D progress 09 p1111 N88-16659
Integrated Application of Active Controls (IAAC) technology to an advanced subsonic transport project: Program review
[NASA-CR-3880] 17 p2301 N88-23763
Computer system for the primary fly-by-wire control of civil transport aircraft (experimental system)
[FBW-TB-2086/88] 21 p2898 N88-27204

FLYBY MISSIONS
NT ASTEROID MISSIONS
NT GIOTTO MISSION
Final phase of Project Vega 01 p0009 N88-10053
Overview of plasma observations during the Halley flybys 01 p0116 N88-10743
The status of the international Halley watch 01 p0116 N88-10744
Correlation between magnetic and electric field fluctuations observed during flyby near Halley's comet 14 p1996 N38-21897
Halley's environments by the Japanese Suisei spacecraft 14 p1999 N88-21915
Determination of the Venus flyby orbits of the Soviet Vega probes using VLBI techniques 22 p3067 N88-28203

FLYING PERSONNEL
NT AIRCRAFT PILOTS
NT ASTRONAUTS
NT COSMONAUTS
NT FLIGHT CREWS
NT ORBITAL WORKERS
NT PILOTS (PERSONNEL)
NT SPACECREWS

FLYING PLATFORM STABILITY
U AERODYNAMIC STABILITY

FLYING QUALITIES
U FLIGHT CHARACTERISTICS

FLYING WING AIRCRAFT
U TAILLESS AIRCRAFT

FLYWHEELS
Apparatus for storing kinetic energy
[EP-PATENT-0-181-736-A1] 01 p0066 N88-10422
Value-assessment of energy storage concepts in burst power systems
[DE87-013756] 09 p1187 N88-17115
An advanced low-cost 2-axis active magnetic bearing flywheel --- satellite attitude control 14 p1877 N88-21213
Qualification of the OLYMPUS reaction wheel 14 p1878 N88-21226
Evolution of large momentum and reaction wheels 14 p1879 N88-21230
Three axis attitude control system
[NASA-CASE-GSC-12970-1] 17 p2308 N88-23808
Assessment of energy storage concepts for use in sprint power 17 p2407 N88-24312
Nuclear Rankine/flywheel MMW space power concept 17 p2413 N88-24349
Energy storage for nuclear burst power systems 17 p2426 N88-24431
Value assessment of energy storage concepts in burst power systems 17 p2426 N88-24432
Rotating-hoop, pulsed-energy converter 17 p2426 N88-24433
Candidate advanced energy storage concepts for multimegawatt burst power systems 17 p2426 N88-24434

FOAMING
Investigations of the stability of the cell opening of soft polyurethane foams
[ETN-88-91481] 11 p1463 N88-18724

FOAMS
A process for producing phenolic foams
[EP-PATENT-0-170-357-A1] 01 p0026 N88-10162
Study of aeropropulsion laboratory pressure drop rig and recommended test procedure
[AD-A184333] 03 p0322 N88-12038
Flame retardant phenolic foams
[EP-PATENT-0-223-489-A2] 05 p0568 N88-13464
The effective elastic properties of low-density foams
[DE87-014629] 06 p0684 N88-14194
Foam generation and air entrainment near a free surface
[AD-A185986] 07 p0848 N88-15149
An experimental investigation of the hydrodynamic and heat-transfer behavior of aqueous foam in laminar tube flow
[DE88-004954] 11 p1483 N88-18855
A study of methods to predict and measure the transmission of sound through the walls of light aircraft
[NASA-CR-182656] 12 p1687 N88-20090
A three-dimensional model for the elastic properties of a foam
[DE88-006197] 15 p2046 N88-22192
Soft-ground aircraft arresting systems
[AD-A190838] 16 p2165 N88-22912
Generation and coalescence of bubbles and stability of foams under microgravity conditions
[BMFT-FB-W-86-020] 16 p2184 N88-23017
Cellular thermosetting fluoropolymers and process for making them
[NASA-CASE-GSC-13008-1] 17 p2326 N88-23894
Determination of radiative properties of fiberglass and foam insulations
[DE88-007845] 21 p2920 N88-27331
Determination of the specific area of liquid gas and the velocity of weak pressure waves in aqueous foams
[NASA-TT-20347] 24 p3373 N88-30087

FOCAL PLANE ARRAYS
U FOCAL PLANE DEVICES
FOCAL PLANE DEVICES
Experiment control and data system for an infrared detector array with maximum sensitivity
[ETN-88-91497] 09 p1136 N88-16813
Integrated focal plane star sensor
[OG-RT/86-0156] 09 p1262 N88-17562
Mid infrared multichannel focal plane breadboard --- pushbroom sensors
[RT-87/014] 14 p1982 N88-21827
The application of an image intensifier to atmospheric Cerenkov gamma ray astronomy
[MPE-PREPRINT-115] 22 p3163 N88-28839
The focal plane reception pattern calculation for a paraboloidal antenna with a nearby fence
[NASA-TM-100691] 24 p3365 N88-30039
Imaging instrument of the vegetation payload (SPOT 4)
[SNIAS-881-440-107] 24 p3386 N88-30169
FOCI
NT PLASMA FOCUS
FOCUSING
NT SELF FOCUSING
A conceptual design of Final Focus Systems for linear colliders
[DE87-012840] 02 p0234 N88-11475
Resolution limitations and optimization of the LLNL streak camera focus
[DE88-001633] 05 p0586 N88-13572
Phenomena at a focus in a laser system
[AD-A185442] 05 p0588 N88-13585
Theory of induced spatial incoherence
[AD-A185005] 05 p0651 N88-13992
Dual mode laser velocimeter
[NASA-CASE-ARC-11634-1] 06 p0709 N88-14350
A directed method for locating the focus of expansion
[AD-A185840] 07 p0906 N88-15491
Study of combination type CO2 laser welding system
[PB87-143764] 08 p0992 N88-16002
Resolution limitations and optimization of the ITT F4157 streak tube focus for fast (10 ps) operation
[DE88-003727] 09 p1169 N88-17007
A-scan ultrasound measurement of ocular changes during accommodation
[AD-A186818] 09 p1198 N88-17181
Visual attention effects on discrimination of line orientation and line arrangement
[AD-A187013] 09 p1200 N88-17190
Trace analysis by MS/MS on a double focussing mass spectrometer
[AD-A187954] 10 p1334 N88-17973
Overview of applications of Laser-Induced Breakdown Spectroscopy (LIBS)
[DE88-004314] 10 p1336 N88-17987
Generalized equations for emittance and field energy of high-current beams in periodic focusing
[DE88-004448] 10 p1404 N88-18372
Geodetic measurement of deformation east of the San Andreas fault in Central California
[NASA-CR-182709] 13 p1798 N88-20754
Focused ion beam fabrication of graded channel FET's in GaAs and Si
[AD-A189166] 13 p1845 N88-21040
Manufacturing of ultrasonic focused probes
[VTT-RR-487] 15 p2074 N88-22368
Hybrid particle simulation for focusing of rotating and propagating LIB 16 p2276 N88-23624
A multi-frame ion pinhole camera for intense ion beam transport and focusing experiments
[DE88-007283] 18 p2516 N88-24926
Aurora status and plans
[DE88-006476] 18 p2521 N88-24955
Aurora status and plans
[DE88-006476] 18 p2521 N88-24955
Heavy ion fusion system assessment: Final focus and transport model
[LBL-23040] 19 p2725 N88-26183
Microfocus X-ray techniques for flaw location
[DE88-008636] 20 p2812 N88-26680
Signal processing software for ground penetrating radar, user's manual
[AD-A194286] 23 p3203 N88-29059
Image focusing in space and time
[AD-A195839] 24 p3429 N88-30410
FOETUSES
U FETUSES
FOG
A proposal of the nowcasting system for sea fog 02 p0202 N88-11264
Forecasting boundary layer clouds and fog: A review of operational numerical models 02 p0208 N88-11307
Two-dimensional numerical modeling of the life cycle of fog 02 p0209 N88-11311
Numerical modeling of radiation fog 08 p1017 N88-16166
Scattering of optical radiation by bursting water particles in fog 09 p1236 N88-17410
Fog, rain and aerosol attenuation in the atmosphere
[AD-A190867] 16 p2235 N88-23350
Rapid-scanning Fourier transform spectrometer for studies of propagation of near-millimeter-wave radiation through clear air and fog
[AD-A193752] 22 p3070 N88-28219
Flow visualization on a small scale
[AD-A194728] 23 p3181 N88-28935
FOIL BEARINGS
Foil gas bearing system endurance testing dynamic isotope power system 17 p2405 N88-24302
FOILS
Chromic acid anodizing of aluminum foil
[NASA-CR-178417] 07 p0837 N88-15077
FOILS (MATERIALS)
NT METAL FOILS
Multilayered foils as radiation entrance windows and spectral filters for image converters in the ultrasoft X-ray wavelength region
[MPE-PREPRINT-90] 02 p0176 N88-11099
RIIM two-pulse injector experiments
[DE88-000926] 05 p0653 N88-14005
FOKKER AIRCRAFT
NT F-27 AIRCRAFT
FOKKER BOND TESTERS
U ADHESION TESTS
FOKKER F 27 AIRCRAFT
U F-27 AIRCRAFT
FOKKER FRIENDSHIP AIRCRAFT
U F-27 AIRCRAFT
FOKKER-PLANCK EQUATION
Nonequilibrium fluctuations and transport in sheared fluids 03 p0316 N88-11999
Boltzmann-Fokker-Planck calculations using standard discrete-ordinates codes
[DE88-005393] 11 p1537 N88-19185
Propagator solutions of partial differential equations applied to plasma transport
[DE88-006432] 13 p1816 N88-20852
Memory efficient evaluations of nonlinear stochastic equations and C3 applications
[AD-A189872] 15 p2110 N88-22569
Multigroup flux-limited asymptotic diffusion Fokker-Planck equation
[DE88-700958] 15 p2118 N88-22615
Nonlinear stochastic interaction in aeroelastic structures
[AD-A193427] 21 p2961 N88-27589
FOLDING
Nonpreemptive run-time scheduling issues on a multitasked, multiprogrammed multiprocessor with dependencies, bidimensional tasks, folding and dynamic graphs
[DE88-003598] 09 p1223 N88-17335
Motion synchronization of a mechanism to deploy and restow a truss beam 14 p1925 N88-21474
Theoretical study of the folded waveguide
[DE88-007877] 19 p2654 N88-25759
FOLDING STRUCTURES
Multisurface control mechanism for a deployable antenna: Far Infrared and Submillimeter Space Telescope (FIRST) technology study
[RP-FA-D003] 09 p1135 N88-16807
Automatic in-orbit payload deployment mechanisms, logistic operations and transport vehicle design compatibilities 12 p1586 N88-19493
The CTM program of masts and the CTM engineering model --- spacecraft mechanism 14 p1874 N88-21196
The development status of the strongback array --- spacecraft structure 14 p1875 N88-21201
The X-beam as a deployable boom for the space station 14 p1925 N88-21473
Alternative module configurations for advanced solar arrays on low orbit and extended lifetime missions (AMOC 2)
[ESA-CR(P)-2581] 24 p3389 N88-30182
FOLIAGE
Stochastic modeling of EM scattering from foliage
[AD-A192258] 20 p2790 N88-26553
Foliar nitrate reductase: A marker for assimilation of atmospheric nitrogen oxides
[DE88-010453] 21 p2971 N88-27648
FOOD
Controlled Ecological Life Support System. Design, Development, and Use of a Ground-Based Plant Growth Module
[NASA-CP-2479] 05 p0630 N88-13852
Irradiation preservation of seafood: Literature review
[DE88-001691] 05 p0631 N88-13858
FOOD INTAKE
The determination of nutritional requirements for Safe Haven Food Supply System (emergency/survival foods) 06 p0792 N88-14856
Operation Everest 2: Nutrition and body composition
[AD-A186449] 08 p1049 N88-16333
FOOD PROCESSING
NT PRESERVING
Food irradiation seminar: Asia and the Pacific
[DE88-700432] 09 p1202 N88-17203
International cooperative effort to establish ASTM (American Society for Testing and Materials) standards for the measurement of radiation dose for food processing
[DE88-002702] 10 p1372 N88-18190
An economic analysis of a multi-commodity fruit and vegetable irradiator
[DE88-003425] 11 p1524 N88-19098
FOOD PRODUCTION (IN SPACE)
Food production and gas exchange system using blue-green alga (spirulina) for CELSS 03 p0358 N88-12253
Biomass recycle as a means to improve the energy efficiency of CELSS algal culture systems 03 p0358 N88-12254
Non-conventional approaches to food processing in CELSS, 1. Algal proteins: Characterization and process optimization 03 p0358 N88-12256
Sunlight supply and gas exchange systems in microalgal bioreactor 03 p0359 N88-12258
A review of recent activities in the NASA CELSS program 03 p0359 N88-12259
Mass balances for a biological life support system simulation model 03 p0361 N88-12272
Modeling the growth dynamics of four candidate crops for Controlled Ecological Life Support Systems (CELSS) 06 p0799 N88-14889
Regenerative life support system research
[NASA-CR-182606] 12 p1671 N88-20006
FOOTPRINTS
Maneuverable reentry vehicle trajectory footprints: Calculation and properties
[DE88-004726] 10 p1292 N88-17726
FORBIDDEN TRANSITIONS
Migration and transfer of triplet energy in selected polymer systems
[DE87-014432] 02 p0152 N88-10953
Theoretical studies of atomic transitions
[DE88-004719] 10 p1407 N88-18389
Macroscopic quantum jumps in a single atom 14 p1975 N88-21784
Forbidden transitions as ion-temperature sensitive lines 17 p2441 N88-24520
FORBUSH DECREASES
Overview of the MONSEE UAG report on STIP intervals No. 15 and 16: The 24-25 April 1984 Forbush decrease period 01 p0111 N88-10712
FORBUSH EFFECT
U FORBUSH DECREASES
FORCE
Repulsive force support system feasibility study
[NASA-CR-178400] 04 p0402 N88-12497
FORCE DISTRIBUTION
Lift distribution and velocity field measurements for a three-dimensional, steady blade/vortex interaction
[NASA-TM-100013] 07 p0815 N88-14962
Computer aided deflection measurement of an aircraft wing
[AD-A187778] 12 p1581 N88-19461
Force distribution and trajectory control for closed kinematic chains with applications to walking machines 13 p1779 N88-20642
Linear force device
[NASA-CASE-MSC-20549-2] 18 p2516 N88-24927
FORCE FIELDS
U FIELD THEORY (PHYSICS)
FORCE-FREE MAGNETIC FIELDS
Coronal magnetic fields produced by photospheric shear
[NASA-CR-181514] 03 p0390 N88-12447
FORCED CONVECTION
Effects of forced and free convections on structural temperatures of space shuttle orbiter during reentry flight
[NASA-TM-86800] 01 p0043 N88-10275
Dynamics and routes to chaos from quasiperiodicity 03 p0312 N88-11974
Regressed relations for forced convection heat transfer in a direct injection stratified charge rotary engine
[NASA-TM-100124] 05 p0549 N88-13345
Review of nucleation and incipient boiling under pool and forced convection conditions 08 p0982 N88-15938
Forced-convective boiling in small diameter tube 20 p2783 N88-26510

Stability experimental results of cable-in-conduit superconductor for fusion
[DE88-753424] 23 p3290 N88-29589
Impact of ETO propellants on the aerothermodynamic analyses of propulsion components
[NASA-TM-101303] 24 p3374 N88-30094

FORCED OSCILLATION
U FORCED VIBRATION

FORCED VIBRATION
Assessment of structural integrity from forced vibration testing
[DE87-014642] 02 p0191 N88-11195
Mechanical and flow excited vibrations of elastic plates and cylindrical shells in dense fluids
03 p0316 N88-11996
Structural frequency functions for an impulsive, distributed forcing function
[DE87-013811] 03 p0333 N88-12101
A review of two-phase flow-induced vibration
[DE88-001955] 09 p1160 N88-16955
Flaw identification from forced vibration testing
[DE88-002641] 10 p1342 N88-18018
Finite element methodology for nonlinear free and harmonic forced vibrations of beam and plate structures
13 p1782 N88-20663
The concept of an impact resonance diagram for characterizing the nonlinear response of impact vibration
[DE88-005475] 15 p2086 N88-22432
Forced response unsteady aerodynamics in a multistage compressor 18 p2512 N88-24903
Experimental and theoretical investigation of passive damping concepts for member forced and free vibration
[NASA-CR-183082] 20 p2814 N88-26693

FORCED VIBRATORY MOTION EQUATIONS
U EQUATIONS
U FORCED VIBRATION

FOREBODIES
NT ABLATIVE NOSE CONES
NT NOSE CONES
NT NOSES (FOREBODIES)
NT ROCKET NOSE CONES
Surface flow visualization of separated flows on the forebody of an F-18 aircraft and wind-tunnel model
[NASA-TM-100436] 14 p1863 N88-21127
Wind-tunnel investigation of actuated forebody strakes for yaw control at high angles of attack
17 p2299 N88-23754
Actuated forebody strakes
[NASA-CASE-LAR-13983-1] 18 p2464 N88-24628

FORECASTING
NT DELPHI METHOD (FORECASTING)
NT LONG RANGE WEATHER FORECASTING
NT NOWCASTING
NT NUMERICAL WEATHER FORECASTING
NT PERFORMANCE PREDICTION
NT PREDICTION ANALYSIS TECHNIQUES
NT STATISTICAL WEATHER FORECASTING
NT TECHNOLOGICAL FORECASTING
NT WEATHER FORECASTING
Testimony to the US Senate on the greenhouse effect
[DE87-013995] 01 p0071 N88-10458
Hanford Meteorological Station computer codes. Volume 2: The PROD computer code
[DE87-014807] 02 p0215 N88-11355
Forecast of current patterns for an eddy tracking experiment in the Norwegian coastal current
[PB87-224853] 06 p0747 N88-14595
Recent Colorado State University tropical cyclone research of interest to forecasters
[AD-A185996] 07 p0879 N88-15332
Forecasting complications of cardiovascular disease in flight personnel 10 p1361 N88-18136
A comparison of projection methods in the forecasting of overhead costs for seven government aerospace contractors
[AD-A187572] 10 p1425 N88-18514
Specific features of emanation, temperature and hydrodynamic fields in the epicentral zone of tectonic earthquake
[DE88-701140] 17 p2373 N88-24114
An investigation of Soviet capabilities in extended range arctic ice forecasting
[AD-A191082] 17 p2376 N88-24127
FAA aviation forecasts fiscal years 1988-1999
[AD-A191711] 18 p2455 N88-24576
Modelling and forecasting deep ocean and near surface mesoscale eddies: Hindcasting and forecasting with, and coupling a surface boundary layer model to, the Harvard quasigeostrophic model 19 p2694 N88-26013
Prospects for hot dry rock in the future
[DE88-010909] 20 p2820 N88-26730
An interagency working group on lightning threat warning
[DE88-009828] 20 p2826 N88-26767

FORECASTS
U FORECASTING

FOREIGN BODIES
The influence of foreign particles on bearing metals
[NASA-TT-20155] 20 p2775 N88-26454

FOREIGN POLICY
NT INTERNATIONAL COOPERATION
NT INTERNATIONAL RELATIONS
Technology transfer to China. Volume 2: Working papers, part 2
[PB88-158712] 14 p1992 N88-21873
Bayesian solutions to a 2 x 2 decision matrix using interval scaled payoffs with an application to foreign policy decisions
[AD-A190863] 16 p2260 N88-23511
Department of Defense Statement on the Balanced Technology Initiative to the Committee on Armed Services, United States Senate, 100th Congress, second session
[AD-A191841] 18 p2588 N88-25378

FOREIGN TRADE
U INTERNATIONAL TRADE

FORENSIC SCIENCES
U LAW (JURISPRUDENCE)

FOREST FIRES
Evaluation of a burned area and the vegetation regeneration affected by the burning in the Parque Nacional de Brazilia through TM/LANDSAT data
17 p2363 N88-24073
History of wildland fires on Vandenberg Air Force Base, California
[NASA-TM-100983] 18 p2549 N88-25134

FOREST MANAGEMENT
Use of SPOT panchromatic imagery to update forest maps of northern Quebec, Canada
03 p0344 N88-12172
Stand based forest inventory from SPOT IMAGE. First experiments 03 p0344 N88-12173
Applicability of SPOT for forest inventory, mapping and change monitoring 03 p0344 N88-12174
Effects of fire on composition, biomass, and nutrients in oak scrub vegetation on John F. Kennedy Space Center, Florida
[NASA-TM-100305] 08 p1020 N88-16182
Investigations on the application of space photographs (Spacelab metric camera) for routine inventories of extensively managed forest areas
[DFVLR-FB-87-22] 09 p1185 N88-17098
Report of the participation in the International Training Course: Remote Sensing in Village Forestry
[INPE-4476-NTE/278] 12 p1637 N88-19802
The radar scattering coefficient as a function of forest stand parameters and viewing angle. An empirical study of the Pinus sylvestris L. in the Kootwijk forest (The Netherlands), extended with observations in the Speulder and Sprielder forest (The Netherlands)
[ETN-88-91348] 13 p1760 N88-20527
Earth resources: A continuing bibliography with indexes (issue 57)
[NASA-SP-7041(57)] 16 p2229 N88-23314
Utilization of TM/LANDSAT images in the implanted forests mapping in the Mogi-Guacu Region (SP-Brazil)
17 p2357 N88-24042
Mobile satellite communications in the Forest Service
19 p2654 N88-25757
Satellite remote sensing for forest management. A review illustrated with research results on SPOT 1 data
22 p3106 N88-28443
An evaluation of the utility of SPOT and Thematic Mapper data for providing forest inventory information
22 p3106 N88-28444
SPOT-1 satellite imagery for forest inventory in Sweden 22 p3106 N88-28445
Forest management applications of SPOT data in Australia 22 p3106 N88-28447
SPOT multispectral data and maritime pine stands in southwest of France 22 p3106 N88-28448
Stand-based forestry inventory from SPOT image
22 p3106 N88-28449
Potential of SPOT imagery as a tool for forest mapping in Quebec 22 p3107 N88-28450
Assessment of large area forest disturbances caused by biotic and abiotic factors on the basis of SPOT images 22 p3107 N88-28451

FORESTS
NT RAIN FORESTS
Investigation of large scale impact of air pollution components on forest ecosystems in Bavaria, West Germany
[DFVLR-FB-87-17] 01 p0068 N88-10434
Correlation between aircraft MSS and LIDAR remotely sensed data on a forested wetland in South Carolina
[NASA-TM-89643] 02 p0193 N88-11204
Development of a method for forest damage inventory using multispectral scanner data
[KFK-PEF-25] 03 p0345 N88-12182
Proceedings of the Third Airborne Imaging Spectrometer Data Analysis Workshop
[NASA-CR-181552] 05 p0611 N88-13755
The use of airborne imaging spectrometer data to determine experimentally induced variation in coniferous canopy chemistry 05 p0612 N88-13761
Overview of Austrian Airborne Imaging Spectrometer (AIS) programme and first results
05 p0612 N88-13762
Improved canopy reflectance modeling and scene inference through improved understanding of scene pattern
[NASA-CR-182488] 10 p1347 N88-18049
Mapping of the mangroves of the Guanabarra Bay through the utilization of remote sensing techniques
[INPE-3942-TDL/229] 12 p1637 N88-19804
Proceedings of the Forest-Atmosphere Interaction Workshop
[CONF-8510250] 12 p1641 N88-19824
Remote sensing of earth terrain
[NASA-CR-182677] 13 p1790 N88-20711
Report of Atmospheric-Canopy Exchange Panel
[DE88-004478] 14 p1944 N88-21597
Aerodynamic aspects of the Amazon Forest
[INPE-4445-TDL/313] 15 p2098 N88-22501
Detection, monitoring and analysis of some environmental effects of fires in the Amazon region through utilization of NOAA and LANDSAT satellite imagery and aircraft data
[INPE-4503-TDL/326] 16 p2230 N88-23322
Radar penetration in the Amazonian rain forest
17 p2352 N88-24015
A proposal for a project entitled assessment of forest resources in Uruguay submitted to the United Nations Industrial Development Organization (UNIDO)
17 p2352 N88-24016
Airborne and spaceborne radar images for geologic and environmental mapping in the Amazon rain forest, Brazil
17 p2353 N88-24021
The use of SLAR and SIRA imagenes for the classification of forest typen in tropical rain forests
17 p2356 N88-24036
Utilization of TM/LANDSAT images in the implanted forests mapping in the Mogi-Guacu Region (SP-Brazil)
17 p2357 N88-24042
Anomalies in the vegetation in the Alto Xingu - MT
17 p2357 N88-24043
Radar penetration in the Amazonian rain forest
17 p2358 N88-24044
Stereoscopic photographs, ground and aerial, of trees used in the arborization of Curitiba (PR)
17 p2366 N88-24091
Mapping of plant associations and the variation of surface water in the Pantanal Mato-Grossense National Park, through remote sensing techniques
17 p2366 N88-24092
Interpreting forest biome productivity and cover utilizing nested scales of image resolution and biogeographical analysis
[NASA-CR-183036] 20 p2817 N88-26711
Spatial and spectral registration of Javanese landscape units with SPOT 22 p3092 N88-28362
Forest mapping by visual interpretation of SPOT images 22 p3106 N88-28446
Contribution to the mapping of forests in an intensively divided area, with the help of SPOT image data
22 p3107 N88-28453
SPOT 1: Image utilization, assessment, results. A study of the Elburgon Forest area (Kenya) showing the spectral responses of different forest tree species
22 p3107 N88-28454
A linear-time algorithm for finding a minimum spanning pseudoforest
[AD-A194029] 23 p3250 N88-29346
Recent measurements of ozone in the Amazon forests
[INPE-4494-PRE/1258] 24 p3389 N88-30185
Investigation of the large-scale impact of air pollution components on forest ecosystems in Bavaria
[ESA-TT-1087] 24 p3390 N88-30187
Some results from the Amazon Forest micrometeorological experiment
[INPE-4631-PRE/1346] 24 p3403 N88-30263

FORGING
Isothermal forging and its effect on the microstructure of powder route nickel alloy AP1
[RAE-TM-P-1094] 01 p0022 N88-10138
Status of titanium alloys R and D described
03 p0298 N88-11876
The effect of deformation rate on JBK-75 stainless steel forgings
[DE88-001696] 07 p0834 N88-15061
Brief evaluation of the alloy 17-4-PH (Z5 CNU 17-04). Semifinished product: 205 mm dia forged roller, test reports
[DF/NH-3616/84] 17 p2322 N88-23866

FORM
U SHAPES

FORM PERCEPTION
U SPACE PERCEPTION
FORMALDEHYDE
Evidence for first polymer in Comet Halley: Polyoxymethylene 14 p1997 N88-21906
FORMALISM
Extending Green's function formalism to general nonlinear equations
[DE87-013541] 02 p0224 N88-11411
Algebraic specification of process algebra, including two examples
[PB88-106729] 07 p0912 N88-15531
Prediction and analysis of basic gravitational microlensing phenomena 11 p1550 N88-19272
A comparative survey of mathematical models for dynamic simulation of in-orbit manipulation operations 12 p1592 N88-19533
Body tensor formalism in finite deformation elasticity and application to the torsion of a circular cylinder 13 p1780 N88-20651
Early reheating and cosmic strings 13 p1855 N88-21103
Hamiltonian formalism in the model of the relativistic string with rigidity
[DE88-701503] 15 p2147 N88-22815
Theoretical and numerical solution of the forward-scattering problem in a circularly cylindrical configuration
[PB88-173489] 16 p2189 N88-23056
Toward a mathematical formalism of performance, task difficulty, and activation 16 p2239 N88-23372
Spatial filtering on digital images 17 p2354 N88-24025
Stochasticity in a Q-machine plasma 18 p2578 N88-25315
FORMAT
UNIX benchmark system
[AD-A184492] 03 p0367 N88-12308
Stress effects and the optimum format of a scrolling seven-line VDT text window
[AD-A185559] 06 p0758 N88-14651
DOE data exchange format specification, mechanical products/drafting: Version 1.2.2: CADCAM-045
[DE88-001923] 07 p0904 N88-15477
Innovative design of composite structures: Further studies in the use of a curvilinear fiber format to improve structural efficiency
[NASA-CR-182576] 11 p1450 N88-18641
Output formatting in Apple-soft BASIC
[DE88-701413] 15 p2108 N88-22559
Parallel binary and parallel coded decimal time code formats
[AD-A190126] 17 p2384 N88-24170
Unified interchange format for computer data (standard file format)
[ESA-STR-225] 17 p2386 N88-24183
A five-layer Open Systems Interconnection (OSI) implementation 17 p2390 N88-24204
A detection theory analysis of visual display performance
[AD-A196291] 24 p3409 N88-30292
Partitioned storage for temporal databases
[AD-A195093] 24 p3436 N88-30451
FORMATION HEAT
U HEAT OF FORMATION
FORMING TECHNIQUES
NT CASTING
NT CENTRIFUGAL CASTING
NT COLD WORKING
NT ELECTROFORMING
NT EXPLOSIVE FORMING
NT EXTRUDING
NT FORGING
NT HOT WORKING
NT INJECTION MOLDING
NT INVESTMENT CASTING
NT PRESSING (FORMING)
NT PULTRUSION
NT ROLL FORMING
NT SLIP CASTING
NT STAMPING
Computer modeling of metal forming
[DE87-013804] 02 p0157 N88-10984
The formation of optical membrane reflector surfaces using uniform pressure loading
[DE87-012275] 03 p0376 N88-12367
Growth of short fatigue cracks in a squeeze formed aluminum alloy 05 p0598 N88-13658
TMA-microrheological testing of polymers (thermomechanical analysis)
[PB87-228805] 06 p0683 N88-14187
Composite ceramic superconducting filaments for superconducting cable
[AD-A187833] 11 p1556 N88-19312
Metals. Preliminary study for an Innovation-Oriented research Program (IOP)
[ETN-88-91317] 14 p1889 N88-21290
Innovation-Oriented research Program (IOP) metals. Annexes
[ETN-88-91318] 14 p1889 N88-21291
Simulation of thermo-mechanical forming processes: A mixed Eulerian-Langrangian finite element method
[PB88-155247] 14 p1933 N88-21530
FORMULAS
Orbit accuracy requirement of GPS for precise positioning and orbit determination within local area 13 p1756 N88-20499
FORMULAS (MATHEMATICS)
On the volume of a n-dimensional simplex
[REPT-87-16] 01 p0086 N88-10557
Incoherent radar spectra 06 p0691 N88-14239
Investigation of the higher-order elements in the SAMSON2 code
[AD-A193638] 23 p3271 N88-29465
FORMULATIONS
The effect of RDX particle size on the shock sensitivity of cast PBX formulations. 2: Bimodal compositions
[DE87-009581] 01 p0031 N88-10198
A procedure for estimating the crystal densities of organic explosives
[AD-A189023] 12 p1613 N88-19646
Investigation of the higher-order elements in the SAMSON2 code
[AD-A193638] 23 p3271 N88-29465
Large displacement and rotational formulation for laminated cylindrical shells including parabolic transverse shear
[AD-A194871] 24 p3384 N88-30158
Formulation and solution of economic equilibrium problems
[AD-A196034] 24 p3439 N88-30470
FORTRAN
Manual for GetData version 3.1: A FORTRAN utility program for time history data
[NASA-TM-88288] 01 p0081 N88-10520
EAGLES: An interactive environment for scientific computing
[DE87-013564] 01 p0084 N88-10541
IMPSOR: A fully vectorized FORTRAN code for three dimensional moving boundary problems with Dirichlet or Neumann boundary conditions
[DE87-014964] 02 p0226 N88-11427
BIMOND3: Monotone piecewise bicubic Hermite interpolation code
[DE87-014612] 02 p0229 N88-11442
Documentation of NCAR (National Center for Atmospheric Research) CCM1 program modules
[PB87-213567] 03 p0352 N88-12220
FORTRAN compiler performance benchmarks for the IBM personal computer
[LA-10883-MS] 03 p0363 N88-12284
Los Alamos National Laboratory computer benchmarking 1986
[LA-10898-MS] 03 p0363 N88-12285
Generating meshes for finite-difference analysis using a solid modeler
[DE88-001458] 04 p0439 N88-12729
A review and analysis of Fortran 8x
[DE88-001320] 04 p0479 N88-12955
Mixing Microsoft C and Microsoft FORTRAN program modules on the IBM Personal Computer
[DE88-001947] 05 p0637 N88-13895
Microprocessor emulating the intermediate code for FORTRAN compiler
[DE88-700540] 07 p0900 N88-15452
FORTRAN 77 programming guidelines
[DFVLR-MITT-87-10] 07 p0905 N88-15487
FORTRAN 77 guidelines for the software projects RASP and ANDECS
[DFVLR-MITT-87-09] 09 p1218 N88-17301
Pattern-recognition software detecting the onset of failures in complex systems
[DE88-002861] 09 p1220 N88-17318
Debugging FORTRAN on a shared memory machine
[DE88-003589] 10 p1386 N88-18276
The Livermore FORTRAN Kernels: A computer test of the numerical performance range --- benchmark tests
[UCRL-53745] 11 p1531 N88-19144
Automatic restructuring of FORTRAN programs for parallel execution
[DE88-003585] 12 p1676 N88-20018
FORTRAN 77 error handling of the RASP library
[DFVLR-MITT-87-14] 14 p1957 N88-21669
User's manual for LINEAR, a FORTRAN program to derive linear aircraft models
[NASA-TP-2768] 14 p1967 N88-21740
Parafrase restructuring of FORTRAN code for parallel processing 16 p2221 N88-23258
A description of an automated database comparison program
[NASA-TM-100609] 16 p2253 N88-23463
CIMAG2: The computer program to generate color images
[AD-A191847] 18 p2557 N88-25175
Advances in personal computers for scientific applications
[DE88-009824] 19 p2713 N88-26107
The MAFIA approach to solving Maxwell's equations in three dimensions
[DE88-007826] 19 p2720 N88-26155
An interactive computer code for preliminary design of solid propellant rocket motors
[AD-A192869] 20 p2766 N88-26399
Directions for programming in FORTRAN 77
[NASA-TT-20317] 20 p2839 N88-26842
An expeditious technique for keyboard input of information to FORTRAN computer programs
[DE88-009617] 20 p2840 N88-26855
FORTRAN 77 implementation of abstract datatype models
[DFVLR-MITT-88-08] 21 p3000 N88-27794
A computer program package for introductory one-dimensional digital signal processing applications
[AD-A194656] 23 p3249 N88-29338
Supermap for Cray FORTRAN: A user's guide
[NASA-CR-177410] 24 p3412 N88-30308
FORWARD LOOKING INFRARED DETECTORS
U FLIR DETECTORS
FORWARD SCATTERING
Theoretical and numerical solution of the forward-scattering problem in a circularly cylindrical configuration
[PB88-173489] 15 p2189 N88-23056
Application of laser diffraction techniques to particle sizing in solid propellant rocket motors
[AD-A193841] 22 p3049 N88-28089
FOSSIL FUELS
NT COAL
NT CRUDE OIL
NT NATURAL GAS
Fluidization mechanisms in slurry flows
[DE88-005191] 13 p1766 N88-20563
FOSSIL METEORITE CRATERS
U FOSSILS
U METEORITE CRATERS
FOSSILS
Disclination structures in carbon and graphite
[AD-A191056] 17 p2322 N88-23868
FOUNDATIONS
NT PILE FOUNDATIONS
Open-graded bases for airfield pavements
[AD-A184461] 04 p0402 N88-12500
A passive vibration-cancelling isolation mount 05 p0595 N88-13636
Significance of foundation-soil separation in dynamic soil-structure interaction 05 p0596 N88-13641
Computer-Aided Structural Engineering (CASE) project. Development of design formulas for ribbed mat foundations on expansive soils
[AD-A194807] 24 p3412 N88-30307
FOURIER ANALYSIS
Ballooning modes or Fourier modes in a toroidal plasma?
[AD-A184299] 04 p0491 N88-13022
The k-grid Fourier analysis of multigrid-type iterative methods
[AD-A186315] 07 p0910 N88-15520
Computerized evaluation of interferograms of the Michelson Interferometer for Passive Atmospheric Sounding (MIPAS) Laboratory Model (LM) 08 p1019 N88-16177
Some applications of surface Raman and infrared spectroscopies to mechanistic electrochemistry involved adsorbed species
[AD-A188777] 12 p1606 N88-19602
FTIR (Fourier Transform Infrared) and FTNMR (Fourier Transform Nuclear Magnetic Resonance) study of organophosphorus surface reactions
[AD-A188337] 12 p1609 N88-19625
Non-oscillatory spectral Fourier methods for shock wave calculations
[NASA-CR-181675] 19 p2720 N88-26148
SARLAC: A relativistic electron beam code
[AD-A193134] 21 p2932 N88-27411
Comparison of 2-D Fourier and spatial techniques for removing noise in real-time X-ray radiography
[AD-A193700] 23 p3187 N88-28962
FOURIER TRANSFORMATION
NT FAST FOURIER TRANSFORMATIONS
Pyroelectric line scanner for remote IR imaging of vehicles
[DE87-012127] 02 p0235 N88-11484

Wavepacket propagation and current startup near the lower hybrid frequency in the torus
[IPPJ-840] 02 p0242 N88-11529
Precise measurement of refractive index and absorption coefficient of near millimeter wave and far infrared materials
[AD-A184538] 03 p0293 N88-11840
Homogeneous turbulence two-point closures and applications to one-point closures
03 p0312 N88-11973
Mutual admittance between slots in cylinders of arbitrary shape
[AD-A184254] 04 p0439 N88-12723
Far infrared Fourier transform spectroscopy of semiconductors
[DE88-000188] 04 p0499 N88-13072
Exploiting the IR: Solar and stellar spectroscopy in the IR 04 p0504 N88-13102
Vectorizing the FFTs on supercomputer SX system
05 p0537 N88-13270
Arrays for discrete Fourier transform
[REPT-87-019] 05 p0632 N88-13861
Development of FTMS methods for the detection of trace chemical species and development of FTMS methods for the analysis of various chemical species
[AD-A185857] 07 p0828 N88-15023
Prognosis using spectral embedding — weather forecasting 08 p1016 N88-16157
Comparison of sensitivity and precision of holographic and speckle-interferometry methods with Fourier-plane recording 08 p1078 N88-16500
Optical Fourier transformation by lensless method with perforated mask and with modified Talbot interferometer for analysis of interferograms 09 p1236 N88-17408
An infra-red investigation of HAN (Hydroxylammonium Nitrate)-based liquid propellants
[AD-A187226] 10 p1307 N88-17815
Explicit approximations for strictly nonlinear oscillators with slowly varying parameters with applications to free electron lasers
[DE88-004116] 10 p1336 N88-17954
Accurate efficient evaluation of Bessel transform: Programs and error analysis
[AD-A187718] 11 p1536 N88-19174
Some applications of surface Raman and infrared spectroscopies to mechanistic electrochemistry involved adsorbed species
[AD-A188777] 12 p1606 N88-19602
FTIR (Fourier Transform Infrared) and FTNMR (Fourier Transform Nuclear Magnetic Resonance) study of organophosphorus surface reactions
[AD-A188337] 12 p1609 N88-19625
Optical signal processing using nonlinear optics
[AD-A188461] 12 p1691 N88-20117
Restoration techniques for redisplay of LANDSAT-5 satellite imagery
[INPE-4189-PRE/1076] 13 p1791 N88-20712
Numerical simulations of multiphoton processes in many electron atoms
[DE88-003293] 13 p1837 N88-20990
Finite elements for the computation of three-dimensional electromagnetic fields in inhomogeneous media (revised)
[PB88-173471] 16 p2190 N88-23057
Computer simulation of a motor pump unit to aid in interpreting vibration data
[DE88-004481] 16 p2223 N88-23270
Finite dimensionality in the complex Ginzburg-Landau equation
[DE88-006480] 16 p2263 N88-23534
Fabry-Perot etalons as prefilters for astronomical far infrared Fourier transform spectroscopy
[MPE-205] 16 p2273 N88-23603
Analysis of binarized Hartley phase-only filter performance with respect to stochastic noise
[DE88-007604] 18 p2519 N88-24945
Integral equation for the laser field: Multimode description of a free-electron laser oscillator
[DE88-007050] 18 p2521 N88-24956
Feature extraction using the Hough transform
[AD-A190679] 18 p2555 N88-25165
On frequency response for nonlinear systems
[RR-323] 18 p2563 N88-25221
Photon limited image processing in the space-time domain
[AD-A193142] 21 p2972 N88-27655
A wideband, high-resolution spectrum analyzer
22 p3066 N88-28194
Goldstone solar system radar performance analysis
22 p3068 N88-28206
Rapid-scanning Fourier transform spectrometer for studies of propagation of near-millimeter-wave radiation through clear air and fog
[AD-A193752] 22 p3070 N88-28219
Fourier transform of gravitational synchrotron radiation
[PREPRINT-588] 22 p3144 N88-28700
Application of the Hilbert transform to Doppler radar signals from a hypervelocity gun
[AD-A193690] 22 p3146 N88-28716
Photoacoustic Fourier transform infrared spectroscopy. An early detection technique for coatings degradation
24 p3354 N88-29968

FOURIER-BESSEL TRANSFORMATIONS
Solution of large order Fourier-Bessel equations
[ARE-TM(UHA)-88504] 23 p3272 N88-29475

FOVEA
Retinotopic mapping of the human visual system with magnetoencephalography
[AD-A189557] 13 p1810 N88-20811

FRACTALS
Processing of fractal functions by linear and nonlinear operators
[RAE-TR-85079] 01 p0088 N88-10571
Phase transition of multifractals
[DE87-014344] 03 p0383 N88-12409
Physics and chemistry 07 p0883 N88-15359
Anomalous scaling laws in multifractal objects
[NOTA-INTERNA-883] 07 p0916 N88-15565
Fractal images: Procedure and theory
[AD-A187014] 09 p1217 N88-17293
Interactive generation of fractal objects
[CWI-CS-R8706] 09 p1218 N88-17302
A fractal analysis of brittle fracture
[AD-A188334] 12 p1635 N88-19788
Image segmentation via fractal dimension
[AD-A188825] 12 p1678 N88-20033
Porosity and fractality of a cometary nucleus
14 p2004 N88-21951
Display and processing of multidimensional signals with the aid of fractal image sequences
[ETN-88-92131] 20 p2806 N88-26642
Survey of the literature on fractals with possible applications to phase change processes
[DE88-012240] 21 p2911 N88-27277
Fractal surface finish
[DE88-007972] 22 p3057 N88-28137
Theory of Laplacian fractals: Diffusion limited aggregation and dielectric breakdown model
[PREPRINT-590] 22 p3144 N88-28701

FRACTIONATION
NT CHEMICAL FRACTIONATION
NT HYDROCRACKING
High-density jet fuels from coal syncrudes, appendix 4
[DE88-003132] 10 p1307 N88-17813
Aviation turbine fuels from tar sands bitumen and heavy oils. Part 3: Laboratory sample production
[AD-A189278] 13 p1753 N88-20484
Impact-induced devolatilization and hydrogen isotopic fractionation of serpentine: Implications for planetary accretion
[NASA-CR-182877] 16 p2175 N88-22966
Turbine fuels from tar sands bitumen and heavy oil. Volume 2, phase 3: Process design specifications for a turbine fuel refinery charging San Ardo heavy crude oil
[AD-A190120] 16 p2183 N88-23011
Photochrome from green plants: Assay, purification and characterization
[DE88-007511] 19 p2702 N88-26067
Real-time measurements of the size fractionation of ambient black carbon aerosols at elevated humidities
[DE88-010870] 23 p3215 N88-29138
Crystal fractionation in the SNC meteorites: Implications for surface units on Mars 23 p3307 N88-29698

FRACTIONS
Mass flow rate influence on void fraction of two-phase helium flow
[DE88-702456] 21 p2945 N88-27495

FRACTOGRAPHY
Failure analysis of composite structure materials
[AD-A184468] 04 p0410 N88-12548
Fractographic study of fiber composites
06 p0677 N88-14146
Fatigue crack growth behavior in hydrogen gas environment 06 p0716 N88-14391
An explanation of the fractography of near-threshold fatigue in FCC metals 06 p0716 N88-14395
Fracture-mechanical, statistics and fractographic investigations on the steel 20 MnMoNi 55 in the ductile-brittle transition domain
[ETN-88-91064] 09 p1144 N88-16856
Nondestructive evaluation of structural ceramics by photoacoustic microscopy
[NASA-CR-180858] 09 p1148 N88-16868
Image correlation on an IBM-PC for characterization of advanced ceramics
[DE88-002829] 09 p1149 N88-16885
Some aspects of the mechanics and mechanisms of dynamic brittle fracture 10 p1343 N88-18028
The intergranular segregation of boron in substoichiometric Ni3Al
[DE88-004783] 11 p1462 N88-18720
Comparative investigations of indirect crack length measurement under fatigue loading in a corrosive environment
[GKSS-86/E/64] 11 p1502 N88-18972
Crack distribution and growth rates for critical fastener holes in Mirage wing RH79
[AD-A189080] 13 p1722 N88-20293
Fracture characteristics of carbon and aramid unidirectional composites in interlaminar shear and open hole tensile tests
[NLR-TR-86083-U] 13 p1735 N88-20371
A study of the dynamics of high temperature brittle intergranular fracture by acoustic emission
[AERE-R-12479] 13 p1780 N88-20650
Fractography of composite delamination
[NASA-CR-182757] 15 p2030 N88-22096
Characterization of sintered SiC by using NDE
15 p2082 N88-22413
Fractographic and microstructural evaluation of 3500-hour durability specimens
17 p2325 N88-23887
The postirradiation tensile properties and microstructure of several vanadium alloys
[DE88-007140] 19 p2615 N88-25515
Research on fractography of heat-resistant alloys
19 p2634 N88-25625

FRACTURE MECHANICS
A quantitative statistical model for cleavage fracture initiation in carbide strengthened steels
[ETN-87-90735] 01 p0025 N88-10157
Low cycle fatigue on isotropic fine-grained graphite
[DE87-702627] 01 p0028 N88-10177
Contribution to the numerical calculation of fracture-mechanical quantities for elastic and elastic-plastic material behavior, especially for mixed loads
[ETN-87-90435] 01 p0062 N88-10399
Fracture mechanical analysis of the initiation and propagation of matrix and surface cracks in thermally loaded fiber composite models
[ETN-87-90439] 01 p0062 N88-10400
New fatigue damage analysis of complex engineering components based on Finite Element Methods (FEM)
[DFVLR-FB-87-15] 01 p0062 N88-10401
Fracture mode research of boron aluminum composite materials by Acoustic Emission (AE)
[NAL-TR-927] 02 p0142 N88-10891
Elevated temperature crack growth
02 p0188 N88-11174
Composite structural materials
[NASA-CR-181416] 02 p0190 N88-11186
Applications of dislocation theory to crack growth problems 02 p0190 N88-11188
Energy changes in transforming solids
[DE87-011257] 02 p0191 N88-11194
Investigation on ductile fracture behavior of 3-inch diameter Type 304 stainless steel pipe with a circumferential through-wall crack
[DE87-753016] 02 p0191 N88-11196
Fracture mechanism of fine grain graphite under high heat fluxes
[IPPJ-842] 02 p0242 N88-11527
The Shock and Vibration Digest, Volume 19, No. 11
03 p0265 N88-11673
The Shock and Vibration Digest, Volume 19, No. 10
03 p0335 N88-12112
Application of fracture mechanics theory in the reliability analysis of structural ceramics in multiaxial loading
03 p0335 N88-12113
Investigation of reliability of strength values measured on CFRP test bars by statistical methods. Part 1: Probability distributions for strength analysis
[ESA-TT-1036] 03 p0336 N88-12115
Computational methods and results for dynamic fracture 03 p0337 N88-12123
Kinetics of crack growth: Thermal/mechanical interaction 03 p0337 N88-12124
Ceramic technology for advanced heat engines project
[DE88-001520] 04 p0420 N88-12605
Work-in-progress presented at the Army Symposium on Solid Mechanics, 1986: Lightening of the Force
[AD-A184791] 04 p0427 N88-12644
Method for the ultrasonic inspection of the soundness of the metal in weld joints in two-ply pipes
[BLL-CE-TRANS-8265-(9022.09)]
04 p0453 N88-12805
Environmentally assisted cracking: Overview of evidence for an adsorption-induced localised-slip process
[AD-A185175] 05 p0565 N88-13443
Stress intensity factors for cracking metal structures under rapid thermal loading, phase 1
[AD-A184112] 05 p0591 N88-13606
Near-threshold growth of defects in engineering materials 05 p0603 N88-13691

Interaction of microstructure and fatigue in tool steels
05 p0603 N88-13693
Environmental fracture toughness and static fatigue crack propagation of silica glass
05 p0606 N88-13716
Deformation, fatigue and fracture behavior of two cast anisotropic superalloys 05 p0608 N88-13732
Strain-energy-release rate analysis of the end-notched flexure specimen using the finite-element method
[NASA-TM-100494] 05 p0608 N88-13735
Fracture analysis of drawn composite dual-phase steel wire
[DE88-001396] 06 p0681 N88-14173
Fatigue 87, volume 2
[AD-A184046] 06 p0715 N88-14381
Fatigue life prediction modeling for turbine hot section materials
[NASA-TM-100291] 06 p0724 N88-14453
Random loading fatigue crack growth: Crack closure considerations 06 p0797 N88-14881
Fracture study of windshield glass panes
06 p0799 N88-14891
Determination of the critical crack length a (sub IC) in turbine discs
[PB87-144812] 07 p0820 N88-14986
J-estimation procedure based on moire interferometry data
[AD-A185965] 07 p0867 N88-15258
Study on fracture behaviour of a joint with a crack in transverse hard layer: Effect of hard layer width on COD
[PB87-143855] 07 p0868 N88-15267
Dislocation free zone model of fracture under reverse loading
[DE88-002676] 07 p0869 N88-15276
Interface characteristics and the mechanical properties of metal matrix composites
[AD-A186441] 08 p0966 N88-15845
Study on the correlation of polystyrene (PS) film craze to its fracture behaviour by TEM (Transmission Electron Microscopy)
[PB87-143343] 08 p0970 N88-15870
Effect of peel angle on peel force
[AD-A186117] 08 p0972 N88-15878
Solid mechanics research for quantitative non-destructive evaluation
[AD-A186599] 08 p0993 N88-16010
The relationship of tensile specimen size and geometry effects to unique constitutive parameters for ductile materials
[AD-A186020] 08 p0994 N88-16012
Elastic-plastic fracture investigation on stable crack growth for plane stress
[PB87-144820] 08 p0995 N88-16022
Study on the fracture behavior of 9 percent Ni steel welded joint
[PB87-143863] 08 p0995 N88-16023
The J-integral concept for elastic-plastic material behavior
[W-5/87] 08 p1000 N88-16059
Summary of HSST wide-plate crack-arrest tests and analyses
[DE88-002601] 08 p1000 N88-16061
NASA/Army Rotorcraft Technology. Volume 2: Materials and Structures, Propulsion and Drive Systems, Flight Dynamics and Control, and Acoustics
[NASA-CP-2495-VOL-2] 09 p1106 N88-16632
Review of fatigue and fracture research at NASA Langley Research Center 09 p1106 N88-16633
Delamination durability of composite materials for rotorcraft 09 p1107 N88-16634
Ceramics for engines 09 p1119 N88-16704
Study of the temperature dependence of the mechanical characteristics of the steels GX 5 CrNi 13 4 and GGG 40 in tensile and bending tests
[DE88-001469] 09 p1143 N88-16850
Fracture-mechanical, statistics and fractographic investigations on the steel 20 MnMoNi 55 in the ductile-brittle transition domain
[ETN-88-91064] 09 p1144 N88-16856
Influence of post-anneal cooling treatments on suppression of cryogenic intergranular fracture in experimental Ni-free high-Mn austenitic steels
[DE88-002766] 09 p1145 N88-16863
The failure and fracture analysis of adhesive bonds
[ETN-87-90713] 09 p1181 N88-17077
Finite element analysis for the calculation of calibration curves of fracture mechanics specimen for semicircular surface cracks with several starting depths, for the crack depth measurement following the dc potential method
[GKSS-87/E/19] 09 p1183 N88-17086
Fracture mechanics characterization of crack growth under creep and fatigue conditions
[W-2/87] 09 p1183 N88-17087
Boundary elements combined with singular fields for three-dimensional cracked solids
[RAE-TR-87038] 09 p1183 N88-17088
Applications of energy density theory in cyclic plasticity
[AD-A186947] 10 p1342 N88-18023
Some aspects of the mechanics and mechanisms of dynamic brittle fracture 10 p1343 N88-18028
Theoretical analysis of adhesive fracture and crack-damage interactions 10 p1343 N88-18030
Fatigue crack growth due to random loading
[DE88-004641] 10 p1345 N88-18038
Institute for Materials Science and Engineering, Fracture and Deformation Division: Technical activities, 1987
[PB88-153622] 10 p1345 N88-18039
Cavitation in model elastomeric composites
[AD-A187401] 11 p1447 N88-18625
Damage mechanics of fiber reinforced plastics: A general view 11 p1448 N88-18631
Study of the mechanical behavior of a 2-D carbon-carbon composite
[NASA-CR-182594] 11 p1451 N88-18649
Effects of sulfur content on the plain strain fracture toughness of inertia welds in 4340 steel
[AD-A188192] 11 p1458 N88-18689
Computer aided testing procedure for stress corrosion cracking investigations
[GKSS-86/E/63] 11 p1460 N88-18706
Synthesis and structure property studies of toughened epoxy resins via functionalized polysiloxanes
[AD-A187984] 11 p1462 N88-18715
Fracture mechanisms and strengthening of slab lasers
[DE88-004002] 11 p1493 N88-18914
Fracture characteristics of a viscoelastic polymer under constant load: Experiments and analysis
11 p1501 N88-18963
Numerical fracture mechanics using finite element method 11 p1501 N88-18966
Determination of the elastic-plastic fracture toughness parameters under special consideration of the activities of the European Group on Fracture (EGF)
[GKSS-87/E/30] 11 p1502 N88-18973
Study of the effects of metallurgical factors on the growth of fatigue microcracks
[AD-A188475] 12 p1608 N88-19615
A simulation of void lining during ductile fracture
[AD-A188404] 12 p1635 N88-19792
Further refinement and applications of the mixed computational algorithm for plane elastic contact problems
[AD-A188308] 12 p1683 N88-20065
High-temperature metal matrix composites
[AD-A189516] 13 p1734 N88-20367
Fracture characteristics of carbon and aramid unidirectional composites in interlaminar shear and open hole tensile tests
[NLR-TR-86083-U] 13 p1735 N88-20371
Materials Research Laboratory at Brown University
[AD-A188006] 13 p1739 N88-20396
Stress corrosion cracking and metal-induced embrittlement: Comparative studies of local chemistries
[DE88-003235] 13 p1742 N88-20419
Non-destructive evaluation techniques applied to the study of fatigue microcrack growth in steel alloys
[DE88-004090] 13 p1742 N88-20420
Fracture mechanics and creep crack growth of 1 percent Cr 1/2 percent Mo steel with and without prior exposure to creep conditions
[NLR-TR-86051-U] 13 p1743 N88-20426
Use of reinforced inorganic cement materials for spark wire and drift chamber wire frames
[NASA-CR-180759] 13 p1746 N88-20438
Fracture criterion of reactor graphite under multiaxial stresses 13 p1746 N88-20442
A study of the dynamics of high temperature brittle intergranular fracture by acoustic emission
[AERE-R-12479] 13 p1780 N88-20650
Theory and experiments of fracture in cyclic compression: Single phase ceramics, transforming ceramics and ceramic composites
[DE88-005792] 13 p1781 N88-20659
Fracture criteria for discontinuously reinforced metal matrix composites
[NASA-CR-182665] 13 p1782 N88-20662
ONR Far East Scientific Bulletin, volume 12, number 3, July-September 1987
[AD-A188554] 13 p1851 N88-21081
JPRS report: Science and technology. USSR: Materials science
[JPRS-UMS-87-009] 14 p1884 N88-21261
Crack resistance of multilayer ceramic-based composite material 14 p1885 N88-21265
The Nordic J-R curve round robin test program --- reactor steel
[VTT-RR-510] 14 p1923 N88-21459
Probabilistic analysis of crack containing structures with the PARIS code
[KFK-4286] 14 p1924 N88-21465
Investigation of the components of the energy-momentum tensor in the neighborhood of crack tips under special materials and loading conditions
[W-4/87] 14 p1934 N88-21531
Effect of loading conditions on environment-sensitive fracture
[BR102697] 14 p1934 N88-21533
Investigation of Super*Zip separation joint
[NASA-TM-4031] 15 p2026 N88-22072
Damage models for delamination and transverse fracture
[AD-A189652] 15 p2029 N88-22088
Fracture toughness testing of a ceramic matrix composite
[AD-A189846] 15 p2029 N88-22089
The effective fracture toughness of aluminum at rapid heating rates
[AD-A189745] 15 p2038 N88-22146
Stress corrosion of ceramic materials
[AD-A190501] 15 p2045 N88-22187
A test for interfacial effects and stress transfer in ceramic matrix composites
[NASA-CR-182758] 15 p2046 N88-22194
Crack opening and extension in inert solid propellant. An experimental study
[AD-A189808] 15 p2048 N88-22201
Environmentally assisted crack growth in structural alloys: Perspectives and new directions
[AD-A190137] 15 p2076 N88-22377
Lewis Structures Technology, 1988. Volume 2: Structural Mechanics
[NASA-CP-3003-VOL-2] 15 p2077 N88-22382
Computational simulation methods for composite fracture mechanics 15 p2079 N88-22396
Lewis Structures Technology, 1988. Volume 3: Structural Integrity Fatigue and Fracture Wind Turbines HOST
[NASA-CP-3003-VOL-3] 15 p2081 N88-22408
Monolithic ceramic analysis using the SCARE program
15 p2081 N88-22409
Fracture technology for brittle materials
15 p2083 N88-22417
Mode 2 fracture mechanics 15 p2083 N88-22418
Elevated temperature crack growth
15 p2084 N88-22421
Large-scale wind turbine structures
15 p2085 N88-22429
Processing defects and strength of alumina substrates
[W-10/87] 15 p2087 N88-22441
A simplified key-curve approach for J-R-curve testing of CT specimens
[VTT-RR-503] 15 p2088 N88-22444
A study of failure characteristics in thermoplastic composite material
[AD-A190613] 16 p2171 N88-22940
Surface crack analysis applied to impact damage in a thick graphite-epoxy composite
[NASA-TM-100600] 16 p2173 N88-22950
A piecewise quadratic strength tensor theory for composites
[AD-A190929] 16 p2173 N88-22952
The adhesive bonding of thermoplastic composites
[AD-A190994] 16 p2173 N88-22953
Dynamic fracture toughness evaluation by measurement of CTOD
[WNS/ASD-88-02] 16 p2178 N88-22982
Fracture morphologies of carbon-black-loaded SBR (Styrene-Butadiene Rubber) subjected to low-cycle, high-stress fatigue
[DE88-006808] 16 p2181 N88-23002
Fatigue crack growth under full-scale cyclic plasticity
[DFVLR-FB-87-48] 16 p2222 N88-23263
Bimodular behavior and crack closure in compression in a brittle material
[AD-A191267] 16 p2224 N88-23275
Strain intensity factor approach for predicting the strength of continuously reinforced metal matrix composites
[NASA-TM-100617] 17 p2317 N88-23838
Structural Ceramics
[NASA-CP-2427] 17 p2323 N88-23872
Friction and wear of ceramics
17 p2323 N88-23874
Some design considerations for ceramic components in heat engine applications 17 p2323 N88-23875
Nondestructive evaluation of structural ceramics
17 p2324 N88-23876
Fracture mechanics 17 p2324 N88-23877
Structural ceramics research
17 p2324 N88-23878
Effect of test sample geometry on the fatigue crack growth of X10NiCrAlTi 32 20 and NiCr22 Co 12Mo
[JUEL-SPEZ-399] 17 p2348 N88-23990
Mechanics of instability-related delimination growth
[NASA-TM-100622] 17 p2349 N88-23998
Design of overlays for rigid airport pavements
[DOT/FAA/PM-87/19] 18 p2468 N88-24652

Mixed-mode fracture of uniaxial fiber reinforced composites
[AD-A191629] 18 p2478 N88-24700
Local delamination buckling in layered structures
18 p2480 N88-24711
Characterization of the 2219 Cegedur alloy. Data acquisition of the fracture mechanics --- aircraft construction materials
[REPT-48-442/F] 18 p2487 N88-24751
Isothermal and bithermal thermomechanical fatigue behavior of a NiCoCrAlY-coated single crystal superalloy
[NASA-TM-100907] 18 p2489 N88-24766
Fracture of solid state lasers
[DE88-007023] 18 p2522 N88-24961
Stress corrosion cracking of A723 steel pressure vessels: Two case studies
[AD-A191741] 18 p2527 N88-24990
Fracture mechanics analysis for short cracks
[AD-A192002] 18 p2527 N88-24992
Investigation of the effect of minimum loads and compression of load spectra on the prediction capacities of the ONERA crack model --- wings
[ONERA-RTS-33/7169-RY-064-R]
18 p2527 N88-24994
Self-consistent model for the brittle response of solids
18 p2528 N88-24999
Analysis and developments of failure concepts in fracture mechanics based on research results in the field of component safety topics: J-integral concept; crack resistance curves; dynamic criterion
[V-19/86] 18 p2530 N88-25009
An assessment of the state of the art in predicting the failure of ceramics
[DE88-008998] 19 p2621 N88-25551
Dimensional analysis and experimental observation of the coupling phenomena between combustion and fracture of damaged propellant samples
19 p2630 N88-25603
Research on fractography of heat-resistant alloys
19 p2634 N88-25625
A simple unified method for predicting the deflections of reinforced concrete structures
19 p2679 N88-25930
The effects of thin compressive films on indentation fracture toughness measurements
[AD-A192243] 20 p2779 N88-26480
Research on the kinetics of phase changes in solids
[AD-A192222] 20 p2814 N88-26696
Prediction of fatigue growth
[NLR-MP-87052-U] 20 p2816 N88-26707
Analytical determination of critical crack size in solar cells
[NASA-CR-183128] 20 p2821 N88-26736
An investigation of soft launch and instability breakup with a two-stage light gas gun
[DE88-010371] 21 p2901 N88-27218
Processing and properties of advanced aluminum alloys
[AD-A193224] 21 p2912 N88-27284
Analysis of crack arrest toughness
[AD-A193340] 21 p2913 N88-27286
Adhesion of hydrated silicate films
[DE88-011250] 21 p2920 N88-27333
Failure analysis of laminated composite angles
21 p2959 N88-27578
Plastic yielding at crack tips
[AD-A192549] 21 p2960 N88-27582
Influence of microstructure and microdamage processes on fracture at high loading rates
[AD-A192957] 21 p2960 N88-27583
Critical issues and directions for fracture mechanics and structural integrity
[AD-A193050] 21 p2960 N88-27584
Soviet dynamic fracture mechanics research
[FASAC-TAR-3140] 21 p2962 N88-27597
Corrosion fatigue of small cracks: Mechanics and chemistry
[DE88-012121] 21 p2964 N88-27605
Size effects in linear elastic fracture mechanics
21 p2964 N88-27609
Applications of fatigue analyses: Aircraft engines
[PNR90439] 22 p3044 N88-28066
Fracture behavior in multidimensional fiber-reinforced composites 22 p3051 N88-28099
Stress corrosion evaluation of powder metallurgy aluminum alloy 7091 with the breaking load test method
22 p3053 N88-28115
Experimental investigation of ductile fracture by white light moire interferometry 22 p3087 N88-28329
Empirical fatigue crack growth data for a tension loaded threaded fastener
[AD-A194112] 22 p3088 N88-28334
Wave and fracture phenomena in impacted ceramics
[AD-A192946] 23 p3196 N88-29020
The use of a surface acoustic wave technique to study the growth behavior of small cracks in a high strength steel alloy 23 p3225 N88-29193
Results on the influence of crack tip plasticity during dynamic crack growth
[AD-A193460] 23 p3225 N88-29194
Critical conditions for failure in materials subjected to high rates of loading
[AD-A194697] 23 p3226 N88-29201
A technique for measuring area under a curve
[AD-A193559] 23 p3271 N88-29463
Constraints on the origin of fractured terrane, Northern Martian plains 23 p3304 N88-29684
Additional fracture and strength test results for A723 steel and 38644 titanium
[AD-A196329] 24 p3353 N88-29960
Stress intensity factors for cracked metallic structures under rapid thermal loading
[AES-8609709F-1] 24 p3353 N88-29962
Modeling of micromechanisms of fatigue and fracture in hybrid materials
[AD-A195604] 24 p3382 N88-30142
Obtaining stress intensity factors on cracks, by means of fitting techniques on numerical results calculated with the finite element method 24 p3384 N88-30153

FRACTURE RESISTANCE
U FRACTURE STRENGTH

FRACTURE STRENGTH
Toughening of alpha-alumina: Preliminary results
[DE87-702776] 01 p0028 N88-10178
Development of a polyimide matrix for filament winding with improved extensibility and fracture toughness for permanent use at 200 C
[BMFT-FB-T-86-118] 01 p0030 N88-10190
Interfacial strength development in thermoplastic resins and fiber-reinforced thermoplastic composites
[NASA-CR-181525] 04 p0411 N88-12549
Plastic strain localization between voids in shear deformation fields 04 p0427 N88-12648
Micromechanisms of fatigue crack growth and fracture toughness in metal matrix composites
[AD-A185200] 05 p0558 N88-13392
Fatigue mechanisms in ARALL, a fatigue resistant hybrid aluminum aramid composite material
05 p0605 N88-13711
Environmental fracture toughness and static fatigue crack propagation of silica glass
05 p0606 N88-13716
Embrittling effect of the plastic zone
05 p0607 N88-13721
Fractographic and microstructural aspects of fracture toughness testing in irradiated 304 stainless steel
[DE88-000795] 06 p0681 N88-14172
Characterization of mechanical damage mechanisms in ceramic composite materials
[AD-A185549] 06 p0686 N88-14205
The effect of non-metallic inclusions on fatigue and fatigue thresholds of 25Mn-5Cr-1Ni steel
06 p0718 N88-14410
Evaluation method of the brittle fracture strength in structurally stress-concentrated regions
[PB87-129490] 06 p0721 N88-14435
Comparison of the strength of single and multiple bolted joints in CFRP
[PB87-123766] 06 p0722 N88-14438
Fatigue, fracture and strain hardening of high carbon hardened alloy steel
[AD-A186101] 07 p0831 N88-15043
Investigation of the auto-tempering of low-carbon martensite
[PB87-143970] 07 p0833 N88-15053
New mechanism of the high temperature (reversible) temper brittleness of alloy steels
[PB87-143954] 07 p0833 N88-15056
Study on the cryogenic toughness of stainless steel weld metals
[PB87-143830] 07 p0834 N88-15057
Static and dynamic determination of aluminum oxide toughness
[PB87-146999] 07 p0869 N88-15275
Improved silicon nitride for advanced heat engines
[NASA-CR-175006] 08 p0973 N88-15886
Fracture-resistant characteristics of medium-strength plates with regard to the initiation, stable and unstable propagation of surface cracks
[PB87-144804] 08 p0996 N88-16025
Micromechanisms of fatigue crack growth and fracture toughness in metal matrix composites
[AD-A186941] 09 p1137 N88-16816
Investigation of microstructural factors that cause low fracture toughness in silicon carbide whisker/Al alloy composites
[AD-A186443] 09 p1137 N88-16817
Microstructures and properties of SiC whisker-reinforced mullite composites
[DE88-002611] 09 p1139 N88-16826
Strength and toughness of a brittle material
[VTT-RR-479] 09 p1183 N88-17089
Finite element substructuring methods for composite mechanics
[NASA-TM-100297] 10 p1296 N88-17745
Some aspects of the mechanics and mechanisms of dynamic brittle fracture 10 p1343 N88-18028
Crack arrest fracture toughness of armor steels
[AD-A187711] 11 p1456 N88-18681
Reduction of residual stresses and distortion in girth welded pipes
[AD-A187728] 11 p1494 N88-18920
Fracture toughness of steel weldments containing lack of penetration defects 11 p1501 N88-18965
Determination of the elastic-plastic fracture toughness parameters under special consideration of the activities of the European Group on Fracture (EGF)
[GKSS-87/E/30] 11 p1502 N88-18973
Microdesigning of lightweight/high strength ceramic materials
[AD-A188526] 12 p1610 N88-19631
A fractal analysis of brittle fracture
[AD-A188334] 12 p1635 N88-19788
Composites strengthening
[AD-A189258] 13 p1734 N88-20364
Fracture criterion of reactor graphite under multiaxial stresses 13 p1746 N88-20442
Degradations of thermal shock resistance and the fracture toughness of reactor graphite subjected to neutron irradiation 13 p1747 N88-20445
Application of ISRM testing methods to fracture toughness testing of graphite 13 p1747 N88-20446
Notch sensitivity of graphite materials for VHTR
13 p1747 N88-20447
Guidelines for estimation and characterization of the thermo-mechanical properties of new optical materials
[DE88-004359] 13 p1840 N88-21010
Structure and strength of boron-aluminum composites
14 p1885 N88-21264
Study of strength characteristics of glass-reinforced plastic by acoustic emissions method
14 p1885 N88-21268
Fracture toughness characterization of SA508 and Sa533B RPB steels
[CISE-3908] 14 p1889 N88-21292
Interface structure and properties of alumina/glass ceramic composites
[DE88-006219] 14 p1892 N88-21302
Growth of fatigue cracks in nickel alloys at high temperatures 14 p1896 N88-21318
The Nordic J-R curve round robin test program --- reactor steel
[VTT-RR-510] 14 p1923 N88-21459
Thermally stable deployable structure
14 p1925 N88-21472
Fracture toughness testing of a ceramic matrix composite
[AD-A189846] 15 p2029 N88-22089
Interlaminar fracture toughness of thermoplastic composites
[NASA-TM-100532] 15 p2030 N88-22097
Postbuckling delamination of a stiffened composite panel using finite element methods
[NASA-CR-182803] 15 p2030 N88-22098
The effective fracture toughness of aluminum at rapid heating rates
[AD-A189745] 15 p2038 N88-22146
Fracture toughness of silicon nitride-silicon nitride joints bonded with oxynitride glass
[DE88-005548] 15 p2043 N88-22172
Strength and microstructure of ceramics
[AD-A190712] 15 p2046 N88-22191
Computational simulation methods for composite fracture mechanics 15 p2079 N88-22396
Processing defects and strength of alumina substrates
[W-10/87] 15 p2087 N88-22441
Increasing strength of graphite/epoxy bolted joints by introducing an adhesively bonded metallic insert
[FFA-TN-1987-45] 15 p2088 N88-22442
A piecewise quadratic strength tensor theory for composites
[AD-A190929] 16 p2173 N88-22952
Dynamic fracture toughness evaluation by measurement of CTOD
[WNS/ASD-88-02] 16 p2178 N88-22982
Strength and cracking resistance of ceramics. Report 3: SiC ceramics 16 p2180 N88-22994
Ceramic matrix composites 17 p2325 N88-23888
Polymer precursors for ceramic composites
17 p2326 N88-23890
High strength/sigh modulus aromatic heterocyclic ABA block copolymers
[AD-A191666] 18 p2491 N88-24774
Effect of Zr or Cr content on the fracture toughness of the high purity Al-Zn-Mg alloys
[NASA-TT-20294] 19 p2616 N88-25518

Research on fractography of heat-resistant alloys
19 p2634 N88-25625
The effects of thin compressive films on indentation fracture toughness measurements
[AD-A192243] 20 p2779 N88-26480
Fracture resistance of a TiB2 particle/SiC matrix composite at elevated temperature
[NASA-TM-100967] 20 p2779 N88-26482
Analysis of transverse strength of composites using percolation theory
[AD-A193204] 21 p2904 N88-27234
Fracture behavior in multidimensional fiber-reinforced composites 22 p3051 N88-28099
Advanced processing and properties of high performance alloys
[AD-A193767] 23 p3194 N88-29010
Additional fracture and strength test results for A723 steel and 38644 titanium
[AD-A196329] 24 p3353 N88-29960
Modeling of micromechanisms of fatigue and fracture in hybrid materials
[AD-A195604] 24 p3382 N88-30142

FRACTURE TOUGHNESS
U FRACTURE STRENGTH

FRACTURES (MATERIALS)
NT CRACK TIPS
NT CRACKS
NT MICROCRACKS
NT SHORT CRACKS
NT SURFACE CRACKS
Shear failure in round bar tensile tests of Al-Zn-Mg-Cu alloys
[PB87-143632] 07 p0869 N88-15271
Institute for Materials Science and Engineering, Fracture and Deformation Division: Technical activities, 1987
[PB88-153622] 10 p1345 N88-18039
The influence of small defects on tensile specimen ductility and symmetry of deformation
[AD-A187983] 10 p1346 N88-18044
A fractal analysis of brittle fracture
[AD-A188334] 12 p1635 N88-19788
Interfacial chemistry-structure and fracture of ceramic composites
[DE88-005516] 13 p1750 N88-20461
Mixed-mode fracture of uniaxial fiber reinforced composites
[AD-A191629] 18 p2478 N88-24700
Fracture physics of delamination of composite materials
[AD-A192021] 19 p2609 N88-25482
Irreversible deformations during fracture in polymers
[W-7/86] 20 p2780 N88-26485
Principles of a nondestructive evaluation process for damage location, damage profile, and damage extension in welded joints by radiometric measurements
[MPA-86-02] 20 p2812 N88-26683
Deformation, fracture and explosive properties of reactive materials
[AD-A193080] 21 p2923 N88-27348
Development of creep fracture modelling in ceramics
[PB88-202825] 23 p3196 N88-29021
Hydrogen embrittlement of iron-nickel alloys
[AD-A195909] 24 p3353 N88-29958

FRACTURING
NT CRACKING (FRACTURING)
NT CRUSTAL FRACTURES
NT STRESS CORROSION CRACKING
Small-diameter wire tensile testing
[DE88-000835] 04 p0455 N88-12815
The influence of the topography of fracture surfaces on crack closure 05 p0598 N88-13657
Fracture analysis of drawn composite dual-phase steel wire
[DE88-001396] 06 p0681 N88-14173
Fatigue crack growth and fracture of copper-bismuth bicrystals 06 p0715 N88-14385
Acoustic emission-microstructural relations in ferritic steels. Part 3: The effect of inclusion content
[AERE-R-12041] 10 p1341 N88-18015
Some aspects of the mechanics and mechanisms of dynamic brittle fracture 10 p1343 N88-18028
Theoretical analysis of adhesive fracture and crack-damage interactions 10 p1343 N88-18030
A study of the mechanical behavior of a 2-D carbon-carbon composite 11 p1449 N88-18638
Fracture mechanisms and strengthening of slab lasers
[DE88-004002] 11 p1493 N88-18914
A study of the dynamics of high temperature brittle intergranular fracture by acoustic emission
[AERE-R-12479] 13 p1780 N88-20650
Crack resistance of multilayer ceramic-based composite material 14 p1885 N88-21265
Fracture of solid state lasers
[DE88-007023] 18 p2522 N88-24961
Lattice theory of fracture of solids with layered structure
[DE88-701867] 20 p2876 N88-27073
Influence of microstructure and microdamage processes on fracture at high loading rates
[AD-A192957] 21 p2960 N88-27583
Evaluation of fracture models through pressurized-thermal-shock testing
[DE88-011834] 21 p2963 N88-27603
Wave and fracture phenomena in impacted ceramics
[AD-A192946] 23 p3196 N88-29020

FRAGMENTATION
Computer simulations of fragmentation
[DE87-900985] 03 p0375 N88-12358
The mechanics of fatigue-crack nucleation in a low-alloy steel under fretting conditions 05 p0597 N88-13649
The role of fragmentation in interaction of meteoroids with the Earth's atmosphere 06 p0737 N88-14532
Analysis and interpretation of satellite fragmentation data 06 p0798 N88-14885
Small-scale structure in solar flare radio emission
08 p1097 N88-16598
Splinter generator
[MBB-UA-1048/87] 11 p1491 N88-18897
Fragmentation and flow in central collisions
[DE88-005386] 13 p1837 N88-20991
Milliwatt generator project
[DE88-011261] 20 p2853 N88-26939
Studies of HZE particle interactions and transport for space radiation protection purposes
[NASA-TM-101159] 20 p2886 N88-27142

FRAMES
NT AIRFRAMES
NT CHASSIS
FABSTRAN: A computer program for frame and beam static and transient response analysis (nonlinear)
[ARE-TR-86205] 09 p1182 N88-17079
Control augmented structural synthesis
[NASA-CR-4132] 13 p1721 N88-20290
Use of reinforced inorganic cement materials for spark wire and drift chamber wire frames
[NASA-CR-180759] 13 p1746 N88-20438

FRAMES (DATA PROCESSING)
A unified framework for approximation in inverse problems for distributed parameter systems
[NASA-CR-181621] 10 p1400 N88-18346
Frame synchronization performance and analysis
11 p1473 N88-18787

FRAMING CAMERAS
Fabrication techniques used in the construction of a high resolution X-ray framing camera
[DE88-002653] 07 p0856 N88-15200

FRANCE
ISAURE: Integration of security and fault tolerance in the REALITE 2000 system 02 p0127 N88-10802
Operational activity and improvements in the services and facilities of the balloon launch centers in France
08 p1030 N88-16238
The use of simulation in the development of the Airbus 12 p1702 N88-20188
Acceleration of prototype development and reduction of cost by multidisciplinary integration
12 p1704 N88-20199
EDF's studies and first choices regarding the design of electrical equipment
[NASA-TT-20222] 13 p1764 N88-20553
Evaluation of annual crop surfaces and territorial inventory in the Paris basin by combining classic statistical inquiries and SPOT data (Preliminary Evaluation Program for SPOT 127) 22 p3094 N88-28372
Detailed geological mapping of the massif of Sainte Victoire (Provence, France) using SPOT imagery. Comparison with other multisource data. New tectonic interpretation of this region 22 p3105 N88-28442
Metrology in France: Industrial aspects and its status in the world
[SNIAS-881-430-109] 22 p3146 N88-28713

FRAUNHOFER LINES
Doppler distortion of solar Fraunhofer lines in zodiacal light by reflection from interplanetary dust
19 p2740 N88-26270

FRAUNHOFER REGION
U FAR FIELDS

FREDHOLM EQUATIONS
An approximation technique for solving a system of Fredholm integral equations for asymmetric detector response functions
[AD-A190577] 15 p2121 N88-22645
Numerical solution of linear integral equations with random forcing terms 18 p2565 N88-25237
Generalized Jordan chains and two bifurcation theorems of Krasnoselskii
[AD-A192353] 21 p3008 N88-27845

FREDHOLM OPERATORS
U FREDHOLM EQUATIONS
U OPERATORS (MATHEMATICS)

FREE ATMOSPHERE
SAGE 1 and SAM 2 measurements of 1 micron aerosol extinction in the free troposphere
[NASA-CR-182945] 17 p2374 N88-24121

FREE BOUNDARIES
The method of lines for time dependent free boundary problems
[DE87-013929] 02 p0226 N88-11423
Total linearisation method for solving viscous free boundary flow problems by the finite element method
[PB87-222337] 04 p0441 N88-12737
Computation of free boundaries
[PB87-226023] 06 p0763 N88-14880
Free-boundary equilibrium problem for helically symmetric plasmas
[DE88-700101] 07 p0934 N88-15674
Free boundary problems arising in the control of a flexible robot arm
[AD-A189124] 12 p1634 N88-19781
Some numerical methods for the computation of capillary free boundaries governed by the Navier-Stokes equations
[REPT-87-69] 16 p2206 N88-23167
Free boundary control of the Markov process
[AD-A192401] 21 p3008 N88-27846

FREE CONVECTION
NT RAYLEIGH-BENARD CONVECTION
Effects of forced and free convections on structural temperatures of space shuttle orbiter during reentry flight
[NASA-TM-86800] 01 p0043 N88-10275
Thin film and gradient-driven instability mechanisms
[PB88-101522] 07 p0853 N88-15182
A Lagrangian model of dry thermals
[DM-50] 09 p1193 N88-17150
Thermosolutal convection in high-aspect-ratio enclosures
[NASA-TM-100803] 11 p1486 N88-18871
Analysis of low gravity tolerance of model experiments for space station: Preliminary results for directional solidification
[NASA-CR-182657] 12 p1614 N88-19648
Thermal cracking and variable properties effects on free boundary layer diffusion flames
[NBS/GCR-88/542] 12 p1614 N88-19652
High Rayleigh number convection in rectangular enclosures with differentially heated vertical walls and aspect ratios between zero and unity
[NASA-TM-100277] 12 p1628 N88-19739
Experimental and analytical studies of compressible vortices 19 p2665 N88-25848

FREE ELECTRON LASERS
Visible free electron laser oscillator
[AD-A183871] 01 p0051 N88-10324
Electron beam requirements for soft X-ray/XUV free-electron lasers
[DE87-011750] 01 p0051 N88-10325
Induction linac-driven free-electron lasers: Status and future prospects
[DE87-012914] 01 p0051 N88-10329
Millimeter wave tokamak heating and current drive with a high power free electron laser
[DE87-011324] 01 p0099 N88-10651
Studies on temporal field emission from stainless steel surfaces
[DE87-014237] 02 p0147 N88-10919
Brightness and coherence of radiation from undulators and high-gain free electron lasers
[DE87-011093] 02 p0177 N88-11102
Sideband suppression by an intracavity optical filter in the Los Alamos free-electron laser oscillator
[DE87-011740] 02 p0177 N88-11103
A high-power RF linear accelerator for FELs (Free-Electron Lasers)
[DE87-011795] 02 p0177 N88-11104
On the collective variables description of a high gain free electron laser
[DE87-013315] 02 p0178 N88-11108
Development of a high-energy crowbar for the Los Alamos free-electron laser
[DE87-014748] 02 p0179 N88-11113
Effects of injection of free electron lasers on axial velocity spread of beams 03 p0299 N88-11878
Status, development of laser devices in China
03 p0303 N88-11907
Analysis of undulator field errors for XUV FELs (Extreme Ultraviolet Free Electron Laser)
[DE87-014734] 03 p0328 N88-12073
A microwave FEL (Free Electron Laser) code using waveguide modes
[DE88-000225] 03 p0330 N88-12084
Spectral evolution equation for the sideband instability in a free-electron laser oscillator
[DE88-000510] 04 p0447 N88-12771

The free electron laser sideband instability reconsidered
[AD-A184269] 04 p0447 N88-12773
High-power RF-pulsed modulators for the Los Alamos free-electron laser
[DE88-000514] 04 p0448 N88-12775
The lasertron RF generator for FEL (Free-Electron Laser) applications
[DE88-000515] 04 p0448 N88-12776
Analysis of sideband spectra from untapered undulator using analytical technique
[DE87-014763] 04 p0448 N88-12778
Output power enhancement of AC Raman free-electron laser
[DE88-000503] 04 p0449 N88-12786
The generation and suppression of synchrotron sidebands
[DE88-000532] 04 p0449 N88-12787
Comparison of sideband spectra obtained from analytical formula and from numerical simulation in free-electron laser
[DE88-000521] 04 p0450 N88-12789
A long electromagnetic wiggler for the paladin free-electron laser experiments
[DE88-000970] 05 p0588 N88-13589
Development of a strong electromagnet wiggler
[DE88-000971] 05 p0645 N88-13952
Development of a laced electromagnetic wiggler
[DE88-000972] 05 p0646 N88-13953
Laser development, evolution of applied technologies described 06 p0689 N88-14221
Strategic Defense Initiative Organization/DARPA (Defense Advanced Research Projects Agency) workshop on laser propulsion. Volume 1: Executive summary
[DE87-003254] 06 p0768 N88-14722
High repetition rate electron beam RF-acceleration and sub-millimeter wave generation via a free electron laser
[AD-A186066] 07 p0858 N88-15209
Chapter 2: Threshold for Raman conversion of FEL laser pulses in the atmosphere
[DE88-002470] 07 p0859 N88-15215
Phase control of the microwave radiation in free electron laser two-beam accelerator
[DE88-001460] 07 p0859 N88-15219
The structure of the sideband spectrum in free electron lasers
[AD-A186952] 09 p1170 N88-17015
Intrinsic corrections to optical guiding in a free-electron laser: Beam Research Program
[DE88-002667] 09 p1172 N88-17026
Mode media interactions in an FEL (Free Electron Laser)
[DE88-003155] 09 p1172 N88-17029
Intense electron beams
[DE88-002456] 09 p1247 N88-17474
Microwave system for the microwave Tokamak experiment (MTX)
[DE88-002391] 09 p1250 N88-17487
Conceptual designs of a 50 NM FEL (Free-Electron Laser) oscillator and a 20-40 NM SASE (Self-Amplified Spontaneous Emission) amplifier
[DE88-003150] 10 p1334 N88-17974
Emittance studies at the Los Alamos National Laboratory Free-Electron Laser (FEL)
[DE88-003146] 10 p1334 N88-17975
Physics modeling support contract
[DE88-004039] 10 p1335 N88-17980
Preliminary injector, accelerator, and beamline design for rf-linac-driven XUV free-electron lasers
[DE88-003185] 10 p1336 N88-17983
Explicit approximations for strictly nonlinear oscillators with slowly varying parameters with applications to free electron lasers
[DE88-004116] 10 p1336 N88-17984
Betatron oscillations in a free electron laser
[DE88-004859] 10 p1337 N88-17990
Tapered wiggler analysis of high gain free electron laser oscillators
[AD-A187997] 10 p1338 N88-17997
Where directed energy stands in strategic defense
[DE88-005092] 10 p1403 N88-18365
The stability of free-electron lasers against filamentation
[DE88-004712] 10 p1414 N88-18435
Microwave radiation from rotating, annular electron beams 11 p1475 N88-18801
Experimental results of a hig.-gain microwave FEL operating at 140 GHz
[DE88-004358] 11 p1492 N88-18907
Development of electrostatic-accelerator free-electron lasers
[AD-A189507] 13 p1774 N88-20614
Wiggler taper optimization for free-electron-laser amplifiers with moderate space-charge effects
[DE88-003758] 13 p1775 N88-20618
Projected performance of RF-linac-driven free-electron lasers in the VUV and soft X-ray regions
[DE88-004294] 13 p1776 N88-20625
Effect of electron beam divergence on the gain of free electron lasers 14 p1902 N88-21358
Research on variable-period wiggler type free electron lasers 14 p1902 N88-21360
Pulsed magnet fields for free-electron lasers
14 p1903 N88-21367
Extension of free-electron lasers into the extreme ultraviolet
[DE88-005373] 15 p2070 N88-22341
Program to research laser-driven thermionic electron sources for free electron lasers
[AD-A190473] 15 p2072 N88-22353
The new UCSB (University of California, Santa Barbara) compact far-infrared FEL
[AD-A190864] 16 p2212 N88-23203
Free electron lasers in strategic defense
[DE88-007024] 17 p2394 N88-24231
Integral equation for the laser field: Multimode description of a free-electron laser oscillator
[DE88-007050] 18 p2521 N88-24956
Reducing sensitivity to errors in free electron laser amplifiers
[DE88-007017] 18 p2522 N88-24960
Progress toward a soft X-ray FEL
[DE88-007669] 19 p2675 N88-25905
Generation of coherent soft X-rays using a single-pass free-electron laser amplifier
[DE88-009137] 19 p2675 N88-25907
Application of pulse compression and shaping to the FEL photoelectric injector
[DE88-007908] 19 p2675 N88-25910
The free-electron laser: Theoretical innovations and gas-loaded experiment 20 p2806 N88-26646
The propagation of irradiance moments of an aberrated, apodized FEL beam
[DE88-008972] 20 p2806 N88-26648
The chirped-pulse free-electron laser
[DE88-009289] 20 p2807 N88-26651
Novel magnetic materials research using free electron lasers
[DE88-009989] 20 p2807 N88-26652
Optical guiding in the separable beam limit
[AD-A192452] 21 p2952 N88-27534
Efficiency optimization for FEL oscillators
[AD-A192541] 21 p2952 N88-27536
Research opportunities below 300 nm at the NBS Free-Electron Laser Facility
[AD-A193100] 21 p2953 N88-27538
Initial electron distributions for free-electron lasers generated by injector and accelerator simulations
[DE88-007022] 21 p2953 N88-27540
Development of a free-electron laser user facility for the extreme ultraviolet
[DE88-007892] 21 p2953 N88-27541
Transverse resistive wall instability in a high-power, short-wavelength free-electron laser
[DE88-011730] 21 p2954 N88-27549
On the small signal gain of free electron lasers in the low-current regime
[DFVLR-FB-88-10] 21 p2955 N88-27552
Genetic effects of low level microwave radiation
[AD-A192687] 21 p2984 N88-27722
Guided radiation beams in free electron lasers
[AD-A194525] 22 p3082 N88-28305
Free electron lasers with small period wigglers
[DE88-011627] 23 p3218 N88-29156
The NBS/NRL (National Bureau of Standards/Naval Research Laboratory) free electron laser facility
[AD-A194214] 23 p3219 N88-29159
Analysis of free electron laser performance utilizing the National Bureau of Standards CW microtron
[AD-A194217] 23 p3219 N88-29160
Research on a two-stage free electron laser oscillator
[AD-A195991] 24 p3377 N88-30115
Bibliography of Soviet laser developments, number 88, March - April 1987
[AD-A195978] 24 p3378 N88-30116
Vanderbilt free electron laser project in biomedical and materials research
[AD-A195961] 24 p3378 N88-30121
Ultrafast processes and spectroscopy with free electron lasers
[AD-A195248] 24 p3379 N88-30126

FREE ELECTRONS

Inelastic mean free paths of electrons and positrons in matter
[DE88-008086] 20 p2851 N88-26929

FREE ENERGY

NT GIBBS FREE ENERGY

Soliton twin boundaries of the cubic-tetragonal martensitic transformations in ferroelastic materials
[DE87-014741] 04 p0495 N88-13047
A study of the free energy of the Lenz-Ising model using the cluster variation method of Morita
[AD-A186023] 08 p1073 N88-16476
Theory of the tetragonal-to-orthorhombic structural phase transition in La2CuO4
[AD-A187141] 09 p1254 N88-17514
Free energy calculation via MD (molecular dynamics): Methodology and application to bicrystals
[DE88-002902] 09 p1256 N88-17532
Surface free energy of laser-produced bond percolators
[PB88-130885] 11 p1493 N88-18913
On the theory of the conversion of metallic mixed phases. 5: Fluctuations and nucleation in sub-cooled phases
[NASA-TT-20249] 14 p1890 N88-21296

FREE FLIGHT

Non-linear maximum likelihood estimation of stability derivatives from range data
[NAL-TM-SE-8608] 05 p0552 N88-13365
Australian aerodynamic design codes for aerial tow bodies
[AD-A189048] 13 p1715 N88-20258
Effect of rotation on the lateral stability of a free-flying column subjected to an axial thrust with directional control
[AD-A188690] 13 p1728 N88-20338
Proof-of-principle high speed electronic imaging system, phase 2
[AD-A193798] 23 p3181 N88-28937
Motion planning for a free-flying robot
23 p3255 N88-29378

FREE FLOW

NASA-VOF3D: A three-dimensional computer program for incompressible flows with free surfaces
[DE87-011849] 01 p0045 N88-10288
Measurement of airfoil heat transfer coefficients on a turbine stage 02 p0186 N88-11158
Effects of free stream turbulence, Reynolds number and incidence angle on axial turbine cascade performance
05 p0548 N88-13339
Measurements of the free stream fluctuations above a turbulent boundary layer
[NASA-TM-100036] 06 p0704 N88-14321
Transport and stability properties of free shear flows
13 p1768 N88-20577
Temperature estimates for a free flowing railgun plasma
[MRL-R-1054] 13 p1843 N88-21032
Instruments for use in experimental studies of complex turbulent shear flow: Three component LDVs
[AD-A190526] 15 p2065 N88-22312
Effect of freestream turbulence on a two dimensional cascade, with different surface roughness, at high Reynolds number
[AD-A190615] 15 p2065 N88-22316
Film cooling effectiveness on a flat plate in high free-stream turbulence using a single row of 30 deg slant-hole injectors
[AD-A190500] 15 p2147 N88-22816
Experimental study of bypass transition in a boundary layer
[NASA-TM-100913] 16 p2209 N88-23186
Stagnating turbulent reacting flows
[AD-A191449] 18 p2508 N88-24877
Study of the structure of turbulence in accelerating transitional boundary layers
[AD-A191698] 19 p2663 N88-25837
Experimental study of unsteady separating turbulent boundary layers
[AD-A192997] 21 p2943 N88-27477
Unsteady water channel
[AD-A194231] 23 p3171 N88-28884
Containment of a silicone fluid free surface in reduced gravity using barrier coatings
[NASA-TM-101314] 24 p3371 N88-30072

FREE JETS

Experimental study of three-dimensional turbulent jet-solid boundary interaction 01 p0046 N88-10293
Heat transfer with very high free stream turbulence
02 p0186 N88-11161
The vertical test section (VMK) of DFVLR in Cologne-Porz, Federal Republic of Germany (status 1986)
[ESA-TT-1053] 03 p0267 N88-11682
Laser Doppler measurements in a turbulent free jet
[ESA-TT-1067] 03 p0315 N88-11994
Rayleigh scattering measurements of a freejet with homogeneous condensation 03 p0319 N88-12020
Numerical simulation and visualization of a flowfield by interaction of two parallel two-dimensional freejets
03 p0320 N88-12021
Numerical analysis of flow characteristics of supersonic free-jets 05 p0538 N88-13274
Investigation of the effect of laterally ejected gas jets on flows
[ISL-R-107/86] 05 p0581 N88-13545

Molecular collision processes in gases and at surfaces
[AD-A189518] 13 p1836 N88-20982
Effect of initial tangential velocity distribution on the mean evolution of a swirling turbulent free jet
[NASA-TM-100934] 18 p2458 N88-24592
Particle-laden weakly swirling free jets: Measurements and predictions
[NASA-TM-100920] 18 p2466 N88-24639
Numerical simulation of supersonic free-jets
19 p2636 N88-25639
Cryogenic free jets
[DFVLR-FB-88-16] 21 p2900 N88-27210

FREE MOLECULAR FLOW
Analysis of free molecular effects on the attitude of satellites in geostationary transfer orbit. Part 1: Theoretical analysis
[DFVLR-IB-222-86-A/08] 01 p0014 N88-10077
Analysis of free molecular effects on the attitude of satellites in geostationary transfer orbit. Part 2: Force and torque measurement in free molecular wind tunnel tests
[DFVLR-IB-222-86-A/07] 01 p0014 N88-10078
Experiences using the Mark IV supersonic hypersonic arbitrary body program 05 p0534 N88-13249
Studies of error in temperature measurement with thermistors in the range between continual and free-molecule flows
[NASA-TT-20302] 19 p2674 N88-25900

FREE OSCILLATIONS
U FREE VIBRATION

FREE RADICALS
NT HYDROXYL RADICALS
Photolytic processes for measurement of combustion heats of formation and reaction rates
[DE87-014047] 02 p0144 N88-10905
Free radical detection and reactions in the decomposition of energetic materials
[AD-A184677] 03 p0296 N88-11858
Physiological and biochemical aspects of toxic effects of oxidants in man's environment (air, water)
07 p0890 N88-15391
Laser studies of the dynamics of free radical reactions
[DE88-004431] 10 p1337 N88-17989
Gas phase reactions of electrons, negative ions and free-radicals with transition metal complexes
11 p1560 N88-19339
Photolytic formation of free radicals and their effect on hydrocarbon pyrolysis chemistry in a concentrated solar environment
[DE88-004129] 13 p1794 N88-20730
Photodissociation lifetimes of CH and CD radicals in comets 14 p1998 N88-21908
Infrared absorption spectroscopy and chemical kinetics of free radicals
[DE88-006536] 15 p2033 N88-22112
Time-resolved studies of free radicals and laser-initiated chain reactions
[DE88-006569] 16 p2266 N88-23553
Energy transfer processes in free radicals: A collaborative experimental and theoretical investigation
[AD-A191264] 16 p2269 N88-23578

FREE STREAM EFFECTS
U FREE FLOW

FREE STREAMS
U FREE FLOW

FREE VIBRATION
Calculation of the eigenvibrations of axisymmetric fluid configurations with a singularity method, taking into account surface tension effects under reduced gravity
[ETN-87-90438] 01 p0048 N88-10304
Finite element methodology for nonlinear free and harmonic forced vibrations of beam and plate structures
13 p1782 N88-20663
Calculation of displacement, constraints and eigenmodes of rotating blades
[ETN-88-92296] 16 p2224 N88-23277
Experimental and theoretical investigation of passive damping concepts for member forced and free vibration
[NASA-CR-183082] 20 p2814 N88-26693
Free vibration of rectangular plates with a small initial curvature
[NASA-CR-179370] 24 p3383 N88-30148

FREE-PISTON ENGINES
Study of free-piston Stirling engine driven linear alternators
[NASA-CR-181425] 01 p0055 N88-10355
RE-1000 free-piston Stirling engine hydraulic output system description
[NASA-TM-100185] 01 p0108 N88-10700
SPRE 1 free-piston Stirling engine testing at NASA Lewis Research Center
[NASA-TM-100241] 03 p0277 N88-11747
Shock tunnels for real gas hypersonics
05 p0530 N88-13223
Description of an oscillating flow pressure drop test rig
[NASA-TM-100905] 16 p2170 N88-22933
The 1988 overview of free-piston Stirling technology for space power at the NASA Lewis Research Center
[NASA-TM-100795] 16 p2170 N88-22934
Overview of NASA Lewis Research Center free-piston Stirling engine technology activities applicable to space power systems 17 p2398 N88-24255
Component improvement of free-piston Stirling engine key technology for space power
[NASA-TM-100950] 19 p2607 N88-25476

FREEZING
NT ZONE MELTING
Nowcasting rain/snow transitions and freezing rain
02 p0202 N88-11265
Experimental evidence for modifying the current physical model for ice accretion on aircraft surfaces
[NASA-TM-87184] 04 p0397 N88-12473
Geochemistry of freezing brines, low-temperature properties of sodium chloride
[AD-A185751] 06 p0680 N88-14168
Evaluation of the magnetic induction conductivity method for detecting frazil ice deposits
[AD-A186940] 09 p1194 N88-17157
Mesoscale monitoring of the soil freeze/thaw boundary from orbital microwave radiometry
[NASA-CR-182659] 12 p1645 N88-19855
Dendritic growth in the presence of convection
18 p2580 N88-25328
Component stress during freeze/thaw cycling
[DE88-011204] 21 p2938 N88-27449
Effect of thermal cycling on CSPL (Chloride Silent Power Ltd.) sodium/sulfur cells
[DE88-011205] 21 p2939 N88-27455

FREEZING POINTS
U MELTING POINTS

FREIGHT
U CARGO

FRENCH SATELLITES
NT SPOT (FRENCH SATELLITE)
The heat pipe network of TDF-1/TV-SAT. Review of the development at completion
[SNIAS-881-440-103] 23 p3213 N88-29127

FRENCH SPACE PROGRAMS
Development of the SPOT commercial service: Preliminary conclusions after six months of operations
03 p0340 N88-12144
SPOT Image Corporation: Early results
03 p0340 N88-12146
The new generation of SPOT satellites
03 p0345 N88-12178
The French balloon and sounding rocket space program 08 p1025 N88-16203
French activities in ocean colour observations
08 p1043 N88-16303
The Earthnet Heat Capacity Mapping Mission (HCMM) data-processing system at Lannion (France)
09 p1127 N88-16761
The French spaceborne oceanography program
19 p2701 N88-26058
Perspectives for the SPOT program
22 p3115 N88-28508
Closing of the Preliminary Evaluation Program for SPOT (PEPS): Assessment of the acquisition, production, and monitoring of PEPS 22 p3115 N88-28509
Organization of the TDF1/TDF2 program
22 p3161 N88-28827
Microwave remote sensing in the French industries
[ETN-88-93081] 24 p3387 N88-30171

FREON
Kinetics of homogeneous nucleation in superheated F-11 and F-21 liquid freons
[NASA-TT-20286] 19 p2613 N88-25503
Investigation on refrigerant R12 critical boiling point in narrow flow pipes considered as model fluid
[ETN-88-92374] 20 p2802 N88-26626

FREQUENCIES
NT ACOUSTIC FREQUENCIES
NT AUDIO FREQUENCIES
NT BEAT FREQUENCIES
NT BROADBAND
NT CARRIER FREQUENCIES
NT CYCLOTRON FREQUENCY
NT EXTREMELY HIGH FREQUENCIES
NT EXTREMELY LOW FREQUENCIES
NT EXTREMELY LOW RADIO FREQUENCIES
NT HIGH FREQUENCIES
NT INFRASONIC FREQUENCIES
NT INTERMEDIATE FREQUENCIES
NT IONIZATION FREQUENCIES
NT LOW FREQUENCIES
NT MAXIMUM USABLE FREQUENCY
NT MICROWAVE FREQUENCIES
NT PLASMA FREQUENCIES
NT RADIO FREQUENCIES
NT RESONANT FREQUENCIES
NT SUPERHIGH FREQUENCIES
NT SWEEP FREQUENCY
NT ULTRAHIGH FREQUENCIES
NT VERY HIGH FREQUENCIES
NT VERY LOW FREQUENCIES
Modeling XV-15 tilt-rotor aircraft dynamics by frequency and time-domain identification techniques
03 p0263 N88-11657
Structural frequency functions for an impulsive, distributed forcing function
[DE87-013811] 03 p0333 N88-12101
Lower bounds on bearing accuracy for closely spaced sources
[AD-A184258] 04 p0486 N88-12997
Program to development an optical transistor and switch
[AD-A185666] 06 p0697 N88-14278
On simultaneous estimation of the number of signals and frequencies under a model with multiple sinusoids
[AD-A186026] 07 p0913 N88-15543
On rate of convergence of equivariation linear prediction estimates of the number of signals and frequencies of multiple sinusoids
[AD-A186034] 07 p0914 N88-15549
Qualification of frequency response functions using the rigid-body response
[DE88-000745] 10 p1344 N88-18033
Frequency response function estimation at level
[DE88-002644] 10 p1344 N88-18034
Frequency-sampling design of two-dimensional FIR digital filters with nonuniform samples
[AD-A187773] 11 p1477 N88-18815
Minimum weight design of rectangular and tapered helicopter rotor blades with frequency constraints
[NASA-TM-100561] 12 p1582 N88-19465
Sensitivity reduction over a frequency band
[AD-A189123] 12 p1621 N88-19694
Wavenumber - frequency structure of turbulent flow in a channel from a direct simulation
[AD-A189079] 12 p1627 N88-19737
Theoretical investigation of EM wave generation and radiation in the ULF, ELF and VLF bands by the electrodynamic orbiting tether
[NASA-CR-182720] 13 p1760 N88-20529
Optimal and conventional space-time processing in flow noise
[AD-A189104] 13 p1833 N88-20965
NBS (National Bureau of Standards) measurement services. GOES (Geostationary Operational Environmental Satellite) time code dissemination: Description and operation
[PB88-168760] 14 p1880 N88-21235
Minimum weight design of rotorcraft blades with multiple frequency and stress constraints
[NASA-TM-100569] 16 p2161 N88-22892
Time-frequency representations for speech signals
[AD-A188661] 18 p2498 N88-24819
Exact tests for variance component models with unequal cell frequencies in the last stage
[AD-A191645] 18 p2568 N88-25253
Frequency Analysis of Acoustic Emission - Application to machining and welding
[DE88-701478] 18 p2570 N88-25262
A microcomputer based frequency-domain processor for laser Doppler anemometry
[NASA-TM-100998] 20 p2803 N88-26634
Investigation of the validity of Reynolds averaged turbulence models at the frequencies that occur in turbomachinery
[NASA-CR-182162] 22 p3048 N88-28087
Effect of phase errors in stepped-frequency radar systems
[AD-A194476] 23 p3203 N88-29061
Contamination and distortion of steady flow field induced by discrete frequency disturbances in aircraft gas engines
[AD-A195440] 24 p3370 N88-30069

FREQUENCY ANALYZERS
An expert system to analyze high frequency dependent data for the space shuttle main engine turbopumps
08 p1060 N88-16399

FREQUENCY ASSIGNMENT
Telemetry, Tracking, and Control Working Group report 01 p0016 N88-10096
HF (High Frequency) broadcasting planning model: A comparison of two versions
[PB87-210282] 01 p0036 N88-10230
High data rate modem simulation for the space station multiple-access communications system
06 p0795 N88-14870
Numerical arc segmentation algorithm for a radio conference-NASARC (version 2.0) technical manual
[NASA-TM-100160] 08 p0977 N88-15910

FREQUENCY BANDS
U FREQUENCIES

FREQUENCY CONTROL
NT AUTOMATIC FREQUENCY CONTROL

Optically tuned MM-wave IMPATT source
[AD-A185250] 05 p0577 N88-13523
Frequency locking of two lasers
[FOA-C-30456-3.1] 08 p0992 N88-16000
Fiber-coupled external-cavity semiconductor high power laser
[AD-A188454] 13 p1774 N88-20611
Investigation of boundary layer disturbances caused by periodic heating of a thin ribbon
[AD-A190572] 15 p2065 N88-22314
Interleaver design for trellis-coded differential 8-PSK modulation with non-coherent detection
19 p2648 N88-25719
Quartz crystal resonators and oscillators for frequency control and timing applications
[AD-A193310] 21 p2937 N88-27443
Three-dimensional vortex interactions
[AD-A194066] 23 p3172 N88-28889
Reduction in mill air compressor power requirements through instalation of a variable frequency speed control
[DE88-008493] 23 p3221 N88-29171

FREQUENCY CONVERSION
U FREQUENCY CONVERTERS

FREQUENCY CONVERTERS
NT FREQUENCY DIVIDERS
NT FREQUENCY MULTIPLIERS
NT FREQUENCY SYNTHESIZERS
NT UP-CONVERTERS
Non-linear materials (TAS)
[AD-A189197] 12 p1633 N88-19775
Electrostatic whistler mode conversion at plasma resonance
[AD-A192951] 20 p2860 N88-26989
Nonlinear materials for frequency conversion
[DE88-008343] 20 p2875 N88-27067

FREQUENCY DISCRIMINATORS
Acoustic emission frequency discrimination
[NASA-CASE-MSC-20467-1] 17 p2342 N88-23966

FREQUENCY DISTRIBUTION
Statistical distribution of solar radiation (hourly sums): Cumulative frequency curves preparation of a European data set and direction for use
[PB87-107454] 04 p0467 N88-12886
Analysis, suppression of land clutter characteristics reported 14 p1903 N88-21369
Wigner distribution function: Relation to short-term spectral estimation, smoothing and performance in noise
[AD-A193865] 23 p3275 N88-29492

FREQUENCY DIVIDERS
Interactive computer programme for the analysis of a two-way Wilkinson divider/combiner
[PB88-105424] 20 p2837 N88-26831

FREQUENCY DIVISION MULTIPLE ACCESS
Mobilestar field test program
19 p2646 N88-25707
Comparison of CDMA and FDMA for the MobileStar(sm) system 19 p2649 N88-25724
A study on the co- and adjacent channel protection requirements for mobile satellite ACSSB modulation
19 p2650 N88-25732
Rivista Tecnica Selenia, volume 10, no. 3, 1987
[ETN-88-92717] 22 p3068 N88-28210
The Frequency Division Multiple Access/Time Domain Multiplex (FDMA/TDM) system reviewed
22 p3069 N88-28214

FREQUENCY DIVISION MULTIPLEXING
The design and testing of an analog optical communication link capable of the simultaneous transmission of four frequency division multiplexed audio signals
[AD-A184695] 03 p0307 N88-11936

FREQUENCY HOPPING
Performance analysis of coded frequency-hopped spread-spectrum systems with unknown interference
[AD-A186069] 07 p0841 N88-15103
Coding for spread-spectrum communications networks
[AD-A185667] 07 p0844 N88-15119
The ratio detector: A method of amplitude insensitive frequency demodulation
[RAE-TR-87008] 09 p1153 N88-16910
Soft decoding of recorded HF data
[FOA-C-30473-3.3] 15 p2058 N88-22269
A Differential Phase Shift Keying (DPSK) modulator for a frequency hopping short wave system
[FOA-C-30460-3.3] 18 p2501 N88-24840

FREQUENCY MEASUREMENT
NO2 heterodyne frequency measurements with a tunable diode laser, a CO laser transfer oscillator and CO2 laser standards
[NASA-CR-182393] 06 p0710 N88-14353
Material parameter measurements at high temperatures
[NASA-CR-182707] 13 p1739 N88-20397
Apparatus for using a time interval counter to measure frequency stability
[NASA-CASE-NPO-17325-1-CU]
18 p2502 N88-24846
Airborne measurement of low frequency atmospheric noise ALFAN 1
[AD-A193056] 21 p2931 N88-27405
A notch filter instrument for measuring ELF (Extremely Low Frequency) MSK (Minimum Shift Keying) signals
[AD-A193324] 21 p2933 N88-27414

FREQUENCY MODULATION
NT FREQUENCY SHIFT KEYING
Large-aperture high-efficiency frequency doubling using tandem KDP crystals 03 p0301 N88-11894
Fast autotuning of a hydrogen maser by cavity Q modulation 04 p0436 N88-12707
Study of vibration relaxation in active medium of CO2-laser using phase-absorption method
07 p0919 N88-15582
Telemetry applications handbook
[AD-A186825] 09 p1132 N88-16789
The ratio detector: A method of amplitude insensitive frequency demodulation
[RAE-TR-87008] 09 p1153 N88-16910
Magnet strength fluctuations in the SSC (Superconducting Super Collider) lattice. Part 2: Frequency modulation
[DE88-006491] 15 p2141 N88-22774
Statistical fine structure in the inhomogeneously broadened electronic origin of pentacene in p-terphenyl
[AD-A191211] 16 p2176 N88-22968
A study on the co- and adjacent channel protection requirements for mobile satellite ACSSB modulation
19 p2650 N88-25732

FREQUENCY MULTIPLIERS
Powerful picosecond ultraviolet laser output at 354.7 nanometers 03 p0327 N88-12063
Frequency doubling conversion efficiencies for deep space optical communications 04 p0434 N88-12691
Optical frequency doubling in Ti:LiMbO3 waveguide resonators
[ETN-88-91486] 11 p1550 N88-19271

FREQUENCY RANGES
NT RADIO RANGE

FREQUENCY REGULATION
U FREQUENCY CONTROL

FREQUENCY RESPONSE
Further development of the dynamic gas temperature measurement system 02 p0184 N88-11141
An efficient frequency response solution for nonproportionally damped systems
05 p0595 N88-13634
Dynamic restructuring of pulsed CO2 laser frequency and multiple-peak generation in a cell with IR-absorbing gas in the resonator 07 p0919 N88-15580
Strategic placement of accelerometers to measure forces by the sum of weighted accelerations
[DE88-002262] 10 p1333 N88-17968
On frequency response for nonlinear systems
[RR-323] 18 p2563 N88-25221

FREQUENCY REUSE
Rearrangement procedures in regenerative multibeammobile communications satellites with frequency reuse 19 p2650 N88-25735

FREQUENCY SHIFT
Frequency chirping in pulse modulated gain and real index guided single quantum well lasers
19 p2658 N88-25798

FREQUENCY SHIFT KEYING
ELF/VLF/LF propagation and system design
[AD-A183261] 01 p0033 N88-10212
The 2 FSK/QPSK (Frequency Shift Keying/Quadrature Phase Shift Keying) transmitter and receiver: Design and performance
[AD-A190028] 15 p2056 N88-22258
An FSK (Frequency Shift Keying) telemetry module for vector measuring current meters
[AD-A192142] 18 p2470 N88-24661
A notch filter instrument for measuring ELF (Extremely Low Frequency) MSK (Minimum Shift Keying) signals
[AD-A193324] 21 p2933 N88-27414

FREQUENCY STABILITY
X-band uplink ground systems development: Part 2
04 p0436 N88-12703
On-orbit frequency stability analysis of the GPS NAVSTAR 8 rubidium clock and NAVSTARs 9 and 10 cesium clocks
[AD-A184984] 05 p0544 N88-13312
Study and construction of a compact hydrogen maser with a high-degree of frequency stability
[PB87-151122] 07 p0859 N88-15216
Investigation of boundary layer disturbances caused by periodic heating of a thin ribbon
[AD-A190572] 15 p2065 N88-22314
Apparatus for using a time interval counter to measure frequency stability
[NASA-CASE-NPO-17325-1-CU]
18 p2502 N88-24846
Laser CO2/TEA frequency-stabilized by phase conjugation 22 p3082 N88-28303
Three-dimensional vortex interactions
[AD-A194066] 23 p3172 N88-28889
The aspect ratio dependence of the attractor dimension in Taylor-Couette flow
[AD-A196297] 24 p3369 N88-30065

FREQUENCY STANDARDS
Study and construction of a compact hydrogen maser with a high-degree of frequency stability
[PB87-151122] 07 p0859 N88-15216
Atomic clocks research: An overview
[AD-A185567] 07 p0930 N88-15648
Recommendations for organising the calibration of pure-tone audiometers
[NPL-AC-112] 09 p1167 N88-16999
The JPL trapped mercury ion frequency standard
11 p1471 N88-18776
Tactical Rubidium Frequency Standard (TRFS)
[AD-A191049] 16 p2193 N88-23078
Tactical Rubidium Frequency Standard (TRFS), volume 2
[AD-A191190] 18 p2503 N88-24850
Tactical Rubidium Frequency Standard (TRFS), volume 1
[AD-A192981] 20 p2805 N88-26640
A three-dimensional model of the gas-cell atomic frequency standard
[AD-A193218] 21 p3011 N88-27868
Electromagnetic metrology 24 p3363 N88-30024

FREQUENCY SYNTHESIZERS
Mechanisms mediating perception of complex acoustic patterns
[AD-A189765] 15 p2102 N88-22520
Instrumentation for ultrafast electronics
[AD-A191379] 16 p2193 N88-23080

FREQUENCY TRANSLATION
U FREQUENCY CONVERTERS

FRESH WATER
Karst and submarine fresh water discharge in the Antalya area, southern Turkey 22 p3102 N88-28421

FRESNEL DIFFRACTION
Diffraction effects during materials treatment with laser beams
[ETN-87-90614] 03 p0328 N88-12075
Precision measurement of the Fresnel drag coefficient using a ring laser
[AD-A196025] 24 p3366 N88-30043

FRESNEL INTEGRALS
Overestimation of on-axis power density by the Fraunhofer (far-field) approximation
[AD-A186399] 07 p0843 N88-15111
Beam quality of stable and unstable resonators: A theoretical approach
[DFVLR-FB-87-35] 14 p1982 N88-21826

FRESNEL LENSES
Construction of gallium arsenide solar concentrator for space use
[AD-A194658] 23 p3230 N88-29222

FRESNEL REGION
An improved method for calculating power density in the Fresnel region of circular parabolic reflector antennas
[AD-A190569] 15 p2060 N88-22284

FRESNEL-KIRCHHOFF INTEGRALS
U FRESNEL INTEGRALS

FRETTING
The mechanics of fatigue-crack nucleation in a low-alloy steel under fretting conditions 05 p0597 N88-13649
Fretting wear and fretting fatigue damage
05 p0603 N88-13697

FRETTING CORROSION
The effect of fretting corrosion on the fatigue strength of steel and cast iron under sinusoidal and random loading
[LBF-FB-177] 01 p0023 N88-10142
The effects of thin polymeric surface films in reducing fretting corrosion and wear
[AD-A188633] 12 p1611 N88-19634

FRICTION
NT AERODYNAMIC DRAG
NT DRY FRICTION
NT FLOW RESISTANCE
NT FRICTION DRAG
NT SKIN FRICTION
NT SLIDING FRICTION
NT STATIC FRICTION
NT SUPERSONIC DRAG
NT VISCOUS DRAG

Research on one-dimensional two-phase flow. Theory on hydrodynamic balance in two fluid model and its application
[DE87-702615] 01 p0045 N88-10290
Piston ring friction and vehicle fuel economy
[DE87-014536] 02 p0181 N88-11127
The wear process during the RUNNING-IN of steel in lubricated sliding
[NAL-TR-922T] 02 p0181 N88-11130
The friction and wear of TPS fibers
[NASA-CR-181496] 03 p0291 N88-11830
Ignition and combustion of metals in oxygen
04 p0407 N88-12530
Canonical transformations and exact invariants for dissipative systems
[DE87-703663] 04 p0485 N88-12985
On a numerical method to solve contact problems --- forming processes
[B8711403] 05 p0642 N88-13930
Development, features of roller rocker arm reported
06 p0689 N88-14219
The tribological properties of MoS2 coatings in vacuum, low relative humidity and high relative humidity environments
[DE88-001611] 06 p0711 N88-14356
Dynamical friction
[DE88-002194] 06 p0711 N88-14358
Mechanisms of rolling contact spalling
[NASA-CR-179243] 06 p0714 N88-14380
Centaur G Prime modal test 09 p1181 N88-17075
Friction and wear of monolithic and fiber reinforced silicon-ceramics sliding against IN-718 alloy at 25 to 800 C in atmospheric air at ambient pressure
[NASA-TM-100294] 10 p1304 N88-17796
Adhesion, friction and micromechanical properties of ceramics
[NASA-TM-100782] 10 p1305 N88-17801
Tribology of ceramics: Report of the Committee on Tribology of Ceramics
[NASA-CR-182506] 10 p1305 N88-17802
One-dimensional leakage-flow vibration instabilities
[DE88-002875] 10 p1330 N88-17947
Aircraft and ground vehicle friction correlation test results obtained under winter runway conditions during joint FAA/NASA Runway Friction Program
[NASA-TM-100506] 11 p1438 N88-18582
Synthesis and structure property studies of toughened epoxy resins via functionalized polysiloxanes. Friction and wear studies
[AD-A188258] 11 p1462 N88-18718
Reaction wheel experimental model of artificial satellite attitude control: Construction, simulation, and tests
[INPE-4274-PRE/1146] 11 p1490 N88-18896
In situ ultrahigh vacuum friction measurement and wear track analysis of ion implanted 304 stainless steel
[DE88-004537] 11 p1494 N88-18922
Quantization of quadratic friction revisited
[DE88-700839] 12 p1686 N88-20081
Particle-dynamics calculations of gravity flow of inelastic, frictional spheres
[DE88-005224] 13 p1770 N88-20586
Structural clearances and internal friction: Simulation by Eigen distortions
[ISSN-0208-5658] 13 p1779 N88-20640
Advances in contact algorithms and their application to tires
[NASA-TP-2781] 14 p1922 N88-21456
Effect of friction and control parameters on the tracking accuracy of a target seeker
[AD-A190010] 15 p2056 N88-22257
Traction model development
[AD-A188450] 15 p2073 N88-22359
Friction and wear of ceramics
17 p2323 N88-23874
LLNL granular solids flow project
[DE88-007492] 18 p2513 N88-24906
LLNL Granular Solids Flow Project
[DE88-008023] 19 p2664 N88-25844
Entrance and exit region friction factor models for annular seal analysis
[NASA-CR-183084] 19 p2678 N88-25921
Friction, wear and electrical contact resistance of precious metal alloys
[DE88-011244] 21 p2938 N88-27450
Granular flow: Particle-dynamics simulations of steady flow
[DE88-011342] 21 p2948 N88-27506
Thermo-mechanical cracking in coated media with a cavity by a moving asperity friction
[AD-A193311] 21 p2961 N88-27586
Development of high temperature, high pressure rotating shaft seals
[DE88-001029] 23 p3221 N88-29172

FRICTION COEFFICIENT
U COEFFICIENT OF FRICTION

FRICTION DRAG
NT AERODYNAMIC DRAG
NT SUPERSONIC DRAG
NT VISCOUS DRAG
Combined riblet and lebu drag reduction system
[NASA-CASE-LAR-13286-1] 06 p0664 N88-14071
Friction drag reduction (a speculative essay)
[INPE-4278-PRE/1150] 08 p0988 N88-15985
An assessment of the drag reduction properties of riblets and the penalties of off-design conditions
[RAE-TM-AERO-2113] 17 p2295 N88-23731

FRICTION FACTOR
Further refinement and applications of the mixed computational algorithm for plane elastic contact problems
[AD-A188308] 12 p1683 N88-20065
Drag reduction of turbulent boundary layers by means of grooved surfaces
[ETN-88-92618] 20 p2802 N88-26630
Investigations of rough surface effects on friction factors in turbulent pipe flow
[AD-A193774] 22 p3075 N88-28255

FRICTION LOSS COEFFICIENT
U FRICTION FACTOR

FRICTION MEASUREMENT
The WAFTER: A versatile wear and friction tester
[MRL-TN-519] 09 p1169 N88-17012
In situ ultrahigh vacuum friction measurement and wear track analysis of ion implanted 304 stainless steel
[DE88-004537] 11 p1494 N88-18922
Water tunnel measurements by an electrochemical method 16 p2203 N88-23146
Boundary layer measurements using hot-film sensors
17 p2297 N88-23743

FRICTION PRESSURE DROP
U SKIN FRICTION

FRICTION REDUCTION
Multipath gear-friction planetary transmissions
04 p0424 N88-12629
Riblets for aircraft skin-friction reduction
07 p0814 N88-14955
Airfoil large eddy breakup devices for turbulent drag reduction 07 p0814 N88-14956
Friction drag reduction (a speculative essay)
[INPE-4278-PRE/1150] 08 p0988 N88-15985
An evaluation of effectiveness of PTFE (polytetrafluoroethylene) type friction reducers on reducing friction and wear
[AD-A187440] 10 p1340 N88-18010
On the torque and wear behavior of selected thin film MOS2 lubricated gimbal bearings
14 p1926 N88-21485

FRICTION WELDING
Effects of sulfur content on the plain strain fracture toughness of inertia welds in 4340 steel
[AD-A188192] 11 p1458 N88-18689
Friction welding: Advanced method of producing end cutting tool 14 p1897 N88-21327
Characteristics of joint formation during friction welding of Ti alloys to Nb alloys 14 p1898 N88-21329
Optimum duration of steady-state stage in friction welding of metals without artificial braking
14 p1898 N88-21330
The effect of notch root radius on the determination of toughness in ultrahigh strength steel friction welds
[AD-A195952] 24 p3384 N88-30156

FRICTIONLESS ENVIRONMENTS
Variational and nonvariational theory of frictionless adhesive contact between bodies
[REPT-87-11] 01 p0054 N88-10345
Nonlinear liquid motion in conical containers
[LRT-WE-9-FB-10(1987)] 22 p3077 N88-28270

FRINGE PATTERNS
U DIFFRACTION PATTERNS

FRIT
Titanium powder frit made during the transformation alpha-beta
[ETN-88-91999] 16 p2177 N88-22976

FROGS
Synopsis of the Spacelab D-1 frog statolith experiment STATEX 12 p1659 N88-19940
Organs and tissues regeneration in amphibia under the space flight conditions 12 p1660 N88-19951

FRONTAL AREAS (METEOROLOGY)
U FRONTS (METEOROLOGY)

FRONTS (METEOROLOGY)
NT COLD FRONTS
Longer-duration post-frontal precipitation at Vancouver International Airport, 1953-1983
02 p0203 N88-11269
Observational analysis of the interaction between fronts and the orography in Taiwan during the late winter monsoon season 02 p0203 N88-11270
Conceptual models of Baiu front and Baiu frontal disturbances in multiscale characteristics --- East Asia
02 p0203 N88-11271
The numerical simulation of the mesoscale characteristics associated with Baiu front. Part 1: Structure, low-level jet and radiation characteristics
02 p0203 N88-11272
A one-dimensional model of thermally-driven coastal front evolution 02 p0204 N88-11274
Properties of the atmospheric boundary layer above a subtropical oceanic front
[AD-A184006] 03 p0351 N88-12215
Interactions between the Asian monsoons, the tropical Pacific and the southern hemisphere extratropics
04 p0470 N88-12907
BARS-1M meteorological complex carried on IL-18 airplane 06 p0725 N88-14458
North Pacific Ocean. Tradewind region east of Hawaii, R/V Thomas G Thompson: 25 September - 1 November 1972. STD data report
[AD-A186566] 08 p1044 N88-16311
North Pacific Ocean. Subarctic front central Pacific, R/V Thomas G. Thompson: 8 September - 9 October 1975. CTD data report
[AD-A186567] 08 p1044 N88-16312
North Pacific Ocean. Northwest Pacific Transition Zone, R/V Thomas G. Thompson: 19 March - 1 May 1971. STD data report
[AD-A186568] 08 p1044 N88-16313
North Pacific Ocean. Central Pacific Transition Zone, R/V Thomas G. Thompson: 25 March - 3 May 1968. STD data report
[AD-A186570] 09 p1195 N88-17160
A paper on horizontal deformation in the frontogenesis in south Brazil
[INPE-4469-TDL/322] 12 p1647 N88-19867
Numerical model of Rayleigh instability and spin-off eddies on fronts 13 p1788 N88-20696
The pressure drag and momentum flux during a cold frontal passage over the Alps 13 p1800 N88-20763
Mixed-layer fronts in the California current
13 p1805 N88-20794
Numerical simulation of medium scale disturbance on meiyu front 14 p1900 N88-21346
Development and testing of the gust front algorithm
[AD-A189722] 14 p1949 N88-21622
The effects of time-dependent winds and ocean eddies on ice motion in a marginal ice zone
[AD-A190105] 15 p2100 N88-22511
Observations of frontal instabilities on an upwelling filament
[AD-A191051] 17 p2375 N88-24122
Meteorological features during the marginal ice zone experiment from 20 March to 10 April 1987
[AD-A193960] 23 p3235 N88-29251

FROST
Measurements of vapor flux, liquid water contents, precipitation rates and riming in a Utah mountain cloud system
[PB87-224945] 04 p0469 N88-12900
Effects of wing simulated ground frost on aircraft performance 08 p0952 N88-15775
Last spring frosts and first autumn frosts in Finland
[FMI-6] 19 p2693 N88-26008

FROST DAMAGE
Application of multitemporal SPOT data for crop monitoring: Effects of frost and drought
03 p0344 N88-12171

FROUDE NUMBER
A complete linearized theory for the analysis and design of two-dimensional hydrofoils near a free surface
[UTIAS-TN-264] 05 p0579 N88-13531
Steady ship waves at low Froude numbers, part 2
[AD-A176805] 09 p1160 N88-16953
Centerplane source distribution for slender bodies
10 p1328 N88-17940

FROZEN FOODS
Low temperature storage container for transporting perishables to space station
[NASA-CASE-MFS-28248-1] 18 p2498 N88-24817

FRUITS
Preliminary study on the application of digital processing of TM-LANDSAT data in the mapping of apple orchards in Fraiburgo (SC) 17 p2367 N88-24093

FUEL CAPSULES
Weldability of general purpose heat source iridium capsules 17 p2426 N88-24429

FUEL CELL CATALYSTS
U ELECTROCATALYSTS

FUEL CELL POWER PLANTS
A 40-kW fuel cell field test summary utilities activities report
[PB88-112800] 06 p0731 N88-14496

FUEL CELLS
NT HYDROGEN OXYGEN FUEL CELLS
NT PHOSPHORIC ACID FUEL CELLS
NT REGENERATIVE FUEL CELLS
DOT fuel-cell-powered bus feasibility study
[DE87-012705] 01 p0107 N88-10699

Battery development and testing at ESA
02 p0164 N88-11027
Highlights of the Chemical Technology Division's research activities
[DE88-000233] 03 p0282 N88-11773
Metal containing polymers as fuel cell catalysts
[AD-A184605] 03 p0347 N88-12194
Internal reforming development for solid oxide fuel cells
[DE87-006518] 04 p0464 N88-12871
Phase purity of NiCo2O4, a catalyst candidate for electrolysis of water
[NASA-TM-100239] 05 p0556 N88-13385
High energy density rechargeable batteries for aerospace power requirements
[AD-A184883] 05 p0577 N88-13519
Fuel cells --- military applications
[PML-1986-43] 05 p0622 N88-13813
Extended abstracts: Eighth Battery and Electrochemical Contractors' Conference
[DE88-000960] 06 p0730 N88-14489
Hydroxide ion conductors as possible electrolytes in intermediate temperature fuel cells
[AD-A185508] 06 p0731 N88-14495
A 40-kW fuel cell field test summary utilities activities report
[PB88-112800] 06 p0731 N88-14496
Value-assessment of energy storage concepts in burst power systems
[DE87-013756] 09 p1187 N88-17115
Determination of optimum electrolyte composition for molten carbonate fuel cells literature review
[DE88-001015] 10 p1348 N88-18058
Advanced materials for solid oxide fuel cells
[DE88-002338] 10 p1350 N88-18071
Fuel cell/battery hybrid vehicle assessment
[DE88-005087] 10 p1427 N88-18520
Flammability characteristics of distillate fuels
[AD-A188497] 12 p1612 N88-19642
Recent advances in solid polymer electrolyte fuel cell technology
[DE88-005380] 15 p2092 N88-22464
Value of energy storage in pulsed space power systems
[AD-A191311] 16 p2170 N88-22938
Monolithic fuel cell based power source for sprint power generation 17 p2407 N88-24313
Thermal and power availability transient responses for the Argonne monolithic solid oxide fuel cell
17 p2419 N88-24384
Energy storage for nuclear burst power systems
17 p2426 N88-24431
Value assessment of energy storage concepts in burst power systems 17 p2426 N88-24432
Polymer fuel cell as an energy storage component for space power applications 17 p2429 N88-24452
Sulfur-tolerant anode materials
[DE88-001034] 18 p2537 N88-25054
Phosphoric acid electric utility fuel cell technology development
[DE88-010187] 20 p2795 N88-26582
Oxygen reduction in fuel cell electrolytes
[DE88-008240] 20 p2819 N88-26723
Electrocatalysts for oxygen electrodes
[DE88-008397] 20 p2819 N88-26724
Fuel cell systems program plan: Fiscal year 1988
[DE88-011060] 20 p2820 N88-26731
Monolithic fuel cells
[DE88-012004] 21 p2969 N88-27638
Development of planar geometry solid oxide fuel cell technology, phase 1
[PB88-210356] 23 p3229 N88-29215
Electrocatalytic reduction of oxygen on modified oxide surfaces
[NASA-TM-101333] 24 p3352 N88-29952
Fuel cells for space use
[FCP-TR-DOS-SY-026] 24 p3389 N88-30183

FUEL COMBUSTION
NT NUCLEAR FUEL BURNUP
SCRAM JET (Supersonic Combustion Ramjet) combustion experiments 04 p0404 N88-12512
Oxygen enriched combustion system performance study
[DE88-001500] 05 p0562 N88-13424
Characterizing particle combustion in a Rijke burner
[AD-A186157] 08 p0966 N88-15847
A holographic investigation of particulates in metallized solid fuel ramjet combustion
[AD-A186887] 09 p1140 N88-16831
The effects of fuel composition on ignition delay in homogeneous charge and direct injection compression ignition engines
[DE88-003691] 09 p1143 N88-16849
Studies of fluorine combustion
[AD-A187646] 11 p1452 N88-18656
Fuels combustion research
[AD-A187688] 11 p1453 N88-18657
Fuels combustion research
[AD-A189114] 13 p1736 N88-20381
Basic research on natural gas combustion phenomena
[PB88-168380] 14 p1887 N88-21278
Application of laser-induced fluorescence in an atmospheric-pressure boron-seeded flame
[AD-A189631] 14 p1889 N88-21287
AFRAPT (Air Force Research in Aero Propulsion Technology) trainee program
[AD-A190525] 15 p2035 N88-22123
Effect of mass-velocity on liquid jet atomization in Mach 1 gasflow
[NASA-TM-100813] 16 p2211 N88-23194
Coal particle behaviour in a counter-current combustor
[TAE-606] 19 p2612 N88-25498
Characteristic time correlations to liquid fuel ramjet combustion efficiency 19 p2624 N88-25566
Combustion rate limits of hydrogen plus hydrocarbon fuel: Air diffusion flames from an opposed jet burner technique 19 p2624 N88-25567
Dual Stokes cars measurements in supersonic combusting flow 19 p2625 N88-25569
Ignition and flammability characteristics of solid fuel ramjets 19 p2626 N88-25575
Pollutant formation in heterogeneous mixtures of fuel drops and air
[DOE/CE-50052/H1] 19 p2689 N88-25986
Laser diagnostics applied to advanced combustion systems
[DE88-753119] 20 p2806 N88-26649
Effects of ceramic surfaces on autoignition in a constant volume combustion apparatus
[AD-A193055] 21 p2909 N88-27266
The application of the two-fluid model of turbulence to the 3-D simulation of turbulent combustion in reciprocating engines
[PDR/CFDU/IC/37] 22 p3052 N88-28110
Modeling of spray combustion in direct injection diesel engine
[AD-A193787] 22 p3084 N88-28314
Combustion studies of acoustically suspended liquid droplets
[AD-A193892] 23 p3192 N88-28998
Experiments and modeling of multi-component fuel behavior in combustion
[AD-A195011] 24 p3343 N88-29896
Alternative fuel spray behavior
24 p3345 N88-29912
Atomization of alternative fuels
24 p3345 N88-29913
Turbulence effects on the droplet distribution behind airblast atomizers 24 p3346 N88-29915
Multiple scattering effects in drop sizing of dense fuel sprays by laser diffraction 24 p3346 N88-29917
Influence of operating conditions on the atomization and distribution of fuel by air blast atomizers
24 p3346 N88-29918
The characterizatin of combustion by fuel composition: Measurements in a small conventional combustor
24 p3346 N88-29920
Flame stabilization in a reheat combustor
24 p3346 N88-29921
High performance turbofan afterburner systems
24 p3347 N88-29922
Comparison of the performance of a reverse flow annular combustion chamber under low and high pressure conditions 24 p3347 N88-29923
Radiation transfer in gas turbine combustors
24 p3348 N88-29929
Gas turbine smoke measurement: A smoke generator for the assessment of current and future techniques
24 p3348 N88-29930
Rates of formation of soot from hydrocarbon flames and its destruction 24 p3349 N88-29933
Modeling the stability of a turbulent premixed flame, downstream from a step by a Lagrangian method
24 p3350 N88-29943
Gaseous premixed flames in non-uniform flows
24 p3351 N88-29945
Modeling and experimental study of a reactive flow confined with well injection 24 p3351 N88-29946
Influence of the convection on evaporation and combustion of a fuel droplet 24 p3351 N88-29948
A small annular combustor of high power density, wide operating range and low manufacturing cost
24 p3351 N88-29951

FUEL CONSERVATION
U FUEL CONSUMPTION

FUEL CONSUMPTION
Japanese industrial research on lean combustion: A case study: International Research Monitoring Program
[DE87-013839] 02 p0144 N88-10904
Automotive Stirling engine: Mod 2 design report
[NASA-CR-175106] 02 p0250 N88-11578
Development of strength in cements
[PB87-232971] 06 p0684 N88-14189
Small engine technology programs
08 p0956 N88-15801
X-wing potential for Navy applications
10 p1271 N88-17604
The advantage of variable geometry for turbine engines at low power 10 p1280 N88-17653
Minimum Energy Routing through Interactive Techniques (MERIT) modeling
[NASA-CR-182535] 10 p1356 N88-18105
Review of the state of the art and projected technology of low heat rejection engines
[PB88-131255] 11 p1496 N88-18934
High shear rate rheometry of low-viscosity liquids
[AD-A188447] 12 p1627 N88-19733
Large-Scale Advanced Prop-Fan (LAP)
[NASA-CR-182112] 13 p1723 N88-20306
Gas consumption estimation of an attitude control system of an artificial satellite (utilizing DRF) in limit cycle phase
[INPE-4338-RPE/553] 13 p1731 N88-20350
Status of alcohol fuels utilization technology for highway transportation: A 1986 perspective. Volume 2: Compression ignition engines
[DE88-006059] 13 p1753 N88-20485
The initial calculation of range and mission fuel during conceptual design --- aircraft design
[LR-525] 16 p2161 N88-22889
NASA advanced turboprop research and concept validation program
[NASA-TM-100891] 16 p2163 N88-22902
The effect of weathering on octane quality for winter-grade and summer-grade gasolines
[AD-A190640] 16 p2183 N88-23012
Sunshine project for FY 1987 outlined
16 p2184 N88-23021
NASA/industry advanced turboprop technology program
[NASA-TM-100929] 18 p2466 N88-24641
Computer simulation of turbulent combustion in reciprocating engines
[CFDU/87/11] 18 p2482 N88-24725

FUEL CONTAMINATION
Formation of sediments in fuels containing added sulphonic acids --- marine diesel fuels
[RAE-TM-NAV-ENG-1163] 09 p1150 N88-16891
Fuel containment concepts: Transport category airplanes
[AD-A189818] 18 p2494 N88-24799
Development of a test method to determine potential peroxide content in turbine fuels. Part 2
[AD-A192244] 23 p3199 N88-29042
Atomization of alternative fuels
24 p3345 N88-29913
Fuel effects on flame radiation and hot-section durability 24 p3347 N88-29925

FUEL CONTROL
Investigation of the need for in-use dispensing rate limits and fuel nozzle geometry standardization
[PB88-102611] 07 p0839 N88-15089
AF cryogenic and fluid management spacecraft technology program 08 p0981 N88-15925
Nozzle airflow influences on fuel patternation
24 p3346 N88-29916

FUEL CORROSION
Molten salt corrosion of SiC and Si3N4
17 p2325 N88-23885
Development of reliable fuel pins for space reactor applications 17 p2409 N88-24326

FUEL ELEMENTS (NUCLEAR REACTORS)
U NUCLEAR FUEL ELEMENTS

FUEL FLOW
NT PROPELLANT TRANSFER
SCRAM JET (Supersonic Combustion Ramjet) combustion experiments 04 p0404 N88-12512
Dynamics of propellant feedline systems
[AD-A184865] 05 p0580 N88-13537
Investigation of the flow and combustion behavior in a solid fuel combustion chamber, including the measuring program
[VTH-LR-460] 09 p1141 N88-16838
Arcjet thruster research and technology, phase 1
[NASA-CR-182107] 17 p2314 N88-23830

FUEL INJECTION
Application of electronic fuel injection to the optimum engine for methanol utilization
[PB87-201950] 02 p0180 N88-11120
Performance and combustion characteristics of direct-injection stratified-charge rotary engines
[NASA-TM-100134] 04 p0400 N88-12490
SCRAM JET (Supersonic Combustion Ramjet) combustion experiments 04 p0404 N88-12512
A three-barrel repeating pneumatic pellet injector for plasma fueling of the Joint European Torus
[DE88-000330] 04 p0491 N88-13026

Regressed relations for forced convection heat transfer in a direct injection stratified charge rotary engine
[NASA-TM-100124] 05 p0549 N88-13345
Ignition and flameholding in supersonic flow by injection of dissociated hydrogen 05 p0560 N88-13410
A study of the interaction of laser light with liquid propellant drops
[AD-A185117] 05 p0587 N88-13582
Fuel-injector/air-swirl characterization
[NASA-CR-180864] 07 p0820 N88-14985
Liquid sprays and flow studies in the direct-injection diesel engine under motored conditions
[NASA-TM-100135] 11 p1440 N88-18594
Concept and analysis of a direct-injection alcohol layer charge motor
[ETN-88-91482] 11 p1495 N88-18925
Practical system for the use of alcohol in diesel engines
[PB88-147863] 12 p1612 N88-19638
Development of a laboratory test for multiport fuel injector deposits - evaluation of the Jet Fuel Thermal Oxidation Test apparatus (JFTOT)
[AD-A191313] 16 p2183 N88-23015
Full electronic control system for diesel engine 16 p2185 N88-23025
Liquid Engine Jet Atomization Workshop report 19 p2627 N88-25584
Direct gas injection with glow plug ignition
[PB88-187323] 19 p2676 N88-25911
Pollutant formation in heterogeneous mixtures of fuel drops and air
[DOE/CE-50052/H1] 19 p2689 N88-25986
Heterogeneous diffusion flame stabilization
[AD-A193014] 20 p2771 N88-26429
Pulsed spray structure and atomisation techniques
[AD-A192280] 20 p2800 N88-26614
The 210-HP diesel engine endurance and performance testing with fire resistant diesel fuel
[AD-A193153] 21 p2956 N88-27558
Modeling of spray combustion in direct injection diesel engine
[AD-A193787] 22 p3084 N88-28314
The dc power control for a liquid-fed resistojet
[NASA-TM-101326] 24 p3338 N88-29869
Combustion and fuels in gas turbine engines
[AGARD-CP-422] 24 p3345 N88-29910
Simulation study of spraying, streaming and vaporization phenomena associated with fuel injection 24 p3345 N88-29914
Spray performance of a vaporizing fuel injector 24 p3346 N88-29919
Modeling and experimental study of a reactive flow confined with well injection 24 p3351 N88-29946

FUEL PRODUCTION
Application of solar technology to fuel production chemical processing, and thermochemical energy transport: Status and future
[DE87-014172] 03 p0346 N88-12189
Design study for asteroidal exploitation 03 p0389 N88-12445
The 210-HP diesel engine endurance and performance testing with fire resistant diesel fuel
[AD-A193153] 21 p2956 N88-27558

FUEL PUMPS
Pumping systems and flow interfaces for rapid response electronic reheat controls 10 p1282 N88-17665
Two phase flow in a rotating screw tube (screw tube pump). Investigation of the function and efficiency of the screw tube pump
[MPIS-16/1987] 23 p3222 N88-29178

FUEL SPRAYS
Fuel-injector/air-swirl characterization 02 p0185 N88-11150
Ignition and flame propagation in sprays
[AD-A184679] 03 p0283 N88-11781
SCRAM JET (Supersonic Combustion Ramjet) combustion experiments 04 p0404 N88-12512
Study of electrostatic modulation of fuel sprays to enhance combustion performance in an aviation gas turbine
[AD-A184967] 05 p0548 N88-13341
Investigation of real-time two-dimensional visualization of fuel spray liquid/vapor distribution via exciplex fluorescence
[AD-A188268] 10 p1307 N88-17816
Liquid sprays and flow studies in the direct-injection diesel engine under motored conditions
[NASA-TM-100135] 11 p1440 N88-18594
Quantitative use of exciplex-based vapor/liquid visualization systems, users' manual
[AD-A191649] 19 p2610 N88-25491
Effects of ceramic surfaces on autoignition in a constant volume combustion apparatus
[AD-A193055] 21 p2909 N88-27266
Modeling of spray combustion in direct injection diesel engine
[AD-A193787] 22 p3084 N88-28314
Alternative fuel spray behavior 24 p3345 N88-29912
Atomization of alternative fuels 24 p3345 N88-29913
Simulation study of spraying, streaming and vaporization phenomena associated with fuel injection 24 p3345 N88-29914
Turbulence effects on the droplet distribution behind airblast atomizers 24 p3346 N88-29915
Nozzle airflow influences on fuel patternation 24 p3346 N88-29916
Multiple scattering effects in drop sizing of dense fuel sprays by laser diffraction 24 p3346 N88-29917
Influence of operating conditions on the atomization and distribution of fuel by air blast atomizers 24 p3346 N88-29918
Spray performance of a vaporizing fuel injector 24 p3346 N88-29919
The characterizatin of combustion by fuel composition: Measurements in a small conventional combustor 24 p3346 N88-29920
The performance of a surrogate blend in simulating JP-4 in a spray-fueled combustor 24 p3347 N88-29926

FUEL SYSTEMS
NT AIRCRAFT FUEL SYSTEMS
Aircraft fire safety research 04 p0406 N88-12526
Safety implications of onboard refueling vapor recovery systems
[PB88-102603] 07 p0839 N88-15088
An irradiation performance data base for nitride fuels 17 p2427 N88-24438
Fuel containment concepts: Transport category airplanes
[AD-A189818] 18 p2494 N88-24799
Servojet retrofit
[AD-A191075] 18 p2522 N88-24964
Mach 2 combustion characteristics of hydrogen/hydrocarbon fuel mixtures 19 p2625 N88-25568

FUEL TANKS
NT WING TANKS
An experimental comparison of two designs of mercury propellant tank for use with an electric propulsion engine
[RAE-TR-75109] 01 p0018 N88-10109
Measurements in large JP-4 pool fires
[DE87-013445] 03 p0284 N88-11783
Performance analysis of advanced spacecraft TPS
[NASA-CR-181532] 04 p0399 N88-12484
Orbital Spacecraft Consumables Resupply System (OSCRS). Volume 1: Executive summary
[NASA-CR-172010] 05 p0553 N88-13368
Development of on-orbit fluid gaging techniques 08 p0982 N88-15936
Development and evaluation of an airplane fuel tank ullage composition model. Volume 2: Experimental determination of airplane fuel tank ullage compositions
[AD-A190408] 15 p2017 N88-22025
Domain decomposition in parallel reservoir simulation
[REPT-87-63] 16 p2254 N88-23469
Fuel containment, lightning protection and damage tolerance in large composite primary aircraft structures
[NASA-CR-3875] 17 p2317 N88-23839
Stressed fabric abrasion test procedure for urethane coated fabric fuel tanks
[AD-A196327] 24 p3356 N88-29982

FUEL TESTS
J85-21 fuel nozzle atomization tests
[AD-A189394] 12 p1613 N88-19647
Development of a laboratory test for multiport fuel injector deposits - evaluation of the Jet Fuel Thermal Oxidation Test apparatus (JFTOT)
[AD-A191313] 16 p2183 N88-23015
Aircraft emissions characterization: TF41-A2, TF30-P103 and TF30-P109 engines
[AD-A192053] 18 p2466 N88-24638
Fuel property effects on the US Navy's TF30 engine 24 p3345 N88-29911

FUELING
U REFUELING

FUELS
NT AIRCRAFT FUELS
NT ANTIMISTING FUELS
NT AUTOMOBILE FUELS
NT CERAMIC NUCLEAR FUELS
NT CHEMICAL FUELS
NT COAL
NT CRUDE OIL
NT DIESEL FUELS
NT FOSSIL FUELS
NT GASEOUS FUELS
NT GASOHOL (FUEL)
NT GASOLINE
NT HYDROCARBON FUELS
NT HYDROGEN FUELS
NT JET ENGINE FUELS
NT JP-4 JET FUEL
NT JP-5 JET FUEL
NT JP-8 JET FUEL
NT KEROSENE
NT LIQUEFIED NATURAL GAS
NT LIQUID FUELS
NT MONOPROPELLANTS
NT NATURAL GAS
NT NUCLEAR FUELS
NT SPENT FUELS
NT SYNTHETIC FUELS
Compendium of significant events in the recent development of alcohol fuels in the United States
[DE87-013355] 01 p0032 N88-10202
Application of electronic fuel injection to the optimum engine for methanol utilization
[PB87-201950] 02 p0180 N88-11120
High pressure autoignition of natural gas/air mixtures and the problem of engine knock
[DE87-013799] 03 p0284 N88-11784
Investigation of fuel additive effects on sooting flames
[AD-A186403] 07 p0829 N88-15026
The effect of microgravity on flame spread over a thin fuel
[NASA-TM-100195] 08 p0967 N88-15853
Bistable cellular flames
[DE88-003074] 09 p1142 N88-16848
The chemistry of the hypochlorite neutralization of hydrazine fuels
[DE88-002971] 10 p1307 N88-17812
J85-21 fuel nozzle atomization tests
[AD-A189394] 12 p1613 N88-19647
Alternative fuels: Information on DOE's (Department of Energy's) methanol vehicle demonstration program
[PB88-118203] 13 p1753 N88-20481
Status of alcohol fuels utilization technology for highway transportation: A 1986 perspective. Volume 2: Compression ignition engines
[DE88-006059] 13 p1753 N88-20485
Molybdenum-base cermet fuel development
[DE88-005529] 13 p1839 N88-21003
Kinetics of combustion of finely divided solid fuel in granules
[BLL-M-37626-(5828.4)] 14 p1888 N88-21283
History of wildland fires on Vandenberg Air Force Base, California
[NASA-TM-100983] 18 p2549 N88-25134
Ethanol as a fuel of a lorry. Use experience from a diesel engine modified to an otto engine
[DE88-752870] 21 p2958 N88-27569
Soot and radiation in a gas turbine combustor
[AD-A191991] 23 p3179 N88-28924

FULL SCALE TESTS
Numerical field model simulation of full scale fire tests in a closed spherical/cylindrical vessel
[AD-A195067] 24 p3359 N88-29998

FUMES
Summary report of the history and events pertinent to the Civil Aeromedical Institute's evaluation of providing smoke/fume protective breathing equipment for airline passenger use
[AD-A184499] 03 p0261 N88-11645

FUMIGATION
Practical system for the use of alcohol in diesel engines
[PB88-147863] 12 p1612 N88-19638

FUNCTION GENERATORS
Normal form of a fully resonant Hamiltonian function
[PB88-100946] 06 p0767 N88-14711
Interactive generation of fractal objects
[CWI-CS-R8706] 09 p1218 N88-17302
High-voltage inverse-square function generator
[DE88-701109] 15 p2058 N88-22270
Calibration technique and study on metrological characteristics of a high-voltage inverse square-law function generator
[DE88-702101] 22 p3072 N88-28236

FUNCTION SPACE
NT BANACH SPACE
NT HILBERT SPACE
Isotropic probability measures in infinite dimensional spaces: Inverse problems/prior information/stochastic inversion
[NASA-CR-181555] 05 p0643 N88-13936
Topological equivalence of certain function spaces 2
[PB88-100904] 06 p0767 N88-14712
Linear spaces, absolute retracts and the compact extension property
[PB88-181110] 18 p2564 N88-25225

FUNCTIONAL ANALYSIS
NT BANACH SPACE
NT CONVOLUTION INTEGRALS
NT FOURIER TRANSFORMATION
NT FREDHOLM EQUATIONS

NT HARMONIC ANALYSIS
NT HILBERT SPACE
NT HILBERT TRANSFORMATION
NT INTEGRAL EQUATIONS
NT INTEGRAL TRANSFORMATIONS
NT J INTEGRAL
NT LAPLACE TRANSFORMATION
NT SINGULAR INTEGRAL EQUATIONS
NT VOLTERRA EQUATIONS
NT ZONAL HARMONICS
On the correlation free forms for nonlinear stochastic systems
[DE87-011169] 05 p0645 N88-13947
Local and global techniques for the tracking of periodic solutions of parameter-dependent functional differential equations
[AD-A185756] 06 p0766 N88-14704
Remark on the multiple Wiener integral
[AD-A186015] 07 p0913 N88-15541
Admissible and singular translates of stable processes
[AD-A186426] 07 p0917 N88-15571
Matrix functions in the stability of higher-order numerical schemes
[INPE-4246-PRE/1119] 08 p1073 N88-16472
Boundary value problems for differential and functional differential equations
[AD-A187378] 10 p1400 N88-18349
Well-posedness and spectral estimation for infinite dimensional systems
[AD-A187621] 10 p1401 N88-18354
On exterior variational calculus
[DE88-700861] 12 p1683 N88-20062
On the equivalence of four-dimensional self-duality equations to continual analog of the main chiral field problem
[DE88-700871] 12 p1686 N88-20083
Further extensions of the choquet-deny and deny theorems with applications in characterization theory
[AD-A193358] 21 p3006 N88-27834
Weak solution of the Langevin equation on a generalized functional space
[AD-A194290] 23 p3270 N88-29456
Robust finite-dimensional LQG (Linear Quadric Gaussian)-based controllers for a class of distributed parameter systems
[AD-A194872] 24 p3425 N88-30382

FUNCTIONAL DESIGN SPECIFICATIONS
Components for cryostat --- spaceborne
[MBB/ISO-TN-CD00.003-REV-A] 01 p0032 N88-10207
Access flight hardware design and development 02 p0139 N88-10873
An introduction to the GOES I-M imager and sounder instruments and the GVAR retransmission format
[NOAA-TR-NESDIS-33] 02 p0140 N88-10884
Research relative to an advanced rod control system for quadrupole mass spectrometry applications
[NASA-CR-181458] 02 p0167 N88-11050
Present status of the high resolution spectrometers
[CEBAF-PR-87-029] 02 p0234 N88-11478
Hard X-ray telescope HAPI-1 and its observation of Crab pulsar 03 p0269 N88-11692
Hollow cathode plasma coupling study, 1986
[NASA-CR-171985] 03 p0309 N88-11949
Assessment of existing specifications against the design-philosophy for grounding and inter-unit wiring (EMCR 20/85)
[EMCR-22/85] 03 p0310 N88-11956
Alternatives to the techniques implicit in the design philosophy, and the penalties in performance associated with them --- grounding and wiring
[EMCR-31/85] 03 p0310 N88-11957
Study of an airborne Doppler radar: Project Asterix
[BLL-MO-TRANS-1667-(9022.552)] 04 p0432 N88-12675
Generic specifications for hybrid microcircuits
[ESA-PSS-01-608-ISSUE-2] 06 p0696 N88-14273
Research sensors 08 p0955 N88-15795
Optical measurement systems 08 p0955 N88-15796
Contribution to the design of flexible manufacturing systems: Modeling, simulation, and evaluation of parameters
[ISAL-IDI1-87-04] 09 p1151 N88-16894
Construction of airborne radars for remote sensing
[PB88-113063] 09 p1154 N88-16916
An approach to the hierarchical specification, design and verification of software
[RSRE-MEMO-4063] 09 p1223 N88-17332
Supercritical fluid extraction-gas chromatography of Volatile Organic Compounds (VOC) from tenax devices
[PB88-124300] 10 p1298 N88-17759
Algebra of Communicating Processes (ACP)tau: A universal axiom system for process specification
[CWI-CS-R8725] 13 p1819 N88-20869
Recommended test specification for the electromagnetic compatibility of aircraft equipment
[RAE-TM-FS(F)-510] 14 p1867 N88-21155
Towards a practical microgravity environment --- isolation mount 14 p1878 N88-21223
Further development of a mathematical model for the specification of immersion clothing insulation
[IAM-653] 14 p1954 N88-21644
Using Colored Stochastic Petri Net (CS-PN) software for protocol specification, validation, and evaluation
[ENST-87C004] 15 p2113 N88-22588
A pyrotechnical opening valve
[SNIAS-MU/TYS-NT-2-06(0)] 16 p2167 N88-22922
Development of a digital sun sensor for a spin-stabilized satellite
[INPE-4508-TDL/327] 16 p2169 N88-22929
Present, future of automotive hybrid IC applications discussed 16 p2185 N88-23024
A PC-based receiver-decoder for remote sensor monitoring
[DE88-004733] 16 p2192 N88-23075
Critical issues for SOAR: The space orbiting advanced fusion power reactor 17 p2433 N88-24474
Low cross-section Mo-Nb thermocouples for nuclear application: The state-of-the-art 17 p2433 N88-24477
Parachute for in-flight training on parachute ejection
[REPT-87-11] 18 p2458 N88-24593
Preparation for microgravity: The role of the microgravity materials science laboratory
[NASA-TM-100906] 18 p2497 N88-24811
Application-specific packaging for custom micromechanical structures 19 p2671 N88-25879
Software engineering guidelines for RASP and ANDECS: Requirements and architectural design
[DFVLR-MITT-88-07] 21 p3000 N88-27793
DSN very long baseline interferometry system Mark IV-88 22 p3067 N88-28199
Atmospheric Lidar Experiment in Space (ALEXIS)
[DFVLR-MITT-88-10] 22 p3118 N88-28526
Reliable onboard computing for critical space systems
[RR-670-I] 22 p3135 N88-28641
On eclecticism in specifications: A case study centered around Petri nets --- software engineering
[REPT-87-008] 22 p3140 N88-28671
Customizing Space Nuclear Power System Analysis Model (SNPSAM): Introducing a secondary coolant loop
[AD-A194620] 22 p3151 N88-28750
Performance and technical tolerance --- space projects 22 p3160 N88-28812
Formal specification of a secure document control system for SMITE
[RSRE-88002] 23 p3245 N88-29309
Specifications and performance of ultrastable oscillators in the DORIS orbitography and positioning system
[ETN-88-92761] 24 p3331 N88-29831
Qualification test levels for units to be derived from mechanical test data analysis --- ESA
[REPT-87-158-EI/ET/AG] 24 p3381 N88-30139
Study of human factors engineering criteria for extravehicular activity (EVA) systems, volume 1
[STF23-F87025-VOL-1] 24 p3410 N88-30298

FUNCTIONALS
A functional interpretation of the logistic equation
[REPT-87-037] 05 p0645 N88-13946
Evaluation of quantum mechanics path integrals by the approximations exact on a class of polynomial functionals
[DE88-702434] 21 p3011 N88-27865
On a class of functionals invariant under a Z(sup n) action
[AD-A193474] 23 p3269 N88-29451
Practical higher-order functional and logic programming based on lambda-calculus and set-abstraction
[AD-A193645] 23 p3271 N88-29466
Critical values of functionals on Banach surfaces
[DE88-702735] 23 p3272 N88-29472

FUNCTIONS (MATHEMATICS)
NT ABEL FUNCTION
NT ANALYTIC FUNCTIONS
NT ASYMPTOTES
NT BOOLEAN FUNCTIONS
NT CONFORMAL MAPPING
NT COORDINATE TRANSFORMATIONS
NT COSINE SERIES
NT DELTA FUNCTION
NT DISCRETE FUNCTIONS
NT DISCRIMINANT ANALYSIS (STATISTICS)
NT DISTRIBUTION FUNCTIONS
NT ELLIPTIC FUNCTIONS
NT ENTIRE FUNCTIONS
NT ERROR FUNCTIONS
NT EXPONENTIAL FUNCTIONS
NT FAST FOURIER TRANSFORMATIONS
NT FOURIER TRANSFORMATION
NT FOURIER-BESSEL TRANSFORMATIONS
NT FRESNEL INTEGRALS
NT GREEN'S FUNCTIONS
NT HAMILTONIAN FUNCTIONS
NT HANKEL FUNCTIONS
NT HYPERBOLIC FUNCTIONS
NT HYPERGEOMETRIC FUNCTIONS
NT KERNEL FUNCTIONS
NT LAGUERRE FUNCTIONS
NT LAPLACE TRANSFORMATION
NT LIAPUNOV FUNCTIONS
NT LINEAR TRANSFORMATIONS
NT LOGARITHMS
NT LORENTZ TRANSFORMATIONS
NT MAXWELL-BOLTZMANN DENSITY FUNCTION
NT MELLIN TRANSFORMS
NT MEROMORPHIC FUNCTIONS
NT MODULATION TRANSFER FUNCTION
NT MONOTONE FUNCTIONS
NT NORMAL DENSITY FUNCTIONS
NT OPTICAL TRANSFER FUNCTION
NT ORTHOGONAL FUNCTIONS
NT ORTHONORMAL FUNCTIONS
NT PENALTY FUNCTION
NT PERIODIC FUNCTIONS
NT POINT SPREAD FUNCTIONS
NT POISSON DENSITY FUNCTIONS
NT PROBABILITY DENSITY FUNCTIONS
NT PROBABILITY DISTRIBUTION FUNCTIONS
NT RAYLEIGH DISTRIBUTION
NT RECURSIVE FUNCTIONS
NT SPACE-TIME FUNCTIONS
NT SPHERICAL HARMONICS
NT SPLINE FUNCTIONS
NT STEP FUNCTIONS
NT STRESS FUNCTIONS
NT TANGENTS
NT TIME FUNCTIONS
NT TRANSCENDENTAL FUNCTIONS
NT TRANSFER FUNCTIONS
NT TRIGONOMETRIC FUNCTIONS
NT WALSH FUNCTION
NT WEIBULL DENSITY FUNCTIONS
NT WEIGHTING FUNCTIONS
Solution of nonlinear least-squares problems
[AD-A184010] 03 p0371 N88-12335
A computational examination of orthogonal distance regression
[AD-A184374] 03 p0371 N88-12337
Strong consistency of M-estimates for the linear model
[AD-A185487] 06 p0764 N88-14696
On the relations between increasing functions associated with two-parameter continuous martingales
[AD-A185572] 06 p0765 N88-14699
Upper bounds on the expected value of a convex function using gradient and conjugate function information
[AD-A186246] 07 p0910 N88-15517
Operator foundation of functional integral in non-Abelian gauge theory
[DE88-700508] 07 p0941 N88-15719
An extended Cobb-Douglas form for use in production economics
[AD-A186372] 07 p0943 N88-15733
Implementation of elementary functions in Ada
[CWI-NM-R8709] 09 p1218 N88-17303
Design and implementation of elementary functions in Ada
[CWI-NM-R8710] 09 p1218 N88-17304
An algebraic approach to a calculus of functional differences: Fixed differences and integrals
[AD-A187079] 09 p1227 N88-17346
Computation of the zeta-function of an algebraic curve with the differentials of the first kind
[PB88-127527] 10 p1399 N88-18339
A view of unconstrained optimization
[AD-A188327] 12 p1684 N88-20066
The inverse problem and the pseudo-empirical orthogonal function method of solution. Part 1: Theory; Part 2: Application
[AD-A188894] 12 p1684 N88-20069
Analiticity in fourth order wave equations
[DE88-700837] 12 p1686 N88-20080
Large momentum pairing in one-dimensional systems
[AD-A189228] 13 p1835 N88-20981
Random processes, turbulence and disordering fields
[AD-A191399] 16 p2209 N88-23181
Proposal for standard mathematical packages in Ada
[CWI-NM-R8718] 16 p2249 N88-23439
Estimation of time- and state-dependent delays and other parameters in functional differential equations
[NASA-CR-181663] 17 p2383 N88-24164
A simple explanation of the Stokes phenomenon
[AD-A193253] 21 p3006 N88-27832
An overview of lattice QCD
[DE88-010867] 21 p3026 N88-27963

An exponential decay estimate for the stationary perturbation of Poiseuille flow
[AD-A193480] 23 p3210 N88-29105
Multicriteria integer programming for problems involving linear and nonlinear utility functions
[AD-A194530] 23 p3249 N88-29336
Algorithms for nonlinear least-squares problems
[AD-A196071] 24 p3411 N88-30305

FUNGAL DISEASES
A solid phase enzyme-linked immunosorbent assay for the antigenic detection of Legionella pneumophila (serogroup 1): A compliment for the space station diagnostic capability 06 p0795 N88-14868

FUNGI
NT YEAST

FUNGICIDES
NT CAFFEINE
NT XANTHINES

FURAN RESINS
NT KEVLAR (TRADEMARK)
NT POLYAMIDE RESINS

FURANS
Novel conductive polymers
[EP-PATENT-0-182-548-A2] 01 p0026 N88-10163
The first gallium-arsenic compound containing a single Ga3As unit: Isolation and crystal structure of ((thf)Br2Ga)3As (thf = tetrahydrofuran)
[AD-A187457] 11 p1555 N88-19309

FURLABLE ANTENNAS
Aerospatiale unfurlable reflector and associated mechanisms 14 p1875 N88-21203

FURNACES
NT IMAGE FURNACES
NT SOLAR FURNACES
Metallurgy laboratory for Columbus, executive summary
[SNIAS-813-CA/TS] 02 p0157 N88-10980
Evaluation of the Mellen EDG furnace for growth of large diameter GaAs single crystals in a horizontal configuration
[DE88-000463] 04 p0498 N88-13068
Oxygen enriched combustion system performance study
[DE88-001500] 05 p0562 N88-13424
High-temperature photoelectron spectroscopy. An increased sensitivity spectrometer for studying vapor-phase species produced at furnace temperatures greater than 2000K
[AD-A186542] 09 p1140 N88-16835
Heat transfer from impinging flame jets
[ETN-88-91610] 09 p1162 N88-16964
Proceedings of the 1987 International Symposium on Condensing Heat Exchangers
[DE88-005230] 13 p1766 N88-20564
High temperature testing of C/C (Carbon/Carbon) composites
[AD-A193012] 20 p2768 N88-26411
Plasma technology: Preliminary studies 2
[DE88-752815] 22 p3154 N88-28763

FUSELAGE MOUNTING
U AIRCRAFT PRODUCTION

FUSELAGES
Controlling the dynamic environment during NOE flight 03 p0264 N88-11661
A 0.15-scale study of configuration effects on the aerodynamic interaction between main rotor and fuselage
[NASA-CR-166577] 04 p0395 N88-12462
Navier-Stokes simulation of transonic transportation aircraft configurations. 1: Flow-field simulation over wing-fuselage combinations 05 p0540 N88-13288
Compressible Euler solution on a multiblock grid around a wing-fuselage configuration
[FFA-TN-1987-46] 05 p0542 N88-13303
Coupled elastic rotor/body vibrations with inplane degrees of freedom 05 p0596 N88-13643
A study of the utilization of advanced composites in fuselage structures of commercial aircraft
[NASA-CR-172405] 06 p0679 N88-14157
Riblets for aircraft skin-friction reduction 07 p0814 N88-14955
Study on utilization of advanced composites in fuselage structures of large transports
[NASA-CR-172406] 07 p0827 N88-15014
Low frequency eddy current detection and evaluation of corrosion in aircraft skins
[ETN-88-91664] 09 p1144 N88-16859
General fuselage coordinates for the calculation of three-dimensional boundary layers
[MBB/LKE-122/S/PUB/244] 13 p1771 N88-20596
Transonic flow field analysis for real fuselage configurations 14 p1864 N88-21133
Experimental comparison of lightning simulation techniques to CV-580 airborne lightning strike measurements
[AD-A190576] 15 p2098 N88-22496
Multi-body aircraft with an all-movable center fuselage actively controlling fuselage pressure drag
[NASA-CASE-LAR-13511-1] 17 p2301 N88-23765
Helicopter anti-torque system using fuselage strakes
[NASA-CASE-LAR-13630-1] 17 p2308 N88-23809
Vibration testing of ACT fuselage 19 p2634 N88-25627
Research investigation of helicopter main rotor/tail rotor interaction noise
[NASA-CR-4143] 19 p2722 N88-26165
Missiles, fuselage and similar bodies 23 p3167 N88-28858
Missiles, fuselages and similar bodies 23 p3169 N88-28869
Test of an 0.8-scale model of the AH-64 Apache in the NASA Langley full-scale wind tunnel
[AD-A196129] 24 p3319 N88-29768

FUSES
The development of diagnostic fuses
[SAND-86-0395] 03 p0311 N88-11963
A comparative assessment of US and UK explosives qualified as replacements for tetryl
[MRL-R-1094] 13 p1754 N88-20486

FUSES (ORDNANCE)
Mechanism of and particle size effects on shock sensitivity of heterogeneous pressed explosives: Preliminary assessment of binderless RDX in fuze trains
[MRL-R-1077] 09 p1150 N88-16892
Recommended replacements for tetryl in Australian production fuzes and related ordnance
[MRL-R-1089] 13 p1754 N88-20489

FUSIFORM SHAPES
U CONES

FUSION (MELTING)
Analytical treatment of the melting and solidification of latent heat store materials in finned tube geometries
[IKE-5-223] 03 p0314 N88-11985

FUSION REACTORS
NT SPHEROMAKS
NT STELLARATORS
Plasma properties
[DE87-013662] 01 p0101 N88-10663
Fusion reactor physics and technology studies
[DE87-013691] 01 p0101 N88-10664
Technical evaluation of major candidate blanket systems for fusion power reactor
[DE87-752989] 02 p0239 N88-11512
Low activation ferritic alloys for nuclear fusion reactors
[DE87-010711] 03 p0286 N88-11801
Reduced-activation ferritic steels: A comparison with Cr-Mo steels
[DE88-000332] 03 p0290 N88-11826
The LPX (Long Pulse Experiment) facility
[DE87-010493] 03 p0311 N88-11964
Applications of neutral beam and rf technologies
[DE87-014936] 03 p0379 N88-12382
Inertial confinement fusion reactor cavity analysis
[DE88-000788] 04 p0492 N88-13028
Refueling and density control in the ZT-40M reversed field pinch
[DE88-000504] 04 p0493 N88-13040
PISCES: Plasma-surface interactions and materials research
[DE88-001323] 04 p0494 N88-13044
ICRF launcher studies
[DE88-001710] 04 p0495 N88-13046
Advanced concepts theory annual report 1986
[AD-A184986] 05 p0651 N88-13991
Dynamic processes in field-reversed-configuration compact toroids
[DE87-014756] 05 p0652 N88-13998
A short introduction to the status and motivation for reversed field pinch and compact toroid research
[DE88-000487] 05 p0652 N88-13999
A review of the experimental and theoretical status of the reversed-field pinch
[DE88-000529] 05 p0652 N88-14000
Economics of fusion reactors
[DE88-000580] 05 p0653 N88-14002
Subcommittee for MHD theory
[DE88-000596] 05 p0653 N88-14003
Transport scaling in the collisionless-detrapping regime in stellarators
[DE88-001511] 05 p0653 N88-14006
Microwave superheaters for fusion
[DE88-001656] 05 p0653 N88-14007
The TITAN oscillating-field current-drive system
[DE88-001823] 06 p0782 N88-14798
Edge plasmas and plasma/wall interactions in an ignition-class reversed field pinch
[DE88-001825] 06 p0782 N88-14799
The TITAN magnet configuration
[DE88-001826] 06 p0782 N88-14800
Reversed field pinch experiments: Summary of progress report
[DE88-002367] 07 p0934 N88-15673
Main physics features driving design concept and physics design constraints. Conceptual design study of FY86 FER
[DE88-750309] 07 p0936 N88-15689
Conceptual design study of Fusion Experimental Reactor (FY86 FER): Safety
[DE88-751071] 10 p1411 N88-18418
Diagnostics for ATF
[DE88-004175] 10 p1414 N88-18438
ATF experimental plans
[DE88-004177] 10 p1414 N88-18439
Zero-dimensional model of a reversed field pinch fusion reactor
[DE88-005213] 10 p1414 N88-18442
Low aspect ratio torsatrons
[DE88-004173] 11 p1552 N88-19284
Potential benefits of a broad magnetic fusion R and D program
[DE88-003288] 11 p1553 N88-19297
Summaries of FY86 research in the Applied Plasma Physics Fusion Theory Program
[DE88-004242] 11 p1554 N88-19298
Proceedings of US-Japan Heliotron-Stellarator Workshop, volume 3
[DE88-004788] 11 p1554 N88-19299
Proceedings of US-Japan Heliotron-Stellarator Workshop, volume 2
[DE88-004789] 11 p1554 N88-19300
Proceedings of US-Japan Heliotron-Stellarator Workshop, volume 4
[DE88-004787] 12 p1693 N88-20126
Improved zero dimensional model of a reversed field pinch fusion device
[DE88-005212] 12 p1693 N88-20127
Application of railgun principle to high-velocity hydrogen pellet injection for magnetic fusion reactor refueling
[DE88-005830] 13 p1728 N88-20334
The Magnetically Insulated Inertial Confinement Fusion (MICF): A novel approach
[DE88-005460] 13 p1842 N88-21026
Outlook for the fusion hybrid and tritium-breeding fusion reactors
[PB88-149281] 13 p1843 N88-21029
Analyses and experiments on the integrity and lifetime predictions of plasma-facing components in fusion reactors
[DE87-702957] 15 p2135 N88-22735
Magnet shielding analysis for SOAR: A space fusion reactor 17 p2400 N88-24269
A fusion based plasma propulsion system 17 p2401 N88-24274
SOAR: Space orbiting advanced fusion power reactor 17 p2416 N88-24366
Energy requirements for HE-3 mining operations on the Moon 17 p2420 N88-24390
Design studies of low aspect-ratio torsatrons
[DE88-007562] 18 p2579 N88-25320
Heavy ion fusion system assessment: Final focus and transport model
[LBL-23040] 19 p2725 N88-26183
The JET (Joint European Torus) multipellet launcher and fueling of JET plasmas by multipellet injection
[DE88-008367] 19 p2729 N88-26206
Inertial fusion in the nineties
[DE88-007913] 19 p2730 N88-26214
Pulsed power driver technologies for inertial confinement fusion power reactors
[DE88-009260] 19 p2731 N88-26221
Development of high current and high brightness negative hydrogen ion sources
[DE88-010882] 20 p2852 N88-26934
Optical imaging diagnostics for fusion plasmas
[DE88-997572] 21 p3018 N88-27910

FUSION WELDING
NT ARC WELDING
NT BRAZING
NT ELECTRON BEAM WELDING
NT GAS TUNGSTEN ARC WELDING
NT GAS WELDING
NT PLASMA ARC WELDING
Gas tungsten arc welding of Al-10Fe-5Ce
[AD-A184202] 03 p0334 N88-12104
Efficiency of fusion during periodic-pulse laser-beam welding 14 p1897 N88-21324

FUSION-FISSION HYBRID REACTORS
Development of fast breeder reactors in China 16 p2186 N88-23032

FUZZY SETS
Modeling of human judgement in multicriteria analysis using pairwise comparison
[REPT-87-01] 01 p0076 N88-10484
Foundations of O-theory 2: Measurements and relation to fuzzy set theory
[DE88-000013] 04 p0485 N88-12986
Multidimensional least squares fitting of fuzzy models
[AD-A185148] 05 p0640 N88-13916

Least squares for fuzzy vector data regression
[AD-A185156] 05 p0640 N88-13917
An application of fuzzy set theory to statistical hypothesis testing
[AD-A186705] 09 p1232 N88-17388
Measures of similarity between fuzzy concepts: A comparative analysis
[AD-A189430] 13 p1825 N88-20910
An expert system model using predicate transition nets
[AD-A191953] 19 p2718 N88-26141

FUZZY SYSTEMS
Measures of diversity based on fuzzy multinomial distributions
[DE87-010617] 02 p0228 N88-11439
Foundations of O-theory 2: Measurements and relation to fuzzy set theory
[DE88-000013] 04 p0485 N88-12986

F4H AIRCRAFT
U F-4 AIRCRAFT

G

G FORCE
U ACCELERATION (PHYSICS)

G STARS
NT SUN
The X-ray orbital lightcurves of AR Lac and TY Pyx 04 p0509 N88-13129
An analysis of the photospheric line profiles in F, G, and K supergiants 04 p0513 N88-13157
Sensitivity of the H alpha line to expansion, geometrical extent and temperature gradient in the G and K supergiant chromospheres 04 p0514 N88-13159
A helium flare on the active G5 dwarf Kappa Ceti 04 p0519 N88-13189
Observations and analysis of the photospheric magnetic fields on dwarf G, K and M stars 04 p0520 N88-13196

GADOLINIUM
Magnetic investigations of the one-dimensional Heisenberg magnet Gd2Cl3
[ETN-88-91083] 09 p1241 N88-17438
Magnetic phase transitions in 90-K superconductors Ho1Ba2Cu3O(7-delta) and Gd1Ba2Cu3O(7-delta) observed by ZF-muon(+)SR
[DE88-752611] 23 p3290 N88-29588
Absorption spectra and energy levels of Gd(3+), Nd(3+) and Cr(3+) in the garnet Gd3Sc2Ga3O12
[AD-A193634] 23 p3292 N88-29599

GAGES
U MEASURING INSTRUMENTS

GAIN (AMPLIFICATION)
U AMPLIFICATION

GALACTIC CLUSTERS
NT LOCAL GROUP (ASTRONOMY)
NT VIRGO GALACTIC CLUSTER
Finnish-Soviet Symposium on Radio Astronomy (1st) held at Otanlemi on August 26-27, 1985
[PB87-140661] 07 p0944 N88-15736
Galaxy evolution in dense clusters 13 p1855 N88-21101
Infrared constraints on the nature of dark matter 13 p1855 N88-21102
Multiple object redshift determinations in clusters of galaxies using OCTOPUS
[INPE-4528-PRE/1278] 15 p2150 N88-22835
New measurements of radial velocities in clusters of galaxies
[INPE-4527-PRE/1277] 15 p2152 N88-22845
Clustering of galaxies and clusters of galaxies in a decaying-particle cosmological model with a massive decay product
[DE88-753434] 23 p3298 N88-29642
Systematic properties of clusters of galaxies in different cosmological scenarios 23 p3299 N88-29646
Catalog of open clusters and associated interstellar matter
[NASA-RP-1202] 23 p3300 N88-29652

GALACTIC COSMIC RAYS
Production of NO by galactic cosmic rays and lightning
[DE87-014613] 02 p0197 N88-11230
Heavy element compositions and energy spectra of galactic and solar cosmic rays 03 p0272 N88-11714
Preliminary estimates of galactic cosmic ray exposures for manned interplanetary missions
[NASA-TM-100519] 05 p0661 N88-14058
Axial anisotropy of the intensity of the cosmic ray nuclear component
[IFSI-87-7] 05 p0662 N88-14061
A benchmark for galactic cosmic ray transport codes
[NASA-TM-101157] 17 p2453 N88-24571
The application of imaging to the atmospheric Cerenkov technique: Observations of the Crab nebula 20 p2884 N88-27126

GALACTIC EVOLUTION
Kinematics and galactic structure
[PREPRINT-18] 03 p0389 N88-12442
Cosmology with decaying vacuum energy
[DE88-000698] 03 p0389 N88-12443
New cosmological scenario
[DE87-703357] 04 p0520 N88-13198
Galaxy formation by gravitational collapse in a universe dominated by cold dark matter 04 p0521 N88-13205
Number count-redshift relation in a perturbed Friedmann universe
[DE88-750302] 07 p0945 N88-15743
Nonequilibrium ionization of pregalactic plasma and lessening of relic radiation anisotropy 08 p1002 N88-16071
Existence of absolutely closed universe 08 p1080 N88-16509
The origin of the diffuse X-ray background and the formation of galaxies and voids 10 p1428 N88-18527
Effects of galactic chemical evolution on thorium/neodymium cosmochronology
[DE88-003829] 11 p1570 N88-19397
Galaxy evolution in dense clusters 13 p1855 N88-21101
Cosmological parameters and evolution of the galaxy luminosity function
[NASA-CR-183081] 21 p3030 N88-27986
Evolution of heavy-element abundances in the galactic halo and disk
[DE88-011736] 22 p3164 N88-28845
Molecular hydrogen in galaxies 23 p3299 N88-29645
Starbursts and their dynamics
[NASA-CR-180227] 24 p3452 N88-30549
Observations of faint field galaxies
[NASA-CR-183251] 24 p3453 N88-30555
A deep redshift survey of field galaxies. Comments on the reality of the Butcher-Oemler effect
[NASA-CR-183255] 24 p3454 N88-30558

GALACTIC MASS
Molecular clouds at high galactic latitudes 11 p1569 N88-19392
Infrared constraints on the nature of dark matter 13 p1855 N88-21102
Global properties of star formation in spiral galaxies 14 p1994 N88-21883

GALACTIC NUCLEI
NT ACTIVE GALACTIC NUCLEI
Extragalactic VLBI objects: Candidates for optical interferometry? 01 p0094 N88-10616
Galactic nuclei and quasars at high angular resolution 01 p0098 N88-10644
Investigations of extragalactic hydroxyl 03 p0389 N88-12441
Investigation of nuclei of active galaxies as well as sources in the Large Magellanic Cloud using the X-ray astronomy satellite EXOSAT
[ETN-88-91494] 11 p1570 N88-19399
The astrophysics of nebulae and active galactic nuclear emission-line regions: New methods and applications 13 p1858 N88-21111
Model-independent requirements to the source of positrons in the galactic centre
[DE88-700968] 14 p1992 N88-21874
The galactic nucleus at mm-, sub-mm and far-infrared wavelengths
[MPE-PREPRINT-102] 16 p2288 N88-23700
The distance to the center of the galaxy: H2O maser proper motions in Sgr B2(N)
[MPE-PREPRINT-104] 16 p2288 N88-23702
Thermal-nonthermal relationships in active galactic nuclei
[B8661482] 16 p2289 N88-23707
IUE evidence on the nature of the innermost broad-line region in Seyfert 1 galaxies 17 p2450 N88-24552

GALACTIC RADIATION
NT GALACTIC COSMIC RAYS
NT GALACTIC RADIO WAVES
Investigations of extragalactic hydroxyl 03 p0389 N88-12441
Galactic interstellar abundance surveys with IUE and IRAS 04 p0522 N88-13206
Observations of the large scale anisotropy in the cosmic background radiation at 3 mm
[INPE-4425-PRE/1229] 12 p1712 N88-20249
Stars, gas and dust in the Andromeda galaxy
[B8679680] 16 p2289 N88-23708
Gamma radiation from center of the galaxy of the order of MeV values
[MPE-207] 21 p3032 N88-27999
Measurement of galactic radio emission at frequency 37 GHz from aboard spacecraft 24 p3448 N88-30520

GALACTIC RADIO WAVES
Measurement of galactic radio emission at frequency 37 GHz from aboard spacecraft 24 p3448 N88-30520

GALACTIC ROTATION
Might dark matter not be concentric with luminous matter
[DE87-703094] 02 p0252 N88-11589
Kinematics and dynamics of barred spiral galaxies 03 p0388 N88-12440
Dipole component of relict radiation determined from Relikt experiment data 08 p1002 N88-16070
The velocity field of the outer galaxy
[B8681472] 20 p2885 N88-27132
The kinematics of late-type supergiants
[SER-C-PREPUBL-FASC-28] 24 p3454 N88-30560
The dynamics of SBO galaxies. Part 1: The data
[SER-C-PREPUBL-FASC-22] 24 p3455 N88-30567

GALACTIC STRUCTURE
Kinematics and galactic structure
[PREPRINT-18] 03 p0389 N88-12442
Comments on H. Arp The persistent problem of spiral galaxies
[TRITA-EPP-87-05] 05 p0660 N88-14052
Prediction and analysis of basic gravitational microlensing phenomena 11 p1550 N88-19272
The comet flux and the 15 Myr galactic cycle 14 p1995 N88-21889
Differential spectral synthesis of the stellar populations in the bulges of spiral galaxies 17 p2451 N88-24558

GALAXIES
NT ACTIVE GALAXIES
NT ANDROMEDA GALAXY
NT BARRED GALAXIES
NT DISK GALAXIES
NT ELLIPTICAL GALAXIES
NT GALACTIC CLUSTERS
NT IRREGULAR GALAXIES
NT LOCAL GROUP (ASTRONOMY)
NT MAGELLANIC CLOUDS
NT MILKY WAY GALAXY
NT RADIO GALAXIES
NT SEYFERT GALAXIES
NT SPIRAL GALAXIES
NT STARBURST GALAXIES
NT VIRGO GALACTIC CLUSTER
Number count-redshift relation in universe models with nonzero cosmological constant
[DE87-703043] 03 p0388 N88-12435
The origin of the diffuse X-ray background and the formation of galaxies and voids 10 p1428 N88-18527
EXOSAT observations of active galaxies in the medium-energy X-ray domain
[ETN-88-91499] 14 p1993 N88-21879
Near-infrared observations of cepheids: The distance to M33 15 p2152 N88-22846
Method of digital surface photometry of galaxies and its application to the edge-on galaxy NGC 5907 16 p2287 N88-23695
Dynamics of interacting galaxies 23 p3299 N88-29647
Observations of faint field galaxies
[NASA-CR-183251] 24 p3453 N88-30555
A deep redshift survey of field galaxies. Comments on the reality of the Butcher-Oemler effect
[NASA-CR-183255] 24 p3454 N88-30558

GALAXY GROUPS
U GALACTIC CLUSTERS

GALERKIN METHOD
Semidiscrete Galerkin method for semilinear evolution equations with a differential operator of third order
[BONNER-MATHE-SCHR-181] 01 p0087 N88-10570
Numerical solution of Euler equations for compressible fluids by the finite element method, volume 3
[ETN-87-90650] 02 p0170 N88-11070
An adaptive pseudo-spectral method for reaction diffusion problems
[NASA-CR-178394] 02 p0224 N88-11414
An evaluation of a translator for finite element data to resistor/capacitor data for the heat diffusion equation
[DE87-013926] 06 p0698 N88-14285
Stabilized Galerkin method for convection-diffusion problems
[PB87-234985] 06 p0764 N88-14694
SRB combustion dynamics analysis computer program (CDA-1)
[NASA-CR-182404] 07 p0830 N88-15032
On the convergence of the p-version of the boundary element Galerkin method
[AD-A186198] 07 p0910 N88-15514

Radiative heat transfer solutions in plane-parallel participating media: Application to multilayer insulations for space vehicles
[INPE-4221-PRE/1101] 08 p0962 N88-15824
Investigation of iterative and spectral Galerkin techniques for solving electromagnetic boundary value problems 09 p1155 N88-16925
Successful mixed formulation for axisymmetric shell analysis employing discontinuous stress fields of the same order as the displacement field
[DE88-700021] 09 p1178 N88-17052
Shuttle rocket booster computational fluid dynamics
[NASA-CR-182518] 10 p1293 N88-17733
Dynamic response of some structural elements fabricated from a non-linear elastic material 10 p1344 N88-18031
Comprehensive analysis of helicopters with bearingless rotors
[NASA-CR-182537] 10 p1390 N88-18300
Finite element methods of analysis for high speed viscous flows
[NASA-CR-182529] 11 p1483 N88-18852
A velocity-pressure integrated, mixed interpolation, Galerkin finite element method for high Reynolds number laminar flows
[NASA-CR-179264] 11 p1486 N88-18868
A posterior error estimation in a finite element method for parabolic partial differential equations
[AD-A190296] 15 p2120 N88-22636
Numerical solution of linear integral equations with random forcing terms 18 p2565 N88-25237
Galerkin approximation for inverse problems for nonautonomous nonlinear distributed systems
[NASA-CR-181676] 18 p2567 N88-25246
New mixed finite element methods 18 p2567 N88-25248
Numerical simulation and stability analysis of the absolutely and convectively unstable wake
[DFVLR-FB-88-09] 21 p2949 N88-27518
Convergence of Galerkin approximations for operator Riccati equations: A nonlinear evolution equation approach
[NASA-CR-181706] 24 p3425 N88-30386

GALILEAN SATELLITES
NT IO

GALILEO MISSION
U GALILEO PROJECT

GALILEO PROBE
Galileo probe parachute test program: Wake properties of the Galileo probe at Mach numbers from 0.25 to 0.95
[NASA-RP-1130] 11 p1488 N88-18884

GALILEO PROJECT
A new code for Galileo 22 p3065 N88-28186
Mission telemetry system monitor: A real-time knowledge-based system 24 p3418 N88-30345

GALILEO SPACECRAFT
Experimental investigation of hypersonic aerodynamics
[NASA-CR-182973] 18 p2458 N88-24591

GALLIUM
IRAC test report. Gallium doped silicon band 2: Read noise and dark current
[NASA-TM-87813] 09 p1159 N88-16945
Angular resolved energy analysis of (69)Ga+ ions from a gallium liquid metal ion source
[AERE-R-12649] 15 p2139 N88-22760
Tunable optical sources/growth and characterization of nonlinear optical materials
[AD-A190874] 16 p2274 N88-23608
Nuclear magnetic resonance spectrometer
[AD-A192928] 21 p2950 N88-27523
Growth and characterization of CuGaS2, CuAlS2 and CuGa0.9Al0.1S2 single crystals
[AD-A192963] 21 p3021 N88-27930
Development of a unit cell for a Ge:Ga detector array
[NASA-CR-177445] 24 p3375 N88-30100

GALLIUM ARSENIDE LASERS
AlGaAs heterojunction lasers
[NASA-CR-4119] 09 p1171 N88-17020
Visible InGaAsP/GaAsP lasers produced by epitaxial growth from liquid phase 09 p1237 N88-17416
High-efficiency GaAs semiconductor laser with longitudinal excitation by scanning electron beam 09 p1238 N88-17421
New semiconductor laser structure for an optical communication system
[ETN-88-92353] 20 p2807 N88-26654
Diode laser ignition of high explosives and pyrotechnics
[DE88-008771] 21 p2923 N88-27352

GALLIUM ARSENIDES
NT ALUMINUM GALLIUM ARSENIDES
Effects of electron and proton irradiations on n/p and p/n GaAs cells grown by MOCVD
[NASA-TM-100199] 01 p0042 N88-10266
Study and realization of Schottky diodes for forthcoming integrated hyperfrequency devices
[LAAS-87-062] 02 p0167 N88-11054
Surface effects and low frequency noises in GaAs field effect transistors
[LAAS-87-179] 02 p0168 N88-11055
Quantum well laser diodes: Modeling and realization of GaAs/GaAlAs
[LAAS-87-105] 02 p0179 N88-11116
Gallium arsenide and multibandgap solar cell research
[DE87-012260] 02 p0194 N88-11215
Ohmic contacting schemes to gallium arsenide devices
[DE87-014627] 02 p0244 N88-11544
Photoluminescence studies of GaAs/AlAs superlattices
[DE87-013817] 02 p0245 N88-11548
Study and optimization of a technological process for the fabrication of heterojunction bipolar transistors. Applications to high speed devices
[LAAS-87-134] 02 p0246 N88-11555
Molecular beam heteroepitaxy: (Ca,Sr)F2-GaAs system
[LAAS-87-168] 02 p0246 N88-11556
Excimer laser-assisted deposition of GaAs, AlAs and (Al,Ga)As from Lewis acid-base adducts
[AD-A184588] 03 p0329 N88-12081
Performance of GaAs and silicon concentrator cells under 37 MeV proton irradiation
[NASA-TM-100144] 04 p0465 N88-12877
Radiation performance of AlGaAs concentrator cells and expected performance of cascade structures
[NASA-TM-100145] 04 p0465 N88-12878
Evaluation of the Mellen EDG furnace for growth of large diameter GaAs single crystals in a horizontal configuration
[DE88-000463] 04 p0498 N88-13068
Fundamental studies in the OM-CVD growth of Ga-In-As-Sb
[AD-A184822] 05 p0655 N88-14014
A GaAs MESFET balanced mixer with very low intermodulation
[AD-A184848] 05 p0655 N88-14015
Resonant level lifetime in GaAs/ AlGaAs double-barrier structures
[AD-A185376] 05 p0655 N88-14020
Analytical investigations of bulk wave resonators in the piezoelectric thin film on gallium-arsenide configuration
[AD-A185716] 06 p0789 N88-14840
GaAs MMIC yield evaluation --- monolithic microwave integrated circuits (MMIC)
[ESA-CR(P)-2470] 08 p0979 N88-15916
Influence of arsenic superficial enrichment on the ohmicity of the n-GaAs:In/Au contact
[ECL-87-09] 08 p1089 N88-16554
Nanoelectronics
[AD-A186969] 09 p1156 N88-16930
Radiant power degradation of silicon-doped gallium arsenide and gallium aluminum arsenide infrared light-emitting diodes
[AD-A186726] 09 p1157 N88-16935
GaAs varactor diode MMIC fabrication technology --- monolithic microwave integrated circuit (MMIC)
[RSRE-MEMO-4022] 09 p1158 N88-16943
Forward-biased current annealing of radiation damaged gallium arsenide and silicon solar cells
[AD-A186904] 09 p1186 N88-17105
A report on the effects of neutron irradiation of GaAs semiconductors
[AD-A186816] 09 p1253 N88-17510
A payload for investigating the influence of convection on GaAs crystal growth 10 p1288 N88-17702
Strength and structure of Ga sub 1-xIn sub xAs alloys
[AD-A188092] 10 p1303 N88-17795
Wafer scale implementation of a GaAs systolic signal processor cell 10 p1381 N88-18247
Grazing incidence X-ray scattering study of defect structures in MBE GaAs/Si using synchrotron radiation
[DE88-004556] 10 p1420 N88-18483
Development of a planar heterojunction bipolar transistor for very high speed logic
[AD-A188137] 11 p1478 N88-18820
Positron annihilation spectroscopy of AlGaAs/GaAs interfaces in MOCVD-grown GaAs heterojunction solar cells
[DE88-003903] 11 p1508 N88-19012
Digital control of the Czochralski growth of Gallium arsenide-controller software reference manual
[AD-A187210] 11 p1528 N88-19127
Development of VLSI optical data link
[AD-A187883] 11 p1549 N88-19265
Development of VLSI optical data link
[AD-A187884] 11 p1549 N88-19266
Radiation effects on gallium arsenide integrated optical devices
[DE88-004107] 11 p1551 N88-19277
Silicon and indium doping of GaAs: Measurements of the effect of doping on mechanical behavior and relation with dislocation formation
[DE88-003862] 11 p1554 N88-19303
Structural characterization of undoped and doped GaAs: A comparative study of four techniques
[DE88-004552] 11 p1555 N88-19304
Autonomous Liquid Encapsulated Czochralski (LEC) growth of single crystal GaAs by intelligent digital control
[AD-A187211] 11 p1555 N88-19305
The first gallium-arsenic compound containing a single Ga3As unit: Isolation and crystal structure of ((thf)Br2Ga)3As (thf = tetrahydrofuran)
[AD-A187457] 11 p1555 N88-19309
Laser measurements of state-resolved Ga and in atom sticking and desorption on metal and semiconductor surfaces
[AD-A187644] 11 p1555 N88-19310
Investigation of defect and electronic interactions associated with GaAs device processing
[AD-A188021] 11 p1556 N88-19313
Ion beam modification of film stress and the effectiveness of thin film encapsulants on GaAs
[DE88-004458] 11 p1558 N88-19328
Comparison of low temperature photoluminescence of bulk MBE (Molecular Beam Epitaxy) grown AlGaAs and GaAs using a graphite generated dimer versus a standard tetramer arsenic group-V source
[DE88-004939] 11 p1558 N88-19329
Development of a multiplexer module for use in a spaceborne cryogenic environment based on GaAs MESFET technology
[RPT/CRY/62463/BOP] 11 p1559 N88-19335
Automatic prober for the dc characterization of gallium arsenide devices. Part 1: The measurement facility
[AD-A187583] 11 p1560 N88-19337
Spatial distribution of carbon and native defects in large-diameter bulk grown GaAs
[DE88-003870] 11 p1562 N88-19348
Emerging technologies program 3-5: Microelectronics Panel report
[AD-A189463] 12 p1624 N88-19716
Development of a high speed InGaAs/InP Schottky barrier photodetector for millimeter-wave fiber optical links
[AD-A188594] 12 p1629 N88-19750
Acoustic phonons, surface plasmons and surface acoustic plasmons in a superlattice and their nonreciprocal device applications
[AD-A188918] 12 p1698 N88-20163
Modeling and transport in semiconductor devices
[AD-A188760] 13 p1844 N88-21037
Research on mercury cadmium telluride
[AD-A189155] 13 p1845 N88-21039
Focused ion beam fabrication of graded channel FET's in GaAs and Si
[AD-A189166] 13 p1845 N88-21040
Optical study of germanium, germanium plus arsenic, and germanium plus gallium implants in gallium arsenide
[AD-A189600] 13 p1845 N88-21045
Electrical characteristics of MBE (Molecular Beam Epitaxyl)-grown GaAs/sub 1-x/Sb/sub x on InP and correlation with film microstructure
[DE88-003841] 13 p1847 N88-21053
X-ray diffraction study of a thin GaAs film on Si(100)
[DE88-005290] 13 p1847 N88-21055
Lattice relaxation of the DX centers in Ga/sub 1-x/Al/sub x/As and of the pressure-induced deep donors in GaAs
[DE88-005452] 13 p1848 N88-21061
Energy loss rates for light holes in InGaAs/GaAs strained layer single quantum wells
[DE88-005744] 13 p1848 N88-21062
Atmospheric attenuation of near infrared radiation propagating through fog 14 p1899 N88-21342
First report on InGaAs hall device 14 p1903 N88-21372
Monolithic microwave integrated circuit technology for advanced space communication
[NASA-TM-100829] 14 p1906 N88-21389
New method of examining microononhomogeneity of local centers in high-resistivity semiconductor materials under scanning electron microscope 14 p1969 N88-21754
Considerations in GaAs standard cell design
[DE88-003310] 14 p1985 N88-21840
In situ TEM observations of heavy ion damage in gallium arsenide
[DE88-005984] 14 p1986 N88-21843
Stress corrosion of ceramic materials
[AD-A190501] 15 p2045 N88-22187
The influence of current stressing on the structure of Ag contacts to GaAs
[DE88-005988] 15 p2140 N88-22771

Examination of temperature effects on gate-to-drain avalanche breakdown in GaAs MESFETs (Metal-Semiconductor Field Effect Transistors) by measuring light emission under RF drive
[AD-A189634] 15 p2141 N88-22778

Autonomous control system for Czochralski growth of LEC GaAs
[AD-A189726] 15 p2141 N88-22779

Design and evaluation of single-lobed far-field pattern laser arrays: AlGaAs/GaAs and InGaAsP/InP systems --- optical communication
[LAAS-88-023] 16 p2214 N88-23211

Local density of states in double-barrier resonant tunneling structures
[AD-A190673] 16 p2281 N88-23656

Initial stages of molecular beam heteroepitaxial growth in GaAs-(Ca,Sr)F2 and GaAs/Si systems
[LAAS-87-355] 16 p2281 N88-23658

Microscopic control of semiconductor interface reactivity
[AD-A191193] 16 p2283 N88-23668

Monolithic integration on a GaAs substrate of a quarter ring laser and an optical guide coupled by an evanescent wave
[ETN-88-92308] 17 p2344 N88-23969

Joint services electronics program research in electronics
[AD-A192206] 18 p2504 N88-24857

A monolithic reduced-size Ku-Band SPOT (Single-Pole Double Throw) FET switch
[DE88-006273] 18 p2505 N88-24858

Monolithic GaAs Ku-band one watt constant phase variable power amplifier
[DE88-006272] 18 p2506 N88-24866

Optical nonlinearities in GaAs/GaAlAs multiple quantum wells fabricated by metalorganic chemical vapor deposition for use in optical signal processing
[AD-A191558] 18 p2582 N88-25337

On the use of convergent beam electron diffraction for identification of antiphase boundaries in GaAs grown on Si
[DE88-008220] 18 p2585 N88-25362

InP/GaInAs/InP PIN photodiode with FWHM less than 18 ps 19 p2658 N88-25799

Monte Carlo investigation of hot photoexcited electron relaxation in GaAs 19 p2659 N88-25805

Picosecond carrier transport in GaAs quantum wells 19 p2660 N88-25813

Quantum-confined stark effect in InGaAs/InP quantum wells grown by metal-organic chemical vapor deposition 19 p2660 N88-25814

Dynamics of below-gap photoexcitation in GaAs quantum wells 19 p2660 N88-25815

Aging behavior of Au-based ohmic contacts to GaAs
[NASA-CR-182146] 19 p2662 N88-25831

Defects in high-mobility semiconductor systems
[AD-A191618] 19 p2732 N88-26224

Digital control of the czochralski growth of gallium arsenide. System reference manual. Valid for Czochralski growth controller software version 2.4
[AD-A191997] 19 p2732 N88-26227

X-ray response of GaAlAs/GaAs radiation hardened double: Heterostructure photodiode compared to Si:PIN photodiodes
[DE88-007425] 19 p2733 N88-26231

Development of a GaAs solid state device model for high power applications
[DE88-009048] 19 p2734 N88-26242

Integrated optoelectronic circuits utilizing InGaAsP grown by molecular beam epitaxy (erbium doping of MBE GaAs)
[AD-A192269] 20 p2795 N88-26584

Transport in GaAs heterojunction ring structures 20 p2864 N88-27011

Pressure-dependent measurement on n+GaAs (Si, Sn): The effect of deep donor (DX) states on the electrical properties and presistant photoconductivity effects 20 p2866 N88-27020

Direct imaging of the columnar structure of GaAs quantum wells 20 p2866 N88-27030

Direct measurement of ultrafast electron-hole plasma expansion at high density at an asymmetric GaAs quantum well 20 p2871 N88-27044

Photoluminescence studies of InGaAlAs quaternary alloys
[DE88-007197] 20 p2874 N88-27062

Defects in high-mobility semiconductor systems
[AD-A192298] 20 p2879 N88-27090

Thermal conductivity of isotopically pure semiconductors, superlattices, semiconductor alloys and semiconductors as a function of temperature; control of the segregation coefficient in LEC crystal growth; and photo-Hall measurements of GaAs 21 p2927 N88-27375

Picosecond optoelectronic sampling of electrical waveforms produced by an optically excited field effect transistor
[AD-A192384] 21 p2935 N88-27428

Studying the physics and operation of multi-terminal near-micron and sub-micron length, hot electron semiconductor devices
[AD-A193380] 21 p2938 N88-27446

A GaAs solid state device model for high power applications
[DE88-011320] 21 p2939 N88-27457

Phase comparator for range imaging laser radar
[DE88-008109] 21 p2954 N88-27545

Photodiodes for optical communication in the near infrared
[ETN-88-92379] 21 p3016 N88-27900

Picosecond transient reflectivity of unpinned gallium arsenide (100) surfaces
[AD-A193242] 21 p3021 N88-27933

Investigations on the MBE (Molecular Beam Epitaxy) growth and properties of Al(sub y)Ga(sub y)In(sub 1-x-y)AsInP and InGaAs-InAlAs superlattices
[DE88-009105] 21 p3022 N88-27941

Large-signal modeling of gallium arsenide field-effect transistors 22 p3073 N88-28242

Development and experimental verification of a two-dimensional numerical model of piezoelectrically induced threshold voltage shifts in GaAs MESFETs
[AD-A193462] 23 p3206 N88-29080

Metal grid base heterojunction transistor operating at 60 and 94 GHz
[AD-A194763] 23 p3207 N88-29087

The diamond as a new electronic material
[NASA-TT-20354] 23 p3209 N88-29098

Construction of gallium arsenide solar concentrator for space use
[AD-A194658] 23 p3230 N88-29222

Studies on strained (In,Ga)As/GaAs semiconductors and optical devices 23 p3287 N88-29575

Laser induced chemical vapor epitaxial growth of gallium arsenide films
[AD-A194254] 23 p3291 N88-29595

Electrical conductivity of GaAs layers implanted on semi-insulator nondoped substrates
[CERT-422000/RF] 23 p3294 N88-29614

High frequency GaAlAs modulator and photodetector for phased array antenna applications
[NASA-TM-101328] 24 p3367 N88-30048

Optoelectronic gain control of a microwave single stage GaAs MESFET amplifier
[NASA-CR-182201] 24 p3368 N88-30055

Automatic prober for the dc characterisation of gallium arsenide devices. Part 2: The data sorting and display facility
[AD-A195408] 24 p3377 N88-30111

Growth of GaAs crystals by the Heat Exchanger Method for microwave device applications
[AD-A196028] 24 p3433 N88-30435

Streaking images that appear only in the plane of diffraction in undoped GaAs single crystals: Diffraction imaging (topography) by monochromatic synchrotron radiation
[NASA-CR-183267] 24 p3433 N88-30437

Joint services electronics program
[AD-A195731] 24 p3434 N88-30439

GALLIUM COMPOUNDS
NT ALUMINUM GALLIUM ARSENIDES
NT GALLIUM ARSENIDES
NT GALLIUM NITRIDES
NT GALLIUM PHOSPHIDES

Phase equilibrium and crystal growth studies on AgGaSe2 and related nonlinear optical materials
[AD-A184768] 03 p0382 N88-12400

GALLIUM NITRIDES

Deposition of device quality epitaxial layers of gallium nitride and indium nitride for electronic applications
[AD-A188001] 11 p1453 N88-18661

GALLIUM PHOSPHIDES

Effect of high-temperature annealing on the microstructure and thermoelectric properties of GaP doped SiGe
[NASA-TM-100164] 01 p0029 N88-10188

Preparation and characterization of members of the system (Zn,Se)1-xGaPx
[AD-A185073] 05 p0655 N88-14019

High-efficiency thin-film silicon-on-GaP solar cell for improved radiation resistance
[AD-A190268] 15 p2091 N88-22460

Improved GaP doped SiGe thermoelectric material 17 p2437 N88-24503

Improved properties of SiGe/GaP alloys
[NASA-CASE-NPO-17259-1-CU] 18 p2585 N88-25358

Molecular beam epitaxy of GaP films on Si substrates
[PB88-131974] 21 p3020 N88-27923

Vibration spectra induced by impurities in 3-5-compounds semiconductors
[DE88-702730] 23 p3293 N88-29610

GALVANIC CELLS
U ELECTROLYTIC CELLS

GALVANIZING
U ZINC COATINGS

GALVANOMAGNETIC EFFECTS

Integrated magnetic field sensor using high magnetotransistors
[ETN-88-92356] 21 p2941 N88-27465

GALVANOMAGNETISM
U GALVANOMAGNETIC EFFECTS

GALVANOMETERS

A twin-mirrored galvanometer laser light sheet generator
[NASA-TM-100587] 19 p2674 N88-25901

GAME THEORY

The isotropic rocket: A surveillance evasion game
[REPT-87-21] 05 p0645 N88-13949

Uncertain knowledge in distributed systems
[AD-A189017] 12 p1685 N88-20076

Perfect knowledge and beyond --- chess endgames
[REPT-87-37] 14 p1967 N88-21738

Interactive, networked moving platform simulators
[AD-A192374] 23 p3182 N88-28940

Stochastic game approach to guidance design
[AD-A194574] 23 p3276 N88-29498

GAMETOCYTES
NT EGGS

GAMMA RADIATION
U GAMMA RAYS

GAMMA RAY ABSORPTION

Gamma-ray optics of multi-beam Borrmann modes with possible applications to nuclear lasing 04 p0449 N88-12784

GAMMA RAY ASTRONOMY

Gamma ray lines from novae 04 p0526 N88-13214

A search for medium energy gamma ray pulsars 11 p1568 N88-19385

Very high energy gamma ray astrophysics
[DE88-005821] 13 p1854 N88-21095

Topics in curved and flat space electromagnetism 13 p1854 N88-21100

External tank gamma ray imaging telescope study. Final review, phase 2
[NASA-CR-179320] 15 p2150 N88-22834

Spectral modelling of the soft gamma ray repeater
[DE88-007027] 17 p2453 N88-24570

The application of imaging to the atmospheric Cerenkov technique: Observations of the Crab nebula 20 p2884 N88-27126

Application of two-dimensional imaging to very high energy gamma ray astronomy
[DE88-010120] 21 p3030 N88-27983

Gamma radiation from center of the galaxy of the order of MeV values
[MPE-207] 21 p3032 N88-27999

The application of an image intensifier to atmospheric Cerenkov gamma ray astronomy
[MPE-PREPRINT-115] 22 p3163 N88-28839

Very high energy cosmic gamma rays from radio and X-ray pulsars 23 p3309 N88-29711

Gamma radiation expected from supernova 1987A in large magellanic cloud 24 p3445 N88-30505

GAMMA RAY BURSTS

HEAO-1 observations of gamma-ray bursts 07 p0947 N88-15756

Observations of gamma bursts from GBS 0526-66 08 p1001 N88-16065

Spectral modelling of the soft gamma ray repeater
[DE88-007027] 17 p2453 N88-24570

Cascade model of gamma-ray bursts: Power-law and annihilation-line components
[NASA-TM-101176] 21 p3032 N88-27998

On the origin of gamma ray bursts
[MPE-PREPRINT-120] 22 p3166 N88-28855

GAMMA RAY LASERS

Gamma-ray optics of multi-beam Borrmann modes with possible applications to nuclear lasing 04 p0449 N88-12784

The gamma-ray laser project
[AD-A184824] 05 p0587 N88-13578

Extension of nuclear structure data base searches for gamma-ray laser candidates
[DE88-004288] 10 p1336 N88-17985

A nuclear structure study of the proposed gamma-ray laser candidate nucleus Re-186
[DE88-004299] 10 p1336 N88-17986

Shape isomers as candidates for the gamma ray laser storage state
[DE88-005228] 11 p1492 N88-18909

SDIO/IST ultrashort wavelength laser: Novel experimental schemes for observing the Mossbauer effect in long-lived nuclear levels
[AD-A190275] 15 p2072 N88-22351
SDIO/IST ultrashort wavelength laser. Mossbauer effect in gamma-ray lasers
[AD-A190306] 15 p2072 N88-22352
Primer on coupling collective electronic oscillations to nuclei
[LA-10878] 19 p2723 N88-26170
Proof of the feasibility of coherent and incoherent schemes for pumping a gamma-ray laser
[AD-A193856] 23 p3220 N88-29165

GAMMA RAY OBSERVATORY
Orbital Spacecraft Consumables Resupply System (OSCRS). Volume 2: Study results
[NASA-CR-172011] 03 p0268 N88-11687
Calibration of the EGRET gamma ray telescope with a back-scattered laser beam 06 p0800 N88-14895

GAMMA RAY SPECTRA
Gamma ray lines from novae 04 p0526 N88-13214
Gamma radiation at the 970 MeV plane positron channeling in diamond crystals
[DE88-700557] 07 p0939 N88-15705
Gamma-ray imaging observations of the Crab and Cygnus regions 10 p1427 N88-18522
Spectral modelling of the soft gamma ray repeater
[DE88-007027] 17 p2453 N88-24570
Characterization of yttrium aluminum garnet/YAG/using 14 MeV neutron activation
[AD-A191925] 18 p2582 N88-25342
VAXGAP: A code for the routine analysis of gamma-ray pulse-height spectra on a VAX computer
[DE88-011702] 22 p3137 N88-28648

GAMMA RAY SPECTROMETERS
Measurement of the gamma-ray response of some commercial silicon detectors
[AD-A187431] 11 p1543 N88-19221
Content of natural radioactive elements in Venusian rocks determined using data from Vega-1 and Vega-2 stations 13 p1726 N88-20323
The gamma-ray spectrometer experiment on the solar maximum mission satellite
[NASA-CR-182977] 17 p2452 N88-24569
Study of comet nucleus gamma-ray spectrometer penetration system
[NASA-CR-177393] 20 p2883 N88-27120
Gamma-ray/neutron spectroscopy from the Mars observer 23 p3302 N88-29671

GAMMA RAY TELESCOPES
Infra-red lamp panel study and assessment application to thermal vacuum testing of sigma telescope 02 p0132 N88-10830
Calibration of the EGRET gamma ray telescope with a back-scattered laser beam 06 p0800 N88-14895
Crystal diffraction lenses for imaging gamma-ray telescope
[DE88-003084] 08 p1083 N88-16529
Gamma-ray imaging observations of the Crab and Cygnus regions 10 p1427 N88-18522

GAMMA RAYS
NT GAMMA RAY BURSTS
Research in particles and fields
[NASA-CR-180412] 01 p0119 N88-10763
Program description of FIBRAM: A radiation attenuation model for optical fibers
[PB87-230686] 06 p0690 N88-14229
Shielding analysis of a small compact space nuclear reactor
[AD-A185566] 06 p0779 N88-14784
Combined effect of microwaves and ionizing radiation 07 p0893 N88-15413
Solar event of 27 April 1981 08 p1004 N88-16084
Gamma-ray and neutron spectroscopy of planetary surfaces and atmospheres
[DE88-004287] 10 p1430 N88-18541
Measurement of the gamma-ray response of some commercial silicon detectors
[AD-A187431] 11 p1543 N88-19221
Emission of gamma rays from various materials pulsed with 14-MeV neutrons
[DE88-003837] 11 p1544 N88-19227
Response characteristics of dual MOSFET gamma-ray sensors produced by Mitel Corporation
[AD-A189026] 12 p1630 N88-19755
The imaging of extra-galactic low-energy gamma-ray sources prospects, techniques, and instrumentation
[NASA-CR-182536] 12 p1713 N88-20251
Proof of the feasibility of coherent and incoherent schemes for pumping a gamma-ray laser
[AD-A189238] 13 p1774 N88-20613
Gamma-ray densitometry: Nondestructive analysis of density evolution during ceramic powder processing
[DE88-006671] 15 p2047 N88-22198
The response of a power MOSFET (N-channel) and a dielectric isolated operational amplifier to the combined environmental effects of high temperature and total dose gamma radiation 17 p2406 N88-24309
MMW shielding design and analysis 17 p2430 N88-24457
The response of selected semiconductor technologies to the combined environmental effects of high temperature and total dose gamma radiation 17 p2431 N88-24462
Utilization of the IR telescope gimbaling system as a stabilized pointing platform for balloon payloads. Volume 1: Technical results
[NASA-CR-179339] 18 p2522 N88-24962
Gamma rays from Cygnus X-1: Modeling and nonthermal pair production
[DE88-006830] 18 p2596 N88-25426
JFET/SOS (Junction Field-Effect Transistor/Silicon-on-Sapphire) devices: Gamma-radiation-induced effects
[AD-A193001] 20 p2795 N88-26586
Research in particle and gamma-ray astrophysics
[NASA-CR-183111] 20 p2887 N88-27146
Gamma radiation from center of the galaxy of the order of MeV values
[MPE-207] 21 p3032 N88-27999
The radiation sensitivity of select metal chelate polymers: Mechanistic changes at higher energies
[AD-A193467] 23 p3196 N88-29019
Phase modulation of recoiless gamma radiation in Mossbauer spectroscopy
[ETN-88-92648] 24 p3428 N88-30403
A coded mask telescope for observations of X and gamma ray sources in the southern sky
[INPE-4580-PRE/1314] 24 p3453 N88-30551
Research in particle and gamma-ray astrophysics
[NASA-CR-183126] 24 p3455 N88-30566
X- and gamma-ray background observations in Antarctic
[INPE-4583-PRE/1317] 24 p3459 N88-30578

GANTRIES
U GANTRY CRANES

GANTRY CRANES
Force servo control of a commercial gantry robot
[DE88-006649] 20 p2808 N88-26660

GAPS
NT ENERGY GAPS (SOLID STATE)
NT SPARK GAPS
Recovery of vacuum gaps after arcing
[DE87-013852] 01 p0039 N88-10250
Fin gaps and body slots of guided projectiles: Effects, data correlation and modeling
[AD-A184440] 03 p0270 N88-11698
The axisymmetric sealing gap with variable viscosity. A variable hydraulic resistance
[ETN-87-90604] 03 p0314 N88-11987
Geometric structure, pseudoband gaps, and surface vibrational resonances on metal surfaces
[AD-A187001] 09 p1143 N88-16851

GARNETS
NT YTTRIUM-ALUMINUM GARNET
Mode locking in Nd-laser by means of Gd-Sc-Ga-garnet shutter 09 p1237 N88-17412
Hydrodynamic simulation of forced convection in the Czochralski process
[INPE-4471-TDL/323] 12 p1697 N88-20158
High-efficiency Y-Sc-Ga:Cr (sup)3+,Tu (sup)3+,Ho (sup)3+ garnet laser (gl= 2.088 gmm at room temperature 14 p1971 N88-21766
Absorption spectra and energy levels of Gd(3+), Nd(3+) and Cr(3+) in the garnet Gd3Sc2Ga3O12
[AD-A193634] 23 p3292 N88-29599

GARP
U GLOBAL ATMOSPHERIC RESEARCH PROGRAM

GAS ANALYSIS
NT OZONOMETRY
Metal-sensing layer-semiconductor and metal-sensing layer-metal heterostructure gas sensors
[DE87-011293] 01 p0103 N88-10674
Developments in optical sensor technologies described 06 p0689 N88-14220
Analysis of gases in the earth's crust
[PB88-141619] 10 p1354 N88-18093
Method for sampling of methyl salicylate vapor in air using passivated stainless steel syringes and analysis by gas chromatography
[AD-A187838] 11 p1447 N88-18624
Breath-by-breath measurement of alveolar gas exchange 12 p1653 N88-19905
A mass spectrometer evolved gas analysis experiment for in-situ analysis of cometary dust volatiles 13 p1854 N88-21097
An automated ozone photometer
[NASA-TM-100064] 14 p1908 N88-21404
CCD-observations of gas and dust jets in the coma of Comet Halley 14 p1998 N88-21912
Profiles of the major gas emissions and distribution of dust particles in the inner coma (0 to 10,000 km) of Comet Halley 14 p1999 N88-21919
Gas coma of Comet Giacobini-Zinner: Emission from grains 14 p2000 N88-21923
Structure/property/reactivity relations among nitramine and other energetic materials
[AD-A190878] 18 p2481 N88-24716
Geological evolution and analysis of confirmed or suspected gas hydrate localities. Volume 2: Basin analysis, formation and stability of gas hydrates in the Black Sea
[DE88-001052] 18 p2532 N88-25023
Method and device for determining heats of combustion of gaseous hydrocarbons
[NASA-CASE-LAR-13528-1] 23 p3193 N88-29002
The behaviour of synthetic fuels in a small transparent combustor 24 p3351 N88-29950
Energy budget and ground temperatures in hot regions
[AD-A196298] 24 p3404 N88-30268

GAS ATOMIZATION
Laboratory scale inert gas atomizer for producing rapidly solidified powders
[DE88-006734] 18 p2497 N88-24812
Theoretical and experimental investigations on the structure of stationary shock waves in gas particle dispersions
[ETN-88-92983] 23 p3213 N88-29122

GAS BAGS
An experimental comparison of two designs of mercury propellant tank for use with an electric propulsion engine
[RAE-TR-75109] 01 p0018 N88-10109

GAS BEARINGS
Design of a spherical air bearing simulator for tests of the attitude control system of artificial satellites
[INPE-4284-PRE/1155] 12 p1595 N88-19551
Foil gas bearing system endurance testing dynamic isotope power system 17 p2405 N88-24302
Dynamic isotope power system critical component verification 17 p2425 N88-24421

GAS CHROMATOGRAPHY
Laser probes of propellant combustion chemistry
[AD-A184854] 05 p0561 N88-13415
Chemical analysis for excimer laser systems
[DE88-001941] 05 p0589 N88-13591
Application of inverse gas chromatography to fluidity studies
[DE88-002896] 10 p1296 N88-17750
Supercritical fluid extraction-gas chromatography of Volatile Organic Compounds (VOC) from tenax devices
[PB88-124300] 10 p1298 N88-17759
Method for sampling of methyl salicylate vapor in air using passivated stainless steel syringes and analysis by gas chromatography
[AD-A187838] 11 p1447 N88-18624
Chromatographic and related reactors
[AD-A188452] 12 p1605 N88-19599
Gas-chromatographic analysis of products of thermal reactions of aerosol in Venusian cloud layer on Vega-1 and Vega-2 automatic interplanetary stations 13 p1725 N88-20318
Fuels combustion research
[AD-A189114] 13 p1736 N88-20381
Chromatographic and mass spectrometric separation and analysis
[AD-A190113] 16 p2174 N88-22958
Selective detection in gas chromatography
[AD-A191499] 18 p2481 N88-24718
Thermal decomposition studies of explosives for component applications
[DE88-007201] 18 p2495 N88-24805
Fundamental studies of separation processes
[DE88-007487] 19 p2611 N88-25494
Determination of relative flammability of materials by pyrolysis and gas-chromatographic light hydrocarbon analysis
[DE88-012449] 24 p3343 N88-29898

GAS COMPOSITION
NT CARBON DIOXIDE CONCENTRATION
The composition of the gas in the loading inlet of the Space Shuttle Orbiter
[ETN-87-90430] 01 p0012 N88-10069
Diagnostics of atmospheric chemistry through ozone measurement
[INPE-4230-PRE/1105] 01 p0068 N88-10437
Role of testing total gas (O2 and CO2) tension of blood plasma in the study of human gas homeostasis 07 p0894 N88-15419
Requirements for temperature and species concentration measurements in microgravity combustion experiments 17 p2329 N88-23903
Laser Diagnostics for combustion temperature and species measurements 17 p2330 N88-23912

GAS COOLED REACTORS
NT HIGH TEMPERATURE GAS COOLED REACTORS
NT HIGH TEMPERATURE NUCLEAR REACTORS

Gas-cooled reactor for space power systems
[DE87-011549] 02 p0233 N88-11471
Gas-cooled reactor power systems for space
[DE88-005220] 11 p1545 N88-19240
IAEA Specialists' Meeting on Graphite Component Structural Design
[DE88-780006] 13 p1746 N88-20439
Basic characteristics of heat-exchanger-type steam reformer heated by high-temperature helium gas (2). Analysis by simulation model (2)
[DE87-702962] 15 p2061 N88-22291
A critique of NERVA based nuclear reactor design and performance for MMW space propulsion applications
17 p2404 N88-24297
Gas-cooled reactor power systems for space
17 p2413 N88-24350
Inherently safe space reactors
17 p2415 N88-24363
Multimegawatt nuclear power system for lunar base applications 17 p2416 N88-24367
Gas core reactors for direct nuclear propulsion
17 p2428 N88-24442
Transient analyses of multimegawatt space reactors
17 p2430 N88-24456
The NERVA derivative reactor and a systematic approach to multiple space power requirements
17 p2430 N88-24458
Burst power gas core reactor with MHD power generation 17 p2433 N88-24472

GAS COOLING
Strain rate effects in fast-gas-cooled uranium-titanium and uranium-niobium alloys
[OUEL-1683/87] 02 p0149 N88-10937
Thermal and mechanical analysis of the Faraday shield for the compact ignition tokamak
[DE88-007855] 20 p2856 N88-26962
Studies of gas turbine heat transfer airfoil surface and end-wall cooling effects
[AD-A195165] 24 p3326 N88-29805

GAS DETECTORS
ECC (Electrochemical Concentration Cell) ozonesonde observations at South Pole, Antarctica during 1986
[PB87-207502] 02 p0197 N88-11228
Combustion control with smart sensors
[DE87-013688] 03 p0281 N88-11768
Fundamental study on gas monitoring in CELSS
03 p0359 N88-12263
Plant Growth Module (PGM) conceptual design
05 p0631 N88-13855
High polymer sensor materials discussed
06 p0676 N88-14140
Computer modeling for optical waveguide sensors
[AD-A187702] 11 p1549 N88-19263
Ultrasonic oxygen sensor
[AD-A189723] 15 p2105 N88-22537
Alternate techniques for noble-gas detection
[DE88-009471] 19 p2613 N88-25507
Pyrolyzed organic polymer nitrogen dioxide sensor
19 p2669 N88-25868
Surface acoustic wave gas sensor based on film conductivity changes 19 p2673 N88-25894
Tin oxide microsensors on thin silicon membranes
19 p2673 N88-25897
Method for the isotopically selective detection of inert gases
[DE88-008370] 20 p2769 N88-26421

GAS DIFFUSION
U GASEOUS DIFFUSION

GAS DISCHARGE COUNTERS
U COUNTERS
U GAS DISCHARGE TUBES

GAS DISCHARGE TUBES
NT THYRATRONS
Gas feed system for the T-15 tokamak discharge chamber
[DE86-700351] 07 p0935 N88-15682

GAS DISCHARGES
Gas flow effects in pulse avalanche discharge XeCl excimer lasers 03 p0328 N88-12070
Measurement of the electron density and the attachment rate coefficient in silane/helium discharges
[AD-A184268] 04 p0496 N88-13051
Electron-impact-ionization and electron-attachment cross sections of radicals important in transient gaseous discharges
[AD-A192248] 20 p2770 N88-26424
Investigations on beam quality of high frequency excited CO2 high performance lasers
[ETN-88-92363] 21 p2954 N88-27550
The study of hydromagnetic waves and RF heating using the TORTUS tokamak, the development of diagnostic techniques based on submillimeter lasers and the gyrotron, and gas discharge 24 p3431 N88-30419

GAS DISSOCIATION
Initial results with the LLNL 2-D chemical-radiative-transport model of the troposphere and stratosphere
[DE88-004355] 11 p1512 N88-19033

GAS DYNAMICS
NT AERODYNAMICS
NT AEROTHERMODYNAMICS
NT INTERACTIONAL AERODYNAMICS
NT RAREFIED GAS DYNAMICS
NT ROTOR AERODYNAMICS
NT SUPERSONICS
NT UNSTEADY AERODYNAMICS
Fundamentals of numerical magnetohydrodynamics
[DE87-011769] 01 p0100 N88-10656
Dynamic effects of stellar winds and associated HII regions on the interstellar medium
[ETN-87-90421] 01 p0109 N88-10706
A simple self-breaking 2 MV gas switch
[DE87-014346] 02 p0166 N88-11047
The calculation of thermal rate constants for gas-phase and heterogeneous reactions in combustion processes
[AD-A184435] 03 p0284 N88-11788
Numerical simulation and visualization of a flowfield by interaction of two parallel two-dimensional freejets
03 p0320 N88-12021
Some aspects of high resolution numerical methods for hyperbolic systems of conservation laws, with applications to gas dynamics
[DMS-86-7] 03 p0321 N88-12031
Gas dynamic characteristics in past axial flow CO2 laser 03 p0327 N88-12067
Some asymptotic modes of transonic vortex flow
04 p0425 N88-12632
Model of solar-wind magnetosphere coupling
04 p0525 N88-13211
Dynamic stability of hypersonic conical lifting vehicles according to Newton-Busemann theory
05 p0534 N88-13247
Influence of shock wave and gas pressure on the behavior of a pyrotechnical device
[SNIAS-872-430-111] 05 p0570 N88-13477
Performance-limiting factors in MPD thrusters
[AD-A185605] 06 p0674 N88-14128
Gasdynamic effects in linear MHD generators
[ETN-88-91372] 06 p0784 N88-14810
Realization of the immediate objectives of the Aero-Gas Dynamics and Vibration Laboratory (LAGG) at the National Center for Research, Science and Technology (PUSPIPTEK) at Serpong, Java (Indonesia), Project TTA-79
[GG/CPR-10] 08 p1092 N88-16572
New techniques in computational aerodynamics
[AD-A186719] 09 p1112 N88-16664
High performance Solid Rocket Motor (SRM) submerged nozzle/combustion cavity flowfield assessment
[NASA-CR-179307] 11 p1446 N88-18622
Upper-thermospheric observations and neutral-gas dynamics at high latitudes during solar maximum
[AD-A188058] 11 p1512 N88-19031
Accurate boundary conditions for exterior problems in gas dynamics
[NASA-TM-100807] 11 p1537 N88-19182
Theoretical studies of the potential surface for the F - H2 greater than HF + H reaction
[NASA-CR-182551] 11 p1557 N88-19319
A modeling analysis program for the JPL table mountain Io sodium cloud data
[NASA-CR-182555] 11 p1570 N88-19400
A method of calculating nonstationary heat flow in hydrogasodynamic processes in closed cryogenic systems
[DE88-700884] 12 p1626 N88-19727
Heat pipe transient analysis: Vapor dynamics
[DE88-005132] 13 p1767 N88-20568
Problems in fluid dynamics
[NASA-CR-182678] 14 p1909 N88-21410
Random-choice based hybrid methods for one and two dimensional gas dynamics
[CAR-88-01] 14 p1910 N88-21415
A model of the anisotropic structure of the neutral gas coma of a comet 14 p1999 N88-21918
The role of hydrogen thermalization in shaping the Lyman-alpha coma --- comets 14 p2007 N88-21971
Investigation of combustion in large vortices
[AD-A190406] 15 p2035 N88-22121
Research sensors 15 p2085 N88-22430
Transient analysis of heat pipe vapor dynamics
17 p2412 N88-24341
Heat pipe transient analysis: Vapor dynamics
17 p2421 N88-24397
Entrance and exit region friction factor models for annular seal analysis
[NASA-CR-183084] 19 p2678 N88-25921
A shock-tube experiment on gases mixing processes associated with CO2/N2 mixing gasdynamic laser
[ISAS-RN-350] 20 p2797 N88-26598
Nozzle lip effects on gas expansion into the plume backflow region
[AD-A192806] 21 p2942 N88-27475
Investigations on beam quality of high frequency excited CO2 high performance lasers
[ETN-88-92363] 21 p2954 N88-27550
Coupling between radiation and gas dynamics
[AD-A194593] 23 p3211 N88-29113

GAS EVOLUTION
Different trapping mechanisms of gases by water ice and their relevance for comet nuclei
14 p2007 N88-21970

GAS EXCHANGE
Contribution of bubbles and waves to air-sea CO2 flux, with implications for remote sensing
[PB87-203980] 01 p0073 N88-10467
The effect of wind and currents on gas exchange in an estuarine system
[NASA-CR-181424] 01 p0073 N88-10468
Environmental life support system technology study --- space flight
[ESA-CR(P)-2432] 02 p0218 N88-11371
Controlled Ecological Life Support System: Regenerative Life Support Systems in Space
[NASA-CP-2480] 03 p0357 N88-12251
Food production and gas exchange system using blue-green alga (spirulina) for CELSS
03 p0358 N88-12253
Operation of an experimental algal gas exchanger for use in a CELSS 03 p0358 N88-12255
Sunlight supply and gas exchange systems in microalgal bioreactor 03 p0359 N88-12258
Preliminary experimental results of gas recycling subsystems except carbon dioxide concentration
03 p0359 N88-12261
Fundamental study on gas monitoring in CELSS
03 p0359 N88-12263
Influence of stratification in near-surface water layer on intensity of gas exchange between atmosphere and water 04 p0459 N88-12841
Influence of gas exchange between ocean and atmosphere on formation of atmospheric pressure field
06 p0726 N88-14467

GAS EXPANSION
A fluid simulation of the AMPTE lithium gas releases in the solar wind
[TRITA-EPP-87-06] 05 p0661 N88-14056
A study of single and binary ion plasma expansion into laboratory-generated plasma wakes
[NASA-CR-4125] 10 p1412 N88-18427
Molecular collision processes in gases and at surfaces
[AD-A189518] 13 p1836 N88-20982
Nozzle lip effects on gas expansion into the plume backflow region
[AD-A192806] 21 p2942 N88-27475

GAS EXPLOSIONS
A transient model for thermal detonation
[IKE-2-75] 03 p0314 N88-11984
Computer code simulations of explosions in flow networks and comparison with experiments
[DE88-001946] 05 p0573 N88-13491
Laser induced ignition of propellants
[AD-A191100] 16 p2168 N88-22927
Application of Particle Image Displacement Velocimetry (PIDV) to complex flows: Velocity field measurements in front of a heavy gas cloud
[VKI-TN-166] 23 p3213 N88-29125

GAS FLOW
NT AIR CURRENTS
NT AIR FLOW
NT CONTINUUM FLOW
NT COOLING FLOWS (ASTROPHYSICS)
NT EQUILIBRIUM FLOW
NT FREE MOLECULAR FLOW
NT JET STREAMS (METEOROLOGY)
NT MERIDIONAL FLOW
NT MOLECULAR FLOW
NT NONEQUILIBRIUM FLOW
NT PIPE FLOW
NT SLIP FLOW
NT TRANSITION FLOW
NT VERTICAL AIR CURRENTS
Blowdown of two-component gas mixtures in branching systems
[DE87-011392] 01 p0045 N88-10287
Vortex/boundary-layer interactions: Data report, volume 1
[NASA-CR-181462] 02 p0121 N88-10768
Optical fiber interferometric sensor to measure temperature in gas flow
[ENST-87E006] 02 p0170 N88-11071
Gas dynamic characteristics in past axial flow CO2 laser 03 p0327 N88-12067

Gas flow effects in pulse avalanche discharge XeCl excimer lasers 03 p0328 N88-12070
Conical wing with maximum lift-to-drag ratio in supersonic gas flow 04 p0425 N88-12633
On the numerical simulation of three-dimensional hypersonic flow 05 p0532 N88-13237
Rarefied gas numerical wind tunnel. 2: Two-dimensional and axially symmetric bodies 05 p0538 N88-13273
Experimental investigation of heterogeneous compressible shear layers 06 p0700 N88-14294
Gas diffusion studies in steady and nonsteady cavities [AD-A185795] 06 p0704 N88-14318
Method of calculations for flow of ideal gas through plane and axisymmetric nozzles with broken-line contour 06 p0771 N88-14737
Programs for calculating transient Darcian flow through non-uniform materials [DE88-001924] 07 p0852 N88-15177
SSME environment database development [NASA-CR-179245] 08 p0964 N88-15836
A comparison of experimental and theoretical results for labyrinth gas seals with honeycomb stators [NASA-CR-182441] 08 p0993 N88-16006
Gasflows in the transition region above sunspot 08 p1095 N88-16586
Design of a gas mass flow control system for the gas inlet installation of a solid fuel combustion chamber [VTH-LR-471] 09 p1141 N88-16839
Modeling of pulsed gas flow lasers [DFVLR-FB-87-19] 09 p1171 N88-17021
Development and application of oxygen flow tagging for velocity measurements and flow visualization in turbulent three-dimensional supersonic flows [AD-A187982] 10 p1289 N88-17714
Self-pumped phase conjugation in a supersonically flowing medium [AD-A188281] 10 p1338 N88-17998
The effect of combustion gas flow on the rotational dynamics of a spinning solid fuel rocket 13 p1732 N88-20358
Innovative, counterflow gas/fine solids, direct contact heat exchanger [DE88-004744] 13 p1770 N88-20585
Low pressure gas flow analysis through an effusive inlet using mass spectrometry [NASA-CR-182712] 14 p1910 N88-21413
Ammonia transfer across rotating joints in space 14 p1927 N88-21492
Effect of mass-velocity on liquid jet atomization in Mach 1 gasflow [NASA-TM-100813] 16 p2211 N88-23194
Compressible flow in a pie-shaped cylinder rotating about the vertex 18 p2460 N88-24604
Measurement of the radiative properties of gas and oil flames [NASA-TT-20299] 19 p2612 N88-25502
Rarefied gas numerical wind tunnel 3. Universal code for three dimensional bodies 19 p2637 N88-25644
Non equilibrium expansion of a radiating gas in a channel of varying section [DE88-702063] 19 p2665 N88-25845
A monolithic gas flow sensor with polyimide as thermal insulator 19 p2669 N88-25864
Remote sensing and satellite applications to the needs of the gas and pipeline industry [PB88-202668] 20 p2817 N88-26714
Some properties of ignition gases. Review of measuring results in the years 1981-1986) [PB88-106968] 21 p2908 N88-27259
Gaseous tracer techniques for pore structure characterization of granular materials [DE88-011542] 21 p2911 N88-27274
Computation of flow and diffusion process in gas centrifuges [ETN-88-92366] 21 p2949 N88-27514
Low density real gas flows about hypersonic vehicles [AD-A194251] 22 p3075 N88-28253
Nonequilibrium flow of a radiating gas in a vertical channel with axial temperature variation [DE88-702535] 23 p3212 N88-29120
Modeling of pulsed gas flow lasers [ESA-TT-1090] 23 p3220 N88-29169
Laser Doppler Velocimeter (LDV) and pressure measurements of gas particle flows in bends [VKI-TN-163] 24 p3372 N88-30083
Nonequilibrium flow of a dissociating gas in a horizontal channel with axial temperature variation [DE88-702536] 24 p3373 N88-30089
Transverse CO2 laser two-dimensional gain distributions [AD-A196240] 24 p3378 N88-30119

GAS GENERATOR ENGINES
U ENGINES
U GAS GENERATORS

GAS GENERATORS
Vapor generation of fuels [PB88-109897] 08 p0974 N88-15892
Experimental evaluation of a translating nozzle sidewall radial turbine 10 p1280 N88-17656
Design and aerodynamic performance of a small mixed-flow gas generator turbine 10 p1281 N88-17662
Speed control of a missile with throttleable ducted rocket propulsion 12 p1597 N88-19561
Preliminary analysis of helium generation and its effects on the SP-100 system performance 17 p2422 N88-24406

GAS GIANT PLANETS
NT JUPITER (PLANET)
NT NEPTUNE (PLANET)
NT URANUS (PLANET)
Numerical evidence that the motion of Pluto is chaotic [AD-A195920] 24 p3455 N88-30568

GAS GUNS
NT LIGHT GAS GUNS
Ultrasonic Time-Of-Flight Diffraction (TOFD) measurements of crack depths in an acceleration reservoir of a high velocity research gun [DE88-006644] 16 p2164 N88-22907
Use of a two-stage light-gas gun as an injector for electromagnetic railguns [DE88-007200] 18 p2469 N88-24657

GAS HEATING
Finite element analysis of three-dimensional steady and unsteady temperature fields (computation of temperature distribution of turbine blade with composite cooling) 03 p0300 N88-11887
Microwave superheaters for fusion [DE88-001656] 05 p0653 N88-14007
Assessment of opportunities for gas-fired sintering in the advanced ceramics and powdered metals industries [PB88-197157] 19 p2620 N88-25545

GAS INJECTION
Direct gas injection with glow plug ignition [PB88-187323] 19 p2676 N88-25911
Three-dimensional viscous flow computations of a circular jet in subsonic and supersonic cross flow [NASA-CR-182153] 20 p2800 N88-26616

GAS IONIZATION
NT ATMOSPHERIC IONIZATION
NT AURORAL IONIZATION
NT FLAME IONIZATION
The study of excited oxygen molecule gas species production and quenching on thermal protection system materials [NASA-CR-172027] 02 p0233 N88-11470
Critical Ionization Velocity (CIV) interaction: Some unsolved questions [TRITA-EPP-87-12] 09 p1250 N88-17491
On the role of the ionization frequency to gyrofrequency ratio in the critical ionization velocity interaction [TRITA-EPP-86-10] 10 p1410 N88-18414
High-order multiphoton ionization of the noble gases [DE88-007489] 18 p2571 N88-25273

GAS JETS
Investigation of the effect of laterally ejected gas jets on flows [ISL-R-107/86] 05 p0581 N88-13545
Mixing and combustion of pulsed gas jets [PB88-112834] 06 p0680 N88-14169
Mixing and combustion of pulsed gas jets [PB88-108014] 06 p0680 N88-14170
Dimensions of ignition zones in blow-outs of combustible gases from rectangular and circular ports 07 p0918 N88-15577
On the start up of supersonic underexpanded jets — Mach disks 11 p1435 N88-18563
Cold gas jet system for satellite attitude control-modeling and simulation [INPE-4279-PRE/1150] 12 p1601 N88-19583
Anisotropic emission from comets: Fans versus jets. 1: Concept and modeling 14 p2001 N88-21927
Noncondensing round turbulent gas jets in liquids [AD-A191191] 16 p2208 N88-23179

GAS LASERS
NT CARBON DIOXIDE LASERS
NT CARBON MONOXIDE LASERS
NT EXCIMER LASERS
NT HCN LASERS
NT HELIUM-NEON LASERS
NT HF LASERS
NT KRYPTON FLUORIDE LASERS
NT NITROGEN LASERS
NT TEA LASERS
NT ULTRAVIOLET LASERS
NT XENON CHLORIDE LASERS
NT XENON FLUORIDE LASERS
Segmented hollow cathode discharges for copper ion lasers [ETN-87-90403] 01 p0052 N88-10333
Status, development of laser devices in China 03 p0303 N88-11907
JPRS Report: Science and Technology. China [JPRS-CST-87-033] 03 p0326 N88-12062
Laser development, evolution of applied technologies described 06 p0689 N88-14221
Neutronics conceptual design of a UF6-fueled gasesous laser system 17 p2422 N88-24405
High power axial flow CO2 laser [ETN-88-91951] 18 p2521 N88-24959
A shock-tube experiment on gases mixing processes associated with CO2/N2 mixing gasdynamic laser [ISAS-RN-350] 20 p2797 N88-26598
Model for pulse amplification by a gaseous laser amplifier [DE88-011729] 20 p2808 N88-26657
MIDIR (Mid-Infrared) laser, phase 1 [AD-A193935] 23 p3220 N88-29166
Bibliography of Soviet laser developments, number 88, March - April 1987 [AD-A195978] 24 p3378 N88-30116

GAS LIQUEFACTION
U CONDENSING

GAS LUBRICANTS
Friction drag reduction (a speculative essay) [INPE-4278-PRE/1150] 08 p0988 N88-15985

GAS LUBRICATED BEARINGS
U GAS BEARINGS

GAS MASERS
NT HYDROGEN MASERS

GAS MIXTURES
NT AIR
NT ALVEOLAR AIR
NT DETONABLE GAS MIXTURES
NT HIGH TEMPERATURE AIR
PRMIXn: A computer program for thermophysical properties of real gases and gas mixtures [GKSS-86/E/59] 01 p0020 N88-10125
Blowdown of two-component gas mixtures in branching systems [DE87-011392] 01 p0045 N88-10287
Detailed mechanism of benzene oxidation [NASA-TM-100202] 03 p0282 N88-11775
Flame acceleration and transition to detonation in channels [DE87-014193] 03 p0284 N88-11786
TOPAZ: The transient one-dimensional pipe flow analyzer: An update on code improvements and increased capabilities [DE88-001781] 04 p0443 N88-12751
Development of a low noise 10 K J-T refrigeration system [AD-A185258] 05 p0571 N88-13484
Chemical analysis for excimer laser systems [DE88-001941] 05 p0589 N88-13591
Nonlinear reflection of sound wave in gas mixture 06 p0769 N88-14728
The carbon dioxide chaperon efficiency for the reaction H + O2 + M yields HO2 + M from ignition delay times behind reflected shock waves [NASA-TM-100125] 07 p0830 N88-15036
Study of vibration relaxation in active medium of CO2-laser using phase-absorption method 07 p0919 N88-15582
Magnetic control of low pressure discharges [AD-A186794] 10 p1322 N88-17900
Basic research on natural gas combustion phenomena [PB88-168380] 14 p1887 N88-21278
Use of nonporous metals membranes for the separation of hydrogen from gas mixtures [BMFT-FB-T-86-206] 14 p1888 N88-21280
Ultrasonic oxygen sensor [AD-A189723] 15 p2105 N88-22537
Trace gas measurements in the troposphere using tunable diode lasers 18 p2540 N88-25072
Antimisting kerosene: Low temperature degradation and blending [NASA-CR-182725] 20 p2781 N88-26495
A shock-tube experiment on gases mixing processes associated with CO2/N2 mixing gasdynamic laser [ISAS-RN-350] 20 p2797 N88-26598
An experimental setup for the study of polarized He3 and dilute He3-He4 mixtures [B8705589] 23 p3193 N88-29001

GAS PHASES
U VAPOR PHASES

GAS PIPES
Technology survey for a robot which will investigate the condition of underground pipe [PB87-209979] 01 p0055 N88-10351
Analysis and application of the constant tensile load test for polyethylene gas pipe materials [DE88-002868] 10 p1345 N88-18037
Characteristics of welds joining parts of high-strength pipe steels and produced by beam of continuous-wave CO2-laser 14 p1897 N88-21325

Trailer shield assembly for a welding torch
[NASA-CASE-MFS-29260-1] 18 p2524 N88-24972
Remote sensing and satellite applications to the needs of the gas and pipeline industry
[PB88-202668] 20 p2817 N88-26714

GAS PRESSURE
Correlation of air pressure drop and flame arrestor characteristics for explosion suppression materials
[AD-A184960] 05 p0548 N88-13340
Gas diffusion studies in steady and nonsteady cavities
[AD-A185795] 06 p0704 N88-14316
On the signal strength dependency on pressure in laser sub-Doppler saturation spectroscopy with special attention to gaseous diatonic molecules
[USIP-87-13] 09 p1171 N88-17023
A control system for maintaining high stability in gas pressure
[DE88-003712] 09 p1175 N88-17042
On the start up of supersonic underexpanded jets --- Mach disks 11 p1435 N88-18563
Measurement of rate constants of elementary gas reactions of importance to upper atmosphere and combustion systems
[AD-A189432] 13 p1737 N88-20386
Gas diffusion studies in steady and nonsteady cavities 18 p2512 N88-24902

GAS RECOVERY
Food production and gas exchange system using blue-green alga (spirulina) for CELSS 03 p0358 N88-12253
An overview of Japanese CELSS research activities 03 p0360 N88-12267
An analysis of gas-steam total power recovery energy system 20 p2784 N88-26512

GAS SPECTROSCOPY
On the signal strength dependency on pressure in laser sub-Doppler saturation spectroscopy with special attention to gaseous diatonic molecules
[USIP-87-13] 09 p1171 N88-17023

GAS STREAMS
Spray deposition: A fundamental study of droplet impingement, spreading and consolidation
[AD-A186627] 08 p0970 N88-15869

GAS TEMPERATURE
Further development of the dynamic gas temperature measurement system 02 p0184 N88-11141
Measurements of gas velocities and temperatures in a large open pool fire
[DE87-005853] 03 p0261 N88-11641
Research sensors 08 p0955 N88-15795
Research sensors 15 p2085 N88-22430
Anomalies in the heat-capacity signatures of submonolayer adsorbates with attractive lateral interactions
[AD-A190736] 15 p2147 N88-22817
Nonequilibrium flow of a radiating gas in a vertical channel with axial temperature variation
[DE88-702535] 23 p3212 N88-29120
Nonequilibrium flow of a dissociating gas in a horizontal channel with axial temperature variation
[DE88-702536] 24 p3373 N88-30089

GAS TRANSPORT
Investigations of the dispersion of spontaneously released heavy gases
[WA-81] 01 p0066 N88-10427
TOPAZ: The transient one-dimensional pipe flow analyzer: An update on code improvements and increased capabilities
[DE88-001781] 04 p0443 N88-12751
Preliminary study of niobium alloy contamination by transport through helium 17 p2402 N88-24279

GAS TUNGSTEN ARC WELDING
Gas tungsten arc welding of Al-10Fe-5Ce
[AD-A184202] 03 p0334 N88-12104
An experimental method for species concentration measurements in a welding arc using laser-induced fluorescence
[DE88-005638] 13 p1778 N88-20636
Development of remote control welding system of large structures
[PB87-219853] 22 p3083 N88-28309

GAS TURBINE ENGINES
NT CONVERTIBLE FAN-SHAFT ENGINES
NT HYDROGEN ENGINES
NT J-57 ENGINE
NT JET ENGINES
NT RAMJET ENGINES
NT SUPERSONIC COMBUSTION RAMJET ENGINES
NT TF-30 ENGINE
NT TURBOFAN ENGINES
NT TURBOJET ENGINES
NT TURBOPROP ENGINES
Turbines with counterrotating runners for aircraft power plants 02 p0158 N88-10992
Diagnosis of flow channel in aircraft gas-turbine engines on basis of vibration spectrum characteristics 02 p0159 N88-10993
Development of a statistically proven injection molding method for reaction bonded silicon nitride, sintering reaction bonded silicon nitride, and sintered silicon nitride
[ETN-87-90575] 02 p0160 N88-11002
Investment foundry melting stock. Rolls Royce requirements and demands in terms of quality and the relationship to end product performance
[PNR90397] 02 p0160 N88-11003
Turbine Engine Hot Section Technology, 1985
[NASA-CP-2405] 02 p0184 N88-11140
The development of a high temperature static strain gage system 02 p0184 N88-11142
The Lewis Strain Gauge Laboratory: Status and plans 02 p0184 N88-11146
Fuel-injector/air-swirl characterization 02 p0185 N88-11150
Combustor-diffuser interaction program 02 p0185 N88-11152
Dilution jet mixing program, phase 3 02 p0185 N88-11153
On the mixing of a row of jets with a confined crossflow 02 p0185 N88-11154
Measurement of airfoil heat transfer coefficients on a turbine stage 02 p0186 N88-11158
Heat transfer in the tip region of a rotor blade simulator 02 p0186 N88-11159
Coolant passage heat transfer with rotation 02 p0186 N88-11160
Heat transfer with very high free stream turbulence 02 p0186 N88-11161
Prediction of turbine blade heat transfer 02 p0187 N88-11162
Flow in a model turbine stator 02 p0187 N88-11163
3D inelastic analysis methods for hot section components 02 p0187 N88-11164
3-D inelastic analysis methods for hot section components 02 p0187 N88-11165
Component specific modeling 02 p0187 N88-11166
Constitutive modeling of superalloy single crystals with verification testing 02 p0188 N88-11169
High temperature stress-strain analysis 02 p0188 N88-11170
Constitutive modeling for isotropic materials 02 p0188 N88-11171
Constitutive modeling for isotropic materials 02 p0188 N88-11172
Creep fatigue life prediction for engine hot section materials (isotropic): Third year progress review 02 p0188 N88-11173
Elevated temperature crack growth 02 p0188 N88-11174
Life prediction and constitutive models for engine hot section anisotropic materials program 02 p0188 N88-11175
Turbine airfoil deposition models and their hot corrosion implications 02 p0189 N88-11178
Experimental verification of vapor deposition rate theory in high velocity burner rigs 02 p0189 N88-11179
Effects of surface chemistry on hot corrosion life 02 p0189 N88-11180
Thermal expansion mismatch and oxidation in thermal barrier coatings 02 p0189 N88-11182
Thermal barrier coating life prediction model development 02 p0190 N88-11183
Composite mechanics for engine structures
[NASA-TM-100178] 04 p0411 N88-12552
A numerical study of the effects of curvature and convergence on dilution jet mixing
[NASA-TM-89878] 05 p0549 N88-13347
Turbine engine supportability study for Army Aviation Systems Command (AVSCOM)
[DE88-002339] 07 p0820 N88-14984
Fuel-injector/air-swirl characterization
[NASA-CR-180864] 07 p0820 N88-14985
Life modeling of thermal barrier coatings for aircraft gas turbine engines
[NASA-TM-100263] 07 p0834 N88-15060
Small gas turbine engine technology 09 p1107 N88-16638
Self-lubricating coatings for high-temperature applications 09 p1119 N88-16703
Advanced Technology for Aero Gas Turbine Components
[AGARD-CP-421] 10 p1279 N88-17647
The advantage of variable geometry for turbine engines at low power 10 p1280 N88-17653
A research program on the aerodynamics of a highly loaded turbine stage 10 p1280 N88-17655
Experimental evaluation of a translating nozzle sidewall radial turbine 10 p1280 N88-17656
An integrated aero/mechanical performance approach to high technology turbine design 10 p1280 N88-17657
Advanced techniques employed in blade cooling research 10 p1281 N88-17659
Design and aerodynamic performance of a small mixed-flow gas generator turbine 10 p1281 N88-17662
Possibilities for on-line surge suppression by fast guide vane adjustment in axial compressors 10 p1283 N88-17674
Ceramic bearings for use in gas turbine engines
[NASA-TM-100288] 10 p1340 N88-18007
Open-cycle centrifugal vapor-compression heat pump
[PB88-157391] 11 p1488 N88-18885
Error evaluation of some practical thermocouple probes for gas turbine combustor tests
[NAL-TR-938] 11 p1489 N88-18886
Effect of spatial inlet temperature and pressure distortion on turbofan engine stability
[NASA-TM-100850] 14 p1868 N88-21162
Review and assessment of the HOST turbine heat transfer program 15 p2086 N88-22431
Evaluation of ceramic thermal barrier coatings for gas turbine engine components
[ETN-88-91947] 16 p2181 N88-22998
Thermal stress minimized, two component, turbine shroud seal
[NASA-CASE-LEW-14212-1] 17 p2345 N88-23978
Corrosion prevention in gas turbines
[NLR-MP-87029-U] 20 p2760 N88-26373
COMPASS ground based engine monitoring program for general application --- Condition Monitoring and Performance Analysis Software System (COMPASS)
[PNR90420] 22 p3044 N88-28064
RB211 developments
[PNR90444] 22 p3045 N88-28069
A review of non-contacting displacement measurement techniques used to monitor the movement of rotor blades in gas turbine aero engines
[PNR90457] 22 p3045 N88-28071
The effect of coatings on fatigue in aerospace materials --- gas turbine engines
[PNR90460] 22 p3059 N88-28150
Managing and controlling change
[PNR90419] 22 p3159 N88-28801
V2500 engine collaboration
[PNR90423] 24 p3326 N88-29803
Constitutive modeling for isotropic materials
[NASA-CR-182132] 24 p3327 N88-29811
Spray automated balancing of rotors: Methods and materials
[NASA-CR-182151] 24 p3330 N88-29825
Radiation transfer in gas turbine combustors 24 p3348 N88-29929
Gas turbine smoke measurement: A smoke generator for the assessment of current and future techniques 24 p3348 N88-29930
Assessment of a 3-D boundary layer analysis to predict heat transfer and flow field in a turbine passage
[NASA-CR-174894] 24 p3370 N88-30066

GAS TURBINES
Optical sizing of soot in gas turbine combustors and exhaust augmentor tubes
[AD-A183785] 01 p0006 N88-10034
Calculation of the damage of highly loaded gas turbine disks under real flight conditions
[ETN-87-90416] 01 p0007 N88-10036
Comparison of different kinds of compact cross flow heat exchangers
[DFVLR-FB-86-63] 01 p0048 N88-10305
The influence of high free stream turbulence, intensive cooling and wake on the external heat transfer of convectively cooled gas turbine blades
[ETN-87-90432] 01 p0056 N88-10360
Development of a statistically proven injection molding method for reaction bonded silicon nitride, sintering reaction bonded silicon nitride, and sintered silicon nitride
[ETN-87-90575] 02 p0160 N88-11002
Blade excitation criteria developed for aero derived engines in Arctic Alaska
[PNR90368] 02 p0182 N88-11131
Marine gas turbines - engine health monitoring, new approaches
[PNR90369] 02 p0182 N88-11132
Combustion characteristics of gas turbine alternative fuels
[NASA-TM-100247] 05 p0548 N88-13338
Effects of free stream turbulence, Reynolds number and incidence angle on axial turbine cascade performance 05 p0548 N88-13339
Study of electrostatic modulation of fuel sprays to enhance combustion performance in an aviation gas turbine
[AD-A184967] 05 p0548 N88-13341

HOST turbine heat transfer program summary
[NASA-TM-100280] 06 p0704 N88-14320
Recent advances in high temperature instrumentation for hot section applications
[NASA-TM-100282] 06 p0707 N88-14339
Small High Pressure Ratio Turbines — conference
[VKI-LS-1987-07] 06 p0712 N88-14364
High pressure ratio turbine design constraints
[TRR-0279] 06 p0712 N88-14365
Mainline performance prediction for radial inflow turbines 06 p0712 N88-14366
Conclusions from a research program on mixed flow gas generator turbines 06 p0713 N88-14368
Highlights from a research program on a very highly loaded axial gas generator turbine
06 p0713 N88-14369
Aerodynamic design of first stage turbines for small aero engines 06 p0713 N88-14370
Aerodynamic testing of small turbines
06 p0713 N88-14371
Aerodynamic design and test performance of supersonic turbines for the Vulcain rocket engine
06 p0713 N88-14373
Report to Congress on the Automotive Technology Development Program
[DE88-003742] 07 p0864 N88-15242
Small engine technology programs
08 p0956 N88-15801
Aircraft engine hot section technology: An overview of the HOST Project 08 p0957 N88-15804
Turbine engine monitoring systems: Can they benefit component improvement program management?
[AD-A186992] 09 p1120 N88-16706
Turbine flow meter with optical fiber pick-up
[NAL-TR-923] 09 p1169 N88-17009
Wake interaction effects on the transition process on turbine blades
[AD-A188020] 10 p1332 N88-17962
Measurements of gas turbine combustor and engine augmentor tube sooting characteristics
[AD-A187831] 11 p1440 N88-18592
Gas cleaning at high temperatures and pressures for gas turbines
[DE88-751171] 11 p1440 N88-18593
Quality assurance of ceramic materials and gas turbine components
[IZFP-850303-TW] 11 p1465 N88-18735
Structural analysis methods development for turbine hot section components
[NASA-TM-100298] 11 p1501 N88-18967
Assessment, development and application of combustor aerothermal models
[NASA-TM-100290] 12 p1582 N88-19469
Hot corrosion in gas turbines: A new, unique and informative technique is EASE (Electronic Absorption Spectroscopy Experiments)
[AD-A188508] 12 p1583 N88-19470
Elevated temperature crack growth studies of advanced titanium aluminides
[AD-A189025] 12 p1608 N88-19618
Advanced Gas Turbine (AGT) Technology Development Project, ceramic component developments
[NASA-CR-180871] 12 p1709 N88-20229
Advanced Gas Turbine (AGT) technology development project
[NASA-CR-180891] 12 p1709 N88-20230
Research as part of the Air Force in aero propulsion technology (AFRAPT) program
[AD-A190336] 15 p2019 N88-22036
Small engine components test facility turbine testing cell
[NASA-TM-100887] 15 p2019 N88-22037
AFRAPT (Air Force Research in Aero Propulsion Technology) trainee program
[AD-A190525] 15 p2035 N88-22123
Experimental determination of the coefficients of the hydraulic resistance of apertures in the rotary disks
[AD-A190627] 15 p2066 N88-22317
Study on shaft seals for potassium turbine
[EL-891] 15 p2074 N88-22364
Comparison of different kinds of compact crossflow heat exchangers
[ESA-TT-1076] 16 p2207 N88-23169
Two-equation low-Reynolds-number turbulence modeling of transitional boundary layer flows characteristic of gas turbine blades
[NASA-CR-4145] 16 p2209 N88-23185
The effects of inlet turbulence and rotor/stator interactions on the aerodynamics and heat transfer of a large-scale rotating turbine model. Part 4: Aerodynamic data tabulation
[NASA-CR-179469] 17 p2339 N88-23956
Hydrogen turbines for space power systems: A simplified axial flow gas turbine model 17 p2419 N88-24385
Research on aero-thermodynamic distortion induced structural dynamic response of multi-stage compressor blading
[AD-A192169] 18 p2456 N88-24584
An empirical model of the effects of curvature and convergence on dilution jet mixing
[NASA-TM-100896] 18 p2466 N88-24640
Evaluation of manure as a feedstock for gas turbines
18 p2536 N88-25050
A 3 MW wood fired gas turbine at Red Boiling Springs, Tennessee 18 p2536 N88-25051
Hydrogen turbines for space power systems: A simplified axial flow gas turbine model
[DE88-009585] 19 p2677 N88-25920
Engine component retirement for cause. Volume 1: Executive summary
[AD-A192730] 20 p2760 N88-26371
Analysis of gas turbine test cell number 1, Lemoore Naval Air Station, California
[AD-A192870] 20 p2762 N88-26380
Use of penetrating radiations for the dynamic examination of aero gas turbines
[PNR90470] 22 p3045 N88-28073
Interaction of creep and fatigue damage in gas turbine blade material
[PNR90440] 22 p3088 N88-28335
AGARD (Advisory Group for Aerospace Research and Development) engine disc material cooperative test (supplementary program)
[AD-A193678] 23 p3179 N88-28925
Failure analysis for gas turbines
[NLR-MP-87037-U] 24 p3326 N88-29808
Gas turbine combustion modeling
24 p3349 N88-29936
Three-dimensional gas turbine combustor modelling
24 p3349 N88-29937
On the application of finite-difference techniques for the computation of the flow field in gas turbine combustors with complex geometries 24 p3349 N88-29938
Numerical modeling of combustion processes in gas turbines 24 p3350 N88-29939
Modelling of CO oxidation in dilution jet flows
24 p3351 N88-29947
Determination of the hydroperoxide potential of jet fuels
[AD-A195975] 24 p3357 N88-29991
User's manual for three dimensional boundary layer (BL3-D) code
[NASA-CR-174899] 24 p3369 N88-30063
Contamination and distortion of steady flow field induced by discrete frequency disturbances in aircraft gas engines
[AD-A195440] 24 p3370 N88-30069

GAS VISCOSITY
Influence of viscosity on the structure of a magnetic neutral layer 08 p1098 N88-16605
Negative viscosity in global circulations
13 p1786 N88-20685

GAS WELDING
NT BRAZING
Weldability of a leaded carbon steel
[PB88-110341] 07 p0861 N88-15225

GAS-GAS INTERACTIONS
NT ASSOCIATION REACTIONS
Vortex/boundary-layer interactions: Data report, volume 1
[NASA-CR-181462] 02 p0121 N88-10768
Vortex/boundary-layer interactions: Data report, volume 2
[NASA-CR-181463] 02 p0122 N88-10769
Experimental study of interacting vortex rings
03 p0318 N88-12007
Experimental study of secondary flow in the presence of two jet arrays on the wall of a turbine blade
[ECL-87-11] 08 p0987 N88-15981
Transition metal cluster chemistry
[AD-A188731] 13 p1740 N88-20405
Numerical and experimental investigation of multiple shock wave/turbulent boundary layer interactions in a rectangular duct
[AD-A190772] 15 p2066 N88-22320
Coupling between radiation and gas dynamics
[AD-A194593] 23 p3211 N88-29113

GAS-LIQUID INTERACTIONS
NT AIR SEA ICE INTERACTIONS
NT AIR WATER INTERACTIONS
Bipropellant combustion in a liquid rocket combustion chamber 13 p1733 N88-20359
Advanced chemical heat pumps using liquid-vapor reactions
[DE88-006760] 16 p2205 N88-23159
Microgravity two-phase fluid flow pattern modeling
17 p2432 N88-24467

GAS-SOLID INTERACTIONS
Wake shield 03 p0298 N88-11871
Feasibility study for gas-grain simulation facility
[NASA-CR-177468] 05 p0646 N88-13954
Theoretical studies of kinetic mechanisms of negative ion formation in plasmas
[AD-A185735] 06 p0784 N88-14812
Different trapping mechanisms of gases by water ice and their relevance for comet nuclei
14 p2007 N88-21970
Microvax networked computer system
[AD-A190308] 15 p2114 N88-22596
An improved external recycle reactor for determining gas-solid reaction kinetics
[NASA-TM-101160] 19 p2611 N88-25492

GASDYNAMIC LASERS
Modeling of pulsed gas flow lasers
[DFVLR-FB-87-19] 09 p1171 N88-17021
Non equilibrium expansion of a radiating gas in a channel of varying section
[DE88-702063] 19 p2665 N88-25845
Modeling of pulsed gas flow lasers
[ESA-TT-1090] 23 p3220 N88-29169

GASEOUS CAVITATION
U CAVITATION FLOW
U GAS FLOW

GASEOUS DIFFUSION
Microgravity nucleation and particle coagulation experiments support
[NASA-CR-181540] 04 p0423 N88-12618
Microgravity nucleation and particle coagulation experiments support
[NASA-CR-181541] 04 p0423 N88-12619
Gas separation using solid electrolytes described
06 p0675 N88-14131
Gas diffusion studies in steady and nonsteady cavities
[AD-A185795] 06 p0704 N88-14318
Investigations of the influence of chemical reactions of the vertical flow of gaseous and particulate compounds
08 p1017 N88-16165
Measuring thin film properties using SAW (Surface Acoustic Wave) devices: Diffusivity and surface area
[DE88-002216] 13 p1834 N88-20970
Synthesis and analysis of novel polymers with potential for providing both high permselectivity and permeability in gas separation applications
[DE88-006533] 15 p2043 N88-22174
Mechanisms of gas permeation through polymer membranes: Renewal proposal for period December 1, 1986 - November 30, 1989
[DE88-007436] 18 p2494 N88-24796
Gas diffusion studies in steady and nonsteady cavities
18 p2512 N88-24902
Computation of flow and diffusion process in gas centrifuges
[ETN-88-92366] 21 p2949 N88-27514
Development of the Simplified Compressor Model (SCM) for performance analysis of gaseous diffusion compressors
[DE88-009066] 23 p3221 N88-29173

GASEOUS FISSION REACTORS
Acoustical gas core reactor with MHD power generation for burst power in a bimodal system
17 p2403 N88-24290

GASEOUS FUELS
NT NATURAL GAS
Feasibility of a complex compound heat pump
[PB88-113022] 07 p0853 N88-15183

GASES
NT AIR
NT ALVEOLAR AIR
NT AMMONIA
NT ARGON
NT ARGON ISOTOPES
NT CARBON DIOXIDE
NT CARBON MONOXIDE
NT COLD GAS
NT COMPRESSED GAS
NT DETONABLE GAS MIXTURES
NT DEUTERIUM
NT DIATOMIC GASES
NT DISSOLVED GASES
NT EXHAUST GASES
NT GAS MIXTURES
NT GAS STREAMS
NT GASEOUS FUELS
NT HELIUM
NT HELIUM ISOTOPES
NT HIGH PRESSURE OXYGEN
NT HIGH TEMPERATURE AIR
NT HIGH TEMPERATURE GASES
NT HYDROGEN
NT HYDROGEN ISOTOPES
NT IDEAL GAS
NT INTERPLANETARY GAS
NT INTERSTELLAR GAS
NT IONIZED GASES
NT KRYPTON

NT KRYPTON ISOTOPES
NT LIQUEFIED NATURAL GAS
NT LIQUID AMMONIA
NT LIQUID HELIUM
NT LIQUID HELIUM 2
NT LIQUID HYDROGEN
NT LIQUID NITROGEN
NT LIQUID OXYGEN
NT MOLECULAR GASES
NT MONATOMIC GASES
NT NATURAL GAS
NT NEON
NT NEUTRAL GASES
NT NITROGEN
NT NITROGEN ISOTOPES
NT OXYGEN
NT OXYGEN ISOTOPES
NT OZONE
NT RADON
NT RADON ISOTOPES
NT RARE GASES
NT RAREFIED GASES
NT REAL GASES
NT TRITIUM
NT XENON

Gases released by surface flashover of insulators
[DE87-013851] 01 p0039 N88-10249

Application of new conformal solution of theories
[PB87-214557] 01 p0105 N88-10684

Lattice gas hydrodynamics 03 p0313 N88-11978

Study of field adsorption using pulsed-laser field ion microscopy
[DE88-000310] 03 p0330 N88-12085

Porosity influence on the strength and elasticity of first-year sea ice
[AD-A184493] 03 p0354 N88-12233

The effect of environment on low cycle fatigue properties in HSLA steel 05 p0605 N88-13705

Gas separation using solid electrolytes described
06 p0675 N88-14131

First flight of the ATMOS instrument during the Spacelab 3 Mission, April 29 through May 6, 1985
[NASA-CR-182360] 06 p0728 N88-14482

European reacting flow research: A final assessment
[AD-A185833] 07 p0828 N88-15022

Dimensions of ignition zones in blow-outs of combustible gases from rectangular and circular ports
07 p0918 N88-15577

Gas feed system for the T-15 tokamak discharge chamber
[DE88-700351] 07 p0935 N88-15682

Operation Everest 2: Comparison of four instruments for measuring blood oxygen saturation
[AD-A186456] 08 p1049 N88-16337

Electron acceleration by laser fields in a gas
[DE88-003337] 08 p1082 N88-16523

Time dependent degradation of energetic electrons in gaseous and condensed media
[DE88-002912] 09 p1246 N88-17465

Atomic and molecular gas phase spectrometry
[AD-A187582] 11 p1452 N88-18655

Gas consumption estimation of an attitude control system of an artificial satellite (utilizing DRF) in limit cycle phase
[INPE-4338-RPE/553] 13 p1731 N88-20350

Stratospheric trace gas distributions from fair infrared thermal emission spectroscopy
13 p1797 N88-20749

Detecting the gas bubbles in a liquid metal coolant by means of magnetic flowmeters
[DE88-701427] 15 p2062 N88-22294

Gas source MBE (Molecular Beam Epitaxy)
[AD-A189763] 15 p2142 N88-22782

User's manual for EULER3DS
[AD-A191048] 16 p2208 N88-23177

Research in nonlinear partial differential equations and bifurcation theory
[AD-A190986] 16 p2260 N88-23514

Heating and evaporation of turbulent liquid films: Measurement of film thickness and the onset of nucleate boiling
[DE88-006388] 18 p2512 N88-24905

Factors which affect operation of a plasma focus in various gases
[DE88-701882] 20 p2858 N88-26975

Infrared detectors based on the photon drag effect and intersubband absorption by a two-dimensional electron gas 20 p2867 N88-27024

Experimental study of planetary gases with applications to planetary interior models
[NASA-CR-183098] 20 p2886 N88-27137

Sinterable ceramic powders from laser-heated gases
[AD-A194162] 23 p3197 N88-29024

The kinematics of Milky Way halo gas
23 p3299 N88-29648

Numerical modelling of premixed flames in gaseous media 24 p3350 N88-29944

GASIFICATION
NT COAL GASIFICATION

The applicability of the catalytic wet-oxidation to CELSS 03 p0360 N88-12264

Bench-scale studies on fluid-bed pyrolysis of wood using different contact gases 18 p2536 N88-25049

Feasibility of producing jet fuel from GPGP (Great Plains Gasification Plant) by-products
[DE88-010233] 20 p2781 N88-26492

GASOHOL (FUEL)

Compendium of significant events in the recent development of alcohol fuels in the United States
[DE87-013355] 01 p0032 N88-10202

Vapor generation of fuels
[PB88-109897] 08 p0974 N88-15892

GASOLINE

Safety implications of onboard refueling vapor recovery systems
[PB88-102603] 07 p0839 N88-15088

Summary and analysis of comments on the recommended practice for the measurement of refueling emissions
[PB88-101530] 07 p0876 N88-15313

Vapor generation of fuels
[PB88-109897] 08 p0974 N88-15892

The effect of weathering on octane quality for winter-grade and summer-grade gasolines
[AD-A190640] 16 p2183 N88-23012

Development of a laboratory test for multiport fuel injector deposits - evaluation of the Jet Fuel Thermal Oxidation Test apparatus (JFTOT)
[AD-A191313] 16 p2183 N88-23015

Upgrading pyrolysis vapors to aromatic gasoline with zeolite catalysis at atmospheric pressure
18 p2536 N88-25045

Research on hydrotreating catalysts to hydrodeoxygenate biocrude oils
18 p2536 N88-25046

Technical and economic evaluation of emerging biomass pyrolysis processes for gasoline production
18 p2536 N88-25048

GASTROINTESTINAL SYSTEM
NT INTESTINES
NT STOMACH

Gastric emptying during walking and running: Effects of varied exercise intensity
[AD-A194025] 23 p3240 N88-29281

GATES (CIRCUITS)

Wide-area communication under Amoeba
[PB87-234431] 06 p0760 N88-14665

Impurity bands in quantum wells
[INPE-4250-PRE/1123] 08 p1089 N88-16552

Effect of the gate oxide thickness on the speed of MOS integrated circuits
[PB88-155783] 10 p1323 N88-17910

Study of quantum mechanical effects in deep submicron, grating-gate field effect transistors
[AD-A188283] 10 p1325 N88-17923

Parts-R-Us
[AD-A188621] 12 p1622 N88-19705

GM: A gate matrix layout generator
[EUT-87-E-179] 13 p1820 N88-20875

GADL: A gate array description language
[EUT-87-E-165] 14 p1907 N88-21396

Design of the Detector 2: A CMOS gate array for the study of concurrent error detection techniques
[AD-A191247] 16 p2193 N88-23079

Planar fully ion-implanted high power InP MISFETs
[AD-A191589] 18 p2582 N88-25338

Development of the field-induced electron injection and impact ionization (F4I) technique for radiation hardness testing of MOS (Metal-Oxide-Semiconductor) gate insulators
[AD-A192114] 18 p2583 N88-25345

The response of ultrathin palladium gate sensors to hydrogen and carbon monoxide
19 p2672 N88-25885

Picosecond optoelectronic sampling of electrical waveforms produced by an optically excited field effect transistor
[AD-A192384] 21 p2935 N88-27428

GATES (OPENINGS)

Test of a prototype gate with fast opening equipping the shock tube 0 2.40 m at CEG
[PB87-227864] 19 p2604 N88-25485

GAUGE INVARIANCE

Anomalies in gauge theories
[DE87-014087] 02 p0229 N88-11444

Inequivalent quantizations and fundamentally perfect spaces
[DE87-014225] 02 p0229 N88-11446

Magnitude-redshift relation in a perturbed Friedmann universe
[DE87-753020] 02 p0252 N88-11590

Comment on the Adler-Bardeen theorem and related problems
[DE88-751051] 10 p1403 N88-18367

Chiral symmetry breaking in finite quantum electrodynamics
[DE88-700860] 12 p1699 N88-20169

Recent developments in the path integral approach to anomalies
[DE87-703032] 15 p2118 N88-22616

Path integral, BRS symmetry, and string and membrane theories
[DE88-752300] 15 p2146 N88-22810

Quantization of axial electrodynamics
[DE88-701498] 15 p2147 N88-22813

General relativity invariance and string field theory
[DE88-702045] 19 p2737 N88-26252

Some remarks on geodesics in gauge groups and harmonic maps
[DE88-702665] 22 p3115 N88-28510

GAUGE THEORY

Anomalies in gauge theories
[DE87-014087] 02 p0229 N88-11444

Research program in elementary particle theory
[DE88-000159] 02 p0233 N88-11468

Finite size scaling and lattice gauge theory
[DE87-014139] 02 p0245 N88-11549

Regular effective action of gauge field theory and quantum gravity
[DE87-703076] 02 p0247 N88-11560

Geometrization of Planck length in composite gravity and supergravity
[DE87-703085] 02 p0251 N88-11588

A supersymmetric Lagrangian for Poincare gauge theories of gravity
[DE88-001670] 04 p0500 N88-13078

Gravity from symmetry breakdown of a gauge affine theory
[DE88-001671] 04 p0500 N88-13079

Operator foundation of functional integral in non-Abelian gauge theory
[DE88-700508] 07 p0941 N88-15719

Secondary gauge conditions in field theory
[DE88-701499] 15 p2147 N88-22814

Rigid symmetries and BRST-invariance in gauge theories
[PB88-180948] 18 p2572 N88-25280

Introduction to lattice gauge theory
[DE88-006073] 18 p2584 N88-25349

Topics in gauge theories and the unification of elementary particle interactions
[DE88-008112] 19 p2738 N88-26256

Closed string fields as parameters of extra gauge symmetry of open string field theory
[DE88-702046] 21 p3026 N88-27960

Theoretical particle physics
[DE88-011499] 23 p3295 N88-29621

Lagrangian of the self-duality equation and d = 10, N = 2b supergravity
[DE88-701554] 24 p3455 N88-30563

GAUSS EQUATION

Local properties of index-alpha stable fields
[AD-A186432] 07 p0912 N88-15530

Application of artificial intelligence to impulsive orbital transfers 08 p1066 N88-16439

Gaussian techniques on shared memory multiprocessor computers
[DE88-005426] 13 p1817 N88-20855

Exact image method for Gaussian beam problems involving a planar interface
[NASA-CR-182702] 14 p1905 N88-21380

Limiting distributions of non-linear vector functions of stationary Gaussian processes
[AD-A194569] 23 p3274 N88-29488

GAUSS FUNCTION
U GAUSS EQUATION

GAUSS-MARKOV THEOREM

Computational behavior of Gauss-Newton methods
[DE87-014486] 02 p0224 N88-11413

Concentration inequalities for Gauss Markov estimators
[CWI-MS-R8706] 14 p1965 N88-21726

A unified approach to estimation in linear models with fixed and mixed effects
[AD-A193060] 21 p3006 N88-27829

GAUSSIAN DISTRIBUTIONS
U NORMAL DENSITY FUNCTIONS

GAUSSIAN ELIMINATION

A graph separator theorem and its application to Gaussian elimination to optimize Boolean expressions for parallel evaluation
[AD-A188527] 14 p1962 N88-21706

Gaussian techniques on shared-memory multiprocessors
[DE88-010594] 19 p2716 N88-26126

Reducing the parallel solution time of sparse circuit matrices using reordered Gaussian elimination and relaxation
[AD-A195152] 24 p3366 N88-30045
GAUSSIAN NOISE
U RANDOM NOISE
GAUSSMETERS
U MAGNETOMETERS
GC-130 AIRCRAFT
U C-130 AIRCRAFT
GCR (REACTORS)
U GAS COOLED REACTORS
GDOP
U GEOMETRIC DILUTION OF PRECISION
GEAR TEETH
A hydrodynamic analysis of fluid flow between meshing spur gear teeth
[AD-A187671] 11 p1482 N88-18844
Spur gears: Optimal geometry, methods for generation and Tooth Contact Analysis (TCA) program
[NASA-CR-4135] 16 p2215 N88-23216
GEARS
Assessment of the COFSI/MAST I project
[NASA-CR-181366] 01 p0053 N88-10340
Improving repairability of gears 02 p0158 N88-10989
Multipath gear-friction planetary transmissions 04 p0424 N88-12629
On dynamic loads in parallel shaft transmissions. 1: Modelling and analysis
[NASA-TM-100180] 04 p0451 N88-12797
On dynamic loads in parallel shaft transmissions. 2: Parameter study
[NASA-TM-100181] 04 p0452 N88-12798
Efficiency testing of a helicopter transmission planetary reduction stage
[NASA-TP-2795] 07 p0861 N88-15224
Pin joints, gears, springs, cranks and other novel micromechanical structures
[DE88-002504] 07 p0864 N88-15245
Rotorcraft transmission 08 p0956 N88-15802
Experimental investigation on the bending fatigue performance of gas carbonitrided and carburized gears
[PB87-147997] 08 p0992 N88-16003
Results of NASA/Army transmission research 09 p1108 N88-16640
Dynamic analysis of multimesh-gear helicopter transmissions
[NASA-TP-2789] 09 p1176 N88-17045
Dynamic response of a geared train of rotors subjected to random support excitations 09 p1181 N88-17073
Gear systems for advanced turboprops 10 p1282 N88-17667
Analysis of possible transmission arrangements applicable for driving single or twin counterrotating fans on propfan engines 10 p1282 N88-17670
Army maintenance: Actions to reduce the likelihood of helicopter gear failures
[PB88-135256] 11 p1433 N88-18551
Finite element methods for quasi-prismatic bodies with application to gears 13 p1779 N88-20644
The performance of thin solid films for satellite gears 14 p1876 N88-21209
Advanced transmission studies
[NASA-TM-100867] 14 p1919 N88-21454
Spur gears: Optimal geometry, methods for generation and Tooth Contact Analysis (TCA) program
[NASA-CR-4135] 16 p2215 N88-23216
Linear force device
[NASA-CASE-MSC-20549-2] 18 p2516 N88-24927
Design, manufacture and spin test of high contact ratio helicopter transmission utilizing Self-Aligning Bearingless Planetary (SABP)
[NASA-CR-4155] 18 p2524 N88-24975
Determination of settings of a tilted head-cutter for generation of hypoid and spiral bevel gears
[NASA-CR-182138] 18 p2524 N88-24976
Surface fatigue life of CBN and vitreous ground carburized and hardened AISI 9310 spur gears
[NASA-TM-100960] 19 p2677 N88-25916
A review of gear housing dynamics and acoustics literature
[NASA-CR-183110] 20 p2811 N88-26675
Optimization of planetary gears
[ETN-88-92375] 21 p2958 N88-27573
An analytical investigation of geared system dynamics containing spur and helical gears 22 p3085 N88-28317
Design and evaluation of high contact ratio gearing
[NASA-CR-174958] 22 p3085 N88-28319
High hot-hardness gear lubricant evaluations, phase 2
[AD-A192309] 23 p3196 N88-29017
GEL PERMEATION CHROMATOGRAPHY
U LIQUID CHROMATOGRAPHY
GELATION
Cure and properties of thermosetting polymers
[AD-A184669] 03 p0293 N88-11843
Molecular engineering of ceramics
[DE88-000174] 04 p0420 N88-12603
Glassy GeO2 obtained by the gel process
[NASA-TT-20125] 06 p0685 N88-14201
The numerical simulation of viscous flows with change of phase and chemical reaction
[DE88-003204] 15 p2062 N88-22292
GELLED PROPELLANTS
NT GELLED ROCKET PROPELLANTS
Characterization of aluminum/RP-1 gel propellant properties
[NASA-TM-100951] 18 p2496 N88-24808
GELLED ROCKET PROPELLANTS
Burning rate measurements of Non-Newtonian Liquid Propellant (NNLP) 19 p2623 N88-25561
GELS
NT DOUBLE BASE ROCKET PROPELLANTS
NT SILICA GEL
Use of sol-gels in the application of ceramic oxide thin films
[DE87-013610] 01 p0028 N88-10176
Molecular engineering of ceramics
[DE88-000174] 04 p0420 N88-12603
T.E.M. study of boehmite gels and of their transformation into alpha-alumina
[SNIAS-872-430-121] 05 p0656 N88-14023
Fluids, gels and glasses under extreme conditions of pressure and temperature
[AD-A190655] 15 p2035 N88-22125
Cellular thermosetting fluoropolymers and process for making them
[NASA-CASE-GSC-13008-1] 17 p2326 N88-23894
Electrode films of porous agarose: The effects of physical structure on electron transport processes
[DE88-007366] 19 p2611 N88-25493
Characterization of the surface area and porosity of sol-gel films using saw devices
[DE88-008794] 20 p2875 N88-27069
Preparation and properties of new inorganic glasses and gel-derived solids
[AD-A192922] 21 p2917 N88-27315
Method of dispensing reagent chemicals in space
[NASA-CASE-LAR-13607-1-CU] 23 p3200 N88-29048
GEMINID METEOROIDS
Some models of the Geminids meteor stream formation 06 p0740 N88-14551
GENERAL AVIATION AIRCRAFT
NT AGRICULTURAL AIRCRAFT
NT DO-28 AIRCRAFT
Wind-tunnel investigation of a full-scale general aviation airplane equipped with an advanced natural laminar flow wing
[NASA-TP-2772] 01 p0002 N88-10009
Aircraft accident reports, brief format, US civil and foreign aviation. Issue number 1: 1986 accidents
[PB87-916903] 02 p0123 N88-10781
Semiempirical method for prediction of aerodynamic forces and moments on a steadily spinning light airplane
[NASA-TM-4009] 04 p0393 N88-12456
Wind tunnel results for a high-speed, natural laminar-flow airfoil designed for general aviation aircraft
[NASA-TM-87602] 06 p0665 N88-14078
Aircraft accident reports: Brief format, US Civil and Foreign Aviation, Issue Number 4 of 1986 accidents
[PB87-916906] 06 p0666 N88-14086
Sudden in-flight incapacitation in general aviation
[AD-A187044] 09 p1115 N88-16682
Investigation of the misfueling of reciprocating piston aircraft engines
[NASA-TP-2803] 14 p1865 N88-21144
It's time to reinvent the general aviation airplane 17 p2294 N88-23726
High-flaps for natural laminar flow airfoils 17 p2296 N88-23739
Certification aspects of airplanes which may operate with significant natural laminar flow 17 p2298 N88-23749
Development of a multipurpose smart recorder for general aviation aircraft
[NASA-CR-168353] 18 p2465 N88-24637
GENERAL DYNAMICS AIRCRAFT
NT F-106 AIRCRAFT
NT F-111 AIRCRAFT
GENERAL DYNAMICS MILITARY AIRCRAFT
U MILITARY AIRCRAFT
GENERATORS
Optimum size of staged flux compression generators
[DE87-011741] 01 p0038 N88-10244
Cast iron-base alloy for cylinder/regenerator housing
[NASA-CR-182116] 12 p1608 N88-19613
GENETIC CODE
The human genome: Computational challenges
[DE88-006465] 18 p2549 N88-25131
GENETIC ENGINEERING
Biopolymers: Protein and nucleic acids
[AD-A185837] 07 p0835 N88-15066
Synthesis of high molecular weight peptide polymers and copolymers containing L-dope residues
[AD-A186462] 08 p0973 N88-15887
Potential use of the bioreactor to determine effects of microgravity and other environmental parameters on growth of hybridoma cells 09 p1198 N88-17178
The use of plant protoplasts in biotechnological space research 12 p1655 N88-19914
Biology and Medicine Division
[DE87-009280] 14 p1952 N88-21632
Saccharification of cellulose by combined fungal and bacterial preparations 17 p2316 N88-23833
The human genome: Computational challenges
[DE88-006465] 18 p2549 N88-25131
Ecological risk factors related to environmental uses of genetically engineered organisms
[DE88-006674] 18 p2549 N88-25132
GENETICS
JPRS report: Science and technology. USSR: Life sciences
[JPRS-ULS-87-009] 04 p0473 N88-12915
Review of cytoskeleton research in cell differentiation and development
[AD-A185832] 07 p0882 N88-15353
A theoretical concept for state changes and shape changes in weightlessness 07 p0884 N88-15365
Physiological and biochemical aspects of toxic effects of oxidants in man's environment (air, water) 07 p0890 N88-15391
Investigation of genetic structures of rat germ cells following flight aboard Cosmos-1514 biosatellite during their prenatal development 10 p1364 N88-18155
Genetic research in space
[NASA-TT-20216] 11 p1518 N88-19066
A Darwinian approach to artificial neural systems
[DE87-013184] 13 p1824 N88-20900
ECUT (Energy Conversion and Utilization Technologies) program: Biocatalysis Project
[NASA-CR-182917] 17 p2370 N88-24110
Genetic effects of low level microwave radiation
[AD-A192687] 21 p2984 N88-27722
The effects of microgravity on genetic recombination in Escherichia coli — Spacelab D1 mission 22 p3060 N88-28157
GENITOURINARY SYSTEM
NT KIDNEYS
NT TESTES
GEO ENVIRONMENTS
U EARTH ORBITAL ENVIRONMENTS
GEOASTROPHYSICS
U ASTROPHYSICS
U GEOPHYSICS
GEOBOTANY
Overview of Austrian Airborne Imaging Spectrometer (AIS) programme and first results 05 p0612 N88-13762
GEOCHEMISTRY
NT BIOGEOCHEMISTRY
Development of an X-ray fluorescence microprobe at the National Synchrotron Light Source, Brookhaven National Laboratory: Early results: Comparison with data from other techniques
[NASA-CR-181468] 02 p0236 N88-11486
A mineral reconnaissance sampling manual for Costa Rica: Central American energy and resource project
[DE87-014997] 04 p0462 N88-12859
Summaries of physical research in the geosciences
[DE88-000833] 04 p0468 N88-12896
RRS DISCOVERY cruise 160, 30 June-25 July, 1986. Geochemical sampling over the Madeira and Porcupine Abyssal Plains
[PB87-222030] 04 p0471 N88-12910
Geochemistry of freezing brines, low-temperature properties of sodium chloride
[AD-A185751] 06 p0680 N88-14168
Research needs for hydrocarbon fuels
[DE87-014555] 06 p0687 N88-14209
Petrogenesis of basalts from the Archean Matachewan Dike Swarm Superior Province of Canada 06 p0796 N88-14878
Nature and origin of mineral coatings on volcanic rocks of the Black Mountain, Stonewall Mountain, and Kane Springs Wash volcanic centers, Southern Nevada
[NASA-CR-181437] 09 p1191 N88-17140
Earth materials research: Report of a Workshop on Physics and Chemistry of Earth Materials
[NASA-CR-182519] 10 p1298 N88-17761
Analysis of gases in the earth's crust
[PB88-141619] 10 p1354 N88-18093
Trace element geochemistry of the South Atlantic Bight
[DE88-003515] 10 p1356 N88-18108

Reports and contributions of the Max-Planck Institute of Chemistry (Otto Hahn Institute)
[REPT-1/87] 11 p1570 N88-19398

Advances in geochemistry and cosmochemistry: Trace element microdistributions with the synchrotron X-ray fluorescence microprobe
[DE88-006355] 15 p2032 N88-22108

Geochemistry of the middle and lower atmosphere: Environmental impact through the deterioration of the ozone layer
[INPE-4477-PRE/1241] 16 p2230 N88-23321

A sedimentological and mineralogical study of the Koogah Formation, New South Wales
18 p2542 N88-25087

SPOT images and geochemical mapping of lateritic covers in southern Mali 22 p3105 N88-28438

MEVTV Workshop on Nature and Composition of Surface Units on Mars
[NASA-CR-183075] 23 p3300 N88-29654

Mars: Spectral signatures seen and unseen
23 p3301 N88-29659

Aqueous alteration in S-N-C meteorites and implications for weathering products on Mars
23 p3303 N88-29673

Pb isotope constaints on the extent of crustal recycling into a steady state mantle 24 p3394 N88-30215

Crustal evolution and the eclogite to granulite phase transition in xenoliths from the West African Craton
24 p3395 N88-30217

Changing styles of crustal growth in Southern Africa: Constraints from geochemical and Sr-Nd isotope studies in Archaean to Pan African terrains
24 p3396 N88-30227

Continental crustal formation and recycling: Evidence from oceanic basalts 24 p3398 N88-30238

Evolution of the Dharwar Craton: A terrain of early Archean crustal stability, long term orogenic cycles and large scale palaeobiological activity
24 p3399 N88-30241

The growth of the continental crust: Constraints from radiogenic isotope geochemistry
24 p3399 N88-30245

Crustal growth in the Archean: The geochemical evidence 24 p3400 N88-30246

Crustal underplating in the North American Craton: Evidence from the Petrogenesis of anorthositic rocks in the Middle Proterozoic Midcontinent Rift System
24 p3400 N88-30252

Terrestrial versus giant planet formation
24 p3451 N88-30543

GEOCHRONOLOGY

Measurements of iridium and the meteoric impact hypothesis at cretaceous end
[DE87-703765] 04 p0521 N88-13200

Tectonics of sedimentary cover and basement of Labrador Sea 06 p0726 N88-14468

New data on the formation conditions and age of the Kamensk and Gusev astroblemes
[NASA-TT-20212] 11 p1513 N88-19040

Workshop on the Growth of Continental Crust
[NASA-CR-183073] 24 p3392 N88-30201

Role of zircon in tracing crustal growth and recycling
24 p3394 N88-30211

Construction of mass-age curves for the continental crust: An empirical model and an example from the western US 24 p3394 N88-30213

Pb isotope constaints on the extent of crustal recycling into a steady state mantle 24 p3394 N88-30215

Metamorphic P-T paths and Precambrian crustal growth in East Antarctica 24 p3395 N88-30218

The early archaean crustal history of West Greenland as recorded by detrital zircons 24 p3395 N88-30221

Growth of early archaean crust in the ancient Gneiss complex of Swaziland and adjacent Barberton Greenstone Belt, Southern Africa 24 p3396 N88-30223

Structure of Southwestern Michipicoten Greenstone Belt, Ontario: Evidence for Archean accretion
24 p3397 N88-30228

Geochronological and lead-isotope evidences for rapid crust formation in middle-proterozoic time: The Labrador example 24 p3398 N88-30239

The growth of the continental crust: Constraints from radiogenic isotope geochemistry
24 p3399 N88-30245

Mineralization through geologic time: Evolution of continental crust 24 p3400 N88-30250

Late-Archaean crustal growth in the Lewisian Complex of Northwest Scotland: Diachroneity in magmatic accretion and implications for models of crustal growth
24 p3401 N88-30253

The effect of thicker oceanic crust in the Archaean on the growth of continental crust through time
24 p3401 N88-30254

Spectral analysis of the Elatina varve series
[NASA-CR-183085] 24 p3402 N88-30260

GEOCORONAL EMISSIONS

Lyman alpha SMM/UVSP absolute calibration and geocoronal correction
[NASA-TM-100314] 03 p0389 N88-12446

GEODESIC LINES

The information metric for univariate linear elliptic models
[AD-A186385] 07 p0911 N88-15527

Some remarks on geodesics in gauge groups and harmonic maps
[DE88-702665] 22 p3115 N88-28510

GEODESY

NT CELESTIAL GEODESY

Strain gages in engineering geodesy
[SER-C-320] 01 p0048 N88-10309

Accuracy of GPS surveying technique and its possible application to the Wegener project --- Mediterranean tectonics
[REPT-85.3] 01 p0063 N88-10407

Study of a satellite-to-satellite tracking gravity mission
[ESA-CR(P)-2419] 02 p0198 N88-11237

Software design for an airborne gravity measurement system
[AD-A185000] 05 p0634 N88-13878

Five-diagonal weighting scheme for geoidal profiles
[AD-A188033] 10 p1347 N88-18054

A smart, mapping, charting and geodesy control generator, phase 1
[AD-A188184] 10 p1347 N88-18055

Estimation of gravity vector components from Bell gravity gradiometer and auxiliary data under consideration of topography and associated analytical upward continuation aspects
[AD-A188146] 10 p1355 N88-18099

Reports on cartography and geodesy. Series 1, report 98
[ISSN-0469-4236] 11 p1506 N88-18993

Geodetic positioning by employment of the GPS-NAVSTAR satellites applying the techniques of VLBI and sequential recursive optimal estimation
[INPE-4438-TDL/311] 12 p1594 N88-19547

Department of Defense World Geodetic System 1984: Its definition and relationships with local geodetic systems
[AD-A188815] 12 p1639 N88-19811

Conformal geometry, Hotine's conjecture, and differential geodesy
[AD-A189265] 13 p1790 N88-20709

Determination of Earth rotation by the combination of data from different space geodetic systems
[NASA-CR-181388] 13 p1791 N88-20713

The Spring 1985 high precision baseline test of the JPL GPS-based geodetic system
[NASA-CR-182686] 14 p1940 N88-21577

Estimation of geopotential from satellite-to-satellite range rate data: Numerical results
[NASA-CR-180771] 14 p1941 N88-21583

Validate algorithms for the determination of rainfall rates from SSM/I microwave satellite imagery
[AD-A191337] 16 p2236 N88-23353

Spectral analysis in the linear geodetic boundary value problem
[B8735056] 16 p2259 N88-23502

Criteria for planimetric and altimetric correction of maps restituted from aerial photographs in 1:100,000 scale
17 p2367 N88-24097

Geodesy by radio interferometry: Optimization of wet path delay algorithms using microwave radiometer data
[PB88-167739] 18 p2498 N88-24820

Research project Loran-C of the Geometric Service of the Ministry of Public Works
[B8735055] 20 p2757 N88-26356

Optimized observation periods required to achieve geodetic accuracies using the global positioning system
[AD-A193844] 22 p3041 N88-28052

GEODETIC ACCURACY

Research in geodesy based upon radio interferometric observations of GPS (Global Positioning System) satellites
[AD-A184040] 03 p0346 N88-12187

A demonstration of high precision GPS orbit determination for geodetic applications
04 p0432 N88-12680

Precision analysis of regular networks
[B8709808] 05 p0620 N88-13806

Determination of TRANET (tracking station coordinates for tracking network) and SMTP (Special Mission Tracking Program) tracking station coordinates for use in the WGS (World Geodetic System) 84
[AD-A185863] 07 p0817 N88-14972

Generalized expression for radio navigation parameter error 13 p1787 N88-20691

Research project Loran-C of the Geometric Service of the Ministry of Public Works
[B8735055] 20 p2757 N88-26356

Optimized observation periods required to achieve geodetic accuracies using the global positioning system
[AD-A193844] 22 p3041 N88-28052

Estimation of short-wavelength gravity on a dense grid using digital terrain elevation data
[AD-A196325] 24 p3391 N88-30196

GEODETIC COORDINATES

Control of the German main triangulation network by macrometer measurement 1983-1985 (KONMAC)
[SER-B-282] 01 p0063 N88-10404

Analytical treatment of the spatial trilateration problem (4, 6, 0, 0)
[SER-A-104] 01 p0085 N88-10548

Method for joint adjustment of satellite and surface geodetic networks 08 p1007 N88-16105

New possibilities for using gravity data in developing geodetic coordinate systems 08 p1009 N88-16116

Reports on cartography and geodesy. Series 1, report 98
[ISSN-0469-4236] 11 p1506 N88-18993

The significance of orientation unknowns in station and net adjustments 11 p1506 N88-18994

The orientation of global satellite networks
11 p1506 N88-18996

GEODETIC SATELLITES

NT GEOS 2 SATELLITE

NT GEOSAT SATELLITES

Control of the German main triangulation network by macrometer measurement 1983-1985 (KONMAC)
[SER-B-282] 01 p0063 N88-10404

Accuracy of GPS surveying technique and its possible application to the Wegener project --- Mediterranean tectonics
[REPT-85.3] 01 p0063 N88-10407

Determination of TRANET (tracking station coordinates for tracking network) and SMTP (Special Mission Tracking Program) tracking station coordinates for use in the WGS (World Geodetic System) 84
[AD-A185863] 07 p0817 N88-14972

GEODETIC SURVEYS

Control of the German main triangulation network by macrometer measurement 1983-1985 (KONMAC)
[SER-B-282] 01 p0063 N88-10404

Accuracy of GPS surveying technique and its possible application to the Wegener project --- Mediterranean tectonics
[REPT-85.3] 01 p0063 N88-10407

Research in geodesy based upon radio interferometric observations of GPS (Global Positioning System) satellites
[AD-A184040] 03 p0346 N88-12187

Considering refraction in leveling with laser plane
04 p0462 N88-12857

Precision analysis of regular networks
[B8709808] 05 p0620 N88-13806

Observations of Earth tides by the German Geodetic Research Institute, division 1, in the period 1979-1985 at the Berchtesgaden and Wettzell stations
[SER-B-280] 07 p0872 N88-15291

Crustal dynamics project data analysis, 1987. Volume 1: Fixed station VLBI geodetic results, 1979-1986
[NASA-TM-100682] 08 p1035 N88-16279

Crustal dynamics project data analysis, 1987. Volume 2: Mobile VLBI geodetic results, 1982-1986
[NASA-TM-100689-VOL-2] 08 p1035 N88-16280

Crustal Dynamics Project: Catalogue of site information
[NASA-RP-1198] 11 p1513 N88-19037

Geodetic measurement of deformation east of the San Andreas fault in Central California
[NASA-CR-182709] 13 p1798 N88-20754

Global Positioning System (GPS) exploitation by ODOT (Ohio Department of Transportation)
[PB88-172796] 16 p2159 N88-22882

Basic research for the geodynamics program
[NASA-CR-183149] 21 p2973 N88-27662

A comparison: Static and future kinematic GPS (Global Positioning System) surveys
[AD-A194666] 23 p3175 N88-28904

DATATRAN: Datum transformation software
[AD-A195723] 24 p3387 N88-30175

Estimation of short-wavelength gravity on a dense grid using digital terrain elevation data
[AD-A196325] 24 p3391 N88-30196

Analytical method for approximate geodetic referencing of scanner images of meteorological artificial earth satellites using control points 24 p3449 N88-30527

GEODYNAMICS

The interpretation of crustal dynamics data in terms of plate motions and regional deformation near plate boundaries
[NASA-CR-181475] 03 p0349 N88-12205

The Telecommunications and Data Acquisition Report
[NASA-CR-181546] 04 p0432 N88-12679

Crustal dynamics project data analysis, 1987. Volume 1: Fixed station VLBI geodetic results, 1979-1986
[NASA-TM-100682] 08 p1035 N88-16279
Crustal dynamics project data analysis, 1987. Volume 2: Mobile VLBI geodetic results, 1982-1986
[NASA-TM-100689-VOL-2] 08 p1035 N88-16280
Crustal Dynamics Project: Catalogue of site information
[NASA-RP-1198] 11 p1513 N88-19037
Proceedings of an ESA-NASA Workshop on a Joint Solid Earth Program
[NASA-CR-182642] 12 p1644 N88-19844
NASA's geodynamics program
12 p1644 N88-19845
Drilling investigation of a young magmatic intrusion beneath the Inyo Domes, Long Valley, California: Structural and textural studies
[DE88-006613] 18 p2541 N88-25078
The interpretation of crustal dynamics data in terms of plate interactions and active tectonics of the Anatolian Plate and surrounding regions in the Middle East
[NASA-CR-183024] 18 p2543 N88-25092
SPOT imagery preliminary contribution to cartography and geodynamics in the Benue trough (Nigeria)
22 p3103 N88-28429

GEOELECTRICITY
Electromagnetic induction in spherical earth containing oceans and continents in electrical contact with underlying section: Theory, method, example
08 p1011 N88-16127
Temporal evolution of ionospheric electric field driven by field-aligned current 11 p1469 N88-18761

GEOFRACTURES
U GEOLOGICAL FAULTS

GEOGRAPHIC INFORMATION SYSTEMS
Problems in integrating geographic data
[DE87-012880] 01 p0106 N88-10689
KBGIS-II: A knowledge-based geographic information system
[NASA-CR-182492] 09 p1261 N88-17559
Air Force geographic information and analysis system
[DE88-001420] 10 p1424 N88-18505
Development of a digital terrain modeling system for microcomputers
[INPE-4406-TDL/303] 12 p1639 N88-19816
An overview of the army GIS (Geographic Information Systems) Research Program
[AD-A189711] 14 p1992 N88-21871
Updating of the municipal official register of real estate through a geographical information system
[INPE-4459-PRE/1238] 15 p2090 N88-22453
Sources of digital spatial data for geographic information systems
[AD-A189788] 15 p2148 N88-22824
Georelational data model
[INPE-4490-PRE/1254] 15 p2149 N88-22829
Inventory of topographic mapping and standardization of geographic names as the basis of a Geographic Information System (GIS) 16 p2225 N88-23281
Remote sensing and data integration: Practical solutions for resource managers 17 p2356 N88-24034
Implantation of a geo-cartographical information system through microcomputers 17 p2361 N88-24064
Research on enhancing the utilization of digital multispectral data and geographic information systems in global habitability studies
[NASA-CR-182799] 17 p2368 N88-24101
Updating of municipal official register of real estate through the geographical information system
19 p2684 N88-25952
Hydrologic models for land-atmosphere retrospective studies of the use of LANDSAT and AVHRR data
[NASA-CR-182861] 20 p2817 N88-26712
Hydrologic models for land-atmosphere retrospective studies of the use of LANDSAT and AVHRR data
[NASA-CR-182862] 20 p2818 N88-26716
Geographical information for design purposes
[NLR-MP-87014-U] 20 p2818 N88-26719
Knowledge representation in geographic information systems
[ETN-88-92470] 20 p2882 N88-27112
Review of geographic processing techniques applicable to regional analysis
[DE88-010759] 21 p2970 N88-27643
An evaluation of the applicability of SPOT stereoscopic imagery to the Canada Land Use Monitoring Program (CLUMP) 22 p3099 N88-28403
Use of SPOT imagery in a geographic information system 22 p3114 N88-28498
SEP/VIPS 32 geographic information system. Processing and thematic analysis of images, maps, and associated data 22 p3114 N88-28499
Contribution of SPOT to geographic information systems 22 p3114 N88-28502
A digital terrain model system for a microcomputer
[INPE-4610-PRE/1333] 24 p3413 N88-30316

GEOGRAPHY
NT HYPSOGRAPHY
NT OROGRAPHY
Advanced techniques for the storage and use of very large, heterogeneous spatial databases. The representation of geographic knowledge: Toward a universal framework — relations (mathematics)
[NASA-CR-181517] 03 p0385 N88-12421
Geographic application of the relational data base system Cantor
[PB87-120945] 06 p0791 N88-14851
Space applications in geography
08 p1007 N88-16104
The Systeme d'Analyse Geographique (SAGE) geographic analysis system 17 p2353 N88-24019
The SAGE geographic analysis system
17 p2361 N88-24063
The Department of Defense report on the merit review process for competitive selection of university research projects and an analysis of the potential for expanding the geographic distribution of research for the Committees on Appropriations, United States Congress
[AD-A191842] 18 p2588 N88-25379
The impact of disorganized occupation of urban sub-basins: Sub-basin of the Cabucu River, metropolitan area of Sao Paulo (SP) 19 p2682 N88-25945
Application of interactive graphic system (CAD/CAM) in the determination of process evolution in land use in the Ribeirao Preto municipality 19 p2684 N88-25956
Aerial photography as an instrument of municipal and regional planning: Metropolitan area of Sao Paulo (SP)
19 p2684 N88-25957
Remote sensing applied to integrated regional development programs 19 p2685 N88-25958

GEOIDS
Five-diagonal weighting scheme for geoidal profiles
[AD-A188033] 10 p1347 N88-18054
Department of Defense World Geodetic System 1984: Its definition and relationships with local geodetic systems
[AD-A188815] 12 p1639 N88-19811
Evaluation of a model of the Earth's gravity field
[EPSHOM-003/87] 17 p2373 N88-24116
The determination of gravity and topography from seismic velocities, accounting for dynamic behavior of the Earth's mantle
[ETN-88-92420] 17 p2374 N88-24117
To relate measurements of gravity and geoid anomalies over the oceans to near surface density distributions
[AD-A192168] 18 p2547 N88-25120

GEOLOGICAL FAULTS
NT AFRICAN RIFT SYSTEM
NT SAN ANDREAS FAULT
Gravity and fault structures, Long Valley Caldera, California
[DE87-014117] 02 p0197 N88-11229
Geological interpretation of a SPOT image over Kenya: The Gregory rift network of faults
03 p0343 N88-12164
The interpretation of crustal dynamics data in terms of plate motions and regional deformation near plate boundaries
[NASA-CR-181475] 03 p0349 N88-12205
Earthquake source mechanisms and transform fault tectonics in the Gulf of California
03 p0349 N88-12206
Interseismic deformation for normal fault earthquakes
03 p0349 N88-12207
Transform fault earthquakes in the North Atlantic: Source mechanisms and depth of faulting
03 p0350 N88-12208
State-of-the-art for assessing earthquake hazards in the United States. Report 26: Parameters for specifying magnitude-related earthquake ground motions
[AD-A185997] 07 p0877 N88-15319
Space photographs of the Onega-Ladoga isthmus and prediction of useful minerals 08 p1008 N88-16108
Use of space photographs for paleoseismogeological studies (on the example of Mongolian Altay)
08 p1008 N88-16110
Geomechanical model of seismofocal zone of active continental margin 08 p1011 N88-16128
State-of-the-art for assessing earthquake hazards in the US. Parameters for specifying intensity-related earthquake ground motions
[AD-A188230] 11 p1512 N88-19032
Naval weapons center active fault map series
[AD-A188425] 12 p1643 N88-19835
Ultrasonic physical modeling of seismic wave propagation from graben-like structures
[AD-A189066] 13 p1796 N88-20744
Study of fracturing for groundwater research in the Sergipe state with remote sensing products
17 p2359 N88-24052
Rate of slip on the Altin Dagh Fault (North Tibet, China) 22 p3102 N88-28420
Geologic applications of SPOT-1, TM, and NOAA-7 data: Finding and defining unmapped structural features
22 p3104 N88-28434
Mechanics of thrust fault formation
23 p3231 N88-29229
Diapirs of the Mediterranean ridge: The tectonic regime of an incipient accreted terrane
24 p3396 N88-30224
Faulting and its relation to volcanism: Mars western equatorial region 24 p3443 N88-30489

GEOLOGICAL SURVEYS
SPOT for earthquake hazard zoning in southern Italy, a provisional report 03 p0342 N88-12161
Application of SPOT-1 data to mineral exploration in Nevada 03 p0343 N88-12163
Geological interpretation of a SPOT image over Kenya: The Gregory rift network of faults
03 p0343 N88-12164
Evolution of remote sensing utilization in geological mapping and ore exploration: Example in Zimbabwe
03 p0343 N88-12165
Modern concept concerning transport of bottom sediments in abyssal regions of world ocean
06 p0728 N88-14478
Remote sensing in mineral exploration
[PB87-138558] 06 p0729 N88-14484
Space photographs of the Onega-Ladoga isthmus and prediction of useful minerals 08 p1008 N88-16108
International role of US geoscience
[NASA-CR-182407] 08 p1035 N88-16281
Solid Earth mission end-to-end data system study
[C04825.08/FR] 17 p2309 N88-23811
The use of SPOT images for water resources surveys in the Kasserine Basin (Tunisia)
22 p3090 N88-28349
Utilizing SPOT data for seismic shot-line mapping and environmental monitoring in oil and gas exploration
22 p3098 N88-28401
First results of international investigations of the applications of SPOT-1 data to geologic problems, mineral and energy exploration 22 p3101 N88-28419
Karst and submarine fresh water discharge in the Antalya area, southern Turkey 22 p3102 N88-28421
Results of the Geosat program to evaluate SPOT data for petroleum and mineral exploration
22 p3102 N88-28422
The application of SPOT data to the structural geology of western Nevada 22 p3102 N88-28423
Evaluation of SPOT imagery for discriminating vegetation communities associated with surficial and bedbrock geology and identifying anomalous and stressed vegetation associated with mineralization
22 p3103 N88-28426
Role of SPOT in geological application of remote sensing 22 p3103 N88-28428
SPOT imagery preliminary contribution to cartography and geodynamics in the Benue trough (Nigeria)
22 p3103 N88-28429
An evaluation of SPOT imagery for Earth science studies in the Antarctic. Preliminary Evaluation Program (PEPS) 289 for SPOT 22 p3103 N88-28430
Methodology for the use of SPOT imagery in petroleum exploration. Example of the Bas-Languedoc area (France) 22 p3104 N88-28432
Spectral and spatial attribute evaluation of SPOT data in geological mapping of precambrian terrains in semiarid environment of Brazil 22 p3104 N88-28436
Detailed geological mapping of the massif of Sainte Victoire (Provence, France) using SPOT imagery. Comparison with other multisource data. New tectonic interpretation of this region 22 p3105 N88-28442
Digital terrain modelling with SPOT data and geological applications 22 p3110 N88-28474
Radiometric analysis and potential of SPOT HRV imagery for applications in urban environments and geology 22 p3112 N88-28486

GEOLOGY
NT GEOCHRONOLOGY
NT GEOMORPHOLOGY
NT GLACIOLOGY
NT HYDROGEOLOGY
NT LITHOLOGY
NT MARS VOLCANOES
NT OROGRAPHY
NT PETROGRAPHY
NT PETROLOGY
NT PHOTOGEOLOGY
NT STRUCTURAL PROPERTIES (GEOLOGY)
NT SUBDUCTION (GEOLOGY)
NT TECTONICS
NT VOLCANOES
NT VOLCANOLOGY
NBS (National Bureau of Standards) research reports (April 1987)
[PB87-210258] 01 p0018 N88-10111

JPRS report: Science and technology. China
[JPRS-CST-87-032] 03 p0376 N88-12365
Summaries of physical research in the geosciences
[DE88-000833] 04 p0468 N88-12896
Research needs for hydrocarbon fuels
[DE87-014555] 06 p0687 N88-14209
The adaption and use of research codes for performance assessment
[DE88-000552] 06 p0756 N88-14639
Earth materials research: Report of a Workshop on Physics and Chemistry of Earth Materials
[NASA-CR-182519] 10 p1296 N88-17761
Geological evolution and analysis of confirmed or suspected gas hydrate localities. Volume 10: Basin analysis, formation and stability of gas hydrates of the Aleutian Trench and the Bering Sea
[DE88-001008] 10 p1346 N88-18048
New data on the formation conditions and age of the Kamensk and Gusev astroblemes
[NASA-TT-20212] 11 p1513 N88-19040
JPRS report: Science and technology. China
[JPRS-CST-88-003] 13 p1755 N88-20495
JPRS report: Science and technology. USSR: Earth sciences
[JPRS-UES-88-001] 13 p1784 N88-20674
Activities and objectives of the Polar Research Board
[DE88-004543] 13 p1797 N88-20747
JPRS report: Science and technology. China
[JPRS-CST-87-041] 14 p1902 N88-21365
Groundwater sapping valleys: Experimental studies, geological controls and implications to the interpretation of valley networks on Mars
[NASA-CR-182718] 15 p2152 N88-22847
A proposal of adaptation of a knowledge-based scene analysis model to some remote sensing problems
17 p2362 N88-24068
Geological evolution and analysis of confirmed or suspected gas hydrate localities. Volume 2: Basin analysis, formation and stability of gas hydrates in the Black Sea
[DE88-001052] 18 p2532 N88-25023
Territorial management program
19 p2682 N88-25942
Vegetation studies on Vandenberg Air Force Base, California
[NASA-TM-100985] 20 p2831 N88-26795
Mars: Near-infrared comparative spectroscopy during the 1986 opposition 23 p3301 N88-29658
Intercrater plains deposits and the origin of Martian valleys 23 p3301 N88-29661
Elemental composition of the Martian surface
23 p3302 N88-29665
Distribution and timing of thick transient air-fall deposits in Electris: Implications for the nature of the upland plains 23 p3303 N88-29674
Geology of six possible Martian landing sites
23 p3304 N88-29682
Documenting volcano-tectonic episodes in Mars' stratigraphic record 23 p3306 N88-29695
NASA MEVTV Program Working Group Meeting: Volcanism on Mars
[NASA-CR-183074] 24 p3442 N88-30487

GEOMAGNETIC ANOMALIES
U MAGNETIC ANOMALIES

GEOMAGNETIC CROTCHETS
U SUDDEN IONOSPHERIC DISTURBANCES

GEOMAGNETIC EFFECTS
U MAGNETIC EFFECTS

GEOMAGNETIC FIELD
U GEOMAGNETISM

GEOMAGNETIC MICROPULSATIONS
Monitoring of Pc3 pulsations in solar wind and at Earth by interplanetary magnetic field
08 p1002 N88-16069
Report on ground-based activity at Andoya (Norway) in relation to the Aureld-VIP high rocket and to the Viking satellite --- Swedish satellite 08 p1026 N88-16212
Field-aligned structure of the storm time Pc 5 wave of November 14-15, 1979
[AD-A193022] 21 p2972 N88-27653

GEOMAGNETIC PULSATIONS
NT GEOMAGNETIC MICROPULSATIONS
Auroral X-ray images during a pulsation event
08 p1026 N88-16214
The effects of a geomagnetic storm on thermospheric circulation
[AD-A186638] 09 p1190 N88-17128

GEOMAGNETIC STORMS
U MAGNETIC STORMS

GEOMAGNETIC TAIL
The tail lobe ion spectrometer: Theory and observations
[IFSI-86-12] 05 p0585 N88-13569
Coupling of microscopic and macroscopic processes in the Earth's magnetotail 08 p1095 N88-16588
Evidence of small-scale reconnection in the magnetosphere 08 p1097 N88-16601
Interpretation of the northward B sub z (NBZ) Birkeland current system and polar cap convection patterns in terms of the impulsive penetration model
[AERONOMICA-ACTA-A-321-1987]
18 p2595 N88-25422
Relationship between characteristics of low-energy electrons and geomagnetic disturbance in geostationary orbit 24 p3444 N88-30501

GEOMAGNETICALLY TRAPPED PARTICLES
U RADIATION BELTS

GEOMAGNETISM
Solar activity, magnetic clouds, and geomagnetic storms 01 p0115 N88-10735
Narsarsuaq (Greenland) Geophysical Observatory. Magnetic results, 1984
[ISBN-87-7478-281-9] 02 p0198 N88-11235
Solar-geophysical data number 514, June 1987. Part 1: (Prompt reports). Data for May 1987, April 1987 and late data
[PB87-217261] 02 p0257 N88-11626
Morphology of the Earth's environment
03 p0272 N88-11706
Radiation belts 03 p0272 N88-11707
Directory of geomagnetic observatories with high-resolution digital results, 1987
[PB87-221156] 03 p0348 N88-12201
Narssarssuaq Geophysical Observatory: Magnetic results, 1980-83. Instrumentation and formulas
[ISBN-87-7478-280-0] 03 p0350 N88-12209
Statistics of the geomagnetic secular variation for the past 5Ma
[NASA-CR-181558] 04 p0467 N88-12890
Tectonics and magmatism of Walvis Ridge and Discovery Rise (Atlantic Ocean)
06 p0726 N88-14463
Radar observations of high-latitude lower-thermospheric and upper-mesospheric winds and their response to geomagnetic activity 06 p0742 N88-14563
Solar-geophysical activity reports for STIP (Study of Travelling Interplanetary Phenomena) interval 15, 12-21 February 1984 ground level event and STIP interval 16, 20 April-4 May 1984 Forbush decrease
[PB88-101274] 06 p0802 N88-14906
A compilation of Sudden Storm Commencements (SSCs), associated interplanetary disturbances, and cosmic ray variations
[IFSI-86-11] 06 p0807 N88-14923
Flare doublet: Interplanetary and geomagnetic effects
08 p1001 N88-16066
FTE like variations in the geomagnetic field at ground based conjugate stations in the cusp regions
[INPE-4345-PRE/1182] 08 p1024 N88-16199
Criteria of interplanetary parameters causing intense magnetic storms (Dst less than -100nT)
[NASA-CR-182423] 08 p1024 N88-16200
Balloon measurement of magnetic field during substorms in auroral zone 08 p1026 N88-16213
Acceleration of auroral particles by magnetic field-aligned electric fields 08 p1031 N88-16246
A study of the magnetic field annihilation process in the magnetosphere and some geotechnical applications
[DE88-004165] 10 p1355 N88-18096
Energetic particle drift motions in the outer dayside magnetosphere
[DE88-005097] 11 p1512 N88-19034
Observation of a hydromagnetic wave in the earth's magnetosphere
[AD-A188942] 12 p1644 N88-19841
Proceedings of an ESA-NASA Workshop on a Joint Solid Earth Program
[NASA-CR-182642] 12 p1644 N88-19844
Spaceborne magnetometry 12 p1644 N88-19846
Magnetic results, 1985
[ISBN-8-77-478262-7] 14 p1944 N88-21600
Simultaneous observation of upward moving field aligned energetic electrons and ions on auroral zone field lines
[IRF-PREPRINT-102] 16 p2231 N88-23326
Solar-geophysical data number 520, December 1987. Part 1: (Prompt reports). Data for November 1987, October 1987 and late data
[PB88-164199] 16 p2290 N88-23712
DOD 1985 world magnetic model: Charts and grid values
[AD-A191484] 18 p2541 N88-25080
Spacecraft requirements for predictions of geomagnetic activity (a tutorial)
[AD-A191943] 19 p2685 N88-25959
Scaling laws for geomagnetic tail current sheet acceleration
[AD-A193379] 19 p2691 N88-25998

GEOMETRIC ACCURACY
Registration of SPOT images
03 p0341 N88-12155

GEOMETRIC DILUTION OF PRECISION
GPS vertical axis performance enhancement for helicopter precision landing approach
[NASA-CR-177443] 04 p0397 N88-12477
Automatic omega station and LOP (Line Of Position) selection
[AD-A193302] 21 p2894 N88-27179

GEOMETRIC RECTIFICATION (IMAGERY)
First assessment of processing and use of SPOT images by the Institut Geographique Nationale --- French National Geographic Institute 03 p0341 N88-12148
Some characteristics in synthetic aperture radar (SAR) raw data and SAR images
[FOA-C-30483-3.2] 22 p3071 N88-28232
The use of SPOT imagery on analytical photogrammetric instruments 22 p3110 N88-28471
A geometrical analysis of SPOT data
22 p3111 N88-28478

GEOMETRICAL ACOUSTICS
Elastodynamic ray theory and asymptotic methods for direct and inverse scattering problems
03 p0335 N88-12108
Application of ray theory to propagation of low frequency noise from wind turbines
[NASA-CR-178367] 03 p0373 N88-12349
Correcting ray field failures caused by focusing in an inhomogeneous duct: A critical look at the Gaussian beam method 12 p1616 N88-19663
Propagation of acoustic disturbances in transonic flow fields of lifting wings
[DFVLR-FB-88-13] 21 p3013 N88-27880

GEOMETRICAL HYDROMAGNETICS
U MAGNETOHYDRODYNAMICS

GEOMETRICAL OPTICS
Intrinsic and extrinsic geometric quality --- SPOT images 03 p0341 N88-12154
A prototype ray tracer
[AD-A184863] 05 p0634 N88-13874
Backscattering from three dimensional conducting bodies
[AD-A187570] 11 p1470 N88-18768
Scattering and depolarization by random rough terrain and vegetation covered terrain-unified full wave approach 12 p1615 N88-19657
Semiclassical theory of injected lasers with arbitrary stable and unstable resonators
[AD-A189514] 13 p1775 N88-20615
Models for electromagnetic scattering from the sea at extremely low grazing angles
[AD-A190472] 15 p2057 N88-22261

GEOMETRICAL THEORY OF DIFFRACTION
Theoretical Aspects of Target Classification
[AGARD-LS-152] 03 p0303 N88-11909
Target strength: An overview of some recent theoretical developments 03 p0303 N88-11910
Uniform geometrical theory of diffraction
03 p0303 N88-11911
Backscattering from three dimensional conducting bodies
[AD-A187570] 11 p1470 N88-18768
Seventy-meter antenna performance predictions: GTD analysis compared with traditional ray-tracing methods
11 p1474 N88-18793
Models for electromagnetic scattering from the sea at extremely low grazing angles
[AD-A190472] 15 p2057 N88-22261
Fields and waves 24 p3363 N88-30025

GEOMETRODYNAMICS
U RELATIVITY

GEOMETRY
NT ANALYTIC GEOMETRY
NT ANGLE OF ATTACK
NT ANGLES (GEOMETRY)
NT BOSE GEOMETRY
NT BRAGG ANGLE
NT CARTESIAN COORDINATES
NT CATENARIES
NT CIRCLES (GEOMETRY)
NT CIRCUMFERENCES
NT COLLINEARITY
NT COMPUTATIONAL GEOMETRY
NT CONICS
NT COPLANARITY
NT CRACK GEOMETRY
NT CUBES (MATHEMATICS)
NT CURVATURE
NT CURVES (GEOMETRY)
NT DESCRIPTIVE GEOMETRY
NT DIFFERENTIAL GEOMETRY
NT DIHEDRAL ANGLE
NT ELEVATION ANGLE
NT ELLIPSES
NT EUCLIDEAN GEOMETRY
NT FIXED POINTS (MATHEMATICS)
NT FLOW GEOMETRY
NT FRACTALS

NT GEODESIC LINES
NT HILBERT SPACE
NT HOMOTOPY THEORY
NT ICOSAHEDRONS
NT INFLECTION POINTS
NT INVARIANT IMBEDDINGS
NT LEADING EDGE SWEEP
NT LIE GROUPS
NT LINES (GEOMETRY)
NT METRIC SPACE
NT NOZZLE GEOMETRY
NT OBLATE SPHEROIDS
NT PARABOLAS
NT POINTS (MATHEMATICS)
NT POLYGONS
NT POLYHEDRONS
NT PROJECTIVE GEOMETRY
NT PROLATE SPHEROIDS
NT PYRAMIDS
NT QUADRANTS
NT RADII
NT RECTANGLES
NT RHOMBOIDS
NT RIEMANN MANIFOLD
NT S CURVES
NT SPECIMEN GEOMETRY
NT SWEEP ANGLE
NT SWEEPBACK
NT TANGENTS
NT TENSOR ANALYSIS
NT TOPOLOGY
NT TORUSES
NT TRIANGLES
NT VECTOR ANALYSIS
NT VORTICITY

TIPS-1 user's manual: Cray-1 version
[DE87-013297] 01 p0081 N88-10522

Aerodynamic design and performance of a bent-axis geometry vehicle
[DE87-013726] 02 p0124 N88-10786

The structure and reactivity of heterogeneous surfaces and study of the geometry of surface complexes
[DE88-000158] 03 p0279 N88-11754

Observations on the hydrodynamic flow visualization at ONERA
[PD-FM-8718] 04 p0444 N88-12753

The linear characteristic method in XYZ geometry
[DE87-011668] 04 p0484 N88-12984

Introduction to string field theory
[DE87-014583] 05 p0657 N88-14032

A zonal approach for the solution of coupled Euler and potential solutions of flows with complex geometries
[AD-A185465] 06 p0702 N88-14310

Eigenvectors of graphs
[AD-A185538] 06 p0765 N88-14698

Application of a full potential method for analysis of complex aircraft geometries 07 p0809 N88-14930

Horn design equations for the NBS (National Bureau of Standards) horn-type noise standards
[PB88-110226] 07 p0844 N88-15122

The information metric for univariate linear elliptic models
[AD-A186385] 07 p0911 N88-15527

A multistage mesh generator for solving the average-passage equation system
[NASA-CR-179539] 08 p0951 N88-15769

Mixed method of finite strip and finite element
[PB87-143467] 08 p0996 N88-16027

Nonlinear evolution of the internal kink mode in toroidal geometry for shaped tokamak plasmas
[DE88-003655] 08 p1087 N88-16550

A project to experimentally and theoretically examine fluid interfacial wave phenomena in a rotating cylindrical geometry: Current results and future plans
[DE88-003738] 09 p1165 N88-16984

Flat-field response and geometric distortion measurements of optical streak cameras
[DE88-002394] 09 p1168 N88-17005

A finite element analysis of adhesively bonded composite joints including geometric nonlinearity, nonlinear viscoelasticity moisture diffusion and delayed failure
[AD-A187455] 10 p1296 N88-17747

Design sensitivity analysis of nonlinear structural systems and numerical implementation with established finite element codes 10 p1344 N88-18032

Computer aided geometric design
[AD-A187324] 10 p1389 N88-18293

Optimal selection of global positioning system set to minimize emitter location errors
[AD-A189559] 12 p1579 N88-19447

An interactive user-friendly approach to surface-fitting three-dimensional geometries
[NASA-CR-4126] 12 p1682 N88-20058

Conformal geometry, Hotine's conjecture, and differential geodesy
[AD-A189265] 13 p1790 N88-20709

Campaign graphs
[DE88-005336] 13 p1831 N88-20952

Advanced probabilistic methods for quantifying the effects of various uncertainties in structural response 15 p2080 N88-22401

Boundary shape identification problems in two-dimensional domains related to thermal testing of materials
[NASA-CR-181654] 15 p2105 N88-22541

The elliptic Sinh-Gordon equation and the construction of toroidal soap bubbles
[DE88-006426] 15 p2113 N88-22585

Geometric methods and the gauge structure of Berry's phase
[DE88-006538] 15 p2127 N88-22682

Matched index laser anemometry systems for flow studies in complex geometries 16 p2203 N88-23145

Spur gears: Optimal geometry, methods for generation and Tooth Contact Analysis (TCA) program
[NASA-CR-4135] 16 p2215 N88-23216

Derivative arrays, geometric control theory and realizations of linear descriptor systems
[AD-A190882] 16 p2260 N88-23513

Hybrid particle simulation for focusing of rotating and propagating LIB 16 p2276 N88-23624

The geometric workstation, a new approach for geometric corrections of remotely sensed data 17 p2352 N88-24017

Internal fluid dynamics within a nonspinning partially liquid-filled shell due to burster rupture
[AD-A191055] 18 p2507 N88-24874

Modeling of geometric reasoning for robot programming
[ETN-88-92290] 18 p2561 N88-25202

Optical investigations of the thermal boundary layer in arc plasmas 18 p2578 N88-25313

The geometry of the Virasoro group for physicists
[DE88-007374] 18 p2586 N88-25366

Control of combustion instabilities in ramjet motors 19 p2625 N88-25574

Effect of burn-path tortuosity on the burn rate of composite propellants 19 p2630 N88-25602

How much do edges affect the ignition of a homogeneous reactive solid: Summary to date 19 p2631 N88-25608

Numerical simulations of aerodynamic contribution of flows about a space-plane-type configuration 19 p2635 N88-25632

Accurate, productive aerodynamic simulation on patched mesh systems
[AD-A192040] 19 p2714 N88-26110

Voyager imaging photometry and radiative transfer modeling of the spoke-like features in Saturn's outer B-ring 19 p2742 N88-26278

Development of liquid metal field-emission sources for use in fast repetitive opening switches
[AD-A192230] 20 p2795 N88-26583

Full-wave calculations in flux coordinates for toroidal geometry
[DE88-010131] 20 p2860 N88-26985

Aharonov-Bohm effects in disordered metals 20 p2864 N88-27008

Design and development of courseware for goniometry
[REPT-87-73] 20 p2881 N88-27106

The influence of weld metal properties, weld geometry and applied load on weld system performance
[AD-A193403] 21 p2961 N88-27588

An investigation of techniques for determination of optimum/self-optimizing systems 21 p2963 N88-27600

Automatic line network extraction from aerial imagery of urban areas through knowledge based image analysis
[AD-A193067] 21 p2965 N88-27615

Parallel solutions to geometric problems on the scan model of computation
[AD-A192321] 21 p3004 N88-27819

Geometry of superconformal manifolds, part 1
[DE88-702405] 21 p3011 N88-27863

Geometry of superconformal manifolds, part 2
[DE88-702406] 21 p3011 N88-27864

Delta wing configurations 23 p3167 N88-28860

Ice detector
[NASA-CASE-LAR-13776-1] 23 p3217 N88-29149

Cooperating knowledge-based systems
[NASA-CR-183109] 23 p3247 N88-29327

Holomorphic geometry of interacting string
[DE88-702714] 23 p3295 N88-29627

Numerical modelling of premixed flames in gaseous media 24 p3350 N88-29944

An automated computerized vision technique for determination of three-dimensional object geometry 24 p3419 N88-30348

GEOMORPHOLOGY

SPOT for earthquake hazard zoning in southern Italy, a provisional report 03 p0342 N88-12161

The impact of varves on solar physics
[NASA-CR-181519] 03 p0390 N88-12448

Geophysical-geomorphological statistical regionalization of North Atlantic 06 p0726 N88-14466

Tectonics of sedimentary cover and basement of Labrador Sea 06 p0726 N88-14468

Use of space photographs for geomorphological studies in southwestern Tajikistan 08 p1008 N88-16109

Use of space photographs for paleoseismogeological studies (on the example of Mongolian Altay) 08 p1008 N88-16110

Geological evolution and analysis of confirmed or suspected gas hydrate localities. Volume 10: Basin analysis, formation and stability of gas hydrates of the Aleutian Trench and the Bering Sea
[DE88-001008] 10 p1346 N88-18048

Geological evolution and analysis of confirmed or suspected gas hydrate localities. Volume 9: Formation and stability of gas hydrates of the Middle America Trench
[DE88-001007] 10 p1347 N88-18050

Martian geomorphology and its relation to subsurface volatiles
[NASA-CR-182428] 12 p1711 N88-20237

Project CODEAMA/FUNCATE (test-area of Barreirinha-AM): Field report
[INPE-4500-RPE/563] 15 p2090 N88-22455

Bilateral symmetry elements of the Zhamanshin impact crater
[NASA-TT-20288] 15 p2096 N88-22490

Airborne and spaceborne radar images for geologic and environmental mapping in the Amazon rain forest, Brazil 17 p2353 N88-24021

Subsurface morphology and geoarchaeology revealed by spaceborne and airborne radar 17 p2353 N88-24022

Utilization of LANDSAT-TM , for aiding in the localization of archeological sites in the state of Sao Paulo 17 p2362 N88-24089

The breaked anticlines, cuesta and crest homoclines, ortoclinal valleys, and other forms of relief outcrops delineated with the help of remote sensing imagery 17 p2366 N88-24089

Geomorphologic sector maps of Niquizanga-Mayares, province of San Juan, Argentina 17 p2368 N88-24098

Geological evolution and analysis of confirmed or suspected gas hydrate localities. Volume 2: Basin analysis, formation and stability of gas hydrates in the Black Sea
[DE88-001052] 18 p2532 N88-25023

Use of remote sensing in the study of superficial formation certifying the development of integrated economy-case example: Rio Claro (SP) region 19 p2683 N88-25950

Remote sensing applied to integrated regional development programs 19 p2685 N88-25958

MEVTV Workshop on Nature and Composition of Surface Units on Mars
[NASA-CR-183075] 23 p3300 N88-29654

The history of Martian volcanism determined from a revised relative chronology 23 p3301 N88-29657

Morphologic contrasts between Nirgal and Auqakuh Valles, Mars: Evidence of different crustal properties 23 p3304 N88-29681

Geology of six possible Martian landing sites 23 p3304 N88-29682

Stratigraphy of the Kasei Valles region, Mars 23 p3305 N88-29690

High resolution Viking Orbiter images: A useful data source for testing the viability of geomorphic processes attributed to Martian landforms 23 p3307 N88-29703

Evaluation of LANDSAT-TM data for geomorphological mapping
[INPE-4593-PRE/1324] 24 p3386 N88-30168

Eruptive viscosity and volcano morphology 24 p3442 N88-30488

The Martian highland paterae: Evidence for explosive volcanism on Mars 24 p3443 N88-30492

Physical properties of surface materials on Martian volcanoes: Dust-covered lava and ash 24 p3443 N88-30493

Rifts of deeply eroded Hawaiian basaltic shields: A structural analog for large Martian volcanoes 24 p3443 N88-30494

Small-scale volcanic landforms indicative of distributary tube systems 24 p3444 N88-30496

GEON (TRADEMARK)

U POLYVINYL CHLORIDE

GEOPHYSICAL OBSERVATORIES

Narsarsuaq (Greenland) Geophysical Observatory. Magnetic results, 1984
[ISBN-87-7478-281-9] 02 p0198 N88-11235

Directory of geomagnetic observatories with high-resolution digital results, 1987
[PB87-221156] 03 p0348 N88-12201
Narssarssuaq Geophysical Observatory: Magnetic results, 1980-83. Instrumentation and formulas
[ISBN-87-7478-280-0] 03 p0350 N88-12209
Magnetic results, 1985
[ISBN-8-77-478282-7] 14 p1944 N88-21600

GEOPHYSICAL SATELLITES
NT COSMOS SATELLITES
NT INTERCOSMOS SATELLITES
Wave structures in thermospheric density from satellite electrostatic triaxial accelerometer measurements
[AD-A194134] 23 p3233 N88-29240

GEOPHYSICS
Mathematics applied to nuclear geophysics
[INPE-4234-PRE/1109] 01 p0086 N88-10561
Solar-geophysical data number 513, May 1987. Part 1: (Prompt reports). Data for April, March 1987 and late data
[PB87-204939] 01 p0119 N88-10760
Solar-geophysical data number 513, May 1987. Part 2: (Comprehensive reports). Data for November 1986 and miscellanea
[PB87-204974] 01 p0119 N88-10761
Institute of Geophysics and Planetary Physics at Lawrence Livermore National Laboratory
[DE87-014618] 02 p0251 N88-11583
Solar-geophysical data number 514, June 1987. Part 1: (Prompt reports). Data for May 1987, April 1987 and late data
[PB87-217261] 02 p0257 N88-11626
Publications and final reports on contracts and grants, 1986 (National Environmental Satellite, Data and Information Service)
[PB87-220810] 03 p0352 N88-12218
Solar-geophysical data number 514, June 1987. Part 2: (Comprehensive reports). Data for December 1986
[PB87-217279] 03 p0390 N88-12450
USSR report: Earth sciences
[JPRS-UES-86-006] 04 p0458 N88-12831
Summaries of physical research in the geosciences
[DE88-000633] 04 p0468 N88-12896
Isotropic probability measures in infinite dimensional spaces: Inverse problems/prior information/stochastic inversion
[NASA-CR-181555] 05 p0643 N88-13936
Research needs for hydrocarbon fuels
[DE87-014555] 06 p0687 N88-14209
USSR report: Earth sciences
[JPRS-UES-87-004] 06 p0725 N88-14455
Tectonics and magmatism of Walvis Ridge and Discovery Rise (Atlantic Ocean)
06 p0726 N88-14463
Geophysical-geomorphological statistical regionalization of North Atlantic
06 p0726 N88-14466
Effective methods of gravimetric and magnetometric data processing 06 p0728 N88-14479
Polar Geophysical Institute's studies of magnetosphere, ionosphere 06 p0728 N88-14480
Solar-geophysical data number 515, July 1987. Part 1: (Prompt reports). Data for June 1987, May 1987 and late data
[PB87-233177] 06 p0805 N88-14912
Solar-geophysical data number 515, July 1987. Part 2: (Comprehensive reports). Data for January 1987 and miscellanea
[PB87-233185] 06 p0805 N88-14913
Solar-geophysical data number 515, July 1987. Supplement (explanation of data reports)
[PB87-233169] 06 p0805 N88-14914
Solar-geophysical activity reports for STIP (Study of Travelling Interplanetary Phenomena) Interval 15, 12-21 February 1984 ground level event and STIP Interval 16, 20 April-4 May 1984 Forbush decrease
[PB87-232658] 06 p0805 N88-14915
USSR report: Earth sciences
[JPRS-UES-87-003] 08 p1009 N88-16119
Processes in the quiet and disturbed equatorial-low latitude ionosphere: Sundial campaign, 1984
[INPE-4152-PRE/1057] 08 p1036 N88-16282
Interplanetary and geophysical effects of a coronal transient 08 p1095 N88-16587
Earth materials research: Report of a Workshop on Physics and Chemistry of Earth Materials
[NASA-CR-182519] 10 p1298 N88-17761
Three-dimensional transient electromagnetic modeling for exploration geophysics 10 p1346 N88-18047
Solar-geophysical data number 517, September 1987. Part 1: (Prompt reports). Data for August, July 1987 and late data
[PB88-128426] 10 p1430 N88-18544
Solar-geophysical data number 517, September 1987. Part 2: (Comprehensive reports). Data for March 1987 and miscellanea
[PB88-128434] 10 p1431 N88-18545
AFGL (Air Force Geophysics Laboratory) fiscal year 1988 Air Force technical objectives document
[AD-A187701] 11 p1503 N88-18977
An adaptive grid finite difference method for time-dependent Magnetohydrodynamic (MHD) flows and its astrogeophysical applications
11 p1553 N88-19294
Geophysical study of the structure and processes of the continental convergence zones: Alpine-Himalayan Belt
[NASA-CR-182647] 12 p1644 N88-19842
Proceedings of an ESA-NASA Workshop on a Joint Solid Earth Program
[NASA-CR-182642] 12 p1644 N88-19844
Solar-geophysical data number 518, October 1987. Part 2: (Comprehensive reports). Data for April 1987
[PB88-138060] 12 p1711 N88-20242
Solar-geophysical data number 518, October 1987. Part 1: (Prompt reports). Data for September 1987, August 1987 and late data
[PB88-138078] 12 p1712 N88-20243
Interactive automated system for testing analog units of digital seismic stations 13 p1789 N88-20702
Inversion algorithms for geophysical problems
[AD-A189252] 13 p1815 N88-20845
Physics of condensed matter at extreme conditions
[DE88-006232] 13 p1832 N88-20958
ONR Far East Scientific Bulletin, volume 12, number 3, July-September 1987
[AD-A188554] 13 p1851 N88-21081
The Spring 1985 high precision baseline test of the JPL GPS-based geodetic system
[NASA-CR-182686] 14 p1940 N88-21577
Solar-geophysical data number 519, November 1987. Part 2: (Comprehensive reports). Data for May 1987 and miscellanea
[PB88-158910] 14 p2011 N88-21997
A hardware/software system for implementing geophysical diffraction tomography
[DE88-006411] 15 p2094 N88-22480
Bilateral symmetry elements of the Zhamanshin impact crater
[NASA-TT-20288] 15 p2096 N88-22490
Solar-geophysical data number 520, December 1987. Part 1: (Prompt reports). Data for November 1987, October 1987 and late data
[PB88-164199] 16 p2290 N88-23712
An integrated study of the Alto Paranaiba Kimberlite Province, Minas Gerais, Brazil: A possible tool for diamond exploration 17 p2355 N88-24031
Remote sensing of acoustic properties of shallow water sediments: A review
[AD-A192107] 18 p2570 N88-25267
Geophysical monitoring for climatic change, number 15
[PB88-180146] 19 p2692 N88-26003
Solar-geophysical data number 521, January 1988. Part 1: (Prompt reports). Data for December 1987, November 1987 and late data
[PB88-179213] 19 p2743 N88-26284
Solar-geophysical data number 521, January 1988. Part 2: (Comprehensive reports). Data for July 1987 and miscellanea
[PB88-179221] 19 p2743 N88-26285
Reports of planetary geology and geophysics program, 1987
[NASA-TM-4041] 20 p2885 N88-27133
Solar-geophysical data number 522, February 1988. Part 2: (Comprehensive reports). Data for August 1987 and miscellanea
[PB88-194741] 20 p2886 N88-27138
Solar-geophysical data number 522, February 1988. Part 1: (Prompt reports). Data for January 1988, December 1987 and late data
[PB88-194733] 20 p2886 N88-27139
Development of radiation and cloud parameterization programs for AFGL (Air Force Geophysics Laboratory) global models
[AD-A193369] 21 p2973 N88-27658
Program to increase the measurement capabilities of the AFGL (Air Force Geophysics Laborstory) fixed and mobile high altitude lidar systems
[AD-A194614] 23 p3203 N88-29063
Solar-geophysical data number 523, March 1988. Part 2: (Comprehensive reports). Data for September 1987 and miscellanea
[PB88-212774] 24 p3458 N88-30576

GEOPOTENTIAL
NT GEOPOTENTIAL HEIGHT
The contraction of satellite orbits under the influence of air drag. Part 8: Orbital lifetime in an oblate atmosphere, when perigee distance is perturbed by odd zonal harmonics in the geopotential
[RAE-TR-86069-PT-8] 01 p0010 N88-10058
A study of a satellite-to-satellite tracking configuration by application of linear perturbation theory
[REPT-86.3] 01 p0011 N88-10059
Estimability of potential coefficients from orbit perturbations — satellite geodesy
[REPT-86.1] 01 p0064 N88-10408
Advanced simulation and analysis of a geopotential research mission
[NASA-CR-182355] 06 p0670 N88-14108
Simulation and analysis of a geopotential research mission
[NASA-CR-182354] 06 p0670 N88-14109
Estimation of geopotential from satellite-to-satellite range rate data: Numerical results
[NASA-CR-180771] 14 p1941 N88-21583
Modeling and estimation of a low degree geopotential model from terrestrial gravity data
[NASA-CR-182808] 16 p2232 N88-23330

GEOPOTENTIAL HEIGHT
Mean pressure distribution and geostrophic circulation in the meteor zone 06 p0734 N88-14513
New possibilities for using gravity data in developing geodetic coordinate systems 08 p1009 N88-16116
Persistence characteristics of 500 mb blocking and zonal flows in the mid-latitudes of the Northern and Southern Hemispheres 10 p1353 N88-18088
Monthly mean global climatology of temperature, wind, geopotential height, and pressure for 0 - 120 km
[NASA-TM-100697] 15 p2099 N88-22503
Global atmospheric circulation statistics, 1000-1 mb
[PB88-168240] 16 p2234 N88-23340
The relative utility of persistence and medium-range dynamical forecasts of monthly mean 700 mb heights
22 p3127 N88-28588

GEOPOTENTIAL RESEARCH MISSION
An orbit simulation study of a geopotential research mission including satellite-to-satellite tracking and disturbance compensation systems
[NASA-CR-182353] 07 p0823 N88-14997

GEOPRESSURE
Geothermal energy technology: Issues, R and D (Research and Development) and cooperative arrangements
[PB88-193107] 21 p2967 N88-27626

GEOS SATELLITES (ESA)
A European apogee boost motor for GEOS
09 p1123 N88-16719

GEOS SATELLITES (ESRO)
U GEOS SATELLITES (ESA)

GEOS 2 SATELLITE
Interplanetary Magnetic Field (IMF) influence on the magnetic configuration and particle fluxes at geostationary orbit and on the substorm onset
08 p1031 N88-16247

GEOS-B SATELLITE
U GEOS 2 SATELLITE

GEOSAT SATELLITES
GEOSAT altimeter geophysical data record user handbook
[PB87-213336] 03 p0276 N88-11743
Geosat crossover analysis in the tropical Pacific. Part 1: Constrained sinusoidal crossover adjustment
[NASA-CR-182391] 07 p0871 N88-15285

GEOSTATIONARY OPERATIONAL ENVIRON SATS
U GOES SATELLITES

GEOSTATIONARY PLATFORMS
U SYNCHRONOUS PLATFORMS

GEOSTATIONARY SATELLITES
U SYNCHRONOUS SATELLITES

GEOSTROPHIC WIND
An improved method of analyzing surface geostrophic winds and pressure 02 p0212 N88-11334
Mean pressure distribution and geostrophic circulation in the meteor zone 06 p0734 N88-14513
A study of the mechanism of internal gravity wave generation by quasigeostrophic meteorological motions
06 p0735 N88-14520
Longitudinal peculiarities of meridional circulation in lower thermosphere and mesosphere
06 p0736 N88-14525
Analysis of quasi-geostrophic forcing during the AIMCS (Airborne Investigations of Mesoscale Convective Systems) Project. Volume 2: Results for June 14 through July 16, 1984
[PB88-123807] 10 p1354 N88-18092
Analysis of quasi-geostrophic forcing during the AIMCS (Airborne Investigations of Mesoscale Convective System) Project. Volume 1: Discussion
[PB88-133095] 12 p1646 N88-19860

Contribution to theory of quasigeostrophic motions of finite amplitude in viscous stratified ocean
13 p1788 N88-20695
Physical process for maintenance of mean meridional and zonal circulation of atmosphere in middle latitudes, volume 2
14 p1900 N88-21345
Geostrophic flow in the central Bering Sea, Fall 1986 and Summer 1987
[PB88-174354] 16 p2237 N88-23360
Three-dimensional temperature fields in the atmosphere up to 50 km altitude
[ETN-88-92150] 18 p2542 N88-25089
Modelling and forecasting deep ocean and near surface mesoscale eddies: Hindcasting and forecasting with, and coupling a surface boundary layer model to, the Harvard quasigeostrophic model
19 p2694 N88-26013

GEOSYNCHRONOUS EARTH ORBITAL ENVIRONMENTS
U EARTH ORBITAL ENVIRONMENTS

GEOSYNCHRONOUS ORBITS
The geosynchronous plasma environment
03 p0273 N88-11716
External surface charging mechanisms — spacecraft
03 p0273 N88-11719
An allotment planning concept and related computer software for planning the fixed satellite service at the 1988 space WARC
[NASA-TM-100244] 03 p0308 N88-11944
Planning for future operational sensors and other priorities
[PB87-220802] 03 p0325 N88-12056
Observation guidelines for a Total Ozone Mapping Spectrometer (TOMS) in geosynchronous orbit
05 p0619 N88-13801
A laser communication experiment utilizing the ACT satellite and an airborne laser transceiver
[NASA-TM-100792] 11 p1492 N88-18910
Study of the optimization of satellite system design for transfer orbit
[MBB-URV-135] 13 p1727 N88-20332
Spacecraft trajectories
[ISBN-2-85-428166-7] 15 p2023 N88-22054
Centaur operations at the space station
[NASA-CR-179593] 19 p2606 N88-25473
Relationship between characteristics of low-energy electrons and geomagnetic disturbance in geostationary orbit
24 p3444 N88-30501

GEOTECHNICAL ENGINEERING
Siting and Geotechnical Program Focus and Directions. Report upon the deliberations of a workshop held at the Illinois Institute of Technology, Chicago, Illinois on August 4-5, 1986
[PB87-206272] 02 p0198 N88-11238
Error analysis for geotechnical engineering
[AD-A186795] 09 p1189 N88-17124
A study of the magnetic field annihilation process in the magnetosphere and some geotechnical applications
[DE88-004165] 10 p1355 N88-18096
Computer Applications in Geotechnical Engineering (CAGE) and Geotechnical aspects of the Computer-Aided Structural Engineering (G-CASE) projects. User's guide. UTEXAS2 slope-stability package. Volume 1: User's manual
[AD-A187674] 11 p1511 N88-19025

GEOTEMPERATURE
Determining deep heat flow under complex geothermal conditions
08 p1011 N88-16130

GEOTHERMAL ANOMALIES
Metamorphic P-T paths and Precambrian crustal growth in East Antarctica
24 p3395 N88-30218

GEOTHERMAL ENERGY CONVERSION
Status of the Magma Energy Project
[DE88-002413] 13 p1792 N88-20719
Overview of recent activities in the Heat Cycle Research Program
[DE88-005544] 13 p1795 N88-20738

GEOTHERMAL ENERGY EXTRACTION
Recent progress in magma energy extraction
[DE87-013083] 01 p0066 N88-10424
Status of the Magma Energy Project
[DE88-002413] 13 p1792 N88-20719

GEOTHERMAL ENERGY UTILIZATION
Tapping the earth's geothermal resources: Hydrothermal today, magma tomorrow
[DE87-014718] 02 p0196 N88-11223
Application of Organic Rankine Cycles (ORCs) to decentralized power generation, preliminary study
[DE87-753331] 03 p0347 N88-12197
Advanced geothermal technologies
[DE88-004307] 15 p2091 N88-22463
Prospects for hot dry rock in the future
[DE88-010909] 20 p2820 N88-26730

GEOTHERMAL RESOURCES
Tapping the earth's geothermal resources: Hydrothermal today, magma tomorrow
[DE87-014718] 02 p0196 N88-11223
Overview of recent activities in the Heat Cycle Research Program
[DE88-005544] 13 p1795 N88-20738
Advanced geothermal technologies
[DE88-004307] 15 p2091 N88-22463
Prospects for hot dry rock in the future
[DE88-010909] 20 p2820 N88-26730
Unstable heat pipes
[DE88-010780] 23 p3229 N88-29217

GEOTHERMAL TECHNOLOGY
Thin films for geothermal sensing
[DE88-000154] 03 p0326 N88-12061
Advanced geothermal technologies
[DE88-004307] 15 p2091 N88-22463
Prospects for hot dry rock in the future
[DE88-010909] 20 p2820 N88-26730
Geothermal energy technology: Issues, R and D (Research and Development) and cooperative arrangements
[PB88-193107] 21 p2967 N88-27626

GEOTHERMOMETRY
U GEOTEMPERATURE

GEP TELESCOPES
U PARTICLE TELESCOPES

GERDIEN ARC HEATERS
U ARC HEATING
U HEATING EQUIPMENT

GERMAN INFRARED LABORATORY
An infrared grating spectrometer for GIRL
[ETN-88-91071] 09 p1167 N88-16997

GERMANIUM
Si - SiO2 interfaces: A High Resolution Transmission Electron Microscopy (HRTEM) study
[DE87-012255] 01 p0028 N88-10181
Effect of high-temperature annealing on the microstructure and thermoelectric properties of GaP doped SiGe
[NASA-TM-100164] 01 p0029 N88-10188
Thermal expansion of some Ge-Se-Te glasses
[PD-MT-8722] 04 p0420 N88-12606
Studies on some Ge-Se-Te glasses
[PD-MT-8721] 04 p0420 N88-12607
The influence of phosphorus on the solid state reaction between copper and silicon or germanium
[ETN-88-91361] 06 p0789 N88-14838
The migration of grain boundaries in ceramic materials with particular reference to the sintering process
[DE88-004085] 10 p1306 N88-17808
Preparation and characterization of Cu2Zn1-xMnxGeS4
[AD-A188113] 11 p1556 N88-19315
Development of Si/SiGe heterostructures
[AD-A189527] 13 p1845 N88-21044
Optical study of germanium, germanium plus arsenic, and germanium plus gallium implants in gallium arsenide
[AD-A189600] 13 p1845 N88-21045
Fundamental properties and devices applications of Ge(x)Si(1-x)/Si superlattices
[AD-A190129] 15 p2143 N88-22787
Interface formation and precursory dynamics
[AD-A190741] 15 p2144 N88-22794
Interaction of slow neutrons with Ge74 single crystals
[DE87-703010] 17 p2445 N88-24536
Defects in high-mobility semiconductor systems
[AD-A191618] 19 p2732 N88-26224
Influence of the interface on the crystallization of amorphous Ge in Pb/Ge multilayers
[DE88-010072] 22 p3156 N88-28776
Low temperature film growth of the oxides of zinc, aluminum and vanadium (and related systems, oxides of gold and germanium, nitrides of aluminum and tungsten) by reactive sputter deposition
[AD-A193497] 23 p3191 N88-28986
Development of a unit cell for a Ge:Ga detector array
[NASA-CR-177445] 24 p3375 N88-30100

GERMANIUM ALLOYS
Factors determining the morphology of precipitation in aluminum-germanium and aluminum-silicon alloys
[DE87-014682] 03 p0287 N88-11806
Stability diagrams for epitaxial strained layers
[DE88-003935] 10 p1418 N88-18470
Optimisation of the thermoelectric figure of merit of modified silicon germanium alloys
[AD-A191347] 16 p2283 N88-23670
Preparation of improved PbSnTe thermoelectric alloys and evaluation of their figure of merit
[AD-A191346] 17 p2445 N88-24538
Improved properties of SiGe/GaP alloys
[NASA-CASE-NPO-17259-1-CU] 18 p2585 N88-25358
Metastability in SiGe/Si strained-layer structures
[DE88-007603] 18 p2585 N88-25361
Hydrogenated amorphous silicon-germanium alloys
[DE88-001147] 19 p2620 N88-25546
Calculation of the specific and volumetric enthalpies of Ge-Si alloys
[DE88-008949] 21 p3026 N88-27965

GERMANIUM COMPOUNDS
Silicon-germanium heterostructures
13 p1844 N88-21034
Improved GaP doped SiGe thermoelectric material
17 p2437 N88-24503
Photorefractive damage mechanism in electro-optic materials
[AD-A194560] 23 p3282 N88-29543

GERMANIUM DIODES
An investigation of the equivalent circuit and carrier lifetimes of Si/SiGe heterostructure p-n diodes for frequencies between 0.5 and 18.5 MHz
[FOA-C-30469-3.2] 09 p1256 N88-17529

GERMANIUM RECTIFIERS
U GERMANIUM DIODES

GERMANY
History of aeroelasticity in Germany from the beginning to 1945
[ESA-TT-1082] 24 p3319 N88-29767

GET AWAY SPECIALS (STS)
Low frequency VLBI in space using GAS-Can satellites: Report on the May 1987 JPL Workshop
[NASA-CR-182362] 06 p0801 N88-14904
The 1987 Get Away Special Experimenter's Symposium
[NASA-CP-2500] 10 p1286 N88-17691
Microgravity research at the University of Mexico: Experiments in payload G-006
10 p1286 N88-17692
Materials processing in space: An introduction to the G-480 payload
10 p1287 N88-17695
Ten past and ten future GAS/MAUS-payloads
10 p1287 N88-17696
An update to the MITRE/WPI Space Shuttle Program GASCAN G-408
10 p1287 N88-17697
Electrochemical growth of linear conducting crystals in microgravity
10 p1287 N88-17698
Planet X probe: A fresh new look at an old familiar place
10 p1287 N88-17699
Protein-crystal growth experiment (planned)
10 p1287 N88-17700
The photons payload, G-494: A learning experience
10 p1288 N88-17701
A payload for investigating the influence of convection on GaAs crystal growth
10 p1288 N88-17702
An advanced microcomputer design for processing of semiconductor materials
10 p1288 N88-17703
Project Explorer takes its second step: GAS-608 in engineering development
10 p1288 N88-17707
GAS 450: A space payload for the People Central Coast Student Experimenters
10 p1289 N88-17709
The NORSTAR Program: Space shuttle to space station
10 p1289 N88-17710
Lightsats and their attraction to budget oriented Federal agencies
10 p1289 N88-17711
GAS eleven node thermal model (GEM)
10 p1289 N88-17712
Aerospace payload support systems
[AFGL-TR-87-0241] 24 p3334 N88-29843

GETTERS
A new polymer-based hydrogen getter
[DE88-004538] 13 p1751 N88-20467

GIACOBINI-ZINNER COMET
An overview of STIP interval 18: September 1985, the G-Z encounter
01 p0116 N88-10741
Comparative plasma tails of Venus and comets
01 p0116 N88-10742
The status of the international Halley watch
01 p0116 N88-10744
Large-scale interaction of the solar wind with comets Halley and Giacobini-Zinner
01 p0117 N88-10745
Solar wind-cometary interaction at the ionopause and associated phenomena
01 p0117 N88-10748
Space missions to Comets Halley and Giacobini-Zinner
03 p0272 N88-11712
Analysis of the ICE combiner for multiple antenna arraying
04 p0436 N88-12704
A comparison between wave observations performed in the environments of Comets Halley and Giacobini-Zinner
14 p1996 N88-21896
Narrow-band photometry of Comet P/Giacobini-Zinner at the time of ICE encounter
14 p1998 N88-21911
Gas coma of Comet Giacobini-Zinner: Emission from grains
14 p2000 N88-21923
Determination of the content of CO(+) and H2O(+) ions in the tail of Comet Giacobini-Zinner and Comet Halley
14 p2006 N88-21964

GIANT STARS
NT ASYMPTOTIC GIANT BRANCH STARS
NT CARBON STARS
NT RED GIANT STARS
Mass loss
02 p0253 N88-11597

A re-examination of the corona-wind dividing line: Diagnostics of non-coronal atmospheres
04 p0504 N88-13101
Atmospheres of stars in the limits of thick and thin convection zones: M giants 04 p0505 N88-13105
Carbon abundances and C12/C13 ratios in M giants
04 p0515 N88-13167
JHK photometry of CN-rich field giants
04 p0516 N88-13175
A comprehensive exploration of late-type stars in the far-ultraviolet 04 p0520 N88-13194
AGB (Asymptotic Giant Branch): Star evolution
[DE88-001829] 07 p0945 N88-15742
Spectroscopic determinations of surface gravities of giant stars, and ultraviolet observations of RR Lyrae and X Arietis 11 p1569 N88-19391
Review of the theoretical changes of surface chemistry during massive star evolution
[SER-C-PREPUBL-FASC-17] 18 p2593 N88-25411
Asymptotic giant branch stars in the Infrared Astronomical Satellite (IRAS) catalogs: Selection and analysis of the population characteristics
[MPE-PREPRINT-116] 22 p3163 N88-28840

GIBBS FREE ENERGY
Certain questions of thermodynamic theory of weak solutions 18 p2586 N88-25368

GIMBALS
Balloon-borne three-meter telescope for far-infrared and submillimeter astronomy
[NASA-CR-182310] 09 p1262 N88-17565
Experience with duplex bearings in narrow angle oscillating applications 14 p1926 N88-21484
On the torque and wear behavior of selected thin film MOS2 lubricated gimbal bearings
14 p1926 N88-21485
Two gimbal bearing case studies: Some lessons learned 14 p1927 N88-21487
Utilization of the IR telescope gimbaling system as a stabilized pointing platform for balloon payloads. Volume 1: Technical results
[NASA-CR-179339] 18 p2522 N88-24962

GIOTTO MISSION
Space missions to Comets Halley and Giacobini-Zinner 03 p0272 N88-11712
Data processing of the JPA instrument. Part 1: Data management
[IFSI-86-15-PT-1] 06 p0757 N88-14645
Giotto: A mission to Halley's Comet
09 p1127 N88-16756
Energy spectra of pick-up ions recorded during the encounter of Giotto with Comet Halley
14 p1997 N88-21901
Observation of energetic particles (E greater than 30 keV) by the Giotto experiment EPA in the magnetic cavity of Comet Halley 14 p1997 N88-21903
Evidence for first polymer in Comet Halley: Polyoxymethylene 14 p1997 N88-21906
The Giotto extended mission
14 p2005 N88-21957
Alternative cometary targets for the Giotto extended mission 14 p2010 N88-21990

GIRDERS
Deformation induced cracking in steel girder bridges and retrofit guidelines
[PB88-102710] 07 p0868 N88-15265

GLACIAL DRIFT
The unsteady ground heat flow at the contact surface between a glacier run and the subsoil
08 p1014 N88-16147
Large ice masses: Characteristics, behaviour and relation to climate 14 p1939 N88-21569

GLACIERS
Energy balance and discharge of an Alpine glacier, illustrated by Mount Vernagtferner in the Oetzal Alps, Tyrol 08 p1014 N88-16145
Vertical sounding of th air layer close to a glacier on Mount Vernagferner in the Oetzal Alps, Tyrol (experiment LUZIVER 1983) 08 p1015 N88-16152
Large ice masses: Characteristics, behaviour and relation to climate 14 p1939 N88-21569
Topography of an Antartic ice stream
22 p3092 N88-28361

GLACIOFLUVIAL DEPOSITS
U GLACIAL DRIFT

GLACIOLOGY
NASA Oceanic Processes Program
[NASA-TM-4025] 10 p1357 N88-18109
SPOT image exploitation for glacial mass balance fluctuation monitoring in the French Alps
22 p3090 N88-28350
Topography of an Antartic ice stream
22 p3092 N88-28361

GLANDS (ANATOMY)
NT ADRENAL GLAND
NT HYPOTHALAMUS
NT PITUITARY GLAND
NT TESTES

GLASS
NT BOROSILICATE GLASS
NT E GLASS
NT GLASS FIBERS
NT METALLIC GLASSES
NT S GLASS
NT SILICA GLASS
NT SPIN GLASS
Ion-implantation-induced stress in glasses: Variation of damage mode efficiency with changes in glass structure
[DE87-013523] 01 p0028 N88-10175
Mechanism of mechanical fatigue of fused silica
[DE87-014199] 02 p0152 N88-10950
Stress measurements in sol-gel films
[DE87-014467] 02 p0153 N88-10955
Study of the micromechanical behavior of a SiO2-Al2O3-Li2O glass ceramic and its relation to the microstructure
[ISAL-ITC1-87-01] 02 p0153 N88-10960
Preparation of oxide glasses from metal alkoxides by sol-gel method
[NASA-TT-20124] 02 p0154 N88-10965
Some speculations on the mechanisms of abrasive grinding and polishing
[DE87-014242] 02 p0181 N88-11126
Carbon fiber reinforced glass matrix composites for space based applications
[AD-A184355] 04 p0410 N88-12546
Thermal expansion of some Ge-Se-Te glasses
[PD-MT-8722] 04 p0420 N88-12606
Reliability of Li/SO2 cells for long-life applications
[DE88-001360] 04 p0440 N88-12735
Composite materials with glass matrix
[SGR/PR-4305/86-SV/JC] 05 p0558 N88-13394
Ionic transport and electrical relaxation in glass
[DE88-000887] 05 p0657 N88-14028
Material design of high-purpose glass discussed
06 p0675 N88-14133
Reactions and bonding between glasses and titanium
[DE88-000603] 06 p0685 N88-14195
Glassy GeO2 obtained by the gel process
[NASA-TT-20125] 06 p0685 N88-14201
Material design of high performance glasses discussed 06 p0688 N88-14216
Photoinduced low-temperature changes in optical losses in fiber optics based on chalcogenide glasses
06 p0770 N88-14731
Fracture study of windshield glass panes
06 p0799 N88-14891
Diffraction by glasses with a layer structure
[DE88-003059] 07 p0837 N88-15078
Development of composite polymer-glass edge claddings for Nova laser disks
[DE88-002389] 07 p0860 N88-15220
The development of test methodology for testing glassy materials 07 p0927 N88-15633
Processing and interfacial analysis of glass-ceramic to metal seals
[DE88-002999] 08 p0971 N88-15873
Review of nucleation and incipient boiling under pool and forced convection conditions
08 p0982 N88-15938
JPRS report: Science and technology. USSR: Physics and mathematics
[JPRS-UPM-87-010] 08 p1075 N88-16485
Study of the micromechanical properties of fluor glasses based on ZrF4
[ISAL-ITC1-87-03] 09 p1148 N88-16882
LFCM (Liquid-Fed Ceramic Melter) vitrification technology
[DE88-003441] 09 p1149 N88-16887
Models for ionic transport in glass
[DE88-002860] 10 p1304 N88-17799
Metal modification for improved glass-ceramic to metal seals: 1. Auger results on ion implantation and vapor deposition films
[DE88-005244] 10 p1339 N88-18006
Crystallization and glass formation in electron and laser beam irradiated Cu-Zr alloys
[DE88-003390] 11 p1464 N88-18729
Phosphorus oxynitride glass for laser applications
[DE88-005413] 12 p1632 N88-19768
Fast protonic conducting solid electrolytes
[AD-A188524] 12 p1698 N88-20160
Materials Research Laboratory at Brown University
[AD-A188006] 13 p1739 N88-20396
Processing of glass to aluminum (low melting metals) seals via an injection molding technique
[DE88-004689] 13 p1751 N88-20468
Nonlinear refractive index measurements of glasses and crystals
[DE88-005673] 13 p1840 N88-21009
Theoretical studies on the electronic structure and properties of complex ceramic crystals and glasses
[DE88-005837] 13 p1846 N88-21049
Interface structure and properties of alumina/glass ceramic composites
[DE88-006219] 14 p1892 N88-21302
Determination of the modulus of elasticity of structural silicone sealants
[PB88-157458] 14 p1893 N88-21307
Anisotropy of light absorption by color centers in waveguides produced on photochromic glasses by diffusion 14 p1896 N88-21320
Radiation absorption in neodymium glasses during passage of strong laser pulse 14 p1969 N88-21757
Fluids, gels and glasses under extreme conditions of pressure and temperature
[AD-A190655] 15 p2035 N88-22125
Fracture toughness of silicon nitride-silicon nitride joints bonded with oxynitride glass
[DE88-005548] 15 p2043 N88-22172
Containerless glass melting 15 p2051 N88-22222
Solar cell cover glasses for satellites
15 p2052 N88-22225
Magnetic anomalies in the rare earth oxide superconductors GdBa2Cu3O(7-x) and YbBa2Cu3O(7-x)
[AD-A190713] 15 p2144 N88-22793
Remarks on solid state amorphizing transformations
[DE88-006452] 15 p2145 N88-22803
Fast ion conducting glasses
[AD-A191412] 16 p2183 N88-23010
Investigation of non-linear optical behavior of semiconductors for optical switching, volume 1
[AD-A191297] 16 p2274 N88-23611
Noncontact temperature measurement in glass and other transparent materials 17 p2328 N88-23900
Apparatus for the measurement of resistivity of glasses and ceramics 17 p2431 N88-24450
Glass forming ranges of amorphous alloys
[DE88-007897] 20 p2772 N88-26438
Statistical mechanics of polymer systems
[DE88-011172] 20 p2778 N88-26477
Semiconductor microcrystallites in porous glass and their applications in optics 20 p2863 N88-27005
Fabrication of SiC fiber reinforced glass matrix by extrusion process and investigation of its mechanical properties
[ETN-88-92367] 21 p2906 N88-27244
Preparation and properties of new inorganic glasses and gel-derived solids
[AD-A192922] 21 p2917 N88-27315
Performance evaluation of large-area glass-mirror heliostats
[DE88-011883] 21 p2969 N88-27636
Metal halide optical glasses
[AD-A193794] 23 p3198 N88-29032
Ion exchange processes for fabrication of integrated optical waveguide structures into glass substrates
[VTT-46] 24 p3429 N88-30405

GLASS COATINGS
Short fiber reinforced thermoplastic composites for armor applications: Interfacial bonding
[DE88-004007] 10 p1295 N88-17742
Improved glass-ceramic to metal seals in actuator and detonator applications with an aluminum-containing austenitic stainless steel
[DE88-004691] 13 p1749 N88-20458
SBIR-Long fluoride fiber
[AD-A188595] 13 p1754 N88-20492
The Time-Temperature-Transformation (TTT) diagram as a basis for relating the formation and properties of reactive coatings
[AD-A190872] 16 p2182 N88-23006

GLASS FIBER REINFORCED PLASTICS
The influence of microvoids on the electrical strength of glass fiber reinforced epoxy resins
[ETN-87-90443] 01 p0030 N88-10189
Interactive buckling effects in stiffened FRP panels
[ARE-TM(UMS)-87204] 01 p0059 N88-10378
Determination of through-plane shear moduli for glass-reinforced plastics
[PB87-106274] 04 p0418 N88-12592
In-situ characterization of the interface of glass reinforced composites
[AD-A185136] 05 p0557 N88-13391
Fractographic study of fiber composites
06 p0677 N88-14146
Experimental and theoretical investigation of mechanically fastened composites
[AD-A185896] 07 p0826 N88-15008

To determine the stress distribution in the vicinity of GRP end pads where the specimen is held and loaded (CFC coupon specimens) --- glass reinforced plastic (GRP) carbon fiber composite (CFC)
[BAE-WST-R-RES-CFC-12023] 09 p1182 N88-17080
Further tests to determine the stress distribution in the vicinity of GRP end pads where the specimen is held and loaded (CFC coupon specimens) --- glass reinforced plastic (GRP) carbon fiber composite (CFC)
[BAE-WST-R-RES-CFC-12023-ADD-1] 09 p1182 N88-17081
Studies of traverse impact damage in composite materials using a Hopkinson pressure-bar technique
[OUEL-1706/87] 14 p1883 N88-21255
Study of strength characteristics of glass-reinforced plastic by acoustic emissions method 14 p1885 N88-21268
Rocket motor case materials. An evaluation of new fibers for composites
[FOA-C-20696-2.1] 21 p2906 N88-27245
Development of a glass fiber wing following the construction regulation FAR Part 23
[ETN-88-92966] 23 p3189 N88-28979

GLASS FIBERS
Effects of solvent exposures on poly(etheretherketone) (PEEK) and PEEK-fiberglass composites
[MLM-3405] 03 p0281 N88-11766
Development and application of composites 03 p0286 N88-11795
A creep measurement of unidirectional epoxy-fiberglass rod
[DE87-014812] 04 p0411 N88-12553
A hybrid fibreglass-CFRP cloth for new furnishings --- aircraft cabins
[SNIAS-872-111-109] 05 p0558 N88-13396
High temperature adhesive
[PB87-109229] 06 p0683 N88-14186
Evaluation of the thermal effectiveness of urethane foam and fiberglass as insulation systems for tank cars
[PB88-100797] 06 p0686 N88-14207
Interfacial shear strength of pitch and high strain pan fibers in an epoxy matrix
[AD-A185966] 07 p0826 N88-15011
The strength of hybrid composites
[BR101991] 09 p1138 N88-16821
Fabrication and materials evaluation of high performance aligned ceramic fibre reinforced glass matrix composite
[AERE-R-12517] 10 p1294 N88-17736
Lunar fiberglass: Properties and process design
[NASA-CR-182580] 11 p1466 N88-18740
Mast material test program (MAMATEP)
[NASA-TM-100821] 12 p1604 N88-19592
Fibrous glass aerosols: A literature review
[AD-A188420] 12 p1672 N88-20008
Use of reinforced inorganic cement materials for spark wire and drift chamber wire frames
[NASA-CR-180759] 13 p1746 N88-20438
SBIR-Long fluoride fiber
[AD-A188595] 13 p1754 N88-20492
Dependence of formation of radiative color centers in optical glass fibers on technological factors 14 p1896 N88-21321
Corrosion and fatique properties of FeCrB/Si metallic glass wires in aqueous environments 17 p2320 N88-23855
Sol/gel processing techniques for glass matrix composites
[AD-A191748] 18 p2478 N88-24701
Calculational model development for fibrous thermal insulation transient test procedures
[DE88-007843] 18 p2493 N88-24789
Novel fiber preforms: Rare earth doping
[AD-A191549] 18 p2575 N88-25294
Investigation of leaks in fiberglass-reinforced pressure vessels by direct observation of hollow fibers in glass cloth
[DE88-006936] 19 p2609 N88-25485
Excitation of single-mode glass fiber by partially coherent sources
[ETN-88-92121] 20 p2854 N88-26951
Effects of electron beam irradiation on mechanical properties at low and high temperature of fiber reinforced composites using PEEK as matrix material
[DE88-753134] 21 p2905 N88-27239
Contribution to the development of coated fiber ceramic insolation material
[ETN-88-92361] 21 p2906 N88-27243
Determination of radiative properties of fiberglass and foam insulations
[DE88-007845] 21 p2920 N88-27331

GLASS LASERS
Large-scale stimulated rotational Raman scattering experiments using the LLNL Nova laser
[DE87-012661] 01 p0051 N88-10328
Thermal stress in the edge cladding of Nova glass laser disks
[DE88-000425] 04 p0448 N88-12780
An investigation of unipolar arcing at atmospheric pressure in aluminum 2024 and aluminum coated glass slides
[AD-A184903] 05 p0577 N88-13521
JPRS report: Science and technology. USSR: Physics and mathematics
[JPRS-UPM-87-008] 06 p0769 N88-14727
Phosphorus oxynitride glass for laser applications
[DE88-005413] 12 p1632 N88-19768
Radiation absorption in neodymium glasses during passage of strong laser pulse 14 p1969 N88-21757
Development of high efficiency q-switched glass laser via sol-gel processing
[AD-A192301] 23 p3218 N88-29154

GLASS TRANSITION TEMPERATURE
Studies on some Ge-Se-Te glasses
[PD-MT-8721] 04 p0420 N88-12607
Correlations of norbornenyl crosslinked polyimide resin structures with resin thermo-oxidative stability, resin glass transition temperature and composite initial mechanical properties
[NASA-TM-100791] 09 p1147 N88-16877
Determination of the glass transition temperature of cured composite materials
[DT-87/62-R] 21 p2906 N88-27248

GLAUERT COEFFICIENT
U AERODYNAMIC FORCES
U MACH NUMBER

GLAZES
A flow visualization study of the leading edge separation bubble on a NACA 0012 airfoil with simulated glaze ice
[NASA-CR-180846] 07 p0816 N88-14966
An experimental mapping of the flow field behind a glaze ice shape on a NACA 0012 airfoil
[NASA-CR-180847] 08 p0950 N88-15766
Laser surface melting
[BMFT-FB-T-86-072] 14 p1914 N88-21435

GLIDE LANDINGS
The effects of RCS jet firing on the isolated Orbiter and mated coast phases of the glide return to launch site maneuver at Mach number 6 (IA302B)
[NASA-CR-180223] 20 p2768 N88-26403

GLIDERS
Investigations of the laminar-turbulent boundary layer transition for the improvement of the performance of powered glider aircraft profiles
[ETN-88-91094] 11 p1436 N88-18569

GLIDING
Computer simulation of pencil glide in B.C.C. metals
[DE88-001802] 07 p0834 N88-15062

GLOBAL AIR POLLUTION
Spatial characterization of acid rain stress in Canadian Shield Lakes
[NASA-CR-181136] 01 p0067 N88-10430
Spatial characterization of acid rain stress in Canadian Shield Lakes
[NASA-CR-180577] 01 p0067 N88-10431
Global environmental change research
[S-HRG-100-301] 03 p0348 N88-12199

GLOBAL ATMOSPHERIC RESEARCH PROGRAM
Statistical relationships between the mesoscale organization of convection and the large-scale wind profiles during GATE --- GARP Atlantic Tropical Experiment (GATE) 02 p0208 N88-11302
Seasonal variations and excitation mechanisms of the equatorially trapped waves 13 p1798 N88-20751
Diagnostic studies of the HxOy-NzOy-O3 photochemical system using data from NASA GTE field expeditions
[NASA-CR-183038] 19 p2689 N88-25984

GLOBAL POSITIONING SYSTEM
Accurate position measuring spacecraft package
[ESA-CR(P)-2398-VOL-1] 01 p0004 N88-10022
Accurate position measuring spacecraft package, executive summary
[ESA-CR(P)-2398-VOL-2] 01 p0004 N88-10023
Accuracy of GPS surveying technique and its possible application to the Wegener project --- Mediterranean tectonics
[REPT-85.3] 01 p0063 N88-10407
Contributions to geodesy, photogrammetry, and cartography. Series 2, number 45
[ISSN-0469-4244] 01 p0065 N88-10416
A method resolving an ambiguity of measured distances by means of NAVSTAR GPS signals 01 p0065 N88-10417
Global positioning satellite-based automatic landing system and wind estimated feedback for the AH-64 helicopter 02 p0124 N88-10784
Ionospheric total electron content estimation for single-frequency global positioning system receivers 02 p0161 N88-11005
Research in geodesy based upon radio interferometric observations of GPS (Global Positioning System) satellites
[AD-A184040] 03 p0346 N88-12187
Balloon track data analysis
[AD-A184750] 03 p0350 N88-12213
Dynamic positioning at sea using the global positioning system
[AD-A184453] 04 p0397 N88-12476
GPS vertical axis performance enhancement for helicopter precision landing approach
[NASA-CR-177443] 04 p0397 N88-12477
A demonstration of high precision GPS orbit determination for geodetic applications 04 p0432 N88-12680
Precise near-earth navigation with GPS: A survey of techniques 04 p0433 N88-12682
On-orbit frequency stability analysis of the GPS NAVSTAR 8 rubidium clock and NAVSTARs 9 and 10 cesium clocks
[AD-A184984] 05 p0544 N88-13312
Use of the global positioning system for trajectory determination of SRAM 2 missiles at the Eastern Test Range
[AD-A185266] 05 p0544 N88-13314
A fully redundant double difference algorithm for obtaining minimum variance estimates from GPS observations
[NASA-CR-182363] 06 p0667 N88-14089
Surveying with GPS in Australia 11 p1504 N88-18986
Application of the Global Positioning System (GPS) time receivers to the fundamental station Wettzell 11 p1506 N88-18995
The global positioning system as an aid to the testing of inertial navigation units (volume 1, addendum 1)
[AD-A185783] 12 p1578 N88-19443
Optimal selection of global positioning system set to minimize emitter location errors
[AD-A189559] 12 p1579 N88-19447
Geodetic positioning by employment of the GPS-NAVSTAR satellites applying the techniques of VLBI and sequential recursive optimal estimation
[INPE-4438-TDL/311] 12 p1594 N88-19547
NAVARES: A prototype expert system for NAVSTAR anomaly resolution
[AD-A189491] 12 p1600 N88-19579
The evaluation and selection of a 5th ground antenna site for the global positioning system
[AD-A189495] 13 p1720 N88-20286
An investigation of Doppler satellite positioning multi-station adjustment software 13 p1730 N88-20345
Orbit accuracy requirement of GPS for precise positioning and orbit determination within local area 13 p1756 N88-20499
Satellite acquisition: Global positioning system acquisition changes after Challenger's accident
[PB88-155536] 14 p1880 N88-21236
The Spring 1985 high precision baseline test of the JPL GPS-based geodetic system
[NASA-CR-182686] 14 p1940 N88-21577
Securing the timescale of the NAVEX-reference clock and rate determinations by time comparisons with the help of the Global Positioning System (GPS) --- Spacelab D1 mission
[DFVLR-MITT-87-20] 16 p2159 N88-22879
Global Positioning System (GPS) exploitation by ODOT (Ohio Department of Transportation)
[PB88-172796] 16 p2159 N88-22882
Investigation of air transportation technology at Ohio University, 1986 17 p2293 N88-23719
Integrated multisensor navigation systems 17 p2294 N88-23722
Development of an airborne facility for advanced avionics research 17 p2307 N88-23801
Adjustment in photogrammetry: Methods, programs and applications
[B8735130] 17 p2369 N88-24105
Inertial reference system with Global Positioning System (GPS) support 18 p2518 N88-24936
Miltipath measurements for land mobile satellite service using global positioning system signals 19 p2645 N88-25700
NAVSTAR global positioning system
[AD-A192609] 20 p2757 N88-26354
Position and velocity determination using a Global Positioning System: An outline
[B8735052] 20 p2757 N88-26355
The Sercel TR5S Global Positioning System (GPS) receiver
[ETN-88-92473] 20 p2757 N88-26357
A positioning system based on NAVSAT
[NLR-MP-87018-U] 20 p2757 N88-26358

Spacecraft applications of advanced global positioning system technology
[NASA-CR-172063] 20 p2757 N88-26359
Spacecraft applications of advanced global positioning system technology
[NASA-CR-172055] 21 p2894 N88-27180
Optimized observation periods required to achieve geodetic accuracies using the global positioning system
[AD-A193844] 22 p3041 N88-28052
The limits of direct satellite tracking with the Global Positioning System (GPS) 22 p3084 N88-28179
Estimation forces acting on an underwater vehicle with G.P.S. (Global Positioning System) and Kalman filtering
[AD-A194339] 23 p3175 N88-28901
Performance of GPS-aided INS during high-dynamic maneuvers
[AD-A194624] 23 p3175 N88-28903
A comparison: Static and future kinematic GPS (Global Positioning System) surveys
[AD-A194666] 23 p3175 N88-28904

GLOBULAR CLUSTERS
The formation of single millisecond pulsars in globular clusters
[MPE-PREPRINT-97] 10 p1428 N88-18525

GLOBULINS
NT FIBRINOGEN

GLOSSARIES
U DICTIONARIES

GLOTTIS
Visualization of the air flowing through a dynamic model of the vocal folds
[ISVR-TR-154] 14 p1952 N88-21634

GLOVES
Constructing Gloved wings for aerodynamic studies
[NASA-TM-100440] 14 p1863 N88-21128
Design, development and evaluation of Stanford/Ames EVA prehensors
[NASA-CR-182688] 15 p2105 N88-22540
Four-axis side-arm flight control simulator investigation
[AD-A196026] 24 p3409 N88-30294

GLOW
U LUMINESCENCE

GLOW DISCHARGES
Magnetic control of low pressure discharges
[AD-A186794] 10 p1322 N88-17900
An experimental and theoretical investigation of optogalvanic effects
[AD-A189618] 12 p1625 N88-19720
Measurement of rate constants of elementary gas reactions of importance to upper atmosphere and combustion systems
[AD-A189432] 13 p1737 N88-20386
In-situ reactive of X-ray optics by glow discharge
[DE88-009840] 20 p2854 N88-26947
Direct determination of part-per-billion levels of volatile organics in water and soil samples using glow discharge mass spectrometry
[DE88-011389] 21 p2910 N88-27272
Low temperature film growth of the oxides of zinc, aluminum and vanadium (and related systems, oxides of gold and germanium, nitrides of aluminum and tungsten) by reactive sputter deposition
[AD-A193497] 23 p3191 N88-28986
Decomposition of hydrazine by high frequency glow electrical discharges
[NASA-TT-20240] 24 p3344 N88-29906

GLUCOSE
Observing effect of laser radiation of low-frequency Raman scattering of light 06 p0772 N88-14742
Saccharification of cellulose by combined fungal and bacterial preparations 17 p2316 N88-23833
Evaluation of the endogenous glucocorticoid hypothesis of denervation atrophy
[NASA-CR-182848] 17 p2381 N88-24157
Design considerations for the development of an implantable sensor for the continuous measurement of glucose in the diabetic patient 17 p2382 N88-24159

GLUCOSIDES
NT NUCLEOSIDES

GLUONS
The approach to equilibrium in a quark-gluon plasma
[DE88-002117] 09 p1251 N88-17499
Computational quantum field theory
[DE88-700918] 16 p2284 N88-23672
Tagging of gamma yields qq bar events and direct measurement of the gluon structure function at HERA
[NOTA-INTERNA-910] 22 p3151 N88-28745

GLUTAMIC ACID
Human blood glutamic acid level with exposure to high ambient concentrations of ammonia 10 p1361 N88-18134

GLUTAMINE
A program for the study of skeletal muscle catabolism following physical trauma
[AD-A189771] 15 p2102 N88-22521
Dexamethasone regulates glutamine synthetase expression in rat skeletal muscles
[NASA-CR-182935] 18 p2549 N88-25129

GLUTATHIONE
The evolution of glutathione metabolism in phototrophic microorganisms
[NASA-CR-182902] 19 p2695 N88-26015

GLYCERINS
U GLYCEROLS

GLYCEROLS
Transparent metal model study of the use of a cellular growth front to form aligned monotectic composite materials
[NASA-CR-182414] 08 p0969 N88-15861
Metabolic and cardiorespiratory parameters during three consecutive days of exhaustive running
[AD-A192598] 21 p2985 N88-27726

GLYCOGENS
Influence of skeletal muscle glycogen on passive rewarming after hypothermia
[AD-A186451] 08 p1049 N88-16334
Manipulation of muscle glycogen concentrations using high and low carbohydrate diets and exercise
[AD-A187732] 11 p1519 N88-19069

GLYCOLS
High ionic conductivity in PEO.PPG block polymer and salt solutions
[AD-A183502] 01 p0026 N88-10168
Physical properties of immiscible polymers 03 p0297 N88-11868
Effects of aircraft deicing/antiicing fluids on airfoil characteristics 08 p0952 N88-15776
Thermogravimetric analysis of polymeric materials for an intermediate temperature solid electrolyte
[DE88-004854] 10 p1306 N88-17809

GNEISS
The timing and mechanism of depletion in Lewisian granulites 24 p3394 N88-30209
Growth of early archaean crust in the ancient Gneiss complex of Swaziland and adjacent Barberton Greenstone Belt, Southern Africa 24 p3396 N88-30223
Reappraisal of the geology of Kangimut Sammisoq, Ameralik Fjord, Southern West Greenland: Crustal structure and interpretation of isotopic data 24 p3398 N88-30234

GOAL THEORY
Plans for discourse
[AD-A192242] 20 p2832 N88-26802

GOALS
Space Assembly, Maintenance, and Servicing Study (SAMSS) 01 p0015 N88-10089
Space technology to meet future needs
[NASA-CR-181473] 02 p0130 N88-10819
Spinoff
[NASA-TM-89651] 03 p0386 N88-12426
Lifting bodies: An attractive aerodynamic configuration choice for hypervelocity vehicles 05 p0534 N88-13248
Recent trends in superconductor development discussed 06 p0688 N88-14215
Supersonic STOVL propulsion technology program: An overview 08 p0957 N88-15808
Present stage of space medicine 10 p1364 N88-18151
Energy-related atomic and molecular structure and scattering studies
[DE88-004246] 10 p1406 N88-18386
Communication satellites: Guidelines for a strategic plan
[NASA-TM-89306] 12 p1599 N88-19569
Defending secrets, sharing data: New locks and keys for electronic information
[PB88-143185] 12 p1706 N88-20210
Johnson Space Center's strategic game plan: Charting a course to the year 2000 and beyond
[NASA-TM-89733] 13 p1850 N88-21076
Orbital transfer vehicle: Concept definition and system analysis study
[NASA-CR-179315] 15 p2024 N88-22060
NASA and the challenge of ISDN: The role of satellites in an ISDN world
[NASA-CR-182749] 15 p2126 N88-22676
Advanced development of double-injection, deep-impurity semiconductor switches
[NASA-CR-182118] 18 p2583 N88-25346
Computer-Aided Engineering (CAE) for engineering design 21 p2929 N88-27390

GODDARD EXPERIMENT PACKAGE TELESCOPE
U PARTICLE TELESCOPES

GOERTLER INSTABILITY
On the onset of three-dimensionality and time-dependence in the Goertler vortex problem
[NASA-CR-178404] 03 p0260 N88-11638
The strong nonlinear interaction of Tollmien-Schlichting waves and Taylor-Goertler vortices in curved channel flow
[NASA-CR-181697] 24 p3311 N88-29716
On the generation of mean flows by the interaction of Goertler vortices and Tollmien-Schlichting waves in curved channel flows
[NASA-CR-181690] 24 p3315 N88-29743

GOES SATELLITES
GOES observations for the FIRE/SRB Wisconsin experiment region from October 11 through November 2, 1986
[NASA-TM-100485] 01 p0071 N88-10453
An introduction to the GOES I-M imager and sounder instruments and the GVAR retransmission format
[NOAA-TR-NESDIS-33] 02 p0140 N88-10884
Improved geostationary satellite soundings for the mesoscale weather analysis/forecast operation 02 p0200 N88-11252
VAS products as indices of thunderstorms and severe local storm potential — Visible and Infrared Spin Scan Radiometer Atmospheric Sounder (VAS) 02 p0201 N88-11253
Operational cloud-clearing techniques of VAS radiance data — Visible and Infrared Spin Scan Radiometer Atmospheric Sounder (VAS) 02 p0201 N88-11256
Automated detection of severe thunderstorms using geosynchronous infrared data 02 p0201 N88-11257
The Pacific Weather Center Satellite Facility: An overview 02 p0205 N88-11286
Suggested severe local storm operational scenario for GOES I-M
[NASA-TM-100688] 11 p1515 N88-19052
NBS (National Bureau of Standards) measurement services. GOES (Geostationary Operational Environmental Satellite) time code dissemination: Description and operation
[PB88-168760] 14 p1880 N88-21235
Solar-geophysical data number 520, December 1987. Part 2: (Comprehensive reports). Data for June 1987 and miscellanea
[PB88-164207] 15 p2152 N88-22849

GOGGLES
Development, testing and evaluation of a night vision goggle compatible BO-105 for night low level operation 03 p0265 N88-11668
Advanced programming and control techniques for complex mechanical systems
[AD-A190238] 15 p2071 N88-22349

GOLD
Far-infrared spectra of lithium deposited on a gold electrode: Interpretation using a cluster model
[AD-A184231] 04 p0495 N88-13050
Some present limitations on the lattice imaging of grain boundaries
[DE87-014665] 09 p1256 N88-17530
Order-disorder transition of Au and Pt (110) surfaces: The significance of relaxations and vibrations
[DE88-004651] 10 p1419 N88-18473
Ion-beam mixing and amorphization in Au/Zr bilayers
[DE88-005999] 15 p2140 N88-22767
Femtosecond nonequilibrium electronic heat transport in thin gold films 19 p2659 N88-25807
Grain boundaries
[DE88-009889] 20 p2773 N88-26448
Low temperature film growth of the oxides of zinc, aluminum and vanadium (and related systems, oxides of gold and germanium, nitrides of aluminum and tungsten) by reactive sputter deposition
[AD-A193497] 23 p3191 N88-28986
Correlations between wettability and structure in monolayers of alkanethiols adsorbed on gold
[AD-A194348] 23 p3191 N88-28991
Potential induced structural transformations of the Au(100) and Au(111) surfaces
[DE88-005446] 23 p3287 N88-29571

GOLD ALLOYS
Aging behavior of Au-based ohmic contacts to GaAs
[NASA-CR-182146] 19 p2662 N88-25831
High resolution detection of solute segregation to the cores of dislocations in grain boundaries
[DE88-009168] 20 p2877 N88-27078

GONADS
NT TESTES

GONDOLAS
Balloon-borne three-meter telescope for far-infrared and submillimeter astronomy
[NASA-CR-182310] 09 p1262 N88-17565
Adaptive control of scientific balloon-borne gondola attitude 13 p1755 N88-20497
Balloon-borne three-meter telescope for far-infrared and submillimeter astronomy
[NASA-CR-182924] 17 p2449 N88-24550

Utilization of the IR telescope gimbaling system as a stabilized pointing platform for balloon payloads. Volume 1: Technical results
[NASA-CR-179339] 18 p2522 N88-24962

GONIOMETERS
Joint angle sensors for closed-loop control
19 p2673 N88-25891

GOODNESS OF FIT
Asymptotic error bounds for power approximations to multinomial tests of fit
[MEMO-640] 08 p1072 N88-16470
The striae in the dust tails of great comets: A formal comparison of the goodness of fit by various theories, and a new proposal 14 p2002 N88-21937
An innovation approach to goodness of fit tests in R sup m
[CWI-MS-R8712] 16 p2259 N88-23501
Fitting a circle to radially suppressed data
[NPL-DITC-103/87] 17 p2392 N88-24223
Fitting an ellipse to data
[NPL-DITC-95/87] 22 p3143 N88-28693

GOVERNMENT PROCUREMENT
Supportability in aircraft systems through technology and acquisition strategy applications
[AD-A186465] 08 p0949 N88-15759
NASA (National Aeronautics and Space Administration) procurement: The 1973 space shuttle solid rocket motor contractor selection
[PB88-135264] 11 p1447 N88-18623
Streamlining invitation for bids
[AD-A188941] 12 p1705 N88-20206
MANPRINT handbook for RFP (Request For Proposal) development
[AD-A188321] 13 p1850 N88-21075
Microvax networked computer system
[AD-A190308] 15 p2114 N88-22596
Department of Defense Statement on the Technology Base to the Subcommittee on Defense Industry and Technology of the Committee on Armed Services, United States Senate, 100th Congress, second session
[AD-A191839] 18 p2588 N88-25376
The use of commercial off-the-shelf equipment and its impact on C3 (Command, Control and Communications EMP (electromagnetic pulse) survivability
[AD-A192614] 20 p2791 N88-26556
The cost and performance implications of reliability improvements in the F-16A/B
[AD-A195096] 24 p3324 N88-29796

GOVERNMENT/INDUSTRY RELATIONS
Structures and Materials Working Group report
01 p0016 N88-10093
The British Technology Group
[ONRL-7-022-R] 01 p0107 N88-10698
Summaries of FY 1987 engineering research
[DE88-002572] 07 p0840 N88-15096
Lightsats and their attraction to budget oriented Federal agencies 10 p1289 N88-17711
A study of technology transfer arrangements for national laboratories
[DE88-005423] 11 p1567 N88-19382
The effects of two Carlucci initiatives concurrency and streamlining, on the test and evaluation phase of system acquisitions 12 p1704 N88-20198
The influence of infrastructure on the costs and timescales of collaborative programmes
12 p1704 N88-20201
The impact of independent research and development regulations on companies not required to negotiate advanced independent research and development agreements
[AD-A190007] 15 p2147 N88-22818
Civil missions applications study
17 p2417 N88-24376
Class 2 design update for the family of commuter airplanes
[NASA-CR-182681] 18 p2464 N88-24629
The Department of Defense report on the merit review process for competitive selection of university research projects and an analysis of the potential for expanding the geographic distribution of research for the Committees on Appropriations, United States Congress
[AD-A191842] 18 p2588 N88-25379
Workshop report and presentations from the Semiconductor Research Corporation-DOE Semiconductor Task Force Workshop
[DE88-007690] 19 p2733 N88-26232
Economic impact of space flight activities in West Germany. Influence of allocations of Bundesministerium fuer Forschung und Technologie
[ETN-88-92106] 21 p2901 N88-27215
Argonne National Laboratory technology transfer report, FY87
[DE88-010091] 23 p3298 N88-29639

GOVERNMENTS
Freedom of Information Act: Fee waiver practices at the FBI (Federal Bureau of Investigation)
[PB87-216727] 02 p0249 N88-11573
Center for Electronics and Electrical Engineering Technical Progress Bulletin covering center programs, January to March 1987 with 1987 CEEE events calendar
[PB87-224648] 03 p0309 N88-11946
University research initiative research program summaries
[AD-A184876] 05 p0658 N88-14035
Role of the technical report in technological innovation
[PB87-232500] 05 p0658 N88-14040
Federal plan for meteorological services and supporting research, fiscal year 1988
[PB88-118716] 07 p0880 N88-15336
A study of federal technology transfer to the commercial sector
[AD-A187017] 09 p1262 N88-17560
Journal of Research of the National Bureau of Standards, volume 92, number 5, September-October 1987
[PB88-124409] 10 p1426 N88-18518
Journal of Research of the National Bureau of Standards, volume 92, number 6, November-December 1987
[PB88-138516] 10 p1426 N88-18519
National Informatics Centre: Profile of services
[PB88-134135] 12 p1706 N88-20211
Technology transfer from US Federal laboratories: Report of a roundtable
[PB88-144803] 12 p1709 N88-20228

GOVERNORS
U SPEED REGULATORS

GRABENS
U GEOLOGICAL FAULTS

GRADIENT INDEX OPTICS
Optical characterization of silica aerogel
[DE88-008916] 20 p2854 N88-26946

GRADIENTS
NT ELECTRON DENSITY PROFILES
NT POTENTIAL GRADIENTS
NT PRESSURE GRADIENTS
NT TEMPERATURE GRADIENTS
NT THERMOCLINES
Monocrystalline silicon gradiometer for gravity experiments in space
[NASA-CR-181452] 01 p0050 N88-10321
High gradient superconducting quadrupoles
[DE87-013590] 02 p0244 N88-11541
Conservation and transport properties of turbulence with large density variations
[LA-10911-MS] 03 p0321 N88-12032
Numerical solution of bound constrained problems
[DE88-000653] 03 p0371 N88-12334
An application of a gradient relaxation method to noisy infrared images
[AD-A184666] 03 p0377 N88-12371
Collider constraints in the choices for wavelength and gradient scaling
[PB87-123691] 06 p0779 N88-14783
Trust regions and projected gradients
[DE88-005829] 15 p2122 N88-22646
Probing the possibility of a (12)C/(13)C abundance gradient from observations of interstellar CH+
[DE88-008908] 20 p2884 N88-27125
The gradient method for interface tracking
[AD-A194477] 23 p3248 N88-29334

GRADUATION
U CALIBRATING

GRAFTING
New method of grafting crystals
16 p2180 N88-22992
Modification of polymers by photografting processes
17 p2323 N88-23871

GRAIN BOUNDARIES
Observations of localized grain boundary dislocations in series of {001} and {110} symmetrical tilt boundaries in aluminum
[DE87-014011] 01 p0025 N88-10156
A simulation study of interfaces in Ni, Al and Ni3Al with and without boron
[DE87-013156] 01 p0102 N88-10667
Grain boundary effects in processing high T/sub c/ superconductors
[DE87-009297] 01 p0103 N88-10673
Dynamical simulation of structural multiplicity in grain boundaries
[DE87-012746] 01 p0103 N88-10676
Understanding the transport properties of silicon grain boundaries and how they relate to I.C. applications of polysilicon
[DE87-013809] 01 p0104 N88-10677
Grain boundary phase equilibria in metallic systems
[DE87-014123] 01 p0104 N88-10679
Analytical electron microscopy characterization of boron in sintered alpha-SiC
[DE87-012532] 02 p0142 N88-10889
Influence of thermocyclic treatment on mobility of grain boundaries
[BLL-M-37329-(5828.4)] 02 p0149 N88-10933
Applications of dislocation theory to crack growth problems 02 p0190 N88-11188
Solute segregation to phase interfaces and grain boundaries: Studies by analytical electron microscopy and profile deconvolution
[DE87-012129] 02 p0243 N88-11537
On the search for experimentally observed grain boundary phase transitions
[DE87-012747] 02 p0244 N88-11539
Slip casting and extruding shapes of rhenium with metal oxide additives. Part 2: Development of grain stabilized rhenium parts for resistojets
[NASA-CR-180851] 03 p0278 N88-11749
Microstructural effects on the fatigue behavior of Fe-C-X alloys
[DE88-000155] 03 p0288 N88-11809
Ultra-fine grained alloy material
[AD-A184500] 03 p0290 N88-11820
International Conference on Microstructology held in Gainesville, Florida on 7-9 May 1986
[AD-A184604] 03 p0290 N88-11822
Microstructural characterization of irradiated PWR steels using the atom probe field-ion microscope
[DE88-000341] 03 p0291 N88-11828
Indentation damage in ceramics
[AD-A184686] 03 p0294 N88-11844
Some stochastic aspects of intergranular creep cavitation
[DE88-000065] 04 p0416 N88-12581
Welding and weldability of ductile intermetallic alloys
[DE87-014061] 04 p0416 N88-12582
Cyclic deformation and crack initiation
05 p0597 N88-13646
Effect of grain orientation on the origination and the initial growth of fatigue cracks in pure iron
05 p0597 N88-13647
Study of boundary structures
[AD-A184808] 05 p0655 N88-14013
Computer simulation of impurities and interfaces in body centered cubic metals
[PB88-108162] 07 p0832 N88-15047
Microstructural observations of the Sn-Pb solder/Cu system and thermal fatigue of the solder joint
[DE88-001392] 07 p0832 N88-15048
The influence of grain boundary chemistry and structure on the intergranular attack and intergranular stress corrosion cracking of austenitic alloys
[DE88-002436] 07 p0835 N88-15063
Grain boundary and surface diffusion in oxides
[DE88-002348] 07 p0938 N88-15697
Influence of post-anneal cooling treatments on suppression of cryogenic intergranular fracture in experimental Ni-free high-Mn austenitic steels
[DE88-002766] 09 p1145 N88-16863
Some present limitations on the lattice imaging of grain boundaries
[DE87-014665] 09 p1256 N88-17530
Molecular dynamics study of high-temperature grain-boundary stability in a (100) sigma = 29 bicrystal model
[DE88-002955] 09 p1258 N88-17546
The migration of grain boundaries in ceramic materials with particular reference to the sintering process
[DE88-004085] 10 p1306 N88-17808
Grain boundaries, planar defects and superconducting properties of YBa2Cu3O7
[DE88-003477] 10 p1419 N88-18475
Simulation and processing of high resolution images of defects and interfaces in superconducting YBa2Cu3O7
[DE88-003856] 10 p1420 N88-18480
Influence of grain boundary phosphorus segregation on hydrogen embrittlement in steel
[DE88-700176] 11 p1459 N88-18696
The intergranular segregation of boron in substoichiometric Ni3Al
[DE88-004783] 11 p1462 N88-18720
Atomistic studies of the structure and properties of grain boundaries with substitutional impurities
[DE88-004161] 11 p1545 N88-19237
Gordon Conference on Intermetallic Compounds held at Tilton, New Hampshire on 20-24 July 1987
[AD-A188502] 13 p1745 N88-20435
JPRS report: Science and technology. USSR: Materials science
[JPRS-UMS-87-007] 14 p1895 N88-21312
Dependence of hydrogen embrittlement of austenitic stainless steels on structural state of grain boundaries
14 p1896 N88-21316
Grain boundaries
[DE88-006628] 14 p1987 N88-21852

On rotating sphere-on-a-plate experiments and the questions of whether high angle grain boundaries melt below bulk melting temperatures
[DE88-006627] 15 p2038 N88-22142
Investigation and synthesis of high temperature and increased stiffness RSP aluminum alloys
[AD-A190407] 15 p2039 N88-22151
Strength and microstructure of ceramics
[AD-A190712] 15 p2046 N88-22191
Grain boundary oxidation and low-cycle fatigue at elevated temperatures 15 p2083 N88-22420
Interface formation and precursory dynamics
[AD-A190741] 15 p2144 N88-22794
SSME single-crystal turbine blade dynamics 16 p2221 N88-23257
Disclination structures in carbon and graphite
[AD-A191056] 17 p2322 N88-23868
The role of oxygen on the mechanical behavior of molybdenum alloys 17 p2401 N88-24278
The morphological stability of continuous intergranular phases: Thermodynamic considerations
[DE88-006328] 18 p2584 N88-25350
The postirradiation tensile properties and microstructure of several vanadium alloys
[DE88-007140] 19 p2615 N88-25515
Phase stability and alloy design of ordered intermetallics
[DE88-007479] 20 p2772 N88-26435
Grain boundary structure in Ni3Al
[DE88-009164] 20 p2773 N88-26444
The effects of gradients on boundary stability
[DE88-009592] 20 p2773 N88-26445
Grain boundaries
[DE88-009889] 20 p2773 N88-26446
The structure and properties of grain boundaries in B2 ordered alloys
[DE88-009890] 20 p2773 N88-26447
Effects of grain boundary composition on properties of YBa2Cu3O/sub 7-x/
[DE88-007679] 20 p2875 N88-27064
High resolution detection of solute segregation to the cores of dislocations in grain boundaries
[DE88-009168] 20 p2877 N88-27078
Analysis of grain refinement and superplasticity in aluminum-magnesium alloys
[AD-A193029] 21 p2912 N88-27283
Processing and properties of advanced aluminum alloys
[AD-A193224] 21 p2912 N88-27284
Microchemical analysis of polycrystalline Ni3Al and other ordered alloys using the field-ion microscope atom probe
[DE88-011519] 21 p2914 N88-27294
Computer simulation of elastic properties of grain boundary materials
[DE88-011965] 21 p2916 N88-27305
Study of feasibility and optimization conditions of laser treatments: Application of the local recrystallization of aluminum
[ISAL-87-0048] 21 p2916 N88-27309
The influence of solute segregation on the dislocation structure of small and large angle (001) twist boundaries in Fe-Sb alloys
[DE88-009166] 22 p3155 N88-28770
Atomistic simulation of silicon grain boundaries
[DE88-009925] 22 p3155 N88-28771
A new model for the simulation of interfaces at high temperature
[DE88-009926] 22 p3155 N88-28772
Transverse expansion of individual carbon and graphite filaments
[AD-A195073] 24 p3342 N88-29891

GRAIN SIZE
Development of ultrafine grains and related properties in Hadfield manganese steels
[DE87-011884] 01 p0024 N88-10154
Microstructural effects in shock initiation of granular explosives
[DE87-011282] 01 p0031 N88-10200
Precision metrology comparing ultrasonic and other techniques for the determination of steel thickness
[DE87-011051] 02 p0230 N88-11452
Structure and grain coarsening during the processing of engineering ceramics
[NASA-TM-100235] 03 p0293 N88-11838
Characterization of catalysts with metal-support effects and of the species adsorbed on their surfaces
[DE87-014836] 04 p0414 N88-12564
Influence of microstructure and aging condition on the fatigue crack propagation in age hardened aluminium alloys 05 p0599 N88-13659
The effect of alpha platelet morphology and beta-grain size on the initiation and growth of short fatigue cracks in Ti6SS 05 p0600 N88-13667
Near-threshold fatigue 06 p0716 N88-14392
Microstructure and magnetic properties of cobalt-chromium alloys
[DE88-002762] 07 p0835 N88-15064
Acoustic backscattering from bottom sediment at normal incidence in the laboratory
[AD-A186905] 09 p1242 N88-17443
Processing of nanophase ceramics
[DE88-005985] 13 p1752 N88-20475
Grain growth behavior of extrusion consolidated centrifugally atomized Type 304 stainless steel powder
[DE88-006788] 15 p2038 N88-22143
JPRS report: Science and technology. Japan
[JPRS-JST-88-002] 15 p2050 N88-22210
Fine grain development by laser CVD 15 p2050 N88-22214
Superfine grain development by laser 15 p2050 N88-22215
Analysis of dust grain properties in two star forming regions through comparison of theoretical models to observations 17 p2451 N88-24559
The first synthesis of chem-prep varistor LAC (Lightning Arrestor Connector) granules
[DE88-008005] 21 p2936 N88-27438

GRAINS (FOOD)
NT CORN
NT RICE
NT WHEAT
Food Irradiation Newsletter, Vol. 11, No. 1
[DE88-700808] 12 p1671 N88-20004

GRAMMARS
Formal grammars and Markov models
[RSRE-MEMO-4051] 09 p1219 N88-17311
Semi-applicative programming 10 p1380 N88-18239
A parser generator for finitely ambiguous context-free grammars
[CWI-CS-R8712] 13 p1818 N88-20864
A cockpit natural language study: Vocabulary and grammar analyses
[AD-A193289] 21 p2993 N88-27753
Linguistic semantics for parallel computation
[PB88-105960] 21 p2995 N88-27761

GRAND UNIFIED THEORY
NT UNIFIED FIELD THEORY
Status of the electroweak theory
[DE88-002342] 10 p1422 N88-18494
Theory of elementary particle studies in weak iteration and grand unification and studies in accelerator design
[DE88-004261] 11 p1545 N88-19238
Diffraction theory in QCD and beyond
[DE88-005958] 13 p1837 N88-20992
Superstrings
[DE87-702982] 19 p2737 N88-26249

GRANITE
Evaluation of AIS-2 (1986) data over hydrothermally altered granitoid rocks of the Singatse Range (Yerington) Nevada and comparison with 1985 AIS-1 data 05 p0613 N88-13767
The timing and mechanism of depletion in Lewisian granulites 24 p3394 N88-30209
Genesis of archean granitoids in the Pilbara block and implications for crustal growth 24 p3394 N88-30210
Crustal evolution and the eclogite to granulite phase transition in xenoliths from the West African Craton 24 p3395 N88-30217

GRANTS
Materials sciences programs: Fiscal Year 1987
[DE88-000672] 04 p0429 N88-12659

GRANULAR MATERIALS
Visible emission from granular explosives during shock initiation
[DE87-012361] 02 p0155 N88-10970
Computer-aided analysis for the Mechanics of Granular Materials (MGM) experiment, part 2 07 p0926 N88-15626
Microscopic modeling of sound waves in granular material
[DE88-000348] 10 p1405 N88-18375
Kinetics of combustion of finely divided solid fuel in granules
[BLL-M-37626-(5828.4)] 14 p1888 N88-21283
Gas coma of Comet Giacobini-Zinner: Emission from grains 14 p2000 N88-21923
P/Halley dust coma: Grains or rocks? 14 p2002 N88-21936
Variation of grain properties at the dust outbursts — Halley's comet 14 p2003 N88-21943
Nature of Comet Halley's organic grains inferred from infrared spectra 14 p2007 N88-21973
Laboratory amorphous carbon: A possible analog of cometary dust 14 p2009 N88-21981
LLNL granular solids flow project
[DE88-007492] 18 p2513 N88-24906
LLNL Granular Solids Flow Project
[DE88-008023] 19 p2664 N88-25844
Granulation of pyrotechnic tracer composition R284T
[MRL-TN-528] 20 p2780 N88-26490
Gaseous tracer techniques for pore structure characterization of granular materials
[DE88-011542] 21 p2911 N88-27274
Granular flow: Particle-dynamics simulations of steady flow
[DE88-011342] 21 p2948 N88-27506
Device physics related to the granular nature of CuInSe2 solar cells
[DE88-001159] 21 p2967 N88-27622

GRAPH THEORY
Strategies for concurrent processing of complex algorithms in data driven architectures
[NASA-CR-181435] 01 p0082 N88-10527
Graph partitioning by eigenvectors
[AD-A184430] 03 p0372 N88-12338
A characterization of separating pairs and triplets in a graph
[AD-A184278] 04 p0477 N88-12941
On the number of minimum size separating vertex sets in a graph
[AD-A184279] 04 p0478 N88-12942
On color polynomials of Fibonacci graphs
[AD-A184133] 04 p0486 N88-12996
Eigenvectors of distance-regular graphs
[AD-A185375] 05 p0641 N88-13919
On the work needed to factor a symmetric positive definite matrix
[AD-A185781] 06 p0759 N88-14660
Eigenvectors of graphs
[AD-A185538] 06 p0765 N88-14698
The perfectly matchable subgraph polytope of an arbitrary graph
[AD-A185993] 07 p0913 N88-15539
Algorithms for transitive reduction of an acyclic graph
[PB87-162822] 09 p1220 N88-17317
Strategies for concurrent processing of complex algorithms 10 p1379 N88-18236
Implementing logical variables on a graph reduction architecture 10 p1382 N88-18252
The clique polytope of a graph
[MEMO-663] 14 p1963 N88-21710
Graph labelings
[AD-A189649] 14 p1964 N88-21722
Compact representation of the separating k-sets of a graph
[AD-A189650] 14 p1965 N88-21723
The total interval of a graph
[AD-A189648] 15 p2119 N88-22625
Structural decomposition of multiple time scale Markov processes
[AD-A189739] 15 p2123 N88-22657
Graphs related to Held's simple group
[CWI-PM-28707] 16 p2264 N88-23536
Edge-disjoint homotopic paths in straight-line planar graphs
[CWI-OS-R8718] 16 p2264 N88-23537
Decomposition of graphs on surfaces and a homotopic circulation theorem
[CWI-OS-R8719] 16 p2264 N88-23538
A mixed-integer linear programming problem which is efficiently solvable
[AD-A191028] 18 p2556 N88-25168
Research in enumeration and graph theory with applications to computer science
[AD-A191567] 18 p2556 N88-25171
Efficient parallel algorithm for the connected component problem and its implementation on the DPP84 (Delft Parallel Processor)
[PB87-225959] 19 p2715 N88-26118
Extensible networks. Part 1: Principles and constructions
[REPT-87-91-PT-1] 20 p2842 N88-26864
Two families of graphs satisfying the cycle basis interpolation property
[PB88-127808] 20 p2846 N88-26890

GRAPHIC ARTS
NT COMPUTER ANIMATION
Active control of jet flowfields
[AD-A186736] 08 p0989 N88-15989
Computer aided geometric design
[AD-A187324] 10 p1389 N88-18293
A digital circuit design environment
[AD-A188831] 12 p1623 N88-19709
MacCAD (Macintosh Computer Aided Design), computer aided design tool for system analysis
[AD-A189241] 13 p1815 N88-20843
Efficient, high resolution computations of projectile and missile flow fields
[AD-A191086] 16 p2158 N88-22873
Algorithms and intuition
[NASA-CR-182900] 16 p2252 N88-23459
The ISI (Information Sciences Institute) grapher manual
[AD-A192198] 18 p2561 N88-25200

Editfont: An interactive font editing system
[AD-A192373] 20 p2838 N88-26836

GRAPHITE
NT PYROLYTIC GRAPHITE
Oxidation of TSX graphite over the temperature range 450 to 1200°C
[DE87-012230] 01 p0020 N88-10127
Low cycle fatigue on isotropic fine-grained graphite
[DE87-702627] 01 p0028 N88-10177
Behavior of graphites under intense heat loads
[DE87-012128] 01 p0028 N88-10179
Comparison of high purity fine grain graphites from different suppliers with regard to physical, mechanical, and thermal properties — Joint European Torus wall protection
[JUEL-SPEZ-401] 02 p0154 N88-10963
Transply crack density detection by acousto-ultrasonics
[NASA-TM-100224] 03 p0279 N88-11758
Corrosion-electrochemical and mechanical properties of composite graphite-carbide metal materials based on titanium and its alloys 03 p0285 N88-11794
Fabrication and testing of fire resistant graphite composite panels
[NASA-CR-177397] 04 p0397 N88-12472
Data base on the high heat flux behaviour of metals and carbon materials for plasma facing components: Experiments at the 10 MW neutral beam injection test stand of the IPP Nagoya
[IPPJ-AM-53] 04 p0492 N88-13031
Proceedings of the Japan-US Workshop P-92 on Plasma Material Interaction/High Heat Flux Data Needs for the Next Step Ignition and Steady State Devices
[DE87-013568] 04 p0494 N88-13042
PISCES: Plasma-surface interactions and materials research
[DE88-001323] 04 p0494 N88-13044
Cyclic deformation behaviour of cast irons with various graphite shapes in the temperature range 20 C less than or = T less than or = 500 C 06 p0715 N88-14384
Effect of point defects on graphite lattice parameters
[DE88-700340] 07 p0827 N88-15019
Performance of a small, graphite electrode, multistage depressed collector with a 500-W, continuous wave, 4.8- to 9.6-GHz traveling wave tube
[NASA-TP-2788] 07 p0848 N88-15146
Review of thermal properties of graphite composite materials
[NASA-TM-100049] 09 p1139 N88-16825
Helium-ion-induced release of hydrogen from graphite
[DE88-002599] 09 p1142 N88-16846
Neutron and X-ray scattering studies of layered solids 09 p1246 N88-17469
Comparison of low temperature photoluminescence of bulk MBE (Molecular Beam Epitaxy) grown AlGaAs and GaAs using a graphite generated dimer versus a standard tetramer arsenic group-V source
[DE88-004939] 11 p1558 N88-19329
An interpretation of the ethylenic, carbidic, and graphite auger lineshapes of chemisorbed carbon species
[AD-A189092] 13 p1736 N88-20379
IAEA Specialists' Meeting on Graphite Component Structural Design
[DE88-780006] 13 p1746 N88-20439
The statistical characterization of tensile strengths for a nuclear-type graphite 13 p1746 N88-20440
Statistical considerations of graphite strength for assessing design allowable stresses 13 p1746 N88-20441
Fracture criterion of reactor graphite under multiaxial stresses 13 p1746 N88-20442
High temperature Young's modulus of IG-110 graphite 13 p1746 N88-20443
Effects of high temperature neutron irradiation on the physical, chemical and mechanical properties of fine-grained isotropic graphite 13 p1747 N88-20444
Degradations of thermal shock resistance and the fracture toughness of reactor graphite subjected to neutron irradiation 13 p1747 N88-20445
Application of ISRM testing methods to fracture toughness testing of graphite 13 p1747 N88-20446
Notch sensitivity of graphite materials for VHTR 13 p1747 N88-20447
Nondestructive testings of HTGR graphites 13 p1747 N88-20448
Recent progress in structure determination by LEED (Low-Energy Electron Diffraction) measure the properties of the deep donors (DX-cent)
[DE88-003851] 13 p1846 N88-21048
Microplasticity phenomena in graphite/magnesium metal matrix composites
[DE88-006772] 15 p2029 N88-22086
Characterization of Mode 1 and Mode 2 delamination growth and thresholds in graphite/peek composites
[NASA-TM-100577] 16 p2172 N88-22947
Disclination structures in carbon and graphite
[AD-A191056] 17 p2322 N88-23868
Interfacial shear phenomena in graphite epoxy composites under impact loading using dynamic moire interferometry
[DE88-006773] 18 p2479 N88-24709
Raman characterization of AsF5-intercalated vapor grown graphite fibers
[AD-A191709] 18 p2491 N88-24778
Stress measurements in graphite fibers by laser raman spectroscopy
[AD-A191710] 18 p2491 N88-24779
Electron-Rayleigh wave interaction in thin film carbons
[AD-A191727] 18 p2492 N88-24781
Photoconductivity in carbon fibers
[AD-A191728] 18 p2492 N88-24782
Effect of uniaxial stress on the Raman spectra of graphite fibers
[AD-A191730] 18 p2492 N88-24783
Microstructure of thin intercalated benezene derived graphite fibers
[AD-A191724] 19 p2618 N88-25534
Graphite as a picosecond laser activated opening switch 19 p2657 N88-25783
Effects of applied stress and temperature on the nonlinear elastic properties of graphite fibers
[AD-A194469] 22 p3050 N88-28093
Transverse expansion of individual carbon and graphite filaments
[AD-A195073] 24 p3342 N88-29891

GRAPHITE-EPOXY COMPOSITES
Effect of adhesive layers on impact damage and dynamic response in composite laminates 02 p0141 N88-10887
A stochastic delamination growth model for fatigue loaded laminated composite materials 02 p0141 N88-10888
The effect of bromination of carbon fibers on the coefficient of thermal expansion of graphite fiber-epoxy composites
[NASA-TM-100236] 02 p0143 N88-10899
Ultrasonic characterization of the nonlinear elastic properties of unidirectional graphite/epoxy composites
[NASA-CR-4100] 03 p0281 N88-11767
Study of zero CTE (Coefficients of Thermal Expansion) of graphite/epoxy composites
[DE87-013557] 04 p0412 N88-12554
Corrosion control by composite material substitution with application to the M-939 5-ton truck 04 p0428 N88-12654
Evaluation of closed cubic failure criterion for graphite/epoxy laminates
[NASA-CR-182375] 06 p0679 N88-14158
Study on utilization of advanced composites in fuselage structures of large transports
[NASA-CR-172406] 07 p0827 N88-15014
Investigation of low velocity impact damage on filamentary composite materials 07 p0923 N88-15607
Postbuckling of laminated anisotropic panels
[NASA-TM-100509] 08 p0994 N88-16011
A fiber-resin micromechanics analysis of the delamination front in a DCB specimen
[NASA-TM-100540] 10 p1294 N88-17737
Radiation and temperature effects on the time-dependent response of T300/934 graphite/epoxy
[NASA-CR-182603] 11 p1451 N88-18646
Effects of moisture, elevated temperature, and fatigue loading on the behavior of graphite/epoxy buffer strip panels with center cracks
[NASA-TM-100558] 12 p1603 N88-19590
Simulated impact damage in a thick graphite/epoxy laminate using spherical indenters
[NASA-TM-100539] 13 p1733 N88-20363
Ply-level failure analysis of a graphite/epoxy laminate under bearing-bypass loading
[NASA-TM-100578] 13 p1735 N88-20372
The buckling and vibration of composite plates using the Levy method considering shear deformation and rotary inertia
[AD-A189743] 15 p2076 N88-22374
Increasing strength of graphite/epoxy bolted joints by introducing an adhesively bonded metallic insert
[FFA-TN-1987-45] 15 p2088 N88-22442
Surface crack analysis applied to impact damage in a thick graphite-epoxy composite
[NASA-TM-100600] 16 p2173 N88-22950
Fuel containment, lightning protection and damage tolerance in large composite primary aircraft structures
[NASA-CR-3875] 17 p2317 N88-23839
Properties of two composite materials made of toughened epoxy resin and high-strain graphite fiber
[NASA-TP-2826] 19 p2609 N88-25480
Loading rate sensitivity of open hole composites in compression
[NASA-TM-100534] 19 p2610 N88-25490
Stiffness degradation of composite laminates 20 p2767 N88-26405
Compression creep of filamentary composites
[NASA-CR-182550] 20 p2798 N88-26601
Damage in a perforated graphite-epoxy plate under monotonic, cyclic biaxial loading
[ONERA-NT-1987-5] 20 p2816 N88-26708
Determination of lumped-mass thermal properties associated with autoclave curing of graphite/epoxy composites 21 p2925 N88-27364
Failure analysis of laminated composite angles 21 p2959 N88-27578
A comprehensive study on damage tolerance properties of notched composite laminates
[AD-A192952] 23 p3188 N88-28968
Analytical study of graphite-epoxy tube response to thermal loads
[NASA-CR-183215] 24 p3341 N88-29884
Experimental aspects of using time-averaged holographic interferometry to detect barely visible impact damage in a graphite/epoxy composite plate
[AD-A194418] 24 p3375 N88-30097

GRAPHITE-POLYIMIDE COMPOSITES
Effect of long-term thermal aging on coated Celion/LARC-160 composites
[NASA-TM-100495] 04 p0410 N88-12544
The 700 F properties of autoclave cured PMR-2 composites
[NASA-TM-100923] 18 p2480 N88-24712
A thermally modified polymer matrix composite material with structural integrity to 371 C
[NASA-TM-100922] 19 p2609 N88-25483
Loading rate sensitivity of open hole composites in compression
[NASA-TM-100634] 19 p2610 N88-25490

GRAPHITIZATION
Electronic and structural studies of carbon/carbon composites
[AD-A191729] 19 p2609 N88-25481
Anomalous temperature-dependent negative magnetoresistance in pregraphitic carbons
[AD-A191725] 19 p2619 N88-25535
Brominated graphite fibers and method of producing the same
[NASA-CASE-LEW-14698-1] 24 p3341 N88-29888

GRAPHS (CHARTS)
NT BOND GRAPHS
The ISI (Information Sciences Institute) grapher: A portable tool for displaying graphs pictorially
[AD-A184354] 04 p0478 N88-12944
Eigenvectors of graphs
[AD-A185538] 06 p0765 N88-14698
Nonpreemptive run-time scheduling issues on a multitasked, multiprogrammed multiprocessor with dependencies, bidimensional tasks, folding and dynamic graphs
[DE88-003598] 09 p1223 N88-17335
Design graphs for the first two bending Eigenvibration forms of rotating beams consisting of two beam points
[IW-86006R] 13 p1783 N88-20570
Campaign graphs
[DE88-005336] 13 p1831 N88-20952
Shape detection in remote sensing through graph isomorphism 17 p2354 N88-24028
A matroid algorithm and its application to the efficient solution of two optimization problems on graphs, revision
[AD-A192709] 20 p2838 N88-26838
Algorithm for generating the minimal cycle basis of a graph
[PB88-126610] 20 p2846 N88-26891
Issues in computer-assisted interpretation of graphs and quantitative information
[PB88-116280] 21 p2998 N88-27783

GRASSES
NT SEA GRASSES
Estimating scattered and absorbed radiation in plant canopies by remote sensing
[NASA-CR-181390] 02 p0193 N88-11205

GRASSLANDS
Estimating regional evapotranspiration from remotely sensed data by surface energy balance models
[NASA-CR-181400] 01 p0064 N88-10411
Evaluation of surface energy and radiation balance systems on the Konza Prairie
[NASA-CR-182534] 10 p1355 N88-18097
Measuring and modeling near surface reflected and emitted radiation fluxes at the FIFE site
[NASA-CR-182660] 12 p1640 N88-19818
Mapping of plant associations and the variation of surface water in the Pantanal Mato-Grossense National Park, through remote sensing techniques 17 p2366 N88-24092
Canopy reflectance modeling in a tropical wooded grassland
[NASA-CR-182981] 19 p2685 N88-25961

Use of SPOT satellite in agrohydrology: Detection of spring water excess in a grassland region
22 p3091 N88-28357
Evaluation of the grassy biomass in the Sahelian zone in the South Tamesna region (Niger): Prospects and limits of use of SPOT data
22 p3092 N88-28359
Changes in species composition of heathland, monitored by means of remote sensing and field mapping: The results of the HEISPOT project
22 p3092 N88-28360
Characterization, topology, and cartography of grasslands for the development of fodder resources. (Preliminary Evaluation Program for SPOT number 26)
22 p3095 N88-28377
Study of savannah formation in the Sudanian zone. Northwest sector of the La Comoe park, Ivory Coast
22 p3097 N88-28391

GRASSMANN ALGEBRA
U VECTOR SPACES

GRATINGS (SPECTRA)
Single-periodic multilayer grating laser Doppler vibrometer
03 p0327 N88-12066
Distributed feedback effects in lasers and high gain laser instabilities in optically pumped CH3F
03 p0329 N88-12079
A theoretical study of enhanced Smith-Purcell radiation from a bigrating
[AD-A184530] 03 p0329 N88-12080
Surface polariton resonances and reflectance on a bigrating
[AD-A184663] 03 p0377 N88-12370
All-optical beam control by forced Rayleigh scattering
[AD-A184315] 04 p0490 N88-13018
The production of ultrasmall and superfine holographic diffraction gratings using synchrotron radiation and lithographic techniques
[AD-A185395] 05 p0585 N88-13562
Efficient computation of periodic Green's functions with application to grating structures
[AD-A184853] 05 p0640 N88-13912
The evaluation of a deformable diffraction grating for a stigmatic EUV spectroheliometer
[NASA-CR-182371] 06 p0707 N88-14337
Use of spherical optics in high resolution soft X-ray grating monochromators
[PB87-125191] 06 p0780 N88-14788
A composite grating for moire interferometry
[AD-A186330] 07 p0832 N88-15044
Study of quantum mechanical effects in deep submicron, grating-gate field effect transistors
[AD-A188283] 10 p1325 N88-17923
Holographically correcting synthetic aperture aberrations
[AD-A189510] 12 p1692 N88-20123
Enhancement of second harmonic generation on silver gratings by resonant excitation of surface plasmon
[ETN-88-92304] 17 p2439 N88-24509
The evaluation of a deformable diffraction grating for a stigmatic EUV spectroheliometer
[NASA-CR-183064] 20 p2853 N88-26941
Precise rotational alignment of X-ray transmission diffraction gratings
[DE88-010599] 21 p2911 N88-27273
On the multiple grating spectrometer resolving power
[PREPRINT-585] 22 p3153 N88-28761
A theoretical and experimental investigation into the use of SAW weighting techniques in optical diffraction gratings
[RSRE-MEMO-4128] 23 p3283 N88-29549

GRAVIMETERS
Allowance for influence of gravity field nonuniformity
08 p1012 N88-16137
The superconducting gravimeter: Application, calibration, and further development
[SER-C-329] 09 p1167 N88-16998
Results of the International Comparison of Absolute Gravimeters (2nd) held in Sevres, France in June-July 1985
[AD-A189869] 15 p2093 N88-22474
Testing of a gravimeter LCR G 765
[B8735061] 20 p2806 N88-26843

GRAVIMETRY
Study of a satellite-to-satellite tracking gravity mission
[ESA-CR(P)-2419] 02 p0198 N88-11237
Solution of three-dimensional inverse problem of gravimetry in contact surfaces class by local corrections method
04 p0460 N88-12848
On deviations from Newton's law and the proposal for a Fifth Force
[DE87-703368] 04 p0487 N88-13001
Effective methods of gravimetric and magnetometric data processing
06 p0728 N88-14479
Results of the International Comparison of Absolute Gravimeters (2nd) held in Sevres, France in June-July 1985
[AD-A189869] 15 p2093 N88-22474
Satellite gradiometry
[B8735057] 16 p2229 N88-23313
Evaluation of a model of the Earth's gravity field
[EPSHOM-003/87] 17 p2373 N88-24116

GRAVIRECEPTORS
NT OTOLITH ORGANS
Morphology and development of the inner ear of Anurans
07 p0886 N88-15378
Gravisensing in lentil seedling roots grown in space (Spacelab D-1 mission)
12 p1654 N88-19911
How does Physarum polycephalum perceive and use gravity?
12 p1655 N88-19918
Synopsis of the Spacelab D-1 frog statolith experiment STATEX
12 p1659 N88-19940
Experiments concerning gravisensitivity of protozoa
12 p1660 N88-19949
Contraction behavior and protoplasmic streaming in the slime mold Physarum polycephalum (Physarum kinetics) — Spacelab D1 mission
22 p3060 N88-28160
Graviperception of lentil seedling roots grown in space
22 p3061 N88-28165

GRAVITATION
NT ARTIFICIAL GRAVITY
NT EARTH GRAVITATION
NT GRAVITY ANOMALIES
NT LUNAR GRAVITATION
NT PLANETARY GRAVITATION
NT REDUCED GRAVITY
NT STELLAR GRAVITATION
Inequivalent quantizations and fundamentally perfect spaces
[DE87-014225] 02 p0229 N88-11446
Regular effective action of gauge field theory and quantum gravity
[DE87-703076] 02 p0247 N88-11560
Analytical average model of studies on orbital resonance
03 p0269 N88-11689
Torsion as a source of expansion in a Bianchi type I universe in the self-consistent Einstein-Cartan theory of a perfect fluid with spin density
[AD-A184200] 03 p0322 N88-12037
New notions about space-time and gravitation
[DE87-703259] 03 p0383 N88-12408
Gravitational accretion of hot dark matter
03 p0388 N88-12439
On deviations from Newton's law and the proposal for a Fifth Force
[DE87-703368] 04 p0487 N88-13001
Homogeneous space-time of Goedel type in higher-derivate gravity
[DE87-703690] 04 p0500 N88-13077
A supersymmetric Lagrangian for Poincare gauge theories of gravity
[DE88-001670] 04 p0500 N88-13078
Software design for an airborne gravity measurement system
[AD-A185000] 05 p0634 N88-13878
Relativistic theory of gravitation and new concepts about space-time
09 p1240 N88-17431
Ambiguity in determining the effective action for string-corrected Einstein gravity
[PB87-166153] 09 p1259 N88-17550
On higher derivative gravity
[DE88-700619] 10 p1354 N88-18090
Applications of Lie group methods to the equations of magnetohydrodynamics
10 p1411 N88-18422
Hamiltonian approach to relativistic theory of gravity and to general relativity theory
[DE88-700404] 10 p1422 N88-18492
Connection between general observers and Lanczos potential
[DE88-700139] 11 p1563 N88-19354
Covariance analysis and post-processing of gravity compensation effects for aided multi-state navigation systems
[PAPER-87-13] 12 p1577 N88-19430
Relativistic theory of gravitation and criticism of General Relativity Theory (GRT)
[DE88-701304] 16 p2284 N88-23673
Gravitation and polarization properties of electromagnetic field
[DE88-702166] 19 p2654 N88-25761
Quantum gravity and new forces
[DE88-007829] 19 p2737 N88-26250
Prediction of velocity and temperature profiles in thermally driven gravity currents applied to stratified thermal storage tanks
[DE88-004452] 21 p2946 N88-27496
Gravitation electromagnetic theory
22 p3158 N88-28790
Newtonian and Einsteinian gravitation
22 p3158 N88-28791
Gravitation and electromagnetism
22 p3158 N88-28792
Electromagnetic theory of the gravitation
22 p3158 N88-28793
Cosmological applications
22 p3158 N88-28794
Gravitation control
22 p3158 N88-28795
Gravitational propulsion
22 p3158 N88-28796
Towards a finite quantum gravity
[DE88-701497] 23 p3294 N88-29619

GRAVITATION THEORY
NT SUPERGRAVITY
Gravity from symmetry breakdown of a gauge affine theory
[DE88-001671] 04 p0500 N88-13079
Non-minimal interaction of gravity with other physical fields: An overview
[DE87-703362] 05 p0624 N88-13819
A theoretical model for neutrino masses and mixing
[PREPRINT-553] 06 p0778 N88-14777
Analysis and synthesis of the Earth's gravity field variable in space and time using vector surface spherical functions
[SER-C-325] 07 p0878 N88-15328
On higher derivative gravity
[DE88-700619] 10 p1354 N88-18090
Qualitative methods in nonhomogeneous cosmology
[DE88-700620] 10 p1417 N88-18458
Modified theory of gravity
[DE88-700835] 12 p1642 N88-19830
Einstein metrics and Brans-Dicke superfields
[DE88-006992] 15 p2146 N88-22809
String driven inflation
[DE88-006994] 15 p2151 N88-22841
Bogolyubov transformation in relativistic theory of gravitation
[DE88-701592] 16 p2232 N88-23329
Inevitable inflation in Einstein-Cartan theory with improved energy-momentum tensor with spin
[NASA-TM-101146] 18 p2586 N88-25365
From general relativity to the theory of superstrings
18 p2587 N88-25369

GRAVITATIONAL COLLAPSE
Core bounce supernovae
[DE87-014910] 04 p0520 N88-13197
Galaxy formation by gravitational collapse in a universe dominated by cold dark matter
04 p0521 N88-13205
Supernova mechanisms: Before and after SN1987a
[DE88-003489] 10 p1429 N88-18533
Hydrodynamical equations for spherical gravitational collapse in terms of a generalized theory of gravitation with higher derivatives
[DE87-703027] 15 p2151 N88-22838
Microwave spectroscopy and gravitational collapse
18 p2594 N88-25413

GRAVITATIONAL CONSTANT
New class of spherically symmetric interior solution with cosmological constant
[DE87-703095] 02 p0226 N88-11422
Crucial cosmological observations
[DE87-703081] 02 p0251 N88-11587
On deviations from Newton's law and the proposal for a Fifth Force
[DE87-703368] 04 p0487 N88-13001
Some considerations on measuring the Newtonian gravitational constant G in an orbiting laboratory
07 p0922 N88-15603
Cosmic wavefunction with induced gravity
[DE88-701873] 20 p2884 N88-27129

GRAVITATIONAL EFFECTS
NT GRAVITATIONAL LENSES
NT LAGRANGIAN EQUILIBRIUM POINTS
Preliminary study of a biotechnology research facility for microgravity, executive summary
[MATRA-EPT/AS/VT209/246/NT]
01 p0032 N88-10204
Preliminary study of a gravitational biology facility for Columbus, executive summary
[MATRA-EPT/AS/VT209/255/NT]
01 p0032 N88-10205
Estimability of potential coefficients from orbit perturbations — satellite geodesy
[REPT-86.1] 01 p0064 N88-10408
Continuous flow electrophoresis system experiments on shuttle flights STS-6 and STS-7
[NASA-TP-2778] 02 p0156 N88-10978
On the role of convective motion during dendrite growth: Experiments under variable gravity, revised
[NASA-CR-179213] 02 p0156 N88-10979
Surface coatings and catalyst production by electrodeposition
03 p0297 N88-11863
Estimations of gravitational effects on thermal denaturation process in a biopolymer
03 p0318 N88-12013
A study of chaos and mixing in Rayleigh-Taylor and Richtmyer-Meshkov unstable interfaces
[AD-A184751] 03 p0320 N88-12026
Steady distortion of shape of geoid and normal gravity field under influence of tidal potential
04 p0459 N88-12839

Two-layer stratified flow analysis of gravity currents and turbidity currents in lakes, reservoirs and the ocean
04 p0463 N88-12864
Research and development of anti-G life support systems. Part 1: Development and evaluation of uniform-pressure anti-G suits
[AD-A185658] 06 p0754 N88-14628
Gravitational interaction of massless fields with higher spins (s greater than 2) 06 p0775 N88-14760
Allowable gravity-levels for Spacelab, Columbus and EURECA --- materials science
[BF-R-66.525-2] 07 p0838 N88-15084
Proceedings and program draft in Gravitational Biology in the Federal Republic of Germany --- Effects of Weightlessness on the Human Organism
[ESA-TT-988] 07 p0884 N88-15363
A theoretical concept for state changes and shape changes in weightlessness 07 p0884 N88-15365
Some remarks on gravitational biology
07 p0884 N88-15366
Investigations of Paramecium cells analyzed under microgravity conditions 07 p0884 N88-15367
The origin of the spicule skeleton of fresh water sponges (Spongillides) 07 p0885 N88-15368
Limb regeneration in amphibians, a suitable model for investigations of the effects of weightlessness as regards evolution and modifications 07 p0885 N88-15369
Investigations of the reproductive physiology of the rainbow trout (Salmo gairdneri Richardson)
07 p0885 N88-15370
Changes in the morphological and molecular biological processes during early embryo development in amphibians under micro-g conditions 07 p0885 N88-15371
A learning model as a basis for investigations of the effects of gravity on the learning processes and memory formulation 07 p0886 N88-15374
Morphology and development of the inner ear of Anurans 07 p0886 N88-15378
Human and animal hypovolemic reactions to increasing +Gz accelerations 07 p0890 N88-15395
JPRS report: Science and technology. USSR: Space Biology and Aerospace Medicine, volume 21, no. 4, July - August 1987
[JPRS-USB-88-002] 07 p0893 N88-15412
Experiments with rats flown aboard Cosmos-1667 biosatellite (main objectives, conditions and results)
07 p0893 N88-15414
JPRS report: Science and technology. USSR: Space
[JPRS-USP-87-006] 08 p1001 N88-16063
Magnetic field of planet Uranus: Predictions, measurements, interpretations 08 p1005 N88-16094
Preliminary Material Science Experiment Rocket (MASER) 1 results and the evolution of the MASER program 08 p1033 N88-16260
Flight results of the ESA experiment modules in Materials Science Experiment Rocket (MASER) 1
08 p1033 N88-16261
Life sciences experiments on stratospheric balloons and sounding rockets 08 p1033 N88-16262
The D-1 Biorack results: A base for further space biological investigations 08 p1033 N88-16263
Scientific objectives and functional requirements of life sciences in the Space Station 08 p1033 N88-16264
The ESA Anthrorack project: Integrated research in human physiology 08 p1033 N88-16265
Contribution of stratospheric balloon flights in space biology 08 p1033 N88-16266
White blood cells in space: An experiment for the first Spacelab mission 09 p1127 N88-16757
Looking for new gravitational forces with antiprotons
[DE88-003154] 09 p1192 N88-17142
Potential use of the bioreactor to determine effects of microgravity and other environmental parameters on growth of hybridoma cells 09 p1198 N88-17178
Research in theoretical physics
[DE88-003201] 09 p1259 N88-17548
Microgravity research at the University of Mexico: Experiments in payload G-006 10 p1286 N88-17692
Ten past and ten future GAS/MAUS-payloads
10 p1287 N88-17696
Drosophila geotaxis as a tool for the study of aging
10 p1288 N88-17706
Embryonic development of guppy in weightlessness
10 p1360 N88-18127
Myosin Ca sup (2+), Mg sup (2+)-adenosine triphosphatase activity in ray myocardium following 30-day expose to 1.1 and 2.0 G 10 p1362 N88-18141
Investigation of genetic structures of rat germ cells following flight aboard Cosmos-1514 biosatellite during their prenatal development 10 p1364 N88-18155
Two-dimensional static otolith model
10 p1367 N88-18167
Hemodynamic effects of beta-adrenergic blocking with obsidan in clinostatic and orthostatic positions
10 p1367 N88-18171
NASA Workshop on Biological Adaptation
[NASA-TM-89468] 10 p1368 N88-18174
Study of the production of some superconducting and magnetic materials by solidification in the drop tube and drop tower
[NASA-CR-182494] 11 p1461 N88-18708
Conceptualization and design of a variable-gravity research facility
[NASA-CR-182574] 12 p1595 N88-19550
Proceedings of the 3rd European Symposium on Life Sciences Research in Space
[ESA-SP-271] 12 p1652 N88-19893
The European Space Agency's role in life sciences and research in space 12 p1652 N88-19894
The ESA facility Biorack 12 p1652 N88-19897
The respiratory system under weightlessness
12 p1653 N88-19901
Plant biology in space 12 p1654 N88-19910
Cardiovascular adaptation to zero-g during a long term flight (237 days) on board the Salyut 7 Soviet space station (1984) 12 p1655 N88-19920
Effects of cosmic heavy ion radiation and space microgravity on plant systems 12 p1658 N88-19936
Experiments concerning gravisensitivity of protozoa
12 p1660 N88-19949
Antibiotic activity in space, results and hypothesis
12 p1660 N88-19952
Biorack experiments in Spacelab D-1 and TML-1: Further developments in gravitational biology
12 p1661 N88-19953
Why life science in space? The next step to go beyond 12 p1661 N88-19954
The suspended Japanese quail as an animal model for experiments related to microgravity
12 p1662 N88-19960
Domain perturbation method in the static equilibrium of masses in rotation
[INPE-4217-PRE/1098] 12 p1686 N88-20085
Mechanical design of a ultrahigh gravity UHV facility to launch and recover a low-speed projectile tested on board KC 135 14 p1877 N88-21216
Space experiment plan FMPT
15 p2051 N88-22220
Amorphous semiconductors made in space
15 p2051 N88-22221
Containerless glass melting 15 p2051 N88-22222
Generation and coalescence of bubbles and stability of foams under microgravity conditions
[BMFT-FB-W-86-020] 16 p2184 N88-23017
The determination of gravity and topography from seismic velocities, accounting for dynamic behavior of the Earth's mantle
[ETN-88-92420] 17 p2374 N88-24117
An experiment to investigate Rankine cycle two-phase microgravity issues 17 p2409 N88-24322
Nucleate pool boiling: High gravity to reduced gravity; liquid metals to cryogens 17 p2431 N88-24464
Flotation processes
[PB88-180302] 18 p2540 N88-25075
Cardiovascular effects of weightlessness and ground-based simulation
[NASA-TM-88314] 18 p2551 N88-25140
Fraction eutectic measurements in slowly cooled Pb - 15 wt percent Sn alloys
[NASA-CR-180830] 19 p2618 N88-25531
Noninvasive examination of bones during long-term hypokinesia 19 p2704 N88-26077
Industrial processes influenced by gravity
[NASA-CR-182140] 20 p2782 N88-26497
Thermostatistical estimations of vapor-state molecules affected by gravity in a heat pipe
20 p2783 N88-26505
An experimental investigation of transient characteristics in a gravity-assisted heat pipe 20 p2783 N88-26506
EEG indices of G-induced Loss Of Consciousness (G-LOC) 21 p2982 N88-27709
The auditory evoked response in military pilots
21 p2984 N88-27721
Biorack on Spacelab D1: An overview of the first flight of Biorack, an ESA facility for life sciences research in microgravity
[ESA-SP-1091] 22 p3059 N88-28154
A brief overview of the results of the experiments using the ESA Biorack Facility on the German Spacelab D1 mission 22 p3060 N88-28155
The Biorack facility and its performance during the D1 Spacelab mission 22 p3060 N88-28156
The effects of microgravity on genetic recombination in Escherichia coli --- Spacelab D1 mission
22 p3060 N88-28157
Growth and differentiation of Bacillus subtilis under microgravity conditions 22 p3060 N88-28158
The Antibio experiment --- Spacelab D1 mission
22 p3060 N88-28159
Contraction behavior and protoplasmic streaming in the slime mold Physarum polycephalum (Physarum kinetics) --- Spacelab D1 mission 22 p3060 N88-28160
The Paramecium experiment --- Spacelab D1 mission
22 p3060 N88-28161
The biological clock of Chlamydomonas reinhardii in space 22 p3061 N88-28162
Effect of microgravity on lymphocyte activation --- Spacelab D1 mission 22 p3061 N88-28163
The effect of microgravity on mammalian cell polarization at the ultrastructural level --- Spacelab D1 mission
22 p3061 N88-28164
Graviperception of lentil seedling roots grown in space
22 p3061 N88-28165
Effects of short spaceflights on Drosophila melanogaster embryogenesis and life span 22 p3061 N88-28166
Embryogenesis and organogenesis of Carausius morosus under spaceflight conditions
22 p3061 N88-28167
The role of gravity in the establishment of the dorso/ventral axis in the amphibian embryo --- Spacelab D1 mission 22 p3062 N88-28168
Interplanetary travel: Is gravity needed to close the loop
[NASA-TM-101013] 22 p3132 N88-28622
Gravitation electromagnetic theory
22 p3158 N88-28790
Newtonian and Einsteinian gravitation
22 p3158 N88-28791
Gravitation control 22 p3158 N88-28795
The origin of the moon: Further studies of the giant impact 24 p3440 N88-30474

GRAVITATIONAL FIELDS

Precise orbit computation, gravity model adjustment and altimeter data processing for the ERS-1 altimetry mission
[ESA-CR(P)-2436] 02 p0130 N88-10820
On the theory of the Michelson-Morley experiment in the Earth's gravitational field
[DE87-703077] 02 p0198 N88-11233
Study of a satellite-to-satellite tracking gravity mission
[ESA-CR(P)-2419] 02 p0198 N88-11237
Spherical harmonic expansion of the Levitus Sea surface topography
[NASA-CR-181448] 02 p0216 N88-11362
Covariant Lorentz anomalies in higher dimensional space
[DE87-753021] 02 p0230 N88-11448
GEOSAT altimeter geophysical data record user handbook
[PB87-213336] 03 p0276 N88-11743
East coast gravity validation study
[AD-A184292] 03 p0351 N88-12217
Non-minimal interaction of gravity with other physical fields: An overview
[DE87-703362] 05 p0624 N88-13819
Advanced simulation and analysis of a geopotential research mission
[NASA-CR-182355] 06 p0670 N88-14108
Analysis and synthesis of the Earth's gravity field variable in space and time using vector surface spherical functions
[SER-C-325] 07 p0878 N88-15328
Assessment of anomalous gravitational field of elastic Earth 07 p0921 N88-15594
Perturbations of the Sun's gravitational field due to solar oscillations
[DE88-002099] 07 p0946 N88-15751
Solar oscillations, gravitational multipole field of the Sun and the solar neutrino paradox
[DE88-002100] 07 p0946 N88-15752
New possibilities for using gravity data in developing geodetic coordinate systems 08 p1009 N88-16116
Qualitative methods in nonhomogeneous cosmology
[DE88-700620] 10 p1417 N88-18458
Hamiltonian approach to relativistic theory of gravity and to general relativity theory
[DE88-700404] 10 p1422 N88-18492
Seventy years of the general theory of relativity
[DE88-700784] 11 p1563 N88-19356
Comparisons of global topographic/isostatic models to the Earth's observed gravity field
[NASA-CR-182696] 13 p1798 N88-20752
Spin precession in stationary gravitational fields
[DE88-701107] 15 p2093 N88-22470
Hydrodynamical equations for spherical gravitational collapse in terms of a generalized theory of gravitation with higher derivatives
[DE87-703027] 15 p2151 N88-22838
Direct numerical simulation of buoyantly driven turbulence 16 p2196 N88-23097
Bogolyubov transformation in relativistic theory of gravitation
[DE88-701592] 16 p2232 N88-23329

Relativistic theory of gravitation and criticism of General Relativity Theory (GRT)
[DE88-701304] 16 p2284 N88-23673
Evaluation of a model of the Earth's gravity field
[EPSHOM-003/87] 17 p2373 N88-24116
Non-Newtonian gravity or gravity anomalies?
[NASA-TM-4030] 17 p2374 N88-24118
Gravitation and polarization properties of electromagnetic field
[DE88-702166] 19 p2654 N88-25761
Symmetry problem of energy-momentum tensor and the creation of gravitational field
[DE88-702442] 21 p3026 N88-27964
Gravitational redshift of self-gravitating systems of dark matter in the universe
[DE88-702688] 23 p3300 N88-29650
General equations for the motions of ice crystals and water drops in gravitational and electric fields
[NASA-CR-183229] 24 p3370 N88-30070
Estimation of short-wavelength gravity on a dense grid using digital terrain elevation data
[AD-A196325] 24 p3391 N88-30196
Relationships among earth's gravity field, magnetic field, crustal structure and the magnetic character of crustal rocks
[AD-A195539] 24 p3392 N88-30198
Gravity anomalies, plate tectonics and the lateral growth of Precambrian North America 24 p3400 N88-30248
Resonance effects accompanying motion with low thrust in earth-moon system 24 p3446 N88-30510

GRAVITATIONAL LENSES
Prediction and analysis of basic gravitational microlensing phenomena 11 p1550 N88-19272
Light propagation through gravitationally perturbed Friedmann universes 18 p2577 N88-25307

GRAVITATIONAL PHYSIOLOGY
Scientific objectives and functional requirements of life sciences in the Space Station 08 p1033 N88-16264
The ESA Anthrorack project: Integrated research in human physiology 08 p1033 N88-16265
ESA's facility for research in human physiology in space: Anthrorack 12 p1652 N88-19896
The respiratory system under weightlessness 12 p1653 N88-19901
Respiratory parameters aboard an aircraft performing parabolic flights 12 p1653 N88-19902
Influence of a 6 hr head-out water immersion on different tests of endurance performance capacity 12 p1653 N88-19903
Second-generation respiratory monitoring system for microgravity studies in man 12 p1653 N88-19906
Lung function in simulated microgravity 12 p1654 N88-19907
Fluid volume changes in astronauts: How they fit our understanding of physiology 12 p1655 N88-19919
Cardiovascular adaptation to zero-g during a long term flight (237 days) on board the Salyut 7 Soviet space station (1984) 12 p1655 N88-19920
Cardiac and peripheral circulation assessment by ultrasound on 3 astronauts during two 7-day space flights (1982 Salyut-7 - 1985 STS 51G) 12 p1656 N88-19921
Load and control of the cardiocirculatory system in weightlessness 12 p1656 N88-19922
Neuro-reflex mechanisms of circulation regulation in simulated microgravity 12 p1656 N88-19923
Physiological reactions upon controlled changes of blood distribution in humans 12 p1656 N88-19924
P-31 Magnetic Resonance Spectroscopy (MRS) of limb muscles during bedrest with exercise countermeasures 12 p1656 N88-19925
Disuse condition stimulates bone resorption in organ culture 12 p1656 N88-19926
An in vitro model system to study the effect of microgravity and loading conditions on the mineralization and resorption of skeletal tissues 12 p1657 N88-19927
Vestibular integrated function and microgravity 12 p1658 N88-19937
Neck receptor stimulation in 0 and 1 g 12 p1658 N88-19938
Synopsis of the Spacelab D-1 frog statolith experiment STATEX 12 p1659 N88-19940
The rate of adaptation to altered g in the human centrifuge: Implications for simulations of mass-discrimination in space flight 12 p1659 N88-19941
Effects of anti-g suit inflation on renin and aldosterone response physical exercise 12 p1659 N88-19944
Medilab: A project of a medical laboratory in space 12 p1660 N88-19946
Experiments concerning gravisensitivity of protozoa 12 p1660 N88-19949
Organs and tissues regeneration in amphibia under the space flight conditions 12 p1660 N88-19951
A new isodynamically-braked arm ergometer including the demonstration of a prototype 12 p1661 N88-19957
Assessment of intercompartment fluid shifts by blood densitometry in astronauts 12 p1661 N88-19958
Application of ARIADNE: A data bank-based information system for human physiology research --- Spacelab Anthrorack 12 p1662 N88-19962
Regulation of hemodynamics upon imitation of the transition to weightlessness (mathematical modeling) 13 p1810 N88-20817
Leg volume change under Lower Body Negative Pressure (LBNP) in dependence on stratification
[DFVLR-FB-87-47] 16 p2238 N88-23367

GRAVITATIONAL POTENTIAL
U GRAVITATIONAL FIELDS

GRAVITATIONAL RADIATION
U GRAVITATIONAL WAVES

GRAVITATIONAL WAVE ANTENNAS
Capacitive resonant transducer for the Frascati gravitational antenna
[IFSI-86-9] 05 p0578 N88-13528
Preliminary comparison of some coincidence methods for gravitational wave detectors
[NOTA-INTERNA-903] 14 p1945 N88-21604

GRAVITATIONAL WAVES
Media calibrations of the Doppler signal for a gravitational wave experiment --- interplanetary medium
[IFSI-86-13] 05 p0625 N88-13825
Activities report in interplanetary space physics
[IFSI-86-5] 05 p0659 N88-14047
Budget and programs for 1986 research
[IFSI-86-16] 05 p0660 N88-14048
Data recorded by the Rome room temperature gravitational wave antenna, during the supernova SN 1987 A in the Large Magellanic Cloud
[NOTA-INTERNA-879] 06 p0806 N88-14922
Dynamic modeling of the middle atmosphere 08 p1028 N88-16227
Observational evidence for saturation of gravity waves and the production of turbulence in the mesosphere 08 p1028 N88-16229
Equation of acoustic and gravitational waves in stratified moving medium 08 p1077 N88-16493
Equation of gravitational-gyroscopic waves: Angular potential and its applications 08 p1079 N88-16504
Preliminary comparison of some coincidence methods for gravitational wave detectors
[NOTA-INTERNA-903] 14 p1945 N88-21604
Light propagation through gravitationally perturbed Friedmann universes 18 p2577 N88-25307
Fourier transform of gravitational synchrotron radiation
[PREPRINT-588] 22 p3144 N88-28700
Acoustic-optical detector of gravitational waves based on high-quality crystals
[DE88-702459] 23 p3232 N88-29232
On the degenerate Ferrari-Ibanez solution for colliding plane gravitational waves
[MATH-REPT-209] 23 p3296 N88-29630

GRAVITONS
Comment on non-renormalization theorem in the four dimensional superstrings
[DE88-752551] 18 p2586 N88-25367

GRAVITROPISM
Gravisensing in lentil seedling roots grown in space (Spacelab D-1 mission) 12 p1654 N88-19911

GRAVITY
U GRAVITATION

GRAVITY ANOMALIES
Gravity and fault structures, Long Valley Caldera, California
[DE87-014117] 02 p0197 N88-11229
Study of a satellite-to-satellite tracking gravity mission
[ESA-CR(P)-2419] 02 p0198 N88-11237
Geophysical-geomorphological statistical regionalization of North Atlantic 06 p0726 N88-14466
Assessment of anomalous gravitational field of elastic Earth 07 p0921 N88-15594
A three-dimensional gravity model of the geologic structure of Long Valley caldera
[DE88-006331] 16 p2231 N88-23324
Modeling and estimation of a low degree geopotential model from terrestrial gravity data
[NASA-CR-182808] 16 p2232 N88-23330
Non-Newtonian gravity or gravity anomalies?
[NASA-TM-4030] 17 p2374 N88-24118
To relate measurements of gravity and geoid anomalies over the oceans to near surface density distributions
[AD-A192168] 18 p2547 N88-25120
Gravity anomalies, plate tectonics and the lateral growth of Precambrian North America 24 p3400 N88-30248

GRAVITY GRADIOMETERS
Monocrystalline silicon gradiometer for gravity experiments in space
[NASA-CR-181452] 01 p0050 N88-10321
Estimation of gravity vector components from Bell gravity gradiometer and auxiliary data under consideration of topography and associated analytical upward continuation aspects
[AD-A188146] 10 p1355 N88-18099
Spaceborne gravity gradiometry characterizing the data type 12 p1644 N88-19847
GRADIO three-axis electrostatic accelerometers 12 p1645 N88-19849
Gradiometer accommodation on board a drag-free satellite 12 p1645 N88-19850
Gradiometer mission spectral analysis and simulation studies: Past and future 12 p1645 N88-19851
Satellite gradiometry
[B8735057] 16 p2229 N88-23313

GRAVITY PROBE B
A 1987 progress report of manufacturing techniques for Gravity Probe B gyroscope rotors
[NASA-TM-100312] 02 p0176 N88-11101

GRAVITY WAVES
NT BAROCLINIC WAVES
Toward operational forecasting and detection of weather-producing gravity waves 02 p0208 N88-11303
Dispersion equation for plane capillary-gravity wave on free surface of viscous incompressible fluid 04 p0459 N88-12842
Influence of surfactants on damping of gravity-capillary waves. 1: Frequency dependence 04 p0459 N88-12843
Meteor observation by the Kyoto meteor radar 06 p0733 N88-14507
A study of the mechanism of internal gravity wave generation by quasigeostrophic meteorological motions 06 p0735 N88-14520
Study of internal gravity waves in the meteor zone 06 p0735 N88-14521
Numerical modeling of troposphere-induced gravity wave propagation 06 p0735 N88-14522
A statistical study of variations of internal gravity wave energy characteristics in meteor zone 06 p0735 N88-14523
Internal gravity waves in the meteor zone in the Tbilisi Region 06 p0736 N88-14528
Observations of inertial period waves and vertical velocities in the tropical middle atmosphere using the MST radar technique 06 p0742 N88-14562
An analysis of apparent-motion vectors in, and the structure of, A mid-latitude sporadic E layer using a 2.66 MHz radar
[AD-A186126] 07 p0877 N88-15321
Rayleigh lidar observations of gravity wave activity in the stratosphere and lower mesosphere
[NASA-CR-182384] 09 p1189 N88-17123
Universal power spectra for wave turbulence: Applications to wind waves, flicker noise, solar wind spectrum and classical second sound 10 p1318 N88-17879
Evolution of acoustic gravity wave packet in spatially and temporally varying wind 11 p1469 N88-18760
Seasonal variations and excitation mechanisms of the equatorially trapped waves 13 p1798 N88-20751
Observations of waves and Langmuir circulation with Doppler sonars 13 p1805 N88-20790
Propagation of acoustic gravity wave spectrum through vertical wind shear region 16 p2186 N88-23035
Gravity currents with heat transfer effects
[PB88-180047] 16 p2205 N88-23158
Propagation of linear gravity waves in a relativistic atmosphere
[DE88-702062] 19 p2691 N88-25995
Propagation of inernio-acoustic gravity waves in a rotating and radiating opaque atmosphere
[DE88-701866] 20 p2823 N88-26750

GRAVSAT SATELLITES
U GEOPOTENTIAL RESEARCH MISSION

GRAY SCALE
Weighted averaging method for image smoothing reported 14 p1901 N88-21352
Visualization of digital terrain models 17 p2364 N88-24081
Applications of differential geometry to the shape analysis of gray-value images 21 p2924 N88-27358

GRAZING
All-optical beam control by forced Rayleigh scattering
[AD-A184315] 04 p0490 N88-13018
Acoustic scattering from composite wind-wave surfaces 3: Forward scatter intensities and spatial coherence at low and high frequencies and small grazing angles for Bubble-free regimes
[AD-A185908] 07 p0881 N88-15345
Models for electromagnetic scattering from the sea at extremely low grazing angles
[AD-A190472] 15 p2057 N88-22261

Characterization, topology, and cartography of grasslands for the development of fodder resources. (Preliminary Evaluation Program for SPOT number 26)
22 p3095 N88-28377

GRAZING FLOW
Measured and calculated acoustic attenuation rates of tuned resonator arrays for two surface impedance distribution models with flow
[NASA-TP-2766] 09 p1241 N88-17440

GRAZING INCIDENCE
Backscatter from a periodic rough surface at near grazing incidence
[NASA-CR-182397] 07 p0845 N88-15128
Grazing incidence X-ray scattering study of defect structures in MBE GaAs/Si using synchrotron radiation
[DE88-004556] 10 p1420 N88-18483
Design, construction and performance of the ROSAT high resolution X-ray mirror assembly
[MPE-PREPRINT-101] 15 p2150 N88-22836
An experimental study of the coherent under-ice reflectivity of sound in the Greenland Sea Marginal Ice Zone 18 p2548 N88-25125
The XRD (X-Ray Diode) array, the grazing incidence spectrometer and the X-ray imaging camera on PBFA 2
[DE88-007282] 19 p2728 N88-26200

GRAZING LANDS
U GRASSLANDS

GREASES
Low extractable wipers for cleaning space flight hardware 02 p0137 N88-10863
Developing an accelerated endurance test for greases: A status report
[AD-A185963] 07 p0836 N88-15072
Improved perfluoroalkylether fluid development
[NASA-CR-180872] 08 p0967 N88-15851
Characteristics and use of lubricating greases
[DE88-751103] 11 p1463 N88-18723
Evaluation of solder flux solvents in a vapor-degreasing application for hybrid microcircuits
[BDX-613-3638] 11 p1468 N88-18752

GREAT BASIN (US)
Historical catalog of Southern Great Basin earthquakes, 1868-1978
[DE87-014340] 02 p0198 N88-11232

GREAT BRITAIN
U UNITED KINGDOM

GREEN THEOREM
U GREEN'S FUNCTIONS

GREEN'S FUNCTIONS
Extending Green's function formalism to general nonlinear equations
[DE87-013541] 02 p0224 N88-11411
The Green's function method for fully unsteady aerodynamics around three-dimensional bodies and its application to flutter analysis
[UTIAS-298] 03 p0260 N88-11639
Efficient computation of periodic Green's functions with application to grating structures
[AD-A184853] 05 p0640 N88-13912
Method of two-time Green functions in molecular hydrodynamics of superfluid liquid
06 p0771 N88-14735
Green's function for a ball
[AD-A186239] 07 p0910 N88-15516
Symbolic, algebraic, and numeric solutions to heat conduction problems using Green's functions
09 p1165 N88-16987
Comment on the Adler-Bardeen theorem and related problems
[DE88-751051] 10 p1403 N88-18367
Investigation of a ray-mode representation of the Green's function in a rectangular cavity
[PB88-131677] 11 p1469 N88-18763
Estimates of green tensors for certain boundary value problems
[NASA-TT-20203] 11 p1535 N88-19172
Finite element calculations for aerodynamic coefficients of a 3-dimensional body in subsonic flow using Green's function method
[NASA-TT-20208] 13 p1718 N88-20272
Monte Carlo modified method for Green function. Algorithm and computer code for calculations in equal mass many-body system
[DE88-701114] 14 p1957 N88-21667
Construction of approximations to acoustic Green's functions for nonhomogeneous oceans using transmutation
[PB88-185384] 18 p2548 N88-25126
Green's function approach to roughening transition of one-dimensional restricted solid on solid model
[DE88-702723] 23 p3278 N88-29512

GREENHOUSE EFFECT
Testimony to the US Senate on the greenhouse effect
[DE87-013995] 01 p0071 N88-10458
Global environmental change research
[S-HRG-100-301] 03 p0348 N88-12199
The effects of minor trace gases on the transfer of thermal infrared radiation through the Earth's atmosphere 04 p0468 N88-12893
Carbon dioxide and climate 14 p1936 N88-21545
Observational and theoretical studies of greenhouse climate effects
[DE88-006237] 14 p1948 N88-21621
A primer on greenhouse gases
[DE88-007576] 19 p2689 N88-25981
Surface energy balance of three general circulation models: Current climate and response to increasing atmospheric CO2
[DE88-010967] 21 p2975 N88-27673
Atmospheric science issues in Congress
22 p3125 N88-28573
Episodic vs. epochal release of SO2 on Mars
23 p3305 N88-29688
Nineteenth Lunar and Planetary Science Conference. Press abstracts
[NASA-CR-183037] 24 p3440 N88-30473
Did the greenhouse effect kill the dinosaurs
24 p3442 N88-30484

GREENLAND
Narsarsuaq (Greenland) Geophysical Observatory. Magnetic results, 1984
[ISBN-87-7478-281-9] 02 p0198 N88-11235
Narssarssuaq Geophysical Observatory: Magnetic results, 1980-83. Instrumentation and formulas
[ISBN-87-7478-280-0] 03 p0350 N88-12209
The ice conditions in the Greenland waters, 1981
[ISBN-87-7478-276-2] 05 p0629 N88-13844
The Greenland Sea Project: The Arctemiz project
14 p1939 N88-21573
Meteorological features during the marginal ice zone experiment from 20 March to 10 April 1987
[AD-A193960] 23 p3235 N88-29251

GREGORIAN ANTENNAS
A new approach for shaping of dual-reflector antennas
[NASA-CR-182581] 11 p1476 N88-18806

GRID GENERATION (MATHEMATICS)
Problem and solution formulations for the generation of 3D block-structured grids --- aircraft design
[NLR-MP-86020-U] 01 p0005 N88-10028
Generation of body-fitted grids for two dimensional interior domains by the solution of a system of Poisson equations using multigrid techniques
[GMD-246] 01 p0044 N88-10281
Generating meshes for finite-difference analysis using a solid modeler
[DE88-001458] 04 p0439 N88-12729
Analytical method for generating computational grids about complete aircraft configurations
05 p0540 N88-13287
Shuttle computational grid generation
06 p0794 N88-14863
A multistage mesh generator for solving the average-passage equation system
[NASA-CR-179539] 08 p0951 N88-15769
Adaptive finite difference methods in fluid dynamics
08 p0985 N88-15958
Mesh generation 08 p0986 N88-15971
An automatic finite element mesh generator
[AD-A186939] 09 p1216 N88-17291
Finite element mesh generation and isoparametric elements
[NPL-DITC-97/87] 09 p1229 N88-17365
Approaches to the automatic generation and control of finite element meshes 11 p1526 N88-19113
Generation of surface grids through elliptic partial differential equations for aircraft and missile configurations
[AD-A186631] 11 p1535 N88-19169
The construction of a three-dimensional finite volume grid generator for a wing in a wind tunnel with application to Navier-Stokes flow solvers
[FFA-TN-1987-58] 13 p1719 N88-20277
A knowledge system for automatic finite element mesh generation: AMEKS
[DE87-014894] 13 p1826 N88-20914
Three-dimensional mesh-generation and plotting routines for use with a boundary element program (BIE3D)
[AD-A188079] 14 p1958 N88-21675
Development of adaptive grid schemes based on Poisson grid generators
[AD-A190953] 16 p2262 N88-23528
Two dimensional hyperbolic grid generation
[VKI-TN-162] 18 p2511 N88-24897
Application of advanced grid generation techniques for flow field computations about complex configurations
[NASA-CR-183049] 18 p2515 N88-24922
Numerical simulations of flow around shuttle orbiter
19 p2635 N88-25633
The role of computational fluid dynamics in aeronautical engineering (5). Improvements and applications of implicit TVD finite volume code 19 p2638 N88-25653
Grid generation of a helicopter rotary-wing
19 p2640 N88-25665
Finite element welding computations using general purpose nonlinear analysis codes
[DE88-005398] 20 p2808 N88-26659
Three-dimensional adaptive grid generation for body-fitted coordinate system
[NASA-CR-182192] 21 p2950 N88-27520
Three dimensional grid generation for complex configurations: Recent progress
[AGARD-AG-309] 23 p3245 N88-29313
Lessons learned in the mesh generation for PN/S calculations 23 p3245 N88-29314
Three-dimensional elliptic grid generation for an F-16
23 p3246 N88-29315
Component adaptive grid generation for aircraft configurations 23 p3246 N88-29316
Generation of multiple block grids for arbitrary 3D geometries 23 p3246 N88-29317
Grid generation on and about a cranked-wing fighter aircraft configuration 23 p3246 N88-29318
Grid generation for an advanced fighter aircraft
23 p3246 N88-29319
Algebraic grid generation for fighter type aircraft
23 p3246 N88-29320
Composite grid generation for aircraft configurations with the EAGLE code 23 p3246 N88-29321
Analytical surfaces and grids
23 p3247 N88-29322
Mesh generation for industrial application of Euler and Navier Stokes solvers 23 p3247 N88-29323
Experience with three dimensional composite grids
23 p3247 N88-29324
Grid generation around transport aircraft configurations using a multi-block structured computational domain
23 p3247 N88-29325
Adaptive mesh generation for viscous flows using Delaunay triangulation
[NASA-CR-181699] 24 p3316 N88-29749
Three-dimensional elliptic grid generation technique with application to turbomachinery cascades
[NASA-TM-101330] 24 p3372 N88-30078
Knowledge-based flow field zoning
[NASA-TM-101023] 24 p3412 N88-30314

GRIDS (MATHEMATICS)
U COMPUTATIONAL GRIDS

GRIGG-SKJELLERUP COMET
The Giotto extended mission
14 p2005 N88-21957
Alternative cometary targets for the Giotto extended mission 14 p2010 N88-21990

GRINDING
Surface fatigue life of CBN and vitreous ground carburized and hardened AISI 9310 spur gears
[NASA-TM-100960] 19 p2677 N88-25916

GRINDING (MATERIAL REMOVAL)
Reaming experiments for the lethality test system
[DE88-007902] 20 p2763 N88-26383

GRINDING MACHINES
Size-reduction and sorting behavior in sieve hammer mills
[ETN-88-91480] 11 p1467 N88-18749

GROOVES
Heat transfer characteristics of arterial heat pipe with axial grooves 03 p0319 N88-12017
Riblets for aircraft skin-friction reduction
07 p0814 N88-14955
An assessment of the drag reduction properties of riblets and the penalties of off-design conditions
[RAE-TM-AERO-2113] 17 p2295 N88-23731
Drag reduction of turbulent boundary layers by means of grooved surfaces
[ETN-88-92618] 20 p2802 N88-26630

GROOVING
Surface gouging by hypervelocity sliding contact between metallic materials
[DE88-001937] 06 p0682 N88-14178
Experimental investigation of turbulent flow in smooth and longitudinal grooved tubes
[NASA-TM-77480] 20 p2800 N88-26615

GROUND BASED CONTROL
NT AIR TRAFFIC CONTROL
Teleoperation and control study --- orbital servicing
[BAE-TP-8268] 01 p0076 N88-10489
Space shuttle onboard navigation console expert/trainer system 09 p1203 N88-17208
An intelligent training system for payload-assist module deploys 09 p1204 N88-17214
Promising concepts for ground-to-orbit experiment teleoperation --- Columbus 12 p1590 N88-19518
Ground based supervisory and programming system for automatic experiment execution in orbit
12 p1590 N88-19519
A teleoperated manipulator system concept for unmanned platforms --- Columbus
12 p1593 N88-19537

Optimization of the dilation characteristic on the control jurisdiction of an area control facility
[AD-A191720] 18 p2461 N88-24615
SP-100 Ground Engineering Systems: Test facility control systems
[DE88-009195] 21 p3015 N88-27895

GROUND CREWS
Training in satellite ground system operations 09 p1129 N88-16775

GROUND EFFECT (AERODYNAMICS)
Dispersion in the wake of aircraft: An investigation of the effects of a ground plane on trailing vortices. Literature survey
[IC-AERO-REP-86-04] 01 p0003 N88-10014
An experimental investigation of dynamic ground effect
[NASA-CR-4105] 04 p0394 N88-12458
Propulsion-induced effects caused by out-of-ground effects
[NASA-TM-100032] 06 p0666 N88-14088
Recommendations for ground effects research for V/STOL and STOL aircraft and associated equipment for large scale testing
[NASA-CR-177429] 10 p1268 N88-17585
Model-scale sound propagation experiment
[NASA-TM-100602] 15 p2130 N88-22709
A numerical study of the hot gas environment around a STOVL aircraft in ground proximity
[NASA-TM-100895] 17 p2295 N88-23729
Aerodynamics in ground effect and predicted landing ground roll of a fighter configuration with a secondary-nozzle thrust reverser
[NASA-TP-2834] 24 p3317 N88-29752

GROUND EFFECT (COMMUNICATIONS)
Discharge prevention of geosynchronous orbit conductive thermal control materials and grounding systems 03 p0274 N88-11732
An investigation of terrain related variables for predicting the multipath fade depth distribution on terrestrial microwave lines 12 p1615 N88-19654
A review of the role of surface reflection in multipath propagation over terrestrial microwave links 12 p1615 N88-19655
Development of a ground-conductivity map for the area of the Federal Republic of Germany from measured field-strength contours 12 p1615 N88-19656
Analysis, suppression of land clutter characteristics reported 14 p1903 N88-21369
Performance study of a unipole antenna with conventional and elevated radial wire ground screens
[AD-A193283] 21 p2933 N88-27413

GROUND EFFECT MACHINES
Feasibility report: Operation of light air cushion vehicle at McMurdo Sound, Antarctica
[AD-A189057] 13 p1755 N88-20494

GROUND HANDLING
EASE/ACCESS ground processing at Kennedy Space Center 02 p0139 N88-10877
Turnaround operations analysis for OTV. Volume 2: Detailed technical report
[NASA-CR-179317] 13 p1729 N88-20341
Turnaround operations analysis for OTV. Volume 3: Technology development plan
[NASA-CR-179318] 13 p1729 N88-20342
Turnaround operations analysis for OTV. Volume 4: WBS and dictionary and cost methodology
[NASA-CR-179319] 13 p1729 N88-20343

GROUND STATE
A mechanism for symmetry breaking in antiferromagnetic Heisenberg systems
[ETN-88-91320] 05 p0657 N88-14031
Ground-state correlations in C12 and the mechanism of the (e,e'p) reaction
[B6729349] 14 p1980 N88-21816
Overview of hydrogen clusters 16 p2267 N88-23557
Energy-transfer properties and mechanisms
[DE88-007107] 18 p2571 N88-25272
Ground state properties and electronic structure of high T sub c superconductors
[DE88-007485] 18 p2585 N88-25380
Contribution to the study of order effects in the Ising model framework: Ground states and phase diagrams
[ONERA-NT-1987] 20 p2880 N88-27095
The 2D Rydberg series in Al I
[NASA-TM-101189] 22 p3150 N88-28740
The ground state of the bosonic string
[USIP-88-01] 22 p3151 N88-28746
Measurements of XeF (Xenon Fluoride) ground state dissociation and vibrational equilibration
[AD-A194611] 23 p3280 N88-29527

GROUND STATIONS
NT INTEGRATED MISSION CONTROL CENTER
NT POLYSTATION DOPPLER TRACKING SYSTEM
Development of response models for the Earth Radiation Budget Experiment (ERBE) sensors. Part 2: Analysis of the ERBE integrating sphere ground calibration
[NASA-CR-178293] 01 p0049 N88-10316
The status of the international Halley watch 01 p0116 N88-10744
Results of the satellite and the Toulouse (France) receiving station operator --- SPOT 03 p0341 N88-12149
The Telecommunications and Data Acquisition Report
[NASA-CR-181546] 04 p0432 N88-12679
A hydrogen/nickel oxide battery for remote applications
[DE87-009048] 04 p0464 N88-12872
Design description report for a photovoltaic power system for a remote satellite earth terminal
[NASA-CR-179586] 04 p0465 N88-12875
Dobson-stations performance assessment using TOMS data 05 p0618 N88-13792
A single-station weather forecasting expert system
[AD-A184889] 05 p0627 N88-13832
Satellite ground-terminal user simulation
[NASA-TM-100234] 06 p0694 N88-14260
AVIRIS ground data-processing system 06 p0707 N88-14333
How ground-based observations contribute to rocket, balloon and space shuttle experiments: Experience from the past and outlook for the future 08 p1026 N88-16216
The Earthnet Heat Capacity Mapping Mission (HCMM) data-processing system at Lannion (France) 09 p1127 N88-16761
The design and implementation of the Technical Facilities Controller (TFC) for the Goldstone deep space communications complex 11 p1474 N88-18794
Application of the Global Positioning System (GPS) time receivers to the fundamental station Wettzell 11 p1506 N88-18995
Crustal Dynamics Project: Catalogue of site information
[NASA-RP-1198] 11 p1513 N88-19037
Multiple-beam ground station reflector antenna system: A preliminary study
[EUT-87-E-171] 14 p1904 N88-21379
An outdoor unit for Direct Broadcast Satellite (DBS) digital sound reception
[BMFT-FB-W-86-016] 16 p2189 N88-23050
A low cost automatic Earth observation satellite tracking ground receiving station 17 p2309 N88-23815
Service offerings and interfaces for the ACTS network of Earth stations
[NASA-TM-100809] 18 p2471 N88-24663
An 8.4-GHz dual maser front end for Parkes reimplementation 22 p3066 N88-28197
DSS 14 antenna calibrations for GSSR/VLA Saturn radar experiments 22 p3068 N88-28207
Business telecommunications using satellite microterminals: Gaining the competitive edge
[ESA-BR-49] 22 p3070 N88-28225
Determination of satcom access power levels within the ground segment
[RSRE-MEMO-4097] 22 p3070 N88-28226

GROUND SUPPORT EQUIPMENT
Research on Electrodynamic Tether Effects (RETE) experiment Electrical Ground Support Equipment (EGSE) --- tethered satellite
[IFSI-87-2] 05 p0555 N88-13378
RETE experiment Assembly, Integration, and Verification (AIV) activities
[IFSI-87-6] 05 p0555 N88-13380
Controlling stress corrosion cracking in mechanism components of ground support equipment 14 p1926 N88-21480
V2500 Condition Monitoring and Performance Analysis Software System (COMPASS): Overview of system --- aircraft engine
[PNR90418] 22 p3139 N88-28666
Artificial intelligence costs, benefits, risks for selected spacecraft ground system automation scenarios 24 p3416 N88-30332
Study on industrial organization for European Ground Support Equipment (EGSE) to support European space programs. Volume 1: Technical reports
[SD-RP-AI-009-VOL-1] 24 p3435 N88-30446
Study on industrial organization for European Ground Support Equipment (EGSE) to support European space programs. Volume 2: Technical reports
[SD-RP-AI-009-VOL-2] 24 p3435 N88-30448

GROUND SUPPORT SYSTEMS
EASE/ACCESS ground processing at Kennedy Space Center 02 p0139 N88-10877
Knowledge-based simulation 08 p1061 N88-16404
Columbus feasibility studies. Volume 4: Integration, test, and operations
[ETN-88-90576] 11 p1445 N88-18614
Microgravity User Support Center (MUSC) for EURECA, Spacelab and Columbus missions 12 p1660 N88-19947
The German processing and archiving facility for ERS-1
[ESA-CR(P)-2531] 13 p1851 N88-21082
Development of a mobile research flight test support capability
[NASA-TM-100428] 16 p2159 N88-22883
Reduced flexibility in processing Titan 4 space launch vehicles at Cape Canaveral Air Force Station
[AD-A194908] 24 p3332 N88-29834
Aerospace payload support systems
[AFGL-TR-87-0241] 24 p3334 N88-29843
Study on industrial organization for European Ground Support Equipment (EGSE) to support European space programs. Volume 1: Technical reports
[SD-RP-AI-009-VOL-1] 24 p3435 N88-30446
Study on industrial organization for European Ground Support Equipment (EGSE) to support European space programs. Volume 2: Technical reports
[SD-RP-AI-009-VOL-2] 24 p3435 N88-30448

GROUND TESTS
NT COLD FLOW TESTS
NT PRELAUNCH TESTS
NT STATIC FIRING
Ground shock profiles for an accidental explosion at the proposed Large Rocket Test Facility at Arnold Engineering Development Center
[DE88-002652] 07 p0853 N88-15180
Pattern recognition techniques for failure trend detection in SSME ground tests 07 p0924 N88-15614
A simulation study of the flight dynamics of elastic aircraft. Volume 2: Data
[NASA-CR-4102-VOL-2] 08 p0959 N88-15813
Coordinated use of European test facilities 09 p1123 N88-16726
The NASA integrated test facility and its impact on flight research
[NASA-TM-100418] 14 p1870 N88-21177
Description of ground motion data processing codes, volume 2
[DE88-007137] 15 p2095 N88-22481
A cyclic ground test of an ion auxiliary propulsion system: Description and operational considerations
[NASA-TM-100870] 17 p2313 N88-23829
Requirements and cost considerations for a combined space nuclear reactor test facility 17 p2401 N88-24277
Conceptual design of the SP-100 GES test site 17 p2402 N88-24284
Selection of a handling and maintenance option for the SP-100 ground engineering system test 17 p2402 N88-24285
SP-100 flight qualification testing assessment 17 p2424 N88-24414
SP-100 ground engineering systems test facility control systems 17 p2436 N88-24496
Australian structures response evaluation: Ground shock and air blast measurements for site investigation survey
[MRL-TN-526] 20 p2813 N88-26685
Successful completion of a cyclic ground test of a mercury ion auxiliary propulsion system
[NASA-TM-101351] 24 p3339 N88-29873

GROUND TRACKS
NT SATELLITE GROUND TRACKS
Radial track of moving objects determined by HF backscatter technique 14 p1901 N88-21354

GROUND TRUTH
From pattern to process: The strategy of the Earth Observing System: Volume 2: EOS Science Steering Committee report
[NASA-TM-89702] 07 p0871 N88-15283
Spectral measurements for correcting LANDSAT data for atmospheric effects 17 p2362 N88-24066
Evaluation of an estimation system for an irrigated area in a tropical region through TM-LANDSAT imagery 17 p2363 N88-24075
Evaluation of the mangrove area at the Piaui River (SE) through remote sensing 17 p2365 N88-24086
Stereoscopic photographs, ground and aerial, of trees used in the arborization of Curitiba (PR) 17 p2366 N88-24091
Integrating multispectral imagery and ground level hyperspectral signature data
[AD-A195976] 24 p3386 N88-30166

GROUND WATER
Water source heat pump: How to get home heating and cooling from your own back yard
[DE88-900180] 07 p0875 N88-15306
Boundary-integral-equation method for computing the three-dimensional flow of groundwater
[PB88-126891] 10 p1330 N88-17951
Reverse osmosis treatment to remove inorganic contaminants from drinking water
[PB88-147780] 12 p1605 N88-19598

Study of fractures as subsidiary research of ground water in the Sergipe state: An approach through remote sensing data
[INPE-4319-TDL/286] 12 p1639 N88-19813
Environmental projects. Volume 5, part 1: Study of subsurface contamination. Part 2: Guide to implement environmental compliance programs
[NASA-CR-182691] 13 p1796 N88-20741
Groundwater sapping valleys: Experimental studies, geological controls and implications to the interpretation of valley networks on Mars
[NASA-CR-182718] 15 p2152 N88-22847
A core hole into the hydrothermal system of the Long Valley caldera
[DE88-006335] 16 p2231 N88-23325
Indentification of shallow groundwater regions in semi-arid Brazil by remote sensing methods
17 p2355 N88-24030
Study of fracturing for groundwater research in the Sergipe state with remote sensing products
17 p2359 N88-24052
A zoomable and adaptable hidden fine-mesh approach to solving advection-dispersion equations
[DE88-006174] 21 p3004 N88-27816
Comparing different images for ground water survey based on lineament analysis 22 p3104 N88-28435

GROUND WAVE PROPAGATION
Surface-wave model uncertainty assessment
[AD-A193094] 21 p2932 N88-27408

GROUND WIND
Statistical very short-range forecasting via analogues
02 p0206 N88-11290
Short-term forecasting of lightning based on the surface wind field at Kennedy Space Center
02 p0208 N88-11306
Mesoscale surface field analysis from routine observations --- pressure, wind fields
02 p0209 N88-11315
High resolution determination of true surface winds at sea from wind and pressure data
02 p0210 N88-11316
A preliminary demonstration of the use of boundary-layer models of flow in complex terrain for high resolution surface wind forecasting 02 p0212 N88-11330
Cross flow in the Alps and flat foehn during the experiment MERKUR --- mesoscale experiment
06 p1013 N88-16142
Simulation of a typical flow in a broad valley
08 p1015 N88-16154
Moscow USSR. Limited surface observations climatic summary (LISOCS), parts A-F
[AD-A188080] 11 p1514 N88-19046

GROUND-TO-AIR MISSILES
U SURFACE TO AIR MISSILES

GROUP BEHAVIOR
U GROUP DYNAMICS

GROUP DYNAMICS
A comparison of the effects of group dynamics on individuals assigned to integral and non-integral aircrews
[AD-A186467] 08 p1051 N88-16345
Group adaptation and individual adjustment in antarctica: A summary of recent research
[AD-A186605] 08 p1051 N88-16347
First encounters of the close kind: The formation process of airline flight crews
[AD-A187977] 11 p1523 N88-19091
De Finetti's approach to group decision making
[AD-A188074] 11 p1536 N88-19177
The relationship between group process and performance 17 p2448 N88-24549
The human element in space: Lessons from Antarctica
[AD-A193440] 21 p2988 N88-27741

GROUP THEORY
NT AUTOMORPHISMS
Group analysis of equations arising in ocean acoustics
04 p0472 N88-12914
Group quantization of constrained systems
[PREPRINT-564] 06 p0790 N88-14844
Non-steady group combustion of a cloud of char particles
[DE87-010773] 08 p0966 N88-15849
The r-rank of the groups of exceptional Lie type
[CWI-PM-R8607] 08 p1072 N88-16468
A note on compactifications of products of semigroups
[CWI-PM-R8701] 08 p1072 N88-16469
Some aspects of control for semilinear distributed parameter systems
[INPE-4147-PRE/1054] 08 p1075 N88-16484
Perturbation theory for dual semigroups 2. Time-dependent perturbations in the sun-reflexive case
[PB88-113097] 09 p1230 N88-17369
Renormalization group analysis of the temperature dependent coupling constant in massless theory
[DE88-751059] 09 p1259 N88-17552
Mathematical foundations of signal processing. 2: The role of group theory
[AD-A188482] 12 p1620 N88-19685
Integrable quantum systems and classical Lie algebras
[DE88-700872] 12 p1683 N88-20063
SUSY anomaly in quantum-mechanical systems
[DE88-700890] 12 p1699 N88-20170
Group theoretic interpretations of Askey's scheme of hypergeometric orthogonal polynomials
[CWI-PM-R8703] 13 p1831 N88-20954
Lie groups in prolongation theory
[B8721781] 14 p1967 N88-21743
On generalized lie-like algebras
[PREPRINT-574] 14 p1968 N88-21748
Lumped model generation and evaluation: Sensitivity and Lie algebraic techniques with applications to combustion
[AD-A190402] 15 p2127 N88-22689
Perturbation theory for dual semigroups. Part 3: Nonlinear Lipschitz continuous perturbations in the Sun-reflexive case
[CWI-AM-R8706-PT-3] 16 p2263 N88-23535
Using Clifford algebras for the geometry of a tube domain (and its corresponding bounded domain) in the complexified Minkowski space of arbitrary dimension
[REPT-87-64] 16 p2264 N88-23540
Special relativity theory (one-dimensional case) without the postulate on the equality of directions
[DE88-701368] 16 p2284 N88-23674
Perturbation theory for dual semigroups. Part 4: The intertwining formula and the canonical pairing
[CWI-AM-R8802-PT-4] 18 p2569 N88-25258
Nontrivial critical points for asymptotically quadratic function
[DE88-101851] 20 p2845 N88-26881
Algebraic and arithmetic geometry in string theory
[CWI-PM-R8708] 20 p2848 N88-26904
Some remarks on geodesics in gauge groups and harmonic maps
[DE88-702665] 22 p3115 N88-28510
Global gauge anomaly of classical groups in even dimension
[DE88-008572] 22 p3158 N88-28797
Invariant ideals of multiplicity free algebraic group actions
[B8803517] 23 p3277 N88-29509

GROUP VELOCITY
Realization of active high pass filters for group velocity correction
[MPE-IN-REPT-47] 08 p0979 N88-15918

GROUP 7A COMPOUNDS
U HALOGEN COMPOUNDS

GROWTH
NT CROP GROWTH
NT CRYSTAL GROWTH
NT CZOCHRALSKI METHOD
NT DIRECTIONAL SOLIDIFICATION (CRYSTALS)
NT EPITAXY
NT LIQUID PHASE EPITAXY
NT MOLECULAR BEAM EPITAXY
NT VAPOR PHASE EPITAXY
NT VEGETATION GROWTH
Long term investigations of the growth, metabolism, and reproduction of fish under conditions close to weightlessness 01 p0074 N88-10473
A stochastic delamination growth model for fatigue loaded laminated composite materials
02 p0141 N88-10888
Molecular beam heteroepitaxy: (Ca,Sr)F2-GaAs system
[LAAS-87-168] 02 p0246 N88-11556
A functional interpretation of the logistic equation
[REPT-87-037] 05 p0645 N88-13946
Maximum likelihood estimates for the discrete application of the AMSAA growth model
[AD-A186921] 09 p1177 N88-17048
Synthesis and characterization of thin films
[AD-A187335] 10 p1421 N88-18485
Thermal oxide growth on silicon: Intrinsic stress and silicon cleaning effects
[AD-A188790] 13 p1736 N88-20377
Some problems of the theory of bubble growth and condensation in bubble chambers
[NASA-TT-20232] 13 p1771 N88-20593
Study of mean free path effects on growth of ultrafine metallic aerosols
[AD-A190206] 15 p2039 N88-22149
Vapor phase deposition and growth of polyimide films on copper
[AD-A189969] 15 p2044 N88-22178
The growth potential of corona discharges from aircraft flying in precipitation
[AD-A190507] 15 p2094 N88-22478
Mechanics of instability-related delimination growth
[NASA-TM-100622] 17 p2349 N88-23998
Biological patterns of growth in postnatal ontogenesis of lower primates 19 p2705 N88-26087
Growth and differentiation of Bacillus subtilis under microgravity conditions 22 p3060 N88-28158
The Paramecium experiment --- Spacelab D1 mission
22 p3060 N88-28161
Lattice-matched HgZnTe epitaxy development
[AD-A193677] 23 p3292 N88-29600
Growth of continental crust: Clues from Nd isotopes and Nb-Th relationships in mantle-derived magmas
24 p3393 N88-30205

GRUMMAN AIRCRAFT
NT F-14 AIRCRAFT
NT F-111 AIRCRAFT
NT OV-1 AIRCRAFT

GRUMMAN OV-1C AIRCRAFT
U OV-1 AIRCRAFT

GUANIDINES
The 1,2,3-triaminoguanidinium nitrate: An alternate explanation of the nitrate anion disorder
[AD-A188386] 12 p1612 N88-19640
Discovery of a low temperature form of TAGN (Triaminoguanidinium Nitrate)
[AD-A196059] 24 p3357 N88-29989

GUARDS (SHIELDS)
Trailer shield assembly for a welding torch
[NASA-CASE-MFS-29260-1] 18 p2524 N88-24972

GUIDANCE (MOTION)
NT AIRCRAFT GUIDANCE
NT COMMAND GUIDANCE
NT INERTIAL GUIDANCE
NT LASER GUIDANCE
NT MAP MATCHING GUIDANCE
NT MIDCOURSE GUIDANCE
NT RENDEZVOUS GUIDANCE
NT SPACECRAFT GUIDANCE
NT STRAPDOWN INERTIAL GUIDANCE
NT TERMINAL GUIDANCE
Fault tolerant considerations and methods for guidance and control systems
[AGARD-AG-289] 02 p0126 N88-10796
Guidance of high-altitude sounding rockets using the S19 and Spinning Rocket Altitude Control (SPINRAC) systems 08 p1034 N88-16273
Sounding rockets/microgravity products and service
08 p1035 N88-16277
Guidance and control of air-launched armaments: An aeroengineer's perspective 12 p1597 N88-19557
Terrestrial Propagation Characteristics in Modern Systems of Communications, Surveillance, Guidance and Control
[AGARD-CP-407] 12 p1614 N88-19653
Local free-space mapping and path guidance for mobile robots
[AD-A192970] 20 p2810 N88-26674
Approximations and implementations of nonlinear filtering schemes
[AD-A194685] 23 p3271 N88-29462
Stochastic game approach to guidance design
[AD-A194574] 23 p3276 N88-29498

GUIDANCE SENSORS
Fine attitude measurement system study. Volume 1: Executive summary
[BAE-TP-7831-VOL-1] 09 p1133 N88-16795
Fine attitude measurement system study, volume 2
[BAE-TP-7831-VOL-2] 09 p1133 N88-16796
Fine attitude measurement system study. Volume 3: Appendices
[BAE-TP-7831-VOL-3] 09 p1133 N88-16797
Advanced guidance algorithms for homing missiles with bearings-only measurements
[AD-A190435] 15 p2017 N88-22026
The optical accelerometer: A novel sensor for vertical flight guidance 18 p2518 N88-24935

GUIDE VANES
NT JET VANES
Test stand performance of a convertible engine for advanced V/STOL and rotorcraft propulsion
[NASA-TM-100211] 03 p0266 N88-11679
Possibilities for on-line surge suppression by fast guide vane adjustment in axial compressors
10 p1283 N88-17674
Experimental evaluation of turning vane designs for high-speed and coupled fan-drive corriers of 0.1-scale model of NASA Lewis Research Center's proposed altitude wind tunnel
[NASA-TP-2681] 10 p1285 N88-17686

GULF OF ALASKA
North Pacific Ocean. Gulf of Alaska, R/V Thomas G. Thompson: 1 February - 8 March 1987. STD data report
[AD-A186569] 08 p1045 N88-16314

GULF OF CALIFORNIA (MEXICO)
The interpretation of crustal dynamics data in terms of plate motions and regional deformation near plate boundaries
[NASA-CR-181475] 03 p0349 N88-12205

Earthquake source mechanisms and transform fault tectonics in the Gulf of California
03 p0349 N88-12206

GULF OF MEXICO
Hurricane climatology for the Atlantic and Gulf coasts of the United States
[PB88-114657] 08 p1039 N88-16288

GULF STREAM
Study of evolution of Gulf Stream cyclinic eddy
06 p0727 N88-14473
Hydrochemical structure of Gulf Stream frontal zone waters 06 p0727 N88-14476
Estimates of ocean-atmosphere thermal interaction in Gulf Stream energy-active test range in winter of 1984
13 p1785 N88-20679
Phenomenological description of eddy registered in Gulf Stream 13 p1787 N88-20694
Studies toward observing and modelling large energetic ocean regions
[AD-A189267] 13 p1803 N88-20778
Application of acoustic-Doppler current profiler and expendable bathythermograph measurements to the study of the velocity structure and transport of the Gulf Stream
[NASA-CR-183188] 22 p3129 N88-28605

GULFS
NT GULF OF ALASKA
NT GULF OF CALIFORNIA (MEXICO)
NT GULF OF MEXICO

GUM VULCANIZATES
U VULCANIZED ELASTOMERS

GUMBEL THEORY
U RANGE (EXTREMES)

GUN LAUNCHERS
Effects of barrel joints on hypervelocity projectiles
[DE87-013447] 02 p0157 N88-10983
Reaming experiments for the lethality test system
[DE88-007902] 20 p2763 N88-26383

GUN PROPELLANTS
Thermoplastic elastomers as LOVA (Low Vulnerability Ammunition) binders
[AD-A184350] 04 p0419 N88-12599
High pressure strand burn rate tests of polyvinylnitrate/nitramine propellants
[AD-A184178] 04 p0422 N88-12615
Thermoplastic elastomers as LOVA binders
[AD-A185864] 07 p0835 N88-15067
Thermoplastic elastomers as LOVA binders
[AD-A185865] 07 p0835 N88-15068
Droplet formation for liquid monopropellant jets
[AD-A187172] 10 p1331 N88-17956
Continued studies of programmed-splitting stick propellant
[AD-A188987] 12 p1613 N88-19644
Electrical ignition of HAN-based liquid propellants
[AD-A191349] 18 p2495 N88-24801
Measurement of burning rates of NOSOL-363 propellants under cross-flow and strand burner conditions using real-time X-ray radiography
19 p2623 N88-25560
Burning rate measurements of Non-Newtonian Liquid Propellant (NNLP) 19 p2623 N88-25561
Gas phase combustion chemistry of nitramine propellants
[AD-A195082] 24 p3344 N88-29902
Flamespreading processes in obliquely loaded stick propellant beds
[AD-A195081] 24 p3352 N88-29956

GUN TURRETS
A piloted simulation investigating handling qualities and performance requirements of a single-pilot helicopter in air combat employing a helmet-driven turreted gun
[AD-A186878] 09 p1116 N88-16689

GUNFIRE
Analysis of a series of electromagnetic launcher firings
[AR-005-131] 04 p0405 N88-12516
Efficiency aspects of short, low velocity railguns
[AR-004-847] 04 p0405 N88-12517

GUNN DIODES
NT TRANSFERRED ELECTRON DEVICES
Focused ion beam fabrication of graded channel FETs in GaAs and Si
[AD-A193098] 21 p2936 N88-27439

GUNPOWDER
U GUN PROPELLANTS

GUNS (ORDNANCE)
NT ARTILLERY
The LLNL 150-mm equation-of-state gun system
[DE88-000423] 04 p0405 N88-12519
A piloted simulation investigating handling qualities and performance requirements of a single-pilot helicopter in air combat employing a helmet-driven turreted gun
[AD-A186878] 09 p1116 N88-16689
Hydrogen embrittlement of gun steel
[AD-A188972] 13 p1740 N88-20407
Preliminary measurements of heat flux in a subsonic gun simulator
[AD-A191090] 16 p2208 N88-23178
An interferometric measurement technique for railgun structures
[AD-A192851] 21 p2901 N88-27217
Combustion diagnostics of propellant with new grain geometries
[AD-A194944] 24 p3342 N88-29895

GUST ALLEVIATORS
Design of an integrated control system for flutter margin augmentation and gust load alleviation, tested on a dynamic windtunnel model
[PB88-149885] 15 p2020 N88-22038
The Flight of Flexible Aircraft in Turbulence: State-of-the-Art in the Description and Modelling of Atmospheric Turbulence
[AGARD-R-734-ADD] 24 p3311 N88-29717
A review of measured gust responses in the light of modern analysis methods 24 p3312 N88-29724
Measurement and analysis of low altitude atmospheric turbulence obtained using a specially instrumented Gnat aircraft 24 p3313 N88-29728

GUST LOADS
Flutter suppression and gust load alleviation. Part 1: Results of phase 1 to 3. Part 2: Description of the Garteur model
[MBB/LKE-292/S/PUB/191] 01 p0007 N88-10038
Acquisition of gust statistics from Aircraft Integrated Data Systems (AIDS) recorded data
[NLR-MP-86048-U-ISS-2] 06 p0745 N88-14586
Turbulence structure during high wind
08 p1014 N88-16149
Extrapolation of extremum values of the wind velocity
08 p1015 N88-16150
Maximum dynamic responses using matched filter theory and random process theory
[NASA-TM-100653] 22 p3042 N88-28059
Current and proposed gust criteria and analysis methods: An FAA overview 24 p3311 N88-29718
Comparison of the influence of different gust models on structural design 24 p3312 N88-29722
A review of measured gust responses in the light of modern analysis methods 24 p3312 N88-29724
The Flight of Flexible Aircraft in Turbulence: State-of-the-Art in the Description and Modelling of Atmospheric Turbulence
[AGARD-R-734] 24 p3312 N88-29725
An interim comparison of operational CG records in turbulence on small and large civil aircraft
24 p3313 N88-29729
Acquisition of gust statistics from AIDS-recorded data
24 p3313 N88-29733
Extreme gusts distribution 24 p3314 N88-29734

GUSTS
Analyses and assessments of span wise gust gradient data from NASA B-57B aircraft
[NASA-CR-178288] 01 p0002 N88-10007
Status of FAA terminal Doppler weather radar programs 10 p1275 N88-17632
Development and testing of the gust front algorithm
[AD-A189722] 14 p1949 N88-21622
Matching P.S.D.: Design loads
24 p3312 N88-29720
A summary of methods for establishing airframe design loads from continuous gust design criteria
24 p3312 N88-29721
An interim comparison of operational CG records in turbulence on small and large civil aircraft
24 p3313 N88-29729
Re-assessment of gust statistics using CAADRP data
24 p3313 N88-29732

GUT
U GRAND UNIFIED THEORY

GUY WIRES
The effect of mass, wind angle and erection technique on the aeroelastic behaviour of a cable-stayed bridge model
[NAE-AN-46] 04 p0455 N88-12819

GYMNASTICS
U PHYSICAL EXERCISE

GYRATION
NT COROTATION
NT COUNTER ROTATION
NT EARTH ROTATION
NT MOLECULAR ROTATION
NT MUON SPIN ROTATION
NT PRECESSION
NT QUENCHING (ATOMIC PHYSICS)
NT REVOLVING
NT ROTATION
NT SATELLITE ROTATION
NT SOLAR ROTATION
NT STELLAR ROTATION

GYRATORS
NT MICROWAVE FILTERS

GYRES
Current velocity and hydrographic observations in the Straits of Florida, the Caribbean Sea and offshore of the Antillean Archipelago: Subtropical Atlantic climate studies (STACS) 1984 and 1985
[PB88-149299] 12 p1649 N88-19874
The WOCE Core Project Planning Meeting on the Gyre Dynamics Experiment --- ocean dynamics
[WCP-139] 16 p2236 N88-23358

GYROFREQUENCY
On the role of the ionization frequency to gyrofrequency ratio in the critical ionization velocity interaction
[TRITA-EPP-86-10] 10 p1410 N88-18414

GYROMAGNETISM
NT GYROFREQUENCY

GYROPLANES
U HELICOPTERS

GYROS
U GYROSCOPES

GYROSCOPE FLUIDS
Equation of gravitational-gyroscopic waves: Angular potential and its applications 08 p1079 N88-16504

GYROSCOPES
NT ATTITUDE GYROS
NT CONTROL MOMENT GYROSCOPES
NT GYROSTABILIZERS
NT LASER GYROSCOPES
NT OPTICAL GYROSCOPES
NT TUNING FORK GYROSCOPES
Contribution to the dynamical analysis of rheolinear nonconservative, gyroscopic systems using finite element methods
[ETN-87-90410] 01 p0050 N88-10320
A 1987 progress report of manufacturing techniques for Gravity Probe B gyroscope rotors
[NASA-TM-100312] 02 p0176 N88-11101
A conceptual design of an inertial navigation system for an autonomous submersible testbed vehicle
[AD-A188038] 11 p1438 N88-18578
Thirteenth Biennial Guidance Test Symposium, volume 1
[AD-A185782] 12 p1576 N88-19427
Robotics applications in the testing of inertial sensors
12 p1577 N88-19433
The optimum solution to instrument quantization effects 12 p1577 N88-19434
Rate and dynamic tests on the Canadian Strapdown Gyroscope (CSG-2) 12 p1578 N88-19439
The German Honeywell ring laser gyro: Development and test results 12 p1578 N88-19440
Advances in Air-Launched Weapon Guidance and Control
[AGARD-CP-431] 12 p1596 N88-19553
A prototype fibre optic gyroscope for missile guidance applications 12 p1596 N88-19554
A fiber optic gyro strapdown reference system for guided weapons 12 p1597 N88-19560
Laser gyro attitude control system feasibility
[AD-A189368] 13 p1720 N88-20285
Application of the Single-Axis rate Table (SAT) of the DFVLR for the evaluation of stationary and dynamic gyro properties
[DFVLR-MITT-88-09] 21 p2952 N88-27533
The anatomy of the gyroscope
[AGARD-AG-313] 22 p3079 N88-28287

GYROSCOPIC DRIFT
U GYROSCOPES
U GYROSCOPIC STABILITY

GYROSCOPIC STABILITY
A comparison between theory and experiment for the yaw moment induced by a loose internal part
[AD-A187053] 09 p1131 N88-16787
An analysis of DREO's (Defence Research Establishment Ottawa) analog rebalance loops for the CSG-2 (Canadian Strapdown Gyroscope) tuned-rotor gyroscope
[AD-A188577] 12 p1629 N88-19749
What is the maximum length of a spin stabilized projectile
[PB88-130919] 13 p1728 N88-20336
Application of the Single-Axis rate Table (SAT) of the DFVLR for the evaluation of stationary and dynamic gyro properties
[DFVLR-MITT-88-09] 21 p2952 N88-27533

GYROSTABILIZERS
Gyrostabilizer system of Kvant module
08 p1006 N88-16099

GYROSTATS
U GYROSCOPES

GYROTRONS
U CYCLOTRON RESONANCE DEVICES

H

H ALPHA LINE
Contemporaneous B,V,R,I photometry and H alpha spectroscopy of YY Gem 04 p0513 N88-13155
Sensitivity of the H alpha line to expansion, geometrical extent and temperature gradient in the G and K supergiant chromospheres 04 p0514 N88-13159

H BETA LINE
The astrophysics of nebulae and active galactic nuclear emission-line regions: New methods and applications 13 p1858 N88-21111

H II REGIONS
High spatial resolution observations of dust and gas in NGC 7027 and the M8 Hourglass 06 p0801 N88-14903
Models of recombination lines in radio H2 regions [INPE-4302-TDL/277] 12 p1710 N88-20232
Narrow-band photographic observations of the HII Region S296 in Canis Major 16 p2288 N88-23696

H LINES
NT H ALPHA LINE
NT H BETA LINE
Experimental study of the role of plasma polarization on line shape in dense laboratory plasmas [ETN-88-92001] 13 p1844 N88-21033
Density diagnostics by hydrogen line intensity ratios: Excitation cross section between excited states 17 p2441 N88-24522

H WAVES
Input-output characterization of fiber composites by SH waves [NASA-CR-4153] 17 p2347 N88-23986

HABITABILITY
Disturbance and recovery of Arctic Alaskan tundra terrain. A review of recent investigations [AD-A184442] 04 p0467 N88-12887
Space station group activities habitability module study: A synopsis 12 p1651 N88-19886
Space station habitability recommendations based on a systematic comparative analysis of analogous conditions [NASA-CR-3943] 18 p2587 N88-25372
Proceedings of the Colloquium on Space and Sea [ESA-SP-280] 19 p2695 N88-26016
Habitability of the Space Station: From vehicle to living space 19 p2697 N88-26033
Recent research on crew wardroom habitability for the Space Station 19 p2698 N88-26039

HABITATS
Compilation of 1986 annual reports of the Navy ELF (Extremely Low Frequency) communications system ecological monitoring program, volume 2 [AD-A184562] 03 p0306 N88-11931
Compilation of 1986 annual reports of the Navy ELF (Extremely Low Frequency) communications system ecological monitoring program, volume 3 [AD-A184563] 03 p0306 N88-11932
Preliminary analysis of an integrated logistics system for OSSA payloads. Volume 4: Supportability analysis of the 1.8m centrifuge 12 p1584 N88-19481
Research on enhancing the utilization of digital multispectral data and geographic information systems in global habitability studies [NASA-CR-182799] 17 p2368 N88-24101

HABITS
Dietary factors related to physical fitness [AD-A190272] 15 p2103 N88-22527

HADRONS
NT BARYONS
NT KAONS
NT MESONS
NT MUONS
Parton densities from deep inelastic scattering to hadronic processes at super collider energies [NOTA-INTERNA-885] 07 p0930 N88-15646
The high resolution spaghetti hadron calorimeter [NIKHEF-H/87-7] 08 p0990 N88-15993
Primordial nucleosynthesis during the keV era [DE88-002233] 08 p1104 N88-16623
Hadron-quark phase transition in dense stars [DE88-003412] 10 p1429 N88-18532
High resolution hadron calorimetry [NIKHEF-H/87-8] 13 p1773 N88-20605
Energy loss of particles in dense matter-calorimetry [NIKHEF-H/87-12] 13 p1836 N88-20988
Hadronic overlap and total multiplicity distributions in high energy physics collisions [NIKHEF-H/87-10] 13 p1838 N88-21001
Gluino branching ratio effects on the search for supersymmetry [PREPRINT-572] 14 p1981 N88-21821
Analysis of hadron production in deep inelastic muon-proton collisions through the fire-string model [PREPRINT-578] 14 p1981 N88-21822
Lattice QCD calculation of K yields pi nonleptonic weak transition and other hadronic weak parameters [PREPRINT-580] 15 p2132 N88-22717
Quark core stars, quark stars and strange stars [DE88-006991] 17 p2450 N88-24555
Experimental elementary particle physics [DE88-007510] 18 p2572 N88-25274
Production of pi(0) mesons and charged hadrons in nu bar neon and nu neon charges current interactions [MPI-PAE/EXP.EL.188] 22 p3150 N88-28743
Hadrons produced in atmospheric interactions [DE88-702492] 23 p3309 N88-29712

HAFNIUM
Hafnia-rich mixed oxide ceramics of the system HfO2-ZrO2-TiO2 for heaters and heat exchangers in electrothermal thrusters: The effects of titania on selected electrical and mechanical properties of Hafnia-rich mixed oxides in the system Hafnia-Zirconia-Titania, volume 1 [NASA-CR-182800-VOL-1] 15 p2047 N88-22197

HAFNIUM COMPOUNDS
NT HAFNIUM OXIDES
Metal intercalation characteristics of n-HfS2 photoelectrodes in non-aqueous electrolytes [AD-A184381] 03 p0383 N88-12407

HAFNIUM OXIDES
On 1064 nm and 350 nm laser damage thresholds of high index oxide films deposited from organic solutions and sols [DE88-001636] 07 p0859 N88-15217

HAILSTORMS
The studies of physical models on hailstorms and their applications in nowcasting 02 p0207 N88-11300

HAIR
Local human skin potential: Spatial distribution, magnitude and origin [DE87-012882] 01 p0075 N88-10480

HALF PLANES
Path integration on the upper half-plane [DE88-751050] 12 p1682 N88-20057
Complex space monofilar approximation of diffraction currents on a conducting half plane [NASA-CR-182883] 16 p2273 N88-23605

HALF SPACES
Electromagnetic scattering by a thick strip on a half-space [PB87-227096] 03 p0306 N88-11928
A finite-amplitude analysis of the buoyant instability of a highly viscous film over a less viscous half-space 13 p1769 N88-20581
Exact image theory for the problem of dielectric/magnetic slab [NASA-CR-182865] 16 p2189 N88-23055

HALIDES
NT ALUMINUM FLUORIDES
NT BORON CHLORIDES
NT BROMIDES
NT CALCIUM FLUORIDES
NT CESIUM IODIDES
NT CHLORIDES
NT CHLORINE FLUORIDES
NT COPPER CHLORIDES
NT DICHLORIDES
NT FLUORIDES
NT HYDROCHLORIC ACID
NT HYDROFLUORIC ACID
NT HYDROGEN CHLORIDES
NT LITHIUM CHLORIDES
NT LITHIUM FLUORIDES
NT MAGNESIUM CHLORIDES
NT METAL HALIDES
NT NITROGEN FLUORIDES
NT POTASSIUM BROMIDES
NT SILVER CHLORIDES
NT SILVER IODIDES
NT SODIUM CHLORIDES
NT SODIUM FLUORIDES
NT SULFUR FLUORIDES
NT URANIUM FLUORIDES
Evaluation and compilation of thermodynamic properties of high temperature chemical species [AD-A187509] 11 p1452 N88-18654
Rare Gas Halide (RGH) kinetics [AD-A192352] 20 p2770 N88-26425

HALL COEFFICIENT
U HALL EFFECT

HALL CURRENTS
U ELECTRIC CURRENT
U HALL EFFECT

HALL EFFECT
Complex scattering dynamics and the integer quantum Hall effect [DE87-011790] 02 p0243 N88-11536
High pressure electronic transport in semiconductors [AD-A187428] 11 p1555 N88-19308
Electrical characteristics of MBE (Molecular Beam Epitaxyl)-grown GaAs/sub 1-x/Sb/sub x on InP and correlation with film microstructure [DE88-003841] 13 p1847 N88-21053
First report on InGaAs hall device 14 p1903 N88-21372
Electrical anisotropy of layered semiconductor ZrSe2 16 p2257 N88-23488
A nuclear powered space based multimegawatt MHD disc power system 17 p2432 N88-24471
Quantum transport in an electron waveguide 20 p2864 N88-27010
Thermal conductivity of isotopically pure semiconductors, superlattices, semiconductor alloys and semiconductors as a function of temperature; control of the segregation coefficient in LEC crystal growth; and photo-Hall measurements of GaAs 21 p2927 N88-27375
DARPA-URI consortium meetings on submicron heterostructures of diluted magnetic semiconductors [AD-A193499] 23 p3206 N88-29081
Temperature dependence of conductivity and of Hall coefficients for noble metal films [ETN-88-92981] 23 p3294 N88-29616

HALLEY'S COMET
Final phase of Project Vega 01 p0009 N88-10053
Overview of plasma observations during the Halley flybys 01 p0116 N88-10743
The status of the international Halley watch 01 p0116 N88-10744
Large-scale interaction of the solar wind with comets Halley and Giacobini-Zinner 01 p0117 N88-10745
Solar wind-cometary interaction at the ionopause and associated phenomena 01 p0117 N88-10748
Solar wind effects on the outer ion coma of Comet Halley 01 p0117 N88-10750
Plasma-tail activity and the interplanetary medium at Halley's Comet during Armada Week: 6-14 March 1986 01 p0118 N88-10752
Occultation of compact radio sources by the ion tail of Halley's Comet 01 p0118 N88-10753
Space missions to Comets Halley and Giacobini-Zinner 03 p0272 N88-11712
Comparative analysis of ultraviolet observations of Halley's comet on ASTRON astrophysical station before and after perihelion 08 p1004 N88-16086
Some ground-based optical observations of Comet Halley during its post-perihelion passage 08 p1033 N88-16259
Giotto: A mission to Halley's Comet 09 p1127 N88-16756
JPRS report: Science and technology. USSR: Space [JPRS-USP-88-002] 13 p1724 N88-20312
Vega-1 and Vega-2 automatic stations: Functioning of landing modules in Venusian atmosphere 13 p1725 N88-20313
Vega-1 and Vega-2 automatic stations: Functioning of flyby vehicles during encounter with Halley's comet 13 p1725 N88-20314
Some periodicities in motion of Halley's Comet relative to center of mass 13 p1726 N88-20324
Results of infrared spectrometer experiment. 1: Infrared radiation of parent molecules in Halley's Comet 13 p1726 N88-20325
Results of infrared spectrometer experiment. 2: Infrared radiometry of nucleus of Halley's Comet 13 p1727 N88-20326
Analysis of hydrocarbon band 3.35 in spectrum of Halley's Comet using data from infrared spectrometer on Vega-1 spacecraft 13 p1727 N88-20327
How typical is Halley's Comet? 14 p1994 N88-21886
Solar wind observation at the time of closest encounter with Comet Halley 14 p1995 N88-21890
Variability of Comet Halley's coma: VEGA-1 and VEGA-2 magnetic field observations 14 p1995 N88-21891
Calculation of the shape of the contact surface at Comet Halley 14 p1995 N88-21892
The foreshock region upstream from the Comet Halley bow shock 14 p1995 N88-21893
Physical processes in the vicinity of the cometopause interpreted on the basis of plasma, magnetic field and plasma wave data measured on board VEGA-2 spacecraft --- Halley's comet 14 p1996 N88-21894
Some new features of plasma wave phenomena at Halley: APV-N observations --- VEGA 14 p1996 N88-21895
A comparison between wave observations performed in the environments of Comets Halley and Giacobini-Zinner 14 p1996 N88-21896
Correlation between magnetic and electric field fluctuations observed during flyby near Halley's comet 14 p1996 N88-21897
Magnetic cavity formation at Comet Halley and at the AMPTE Li release 14 p1996 N88-21898

Plasma phenomena in the vicinity of the closest approach of VEGA-1, 2 spacecraft to the Comet Halley nucleus 14 p1996 N88-21899
Energy spectra of pick-up ions recorded during the encounter of Giotto with Comet Halley 14 p1997 N88-21901
Stochastic acceleration of cometary ions: The effects of composition and source strength distributions 14 p1997 N88-21902
Observation of energetic particles (E greater than 30 keV) by the Giotto experiment EPA in the magnetic cavity of Comet Halley 14 p1997 N88-21903
Evidence for first polymer in Comet Halley: Polyoxymethylene 14 p1997 N88-21906
Photometry of P/Halley (1982i): Is what we have learned useful for other comets? 14 p1998 N88-21909
Water vapor and hydroxyl distributions in the inner coma of Comet Halley measured by the VEGA-2 three channel spectrometer TKS 14 p1998 N88-21910
CCD-observations of gas and dust jets in the coma of Comet Halley 14 p1998 N88-21912
Spatial distribution of O(supra 1D) from Comet Halley 14 p1999 N88-21913
Distribution of neutral gas molecules at large distances from Halley's comet 14 p1999 N88-21914
Halley's environments by the Japanese Suisei spacecraft 14 p1999 N88-21915
Recent observations of the OH radio lines in comets 14 p1999 N88-21917
A model of the anisotropic structure of the neutral gas coma of a comet 14 p1999 N88-21918
Profiles of the major gas emissions and distribution of dust particles in the inner coma (0 to 10,000 km) of Comet Halley 14 p1999 N88-21919
Analysis of the coma outburst of Comet Halley, March 24 to 25 (UT), 1986 14 p2000 N88-21920
Dust coma morphology of Comet Halley during the Giotto encounter 14 p2000 N88-21921
Cometary MHD and chemistry: Application to Halley 14 p2000 N88-21922
Objective-prism spectra of the Comets Honda (1968 e), Hartley-Good (1985 l) and Halley 14 p2000 N88-21924
Color fluctuations in the inner coma of Comet Halley as measured from VEGA-2 14 p2000 N88-21925
New properties of cometary dust 14 p2001 N88-21926
Comet P/Halley's near-nucleus jet activity 14 p2001 N88-21929
Dust photometry in the near nucleus region of Comet Halley from VEGA-2 observations 14 p2001 N88-21930
Dynamics of charged submicron grains in Halley's coma 14 p2001 N88-21931
Composition of cometary dust particles --- Halley 14 p2001 N88-21932
Isotopic composition of Halley dust 14 p2002 N88-21933
On the interpretation of the 3 micron emission feature in the spectrum of Comet Halley: Abundances in Comet Halley and in interstellar matter 14 p2002 N88-21935
P/Halley dust coma: Grains or rocks? 14 p2002 N88-21936
The origin of low mass particles within and beyond the dust coma envelopes of Comet Halley 14 p2002 N88-21938
Optical and hydrodynamic implications of Comet Halley dust size distribution 14 p2003 N88-21939
Cometary grains and interplanetary dust: A polarimetric sensing --- Halley 14 p2003 N88-21941
The dust around the nucleus of Comet Halley 14 p2003 N88-21942
Variation of grain properties at the dust outbursts --- Halley's comet 14 p2003 N88-21943
On orbits and association of meteor streams with Comets P/Halley and P/Encke 14 p2003 N88-21945
The evolution of the mass distribution of cometary particles 14 p2004 N88-21946
The nucleus of Comet Halley 14 p2004 N88-21947
Comparison of active regions on the nucleus of Comet Halley 14 p2004 N88-21948
Reconstruction of the orientation and shape of the nucleus of Comet Halley 14 p2004 N88-21949
Properties of the nucleus of P/Halley 14 p2004 N88-21952
Plasma tail of Comet Halley in January 1986 14 p2006 N88-21960
The evolution of CN emission in Halley's comet with heliocentric distance 14 p2006 N88-21961
Study of the ionic and neutral species in the coma of Comet Halley with an image intensifier camera 14 p2006 N88-21962
Determination of the content of CO(+) and H2O(+) ions in the tail of Comet Giacobini-Zinner and Comet Halley 14 p2006 N88-21964
Comparison of Halley's monochromatic comae with others 14 p2006 N88-21965
P/Halley activity in November 1985 14 p2006 N88-21966
Outburst of Halley's comet 14 p2007 N88-21967
Comet P/Halley: Visual magnitude estimates and gas production 14 p2007 N88-21968
Spectrophotometric observations of Comet Halley 14 p2007 N88-21972
Nature of Comet Halley's organic grains inferred from infrared spectra 14 p2007 N88-21973
The dust tail of Comet Halley 14 p2008 N88-21974
The structure of the Halley meteor stream and the orbital history of the comet 14 p2008 N88-21975
On the periodic southward jets of Comet Halley before perihelion passage 14 p2008 N88-21978
Dust tail streamers and Halley's nucleus rotation 14 p2008 N88-21979
Near-infrared imaging of Comet Halley: Discovery of a color gradient in the inner coma 14 p2009 N88-21980
Laboratory amorphous carbon: A possible analog of cometary dust 14 p2009 N88-21981
Linear and circular polarization of Comet Halley light 14 p2009 N88-21982
Image processing on VEGA pictures 14 p2009 N88-21983
The light curve of P/Halley and the rotation of its nucleus 14 p2009 N88-21984
Temperature of the nucleus of Comet Halley 14 p2009 N88-21985
Consequences of the size determination of P/Halley by space probes on the scale of sizes of cometary nuclei 14 p2009 N88-21986
The splitting of Comet Halley 1986 14 p2010 N88-21989
Three approaches to the modeling of Comet Halley's motion over long periods of time 14 p2010 N88-21992
Memoirs of the Faculty of Science, Kyoto University. Series of Physics, Astrophysics, Geophysics and Chemistry, volume 37, no. 2 [ISSN-0368-9689] 16 p2287 N88-23694
Dust and C2-contents in the coma of Halley's Comet (1986III) 16 p2288 N88-23697
The evolution of cometary activity 18 p2594 N88-25416
Processing and analysis of images transmitted by Vega space probes over Halley's comet [ETN-88-92291] 20 p2885 N88-27131
A theoretical determination of the density at a traveling source that emitts particles [ISAS-RN-351] 21 p3013 N88-27883

HALOCARBONS
NT CHLOROCARBONS
NT FLUOROCARBONS

HALOGEN COMPOUNDS
NT ALUMINUM FLUORIDES
NT AMMONIUM PERCHLORATES
NT BORON CHLORIDES
NT BROMIDES
NT BROMINE COMPOUNDS
NT CALCIUM FLUORIDES
NT CESIUM IODIDES
NT CHLORIDES
NT CHLORINE COMPOUNDS
NT CHLORINE FLUORIDES
NT CHLOROCARBONS
NT COPPER CHLORIDES
NT DICHLORIDES
NT DIFLUORO COMPOUNDS
NT FLUORIDES
NT FLUORINE COMPOUNDS
NT FLUORINE ORGANIC COMPOUNDS
NT FLUORO COMPOUNDS
NT FLUOROCARBONS
NT FLUOROHYDROCARBONS
NT FLUOROPOLYMERS
NT HALIDES
NT HYDROCHLORIC ACID
NT HYDROFLUORIC ACID
NT HYDROGEN CHLORIDES
NT IODIDES
NT LITHIUM CHLORIDES
NT LITHIUM FLUORIDES
NT LITHIUM IODATES
NT LITHIUM PERCHLORATES
NT MAGNESIUM CHLORIDES
NT METAL HALIDES
NT NITROGEN FLUORIDES
NT POLYTETRAFLUOROETHYLENE
NT POLYVINYL FLUORIDE
NT POTASSIUM BROMIDES
NT SILVER CHLORIDES
NT SILVER IODIDES
NT SODIUM CHLORIDES
NT SODIUM FLUORIDES
NT SULFUR FLUORIDES
NT TEFLON (TRADEMARK)
NT URANIUM FLUORIDES
Spectroscopy and energy transfer kinetics of the interhalogens [AD-A192103] 18 p2583 N88-25344

HALOGENATION
NT BROMINATION
NT CHLORINATION
NT FLUORINATION
Measurement of vertical distributions of halogenated hydrocarbons in the stratosphere [ETN-88-91065] 09 p1191 N88-17135

HALOGENS
NT BROMINE ISOTOPES
NT CHLORINE
NT FLUORINE
NT IODINE
NT IODINE ISOTOPES

HALOS
Experimental model of halo plasma observed in small-aspect FRC plasma [INPE-4159-PRE/1061] 08 p1085 N88-16534
A global model for planetary nebulae, taking into account central stellar evolution and influence on halo ionization [ETN-88-91491] 11 p1568 N88-19389

HAMILTON-JACOBI EQUATION
Fronts propagating with curvature dependent speed: Algorithms based on Hamilton-Jacobi formulations [NASA-CR-178382] 01 p0077 N88-10495
Introduction to classical mechanics of systems with constraints, part 2 [DE88-701056] 13 p1849 N88-21072

HAMILTONIAN FUNCTIONS
A quantum theoretical study of polyimides [NASA-CR-181495] 03 p0292 N88-11831
Equilibria, lattices and chaotic dynamics of point vortices 04 p0444 N88-12758
Recursion operator and bihamiltonian structure for integrable multi-dimensional lattices [PREPRINT-552] 06 p0764 N88-14688
Normal form of a fully resonant Hamiltonian function [PB88-100946] 06 p0767 N88-14711
A study to evaluate STS heads-up ascent trajectory performance employing a minimum-Hamiltonian optimization strategy [NASA-TP-2793] 08 p0960 N88-15820
Coulomb interactions and effective strong coupling Hamiltonians in Cu-O superconductors [DE88-002942] 08 p1090 N88-16561
The structure of the sideband spectrum in free electron lasers [AD-A186952] 09 p1170 N88-17015
Hamiltonian approach to relativistic theory of gravity and to general relativity theory [DE88-700404] 10 p1422 N88-18492
The Hamiltonian structure of nonlinear elasticity: The convective representation of solids, rods, and plates [AD-A187200] 11 p1498 N88-18943
Systems near the onset and in the well-developed regimes of turbulence [DE88-005365] 13 p1766 N88-20565
Hamiltonian description of the interaction of surface waves with mixed-layer currents 13 p1806 N88-20799
Stochasticity in nonlinear Hamiltonian systems [DE88-005499] 13 p1826 N88-20915
Introduction to classical mechanics of systems with constraints, part 2 [DE88-701056] 13 p1849 N88-21072
The biHamiltonian formulations of integrable evolution equations in multidimensions [PREPRINT-568] 14 p1968 N88-21745
Mixing coefficients of the lattice weak Hamiltonian with dimension five operators [PREPRINT-576] 14 p1968 N88-21749
Periodic orbits around a satellite modelled as a triaxial ellipsoid [AD-A190592] 15 p2022 N88-22051
Geometric methods and the gauge structure of Berry's phase [DE88-006538] 15 p2127 N88-22682
Quantization of axial electrodynamics [DE88-701498] 15 p2147 N88-22813
Hamiltonian formalism in the model of the relativistic string with rigidity [DE88-701503] 15 p2147 N88-22815
Integrability of fermionic string in superfluid Hamiltonian approach [DE88-701662] 16 p2284 N88-23678

Existence of periodic solutions in n-dimensional retarded functional differential equations
[RR-325] 17 p2392 N88-24221
Non-effective-mass matching in superlattices
20 p2872 N88-27049
Finitely many delta-interactions with supports on concentric spheres
[DE88-701834] 20 p2880 N88-27101
A minimax method for a class of Hamiltonian systems with singular potentials
[AD-A193478] 23 p3270 N88-29453
Periodic solutions of perturbed superquadratic Hamiltonian systems
[AD-A194282] 23 p3270 N88-29457
On the periodic nonlinearity and the multiplicity of solutions
[AD-A194295] 23 p3270 N88-29459
Bifurcations of periodic solutions of non-integrable Hamiltonians with two degrees of freedom: Numerical and analytical results
[DE88-702747] 23 p3272 N88-29473

HAMMERS
Size-reduction and sorting behavior in sieve hammer mills
[ETN-88-91480] 11 p1467 N88-18749

HAND (ANATOMY)
NT FINGERS
Design, development and evaluation of Stanford/Ames EVA prehensors
[NASA-CR-182688] 15 p2105 N88-22540
A standard architecture for controlling robots
[AD-A195929] 24 p3423 N88-30371

HANDBOOKS
NT USER MANUALS (COMPUTER PROGRAMS)
Middle Atmosphere Program: Handbook for MAP, volume 24
[NASA-CR-181451] 01 p0069 N88-10444
Uniform laws and regulations as adopted by the National Conference on Weights and Measures (72nd), 1987
[PB88-123724] 06 p0689 N88-14225
Development of Soviet state ergonomic standards (GOST)
[AD-A185536] 07 p0899 N88-15449
Evaluation and compilation of thermodynamic properties of high temperature chemical species
[AD-A187509] 11 p1452 N88-18654
Air traffic control
[FAA-ORDER-7110.65E] 12 p1576 N88-19426
MANPRINT handbook for RFP (Request For Proposal) development
[AD-A188321] 13 p1850 N88-21075
The official handbook of MASCOT, version 3.1, issue 1 — software tool
[BR103975] 16 p2246 N88-23419
Soviet space program handbook
[AD-A194332] 22 p3046 N88-28077

HANDICAPS
Ergonomics of car controls for disabled people, phase 1. Part 1: Chapters 1-7. Part 2: Appendices. Part 3: References
[ISBN-0-947767-82-7] 09 p1202 N88-17204

HANDLEY PAGE AIRCRAFT
Sound transmission through the walls of light aircraft: An investigation of structure-borne noise in a Handley Page 137 Jetstream 3 aircraft
[NASA-CR-182509] 10 p1405 N88-18376

HANDLING EQUIPMENT
NT CRANES
NT GANTRY CRANES
Human factors in robotic system design discussed
02 p0158 N88-10988
Tether Elevator Crawler Systems (TECS)
07 p0927 N88-15631

HANDLING QUALITIES
U CONTROLLABILITY

HANGARS
Investigation of the nature and concentration of vapor and mist during the cleaning of aircraft
[PML-1985-29] 05 p0623 N88-13817

HANKEL FUNCTIONS
Incomplete Lipschitz-Hankel integrals of MacDonald functions
[AD-A191034] 16 p2261 N88-23515

HARDENING
The effects of thin anodic films on the cyclic microstrain/macrostrain behavior of tungsten
05 p0597 N88-13650
Study of the characteristic curve of hardening and softening during low-cycle fatigue process
06 p0719 N88-14414
Laser transformation hardening of precision V-slide way
[PB87-144028] 08 p0991 N88-15999

HARDENING (MATERIALS)
NT CARBURIZING
NT HOT ISOSTATIC PRESSING
NT HOT PRESSING
NT NITRIDING
NT PRECIPITATION HARDENING
NT PULSE HEATING
NT STRAIN HARDENING
NT WORK HARDENING
An expert system for materials design
[DE88-000191] 04 p0483 N88-12974
Master plots for predicting the case-depth in laser surface treatments
[PB87-221875] 05 p0586 N88-13574
Influence of microstructure and aging condition on the fatigue crack propagation in age hardened aluminium alloys 05 p0599 N88-13659
Analysis of stable crack growth with isotropic and kinematic hardening
[PB87-144911] 07 p0868 N88-15266
Nonlinear line-spring model for surface crack analysis with particular reference to work hardening materials
[PB87-144838] 08 p0994 N88-16016
Nondestructive magnetic testing of laser hardening parameters (hardening depth, hardness profile, retained austenite)
[ETN-88-91070] 09 p1144 N88-16857
Evolution of hardening and damage during viscoplastic deformation
[AD-A190714] 15 p2077 N88-22381
Disclination structures in carbon and graphite
[AD-A191056] 17 p2322 N88-23868
Theory of viscoplasticity based on overstress with applications 18 p2529 N88-25007
Development of fine-grained carbide-particle hardened Hadfield manganese steels
[DE88-008919] 19 p2617 N88-25523
Surface fatigue life of CBN and vitreous ground carburized and hardened AISI 9310 spur gears
[NASA-TM-100960] 19 p2677 N88-25916

HARDENING (SYSTEMS)
The electromagnetic threat to future avionic systems
17 p2305 N88-23790
Shielding effectiveness of metallic joints versus corrosion prevention 22 p3054 N88-28120

HARDNESS
NT MICROHARDNESS
Investigation of the structure of coatings of self fluxing alloys fused by laser energy
[BLL-M-37301-(5828.4)] 02 p0148 N88-10930
Ion plating: Fundamental processing studies and synthesis of high performance coatings
[AD-A184766] 03 p0303 N88-11908
Weldability of 2219-T851 and 2519-T87 aluminum armor alloys for use in Army vehicle systems
[AD-A184296] 04 p0451 N88-12792
Analysis of load-bearing capacity of nitrided layer
[PB87-144176] 08 p0968 N88-15857
Response of aluminum alloys to erosive particle impacts
[DE88-005910] 15 p2041 N88-22159
Hydrogen embrittlement susceptibility of high strength ESR 4340 steel alloys for ballistically resistant/tolerant components 17 p2319 N88-23848
Initial development of high-temperature titanium silicide alloys
[DE88-007860] 20 p2772 N88-26437
Study of the friction and wear-related properties of ceramic superconductors
[DE88-011844] 21 p3024 N88-27950

HARDNESS TESTS
Critical cooling rates on solution treatment of Cu-Cr and Cu-Be alloys
[NASA-TT-20163] 18 p2488 N88-24760

HARDWARE
Hardware fault insertion and instrumentation system: Mechanization and validation
[NASA-CR-181445] 01 p0078 N88-10497
Experimental assembly of structures in EVA: Hardware morphology and development issues
02 p0139 N88-10872
Access flight hardware design and development
02 p0139 N88-10873
The development of ODE methods: A symbiosis between hardware and numerical analysis
[DE87-014925] 03 p0370 N88-12325
Plant Growth Module (PGM) conceptual design
05 p0631 N88-13855
Benchmarking and evaluation of hardware description languages for design of VLSI systems
[PB87-134557] 06 p0758 N88-14648
Virtual image processor: A prototype implementation
[AD-A185560] 06 p0758 N88-14652
Software-implemented fault insertion: An FTMP example
[NASA-CR-178423] 06 p0761 N88-14668
Major spacecraft hardware testing in Europe
09 p1125 N88-16740
Hardware/software reliability study — space programs
[REPT-65.5686] 09 p1218 N88-17307
An applicative programmer's approach to matrix algebra, lessons for hardware and software
10 p1382 N88-18251
A programmable global system for the manipulation of residue numbers
[ETN-88-91476] 11 p1530 N88-19139
Computer architecture for efficient algorithmic executions in real-time systems: New technology for avionics systems and advanced space vehicles
[NASA-CR-182650] 12 p1675 N88-20016
Portability of software. The use of software in the hardware mixture
[MBB/LWD-11/S/PUB/253] 16 p2246 N88-23416
An application of the Bayesian method to the estimation and forecast of system hardware components MTBF
22 p3068 N88-28211

HARMONIC ANALYSIS
NT ZONAL HARMONICS
Wave group analysis based on Kimura's method
[AD-A187610] 11 p1516 N88-19055
Comparisons of global topographic/isostatic models to the Earth's observed gravity field
[NASA-CR-182696] 13 p1798 N88-20752

HARMONIC CONTROL
Analytic investigation of helicopter rotor blade appended aeroelastic devices
[NASA-CR-166525] 03 p0266 N88-11676
Investigations on higher harmonic blade pitch control at helicopters
[DFVLR-FB-87-36] 14 p1868 N88-21165
Dual adaptive control: Design principles and applications
[NASA-CR-177485] 22 p3038 N88-28038

HARMONIC EXCITATION
A system identification technique based on the random decrement signatures. Part 1: Theory and simulation
05 p0594 N88-13625
A system identification technique based on the random decrement signatures. Part 2: Experimental results
05 p0594 N88-13626
Dynamic analysis of a structure with sliding base
08 p0998 N88-16045
Experimental and theoretical study on cavitation inception and bubbly flow dynamics. Part 1: Design, development and operation of a cavitation susceptibility meter. Part 2: Linearized dynamics of bubbly and cavitating flows with bubble dynamics effects
[AD-A187133] 09 p1160 N88-16952
Dynamic response of a geared train of rotors subjected to random support excitations 09 p1181 N88-17073
Harmonic and rectangular pulse reproduction through current transformers
[EUT-86-E-159] 14 p1907 N88-21395

HARMONIC GENERATIONS
Third-harmonic generation and multiphoton ionization spectroscopy
[DE87-013545] 03 p0281 N88-11769
Higher harmonic generation in the induced resonance electron cyclotron maser
[AD-A186236] 07 p0858 N88-15210
Enhancement of second harmonic generation on silver gratings by resonant excitation of surface plasmon
[ETN-88-92304] 17 p2439 N88-24509

HARMONIC GENERATORS
Coherent states for the damped harmonic oscillator
[AD-A186111] 07 p0922 N88-15599
Digital control of high frequency pulse-width modulated inverters
[ETN-87-90711] 09 p1157 N88-16936
Frequency doubling at 1.315 micrometers
[AD-A193902] 23 p3208 N88-29092

HARMONIC MOTION
Theory of laser cooling and spectroscopy of harmonically trapped single atoms
[AD-A189576] 13 p1775 N88-20617

HARMONIC OSCILLATION
On the pairing process in an excited, plane, turbulent mixing layer
[AD-A186355] 07 p0850 N88-15157
A panel method based on velocity potential to compute harmonically oscillating lift surface systems
[ETN-88-91886] 15 p2061 N88-22290
Cascades with harmonically oscillating blades in supersonic flow
[NASA-TT-20323] 19 p2599 N88-25446
Off-boundary approach to the boundary element method
[AD-A192931] 20 p2815 N88-26701

HARMONIC OSCILLATORS
Visible free electron laser oscillator
[AD-A183871] 01 p0051 N88-10324

Coherent states for the damped harmonic oscillator
[AD-A186111] 07 p0922 N88-15599
Gigantic optical nonlinearity in low dimensional systems 14 p1975 N88-21786
Squeezed state in degenerate parametric amplification discussed by H. Takahasi in 1963 14 p1976 N88-21790
Thermo field dynamics and para statistical mechanics
[DE88-702057] 19 p2737 N88-26253
Research opportunities below 300 nm at the NBS Free-Electron Laser Facility
[AD-A193100] 21 p2953 N88-27538

HARMONICS
NT HARMONIC EXCITATION
NT HARMONIC GENERATIONS
NT HARMONIC OSCILLATION
NT SPHERICAL HARMONICS
NT SUPERHARMONICS
NT ZONAL HARMONICS
A deterministic approach to turbulence: Chaos in Rayleigh-Benard convection 03 p0313 N88-11975
A study of rotor broadband noise mechanisms and helicopter tail rotor noise 06 p0777 N88-14766
Characteristics of LKI-501 tunable dye laser with dyes in solid matrix 07 p0920 N88-15587
Harmonic expansion for the magnetic field of the helical solenoid
[DE88-700100] 07 p0928 N88-15638
Demonstration of efficient full aperture Type 1/Type 2 third harmonic conversion on Nova
[DE88-003834] 14 p1914 N88-21438
Subharmonic aliasing and its effects on the AFTI/F-16 digital flight control system
[AD-A190614] 15 p2020 N88-22042
Observation of synchronously transient pumped mode-locking dye laser under negative cavity detuning 16 p2187 N88-23041
Secondary instability of compressible boundary layer to subharmonic three-dimensional disturbances
[NASA-CR-4144] 16 p2200 N88-23122
Fluxons and order in long Josephson junctions
[AD-A190879] 16 p2282 N88-23665
Harmonic considerations for electrical distribution feeders
[DE88-007849] 18 p2505 N88-24860
Motor theory of auditory perception
[AD-A192095] 18 p2550 N88-25136
Analysis of the electrical harmonic characteristics of a slip recovery variable speed generating system for wind turbine applications
[DE88-001140] 19 p2687 N88-25972
Primer on coupling collective electronic oscillations to nuclei
[LA-10878] 19 p2723 N88-26170
Theoretical and experimental study of a mode-converting coupler for application to a harmonic gyrotron amplifier
[AD-A193760] 22 p3081 N88-28294
CryoSQUID: A SQUID-based magnetic field sensor
[AD-A194237] 23 p3239 N88-29275

HARNESSES
Human response to prolonged motionless suspension in four types of full body harnesses 21 p2929 N88-27387

HARRIER AIRCRAFT
Full-envelope aerodynamic modeling of the Harrier aircraft
[NASA-TM-88376] 05 p0552 N88-13363
Derivation of equipment vibration requirements for AV-8B 08 p0997 N88-16037
Manoeuvres by default, by demand and by design 12 p1580 N88-19455

HARTREE APPROXIMATION
The finite element method for electronic structure
[DE88-001708] 04 p0485 N88-12989
Theoretical studies of atomic transitions
[DE88-004719] 10 p1407 N88-18389
Numerical simulations of multiphoton processes in many electron atoms
[DE88-003293] 13 p1837 N88-20990

HARTREE-APPLETON APPROXIMATION
U HARTREE APPROXIMATION

HARTREE-FOCK APPROXIMATION
U HARTREE APPROXIMATION

HASTELLOY (TRADEMARK)
Resistance of welded joints in high temperature Hastelloy N-type nickel alloy to hot crack formation 03 p0286 N88-11798
Fatigue and uniaxial deformation behavior of Hastelloy XR at elevated temperatures
[DE88-751058] 09 p1145 N88-16862
Some implications for cyclic plastic and viscoplastic equations based on nonproportional loading experiments 14 p1931 N88-21515
Effect of strain rate on high-temperature low-cycle fatigue behavior of Hastelloy X and Hastelloy XR
[DE88-752302] 15 p2037 N88-22140
Creep behavior for Hastelloy-XR
[DE88-753428] 21 p2914 N88-27295

HATCHES
Hatch cover
[NASA-CASE-MSC-21356-1] 18 p2472 N88-24671

HAWAII
North Pacific Ocean. Tradewind region east of Hawaii, R/V Thomas G Thompson: 25 September - 1 November 1972. STD data report
[AD-A186566] 08 p1044 N88-16311
North Pacific Ocean. Subarctic front central Pacific, R/V Thomas G. Thompson: 8 September - 9 October 1975. CTD data report
[AD-A186567] 08 p1044 N88-16312
North Pacific Ocean. Central Pacific Transition Zone, R/V Thomas G. Thompson: 25 March - 3 May 1968: STD data report
[AD-A186570] 09 p1195 N88-17160

HAWKER SIDDELEY AIRCRAFT
NT HARRIER AIRCRAFT

HAZ (METALLURGY)
U HEAT AFFECTED ZONE

HAZARDOUS MATERIAL DISPOSAL (IN SPACE)
A proposed national policy concerning the reentry of space reactors 17 p2415 N88-24359

HAZARDS
NT AIRCRAFT HAZARDS
NT FLIGHT HAZARDS
NT METEOROID HAZARDS
NT RADIATION HAZARDS
NT TOXIC HAZARDS
Airborne lidar experiments at the Savannah River Plant
[NASA-TM-4007] 02 p0194 N88-11209
Human motor reactions to dangerous motions in robot operations
[PB87-222196] 03 p0361 N88-12275
Committee on Interagency Radiation Research and Policy Coordination
[DE88-003358] 09 p1188 N88-17121
Modeling of the non-auditory response to blast overpressure
[AD-A187397] 10 p1369 N88-18184
Toxic effects of man-made mineral fibers with particular reference to ceramic fibers
[AD-A187949] 11 p1519 N88-19072
Post-Challenger evaluation of space shuttle risk assessment and management
[NASA-CR-182461] 12 p1705 N88-20202
Atmospheric electrical modeling in support of the NASA F-106 storm hazards project
[NASA-CR-181639] 13 p1799 N88-20758
Bathymetric hazard survey test
[AD-A189150] 13 p1803 N88-20775
SPOT for earthquake hazard zoning in southern Italy 22 p3093 N88-28365

HAZE
Analysis of meteorological conditions and haze distribution for the Second Arctic Gas and Aerosol Sampling Program (AGASP 2), March-April 1986
[PB88-164140] 14 p1948 N88-21618

HCMM
U HEAT CAPACITY MAPPING MISSION

HCN LASERS
Electron density profile reconstruction by maximum entropy method with multichannel HCN laser interferometer system on SPAC 7
[IPPJ-858] 11 p1553 N88-19295

HEAD (ANATOMY)
NT SKULL
Analysis of head response to torso acceleration. Volume 1: Development of performance requirements
[PB88-156757] 14 p1953 N88-21640
Basic research on flame radiation
[PB88-168372] 15 p2032 N88-22105
Analysis of head response to torso acceleration. Volume 2: Description of data retrieval, analysis and display software
[PB88-156765] 15 p2104 N88-22536

HEAD DOWN TILT
Biorhythmological analysis of dynamics of pulmonary ventilation parameters during orthostatic tests 07 p0891 N88-15400
Changes in regional and central hemodynamics during seven-day water immersion 07 p0895 N88-15421
Effect of antiorthostatic position and different illumination on sensitivity of skin in upper half of the body to ultraviolet radiation 10 p1363 N88-18145
Does 7-day hindquarters unloading simulate 7 days of weightlessness exposure in rat trabecular bone? 12 p1657 N88-19928
Is ANF implied in the night attenuated renal response to central hypervolemia? 12 p1659 N88-19945
Determination of settings of a tilted head-cutter for generation of hypoid and spiral bevel gears
[NASA-CR-182138] 18 p2524 N88-24976
Human hemodynamics during water immersion as related to position during submersion 19 p2703 N88-26071
Human erykthrocyte metabolism in the presence of hyperoxygenation during antiorthostatic hypokinesia 19 p2706 N88-26092
An evaluation of flight path formats head-up and head-down
[NASA-CR-4176] 21 p2897 N88-27196

HEAD-UP DISPLAYS
The deviation of light rays passing through a curved windscreen — aircraft
[BAE-MSC.115] 01 p0093 N88-10610
Multi-crew pictorial format display evaluation
[AD-A189349] 13 p1812 N88-20824
First flight simulator test of the head-up display for NAL QSTOL experimental aircraft (ASUKA)
[DE88-751804] 16 p2162 N88-22896
An evaluation of three linear scale radar altimeter displays
[AD-A192173] 18 p2485 N88-24636
Improvement of head-up display standards. Volume 1: Head-up display design guide, appendix
[AD-A192973] 20 p2834 N88-26809
An evaluation of flight path formats head-up and head-down
[NASA-CR-4176] 21 p2897 N88-27196
Improvement of head-up display standards. Volume 4: Head-up display dynamics flight tests
[AD-A193617] 22 p3042 N88-28060
Improvement of head-up display standards. Volume 2: Evaluation of head-up displays to enhance unusual attitude recovery
[AD-A194601] 23 p3178 N88-28921
Improvement of head-up display standards. Volume 5: Head up display ILS (Instrument Landing System) accuracy flight tests
[AD-A194602] 23 p3178 N88-28922
Vision through aircraft transparencies 23 p3242 N88-29294
Maintenance of vision-related components 23 p3242 N88-29296
Display system image quality 23 p3242 N88-29298
Improvement of head-up display standards. Volume 3: An evaluation of head-up display safety
[AD-A195787] 24 p3410 N88-30300

HEALTH
NT HEALTH PHYSICS
NT PUBLIC HEALTH
An assessment of clinical chemical sensing technology for potential use in space station health maintenance facility
[NASA-CR-172013] 04 p0475 N88-12926
Fibrous glass aerosols: A literature review
[AD-A188420] 12 p1672 N88-20008
The effects of normal and therapeutic baths on the central vascular organs of persons with healthy hearts, as measured by X-ray
[NASA-TT-20252] 13 p1811 N88-20818
The impact of hyperthermia and hypohydration on circulation, strength, endurance and health
[AD-A192657] 22 p3131 N88-28615
Physiological effects of extremely low frequency electric and magnetic fields
[DE88-752814] 22 p3132 N88-28620
Evaluation of the potential health hazards associated with the machining of carbon fiber composites
[AD-A194835] 24 p3408 N88-30286

HEALTH PHYSICS
NT PUBLIC HEALTH
Health hazards of video display terminals. A comprehensive, annotated bibliography on a critical issue of workplace health and safety with sources for obtaining items and list of terminal suppliers
[RSI-IAS-4] 03 p0355 N88-12240
Trends in research and development in the Netherlands. The influence of national science policy between 1973 and 1986
[B8701588] 08 p1094 N88-16580

HEAO
NT HEAO 2

HEAO B
U HEAO 2

HEAO 2
Soft X-ray observations of pre-main sequence stars in the chamaeleon dark cloud
[NASA-CR-181457] 02 p0250 N88-11579
Exosat results on the dMe flare Star Wolf 630AB and on VB 8 04 p0512 N88-13151

HEARING
Mechanisms mediating the perception of complex acoustic patterns
[AD-A190112] 15 p2130 N88-22705
Predicting Air Combat Maneuvering (ACM) performance: Fleet fighter ACM readiness program grades as performance criteria
[AD-A191605] 19 p2710 N88-26099
Auditory evoked magnetic fields in man
[PB88-193446] 20 p2831 N88-26796
Dissecting the visual and auditory pathways by means of the two-input technique 21 p2978 N88-27690
Neuromagnetic evidence of place mechanisms for frequency and intensity coding in the human auditory cortex 21 p2979 N88-27693
HEART
NT CARDIAC VENTRICLES
NT MYOCARDIUM
Dimensional analysis of nonlinear oscillations in brain, heart and muscle
[DE87-014749] 06 p0751 N88-14614
Ballistocardiography in weightlessness research 11 p1521 N88-19080
Response of coronary blood flow to step changes in plasma protein concentration in the isolated rat heart 12 p1651 N88-19892
The effects of normal and therapeutic baths on the central vascular organs of persons with healthy hearts, as measured by X-ray
[NASA-TT-20252] 13 p1811 N88-20818
HEART DISEASES
NT CORONARY ARTERY DISEASE
NT MYOCARDIAL INFARCTION
Relationships between coronary heart disease risk factors and serum ionized calcium in Kennedy Space Center Cohort
[NASA-TM-100979] 10 p1368 N88-18177
HEART FUNCTION
Maximal cardiorespiratory responses to one- and two-legged cycling during acute and long-term exposure to 4300m
[AD-A185730] 06 p0752 N88-14621
Cardiac contractility in weightlessness according to spatial ballistocardiography 07 p0890 N88-15393
Distinctions and mechanisms of effects of epinephrine and norepinephrine on cardiac pumping function under hypokinetic conditions 07 p0891 N88-15399
Respiratory and cardiovascular responses to cold stress following repeated cold water immersion
[AD-A186460] 08 p1050 N88-16340
Sudden in-flight incapacitation in general aviation
[AD-A187044] 09 p1115 N88-16682
Validation of a modified one-step rebreathing technique for measuring exercise cardiac output
[AD-A192600] 21 p2986 N88-27729
HEART RATE
NT ARRHYTHMIA
NT TACHYCARDIA
Assessment of physical activity intensity by heart rate during sleep limited military operations
[AD-A185913] 07 p0888 N88-15382
Distinctions and mechanisms of effects of epinephrine and norepinephrine on cardiac pumping function under hypokinetic conditions 07 p0891 N88-15399
Biorhythmic aspects of intercontinental Antarctic adaptation 08 p1046 N88-16321
The use of heart rate in the prescription and evaluation of exercise programs
[AD-A186454] 08 p1049 N88-16336
Vital signs rate meter
[AD-A187015] 09 p1198 N88-17183
Electromagnetic metrics of mental workload
[AD-A188205] 11 p1523 N88-19093
The effect of orthostatic changes in central blood volume on the heart rate response to graded Valsalva maneuvers 12 p1653 N88-19904
Desynchronization of heart rate and breathing frequency after transmeridional flight across three time zones 12 p1663 N88-19968
Interrelationship of heart rhythm indicators and resistance to hypoxia in Antarctic polar workers 12 p1664 N88-19974
Vagal tone as an index of mental state 16 p2239 N88-23373
Estimating the cost of mental loading in a bimodal divided-attention task: Combining reaction time, heart-rate variability and signal-detection theory 16 p2241 N88-23385
Cardiac rhythm of animals consuming reclaimed water differing in concentration of sodium and potassium ions 19 p2705 N88-26085
Fighter pilot performance during airborne and simulator missions: Physiological comparisons 21 p2981 N88-27704
Metabolic and cardiorespiratory parameters during three consecutive days of exhaustive running
[AD-A192598] 21 p2985 N88-27728
Validation of a modified one-step rebreathing technique for measuring exercise cardiac output
[AD-A192600] 21 p2986 N88-27729
Validation of a modified one-step rebreathing technique for non-invasive measurement of submaximal cardiac output
[AD-A192852] 21 p2987 N88-27735
Effects of psychophysical lifting training on maximal repetitive lifting capacity
[AD-A192605] 23 p3238 N88-29271
HEAT
NT DRY HEAT
NT ENTHALPY
NT GIBBS FREE ENERGY
NT HEAT OF COMBUSTION
NT HEAT OF FORMATION
NT HEAT OF FUSION
NT LATENT HEAT
NT NUCLEAR HEAT
NT SPECIFIC HEAT
Structural reliability and damage tolerance of ceramic composites for high-temperature applications
[PB87-208310] 01 p0019 N88-10119
Heat engine regenerators: Research status and needs
[DE87-013581] 01 p0054 N88-10348
Needs assessment for nondestructive testing and materials characterization for improved reliability in structural ceramics for heat engines
[DE88-000040] 02 p0153 N88-10957
Assessment of the reliability of a correction procedure for WGT (Wet Globe Thermometer) (Botsball) measurements of heat stress
[AD-A185193] 05 p0584 N88-13559
Polymer material for heat sensors 06 p0676 N88-14142
Ceramic technology for advanced heat engines program data base
[DE88-003922] 11 p1464 N88-18730
Gastric emptying during exercise: Effects of acute heat stress, acclimation and hypohydration
[AD-A188008] 11 p1519 N88-19073
HEAT ACCLIMATIZATION
Determination of the individual state of acclimatization
[IZF-1986-27] 01 p0075 N88-10478
Daily dynamics of some physiological indicators of man under desert condition 06 p0750 N88-14605
Polycythemia and hydration status: Effects on blood volume and thermoregulation during exercise-heat stress
[AD-A185946] 07 p0888 N88-15383
Gastric emptying during exercise: Effects of acute heat stress, acclimation and hypohydration
[AD-A188008] 11 p1519 N88-19073
Heat acclimatization under controlled hyperthermia 12 p1665 N88-19981
Plasma cortisol, renin and aldosterone during an intense heat acclimation program
[AD-A189387] 13 p1809 N88-20810
Physiological and hematological responses of matched older and younger men during dry-heat acclimation
[AD-A186450] 18 p2550 N88-25139
Variability in intake and dehydration in young men during a simulated desert walk
[AD-A192654] 22 p3131 N88-28613
Hormonal regulation of fluid and electrolytes: Effects of heat exposure and exercise in the heat
[AD-A192655] 22 p3131 N88-28614
HEAT AFFECTED ZONE
A physical metallurgical basis for heat-affected zone and base-plate properties of a microalloyed HSLA steel
[AD-A180200] 01 p0022 N88-10137
Effects of stress-relieving on the mechanical properties and the structure of specimens of high-temperature fine-grained structural steels heat-treated to simulate welding
[BLL-CE-TRANS-8258-(9022.09)] 04 p0417 N88-12586
Study on fracture behaviour of a joint with a crack in transverse hard layer: Effect of hard layer width on COD
[PB87-143855] 07 p0868 N88-15267
Microstructural characterization of the heat affected zone of HSLA (High Strength Low Alloy)-100 steel GMA (Gas Metal Arc)-weldment
[AD-A187825] 11 p1457 N88-18686
Transformation, metallurgical response and behavior of the weld fusion zone and heat affected zone in Cr-Mo steels for fossil energy application
[DE88-006037] 13 p1744 N88-20430
Efficiency of fusion during periodic-pulse laser-beam welding 14 p1897 N88-21324
HEAT BALANCE
Approximate solutions of heat conduction in a medium with variable properties
[AD-A186933] 10 p1326 N88-17925
The active layer of the upper Atlantic Ocean 22 p3124 N88-28566
HEAT BUDGET
NT ATMOSPHERIC HEAT BUDGET
The ocean heat budget
[AD-A186130] 07 p0881 N88-15346
Measurement from satellites of land surface parameters and fluxes in the thermal infrared bands: Problems and methods 14 p1937 N88-21557
Energy budget and ground temperatures in hot regions
[AD-A196298] 24 p3404 N88-30268
HEAT CAPACITY
U SPECIFIC HEAT
HEAT CAPACITY MAPPING MISSION
The Earthnet Heat Capacity Mapping Mission (HCMM) data-processing system at Lannion (France) 09 p1127 N88-16761
HEAT CONDUCTION
U CONDUCTIVE HEAT TRANSFER
HEAT CONTENT
U ENTHALPY
HEAT DISSIPATION
U COOLING
HEAT DISSIPATION CHILLING
U COOLING
HEAT EFFECTS
U TEMPERATURE EFFECTS
HEAT EQUATIONS
U THERMODYNAMICS
HEAT EXCHANGERS
NT TUBE HEAT EXCHANGERS
Performance of rotary regenerative heat exchanger: A numerical simulation 01 p0046 N88-10292
Comparison of different kinds of compact cross flow heat exchangers
[DFVLR-FB-86-63] 01 p0048 N88-10305
Recent progress in magma energy extraction
[DE87-013083] 01 p0066 N88-10424
Continued research on direct contact heat exchangers: Effects of crystallization
[DE87-014931] 03 p0322 N88-12035
Overview of free-piston Stirling engine technology for space power application
[NASA-TM-88886] 03 p0386 N88-12427
Two-watt, 4-Kelvin closed cycle refrigerator performance 04 p0437 N88-12709
Theory of one and two-pass cross-flow heat exchanger
[PB87-225157] 04 p0441 N88-12736
Measured performance of the heat exchanger in the NASA icing research tunnel under severe icing and dry-air conditions
[NASA-TM-100116] 04 p0451 N88-12796
Design and development of absorption heat pumps
[DE88-900082] 04 p0466 N88-12885
Advanced condensing heat exchangers
[DE88-001485] 06 p0699 N88-14288
Development of a low noise 10 K J-T refrigeration system
[AD-A186004] 07 p0838 N88-15085
Evaluation of thermal storage for solar heating systems: Executive summary
[DE88-900219] 07 p0874 N88-15304
A quasi-three-dimensional calculation procedure for the prediction of flow and heat transfer in heat exchanger passages 09 p1165 N88-16985
Microcomputer analysis of regenerative heat exchangers for oscillating flow
[DE88-001773] 10 p1329 N88-17945
A solar receiver-reactor with specularly reflecting walls for high-temperature thermoelectrochemical and thermochemical processes
[AD-A187612] 10 p1351 N88-18077
Performance evaluation of plate-fin heat exchangers
[AD-A187798] 11 p1482 N88-18845
Ultrasonic testing of heat exchanger tubes
[DE88-751172] 11 p1497 N88-18939
Growth of Cr,Nd:Gd3Sc2Al3O12 (Cr,Nd:GSAG) crystals by the Heat Exchanger Method (HEM)(trademark)
[DE88-004041] 11 p1558 N88-19326
Proceedings of the 1987 International Symposium on Condensing Heat Exchangers
[DE88-005230] 13 p1766 N88-20564
Innovative, counterflow gas/fine solids, direct contact heat exchanger
[DE88-004744] 13 p1770 N88-20585
Study on the burnout with variations of flow twisting over tube length
[DE87-703170] 14 p1909 N88-21405
Hafnia-rich mixed oxide ceramics of the system HfO2-ZrO2-TiO2 for heaters and heat exchangers in electrothermal thrusters: The effects of titania on selected electrical and mechanical properties of Hafnia-rich mixed oxides in the system Hafnia-Zirconia-Titania, volume 1
[NASA-CR-182800-VOL-1] 15 p2047 N88-22197

Basic characteristics of heat-exchanger-type steam reformer heated by high-temperature helium gas (2). Analysis by simulation model (2)
[DE87-702962] 15 p2061 N88-22291
Comparison of entropy generation and conventional design methods for heat exchangers
[AD-A190256] 15 p2064 N88-22306
A survey of oscillating flow in Stirling engine heat exchangers
[NASA-CR-182108] 15 p2067 N88-22322
An evaluation of nondestructive methods for ceramic heat exchanger applications
[DE88-006731] 15 p2068 N88-22328
Comparison of different kinds of compact crossflow heat exchangers
[ESA-TT-1076] 16 p2207 N88-23169
Computational fluid dynamics applied to the prediction of the heat-transfer, mechanical and thermal-stress behavior of heat exchangers
[CFDU/87/7] 18 p2510 N88-24893
Moving belt radiator development status
[NASA-TM-100909] 19 p2607 N88-25477
Cross flow induced vibrations in tube bundle by displaced and misaligned tube configurations
[ETN-88-92132] 20 p2801 N88-26621
The design and fabrication of a Stirling engine heat exchanger module with an integral heat pipe
[NASA-TM-101296] 20 p2820 N88-26732
Heat exchanger demonstration expert system
22 p3066 N88-28193
High effectiveness contour matching contact heat exchanger
[NASA-CASE-MSC-20640-1] 23 p3214 N88-29132
Oxidizer heat exchanger component test
[NASA-CR-182159] 24 p3339 N88-29876
Theories of comparative analysis
[AD-A196328] 24 p3427 N88-30395
Growth of GaAs crystals by the Heat Exchanger Method for microwave device applications
[AD-A196028] 24 p3433 N88-30435

HEAT FLOW
U HEAT TRANSMISSION

HEAT FLUX
Effect of NASA advanced designs on thermal behavior of Ni-H2 cells
[NASA-TM-100197] 01 p0021 N88-10132
Locating parallel numerical tasks in the solution of viscous fluid flows
[DE87-013510] 02 p0169 N88-11064
Development of heat flux sensors for turbine airfoils
02 p0184 N88-11143
Enhancement of surface-atmosphere fluxes by desert-fringe vegetation through reduction of surface albedo and of soil heat flux
[NASA-CR-181442] 02 p0197 N88-11231
Measurements of gas velocities and temperatures in a large open pool fire
[DE87-005853] 03 p0261 N88-11641
Measurements in large JP-4 pool fires
[DE87-013445] 03 p0284 N88-11783
Experimental study of thermocapillary flows in a thin liquid layer with heat fluxes imposed on the free surface
[NASA-TM-100252] 04 p0445 N88-12763
Data base on the high heat flux behaviour of metals and carbon materials for plasma facing components: Experiments at the 10 MW neutral beam injection test stand of the IPP Nagoya
[IPPJ-AM-53] 04 p0492 N88-13031
Proceedings of the Japan-US Workshop P-92 on Plasma Material Interaction/High Heat Flux Data Needs for the Next Step Ignition and Steady State Devices
[DE87-013568] 04 p0494 N88-13042
Hypersonic laminar boundary layer: Parametric study for the representation of real gas effects
05 p0532 N88-13236
Use of a local heat source for determining temperature of inlet heat section in ring channels
[DE88-700332] 07 p0854 N88-15187
The effect of asymmetric heating on flow stability and heat transfer for flow in a vertical tube
[DE88-003242] 07 p0855 N88-15193
Particle-gas temperature differentials resulting from time-dependent radiative-conductive heat flux divergences in the tenuous dust-laden atmosphere of mars
[AD-A185888] 07 p0945 N88-15747
Bidirectional electron heat flux events in space
[DE88-001791] 08 p1084 N88-16531
Heat transfer from impinging flame jets
[ETN-88-91610] 09 p1162 N88-16964
Investigation of critical heating in narrow flow channels with R12 refrigerant as model fluid
[GKSS-87/E/25] 09 p1163 N88-16972
Numerical solutions of two moving boundary problems by both finite difference and finite element methods with applications
[DE88-002867] 09 p1230 N88-17374
Approximate solutions of heat conduction in a medium with variable properties
[AD-A186933] 10 p1326 N88-17925
Experimental study of thermal loading at the wall of an industrial Diesel motor
[ISAL-IDI1-87-10] 10 p1339 N88-18000
Experimental determination of the heat flux inside a tubular projectile for the velocity range M = 3 and M = 6
[ISL-R-118/86] 11 p1443 N88-18605
Prototype thin-film thermocouple/heat-flux sensor for a ceramic-insulated diesel engine
[NASA-TM-100798] 11 p1490 N88-18892
Test methodology for infrared tubular heaters
[PB88-160916] 12 p1626 N88-19728
Current velocity and hydrographic observations in the Straits of Florida, the Caribbean Sea and offshore of the Antillean Archipelago: Subtropical Atlantic climate studies (STACS) 1984 and 1985
[PB88-149299] 12 p1649 N88-19874
Some effects of heating on the wind-driven velocity in the upper ocean 13 p1805 N88-20792
Study on the burnout with variations of flow twisting over tube length
[DE87-703170] 14 p1909 N88-21405
The turbulent heat flux in low Mach number flows with large density variations
[DE88-006445] 14 p1911 N88-21419
Mass, heat and nutrient fluxes in the Atlantic Ocean determined by inverse methods
[NASA-CR-180535] 14 p1950 N88-21626
Thermostructural analysis of simulated cowl lips
15 p2080 N88-22403
Research sensors 15 p2085 N88-22430
Magnetic fusion energy plasma interactive and high heat flux components. Volume 5: Technical assessment of critical issues in the steady state operation of fusion confinement devices
[DE88-006920] 15 p2136 N88-22744
Preliminary measurements of heat flux in a subsonic gun simulator
[AD-A191090] 16 p2208 N88-23178
REFLEX: An energy deposition code that models the effects of electron reflection during electron beam heating tests
[DE88-009789] 19 p2726 N88-26186
Vaporization studies of plasma interactive materials in simulated plasma disruption events
[DE88-010100] 19 p2731 N88-26222
Surface temperature thermal fluxmeters for shock tubes
[NASA-TT-20319] 20 p2762 N88-26381
Evaluation of surface energy and radiation balance systems for FIFE
[NASA-CR-183118] 20 p2828 N88-26778
Optical imaging diagnostics for fusion plasmas
[DE88-997572] 21 p3018 N88-27910
Development of sensors for ceramic components in advanced propulsion systems: Survey and evaluation of measurement techniques for temperature, strain and heat flux for ceramic components in advanced propulsion systems
[NASA-CR-182111] 22 p3081 N88-28299
Study on iron disilicide thermoelectric generator
[AD-A193082] 22 p3116 N88-28517
The thermal behavior of film cooled turbulent boundary layers as affected by longitudinal vortices
[AD-A195155] 24 p3374 N88-30095
Measurement of local high-level, transient surface heat flux
[NASA-TP-2840] 24 p3375 N88-30099

HEAT GAIN
U HEATING

HEAT GENERATION
Nitrogen scale-up
[AD-A185702] 06 p0709 N88-14351
Investigation of self-discharge characteristics of spacecraft nickel-cadmium cells at elevated temperatures
[AD-A186497] 08 p0979 N88-15919

HEAT MEASUREMENT
On the stressing of annealed NITINOL: The electrical resistance and calorimetric effects
[AD-A184465] 04 p0414 N88-12569
Investigation by differential scanning calorimetry of microstructure in a superplastic Al-Mg-Zr alloy
[AD-A184902] 05 p0564 N88-13439
Investigation of energy metabolism of biological systems in weightlessness 07 p0893 N88-15409
Investigation of critical heating in narrow flow channels with R12 refrigerant as model fluid
[GKSS-87/E/25] 09 p1163 N88-16972
Time-resolved heat transfer measurements and analysis in the wage region of a cylinder in crossflow
10 p1328 N88-17939
Experimental study of thermal loading at the wall of an industrial Diesel motor
[ISAL-IDI1-87-10] 10 p1339 N88-18000
Specific heat of novel thin-film material systems
10 p1415 N88-18446
Experimental determination of the heat flux inside a tubular projectile for the velocity range M = 3 and M = 6
[ISL-R-118/86] 11 p1443 N88-18605
Multilayer thermal insulation tests
[INPE-4475-PRE/1243] 12 p1626 N88-19729
A calorimetric determination of the enthalpy of formation and a description of the defect structure of the ordered beta-phase /Ni, Cu/ /1-x/ Al/x/
[NASA-TT-20157] 13 p1745 N88-20434
High resolution hadron calorimetry
[NIKHEF-H/87-8] 13 p1773 N88-20605
Anomalies in the heat-capacity signatures of submonolayer adsorbates with attractive lateral interactions
[AD-A190736] 15 p2147 N88-22817
Note on the double crystal method of measuring heat transfer coefficient
[OUEL-1710/87] 17 p2338 N88-23950
Calorimetry applied to nucleus-nucleus collisions at ultrarelativistic energies
[DE88-006173] 18 p2573 N88-25282
Surface temperature thermal fluxmeters for shock tubes
[NASA-TT-20319] 20 p2762 N88-26381
Method and device for determining heats of combustion of gaseous hydrocarbons
[NASA-CASE-LAR-13528-1] 23 p3193 N88-29002

HEAT OF COMBUSTION
Photolytic processes for measurement of combustion heats of formation and reaction rates
[DE87-014047] 02 p0144 N88-10905
Correlation between flammability and heat of combustion of polymers
[NASA-TT-20116] 08 p0973 N88-15884
Numerical simulation of turbulent flames using vortex methods
[AD-A189813] 15 p2034 N88-22116
Application of Rayleigh scattering to turbulent flow with heat transfer and combustion
[AD-A191565] 18 p2481 N88-24720
On-line measurement of heat of combustion
[NASA-CR-183076] 19 p2738 N88-26255
Method and device for determining heats of combustion of gaseous hydrocarbons
[NASA-CASE-LAR-13528-1] 23 p3193 N88-29002

HEAT OF FORMATION
A calorimetric determination of the enthalpy of formation and a description of the defect structure of the ordered beta-phase /Ni, Cu/ /1-x/ Al/x/
[NASA-TT-20157] 13 p1745 N88-20434
Evaluation of direct methane conversion to higher hydrocarbons and oxygenates
[DE88-003812] 15 p2049 N88-22204

HEAT OF FUSION
Analytical treatment of the melting and solidification of latent heat store materials in finned tube geometries
[IKE-5-223] 03 p0314 N88-11985

HEAT PIPES
Membrane heat pipe development for space radiator applications
[DE86-006015] 01 p0045 N88-10285
Transient modeling of the thermohydraulic behavior of high temperature heat pipes for space reactor applications 02 p0136 N88-10857
Applications of heat pipes to cool PWBS and hybrid microcircuits 02 p0136 N88-10858
The Proceedings of the Symposium on Mechanics for Space Flight
[ISAS-SP-5] 03 p0317 N88-12006
Heat transfer performance of axially grooved heat pipes 03 p0319 N88-12016
Heat transfer characteristics of arterial heat pipe with axial grooves 03 p0319 N88-12017
Pump assisted heat pipe 03 p0319 N88-12018
Overview of free-piston Stirling engine technology for space power application
[NASA-TM-88886] 03 p0386 N88-12427
Advanced radiator concepts utilizing honeycomb panel heat pipes
[NASA-CR-172017] 04 p0443 N88-12747
Testing of heat pipes on SPAS-01
[BMFT-FB-W-86-014] 06 p0672 N88-14119
Orbital Replaceable Unit (ORU)/cold plate thermal interface study. Volume 1: Executive Summary
[BAE-TP-8430] 07 p0855 N88-15195
Heat pipes for space use 09 p1124 N88-16736
Compressible friction coefficients in a simulated heat pipe
[AD-A188818] 12 p1627 N88-19735

Moveable thermal joints for deployable or steerable spacecraft radiator systems
[NLR-MP-87016-U] 13 p1730 N88-20347
Heat pipe transient analysis: Vapor dynamics
[DE88-005132] 13 p1767 N88-20568
Development, manufacturing and testing of a gas-loaded variable conductance methanol heat pipe
[NLR-MP-87010-U] 13 p1767 N88-20571
Design of the Sandia-Israel 20-kW reflux heat-pipe solar receiver/reactor
[DE88-001312] 13 p1794 N88-20729
Development of an integrated heat pipe-thermal storage system for a solar receiver
[NASA-TM-101099] 15 p2091 N88-22458
Solar dynamic heat rejection technology. Task 2: Heat pipe radiator development
[NASA-CR-182141] 16 p2209 N88-23182
Transient analysis of heat pipe vapor dynamics
17 p2412 N88-24341
Progress in the computer modeling of the liquid phase behavior of a liquid metal heat pipe
17 p2412 N88-24342
A compressible vapor flux model for transient heat pipe analysis 17 p2412 N88-24343
ATHENA heat pipe transient model
17 p2412 N88-24344
Detailed transient model of a liquid-metal heat pipe
17 p2412 N88-24345
Thermochemical analysis of mass transfer in a NB-1ZR-potassium heat pipe 17 p2412 N88-24346
Transient thermohydraulic heat pipe modeling
17 p2413 N88-24347
The Lewis heat pipe code with application to SP-100 GES heat pipes 17 p2421 N88-24395
HTPIPE: A steady state heat pipe analysis program
17 p2421 N88-24396
Heat pipe transient analysis: Vapor dynamics
17 p2421 N88-24397
A transient model for liquid metal heat pipes
17 p2421 N88-24398
The THROHPUT code: Thermohydraulic heat pipe modeling 17 p2421 N88-24399
MACRAD: A mass analysis code for radiators
17 p2424 N88-24418
Fabric radiators 17 p2427 N88-24435
Trade study for kWe class space reactors
17 p2430 N88-24454
Performance of vapor-fed sodium heat engine/AMTEC systems 17 p2437 N88-24502
Moving belt radiator development status
[NASA-TM-100909] 19 p2607 N88-25477
The Proceedings of the Symposium on Mechanics for Space Flight 1987
[ISAS-SP-6] 20 p2782 N88-26499
Thermostatistical estimations of vapor-state molecules affected by gravity in a heat pipe
20 p2783 N88-26505
An experimental investigation of transient characteristics in a gravity-assisted heat pipe 20 p2783 N88-26506
Heat transfer of mesh-wick heat-pipes (bottom heat mode) 20 p2783 N88-26507
A statistical treatment of accelerated life test data for copper-water heat pipes 20 p2783 N88-26509
The design and fabrication of a Stirling engine heat exchanger module with an integral heat pipe
[NASA-TM-101296] 20 p2820 N88-26732
Reflux heat-pipe solar receivers for dish-electric systems
[DE88-008671] 21 p2968 N88-27631
The heat pipe network of TDF-1/TV-SAT. Review of the development at completion
[SNIAS-881-440-103] 23 p3213 N88-29127
Development of a space deployable radiator using heat pipes
[SNIAS-881-440-104] 23 p3214 N88-29128
Polymeric heat pipe wick
[NASA-CASE-GSC-13019-1] 23 p3214 N88-29133
Unstable heat pipes
[DE88-010780] 23 p3229 N88-29217
Effect of interfacial phenomena on contact line heat Transfer-3
[AD-A194941] 24 p3343 N88-29901

HEAT PUMPS
Double-effect absorption heat pump, phase 3
[PB87-232195] 03 p0317 N88-12005
Optimized ground coupled heat pump mechanical package
[DE87-014899] 04 p0441 N88-12738
Design and development of absorption heat pumps
[DE88-900082] 04 p0466 N88-12885
Life-cycle cost analysis of residential heat pumps and alternative HVAC (Heating, Ventilating and Air-Conditioning) systems
[DE88-003701] 07 p0839 N88-15090
Feasibility of a complex compound heat pump
[PB88-113022] 07 p0853 N88-15183
Heat pump and appliance research
[PB88-102462] 07 p0853 N88-15184
Working fluids for sorption heat pumps
[DE88-900203] 07 p0874 N88-15301
Water source heat pump: How to get home heating and cooling from your own back yard
[DE88-900180] 07 p0875 N88-15306
Comparison of a thermoelectric cooling system and a groundwater heat pump
[DE88-001753] 08 p0984 N88-15950
Solar assisted absorption or motor driven heat pump with earth seasonal storage, part 1
[DE88-900191] 09 p1187 N88-17114
Free-piston Stirling engine diaphragm-coupled heat-actuated heat pump component technology program, phase 1C
[DE88-003654] 10 p1330 N88-17949
Analysis of the performance of an air-water heat pump: Regulation of intrinsic performances
[DE88-900241] 10 p1349 N88-18061
Free-piston Stirling engine diaphragm-coupled heat-actuated heat pump component technology program, phase 1B
[DE88-003653] 11 p1483 N88-18854
Open-cycle centrifugal vapor-compression heat pump
[PB88-157391] 11 p1488 N88-18885
Proceedings of the 1987 International Symposium on Condensing Heat Exchangers
[DE88-005230] 13 p1766 N88-20564
Efficiency characteristics of speed modulated drives at predicted torque conditions for air-to-air heat pumps
[DE88-005846] 13 p1770 N88-20588
Overview of 1987 moonlight project
15 p2052 N88-22231
Application and technology requirements for heat pumps at the process industries
[DE88-006740] 15 p2062 N88-22293
Advanced chemical heat pumps using liquid-vapor reactions
[DE88-006760] 16 p2205 N88-23159
Heat pump-augmented systems for spacecraft thermal management 17 p2424 N88-24419
Solar assisted absorption or motor driven heat pump with earth seasonal storage. Part 2: Tables and figures
[DE88-900226] 19 p2686 N88-25964
Heat pump augmented radiators for spacecraft thermal management
[DE88-007890] 20 p2764 N88-26392
Heat pump augmented radiator for low-temperature space applications
[DE88-008369] 20 p2765 N88-26393
Magnetic heat pump design
[DE88-007730] 20 p2798 N88-26605
The Oak Ridge Heat Pump Design Model: Mark 3 version program documentationon
[DE88-007863] 20 p2799 N88-26607
Thermodynamic analysis of chemical heat storage system for heat pump
[DE88-753121] 20 p2820 N88-26728
Magnetic heat pumps
[DE88-012058] 21 p2969 N88-27639
A comparative economic evaluation of industrial heat pumps. Part 2: Addendum
[DE88-011701] 22 p3117 N88-28519
Absorption heat pumps
[DE88-752820] 23 p3229 N88-29218

HEAT RADIATORS
NT SPACECRAFT RADIATORS
Estimating payload internal temperatures and radiator size for multimegawatt space platforms
[DE88-000244] 03 p0275 N88-11738
Adiabatic diesel engine component development: Reference engine for on-highway applications
[NASA-CR-179531] 03 p0386 N88-12428
Advanced radiator concepts utilizing honeycomb panel heat pipes
[NASA-CR-172017] 04 p0443 N88-12747
AF cryogenic and fluid management spacecraft technology program 08 p0981 N88-15925
Indirect measurement of local condensing heat-transfer coefficient around horizontal finned tubes
[AD-A186929] 09 p1160 N88-16950
Solar dynamic heat rejection technology. Task 2: Heat pipe radiator development
[NASA-CR-182141] 16 p2209 N88-23182
Thermal management for multi-modal nuclear power plants 17 p2410 N88-24331
A review of impact design criteria for space power heat rejection systems 17 p2410 N88-24333
Progress in the computer modeling of the liquid phase behavior of a liquid metal heat pipe
17 p2412 N88-24342
A generalized method for optimizing the mass of space power systems 17 p2416 N88-24369
The Curie point radiator 17 p2424 N88-24420
Development of materials for fabric radiators
17 p2429 N88-24448
High power density alkaline fuel cell technology for MMW space burst power 17 p2429 N88-24451
Trade study for kWe class space reactors
17 p2430 N88-24454

HEAT REGULATION
U TEMPERATURE CONTROL

HEAT REJECTION DEVICES
U HEAT RADIATORS

HEAT RESISTANCE
U THERMAL RESISTANCE

HEAT RESISTANT ALLOYS
NT MOLYBDENUM ALLOYS
NT NIMONIC ALLOYS
NT NIOBIUM ALLOYS
NT REFRACTORY METAL ALLOYS
NT RHENIUM ALLOYS
NT TANTALUM ALLOYS
NT TUNGSTEN ALLOYS
Investigation of rapidly-solidified dispersion strengthened titanium alloys
[AD-A183882] 01 p0022 N88-10140
The development of a high temperature static strain gage system 02 p0184 N88-11142
Constitutive modeling for single crystal superalloys
02 p0187 N88-11168
Constitutive modeling of superalloy single crystals with verification testing 02 p0188 N88-11169
Constitutive modeling for isotropic materials
02 p0188 N88-11171
Constitutive modeling for isotropic materials
02 p0188 N88-11172
Creep-fatigue behavior of NiCoCrAlY coated PWA 1480 02 p0189 N88-11176
Quantitative electron probe microanalysis investigation of the oxidation of high temperature alloys at low oxygen partial pressures
[JUEL-2120] 03 p0288 N88-11811
Investigation of the deformation behavior of ferritic two-phase Fe-Ni-Al alloys with high concentrations of the intermetallic (Fe, Ni)Al phase at high temperatures
[ETN-87-90605] 03 p0288 N88-11812
Cast iron freezing mechanisms
03 p0298 N88-11870
Influence of boron on porosity in nickel-base superalloy castings 03 p0299 N88-11877
Deformation mechanisms of thermostructural materials
[AD-A184070] 03 p0338 N88-12128
A mathematical model of high alloy nickel base high temperature alloys
[BLL-M-37381-(5828.4)] 05 p0564 N88-13436
Behavior of long and short fatigue cracks in a powder metallurgy superalloy at room and at high temperature
05 p0601 N88-13677
Fatigue strength of alloy A286 at cryogenic temperature 05 p0603 N88-13695
Low cycle fatigue behaviour of notched specimens of nickel based superalloy single crystal
05 p0605 N88-13712
An overview of fatigue 05 p0608 N88-13729
Deformation, fatigue and fracture behavior of two cast anisotropic superalloys 05 p0608 N88-13732
Characterization of the microstructures of various materials
[AD-A184961] 05 p0655 N88-14017
High temperature low cycle fatigue of oxide dispersion strengthened and single crystal nickel base superalloys
06 p0720 N88-14422
High temperature low cycle fatigue behavior and creep-fatigue interation of MA 6000 ODS alloy
06 p0720 N88-14425
The effect of temperature on fatigue crack initiation from aluminosilicate inclusions 06 p0720 N88-14427
Dependence of strainrange partitioned fatigue life at elevated temperature on monotonic stress-strain properties 06 p0721 N88-14428
An analysis of temperature effect on LCF crack growth rates in superalloy GH36 06 p0721 N88-14431
Metallurgical processes in multi-component rare earth-transition metal permanent magnet alloys
[AD-A186401] 07 p0832 N88-15045
Center for the Space Processing of Engineering Materials 07 p0838 N88-15083
Development of a new generation of high-temperature composite materials 09 p1119 N88-16702
Investigation of the deformation behavior of the intermetallic phase (Fe,Ni)Al at high temperatures
[ETN-88-91062] 09 p1143 N88-16854
Effects of ion implantation on cavitation erosion of a cobalt based metal/carbide alloy
[AD-A187239] 10 p1303 N88-17793
Hot corrosion in gas turbines: A new, unique and informative technique is EASE (Electronic Absorption Spectroscopy Experiments)
[AD-A188508] 12 p1583 N88-19470

The cyclic stress-strain behavior of a single crystal nickel-base superalloy
[NASA-TM-100260] 12 p1607 N88-19610
Development of metastable processing paths for high temperature alloys
[AD-A188682] 12 p1608 N88-19617
Gordon Conference on Intermetallic Compounds held at Tilton, New Hampshire on 20-24 July 1987
[AD-A188502] 13 p1745 N88-20435
Activities report of the Materials Department
[ETN-88-91984] 13 p1745 N88-20436
Effect of nonuniform state of thermal stress on resistance of EI826 alloy to thermal fatigue
14 p1895 N88-21313
Effect of protective coatings on high-temperature fatigue of heat-resistant alloys 14 p1895 N88-21314
Experiments on the creep behavior of semifinished X10NiCrAlTi 32 20 (Nicrofer 32 20) tubes under multiaxial loading --- nuclear reactors
[JUEL-2127] 14 p1923 N88-21464
The viscoplasticity theory based on overstress applied to the modeling of a nickel base superalloy at 815 C
14 p1928 N88-21499
Development of a unified constitutive model for an isotropic nickel base superalloy Rene 80
14 p1929 N88-21501
Modeling the viscoplastic behavior of Inconel 718 at 1200 F 14 p1929 N88-21502
A theory of viscoplasticity accounting for internal damage 14 p1930 N88-21508
A constitutive model with damage for high temperature superalloys 14 p1930 N88-21510
The effects of temperature and strain rate on the yielding behavior of the single crystal superalloy PWA 1480
14 p1931 N88-21517
Investigation and synthesis of high temperature and increased stiffness RSP aluminum alloys
[AD-A190407] 15 p2039 N88-22151
High temperature oxidation and electrochemical studies related to hot corrosion
[AD-A190699] 15 p2040 N88-22156
Characterization of HYTUF steel. Semifinished product: 160 mm dia forging block. Processor: C3f. Test Report M3-434600
[M3-434600] 15 p2041 N88-22164
Bithermal fatigue of a nickel-base superalloy single crystal
[NASA-TM-100885] 15 p2042 N88-22168
Life prediction modeling based on cyclic damage accumulation 15 p2085 N88-22426
Fatigue damage modeling for coated single crystal superalloys 15 p2085 N88-22427
Fatigue crack growth behavior of a single crystal alloy as observed through an in situ fatigue loading stage
[NASA-TM-100863] 16 p2179 N88-22986
Model study of thermal stresses in gas-turbine blades with protective coating 16 p2179 N88-22989
Effect of alloying, rapid solidification, and surface kinetics on the high temperature environmental resistance of niobium
[AD-A192093] 18 p2485 N88-24743
Isothermal and bithermal thermomechanical fatigue behavior of a NiCoCrAlY-coated single crystal superalloy
[NASA-TM-100907] 18 p2489 N88-24766
JPRS report: Science and technology. Japan
[JPRS-JST-88-005] 19 p2633 N88-25619
Research on fractography of heat-resistant alloys
19 p2634 N88-25625
New super alloys used in turbochargers
19 p2634 N88-25626
A constitutive model with damage for high-temperature superalloys 20 p2771 N88-26434
Accelerated fatigue crack growth behavior of PWA 1480 single crystal alloy and its dependence on the deformation mode
[NASA-TM-100943] 20 p2772 N88-26436
Initial development of high-temperature titanium silicide alloys
[DE88-007860] 20 p2772 N88-26437
A fundamental understanding of the interfacial compatibility in hybrid material systems
[AD-A192921] 21 p2909 N88-27264
A review of solid particle erosion of engineering materials
[DE88-010065] 22 p3054 N88-28124
Advanced processing and properties of high performance alloys
[AD-A193767] 23 p3194 N88-29010
Anisotropic constitutive modeling for nickel-base single crystal superalloys
[NASA-CR-182157] 24 p3353 N88-29961

HEAT SHIELDING
NT REENTRY SHIELDING
Raman spectra of adsorbed layers on space shuttle and AOTV thermal protection system surface
06 p0799 N88-14890
OLYMPUS shuttle specific radiator shield
14 p1879 N88-21234
New concepts for atmospheric braking deceleration in planetary atmosphere entry
[SNIAS-CAS-DECE-P003-DPAA]
16 p2168 N88-22923
Dependence of structure of stabilized ZrO2 coatings on condensation rate 16 p2180 N88-22990
Space vehicle/nuclear reactor thermal radiation integration issues 17 p2424 N88-24417
Thermal and mechanical analysis of the Faraday shield for the compact ignition tokamak
[DE88-007855] 20 p2858 N88-26962
Far infrared spectroscopy telescope (FIRST) inflatable thermal shield, phase 1
[SR/FIS/108(87)CZ] 24 p3453 N88-30552

HEAT SINKS
Low-pressure eutectic bonding of depleted uranium to copper
[DE87-014625] 02 p0181 N88-11128
The global balance of dynamic vorticity in relation to heat sources and sinks 07 p0876 N88-15316
Surface-emitting two-dimensional laser diode arrays constructed on zig-zag heat sink surface
[DE88-005215] 14 p1915 N88-21439
Assessment of energy storage concepts for use in sprint power 17 p2407 N88-24312
Transient analysis of Li and LiH thermal storage spheres 17 p2411 N88-24334
The effect of maximum allowable payload temperature on the mass of a multimegawatt space based platform
17 p2424 N88-24416
Forced-convection, liquid-cooled, microchannel heat sinks
[AD-A193337] 21 p2937 N88-27444

HEAT SOURCES
NT GEOTHERMAL RESOURCES
A 40-kW fuel cell field test summary utilities activities report
[PB88-112800] 06 p0731 N88-14496
Use of a local heat source for determining temperature of inlet heat section in ring channels
[DE88-700332] 07 p0854 N88-15187
The global balance of dynamic vorticity in relation to heat sources and sinks 07 p0876 N88-15316
Dynamics Explorer guest investigator
[NASA-CR-181494] 07 p0878 N88-15325
A case study of the development of a military specification - zirconium powder for thermal batteries
[AD-A188751] 13 p1792 N88-20717
Tropical and monsoonal studies
[AD-A188387] 14 p1947 N88-21611
Superfine grain development by laser
15 p2050 N88-22215
The Light-Weight Radioisotope Heater Unit (LWRHU): Development and application 17 p2405 N88-24299
The application of high-rate biaxial testing to the design of containment vessels for radioisotope heat sources
17 p2426 N88-24428
Milliwatt generator project
[DE88-011261] 20 p2853 N88-26939
Storage of thermal energy by means of an absorption cycle
[PB88-190814] 21 p2966 N88-27619
High temperature electric arc furnace
[NASA-CASE-MFS-28281-1] 23 p3181 N88-28938

HEAT STORAGE
DTA/DSC studies of phase equilibria in binary mixtures of barium carbonate with alkali carbonates
[DE87-001195] 02 p0194 N88-11213
Analytical treatment of the melting and solidification of latent heat store materials in finned tube geometries
[IKE-5-223] 03 p0314 N88-11985
Evaluation of thermal storage for solar heating systems: Executive summary
[DE88-900219] 07 p0874 N88-15304
Thermal energy storage by means of an absorption cycle
[ETN-88-91614] 09 p1186 N88-17108
Effect of storage thermal behavior in seasonal storage solar heating systems
[PB88-114236] 10 p1350 N88-18067
Development of encapsulated lithium hydride thermal energy storage for space power systems
[DE88-004762] 11 p1507 N88-19001
An assessment methodology for thermal energy storage evaluation
[DE88-004642] 13 p1794 N88-20732
Thermal analysis of heat storage canisters for a solar dynamic, space power system
[DE88-004199] 15 p2027 N88-22075
Structural assessment of a space station solar dynamic heat receiver thermal energy storage canister
15 p2081 N88-22406
Development of an integrated heat pipe-thermal storage system for a solar receiver
[NASA-TM-101099] 15 p2091 N88-22458
Value of energy storage in pulsed space power systems
[AD-A191311] 16 p2170 N88-22938
Material degradation in a barium hydroxide latent heat storage pilot unit
[DFVLR-FB-87-49] 16 p2175 N88-22961
Assessment of energy storage concepts for use in sprint power 17 p2407 N88-24312
Transient analysis of Li and LiH thermal storage spheres 17 p2411 N88-24334
Field experience with aquifer thermal energy storage
[DE88-007075] 18 p2538 N88-25058
Advanced heat receiver conceptual design study
[NASA-CR-180901] 19 p2688 N88-25977
Thermodynamic analysis of chemical heat storage system for heat pump
[DE88-753121] 20 p2820 N88-26726
Transient thermal analysis of three latent heat storage configurations for rapid thermal charging
[DE88-008943] 20 p2881 N88-27104
Prediction of velocity and temperature profiles in thermally driven gravity currents applied to stratified thermal storage tanks
[DE88-004452] 21 p2946 N88-27496
Transient thermal analysis of three fast-charging latent heat storage configurations for a space-based power system
[DE88-009714] 23 p3186 N88-28960

HEAT STROKE
Rapid hypothermia subsequent to oral nicotinic acid and immersion in warm (30C) water
[AD-A186458] 08 p1050 N88-16339

HEAT TESTS
U HIGH TEMPERATURE TESTS

HEAT TOLERANCE
Assessment of the reliability of a correction procedure for WGT (Wet Globe Thermometer) (Botsball) measurements of heat stress
[AD-A185193] 05 p0584 N88-13559
Effects of moderate cold and heat stress on the potential work performance of industrial workers. Part 6: The effects of increasing vapour pressure at four air temperatures on the performance and physiology of white females
[PB88-124854] 18 p2550 N88-25137
Satellite remote sensing of the wet bulb globe temperature heat stress index, phase 2
[AD-A192798] 20 p2818 N88-26717
Hyperthermia: New thoughts on an old problem
[AD-A192602] 21 p2986 N88-27731
Plasma volume expansion in rats: Effects on thermoregulation and exercise
[AD-A192656] 22 p3130 N88-28606

HEAT TRANSFER
NT AERODYNAMIC HEAT TRANSFER
NT CONDUCTIVE HEAT TRANSFER
NT CONVECTIVE HEAT TRANSFER
NT LAMINAR HEAT TRANSFER
NT RADIATIVE HEAT TRANSFER
NT TURBULENT HEAT TRANSFER
Modeling and measurement of heat transfer on turbine blade tips 01 p0006 N88-10032
Thermal Control Working Group report
01 p0016 N88-10094
Effects of forced and free convections on structural temperatures of space shuttle orbiter during reentry flight
[NASA-TM-86800] 01 p0043 N88-10275
Membrane heat pipe development for space radiator applications
[DE86-006015] 01 p0045 N88-10285
Heat engine regenerators: Research status and needs
[DE87-013581] 01 p0054 N88-10348
The reliability of numerical solutions of ordinary differential equations, obtained by implicit calculation schemes
[PTB-W-30] 01 p0085 N88-10549
Error estimates for finite element approximations of parabolic variational equations
[BONNER-MATHE-SCHR-179]
01 p0087 N88-10569
The aerothermodynamic environment for holes in hypersonic configurations
[DE87-014651] 02 p0121 N88-10767
Thermal resistance of contacting metal surfaces at helium temperatures
[BLL-RISLEY-TR-5500-(9091.9F)]
02 p0148 N88-10929
Flow and heat transfer with impinging jets and rough surfaces
[DE87-014162] 02 p0169 N88-11065
Heat transfer in a real engine environment
02 p0186 N88-11155

Film cooling heat transfer on a turbine airfoil
02 p0186 N88-11156
Coolant passage heat transfer with rotation
02 p0186 N88-11160
Prediction of turbine blade heat transfer
02 p0187 N88-11162
Flow in a model turbine stator
02 p0187 N88-11163
Component specific modeling
02 p0187 N88-11166
New directions in Vlasov plasma turbulence and anomalous transport
[DE87-014425] 02 p0238 N88-11500
A heat transfer model for a heated helium airship
[AD-A183786] 03 p0259 N88-11629
Heat transfer in laminar flow for mass inlet into an annular channel
[DE87-702890] 03 p0314 N88-11983
A transient model for thermal detonation
[IKE-2-75] 03 p0314 N88-11984
Numerical analysis of Marangoni convection in Bridgman method
03 p0319 N88-12014
Heat transfer performance of axially grooved heat pipes
03 p0319 N88-12016
Heat transfer characteristics of arterial heat pipe with axial grooves
03 p0319 N88-12017
Pump assisted heat pipe
03 p0319 N88-12018
Local heat/mass transfer and pressure drop in a two-pass rib-roughened channel for turbine airfoil cooling
[NASA-CR-179635] 03 p0322 N88-12039
Heats of mixing for thermal energy storage systems. Phase 1: Selection of suitable liquid-liquid mixtures
[DE87-014971] 03 p0347 N88-12196
Performance analysis of advanced spacecraft TPS
[NASA-CR-181532] 04 p0399 N88-12484
Thermal analysis of electromagnetic launcher rails
[DE88-000166] 04 p0405 N88-12514
Ceramic technology for advanced heat engines project
[DE88-001520] 04 p0420 N88-12605
Resistor cooling in a vacuum
[DE88-000696] 04 p0440 N88-12733
NACHOS 2: A finite element computer program for incompressible flow problems. Part 2: User's manual
[DE88-001451] 04 p0443 N88-12750
Steady shearing in a viscoplastic solid
[AD-A184341] 04 p0454 N88-12810
Theory of heat and moisture exchange between finely disperse storm-generated spray and turbulent air flow
04 p0461 N88-12851
Structure of stably stratified atmospheric surface layer in presence of heat-releasing admixture
04 p0462 N88-12856
Influence of bond dilution on the free surface and interface Potts ferromagnetism
[DE87-703360] 04 p0497 N88-13061
Experimental investigations on blunt bodies and corner configurations in hypersonic flow
05 p0530 N88-13225
An evaluation of a translator for finite element data to resistor/capacitor data for the heat diffusion equation
[DE87-013926] 06 p0698 N88-14285
Heat transfer investigations in a slurry bubble column
[DE88-001445] 06 p0699 N88-14286
International workshop on two-phase flow fundamentals
[DE88-001478] 06 p0699 N88-14287
Advanced condensing heat exchangers
[DE88-001485] 06 p0699 N88-14288
Model development for induction heating
[DE88-002376] 06 p0699 N88-14289
HOST turbine heat transfer program summary
[NASA-TM-100280] 06 p0704 N88-14320
Role of anomalous currents in formation of ocean surface temperature field
06 p0727 N88-14474
Wall turbulence control
07 p0812 N88-14943
Numerical computations of natural convection heat transfer in irregular geometries
[DE88-002358] 07 p0852 N88-15178
The effect of asymmetric heating on flow stability and heat transfer for flow in a vertical tube
[DE88-003242] 07 p0855 N88-15193
A numerical study of transient heat and mass transfer in crystal growth
07 p0925 N88-15619
Particle-gas temperature differentials resulting from time-dependent radiative-conductive heat flux divergences in the tenuous dust-laden atmosphere of mars
[AD-A185888] 07 p0945 N88-15747
Turbomachinery
08 p0955 N88-15792
Finite element fundamentals, part 2
08 p0985 N88-15962
Review of the equations of fluid mechanics and heat transfer
08 p0986 N88-15970
The effect of eddy distribution on momentum and heat transfer near the wall in turbulent pipe flow
[NASA-TM-100257] 08 p0988 N88-15984
Comparative performance of the conjugate gradient and SOR (Successive Over Relaxation) methods for computational thermal hydraulics
[DE88-002553] 08 p0988 N88-15986
Influence of skeletal muscle glycogen on passive rewarming after hypothermia
[AD-A186451] 08 p1049 N88-16334
Numerical simulation of heat transfer turbulence, volume 4
[AD-A185132] 09 p1159 N88-16947
Indirect measurement of local condensing heat-transfer coefficient around horizontal finned tubes
[AD-A186929] 09 p1160 N88-16950
The dynamics of heat transfer at a turbulent pipe flow
[OEFZS-4400] 09 p1164 N88-16975
A quasi-three-dimensional calculation procedure for the prediction of flow and heat transfer in heat exchanger passages
09 p1165 N88-16985
Interaction of the cold conveyor belt with polar jet streaks
[AD-A186774] 09 p1192 N88-17145
Investigation of thermoacoustic heat transport using a thermoacoustic couple
[AD-A186889] 09 p1242 N88-17442
Two-phase reduced gravity experiments for a space reactor design
[DE86-015530] 09 p1247 N88-17475
Nonequilibrium superconductivity for particle detectors
[DE88-002876] 09 p1257 N88-17539
Overview of heat transfer and fluid flow problem areas encountered in Stirling engine modeling
[NASA-TM-100131] 09 p1262 N88-17561
Application of Hoffman modulation contrast microscopy coupled with three-wavelength two-beam interferometry to the in situ direct observation of the growth process of a crystal in microgravity
10 p1288 N88-17704
Effect of translucence of engineering ceramics on heat transfer in diesel engines
[DE88-003732] 10 p1305 N88-17804
An experiment to investigate Rankine cycle two-phase microgravity issues
[DE88-004197] 10 p1308 N88-17818
Mechanistic model for void distribution in flashing flow
[DE88-002948] 10 p1326 N88-17928
Time-resolved heat transfer measurements and analysis in the wage region of a cylinder in crossflow
10 p1328 N88-17939
Periodic natural convection in a rectangular enclosure of low aspect ratio
10 p1329 N88-17941
Microcomputer analysis of regenerative heat exchangers for oscillating flow
[DE88-001773] 10 p1329 N88-17945
Experimental studies of heat and mass exchange in parallel-passage rotary desiccant dehumidifiers for solar cooling applications
[DE88-001119] 10 p1350 N88-18069
Physiological and ecological implications of coupled heat- and water-transport mechanisms of endotherms and vegetation
[DE88-004170] 10 p1352 N88-18081
Disk pumping test
[AD-A187199] 11 p1440 N88-18591
Investigation of surface tension driven convection as a feasibility study for a micro-gravity experiment
[NASA-CR-182504] 11 p1466 N88-18739
Laminar flow heat transfer downstream from U-bends
11 p1484 N88-18859
Two and three dimensional elliptic flows
11 p1485 N88-18866
Unsteady heat transfer in turbine blade ducts: Focus on combustor sources
[NASA-TM-100815] 11 p1486 N88-18870
Thermosolutal convection in high-aspect-ratio enclosures
[NASA-TM-100803] 11 p1486 N88-18871
Effect of experimental variables on flash thermal diffusivity data analysis
[DE88-003631] 11 p1487 N88-18877
Effect of density change on rapid liquid-solid interface kinetics and heat flow
[DE88-004286] 11 p1487 N88-18878
Ultrasonic testing of heat exchanger tubes
[DE88-751172] 11 p1497 N88-18939
Effect of element size on the solution accuracies of finite-element heat transfer and thermal stress analyses of space shuttle orbiter
[NASA-TM-88292] 11 p1502 N88-18971
Mechanical design and construction of a 200 mA, 100 keV, dc, negative ion accelerator
[DE88-003855] 11 p1548 N88-19257
A method of calculating nonstationary heat flow in hydrogasodynamic processes in closed cryogenic systems
[DE88-700884] 12 p1626 N88-19727
Vapor-mist for lightweight high voltage space insulation systems
[DE87-011704] 13 p1762 N88-20538
Investigation of heat transfer to a flat plate in a shock tube
[AD-A189538] 13 p1766 N88-20561
Heat pipe transient analysis: Vapor dynamics
[DE88-005132] 13 p1767 N88-20568
The influence of Mach number and heat transfer on the turbulent flow wall law
[NASA-TT-20230] 13 p1771 N88-20594
Estimates of ocean-atmosphere thermal interaction in Gulf Stream energy-active test range in winter of 1984
13 p1785 N88-20679
Compatibility in space reactor fuel systems
[DE88-005698] 13 p1839 N88-21004
Study on the burnout with variations of flow twisting over tube length
[DE87-703170] 14 p1909 N88-21405
Ocean eddies
14 p1938 N88-21566
Thermal modeling of solar central receiver cavities
[DE88-004940] 14 p1943 N88-21594
Mass, heat and nutrient fluxes in the Atlantic Ocean determined by inverse methods
[NASA-CR-180535] 14 p1950 N88-21626
The role of water in the thermal balance of the coma
14 p1999 N88-21916
The numerical simulation of viscous flows with change of phase and chemical reaction
[DE88-003204] 15 p2062 N88-22292
Enhancement of data acquisition and numerical computation capabilities for unsteady fluid dynamics
[AD-A190115] 15 p2063 N88-22302
FLOSIN: A fluid loop analyzer for SINDA
15 p2066 N88-22321
Thermal-structural analyses of Space Shuttle Main Engine (SSME) hot section components
15 p2081 N88-22404
Review and assessment of the HOST turbine heat transfer program
15 p2086 N88-22431
Performance evaluation of molten salt thermal storage systems
[DE87-014645] 15 p2091 N88-22461
Peculiarities of non-stationary heat transfer to superfluid helium
[DE88-701174] 16 p2200 N88-23124
Gravity currents with heat transfer effects
[PB88-180047] 16 p2205 N88-23158
Preliminary measurements of heat flux in a subsonic gun simulator
[AD-A191090] 16 p2208 N88-23178
Boundary layer measurements using hot-film sensors
17 p2297 N88-23743
Studies of heat and mass transfer during chemical vapor deposition
17 p2338 N88-23953
The effects of inlet turbulence and rotor/stator interactions on the aerodynamics and heat transfer of a large-scale rotating turbine model. Part 4: Aerodynamic data tabulation
[NASA-CR-179469] 17 p2339 N88-23956
Heat transfer in aerospace propulsion
[NASA-TM-100874] 17 p2339 N88-23957
Pumped two-phase heat transfer loop
[NASA-CASE-MSC-20841-2] 17 p2339 N88-23958
Botany Facility: Test report on breadboard tests for the determination of the heat transfer at the glass disk and of the temperature distribution in the fluorescent tube
[BF-TN-ER-053] 17 p2378 N88-24136
An experiment to investigate Rankine cycle two-phase microgravity issues
17 p2409 N88-24322
Transient analysis of Li and LiH thermal storage spheres
17 p2411 N88-24334
A liquid metal MHD concept for multimegawatt space power application
17 p2413 N88-24348
Development of a lightweight structure with load bearing capability and high thermal conductance
17 p2420 N88-24393
A reflux tube fabric radiator
17 p2421 N88-24394
Heat pipe transient analysis: Vapor dynamics
17 p2421 N88-24397
The Curie point radiator
17 p2424 N88-24420
The liquid droplet radiator in space: A parametric approach
17 p2427 N88-24437
Nucleate pool boiling: High gravity to reduced gravity; liquid metals to cryogens
17 p2431 N88-24464
Reduced-gravity two-phase flow experiments in the NASA KC-135
17 p2431 N88-24465
Microgravity two-phase fluid flow pattern modeling
17 p2432 N88-24467
Method and apparatus for growing crystals
[NASA-CASE-MFS-28137-1] 17 p2446 N88-24544
Analytic and numerical modeling of heat and material transport in electrical hypervelocity guns
[AD-A192178] 18 p2469 N88-24655
Designing to safe power limits in hybrid circuits
[DE88-005533] 18 p2506 N88-24865

Heat transfer from a negatively buoyant wall jet
[PB88-181953] 18 p2507 N88-24873
Computational fluid dynamics applied to the prediction of the heat-transfer, mechanical and thermal-stress behavior of heat exchangers
[CFDU/87/7] 18 p2510 N88-24893
Similarity solutions of nonlinear partial differential equations invariant to a family of affine groups
[DE88-003404] 18 p2567 N88-25245
Modelling of thermal plasma systems
18 p2578 N88-25314
Correlations of velocity and temperature fluctuations in the stagnation-point flow of circular cylinder in turbulent flow
[NASA-TM-100930] 19 p2597 N88-25435
Liquid phase decomposition in slurry fuels
19 p2624 N88-25564
Femtosecond nonequilibrium electronic heat transport in thin gold films 19 p2659 N88-25807
Pressure drop and heat transfer in turbulent non-Newtonian pipe flow of advanced energy transmission fluids
[DE88-010021] 19 p2666 N88-25853
Design and testing of a high power spacecraft thermal management system
[NASA-TM-4051] 20 p2764 N88-26389
Heat transfer of mesh-wick heat-pipes (bottom heat mode) 20 p2783 N88-26507
Magnetic heat pump design
[DE88-007730] 20 p2798 N88-26605
Multigrid computation of practical fluid flows and heat transfer
[DE88-010064] 20 p2799 N88-26609
Boundary element method for contact heat transfer
[DE88-011013] 20 p2800 N88-26613
Overview of the TITAN-2 reversed-field pinch aqueous fusion power core design
[DE88-008170] 20 p2857 N88-26966
Development of an experimental system for studying fast transient ignition phenomena
[DE88-011917] 21 p2911 N88-27276
Ceramic technology for advanced heat engines project
[DE88-008945] 21 p2919 N88-27323
Determination of lumped-mass thermal properties associated with autoclave curing of graphite/epoxy composites 21 p2925 N88-27364
Heat and mass transfer in a transport channel
[DE88-701968] 21 p2945 N88-27493
Determination of the local heat-transfer characteristics on glaze ice accretions on a cylinder and a NACA 0012 airfoil 21 p2946 N88-27500
Heat and mass transfer in laminar wavy film absorption with the presence of non-absorbable gases
21 p2947 N88-27502
Plasma behavior in the boundary layer near a railgun surface
[DE88-008889] 21 p3017 N88-27909
On the impact of low-latitude anomalous forcing on local and remote circulation: Winters(DJF) 1978/79 to 1986/87 22 p3123 N88-28560
The effects of inlet turbulence and rotor/stator interactions on the aerodynamics and heat transfer of a large-scale rotating turbine model. Volume 3: Heat transfer data tabulation 65 percent axial spacing
[NASA-CR-179468] 23 p3180 N88-28930
Transient thermal analysis of three fast-charging latent heat storage configurations for a space-based power system
[DE88-009714] 23 p3186 N88-28960
Combustion dynamics and thermal structure of a planar spray flame 23 p3190 N88-28985
Numerical investigations in three-dimensional internal flows
[NASA-CR-183108] 23 p3210 N88-29106
Aerodynamic heating of missiles
24 p3319 N88-29764
The use of hot-film technique for boundary layer studies on a 21 percent thick airfoil
[NAE-AN-45] 24 p3321 N88-29781
The effects of inlet turbulence and rotor/stator interactions on the aerodynamics and heat transfer of a large-scale rotating turbine model. Volume 2: Heat transfer data tabulation. 15 percent axial spacing
[NASA-CR-179467] 24 p3326 N88-29804
Effect of interfacial phenomena on contact line heat Transfer-3
[AD-A194941] 24 p3343 N88-29901
Radiation from soot-containing flames
24 p3347 N88-29927
Transition at hypersonic speeds
[NASA-CR-178315] 24 p3368 N88-30058
Assessment of a 3-D boundary layer analysis to predict heat transfer and flow field in a turbine passage
[NASA-CR-174894] 24 p3370 N88-30066
The use of upwind schemes at high Reynolds number: A cautionary note
[AD-A196227] 24 p3371 N88-30074
The thermal behavior of film cooled turbulent boundary layers as affected by longitudinal vortices
[AD-A195155] 24 p3374 N88-30095

HEAT TRANSFER COEFFICIENTS

Jet impingement heat transfer: A literature study
[PNR90404] 02 p0172 N88-11083
Measurement of airfoil heat transfer coefficients on a turbine stage 02 p0186 N88-11158
Heat transfer with very high free stream turbulence
02 p0186 N88-11161
Regressed relations for forced convection heat transfer in a direct injection stratified charge rotary engine
[NASA-TM-100124] 05 p0549 N88-13345
Determination of the heat conduction coefficient of the soil from the advance of the diurnal temperature wave
08 p1015 N88-16151
Indirect measurement of local condensing heat-transfer coefficient around horizontal finned tubes
[AD-A186929] 09 p1160 N88-16950
Heat transfer modeling of jet vane Thrust Vector Control (TVC) systems
[AD-A190106] 15 p2019 N88-22034
Note on the double crystal method of measuring heat transfer coefficient
[OUEL-1710/87] 17 p2338 N88-23950
Characteristics of long size thermosyphons made of corrugated tube 20 p2784 N88-26511
Estimation of transient heat transfer coefficients in multidimensional problems by using inverse heat transfer methods 23 p3210 N88-29108
Experimental and analytical study of two-phase flow in zero gravity
[AD-A195223] 24 p3358 N88-29993

HEAT TRANSMISSION

NT AERODYNAMIC HEAT TRANSFER
NT CONDUCTIVE HEAT TRANSFER
NT CONVECTIVE HEAT TRANSFER
NT HEAT TRANSFER
NT LAMINAR HEAT TRANSFER
NT RADIATIVE HEAT TRANSFER
NT TURBULENT HEAT TRANSFER
Nitrogen scale-up
[AD-A185702] 06 p0709 N88-14351
Determining deep heat flow under complex geothermal conditions 08 p1011 N88-16130
Effect of density change on rapid liquid-solid interface kinetics and heat flow
[DE88-004286] 11 p1487 N88-18878
A method of calculating nonstationary heat flow in hydrogasodynamic processes in closed cryogenic systems
[DE88-700684] 12 p1626 N88-19727

HEAT TREATMENT

NT ANNEALING
NT LASER ANNEALING
NT NITRIDING
NT PULSE HEATING
NT TEMPERING
Outgassing data for selecting spacecraft materials
[NASA-RP-1124] 01 p0019 N88-10117
Microstructural evolution and response to double-loop reactivation testing of heat-treated pH 13-8 Mo martensitic stainless steel
[DE87-009058] 02 p0146 N88-10915
Influence of thermocyclic treatment on mobility of grain boundaries
[BLL-M-37329-(5828.4)] 02 p0149 N88-10933
High temperature superconductors
03 p0297 N88-11869
Gas tungsten arc welding of Al-10Fe-5Ce
[AD-A184202] 03 p0334 N88-12104
Effect of long-term thermal aging on coated Celion/LARC-160 composites
[NASA-TM-100495] 04 p0410 N88-12544
Effect of time and temperature on transformation toughened zirconias
[AD-A184356] 04 p0419 N88-12600
Study of the influence of mechanical - thermal treatments on the creep behavior of a niobium stainless steel
[DE87-703506] 05 p0563 N88-13431
The effect of heat treatment on fatigue crack growth in polycarbonate 05 p0606 N88-13714
Characterization of current steels. The 35 NCD 16 alloy in 30 mm diam laminated bars made by Aubert and Duval
[CEAT-41/N/76] 07 p0832 N88-15046
Rare earth elements in heat treatable steels
[PB87-144002] 08 p0968 N88-15858
Laser transformation hardening of precision V-slide way
[PB87-144028] 08 p0991 N88-15999
Modification of properties of metals by high-power ion beams 08 p1079 N88-16507
Effects of a regenerating heat treatment on the creep behavior and the lifetime during creep test loading
[ETN-88-91063] 09 p1144 N88-16855
Effect of post-cure heat-treatment on static and fatigue behaviour of XAS-914C carbon fibre composite
[AD-A186943] 10 p1294 N88-17735
Effects of thermal and thermo-mechanical treatments on the mechanical properties of centrifugally cast alloy 718
[AD-A188195] 11 p1458 N88-18690
Influence of heat treatment on the properties of boroaluminum 14 p1886 N88-21270
Increasing the rate at which ceramic castings undergo preliminary heat-treatment in an ultra-high frequency magnetic field 14 p1886 N88-21275
Cellular thermosetting fluoropolymers and process for making them
[NASA-CASE-GSC-13008-1] 17 p2326 N88-23894
A study on the precipitation and reversion behaviors of Cu-0.3 percent Cr alloy by the step annealing method
[NASA-TT-20169] 18 p2489 N88-24764
Development of protective coatings for ceramic tubular components
[PB88-197165] 20 p2776 N88-26483
Stress corrosion of C ring specimen in salt spray tests
[I-186/87] 21 p2916 N88-27307
High-speed, precision processing using an electron beam 21 p2929 N88-27391
Preparation and development of advanced battery catalysts
[AD-A193208] 21 p2937 N88-27441

HEATERS

Research and development on high strength ceramic heaters discussed 04 p0404 N88-12508

HEATING

NT AERODYNAMIC HEATING
NT ARC HEATING
NT ATMOSPHERIC HEATING
NT ELECTRON CYCLOTRON HEATING
NT GAS HEATING
NT INDUCTION HEATING
NT IONOSPHERIC HEATING
NT KINETIC HEATING
NT LASER HEATING
NT PLASMA HEATING
NT PULSE HEATING
NT RADIANT HEATING
NT RADIO FREQUENCY HEATING
NT SHOCK HEATING
NT SOLAR HEATING
NT SPACE HEATING (BUILDINGS)
NT SUPERHEATING
NT TRANSIENT HEATING
NT WATER HEATING
Millimeter wave tokamak heating and current drive with a high power free electron laser
[DE87-011324] 01 p0099 N88-10651
Thermal testing by internal IR heating of the FEP module 02 p0136 N88-10854
Overview of free-piston Stirling engine technology for space power application
[NASA-TM-88886] 03 p0386 N88-12427
A large X-ray flare on Sigma 2 coronae borealis observed with exosat 04 p0508 N88-13121
Chromospheric and coronal heating in a bias-free sample of K dwarfs 04 p0518 N88-13184
Pumping systems and flow interfaces for rapid response electronic reheat controls 10 p1282 N88-17665
The influence of the heating procedure on the oxidation behaviour of NiAl studied by XPS
[AERE-R-12498] 10 p1300 N88-17776
A study of the magnetic field annihilation process in the magnetosphere and some geotechnical applications
[DE88-004165] 10 p1355 N88-18096
Coronal heating by means of helical magnetohydrodynamic turbulence
[AD-A187084] 10 p1410 N88-18413
An application of active surface heating for augmenting lift and reducing drag of an airfoil
[NASA-TM-100563] 11 p1436 N88-18570
Removal of out-of-plane distortion in mild steel panels using flame heating, volume 1
[AD-A187802] 11 p1457 N88-18684
Removal of out-of-plane distortion in mild steel panels using flame heating, volume 2
[AD-A187803] 11 p1457 N88-18685
Some effects of heating on the wind-driven velocity in the upper ocean 13 p1805 N88-20792
Rapid e-beam heating for measuring thermodynamics of metastable materials
[DE88-003565] 13 p1849 N88-21066
Early reheating and cosmic strings
13 p1855 N88-21103
Response of aluminum alloys to erosive particle impacts
[DE88-005910] 15 p2041 N88-22159

Investigation of boundary layer disturbances caused by periodic heating of a thin ribbon
[AD-A190572] 15 p2065 N88-22314
Tactical Rubidium Frequency Standard (TRFS)
[AD-A191049] 16 p2193 N88-23078
Heating at a propagating crack tip in a viscoplastic material
[AD-A190952] 16 p2224 N88-23274
Acoustic convective system
[NASA-CASE-NPO-17278-1-CU] 18 p2498 N88-24818
Heating and evaporation of turbulent liquid films: Measurement of film thickness and the onset of nucleate boiling
[DE88-006388] 18 p2512 N88-24905
Dynamics explorer data analysis
[NASA-CR-181428] 19 p2691 N88-25996
Numerical calculations of dopent diffusion involving flashlamp heating of silicon 21 p2929 N88-27384
Thermal-sensation control: A new method of controlling cooled/heated environments 21 p2930 N88-27394
Effects of surface tension and contact angle on sensible heating and boiling incipience in dielectric falling films
[DE88-007057] 21 p2945 N88-27492
Thermocouple for heating and cooling of memory metal actuators
[NASA-CASE-NPO-17068-1-CU] 23 p3217 N88-29151

HEATING EQUIPMENT
NT BOILERS
NT EVAPORATORS
NT FURNACES
NT IMAGE FURNACES
NT SOLAR FURNACES
NT VAPORIZERS
Development of creep resistant austenitic stainless steels for advanced steam cycle superheater application
[DE87-012929] 01 p0023 N88-10147
Electrical heating method --- pipelines, metal tanks
[GB-PATENT-2-137-059-A] 01 p0043 N88-10274
Development of an innovative, low-cost solar collector
[PB87-206819] 02 p0194 N88-11210
Modified 14Cr-16Ni stainless steels with improved creep resistance at 700 C due to tailored precipitate microstructures
[DE87-014788] 03 p0290 N88-11825
SCRAM JET (Supersonic Combustion Ramjet) combustion experiments 04 p0404 N88-12512
Plant Growth Module (PGM) conceptual design 05 p0631 N88-13855
Research on fluid dynamic energy separation
[DE88-002776] 10 p1339 N88-18001

HEAVING
The impact of vertical axis characteristics on helicopter handling qualities
[AD-A188964] 12 p1583 N88-19474

HEAVY COSMIC RAY PRIMARIES
U HEAVY NUCLEI
U PRIMARY COSMIC RAYS

HEAVY ELEMENTS
Heavy element compositions and energy spectra of galactic and solar cosmic rays 03 p0272 N88-11714
New nuclear structure calculations and the astrophysical r-process
[DE88-000979] 08 p1082 N88-16518
Molecular orbital studies of the bonding in heavy element organometallics: Progress report
[DE88-007765] 19 p2723 N88-26168

HEAVY IONS
Proceedings of the Workshop on Opportunities for Atomic Physics Using Slow, Highly-Charged Ions
[DE87-013991] 02 p0231 N88-11457
Proceedings of the Workshop on Opportunities for Atomic Physics Using Slow, Highly-Charged Ions
[DE87-013991] 02 p0231 N88-11457
Relativisitic heavy ion collisions
[DE87-014292] 02 p0232 N88-11462
Irradiations. Accumulated doses. Heavy ions --- space environment 03 p0272 N88-11708
Wavelengths of the 3p-3d transitions of the Co- and Fe-like ions: The effects of electron correlation
[DE88-000219] 04 p0498 N88-13067
Heavy-ion accelerator research for inertial fusion
[DE88-000541] 05 p0653 N88-14001
Method of plasma diagnostics by a heavy ion beam for the T-15 tokamak
[DE88-700342] 07 p0935 N88-15678
Particle desorption from nonconducting surfaces by high energy heavy ions
[ETN-88-91088] 09 p1245 N88-17461
Magnetic properties of heavy fermion superconductors
[ETN-88-91078] 09 p1255 N88-17524
Cellular effects of heavy ions: Experimental results and theoretical approaches --- space radiation 12 p1658 N88-19933
Effects of heavy ions on egg-developing systems 12 p1658 N88-19935
Effects of cosmic heavy ion radiation and space microgravity on plant systems 12 p1658 N88-19936
QED description of relativistic Coulomb excitation in heavy ion collisions
[DE88-700834] 12 p1689 N88-20100
In situ TEM observations of heavy ion damage in gallium arsenide
[DE88-005984] 14 p1986 N88-21843
Stochastic acceleration of cometary ions: The effects of composition and source strength distributions 14 p1997 N88-21902
An evaluation of energy-independent heavy ion transport coefficient approximations
[NASA-TM-101158] 17 p2397 N88-24251
The precipitation of energetic heavy ions into the upper atmosphere of Jupiter
[NASA-TM-101155] 17 p2452 N88-24565
The Jovian aurora: Electron or ion precipitation
[NASA-TM-101153] 17 p2452 N88-24566
The multistring model VENUS for ultrarelativistic heavy ion collisions
[DE88-007666] 18 p2573 N88-25284
Experiments with high energy nuclear beams at Brookhaven: From AGS to RHIC (Relativistic Heavy Ion Collider)
[DE88-007042] 18 p2574 N88-25287
Heavy ion fusion system assessment: Final focus and transport model
[LBL-23040] 19 p2725 N88-26183
Heavy ion collisions with A = 10(sup 57): Aspects of nuclear stability and the nuclear equation of state in coalescing neutron-star binary systems
[DE88-008029] 19 p2741 N88-26277
Charged pion production and projectile breakup in 85A MeV(sup)12C induced heavy ion reactions
[LUIP-8802] 20 p2850 N88-26920
Fluid dynamical model of ultrarelativistic heavy ion collisions
[DE88-007905] 20 p2850 N88-26921
Studies of HZE particle interactions and transport for space radiation protection purposes
[NASA-TM-101159] 20 p2886 N88-27142
Eikonal solutions to optical model coupled-channel equations
[NASA-TP-2830] 24 p3428 N88-30402

HEAVY LIFT HELICOPTERS
General equilibrium characteristics of a dual-lift helicopter system
[NASA-TP-2615] 12 p1573 N88-19407

HEAVY LIFT LAUNCH VEHICLES
Department of Housing and Urban Development-Independent Agencies Appropriations for fiscal year 1988, Thursday, 9 April 1987: National Aeronautics and Space Administration 03 p0386 N88-12424
Department of Housing and Urban Development-Independent Agencies Appropriations for fiscal year 1988, Friday, 10 April 1987: National Aeronautics and Space Administration 03 p0386 N88-12425
Assessment of mixed fleet potential for space station launch and assembly
[NASA-TM-100550] 11 p1443 N88-18608
Space station heavy lift launch vehicle utilization
[NASA-TM-100604] 14 p1873 N88-21188

HEAVY NUCLEI
Heavy-particle collisions in the plasma edge
[DE87-012928] 02 p0237 N88-11493
Neutron capture nucleosynthesis in low mass AGB stars 04 p0517 N88-13178
Investigation of a new magnetic dipole mode in the heavy, deformed nuclei 154 Sm, 156 Gd, 158 Gd, 164 Dy, 168 Er, and 174 Yb with high resolution electron scattering
[ETN-88-91084] 09 p1245 N88-17460
Production of heavy antinuclei: Review of experimental results 16 p2269 N88-23574
Cosmions and stars
[DE88-010886] 20 p2887 N88-27145
Charge composition of primary cosmic ray nuclei with z greater than or equal to 2 in energy region greater than or equal to 2 TeV 24 p3448 N88-30519

HEIGHT
NT SCALE HEIGHT
The end height of fireball as a function of their residual kinetic energy 06 p0737 N88-14535
Some measurements of height gain at V.H.F. 12 p1617 N88-19671
WAVFLD: A program to compute ionospheric height gain functions and field strengths at VLF
[AD-A191159] 16 p2191 N88-23066
Antenna heights for the optimum utilization of the oceanic evaporation duct. Part 1: Results from the Pacific measurements. Part 2: Results from the Key West measurements, volume 1
[AD-A192358] 20 p2791 N88-26555
TE/TM (Transverse Electric/Transverse Magnetic) height profile measurements of transpolar VLF (Very Low Frequency) signals
[AD-A194503] 22 p3069 N88-28216
Determination of most probable predicted 50 kPa pattern by empirical orthogonal functions 22 p3128 N88-28593
Analysis of environmental parameters from the Panama City tower radar experiment
[AD-A194994] 24 p3404 N88-30264

HEISENBERG THEORY
A study of mechanisms of hydrogen diffusion in separation devices
[DE88-000328] 04 p0416 N88-12584
A mechanism for symmetry breaking in antiferromagnetic Heisenberg systems
[ETN-88-91320] 05 p0657 N88-14031

HELICAL ANTENNAS
Short experiment study of four-wire helical antennas (half turn half wave)
[CNES-CT/DRT/TIT/AN-249-T] 15 p2058 N88-22266

HELICAL FLOW
Computational study of three-dimensional magnetohydrodynamic equilibria in toroidal helical systems
[DE87-753007] 02 p0240 N88-11514
On helicity fluctuations and the energy cascade in turbulence
[NASA-CR-178403] 03 p0321 N88-12028
Helicity dissipation in the plasma edge
[DE87-014762] 03 p0378 N88-12376

HELICAL INDUCERS
Symmetrized magnetic field configuration of low aspect ratio helical system
[IPPJ-869] 20 p2855 N88-26956

HELICAL WINDINGS
On some asymptotics of laminar flow in a coiled pipe 10 p1328 N88-17936

HELICOPTER ATTITUDE INDICATORS
U ATTITUDE INDICATORS
U HELICOPTERS

HELICOPTER CONTROL
Engine/airframe response evaluation of the HH-60A helicopter equipped with the T700-GE-701 transient droop improvement electronic control unit
[AD-A184443] 04 p0401 N88-12492
Rotor SAR (ROSAR): A new high-resolution all-weather vision method for helicopters
[MBB-UA-1046/87] 10 p1314 N88-17855
The impact of vertical axis characteristics on helicopter handling qualities
[AD-A188964] 12 p1583 N88-19474
Automatic flight control system for modern helicopters 12 p1597 N88-19558
Servo-actuator control for sampled-data feedback disturbance rejection --- helicopters
[ESA-TT-1002] 16 p2163 N88-22903
Helicopter anti-torque system using fuselage strakes
[NASA-CASE-LAR-13630-1] 17 p2308 N88-23809
Simultaneous multiple control force exertion capabilities of males and females versus helicopter control force design limits
[AD-A191653] 18 p2553 N88-25153
Frequency domain identification of the dynamics of a scaled remotely-piloted helicopter 20 p2786 N88-26524
Minimum-complexity helicopter simulation math model
[NASA-CR-177476] 24 p3328 N88-29819

HELICOPTER DESIGN
Integration of dynamic, aerodynamic and structural optimization of helicopter rotor blades
[NASA-CR-181441] 01 p0002 N88-10012
Results of the 1986 NASA/FAA/DFVLR main rotor test entry in the German-Dutch wind tunnel (DNW)
[NASA-TM-100507] 04 p0487 N88-13003
Model helicopter rotor rig and associated strain gauge balance for performance studies
[NAL-TM-AE-8704] 05 p0552 N88-13364
Sitting posture of helicopter pilots of the Royal Netherlands Air Force; preliminary recommendations
[IZF-1986-16] 05 p0631 N88-13857
Rotorcraft transmission 08 p0956 N88-15802
Accomplishments at NASA Langley Research Center in rotorcraft aerodynamics technology 09 p1105 N88-16626
Rotorcraft aeroelastic stability 09 p1106 N88-16631
System analysis in rotorcraft design: The past decade 09 p1110 N88-16652

An integrated approach to rotorcraft human factors research 09 p1110 N88-16653
An overview of key technology thrusts at Bell Helicopter Textron 09 p1111 N88-16657
Rotorcraft technology at Boeing Vertol: Recent advances 09 p1111 N88-16658
Recent Sikorsky R and D progress 09 p1111 N88-16659
Analysis of tasks for dynamic man/machine load balancing in advanced helicopters [DE88-003735] 09 p1117 N88-16696
Helicopter activities in Germany [MBB-UD-487/86] 10 p1314 N88-17853
Testing of a tail rotor system in a fiber composite type of construction [MBB-UD-472/86] 10 p1314 N88-17854
Computer program for conceptual tandem rotor helicopter design [AD-A187832] 11 p1439 N88-18584
Verification of the momemtum theory for rotors using measurements on a model helicopter [R-840-S] 13 p1718 N88-20275
Helicopter anti-torque system using fuselage strakes [NASA-CASE-LAR-13630-1] 17 p2308 N88-23809
Structurally tailorable non-linear snap-through spring system [NASA-CASE-LAR-13729-1] 18 p2523 N88-24970
Aeroelastic characteristics of the AH-64 bearingless tail rotor 21 p2891 N88-27162
Program user's manual for an unsteady helicopter rotor-fuselage aerodynamic analysis [NASA-CR-181701] 22 p3039 N88-28047

HELICOPTER ENGINES

Efficiency testing of a helicopter transmission planetary reduction stage [NASA-TP-2795] 07 p0661 N88-15224
Dynamic analysis of multimesh-gear helicopter transmissions [NASA-TP-2789] 09 p1176 N88-17045
Army maintenance: Actions to reduce the likelihood of helicopter gear failures [PB88-135256] 11 p1433 N88-18551
Artificial and natural icing tests of AH-64, phase 2 [AD-A188231] 11 p1439 N88-18585

HELICOPTER IMPULSIVE NOISE

U BLADE SLAP NOISE

HELICOPTER PERFORMANCE

An observer approach to the estimation of helicopter airspeed [DFVLR-FB-87-13] 01 p0005 N88-10029
Engine/airframe response evaluation of the HH-60A helicopter equipped with the T700-GE-701 transient droop improvement electronic control unit [AD-A184443] 04 p0401 N88-12492
Impact of flying qualities on mission effectiveness for helicopter air combat, volume 1 [NASA-CR-166568] 06 p0669 N88-14100
NASA/Army Rotorcraft Technology. Volume 3: Systems Integration, Research Aircraft, and Industry [NASA-CP-2495-VOL-3] 09 p1110 N88-16650
System analysis in rotorcraft design: The past decade 09 p1110 N88-16652
Rotorcraft flight research with emphasis on rotor systems 09 p1111 N88-16656
Helicopters as test carriers for avionics systems (HETAS) [DFVLR-IB-112-85/18] 09 p1116 N88-16692
Optimizing HF antenna systems on the Dolphin and Sea Hawk helicopters [AD-A186552] 09 p1152 N88-16901
Rotorcraft weight trends in light of structural material characteristics [AD-A186576] 10 p1276 N88-17642
Helicopter activities in Germany [MBB-UD-487/86] 10 p1314 N88-17853
Robust digital model following controller for helicopters [DFVLR-FB-88-07] 21 p2898 N88-27203
Preliminary airworthiness evaluation of the UH-60A/ESSS (External Stores Support System) with HELLFIRE launcher installed [AD-A196187] 24 p3323 N88-29793

HELICOPTER ROTORS

U ROTARY WINGS

HELICOPTER TAIL ROTORS

A study of rotor broadband noise mechanisms and helicopter tail rotor noise 06 p0777 N88-14766
An experimental investigation of the chopping of helicopter main rotor tip vortices by the tail rotor. Part 2: High speed photographic study [NASA-CR-177457] 09 p1114 N88-16678
Testing of a tail rotor system in a fiber composite type of construction [MBB-UD-472/86] 10 p1314 N88-17854

HELICOPTERS

NT AH-64 HELICOPTER
NT BO-105 HELICOPTER
NT CH-46 HELICOPTER
NT COMPOUND HELICOPTERS
NT HEAVY LIFT HELICOPTERS
NT MILITARY HELICOPTERS
NT OH-58 HELICOPTER
NT RIGID ROTOR HELICOPTERS
NT TANDEM ROTOR HELICOPTERS
NT UH-1 HELICOPTER
NT UH-60A HELICOPTER

Detection of targets in the presence of clutter using target echo modulations caused by rotating structures [REPT-12-86] 01 p0036 N88-10231
Analytical modeling of helicopter static and dynamic induced velocity in GRASP [NASA-TM-100026] 02 p0123 N88-10777
Global positioning satellite-based automatic landing system and wind estimated feedback for the AH-64 helicopter 02 p0124 N88-10784
Improved oil-off survivability of tapered roller bearings [NASA-CR-180804] 02 p0182 N88-11135
Helicopter main-rotor speed effects on far-field acoustic levels [NASA-TM-100512] 02 p0230 N88-11451
Rotorcraft Design for Operations [AGARD-CP-423] 03 p0262 N88-11649
Design requirements for future commercial operations 03 p0262 N88-11651
Mission-oriented flying qualities criteria for helicopter design via in-flight simulation 03 p0263 N88-11652
Handling qualities criterion for very low visibility rotorcraft 03 p0263 N88-11654
The flight evaluation of an advanced engine display and monitoring system 03 p0264 N88-11659
Active control of helicopter vibration using multiloop self-adaptive control 03 p0264 N88-11660
Controlling the dynamic environment during NOE flight 03 p0264 N88-11661
Minimisation of helicopter vibration through active control of structural response 03 p0264 N88-11662
New aerodynamic design of the fenestron for improved performance 03 p0264 N88-11664
System for SAR missions 03 p0265 N88-11671
The EH-101 integrated project: A naval, utility and commercial helicopter system 03 p0265 N88-11672
Analytic investigation of helicopter rotor blade appended aeroelastic devices [NASA-CR-166525] 03 p0266 N88-11676
Integrated voice and visual systems research topics [NASA-CR-177417] 03 p0356 N88-12246
Report of the helicopter human factors working group — accident prevention [CAA-PAPER-87007] 03 p0361 N88-12274
A full potential flow analysis with realistic wake influence for helicopter rotor airload prediction [NASA-CR-4007] 04 p0393 N88-12452
A 0.15-scale study of configuration effects on the aerodynamic interaction between main rotor and fuselage [NASA-CR-166577] 04 p0395 N88-12462
GPS vertical axis performance enhancement for helicopter precision landing approach [NASA-CR-177443] 04 p0397 N88-12477
Hovering helicopter flight dynamics: A study of vertical motion [AR-004-526] 04 p0399 N88-12485
Some data processing requirements for precision Nap-Of-the-Earth (NOE) guidance and control of rotorcraft [NASA-CR-177453] 04 p0401 N88-12493
Flap-lag equations of motion of rigid, articulated rotor blades with three hinge sequences [NASA-TM-100023] 04 p0401 N88-12495
Calculation of helicopter rotor blade/vortex interaction by Navier-Stokes procedures [NASA-CR-177441] 05 p0540 N88-13291
Coupled elastic rotor/body vibrations with inplane degrees of freedom 05 p0596 N88-13643
Sitting posture of helicopter pilots of the Royal Netherlands Air Force; preliminary recommendations [IZF-1986-16] 05 p0631 N88-13857
Development of an unsteady wake theory appropriate for aeroelastic analyses of rotors in hover and forward flight [NASA-CR-182357] 06 p0664 N88-14075
Aircraft accident report: Grand Canyon Airlines, Inc., and Helitech, Inc., midair collision over Grand Canyon National Park, June 18, 1986 [PB87-910403] 06 p0666 N88-14087
Euler solution of multiblade rotor flow [NASA-TM-100014] 06 p0704 N88-14322
Development of rotorcraft interior noise control concepts. Phase 3: Development of noise control concepts [NASA-CR-178172] 06 p0776 N88-14762
Development of a prototype H-46 helicopter diagnostic expert system [AD-A186077] 07 p0809 N88-14924
Lift distribution and velocity field measurements for a three-dimensional, steady blade/vortex interaction [NASA-TM-100013] 07 p0815 N88-14962
Digital processing of flight test data without using anti-aliasing filters, using a helicopter as an example [DFVLR-MITT-87-12] 07 p0819 N88-14981
Experimental design of a piloted helicopter off-axis-tracking simulation using a helmet mounted display [AD-A186228] 07 p0820 N88-14982
Turbine engine supportability study for Army Aviation Systems Command (AVSCOM) [DE88-002339] 07 p0820 N88-14984
Application of the analysis phase of the instructional system development to the MK-105 magnetic minesweeping mission of the MH-53E helicopter [AD-A186282] 07 p0822 N88-14994
The development of laboratory vibration test schedules: Philosophies and techniques 08 p0999 N88-16049
NASA/Army Rotorcraft Technology. Volume 1: Aerodynamics, and Dynamics and Aeroelasticity [NASA-CP-2495-VOL-1] 09 p1105 N88-16625
The development of CFD methods for rotor applications 09 p1105 N88-16627
A summary of recent NASA/Army contributions to rotorcraft vibrations and structural dynamics technology 09 p1105 N88-16628
NASA/Army Rotorcraft Technology. Volume 2: Materials and Structures, Propulsion and Drive Systems, Flight Dynamics and Control, and Acoustics [NASA-CP-2495-VOL-2] 09 p1106 N88-16632
Review of fatigue and fracture research at NASA Langley Research Center 09 p1106 N88-16633
Helicopter crashworthiness research program 09 p1107 N88-16635
Results of NASA/Army transmission research 09 p1108 N88-16640
NASA's rotorcraft icing research program 09 p1108 N88-16641
Helicopter mathematical models and control law development for handling qualities research 09 p1108 N88-16642
Rotorcraft flight-propulsion control integration 09 p1108 N88-16643
Helicopter human factors research 09 p1109 N88-16644
Rotorcraft handling-qualities design criteria development 09 p1109 N88-16645
A decade of aeroacoustic research at NASA Ames Research Center 09 p1109 N88-16648
Aeroacoustic research programs at the Army Aviation Research and Technology Activity 09 p1109 N88-16649
Status of NASA/Army rotorcraft research and development piloted flight simulation 09 p1110 N88-16651
Helicopters as test carriers for avionics systems (HETAS) [DFVLR-IB-112-85/18] 09 p1116 N88-16692
Optimizing HF antenna systems on the Dolphin and Sea Hawk helicopters [AD-A186552] 09 p1152 N88-16901
Refinement of eye-point-of-regard measurement with helicopter pilots in a flight experiment [ESA-TT-1073] 09 p1200 N88-17195
Comparison of alphanumeric data entry methods for advanced helicopter cockpits [AD-A186934] 09 p1201 N88-17201
General Rotorcraft Aeromechanical Stability Program (GRASP) version 1.03: User's manual [NASA-TM-100043] 09 p1219 N88-17313
Helicopter external vision requirements and visual display characteristics: A report/bibliography, revision A [AD-A187075] 10 p1276 N88-17641
Research and development. Technical-scientific publications (1956-1987): Retrospective view and prospects. Jubilee edition on the occasion of the 75th birthday of Dipl.-Engr. Dr.-Engr. E. H. Ludwig Boelkow [ISSN-0931-9751] 10 p1309 N88-17819
Special flight mechanical features of the bearingless helicopter rotor [MBB-FM-315/O] 10 p1309 N88-17825
Comprehensive analysis of helicopters with bearingless rotors [NASA-CR-182537] 10 p1390 N88-18300
The maximum entropy method for the analysis of radar echoes from hovering helicopters in clutter [FB-2-87] 11 p1475 N88-18799

Acoustic measurements from a rotor blade-vortex interaction noise experiment in the German-Dutch Wind Tunnel (DNW)
[NASA-TM-4024] 11 p1542 N88-19218
Safety study: Commercial emergency medical service helicopter operation
[PB88-917001] 12 p1575 N88-19422
Minimum weight design of rectangular and tapered helicopter rotor blades with frequency constraints
[NASA-TM-100561] 12 p1582 N88-19465
Automatic flight control system for modern helicopters 12 p1597 N88-19558
Organization of helicopter development activities with a view toward reduction of costs and cycles 12 p1704 N88-20200
An experimental investigation of the flap-lag-torsion aeroelastic stability of a small-scale hingeless helicopter rotor in hover
[NASA-TP-2546] 13 p1715 N88-20257
Procedure for detection and identification of a helicopter
[NASA-TT-20234] 13 p1722 N88-20297
Time-domain system for identification of the natural resonant frequencies of aircraft relevant to electromagnetic compatibility testing
[PB88-164520] 13 p1759 N88-20519
Optimal placement of tuning masses for vibration reduction in helicopter rotor blades
[NASA-TM-100562] 13 p1782 N88-20685
Inflow measurement made with a laser velocimeter on a helicopter model in forward flight. Volume 2: Rectangular planform blades at an advance ratio of 0.23
[NASA-TM-100542] 14 p1864 N88-21139
Advanced transmission studies
[NASA-TM-100867] 14 p1919 N88-21454
Inflow measurement made with a laser velocimeter on a helicopter model in forward flight. Volume 3: Rectangular planform blades at an advance ratio of 0.30
[NASA-TM-100543] 15 p2015 N88-22015
The effects of torque response and time delay on rotorcraft vertical axis handling qualities
[AD-A189873] 15 p2017 N88-22023
Preliminary airworthiness evaluation of the UH-60A equipped with the XM-139 VOLCANO mine dispensing system
[AD-A190604] 15 p2018 N88-22029
Method and device for the detection and identification of a helicopter
[NASA-TT-20251] 15 p2129 N88-22698
Acoustic propagation in the low atmosphere. Experimental study and modeling by the radius method
[ISL-CO-247/86] 15 p2131 N88-22713
Inflow measurements made with a laser velocimeter on a helicopter model in forward flight. Volume 4: Tapered planform blades at an advance ratio of 0.15
[NASA-TM-100544] 16 p2156 N88-22863
Tip vortices of isolated wings and helicopter rotor blades
[AD-A191336] 16 p2158 N88-22874
Development of a flexible and economic helicopter engine monitoring system
[PB88-185147] 16 p2160 N88-22887
Digital processing of flight data of a helicopter without using anti-aliasing filters
[ESA-TT-1094] 16 p2161 N88-22890
Minimum weight design of rotorcraft blades with multiple frequency and stress constraints
[NASA-TM-100569] 16 p2161 N88-22892
The application of linear maximum likelihood estimation of aerodynamic derivatives for the Bell-205 and Bell-206
[AD-A191279] 16 p2161 N88-22894
Airworthiness and flight characteristics test of a ski assembly for the UH-60A Black Hawk helicopter
[AD-A191414] 16 p2162 N88-22895
Experimental investigation of Hover flowfields in water at the McDonnell Douglas Research Laboratories 16 p2202 N88-23135
Acoustic characteristics of 1/20-scale model helicopter rotors
[NASA-CR-177355] 16 p2265 N88-23548
Inflow measurement made with a laser velocimeter on a helicopter model in forward flight. Volume 5: Tapered planform blades at an advance ratio of 0.23
[NASA-TM-100545] 17 p2299 N88-23755
Design and development of an avionics system adapted to helicopter missions 17 p2305 N88-23786
Competitive assessment of the U.S. civil helicopter industry
[PB88-186325] 18 p2455 N88-24574
Passive shock wave-boundary layer control for the Bell FX69-H-098 airfoil 18 p2457 N88-24588
Some rotorcraft applications of computational fluid dynamics
[NASA-TM-100066] 18 p2459 N88-24601
Inflow measurements made with a laser velocimeter on a helicopter model in forward flight. Volume 1: Rectangular planform blades at an advance ration of 0.15
[NASA-TM-100541] 18 p2460 N88-24607
Rotorcraft TCAS (traffic alert and collision avoidance system) evaluation: Group 3 results
[AD-A191719] 18 p2461 N88-24614
An enumeration of research to determine the optimal design and use of Army flight training simulators
[AD-A191242] 18 p2468 N88-24649
Design, manufacture and spin test of high contact ratio helicopter transmission utilizing Self-Aligning Bearingless Planetary (SABP)
[NASA-CR-4155] 18 p2524 N88-24975
Zero/zero rotorcraft certification issues. Volume 1: Executive summary
[NASA-CR-177483-VOL-1] 19 p2602 N88-25453
Zero/zero rotorcraft certification issues. Volume 2: Plenary session presentations
[NASA-CR-177483-VOL-2] 19 p2602 N88-25454
Zero/zero rotorcraft certification issues. Volume 3: Working group results
[NASA-CR-177483-VOL-3] 19 p2602 N88-25455
Grid generation of a helicopter rotary-wing 19 p2640 N88-25665
Aircraft accident report: Joe Foster Excavating, Inc., Bell 206B, N49606, in-flight collision with trees, Alamo, California, August 3, 1986
[PB88-910405] 20 p2755 N88-26345
Flight Mechanics Panel Symposium on Rotorcraft Design for Operations: Technical evaluation report
[AGARD-AR-243] 20 p2758 N88-26362
Computer simulation of a single pilot flying a modern high-performance helicopter
[NASA-TM-100182] 20 p2761 N88-26376
Computer simulation of multiple pilots flying a modern high performance helicopter
[NASA-TM-100183] 20 p2761 N88-26377
A high fidelity real-time simulation of a small turboshaft engine
[NASA-TM-100991] 20 p2761 N88-26378
A general-purpose approach to computer-aided dynamic analysis of a flexible helicopter
[NASA-TM-101002] 20 p2816 N88-26709
A comparison of the various helicopter mathematical models used in the methodology assessment 21 p2889 N88-27149
A comparison of theory and experiment for aeroelastic stability of a hingeless rotor model in hover 21 p2889 N88-27150
A comparison of theory and flight test of the BO 105/BMR in hover and forward flight 21 p2890 N88-27155
Comparison of experimental coupled helicopter rotor/body stability results with a simple analytical model 21 p2891 N88-27160
Transonic blade-vortex interactions 22 p3037 N88-28035
Euler equation computations for the flow over a hovering helicopter rotor
[NASA-CR-177493] 22 p3038 N88-28037
Dual adaptive control: Design principles and applications
[NASA-CR-177485] 22 p3038 N88-28038
Proceedings of the French-German Colloquium on Helicopter Detection
[ISL-R-104/87] 22 p3147 N88-28723
Acoustic helicopter positioning 22 p3148 N88-28726
Acoustic detection of helicopters: Experiments 22 p3148 N88-28727
Acoustic direction finding of flying helicopters 22 p3148 N88-28728
Detection of helicopters using ground-controlled microphones 22 p3148 N88-28730
Sensors adapted for acoustic detection 22 p3148 N88-28731
Correlation method and sensors adapted to the environment 22 p3149 N88-28732
Helicopter Warning Sensor (HWS) 22 p3149 N88-28735
Helicopter recognition using laser radars 22 p3149 N88-28736
The maximum entropy method for the analysis of short-time radar echoes from hovering helicopters 22 p3149 N88-28737
The VHF experimental radar LARA. A long-wavelength radar for helicopter detection 22 p3149 N88-28738
The radar detection of hovering helicopters 22 p3150 N88-28739
Investigation of helicopter rotor blade/wake interactive impulsive noise
[NASA-CR-177435] 23 p3171 N88-28882
JUH-1H redesigned pneumatic boot deicing system flight test evaluation
[AD-A194918] 24 p3322 N88-29785
Threat expert system technology advisor
[NASA-CR-177479] 24 p3328 N88-29816
Development and demonstration of an on-board mission planner for helicopters
[NASA-CR-177482] 24 p3328 N88-29817
A fiber optic collective flight control system for helicopters
[AD-A195406] 24 p3328 N88-29818

HELIOCENTRIC ORBITS
U SOLAR ORBITS

HELIOGRAPHS
U SPECTROHELIOGRAPHS

HELIOGRAPHY
U SPECTROHELIOGRAPHS

HELIOMAGNETISM
U SOLAR MAGNETIC FIELD

HELIOS SATELLITES
NT HELIOS 1
NT HELIOS 2
Comet West: A view from the HELIOS zodiacal light photometers 01 p0117 N88-10749

HELIOS 1
Magnetic field hourly averages from the Rome-GSFC experiment aboard Helios 1 and Helio 2
[NASA-TM-89782] 14 p2011 N88-21995

HELIOS 2
Magnetic field hourly averages from the Rome-GSFC experiment aboard Helios 1 and Helio 2
[NASA-TM-89782] 14 p2011 N88-21995

HELIOSEISMOLOGY
Perturbations of the Sun's gravitational field due to solar oscillations
[DE88-002099] 07 p0946 N88-15751
Solar oscillations, gravitational multipole field of the Sun and the solar neutrino paradox
[DE88-002100] 07 p0946 N88-15752

HELIOSPHERE
Solar modulation of the cosmic radiation in the heliosphere 01 p0112 N88-10720
Evolution of the solar wind structure in the outer heliosphere 01 p0112 N88-10721
Observations of turbulence and fluctuations in the solar wind 04 p0525 N88-13212
Observations of cosmic rays in the outer heliosphere
[NASA-CR-182942] 18 p2596 N88-25425

HELIOSTATS
Solar thermal technology
[DE87-001171] 02 p0195 N88-11218
Polymers in solar technologies
[DE88-001102] 03 p0294 N88-11849
Mean and peak wind load reduction on heliostats
[DE87-012281] 07 p0873 N88-15296
Performance evaluation of large-area glass-mirror heliostats
[DE88-011883] 21 p2969 N88-27636
Optical evaluation of prototype stretched-membrane mirror modules for solar central receivers
[DE88-011884] 21 p2969 N88-27637

HELIPORTS
Analyses of heliport system plans
[DOT/FAA/PM-87/31] 17 p2308 N88-23810
Four urban heliport case studies
[DOT/FAA/PM-87/32] 19 p2604 N88-25463

HELIUM
NT HELIUM ISOTOPES
NT LIQUID HELIUM
NT LIQUID HELIUM 2
Impact behavior of 9-Cr and 12-Cr ferritic steels after low-temperature irradiation
[DE88-000333] 03 p0291 N88-11827
Experimental study of stabilizing He-Ne laser output power with transverse magnetic field 03 p0303 N88-11906
A cold ejector for closed-cycle helium refrigerators 04 p0434 N88-12690
Design concepts for the ASTROMAG cryogenic system
[NASA-CR-181505] 04 p0497 N88-13060
A helium flare on the active G5 dwarf Kappa Ceti 04 p0519 N88-13189
An investigation into flow regimes for two-phase helium flow
[DE88-002834] 07 p0853 N88-15181
Tests of cold helium compressors at Fermilab
[DE88-002837] 07 p0862 N88-15230
A refractometer for the interferometric determination of the helium abundance in the Jupiter atmosphere
[BONN-IR-86-23] 07 p0946 N88-15749
New technique for enhancing helium production in ferritic materials
[DE88-003048] 09 p1142 N88-16847
State-to-state dynamics of molecular energy transfer
[DE88-003282] 10 p1406 N88-18382
Superfluid turbulence in He II at elevated pressures 10 p1422 N88-18493

Weldability of tritium-charged 304L stainless steel
[DP-1740] 12 p1607 N88-19611
An experimental and theoretical investigation of optogalvanic effects
[AD-A189618] 12 p1625 N88-19720
Creep behavior of consolidated rapidly solidified Type 304 stainless steel powder containing helium
[DE88-005536] 13 p1743 N88-20424
Experimental and theoretical methods for investigating helium effects in rapidly solidified metals
[DE88-005542] 13 p1743 N88-20425
Increase in influence of oxygen on the body in the presence of helium 13 p1810 N88-20816
The astrophysics of nebulae and active galactic nuclear emission-line regions: New methods and applications
13 p1858 N88-21111
Spectrographic detection of nitrogen impurity in helium
[DE88-752301] 15 p2033 N88-22111
Long-time tunneling in amorphous metals at helium temperatures
[DE88-701150] 16 p2281 N88-23654
Preliminary analysis of helium generation and its effects on the SP-100 system performance
17 p2422 N88-24406
Helium induced degradation in the weldability of an austenitic stainless steel
[DE88-009062] 20 p2773 N88-26443
HeFlow: A program for calculating pressure and temperature of helium in forced-flow superconductors. Part 1: Numerical solutions. Part 2: HeFlow user's manual
[DE88-008941] 20 p2876 N88-27071
Cosmological helium production simplified
[DE88-009578] 20 p2885 N88-27130
Improved adhesion for SiO2 particles in silica substrates using helium-ion irradiation
[DE88-008915] 21 p2920 N88-27332
Mass flow rate influence on void fraction of two-phase helium flow
[DE88-702456] 21 p2945 N88-27495
Temperature rise in superfluid helium pumps
[NASA-TM-100997] 21 p2948 N88-27507
An upper limit on the primordial He4 abundance from speckle interferometric observations of muon Cassiopeiae 23 p3298 N88-29641
Crystal structure and density of helium to 232 kbar
24 p3441 N88-30481
Evolutionary helium and CNO anomalies in the atmospheres and winds of massive hot stars
[NASA-CR-183254] 24 p3452 N88-30550

HELIUM ATOMS
Helium atom surface scattering apparatus for studies of crystalline surface dynamics
[DE88-002104] 06 p0787 N88-14826

HELIUM FILM
Dilution refrigerator with non-valve adsorption system of sup 3/He circulation
[DE88-700974] 15 p2050 N88-22209

HELIUM IONS
Experimental method for investigating helium effects in irradiated vanadium
[DE88-002891] 06 p0969 N88-15865

HELIUM ISOTOPES
Dilution refrigerator with non-valve adsorption system of sup 3/He circulation
[DE88-700974] 15 p2050 N88-22209
Basic characteristics of heat-exchanger-type steam reformer heated by high-temperature helium gas (2). Analysis by simulation model (2)
[DE87-702962] 15 p2061 N88-22291
Peculiarities of non-stationary heat transfer to superfluid helium
[DE88-701174] 16 p2200 N88-23124
Helium-3 fusion fuel resources for space power
17 p2410 N88-24330
Energy requirements for HE-3 mining operations on the Moon 17 p2420 N88-24390

HELIUM PLASMA
SOAR: Space orbiting advanced fusion power reactor
[AD-A189234] 13 p1732 N88-20356
Properties of hydrogen/helium accretion plasmas
[DE88-006831] 19 p2728 N88-26197

HELIUM STARS
U B STARS

HELIUM 2
U HELIUM ISOTOPES
U LIQUID HELIUM

HELIUM 3
U HELIUM ISOTOPES

HELIUM 4
U HELIUM ISOTOPES

HELIUM-NEON LASERS
Measuring stability of optical reference cavities by analyzing polarization spectrum
03 p0327 N88-12065
Laser system for automating topographic terrain survey 08 p1012 N88-16136
Fuels combustion research
[AD-A189114] 13 p1736 N88-20381
Failure mechanism of He-Ne lasers
14 p1902 N88-21362
Particle beam alignment system for single event upset-Van de Graaf experiments
[AD-A189695] 15 p2132 N88-22721
Fast acting optical beam detection and deflection system
[AD-A192161] 18 p2521 N88-24954
Precise beam alignment He-Ne laser tubes
[PB87-228334] 19 p2675 N88-25906

HELIUM-OXYGEN ATMOSPHERES
Structure and properties of welded joints produced between niobium parts in controllable helium atmosphere 14 p1897 N88-21326
Life in a hyperbaric environment. A new O2-H2 breathing mixture for industrial diving 19 p2695 N88-26019

HELIX TUBES
U TRAVELING WAVE TUBES

HELMET MOUNTED DISPLAYS
Experimental design of a piloted helicopter off-axis-tracking simulation using a helmet mounted display
[AD-A186228] 07 p0820 N88-14982
A piloted simulation investigating handling qualities and performance requirements of a single-pilot helicopter in air combat employing a helmet-driven turreted gun
[AD-A186878] 09 p1116 N88-16689
Refinement of eye-point-of-regard measurement with helicopter pilots in a flight experiment
[ESA-TT-1073] 09 p1200 N88-17195
Helicopter external vision requirements and visual display characteristics: A report/bibliography, revision A
[AD-A187075] 10 p1276 N88-17641
Virtual interface environment
17 p2381 N88-24153
Evaluation of the US Army fitting program for the integrated helmet unit of the integrated helmet and display sighting system
[AD-A191616] 18 p2465 N88-24635
Assessments of maneuverability with the TeleOperated Vehicle (TOV)
[AD-A191584] 21 p2993 N88-27751
Display system image quality
23 p3242 N88-29298

HELMHOLTZ EQUATIONS
On a boundary data operator and generalized exterior Robin problems for the Helmholtz equation
[AD-A185124] 05 p0640 N88-13915

HELMHOLTZ VORTICITY EQUATION
Point vortex dynamics: Recent results and open problems
[DE87-014759] 03 p0314 N88-11982
Group analysis of equations arising in ocean acoustics
04 p0472 N88-12914
Coupled FE and HIE method for exterior acoustics of axisymmetric shells --- finite element (FE) Helmholtz integral equation (HIE)
[ARE-TM(UHA)-87506] 09 p1243 N88-17448

HELOS (SATELLITE)
U EXOSAT SATELLITE

HEMATITE
Photoacoustic measurements of atmospheric aerosol absorption coefficients at ultraviolet, visible and infrared wavelengths 11 p1512 N88-19036

HEMATOLOGY
Polycythemia and hydration status: Effects on blood volume and thermoregulation during exercise-heat stress
[AD-A185946] 07 p0888 N88-15383
Changes in hemostasis system of animals under conditions of granulocytopoiesis inhibition under effect of decreased barometric pressure
12 p1651 N88-19890
Physiological and hematological responses of matched older and younger men during dry-heat acclimation
[AD-A186450] 18 p2550 N88-25139

HEMATOPOIESIS
Hypoxic hypoxia as a stimulus of erythropoiesis in vivo and in vitro 07 p0885 N88-15373
Differentiation of hemopoietic stem cells during adaptation to high altitude 07 p0893 N88-15410

HEMISPHERES
The corrosion of iron rotating hemispheres in 1 M sulfuric acid: An electrochemical impedance study
[DE87-014679] 02 p0148 N88-10925

HEMODYNAMIC RESPONSES
Effect of spaceflight factors on primate's blood circulation 10 p1359 N88-18124
Central hemodynamics in antiorthostatic hypokinesia and immersion models of weightlessness
11 p1521 N88-19081
Neuro-reflex mechanisms of circulation regulation in simulated microgravity 12 p1656 N88-19923
Physiological reactions upon controlled changes of blood distribution in humans 12 p1656 N88-19924
Is ANF implied in the night attenuated renal response to central hypervolemia? 12 p1659 N88-19945
Regulation of hemodynamics upon imitation of the transition to weightlessness (mathematical modeling)
13 p1810 N88-20817
Propranolol and the compensatory circulatory responses to orthostasis at high altitude
[AD-A192675] 22 p3131 N88-28618
Human performance and acute hypoxia, chapter 12
[AD-A192604] 23 p3238 N88-29270

HEMODYNAMICS
NT LOWER BODY NEGATIVE PRESSURE
Human metabolism and peripheral circulation during antiorthostatic hypokinesia 07 p0891 N88-15398
Acid-base equilibrium and some rat blood parameters following exposure to hyperbaric oxygenation
07 p0894 N88-15420
Changes in regional and central hemodynamics during seven-day water immersion 07 p0895 N88-15421
Comparative evaluation of orthostatic stability following immersion in horizontal and vertical positions
10 p1363 N88-18143
JPRS Report: Science and Technology. USSR: Space Biology and Aerospace Medicine, volume 21, no. 6, November - December 1987
[JPRS-USB-88-004] 10 p1364 N88-18150
Effect of exogenous cardiosynchronized counterpulsation on human regional and central hemodynamics 10 p1366 N88-18163
Hemodynamic effects of beta-adrenergic blocking with obsidan in clinostatic and orthostatic positions
10 p1367 N88-18171
Central hemodynamics in antiorthostatic hypokinesia and immersion models of weightlessness
11 p1521 N88-19081
Cardiovascular adaptation to zero-g during a long term flight (237 days) on board the Salyut 7 Soviet space station (1984) 12 p1655 N88-19920
Cardiac and peripheral circulation assessment by ultrasound on 3 astronauts during two 7-day space flights (1982 Salyut-7 - 1985 STS 51G)
12 p1656 N88-19921
Nitrogen's biological effect on oxygen transport through hematoparenchymal barrier 12 p1662 N88-19967
Effects of intense, time-constrained mental effort on hemodynamics and cardiovascular function
12 p1664 N88-19975
Human hemodynamics during water immersion as related to position during submersion
19 p2703 N88-26071

HEMOGLOBIN
Role of hemoglobin affinity for oxygen in efficiency of blood respiratory function 07 p0892 N88-15406
Air quality and human performance, chapter 16
[AD-A188335] 12 p1666 N88-19988
Effects of pulsed and CW (Continuous Wave) 2450 MHz radiation on transformation and chromosomes of human lymphocytes in vitro
[AD-A193104] 21 p2987 N88-27736

HEMORRHAGES
Hemorrhages and hemostasis in guinea pigs exposed to radiation at high altitude 19 p2705 N88-26083

HEMOSTASIS
U HEMOSTATICS

HEMOSTATICS
Role of carbon dioxide in correction of coagulation hemostasis under hypoxic conditions
10 p1365 N88-18160
Changes in hemostasis system of animals under conditions of granulocytopoiesis inhibition under effect of decreased barometric pressure
12 p1651 N88-19890
Hemostasis parameters of individuals with neurocirculatory dystonia submitted to dry immersion
19 p2703 N88-26072
Distinctive features in blood clotting and fibrinolytic properties under effect of epinephrine in presence of hypoxia and hypercapnia 19 p2705 N88-26082
Hemorrhages and hemostasis in guinea pigs exposed to radiation at high altitude 19 p2705 N88-26083

HENRY LAW
Evaluation and prediction of Henry's law constants and aqueous solubilities for solvents and hydrocarbon fuel components. Volume 1: Technical discussion
[AD-A188571] 12 p1613 N88-19643
Certain questions of thermodynamic theory of weak solutions 18 p2586 N88-25368

HERBIG-HARO OBJECTS
Finnish-Soviet Symposium on Radio Astronomy (1st) held at Otanlemi on August 26-27, 1985
[PB87-140661] 07 p0944 N88-15736

HERCULES AIRCRAFT
U C-130 AIRCRAFT

HERCULES NOVA
The 35-day cycle of Hercules X-1
[MPE-204] 11 p1571 N88-19405

HERMES MANNED SPACEPLANE
Preparation of qualification tests of a plasma generator for the feeding of a hypersonic wind tunnel
05 p0530 N88-13222
General aerodynamic-aerothermodynamic concepts for Hermes 05 p0535 N88-13251
Hermes propulsion system
[SNIAS-872-422-109] 05 p0556 N88-13383
Nonequilibrium reacting flows
08 p0985 N88-15959
The Hermes robot arm, its design and verification
12 p1588 N88-19508
The Hermes manipulation system (HERA) simulation facility development 12 p1591 N88-19524
HERMES Program: Airlock swimming pool tests
12 p1591 N88-19525
EVA, the technological challenge
12 p1592 N88-19535
Modelling and simulation of a rate controlled manipulator arm — Hermes
[NLR-TR-87010-U] 13 p1778 N88-20639
Management of large space projects. Case study: The Hermes program 22 p3162 N88-28830
Case study: The Hermes program product assurance
22 p3162 N88-28831
Ariane 5, HERMES and European vehicles for space station servicing
[SNIAS-881-422-102] 23 p3183 N88-26943
Hermes: Study of propulsion system for reusable man-rated spacecraft
[PSRM-TN-0000-00-04A] 24 p3337 N88-29866
Fuel cells for space use
[FCP-TR-DOS-SY-026] 24 p3389 N88-30183
The LTPP communication processor — Columbus and Hermes
[CL/CP/SES/FR/004] 24 p3415 N88-30328

HERMETIC SEALS
Improved glass-ceramic to metal seals in actuator and detonator applications with an aluminum-containing austenitic stainless steel
[DE88-004691] 13 p1749 N88-20458
Hermetic coating of optical fibers
[AD-A189886] 15 p2044 N88-22177
Hermetically sealable package for hybrid solid-state electronic devices and the like
[NASA-CASE-MSC-20181-1] 17 p2335 N88-23941
Sinterable ceramic powders from laser-heated gases
[AD-A194162] 23 p3197 N88-29024

HERMITIAN POLYNOMIAL
REDUCE-aided study of a problem in Hermitian matrix theory
[DE87-014331] 02 p0229 N88-11445
A taxonomy for conjugate gradient methods
[DE88-008574] 21 p3004 N88-27817

HERTZSPRUNG-RUSSELL DIAGRAM
A re-examination of the corona-wind dividing line: Diagnostics of non-coronal atmospheres
04 p0504 N88-13101

HERZBERG BANDS
Aeronomic problems of the molecular oxygen photodissociation. Part 3: Solar spectral irradiances in the region of the O2 Herzberg continuum, Schumann-Runge bands and continuum
[AERONOMICA-ACTA-A-332-1988]
24 p3343 N88-29897
Aeronomic problems of molecular oxygen photodissociation. Part 4: The various parameters for the Herzberg continuum
[AERONOMICA-ACTA-A-333-1988]
24 p3352 N88-29955

HESSIAN MATRICES
Conic algorithms for unconstrained minimization with special consideration of problems with large sparse Hessians: A summary of research performed
[DE88-002549] 13 p1816 N88-20850

HETEROCYCLIC COMPOUNDS
NT ADENOSINE TRIPHOSPHATE
NT ADENOSINES
NT ATROPINE
NT AZOLES
NT AZULENE
NT CAFFEINE
NT CARBAZOLES
NT ERGOTAMINE
NT FURANS
NT HMX
NT MORPHINE
NT NICOTINIC ACID
NT PHTHALOCYANIN
NT PYRIDINES
NT PYRROLES
NT RDX
NT THYMINE
NT URACIL
NT XANTHINES

X-ray structure analyses and molecular mechanics analyses of dense energetic materials
[AD-A185462] 06 p0779 N88-14781
Thermogravimetric analysis of polymeric materials for an intermediate temperature solid electrolyte
[DE88-004854] 10 p1306 N88-17809
Electronic and ionic transport in polymers
[AD-A187253] 11 p1452 N88-18651
Electronic and ionic transport in polymers
[AD-A190434] 15 p2045 N88-22185
High-performance polymeric materials
[AD-A190708] 15 p2046 N88-22190
High strength/sigh modulus aromatic heterocyclic ABA block copolymers
[AD-A191666] 18 p2491 N88-24774

HETERODYNING
NT OPTICAL HETERODYNING
Mid infrared LHS system packaging using flexible waveguides
[NASA-CR-181192] 01 p0093 N88-10607
Exploiting the IR: Solar and stellar spectroscopy in the IR 04 p0504 N88-13102
NO2 heterodyne frequency measurements with a tunable diode laser, a CO laser transfer oscillator and CO2 laser standards
[NASA-CR-182393] 06 p0710 N88-14353
Investigation of vibration problems with heterodyne holographic interferometer 08 p1000 N88-16058
Comparative investigation of heterodyne mixers at 1000 GHz
[FTL-068627] 09 p1158 N88-16940
Comparison of direct and heterodyne detection optical intersatellite communication links
09 p1169 N88-17013
Quantum limits of superconducting heterodyne receivers
[AD-A188014] 11 p1478 N88-18817
Diagnostics for research in atomization and turbulent two-phase flows
[AD-A187338] 11 p1482 N88-18843
Laser-heterodyne interferometry with streak camera detection
[DE88-003292] 14 p1914 N88-21437
Heterodyne spectrometer for the very high frequency range between 300 and 3000 GHz (1 mm to 0.1 mm) using a mixer in open structure
16 p2271 N88-23589
Design and calibration of a two-channel low-noise heterodyne receiver for use in a CO2 laser Thomson scattering alpha particle diagnostic
[DE88-007866] 19 p2728 N88-26201
Performance analysis of a noncoherently combined large aperture optical heterodyne receiver
22 p3065 N88-28189

HETEROGENEITY
Current experimental and theoretical understanding of detonation waves in heterogeneous solid explosives
[DE87-012177] 01 p0032 N88-10201
The calculation of thermal rate constants for gas-phase and heterogeneous reactions in combustion processes
[AD-A184435] 03 p0284 N88-11788
Heterogeneous multi-trunking queueing systems
[AD-A184255] 04 p0431 N88-12668
A data translation method for heterogeneous database systems 04 p0501 N88-13081
A raytrace method for a laterally heterogeneous environment
[AD-A186525] 08 p0978 N88-15912
Upper mantle heterogeneity and composition of primary ocean island magmas 08 p1009 N88-16120
Mechanism of and particle size effects on shock sensitivity of heterogeneous pressed explosives: Preliminary assessment of binderless RDX in fuze trains
[MRL-R-1077] 09 p1150 N88-16892
Software support for heterogeneous machines
10 p1378 N88-18224
Static dielectric breakdown strength of condensed heterogeneous high explosives
[AD-A191035] 16 p2183 N88-23014
Nanosecond laser photolysis of opaque heterogeneous photosensitizers
[AD-A191424] 16 p2213 N88-23209
Distributed mathematics in a heterogeneous environment
[DE88-009128] 19 p2716 N88-26124
Sintering of the heterogeneous MgO compacts
[DE88-010357] 20 p2767 N88-26408
Off-boundary approach to the boundary element method
[AD-A192931] 20 p2815 N88-26701
Mathematical problems of nonlinear wave propagation and of waves in heterogeneous media
[AD-A195970] 24 p3368 N88-30057

HETEROJUNCTION DEVICES
NT HIGH ELECTRON MOBILITY TRANSISTORS
NT MODFETS

Study and optimization of a technological process for the fabrication of heterojunction bipolar transistors. Applications to high speed devices
[LAAS-87-134] 02 p0246 N88-11555
Novel heterojunction devices
[DE87-013716] 05 p0656 N88-14026
AlGaAs heterojunction lasers
[NASA-CR-4119] 09 p1171 N88-17020
Positron annihilation spectroscopy of AlGaAs/GaAs interfaces in MOCVD-grown GaAs heterojunction solar cells
[DE88-003903] 11 p1508 N88-19012
Low threshold ridge waveguide single quantum well lasers 13 p1777 N88-20631
Cadmium sulfide/copper ternary heterojunction cell research
[DE88-001122] 13 p1793 N88-20727
InP/GaInAs/InP PIN photodiode with FWHM less than 18 ps 19 p2658 N88-25799
Non-stationary transport in MODFET's and heterojunction devices 19 p2659 N88-25804
Transport in GaAs heterojunction ring structures
20 p2864 N88-27011
Vertical electronic transport in novel semiconductor heterojunction structures 20 p2871 N88-27045
Theoretical investigation on heterojunction solar cell
[DE88-701837] 23 p3229 N88-29219
On 3-5 heterojunction structures and high speed devices
[AD-A195464] 24 p3433 N88-30438
Joint services electronics program
[AD-A195731] 24 p3434 N88-30439

HETEROJUNCTIONS
Metal-sensing layer-semiconductor and metal-sensing layer-metal heterostructure gas sensors
[DE87-011293] 01 p0103 N88-10674
X-ray studies of strain, interface and impurity in semiconductors
[DE87-013856] 01 p0104 N88-10678
Phase-locked semiconductor quantum well laser arrays
[AD-A185155] 05 p0588 N88-13583
Structural relaxation in strained-layer heterostructures
[DE88-002326] 07 p0868 N88-15264
Influence of arsenic superficial enrichment on the ohmicity of the n-GaAs:In/Au contact
[ECL-87-09] 08 p1089 N88-16554
Visible InGaAsP/GaAsP lasers produced by epitaxial growth from liquid phase 09 p1237 N88-17416
Solid state research
[AD-A185987] 09 p1253 N88-17508
MBE growth, characterization and electronic device processing of HgCdTe, HgZnTe related heterojunctions and HgCdTe-CdTe superlattices
[AD-A187456] 10 p1421 N88-18486
Development of a planar heterojunction bipolar transistor for very high speed logic
[AD-A188137] 11 p1478 N88-18820
MBE (Molecular Beam Epitaxial) growth characterization and electronic device processing of HgCdTe, HgZnTe related heterojunctions and HgCdTe-CdTe superlattices
[AD-A187416] 11 p1555 N88-19307
Acoustic phonons, surface plasmons and surface acoustic plasmons in a superlattice and their nonreciprocal device applications
[AD-A188918] 12 p1698 N88-20163
Silicon-germanium heterostructures
13 p1844 N88-21034
Development of Si/SiGe heterostructures
[AD-A189527] 13 p1845 N88-21044
First-principles calculations of quasiparticle energies at surfaces and interfaces: Semiconductor surface-state spectra and band offsets
[DE88-006340] 15 p2141 N88-22773
Fundamental properties and devices applications of Ge(x)Si(1-x)/Si superlattices
[AD-A190129] 15 p2143 N88-22787
MBE of HgCdTe
[AD-A191423] 16 p2283 N88-23671
Joint services electronics program research in electronics
[AD-A192206] 18 p2504 N88-24857
Optical properties of heterostructures and superlattices
[AD-A191542] 18 p2581 N88-25335
X-ray response of GaAlAs/GaAs radiation hardened double: Heterostructure photodiode compared to Si:PIN photodiodes
[DE88-007425] 19 p2733 N88-26231
Theoretical aspects of electron transport in modulated structures 20 p2865 N88-27016
Metal grid base heterojunction transistor operating at 60 and 94 GHz
[AD-A194763] 23 p3207 N88-29087

Intrinsic and extrinsic energy states of semiconductors and heterostructures using novel techniques
[DE88-008560] 23 p3289 N88-29582
Spectroscopic studies with multiple quantum well materials with applications to optical signal processing at room temperature
[AD-A194171] 24 p3429 N88-30409

HEURISTIC METHODS
Adaptive line of sight algorithms
[DE87-014275] 01 p0081 N88-10523
An expert system for aircraft conflict resolution in dense airspaces 02 p0129 N88-10810
A review of the knowledge engineering process 02 p0129 N88-10814
Autonomous Land Vehicle (ALV) planning and navigation system
[AD-A184243] 04 p0397 N88-12475
On the work needed to factor a symmetric positive definite matrix
[AD-A185781] 06 p0759 N88-14660
Heuristic control of the Utah/MIT dextrous robot hand 06 p0793 N88-14858
Heuristic search in robot configuration space using variable metric 08 p1059 N88-16389
Iterative-deepening heuristic search for optimal and semi-optimal resource allocation 08 p1062 N88-16410
Discovery and problem solving: Triangulation as a weak heuristic 08 p1062 N88-16412
Commonality analysis as a knowledge acquisition problem 08 p1062 N88-16413
Operational aspects of a spacecraft planning/scheduling expert system 08 p1062 N88-16415
Planning activities in space 08 p1063 N88-16417
Scheduling spacecraft operations 08 p1064 N88-16426
Automatic program generation from specifications using Prolog 08 p1065 N88-16437
Range and mission scheduling automation using combined AI and operations research techniques 09 p1209 N88-17249
An evaluation of project scheduling techniques in a dynamic environment
[AD-A187057] 09 p1260 N88-17554
A comparative study of heurstic algorithms for task assignment in distributed computing systems 10 p1376 N88-18211
Two new frameworks for learning
[AD-A187723] 11 p1534 N88-19162
Stochastic heuristics in network design: Parameter tuning and performance evaluation
[REPT-87-017] 11 p1541 N88-19210
Compilation of preprints
[AD-A191245] 16 p2252 N88-23460
Low altitude remote sensing data in the implementation of a mathematical model for the planning of urban equipment networks 17 p2363 N88-24074
Genetic algorithms for adaptive real-time control in space systems 17 p2388 N88-24195
Automatic program generation from specifications using PROLOG 17 p2388 N88-24196
Design of partially replicated distributed database systems: An integrated methodology 18 p2589 N88-25383
Automatic routing in symbolic IC design environment 19 p2714 N88-26112
Primer on coupling collective electronic oscillations to nuclei
[LA-10878] 19 p2723 N88-26170
Three-dimensional scene analysis using stero based imaging
[AD-A193120] 21 p2894 N88-27178
An investigation of performance improvement in knowledge-based control systems 21 p2928 N88-27382
An approach to combining heuristic and qualitative reasoning in an expert system 23 p3253 N88-29362
NOA: A Network Operator Assistant for scheduling Tracking and Data Relay Satellite System (TDRSS) 23 p3259 N88-29403
Identification and control of time-varying flexible structures: An artificial intelligence approach 23 p3265 N88-29437

HEWLETT-PACKARD COMPUTERS
A data analysis environment for HP (Hewlett-Packard) 1000 computers
[DE87-010511] 04 p0477 N88-12936

HEXAGONAL CELLS
An orthogonal oriented quadrature hexagonal image pyramid
[NASA-TM-100054] 06 p0755 N88-14630

HEXOSES
NT GLUCOSE

HF LASERS
Computer simulation of cw HF chemical laser unstable resonator performance
[AD-A185059] 05 p0587 N88-13581
An experimental study of CW HF chemical laser amplifier performance and zero power gain
[AD-A185241] 05 p0588 N88-13584
Preliminary studies of NF3+H2 production of N2(A3 sigma(+)u) in a supersonic flow
[AD-A194479] 23 p3219 N88-29162

HIBERNATION
Neurochemical changes in hibernation 08 p1046 N88-16322

HIERARCHIES
A heteroscedastic hierarchical model
[AD-A184258] 03 p0372 N88-12340
Advanced Information Processing System (AIPS) proof-of-concept system functional design I/O network system services
[NASA-CR-181488] 03 p0384 N88-12413
Source hierarchy list. Volume 1: A through D
[AD-A185900] 07 p0941 N88-15722
Source hierarchy list. Volume 2: E through O
[AD-A185901] 07 p0941 N88-15723
Cirrus: An automated protocol analysis tool
[AD-A186648] 08 p1052 N88-16348
Media independent interface. Interface control document
[NASA-CR-172032] 08 p1067 N88-16447
An approach to the hierarchical specification, design and verification of software
[RSRE-MEMO-4063] 09 p1223 N88-17332
Research and development trends for memory hierarchies — cache memories 10 p1374 N88-18198
Hierachical object recognition using libraries of parameterized model sub-parts
[AD-A187476] 10 p1396 N88-18322
A hierarchical structure for automatic meshing and adaptive FEM analysis 11 p1527 N88-19119
The construction of a pedagogy to promote meaningful learning of strategies and tactics for solving problems of elementary combinatorics
[AD-A187928] 11 p1542 N88-19216
Update on the meso-microscale meteorological hierarchy
[DE88-009133] 21 p2975 N88-27670
An introduction to the nested sequence of tuples data model and algebra
[REPT-87-049] 22 p3145 N88-28702
Hierarchical organization for large, dynamic radio networks
[AD-A193942] 23 p3204 N88-29067
Motion planning for legged locomotion systems on uneven terrain 23 p3221 N88-29170

HIGH ALTITUDE
Maximal cardiorespiratory responses to one- and two-legged cycling during acute and long-term exposure to 4300m
[AD-A185730] 06 p0752 N88-14621
Guidance of high-altitude sounding rockets using the S19 and Spinning Rocket Altitude Control (SPINRAC) systems 08 p1034 N88-16273
Dexamethasone as prophylaxis for acute mountain sickness: Effect of dose level
[AD-A185848] 08 p1047 N88-16325
Operation Everest 2: Nutrition and body composition
[AD-A186449] 08 p1049 N88-16333
A methodology to assess the effects of high altitude electromagnetic pulse (HEMP) on electric power systems
[DE88-000338] 11 p1476 N88-18808
Results of the 1987 NASA/JPL balloon flight solar cell calibration program
[NASA-CR-182617] 12 p1574 N88-19413
High altitude chemical release systems for project BIME (Brazilian Ionospheric Modification Experiments) project IMS (Ionospheric Modification Studies) project PIIE (Polar Ionospheric Irregularities Experiment) project polar arcs
[AD-A188299] 12 p1642 N88-19833
Status of microcirculation in high-altitude blood loss 12 p1663 N88-19973
Current induced by high-altitude electromagnetic pulse (HEMP) on wire above ground
[FOA-C-30485-4.2] 22 p3072 N88-28235
Design, development, fabrication and launch support for a high altitude release of neodymium vapor
[AD-A194196] 22 p3118 N88-28527

HIGH ALTITUDE BALLOONS
NT JIMSPHERE BALLOONS
Balloon track data analysis
[AD-A184750] 03 p0350 N88-12213
Life sciences experiments on stratospheric balloons and sounding rockets 08 p1033 N88-16262
Contribution of stratospheric balloon flights in space biology 08 p1033 N88-16266

HIGH ALTITUDE BREATHING
Effects of breathing air containing contaminants such as CO2, CO and hydrocarbons at 1 and 5 atmospheres
[PB88-132915] 11 p1521 N88-19084
Acute mountain sickness at 4500 m is not altered by repeated eight-hour exposures to 3200-3550 m normobaric hypoxic equivalent
[AD-A188358] 12 p1666 N88-19990
Effect of different modes of voluntary control of breathing on human electroencephalogram with exposure to acute hypoxic hypoxia 19 p2707 N88-26093

HIGH ALTITUDE ENVIRONMENTS
Biorhythmic aspects of intercontinental Antarctic adaptation 08 p1046 N88-16321
Polar worker adaptability to Antarctic high altitudes 10 p1366 N88-18165
Medical problems related to altitude in: Human performance physiology and environmental medicine at terrestrial extremes, chapter 14
[AD-A188340] 12 p1666 N88-19989
Hemorrhages and hemostasis in guinea pigs exposed to radiation at high altitude 19 p2705 N88-26083
Alterations in upper extremity motor function in soldiers during acute high altitude exposure
[AD-A192676] 23 p3238 N88-29272

HIGH ALTITUDE FLIGHT
U HIGH ALTITUDE

HIGH ASPECT RATIO
Design verification and fabrication of active control systems for the DAST ARW-2 high aspect ratio wing, part 1
[NASA-CR-177959-PT-1] 06 p0669 N88-14101
Design verification and fabrication of active control systems for the DAST ARW-2 high aspect ratio wing. Part 2: Appendices
[NASA-CR-177959-PT-2] 06 p0669 N88-14102
Testing of a schematic transport plane model in several European windtunnels
[PB87-170270] 09 p1113 N88-16671
Experimental study on the effect of fiber orientation on flutter characteristics of high-aspect-ratio transport wing
[NAL-TR-936] 09 p1120 N88-16708
Thermosolutal convection in high-aspect-ratio enclosures
[NASA-TM-100803] 11 p1486 N88-18871
A detailed description of the uncertainty analysis for high area ratio rocket nozzle tests at the NASA Lewis Research Center 19 p2626 N88-25580

HIGH ASPECT RATIO WINGS
U SLENDER WINGS

HIGH CURRENT
New concepts for high current self-sustained diffuse discharge closing switches
[DE87-011678] 01 p0040 N88-10252
High midplane accessibility stellarator windings for high current toroidal accelerators
[AD-A186235] 07 p0933 N88-15665

HIGH ECCENTRIC LUNAR OCCULTATION SATELLITE
U EXOSAT SATELLITE

HIGH ELECTRON MOBILITY TRANSISTORS
NT MODFETS
A 2.3-GHz cryogenically cooled HEMT amplifier for DSS 13 04 p0434 N88-12689
Numerical studies of the dual HEMT/algorithm development and numerical studies of Schrodinger's equation
[AD-A184471] 04 p0478 N88-12946
Microwave response of an HEMT photoconductor
[NASA-TM-100819] 11 p1480 N88-18835
Computer aided design of monolithic microwave and millimeter wave integrated circuits and subsystems
[AD-A191593] 18 p2503 N88-24852
Light-millimeter wave interactions in semiconductor devices
[AD-A195898] 24 p3432 N88-30428

HIGH ENERGY ASTRONOMY OBSERVATORY B
U HEAO 2

HIGH ENERGY ASTRONOMY OBSERVATORY 2
U HEAO 2

HIGH ENERGY ELECTRONS
NT RELATIVISTIC ELECTRON BEAMS
Simulation of tokamak runaway-electron events. Study of the response of materials by use of an electron linear accelerator
[IPPJ-841] 02 p0242 N88-11528
A generalized description of the anomalous Doppler resonance and the stabilizing role of ion dynamics
[INPE-4384-PRE/1204] 08 p1081 N88-16513
Energy distribution of Cerenkov radiation for finite frequency intervals
[AD-A186901] 09 p1244 N88-17454
Simulation and modeling of whistler mode wave growth through cyclotron resonance with energetic electrons in the magnetosphere 10 p1353 N88-18089

Investigations of stimulated Raman scattering from high density underdense plasmas irradiated by a 0.35 micron laser 10 p1411 N88-18421
Modeling and transport in semiconductor devices [AD-A188760] 13 p1844 N88-21037
Deep dielectric charging effects due to high energy electrons in earth's outer magnetosphere [AD-A192154] 18 p2541 N88-25083
A study of electronic transport and breakdown in SiO2 [AD-A194258] 22 p3156 N88-28780

HIGH ENERGY INTERACTIONS
NT STRONG INTERACTIONS (FIELD THEORY)
Research program in elementary particle theory [DE88-000159] 02 p0233 N88-11468
High energy experimental physics [DE87-013516] 03 p0376 N88-12363
Analysis of geophysical data bases and models for spacecraft interactions [AD-A184809] 05 p0555 N88-13375
TIBER 2 (Tokamak Ignition/Burn Experimental Reactor) parameters with neutral beams at high energies [DE88-001891] 06 p0783 N88-14803
Scanning and measuring peculiarities with high-space resolution objects recorded at the Gabor holograms [DE88-700373] 07 p0857 N88-15203
Energy distribution of Cerenkov radiation for finite frequency intervals [AD-A186901] 09 p1244 N88-17454
Properties of nuclei and elementary particles at low and intermediate energies [DE88-001913] 09 p1244 N88-17456
High Z interaction physics on Nova [DE88-004397] 10 p1413 N88-18433
Design and fabrication of advanced hybrid circuits for high energy physics [DE88-004392] 11 p1479 N88-18825
Pion nucleus single charge exchange reactions above the delta(1232) resonance [LA-11004-T] 11 p1544 N88-19231
Medium high energy physics at Syracuse University [DE88-003670] 11 p1545 N88-19235
High energy polarized electron beams [CEBAF-R-87-002] 11 p1546 N88-19244
Induction linacs: A technology come of age for international cooperation [DE88-003953] 11 p1548 N88-19258
Channeling and dechanneling at high energy [DE88-003989] 11 p1548 N88-19259
Freund-Rubin type solutions for different compactifications of the eleven-dimensional space [DE88-700869] 12 p1686 N88-20082
Energy loss of particles in dense matter-calorimetry [NIKHEF-H/87-12] 13 p1836 N88-20988
Hadronic overlap and total multiplicity distributions in high energy physics collisions [NIKHEF-H/87-10] 13 p1838 N88-21001
Modeling and transport in semiconductor devices [AD-A188760] 13 p1844 N88-21037
Systematics on neutron-induced isomeric cross-section ratios at 14.5 MeV [ECN-200] 14 p1980 N88-21815
Particle acceleration to high energies and amplification of coherent radiation by electromagnetic interactions in plasmas [DE88-701020] 15 p2135 N88-22737
Subthreshold pion production in proton induced reactions at 180 to 201 MeV and He3 at 283 MeV [ETN-88-92303] 17 p2397 N88-24250
Energy measurements in oxygen-induced reactions at 60 A GeV and 200 A GeV [DE88-006420] 18 p2573 N88-25283
Products from cosmic-ray interactions in extraterrestrial matter: What they tell us about radiation backgrounds in space [DE88-009143] 19 p2743 N88-26288
Theoretical studies in elementary particle physics [DE88-006929] 20 p2651 N88-26926
Studying the physics and operation of multi-terminal near-micron and sub-micron length, hot electron semiconductor devices [AD-A193380] 21 p2938 N88-27446
High energy and high intensity laser effects on aerosols: Changes in droplet morphology, surrounding temperature and vapor concentration [AD-A193825] 23 p3220 N88-29164
Theoretical studies in high energy physics [DE88-011606] 23 p3281 N88-29538
A coded mask telescope for observations of X and gamma ray sources in the southern sky [INPE-4580-PRE/1314] 24 p3453 N88-30551

HIGH FREQUENCIES
High-frequency limit of the longitudinal impedance [CEBAF-PR-87-030] 02 p0234 N88-11479
Height profile inversion of ionospheric movement from observed parameters of HF radio echoes 03 p0299 N88-11884
Target strength: An overview of some recent theoretical developments 03 p0303 N88-11910
Effect of electrostatic field on behaviour of peripheric plasma at high-frequency heating [DE87-703328] 03 p0378 N88-12378
High frequency periodic time domain waveform measurement system [PB87-225256] 06 p0695 N88-14264
A contribution to the realization of active filters for high frequency applications [ETN-88-90811] 06 p0696 N88-14272
Studies on parametric instabilities in high-frequency wave heating of fusion plasmas [PH-156] 07 p0933 N88-15667
An expert system to analyze high frequency dependent data for the space shuttle main engine turbopumps 08 p1060 N88-16399
An investigation of the equivalent circuit and carrier lifetimes of Si/SiGe heterostructure p-n diodes for frequencies between 0.5 and 18.5 MHz [FOA-C-30469-3.2] 09 p1256 N88-17529
Wideband HF (High Frequency) modeling and simulation [PB88-116116] 10 p1317 N88-17874
User's guide for the HF (High Frequency) broadcast antenna design and validation summary programs [PB88-116124] 10 p1317 N88-17875
Dynamics of small and large scale irregularities at sub-auroral latitudes [AD-A189052] 12 p1645 N88-19853
HF (High Frequency) Maximum Usable Frequency (MUF) model uncertainty assessment [AD-A189132] 13 p1757 N88-20513
Adaptive algorithms for HF antenna arrays [AD-A189329] 13 p1761 N88-20534
Soft decoding of recorded HF data [FOA-C-30473-3.3] 15 p2058 N88-22269
IREPS (Integrated Refractive Effects Prediction System) 3.0, user's manual [AD-A190398] 16 p2188 N88-23045
High frequency power distribution system [NASA-CR-175071] 17 p2335 N88-23939
High frequency ultrasonic characterization of sintered SiC [NASA-TM-100825] 17 p2347 N88-23985
Communications using channels formed by meteor bursts [AD-A192088] 18 p2501 N88-24834
Radio-wave scintillations and ionospheric irregularities at high latitudes [AD-A192140] 18 p2501 N88-24837
Improved description of base dynamics in the modeling of bipolar transistors [PB88-181516] 19 p2732 N88-26229
Performance study of a unipole antenna with conventional and elevated radial wire ground screens [AD-A193283] 21 p2933 N88-27413
Calculations of high-frequency parameters of disc-loaded waveguides [DE88-702178] 21 p2933 N88-27417
Decomposition of hydrazine by high frequency glow electrical discharges [NASA-TT-20240] 24 p3344 N88-29906
Long haul communications in the HF spectrum utilizing high speed modems [AD-A194683] 24 p3360 N88-30003
Comparative analysis of passive communications satellites employing the SHF and HF spectrum for use in a strategic role [AD-A194682] 24 p3362 N88-30019
Modeling and performance of HF/OTH (High-Frequency/Over-the-Horizon) radar target identification systems [AD-A196267] 24 p3365 N88-30038
High frequency GaAlAs modulator and photodetector for phased array antenna applications [NASA-TM-101328] 24 p3367 N88-30048
In situ fault detection by the hybrid ray mode method [AD-A195226] 24 p3381 N88-30137

HIGH GAIN
High power phased array and tailored gain semiconductor lasers 03 p0329 N88-12078
Distributed feedback effects in lasers and high gain laser instabilities in optically pumped CH3F 03 p0329 N88-12079
Periodically pulsed excimer master oscillator-regenerative amplifier laser set 06 p0772 N88-14741
Tapered wiggler analysis of high gain free electron laser oscillators [AD-A187997] 10 p1338 N88-17997
Research studies on extreme ultraviolet and soft X-ray lasers [AD-A189163] 12 p1633 N88-19773
The off-axis channel macroplate [NASA-CR-182938] 18 p2505 N88-24861

HIGH GRAVITY (ACCELERATION)
U HIGH GRAVITY ENVIRONMENTS

HIGH GRAVITY ENVIRONMENTS
The rate of adaptation to altered g in the human centrifuge: Implications for simulations of mass-discrimination in space flight 12 p1659 N88-19941

HIGH IMPULSE
Production of intensive electron beam impulsions by setup of pseudoglare discharges [ISL-CO-210/87] 21 p3019 N88-27920

HIGH INTENSITY LASERS
U HIGH POWER LASERS

HIGH LATITUDES
U POLAR REGIONS

HIGH LEVEL LANGUAGES
NT ADA (PROGRAMMING LANGUAGE)
NT C (PROGRAMMING LANGUAGE)
Data Management Working Group report 01 p0016 N88-10097
The warp computer: Architecture, implementation, and performance [AD-A184329] 03 p0363 N88-12286
ERIC: An object-oriented simulation language [AD-A184757] 03 p0364 N88-12293
ADAMEASURE: An implementation of the Halstead and Henry metrics [AD-A184005] 03 p0365 N88-12299
Comparison of pascal and the dBASE 3 PLUS language in programming an inventory management system [AD-A184027] 03 p0365 N88-12300
A survey of object oriented languages in programming environments [AD-A184127] 04 p0477 N88-12937
LISP: A language for stratified design [AD-A185606] 06 p0759 N88-14654
Types and effects towards the integration of functional and imperative programming [AD-A186930] 09 p1216 N88-17290
Occam/Ada parallel programming system [ISAL-IDI1-87-11] 09 p1219 N88-17312
Optical symbolic processor for expert system execution [AD-A187494] 10 p1385 N88-18268
BLITZ: Blitzen's micron-code assembly language design document, version 1.0 [TR88-14] 12 p1676 N88-20019
Design of the CONSUL programming language [AD-A189202] 13 p1815 N88-20841
An integrated data description language for coding design knowledge [CWI-CS-R8731] 13 p1819 N88-20871
New generation knowledge processing, volume 1 [AD-A190165] 15 p2149 N88-22826
Adapting high-level language programs for parallel processing using data flow 16 p2218 N88-23234
New generation knowledge processing, volume 2 [AD-A190166] 16 p2285 N88-23681
New generation knowledge processing, volume 3 [AD-A190167] 16 p2285 N88-23682
A software life cycle support environment 17 p2306 N88-23800
A robotic language for cooperative multi-robots 17 p2387 N88-24186
New York TRACON demonstration of program recoding requirements analysis document [DOT/FAA/CT-87/34] 18 p2462 N88-24622
EPL (Equational Programing Language) system design: Intermediate processing steps [AD-A191203] 18 p2556 N88-25169
Definition of an auxiliary processor dedicated to real-time operating system kernels [NASA-CR-183070] 20 p2841 N88-26880
Subset-logic programming: Application and implementation [AD-A193647] 22 p3138 N88-28655
Combined and-or parallel execution of logic programs [AD-A193648] 22 p3138 N88-28656
Investigation of the use of High Order Languages (HOLs) for on-board software [CRI/FR/HOL-C/1/87] 23 p3251 N88-29349
Archetyping: A software generation and management methodology 23 p3256 N88-29382
The FORCE [AD-A193463] 23 p3264 N88-29429
Strategic defense initiative architecture dataflow modeling technique version 1.5 [AD-A194356] 23 p3275 N88-29494
Conversion of productions in OPS5 to their equivalent English [ORNL/TM-10246] 24 p3411 N88-30306

HIGH MELTING COMPOUNDS
U REFRACTORY MATERIALS

HIGH PASS FILTERS
Realization of active high pass filters for group velocity correction
[MPE-IN-REPT-47] 08 p0979 N88-15918
HIGH POLYMERS
Polymer modified binders for bituminous or asphaltic paving layers
[PC-5] 02 p0153 N88-10958
JPRS report: Science and technology. Japan
[JPRS-JST-87-028] 06 p0675 N88-14130
High polymer sensor materials discussed 06 p0676 N88-14140
Synthesis of high molecular weight peptide polymers and copolymers containing L-dope residues
[AD-A186462] 08 p0973 N88-15887
Soluble polysilane derivatives: Chemistry and spectroscopy
[AD-A187889] 11 p1461 N88-18713
Photophysics and photochemistry of poly(di-n-hexylsilane) in room temperature solution
[AD-A187890] 11 p1462 N88-18714
Investigations on drag reduction in turbulent pipe flows by addition of ionic and nonionic high polymers
[ETN-88-92380] 21 p2949 N88-27515
HIGH POWER LASERS
NT NOVA LASER SYSTEM
Millimeter wave tokamak heating and current drive with a high power free electron laser
[DE87-011324] 01 p0099 N88-10651
Laser-plasma-interaction experiments using multikilojoule lasers
[DE87-013483] 01 p0100 N88-10658
Status, development of laser devices in China 03 p0303 N88-11907
High average power solid state laser power conditioning system
[DE87-013558] 03 p0328 N88-12071
Diffraction effects during materials treatment with laser beams
[ETN-87-90614] 03 p0328 N88-12075
High-power RF-pulsed modulators for the Los Alamos free-electron laser
[DE88-000514] 04 p0448 N88-12775
Phenomena at a focus in a laser system
[AD-A185442] 05 p0588 N88-13585
Lawrence Livermore National Laboratory Soft X-ray Laser Program
[DE88-001868] 07 p0859 N88-15218
Nondestructive magnetic testing of laser hardening parameters (hardening depth, hardness profile, retained austenite)
[ETN-88-91070] 09 p1144 N88-16857
Dielectric behavior of electromagnetic (EM) windows materials irradiated by a CW CO2 high-power laser --- hypersonic/reentry vehicles
[ISL-CO-239/86] 09 p1154 N88-16913
A crude scaling law for lasertrons
[DE88-003880] 09 p1173 N88-17032
Mirrors for high-power continuous-wave Ar-lasers 09 p1235 N88-17404
High-power periodic-pulse YAG:Nd3+-laser system with telescopic unstable resonator and two-stage amplifier 09 p1237 N88-17414
Dye lasers pumped by radiation from high-power semiconductor lasers 09 p1237 N88-17417
High power, high efficiency 770 nm laser diode array
[DE88-004043] 12 p1631 N88-19762
Optical properties of compressible inhomogeneous shear layers relevant to high power lasers
[AD-A189299] 12 p1633 N88-19774
Phase preservation cleanup in a double-pass Raman amplifier SBS (Stimulated Brillouin Scattering) conjugator
[AD-A189428] 13 p1761 N88-20536
Fiber-coupled external-cavity semiconductor high power laser
[AD-A188454] 13 p1774 N88-20611
Causes of damage in multilayer dielectric coatings exposed to high average power visible laser radiation
[DE88-005363] 13 p1775 N88-20619
High power, high efficiency, 2D laser diode arrays for pumping solid state lasers
[DE88-004042] 13 p1777 N88-20632
Laser technology: CO2 lasers and laser optics
[ETN-88-91469] 14 p1915 N88-21441
JPRS report: Science and technology. China
[JPRS-CST-87-043] 15 p2053 N88-22233
Magic light high-power laser passes state certification 15 p2053 N88-22236
Coupled high power waveguide laser research
[AD-A189800] 15 p2071 N88-22345
Laser evaporation studies
[AD-A189815] 15 p2071 N88-22346
High power axial flow CO2 laser
[ETN-88-91951] 18 p2521 N88-24959
Optical coatings for high average power XeF lasers
[DE88-011356] 20 p2807 N88-26656
High energy and high intensity laser effects on aerosols: Changes in droplet morphology, surrounding temperature and vapor concentration
[AD-A193825] 23 p3220 N88-29164
Energy conversion measurements in laser-sustained argon plasmas for application to rocket propulsion
[AD-A194931] 24 p3337 N88-29861
HIGH PRESSURE
Nitrogen at high pressure
[DE87-013797] 01 p0021 N88-10130
Nitrogen at very high pressure
[DE87-013800] 01 p0021 N88-10131
Chemical equilibrium calculations for the high pressure and temperature dissociation of liquid nitrogen
[DE87-013788] 01 p0021 N88-10135
Theory of the carbon phase diagram at high pressures and temperatures
[DE87-012245] 01 p0028 N88-10180
The effect of additives on the reactivity of palladium surfaces for the chemisorption and hydrogenation of carbon monoxide: A surface science and catalytic study
[DE87-014685] 02 p0145 N88-10909
Electrical properties of high T/sub c/ superconductors under high pressures
[DE87-012818] 02 p0245 N88-11546
High pressure strand burn rate tests of polyvinylnitrate/nitramine propellants.
[AD-A184178] 04 p0422 N88-12615
Studies of tunneling in metals under high pressure 06 p0775 N88-14757
Programs for calculating transient Darcian flow through non-uniform materials
[DE88-001924] 07 p0852 N88-15177
An automated flow calorimeter for heat capacity and enthalpy measurements at elevated temperatures and pressures
[DE88-002357] 07 p0857 N88-15206
Welding in high pressure CO2 atmosphere --- underwater welding
[PB87-144044] 07 p0862 N88-15232
The determination of equivalent bearing loading for the BSMT that simulate SSME high pressure oxidizer turbopump conditions using the SHABERTH/SINDA computer programs 07 p0925 N88-15623
Excess thermodynamic properties of aqueous electrolytes to high temperatures and pressures
[DE88-001768] 07 p0940 N88-15712
Superconductivity and crystal structure of high-pressure phases in V-Ru-H system 09 p1239 N88-17426
Radial compressor design using an Euler solver 10 p1283 N88-17675
Design and testing of a front stage for an advanced high pressure compressor 10 p1283 N88-17679
Gas cleaning at high temperatures and pressures for gas turbines
[DE88-751171] 11 p1440 N88-18593
Operation of electron-beam controlled CO2 laser at 6 atmospheres 11 p1468 N88-18758
High pressure electronic transport in semiconductors
[AD-A187428] 11 p1555 N88-19308
Properties of molecular solids and fluids at high pressure and temperature
[DE88-004195] 13 p1738 N88-20391
Fluids, gels and glasses under extreme conditions of pressure and temperature
[AD-A190655] 15 p2035 N88-22125
Cracking tendencies of restrained welds in high strength low alloy steels under hyperbaric conditions
[AD-A190255] 15 p2039 N88-22150
Synthesis of metastable superconductors by high dynamic pressure
[DE88-005620] 15 p2139 N88-22764
Electronic structure of matter at high compression: Isostructural transitions and approach of the Fermi-gas limit
[MPQ-124] 16 p2266 N88-23551
High pressure operation of beam diodes for generating relativistic electron beams 16 p2279 N88-23643
The high pressure sound velocity and equation of state of aqueous solutions of hydroxylammonium nitrate and triethanolammonium nitrate
[AD-A191740] 18 p2570 N88-25266
Kinetic measurements of thermal decomposition of energetic materials at high pressures
[AD-A191612] 19 p2622 N88-25552
Experimental study of protective effect of antioxidant enzymes-superoxide dismutase and catalase-when using intermittent toxic modes of hyperbaric oxygenation 19 p2707 N88-26094
Asynchronous optical sampling for laser-based combustion diagnostics in high pressure flames
[AD-A192920] 20 p2770 N88-26428
Respiration and oxygen tension in the blood of animals exposed to high pressures 20 p2830 N88-26790
Electronic structure of quantum-well states revealed under high pressures 20 p2870 N88-27038
Experimental study of planetary gases with applications to planetary interior models
[NASA-CR-183098] 20 p2886 N88-27137
Investigation of hydrogen isotope penetration through stainless steels Kh18N10T and Kh3M2BFR
[DE88-702189] 21 p2915 N88-27297
Reaction products of solid propellants after burning at pressures up to 1000 MPa: Comparison between theoretical and experimental results
[ISL-CO-227/87] 22 p3059 N88-28153
E3 10C compressor test analysis of high-speed post-stall data
[NASA-CR-179521] 23 p3179 N88-28929
Development of high temperature, high pressure rotating shaft seals
[DE88-001029] 23 p3221 N88-29172
HIGH PRESSURE OXYGEN
Effect of high pressure oxygen loading on the superconductivity of La2CuO4
[DE88-002108] 06 p0787 N88-14827
USAF hyperbaric animal transfer chamber system
[AD-A193633] 23 p3237 N88-29265
HIGH Q
U Q FACTORS
HIGH RESOLUTION
CERGA high angular resolution optical network --- astronomical interferometry 01 p0096 N88-10633
Solar interferometry with a 4-aperture nonredundant and stabilized network 01 p0097 N88-10639
Galactic nuclei and quasars at high angular resolution 01 p0098 N88-10644
Assimilation of high resolution TOVS data into a mesoscale NWP model --- numerical weather prediction (NWP) 02 p0213 N88-11338
Present status of the high resolution spectrometers
[CEBAF-PR-87-029] 02 p0234 N88-11478
Theoretical Problems in High Resolution Solar Physics, 2
[NASA-CP-2483] 02 p0254 N88-11609
Some aspects of high resolution numerical methods for hyperbolic systems of conservation laws, with applications to gas dynamics
[DMS-86-7] 03 p0321 N88-12031
Conceptual design of a high-resolution pion (0) spectrometer
[DE87-014757] 03 p0324 N88-12047
Numerical experiments with a symmetric high-resolution shock-capturing scheme
[NASA-TM-88325] 03 p0370 N88-12332
Implementation and performance of a complex vision system on a systolic array machine
[AD-A184331] 04 p0482 N88-12971
High resolution finite volume methods on arbitrary grids via wave propagation
[NASA-CR-178397] 04 p0484 N88-12979
Exosat results on the dMe flare Star Wolf 630AB and on VB 8 04 p0512 N88-13151
New results from high angular resolution observations of alpha Ori 04 p0514 N88-13161
High resolution satellite imagery simulation --- treaty verification
[FOA-C-30462-3.3,9.3] 05 p0620 N88-13610
High resolution ultraviolet filter development
[AD-A184183] 05 p0649 N88-13979
High-spatial-resolution TOVS observations for the FIRE/SRB Wisconsin experiment region from October 14 through November 2, 1986
[NASA-TM-100522] 06 p0747 N88-14593
Use of spherical optics in high resolution soft X-ray grating monochromators
[PB87-125191] 06 p0780 N88-14788
High spatial resolution observations of dust and gas in NGC 7027 and the M8 Hourglass 06 p0801 N88-14903
High resolution simulation of turbulent flow in a channel
[AD-A186022] 07 p0848 N88-15150
Fabrication techniques used in the construction of a high resolution X-ray framing camera
[DE88-002653] 07 p0856 N88-15200
Determination of network attributes from a high resolution terrain data base
[AD-A186078] 07 p0870 N88-15279
Estimation of broadband planetary albedo from operational narrowband satellite measurements
[PB88-107644] 07 p0945 N88-15748
The high resolution spaghetti hadron calorimeter
[NIKHEF-H/87-7] 08 p0990 N88-15993
High-speed assembly language (80386/80387) programming for laser spectra scan control and data acquisition providing improved resolution water vapor spectroscopy
[NASA-CR-4117] 08 p1053 N88-16355
Application of a simple rotational spherical grating mounting to high resolution soft X-ray spectroscopy
[PB87-164836] 09 p1142 N88-16845

Investigation of a new magnetic dipole mode in the heavy, deformed nuclei 154 Sm, 156 Gd, 158 Gd, 164 Dy, 168 Er, and 174 Yb with high resolution electron scattering
[ETN-88-91084] 09 p1245 N88-17460
Rotor SAR (ROSAR): A new high-resolution all-weather vision method for helicopters
[MBB-UA-1046/87] 10 p1314 N88-17855
Experiments for the high resolution detection of moving targets using a CO2 laser radar
[MBB-UA-1044/87] 10 p1316 N88-17864
New generation imager system
[NASA-CR-180464] 10 p1408 N88-18398
High-resolution X-ray microstructural study of single crystals of YBa2Cu3O/sub 7-y/
[DE88-004856] 10 p1421 N88-18484
An evaluation of the impact of variable temporal and spatial data resolution upon IREPS (Integrated Refractive Effects Prediction System)
[AD-A187764] 11 p1470 N88-18769
General determination of Earth surface type and cloud amount using multispectral AVHRR data
[NOAA-TR-NESDIS-39] 11 p1506 N88-18997
Suggested severe local storm operational scenario for GOES I-M
[NASA-TM-100688] 11 p1515 N88-19052
High resolution hadron calorimetry
[NIKHEF-H/87-8] 13 p1773 N88-20605
Improved methods for high resolution electron microscopy
[DE88-005731] 13 p1774 N88-20609
Simulating high-resolution vertical plane array wind characteristics using lower-spatial-resolution wind measurements
[DE88-005626] 13 p1800 N88-20761
Velocity resolved far-infrared spectroscopy of galactic sources 13 p1854 N88-21099
Pre-launch calibration of channels 1 and 2 of the advanced very high resolution radiometer
[PB88-157169] 14 p1913 N88-21427
What has been done and what will be done by subnatural linewidth spectroscopy 14 p1978 N88-21807
Fluids, gels and glasses under extreme conditions of pressure and temperature
[AD-A190655] 15 p2035 N88-22125
Design, construction and performance of the ROSAT high resolution X-ray mirror assembly
[MPE-PREPRINT-101] 15 p2150 N88-22836
Navigation system from AVHRR data from NOAA series satellites 17 p2359 N88-24054
High resolution radar techniques: Five contributions to MILINF 86
[PB88-172721] 18 p2498 N88-24821
DMSP-SSM/1 NASA algorithm validation using primarily LANDSAT and secondarily DMSP and/or AVHRR visible and thermal infrared satellite imagery
[NASA-CR-182979] 18 p2532 N88-25024
New duplicating paper with high resolution for aerial photography
[PB87-228706] 19 p2685 N88-25962
Contribution of spaceborne high resolution radiometers to mapping of precoastal depths 19 p2701 N88-26063
High resolution detection of solute segregation to the cores of dislocations in grain boundaries
[DE88-009168] 20 p2877 N88-27078
Enhancement of modeling and image generation techniques for high-resolution 3-dimensional imagery
[DE88-008923] 21 p2998 N88-27782
Research for reducing the labor intensive nature of high-resolution terrain analysis feature extraction
[AD-A192661] 22 p3089 N88-28345
High resolution orthoimage quadrangle maps using SPOT satellite data 22 p3112 N88-28488
Automatic extraction of high resolution elevation data from SPOT stereo images 22 p3113 N88-28489
High definition television: Evaluation for remote task performance
[DE88-011573] 23 p3202 N88-29057
Signal processing software for ground penetrating radar, user's manual
[AD-A194286] 23 p3203 N88-29059
An analysis of results of a high-resolution world ocean circulation model
[AD-A195760] 24 p3405 N88-30272

HIGH REYNOLDS NUMBER

Wall interference tests of a CAST 10-2/DOA 2 airfoil in an adaptive-wall test section
[NASA-TM-4015] 02 p0122 N88-10772
Asymptotic form of stationary solutions of the Navier-Stokes equations for large Reynolds numbers 04 p0459 N88-12838
Practical application of two-dimensional viscous flow computation 05 p0535 N88-13257
Numerical analysis of cascade flow solving Navier-Stokes equations 05 p0536 N88-13262
The aerodynamic design of hypersonic contoured axisymmetric nozzles including real gas effects
[VKI-TM-43] 06 p0665 N88-14076
Unsteady stall penetration experiments at high Reynolds number
[AD-A186120] 07 p0814 N88-14958
Pressure distributions from high Reynolds number transonic tests of an NACA 0012 airfoil in the Langley 0.3-meter transonic cryogenic tunnel
[NASA-TM-100526] 11 p1435 N88-18565
High Reynolds number transonic tests on a NACA 0012 airfoil in the Langley 0.3-meter transonic cryogenic tunnel
[NASA-TM-100527] 11 p1436 N88-18571
High Reynolds number pump facility for cavitation research
[AD-A189310] 13 p1765 N88-20558
High Reynolds number, low Mach number, steady flow field calculations over a NACA 0012 airfoil using Navier-Stokes and interactive boundary layer theory
[AD-A189871] 15 p2013 N88-22005
Effect of freestream turbulence on a two dimensional cascade, with different surface roughness, at high Reynolds number
[AD-A190615] 15 p2065 N88-22316
High Reynolds number tests of a Douglas DLBA 032 airfoil in the Langley 0.3-meter transonic cryogenic tunnel
[NASA-TM-87663] 17 p2296 N88-23734
Velocity-pressure integrated versus penalty finite element methods for high Reynolds number flows
[NASA-CR-179357] 20 p2803 N88-26635
Analysis of experimental data for cast 10-2/DOA2 supercritical airfoil at high Reynolds numbers
[AD-A192827] 21 p2892 N88-27166
Field methods for computing high Reynolds number viscous flow
[FFA-TN-1988-01] 22 p3039 N88-28046
The use of upwind schemes at high Reynolds number: A cautionary note
[AD-A196227] 24 p3371 N88-30074

HIGH SPEED

Response of helical structures to high speed pulses or when can a helix be called an inductor
[DE87-014347] 01 p0090 N88-10587
Civil applications of high-speed rotorcraft and powered-lift aircraft configurations
[NASA-TM-100035] 03 p0261 N88-11643
Analysis of 7- X 10-foot high speed wind tunnel shaft loads in support of fan blade failure investigation
[NASA-TM-100504] 04 p0402 N88-12496
Progress in the development of niobium alloyed high speed steel
[DE87-703549] 04 p0415 N88-12576
Thermomechanical cracking in coated media due to high speed asperity excitation
[AD-A184176] 04 p0454 N88-12809
Fluctuating pressure loads under high speed boundary layers
[NASA-TM-100517] 05 p0647 N88-13962
Tribological studies on high speed steel cutting tools
[DE88-002550] 07 p0864 N88-15246
High-speed inlet research program and supporting analyses 08 p0958 N88-15811
Experimental evaluation of turning vane designs for high-speed and coupled fan-drive corners of 0.1-scale model of NASA Lewis Research Center's proposed altitude wind tunnel
[NASA-TP-2681] 10 p1285 N88-17686
Dynamics of high-speed mechanisms with elastic members 13 p1779 N88-20643
High speed, bandpass sampling of digital communications waveforms
[AD-A189842] 15 p2056 N88-22254
Application of high speed holography to aerodynamic and hydrodynamic three-dimensional velocimetry 16 p2203 N88-23144
Pressure measuring probe
[NASA-CASE-LAR-13853-1] 17 p2341 N88-23961
High-speed optical logic using GaAs 19 p2656 N88-25773
High speed opto-isolator for radar applications 19 p2658 N88-25795
Effective communication between a microVAX and a specialized high-speed subprocessor
[DE88-007967] 19 p2714 N88-26115
Development of a GaAs solid state device model for high power applications
[DE88-009048] 19 p2734 N88-26242
High speed inlet calculations with real gas effects
[NASA-CR-182167] 20 p2752 N88-26336
A high speed serial link interface for SANDAC-V
[DE88-007694] 20 p2842 N88-26861
A survey of the Ap stars for rapid variability 20 p2884 N88-27127
The MELMUX MX-7100 series high-speed digital multiplexers 21 p2930 N88-27396
E3 10C compressor test analysis of high-speed post-stall data
[NASA-CR-179521] 23 p3179 N88-28929
Proof-of-principle high speed electronic imaging system, phase 2
[AD-A193798] 23 p3181 N88-28937
Ultrafast processes and spectroscopy with free electron lasers
[AD-A195248] 24 p3379 N88-30126
On 3-5 heterojunction structures and high speed devices
[AD-A195464] 24 p3433 N88-30438

HIGH SPEED CAMERAS

NT FRAMING CAMERAS
Optically time-resolved detonation break out
[DE87-010340] 01 p0031 N88-10199
A high-speed, eight-frame image intensified electro-optic camera with 200-800mm zoom objective capability
[DE88-000229] 03 p0326 N88-12059
Simple high speed camera with CCD-sensor
[MPIS-8/1987] 18 p2518 N88-24940

HIGH SPEED FLIGHT

U HIGH SPEED

HIGH SPEED PHOTOGRAPHY

Reduction of temperature rise in high-speed photography
[NASA-TM-100222] 02 p0176 N88-11100
An ultra-high-speed cinematographic method for the study of wakes in hypersonic ballistic ranges 05 p0531 N88-13228
Analysis of photopole data reduction models 05 p0593 N88-13616
Synchronous multi-image high speed photography of welding arc by optical fibers
[PB87-143939] 07 p0857 N88-15202
Measurements of particulates in solid propellant rocket motors
[AD-A187777] 11 p1446 N88-18621
Ignition and high speed photography of energetic materials with a copper vapor laser
[DE88-004831] 12 p1631 N88-19785

HIGH SPEED TRANSPORTATION

U RAPID TRANSIT SYSTEMS

HIGH STRENGTH

Composite reliability enhancement via preloading
[AD-A185938] 07 p0826 N88-15010
Structure and surface characterizations of high strength carbon fibers
[AD-A189642] 15 p2029 N88-22087
High-strength ceramic based on tetragonal ZrO2 with Al2O3 admixture 16 p2180 N88-22996

HIGH STRENGTH ALLOYS

NT ASTROLOY (TRADEMARK)
NT HIGH STRENGTH STEELS
NT MARAGING STEELS
Investigation of rapidly-solidified dispersion strengthened titanium alloys
[AD-A183882] 01 p0022 N88-10140
The effect of temperature on the tensile properties of HSLA-100 steel
[AD-A184951] 05 p0565 N88-13441
Microstructural characterization of HSLA-100 GMA-weldments
[AD-A187782] 11 p1457 N88-18683
Microstructural characterization of the heat affected zone of HSLA (High Strength Low Alloy)-100 steel GMA (Gas Metal Arc)-weldment
[AD-A187825] 11 p1457 N88-18686
Deformation of rapidly solidified dispersion strengthened titanium alloys
[AD-A190793] 16 p2179 N88-22984
Evaluation of a diffusion/trapping model for hydrogen ingress in high-strength alloys
[AD-A194301] 23 p3194 N88-29008

HIGH STRENGTH STEELS

NT MARAGING STEELS
The fatigue properties of aerospace steels under constant amplitude and flight-by-flight simulated loading
[BAE-MSM-R-GEN-0566] 01 p0059 N88-10377
Stress corrosion cracking of high-strength steels in aqueous environments 03 p0289 N88-11818
Computational methods and results for dynamic fracture 03 p0337 N88-12123
Mechanical behavior of a controlled rolled high-strength low alloy steeel plate, microalloyed with Nb and V
[DE87-703507] 04 p0415 N88-12571
The effect of temperature on the tensile properties of HSLA-100 steel
[AD-A184951] 05 p0565 N88-13441
Fatigue characteristics of ion treated surfaces 05 p0606 N88-13713
Environmentally assisted fatigue crack growth 05 p0608 N88-13731

Numerical simulations of impact tests on a rigid wall --- armor steel
[SNIAS-872-320-102] 05 p0610 N88-13744
Effect of rare earth elements on the hydrogen-induced cracking in high strength low alloy steel
[PB87-143806] 07 p0833 N88-15052
Multipurpose corrosion inhibitors for aerospace materials in Naval environments
[AD-A186728] 09 p1143 N88-16853
Crack arrest fracture toughness of armor steels
[AD-A187711] 11 p1456 N88-18681
Microstructural characterization of HSLA-100 GMA weldments
[AD-A187782] 11 p1457 N88-18683
The influence of strain on hydrogen entry, transport, and embrittlement of a high strength steel in aqueous sodium chloride solution
[AD-A189302] 12 p1608 N88-19619
Development of a constitutive equation for HSLA (High-Strength Low-Alloy)-100 at cryogenic temperatures
[AD-A189243] 13 p1740 N88-20408
Cracking tendencies of restrained welds in high strength low alloy steels under hyperbaric conditions
[AD-A190255] 15 p2039 N88-22150
Hydrogen embrittlement susceptibility of high strength ESR 4340 steel alloys for ballistically resistant/tolerant components 17 p2319 N88-23848
Brief evaluation of the alloy 17-4-PH (Z5 CNU 17-04). Semifinished product: 205 mm dia forged roller, test reports
[DF/NH-3616/84] 17 p2322 N88-23866
Analysis of crack arrest toughness
[AD-A193340] 21 p2913 N88-27286
Development of high strength and toughness microcomposite HSLA Fe/Cr/Mn/C steel with and without Nb
[DE88-009813] 21 p2913 N88-27290
A review of solid particle erosion of engineering materials
[DE88-010065] 22 p3054 N88-28124
Additional fracture and strength test results for A723 steel and 38644 titanium
[AD-A196329] 24 p3353 N88-29960

HIGH TEMPERATURE

Optimizing the application of high temperature corrosion resistant aluminium-silicon-base coatings
[BLL-M-37222-(5828.4)] 01 p0018 N88-10112
Oxidation of TSX graphite over the temperature range 450 to 1200°C
[DE87-012230] 01 p0020 N88-10127
Chemical equilibrium calculations for the high pressure and temperature dissociation of liquid nitrogen
[DE87-013788] 01 p0021 N88-10135
Large-strain softening of aluminum at elevated temperature
[DE87-011559] 01 p0024 N88-10153
Theory of the carbon phase diagram at high pressures and temperatures
[DE87-012245] 01 p0028 N88-10180
Effect of high-temperature annealing on the microstructure and thermoelectric properties of GaP doped SiGe
[NASA-TM-100164] 01 p0029 N88-10188
High temperature metal matrix composites for future aerospace systems
[NASA-TM-100212] 02 p0149 N88-10938
High temperature stress-strain analysis 02 p0188 N88-11170
Elevated temperature crack growth 02 p0188 N88-11174
Lewis' enhanced laboratory for research into the fatigue and constitutive behavior of high temperature materials 02 p0189 N88-11177
Organic Rankine-cycle power systems working fluids study. Topical report No. 1: Fluorinol 85
[DE87-014604] 02 p0195 N88-11217
The effect of strain rate on the yield behavior of iron-base LRO alloys at elevated temperatures
[DE87-014893] 03 p0288 N88-11808
A fundamental study of the mechanical and microstructural response of elevated temperature PM aluminum-titanium alloys 03 p0289 N88-11819
Modified 14Cr-16Ni stainless steels with improved creep resistance at 700 C due to tailored precipitate microstructures
[DE87-014788] 03 p0290 N88-11825
Impact behavior of 9-Cr and 12-Cr ferritic steels after low-temperature irradiation
[DE88-000333] 03 p0291 N88-11827
High temperature superconductors 03 p0297 N88-11869
Gas tungsten arc welding of Al-10Fe-5Ce
[AD-A184202] 03 p0334 N88-12104
Adiabatic diesel engine component development: Reference engine for on-highway applications
[NASA-CR-179531] 03 p0386 N88-12428
Research and development on high strength ceramic heaters discussed 04 p0404 N88-12508
Pipe and bend erosion by pneumatic transport of solids at high temperature
[DE88-001345] 04 p0429 N88-12658
A fundamental study of P/M processed elevated temperature aluminum alloys
[AD-A185393] 05 p0565 N88-13445
Coatings for high-temperature bearings and seals
[NASA-TM-100249] 05 p0567 N88-13453
Behavior of long and short fatigue cracks in a powder metallurgy superalloy at room and at high temperature 05 p0601 N88-13677
Thermo-mechanical behavior of high temperature fiber composites 06 p0678 N88-14149
Cyclic fatigue of ceramics at high temperatures
[PB87-127700] 06 p0685 N88-14200
Recent advances in high temperature instrumentation for hot section applications
[NASA-TM-100282] 06 p0707 N88-14339
High temperature low cycle fatigue of oxide dispersion strengthened and single crystal nickel base superalloys 06 p0720 N88-14422
Orientation effects in copper single crystals fatigued at elevated temperatures 06 p0720 N88-14423
Elevated temperature fatigue crack propagation 06 p0720 N88-14424
High temperature low cycle fatigue behavior and creep-fatigue interation of MA 6000 ODS alloy 06 p0720 N88-14425
Creep-fatigue cracking in high temperature turbine rotors 06 p0720 N88-14426
Hot piston ring tests
[NASA-TM-100256] 06 p0729 N88-14486
Precipitation in alumina-rich spinel: A transformation-toughened ceramic single crystal
[DE87-012380] 06 p0785 N88-14815
High temperature stability of superconducting YBa2Cu3O subx as characterized by X-ray diffraction
[DE88-001856] 06 p0787 N88-14824
An automated flow calorimeter for heat capacity and enthalpy measurements at elevated temperatures and pressures
[DE88-002357] 07 p0857 N88-15206
Excess thermodynamic properties of aqueous electrolytes to high temperatures and pressures
[DE88-001768] 07 p0940 N88-15712
Determination of thermodynamic function of minerals at high temperatures
[DE88-001911] 07 p0940 N88-15713
Determination of thermodynamic function of minerals at high temperatures
[DE88-002311] 07 p0940 N88-15714
High-temperature electronics 08 p0956 N88-15797
Aircraft engine hot section technology: An overview of the HOST Project 08 p0957 N88-15804
Hot piston ring/cylinder liner materials: Selection and evaluation
[NASA-TM-100276] 08 p0971 N88-15872
Sputtered silver films to improve chromium carbide based solid lubricant coatings for use to 900 C
[NASA-TM-100783] 08 p0973 N88-15885
Investigation of self-discharge characteristics of spacecraft nickel-cadmium cells at elevated temperatures
[AD-A186497] 08 p0979 N88-15919
High temperature polymer matrix composites 09 p1119 N88-16700
Development of a new generation of high-temperature composite materials 09 p1119 N88-16702
A rapid method for the computation of equilibrium chemical composition of air to 15000 K
[NASA-TP-2792] 09 p1140 N88-16830
High-temperature photoelectron spectroscopy. An increased sensitivity spectrometer for studying vapor-phase species produced at furnace temperatures greater than 2000K
[AD-A186542] 09 p1140 N88-16835
Fatigue and uniaxial deformation behavior of Hastelloy XR at elevated temperatures
[DE88-751058] 09 p1145 N88-16862
Evaluation of high temperature structural adhesives for extended service, phase 5
[NASA-CR-178176] 09 p1149 N88-16884
Molecular dynamics study of high-temperature grain-boundary stability in a (100) sigma = 29 bicrystal model
[DE88-002955] 09 p1258 N88-17546
A review of pitting corrosion in high temperature aqueous solutions
[DE88-003547] 10 p1302 N88-17787
Dynamic recrystallization during high temperature low cycle fatigue of nickel
[DE88-003224] 10 p1302 N88-17788
A solar receiver-reactor with specularly reflecting walls for high-temperature thermoelectrochemical and thermochemical processes
[AD-A187612] 10 p1351 N88-18077
High temperature processing of superconducting Y1Ba2Cu3O6.9
[DE88-003002] 10 p1416 N88-18449
Electronic structure, charge transfer excitations and high temperature superconductivity
[DE88-003096] 10 p1416 N88-18453
Innovative arrangements for industry/DOE laboratory collaboration in high temperature superconductivity
[DE88-004320] 10 p1420 N88-18482
Gas cleaning at high temperatures and pressures for gas turbines
[DE88-751171] 11 p1440 N88-18593
An electron spectroscopic investigation of high-temperature superconducting oxides
[DE88-003807] 11 p1558 N88-19325
Research briefing on high-temperature superconductivity
[PB88-133004] 11 p1561 N88-19344
To the problem of determining true volume steam content by measured values of mean density of a mixture in thermally unsteady two-phase flows
[DE88-700840] 12 p1626 N88-19726
Properties of molecular solids and fluids at high pressure and temperature
[DE88-004195] 13 p1738 N88-20391
Material parameter measurements at high temperatures
[NASA-CR-182707] 13 p1739 N88-20397
Effects of high temperature neutron irradiation on the physical, chemical and mechanical properties of fine-grained isotropic graphite 13 p1747 N88-20444
A study of the dynamics of high temperature brittle intergranular fracture by acoustic emission
[AERE-R-12479] 13 p1780 N88-20650
Power from the sun: Principles of high temperature solar thermal technology
[DE87-001104] 13 p1795 N88-20736
Discussion of radiation effects and high-temperature oxide superconductors
[DE88-001427] 13 p1846 N88-21046
Prediction of high-temperature thermodynamic properties of mixed electrolyte solutions including solubility equilibria, vapor pressure depression and boiling point elevation
[DE88-006344] 13 p1849 N88-21069
A viscoplastic constitutive theory for metal matrix composites at high temperature 14 p1929 N88-21500
Effects of state recovery on creep buckling under variable loading 14 p1933 N88-21527
On 3-D inelastic analysis methods for hot section components. Volume 1: Special finite element models
[NASA-CR-180893] 14 p1934 N88-21535
Prediction of thermodynamic properties, including solubility equilibria and vapor pressures, for mixed aqueous electrolytes to high temperatures
[DE88-006317] 14 p1990 N88-21863
Fluids, gels and glasses under extreme conditions of pressure and temperature
[AD-A190655] 15 p2035 N88-22125
Advanced B and Al combustion kinetics over wide temperature ranges
[AD-A190752] 15 p2036 N88-22128
Effect of strain rate on high-temperature low-cycle fatigue behavior of Hastelloy X and Hastelloy XR
[DE88-752302] 15 p2037 N88-22140
The thermal radiative properties of metals at high temperature
[DE88-006625] 15 p2038 N88-22141
High temperature oxidation and electrochemical studies related to hot corrosion
[AD-A190699] 15 p2040 N88-22156
Developments in ceramic superconducting materials 15 p2052 N88-22229
Fracture technology for brittle materials 15 p2083 N88-22417
Elevated temperature crack growth 15 p2084 N88-22421
Thermal stress in high temperature cylindrical fasteners
[NASA-TM-100611] 15 p2087 N88-22438
Synthesis of metastable superconductors by high dynamic pressure
[DE88-005620] 15 p2139 N88-22764
A theoretical and experimental study of the thermophysical properties of lithium hydride
[NASA-TT-20179] 16 p2175 N88-22965
The analysis of fatigue crack growth mechanism and oxidation and fatigue life at elevated temperatures
[NASA-CR-182129] 16 p2179 N88-22987

High temperature solid lubrication by catalytically generated carbon
[AD-A190804] 16 p2182 N88-23004
Laser cladding of Ni, Nb and Mg alloys for improved environmental resistance at high temperature
[AD-A191274] 16 p2213 N88-23208
Study of mechanisms of time-dependent crack growth at elevated temperature
[DE88-006918] 16 p2223 N88-23271
Creep behavior of tungsten/niobium and tungsten/niobium-1 percent zirconium composites 17 p2425 N88-24427
Fabric radiators 17 p2427 N88-24435
The variation of torsional ductility of high-purity aluminum with temperature and strain rate
[DE88-005618] 18 p2487 N88-24755
A thermally modified polymer matrix composite material with structural integrity to 371 C
[NASA-TM-100922] 19 p2609 N88-25483
Extended ductility of Al and alpha-Fe alloys through dynamic recovery mechanisms
[DE88-008679] 19 p2616 N88-25522
Metals and Ceramics Division
[DE88-008955] 19 p2618 N88-25530
Uniaxial tensile strain measurement for ceramic testing at elevated temperature: Requirements, problems and solutions
[DE88-008090] 19 p2621 N88-25550
Hot carrier effects in CMOS field effect transistors at cryogenic temperatures 19 p2662 N88-25829
Pulsatile fluidic pump performance at elevated temperatures
[DE88-008046] 19 p2677 N88-25919
The adherence of nickel oxide on nickel during high temperature oxidation
[DE88-011194] 20 p2774 N88-26450
Fracture resistance of a TiB2 particle/SiC matrix composite at elevated temperature
[NASA-TM-100967] 20 p2779 N88-26482
Feasibility of producing jet fuel from GPGP (Great Plains Gasification Plant) by-products
[DE88-010233] 20 p2781 N88-26492
Molten salt electrolytes for high-temperature lithium cells
[DE88-010058] 20 p2794 N88-26581
On the chemistry of superconductivity
[DE88-010714] 20 p2880 N88-27096
Creep behavior for Hastelloy-XR
[DE88-753428] 21 p2914 N88-27295
Investigation of hydrogen isotope penetration through stainless steels Kh18N10T and Kh3M2BFR
[DE88-702189] 21 p2915 N88-27297
Kinetic of oxidation to air of a Fe-Al-Mn alloy system at 600-800(sup 0)C temperature range
[DE88-702309] 21 p2920 N88-27330
Properties of new low dimensional materials and mechanisms of high T(sub c) superconductivity
[DE88-012026] 21 p3024 N88-27951
The High Temperature Materials Laboratory: A new research and user facility at the Oak Ridge National Laboratory
[DE88-010792] 22 p3057 N88-28138
A new model for the simulation of interfaces at high temperature
[DE88-009926] 22 p3155 N88-28772
Possible occurrence of band interplay in high Tc superconductor
[PREPRINT-593] 22 p3157 N88-28789
The effects of moisture loss and elevated temperature upon the material damping of fibre reinforced polymer matrix composites
[UTIAS-324] 23 p3188 N88-28970
The high temperature creep deformation of Si3N4-6Y2O3-2Al2O3
[NASA-CR-183204] 23 p3190 N88-28981
A fundamental study of P/M processed elevated temperature aluminum alloys
[AD-A192958] 23 p3194 N88-29005
Development of high temperature, high pressure rotating shaft seals
[DE88-001029] 23 p3221 N88-29172
Creep of carbon yarn and carbon-carbon composites at high temperatures and high stresses
[AD-A195224] 24 p3340 N88-29878
A study of the critical factors controlling the synthesis of ceramic matrix composites from preceramic polymers
[AD-A195405] 24 p3340 N88-29881
Electrical properties of materials for elevated temperature resistance strain gage application
[NASA-CR-182214] 24 p3376 N88-30106

HIGH TEMPERATURE AIR
SCRAM JET (Supersonic Combustion Ramjet) combustion experiments 04 p0404 N88-12512

HIGH TEMPERATURE ALLOYS
U HEAT RESISTANT ALLOYS

HIGH TEMPERATURE ENVIRONMENTS
Calculation of the tribological properties of surfaces by semi-empirical methods
[AD-A184283] 04 p0450 N88-12791
Daily dynamics of some physiological indicators of man under desert condition 06 p0750 N88-14605
Portable, ambient air microclimate cooling in simulated desert and tropic conditions
[AD-A186457] 08 p1050 N88-16338
An integrated aero/mechanical performance approach to high technology turbine design 10 p1280 N88-17657
Johnson noise thermometer for high radiation and high temperature environments
[DE88-003770] 10 p1323 N88-17911
Johnson noise thermometer for high-radiation and high-temperature environments 17 p2434 N88-24480
Effect of alloying, rapid solidification, and surface kinetics on the high temperature environmental resistance of niobium
[AD-A192093] 18 p2485 N88-24743
High speed inlet calculations with real gas effects
[NASA-CR-182167] 20 p2752 N88-26336
Finite-rate water condensation in combustion-heated wind tunnels
[NASA-TP-2833] 22 p3046 N88-28075
Development of computer-controlled thermogravimetric instrumentation for measurement of environmental and high temperature volatilization and desorption of contaminants from polymeric materials
[AD-A195934] 24 p3343 N88-29900

HIGH TEMPERATURE FLUIDS
NT HIGH TEMPERATURE AIR
NT HIGH TEMPERATURE GASES
Birch's law and the properties of high temperature fluid metals
[DE87-014744] 03 p0288 N88-11807

HIGH TEMPERATURE GAS COOLED REACTORS
Effect of fuel burnup and cross sections on modular HTGR (High-Temperature Gas-cooled Reactor) reactivity coefficients
[DE88-006656] 22 p3151 N88-28748

HIGH TEMPERATURE GASES
NT HIGH TEMPERATURE AIR
KR+ laser excitation of NH2 in atmospheric pressure flames
[AD-A183421] 01 p0050 N88-10322
High temperature CO2 study: Anti-Stokes coherent Raman diffusion and infrared spectroscopy
[ESA-TT-1048] 03 p0282 N88-11777
HOST turbine heat transfer program summary
[NASA-TM-100280] 06 p0704 N88-14320
Evaluation of a temperature remote sensing technique
[AD-A187885] 10 p1347 N88-18053
Evaluation and compilation of thermodynamic properties of high temperature chemical species
[AD-A187509] 11 p1452 N88-18654
Basic characteristics of heat-exchanger-type steam reformer heated by high-temperature helium gas (2). Analysis by simulation model (2)
[DE87-702962] 15 p2061 N88-22291
A numerical study of the hot gas environment around a STOVL aircraft in ground proximity
[NASA-TM-100895] 17 p2295 N88-23729
Laser Diagnostics for combustion temperature and species measurements 17 p2330 N88-23912

HIGH TEMPERATURE LUBRICANTS
High hot-hardness gear lubricant evaluations, phase 2
[AD-A192309] 23 p3196 N88-29017

HIGH TEMPERATURE MATERIALS
U REFRACTORY MATERIALS

HIGH TEMPERATURE NUCLEAR REACTORS
NT HIGH TEMPERATURE GAS COOLED REACTORS
IAEA Specialists' Meeting on Graphite Component Structural Design
[DE88-780006] 13 p1746 N88-20439

HIGH TEMPERATURE PLASMAS
Fast wave injection into high temperature tokamak plasmas in the lower-hybrid-density regime of JIPP T-IIU
[ISSN-0469-4732] 01 p0099 N88-10649
Diagnostic technique for monitoring high temperature plasma dynamics
[DE87-011786] 01 p0099 N88-10653
Study of ionization equilibrium of high temperature and low density plasma
[DE87-703070] 02 p0238 N88-11502
Solar transition region and coronal response to heating rate perturbations 02 p0256 N88-11620
Hot plasmas in the Earth's magnetosphere 03 p0272 N88-11710
Advanced concepts theory annual report 1986
[AD-A184986] 05 p0651 N88-13991
Relativistic plasma concentration measuring by Bremsstrahlung
[DE88-700560] 07 p0936 N88-15685
Simple model for hot ion plasmas
[DE88-750045] 07 p0936 N88-15688
Energetics and dynamics of simple impulsive solar flares
[NASA-TM-87816] 07 p0947 N88-15755
Acceleration/heating processes on auroral field lines as observed by the Viking spacecraft 08 p1096 N88-16596
X-ray lithographic research: A collection of NRL contributions
[AD-A188313] 12 p1695 N88-20140
Effects of toroidal forces in current loops embedded in a background plasma
[AD-A188878] 12 p1695 N88-20143
Fundamental studies and device development in beta silicon carbide
[AD-A189540] 12 p1699 N88-20165
Modeling and transport in semiconductor devices
[AD-A188760] 13 p1844 N88-21037
X-ray lasers: State of art and prospect
[ETN-88-92003] 14 p1914 N88-21434
Ionization equilibrium and radiative energy losses in a stationary plasma
[DE88-700856] 14 p1984 N88-21832
Advanced diagnostics for reacting flows
[AD-A190485] 15 p2035 N88-22122
Measurement of time evolution of plasma electron component parameters on the Ogra-4 device by the Thomson scattering method
[DE88-701575] 16 p2282 N88-23662
Bremsstrahlung from high Z impurities in hot plasmas
[DE88-011755] 20 p2861 N88-26994
Apparatus for submillimeter laser diagnostics of high-temperature plasma
[DE88-702464] 23 p3285 N88-29563

HIGH TEMPERATURE PROPELLANTS
KR+ laser excitation of NH2 in atmospheric pressure flames
[AD-A183421] 01 p0050 N88-10322
Durability testing of an iridium-plated storable rocket engine injector
[AD-A190707] 15 p2027 N88-22078

HIGH TEMPERATURE SUPERCONDUCTORS
Grain boundary effects in processing high T/sub c/ superconductors
[DE87-009297] 01 p0103 N88-10673
Progress toward a superconducting opening switch
[DE87-014170] 02 p0167 N88-11051
Electrical properties of high T/sub c/ superconductors under high pressures
[DE87-012818] 02 p0245 N88-11546
High temperature superconductors 03 p0297 N88-11869
A role for national laboratories in enhancing economic competitiveness. The example of high-temperature superconductors: CNSS papers, No. 1
[DE87-013833] 03 p0379 N88-12386
Shock-induced chemical synthesis of phases similar to the high temperature superconductor oxides
[DE87-013725] 03 p0380 N88-12387
Shock-induced chemical synthesis of phases similar to the high temperature superconductor oxides
[DE87-013725] 03 p0380 N88-12387
Specific heat of the high T/sub c superconductors (La,M)2CuO4 and YBa2Cu3O7 in magnetic fields
[DE87-014680] 03 p0380 N88-12388
The chemical bond and superconductivity
[AD-A184275] 04 p0496 N88-13053
Hitachi develops ceramic superconducting device 06 p0688 N88-14214
Superconducting material development 06 p0688 N88-14217
Study of some superconducting and magnetic materials on high T sub c oxide superconductors
[NASA-CR-182330] 06 p0785 N88-14813
L2,3 XANES of the high T sub c superconductor YBa2Cu3O7 with variable oxygen content
[NOTA-INTERNA-888] 06 p0788 N88-14837
On the coexistence of phonon and non-phonon (plasmon) mechanisms in new high T/sub c/ superconductors
[DE88-003188] 07 p0938 N88-15703
Localization of Cu 3d levels in the high Tc superconductor YBa2Cu3O approximately 7 by Cu2p X-ray photoelectron spectroscopy
[NOTA-INTERNA-887] 07 p0939 N88-15710
Structural relationships in high temperature superconductors
[DE88-002924] 09 p1257 N88-17534
Application of high temperature ceramic superconductors (CSC) to commercial tokamak reactors
[DE88-003973] 09 p1257 N88-17538
High temperature superconductivity research at Argonne National Laboratory
[DE88-003055] 09 p1258 N88-17541

The relationship of the chemical bonding topology of high critical temperature copper oxide superconductors to that of the chevrel phases and the ternary lanthanide rhodium borides
[AD-A189255] 13 p1845 N88-21042
Thermochemistry and high temperature thermodynamic properties of rare earth-alkaline earth-copper oxide superconductors
[DE88-005976] 15 p2140 N88-22770
High-T(sub c) superconducting wire fabrication and testing
[DE88-005989] 15 p2144 N88-22798
High temperature superconductors in the La(sub 1+x)Ba(sub 2-x)Cu O(sub y system
[DE88-006367] 15 p2145 N88-22802
The application of high temperature superconductors to space electrical power distribution components
[NASA-TM-100901] 16 p2171 N88-22939
High temperature superconductivity
[AD-A190259] 16 p2281 N88-23655
Materials science with muon spin rotation
[NASA-CR-182891] 17 p2396 N88-24242
Systematic variation of magnetic-field penetration depth in high-T(c) superconductors studied by muon spin relaxation 17 p2396 N88-24243
Crystalline metal-semiconductor superlattices
[DE88-007063] 18 p2581 N88-25332
Ground state properties and electronic structure of high T sub c superconductors
[DE88-007485] 18 p2585 N88-25360
Systematics of excimer laser ablation: Thin film preparation of high T(sub c) material
[DE88-010569] 19 p2675 N88-25909
Search for new high-temperature superconducting copper oxides
[DE88-009922] 19 p2735 N88-26245
Compilation of NRL publications on high temperature superconductivity
[AD-A189137] 21 p3019 N88-27921
Anharmonic model for high-Tc superconductors
[DE88-702196] 21 p3020 N88-27924
Superconducting properties of oxygen deficient YBa2Cu3O(sub 7-delta)
[DE88-009969] 22 p3155 N88-28774
La2CuO(sub 4 + delta): A superconducting superoxide
[DE88-010325] 23 p3288 N88-29578
Dependence of high critical temperature of ceramic superconductors on the nominal Cu(sup 3+)/Cu(sup 2+) ratio
[DE88-702734] 23 p3293 N88-29611
Theory of superconductivity in oxides
[AD-A195647] 24 p3433 N88-30432
Theoretical model of high temperature superconductors
[DE88-702707] 24 p3434 N88-30441

HIGH TEMPERATURE TESTS
Viscosity measurements at high temperatures on a standard reference material supplied by BCR --- Bureau Communite de Reference (BCR)
[NPL-DMA(A)-146] 01 p0020 N88-10126
High temperature characterization of ceramic materials
[REPT-NT-3403] 03 p0292 N88-11837
High temperature tensile testing of ceramic composites
[NASA-CR-180886] 08 p0990 N88-15996
High temperature Young's modulus of IG-110 graphite 13 p1746 N88-20443
Development, high temperature properties, and microanalysis of nonoxide ceramics
[ETN-88-92103] 14 p1893 N88-21304
An experimental comparison of several current viscoplastic constitutive models at elevated temperature 14 p1931 N88-21516
Unified constitutive model development for metal matrix composites at high temperature 15 p2078 N88-22387
Examination of temperature effects on gate-to-drain avalanche breakdown in GaAs MESFETs (Metal-Semiconductor Field Effect Transistors) by measuring light emission under RF drive
[AD-A189634] 15 p2141 N88-22778
Strength and cracking resistance of ceramics. Report 3: SiC ceramics 16 p2180 N88-22994
Strength and failure rate of composite materials with carbon in ceramic matrix 16 p2180 N88-22995
Combustion behavior of the vitiator. Experimental results of a second test series
[VTH-LR-509] 18 p2484 N88-24734
Automated measurement of crack length and load line displacement at elevated temperature
[NLR-MP-87049-U] 20 p2816 N88-26706
Determination of multiaxial flow surfaces at elevated temperatures using the concept of dissipation potential
[ORNL/TM-10787] 24 p3383 N88-30149

HIGH THRUST
Development of circulation control technology for powered-lift STOL aircraft 10 p1272 N88-17608

HIGH VACUUM
Fatigue crack propagation of low-alloy steel in a vacuum environment
[DE87-013770] 01 p0061 N88-10393

HIGH VOLTAGES
A high-voltage multistage laser-triggered gas switch
[DE87-011725] 01 p0040 N88-10253
A tutorial on Rogowski coil theory and operation
[DE88-000006] 02 p0230 N88-11449
The LPX (Long Pulse Experiment) facility
[DE87-010493] 03 p0311 N88-11964
Measurements in an electromagnetic test laboratory
[SNIAS-872-430-102] 05 p0575 N88-13507
Low jitter laser-triggered high-voltage vacuum switch using low laser energies
[DE88-001922] 05 p0587 N88-13576
Evaluation of high-voltage, high-power, solid-state remote power controllers for amps 07 p0924 N88-15612
Vapor-mist for lightweight high voltage space insulation systems
[DE87-011704] 13 p1762 N88-20538
Partial discharges and the electrical aging of cross linked polyethene (XLPE) cable insulation
[EUT-86-E-160] 14 p1892 N88-21300
Test results of high-voltage, high-power, solid-state remote power controllers
[NASA-TM-100322] 16 p2194 N88-23085
High frequency power distribution system
[NASA-CR-175071] 17 p2335 N88-23939
Studies on the use of propylene carbonate as a high-voltage insulator
[DE88-011786] 22 p3057 N88-28141
Calibration technique and study on metrological characteristics of a high-voltage inverse square-law function generator
[DE88-702101] 22 p3072 N88-28236

HIGHLANDS
Topography of large craters on Mars: Implications for the highlands resurfacing history 23 p3306 N88-29691
Ridged and gullied terrains in the Martian uplands 23 p3307 N88-29700

HIGHLY MANEUVERABLE AIRCRAFT
HiMAT flight program: Test results and program assessment overview
[NASA-TM-86725] 01 p0005 N88-10026
Development and flight test of an experimental maneuver autopilot for a highly maneuverable aircraft
[NASA-TP-2618] 14 p1867 N88-21153

HIGHWAYS
Seasonal variation for structural strength value
[PB88-169248] 16 p2222 N88-23260

HILBERT SPACE
Stochastic integration for operator valued processes on Hilbert spaces and on nuclear spaces
[ENST-87D002] 01 p0089 N88-10580
Irreducible *-representations of the Lie superalgebra osp(1,4) with finite-degenerated vacuum
[DE87-703069] 02 p0225 N88-11420
Families of Bose rays in quantum optics
[DE87-014584] 02 p0236 N88-11489
Compactness of quasi-conforming element spaces, convergence of quasi-conforming element method 03 p0301 N88-11896
Stochastic filtering solutions for ill-posed linear problems and their extension to measurable transformations
[AD-A186016] 07 p0909 N88-15506
Strong laws of large numbers for arrays of orthogonal random variables
[AD-A186159] 07 p0910 N88-15513
Characterization of all controlled invariant sub-spaces for spectral systems
[PB88-106638] 07 p0912 N88-15532
Admissible and singular translates of stable processes
[AD-A186426] 07 p0917 N88-15571
Strong convergence and convergence rates of approximating solutions for algebraic Riccati equations in Hilbert spaces
[AD-A186190] 08 p1072 N88-16464
Computation of the zeta-function of an algebraic curve with the differentials of the first kind
[PB88-127527] 10 p1399 N88-18339
Eigenvalue problems
[AD-A186069] 10 p1401 N88-18356
The global convergence of partitioned BFGS on problems with convex decompositions and Lipschitzian gradients
[DE88-006249] 14 p1968 N88-21744
Stochastic evolution equations driven by nuclear space valued martingales
[AD-A189342] 15 p2126 N88-22677
Geometric methods and the gauge structure of Berry's phase
[DE88-006538] 15 p2127 N88-22682
Coding capacity of generalized additive channels
[AD-A190315] 15 p2127 N88-22685
On the Hilbert space of supersymmetric quantum systems
[DE88-701648] 16 p2284 N88-23677
Theory of pseudo-differential operators over C*-algebras
[DE88-701860] 20 p2845 N88-26883
Backlund transformations associated with a Riemann-Hilbert spectral problem
[PREPRINT-596] 22 p3148 N88-28712
The Hilbert space of the closed bosonic string
[USIP-88-04] 22 p3151 N88-28747
Feedback stabilization of du/dt=Au + bf in Hilbert space when the normalization function is less than or equal to r
[AD-A193510] 23 p3277 N88-29506
The Hilbert space of the open bosonic string
[USIP-88-02] 23 p3295 N88-29628

HILBERT TRANSFORMATION
Some properties of the Hilbert transform
[DE88-002465] 09 p1227 N88-17350
Approximation problems of the Hilbert transform to identify minimum phase linear systems
[FUB-42-1986] 21 p2999 N88-27790
Application of the Hilbert transform to Doppler radar signals from a hypervelocity gun
[AD-A193690] 22 p3148 N88-28716

HILLER MILITARY AIRCRAFT
U MILITARY AIRCRAFT

HIMAT
U HIGHLY MANEUVERABLE AIRCRAFT

HINDRANCE
U CONSTRAINTS

HINGE MOMENTS
U TORQUE

HINGED ROTOR BLADES
U HINGES
U ROTARY WINGS

HINGELESS ROTORS
U RIGID ROTORS

HINGES
NT FLAPPING HINGES
Locking hinge
[NASA-CASE-MSC-21056-1] 17 p2312 N88-23827
Payload deployment method and system
[NASA-CASE-MSC-21330-1] 18 p2470 N88-24660

HIP (PROCESS)
U HOT ISOSTATIC PRESSING

HIPPARCOS SATELLITE
Deep space target location with Hubble Space Telescope (HST) and Hipparcos data
[NASA-CR-182520] 10 p1427 N88-18524
Preparation of photometric measurements on a million stars in the framework of the satellite project HIPPARCOS/TYCHO
[ETN-88-91502] 13 p1853 N88-21093

HIPPOCAMPUS
Long term synaptic plasticity and learning in neuronal networks
[AD-A186834] 09 p1199 N88-17188

HISTOCHEMICAL ANALYSIS
Histomorphometric analysis of rat bones after spaceflight aboard Cosmos-1667 biosatellite 10 p1360 N88-18126
Muscle preservation in the study of bioenergetic effects of hypokinesia 10 p1362 N88-18139
Investigation of rat skeletal muscles following short-term spaceflight aboard Cosmos-1667 biosatellite 10 p1365 N88-18157

HISTOGRAMS
Necessary and sufficient conditions for the convergence of integrated and mean-integrated r-th order error of histogram density estimates
[AD-A186037] 07 p0914 N88-15550
Almost sure L(gamma)-norm convergence for data-based histogram density estimates
[AD-A189944] 17 p2393 N88-24228

HISTOLOGY
Status of microcirculation in high-altitude blood loss 12 p1663 N88-19973

HISTORIES
The history of aeroelasticity research in Germany from the beginning until 1945 --- airframes
[DFVLR-MITT-86-25] 01 p0001 N88-10003
Overview of STIP intervals 15-19 01 p0110 N88-10710
On the occasion of the 50th anniversary of the death of Professor Hugo Junkers
[MBB/LW-3016/S/PUB/201] 02 p0257 N88-11627
Hypocenters (1977-1984) around the Richton Dome and the Melvin, Alabama, 1978 earthquake
[DE87-014336] 03 p0351 N88-12214

The development of ODE methods: A symbiosis between hardware and numerical analysis
[DE87-014925] 03 p0370 N88-12325
How space, the fourth operational medium, supports operational maneuver
[AD-A184742] 03 p0373 N88-12346
Hypersonic airbreathing propulsion: Evolution and opportunities 05 p0531 N88-13231
The technical evolution of the Wilson camera: The beginnings (1895-1925)
[NOTA-INTERNA-876] 05 p0585 N88-13568
The birth of big science: Nuclear physics as advanced technology source
[NOTA-INTERNA-881] 05 p0648 N88-13967
The history and development of nonlinear stellar pulsation codes
[DE88-001828] 06 p0801 N88-14899
Measurements in centrifugal compressors 07 p0850 N88-15161
Lewis materials research and technology: An overview 09 p1119 N88-16699
A comparison of fitting techniques for the cumulative average learning curves with historical lot cost data
[AD-A187127] 09 p1227 N88-17349
The coming revolution in turbine engine technology 10 p1279 N88-17648
Airbus, the successful European cooperation
[MBB-UT-005/87] 10 p1313 N88-17847
Messerschmitt-Boelkow-Blohm: A company with a tradition 10 p1316 N88-17866
Messerschmitt-Boelkow-Blohm: Biography and history of a company 10 p1316 N88-17867
Present stage of space medicine 10 p1364 N88-18151
Antimatter: Its history and its properties
[DE88-004308] 10 p1423 N88-18498
Spacecraft fire detection and extinguishment: A bibliography
[NASA-CR-180880] 11 p1444 N88-18612
Announced United States nuclear tests: July 1945 through December 1986
[NVO-209-REV-7] 11 p1545 N88-19247
The early years of string theory: The dual resonance model
[DE88-003521] 11 p1563 N88-19359
An evaluation in a modern wind tunnel of the transonic adaptive wall adjustment strategy developed by NPL in the 1940's
[NASA-CR-181623] 12 p1575 N88-19417
Historical electromagnetic propagation condition database description
[AD-A189157] 12 p1621 N88-19695
An evaluation of historical algebras
[AD-A188350] 12 p1684 N88-20067
HISPLT: A history graphics post processor for wave propagation codes
[DE88-005507] 13 p1817 N88-20857
Electronics and communications in air traffic control: The Presidential Address
[ETN-88-92057] 14 p1865 N88-21146
Sunspot frequency and solar activity
[PUBL-17/87] 14 p2011 N88-21996
Chronology of KSC and KSC related events for 1987
[NASA-CR-182754] 14 p2012 N88-22002
Energy from the wind
[DE88-006897] 15 p2091 N88-22459
Marshall Space Flight Center 1960-1985: 25th anniversary report
[NASA-TM-100328] 15 p2153 N88-22852
Two decades of achievement in the ocean, 1968-1988
[PB88-167077] 16 p2236 N88-23356
Presentation of the METEOSAT system and the roles of EUMETSAT within the meteorological community 17 p2357 N88-24039
Sea ice kinematics: Space and time scales
[AD-A191162] 17 p2376 N88-24128
The application of hydrocarbon bioconversion technology to aerospace materials production 18 p2478 N88-24698
History of wildland fires on Vandenberg Air Force Base, California
[NASA-TM-100983] 18 p2549 N88-25134
NASA history data book. Volume 1: NASA resources 1958-1968
[NASA-SP-4012-VOL-1] 18 p2596 N88-25428
NASA historical data book. Volume 2: Programs and projects 1958-1968
[NASA-SP-4012-VOL-2] 18 p2596 N88-25429
NASA historical data book. Volume 3: Programs and projects 1969-1978
[NASA-SP-4012-VOL-3] 18 p2596 N88-25430
High-temperature superconductivity: An overview
[DE88-702051] 21 p3020 N88-27925
History of manned spaceflight
[CNES-NT-121] 21 p3032 N88-28000
Soviet space program handbook
[AD-A194332] 22 p3046 N88-28077
Review of past and current trials and uses of unmanned vehicles
[AD-A194527] 22 p3084 N88-28311
Newtonian and Einsteinian gravitation 22 p3158 N88-28791
Regional intercomparisons of General Circulation Model predictions and historical climate data: CO2
[DE88-010416] 23 p3235 N88-29248
SDI (Strategic Defense Initiative): A policy analysis
[AD-A194240] 23 p3275 N88-29493
An introduction to the historical records of China about Mars 23 p3301 N88-29664
History of aeroelasticity in Germany from the beginning to 1945
[ESA-TT-1082] 24 p3319 N88-29767
Analysis of environmental parameters from the Panama City tower radar experiment
[AD-A194994] 24 p3404 N88-30264

HLLV
U HEAVY LIFT LAUNCH VEHICLES

HMX
High pressure strand burn rate tests of polyvinylnitrate/nitramine propellants
[AD-A184178] 04 p0422 N88-12615
The correlation of HMX (cyclotetramethylenetetranitramine) particle characterization techniques to propellant burn rate
[AD-A187119] 09 p1140 N88-16833
Kinetic measurements of thermal decomposition of energetic materials at high pressures
[AD-A191612] 19 p2622 N88-25552
Temperature and species profiles in propellant ignition and combustion 19 p2633 N88-25616
Chemical kinetics modeling of HMX combustion 19 p2633 N88-25617
Descriptive characterization of propellant particles
[AD-A195176] 24 p3356 N88-29985

HOGBACKS
U RIDGES

HOHMANN TRAJECTORIES
U ELLIPTICAL ORBITS
U TRANSFER ORBITS

HOHMANN TRANSFER ORBITS
U ELLIPTICAL ORBITS
U TRANSFER ORBITS

HOLDERS
NT FLAME HOLDERS
An optically strobed sample and hold circuit 19 p2656 N88-25772
Evaluation of transfer films of Salox M on 440C for HPOTP bearing cage applications, task 119
[NASA-CR-179020] 23 p3223 N88-29184

HOLE BURNING
Applications of nonlinear hole burning spectroscopy
[AD-A184943] 05 p0587 N88-13580

HOLE DISTRIBUTION (ELECTRONICS)
Electrical and optical properties of Hg/sub 1-x/Cd/sub x/Te doped layers grown by Liquid Phase Epitaxy (LPE)
[DE88-701023] 16 p2281 N88-23653

HOLE DISTRIBUTION (MECHANICS)
Crack distribution and growth rates for critical fastener holes in Mirage wing RH79
[AD-A189080] 13 p1722 N88-20293
Stress concentration around circular hole in a composite material specimen representative of the X-29A forward-swept wing aircraft
[NASA-CR-179435] 20 p2814 N88-26694

HOLE GEOMETRY (MECHANICS)
Device for measuring hole elongation in a bolted joint
[NASA-CASE-LAR-13453-1] 06 p0712 N88-14361
Life and reliability of rotating disks 15 p2085 N88-22428
Dynamical stress concentration problems, from every side, bordered and perforated plates
[ETN-88-92128] 20 p2815 N88-26703

HOLE MOBILITY
Electrical and optical properties of Hg/sub 1-x/Cd/sub x/Te doped layers grown by Liquid Phase Epitaxy (LPE)
[DE88-701023] 16 p2281 N88-23653

HOLES
Loading rate sensitivity of open hole composites in compression
[NASA-TM-100634] 19 p2610 N88-25490
Compression creep of filamentary composites
[NASA-CR-182550] 20 p2798 N88-26601

HOLES (ELECTRON DEFICIENCIES)
Modeling and transport in semiconductor devices
[AD-A188760] 13 p1844 N88-21037
Nonlinear optical properties and subpicosecond dynamics of excitons and electron-hole plasmas in multiple quantum well structures
[AD-A191926] 19 p2727 N88-26196
Direct measurement of ultrafast electron-hole plasma expansion at high density at an asymmetric GaAs quantum well 20 p2871 N88-27044
Oxygen vacancy ordering and superconductivity in YBa2Cu3O(sub 7-x)
[DE88-010005] 20 p2877 N88-27083
Inelastic electron scattering and electron-hole excitations in iron and nickel
[DE88-011843] 21 p2915 N88-27303

HOLES (MECHANICS)
Hole diameters in plates impacted by projectiles 21 p2929 N88-27386
Two-dimensional sequential and concurrent finite element analysis of unstiffened and stiffened aluminum and composite panels with hole
[NASA-CR-183083] 22 p3086 N88-28325

HOLLAND
U NETHERLANDS

HOLLOW CATHODES
Segmented hollow cathode discharges for copper ion lasers
[ETN-87-90403] 01 p0052 N88-10333
Hollow cathode plasma coupling study, 1986
[NASA-CR-171985] 03 p0309 N88-11949
Advanced electric propulsion and space plasma contactor research
[NASA-CR-180862] 06 p0674 N88-14126
Space plasma contactor research, 1987
[NASA-CR-182148] 16 p2280 N88-23649

HOLMIUM
Magnetic phase transitions in 90-K superconductors Ho1Ba2Cu3O(7-delta) and Gd1Ba2Cu3O(7-delta) observed by ZF-muon(+)SR
[DE88-752611] 23 p3290 N88-29588

HOLOGRAPHIC INTERFEROMETRY
ISIS: Imaging Speckle Interfereometer in Space 01 p0095 N88-10625
Optical flow diagnostic measurements in turbomachinery
[PNR90396] 02 p0172 N88-11081
Development and testing of a system for the partially automated evaluation of holographic interferograms in the experimental stress analysis of reactor components
[ETN-87-90574] 02 p0175 N88-11095
The use of holographic interferometry for turbomachinery fan evaluation during rotating tests
[PNR90390] 02 p0176 N88-11098
Diffraction moire: The dynamic regime
[DE87-014883] 03 p0335 N88-12111
Determination of the origin of self-pumped phase conjugation in barium titanate
[AD-A184697] 03 p0377 N88-12372
Interferometric data for a shock-wave/boundary-layer interaction
[NASA-TM-88227] 05 p0543 N88-13306
Full field visualization of surface and bulk acoustic waves using heterodyne holographic interferometry
[AD-A185071] 05 p0646 N88-13958
Dye laser for holographic interferometry 07 p0920 N88-15588
Investigation of vibration problems with heterodyne holographic interferometer 08 p1000 N88-16058
JPRS report: Science and technology. USSR: Physics and mathematics
[JPRS-UPM-87-010] 08 p1075 N88-16485
Formation of high-coherence radiation in free-running mode ruby laser for pulse holography 08 p1077 N88-16497
Comparison of sensitivity and precision of holographic and speckle-interferometry methods with Fourier-plane recording 08 p1078 N88-16500
Holographic phase correction
[RSRE-MEMO-4036] 09 p1167 N88-17000
A review on holography, its principles and applications
[ISL-CO-242/86] 15 p2069 N88-22338
Computer tomography and hybrid optical/digital methods for aerodynamic measurements
[AD-A190909] 16 p2157 N88-22872
Dual wavelength holographic interferometry system
[NASA-CASE-MFS-28242-1] 17 p2341 N88-23960
Simultaneously time- and space-resolved spectroscopic characterization of laser-produced plasmas
[DE88-008038] 19 p2728 N88-26202
Turbulent flow field visualization with integral interferometric imaging and computed tomography 21 p2950 N88-27521
Holographic interferometry for flow visualization studies in high speed fans
[PNR90459] 22 p3045 N88-28072
Holographic flow visualization
[PNR90466] 22 p3079 N88-28283
Experimental aspects of using time-averaged holographic interferometry to detect barely visible impact damage in a graphite/epoxy composite plate
[AD-A194418] 24 p3375 N88-30097

Use of holography in vibration and flutter study of fans
[PNR90458] 24 p3375 N88-30098

HOLOGRAPHY
NT SPECKLE HOLOGRAPHY
NT WHITE LIGHT HOLOGRAPHY
Implementation of a digital optical matrix-vector multiplier using a holographic look-up table and residue arithmetic
[NASA-CR-180431] 01 p0078 N88-10496
Ultrafast holography using optical fibers
[ISL-R-101/86] 02 p0176 N88-11096
Computed neutron tomography and coded aperture holography from real time neutron images
04 p0427 N88-12645
Measurement and control of damage in composite materials: Nondestructive controls by thermography, holography, and radiography
[SNIAS-872-430-110] 05 p0559 N88-13403
The production of ultrasmall and superfine holographic diffraction gratings using synchrotron radiation and lithographic techniques
[AD-A185395] 05 p0585 N88-13562
Determination of a flow velocity field using four-exposure laser holography
[IMFL-3114-85/32] 05 p0585 N88-13565
Selection of holographic screen for projection of images reconstructed by multiaspect holograms of focused images
06 p0773 N88-14745
Online monitoring of laserpulses using the GPIB-interface of a Tektronix 2430 Digital Storage Oscilloscope
[DE88-002836] 07 p0856 N88-15201
Scanning and measuring peculiarities with high-space resolution objects recorded at the Gabor holograms
[DE88-700373] 07 p0857 N88-15203
Holography of the ionosphere at HIPAS
[AD-A186237] 07 p0877 N88-15322
Multilayer holographic functional element in analog-digital converter 07 p0921 N88-15593
Resolution of holograms produced by the fluid experiment system and the holography ground system
07 p0923 N88-15609
Cavitation inception scale effects. 1. Nuclei distributions in natural waters. 2. Cavitation inception in a turbulent shear flow
[AD-A186553] 08 p0988 N88-15987
Formation of high-coherence radiation in free-running mode ruby laser for pulse holography
08 p1077 N88-16497
A holographic investigation of particulates in metallized solid fuel ramjet combustion
[AD-A186887] 09 p1140 N88-16831
Holographic investigation of metallized solid propellant combustion in two-dimensional and three-dimensional rocket motors
[AD-A187000] 09 p1140 N88-16832
Calculation of noise in spatial speckle-field holograms under conditions of saturated photoresponse
09 p1235 N88-17403
Color shadow methods of analyzing reconstructed wave front 09 p1236 N88-17407
Kinetics and spectrum of light pulse used in picosecond holography 09 p1236 N88-17409
Measuring accuracy of 3-dimensional bodies by the GOMER-1 device
[DE87-703230] 12 p1628 N88-19744
Holographically correcting synthetic aperture aberrations
[AD-A189510] 12 p1692 N88-20123
Development of fiber optic systems for recording and transmitting holographic information
[AD-A189406] 13 p1773 N88-20603
ONR Far East Scientific Bulletin, volume 12, number 3, July-September 1987
[AD-A188554] 13 p1851 N88-21081
Holographic disk for data storage
14 p1972 N88-21771
MIG-1 on-line measuring holographic microscope
[DE88-701103] 15 p2068 N88-22332
Focused image holography abberations
[DE88-701105] 15 p2068 N88-22333
A review on holography, its principles and applications
[ISL-CO-242/86] 15 p2069 N88-22338
Space-variant optical systems
[AD-A189967] 15 p2133 N88-22724
The use of a water towing tank for aerodynamic testing and methods for quantitative evaluation of photographs
16 p2202 N88-23140
Flow measurements in a water tunnel using a holocinematographic velocimeter
16 p2203 N88-23141
Application of high speed holography to aerodynamic and hydrodynamic three-dimensional velocimetry
16 p2203 N88-23144
Study of flow tracer behavior models and experimental validation with multiple exposure holographic velocimetry
[IMFL-87/30] 20 p2801 N88-26622
Interferometric recording of holographic optical elements using partially coherent light
20 p2805 N88-26636
Active phase compensation system for fiber optic holography
[NASA-TM-101295] 20 p2805 N88-26641
Optical data processing
[AD-A193024] 20 p2839 N88-26841
Precise rotational alignment of X-ray transmission diffraction gratings
[DE88-010599] 21 p2911 N88-27273
Holographic determination of droplet size distributions
[DFVLR-MITT-88-05] 22 p3074 N88-28250
Noise generation and boundary layer effects in vortex-airfoil interaction and methods of digital hologram analysis for these flow fields
[AD-A194191] 23 p3171 N88-28883
Hologram representation of design data in an expert system knowledge base 23 p3251 N88-29354
Automatic data retrieval from rocket motor holograms
[AD-A195586] 24 p3337 N88-29864
Evaluation of multi-focus holographic lenses
[AD-A196167] 24 p3377 N88-30110
High-resolution (30 m) lunar radar images
24 p3442 N88-30486

HOLOMORPHISM
U ANALYTIC FUNCTIONS

HOMEOSTASIS
Physicochemical correlates of human adaptation to extreme environments 06 p0750 N88-14607
Mother-fetus system as object for investigation of mechanisms of physiological effect of weightlessness
07 p0891 N88-15402
Spleen lymphocyte nucleic acids in pregnant rats flown in space and their offspring 07 p0892 N88-15403
Role of testing total gas (O2 and CO2) tension of blood plasma in the study of human gas homeostasis
07 p0894 N88-15419
JPRS Report: Science and Technology. USSR: Space Biology and Aerospace Medicine, volume 21, no. 5, September - October 1987
[JPRS-USB-88-003] 10 p1359 N88-18122
Effect of spaceflight factors on primate hydration homeostasis 10 p1360 N88-18126
Discrete adaptation to sensory conflict
10 p1363 N88-18146
The influence of space flight on water-salt homeostasis in man and animals 12 p1659 N88-19943
Human adaptation to various hypercapnic conditions in relation to salivary electrolyte dynamics and renal function 12 p1664 N88-19977

HOMING
Optimal guidance of homing missiles
06 p0671 N88-14111
Effects of closing speed uncertainty on optimal guidance 12 p1597 N88-19556

HOMING DEVICES
The impact of environmental factors on the performance of millimeter wave seekers in smart munitions
[DE87-014277] 03 p0270 N88-11697
Optimal guidance of homing missiles
06 p0671 N88-14111
Advanced guidance algorithms for homing missiles with bearings-only measurements
[AD-A190435] 15 p2017 N88-22026

HOMODYNE RECEPTION
Coherent infrared detection, volume B — CO2 laser intersatellite data link
[ESA-CR(P)-2392-VOL-1] 01 p0034 N88-10218
Coherent infrared detection, volume D — CO2 laser intersatellite data link
[ESA-CR(P)-2392-VOL-2] 01 p0034 N88-10219

HOMOGENEITY
The dishomogeneity of the degree of sensitization in large recirculation pipes in Boiling Water Reactor (BWR) power plants
[CISE-3955] 09 p1247 N88-17473
The h-p version of the finite element method for problems with nonhomogeneous essential boundary condition
[AD-A187356] 10 p1400 N88-18348
Inversion of parabolic and paraboloidal projections
[AD-A187538] 10 p1405 N88-18380
Notes on a class of homogeneous space-times
[DE88-700138] 11 p1562 N88-19353
Decomposition of hypochlorite in the presence of copper in a homogeneous medium
[NASA-TT-20199] 13 p1740 N88-20403
Local structure of intercomponent energy transfer in homogeneous turbulent shear flow
16 p2197 N88-23103
Kinetics of homogeneous nucleation in superheated F-11 and F-21 liquid freons
[NASA-TT-20286] 19 p2613 N88-25503
Off-boundary approach to the boundary element method
[AD-A192931] 20 p2815 N88-26701
Homogeneity of glasses: Experiment WL-IHF-05 in D1 mission — Spacelab
[ETN-88-92339] 21 p2924 N88-27353

HOMOGENEOUS TURBULENCE
Center for Turbulence Research 1987 activities
[NASA-CR-182693] 13 p1769 N88-20583
Dense-spray structure and phenomena. Part 1. Turbulence/dispersed-phase interactions
[AD-A190606] 15 p2065 N88-22315
Reynolds stress models of homogeneous turbulence
16 p2197 N88-23106
Evaluation of a theory for pressure-strain rate
16 p2198 N88-23108
Relations between two-point correlations and pressure strain terms 16 p2198 N88-23109
Coherent structures: Comments on mechanisms
16 p2199 N88-23118
On the prediction of equilibrium states in homogeneous turbulence
[NASA-CR-181659] 16 p2207 N88-23174
Numerical simulation of compressible homogeneous turbulence: Effects of fluid compressibility
[PB88-127154] 19 p2597 N88-25433
Development of a more general Reynolds stress closure for swirling flow
[AD-A195121] 24 p3374 N88-30092

HOMOGENIZATION
U HOMOGENIZING

HOMOGENIZING
Homogenization study of matrix behavior in a composite material
[ONERA-RT-1/7256-RY-060-R]
16 p2172 N88-22943
Functional and mechanical analysis of continuous media-application to the study of elastic composites with periodic structure: Homogenization
[NASA-TT-20188] 18 p2480 N88-24710

HOMOMORPHISMS
NT AUTOMORPHISMS

HOMOTOPY THEORY
A polynomial approach to the H sub infinity control design method
[MEMO-662] 14 p1962 N88-21701
Edge-disjoint homotopic paths in straight-line planar graphs
[CWI-OS-R8718] 16 p2264 N88-23537
Decomposition of graphs on surfaces and a homotopic circulation theorem
[CWI-OS-R8719] 16 p2264 N88-23538

HONEYCOMB CORES
Core material — honeycombs
[EP-PATENT-0-196-926-A2] 05 p0558 N88-13393

HONEYCOMB STRUCTURES
NT HONEYCOMB CORES
Solar converging method 04 p0403 N88-12504
Advanced radiator concepts utilizing honeycomb panel heat pipes
[NASA-CR-172017] 04 p0443 N88-12747
Influence of bonding shop moisture on metal-honeycomb junctions bonded with ultra-thin adhesive films
[SNIAS-872-422-112] 05 p0558 N88-13399
A comparison of experimental and theoretical results for labyrinth gas seals with honeycomb stators
[NASA-CR-182441] 08 p0993 N88-16006
Experimental rotordynamic coefficient results for honeycomb seals
[NASA-CR-182440] 08 p0993 N88-16007

HOOKES LAW
Kinematics of Hooke universal joint robot wrists
[NASA-TM-100567] 20 p2843 N88-26870

HOOP COLUMN ANTENNAS
Studies of the structural dynamic behavior of satellite antenna system
[AD-A185526] 06 p0673 N88-14121
The 15-meter diameter hoop/column antenna surface control actuator system 14 p1924 N88-21469

HOPPERS
Energy efficient continuous flow ash lockhopper
[NASA-CASE-NPO-16985-1-CU]
18 p2497 N88-24814

HORIZON
Satellite autonomous navigation with SHAD (Stellar Horizon Atmospheric Dispersion)
[AD-A184988] 05 p0544 N88-13313

HORIZON SCANNERS
High lifetime mechanisms implemented in infrared horizon scanning sensors — SPOT
14 p1877 N88-21214

HORIZON SENSING
U HORIZON SCANNERS

HORIZONTAL FLIGHT
Flap-lag-torsion aeroelastic stability of a circulation control rotor in forward flight 10 p1271 N88-17600
HORIZONTAL ORIENTATION
Large-scale horizontal flows from SOUP observations of solar granulation 02 p0256 N88-11621
Effects of combining vertical and horizontal information into a primary flight display
[NASA-TP-2783] 04 p0399 N88-12487
Aircraft engine exhaust plume dynamics
[AD-A184238] 04 p0400 N88-12488
Study on a rotor speed control system for a horizontal axis windmill
[NAL-TR-931] 10 p1349 N88-18062
State-of-the-art for assessing earthquake hazards in the US. Parameters for specifying intensity-related earthquake ground motions
[AD-A188230] 11 p1512 N88-19032
A polarization diversity meteorological radar system
[AD-A189291] 13 p1758 N88-20515
Fatigue load measurements and evaluation of the 25m Horizontal Axis Wind Turbine (HAWT) at Petten, The Netherlands
[NLR-MP-86054-U] 13 p1782 N88-20660
HORIZONTAL STABILIZERS
U STABILIZERS (FLUID DYNAMICS)
HORMONE METABOLISMS
Is ANF implied in the night attenuated renal response to central hypervolemia? 12 p1659 N88-19945
Renal effects of anti-gravity suit inflation in man in relation to cardiovascular and hormonal changes 12 p1661 N88-19959
HORMONES
NT ALDOSTERONE
NT CORTICOSTEROIDS
NT PITUITARY HORMONES
Cosmonauts' hormonal responses after brief spaceflights 07 p0890 N88-15394
Effect of steroid hormones on biogenic amine levels in lungs during development of pulmonary hypertension in rats submitted to chronic hypobaric hypoxia 07 p0896 N88-15430
Certain aspects of human metabolism during spaceflights of varying duration
[NASA-TT-20215] 10 p1369 N88-18181
Endocrine responses to resistance exercise
[AD-A188681] 12 p1667 N88-19993
Hormonal regulation of fluid and electrolytes: Effects of heat exposure and exercise in the heat
[AD-A192655] 22 p3131 N88-28614
HORNS
Horn design equations for the NBS (National Bureau of Standards) horn-type noise standards
[PB88-110226] 07 p0844 N88-15122
HOSES
Variable collision frequency effects on hose and sausage instabilities in relativistic electron beams
[AD-A184206] 04 p0490 N88-13021
HOT AIR
U HIGH TEMPERATURE AIR
HOT CORROSION
Optimizing the application of high temperature corrosion resistant aluminium-silicon-base coatings
[BLL-M-37222-(5828.4)] 01 p0018 N88-10112
Turbine airfoil deposition models and their hot corrosion implications 02 p0189 N88-11178
Experimental verification of vapor deposition rate theory in high velocity burner rigs 02 p0189 N88-11179
Effects of surface chemistry on hot corrosion life 02 p0189 N88-11180
Reaction mechanism of sulfur dioxide with single crystal cobalt and chromium and CoCrAlY coatings
[AD-A185989] 09 p1253 N88-17509
High temperature oxidation and electrochemical studies related to hot corrosion
[AD-A190699] 15 p2040 N88-22156
Corrosion Research Center, University of Minnesota
[DE88-006681] 15 p2041 N88-22160
High temperature corrosion of ceramics
[DE88-006567] 15 p2046 N88-22193
Vanadic hot corrosion of gas turbine blade coating materials 17 p2321 N88-23864
Molten salt corrosion of SiC and Si3N4 17 p2325 N88-23885
Guide to the control of high temperature corrosion and protection of gas turbine materials
[PB88-107412] 20 p2760 N88-26370
HOT ELECTRONS
Long wavelength vortices of low frequency interchange modes
[IPPJ-844] 02 p0241 N88-11525
A ray-tracing study of electron cyclotron resonance heating in tokamak plasmas with a superthermal electron tail
[INPE-4381-PRE/1201] 08 p1085 N88-16536
Absorption of electron cyclotron radiation in tokamak plasmas with a superthermal tail in the electron velocity distribution
[INPE-4391-PRE/1211] 08 p1086 N88-16541
Investigations of stimulated Raman scattering from high density underdense plasmas irradiated by a 0.35 micron laser 10 p1411 N88-18421
Hot electron diagnostics using X-ray imaging on GAMMA10 17 p2443 N88-24530
Resonant tunneling electron spectroscopy 19 p2660 N88-25811
Third International Conference on Superlattices, Microstructures and Microdevices
[AD-A191416] 20 p2861 N88-26995
Hot electron transistors grown by MOCVD 20 p2861 N88-26996
Hot electrons in silicon dioxide: Ballistic to steady-state transport 20 p2871 N88-27042
Recent applications of Monte Carlo methods for semiconductor microdevice simulation 20 p2871 N88-27046
Studying the physics and operation of multi-terminal near-micron and sub-micron length, hot electron semiconductor devices
[AD-A193380] 21 p2938 N88-27446
Hot electron emission in semiconductors
[AD-A194101] 23 p3292 N88-29601
HOT EXTRUDING
U EXTRUDING
HOT FORMING
U HOT WORKING
HOT GAS SYSTEMS
U HIGH TEMPERATURE GASES
HOT GASES
U HIGH TEMPERATURE GASES
HOT ISOSTATIC PRESSING
Hot isostatic pressing of nickel aluminide powders
[DE88-009677] 19 p2617 N88-25525
HOT JET EXHAUST
U HIGH TEMPERATURE GASES
U JET EXHAUST
HOT JETS
U JET FLOW
HOT PLASMAS
U HIGH TEMPERATURE PLASMAS
HOT PRESSING
NT HOT ISOSTATIC PRESSING
Isothermal forging and its effect on the microstructure of powder route nickel alloy AP1
[RAE-TM-P-1094] 01 p0022 N88-10138
Characterization and thermal conductivity of hot-pressed silicon carbide
[DKG-25] 03 p0292 N88-11834
Deformation mechanisms of thermostructural materials
[AD-A184070] 03 p0338 N88-12128
Fabrication and materials evaluation of high performance aligned ceramic fibre reinforced glass matrix composite
[AERE-R-12517] 10 p1294 N88-17736
Molybdenum-base cermet fuel development
[DE88-005529] 13 p1839 N88-21003
Processing, physical metallurgy and creep of NiAl + Ta and NiAl + Nb alloys
[NASA-CR-182113] 14 p1890 N88-21295
Processing, microstructure, and mechanical properties of silicon carbide particulate reinforced aluminum alloys
[AD-A188981] 15 p2037 N88-22136
Strength optimization of alpha-SiC by improved processing 17 p2324 N88-23880
Improved silicon nitride for advanced heat engines 17 p2324 N88-23881
Molybdenum-base cermet fuel development 17 p2434 N88-24481
Martensitic transformation and microstructures in sintered NiAl alloys
[NASA-TT-20178] 18 p2488 N88-24761
Martensitic transformation and microstructures in sintered NiAl alloys
[NASA-TT-20192] 19 p2616 N88-25519
Hot isostatic pressing of tungsten-nickel-iron composites
[FOA-C-20698-2.1] 22 p3056 N88-28135
HOT STARS
NT A STARS
NT B STARS
NT O STARS
NT WHITE DWARF STARS
NT WOLF-RAYET STARS
Literature survey relating to the absorption properties of ozone in the near ultraviolet
[ESRO-SM-81] 09 p1190 N88-17129
Time-dependent mass loss from hot stars with and without radiative driving
[DE88-008899] 20 p2884 N88-27128
Evolutionary helium and CNO anomalies in the atmospheres and winds of massive hot stars
[NASA-CR-183254] 24 p3452 N88-30550
HOT SURFACES
Recent advances in high temperature instrumentation for hot section applications
[NASA-TM-100282] 06 p0707 N88-14339
Structural analysis methods development for turbine hot section components
[NASA-TM-100298] 11 p1501 N88-18967
On 3-D inelastic analysis methods for hot section components. Volume 1: Special finite element models
[NASA-CR-180893] 14 p1934 N88-21535
Diamond film by hot filament CVD method
[NASA-TT-20335] 23 p3294 N88-29618
Constitutive modeling for isotropic materials
[NASA-CR-182132] 24 p3327 N88-29811
HOT WORKING
Advances in processing techniques for nickel aluminides
[DE87-014571] 05 p0566 N88-13449
Method of obtaining of fire resistant polyacrylonitrile fiber or cloth from it
[AD-A185941] 07 p0836 N88-15071
Statistical analysis of feasibility of non-destructive inspection of mechanical properties of hot worked pipes of alloy steels
[BLL-M-37598-(5828.4)] 14 p1922 N88-21455
HOT-FILM ANEMOMETERS
The design and use of a temperature-compensated hot-film anemometer system for boundary-layer flow transition detection on supersonic aircraft
[NASA-TM-100421] 13 p1723 N88-20304
Crossflow vorticity sensor
[NASA-CASE-LAR-13436-1-CU] 17 p2300 N88-23759
Method of forming a multiple layer dielectric and a hot film sensor therewith
[NASA-CASE-LAR-13678-1] 18 p2584 N88-25355
The use of hot-film technique for boundary layer studies on a 21 percent thick airfoil
[NAE-AN-45] 24 p3321 N88-29781
HOT-WIRE ANEMOMETERS
Turbulence measurement in hypersonic flow 05 p0530 N88-13224
Hot wire and laser velocimeter studies of turbulent flow at supersonic velocities
[ETN-88-91172] 05 p0585 N88-13566
Studies of supersonic turbulence and hot-wire response using Laser-Induced Fluorescence (LIF) 06 p0664 N88-14072
Flow field measurements using hotwire anemometry
[AD-A187029] 09 p1160 N88-16951
Calibration of a hot-wire/hot-film anemometer over a range of temperatures, velocities and pressures
[AD-A189717] 14 p1913 N88-21430
Development of a hot-wire measurement technique for moderate intensity three-dimensional flows 22 p3080 N88-28289
Calibration of a triple wire probe for turbulence measurements
[AD-A193956] 22 p3081 N88-28296
HOT-WIRE FLOWMETERS
Development of subminiature multi-sensor hot-wire probes
[NASA-TM-100052] 15 p2069 N88-22336
On experiences with two hot-wire instruments for measuring the liquid water content in clouds
[ESA-TT-1085] 23 p3236 N88-29255
HOT-WIRE TURBULENCE METERS
U HOT-WIRE FLOWMETERS
U TURBULENCE METERS
HOTOL LAUNCH VEHICLE
Hypersonic aerodynamics: Applications for HOTOL 05 p0535 N88-13252
HOTSHOT WIND TUNNELS
The aerodynamic design of hypersonic contoured axisymmetric nozzles including real gas effects
[VKI-TM-43] 06 p0665 N88-14076
HOUSEKEEPING (SPACECRAFT)
Contamination control of the space shuttle Orbiter crew compartment 02 p0133 N88-10834
Development of response models for the Earth Radiation Budget Experiment (ERBE) sensors. Part 3: ERBE scanner measurement accuracy analysis due to reduced housekeeping data
[NASA-CR-178294] 05 p0583 N88-13553
HOUSINGS
NT COWLINGS
Gas erosion of impeller housing in the operation of a high-temperature, high-pressure helium circulator
[DE88-002607] 09 p1175 N88-17041
Cast iron-base alloy for cylinder/regenerator housing
[NASA-CR-182116] 12 p1608 N88-19613

A review of gear housing dynamics and acoustics literature
[NASA-CR-183110] 20 p2811 N88-26675
HOVERCRAFT
U GROUND EFFECT MACHINES
HOVERING
Detection of targets in the presence of clutter using target echo modulations caused by rotating structures
[REPT-12-86] 01 p0036 N88-10231
Investigation of vertical axis handling qualities for helicopter hover and NOE flight 03 p0263 N88-11653
Handling qualities criterion for very low visibility rotorcraft 03 p0263 N88-11654
Modeling XV-15 tilt-rotor aircraft dynamics by frequency and time-domain identification techniques 03 p0263 N88-11657
Hovering helicopter flight dynamics: A study of vertical motion
[AR-004-526] 04 p0399 N88-12485
Solution procedure for the Navier-Stokes equations applied to rotors 05 p0579 N88-13533
Development of an unsteady wake theory appropriate for aeroelastic analyses of rotors in hover and forward flight
[NASA-CR-182357] 06 p0664 N88-14075
Preliminary airworthiness evaluation of a UH-1 equipped with a terrain mapping receiver antenna
[AD-A186274] 07 p0819 N88-14980
A dynamic simulation and feedback control scheme for the U.S. Marine Corps' Airborne Remotely Operated Device (AROD)
[AD-A186597] 08 p0953 N88-15784
The maximum entropy method for the analysis of radar echoes from hovering helicopters in clutter
[FB-2-87] 11 p1475 N88-18799
An experimental investigation of the flap-lag-torsion aeroelastic stability of a small-scale hingeless helicopter rotor in hover
[NASA-TP-2546] 13 p1715 N88-20257
Experimental investigation of Hover flowfields in water at the McDonnell Douglas Research Laboratories 16 p2202 N88-23135
Method for prediction and determination of takeoff performance for vectored thrust vehicles
[AD-A191809] 18 p2463 N88-24626
Operational noise data for CH-47D and AH-64 army helicopters
[AD-A191059] 18 p2570 N88-25263
Hover performance tests of baseline metal and Advanced Technology Blade (ATB) rotor systems for the XV-15 tilt rotor aircraft
[NASA-CR-177436] 20 p2759 N88-26367
A comparison of theory and experiment for coupled rotor-body stability of a hingeless rotor model in hover 21 p2889 N88-27152
A comparison of theory and experiment for coupled rotor body stability of a bearingless rotor model in hover and forward flight 21 p2890 N88-27154
Effects of static equilibrium and higher-order nonlinearities on rotor blade stability in hover 21 p2890 N88-27157
A conceptual design study of a hovering system controller for an autonomous underwater vehicle
[AD-A193423] 21 p2930 N88-27399
Euler equation computations for the flow over a hovering helicopter rotor
[NASA-CR-177493] 22 p3038 N88-28037
The maximum entropy method for the analysis of short-time radar echoes from hovering helicopters 22 p3149 N88-28737
The radar detection of hovering helicopters 22 p3150 N88-28739
HR DIAGRAM
U HERTZSPRUNG-RUSSELL DIAGRAM
HRB-1 HELICOPTER
U CH-46 HELICOPTER
HTGR
U HIGH TEMPERATURE GAS COOLED REACTORS
HTPB PROPELLANTS
Review of research concerning Solid Fuel Ramjet (SOFRAM) at the Research Institute of National Defence (FOA) 2
[FOA-C-20714-2.1] 24 p3327 N88-29813
Thermomechanical computations for GAP, a high energy binder for composite propellants
[FOA-C-20718-2.1] 24 p3357 N88-29988
HU-1 HELICOPTER
U UH-1 HELICOPTER
HUBBLE CONSTANT
Crucial cosmological observations
[DE87-703081] 02 p0251 N88-11587
String driven inflation
[DE88-006994] 15 p2151 N88-22841
HUBBLE SPACE TELESCOPE
Department of Housing and Urban Development-Independent Agencies Appropriations for fiscal year 1988, Friday, 10 April 1987: National Aeronautics and Space Administration 03 p0386 N88-12425
HSTDEK: Developing a methodology for construction of large-scale, multi-use knowledge bases 08 p1057 N88-16377
Knowledge-based monitoring of the pointing control system on the Hubble space telescope 08 p1057 N88-16378
A distributed architecture for intelligent monitoring and anomaly diagnosis of the Hubble Space Telescope 08 p1057 N88-16379
A knowledge-based system for monitoring the electrical power system of the Hubble Space Telescope 08 p1058 N88-16380
Artificial intelligence and space power systems automation 08 p1058 N88-16381
A multiprocessing architecture for real-time monitoring 08 p1059 N88-16390
ESA Bulletin No. 8
[ETN-87-90513] 09 p1122 N88-16718
The 2.4 m Space Telescope and ESA participation in the program 09 p1123 N88-16721
Deep space target location with Hubble Space Telescope (HST) and Hipparcos data
[NASA-CR-182520] 10 p1427 N88-18524
TALOS: A distributed architecture for intelligent monitoring and anomaly diagnosis of the Hubble Space Telescope 17 p2388 N88-24193
Automated generation of spacecraft activity plans 23 p3258 N88-29396
Knowledge based tools for Hubble Space Telescope planning and scheduling: Constraints and strategies 24 p3417 N88-30338
The proposal entry processor: Telescience applications for Hubble Space Telescope science operations 24 p3417 N88-30339
Lisp Object State Saver (LOSS): A facility used to save partial schedules of the Hubble Space Telescope 24 p3421 N88-30360
HUBS
Impacts of rotor hub design criteria on the operational capabilities of rotorcraft systems 03 p0264 N88-11663
A129 advanced solutions for meeting today's combat helicopter requirement 03 p0265 N88-11669
A comparison of theory and flight test of the BO 105/BMR in hover and forward flight 21 p2890 N88-27155
HUGHES AIRCRAFT
NT AH-64 HELICOPTER
HUGHES MILITARY AIRCRAFT
U MILITARY AIRCRAFT
HULLS (STRUCTURES)
NT SHIP HULLS
Response of SMA (Shielded Metal Arc) and narrow gap HY80 weldments to explosive shock loading
[AD-A195994] 24 p3385 N88-30162
HUMAN BEHAVIOR
Studies of the processing of single words using positron tomographic measures of cerebral blood flow change
[AD-A184058] 03 p0356 N88-12244
Human adaptation to isolated and confined environments
[NASA-CR-181502] 03 p0357 N88-12248
A simulation study of a speed control system for autonomous on-road operation of automotive vehicles
[AD-A184030] 03 p0362 N88-12279
Complex sound processing: An interdisciplinary approach
[AD-A189782] 15 p2102 N88-22523
The representational code of the internal model of dynamic systems: An individual differences and dual task approach
[AD-A190876] 16 p2244 N88-23403
Performance effectiveness and the work/rest cycle
[AD-A191448] 18 p2551 N88-25145
Attitudes towards the cold: Effects on psychological mood and subjective reports of illness during cold weather training
[AD-A194777] 23 p3239 N88-29274
Contributions to engineering models of human-computer interaction, volume 1
[AD-A195590] 24 p3409 N88-30295
HUMAN BEINGS
Cirrus: An automated protocol analysis tool
[AD-A186646] 08 p1052 N88-16348
Experimental measurements of the uptake of ozone in rats and human subjects
[PB88-125422] 10 p1364 N88-18149
Certain aspects of human metabolism during spaceflights of varying duration
[NASA-TT-20215] 10 p1369 N88-18181
Modeling of the non-auditory response to blast overpressure
[AD-A187397] 10 p1369 N88-18184
Methods of eliciting information from experts
[AD-A187468] 10 p1372 N88-18189
Critical phenomena and electromagnetic effects in biological membranes
[AD-A188156] 11 p1518 N88-19064
Motor control in man and monkey 11 p1518 N88-19065
Motion sickness: A study of its effects on human physiology
[AD-A188821] 12 p1667 N88-19995
Pursuit tracking performance decrements associated with decreasing ambient illumination
[AD-A189336] 13 p1809 N88-20809
Evaluation of existing total human exposure models
[PB88-146840] 15 p2101 N88-22517
Auditory pattern memory: Mechanisms of tonal sequence discrimination by human observers
[AD-A190337] 15 p2104 N88-22534
Extension of computer based algorithms by operator analysts
[NASA-CR-182798] 15 p2111 N88-22575
The event-related brain potential as an index of information processing and cognitive activity: A program of basic research
[AD-A191244] 16 p2243 N88-23400
Activation, strength and endurance of human respiratory and limb muscles 17 p2381 N88-24158
Effects of pulsed and CW (Continuous Wave) 2450 MHz radiation on transformation and chromosomes of human lymphocytes in vitro
[AD-A193104] 21 p2987 N88-27736
Demodulation processes in auditory perception
[AD-A193421] 21 p2988 N88-27740
SQUID (superconducting quantum interference device) arrays for simultaneous magnetic measurements: Calibration and source localization performance
[AD-A193815] 23 p3216 N88-29143
Currents induced in a human being for electromagnetic fields to 10 kHz-50 MHz
[AD-A191977] 23 p3238 N88-29268
Human auditory and visual continuous evoked potentials 23 p3238 N88-29269
Limits of pattern discrimination in human vision
[AD-A193449] 23 p3239 N88-29273
Methods and instrumentation for biomagnetism
[AD-A193811] 23 p3239 N88-29278
Visual motion perception and visual attentive processes
[AD-A193640] 23 p3241 N88-29288
Multilevel computational theory of stereoscopic visual image processing
[AD-A195331] 24 p3408 N88-30288
Eye movements and spatial pattern vision
[AD-A195496] 24 p3408 N88-30290
Haptic exploration in humans and machines: Attribute integration and machine recognition/implementation
[AD-A193692] 24 p3410 N88-30299
HUMAN BODY
Human physical fields 06 p0750 N88-14609
Proceedings and program draft in Gravitational Biology in the Federal Republic of Germany --- Effects of Weightlessness on the Human Organism
[ESA-TT-988] 07 p0884 N88-15363
Operation Everest 2: Nutrition and body composition
[AD-A186449] 08 p1049 N88-16333
Lifting and carrying capacities relative to physical fitness measures
[AD-A189305] 13 p1809 N88-20808
Anthropomorphic phantom radiation dosimetry at the NATO standard reference point at Aberdeen Proving Ground
[AD-A190508] 15 p2103 N88-22528
Experimental research on skin reflection, transmission, absorption of light rays 16 p2187 N88-23039
Physiological effects on man of long duration confinement in a carbon dioxide enriched environment 19 p2695 N88-26017
Behavioral, psychological and demographic predictors of physical fitness
[AD-A192697] 21 p2986 N88-27733
HUMAN CENTRIFUGES
The rate of adaptation to altered g in the human centrifuge: Implications for simulations of mass-discrimination in space flight 12 p1659 N88-19941
Physiological monitoring methodology in the USAFSAM centrifuge 21 p2924 N88-27356
HUMAN ENGINEERING
U HUMAN FACTORS ENGINEERING
HUMAN FACTORS ENGINEERING
NT MOTION SIMULATION
Human factors in robotic system design discussed 02 p0158 N88-10988

A research on pilot performance in a flight incident situation
[ETN-87-90653] 02 p0217 N88-11370
Computer-controlled testing of visual-spatial ability
[AD-A183971] 03 p0357 N88-12249
Report of the helicopter human factors working group --- accident prevention
[CAA-PAPER-87007] 03 p0361 N88-12274
A scientific workstation operator-interface for accelerator control
[DE87-014689] 03 p0362 N88-12278
Research papers and publications (1981-1987): Workload research program
[NASA-TM-100016] 04 p0474 N88-12924
Human engineering laboratory grounding analysis (HELGA)-2
[AD-A185367] 05 p0578 N88-13524
Sitting posture of helicopter pilots of the Royal Netherlands Air Force; preliminary recommendations
[IZF-1986-16] 05 p0631 N88-13857
Research and development of anti-G life support systems. Part 1: Development and evaluation of uniform-pressure anti-G suits
[AD-A185658] 06 p0754 N88-14628
Tools and technologies for expert systems: A human factors perspective 06 p0797 N88-14882
New US book on aviation psychology reviewed 07 p0896 N88-15433
Human performance data needed for training device design decisions
[AD-A185988] 07 p0898 N88-15441
Using multiple dialog modes in a user-system interface to accomodate different levels of user experience: An experimental study
[AD-A186115] 07 p0899 N88-15444
Development of Soviet state ergonomic standards (GOST)
[AD-A185536] 07 p0899 N88-15449
Soviet state ergonomic standards (GOST)
[AD-A185537] 07 p0900 N88-15450
Proceedings of the DOD Workload Assessment Workshop on Workload Assessment Techniques and Tools held in Dayton, Ohio on 27-28 September 1986
[AD-A185650] 08 p1052 N88-16352
Development of a menu of performance tests self-administered on a portable microcomputer
[NASA-CR-172040] 08 p1067 N88-16452
Helicopter human factors research 09 p1109 N88-16644
An integrated approach to rotorcraft human factors research 09 p1110 N88-16653
Dynamic function allocation in fighter cockpits
[AD-A185397] 09 p1201 N88-17199
Air Force Human Resources Laboratory technical reports and technical papers
[AD-A186830] 09 p1201 N88-17200
Comparison of alphanumeric data entry methods for advanced helicopter cockpits
[AD-A186934] 09 p1201 N88-17201
Ergonomics of car controls for disabled people, phase 1. Part 1: Chapters 1-7. Part 2: Appendices. Part 3: References
[ISBN-0-947767-82-7] 09 p1202 N88-17204
Systems integrated human engineering on the Navy's rapid acquisition of manufactured parts/test and integration facility 09 p1206 N88-17226
User engineering: A new look at system engineering 09 p1206 N88-17231
Surrogate measures: A proposed alternative in human factors assessment of operational measures of performance 09 p1215 N88-17281
Information transfer in the National Airspace System 10 p1275 N88-17634
Cockpit data management
[NASA-CR-178407] 11 p1438 N88-18579
Spacecraft fire detection and extinguishment: A bibliography
[NASA-CR-180880] 11 p1444 N88-18612
A worked example of an application of the SAINT simulation program
[AD-A188198] 11 p1524 N88-19097
Night Vision: Current Research and Future Directions, symposium proceedings
[PB88-132006] 11 p1550 N88-19274
Characteristics of the thermal environment
[AD-A188359] 12 p1641 N88-19827
Space Station Human Factors Research Review. Volume 3: Space Station Habitability and Function: Architectural Research
[NASA-CP-2426-VOL-3] 12 p1650 N88-19883
Space station architectural elements model study. Space station human factors research review 12 p1650 N88-19884
Space station group activities habitability module study: A synopsis 12 p1651 N88-19886
Full scale architectural simulation techniques for space stations 12 p1651 N88-19887
Social factors in space station interiors 12 p1651 N88-19888
Human factor in engineering work 12 p1663 N88-19970
JPRS report: Science and technology. USSR: Life sciences
[JPRS-ULS-88-002] 12 p1665 N88-19982
User perceptions of side-arm flight control in rotary-wing aircraft
[AD-A188519] 12 p1672 N88-20009
Multi-crew pictorial format display evaluation
[AD-A189349] 13 p1812 N88-20824
Advanced human factors engineering tool technologies
[AD-A189390] 13 p1812 N88-20825
Incorporation of privacy elements in space station design
[NASA-CR-182748] 14 p1881 N88-21242
Human interfaces in remote driving
[DE88-006843] 14 p1953 N88-21643
Napping and human functioning during prolonged work
[AD-A190228] 15 p2102 N88-22525
Psychosensory cockpit ergonomics, advantages of intelligent information systems 17 p2304 N88-23784
Designing for design effectiveness of complex avionics systems 17 p2305 N88-23788
Experience in the integration of human engineering effort with avionics systems development 17 p2305 N88-23793
A look toward the future of complex avionics systems development using the USAF Test Pilot School's avionics systems test training aircraft 17 p2306 N88-23797
Space Station Human Factors Research Review. Volume 1: EVA Research and Development
[NASA-CP-2426-VOL-1] 17 p2379 N88-24145
Space Station Human Factors Research Review. Volume 4: Inhouse Advanced Development and Research
[NASA-CP-2426-VOL-4] 17 p2380 N88-24148
Teleoperator human factors study
[NASA-CR-178930] 17 p2382 N88-24162
SP-100 ground engineering systems test facility control systems 17 p2436 N88-24496
Space station architectural elements model study
[NASA-CR-4027] 18 p2464 N88-24632
Evaluation of the US Army fitting program for the integrated helmet unit of the integrated helmet and display sighting system
[AD-A191616] 18 p2465 N88-24635
Human problem solving in complex dynamic environments
[AD-A190788] 18 p2551 N88-25142
An advanced prototyping tool for human factors design
[AD-A187290] 18 p2552 N88-25149
Human performance issues arising from manned space station missions
[NASA-CR-3942] 18 p2553 N88-25156
Space station habitability recommendations based on a systematic comparative analysis of analogous conditions
[NASA-CR-3943] 18 p2587 N88-25372
Similarities between diving operations and space missions 19 p2697 N88-26027
Ergonomy and interior furnishing of the cabins of deep diving manned submarines: The Nautile example --- couch 19 p2697 N88-26032
Habitability of the Space Station: From vehicle to living space 19 p2697 N88-26033
Recent research on crew wardroom habitability for the Space Station 19 p2698 N88-26039
Introduction to human factors
[DE88-009021] 19 p2711 N88-26103
Computer simulation of multiple pilots flying a modern high performance helicopter
[NASA-TM-100183] 20 p2761 N88-26377
A human factors evaluation of the Advanced Visual Technology System (AVTS) eye tracking oculometer 21 p2925 N88-27361
The human element in space: Lessons from Antarctica
[AD-A193440] 21 p2988 N88-27741
The assessment of human/computer performance using human productivity measures: MIPS and BIPS are MEGAFLOPS
[DE87-013491] 21 p2993 N88-27750
Issues in computer-assisted interpretation of graphs and quantitative information
[PB88-116280] 21 p2998 N88-27783
NASA information sciences and human factors program
[NASA-TM-4064] 22 p3166 N88-28856
Visual Effects in the High Performance Aircraft Cockpit
[AGARD-LS-156] 23 p3241 N88-29291
Advances in Flying Qualities
[AGARD-LS-157] 24 p3314 N88-29735
Pilot modeling 24 p3314 N88-29736
Human factors report on information management requirements for next-generation manned bombers
[AD-A195870] 24 p3409 N88-30296
Study of human factors engineering criteria for extravehicular activity (EVA) systems, volume 1
[STF23-F87025-VOL-1] 24 p3410 N88-30298
Haptic exploration in humans and machines: Attribute integration and machine recognition/implementation
[AD-A193692] 24 p3410 N88-30299
Space station proximity operations windows: Human factors design guidelines
[NASA-TM-88233] 24 p3410 N88-30301

HUMAN PATHOLOGY
Further investigation of tests for susceptibility to noise-induced hearing loss
[ISVR-TR-149] 14 p1952 N88-21633

HUMAN PERFORMANCE
NT ASTRONAUT PERFORMANCE
NT OPERATOR PERFORMANCE
NT PILOT PERFORMANCE
Modeling of human judgement in multicriteria analysis using pairwise comparison
[REPT-87-01] 01 p0076 N88-10484
Masking effects of fine and coarse grain pictorial noise
[IZF-1985-21] 01 p0076 N88-10485
Loss of performance due to military clothing and equipment
[IZF-1986-13] 01 p0077 N88-10490
Integrated voice and visual systems research topics
[NASA-CR-177417] 03 p0356 N88-12246
Research papers and publications (1981-1987): Workload research program
[NASA-TM-100016] 04 p0474 N88-12924
Examining the relative efficiency of Part- versus whole-task practice for multiple-task situations
[AD-A185056] 05 p0631 N88-13856
Vision of details in space and time
[B8711402] 06 p0753 N88-14624
Stress effects and the optimum format of a scrolling seven-line VDT text window
[AD-A185559] 06 p0758 N88-14651
Regulation of energy metabolism during parachute jumps 07 p0896 N88-15428
Evoked brain activity and personnel performance
[AD-A185922] 07 p0897 N88-15436
Human performance data needed for training device design decisions
[AD-A185988] 07 p0898 N88-15441
Antarctica as a model for the human exploration of Mars
[AD-A185835] 08 p1051 N88-16342
Overlearning and positive thinking alleviate negative effects of stress on performance
[FOA-C-50051-5.3] 08 p1051 N88-16344
Stability, reliability and cross-mode correlations of tests in a recommended 8-minute performance assessment battery
[NASA-CR-172039] 08 p1052 N88-16351
Team problem solving: Effects of communication and function overlap
[AD-A187010] 09 p1152 N88-16898
Air Force Human Resources Laboratory technical reports and technical papers
[AD-A186830] 09 p1201 N88-17200
Tutoring electronic troubleshooting in a simulated maintenance work environment 09 p1204 N88-17215
A human performance modelling approach to intelligent decision support systems 09 p1208 N88-17242
Surrogate measures: A proposed alternative in human factors assessment of operational measures of performance 09 p1215 N88-17281
Second All-Union Conference on Physiology of Extreme States and Individual Protection of Man 10 p1363 N88-18147
Development of a coping strategies questionnaire to assess endurance performance
[AD-A188010] 11 p1520 N88-19074
Influence of a 6 hr head-out water immersion on different tests of endurance performance capacity 12 p1653 N88-19903
JPRS report: Science and technology. USSR: Life sciences
[JPRS-ULS-88-002] 12 p1665 N88-19982
Measuring functional feasibility of human visual system 12 p1665 N88-19983
Training in time interval discrimination using verbal feedback 12 p1665 N88-19985

Efficiency of human workers and means to increase it
12 p1666 N88-19986
Air quality and human performance, chapter 16
[AD-A188335] 12 p1666 N88-19988
Medical problems related to altitude in: Human performance physiology and environmental medicine at terrestrial extremes, chapter 14
[AD-A188340] 12 p1666 N88-19989
Human efficiency for visual detection of targets on CRT displays using a two-level multiple channel time history format
[AD-A188419] 12 p1670 N88-20001
Task allocation for efficient performance of a decentralized organization
[AD-A188699] 12 p1705 N88-20204
Management information systems design implications: The effect of cognitive style and information presentation on problem solving
[AD-A188850] 12 p1705 N88-20205
Lifting and carrying capacities relative to physical fitness measures
[AD-A189305] 13 p1809 N88-20808
Proceedings of the Workshop on the Assessment of Crew Workload Measurements Methods, Techniques and Procedures. Volume 1: Preliminary Selection of Measures
[AD-A189004] 13 p1812 N88-20827
A comparison of two chord keyboard coding systems for alphanumeric data entry
[AD-A189230] 13 p1813 N88-20834
Construction of a multidimensional questionnaire to determine interindividual differences in controlling attention
[DFVLR-FB-87-45] 14 p1952 N88-21637
Masking of motion cues by random motion: Comparison of human performance with a signal detection model
[UTIAS-313] 14 p1953 N88-21639
Age, alcohol, and simulated altitude: Effects on performance and breathalyzer scores
[AD-A190642] 15 p2103 N88-22531
An evaluation of the effects of high visual taskload on the separate behaviors involved in complex monitoring performance
[AD-A190641] 15 p2105 N88-22538
Dynamic properties of human brightness perception
[ETN-88-92243] 16 p2238 N88-23366
Mental-State Estimation, 1987
[NASA-CP-2504] 16 p2239 N88-23370
Challenges of physiological monitoring in a Navy operational setting 16 p2239 N88-23374
The N2-P3 complex of the evoked potential and human performance 16 p2241 N88-23388
The relationship between group process and performance 17 p2448 N88-24549
Effects of moderate cold and heat stress on the potential work performance of industrial workers. Part 6: The effects of increasing vapour pressure at four air temperatures on the performance and physiology of white females
[PB88-124854] 18 p2550 N88-25137
Eye and head response to an attention cue in a dual task paradigm
[AD-A191052] 18 p2551 N88-25143
Optimizing feedback utilization in motor skill training
[AD-A191559] 18 p2552 N88-25146
Performance estimates for operations conducted while wearing individual protective equipment: User manual
[AD-A191871] 18 p2553 N88-25154
Modeling and evaluation of variable structure organizations
[AD-A191947] 18 p2588 N88-25381
Monitoring of divers/astronauts during missions
19 p2698 N88-26036
Contra- and ipsilateral auditory stimuli produce different activation patterns at the human auditory cortex: A neuromagnetic study
[PB88-181490] 19 p2708 N88-26098
Proceedings of the Workshop on the Assessment of Crew Workload Measurement Methods, Techniques and Procedures. Volume 2: Library references
[AD-A191209] 19 p2710 N88-26101
Electric and Magnetic Activity of the Central Nervous System: Research and Clinical Applications in Aerospace Medicine
[AGARD-CP-432] 21 p2977 N88-27683
Studies of the intact human brain: Implications for performance 21 p2977 N88-27684
The effects of hypoxia on P300 and reaction time
[DCIEM-87-RR-12] 21 p2979 N88-27697
Can CNV amplitude predict ability to accomplish a demanding task? 21 p2980 N88-27700
Physiological responses to acute exercise-heat stress
[AD-A192606] 21 p2986 N88-27732
Determinants of dual-task interference and resource theories in cognitive psychology
[DFVLR-FB-88-14] 21 p2992 N88-27748
The effects of acute cold exposure on exercise performance
[AD-A192650] 22 p3130 N88-28610
Human acclimatization and physical performance at high altitude
[AD-A192651] 22 p3130 N88-28611
The impact of hyperthermia and hypohydration on circulation, strength, endurance and health
[AD-A192657] 22 p3131 N88-28615
Effects of air polution on human exercise performance
[AD-A192660] 22 p3131 N88-28617
Engineering data compendium. Human perception and performance, volume 2
[LC-87-19560] 22 p3134 N88-28631
Engineering data compendium. Human perception and performance, volume 3
[LC-87-19560] 22 p3134 N88-28632
Human performance and acute hypoxia, chapter 12
[AD-A192604] 23 p3238 N88-29270
Literature review: Validity and potential usefulness of psychomotor ability tests for personnel selection and classification
[AD-A193558] 23 p3241 N88-29287

HUMAN REACTIONS
Human motor reactions to dangerous motions in robot operations
[PB87-222196] 03 p0361 N88-12275
Life sciences experiments on stratospheric balloons and sounding rockets 08 p1033 N88-16262
The ESA Anthrorack project: Integrated research in human physiology 08 p1033 N88-16265
Evidence for human adaptive response to dehydration: Increase of circulating protein mass
[AD-A186225] 08 p1048 N88-16328
White blood cells in space: An experiment for the first Spacelab mission 09 p1127 N88-16757
Cardiovascular adaptation to zero-g during a long term flight (237 days) on board the Salyut 7 Soviet space station (1984) 12 p1655 N88-19920
Load and control of the cardiocirculatory system in weightlessness 12 p1656 N88-19922
Computer simulation of a single pilot flying a modern high-performance helicopter
[NASA-TM-100182] 20 p2761 N88-26376
Effect of microgravity on lymphocyte activation — Spacelab D1 mission 22 p3061 N88-28163

HUMAN RELATIONS
A comparison of the effects of group dynamics on individuals assigned to integral and non-integral aircrews
[AD-A186467] 08 p1051 N88-16345

HUMAN RESOURCES
A software planning and development methodology with resource allocation capability
[AD-A186088] 07 p0902 N88-15462

HUMAN TOLERANCES
Determination of the individual state of acclimatization
[IZF-1986-27] 01 p0075 N88-10478
Measurement of suspension and ride characteristics of the M1 main battle tank 05 p0596 N88-13637
Investigation of the exposure to harmful compounds in the workshop of nondestructive materials testing at Gilze-Rijen (Netherlands)
[PML-1985-42] 05 p0623 N88-13816
Improvement of human tolerance to head-pelvis (+Gz) accelerations by increasing hydration
10 p1364 N88-18153
Influence of a 6 hr head-out water immersion on different tests of endurance performance capacity
12 p1653 N88-19903
Advanced turboprop aircraft flyover noise: Annoyance to counter-rotating-propeller configurations with an equal number of blades on each rotor, preliminary results
[NASA-TM-100612] 16 p2265 N88-23547
Human response to prolonged motionless suspension in four types of full body harnesses
21 p2929 N88-27387

HUMAN WASTES
NT URINE
Specific organic compounds in excreta
07 p0895 N88-15422

HUMAN-COMPUTER INTERFACE
U MAN-COMPUTER INTERFACE

HUMIDITY
The effect of organic inhibitors on the atmospheric corrosion and solderability of copper
[DE88-000261] 04 p0414 N88-12565
Estimation of marine boundary layer depth and relative humidity with multispectral satellite measurements
[AD-A184881] 05 p0620 N88-13804
Controlled ecological life support systems: Development of a plant growth module 05 p0630 N88-13854
Corrosion and deterioration testing in humid tropic environments
[AD-A186917] 10 p1302 N88-17783
Determination of atmospheric moisture structure from high resolution MAMS radiance data
11 p1515 N88-19049
Review of recent developments in evaporation ducting assessment 12 p1616 N88-19664
Remote sensing of meteorological parameters with the aid of a clear-air Doppler radar
[PB88-142518] 12 p1647 N88-19864
Perspectives in microclimate cooling involving protective clothing in hot environments
[AD-A188370] 12 p1671 N88-20007
The effects of humidity on the profile of photographic plates
[NPL-DMOM-88] 14 p1913 N88-21429
Aerodynamic aspects of the Amazon Forest
[INPE-4445-TDL/313] 15 p2098 N88-22501
Intercomparison of NMC (National Meteorological Center) and ECMWF (European Centre for Medium Range Weather Forecasts) global analyses: 1980-1986
[PB88-196548] 21 p2974 N88-27668
Corrosion problems associated with computer disk packs 22 p3054 N88-28121
Advancements in oxygen generation and humidity control by water vapor electrolysis
[NASA-CR-172073] 22 p3134 N88-28633
Real-time measurements of the size fractionation of ambient black carbon aerosols at elevated humidities
[DE88-010870] 23 p3215 N88-29138
Fatigue crack growth characteristics of ARALL (trademark)-1
[AD-A196185] 24 p3341 N88-29889

HUMIDITY MEASUREMENT
Lidar-radiometric method for determining liquid-water content of cirrus clouds 04 p0461 N88-12854
Estimation of marine boundary layer depth and relative humidity with multispectral satellite measurements
[AD-A184881] 05 p0620 N88-13804
Method of determining atmospheric moisture content by measurement of upward radiation intensity in near IR
08 p1007 N88-16106
Ion content and infrared absorption of moist atmospheric air
[AD-A188839] 12 p1643 N88-19838
Thermodynamic study of hygroscopic polymers using surface acoustic waves 19 p2672 N88-25882

HUNGARY
Proceedings of the 17th International Conference on Phenomena in Ionized Gases held in Budapest, Hungary, July 8-12, 1985: Invited papers
[DE87-703562] 05 p0651 N88-13987

HURRICANES
Hurricane Elena storm surge data
[AD-A184573] 03 p0353 N88-12228
Hurricane Danny storm surge data, report 4
[AD-A186373] 07 p0879 N88-15334
Hurricane Kate storm surge data, report 5
[AD-A186374] 07 p0880 N88-15335
Hurricane climatology for the Atlantic and Gulf coasts of the United States
[PB88-114657] 08 p1039 N88-16288
Annual data summary and climatological evaluation CERC (Coastal Engineering Research Center) field research facility, 1985. Volume 1. Main text and appendixes A and B
[AD-A186442] 08 p1039 N88-16289
Forecast of Atlantic seasonal hurricane activity for 1988 15 p2098 N88-22500
Suggested hurricane operational scenario for GOES I-M
[NASA-TM-89729] 19 p2692 N88-26002
Observational/numerical study of the upper ocean response to hurricanes
[AD-A193592] 22 p3128 N88-28598

HYBRID CIRCUITS
Wire interconnection reliability and moisture levels in hybrid microcircuits with epoxy-attached components
[DE87-012987] 01 p0039 N88-10247
Applications of heat pipes to cool PWBS and hybrid microcircuits 02 p0136 N88-10858
Generic specifications for hybrid microcircuits
[ESA-PSS-01-608-ISSUE-2] 06 p0696 N88-14273
Evaluation of solder flux solvents in a vapor-degreasing application for hybrid microcircuits
[BDX-613-3638] 11 p1468 N88-18752
Design and fabrication of advanced hybrid circuits for high energy physics
[DE88-004392] 11 p1479 N88-18825
Hermetically sealable package for hybrid solid-state electronic devices and the like
[NASA-CASE-MSC-20181-1] 17 p2335 N88-23941
Designing to safe power limits in hybrid circuits
[DE88-005533] 18 p2506 N88-24865

HYBRID COMPUTERS
Simulation of real time problem solving
[AD-A193436] 21 p2997 N88-27778

HYBRID PROPULSION
The convertible engine: A dual-mode propulsion system 09 p1108 N88-16639
HYBRID STRUCTURES
Design description report for a photovoltaic power system for a remote satellite earth terminal [NASA-CR-179586] 04 p0465 N88-12875
Fatigue behaviour of hybrid composites [BR102236] 09 p1138 N88-16819
The strength of hybrid composites [BR101991] 09 p1138 N88-16821
Outlook for the fusion hybrid and tritium-breeding fusion reactors [PB88-149281] 13 p1843 N88-21029
HYBRIDS (BIOLOGY)
U GENETIC ENGINEERING
HYDRATES
Development of highly porous calcium silicate hydrate materials with extremely low thermal conductivity [BMFT-FB-T-86-164] 02 p0150 N88-10941
Gas hydrate model development and validation [DE88-001004] 10 p1298 N88-17762
Geological evolution and analysis of confirmed or suspected gas hydrate localities. Volume 9: Formation and stability of gas hydrates of the Middle America Trench [DE88-001007] 10 p1347 N88-18050
Geological evolution and analysis of confirmed or suspected gas hydrate localities. Volume 2: Basin analysis, formation and stability of gas hydrates in the Black Sea [DE88-001052] 18 p2532 N88-25023
HYDRATION
Effect of spaceflight factors on primate hydration homeostasis 10 p1360 N88-18126
Improvement of human tolerance to head-pelvis (+Gz) accelerations by increasing hydration 10 p1364 N88-18153
Morphological and functional state of the hypothalamo-hypophyseal neurosecretory system of rats flown aboard Cosmos-1667 10 p1365 N88-18156
Gastric emptying during exercise: Effects of acute heat stress, acclimation and hypohydration [AD-A188008] 11 p1519 N88-19073
The impact of hyperthermia and hypohydration on circulation, strength, endurance and health [AD-A192657] 22 p3131 N88-28615
HYDRAULIC ACTUATORS
U ACTUATORS
U HYDRAULIC EQUIPMENT
HYDRAULIC CONTROL
Adaptive control of hydraulic devices [FB-1/85] 01 p0084 N88-10543
Control system simulation for a single-link flexible arm [AD-A187037] 09 p1174 N88-17035
HYDRAULIC EQUIPMENT
Adaptive control of hydraulic devices [FB-1/85] 01 p0084 N88-10543
RE-1000 free-piston Stirling engine hydraulic output system description [NASA-TM-100185] 01 p0108 N88-10700
Human factors in robotic system design discussed 02 p0158 N88-10988
The axisymmetric sealing gap with variable viscosity. A variable hydraulic resistance [ETN-87-90604] 03 p0314 N88-11987
Calculation of the three dimensional flow in the impeller of hydraulic turbomachines using a finite element method [ETN-87-90612] 03 p0315 N88-11988
A cost and benefit analysis of hydraulic fluid systems for the next generation of tactical aircraft [AD-A186911] 09 p1116 N88-16690
Control system simulation for a single-link flexible arm [AD-A187037] 09 p1174 N88-17035
Reduction of residual stresses and distortion in girth welded pipes [AD-A187728] 11 p1494 N88-18920
Electrical/pneudraulic design considerations [AD-A188097] 12 p1581 N88-19462
High Reynolds number pump facility for cavitation research [AD-A189310] 13 p1765 N88-20558
Modelling of a hydraulic motor and servo-valve to produce a desired system response using analogue and digital compensation techniques [ETN-88-92079] 14 p1899 N88-21337
A 150,000 pounds per square inch dynamic pressure calibrator [AD-A190659] 15 p2069 N88-22335
Hydraulic pumps and hydraulic equipment at low temperatures [DE88-752871] 21 p2958 N88-27570
HYDRAULIC FLUIDS
A cost and benefit analysis of hydraulic fluid systems for the next generation of tactical aircraft [AD-A186911] 09 p1116 N88-16690
Evaluation of the acute toxicity of a synthetic polyalphaolefin-based hydraulic fluid [AD-A190412] 15 p2045 N88-22184
Experimental determination of the coefficients of the hydraulic resistance of apertures in the rotary disks [AD-A190627] 15 p2066 N88-22317
Hydraulic pumps and hydraulic equipment at low temperatures [DE88-752871] 21 p2958 N88-27570
HYDRAULIC HEATING SOURCES
U HEAT SOURCES
U HYDRAULIC EQUIPMENT
HYDRAULIC JETS
Pressure distributions and losses in a waterjet propulsion system [AD-A188423] 12 p1633 N88-19777
Dense-spray structure and phenomena. Part 2: Pressure-atomized sprays [AD-A190312] 15 p2064 N88-22307
Deflection of a circular liquid jet on a flat plate perpendicular to the flow direction [NASA-TT-20279] 18 p2207 N88-23173
Hydroacoustic pulsating jet generator [MPIS-7/1987] 18 p2510 N88-24891
HYDRAULIC PUMPS
U HYDRAULIC EQUIPMENT
U PUMPS
HYDRAULIC SYSTEMS
U HYDRAULIC EQUIPMENT
HYDRAULIC TEST TUNNELS
Main features of the 0.43m x 0.43m wind tunnel [AXM-132] 14 p1870 N88-21175
Aerodynamic and Related Hydrodynamic Studies Using Water Facilities [AGARD-CP-413] 16 p2200 N88-23125
Vortex breakdown and control experiments in the Ames-Dryden water tunnel 16 p2200 N88-23127
The use of the NRC/NAE water facilities in Canadian aeronautical research and development 16 p2201 N88-23132
Description of a water tank facility: Study of a missile at high incidence 16 p2201 N88-23133
The ONERA water tunnels test possibilities for flow visualization in aeronautical and Naval domains 16 p2202 N88-23139
A new laminar water tunnel to study the transition process in a blasius layer and in a separation bubble and a new tool for industrial aerodynamics and hydrodynamic research 16 p2204 N88-23150
A comparative study of vortex flows in wind and water tunnels 16 p2204 N88-23151
HYDRAULIC VALVES
U HYDRAULIC EQUIPMENT
U VALVES
HYDRAZINE ENGINES
Development and qualification of an Augmented Electro-Thermal Hydrazine-Thruster (AEHT) with 0.1 to 0.2 N vacuum thrust [BMFT-FB-W-86-012] 16 p2169 N88-22931
HYDRAZINE NITRATE
Detonation velocity of the hydrazinum nitrate-hydrazine water system [NASA-TT-20213] 13 p1770 N88-20590
HYDRAZINES
Products of the neutralization of hydrazine fuels with hypochlorite, 2 [DE87-011454] 01 p0030 N88-10193
A life test of a 22-Newton (5-lbf) hydrazine rocket [NASA-TM-100232] 03 p0278 N88-11750
Low-g propellant gaging 08 p0982 N88-15937
The chemistry of the hypochlorite neutralization of hydrazine fuels [DE88-002971] 10 p1307 N88-17812
Decomposition of hydrazine by high frequency glow electrical discharges [NASA-TT-20240] 24 p3344 N88-29906
HYDRAZINIUM COMPOUNDS
Detonation velocity of the hydrazinum nitrate-hydrazine water system [NASA-TT-20213] 13 p1770 N88-20590
HYDRIDES
NT BORANES
NT BORON HYDRIDES
NT LITHIUM HYDRIDES
NT METAL HYDRIDES
NT NITROGEN HYDRIDES
NT SILANES
NT SODIUM HYDRIDES
Hydride generation from the Exide load-leveling cells [DE87-011361] 01 p0041 N88-10259
Metal hydrides [DE88-005083] 10 p1299 N88-17766
Quantitative determination of a hydrogen impurity in a sodium coolant by hydride thermal dissociation [NASA-TT-20239] 13 p1740 N88-20402
HYDROACOUSTICS
U UNDERWATER ACOUSTICS
HYDROAEROMECHANICS
U AERODYNAMICS
HYDROBALLISTICS
Investigation and implementation of an algorithm for computing optimal search paths [AD-A185927] 07 p0902 N88-15461
HYDROBAROPHONES
U HYDROPHONES
HYDROCARBON COMBUSTION
Detailed kinetic modeling of autoignition chemistry [DE87-013226] 03 p0283 N88-11782
Laser probes of propellant combustion chemistry [AD-A184854] 05 p0561 N88-13415
Investigation of fuel additive effects on sooting flames [AD-A186403] 07 p0829 N88-15026
Combustion of hydrogen and hydrocarbons in fluorine [AD-A188018] 11 p1453 N88-18662
Chemical kinetics of nitramine propellant combustion [AD-A191556] 18 p2495 N88-24802
Laser probes of natural gas ignition chemistry [PB88-212568] 21 p2910 N88-27271
HYDROCARBON FUEL PRODUCTION
Research on hydrotreating catalysts to hydrodeoxygenate biocrude oils 18 p2536 N88-25046
HYDROCARBON FUELS
NT CRUDE OIL
NT DIESEL FUELS
NT FOSSIL FUELS
NT GASOLINE
NT JET ENGINE FUELS
NT JP-4 JET FUEL
NT JP-5 JET FUEL
NT JP-8 JET FUEL
NT LIQUEFIED NATURAL GAS
NT NATURAL GAS
Detection of vapors of flammable liquids in air by atmospheric sampling mass spectrometry/mass spectrometry [DE88-000030] 02 p0196 N88-11227
An experimental investigation of the ignition and flammability limits of various hydrocarbon fuels in a two-dimensional solid fuel ramjet [AD-A184968] 05 p0549 N88-13342
Evaluation and prediction of Henry's law constants and aqueous solubilities for solvents and hydrocarbon fuel components. Volume 1: Technical discussion [AD-A188571] 12 p1613 N88-19643
Dual-fuel, dual-mode rocket engine [NASA-CASE-LAR-13773-1] 18 p2475 N88-24685
Production costs of hydrocarbon fuels from biomass [DE88-006667] 18 p2495 N88-24804
Motor vehicles as sources of compounds important to tropospheric and stratospheric ozone [PB88-195219] 18 p2540 N88-25076
Combustion rate limits of hydrogen plus hydrocarbon fuel: Air diffusion flames from an opposed jet burner technique 19 p2624 N88-25567
Mach 2 combustion characteristics of hydrogen/hydrocarbon fuel mixtures 19 p2625 N88-25568
Pollutant formation in heterogeneous mixtures of fuel drops and air [DOE/CE-50052/H1] 19 p2689 N88-25986
Carbon deposition model for oxygen-hydrocarbon combustion, volume 1 [NASA-CR-179375] 21 p2908 N88-27254
Carbon deposition model for oxygen-hydrocarbon combustion, volume 2 [NASA-CR-179376] 21 p2908 N88-27255
Hydrocarbon fuel spill dispersion on water: Literature review [AD-A192486] 21 p2922 N88-27346
Experiments and modeling of multi-component fuel behavior in combustion [AD-A195011] 24 p3343 N88-29896
HYDROCARBONS
NT ACETYLENE
NT ALKANES
NT ALKENES
NT ANTHRACENE
NT BENZENE
NT BUTADIENE
NT BUTANES
NT BUTENES
NT CAROTENE
NT CETANE
NT CUBANE
NT CYCLIC HYDROCARBONS
NT CYCLOBUTANE
NT CYCLOHEXANE
NT ETHANE
NT ETHYLENE
NT LIQUEFIED NATURAL GAS

NT METHANE
NT METHYLENE
NT NAPHTHALENE
NT NAPHTHENES
NT NATURAL GAS
NT OXYACETYLENE
NT PARAFFINS
NT POLYBUTADIENE
NT PROPANE
NT PROPYLENE
NT PYRENES
NT TOLUENE
NT VINYLIDENE
The photophysics and chemistry of PAH (Polycyclic Aromatic Hydrocarbons) compounds
[DE87-014455] 02 p0153 N88-10954
The structure of adsorbed sulfur and carbon on molybdenum and rhenium single crystal surfaces, and their influence on carbon monoxide and hydrocarbon chemisorption
[DE88-001393] 04 p0499 N88-13073
Development of a low noise 10 K J-T refrigeration system
[AD-A185258] 05 p0571 N88-13484
Molecular dynamics studies of aromatic hydrocarbon liquids
[DE88-001473] 05 p0648 N88-13973
Summary and analysis of comments on the recommended practice for the measurement of refueling emissions
[PB88-101530] 07 p0876 N88-15313
Van der Waals clusters of aromatic molecules studied using supersonic molecular jet spectroscopy
[AD-A186087] 07 p0929 N88-15644
A review of methanol vehicles and air quality impacts
[DE88-002846] 08 p1023 N88-16194
Measurement of vertical distributions of halogenated hydrocarbons in the stratosphere
[ETN-88-91065] 09 p1191 N88-17135
Degradation of jet and missile fuels by aquatic microbial communities
[AD-A188065] 11 p1465 N88-18737
Effects of breathing air containing contaminants such as CO2, CO and hydrocarbons at 1 and 5 atmospheres
[PB88-132915] 11 p1521 N88-19084
Analysis of hydrocarbon band 3.35 in spectrum of Halley's Comet using data from infrared spectrometer on Vega-1 spacecraft 13 p1727 N88-20327
On the interpretation of the CH cometary spectrum 14 p2007 N88-21969
The application of hydrocarbon bioconversion technology to aerospace materials production 18 p2478 N88-24698
Diamond like carbon coatings: Categorization by atomic number density
[NASA-CR-174895] 22 p3059 N88-28151
Method and device for determining heats of combustion of gaseous hydrocarbons
[NASA-CASE-LAR-13528-1] 23 p3193 N88-29002
Nonseismic, surface geophysical and geochemical prospecting technology
[PB88-196613] 23 p3227 N88-29207
Determination of relative flammability of materials by pyrolysis and gas-chromatographic light hydrocarbon analysis
[DE88-012449] 24 p3343 N88-29898
Rates of formation of soot from hydrocarbon flames and its destruction 24 p3349 N88-29933

HYDROCHLORIC ACID
Monitoring biological impacts of space shuttle launches from Vandenberg Air Force Base: Establishment of baseline conditions
[NASA-TM-100982] 18 p2549 N88-25133

HYDROCRACKING
High-density jet fuels from coal syncrudes, appendix 4
[DE88-003132] 10 p1307 N88-17813
Research on hydrotreating catalysts to hydrodeoxygenate biocrude oils 18 p2536 N88-25046

HYDRODYNAMIC COEFFICIENTS
Free Lagrange reconnection algorithms for hydrocodes using a quadrilateral mesh
[DE88-001580] 05 p0611 N88-13752

HYDRODYNAMIC EQUATIONS
NT HELMHOLTZ VORTICITY EQUATION
Lattice gas hydrodynamics 03 p0313 N88-11978
Induced turbulence in aerosol-loaded atmospheres, Jun. 1987
[DE87-014724] 09 p1192 N88-17141
Hydrodynamical regimes in molten metals under a horizontal temperature gradient 14 p1988 N88-21859

HYDRODYNAMIC STABILITY
U FLOW STABILITY

HYDRODYNAMICS
NT ELASTOHYDRODYNAMICS
NT ELECTROHYDRODYNAMICS
NT MAGNETOHYDRODYNAMICS
NASA-VOF3D: A three-dimensional computer program for incompressible flows with free surfaces
[DE87-011849] 01 p0045 N88-10288
Research on one-dimensional two-phase flow. Theory on hydrodynamic balance in two fluid model and its application
[DE87-702615] 01 p0045 N88-10290
Two-phase non-Newtonian hydrodynamic modeling of slurries
[DE87-011519] 01 p0047 N88-10298
Phase dynamics: A review and a perspective
[DE87-013173] 01 p0048 N88-10306
Technical evaluation report on the Fluid Dynamics Panel Symposium on aerodynamic and related hydrodynamic studies using water facilities
[AGARD-AR-225] 03 p0312 N88-11968
Lattice gas hydrodynamics 03 p0313 N88-11978
The evolution of HOBO
[DE87-014742] 03 p0313 N88-11980
Nonequilibrium fluctuations and transport in sheared fluids 03 p0316 N88-11999
Breaking wave forces on vertical cylinders
[RR-CE71] 03 p0338 N88-12126
Coastal dynamics of the mouth of the Saloum (Senegal) --- SPOT imagery 03 p0345 N88-12177
Kinematics and dynamics of barred spiral galaxies 03 p0388 N88-12440
Three-dimensional, free-Lagrange hydrodynamics
[DE88-000494] 04 p0443 N88-12749
Observations on the hydrodynamic flow visualization at ONERA
[PD-FM-8718] 04 p0444 N88-12753
Dynamics of isolated intrathermocline eddy 04 p0460 N88-12845
Variations of the vertical and horizontal velocities of the small-scale structures and the physical problems related to overshoot layers 04 p0507 N88-13115
A complete linearized theory for the analysis and design of two-dimensional hydrofoils near a free surface
[UTIAS-TN-264] 05 p0579 N88-13531
Advanced concepts theory annual report 1986
[AD-A184986] 05 p0651 N88-13991
Hydroburst test of a carbon-carbon involute exit cone
[NASA-TP-2556] 06 p0671 N88-14112
Methods for reducing computational costs of typical finite element unsteady hydrodynamic models
[AD-A185499] 06 p0702 N88-14312
Method of two-time Green functions in molecular hydrodynamics of superfluid liquid 06 p0771 N88-14735
Fundamental studies of surfaces processes and trace analysis using solid electrodes
[AD-A186156] 07 p0828 N88-15024
A variational formulation of a hydrodynamic lubrication problem
[MEMO-642] 08 p0987 N88-15979
The use of optical fibers for shock pressure and timing measurements at high pressures
[DE88-004012] 10 p1334 N88-17971
Energy transfers for multilayer hydrodynamic ocean models: General formulation and specific examples
[AD-A187604] 10 p1358 N88-18116
A method of calculating nonstationary heat flow in hydrogasodynamic processes in closed cryogenic systems
[DE88-700864] 12 p1626 N88-19727
Dynamic modelling of flexible rotor shafts mounted on hydrodynamic bearings 13 p1779 N88-20641
Model of hydrodynamic adjustment of temperature, salinity and current fields, 13 p1789 N88-20700
Proceedings of the Seminar on Hydrodynamics and Crystal Growth
[ETN-88-92025] 14 p1987 N88-21853
Optical and hydrodynamic implications of Comet Halley dust size distribution 14 p2003 N88-21939
PLASMOR: A laser-plasma simulation code, part 2
[DE88-701289] 15 p2135 N88-22736
Hydrodynamical equations for spherical gravitational collapse in terms of a generalized theory of gravitation with higher derivatives
[DE87-703027] 15 p2151 N88-22838
Aerodynamic and Related Hydrodynamic Studies Using Water Facilities
[AGARD-CP-413] 16 p2200 N88-23125
Water facilities in retrospect and prospect: An illuminating tool for vehicle design 16 p2200 N88-23126
Application of high speed holography to aerodynamic and hydrodynamic three-dimensional velocimetry 16 p2203 N88-23144
Use of water towing tanks for aerodynamics and hydrodynamics 16 p2204 N88-23149
A new laminar water tunnel to study the transition process in a blasius layer and in a separation bubble and a new tool for industrial aerodynamics and hydrodynamic research 16 p2204 N88-23150
Initial condition effect on pressure waves in an axisymmetric jet
[NASA-TM-100915] 16 p2209 N88-23184
Pump rod forces due to hydrodynamic effects in piston pumps
[PB88-164850] 16 p2214 N88-23212
Periodic response of nonlinear systems 16 p2217 N88-23228
Self-similar expansions in ion beam fusion 16 p2278 N88-23635
The structure and stability of spherically expanding flames 17 p2318 N88-23842
Specific features of emanation, temperature and hydrodynamic fields in the epicentral zone of tectonic earthquake
[DE88-701140] 17 p2373 N88-24114
The influence of cathodic protection on erosion-corrosion of metals and model alloys
[AD-A191613] 18 p2485 N88-24742
Dynamics and control of turbulent shear flows
[AD-A191527] 18 p2508 N88-24879
Heating and evaporation of turbulent liquid films: Measurement of film thickness and the onset of nucleate boiling
[DE88-006388] 18 p2512 N88-24905
LLNL granular solids flow project
[DE88-007492] 18 p2513 N88-24906
Droplet formation for liquid monopropellant jets 19 p2623 N88-25557
Dissipative relativistic radiation hydrodynamics
[DE88-702092] 19 p2665 N88-25846
Electron-acoustic waves in a beam-plasma system
[DE88-702053] 19 p2729 N88-26207
Ludwig Prandtl collected treatises on applied mechanics, hydro- and aerodynamics, part 2, IV interfaces and resistance
[NASA-TT-20315] 20 p2752 N88-26338
Modelling of premixed combustion using a thin flame sheet and the effect of the hydrodynamic instability
[DE88-009467] 20 p2770 N88-26423
Numerical modeling of the effect of particle size of explosives on shock initiation properties
[DE88-010479] 20 p2780 N88-26491
Vertical ship motions and sea loads considering nonlinear effects
[TAE-592] 20 p2784 N88-26515
Freely expanding detonation products: Scaling of rate processes
[DE88-007827] 20 p2799 N88-26606
A study of fluid-structure problems 21 p2941 N88-27468
Numerical simulation of fuel droplet interactions and breakup
[AD-A192431] 21 p2941 N88-27470
Research on ocean forecasting and nonlinear wave propagation and numerical hydrodynamics in the ocean
[AD-A193363] 21 p2976 N88-27680
Surface tension and viscosity with Lagrangian hydrodynamics on a triangular mesh
[AD-A194120] 22 p3075 N88-28258
Nonseismic, surface geophysical and geochemical prospecting technology
[PB88-196613] 23 p3227 N88-29207
Piecewise-parabolic methods for systems of hyperbolic conservation laws in multiprocessing environments
[DE88-010202] 23 p3248 N88-29329
Gaseous premixed flames in non-uniform flows 24 p3351 N88-29945

HYDROELASTICITY
Traction model development
[AD-A188450] 15 p2073 N88-22359
Nonlinear hydroelastic vibrations in rectangular containers
[LRT-WE-9-FB-7(1987)] 22 p3088 N88-28340

HYDROELECTRIC POWER STATIONS
Utilization of LANDSAT-TM imagery in the hydroenergetic inventory of the Paraiba do Sul River Basin 17 p2364 N88-24077

HYDROFLUORIC ACID
Evaluation of the sensidyne toxic gas sensor for HF (Hydrogen Fluoride) vapor
[DE88-000647] 04 p0446 N88-12767

HYDROFOILS
NT KEELS
A complete linearized theory for the analysis and design of two-dimensional hydrofoils near a free surface
[UTIAS-TN-264] 05 p0579 N88-13531

HYDROFORMING
A finite element analysis for the hydroforming of aluminum
[DE88-008050] 20 p2784 N88-26516

HYDROGEN
NT DEUTERIUM
NT HYDROGEN ISOTOPES
NT LIQUID HYDROGEN
NT TRITIUM
Hydrogen annealing of P(sub) b and E prime defect centers in oxidized silicon wafers
[DE87-014293] 02 p0152 N88-10951
Flame acceleration and transition to detonation in channels
[DE87-014193] 03 p0284 N88-11786
Characterization of catalysts with metal-support effects and of the species adsorbed on their surfaces
[DE87-014836] 04 p0414 N88-12564
A hydrogen/nickel oxide battery for remote applications
[DE87-009048] 04 p0464 N88-12872
Excess emission in the wings of the Hydrogen Balmer lines during a flare on the late-type dMe star YZ CMi 04 p0511 N88-13146
Hydrogen and deuterium in the local interstellar medium 04 p0521 N88-13204
Fatigue crack growth behavior in hydrogen gas environment 06 p0716 N88-14391
Threshold behaviour of semi-elliptic hydrogen-induced and fatigue-induced cracks 06 p0717 N88-14397
Experimental observation of photoresonance of electrons localized above surface of solid hydrogen 06 p0774 N88-14755
Hydrogen retention and release from uranium dioxide
[DE88-002042] 07 p0829 N88-15030
The carbon dioxide chaperon efficiency for the reaction H + O2 + M yields HO2 + M from ignition delay times behind reflected shock waves
[NASA-TM-100125] 07 p0830 N88-15036
Helium-ion-induced release of hydrogen from graphite
[DE88-002599] 09 p1142 N88-16846
Hydrogen in niobium-tantalum superlattices 09 p1146 N88-16867
Blast waves generated by planar detonations
[DE88-002219] 09 p1164 N88-16979
Feasibility of chemical lasers based on chain reaction involving hydrogen fluorination with thermal branching mechanism 09 p1238 N88-17420
Oscillations of solar models with internal element diffusion
[DE88-003156] 09 p1264 N88-17573
Hydrogen Energy Coordinating Committee: Summary of DOE hydrogen programs for FY 1987
[DE88-003960] 10 p1306 N88-17811
Two-photon (VUV and visible) resonant ionization spectroscopy of atoms and molecules
[DE88-004332] 10 p1407 N88-18388
Combustion of hydrogen and hydrocarbons in fluorine
[AD-A188018] 11 p1453 N88-18662
Calculations of rate constants for the three-body recombination of H2 in the presence of H2
[NASA-CR-182548] 11 p1454 N88-18664
Spatial and temporal monitoring of the Jovian atmosphere 12 p1711 N88-20240
Uncertainties in hydrogen combustion
[DE88-005354] 13 p1739 N88-20395
Quantitative determination of a hydrogen impurity in a sodium coolant by hydride thermal dissociation
[NASA-TT-20239] 13 p1740 N88-20402
Hydrogen induced cracks in armor steel weldments fabricated with austenitic filler alloys
[AD-A188733] 13 p1740 N88-20406
Influence of hydrogen on crack formation tendency in heat-affected zone with stress concentrator 14 p1887 N88-21276
Use of nonporous metals membranes for the separation of hydrogen from gas mixtures
[BMFT-FB-T-86-206] 14 p1888 N88-21280
The effect of H2S concentration and pH on hydrogen permeation in AISI 410 stainless steel in 5 percent NaCl
[NPL-DMA(A)-148] 14 p1890 N88-21293
Theory of Muon method for study of solid and liquid hydrogen 14 p1972 N88-21770
The role of hydrogen thermalization in shaping the Lyman-alpha coma --- comets 14 p2007 N88-21971
The structure of the boron-hydrogen complex in silicon
[DE88-005433] 15 p2144 N88-22795
Some visualization studies on turbulent boundary layers using multiwire hydrogen bubble generation 16 p2204 N88-23153
Hydrogen turbines for space power systems: A simplified axial flow gas turbine model 17 p2419 N88-24385
Effect of hydrogen, deuterium and oxygen on the anelastic properties of refractory alloys
[DE88-007349] 18 p2484 N88-24736
The response of ultrathin palladium gate sensors to hydrogen and carbon monoxide 19 p2672 N88-25885
Life in a hyperbaric environment. A new O2-H2 breathing mixture for industrial diving 19 p2695 N88-26019
Ultraviolet imaging of hydrogen flames
[DE88-009152] 20 p2769 N88-26422
Production of powdered sodium hydride with large specific surface by the catalyzed reaction of molten sodium with hydrogen-1
[NASA-TT-20185] 20 p2776 N88-26462
Shock wave compression and metallization of simple molecules
[DE88-008031] 20 p2851 N88-26925
Enhancement of volume H(-) production by vibrationally pre-exciting the hydrogen molecules
[DE88-010783] 20 p2853 N88-26937
A method for determining the solubility of hydrogen in molten aluminum-lithium alloys
[DE88-009807] 21 p2910 N88-27270
Theory of the dissociation dynamics of small molecules on metal surfaces: Finite temperature studies
[DE88-007763] 21 p3013 N88-27882
Hydrogen storage by molecular polyhydrides
[AD-A194207] 23 p3191 N88-28989
Measure of hydrogen concentration profile in materials by resonant nuclear reactions
[DE88-702599] 23 p3193 N88-28999
Hydrogen permeation through metallic foils
[DE88-702600] 23 p3193 N88-29000
Kinetic of martensitic transformations induced by hydrogen in the austenite
[DE88-701623] 23 p3194 N88-29007
N2(A3epsilon u+) by reaction of N2F4+H2 in a supersonic flow
[AD-A194493] 23 p3219 N88-29163
Chemical kinetics of hydrogen and P(sub b) centers
[DE88-010528] 23 p3291 N88-29594
Theoretical investigation of image states of the hydrogen covered Cu (100)
[DE88-702662] 23 p3292 N88-29604
Extended atmospheres of outer planet satellites and comets
[NASA-CR-183157] 24 p3457 N88-30572
HYDROGEN AIR FUEL CELLS
U HYDROGEN OXYGEN FUEL CELLS
HYDROGEN ATOMS
Design study for measurement of neutral hydrogen atom density by laser induced fluorescence method
[DE87-752964] 02 p0179 N88-11114
A study of mechanisms of hydrogen diffusion in separation devices
[DE88-000328] 04 p0416 N88-12584
Atomic data for hydrogens in collisions with electrons: Addenda
[IPPJ-AM-55-ADD] 09 p1252 N88-17502
On the dynamical supersymmetry of atomic hydrogen
[DE88-700713] 10 p1422 N88-18495
The astrophysics of nebulae and active galactic nuclear emission-line regions: New methods and applications 13 p1858 N88-21111
Determination of beam orientation of optical diagnostics of excited 200-MeV hydrogen atoms resulting from photodetachment of H(-)ions
[AD-A189976] 14 p1981 N88-21823
Analysis of reversible and irreversible hydrogen trapping in metals
[NPL-DMA(A)-154] 16 p2177 N88-22977
Stark effect in intense field. Perturbation theory and 1/n-expansion
[DE87-702947] 16 p2266 N88-23550
Associative two-body condensation in laser-cooled sodium and hydrogen 16 p2267 N88-23559
Electromagnetic manipulation of atomic hydrogen 16 p2268 N88-23568
Magnetic traps for an anti-hydrogen gas 16 p2269 N88-23572
Key problems and hydrogen atom formation 16 p2269 N88-23573
Small molecule and small cluster ion formation in a low-density containerless mixture of electrons, protons and hydrogen atoms 16 p2269 N88-23577
Nascent vibrational/rotational distribution produced by hydrogen atom recombination
[AD-A193005] 20 p2852 N88-26933
Electronic states of the Xe(sub n)HCl systems in gas and condensed phases
[AD-A193881] 23 p3192 N88-28997
Computed potential energy surfaces for chemical reactions
[NASA-CR-183168] 24 p3342 N88-29893
HYDROGEN BONDS
High pressure strand burn rate tests of polyvinylnitrate/nitramine propellants
[AD-A184178] 04 p0422 N88-12615
Observing effect of laser radiation of low-frequency Raman scattering of light 06 p0772 N88-14742
Van der Waals clusters of aromatic molecules studied using supersonic molecular jet spectroscopy
[AD-A186087] 07 p0929 N88-15644
HYDROGEN CHLORIDES
NT HYDROCHLORIC ACID
Hydrogen chloride measurements in launch-vehicle exhaust clouds
[DE87-011552] 08 p0964 N88-15837
HYDROGEN CLOUDS
NT H II REGIONS
NT ORION NEBULA
Detection of abundant molecular gas in the UV-excess quasar Mrk 1014 22 p3164 N88-28842
HYDROGEN COMPOUNDS
NT BORANES
NT BORON HYDRIDES
NT DEUTERIUM COMPOUNDS
NT HYDRIDES
NT HYDROGEN PEROXIDE
NT HYDROGEN SULFIDE
NT LITHIUM HYDRIDES
NT METAL HYDRIDES
NT NITROGEN HYDRIDES
NT SILANES
NT SODIUM HYDRIDES
HYDROGEN CYANIDE LASERS
U HCN LASERS
HYDROGEN EMBRITTLEMENT
Environmentally assisted cracking: Overview of evidence for an adsorption-induced localised-slip process
[AD-A185175] 05 p0565 N88-13443
The influence of crack conditions on hydrogen uptake by steels 05 p0604 N88-13702
the influence of temper embrittlement on fatigue crack growth in hydrogen 05 p0605 N88-13709
Crack initiation studies in hydrogen embrittled spring steel strip 05 p0605 N88-13710
Embrittling effect of the plastic zone 05 p0607 N88-13721
The factors which govern the acceleration of corrosion fatigue crack growth rate of a ferritic stainless steel 06 p0717 N88-14402
Effect of rare earth elements on the hydrogen-induced cracking in high strength low alloy steel
[PB87-143806] 07 p0833 N88-15052
Multipurpose corrosion inhibitors for aerospace materials in Naval environments
[AD-A186728] 09 p1143 N88-16853
Detection of hydrogen-assisted-cracking in U-0.8Ti alloy weldments by acoustic emission monitoring
[DE88-003221] 09 p1184 N88-17093
Influence of grain boundary phosphorus segregation on hydrogen embrittlement in steel
[DE88-700176] 11 p1459 N88-18696
The influence of strain on hydrogen entry, transport, and embrittlement of a high strength steel in aqueous sodium chloride solution
[AD-A189302] 12 p1608 N88-19619
Hydrogen embrittlement of gun steel
[AD-A188972] 13 p1740 N88-20407
Dependence of hydrogen embrittlement of austenitic stainless steels on structural state of grain boundaries 14 p1896 N88-21316
Hydrogen embrittlement susceptibility of high strength ESR 4340 steel alloys for ballistically resistant/tolerant components 17 p2319 N88-23848
Investigation of structure and surface state effect on hydrogen embrittlement of steels, under consideration of acoustic emission analysis
[ETN-88-92350] 20 p2775 N88-26457
Research on the kinetics of phase changes in solids
[AD-A192222] 20 p2814 N88-26696
Evaluation of a diffusion/trapping model for hydrogen ingress in high-strength alloys
[AD-A194301] 23 p3194 N88-29008
Hydrogen embrittlement of iron-nickel alloys
[AD-A195909] 24 p3353 N88-29958
HYDROGEN ENGINES
Advanced fabrication techniques for hydrogen-cooled engine structures
[NASA-CR-3949] 06 p0723 N88-14447
HYDROGEN FLUORIDES
U HYDROFLUORIC ACID
HYDROGEN FUELS
Hydrogen Energy Coordinating Committee: Summary of DOE hydrogen programs for FY 1987
[DE88-003960] 10 p1306 N88-17811
Fusion, and advanced fuel, reaction bibliography: Particle reactions from H1 to B11
[AD-A187420] 11 p1552 N88-19286
Electrochemical hydrogen concentrator for phosphoric acid fuel cells
[AD-A191355] 16 p2229 N88-23317
Ultra high temperature direct propulsion 17 p2401 N88-24275

Performance of a hydrogen pulsed electrothermal thruster. Strategic defense initiative organization innovative science and technology. SBIR, phase 1
[AD-A191999] 18 p2475 N88-24679
Dual-fuel, dual-mode rocket engine
[NASA-CASE-LAR-13773-1] 18 p2475 N88-24685
Catalytic ignition of hydrogen and oxygen propellants
[NASA-TM-100957] 18 p2476 N88-24689
Mach 2 combustion characteristics of hydrogen/hydrocarbon fuel mixtures
19 p2625 N88-25568
Numerical simulation of ignition of hydrogen jet in hot air 19 p2637 N88-25647
Chemical/hydrogen energy systems
[DE88-007013] 19 p2687 N88-25969

HYDROGEN IONS
Dynamic effects of stellar winds and associated HII regions on the interstellar medium
[ETN-87-90421] 01 p0109 N88-10706
Studies on surface chemical states of some metals and ceramics bombarded with energetic light-ions
[DE87-752975] 02 p0145 N88-10910
The dc conductivity studies of an hydroxide ion conductor at intermediate temperatures
[AD-A186044] 07 p0847 N88-15142
Atomic data for hydrogens in collisions with electrons: Addenda
[IPPJ-AM-55-ADD] 09 p1252 N88-17502
Optimization of volume produced H(-) ions in a low-pressure hydrogen plasma
[IPPJ-853] 09 p1252 N88-17505
An infra-red investigation of HAN (Hydroxylammonium Nitrate)-based liquid propellants
[AD-A187226] 10 p1307 N88-17815
The magnitude of secondary electron contributions in photon stimulated desorption
[AD-A189094] 13 p1835 N88-20980
Determination of beam orientation of optical diagnostics of excited 200-MeV hydrogen atoms resulting from photodetachment of H(-)ions
[AD-A189976] 14 p1981 N88-21823
Proceedings of the Cooling, Condensation, and Storage of Hydrogen Cluster Ions Workshop
[AD-A189857] 16 p2268 N88-23555
Overview of hydrogen clusters
16 p2267 N88-23557
Large hydrogen cluster ions 16 p2267 N88-23558
Formation and reactivity of small hydrogen cluster ions 16 p2267 N88-23560
Electronic structure and stability of small cation and anion hydrogen clusters 16 p2267 N88-23562
Photon-assisted formation and cooling of molecular hydrogen
[MP-87-102] 16 p2267 N88-23563
Vibrational spectroscopy of the hydrogen and hydrated hydronium cluster ions 16 p2268 N88-23566
First capture of antiprotons in an ion trap and the possibility of antihydrogen 16 p2268 N88-23569
Analysis of containerless condensation of polyatomic hydrogen ions, with emphasis on H3(+,-) association channels and a future workshop to study related topics
16 p2269 N88-23576
An optical technique for measuring divergence, beam profile, and aiming direction, of relativistic negative hydrogen ions
[DE88-007049] 18 p2572 N88-25278
Development of high current and high brightness negative hydrogen ion sources
[DE88-010882] 20 p2852 N88-26934

HYDROGEN ISOTOPES
NT DEUTERIUM
NT TRITIUM
Impact-induced devolatilization and hydrogen isotopic fractionation of serpentine: Implications for planetary accretion
[NASA-CR-182877] 16 p2175 N88-22966
Investigation of hydrogen isotope penetration through stainless steels Kh18N10T and Kh3M2BFR
[DE88-702189] 21 p2915 N88-27297

HYDROGEN MASERS
Fast autotuning of a hydrogen maser by cavity Q modulation 04 p0436 N88-12707
Study and construction of a compact hydrogen maser with a high-degree of frequency stability
[PB87-151122] 07 p0859 N88-15216
Atomic clocks research: An overview
[AD-A185567] 07 p0930 N88-15648
Hydrogen maser
[PB87-171617] 09 p1172 N88-17025

HYDROGEN OXYGEN ENGINES
Space station propulsion
[NASA-TM-100216] 03 p0277 N88-11746
Auxiliary propulsion technology for advanced Earth-to-orbit vehicles
[NASA-TM-100237] 06 p0674 N88-14127
Equilibrium retention in the nozzle of oxygen hydrogen propulsion systems 07 p0924 N88-15616
Space station propulsion technology
[NASA-CR-179260] 08 p0964 N88-15835
An analytical study of the hydrogen-air reaction mechanism with application to scramjet combustion
[NASA-TP-2791] 08 p0966 N88-15846
Recent advances in low-thrust propulsion technology
[NASA-TM-100959] 18 p2569 N88-25260

HYDROGEN OXYGEN FUEL CELLS
Electrochemical characteristics of acid electrolytes for fuel cells
[PB88-104641] 06 p0731 N88-14497
Regenerative fuel cell energy storage system for a low earth orbit space station
[NASA-CR-174802] 24 p3389 N88-30184

HYDROGEN PEROXIDE
The redox chemistry of some peroxo and superoxo metal ion complexes
[AD-A189159] 12 p1806 N88-19606
Sulfur dioxide-hydrogen peroxide relationships in clean air, clouds, and precipitation
[DE88-006352] 19 p2690 N88-25990
Liquid-phase oxidation of acetone with hydrogen peroxide on oxide catalysts 19 p2706 N88-26091

HYDROGEN PLASMA
NT DEUTERIUM PLASMA
Theoretical studies of kinetic mechanisms of negative ion formation in plasmas
[AD-A185735] 06 p0784 N88-14812
Hydrogen pumping and release by graphite under high flux plasma bombardment
[DE88-005880] 13 p1842 N88-21021
Properties of hydrogen/helium accretion plasmas
[DE88-006831] 19 p2728 N88-26197
Plasma armature formation in high-pressure, high-velocity hydrogen
[DE88-008347] 20 p2857 N88-26967

HYDROGEN PRODUCTION
The developmental status of solar thermochemical hydrogen production
[DE88-001778] 04 p0466 N88-12884
Intramolecular energy transfer reactions as a method for metal complex assisted production of hydrogen
[DE88-001621] 05 p0562 N88-13425
Nitrogen scale-up
[AD-A185702] 06 p0709 N88-14351
Study of the vapor-liquid equilibria used in the fabrication process of hydrogen by thermochemistry
[DE88-900239] 07 p0830 N88-15035
Organic coatings to improve the storageability and safety of pyrotechnic compositions
[AD-A187158] 09 p1150 N88-16889
Optimization of volume produced H(-) ions in a low-pressure hydrogen plasma
[IPPJ-853] 09 p1252 N88-17505
Solar-assisted hydrogen generation by photoelectrocatalysis
[PB88-160932] 12 p1605 N88-19597
Basic characteristics of heat-exchanger-type steam reformer heated by high-temperature helium gas (2). Analysis by simulation model (2)
[DE87-702962] 15 p2061 N88-22291
Chemical/hydrogen energy systems
[DE88-007013] 19 p2687 N88-25969
Photosynthetic water splitting
[DE88-007809] 20 p2830 N88-26791

HYDROGEN RECOMBINATIONS
Test summary for advanced H2 cycle NI-CD cell
02 p0165 N88-11040
Nascent vibrational/rotational distribution produced by hydrogen atom recombination
[AD-A193005] 20 p2852 N88-26933

HYDROGEN SULFIDE
The effect of H2S concentration and pH on hydrogen permeation in AISI 410 stainless steel in 5 percent NaCl
[NPL-DMA(A)-148] 14 p1890 N88-21293
The effect of H2S concentration and pH on the cracking resistance of AISI 410 stainless steel in 5 percent brine
[NPL-DMA(A)-149] 14 p1890 N88-21294

HYDROGEN 2
U DEUTERIUM

HYDROGEN 3
U TRITIUM

HYDROGENATION
The effect of additives on the reactivity of palladium surfaces for the chemisorption and hydrogenation of carbon monoxide: A surface science and catalytic study
[DE87-014685] 02 p0145 N88-10909
Characterization of catalysts with metal-support effects and of the species adsorbed on their surfaces
[DE87-014636] 04 p0414 N88-12564
Detection of minimum-ionizing particles in hydrogenated amorphous silicon
[DE88-002769] 07 p0837 N88-15081
Surface composition-reactivity relationships in heterogeneous catalysis
[DE87-003450] 09 p1140 N88-16834
Superconductivity and crystal structure of high-pressure phases in V-Ru-H system 09 p1239 N88-17426
High-density jet fuels from coal syncrudes, appendix 4
[DE88-003132] 10 p1307 N88-17813
A new polymer-based hydrogen getter
[DE88-004538] 13 p1751 N88-20487
Investigations of the origins of metastable, light-induced changes in hydrogenated amorphous silicon
[DE88-001117] 13 p1846 N88-21051
Improvements to Raney copper zinc methanol synthesis catalysts 17 p2318 N88-23844
Surface composition-reactivity relationships in heterogeneous catalysis
[DE88-006679] 18 p2480 N88-24714
Research on hydrotreating catalysts to hydrodeoxygenate biocrude oils
18 p2536 N88-25046
Hydrogenated amorphous silicon-germanium alloys
[DE88-001147] 19 p2620 N88-25546

HYDROGENOLYSIS
NT HYDROCRACKING

HYDROGEOLOGY
Study of Earth from space and strengthening of economy 01 p0010 N88-10055
The contribution of remote sensing to hydrology and hydrogeology 22 p3090 N88-28347
The use of SPOT images for water resources surveys in the Kasserine Basin (Tunisia)
22 p3090 N88-28349

HYDROGRAPHY
Varifront 3 expedition data report (USNS DE STEIGUER CRUISE 1202-82). Bioluminescence, hydrographic, nutrient, and satellite data from the Gulf of California (November-December 1981)
[AD-A185011] 05 p0620 N88-13805
Hurricane Danny storm surge data, report 4
[AD-A186373] 07 p0879 N88-15334
Hurricane Kate storm surge data, report 5
[AD-A186374] 07 p0880 N88-15335
North Pacific Ocean. Subtropical front north of Hawaii, R/V Thomas G. Thompson: 7 January - 10 February 1974. CTD data report
[AD-A186565] 08 p1044 N88-16310
North Pacific Ocean. Tradewind region east of Hawaii, R/V Thomas G Thompson: 25 September - 1 November 1972. STD data report
[AD-A186566] 08 p1044 N88-16311
North Pacific Ocean. Subarctic front central Pacific, R/V Thomas G. Thompson: 8 September - 9 October 1975. CTD data report
[AD-A186567] 08 p1044 N88-16312
North Pacific Ocean. Central Pacific Transition Zone, R/V Thomas G. Thompson: 25 March - 3 May 1968. STD data report
[AD-A186570] 09 p1195 N88-17160
North Pacific Ocean. Northeast Pacific Transition Zone, R/V Thomas G. Thompson: 1 November - 6 December 1969. STD data report
[AD-A186574] 09 p1195 N88-17161
Hydrographic and current measurements in the North-East Atlantic Ocean. Data report on F.S. Meteor cruises 69/5 and 69/6, October to November 1984
[REPT-166] 09 p1196 N88-17164
Current velocity and hydrographic observations in the Straits of Florida, the Caribbean Sea and offshore of the Antillean Archipelago: Subtropical Atlantic climate studies (STACS) 1984 and 1985
[PB88-149299] 12 p1649 N88-19874
Mass, heat and nutrient fluxes in the Atlantic Ocean determined by inverse methods
[NASA-CR-180535] 14 p1950 N88-21626
Hydrographic data from the OPTOMA (Ocean Prediction Through Observation, Modeling and Analysis) program: OPTOMA 23, 9-19 November 1986
[AD-A189868] 15 p2099 N88-22506
Physical, chemical and CTD (Conductivity/Temperature/Depth) data from the Marathon 2 expedition
[AD-A189930] 15 p2099 N88-22507
Hydrographic observations in the northwestern Weddell Sea Marginal Ice Zone during March 1986
[PB88-173240] 16 p2237 N88-23359
The impact of hemp production on the development of the municipalities of Araras, Leme, Santa Cruz da Conceicao and Pirassununga 19 p2683 N88-25948
Aerial photography as an instrument of atmospheric analysis: Maps of the middle atmosphere and its dynamics, Baixada Santista (SP) 19 p2684 N88-25955
Beaufort sea mesoscale circulation study: Hydrography helicopter operations, April 1987
[PB88-203658] 21 p2976 N88-27681
Utilization of SPOT in hydrography
22 p3108 N88-28459

A method for determining absolute velocities from hydrographic data: The numerical code
[AD-A193997] 22 p3129 N88-28603
An analysis of results of a high-resolution world ocean circulation model
[AD-A195760] 24 p3405 N88-30272
HYDROKINETICS
U HYDROMECHANICS
HYDROLOGICAL CYCLE
Report of the Workshop on Space Systems Possibilities for a Global Energy and Water Cycle Experiment
[WCP-137] 09 p1193 N88-17147
HYDROLOGY
NT HYDROGEOLOGY
Remote Sensing-Arid Lands Workshop, Page, Arizona, June 10-12, 1986
[DE87-012368] 01 p0064 N88-10412
Description of NCAR (National Center for Atmospheric Research) Community Climate Model (CCM1)
[PB87-203782] 01 p0072 N88-10462
Study of evolution of Gulf Stream cyclinic eddy 06 p0727 N88-14473
Errors in retrieving hydrological fields and fields of their differential characteristics by method of approximation by orthogonal functions 06 p0727 N88-14475
Hydrochemical structure of Gulf Stream frontal zone waters 06 p0727 N88-14476
Modern concept concerning transport of bottom sediments in abyssal regions of world ocean 06 p0728 N88-14478
Tropical hydrology
[WMO-655] 06 p0745 N88-14584
Evaluation of the flooding areas of the Sao Goncalo Canal through LANDSAT 5 thematic mapper images
[INPE-4118-PRE/1039] 08 p1020 N88-16185
Hydrological models 14 p1937 N88-21559
The Hapex-Mobilhy program 14 p1938 N88-21560
Project CODEAMA/FUNCATE (test-area of Barreirinha-AM): Field report
[INPE-4500-RPE/563] 15 p2090 N88-22455
A core hole into the hydrothermal system of the Long Valley caldera
[DE88-006335] 16 p2231 N88-23325
Evaluation of the floodable area of the canal of Sao Goncalo through TM-LANDSAT 5 imagery 17 p2364 N88-24078
Evaluation of a flood period (June, 1984) in the southern region of Laguna dos Patos, through remote sensing data, meteorological and oceanographic 17 p2365 N88-24083
Aerial photography as an instrument of atmospheric analysis: Maps of the middle atmosphere and its dynamics, Baixada Santista (SP) 19 p2684 N88-25955
Surface hydrology, sediment transport dynamics and remote sensing of disturbed watersheds in a humid temperate region
[DE88-006719] 20 p2817 N88-26715
Vegetation studies on Vandenberg Air Force Base, California
[NASA-TM-100985] 20 p2831 N88-26795
Use of SPOT satellite in agrohydrology: Detection of spring water excess in a grassland region 22 p3091 N88-28357
The world's water resources: A major neglect. A study in remote sensing in hydrology and water management
[ESA-BR-40] 22 p3116 N88-28511
Use of LANDSAT images of vegetation cover to estimate effective hydraulic properties of soils
[NASA-CR-183185] 22 p3116 N88-28514
HYDROLOGY MODELS
Regularity properties of a doubly degenerate equation in hydrology
[REPT-87-07] 01 p0064 N88-10409
Use of the thermodynamic evaporation formula of Hoffmann in energy balance models for flowing water 08 p1013 N88-16143
Hydrologic models for land-atmosphere retrospective studies of the use of LANDSAT and AVHRR data
[NASA-CR-182861] 20 p2817 N88-26712
Hydrologic models for land-atmosphere retrospective studies of the use of LANDSAT and AVHRR data
[NASA-CR-182862] 20 p2818 N88-26716
HYDROLYSIS
Preparation of oxide glasses from metal alkoxides by sol-gel method
[NASA-TT-20124] 02 p0154 N88-10965
Effects of hydrolysis on metallo-organic solution deposition of PZT films
[ATR-86(8443)-1] 06 p0679 N88-14160
On copper peroxide
[NASA-TT-20263] 15 p2037 N88-22135
Identification of hydroxypropyl starch hydrolysate components 17 p2315 N88-23832
Saccharification of cellulose by combined fungal and bacterial preparations 17 p2316 N88-23833
Complexation and hydrolysis reactions of iron(III) 17 p2322 N88-23867
A study of solvent effects on the synthesis of pure component and composite ceramic powders by metal alkoxide hydrolysis
[DE88-008381] 20 p2777 N88-26470
HYDROMAGNETIC FLOW
U MAGNETOHYDRODYNAMIC FLOW
HYDROMAGNETIC STABILITY
U MAGNETOHYDRODYNAMIC STABILITY
HYDROMAGNETIC WAVES
U MAGNETOHYDRODYNAMIC WAVES
HYDROMAGNETICS
U MAGNETOHYDRODYNAMICS
HYDROMAGNETISM
U MAGNETOHYDRODYNAMICS
HYDROMECHANICS
NT ELASTOHYDRODYNAMICS
NT ELECTROHYDRODYNAMICS
NT HYDRODYNAMICS
NT HYDROSTATICS
NT MAGNETOHYDRODYNAMICS
A review of the NATO special group of experts on Naval hydromechanics and related problems 16 p2205 N88-23157
HYDROMETEOROLOGY
NT MARINE METEOROLOGY
The application of doubly-truncated hydrometeor distributions to numerical cloud models
[AD-A185273] 05 p0627 N88-13836
Influence of hydrometeorological factors on visibility of objects detected by radar 13 p1790 N88-20707
HYDRONIUM IONS
Vibrational spectroscopy of the hydrogen and hydrated hydronium cluster ions 16 p2268 N88-23566
HYDROPHONES
Bodies in unsteady flow
[AD-A190416] 15 p2064 N88-22308
Remote sensing of acoustic properties of shallow water sediments: A review
[AD-A192107] 18 p2570 N88-25267
HYDROPOWER STATIONS
U HYDROELECTRIC POWER STATIONS
HYDROSTATIC PRESSURE
Experimental studies on the tripping behavior of narrow T-stiffened flat plates subjected to hydrostatic pressure and underwater shock 05 p0592 N88-13613
Quantum wells and bulk AlGaAs under hydrostatic pressure 20 p2862 N88-27000
Pressure-dependent measurement on n+ GaAs (Si, Sn): The effect of deep donor (DX) states on the electrical properties and presistent photoconductivity effects 20 p2866 N88-27020
HYDROSTATICS
Composites strengthening
[AD-A189258] 13 p1734 N88-20364
Active control and system identification of rotordynamic structure 16 p2218 N88-23230
HYDROTHERMAL STRESS ANALYSIS
STAEBL/general composites with hygrothermal effects (STAEBL/GENCOM)
[NASA-TM-100266] 05 p0611 N88-13754
HYDROTHERMAL SYSTEMS
Tapping the earth's geothermal resources: Hydrothermal today, magma tomorrow
[DE87-014718] 02 p0196 N88-11223
Effective use of principal component analysis with high resolution remote sensing data to delineate hydrothermal alteration and carbonate rocks 05 p0612 N88-13758
Evaluation of AIS-2 (1986) data over hydrothermally altered granitoid rocks of the Singatse Range (Yerington) Nevada and comparison with 1985 AIS-1 data 05 p0613 N88-13767
Mapping hydrothermally altered rocks in the Northern Grapevine Mountains, Nevada and California with the airborne imaging spectrometer 05 p0614 N88-13772
Experimental and theoretical constraints on the origin of mid-ocean ridge geothermal fluids 13 p1804 N88-20784
A core hole into the hydrothermal system of the Long Valley caldera
[DE88-006335] 16 p2231 N88-23325
Geothermal energy technology: Issues, R and D (Research and Development) and cooperative arrangements
[PB86-193107] 21 p2967 N88-27626
HYDROX ENGINES
U HYDROGEN OXYGEN ENGINES
HYDROXIDES
NT LITHIUM HYDROXIDES
NT SODIUM HYDROXIDES
Toughening of alpha-alumina: Preliminary results
[DE87-702776] 01 p0028 N88-10178
Hydroxide ion conductors as possible electrolytes in intermediate temperature fuel cells
[AD-A185508] 06 p0731 N88-14495
Investigation of OH reaction products. Excimer laser photolysis/slab laser fluorescence under tropospheric conditions
[REPT-8] 09 p1191 N88-17137
Electron transfer to iron(3) oxide colloids
[DE88-002885] 10 p1416 N88-18448
Dynamics of production and oxidation of boranes
[AD-A188988] 12 p1606 N88-19605
Characterization of redox states of nickel hydroxide film electrodes by in-situ Raman spectroscopy
[AD-A189288] 13 p1741 N88-20411
Material degradation in a barium hydroxide latent heat storage pilot unit
[DFVLR-FB-87-49] 16 p2175 N88-22961
Transition probabilities in OH A 2 sigma + - X 2 pi i: Bands with v prime = 0 and 1, v double prime = 0 to 4
[NASA-CR-182946] 18 p2584 N88-25353
Crystallization of aluminum hydroxide in the aluminum-air battery: Literature review, crystallizer design and results of integrated system tests
[DE88-010510] 20 p2797 N88-26594
HYDROXYL COMPOUNDS
NT ALCOHOLS
NT ETHYL ALCOHOL
NT GLYCOLS
NT ISOPROPYL ALCOHOL
NT METHYL ALCOHOL
NT PHENOLS
NT POLYVINYL ALCOHOL
High pressure strand burn rate tests of polyvinylnitrate/nitramine propellants
[AD-A184178] 04 p0422 N88-12615
An infra-red investigation of HAN (Hydroxylammonium Nitrate)-based liquid propellants
[AD-A187226] 10 p1307 N88-17815
Identification of hydroxypropyl starch hydrolysate components 17 p2315 N88-23832
The burning of HAN-based (hydroxylammonium nitrate) liquid propellants
[DE88-006863] 18 p2494 N88-24800
HYDROXYL EMISSION
Lyman-alfa/OH-resonance-absorbtion measurements and simulation calculations for the investigation of the induction behavior of methane/ethane/oxygen mixtures in reflected shock waves
[ETN-88-90806] 07 p0831 N88-15042
VLBI research on OH-maser IN W33 08 p1001 N88-16064
HYDROXYL RADICALS
Preparation of polymer polyols
[EP-PATENT-0-162-589-A1] 01 p0102 N88-10665
Investigations of extragalactic hydroxyl 03 p0389 N88-12441
Photon stimulated desorption from oxidized Al(110)
[DE88-002209] 06 p0787 N88-14828
Measurement of rate constants of elementary gas reactions of importance to upper atmosphere and combustion systems
[AD-A189432] 13 p1737 N88-20386
Ground-based column abundance measurements of atmospheric hydroxyl
[NASA-CR-182676] 14 p1944 N88-21598
Water vapor and hydroxyl distributions in the inner coma of Comet Halley measured by the VEGA-2 three channel spectrometer TKS 14 p1998 N88-21910
Ultraviolet measurements: Measurements of photolysis rates 18 p2539 N88-25065
Laboratory experiments on atmospheric OH reactions 18 p2539 N88-25066
Effect of carbohydrate oxidation on the tropospheric HOx-system 18 p2539 N88-25067
Measurement of atmospheric OH with laser differential optical absorption spectroscopy (LDOAS) 18 p2539 N88-25068
Tropospheric OH measurements by long path absorption with rapid spectral concordance 18 p2539 N88-25069
Determination of tropospheric H concentrations by a double-pulsed UV laser method 18 p2539 N88-25070
Tropospheric OH measurement by Laser Induced Fluorescence (LIF) 18 p2540 N88-25071
Development of continuous wave laser frequency modulation of OH in tropospheric concentrations range 18 p2540 N88-25073
The evolution of cometary activity 18 p2594 N88-25416
Ground level hydroxyl (OH) concentration measurements by long path differential optical laser absorption
[ETN-88-92124] 20 p2855 N88-26952
Distribution of hydroxyl clouds in the galaxy
[DE88-702415] 22 p3164 N88-28844

HYGRAL PROPERTIES
STAEBL/general composites with hygrothermal effects (STAEBL/GENCOM)
[NASA-TM-100266] 05 p0611 N88-13754
HYGROSCOPICITY
Thermodynamic study of hygroscopic polymers using surface acoustic waves 19 p2672 N88-25882
HYPERBARIC CHAMBERS
Space station internal environmental and safety concerns 04 p0407 N88-12527
USAF hyperbaric animal transfer chamber system
[AD-A193633] 23 p3237 N88-29265
HYPERBOLIC COORDINATES
Two dimensional hyperbolic grid generation
[VKI-TN-162] 18 p2511 N88-24897
HYPERBOLIC DIFFERENTIAL EQUATIONS
A study of numerical methods for hyperbolic conservation laws with stiff source terms
[NASA-TM-100075] 10 p1399 N88-18343
Accurate boundary conditions for exterior problems in gas dynamics
[NASA-TM-100807] 11 p1537 N88-19182
Conservative finite volume solutions of a linear hyperbolic transport equation in two and three dimensions using multiple grids
[NASA-CR-182715] 13 p1828 N88-20934
Feedback control of a hyperbolic partial-differential equation with viscoelastic damping
[AD-A192896] 21 p3003 N88-27810
HYPERBOLIC FUNCTIONS
Inhomogeneous conditions at open boundaries for wave propagation problems
[AD-A183647] 01 p0033 N88-10214
Smooth dynamics on the interval (with an emphasis on unimodal maps)
[REPT-87-09] 01 p0086 N88-10555
Stability of semidiscrete approximations for hyperbolic initial-boundary-value problems: An eigenvalue analysis
[NASA-TM-88328] 02 p0227 N88-11434
Some aspects of high resolution numerical methods for hyperbolic systems of conservation laws, with applications to gas dynamics
[DMS-86-7] 03 p0321 N88-12031
Nonlinear hyperbolic conservation laws
[AD-A184963] 05 p0580 N88-13538
Stability analysis of finite difference schemes for hyperbolic systems, and problems in applied and computational linear algebra
[AD-A185824] 07 p0908 N88-15499
Hyperbolicity and invariant measures for general C sq interval maps satisfying the Misiurewicz condition
[REPT-87-46] 14 p1966 N88-21733
La Recherche Aerospatiale, bimonthly bulletin, no. 1986-5, 234/September-October
[ESA-TT-1032] 19 p2641 N88-25671
Stability of semidiscrete approximations for hyperbolic initial-boundary-value problems: Stationary modes
[NASA-TM-100994] 23 p3270 N88-29455
HYPERBOLIC NAVIGATION
NT LORAN C
HYPERBOLIC SPACE
U HYPERBOLIC COORDINATES
HYPERBOLIC TRAJECTORIES
Solution of the hyperbolic Kepler's equation
[RAE-TR-87042] 09 p1229 N88-17368
HYPERCAPNIA
Effect of intermittent hypercapnia on visual analyzer function 07 p0896 N88-15431
Effect of hypercapnic-hypoxic test on cariorespiratory parameters of individuals with neurocirculatory dystonia 10 p1387 N88-18169
Human adaptation to various hypercapnic conditions in relation to salivary electrolyte dynamics and renal function 12 p1664 N88-19977
Physiological effects on man of long duration confinement in a carbon dioxide enriched environment 19 p2695 N88-26017
Distinctive features in blood clotting and fibrinolytic properties under effect of epinephrine in presence of hypoxia and hypercapnia 19 p2705 N88-26082
HYPERCUBE MULTIPROCESSORS
A portable hypercube simulator
[DE87-013369] 04 p0478 N88-12947
Implementation of a 3-D nonlinear MHD calculation on the Intel hypercube
[DE87-014637] 04 p0479 N88-12949
Parallelization of hydrocodes on the Intel Hypercube, part 2
[DE88-001591] 04 p0480 N88-12957
Performance analysis of parallel branch and bound search with the hypercube architecture 09 p1206 N88-17229
The next generation of hypercube computers 10 p1378 N88-18226
Investigations on the usefulness of the Massively Parallel Processor for study of electronic properties of atomic and condensed matter systems
[NASA-CR-182514] 10 p1383 N88-18259
Experiences with serial and parallel algorithms for channel routing using simulated annealing
[NASA-CR-182530] 10 p1388 N88-18289
Implementation of a 3-D nonlinear MHD (magnetohydrodynamics) calculation on the Intel hypercube
[DE88-000625] 13 p1816 N88-20848
Cholesky downdating on a hypercube
[DE88-006780] 15 p2113 N88-22586
Simulation of fault tolerance in a hypercube arrangement of discrete processors
[AD-A189682] 15 p2114 N88-22594
Implementation and performance analysis of parallel assignment algorithms on a hypercube computer
[AD-A190678] 15 p2115 N88-22600
Multi-sensor integration on the NCUBE hypercube computer
[DE88-007472] 18 p2554 N88-25182
QR factorization of a dense matrix on a hypercube multiprocessor
[DE88-009187] 19 p2716 N88-26129
Relay approach message routing in hypercube multiprocessors
[DE88-009973] 20 p2835 N88-26814
Distributed fault tolerant embeddings of binary trees in hypercubes
[AD-A192929] 20 p2839 N88-26840
Motor-response learning at a process control panel by an autonomous robot
[DE88-005055] 21 p2955 N88-27554
Parallel implementation of the boundary element method
[DE88-011846] 21 p3007 N88-27839
Solving the symmetric tridiagonal eigenvalue problem on the hypercube
[AD-A193905] 23 p3250 N88-29344
A performance study of the hypercube architecture
[AD-A194361] 23 p3264 N88-29433
HYPERFINE STRUCTURE
Fundamental properties of spin-polarized quantum systems
[DE88-004425] 10 p1423 N88-18499
Sources of polarized ions and atoms
[DE88-010910] 20 p2852 N88-26931
Experimental and theoretical investigations of isotope shift and hyperfine structure on 5d elements (especially platinum, iridium and rhenium)
[ETN-88-93121] 24 p3353 N88-29957
HYPERGEOMETRIC FUNCTIONS
Peetre's Theorem and generalized functions
[MEMO-661] 14 p1967 N88-21742
Jacobi polynomials as generalized Faber polynomials
[CWI-PM-R8706] 16 p2258 N88-23498
Incomplete Lipschitz-Hankel integrals of MacDonald functions
[AD-A191034] 16 p2261 N88-23515
HYPERGEOMETRY
U HYPERSPACES
HYPERNUCLEI
Physics of few-body lambda hypernuclei
[DE87-014746] 03 p0375 N88-12357
Few body hypernuclear systems: Weak decays
[DE87-014920] 04 p0488 N88-13010
Experimental aspects of hypernuclear physics at CEBAF
[CEBAF-R-86-013] 11 p1546 N88-19245
HYPEROXIA
Human metabolism and peripheral circulation during antiorthostatic hypokinesia 07 p0891 N88-15398
Effect of oxygen inhalation on respiratory function during exercise and exposure to added resistance to respiration 10 p1366 N88-18164
Increase in influence of oxygen on the body in the presence of helium 13 p1810 N88-20816
The evolution of glutathione metabolism in phototrophic microorganisms
[NASA-CR-182902] 19 p2695 N88-26015
Human erykthrocyte metabolism in the presence of hyperoxygenation during antiorthostatic hypokinesia 19 p2706 N88-26092
HYPERPLANES
On the volume of a n-dimensional simplex
[REPT-87-16] 01 p0086 N88-10557
HYPERSONIC AIRCRAFT
Experimental aerothermodynamic research of hypersonic aircraft
[NASA-CR-181533] 04 p0399 N88-12483
The off-design performance of hypersonic waveriders 05 p0533 N88-13244
Numerical optimization of conical flow waveriders including detailed viscous effects 05 p0533 N88-13245
Dynamic stability of hypersonic conical lifting vehicles according to Newton-Busemann theory 05 p0534 N88-13247
Lifting bodies: An attractive aerodynamic configuration choice for hypervelocity vehicles 05 p0534 N88-13248
Aeropropulsion '87. Session 6: High-Speed Propulsion Technology
[NASA-CP-10003-SESS-6] 08 p0957 N88-15807
Hypersonic propulsion research 08 p0958 N88-15812
Accuracies of southwell and force/stiffness methods in the prediction of buckling strength of hypersonic aircraft wing tubular panels
[NASA-TM-88295] 09 p1183 N88-17090
Aerothermal tests of quilted dome models on a flat plate at a Mach number of 6.5
[NASA-TP-2804] 15 p2067 N88-22325
National aero-space plane: A technology development and demonstration program to build the X-30
[GAO/NSIAD-88-122] 17 p2301 N88-23764
Application of integrated fluid-thermal-structural analysis methods
[NASA-TM-100625] 17 p2350 N88-24001
Supersonic transport/hypersonic transport (SST/HST) development
[REPT-881-111-101] 21 p2896 N88-27192
HYPERSONIC BOUNDARY LAYER
Turbulence in hypersonic flow
[AD-A185624] 07 p0815 N88-14961
Shock wave/turbulent boundary layer interaction in high-Reynolds-number hypersonic flows
[AD-A188029] 11 p1434 N88-18555
Hypersonic turbulent wall boundary layer computations
[NASA-CR-182147] 18 p2514 N88-24917
Low density real gas flows about hypersonic vehicles
[AD-A194251] 22 p3075 N88-28253
The effects of incoming boundary layer thickness on unsteady shock-induced turbulent separations induced by cylinders
[AD-A196190] 24 p3368 N88-30060
HYPERSONIC FLIGHT
Shock tunnels for real gas hypersonics 05 p0530 N88-13223
Driving mechanism of unsteady separation shock motion in hypersonic interactive flow 05 p0530 N88-13226
Upgrading of NASA-Ames high-energy hypersonic facilities: A Study
[NASA-CR-182475] 09 p1122 N88-16717
Review of convectively cooled structures for hypersonic flight
[NASA-TM-87740] 17 p2310 N88-23817
Compressible boundary layers — atmospheric reentry
[CERT-OA-13/5005-AYD] 20 p2801 N88-26823
Hypersonic flight testing
[DE88-001655] 21 p3015 N88-27894
HYPERSONIC FLOW
Fast shock tube assemblies
[DE87-011732] 01 p0008 N88-10042
The aerothermodynamic environment for holes in hypersonic configurations
[DE87-014651] 02 p0121 N88-10767
Similar solutions for viscous hypersonic flow over a slender three-fourths-power body of revolution
[NASA-TM-100205] 04 p0443 N88-12752
Experimental investigations on blunt bodies and corner configurations in hypersonic flow 05 p0530 N88-13225
An ultra-high-speed cinematographic method for the study of wakes in hypersonic ballistic ranges 05 p0531 N88-13228
Numerical simulation of the hypersonic flow around lifting vehicles 05 p0532 N88-13234
Hypersonic laminar boundary layer: Parametric study for the representation of real gas effects 05 p0532 N88-13236
On the numerical simulation of three-dimensional hypersonic flow 05 p0532 N88-13237
Numerical experiments with hypersonic flows beneath a cone-delta-wing combination 05 p0532 N88-13238
A spatial marching technique for the inviscid blunt body problem 05 p0533 N88-13239
A 3-D Euler solution for hypersonic Mach numbers 05 p0533 N88-13240
Computation of flow past conical hypersonic wings using a second order Godunov method 05 p0533 N88-13241
Time-dependent hypersonic viscous interactions
[AD-A185764] 06 p0665 N88-14082
Turbulence in hypersonic flow
[AD-A185624] 07 p0815 N88-14961
Three-dimensional Euler solutions for hypersonic Mach numbers
[MBB-UR-944/87] 10 p1315 N88-17859

A study of numerical methods for hyperbolic conservation laws with stiff source terms
[NASA-TM-100075] 10 p1399 N88-18343
Hypersonic blunt body computations including real gas effects
[NASA-TM-100074] 10 p1400 N88-18344
Analysis of shear-layer probe data for holes in hypersonic configurations
[DE88-003992] 11 p1435 N88-18564
Topology and grid adaption for high-speed flow computations
[NASA-CR-182586] 11 p1487 N88-18875
A new parabolized Navier-Stokes code for chemically reacting flow fields 12 p1625 N88-19721
Documentation and installation of the hypersonic arbitrary-body computer program (Mark 3 version) of A.E. Gentry on the IBM computer system
[MBB/LKE-127/S/PUB/256] 13 p1719 N88-20276
High-resolution shock-capturing schemes for inviscid and viscous hypersonic flows
[NASA-TM-100097] 15 p2122 N88-22651
Experimental investigation of the hypersonic flow over a six finned configuration
[AD-A190870] 16 p2157 N88-22871
Application of integrated fluid-thermal-structural analysis methods
[NASA-TM-100625] 17 p2350 N88-24001
Boundary layer transition
[CERT-OA-37/5018-AYD] 18 p2458 N88-24595
Hypersonic turbulent wall boundary layer computations
[NASA-CR-182147] 18 p2514 N88-24917
Aerodynamics of lifting bodies with combined transverse and longitudinal curvature 19 p2598 N88-25436
Two-dimensional viscous flow computations of hypersonic scramjet nozzle flowfields at design and off-design conditions
[NASA-CR-182150] 19 p2603 N88-25459
The Proceedings of the Symposium on Mechanics for Space Flight 1987
[ISAS-SP-6] 20 p2782 N88-26499
Numerical computation of space shuttle orbiter flow field
[NASA-CR-183193] 22 p3040 N88-28048
Fellowships in hypersonic aerodynamics
[AD-A194265] 23 p3172 N88-28885
A numerical study of the test time in a hypersonic shock tunnel
[AD-A194057] 23 p3172 N88-28888

HYPERSONIC REENTRY
The aerodynamic design of hypersonic contoured axisymmetric nozzles including real gas effects
[VKI-TM-43] 06 p0665 N88-14076
Three-dimensional Euler solutions for hypersonic Mach numbers
[MBB-UR-944/87] 10 p1315 N88-17859
Study of hypersonic boundary layers
[CERT-RSF-OA-17/5005-AYD] 23 p3213 N88-29121

HYPERSONIC SHOCK
A numerical study of the test time in a hypersonic shock tunnel
[AD-A194057] 23 p3172 N88-28888

HYPERSONIC SPEED
SCRAM JET (Supersonic Combustion Ramjet) combustion experiments 04 p0404 N88-12512
Aerodynamic characteristics of wings designed with a combined-theory method to cruise at a Mach number of 4.5
[NASA-TP-2799] 12 p1575 N88-19420
Numerical study of unsteady viscous hypersonic blunt body flows with an impinging shock
[NASA-TM-100096] 15 p2122 N88-22650
A computational analysis of under-expanded jets in the hypersonic regime
[NASA-TM-101319] 21 p2893 N88-27174
Fellowships in hypersonic aerodynamics
[AD-A194265] 23 p3172 N88-28885
Transition at hypersonic speeds
[NASA-CR-178315] 24 p3368 N88-30058

HYPERSONIC VEHICLES
NT HYPERSONIC AIRCRAFT
NT X-30 VEHICLE
The aerothermodynamic environment for holes in hypersonic configurations
[DE87-014651] 02 p0121 N88-10767
The effects of sweep and bluntness on a glancing shock wave turbulent boundary layer interaction 05 p0531 N88-13227
Hypersonic static and dynamic stability of axisymmetric shapes: A comparison of prediction methods and experiment 05 p0534 N88-13246
Hypervelocity Technology (HVT) crew escape 09 p1214 N88-17280
Thermal stress in high temperature cylindrical fasteners
[NASA-TM-100611] 15 p2087 N88-22438
Aerodynamics of Hypersonic Lifting Vehicles: Fluid Dynamics Panel AGARD Symposium
[AGARD-AR-246] 21 p2943 N88-27480
Low density real gas flows about hypersonic vehicles
[AD-A194251] 22 p3075 N88-28253
Fellowships in hypersonic aerodynamics
[AD-A194265] 23 p3172 N88-28885

HYPERSONIC WIND TUNNELS
NT CASCADE WIND TUNNELS
NT HOTSHOT WIND TUNNELS
NT SHOCK TUNNELS
The 0.6m x 0.6m trisonic test section (TMK) of DFVLR in Cologne-Porz, Federal Republic of Germany (status 1986)
[ESA-TT-1052] 03 p0267 N88-11681
A survey of existing hypersonic ground test facilities: North America 05 p0529 N88-13220
European hypersonic wind tunnels 05 p0530 N88-13221
Preparation of qualification tests of a plasma generator for the feeding of a hypersonic wind tunnel 05 p0530 N88-13222
Turbulence measurement in hypersonic flow 05 p0530 N88-13224
The drag of slender axisymmetric cones in rarefied hypersonic flow 05 p0531 N88-13229
Low Reynolds number influence on aerodynamic performance of hypersonic lifting vehicles 05 p0531 N88-13230
Aerothermodynamics research at NASA Ames 05 p0533 N88-13242
The performance of the VKI longshot hypersonic wind tunnel
[VKI-TN-161] 18 p2468 N88-24650
A numerical study of the test time in a hypersonic shock tunnel
[AD-A194057] 23 p3172 N88-28888
Quantitative surface temperature measurement using two-color thermographic phosphors and video equipment
[NASA-CASE-LAR-13740-1] 24 p3376 N88-30105

HYPERSPACES
Group theoretic interpretations of Askey's scheme of hypergeometric orthogonal polynomials
[CWI-PM-R8703] 13 p1831 N88-20954
Hyperelliptic statsums in superstring theory
[DE88-701646] 16 p2284 N88-23676

HYPERTENSION
Effect of steroid hormones on biogenic amine levels in lungs during development of pulmonary hypertension in rats submitted to chronic hypobaric hypoxia 07 p0896 N88-15430
Hemodynamic effects of beta-adrenergic blocking with obsidan in clinostatic and orthostatic positions 10 p1367 N88-18171
Risk of hypertension and functional cerebral laterality in oil expedition works in far north 12 p1665 N88-19980

HYPERTHERMIA
Heat acclimatization under controlled hyperthermia 12 p1665 N88-19981
Analysis of annular microstrip antennas for hyperthermic applicators
[PB88-181508] 19 p2643 N88-25679
Hyperthermia: New thoughts on an old problem
[AD-A192602] 21 p2986 N88-27731
The impact of hyperthermia and hypohydration on circulation, strength, endurance and health
[AD-A192657] 22 p3131 N88-28615
Improvements in techniques of microwave thermography
[AD-A193620] 23 p3239 N88-29276

HYPERTONIA
U OSMOSIS

HYPERTROPHY
U GROWTH

HYPERVELOCITY ACCELERATORS
U HYPERVELOCITY GUNS

HYPERVELOCITY CRATERING
U HYPERVELOCITY PROJECTILES
U PROJECTILE CRATERING

HYPERVELOCITY FLOW
Acceleration to hypervelocities using minimum energy concepts
[DE87-011796] 01 p0089 N88-10583

HYPERVELOCITY GUNS
Effects of barrel joints on hypervelocity projectiles
[DE87-013447] 02 p0157 N88-10983
Current-filamentation instability in railgun arcs
[AD-A184618] 03 p0269 N88-11693
Experimental investigation of a three-stage railgun incorporating puff-switching
[MRL-R-1056] 09 p1130 N88-16785
Pulsed current transformer for low inductive loads
[AD-A187224] 10 p1324 N88-17913
A laboratory railgun for terminal ballistics and arc armature research studies
[AD-A187225] 11 p1442 N88-18603
Structural integrity of metallic armature rail guns
[AD-A188735] 13 p1728 N88-20333
Launchability of base-driven electromagnetic projectiles
[AD-A189635] 15 p2023 N88-22055
Ultrasonic Time-Of-Flight Diffraction (TOFD) measurements of crack depths in an acceleration reservoir of a high velocity research gun
[DE88-006644] 16 p2164 N88-22907
Experimental investigation of a three-stage railgun incorporating puff-switching
[AD-A191044] 16 p2166 N88-22918
Analytic and numerical modeling of heat and material transport in electrical hypervelocity guns
[AD-A192178] 18 p2469 N88-24655
STARFIRE: Hypervelocity railgun development for high-pressure research
[DE88-008348] 19 p2605 N88-25469
Application of the Hilbert transform to Doppler radar signals from a hypervelocity gun
[AD-A193690] 22 p3146 N88-28716

HYPERVELOCITY IMPACT
Shock-wave studies using plastic flyers driven by an electric gun for hypervelocity impact on selected materials
[DE87-012631] 01 p0008 N88-10046
Computations of hypervelocity impact using the CTH shock wave physics code
[DE87-013067] 02 p0169 N88-11062
Measurements of iridium and the meteoric impact hypothesis at cretaceous end
[DE87-703765] 04 p0521 N88-13200
Conditions for geomagnetically trapping sub-micron lunar ejecta between L = 1.2 and L = 3.1 04 p0521 N88-13203
An investigation of oblique hypervelocity impact 07 p0927 N88-15629
An analysis of penetration and ricochet phenomena in oblique hypervelocity impact
[NASA-TM-100319] 10 p1339 N88-18004
Sub-scaling of projectile/target system damaged by hypervelocity
[AD-A188683] 12 p1634 N88-19779
Effects of meteoroids and space debris on the particulate environment for space station 18 p2591 N88-25399
Hypervelocity impact analysis with supercomputers
[DE88-008907] 21 p3001 N88-27797
The effect of the near earth micrometeoroid environment on a highly reflective mirror surface
[NASA-TM-101307] 24 p3332 N88-29833

HYPERVELOCITY LAUNCHERS
A feasibility study of a hypersonic real-gas facility
[NASA-CR-180423] 01 p0008 N88-10043
Ultimate velocities for induction launchers
[DE87-012360] 04 p0404 N88-12513
Analysis of a series of electromagnetic launcher firings
[AR-005-131] 04 p0405 N88-12516
The railgun and its power source
[MRL-R-1058] 09 p1130 N88-16786
Continuous measurements of in-bore projectile velocity
[DE88-006841] 15 p2023 N88-22056
A chemical method for achieving acceleration of macroparticles to ultrahigh velocities
[DE88-006377] 15 p2128 N88-22695
Power and energy requirements for electromagnetic launchers 17 p2420 N88-24391
Fabrication issues and technology development for HELEOS (Hypervelocity Electromagnetic Launcher for Equation Of State)
[DE88-007419] 18 p2470 N88-24658
Application of superconducting technology to earth-to-orbit electromagnetic launch systems
[NASA-TM-101134] 20 p2763 N88-26385
Application of superconducting technology to earth-to-orbit electromagnetic launch systems
[DE88-010022] 20 p2763 N88-26386

HYPERVELOCITY PROJECTILES
Effects of barrel joints on hypervelocity projectiles
[DE87-013447] 02 p0157 N88-10983
Efficiency aspects of short, low velocity railguns
[AR-004-847] 04 p0405 N88-12517
A laboratory railgun for terminal ballistics and arc armature research studies
[AD-A187225] 11 p1442 N88-18603
Experimental determination of the heat flux inside a tubular projectile for the velocity range M = 3 and M = 6
[ISL-R-118/86] 11 p1443 N88-18605
Numerical simulation of the perforation of thin plates
[ISL-R-122/86] 11 p1495 N88-18926

Trajectory characteristics and heating of hypervelocity projectiles having large ballistic coefficients
[NASA-TP-2614] 12 p1574 N88-19412
Aerodynamic possibilities for the realization of trajectory corrections
[ISL-CO-251/86] 14 p1862 N88-21120
Variable Mach number wall jets for control/propulsion on hypervelocity projectiles/interceptors: Tests with an existing model
[AD-A192845] 21 p2892 N88-27167

HYPERVELOCITY WIND TUNNELS
NT CASCADE WIND TUNNELS
NT HOTSHOT WIND TUNNELS
NT SHOCK TUNNELS
Experience about the application and valuation of roughness strips for boundary layer transition control in wind tunnel tests in the high-speed range
[ESA-TT-1028] 01 p0044 N88-10278

HYPERVENTILATION
Detection of hyperventilation of parachutists
[DFVLR-FB-87-11] 01 p0075 N88-10482

HYPNOSIS
Hypnosis: Possible applications for cosmonauts
12 p1665 N88-19984

HYPOBARIC ATMOSPHERES
Cooling electronic equipment at simulated high altitude in hypobaric chambers
[AD-A185196] 05 p0584 N88-13560
Dexamethasone as prophylaxis for acute mountain sickness: Effect of dose level
[AD-A185848] 08 p1047 N88-16325
Operation Everest 2: Alterations in the immune system at high altitude
[AD-A188011] 11 p1520 N88-19075
Changes in hemostasis system of animals under conditions of granulocytopoiesis inhibition under effect of decreased barometric pressure
12 p1651 N88-19890
Acute mountain sickness at 4500 m is not altered by repeated eight-hour exposures to 3200-3550 m normobaric hypoxic equivalent
[AD-A188358] 12 p1666 N88-19990
Visual sensitivities under reduced oxygen
[AD-A195628] 24 p3406 N88-30279

HYPOCAPNIA
Biofeedback control of alveolar carbon dioxide tension to eliminate hypocapnia in man in the presence of hypoxia 07 p0892 N88-15405

HYPOGLYCEMIA
Spontaneous cerebral electrical activity during prolonged hypoglycemia: A quantitative study in humans
21 p2983 N88-27717

HYPOKINESIA
Human metabolism and peripheral circulation during antiorthostatic hypokinesia 07 p0891 N88-15398
Distinctions and mechanisms of effects of epinephrine and norepinephrine on cardiac pumping function under hypokinetic conditions 07 p0891 N88-15399
Circulatory response of males 45-52 years of age to antiorthostatic hypokinesia 07 p0894 N88-15416
Morphometric analysis of rat aorta endothelium during long-term hypokinesia 07 p0894 N88-15417
Nucleic acid content of skeletal muscles during hypokinesia and in the recovery period
07 p0894 N88-15418
JPRS Report: Science and Technology. USSR: Space Biology and Aerospace Medicine, volume 21, no. 5, September - October 1987
[JPRS-USB-88-003] 10 p1359 N88-18122
Isotope methods of determining distribution and movement of blood in the body
10 p1362 N88-18138
JPRS Report: Science and Technology. USSR: Space Biology and Aerospace Medicine, volume 21, no. 6, November - December 1987
[JPRS-USB-88-004] 10 p1364 N88-18150
Morphological study of early changes in rat bones in simulated weightlessness 10 p1365 N88-18158
Lipid peroxidation in rat tissues with exposure to antiorthostatic hypokinesia, exercise and immobilization stress 10 p1365 N88-18159
New book on metabolic aspects of spaceflight stress
10 p1367 N88-18172
Central hemodynamics in antiorthostatic hypokinesia and immersion models of weightlessness
11 p1521 N88-19081
Regulation of calcium metabolism during prolonged antiorthostatic hypokinesia
[NASA-TT-20219] 11 p1521 N88-19085
Use of diphosphonates to correct disorders in calcium metabolism and mineral composition of bone tissue with 60-day hypokinesia in rats
[NASA-TT-20220] 13 p1809 N88-20807
Changes in the status of the human tibia during antiorthostatic hypokinesia
[NASA-TT-20221] 13 p1810 N88-20813
JPRS report: Science and technology. USSR: Space Biology and Aerospace Medicine, volume 22, no. 1, January - February 1988
[JPRS-USB-88-005] 19 p2702 N88-26069
Noninvasive examination of bones during long-term hypokinesia 19 p2704 N88-26077
Human erykthrocyte metabolism in the presence of hyperoxygenation during antiorthostatic hypokinesia
19 p2706 N88-26092

HYPOPHYSIS
U PITUITARY GLAND

HYPOTHALAMUS
Neurophysiological analysis of hypothalamic regulation mechanisms of primary sleep and hypobiosis
06 p0751 N88-14611
Morphological and functional state of the hypothalamo-hypophyseal neurosecretory system of rats flown aboard Cosmos-1667 10 p1365 N88-18156
Hypothalamic-pituitary-adrenal responses to short duration high intensity cycle exercise
[AD-A192597] 21 p2985 N88-27727

HYPOTHERMIA
Influence of skeletal muscle glycogen on passive rewarming after hypothermia
[AD-A186451] 08 p1049 N88-16334
Rapid hypothermia subsequent to oral nicotinic acid and immersion in warm (30C) water
[AD-A186458] 08 p1050 N88-16339
Respiratory and cardiovascular responses to cold stress following repeated cold water immersion
[AD-A186460] 08 p1050 N88-16340
The role of hydration on peripheral response to cold
[AD-A186448] 09 p1199 N88-17186
Accidental hypothermia
[AD-A194967] 24 p3406 N88-30278

HYPOTHESES
NT EXPECTANCY HYPOTHESIS
NT LAGRANGE SIMILARITY HYPOTHESIS
Lower bounds on bearing accuracy for closely spaced sources
[AD-A184258] 04 p0486 N88-12997
Measurements of iridium and the meteoric impact hypothesis at cretaceous end
[DE87-703765] 04 p0521 N88-13200
Testing and interval estimation in a change-point model allowing at most one change
[AD-A185525] 06 p0767 N88-14716
Changing the layers of mind
[AD-A186648] 08 p1052 N88-16350
Exploring hypotheses in attitude control fault diagnosis
08 p1058 N88-16384
Discovery and problem solving: Triangulation as a weak heuristic 08 p1062 N88-16412
Practical applicability of exact and approximate forms of the randomization test for two independent samples
[AD-A186815] 09 p1231 N88-17381
An application of fuzzy set theory to statistical hypothesis testing
[AD-A186705] 09 p1232 N88-17386
Natural object categorization
[AD-A194103] 22 p3139 N88-28662

HYPOVOLEMIA
Human and animal hypovolemic reactions to increasing +Gz accelerations 07 p0890 N88-15395

HYPOXIA
Superoxide dismutase assays
[AD-A183972] 03 p0356 N88-12242
Scotopic sensitivity with 10 percent oxygen
[AD-A183973] 03 p0356 N88-12243
Hypoxic hypoxia as a stimulus of erythropoiesis in vivo and in vitro 07 p0885 N88-15373
Trace-element metabolism in man and animals in the presence of hypoxic states of diverse etiology
07 p0889 N88-15390
Biofeedback control of alveolar carbon dioxide tension to eliminate hypocapnia in man in the presence of hypoxia 07 p0892 N88-15405
Differentiation of hemopoietic stem cells during adaptation to high altitude 07 p0893 N88-15410
Effect of pyrocetam on mouse resistance to hypoxic hypoxia 2-3 months after exposure to X-radiation
07 p0895 N88-15425
Effect of steroid hormones on biogenic amine levels in lungs during development of pulmonary hypertension in rats submitted to chronic hypobaric hypoxia
07 p0896 N88-15430
Mononuclear phagocytes during adaptation of essentially healthy people to high altitudes
07 p0896 N88-15432
Effects of extreme hypoxia on phospholipid metabolism in subcellular structures of rat brain
08 p1046 N88-16323
Operation Everest 2: Nutrition and body composition
[AD-A186449] 08 p1049 N88-16333
Role of carbon dioxide in correction of coagulation hemostasis under hypoxic conditions
10 p1365 N88-18160
Polar worker adaptability to Antarctic high altitudes
10 p1366 N88-18165
Combined effect of ionizing radiation and altered gas atmosphere on central nervous system
10 p1367 N88-18168
Effect of hypercapnic-hypoxic test on cariorespiratory parameters of individuals with neurocirculatory dystonia
10 p1367 N88-18169
Operation Everest 2: Alterations in the immune system at high altitude
[AD-A188011] 11 p1520 N88-19075
Interrelationship of heart rhythm indicators and resistance to hypoxia in Antarctic polar workers
12 p1664 N88-19974
Human adaptation to various hypercapnic conditions in relation to salivary electrolyte dynamics and renal function 12 p1664 N88-19977
Medical problems related to altitude in: Human performance physiology and environmental medicine at terrestrial extremes, chapter 14
[AD-A188340] 12 p1666 N88-19989
Acute mountain sickness at 4500 m is not altered by repeated eight-hour exposures to 3200-3550 m normobaric hypoxic equivalent
[AD-A188358] 12 p1666 N88-19990
Distinctive features in blood clotting and fibrinolytic properties under effect of epinephrine in presence of hypoxia and hypercapnia 19 p2705 N88-26082
Effect of different modes of voluntary control of breathing on human electroencephalogram with exposure to acute hypoxic hypoxia 19 p2707 N88-26093
Experimental study of protective effect of antioxidant enzymes-superoxide dismutase and catalase-when using intermittent toxic modes of hyperbaric oxygenation
19 p2707 N88-26094
The effects of hypoxia on P300 and reaction time
[DCIEM-87-RR-12] 21 p2979 N88-27697
The effect of mild hypoxia on the vestibular evoked response 21 p2982 N88-27713
Alterations in cutaneous vasomotor regulation during acute and chronic hypoxia
[AD-A192653] 22 p3131 N88-28612
Biomedical aspects of military operations at high altitude
[AD-A192677] 22 p3132 N88-28619
Human performance and acute hypoxia, chapter 12
[AD-A192604] 23 p3238 N88-29270
Visual sensitivities under reduced oxygen
[AD-A195628] 24 p3406 N88-30279

HYPSOGRAPHY
Vectorization of raster algorithms for elevation data processing 18 p2534 N88-25036

HYSTERESIS
Temperature hysteresis and magnetic transitions in amorphous Fe-Ni-Zr alloys
[DE88-000228] 03 p0294 N88-11848
Applications of a theory of ferromagnetic hysteresis
[DE87-014725] 03 p0373 N88-12348
The consequences of intergrain Josephson coupling in ceramic high-temperature superconductors
[DE87-013713] 06 p0785 N88-14816
RCL model for the development of hysteresis in superconductors
[DE88-702061] 19 p2733 N88-26234
Experimental and theoretical study of the dynamic operational behavior of a three stage radial compressor
[ETN-88-92129] 20 p2611 N88-26676
Mathematical theory and calculations of magnetic hysteresis curves
[DE88-011055] 23 p3277 N88-29510
The aspect ratio dependence of the attractor dimension in Taylor-Couette flow
[AD-A196297] 24 p3369 N88-30065
Nonlinear stress-strain and inelastic rebound with exponential stiffness
[AD-A195667] 24 p3384 N88-30159
Behaviour and hysteresis losses of irreversible type-2 superconducting cylindrical shell
[DE88-702708] 24 p3433 N88-30434

I

I BEAMS
Partially braced inelastic beam buckling experiments
[PB87-133831] 06 p0723 N88-14444

IBM COMPUTERS
A CAMAC system controlled by an IBM AT computer for time-resolved spectroscopy
[DE87-010111] 01 p0080 N88-10514
FORTRAN compiler performance benchmarks for the IBM personal computer
[LA-10883-MS] 03 p0363 N88-12284

An IBM PC version of ASENT
[DE88-004244] 11 p1532 N88-19150
Documentation and installation of the hypersonic arbitrary-body computer program (Mark 3 version) of A.E. Gentry on the IBM computer system
[MBB/LKE-127/S/PUB/256] 13 p1719 N88-20276
The PC/AT compatible computer as a mission control center display processor at Ames-Dryden Flight Research Facility
[NASA-TM-100426] 14 p1955 N88-21654
Specification for IBM/IBM compatible 3480 tape cartridge
[NASA-TM-100702] 17 p2384 N88-24168
Aircraft noise prediction program propeller analysis system IBM-PC version user's manual version 2.0
[NASA-CR-181689] 24 p3428 N88-30399

ICE
NT GLACIERS
NT ICE FLOES
NT ICEBERGS
NT LAND ICE
NT PRESSURE ICE
NT SEA ICE
On the surging potential of polar ice streams. Antarctic surges: A clear and present danger
[DE87-013980] 02 p0216 N88-11363
Altered and enhanced iodargyrite with bismuth triiodide for use in precipitation enhancement operations
[AD-A185229] 05 p0561 N88-13419
Automated satellite cloud analysis: A multispectral approach to the problem of snow/cloud discrimination
[AD-A185672] 06 p0746 N88-14591
Planetary science 07 p0883 N88-15356
Atmospheric science 07 p0883 N88-15357
Recommendations for a US ice coring program
[PB88-115043] 09 p1185 N88-17102
Radar reflectivity and attenuation of radio waves in the melting layer of precipitation
[PB88-121553] 10 p1318 N88-17882
Aircraft and ground vehicle friction correlation test results obtained under winter runway conditions during joint FAA/NASA Runway Friction Program
[NASA-TM-100506] 11 p1438 N88-18582
Multiple scattering of polarized light in cirrus clouds
13 p1801 N88-20768
Predictions and studies with a one-dimensional ice/ocean model
[AD-A189158] 13 p1803 N88-20776
Diversity of comets, synergic temperature effects and the stability of organic compounds in icy nuclei
14 p2005 N88-21955
Different trapping mechanisms of gases by water ice and their relevance for comet nuclei
14 p2007 N88-21970
Sublimation characteristics of H2O comet nucleus with CO2 impurities 14 p2010 N88-21988
Thermal instability and heat transfer characteristics in water/ice systems
[AD-A189627] 15 p2062 N88-22297
Microgravity thaw experiment (MITEX)
17 p2427 N88-24439
Analysis of dust grain properties in two star forming regions through comparison of theoretical models to observations 17 p2451 N88-24559
MIZPAC (marginal ice zone Pacific) 84-86 CTD (Conductivity, Temperature, Depth) data report
[AD-A192478] 21 p2976 N88-27679
Reduce uncertainty in projection of future sea-level changes due to ice wastage
[DE88-009883] 22 p3129 N88-28601
Ice detector
[NASA-CASE-LAR-13776-1] 23 p3217 N88-29149
General equations for the motions of ice crystals and water drops in gravitational and electric fields
[NASA-CR-183229] 24 p3370 N88-30070

ICE ENVIRONMENTS
Blade excitation criteria developed for aero derived engines in Arctic Alaska
[PNR90368] 02 p0182 N88-11131
JPRS report: Science and technology. USSR: Earth sciences
[JPRS-UES-88-001] 13 p1784 N88-20674
Real-time environmental Arctic monitoring (R-TEAM)
[AD-A189948] 15 p2099 N88-22508

ICE FLOES
Underwater acoustic backscatter from a model of arctic ice open leads and pressure ridges
[AD-A184693] 03 p0354 N88-12234
Navarin Basin Ice Drift Program
[PB88-104021] 06 p0748 N88-14599

ICE FORMATION
NT CLOUD GLACIATION
Conception and discussion of a model describing ice formation on various obstacles
[ONERA-NT-1986-6] 01 p0072 N88-10460
The dependence of the normalized ice accretion thickness on cloud-physical parameters
[DFVLR-FB-87-08] 01 p0072 N88-10464
Stability relationship for water droplet crystallization with the NASA Lewis icing spray
[NASA-TM-100220] 02 p0125 N88-10790
On the role of convective motion during dendrite growth: Experiments under variable gravity, revised
[NASA-CR-179213] 02 p0156 N88-10979
Analysis of counting errors in the phase/Doppler particle analyzer
[NASA-TM-100231] 03 p0323 N88-12043
Icing detector with early warning capability
[AOA-4.1.0055] 03 p0325 N88-12050
Experimental evidence for modifying the current physical model for ice accretion on aircraft surfaces
[NASA-TM-87184] 04 p0397 N88-12473
Measured performance of the heat exchanger in the NASA icing research tunnel under severe icing and dry-air conditions
[NASA-TM-100116] 04 p0451 N88-12796
Computation of rime ice accretion on airfoils
[FFA-TN-1987-08] 05 p0542 N88-13301
Measurement of local convective heat transfer coefficients from a smooth and roughened NACA-0012 airfoil: Flight test data
[NASA-TM-100284] 05 p0582 N88-13552
Operating envelopes of particle sizing instrumentation used for icing research
[NASA-CR-180870] 05 p0586 N88-13573
The ice conditions in the Greenland waters, 1981
[ISBN-87-7478-276-2] 05 p0629 N88-13844
A flow visualization study of the leading edge separation bubble on a NACA 0012 airfoil with simulated glaze ice
[NASA-CR-180846] 07 p0816 N88-14966
An experimental mapping of the flow field behind a glaze ice shape on a NACA 0012 airfoil
[NASA-CR-180847] 08 p0950 N88-15766
The NASA aircraft icing research program
08 p0957 N88-15803
NASA's rotorcraft icing research program
09 p1108 N88-16641
Calibration of the ARL (Aeronautical Research Laboratories) rain and icing facility
[AD-A186776] 09 p1121 N88-16710
Evaluation of the magnetic induction conductivity method for detecting frazil ice deposits
[AD-A186940] 09 p1194 N88-17157
Physical and structural characteristics of Weddell Sea pack ice
[AD-A188189] 10 p1358 N88-18119
Three-dimensional trajectory analyses of two drop sizing instruments: PMS OAP and PMS FSSP
[NASA-CR-4113] 11 p1437 N88-18574
Artificial and natural icing tests of AH-64, phase 2
[AD-A188231] 11 p1439 N88-18585
Layered-capacitor method for dielectric bridge measurements. Algorithms for inversion and parameter fitting: Documentation, verification, data analysis
[PB88-131479] 11 p1505 N88-18989
An experimental and theoretical study of the ice accretion process during artificial and natural icing conditions
[NASA-CR-182119] 14 p1865 N88-21143
Bibliography of icing on aircraft (status 1987)
[DFVLR-MITT-87-18] 16 p2158 N88-22876
Reclamation of water contaminated with fuel system icing inhibitor. Phase 1: Literature review and information compilation
[DE88-006575] 16 p2183 N88-23013
Investigation of air transportation technology at Massachusetts Institute of Technology, 1986
17 p2293 N88-23716
In-flight measurement of ice growth on an airfoil using an array of ultrasonic transducers
[AIAA-PAPER-87-0178] 17 p2293 N88-23717
Experimental measurements of heat transfer from an iced surface during artificial and natural cloud icing conditions
[AIAA-PAPER-86-1352] 17 p2293 N88-23718
Ice formation on aircraft
[ETN-88-92154] 18 p2545 N88-25104
National plans for aircraft icing and improved aircraft icing forecasts and associated warning services
18 p2546 N88-25113
Determination of the local heat-transfer characteristics on glaze ice accretions on a cylinder and a NACA 0012 airfoil 21 p2946 N88-27500
New ice detection system 22 p3037 N88-28030
JUH-1H redesigned pneumatic boot deicing system flight test evaluation
[AD-A194918] 24 p3322 N88-29785
Cloud/mesoscale model development and application studies
[AFGL-TR-87-0219] 24 p3404 N88-30269

ICE MAPPING
Navarin Basin Ice Drift Program
[PB88-104021] 06 p0748 N88-14599
Marginal Ice Zone Experiment (MIZEX) 1984 VARAN-S data set
[ETN-88-92032] 14 p1950 N88-21625

ICE OBSERVATION
U ICE REPORTING

ICE PACKS
U SEA ICE

ICE PREVENTION
Boundary layer profile investigations downstream of an aero-engine intake anti-icing air exhaust slot
[PNR90378] 02 p0171 N88-11080
Theoretical analysis of the electrical aspects of the basic electro-impulse problem in aircraft de-icing applications
[NASA-CR-180845] 05 p0543 N88-13310
Laminar flow control leading edge glove flight test article development
[NASA-CR-172137] 07 p0815 N88-14960
Effects of aircraft deicing/antiicing fluids on airfoil characteristics 08 p0952 N88-15776
NASA's rotorcraft icing research program
09 p1108 N88-16641
Artificial and natural icing tests of AH-64, phase 2
[AD-A188231] 11 p1439 N88-18585

ICE REPORTING
Eastern - western Arctic Sea ice analysis 1986
[AD-A184016] 03 p0355 N88-12235
The ice conditions in the Greenland waters, 1981
[ISBN-87-7478-276-2] 05 p0629 N88-13844
The Greenland Sea Project: The Arctemiz project
14 p1939 N88-21573
ERS-1 data products and services and their value for tropical countries 17 p2357 N88-24040
Ice conditions along the Ohio River as observed on LANDSAT images, 1972-1985
[AD-A191172] 18 p2531 N88-25018
An experimental study of the coherent under-ice reflectivity of sound in the Greenland Sea Marginal Ice Zone 18 p2548 N88-25125

ICE SHELVES
U LAND ICE

ICEBERGS
Arctic ice island and sea ice movements and mechanical properties
[DE88-004267] 20 p2829 N88-26782

ICELAND
SeaSoar profiles in the Iceland-Scotland area, May 1987
[IOS-253] 18 p2548 N88-25124
Meteorological features during the marginal ice zone experiment from 20 March to 10 April 1987
[AD-A193960] 23 p3235 N88-29251

ICING
U ICE FORMATION

ICOSAHEDRONS
Structural relationship between icosahedral and Frank-Kasper phases of Al-Li-Cu
[AD-A193768] 23 p3195 N88-29011

ICY SATELLITES
NT TITANIA

IDEAL FLUIDS
Instability of steady flow with constant vorticity in vessels with elliptical cross-section 02 p0159 N88-10997
Torsion as a source of expansion in a Bianchi type I universe in the self-consistent Einstein-Cartan theory of a perfect fluid with spin density
[AD-A184200] 03 p0322 N88-12037
Mass transport in annular spherical system
[LRT-WE-9-FB-11(1987)] 22 p3077 N88-28271

IDEAL GAS
Method of calculations for flow of ideal gas through plane and axisymmetric nozzles with broken-line contour
06 p0771 N88-14737
Some performance comparisons for a fluid dynamics code
[PB88-113709] 07 p0852 N88-15175
A new parabolized Navier-Stokes code for chemically reacting flow fields 12 p1625 N88-19721

IDENTIFYING
NT CROP IDENTIFICATION
NT PARAMETER IDENTIFICATION
NT SYSTEM IDENTIFICATION
Foreign language identification: First step in the translation process
[DE87-011065] 02 p0248 N88-11585
Recognition of isolated non-speech sounds
[AD-A184800] 03 p0306 N88-11933
A search for X-ray luminous late type stars in NIPSS data 04 p0511 N88-13143
Bar code document accountability system performance update
[DE88-002256] 06 p0791 N88-14849

Application of knowledge based systems to the maintenance of inertial system electronics
12 p1578 N88-19441
A texture analysis approach to computer vision for identification of roads in aerial photographs
[AD-A189340] 12 p1639 N88-19815
Estimation-correlation, modeling, and identification in adaptive array processors
[AD-A189130] 13 p1757 N88-20512
A comparison of terrain association and resection as methods of position location
[AD-A189480] 13 p1790 N88-20710
Passive DF: A tutorial, part 1
[NASA-CR-182669] 13 p1815 N88-20846
On categorizing sounds
[AD-A189784] 15 p2129 N88-22700
K-pulse estimation from incomplete multiple-frequency scattering data and target identification
[AD-A190827] 16 p2190 N88-23061
An approximation theory for the identification of nonlinear distributed parameter systems
[NASA-CR-181658] 18 p2260 N88-23510
Modeling and performance of HF/OTH (High-Frequency/Over-the-Horizon) radar target identification systems
[AD-A196287] 24 p3365 N88-30038

IDENTITIES
Effects of divided attention on identity and semantic priming
[AD-A184289] 03 p0357 N88-12250
Decoupling identities and predictable transformations in exchangeability
[AD-A186013] 07 p0913 N88-15540

IFR (RULES)
U INSTRUMENT FLIGHT RULES

IGFET
U FIELD EFFECT TRANSISTORS

IGNEOUS ROCKS
NT ANORTHOSITE
NT BASALT
NT ECLOGITE
NT GRANITE
NT PERIDOTITE
Abundance and distribution of ultramafic microbreccia in Moses Rock Dike: Quantitative application of AIS data
05 p0613 N88-13766
Weathering of sulfides on Mars
23 p3301 N88-29662
Volcano evolution on Mars 23 p3305 N88-29686
Pluton emplacement and magmatic arc construction: A model from the Patagonian batholith
24 p3393 N88-30206

IGNIMBRITE
U IGNEOUS ROCKS

IGNITERS
NT BOOSTERS (EXPLOSIVES)
NT DETONATORS
NT INITIATORS (EXPLOSIVES)
NT PRIMERS (EXPLOSIVES)
Pulsed plasma jet igniters: Species measurements in methane combustion
[DE88-001389] 05 p0562 N88-13422
Ignition studies in a two-stage closed vessel using various igniter materials
[ISL-CO-231/86] 09 p1142 N88-16843
An electro-optic explosive igniter
[DE88-004728] 11 p1466 N88-18738
Catalytic ignition of hydrogen and oxygen propellants
[NASA-TM-100957] 18 p2476 N88-24689
Some properties of ignition gases. Review of measuring results in the years 1961-1986)
[PB88-106966] 21 p2908 N88-27259

IGNITION
NT ELECTRIC IGNITION
NT SOLID PROPELLANT IGNITION
NT SPARK IGNITION
Laser probes of natural gas ignition chemistry
[PB87-209599] 01 p0021 N88-10129
Pyrotechnic component development at Sandia National Laboratory
[DE87-006899] 02 p0154 N88-10967
System studies of compact ignition tokamaks
[DE87-014976] 02 p0239 N88-11508
Planning for US ion cyclotron heating research relevant to the compact ignition tokamak and Alcator C-Mod
[DE88-000022] 02 p0241 N88-11520
Relative merits of size, field, and current on ignited Tokamak performance: A comparison of CITs and Super-JETs
[DE88-000038] 02 p0241 N88-11521
Detailed mechanism of benzene oxidation
[NASA-TM-100202] 03 p0282 N88-11775
Photochemical ignition studies. 3: Ignition by efficient and resonant multiphoton photochemical formation of microplasmas
[AD-A184644] 03 p0283 N88-11780
Detailed kinetic modeling of autoignition chemistry
[DE87-013226] 03 p0283 N88-11782
High pressure autoignition of natural gas/air mixtures and the problem of engine knock
[DE87-013799] 03 p0284 N88-11784
Ignition and combustion of metals in oxygen
04 p0407 N88-12530
Proceedings of the Japan-US Workshop P-92 on Plasma Material Interaction/High Heat Flux Data Needs for the Next Step Ignition and Steady State Devices
[DE87-013568] 04 p0494 N88-13042
An experimental investigation of the ignition and flammability limits of various hydrocarbon fuels in a two-dimensional solid fuel ramjet
[AD-A184968] 05 p0549 N88-13342
Ignition and flameholding in supersonic flow by injection of dissociated hydrogen 05 p0560 N88-13410
Pulsed plasma jet igniters: Species measurements in methane combustion
[DE88-001389] 05 p0562 N88-13422
Detailed mechanism of toluene oxidation and comparison with benzene
[NASA-TM-100261] 05 p0563 N88-13428
Jet initiation of PBX 9502
[DE88-000493] 05 p0571 N88-13481
A study of the interaction of laser light with liquid propellant drops
[AD-A185117] 05 p0587 N88-13582
Edge plasmas and plasma/wall interactions in an ignition-class reversed field pinch
[DE88-001825] 06 p0782 N88-14799
TIBER 2 (Tokamak Ignition/Burn Experimental Reactor) parameters with neutral beams at high energies
[DE88-001891] 06 p0783 N88-14803
Overview of the TIBER 2 (Thermal Ignition/Burn Experimental Reactor) design
[DE88-001892] 06 p0783 N88-14804
The carbon dioxide chaperon efficiency for the reaction H + O2 + M yields HO2 + M from ignition delay times behind reflected shock waves
[NASA-TM-100125] 07 p0830 N88-15036
Dimensions of ignition zones in blow-outs of combustible gases from rectangular and circular ports
07 p0918 N88-15577
Poloidal magnetics of compact ignition tokamaks
[DE88-001774] 07 p0934 N88-15672
Calculation evaluation of the boundary conditions of autoinflammation of propulsive charges
[PB87-139044] 08 p0974 N88-15890
DSC (Differential Scanning Calorimeter) stability test for liquid propellants: A preliminary report
[AD-A187115] 09 p1150 N88-16888
EXPLO: Explosives thermal analysis computer code
[DE88-001938] 10 p1307 N88-17814
Flash threshold of shocked aluminum silicofluoride
[DE88-003978] 10 p1339 N88-18005
D-3He fuels in a field-reversed configuration
[IPPJ-855] 10 p1411 N88-18419
On the possibility of high velocity deflagration front propagation by radiative energy transfer
[AD-A189022] 12 p1613 N88-19645
J85-21 fuel nozzle atomization tests
[AD-A189394] 12 p1613 N88-19647
CIT (Compact Ignition Tokamak) fueling
[DE88-002709] 12 p1692 N88-20125
A pyrotechnic delay ignition system for a submarine launched marine signal
[MRL-R-1079] 13 p1754 N88-20487
Numerical modeling of divergent detonation wave
14 p1903 N88-21373
Environmental assessment for the compact ignition Tokamak
[DE88-005633] 15 p2135 N88-22740
Transport simulations of ohmic ignition experiment: IGNITEX
[DE88-006055] 15 p2138 N88-22757
Laser induced ignition of propellants
[AD-A191100] 16 p2168 N88-22927
Laser induced ignition of propellants
[AD-A191099] 16 p2213 N88-23206
Numerical analysis for effects of irradiation nonuniformities on target implosion
16 p2276 N88-23621
Pusherless implosion, pulse tailoring and ignition scaling law for laser fusion 16 p2277 N88-23629
Stability requirement FOT ignition and high gain implosion = 2-D simulation for high neutron yield experiment = 16 p2278 N88-23633
On selfsimilar thermonuclear ignition of a plasma in necks of zeta devices
[DE88-701640] 16 p2280 N88-23647
Catalytic ignition of hydrogen and oxygen propellants
[NASA-TM-100957] 18 p2476 N88-24689
The burning of HAN-based (hydroxylammonium nitrate) liquid propellants
[DE88-006863] 18 p2494 N88-24800
On the use of thermal degradation data to predict cable ignition performance
[DE88-002276] 19 p2621 N88-25549
The 24th JANNAF Combustion Meeting, volume 2
[AD-A190164] 19 p2622 N88-25554
The combustion of hydroxylammonium nitrate based liquid propellants 19 p2622 N88-25555
Comparison of calculated and measured ignition times for boron agglomerates 19 p2624 N88-25563
Recent advances in photochemical techniques for ignition and combustion enhancement
19 p2625 N88-25570
Ignition and flammability characteristics of solid fuel ramjets 19 p2626 N88-25575
The 24th JANNAF Combustion Meeting, volume 1
[AD-A190163] 19 p2627 N88-25585
Dynamics of propellant ignition
19 p2628 N88-25590
How much do edges affect the ignition of a homogeneous reactive solid: Summary to date
19 p2631 N88-25608
Theoretical studies of the chemical reactions involved in the ignition of nitramines 19 p2632 N88-25615
Temperature and species profiles in propellant ignition and combustion 19 p2633 N88-25616
Ignition and flame spread of PMMA
[NASA-TT-20290] 20 p2771 N88-26431
Thermal and mechanical analysis of the Faraday shield for the compact ignition tokamak
[DE88-007855] 20 p2856 N88-26962
Effects of ceramic surfaces on autoignition in a constant volume combustion apparatus
[AD-A193055] 21 p2909 N88-27266
Laser probes of natural gas ignition chemistry
[PB88-212568] 21 p2910 N88-27271
Development of an experimental system for studying fast transient ignition phenomena
[DE88-011917] 21 p2911 N88-27276
Shock initiation studies on heterogeneous explosives
[DE88-008681] 21 p2923 N88-27351
Diode laser ignition of high explosives and pyrotechnics
[DE88-008771] 21 p2923 N88-27352
Combustion dynamics and thermal structure of a planar spray flame 23 p3190 N88-28985
Semiconductor bridge (SCB) igniter studies. 1: Comparison of SCB and hot-wire pyrotechnic actuators
[DE88-008802] 23 p3200 N88-29046
Ignition and extinguishing of a Solid Fuel Ramjet (SOFRAM)
[FOA-C-20713-2.1] 24 p3337 N88-29885
Gas phase combustion chemistry of nitramine propellants
[AD-A195082] 24 p3344 N88-29902
Flamespreading processes in obliquely loaded stick propellant beds
[AD-A195081] 24 p3352 N88-29956

IGNITION LIMITS
An experimental investigation of the ignition and flammability limits of various hydrocarbon fuels in a two-dimensional solid fuel ramjet
[AD-A184968] 05 p0549 N88-13342
Numerical simulation of ignition of hydrogen jet in hot air 19 p2637 N88-25647

IGNITION SYSTEMS
High pressure autoignition of natural gas/air mixtures and the problem of engine knock
[DE87-013799] 03 p0284 N88-11784
An electro-optic explosive igniter
[DE88-004728] 11 p1466 N88-18738
Flamespreading processes in obliquely loaded stick propellant beds
[AD-A195081] 24 p3352 N88-29956

IGNITION TEMPERATURE
NT FLASH POINT
Ignition and flame propagation in sprays
[AD-A184679] 03 p0283 N88-11781
A neutral-beam diagnostic for fast confined alpha particles in a burning plasma: Applicatoin on CIT (Compact Ignition Tokamak)
[DE88-004890] 11 p1554 N88-19301

ILLINOIS
TABLET: The personal computer of the year 2000
[NASA-CR-182528] 10 p1384 N88-18267

ILLUMINANCE
Monte Carlo method calculation of spectral brightness coefficient of vegetation cover as function of illumination conditions 08 p1008 N88-16113
Influence of solar illumination conditions on TM/Landsat data
[INPE-4463-TDL/320] 12 p1638 N88-19806
Analysis of the parameters responsible for the variations of the illumination conditions in the LANSAT data
17 p2362 N88-24070

ILLUMINATING
The optimum illumination conditions for EXELFS studies in a CTEM
[USIP-87-08] 01 p0092 N88-10600
Photoinduced low-temperature changes in optical losses in fiber optics based on chalcogenide glasses
06 p0770 N88-14731
Fish as a tool for testing fitness in space
12 p1662 N88-19963
Botany Facility: Breadboarding results of the illumination system
[SIRA-A/7373/WP110/MAC003]
17 p2378 N88-24137
Optical system of laser illuminated streamer chamber
[DE88-702127] 18 p2577 N88-25306
Maintenance of vision-related components
23 p3242 N88-29296
Night lighting and night vision goggle compatibility
23 p3242 N88-29297

ILLUMINATION
Plant Growth Module (PGM) conceptual design
05 p0631 N88-13855

ILLUSIONS
Eye movements and spatial pattern vision
[AD-A195496] 24 p3408 N88-30290

ILS (LANDING SYSTEMS)
U INSTRUMENT LANDING SYSTEMS

IMAGE ANALYSIS
Masking effects of fine and coarse grain pictorial noise
[IZF-1985-21] 01 p0076 N88-10485
Input/output technologies: An overview of image scanning, storage, and display
[DE87-014837] 04 p0476 N88-12933
On the recognition of curved objects
[AD-A184441] 04 p0478 N88-12945
Determination of the fiber ratio in carbon fiber/resin composites by means of image analysis
[SNIAS-872-422-101] 05 p0558 N88-13398
Land cover/use classification of Cairns, Queensland, Australia: A remote sensing study involving the conjunctive use of the airborne imaging spectrometer, the large format camera and the thematic mapper simulator
05 p0612 N88-13759
A unified mathematical approach to image analysis
[AD-A185719] 06 p0765 N88-14703
Some vision algorithms 06 p0795 N88-14871
An investigation of offshore circulation using satellite data and feature tracking techniques
[AD-A186271] 07 p0881 N88-15347
A knowledge-based object recognition system for applications in the space station
[NASA-CR-182411] 08 p0989 N88-15991
Space photographs of the Onega-Ladoga isthmus and prediction of useful minerals 08 p1008 N88-16108
Study of relief of ore regions using space images (on the example of Eastern Yakutia)
08 p1008 N88-16111
Processing of radar images of Venus on the Magiscan-2 analyzer 08 p1009 N88-16117
Thematic mapper research in the earth sciences: Small scale patches of suspended matter and phytoplankton in the Elbe River Estuary, German Bight and Tidal Flats
[NASA-CR-182378] 08 p1019 N88-16180
Textural features for image classification in remote sensing
[INPE-4169-PRE/1066] 08 p1020 N88-16181
Digital image processing
[INPE-4131-TDL/264] 08 p1083 N88-16527
Nature and origin of mineral coatings on volcanic rocks of the Black Mountain, Stonewall Mountain, and Kane Springs Wash volcanic centers, Southern Nevada
[NASA-CR-181437] 09 p1191 N88-17140
A procedure for automatic classification of crop areas
[INPE-4467-PRE/1240] 13 p1790 N88-20708
Exact image method for Gaussian beam problems involving a planar interface
[NASA-CR-182702] 14 p1905 N88-21380
Classification of small image areas by digital correlation for the connection of different images in photogrammetry and long-range reconnaissance
[ETN-88-91506] 14 p1940 N88-21578
On the geometric interpretation of image contours
[RR-647-I-IMAG-57-LIFIA] 15 p2109 N88-22563
Conversational Analysis of Color Images (CAICOU): An interactive development system for the analysis of color images
[RR-641-I-IMAG-39-LIFIA] 17 p2342 N88-23964
Textural features for image classification in remote sensing 17 p2354 N88-24027
Practical image analysis using personal computers: The Canadian experience 17 p2356 N88-24037
A proposal of adaptation of a knowledge-based scene analysis model to some remote sensing problems
17 p2362 N88-24068
Interpretation of MSS/LANDSAT data for evaluation of physical distribution of mangroves in Cananeia-Iguape (SP) 17 p2363 N88-24072
An update on remote measurement of soil moisture over vegetation using infrared temperature measurements: A FIFE perspective
[NASA-CR-182926] 17 p2370 N88-24109
Generic cueing in image understanding
[RSRE-MEMO-4109] 17 p2386 N88-24181
Linguistic definition of generic models in computer vision
[RSRE-MEMO-4110] 17 p2386 N88-24182
Mathematical morphology for structures without translation symmetry
[CWI-AM-R8803] 18 p2566 N88-25241
Real-time image difference detection using a polarization rotation spacial light modulator
[NASA-CASE-NPO-17144-1-CU]
18 p2576 N88-25305
Separability of cultivation through digital analysis of SPOT and TM data
[INPE-4541-PRE/1287] 19 p2685 N88-25963
Bathymetry estimation by analyzing swell on SPOT images 19 p2701 N88-26062
Image pyramid motion detection applied to sea ice
20 p2817 N88-26713
Processing and analysis of images transmitted by Vega space probes over Halley's comet
[ETN-88-92291] 20 p2885 N88-27131
Automatic line network extraction from aerial imagery of urban areas through knowledge based image analysis
[AD-A193067] 21 p2965 N88-27615
Remote sensing of wetlands: Applications overview
[DE88-010895] 21 p2966 N88-27618
Mapping of streamflow and soil infiltration of a Sahelian catchment area by SPOT image interpretation: The Oursi pond catchment area in Burkino Faso
22 p3090 N88-28348
Evaluation of automatic texture analysis for increased crop identification accuracy with SPOT data
22 p3094 N88-28373
Digital and visual analysis of SPOT and TM data for crop discrimination in southern Brazil
22 p3096 N88-28385
Discrimination methods of traditional fields in a humid tropical region (Shaba, Zaire) using digital classification on SPOT data 22 p3096 N88-28387
Identification of farming systems in the cotton area of West Burkina Faso from SPOT-1 data
22 p3097 N88-28389
Monitoring urban land cover changes at the urban fringe from SPOT HRV imagery in south-east England
22 p3099 N88-28406
Analysis of SPOT multispectral data concerning a border zone between two geographical regions in southern Belgium 22 p3100 N88-28411
Applications of SPOT data for urban real estate investment information systems
22 p3101 N88-28414
Mapping and urban multi-experimental assessment of SPOT: Urban results 22 p3101 N88-28415
SPOT-1 over New Zealand: Analysis of SPOT imagery for land use investigations 22 p3101 N88-28416
Comparison of SPOT, LANDSAT TM and combined data for urban studies 22 p3101 N88-28417
Utilization of SPOT multispectral data for urban planning 22 p3101 N88-28418
First results of international investigations of the applications of SPOT-1 data to geologic problems, mineral and energy exploration 22 p3101 N88-28419
Rate of slip on the Altin Dagh Fault (North Tibet, China) 22 p3102 N88-28420
Karst and submarine fresh water discharge in the Antalya area, southern Turkey 22 p3102 N88-28421
Results of the Geosat program to evaluate SPOT data for petroleum and mineral exploration
22 p3102 N88-28422
The application of SPOT data to the structural geology of western Nevada 22 p3102 N88-28423
Application SPOT-1 data to mining activity: Example of the Imiter Silver Mine, Morocco
22 p3102 N88-28424
Evaluation of SPOT imagery contribution to petroleum exploration: The Suez Rift (Egypt)
22 p3102 N88-28425
Evaluation of SPOT imagery for discriminating vegetation communities associated with surficial and bedbrock geology and identifying anomalous and stressed vegetation associated with mineralization
22 p3103 N88-28426
SPOT imagery as an aid to understanding volcanism and tectonics: Examples from the Chilean Andes and the Tibetan Plateau 22 p3103 N88-28427
Role of SPOT in geological application of remote sensing 22 p3103 N88-28428
SPOT imagery preliminary contribution to cartography and geodynamics in the Benue trough (Nigeria)
22 p3103 N88-28429
An evaluation of SPOT imagery for Earth science studies in the Antarctic. Preliminary Evaluation Program (PEPS) 289 for SPOT 22 p3103 N88-28430
Structural analysis of the Jura mountains-Rhine Graben intersection (Switzerland) for petroleum exploration using SPOT stereoscopic data 22 p3103 N88-28431
Methodology for the use of SPOT imagery in petroleum exploration. Example of the Bas-Languedoc area (France) 22 p3104 N88-28432
Analyzing the stratigraphy, tectonism, and mineralization at the Spanish side of the pyrite belt, Huelva province, Spain, using SPOT imagery 22 p3104 N88-28433
Geologic applications of SPOT-1, TM, and NOAA-7 data: Finding and defining unmapped structural features
22 p3104 N88-28434
Spectral and spatial attribute evaluation of SPOT data in geological mapping of precambrian terrains in semiarid environment of Brazil 22 p3104 N88-28436
Geologic results obtained from the use of SPOT imagery along plate boundaries: Examples in the East African rift and of the northern-Caribbean collision
22 p3105 N88-28437
SPOT images and geochemical mapping of lateritic covers in southern Mali 22 p3105 N88-28438
Analysis of the multispectral content and of SPOT subscenes in two regions of Burundi. Lithologic and tectonic interpretations 22 p3105 N88-28439
SPOT imagery for landslide cartography in mountainous areas. Example of the French Maritime Alps
22 p3105 N88-28440
SPOT for slope instability survey in Nepal
22 p3105 N88-28441
Detailed geological mapping of the massif of Sainte Victoire (Provence, France) using SPOT imagery. Comparison with other multisource data. New tectonic interpretation of this region 22 p3105 N88-28442
An evaluation of the utility of SPOT and Thematic Mapper data for providing forest inventory information
22 p3106 N88-28444
SPOT-1 satellite imagery for forest inventory in Sweden 22 p3106 N88-28445
Forest mapping by visual interpretation of SPOT images 22 p3106 N88-28446
SPOT multispectral data and maritime pine stands in southwest of France 22 p3106 N88-28448
Stand-based forestry inventory from SPOT image
22 p3106 N88-28449
Potential of SPOT imagery as a tool for forest mapping in Quebec 22 p3107 N88-28450
Assessment of large area forest disturbances caused by biotic and abiotic factors on the basis of SPOT images 22 p3107 N88-28451
Study of deforestation in the Vosges (France) by remote sensing 22 p3107 N88-28452
Contribution to the mapping of forests in an intensively divided area, with the help of SPOT image data
22 p3107 N88-28453
SPOT 1: Image utilization, assessment, results. A study of the Elburgon Forest area (Kenya) showing the spectral responses of different forest tree species
22 p3107 N88-28454
SPOT investigations of estuaries and coastal zones: An overview 22 p3107 N88-28455
SPOT: A tool to aid preselection of sites favorable for aquiculture. Evaluation and perspectives of the Preliminary Evaluation Program for SPOT (PEPS) ALIAS Caledonie
22 p3108 N88-28456
The monitoring of sediment transport, water circulation and mixing in estuaries and coastal waters
22 p3108 N88-28457
Evaluation of SPOT data for remote sensing of physical and biological properties of estuaries and coastal zones
22 p3108 N88-28458
Physiography and kinematics of the western coast of the province of Huelva (Andalousia, Spain)
22 p3109 N88-28465
The use of SPOT imagery on analytical photogrammetric instruments 22 p3110 N88-28471
SPOT images features extraction
22 p3114 N88-28496
SEP/VIPS 32 geographic information system. Processing and thematic analysis of images, maps, and associated data 22 p3114 N88-28499
Summary of analysis and processing techniques used on SPOT imagery 22 p3115 N88-28503
Automatic line network extraction from aerial imagery of urban areas through knowledge-based image analysis
[AD-A192399] 23 p3227 N88-29208
Evaluation of LANDSAT-TM data for geomorphological mapping
[INPE-4593-PRE/1324] 24 p3386 N88-30168
Autonomous image data reduction by analysis and interpretation 24 p3418 N88-30347

IMAGE CONTRAST
Performances of an Actively Stabilized Stellar Interferometer (ASSI): Faint magnitudes, low fringe contrast measurements and operationality
01 p0097 N88-10641
Development and validation of transmission measurements techniques of image contrast, utilizing existing IR imagers
[AD-A191471] 18 p2541 N88-25079
The FEL CCD-camera: Experimental system for camera and image processing research
[FEL-1987-34] 21 p2952 N88-27532
IMAGE CONVERTERS
NT IMAGE TUBES
Multilayered foils as radiation entrance windows and spectral filters for image converters in the ultrasoft X-ray wavelength region
[MPE-PREPRINT-90] 02 p0176 N88-11099
Dynamics Explorer guest investigator
[NASA-CR-181494] 07 p0878 N88-15325
Suspension of small metallic plates: A versatile sensor
[PB88-130901] 11 p1487 N88-18874
IMAGE CORRELATORS
Statistical investigations of the behavior of a product correlator and an edge detector in critical situations
[MBB-UA-1034/87] 06 p0781 N88-14793
Image correlation on an IBM-PC for characterization of advanced ceramics
[DE88-002829] 09 p1149 N88-16885
Classification of small image areas by digital correlation for the connection of different images in photogrammetry and long-range reconnaissance
[ETN-88-91506] 14 p1940 N88-21578
A high dynamic range acousto-optic image correlator for real-time pattern recognition
[DE88-007933] 19 p2726 N88-26191
IMAGE DISSECTOR TUBES
Visual display representation of multidimensional systems: The effect of information correlation and display integrality
[AD-A188655] 12 p1672 N88-20010
IMAGE ENHANCEMENT
A general solution to the silhouette problem
[NASA-TP-2695] 06 p0755 N88-14629
Digital enhancement of flow field images
[NASA-TP-2770] 13 p1813 N88-20833
Weighted averaging method for image smoothing reported 14 p1901 N88-21352
Utilization of space color transformation, linear contrast and filtration for enhancement of colored digital images
[INPE-4310-PRE/1176] 14 p1983 N88-21831
Dynamic range compression/expansion of light beams by photorefractive crystals
[NASA-CASE-NPO-17140-1-CU] 17 p2438 N88-24508
Enhancement of modeling and image generation techniques for high-resolution 3-dimensional imagery
[DE88-008923] 21 p2998 N88-27782
IMAGE FILTERS
Multilayered foils as radiation entrance windows and spectral filters for image converters in the ultrasoft X-ray wavelength region
[MPE-PREPRINT-90] 02 p0176 N88-11099
Parallel algorithms for computer vision on the connection machine
[AD-A185842] 07 p0901 N88-15456
Optimization of imaging energy filters for analytical electron microscopy
[ETN-88-91079] 09 p1248 N88-17483
Photographic filters
[INPE-4448-RPE/558] 12 p1692 N88-20124
IMAGE FURNACES
Zone crystallization experiments in mirror heating facilities
[BMFT-FB-W-86-023] 16 p2184 N88-23016
IMAGE INTENSIFIERS
Development, testing and evaluation of a night vision goggle compatible BO-105 for night low level operation
03 p0265 N88-11668
A high-speed, eight-frame image intensified electro-optic camera with 200-800mm zoom objective capability
[DE88-000229] 03 p0326 N88-12059
Determination of the origin of self-pumped phase conjugation in barium titanate
[AD-A184697] 03 p0377 N88-12372
Increased gain of channel intensifier tubes by pulsed biasing
[DE88-000512] 04 p0490 N88-13019
A focussed MCP (microchannel plate) image intensifier type for high speed gating
[DE88-000480] 05 p0583 N88-13555
Streak camera dynamic range optimization
[DE88-001632] 05 p0586 N88-13571
High-resolution Real-Time Radiography (RTR) system design
[AD-A187107] 09 p1166 N88-16992
Signal processing studies program optical signal amplification, volume 1
[AD-A188055] 10 p1321 N88-17897
Performance of a photon counting microchannel plate intensifier with wedge and strip image readout
[DE88-003831] 10 p1334 N88-17970
Study of the ionic and neutral species in the coma of Comet Halley with an image intensifier camera
14 p2006 N88-21962
Four-frame gated optical imager with 120-ps resolution
[DE88-011735] 22 p3080 N88-28288
The application of an image intensifier to atmospheric Cerenkov gamma ray astronomy
[MPE-PREPRINT-115] 22 p3163 N88-28839
IMAGE MOTION COMPENSATION
Self calibration of motion and stereo vision for mobile robot navigation
[AD-A185602] 06 p0781 N88-14794
A directed method for locating the focus of expansion
[AD-A185840] 07 p0906 N88-15491
Relaxing the brightness constancy assumption in computing optical flow
[AD-A187437] 10 p1410 N88-18410
IMAGE PROCESSING
NT GEOMETRIC RECTIFICATION (IMAGERY)
Study, design, and evaluation of data reduction by encoding or information extraction. Part 1: Data generation analysis --- multispectral satellite imagery
[NLR-TR-85094-L-PT-1] 01 p0078 N88-10501
Study, design and evaluation of data reduction by encoding or information extraction. Part 2: Operational considerations --- multispectral satellite imagery
[NLR-TR-85094-L-PT-2] 01 p0079 N88-10502
Study, design and evaluation of data reduction by encoding or information extraction. Part 4: Performance demonstration --- multispectral satellite imagery
[NLR-TR-85094-L-PT-4] 01 p0079 N88-10504
Estimation of the position and orientation of objects using associative memories
[ESA-TT-1034] 01 p0079 N88-10507
Report outline of a programming variable and application through example
[INPE-4211-PRE/1092] 01 p0081 N88-10521
Unified Sun and sky illumination for shadows under trees
[DE87-014232] 01 p0083 N88-10535
Imaging at radio wavelengths
01 p0094 N88-10618
Diagnostic technique for monitoring high temperature plasma dynamics
[DE87-011786] 01 p0099 N88-10653
Personal Computer (PC) based image processing applied to fluid mechanics
[NASA-TM-100024] 02 p0172 N88-11087
How we get pictures from space, revised edition
[NF-151/7-87-REV] 02 p0193 N88-11203
Operational cloud-clearing techniques of VAS radiance data --- Visible and Infrared Spin Scan Radiometer Atmospheric Sounder (VAS) 02 p0201 N88-11256
Automated detection of severe thunderstorms using geosynchronous infrared data 02 p0201 N88-11257
The use of McIDAS as a Mesoscale forecasting tool during the Canadian Atlantic storms programs --- Man-computer Interactive Data Access System (McIDAS) 02 p0205 N88-11284
A preliminary taxonomy of visible surface algorithms
[DE87-013559] 02 p0220 N88-11386
Projection-space iterative interpolation for limited-angle tomography in parallel- and fan-beam geometry, part 1
[DE87-013965] 02 p0221 N88-11391
Pyroelectric line scanner for remote IR imaging of vehicles
[DE87-012127] 02 p0235 N88-11484
Description of a multiframe optical probing system
[DE87-014255] 02 p0236 N88-11487
Fundamentals and techniques of nonimaging optics research
[DE87-014544] 02 p0236 N88-11488
Preliminary estimation of color inhomogeneities on the surface of Venus according to the television images obtained by the VENERA-13 and VENERA-14 automated space probes
[NASA-TT-20114] 02 p0254 N88-11608
Dynamic image interpretation for autonomous vehicle navigation
[AD-A184043] 03 p0262 N88-11647
Helicopter fire control: Advantages of an automatic target tracker 03 p0264 N88-11667
Delay-Doppler radar imaging
[AD-A184165] 03 p0308 N88-11943
SPOT 1: First In-Flight Results --- conferences
[ISBN-2-85428-177-2] 03 p0340 N88-12143
Results of the satellite and the Toulouse (France) receiving station operator --- SPOT
03 p0341 N88-12149
Detector normalization --- SPOT remote sensors
03 p0341 N88-12151
Registration of SPOT images
03 p0341 N88-12155
Adaptation of numerical SPOT data to an urban environment 03 p0342 N88-12158
Geological interpretation of a SPOT image over Kenya: The Gregory rift network of faults
03 p0343 N88-12164
SPOT data for crop discrimination in southern Brazil
03 p0343 N88-12169
A review of computer-assisted photo interpretation research at USAETL (US Army Engineer Topographic Laboratories)
[AD-A184034] 03 p0346 N88-12186
Algorithms and hardware for efficient image smoothing
[TR-149] 03 p0365 N88-12296
Issues in image processing software development for a multi-user, multi-programming environment
[DE88-000358] 03 p0365 N88-12298
End of year report for parallel vision algorithm design and implementation
[AD-A184327] 03 p0366 N88-12301
Recognizing rigid objects by aligning them with an image
[AD-A184253] 03 p0368 N88-12318
Low-level vision on warp and the apply programming model
[AD-A184330] 03 p0369 N88-12320
Image processing for optical engineering applications
[PB87-210035] 03 p0376 N88-12364
An application of a gradient relaxation method to noisy infrared images
[AD-A184666] 03 p0377 N88-12371
Programmable real-time digital video image processing
[PB87-104162] 04 p0430 N88-12661
Design of source coders and joint source/channel coders for noisy channels
[NASA-CR-181547] 04 p0432 N88-12678
Tracking through turbulence at the Tonopah Test Range
[DE88-001448] 04 p0446 N88-12766
Cloud cover determination in polar regions from satellite imagery
[NASA-CR-181544] 04 p0471 N88-12908
Input/output technologies: An overview of image scanning, storage, and display
[DE87-014837] 04 p0476 N88-12933
Computer-aided X-ray image system design and evaluation
[DE88-000997] 04 p0481 N88-12965
Correction of inertial navigation system drift errors for an autonomous land vehicle using optical radar terrain data
[AD-A184973] 05 p0544 N88-13311
Television motion measurement for DATV and other applications
[BBC-RD-1987/11] 05 p0573 N88-13496
Italy's Institute of Research on Electromagnetic Waves--the Istituto di Ricerca sulle Onde Elettromagnetiche
[AD-A185020] 05 p0574 N88-13501
Study on data compression systems for operational remote sensing --- meteosat imagery
[NLR-TR-86029-L] 05 p0620 N88-13808
Matching segments from a map and an aerial image using relaxation techniques
[SNIAS-872-422-103] 05 p0620 N88-13809
Learning a color algorithm from examples
[AD-A184385] 05 p0632 N88-13862
A prototype ray tracer
[AD-A184863] 05 p0634 N88-13874
The use of color in electronic maps. Part 1: Generation and analysis of color on the Gould/DeAnza image processing system
[IZF-1986-32] 05 p0635 N88-13882
The maximum likelihood estimator method of image reconstruction: Its fundamental characteristics and their origin
[DE88-000462] 05 p0636 N88-13892
Full field visualization of surface and bulk acoustic waves using heterodyne holographic interferometry
[AD-A185071] 05 p0646 N88-13958
X-ray imaging: Status and trends
[DE88-000756] 05 p0649 N88-13980
Two digital X-ray imaging systems for applications in X-ray diffraction
[PB87-123683] 06 p0669 N88-14103
Optical seam tracking in robotic arc welding
[VTT-RR-463] 06 p0713 N88-14376
A general solution to the silhouette problem
[NASA-TP-2695] 06 p0755 N88-14629
An orthogonal oriented quadrature hexagonal image pyramid
[NASA-TM-100054] 06 p0755 N88-14630

Algorithms and programming tools for image processing on the MPP:3
[NASA-CR-182349] 06 p0757 N88-14641
Virtual image processor: A prototype implementation
[AD-A185560] 06 p0758 N88-14652
A unified mathematical approach to image analysis
[AD-A185719] 06 p0765 N88-14703
New description of Lau effect based on theory of raster image forming process 06 p0772 N88-14744
Selection of holographic screen for projection of images reconstructed by multiaspect holograms of focused images 06 p0773 N88-14745
Self calibration of motion and stereo vision for mobile robot navigation
[AD-A185602] 06 p0781 N88-14794
Characterization of microstructure in metallic and composite materials
[AD-A186193] 07 p0826 N88-15012
Texture study of Synthetic Aperture Radar (SAR) images of ocean surfaces
[AD-A186021] 07 p0841 N88-15101
Electronic imaging technique for welding and other high-luminosity processes
[DE88-002199] 07 p0862 N88-15227
Model-based building verification in aerial photographs
[AD-A186010] 07 p0870 N88-15278
Optimization of photogrammetric image adjustment
[SER-C-323] 07 p0872 N88-15289
Theory and research on the disjunction of cross passage errors and systematic image errors in photogrammetric point determination
[SER-C-324] 07 p0872 N88-15290
Parallel algorithms for computer vision on the connection machine
[AD-A185842] 07 p0901 N88-15456
Proceedings of Image Understanding Workshop, volume 1
[AD-A186103] 07 p0902 N88-15463
Proceedings of Image Understanding Workshop, volume 2
[AD-A186104] 07 p0902 N88-15464
Image processing language development
[AD-A186251] 07 p0903 N88-15467
Sound pressure distribution in front of a serrated boundary: Standing wave suppression and diffusion 07 p0928 N88-15639
Feasibility studies of optical processing of image bandwidth compression schemes
[AD-A186073] 07 p0932 N88-15660
Active control of jet flowfields
[AD-A186736] 08 p0989 N88-15989
A knowledge-based object recognition system for applications in the space station
[NASA-CR-182411] 08 p0989 N88-15991
Modeling of architecture of a problem-oriented on-board processor 08 p1008 N88-16114
Textural features for image classification in remote sensing
[INPE-4169-PRE/1066] 08 p1020 N88-16181
Evaluation of the flooding areas of the Sao Goncalo Canal through LANDSAT 5 thematic mapper images
[INPE-4118-PRE/1039] 08 p1020 N88-16185
The power of neural nets 08 p1064 N88-16430
Digital image processing: A summary of main techniques
[INPE-4404-PRE/1220] 08 p1068 N88-16454
Digital image processing
[INPE-4131-TDL/264] 08 p1083 N88-16527
Earthnet's experience with Seasat SAR image processing 09 p1127 N88-16760
The Earthnet Heat Capacity Mapping Mission (HCMM) data-processing system at Lannion (France) 09 p1127 N88-16761
Parallel-processing computer systems and their possible applications in the agency 09 p1128 N88-16774
Technical assessment of the joint CSIRO/Bureau of Meteorology proposal for a geostationary imager/sounder over the Australian region
[RTP-15] 09 p1135 N88-16811
Image correlation on an IBM-PC for characterization of advanced ceramics
[DE88-002829] 09 p1149 N88-16885
Backscattering signal analysis concerning a three-dimensional object configuration on the basis of object motion
[ESA-TT-1044] 09 p1154 N88-16915
Unsteady behavior of three-dimensional vortices relevant to turbulent boundary layers
[AD-A186767] 09 p1161 N88-16958
Techniques of flow visualization
[AGARD-AG-302] 09 p1164 N88-16977
Flat-field response and geometric distortion measurements of optical streak cameras
[DE88-002394] 09 p1168 N88-17005
Performance of a digital real time radiographic imaging system
[MRL-R-1068] 09 p1169 N88-17011
Nature and origin of mineral coatings on volcanic rocks of the Black Mountain, Stonewall Mountain, and Kane Springs Wash volcanic centers, Southern Nevada
[NASA-CR-181437] 09 p1191 N88-17140
Meteorological Information Extraction Center (MIEC) processing --- Meteosat imagery
[ESA-STR-224] 09 p1192 N88-17143
Sea surface current estimates off central California as derived from enhanced AVHRR (Advanced Very High Resolution Radiometer) infrared images
[AD-A186867] 09 p1194 N88-17155
Image chunking: Defining spatial building blocks for scene analysis
[AD-A187072] 09 p1200 N88-17191
Vision algorithms and psychophysics
[AD-A186773] 09 p1200 N88-17193
Handbook of the GEMS image processing system
[RAE-TR-86062] 09 p1219 N88-17310
A comparison of algorithms for the analysis of images generated by two-dimensional electrophoresis
[DE88-003730] 09 p1220 N88-17319
Comparison of a few methods of restoring images distorted by atmospheric turbulence
[ESA-TT-1065] 09 p1248 N88-17481
Transport delay compensation for computer-generated imagery systems
[NASA-TM-100084] 10 p1277 N88-17645
Instrumentation and quantitative methods of evaluation
[DE87-013639] 10 p1342 N88-18017
A smart, mapping, charting and geodesy control generator, phase 1
[AD-A188184] 10 p1347 N88-18055
Autocorrelation of control points on 11-band multispectral imagery
[AD-A188185] 10 p1348 N88-18056
Image texture classification with an optical crossbar interconnected processor 10 p1375 N88-18202
New generation imager system
[NASA-CR-180464] 10 p1408 N88-18398
Multidimensional system analysis of electro-optic sensors with sampled deterministic output
[AD-A187083] 10 p1408 N88-18399
Simulation and processing of high resolution images of defects and interfaces in superconducting YBa2Cu3O7
[DE88-003856] 10 p1420 N88-18480
Air Force geographic information and analysis system
[DE88-001420] 10 p1424 N88-18505
Fixed and adaptive interframe image prediction for remote piloting application
[AD-A187987] 11 p1471 N88-18771
Imaging methods for nondestructive materials testing
[ETN-88-91477] 11 p1497 N88-18940
Three-dimensional image generation from an aerial photograph
[AD-A188039] 11 p1503 N88-18979
The Quick Response Multicolor Printer (QRMP) system
[AD-A188140] 11 p1504 N88-18982
Geophysical diffraction tomography for imaging isolated subsurface inclusions
[DE88-003918] 11 p1505 N88-18990
Ideal shrinking and expansion of discrete sequences
[NASA-TM-88202] 11 p1524 N88-19100
A unified approach for digital image processing problems: Mathematical morphology
[INPE-4311-TDL/278] 11 p1537 N88-19183
Solar radioimage restoration
[INPE-4312-TDL/279] 11 p1571 N88-19402
Three-dimensional information from stereovision process 12 p1593 N88-19540
Measuring accuracy of 3-dimensional bodies by the GOMER-1 device
[DE87-703230] 12 p1628 N88-19744
Automated stereophotogrammetry
[AD-A189617] 12 p1630 N88-19757
Report on phase 1 of the project estimate development of a model for yield estimation of sugar cane based on LANDSAT and agromet data
[INPE-4466-RPE/560] 12 p1638 N88-19807
Automatic knowledge acquisition for aerial image interpretation
[AD-A188616] 12 p1638 N88-19810
Visual display representation of multidimensional systems: The effect of information correlation and display integrality
[AD-A188655] 12 p1672 N88-20010
Procedure for initial data input and checkup in the system for film data mathematical processing
[DE88-700926] 12 p1676 N88-20022
Image segmentation via fractal dimension
[AD-A188825] 12 p1678 N88-20033
Applications of mathematical morphology to range imagery
[AD-A189316] 12 p1684 N88-20072
Three-dimensional image reconstruction in object space
[DE88-900279] 12 p1712 N88-20246
Recent developments in nondestructive evaluation for structural ceramics
[DE88-005889] 13 p1751 N88-20473
A hybrid transform/DPCM encoder for data compression
[DE87-014852] 13 p1758 N88-20518
Dynamics of high-speed mechanisms with elastic members 13 p1779 N88-20643
Analysis for architecture for image processing
[INPE-4294-PRE/1165] 13 p1791 N88-20715
Bathymetric hazard survey test
[AD-A189150] 13 p1803 N88-20775
Retinotopic mapping of the human visual system with magnetoencephalography
[AD-A189557] 13 p1810 N88-20811
Digital enhancement of flow field images
[NASA-TP-2770] 13 p1813 N88-20833
On relaxation algorithms based on Markov random fields
[AD-A189043] 13 p1814 N88-20840
Method to evaluate image-recovery algorithms based on task performance
[DE88-005382] 13 p1816 N88-20853
Parallel graphical output from dialogue cells
[CWI-CS-R8719] 13 p1818 N88-20867
On effectively labeling planar projections of polyhedra
[CWI-CS-R8715] 13 p1826 N88-20917
Passive autonomous infrared sensor technology
[AD-A188898] 13 p1839 N88-21005
Weighted averaging method for image smoothing reported 14 p1901 N88-21352
Classification of small image areas by digital correlation for the connection of different images in photogrammetry and long-range reconnaissance
[ETN-88-91506] 14 p1940 N88-21578
Generalised threshold selection for edge detection
[RAE-TR-87035] 14 p1941 N88-21581
Oceanographic export system development, year 1
[AD-A189134] 14 p1950 N88-21623
Definition and display of profiled sweep-objects --- computer graphics
[REPT-87-45] 14 p1957 N88-21665
Proposal for a parallel system with image processing applications
[INPE-4793-PRE/1164] 14 p1961 N88-21696
The application of thermal imaging sensors and image processing techniques to a short range surface-to-air missile system
[ETN-88-92080] 14 p1962 N88-21829
Utilization of space color transformation, linear contrast and filtration for enhancement of colored digital images
[INPE-4310-PRE/1176] 14 p1983 N88-21831
Image processing on VEGA pictures 14 p2009 N88-21983
Focused image holography abberations
[DE88-701105] 15 p2068 N88-22333
Systems for ultrasonic scanning, analysis and imagery 15 p2082 N88-22414
Satellite UV image processing
[AD-A190466] 15 p2089 N88-22451
Method for restoration and resampling of TM sensor imagery
[INPE-4491-PRE/1255] 15 p2090 N88-22454
A hardware/software system for implementing geophysical diffraction tomography
[DE88-006411] 15 p2094 N88-22480
Calibration and processing of AVHRR data for temperature estimation
[INPE-4493-PRE/1257] 15 p2095 N88-22485
Multiple-transform pipelines for image coding
[REPT-87-038] 15 p2108 N88-22561
On the geometric interpretation of image contours
[RR-647-I-IMAG-57-LIFIA] 15 p2109 N88-22563
Rapid feature extraction via the radon transform
[AD-A190032] 15 p2110 N88-22573
Design and implementation of VLSI prime factor algorithm processor
[AD-A190483] 15 p2112 N88-22580
Contour interactive extraction using image numerical treatment
[ISL-R-114/86] 15 p2113 N88-22587
Modeling a parallel architecture for image processing
[RR-646-I] 15 p2114 N88-22593
Finding texture boundaries in images
[AD-A190554] 15 p2117 N88-22609
Multi-disciplinary techniques for understanding time-varying space-based imagery
[AD-A190711] 15 p2117 N88-22610

Concurrent algorithms for a mobile robot vision system
[DE88-005850] 15 p2117 N88-22614
Rigidity and smoothness of motion
[AD-A190555] 15 p2128 N88-22694
ROVER: A prototype active vision system
[AD-A189246] 15 p2133 N88-22722
Flow velocity measurements by image processing of optically modulated traces 16 p2203 N88-23147
The radiometric processing of SLAR measuring values using the PARES program
[BCRS-88-04] 16 p2227 N88-23301
Results of the testing of the segmentation program on RESEDA
[BCRS-87-01] 16 p2228 N88-23304
Stochastic approach of image segmentation. A model of cooperation between region primitives and boundaries
[ETN-88-92192] 16 p2262 N88-23523
Activities report of the Imagery Department
[ENST-87D008] 16 p2273 N88-23604
Visual enhancement of digital color imagery utilizing transformation in color coordinates (IHS transformation)
[INPE-4482-PRE/1248] 16 p2273 N88-23606
Adaptive segmentation evaluation
[AD-A190965] 16 p2274 N88-23609
Sensitivity of F-106B leading-edge-vortex images to flight and vapor-screen parameters
[NASA-TP-2818] 17 p2300 N88-23760
Nondestructive Evaluation (NDE) of structural ceramics by photoacoustic microscopy 17 p2325 N88-23884
Conversational Analysis of Color Images (CAICOU): An interactive development system for the analysis of color images
[RR-641-I-IMAG-39-LIFIA] 17 p2342 N88-23964
Some problems with regard to the TOVS processing detected by using NOAA-HRPT data check program
17 p2351 N88-24009
Enhanced infra-red picture of LR-FAX for spring and autumn seasons 17 p2351 N88-24011
Latin American Symposium on Remote Sensing. 4th Brazilian Remote Sensing Symposium and 6th SELPER Plenary Meeting, volume 1 17 p2352 N88-24013
Textural features for image classification in remote sensing 17 p2354 N88-24027
The USSR space systems for remote sensing of earth resources and the environment (sensor systems, processing techniques, applications)
17 p2356 N88-24035
Evolution of a family of image processing systems at INPE 17 p2361 N88-24065
Study of methods of post-processing applied to a problem of standard classification
17 p2362 N88-24067
Interpretation of MSS/LANDSAT data for evaluation of physical distribution of mangroves in Cananeia-Iguape (SP) 17 p2363 N88-24072
COMTAL vision one/20 programming processor system from the VAX 11/780 17 p2364 N88-24079
Automatic registration of satellite imagery
17 p2364 N88-24080
Application of its transformation in color enhancement of LANDSAT imagery 17 p2365 N88-24082
Restrictions in activity monitoring through remote sensing 17 p2365 N88-24084
Preliminary study on the application of digital processing of TM-LANDSAT data in the mapping of apple orchards in Fraiburgo (SC) 17 p2367 N88-24093
Evaluation of TM false color composites for crop discrimination 17 p2367 N88-24096
Terrain classification using SPOT images and the computer system GOP-300
[FOA-C-20677-2.7] 17 p2368 N88-24102
Adjustment in photogrammetry: Methods, programs and applications
[B8735130] 17 p2369 N88-24105
Image management research
17 p2380 N88-24150
Generic cueing in image understanding
[RSRE-MEMO-4109] 17 p2386 N88-24181
Orbital navigation, docking and obstacle avoidance as a form of three dimensional model-based image understanding 17 p2388 N88-24194
Application of spline functions to digital image processing
[ETN-88-92194] 17 p2392 N88-24218
Analysis of binarized Hartley phase-only filter performance with respect to stochastic noise
[DE88-007604] 18 p2519 N88-24945
High-energy laser-assisted imaging through vaporizing aerosols
[DE88-007911] 18 p2521 N88-24957
Visual information processing in the perception of features and objects
[AD-A192026] 18 p2552 N88-25148
CIMAG2: The computer program to generate color images
[AD-A191847] 18 p2557 N88-25175
System overview: Teragon 4000, an image processing equipment at FOA 3
[FOA-C-30465-3.3] 18 p2557 N88-25179
Shape from shading, occlusion and texture
[AD-A184840] 18 p2571 N88-25269
Optical system of laser illuminated streamer chamber
[DE88-702127] 18 p2577 N88-25306
An image processing system for research in solar physics
[AD-A191673] 18 p2595 N88-25421
Analysis and modeling of complex non-stationary flows
[PB88-127188] 19 p2664 N88-25842
A concurrent on-board vision system for a mobile robot
[DE88-007475] 19 p2676 N88-25914
Model-based computed tomography for nondestructive evaluation: An overview and proposal
[DE88-010600] 19 p2679 N88-25926
Model-based computed tomography for nondestructive evaluation: An overview and proposal
[DE88-010600] 19 p2679 N88-25926
Separability of cultivation through digital analysis of SPOT and TM data
[INPE-4541-PRE/1287] 19 p2685 N88-25963
Underwater optical trajectography and video image mosaics 19 p2700 N88-26051
Image processing applied to quantitative numerical cartography of ocean circulation
19 p2702 N88-26065
Methods for processing satellite images and their application to underwater operations
19 p2702 N88-26066
Intermediate level computer vision processing algorithm development for the content addressable array parallel processor
[AD-A192086] 19 p2714 N88-26111
PHOTODIGITIZE: A software/hardware system
[DE88-009575] 19 p2716 N88-26125
An instrument control and data analysis program for NMR imaging and spectroscopy
[DE88-007377] 19 p2717 N88-26132
SLAPP: A special multiprocessor array for signal processing and linear algebra
[AD-A191587] 19 p2719 N88-26146
Data volume reduction for imaging radar polarimetry
[NASA-CASE-NPO-17184-1-CU]
20 p2788 N88-26541
Microwave image understanding and its application to radar cross section management
20 p2788 N88-26542
Microfocus X-ray techniques for flaw location
[DE88-008636] 20 p2812 N88-26680
The interaction of sensory and perceptual variables: Spatial, temporal and orientation response to figure and ground
[AD-A192897] 20 p2832 N88-26798
Research in computer science 1985/6
[PB88-113840] 20 p2835 N88-26815
Automated system for mathematical processing of the data from a hybrid spectrometer
[DE87-702995] 20 p2836 N88-26820
Common Data Format (CDF) to store images
[NASA-CR-179366] 20 p2836 N88-26825
SEGMERGE: A scanline visible surface algorithm with adaptive span selection and inexpensive antialiasing
[DE88-009186] 20 p2836 N88-26826
A new approach to machine-based perception of monocular images
[DE88-002418] 20 p2853 N88-26942
Digital image processing from speckle interferograms by correlation methods: Application in atmospheric optics, astronomy, and biology
[ETN-88-92125] 20 p2855 N88-26953
Direct imaging of the columnar structure of GaAs quantum wells 20 p2868 N88-27030
Methods for indirect imaging through the atmosphere
[ONERA-NT-1987-4] 20 p2884 N88-27124
The application of imaging to the atmospheric Cerenkov technique: Observations of the Crab nebula
20 p2884 N88-27126
Processing and analysis of images transmitted by Vega space probes over Halley's comet
[ETN-88-92291] 20 p2885 N88-27131
Three-dimensional scene analysis using stero based imaging
[AD-A193120] 21 p2894 N88-27178
Applications of differential geometry to the shape analysis of gray-value images 21 p2924 N88-27358
Optical interconnections for digital image coding
21 p2928 N88-27381
Linear feature extraction from radar imagery. Phase 2: Base contract report
[AD-A192828] 21 p2931 N88-27404
The design of a digital Eprom oscillator for electrical impedance tomography
[DE88-012243] 21 p2940 N88-27462
The FEL CCD-camera: Experimental system for camera and image processing research
[FEL-1987-34] 21 p2952 N88-27532
Phase comparator for range imaging laser radar
[DE88-008109] 21 p2954 N88-27545
Interface control using low frequency (3 to 20 MHz) acoustic microscopy
[REPT-48-411/F] 21 p2959 N88-27577
Automatic line network extraction from aerial imagery of urban areas through knowledge based image analysis
[AD-A193067] 21 p2965 N88-27615
Review of geographic processing techniques applicable to regional analysis
[DE88-010759] 21 p2970 N88-27643
Photon limited image processing in the space-time domain
[AD-A193142] 21 p2972 N88-27655
Effects of pulsed and CW (Continuous Wave) 2450 MHz radiation on transformation and chromosomes of human lymphocytes in vitro
[AD-A193104] 21 p2987 N88-27736
Texture perception and shape from texture
[AD-A192923] 21 p2996 N88-27771
Research into the architecture of CAD based robot vision systems
[AD-A193330] 21 p2997 N88-27776
Enhancement of modeling and image generation techniques for high-resolution 3-dimensional imagery
[DE88-008923] 21 p2998 N88-27782
Maximum entropy signal restoration with linear programming
[DE88-011740] 21 p2999 N88-27787
Contribution to almost realistic picture processing by a computer graphics procedure
[ETN-88-92372] 21 p2999 N88-27789
Image processing using a parallel architecture
[AD-A192833] 21 p3002 N88-27803
Optical method to measure the deformations of structures loaded by hydraulic pressure
[SNIAS-881-430-111] 22 p3088 N88-28338
Methodological developments on crop inventories using SPOT and ground surveys 22 p3094 N88-28371
An evaluation of multidate SPOT data for agriculture and land use mapping in the United Kingdom
22 p3094 N88-28375
Topographic suppression and advances in classification for land cover mapping using SPOT-1 HRV imagery
22 p3099 N88-28404
Assessment of SPOT satellite based system in humid tropical vegetation identification, classification and monitoring 22 p3100 N88-28408
SPOT-1 satellite imagery for forest inventory in Sweden 22 p3106 N88-28445
Rigorous stereophotogrammetric treatment of SPOT images 22 p3111 N88-28482
Automatic extraction of high resolution elevation data from SPOT stereo images 22 p3113 N88-28489
Digital SPOT stereoplotting: An original approach to the formation of epipolar images and matching
22 p3113 N88-28493
Summary of analysis and processing techniques used on SPOT imagery 22 p3115 N88-28503
Research on wide area workstations
[AD-A192529] 22 p3136 N88-28643
Natural object categorization
[AD-A194103] 22 p3139 N88-28662
Implementation of nonsquare tilings on an image processing system
[FOA-C-30487-3.3] 22 p3140 N88-28669
Survey of neural net paradigms for specification of discrete networks
[AD-A192682] 22 p3141 N88-28674
Rendering of surfaces from volume data
[AD-A193649] 22 p3143 N88-28689
Direct visualization of surfaces from computed tomography data
[AD-A193646] 22 p3153 N88-28758
Noise generation and boundary layer effects in vortex-airfoil interaction and methods of digital hologram analysis for these flow fields
[AD-A194191] 23 p3171 N88-28883
Three-dimensional vortex interactions
[AD-A194066] 23 p3172 N88-28889
Analysis of edge detection techniques for radiographic image measurement
[AD-A193650] 23 p3186 N88-28961
Comparison of 2-D Fourier and spatial techniques for removing noise in real-time X-ray radiography
[AD-A193700] 23 p3187 N88-28962

Visual motion perception and visual attentive processes
[AD-A193640] 23 p3241 N88-29288
Automatic object recognition
23 p3254 N88-29368
Two dimensional convolute integers for machine vision and image recognition 23 p3254 N88-29369
Object discrimination via bulk temperature/velocity filtering, phase 1
[AD-A194533] 23 p3274 N88-29487
Accuracy of satellite data navigation
[AD-A195877] 24 p3322 N88-29787
Automatic data retrieval from rocket motor holograms
[AD-A195586] 24 p3337 N88-29864
Degradation of protective coatings on steel in corrosive environments 24 p3354 N88-29969
Integrating multispectral imagery and ground level hyperspectral signature data
[AD-A195976] 24 p3386 N88-30166
LANDSAT-TM data to map flooded areas
[INPE-4594-PRE/1324] 24 p3387 N88-30177
Multilevel computational theory of stereoscopic visual image processing
[AD-A195331] 24 p3408 N88-30288
Using primal sketch primitives as the basis for the Hough transform
[INPE-4564-PRE/1305] 24 p3412 N88-30310
A digital terrain model system for a microcomputer
[INPE-4610-PRE/1333] 24 p3413 N88-30316
Compression and decompression of imaging sensor signals (CADISS): A multiprocessor system for image compression/decompression on board scientific satellites
[NLR-TR-87076-L] 24 p3414 N88-30323
The 1988 Goddard Conference on Space Applications of Artificial Intelligence
[NASA-CP-3009] 24 p3415 N88-30330
Low level image processing techniques using the pipeline image processing engine in the flight telerobotic servicer 24 p3418 N88-30346
An interactive testbed for development of expert tools for pattern recognition 24 p3419 N88-30349
The combinatorics of object recognition in cluttered environments using constrained search
[AD-A196224] 24 p3422 N88-30364
Symbolic construction of a 2D scale-space image
[AD-A195926] 24 p3423 N88-30374
Image focusing in space and time
[AD-A195839] 24 p3429 N88-30410
Activities in astrophysics
[INPE-4582-PRE/1316] 24 p3456 N88-30570

IMAGE RECONSTRUCTION

Imaging strategies for a spaceborne interferometer
01 p0094 N88-10617
ISIS: Image reconstruction methods and signal-to-noise ratio investigations --- spaceborne interferometry
01 p0094 N88-10619
ISIS: Image reconstruction experiments and comparison of various array configurations --- spaceborne interferometry 01 p0095 N88-10620
Milliarcsecond ground-based imaging with single telescopes 01 p0097 N88-10637
Three dimensional reconstruction of optical microscope pictures using the three dimensional microscopic inverse point spread function
[ETN-87-90420] 01 p0098 N88-10646
Study of the distribution of a multi-electrode circular system sensitivity for the reconstruction of bioelectrical impedance images
[ISAL-IDI1-87-01] 02 p0217 N88-11368
The maximum likelihood estimator method of image reconstruction: Its fundamental characteristics and their origin
[DE88-000462] 05 p0636 N88-13892
Computing 3-D structure of rigid objects using stereo and motion 08 p1061 N88-16407
Comparison of a few methods of restoring images distorted by atmospheric turbulence
[ESA-TT-1065] 09 p1248 N88-17481
Ideal shrinking and expansion of discrete sequences
[NASA-TM-88202] 11 p1524 N88-19100
Solar radioimage restoration
[INPE-4312-TDL/279] 11 p1571 N88-19402
Three-dimensional image reconstruction in object space
[DE88-900279] 12 p1712 N88-20246
Restoration techniques for redisplay of LANDSAT-5 satellite imagery
[INPE-4189-PRE/1076] 13 p1791 N88-20712
Method to evaluate image-recovery algorithms based on task performance
[DE88-005382] 13 p1816 N88-20853
Rainbow holographic image reconstructed by spatially extended white light source 15 p2055 N88-22249
Focused image holography abberations
[DE88-701105] 15 p2068 N88-22333
Geometric restoration of satellite image data
[AD-A190462] 15 p2089 N88-22450
Stochastic approach of image segmentation. A model of cooperation between region primitives and boundaries
[ETN-88-92192] 16 p2262 N88-23523
Activities report of the Imagery Department
[ENST-87D008] 16 p2273 N88-23604
Application of dynamic programming to image registration
[ENST-87E022] 18 p2557 N88-25180
A fast and efficient procedure for generalized cross-validation with large data sets. Application to image reconstruction
[RR-669-M] 18 p2563 N88-25220
Display and processing of multidimensional signals with the aid of fractal image sequences
[ETN-88-92131] 20 p2806 N88-26642
A new approach to machine-based perception of monocular images
[DE88-002418] 20 p2853 N88-26942
Reconstruction of multidimensional signals from multiple level threshold crossings
[AD-A195561] 24 p3425 N88-30383

IMAGE RESOLUTION

On the concept of resolution ellipse in aperture synthesis matched deconvolution with error analysis --- astronomical interferometry 01 p0095 N88-10621
Galactic nuclei and quasars at high angular resolution
01 p0098 N88-10644
Intrinsic and extrinsic geometric quality --- SPOT images 03 p0341 N88-12154
Registration of SPOT images
03 p0341 N88-12155
Input/output technologies: An overview of image scanning, storage, and display
[DE87-014837] 04 p0476 N88-12933
High resolution ultraviolet filter development
[AD-A184183] 05 p0649 N88-13979
Study of synthetic aperture radar data compression and encoding. Part 1: SAR image data analysis
[NLR-TR-85085-L-PT-1] 07 p0843 N88-15115
Multiple-object motion estimation by maximal matching of 3-D point and line features 09 p1220 N88-17322
Investigations of high resolution imaging through the Earth's atmosphere using speckle interferometry
[AD-A189295] 12 p1692 N88-20121
Generalised threshold selection for edge detection
[RAE-TR-87035] 14 p1941 N88-21581
Rainbow holographic image reconstructed by spatially extended white light source 15 p2055 N88-22249
An investigation into the precision of a digital camera
[B8735054] 16 p2210 N88-23193
Instrumentation for turbulent reacting flows
[AD-A191671] 18 p2515 N88-24923
Ultraviolet imaging of hydrogen flames
[DE88-009152] 20 p2769 N88-26422
Interpreting forest biome productivity and cover utilizing nested scales of image resolution and biogeographical analysis
[NASA-CR-183036] 20 p2817 N88-26711
Comparison of 2-D Fourier and spatial techniques for removing noise in real-time X-ray radiography
[AD-A193700] 23 p3187 N88-28962
High definition television: Evaluation for remote task performance
[DE88-011573] 23 p3202 N88-29057

IMAGE ROTATION

Position, scale, and rotation invariant target recognition using range imagery
[AD-A188828] 12 p1633 N88-19772

IMAGE TRANSDUCERS

Cryogenic acoustic microscopy
[AD-A187274] 10 p1299 N88-17767

IMAGE TUBES

Resolution limitations and optimization of the LLNL streak camera focus
[DE88-001633] 05 p0586 N88-13572
Resolution limitations and optimization of the ITT F4157 streak tube focus for fast (10 ps) operation
[DE88-003727] 09 p1169 N88-17007
The 5-GHz operation of the ITT and RCA streak tubes with a 7.5-ns time window
[DE88-003342] 09 p1169 N88-17008

IMAGERY

NT AERIAL PHOTOGRAPHY
NT ASTRONOMICAL PHOTOGRAPHY
NT AUTORADIOGRAPHY
NT BLACK AND WHITE PHOTOGRAPHY
NT CINEMATOGRAPHY
NT CLOUD PHOTOGRAPHY
NT COLOR PHOTOGRAPHY
NT COMPUTER AIDED TOMOGRAPHY
NT ELECTRO-OPTICAL PHOTOGRAPHY
NT HOLOGRAPHY
NT INFRARED IMAGERY
NT INFRARED PHOTOGRAPHY
NT MICROWAVE IMAGERY
NT NEUTRON RADIOGRAPHY
NT PHOTOMICROGRAPHY
NT PHOTORECONNAISSANCE
NT PIXELS
NT RADAR IMAGERY
NT RADAR PHOTOGRAPHY
NT RADIOGRAPHY
NT REPRODUCTION (COPYING)
NT SATELLITE IMAGERY
NT SATELLITE-BORNE PHOTOGRAPHY
NT SCHLIEREN PHOTOGRAPHY
NT SHADOWGRAPH PHOTOGRAPHY
NT SPACEBORNE PHOTOGRAPHY
NT SPECKLE HOLOGRAPHY
NT SPECTROHELIOGRAPHS
NT SPECTROPHOTOGRAPHY
NT STEREOPHOTOGRAPHY
NT STEREOSCOPY
NT TOMOGRAPHY
NT ULTRAVIOLET PHOTOMETRY
NT WHITE LIGHT HOLOGRAPHY
NT X RAY IMAGERY
NT XEROGRAPHY

Two dimensional imaging observations of meter-decameter bursts associated with the February 1986 flare activity 01 p0113 N88-10723
Modeling cloudy and clear interval length probabilities using space shuttle imagery
[AD-A185290] 05 p0627 N88-13837
Range imagery algorithms for the detection of obstacles by autonomous vehicles
[AD-A185421] 05 p0659 N88-14045
Imaging subtle microstructural variations in ceramics with precision ultrasonic velocity and attenuation measurements
[NASA-TM-100129] 07 p0867 N88-15257
Theory and research on the disjunction of cross passage errors and systematic image errors in photogrammetric point determination
[SER-C-324] 07 p0872 N88-15290
Proceedings of Image Understanding Workshop, volume 2
[AD-A186104] 07 p0902 N88-15464
Orbital navigation, docking and obstacle avoidance as a form of three dimensional model-based image understanding 08 p1061 N88-16406
Computing 3-D structure of rigid objects using stereo and motion 08 p1061 N88-16407
Comparison of UNL laser imaging and sizing system and a phase/Doppler system for analyzing sprays from a NASA nozzle
[NASA-CR-182437] 09 p1161 N88-16956
Performance of a photon counting microchannel plate intensifier with wedge and strip image readout
[DE88-003831] 10 p1334 N88-17970
Autocorrelation of control points on 11-band multispectral imagery
[AD-A188185] 10 p1348 N88-18056
Three-dimensional image generation from an aerial photograph
[AD-A188039] 11 p1503 N88-18979
Applications of mathematical morphology to range imagery
[AD-A189316] 12 p1684 N88-20072
Multi-disciplinary techniques for understanding time-varying space-based imagery
[AD-A190711] 15 p2117 N88-22610
Television monitor field shifter and an opto-electronic method for obtaining a stereo image of optimal depth resolution and reduced depth distrotion on a single screen
[NASA-CASE-NPO-17249-1-CU] 17 p2332 N88-23924
Atmospheric autorotating imaging device
[NASA-CASE-NPO-17390-1-CU] 18 p2519 N88-24944
Investigation of the diffuse ultraviolet background with DE data
[NASA-CR-182863] 19 p2741 N88-26271
Description of a tool for the simulation of imagery systems 22 p3147 N88-28724
Determining vehicle motion from stereo image sequences
[AD-A194371] 23 p3216 N88-29140
Microcircuit trace cutting with focused ion beams
[AD-A196030] 24 p3367 N88-30050
Integrating multispectral imagery and ground level hyperspectral signature data
[AD-A195976] 24 p3386 N88-30166
Symbolic construction of a 2D scale-space image
[AD-A195926] 24 p3423 N88-30374
Kalman filter-based algorithms for estimating depth from image sequences
[AD-A195818] 24 p3424 N88-30380

Diffraction imaging (topography) with monochromatic synchrotron radiation
[NASA-CR-183264] 24 p3433 N88-30431
Applications of synchrotron radiation to materials science: Diffraction imaging (topography) and microradiography
[NASA-CR-183265] 24 p3434 N88-30440

IMAGES
Design of source coders and joint source/channel coders for noisy channels
[NASA-CR-181547] 04 p0432 N88-12678
Interaction of different modules in depth perception: Stereo and shading
[AD-A185607] 06 p0759 N88-14655
Three dimensional display of meteorological scientific data
[DE88-000776] 07 p0880 N88-15339
Research on visual information processing with special reference to oculomotor behavior in the areas of exploration, recognition and search
[AD-A186598] 08 p1051 N88-16346
Image correlation on an IBM-PC for characterization of advanced ceramics
[DE88-002829] 09 p1149 N88-16885
Fractal images: Procedure and theory
[AD-A187014] 09 p1217 N88-17293
The role of photodetectors in optical signal processing
[AD-A186804] 09 p1247 N88-17476
Management Information and Downloader Interface System (MIDIS)
[AD-A186978] 09 p1261 N88-17557
Visual integration and detection of discontinuities: The key role of intensity edges
[AD-A188012] 11 p1520 N88-19076
Soft maps for US Army electronic map background applications
[AD-A188427] 12 p1638 N88-19809
Reduced tolerance imaging 2, volume 2
[AD-A189604] 13 p1829 N88-20939
Aberrations: Their effect on off-axis beam steering
[AD-A189601] 13 p1840 N88-21008
Finding texture boundaries in images
[AD-A190554] 15 p2117 N88-22609
Finding wheels of vehicles in stereo images
[AD-A194372] 22 p3080 N88-28292
Transformations of short-term visual memory
[AD-A193873] 23 p3241 N88-29290
Particle sizing in combustion systems, using scattered laser light
[AD-A196231] 24 p3352 N88-29953
Comparative aspects of multiple processes of attention
[AD-A195805] 24 p3408 N88-30291
Dynamical systems and motion vision
[AD-A195932] 24 p3422 N88-30366
Symbolic construction of a 2D scale-space image
[AD-A195926] 24 p3423 N88-30374
Kalman filter-based algorithms for estimating depth from image sequences
[AD-A195818] 24 p3424 N88-30380
Streaking images that appear only in the plane of diffraction in undoped GaAs single crystals: Diffraction imaging (topography) by monochromatic synchrotron radiation
[NASA-CR-183267] 24 p3433 N88-30437

IMAGING RADAR
Principal space programs in the area of microwaves
[INPE-4164-PRE/1064] 12 p1618 N88-19677
The superconducting phase shifter in the development of a terahertz imaging radar system
[AD-A190666] 16 p2188 N88-23046
Investigation of the usefulness of speckle analysis in imaging radar systems
[BCRS-86-05] 16 p2227 N88-23302
The role of space borne imaging radars in environmental monitoring: Some shuttle imaging radar results in Asia
[NASA-TM-101178] 18 p2502 N88-24844
Data volume reduction for imaging radar polarimetry
[NASA-CASE-NPO-17184-1-CU] 20 p2788 N88-26541
Phase comparator for range imaging laser radar
[DE88-006109] 21 p2954 N88-27545
A submillimeter wavelength space-based imaging radar
[AD-A195846] 24 p3364 N88-30033

IMAGING SPECTROMETERS
Radiometric calibration of the Earth observing system's imaging sensors
[NASA-CR-181542] 04 p0463 N88-12665
Proceedings of the Third Airborne Imaging Spectrometer Data Analysis Workshop
[NASA-CR-181552] 05 p0611 N88-13755
The Portable Instant Display and Analysis Spectrometer (PIDAS) 05 p0611 N88-13756
AIS-2 radiometry and a comparison of methods for the recovery of ground reflectance 05 p0611 N88-13757
Effective use of principal component analysis with high resolution remote sensing data to delineate hydrothermal alteration and carbonate rocks 05 p0612 N88-13758
Land cover/use classification of Cairns, Queensland, Australia: A remote sensing study involving the conjunctive use of the airborne imaging spectrometer, the large format camera and the thematic mapper simulator 05 p0612 N88-13759
Calibrating AIS images using the surface as a reference 05 p0612 N88-13760
The use of airborne imaging spectrometer data to determine experimentally induced variation in coniferous canopy chemistry 05 p0612 N88-13761
Overview of Austrian Airborne Imaging Spectrometer (AIS) programme and first results 05 p0612 N88-13762
AIS-2 spectra of California wetland vegetation 05 p0613 N88-13763
Toward detecting California shrubland canopy chemistry with AIS data 05 p0613 N88-13764
Measuring near infrared spectral reflectance changes from water stressed conifer stands with AIS-2 05 p0613 N88-13765
Abundance and distribution of ultramafic microbreccia in Moses Rock Dike: Quantitative application of AIS data 05 p0613 N88-13766
Evaluation of AIS-2 (1986) data over hydrothermally altered granitoid rocks of the Singatse Range (Yerington) Nevada and comparison with 1985 AIS-1 data 05 p0613 N88-13767
Preliminary results from an investigation of AIS-1 data over an area of epithermal alteration: Plateau, Northern Queensland, Australia 05 p0613 N88-13768
Causes of spurious features in spectral reflectance data 05 p0614 N88-13769
Automatic continuum analysis of reflectance spectra 05 p0614 N88-13770
Analysis of airborne imaging spectrometer data for the Ruby Mountains, Montana, by use of absorption-band-depth images 05 p0614 N88-13771
Mapping hydrothermally altered rocks in the Northern Grapevine Mountains, Nevada and California with the airborne imaging spectrometer 05 p0614 N88-13772
A geostationary imaging spectrometer TOMS instrument 05 p0619 N88-13802
HIRIS (High-Resolution Imaging Spectrometer: Science opportunities for the 1990s. Earth observing system. Volume 2C: Instrument panel report
[NASA-TM-89703] 07 p0871 N88-15282
Technical assessment of the joint CSIRO/Bureau of Meteorology proposal for a geostationary imager/sounder over the Australian region
[RTP-15] 09 p1135 N88-16811

IMAGING TECHNIQUES
NT RASTER SCANNING
NT SPECKLE HOLOGRAPHY
Laser probes of natural gas ignition chemistry
[PB87-209599] 01 p0021 N88-10129
Imaging of planar defects with synthetic aperture focusing technique (LSAFT) — ultrasonic inspection
[VTT-468] 01 p0058 N88-10370
Image sharpening observations of active galactic nuclei 01 p0098 N88-10643
How we get pictures from space, revised edition
[NF-151/7-87-REV] 02 p0193 N88-11203
Study of the distribution of a multi-electrode circular system sensitivity for the reconstruction of bioelectrical impedance images
[ISAL-IDI1-87-01] 02 p0217 N88-11368
A preliminary taxonomy of visible surface algorithms
[DE87-013559] 02 p0220 N88-11386
Fundamentals and techniques of nonimaging optics research
[DE87-014544] 02 p0236 N88-11488
Delay-Doppler radar imaging
[AD-A184165] 03 p0308 N88-11943
Planning for future operational sensors and other priorities
[PB87-220802] 03 p0325 N88-12056
Some new ideas in liquid detectors
[DE88-000732] 04 p0446 N88-12768
Simultaneous, cospatial imaging of the Sun in cyanogen and singly-ionized calcium 04 p0507 N88-13114
Doppler snapshots 04 p0508 N88-13125
Photon counting image sensor development for astronomical applications
[NASA-CR-181507] 05 p0660 N88-14049
Statistical investigations of the behavior of a product correlator and an edge detector in critical situations
[MBB-UA-1034/87] 06 p0781 N88-14793
Time-domain robotic vision application 06 p0798 N88-14886
Scanning and measuring peculiarities with high-space resolution objects recorded at the Gabor holograms
[DE88-700373] 07 p0857 N88-15203
Electronic imaging technique for welding and other high-luminosity processes
[DE88-002199] 07 p0862 N88-15227
Recognition of polyhedral objects under structured illumination
[PB88-106703] 07 p0932 N88-15661
The use of NMR imaging to measure porosity and binder distributions in green-state and partially sintered ceramics
[DE88-003099] 08 p0972 N88-15881
Textural features for image classification in remote sensing
[INPE-4169-PRE/1066] 08 p1020 N88-16181
Developments in instrumental techniques for observations of magnetospheric and ionospheric shaped charge releases 08 p1031 N88-16248
Computing 3-D structure of rigid objects using stereo and motion 08 p1061 N88-16407
Crystal diffraction lenses for imaging gamma-ray telescope
[DE88-003084] 08 p1083 N88-16529
Future television systems: Comparison of sequent ial and interlaced scanning
[BBC-RD-1987/18] 09 p1155 N88-16923
Thermal wave imaging
[AD-A186810] 09 p1177 N88-17048
Comparison of a few methods of restoring images distorted by atmospheric turbulence
[ESA-TT-1065] 09 p1248 N88-17481
Some present limitations on the lattice imaging of grain boundaries
[DE87-014665] 09 p1256 N88-17530
NMR (Nuclear Magnetic Resonance) imaging for detecting binder/plasticizers in green-state structural ceramics
[DE88-003111] 10 p1304 N88-17800
Digital imaging techniques for single- and multi-phase reacting flowfields 10 p1327 N88-17933
Instrumentation and quantitative methods of evaluation
[DE87-013639] 10 p1342 N88-18017
Investigation of a ray-mode representation of the Green's function in a rectangular cavity
[PB88-131677] 11 p1469 N88-18763
Multisource context classification methods in remote sensing 11 p1504 N88-18985
Geophysical diffraction tomography for imaging isolated subsurface inclusions
[DE88-003918] 11 p1505 N88-18990
Scanning tunneling microscopy of silver, gold, and aluminium monomers and small clusters on graphite
[DE88-003871] 11 p1562 N88-19349
Spectral images and multi-component models of the chromospheres of AR Lacertae 11 p1568 N88-19384
A method to detect and digitize small plant movements 12 p1654 N88-19912
Image segmentation via fractal dimension
[AD-A188825] 12 p1678 N88-20033
Investigations of high resolution imaging through the Earth's atmosphere using speckle interferometry
[AD-A189295] 12 p1692 N88-20121
Photographic filters
[INPE-4448-RPE/558] 12 p1692 N88-20124
The imaging of extra-galactic low-energy gamma-ray sources prospects, techniques, and instrumentation
[NASA-CR-182536] 12 p1713 N88-20251
Bathymetric hazard survey test
[AD-A189150] 13 p1803 N88-20775
Parallel image compression
[NASA-CR-180758] 13 p1814 N88-20837
Reduced tolerance imaging 2, volume 2
[AD-A189604] 13 p1829 N88-20939
Effects of update and refresh rates on flight simulation visual displays
[NASA-TM-100415] 15 p2018 N88-22033
Polarimetric ISAR imaging using either measured or calculated transient signatures
[AD-A190077] 15 p2056 N88-22259
Range image segmentation and surface parameter extraction for a mobile robot
[DE87-013877] 15 p2073 N88-22360
Systems for ultrasonic scanning, analysis and imagery 15 p2082 N88-22414
Method for restoration and resampling of TM sensor imagery
[INPE-4491-PRE/1255] 15 p2090 N88-22454
Comparative utilization of analog and digital processes in the treatment of MSS-LANDSAT data for studying the national parks of Brazil
[INPE-4011-TDL/240] 15 p2090 N88-22456

Stochastic approach of image segmentation. A model of cooperation between region primitives and boundaries
[ETN-88-92192] 16 p2262 N88-23523
Activities report of the Imagery Department
[ENST-87D008] 16 p2273 N88-23604
Latin American Symposium on Remote Sensing. 4th Brazilian Remote Sensing Symposium and 6th SELPER Plenary Meeting, volume 1 17 p2352 N88-24013
The geometric workstation, a new approach for geometric corrections of remotely sensed data 17 p2352 N88-24017
Subsurface morphology and geoarchaeology revealed by spaceborne and airborne radar 17 p2353 N88-24022
Mapping soil and rock variation from satellite images in the Sahel 17 p2354 N88-24023
Textural features for image classification in remote sensing 17 p2354 N88-24027
Shape detection in remote sensing through graph isomorphism 17 p2354 N88-24028
The modeling of error budget analysis and tolerance specifications for BRESEX multiband linear array CCD camera 17 p2355 N88-24029
Practical image analysis using personal computers: The Canadian experience 17 p2356 N88-24037
Comparison of the solar radiation estimation method by satellites 17 p2360 N88-24055
Study of methods of post-processing applied to a problem of standard classification 17 p2362 N88-24067
Analysis of the parameters responsible for the variations of the illumination conditions in the LANSAT data 17 p2362 N88-24070
COMTAL vision one/20 programming processor system from the VAX 11/780 17 p2364 N88-24079
Automatic registration of satellite imagery 17 p2364 N88-24080
Application of its transformation in color enhancement of LANDSAT imagery 17 p2365 N88-24082
Evaluation of TM false color composites for crop discrimination 17 p2367 N88-24096
Novel silicon Schottky barrier infrared imaging arrays 17 p2439 N88-24510
Delay-doppler radar imaging
[AD-A191509] 18 p2499 N88-24826
High-energy laser-assisted imaging through vaporizing aerosols
[DE88-007911] 18 p2521 N88-24957
Utilization of the IR telescope gimbaling system as a stabilized pointing platform for balloon payloads. Volume 1: Technical results
[NASA-CR-179339] 18 p2522 N88-24962
Instantaneous two-dimensional multiple particle sizing diagnostic 19 p2630 N88-25600
Design and preliminary evaluation of an underwater laser-based imaging system
[DE88-010560] 19 p2675 N88-25908
The use of satellite imagery for municipal conditions in rural recording in Pereira Barreto (SP) 19 p2682 N88-25944
The impact of disorganized occupation of urban sub-basins: Sub-basin of the Cabucu River, metropolitan area of Sao Paulo (SP) 19 p2682 N88-25945
Application of 35mm EM aerial reconnaissance photographic format of the municipality of Ubatuba (SP) 19 p2684 N88-25953
An instrument control and data analysis program for NMR imaging and spectroscopy
[DE88-007377] 19 p2717 N88-26132
Ultraviolet imaging of hydrogen flames
[DE88-009152] 20 p2769 N88-26422
Methods for indirect imaging through the atmosphere
[ONERA-NT-1987-4] 20 p2864 N88-27124
Optical diagnostics for metallurgical processes
[DE88-009255] 21 p2913 N88-27289
Ellipsometric imaging of drying sol-gel films
[DE88-011785] 21 p2921 N88-27335
Turbulent flow field visualization with integral interferometric imaging and computed tomography 21 p2950 N88-27521
Optical imaging diagnostics for fusion plasmas
[DE88-997572] 21 p3018 N88-27910
Application of two-dimensional imaging to very high energy gamma ray astronomy
[DE88-010120] 21 p3030 N88-27983
Characterization of new FPS (Focus Projection and Scale) vidicons for scientific imaging applications
[DE88-011213] 22 p3080 N88-28290
Proof-of-principle high speed electronic imaging system, phase 2
[AD-A193798] 23 p3181 N88-28937
Visual Effects in the High Performance Aircraft Cockpit
[AGARD-LS-156] 23 p3241 N88-29291
Display system image quality 23 p3242 N88-29298
Optimization-driven machine-oriented motion measurement 23 p3245 N88-29312
ZT imaging system for layered thin wall structures
[AD-A195486] 24 p3352 N88-29954
Quantitative surface temperature measurement using two-color thermographic phosphors and video equipment
[NASA-CASE-LAR-13740-1] 24 p3376 N88-30105
Method for combined image interpolation-restoration through a fir filter design technique
[INPE-4561-PRE/1302] 24 p3413 N88-30315
A coded mask telescope for observations of X and gamma ray sources in the southern sky
[INPE-4580-PRE/1314] 24 p3453 N88-30551

IMBEDDINGS (MATHEMATICS)
NT INVARIANT IMBEDDINGS

IMCC (CONTROL CENTER)
U INTEGRATED MISSION CONTROL CENTER

IMIDES
Aromatic cyclotriphosphazenes
[NASA-CASE-ARC-11428-3] 18 p2477 N88-24692

IMINES
Polymerization of azaethylenes (imines) and aza-1,3-dienes: Potential reactive monomers
[AD-A194717] 23 p3197 N88-29028

IMMERSION
U SUBMERGING

IMMISCIBILITY
U SOLUBILITY

IMMITTANCE
U ELECTRICAL IMPEDANCE

IMMOBILIZATION
Lipid peroxidation in rat tissues with exposure to antiorthostatic hypokinesia, exercise and immobilization stress 10 p1365 N88-18159
New book on metabolic aspects of spaceflight stress 10 p1367 N88-18172
Human response to prolonged motionless suspension in four types of full body harnesses 21 p2929 N88-27387

IMMUNE SYSTEMS
Mononuclear phagocytes during adaptation of essentially healthy people to high altitudes 07 p0896 N88-15432
White blood cells in space: An experiment for the first Spacelab mission 09 p1127 N88-16757
Operation Everest 2: Alterations in the immune system at high altitude
[AD-A188011] 11 p1520 N88-19075
Direct interaction between autonomic nerves and the immune system
[AD-A188576] 12 p1667 N88-19991
Immunofluorescence localization of dissociation supernatant and extracellular matrix components in Lytechinus pictus sectioned embryos
[NASA-CR-183137] 24 p3406 N88-30276

IMMUNITY
Mononuclear phagocytes during adaptation of essentially healthy people to high altitudes 07 p0896 N88-15432
Operation Everest 2: Alterations in the immune system at high altitude
[AD-A188011] 11 p1520 N88-19075

IMMUNOASSAY
A solid phase enzyme-linked immunosorbent assay for the antigenic detection of Legionella pneumophila (serogroup 1): A compliment for the space station diagnostic capability 06 p0795 N88-14868
Effects of anti-g suit inflation on renin and aldosterone response physical exercise 12 p1659 N88-19944
Is ANF implied in the night attenuated renal response to central hypervolemia? 12 p1659 N88-19945
Photochrome from green plants: Assay, purification and characterization
[DE88-007511] 19 p2702 N88-26067

IMMUNOLOGY
JPRS report: Science and technology. USSR: Life sciences
[JPRS-ULS-87-009] 04 p0473 N88-12915
TOMS as a monitor of the ultraviolet radiation environment: Applications to photobiology 05 p0617 N88-13785
Physiological and immunological aspects of human adaptation to temperature elevation in a closed environment 07 p0895 N88-15424
Supersonic and subsonic aircraft noise effects on animals: A literature survey
[AD-A186922] 10 p1404 N88-18373
Neurohumoral aspects of sleep
[AD-A188653] 12 p1667 N88-19992
JPRS report: Science and technology. USSR: Life sciences
[JPRS-ULS-88-004] 13 p1810 N88-20815
Bioeffects of electromagnetic waves 24 p3364 N88-30032

IMP-H
U EXPLORER 47 SATELLITE

IMP-7
U EXPLORER 47 SATELLITE

IMPACT
NT ECONOMIC IMPACT
NT ELECTRON IMPACT
NT HYPERVELOCITY IMPACT
NT POINT IMPACT
Assessment of the impacts of transferring certain nuclear reactor technologies to the Soviet Union and Eastern Europe
[DE87-014388] 02 p0249 N88-11576
The impact of environmental factors on the performance of millimeter wave seekers in smart munitions
[DE87-014277] 03 p0270 N88-11697
Simulation of effect on biological systems of impact wave from heavy charged particle track 07 p0896 N88-15429
A review of methanol vehicles and air quality impacts
[DE88-002846] 08 p1023 N88-16194
Factors affecting the sticking of insects on modified aircraft wings
[NASA-CR-182451] 09 p1148 N88-16878
A substructure method for dynamic simulation of flexible mechanical systems with geometric nonlinearities 09 p1176 N88-17044
Quantitative and qualitative assessments of the impact of linguistic theory on information science 10 p1424 N88-18507
The concept of an impact resonance diagram for characterizing the nonlinear response of impact vibration
[DE88-005475] 15 p2086 N88-22432
Revised Impact Dynamic Design-Analysis Method (RIDDAM)
[AD-A190479] 16 p2217 N88-23225
Survey of impact damper performance 16 p2217 N88-23227
Nineteenth Lunar and Planetary Science Conference. Press abstracts
[NASA-CR-183037] 24 p3440 N88-30473
Exotic minerals in 3,500 million year old rocks: Evidence for large meteorite impacts 24 p3440 N88-30475
LSU scientists discover evidence of large meteorite impacts on the early earth 24 p3441 N88-30480

IMPACT ACCELERATION
Peak Acceleration Device (PAD)
[AD-A191639] 18 p2461 N88-24611

IMPACT DAMAGE
NT METEORITIC DAMAGE
NT RAIN IMPACT DAMAGE
Effect of adhesive layers on impact damage and dynamic response in composite laminates 02 p0141 N88-10887
Simulation of tokamak runaway-electron events. Study of the response of materials by use of an electron linear accelerator
[IPPJ-841] 02 p0242 N88-11528
Impact of solids on composite materials
[NASA-CR-182395] 07 p0827 N88-15015
Behavior of a steel cylinder under the influence of a local load in the elastic and elasto-plastic area
[PB87-154787] 07 p0869 N88-15272
Investigation of low velocity impact damage on filamentary composite materials 07 p0923 N88-15607
Through-transmission/pulse-echo ultrasonic equipment evaluation
[AD-A186340] 07 p0929 N88-15641
Space station integrated wall damage and penetration damage control. Task 5: Space debris measurement, mapping and characterization system
[NASA-CR-179281] 10 p1285 N88-17688
An analysis of penetration and ricochet phenomena in oblique hypervelocity impact
[NASA-TM-100319] 10 p1339 N88-18004
Analysis of impact crater arrangement on the Venutian surface (from photographic materials of the Venera-15 and -16 spacecraft)
[NASA-TT-20211] 11 p1571 N88-19401
Simulated impact damage in a thick graphite/epoxy laminate using spherical indenters
[NASA-TM-100539] 13 p1733 N88-20363
Studies of traverse impact damage in composite materials using a Hopkinson pressure-bar technique
[OUEL-1706/87] 14 p1883 N88-21255
Analysis of head response to torso acceleration. Volume 1: Development of performance requirements
[PB88-156757] 14 p1953 N88-21640
Impact damage in composite laminates 15 p2080 N88-22402
Bilateral symmetry elements of the Zhamanshin impact crater
[NASA-TT-20288] 15 p2096 N88-22490

Surface crack analysis applied to impact damage in a thick graphite-epoxy composite
[NASA-TM-100600] 16 p2173 N88-22950
GARTEUR TP-037: Impact damage tolerance of carbon fiber and hybrid laminates
[RAE-TR-87057] 17 p2316 N88-23837
The application of high-rate biaxial testing to the design of containment vessels for radioisotope heat sources 17 p2426 N88-24428
Design manual for impact damage tolerant aircraft structure, addendum
[AGARD-AG-238-ADD] 21 p2895 N88-27185
Hole diameters in plates impacted by projectiles 21 p2929 N88-27386
Assessment of the effects of space debris and meteoroids environment on the space station solar array assembly
[NASA-TM-101315] 23 p3185 N88-28959
Wave and fracture phenomena in impacted ceramics
[AD-A192946] 23 p3196 N88-29020
Experimental aspects of using time-averaged holographic interferometry to detect barely visible impact damage in a graphite/epoxy composite plate
[AD-A194418] 24 p3375 N88-30097
A compilation of information and data on the Manson impact structure
[NASA-CR-183169] 24 p3401 N88-30258

IMPACT DECELERATION
U DECELERATION
U IMPACT ACCELERATION

IMPACT LOADS
Time-resolved measurements of shock-induced vapor-pressure profiles
[DE87-012972] 01 p0045 N88-10289
Fabrication of standardized piezoelectric polymer shock gauges by the Bauer method
[DE87-012738] 01 p0049 N88-10315
Experimental measurements and numerical simulations of metal spallation by detonating solid explosives
[DE87-013227] 01 p0054 N88-10347
Experimental molecular spectroscopy in shock-compressed materials
[DE87-013139] 02 p0144 N88-10903
Rarefaction velocities in shocked lead
[DE87-013141] 02 p0146 N88-10917
Computations of hypervelocity impact using the CTH shock wave physics code
[DE87-013067] 02 p0169 N88-11062
Shock-chemistry in natural materials and evolution of planetary surfaces
[DE87-012737] 02 p0254 N88-11604
Conservatism implications of shock test tailoring for multiple design environments
[DE87-013927] 03 p0338 N88-12127
The nonlinear dynamic response of an elastic-plastic thin plate under impulse loading
[AD-A182147] 08 p0994 N88-16013
Dynamic finite element with diagonalized consistent mass matrix and elastic-plastic impact calculation
[PB87-143376] 08 p0995 N88-16020
Mechanical impact: Theoretical simulation and correlation 09 p1179 N88-17060
Spatial pressure variations and three-dimensional effects on liquid sloshing loads
[PB88-120134] 10 p1326 N88-17926
Use of the LLNL 40 kV electric gun to study the shock response of 21-6-9 stainless steel
[DE87-014550] 13 p1742 N88-20418
An investigation of the spray produced by a yawed wheel, including measurement of impact forces --- aircraft wheels
[BU-363] 14 p1866 N88-21150
Inertia welding with variable magnitude of impact load 14 p1897 N88-21328
Response of aluminum alloys to erosive particle impacts
[DE88-005910] 15 p2041 N88-22159
Impact damage in composite laminates 15 p2080 N88-22402
Behavior of a two-layered beam under impact loading
[OUEL-1716/87] 17 p2349 N88-23993
Interfacial shear phenomena in graphite epoxy composites under impact loading using dynamic moire interferometry
[DE88-006773] 18 p2479 N88-24709
Contact force histor, and dynamic response due to the impact of a soft projectile
[NASA-TM-100961] 20 p2811 N88-26679
Control systems for platform landings cushioned by air bags
[AD-A196154] 24 p3358 N88-29996
Impact force as a part of the total breaking wave force on a vertical cylinder
[RR-CE78] 24 p3384 N88-30154

IMPACT MELTS
Spray deposition: A fundamental study of droplet impingement, spreading and consolidation
[AD-A186627] 08 p0970 N88-15869

IMPACT PREDICTION
Utilization of dynamic characteristics of materials to optimize military explosive charges. Application to antiship devices
[SNIAS-872-320-101] 05 p0610 N88-13743
Survey of impact damper performance 16 p2217 N88-23227

IMPACT PRESSURES
U IMPACT LOADS

IMPACT RESISTANCE
Impact behavior of 9-Cr and 12-Cr ferritic steels after low-temperature irradiation
[DE88-000333] 03 p0291 N88-11827
Development of an impact- and solvent-resistant thermoplastic composite matrix, phase 4
[NASA-CR-178413] 06 p0677 N88-14145
Behavior of a steel cylinder under the influence of a local load in the elastic and elasto-plastic area
[PB87-154787] 07 p0869 N88-15272
Abrasion and impact resistant coatings
[DE88-003562] 13 p1750 N88-20464
KRASH parametric sensitivity study: Transport category airplanes
[AD-A189962] 15 p2017 N88-22024
Evaluation of the US Army fitting program for the integrated helmet unit of the integrated helmet and display sighting system
[AD-A191616] 18 p2465 N88-24635
Improved procedure for impact probability computation of aircraft crash based on Balfanz model
[JUEL-SPEZ-425] 21 p2894 N88-27176
Deformation, fracture and explosive properties of reactive materials
[AD-A193080] 21 p2923 N88-27348

IMPACT SENSITIVITY
U IMPACT RESISTANCE

IMPACT STRENGTH
Laminated ferrous composites based on ultrahigh carbon (UHC) steels
[AD-A184617] 03 p0280 N88-11764
Impact behavior of 9-Cr and 12-Cr ferritic steels after low-temperature irradiation
[DE88-000333] 03 p0291 N88-11827
Models for penetration of thin plates
[DE87-013727] 03 p0332 N88-12090
Computer simulations of ballistic experiments
[DE87-005835] 07 p0862 N88-15226
Effect of low velocity impact on compression strength of a quasi-isotropic laminate
[FFA-TN-1987-38] 09 p1138 N88-16822
Effect of low-temperature aging on the mechanical properties of cast stainless steels
[DE88-002872] 10 p1300 N88-17774
A direct correlation of strength with impact velocity
[AD-A189251] 13 p1741 N88-20409
Structure and properties of welded joints produced between niobium parts in controllable helium atmosphere 14 p1897 N88-21326
A study of damage tolerance in curved composite panels
[AD-A190617] 15 p2029 N88-22092
Relation between the mechanical characteristics of carbon-resin composites and their impact strength
[REPT-48-284/F] 21 p2907 N88-27249

IMPACT TESTS
NT CHARPY IMPACT TEST
Full-scale transport controlled impact demonstration program
[NASA-TM-89642] 01 p0004 N88-10021
Shock-wave studies using plastic flyers driven by an electric gun for hypervelocity impact on selected materials
[DE87-012631] 01 p0008 N88-10046
High velocity erosion of metal interfaces
[DE87-013937] 01 p0025 N88-10155
Computations of hypervelocity impact using the CTH shock wave physics code
[DE87-013067] 02 p0169 N88-11062
A direct method to obtain constitutive model constants from cylinder impact test results 04 p0427 N88-12647
High explosive moulding powders from RDX and aqueous polyurethane dispersions
[AD-A185026] 05 p0568 N88-13458
Numerical simulations of impact tests on a rigid wall --- armor steel
[SNIAS-872-320-102] 05 p0610 N88-13744
New mechanism of the high temperature (reversible) temper brittleness of alloy steels
[PB87-143954] 07 p0833 N88-15056
Study on the cryogenic toughness of stainless steel weld metals
[PB87-143830] 07 p0834 N88-15057
Residual stiffness and strength of Kevlar/epoxy laminated impulsively loaded to 7.9 ktaps
[DE88-003724] 09 p1149 N88-16886
High-velocity reverse ballistic rocket sled testing at Sandia National Laboratories 09 p1179 N88-17059
A direct correlation of strength with impact velocity
[AD-A189251] 13 p1741 N88-20409
Mechanical design of a ultrahigh gravity UHV facility to launch and recover a low-speed projectile tested on board KC 135 14 p1877 N88-21216
Studies of traverse impact damage in composite materials using a Hopkinson pressure-bar technique
[OUEL-1706/87] 14 p1883 N88-21255
Environmental effects on the post-impact compressive strength of CFC
[RAE-TM-MAT-STR-1088] 14 p1884 N88-21258
An investigation of the mechanical properties of improved carbon fibre composite materials
[RAE-TR-86021] 14 p1884 N88-21259
Phenomenological piercing characteristics of composite materials 14 p1895 N88-21315
Impact shock generator from explosively driven plates
[DE88-003596] 14 p1918 N88-21452
KRASH parametric sensitivity study: Transport category airplanes
[AD-A189962] 15 p2017 N88-22024
Response of aluminum alloys to erosive particle impacts
[DE88-005910] 15 p2041 N88-22159
Finite element simulation of perforation of aluminum plates
[DE88-002092] 15 p2073 N88-22362
Behaviour of fibre-reinforced composites under dynamic loading
[AD-A191310] 16 p2174 N88-22955
Peak Acceleration Device (PAD)
[AD-A191639] 18 p2461 N88-24611
Fuel containment and damage tolerance in large composite primary aircraft structures. Phase 2: Testing
[NASA-CR-172519] 19 p2601 N88-25452
Contact force history and dynamic response due to the impact of a soft projectile
[NASA-TM-100961] 20 p2811 N88-26679
Analysis of the perforation of monolithic and simple laminate aluminium targets as a test of analytical deformation models
[MRL-R-1111] 20 p2813 N88-26686
Milliwatt generator project
[DE88-011261] 20 p2853 N88-26939
Hypervelocity impact analysis with supercomputers
[DE88-008907] 21 p3001 N88-27797
Decomposition of energetic materials on the drop-weight impact machine
[DE88-009154] 22 p3059 N88-28152
Calibration of quartz load cells: An in-situ procedure for instrumented falling weight impact machines
[NPL-DMA(A)-155] 22 p3081 N88-28297
Experimental aspects of using time-averaged holographic interferometry to detect barely visible impact damage in a graphite/epoxy composite plate
[AD-A194418] 24 p3375 N88-30097

IMPACT TOLERANCES
Fuel containment, lightning protection and damage tolerance in large composite primary aircraft structures
[NASA-CR-3875] 17 p2317 N88-23839
Design manual for impact damage tolerant aircraft structure, addendum
[AGARD-AG-238-ADD] 21 p2895 N88-27185

IMPACTORS
Measurement of combustion aerosol size distributions with multistage inertial impactors
[DE88-751101] 11 p1454 N88-18669

IMPATT DIODES
U AVALANCHE DIODES

IMPEDANCE
NT ACOUSTIC IMPEDANCE
NT CONTACT RESISTANCE
NT ELECTRICAL IMPEDANCE
NT ELECTRICAL RESISTANCE
NT MECHANICAL IMPEDANCE
NT SKIN RESISTANCE
NT TRANSCONDUCTANCE
Impedance of passive lithium anodes in SOCl2 solutions under low-field polarization
[DE88-000922] 04 p0439 N88-12728
Interior impedance wedge diffraction with surface waves
[NASA-CR-182405] 07 p0854 N88-15186
Minimum necessary intensity of source of preionization for stabilization of a self-sustaining laser discharge with mean power raised by electron beam or X-rays
[PB87-178158] 09 p1171 N88-17024

Model-scale sound propagation experiment
[NASA-TM-100602] 15 p2130 N88-22709
Study on the flashover ion diode with cryogenic anode
16 p2279 N88-23642
AC impedance analysis of corrosion fatigue in naval aircraft alloys
[AD-A190822] 17 p2322 N88-23865
Scattering patterns of dihedral corner reflectors with impedance surface impedances
[NASA-CR-183078] 20 p2789 N88-26545
Some equivalent circuit models for AC impedance analysis of pyrite/solution interface
[DE88-010574] 21 p2939 N88-27452
Power supply conditioning circuit
[NASA-CASE-NPO-17233-1-CU]
23 p3208 N88-29095

IMPEDANCE MATCHING
Electromagnetic tests
[SNIAS-872-430-103] 05 p0575 N88-13508
The design of Impedance- matching networks for broadband antennas
[AD-A187600] 10 p1320 N88-17895
Vortices in long Josephson junctions
[AD-A190338] 15 p2059 N88-22279

IMPEDANCE MEASUREMENT
High-frequency limit of the longitudinal impedance
[CEBAF-PR-87-030] 02 p0234 N88-11479
Operators manual for a computer controlled impedance measurement system
[AD-A187513] 10 p1324 N88-17917
Estimation of body fluid shift by electrical impedance in various postures 12 p1661 N88-19956
A simulation analysis of errors in the measurement of standard electrochemical rate constants from phase-selective impedance data
[AD-A192739] 20 p2770 N88-26426
Ultrasonic detection of diffusion and adhesion loss
24 p3354 N88-29967

IMPEDANCE PROBES
Evaluation of a multi-point method for determining acoustic impedance
[NASA-TM-100637] 20 p2849 N88-26913

IMPELLER BLADES
U ROTOR BLADES (TURBOMACHINERY)

IMPELLERS
NT PUMP IMPELLERS
Calculation of the three dimensional flow in the impeller of hydraulic turbomachines using a finite element method
[ETN-87-90612] 03 p0315 N88-11988
Centrifugal compressors 07 p0850 N88-15162
Gas erosion of impeller housing in the operation of a high-temperature, high-pressure helium circulator
[DE88-002607] 09 p1175 N88-17041
Secondary flow measurements with L2F-technique in centrifugal compressors 10 p1283 N88-17676
A study of fluid-structure problems
21 p2941 N88-27468
JTDE 1 XTE34 materials research and development report
[AD-A194268] 22 p3044 N88-28063

IMPERFECTIONS
U DEFECTS

IMPINGEMENT
NT JET IMPINGEMENT
Performance of supersonic impingement radial turbines 06 p0712 N88-14367
Spray deposition: A fundamental study of droplet impingement, spreading and consolidation
[AD-A186627] 08 p0970 N88-15869
Studies on rocket exhaust plumes and impingement effects related to the Columbus Space Station program: Executive summary
[DFVLR-IB-222-88-A-12] 24 p3337 N88-29862

IMPLANTATION
NT ION IMPLANTATION
Design considerations for the development of an implantable sensor for the continuous measurement of glucose in the diabetic patient 17 p2382 N88-24159
Investigation of photoconductive picosecond microstripline switches on self-implanted Silicon On Sapphire (SOS) 19 p2657 N88-25789
Transport study on Si/Si(1-x)Ge(x) superlattices selectively doped by secondary implantation of Sb
20 p2867 N88-27027
NDP (Neutron Depth Profiling) evaluations of boron-implanted compound semiconductors
[AD-A192306] 21 p2934 N88-27425

IMPLICATION
Conservatism implications of shock test tailoring for multiple design environments
[DE87-013927] 03 p0338 N88-12127
Phenomenological implications of the blown-up orbifolds
[DE87-014608] 03 p0373 N88-12347
Implications of the trapping-desorption and direct inelastic scattering channels on Dicke-narrowed lineshapes
[AD-A191410] 16 p2270 N88-23581
The cost and performance implications of reliability improvements in the F-16A/B
[AD-A195096] 24 p3324 N88-29796

IMPLOSIONS
Time-resolved ablation measurements of imploding targets
[DE87-014464] 02 p0178 N88-11111
Time-resolved absorption measurements on OMEGA
[DE87-014465] 02 p0179 N88-11112
Analytic model of an imploding Z-pinch plasma colliding inelastically with a thin-shelled cylindrical target
[DE88-000051] 03 p0378 N88-12379
Advanced concepts theory annual report 1986
[AD-A184986] 05 p0651 N88-13991
Analysis for high compressible supersonic flow in converging nozzle
[IPPJ-860] 16 p2157 N88-22869
Proceedings of Symposium on Physics of Target Implosion and Pulsed Power Techniques
[IPPJ-859] 16 p2276 N88-23619
Analysis for fuel implosion in ICF target and pellet gain 16 p2276 N88-23620
Numerical analysis for effects of irradiation nonuniformities on target implosion
16 p2276 N88-23621
Numerical analysis of target implosion in LIB ICF
16 p2277 N88-23628
Pusherless implosion, pulse tailoring and ignition scaling law for laser fusion 16 p2277 N88-23629
Efficient shell implosion and target design
16 p2277 N88-23630
Stability requirement FOT ignition and high gain implosion = 2-D simulation for high neutron yield experiment = 16 p2278 N88-23633
Finite ion-relaxation and nonequilibrium radiation effects on laser-driven implosions 16 p2278 N88-23636
The application of Rutherford backscattering for analyzing multilayered structure change induced by pulsed ion beam bombardment 16 p2278 N88-23638

IMPROVEMENT
Performance improvements of an F-15 airplane with an integrated engine-flight control system
[NASA-TM-100431] 14 p1867 N88-21159
Parameter identification methods for improving structural dynamic models
[NASA-TM-100812] 17 p2349 N88-23994

IMPULSE GENERATORS
Development of a repetitive 1-MV, 22-kJ Marx generator
[DE87-011286] 01 p0038 N88-10242
The light pulse generator 869 for high speed investigations
[MPIS-9/1987] 11 p1491 N88-18898

IMPULSES
Structural frequency functions for an impulsive, distributed forcing function
[DE87-013811] 03 p0333 N88-12101
Analysis of photopole data reduction models
05 p0593 N88-13616
Dynamic evolution of the source volumes of gradual and impulsive solar flare emissions
[NASA-TM-87815] 08 p1102 N88-16621
Fiber-optics used to record high-speed photographs inside a pressurized tank during lethality testing
[DE88-011283] 21 p2951 N88-27529

IMPURITIES
X-ray studies of strain, interface and impurity in semiconductors
[DE87-013856] 01 p0104 N88-10678
Interaction between defects and the formation of dissipative structures in irradiated impure crystals
[DE87-703125] 02 p0246 N88-11552
Far infrared Fourier transform spectroscopy of semiconductors
[DE88-000188] 04 p0499 N88-13072
Chemical analysis for excimer laser systems
[DE88-001941] 05 p0589 N88-13591
Vibrational properties of disordered solids. Far infrared studies: Performance report
[DE88-001474] 06 p0786 N88-14821
Computer simulation of impurities and interfaces in body centered cubic metals
[PB88-108162] 07 p0832 N88-15047
Investigation of impurity defects in alpha-iron by molecular dynamics method
[DE88-700355] 07 p0834 N88-15058
Interface characteristics and the mechanical properties of metal matrix composites
[AD-A186441] 08 p0986 N88-15845
Effect of extraneous factors on optical one-phonon transitions in impurity centers with cubic symmetry
08 p1077 N88-16496
Impurity bands in quantum wells
[INPE-4250-PRE/1123] 08 p1089 N88-16552
Diagonal and off-diagonal disorder in doped quantum wells
[INPE-4255-PRE/1128] 08 p1089 N88-16556
Density of states of electrons bound to impurities in quantum wells of GaAlAs/GaAs
[INPE-4257-PRE/1130] 08 p1089 N88-16557
Modeling considerations for selected rf-plasma edge effects
[DE88-003285] 09 p1252 N88-17500
Superconductivity in La/sub 1.85-x/Nd/sub x/Sr/sub .15/CuO
[DE88-003014] 09 p1258 N88-17540
Mechanisms of intergranular attack and stress corrosion cracking of alloy 600 by high-temperature caustic solutions containing impurities
[DE87-012820] 10 p1300 N88-17773
Influence of non-metallic elements in the mechanical properties of 20 Mn Mo Ni 55 steel
[DE88-700412] 10 p1300 N88-17775
The effect of magnetic impurities and barriers on the magnetization and critical current of fine filament NbTi composites
[DE88-004443] 10 p1419 N88-18472
Deactivation of alumina based catalysts
11 p1455 N88-18673
Study of adherent oxide scales
[AD-A187368] 11 p1456 N88-18680
Influence of grain boundary phosphorus segregation on hydrogen embrittlement in steel
[DE88-700176] 11 p1459 N88-18696
Atomistic studies of the structure and properties of grain boundaries with substitutional impurities
[DE88-004161] 11 p1545 N88-19237
Spatial distribution of carbon and native defects in large-diameter bulk grown GaAs
[DE88-003870] 11 p1562 N88-19348
Laser raman studies related to liquid propellants: Structural characteristics inferred from the nitrate anion spectra
[AD-A188462] 12 p1612 N88-19641
Thermal oxide growth on silicon: Intrinsic stress and silicon cleaning effects
[AD-A188790] 13 p1736 N88-20377
Quantitative determination of a hydrogen impurity in a sodium coolant by hydride thermal dissociation
[NASA-TT-20239] 13 p1740 N88-20402
Study of activationless reactions of point defects with impurities and impurity-defect complexes in alpha-iron
[DE88-701028] 13 p1745 N88-20433
Research on multibandgap solar cells
[DE87-012261] 13 p1792 N88-20721
Evolution of poloidal variation of impurity density and ambipolar potential in rotating tokamak plasma, part 1
[DE88-006263] 13 p1842 N88-21022
Effect of Mg impurity on local vibrations of U-centers in LiF lattice 14 p1969 N88-21753
Magnetic impurities in superconductors
[DE88-006917] 14 p1986 N88-21846
Sublimation characteristics of H2O comet nucleus with CO2 impurities 14 p2010 N88-21988
Spectrographic detection of nitrogen impurity in helium
[DE88-752301] 15 p2033 N88-22111
Activities of As, Sb, Bi and Pb in copper mattes and their effects on impurity elimination
[TKK-V-A10(1988)] 15 p2041 N88-22165
High temperature corrosion of ceramics
[DE88-006567] 15 p2046 N88-22193
Long-time impurity confinement as a precursor to disruptions in ohmically heated tokamaks
[DE88-006183] 15 p2136 N88-22742
Observation of injected silicon in heliotron E
17 p2441 N88-24524
Flux density measurements of neutral iron in TEXTOR with laser induced fluorescence
17 p2442 N88-24528
Recent data on Si:As impurity band conduction multiplexed arrays
[AD-A191752] 18 p2582 N88-25340
Advanced development of double-injection, deep-impurity semiconductor switches
[NASA-CR-182118] 18 p2583 N88-25346
A general qualitative study of point and extended defects and their interactions in non-metallic systems
[AD-A191687] 19 p2618 N88-25532
Zero-dimensional calculation for ZT-H
[DE88-009175] 19 p2731 N88-26217
Evolution of poloidal variation of impurity density and ambipolar potential in rotating tokamak plasma, part 2
[DE88-009882] 19 p2731 N88-26218
Structural and magnetic properties of Fe impurities in YBa2Cu3O(sub 7-delta)
[DE88-009961] 19 p2735 N88-26247

Surface crack analysis applied to impact damage in a thick graphite-epoxy composite
[NASA-TM-100600] 16 p2173 N88-22950
GARTEUR TP-037: impact damage tolerance of carbon fiber and hybrid laminates
[RAE-TR-87057] 17 p2316 N88-23837
The application of high-rate biaxial testing to the design of containment vessels for radioisotope heat sources
17 p2426 N88-24428
Design manual for impact damage tolerant aircraft structure, addendum
[AGARD-AG-238-ADD] 21 p2895 N88-27185
Hole diameters in plates impacted by projectiles
21 p2929 N88-27386
Assessment of the effects of space debris and meteoroids environment on the space station solar array assembly
[NASA-TM-101315] 23 p3185 N88-28959
Wave and fracture phenomena in impacted ceramics
[AD-A192946] 23 p3196 N88-29020
Experimental aspects of using time-averaged holographic interferometry to detect barely visible impact damage in a graphite/epoxy composite plate
[AD-A194418] 24 p3375 N88-30097
A compilation of information and data on the Manson impact structure
[NASA-CR-183169] 24 p3401 N88-30258

IMPACT DECELERATION
U DECELERATION
U IMPACT ACCELERATION

IMPACT LOADS
Time-resolved measurements of shock-induced vapor-pressure profiles
[DE87-012972] 01 p0045 N88-10289
Fabrication of standardized piezoelectric polymer shock gauges by the Bauer method
[DE87-012738] 01 p0049 N88-10315
Experimental measurements and numerical simulations of metal spallation by detonating solid explosives
[DE87-013227] 01 p0054 N88-10347
Experimental molecular spectroscopy in shock-compressed materials
[DE87-013139] 02 p0144 N88-10903
Rarefaction velocities in shocked lead
[DE87-013141] 02 p0146 N88-10917
Computations of hypervelocity impact using the CTH shock wave physics code
[DE87-013067] 02 p0169 N88-11062
Shock-chemistry in natural materials and evolution of planetary surfaces
[DE87-012737] 02 p0254 N88-11604
Conservatism implications of shock test tailoring for multiple design environments
[DE87-013927] 03 p0338 N88-12127
The nonlinear dynamic response of an elastic-plastic thin plate under impulse loading
[AD-A182147] 08 p0994 N88-16013
Dynamic finite element with diagonalized consistent mass matrix and elastic-plastic impact calculation
[PB87-143378] 08 p0995 N88-16020
Mechanical impact: Theoretical simulation and correlation 09 p1179 N88-17060
Spatial pressure variations and three-dimensional effects on liquid sloshing loads
[PB88-120134] 10 p1326 N88-17926
Use of the LLNL 40 kV electric gun to study the shock response of 21-6-9 stainless steel
[DE87-014550] 13 p1742 N88-20418
An investigation of the spray produced by a yawed wheel, including measurement of impact forces --- aircraft wheels
[BU-363] 14 p1866 N88-21150
Inertia welding with variable magnitude of impact load
14 p1897 N88-21328
Response of aluminum alloys to erosive particle impacts
[DE88-005910] 15 p2041 N88-22159
Impact damage in composite laminates
15 p2080 N88-22402
Behavior of a two-layered beam under impact loading
[OUEL-1716/87] 17 p2349 N88-23993
Interfacial shear phenomena in graphite epoxy composites under impact loading using dynamic moire interferometry
[DE88-006773] 18 p2479 N88-24709
Contact force histor, and dynamic response due to the impact of a soft projectile
[NASA-TM-100961] 20 p2811 N88-26679
Control systems for platform landings cushioned by air bags
[AD-A196154] 24 p3358 N88-29996
Impact force as a part of the total breaking wave force on a vertical cylinder
[RR-CE76] 24 p3384 N88-30154

IMPACT MELTS
Spray deposition: A fundamental study of droplet impingement, spreading and consolidation
[AD-A186627] 08 p0970 N88-15869

IMPACT PREDICTION
Utilization of dynamic characteristics of materials to optimize military explosive charges. Application to antiship devices
[SNIAS-872-320-101] 05 p0610 N88-13743
Survey of impact damper performance
16 p2217 N88-23227

IMPACT PRESSURES
U IMPACT LOADS

IMPACT RESISTANCE
Impact behavior of 9-Cr and 12-Cr ferritic steels after low-temperature irradiation
[DE88-000333] 03 p0291 N88-11827
Development of an impact- and solvent-resistant thermoplastic composite matrix, phase 4
[NASA-CR-178413] 06 p0677 N88-14145
Behavior of a steel cylinder under the influence of a local load in the elastic and elasto-plastic area
[PB87-154787] 07 p0869 N88-15272
Abrasion and impact resistant coatings
[DE88-003562] 13 p1750 N88-20464
KRASH parametric sensitivity study: Transport category airplanes
[AD-A189962] 15 p2017 N88-22024
Evaluation of the US Army fitting program for the integrated helmet unit of the integrated helmet and display sighting system
[AD-A191616] 18 p2465 N88-24635
Improved procedure for impact probability computation of aircraft crash based on Balfanz model
[JUEL-SPEZ-425] 21 p2894 N88-27176
Deformation, fracture and explosive properties of reactive materials
[AD-A193080] 21 p2923 N88-27348

IMPACT SENSITIVITY
U IMPACT RESISTANCE

IMPACT STRENGTH
Laminated ferrous composites based on ultrahigh carbon (UHC) steels
[AD-A184617] 03 p0280 N88-11764
Impact behavior of 9-Cr and 12-Cr ferritic steels after low-temperature irradiation
[DE88-000333] 03 p0291 N88-11827
Models for penetration of thin plates
[DE87-013727] 03 p0332 N88-12090
Computer simulations of ballistic experiments
[DE87-005835] 07 p0862 N88-15226
Effect of low velocity impact on compression strength of a quasi-isotropic laminate
[FFA-TN-1987-38] 09 p1138 N88-16822
Effect of low-temperature aging on the mechanical properties of cast stainless steels
[DE88-002872] 10 p1300 N88-17774
A direct correlation of strength with impact velocity
[AD-A189251] 13 p1741 N88-20409
Structure and properties of welded joints produced between niobium parts in controllable helium atmosphere 14 p1897 N88-21326
A study of damage tolerance in curved composite panels
[AD-A190617] 15 p2029 N88-22092
Relation between the mechanical characteristics of carbon-resin composites and their impact strength
[REPT-48-284/F] 21 p2907 N88-27249

IMPACT TESTS
NT CHARPY IMPACT TEST
Full-scale transport controlled impact demonstration program
[NASA-TM-89642] 01 p0004 N88-10021
Shock-wave studies using plastic flyers driven by an electric gun for hypervelocity impact on selected materials
[DE87-012631] 01 p0008 N88-10046
High velocity erosion of metal interfaces
[DE87-013937] 01 p0025 N88-10155
Computations of hypervelocity impact using the CTH shock wave physics code
[DE87-013067] 02 p0169 N88-11062
A direct method to obtain constitutive model constants from cylinder impact test results
04 p0427 N88-12647
High explosive moulding powders from RDX and aqueous polyurethane dispersions
[AD-A185026] 05 p0568 N88-13458
Numerical simulations of impact tests on a rigid wall --- armor steel
[SNIAS-872-320-102] 05 p0610 N88-13744
New mechanism of the high temperature (reversible) temper brittleness of alloy steels
[PB87-143954] 07 p0833 N88-15056
Study on the cryogenic toughness of stainless steel weld metals
[PB87-143830] 07 p0834 N88-15057
Residual stiffness and strength of Kevlar/epoxy laminated impulsively loaded to 7.9 ktaps
[DE88-003724] 09 p1149 N88-16886
High-velocity reverse ballistic rocket sled testing at Sandia National Laboratories 09 p1179 N88-17059
A direct correlation of strength with impact velocity
[AD-A189251] 13 p1741 N88-20409
Mechanical design of a ultrahigh gravity UHV facility to launch and recover a low-speed projectile tested on board KC 135 14 p1877 N88-21216
Studies of traverse impact damage in composite materials using a Hopkinson pressure-bar technique
[OUEL-1706/87] 14 p1883 N88-21255
Environmental effects on the post-impact compressive strength of CFC
[RAE-TM-MAT-STR-1088] 14 p1884 N88-21258
An investigation of the mechanical properties of improved carbon fibre composite materials
[RAE-TR-86021] 14 p1884 N88-21259
Phenomenological piercing characteristics of composite materials 14 p1895 N88-21315
Impact shock generator from explosively driven plates
[DE88-003596] 14 p1918 N88-21452
KRASH parametric sensitivity study: Transport category airplanes
[AD-A189962] 15 p2017 N88-22024
Response of aluminum alloys to erosive particle impacts
[DE88-005910] 15 p2041 N88-22159
Finite element simulation of perforation of aluminum plates
[DE88-002092] 15 p2073 N88-22362
Behaviour of fibre-reinforced composites under dynamic loading
[AD-A191310] 16 p2174 N88-22955
Peak Acceleration Device (PAD)
[AD-A191639] 18 p2461 N88-24611
Fuel containment and damage tolerance in large composite primary aircraft structures. Phase 2: Testing
[NASA-CR-172519] 19 p2601 N88-25452
Contact force history and dynamic response due to the impact of a soft projectile
[NASA-TM-100961] 20 p2811 N88-26679
Analysis of the perforation of monolithic and simple laminate aluminium targets as a test of analytical deformation models
[MRL-R-1111] 20 p2813 N88-26686
Milliwatt generator project
[DE88-011261] 20 p2853 N88-26939
Hypervelocity impact analysis with supercomputers
[DE88-008907] 21 p3001 N88-27797
Decomposition of energetic materials on the drop-weight impact machine
[DE88-009154] 22 p3059 N88-28152
Calibration of quartz load cells: An in-situ procedure for instrumented falling weight impact machines
[NPL-DMA(A)-155] 22 p3081 N88-28297
Experimental aspects of using time-averaged holographic interferometry to detect barely visible impact damage in a graphite/epoxy composite plate
[AD-A194418] 24 p3375 N88-30097

IMPACT TOLERANCES
Fuel containment, lightning protection and damage tolerance in large composite primary aircraft structures
[NASA-CR-3875] 17 p2317 N88-23839
Design manual for impact damage tolerant aircraft structure, addendum
[AGARD-AG-238-ADD] 21 p2895 N88-27185

IMPACTORS
Measurement of combustion aerosol size distributions with multistage inertial impactors
[DE88-751101] 11 p1454 N88-18669

IMPATT DIODES
U AVALANCHE DIODES

IMPEDANCE
NT ACOUSTIC IMPEDANCE
NT CONTACT RESISTANCE
NT ELECTRICAL IMPEDANCE
NT ELECTRICAL RESISTANCE
NT MECHANICAL IMPEDANCE
NT SKIN RESISTANCE
NT TRANSCONDUCTANCE
Impedance of passive lithium anodes in SOCl2 solutions under low-field polarization
[DE88-000922] 04 p0439 N88-12726
Interior impedance wedge diffraction with surface waves
[NASA-CR-182405] 07 p0854 N88-15186
Minimum necessary intensity of source of preionization for stabilization of a self-sustaining laser discharge with mean power raised by electron beam or X-rays
[PB87-178158] 09 p1171 N88-17024

Model-scale sound propagation experiment
[NASA-TM-100602] 15 p2130 N88-22709
Study on the flashover ion diode with cryogenic anode
16 p2279 N88-23642
AC impedance analysis of corrosion fatigue in naval aircraft alloys
[AD-A190822] 17 p2322 N88-23865
Scattering patterns of dihedral corner reflectors with impedance surface impedances
[NASA-CR-183078] 20 p2789 N88-26545
Some equivalent circuit models for AC impedance analysis of pyrite/solution interface
[DE88-010574] 21 p2939 N88-27452
Power supply conditioning circuit
[NASA-CASE-NPO-17233-1-CU]
23 p3208 N88-29095

IMPEDANCE MATCHING
Electromagnetic tests
[SNIAS-872-430-103] 05 p0575 N88-13508
The design of Impedance- matching networks for broadband antennas
[AD-A187600] 10 p1320 N88-17895
Vortices in long Josephson junctions
[AD-A190336] 15 p2059 N88-22279

IMPEDANCE MEASUREMENT
High-frequency limit of the longitudinal impedance
[CEBAF-PR-87-030] 02 p0234 N88-11479
Operators manual for a computer controlled impedance measurement system
[AD-A187513] 10 p1324 N88-17917
Estimation of body fluid shift by electrical impedance in various postures 12 p1661 N88-19956
A simulation analysis of errors in the measurement of standard electrochemical rate constants from phase-selective impedance data
[AD-A192739] 20 p2770 N88-26426
Ultrasonic detection of diffusion and adhesion loss
24 p3354 N88-29967

IMPEDANCE PROBES
Evaluation of a multi-point method for determining acoustic impedance
[NASA-TM-100637] 20 p2849 N88-26913

IMPELLER BLADES
U ROTOR BLADES (TURBOMACHINERY)

IMPELLERS
NT PUMP IMPELLERS
Calculation of the three dimensional flow in the impeller of hydraulic turbomachines using a finite element method
[ETN-87-90612] 03 p0315 N88-11988
Centrifugal compressors 07 p0850 N88-15162
Gas erosion of impeller housing in the operation of a high-temperature, high-pressure helium circulator
[DE88-002607] 09 p1175 N88-17041
Secondary flow measurements with L2F-technique in centrifugal compressors 10 p1283 N88-17676
A study of fluid-structure problems
21 p2941 N88-27468
JTDE 1 XTE34 materials research and development report
[AD-A194268] 22 p3044 N88-28063

IMPERFECTIONS
U DEFECTS

IMPINGEMENT
NT JET IMPINGEMENT
Performance of supersonic impingement radial turbines 06 p0712 N88-14367
Spray deposition: A fundamental study of droplet impingement, spreading and consolidation
[AD-A186627] 08 p0970 N88-15869
Studies on rocket exhaust plumes and impingement effects related to the Columbus Space Station program: Executive summary
[DFVLR-IB-222-88-A-12] 24 p3337 N88-29862

IMPLANTATION
NT ION IMPLANTATION
Design considerations for the development of an implantable sensor for the continuous measurement of glucose in the diabetic patient 17 p2382 N88-24159
Investigation of photoconductive picosecond microstripline switches on self-implanted Silicon On Sapphire (SOS) 19 p2657 N88-25789
Transport study on Si/Si(1-x)Ge(x) superlattices selectively doped by secondary implantation of Sb
20 p2867 N88-27027
NDP (Neutron Depth Profiling) evaluations of boron-implanted compound semiconductors
[AD-A192306] 21 p2934 N88-27425

IMPLICATION
Conservatism implications of shock test tailoring for multiple design environments
[DE87-013927] 03 p0338 N88-12127
Phenomenological implications of the blown-up orbifolds
[DE87-014608] 03 p0373 N88-12347
Implications of the trapping-desorption and direct inelastic scattering channels on Dicke-narrowed lineshapes
[AD-A191410] 16 p2270 N88-23581
The cost and performance implications of reliability improvements in the F-16A/B
[AD-A195096] 24 p3324 N88-29796

IMPLOSIONS
Time-resolved ablation measurements of imploding targets
[DE87-014464] 02 p0178 N88-11111
Time-resolved absorption measurements on OMEGA
[DE87-014465] 02 p0179 N88-11112
Analytic model of an imploding Z-pinch plasma colliding inelastically with a thin-shelled cylindrical target
[DE88-000051] 03 p0378 N88-12379
Advanced concepts theory annual report 1986
[AD-A184986] 05 p0651 N88-13991
Analysis for high compressible supersonic flow in converging nozzle
[IPPJ-880] 16 p2157 N88-22869
Proceedings of Symposium on Physics of Target Implosion and Pulsed Power Techniques
[IPPJ-859] 16 p2276 N88-23619
Analysis for fuel implosion in ICF target and pellet gain 16 p2276 N88-23620
Numerical analysis for effects of irradiation nonuniformities on target implosion
16 p2276 N88-23621
Numerical analysis of target implosion in LIB ICF
16 p2277 N88-23628
Pusherless implosion, pulse tailoring and ignition scaling law for laser fusion 16 p2277 N88-23629
Efficient shell implosion and target design
16 p2277 N88-23630
Stability requirement FOT ignition and high gain implosion = 2-D simulation for high neutron yield experiment = 16 p2278 N88-23633
Finite ion-relaxation and nonequilibrium radiation effects on laser-driven implosions 16 p2278 N88-23636
The application of Rutherford backscattering for analyzing multilayered structure change induced by pulsed ion beam bombardment 16 p2278 N88-23638

IMPROVEMENT
Performance improvements of an F-15 airplane with an integrated engine-flight control system
[NASA-TM-100431] 14 p1867 N88-21159
Parameter identification methods for improving structural dynamic models
[NASA-TM-100812] 17 p2349 N88-23994

IMPULSE GENERATORS
Development of a repetitive 1-MV, 22-kJ Marx generator
[DE87-011286] 01 p0038 N88-10242
The light pulse generator 869 for high speed investigations
[MPIS-9/1987] 11 p1491 N88-18898

IMPULSES
Structural frequency functions for an impulsive, distributed forcing function
[DE87-013811] 03 p0333 N88-12101
Analysis of photopole data reduction models
05 p0593 N88-13616
Dynamic evolution of the source volumes of gradual and impulsive solar flare emissions
[NASA-TM-87815] 08 p1102 N88-16621
Fiber-optics used to record high-speed photographs inside a pressurized tank during lethality testing
[DE88-011283] 21 p2951 N88-27529

IMPURITIES
X-ray studies of strain, interface and impurity in semiconductors
[DE87-013856] 01 p0104 N88-10678
Interaction between defects and the formation of dissipative structures in irradiated impure crystals
[DE87-703125] 02 p0246 N88-11552
Far infrared Fourier transform spectroscopy of semiconductors
[DE88-000188] 04 p0499 N88-13072
Chemical analysis for excimer laser systems
[DE88-001941] 05 p0589 N88-13591
Vibrational properties of disordered solids. Far infrared studies. Performance report
[DE88-001474] 06 p0786 N88-14821
Computer simulation of impurities and interfaces in body centered cubic metals
[PB88-108162] 07 p0832 N88-15047
Investigation of impurity defects in alpha-iron by molecular dynamics method
[DE88-700355] 07 p0834 N88-15058
Interface characteristics and the mechanical properties of metal matrix composites
[AD-A186441] 08 p0966 N88-15845
Effect of extraneous factors on optical one-phonon transitions in impurity centers with cubic symmetry
08 p1077 N88-16496
Impurity bands in quantum wells
[INPE-4250-PRE/1123] 08 p1089 N88-16552
Diagonal and off-diagonal disorder in doped quantum wells
[INPE-4255-PRE/1126] 08 p1089 N88-16556
Density of states of electrons bound to impurities in quantum wells of GaAlAs/GaAs
[INPE-4257-PRE/1130] 08 p1089 N88-16557
Modeling considerations for selected rf-plasma edge effects
[DE88-003285] 09 p1252 N88-17500
Superconductivity in La/sub 1.85-x/Nd/sub x/Sr/sub .15/CuO
[DE88-003014] 09 p1258 N88-17540
Mechanisms of intergranular attack and stress corrosion cracking of alloy 600 by high-temperature caustic solutions containing impurities
[DE87-012820] 10 p1300 N88-17773
Influence of non-metallic elements in the mechanical properties of 20 Mn Mo Ni 55 steel
[DE88-700412] 10 p1300 N88-17775
The effect of magnetic impurities and barriers on the magnetization and critical current of fine filament NbTi composites
[DE88-004443] 10 p1419 N88-18472
Deactivation of alumina based catalysts
11 p1455 N88-18673
Study of adherent oxide scales
[AD-A187368] 11 p1456 N88-18680
Influence of grain boundary phosphorus segregation on hydrogen embrittlement in steel
[DE88-700176] 11 p1459 N88-18696
Atomistic studies of the structure and properties of grain boundaries with substitutional impurities
[DE88-004161] 11 p1545 N88-19237
Spatial distribution of carbon and native defects in large-diameter bulk grown GaAs
[DE88-003870] 11 p1562 N88-19348
Laser raman studies related to liquid propellants: Structural characteristics inferred from the nitrate anion spectra
[AD-A188462] 12 p1612 N88-19641
Thermal oxide growth on silicon: Intrinsic stress and silicon cleaning effects
[AD-A188790] 13 p1736 N88-20377
Quantitative determination of a hydrogen impurity in a sodium coolant by hydride thermal dissociation
[NASA-TT-20239] 13 p1740 N88-20402
Study of activationless reactions of point defects with impurities and impurity-defect complexes in alpha-iron
[DE88-701028] 13 p1745 N88-20433
Research on multibandgap solar cells
[DE87-012261] 13 p1792 N88-20721
Evolution of poloidal variation of impurity density and ambipolar potential in rotating tokamak plasma, part 1
[DE88-006263] 13 p1842 N88-21022
Effect of Mg impurity on local vibrations of U-centers in LiF lattice 14 p1969 N88-21753
Magnetic impurities in superconductors
[DE88-006917] 14 p1986 N88-21846
Sublimation characteristics of H2O comet nucleus with CO2 impurities 14 p2010 N88-21988
Spectrographic detection of nitrogen impurity in helium
[DE88-752301] 15 p2033 N88-22111
Activities of As, Sb, Bi and Pb in copper mattes and their effects on impurity elimination
[TKK-V-A10(1988)] 15 p2041 N88-22165
High temperature corrosion of ceramics
[DE88-006567] 15 p2046 N88-22193
Long-time impurity confinement as a precursor to disruptions in ohmically heated tokamaks
[DE88-006183] 15 p2136 N88-22742
Observation of injected silicon in heliotron E
17 p2441 N88-24524
Flux density measurements of neutral iron in TEXTOR with laser induced fluorescence
17 p2442 N88-24528
Recent data on Si:As impurity band conduction multiplexed arrays
[AD-A191752] 18 p2582 N88-25340
Advanced development of double-injection, deep-impurity semiconductor switches
[NASA-CR-182118] 18 p2583 N88-25346
A general qualitative study of point and extended defects and their interactions in non-metallic systems
[AD-A191687] 19 p2618 N88-25532
Zero-dimensional calculation for ZT-H
[DE88-009175] 19 p2731 N88-26217
Evolution of poloidal variation of impurity density and ambipolar potential in rotating tokamak plasma, part 2
[DE88-009882] 19 p2731 N88-26218
Structural and magnetic properties of Fe impurities in YBa2Cu3O(sub 7-delta)
[DE88-009961] 19 p2735 N88-26247

Impurity transport calculations for a drift-dependent tokamak scrape-off plasma
[DE88-010053] 20 p2859 N88-26984
Bremsstrahlung from high Z impurities in hot plasmas
[DE88-011755] 20 p2861 N88-26994
Diffusion and solubility of some interstitial impurities in deformed metals
[DE88-701859] 21 p2914 N88-27296
Application of Auger electron spectroscopy to the study of trace element effects on weldability
[DE88-010457] 21 p2915 N88-27301
Prediction of deep levels and equilibrium concentrations of defects in semiconductors 21 p3023 N88-27945
X-ray studies of strain, interface and impurities in semiconductors
[DE88-012460] 21 p3025 N88-27954
Determination of impurities in silicon carbide by ICP AES (inductively coupled plasma atomic emission spectrometry) after coprecipitation with lanthanum hydroxide
[NASA-TT-20332] 23 p3193 N88-29003
Vibration spectra induced by impurities in 3-5-compounds semiconductors
[DE88-702730] 23 p3293 N88-29610
Impurity analysis in SIMOX samples by high-efficiency resonance ionization time-of-flight mass spectrometry
[DE88-012061] 24 p3367 N88-30051

IN-FLIGHT MONITORING
Acquisition of gust statistics from Aircraft Integrated Data Systems (AIDS) recorded data
[NLR-MP-86048-U-ISS-2] 06 p0745 N88-14586
Measurement and modification of sensorimotor system function during visual-motor performance
[AD-A186351] 07 p0889 N88-15387
Refinement of eye-point-of-regard measurement with helicopter pilots in a flight experiment
[ESA-TT-1073] 09 p1200 N88-17195
Flight testing of fighter aircraft
[MBB/LKE-62/S/PUB/292] 10 p1312 N88-17844
A system status monitor for the National Aerospace Plane
[AD-A190681] 18 p2463 N88-24624
In-flight load measurements of the Robot-X canards
[AD-A193428] 21 p2895 N88-27187
Robust digital model following controller for helicopters
[DFVLR-FB-88-07] 21 p2898 N88-27203
Proceedings of the 14th Symposium on Aircraft Integrated Monitoring Systems
[DFVLR-MITT-88-04] 22 p3033 N88-28001
From turboprop aircraft to multi-engined jet aircraft Aircraft Integrated Monitoring Systems (AIMS)
22 p3033 N88-28003
Aircraft component health monitoring: An effective approach 22 p3033 N88-28006
German Air Force requirements for the on-board life monitoring system (OLMOS) on Tornado
22 p3033 N88-28007
Onboard Life Monitoring System (OLMOS), hardware equipment onboard and on ground
22 p3034 N88-28009
A solution to improve a military aircraft's Onboard-Checkout-And-Monitoring-System (OCAMS)
22 p3034 N88-28013
Proposal for the on-board part of a future aircraft integrated monitoring system 22 p3035 N88-28016
V2500 Condition Monitoring and Performance Analysis Software System (COMPASS): Overview of system --- aircraft engine
[PNR90418] 22 p3139 N88-28666
Acquisition of gust statistics from AIDS-recorded data
24 p3313 N88-29733
The development of acoustic emission for structural integrity monitoring of aircraft
[AD-A196264] 24 p3427 N88-30396

INACTIVATION
U DEACTIVATION

INCENDIARY AMMUNITION
Granulation of pyrotechnic tracer composition R264T
[MRL-TN-528] 20 p2780 N88-26490

INCENTIVE TECHNIQUES
Anatomy of an organizational change effort at the Lewis Research Center
[NASA-CR-4146] 19 p2739 N88-26264

INCIDENCE
NT GRAZING INCIDENCE
Effects of free stream turbulence, Reynolds number and incidence angle on axial turbine cascade performance
05 p0548 N88-13339
An investigation of oblique hypervelocity impact
07 p0927 N88-15629
Influence of solar illumination conditions on TM/Landsat data
[INPE-4463-TDL/320] 12 p1638 N88-19806
Experimental investigation of the transonic flow at the leeward side of a delta wing at high incidence
[LR-518] 16 p2156 N88-22861
Description of a water tank facility: Study of a missile at high incidence 16 p2201 N88-23133
Curvature of blended rolled edge reflectors at the shadow boundary contour
[NASA-CR-182974] 18 p2578 N88-25300
On the global radiation incident variously orientated surfaces on the South Coast of Finland
[FMI-5] 20 p2823 N88-26746
A calculation of the turbulent boundary layer on a slender ellipsoid at low incidence
[FFA-TN-1988-02] 23 p3213 N88-29126

INCIDENT RADIATION
A method of long-term radar shower data analysis
06 p0738 N88-14541
Incident meteoroid flux density
06 p0739 N88-14542
On meteor stream spatial structure theory
06 p0739 N88-14544
Scattering of longitudinal wave normally incident on discal cavity in elastic body 08 p1077 N88-16492
Radiation balance components above the tropical evergreen Amazon forests (3rd campaign of data collection)
[INPE-4195-PRE/1079] 11 p1513 N88-19039

INCINERATION
U INCINERATORS

INCINERATORS
Government research on ceramics coating technology
16 p2184 N88-23019

INCLUSIONS
The effect of temperature on fatigue crack initiation from aluminosilicate inclusions
[PNR90377] 02 p0154 N88-10962
The effect of non-metallic inclusions on fatigue and fatigue thresholds of 25Mn-5Cr-1Ni steel
06 p0718 N88-14410
A comparison of film-based tomography and computed tomography for advanced ceramic materials
[DE88-003114] 07 p0837 N88-15079
Acoustic emission-microstructural relations in ferritic steels. Part 3: The effect of inclusion content
[AERE-R-12041] 10 p1341 N88-18015
Geophysical diffraction tomography for imaging isolated subsurface inclusions
[DE88-003918] 11 p1505 N88-18990
Resolution of the magnetotelluric method for determining local inhomogeneities in the sedimentary cover 13 p1789 N88-20701
An evaluation of nondestructive methods for ceramic heat exchanger applications
[DE88-006731] 15 p2068 N88-22328

INCOHERENCE
Theory of induced spatial incoherence
[AD-A185005] 05 p0651 N88-13992

INCOHERENT SCATTER RADAR
NT EISCAT RADAR SYSTEM (EUROPE)
High latitude problems to be studied by incoherent scatter radars
[DMI-GEOPHYS-PAPERS-R-77]
03 p0350 N88-12211
Radar observations of high-latitude lower-thermospheric and upper-mesospheric winds and their response to geomagnetic activity 06 p0742 N88-14563
EISCAT (European incoherent scatter radar) electron density studies
[AD-A185998] 07 p0841 N88-15099
Investigation of the Sun-aligned F-region walls and related phenomena in the auroral latitude range
[AFGL-TR-87-0248] 19 p2692 N88-26000

INCOHERENT SCATTERING
Lower bounds on bearing accuracy for closely spaced sources
[AD-A184258] 04 p0486 N88-12997
The solution of large linear inverse problems
06 p0691 N88-14238
Incoherent radar spectra 06 p0691 N88-14239
Characteristics of coherent and incoherent waves in snow at microwave and millimeter wave frequencies
[AD-A188990] 12 p1620 N88-19692
Spectrophotometric remote sensing of the diffuse aurora
[AD-A188599] 12 p1643 N88-19837
Dynamics of small and large scale irregularities at sub-auroral latitudes
[AD-A189052] 12 p1645 N88-19853
The effects of optical smoothing techniques on filamentation in laser plasmas
[AD-A188719] 16 p2275 N88-23614
Multiple scattering of waves in discrete random media
[AD-A191068] 18 p2499 N88-24823
Ionospheric radio and propagation: Waves in plasmas
24 p3364 N88-30030

INCOMPRESSIBILITY
A critical review of the development of several viscoplastic constitutive theories
[AD-A185652] 07 p0867 N88-15262
Generalized displacement method in the finite element analysis of incompressible material
[PB87-143434] 08 p0995 N88-16018
Vibrations of shells containing fluid
12 p1635 N88-19787
Equilibrium shocks in plane deformations of incompressible elastic materials
[AD-A188696] 12 p1636 N88-19796

INCOMPRESSIBLE BOUNDARY LAYER
Breakdown of steady and unsteady interacting boundary layers
[NLR-MP-86047-U] 01 p0045 N88-10284
A method for the approximate calculation of the skin friction coefficient of horizontal wavy plates
[VKI-TN-160] 07 p0851 N88-15172
Boundary layer calculation using digital computers
[REPT-MM-4] 10 p1309 N88-17821
Study of the boundary layer of a flow pulsed by acoustic waves
[ETN-88-91998] 16 p2206 N88-23163
Nonlinear Tollmien-Schlichting/vortex interaction in boundary layers
[NASA-CR-181698] 24 p3311 N88-29715

INCOMPRESSIBLE FLOW
NT STOKES FLOW
An inviscid model of planar, separated flows of finite extent
[RAE-TR-86070] 01 p0044 N88-10279
ARSPNS: A method to calculate steady and unsteady potential flow about fixed and rotational lifting and nonlifting bodies
[NLR-TR-85114-U] 01 p0044 N88-10282
NASA-VOF3D: A three-dimensional computer program for incompressible flows with free surfaces
[DE87-011849] 01 p0045 N88-10288
Instability of steady flow with constant vorticity in vessels with elliptical cross-section 02 p0159 N88-10997
Point vortex dynamics: Recent results and open problems
[DE87-014759] 03 p0314 N88-11982
The diffusion-convection vortex method for solving two-dimensional incompressible Navier-Stokes equation
03 p0317 N88-12001
The dynamics of bubble growth for Rayleigh-Taylor unstable interfaces
[AD-A184752] 03 p0321 N88-12027
On the instability of thin circular shear layers
04 p0395 N88-12467
Calculation of aerodynamic characteristics of three-dimensional finite span wings in potential incompressible flow 04 p0425 N88-12631
Studies of pressure-velocity coupling schemes for analysis of incompressible and compressible flows
[NASA-CR-181526] 04 p0443 N88-12748
NACHOS 2: A finite element computer program for incompressible flow problems. Part 2: User's manual
[DE88-001451] 04 p0443 N88-12750
Analytical studies of axially symmetric motion of an incompressible viscous fluid between two concentric rotating spheres 04 p0444 N88-12757
INS3D: An incompressible Navier-Stokes code in generalized three-dimensional coordinates
[NASA-TM-100012] 04 p0485 N88-12991
Numerical prediction of turbulent flows in dump diffusers 05 p0537 N88-13265
Computation of flow around 2-D circular cylinder
05 p0539 N88-13284
The development of a computer code (U2DIIF) for the numerical solution of unsteady, inviscid and incompressible flow over an airfoil
[AD-A185033] 05 p0541 N88-13293
Delta wing in incompressible flow. Experimental study in F2
[ONERA-RT-36/1147-AN-249-G]
05 p0541 N88-13298
Statistical theory of turbulent incompressible multimaterial flow
[DE88-000435] 05 p0579 N88-13535
Incompressible viscous flow simulations of the NFAC wind tunnel
[NASA-CR-177431] 07 p0816 N88-14969
Analysis of three-dimensional viscous internal flows
[AD-A186254] 07 p0849 N88-15155
Spectral methods: Analysis and applications to flow problems
[AD-A186265] 07 p0850 N88-15156
Nonlinear and nonparallel stability problems
[AD-A186406] 07 p0850 N88-15159
Mean velocities and Reynolds stresses in the juncture flow and in the shear layer downstream of an appendage
[AD-A185819] 08 p0980 N88-15923
Navier-Stokes solutions for laminar incompressible flow over a NACA 0012 airfoil and a backward facing step
[FFA-TN-1987-50] 09 p1162 N88-16966

A project to experimentally and theoretically examine fluid interfacial wave phenomena in a rotating cylindrical geometry: Current results and future plans
[DE88-003738] 09 p1165 N88-16984
Implicit solution of the incompressible Navier-Stokes equations in primitive variables on non-staggered grids
10 p1326 N88-17930
On the smallest scale for the incompressible Navier-Stokes equations
[NASA-CR-181628] 11 p1434 N88-18558
A hydrodynamic analysis of fluid flow between meshing spur gear teeth
[AD-A187671] 11 p1482 N88-18844
A new computational technique for generating algorithms, with application to the solution of the time-dependent incompressible Navier-Stokes equations
11 p1485 N88-18864
Transient radiative energy transfer in incompressible laminar flows
[NASA-CR-182605] 11 p1488 N88-18883
Three-dimensional incompressible Navier-Stokes computations of internal flows
[NASA-TM-100076] 12 p1576 N88-19425
High Reynolds number pump facility for cavitation research
[AD-A189310] 13 p1765 N88-20558
Potential applications of computational fluid dynamics to biofluid analysis
[NASA-TM-100089] 14 p1911 N88-21422
On the use of nonstaggered pressure-velocity arrangement for the numerical solution of incompressible flows
[KU-SFB-210/T/35] 16 p2206 N88-23165
Investigation of subgrid models in homogeneous incompressible turbulence
[ONERA-RSF-13/3419-AY-106-A]
16 p2209 N88-23183
The exact calculation of quadrupole sources for some incompressible flows
[NASA-TM-100623] 17 p2395 N88-24240
Incompressible Euler solution on a multiblock grid around a car configuration
[FFA-TN-1987-65] 18 p2457 N88-24586
Prediction of laminar and turbulent flows past single and twin airfoils 18 p2457 N88-24589
Continuum theories for fluid-particle flows: Some aspects of lift forces and turbulence
[DE88-007038] 18 p2511 N88-24898
Theoretical analysis of laminar incompressible flow in slender channels
[VTH-LR-517] 18 p2513 N88-24909
Finite element analysis of incompressible viscous flow around multi-element aerofoils 19 p2635 N88-25634
Computational boundary conditions for the incompressible Navier-Stokes equations in channels and pipes
[AD-A193356] 21 p2944 N88-27487
Numerical treatment of the pressure singularity at a re-entrant corner
[AD-A193357] 21 p2944 N88-27488
A fast vortex code for computing 2-D flow in a box
[DE88-011732] 21 p2946 N88-27498
Numerical methods for incompressible viscous flows with engineering applications
[NASA-CR-183143] 21 p2948 N88-27508
Surface tension and viscosity with Lagrangian hydrodynamics on a triangular mesh
[AD-A194120] 22 p3075 N88-28258
Steady and unsteady internal flow computations via the solution of the compressible Navier Stokes equations for low Mach numbers 23 p3209 N88-29100
Computation of the eigenvalues for perturbations of Poiseuille flow using a two-point boundary value method
[AD-A193479] 23 p3210 N88-29104
An exponential decay estimate for the stationary perturbation of Poiseuille flow
[AD-A193480] 23 p3210 N88-29105
Computational fluid dynamics methods for low Reynolds number precessing/spinning incompressible flows
[AD-A193891] 23 p3212 N88-29119
Numerical simulation of unsteady incompressible flow in a partially-filled rotating cylinder
[AD-A196001] 24 p3371 N88-30073
Numerical simulation of unsteady incompressible viscous flows in generalized coordinate systems
[NASA-TM-101016] 24 p3373 N88-30085

INCOMPRESSIBLE FLUIDS
NT MICROPOLAR FLUIDS
Determination of the dynamic parameters of annular clearances with turbulent flow and incompressible media
[ETN-87-90434] 01 p0047 N88-10303
Viscous damped space structure for reduced jitter
05 p0594 N88-13623
Well-posedness and spectral estimation for infinite dimensional systems
[AD-A187621] 10 p1401 N88-18354
Vibrations of shells containing fluid
12 p1635 N88-19787
Incompressible theory of interaction between moving bodies and vorticity field: Force on moving bodies by vorticity field 14 p1863 N88-21132
Theoretical studies of solar lasers and converters
[NASA-CR-182927] 17 p2344 N88-23972
Higher order vortex methods with rezoning
[DE88-010777] 21 p2947 N88-27505
Distributive iteration for indefinite systems as smoothing method in multigrid process on example of Stokes and Navier-Stokes equations with emphasis on incomplete decompositions
[ETN-88-92127] 21 p2948 N88-27509
Nonlinear oscillations of a nonviscous cylindrical liquid system in weightlessness condition
[LRT-WE-9-FB-14(1987)] 22 p3063 N88-28175
Nonlinear liquid motion in conical containers
[LRT-WE-9-FB-10(1987)] 22 p3077 N88-28270
Nonlinear oscillations in paraboloidal containers
[LRT-WE-9-FB-3(1988)] 22 p3078 N88-28275

INCONEL (TRADEMARK)
Near-threshold fatigue crack growth behavior at cryogenic temperature 06 p0718 N88-14409
Grain refinement during primary breakdown of alloy 718
[DE88-005193] 13 p1743 N88-20423
Modeling the viscoplastic behavior of Inconel 718 at 1200 F 14 p1929 N88-21502
An experimental comparison of several current viscoplastic constitutive models at elevated temperature
14 p1931 N88-21516
Milliwatt generator project
[DE88-011261] 20 p2853 N88-26939

INDEPENDENT VARIABLES
NT LATTICE PARAMETERS
Group analysis of equations arising in ocean acoustics
04 p0472 N88-12914
Investigation, development and application of optimal output feedback theory. Vol. 4: Measures of eigenvalue/eigenvector sensitivity to system parameters and unmodeled dynamics
[NASA-CR-4108] 04 p0482 N88-12969
The bimodality of large scale averaged flow parameters --- statistical weather forecasting
08 p1016 N88-16159
On error equations for determining Earth rotation parameters with VLBI network 13 p1756 N88-20500
Comparative analysis
[AD-A190556] 15 p2065 N88-22313
Effects of randomness of parameters on mean wave propagation in a viscoelastic medium
[REPT-87-60] 16 p2206 N88-23166
Improved estimators in simultaneous estimation of scale parameters
[AD-A191108] 17 p2392 N88-24216
Studies of HZE particle interactions and transport for space radiation protection purposes
[NASA-TM-101159] 20 p2886 N88-27142
Superconducting thin films, composites and junctions
[AD-A193123] 21 p2937 N88-27440
A minitab macro for the Kaplan-Meier product limit estimator and the Tarone-Ware class of tests
[AD-A194298] 23 p3248 N88-29331
A nonparametric multidimensional IRT approach with applications to ability estimation and test bias
[AD-A194212] 23 p3273 N88-29483
High power storage system based on thin film solid ionics
[AD-A193623] 23 p3291 N88-29598
Canonical variables and canonical integrals for motion in near-circular orbits 24 p3446 N88-30512

INDEXES (DOCUMENTATION)
Master index for the carbon dioxide research state-of-the-art report series
[DE87-012757] 01 p0072 N88-10459
Source header list. Volume 1: A through D
[AD-A184000] 04 p0501 N88-13086
USSR Space Life Sciences Digest index to issues 10-14
[NASA-CR-3922(17)] 07 p0883 N88-15361
TeXting the FORMULARY: A collection of examples of the use of TeX to produce ruled tables and displayed equations
[AD-A185920] 07 p0921 N88-15598
Source hierarchy list. Volume 1: A through D
[AD-A185900] 07 p0941 N88-15722
Source hierarchy list. Volume 2: E through O
[AD-A185901] 07 p0941 N88-15723
Source hierarchy list. Volume 3: P through Z
[AD-A185902] 07 p0942 N88-15724
A performance index approach to aerodynamic design with the use of analysis codes only
[NASA-TP-2805] 11 p1433 N88-18552
NASA scientific and technical publications: A catalog of Special Publications, Reference Publications, Conference Publications, and Technical Papers, 1987
[NASA-SP-7063(02)] 15 p2149 N88-22830
Engine structures: A bibliography of Lewis Research Center's research for 1980-1987
[NASA-TM-100842] 17 p2350 N88-24002
NASA combined file postings statistics based on NASA thesaurus, Jan. 1968 - July 1988
[NASA-CR-182985] 18 p2589 N88-25384
An assessment of index term ranking
21 p3028 N88-27974
A design for a ground-based data management system 24 p3420 N88-30355

INDEXES (RATIOS)
NT LEAF AREA INDEX
Vagal tone as an index of mental state
16 p2239 N88-23373

INDIA
Director of R and D institutions (Government of India)
[PB88-127162] 10 p1285 N88-17685
Science and technology in India
[PB88-134747] 11 p1564 N88-19362
District information system of National Information Centre
[PB88-134739] 11 p1565 N88-19373
National informatics Centre: Profile of services
[PB88-134135] 12 p1706 N88-20211
Indian monsoon rainfall, 1986-1987
22 p3120 N88-28536
Differences in radiation budget parameters over Asia in relation to contrasting Indian monsoons
22 p3125 N88-28574
On climate prediction for India
22 p3127 N88-28590

INDIAN OCEAN
Interactions between the Asian monsoons, the tropical Pacific and the southern hemisphere extratropics
04 p0470 N88-12907
Modes of surface circulation and climate over the tropical Atlantic, Eastern Pacific, and Indian Oceans
06 p0742 N88-14564
New data on structure of earth's crust and seismicity of basins in Atlantic and Indian Oceans
08 p1010 N88-16123
Oceanographic features of the east and southeast Indian Ocean for June 1983
[AD-A186948] 09 p1195 N88-17158
Interannual variability in the Atlantic and Indian Oceans and its relationship to the southern oscillation
22 p3121 N88-28548
Indian Ocean validation
[AD-A194458] 23 p3175 N88-28902

INDIAN SPACECRAFT
Radio frequency compatibility between IRS and SPOT 3: Preliminary study
[CNES-86/CT/DRT/TIT/TR/011]
14 p1905 N88-21383

INDICATING INSTRUMENTS
NT ATTITUDE INDICATORS
NT CLOUD HEIGHT INDICATORS
NT POSITION INDICATORS
NT TACHOMETERS
NT WEIGHT INDICATORS
The P delta V fundamental gas leak calibration system qualification report
[DE88-008964] 21 p2951 N88-27526

INDIUM
Visible InGaAsP/GaAsP lasers produced by epitaxial growth from liquid phase 09 p1237 N88-17416
Strength and structure of Ga sub 1-xIn sub xAs alloys
[AD-A188092] 10 p1303 N88-17795
Silicon and indium doping of GaAs: Measurements of the effect of doping on mechanical behavior and relation with dislocation formation
[DE88-003862] 11 p1554 N88-19303
New method of examining microonhomogeneity of local centers in high-resistivity semiconductor materials under scanning electron microscope 14 p1969 N88-21754
Giant Josephson signal in wide superconducting films
14 p1973 N88-21777
Device physics related to the granular nature of CuInSe2 solar cells
[DE88-001159] 21 p2967 N88-27622
Studies on strained (In,Ga)As/GaAs semiconductors and optical devices 23 p3287 N88-29575
Muon-spin rotation experiment (micro + SR) on aluminum and indium after low temperature electron irradiation
[ETN-88-92985] 23 p3294 N88-29617

INDIUM ALLOYS
Nonlinear absorption of CO2 laser radiation in p-type InSb
[DE88-004055] 11 p1492 N88-18906

Studies of transverse phonon modes in premartensitic indium-thallium alloys
[DE88-003481] 13 p1744 N88-20428
Aluminum alloy
[NASA-CASE-LAR-13924-1-CU] 18 p2487 N88-24753

INDIUM ANTIMONIDES
MBE of HgCdTe
[AD-A191423] 16 p2283 N88-23671
Spectroscopy of one-dimensional subbands on InSb 20 p2864 N88-27007

INDIUM ARSENIDES
MBE growth of InAsSb strained-layer superlattices
[DE88-000365] 05 p0654 N88-14011
Development of a high speed InGaAs/InP Schottky barrier photodetector for millimeter-wave fiber optical links
[AD-A188594] 12 p1629 N88-19750
First report on InGaAs hall device 14 p1903 N88-21372
Photoluminescence studies of InGaAlAs quaternary alloys
[DE88-007197] 20 p2874 N88-27062
Photodiodes for optical communication in the near infrared
[ETN-88-92379] 21 p3016 N88-27900

INDIUM COMPOUNDS
NT INDIUM ANTIMONIDES
NT INDIUM ARSENIDES
NT INDIUM PHOSPHATES
NT INDIUM PHOSPHIDES
Deposition of device quality epitaxial layers of gallium nitride and indium nitride for electronic applications
[AD-A188001] 11 p1453 N88-18661
The synthesis, characterization and structural studies of In(C5H4Me) by X-ray diffraction and electron diffraction techniques and a reinvestigation of the crystalline state of In(C5H5) by X-ray diffraction studies
[AD-A189110] 13 p1844 N88-21038

INDIUM PHOSPHATES
Design and evaluation of single-lobed far-field pattern laser arrays: AlGaAs/GaAs and InGaAsP/InP systems --- optical communication
[LAAS-88-023] 16 p2214 N88-23211
Power MISFETs on OnP
[AD-A195242] 24 p3433 N88-30436

INDIUM PHOSPHIDES
Photoluminescence study of InP surfaces and InP-insulator interfaces
[ECL-87-13] 08 p1089 N88-16555
Progress in InP solar cell research
[NASA-TM-100914] 18 p2507 N88-24870
Planar fully ion-implanted high power InP MISFETs
[AD-A191589] 18 p2582 N88-25338
InP/GaInAs/InP PIN photodiode with FWHM less than 18 ps 19 p2658 N88-25799
Quantum-confined stark effect in InGaAs/InP quantum wells grown by metal-organic chemical vapor deposition 19 p2660 N88-25814
Investigations on the MBE (Molecular Beam Epitaxy) growth and properties of Al(sub y)Ga(sub y)In(sub 1-x-y)AsInP and InGaAs-InAlAs superlattices
[DE88-009105] 21 p3022 N88-27941

INDONESIA
Spatial and spectral registration of Javanese landscape units with SPOT 22 p3092 N88-28362
Thematic mapping of central Java (Indonesia) 22 p3100 N88-28412

INDOOR AIR POLLUTION
Committee on Interagency Radiation Research and Policy Coordination
[DE88-003358] 09 p1188 N88-17121

INDUCED FLUID FLOW
U FLUID FLOW

INDUCTANCE
NT PROXIMITY EFFECT (ELECTRICITY)
Inductance effects in the high-power transmitter crowbar system 04 p0433 N88-12687
Pulsed current transformer for low inductive loads
[AD-A187224] 10 p1324 N88-17913
Comparative evaluation of resistive and inductive techniques for measuring temperature of superconducting transition
[DE88-700603] 10 p1417 N88-18457
Inductive spurious coupling of a dc-SQUID to resonant input circuit
[NOTA-INTERNA-894] 14 p1908 N88-21401
Linear thyratron
[AD-A194111] 23 p3208 N88-29094

INDUCTION (MATHEMATICS)
Constructive version of the approximation induction principle
[PB88-165477] 15 p2122 N88-22647
The use of rule induction to assist in the diagnosis of avionic circuit board defects
[ETN-88-92077] 16 p2162 N88-22899
Induction of models under uncertainty
[NASA-TM-101173] 17 p2394 N88-24230
Induction instrument for logic conclusion
[LRT-WE-9-FB-5(1987)] 22 p3144 N88-28697

INDUCTION HEATING
A finite element model for induction heating of a metal crucible
[DE87-014246] 02 p0246 N88-11551
Model development for induction heating
[DE88-002376] 06 p0699 N88-14289

INDUCTION MOTORS
Process support compressor motor electromagnetic design summary
[DE87-014359] 02 p0167 N88-11048
The theory and implementation of a high quality pulse width modulated waveform synthesiser applicable to voltage FED inverters
[ETN-87-90712] 09 p1157 N88-16937
Industrial electric motors and controllers
[PB88-139589] 14 p1907 N88-21394
Analysis of induction motors based on the numerical solution of the magnetic field and circuit equations
[EL-59] 14 p1907 N88-21398

INDUCTION SYSTEMS
U INTAKE SYSTEMS

INDUCTORS
Response of helical structures to high speed pulses or when can a helix be called an inductor
[DE87-014347] 01 p0090 N88-10587
Advanced thermionic converter technology for inductive output coupling 17 p2407 N88-24311

INDUSTRIAL MANAGEMENT
NT ENGINEERING MANAGEMENT
NT INVENTORY CONTROLS
NT INVENTORY MANAGEMENT
NT PERSONNEL MANAGEMENT
The ESA centralized management system for satellite electronic test and checkout instrumentation 09 p1124 N88-16731
Research, development, and growth strategy 10 p1309 N88-17820
Operations research in management?
[MBB-Z-138/87] 10 p1311 N88-17835
Messerschmitt-Boelkow-Blohm, the company today. Data, numbers and facts 10 p1316 N88-17868
Soviet high-technology restructuring drive: the MNTK network
[AD-A188138] 11 p1565 N88-19370
Managing and controlling change
[PNR90419] 22 p3159 N88-28801
Human organization --- space projects 22 p3160 N88-28808

INDUSTRIAL PLANTS
Contribution to the design of flexible manufacturing systems: Modeling, simulation, and evaluation of parameters
[ISAL-IDI1-87-04] 09 p1151 N88-16894
Stable discrete-time adaptive control 19 p2719 N88-26142

INDUSTRIAL SAFETY
Safety guidelines and procedures for bioscience-based industry and other applied microbiology
[PB87-140521] 08 p1045 N88-16316
Toxic effects of man-made mineral fibers with particular reference to ceramic fibers
[AD-A187949] 11 p1519 N88-19072
Spectroradiometry in industrial safety 16 p2272 N88-23600
Evaluation of the potential health hazards associated with the machining of carbon fiber composites
[AD-A194835] 24 p3408 N88-30286

INDUSTRIAL WASTES
Global mixed-layer natural and anthropogenic fluxes 13 p1807 N88-20803
Waste destruction by plasma
[SNIAS-881-430-113] 21 p2971 N88-27651

INDUSTRIES
NT AEROSPACE INDUSTRY
NT AIRCRAFT INDUSTRY
NT DEFENSE INDUSTRY
Japanese industrial research on lean combustion: A case study: International Research Monitoring Program
[DE87-013839] 02 p0144 N88-10904
Spinoff, 1987
[NASA-TM-89652] 02 p0250 N88-11577
Composite materials in western Europe
[PB87-102943] 03 p0279 N88-11759
A national model at Howard University demonstrating private sector interrelationships that facilitate research in predominantly Black colleges and universities
[DE88-000160] 04 p0502 N88-13089
Impacts of world development on selected characteristics of the atmosphere: An integrative approach. Volume 1: Main report
[DE88-001495] 07 p0875 N88-15309
Impacts of world development on selected characteristics of the atmosphere: An integrative approach. Volume 2: Appendices
[DE88-001496] 07 p0875 N88-15310
An extended Cobb-Douglas form for use in production economics
[AD-A186372] 07 p0943 N88-15733
The development of emission tomography for the nuclear industry
[AERE-R-12319] 10 p1341 N88-18014
International Conference on Industrial and Applied Mathematics
[AD-A188251] 11 p1483 N88-18851
Status of emerging technologies: An economic/technological assessment to the year 2000
[PB88-155775] 11 p1567 N88-19381
Safety study: Commercial emergency medical service helicopter operation
[PB88-917001] 12 p1575 N88-19422
Basic research in ceramic and semiconductor science at selected Japanese laboratories, based on a September 1986 visit: Highlights, summary and overview and detailed notes from selected Japanese laboratories
[DOE/ER-0314] 12 p1696 N88-20150
A project to transfer technology from NASA centers in support of industrial innovation in the midwest
[NASA-CR-180360] 12 p1708 N88-20224
Development of a nationwide network for technology transfer
[NASA-CR-181058] 12 p1709 N88-20225
Technology transfer from US Federal laboratories: Report of a roundtable
[PB88-144803] 12 p1709 N88-20228
Some properties of Australian produced explosive composition H-6
[MRL-TN-525] 13 p1754 N88-20490
Industrial electric motors and controllers
[PB88-139589] 14 p1907 N88-21394
Lasers: Invention to application
[PB88-161583] 14 p1914 N88-21436
Preliminary market analysis for large zeolite crystals
[NASA-CR-182882] 15 p2049 N88-22207
The necessity of automation in Brazil
[INPE-4346-PRE/1183] 15 p2150 N88-22832
Status of CAD/CAM in medium-sized industries described 16 p2184 N88-23022
DOE (Department of Energy) national laboratories and the semiconductor industry: Continuing the joint planning
[PB88-170295] 16 p2281 N88-23657
Data management strategies in the industrial environment
[NLR-MP-87002-U] 16 p2286 N88-23684
Defense Small Business Innovation Research Program (SBIR). Volume 3: Air Force abstracts of phase 1 awards, 1987 17 p2448 N88-24548
Competitive assessment of the U.S. civil helicopter industry
[PB88-186325] 18 p2455 N88-24574
The application of hydrocarbon bioconversion technology to aerospace materials production 18 p2478 N88-24698
Determining system maintainability as a probability
[DE88-007722] 19 p2679 N88-25927
Photointerpretation with instrumentation for evaluation of environmental impact: Mata Atlantica in Cubatao 19 p2683 N88-25946
Study of evolution of vegetal cover and slide scars in the Cubatao municipality-Sao Paulo 19 p2683 N88-25947
Workshop report and presentations from the Semiconductor Research Corporation-DOE Semiconductor Task Force Workshop
[DE88-007690] 19 p2733 N88-26232
Resources: NASA for entrepreneurs
[NASA-CR-182152] 20 p2883 N88-27119
Federal Council on Science, Engineering and Technology: Committee on Computer Research and Applications, Subcommittee on Science and Engineering Computing: The US Supercomputer Industry
[DE88-011262] 21 p2994 N88-27756
Absorption heat pumps
[DE88-752820] 23 p3229 N88-29218

INELASTIC BODIES
U RIGID STRUCTURES

INELASTIC COLLISIONS
An interactive computer program for materials analysis by means of ion scattering
[MRL-R-1040] 01 p0091 N88-10596
Physics and chemistry 07 p0883 N88-15359
Particle-dynamics calculations of gravity flow of inelastic, frictional spheres
[DE88-005224] 13 p1770 N88-20586
Survey of impact damper performance 16 p2217 N88-23227
Forbidden transitions as ion-temperature sensitive lines 17 p2441 N88-24520

INELASTIC SCATTERING
Experimental studies of electromagnetic properties of few body systems
[DE87-014610] 02 p0161 N88-11008
Electron interactions with nuclei
[DE87-014587] 02 p0232 N88-11460
Consistency question in the renormalization group analysis of deep inelastic scattering
[DE87-703372] 04 p0487 N88-12999
Parton densities from deep inelastic scattering to hadronic processes at super collider energies
[NOTA-INTERNA-885] 07 p0930 N88-15646
Pion elastic and inelastic scattering near N=28
[LA-10968-T] 11 p1544 N88-19232
Advanced electron optics for vibrational spectroscopy
[AD-A188469] 12 p1629 N88-19747
On (p,n) systematics and the cosmological connection
[DE88-005031] 12 p1712 N88-20245
Analysis of hadron production in deep inelastic muon-proton collisions through the fire-string model
[PREPRINT-578] 14 p1981 N88-21822
Implications of the trapping-desorption and direct inelastic scattering channels on Dicke-narrowed lineshapes
[AD-A191410] 16 p2270 N88-23581
Memoirs of the Faculty of Science, Kyoto University. Series of Physics, Astrophysics, Geophysics and Chemistry, volume 37, no. 2
[ISSN-0368-9689] 16 p2287 N88-23694
Nuclear structure studies at intermediate energies
[DE88-006683] 18 p2571 N88-25271
Influence of scattering on seismic waves: Physical mechanisms contributing to attenuation in the crust
[AD-A191699] 19 p2690 N88-25992
Inelastic ion-surface collisions
[AFGL-TR-87-0206] 19 p2724 N88-26174
Half collision studies of inelastic energy transfer processes
[DE88-008096] 19 p2724 N88-26178
Inelastic two composite particle systems scattering at high energy
[DE88-701841] 20 p2851 N88-26928
Inelastic electron scattering and electron-hole excitations in iron and nickel
[DE88-011843] 21 p2915 N88-27303
Tagging of gamma yields qq bar events and direct measurement of the gluon structure function at HERA
[NOTA-INTERNA-910] 22 p3151 N88-28745
Effect of a laser field in the electron inelastic scattering into plasma fields
[DE88-702295] 23 p3218 N88-29157
On selection rules and inelastic electron scattering at intermediate energies
[DE88-701833] 23 p3280 N88-29526
Eikonal solutions to optical model coupled-channel equations
[NASA-TP-2830] 24 p3428 N88-30402

INELASTIC STRESS
Experimental determination of flow potential surfaces supporting a multiaxial formulation of viscoplasticity 02 p0187 N88-11167
Constitutive modeling of superalloy single crystals with verification testing 02 p0188 N88-11169
Unified constitutive models for high-temperature structural applications 14 p1932 N88-21523
A constitutive model for an overlay coating 14 p1933 N88-21525
On 3-D inelastic analysis methods for hot section components. Volume 1: Special finite element models
[NASA-CR-180893] 14 p1934 N88-21535
Experiments investigating advanced materials under thermomechanical loading 15 p2077 N88-22385
Three-dimensional inelastic approximate analysis code (MOMM) 15 p2079 N88-22392
Specialty three-dimensional finite element analysis codes 15 p2079 N88-22393
MHOST: An efficient finite element program for inelastic analysis of solids and structures 15 p2079 N88-22394
An experimental study of biaxial yield in modified 9Cr-1Mo steel at room temperature
[NASA-CR-175012] 24 p3385 N88-30164

INEQUALITIES
NT SCHWARTZ INEQUALITY
Feedback in LQCP (Linear Quadratic Control Problem) with a terminal inequality constraint
[PB87-220034] 06 p0762 N88-14676
On hypercontractivity of alpha-stable random variables, 0 less than alpha less than 2
[AD-A186425] 07 p0915 N88-15559
Norm inequalities for derivatives and differences
[DE86-002920] 09 p1230 N88-17371
Some majorization inequalities for functions of exchangeable random variables
[AD-A188207] 11 p1536 N88-19178
Additive prophet inequalities for transforms of uniformly bounded pairwise independent random variables
[PB88-173513] 18 p2588 N88-25250
Conditions for finite convergence of algorithms for nonlinear programs and variational inequalities
[AD-A192355] 20 p2838 N88-26834

INERT ATMOSPHERE
Spacecraft Fire Safety
[NASA-CP-2476] 04 p0406 N88-12520
Fire extinguishment and inhibition in spacecraft environments 04 p0406 N88-12523
Inerting and atmospheres 04 p0406 N88-12524

INERT GASES
U RARE GASES

INERTIA
WKBJ method and strained coordinates for high frequency inertial wave filtering
[INPE-4214-PRE/1095] 11 p1537 N88-19186
Horizontal scales of wind forced inertial motions 13 p1806 N88-20795
The buckling and vibration of composite plates using the Levy method considering shear deformation and rotary inertia
[AD-A189743] 15 p2076 N88-22374
Napping and human functioning during prolonged work
[AD-A190228] 15 p2102 N88-22525
A new method for the estimation of aircraft inertia characteristics 20 p2787 N88-26530

INERTIA BONDING
Inertia welding with variable magnitude of impact load 14 p1897 N88-21328

INERTIA MOMENTS
U MOMENTS OF INERTIA

INERTIA WHEELS
U REACTION WHEELS

INERTIAL CONFINEMENT FUSION
Status of inertial fusion
[DE87-010988] 01 p0099 N88-10654
Laser-plasma-interaction experiments using multikilojoule lasers
[DE87-013483] 01 p0100 N88-10658
Compact torus studies
[DE87-014254] 02 p0237 N88-11496
Filamentation instability of rotating light ion beams in fusion target chambers
[IPPJ-839] 02 p0242 N88-11530
Analysis of an induction linac driver system for inertial fusion
[DE88-000681] 03 p0379 N88-12384
Interplanetary propulsion using inertial fusion
[NASA-TM-89661] 04 p0409 N88-12540
The VISTA spacecraft: Advantages of ICF (Inertial Confinement Fusion) for interplanetary fusions propulsion applications
[NASA-CR-181549] 04 p0491 N88-13024
Inertial confinement fusion reactor cavity analysis
[DE88-000788] 04 p0492 N88-13028
ICRF launcher studies
[DE88-001710] 04 p0495 N88-13046
The Rayleigh-Taylor instability in ablatively accelerated targets with 1, 1/2 and 1/4 micrometers laser light
[AD-A185945] 07 p0858 N88-15208
Laser Program
[DE87-011009] 07 p0858 N88-15212
High Z interaction physics on Nova
[DE88-004397] 10 p1413 N88-18433
The stability of free-electron lasers against filamentation
[DE88-004712] 10 p1414 N88-18435
Diagnostics for ATF
[DE88-004175] 10 p1414 N88-18438
ATF experimental plans
[DE88-004177] 10 p1414 N88-18439
ICF research at Los Alamos
[DE88-005394] 11 p1493 N88-18916
ICF special studies
[DE88-004057] 11 p1551 N88-19281
Magnetic and inertial fusion status and development plans
[DE88-004405] 11 p1552 N88-19288
Potential benefits of a broad magnetic fusion R and D program
[DE88-003288] 11 p1553 N88-19297
The Magnetically Insulated Inertial Confinement Fusion (MICF): A novel approach
[DE88-005460] 13 p1842 N88-21026
Activities report in laser-matter interaction
[ETN-88-92007] 15 p2129 N88-22696
Environmental assessment for the compact ignition Tokamak
[DE88-005633] 15 p2135 N88-22740
Magnetic fusion energy plasma interactive and high heat flux components. Volume 5: Technical assessment of critical issues in the steady state operation of fusion confinement devices
[DE88-006920] 15 p2136 N88-22744
Rayleigh-Taylor instability in inertial confinement fusion
[DE88-701411] 15 p2137 N88-22750
Development of Electromagnetic PIC code for LIB diode 16 p2276 N88-23622
Kinetic theoretical analysis for propagation of rotating ion beam in ICF 16 p2276 N88-23623
Hybrid particle simulation for focusing of rotating and propagating LIB 16 p2276 N88-23624
Simulation code for ICF including radiative energy transfer 16 p2277 N88-23627
Efficient shell implosion and target design 16 p2277 N88-23630
Microinstabilities in ion beam propagation 16 p2277 N88-23631
Self-similar expansions in ion beam fusion 16 p2278 N88-23635
Two-dimensional focusing of self-magnetically insulated plasma focus diode 16 p2278 N88-23639
Research on anode plasma behavior of flashover pulsed ion sources 16 p2279 N88-23640
Study on the flashover ion diode with cryogenic anode 16 p2279 N88-23642
Interplanetary propulsion using inertial fusion 17 p2401 N88-24273
Inertial fusion in the nineties
[DE88-007913] 19 p2730 N88-26214
Pulsed power driver technologies for inertial confinement fusion power reactors
[DE88-009260] 19 p2731 N88-26221
The effect of ICRF on the Alcator C Scrape-Off Layer plasma
[DE88-009821] 20 p2858 N88-26972

INERTIAL FORCES
U INERTIA

INERTIAL FUSION (REACTOR)
Status of inertial fusion
[DE87-010988] 01 p0099 N88-10654
LLE Review, volume 30
[DE87-014469] 02 p0178 N88-11109
Analysis of an induction linac driver system for inertial fusion
[DE88-000681] 03 p0379 N88-12384
Interplanetary propulsion using inertial fusion
[NASA-TM-89661] 04 p0409 N88-12540
Heavy-ion accelerator research for inertial fusion
[DE88-000541] 05 p0653 N88-14001
Particle transport in microdetonations --- inertial confinement fusion pellets
[OEFZS-4402] 09 p1164 N88-16976
Magneto-Inertia Confinement Approach (MICA) to fusion in dynamic Z-pinch formed from a frozen deuterium-tritium tube
[IPPJ-856] 09 p1252 N88-17504
Design issues for a laboratory high gain fusion facility
[DE88-004406] 10 p1413 N88-18434
Interplanetary propulsion using inertial fusion 17 p2401 N88-24273

INERTIAL GUIDANCE
NT STRAPDOWN INERTIAL GUIDANCE
Optical alignment of Centaur's inertial guidance system
[NASA-TM-88844] 04 p0405 N88-12515
Gyrostabilizer system of Kvant module 08 p1006 N88-16099
Development of a facility using robotics for testing automation of inertial instruments 09 p1213 N88-17271
Reference position vector 12 p1577 N88-19432
Rate and dynamic tests on the Canadian Strapdown Gyroscope (CSG-2) 12 p1578 N88-19439
Convective heat transfer and its effect on inertial measurement units 12 p1578 N88-19442
Features of Soyuz TM spacecraft 13 p1727 N88-20329
Inertial reference system with Global Positioning System (GPS) support 18 p2518 N88-24936

INERTIAL MEASURING UNITS
U INERTIAL PLATFORMS

INERTIAL NAVIGATION
Test equipment with fiber optic data bus and laser gyro strapdown system LTN-90 for the helicopter BO-105
[ESA-TT-1038] 01 p0005 N88-10025
NAVSIM 2: A computer program for simulating aided-inertial navigation for aircraft
[NASA-CR-177438] 04 p0398 N88-12478
Correction of inertial navigation system drift errors for an autonomous land vehicle using optical radar terrain data
[AD-A184973] 05 p0544 N88-13311

A conceptual design of an inertial navigation system for an autonomous submersible testbed vehicle
[AD-A188038] 11 p1438 N88-18578
Thirteenth Biennial Guidance Test Symposium, volume 1
[AD-A185782] 12 p1576 N88-19427
Calibration of a ring laser gyro inertial navigation system 12 p1576 N88-19428
Simultaneous estimation and detection of bias shifts for inertial navigation systems 12 p1576 N88-19429
Covariance analysis and post-processing of gravity compensation effects for aided multi-state navigation systems
[PAPER-87-13] 12 p1577 N88-19430
Commonality in the design and production of the H-423 (F3) and H-770 (F-15) RLG inertial navigation systems 12 p1577 N88-19431
The global positioning system as an aid to the testing of inertial navigation units (volume 1, addendum 1)
[AD-A185783] 12 p1578 N88-19443
An evaluation of perceptions of form, fit, function (F3) standardization on the Standard Inertial Navigation Unit (STD INU) program
[AD-A188955] 12 p1579 N88-19446
Optics: Perspectives for Measurement Techniques and Signal Processing for Flight Guidance — conference
[DFVLR-MITT-87-21] 18 p2516 N88-24928
Laboratory tests of laser gyroscopes for future utilization in multifunction systems for precision navigation and flight guidance 18 p2517 N88-24932
The optical accelerometer: A novel sensor for vertical flight guidance 18 p2518 N88-24935
On-board data processing of navigation data at high latitudes in Antarctica 22 p3036 N88-28027
Performance of GPS-aided INS during high-dynamic maneuvers
[AD-A194624] 23 p3175 N88-28903
Angle of attack and sideslip estimation using an inertial reference platform
[AD-A194876] 24 p3319 N88-29769
Observed track-keeping performance of DC10 aircraft equipped with the Collins AINS-70 area navigation system: Karlsruhe and Masstricht UACs (Upper Area Control centres)
[EEC-202] 24 p3323 N88-29768
Estimation of short-wavelength gravity on a dense grid using digital terrain elevation data
[AD-A196325] 24 p3391 N88-30196

INERTIAL PLATFORMS
Application of the Single-Axis rate Table (SAT) of the DFVLR for the evaluation of stationary and dynamic gyro properties
[DFVLR-MITT-88-09] 21 p2952 N88-27533
Angle of attack and sideslip estimation using an inertial reference platform
[AD-A194876] 24 p3319 N88-29769

INERTIAL REFERENCE SYSTEMS
The global positioning system as an aid to the testing of inertial navigation units (volume 1, addendum 1)
[AD-A185783] 12 p1578 N88-19443
A study on local level inertial surveying systems. Error model for the stationary system
[B8736714] 16 p2229 N88-23312
Laboratory tests of laser gyroscopes for future utilization in multifunction systems for precision navigation and flight guidance 18 p2517 N88-24932
Inertial reference system with Global Positioning System (GPS) support 18 p2518 N88-24936

INERTIAL UPPER STAGE
Qualification by analysis of IUS plume deflectors 09 p1179 N88-17063

INFARCTION
NT MYOCARDIAL INFARCTION

INFECTIONS
U INFECTIOUS DISEASES

INFECTIOUS DISEASES
NT BACTERIAL DISEASES
NT FUNGAL DISEASES
NT PARASITIC DISEASES
Illustrations of a density-equalizing map projection technique
[DE87-013992] 03 p0339 N88-12130

INFERENCE
Analogical inference and analogical access
[AD-A184345] 03 p0369 N88-12321
Statistical inference: Computer oriented algorithmic approach
[DE87-013874] 04 p0478 N88-12948
An APL workspace for conducting nonparametric statistical inference
[AD-A184971] 05 p0634 N88-13877
Genie inference engine rule writer's guide
[AD-A185709] 06 p0762 N88-14675
An inference engine for embedded diagnostic systems 08 p1056 N88-16367
The empirical accuracy of uncertain inference models 09 p1208 N88-17243
TYPICAL: A knowledge representation system for automated discovery and inference
[AD-A187483] 11 p1533 N88-19160
Expert systems: Their impact on performance and cognitive strategies in diagnostic inference
[AD-A188518] 12 p1677 N88-20027
Knowledge retrieval as specialized inference
[AD-A189042] 13 p1823 N88-20899
Inference engine for expert systems
[INPE-4485-TDL/321] 15 p2113 N88-22590
Statistical inference for stochastic processes
[AD-A190491] 15 p2126 N88-22673
Studies in reliability and inference
[AD-A191389] 16 p2217 N88-23223
Capitalizing on failure through case-based inference
[AD-A190927] 16 p2255 N88-23480
Inference for a nonlinear semimartingale regression model
[AD-A190857] 16 p2262 N88-23527
Induction of models under uncertainty
[NASA-TM-101173] 17 p2394 N88-24230
User's guide to the Fault Inferring Nonlinear Detection System (FINDS) computer program
[NASA-CR-178410] 18 p2462 N88-24619
Adaptive time series analysis using predictive inference and entropy
[AD-A191858] 18 p2560 N88-25199
A network approach to the certainty factor model — expert systems
[CWI-CS-R8757] 20 p2840 N88-26852
Topics in adaptive control and inference
[AD-A194718] 23 p3266 N88-29443
Theories of comparative analysis
[AD-A196328] 24 p3427 N88-30395

INFILTRATION
Ceramic composites by chemical vapor infiltration
[DE87-009128] 01 p0029 N88-10185
Cast iron freezing mechanisms 03 p0298 N88-11870

INFINITY
Equivalence of input-output stability and exponential stability for infinite dimensional systems
[TW-276] 05 p0638 N88-13903
Conditions at infinity for theories of oscillating wings and propellers in subsonic flow
[NAL-TR-937] 11 p1434 N88-18556
Algorithm for accounting the conditions in infinity for two-dimensional magnetostatics problems
[DE88-701673] 16 p2264 N88-23541

INFLATABLE DEVICES
U INFLATABLE STRUCTURES

INFLATABLE STRUCTURES
NT BALLOONS
NT GAS BAGS
NT HIGH ALTITUDE BALLOONS
NT JIMSPHERE BALLOONS
Far infrared spectroscopy telescope (FIRST) inflatable thermal shield, phase 1
[SR/FIS/108(87)CZ] 24 p3453 N88-30552

INFLATING
Rheological behaviors of an elastomeric membrane
[DE87-013105] 01 p0061 N88-10392
Renal effects of anti-gravity suit inflation in man in relation to cardiovascular and hormonal changes 12 p1661 N88-19959

INFLECTION POINTS
Boundary value problems for ordinary differential equations with multiple turning points
[CWI-AM-R8701] 09 p1228 N88-17354

INFLUENCE COEFFICIENT
NT STRUCTURAL INFLUENCE COEFFICIENTS
An initial investigation into methods of computing transonic aerodynamics sensitivity coefficients
[NASA-CR-182444] 09 p1112 N88-16663
The experimental verification of wall movement influence coefficients for an adaptive walled test section
[NASA-CR-181681] 19 p2598 N88-25439
Investigation of oscillating cascade aerodynamics by an experimental influence coefficient technique
[NASA-TM-101313] 22 p3039 N88-28041
Comparison of the influence of different gust models on structural design 24 p3312 N88-29722
An experimental study of an adaptive-wall wind tunnel
[NASA-CR-183152] 24 p3329 N88-29821

INFORMATION
Summaries of the FY 1987 applied mathematical sciences research program
[DE87-014447] 02 p0225 N88-11416
Wave and wind data sources, environmental conditions committee report, International Ship and Offshore Structures Congress
[PB87-234902] 06 p0746 N88-14588
Conceptual information processing: A robust approach to KBS-DBMS integration 08 p1063 N88-16422
Resonance, information, and the primacy of process: Ancient light on modern information and communication theory and technology 10 p1424 N88-18506
The optimum solution to instrument quantization effects 12 p1577 N88-19434
Interfacing and integrating hardware and software design systems 17 p2306 N88-23796

INFORMATION ADAPTIVE SYSTEM
An interactive computer graphics network monitor for a tactical communications network
[AD-A184131] 04 p0477 N88-12938

INFORMATION DISSEMINATION
NT MESSAGES
Spacecraft 2000 program overview 01 p0015 N88-10085
NASA's new technology reporting system: A review and future prospects
[NASA-CR-180954] 01 p0105 N88-10686
Freedom of Information Act: Fee waiver practices at the FBI (Federal Bureau of Investigation)
[PB87-216727] 02 p0249 N88-11573
Automatic photometric monitoring of cool stars 04 p0504 N88-13103
Role of technical information in innovation
[PB87-235388] 05 p0658 N88-14039
Role of the technical report in technological innovation
[PB87-232500] 05 p0658 N88-14040
Inexpensive solution for the mass distribution of satellite images
[PB88-114038] 10 p1317 N88-17873
NASA/UK TAP
[NASA-CR-180350] 12 p1708 N88-20223
Applicability of aerospace thermal insulation technologies to the civilian sector
[DE88-003717] 13 p1852 N88-21086
Sigma system: Overview, prospects 15 p2052 N88-22230
Presentation of the METEOSAT system and the roles of EUMETSAT within the meteorological community 17 p2357 N88-24039
Computer resource management technology program (PE 64740F). Task no. 9: Advanced user authentication
[PB88-183066] 18 p2555 N88-25163
Technology transfer, Sandia National Laboratories
[DE88-009790] 19 p2740 N88-26268
Context of national information systems in developing countries: India and China in a comparative perspective
[PB88-109954] 20 p2882 N88-27111
Flight information publication (FLIP) feedback
[AD-A194462] 23 p3174 N88-28897
Barriers to Information Transfer and Approaches Toward Their Reduction
[AGARD-CP-430] 24 p3437 N88-30458
Linguistic and cultural barriers to the transfer of information 24 p3437 N88-30459

INFORMATION FLOW
Application of artificial intelligence to impulsive orbital transfers 08 p1066 N88-16439
Data flow graph optimization in IF1
[DE88-004396] 11 p1532 N88-19151
Rapid prototyping of complex avionic system architectures 17 p2302 N88-23771
A multiprocessor data flow accelerator module
[DE88-007587] 18 p2554 N88-25161
Technology transfer, Sandia National Laboratories
[DE88-009790] 19 p2740 N88-26268
Context of national information systems in developing countries: India and China in a comparative perspective
[PB88-109954] 20 p2882 N88-27111
Hiding in stream semantics of uniform concurrency
[PB88-121579] 20 p2882 N88-27114
Large-grain pipelining on distributed-memory multiprocessors
[DE88-009974] 23 p3264 N88-29432

INFORMATION MANAGEMENT
Implementing and managing change: A guide for assessing information technology
[DE88-000035] 02 p0249 N88-11571
Advanced Information Processing System (AIPS) proof-of-concept system functional design I/O network system services
[NASA-CR-181488] 03 p0384 N88-12413
Electronic Records Administration at the Savannah River Plant
[DE87-014842] 03 p0384 N88-12415
Information analysis centers in the department of defense, revision
[AD-A184002] 03 p0385 N88-12420
Foundation: Transforming data bases into knowledge bases 08 p1063 N88-16423
The intelligent user interface for NASA's advanced information management systems 08 p1063 N88-16424
Media independent interface. Interface control document
[NASA-CR-172032] 08 p1067 N88-16447

Information handling architecture and software for CIM (Computer Integrated Manufacturing)
[PB88-105820] 08 p1067 N88-16453
Distributed transaction processing and the Camelot system
[AD-A188614] 13 p1821 N88-20885
Laboratory Information Management System (LIMS): A case study
[NASA-TM-100835] 14 p1961 N88-21697
Information systems for quality. Experience at the Nerviano Aeritalia plant. Avionic systems and equipment group
[ETN-88-92274] 15 p2148 N88-22821
Crewstation Information and Development System (CIDS) 17 p2304 N88-23781
Designing for design effectiveness of complex avionics systems 17 p2305 N88-23788
Space Power Reference Source (SPRS): A user's guide to SDI Space Power Technology Programs 17 p2427 N88-24440
Developing a connector selection DBMS (database management system) using NIAM (Nijssen's Information Analysis Methodology)
[DE88-008110] 21 p3028 N88-27972
Pattern information processing and multimedia database system: Current research on multimedia information system
[PB88-131917] 21 p3028 N88-27973
Information retrieval systems evolve-advances for easier and more successful use 24 p3438 N88-30462

INFORMATION PROCESSING (BIOLOGY)
A survey of artificial neural systems
[AD-A184759] 03 p0368 N88-12312
Taskomat, a task battery for information processing
[IZF-1987-2] 05 p0630 N88-13851
Genie inference engine rule writer's guide
[AD-A185709] 06 p0762 N88-14675
Probabilistic neural networks: In or out of equilibrium
[DE88-002907] 09 p1201 N88-17198
A situation-response model for intelligent pilot aiding 09 p1208 N88-17241
A conceptual framework for intelligent real-time information processing 09 p1211 N88-17257
Two attentional models of classical conditioning: Variations in CS effectiveness revisited
[AD-A187697] 11 p1522 N88-19088
Electromagnetic metrics of mental workload
[AD-A188205] 11 p1523 N88-19093
When decision aids fail
[AD-A187531] 11 p1523 N88-19095
A personalized and prescriptive decision aid for choice from a database of options
[AD-A188726] 13 p1811 N88-20820
Synapses that compute motion
[AD-A190389] 15 p2116 N88-22607
Processing deficits in monitoring analog and digital displays: Implications for attentional theory and mental-state estimation research 16 p2241 N88-23389
Information processing deficits in psychiatric populations: Implications for normal workload assessment 16 p2241 N88-23390
Novel nonlinear signal processing principles
[AD-A191644] 19 p2707 N88-26097
Contra- and ipsilateral auditory stimuli produce different activation patterns at the human auditory cortex: A neuromagnetic study
[PB88-181490] 19 p2708 N88-26098
Working memory capacity: An individual differences approach
[AD-A192359] 20 p2833 N88-26803
A review of workload measurement in relation to verbal comprehension 21 p2925 N88-27360
The effects of increased cognitive demands on autonomic self-regulation: An indicator of parallel processing in the brain 21 p2925 N88-27362
Mitsubishi Electric Advance (R and D Edition), Volume 41
[PB88-194162] 21 p2929 N88-27388
Basic research on optical neural computers 21 p2929 N88-27389
Electric and Magnetic Activity of the Central Nervous System: Research and Clinical Applications in Aerospace Medicine
[AGARD-CP-432] 21 p2977 N88-27683
Dissecting the visual and auditory pathways by means of the two-input technique 21 p2978 N88-27690
Electric and magnetic brain activity related to cognitive performance 21 p2979 N88-27692
Neuromagnetic evidence of place mechanisms for frequency and intensity coding in the human auditory cortex 21 p2979 N88-27693
A study of sources in the human brain associated with stereopsis 21 p2979 N88-27695
The effects of hypoxia on P300 and reaction time
[DCIEM-87-RR-12] 21 p2979 N88-27697
Using ERPS to study human information processing 21 p2980 N88-27698
The effect of mild hypoxia on the vestibular evoked response 21 p2982 N88-27713
Transformations of short-term visual memory
[AD-A193873] 23 p3241 N88-29290
Nested neural networks
[NASA-TM-101032] 24 p3423 N88-30373

INFORMATION RETRIEVAL
A parallel model of the kinetic depth effect using local computations
[AD-A181945] 01 p0083 N88-10536
On perfect hash functions
[ENST-86D008] 01 p0087 N88-10565
High performance clause indexing
[DE87-011399] 01 p0106 N88-10688
Optical laser technology, specifically CD-ROM (Compact Disc - Read Only Memory) and its application to the storage and retrieval of information
[AD-A184111] 03 p0330 N88-12086
Electronic Records Administration at the Savannah River Plant
[DE87-014842] 03 p0384 N88-12415
Source header list. Volume 2: L through Z
[AD-A184001] 03 p0385 N88-12419
Towards automated consulting: Design feedback from the performance of online documentation
[DE87-012243] 04 p0501 N88-13082
Subjective probability, combination of expert opinion and probabilistic approaches to information retrieval 04 p0501 N88-13085
Storing and retrieving data in a parallel distributed memory system
[AD-A185177] 05 p0637 N88-13897
Status, outlook of optical technology in information equipment field 06 p0689 N88-14222
Using user models and automatic expertise acquisition in data base interactions
[PB87-234357] 06 p0791 N88-14848
A review of hypertext in a NASA project management context 06 p0793 N88-14859
Source hierarchy list. Volume 1: A through D
[AD-A185900] 07 p0941 N88-15722
Source hierarchy list. Volume 2: E through O
[AD-A185901] 07 p0941 N88-15723
Source hierarchy list. Volume 3: P through Z
[AD-A185902] 07 p0942 N88-15724
Problem solving as intelligent retrieval from distributed knowledge sources 08 p1059 N88-16392
User's guide to a data base of current environmental monitoring projects in the US-Canadian transboundary region
[DE88-002476] 09 p1188 N88-17119
Recovery using virtual memory
[AD-A187098] 09 p1217 N88-17296
Inexpensive solution for the mass distribution of satellite images
[PB88-114038] 10 p1317 N88-17873
A hypertext writing environment and its cognitive basis
[AD-A188179] 10 p1389 N88-18298
Using SIR (Scientific Information Retrival) system for data management during a field program
[DE88-001555] 10 p1424 N88-18508
The acoustic-modeling problem in automatic speech recognition
[AD-A188529] 13 p1757 N88-20510
Knowledge retrieval as specialized inference
[AD-A189042] 13 p1823 N88-20899
A menu-driven knowledge retrieval system accessing ASCII data
[DE88-001742] 13 p1851 N88-21079
Baseline observing system experiments using the AFGL global data assimilation system
[AD-A188861] 15 p2024 N88-22062
Relationship of encoding speed and memory tests to flight training performance
[AD-A190670] 15 p2105 N88-22539
The Scientific and Technical Information Network (STINET). Foundation for evolution
[AD-A189750] 15 p2148 N88-22822
The Engineer Studies Center guide to research and data collection
[AD-A189971] 16 p2285 N88-23680
Translations of scientific and technical literature: A guide to their location 16 p2286 N88-23686
Extracting information from problem solving experience
[AD-A191331] 16 p2286 N88-23688
Defense Technical Information Center cataloging guidelines
[AD-A192200] 18 p2589 N88-25382
Engineering drawings and changes: Storing and controlling by the tens of terrabytes
[DE88-007605] 18 p2589 N88-25387
Computer-aided research
[DE88-007771] 19 p2714 N88-26114
MVS (Multiple Virtual Storage) batch computing and data management at ANL
[DE88-007342] 19 p2718 N88-26137
A cockpit natural language study - selected transcripts
[AD-A192972] 20 p2834 N88-26808
Use of optical disk technology at the Air Command and Staff College
[AD-A192424] 21 p3027 N88-27969
Capitalizing on experience with intelligence gateway software
[AD-A193362] 21 p3028 N88-27971
An assessment of index term ranking 21 p3028 N88-27974
Walter user's manual (Version 1.0)
[AD-A192542] 22 p3136 N88-28644
Optimization techniques for relational database systems 22 p3137 N88-28650
Distributed knowledge base systems for diagnosis and information retrieval
[AD-A193107] 23 p3296 N88-29633
Experiments in automatic phrase indexing for document retrieval: A comparison of syntactic and non-syntactic methods 23 p3296 N88-29634
Information retrieval systems evolve-advances for easier and more successful use 24 p3438 N88-30462

INFORMATION SYSTEMS
NT GEOGRAPHIC INFORMATION SYSTEMS
NT INFORMATION ADAPTIVE SYSTEM
NT MANAGEMENT INFORMATION SYSTEMS
NT NUMERICAL DATA BASES
Compilation and analysis of air quality data in support of acid deposition research
[DE87-014428] 02 p0196 N88-11226
The microcomputer as an engineering management tool
[DE87-014882] 02 p0219 N88-11378
Design and development of a database for spectral data and analysis results
[DE87-011323] 02 p0247 N88-11564
Implementing and managing change: A guide for assessing information technology
[DE88-000035] 02 p0249 N88-11571
Lewis Information Network (LINK): Background and overview
[NASA-TM-100162] 03 p0305 N88-11925
Advanced Information Processing System (AIPS) proof-of-concept system functional requirements I/O network system services
[NASA-CR-181481] 03 p0384 N88-12412
Advanced Information Processing System (AIPS) proof-of-concept system functional design I/O network system services
[NASA-CR-181488] 03 p0384 N88-12413
The impact of information technology on research in science and engineering
[DE88-000342] 03 p0385 N88-12417
Information analysis centers in the department of defense, revision
[AD-A184002] 03 p0385 N88-12420
Advanced techniques for the storage and use of very large, heterogeneous spatial databases. The representation of geographic knowledge: Toward a universal framework -- relations (mathematics)
[NASA-CR-181517] 03 p0385 N88-12421
Materials sciences programs: Fiscal Year 1987
[DE88-000672] 04 p0429 N88-12659
Space station software reliability analysis based on failures observed during testing at the multisystem integration facility 06 p0798 N88-14884
Facility design validation of the information systems laboratory
[AD-A186309] 07 p0906 N88-15488
Compilation and development of K-6 aerospace materials for implementation in NASA spacelink electronic information system 07 p0922 N88-15605
DoD Gateway Information System (DGIS) common command language: The first prototyping and the decision for artificial intelligence
[AD-A185950] 07 p0942 N88-15725
DoD Gateway Information System (DGIS): Common command language mapping
[AD-A185951] 07 p0942 N88-15726
Problem solving as intelligent retrieval from distributed knowledge sources 08 p1059 N88-16392
Conceptual information processing: A robust approach to KBS-DBMS integration 08 p1063 N88-16422
The intelligent user interface for NASA's advanced information management systems 08 p1063 N88-16424
DOD Gateway Information System (DGIS) common command language: Prolog knowledge base profile. Common command language report no. 3
[AD-A186150] 08 p1092 N88-16574
Critical issues in NASA information systems
[NASA-CR-182380] 08 p1093 N88-16577

IMIS: Integrated Maintenance Information System. A maintenance information delivery concept
09 p1203 N88-17207
Interchange of electronic design through VHDL and EIS 09 p1205 N88-17222
Management of complex information in support of evolving autonomous expert systems
[AD-A186680] 09 p1224 N88-17337
Wind turbine acoustics research bibliography with selected annotation
[NASA-TM-100528] 09 p1243 N88-17450
Code division multiple access applied to fiber optic data transmission
[AD-A186873] 09 p1247 N88-17477
Information needs analysis for the Aeronautical Systems Division Executive Information System
[AD-A186912] 09 p1261 N88-17556
Wide band data transmission system using optical fibers
[DE88-004555] 10 p1319 N88-17889
Methods of eliciting information from experts
[AD-A187468] 10 p1372 N88-18189
Automated data flow diagram verification
10 p1382 N88-18255
Air Force geographic information and analysis system
[DE88-001420] 10 p1424 N88-18505
Computer-Aided Design Information System (CADIS): User's manual
[DE88-004365] 10 p1424 N88-18509
Guidelines for exchanging computerized information
[DE88-004736] 10 p1425 N88-18510
International geosphere-biosphere program: A study of global change
[PB88-142393] 11 p1510 N88-19021
AITI Test Report 87-002: Pratt and Whitney technical order transfer tests
[DE88-004045] 11 p1564 N88-19363
AITI Report 87-003: Honeywell technical order transfer tests
[DE88-004046] 11 p1564 N88-19364
District information system of National Information Centre
[PB88-134739] 11 p1565 N88-19373
Application of ARIADNE: A data bank-based information system for human physiology research --- Spacelab Anthrorack 12 p1662 N88-19962
KREME (Knowledge Representation, Editing and Modeling Environment): A user's introduction, phase 1
[AD-A188906] 12 p1681 N88-20052
Defending secrets, sharing data: New locks and keys for electronic information
[PB88-143185] 12 p1706 N88-20210
National Informatics Centre: Profile of services
[PB88-134135] 12 p1706 N88-20211
Design methodology for allocating data in a distributed database
[AD-A188826] 12 p1706 N88-20215
Implementing information systems/office automation in an Air Force environment
[AD-A188956] 12 p1707 N88-20218
A comparison of information system development methodologies
[AD-A188957] 12 p1707 N88-20219
Towards a tribology information system: The results of a Planning Workshop held at the National Bureau of Standards, July-August 1985
[PB88-168604] 14 p1918 N88-21448
Geometric modeling of flight information for graphical cockpit display
[AD-A190484] 15 p2021 N88-22043
Information systems for quality. Experience at the Nerviano Aeritalia plant. Avionic systems and equipment group
[ETN-88-92274] 15 p2148 N88-22821
The Scientific and Technical Information Network (STINET). Foundation for evolution
[AD-A189750] 15 p2148 N88-22822
Sources of digital spatial data for geographic information systems
[AD-A189788] 15 p2148 N88-22824
Data base design and implementation
[AD-A190414] 15 p2149 N88-22827
PPDS compas-primer
[DE88-701569] 16 p2266 N88-23554
Information and stochastic systems
[AD-A192167] 18 p2501 N88-24838
The human genome: Computational challenges
[DE88-006465] 18 p2549 N88-25131
Application of interactive graphic system (CAD/CAM) in the determination of process evolution in land use in the Ribeirao Preto municipality 19 p2684 N88-25956
The role of working memory in language comprehension
[AD-A192721] 20 p2833 N88-26805
SIMS: Single Interface to Multiple Systems
[AD-A192264] 20 p2837 N88-26832
Computer-aided writing
[AD-A192516] 20 p2838 N88-26837
Context of national information systems in developing countries: India and China in a comparative perspective
[PB88-109954] 20 p2882 N88-27111
Capitalizing on experience with intelligence gateway software
[AD-A193362] 21 p3028 N88-27971
Walter user's manual (Version 1.0)
[AD-A192542] 22 p3136 N88-28644
NASA information sciences and human factors program
[NASA-TM-4064] 22 p3166 N88-28856
A comparison of typical meteorological year solar radiation information with the SOLMET data base
[DE88-009242] 23 p3234 N88-29247
Advanced information processing system: Input/output network management software
[NASA-CR-181678] 23 p3264 N88-29431
Experiments in automatic phrase indexing for document retrieval: A comparison of syntactic and non-syntactic methods 23 p3296 N88-29634
EMPTAC (Electromagnetic Pulse Test Aircraft) user's guide
[AD-A195072] 24 p3360 N88-30006
Human factors report on information management requirements for next-generation manned bombers
[AD-A195870] 24 p3409 N88-30296
Telescience testbed pilot program
[NASA-CR-183207] 24 p3412 N88-30309
A shared-world conceptual model for integrating space station life sciences telescience operations
24 p3416 N88-30333
The second generation intelligent user interface for the crustal dynamics data information system
24 p3419 N88-30352
Knowledge-based integrated information systems engineering: Highlights and bibliography. Knowledge-Based Integrated Information Systems Engineering (KBIISE) Project, volume 1
[AD-A195850] 24 p3435 N88-30449
Technical opinions regarding knowledge-based integrated information systems engineering, volume 8
[AD-A195857] 24 p3436 N88-30454
Knowledge-Based Integrated Information Systems Development Methodologies Plan. Knowledge-Based Integrated Information Systems Engineering (KBIISE) report, volume 2
[AD-A195851] 24 p3436 N88-30455
Strategic, organizational and standardization aspects of integrated information systems, volume 6
[AD-A195855] 24 p3437 N88-30457
Integrating information systems in a major decentralized international organization, volume 7
[AD-A195856] 24 p3439 N88-30468

INFORMATION THEORY

Study, design, and evaluation of data reduction by encoding or information extraction. Part 1: Data generation analysis --- multispectral satellite imagery
[NLR-TR-85094-L-PT-1] 01 p0078 N88-10501
Study, design and evaluation of data reduction by encoding or information extraction. Part 2: Operational considerations --- multispectral satellite imagery
[NLR-TR-85094-L-PT-2] 01 p0079 N88-10502
Study, design and evaluation of data reduction by encoding or information extraction. Part 3: Algorithm design --- multispectral satellite imagery
[NLR-TR-85094-L-PT-3] 01 p0079 N88-10503
Study, design and evaluation of data reduction by encoding or information extraction. Part 4: Performance demonstration --- multispectral satellite imagery
[NLR-TR-85094-L-PT-4] 01 p0079 N88-10504
Study, design and evaluation of data reduction by encoding or information extraction. Part 5: Algorithm implementation aspects --- multispectral satellite imagery
[NLR-TR-85094-L-PT-5] 01 p0079 N88-10505
General potential surfaces and neural networks
[AD-A184484] 03 p0367 N88-12311
Bandwidth efficient block codes for M-ary PSK modulation
[NASA-CR-181543] 04 p0437 N88-12712
On detection of change points using mean vectors
[AD-A185581] 06 p0767 N88-14717
Local likelihood method in the problems related to change points
[AD-A185604] 06 p0768 N88-14718
Variable selection in logistic regression
[AD-A186032] 07 p0914 N88-15547
Discovery and problem solving: Triangulation as a weak heuristic 08 p1062 N88-16412
Conceptual information processing: A robust approach to KBS-DBMS integration 08 p1063 N88-16422
The linear dependency structure of covariance nonstationary time series
[AD-A186548] 09 p1232 N88-17383
Strong consistency of certain information theoretic criteria for model selection in calibration, discriminant analysis and canonical correlation analysis
[AD-A186584] 09 p1232 N88-17385
Resonance, information, and the primacy of process: Ancient light on modern information and communication theory and technology 10 p1424 N88-18506
Quantitative and qualitative assessments of the impact of linguistic theory on information science
10 p1424 N88-18507
Two new frameworks for learning
[AD-A187723] 11 p1534 N88-19162
A comparison of information system development methodologies
[AD-A188957] 12 p1707 N88-20219
Research in applied mathematics related to identification of noisy systems
[AD-A189355] 13 p1825 N88-20908
Instrumentation for scientific computing in neural networks, information science, artificial intelligence and applied mathematics
[AD-A189981] 15 p2106 N88-22549
Information and coding capacities of mismatched Gaussian channels
[AD-A190321] 15 p2124 N88-22665
Information capacity of Gaussian channels
[AD-A190316] 15 p2127 N88-22686
Coding capacity of discrete-time Gaussian and nonGaussian channels
[AD-A190318] 15 p2127 N88-22688
Error control techniques for satellite and space communications
[NASA-CR-182886] 17 p2332 N88-23922
Analysis and synthesis of decision-making organizations
[AD-A191948] 19 p2738 N88-26258
Modeling and evaluation of expert systems in decisionmaking organizations
[AD-A191951] 19 p2739 N88-26260
Survey of neural net paradigms for specification of discrete networks
[AD-A192682] 22 p3141 N88-28674
NASA information sciences and human factors program
[NASA-TM-4064] 22 p3166 N88-28856
On the design and optimization of distributed signal detection and parameter estimation systems
[AD-A193934] 23 p3266 N88-29446
Signals and systems 24 p3363 N88-30026
The bounded rationality constraint: Experimental and analytical results
[AD-A195897] 24 p3413 N88-30318

INFORMATION TRANSFER

Impressions, observations and comments on science and technology in Japan
[PB87-235743] 06 p0799 N88-14893
Computer aided design for Petri Nets
[AD-A186109] 07 p0902 N88-15465
DOE data exchange format specification, mechanical products/drafting: Version 1.2.2: CADCAM-045
[DE88-001923] 07 p0904 N88-15477
Information needs analysis for the Aeronautical Systems Division Executive Information System
[AD-A186912] 09 p1261 N88-17556
Airborne Wind Shear Detection and Warning Systems: First Combined Manufacturers' and Technologists' Conference
[NASA-CP-10006] 10 p1273 N88-17616
Information transfer in the National Airspace System
10 p1275 N88-17634
Minutes of the meeting of the Indo-US Subcommission on Science and Technology (8th) held at Washington, D.C. on September 22-24, 1986
[PB88-130158] 10 p1423 N88-18503
District information system of National Information Centre
[PB88-134739] 11 p1565 N88-19373
Design and implementation of VLSI prime factor algorithm processor
[AD-A190483] 15 p2112 N88-22580
Sky radiance distributions for thermal imaging backgrounds
[AD-A191135] 17 p2373 N88-24115
A cockpit natural language study - selected transcripts
[AD-A192972] 20 p2834 N88-26808
Barriers to Information Transfer and Approaches Toward Their Reduction
[AGARD-CP-430] 24 p3437 N88-30458
Linguistic and cultural barriers to the transfer of information 24 p3437 N88-30459
Political and economic barriers to information transfer
24 p3437 N88-30460
Information retrieval systems evolve-advances for easier and more successful use 24 p3438 N88-30462
Words: Keys or barriers to information transfer
24 p3438 N88-30464

Technical change needs organizational change
24 p3438 N88-30466
Using standards to break down information transfer barriers
24 p3439 N88-30467
INFORMATION TRANSMISSION
U DATA TRANSMISSION
INFRARED ABSORPTION
Reduction of temperature rise in high-speed photography
[NASA-TM-100222] 02 p0176 N88-11100
Direct infrared absorption of clusters in pulsed molecular beams
[DE87-014802] 02 p0236 N88-11490
Absorption of far IR-radiation by H2O-N2 complexes under atmospheric conditions 04 p0462 N88-12855
Radiation absorption in the infrared spectral range: A comparison between laboratory measurements and theoretical calculation illustrated by a H2O 2.7 micrometer 08 p1018 N88-16170
Ion content and infrared absorption of moist atmospheric air
[AD-A188839] 12 p1643 N88-19838
Infrared absorption spectroscopy and chemical kinetics of free radicals
[DE88-006536] 15 p2033 N88-22112
Infrared differential absorption lidar for vapor detection
[AD-A190600] 15 p2098 N88-22497
Calculation of far infrared absorption in B poly(dA).poly(dT)
[AD-A193128] 21 p2918 N88-27318
Survey of material for an infrared-opaque coating
[NASA-TM-88204] 22 p3153 N88-28757
INFRARED ASTRONOMY
Circumstellar radio molecular lines
02 p0252 N88-11595
Study of solid state photomultiplier
[NASA-CR-177465] 05 p0583 N88-13556
Activities report in interplanetary space physics
[IFSI-86-5] 05 p0659 N88-14047
A new liquid helium-cooled Fabry-Perot spectrometer used in a far infrared astronomical balloon experiment
08 p1028 N88-16224
Justification and prospects of observations of interstellar, far-infrared emission lines, using a small-sized balloon-borne telescope 08 p1032 N88-16254
PRONAOS: A submillimeter facility --- astronomical balloon 08 p1032 N88-16255
ESA Bulletin No. 8
[ETN-87-90513] 09 p1122 N88-16718
Infrared astronomy: Why and how?
09 p1123 N88-16722
Experiment control and data system for an infrared detector array with maximum sensitivity
[ETN-88-91497] 09 p1136 N88-16813
Integrated focal plane star sensor
[OG-RT/86-0156] 09 p1262 N88-17562
Workshop on Technology Development Issues for the Large Deployable Reflector (LDR)
[NASA-CP-2407] 12 p1710 N88-20235
Advanced components for spaceborne infrared astronomy
[NASA-CR-177470] 13 p1772 N88-20601
Analysis of deep sky sources found by the infrared astronomy satellite
[AD-A189605] 13 p1853 N88-21089
Far-infrared (120-300 micron) observations of the Carina Nebula 14 p1993 N88-21876
The galactic nucleus at mm-, sub-mm and far-infrared wavelengths
[MPE-PREPRINT-102] 16 p2288 N88-23700
Submillimeter and far infrared line observations of M17 SW: A clumpy molecular cloud penetrated by UV radiation
[NASA-CR-182866] 16 p2288 N88-23701
Balloon-borne three-meter telescope for far-infrared and submillimeter astronomy
[NASA-CR-182924] 17 p2449 N88-24550
Infrared astronomy at extremely faint light levels in support of the LAIRTS program
[AD-A191497] 18 p2592 N88-25404
Study of a safe attitude for the Infrared Space Observatory (ISO) during perigee pass
[SNIAS-881-440-113] 23 p3185 N88-28954
Far infrared supplement: Catalog of infrared observations, second edition
[NASA-RP-1205] 24 p3452 N88-30545
INFRARED ASTRONOMY SATELLITE
Optical spectroscopy of IRAS sources with infrared emission bands. 1: IRAS 21282+5050 and the diffuse interstellar bands
[NASA-CR-181387] 01 p0094 N88-10611
Emission features in IRAS LRS spectra of MS, S and CS stars 04 p0514 N88-13163
IRAS and cool stellar mass loss
04 p0515 N88-13166
Study of interactional effects in the chemisorbed layer by Infrared Reflection Absorption Spectroscopy (IRAS)
[DE88-001808] 06 p0680 N88-14164
Analysis of deep sky sources found by the infrared astronomy satellite
[AD-A189605] 13 p1853 N88-21089
INFRARED DETECTORS
NT FLIR DETECTORS
Coherent infrared detection, volume B --- CO2 laser intersatellite data link
[ESA-CR(P)-2392-VOL-1] 01 p0034 N88-10218
Coherent infrared detection, volume D --- CO2 laser intersatellite data link
[ESA-CR(P)-2392-VOL-2] 01 p0034 N88-10219
Automatic seam welding with infrared sensor feedback
[DE87-013556] 01 p0055 N88-10352
A study of infrared missile seekers and the countermeasure techniques employed to defeat them
[ETN-87-90927] 02 p0131 N88-10622
Monitored background radiometer
02 p0133 N88-10831
Exosat results on the dMe flare Star Wolf 630AB and on VB 8 04 p0512 N88-13151
Evaluation of a cryogenic refrigerator for cooling focal plane instrumentation --- satellite instruments
[BAE-TP-8095-VOL-1] 05 p0572 N88-13485
Evaluation of a cryogenic refrigerator for cooling focal plane instrumentation. Appendix B: Accommodation study --- satellite instruments
[BAE-TP-8095-VOL-2] 05 p0572 N88-13486
Integrated photo-responsive metal oxide semiconductor circuit
[NASA-CASE-GSC-12782-1] 06 p0696 N88-14271
Visible and infrared linear detector arrays for the Airborne Visible/Infrared Imaging Spectrometer (AVIRIS)
06 p0706 N88-14329
AVHRR/HIRS (Advanced Very High Resolution Radiometer/High Resolution Infra-Red Sounder) operational method for satellite based sea surface temperature determination
[PB88-107594] 06 p0708 N88-14340
Description of data on the Nimbus 7 LIMS map archive tape: Water vapor and nitrogen dioxide
[NASA-TP-2761] 06 p0744 N88-14572
Experiment control and data system for an infrared detector array with maximum sensitivity
[ETN-88-91497] 09 p1136 N88-16813
Fabrication and packaging of discontinuous MIM (Metal-Insulator-Metal) film arrays for efficient MM wave and IR detection and mixing
[AD-A186809] 09 p1146 N88-16869
IRAC test report. Gallium doped silicon band 2: Read noise and dark current
[NASA-TM-87813] 09 p1159 N88-16945
Integrated focal plane star sensor
[OG-RT/86-0156] 09 p1262 N88-17562
Depolarized infrared reflectance from dry and wetted surfaces
[AD-A188213] 11 p1492 N88-18903
Project SKYLITE: A design exploration
[AD-A187906] 11 p1511 N88-19030
HP-41CX programs for HgCdTe detectors and IR systems
[AD-A188935] 12 p1692 N88-20120
Procedure for detection and identification of a helicopter
[NASA-TT-20234] 13 p1722 N88-20297
Advanced components for spaceborne infrared astronomy
[NASA-CR-177470] 13 p1772 N88-20601
Passive autonomous infrared sensor technology
[AD-A188698] 13 p1839 N88-21005
Analysis of deep sky sources found by the infrared astronomy satellite
[AD-A189605] 13 p1853 N88-21089
Laser pulse detection with infrared range semiconductor detectors
[DE88-700857] 14 p1914 N88-21432
Mid infrared multichannel focal plane breadboard --- pushbroom sensors
[RT-87/014] 14 p1982 N88-21827
Hybrid PV HgCdTe IR detectors technology reliability and failure program: Environmental stress testing plan
[AD-A191165] 16 p2211 N88-23195
Novel silicon Schottky barrier infrared imaging arrays
17 p2439 N88-24510
Infrared detectors based on the photon drag effect and intersubband absorption by a two-dimensional electron gas 20 p2867 N88-27024
Photodiodes for optical communication in the near infrared
[ETN-88-92379] 21 p3016 N88-27900
Development of 30 micrometers extrinsic silicon multiplexed infrared deterctor array
[NASA-CR-177446] 22 p3082 N88-28301
Infrared detection using Rydberg atoms
[AD-A194308] 23 p3191 N88-28990
Evaluation of atmospheric effects for operational tactical decision aid
[AD-A194205] 23 p3232 N88-29236
Multi-sensory tracking mount control
[AD-A194675] 23 p3249 N88-29339
Integration of LANTIRN (Low Altitude Navigation and Targeting Infrared for Night) into operational fighter training
[AD-A194906] 24 p3325 N88-29799
Development of a unit cell for a Ge:Ga detector array
[NASA-CR-177445] 24 p3375 N88-30100
A system study with an infrared sensitive microelectronic image sensor
[FOA-C-30481-3.1] 24 p3429 N88-30407
Principles of the optical differential thermal analysis
[AD-A195951] 24 p3429 N88-30408
Estimation of soil temperature profile from remote microwave and IR measurements
24 p3450 N88-30532
INFRARED HORIZON SCANNERS
U HORIZON SCANNERS
U INFRARED SCANNERS
INFRARED IMAGERY
Tropical cyclone center locations from enhanced infrared satellite imagery
[PB87-213450] 01 p0071 N88-10455
Psychophysical considerations in measuring MRTD with staring arrays --- minimum resolvable temperature difference (MRTD)
[RSRE-MEMO-4031] 01 p0076 N88-10487
The use of satellite IR data in the enhancement of surface thermal fields 02 p0202 N88-11260
Pyroelectric line scanner for remote IR imaging of vehicles
[DE87-012127] 02 p0235 N88-11484
An application of a gradient relaxation method to noisy infrared images
[AD-A184666] 03 p0377 N88-12371
Aircraft engine exhaust plume dynamics
[AD-A184238] 04 p0400 N88-12488
Airborne Visible/Infrared Imaging Spectrometer (AVIRIS). A description of the sensor, ground data processing facility, laboratory calibration, and first results
[NASA-CR-182365] 06 p0705 N88-14325
A system overview of the Airborne Visible/Infrared Imaging Spectrometer (AVIRIS)
06 p0705 N88-14326
AVIRIS ground data-processing system
06 p0707 N88-14333
Spectral and radiometric calibration of the Airborne Visible/Infrared Imaging Spectrometer
06 p0707 N88-14334
First results from the Airborne Visible/Infrared Imaging Spectrometer (AVIRIS) 06 p0707 N88-14335
Experimental design of a piloted helicopter off-axis-tracking simulation using a helmet mounted display
[AD-A186228] 07 p0820 N88-14982
Commercial applications and scientific research requirements for thermal-infrared observations of terrestrial surfaces
[NASA-TM-89704] 08 p1019 N88-16179
Technical assessment of the joint CSIRO/Bureau of Meteorology proposal for a geostationary imager/sounder over the Australian region
[RTP-15] 09 p1135 N88-16811
Thermal wave imaging
[AD-A186810] 09 p1177 N88-17046
Sea surface current estimates off central California as derived from enhanced AVHRR (Advanced Very High Resolution Radiometer) infrared images
[AD-A186867] 09 p1194 N88-17155
Passive autonomous infrared sensor technology
[AD-A188698] 13 p1839 N88-21005
The application of thermal imaging sensors and image processing techniques to a short range surface-to-air missile system
[ETN-88-92080] 14 p1982 N88-21829
Infrared-sensitive spatial light modulator
[AD-A190391] 15 p2134 N88-22729
Validate algorithms for the determination of rainfall rates from SSM/I microwave satellite imagery
[AD-A188769] 16 p2233 N88-23337
Infrared radiometric technique in temperature measurement 17 p2330 N88-23913
Real time thermal imaging of high temperature semiconductor melts 17 p2330 N88-23914
Enhanced infra-red picture of LR-FAX for spring and autumn seasons 17 p2351 N88-24011
An update on remote measurement of soil moisture over vegetation using infrared temperature measurements: A FIFE perspective
[NASA-CR-182926] 17 p2370 N88-24109

Sky radiance distributions for thermal imaging backgrounds
[AD-A191135] 17 p2373 N88-24115
Thermographic detection of buried debonds
[AD-A192115] 18 p2475 N88-24680
Stress analysis using infrared thermography
[ETN-88-92169] 20 p2816 N88-26705
Cyrogenic test facilities for an optical cryomechanism qualification
[REPT-881-440-116] 21 p2901 N88-27219
IR (infrared) sky radiance distributions in the marine boundary layer
[AD-A193683] 22 p3119 N88-28531
A probabilistic model of the apparent radiance of a rough sea
[AD-A193867] 22 p3129 N88-28602
An objective technique for Arctic cloud analysis using multispectral AVHRR (Advanced Very High Resolution Radiometer) satellite imagery
[AD-A194732] 23 p3235 N88-29250
A system study with an infrared sensitive microelectronic image sensor
[FOA-C-30481-3.1] 24 p3429 N88-30407
Common modules: A success story
[AD-A195937] 24 p3430 N88-30415

INFRARED INSTRUMENTS
NT FLIR DETECTORS
NT INFRARED DETECTORS
NT INFRARED INTERFEROMETERS
NT INFRARED SCANNERS
NT INFRARED SPECTROMETERS
NT INFRARED SPECTROPHOTOMETERS
Scene simulation for passive IR systems
02 p0137 N88-10861
Infrared low-level wind shear work
10 p1275 N88-17628
Specification for an infrared satellite surveillance system for the detection of aircraft
[AD-A189592] 13 p1797 N88-20746
Infrared simulation model Sensor Atmosphere Target (SENSAT)-2A
[DFVLR-FB-88-01] 16 p2165 N88-22910
A disposable liquid microcell for near-infrared reflectance analysis
[AD-A192190] 18 p2575 N88-25298
Infrared devices using semiconductor quantum wells
[RSRE-MEMO-4018] 22 p3157 N88-28788
Common modules: A success story
[AD-A195937] 24 p3430 N88-30415

INFRARED INTERFEROMETERS
A two-wavelength infrared interferometer/polarimeter system for CIT (Compact Ignition Tokamak)
[DE88-007681] 18 p2579 N88-25321

INFRARED LASERS
IR laser excitation in molecules: Chaos and diffusive energy growth
[DE87-013147] 02 p0178 N88-11105
Distributed feedback effects in lasers and high gain laser instabilities in optically pumped CH3F
03 p0329 N88-12079
Dynamic restructuring of pulsed CO2 laser frequency and multiple-peak generation in a cell with IR-absorbing gas in the resonator 07 p0919 N88-15580
Dielectric behavior of electromagnetic (EM) windows materials irradiated by a CW CO2 high-power laser --- hypersonic/reentry vehicles
[ISL-CO-239/86] 09 p1154 N88-16913
Continuously frequency-tunable high-pressure CO2-laser with plasmatic cathode
09 p1238 N88-17418
Energy transfer studies with lasers
[DE88-004864] 10 p1337 N88-17991
Influence of nonlinear spectroscopic effects on atmospheric propagation of intense laser radiation at 10.6 microns wavelength 13 p1789 N88-20705
Effect of atmospheric turbulence on the bit error probability of a space to ground near infrared laser communications link using binary pulse position modulation and an avalanche photodiode detector
[NASA-TM-100699] 14 p1873 N88-21189
Laser technology: CO2 lasers and laser optics
[ETN-88-91469] 14 p1915 N88-21441
Nonlinearly tunable wideband emission of infrared radiation by Al2O3:Ti laser 14 p1970 N88-21758
Diode laser spectroscopy of chemical moieties at surfaces
[AD-A190710] 15 p2036 N88-22127
Generation of tunable coherent radiation in 3 micrometers-5 micrometers region using semiconductor lasers in external cavities
[AD-A190860] 16 p2212 N88-23202
The new UCSB (University of California, Santa Barbara) compact far-infrared FEL
[AD-A190864] 16 p2212 N88-23203
Infrared and far-infrared laser development for plasma diagnostics at Oak Ridge National Laboratory
[DE88-007262] 19 p2674 N88-25904
Predicting the durability of adhesives and coatings by remote detection of hidden defects and coating-thickness irregularities: A theoretical and numerical study
24 p3355 N88-29972

INFRARED MASERS
U INFRARED LASERS

INFRARED PHOTOGRAPHY
IRAC test report. Gallium doped silicon band 2: Read noise and dark current
[NASA-TM-87813] 09 p1159 N88-16945

INFRARED PHOTOMETRY
A search for very low mass (brown dwarf) stars as wide binaries using a seven element infrared camera-photometer 04 p0512 N88-13150
IRAS and near IR observations of active binaries
04 p0518 N88-13186
Tailorable infrared sensing device with strain layer superlattice structure
[NASA-CASE-NPO-16607-1-CU]
06 p0788 N88-14836
Infrared constraints on the nature of dark matter
13 p1855 N88-21102
Near-infrared observations of cepheids: The distance to M33 15 p2152 N88-22846

INFRARED RADAR
A very wide frequency band pulsed/IF radar system
[NASA-CR-182889] 16 p2190 N88-23059

INFRARED RADIATION
NT FAR INFRARED RADIATION
NT NEAR INFRARED RADIATION
Status of the solar and infrared radiation submodels in the LLNL 1-D and 2-D chemical-transport models
[DE87-014320] 01 p0069 N88-10441
GOES observations for the FIRE/SRB Wisconsin experiment region from October 11 through November 2, 1986
[NASA-TM-100485] 01 p0071 N88-10453
Mid infrared LHS system packaging using flexible waveguides
[NASA-CR-181192] 01 p0093 N88-10607
Infra-red lamp panel study and assessment application to thermal vacuum testing of sigma telescope
02 p0132 N88-10830
Thermal testing by internal IR heating of the FEP module 02 p0136 N88-10854
A new type of lamp and reflector for I.R. simulation
02 p0136 N88-10855
Evaluation of the infrared test method for the olympus thermal balance tests 02 p0136 N88-10856
IR laser excitation in molecules: Chaos and diffusive energy growth
[DE87-013147] 02 p0178 N88-11105
The effects of minor trace gases on the transfer of thermal infrared radiation through the Earth's atmosphere 04 p0488 N88-12893
The giant spot on Il Peg in 1986
04 p0508 N88-13120
Macroscopic distribution of fiber finish
[DCQ/L-48-263/F] 07 p0827 N88-15013
Satellite techniques of solar resource assessment for focusing and non-focusing solar collector systems
[DE88-001657] 07 p0874 N88-15298
Intracavity spectrum analyzer with NaF:F2(+):F3(-) crystal laser for long-wave IR wave band
07 p0919 N88-15584
Infrared emission and tidal interactions of spiral galaxies 07 p0923 N88-15611
Catalog of infrared observations. Part 2: Appendixes
[NASA-RP-1196-PT-2-ED-2] 08 p1099 N88-16615
Development of infrared techniques for testing spacecraft 09 p1128 N88-16772
Radiant power degradation of silicon-doped gallium arsenide and gallium aluminum arsenide infrared light-emitting diodes
[AD-A186726] 09 p1157 N88-16935
Variable band gap materials for thermophotovoltaic generators
[AD-A186858] 09 p1186 N88-17104
PbSnTe photovoltaic detectors for operation in the 2-14 micron band
[INPE-4252-PRE/1125] 11 p1506 N88-19008
Some applications of surface Raman and infrared spectroscopies to mechanistic electrochemistry involved adsorbed species
[AD-A188777] 12 p1606 N88-19602
Test methodology for infrared tubular heaters
[PB88-160916] 12 p1626 N88-19728
DIRBE External Calibrater (DEC)
[NASA-CR-180761] 12 p1631 N88-19760
Results of infrared spectrometer experiment. 1: Infrared radiation of parent molecules in Halley's Comet
13 p1726 N88-20325
Analysis of hydrocarbon band 3.35 in spectrum of Halley's Comet using data from infrared spectrometer on Vega-1 spacecraft 13 p1727 N88-20327
Dynamical modeling of marine boundary layer convection 13 p1797 N88-20750
Analysis of deep sky sources found by the infrared astronomy satellite
[AD-A189605] 13 p1853 N88-21089
Infrared differential absorption lidar for vapor detection
[AD-A190600] 15 p2098 N88-22497
Studies of surfaces using optical sum-frequency generation
[DE88-006334] 15 p2131 N88-22715
Dispersion measurements of microcrystals in the near ultraviolet and infrared
[DE88-006234] 15 p2145 N88-22800
Tunable optical sources/growth and characterization of nonlinear optical materials
[AD-A190874] 16 p2274 N88-23608
Estimation of total Outgoing Longwave Radiation (OLR) flux from geostationary meteorological satellite infrared window radiance 17 p2351 N88-24006
Bimolecular reactions and energy-transfer processes of highly vibrationally excited molecules related to energetic materials
[AD-A189013] 18 p2571 N88-25270
Calculation of space station infrared irradiance from atmosphere-induced emissions
18 p2591 N88-25396
Regulatory biochemical and metabolic responses in photoreceptors
[AD-A192898] 20 p2831 N88-26794
Far- and mid-infrared properties of metal-insulator composite materials
[AD-A193227] 21 p2905 N88-27236
Development of radiation and cloud parameterization programs for AFGL (Air Force Geophysics Laboratory) global models
[AD-A193369] 21 p2973 N88-27658
A probabilistic model of the apparent radiance of a rough sea
[AD-A193867] 22 p3129 N88-28602
MIDIR (Mid-Infrared) laser, phase 1
[AD-A193935] 23 p3220 N88-29166
Miniature respiratory sensor
[AD-A193430] 23 p3243 N88-29300
Principles of the optical differential thermal analysis
[AD-A195951] 24 p3429 N88-30408
Radio and infrared properties of young stars
[NASA-CR-183252] 24 p3459 N88-30579

INFRARED RADIOMETERS
NT ADVANCED VERY HIGH RESOLUTION RADIOMETER
Forward looking wind shear detection
10 p1275 N88-17629
Noncontact Temperature Measurement
[NASA-CP-2503] 17 p2327 N88-23895
Radiation thermometry: The measurement problem
17 p2328 N88-23896
The role of fiberoptics in remote temperature measurement 17 p2329 N88-23909
Infrared radiometric technique in temperature measurement 17 p2330 N88-23913

INFRARED REFLECTION
Reduction of temperature rise in high-speed photography
[NASA-TM-100222] 02 p0176 N88-11100
Study of interactional effects in the chemisorbed layer by Infrared Reflection Absorption Spectroscopy (IRAS)
[DE88-001808] 06 p0680 N88-14164
Some applications of surface Raman and infrared spectroscopies to mechanistic electrochemistry involved adsorbed species
[AD-A188777] 12 p1606 N88-19602

INFRARED SCANNERS
Improved geostationary satellite soundings for the mesoscale weather analysis/forecast operation
02 p0200 N88-11252
VAS products as indices of thunderstorms and severe local storm potential --- Visible and Infrared Spin Scan Radiometer Atmospheric Sounder (VAS)
02 p0201 N88-11253
Operational cloud-clearing techniques of VAS radiance data --- Visible and Infrared Spin Scan Radiometer Atmospheric Sounder (VAS) 02 p0201 N88-11256
Measurement from satellites of land surface parameters and fluxes in the thermal infrared bands: Problems and methods 14 p1937 N88-21557

INFRARED SIGNATURES
A probabilistic model of the apparent radiance of a rough sea
[AD-A193867] 22 p3129 N88-28602

INFRARED SOURCES (ASTRONOMY)
NT INFRARED STARS

Optical spectroscopy of IRAS sources with infrared emission bands. 1: IRAS 21282+5050 and the diffuse interstellar bands
[NASA-CR-181387] 01 p0094 N88-10611
Catalog of infrared observations. Part 1: Data
[NASA-RP-1196-PT-1-ED-2] 07 p0944 N88-15738
Catalog of infrared observations. Part 2: Appendixes
[NASA-RP-1196-PT-2-ED-2] 08 p1099 N88-16615
Far infrared supplement: Catalog of infrared observations, second edition
[NASA-RP-1205] 24 p3452 N88-30545

INFRARED SPACE OBSERVATORY (ISO)
Development of a cryogenic stepping drive for ISO/LWS 14 p1878 N88-21220
Cryogenic mechanism for ISO camera 14 p1878 N88-21221

INFRARED SPECTRA
Picosecond CO2 laser interactions with polyatomic molecules
[DE87-012072] 01 p0051 N88-10327
Development of many-body methods for flame chemistry and large molecule applications
[AD-A184451] 03 p0284 N88-11789
Spectroscopic and retrieval studies in support of SCRIBE (Stratospheric Cryogenic Interferometer Balloon Experiment)
[AD-A184037] 03 p0351 N88-12216
Far-infrared spectra of lithium deposited on a gold electrode: Interpretation using a cluster model
[AD-A184231] 04 p0495 N88-13050
Infrared excesses of barium stars 04 p0516 N88-13174
The contribution of accretion luminosity to the infrared spectra of T Tauri stars: A possible test 04 p0518 N88-13183
IRAS and near IR observations of active binaries 04 p0518 N88-13186
Measuring near infrared spectral reflectance changes from water stressed conifer stands with AIS-2 05 p0613 N88-13765
High energy molecules of high symmetry
[AD-A185385] 05 p0647 N88-13965
Extinction by dielectric particles at optical and infrared wavelength
[AD-A184818] 05 p0650 N88-13981
Study of interactional effects in the chemisorbed layer by Infrared Reflection Absorption Spectroscopy (IRAS)
[DE88-001808] 06 p0680 N88-14164
Lightning spectra in the near infrared
[DE88-002218] 07 p0880 N88-15341
Christiansen effect in infrared spectra of soil-derived atmospheric dusts
[AD-A187071] 09 p1248 N88-17479
Memory effects on infrared adsorbate spectra
[AD-A186976] 09 p1253 N88-17512
Crystalline sulfur dioxide: Crystal field splittings, absolute band intensities and complex refractive indices derived from infrared spectra
[NASA-CR-182502] 09 p1258 N88-17547
Simulation of infrared spectra
[AD-A187881] 11 p1453 N88-18658
Growth and characteristics of materials for tunable lasers in the near infrared spectral region
[NASA-CR-182501] 11 p1491 N88-18901
In-situ vibrational spectroscopy of specifically adsorbed azide on silver electrodes
[AD-A188511] 12 p1605 N88-19600
FTIR (Fourier Transform Infrared) and FTNMR (Fourier Transform Nuclear Magnetic Resonance) study of organophosphorus surface reactions
[AD-A188337] 12 p1609 N88-19625
Synchronous measurements of effective photon path length in visible and near-IR spectral regions in real cloud systems 13 p1790 N88-20706
Stratospheric trace gas distributions from fair infrared thermal emission spectroscopy 13 p1797 N88-20749
An investigation of the infrared emission spectra of carbon condensates 14 p1886 N88-21272
Measurement of the water content of soil from space and application to the regional water balance 14 p1938 N88-21561
Effect of Mg impurity on local vibrations of U-centers in LiF lattice 14 p1969 N88-21753
Optical and hydrodynamic implications of Comet Halley dust size distribution 14 p2003 N88-21939
Nature of Comet Halley's organic grains inferred from infrared spectra 14 p2007 N88-21973
Extension of the vegetation mission to thermal infrared spectral bands
[CNES-T-86/224-CT/DRT/TIT/IO] 16 p2227 N88-23299
Time-resolved studies of free radicals and laser-initiated chain reactions
[DE88-006569] 16 p2266 N88-23553
Optical constants of minerals and other materials from the millimeter to the ultraviolet
[AD-A192210] 18 p2482 N88-24724
Development of an experimental system for studying fast transient ignition phenomena
[DE88-011917] 21 p2911 N88-27276

INFRARED SPECTROMETERS
Balloon-based infrared solar occultation measurements of stratospheric O3, H2O, HNO3 and CFC-12
[NOAA-TR-NESDIS-34] 01 p0068 N88-10438
Direct infrared absorption of clusters in pulsed molecular beams
[DE87-014802] 02 p0236 N88-11490
Complementary information between UV and IR for remote sensing of total ozone 05 p0619 N88-13800
Airborne Visible/Infrared Imaging Spectrometer (AVIRIS) spectrometer design and performance 06 p0706 N88-14327
AVIRIS foreoptics, fiber optics and on-board calibrator 06 p0706 N88-14328
Visible and infrared linear detector arrays for the Airborne Visible/Infrared Imaging Spectrometer (AVIRIS) 06 p0706 N88-14329
AVIRIS scan drive design and performance 06 p0706 N88-14330
Signal chain for the Airborne Visible/Infrared Imaging Spectrometer (AVIRIS) 06 p0706 N88-14331
AVIRIS onboard data handling and control 06 p0706 N88-14332
AVIRIS ground data-processing system 06 p0707 N88-14333
Spectral and radiometric calibration of the Airborne Visible/Infrared Imaging Spectrometer 06 p0707 N88-14334
First results from the Airborne Visible/Infrared Imaging Spectrometer (AVIRIS) 06 p0707 N88-14335
A new liquid helium-cooled Fabry-Perot spectrometer used in a far infrared astronomical balloon experiment 08 p1028 N88-16224
The Cryogenic Infrared Spectrometer and Telescope for the Atmosphere (CRISTA) experiment on Astro-SPAS 08 p1034 N88-16270
Characteristics of an Ebert monochromator for an infrared spectrometer in the wavelength range 1 micrometer to 15 micrometers
[AD-A186945] 09 p1166 N88-16991
Results of infrared spectrometer experiment. 1: Infrared radiation of parent molecules in Halley's Comet 13 p1726 N88-20325
Velocity resolved far-infrared spectroscopy of galactic sources 13 p1854 N88-21099
Calibration and data reduction techniques for the AFGL infrared array spectrometer 21 p2927 N88-27374

INFRARED SPECTROPHOTOMETERS
NBS (National Bureau of Standards) measurement services: Spectral reflectance
[PB88-109905] 06 p0779 N88-14785
Extension of the vegetation mission to thermal infrared spectral bands
[CNES-T-86/224-CT/DRT/TIT/IO] 16 p2227 N88-23299

INFRARED SPECTROSCOPY
Far infrared Fourier transform spectroscopy of semiconductors
[DE88-000188] 04 p0499 N88-13072
Time series infrared spectroscopy of long period variables 04 p0516 N88-13172
Use of lasers with F sub A(II)-color center KCl:Li crystals in the intraresonator laser spectroscopy method 06 p0769 N88-14729
Photoacoustic infrared laser spectroscopy for analyzing gaseous contaminants
[ETN-88-90805] 07 p0831 N88-15041
Long range reconnaissance of trace gases: A special aspect of emission spectroscopy 08 p1018 N88-16172
Monolayer films prepared by the spontaneous self-assembly of symmetrical and unsymmetrical dialkyl sulfides from solution onto gold substrates: Structure, properties, and reactivity of constituent functional groups
[AD-A186717] 09 p1137 N88-16814
An infra-red investigation of HAN (Hydroxylammonium Nitrate)-based liquid propellants
[AD-A187226] 10 p1307 N88-17815
Study of the vibrational modes of subsurface oxygen on Al (111) using diode laser infrared reflection-absorption spectroscopy
[AD-A188322] 12 p1632 N88-19769
Results of infrared spectrometer experiment. 2: Infrared radiometry of nucleus of Halley's Comet 13 p1727 N88-20326
Analysis of hydrocarbon band 3.35 in spectrum of Halley's Comet using data from infrared spectrometer on Vega-1 spacecraft 13 p1727 N88-20327
Molecular collision processes in gases and at surfaces
[AD-A189518] 13 p1836 N88-20982
Infrared reflection-absorption spectroscopy of hyperfine layers on surfaces of semiconductors and dielectrics 14 p1969 N88-21755
The spectroscopy and reaction kinetics of coordinatively unsaturated metal carbonyls
[AD-A190533] 15 p2035 N88-22124
Diode laser spectroscopy of chemical moieties at surfaces
[AD-A190710] 15 p2036 N88-22127
Excitations in magnetic low-dimensional systems: A spectroscopic study
[ETN-88-92230] 15 p2129 N88-22697
Infrared spectroscopy of H3(+) 16 p2268 N88-23585
Spectral radiometry: Methods, measuring techniques, and applications --- conference
[PTB-OPT-24] 16 p2271 N88-23585
Multiplex methods in infrared spectrometry 16 p2271 N88-23588
Spectroscopy of one-dimensional subbands on InSb 20 p2864 N88-27007
Attenuated total reflectance FT-IR spectroscopy to measure interfacial reaction kinetics at silica surfaces
[AD-A196330] 24 p3344 N88-29908
Photoacoustic Fourier transform infrared spectroscopy. An early detection technique for coatings degradation 24 p3354 N88-29968

INFRARED STARS
A search for very low mass (brown dwarf) stars as wide binaries using a seven element infrared camera-photometer 04 p0512 N88-13150
Analysis of deep sky sources found by the infrared astronomy satellite
[AD-A189605] 13 p1853 N88-21089

INFRARED SUPPRESSION
A technique for wing suppressed IR sampling 19 p2658 N88-25794

INFRARED TELESCOPES
NT SPACE INFRARED TELESCOPE FACILITY
PRONAOS: A submillimeter facility --- astronomical balloon 08 p1032 N88-16255
The Cryogenic Infrared Spectrometer and Telescope for the Atmosphere (CRISTA) experiment on Astro-SPAS 08 p1034 N88-16270
Multisurface control mechanism for a deployable antenna: Far Infrared and Submillimeter Space Telescope (FIRST) technology study
[RP-FA-D003] 09 p1135 N88-16807
Workshop on Technology Development Issues for the Large Deployable Reflector (LDR)
[NASA-CP-2407] 12 p1710 N88-20235
Design of a linear actuator and breadboard test result --- far IR telescope 14 p1877 N88-21217
Photoelastic model tests of the Dornier linear actuator --- far IR telescope 14 p1877 N88-21218
Fine adjustment mechanism for FIRST 14 p1878 N88-21219
Far-infrared (120-300 micron) observations of the Carina Nebula 14 p1993 N88-21876
Telescope illumination and beam measurements for submillimeter astronomy
[MPE-PREPRINT-88] 16 p2288 N88-23699
Balloon-borne three-meter telescope for far-infrared and submillimeter astronomy
[NASA-CR-182924] 17 p2449 N88-24550
Utilization of the IR telescope gimbaling system as a stabilized pointing platform for balloon payloads. Volume 1: Technical results
[NASA-CR-179339] 18 p2522 N88-24962
Far infrared spectroscopy telescope (FIRST) inflatable thermal shield, phase 1
[SR/FIS/108(87)CZ] 24 p3453 N88-30552

INFRARED TRACKING
Passive autonomous infrared sensor technology
[AD-A188[illegible]] 13 p1839 N88-21005

INFRARED WINDOWS
A rapid polishing method for KBr and NaCl infrared windows
[DE88-002480] 07 p0862 N88-15229
Estimation of total Outgoing Longwave Radiation (OLR) flux from geostationary meteorological satellite infrared window radiance 17 p2351 N88-24006
Growth and characterization of CuGaS2, CuAlS2 and CuGa0.9Al0.1S2 single crystals
[AD-A192963] 21 p3021 N88-27930
An organometallic route to micron-sized whiskers of zinc sulfide
[AD-A195889] 24 p3430 N88-30414

INFRASONIC FREQUENCIES
Mechanisms mediating the perception of complex acoustic patterns
[AD-A190112] 15 p2130 N88-22705
Surface disturbances produced by low-level, subsonic B-1 aircraft
[AD-A192257] 20 p2824 N88-26752

INGESTION (BIOLOGY)
NT DRINKING
NT GRAZING

INGESTION (ENGINES)
A numerical study of the hot gas environment around a STOVL aircraft in ground proximity
[NASA-TM-100895] 17 p2295 N88-23729

INGOTS
Compositional redistribution during casting of Hg sub 0.8 Cd sub 0.2 Te alloys
[NASA-TM-101151] 17 p2326 N88-23893

INHALATION
U RESPIRATION

INHIBITION (PSYCHOLOGY)
Distraction and inhibition in continuous CRT performance: A replication and some new findings
[PB88-150941] 13 p1811 N88-20821

INHIBITORS
NT WEAR INHIBITORS
Proceedings of the 1987 Tri-Service Conference on Corrosion, Volume 2
[AD-A189660] 17 p2319 N88-23847
Development of microencapsulated DNBM quaternary ammonium inhibitors for paints
17 p2319 N88-23851
Low doses of atropine sulfate impair retention of a well-learned spatial task
[AD-A194065] 23 p3237 N88-29266

INHOMOGENEITY
Eddy current density in wedge-shaped conducting cylinders with inhomogeneous conductivity
[ETN-87-90404] 01 p0042 N88-10268
Effect of optical inhomogeneities on space coherence of radiation emitted by laser with unstable resonator
06 p0771 N88-14738
Evolution of spectral densities in weakly inhomogeneous plasmas
[PB87-137402] 06 p0784 N88-14811
Analysis of electromagnetic wave propagation in slightly inhomogeneous hollow waveguides
[DFVLR-FB-87-23] 09 p1152 N88-16904
New method of examining micrononhomogeneity of local centers in high-resistivity semiconductor materials under scanning electron microscope 14 p1969 N88-21754
Wave energy flow conservation for propagation in inhomogeneous Vlasov-Maxwell equilibria
[DE88-006705] 15 p2055 N88-22251
Parametric instabilities of inhomogeneous plasma near the lower-hybrid resonance
[DE88-701201] 15 p2137 N88-22748
Statistical fine structure in the inhomogeneously broadened electronic origin of pentacene in p-terphenyl
[AD-A191211] 16 p2176 N88-22968
Experimental investigation of simplest inhomogeneities in cylindrical slit line
[DE88-702388] 21 p2933 N88-27418

INITIAL VALUE PROBLEMS
U BOUNDARY VALUE PROBLEMS

INITIATION
A nondissipative Pyrotechnic Arming and Firing Unit (PAFU)
[CRA/REPO/8019] 02 p0155 N88-10974
Shock initiation studies on heterogeneous explosives
[DE88-008661] 21 p2923 N88-27351

INITIATORS (EXPLOSIVES)
NT BOOSTERS (EXPLOSIVES)
NT DETONATORS
NT PRIMERS (EXPLOSIVES)
Development and verification of NASA Standard Initiator-2 (NSI-2)
[NASA-CR-172069] 23 p3200 N88-29044
Development and verification of NASA Standard Initiator-2 (NSI-2): Appendix
[NASA-CR-172070] 23 p3200 N88-29045

INJECTION
NT CARRIER INJECTION
NT FLUID INJECTION
NT FUEL INJECTION
NT GAS INJECTION
NT ION INJECTION
NT WATER INJECTION
The injector for the CEBAF CW superconducting linac
[CEBAF-PR-87-011] 11 p1546 N88-19241
Application of railgun principle to high-velocity hydrogen pellet injection for magnetic fusion reactor refueling
[DE88-005830] 13 p1728 N88-20334
Design of divertor plate and measurements of double-null open divertor plasma in the JFT-2M tokamak
[DE88-753130] 21 p3018 N88-27914
Influence of plasma parameters on VLF radiation in near-rocket region 24 p3448 N88-30518

INJECTION CARBURETORS
U CARBURETORS
U FUEL INJECTION

INJECTION LOCKING
An analytical and experimental study of injection-locked two-port oscillators
[NASA-TM-100119] 04 p0439 N88-12727

INJECTION MOLDING
Fabrication of microstructures with extreme structural heights by vacuum reaction injection molding and electroforming
[KFK-4267] 01 p0033 N88-10210
Development of a statistically proven injection molding method for reaction bonded silicon nitride, sintering reaction bonded silicon nitride, and sintered silicon nitride
[ETN-87-90575] 02 p0160 N88-11002
Improved silicon nitride for advanced heat engines
[NASA-CR-175006] 08 p0973 N88-15886
Processing of glass to aluminum (low melting metals) seals via an injection molding technique
[DE88-004689] 13 p1751 N88-20468
Improved silicon carbide for advanced heat engines
17 p2324 N88-23879
Improved silicon nitride for advanced heat engines
17 p2324 N88-23881
High temperature resins for injection. High temperature pre-impregnated
[RC-648676] 20 p2780 N88-26486

INJECTORS
Aerothermal modeling program, phase 2
02 p0185 N88-11149
Fuel-injector/air-swirl characterization
02 p0185 N88-11150
A three-barrel repeating pneumatic pellet injector for plasma fueling of the Joint European Torus
[DE88-000330] 04 p0491 N88-13026
RIIM two-pulse injector experiments
[DE88-000926] 05 p0653 N88-14005
Preliminary injector, accelerator, and beamline design for rf-linac-driven XUV free-electron lasers
[DE88-003185] 10 p1336 N88-17983
Proposal for construction of an Energetic Particle Injector (EPI)
[INPE-4242-RPE/548] 12 p1690 N88-20112
Durability testing of an iridium-plated storable rocket engine injector
[AD-A190707] 15 p2027 N88-22078
Development of a laboratory test for multiport injector deposits: Approaches 1 and 2
[AD-A190697] 15 p2048 N88-22203
Dense-spray structure and phenomena. Part 2: Pressure-atomized sprays
[AD-A190312] 15 p2064 N88-22307
Program to research laser-driven thermionic electron sources for free electron lasers
[AD-A190473] 15 p2072 N88-22353
Film cooling effectiveness on a flat plate in high free-stream turbulence using a single row of 30 deg slant-hole injectors
[AD-A190500] 15 p2147 N88-22816
Application of pulse compression and shaping to the FEL photoelectric injector
[DE88-007908] 19 p2675 N88-25910
Initial electron distributions for free-electron lasers generated by injector and accelerator simulations
[DE88-007022] 21 p2953 N88-27540

INJURIES
NT BACK INJURIES
NT BRAIN DAMAGE
NT LESIONS
NT NOISE INJURIES
NT RADIATION INJURIES
Modeling of the non-auditory response to blast overpressure
[AD-A187397] 10 p1369 N88-18184
Causes and prevention of occupational Repetition Strain Injuries (RSI) 11 p1521 N88-19083
Analysis of head response to torso acceleration. Volume 1: Development of performance requirements
[PB88-156757] 14 p1953 N88-21640

INLAND WATERS
NT GROUND WATER
An exploratory study of inland water and land altimetry using Seasat data
[ESA-CR(P)-2433] 02 p0193 N88-11208
Research in Switzerland on ocean and inland-water colour monitoring 08 p1043 N88-16301

INLET FLOW
Numerical computation of transonic potential flow about 3-dimensional inlets
[NAL-TR-924] 02 p0122 N88-10770
Combustor-diffuser interaction program
02 p0185 N88-11152
Measurement of airfoil heat transfer coefficients on a turbine stage 02 p0186 N88-11158
Heat transfer in laminar flow for mass inlet into an annular channel
[DE87-702890] 03 p0314 N88-11983
Analysis and performance prediction of scramjet inlets utilizing a three-dimensional Navier-Stokes code
07 p0811 N88-14936
Aeropropulsion '87. Session 3: Internal Fluid Mechanics Research
[NASA-CP-10003-SESS-3] 08 p0954 N88-15790
Propulsion challenges and opportunities for high-speed transport aircraft 08 p0958 N88-15809
Supersonic throughflow fans for high-speed aircraft
08 p0958 N88-15810
High-speed inlet research program and supporting analyses 08 p0958 N88-15811
Parametric study of choke flutter with a linear theory
10 p1283 N88-17673
Experimental investigation of a supercritical compressor rotor blade section 10 p1284 N88-17680
Numerical simulation of scramjet inlet flow fields
[NASA-TP-2517] 17 p2296 N88-23735
Low frequency pressure oscillations in a model ramjet combustor 19 p2625 N88-25571
Effects of Mach number on acoustic-vortex interactions in a ramjet 19 p2625 N88-25573
High speed inlet calculations with real gas effects
[NASA-CR-182167] 20 p2752 N88-26336
The calculation of the flow through a two-dimensional faired diffuser
[PNR90433] 22 p3076 N88-28259
Prediction of the pressure distribution for radial inflow between co-rotating discs
[PNR90464] 22 p3076 N88-28261
The use of fins to reduce the pressure drop in a rotating cavity with a radial flow
[PNR90465] 22 p3079 N88-28282
The effects of inlet turbulence and rotor/stator interactions on the aerodynamics and heat transfer of a large-scale rotating turbine model. Volume 3: Heat transfer data tabulation 65 percent axial spacing
[NASA-CR-179468] 23 p3180 N88-28930
The effects of inlet turbulence and rotor/stator interactions on the aerodynamics and heat transfer of a large-scale rotating turbine model. Volume 2: Heat transfer data tabulation. 15 percent axial spacing
[NASA-CR-179467] 24 p3326 N88-29804

INLET NOZZLES
Test stand performance of a convertible engine for advanced V/STOL and rotorcraft propulsion
[NASA-TM-100211] 03 p0266 N88-11679
Theoretical and experimental study of flow-control devices for inlets of indraft wind tunnels
03 p0268 N88-11684
Electromagnetic fields backscattered from an s-shaped inlet cavity with an absorber coating on its inner walls
[NASA-CR-182401] 07 p0845 N88-15130
Low pressure gas flow analysis through an effusive inlet using mass spectrometry
[NASA-CR-182712] 14 p1910 N88-21413
The effects of inlet turbulence and rotor/stator interactions on the aerodynamics and heat transfer of a large-scale rotating turbine model. Part 4: Aerodynamic data tabulation
[NASA-CR-179469] 17 p2339 N88-23956
Rotation symmetric inside flow with diametric expansion resolution
[ILR-MITT-193] 23 p3213 N88-29123

INLET PRESSURE
Soot and radiation in a gas turbine combustor
[AD-A191991] 23 p3179 N88-28924
Simulation of Vulcain engine operation at low inlet pressure
[ETN-88-93083] 24 p3339 N88-29875

INLET TEMPERATURE
Use of a local heat source for determining temperature of inlet heat section in ring channels
[DE88-700332] 07 p0854 N88-15187
Effect of spatial inlet temperature and pressure distortion on turbofan engine stability
[NASA-TM-100850] 14 p1868 N88-21162

INLETS (DEVICES)
U INTAKE SYSTEMS

INNER RADIATION BELT
Approximate analytical formulae for electron density and collision frequency in the natural and nuclear-disturbed ionosphere and inner magnetosphere
[AD-A193129] 21 p2972 N88-27654

INORGANIC COATINGS
NT ANODIC COATINGS
NT CERAMIC COATINGS

INORGANIC COMPOUNDS
NT AMMONIA
NT LIQUID AMMONIA

INORGANIC MATERIALS
Highly Non-Linear Optical (NLO) organic crystals and films. Electrooptical organic materials
03 p0297 N88-11866

INORGANIC NITRATES
NT AMMONIUM NITRATES
NT HYDRAZINE NITRATE
NT SODIUM NITRATES
INORGANIC PEROXIDES
NT HYDROGEN PEROXIDE
INORGANIC SULFIDES
NT BISMUTH SULFIDES
NT CADMIUM SULFIDES
NT COPPER SULFIDES
NT HYDROGEN SULFIDE
NT LEAD SULFIDES
NT MOLYBDENUM DISULFIDES
NT MOLYBDENUM SULFIDES
NT POLYSULFIDES
NT ZINC SULFIDES
INPUT
Equivalence of input-output stability and exponential stability for infinite dimensional systems
[TW-276] 05 p0638 N88-13903
Modeling and generating input processes
[DE87-013162] 05 p0645 N88-13948
A queueing system with independent Markov input streams
[AD-A187601] 10 p1402 N88-18363
High bit rate serial input mutipliers
[REPT-87-012] 11 p1530 N88-19140
A serial input pipelined multiplier
[REPT-87-030] 11 p1530 N88-19141
On serial-input multipliers for two-complement numbers
[REPT-86-035] 11 p1536 N88-19181
Logical input devices and interaction --- computer graphics
[CWI-CS-R8738] 13 p1814 N88-20836
Why is it difficult to program in von Neumann languages
[AD-A192830] 20 p2838 N88-26839
A study of the effect of random input motion on low Reynolds number flows
[AD-A195559] 24 p3316 N88-29747
INPUT/OUTPUT ROUTINES
Integrated voice and visual systems research topics
[NASA-CR-177417] 03 p0356 N88-12246
Advanced Information Processing System (AIPS) proof-of-concept system functional requirements I/O network system services
[NASA-CR-181481] 03 p0384 N88-12412
Advanced Information Processing System (AIPS) proof-of-concept system functional design I/O network system services
[NASA-CR-181488] 03 p0384 N88-12413
Rationale for the design of the Ada (tradename) programming language
[AD-A187106] 09 p1217 N88-17297
Data acquisition and processing for surface plate calibration
[AD-A187264] 11 p1564 N88-19366
The TempIS Project: Performance analysis of temporal queries
[AD-A188354] 12 p1706 N88-20213
A comparison of two chord keyboard coding systems for alphanumeric data entry
[AD-A189230] 13 p1813 N88-20834
A proof of the Kahn principle for input/output automata
[AD-A194454] 23 p3248 N88-29333
INSAT SATELLITES
U INDIAN SPACECRAFT
INSECTICIDES
NT CARBAMATES (TRADENAME)
NT URETHANES
INSECTS
NT DROSOPHILA
Insect contamination protection for laminar flow surfaces 07 p0814 N88-14954
Factors affecting the sticking of insects on modified aircraft wings
[NASA-CR-182451] 09 p1148 N88-16878
Factors affecting the sticking of insects on modified aircraft wings
[NASA-CR-182615] 12 p1575 N88-19421
INSENSITIVITY
U SENSITIVITY
INSERTION
Hardware fault insertion and instrumentation system: Mechanization and validation
[NASA-CR-181445] 01 p0078 N88-10497
Software-implemented fault insertion: An FTMP example
[NASA-CR-178423] 06 p0761 N88-14668
Insertions using geometric analysis and hybrid force-position control: Method and analysis
[DE87-013652] 15 p2117 N88-22611
INSERTS
A low volume insert for solid state magic angle spinning NMR of small samples
[AD-A184359] 04 p0419 N88-12601
Increasing strength of graphite/epoxy bolted joints by introducing an adhesively bonded metallic insert
[FFA-TN-1987-45] 15 p2088 N88-22442
Insert design handbook
[ESA-PSS-03-1202-ISSUE-1] 17 p2311 N88-23822
INSOLATION
A quasi-physical model for converting hourly global horizontal to direct normal insolation
[DE87-012273] 03 p0349 N88-12204
Calendar year 1985 solar and weather data for Austin, Texas
[PB87-220174] 03 p0352 N88-12219
Satellite techniques of solar resource assessment for focusing and non-focusing solar collector systems
[DE88-001657] 07 p0874 N88-15298
Short Reference Years: Short weather data sets for faster simulations of solar energy systems and energy consumption in buildings
[DE88-900198] 07 p0881 N88-15343
The use of the direct measurement of solar radiation for the determination of Pasquill Stability Parameter
[AD-A186084] 07 p0946 N88-15750
Calibration of the solar radiation estimation method by satellites
[INPE-4349-PRE/1185] 12 p1646 N88-19861
Global solar radiation in Sierra Leone (West Africa)
[DE88-702725] 23 p3235 N88-29252
INSPECTION
NT X RAY INSPECTION
Technology survey for a robot which will investigate the condition of underground pipe
[PB87-209979] 01 p0055 N88-10351
Nondestructive inspection of the pressure vessel in Stuttgart. ALOK part. Phase 1: ALOK combined with conventional probes
[REPT-860113-TW] 01 p0057 N88-10367
Needs assessment for NDT and characterization of ceramics: Assessment of inspection technology for green state and sintered ceramics
[DE87-013550] 02 p0151 N88-10947
Ultrasonic method of imspecting austenitic weld joints in nuclear power station equipment
[BLL-CE-TRANS-8281-(9022.09)] 04 p0453 N88-12806
Pulsed eddy-current inspection of thin-walled stainless steel tubing
[DE88-001492] 04 p0457 N88-12830
Computerized certification of digital ultrasonic instrumentation
[DE88-000820] 04 p0488 N88-13008
A pulsed eddy current method for examining thin-walled stainless steel tubing
[DE88-002294] 07 p0866 N88-15255
Through-transmission/pulse-echo ultrasonic equipment evaluation
[AD-A188340] 07 p0929 N88-15641
Analysis of the reliability of Royal Australian Air force non-destructive inspection
[AD-A186979] 09 p1177 N88-17049
Micro PAVER concept and development airport pavement management system
[AD-A187360] 11 p1441 N88-18598
Ultrasonic inspection of irregular surfaces
[AERE-R-12465] 13 p1780 N88-20648
Quick actuating closure and handling system 14 p1925 N88-21476
Eddy current nondestructive inspection of graphite epoxy using ferrite cup core probes
[AD-A189823] 15 p2074 N88-22365
Nondestructive evaluation of large scale composite components
[AD-A190998] 16 p2173 N88-22954
Method of radiographic inspection of wooden members
[NASA-CASE-LAR-13724-1] 17 p2346 N88-23983
Knowledge based systems in nondestructive evaluation
[DE88-006653] 18 p2525 N88-24981
The inspection of metallurgical bounds in electronic systems
[AD-A192064] 18 p2582 N88-25343
Inspection methods in programming: Cliches and plans
[AD-A192782] 21 p2996 N88-27767
Use of Moessbauer spectroscopy to study implanted surfaces
[DE88-010452] 21 p3023 N88-27942
Evaluation of bond testing equipment for inspection of Army advanced composite airframe structures
[AD-A195795] 24 p3341 N88-29885
INSPIRATION
Discovery and problem solving: Triangulation as a weak heuristic 08 p1062 N88-16412
INSTABILITY
U STABILITY
INSTALLATION
U INSTALLING
INSTALLING
Advanced turboprop wing installation effects measured by unsteady blade pressure and noise
[NASA-TM-100200] 01 p0002 N88-10008
Airframe/store compatibility 05 p0545 N88-13323
Human engineering laboratory grounding analysis (HELGA)-2
[AD-A185367] 05 p0579 N88-13524
Facility design validation of the information systems laboratory
[AD-A186309] 07 p0906 N88-15488
The design and implementation of the Technical Facilities Controller (TFC) for the Goldstone deep space communications complex 11 p1474 N88-18794
Airworthiness and flight characteristics test of a ski assembly for the UH-60A Black Hawk helicopter
[AD-A191414] 16 p2162 N88-22895
The Environment for Application Software Integration and Execution (EASIE) version 1.0. Volume 4: System installation and maintenance guide
[NASA-TM-100576] 17 p2386 N88-24185
Aircraft avionics and missile system installation cost study. Volume 2: Appendices F and G
[AD-A195372] 24 p3325 N88-29801
Electronic materials and devices prepared by molecular beam epitaxy
[AD-A195694] 24 p3433 N88-30433
INSTANTONS
Instanton in supersymmetric theory with static disorder
[DE88-700357] 07 p0940 N88-15716
Recent developments in the path integral approach to anomalies
[DE87-703032] 15 p2118 N88-22616
INSTRUCTIONS
U EDUCATION
INSTRUCTORS
Elementary and middle school science improvement project
[NASA-CR-179328] 16 p2285 N88-23679
US civil airmen statistics, 1987
[AD-A191714] 18 p2455 N88-24577
INSTRUMENT APPROACH
Boeing 727 MLS (Microwave Landing System) terminal instrument procedures (TERPS) approach data collection and processing, data report
[AD-A185523] 06 p0667 N88-14090
Investigation of air transportation technology at Massachusetts Institute of Technology, 1986 17 p2293 N88-23716
Loran-C monitor correlation over a 92-mile baseline in Ohio 17 p2293 N88-23720
Cessna 172 MLS (Microwave Landing System) terminal instrument procedures (TERPS) approach data collection and processing data report
[AD-A191241] 18 p2461 N88-24613
INSTRUMENT COMPENSATION
NT TEMPERATURE COMPENSATION
CGI delay compensation
[NASA-TM-86703] 04 p0476 N88-12932
Corner compensation structures for (110) oriented silicon
[DE88-003300] 10 p1417 N88-18455
INSTRUMENT DRIFT
U DRIFT (INSTRUMENTATION)
INSTRUMENT ERRORS
Effect of installation and calibration errors of sensors on system identification results of an aircraft
[ESA-TT-1059] 03 p0266 N88-11678
Flightpath reconstruction and systematic radar error estimation from multiradar range-azimuth measurements
[NLR-MP-85064-U] 06 p0693 N88-14251
Determination of cloud base height and emissivity from downwelling angular radiances
[AD-A185985] 07 p0879 N88-15331
Zeroshift of piezoelectric accelerometers in pyroshock measurements 08 p0997 N88-16039
Common but unappreciated sources of error in one, two, and multiple-color pyrometry 17 p2329 N88-23907
INSTRUMENT FLIGHT RULES
Estimates of potential increases in airport capacity through ATC (Air Traffic Control) system improvements in the airport and terminal areas
[AD-A188533] 12 p1578 N88-19444
Rule-based fault-tolerant flight control 17 p2294 N88-23725
Aircraft accident/incident, Copperhill, Tennessee, February 22, 1986
[PB88-910407] 18 p2461 N88-24612

Improvement of head-up display standards. Volume 3: An evaluation of head-up display safety
[AD-A195787] 24 p3410 N88-30300

INSTRUMENT LANDING SYSTEMS
NT AUTOMATIC LANDING CONTROL
Improvement of head-up display standards. Volume 5: Head up display ILS (Instrument Landing System) accuracy flight tests
[AD-A194602] 23 p3178 N88-28922

INSTRUMENT PACKAGES
NT EREP
Instrumentation package for a shrouded SWERVE/EPW rocket sled test
[DE87-014267] 01 p0008 N88-10045

INSTRUMENT TRANSFORMERS
Low frequency IF transformer designs having variable coupling
[RAE-TM-RAD-NAV-291] 01 p0043 N88-10272

INSTRUMENTAL ANALYSIS
U AUTOMATION

INSULATING MATERIALS
U INSULATION

INSULATION
NT ELECTRICAL INSULATION
NT MULTILAYER INSULATION
NT THERMAL INSULATION
Elimination of subboundaries in 0.5-micron-thick Si-on-insulation films produced by ZMR
[AD-A184590] 03 p0381 N88-12396
The assessment of the sound insulation requirements for a large broadcasting studio, using a scale model: Theoretical considerations
[BBC-RD-1987/20] 09 p1155 N88-16921
Some investigations of electrical discharges at the surfaces of solid cathodes immersed in aqueous electrolyte solutions
[PB87-168209] 09 p1159 N88-16946
Indirect measurement of local condensing heat-transfer coefficient around horizontal finned tubes
[AD-A186929] 09 p1160 N88-16950
The assessment of the sound insulation requirements for a large broadcasting studio, using a scale model: Practical details
[BBC-RD-1987/21] 10 p1318 N88-17878
Prototype thin-film thermocouple/heat-flux sensor for a ceramic-insulated diesel engine
[NASA-TM-100798] 11 p1490 N88-18892
Review of the state of the art and projected technology of low heat rejection engines
[PB88-131255] 11 p1496 N88-18934
Safety research of insulating materials of cable for nuclear power generating station
[NASA-TT-20202] 13 p1752 N88-20477
Aging properties of cable polmers (2)
[NASA-TT-20228] 13 p1752 N88-20479
The Magnetically Insulated Inertial Confinement Fusion (MICF): A novel approach
[DE88-005460] 13 p1842 N88-21026
Experiments on insulation of relativistic electron flows in oblique and tapered magnetic fields
[DE88-007199] 19 p2724 N88-26176
SIS (Superconductor-Insulator-Superconductor) mixer research
[AD-A192908] 20 p2879 N88-27092
Far- and mid-infrared properties of metal-insulator composite materials
[AD-A193227] 21 p2905 N88-27236

INSULATORS
Gases released by surface flashover of insulators
[DE87-013851] 01 p0039 N88-10249
Thermionic Technology Program. A: Insulator test and evaluation
[DE88-004707] 13 p1795 N88-20735
Generation of high brightness ion beam from insulated anode PED 18 p2278 N88-23637
Development of the field-induced electron injection and impact ionization (F4I) technique for radiation hardness testing of MOS (Metal-Oxide-Semiconductor) gate insulators
[AD-A192114] 18 p2583 N88-25345
Data compilation for radiation damage on ceramic insulators. Revised with updated data and reviews
[DE88-753426] 21 p2920 N88-27329
Studies on the use of propylene carbonate as a high-voltage insulator
[DE88-011786] 22 p3057 N88-28141

INSURANCE (CONTRACTS)
Review of commercial spacecraft: Recovery and repair experiences. Implications for future spacecraft designs and operations 12 p1591 N88-19528
The role and the place of insurance of large space projects 22 p3161 N88-28826

INTAKE SYSTEMS
NT AIR INTAKES
NT ENGINE INLETS
NT HELICAL INDUCERS
NT SIDE INLETS
NT SUPERSONIC INLETS
Theoretical and experimental study of flow-control devices for inlets of indraft wind tunnels 03 p0268 N88-11684
Dynamics of reverse flows at pump inlet 04 p0425 N88-12636
Fundamentals of fighter aircraft design: Engine intake and afterbody 05 p0545 N88-13322
Fluid mass and thermal loading effects on the modal characteristics of space shuttle main engine liquid oxygen inlet splitter vanes 05 p0594 N88-13628
Inlets, ducts and nozzles 08 p0955 N88-15791
The advantage of variable geometry for turbine engines at low power 10 p1280 N88-17653
Investigation of dihedral effects in compressor cascades 10 p1282 N88-17672
Wake interaction effects on the transition process on turbine blades
[AD-A188020] 10 p1332 N88-17962
Measurement and analysis of the noise radiated by low Mach numbers centrifugal blowers
[AD-A189226] 13 p1833 N88-20966
Flow/acoustic interaction in duct inflow
[AD-A189264] 13 p1833 N88-20967
Inflow measurement made with a laser velocimeter on a helicopter model in forward flight. Volume 2: Rectangular planform blades at an advance ratio of 0.23
[NASA-TM-100542] 14 p1864 N88-21139
Inflow measurements made with a laser velocimeter on a helicopter model in forward flight. Volume 4: Tapered planform blades at an advance ratio of 0.15
[NASA-TM-100544] 16 p2156 N88-22863
A numerical study of the hot gas environment around a STOVL aircraft in ground proximity
[NASA-TM-100895] 17 p2295 N88-23729
Inflow measurement made with a laser velocimeter on a helicopter model in forward flight. Volume 5: Tapered planform blades at an advance ratio of 0.23
[NASA-TM-100545] 17 p2299 N88-23755
Inflow measurements made with a laser velocimeter on a helicopter model in forward flight. Volume 1: Rectangular planform blades at an advance ration of 0.15
[NASA-TM-100541] 18 p2460 N88-24607
The effects of different combinations of inlet air conditions used for cooling as measured on a heated manikin
[AD-A191116] 18 p2552 N88-25151
Air intake aerodynamics 24 p3318 N88-29762

INTEGERS
Discrete generalized networks: Application to integer constrained flow problems
[AD-A190823] 16 p2190 N88-23060
A mixed-integer linear programming problem which is efficiently solvable
[AD-A191028] 18 p2556 N88-25168
Factorization of large integers on a massively parallel computer
[DE88-011625] 21 p2999 N88-27786
Multicriteria integer programming for problems involving linear and nonlinear utility functions
[AD-A194530] 23 p3249 N88-29336
Two dimensional convolute integers for machine vision and image recognition 23 p3254 N88-29369
Bifurcations of periodic solutions of non-integrable Hamiltonians with two degrees of freedom: Numerical and analytical results
[DE88-702747] 23 p3272 N88-29473

INTEGRAL CALCULUS
An algebraic approach to a calculus of functional differences: Fixed differences and integrals
[AD-A187079] 09 p1227 N88-17346
Martingale representation and the Malliavin calculus
[AD-A189721] 15 p2119 N88-22626

INTEGRAL EQUATIONS
NT FREDHOLM EQUATIONS
NT J INTEGRAL
NT SINGULAR INTEGRAL EQUATIONS
NT VOLTERRA EQUATIONS
On oscillation of a kind of integro-differential equation with delay
[DE87-703059] 02 p0225 N88-11417
Parallel methods for ordinary differential equations
[DE87-014667] 02 p0226 N88-11425
Numerical modeling: Integral equation method 03 p0304 N88-11919
An integral equation analysis of inelastic shells 03 p0336 N88-12118
Mutual admittance between slots in cylinders of arbitrary shape
[AD-A184254] 04 p0439 N88-12723
Steady waves in a nonlinear theory of viscoelasticity
[AD-A185548] 06 p0723 N88-14448
On the convergence of the p-version of the boundary element Galerkin method
[AD-A186198] 07 p0910 N88-15514
Computational analysis of propagation properties of integrated-optical waveguides using a domain integral equation
[PB87-163358] 09 p1154 N88-16917
Retarded potential technique applied for shock wave loading of doubly symmetric submerged structures 09 p1179 N88-17058
Theory of the generalized Abel integral equations
[ETN-88-91086] 09 p1229 N88-17362
Conjugate gradient spectral iterative technique
[PB88-126917] 10 p1398 N88-18337
Small degree solutions for the polynomial Bezout equation
[AD-A187630] 10 p1401 N88-18355
Integral equations with modified fundamental solutions for exterior boundary value problems from electromagnetic wave theory
[ETN-88-91483] 11 p1475 N88-18800
A discretization of the integral equation for the time dependent linearized subsonic potential flow over a wing
[AD-A188534] 12 p1574 N88-19411
Study of inhomogeneously filled cylindrical resonant cavities by the finite integration technique
[PB88-133707] 12 p1697 N88-20156
Computational technique for compressible vortex flows using the integral equation solution
[NASA-CR-182695] 13 p1718 N88-20271
Integral equation theory of homopolymer melts
[DE88-005304] 13 p1751 N88-20470
Integral equation theory of polymer blends
[DE88-005305] 13 p1751 N88-20471
Inversion algorithms for geophysical problems
[AD-A189252] 13 p1815 N88-20845
WKB theory of wave tunneling for Hermitian vector systems of integral equations
[DE88-005332] 13 p1831 N88-20951
Global spatial periodic solutions to the Ginzburg-Landau equations
[DE88-006424] 15 p2119 N88-22623
An integral equation for the linearized supersonic flow over a wing
[AD-A191408] 16 p2158 N88-22875
Determination of characteristic radiation properties of a torus antenna: Integral equation method
[DFVLR-FB-87-46] 16 p2188 N88-23049
Parameter estimation for boundary value problems by integral equations of the second kind
[NASA-CR-181660] 17 p2332 N88-23918
A new collocation-type method for the numerical solution of Hammerstein equations 17 p2393 N88-24226
Joint services electronics program
[AD-A191749] 18 p2504 N88-24853
Cross stream differencing for integral boundary layer equations
[AD-A191744] 18 p2509 N88-24886
Integral equation for the laser field: Multimode description of a free-electron laser oscillator
[DE88-007050] 18 p2521 N88-24956
Fracture mechanics analysis for short cracks
[AD-A192002] 18 p2527 N88-24992
Information analysis of integral equations in remote sensing of atmospheric aerosols 18 p2532 N88-25022
A mixed min-max control problem governed by integral equations 18 p2564 N88-25228
Optimal processes governed by integral equations with unilateral constraint 18 p2565 N88-25231
Numerical solution of random Love's integral equation 18 p2565 N88-25235
New hybrid method for solving time-domain integral equations (one-dimensional scattering problems)
[PB88-186192] 20 p2789 N88-26547
Time-domain boundary element analysis of dynamic near-tip fields for impact-loaded collinear cracks
[AD-A192930] 20 p2815 N88-26700
A new boundary integral equation formulation for elastodynamic and elastostatic crack analysis
[AD-A192967] 20 p2815 N88-26702
Ill-posed problems and integral equations
[AD-A193709] 22 p3143 N88-28691
An integral equation for the linearized unsteady supersonic flow over a wing
[AD-A193773] 23 p3172 N88-28887
Resonance excitation of linear and non-linear spiral density waves in a gaseous disk 23 p3299 N88-29643
Initial value problems in viscoelasticity
[AD-A196052] 24 p3382 N88-30145

INTEGRAL FUNCTIONS
U ENTIRE FUNCTIONS

INTEGRAL TRANSFORMATIONS
NT FAST FOURIER TRANSFORMATIONS
NT FOURIER TRANSFORMATION
NT FOURIER-BESSEL TRANSFORMATIONS
NT HILBERT TRANSFORMATION
NT LAPLACE TRANSFORMATION
Thermomechanical cracking in coated media due to high speed asperity excitation
[AD-A184176] 04 p0454 N88-12809
Theory of the generalized Abel integral equations
[ETN-88-91086] 09 p1229 N88-17362
INTEGRALS
NT CONVOLUTION INTEGRALS
Elevated temperature crack growth
02 p0188 N88-11174
Method estimating integral mean value of enhancement factor and path latitude for whistlers below magnetic latitude 10 deg
03 p0300 N88-11885
Operator foundation of functional integral in non-Abelian gauge theory
[DE88-700508] 07 p0941 N88-15719
Theory of the generalized Abel integral equations
[ETN-88-91086] 09 p1229 N88-17362
Path integration on the upper half-plane
[DE88-751050] 12 p1682 N88-20057
Product-integrals and counting processes
[CWI-MS-R8707] 14 p1965 N88-21727
Recent developments in the path integral approach to anomalies
[DE87-703032] 15 p2118 N88-22616
Remarks on the time transformation of path-integral measures
[DE87-703040] 15 p2118 N88-22617
Path integral, BRS symmetry, and string and membrane theories
[DE88-752300] 15 p2146 N88-22810
Computation of a complete elliptic integral of the first kind using q-expansion
16 p2257 N88-23490
Incomplete Lipschitz-Hankel integrals of MacDonald functions
[AD-A191034] 16 p2261 N88-23515
Evaluation of quantum mechanics path integrals by the approximations exact on a class of polynomial functionals
[DE88-702434] 21 p3011 N88-27865
An asymptotic evaluation of the tail of a multiple symmetric alpha-stable integral
[AD-A194570] 23 p3270 N88-29460
Numerical calculations of the response of a spinning spheroidal payload to coning motion
[AD-A195890] 24 p3368 N88-30059
On the Nash point equilibria in the calculus of variations
[AD-A194959] 24 p3424 N88-30381
Canonical variables and canonical integrals for motion in near-circular orbits
24 p3446 N88-30512
INTEGRATED CIRCUITS
NT ENCAPSULATED MICROCIRCUITS
NT LARGE SCALE INTEGRATION
NT LINEAR INTEGRATED CIRCUITS
NT VERY LARGE SCALE INTEGRATION
NT VHSIC (CIRCUITS)
Physics and device design of vacuum integrated circuits
01 p0039 N88-10251
An interactive optimization procedure for the computer aided dimensioning of integrated circuits
[ETN-87-90414] 01 p0082 N88-10531
Understanding the transport properties of silicon grain boundaries and how they relate to I.C. applications of polysilicon
[DE87-013809] 01 p0104 N88-10677
Voltammetric investigation of porous silicon for integrated circuit applications
[DE87-009287] 02 p0166 N88-11042
Low noise-low power monolithic multiplexing readout electronics for silicon strip detectors
[MPI-PAE/EXP.EL.178] 02 p0168 N88-11057
Some 2-D WSI array architectures --- wafer scale integration (WSI)
[OUEL-1672/87] 02 p0219 N88-11381
Development of standard cells in NMOS technology for the design of digital integrated circuits
[FI-62-TB-6] 03 p0310 N88-11953
Integrated circuit design
[AD-A184486] 03 p0311 N88-11960
Research in monolithic signal-processing circuits
[AD-A184680] 03 p0311 N88-11962
Dramatically improved radiation hardness for CMOS silicon gate integrated circuits even down to cryogenic temperatures
[AD-A184672] 03 p0381 N88-12398
A procedural method for the efficient implementation of full-custom VLSI designs
04 p0436 N88-12701
Programmable Logic Arrays (PLA's) design for testability
[PB87-102935] 04 p0438 N88-12718
Electromagnetics and electrothermal approach to evaluate failures in microelectronic devices caused by electrostatic discharges: Stochastical aspects of the device reliability
[AD-A184906] 05 p0577 N88-13522
An extension to the multilevel logic simulator for microcomputers
[AD-A185032] 05 p0634 N88-13879
Computer modeling of complete IC fabrication process
[AD-A184807] 05 p0654 N88-14012
Technology upgrade of a silicon compiler
[AD-A184873] 05 p0655 N88-14016
Integrated photo-responsive metal oxide semiconductor circuit
[NASA-CASE-GSC-12782-1] 06 p0696 N88-14271
An analysis of simplified feed architectures for MMIC (Monolithic Microwave Integrated Circuit) T/R (Transmit/Receive) module arrays
[AD-A185474] 06 p0697 N88-14275
Investigations on an RF plasma related to plasma etching
[ETN-88-91366] 06 p0784 N88-14809
Correctness proofs for systolic algorithms: Palindromes and sorting
[PB88-106075] 07 p0912 N88-15534
GaAs MMIC yield evaluation --- monolithic microwave integrated circuits (MMIC)
[ESA-CR(P)-2470] 08 p0979 N88-15916
Single-layer wire routing
[AD-A186990] 09 p1157 N88-16932
Plasma and ion etching for failure analysis. Part 2. The etching of plastic encapsulant and other semiconductor device materials, using the Technics Giga Etch 100-E plasma etch system
[AERE-R-12212] 09 p1177 N88-17050
Interchange of electronic design through VHDL and EIS
09 p1205 N88-17222
Effect of the gate oxide thickness on the speed of MOS integrated circuits
[PB88-155783] 10 p1323 N88-17910
Time domain wave propagation in multilayered integrated circuits
[AD-A187462] 10 p1324 N88-17916
Formal multilevel hierarchical verification of synchronous MOS VLSI circuits
[AD-A187532] 10 p1324 N88-17918
The soft/hard wet anodization of aluminum oxide and its use in a thin film multilayered capacitor
[AD-A187575] 10 p1325 N88-17919
Signal processing studies program VLSI designs for unary functions
[AD-A188053] 10 p1325 N88-17922
The arithmetic cube and its associated algorithms
10 p1374 N88-18195
Voltammetric investigation of porous silicon for integrated circuit applications
[DE88-004024] 11 p1456 N88-18677
RELIC: A reliability simulator for integrated circuits
[AD-A187493] 11 p1477 N88-18811
Modules of nanosecond logic electronics system with computer control
[DE88-700190] 11 p1479 N88-18828
Polymeric materials for electro-optic testing
[AD-A188382] 12 p1610 N88-19627
Intergrated circuit design, phase 2
[AD-A189060] 13 p1760 N88-20530
Laser programming integrated circuits
[AD-A189590] 13 p1762 N88-20537
Optical RF distribution links for MMIC phased array antennas
[NASA-TM-100841] 13 p1764 N88-20555
Monolithic microwave integrated circuit technology for advanced space communication
[NASA-TM-100829] 14 p1906 N88-21389
Monolithic phase shifter study
[AD-A190213] 15 p2059 N88-22278
Fabrication and electrical characterization of multilevel aluminum interconnects used to achieve silicon-hybrid wafer-scale integration
[AD-A190519] 15 p2060 N88-22282
Fast analog-to-digital converter
[DE88-701488] 15 p2106 N88-22543
Beam assisted fabrication of 3-5/Si monolithic devices
[AD-A189979] 15 p2142 N88-22785
Present, future of automotive hybrid IC applications discussed
16 p2185 N88-23024
Algorithms and architectures for acoustic phonetical detection of continuous speech
[ENST-87E016] 16 p2189 N88-23054
Instrumentation for ultrafast electronics
[AD-A191379] 16 p2193 N88-23080
A 30 GHz monolithic receive module technology assessment
[NASA-CR-180825] 16 p2194 N88-23084
Computer aided design tools for integrated silicon system structures
[ETN-88-92186] 16 p2247 N88-23424
Contribution to the automatic generation of floor plan placing --- integrated circuit design
[ETN-88-92193] 16 p2247 N88-23426
Millimeter and submillimeter waves and frequency selective surfaces
[AD-A191511] 18 p2500 N88-24827
Joint services electronics program
[AD-A190239] 18 p2503 N88-24848
Computer aided design of monolithic microwave and millimeter wave integrated circuits and subsystems
[AD-A191593] 18 p2503 N88-24852
The inspection of metallurgical bounds in electronic systems
[AD-A192064] 18 p2582 N88-25343
A non-contact picosecond prober for integrated circuit testing
19 p2655 N88-25766
Picosecond sampling of integrated circuits
19 p2655 N88-25767
Electro-optic sampling of high-speed, InP-based integrated circuits
19 p2655 N88-25769
Millimeter-wave integrated circuits
19 p2656 N88-25774
Enhanced performance ultrabroadband distributed amplifiers
19 p2656 N88-25775
Thermionic integrated circuit program
[DE88-010119] 19 p2662 N88-25833
The 1988 IEEE Solid-State Sensor Workshop
[AD-A190922] 19 p2668 N88-25860
An integrated on-chip pressure sensor for accurate control applications
19 p2671 N88-25880
Resonant structures for integrated sensors
19 p2673 N88-25893
Zinc-oxide thin films for integrated-sensor applications
19 p2673 N88-25896
Effects of cosmic rays on single event upsets
[NASA-CR-183053] 20 p2793 N88-26569
Analysis of networks with parameters S: Generalization of junction matrix
[INPE-4535-PRE/1282] 20 p2793 N88-26570
Integrated optoelectronic circuits utilizing InGaAsP grown by molecular beam epitaxy (erbium doping of MBE GaAs)
[AD-A192269] 20 p2795 N88-26584
An integrated circuit for error protection in modern data communication systems conforming to Eurocom specifications
[FEL-1987-48] 20 p2796 N88-26593
Research in VLSI computer systems
[AD-A192^15] 20 p2835 N88-26816
Defects in high-mobility semiconductor systems
[AD-A192298] 20 p2879 N88-27090
Picosecond optoelectronic sampling of electrical waveforms produced by an optically excited field effect transistor
[AD-A192384] 21 p2935 N88-27428
A planar IC-compatible transferred electron device for millimeter-wave operation
[AD-A192692] 21 p2936 N88-27433
Guided wave interactions in millimeter-wave integrated circuits
[AD-A193017] 21 p2936 N88-27437
Very High Speed Integrated Circuits (VHSIC)
[AD-A193225] 21 p2937 N88-27442
Silicon-on-insulator pin diodes
[AD-A193359] 21 p2937 N88-27445
STAR: Sandia Timing Analyzer Routine
[DE88-012412] 21 p2940 N88-27463
Molecular beam epitaxy of GaP films on Si substrates
[PB88-131974] 21 p3020 N88-27923
Dose-enhancement effects in TaSi/Al- and Al-gate MOS devices
[DE88-005483] 21 p3020 N88-27926
*Array trade-off study using multilayer parasitic subarrays
[NASA-TM-101321] 22 p3070 N88-28222
Time domain wave propagation in multilayered integrated circuits
[AD-A193821] 22 p3073 N88-28241
Signals and systems
24 p3363 N88-30026
Electronic and optical devices and applications
24 p3363 N88-30027
Circuit design criteria for stable lateral inhibition neural networks
[AD-A195066] 24 p3366 N88-30046
Impurity analysis in SIMOX samples by high-efficiency resonance ionization time-of-flight mass spectrometry
[DE88-012061] 24 p3367 N88-30051
Stress related failures causing open metallization
[AD-A195061] 24 p3383 N88-30150
INTEGRATED ENERGY SYSTEMS
Integrated analysis and applications
08 p0954 N88-15789

Assessment of VAS-derived products created by a simultaneous algorithm on a convectively active day
[AD-A186158] 08 p1054 N88-16359

INTEGRATED MISSION CONTROL CENTER
Optimization of the dilation characteristic on the control jurisdiction of an area control facility
[AD-A191720] 18 p2461 N88-24615

INTEGRATED OPTICS
Computational analysis of propagation properties of integrated-optical waveguides using a domain integral equation
[PB87-163358] 09 p1154 N88-16917
Monolithic integration on a GaAs substrate of a quarter ring laser and an optical guide coupled by an evanescent wave
[ETN-88-92308] 17 p2344 N88-23969
Nonlinear surface polaritons
[AD-A191048] 18 p2499 N88-24822
Research in the optical sciences
[AD-A192175] 18 p2575 N88-25297
Investigations on periodically perturbed optical waveguides
[88712725] 23 p3283 N88-29548
Ion exchange processes for fabrication of integrated optical waveguide structures into glass substrates
[VTT-46] 24 p3429 N88-30405

INTEGRATION (REAL VARIABLES)
U MEASURE AND INTEGRATION

INTEGRATORS
Rotorcraft flight-propulsion control integration: An eclectic design concept
[NASA-TP-2815] 12 p1584 N88-19475

INTEGRITY
NT COMPUTER PROGRAM INTEGRITY

INTEGRODIFFERENTIAL EQUATIONS
U DIFFERENTIAL EQUATIONS
U INTEGRAL EQUATIONS

INTELLIGENCE
NT ARTIFICIAL INTELLIGENCE
NT EXPERT SYSTEMS
NT EXTRATERRESTRIAL INTELLIGENCE
Intelligent tutoring systems as tools for investigating individual differences in learning
09 p1204 N88-17216
An intelligent processing environment for real-time simulation
[NASA-CR-183056] 19 p2715 N88-26119
Reliability and construct validity of reaction time, inspection time and machine-paced tests of cognitive speed
[AD-A193779] 23 p3241 N88-29289

INTELLIGIBILITY
NT SPEECH RECOGNITION

INTENSIFICATION
U AMPLIFICATION

INTENSIFIER TUBES
U IMAGE INTENSIFIERS

INTENSIFIERS
NT IMAGE INTENSIFIERS

INTERACTIONAL AERODYNAMICS
Breakdown of steady and unsteady interacting boundary layers
[NLR-MP-86047-U] 01 p0045 N88-10284
An experimental investigation of the chopping of helicopter main rotor tip vortices by the tail rotor. Part 2: High speed photographic study
[NASA-CR-177457] 09 p1114 N88-16678
Propulsion and airframe aerodynamic interactions of supersonic V/STOL configurations. Volume 1: Wind tunnel test pressure data report
[NASA-CR-177343-VOL-1] 16 p2157 N88-22866
Propulsion and airframe aerodynamic interactions of supersonic V/STOL configurations. Volume 2: Wind tunnel test force and moment data report
[NASA-CR-177343-VOL-2] 16 p2157 N88-22867
Propulsion and airframe aerodynamic interactions of supersonic V/STOL configurations. Volume 4: Summary
[NASA-CR-177343-VOL-4] 16 p2157 N88-22868
Forced response unsteady aerodynamics in a multistage compressor 18 p2512 N88-24903
Research investigation of helicopter main rotor/tail rotor interaction noise
[NASA-CR-4143] 19 p2722 N88-26165
Theory of sound production by vortex-airfoil interaction
[AD-A193386] 21 p3012 N88-27875
An unsteady helicopter rotor: Fuselage interaction analysis
[NASA-CR-4178] 23 p3171 N88-28880
Experience with three dimensional composite grids
23 p3247 N88-29324
Three-dimensional Navier-Stokes simulations of turbine rotor-stator interaction
[NASA-TM-100081] 24 p3316 N88-29750
Experimental and numerical investigation of the effect of distributed suction on oblique shock wave/turbulent boundary layer interaction
[NASA-TM-101334] 24 p3372 N88-30084

INTERACTIONS
Interaction between a module cluster and a plasma in a magnetic field
[PB87-148276] 07 p0934 N88-15675
Process migration in UNIX environments
[NASA-CR-182951] 23 p3245 N88-29311

INTERACTIVE CONTROL
An interactive optimization procedure for the computer aided dimensioning of integrated circuits
[ETN-87-90414] 01 p0082 N88-10531
Interactive Design of Accelerators (IDA)
[DE87-013298] 02 p0234 N88-11476
Microcomputer control of spectroscopic instruments
[ATR-86(8431)-4] 03 p0326 N88-12058
A computer code to process and plot laser altimetry data interactively on a microcomputer
[NASA-TM-100687] 05 p0554 N88-13371
GENLPLOT: An interactive program for display and analysis of data, user's manual
[DE88-002292] 07 p0905 N88-15485
Development and testing of an interactive procedure for the improvement of objective analyses
[AD-A186595] 08 p1040 N88-16290
An interactive user-friendly approach to surface-fitting three-dimensional geometries
[NASA-CR-4126] 12 p1682 N88-20058
A description of an automated database comparison program
[NASA-TM-100609] 16 p2253 N88-23463
EnviroNET: An interactive space-environment information resource
[NASA-TM-101137] 17 p2309 N88-23812
A computer-aided approach to nonlinear control synthesis
[NASA-CR-179391] 22 p3140 N88-28673
Mesh generation for industrial application of Euler and Navier Stokes solvers 23 p3247 N88-29323
Numerical simulation of nozzle flows
[AD-A195144] 24 p3369 N88-30064

INTERACTIVE GRAPHICS
U COMPUTER GRAPHICS

INTERATOMIC FORCES
Investigation of impurity defects in alpha-iron by molecular dynamics method
[DE88-700355] 07 p0834 N88-15058

INTERCALATION
Metal intercalation characteristics of n-HfS2 photoelectrodes in non-aqueous electrolytes
[AD-A184381] 03 p0383 N88-12407
Neutron and X-ray scattering studies of layered solids
09 p1246 N88-17469

INTERCEPTION
Optimal thrust vector control of coplanar orbital evasive maneuvers
[AD-A189544] 13 p1730 N88-20346
Passive DF: A tutorial, part 1
[NASA-CR-182669] 13 p1815 N88-20846

INTERCEPTOR AIRCRAFT
U FIGHTER AIRCRAFT

INTERCONNECTION
U JOINING

INTERCONTINENTAL BALLISTIC MISSILES
NT MX MISSILE

INTERCOSMOS SATELLITES
Intershock observations during STIP intervals 17 and 18 01 p0119 N88-10759

INTERDIGITAL TRANSDUCERS
MESFET compatible IMSM detectors
19 p2659 N88-25801

INTERFACE STABILITY
Lithium/polymer electrolyte interfacial instability
[AD-A187164] 09 p1147 N88-16874
Microscopic control of metallization stability
[AD-A187553] 10 p1421 N88-18487
CdTe(110)-Mn interface reaction and the formation of non-equilibrium ternary semimagnetic semiconductor alloys
[AD-A187593] 10 p1422 N88-18491
The influence of current stressing on the structure of Ag contacts to GaAs
[DE88-005988] 15 p2140 N88-22771
Agenda for advancing electrochemical science and technology 17 p2321 N88-23861
The morphological stability of continuous intergranular phases: Thermodynamic considerations
[DE88-006328] 18 p2584 N88-25350
Stability of a coastal upwelling front over topography
[AD-A192354] 20 p2829 N88-26784
Natural frequencies and stability of immiscible spherical liquid systems
[LRT-WE-9-FB-2(1987)] 22 p3053 N88-28113
Natural frequencies and stability of circular cylindrical immiscible liquid systems
[LRT-WE-9-FB-3(1987)] 22 p3062 N88-28172

INTERFACES
NT FLUID BOUNDARIES
NT LIQUID-LIQUID INTERFACES
NT LIQUID-SOLID INTERFACES
NT LIQUID-VAPOR INTERFACES
NT SOLID-SOLID INTERFACES
Polyitaconic acid macromolecule primer for adhesive bonding and corrosion control of aluminum
[DE87-013306] 01 p0027 N88-10173
Si - SiO2 interfaces: A High Resolution Transmission Electron Microscopy (HRTEM) study
[DE87-012255] 01 p0028 N88-10181
A simulation study of interfaces in Ni, Al and Ni3Al with and without boron
[DE87-013156] 01 p0102 N88-10667
X-ray studies of strain, interface and impurity in semiconductors
[DE87-013856] 01 p0104 N88-10678
Photocatalytic electrochemistry at a biological-membrane metal-colloid interface
[DE87-009122] 02 p0166 N88-11041
Surface topography and electrical response of metal-electrolyte interface
[DE87-013553] 02 p0166 N88-11046
Tutorial and hands-on demonstration of a fluent interpreter for CARE 3
[NASA-TM-4011] 02 p0220 N88-11383
Taper sectioning to magnify the interface thickness of a dissimilar metal joint
[RFP-3890-REV] 03 p0333 N88-12099
Gas tungsten arc welding of Al-10Fe-5Ce
[AD-A184202] 03 p0334 N88-12104
Durability (lifetime) predictions adhesively bonded structures
[AD-A184069] 03 p0335 N88-12110
A scientific workstation operator-interface for accelerator control
[DE87-014689] 03 p0362 N88-12278
Materials sciences programs: Fiscal Year 1987
[DE88-000672] 04 p0429 N88-12659
On computing environments in data analysis
[DE88-000078] 04 p0480 N88-12961
Influence of bond dilution on the free surface and interface Potts ferromagnetism
[DE87-703360] 04 p0497 N88-13061
Non-lattice matched metallic superlattices
[DE87-011512] 04 p0497 N88-13062
Development of an interface for an ultrareliable fault-tolerant control system and an electronic servo-control unit
[NASA-TM-88236] 05 p0553 N88-13367
Reactions of porphyrins in surfactant assemblies, microemulsions and in solutions
[AD-A184797] 05 p0560 N88-13412
Water disbondment characterization of organic Coating/metal substrate systems
[AD-A184847] 05 p0567 N88-13454
Molecular-level synthesis and characterization of metal-polymer interfaces
[AD-A184956] 05 p0567 N88-13455
Bending of a bonded beam as a test method for adhesive properties
[AD-A184813] 05 p0609 N88-13736
Molecular beam epitaxial growth and characterization of 3-5 compound semiconductor single and multiple interface structures
[AD-A185400] 05 p0656 N88-14021
Reactions and bonding between glasses and titanium
[DE88-000603] 06 p0685 N88-14195
Some investigations of molecular beam epitaxial growth of 3-5 semiconductor films via Monte-Carlo computer simulations, carrier tunnelling and spectroscopic ellipsometry
[AD-A185520] 06 p0789 N88-14839
Scientific data manipulation in a relational database system
[PB87-124400] 06 p0791 N88-14850
Interface effects on the mechanical properties of ceramic composites
[AD-A185899] 07 p0826 N88-15009
Orbital Replaceable Unit (ORU)/cold plate thermal interface study. Volume 1: Executive Summary
[BAE-TP-8430] 07 p0855 N88-15195
Online monitoring of laserpulses using the GPIB-interface of a Tektronix 2430 Digital Storage Oscilloscope
[DE88-002836] 07 p0856 N88-15201
An interactive visual interface for Fastbus diagnostics
[DE88-002569] 07 p0900 N88-15453
The feasibility of using TAE as the UIL for the space station and for other internal NASA tasks and projects
07 p0925 N88-15618

Interface between astrophysical datasets and distributed database management systems (DAVID)
[NASA-CR-182394] 07 p0942 N88-15731
Interfacing the expert: Characteristics and requirements for the user interface in expert systems
08 p1063 N88-16419
Media independent interface
[NASA-CR-172033] 08 p1066 N88-16446
Media independent interface. Interface control document
[NASA-CR-172032] 08 p1067 N88-16447
Moving Target Indicator (MTI) interface for simple radar
[FOA-C-30463-3.2] 09 p1154 N88-16914
Study of pattern formation at liquid interfaces
[DE88-001399] 09 p1160 N88-16954
User interface devices for mission control
09 p1205 N88-17224
The desktop interface in intelligent tutoring systems
09 p1205 N88-17225
Interfacing slave designs to Fastbus: Practical experience
[DE88-002807] 09 p1215 N88-17286
A proposal for a feasibility study on the design of software interfaces in large systems
[NPL-DITC-89/87] 09 p1222 N88-17330
Electronic and chemical structure of 3-5/metal and Si/metal interfaces
[AD-A186579] 09 p1254 N88-17518
Surface and interface electronic structure
[DE88-003363] 09 p1258 N88-17545
Molecular dynamics study of high-temperature grain-boundary stability in a (100) sigma = 29 bicrystal model
[DE88-002955] 09 p1258 N88-17546
POCC capabilities document. Payload support capabilities description: MCC, JSC POCC, remote POCC interface
[NASA-TM-89708] 09 p1260 N88-17555
Crew interface with windshear systems
10 p1275 N88-17631
Short fiber reinforced thermoplastic composites for armor applications: Interfacial bonding
[DE88-004007] 10 p1295 N88-17742
Ytterbium monolayer diffusion barriers at Hg(1-x)Cd(x)Te/Al junctions
[AD-A188013] 10 p1299 N88-17768
A detailed microstructural examination of the cause of HAZ cracking in type 316 steel
[AERE-R-12428] 10 p1301 N88-17777
Monitoring interfacial dynamics by pulsed laser techniques
[DE88-003362] 10 p1335 N88-17976
Energy transfers for multilayer hydrodynamic ocean models: General formulation and specific examples
[AD-A187604] 10 p1358 N88-18116
Chips: A tool for developing software interfaces interactively
[AD-A187499] 10 p1389 N88-18295
Application of Onsager's reciprocity relations to interface motion
[DE88-003286] 10 p1397 N88-18327
Local stoichiometry and atomic interdiffusion during reactive metal/mercury-cadmium-telluride junction formation
[AD-A187554] 10 p1421 N88-18488
Nonmonotonic evolution and thermodynamic trends at metal/(Hg,Cd)Te interfaces: Yb/Hg0.78Cd0.22Te
[AD-A187591] 10 p1422 N88-18490
CdTe(110)-Mn interface reaction and the formation of non-equilibrium ternary semimagnetic semiconductor alloys
[AD-A187593] 10 p1422 N88-18491
Void formation in solidification
[DE88-003895] 11 p1452 N88-18650
Parallel pseudospectral domain decomposition techniques
[NASA-CR-181629] 11 p1524 N88-19101
Theoretical studies of the interface electronic properties of tetrahedrally coordinated semiconductors
[AD-A187216] 11 p1555 N88-19306
Formation of buried nitride layers in (110) silicon
[DE88-003255] 11 p1557 N88-19323
Interfacial adhesion: Theory and experiment
[NASA-TM-100830] 13 p1742 N88-20417
Interfacial chemistry-structure and fracture of ceramic composites
[DE88-005516] 13 p1750 N88-20461
Component mode synthesis using experimental modes enhanced by mass loading
[DE88-006097] 13 p1781 N88-20657
An interface between object-oriented systems
[AD-A189245] 13 p1815 N88-20844
Exploring the relation between interface structure and mechanical properties in multilayer structures
[DE88-005428] 13 p1848 N88-21060
Human interfaces in remote driving
[DE88-006843] 14 p1953 N88-21643
Proceedings of the Seminar on Hydrodynamics and Crystal Growth
[ETN-88-92025] 14 p1987 N88-21853
Problems appearing at interface balances --- flames
14 p1987 N88-21855
Common database interface for heterogeneous software engineering tools
[AD-A189628] 14 p1991 N88-21870
Vapor phase deposition and growth of polyimide films on copper
[AD-A189969] 15 p2044 N88-22178
Thermal instability and heat transfer characteristics in water/ice systems
[AD-A189627] 15 p2062 N88-22297
CK-LOG system conversion (user's manual and user interface)
[AD-A190273] 15 p2111 N88-22577
Studies of surfaces using optical sum-frequency generation
[DE88-006334] 15 p2131 N88-22715
Interface formation and precursory dynamics
[AD-A190741] 15 p2144 N88-22794
Surface and interfacial properties of carbon fibers
[NASA-CR-182890] 16 p2173 N88-22951
High temperature solid lubrication by catalytically generated carbon
[AD-A190804] 16 p2182 N88-23004
Laser cladding of Ni, Nb and Mg alloys for improved environmental resistance at high temperature
[AD-A191274] 16 p2213 N88-23208
Microscopic control of semiconductor interface reactivity
[AD-A191193] 16 p2283 N88-23668
Test philosophy of the EH101 integrated avionic
17 p2303 N88-23775
Interfacing and integrating hardware and software design systems
17 p2306 N88-23796
Polyitaconic acid macromolecule primer for adhesive bonding and corrosion control of aluminum
17 p2319 N88-23849
Service offerings and interfaces for the ACTS network of Earth stations
[NASA-TM-100809] 18 p2471 N88-24663
Interfacial shear phenomena in graphite epoxy composites under impact loading using dynamic moire interferometry
[DE88-006773] 18 p2479 N88-24709
Auger analysis of a fiber/matrix interface in a ceramic matrix composite
[NASA-TM-100892] 19 p2610 N88-25487
The development of an intelligent interface to a computational fluid dynamics flow-solver code
[NASA-TM-100908] 19 p2716 N88-26127
Report on the Second Catalog Interoperability Workshop
[NASA-TM-100701] 19 p2718 N88-26135
Ludwig Prandtl collected treatises on applied mechanics, hydro- and aerodynamics, part 2, IV interfaces and resistance
[NASA-TT-20315] 20 p2752 N88-26338
Interface modification in Nicalon (trademark)/SiC composites
[DE88-009708] 20 p2767 N88-26409
Surface phases and their influence on metal-oxide interfaces
[DE88-007938] 20 p2769 N88-26420
Direct manipulation and the design of user interfaces
[PB88-126354] 20 p2834 N88-26810
Common Data Format (CDF) to store images
[NASA-CR-179366] 20 p2836 N88-26825
A high speed serial link interface for SANDAC-V
[DE88-007694] 20 p2842 N88-26861
Superlattice doping interfaces
20 p2866 N88-27019
Fermi level dependent native defect formation: Consequences for metal-semiconductor and semiconductor-semiconductor interfaces
[DE88-008247] 20 p2875 N88-27066
Fundamental optical studies of competitive adsorption and thin film phenomena
[DE88-008780] 20 p2875 N88-27068
Twin boundaries and heterophase interfaces in ferroelastic martensites
[DE88-011894] 21 p2916 N88-27304
Effects of near interfacial microstructure on toughness and subcritical crack growth in ceramic/metal systems
[DE88-009842] 21 p2919 N88-27325
Application of controlled interfacial pore structures to kinetic studies in alumina
[DE88-010884] 21 p2919 N88-27326
Some equivalent circuit models for AC impedance analysis of pyrite/solution interface
[DE88-010574] 21 p2939 N88-27452
Synopsis of a computer program designed to interface a personal computer with the fast data acquisition system of a time-of-flight mass spectrometer
[NASA-CR-177474] 21 p3001 N88-27798
X-ray studies of strain, interface and impurities in semiconductors
[DE88-012460] 21 p3025 N88-27954
Capitalizing on experience with intelligence gateway software
[AD-A193362] 21 p3028 N88-27971
Interface techniques and systems for standard aircraft data buses 22 p3036 N88-28028
Corrosion control through a better understanding of the metallic substrate/organic coating/interface
[AD-A193981] 22 p3056 N88-28132
Chemistry of adhesion at the polyimide-metal interface
[AD-A194647] 22 p3058 N88-28143
An interface for the connection of the SCP2160A pulse analyser to a Hewlett-Packard desk-top computer
[RSRE-MEMO-4030] 22 p3073 N88-28245
Review of past and current trials and uses of unmanned vehicles
[AD-A194527] 22 p3084 N88-28311
A new model for the simulation of interfaces at high temperature
[DE88-009926] 22 p3155 N88-28772
Influence of the interface on the crystallization of amorphous Ge in Pb/Ge multilayers
[DE88-010072] 22 p3156 N88-28776
Model for bimetallic interfaces, part 2
[DE88-702672] 22 p3157 N88-28787
Expandable pallet for space station interface attachments
[NASA-CASE-MSC-21117-1] 23 p3185 N88-28958
Elastic behavior of a rubber layer bonded between two rigid spheres
[AD-A193698] 23 p3198 N88-29030
Experimental investigation of the effects of underwater exposure on the damping characteristics of bolted structural connections for plates and shells
[AD-A194486] 23 p3226 N88-29200
The gradient method for interface tracking
[AD-A194477] 23 p3248 N88-29334
Definition of common support equipment and space station interface requirements for IOC model technology experiments
[NASA-TM-100656] 24 p3336 N88-29856

INTERFACIAL ENERGY

On rotating sphere-on-a-plate experiments and the questions of whether high angle grain boundaries melt below bulk melting temperatures
[DE88-006627] 15 p2038 N88-22142
First-principles calculations of quasiparticle energies at surfaces and interfaces: Semiconductor surface-state spectra and band offsets
[DE88-006340] 15 p2141 N88-22773
Adhesion of hydrated silicate films
[DE88-011250] 21 p2920 N88-27333

INTERFACIAL STRAIN

U INTERFACIAL TENSION

INTERFACIAL TENSION

Calculation of the eigenvibrations of axisymmetric fluid configurations with a singularity method, taking into account surface tension effects under reduced gravity
[ETN-87-90438] 01 p0048 N88-10304
The infiltration kinetics of aluminum in silicon carbide compacts
[AD-A184682] 03 p0290 N88-11823
Double-effect absorption heat pump, phase 3
[PB87-232195] 03 p0317 N88-12005
Numerical analysis of Marangoni convection in Bridgman method 03 p0319 N88-12014
Interfacial strength development in thermoplastic resins and fiber-reinforced thermoplastic composites
[NASA-CR-181525] 04 p0411 N88-12549
Effect of interface on mechanical properties of graphite/201 aluminum composites
05 p0606 N88-13717
Crack opening displacement test in tension
[PB87-143848] 08 p0996 N88-16026
Investigation of surface tension driven convection as a feasibility study for a micro-gravity experiment
[NASA-CR-182504] 11 p1466 N88-18739
The effect of surface tension in the weld pool on seam formation when welding thin sheet with light rays
14 p1898 N88-21334
Electrohydrodynamic migration of charged droplets in an insulating fluid
[NASA-TM-100849] 14 p1912 N88-21424
Selective growth velocity in needle crystals
14 p1988 N88-21858
Methods of measurement for the evaluation of monolayer properties. Development and applications --- lung surfactants
[ETN-88-92229] 15 p2104 N88-22532

A study of surface tension driven segregation in monotectic alloy systems
[NASA-CR-182894] 16 p2178 N88-22983
Dendritic growth in the presence of convection
18 p2580 N88-25328
Interfacial tension of immiscible polymer blends: Temperature and molecular weight dependence
[AD-A192463] 21 p2917 N88-27312
Rubber-modified epoxies: Interfacial tension and morphology
[AD-A192464] 21 p2917 N88-27313
Plasma treatment of polymers for improved adhesion
[DE88-011623] 21 p2921 N88-27334
Effects of surface tension and contact angle on sensible heating and boiling incipience in dielectric falling films
[DE88-007057] 21 p2945 N88-27492
Surface tension and viscosity with Lagrangian hydrodynamics on a triangular mesh
[AD-A194120] 22 p3075 N88-28258
Orbital Propulsion Module (OPM). Study on coni-spherical surface tension tanks (COSTA)
[MBB-URV-170/87] 23 p3187 N88-28963
Surface Tension Confined Liquid Cryogen Cooler (STCLCC)
[NASA-CASE-GSC-13112-1] 23 p3201 N88-29050
Shear stress at a film-substrate interface due to mismatch strain
[AD-A193461] 23 p3288 N88-29577
A test for interfacial effects and stress transfer in ceramic matrix composites
[NASA-CR-182873] 24 p3340 N88-29880
Some theoretical considerations of the surface tension of liquid metals for metal matrix composites
[AD-A195999] 24 p3340 N88-29882
Effect of interfacial phenomena on contact line heat Transfer-3
[AD-A194941] 24 p3343 N88-29901

INTERFERENCE
Wind tunnel wall interference
07 p0811 N88-14938
Status of magnetic suspension technology
07 p0811 N88-14939
Effect of a model support strut on measurement of aerodynamic longitudinal and lateral coefficients
[PB87-170288] 09 p1113 N88-16670
Wideband HF (High Frequency) modeling and simulation
[PB86-116116] 10 p1317 N88-17874
Simulated performance of an order statistic threshold strategy for detection of narrowband signals
11 p1474 N88-18796
Wind tunnel wall interference (January 1980 - May 1988): A selected, annotated bibliography
[NASA-TM-4061] 19 p2604 N88-25466

INTERFERENCE DRAG
Laser velocimeter measurements in a wing-fuselage type juncture
[NASA-TM-100588] 15 p2014 N88-22012

INTERFERENCE FIT
A finite element procedure for interference-fit and cold-working problems with limited yielding
[AR-004-517] 04 p0485 N88-12992
Computed stress and strain distributions under interference fit and after coldworking
[AD-A186950] 10 p1342 N88-18024

INTERFERENCE GRATING
An infrared grating spectrometer for GIRL
[ETN-88-91071] 09 p1167 N88-16997

INTERFERENCE IMMUNITY
Electromagnetic compatibility. View of the near future
[SNIAS-881-422-104] 22 p3071 N88-28229

INTERFERENCE LIFT
An engineering study of hybrid adaptation of wind tunnel walls for three-dimensional testing
[NASA-CR-178374] 07 p0814 N88-14957

INTERFERENCE MONOCHROMATIZATION
U DIFFRACTION

INTERFEROGRAMS
U INTERFEROMETRY

INTERFEROMETERS
NT ETALONS
NT FABRY-PEROT INTERFEROMETERS
NT INFRARED INTERFEROMETERS
NT MACH-ZEHNDER INTERFEROMETERS
NT MICHELSON INTERFEROMETERS
NT MICROWAVE INTERFEROMETERS
NT PHASE SWITCHING INTERFEROMETERS
NT RADIO INTERFEROMETERS
Description of a multiframe optical probing system
[DE87-014255] 02 p0236 N88-11487
Vibrational properties of disordered solids. Far infrared studies: Performance report
[DE88-001474] 06 p0786 N88-14821
Middle atmospheric wind measurements using a medium frequency radar
[AD-A185931] 07 p0879 N88-15330
Optical Fourier transformation by lensless method with perforated mask and with modified Talbot interferometer for analysis of interferograms 09 p1236 N88-17408
Electron density profile reconstruction by maximum entropy method with multichannel HCN laser interferometer system on SPAC 7
[IPPJ-858] 11 p1553 N88-19295
Applications of the lateral shearing interferometer in measurement of synchrotron radiation optical elements
[DE88-005184] 13 p1840 N88-21011
Development of an optical diagnostic instrument. Part 2: Instrument development — space laboratories
[NLR-TR-87079-L-PT-2] 13 p1841 N88-21016
Synthetic-aperture radars viewed as interferometers with matched filter processing of the collected data
[AD-A190608] 15 p2057 N88-22262
Equipment for an advanced electron beam lithography system
[AD-A192956] 21 p2936 N88-27435
Optical bistable behavior of a planar quasi-waveguide interferometer made with a conjugated organic polymer film
[AD-A194349] 22 p3152 N88-28756

INTERFEROMETRY
NT DIFFERENTIAL INTERFEROMETRY
NT HOLOGRAPHIC INTERFEROMETRY
NT LASER INTERFEROMETRY
NT MOIRE INTERFEROMETRY
NT SPECKLE INTERFEROMETRY
NT VERY LONG BASE INTERFEROMETRY
Time-resolved measurements of shock-induced vapor-pressure profiles
[DE87-012972] 01 p0045 N88-10289
ESA Workshop on Optical Interferometry in Space
[ESA-SP-273] 01 p0094 N88-10613
A comparison of interferometry from space and ground 01 p0094 N88-10614
About the interest of solar interferometric observations
01 p0094 N88-10615
Imaging strategies for a spaceborne interferometer
01 p0094 N88-10617
Imaging at radio wavelengths
01 p0094 N88-10618
ISIS: Image reconstruction methods and signal-to-noise ratio investigations — spaceborne interferometry
01 p0094 N88-10619
ISIS: Image reconstruction experiments and comparison of various array configurations — spaceborne interferometry 01 p0095 N88-10620
On the concept of resolution ellipse in aperture synthesis matched deconvolution with error analysis — astronomical interferometry 01 p0095 N88-10621
OASIS: A mission concept — Optical Aperture Synthesis Space Interferometry (OASIS) 01 p0095 N88-10622
COSMIC — Coherent Optical System of Modular Image Collectors (COSMIC); spaceborne telescope
01 p0095 N88-10623
Binary Star Explorer 01 p0095 N88-10624
Fiber-linked telescope arrays on the ground and in space 01 p0095 N88-10626
Space station based interferometry
01 p0096 N88-10628
ESA technological research activities on lightweight mirrors — spaceborne interferometry
01 p0096 N88-10629
NASA/JPL study on optical imaging interferometry in space 01 p0096 N88-10630
Ground-based optical interferometry
01 p0096 N88-10631
Ground-based interferometry with the European Very Large Telescope (VLT) 01 p0096 N88-10632
CERGA high angular resolution optical network — astronomical interferometry 01 p0096 N88-10633
Practical limits to ground based interferometry and its impact on space interferometry
01 p0096 N88-10634
Solar interferometry with a 4-aperture nonredundant and stabilized network 01 p0097 N88-10639
Diagnostics of solar coronal loops at interferometric angular resolution 01 p0098 N88-10642
Short baseline phase delay interferometry
04 p0433 N88-12683
Interferometry theory for the block 2 processor
[NASA-CR-181551] 04 p0440 N88-12730
An optical interferometry technique to evaluate closure along a crack front 05 p0607 N88-13726
Realization of an instrument to measure temperature and concentration gradients in fluids — microgravity
[CISE-3128] 09 p1168 N88-17003
Application of Hoffman modulation contrast microscopy coupled with three-wavelength two-beam interferometry to the in situ direct observation of the growth process of a crystal in microgravity 10 p1286 N88-17704
Interferometric study of natural convection heat transfer from a vertical flat plate with transverse roughness elements 10 p1327 N88-17935
Diagnostics for research in atomization and turbulent two-phase flows
[AD-A187338] 11 p1482 N88-18843
An interferometric investigation of the diffraction of planar shock waves over a half-diamond cylinder in air
[UTIAS-322] 13 p1768 N88-20575
Passive DF: A tutorial, part 1
[NASA-CR-182669] 13 p1815 N88-20846
Optics for large telescope 13 p1840 N88-21014
Continuous measurements of in-bore projectile velocity
[DE88-006841] 15 p2023 N88-22056
Development and applications of optical interferometric micrometrology in the angstrom and subangstrom range
[NASA-TM-100299] 16 p2211 N88-23196
Geodesy by radio interferometry: Optimization of wet path delay algorithms using microwave radiometer data
[PB88-167739] 18 p2498 N88-24820
Interferometric recording of holographic optical elements using partially coherent light
20 p2805 N88-26636
Digital image processing from speckle interferograms by correlation methods: Application in atmospheric optics, astronomy, and biology
[ETN-88-92125] 20 p2855 N88-26953
Is the 3C273 quasar Mach nearer
[DE88-702235] 21 p3030 N88-27988
Interferometric tomography of continuous fields with incomplete projections
[NASA-CR-183181] 22 p3081 N88-28295

INTERGALACTIC MEDIA
Royal Observatory, Edinburgh: Research and Facilities
[ISSN-0267-6281] 14 p1993 N88-21881

INTERGRANULAR CORROSION
Microstructural evolution and response to double-loop reactivation testing of heat-treated pH 13-8 Mo martensitic stainless steel
[DE87-009058] 02 p0146 N88-10915
Study of stainless steel time-temperature sensitization diagrams, part 1
[ETN-87-90762] 03 p0289 N88-11815
The influence of grain boundary chemistry and structure on the intergranular attack and intergranular stress corrosion cracking of austenitic alloys
[DE88-002436] 07 p0835 N88-15063
Mechanisms of intergranular attack and stress corrosion cracking of alloy 600 by high-temperature caustic solutions containing impurities
[DE87-012820] 10 p1300 N88-17773
Stress corrosion cracking properties of Al-Li alloys
17 p2320 N88-23853
The effect of titanium reinforcement on the life of positive grids in lead-acid batteries 17 p2320 N88-23857
Hydrogen embrittlement of iron-nickel alloys
[AD-A195909] 24 p3353 N88-29958

INTERIM STAGES (SPACECRAFT)
NT INERTIAL UPPER STAGE

INTERIM UPPER STAGE (STS)
U INERTIAL UPPER STAGE

INTERIOR BALLISTICS
A study of the interaction of laser light with liquid propellant drops
[AD-A185117] 05 p0587 N88-13582
Experimental determination of the heat flux inside a tubular projectile for the velocity range M = 3 and M = 6
[ISL-R-118/86] 11 p1443 N88-18605
Continued studies of programmed-splitting stick propellant
[AD-A188987] 12 p1613 N88-19644
A study of combustion and flow behaviour in solid-propellant rocket motors
[UTIAS-280] 13 p1732 N88-20357
Two-phase flows in the wake of in-cylinder projectiles
[AD-A189422] 13 p1765 N88-20559
Flamespreading processes in obliquely loaded stick propellant beds
[AD-A195081] 24 p3352 N88-29956

INTERLACING DRAINAGE
U DRAINAGE PATTERNS

INTERLAYERS
NT MULTILAYER INSULATION
Effect of adhesive layers on impact damage and dynamic response in composite laminates
02 p0141 N88-10887
Improving the interlaminar shear strength of carbon fiber-epoxy composites through carbon fiber bromination
[NASA-TM-100248] 07 p0827 N88-15018
Interlaminar fracture toughness of thermoplastic composites
[NASA-TM-100532] 15 p2030 N88-22097
Dimensional crossover in layered superconductors
19 p2734 N88-26237

INTERLOCKING
U LOCKING

INTERMEDIATE FREQUENCIES
Low frequency IF transformer designs having variable coupling
[RAE-TM-RAD-NAV-291] 01 p0043 N88-10272
Performance study of a unipole antenna with conventional and elevated radial wire ground screens
[AD-A193283] 21 p2933 N88-27413
INTERMETALLICS
High temperature metal matrix composites for future aerospace systems
[NASA-TM-100212] 02 p0149 N88-10938
Modelling and theories of alloy phase behavior
[DE87-014399] 03 p0287 N88-11804
Investigation of the deformation behavior of ferritic two-phase Fe-Ni-Al alloys with high concentrations of the intermetallic (Fe, Ni)Al phase at high temperatures
[ETN-87-90605] 03 p0288 N88-11812
Welding and weldability of ductile intermetallic alloys
[DE87-014061] 04 p0416 N88-12582
Experimental perspectives on heavy electron metals
[DE87-014766] 04 p0416 N88-12583
Investigation of the deformation behavior of the intermetallic phase (Fe,Ni)Al at high temperatures
[ETN-88-91062] 09 p1143 N88-16854
Superconductivity of thin film intermetallic compounds
[AD-A187563] 10 p1421 N88-18489
The intergranular segregation of boron in substoichiometric Ni3Al
[DE88-004783] 11 p1462 N88-18720
Thermodynamics of wetting by liquid metals
[DE88-003634] 11 p1563 N88-19360
Development of metastable processing paths for high temperature alloys
[AD-A188682] 12 p1608 N88-19617
Elevated temperature crack growth studies of advanced titanium aluminides
[AD-A189025] 12 p1608 N88-19618
Gordon Conference on Intermetallic Compounds held at Tilton, New Hampshire on 20-24 July 1987
[AD-A188502] 13 p1745 N88-20435
Processing, physical metallurgy and creep of NiAl + Ta and NiAl + Nb alloys
[NASA-CR-182113] 14 p1890 N88-21295
Brillouin scattering and transmission electron microscopy studies of radiation-induced elastic softening, disordering and amorphization of intermetallic compounds
[DE88-005927] 14 p1987 N88-21850
Coexisting static magnetic ordering and superconductivity in CeCu2.1Si2 found by muon spin relaxation 17 p2396 N88-24245
Static magnetic ordering of CeCu2.1Si2 found by muon spin relaxation 17 p2396 N88-24246
Chemical compatibility between silicon carbide and a nickel aluminide
[DE88-006188] 18 p2479 N88-24708
Martensitic transformation and microstructures in sintered NiAl alloys
[NASA-TT-20178] 18 p2488 N88-24761
Martensitic transformation and microstructures in sintered NiAl alloys
[NASA-TT-20192] 19 p2616 N88-25519
Extended ductility of Al and alpha-Fe alloys through dynamic recovery mechanisms
[DE88-008679] 19 p2616 N88-25522
Exploratory development in the system Al-Sc-X
[DE88-008242] 19 p2618 N88-25529
Phase stability and alloy design of ordered intermetallics
[DE88-007479] 20 p2772 N88-26435
Nickel aluminides: A new family of nickel + aluminum alloys featuring simple composition, low density, excellent oxidation resistance and high yield strength that increases with temperature
[DE88-010892] 20 p2776 N88-26461
Superconductivity of heavy-electron uranium compounds
[DE88-007901] 20 p2875 N88-27065
A fundamental understanding of the interfacial compatibility in hybrid material systems
[AD-A192921] 21 p2909 N88-27264
Microchemical analysis of polycrystalline Ni3Al and other ordered alloys using the field-ion microscope atom probe
[DE88-011519] 21 p2914 N88-27294
INTERMITTENCY
Anomalous scaling laws in multifractal objects
[NOTA-INTERNA-883] 07 p0916 N88-15565
Intermittency of atmospheric turbulence--applicatin of Lyapunov exponents and fractional dimension
14 p1900 N88-21348
INTERMODULATION
A GaAs MESFET balanced mixer with very low intermodulation
[AD-A184848] 05 p0655 N88-14015
INTERMONTANE FLOORS
U VALLEYS
INTERNAL COMBUSTION ENGINES
NT CONVERTIBLE FAN-SHAFT ENGINES
NT DIESEL ENGINES
NT GAS TURBINE ENGINES
NT HELICOPTER ENGINES
NT HYDROGEN ENGINES
NT J-57 ENGINE
NT JET ENGINES
NT RAMJET ENGINES
NT ROTARY ENGINES
NT SUPERSONIC COMJUSTION RAMJET ENGINES
NT TF-30 ENGINE
NT TURBOFAN ENGINES
NT TURBOJET ENGINES
NT TURBOPROP ENGINES
NT WANKEL ENGINES
Multidimensional modeling of convective heat transfer with application to IC engines
[DE87-011046] 01 p0055 N88-10353
Japanese industrial research on lean combustion: A case study: International Research Monitoring Program
[DE87-013839] 02 p0144 N88-10904
Needs assessment for nondestructive testing and materials characterization for improved reliability in structural ceramics for heat engines
[DE88-000040] 02 p0153 N88-10957
Development of a light duty gas engine for cogeneration service
[PB87-221297] 02 p0180 N88-11119
Coatings for Advanced Heat Engines Workshop: Book of abstracts
[DE87-012623] 02 p0180 N88-11121
High pressure autoignition of natural gas/air mixtures and the problem of engine knock
[DE87-013799] 03 p0284 N88-11784
Multidimensional modeling of convective heat transfer with application to I.C. engines
[DE87-014983] 03 p0322 N88-12036
Numerical simulation of internal combustion engine flows: Development and users guide for MAGIC radial-azimuthal version
[DE87-014453] 03 p0332 N88-12091
Development, construction and testing of a novel internal combustion engine with conical rotating slide valve
[DE88-900071] 05 p0589 N88-13583
The development and evaluation of three-dimensional models of cold flow in internal combustion engines
[DE88-900077] 05 p0589 N88-13594
The role of low temperature chemistry in the autoignition of n-butane
[DE88-002385] 07 p0829 N88-15031
Multidimensional modeling of convective heat transfer with application to IC engines
[DE88-003398] 10 p1330 N88-17948
An evaluation of effectiveness of PTFE (polytetrafluoroethylene) type friction reducers on reducing friction and wear
[AD-A187440] 10 p1340 N88-18010
Fuel cell/battery hybrid vehicle assessment
[DE88-005087] 10 p1427 N88-18520
Review of the state of the art and projected technology of low heat rejection engines
[PB88-131255] 11 p1496 N88-18934
Status of alcohol fuels utilization technology for highway transportation: A 1986 perspective. Volume 2: Compression ignition engines
[DE88-006059] 13 p1753 N88-20485
Combustion and performance characteristics of methanol plus higher alcohols in a spark ignition engine
[PB88-147962] 14 p1918 N88-21451
JPRS report: Science and technology. Japan
[JPRS-JST-87-030] 16 p2185 N88-23026
Status, trends in research on internal combustion engines 16 p2185 N88-23027
Composite piston
[NASA-CASE-LAR-13435-1] 17 p2346 N88-23981
Multidimensional modeling of convective heat transfer with application to I.C. engines
[DE88-007446] 19 p2738 N88-26257
The outlook for ceramics in heat engines, 1990-2010: Results of a worldwide Delphi survey
[DE88-010075] 20 p2778 N88-26475
Ceramic Technology for Advanced Heat Engines Program data base
[DE88-008954] 20 p2780 N88-26489
Analytical and experimental investigation of ringless piston concept
[AD-A193213] 21 p2956 N88-27559
INTERNAL CONVERSION
The effect of internal relaxation on optoacoustic conversion in liquids
[AD-A191307] 16 p2176 N88-22970
INTERNAL ENERGY
Product kinetic and internal energy distributions via velocity-aligned Doppler spectroscopy
[DE88-003510] 10 p1298 N88-17764
INTERNAL PRESSURE
Durability of compound cylinder under static internal-pressure repeat load of long duration
16 p2180 N88-22991
INTERNAL STRESS
U RESIDUAL STRESS
INTERNAL WAVES
NT PLANETARY WAVES
The effect of ocean fluctuations on sound transmission in the ocean
[AD-A184382] 03 p0355 N88-12236
AFAR (Azores Fixed Acoustic Range) measurements of intensity and intensity moments
[AD-A184431] 03 p0355 N88-12237
A study of the mechanism of internal gravity wave generation by quasigeostrophic meteorological motions
06 p0735 N88-14520
Study of internal gravity waves in the meteor zone
06 p0735 N88-14521
Numerical modeling of troposphere-induced gravity wave propagation 06 p0735 N88-14522
A statistical study of variations of internal gravity wave energy characteristics in meteor zone
06 p0735 N88-14523
Internal gravity waves in the meteor zone in the Tbilisi Region 06 p0736 N88-14528
An analysis of apparent-motion vectors in, and the structure of, A mid-latitude sporadic E layer using a 2.66 MHz radar
[AD-A186126] 07 p0877 N88-15321
Interpretation of equatorial current meter data as internal waves
[PB88-108113] 08 p1044 N88-16309
Wind forcing and observed oceanic wavenumber spectra 13 p1806 N88-20797
Nonlinear surface and internal waves on shear flow
[PREPRINT-584] 22 p3129 N88-28604
INTERNATIONAL COMETARY EXPLORER
U INTERNATIONAL SUN EARTH EXPLORER 3
INTERNATIONAL COOPERATION
Space station: Leadership for the future
[NASA-PAM-509/8-87] 01 p0013 N88-10072
The criterion of equal integrated quality: An improved method of planning DBS systems
[BBC-RD-1987/10] 02 p0161 N88-11012
Materials studies for magnetic fusion energy applications at low temperatures-X
[PB87-232575] 03 p0381 N88-12395
Solar energy: European research and development
[PB87-107645] 04 p0463 N88-12866
Technology transfer to China
[PB87-223418] 04 p0502 N88-13087
The A320 Airbus program
[SNIAS-872-111-105] 05 p0529 N88-13215
Dutch-German wind tunnel's tenth anniversary
[ETN-88-91350] 06 p0670 N88-14105
EISCAT research in Finland in 1986
06 p0691 N88-14234
Current status of world weather service
06 p0725 N88-14459
Integrated Global Background Monitoring Network
[DE88-001503] 06 p0731 N88-14499
Interim review of the possibilities and opportunities for the ONR tropical cyclone motion research initiative
[AD-A185679] 06 p0746 N88-14592
The results of the 1984/1985 Round-Robin Calibration of Reference Solar Cells for the Summit Working Group on Technology, Growth and Employment
[DE88-900215] 07 p0874 N88-15303
International role of US geoscience
[NASA-CR-182407] 08 p1035 N88-16281
The European space physics analysis network
08 p1099 N88-16613
The 2.4 m Space Telescope and ESA participation in the program 09 p1123 N88-16721
A policy for international relations
09 p1123 N88-16724
Unispace 82 09 p1128 N88-16766
Entry into force of the ESA convention
09 p1128 N88-16768
Satellite power systems under consideration by the United Nations 09 p1128 N88-16773
The NORSTAR Program: Space shuttle to space station 10 p1289 N88-17710
Cooperation know-how in high-tech products
[MBB-Z-101/86] 10 p1311 N88-17833
Airbus, the successful European cooperation
[MBB-UT-005/87] 10 p1313 N88-17847
Messerschmitt-Boelkow-Blohm, the company today. Data, numbers and facts 10 p1316 N88-17868
Minutes of the meeting of the Indo-US Subcommission on Science and Technology (8th) held at Washington, D.C. on September 22-24, 1986
[PB88-130158] 10 p1423 N88-18503

Journal of Research of the National Bureau of Standards, volume 92, number 5, September-October 1987
[PB88-124409] 10 p1426 N88-18518
Journal of Research of the National Bureau of Standards, volume 92, number 6, November-December 1987
[PB88-138516] 10 p1426 N88-18519
International geosphere-biosphere program: A study of global change
[PB88-142393] 11 p1510 N88-19021
Proceedings of the First International Symposium on Physical and Technical Problems of Superconductivity Application in Power Generation
[DE88-700818] 11 p1559 N88-19332
Science and technology in India
[PB88-134747] 11 p1584 N88-19362
System-wide medium-term environment programme for the period 1990-1995: Strategies of the United Nations system for the environment
[UNEP/GCSS.I/2] 12 p1641 N88-19826
The influence of infrastructure on the costs and timescales of collaborative programmes
12 p1704 N88-20201
Space projects for the 90's relevant to climatology
14 p1935 N88-21539
The International Satellite Land-Surface Climatology Project (ISLSCP) 14 p1937 N88-21558
Japanese space station module
15 p2052 N88-22224
Overview of 1987 moonlight project
15 p2052 N88-22231
A review of the NATO special group of experts on Naval hydromechanics and related problems
16 p2205 N88-23157
International cooperation in remote sensing: The ESA experience 17 p2356 N88-24038
Discussions and agreements in the United Nations on important issues associated with nuclear power in space
17 p2423 N88-24411
CFD benefits, goals, stepping-stones and techniques. Proposals for the scientific programme of the European Reserch Centre on flow, turbulence and combustion — computational fluid dynamics
[CFDU/88/1] 18 p2510 N88-24894
Centre for International Co-Operation and Approriate Technology (CICAT)
[PB88-165501] 18 p2590 N88-25389
Mobile satellite services: International co-ordination, co-operation and competition 19 p2644 N88-25691
International and domestic regulator issues facing the Canadian MSAT system 19 p2644 N88-25692
Satellites at sea — INMARSAT
19 p2700 N88-26054
Realistic planning scenarios
[AD-A191640] 19 p2740 N88-26267
An agenda for the strategic defense initiative
[RAND-P-7404] 20 p2847 N88-26898
Simulation of the neutronic characteristics of large fast neutron reactors
[ETN-88-92305] 20 p2853 N88-26940
European transonic wind tunnel project: Assistance to the design group
[ONERA-RSF-11/0694-GY-010-G]
21 p2900 N88-27208
Studies concerning the European transonic wind tunnel
[ONERA-RSF-10/0694-GY-010-G]
21 p2900 N88-27209
Metrology in France: Industrial aspects and its status in the world
[SNIAS-881-430-109] 22 p3146 N88-28713
Using standards to break down information transfer barriers 24 p3439 N88-30467

INTERNATIONAL GEOSPHERE-BIOSPHERE PROGRAM
International geosphere-biosphere program: A study of global change
[PB88-142393] 11 p1510 N88-19021

INTERNATIONAL LAW
NT SPACE LAW

INTERNATIONAL PRACTICAL TEMPERATURE
U TEMPERATURE SCALES

INTERNATIONAL RELATIONS
NT INTERNATIONAL COOPERATION
SDI (Strategic Defense Initiative). Where do we go from here
[AD-A194544] 23 p3275 N88-29497

INTERNATIONAL SATS FOR IONOSPHERIC STUDY
U ISIS SATELLITES

INTERNATIONAL SOLAR POLAR MISSION
U ULYSSES MISSION

INTERNATIONAL SUN EARTH EXPLORER 3
Space missions to Comets Halley and Giacobini-Zinner 03 p0272 N88-11712
A comparison between wave observations performed in the environments of Comets Halley and Giacobini-Zinner 14 p1996 N88-21896

INTERNATIONAL SUN EARTH EXPLORERS
NT INTERNATIONAL SUN EARTH EXPLORER 3
Nuclear and ionic charge distribution experiment on ISEE-1 and ISEE-3
[NASA-CR-180776] 23 p3183 N88-28947

INTERNATIONAL SYSTEM OF UNITS
Metrology in France: Industrial aspects and its status in the world
[SNIAS-881-430-109] 22 p3146 N88-28713

INTERNATIONAL TRADE
Aircraft accident reports: Brief format, US Civil and Foreign Aviation, Issue Number 5 of 1986 accidents
[PB87-916907] 08 p0952 N88-15780
Aircraft accident reports: Brief format, US Civil and Foreign Aviation, Issue Number 8 of 1986 accidents
[PB87-916910] 08 p0953 N88-15782
Cooperation know-how in high-tech products
[MBB-Z-101/86] 10 p1311 N88-17833
Status of emerging technologies: An economic/technological assessment to the year 2000
[PB88-155775] 11 p1567 N88-19381
Oceanographic export system development, year 1
[AD-A189134] 14 p1950 N88-21623
Competitive assessment of the U.S. civil helicopter industry
[PB88-186325] 18 p2455 N88-24574
A basis of settlement: Economic foundations of permanent pioneer communities
[DE88-010907] 20 p2762 N88-26382
Commercialization and export — aerospace industry
22 p3161 N88-28824

INTERNATIONAL ULTRAVIOLET EXPLORER
U IUE

INTERPERSONAL RELATIONS
U HUMAN RELATIONS

INTERPLANETARY DUST
NT ZODIACAL DUST
Analysis of laser extracted volatiles in carbonaceous chondrites 06 p0793 N88-14861
Planetary science 07 p0883 N88-15356
Mass loss from evolved stars
11 p1569 N88-19394
Cometary evolution: Clues from chondritic interplanetary dust particles 14 p2002 N88-21934
Cometary grains and interplanetary dust: A polarimetric sensing — Halley 14 p2003 N88-21941
Particles injected by comets 14 p2003 N88-21944
Doppler distortion of solar Fraunhofer lines in zodiacal light by reflection from interplanetary dust
19 p2740 N88-26270

INTERPLANETARY FLIGHT
Preliminary estimates of galactic cosmic ray exposures for manned interplanetary missions
[NASA-TM-100519] 05 p0661 N88-14058
Trade study for kWe class space reactors
17 p2430 N88-24454
Preliminary estimates of radiation exposures for manned interplanetary missions from anomalously large solar flare events
[NASA-TM-100620] 18 p2596 N88-25427
Interplanetary travel: Is gravity needed to close the loop
[NASA-TM-101013] 22 p3132 N88-28622
JPRS report: Science and technology. USSR: Space
[JPRS-USP-88-001] 24 p3444 N88-30498

INTERPLANETARY GAS
Mass loss from evolved stars
11 p1569 N88-19394
Extended atmospheres of outer planet satellites and comets
[NASA-CR-183157] 24 p3457 N88-30572

INTERPLANETARY MAGNETIC FIELDS
Dynamics of magnetic clouds in interplanetary space
01 p0115 N88-10736
Model of solar-wind magnetosphere coupling
04 p0525 N88-13211
Observations of turbulence and fluctuations in the solar wind 04 p0525 N88-13212
The polar ionosphere and interplanetary field
[AD-A185386] 05 p0624 N88-13822
Magnetic field draping about coronal mass ejecta
[DE88-001805] 05 p0661 N88-14057
Interplanetary magnetic field effects on the interaction of the solar wind with Venus 06 p0805 N88-14910
A compilation of Sudden Storm Commencements (SSCs), associated interplanetary disturbances, and cosmic ray variations
[IFSI-86-11] 06 p0807 N88-14923
Monitoring of Pc3 pulsations in solar wind and at Earth by interplanetary magnetic field
08 p1002 N88-16069
Criteria of interplanetary parameters causing intense magnetic storms (Dst less than -100nT)
[NASA-CR-182423] 08 p1024 N88-16200
Polar cusp electrodynamics 08 p1030 N88-16242
Interplanetary Magnetic Field (IMF) influence on the magnetic configuration and particle fluxes at geostationary orbit and on the substorm onset
08 p1031 N88-16247
Bidirectional electron heat flux events in space
[DE88-001791] 08 p1084 N88-16531
Proceedings of the 21st ESLAB Symposium on Small Scale Processes in the Chromosphere/Corona, Interplanetary Medium and Planetary Magnetospheres
[ESA-SP-275] 08 p1094 N88-16582
Interplanetary and geophysical effects of a coronal transient 08 p1095 N88-16587
Transverse flow deflections associated with fast coronal mass ejecta in interplanetary space
[DE88-003180] 09 p1263 N88-17566
Electric fields in Earth orbital space. Magnetospheric structural dynamic response to external variables
[AD-A188592] 12 p1643 N88-19836
Variability of Comet Halley's coma: VEGA-1 and VEGA-2 magnetic field observations 14 p1995 N88-21891
Correlation between magnetic and electric field fluctuations observed during flyby near Halley's comet
14 p1996 N88-21897
Magnetic cavity formation at Comet Halley and at the AMPTE Li release 14 p1996 N88-21898
Time dependent MHD models for the cometary magnetosphere 14 p1997 N88-21900
Observation of energetic particles (E greater than 30 keV) by the Giotto experiment EPA in the magnetic cavity of Comet Halley 14 p1997 N88-21903
Dynamics Explorer-2 measurements during an isolated auroral substorm
[AD-A191202] 18 p2543 N88-25091
On the conjugacy of the aurora: High and low latitudes
[AD-A193008] 20 p2824 N88-26755

INTERPLANETARY MEDIUM
NT INTERPLANETARY DUST
NT INTERPLANETARY GAS
NT ZODIACAL DUST
STIP Symposium on Physical Interpretation of Solar/Interplanetary and Cometary Intervals
[NASA-CR-181201] 01 p0110 N88-10709
Solar-terrestrial observations during STIP interval 15 (12-21 February 1984) 01 p0111 N88-10711
Overview of the MONSEE UAG report on STIP intervals No. 15 and 16: The 24-25 April 1984 Forbush decrease period 01 p0111 N88-10712
The largest white light flare ever observed: 25 April 1984, 0001 UT 01 p0111 N88-10714
Probable detection of solar neutrons by ground-level neutron monitors during STIP interval 16
01 p0111 N88-10715
Solar energetic particles events observed by Prognoz-10 Intercosmos (May-October 1985)
01 p0111 N88-10716
The large Type 4 radio burst event of 24 April 1985 interpreted by dynamic spectral recordings and associated recordings 01 p0112 N88-10717
Propagating shocks in the corona
01 p0112 N88-10718
Change in interplanetary shock acceleration preceding STIP Interval 17 01 p0112 N88-10719
Solar modulation of the cosmic radiation in the heliosphere 01 p0112 N88-10720
Comparison of MHD simulation for the February 1986 events with interplanetary observations by the spacecraft Sakigake 01 p0113 N88-10722
Two dimensional imaging observations of meter-decameter bursts associated with the February 1986 flare activity 01 p0113 N88-10723
Solar origins of coronal mass ejections
01 p0113 N88-10726
Radio studies of large scale structures of the Sun's corona and transient activity 01 p0114 N88-10728
Observations of the brightness temperature distribution of the quiet solar corona at decametric wavelengths
01 p0114 N88-10729
Meterwave observations of a coronal hole
01 p0114 N88-10730
Coronal and interplanetary Type 2 radio emission
01 p0114 N88-10731
Coronal mass ejections: The long-term variation of their occurrence rate and the solar wind mass flux
01 p0114 N88-10732
Was the eclipse comet of 1893 a disconnected coronal transient? 01 p0115 N88-10733
Solar events and their influence on the interplanetary medium 01 p0115 N88-10734
Solar activity, magnetic clouds, and geomagnetic storms 01 p0115 N88-10735
Dynamics of magnetic clouds in interplanetary space
01 p0115 N88-10736
The expansion of magnetic clouds
01 p0115 N88-10737
A numerical study of transient, thermally-conductive solar wind 01 p0115 N88-10738

A two-fluid model for solar wind fluid with higher order moments 01 p0116 N88-10739
Interaction of interplanetary shocks with nonuniform ambient solar wind 01 p0116 N88-10740
An overview of STIP interval 18: September 1985, the G-Z encounter 01 p0116 N88-10741
Comparative plasma tails of Venus and comets 01 p0116 N88-10742
Overview of plasma observations during the Halley flybys 01 p0116 N88-10743
The status of the international Halley watch 01 p0116 N88-10744
Large-scale interaction of the solar wind with comets Halley and Giacobini-Zinner 01 p0117 N88-10745
The global interaction of comets with the solar wind 01 p0117 N88-10746
Solar-terrestrial research in the space station era 01 p0117 N88-10747
Solar wind-cometary interaction at the ionopause and associated phenomena 01 p0117 N88-10748
Comet West: A view from the HELIOS zodiacal light photometers 01 p0117 N88-10749
Solar wind effects on the outer ion coma of Comet Halley 01 p0117 N88-10750
The solar wind interaction with comets: A post encounter view 01 p0118 N88-10751
Plasma-tail activity and the interplanetary medium at Halley's Comet during Armada Week: 6-14 March 1986 01 p0118 N88-10752
Occultation of compact radio sources by the ion tail of Halley's Comet 01 p0118 N88-10753
Equilibrium and tearing stability of thin current layers in magnetic arcades 01 p0118 N88-10754
A simulation of the IPS variations from a magnetohydrodynamical simulation 01 p0118 N88-10755
Study of the mechanism for solar wind formation 01 p0118 N88-10756
An account of a flare related shock event recorded by the energetic particle detector EPONA of the Giotto spacecraft during September 1985 (STIP interval 18) 01 p0118 N88-10757
Interactions of oblique interplanetary discontinuities and their manifestations during STIP intervals 15-19 01 p0119 N88-10758
Intershock observations during STIP intervals 17 and 18 01 p0119 N88-10759
Research in particles and fields [NASA-CR-180412] 01 p0119 N88-10763
Media calibrations of the Doppler signal for a gravitational wave experiment — interplanetary medium [IFSI-86-13] 05 p0625 N88-13825
JPRS report: Science and technology. USSR: Space [JPRS-USP-87-006] 08 p1001 N88-16063
Flare doublet: Interplanetary and geomagnetic effects 08 p1001 N88-16066
Unusually strong density decrease in near-Earth interplanetary plasma and magnetically quiet day as effects of isolated solar flare 08 p1002 N88-16072
Extended atmospheres of outer planet satellites and comets [NASA-CR-181449] 10 p1430 N88-18540
Physical processes in the vicinity of the cometopause interpreted on the basis of plasma, magnetic field and plasma wave data measured on board VEGA-2 spacecraft — Halley's comet 14 p1996 N88-21894

INTERPLANETARY PROPULSION
U INTERPLANETARY SPACECRAFT
U ROCKET ENGINES

INTERPLANETARY SPACE
Overview of STIP intervals 15-19 01 p0110 N88-10710
Satellite environment: Polar orbits 03 p0272 N88-11713
Environmental interactions of solar generators in space 03 p0274 N88-11730
Activities report in interplanetary space physics [IFSI-86-5] 05 p0659 N88-14047
Low-frequency VLBI in space and interstellar refraction [PB87-127643] 06 p0896 N88-14267
Personal overview of solar wind 8 [DE88-003147] 10 p1430 N88-18543
Activities report of the Institute for Extraterrestrial Physics [MPE-206] 21 p3029 N88-27981
Solar flares and magnetospheric particles: Investigations based upon the ONR-602 and ONR-604 experiments [AD-A193396] 21 p3031 N88-27994

INTERPLANETARY SPACECRAFT
NT GALILEO PROBE
NT GALILEO SPACECRAFT
NT MARS OBSERVER
NT MARS PROBES
NT PIONEER VENUS SPACECRAFT
The VISTA spacecraft: Advantages of ICF (Inertial Confinement Fusion) for interplanetary fusions propulsion applications [NASA-CR-181549] 04 p0491 N88-13024
A technique for capture analysis of low thrust missions in a planetary system [AD-A188934] 12 p1594 N88-19544

INTERPLANETARY TRAJECTORIES
Design study for asteroidal exploitation 03 p0389 N88-12445

INTERPOLATION
BIMOND3: Monotone piecewise bicubic Hermite interpolation code [DE87-014612] 02 p0229 N88-11442
A shape preserving interpolant which has tension controls [DE87-014615] 02 p0229 N88-11443
Robust prediction and interpolation for vector stationary processes, 2d enriched version [AD-A185875] 07 p0865 N88-15247
Fast and practical parallel polynomial interpolation [DE88-003530] 10 p1397 N88-18328
Contour-to-grid interpolation with nonlinear finite elements: A feasibility study [AD-A188108] 11 p1503 N88-18980
Interpolation algorithms for digital terrain models [INPE-4373-PRE/1196] 13 p1820 N88-20877
Synthetic-aperture radars viewed as interferometers with matched filter processing of the collected data [AD-A190608] 15 p2057 N88-22262
Derivation of consistent surface fixed fields for use in a global NWP model [AD-A190131] 15 p2093 N88-22475
Multigrid for structures analysis 16 p2218 N88-23232
High degree interpolation polynomial in Newton form [NASA-CR-181677] 18 p2567 N88-25249
A practical shifted Adams algorithm [DE88-008573] 20 p2837 N88-26830
Prolongation, restriction and coarse grid approximation in a three-dimensional cell-centered multigrid method [REPT-88-02] 20 p2846 N88-26889
Two families of graphs satisfying the cycle basis interpolation property [PB88-127808] 20 p2846 N88-26890
Analytical surfaces and grids 23 p3247 N88-29322
Radial basis functions, multi-variable functional interpolation and adaptive networks [RSRE-MEMO-4148] 23 p3265 N88-29436
Method for combined image interpolation-restoration through a fir filter design technique [INPE-4561-PRE/1302] 24 p3413 N88-30315
Reconstruction of multidimensional signals from multiple level threshold crossings [AD-A195561] 24 p3425 N88-30383

INTERPOLATORS
U REPEATERS

INTERPROCESSOR COMMUNICATION
Data Management Working Group report 01 p0016 N88-10097
Study and design of a communication processor unit [RIDU/TREP/1002/SAAB] 01 p0083 N88-10538
Communications for the DTroll distributed database system [AD-A185579] 06 p0791 N88-14853
Study of communication options in a distributed data handling system and survey of advanced man machine communications schemes. Work package 1: Interprocess communication [ESA-CR(P)-2447] 07 p0843 N88-15114
DoD Gateway Information System (DGIS) common command language: The first prototyping and the decision for artificial intelligence [AD-A185950] 07 p0942 N88-15725
DoD Gateway Information System (DGIS): Common command language mapping [AD-A185951] 07 p0942 N88-15726
SAHAYOG: A testbed for load sharing under failure [AD-A186615] 08 p1069 N88-16480
Interdisciplinary research in applied mathematics [AD-A186793] 09 p1226 N88-17344
Multi-processor reduction machines 10 p1382 N88-18253
Air Force Institute of Technology (AFIT) Local Area Network (LAN) performance evaluation model: An analytic model for assessing the impact of changing LAN hardware and software configurations [AD-A187191] 11 p1469 N88-18784
Experience with Berkeley UNIX interprocess communications [AD-A188353] 12 p1680 N88-20041
MultiRPC: A parallel remote procedure call mechanism [AD-A188613] 12 p1680 N88-20046
Locality, communication and interconnect length in multicomputers [CWI-CS-R8708] 13 p1822 N88-20890
Atomic multireader register — computer storage [CWI-CS-R8722] 14 p1954 N88-21648
Enhancement of data acquisition and numerical computation capabilities for unsteady fluid dynamics [AD-A190115] 15 p2063 N88-22302
Alpha structure based B-HIVE multicomputer [AD-A188708] 16 p2244 N88-23405
Reasoning about networks with many identical finite-state processes [AD-A188743] 16 p2245 N88-23413
IPC for modular software requires a third party connect [AD-A189199] 16 p2246 N88-23414
Intelligent systems interconnection: What should come after open systems interconnection? [CWI-CS-R8742] 16 p2253 N88-23465
Locality, communication and interconnect length in multicomputers [CWI-CS-R8743] 16 p2254 N88-23466
A five-layer Open Systems Interconnection (OSI) implementation 17 p2390 N88-24204
Interconnection of high-speed local area networks 17 p2390 N88-24205
Cellular Array Processor (CAP) and its application to computer graphics 19 p2641 N88-25667
Effective communication between a microVAX and a specialized high-speed subprocessor [DE88-007967] 19 p2714 N88-26115
Real time data base management [AD-A191758] 19 p2739 N88-26265
Relay approach message routing in hypercube multiprocessors [DE88-009973] 20 p2835 N88-26814
Correctness criteria for process migration [NASA-CR-182939] 20 p2836 N88-26823
Constructing a highly-available location service for a distributed environment [AD-A192723] 21 p3001 N88-27801
A modular proof of correctness for a network synchronizer [AD-A192726] 21 p3002 N88-27802
LO-CO-GRAF (low cost graphics): Generating maps to support command and control/crisis management using small computers [AD-A193964] 22 p3139 N88-28661
Random-access algorithms for environments with capture [AD-A194303] 23 p3203 N88-29060
Process migration in UNIX environments [NASA-CR-182951] 23 p3245 N88-29311
Design of a self-timed VLSI multicomputer communication controller [AD-A194567] 24 p3361 N88-30014

INTERSTELLAR CHEMISTRY
Circumstellar chemistry 02 p0253 N88-11598
On the interpretation of the 3 micron emission feature in the spectrum of Comet Halley: Abundances in Comet Halley and in interstellar matter 14 p2002 N88-21935
A spectroscopic study of absorption and emission features of interstellar dust components [B8681462] 16 p2289 N88-23706
Observations of star formation 24 p3451 N88-30538

INTERSTELLAR EXTINCTION
A spectroscopic study of absorption and emission features of interstellar dust components [B8681462] 16 p2289 N88-23706

INTERSTELLAR GAS
NT NEUTRAL GASES
Dynamic effects of stellar winds and associated HII regions on the interstellar medium [ETN-87-90421] 01 p0109 N88-10706

INTERSTELLAR MASERS
The distance to the center of the galaxy: H2O maser proper motions in Sgr B2(N) [MPE-PREPRINT-104] 16 p2288 N88-23702

INTERSTELLAR MATTER
NT DARK MATTER
NT INTERSTELLAR GAS
NT NEUTRAL GASES
Composition, structure and chemistry of interstellar dust [NASA-TM-88350] 02 p0253 N88-11603
Adiabatic supernova expansion into the circumstellar medium [DE87-014241] 03 p0387 N88-12433
Hydrogen and deuterium in the local interstellar medium 04 p0521 N88-13204
Galactic interstellar abundance surveys with IUE and IRAS 04 p0522 N88-13206
Exobiology and life science 07 p0883 N88-15358

Molecular clouds at high galactic latitudes
11 p1589 N88-19392
HNC: A detector to study ultraheavy cosmic rays
12 p1713 N88-20252
On the interpretation of the 3 micron emission feature in the spectrum of Comet Halley: Abundances in Comet Halley and in interstellar matter
14 p2002 N88-21935
A spectroscopic study of absorption and emission features of interstellar dust components
[B8681482] 16 p2289 N88-23706
Optical and infrared observations of high latitude dust clouds --- interstellar matter
[B8621135] 16 p2289 N88-23709
Probing the possibility of a (12)C/(13)C abundance gradient from observations of interstellar CH+
[DE88-008908] 20 p2884 N88-27125
Catalog of open clusters and associated interstellar matter
[NASA-RP-1202] 23 p3300 N88-29652

INTERSTELLAR MICROWAVE SPECTRA
U INTERSTELLAR RADIATION
U MICROWAVE SPECTRA

INTERSTELLAR RADIATION
Optical spectroscopy of IRAS sources with infrared emission bands. 1: IRAS 21282+5050 and the diffuse interstellar bands
[NASA-CR-181387] 01 p0094 N88-10611
Photoabsorption and phototdissociation of molecules important in the interstellar medium
[NASA-CR-182435] 08 p1100 N88-16617
Observations of the large scale anisotropy in the cosmic background radiation at 3 mm
[INPE-4425-PRE/1229] 12 p1712 N88-20249

INTERSTELLAR REDDENING
U INTERSTELLAR EXTINCTION

INTERSTELLAR SPACE
Justification and prospects of observations of interstellar, far-infrared emission lines, using a small-sized balloon-borne telescope 08 p1032 N88-16254

INTERSTELLAR SPACECRAFT
Advanced space propulsion study - antiproton and beamed power propulsion
[AD-A189218] 13 p1732 N88-20355

INTERSTELLAR TRAVEL
Engineering planetary lasers for interstellar communication
[NASA-CR-180780] 17 p2311 N88-23825

INTERSTITIALS
Theory of interstitial solutions
[BLL-M-37314-(5828.4)] 02 p0233 N88-11469
Diffusion studies in amorphous NiZr alloys
[DE88-003009] 10 p1301 N88-17781
The intergranular segregation of boron in substoichiometric Ni3Al
[DE88-004783] 11 p1462 N88-18720
Does the pipe diffusion of self-interstitials in crystals under stresses exist
[DE88-701027] 15 p2139 N88-22762
Migration and stability of HgCdTe lattice defects
[AD-A193293] 21 p3021 N88-27935

INTERVALS
STIP Symposium on Physical Interpretation of Solar/Interplanetary and Cometary Intervals
[NASA-CR-181201] 01 p0110 N88-10709
Solar energetic particles events observed by Prognoz-10 Intercosmos (May-October 1985)
01 p0111 N88-10716
The large Type 4 radio burst event of 24 April 1985 interpreted by dynamic spectral recordings and associated recordings 01 p0112 N88-10717
Propagating shocks in the corona
01 p0112 N88-10718
Change in interplanetary shock acceleration preceding STIP Interval 17 01 p0112 N88-10719
Solar modulation of the cosmic radiation in the heliosphere 01 p0112 N88-10720
Comparison of MHD simulation for the February 1986 events with interplanetary observations by the spacecraft Sakigake 01 p0113 N88-10722
Solar origins of coronal mass ejections
01 p0113 N88-10726
Radio studies of large scale structures of the Sun's corona and transient activity 01 p0114 N88-10728
Observations of the brightness temperature distribution of the quiet solar corona at decametric wavelengths
01 p0114 N88-10729
Meterwave observations of a coronal hole
01 p0114 N88-10730
Coronal and interplanetary Type 2 radio emission
01 p0114 N88-10731
Coronal mass ejections: The long-term variation of their occurrence rate and the solar wind mass flux
01 p0114 N88-10732
Was the eclipse comet of 1893 a disconnected coronal transient? 01 p0115 N88-10733
Solar events and their influence on the interplanetary medium 01 p0115 N88-10734
Solar activity, magnetic clouds, and geomagnetic storms 01 p0115 N88-10735
Dynamics of magnetic clouds in interplanetary space
01 p0115 N88-10736
The expansion of magnetic clouds
01 p0115 N88-10737
A numerical study of transient, thermally-conductive solar wind 01 p0115 N88-10738
A two-fluid model for solar wind fluid with higher order moments 01 p0116 N88-10739
Interaction of interplanetary shocks with nonuniform ambient solar wind 01 p0116 N88-10740
An overview of STIP interval 18: September 1985, the G-Z encounter 01 p0116 N88-10741
Comparative plasma tails of Venus and comets
01 p0116 N88-10742
Overview of plasma observations during the Halley flybys 01 p0116 N88-10743
The status of the international Halley watch
01 p0116 N88-10744
Large-scale interaction of the solar wind with comets Halley and Giacobini-Zinner 01 p0117 N88-10745
The global interaction of comets with the solar wind
01 p0117 N88-10746
Solar-terrestrial research in the space station era
01 p0117 N88-10747
Solar wind-cometary interaction at the ionopause and associated phenomena 01 p0117 N88-10748
Comet West: A view from the HELIOS zodiacal light photometers 01 p0117 N88-10749
Solar wind effects on the outer ion coma of Comet Halley 01 p0117 N88-10750
The solar wind interaction with comets: A post encounter view 01 p0118 N88-10751
Occultation of compact radio sources by the ion tail of Halley's Comet 01 p0118 N88-10753
Equilibrium and tearing stability of thin current layers in magnetic arcades 01 p0118 N88-10754
A simulation of the IPS variations from a magnetohydrodynamical simulation
01 p0118 N88-10755
Study of the mechanism for solar wind formation
01 p0118 N88-10756
An account of a flare related shock event recorded by the energetic particle detector EPONA of the Giotto spacecraft during September 1985 (STIP interval 18)
01 p0118 N88-10757
Interactions of oblique interplanetary discontinuities and their manifestations during STIP intervals 15-19
01 p0119 N88-10758
Intershock observations during STIP intervals 17 and 18 01 p0119 N88-10759
Testing and interval estimation in a change-point model allowing at most one change
[AD-A185525] 06 p0767 N88-14716
Detecting and interval estimation about a slope change point
[AD-A186030] 07 p0909 N88-15509
Training in time interval discrimination using verbal feedback 12 p1665 N88-19985
The total interval of a graph
[AD-A189648] 15 p2119 N88-22625

INTERVERTEBRAL DISKS
Hierarchical structure in polymeric solids and its influence on properties
[AD-A194720] 23 p3197 N88-29029

INTESTINES
Use of bifidumbacterin for correction of intestinal dysbacteriosis 07 p0895 N88-15427

INTOXICATION
Age, alcohol, and simulated altitude: Effects on performance and breathalyzer scores
[AD-A190642] 15 p2103 N88-22531

INTRACRANIAL PRESSURE
Neuropeptides in experimental head injury
[AD-A188067] 11 p1520 N88-19077

INTRAMOLECULAR STRUCTURES
Intramolecular dynamics: A study of molecules at high levels of vibrational excitation
[AD-A195285] 24 p3428 N88-30400

INTRUSION
Volcanic contribution to crustal growth in the Central Andes: A new estimate and a discussion of uncertainties
24 p3401 N88-30255

INVALIDITY
U ERRORS

INVARIANCE
NT GAUGE INVARIANCE
Superconformal invariance and superstring in background fields
[DE87-703097] 02 p0247 N88-11581
Carbon-fiber reinforced plastics
04 p0403 N88-12506
Global bifurcation of periodic solutions with symmetry
[AD-A185881] 07 p0908 N88-15501
Relativistic Calogero-Moser systems and solutions
[CWI-PM-R8702] 08 p1092 N88-16570
Status of the electroweak theory
[DE88-002342] 10 p1422 N88-18494
Topics in string theory: Task D
[DE88-004532] 12 p1699 N88-20167
Invariant characteristics of acoustic field in stratified ocean 13 p1788 N88-20698
Chronometrically invariant formulation of electrodynamics equation
[DE88-701030] 13 p1849 N88-21071
Efficient monotone sequential design
[CWI-MS-R8705] 14 p1962 N88-21707
Hyperbolicity and invariant measures for general C sq interval maps satisfying the Misiurewicz condition
[REPT-87-46] 14 p1966 N88-21733
Absolutely continuous invariant measures for C sq unimodal maps satisfying the Collet-Eckmann conditions
[REPT-87-55] 14 p1966 N88-21735
Similarity solutions of nonlinear partial differential equations invariant to a family of affine groups
[DE88-003404] 18 p2567 N88-25245
Rigid symmetries and BRST-invariance in gauge theories
[PB88-180948] 18 p2572 N88-25280
Gravitation and polarization properties of electromagnetic field
[DE88-702166] 19 p2654 N88-25761
Generalized Jordan chains and two bifurcation theorems of Krasnoselskii
[AD-A192353] 21 p3008 N88-27845
On the estimation of a variance ratio
[AD-A193190] 21 p3009 N88-27854
On the computation of finite invariant sets of mappings
[AD-A193670] 22 p3143 N88-28690
Theory of quark mixing matrix and invariant functions of mass matrices
[USIP-87-14] 22 p3159 N88-28800
A nonparametric multidimensional IRT approach with applications to ability estimation and test bias
[AD-A194212] 23 p3273 N88-29483
Invariant ideals of multiplicity free algebraic group actions
[B8803517] 23 p3277 N88-29509
Non-linear scale invariance in a cold-dark-matter universe
[DE88-011725] 23 p3299 N88-29644

INVARIANT IMBEDDINGS
Vortices on the world sheet and string's critical dynamics
[DE88-702116] 21 p3026 N88-27961

INVENTIONS
Identifying areas of leading edge Japanese science and technology: Activity analysis using SIC (Standard Industrial Classes) categories and scientific subfields
[PB87-204087] 02 p0249 N88-11574
Identifying areas of leading edge Japanese science and technology: Patent activity and citation analysis using US POC (Patent Office Classification) classification
[PB87-204095] 02 p0249 N88-11575
Metals. Preliminary study for an Innovation-Oriented research Program (IOP)
[ETN-88-91317] 14 p1889 N88-21290
Innovation-Oriented research Program (IOP) metals. Annexes
[ETN-88-91318] 14 p1889 N88-21291

INVENTORIES
NT CROP INVENTORIES
NT TIMBER INVENTORY
The Aquarack as a potential instrument for basic research work in space biology: Inventory and scientific dispositions 01 p0073 N88-10470
A general approach to error propagation
[DE87-014287] 02 p0224 N88-11412
Inventory of weather stations. Climatological data from Dutch stations, no. 26
[KNMI-150-26] 05 p0628 N88-13841
Investigations on the application of space photographs (Spacelab metric camera) for routine inventories of extensively managed forest areas
[DFVLR-FB-87-22] 09 p1185 N88-17098
Inventory of topographic mapping and standardization of geographic names as the basis of a Geographic Information System (GIS) 16 p2225 N88-23281
Utilization of LANDSAT-TM imagery in the hydroenergetic inventory of the Paraiba de Sul River Basin 17 p2364 N88-24077
Application of SPOT multidate data to wheat yield estimation in Beauce (France) 22 p3094 N88-28374
An evaluation of the utility of SPOT and Thematic Mapper data for providing forest inventory information
22 p3106 N88-28444

Stand-based forestry inventory from SPOT image
22 p3106 N88-28449
The dynamics of transuranics and other radionuclides in natural environments, December 1985
[DE87-014456] 24 p3390 N88-30189

INVENTORY CONTROLS
Comparison of pascal and the dBASE 3 PLUS language in programming an inventory management system
[AD-A184027] 03 p0365 N88-12300
Application of a database system for inventory management of classified material
[AD-A186986] 09 p1261 N88-17558

INVENTORY MANAGEMENT
NT INVENTORY CONTROLS
Comparison of pascal and the dBASE 3 PLUS language in programming an inventory management system
[AD-A184027] 03 p0365 N88-12300
Inventory behavior at remote sites
06 p0796 N88-14873
Application of a database system for inventory management of classified material
[AD-A186986] 09 p1261 N88-17558
A robotic system for automation of logistics functions on the Space Station 23 p3260 N88-29407

INVERSE SCATTERING
Theoretical aspects of target classification: Physical optics and radon transform methods
03 p0304 N88-11915
Elastodynamic ray theory and asymptotic methods for direct and inverse scattering problems
03 p0335 N88-12108
Inverse scattering analysis of diffraction limited SAR
[FOA-C-30459-3.2] 05 p0576 N88-13512
Solitons in stimulated Raman scattering: Generation and control of ultrashort optical pulses
[AD-A185141] 05 p0650 N88-13983
The inverse back scattering problem for the Schroedinger equation in two space dimensions
[AD-A185603] 06 p0765 N88-14701
Direct scattering of electromagnetic waves by one- and two-dimensional objects and its use for inverse profiling
[PB88-126909] 10 p1319 N88-17887
An efficient numerical algorithm for solving scattering and inverse scattering problems of electromagnetic waves
[AD-A188479] 12 p1619 N88-19684
Born-type reconstruction of material parameters of an inhomogeneous, lossy dielectric slab from reflected-field data
[PB88-188958] 18 p2569 N88-25261
Fields and waves 24 p3363 N88-30025

INVERSIONS
NT POPULATION INVERSION
NT TEMPERATURE INVERSIONS
Review of inversion techniques for spaceborne lidar systems
[AD-A184164] 04 p0447 N88-12772
Lower bounds on bearing accuracy for closely spaced sources
[AD-A184258] 04 p0486 N88-12997
Comparing hard and soft prior bounds in geophysical inverse problems
[NASA-CR-181557] 05 p0624 N88-13820
The solution of large linear inverse problems
06 p0691 N88-14238
Development of direct-inverse 3-D methods for applied aerodynamic design and analysis
[NASA-CR-182436] 08 p0950 N88-15767
Inversion of simulated satellite signals
08 p1017 N88-16168
Aerosol size distribution from measurements of the radiance in the solar aureole 08 p1019 N88-16176
Improved canopy reflectance modeling and scene inference through improved understanding of scene pattern
[NASA-CR-182488] 10 p1347 N88-18049
Inversion of parabolic and paraboloidal projections
[AD-A187538] 10 p1405 N88-18380
Regional wave attenuation and seismic moment from the inversion of NORESS spectra
[AD-A187399] 11 p1510 N88-19023
Recursive inversion of externally defined linear systems
[NASA-TM-100070] 11 p1541 N88-19215
The inverse problem and the pseudo-empirical orthogonal function method of solution. Part 1: Theory; Part 2: Application
[AD-A188894] 12 p1684 N88-20069
Electronic properties of semiconductor inversion layers in sub-micron structures
[AD-A188635] 12 p1698 N88-20161
Tectonics and three-dimensional structure of spreading centers: Microearthquake studies and tomographic inversions
[PB88-163290] 14 p1945 N88-21602
Mass, heat and nutrient fluxes in the Atlantic Ocean determined by inverse methods
[NASA-CR-180535] 14 p1950 N88-21626
Seismic inversion by a RMS (Root-Mean-Square) Born approximation in the space-time domain
[PB88-165402] 15 p2131 N88-22711
A diagonally inverted LU implicit multigrid scheme
[NASA-TM-100911] 20 p2753 N88-26340
Sidelobe level of an adaptive array using the SMI (Sampled Matrix Inversion) algorithm
[AD-A193131] 21 p2932 N88-27409
A method for determining absolute velocities from hydrographic data: The numerical code
[AD-A193997] 22 p3129 N88-28603

INVERTEBRATES
NT ARTEMIA
NT DROSOPHILA
NT INSECTS
NT MOLLUSKS
NT SEA URCHINS
NT SNAILS
Five New South Wales barrier lagoons: Their macrobenthic fauna and seagrass communities
11 p1517 N88-19059

INVERTED CONVERTERS (DC TO AC)
Digital control of a direct current converter for a hybrid vehicle
[LAAS-87-266] 05 p0578 N88-13527
Mathematical model for the dc-ac inverter for the Space Shuttle 06 p0793 N88-14860
Costs and benefits of AC propulsion
[PB88-173380] 16 p2287 N88-23691

INVERTERS
Evaluation of stand-alone inverters for remote applications
[DE87-010957] 01 p0040 N88-10257
Digital control of high frequency pulse-width modulated inverters
[ETN-87-90711] 09 p1157 N88-16936
The operational behavior of microprocessor-controlled and pulsed inverter-fed synchronous machines with permanent magnet excitation
[ETN-88-91479] 11 p1480 N88-18833
A high performance inverter-fed drive system of an interior permanent magnet synchronous machine
[DE88-006753] 15 p2061 N88-22288
A microcomputer-based control and simulation of an advanced IPM (Interior Permanent Magnet) synchronous machine drive system for electric vehicle propulsion
[DE88-006735] 18 p2505 N88-24859
Reduced order modeling of grid-connected photovoltaic inverter systems
[DE88-010603] 21 p2969 N88-27635

INVESTIGATION
NT ACCIDENT INVESTIGATION
NT AIRCRAFT ACCIDENT INVESTIGATION
Analysis of 7- X 10-foot high speed wind tunnel shaft loads in support of fan blade failure investigation
[NASA-TM-100504] 04 p0402 N88-12496
The effect of mass, wind angle and erection technique on the aeroelastic behaviour of a cable-stayed bridge model
[NAE-AN-46] 04 p0455 N88-12819
Method for investigating the formation of crystals in a transparent material
[NASA-CASE-MFS-26008-1-CU]
06 p0788 N88-14835
CTD observations in the coastal transition zone off northern California, 16-25 February 1987
[AD-A187283] 10 p1357 N88-18111
Experimental and theoretical methods for investigating helium effects in rapidly solidified metals
[DE88-005542] 13 p1743 N88-20425
A defect investigation of Thunderflash MK N5 (Navy)
[MRL-TN-522] 13 p1754 N88-20488

INVESTMENT CASTING
Investment foundry melting stock. Rolls Royce requirements and demands in terms of quality and the relationship to end product performance
[PNR90397] 02 p0160 N88-11003

INVESTMENTS
The judgement and evaluation of long-term investments demonstrated by means of a civil aircraft program
12 p1701 N88-20180

INVISCID FLOW
NT STAGNATION FLOW
An inviscid model of planar, separated flows of finite extent
[RAE-TR-86070] 01 p0044 N88-10279
Mechanical and flow excited vibrations of elastic plates and cylindrical shells in dense fluids
03 p0316 N88-11996
Some experiences with the viscous-inviscid interaction approach
[NASA-TM-100015] 04 p0395 N88-12466
Solution of the two-dimensional Euler equations on unstructured triangular meshes
04 p0396 N88-12469
Optimization of explicit time-stepping algorithms and Stream-Function-Coordinate (SFC) concept for fluid dynamics problems 04 p0445 N88-12762
Mesoscale eddy dynamics by the method of point vortices 04 p0463 N88-12863
A spatial marching technique for the inviscid blunt body problem 05 p0533 N88-13239
Numerical optimization of conical flow waveriders including detailed viscous effects
05 p0533 N88-13245
The role of computation fluid dynamics in aeronautical engineering (4). The development and applications of implicit TVD finite volume code
05 p0536 N88-13259
The development of a computer code (U2DIIF) for the numerical solution of unsteady, inviscid and incompressible flow over an airfoil
[AD-A185033] 05 p0541 N88-13293
A Cartesian finite-volume method for the Euler equations 05 p0579 N88-13532
A note on the use of symmetric line Gauss-Seidel for the steady upwind differenced Euler equations
[AD-A185223] 05 p0580 N88-13540
Investigation of viscous/inviscid interaction in transonic flow over airfoils with suction 06 p0664 N88-14074
Numerical simulation of flows in axial and radial turbomachines using Euler solvers
06 p0713 N88-14372
Turbulence in hypersonic flow
[AD-A185624] 07 p0815 N88-14961
Inviscid flows, part 1: Formulation of inviscid rotational flow problems by velocity potential and stream function methods. Applications to turbomachines
08 p0985 N88-15964
Viscous flows, part 1 08 p0986 N88-15967
Supersonic aerodynamics of delta wings
[NASA-TP-2771] 10 p1273 N88-17615
The unsteady gas flow through stator and rotor of a turbomachine 10 p1281 N88-17660
Well-posedness and spectral estimation for infinite dimensional systems
[AD-A187621] 10 p1401 N88-18354
Vibrations of shells containing fluid
12 p1635 N88-19787
Application of a flux vector splitting methodology towards the solution of unsteady transonic flows, with future emphasis on the blade flutter problem
[AD-A189500] 13 p1716 N88-20260
Multigrid solution of the Euler equations
13 p1769 N88-20582
Utilization of parallel processing in solving the inviscid form of the average-passage equation system for multistage turbomachinery
[NASA-TM-89845] 14 p1868 N88-21160
Splitting of inviscid fluxes for real gases
[NASA-TM-100856] 14 p1964 N88-21717
Enhanced viscous flow drag reduction using acoustic excitation
[NASA-CR-182734] 15 p2062 N88-22295
High-resolution shock-capturing schemes for inviscid and viscous hypersonic flows
[NASA-TM-100097] 15 p2122 N88-22651
User's manual for EULER3DS
[AD-A191048] 16 p2208 N88-23177
Numerical method for unsteady viscous-inviscid interaction to calculate buffeting
[ONERA-RSF-02/3617-AY-006-A]
17 p2338 N88-23949
Accurate multigrid solution of the Euler equations on unstructured and adaptive meshes
[NASA-CR-181679] 18 p2460 N88-24608
Composite reduced Navier-Stokes procedures for flow problems with strong pressure interactions
[AD-A191127] 18 p2508 N88-24875
Theoretical investigation of 3-D shock wave-turbulent boundary layer interactions, part 6
[AD-A191546] 18 p2509 N88-24882
Axisymmetric viscid-inviscid interaction by a frozen vorticity approximation
[AD-A191743] 18 p2509 N88-24885
Open channel flow near the resonance speed
18 p2514 N88-24918
A study of flow separation in transonic flow using inviscid and viscous computational fluid dynamics (CFD) schemes
[NASA-CR-183119] 20 p2801 N88-26618
Higher order vortex methods with rezoning
[DE88-010777] 21 p2947 N88-27505
Nonlinear oscillations of an inviscid liquid column under zero-gravity
[LRT-WE-9-FB-8(1987)] 22 p3063 N88-28173

Stability of parallel inviscid shear flow with mean spanwise variation
[FFA-TN-1987-57] 22 p3079 N88-28285
Numerical solutions of unsteady inviscid transonic turbine cascade flows
[AD-A196111] 24 p3316 N88-29748

INVISIBILITY
U VISIBILITY

IO
A modeling analysis program for the JPL table mountain Io sodium cloud data
[NASA-CR-182555] 11 p1570 N88-19400
The Io sulfur torus in 1981
[NASA-TM-101139] 18 p2595 N88-25419
The interaction of Io with the plasma torus
23 p3308 N88-29704

IODATES
NT LITHIUM IODATES

IODIDES
NT CESIUM IODIDES
NT SILVER IODIDES
Altered and enhanced iodargyrite with bismuth triiodide for use in precipitation enhancement operations
[AD-A185229] 05 p0561 N88-13419
The kinetics and dynamics of iodine monofluoride formation in gas-phase collisions
[AD-A185715] 06 p0709 N88-14352

IODINE
NT IODINE ISOTOPES
State-to-state dynamics of molecular energy transfer
[DE88-003282] 10 p1406 N88-18382
Preparation and characterization of Cu2Zn1-xMnxGeS4
[AD-A188113] 11 p1556 N88-19315
Measurement of pressure fluctuations in a resonant chamber with laser-induced iodine fluorescence
[DFVLR-FB-87-53] 21 p2955 N88-27551
Growth and characterization of CuGaS2, CuAlS2 and CuGa0.9Al0.1S2 single crystals
[AD-A192963] 21 p3021 N88-27930

IODINE COMPOUNDS
NT CESIUM IODIDES
NT IODIDES
NT LITHIUM IODATES
NT SILVER IODIDES

IODINE ISOTOPES
The Moessbauer effect of SnI4 at high pressure
[DE87-014771] 04 p0495 N88-13048

IODINE LASERS
Theoretical studies of solar lasers and converters
[NASA-CR-181569] 05 p0587 N88-13577
O2-I laser (Oxygen-iodine) mixing studies using LIF (Laser Induced Fluorescence)
[AD-A186667] 09 p1171 N88-17018
Theoretical studies of solar lasers and converters
[NASA-CR-182927] 17 p2344 N88-23972
Frequency doubling at 1.315 micrometers
[AD-A193902] 23 p3208 N88-29092

ION ACCELERATORS
Mechanical design and construction of a 200 mA, 100 keV, dc, negative ion accelerator
[DE88-003855] 11 p1548 N88-19257
Bevalac external beamline optics
[LBL-23240] 19 p2727 N88-26194
Plasma theory and simulation
[AD-A194674] 23 p3286 N88-29565

ION ACOUSTIC WAVES
Observations of an ion acoustic oscillation near a pulsed sheath
[INPE-4386-PRE/1206] 08 p0979 N88-15915
Experiments on ion-acoustic rarefactive solitons in a multi-component plasma with negative ions
[INPE-4393-PRE/1213] 08 p1086 N88-16542
Double layer formed by beam driven ion-acoustic turbulence
[INPE-4292-PRE/1163] 08 p1086 N88-16543
Experimental investigation of double layers formed by ion-acoustic turbulence
[INPE-4296-PRE/1167] 08 p1086 N88-16544
Basic physics of laser-plasma interactions
[ETN-88-92055] 14 p1984 N88-21838

ION BEAMS
Direct formation of thin films and epitaxial overlayers at low temperatures using a low-energy (10-500 eV) ion beam deposition system
[DE87-012291] 01 p0103 N88-10675
Degradation mechanisms of materials for large space systems in low Earth orbit
[NASA-CR-181472] 02 p0143 N88-10896
Multidimensional elemental analysis with the Sandia nuclear microprobe
[DE87-014158] 02 p0183 N88-11136
Fusion reactivity enhancement due to ion tail formation by beam and ion cyclotron heating
[DE87-753018] 02 p0240 N88-11518
Filamentation instability of rotating light ion beams in fusion target chambers
[IPPJ-839] 02 p0242 N88-11530
Analysis of an induction linac driver system for inertial fusion
[DE88-000681] 03 p0379 N88-12384
Negative ion beams for heating and current-drive in NET
[AD-A184390] 04 p0489 N88-13012
PISCES: Plasma-surface interactions and materials research
[DE88-001323] 04 p0494 N88-13044
ICRF launcher studies
[DE88-001710] 04 p0495 N88-13046
Extreme ultraviolet beam-foil spectroscopy of highly ionized neon and argon
[AD-A185197] 05 p0561 N88-13418
The effect of ion beam mixed Ni-Al surface layers on PSB extrusion morphology in fatigued nickel
05 p0598 N88-13652
Ion-beam nitriding of steels
[NASA-CASE-LEW-14104-2] 06 p0682 N88-14179
Surface modification using ion beams: Recent developments at ORNL
[DE88-000951] 06 p0786 N88-14819
Extending the range of Low Energy Electron Diffraction (LEED) surface structure determination: Co-adsorbed molecules, incommensurate overlayers and alloy surface order studied by new video and electron counting LEED techniques
[DE88-001401] 06 p0786 N88-14820
Structure of layered crystals studied by high energy ion beams
[DE88-001675] 06 p0786 N88-14822
Ion mixing and surface modification in metal-semiconductor systems
[DE88-001702] 06 p0786 N88-14823
On a possibility of ion acceleration up to high energies in a high-current electron beam
[DE88-700532] 07 p0931 N88-15657
Method of plasma diagnostics by a heavy ion beam for the T-15 tokamak
[DE88-700342] 07 p0935 N88-15678
Evolution of radiation-induced voids and dislocations at low temperature
[DE88-700350] 07 p0939 N88-15704
Modification of properties of metals by high-power ion beams 08 p1079 N88-16507
Design considerations for a negative ion source for DC operation of high-power, multi-megaelectron-volt neutral beams
[DE88-002692] 08 p1083 N88-16525
Conceptual design of a radio-frequency driven compact tokamak
[INPE-4364-PRE/1190] 08 p1085 N88-16535
Magnetically insulated ion diode with a gas-breakdown plasma anode
[INPE-4382-PRE/1202] 08 p1085 N88-16537
Double layer formed by beam driven ion-acoustic turbulence
[INPE-4292-PRE/1163] 08 p1086 N88-16543
Experimental investigation of double layers formed by ion-acoustic turbulence
[INPE-4296-PRE/1167] 08 p1086 N88-16544
Energy disposal in ion-molecule reactions
[AD-A186772] 09 p1171 N88-17019
Determination of molecular-ion structures through the use of accelerated beams
[DE88-002960] 09 p1246 N88-17467
Application of ECR ion source beams in atomic physics
[DE88-003767] 10 p1406 N88-18384
Optimization of outlet channel of plasma ion source
[DE88-700471] 10 p1410 N88-18415
Composition and thickness of multilayer foils using MeV ion-beam techniques
[DE88-004360] 11 p1448 N88-18629
Ion energy diagnostics for voltage determinations in plasma-erosion-opening-switch experiments
[DE88-004822] 11 p1479 N88-18827
Charge exchange in low energy (keV) and hyperthermal energy (10-100 eV) ion scattering
[AD-A187643] 11 p1543 N88-19222
Ion beam modification of film stress and the effectiveness of thin film encapsulants on GaAs
[DE88-004458] 11 p1558 N88-19328
Silicon containing photoresists
[AD-A188666] 12 p1605 N88-19601
Focused ion beam fabrication of graded channel FET's in GaAs and Si
[AD-A189166] 13 p1845 N88-21040
A novel method for sputter-deposition of high T(sub c) superconductor films via a computer-controlled mass analyzed ion beam
[DE88-006001] 13 p1848 N88-21064
Improvements in end point detection --- semiconductor fabrication
[RSRE-MEMO-4035/A] 14 p1899 N88-21336
In situ TEM observations of heavy ion damage in gallium arsenide
[DE88-005984] 14 p1986 N88-21843
Ion-beam mixing and amorphization in Au/Zr bilayers
[DE88-005999] 15 p2140 N88-22767
Question on the measurement of the metal work function in an electron spectrometer by the secondary-electron emission threshold method
[NASA-TT-20190] 16 p2178 N88-22979
Proceedings of Symposium on Physics of Target Implosion and Pulsed Power Techniques
[IPPJ-859] 16 p2276 N88-23619
Numerical analysis for effects of irradiation nonuniformities on target implosion
16 p2276 N88-23621
Kinetic theoretical analysis for propagation of rotating ion beam in ICF 16 p2276 N88-23623
Hybrid particle simulation for focusing of rotating and propagating LIB 16 p2276 N88-23624
Electron current effect on stability of plasma channel
16 p2276 N88-23625
Numerical analysis of target implosion in LIB ICF
16 p2277 N88-23626
Microinstabilities in ion beam propagation
16 p2277 N88-23631
Self-similar expansions in ion beam fusion
16 p2278 N88-23635
Generation of high brightness ion beam from insulated anode PED 16 p2278 N88-23637
The application of Rutherford backscattering for analyzing multilayered structure change induced by pulsed ion beam bombardment 16 p2278 N88-23638
Two-dimensional focusing of self-magnetically insulated plasma focus diode 16 p2278 N88-23639
Time-resolved spectroscopic measurement of anode plasma in magnetically-insulated diode
16 p2279 N88-23641
Study on the flashover ion diode with cryogenic anode
16 p2279 N88-23642
Ion beam alloying of aluminum for corrosion resistance 17 p2321 N88-23860
A multi-frame ion pinhole camera for intense ion beam transport and focusing experiments
[DE88-007283] 18 p2516 N88-24926
A new approach to generating negative ion beams
[AD-A191119] 18 p2572 N88-25276
An optical technique for measuring divergence, beam profile, and aiming direction, of relativistic negative hydrogen ions
[DE88-007049] 18 p2572 N88-25278
Trochoidal analysis of scattered electrons in a merged electron-ion beam
[NASA-CASE-NPO-16789-1-CU]
18 p2573 N88-25281
Experiments with high energy nuclear beams at Brookhaven: From AGS to RHIC (Relativistic Heavy Ion Collider)
[DE88-007042] 18 p2574 N88-25287
Propagation of neutralized ion beams
[AD-A191599] 18 p2574 N88-25289
Intense ion beam diagnostics for particle beam fusion experiments on PBFA 2
[DE88-007279] 18 p2577 N88-25308
Rutherford magnetic spectrograph for intense ion beam measurements on PBFA 2
[DE88-007281] 19 p2725 N88-26181
Pulsed power driver technologies for inertial confinement fusion power reactors
[DE88-009260] 19 p2731 N88-26221
Equipment for building and testing superconductive flux flow electronic devices
[AD-A192959] 21 p2936 N88-27436
Propagation of charged particle beams in the atmosphere
[AD-A193185] 21 p3014 N88-27887
Plasmoid propagation
[AD-A192378] 23 p3284 N88-29555
Nonlinear analysis of non-neutral plasmas
[AD-A192506] 23 p3284 N88-29556
An HVEM study of displacement cascade damage in Nb3Sn at 13 K
[DE88-009997] 23 p3289 N88-29584
Ion gun generated electromagnetic interference on the SCATHA satellite
[AD-A195179] 24 p3335 N88-29853
Microcircuit trace cutting with focused ion beams
[AD-A196030] 24 p3367 N88-30050
The Single Event Upset (SEU) test facility on the Hardwell tandem generator for cosmic ray simulation
[AERE-R-12896] 24 p3459 N88-30580

ION CHAMBERS
U IONIZATION CHAMBERS

ION CHARGE
Measurements of vacuum arc ion charge state distributions
[DE88-008249] 23 p3284 N88-29558
ION CONCENTRATION
Ion composition measurements in the upper stratosphere — parachute-borne mass spectrometer
[ETN-87-90423] 01 p0069 N88-10442
The formation and thermochemical properties of multiligand complexes
[AD-A184935] 05 p0561 N88-13416
Activated metal oxide surfaces as highly basic and reducing environments
[AD-A184958] 05 p0561 N88-13417
ION CURRENTS
NT ION BEAMS
High ionic conductivity in PEO.PPG block polymer and salt solutions
[AD-A183502] 01 p0026 N88-10168
New materials for electrochemical cells
[AD-A183659] 01 p0037 N88-10238
Ionically conductive polymers: Application to solid state batteries
[AD-A183733] 01 p0037 N88-10239
Dielectric response of ionic conductors
[DE87-013552] 02 p0166 N88-11045
Applications of multivalent ionic conductors to polymeric electrolyte batteries
[AD-A184252] 04 p0439 N88-12722
Effect of sidechain length and crosslinking on ionic conductivity in polyphosphazene solid electrolytes
[AD-A184419] 04 p0497 N88-13058
Ionically conducting polymers: Principles and properties of solid electrolytes
[DE88-001552] 06 p0684 N88-14190
Conductivity studies on hydroxide ion conductors in the Li-Al-O-H system at intermediate temperatures
[AD-A185714] 06 p0697 N88-14279
Phase behavior in the Li-Al-O-H system at intermediate temperatures
[AD-A185732] 06 p0697 N88-14280
The dc conductivity studies of an hydroxide ion conductor at intermediate temperatures
[AD-A186044] 07 p0847 N88-15142
Studies of model ion channels in defect-free multibilayers of phospholipids
[AD-A186740] 16 p2238 N88-23365
Internal erosion rates of a 10-kW xenon ion thruster
[NASA-TM-100954] 18 p2476 N88-24688
Electrical and chemical sensors for biological cell research 19 p2669 N88-25866
Ion thermal conductivity and ion distribution function in the banana regime
[IPPJ-865] 19 p2729 N88-26208
Polymeric electrolytes
[AD-A193766] 23 p3198 N88-29031
ION CYCLOTRON RADIATION
Fusion reactivity enhancement due to ion tail formation by beam and ion cyclotron heating
[DE87-753018] 02 p0240 N88-11518
Planning for US ion cyclotron heating research relevant to the compact ignition tokamak and Alcator C-Mod
[DE88-000022] 02 p0241 N88-11520
Applications of neutral beam and rf technologies
[DE87-014936] 03 p0379 N88-12382
Theoretical atomic and molecular physics
[DE88-001625] 05 p0649 N88-13974
Parallel gradient effects on ICRH (Ion Cyclotron Resonance Heating) in tokamaks
[DE88-009038] 19 p2730 N88-26216
ION DENSITY (CONCENTRATION)
NT IONOSPHERIC ION DENSITY
NT MAGNETOSPHERIC ION DENSITY
NT PROTON DENSITY (CONCENTRATION)
Self-consistent modification of a fast tail distribution by resonant fields in nonuniform plasmas
[AD-A183790] 01 p0099 N88-10650
The effect of object potentials on the wake of a flowing plasma
[AD-A184038] 03 p0379 N88-12385
Data processing of the JPA instrument. Part 1: Data management
[IFSI-88-15-PT-1] 06 p0757 N88-14645
Ionic mechanisms of soot formation in flames
[AD-A186195] 08 p0966 N88-15848
Anthropogenic effects on the droplet formation process, and ion concentrations in droplets --- clouds
08 p1018 N88-16175
Characteristics of laser-plasma X-radiation source (review) 09 p1239 N88-17428
Electrosorptive detection based on double-layer capacitance for selective anion monitoring in ion chromatography. Part 1: Mercury electrodes
[AD-A188780] 12 p1606 N88-19603
Nonlinear resonance of two-dimensional ion layers
[AD-A188890] 12 p1695 N88-20145
Spectral diagnostics for temperature and density measurements on ATF 17 p2442 N88-24525
ION DISTRIBUTION
Measurement of parallel ion energy distribution function in PISCES plasma
[DE88-000108] 03 p0378 N88-12380
Ion thermal conductivity and ion distribution function in the banana regime
[IPPJ-865] 19 p2729 N88-26208
Moment approach to neoclassical flows, currents and transport in auxiliary heated tokamaks
[DE88-008024] 21 p3016 N88-27901
Nuclear and ionic charge distribution experiment on ISEE-1 and ISEE-3
[NASA-CR-180776] 23 p3183 N88-28947
ION EMISSION
Characterization of Er,Cr:YSGG
[AD-A185885] 07 p0932 N88-15659
Observation of nonlinear wave decay processes in the solar wind by the AMPTE IRM plasma wave experiment
[AD-A191409] 16 p2290 N88-23713
Ion gun generated electromagnetic interference on the SCATHA satellite
[AD-A195179] 24 p3335 N88-29853
ION ENGINES
NT MERCURY ION ENGINES
An 8-cm ion thruster characterization
[NASA-CR-180819] 01 p0017 N88-10106
Megawatt level electric propulsion perspectives
17 p2404 N88-24294
Electric propulsion options for the SP-100 reference mission 17 p2404 N88-24296
TRICE design, evaluation and feasibility tests
17 p2437 N88-24498
Internal erosion rates of a 10-kW xenon ion thruster
[NASA-TM-100954] 18 p2476 N88-24688
Performance of 10-kW class xenon ion thrusters
[NASA-TM-101292] 22 p3049 N88-28088
The NASA Electric Propulsion Program
[NASA-TM-101324] 24 p3336 N88-29859
ION EXCHANGE MEMBRANE ELECTROLYTES
Studies of transport processes in porous and ion exchange membranes
[ISBN-951-99847-0-4] 01 p0021 N88-10133
ION EXCHANGING
Heterogeneous isotope exchange between solid cesium iodide and gaseous methyl iodide
[ETN-88-91085] 09 p1141 N88-16840
Molecular and electronic mechanism in the control of Na+ and K+ permeability of excitable cell membrane by ligand binding on receptor sites
[AD-A188725] 13 p1808 N88-20805
Solid-state electrochemical processes in dye films
[AD-A188756] 13 p1844 N88-21036
Electronic and ionic transport in polymers
[AD-A190434] 15 p2045 N88-22185
Computer simulation of uphill diffusion in ternary ionic system
[NASA-TT-20194] 18 p2573 N88-25285
Dual mechanism bifunctional polymers: Design, synthesis and application of a new category of metal ion complexing agents
[DE88-008233] 20 p2777 N88-26468
Ion exchange processes for fabrication of integrated optical waveguide structures into glass substrates
[VTT-46] 24 p3429 N88-30405
ION EXTRACTION
Application of magnetic barrier for increasing the efficiency of laser ion source
[DE88-701669] 16 p2212 N88-23200
Ion generator and ion application system
[NASA-CASE-MFS-28122-1] 17 p2397 N88-24253
ION GAGES
U IONIZATION GAGES
ION IMPLANTATION
Ion-implantation-induced stress in glasses: Variation of damage mode efficiency with changes in glass structure
[DE87-013523] 01 p0028 N88-10175
Electrical behavior of layers implanted with low energy pions in Si
[INPE-4199-PRE/1051] 01 p0102 N88-10670
Studies on surface chemical states of some metals and ceramics bombarded with energetic light-ions
[DE87-752975] 02 p0145 N88-10910
DSA RuO2/TiO2 electrode modeled by ion implantation: An in situ characterization by photoacoustic and photocurrent spectroscopy
[DE87-009129] 02 p0245 N88-11545
Modeling of irradiation-induced amorphization in a titanate ceramic
[DE87-014751] 03 p0292 N88-11833
Microstructural change of Al on H implantation
[IPPJ-847] 04 p0493 N88-13036
Fatigue characteristics of ion treated surfaces
05 p0606 N88-13713
Develop techniques for ion implantation of (lead-lanthanum-zirconate-titanate) for adaptive optics
[DE88-000642] 05 p0650 N88-13986
Structural characterization of ion implanted beta-SiC thin films
[DE87-014567] 05 p0656 N88-14027
Basic energy sciences research in the Metals and Ceramics Division of Oak Ridge National Laboratory
[DE87-013538] 06 p0681 N88-14171
The effect of ion implantation on the corrosion behavior of a high-density sintered tungsten alloy
[AD-A185713] 06 p0683 N88-14185
Theoretical aspects of channeling, damage, and range distributions for low (keV) and high (MeV) energy implantation
[DE88-000949] 06 p0786 N88-14818
Surface modification using ion beams: Recent developments at ORNL
[DE88-000951] 06 p0786 N88-14819
Ion mixing and surface modification in metal-semiconductor systems
[DE88-001702] 06 p0786 N88-14823
X-ray measurements of phason distortion in ion-implanted Al-Mn
[DE87-014566] 07 p0937 N88-15694
Analysis of load-bearing capacity of nitrided layer
[PB87-144176] 08 p0968 N88-15857
Control of solid-excitation-based photochemical dry etching of semiconductors by ion-bombardment-induced damage
[DE88-003214] 09 p1257 N88-17537
Effects of ion implantation on cavitation erosion of a cobalt based metal/carbide alloy
[AD-A187239] 10 p1303 N88-17793
Metal modification for improved glass-ceramic to metal seals: 1. Auger results on ion implantation and vapor deposition films
[DE88-005244] 10 p1339 N88-18006
Formation of optical waveguides by ion implantation
[DE88-003894] 10 p1409 N88-18407
Electrochemical and optical investigations on ion-implanted TiO2 samples
[ETN-88-91485] 11 p1455 N88-18670
In situ ultrahigh vacuum friction measurement and wear track analysis of ion implanted 304 stainless steel
[DE88-004537] 11 p1494 N88-18922
Optical waveguide formation by ion implantation of Ti or Ag
[DE88-004595] 11 p1551 N88-19278
Formation of buried nitride layers in (110) silicon
[DE88-003255] 11 p1557 N88-19323
Ion beam modification of film stress and the effectiveness of thin film encapsulants on GaAs
[DE88-004458] 11 p1558 N88-19328
An in situ annealing study of lead implanted single crystal calcium titanate
[DE88-005435] 11 p1562 N88-19351
Fundamental studies and device development in beta silicon carbide
[AD-A189540] 12 p1699 N88-20165
Temperature dependence of Kr precipitation in Ni
[DE88-005953] 13 p1744 N88-20429
Focused ion beam fabrication of graded channel FET's in GaAs and Si
[AD-A189166] 13 p1845 N88-21040
Optical study of germanium, germanium plus arsenic, and germanium plus gallium implants in gallium arsenide
[AD-A189600] 13 p1845 N88-21045
Secondary electron emission characteristics improved by ion implantation 14 p1903 N88-21370
Effect of P implantation on the corrosion behavior of Fe-Cr alloys
[DE88-005732] 15 p2040 N88-22158
Ion-beam mixing and amorphization in Au/Zr bilayers
[DE88-005999] 15 p2140 N88-22767
High density ion implanted contiguous disk bubble technology
[AD-A190169] 15 p2143 N88-22789
Microelectronics the next fifteen years
17 p2305 N88-23792
Ion beam alloying of aluminum for corrosion resistance 17 p2321 N88-23860
Planar fully ion-implanted high power InP MISFETs
[AD-A191589] 18 p2582 N88-25338
Studies of boron implantation through photochemically deposited SiO2 films on Hg(sub 1-x)Cd(sub x)Te
[SD-TR-87-26] 19 p2621 N88-25548
Carrier lifetime versus ion-implantation dose in Silicon On Sapphire 19 p2658 N88-25791
High dose uranium ion implantation into silicon
[LBL-23509] 19 p2725 N88-26182
Ion implantation processing of 3-5 strained-layer semiconductors
[DE88-005270] 19 p2734 N88-26240

Development of high current and high brightness negative hydrogen ion sources
[DE88-010882] 20 p2852 N88-26934
A fundamental understanding of the interfacial compatibility in hybrid material systems
[AD-A192921] 21 p2909 N88-27264
Thin film and near-surface characterization using a mechanical properties microprobe
[DE88-011399] 21 p2915 N88-27302
Focused ion beam fabrication of graded channel FETs in GaAs and Si
[AD-A193098] 21 p2936 N88-27439
Friction, wear and electrical contact resistance of precious metal alloys
[DE88-011244] 21 p2938 N88-27450
Use of Moessbauer spectroscopy to study implanted surfaces
[DE88-010452] 21 p3023 N88-27942
Rivista Tecnica Selenia, volume 10, no. 3, 1987
[ETN-88-92717] 22 p3068 N88-28210
A 400 kV ion implanter: Operating principles and applications 22 p3069 N88-28213
Rapid thermal annealing of silicon layers amorphized by ion implantation
[DE88-702307] 23 p3290 N88-29591
Electrical conductivity of GaAs layers implanted on semi-insulator nondoped substrates
[CERT-422000/RF] 23 p3294 N88-29614

ION INJECTION
Particle injection and cosmic ray acceleration at collisionless parallel shocks
[DE88-000507] 04 p0430 N88-12665
Status of RF superconductivity at Argonne National Laboratory
[DE88-005913] 15 p2144 N88-22796
Dynamics explorer data analysis
[NASA-CR-181428] 19 p2691 N88-25996

ION IRRADIATION
NT DEUTERON IRRADIATION
NT PROTON IRRADIATION
Monte Carlo calculations for the simulation of channeling experiments on irradiated aluminum alloys. Calculation of angle-dependent efficiency curves
[HMI-B-433] 01 p0092 N88-10597
Ion-beam nitriding of steels
[NASA-CASE-LEW-14104-2] 06 p0682 N88-14179
Theoretical aspects of channeling, damage, and range distributions for low (keV) and high (MeV) energy implantation
[DE88-000949] 06 p0786 N88-14818
Laser fluorescence spectroscopy of zinc neutrals originating from laser-irradiated and ion-bombarded zinc sulfide and zinc surfaces
[DE88-006033] 13 p1776 N88-20620

ION MICROSCOPES
Field ion microscope studies of surface reconstructions
[DE87-014644] 02 p0147 N88-10924
Atomic-level studies of superconducting YBa2Cu3O sub 7-x
[DE88-002522] 06 p0788 N88-14831
Characterization of duplex stainless steel by TEM (Transmission Electron Microscopy), SANS (Small-Angle Neutron Scattering) and APFIM (Atom-Probe Field Ion Microscopy) techniques
[DE88-002916] 09 p1145 N88-16865
SHaRE: Collaborative materials science research
[DE88-007175] 18 p2467 N88-24648

ION MOTION
Nuclear magnetic resonance studies of ion motion in solid electrolytes
[DE87-014547] 02 p0232 N88-11464
A generalized description of the anomalous Doppler resonance and the stabilizing role of ion dynamics
[INPE-4384-PRE/1204] 08 p1081 N88-16513
Advanced studies of integrable systems
[AD-A186792] 09 p1151 N88-16895
Theory of laser cooling and spectroscopy of harmonically trapped single atoms
[AD-A189576] 13 p1775 N88-20617

ION OSCILLATION
U PLASMA OSCILLATIONS

ION PLATING
Ion plating: Fundamental processing studies and synthesis of high performance coatings
[AD-A184766] 03 p0303 N88-11908
Ion plating for corrosion control
[AD-A185061] 05 p0565 N88-13442
Tin activated reactive ion plating and its application
[PB87-144036] 08 p0970 N88-15871
Structure and properties of titanium nitride and zirconium nitride thin films prepared by reactive ion plating — cutting tools
[ETN-88-92218] 15 p2042 N88-22167
Status and directions of modified tribological surfaces by ion processes
[NASA-TM-101304] 22 p3063 N88-28176

ION PROBES
Studies of fluorine combustion
[AD-A187646] 11 p1452 N88-18656
Electronic and ionic transport in polymers
[AD-A190434] 15 p2045 N88-22185
Laser spectoscopy of plasmas
[AD-A193009] 20 p2861 N88-26991
Role of zircon in tracing crustal growth and recycling 24 p3394 N88-30211

ION PRODUCTION RATES
On formulating a simple D-region model
[AD-A195841] 24 p3392 N88-30197

ION PROPULSION
An 8-cm ion thruster characterization
[NASA-CR-180819] 01 p0017 N88-10106
Auxiliary propulsion system flight package
[NASA-CR-180828] 02 p0141 N88-10886
Design study for asteroidal exploitation 03 p0389 N88-12445
High power ion thruster performance
[NASA-TM-100127] 04 p0409 N88-12542
Intelligent on board control for field emission electric propulsion system 12 p1589 N88-19513
Plasma-gas interaction studies in a hybrid plume plasma rocket
[AD-A190310] 15 p2138 N88-22755
Advanced electric propulsion research
[NASA-CR-182130] 16 p2170 N88-22937
A cyclic ground test of an ion auxiliary propulsion system: Description and operational considerations
[NASA-TM-100870] 17 p2313 N88-23829
High power ion thruster performance 17 p2404 N88-24295

ION RECOMBINATION
Wavelength scaling of lithium-like recombination scheme for X-UV gain production — X-ray lasers
[ETN-88-92002] 13 p1778 N88-20634

ION SCATTERING
An interactive computer program for materials analysis by means of ion scattering
[MRL-R-1040] 01 p0091 N88-10596
Atomic physics with highly charged ions
[DE88-000894] 05 p0648 N88-13972
Charge exchange in low energy (keV) and hyperthermal energy (10-100 eV) ion scattering
[AD-A187643] 11 p1543 N88-19222
Studies of model ion channels in defect-free multibilayers of phospholipids
[AD-A188740] 16 p2238 N88-23365
Inelastic ion-surface collisions
[AFGL-TR-87-0206] 19 p2724 N88-26174

ION SELECTIVE ELECTRODES
Thin films for geothermal sensing
[DE88-000154] 03 p0326 N88-12061
High polymer sensor materials discussed 06 p0676 N88-14140
Chemical multisensors with selective encapsulation of ion-selective membranes 19 p2670 N88-25869
Silver multi-layers for planar Ag/AgCl reference electrodes 19 p2672 N88-25883
Functional study of the Si/SiO2 structures. Application to the implementation of an integrated ion sensor
[ECL-87-16] 22 p3073 N88-28246

ION SHEATHS
Irradiation test results on thermionic fuel element sheath insulators 17 p2402 N88-24280

ION SOURCES
Theoretical atomic and molecular physics
[DE88-001625] 05 p0649 N88-13974
Design considerations for a negative ion source for DC operation of high-power, multi-megaelectron-volt neutral beams
[DE88-002692] 08 p1083 N88-16525
A fiber-optic link for pressure control of ion sources
[DE88-001782] 09 p1248 N88-17484
Application of ECR ion source beams in atomic physics
[DE88-003767] 10 p1406 N88-18384
Optimization of outlet channel of plasma ion source
[DE88-700471] 10 p1410 N88-18415
Magnetic and inertial fusion status and development plans
[DE88-004405] 11 p1552 N88-19288
A moment approach to modeling negative ion sources
[AD-A188858] 12 p1691 N88-20114
Application of magnetic barrier for increasing the efficiency of laser ion source
[DE88-701669] 16 p2212 N88-23200
Multiply stripped ion generation in the metal vapor vacuum arc
[DE88-008418] 19 p2725 N88-26179
A low divergence, high brightness lithium ion source for plasma diagnostics
[DE88-008063] 19 p2729 N88-26203
Sources of polarized ions and atoms
[DE88-010910] 20 p2852 N88-26931
Development of high current and high brightness negative hydrogen ion sources
[DE88-010882] 20 p2852 N88-26934
Enhancement of volume H(-) production by vibrationally pre-exciting the hydrogen molecules
[DE88-010783] 20 p2853 N88-26937
Field-enhanced lithium ion sources for PBFA 2
[DE88-007195] 20 p2856 N88-26960

ION SPECTROMETERS
U MASS SPECTROMETERS

ION STORAGE
Ion traps for large storage capacity 16 p2268 N88-23570

ION STRIPPING
Neutral beam propagation through the atmosphere
[AD-A188984] 12 p1691 N88-20115

ION TEMPERATURE
High ionic conductivity in PEO,PPG block polymer and salt solutions
[AD-A183502] 01 p0026 N88-10168
Hydroxide ion conductors as possible electrolytes in intermediate temperature fuel cells
[AD-A185508] 06 p0731 N88-14495
Magnetic and inertial fusion status and development plans
[DE88-004405] 11 p1552 N88-19288
Alfven waves in plasma with finite ion temperatures 14 p1972 N88-21769
Ion temperature measurement with spectroscopy in JT-60 17 p2439 N88-24513
Ion temperature profile measurement using charge exchange recombination spectroscopy on JIPP T-IIU 17 p2440 N88-24518
Spectroscopic measurements of ion temperature, rotation speed and beam deposition profile on DIII-D 17 p2440 N88-24519
Forbidden transitions as ion-temperature sensitive lines 17 p2441 N88-24520
Spectroscopic study of heliotron E plasmas: Stark profile, CXR, poloidal rotation and carbon coating 17 p2441 N88-24523
Spectral diagnostics for temperature and density measurements on ATF 17 p2442 N88-24525
Properties of hydrogen/helium accretion plasmas
[DE88-006831] 19 p2728 N88-26197
Effects of secondary electron emission on the collector and source sheaths of a finite ion temperature plasma
[DE88-008930] 20 p2858 N88-26971
Effects of low reflection on the collector and source sheaths of a finite ion temperature plasma
[DE88-008929] 21 p3017 N88-27908
Collector and source sheaths of a finite ion temperature plasma
[DE88-008934] 23 p3286 N88-29564

ION TRAPS (INSTRUMENTATION)
Large hydrogen cluster ions 16 p2267 N88-23558
First capture of antiprotons in an ion trap and the possibility of antihydrogen 16 p2268 N88-23569
Ion traps for large storage capacity 16 p2268 N88-23570
Long duration coherent Lyman-alpha sources 16 p2268 N88-23571
Magnetic traps for an anti-hydrogen gas 16 p2269 N88-23572
Examination of the termalization of confined ions
[PB87-227815] 19 p2723 N88-26171

IONIC COLLISIONS
Radiation induced collapse of the crystalline structure
[DE87-014407] 04 p0498 N88-13064
Atomic physics with highly charged ions
[DE88-000894] 05 p0648 N88-13972
The approach to equilibrium in a quark-gluon plasma
[DE88-002117] 09 p1251 N88-17499
Control of solid-excitation-based photochemical dry etching of semiconductors by ion-bombardment-induced damage
[DE88-003214] 09 p1257 N88-17537
Large hydrogen cluster ions 16 p2267 N88-23558
Associative two-body condensation in laser-cooled sodium and hydrogen 16 p2267 N88-23559
Distorted-wave-method calculation of electron-impact excitation of atomic ions 17 p2443 N88-24532
Plasma neutralizer work at BNL (Brookhaven National Laboratory)
[DE88-007046] 18 p2579 N88-25317
Inelastic ion-surface collisions
[AFGL-TR-87-0206] 19 p2724 N88-26174
Theoretical atomic and molecular physics
[DE88-007122] 19 p2724 N88-26175
Atomic physics of strongly correlated systems
[DE88-007789] 19 p2724 N88-26177

Fluid dynamical model of ultrarelativistic heavy ion collisions
[DE88-007905] 20 p2850 N88-26921
Eikonal solutions to optical model coupled-channel equations
[NASA-TP-2830] 24 p3428 N88-30402

IONIC CONDUCTIVITY
U ION CURRENTS

IONIC DIFFUSION
GAS 450: A space payload for the People Central Coast Student Experimenters 10 p1289 N88-17709
Anisotropy of light absorption by color centers in waveguides produced on photochromic glasses by diffusion 14 p1896 N88-21320
Computer simulation of uphill diffusion in ternary ionic system
[NASA-TT-20194] 18 p2573 N88-25285
Inner-shell X-ray line spectra of highly ionized titanium, chromium, iron and nickel and their appliation to laboratory plasmas
[PB87-225181] 19 p2730 N88-26212

IONIC MOBILITY
Ionic transport and electrical relaxation in glass
[DE88-000887] 05 p0657 N88-14028
Ionically conducting polymers: Principles and properties of solid electrolytes
[DE88-001552] 06 p0684 N88-14190
Some aspects of metallic ion chemistry and dynamics in the mesosphere and thermosphere 06 p0737 N88-14534
High power storage system based on thin film solid ionics
[AD-A193623] 23 p3291 N88-29598

IONIC PROPELLANTS
U ION ENGINES

IONIC REACTIONS
Relativisitic heavy ion collisions
[DE87-014292] 02 p0232 N88-11462
Atomic physics with highly charged ions
[DE88-000894] 05 p0648 N88-13972
Studies in solid state ionics
[DE88-700830] 11 p1559 N88-19333

IONIC WAVES
A possible role for ionospheric ions in triggering a geomagnetic substorm onset 08 p1096 N88-16594
Low frequency waves and small scale solitary structures observed by Viking --- Swedish satellite; auroras 08 p1099 N88-16611

IONIZATION
NT ATMOSPHERIC IONIZATION
NT AURORAL IONIZATION
NT AUTOIONIZATION
NT FLAME IONIZATION
NT GAS IONIZATION
NT ION PRODUCTION RATES
NT NONEQUILIBRIUM IONIZATION
NT PHOTOIONIZATION
NT SURFACE IONIZATION
Study of ionization equilibrium of high temperature and low density plasma
[DE87-703070] 02 p0238 N88-11502
JPRS report: Science and technology. China
[JPRS-CST-87-031] 03 p0299 N88-11880
XeCl excimer laser induced multiphoton ionization of ammonia molecule 03 p0299 N88-11883
Equilibrium calculations of ionization in tracer flames
[PB87-104154] 04 p0412 N88-12555
High efficiency generation of 130-nm radiation from sum-frequency mixing in Hg
[DE87-013714] 04 p0431 N88-12674
Radio continuum emission from the ionized stellar winds of the cool supergiants in zeta Aurigae-like systems 04 p0514 N88-13160
Anti-Stokes generation of 226 nm light
[DE88-001612] 05 p0589 N88-13590
Ionization losses in BGO
[NOTA-INTERNA-889] 07 p0856 N88-15198
Method of plasma diagnostics by a heavy ion beam for the T-15 tokamak
[DE88-700342] 07 p0935 N88-15678
Minimum necessary intensity of source of preionization for stabilization of a self-sustaining laser discharge with mean power raised by electron beam or X-rays
[PB87-178158] 09 p1171 N88-17024
An analytic model for ionization distributions produced in nanometer sites by protons
[DE88-003943] 10 p1406 N88-18385
Chemical activation of molecules by metals: Experimental studies of electron distributions and bonding
[DE88-004465] 10 p1407 N88-18393
Synthesis and characterization of thin films
[AD-A187335] 10 p1421 N88-18485
Numerical simulation of the propagation and absorption due to air breakdown of long microwave pulses
[DE88-005227] 11 p1475 N88-18798
Resonantly-enhanced, four-photon ionization of krypton at laser intensities exceeding 10(12) W/sq cm
[DE88-005038] 11 p1544 N88-19229
Spectroscopic determinations of surface gravities of giant stars, and ultraviolet observations of RR Lyrae and X Arietis 11 p1569 N88-19391
Discharge excitation of dye vapors
[AD-A188428] 12 p1632 N88-19770
Kinetic mechanisms for ionization and afterburning suppression
[AD-A189219] 13 p1737 N88-20383
Studies of compound states of negative ions using laser beams
[DE88-004708] 13 p1777 N88-20627
Ionization equilibrium and radiative energy losses in a stationary plasma
[DE88-700856] 14 p1984 N88-21832
Narrow-band photographic observations of the HII Region S296 in Canis Major 16 p2288 N88-23696
Ion generator and ion application system
[NASA-CASE-MFS-28122-1] 17 p2397 N88-24253
Contributions of autoionizing resonances to the electron collisional excitation rates for Be-like ions
[AD-A190924] 18 p2572 N88-25275
High-fidelity in isotope ratio measurements for resonance ionization mass spectrometry
[DE88-009129] 19 p2613 N88-25506
A mass spectrometer for the analysis of thermally labile compounds 19 p2668 N88-25859
Space and sea: Is there a place for ionization? 19 p2699 N88-26043
Interactions of molecules with surfaces
[DE88-007950] 19 p2723 N88-26169
Theoretical atomic and molecular physics
[DE88-007122] 19 p2724 N88-26175
Rare Gas Halide (RGH) kinetics
[AD-A192352] 20 p2770 N88-26425
Laser desorption/ablation studies by resonance ionization mass spectrometry
[DE88-009124] 20 p2807 N88-26650
A 10 microns photoexcited avalanche gain due to electron impact ionization from GaAs quantum well superlattices 20 p2867 N88-27026
Multiphoton ionization of alkaline earth atoms in an intense laser field
[DE88-008078] 21 p3014 N88-27884
The influence of ionization within a plasma opening switch
[AD-A193147] 21 p3017 N88-27906
The 2D Rydberg series in Al I
[NASA-TM-101189] 22 p3150 N88-28740
Breakdown of molecular oxygen by brief pulses of laser radiation
[DE88-702687] 23 p3220 N88-29168
Electron impact ionization cross-section of some organic compounds
[DE88-702044] 23 p3280 N88-29525
The kinematics of Milky Way halo gas 23 p3299 N88-29648
Impurity analysis in SIMOX samples by high-efficiency resonance ionization time-of-flight mass spectrometry
[DE88-012061] 24 p3367 N88-30051
Cluster beam studies
[AD-A195182] 24 p3434 N88-30443

IONIZATION CHAMBERS
NT BUBBLE CHAMBERS
NT CLOUD CHAMBERS
NT PROPORTIONAL COUNTERS
NT SPARK CHAMBERS
Development and evaluation of a Monte Carlo code system for analysis of ionization chamber responses
[AD-A183970] 03 p0375 N88-12359
High efficiency generation of 130-nm radiation from sum-frequency mixing in Hg
[DE87-013714] 04 p0431 N88-12674
Single wire drift chamber design
[DE87-011002] 07 p0857 N88-15205

IONIZATION COEFFICIENTS
Detection of minimum-ionizing particles in hydrogenated amorphous silicon
[DE88-002769] 07 p0837 N88-15081
On formulating a simple D-region model
[AD-A195841] 24 p3392 N88-30197

IONIZATION COUNTERS
U IONIZATION CHAMBERS
U RADIATION COUNTERS

IONIZATION CROSS SECTIONS
Photoionization of atoms and ions: Application of time-dependent response method within the density functional theory
[AD-A185686] 07 p0930 N88-15649
Neutral beam propagation through the atmosphere
[AD-A188984] 12 p1691 N88-20115
Photoionization dynamics and abundance patterns in laser vaporized tin and lead clusters
[AD-A191604] 18 p2482 N88-24722
Molecular sources of ionospheric holes
[AD-A191857] 18 p2541 N88-25082
High-order multiphoton ionization of the noble gases
[DE88-007489] 18 p2571 N88-25273
A new approach to generating negative ion beams
[AD-A191119] 18 p2572 N88-25276
Trochoidal analysis of scattered electrons in a merged electron-ion beam
[NASA-CASE-NPO-16789-1-CU] 18 p2573 N88-25281
Electron impact ionization cross-section of some organic compounds
[DE88-702044] 23 p3280 N88-29525

IONIZATION FREQUENCIES
On the role of the ionization frequency to gyrofrequency ratio in the critical ionization velocity interaction
[TRITA-EPP-86-10] 10 p1410 N88-18414
Photoionization dynamics and abundance patterns in laser vaporized tin and lead clusters
[AD-A191604] 18 p2482 N88-24722

IONIZATION GAGES
TOTAL: A new instrument to study turbulent parameters in the mesosphere and lower thermosphere 08 p1029 N88-16234

IONIZATION POTENTIALS
Critical Ionization Velocity (CIV) interaction: Some unsolved questions
[TRITA-EPP-87-12] 09 p1250 N88-17491

IONIZED GASES
Proceedings of the 17th International Conference on Phenomena in Ionized Gases held in Budapest, Hungary, July 8-12, 1985: Invited papers
[DE87-703562] 05 p0651 N88-13987
A plasma wave instrument on the AMPTE/IRM (Active Magnetospheric Particle Tracing Explorers/Ion Release Module) spacecraft
[AD-A191216] 16 p2233 N88-23336

IONIZED PLASMAS
U PLASMAS (PHYSICS)

IONIZING RADIATION
NT ALPHA PARTICLES
NT BETA PARTICLES
NT COSMIC RAY SHOWERS
NT COSMIC RAYS
NT COSMIC X RAYS
NT EXTREME ULTRAVIOLET RADIATION
NT FAR ULTRAVIOLET RADIATION
NT GALACTIC COSMIC RAYS
NT GAMMA RAY BURSTS
NT GAMMA RAYS
NT LYMAN ALPHA RADIATION
NT NEAR ULTRAVIOLET RADIATION
NT PRIMARY COSMIC RAYS
NT SOLAR COSMIC RAYS
NT SOLAR X-RAYS
NT ULTRAVIOLET RADIATION
NT X RAYS
Ion-implantation-induced stress in glasses: Variation of damage mode efficiency with changes in glass structure
[DE87-013523] 01 p0028 N88-10175
Instrument for radiation testing/screening electronic devices over an extended temperature range
[AD-A184245] 03 p0326 N88-12060
Reevaluating the worst-case radiation response of MOS transistors
[DE87-014157] 04 p0497 N88-13059
Karyometric evaluation of neuronal reactions of rat cerebral cortex to the combined effect of ionizing radiation, longitudinal accelerations and vibration 07 p0890 N88-15396
Combined effect of microwaves and ionizing radiation 07 p0893 N88-15413
Simulation of effect on biological systems of impact wave from heavy charged particle track 07 p0896 N88-15429
Combined effect of ionizing radiation and altered gas atmosphere on central nervous system 10 p1367 N88-18168
Characterization of space radiation environment in terms of the energy deposition in functionally important volumes
[DE88-005627] 15 p2100 N88-22513
Point defects in irradiated silicates 17 p2408 N88-24319
Modeling of radiation dose dependence of MOSFETs 17 p2416 N88-24370
Extremely Low Frequency (ELF) communications program: Non-ionizing electromagnetic radiation literature evaluation and assessment, 1966-1987 literature review
[AD-A192024] 19 p2642 N88-25677
Stress corrosion of ceramic materials
[AD-A191979] 23 p3195 N88-29016
Emetic mechanism in acute radiation sickness
[AD-A194102] 23 p3238 N88-29267

IONOGRAMS
Trajectory synthesis of ionograms in presence of artificial ionospheric inhomogeneities 08 p1002 N88-16067
Trajectory synthesis of ionograms in presence of artificial ionospheric inhomogeneities 13 p1789 N88-20703
IONOSONDES
Height profile inversion of ionospheric movement from observed parameters of HF radio echoes 03 p0299 N88-11884
Ionospheric convection and structure using ground-based digital ionosondes [AD-A194246] 23 p3233 N88-29237
Ionosonde studies of field-aligned irregularities during high-power HF heating at Arecibo [AD-A195848] 24 p3401 N88-30256
IONOSPHERE-MAGNETOSPHERE COUPLING
U MAGNETOSPHERE-IONOSPHERE COUPLING
IONOSPHERES
Solar wind effects on the outer ion coma of Comet Halley 01 p0117 N88-10750
Processes in the quiet and disturbed equatorial-low latitude ionosphere: Sundial campaign, 1984 [INPE-4152-PRE/1057] 08 p1036 N88-16282
A proposal for the establishment of a center of excellence in theoretical geoplasma research [AD-A189742] 16 p2231 N88-23327
The effects of solar cycle and latitude dependence on the formation of ionospheric C layer [INPE-4342-TDL/293] 16 p2232 N88-23332
IONOSPHERIC ABSORPTION
U ELECTROMAGNETIC ABSORPTION
U IONOSPHERIC PROPAGATION
IONOSPHERIC COMPOSITION
The new CP3 06 p0691 N88-14237
Investigations into the properties, conditions and effects of the ionosphere [AD-A194245] 22 p3118 N88-28528
Photochemistry of ionospheric D-region with injection of nitrogen oxides 24 p3444 N88-30499
IONOSPHERIC CURRENTS
NT AURORAL ELECTROJETS
NT EQUATORIAL ELECTROJET
Area of reduced electron concentration in terrestrial plasmasphere 08 p1003 N88-16078
IONOSPHERIC DISTURBANCES
NT SUDDEN IONOSPHERIC DISTURBANCES
NT TRAVELING IONOSPHERIC DISTURBANCES
Height profile inversion of ionospheric movement from observed parameters of HF radio echoes 03 p0299 N88-11884
High latitude F-region drift studies [AD-A184466] 04 p0467 N88-12889
Internal gravity waves in the meteor zone in the Tbilisi Region 06 p0736 N88-14528
Electron acceleration by wave processes in the earth's ionosphere [AD-A186110] 07 p0877 N88-15320
Trajectory synthesis of ionograms in presence of artificial ionospheric inhomogeneities 08 p1002 N88-16067
High altitude chemical release systems for project BIME (Brazilian Ionospheric Modification Experiments) project IMS (Ionospheric Modification Studies) project PIIE (Polar Ionospheric Irregularities Experiment) project polar arcs [AD-A188299] 12 p1642 N88-19833
Trajectory synthesis of ionograms in presence of artificial ionospheric inhomogeneities 13 p1789 N88-20703
Support for FY87 midlatitude electron-density calibration campaign [AD-A190174] 15 p2094 N88-22476
Radio-wave scintillations and ionospheric irregularities at high latitudes [AD-A192140] 18 p2501 N88-24837
The Effect of the Ionosphere on Communication, Navigation and Surveillance Systems Based on Ionospheric Effects Symposium held on 5-7 May 1987 in Springfield, Virginia [AD-A191855] 18 p2541 N88-25081
Approximate analytical formulae for electron density and collision frequency in the natural and nuclear-disturbed ionosphere and inner magnetosphere [AD-A193129] 21 p2972 N88-27654
The effect of equatorial ionospheric irregularities on the performance of a south-looking OTH-B (Over-The-Horizon-Backscatter) radar [AD-A195090] 24 p3362 N88-30018
IONOSPHERIC DRIFT
High latitude F-region drift studies [AD-A184466] 04 p0467 N88-12889
On connection between evolution of troposphere fronts and changes of circulation regime in meteor zone 06 p0735 N88-14519
Atmosphere dynamic processes structure at 80-105 km altitude 06 p0736 N88-14527
Studies of ionosphere/magnetosphere dynamics using SABRE and HILAT [AD-A190947] 16 p2232 N88-23333
High latitude ionospheric radio studies [AD-A192270] 20 p2824 N88-26753
Ionospheric convection and structure using ground-based digital ionosondes [AD-A194246] 23 p3233 N88-29237
IONOSPHERIC ELECTRON DENSITY
Trajectory synthesis of ionograms in presence of artificial ionospheric inhomogeneities 08 p1002 N88-16067
Electrostatic VLF emission determined from rocket and satellite experiments 08 p1002 N88-16068
Longitudinal variations of equatorial ionosphere determined from Intercosmos-19 artificial Earth satellite data 08 p1003 N88-16074
Area of reduced electron concentration in terrestrial plasmasphere 08 p1003 N88-16078
Application of correlation method of reception of direct and reflected cosmic radiation to study of plasmaspheres of planet and distribution of radiation brightness 08 p1004 N88-16085
Distribution of electron concentration in nighttime atmosphere of Venus based on radio transmission data 08 p1005 N88-16092
Multispectral optical observations of ionospheric F-region storm effects at low latitude [INPE-4231-PRE/1105] 08 p1024 N88-16198
Trajectory synthesis of ionograms in presence of artificial ionospheric inhomogeneities 13 p1789 N88-20703
Effect of nitrogen dioxide release on thermosphere 13 p1789 N88-20704
A model of the ionosphere in the altitude interval 50 to 4000 km. Part 2: Molecular ions (N2(+), NO(+), O2(+)) and electron density [DFVLR-FB-88-12-PT-2] 23 p3234 N88-29242
One equatorial anomaly in nighttime ionospheric F region 24 p3447 N88-30517
IONOSPHERIC HEATING
The effects of a geomagnetic storm on thermospheric circulation [AD-A186638] 09 p1190 N88-17128
Role of ordinary to extraordinary mode wave coupling in ionospheric heating experiments [AD-A195335] 24 p3362 N88-30017
IONOSPHERIC ION DENSITY
A possible role for ionospheric ions in triggering a geomagnetic substorm onset 08 p1096 N88-16594
Rocket-borne low energy ion measurements in space 18 p2593 N88-25412
A model of the ionosphere in the altitude interval 50 to 4000 km. Part 1: Atomic ions (H(+), He(+), N(+), O(+)) [DFVLR-FB-88-11-PT-1] 23 p3233 N88-29241
A model of the ionosphere in the altitude interval 50 to 4000 km. Part 2: Molecular ions (N2(+), NO(+), O2(+)) and electron density [DFVLR-FB-88-12-PT-2] 23 p3234 N88-29242
IONOSPHERIC NOISE
NT WHISTLERS
Ionospheric research in Antarctica [INPE-4521-PRE/1273] 16 p2232 N88-23331
IONOSPHERIC PROPAGATION
Report of the 3rd Finnish EISCAT Workshop — European Incoherent Scatter Radar (EISCAT) [REPT-111] 06 p0691 N88-14233
Finnish contributions to EISCAT science in 1986 06 p0691 N88-14235
CP-1-H analysis tests 06 p0691 N88-14236
EISCAT research programs for 1987 06 p0692 N88-14244
Polar Geophysical Institute's studies of magnetosphere, ionosphere 06 p0728 N88-14480
Wideband HF (High Frequency) modeling and simulation [PB88-116116] 10 p1317 N88-17874
User's guide for the HF (High Frequency) broadcast antenna design and validation summary programs [PB88-116124] 10 p1317 N88-17875
Correcting ray field failures caused by focusing in an inhomogeneous duct: A critical look at the Gaussian beam method 12 p1616 N88-19663
An assessment of the application of in situ ion-density data from DMSP to modeling of transionospheric scintillation [AD-A188919] 12 p1643 N88-19840
Upward propagating electric fields from thunderstorms and VLF transmitters 13 p1801 N88-20767
Radial track of moving objects determined by HF backscatter technique 14 p1901 N88-21354
WAVFLD: A program to compute ionospheric height gain functions and field strengths at VLF [AD-A191159] 16 p2191 N88-23066
The Effect of the Ionosphere on Communication, Navigation and Surveillance Systems Based on Ionospheric Effects Symposium held on 5-7 May 1987 in Springfield, Virginia [AD-A191855] 18 p2541 N88-25081
Role of ordinary to extraordinary mode wave coupling in ionospheric heating experiments [AD-A195335] 24 p3362 N88-30017
Review of Radio Science, 1984-1986 24 p3363 N88-30023
Ionospheric radio and propagation: Waves in plasmas 24 p3364 N88-30030
IONOSPHERIC REFLECTION
U IONOSPHERIC PROPAGATION
IONOSPHERIC SOUNDING
First results from the Viking associated Aureld-VIP rocket and EISCAT campaign — auroras; Swedish satellite 08 p1026 N88-16211
A model of the ionosphere in the altitude interval 50 to 4000 km. Part 1: Atomic ions (H(+), He(+), N(+), O(+)) [DFVLR-FB-88-11-PT-1] 23 p3233 N88-29241
Ionospheric radio and propagation: Waves in plasmas 24 p3364 N88-30030
IONOSPHERIC STORMS
NT SUDDEN IONOSPHERIC DISTURBANCES
IONOSPHERIC TEMPERATURE
Support for FY87 midlatitude electron-density calibration campaign [AD-A190174] 15 p2094 N88-22476
IONS
NT ANIONS
NT CATIONS
NT CESIUM IONS
NT DEUTERONS
NT FERRIC IONS
NT HEAVY IONS
NT HELIUM IONS
NT HYDROGEN IONS
NT HYDRONIUM IONS
NT LIGHT IONS
NT METAL IONS
NT MOLECULAR IONS
NT NEGATIVE IONS
NT NITROGEN IONS
NT OXYGEN IONS
NT POSITIVE IONS
NT RECOIL IONS
NT TRITONS
Study of pickup of cometary ions in turbulent solar winds 01 p0113 N88-10725
The analysis of metal finishing solutions by ion chromatography [AD-A184812] 05 p0561 N88-13414
Survey state of the art: Electrical load management techniques and equipment [AD-A184083] 05 p0577 N88-13517
Atomic physics with highly charged ions [DE88-000894] 05 p0648 N88-13972
Ionic transport and electrical relaxation in glass [DE88-000887] 05 p0657 N88-14028
Self-alignment of ions drifting in plasma 06 p0774 N88-14752
Ion mixing and surface modification in metal-semiconductor systems [DE88-001702] 06 p0786 N88-14823
Correlation effects on double electron capture in highly-charged, low-energy ion-atom collisions [DE87-013179] 07 p0930 N88-15651
EISCAT measurements of ion velocities during Coordinated Auroral Experiment using Scatter And Rockets (CAESAR) campaign 08 p1031 N88-16251
Ion flows in magnetospheric flux transfer events 08 p1098 N88-16607
Models for ionic transport in glass [DE88-002860] 10 p1304 N88-17799
Ion chromatography in the manufacture of multilayer circuit boards [DE88-002428] 10 p1322 N88-17902
A study of the magnetic field annihilation process in the magnetosphere and some geotechnical applications [DE88-004165] 10 p1355 N88-18096
Lithium fast-ion conductors: Polymer based materials [AD-A187879] 11 p1461 N88-18712
The JPL trapped mercury ion frequency standard 11 p1471 N88-18776
Ion energy diagnostics for voltage determinations in plasma-erosion-opening-switch experiments [DE88-004822] 11 p1479 N88-18827
Spectral line-broadening codes for hydrogen-, helium- and lithium-like ions in plasmas [DE88-005238] 11 p1552 N88-19289
The redox chemistry of some peroxo and superoxo metal ion complexes [AD-A189159] 12 p1606 N88-19606
Ion content and infrared absorption of moist atmospheric air [AD-A188839] 12 p1643 N88-19838
Laser photoelectron spectroscopy of ions [DE88-006860] 15 p2033 N88-22113

Angular resolved energy analysis of (69)Ga+ ions from a gallium liquid metal ion source
[AERE-R-12649] 15 p2139 N88-22760
Universal detection of ions by replacement-ion chromatography employing an anion-replacement method and an ultraviolet-visible spectrophotometric detector
[AD-A191326] 16 p2176 N88-22971
Studies of model ion channels in defect-free multibilayers of phospholipids
[AD-A188740] 16 p2238 N88-23365
A new fiber-optic-based ion sensor
[AD-A191322] 16 p2274 N88-23612
Centrifugal acceleration of ions in the polar magnetosphere
[NASA-TM-101148] 17 p2374 N88-24120
Contributions of autoionizing resonances to the electron collisional excitation rates for Be-like ions
[AD-A190924] 18 p2572 N88-25275
Contaminant ions and waves in the space station environment 18 p2590 N88-25393
Rocket-borne low energy ion measurements in space 18 p2593 N88-25412
A mass spectrometer for the analysis of thermally labile compounds 19 p2668 N88-25859
Dynamics explorer data analysis
[NASA-CR-181428] 19 p2691 N88-25996
Sources of polarized ions and atoms
[DE88-010910] 20 p2852 N88-26931
Recent advances in atom-probe field ion microscopy
[DE88-008799] 20 p2876 N88-27070
Ion Bernstein modes in current-carrying plasmas 21 p3017 N88-27903
Theory and simulation of relaxed plasmoids
[AD-A192884] 21 p3032 N88-27997
Hydrogen concentration cells as converters of heat into electricity
[DE88-009662] 23 p3229 N88-29216
Large ionic species in sooting acetylene and benzene flames 24 p3348 N88-29932
Particle trajectories and potentials in a plane sheath moving in a magnetoplasma
[AD-A196228] 24 p3390 N88-30190
Ion kinetics in silane plasmas
[AD-A196202] 24 p3431 N88-30423
Ring current role in dynamics of fluctuating electron and ion fluxes in low-latitude magnetosphere 24 p3447 N88-30514

IP (IMPACT PREDICTION)
U COMPUTERIZED SIMULATION

IRAS
U INFRARED ASTRONOMY SATELLITE

IRASERS
U INFRARED LASERS

IRIDIUM
NT IRIDIUM ISOTOPES
Measurements of iridium and the meteoric impact hypothesis at cretaceous end
[DE87-703765] 04 p0521 N88-13200
Oxide-bound transition metal complexes for methane activation
[PB88-169719] 14 p1887 N88-21277
Weldability of general purpose heat source iridium capsules 17 p2426 N88-24429
The structure and properties of RF reactive sputtered IrO2 films 19 p2672 N88-25884
Catalytic activation of carbon dioxide by metal complexes
[AD-A192310] 21 p2909 N88-27262
Iridium-coated rhenium thrusters by CVD
[NASA-TM-101309] 24 p3339 N88-29874

IRIDIUM ISOTOPES
Experimental and theoretical investigations of isotope shift and hyperfine structure on 5d elements (especially platinum, iridium and rhenium)
[ETN-88-93121] 24 p3353 N88-29957

IRON
NT IRON ISOTOPES
NT IRON 57
Lithium/iron sulfide batteries: Development and demonstration
[DE87-014222] 01 p0042 N88-10265
The corrosion of iron rotating hemispheres in 1 M sulfuric acid: An electrochemical impedance study
[DE87-014679] 02 p0148 N88-10925
Wear of iron and nickel in corrosive liquid environments
[NASA-TM-100246] 03 p0289 N88-11817
Post-test analyses of aqueous batteries developed for electric propulsion
[DE88-000655] 03 p0311 N88-11965
Plasticity of aluminum and iron at high shear strain rate and high pressure 05 p0563 N88-13430
The mechanism by which sigma-phase forms in Fe-Cr-Ni system alloys
[BLL-M-37380-(5828.4)] 05 p0564 N88-13437
Effect of grain orientation on the origination and the initial growth of fatigue cracks in pure iron 05 p0597 N88-13647
Surface deformation and fatigue crack initiation of alpha-iron 05 p0598 N88-13651
Determination, by X-ray fluorescence, of platinum, palladium, ruthenium, iron and chromium in special steels
[PB87-132114] 06 p0683 N88-14183
Cyclic deformation behaviour of cast irons with various graphite shapes in the temperature range 20 C less than or = T less than or = 500 C 06 p0715 N88-14384
The relationship between microstructural size and fatigue threshold in iron and steel 06 p0716 N88-14396
Threshold and crack-growth tests on pre-cracked specimens produced in cyclic compression 06 p0718 N88-14412
Investigation of impurity defects in alpha-iron by molecular dynamics method
[DE88-700355] 07 p0834 N88-15058
Seasonal cycling of sulfur and iron in porewaters of a Delaware salt marsh
[NASA-CR-182385] 07 p0876 N88-15311
Studies of the electron spectrum with reference to the clean surfaces of iron, cobalt and nickel and their subsequent exposure to oxygen 11 p1459 N88-18700
Study of activationless reactions of point defects with impurities and impurity-defect complexes in alpha-iron
[DE88-701028] 13 p1745 N88-20433
Use of long-distance pair potentials in calculations of defect characteristics in metals
[DE88-701039] 15 p2037 N88-22138
Effect of P implantation on the corrosion behavior of Fe-Cr alloys
[DE88-005732] 15 p2040 N88-22158
Complexation and hydrolysis reactions of iron(III) 17 p2322 N88-23867
Flux density measurements of neutral iron in TEXTOR with laser induced fluorescence 17 p2442 N88-24528
Calculation of oxidation rates for iron in CO-CO2
[DE88-007313] 18 p2487 N88-24757
Epitaxial iron films
[AD-A191815] 19 p2732 N88-26225
Inelastic electron scattering and electron-hole excitations in iron and nickel
[DE88-011843] 21 p2915 N88-27303
Kinetic of oxidation to air of a Fe-Al-Mn alloy system at 600-800(sup 0)C temperature range
[DE88-702309] 21 p2920 N88-27330
Perfluoropolyalkylether lubricants under boundary conditions: Iron catalysis of lubricant degradation
[AD-A193241] 21 p2956 N88-27560
Study on iron disilicide thermoelectric generator
[AD-A193082] 22 p3116 N88-28517
Radial velocity measurements of a sample of northern metal-deficient stars
[SER-C-PREPUBL-FASC-25] 24 p3455 N88-30564

IRON ALLOYS
NT AUSTENITIC STAINLESS STEELS
NT BAINITIC STEEL
NT CARBON STEELS
NT CHROMIUM STEELS
NT FERRITIC STAINLESS STEELS
NT HIGH STRENGTH STEELS
NT LOW CARBON STEELS
NT MARAGING STEELS
NT MARTENSITIC STAINLESS STEELS
NT NICKEL STEELS
NT STAINLESS STEELS
NT STEELS
Relationships governing change in density in liquid ferrous alloys
[BLL-M-37305-(5828.4)] 02 p0149 N88-10935
The effect of strain rate on the yield behavior of iron-base LRO alloys at elevated temperatures
[DE87-014893] 03 p0288 N88-11808
Microstructural effects on the fatigue behavior of Fe-C-X alloys
[DE88-000155] 03 p0288 N88-11809
Investigations of crystallization velocity and boron diffusion in glassy iron-boron alloys and of activity coefficients of boron in crystalline iron-boron alloys
[ETN-87-90613] 03 p0381 N88-12393
A comparison of high damping shape memory alloys with Cu-Mn-based and Fe-Cr-based alloys
[AD-A184110] 04 p0414 N88-12566
Fatigue strength of alloy A286 at cryogenic temperature 05 p0603 N88-13695
Undercooling and nucleation in iron nickel alloys
[AD-A185500] 06 p0683 N88-14184
Structural relaxation and mechanical properties of amorphous Fe-Zr alloys 07 p0840 N88-15094
Response of Fe-Cr-Mn austenitic alloys to thermal aging neutron irradiation
[DE88-003415] 10 p1302 N88-17785
Cast iron-base alloy for cylinder/regenerator housing
[NASA-CR-182116] 12 p1608 N88-19613
Magnetic studies of iron-rare-earth-metalloid alloys
[DE88-006801] 16 p2282 N88-23660
On the abnormal phenomena observed in the electrical resistivity measurement during the decomposition process of saturated Cu-Fe alloys
[NASA-TT-20183] 18 p2507 N88-24869
Reduced-activation austenitic stainless steels: The Fe-Cr-C system
[DE88-008091] 20 p2773 N88-26442
Hot isostatic pressing of tungsten-nickel-iron composites
[FOA-C-20698-2.1] 22 p3056 N88-28135
The influence of solute segregation on the dislocation structure of small and large angle (001) twist boundaries in Fe-Sb alloys
[DE88-009166] 22 p3155 N88-28770
Hydrogen embrittlement of iron-nickel alloys
[AD-A195909] 24 p3353 N88-29958

IRON COMPOUNDS
NT FERRITES
NT FERROCENES
NT HEMATITE
NT IRON OXIDES
NT PYRITES
Development of iron aluminides
[AD-A185190] 05 p0568 N88-13461
Electron microscopy study of morphology and composition of a ferrisilicate catalyst
[DE88-005754] 11 p1562 N88-19352

IRON ISOTOPES
NT IRON 57
New technique for enhancing helium production in ferritic materials
[DE88-003048] 09 p1142 N88-16847

IRON METEORITES
Moessbauer study of shock induced effects in the Fe-Ni 50/50 ordered alloy in meteorites
[DE87-703364] 04 p0521 N88-13199

IRON ORES
NT HEMATITE

IRON OXIDES
NT HEMATITE
Grain boundary and surface diffusion in oxides
[DE88-002348] 07 p0938 N88-15697
Electron transfer to iron(3) oxide colloids
[DE88-002885] 10 p1416 N88-18448
High Tc superconducting HoBa2Cu(sub 1-x)Fe(sub x)3O(sub 7-y)
[DE88-008909] 22 p3155 N88-28768
Reflectance pattern and the physical and chemical characteristics of three Brazilian Oxisols
[INPE-4590-PRE/1320] 24 p3387 N88-30172

IRON 57
A sup 57 Fe Mossbauer study of the superconductor YBa sub 2 (Fe sub x Cu sub 1-x) sub 3 O sub y
[DE88-701543] 16 p2282 N88-23661

IROQUOIS HELICOPTER
U UH-1 HELICOPTER

IRRADIANCE
NT ILLUMINANCE
NT SOLAR CONSTANT
Radiometric calibration of the Earth observing system's imaging sensors
[NASA-CR-181542] 04 p0463 N88-12865
Statistical distribution of solar radiation (hourly sums): Cumulative frequency curves preparation of a European data set and direction for use
[PB87-107454] 04 p0467 N88-12886
Short-term temporal variations of Nimbus-7 measurements of the solar UV spectral irradiance
[PB88-102132] 07 p0946 N88-15753
Bright source lasers and experiments at very high irradiance
[DE88-004317] 10 p1337 N88-17988
Calculation of space station infrared irradiance from atmosphere-induced emissions 18 p2591 N88-25396
The propagation of irradiance moments of an aberrated, apodized FEL beam
[DE88-008972] 20 p2806 N88-26648
Short term variability between 120 and 300 mm from Solar Mesosphere Explorer (SME) observations
[AERONOMICA-ACTA-A-328-1988] 23 p3308 N88-29709
Aeronomic problems of the molecular oxygen photodissociation. Part 3: Solar spectral irradiances in the region of the O2 Herzberg continuum, Schumann-Runge bands and continuum
[AERONOMICA-ACTA-A-332-1988] 24 p3343 N88-29897

IRRADIATION
NT DEUTERON IRRADIATION
NT ELECTRON IRRADIATION
NT ION IRRADIATION
NT NEUTRON IRRADIATION
NT PROTON IRRADIATION
NT X RAY IRRADIATION
Surface modification by metal deposition and laser irradiation 01 p0023 N88-10148
Effects of electron and proton irradiations on n/p and p/n GaAs cells grown by MOCVD
[NASA-TM-100199] 01 p0042 N88-10266
Electron beam irradiation effects on carbon fiber reinforced PEEK composite
[DE87-753001] 02 p0142 N88-10890
Degradation mechanisms of materials for large space systems in low Earth orbit
[NASA-CR-181472] 02 p0143 N88-10896
Time-resolved absorption measurements on OMEGA
[DE87-014465] 02 p0179 N88-11112
Effects of radiation damage in optical fibers: A tutorial
[PB87-210308] 02 p0235 N88-11482
Time-resolved temperature and density measurements in ionizing, uniformly irradiated UV-laser-produced plasmas
[DE87-014649] 02 p0238 N88-11504
Irradiations. Accumulated doses. Heavy ions --- space environment 03 p0272 N88-11708
Effect of irradiation on the tensile properties of niobium-base alloys
[DE87-002409] 03 p0285 N88-11790
Superconductivity of pseudobinary compounds Al5 (V-Cr)3Si, (V-MO)3Si, Mo3(Si-Re), bombarded with fast neutrons 03 p0285 N88-11792
Effect of helium on irradiation creep in an austenitic stainless steel
[DE87-013754] 03 p0290 N88-11824
Impact behavior of 9-Cr and 12-Cr ferritic steels after low-temperature irradiation
[DE88-000333] 03 p0291 N88-11827
Impact behavior of 9-Cr and 12-Cr ferritic steels after low-temperature irradiation
[DE88-000333] 03 p0291 N88-11827
Microstructural characterization of irradiated PWR steels using the atom probe field-ion microscope
[DE88-000341] 03 p0291 N88-11828
Temperature hysteresis and magnetic transitions in amorphous Fe-Ni-Zr alloys
[DE88-000228] 03 p0294 N88-11848
Computerized system for studies on creep of irradiated materials in the BR-10 reactor. Control system for electric motor
[DE87-702888] 03 p0310 N88-11952
Utilization of potatoes in bioregenerative life support systems 03 p0360 N88-12269
Performance of GaAs and silicon concentrator cells under 37 MeV proton irradiation
[NASA-TM-100144] 04 p0465 N88-12877
PISCES: Plasma-surface interactions and materials research
[DE88-001323] 04 p0494 N88-13044
Reevaluating the worst-case radiation response of MOS transistors
[DE87-014157] 04 p0497 N88-13059
An investigation of unipolar arcing at atmospheric pressure in aluminum 2024 and aluminum coated glass slides
[AD-A184903] 05 p0577 N88-13521
Raman microprobe characterization of dielectric films following high-energy pulsed laser irradiation
[DE88-000559] 05 p0586 N88-13587
Pure dephasing of a vibrational adbond
[AD-A185222] 05 p0609 N88-13740
Controlled ecological life support systems: Development of a plant growth module 05 p0630 N88-13854
Irradiation preservation of seafood: Literature review
[DE88-001691] 05 p0631 N88-13858
Fractographic and microstructural aspects of fracture toughness testing in irradiated 304 stainless steel
[DE88-000795] 06 p0681 N88-14172
Combined effect of microwaves and ionizing radiation 07 p0893 N88-15413
Effect of irradiation on the diffusion evolution of void ensemble in crystals
[DE88-700558] 07 p0939 N88-15706
Space environmental effects on polymeric materials
[NASA-CR-182454] 09 p1148 N88-16879
Food irradiation seminar: Asia and the Pacific
[DE88-700432] 09 p1202 N88-17203
Irradiation effects in metals
[DE88-004272] 10 p1303 N88-17789
International cooperative effort to establish ASTM (American Society for Testing and Materials) standards for the measurement of radiation dose for food processing
[DE88-002702] 10 p1372 N88-18190
NBS (National Bureau of Standards) measurement services: Spectral irradiance calibrations
[PB88-123781] 10 p1408 N88-18401
Investigations of stimulated Raman scattering from high density underdense plasmas irradiated by a 0.35 micron laser 10 p1411 N88-18421
Effects of X irradiation and high field electron injection on the electrical properties of rapid thermal oxides
[DE86-002642] 10 p1417 N88-18461
The effects of low doses of 14 MeV neutrons on the tensile properties of three binary copper alloys
[DE88-003400] 11 p1458 N88-18691
Crystallization and glass formation in electron and laser beam irradiated Cu-Zr alloys
[DE88-003390] 11 p1464 N88-18729
Ceramic decomposition under irradiation
[DE88-004327] 11 p1464 N88-18732
Metastable materials by laser irradiation
[PB88-130364] 11 p1493 N88-18912
An economic analysis of a multi-commodity fruit and vegetable irradiator
[DE88-003425] 11 p1524 N88-19098
Studies in solid state ionics
[DE88-700830] 11 p1559 N88-19333
Radiation response of thin oxides grown by rapid thermal oxidation and rapid thermal annealing techniques
[DE88-003632] 11 p1561 N88-19347
Food Irradiation Newsletter, Vol. 11, No. 1
[DE88-700808] 12 p1671 N88-20004
Hydrogen pumping and release by graphite under high flux plasma bombardment
[DE88-005880] 13 p1842 N88-21021
Coronal fluid-dynamics in laser fusion 16 p2278 N88-23634
The application of Rutherford backscattering for analyzing multilayered structure change induced by pulsed ion beam bombardment 16 p2278 N88-23638
Effects of irradiation on thermal coalescence of pores in real crystals
[DE88-701683] 16 p2282 N88-23663
Irradiation test results on thermionic fuel element sheath insulators 17 p2402 N88-24280
The effect of elevated temperature on irradiated MOS devices 17 p2406 N88-24308
An irradiation performance data base for nitride fuels 17 p2427 N88-24438
Material property and irradiation performance correlations for nitride fuels 17 p2434 N88-24483
Arcing and rf signal generation during target irradiation by a high-energy, pulsed neutral particle beam
[DE88-007169] 18 p2471 N88-24664
Behavioral response of rats exposed to high-power microwave radiation
[AD-A192199] 18 p2548 N88-25128
Self shielding of surfaces irradiated by intense energy fluxes
[DE88-007094] 18 p2579 N88-25318
Molecular characterization of structure and bonding in thin film materials
[DE88-006811] 18 p2584 N88-25351
High-speed phenomena in GaAs multiple-quantum-wells 19 p2660 N88-25812
Laser fluorescence spectroscopy of zinc neutrals originating from laser-irradiated and ion-bombarded zinc sulfide and zinc surfaces
[DE88-008037] 20 p2769 N88-26418
Fast atom bombardment study on interaction of anticodonic nucleotides and their cognate amino acid
[ISAS-RN-355] 20 p2850 N88-26918
Effects of electron beam irradiation on mechanical properties at low and high temperature of fiber reinforced composites using PEEK as matrix material
[DE88-753134] 21 p2905 N88-27239
Improved adhesion for SiO2 particles in silica substrates using helium-ion irradiation
[DE88-008915] 21 p2920 N88-27332
Assessment of cochlear damage after microwave irradiation
[AD-A193237] 21 p2987 N88-27737
Short pulse X-ray diffraction studies of shocked and annealed crystals using the JANUS research laser
[DE88-011329] 23 p3288 N88-29579
Functional assessment of laser irradiation
[AD-A195735] 24 p3408 N88-30287
IRREGULAR GALAXIES
Asymptotic giant branch populations in composite stellar systems 13 p1854 N88-21098
Infrared astronomy at extremely faint light levels in support of the LAIRTS program
[AD-A191497] 18 p2592 N88-25404
IRREGULARITIES
Numerical solution of partial differential equations on irregular grids
[DE87-014760] 03 p0369 N88-12324
Dynamics of small and large scale irregularities at sub-auroral latitudes
[AD-A189052] 12 p1645 N88-19853
Ultrasonic inspection of irregular surfaces
[AERE-R-12485] 13 p1780 N88-20648
IRREVERSIBLE PROCESSES
Two studies of nonlinear processes in irreversible thermodynamics
[DE88-005794] 13 p1849 N88-21067
Applications of some new ideas on irreversible processes to particular fluids
[AD-A191610] 19 p2663 N88-25836
Behaviour and hysteresis losses of irreversible type-2 superconducting cylindrical shell
[DE88-702708] 24 p3433 N88-30434
IRRIGATION
Stirling engines and irrigation pumping
[DE88-000020] 02 p0181 N88-11125
Use of energy emission for detecting the necessity of irrigation in wheat in field conditions
[INPE-4461-TDL/318] 16 p2229 N88-23315
Evaluation of an estimation system for an irrigated area in a tropical region through TM-LANDSAT imagery 17 p2363 N88-24075
Evaluation of SPOT imagery for monitoring irrigated lands 22 p3090 N88-28352
IRRITATION
NT TOXICITY AND SAFETY HAZARD
IRROTATIONAL FLOW
U POTENTIAL FLOW
IRS (INDIAN SPACECRAFT)
U INDIAN SPACECRAFT
ISCHEMIA
Diagnostic value of some load tests in evaluation of nonspecific electrocardiographic changes 07 p0895 N88-15426
ISEE
U INTERNATIONAL SUN EARTH EXPLORERS
ISENTROPE
Isentropic analysis and interpretation: Operational applications to synoptic and mesoscale forecast problems
[AD-A184814] 05 p0626 N88-13830
ISENTROPIC PROCESSES
An isentropic mesoscale analysis system 02 p0212 N88-11332
An isentropic coordinate model used in a mesoscale data assimilation system 02 p0212 N88-11333
A semigroup for Lagrangian 1D isentropic flow
[DE88-006464] 18 p2513 N88-24912
ISIS SATELLITES
Alouette-ISIS program summary
[NASA-CR-180747] 08 p1023 N88-16195
ISLAND ARCS
Pluton emplacement and magmatic arc construction: A model from the Patagonian batholith 24 p3393 N88-30206
An illustration of the complexity of continent formation 24 p3393 N88-30207
ISLANDS
NT ALEUTIAN ISLANDS (US)
NT GREENLAND
NT HAWAII
NT ICELAND
NT INDONESIA
NT JAPAN
NT MALDIVE ISLANDS
NT NEW ZEALAND
Coastal winds of the southeast Alaska Peninsula
[PB87-206173] 02 p0215 N88-11354
Upper mantle heterogeneity and composition of primary ocean island magmas 08 p1009 N88-16120
Zonal wind observations at Christmas Island (2 deg N, 157 deg W) during the 1986-1987 El-Nino 22 p3120 N88-28539
ISOBUTANE
U BUTANES
ISOBUTYLENE
U BUTENES
ISOCYANATES
Research in energetic compounds
[AD-A192953] 20 p2781 N88-26494
ISOLATION
NT SOCIAL ISOLATION
Human adaptation to isolated and confined environments
[NASA-CR-181502] 03 p0357 N88-12248
Analytical study of the effect of early warning on optimal shock isolation 08 p0998 N88-16047
Antarctica as a model for the human exploration of Mars
[AD-A185835] 08 p1051 N88-16342
Expanded envelope concepts for aircraft control-element failure detection and identification
[NASA-CR-181664] 16 p2160 N88-22886

Biological rhythms, sleep, and wakefulness in prolonged confinement 19 p2696 N88-26022
Selection and training of subjects to live and work in hostile and unusual environments 19 p2696 N88-26026
Selection of isolated space crews 19 p2697 N88-26028
The human element in space: Lessons from Antarctica [AD-A193440] 21 p2988 N88-27741

ISOLATORS
NT VIBRATION ISOLATORS
Development of isostatic mounts and associated guidelines --- spacecraft payloads [CASA-IM-WP-301] 13 p1731 N88-20354
Low-loss, high-isolation, fiber-optic isolator [NASA-CASE-NPO-17207-1-CU] 18 p2576 N88-25304
High speed opto-isolator for radar applications 19 p2658 N88-25795

ISOMERIZATION
New polyisoimides: An approach to in situ rigid-rod polyimide formation [AD-A191665] 18 p2490 N88-24773
Active sites and roles of solid acid base catalysts [NASA-TT-20333] 24 p3345 N88-29909

ISOMERS
NT ISOPROPYL ALCOHOL
Development of FTMS methods for the detection of trace chemical species and development of FTMS methods for the analysis of various chemical species [AD-A185857] 07 p0828 N88-15023
Shape isomers as candidates for the gamma ray laser storage state [DE88-005228] 11 p1492 N88-18909
Systematics on neutron-induced isomeric cross-section ratios at 14.5 MeV [ECN-200] 14 p1980 N88-21815
Fundamental studies of separation processes [DE88-007487] 19 p2611 N88-25494

ISOMORPHISM
Complexity of some problems in module algebra [PB88-165386] 15 p2122 N88-22648

ISOPARAMETRIC FINITE ELEMENTS
Finite element mesh generation and isoparametric elements [NPL-DITC-97/87] 09 p1229 N88-17365
Mathematical stress analysis of composite materials 14 p1900 N88-21349
Distortion effects in isoparametric elements, an analytic approach [PNR90454] 22 p3145 N88-28703
Investigation of the higher-order elements in the SAMSON2 code [AD-A193638] 23 p3271 N88-29465

ISOPROPYL ALCOHOL
Characterization of catalysts with metal-support effects and of the species adsorbed on their surfaces [DE87-014636] 04 p0414 N88-12564

ISOPROPYL COMPOUNDS
NT ISOPROPYL ALCOHOL

ISOPYCNIC PROCESSES
Contribution to theory of quasigeostrophic motions of finite amplitude in viscous stratified ocean 13 p1788 N88-20695

ISOSTASY
Comparisons of global topographic/isostatic models to the Earth's observed gravity field [NASA-CR-182696] 13 p1798 N88-20752

ISOSTATIC PRESSURE
Deformation mechanisms of thermostructural materials [AD-A184070] 03 p0338 N88-12128
Strength optimization of alpha-SiC by improved processing 17 p2324 N88-23880
Improved silicon nitride for advanced heat engines 17 p2324 N88-23881
Fabrication of reactor shields at the Y-12 plant 17 p2402 N88-24283

ISOSTERIC PROCESSES
U ISOPYCNIC PROCESSES

ISOTHERMAL FLOW
Determining Langmuir circulation parameters on basis of similarity theory 13 p1785 N88-20680
Heat transfer from a negatively buoyant wall jet [PB88-181953] 18 p2507 N88-24873
Liquid crystals for unsteady surface shear stress visualization [DE88-010570] 21 p2951 N88-27527

ISOTHERMAL PROCESSES
Equation of state of condensed materials physical principles and applications [NASA-TT-20007] 08 p0968 N88-15855
Isothermal and bithermal thermomechanical fatigue behavior of a NiCoCrAlY-coated single crystal superalloy [NASA-TM-100907] 18 p2489 N88-24766
Isothermal measurement and thermal desorption using SAW devices 19 p2671 N88-25881
The crystallization of tough thermoplastic resins in the presence of carbon fibers [NASA-CR-182984] 20 p2776 N88-26464

ISOTOPE EFFECT
Fusion, and advanced fuel, reaction bibliography: Particle reactions from H1 to B11 [AD-A187420] 11 p1552 N88-19286
XUV source for ultra-high resolution photoionization spectroscopy [DE88-007531] 19 p2614 N88-25510
Thermal conductivity of isotopically pure semiconductors, superlattices, semiconductor alloys and semiconductors as a function of temperature; control of the segregation coefficient in LEC crystal growth; and photo-Hall measurements of GaAs 21 p2927 N88-27375
Experimental and theoretical investigations of isotope shift and hyperfine structure on 5d elements (especially platinum, iridium and rhenium) [ETN-88-93121] 24 p3353 N88-29957

ISOTOPE SEPARATION
A study of mechanisms of hydrogen diffusion in separation devices [DE88-000328] 04 p0416 N88-12584
Plasma centrifuge development at INPE [INPE-4243-PRE/1117] 08 p1087 N88-16546
Isotope separation using tuned laser and electron beam [NASA-CASE-NPO-16907-1-CU] 18 p2483 N88-24732

ISOTOPE SHIFT
U ISOTOPE EFFECT

ISOTOPES
NT ARGON ISOTOPES
NT BORON ISOTOPES
NT BROMINE ISOTOPES
NT CALCIUM ISOTOPES
NT CARBON 12
NT CARBON 13
NT COBALT 60
NT DEUTERIUM
NT HELIUM ISOTOPES
NT HYDROGEN ISOTOPES
NT IODINE ISOTOPES
NT IRIDIUM ISOTOPES
NT IRON ISOTOPES
NT IRON 57
NT KRYPTON ISOTOPES
NT LAWRENCIUM
NT LEAD ISOTOPES
NT LITHIUM ISOTOPES
NT MAGNESIUM ISOTOPES
NT MERCURY ISOTOPES
NT NEODYMIUM ISOTOPES
NT NEPTUNIUM
NT NIOBIUM ISOTOPES
NT NITROGEN ISOTOPES
NT OXYGEN ISOTOPES
NT PLATINUM ISOTOPES
NT PLUTONIUM ISOTOPES
NT PLUTONIUM 238
NT RADIOACTIVE ISOTOPES
NT RADON ISOTOPES
NT RUBIDIUM ISOTOPES
NT SAMARIUM ISOTOPES
NT TELLURIUM
NT TRITIUM
NT URANIUM ISOTOPES
NT URANIUM 238
Electron scattering off palladium isotopes. An investigation of the equivalence of the anharmonic vibrator model and the interacting boson model [B8671274] 07 p0931 N88-15654
Heterogeneous isotope exchange between solid cesium iodide and gaseous methyl iodide [ETN-88-91085] 09 p1141 N88-16840
Analysis of gases in the earth's crust [PB88-141619] 10 p1354 N88-18093
Isotopic and chemical studies of early crustal metasedimentary rocks [NASA-CR-182711] 14 p1944 N88-21601
The dynamic isotope power system: Technology status and demonstration program 17 p2422 N88-24400
Characteristics of the closed Brayton cycle for dynamic isotope power systems 17 p2422 N88-24401
Dynamic isotope power system critical component verification 17 p2425 N88-24421
SNAP-DYN: Proven technology for wear-term, higher power in space 17 p2425 N88-24422
The application of high-rate biaxial testing to the design of containment vessels for radioisotope heat sources 17 p2426 N88-24428
High-fidelity in isotope ratio measurements for resonance ionization mass spectrometry [DE88-009129] 19 p2613 N88-25506
Lithospheric evolution of the Northern Arabian Shield: Chemical and isotopic evidence from basalts, xenoliths and granites 24 p3399 N88-30242
The growth of the continental crust: Constraints from radiogenic isotope geochemistry 24 p3399 N88-30245
Noble gases, C,N, and Si isotopes in interstellar SiC form the Murchison carbonaceous chondrite 24 p3442 N88-30483

ISOTOPIC ENRICHMENT
New nuclear structure calculations and the astrophysical r-process [DE88-000979] 08 p1082 N88-16518
Vacuum-arc plasma centrifuge experiment [INPE-4509-PRE/1263] 15 p2138 N88-22758

ISOTOPIC LABELING
The effect of wind and currents on gas exchange in an estuarine system [NASA-CR-181424] 01 p0073 N88-10468
Applications and limitations of deuterium labeling methods to neutron scattering studies of polymers [DE87-012936] 02 p0151 N88-10945
Isotope methods of determining distribution and movement of blood in the body 10 p1362 N88-18138
Method for the isotopically selective detection of inert gases [DE88-008370] 20 p2769 N88-26421
The timing and mechanism of depletion in Lewisian granulites 24 p3394 N88-30209
Genesis of archean granitoids in the Pilbara block and implications for crustal growth 24 p3394 N88-30210
Decoupled Rb-Sr and Sm-Nd isotopic evolution of the continental crust 24 p3395 N88-30216
The early archaean crustal history of West Greenland as recorded by detrital zircons 24 p3395 N88-30221

ISOTOPIC SPIN
Few body hypernuclear systems: Weak decays [DE87-014920] 04 p0488 N88-13010
Double beta decay and nuclear structure [DE88-001966] 07 p0931 N88-15652

ISOTROPIC MEDIA
Existence of absolutely closed universe 08 p1080 N88-16509
Ultrasonic beam distortion in transversely isotropic media [DE88-005937] 15 p2129 N88-22699
Acousto-ultrasonic input-output characterization of unidirectional fiber composite plate by SV waves [NASA-CR-4152] 16 p2217 N88-23224
Wave propagation in locally isotropic turbulent medium with smoothly changing characteristics [NASA-TT-20312] 20 p2800 N88-26617
A transversely isotropic thermoelastic theory [NASA-TM-101302] 22 p3087 N88-28332
Constitutive modeling for isotropic materials [NASA-CR-182132] 24 p3327 N88-29811

ISOTROPIC TURBULENCE
The generation of nearly isotropic turbulence by means of grids [PNR90411] 02 p0172 N88-11084
Center for Turbulence Research 1987 activities [NASA-CR-182693] 13 p1769 N88-20583
EDQNM closure: A homogeneous simulation to support it. A quasi-homogeneous simulation to disprove it 16 p2195 N88-23091
Angular distribution of turbulence in wave space 16 p2195 N88-23093
Big whorls carry little whorls 16 p2195 N88-23094
Analysis of non-premixed turbulent reacting flows 16 p2196 N88-23100
The decay of isotropic turbulence in a rapidly rotating frame 16 p2197 N88-23107
Wave propagation in locally isotropic turbulent medium with smoothly changing characteristics [NASA-TT-20312] 20 p2800 N88-26617

ISOTROPISM
Equilibrium shocks in plane deformations of incompressible elastic materials [AD-A188696] 12 p1636 N88-19796
Wave curves for simple isotropic elastic solids [AD-A188865] 12 p1636 N88-19798
The two isotropic asymptotes of fiber composites [AD-A192305] 21 p2904 N88-27231

ISOTROPY
NT ISOTROPIC MEDIA
Low cycle fatigue on isotropic fine-grained graphite [DE87-702627] 01 p0028 N88-10177
Effect of low velocity impact on compression strength of a quasi-isotropic laminate [FFA-TN-1987-38] 09 p1138 N88-16822
Wave curves for simple isotropic elastic solids [AD-A188865] 12 p1636 N88-19798

Changes in seismic velocity and apparent attenuation due to isotropic and anisotropic scattering: Results from physical modeling
19 p2691 N88-25997

Failure analysis of quasi-isotropic composite laminates with free edges under off-axis loading
22 p3049 N88-28092

ISRAEL

Design of the Sandia-Israel 20-kW reflux heat-pipe solar receiver/reactor
[DE88-001312] 13 p1794 N88-20729

ITALY

Italian activities in ocean colour remote sensing
08 p1043 N88-16304

The 1985 Meteorological Yearbook of Ispra (27th)
[PB88-125729] 20 p2828 N88-26777

Utilization of a satellite communication system to protect the national communication network
[FUB-33-1986] 21 p2934 N88-27423

SPOT for earthquake hazard zoning in southern Italy
22 p3093 N88-28365

ITERATION

NT CONJUGATE GRADIENT METHOD
NT ITERATIVE SOLUTION
NT NEWTON METHODS

An exponential example for Terlaky's pivoting rule for the criss-cross simplex method
[REPT-87-18] 01 p0080 N88-10512

Nonlinear parametric least-squares adjustment
[AD-A184039] 03 p0371 N88-12336

A new method to real-normalize measured complex modes
05 p0593 N88-13618

Near-horn prolog
[AD-A185172] 05 p0634 N88-13880

Research and development of finite elements and iterative algorithms for elliptic partial differential equations
[DE88-001381] 05 p0643 N88-13934

Freidlin-Wentzell type estimates and the law of the iterated logarithm for a class of stochastic processes related to symmetric statistics
[AD-A185366] 05 p0644 N88-13944

Spectral- and spatial-domain filtering and sampling approach to the numerical solution of electromagnetic scattering problems
[PB88-106711] 06 p0694 N88-14261

Study of extended least-square iterative techniques in electromagnetic scattering by penetrable objects
[PB88-105879] 06 p0694 N88-14262

Computing block-angular Karmarker projections with applications to stochastic programming, revision
[AD-A185647] 06 p0759 N88-14656

A multicut algorithm for two-stage stochastic linear programs
[AD-A186148] 07 p0903 N88-15466

A Schur-complement method for sparse quadratic programming
[DE88-002520] 07 p0904 N88-15479

An O(n3L) interior point algorithm for convex quadratic programming
[AD-A186001] 07 p0909 N88-15504

Remark on the multiple Wiener integral
[AD-A186015] 07 p0913 N88-15541

The iterative radiance model of the Meteorological Institute of the University of Munich (West Germany)
08 p1019 N88-16178

Iterative-deepening heuristic search for optimal and semi-optimal resource allocation
08 p1062 N88-16410

Method of iterative coupling between periodic aerodynamic and dynamic fields
[PB87-169934] 09 p1113 N88-16669

Theory of elementary particle studies in weak iteration and grand unification and studies in accelerator design
[DE86-004261] 11 p1545 N88-19238

An improved data reduction procedure for accelerometer centrifuge data
12 p1577 N88-19436

Statistical signal processing using a class of iterative estimation algorithms
[AD-A189050] 13 p1757 N88-20511

Nonlinear differential equations
[DE88-006047] 13 p1828 N88-20933

Iteration of transformation passes over attributed program trees --- compilers
[INF-87-28] 14 p1956 N88-21661

Application of Moment Iteration Method (MIM) to electromagnetic field computation
[PB88-194139] 20 p2789 N88-26546

SARLAC: A relativistic electron beam code
[AD-A193134] 21 p2932 N88-27411

KRYSI, an ODE solver combining a semi-implicit Runge-Kutta method and a preconditioned Krylov method
[DE88-012245] 21 p3008 N88-27841

ITERATIVE NETWORKS

Contribution to optimal flow in networks. A experimental multiprocessor for asynchronous iteration implementation
[LAAS-87-269] 05 p0576 N88-13510

Investigation and implementation of an algorithm for computing optimal search paths
[AD-A185927] 07 p0902 N88-15461

ITERATIVE SOLUTION

Exact solution of the inverse problem for a six-link manipulator with a mechanical offset
[DE87-702646] 01 p0054 N88-10349

S-step iterative methods for symmetric linear systems
[DE87-010819] 01 p0086 N88-10559

Preconditioned iterative methods applied to singularly perturbed elliptic boundary value problems: Volume 2
[DE87-014337] 02 p0225 N88-11415

Parallel methods for ordinary differential equations
[DE87-014667] 02 p0226 N88-11425

Iterative solution of a nonlinear system arising in phase change problems
[DE87-014672] 02 p0226 N88-11426

Efficient numerical approaches for predicting supersonic flows with viscous/inviscid interaction
03 p0260 N88-11637

Three-dimensional finite element based, interative approach for analysis of laminated composites
03 p0280 N88-11763

Steady waves in a nonlinear theory of viscoelasticity
[AD-A185548] 06 p0723 N88-14448

Solution of non-symmetric linear systems by biconjugate gradients or conjugate gradients squared
[PB87-226387] 06 p0763 N88-14679

On the parabolized Navier-Stokes equations without sublayer assumptions
[AD-A186127] 07 p0849 N88-15152

The k-grid Fourier analysis of multigrid-type iterative methods
[AD-A186315] 07 p0910 N88-15520

Investigation of iterative and spectral Galerkin techniques for solving electromagnetic boundary value problems
09 p1155 N88-16925

Improving the stability of predictor-corrector methods by residue smoothing
[CWI-NM-R8707] 09 p1228 N88-17359

Solution of the hyperbolic Kepler's equation
[RAE-TR-87042] 09 p1229 N88-17368

Preconditioned iterative methods for partial differential equations
[DE88-003071] 09 p1230 N88-17372

Optimal application of Morrison's iterative noise removal for deconvolution. Appendices
[NASA-CR-182477] 09 p1231 N88-17376

Centerplane source distribution for slender bodies
10 p1328 N88-17940

Quasigroup approach to solution of linear algebraic equation systems
[DE88-700595] 10 p1398 N88-18330

Leapfrog variants of iterative methods for linear algebra equations
[NASA-CR-181616] 10 p1398 N88-18332

Conjugate gradient spectral iterative technique
[PB88-126917] 10 p1398 N88-18337

Spectral iterative technique with Gram-Schmidt orthoganalization
[PB88-127451] 10 p1399 N88-18338

The application of the hybrid iterative method to scattering by perfectly conducting bodies of revolution
11 p1475 N88-18802

Further refinement and applications of the mixed computational algorithm for plane elastic contact problems
[AD-A188308] 12 p1683 N88-20065

Data traffic reduction schemes for sparse Cholesky factorizations
[NASA-CR-181626] 13 p1813 N88-20831

Inversion algorithms for geophysical problems
[AD-A189252] 13 p1815 N88-20845

A constitutive material model for nonlinear finite element structural analysis using an iterative matrix approach
14 p1932 N88-21521

Assimilation of meteorological observations
14 p1936 N88-21544

Contraction design for small low-speed wind tunnels
[NASA-CR-182747] 15 p2021 N88-22045

Smoothing technique to resolve X-ray spectra in laser nuclear fusion
15 p2053 N88-22235

Relative orientation
[AD-A190385] 15 p2089 N88-22449

Trust regions and projected gradients
[DE88-005829] 15 p2122 N88-22646

Efficiency of some computational techniques for electromagnetic scattering problems
[PB88-148895] 16 p2187 N88-23043

Iterative finite element solver on transputer networks
16 p2218 N88-23235

Vectorization of the odd-even hopscotch scheme and the alternating direction implicit scheme for the two-dimensional Burgers' equations
[CWI-NM-R8720] 16 p2249 N88-23440

Parallelization of Gauss-Seidel algorithms as an example of parallel iterative equation solving
[REPT-87-76] 16 p2254 N88-23471

Residual smoothing for accelerating the Alternating Direction Implicit (ADI) iteration method for elliptic difference equations
[CWI-NM-R8721] 16 p2259 N88-23500

A practical termination criterion for the conjugate gradient method
[REPT-87-62] 16 p2259 N88-23506

Algorithm for accounting the conditions in infinity for two-dimensional magnetostatics problems
[DE88-701673] 16 p2264 N88-23541

Electromagnetic scattering from nonlinear anisotropic cylinders
17 p2333 N88-23930

Fitting a circle to radially suppressed data
[NPL-DITC-103/87] 17 p2392 N88-24223

Adaptive local grid refinement in computational fluid mechanics
[AD-A192215] 18 p2510 N88-24890

Two domain decomposition techniques for Stokes problems
[DE88-008724] 19 p2720 N88-26149

Distributive iteration for indefinite systems as smoothing method in multigrid process on example of Stokes and Navier-Stokes equations with emphasis on incomplete decompositions
[ETN-88-92127] 21 p2948 N88-27509

Grid generation around transport aircraft configurations using a multi-block structured computational domain
23 p3247 N88-29325

Convergence acceleration for vector sequences and applications to computational fluid dynamics
[NASA-TM-101327] 24 p3424 N88-30377

IUE

Active phases on II Peg
04 p0507 N88-13119

The onset of chromospheric activity among the A- and F- type stars
04 p0511 N88-13144

IUE/Optical/VLA flares on AD Leo
04 p0512 N88-13152

A flash spectrum of Cl I, C I, N I, and Ni II absorption in 31 Cygni: A direct observation of the reversing layer
04 p0513 N88-13158

Hydrogen and deuterium in the local interstellar medium
04 p0521 N88-13204

IUE evidence on the nature of the innermost broad-line region in Seyfert 1 galaxies
17 p2450 N88-24552

International ultraviolet explorer observatory operations
[NASA-CR-180775] 22 p3145 N88-28708

International ultraviolet explorer spectral atlas of planetary nebulae, central stars, and related objects
[NASA-RP-1203] 22 p3164 N88-28843

Beyond the visible: A decade of observations with the International Ultraviolet Explorer (IUE)
[ESA-F09] 24 p3331 N88-29828

IUS

U INERTIAL UPPER STAGE

IZSAK ELLIPSOID

U ELLIPSOIDS
U GEODESY

J

J INTEGRAL

Determination of the critical crack length a (sub IC) in turbine discs
[PB87-144812] 07 p0820 N88-14986

J-estimation procedure based on moire interferometry data
[AD-A185965] 07 p0867 N88-15258

The J-integral concept for elastic-plastic material behavior
[W-5/87] 08 p1000 N88-16059

Fracture mechanics and creep crack growth of 1 percent Cr 1/2 percent Mo steel with and without prior exposure to creep conditions
[NLR-TR-86051-U] 13 p1743 N88-20426

The Nordic J-R curve round robin test program --- reactor steel
[VTT-RR-510] 14 p1923 N88-21459

A simplified key-curve approach for J-R-curve testing of CT specimens
[VTT-RR-503] 15 p2088 N88-22444

Method and models for R-curve instability calculations
[NASA-TM-100935] 16 p2224 N88-23278

Analysis and developments of failure concepts in fracture mechanics based on research results in the field of component safety topics: J-integral concept; crack resistance curves; dynamic criterion
[V-19/86] 18 p2530 N88-25009

Experimental investigation of ductile fracture by white light moire interferometry 22 p3087 N88-28329
J-integral measurement using moire interferometry [AD-A193751] 23 p3226 N88-29202

J-57 ENGINE
Operation of gas turbine engines in dust-laden environments 10 p1280 N88-17654

JACKS (ELECTRICAL)
U ELECTRIC CONNECTORS

JACOBI MATRIX METHOD
Analysis of smoothing matrices for the preconditioning of elliptic difference equations [CWI-NM-R8705] 09 p1228 N88-17357
Problems in fluid dynamics [NASA-CR-182678] 14 p1909 N88-21410

JACOBI POLYNOMIALS
U HYPERGEOMETRIC FUNCTIONS

JAMMING
Monitoring of harmful interference to the HF (High Frequency) broadcasting service. 3: Results of the June 1986 coordinated monitoring period [PB87-210274] 01 p0036 N88-10229
Radar ECCM's new area: Anti-STEALTH and anti-ARM 03 p0299 N88-11881
Performance analysis of coded frequency-hopped spread-spectrum systems with unknown interference [AD-A186069] 07 p0841 N88-15103
Adaptive spread spectrum networks [AD-A187154] 09 p1152 N88-16900
Static and dynamic jamming of networks [AD-A188921] 12 p1620 N88-19690
Visual recognition training: Effectiveness of computer graphics [AD-A188302] 12 p1669 N88-19997
Distortions in processed signals and their application in electronic design. Part 3: An automated generator of communication jamming signals [DE88-702733] 23 p3205 N88-29072
MIDIR (Mid-Infrared) laser, phase 1 [AD-A193935] 23 p3220 N88-29166

JAPAN
Japanese industrial research on lean combustion: A case study: International Research Monitoring Program [DE87-013839] 02 p0144 N88-10904
JPRS report: Science and technology. Japan [JPRS-JST-87-025] 04 p0403 N88-12502
Impressions, observations and comments on science and technology in Japan [PB87-235743] 06 p0799 N88-14893
North Pacific Ocean. Northwest Pacific Transition Zone, R/V Thomas G. Thompson: 19 March - 1 May 1971. STD data report [AD-A186568] 08 p1044 N88-16313
NASDA's new test facilities for satellites and rockets 11 p1499 N88-18951
Proceedings of US-Japan Heliotron-Stellarator Workshop, volume 3 [DE88-004788] 11 p1554 N88-19299
Proceedings of US-Japan Heliotron-Stellarator Workshop, volume 2 [DE88-004789] 11 p1554 N88-19300
Directory of Japanese technical resources, 1987 [PB87-205258] 12 p1706 N88-20212
Sunshine project for FY 1987 outlined 16 p2184 N88-23021
Survey on utility technology of a tidal and ocean current energy [DE88-770148] 20 p2819 N88-26722

JAPANESE SPACE PROGRAM
Space missions to Comets Halley and Giacobini-Zinner 03 p0272 N88-11712
An overview of the current Earth observation programs (Europe, USA, and Japan) 09 p1129 N88-16778
Space utilization plans 15 p2051 N88-22219
Space experiment plan FMPT 15 p2051 N88-22220
Japanese space station module 15 p2052 N88-22224
High speed and high angle of attack wind tunnel test results of the winged space vehicle C-2 [ISAS-RN-623] 20 p2751 N88-26329

JAPANESE SPACECRAFT
Comparison of MHD simulation for the February 1986 events with interplanetary observations by the spacecraft Sakigake 01 p0113 N88-10722
Investigation of European remote sensing user needs in accessing MOS-1 payload [ESA-CR(P)-2535] 14 p1940 N88-21580
Halley's environments by the Japanese Suisei spacecraft 14 p1999 N88-21915

JARRING
U MECHANICAL SHOCK

JC-130 AIRCRAFT
U C-130 AIRCRAFT

JEEPS
U AUTOMOBILES

JET AIRCRAFT
NT A-300 AIRCRAFT
NT A-320 AIRCRAFT
NT B-57 AIRCRAFT
NT B-70 AIRCRAFT
NT BOEING 737 AIRCRAFT
NT BOEING 747 AIRCRAFT
NT C-130 AIRCRAFT
NT C-135 AIRCRAFT
NT CONCORDE AIRCRAFT
NT DC 9 AIRCRAFT
NT EUROPEAN AIRBUS
NT F-4 AIRCRAFT
NT F-14 AIRCRAFT
NT F-15 AIRCRAFT
NT F-16 AIRCRAFT
NT F-18 AIRCRAFT
NT F-27 AIRCRAFT
NT F-106 AIRCRAFT
NT F-111 AIRCRAFT
NT MIRAGE AIRCRAFT
NT OV-1 AIRCRAFT
NT P-3 AIRCRAFT
NT T-33 AIRCRAFT
NT TURBOFAN AIRCRAFT
NT TURBOPROP AIRCRAFT
NT U-2 AIRCRAFT
NT VC-10 AIRCRAFT
Effect of empennage arrangement on single-engine nozzle/afterbody static pressures at transonic speeds [NASA-TP-2753] 02 p0122 N88-10771
Soviet aviation technology's state of the art SU-27 fighter [AD-A184121] 03 p0259 N88-11628
Improvements to the adaptive maneuvering logic program [NASA-CR-3985] 03 p0262 N88-11648
Aircraft engine exhaust plume dynamics [AD-A184238] 04 p0400 N88-12488
Computation of nacelle interference using boundary element method 05 p0537 N88-13267
AFRAPT (Air Force Research in Aero Propulsion Technology) trainee program [AD-A190525] 15 p2035 N88-22123
Pilot report: AFTI (Advanced Fighter Technology Integration) F-111 [AD-A192937] 21 p2895 N88-27184
Integration of LANTIRN (Low Altitude Navigation and Targeting Infrared for Night) into operational fighter training [AD-A194906] 24 p3325 N88-29799

JET AIRCRAFT NOISE
Shock structure and noise of supersonic jets in simulated flight to Mach 0.4 [NASA-TP-2785] 08 p1080 N88-16510
Annoyance caused by advanced turboprop aircraft flyover noise: Single-rotating propeller configuration [NASA-TP-2782] 09 p1242 N88-17441
Noise levels from a jet-engined aircraft measured at ground level and at 1.2 m above the ground [NPL-AC-114] 23 p3279 N88-29524

JET AIRSTREAMS
U JET STREAMS (METEOROLOGY)

JET AUGMENTED WING FLAPS
U JET FLAPS
U WING FLAPS

JET CONTROL
Active control of jet flowfields [AD-A186736] 08 p0989 N88-15989
Research on flow control [AD-A189014] 12 p1627 N88-19736
Aerodynamic possibilities for the realization of trajectory corrections [ISL-CO-251/86] 14 p1862 N88-21120
Experimental investigation of two-dimensional confined jet thrust vector control [AD-A189845] 15 p2027 N88-22077
Variable Mach number wall jets for control/propulsion on hypervelocity projectiles/interceptors: Tests with an existing model [AD-A192845] 21 p2892 N88-27167

JET DAMPING
U DAMPING
U SPIN REDUCTION

JET DRIVE
U JET PROPULSION

JET ENGINE FUELS
NT JP-4 JET FUEL
NT JP-5 JET FUEL
NT JP-8 JET FUEL
Study of electrostatic modulation of fuel sprays to enhance combustion performance in an aviation gas turbine [AD-A184967] 05 p0548 N88-13341
An experimental investigation of the ignition and flammability limits of various hydrocarbon fuels in a two-dimensional solid fuel ramjet [AD-A184968] 05 p0549 N88-13342
Production of jet fuels from coal derived liquids. Volume 1: Market assessment for liquid by-products from the Great Plains gasification plant [AD-A184846] 05 p0570 N88-13475
Aviation turbine fuels from tar sands bitumen and heavy oils. Part 2: Laboratory sample production [AD-A185744] 06 p0687 N88-14211
Military jet fuels, 1944-1987 [AD-A186752] 09 p1150 N88-16890
High-density jet fuels from coal syncrudes, appendix 4 [DE88-003132] 10 p1307 N88-17813
Degradation of jet and missile fuels by aquatic microbial communities [AD-A188065] 11 p1465 N88-18737
Flammability characteristics of distillate fuels [AD-A188497] 12 p1612 N88-19642
Availability and cost estimate of a high naphthene, modified aviation turbine fuel [NASA-TM-100823] 13 p1749 N88-20455
Aviation turbine fuels from tar sands bitumen and heavy oils. Part 3: Laboratory sample production [AD-A189278] 13 p1753 N88-20484
Turbine fuels from tar sands bitumen and heavy oil. Volume 2, phase 3: Process design specifications for a turbine fuel refinery charging San Ardo heavy crude oil [AD-A190120] 16 p2183 N88-23011
Development of a laboratory test for multiport fuel injector deposits - evaluation of the Jet Fuel Thermal Oxidation Test apparatus (JFTOT) [AD-A191313] 16 p2183 N88-23015
Selective detection in gas chromatography [AD-A191499] 18 p2481 N88-24718
Reference filters for electrostatic charging tendency measurements of fuels [AD-A191717] 18 p2495 N88-24803
Feasibility of producing jet fuel from GPGP (Great Plains Gasification Plant) by-products [DE88-010233] 20 p2781 N88-26492
Biodegradation of JP-5 aviation fuel by subsurface microbial communities [AD-A192743] 20 p2781 N88-26493
A study relating to the fog oil repiacement program [AD-A192536] 21 p2923 N88-27347
Development of a test method to determine potential peroxide content in turbine fuels. Part 2 [AD-A192244] 23 p3199 N88-29042
Fuel property effects on the US Navy's TF30 engine 24 p3345 N88-29911
Determination of the hydroperoxide potential of jet fuels [AD-A195975] 24 p3357 N88-29991

JET ENGINES
NT CONVERTIBLE FAN-SHAFT ENGINES
NT J-57 ENGINE
NT RAMJET ENGINES
NT SUPERSONIC COMBUSTION RAMJET ENGINES
NT TF-30 ENGINE
NT TURBOFAN ENGINES
NT TURBOJET ENGINES
NT TURBOPROP ENGINES
First article test noise survey of the A/F32T-9 large turbo fan engine enclosed noise suppressor system, Sky Harbor IAP (International Airport), Phoenix, Arizona [AD-A183799] 01 p0090 N88-10588
Effect of empennage arrangement on single-engine nozzle/afterbody static pressures at transonic speeds [NASA-TP-2753] 02 p0122 N88-10771
The use of Kevlar on aero-engine fan containment casings [PNR90410] 02 p0182 N88-11134
Qualitative and temporal reasoning in engine behavior analysis 08 p1058 N88-16383
Optimisation of military compressors for weight and volume 10 p1279 N88-17649
An examination of the impact of potential advances in component technology for future military engines 10 p1279 N88-17650
Specification of an engine and its components starting from a consideration of aircraft missions 10 p1279 N88-17651
Application of highly loaded single-stage mixed-flow compressors in small jet-engines 10 p1280 N88-17652
Aerodynamic performance of a scale-model, counter-rotating unducted fan 10 p1282 N88-17666
Design and development of an advanced F100 compressor 10 p1283 N88-17678
Noise assessment of unsuppressed TF-34-GE-100A engine at Warfield ANG, Baltimore, Maryland [AD-A189966] 15 p2129 N88-22702

Engine component retirement for cause. Volume 1: Executive summary
[AD-A192730] 20 p2760 N88-26371
A fundamental understanding of the interfacial compatibility in hybrid material systems
[AD-A192921] 21 p2909 N88-27264
An investigation of constitutive models for predicting viscoplastic response during cyclic loading
[AD-A194875] 24 p3385 N88-30163

JET EXHAUST
Optical sizing of soot in gas turbine combustors and exhaust augmentor tubes
[AD-A183785] 01 p0006 N88-10034
Aircraft engine exhaust plume dynamics
[AD-A184238] 04 p0400 N88-12488
Influence of base modifications on in-flight base drag in the presence of jet exhaust for Mach numbers from 0.7 to 1.5
[NASA-TP-2802] 11 p1488 N88-18881
Fully-coupled analysis of jet mixing problems. Three-dimensional PNS model, SCIP3D
[NASA-CR-4139] 13 p1715 N88-20256
Techniques utilized in the simulated altitude testing of a 2D-CD vectoring and reversing nozzle
[NASA-TM-100872] 19 p2604 N88-25464

JET FLAMES
U FLAMES
U JET FLOW

JET FLAPS
Investigations of aircraft control with jet spoilers
[ISL-R-112/87] 21 p2898 N88-27202

JET FLIGHT
U JET AIRCRAFT

JET FLOW
NT AIR JETS
NT SUPERSONIC JET FLOW
Experimental and theoretical studies of vertical annular liquid jets
[DE87-013907] 01 p0047 N88-10299
Flow and heat transfer with impinging jets and rough surfaces
[DE87-014162] 02 p0169 N88-11065
A calculation method for the propulsive jet and its aerodynamic interaction with an afterbody
[ESA-TT-1039] 03 p0259 N88-11632
On the instability of thin circular shear layers
04 p0395 N88-12467
Comparative studies in the near-field of turbulent transports of heated and unheated jets normal to a cross stream 04 p0444 N88-12756
Mesoscale eddy dynamics by the method of point vortices 04 p0463 N88-12863
Combustion related shear-flow dynamics in elliptic supersonic jets 05 p0531 N88-13232
Jet initiation of PBX 9502
[DE88-000493] 05 p0571 N88-13481
Trajectory control using laterally ejected jets. Literature review
[ISL-R-117/85] 05 p0581 N88-13544
Raman spectra of adsorbed layers on space shuttle and AOTV thermal protection system surface
06 p0799 N88-14890
Experimental study of secondary flow in the presence of two jet arrays on the wall of a turbine blade
[ECL-87-11] 08 p0987 N88-15981
On the correlation of plume centerline velocity decay of turbulent acoustically excited jets
[NASA-TM-100193] 09 p1114 N88-16681
Wind tunnel studies of circulation control elliptical airfoils 10 p1270 N88-17598
Investigation of non-symmetric jets in cross flow
10 p1327 N88-17932
Droplet formation for liquid monopropellant jets
[AD-A187172] 10 p1331 N88-17956
Numerical simulations of the California current: Filament formation as related to baroclinic instability
[AD-A187573] 10 p1358 N88-18115
A hydrodynamic analysis of fluid flow between meshing spur gear teeth
[AD-A187671] 11 p1482 N88-18844
Studies on homogeneous and heterogeneous reactive flows 11 p1484 N88-18861
Reynold stress closure in jet flows using wave models
[NASA-CR-182662] 12 p1628 N88-19741
Mushroom-shaped currents (eddy dipoles) under rotation and stratification conditions
13 p1784 N88-20678
Interaction of a two-dimensional bluff body and incompressible jet and annulus flows
[AD-A190503] 15 p2064 N88-22310
The structure of sonic underexpanded turbulent air jets in still air
[AD-A190856] 16 p2157 N88-22870
Numerical analysis of critical penetration velocity for jet perpendicular penetration 16 p2186 N88-23037
Initial condition effect on pressure waves in an axisymmetric jet
[NASA-TM-100915] 16 p2209 N88-23184
Acoustically excited heated jets. 1: Internal excitation
[NASA-CR-4129-PT-1] 17 p2298 N88-23751
Acoustically excited heated jets. 2: In search of a better understanding
[NASA-CR-4129-PT-2] 17 p2299 N88-23752
Heat transfer from a negatively buoyant wall jet
[PB88-181953] 18 p2507 N88-24873
Hydroacoustic pulsating jet generator
[MPIS-7/1987] 18 p2510 N88-24891
Numerical solutions of the complete Navier-Stokes equations
[NASA-CR-183023] 18 p2514 N88-24914
Aerodynamic focusing of particles and heavy molecules
[DE88-007145] 19 p2598 N88-25440
Numerical simulations of astrophysical jets
19 p2636 N88-25635
Three-dimensional viscous flow computations of a circular jet in subsonic and supersonic cross flow
[NASA-CR-182153] 20 p2800 N88-26616
A computational analysis of under-expanded jets in the hypersonic regime
[NASA-TM-101319] 21 p2893 N88-27174
Coupled experimental and theoretical investigations of instability, chaos and turbulence in an axisymmetric jet flow
[AD-A192943] 21 p2942 N88-27476
Turbulence structure of mixing swirling flows
[AD-A193063] 21 p2943 N88-27478
A numerical study of turbulent plane jets in still and flowing environments employing two-equation k-epsilon model 23 p3211 N88-29109
The influence of delay effects on the decay of liquid jets
[MPIS-14/1987] 23 p3214 N88-29130
Modelling of CO oxidation in dilution jet flows
24 p3351 N88-29947

JET FUELS
U JET ENGINE FUELS

JET IMPINGEMENT
Flow and heat transfer with impinging jets and rough surfaces
[DE87-014162] 02 p0169 N88-11065
Jet impingement heat transfer: A literature study
[PNR90404] 02 p0172 N88-11083
Heat transfer from impinging flame jets
[ETN-88-91610] 09 p1162 N88-16964

JET LAG
Pharmacological resetting of the Circadian sleep-wake cycle
[AD-A186194] 07 p0889 N88-15385
Desynchronization of heart rate and breathing frequency after transmeridional flight across three time zones
12 p1663 N88-19968

JET LIFT
A jet in a crossflow
[NASA-CR-182469] 09 p1113 N88-16674
Numerical study of delta wing leading edge blowing
[NASA-CR-183101] 20 p2752 N88-26335

JET MIXING FLOW
Dilution jet mixing program, phase 3
02 p0185 N88-11153
On the mixing of a row of jets with a confined crossflow 02 p0185 N88-11154
A numerical study of the effects of curvature and convergence on dilution jet mixing
[NASA-TM-89878] 05 p0549 N88-13347
Chemical reactions in turbulent mixing flows
[AD-A186141] 07 p0849 N88-15153
Fully-coupled analysis of jet mixing problems. Three-dimensional PNS model, SCIP3D
[NASA-CR-4139] 13 p1715 N88-20256
Control of structure in turbulent flows: Bifurcating and blooming jets
[AD-A189607] 13 p1766 N88-20562
Chemically reacting turbulent flow
[AD-A190522] 15 p2065 N88-22311
Saturation and the limit of jet mixing enhancement by single frequency plane wave excitation: Experiment and theory
[NASA-TM-100882] 17 p2295 N88-23732
Acoustically excited heated jets. 1: Internal excitation
[NASA-CR-4129-PT-1] 17 p2298 N88-23751
Acoustically excited heated jets. 2: In search of a better understanding
[NASA-CR-4129-PT-2] 17 p2299 N88-23752
Acoustically excited heated jets. 3: Mean flow data
[NASA-CR-4129-PT-3] 17 p2299 N88-23753
Effect of initial tangential velocity distribution on the mean evolution of a swirling turbulent free jet
[NASA-TM-100934] 18 p2458 N88-24592
An empirical model of the effects of curvature and convergence on dilution jet mixing
[NASA-TM-100896] 18 p2466 N88-24640
Numerical simulation of ignition of hydrogen jet in hot air 19 p2637 N88-25647
Three-dimensional vortex interactions
[AD-A194066] 23 p3172 N88-28889
Small scale mixing in the initial region of a jet
[AD-A193500] 23 p3192 N88-28994

JET NOISE
U JET AIRCRAFT NOISE

JET NOZZLES
Design of supersonic Coanda jet nozzles
10 p1270 N88-17599

JET PILOTS
U AIRCRAFT PILOTS

JET PROPULSION
A calculation method for the propulsive jet and its aerodynamic interaction with an afterbody
[ESA-TT-1039] 03 p0259 N88-11632
Rocket and airjet propulsion for ballistic and aerodynamic space probes
[REPT-TR-527] 10 p1310 N88-17826
Pressure distributions and losses in a waterjet propulsion system
[AD-A188423] 12 p1633 N88-19777
Variable Mach number wall jets for control/propulsion on hypervelocity projectiles/interceptors: Tests with an existing model
[AD-A192845] 21 p2892 N88-27167

JET STREAMS (METEOROLOGY)
Ozone, jet streaks and severe weather
05 p0616 N88-13781
Northern winter circulations for the period 1974-1983
[AD-A187779] 11 p1511 N88-19028

JET THRUST
Aircraft engine exhaust plume dynamics
[AD-A184238] 04 p0400 N88-12488
Pressure measurements of impinging jet with asymmetric nozzle
[NASA-CR-182759] 15 p2014 N88-22011
Experimental investigation of two-dimensional confined jet thrust vector control
[AD-A189845] 15 p2027 N88-22077

JET VANES
Effects of the installation and operation of jet-exhaust yaw vanes on the longitudinal and lateral-directional characteristics of the F-14 airplane
[NASA-TP-2769] 04 p0393 N88-12455
Heat transfer modeling of jet vane Thrust Vector Control (TVC) systems
[AD-A190106] 15 p2019 N88-22034
TVC (Thrust Vector Control) jet vane thermal modeling using parametric system identification
[AD-A191518] 18 p2474 N88-24678

JETAVATORS
U GUIDE VANES

JETS
Jet formation and characterization of a conical shaped charge
[DE87-012102] 02 p0155 N88-10969

JETTIES
U BREAKWATERS

JFET
Advanced components for spaceborne infrared astronomy
[NASA-CR-177470] 13 p1772 N88-20601
JFET/SOS (Junction Field-Effect Transistor/Silicon-on-Sapphire) devices: Gamma-radiation-induced effects
[AD-A193001] 20 p2795 N88-26586

JIMSPHERE BALLOONS
Analysis of the bivariate parameter wind differences between Jimsphere and Windsonde
[NASA-TM-4014] 01 p0072 N88-10461

JITTER
U VIBRATION

JOBS
U TASKS

JOINING
Optically interconnected phased arrays
[NASA-TM-100855] 14 p1908 N88-21400

JOINT EUROPEAN TORUS
Comparison of high purity fine grain graphites from different suppliers with regard to physical, mechanical, and thermal properties --- Joint European Torus wall protection
[JUEL-SPEZ-401] 02 p0154 N88-10963
A three-barrel repeating pneumatic pellet injector for plasma fueling of the Joint European Torus
[DE88-000330] 04 p0491 N88-13026
The JET (Joint European Torus) multipellet launcher and fueling of JET plasmas by multipellet injection
[DE88-008367] 19 p2729 N88-26206

JOINTS (ANATOMY)
NT WRIST

Joint angle sensors for closed-loop control
19 p2673 N88-25891

JOINTS (JUNCTIONS)
NT BOLTED JOINTS
NT BUTT JOINTS
NT INTERFERENCE FIT
NT LAP JOINTS
NT METAL JOINTS
NT RIVETED JOINTS
NT SEAMS (JOINTS)
NT SOLDERED JOINTS
NT SPOT WELDS
NT WELDED JOINTS

Joints in carbon fibre reinforced composites
[BR99969] 01 p0019 N88-10114
Metallic superlattices with monolayer modulation
[DE87-012724] 01 p0023 N88-10145
Superconducting properties of metallic superlattices
[DE87-012725] 01 p0023 N88-10146
Exact solution of the inverse problem for a six-link manipulator with a mechanical offset
[DE87-702646] 01 p0054 N88-10349
Effects of barrel joints on hypervelocity projectiles
[DE87-013447] 02 p0157 N88-10983
Process and equipment capabilities materials joining laboratory, 1987
[DE87-014534] 02 p0180 N88-11122
Low-pressure eutectic bonding of depleted uranium to copper
[DE87-014625] 02 p0181 N88-11128
Assessment of structural integrity from forced vibration testing
[DE87-014642] 02 p0191 N88-11195
Direction dependent connections of complex manifolds and their submanifolds
[DE87-703073] 02 p0225 N88-11419
Stability of mechanical joints in launching vehicles: Local and global stationary values of energy density
03 p0270 N88-11696
Considerations concerning a thermal joint for a deployable or steerable battery radiator for the Columbus Polar Platform
[NLR-TR-86055-U] 03 p0276 N88-11739
Joining of silicon carbide reinforced ceramics
[DE87-014881] 03 p0294 N88-11847
Durability (lifetime) predictions adhesively bonded structures
[AD-A184069] 03 p0335 N88-12110
Overview of free-piston Stirling engine technology for space power application
[NASA-TM-88886] 03 p0386 N88-12427
Reduced complexity structural modeling for automated airframe synthesis
[NASA-CR-177440] 04 p0393 N88-12453
Influence of bond dilution on the free surface and interface Potts ferromagnetism
[DE87-703360] 04 p0497 N88-13061
Advanced joining concepts for passive vibration control 05 p0596 N88-13638
Behavior of bolted joints in composite laminates
06 p0677 N88-14148
Pin joints, gears, springs, cranks and other novel micromechanical structures
[DE88-002504] 07 p0864 N88-15245
Through-transmission/pulse-echo ultrasonic equipment evaluation
[AD-A186340] 07 p0929 N88-15641
Effect of peel angle on peel force
[AD-A186117] 08 p0972 N88-15878
Two-phase flow forms and pressure drop in horizontal T tube joints with vertical branch
[GKSS-87/E/12] 09 p1163 N88-16969
Development of methods for low temperature diffusion bonding
[AD-A186875] 09 p1174 N88-17033
A finite element analysis of adhesively bonded composite joints including geometric nonlinearity, nonlinear viscoelasticity moisture diffusion and delayed failure
[AD-A187455] 10 p1296 N88-17747
Design conditions and workspace for the generally-proportioned 3-hinge spherical wrist for robots
10 p1339 N88-18003
Computed stress and strain distributions under interference fit and after coldworking
[AD-A186950] 10 p1342 N88-18024
Finite element analysis of adhesively bonded composite joints including geometric nonlinearity, nonlinear viscoelasticity, moisture diffusion and delayed failure
[PB88-147822] 11 p1451 N88-18648
Characterization of damped structural connections for multi-component systems
[NASA-TM-100801] 11 p1502 N88-18974
The Shock and Vibration Digest, volume 20, no. 3
12 p1635 N88-19786
Further refinement and applications of the mixed computational algorithm for plane elastic contact problems
[AD-A188308] 12 p1683 N88-20065
Reduction of erosion in elbows due to flow modifications, phase 1
[DE88-001028] 13 p1769 N88-20584
Structural clearances and internal friction: Simulation by Eigen distortions
[ISSN-0208-5658] 13 p1779 N88-20640
Robotic joint prototype for space applications
14 p1878 N88-21222
An efficient gradient projection optimization scheme for a seven-degree-of-freedom redundant robot with spherical wrist
[DE88-005440] 14 p1919 N88-21453
Robotic joint experiments under ultravacuum
14 p1927 N88-21490
Ammonia transfer across rotating joints in space
14 p1927 N88-21492
Space shuttle solid rocket motor Profile Measuring Device (PMD) 14 p1928 N88-21495
Fracture toughness of silicon nitride-silicon nitride joints bonded with oxynitride glass
[DE88-005548] 15 p2043 N88-22172
Ultrasonic characterization of ceramic joints
[DE88-005844] 15 p2043 N88-22173
Stabilization and control problems in structural dynamics
[AD-A190197] 15 p2073 N88-22361
Increasing strength of graphite/epoxy bolted joints by introducing an adhesively bonded metallic insert
[FFA-TN-1987-45] 15 p2088 N88-22442
A three dimensional non-singular modelling of rigid manipulators
[AD-A189707] 15 p2116 N88-22604
Design and test of a new coaxial air joints
[DE88-751808] 16 p2164 N88-22908
Characterization of structural connections for multicomponent systems 16 p2220 N88-23251
On the calculation of stresses in pin-loaded anisotropic plates
[LR-529] 16 p2223 N88-23268
Manufacturing requirements 17 p2297 N88-23745
Bearing-bypass material system test
[NASA-CASE-LAR-13458-1] 17 p2342 N88-23967
The inspection of metallurgical bounds in electronic systems
[AD-A192064] 18 p2582 N88-25343
Optimization of performance criteria with bounded joint velocities for robots with one degree of redundancy
[DE88-003915] 20 p2810 N88-26670
FEB structural analysis, revision H
[AD-A192302] 20 p2814 N88-26698
Kinematics of Hooke universal joint robot wrists
[NASA-TM-100567] 20 p2843 N88-26870
General expression of manipulator kinematics
[DE88-753430] 21 p2957 N88-27567
Chemistry of adhesion at the polyimide-metal interface
[AD-A194647] 22 p3058 N88-28143
Critical joints in large composite primary aircraft structures. Volume 2: Technology demonstration test report
[NASA-CR-172587] 23 p3177 N88-28915
Critical joints in large composite primary aircraft structures. Volume 3: Ancillary test results
[NASA-CR-172588] 23 p3177 N88-28916
Soot and radiation in a gas turbine combustor
[AD-A191991] 23 p3179 N88-28924
Critical joints in large composite primary aircraft structures. Volume 1: Technical summary
[NASA-CR-3914] 23 p3190 N88-28983
Elastic behavior of a rubber layer bonded between two rigid spheres
[AD-A193698] 23 p3198 N88-29030
Stability control of leakage flow channels
[DE88-009995] 23 p3210 N88-29107
Recursive mass matrix factorization and inversion: An operator approach to open- and closed-chain multibody dynamics
[NASA-CR-182516] 23 p3247 N88-29328
Criteria for matrix dominated failure
[AD-A196263] 24 p3341 N88-29887

JOSEPHSON JUNCTIONS
Abrikosov vortex motion and elementary pinning force in a SNS Josephson junction
[DE87-013607] 01 p0105 N88-10683
Hitachi develops ceramic superconducting device
06 p0688 N88-14214
The consequences of intergrain Josephson coupling in ceramic high-temperature superconductors
[DE87-013713] 06 p0785 N88-14816
Macroscopic quantum effects in a Josephson tunnel junction
[DE88-002239] 06 p0787 N88-14830
Comparative investigation of heterodyne mixers at 1000 GHz
[FTL-068627] 09 p1158 N88-16940
Studies of nonlinear and chaotic phenomena in solid state systems
[DE88-002330] 09 p1254 N88-17515
Effect of the subgap conductance on the metastable states in a Josephson tunnel junction
[DE88-003102] 09 p1258 N88-17543
Bloch oscillations in small Josephson junctions: Their manifestation in switching effects
14 p1969 N88-21756
Vortices in long Josephson junctions
[AD-A190338] 15 p2059 N88-22279
Preparation of large area NbN/AlN/NbN Josephson junctions
[DE88-006074] 15 p2145 N88-22799
Fluxons and order in long Josephson junctions
[AD-A190879] 16 p2282 N88-23665
Picosecond switching in Josephson tunnel junctions
19 p2657 N88-25780
Noise and chaos in driven Josephson junctions
19 p2734 N88-26238
Phase sensitive amplification with SIS (Superconductor-Insulator-Superconductor) quasiparticle mixers
[AD-A194594] 23 p3291 N88-29596
Planar thin film SQUID with integral flux concentrator
[NASA-CASE-MFS-28282-1] 23 p3292 N88-29602

JOUKOWSKI TRANSFORMATION
An efficient patched grid Navier-Stokes solution for multiple bodies, phase 1
[AD-A194166] 23 p3211 N88-29110

JOULE HEATING
U OHMIC DISSIPATION

JOULE-THOMSON EFFECT
Development of a low noise 10 K J-T refrigeration system
[AD-A185258] 05 p0571 N88-13484
Cryocooler systems demonstration
[AD-A188025] 11 p1467 N88-18745

JOURNAL BEARINGS
Determination of the fatigue strength of mechanically, thermally and corrosively loaded multilayer materials
[ETN-87-90375] 01 p0058 N88-10372
On the performance of finite journal bearings lubricated with micropolar fluids
[NASA-TM-100293] 08 p0988 N88-15983
The use of multigrid techniques in the solution of the Elrod algorithm for a dynamically loaded journal bearing
[NASA-CR-180873] 10 p1331 N88-17954
Table with aerostatic bearings for simulation in one degree of freedom attitude control systems of artificial satellites
[INPE-4272-PRE/1144] 12 p1595 N88-19552
Dynamic modelling of flexible rotor shafts mounted on hydrodynamic bearings 13 p1779 N88-20641
The solution of the Elrod algorithm for a dynamically loaded journal bearing using multigrid techniques
[NASA-TM-100941] 19 p2666 N88-25854
A lubrication study of engine bearings
21 p2958 N88-27574

JOURNALS (DOCUMENTS)
U PERIODICALS

JOURNALS (SHAFTS)
U SHAFTS (MACHINE ELEMENTS)

JP-4 JET FUEL
Measurements in large JP-4 pool fires
[DE87-013445] 03 p0284 N88-11783
The performance of a surrogate blend in simulating JP-4 in a spray-fueled combustor 24 p3347 N88-29926

JP-5 JET FUEL
Biodegradation of JP-5 aviation fuel by subsurface microbial communities
[AD-A192743] 20 p2781 N88-26493

JP-8 JET FUEL
Cost savings possible with Air Force conversion to JP-8 as its primary fuel
[AD-A183784] 01 p0030 N88-10192

JUDGMENTS
Effects of stress on judgement and decision making in dynamic tasks
[AD-A188203] 11 p1523 N88-19092
Space vehicle approach velocity judgments under simulated visual space conditions
[NASA-TM-89437] 11 p1523 N88-19094
Training in time interval discrimination using verbal feedback 12 p1665 N88-19985
Science, technology and the Constitution: Background paper
[PB88-142534] 12 p1708 N88-20222
On categorizing sounds
[AD-A189784] 15 p2129 N88-22700
A framework for a theory of mapping
[AD-A191071] 18 p2551 N88-25144

Rules, schema and decision making
[AD-A193389] 21 p3027 N88-27967
JUNCTION DIODES
NT MIM DIODES
Metal-sensing layer-semiconductor and metal-sensing layer-metal heterostructure gas sensors
[DE87-011293] 01 p0103 N88-10674
JUNCTION FIELD EFFECT TRANSISTORS
U JFET
JUNCTION TRANSISTORS
NT JFET
Mechanically stacked multijunction solar cells: An update on Sandia programs
[DE87-014641] 03 p0347 N88-12190
JUNGLES
U TROPICAL REGIONS
JUPITER (PLANET)
A Jupiter Data Analysis Program (JDAP) research grant on wave accessibility and attributes
[NASA-CR-182348] 06 p0804 N88-14908
Ray tracing of Jovian low frequency radiation
[NASA-CR-179262] 08 p1101 N88-16620
The precipitation of energetic heavy ions into the upper atmosphere of Jupiter
[NASA-TM-101155] 17 p2452 N88-24565
The Jovian aurora: Electron or ion precipitation
[NASA-TM-101153] 17 p2452 N88-24566
Interpretation of the polarimetric observations of Jupiter
[DE88-702414] 21 p3031 N88-27991
JUPITER ATMOSPHERE
A refractometer for the interferometric determination of the helium abundance in the Jupiter atmosphere
[BONN-IR-86-23] 07 p0946 N88-15749
Study of descent of probes with high lift-drag ratio into the atmosphere of Jupiter 08 p1006 N88-16101
Spatial and temporal monitoring of the Jovian atmosphere 12 p1711 N88-20240
Model of Jovian F region ionosphere
[NASA-CR-182587] 13 p1855 N88-21105
The precipitation of energetic heavy ions into the upper atmosphere of Jupiter
[NASA-TM-101155] 17 p2452 N88-24565
JUPITER PROBES
NT GALILEO PROBE
NT GALILEO SPACECRAFT
JUPITER SATELLITES
NT IO
A modeling analysis program for the JPL table mountain Io sodium cloud data
[NASA-CR-182555] 11 p1570 N88-19400
The 1985 mutual phenomena of Jupiter's satellites observed in Brazil
[INPE-4526-PRE/1276] 15 p2152 N88-22848

K

K BAND
U EXTREMELY HIGH FREQUENCIES
K LINES
Simultaneous, cospatial imaging of the Sun in cyanogen and singly-ionized calcium 04 p0507 N88-13114
K STARS
Magnetic fields on K and M stars 04 p0510 N88-13137
An analysis of the photospheric line profiles in F, G, and K supergiants 04 p0513 N88-13157
Sensitivity of the H alpha line to expansion, geometrical extent and temperature gradient in the G and K supergiant chromospheres 04 p0514 N88-13159
Chromospheric and coronal heating in a bias-free sample of K dwarfs 04 p0518 N88-13184
Observations and analysis of the photospheric magnetic fields on dwarf G, K and M stars 04 p0520 N88-13196
Spectral images and multi-component models of the chromospheres of AR Lacertae 11 p1568 N88-19384
Spectroscopic determinations of surface gravities of giant stars, and ultraviolet observations of RR Lyrae and X Arietis 11 p1569 N88-19391
K-EPSILON TURBULENCE MODEL
A numerical study of turbulent plane jets in still and flowing environments employing two-equation k-epsilon model 23 p3211 N88-29109
Three-dimensional gas turbine combustor modelling 24 p3349 N88-29937
Numerical modeling of combustion processes in gas turbines 24 p3350 N88-29939
Three-dimensional combustor predictors: A comparison of equilibrium and laminar flamelet chemistry models 24 p3350 N88-29940
Analysis of the flow through double swirl airblast atomizers 24 p3351 N88-29949
K-MESONS
U KAONS
KA BAND
U EXTREMELY HIGH FREQUENCIES
KALMAN FILTERS
Estimation filters with adaptive scanning time for flying target tracking
[ETN-87-90401] 01 p0036 N88-10232
Development of response models for the Earth Radiation Budget Experiment (ERBE) sensors. Part 4: Preliminary nonscanner models and count conversion algorithms
[NASA-CR-178295] 01 p0050 N88-10317
GPS vertical axis performance enhancement for helicopter precision landing approach
[NASA-CR-177443] 04 p0397 N88-12477
Investigation, development, and application of optimal output feedback theory. Volume 3: The relationship between dynamic compensators and observers and Kalman filters
[NASA-CR-4107] 05 p0638 N88-13900
Optimal guidance of homing missiles 06 p0671 N88-14111
Improved understanding of the loss-of-symmetry phenomenon in the conventional Kalman filter
[NASA-TM-100041] 06 p0766 N88-14709
Tracking procedure for non-normally distributed measurement errors
[AD-A186287] 07 p0903 N88-15468
Simultaneous estimation and detection of bias shifts for inertial navigation systems 12 p1576 N88-19429
Covariance analysis and post-processing of gravity compensation effects for aided multi-state navigation systems
[PAPER-87-13] 12 p1577 N88-19430
A cause of divergence in the Kalman gain equation 12 p1578 N88-19438
Utilization of strapdown inertial and non-inertial sensors in determination of satellite attitude by Kalman filters
[INPE-4313-TDL/280] 13 p1731 N88-20349
Robustifying the Kalman filter
[AD-A189240] 13 p1825 N88-20907
Kalman filter residual expert system
[AD-A190520] 15 p2020 N88-22041
Moving-bank multiple model adaptive estimation applied to flexible spacestructure control
[AD-A190761] 15 p2026 N88-22071
New stable, vectorisable Kalman filter algorithms based on orthogonal transformations
[DFVLR-FB-87-52] 16 p2258 N88-23494
A positioning system based on NAVSAT
[NLR-MP-87018-U] 20 p2757 N88-26358
Control, stability and filter for a discrete linear stochastic system with correlated noise
[PB88-109525] 21 p3004 N88-27818
Estimation forces acting on an underwater vehicle with G.P.S. (Global Positioning System) and Kalman filtering
[AD-A194339] 23 p3175 N88-28901
Estimation of aircraft parameters using filter error methods and extended Kalman filter
[DFVLR-FB-88-15] 23 p3176 N88-28911
Multi-sensory tracking mount control
[AD-A194675] 23 p3249 N88-29339
Dynamical systems and motion vision
[AD-A195932] 24 p3422 N88-30366
Kalman filter-based algorithms for estimating depth from image sequences
[AD-A195818] 24 p3424 N88-30380
KANSAS
Evaluation of surface energy and radiation balance systems on the Konza Prairie
[NASA-CR-182534] 10 p1355 N88-18097
KAONS
Study of the production of Ko mesons in proton antiproton interactions at 630 GeV
[NOTA-INTERNA-908] 21 p3015 N88-27892
KAPPA-EPSILON TURBULENCE MODEL
U K-EPSILON TURBULENCE MODEL
KARMAN VORTEX STREET
The phenomenology of Karman vortex streets via sound in oscillatory flow
[MPIS-MITT-84-1987] 02 p0122 N88-10775
Dynamics of the von Karman vortex street 03 p0316 N88-11998
ESA Bulletin No. 25
[ISSN-0376-4265] 09 p1128 N88-16767
Meteosat tracks Karman vortex streets in the atmosphere 09 p1128 N88-16770
KC-130 AIRCRAFT
U C-130 AIRCRAFT
KC-135 AIRCRAFT
U C-135 AIRCRAFT
KEELS
Ray scattering from a collection of ice keels
[AD-A191757] 19 p2722 N88-26163
Reflection and scattering of acoustic rays computed for parabolic ice keel models
[AD-A193898] 23 p3278 N88-29517
KELP
U SEAWEEDS
KELVIN-HELMHOLTZ INSTABILITY
Numerical simulation of solar wind and magnetospheric phenomena 08 p1097 N88-16600
The Kelvin-Helmholtz instability in a stratified shear flow
[CFD/88/2] 22 p3076 N88-28265
Vortex formation and particle transport in a cross-field plasma sheath
[AD-A194838] 24 p3432 N88-30425
KENTUCKY
NASA/UK TAP
[NASA-CR-180350] 12 p1708 N88-20223
KENYA
Use of SPOT imagery for vegetation/biomass mapping, geotechnical mapping, catchment area determination, and settlement location in the Turkana district, northern Kenya 22 p3096 N88-28384
KEPLER LAWS
Solution of the hyperbolic Kepler's equation
[RAE-TR-87042] 09 p1229 N88-17368
KERNEL FUNCTIONS
Steady waves in a nonlinear theory of viscoelasticity
[AD-A185548] 06 p0723 N88-14448
Pseudodifferential operators on the circle and finite differences
[PB87-222352] 06 p0763 N88-14681
A modified kernel quantile estimator under censoring
[AD-A186364] 07 p0911 N88-15525
A smooth nonparametric quantile estimator from right-censored data
[AD-A186180] 07 p0915 N88-15552
Admissible and singular translates of stable processes
[AD-A188426] 07 p0917 N88-15571
A note on the analyticity of the Neumann Kernel and an associated quadrature problem in two-dimensional boundary element methods
[ETN-88-92054] 14 p1964 N88-21719
Inference for a nonlinear semimartingale regression model
[AD-A190857] 16 p2262 N88-23527
Symmetrized nearest neighbor regression estimates
[AD-A191998] 18 p2568 N88-25254
Definition of an auxiliary processor dedicated to real-time operating system kernels
[NASA-CR-183070] 20 p2841 N88-26860
KEROSENE
High-density jet fuels from coal syncrudes, appendix 4
[DE88-003132] 10 p1307 N88-17813
Availability and cost estimate of a high naphthene, modified aviation turbine fuel
[NASA-TM-100823] 13 p1749 N88-20455
Antimisting kerosene: Low temperature degradation and blending
[NASA-CR-182725] 20 p2781 N88-26495
KERR ELECTROOPTICAL EFFECT
Double layer polarization of nonconducting spheroidal particles and its application to Kerr effect
[ISSN-0208-5658] 13 p1832 N88-20960
KERR MAGNETOOPTICAL EFFECT
Studies of coherent beam processing concepts, phase 1
[AD-A194749] 22 p3083 N88-28306
KETONES
NT ACETONE
KEVLAR (TRADEMARK)
An experimental and theoretical study of the bending behavior of Kevlar 49/epoxy beams and rings
[DE87-010430] 01 p0061 N88-10394
The use of Kevlar on aero-engine fan containment casings
[PNR90410] 02 p0182 N88-11134
Flammability test on aircraft seats equipped with fire barrier fabrics for the Porcher company
[CEAT-M5-525200] 06 p0666 N88-14084
Flammability, smoke and toxicity test on fire barrier fabric from the Porcher company --- Airbus aircraft
[ETN-88-91168] 06 p0666 N88-14085
Comparison of ultrasonic flaw detection analysis for spherical composite test specimens using two data acquisition techniques
[DE88-005002] 12 p1634 N88-19782
Fracture characteristics of carbon and aramid unidirectional composites in interlaminar shear and open hole tensile tests
[NLR-TR-86083-U] 13 p1735 N88-20371
Thermoviscoelastic characterization and predictions of Kevlar/epoxy composite laminates
[NASA-CR-182878] 16 p2172 N88-22946
On the bending response of Kevlar 49/epoxy beams and rings
[DE88-006824] 18 p2530 N88-25012

NDE performance in predicting failure strength of spherical composite specimens with implanted flaws
[DE88-008223] 21 p2959 N88-27575
Use of microwave measuring systems for the nondestructive control of resins and composites
[REPT-881-430-123] 21 p2959 N88-27576
Nondestructive tests and high performance composite structures
[SNIAS-881-430-119] 23 p3188 N88-28969

KEYING
NT FREQUENCY SHIFT KEYING
NT PHASE SHIFT KEYING
Reconfigurable work station for a video display unit and keyboard
[NASA-CASE-MFS-26009-1-SB] 17 p2382 N88-24163
WIPP (Wave Induced Particle Precipitation) experiment logistic support
[AD-A191184] 18 p2499 N88-24824

KIDNEYS
Nutrient requirements and other factors involved in the culture of human kidney cells on microcarrier beads 09 p1197 N88-17176

KILOMETRIC WAVES
A Jupiter Data Analysis Program (JDAP) research grant on wave accessibility and attributes
[NASA-CR-182348] 06 p0804 N88-14908

KIMBERLITE
U BIOTITE
U PERIDOTITE

KINEMATIC EQUATIONS
Structure-dependent matrix representation of manipulator kinematics and its inverse solution
[DE87-752966] 02 p0229 N88-11447

KINEMATICS
NT BODY KINEMATICS
Use of simulated satellite radiances from a mesoscale numerical model to understand kinematic and dynamic processes 02 p0202 N88-11261
Spectroscopy and nonthermal processes 02 p0252 N88-11594
Kinematics and dynamics of barred spiral galaxies 03 p0388 N88-12440
Kinematics and galactic structure
[PREPRINT-18] 03 p0389 N88-12442
Static standing and dynamic walking of a practical biped robot
[DE88-001367] 04 p0451 N88-12795
Kinematic formulation of finite elements for plate bending 04 p0455 N88-12821
Extremum methods of structural analysis for system reliability assessment 04 p0456 N88-12824
Non-linear maximum likelihood estimation of stability derivatives from range data
[NAL-TM-SE-8608] 05 p0552 N88-13365
SHARP simulation of discontinuities in highly convective steady flow
[NASA-TM-100240] 05 p0642 N88-13931
Robot accuracy improvement through kinematic parameter identification 06 p0712 N88-14363
Dynamics, control and sensor issues pertinent to robotic hands for the EVA retriever system 06 p0796 N88-14876
Analysis of stable crack growth with isotropic and kinematic hardening
[PB87-144911] 07 p0868 N88-15266
Theory of deformation. Part 1: Kinematics
[DE88-003007] 08 p1001 N88-16062
Goal driven kinematic simulation of flexible arm robot for space station missions 08 p1059 N88-16388
Kinematic optimization of mechanisms, a finite element approach
[ISBN-90-370-0012-6] 09 p1175 N88-17039
A substructure method for dynamic simulation of flexible mechanical systems with geometric nonlinearities 09 p1176 N88-17044
An optimal resolved rate law for kinematically redundant manipulators 09 p1212 N88-17268
Considerations of acceleration effects in relativistic kinematics 09 p1260 N88-17553
Kinematic and dynamic analyses of the Stanford/JPL robot hand
[DE88-004637] 11 p1495 N88-18923
Real-time kinematic and dynamic analysis and adaptive model following control of manipulator arms 11 p1495 N88-18927
Improvement in robot positioning accuracy by a kinematic identification model 11 p1496 N88-18931
Electro-mechanical vibratory system 11 p1500 N88-18958
Mass loss from evolved stars 11 p1569 N88-19394
Synthesis of finite displacements and displacements in continental margins
[NASA-CR-182616] 12 p1642 N88-19832
Force distribution and trajectory control for closed kinematic chains with applications to walking machines 13 p1779 N88-20642
Subduction 13 p1806 N88-20796
New representation for kinematics of manipulator
[DE88-751446] 14 p1917 N88-21445
Kinematic support using elastic elements 14 p1926 N88-21481
Analysis of head response to torso acceleration. Volume 1: Development of performance requirements
[PB88-156757] 14 p1953 N88-21640
The striae in the dust tails of great comets: A formal comparison of the goodness of fit by various theories, and a new proposal 14 p2002 N88-21937
A three dimensional non-singular modelling of rigid manipulators
[AD-A189707] 15 p2116 N88-22604
Wave-growth associated with turbulent spot in plane Poiseuille flow 16 p2199 N88-23116
Base reaction optimization of manipulators with redundant kinematics 16 p2219 N88-23238
Sea ice kinematics: Space and time scales
[AD-A191162] 17 p2376 N88-24128
Kinematics, dynamics and control of a closed chain mechanism manipulator 18 p2523 N88-24967
Real-time implementation of a kinematic optimization scheme for seven-degree-of-freedom redundant robots with spherical wrists
[DE88-006785] 18 p2524 N88-24974
Determination of settings of a tilted head-cutter for generation of hypoid and spiral bevel gears
[NASA-CR-182138] 18 p2524 N88-24976
MHD bending waves in a current sheet
[NASA-TM-101149] 18 p2579 N88-25323
Automatic calibration of space based manipulators and mechanisms
[NASA-CR-182804] 19 p2676 N88-25912
Spatial dynamics of deformable multibody systems with variable kinematic structure 20 p2813 N88-26687
Kinematics of Hooke universal joint robot wrists
[NASA-TM-100567] 20 p2843 N88-26870
Theory of relativity and super-light-speeds-I: Kinematical part
[DE88-701832] 20 p2880 N88-27100
Aeroelastic modeling of rotor blades with spanwise variable elastic axis offset: Classic issues revisited and new formulations 21 p2890 N88-27158
Control and use of unsteady flows: Insect use of various wing kinematics and related pressure measurements using a pitching airfoil 21 p2926 N88-27366
Control of free-flying space robot manipulator systems
[NASA-CR-183017] 21 p2956 N88-27562
General expression of manipulator kinematics
[DE88-753430] 21 p2957 N88-27567
Dexterous hands: Optimizing grasp by design and planning 21 p2958 N88-27572
Flow dynamics stimulated by hairpin-like vortices in initially laminar boundary layers
[AD-A194253] 22 p3075 N88-28254
The analysis and control of robotic manipulators operating at or near kinematically singular configurations 22 p3084 N88-28315
A comparison: Static and future kinematic GPS (Global Positioning System) surveys
[AD-A194666] 23 p3175 N88-28904
Shock waves in unsteady flows
[NASA-TT-20329] 23 p3214 N88-29134
Sea ice processes
[AD-A193980] 23 p3237 N88-29262
The kinematics of Milky Way halo gas 23 p3299 N88-29648
A review: Quantitative models for lava flows on Mars 23 p3301 N88-29656
Approximation of viscoelastic stresses from Newtonian turbulent kinematics
[AD-A194317] 24 p3371 N88-30077
The kinematics of late-type supergiants
[SER-C-PREPUBL-FASC-28] 24 p3454 N88-30560

KINESTHESIS
U PROPRIOCEPTION

KINETIC ENERGY
Apparatus for storing kinetic energy
[EP-PATENT-0-181-736-A1] 01 p0066 N88-10422
Navier-Stokes cascade analysis with a stiff Kappa-Epsilon turbulence solver
[NASA-TM-100218] 02 p0123 N88-10778
A multiple-time-scale turbulence model based on variable partitioning of turbulent kinetic energy spectrum
[NASA-CR-179222] 04 p0444 N88-12754
Mechanical property evaluation of a series of commercial tungsten alloys
[AD-A185440] 05 p0565 N88-13446
The end height of fireball as a function of their residual kinetic energy 06 p0737 N88-14535
Theoretical aspects of channeling, damage, and range distributions for low (keV) and high (MeV) energy implantation
[DE88-000949] 06 p0786 N88-14818
New model to estimate the perforation power of kinetic energy projectiles
[PB87-166757] 09 p1175 N88-17040
Product kinetic and internal energy distributions via velocity-aligned Doppler spectroscopy
[DE88-003510] 10 p1298 N88-17764
Energy transfers for multilayer hydrodynamic ocean models: General formulation and specific examples
[AD-A187604] 10 p1358 N88-18116
Unsteady shallowing mixed layer 13 p1805 N88-20791
Launchability of base-driven electromagnetic projectiles
[AD-A189635] 15 p2023 N88-22055
Rocket measurements of ionospheric electron temperature over Natal
[INPE-4485-PRE/1250] 15 p2096 N88-22489
Experimental investigation of a three-stage railgun incorporating puff-switching
[AD-A191044] 16 p2166 N88-22918
Coherent structures and modeling: Some background comments 16 p2199 N88-23120
Inevitable inflation in Einstein-Cartan theory with improved energy-momentum tensor with spin
[NASA-TM-101146] 18 p2586 N88-25365

KINETIC EQUATIONS
NT HELMHOLTZ VORTICITY EQUATION
NT HYDRODYNAMIC EQUATIONS
NT KINEMATIC EQUATIONS
Equations for determining CVD tungsten-rhenium alloy composition and plating rate
[DE87-008831] 01 p0024 N88-10152
Computer models for kinetic equations of magnetically confined plasmas
[DE87-011571] 02 p0236 N88-11492
Current generation and induced conductivity of a plasma under common action of constant electric field and lower-hybrid or ECR waves
[DE88-700345] 07 p0935 N88-15680
Application of Onsager's reciprocity relations to interface motion
[DE88-003286] 10 p1397 N88-18327
Applied mathematics of transport theory
[DE88-004098] 10 p1404 N88-18369
Kinetic and turbulence models for granular and two-phase flows 11 p1484 N88-18862
Plasma rotation in a tokamak
[DE88-700855] 12 p1693 N88-20128
Consistent transport coefficients in astrophysics
[NASA-TM-101154] 17 p2451 N88-24580

KINETIC FRICTION
NT SLIDING FRICTION

KINETIC HEATING
NT AERODYNAMIC HEATING
NT SHOCK HEATING
Sinterable ceramic powders from laser-heated gases
[AD-A194162] 23 p3197 N88-29024

KINETIC THEORY
NT MIXING LENGTH FLOW THEORY
NT TRANSPORT THEORY
Physics and chemistry 07 p0883 N88-15359
Resonance cones in nonthermal plasmas: Laboratory experiments 08 p1027 N88-16223
Kinetic theory for plane flows of rough, inelastic, circular disks 21 p2946 N88-27499
Kinetic theory for electrostatic waves due to transverse velocity shears
[AD-A193404] 23 p3284 N88-29557

KINETICS
NT ELECTROKINETICS
NT KINETIC ENERGY
NT NEWTON SECOND LAW
NT NEWTON THEORY
NT REACTION KINETICS
Exact solution of the inverse problem for a six-link manipulator with a mechanical offset
[DE87-702646] 01 p0054 N88-10349
A parallel model of the kinetic depth effect using local computations
[AD-A181945] 01 p0083 N88-10536
The infiltration kinetics of aluminum in silicon carbide compacts
[AD-A184682] 03 p0290 N88-11823
Molecular engineering of ceramics
[DE88-000174] 04 p0420 N88-12603
An analysis of the effect of system variables on the quality of thin films and powders produced by laser-breakdown chemical vapor deposition
[DE88-001793] 06 p0708 N88-14342
Fundamental studies of surfaces processes and trace analysis using solid electrodes
[AD-A186156] 07 p0828 N88-15024

TEA-TE: Powerful nitrogen-based laser system
07 p0919 N88-15583
Study of kinetics of intracavity absorption in pulsed dye lasers
07 p0919 N88-15585
Investigations in field of surface forces in metallurgy
[BLL-M-47406-(5828.4)] 08 p0969 N88-15860
Kinetics and mechanism of thermal aging embrittlement of duplex stainless steels
[DE88-002987] 08 p0969 N88-15866
Influence of skeletal muscle glycogen on passive rewarming after hypothermia
[AD-A186451] 08 p1049 N88-16334
Kinetics and spectrum of light pulse used in picosecond holography
09 p1236 N88-17409
Deactivation of alumina based catalysts
11 p1455 N88-18673
Effect of density change on rapid liquid-solid interface kinetics and heat flow
[DE88-004286] 11 p1487 N88-18878
Thermodynamic theory of fluctuations and Rayleigh light scattering in solutions
13 p1785 N88-20681
Kinetics of combustion of finely divided solid fuel in granules
[BLL-M-37626-(5828.4)] 14 p1888 N88-21283
Kinetics of slow electrons in excimer laser with electron-beam pumping
14 p1970 N88-21760
Free carrier nonlinear optics
14 p1977 N88-21796
Reactions of N2(A sup 3 sigma sup + sub u) candidates for short wavelength lasers
[DE88-007018] 15 p2070 N88-22342
The kinetics of contact noise in NaBeta alumina
[AD-A190651] 15 p2130 N88-22707
Theoretical calculations of XeF ground state kinetics
[AD-A191398] 16 p2270 N88-23580
Kinetic theoretical analysis for propagation of rotating ion beam in ICF
16 p2276 N88-23623
Thomson scattering for determining electron concentrations and temperatures in an inductively coupled plasma. 2: Description and evaluation of a multichannel instrument
[AD-A191324] 16 p2280 N88-23652
Effect of alloying, rapid solidification, and surface kinetics on the high temperature environmental resistance of niobium
[AD-A192093] 18 p2485 N88-24743
Kinetics of homogeneous nucleation in superheated F-11 and F-21 liquid freons
[NASA-TT-20286] 19 p2613 N88-25503
Kinetics of CO oxidation over a deactivated Rh(111) single crystal catalyst
[DE88-003000] 19 p2613 N88-25504
Irreversible dissolution of solid solutions: A kinetic and stoichiometric model
[DE88-009194] 19 p2614 N88-25513
The crystallization of tough thermoplastic resins in the presence of carbon fibers
[NASA-CR-182984] 20 p2776 N88-26464
Research on the kinetics of phase changes in solids
[AD-A192222] 20 p2814 N88-26696
Proceedings of the 2nd US-Japan Workshop on Advanced Plasma Modeling, volume 3
[IPPJ-867] 20 p2855 N88-26957
Modeling of subtle kinetic processes in plasma simulation
20 p2856 N88-26959
Kinetic of oxidation to air of a Fe-Al-Mn alloy system at 600-800(sup 0)C temperature range
[DE88-702309] 21 p2920 N88-27330
Sol-gel kinetics: Si(sup)29 NMR and a statistical reaction model
[DE88-011545] 23 p3191 N88-28988
Kinetic of martensitic transformations induced by hydrogen in the austenite
[DE88-701623] 23 p3194 N88-29007
Reaction-theoretical aspects of the thermal behavior of lubricating oils and working fluids
[NASA-TT-20304] 23 p3199 N88-29041
Chemical kinetics of hydrogen and P(sub b) centers
[DE88-010528] 23 p3291 N88-29594
Ion kinetics in silane plasmas
[AD-A196202] 24 p3431 N88-30423

KIRCHHOFF LAW OF RADIATION
Beam quality of stable and unstable resonators: A theoretical approach
[DFVLR-FB-87-35] 14 p1982 N88-21826

KIRCHHOFF-HELMHOLTZ FLOW
U PIPE FLOW

KIRCHHOFF-HUYGENS PRINCIPLE
U DIFFRACTION
U WAVE PROPAGATION

KLYSTRONS
Performance of high power S-band klystrons focused with permanent magnet
[DE87-753024] 02 p0167 N88-11053
Development of a high-energy crowbar for the Los Alamos free-electron laser
[DE87-014748] 02 p0179 N88-11113
Inductance effects in the high-power transmitter crowbar system
04 p0433 N88-12687
Microwave system for the microwave Tokamak experiment (MTX)
[DE88-002391] 09 p1250 N88-17487
The numerical simulation of accelerator components
[DE87-011597] 10 p1412 N88-18423
RF pulse compression development
[DE88-004818] 11 p1479 N88-18826
Accelerator research studies
[DE88-008236] 19 p2726 N88-26187

KNIGHT SHIFT
U NUCLEAR MAGNETIC RESONANCE

KNOWLEDGE
NT PARADOXES
NT PHILOSOPHY
Data Model of Objects and Relations (DAMOR): A data model for knowledge representation
[REPT-87-05] 01 p0085 N88-10553
Towards the unmanned cockpit
02 p0129 N88-10812
Generating diagnostic knowledge from a structural and functional description
02 p0129 N88-10813
A review of the knowledge engineering process
02 p0129 N88-10814
Third Conference on Artificial Intelligence for Space Applications, part 1
[NASA-CP-2492-Pt-1] 08 p1055 N88-16360
Methodology for testing and validating knowledge bases
08 p1055 N88-16364
HSTDEK: Developing a methodology for construction of large-scale, multi-use knowledge bases
08 p1057 N88-16377
Interactive knowledge acquisition tools
08 p1060 N88-16401
Knowledge-based simulation
08 p1061 N88-16404
Similarity networks as a knowledge representation for space applications
08 p1062 N88-16411
Commonality analysis as a knowledge acquisition problem
08 p1062 N88-16413
Qualitative models for planning: A gentle introduction
08 p1062 N88-16414
Interfacing the expert: Characteristics and requirements for the user interface in expert systems
08 p1063 N88-16419
Foundation: Transforming data bases into knowledge bases
08 p1063 N88-16423
Case-based reasoning for space applications: Utilization of prior experience in knowledge-based systems
08 p1065 N88-16433
Substructure discovery in executed action sequences
[AD-A186446] 08 p1069 N88-16462
Simplifying the construction of domain-specific automatic programming systems: The NASA automated software development workstation project
09 p1204 N88-17212
Tutoring electronic troubleshooting in a simulated maintenance work environment
09 p1204 N88-17215
The representation of knowledge within model-based control systems
[DE88-004863] 10 p1396 N88-18319
Automatic knowledge acquisition for aerial image interpretation
[AD-A188616] 12 p1638 N88-19810
Rapid prototyping of simulations in artificial intelligence environments
[DE88-004295] 15 p2117 N88-22612
Minimum disclosure proofs of knowledge
[CWI-PM-R8710] 20 p2840 N88-26854
Knowledge representation in geographic information systems
[ETN-88-92470] 20 p2882 N88-27112
A model of information growth
23 p3265 N88-29440

KNOWLEDGE ENGINEERING
U EXPERT SYSTEMS

KNOWLEDGE REPRESENTATION
A survey of artificial neural systems
[AD-A184759] 03 p0368 N88-12312
Advanced techniques for the storage and use of very large, heterogeneous spatial databases. The representation of geographic knowledge: Toward a universal framework --- relations (mathematics)
[NASA-CR-181517] 03 p0385 N88-12421
The characterization of diagnostic tasks for engineering systems
[DE88-000093] 04 p0483 N88-12973
Investigation of candidate data structures and search algorithms to support a knowledge based fault diagnosis system
07 p0923 N88-15606
Expert system technology
07 p0926 N88-15628
A formal approach to validation and verification for knowledge-based control systems
09 p1207 N88-17233
Building validation tools for knowledge-based systems
09 p1207 N88-17235
Diagnosis: Reasoning from first principles and experiential knowledge
09 p1207 N88-17236
Beyond rules: The next generation of expert systems
09 p1210 N88-17256
An efficient representation of spatial information for expert reasoning in robotic vehicles
09 p1214 N88-17278
KBGIS-II: A knowledge-based geographic information system
[NASA-CR-182492] 09 p1261 N88-17559
Knowledge base refinement by monitoring abstract control knowledge, revision 1
[AD-A187502] 10 p1397 N88-18323
Research in knowledge representation for natural language communication and planning assistance
[AD-A187355] 11 p1522 N88-19087
KR: An efficient knowledge representation system
[AD-A187705] 11 p1529 N88-19129
KREME (Knowledge Representation, Editing and Modeling Environment): A user's introduction, phase 1
[AD-A188906] 12 p1681 N88-20052
A knowledge system for automatic finite element mesh generation: AMEKS
[DE87-014894] 13 p1826 N88-20914
Conception of a knowledge-based system for designing distributed systems
[DFVLR-MITT-87-16] 14 p1961 N88-21694
Representing knowledge in two distinct descriptions: Extensional vs. intensional
[CWI-CS-R8728] 14 p1961 N88-21699
Memory-based expert systems
[AD-A190203] 15 p2116 N88-22606
Knowledge engineering in design
[CWI-CS-R8745] 16 p2248 N88-23432
Representation and decision mechanisms in artificial intelligence
[AD-A191083] 18 p2560 N88-25197
Application of flight systems methodologies to the validation of knowledge-based systems
[NASA-TM-100442] 18 p2561 N88-25207
An expert system model using predicate transition nets
[AD-A191953] 19 p2718 N88-26141
The knowledge based automatic extraction of the machinable surfaces for automatic CAD-CAM system
[INPE-4542-PRE/1288] 20 p2836 N88-26824
Delfi-3 as a development environment for expert systems
[REPT-8767] 20 p2839 N88-26845
Computer science and technology: Knowledge-based system for physical database design
[PB88-193289] 20 p2882 N88-27109
Knowledge-based cost estimating vs traditional software cost models
[DE88-009707] 20 p2883 N88-27116
Cooperating knowledge-based systems
[NASA-CR-183109] 23 p3247 N88-29327
Hologram representation of design data in an expert system knowledge base
23 p3251 N88-29354
Knowledge-based fault diagnosis on future space vehicles
23 p3254 N88-29374
AI and simulation: What can they learn from each other
23 p3257 N88-29391
Knowledge acquisition and rapid protyping of an expert system: Dealing with real world problems
23 p3258 N88-29394
Requirements for a tool to aid in the development of expert systems for space station applications
23 p3258 N88-29398
A methodology for multiple rule system integration and resolution within a singular knowledge base
23 p3261 N88-29413
Semantic based man-machine interface for real-time communication
23 p3262 N88-29421
Distributed knowledge base systems for diagnosis and information retrieval
[AD-A193107] 23 p3296 N88-29633
Knowledge-based flow field zoning
[NASA-TM-101023] 24 p3412 N88-30314
Knowledge based simulation: An artificial intelligence approach to system modeling and automating the simulation life cycle
[AD-A195838] 24 p3423 N88-30372

KOLMOGOROFF THEORY
The velocity structure and turbulence at the center of the Orion Nebula
04 p0521 N88-13201
An elementary approach to the Daniell-Kolmogorov theorem and some related results
[AD-A186011] 07 p0909 N88-15505

KONDO EFFECT
Heavy Fermions and coherence in Kondo lattices: Specific heat of low energy excitation in Cer systems
[ETN-88-91080] 09 p1255 N88-17525

Interactions between superconductivity and Kondo-grid properties in CeCu2Si2. Measurement results of specific heat under high pressure
[ETN-88-92377] 21 p3025 N88-27958
Possible occurrence of band interplay in high Tc superconductor
[PREPRINT-593] 22 p3157 N88-28789

KORTEWEG-DEVRIES EQUATION
Variation of wave action: Modulations of the phase shift for strongly nonlinear dispersive waves with weak dissipation. A new adiabatic invariant involving the modulated phase shift for strongly nonlinear, slowly varying, and weakly damped oscillators. The modulated phase shift for weakly dissipated nonlinear oscillatory waves of the Korteweg-de vries type
[AD-A185630] 06 p0765 N88-14702
Baecklund transformation and the Schwarzian derivative
[AD-A190277] 15 p2127 N88-22684
Nonlinear surface and internal waves on shear flow
[PREPRINT-584] 22 p3129 N88-28604

KRAMERS-KRONIG FORMULA
Optical constants of minerals and other materials from the millimeter to the ultraviolet
[AD-A192210] 18 p2482 N88-24724

KRONECKER PRODUCT
U ORTHOGONALITY

KRYPTON
NT KRYPTON ISOTOPES
KR+ laser excitation of NH2 in atmospheric pressure flames
[AD-A183421] 01 p0050 N88-10322
Two-photon (VUV and visible) resonant ionization spectroscopy of atoms and molecules
[DE88-004332] 10 p1407 N88-18388
Resonantly-enhanced, four-photon ionization of krypton at laser intensities exceeding 10(12) W/sq cm
[DE88-005038] 11 p1544 N88-19229
Temperature dependence of Kr precipitation in Ni
[DE88-005953] 13 p1744 N88-20429
Electron stimulated desorption and coherent electron scattering
[AD-A189091] 13 p1835 N88-20978
Numerical modelling specific energy charcteristics of excimer KrF lasers with electron beam excitation
[DE88-701525] 15 p2070 N88-22344
Krypton based adsorption type cryogenic refrigerator
[NASA-CASE-NPO-17334-1-CU] 17 p2331 N88-23917

KRYPTON FLUORIDE LASERS
Operational performance of repetitive KrF, XeCl excimer lasers 03 p0327 N88-12068
Narrow linewidth gain measurements in a KrF excimer amplifier pumped longitudinally by a high-power electron beam
[DE88-001365] 05 p0586 N88-13575
ICF research at Los Alamos
[DE88-005394] 11 p1493 N88-18916
Pulse-train amplification of subnanosecond near-transform-limited KrF laser pulses
[DE88-004460] 12 p1631 N88-19764
The development of high power KrF laser systems for plasma research by the application of stimulated Raman scattering
[ETN-88-92220] 15 p2073 N88-22358
Aurora status and plans
[DE88-006476] 18 p2521 N88-24955

KRYPTON ISOTOPES
Prospects for large dynamic range isotope analysis using photon burst mass spectrometry
[DE88-009110] 19 p2613 N88-25505

KU BAND
U SUPERHIGH FREQUENCIES

KUTTA-JOUKOWSKI CONDITION
On the Kutta condition for flows around lifting airfoils and wings
[DFVLR-FB-87-40] 13 p1717 N88-20268

L

L BAND
U ULTRAHIGH FREQUENCIES

L-SAT
The role of the L-Sat program in the evolution of European communications satellites 09 p1127 N88-16758
Qualification of the OLYMPUS reaction wheel 14 p1878 N88-21226
Development and qualification of the OLYMPUS antenna pointing mechanism 14 p1879 N88-21227
OLYMPUS shuttle specific radiator shield 14 p1879 N88-21234
A 30/20 GHz multibeam array antenna suitable for future high rate TDMA European satellite networks
[ETN-88-93079] 24 p3365 N88-30037

LABELING (MARKING)
U MARKING

LABOR
An extended Cobb-Douglas form for use in production economics
[AD-A186372] 07 p0943 N88-15733

LABORATORIES
NT ENVIRONMENTAL LABORATORIES
NT MANNED ORBITAL LABORATORIES
NT SPACE LABORATORIES
NT SPACELAB
Dynamics of spacecraft control laboratory experiment (SCOLE) slew maneuvers
[NASA-CR-4098] 01 p0014 N88-10082
Transactions of the 4th Army Conference on Applied Mathematics and Computing
[AD-A183544] 01 p0085 N88-10547
Stirling engine research at national and university laboratories in Japan
[DE87-014622] 02 p0180 N88-11123
The Lewis Strain Gauge Laboratory: Status and plans 02 p0184 N88-11146
Lewis' enhanced laboratory for research into the fatigue and constitutive behavior of high temperature materials 02 p0189 N88-11177
Control design challenges of large space systems and spacecraft control laboratory experiment (SCOLE)
[NASA-CR-178392] 03 p0275 N88-11735
Electronics engineering thrust area report, FY86
[DE87-014616] 03 p0309 N88-11950
LLE (Laboratory for Laser Energetics) review, volume 31
[DE87-013732] 03 p0328 N88-12072
Materials sciences programs: Fiscal Year 1987
[DE88-000672] 04 p0429 N88-12659
Realization of the immediate objectives of the Aero-Gas Dynamics and Vibration Laboratory (LAGG) at the National Center for Research, Science and Technology (PUSPIPTEK) at Serpong, Java (Indonesia), Project TTA-79
[GG/QPR-10] 08 p1092 N88-16572
Experience of developing an integrated nondestructive assay system
[DE88-003149] 09 p1184 N88-17092
A study of federal technology transfer to the commercial sector
[AD-A187017] 09 p1262 N88-17560
Helsinki University of Technology Communications Laboratory
[PB88-112974] 10 p1318 N88-17881
Laboratory evaluation and analysis of advanced lead-acid load-leveling batteries
[DE88-002851] 10 p1349 N88-18064
Engineering thrust areas, 1988
[DE88-005103] 11 p1468 N88-18753
Aviation turbine fuels from tar sands bitumen and heavy oils. Part 3: Laboratory sample production
[AD-A189278] 13 p1753 N88-20484
Laboratory Information Management System (LIMS): A case study
[NASA-TM-100835] 14 p1961 N88-21697
Study of lightning and lightning protection (selected pages)
[AD-A190623] 15 p2098 N88-22498
DOE (Department of Energy) national laboratories and the semiconductor industry: Continuing the joint planning
[PB88-170295] 16 p2281 N88-23657
An overview of advanced battery development at Sandia National Laboratories
[DE88-006823] 18 p2506 N88-24867
Inference and discovery in an exploratory laboratory
[AD-A192231] 20 p2832 N88-26801
Experimental study of planetary gases with applications to planetary interior models
[NASA-CR-183098] 20 p2886 N88-27137
Development of radiation and cloud parameterization programs for AFGL (Air Force Geophysics Laboratory) global models
[AD-A193369] 21 p2973 N88-27658
Activities report of the Werner-Heisenberg Institute of Physics
[ETN-88-92946] 21 p3015 N88-27893
An evaluation of Interactive Laboratory System software, ILS-PC/DOS: A digital signal processing software package
[AD-A193838] 22 p3138 N88-28657
Laboratory feasibility study of a composite embedded fiber optic sensor for measurement of structural vibrations
[AD-A194270] 22 p3152 N88-28754
Center for opto-electronic systems research
[AD-A195159] 24 p3429 N88-30411
Electronic materials and devices prepared by molecular beam epitaxy
[AD-A195694] 24 p3433 N88-30433

LABORATORY EQUIPMENT
NT IMAGE FURNACES
A preliminary study of a fluid science laboratory for space station (Columbus). Part 4: Executive summary
[NLR-TR-87023-L-PT-4] 02 p0170 N88-11072
A low volume insert for solid state magic angle spinning NMR of small samples
[AD-A184359] 04 p0419 N88-12601
Measurements in an electromagnetic test laboratory
[SNIAS-872-430-102] 05 p0575 N88-13507
Electromagnetic tests
[SNIAS-872-430-103] 05 p0575 N88-13508
Controlled Ecological Life Support System. Design, Development, and Use of a Ground-Based Plant Growth Module
[NASA-CP-2479] 05 p0630 N88-13852
CELSS Program Meeting 05 p0630 N88-13853
Metrology and calibrating laboratories
[ETN-88-90761] 06 p0670 N88-14104
Data analysis at the Oulu (Finland) EISCAT laboratory 06 p0691 N88-14241
Practical photochemistry: General considerations
[PB87-123386] 06 p0730 N88-14491
Design of a velocity and position control laboratory servo system
[AD-A186596] 08 p0990 N88-15997
The ESA Anthrorack project: Integrated research in human physiology 08 p1033 N88-16265
A laboratory railgun for terminal ballistics and arc armature research studies
[AD-A187225] 11 p1442 N88-18603
ESA's facility for research in human physiology in space: Anthrorack 12 p1652 N88-19896
The ESA facility Biorack 12 p1652 N88-19897
Exobiology and botany facilities for EURECA 12 p1652 N88-19898
BIOTEX, a project for biotechnological basic experiments under microgravity --- Spacelab 12 p1652 N88-19899
Life science techonology --- space applications 12 p1653 N88-19900
Second-generation respiratory monitoring system for microgravity studies in man 12 p1653 N88-19906
Development of an optical diagnostic instrument. Part 2: Instrument development --- space laboratories
[NLR-TR-87079-L-PT-2] 13 p1841 N88-21016
Environment test laboratory
[ETN-88-91885] 14 p1869 N88-21166
Interfacial structure-property relationships at the fiber-matrix interphase in advanced composites
[AD-A190649] 15 p2030 N88-22093
The CRREL (Cold Regions Research and Engineering Laboratory) Hopkinson bar apparatus
[AD-A190599] 15 p2077 N88-22380
Mechanisms mediating perception of complex acoustic patterns
[AD-A189765] 15 p2102 N88-22520
Laboratory equipment update
[AD-A189781] 15 p2102 N88-22522
Microgravity mechanisms and robotics program 16 p2219 N88-23237
Spectroradiometry in the industrial test laboratory 16 p2272 N88-23598
Impact of control errors on the volume/weight demand of the Ventilation and Dryer (VAD) concept --- EURECA Botany Facility
[TN-RB524-006/87] 17 p2377 N88-24132
Botany Facility pre-phase C/D. Core payload for EURECA, volume 1
[BF-RP-ER-015-VOL-1] 17 p2379 N88-24144
SHaRE: Collaborative materials science research
[DE88-007175] 18 p2467 N88-24646
Laboratory experiments on atmospheric OH reactions 18 p2539 N88-25066
Hanging drop crystal growth apparatus and method
[NASA-CASE-MFS-28206-1-SB] 18 p2585 N88-25356
Biorack on Spacelab D1: An overview of the first flight of Biorack, an ESA facility for life sciences research in microgravity
[ESA-SP-1091] 22 p3059 N88-28154
A brief overview of the results of the experiments using the ESA Biorack Facility on the German Spacelab D1 mission 22 p3060 N88-28155
The Biorack facility and its performance during the D1 Spacelab mission 22 p3060 N88-28156
Dosimetric mapping inside Biorack --- Spacelab D1 mission 22 p3062 N88-28169
Biorack thermal performance during the D1 mission --- Spacelab 22 p3062 N88-28170
A 400 kV ion implanter: Operating principles and applications 22 p3069 N88-28213
An evaluation of Interactive Laboratory System software, ILS-PC/DOS: A digital signal processing software package
[AD-A193838] 22 p3138 N88-28657

Research and development objectives: Installation, startup, and test operation of a remote and program controlled measuring table for the calibration of EGRET experiment
[ETN-88-92105] 22 p3152 N88-28752
Biosample: Preservation, handling and observation system synthesis and breadboarding — Spacelab
[ESA-CR(P)-2609] 24 p3336 N88-29857
Crystal structures of ordered carbon metal alloys
[AD-A195597] 24 p3353 N88-29959
Accommodation concept for fluid physics facilities, volume 2 — Spacelab
[SG-TN-AI-027-VOL-2] 24 p3358 N88-29994

LABYRINTH
NT COCHLEA
NT OTOLITH ORGANS
NT SEMICIRCULAR CANALS
NT VESTIBULES

LABYRINTH SEALS
Three-dimensional dynamic labyrinth seal analysis
[AD-A185353] 05 p0590 N88-13599
Flow in labyrinth seals and its influence on rotor stability of turbocompressors 07 p0851 N88-15168
A comparison of experimental and theoretical results for labyrinth gas seals with honeycomb stators
[NASA-CR-182441] 08 p0993 N88-16006
Experimental rotordynamic coefficient results for honeycomb seals
[NASA-CR-182440] 08 p0993 N88-16007

LACE (ENGINE)
U LIQUID AIR CYCLE ENGINES

LACTATES
Oxygen transport during exercise at extreme simulated altitude: Operation Everest 2
[AD-A185720] 06 p0752 N88-14620

LAG (DELAY)
U TIME LAG

LAGEOS (SATELLITE)
The Monte Generoso-Zimmerwald (Switzerland) baseline from satellite laser ranging data using various analysis techniques
[LR-533] 14 p1940 N88-21576
Determining earth's rotation from laser observations of Lageos artificial earth satellite (during period of main merit campaign) 24 p3449 N88-30528

LAGOONS
Five New South Wales barrier lagoons: Their macrobenthic fauna and seagrass communities 11 p1517 N88-19059

LAGRANGE COORDINATES
The evolution of HOBO
[DE87-014742] 03 p0313 N88-11980
A Lagrangian moving grid scheme for one-dimensional evolutionary partial differential equations
[CWI-NM-R8713] 13 p1827 N88-20922
Singular Lagrangians. Classical dynamics and quantization. Lectures for young scientists
[DE88-701158] 15 p2146 N88-22806
A nonlinear computation for composite structures
[ONERA-RT-15/3542-RY-062-R] 16 p2222 N88-23265
Classical non-Abelian solutions for nonstandard Lagrangians
[DE88-701305] 16 p2263 N88-23532

LAGRANGE EQUATIONS OF MOTION
U EULER-LAGRANGE EQUATION

LAGRANGE MULTIPLIERS
Generalized hybrid variational principle, corresponding finite element model 03 p0301 N88-11895
Lagrangian procedures for higher order field equations
[DE87-703365] 05 p0640 N88-13911
A substructure method for dynamic simulation of flexible mechanical systems with geometric nonlinearities 09 p1176 N88-17044
A concurrent neural network algorithm for the traveling salesman problem
[DE88-006981] 18 p2562 N88-25208
The use of Lagrange multipliers and Kuhn-Tucker's theory in optimization problems 16 p2565 N88-25236
Surface tension and viscosity with Lagrangian hydrodynamics on a triangular mesh
[AD-A194120] 22 p3075 N88-28258
Lagrangian of the self-duality equation and d = 10, N = 2b supergravity
[DE88-701554] 24 p3455 N88-30563

LAGRANGE SIMILARITY HYPOTHESIS
Fully Lagrangian Renormalized Approximation theory of fluid turbulence
[DE86-004960] 10 p1330 N88-17952
Center for Turbulence Research 1987 activities
[NASA-CR-182693] 13 p1769 N88-20583

LAGRANGIAN EQUILIBRIUM POINTS
Single-burn transfer to nominally periodic orbit in the vicinity of point L2 of Earth-Sun system and related problems 08 p1006 N88-16100

LAGUERRE FUNCTIONS
Generalizations of Laguerre (type) polynomials
[REPT-87-58] 14 p1963 N88-21714

LAKE ICE
NT ICE FLOES

LAKES
Using space photography of the Earth in the classroom: Drought in Africa
[NASA-CR-182948] 19 p2685 N88-25960
Eigenmatrix representations of radiance distributions in layered natural waters with wind-roughened surfaces
[PB88-188701] 20 p2828 N88-26780
SPOT on land and lakes in the Hubei Province (China) 22 p3090 N88-28351

LAMB WAVES
Different ways of looking at the electromagnetic vacuum
[DE87-013150] 01 p0089 N88-10584
Thin-membrane Lamb-mode acoustic oscillators for chemical detection 19 p2673 N88-25895
Relativistic theory of the Lamb shift based on self energy
[DE88-702658] 23 p3295 N88-29626

LAMINA
U LAYERS

LAMINAR BOUNDARY LAYER
Excitation of natural oscillations of a boundary layer by an external acoustic field 04 p0425 N88-12634
Hypersonic laminar boundary layer: Parametric study for the representation of real gas effects 05 p0532 N88-13236
Navier-Stokes analysis of laminar flow control of a two-dimensional airfoil 05 p0540 N88-13286
Structural tests and development of a laminar flow control wing surface composite chordwise joint
[NASA-CR-172462] 06 p0663 N88-14066
Investigation of viscous/inviscid interaction in transonic flow over airfoils with suction 06 p0664 N88-14074
Upwind relaxation algorithms for Euler/Navier-Stokes equations 07 p0810 N88-14931
Numerical simulation of a controlled boundary layer 07 p0810 N88-14933
Computational design of natural laminar flow wings for transonic transport application 07 p0813 N88-14948
Flight research on natural laminar flow 07 p0813 N88-14950
Design and experimental evaluation of a swept supercritical Laminar Flow Control (LFC) airfoil 07 p0813 N88-14951
Laminar flow integration: Flight tests status and plans 07 p0813 N88-14952
Roughness and waviness requirements for laminar flow surfaces 07 p0813 N88-14953
Nonlinear and nonparallel stability problems
[AD-A186406] 07 p0850 N88-15159
A computationally efficient modelling of laminar separation bubbles
[NASA-CR-182417] 08 p0984 N88-15949
Numerical simulation of the interaction of pressure waves with laminar and turbulent boundary layers
[DFVLR-FB-87-18] 09 p1161 N88-16960
Boundary layer calculation using digital computers
[REPT-MM-4] 10 p1309 N88-17821
Velocity measurements in a 3D (three dimensional) shock wave laminar boundary layer interaction
[AD-A187334] 10 p1332 N88-17959
A simplified streamline swallowing procedure for the windward meridian of axisymmetric blunt bodies
[AD-A188413] 12 p1626 N88-19732
Development of disturbances in swept wing flows
[NASA-CR-182675] 13 p1768 N88-20574
The NASA Langley Laminar-Flow-Control (LFC) experiment on a swept, supercritical airfoil: Design overview
[NASA-TP-2809] 14 p1861 N88-21117
Application of hybrid laminar flow control to global range military transport aircraft
[NASA-CR-181638] 14 p1862 N88-21124
Modifications to the Langley 8-foot transonic pressure tunnel for the laminar flow control experiment
[NASA-TM-4032] 15 p2021 N88-22047
Investigation of boundary layer disturbances caused by periodic heating of a thin ribbon
[AD-A190572] 15 p2065 N88-22314
Aerothermal tests of quilted dome models on a flat plate at a Mach number of 6.5
[NASA-TP-2804] 15 p2067 N88-22325
Design method for laminar flow control of two-dimensional airfoils in incompressible flow. Numerical study of LFC design concepts
[DE88-751809] 16 p2155 N88-22859
The simulation of coherent structures in a laminar boundary layer 16 p2198 N88-23111
A new laminar water tunnel to study the transition process in a blasius layer and in a separation bubble and a new tool for industrial aerodynamics and hydrodynamic research 16 p2204 N88-23150
Solution of the compressible Navier-Stokes equations of motion by Chebyshev polynomials for laminar shock-boundary layer flow
[AD-A191033] 16 p2208 N88-23176
Boundary-layer stability and airfoil design 17 p2296 N88-23738
Numerical simulations of the flat-plate laminar boundary layer in subsonic and supersonic flow
[PDR/CFDU/IC/36] 18 p2511 N88-24895
Aerodynamic analysis of natural laminar flow airfoil 19 p2634 N88-25624
Active control of 2-D instability waves on an axisymmetric body
[AD-A191578] 19 p2663 N88-25835
Comparison of the wall pressure fluctuations in artificially generated turbulent spots, natural transition and turbulent boundary layers
[AD-A191777] 19 p2663 N88-25838
Boundary layer development as a function of chamber pressure in the NASA Lewis 1030:1 area ratio rocket nozzle
[NASA-TM-100917] 19 p2664 N88-25841
Analysis of experimental data for cast 10-2/DOA2 supercritical airfoil at high Reynolds numbers
[AD-A192627] 21 p2892 N88-27166
Flow dynamics stimulated by hairpin-like vortices in initially laminar boundary layers
[AD-A194253] 22 p3075 N88-28254
Solution to the compressible Navier-Stokes equations of motion by Chebyshev polynomials with implicit time stepping
[AD-A194119] 22 p3075 N88-28257
Coupled inviscid - boundary layer methods for turbomachinery blading design
[PNR90437] 22 p3076 N88-28260
Techniques for boundary layer tripping and control 23 p3168 N88-28863
Numerical simulation of the interaction of pressure waves with laminar and turbulent boundary layers
[ESA-TT-1089] 24 p3371 N88-30075

LAMINAR BOUNDARY LAYER SEPARATION
U BOUNDARY LAYER SEPARATION
U LAMINAR BOUNDARY LAYER

LAMINAR FLAMES
U FLAMES
U LAMINAR FLOW

LAMINAR FLOW
NT BLASIUS FLOW
NT STRATIFIED FLOW
Laminar flow over a spinning projectile at an angle of attack 02 p0121 N88-10766
Radiative and free-convective heat transfer from a finite horizontal plate inside an enclosure 02 p0133 N88-10833
Transition to turbulence via spatio-temporal intermittency 03 p0313 N88-11976
Heat transfer in laminar flow for mass inlet into an annular channel
[DE87-702890] 03 p0314 N88-11983
Numerical study of the entrance flow and its transition in a circular pipe (2) 03 p0318 N88-12011
Experiments on densely-loaded non-Newtonian slurries in laminar and turbulent pipe flows
[DE88-000719] 04 p0442 N88-12746
Studies of pressure-velocity coupling schemes for analysis of incompressible and compressible flows
[NASA-CR-181526] 04 p0443 N88-12748
On the numerical simulation of three-dimensional hypersonic flow 05 p0532 N88-13237
Structural tests and development of a laminar flow control wing surface composite chordwise joint
[NASA-CR-172462] 06 p0663 N88-14066
Visible boundary layer transition points through flight tests 06 p0675 N88-14136
Numerical simulation of boundary layers. Part 3: Turbulence and relaminarization in sink flows
[NASA-TM-88220] 06 p0698 N88-14283
Experimental investigation of heterogeneous compressible shear layers 06 p0700 N88-14294
Three-dimensional structure of boundary layers in transition to turbulence
[AD-A185466] 06 p0702 N88-14311
A multistage time-stepping scheme for the thin-layer Navier-Stokes equations 07 p0810 N88-14932
Flow diagnostics and visualization in wind tunnels and flight 07 p0811 N88-14940
Overview of the Langley viscous drag reduction program 07 p0812 N88-14946
Advanced natural laminar flow airfoil with high lift to drag ratio 07 p0812 N88-14947
Natural laminar flow nacelle for transport aircraft 07 p0813 N88-14949

Flight research on natural laminar flow
07 p0813 N88-14950
Laminar flow integration: Flight tests status and plans
07 p0813 N88-14952
Insect contamination protection for laminar flow surfaces 07 p0814 N88-14954
Laminar flow control leading edge glove flight test article development
[NASA-CR-172137] 07 p0815 N88-14960
Viscous drag reduction of horizontal plates
[VKI-TN-159] 07 p0851 N88-15171
Experimental and theoretical study on cavitation inception and bubbly flow dynamics. Part 1: Design, development and operation of a cavitation susceptibility meter. Part 2: Linearized dynamics of bubbly and cavitating flows with bubble dynamics effects
[AD-A187133] 09 p1160 N88-16952
Navier-Stokes solutions for laminar incompressible flow over a NACA 0012 airfoil and a backward facing step
[FFA-TN-1987-50] 09 p1162 N88-16966
Solution of the three-dimensional Navier-Stokes equations for transonic flow using a multigrid method
10 p1267 N88-17579
On some asymptotics of laminar flow in a coiled pipe
10 p1328 N88-17936
An experimental investigation of the hydrodynamic and heat-transfer behavior of aqueous foam in laminar tube flow
[DE88-004954] 11 p1483 N88-18855
Laminar flow heat transfer downstream from U-bends
11 p1484 N88-18859
A velocity-pressure integrated, mixed interpolation, Galerkin finite element method for high Reynolds number laminar flows
[NASA-CR-179264] 11 p1486 N88-18868
Transient radiative energy transfer in incompressible laminar flows
[NASA-CR-182605] 11 p1488 N88-18883
Solution of a rotating Navier-Stokes problem by a nonlinear multigrid algorithm 11 p1538 N88-19194
The NASA Langley Laminar-Flow-Control (LFC) experiment on a swept, supercritical airfoil: Design overview
[NASA-TP-2809] 14 p1861 N88-21117
Application of hybrid laminar flow control to global range military transport aircraft
[NASA-CR-181638] 14 p1862 N88-21124
Constructing Gloved wings for aerodynamic studies
[NASA-TM-100440] 14 p1863 N88-21128
Duct flow nonuniformities: Effect of struts in SSME HGM II(+)
[NASA-CR-179285] 15 p2062 N88-22296
Experiments on densely-loaded non-Newtonian slurries in laminar and turbulent pipe flows
[DE88-006209] 15 p2067 N88-22323
Wave-growth associated with turbulent spot in plane Poiseuille flow 16 p2199 N88-23116
Experimental study of vortex sheets in plane flow
16 p2203 N88-23142
Simulation of laminar-turbulent transition in the vicinity of a wall
[AD-A191380] 16 p2208 N88-23180
Laminar Flow Aircraft Certification
[NASA-CP-2413] 17 p2296 N88-23737
Boundary-layer stability and airfoil design
17 p2296 N88-23738
High-flaps for natural laminar flow airfoils
17 p2296 N88-23739
Computational wing design studies relating to natural laminar flow 17 p2297 N88-23740
Wind tunnel testing of low-drag airfoils
17 p2297 N88-23741
Flight experiences with laminar flow
17 p2297 N88-23744
Manufacturing requirements 17 p2297 N88-23745
Preliminary aerodynamic design considerations for advanced laminar flow aircraft configurations
17 p2297 N88-23746
Natural laminar flow and airplane stability and control
17 p2298 N88-23747
Operational considerations for laminar flow aircraft
17 p2298 N88-23748
Certification aspects of airplanes which may operate with significant natural laminar flow 17 p2298 N88-23749
Wave growth associated with turbulent spots in plane Poiseuille flow
[FFA-TN-1988-08] 18 p2457 N88-24587
Prediction of laminar and turbulent flows past single and twin airfoils 18 p2457 N88-24589
Theoretical analysis of laminar incompressible flow in slender channels
[VTH-LR-517] 18 p2513 N88-24909
Method and apparatus for detecting laminar flow separation and reattachment
[NASA-CASE-LAR-13952-1-SB]
18 p2513 N88-24910
Method of forming a multiple layer dielectric and a hot film sensor therewith
[NASA-CASE-LAR-13678-1] 18 p2584 N88-25355
Drag measurements on a laminar flow body of revolution in Langley's 13 inch magnetic suspension and balance system
[NASA-CR-182909] 19 p2597 N88-25432
Structure of laminar, premixed flames of CH2O/NO2/O2 mixtures 19 p2632 N88-25613
Finite element analysis of incompressible viscous flow around multi-element aerofoils 19 p2635 N88-25634
Numerical simulation of transition to turbulence in plane Poiseuille flow by a spectral method
19 p2640 N88-25661
Boundary layer development as a function of chamber pressure in the NASA Lewis 1030:1 area ratio rocket nozzle
[NASA-TM-100917] 19 p2664 N88-25841
Numerical simulation studies of laminar-turbulent transition in the plan channel 19 p2665 N88-25850
Navier-Stokes code NS3D for blunt bodies. Part 1: Analysis, results and verification
[DE88-010105] 19 p2666 N88-25855
Experiments on densely-loaded non-Newtonian slurries in laminar and turbulent pipe flows
[DE88-010579] 20 p2800 N88-26612
Velocity-pressure integrated versus penalty finite element methods for high Reynolds number flows
[NASA-CR-179357] 20 p2803 N88-26635
The structure and stability of nonpremixed gas jet flames 21 p2908 N88-27257
Turbulent flow field visualization with integral interferometric imaging and computed tomography
21 p2950 N88-27521
Runge-Kutta finite-volume simulation of laminar transonic flow over the ONERA M6 wing using the Navier-Stokes equations
[FFA-TN-1987-06] 22 p3039 N88-28045
Theoretical study and numerical simulation of flame fronts
[PB88-122932] 22 p3051 N88-28104
Application of rectangular co-ordinates to the problem of laminar combined convection in a straight horizontal tube whose circumference is heated nonuniformly
[PDR/CFDU/IC/33] 22 p3076 N88-28263
The Kelvin-Helmholtz instability in a stratified shear flow
[CFD/88/2] 22 p3076 N88-28265
Mass transport in annular spherical system
[LRT-WE-9-FB-11(1987)] 22 p3077 N88-28271
Variable Sweep Transition Flight Experiment (VSTFE)-parametric pressure distribution boundary layer stability study and wing glove design task
[NASA-CR-3992] 23 p3173 N88-28894
Pressure distributions from subsonic tests of an advanced laminar-flow-control wing with leading- and trailing-edge flaps
[NASA-TM-4040-PT-2] 24 p3321 N88-29776
Radiation from soot-containing flames
24 p3347 N88-29927
Techniques used in the F-14 variable-sweep transition flight experiment
[NASA-TM-100444] 24 p3374 N88-30093

LAMINAR FLOW AIRFOILS
Wind-tunnel investigation of a full-scale general aviation airplane equipped with an advanced natural laminar flow wing
[NASA-TP-2772] 01 p0002 N88-10009
Wind tunnel results for a high-speed, natural laminar-flow airfoil designed for general aviation aircraft
[NASA-TM-87602] 06 p0665 N88-14078
Oscillating airfoils: Achievements and conjectures
[AD-A190490] 15 p2014 N88-22008
Design method for laminar flow control of two-dimensional airfoils in incompressible flow. Numerical study of LFC design concepts
[DE88-751809] 16 p2155 N88-22859
Laminar Flow Aircraft Certification
[NASA-CP-2413] 17 p2296 N88-23737
Pressure distributions from subsonic tests of an advanced laminar-flow-control wing with leading- and trailing-edge flaps
[NASA-TM-4040-PT-1] 17 p2300 N88-23758
Instability of laminar separation bubbles: Causes and effects
[AD-A191168] 18 p2508 N88-24876
Calibration of averaging total pressure flight wake rake and natural-laminar-flow airfoil drag certification
[NASA-CR-181630] 19 p2599 N88-25443
JPRS report: Science and technology. Japan
[JPRS-JST-88-005] 19 p2633 N88-25619
Aerodynamic analysis of natural laminar flow airfoil
19 p2634 N88-25624
Solution to the compressible Navier-Stokes equations of motion by Chebyshev polynomials with implicit time stepping
[AD-A194119] 22 p3075 N88-28257

LAMINAR FLOW CONTROL
U BOUNDARY LAYER CONTROL
U LAMINAR BOUNDARY LAYER

LAMINAR HEAT TRANSFER
Heat transfer in laminar flow for mass inlet into an annular channel
[DE87-702890] 03 p0314 N88-11983
An experimental investigation of the hydrodynamic and heat-transfer behavior of aqueous foam in laminar tube flow
[DE88-004954] 11 p1483 N88-18855
Heat transfer modeling of jet vane Thrust Vector Control (TVC) systems
[AD-A190106] 15 p2019 N88-22034
Forced-convection, liquid-cooled, microchannel heat sinks
[AD-A193337] 21 p2937 N88-27444

LAMINAR JETS
U JET FLOW
U LAMINAR FLOW

LAMINAR WAKES
A mapping of the viscous flow behavior in a controlled diffusion compressor cascade using laser Doppler velocimetry and preliminary evaluation of codes for the prediction of stall
[AD-A194490] 23 p3211 N88-29112

LAMINATED MATERIALS
U LAMINATES

LAMINATES
Joints in carbon fibre reinforced composites
[BR99969] 01 p0019 N88-10114
Effect of adhesive layers on impact damage and dynamic response in composite laminates
02 p0141 N88-10887
A stochastic delamination growth model for fatigue loaded laminated composite materials
02 p0141 N88-10888
Cumulative fatigue and life prediction of fibre composites. Part 1: Literature reviews
[BR101013] 02 p0142 N88-10893
Cumulative fatigue and life prediction of fibre composites. Part 2: Experimental techniques and results
[BR101014] 02 p0142 N88-10894
Contribution to the study of composite materials and their damage
[NASA-TT-20107] 02 p0143 N88-10897
Theoretical investigation of stress concentrations in damaged carbon fibre reinforced plastic plate structures. Volume 1: Main text
[BR99872-VOL-1] 03 p0280 N88-11761
Theoretical investigation of stress concentrations in damaged carbon fibre reinforced plastic plate structures. Volume 2: Tables, figures and plates
[BR99873-VOL-2] 03 p0280 N88-11762
Carbon-fiber reinforced plastics
04 p0403 N88-12506
Thixotropic surface composition for phenolaldehyde resin laminates
[GB-PATENT-2-180-251-A] 04 p0410 N88-12545
Study of zero CTE (Coefficients of Thermal Expansion) of graphite/epoxy composites
[DE87-013557] 04 p0412 N88-12554
Spatial strength variation and statistical size effect of laminated orthotropic composite materials
04 p0427 N88-12646
A refined nonlinear analysis of laminated composite plates and shells
[AD-A184436] 04 p0454 N88-12811
Vibration and buckling of geometrically imperfect laminated cylindrical shells 04 p0456 N88-12822
Dynamic response of laminated composite plates using a three-dimensional hybrid-stress finite-element formulation 05 p0596 N88-13639
Fatigue mechanisms in ARALL, a fatigue resistant hybrid aluminum aramid composite material
05 p0605 N88-13711
Behavior of bolted joints in composite laminates
06 p0677 N88-14148
Evaluation of closed cubic failure criterion for graphite/epoxy laminates
[NASA-CR-182375] 06 p0679 N88-14158
Stresses and displacements in two, three and four layered structures submitted to flexible or rigid loads
[AD-A185707] 06 p0723 N88-14450
Experimental and theoretical investigation of mechanically fastened composites
[AD-A185896] 07 p0826 N88-15008
Investigation of low velocity impact damage on filamentary composite materials
07 p0923 N88-15607
Postbuckling of laminated anisotropic panels
[NASA-TM-100509] 08 p0994 N88-16011

Failure modes of laminate structures
[DE88-002579] 08 p0996 N88-16033
Sublaminate damage mechanisms in composite structures
[AD-A186807] 09 p1137 N88-16815
Fatigue and damage tolerance design data for carbon fibre composites
[BAE-MSM-R-GEN-0454] 09 p1138 N88-16818
Fatigue behaviour of hybrid composites
[BR102236] 09 p1138 N88-16819
Effects of processing variables on the behavior of E-glass/913 and XAS carbon fibre/913 laminates subjected to hot/wet environmental conditions
[BR101940] 09 p1138 N88-16820
Effect of low velocity impact on compression strength of a quasi-isotropic laminate
[FFA-TN-1987-38] 09 p1138 N88-16822
Finite element analysis of damaged cross-ply composite laminates
[CCMS-87-10] 09 p1139 N88-16829
An analytical study of the effects of transverse shear deformation and anisotropy on natural vibration frequencies of laminated cylinders
[NASA-TM-100554] 10 p1295 N88-17739
Analytical and experimental characterization of damage processes in composite laminates
[AD-A187221] 10 p1296 N88-17746
Piezoelectric laminates for torsional and bending model control: Theory and experiment
10 p1343 N88-18029
Ultrasonic characterization of layered composite systems 10 p1404 N88-18374
On delamination of (+ or - theta sub m/90 sub n/2) sub s laminates subject to tensile loading
[AD-A188095] 11 p1447 N88-18626
Colloquium on damage mechanics of graphite/expoxy laminates during fatigue
[DFVLR-MITT-87-08] 11 p1448 N88-18630
Influence of different parameters on damage development --- carbon fiber reinforced plastics
11 p1448 N88-18632
Initiation and propagation of damage in notched unidirectional and multidirectional CFRE resin laminates
11 p1449 N88-18633
Damage initiation and growth in sateen laminates under static and cyclic loading 11 p1449 N88-18634
Damage mechanisms of CFRP riveted joints
11 p1449 N88-18636
Damage mechanisms and fatigue life prediction of graphite/epoxy laminates 11 p1449 N88-18637
Innovative design of composite structures: Further studies in the use of a curvilinear fiber format to improve structural efficiency
[NASA-CR-182576] 11 p1450 N88-18641
An experimental and numerical study of notch sensitivity of ARALL laminates
[CCMS-88-04] 11 p1450 N88-18644
Analysis of composite laminates with matrix cracks
[CCMS-88-03] 11 p1451 N88-18645
A nonlinear computational model for the strength and failure of composite plates and shells
11 p1501 N88-18964
An experimental measurement of metal multilayer X-ray reflectivity degradation due to intense X-ray flux
[LA-10969-T] 11 p1547 N88-19255
Wave propagation in laminated composite plates
[AD-A188999] 12 p1604 N88-19594
Ultrasonic-velocity studies of composite and heterogeneous materials
[AD-A189000] 12 p1604 N88-19595
Multilayer thermal insulation tests
[INPE-4475-PRE/1243] 12 p1626 N88-19729
Simulated impact damage in a thick graphite/epoxy laminate using spherical indenters
[NASA-TM-100539] 13 p1733 N88-20363
Transient dynamics of fibre reinforced composite plates
[IIT-B/CE/RR/87-1] 13 p1734 N88-20370
Delamination stresses in semicircular laminated composite bars
[NASA-TM-4026] 13 p1735 N88-20375
Nondestructive evaluation of carbon-carbon coatings
[AD-A189524] 13 p1748 N88-20453
Exploring the relation between interface structure and mechanical properties in multilayer structures
[DE88-005428] 13 p1848 N88-21060
Studies of traverse impact damage in composite materials using a Hopkinson pressure-bar technique
[OUEL-1706/87] 14 p1883 N88-21255
Environmental effects on the post-impact compressive strength of CFC
[RAE-TM-MAT-STR-1088] 14 p1884 N88-21256
Strength and failure analysis of composite laminate containing a circular hole with reinforcement
[AD-A189629] 14 p1884 N88-21260
Crack resistance of multilayer ceramic-based composite material 14 p1885 N88-21265
Influence of heat treatment on the properties of boroaluminum 14 p1886 N88-21270
Stress-strain behaviour of a bolt hole in carbon fibre composite plates
[BU-354] 14 p1923 N88-21460
An investigation of the failure response of laminates under biaxial stress
[AD-A190039] 15 p2029 N88-22090
Interlaminar fracture toughness of thermoplastic composites
[NASA-TM-100532] 15 p2030 N88-22097
A system to measure damage in composite materials by the ultrasonic method
[ONERA-RT-2/7256-RY-061-R]
15 p2031 N88-22103
Donor acceptor polymerization chemistry as a vehicle to low energy cure matrix resins
[AD-A190119] 15 p2044 N88-22179
The buckling and vibration of composite plates using the Levy method considering shear deformation and rotary inertia
[AD-A189743] 15 p2076 N88-22374
Impact damage in composite laminates
15 p2080 N88-22402
Design studies of primary aircraft structures in ARALL laminates
[LR-520] 16 p2160 N88-22868
A study of failure characteristics in thermoplastic composite material
[AD-A190613] 16 p2171 N88-22940
Fatigue damage development of various CFRP-laminates
[NASA-TT-20247] 16 p2172 N88-22945
Behaviour of fibre-reinforced composites under dynamic loading
[AD-A191310] 16 p2174 N88-22955
On the calculation of stresses in pin-loaded anisotropic plates
[LR-529] 16 p2223 N88-23268
GARTEUR TP-037: Impact damage tolerance of carbon fiber and hybrid laminates
[RAE-TR-87057] 17 p2316 N88-23837
Local delamination buckling in layered structures
18 p2480 N88-24711
Damage by creep fatigue: Influence of the visco-elasticity of the matrix
[PB88-124706] 18 p2528 N88-24998
On the bending response of Kevlar 49/epoxy beams and rings
[DE88-006824] 18 p2530 N88-25012
Method of forming a multiple layer dielectric and a hot film sensor therewith
[NASA-CASE-LAR-13678-1] 18 p2584 N88-25355
Metastability in SiGe/Si strained-layer structures
[DE88-007603] 18 p2585 N88-25361
Fuel containment and damage tolerance in large composite primary aircraft structures. Phase 2: Testing
[NASA-CR-172519] 19 p2601 N88-25452
Fracture physics of delamination of composite materials
[AD-A192021] 19 p2609 N88-25482
Loading rate sensitivity of open hole composites in compression
[NASA-TM-100534] 19 p2610 N88-25490
Silver multi-layers for planar Ag/AgCl reference electrodes 19 p2672 N88-25883
Stiffness degradation of composite laminates
20 p2767 N88-26405
Instability-related delamination growth of embedded and edge delaminations 20 p2767 N88-26406
Computation equipment for damage simulation in laminated composites
[AD-A193013] 20 p2768 N88-26412
A micromechanics model of the stiffness and strength of laminates with fiber waviness
[NASA-CR-181670] 20 p2768 N88-26413
Compression creep of filamentary composites
[NASA-CR-182550] 20 p2798 N88-26601
Three-dimensional analysis of a postbuckled embedded delamination
[NASA-TP-2823] 20 p2812 N88-26684
Analysis of the perforation of monolithic and simple laminate aluminium targets as a test of analytical deformation models
[MRL-R-1111] 20 p2813 N88-26686
Properties of multilayers for soft X-ray optics
20 p2867 N88-27025
The two isotropic asymptotes of fiber composites
[AD-A192305] 21 p2904 N88-27231
An experimental and analytical evaluation of a biaxial test for determining shear properties of composite materials
[NASA-CR-182928] 21 p2962 N88-27593
Failure analysis of quasi-isotropic composite laminates with free edges under off-axis loading
22 p3049 N88-28092
Analysis of stiffness reduction, failure and stress concentration in fiber composite laminates
[AD-A193519] 22 p3050 N88-28096
Micromechanics of composite laminate compression failures
[NASA-CR-183179] 22 p3050 N88-28098
Wave propagation and vibration of fibre reinforced laminates
[AD-A194144] 22 p3051 N88-28101
Array trade-off study using multilayer parasitic subarrays
[NASA-TM-101321] 22 p3070 N88-28222
Elastic wave dispersion in laminated composite plate
[AD-A192289] 23 p3188 N88-28967
A comprehensive study on damage tolerance properties of notched composite laminates
[AD-A192952] 23 p3188 N88-28968
Thermal stress analysis in PMR-15 carbon fibre laminates
[ETN-88-93123] 24 p3341 N88-29886
ZT imaging system for layered thin wall structures
[AD-A195466] 24 p3352 N88-29954
Modeling of micromechanisms of fatigue and fracture in hybrid materials
[AD-A195604] 24 p3382 N88-30142
Large displacement and rotational formulation for laminated cylindrical shells including parabolic transverse shear
[AD-A194871] 24 p3384 N88-30158

LAMINATIONS
U LAMINATES

LAMPS
U LUMINAIRES

LAN (COMPUTER NETWORKS)
U LOCAL AREA NETWORKS

LAND
NT ARID LANDS
NT COASTAL PLAINS
NT DESERTS
NT FARMLANDS
NT FLOOD PLAINS
NT GRASSLANDS
NT MARSHLANDS
NT PARKS
NT PLAINS
NT PLAYAS
NT SAHARA DESERT (AFRICA)
NT TUNDRA
NT WETLANDS
An exploratory study of inland water and land altimetry using Seasat data
[ESA-CR(P)-2433] 02 p0193 N88-11208
Automated satellite cloud analysis: A multispectral approach to the problem of snow/cloud discrimination
[AD-A185672] 06 p0746 N88-14591
The role of anisotropy in the long range reconnaissance of the albedo of land surfaces 08 p1017 N88-16169
The anisotropy of reflected solar radiation over several types of land surface 08 p1018 N88-16171
Assessment of the differential technique for land navigation within 1000 km of Omega Australia
[AD-A191036] 16 p2160 N88-22885
Non-Gaussian models for surface clutter
22 p3068 N88-28212
Global-scale temperature changes to August 1987 and a comparison of satellite and conventional data
22 p3125 N88-28572

LAND ICE
Large ice masses: Characteristics, behaviour and relation to climate 14 p1939 N88-21569
The role of remote sensing in the study of polar ice sheets 14 p1939 N88-21570

LAND MANAGEMENT
Characterization, topology, and cartography of grasslands for the development of fodder resources. (Preliminary Evaluation Program for SPOT number 26)
22 p3095 N88-28377

LAND MOBILE SATELLITE SERVICE
Communication satellite technology trends
01 p0015 N88-10088
Study of mobile communications payload for Columbus Polar Platforms
[ITS-TR-056A/86] 01 p0034 N88-10220
Study of the feasibility of a satellite communication system for road transportation home office to vehicle communication. Volume 1: Conceptual analysis
[SC/87-E/6-VOL-1] 05 p0575 N88-13505
Study of the feasibility of a satellite communication system for road transportation home office to vehicle communication. Volume 2: Market study
[SC/87-E/6-VOL-2] 05 p0575 N88-13506

Receiver susceptibility measurements relating to interference between UHF (Ultra High Frequency) television and land mobile radio services
[PB87-228029] 06 p0690 N88-14228
Land mobile satellite transmission measurements at 869 MHz. A comparison of error probabilities for various message block durations and fade margins as a function of vegetation shadowing
[NASA-CR-179929] 06 p0693 N88-14255
Multicarrier demodulator design, volume 1 — communication satellites
[ESA-CR(P)-2468-VOL-1] 09 p1158 N88-16941
Multicarrier demodulator design. Volume 2: Executive summary — communication satellites
[ESA-CR(P)-2468-VOL-2] 09 p1158 N88-16942
A microstrip array feed for MSAT spacecraft reflector antenna 19 p2652 N88-25747

LAND USE
NT RURAL LAND USE
Vegetation classification, land systems and mapping using SPOT multispectral data: Preliminary results 03 p0342 N88-12160
Land cover/use classification of Cairns, Queensland, Australia: A remote sensing study involving the conjunctive use of the airborne imaging spectrometer, the large format camera and the thematic mapper simulator 05 p0612 N88-13759
Overview of Austrian Airborne Imaging Spectrometer (AIS) programme and first results 05 p0612 N88-13762
Design and implementation of a data base system for Digital Land Mass System (DLMS) data
[FEL-IR-1987-19] 09 p1185 N88-17101
Air Force geographic information and analysis system
[DE88-001420] 10 p1424 N88-18505
Land-use classification in a region north-west of Wuerzburg (Federal Republic of Germany) using digital, multispectral LANDSAT 5 Thematic Mapper data
[DFVLR-FB-87-37] 14 p1940 N88-21579
Updating of the municipal official register of real estate through a geographical information system
[INPE-4459-PRE/1238] 15 p2090 N88-22453
Comparative utilization of analog and digital processes in the treatment of MSS-LANDSAT data for studying the national parks of Brazil
[INPE-4011-TDL/240] 15 p2090 N88-22456
Orbital remote sensing: An instrument for monitoring urban growth
[INPE-4456-PRE/1287] 15 p2150 N88-22833
Applications of multitemporal compositions obtained from LANDSAT data in the study of urban growth
[INPE-4480-PRE/1246] 16 p2287 N88-23692
Updating land-use of the Sao Jose dos Campos municipality through remote sensing data
[INPE-4479-RPE/562] 16 p2287 N88-23693
Landuse and landform studies of the Mahanadi River Delta with the help of satellite MSS band 17 p2355 N88-24033
Remote sensing techniques in the estimation of the area cultivated with beans, corn, and castor beans in the Irece County (Bahia State) 17 p2358 N88-24045
CANASATE: Sugar cane mapping by satellite 17 p2358 N88-24046
Utilization of LANDSAT-TM imagery in the hydroenergetic inventory of the Paraiba de Sul River Basin 17 p2364 N88-24077
Preliminary study on the application of digital processing of TM-LANDSAT data in the mapping of apple orchards in Fraiburgo (SC) 17 p2367 N88-24093
Research on enhancing the utilization of digital multispectral data and geographic information systems in global habitability studies
[NASA-CR-182799] 17 p2368 N88-24101
Coupling of satellite remote sensing to digitized topographic map to detect changes in land use
[B8735129] 17 p2369 N88-24104
National Meeting on Remote Sensing Applied to Municipal Planning 19 p2681 N88-25939
Mapping of land use in Sao Jose dos Campos municipality by remote sensing, an aid for the elaboration of its PDDI 19 p2681 N88-25940
Remote sensing techniques applied to the study of metropolitan regions: The west sector of the Sao Paulo metropolitan area 19 p2681 N88-25941
The use of satellite imagery for municipal conditions in rural recording in Pereira Barreto (SP) 19 p2682 N88-25944
The impact of disorganized occupation of urban sub-basins: Sub-basin of the Cabucu River, metropolitan area of Sao Paulo (SP) 19 p2682 N88-25945
The impact of hemp production on the development of the municipalities of Araras, Leme, Santa Cruz da Conceicao and Pirassununga 19 p2683 N88-25948
Application of interactive graphic system (CAD/CAM) in the determination of process evolution in land use in the Ribeirao Preto municipality 19 p2684 N88-25956
Hydrologic models for land-atmosphere retrospective studies of the use of LANDSAT and AVHRR data
[NASA-CR-182861] 20 p2817 N88-26712
SPOT on land and lakes in the Hubei Province (China) 22 p3090 N88-28351
Review of the studies of geography and environment and studies on spectral characteristics of SPOT HRV data 22 p3091 N88-28358
Comparison between the respective contributions of the TM LANDSAT-4 and HRV SPOT-1 data to the land use mapping of Mediterranean coastal zone 22 p3092 N88-28363
Evaluation of annual crop surfaces and territorial inventory in the Paris basin by combining classic statistical inquiries and SPOT data (Preliminary Evaluation Program for SPOT 127) 22 p3094 N88-28372
SPOT-1 HRV data and vegetation amount 22 p3095 N88-28379
Use of SPOT imagery for vegetation/biomass mapping, geotechnical mapping, catchment area determination, and settlement location in the Turkana district, northern Kenya 22 p3096 N88-28384
An evaluation of the applicability of SPOT stereoscopic imagery to the Canada Land Use Monitoring Program (CLUMP) 22 p3099 N88-28403
Topographic suppression and advances in classification for land cover mapping using SPOT-1 HRV imagery 22 p3099 N88-28404
Accuracy of land use classification for SPOT image data 22 p3100 N88-28410
Utilization of SPOT-1 multispectral data for mapping land cover and phytohygiene monitoring in the central zone of the Mercantour National Park (France) 22 p3100 N88-28413
Applications of SPOT data for urban real estate investment information systems 22 p3101 N88-28414
Mapping and urban multi-experimental assessment of SPOT: Urban results 22 p3101 N88-28415
Utilization of SPOT multispectral data for urban planning 22 p3101 N88-28418
An analysis of time and space requirements for aircraft turnrounds
[TT-8705] 24 p3322 N88-29783

LANDAU DAMPING
Fast wave injection into high temperature tokamak plasmas in the lower-hybrid-density regime of JIPP T-IIU
[ISSN-0469-4732] 01 p0099 N88-10649
Plasma wave radiative damping of a new type in a relativistic one-dimensional plasma
[DE88-701191] 15 p2135 N88-22739
Improvement of plasma confinement due to electron Landau damping in tokamaks
[DE88-752339] 15 p2136 N88-22747

LANDAU-GINZBURG EQUATIONS
Global spatial periodic solutions to the Ginzburg-Landau equations
[DE88-006424] 15 p2119 N88-22623

LANDFORMS
NT ALEUTIAN ISLANDS (US)
NT ALPS MOUNTAINS (EUROPE)
NT ANDES MOUNTAINS (SOUTH AMERICA)
NT CALDERAS
NT CAPE HATTERAS (NC)
NT CARPATHIAN MOUNTAINS (EUROPE)
NT DELAWARE RIVER BASIN (US)
NT DELTAS
NT DUNES
NT GREAT BASIN (US)
NT GREENLAND
NT HAWAII
NT ICELAND
NT INDONESIA
NT ISLAND ARCS
NT ISLANDS
NT JAPAN
NT LAGOONS
NT MALDIVE ISLANDS
NT MARS VOLCANOES
NT MOUNTAINS
NT NEW ZEALAND
NT PIEDMONTS
NT PLATEAUS
NT PLAYAS
NT RIVER BASINS
NT SIERRA NEVADA MOUNTAINS (CA)
NT STEPPES
NT STRUCTURAL BASINS
NT TUNDRA
NT VOLCANOES
NT WATERSHEDS
Tectonics and magmatism of Walvis Ridge and Discovery Rise (Atlantic Ocean) 06 p0726 N88-14463
The digital landmass simulation production overview
[AD-A187978] 11 p1503 N88-18978

LANDING
NT AIRCRAFT LANDING
NT CRASH LANDING
NT DITCHING (LANDING)
NT GLIDE LANDINGS
NT MARS LANDING
NT PLANETARY LANDING
NT SPACECRAFT LANDING
NT VERTICAL LANDING
Effect of motion cues during complex curved approach and landing tasks: A piloted simulation study
[NASA-TP-2773] 04 p0398 N88-12480
High speed propeller performance and noise predictions at takeoff/landing conditions
[NASA-TM-100267] 05 p0646 N88-13960
Aerodynamic and acoustic characteristics of an advanced propeller under take-off and landing conditions
[NAL-TR-935] 09 p1243 N88-17453
Radar returns from ground clutter in vicinity of airports 10 p1274 N88-17624

LANDING AIDS
NT ARRESTING GEAR
NT AUTOMATIC LANDING CONTROL
NT INSTRUMENT LANDING SYSTEMS
NT MICROWAVE LANDING SYSTEMS
Boeing 727 MLS (Microwave Landing System) terminal instrument procedures (TERPS) approach data collection and processing, data report
[AD-A185523] 06 p0667 N88-14090
First flight simulator test of the head-up display for NAL QSTOL experimental aircraft (ASUKA)
[DE88-751804] 16 p2162 N88-22896
Cessna 172 MLS (Microwave Landing System) terminal instrument procedures (TERPS) approach data collection and processing data report
[AD-A191241] 18 p2461 N88-24613
Microwave landing system mathematical modeling study for Midway Airport Runway 22L, Chicago, Illinois
[AD-A191721] 18 p2462 N88-24616
Simulator evaluation of lineup visual landing aids for night carrier landing
[AD-A191212] 18 p2468 N88-24648
Control systems for platform landings cushioned by air bags
[AD-A196154] 24 p3358 N88-29996

LANDING GEAR
Cornering characteristics of the main-gear tire of the space shuttle orbiter
[NASA-TP-2790] 11 p1438 N88-18583
Metallurgical analysis of fractured F-27 aircraft landing gear
[DE88-005885] 11 p1460 N88-18705
An investigation of classical dynamic scaling techniques applied to an oleo-pneumatic landing gear strut
[AD-A187664] 13 p1721 N88-20292
Aircraft corrosion problems and research in the Netherlands
[NLR-MP-88066-U] 13 p1744 N88-20427
In-service measurements of SAAB SF-340 landing gear loads
[FFA-TN-1987-48] 15 p2018 N88-22032
Soft-ground aircraft arresting systems
[AD-A190838] 16 p2165 N88-22912

LANDING LOADS
In-service measurements of SAAB SF-340 landing gear loads
[FFA-TN-1987-48] 15 p2018 N88-22032
Control systems for platform landings cushioned by air bags
[AD-A196154] 24 p3358 N88-29996

LANDING MODULES
NT LUNAR LANDING MODULES
Mars Lander/Rover vehicle development: An advanced space design project for USRA and NASA/OAST
[NASA-CR-182570] 11 p1567 N88-19380
Mars Lander/Rover vehicle development: An advanced space design project for USRA and NASA/OAST
[NASA-CR-182562] 12 p1709 N88-20226

LANDING SIMULATION
Additional investigations in landing process of aircraft: Test distributions
[DFVLR-MITT-87-13] 09 p1115 N88-16686
First flight simulator test of the head-up display for NAL QSTOL experimental aircraft (ASUKA)
[DE88-751804] 16 p2162 N88-22896
Automatic landing by computer vision
[ETN-88-92991] 23 p3175 N88-28905
Additional investigations into the aircraft landing process: Test distributions
[ESA-TT-1099] 23 p3177 N88-28913

LANDING SITES
A Workshop on Desert Processes, September 24-28, 1984: Report on the conference
[AD-A184599] 03 p0345 N88-12184

The Viking landing sites: A cartographic perspective
[NASA-CR-177486] 19 p2742 N88-26282

LANDING SYSTEMS
U LANDING AIDS

LANDSAT SATELLITES
NT LANDSAT 5
Object-dependent atmospheric influence on LANDSAT recordings 01 p0065 N88-10420
Remote sensing in mineral exploration
[PB87-138558] 06 p0729 N88-14484
LANDSAT thematic mapper radiometric calibration study
[NASA-CR-182410] 07 p0872 N88-15287
Space-based remote sensing of the Earth: A report to the Congress
[NASA-TM-89709] 10 p1346 N88-18046
Thematic mapper study of Alaskan ophiolites
[NASA-CR-182554] 11 p1504 N88-18984
An application of digital cartography updating middle and small scale thematic maps using orbital data
[INPE-4460-TDL/317] 12 p1637 N88-19805
The use of LANDSAT-TM pictures for the detection of space-limiting elements for the benefit of landscape photomapping
[BCRS-87-02] 16 p2226 N88-23305
Applications of multitemporal compositions obtained from LANDSAT data in the study of urban growth
[INPE-4480-PRE/1246] 16 p2287 N88-23692
Mapping soil and rock variation from satellite images in the Sahel 17 p2354 N88-24023
DMSP-SSM/1 NASA algorithm validation using primarily LANDSAT and secondarily DMSP and/or AVHRR visible and thermal infrared satellite imagery
[NASA-CR-182979] 18 p2532 N88-25024
Comparative study of crop and soil mapping using multitemporal and multispectral SPOT and LANDSAT data 22 p3091 N88-28354
Monitoring of agricultural production in West Africa. The need to integrate different satellite platforms 22 p3096 N88-28383
Use of SPOT imagery for vegetation/biomass mapping, geotechnical mapping, catchment area determination, and settlement location in the Turkana district, northern Kenya 22 p3096 N88-28384
Accuracy of land use classification for SPOT image data 22 p3100 N88-28410
Utilization of SPOT-1 multispectral data for mapping land cover and phytohygiene monitoring in the central zone of the Mercantour National Park (France) 22 p3100 N88-28413
Use of LANDSAT images of vegetation cover to estimate effective hydraulic properties of soils
[NASA-CR-183185] 22 p3116 N88-28514

LANDSAT 5
Remote sensing with LANDSAT 5 Thematic Mapper (TM) and its application to various planning levels: A case study from the Wuerzburg area, West Germany
[DFVLR-FB-86-62] 01 p0065 N88-10421
Evaluation of digital, multitemporal LANDSAT 5 thematic mapper data for the determination of the aerial snowcover extent and spectral separation of various surface types in the inner Oetztal (West Germany) with special regard to the significance of aerial snowcover information for water resources management
[DFVLR-FB-86-46] 03 p0345 N88-12180
Land-use classification in a region north-west of Wuerzburg (Federal Republic of Germany) using digital, multispectral LANDSAT 5 Thematic Mapper data
[DFVLR-FB-87-37] 14 p1940 N88-21579
Comparison between the respective contributions of the TM LANDSAT-4 and HRV SPOT-1 data to the land use mapping of Mediterranean coastal zone 22 p3092 N88-28363

LANDSCAPE
U TERRAIN
U TOPOGRAPHY

LANDSLIDES
Photointerpretation with instrumentation for evaluation of environmental impact: Mata Atlantica in Cubatao 19 p2683 N88-25946
Study of evolution of vegetal cover and slide scars in the Cubatao municipality-Sao Paulo 19 p2683 N88-25947
SPOT imagery for landslide cartography in mountainous areas. Example of the French Maritime Alps 22 p3105 N88-28440
SPOT for slope instability survey in Nepal 22 p3105 N88-28441

LANES
U PATHS

LANGEVIN FORMULA
Weak solution of the Langevin equation on a generalized functional space
[AD-A194290] 23 p3270 N88-29456

LANGMUIR PROBES
U ELECTROSTATIC PROBES

LANGUAGE PROGRAMMING
Applicative parallelism: Potential and challenge
[DE87-011885] 08 p1068 N88-16459
Design for a TPL complier system: A system for retargeting high level language programs 10 p1381 N88-18248

LANGUAGES
NT ADA (PROGRAMMING LANGUAGE)
NT APL (PROGRAMMING LANGUAGE)
NT ASSEMBLY LANGUAGE
NT BASIC (PROGRAMMING LANGUAGE)
NT C (PROGRAMMING LANGUAGE)
NT COBOL
NT COMMAND LANGUAGES
NT CONTEXT FREE LANGUAGES
NT ENGLISH LANGUAGE
NT FORTRAN
NT HIGH LEVEL LANGUAGES
NT LISP (PROGRAMMING LANGUAGE)
NT NATURAL LANGUAGE (COMPUTERS)
NT PASCAL (PROGRAMMING LANGUAGE)
NT PROGRAMMING LANGUAGES
NT PROLOG (PROGRAMMING LANGUAGE)
NT QUERY LANGUAGES
NT SYLLABLES
NT WORDS (LANGUAGE)
Foreign language identification: First step in the translation process
[DE87-011065] 02 p0248 N88-11565
Errors associated with Russian name transliteration
[DE87-011717] 02 p0248 N88-11566
LISP as a rapid prototyping environment: The chinese tutor
[AD-A184328] 03 p0369 N88-12319
Space languages 08 p1063 N88-16420
Linguistic-technical aspects of machine translation 24 p3438 N88-30461
Linguistic barriers: Translation problems 24 p3438 N88-30465

LANTHANIDE SERIES METALS
U RARE EARTH ELEMENTS

LANTHANUM
Develop techniques for ion implantation of (lead-lanthanum-zirconate-titanate) for adaptive optics
[DE88-000642] 05 p0650 N88-13986
Theory of the tetragonal-to-orthorhombic structural phase transition in La2CuO4
[AD-A187141] 09 p1254 N88-17514
Paramagnetic spins in oxygen-loaded ceramic La2CuO4/sub 4+delta/
[DE88-007114] 19 p2619 N88-25539
PLZT (Lead-Lathanium-Zirconium-Titanium) electro-optic photographic system
[AD-A193473] 23 p3215 N88-29137

LANTHANUM COMPOUNDS
NT LANTHANUM OXIDES
NT LANTHANUM TELLURIDES
A synthetic plasma source
[TRITA-EPP-86-15] 05 p0652 N88-13995
Properties of lanthanide oxides as supports for transition metal catalysts
[DE88-004520] 11 p1456 N88-18678
High-current density, high-brightness electron beams from large-area lanthanum hexaboride cathodes
[AD-A187700] 11 p1477 N88-18813
Compilation of NRL publications on high temperature superconductivity
[AD-A189137] 21 p3019 N88-27921
Anharmonic model for high-Tc superconductors
[DE88-702196] 21 p3020 N88-27924

LANTHANUM OXIDES
Superconductivity in La/sub 1.85-x/Nd/sub x/Sr/sub .15/CuO
[DE88-003014] 09 p1258 N88-17540
Single-crystal structural study of La2Cu/sub 0.95/Li/sub 0.05/O4
[DE88-003482] 11 p1554 N88-19302
High temperature superconductors in the La(sub 1+x)Ba(sub 2-x)Cu O(sub y system
[DE88-006367] 15 p2145 N88-22802
Comparison between muon spin rotation and neutron scattering studies on the 3-dimensional magnetic ordering of La2CuO(4-y) 17 p2396 N88-24244
Superconducting properties of LaBa2Cu3O(sub x) and YBa2Cu3O(sub y)
[DE88-012038] 21 p3024 N88-27952
Possible mechanism for high-temperature superconductivity in the BaSr-La(Y)-CuO systems
[DE88-702060] 23 p3288 N88-29576
La2CuO(sub 4 + delta): A superconducting superoxide
[DE88-010325] 23 p3288 N88-29578
Theory of superconductivity in oxides
[AD-A195647] 24 p3433 N88-30432

LANTHANUM TELLURIDES
Crystalline metal-semiconductor superlattices
[DE88-007063] 18 p2581 N88-25332

LAOS
A comparative thematic mapping analysis of SPOT data: The Vientiane Plain (Lao PDR) 22 p3096 N88-28386

LAP JOINTS
Device for measuring hole elongation in a bolted joint
[NASA-CASE-LAR-13453-1] 06 p0712 N88-14361

LAPLACE EQUATION
Contributions to a numerical library in Ada
[NPL-DITC-98/87] 09 p1219 N88-17309
Finite element mesh generation and isoparametric elements
[NPL-DITC-97/87] 09 p1229 N88-17365
Performance of a multigrid method on parallel architecture 11 p1539 N88-19200
Double layer polarization of nonconducting spheroidal particles and its application to Kerr effect
[ISSN-0208-5658] 13 p1832 N88-20960
The calculation of transonic flow over the shuttle orbiter using slender body theory 18 p2460 N88-24606
Theory of Laplacian fractals: Diffusion limited aggregation and dielectric breakdown model
[PREPRINT-590] 22 p3144 N88-28701

LAPLACE OPERATORS
U LAPLACE TRANSFORMATION

LAPLACE TRANSFORMATION
Frozen-field, rigid-beam, uniform-conductivity-channel tracking force calculation
[DE87-012510] 02 p0190 N88-11190
Numerica calculation in the Laplace domain for subsonic unsteady aerodynamic forces acting on a finite wing 05 p0535 N88-13256
Symbolic, algebraic, and numeric solutions to heat conduction problems using Green's functions 09 p1165 N88-16987
Free Laplacian with attractive boundary conditions
[DE87-702971] 16 p2256 N88-23482

LARGE SCALE INTEGRATION
Introducing new technology into onboard handling systems 09 p1124 N88-16733
Characteristics of LSI-wiring expert system discussed 15 p2052 N88-22226
Progress and challenges in HEMT LSI technology 19 p2656 N88-25779
Diffraction by a simple deep phase object — integrated circuit measurement
[RSRE-MEMO-4039] 22 p3070 N88-28224

LARGE SPACE STRUCTURES
Assessment of the COFSI/MAST I project
[NASA-CR-181366] 01 p0053 N88-10340
A DMAP for updating dynamic mathematical models with measured data
[NLR-MP-86027-U] 01 p0060 N88-10387
Recent advances in structural dynamics of large space structures
[NASA-TM-100513] 02 p0138 N88-10867
Structural Assembly Demonstration Experiment (SADE)
[NASA-CR-179205] 02 p0138 N88-10868
Experimental assembly of structures in EVA: Hardware morphology and development issues 02 p0139 N88-10872
Marshall Space Flight Center's role in EASE/ACCESS mission management 02 p0139 N88-10875
A monograph of the National Space Transportation System Office (NSTSO) integration activities conducted at the NASA Lyndon B. Johnson Space Center for the EASE/ACCESS payload flown on STS 61-B 02 p0139 N88-10876
Research and development at the Marshall Space Flight Center Neutral Buoyancy Simulator 02 p0139 N88-10878
A synopsis of the EVA training conducted on EASE/ACCESS for STS-61-B 02 p0140 N88-10879
Results of the ACCESS experiment 02 p0140 N88-10880
EASE (Experimental Assembly of Structures in EVA) overview of selected results 02 p0140 N88-10881
Overview of crew member energy expenditure during Shuttle Flight 61-B EASE/ACCESS task performance 02 p0140 N88-10882
Pinhole occulter experiment
[NASA-CR-179206] 02 p0235 N88-11481
Control design challenges of large space systems and spacecraft control laboratory experiment (SCOLE)
[NASA-CR-178392] 03 p0275 N88-11735
Adaptive control of Large Space Structure (LSS)
[ISAS-R-621] 03 p0276 N88-11740
Wavefront error sensing
[NASA-CR-181504] 03 p0321 N88-12030

Stochastic model of the NASA/MSFC ground facility for large space structures with uncertain parameters: The maximum entropy approach
[NASA-CR-181489] 03 p0372 N88-12343
New feedback design methodologies for large space structures: A multi-criterion optimization approach
04 p0408 N88-12535
Computational methods for problems in aerodynamics and large space structure using parallel and vector architectures
[AD-A185401] 05 p0541 N88-13294
Survey on large scale system control methods
[NASA-CR-181556] 05 p0554 N88-13374
Design of low order controllers for robust disturbance rejection in large space structures
[AD-A185202] 05 p0555 N88-13376
Modeling and control of large flexible vehicles in the atmosphere and space
[AD-A185368] 05 p0555 N88-13377
Potential for on-orbit manufacture of large space structures using the pultrusion process
[NASA-TM-4016] 05 p0557 N88-13388
Optimal control of large space structures via generalized inverse matrix
[NASA-CR-182336] 05 p0639 N88-13907
Approaches and possible improvements in the area of multibody dynamics modeling
[NASA-CR-179227] 06 p0663 N88-14067
Investigation of design concepts for large space structures to support military applications
[AD-A186098] 07 p0824 N88-15000
Natural frequencies and structural integrity assessment of large space structures
[AD-A186139] 07 p0824 N88-15001
Wave propagation experiments on 22-bay lattice
[AD-A186140] 07 p0824 N88-15002
Maximum entropy/optimal projection design synthesis for decentralized control of large space structures
[AD-A186359] 07 p0824 N88-15003
Large-angle slewing maneuvers for flexible spacecraft
[NASA-CR-4123] 08 p1000 N88-16060
Emulating a flexible space structure: Modeling
[NASA-TM-100320] 09 p1135 N88-16812
Optimized structure design using reanalysis techniques 09 p1180 N88-17067
Sensitivity of active vibration control to structural changes and model reduction 10 p1284 N88-17683
Formulation methods of rigid multibody systems for large space structures and some results of computer simulation
[NAL-TR-942] 10 p1293 N88-17730
Preliminary investigation of stability of a fin-stiffened slender strut
[NASA-TM-4034] 12 p1599 N88-19568
Cost effective development of a national test bed
[NASA-TM-100321] 12 p1601 N88-19585
Workshop on Technology Development Issues for the Large Deployable Reflector (LDR)
[NASA-CP-2407] 12 p1710 N88-20235
Robust decentralized control of large flexible structures
[DE88-005416] 13 p1824 N88-20902
A sequentially deployable structure for space applications 14 p1875 N88-21202
Optimal control and identification of space structures
[AD-A190033] 15 p2025 N88-22065
Wave propagation and dynamics of lattice structures
[AD-A190037] 15 p2025 N88-22066
Feedback control of distributed parameter systems with applications to large space structures
[AD-A190536] 15 p2025 N88-22068
Wave propagation and dynamics of lattice structures
[AD-A190611] 15 p2025 N88-22069
Vibrations of structures with parametric uncertainties
[AD-A190400] 15 p2076 N88-22378
Travelling wave concepts for the modeling and control of space structures
[AD-A191235] 17 p2310 N88-23819
Soviet spacecraft engineering research
[FASAC-TAR-3090] 17 p2311 N88-23823
LDR structural experiment definition
[NASA-TM-100618] 17 p2312 N88-23826
Space spider crane
[NASA-CASE-LAR-13411-1-SB]
17 p2312 N88-23828
Continuum modeling and dynamic analysis of large truss structures 17 p2349 N88-23995
Electromagnetic damping and vibration isolation of space structures
[AD-A191492] 18 p2471 N88-24665
Estimation and control of distributed models for certain elastic systems arising in large space structures
[AD-A192120] 18 p2472 N88-24666
Low authority control of large space structures using a constrained threshold control formulation
18 p2472 N88-24667
Experimental study of active vibration control
[AD-A191454] 18 p2526 N88-24989
Large antenna experiments aboard the space shuttle: Application of nonuniform sampling techniques
19 p2652 N88-25745
The 15-meter antenna performance optimization using an interdisciplinary approach 19 p2652 N88-25746
Adaptive residual mode filter control of distributed parameter systems for large space structure applications
19 p2719 N88-26143
L(sub infinity symbol)-approximations of complex functions and robust controllers for large flexible space structures
[PB88-186226] 20 p2764 N88-26390
Mobile remote manipulator system for a tetrahedral truss
[NASA-CASE-MSC-20985-1] 20 p2765 N88-26398
Experimental and theoretical investigation of passive damping concepts for member forced and free vibration
[NASA-CR-183082] 20 p2814 N88-26693
Spacecraft applications of advanced global positioning system technology
[NASA-CR-172055] 21 p2894 N88-27180
Technology for large space systems: A bibliography with indexes (supplement 18)
[NASA-SP-7046(18)] 21 p2901 N88-27214
Vibration control of large structures
[AD-A193317] 21 p2961 N88-27587
Sensor and actuator selection for large space structure control
[AD-A194912] 24 p3333 N88-29842
Space structure (dynamics and control) theme development
[NASA-TM-100597] 24 p3335 N88-29850
Theory of filtering and control with application to control of large space structures
[AD-A195500] 24 p3335 N88-29851
Clevis joint for deployable space structures
[NASA-CASE-LAR-13898-1] 24 p3380 N88-30130
Robust design of distributed controllers for large flexible space structures
[NASA-CR-183202] 24 p3380 N88-30134

LARGE SPACE TELESCOPE
U HUBBLE SPACE TELESCOPE

LARVAE
Embryogenesis and organogenesis of Carausius morosus under spaceflight conditions
22 p3061 N88-28167

LARYNX
NT GLOTTIS
Visualization of the air flowing through a dynamic model of the vocal folds
[ISVR-TR-154] 14 p1952 N88-21634

LASER ALTIMETERS
Considering refraction in leveling with laser plane
04 p0462 N88-12857
A computer code to process and plot laser altimetry data interactively on a microcomputer
[NASA-TM-100687] 05 p0554 N88-13371

LASER ANEMOMETERS
Optical flow diagnostic measurements in turbomachinery
[PNR90396] 02 p0172 N88-11081
The four spot time-of-flight laser anemometer
02 p0184 N88-11145
Three-dimensional calculation in high subsonic axial compressor rotor and its comparison with L2F velocity measurement 03 p0300 N88-11886
A FORTRAN code for the calculation of probe volume geometry changes in a laser anemometry system caused by window refraction
[NASA-TM-100210] 03 p0364 N88-12288
Turbulence measurement in hypersonic flow
05 p0530 N88-13224
Optical measurement systems
08 p0955 N88-15796
Correlation and spectral density measurements by LDA --- flow measurement
[ISL-CO-244/86] 14 p1910 N88-21412
Matched index laser anemometry systems for flow studies in complex geometries 16 p2203 N88-23145
Laser Doppler anemometry
[NASA-TM-100072] 16 p2210 N88-23187
Study of the local behavior of a flame
[ETN-88-92300] 20 p2771 N88-26433

LASER ANNEALING
Nondestructive magnetic testing of laser hardening parameters (hardening depth, hardness profile, retained austenite)
[ETN-88-91070] 09 p1144 N88-16857
Laser spectroscopy investigations of materials for solid state laser systems
[AD-A192514] 21 p2952 N88-27535

LASER APPLICATIONS
NT LASER CUTTING
NT LASER FUSION
Experimental investigation in a wind tunnel of the stability and vorticity of the vortex breakdown phenomenon above delta wings, using the ultrasonic laser method
[DFVLR-FB-87-06] 01 p0003 N88-10017
Low temperature deposition by laser induced breakdown in the vapor phase
[DE87-007509] 01 p0024 N88-10151
Laser chemically vapor deposited silicon-carbide: Growth features, topography, microstructure, and composition
[DE87-013767] 01 p0029 N88-10184
A high-voltage multistage laser-triggered gas switch
[DE87-011725] 01 p0040 N88-10253
Monocrystalline silicon gradiometer for gravity experiments in space
[NASA-CR-181452] 01 p0050 N88-10321
KR+ laser excitation of NH2 in atmospheric pressure flames
[AD-A183421] 01 p0050 N88-10322
Diode pumped solid-state laser oscillators for spectroscopic applications
[NASA-CR-180576] 01 p0052 N88-10331
Mid infrared LHS system packaging using flexible waveguides
[NASA-CR-181192] 01 p0093 N88-10607
Improving coherent visualization by means of film optical filtering --- projectile visualization
[ISL-R-116/86] 02 p0176 N88-11097
Method for single-shot measurement of picosecond laser pulse-lengths without electronic time dispersion
[DE87-013171] 02 p0178 N88-11107
A study of the performance of airborne laser radar systems and techniques
[ETN-87-90928] 02 p0179 N88-11117
Description of a multiframe optical probing system
[DE87-014255] 02 p0236 N88-11487
JPRS report: Science and technology. China
[JPRS-CST-87-026] 03 p0269 N88-11688
China report: Science and technology
[JPRS-CST-87-015] 03 p0298 N88-11873
JPRS report: Science and technology. China
[JPRS-CST-87-025] 03 p0300 N88-11888
Study of IR laser photoacoustic spectra of organic molecules adsorbed on metal surface
03 p0301 N88-11891
Ultra-short pulse laser system used for lageos range finding 03 p0301 N88-11893
Performance and operating envelope of imaging and scattering particle sizing instruments
[NASA-CR-180859] 03 p0323 N88-12042
JPRS Report: Science and Technology. China
[JPRS-CST-87-033] 03 p0326 N88-12062
Single-periodic multilayer grating laser Doppler vibrometer 03 p0327 N88-12066
Laser sources today and tomorrow
[DE87-014247] 03 p0330 N88-12083
Optical laser technology, specifically CD-ROM (Compact Disc - Read Only Memory) and its application to the storage and retrieval of information
[AD-A184111] 03 p0330 N88-12086
A simplified CARS measurement system for rapid determination of temperature and oxygen concentration
[NASA-TM-100498] 03 p0374 N88-12353
High efficiency generation of 130-nm radiation from sum-frequency mixing in Hg
[DE87-013714] 04 p0431 N88-12674
Lasers measure atmosphere
04 p0461 N88-12849
Multiwave laser soundings of atmospheric aerosol: Experimental research (review)
04 p0461 N88-12852
JPRS report: Science and technology. USSR: Life sciences
[JPRS-ULS-87-009] 04 p0473 N88-12915
Theoretical plasma physics
[DE88-001475] 04 p0492 N88-13029
An ultra-high-speed cinematographic method for the study of wakes in hypersonic ballistic ranges
05 p0531 N88-13228
Master plots for predicting the case-depth in laser surface treatments
[PB87-221875] 05 p0586 N88-13574
Measurement of particle size distribution in a solid propellant rocket motor using light scattering
[AD-A184875] 06 p0673 N88-14124
Recording materials for optical disk memory discussed
06 p0684 N88-14193
JPRS report: Science and technology. Japan
[JPRS-JST-87-027] 06 p0688 N88-14213
Developments in optical sensor technologies described 06 p0689 N88-14220
Laser development, evolution of applied technologies described 06 p0689 N88-14221
Status, outlook of optical technology in information equipment field 06 p0689 N88-14222

USSR report: Physics and mathematics
[JPRS-UPM-87-006] 06 p0708 N88-14344
Uses of airborne laser Chayka-1 for probing water, land surfaces 06 p0725 N88-14461
Super-short yttrium aluminate pulse generator with controlled resonator Q-factor 06 p0772 N88-14740
Nonuniformity of electromagnetic field at Lambda = 10.6 micron wavelength inside atmospheric aerosol particles 06 p0772 N88-14743
Development of crack under periodically pulsed laser radiation 06 p0774 N88-14754
Analysis of laser extracted volatiles in carbonaceous chondrites 06 p0793 N88-14861
Lawrence Livermore National Laboratory Soft X-ray Laser Program
[DE88-001888] 07 p0859 N88-15218
Intracavity spectrum analyzer with NaF:F2(+):F3(-) crystal laser for long-wave IR wave band 07 p0919 N88-15584
Laser thermal propulsion
[AD-A186407] 07 p0933 N88-15666
The application of photoconductive detectors to the measurement of X-ray production in laser produced plasmas
[DE88-001630] 07 p0934 N88-15671
Laser transformation hardening of precision V-slide way
[PB87-144028] 08 p0991 N88-15999
Laser system for automating topographic terrain survey 08 p1012 N88-16136
High-speed assembly language (80386/80387) programming for laser spectra scan control and data acquisition providing improved resolution water vapor spectroscopy
[NASA-CR-4117] 08 p1053 N88-16355
Pulsed laser stereophotography of plasmas and dynamically moving surfaces
[DE88-003170] 09 p1173 N88-17031
Laser simulation of light and plasma action on comets and planets 09 p1237 N88-17413
Energy transmission using coherent, quasimonochromatic light beams 09 p1241 N88-17436
Solid antimatter
[PB87-166146] 09 p1259 N88-17549
Laser investigations for payload G-652 prior to filing pre-flight accommodation requirements 10 p1286 N88-17694
High resolution electron and ion microscopy
[AERE-R-12502] 10 p1297 N88-17754
A ring model of the lasertron
[DE88-004656] 10 p1323 N88-17908
Digital imaging techniques for single- and multi-phase reacting flowfields 10 p1327 N88-17933
Monitoring interfacial dynamics by pulsed laser techniques
[DE88-003362] 10 p1335 N88-17976
Overview of applications of Laser-Induced Breakdown Spectroscopy (LIBS)
[DE88-004314] 10 p1336 N88-17987
Optically controlled devices and ultrafast laser sources for signal processing
[AD-A187417] 10 p1338 N88-17995
Evaluation of a temperature remote sensing technique
[AD-A187885] 10 p1347 N88-18053
A laser communication experiment utilizing the ACT satellite and an airborne laser transceiver
[NASA-TM-100792] 11 p1492 N88-18910
The Quick Response Multicolor Printer (QRMP) system
[AD-A188140] 11 p1504 N88-18982
JPRS report. Science and technology: Europe and Latin America
[JPRS-ELS-87-054] 12 p1573 N88-19406
JPRS report. Science and technology: Europe and Latin America
[JPRS-ELS-87-055] 12 p1686 N88-20086
Optically stimulated sound from gas bubbles in water 12 p1686 N88-20087
Molecular dynamics of laser ablation of a polymer coating
[DE88-004337] 13 p1750 N88-20466
Studies of compound states of negative ions using laser beams
[DE88-004708] 13 p1777 N88-20627
Noncontact thermometry via laser pumped, thermographic phosphors: Characterization of systematic errors and industrial applications
[DE88-005599] 13 p1777 N88-20628
Low threshold ridge waveguide single quantum well lasers 13 p1777 N88-20631
Study of photochromic materials for use in optical signal processing
[AD-A189068] 13 p1839 N88-21006
Vortex flow over a delta wing with apex flaps using laser flow visualisation
[BU-356] 14 p1862 N88-21121
Influence of hydrogen on crack formation tendency in heat-affected zone with stress concentrator 14 p1887 N88-21276
Measurement of species concentrations in flames by laser-induced fluorescence
[DE88-007096] 14 p1889 N88-21286
JPRS report: Science and technology. China
[JPRS-CST-87-038] 14 p1901 N88-21350
Applications of lasers to semiconductor studies 14 p1901 N88-21356
JPRS report: Science and technology. China
[JPRS-CST-87-041] 14 p1902 N88-21365
Laser surface melting
[BMFT-FB-T-86-072] 14 p1914 N88-21435
Lasers: Invention to application
[PB88-161583] 14 p1914 N88-21436
Lidar active remote sensing. Applications to the atmosphere 14 p1936 N88-21547
Optical cooling and trapping 14 p1974 N88-21782
Optical trapping of neutral atoms and dielectric particles by radiation pressure 14 p1974 N88-21783
Laser cooling of neon metastable states 14 p1975 N88-21785
Femtosecond studies in hot carrier relaxation in GaAs and AlGaAs 14 p1977 N88-21801
Diode laser spectroscopy of chemical moieties at surfaces
[AD-A190710] 15 p2036 N88-22127
Laser enhanced adhesion of copper films to sapphire substrates
[DE88-006802] 15 p2038 N88-22144
Laser photodeposition and etching study
[AD-A190535] 15 p2040 N88-22153
Oxide optical coatings prepared by metal-organic vapor deposition
[DE88-006809] 15 p2043 N88-22175
JPRS report: Science and technology. Japan
[JPRS-JST-88-002] 15 p2050 N88-22210
Laser processing-status, perspectives 15 p2050 N88-22211
Compound ceramic processing 15 p2050 N88-22212
Fine grain development by laser CVD 15 p2050 N88-22214
Material surface improvement by laser 15 p2051 N88-22217
Laser evaporation studies
[AD-A189815] 15 p2071 N88-22346
Research on certain aspects of laser diffraction particle sizing relevant to autonomous self-diagnosing instrumentation
[AD-A190220] 15 p2071 N88-22348
A laser-based photoacoustic spectrometer for direct breath C-13O2/C-12O2 measurement
[DE88-004915] 15 p2101 N88-22516
Activities report in laser-matter interaction
[ETN-88-92007] 15 p2129 N88-22696
Characteristics of distributed feedback lasers discussed 16 p2185 N88-23028
Three-dimensional flow visualization using laser-sheet scanning 16 p2203 N88-23143
Comparison of electrically driven lasers for space power transmission
[NASA-TM-4045] 16 p2212 N88-23197
Laser induced ignition of propellants
[AD-A191099] 16 p2213 N88-23206
Laser cladding of Ni, Nb and Mg alloys for improved environmental resistance at high temperature
[AD-A191274] 16 p2213 N88-23208
Proceedings of the Cooling, Condensation, and Storage of Hydrogen Cluster Ions Workshop
[AD-A189857] 16 p2266 N88-23555
Pusherless implosion, pulse tailoring and ignition scaling law for laser fusion 16 p2277 N88-23629
Efficient shell implosion and target design 16 p2277 N88-23630
Research on anode plasma behavior of flashover pulsed ion sources 16 p2279 N88-23640
Laser pyrometry 17 p2330 N88-23910
Noncontact true temperature measurement, 2 17 p2330 N88-23911
Laser Diagnostics for combustion temperature and species measurements 17 p2330 N88-23912
Research investigation directed toward extending the useful range of the electromagnetic spectrum
[AD-A190198] 17 p2332 N88-23920
Research investigation directed toward extending the useful range of the electromagnetic spectrum, appendix
[AD-A190199] 17 p2332 N88-23921
Cascade fluorescences from laser-excited lithium atom for plasma diagnostics 17 p2442 N88-24526
Flux density measurements of neutral iron in TEXTOR with laser induced fluorescence 17 p2442 N88-24528
Isotope separation using tuned laser and electron beam
[NASA-CASE-NPO-16907-1-CU] 18 p2483 N88-24732
Bibliography of Soviet laser developments, number 83, May - June 1986
[AD-A190969] 18 p2520 N88-24950
Optical diagnostics for a high power, rf-inductively coupled plasma
[DE88-007822] 18 p2579 N88-25322
Propellant combustion response to oscillatory radiant heat flux 19 p2628 N88-25589
Minimum ignition energy measurements using laser induced spark initiation 19 p2632 N88-25610
Laser-RDX aerosol pyrolysis with matrix isolation of unstable intermediates 19 p2632 N88-25614
Organization of a Topical Meeting on Picosecond Electronics and Optoelectronics
[AD-A187136] 19 p2655 N88-25765
Picosecond electrical pulses for VLSI electronics characterization 19 p2655 N88-25768
A mass spectrometer for the analysis of thermally labile compounds 19 p2668 N88-25859
Asynchronous optical sampling for laser-based combustion diagnostics in high pressure flames
[AD-A192920] 20 p2770 N88-26428
Interferometric recording of holographic optical elements using partially coherent light 20 p2805 N88-26636
Study of feasibility and optimization conditions of laser treatments: Application of the local recrystallization of aluminum
[ISAL-87-0048] 21 p2916 N88-27309
Attachable interferometric strain gages
[AD-A192390] 21 p2950 N88-27522
Measurement of pressure fluctuations in a resonant chamber with laser-induced iodine fluorescence
[DFVLR-FB-87-53] 21 p2955 N88-27551
Laser and electrochemical studies of metallizations in electronic devices
[AD-A193786] 23 p3208 N88-29090
Flow visualization by laser sheet
[AD-A194481] 23 p3211 N88-29111
N2(A3epsilon u+) by reaction of N2F4+H2 in a supersonic flow
[AD-A194493] 23 p3219 N88-29163
Optical measurements of soot and temperature profiles in premixed propane-oxygen flames
[NASA-TM-101343] 24 p3358 N88-29997
Optical measurements of soot in premixed flames
[NASA-TM-101305] 24 p3373 N88-30090
Spontaneous force optical traps
[AD-A196103] 24 p3377 N88-30114
Bibliography of Soviet laser developments, number 88, March - April 1987
[AD-A195978] 24 p3378 N88-30116
Laser sensing for identification and control of distributed parameter systems
[AD-A195886] 24 p3379 N88-30124

LASER BEAM DEFOCUSING
U THERMAL BLOOMING

LASER BEAMS
Laser CO2/TEA frequency-stabilized by phase conjugation 22 p3082 N88-28303
Application of optical correlation techniques to particle imaging velocimetry
[NASA-TM-101306] 23 p3218 N88-29152

LASER CAVITIES
JPRS report: Science and technology. China
[JPRS-CST-87-034] 03 p0301 N88-11897
Measuring stability of optical reference cavities by analyzing polarization spectrum 03 p0327 N88-12065
Nonconventional optical techniques for optical wavefront processing
[AD-A185099] 05 p0650 N88-13982
Active medium formation in lasers using mixtures of inert gases and optical breakdown pumping 06 p0709 N88-14347
Dynamic restructuring of pulsed CO2 laser frequency and multiple-peak generation in a cell with IR-absorbing gas in the resonator 07 p0919 N88-15580
Study of kinetics of intracavity absorption in pulsed dye lasers 07 p0919 N88-15585
Characteristics of LKI-501 tunable dye laser with dyes in solid matrix 07 p0920 N88-15587
High peak power Ka-band gyrotron oscillator experiments with slotted and unslotted cavities
[AD-A188109] 11 p1478 N88-18819
Soft X-ray beamsplitters and highly dispersive multilayer mirrors for use as soft X-ray laser cavity components
[DE88-004003] 11 p1549 N88-19270

Fiber-coupled external-cavity semiconductor high power laser
[AD-A188454] 13 p1774 N88-20611
Resonator coupling of two ring cavity, argon-ion lasers
[AD-A189558] 13 p1775 N88-20616
JPRS report: Science and technology. China
[JPRS-CST-87-038] 14 p1901 N88-21350
A picosecond tunable ultrashort cavity dye laser
14 p1902 N88-21361
Generation of tunable coherent radiation in 3 micrometers-5 micrometers region using semiconductor lasers in external cavities
[AD-A190860] 16 p2212 N88-23202
Mode locking of semiconductor laser with external cavity
[AD-A196018] 24 p3378 N88-30117

LASER COMMUNICATION
U OPTICAL COMMUNICATION

LASER CUTTING
Geometry and reproducibility of a plasma-supported removal of material by laser radiation
[ETN-87-90436] 01 p0052 N88-10335
Diffraction effects during materials treatment with laser beams
[ETN-87-90614] 03 p0328 N88-12075
Laser programming integrated circuits
[AD-A189590] 13 p1762 N88-20537

LASER DAMAGE
Optical damage in polymers by millisecond light pulses
[DE87-013106] 02 p0151 N88-10943
Long-range pulselength scaling of 351nm laser damage thresholds
[DE87-014754] 04 p0448 N88-12777
Dependence of acoustical characteristics of laser-induced breakdown in dielectric materials on shape of inelastic region 06 p0774 N88-14753
On 1064 nm and 350 nm laser damage thresholds of high index oxide films deposited from organic solutions and sols
[DE88-001636] 07 p0859 N88-15217
Dielectric behavior of electromagnetic (EM) windows materials irradiated by a CW CO2 high-power laser --- hypersonic/reentry vehicles
[ISL-CO-239/86] 09 p1154 N88-16913
Psychophysical, biochemical and histological studies of spectrally selective photic damage to primate retina
[AD-A188115] 11 p1517 N88-19063
Causes of damage in multilayer dielectric coatings exposed to high average power visible laser radiation
[DE88-005363] 13 p1775 N88-20619
Database of average-power damage thresholds at 1064 nm
[DE88-004352] 13 p1776 N88-20626
Protection against laser damage to human body reviewed 15 p2053 N88-22237
A preliminary comparison of the transient effects of single versus multiple q-switched doubled-neodymium laser pulses
[AD-A189855] 15 p2071 N88-22347
Advanced programming and control techniques for complex mechanical systems
[AD-A190238] 15 p2071 N88-22349
A comparison of visual evoked potential and behavioral measures of flashblindness in humans
[AD-A189757] 15 p2101 N88-22519
New acousto-ultrasonic techniques applied to aerospace materials
[NASA-TM-101299] 22 p3086 N88-28323
Spallation and dynamic fracture as an effect of laser induced shock-waves
[AD-A193513] 23 p3188 N88-28971
Functional assessment of laser irradiation
[AD-A195735] 24 p3408 N88-30287

LASER DOPPLER VELOCIMETERS
Laser Doppler measurements in a turbulent free jet
[ESA-TT-1067] 03 p0315 N88-11994
Methods for a coherent CO2 laser heterodyne radar system
[ESA-TT-1035] 03 p0328 N88-12076
A FORTRAN code for the calculation of probe volume geometry changes in a laser anemometry system caused by window refraction
[NASA-TM-100210] 03 p0364 N88-12288
Determination of a flow velocity field using four-exposure laser holography
[IMFL-3114-85/32] 05 p0585 N88-13565
Hot wire and laser velocimeter studies of turbulent flow at supersonic velocities
[ETN-88-91172] 05 p0585 N88-13566
Dual cylindrical wave Laser-Doppler method for measurement of skin friction in fluid flow
06 p0700 N88-14297
Dual mode laser velocimeter
[NASA-CASE-ARC-11634-1] 06 p0709 N88-14350
Velocity interferometry in shock tubes and shock tunnels
[ISL-CO-203/87] 09 p1122 N88-16713
Investigation of dynamic stall using LDV (Laser Doppler Velocimetry): Mean flow studies
[AD-A187629] 10 p1272 N88-17611
Laser velocimeter measurements of solids in multiphase flow
[DE88-000196] 11 p1487 N88-18876
New monostatic balanced Doppler velocimeter using a polarization preserving fiber
[PB88-130869] 11 p1490 N88-18895
Laser fluorescence velocimeter
[AD-A189010] 12 p1630 N88-19753
Laser Doppler velocimetry primer
[NASA-CR-177386] 12 p1631 N88-19761
Inflow measurement made with a laser velocimeter on a helicopter model in forward flight. Volume 2: Rectangular planform blades at an advance ratio of 0.23
[NASA-TM-100542] 14 p1864 N88-21139
Correlation and spectral density measurements by LDA --- flow measurement
[ISL-CO-244/86] 14 p1910 N88-21412
Laser velocimeter measurements in a wing-fuselage type juncture
[NASA-TM-100588] 15 p2014 N88-22012
Inflow measurement made with a laser velocimeter on a helicopter model in forward flight. Volume 3: Rectangular planform blades at an advance ratio of 0.30
[NASA-TM-100543] 15 p2015 N88-22015
Unsteady flow field measurements using LDV (Laser Doppler Velocimetry)
[AD-A189907] 15 p2063 N88-22298
Instruments for use in experimental studies of complex turbulent shear flow: Three component LDVs
[AD-A190526] 15 p2065 N88-22312
Inflow measurements made with a laser velocimeter on a helicopter model in forward flight. Volume 4: Tapered planform blades at an advance ratio of 0.15
[NASA-TM-100544] 16 p2156 N88-22863
Flow measurements in a water tunnel using a holocinematographic velocimeter
16 p2203 N88-23141
Experimental studies of vortex flows
[NASA-CR-182874] 16 p2207 N88-23171
Inflow measurement made with a laser velocimeter on a helicopter model in forward flight. Volume 5: Tapered planform blades at an advance ratio of 0.23
[NASA-TM-100545] 17 p2299 N88-23755
Inflow measurements made with a laser velocimeter on a helicopter model in forward flight. Volume 1: Rectangular planform blades at an advance ration of 0.15
[NASA-TM-100541] 18 p2460 N88-24607
Propellant combustion response to oscillatory radiant heat flux 19 p2628 N88-25589
Influence of rear body geometry on the velocity characteristics of the near wake
[ISL-R-113/87] 20 p2753 N88-26339
Experiments on densely-loaded non-Newtonian slurries in laminar and turbulent pipe flows
[DE88-010579] 20 p2800 N88-26612
Study of flow tracer behavior models and experimental validation with multiple exposure holographic velocimetry
[IMFL-87/30] 20 p2801 N88-26622
A microcomputer based frequency-domain processor for laser Doppler anemometry
[NASA-TM-100998] 20 p2803 N88-26634
Laser-Doppler measurements of turbulence structures in free streams behind flat and rotation symmetrical profiles
[ETN-88-92336] 21 p2948 N88-27510
Velocity measurements downstream of a sudden expansion using the Laser Doppler Velocimeters (LDV) technique. Part 1: Method of measurement and experimental facility
[FOA-C-20700-2.1-PT-1] 22 p3076 N88-28262
Hot-wire measurements of compressor blade wakes in a cascade wind tunnel
[AD-A194737] 23 p3181 N88-28936
Three-dimensional laser Doppler velocimeter studies of flow in a 90 deg curved duct having a square cross-section 23 p3209 N88-29101
Construction of a laser Doppler anemometer and its use for the testing of a novel probe for the measurement of the variations of the lateral component of the vortex vector
[MPIS-13/1987] 23 p3217 N88-29147
Laser Doppler Velocimeter (LDV) and pressure measurements of gas particle flows in bends
[VKI-TN-163] 24 p3372 N88-30083

LASER FUSION
Laser-plasma-interaction experiments using multikilojoule lasers
[DE87-013483] 01 p0100 N88-10658
Investigation of the structure of coatings of self fluxing alloys fused by laser energy
[BLL-M-37301-(5828.4)] 02 p0148 N88-10930
LLE Review, volume 30
[DE87-014469] 02 p0178 N88-11109
X-ray emission from high-Z spherical laser plasmas: Implications for plasma dynamics
[DE87-014722] 02 p0239 N88-11506
Interplanetary propulsion using inertial fusion
[NASA-TM-89661] 04 p0409 N88-12540
Thermal stress in the edge cladding of Nova glass laser disks
[DE88-000425] 04 p0448 N88-12780
Inertial confinement fusion reactor cavity analysis
[DE88-000788] 04 p0492 N88-13028
Theory of induced spatial incoherence
[AD-A185005] 05 p0651 N88-13992
The Rayleigh-Taylor instability in ablatively accelerated targets with 1, 1/2 and 1/4 micrometers laser light
[AD-A185945] 07 p0858 N88-15208
High Z interaction physics on Nova
[DE88-004397] 10 p1413 N88-18433
Smoothing technique to resolve X-ray spectra in laser nuclear fusion 15 p2053 N88-22235
Magic light high-power laser passes state certification
15 p2053 N88-22236
Coronal fluid-dynamics in laser fusion
16 p2278 N88-23634
Finite ion-relaxation and nonequilibrium radiation effects on laser-driven implosions 16 p2278 N88-23636
Interplanetary propulsion using inertial fusion
17 p2401 N88-24273

LASER GEODYNAMIC SATELLITE
U LAGEOS (SATELLITE)

LASER GUIDANCE
Range imagery algorithms for the detection of obstacles by autonomous vehicles
[AD-A185421] 05 p0659 N88-14045
Optics: Perspectives for Measurement Techniques and Signal Processing for Flight Guidance --- conference
[DFVLR-MITT-87-21] 18 p2516 N88-24928
Tracking a monochromatic light source
[DE88-011260] 20 p2807 N88-26653

LASER GYROSCOPES
Test equipment with fiber optic data bus and laser gyro strapdown system LTN-90 for the helicopter BO-105
[ESA-TT-1038] 01 p0005 N88-10025
Investigation of the fabrication parameters of laser mirrors with hard oxide interference coatings
[ESA-TT-1064] 03 p0329 N88-12077
Study on a unidirectional ring laser gyro. Part 1: Proposition of the principle and studies on the components
[NAL-TR-933] 09 p1169 N88-17010
Laser gyro attitude control system feasibility
[AD-A189368] 13 p1720 N88-20285
Principles of a low-cost laser gyro for rotating vehicles and platforms
[DFVLR-MITT-87-15] 14 p1912 N88-21425
Optimization of metal-dielectric laser mirrors of TiO2/SiO2 and silver
[ESA-TT-1068] 16 p2212 N88-23199
Concepts for a laser gyroscope of the highest precision 18 p2517 N88-24929
Laser gyroscopes using the rate-bias technique
18 p2517 N88-24930
Development of mirrors for high-precision laser gyroscopes 18 p2517 N88-24931
Laboratory tests of laser gyroscopes for future utilization in multifunction systems for precision navigation and flight guidance 18 p2517 N88-24932
Precision measurement of the Fresnel drag coefficient using a ring laser
[AD-A196025] 24 p3366 N88-30043

LASER HEATING
Mechanisms in thermal mechanical forming of plates
[AD-A187797] 11 p1466 N88-18744
Effect of experimental variables on flash thermal diffusivity data analysis
[DE88-003631] 11 p1487 N88-18877
Particle simulation research by plasma parametric heating caused by strong laser
14 p1903 N88-21368
Laser surface melting
[BMFT-FB-T-86-072] 14 p1914 N88-21435
Superfine grain development by laser
15 p2050 N88-22215
Material surface improvement by laser
15 p2051 N88-22217
Laser-RDX aerosol pyrolysis with matrix isolation of unstable intermediates 19 p2632 N88-25614
Laser-heated CVD process for depositing thin films for low-cost solar-cell applications
[DE88-001162] 21 p2967 N88-27623

LASER INDUCED FLUORESCENCE

Design study for measurement of neutral hydrogen atom density by laser induced fluorescence method
[DE87-752964] 02 p0179 N88-11114

Laser induced fluorescent study of relativistic electron beams
[AD-A184456] 04 p0447 N88-12774

Calibration of a laser-pumped, thermographic phosphor remote thermometry system
[DE88-000452] 04 p0449 N88-12781

Nitrogen energy transfer study
[AD-A184457] 04 p0464 N88-12869

Laser probes of propellant combustion chemistry
[AD-A184854] 05 p0581 N88-13415

Studies of supersonic turbulence and hot-wire response using Laser-Induced Fluorescence (LIF)
06 p0664 N88-14072

The kinetics and dynamics of iodine monofluoride formation in gas-phase collisions
[AD-A185715] 06 p0709 N88-14352

The use of chlorophyll fluorescence measurements from space for separating constituents of sea water. Volume 1: Summary
[ESA-CR(P)-2444-VOL-1] 07 p0873 N88-15294

The use of chlorophyll fluorescence measurements from space for separating constituents of sea water. Volume 2: Appendices
[ESA-CR(P)-2444-VOL-2] 07 p0873 N88-15295

O2-I laser (Oxygen-iodine) mixing studies using LIF (Laser Induced Fluorescence)
[AD-A186667] 09 p1171 N88-17018

The YAlO(sub 3):Er laser
[PB88-130877] 11 p1493 N88-18911

Dynamics of production and oxidation of boranes
[AD-A188988] 12 p1606 N88-19605

Laser fluorescence velocimeter
[AD-A189010] 12 p1630 N88-19753

An experimental method for species concentration measurements in a welding arc using laser-induced fluorescence
[DE88-005638] 13 p1778 N88-20636

Measurement of species concentrations in flames by laser-induced fluorescence
[DE88-007096] 14 p1889 N88-21286

Application of laser-induced fluorescence in an atmospheric-pressure boron-seeded flame
[AD-A189631] 14 p1889 N88-21287

Turbulent reacting flows and supersonic combustion
[AD-A189690] 15 p2034 N88-22115

Advanced diagnostics for reacting flows
[AD-A190485] 15 p2035 N88-22122

Visualization of flows in turbomachinery
[AD-A189927] 15 p2063 N88-22299

Instrumentation for turbulent reacting flows
[AD-A191671] 18 p2515 N88-24923

Tropospheric OH measurement by Laser Induced Fluorescence (LIF) 18 p2540 N88-25071

Quantitative use of exciplex-based vapor/liquid visualization systems, users' manual
[AD-A191649] 19 p2610 N88-25491

Developing diagnostic methods for plasma-particle interaction
[DE88-007726] 20 p2858 N88-26973

Velocity measurements and flow visualization in turbulent three-dimensional supersonic flows using oxygen flow tagging
[AD-A192551] 21 p2892 N88-27165

Laser probes of natural gas ignition chemistry
[PB88-212568] 21 p2910 N88-27271

Measurement of pressure fluctuations in a resonant chamber with laser-induced iodine fluorescence
[DFVLR-FB-87-53] 21 p2955 N88-27551

LASER INTERFEROMETRY

Microstructural effects in shock initiation of granular explosives
[DE87-011282] 01 p0031 N88-10200

Proposed studies of a 30 meter imaging interferometer concept --- spaceborne astronomy
01 p0096 N88-10627

Optical flow diagnostic measurements in turbomachinery
[PNR90396] 02 p0172 N88-11081

LLE (Laboratory for Laser Energetics) review, volume 31
[DE87-013732] 03 p0328 N88-12072

Phase-coherent astrometric interferometry
[AD-A184428] 04 p0439 N88-12725

Velocity interferometry in shock tubes and shock tunnels
[ISL-CO-203/87] 09 p1122 N88-16713

Determination of the equilibrium concentration of characteristic defects by the measurement of thermal expansion using neutron scattering and laser interferometry
[ETN-88-91489] 11 p1490 N88-18890

A rubidium-stabilised laser diode for interferometry
[NPL-MOM-85] 14 p1914 N88-21433

Laser-heterodyne interferometry with streak camera detection
[DE88-003292] 14 p1914 N88-21437

Attachable interferometric strain gages
[AD-A192390] 21 p2950 N88-27522

LASER MATERIALS

Laser sources today and tomorrow
[DE87-014247] 03 p0330 N88-12083

JPRS report: Science and technology. USSR: Life sciences
[JPRS-ULS-87-012] 03 p0355 N88-12238

400-nm photoluminescence of a color center in undoped YAG grown under reducing atmosphere
[DE88-001760] 07 p0858 N88-15213

Development of composite polymer-glass edge claddings for Nova laser disks
[DE88-002389] 07 p0860 N88-15220

Photodetachment neutralizer development: Laser window design study. Volume 2: Window design details
[DE88-000783] 09 p1170 N88-17014

JPRS report: Science and technology. USSR: Physics and mathematics
[JPRS-UPM-87-009] 09 p1233 N88-17395

Efficiency of ionic noble gas and alkali metal molecules as ultraviolet and far-ultraviolet lasers
09 p1238 N88-17419

A nuclear structure study of the proposed gamma-ray laser candidate nucleus Re-186
[DE88-004299] 10 p1336 N88-17986

Growth and characteristics of materials for tunable lasers in the near infrared spectral region
[NASA-CR-182501] 11 p1491 N88-18901

Fracture mechanisms and strengthening of slab lasers
[DE88-004002] 11 p1493 N88-18914

High power, high efficiency 770 nm laser diode array
[DE88-004043] 12 p1631 N88-19762

Reactions of N2(A(3)(SIGMA)/sub u/(+)) and candidates for short wavelength lasers
[DE88-005366] 12 p1632 N88-19767

Phosphorus oxynitride glass for laser applications
[DE88-005413] 12 p1632 N88-19768

Database of average-power damage thresholds at 1064 nm
[DE88-004352] 13 p1776 N88-20626

Design studies for a solar pumped laser device
[DFVLR-FB-87-39] 13 p1777 N88-20629

Guidelines for estimation and characterization of the thermo-mechanical properties of new optical materials
[DE88-004359] 13 p1840 N88-21010

Reactions of N2(A sup 3 sigma sup + sub u) candidates for short wavelength lasers
[DE88-007018] 15 p2070 N88-22342

Solid hosts for dye laser rods. Part 1: Criteria for choosing a host material
[DE88-006478] 15 p2072 N88-22355

Development program for 1.93-micron lasers
[NASA-CR-4148] 16 p2212 N88-23198

Laser comparison study of Nd:BEL and Nd:YAG
[AD-A191084] 16 p2213 N88-23205

Fracture of solid state lasers
[DE88-007023] 18 p2522 N88-24961

Liquid crystal optics for laser systems
[DE88-008475] 20 p2854 N88-26948

Nonlinear materials for frequency conversion
[DE88-008343] 20 p2875 N88-27067

Growth and characterization of materials for tunable lasers in the near infrared spectral region
[NASA-CR-183132] 24 p3377 N88-30113

Bibliography of Soviet laser developments, number 88, March - April 1987
[AD-A195978] 24 p3378 N88-30116

LASER MICROSCOPY

Flaw characterization in structural ceramics using scanning laser acoustic microscopy
15 p2082 N88-22415

Nondestructive evaluation of sintered ceramics
15 p2083 N88-22416

LASER MODE LOCKING

A mode-locked ruby laser with chlorophyll d as saturable absorber 03 p0327 N88-12064

Mode locking in Nd-laser by means of Gd-Sc-Ga-garnet shutter 09 p1237 N88-17412

Theoretical study of colliding pulse mode-locking in dye lasers 14 p1903 N88-21366

Laser gyroscopes using the rate-bias technique
18 p2517 N88-24930

LASER MODES

Distributed feedback effects in lasers and high gain laser instabilities in optically pumped CH3F
03 p0329 N88-12079

Lasers with wavefront-reversing mirrors (review article)
06 p0709 N88-14349

Burst mode Nd:YLF laser oscillator
[DE88-004040] 11 p1492 N88-18905

Beam quality of stable and unstable resonators: A theoretical approach
[DFVLR-FB-87-35] 14 p1982 N88-21826

Discussion of two-mode two-photon CW laser oscillation 16 p2187 N88-23042

Distributed feedback lasers
[NASA-CR-4154] 18 p2520 N88-24948

Spectral properties of semiconductor lasers with external resonators
[ETN-88-93119] 24 p3379 N88-30125

LASER OUTPUTS

Thermo-optical modeling of flashlamp-pumped zig-zag slabs
[DE87-011878] 01 p0051 N88-10326

Models of high spatial frequency thermal blooming instabilities
[DE87-014280] 01 p0052 N88-10330

High energy efficient solid state laser sources
[NASA-CR-181362] 01 p0052 N88-10332

Optical damage in polymers by millisecond light pulses
[DE87-013106] 02 p0151 N88-10943

Quantum-mechanical aspects of classically chaotic driven systems
[DE87-013152] 02 p0178 N88-11106

An acoustic emission digital data acquisition workstation
[DE87-012425] 02 p0191 N88-11191

Feasibility of alpha particle measurement in a magnetically confined plasma by CO2 laser Thomson scattering
[DE88-000039] 02 p0241 N88-11522

Ultra-short pulse laser system used for lageos range finding 03 p0301 N88-11893

Large-aperture high-efficiency frequency doubling using tandem KDP crystals 03 p0301 N88-11894

A 10 W transverse flow excimer laser
03 p0302 N88-11901

Excimer laser cell with longitudinal electron-beam excitation 03 p0302 N88-11903

Experimental study of stabilizing He-Ne laser output power with transverse magnetic field
03 p0303 N88-11906

Thrust and specific impulse of repetitively-pulsed-laser propulsion rocket 03 p0318 N88-12012

Instrument for radiation testing/screening electronic devices over an extended temperature range
[AD-A184245] 03 p0326 N88-12060

Powerful picosecond ultraviolet laser output at 354.7 nanometers 03 p0327 N88-12063

Gas dynamic characteristics in past axial flow CO2 laser 03 p0327 N88-12067

Investigation of two laser beam coupling and amplification in Ce-doped SBN single crystals
03 p0327 N88-12069

Production of atom flows at materials evaporation by laser radiation
[DE87-703327] 03 p0328 N88-12074

Distributed feedback effects in lasers and high gain laser instabilities in optically pumped CH3F
03 p0329 N88-12079

Plume mechanics and aerosol growth processes
[AD-A184467] 04 p0442 N88-12742

The lasertron RF generator for FEL (Free-Electron Laser) applications
[DE88-000515] 04 p0448 N88-12776

Low jitter laser-triggered high-voltage vacuum switch using low laser energies
[DE88-001922] 05 p0587 N88-13576

Theoretical studies of solar lasers and converters
[NASA-CR-181569] 05 p0587 N88-13577

A study of the interaction of laser light with liquid propellant drops
[AD-A185117] 05 p0587 N88-13582

An experimental study of CW HF chemical laser amplifier performance and zero power gain
[AD-A185241] 05 p0588 N88-13584

Raman microprobe characterization of dielectric films following high-energy pulsed laser irradiation
[DE88-000559] 05 p0588 N88-13587

Development of a data analysis system for the detection of lower level atmospheric turbulence with an acoustic sounder
[AD-A184972] 05 p0624 N88-13821

Repetitively pulsed and continuous wave CO2 lasers pumped by a pulsed self-sustained discharge for thermal processing 06 p0709 N88-14346

Observation of instabilities in time during dynamic self-diffraction of light in anisotropic nonhomogeneous medium 06 p0769 N88-14730

Effect of optical inhomogeneities on space coherence of radiation emitted by laser with unstable resonator
06 p0771 N88-14738

Super-short yttrium aluminate pulse generator with controlled resonator Q-factor 06 p0772 N88-14740

Periodically pulsed excimer master oscillator-regenerative amplifier laser set
06 p0772 N88-14741
Observing effect of laser radiation of low-frequency Raman scattering of light 06 p0772 N88-14742
The Rayleigh-Taylor instability in ablatively accelerated targets with 1, 1/2 and 1/4 micrometers laser light
[AD-A185945] 07 p0858 N88-15208
Laser action from syn-(methyl,methyl) bimane
[AD-A186314] 07 p0858 N88-15211
Chapter 2: Threshold for Raman conversion of FEL laser pulses in the atmosphere
[DE88-002470] 07 p0859 N88-15215
Lawrence Livermore National Laboratory Soft X-ray Laser Program
[DE88-001888] 07 p0859 N88-15218
Phase phenomena in parametric generators and amplifiers of ultrashort light pulses
07 p0918 N88-15576
Effect of multiplication of spectral components of multi-frequency lasing of pulsed tunable laser
07 p0920 N88-15586
Characteristics of LKI-501 tunable dye laser with dyes in solid matrix 07 p0920 N88-15587
Explosive absorption of laser beam of finite diameter
07 p0921 N88-15597
Characterization of Er,Cr:YSGG
[AD-A185885] 07 p0932 N88-15659
Laser thermal propulsion
[AD-A186407] 07 p0933 N88-15666
Effect of the band-gap characteristics on laser-induced dry etching of semiconductors
[DE88-001853] 07 p0937 N88-15695
Characteristics of thermooptical sound excitation in metals 08 p1076 N88-16486
Instability of strong-absorption domain in semiconductor 08 p1077 N88-16495
Stimulated Raman scattering of picosecond light pulses in long dispersive medium 08 p1078 N88-16498
Electron acceleration by laser fields in a gas
[DE88-003337] 08 p1082 N88-16523
Analysis of the decomposition of transparent polymer materials (blocks) under the action of laser beams in free generation mode
[AD-A187090] 09 p1147 N88-16873
Studies on nonlinear mechanisms of excimer laser propagation in fused silica fibers
[AD-A186822] 09 p1156 N88-16929
Comparison of UNL laser imaging and sizing system and a phase/Doppler system for analyzing sprays from a NASA nozzle
[NASA-CR-182437] 09 p1161 N88-16956
Solar pumped, alkali vapor laser
[AD-A187156] 09 p1170 N88-17016
Nuclear excitation via the motion of electrons in a strong laser field
[AD-A187166] 09 p1171 N88-17017
Investigations of solid state slab lasers
[ETN-88-91055] 09 p1171 N88-17022
Minimum necessary intensity of source of preionization for stabilization of a self-sustaining laser discharge with mean power raised by electron beam or X-rays
[PB87-178158] 09 p1171 N88-17024
Semiconductor laser with electron-beam pumping and fiber-optic output waveguide 09 p1235 N88-17405
Parametric interaction of optical modes in fiber-optic light guide 09 p1235 N88-17406
Statistics of breakdown centers appearing during propagation of laser radiation through turbulent atmosphere 09 p1236 N88-17411
High-power periodic-pulse YAG:Nd3+-laser system with telescopic unstable resonator and two-stage amplifier
09 p1237 N88-17414
Spatially resolved X-ray laser spectra and demonstration of gain in nickel-like systems
[DE88-003957] 10 p1335 N88-17979
Dynamics of coupled electron-nucleon motion in a laser field
[DE88-005063] 10 p1337 N88-17994
Evaluation of a temperature remote sensing technique
[AD-A187885] 10 p1347 N88-18053
Laser-induced desorption determinations of surface diffusion on Rh(111)
[DE88-005159] 11 p1454 N88-18667
Operation of electron-beam controlled CO2 laser at 6 atmospheres 11 p1468 N88-18758
Burst mode Nd:YLF laser oscillator
[DE88-004040] 11 p1492 N88-18905
Metastable materials by laser irradiation
[PB88-130364] 11 p1493 N88-18912
Surface free energy of laser-produced bond percolators
[PB88-130885] 11 p1493 N88-18913
Quenched-laser operation of a Littman dye oscillator
[DE88-004020] 11 p1493 N88-18915
Project SKYLITE: A design exploration
[AD-A187906] 11 p1511 N88-19030
Laser flash effects on chromatic discrimination in monkeys
[AD-A187703] 11 p1517 N88-19061
An experimental and theoretical investigation of optogalvanic effects
[AD-A189618] 12 p1625 N88-19720
Non-linear materials (TAS)
[AD-A189197] 12 p1633 N88-19775
Magnetic trapping of neutral atoms
[AD-A188473] 12 p1689 N88-20103
Advanced space propulsion study - antiproton and beamed power propulsion
[AD-A189218] 13 p1732 N88-20355
Laser ignition of nitramine composite propellants and crack propagation and branching in burning solid propellants
[AD-A189260] 13 p1753 N88-20483
Laser fluorescence spectroscopy of zinc neutrals originating from laser-irradiated and ion-bombarded zinc sulfide and zinc surfaces
[DE88-006033] 13 p1776 N88-20620
Refractive index gradients in nuclear-reactor-pumped lasers: Gasdynamic effects
[DE88-006099] 13 p1776 N88-20621
Multimode-waveguide laser beam deflector
[DE88-006222] 13 p1776 N88-20622
Database of average-power damage thresholds at 1064 nm
[DE88-004352] 13 p1776 N88-20626
Studies of compound states of negative ions using laser beams
[DE88-004708] 13 p1777 N88-20627
Direct solar-pumped iodine laser amplifier
[NASA-CR-182674] 13 p1777 N88-20630
Low threshold ridge waveguide single quantum well lasers 13 p1777 N88-20631
Doubly periodic output from a dye laser pumped by a free-running argon laser
[DE88-005027] 13 p1778 N88-20633
Initial stages of silicon growth on the (100) surface of silicon by localized laser CVD
[DE88-005420] 13 p1848 N88-21059
Folded long-pulse XeCl excimer laser described
14 p1901 N88-21357
Theoretical study of colliding pulse mode-locking in dye lasers 14 p1903 N88-21366
Exact image method for Gaussian beam problems involving a planar interface
[NASA-CR-182702] 14 p1905 N88-21380
Nonlinearly tunable wideband emission of infrared radiation by Al2O3:Ti laser 14 p1970 N88-21758
Time characteristics of ultrashort light pulses from dye lasers with distributed feedback
14 p1970 N88-21759
Emission characteristics of XeCl-laser excited by electron beam of microsecond duration
14 p1970 N88-21762
Effects of emission energy transient in periodic-pulse XeCl excimer laser of approximately 400 W average power 14 p1971 N88-21763
Nonlinear stage of ultrashort-pulse formation in solid-state laser 14 p1971 N88-21765
High-efficiency Y-Sc-Ga:Cr (sup)3+,Tu (sup)3+,Ho (sup)3+ garnet laser (gl= 2.088 gmm at room temperature 14 p1971 N88-21766
Space-time structure of ultrashort light pulses formed during stimulated backscattering of laser beam
14 p1972 N88-21767
Free carrier nonlinear optics 14 p1977 N88-21796
Beam quality of stable and unstable resonators: A theoretical approach
[DFVLR-FB-87-35] 14 p1982 N88-21826
Laser processing-status, perspectives
15 p2050 N88-22211
Magic light high-power laser passes state certification
15 p2053 N88-22236
A preliminary comparison of the transient effects of single versus multiple q-switched doubled-neodymium laser pulses
[AD-A189855] 15 p2071 N88-22347
Research on certain aspects of laser diffraction particle sizing relevant to autonomous self-diagnosing instrumentation
[AD-A190220] 15 p2071 N88-22348
Characterization of space radiation environment in terms of the energy deposition in functionally important volumes
[DE88-005627] 15 p2100 N88-22513
Collective rotation of molecules driven by the angular momentum of light in a nematic film
[FUB-6-1986] 15 p2131 N88-22714
Particle beam alignment system for single event upset-Van de Graaf experiments
[AD-A189695] 15 p2132 N88-22721
Optical switching and control techniques using nonlinear optical wave mixing
[AD-A190467] 15 p2134 N88-22730
Characteristics of distributed feedback lasers discussed 16 p2185 N88-23028
Experimental investigation on stimulated Raman scattering in high-pressure hydrogen by ruby laser
16 p2186 N88-23034
Efficient narrow linewidth waveguide dye laser pumped by CuCl laser 16 p2187 N88-23038
Investigation of ultrashort traveling-wave amplified spontaneous emission 16 p2187 N88-23040
Observation of synchronously transient pumped mode-locking dye laser under negative cavity detuning
16 p2187 N88-23041
Discussion of two-mode two-photon CW laser oscillation 16 p2187 N88-23042
Development program for 1.93-micron lasers
[NASA-CR-4148] 16 p2212 N88-23198
Application of magnetic barrier for increasing the efficiency of laser ion source
[DE88-701669] 16 p2212 N88-23200
Realization of an XeCl laser producing 100W on average
[ETN-88-92541] 17 p2344 N88-23970
Magnetically switched power supply system for lasers
[NASA-CASE-NPO-16402-2] 18 p2505 N88-24862
Distributed feedback lasers
[NASA-CR-4154] 18 p2520 N88-24948
An optical preamplifier for detection of CO2 laser radiation
[AD-A190790] 18 p2520 N88-24949
Atmospheric propagation of laser beams
[AD-A191447] 18 p2520 N88-24952
Fast acting optical beam detection and deflection system
[AD-A192161] 18 p2521 N88-24954
Integral equation for the laser field: Multimode description of a free-electron laser oscillator
[DE88-007050] 18 p2521 N88-24956
An optical technique for measuring divergence, beam profile, and aiming direction, of relativistic negative hydrogen ions
[DE88-007049] 18 p2572 N88-25278
Optical system of laser illuminated streamer chamber
[DE88-702127] 18 p2577 N88-25306
Characteristics, packaging and physics of ultra high speed diode lasers and detectors
19 p2658 N88-25797
A new optoelectronic CW microwave source
19 p2660 N88-25818
A twin-mirrored galvanometer laser light sheet generator
[NASA-TM-100587] 19 p2674 N88-25901
Precise beam alignment He-Ne laser tubes
[PB87-228334] 19 p2675 N88-25906
Laser induced surface emission of neutral species and its relationship to optical surface damage processes
[DE88-008035] 19 p2726 N88-26192
The use of liquid films for spacecraft survivability to laser radiation
[AD-A192954] 20 p2765 N88-26395
Laser fluorescence spectroscopy of zinc neutrals originating from laser-irradiated and ion-bombarded zinc sulfide and zinc surfaces
[DE88-008037] 20 p2769 N88-26418
Electron-impact-ionization and electron-attachment cross sections of radicals important in transient gaseous discharges
[AD-A192248] 20 p2770 N88-26424
Results from the SLAC lasertron
[DE88-007816] 20 p2806 N88-26647
The propagation of irradiance moments of an aberrated, apodized FEL beam
[DE88-008972] 20 p2806 N88-26648
Laser desorption/ablation studies by resonance ionization mass spectrometry
[DE88-009124] 20 p2807 N88-26650
Poloidal field measurements using laser enhanced attenuation of an energetic lithium beam
[DE88-008360] 20 p2856 N88-26863
Predicting optical degradation of a laser beam through a turbulent shear layer 21 p2927 N88-27376
Wave equations for pulse propagation
[DE88-011760] 21 p2954 N88-27548
Multiphoton ionization of alkaline earth atoms in an intense laser field
[DE88-008078] 21 p3014 N88-27884
Theory and simulation of relaxed plasmoids
[AD-A192684] 21 p3032 N88-27997
Frequency doubling at 1.315 micrometers
[AD-A193902] 23 p3208 N88-29092
Flow visualization by laser sheet
[AD-A194481] 23 p3211 N88-29111
Coupling between radiation and gas dynamics
[AD-A194593] 23 p3211 N88-29113

Effect of a laser field in the electron inelastic scattering into plasma fields
[DE88-702295] 23 p3218 N88-29157
Analysis of free electron laser performance utilizing the National Bureau of Standards CW microtron
[AD-A194217] 23 p3219 N88-29160
High energy and high intensity laser effects on aerosols: Changes in droplet morphology, surrounding temperature and vapor concentration
[AD-A193825] 23 p3220 N88-29164
Evidence for laser emission from the TICT exciplex of coumarin dyes
[DE88-702544] 23 p3220 N88-29167
Theory of filtering and control with application to control of large space structures
[AD-A195500] 24 p3335 N88-29851
Bibliography of Soviet laser developments, number 88, March - April 1987
[AD-A195978] 24 p3378 N88-30116
Transverse CO2 laser two-dimensional gain distributions
[AD-A196240] 24 p3378 N88-30119
Nonlinear optical phase conjugation techniques to reduce the physical size of lasers
[AD-A196170] 24 p3379 N88-30122
Functional assessment of laser irradiation
[AD-A195735] 24 p3408 N88-30287
Spectroscopic studies with multiple quantum well materials with applications to optical signal processing at room temperature
[AD-A194171] 24 p3429 N88-30409

LASER PLASMA INTERACTIONS
Transient absorption behavior of metals at the onset of the laser welding process
[DFVLR-FB-87-12] 01 p0025 N88-10160
Laser-plasma-interaction experiments using multikilojoule lasers
[DE87-013483] 01 p0100 N88-10658
Laser blow-off experiments on ASDEX --- tokamak
[IPP-III/119] 02 p0243 N88-11535
Relativistic electromagnetic waves in an electron-ion plasma
[NASA-CR-182421] 08 p1085 N88-16532
Activities report in quantum optics
[ISSN-0177-0101] 09 p1248 N88-17482
Basic physics of laser-plasma interactions
[ETN-88-92055] 14 p1984 N88-21838
The development of high power KrF laser systems for plasma research by the application of stimulated Raman scattering
[ETN-88-92220] 15 p2073 N88-22358
Activities report in laser-matter interaction
[ETN-88-92007] 15 p2129 N88-22696
Unified study of plasma/surface interactions for space power and propulsion
[AD-A195971] 24 p3338 N88-29870

LASER PLASMAS
Geometry and reproducibility of a plasma-supported removal of material by laser radiation
[ETN-87-90436] 01 p0052 N88-10335
Enhanced noise and Raman scattering in plasma
[DE87-014466] 02 p0238 N88-11501
Enhanced Thomson scattering from laser plasmas
[DE87-014463] 02 p0238 N88-11503
X-ray emission from high-Z spherical laser plasmas: Implications for plasma dynamics
[DE87-014722] 02 p0239 N88-11506
Review of X-ray spectroscopy from laser-produced plasmas
[DE88-000755] 04 p0494 N88-13043
An investigation of unipolar arcing at atmospheric pressure in aluminum 2024 and aluminum coated glass slides
[AD-A184903] 05 p0577 N88-13521
Active medium formation in lasers using mixtures of inert gases and optical breakdown pumping
06 p0709 N88-14347
The application of photoconductive detectors to the measurement of X-ray production in laser produced plasmas
[DE88-001630] 07 p0934 N88-15671
Pulsed laser stereophotography of plasmas and dynamically moving surfaces
[DE88-003170] 09 p1173 N88-17031
Characteristics of laser-plasma X-radiation source (review) 09 p1239 N88-17428
Activities report in quantum optics
[ISSN-0177-0101] 09 p1248 N88-17482
Spatially resolved X-ray laser spectra and demonstration of gain in nickel-like systems
[DE88-003957] 10 p1335 N88-17979
Overview of applications of Laser-Induced Breakdown Spectroscopy (LIBS)
[DE88-004314] 10 p1336 N88-17987
Spectroscopic studies of a laser-produced carbon plasma in the near and extreme ultraviolet
11 p1553 N88-19292
Photoenhanced attachment for optical control of diffuse discharges
[AD-A188989] 12 p1696 N88-20147
Wavelength scaling of lithium-like recombination scheme for X-UV gain production --- X-ray lasers
[ETN-88-92002] 13 p1778 N88-20634
Experimental study of the role of plasma polarization on line shape in dense laboratory plasmas
[ETN-88-92001] 13 p1844 N88-21033
Progress in X-ray laser experiments
[ETN-88-92004] 14 p1915 N88-21442
Review of X-ray laser studies at the GRECO: Laser-matter interaction
[ETN-88-92005] 14 p1915 N88-21443
Kinetics of slow electrons in excimer laser with electron-beam pumping 14 p1970 N88-21760
One dimensional calculation model for laser produced plasmas expanding in vacuum
[ISL-R-128/86] 14 p1984 N88-21836
PLASMOR: A laser-plasma simulation code, part 2
[DE88-701289] 15 p2135 N88-22736
Particle acceleration to high energies and amplification of coherent radiation by electromagnetic interactions in plasmas
[DE88-701020] 15 p2135 N88-22737
Application of magnetic barrier for increasing the efficiency of laser ion source
[DE88-701669] 16 p2212 N88-23200
The effects of optical smoothing techniques on filamentation in laser plasmas
[AD-A188719] 16 p2275 N88-23614
Thomson scattering for determining electron concentrations and temperatures in an inductively coupled plasma. 2: Description and evaluation of a multichannel instrument
[AD-A191324] 16 p2280 N88-23652
Laser measurement of particle velocities in vacuum plasma spray deposition
[DE88-007111] 19 p2728 N88-26198
On the self-focusing of electric helicons
[DE88-701870] 20 p2848 N88-26905
Thermal inhibition by megagauss field due to variation of electron temperature in laser plasma
[DE88-701887] 20 p2859 N88-26977
Megagauss field variation along axis of wire target in laser produced plasma
[DE88-701895] 20 p2859 N88-26979
Ultraviolet-visible spectroscopy of laser-produced aluminum plasmas
[AD-A193004] 20 p2860 N88-26990
Laser spectoscopy of plasmas
[AD-A193009] 20 p2861 N88-26991
Target designs for plasma-implosion-driven, photoionization-pumped soft X-ray lasers
[DE88-011278] 21 p2954 N88-27547
Introduction to laser plasma diagnostics
[DE88-011056] 23 p3285 N88-29560
Apparatus for submillimeter laser diagnostics of high-temperature plasma
[DE88-702464] 23 p3285 N88-29563
Modeling of atomic processes in X-ray laser plasmas
[AD-A194118] 23 p3286 N88-29567
Energy conversion measurements in laser-sustained argon plasmas for application to rocket propulsion
[AD-A194931] 24 p3337 N88-29861
Bibliography of Soviet laser developments, number 88, March - April 1987
[AD-A195978] 24 p3378 N88-30116
Structuring processes in expanding laser-produced plasmas
[AD-A195249] 24 p3431 N88-30424

LASER PROPULSION
Thrust and specific impulse of repetitively-pulsed-laser propulsion rocket 03 p0318 N88-12012
Proceedings: SDIO/DARPA Workshop on Laser Propulsion. Volume 3: Viewgraphs
[DE88-000964] 04 p0450 N88-12790
Strategic Defense Initiative Organization/DARPA (Defense Advanced Research Projects Agency) workshop on laser propulsion. Volume 1: Executive summary
[DE87-003254] 06 p0768 N88-14722
Laser thermal propulsion
[AD-A186407] 07 p0933 N88-15666
Solar pumped, alkali vapor laser
[AD-A187156] 09 p1170 N88-17016
Advanced energy conversion concept for beamed-energy propulsion
[AD-A187336] 10 p1324 N88-17914
Advanced space propulsion study - antiproton and beamed power propulsion
[AD-A189218] 13 p1732 N88-20355
Possibilities and limits for use of laser propulsion systems in interorbital space flight
[ILR-MITT-185] 18 p2475 N88-24683
A numerical analysis of flow characteristics in laser propulsion system 19 p2637 N88-25645

LASER PUMPING
Diode pumped solid-state laser oscillators for spectroscopic applications
[NASA-CR-180576] 01 p0052 N88-10331
High energy efficient solid state laser sources
[NASA-CR-181362] 01 p0052 N88-10332
Generation of IR stimulated radiation, UV visible violet coherent radiation by two-photon resonance pumping in K vapor 03 p0301 N88-11892
Operational performance of repetitive KrF, XeCl excimer lasers 03 p0327 N88-12068
Distributed feedback effects in lasers and high gain laser instabilities in optically pumped CH3F
03 p0329 N88-12079
Nonconventional optical techniques for optical wavefront processing
[AD-A185099] 05 p0650 N88-13982
Theory of induced spatial incoherence
[AD-A185005] 05 p0651 N88-13992
Compensation of small-scale phase distortions by means of a Fourier phase corrector
06 p0708 N88-14345
Active medium formation in lasers using mixtures of inert gases and optical breakdown pumping
06 p0709 N88-14347
Periodically pulsed excimer master oscillator-regenerative amplifier laser set
06 p0772 N88-14741
Time characteristics of travelling wave lasing with two-photon picosecond optical pumping
07 p0918 N88-15578
Study of kinetics of intracavity absorption in pulsed dye lasers 07 p0919 N88-15585
High-sensitivity recording of weak reflected or scattered radiation by method of coherent intracavity reception with YAG:Nd(3+) laser 08 p1078 N88-16502
Energy disposal in ion-molecule reactions
[AD-A186772] 09 p1171 N88-17019
Investigations of solid state slab lasers
[ETN-88-91055] 09 p1171 N88-17022
The suppression of stimulated hyper-Raman emission in Na due to parametric four-wave mixing
[DE88-003290] 09 p1172 N88-17030
Dye lasers pumped by radiation from high-power semiconductor lasers 09 p1237 N88-17417
Diode pumped fiber laser
[AD-A187694] 11 p1491 N88-18902
Reactions of N2(A(3)(SIGMA)/sub u/(+)) and candidates for short wavelength lasers
[DE88-005366] 12 p1632 N88-19767
Instrumentation for collisional energy transfer studies
[AD-A188495] 12 p1689 N88-20105
Proof of the feasibility of coherent and incoherent schemes for pumping a gamma-ray laser
[AD-A189238] 13 p1774 N88-20613
Design studies for a solar pumped laser device
[DFVLR-FB-87-39] 13 p1777 N88-20629
XeF excimer laser pumped by high-intensity relativistic electron beam 14 p1901 N88-21355
Folded long-pulse XeCl excimer laser described
14 p1901 N88-21357
XeCl laser-pumped nanosecond dye lasers
14 p1902 N88-21359
A picosecond tunable ultrashort cavity dye laser
14 p1902 N88-21361
X-ray lasers: State of art and prospect
[ETN-88-92003] 14 p1914 N88-21434
Review of X-ray laser studies at the GRECO: Laser-matter interaction
[ETN-88-92005] 14 p1915 N88-21443
Nonlinearly tunable wideband emission of infrared radiation by Al2O3:Ti laser 14 p1970 N88-21758
Kinetics of slow electrons in excimer laser with electron-beam pumping 14 p1970 N88-21760
High-efficiency Y-Sc-Ga:Cr (sup)3+,Tu (sup)3+,Ho (sup)3+ garnet laser (gl= 2.088 gmm at room temperature 14 p1971 N88-21766
Pulsed squeezed light 14 p1976 N88-21792
Fundamental noise processes in a laser excited optical filter
[DE88-006460] 15 p2070 N88-22340
Investigation of ultrashort traveling-wave amplified spontaneous emission 16 p2187 N88-23040
Comparison of electrically driven lasers for space power transmission
[NASA-TM-4045] 16 p2212 N88-23197
Effects of translational and rotational nonequilibrium on CW (Continuous Wave) chemical laser performance
[AD-A191425] 16 p2214 N88-23210

The effects of optical smoothing techniques on filamentation in laser plasmas
[AD-A188719] 16 p2275 N88-23614
Space based nuclear-pumped laser/reactor concepts
17 p2403 N88-24289
Application of particle simulations to the NRL laser experiment
[AD-A191641] 18 p2520 N88-24953
A plasma ultraviolet source for short wavelength lasers
[AD-A192844] 21 p2952 N88-27537
Overview and future direction for blackbody solar-pumped lasers
[NASA-TM-100321] 21 p2955 N88-27553
Spectroscopic studies with multiple quantum well materials with applications to optical signal processing at room temperature
[AD-A194171] 24 p3429 N88-30409

LASER RADAR
U OPTICAL RADAR

LASER RADIATION
U LASER BEAMS

LASER RANGE FINDERS
Ultra-short pulse laser system used for lageos range finding 03 p0301 N88-11893
Evaluation of a satellite laser ranging technique using pseudonoise code modulated laser diodes
[NASA-CR-182347] 06 p0708 N88-14343
The Monte Generoso-Zimmerwald (Switzerland) baseline from satellite laser ranging data using various analysis techniques
[LR-533] 14 p1940 N88-21576
Limits of accuracy and range of laser radars
18 p2517 N88-24934
Range and range rate system
[NASA-CASE-MSC-20867-1] 18 p2521 N88-24958
Laser ranging data analysis
[NASA-CR-183115] 20 p2792 N88-26567
Phase comparator for range imaging laser radar
[DE88-008109] 21 p2954 N88-27545
IEMIS (Integrated Emergency Management Information System) floodplain mapping based on a LIDAR derived data set
[AD-A193071] 21 p2966 N88-27616
Determining earth's rotation from laser observations of Lageos artificial earth satellite (during period of main merit campaign) 24 p3449 N88-30528

LASER RANGER/TRACKER
Orbital navigation, docking and obstacle avoidance as a form of three dimensional model-based image understanding 06 p1061 N88-16406
Baseline estimation from simultaneous satellite laser tracking
[NASA-CR-182750] 15 p2022 N88-22052
Solid Earth mission end-to-end data system study
[C04825.06/FR] 17 p2309 N88-23811

LASER SPECTROMETERS
On the multiple grating spectrometer resolving power
[PREPRINT-585] 22 p3153 N88-28761
The 1985-86 measurements with the tunable diode laser absorption spectrometer
[PB88-214002] 23 p3231 N88-29226

LASER SPECTROSCOPY
Laser spectroscopy and gas-phase chemistry in CVD
[DE87-013715] 03 p0281 N88-11770
Energy transformation in molecular electronic systems
[DE87-013916] 03 p0282 N88-11771
Ro-vibrational laser spectroscopy of ESD neutrals from chemisorbed species
[DE87-013011] 04 p0447 N88-12770
Use of lasers with F sub A(II)-color center KCl:Li crystals in the intraresonator laser spectroscopy method
06 p0769 N88-14729
TEA-TE: Powerful nitrogen-based laser system
07 p0919 N88-15583
Laser post-ionization secondary neutral mass spectroscopy
[DE88-002979] 09 p1172 N88-17027
Picosecond laser spectroscopy of charge-separation in photosynthetic model systems
[DE88-003122] 09 p1172 N88-17028
Energy transfer studies with lasers
[DE88-004864] 10 p1337 N88-17991
Two-photon (VUV and visible) resonant ionization spectroscopy of atoms and molecules
[DE88-004332] 10 p1407 N88-18388
Pulsed laser photothermal spectroscopy of liquids and solids
[DE88-003839] 11 p1455 N88-18675
Study of the vibrational modes of subsurface oxygen on Al (111) using diode laser infrared reflection-absorption spectroscopy
[AD-A188322] 12 p1632 N88-19769
Research studies on extreme ultraviolet and soft X-ray lasers
[AD-A189163] 12 p1633 N88-19773
Resonance energy transfer between carbon monoxide and oxygen molecules using dye laser intracavity absorption spectroscopy
[AD-A188488] 12 p1689 N88-20104
Theory of laser cooling and spectroscopy of harmonically trapped single atoms
[AD-A189576] 13 p1775 N88-20617
Laser fluorescence spectroscopy of zinc neutrals originating from laser-irradiated and ion-bombarded zinc sulfide and zinc surfaces
[DE88-006033] 13 p1776 N88-20620
What has been done and what will be done by subnatural linewidth spectroscopy 14 p1978 N88-21807
Laser spectroscopy and dynamics of combustion intermediates
[DE88-006541] 15 p2033 N88-22110
Infrared absorption spectroscopy and chemical kinetics of free radicals
[DE88-006536] 15 p2033 N88-22112
Laser photoelectron spectroscopy of ions
[DE88-006860] 15 p2033 N88-22113
The spectroscopy and reaction kinetics of coordinatively unsaturated metal carbonyls
[AD-A190533] 15 p2035 N88-22124
Diode laser spectroscopy of chemical moieties at surfaces
[AD-A190710] 15 p2036 N88-22127
Statistical fine structure in the inhomogeneously broadened electronic origin of pentacene in p-terphenyl
[AD-A191211] 16 p2176 N88-22968
Laser Diagnostics for combustion temperature and species measurements 17 p2330 N88-23912
Time resolved spectroscopy facility for the study of nonlinear optical properties of semiconducting polymers
[AD-A191221] 18 p2490 N88-24768
Stress measurements in graphite fibers by laser raman spectroscopy
[AD-A191710] 18 p2491 N88-24779
Workshop on Atmospheric OH
[BPT-7/87] 18 p2538 N88-25063
Determination of tropospheric H concentrations by a double-pulsed UV laser method
18 p2539 N88-25070
Tropospheric OH measurement by Laser Induced Fluorescence (LIF) 18 p2540 N88-25071
Trace gas measurements in the troposphere using tunable diode lasers 18 p2540 N88-25072
Development of continuous wave laser frequency modulation of OH in tropospheric concentrations range
18 p2540 N88-25073
Laser fluorescence spectroscopy of zinc neutrals originating from laser-irradiated and ion-bombarded zinc sulfide and zinc surfaces
[DE88-008037] 20 p2769 N88-26418
Laser diagnostics applied to advanced combustion systems
[DE88-753119] 20 p2806 N88-26649
Ground level hydroxyl (OH) concentration measurements by long path differential optical laser absorption
[ETN-88-92124] 20 p2855 N88-26952
An elliptical spectrograph/gated microchannel plate detector for time-resolved spectral measurements in the X-ray region
[DE88-007590] 20 p2856 N88-26961
Laser spectroscopy investigations of materials for solid state laser systems
[AD-A192514] 21 p2952 N88-27535
Laser spectroscopy of quantum well and superlattice structures
[AD-A193336] 21 p3022 N88-27937
Particle sizing in combustion systems, using scattered laser light
[AD-A196231] 24 p3352 N88-29953

LASER STABILITY
Experimental study of stabilizing He-Ne laser output power with transverse magnetic field
03 p0303 N88-11906
Measuring stability of optical reference cavities by analyzing polarization spectrum
03 p0327 N88-12065
Distributed feedback effects in lasers and high gain laser instabilities in optically pumped CH3F
03 p0329 N88-12079
High-power periodic-pulse YAG:Nd3+ -laser system with telescopic unstable resonator and two-stage amplifier
09 p1237 N88-17414
Semiclassical theory of injected lasers with arbitrary stable and unstable resonators
[AD-A189514] 13 p1775 N88-20615
A rubidium-stabilised laser diode for interferometry
[NPL-MOM-85] 14 p1914 N88-21433
Analysis of free electron laser performance utilizing the National Bureau of Standards CW microtron
[AD-A194217] 23 p3219 N88-29180

LASER TARGET INTERACTIONS
Geometry and reproducibility of a plasma-supported removal of material by laser radiation
[ETN-87-90436] 01 p0052 N88-10335
Time-resolved ablation measurements of imploding targets
[DE87-014464] 02 p0178 N88-11111
Time-resolved absorption measurements on OMEGA
[DE87-014465] 02 p0179 N88-11112
Numerical simulation of laser filamentation experiments
[ETN-87-90959] 02 p0179 N88-11118
Transient processes in the interaction between pulsed laser radiation and matter
[ISL-R-115/86] 05 p0588 N88-13586
Review of X-ray laser studies at the GRECO: Laser-matter interaction
[ETN-88-92005] 14 p1915 N88-21443
Activities report in laser-matter interaction
[ETN-88-92007] 15 p2129 N88-22696
Spallation and dynamic fracture as an effect of laser induced shock-waves
[AD-A193513] 23 p3188 N88-28971
Interaction of high power laser radiation with metals in laser welding
[ISL-PU-304/87] 24 p3381 N88-30135

LASER TARGETS
LLE Review, volume 30
[DE87-014469] 02 p0178 N88-11109
Low jitter laser-triggered high-voltage vacuum switch using low laser energies
[DE88-001922] 05 p0587 N88-13576
Proceedings of Symposium on Physics of Target Implosion and Pulsed Power Techniques
[IPPJ-859] 16 p2276 N88-23619
Efficient shell implosion and target design
16 p2277 N88-23630
Coronal fluid-dynamics in laser fusion
16 p2278 N88-23634
Finite ion-relaxation and nonequilibrium radiation effects on laser-driven implosions 16 p2278 N88-23636
Aurora status and plans
[DE88-006476] 18 p2521 N88-24955
Target designs for plasma-implosion-driven, photoionization-pumped soft X-ray lasers
[DE88-011278] 21 p2954 N88-27547
LLE (Laboratory for Laser Energetics) review
[DE88-008065] 23 p3219 N88-29158

LASER WEAPONS
Large-scale stimulated rotational Raman scattering experiments using the LLNL Nova laser
[DE87-012661] 01 p0051 N88-10328
Relating service doctrine to space system requirements
[AD-A186620] 08 p1074 N88-16483
Where directed energy stands in strategic defense
[DE88-005092] 10 p1403 N88-18365
Constellation sizing for modest directed energy platforms
[DE88-007033] 15 p2070 N88-22343
Power source selection for neutral particle beam systems 17 p2407 N88-24314
Nuclear reactor magnetohydrodynamic power generator for directed energy weapons 17 p2411 N88-24336
Fundamental analysis of space nuclear-MHD generator for gigawatt-level power 17 p2411 N88-24337
Rotating-hoop, pulsed-energy converter
17 p2426 N88-24433
Space Power Reference Source (SPRS): A user's guide to SDI Space Power Technology Programs
17 p2427 N88-24440
Monolithic fuel cell based power source for burst power generation 17 p2429 N88-24450
Laser countermeasure impacts and penalties
[DE88-006871] 18 p2520 N88-24947
High spatial frequency thermal blooming instability: A linear stability analysis
[DE88-010711] 20 p2807 N88-26655
SDI (Strategic Defense Initiative) battle management/C3 (Command, Control and Communications) algorithms technology program plan
[AD-A194357] 23 p3275 N88-29495
Looking beyond the strategic defense initiative
[AD-A195079] 24 p3427 N88-30394

LASER WELDING
NT BRAZING
NT FUSION WELDING
NT GAS WELDING
Transient absorption behavior of metals at the onset of the laser welding process
[DFVLR-FB-87-12] 01 p0025 N88-10160
Effect of rapid solidification on stainless steel weld metal microstructures and its implications on the Schaeffler diagram
[DE88-001489] 05 p0566 N88-13451

Production-process CO2 laser with amplified pulse-repetition operation 06 p0771 N88-14739
Study of combination type CO2 laser welding system [PB87-143764] 08 p0992 N88-16002
Microstructural modification during laser welding [DE88-002344] 09 p1144 N88-16860
Joining of dissimilar materials with the pulsed Nd-YAG laser [DE88-003757] 11 p1458 N88-18693
Calibration of beam power monitors for laser welding [DE88-004687] 11 p1492 N88-18908
Modeling of laser ultrasound generation in a weld pool [DE88-005546] 13 p1834 N88-20971
The technical feasibility of using spiked-radiation lasers to cut out and weld metals 14 p1898 N88-21332
Reduced thermal input by proper selection of YAG laser welding parameters [DE88-000730] 15 p2072 N88-22356
Process control improvements in pulsed Nd:YAG laser closure welding of electromechanical relays [DE88-006275] 21 p2957 N88-27564
Interaction of high power laser radiation with metals in laser welding [ISL-PU-304/87] 24 p3381 N88-30135

LASER WINDOWS
Photodetachment neutralizer development: Laser window design study. Volume 2: Window design details [DE88-000783] 09 p1170 N88-17014

LASERS
NT AIRBORNE LASERS
NT ARGON LASERS
NT ATMOSPHERIC LASERS
NT CARBON DIOXIDE LASERS
NT CARBON MONOXIDE LASERS
NT CHEMICAL LASERS
NT CONTINUOUS WAVE LASERS
NT DISTRIBUTED FEEDBACK LASERS
NT DYE LASERS
NT EXCIMER LASERS
NT FREE ELECTRON LASERS
NT GALLIUM ARSENIDE LASERS
NT GAMMA RAY LASERS
NT GAS LASERS
NT GASDYNAMIC LASERS
NT GLASS LASERS
NT HCN LASERS
NT HELIUM-NEON LASERS
NT HF LASERS
NT HIGH POWER LASERS
NT INFRARED LASERS
NT IODINE LASERS
NT KRYPTON FLUORIDE LASERS
NT LIQUID LASERS
NT METAL VAPOR LASERS
NT NEODYMIUM LASERS
NT NITROGEN LASERS
NT NOVA LASER SYSTEM
NT NUCLEAR PUMPED LASERS
NT PULSED LASERS
NT Q SWITCHED LASERS
NT RAMAN LASERS
NT RARE GAS-HALIDE LASERS
NT RING LASERS
NT RUBY LASERS
NT SEMICONDUCTOR LASERS
NT SOLAR-PUMPED LASERS
NT SOLID STATE LASERS
NT SPACEBORNE LASERS
NT TEA LASERS
NT TUNABLE LASERS
NT TWO-WAVELENGTH LASERS
NT ULTRASHORT PULSED LASERS
NT ULTRAVIOLET LASERS
NT WAVEGUIDE LASERS
NT X RAY LASERS
NT XENON CHLORIDE LASERS
NT XENON FLUORIDE LASERS
NT YAG LASERS
LLE Review, volume 30 [DE87-014469] 02 p0178 N88-11109
LLE review [DE87-014468] 02 p0178 N88-11110
Quantum well laser diodes: Modeling and realization of GaAs/GaAlAs [LAAS-87-165] 02 p0179 N88-11116
JPRS report: Science and technology. China [JPRS-CST-87-025] 03 p0300 N88-11888
Experimental study of stabilizing He-Ne laser output power with transverse magnetic field 03 p0303 N88-11906
LLE (Laboratory for Laser Energetics) review, volume 31 [DE87-013732] 03 p0328 N88-12072
Storing photomicrographs on optical laser disks [DE87-013747] 04 p0449 N88-12785
Lasers measure atmosphere 04 p0461 N88-12849
An analysis of the effect of system variables on the quality of thin films and powders produced by laser-breakdown chemical vapor deposition [DE88-001793] 06 p0708 N88-14342
JPRS report: Science and technology. USSR: Physics and mathematics [JPRS-UPM-87-008] 06 p0769 N88-14727
USSR report: Physics and mathematics [JPRS-UPM-87-002] 07 p0918 N88-15575
Bright source lasers and experiments at very high irradiance [DE88-004317] 10 p1337 N88-17988
Laser studies of the dynamics of free radical reactions [DE88-004431] 10 p1337 N88-17989
Absolute rate measurements of two-photon process of gases, liquids, and solids [DE88-003800] 10 p1407 N88-18391
Investigations of stimulated Raman scattering from high density underdense plasmas irradiated by a 0.35 micron laser 10 p1411 N88-18421
Atomic and molecular gas phase spectrometry [AD-A187562] 11 p1452 N88-18655
Laser velocimeter measurements of solids in multiphase flow [DE88-000196] 11 p1487 N88-18876
Calibration of beam power monitors for laser welding [DE88-004687] 11 p1492 N88-18908
Reactions of N2(A(3)(SIGMA)/sub u/(+)) and candidates for short wavelength lasers [DE88-005366] 12 p1632 N88-19767
JPRS report: Science and technology. USSR: Life sciences [JPRS-ULS-88-002] 12 p1665 N88-19982
Superconductors with structured surfaces: Fields and currents [AD-A189353] 12 p1699 N88-20164
Solid state research [AD-A188388] 12 p1699 N88-20166
Laser programming integrated circuits [AD-A189590] 13 p1762 N88-20537
Proof of the feasibility of coherent and incoherent schemes for pumping a gamma-ray laser [AD-A189238] 13 p1774 N88-20613
Semiclassical theory of injected lasers with arbitrary stable and unstable resonators [AD-A189514] 13 p1775 N88-20615
Lasers: Invention to application [PB88-161583] 14 p1914 N88-21436
Demonstration of efficient full aperture Type 1/Type 2 third harmonic conversion on Nova [DE88-003834] 14 p1914 N88-21438
Surface-emitting two-dimensional laser diode arrays constructed on zig-zag heat sink surface [DE88-005215] 14 p1915 N88-21439
Nonlinearly tunable wideband emission of infrared radiation by Al2O3:Ti laser 14 p1970 N88-21758
High-efficiency Y-Sc-Ga:Cr (sup)3+,Tu (sup)3+,Ho (sup)3+ garnet laser (gl= 2.088 gmm at room temperature 14 p1971 N88-21766
United States - Japan Seminar on Quantum Mechanical Aspects of Quantum Electronics [AD-A186938] 14 p1974 N88-21781
Pulsed squeezed light 14 p1976 N88-21792
Quantum nondemolition detection and squeezing in optical fibers 14 p1976 N88-21793
Recent progress in optical bistability and tristability 14 p1979 N88-21809
Investigation of laser diagnostics of PACVD processes for depositing hard face coatings [DE88-007083] 15 p2043 N88-22176
JPRS report: Science and technology. Japan [JPRS-JST-87-030] 16 p2185 N88-23026
Noncondensing round turbulent gas jets in liquids [AD-A191191] 16 p2208 N88-23179
Theoretical studies of Resonance Enhanced Stimulated Raman Scattering (RESRS) of frequency doubled Alexandrite laser wavelength in cesium vapor [NASA-CR-182871] 17 p2317 N88-23841
Magnetically switched power supply system for lasers [NASA-CASE-NPO-16402-2] 18 p2505 N88-24862
Bibliography of Soviet laser developments, number 83, May - June 1986 [AD-A190969] 18 p2520 N88-24950
Laser desorption/ablation studies by resonance ionization mass spectrometry [DE88-009124] 20 p2807 N88-26650
Liquid crystal optics for laser systems [DE88-008475] 20 p2854 N88-26948
Direct measurement of solids: High temperature sensing. Experimental development and testing of high temperature pulsed EMATs [DE88-009659] 21 p2954 N88-27548
Finite element methodology for integrated flow-thermal-structural analysis [NASA-CR-183144] 21 p2964 N88-27606
Future SDI (Strategic Defense Initiative) decision making [AD-A192794] 21 p3010 N88-27860
Application of laser diffraction techniques to particle sizing in solid propellant rocket motors [AD-A193841] 22 p3049 N88-28089
Apparent brightness of stars and lasers 22 p3065 N88-28188
Effect of fiber diameter on the reliability of composites - automated laser diffraction implementation [AD-A193524] 23 p3188 N88-28972
Tolerances for phase locking of semiconductor laser arrays [AD-A195974] 24 p3378 N88-30120
Nonlinear optical phase conjugation techniques to reduce the physical size of lasers [AD-A196170] 24 p3379 N88-30122
The study of hydromagnetic waves and RF heating using the TORTUS tokamak, the development of diagnostic techniques based on submillimeter lasers and the gyrotron, and gas discharge 24 p3431 N88-30419

LASING
XeCi excimer laser with magnetic compressor 03 p0299 N88-11879
Intracavity absorption spectroscopy with ring traveling-wave dye laser 03 p0300 N88-11890
Distributed feedback effects in lasers and high gain laser instabilities in optically pumped CH3F 03 p0329 N88-12079
Repetitively pulsed and continuous wave CO2 lasers pumped by a pulsed self-sustained discharge for thermal processing 06 p0709 N88-14346
The suppression of stimulated hyper-Raman emission in Na due to parametric four-wave mixing [DE88-003290] 09 p1172 N88-17030
Progress in X-ray laser experiments [ETN-88-92004] 14 p1915 N88-21442
Recent progress in optical bistability and tristability 14 p1979 N88-21809
Characteristics of distributed feedback lasers discussed 16 p2185 N88-23028
Isotope separation using tuned laser and electron beam [NASA-CASE-NPO-16907-1-CU] 18 p2483 N88-24732
Characteristics, packaging and physics of ultra high speed diode lasers and detectors 19 p2658 N88-25797

LASV
U F-111 AIRCRAFT

LATCH-UP
Electric design rules related to latch-up and radiation --- simulation [FOA-E-30006-3.1] 08 p0979 N88-15917
High density CMOS technology 11 p1561 N88-19342

LATCHES
Docking/Berthing Subsystem (DBS). Development part 1: Latching analysis --- Columbus [ESA-CR(P)-2479] 08 p0962 N88-15825
Centaur G Prime modal test 09 p1181 N88-17075
System and concept design of the SSRMS latching end effector --- Space Station 14 p1875 N88-21204
Latching mechanisms for IOC --- EURECA 14 p1875 N88-21205
Structural latches for modular assembly of spacecraft and space mechanisms 14 p1925 N88-21471
Toggle release [NASA-CASE-MSC-21354-1] 18 p2523 N88-24969

LATE STARS
NT CARBON STARS
NT COOL STARS
NT FLARE STARS
NT K STARS
NT M STARS
NT MIRA VARIABLES
NT S STARS
Circumstellar radio molecular lines 02 p0252 N88-11595
Measurements of stellar magnetic fields 04 p0503 N88-13093
Magnetic fields on K and M stars 04 p0510 N88-13137
Broadband linear polarization and chromospheric CaII H and K line emission in late-type main sequence stars 04 p0511 N88-13140
A search for X-ray luminous late type stars in NIPSS data 04 p0511 N88-13143
Excess emission in the wings of the Hydrogen Balmer lines during a flare on the late-type dMe star YZ CMi 04 p0511 N88-13146
MHD energy fluxes for late type dwarfs 04 p0512 N88-13148

Sensitivity of the H alpha line to expansion, geometrical extent and temperature gradient in the G and K supergiant chromospheres 04 p0514 N88-13159
The delta upsilon = 1 fundamental bands of carbon monoxide in late-type stars 04 p0517 N88-13177
A comprehensive exploration of late-type stars in the far-ultraviolet 04 p0520 N88-13194
Hydrogen and deuterium in the local interstellar medium 04 p0521 N88-13204
Duplicity in the solar neighborhood. Part 3: New spectroscopic elements for nine solar-type binary stars [SER-C-PREPUBL-FASC-18-PT-3] 18 p2592 N88-25405
Asymptotic giant branch stars in the Infrared Astronomical Satellite (IRAS) catalogs: Selection and analysis of the population characteristics [MPE-PREPRINT-116] 22 p3163 N88-28840
The kinematics of late-type supergiants [SER-C-PREPUBL-FASC-28] 24 p3454 N88-30560

LATENT HEAT
NT HEAT OF FUSION
Transient thermal analysis of three latent heat storage configurations for rapid thermal charging [DE88-008943] 20 p2881 N88-27104

LATENT HEAT OF FUSION
U HEAT OF FUSION

LATERAL CONTROL
Investigation of interactions between limb-manipulator dynamics and effective vehicle roll control characteristics [NASA-CR-3983] 01 p0007 N88-10039
A preliminary investigation into the feasibility of implementing a direct sideforce control system on the Astra Hawk by means of an active control surface --- aircraft control [ETN-87-90924] 02 p0126 N88-10795
A study into the effects and viability of applying lateral force control to an air to ground rocket [ETN-87-90925] 02 p0131 N88-10821
Determination of the drag of missiles with variable lateral acceleration possibility [REPT-FM15] 10 p1310 N88-17831
Lateral and longitudinal stability and control parameters for the space shuttle discovery as determined from flight test data [NASA-TM-100555] 13 p1724 N88-20309
Control law parameterization for an aeroelastic wind-tunnel model equipped with an active roll control system and comparison with experiment [NASA-TM-100593] 17 p2308 N88-23807

LATERAL STABILITY
Effects of the installation and operation of jet-exhaust yaw vanes on the longitudinal and lateral-directional characteristics of the F-14 airplane [NASA-TP-2769] 04 p0393 N88-12455
Effect of a model support strut on measurement of aerodynamic longitudinal and lateral coefficients [PB87-170288] 09 p1113 N88-16670
Lateral stability and control derivatives extracted from space shuttle Challenger flight data [NASA-TM-100520] 09 p1132 N88-16788
Investigation of dihedral effects in compressor cascades 10 p1282 N88-17672
Natural laminar flow and airplane stability and control 17 p2298 N88-23747

LATERALITY
U LATERAL STABILITY

LATERALIZATION
U LATERAL CONTROL

LATERITES
SPOT images and geochemical mapping of lateritic covers in southern Mali 22 p3105 N88-28438

LATEX
The morphology of emulsion polymerized latex particles [DE88-002672] 08 p0972 N88-15879

LATHES
Universal precision sine bar attachment [NASA-CASE-MFS-28253-1] 18 p2523 N88-24971

LATITUDE
Method estimating integral mean value of enhancement factor and path latitude for whistlers below magnetic latitude 10 deg 03 p0300 N88-11885
Radar observations of high-latitude lower-thermospheric and upper-mesospheric winds and their response to geomagnetic activity 06 p0742 N88-14563
The effect of latitude on the development of tropical cyclones [AD-A185670] 06 p0746 N88-14590
The solar radiation incident at the top of the atmosphere of Uranus and Neptune [AERONOMICA-ACTA-A-317-1987] 07 p0878 N88-15323
Effect of neutral wind on the latitudinal variation of nighttime F-layer vertical movements 08 p1030 N88-16244
Latitudinal and seasonal variation of the cloud characteristic parameters and their effects on the cloud classification 17 p2351 N88-24005
Navigation system from AVHRR data from NOAA series satellites 17 p2359 N88-24054

LATTICE IMPERFECTIONS
U CRYSTAL DEFECTS

LATTICE PARAMETERS
Interaction between defects and the formation of dissipative structures in irradiated impure crystals [DE87-703125] 02 p0246 N88-11552
Effect of point defects on graphite lattice parameters [DE88-700340] 07 p0827 N88-15019
Change of europium crystallographic symmetry at helicoidal magnetic ordering [DE88-700559] 07 p0939 N88-15707
Bulk superconductivity in La2CuO4 [DE88-002509] 09 p1254 N88-17516
Structural studies on La/sub 2/CuO/sub 4+delta/ [DE88-006828] 18 p2581 N88-25330

LATTICE VIBRATIONS
Improper ferroelectricity: A theoretical and experimental study [AD-A184614] 03 p0381 N88-12397
Pure dephasing of a vibrational adbond [AD-A185222] 05 p0609 N88-13740
Computation of natural frequencies of planar lattice structure [AD-A185387] 05 p0641 N88-13920
Study of boundary structures [AD-A184808] 05 p0655 N88-14013
Geometric structure, pseudoband gaps, and surface vibrational resonances on metal surfaces [AD-A187001] 09 p1143 N88-16851
The convergence rate for the strong law of large numbers: General lattice distributions [AD-A187560] 10 p1402 N88-18362
Order-disorder transition of Au and Pt (110) surfaces: The significance of relaxations and vibrations [DE88-004651] 10 p1419 N88-18473
Vibration spectra of oxygen and vanadium atoms in vanadium-oxygen disordered interstitial alloys [DE87-703166] 13 p1740 N88-20404
Effect of Mg impurity on local vibrations of U-centers in LiF lattice 14 p1969 N88-21753
Defects and disorder in amorphous and damaged silicon [AD-A192277] 20 p2879 N88-27089
Coupled even-parity superconducting states: Square lattice [AD-A193432] 21 p3022 N88-27938

LATTICES
Continuum modeling of large lattice structures: Status and projections [NASA-TP-2767] 06 p0672 N88-14115
An orthogonal oriented quadrature hexagonal image pyramid [NASA-TM-100054] 06 p0755 N88-14630

LATTICES (MATHEMATICS)
NT BOOLEAN ALGEBRA
NT BOOLEAN FUNCTIONS
A microstructural lattice model for strain oriented problems: A combined Monte Carlo finite element technique [NASA-TM-100215] 02 p0150 N88-10939
Finite size scaling and lattice gauge theory [DE87-014139] 02 p0245 N88-11549
Transition to turbulence via spatio-temporal intermittency 03 p0313 N88-11976
Lattice gas hydrodynamics 03 p0313 N88-11978
Application of lattice filtering techniques to CW measured time domain data [AD-A184351] 04 p0431 N88-12671
Recursion operator and bihamiltonian structure for integrable multi-dimensional lattices [PREPRINT-552] 06 p0764 N88-14688
Darboux transformation and special solutions for the two-dimensional Toda-lattice [PREPRINT-562] 06 p0764 N88-14692
Integrable quantum systems and classical Lie algebras [DE88-700872] 12 p1683 N88-20063
Mixing properties for random walk in random scenery [REPT-87-48] 14 p1966 N88-21734
The two-dimensional Toda-lattice and its recursion operators [PREPRINT-571] 14 p1968 N88-21746
Mixing coefficients of the lattice weak Hamiltonian with dimension five operators [PREPRINT-576] 14 p1968 N88-21749
Recursion operator and Backlund Transformation for the Ruijsenaars-Toda lattice [PREPRINT-577] 14 p1968 N88-21750
Lattice QCD calculation of K yields pi nonleptonic weak transition and other hadronic weak parameters [PREPRINT-580] 15 p2132 N88-22717
A numerical model of unsteady, subsonic aeroelastic behavior [NASA-TM-101126] 16 p2156 N88-22862
Fixpoint representations of characteristic sets of linear-time temporal formulas [CWI-CS-R8754] 20 p2840 N88-26849
Eigenmodes of a random walk on a 2-D lattice torus with one trap [DE88-007830] 20 p2844 N88-26874
Challenge equality problems in lattice theory [DE88-010094] 20 p2876 N88-27072
An overview of lattice QCD [DE88-010867] 21 p3026 N88-27963
Lax representation and complete integrability for the periodic relativistic Toda lattice [PREPRINT-594] 22 p3146 N88-28711

LAUNCH COMPLEXES
U LAUNCHING BASES

LAUNCH VEHICLE CONFIGURATIONS
ESA Bulletin No. 15: Ariane, the European launcher for the 1980's [ESA-BULLETIN-NO-15] 09 p1125 N88-16741
The Ariane launcher and its progress 09 p1125 N88-16742
Increased performance for Ariane 09 p1125 N88-16744
The Ariane-3 program 09 p1128 N88-16771

LAUNCH VEHICLES
NT ARIANE LAUNCH VEHICLE
NT CENTAUR LAUNCH VEHICLE
NT HEAVY LIFT LAUNCH VEHICLES
NT HOTOL LAUNCH VEHICLE
NT RECOVERABLE LAUNCH VEHICLES
NT REUSABLE LAUNCH VEHICLES
NT TITAN LAUNCH VEHICLES
Configuration evaluation and criteria plan. Volume 2: Evaluation criteria plan (update). Space Transportation Main Engine (STME) configuration study [NASA-CR-181429] 03 p0270 N88-11699
Control of an unstable launcher in atmospheric flight using minimax optimal control laws [SNIAS-872-422-107] 05 p0638 N88-13901
The ILV: A new commercial expendable launch vehicle --- Industrial Launch Vehicle (ILV) 08 p1035 N88-16275
Soviet space transport systems 13 p1727 N88-20328
Expected value analysis for an unmanned expendable launch vehicle payload escape system [AD-A189494] 13 p1728 N88-20337
Satellite acquisition: Global positioning system acquisition changes after Challenger's accident [PB88-155536] 14 p1880 N88-21236
Application of superconducting technology to earth-to-orbit electromagnetic launch systems [DE88-010022] 20 p2763 N88-26386
In-flight motor torque estimates for the second-stage Strypi 9 launch vehicle [DE88-010833] 21 p2902 N88-27222
LRS-2: A specialized knowledge system for launch resource scheduling [AD-A194625] 23 p3182 N88-28941
Wind measurements by electromagnetic probes [NASA-TM-4066] 23 p3236 N88-29256
Reduced flexibility in processing Titan 4 space launch vehicles at Cape Canaveral Air Force Station [AD-A194908] 24 p3332 N88-29834

LAUNCHERS
NT GUN LAUNCHERS
NT HYPERVELOCITY LAUNCHERS
NT MISSILE LAUNCHERS
Thermal analysis of electromagnetic launcher rails [DE88-000166] 04 p0405 N88-12514
ICRF launcher studies [DE88-001710] 04 p0495 N88-13046
Experimental investigation of a three-stage railgun incorporating puff-switching [AD-A191044] 16 p2166 N88-22918
The JET (Joint European Torus) multipellet launcher and fueling of JET plasmas by multipellet injection [DE88-008367] 19 p2729 N88-26206

LAUNCHING
NT AIR LAUNCHING
NT ORBITAL LAUNCHING
NT ROCKET LAUNCHING
NT SEA LAUNCHING
NT SPACECRAFT LAUNCHING
Non-linear shipboard shock analysis of the Tomahawk missile shock isolation system 05 p0592 N88-13614
Operational activity and improvements in the services and facilities of the balloon launch centers in France 08 p1030 N88-16238
A pyrotechnic delay ignition system for a submarine launched marine signal [MRL-R-1079] 13 p1754 N88-20487

Simulations of a missile with liquid payload under launch conditions
[AD-A191479] 18 p2463 N88-24625
Design, development, fabrication and launch support for a high altitude release of neodymium vapor
[AD-A194196] 22 p3118 N88-28527

LAUNCHING BASES
NT CAPE KENNEDY LAUNCH COMPLEX
Esrange (Sweden): New installations, future plans and investments — rocket range 08 p1029 N88-16235
Facilities and plans for improvements at Andoya (Norway) rocket range 08 p1029 N88-16236
The DFVLR-German Space Operations Center (GSOC) mobile rocket base 08 p1029 N88-16237
The Ariane launch base 09 p1126 N88-16746
Description of MSFC engineering photographic analysis
[NASA-TM-4035] 11 p1491 N88-18900
Chronology of KSC and KSC related events for 1987
[NASA-CR-182754] 14 p2012 N88-22002
Lunar base launch and landing facility conceptual design, 2nd edition
[NASA-CR-172049] 20 p2885 N88-27135
Space shuttle natural environment analysis
[NASA-CR-179337] 21 p2976 N88-27676

LAUNCHING DEVICES
U LAUNCHERS

LAUNCHING PADS
Orbiter processing facility service platform failure and redesign 14 p1928 N88-21494

LAUNCHING SITES
NT LAUNCHING PADS
The Ariane launch base 09 p1126 N88-16746
Description of MSFC engineering photographic analysis
[NASA-TM-4035] 11 p1491 N88-18900
High altitude chemical release systems for project BIME (Brazilian Ionospheric Modification Experiments) project IMS (Ionospheric Modification Studies) project PIIE (Polar Ionospheric Irregularities Experiment) project polar arcs
[AD-A188299] 12 p1642 N88-19833
Soil erosion and causative factors at Vandenberg Air Force Base, California
[NASA-TM-100981] 17 p2381 N88-24156

LAVA
A review: Quantitative models for lava flows on Mars 23 p3301 N88-29656
Mapping of volcanic units at Alba Patera, Mars 23 p3301 N88-29663
Lava flow-field morphology: A case study from Mount Etna, Sicily 23 p3303 N88-29676
Lava thicknesses: Implications for rheological and crustal development 24 p3443 N88-30490
Simulations of lava flows on Mars 24 p3443 N88-30495
Small-scale volcanic landforms indicative of distributary tube systems 24 p3444 N88-30496
Volcanic styles at Alba Patera, Mars: Implications of lava flow morphology to the volcanic history 24 p3444 N88-30497

LAW (JURISPRUDENCE)
NT LEGAL LIABILITY
NT SPACE LAW
Science, technology and the Constitution: Background paper
[PB88-142534] 12 p1708 N88-20222

LAWRENCIUM
Bulk superconductivity in La2CuO4
[DE88-002509] 09 p1254 N88-17516

LAWS
NT CLOSURE LAW
NT CONSERVATION LAWS
NT HOOKES LAW
NT KEPLER LAWS
NT KIRCHHOFF LAW OF RADIATION
NT NEWTON SECOND LAW
NT OHMS LAW
NT SCALING LAWS
NT SIMILITUDE LAW
Three-halves law in sunspot cycle shape
[NASA-CR-181520] 04 p0525 N88-13210

LAY-UP
Factors affecting strength in composite materials used for aircraft
[DT-212/87] 21 p2907 N88-27248

LAYERS
Formation of buried nitride layers in (110) silicon
[DE88-003255] 11 p1557 N88-19323
Equilibrium stability of strained epitaxial layers on a rigid substrate
[INPE-4254-PRE/1127] 15 p2145 N88-22804
Ion implantation processing of 3-5 strained-layer semiconductors
[DE88-005270] 19 p2734 N88-26240
Eigenmatrix representations of radiance distributions in layered natural waters with wind-roughened surfaces
[PB88-188701] 20 p2828 N88-26780

LAYOUTS
A procedural method for the efficient implementation of full-custom VLSI designs 04 p0436 N88-12701
Very thin VLSI-layouts (Very Large Scale Integration-Layouts) of complete binary trees
[PB88-100847] 06 p0789 N88-14841
A quantitative method for evaluating sensor layouts 09 p1178 N88-17056
Aerodynamic aspects of the configurational systems layout of a dispenser
[MBB-UA-1047/87] 10 p1315 N88-17863
Gridless routing for generalized cell assemblies: Report and user manual
[EUT-87-E-180] 13 p1784 N88-20549
GM: A gate matrix layout generator
[EUT-87-E-179] 13 p1820 N88-20875
Generating layouts for random logic: Cell generation schemes
[EUT-86-E-164] 14 p1956 N88-21658
Computer aided design tools for integrated silicon system structures
[ETN-88-92186] 16 p2247 N88-23424

LEACHING
Improvements to Raney copper zinc methanol synthesis catalysts 17 p2318 N88-23844

LEAD (METAL)
NT LEAD ISOTOPES
Rarefaction velocities in shocked lead
[DE87-013141] 02 p0146 N88-10917
Analysis of free cutting brass by A.C. polarography
[PD-MT-8728] 04 p0417 N88-12587
Develop techniques for ion implantation of (lead-lanthanum-zirconate-titanate) for adaptive optics
[DE88-000642] 05 p0650 N88-13986
Effect of hold time on fatigue of lead rich PbSn solder 06 p0715 N88-14387
Weldability of a leaded carbon steel
[PB88-110341] 07 p0861 N88-15225
Photoionization dynamics and abundance patterns in laser vaporized tin and lead clusters
[AD-A191604] 18 p2482 N88-24722
Influence of the interface on the crystallization of amorphous Ge in Pb/Ge multilayers
[DE88-010072] 22 p3156 N88-28776
PLZT (Lead-Lathanium-Zirconium-Titanium) electro-optic photographic system
[AD-A193473] 23 p3215 N88-29137

LEAD ACID BATTERIES
Hydride generation from the Exide load-leveling cells
[DE87-011361] 01 p0041 N88-10259
DOT fuel-cell-powered bus feasibility study
[DE87-012705] 01 p0107 N88-10699
Results of a wind turbine/sealed lead-acid battery experiment
[DE87-012720] 02 p0166 N88-11044
Post-test analyses of aqueous batteries developed for electric propulsion
[DE88-000655] 03 p0311 N88-11965
Research and development of advanced lead-acid batteries for electric vehicle propulsion
[DE87-014661] 07 p0873 N88-15297
Laboratory evaluation and analysis of advanced lead-acid load-leveling batteries
[DE88-002851] 10 p1349 N88-18064
Lead-acid load-leveling battery testing at Argonne National Laboratory
[DE88-002853] 11 p1480 N88-18837
Evaluation of advanced lead-acid batteries developed for load-leveling applications
[DE88-002871] 11 p1481 N88-18838
The effect of titanium reinforcement on the life of positive grids in lead-acid batteries 17 p2320 N88-23857

LEAD ALLOYS
Thermomechanical fatigue of lead-base low tin solder 06 p0721 N88-14432
PbSnTe photovoltaic detectors for operation in the 2-14 micron band
[INPE-4252-PRE/1125] 11 p1508 N88-19008
Fraction eutectic measurements in slowly cooled Pb - 15 wt percent Sn alloys
[NASA-CR-180830] 19 p2618 N88-25531

LEAD COMPOUNDS
NT LEAD OXIDES
NT LEAD SULFIDES
NT LEAD TELLURIDES
NT LEAD TITANATES

LEAD ISOTOPES
The elastic scattering of intermediate energy protons from (40)Ca and (208)Pb 01 p0092 N88-10599
Pb isotope constaints on the extent of crustal recycling into a steady state mantle 24 p3394 N88-30215
Geochronological and lead-isotope evidences for rapid crust formation in middle-proterozoic time: The Labrador example 24 p3398 N88-30239

LEAD OXIDES
Properties of superconductors with strong electron-phonon interaction 14 p1974 N88-21779

LEAD SULFIDES
Integrated photo-responsive metal oxide semiconductor circuit
[NASA-CASE-GSC-12782-1] 06 p0696 N88-14271
Activities of As, Sb, Bi and Pb in copper mattes and their effects on impurity elimination
[TKK-V-A10(1988)] 15 p2041 N88-22165

LEAD TELLURIDES
Fabrication and characterization of semiconductor lasers of Pb(1-x)Sn(x)Te
[INPE-4253-PRE/1126] 15 p2072 N88-22357
Growth of Pb/sub 1-x/Eu/sub x/Te epitaxial layers by the liquid phase epitaxy technique
[DE88-701022] 15 p2139 N88-22763
Preparation of improved PbSnTe thermoelectric alloys and evaluation of their figure of merit
[AD-A191346] 17 p2445 N88-24538
Crystalline metal-semiconductor superlattices
[DE88-007063] 18 p2581 N88-25332

LEAD TITANATES
An in situ annealing study of lead implanted single crystal calcium titanate
[DE88-005435] 11 p1562 N88-19351

LEAD ZIRCONATE TITANATES
Effects of hydrolysis on metallo-organic solution deposition of PZT films
[ATR-86(8443)-1] 06 p0679 N88-14160

LEADERSHIP
Space station: Leadership for the future
[NASA-PAM-509/8-87] 01 p0013 N88-10072
Networking requirements and future alternatives
[NASA-TM-89711] 10 p1426 N88-18517
First encounters of the close kind: The formation process of airline flight crews
[AD-A187977] 11 p1523 N88-19091
Meta-analysis of leadership differences between males and females and the effect on performance
[AD-A187769] 11 p1564 N88-19361
Report of the Defense Science Board Summer Study on Technology Base Management
[AD-A188560] 13 p1851 N88-21078
Management and the executive
[AD-A190778] 18 p2587 N88-25374
Stress/fatigue and the ARNG (Army National Guard) aviator
[AD-A194184] 22 p3132 N88-28821
The time of leaders 22 p3160 N88-28809

LEADING EDGE FLAPS
High-flaps for natural laminar flow airfoils 17 p2296 N88-23739
Pressure distributions from subsonic tests of an advanced laminar-flow-control wing with leading- and trailing-edge flaps
[NASA-TM-4040-PT-1] 17 p2300 N88-23758
A low speed wind tunnel investigation of Reynolds number effects on a 60-deg swept wing configuration with leading and trailing edge flaps
[NASA-CR-181684] 19 p2598 N88-25441
Pressure distributions from subsonic tests of an advanced laminar-flow-control wing with leading- and trailing-edge flaps
[NASA-TM-4040-PT-2] 24 p3321 N88-29776

LEADING EDGE SWEEP
Large-Scale Advanced Prop-Fan (LAP)
[NASA-CR-182112] 13 p1723 N88-20306

LEADING EDGES
NT SHARP LEADING EDGES
The structure of separated flow regions occurring near the leading edge of airfoils including transition
[NASA-CR-181434] 01 p0002 N88-10011
Vortex interaction with a leading-edge of finite thickness
[NASA-CR-182341] 05 p0543 N88-13307
A theory for the core flow of leading-edge vortices 07 p0810 N88-14935
Insect contamination protection for laminar flow surfaces 07 p0814 N88-14954
Laminar flow control leading edge glove flight test article development
[NASA-CR-172137] 07 p0815 N88-14960
A flow visualization study of the leading edge separation bubble on a NACA 0012 airfoil with simulated glaze ice
[NASA-CR-180846] 07 p0816 N88-14966
Three-dimensional unsteady flow elicited by finite wings and complex configurations
[AD-A186464] 08 p0951 N88-15770
Mean velocities and Reynolds stresses in the juncture flow and in the shear layer downstream of an appendage
[AD-A185819] 08 p0980 N88-15923

On the effect of leading edge blowing on circulation control airfoil aerodynamics
10 p1270 N88-17595
The international vortex flow experiment: A test case for compressible Euler codes
[NLR-MP-86076-U] 13 p1717 N88-20267
Fluid-thermal-structural study of aerodynamically heated leading edges
[NASA-TM-100579] 13 p1783 N88-20666
Wave interactions in a three-dimensional attachment line boundary layer
[NASA-CR-181653] 14 p1910 N88-21414
Thermostructural analysis of simulated cowl lips
15 p2080 N88-22403
Structure of unsteady flows at leading- and trailing-edges: Flow visualization and its interpretation
16 p2205 N88-23154
Operational considerations for laminar flow aircraft
17 p2298 N88-23748
Sensitivity of F-106B leading-edge-vortex images to flight and vapor-screen parameters
[NASA-TP-2818] 17 p2300 N88-23760
A comparison of experimental and calculated thin-shell leading-edge buckling due to thermal stresses
[NASA-TM-100416] 17 p2349 N88-23999
Numerical study of delta wing leading edge blowing
[NASA-CR-183101] 20 p2752 N88-26335

LEAF AREA INDEX

Estimating scattered and absorbed radiation in plant canopies by remote sensing
[NASA-CR-181390] 02 p0193 N88-11205

LEAKAGE

Experimental rotordynamic coefficient results for honeycomb seals
[NASA-CR-182440] 08 p0993 N88-16007
One-dimensional leakage-flow vibration instabilities
[DE88-002875] 10 p1330 N88-17947
The use of least squares in undetermined problems
[DE88-004473] 12 p1682 N88-20059
Ammonia transfer across rotating joints in space
14 p1927 N88-21492
Development of a rotary fluid transfer coupling and support mechanism for space station
14 p1928 N88-21493
Visualization of flows in turbomachinery
[AD-A189927] 15 p2063 N88-22299
Reduced thermal input by proper selection of YAG laser welding parameters
[DE88-000730] 15 p2072 N88-22356
Study on shaft seals for potassium turbine
[EL-891] 15 p2074 N88-22364
Monte Carlo analysis of lateral collection diode arrays
[RSRE-MEMO-4080] 17 p2335 N88-23938
Fuel containment and damage tolerance in large composite primary aircraft structures. Phase 2: Testing
[NASA-CR-172519] 19 p2601 N88-25452
Investigation of leaks in fiberglass-reinforced pressure vessels by direct observation of hollow fibers in glass cloth
[DE88-006936] 19 p2609 N88-25485
Evaluation of engineering leak before break assessment methods by piping tests
[PB88-126982] 20 p2788 N88-26538
Remote sensing and satellite applications to the needs of the gas and pipeline industry
[PB88-202668] 20 p2817 N88-26714
The P delta V fundamental gas leak calibration system qualification report
[DE88-008964] 21 p2951 N88-27526
Stability control of leakage flow channels
[DE88-009995] 23 p3210 N88-29107

LEARNING

NT ASTRONAUT TRAINING
NT CONDITIONING (LEARNING)
NT MAZE LEARNING
NT TRANSFER OF TRAINING

Analogical inference and analogical access
[AD-A184345] 03 p0369 N88-12321
Learning a color algorithm from examples
[AD-A184385] 05 p0632 N88-13862
A learning model as a basis for investigations of the effects of gravity on the learning processes and memory formulation
07 p0886 N88-15374
Computing support for basic research in perception and cognition
[AD-A186192] 07 p0897 N88-15437
Roles of knowledge in motor learning
[AD-A186420] 07 p0897 N88-15438
Substructure discovery in executed action sequences
[AD-A186446] 08 p1069 N88-16462
Long term synaptic plasticity and learning in neuronal networks
[AD-A186834] 09 p1199 N88-17188
Intelligent tutoring systems as tools for investigating individual differences in learning
09 p1204 N88-17216
Computer assisted instruction: Two decades in perspective
[AD-A186813] 09 p1216 N88-17289
Experiments with the back propagation algorithm: A systematic look at a small problem
[RSRE-MEMO-4049] 09 p1224 N88-17340
Analysis and synthesis of adaptive neural elements
[AD-A187047] 10 p1395 N88-18316
The choice of learning strategy in an autonomous system
[AD-A187707] 11 p1534 N88-19161
Two new frameworks for learning
[AD-A187723] 11 p1534 N88-19162
Learning functions from examples
[AD-A187725] 11 p1534 N88-19163
Soar: An architecture for general intelligence
[AD-A188742] 13 p1823 N88-20898
Optimizing feedback utilization in motor skill training
[AD-A191559] 18 p2552 N88-25146
Models of incremental concept formation
[AD-A191597] 18 p2552 N88-25147
Visual information processing in the perception of features and objects
[AD-A192026] 18 p2552 N88-25148
Representation and decision mechanisms in artificial intelligence
[AD-A191083] 18 p2560 N88-25197
Generalization and the backward propagation neural network
[AD-A191634] 19 p2710 N88-26100
Inference and discovery in an exploratory laboratory
[AD-A192231] 20 p2832 N88-26801
Script editor: An editor for the specification phase in the development of computer based learning
[REPT-87-68] 20 p2839 N88-26846
The sine and cosine function for class 4-VWO. Exploration of possible bottlenecks
[REPT-87-72] 20 p2881 N88-27105
Motor-response learning at a process control panel by an autonomous robot
[DE88-005055] 21 p2955 N88-27554
What's on the menu? Friendlier computers
[AD-A194393] 22 p3135 N88-28637
Effect of hypoxia on speech recognition in noise
[AD-A193943] 23 p3240 N88-29280
Some learnability results for analogical generation
[AD-A193669] 23 p3250 N88-29342
Design of a feeling-thinking machine
[AD-A194107] 23 p3267 N88-29448

LEARNING CURVES

A comparison of fitting techniques for the cumulative average learning curves with historical lot cost data
[AD-A187127] 09 p1227 N88-17349
Analysis of learning curve fitting techniques
[AD-A187680] 11 p1535 N88-19173

LEARNING MACHINES

Analysis and synthesis of abstract data types through generalization from examples
[NASA-CR-178369] 01 p0081 N88-10519
The structure-mapping engine: Algorithm and examples
[AD-A184042] 03 p0388 N88-12315
Deriving descriptions of the mind
[AD-A186647] 08 p1052 N88-16349
Neural network based speech synthesizer: A preliminary report
08 p1064 N88-16429
The power of neural nets
08 p1064 N88-16430
The choice of learning strategy in an autonomous system
[AD-A187707] 11 p1534 N88-19161
Learning by experimentation
[AD-A188912] 12 p1681 N88-20053
Generalizing the structure of explanations in explanation-based learning
[AD-A191327] 16 p2256 N88-23481
Radial basis functions, multi-variable functional interpolation and adaptive networks
[RSRE-MEMO-4148] 23 p3265 N88-29436
Active explanation reduction: An approach to the multiple explanations problem
[AD-A194127] 23 p3276 N88-29501

LEARNING THEORY

Knowledge base refinement by monitoring abstract control knowledge, revision 1
[AD-A187502] 10 p1397 N88-18323
The construction of a pedagogy to promote meaningful learning of strategies and tactics for solving problems of elementary combinatorics
[AD-A187928] 11 p1542 N88-19216
Text organization and comprehensibility in technical writing
[AD-A188913] 12 p1707 N88-20217
Topics in adaptive control and inference
[AD-A194718] 23 p3266 N88-29443

LEAST SQUARES METHOD

A generalized least-squares determination of triaxial stress states by X-ray diffraction and the associated errors
[AD-A183851] 01 p0058 N88-10371
The use of splines in the modelling of a photodiode response
[NPL-DITC-88/87] 01 p0085 N88-10550
Computational behavior of Gauss-Newton methods
[DE87-014486] 02 p0224 N88-11413
Solution of nonlinear least-squares problems
[AD-A184010] 03 p0371 N88-12335
Nonlinear parametric least-squares adjustment
[AD-A184039] 03 p0371 N88-12336
A computational examination of orthogonal distance regression
[AD-A184374] 03 p0371 N88-12337
Least squares linear lags and limited memory filters
[NASA-CR-178381] 03 p0372 N88-12339
Model-based motion estimation and its application to restoration and interpolation of motion pictures
[AD-A185054] 05 p0584 N88-13558
A system identification technique based on the random decrement signatures. Part 1: Theory and simulation
05 p0594 N88-13625
A system identification technique based on the random decrement signatures. Part 2: Experimental results
05 p0594 N88-13626
Multidimensional least squares fitting of fuzzy models
[AD-A185148] 05 p0640 N88-13916
Least squares for fuzzy vector data regression
[AD-A185156] 05 p0640 N88-13917
Study of extended least-square iterative techniques in electromagnetic scattering by penetrable objects
[PB88-105879] 06 p0694 N88-14262
Knot selection for least squares thin plate splines
[AD-A185681] 06 p0759 N88-14657
Interactive nonlinear least squares program
[PB88-109855] 06 p0760 N88-14661
Stabilized Galerkin method for convection-diffusion problems
[PB87-234985] 06 p0764 N88-14694
Round-off error propagation in four generally applicable, recursive, least-squares-estimation schemes
[NASA-TM-100055] 06 p0766 N88-14708
A survey study of energy distribution in component stars of Algol-type binary systems
06 p0801 N88-14901
On the least squares estimator in moving average models of order one
[AD-A186028] 07 p0909 N88-15508
A simultaneous M-ary channel hypothesis test with least-mean-square signal amplitude estimation
[AD-A186526] 08 p0978 N88-15913
Estimation and comparison of changes in the presence of information right censoring by modeling the censoring process
[AD-A186320] 08 p1074 N88-16478
A note on computing robust regression estimates via iteratively reweighted least squares
[AD-A186709] 09 p1227 N88-17352
Fitting a generalized parabola to data
[NPL-DITC-96/87] 09 p1229 N88-17364
Strategies for knot placement in least squares data fitting by splines
[NPL-DITC-101/87] 09 p1229 N88-17366
Analysis of learning curve fitting techniques
[AD-A187680] 11 p1535 N88-19173
Position finding and tolerances
[AD-A187685] 11 p1540 N88-19205
Realtime pilot model parameter identification
[AD-A188873] 12 p1584 N88-19478
The use of least squares in undetermined problems
[DE88-004473] 12 p1682 N88-20059
Computation of LMS (Least-Mean-Square) and matched digital filters for optical clutter suppression
[AD-A188885] 12 p1687 N88-20093
Analysis of pre-flight modulator voltage calibration data for the Voyager plasma science experiment
[NASA-CR-182577] 12 p1710 N88-20236
Two dimensional uncorrelated bias in fix algorithms
[NASA-CR-182683] 13 p1815 N88-20847
Survival analysis using additive risk models
[AD-A189053] 13 p1825 N88-20906
Identification of nonlinear output-affine systems using an orthogonal least squares algorithm
[RR-313] 14 p1958 N88-21678
Motion sickness: Quantitative, algorithmic malaise indication in real time
[AD-A189674] 15 p2101 N88-22518
Cholesky downdating on a hypercube
[DE88-006780] 15 p2113 N88-22586
The 1 and 2D symmetric Helmert transformation: An exact nonlinear least squares solution
[REPT-87-1] 16 p2259 N88-23503
Calculation of root-mean-square loads
[BLL-M-37776-(5828.4)] 18 p2531 N88-25015

Asymptotic theory for weighted least squares estimators in Aalen's additive risk model
[AD-A191085] 18 p2562 N88-25210
New mixed finite element methods
18 p2567 N88-25248
Signal processing computational needs
[AD-A191756] 19 p2642 N88-25674
Parameter estimation of dynamical systems
20 p2785 N88-26519
A deconvolution technique using least-squares model-fitting and its application to optical pulse measurement
[NPL-DES-87] 22 p3144 N88-28694
Automatic classification of digitally modulated signals
[AD-A194623] 23 p3203 N88-29064
Obtaining stress intensity factors on cracks, by means of fitting techniques on numerical results calculated with the finite element method 24 p3384 N88-30153
Algorithms for nonlinear least-squares problems
[AD-A196071] 24 p3411 N88-30305
New methods for nonlinear optimization
[AD-A195982] 24 p3412 N88-30313

LEAVES
Estimation of aerial deposition and foliar uptake of xenobiotics: Assessment of current models
[DE88-000993] 09 p1188 N88-17117
Sources of scattering in vegetarian and other surfaces and objects
[NASA-CR-182975] 20 p2816 N88-26710

LEBESGUE THEOREM
A study on Lebesgue decomposition of measures induced by stable processes
[AD-A192893] 21 p3009 N88-27850

LECTURES
A lecture on detonation-shock dynamics
[DE88-004313] 11 p1487 N88-18879
A practical guide to modern high energy particle accelerators
[DE88-004035] 11 p1548 N88-19260

LED (DIODES)
U LIGHT EMITTING DIODES

LEE WAVES
Simulation of a lee cyclogenesis using a numerical model 08 p1016 N88-16162

LEG (ANATOMY)
Determination of the effect of walking on the forced convective heat transfer coefficient using an articulated mannikin
[AD-A186452] 08 p1049 N88-16335
Morphological manifestations of primate adaptation to orthograde statics and walking erect
10 p1366 N88-18162
Currents induced in a human being for electromagnetic fields to 10 kHz-50 MHz
[AD-A191977] 23 p3238 N88-29268

LEGAL LIABILITY
New technologies and intellectual property: An economic analysis
[N-2601-NSF] 01 p0107 N88-10695

LEGENDRE CODE
U COMPUTER PROGRAMMING
U NEUTRON SCATTERING

LEGUMINOUS PLANTS
NT SOYBEANS
Remote sensing techniques in the estimation of the area cultivated with beans, corn, and castor beans in the Irece County (Bahia State) 17 p2358 N88-24045
TM/LANDSAT-5 data to evaluate wheat and bean percent soil cover and leaf area index
[INPE-4609-PRE/1332] 24 p3385 N88-30165

LEMMAS
U THEOREMS

LENGTH
NT DIFFUSION LENGTH
The effect of microstructure on the surface crack length: Crack depth relationship for short cracks
05 p0600 N88-13670
Mixing and combustion of pulsed gas jets
[PB88-108014] 06 p0680 N88-14170
Development and calibration of Direct Current Potential Difference (DCPD) crack length measurement equipment
[VTT-RR-480] 09 p1182 N88-17083
Locality, communication and interconnect length in multicomputers
[CWI-CS-R8708] 13 p1822 N88-20890
Automated measurement of crack length and load line displacement at elevated temperature
[AGARD-R-751] 20 p2814 N88-26695

LENNARD-JONES POTENTIAL
Free energy calculation via MD (molecular dynamics): Methodology and application to bicrystals
[DE88-002902] 09 p1256 N88-17532

LENSES
NT CONTACT LENSES
NT FRESNEL LENSES
NT GRAVITATIONAL LENSES
NT MAGNETIC LENSES
NT WIDE ANGLE LENSES
NT ZOOM LENSES
Design concepts to improve high performance solar simulator 02 p0136 N88-10852
Dual mode laser velocimeter
[NASA-CASE-ARC-11634-1] 06 p0709 N88-14350
Selection of polymer materials for manufacturing optical parts
[AD-A185898] 07 p0836 N88-15060
Optical Fourier transformation by lensless method with perforated mask and with modified Talbot interferometer for analysis of interferograms 09 p1235 N88-17408
Aberrations: Their effect on off-axis beam steering
[AD-A189601] 13 p1840 N88-21008
Nonlinear wave and diffusion equations
[AD-A191421] 16 p2265 N88-23544
Evaluation of multi-focus holographic lenses
[AD-A196167] 24 p3377 N88-30110

LEO ENVIRONMENTS
U EARTH ORBITAL ENVIRONMENTS

LEPTONS
NT ANTINEUTRINOS
NT CONDUCTION ELECTRONS
NT ELECTRONS
NT MUONS
NT NEUTRINOS
NT POSITRONS
NT SOLAR NEUTRINOS
Study of tau pairs and search for new particles
[B8680488] 07 p0931 N88-15655
Semileptonic weak interactions in nuclei: A relativistic analysis
[CEBAF-PR-87-024] 11 p1547 N88-19249

LESIONS
Relation between VEP and visual function in lesions of the optic nerve and visual pathway
21 p2983 N88-27718

LETHALITY
Switching devices used in the Lethality Test System
[DE87-011734] 01 p0011 N88-10062
Reaming experiments for the lethality test system
[DE88-007902] 20 p2763 N88-26383
Fiber-optics used to record high-speed photographs inside a pressurized tank during lethality testing
[DE88-011283] 21 p2951 N88-27529

LETTERS (SYMBOLS)
U SYMBOLS

LEUKOCYTES
NT LYMPHOCYTES
Mononuclear phagocytes during adaptation of essentially healthy people to high altitudes
07 p0896 N88-15432
White blood cells in space: An experiment for the first Spacelab mission 09 p1127 N88-16757
Effects of whole-body irradiation with low-intensity microwaves on morphological, functional and cytochemical characteristics of leukocytes 12 p1663 N88-19971

LEVEL (QUANTITY)
NT ATOMIC ENERGY LEVELS
NT ELECTRON STATES
NT ENERGY LEVELS
NT GROUND STATE
NT MOLECULAR ENERGY LEVELS
Rain attenuation at 35 GHz over an 18 km path
[AD-A194504] 22 p3069 N88-28217
Exact lower confidence limits for the reliability of k of n systems for zero failures and nonconservativeness of the maximus method
[AD-A194299] 23 p3274 N88-29485
Validate algorithms for the determination of rainfall rates from SSM/I microwave satellite imagery
[AD-A195428] 24 p3404 N88-30270

LEVITATION
NT ACOUSTIC LEVITATION
The interaction of small particles with laser beams
[AD-A190716] 15 p2072 N88-22354

LIABILITIES
NT LEGAL LIABILITY

LIAPUNOV FUNCTIONS
The periodic Lyapunov equations
[REPT-86-007] 01 p0087 N88-10567
Closed-loop system analysis using Lyapunov stability theory 04 p0483 N88-12978
Investigation of the spin stability of the NPS (Naval Postgraduate School) mini-satellite (Orion)
[AD-A187781] 11 p1445 N88-18613
Intermittency of atmospheric turbulence--applicatin of Lyapunov exponents and fractional dimension
14 p1900 N88-21348
Markov processes applied to control, replacement and signal analysis
[AD-A190563] 15 p2126 N88-22674
Finite dimensionality in the complex Ginzburg-Landau equation
[DE88-006480] 16 p2263 N88-23534
Dynamic stability of elastic rotor-bearing systems via Liapunov's direct method 21 p2956 N88-27571
Generalized Jordan chains and two bifurcation theorems of Krasnoselskii
[AD-A192353] 21 p3008 N88-27845
Stability, stochastic stationarity and generalized Lyapunov equations for two-point boundary-value descriptor systems
[AD-A195645] 24 p3425 N88-30385

LIBRARIES
Information analysis centers in the department of defense, revision
[AD-A184002] 03 p0385 N88-12420
The SUPRENUM communications subroutine library for grid-oriented problems
[DE88-000137] 04 p0479 N88-12950
LISP: A language for stratified design
[AD-A185806] 06 p0759 N88-14654
Bibliographic relationships: Toward a conceptual structure of bibliographic information used in cataloging
06 p0791 N88-14852
Treatment of small wire loops in the method of moments code NEC (Numerical Electromagnetics Code)
[DE88-002995] 07 p0846 N88-15136
Prospectus for the development of a linear algebra library for high-performance computers
[DE88-003715] 08 p1068 N88-16457
Hierachical object recognition using libraries of parameterized model sub-parts
[AD-A187476] 10 p1396 N88-18322
DataViews: A personalizable, interactive, data display system for the decisionmaker
[AD-A188509] 14 p1991 N88-21868
Data base design and implementation
[AD-A190414] 15 p2149 N88-22827
A standard library for modeling satellite orbits on a microcomputer
[AD-A195759] 24 p3331 N88-29830

LIBRATION
Relative motion near the triangular libration points in the Earth-Moon system 01 p0097 N88-10636
Study on orbits near the triangular libration points in the perturbed restricted three body problem
[ESA-CR(P)-2440] 07 p0944 N88-15741
Limitation of spacecraft orbit near colinear libration center of limited elliptical three body problem
08 p1003 N88-16075
The dust ring of the Earth
[RAE-TRANS-2163] 22 p3119 N88-28530
Plane periodic satellite motions relative to center of mass in neighborhood of collinear libration point
24 p3445 N88-30507

LIBRATIONAL MOTION
Study on orbits near the triangular libration points in the perturbed restricted three body problem
[ESA-CR(P)-2440] 07 p0944 N88-15741
Periodic orbits of limited elliptical three body problem
08 p1004 N88-16081
Families of periodic solutions in problem of solid body rotation at triangular libration point in restricted three-body problem 24 p3446 N88-30508

LIDAR
U OPTICAL RADAR

LIE GROUPS
Irreducible *-representations of the Lie superalgebra osp(1,4) with finite-degenerated vacuum
[DE87-703089] 02 p0225 N88-11420
Class of N-associative rings
[PB87-230421] 06 p0769 N88-14724
Lie algebraic method in filtering and identification
[CWI-PM-R8606] 08 p1072 N88-16467
The r-rank of the groups of exceptional Lie type
[CWI-PM-R8607] 08 p1072 N88-16468
Applications of Lie group methods to the equations of magnetohydrodynamics 10 p1411 N88-18422
Integrable quantum systems and classical Lie algebras
[DE88-700872] 12 p1683 N88-20063
Freund-Rubin type solutions for different compactifications of the eleven-dimensional space
[DE88-700869] 12 p1686 N88-20082
On the equivalence of four-dimensional self-duality equations to continual analog of the main chiral field problem
[DE88-700871] 12 p1686 N88-20083
Nonlinear differential equations
[DE88-006047] 13 p1828 N88-20933
Galilei relativity principle in classical electrodynamics
[DE87-703203] 14 p1904 N88-21376
Lie groups in prolongation theory
[B8721781] 14 p1967 N88-21743
Algebraic structure of linear and nonlinear models of open quantum systems
[PREPRINT-573] 14 p1968 N88-21747
On generalized lie-like algebras
[PREPRINT-574] 14 p1968 N88-21748

Markov processes applied to control, replacement and signal analysis
[AD-A190563] 15 p2126 N88-22674
Lumped model generation and evaluation: Sensitivity and Lie algebraic techniques with applications to combustion
[AD-A190402] 15 p2127 N88-22689
Introduction to nilpotent approximation filtering
[CWI-PM-R8709] 16 p2262 N88-23524
Canonical construction of differential operators intertwining representations of real semisimple Lie groups
[DE88-701852] 20 p2845 N88-26882
Superalgebras with Grassmann algebra-valued structure constants from superfields
[DE88-702239] 21 p3011 N88-27862

LIF (FLUORESCENCE)
U LASER INDUCED FLUORESCENCE

LIFE (BIOLOGY)
U LIFE SCIENCES

LIFE (DURABILITY)
NT CARRIER LIFETIME
NT FATIGUE LIFE
NT SATELLITE LIFETIME
NT SERVICE LIFE
NT STORAGE STABILITY
High intensity 5 eV O-atom exposure facility for material degradation studies 02 p0135 N88-10847
Advances in nickel hydrogen technology at Yardney Battery Division 02 p0164 N88-11029
International Ultraviolet Explorer (IUE) spacecraft battery performance update 02 p0164 N88-11033
Life prediction and constitutive models for engine hot section anisotropic materials program 02 p0188 N88-11175
Lewis' enhanced laboratory for research into the fatigue and constitutive behavior of high temperature materials 02 p0189 N88-11177
Turbine airfoil deposition models and their hot corrosion implications 02 p0189 N88-11178
Effects of surface chemistry on hot corrosion life 02 p0189 N88-11180
Coating life prediction 02 p0189 N88-11181
Thermal barrier coating life prediction model development 02 p0190 N88-11183
Thermal barrier coating life prediction model development 02 p0190 N88-11184
Thermal barrier coating life prediction model development 02 p0190 N88-11185
Airworthiness of long-life jet transport structures 03 p0265 N88-11674
A low-power arcjet cyclic lifetest
[NASA-TM-100233] 03 p0278 N88-11748
A life test of a 22-Newton (5-lbf) hydrazine rocket
[NASA-TM-100232] 03 p0278 N88-11750
Materials preparation and longevity in hyperthermal atomic oxygen 03 p0297 N88-11862
Advanced natural gas fueled engine development. Part 2: Materials investigation
[PB87-223160] 03 p0331 N88-12088
Durability (lifetime) predictions adhesively bonded structures
[AD-A184069] 03 p0335 N88-12110
Reliability of Li/SO2 cells for long-life applications
[DE88-001360] 04 p0440 N88-12735
Fiber composite structural durability and damage tolerance: Simplified predictive methods
[NASA-TM-100179] 05 p0560 N88-13409
Significance of fatigue crack closure under spectrum loading 05 p0599 N88-13662
Further studies in estimation of life distribution characteristics from censored data
[AD-A184862] 05 p0643 N88-13937
Life prediction of steel cords 06 p0715 N88-14386
Life modeling of thermal barrier coatings for aircraft gas turbine engines
[NASA-TM-100263] 07 p0834 N88-15060
Life prediction of thermomechanical fatigue using total strain version of strainrange partitioning (SRP): A proposal
[NASA-TP-2779] 07 p0867 N88-15263
Documentation in a software maintenance environment
[AD-A185892] 07 p0901 N88-15459
Life prediction technologies for aeronautical propulsion systems 08 p0954 N88-15788
Rotorcraft transmission 08 p0956 N88-15802
Aircraft engine hot section technology: An overview of the HOST Project 08 p0957 N88-15804
Space Infrared Telescope Facility (SIRTF) design and thermal analysis 08 p0982 N88-15934
KBS V and V as related to automation of space station subsystems: Rationale for a KBS lifecycle 08 p1057 N88-16375
Delamination durability of composite materials for rotorcraft 09 p1107 N88-16634
Creep and fatigue research efforts on advanced materials 09 p1119 N88-16701
Ceramics for engines 09 p1119 N88-16704
Mechanics of composite materials: Past, present and future
[NASA-TM-100793] 10 p1295 N88-17744
Lead-acid load-leveling battery testing at Argonne National Laboratory
[DE88-002853] 11 p1480 N88-18837
Review of the state of the art and projected technology of low heat rejection engines
[PB88-131255] 11 p1496 N88-18934
Improve the lifetime of the hollow fiber sodium sulfur cell
[DE88-004881] 13 p1751 N88-20469
In situ fatigue loading stage inside scanning electron microscope 15 p2083 N88-22419
Cumulative fatigue damage models 15 p2084 N88-22422
Life prediction modeling based on strainrange partitioning 15 p2084 N88-22425
Life prediction modeling based on cyclic damage accumulation 15 p2085 N88-22426
Fatigue damage modeling for coated single crystal superalloys 15 p2085 N88-22427
Life and reliability of rotating disks 15 p2085 N88-22428
Status, trends in research on internal combustion engines 16 p2185 N88-23027
Seasonal variation for structural strength value
[PB88-169248] 16 p2222 N88-23260
Rainfall rates and drop-size distributions for environmental testing
[AD-A191342] 16 p2236 N88-23354
Lifetime of pristine optical fibers
[ETN-88-92246] 16 p2273 N88-23602
Ceramics for turbine engines 17 p2323 N88-23873
Thermal cyclic durability testing of ceramic materials for turbine engines 17 p2325 N88-23886
Fractographic and microstructural evaluation of 3500-hour durability specimens 17 p2325 N88-23887
Space reactor end of life issues 17 p2424 N88-24413
Internal erosion rates of a 10-kW xenon ion thruster
[NASA-TM-100954] 18 p2476 N88-24688
Environment assisted degradation mechanisms in advanced light metals
[NASA-CR-182907] 18 p2486 N88-24746
The relationship between observed fatigue damage and life estimation models
[NASA-CR-182191] 21 p2965 N88-27611
Thermal barrier coating life-prediction model development
[NASA-CR-179507] 22 p3058 N88-28142
Vapor Compression Distillation Subsystem (VCDS) component enhancement, testing and expert fault diagnostics development, volume 1
[NASA-CR-172072] 22 p3134 N88-28634
Influence of the temperature-dependence of recombination life-time of free carriers in amorphous semiconductors on thermostimulated photocurrent spectra
[DE88-702728] 23 p3293 N88-29609
Performance and lifetime assessment of MPD arc thruster technology
[NASA-TM-101293] 24 p3336 N88-29860
Successful completion of a cyclic ground test of a mercury ion auxiliary propulsion system
[NASA-TM-101351] 24 p3339 N88-29873
Morphological changes in polymer electrolyte cells
[AD-A195821] 24 p3368 N88-30054
A static scheduler for the computer aided prototyping system: An implementation guide
[AD-A194340] 24 p3414 N88-30322
Knowledge based simulation: An artificial intelligence approach to system modeling and automating the simulation life cycle
[AD-A195838] 24 p3423 N88-30372
Space systems cost study
[AD-A196024] 24 p3439 N88-30469

LIFE CYCLE COSTS
DOT fuel-cell-powered bus feasibility study
[DE87-012705] 01 p0107 N88-10699
A design methodology for the utilization of metrics within various phases of software lifecycle models
[DE87-010519] 02 p0220 N88-11385
Determination of life cycle costs in astronautics
[MBB-UR-E-910/86-PUB] 02 p0249 N88-11572
Optimized ground coupled heat pump mechanical package
[DE87-014899] 04 p0441 N88-12738
Technology Base Research Project for electrochemical energy storage
[DE88-000649] 04 p0464 N88-12868
Simulated service test behavior of various internal and external coatings applied on CF6-50 first stage turbine blades
[NLR-MP-86018-U] 05 p0549 N88-13343
Life-cycle cost analysis of residential heat pumps and alternative HVAC (Heating, Ventilating and Air-Conditioning) systems
[DE88-003701] 07 p0839 N88-15090
Documentation in a software maintenance environment
[AD-A185892] 07 p0901 N88-15459
Supportability in aircraft systems through technology and acquisition strategy applications
[AD-A186465] 08 p0949 N88-15759
Proposal of a methodology for the conceptual design of the Distributed Data Base
[INPE-4315-TDL/282] 08 p1093 N88-16576
A cost and benefit analysis of hydraulic fluid systems for the next generation of tactical aircraft
[AD-A186911] 09 p1116 N88-16690
STS propellant scavenging systems study. Part 2, volume 2: Cost and WBS/dictionary
[NASA-CR-179276] 10 p1290 N88-17717
Future directions in computer architecture 10 p1383 N88-18257
The space station assembly phase: Flight telerobotic servicer feasibility. Volume 2: Methodology and case study
[NASA-CR-182690] 13 p1731 N88-20352
Costs and benefits of AC propulsion
[PB88-173380] 16 p2287 N88-23691
The multi-disciplinary design study: A life cycle cost algorithm
[NASA-CR-4156] 17 p2385 N88-24172
Engine component retirement for cause. Volume 1: Executive summary
[AD-A192730] 20 p2760 N88-26371
PAX ECONOPACK economic analysis package users manual
[AD-A192949] 20 p2883 N88-27117

LIFE SCIENCES
NT EXTRATERRESTRIAL LIFE
NT MOLECULAR BIOLOGY
JPRS report: Science and technology. USSR: Life sciences
[JPRS-ULS-87-009] 04 p0473 N88-12915
JPRS report: Science and technology. USSR: Life sciences
[JPRS-ULS-87-011] 06 p0749 N88-14601
Life sciences flight experiments microcomputer 06 p0792 N88-14857
USSR Space Life Sciences Digest index to issues 10-14
[NASA-CR-3922(17)] 07 p0883 N88-15361
USSR Space Life Sciences Digest, issue 14
[NASA-CR-3922(16)] 08 p1045 N88-16317
USSR report: Life sciences. Biomedical and behavioral sciences
[JPRS-UBB-86-022] 08 p1045 N88-16318
Trends in research and development in the Netherlands. The influence of national science policy between 1973 and 1986
[B8701588] 08 p1094 N88-16580
System analysis study of space platform and station accommodations for life sciences research facilities. Volume 1: Executive summary. Phase A: Conceptual design and programmatics
[NASA-CR-179268] 10 p1291 N88-17721
System analysis study of space platform and station accommodations for life sciences research facilities. Volume 2: Study results, attachment 2. Phase A: Conceptual design and programmatics
[NASA-CR-179272] 10 p1291 N88-17722
System analysis study of space platform and station accommodations for life sciences research facilities. Volume 2: Study results. Appendix E: Work breakdown structure and dictionary
[NASA-CR-179274] 10 p1292 N88-17723
System analysis study of space platform and station accommodations for life sciences research facilities. Volume 2: Study results. Appendix D: Life sciences research facility requirements
[NASA-CR-179273] 10 p1292 N88-17724
USSR Space Life Sciences Digest, issue 15
[NASA-CR-3922(18)] 10 p1368 N88-18175
Minutes of the meeting of the Indo-US Subcommission on Science and Technology (8th) held at Washington, D.C. on September 22-24, 1986
[PB88-130158] 10 p1423 N88-18503
JPRS report: Science and technology. USSR: Life sciences
[JPRS-ULS-88-001] 11 p1520 N88-19079

Conceptual design and programmatics studies of space station accommodations for Life Sciences Research Facilities (LSRF)
[NASA-CR-179270] 12 p1598 N88-19567
Space station accommodations for life sciences research facilities: Phase A conceptual design and programmatics studies for Missions SAAX0307, SAAX0302 and the transition from SAAX0307 to SAAX0302. Volume 1: Executive summary
[NASA-CR-179267] 12 p1599 N88-19571
Proceedings of the 3rd European Symposium on Life Sciences Research in Space
[ESA-SP-271] 12 p1652 N88-19893
The European Space Agency's role in life sciences and research in space 12 p1652 N88-19894
Life sciences in the framework of the ESA microgravity program and future flight opportunities
12 p1652 N88-19895
Life science techonology --- space applications
12 p1653 N88-19900
Why life science in space? The next step to go beyond 12 p1661 N88-19954
Application of ARIADNE: A data bank-based information system for human physiology research --- Spacelab Anthrorack 12 p1662 N88-19962
JPRS report: Science and technology. USSR: Life sciences
[JPRS-ULS-88-004] 13 p1810 N88-20815
JPRS report: Science and technology. China
[JPRS-CST-87-041] 14 p1902 N88-21365
USSR Space Life Sciences Digest, issue 16
[NASA-CR-3922(19)] 15 p2101 N88-22515
JPRS report: Science and technology. China
[JPRS-CST-88-001] 16 p2186 N88-23036
USSR Space Life Sciences Digest, Issue 17
[NASA-CR-3922(20)] 17 p2361 N88-24155
USSR space life sciences digest, issue 18
[NASA-CR-3922(21)] 19 p2707 N88-26096
A shared-world conceptual model for integrating space station life sciences telescience operations
24 p3416 N88-30333

LIFE SPAN
Drosophila geotaxis as a tool for the study of aging
10 p1288 N88-17706

LIFE SUPPORT SYSTEMS
NT CLOSED ECOLOGICAL SYSTEMS
The usefulness of microalgal structures as an element of closed ecological systems like Aquarack and CELSS --- Controlled Ecological Life Support System (CELSS)
01 p0074 N88-10476
Life support systems for biological experiments under weightlessness in the German and European space programs 01 p0074 N88-10477
Controlled Ecological Life Support Systems (CELSS) conceptual design option study
[NASA-CR-177421] 06 p0754 N88-14625
Research and development of anti-G life support systems. Part 1: Development and evaluation of uniform-pressure anti-G suits
[AD-A185658] 06 p0754 N88-14628
Development of a graphical display on the DMS test bed 06 p0794 N88-14864
Monitoring of space station life support systems with miniature mass spectrometry and artificial intelligence
08 p1057 N88-16376
Prototype space station automation system delivered and demonstrated at NASA 08 p1066 N88-16442
Aspects of bioregenerative life support systems
12 p1655 N88-19917
Regenerative life support system research
[NASA-CR-182606] 12 p1671 N88-20006
Life Support Subsystem (LSS). Concept for the Botany Facility --- EURECA
[TN-RB524-107/86] 17 p2377 N88-24131
Summary of the activities performed during the Botany Facility (BF) predevelopment phase for the Life Support S/S (LSS)
[TB-RB524-002/87] 17 p2378 N88-24133
Subsea approach to work systems development
17 p2379 N88-24146
Advanced life support control/monitor instrumentation concepts for flight application
[NASA-CR-177378] 20 p2633 N88-26807
Advanced EMU electrochemically regenerable CO2 and moisture absorber module breadboard
[NASA-CR-172054] 21 p2993 N88-27754
ARGES: An expert system for fault diagnosis within space-based ECLS systems 23 p3255 N88-29380
Maintenance and supply options
[NASA-CR-172062] 24 p3332 N88-29837

LIFETIME (DURABILITY)
U LIFE (DURABILITY)

LIFT
NT INTERFERENCE LIFT
NT JET LIFT
NT ZERO LIFT
On the prospects for increasing dynamic lift
[RAE-TM-AERO-2068] 01 p0003 N88-10018
A heat transfer model for a heated helium airship
[AD-A183786] 03 p0259 N88-11629
An experimental evaluation of advanced rotorcraft airfoils in the NASA Ames eleven-foot transonic wind tunnel
[NASA-CR-166587] 03 p0261 N88-11640
Aerodynamic sensitivities from subsonic, sonic and supersonic unsteady, nonplanar lifting-surface theory
[NASA-TM-100502] 04 p0394 N88-12459
Nonlinear lift control at high speed and high angle of attack using vortex flow technology
05 p0545 N88-13319
Prediction of wing aeroelastic effects on aircraft life and pitching moment characteristics
05 p0551 N88-13356
Wind tunnel results for a high-speed, natural laminar-flow airfoil designed for general aviation aircraft
[NASA-TM-87602] 06 p0665 N88-14078
Lift distribution and velocity field measurements for a three-dimensional, steady blade/vortex interaction
[NASA-TM-100013] 07 p0815 N88-14962
Wind tunnel studies of circulation control elliptical airfoils 10 p1270 N88-17598
Lifting-surface theory of oscillating propellers in compressible flow
[NAL-TR-943] 10 p1273 N88-17613
Calculation of the distributed loads on the blades of individual multiblade propellers in axial flow using linear and nonlinear lifting surface theories
[NASA-TT-20173] 13 p1719 N88-20278
Zero-lift drag predictions in supersonic flow for complex configurations 15 p2054 N88-22246
Stall flutter analysis of propfans
16 p2221 N88-23256
Propulsive performance of a lifting flapping wing
17 p2295 N88-23733
Continuum theories for fluid-particle flows: Some aspects of lift forces and turbulence
[DE88-007038] 18 p2511 N88-24898
FEB (Multifilter Electronics Box) lifting device analysis, revision A
[AD-A192313] 21 p2935 N88-27427
Effects of psychophysical lifting training on maximal repetitive lifting capacity
[AD-A192605] 23 p3238 N88-29271

LIFT AUGMENTATION
On the prospects for increasing dynamic lift
[RAE-TM-AERO-2068] 01 p0003 N88-10018
Validation elements of the computation methods and measurement techniques for high lift aerodynamic systems
[SNIAS-872-111-101] 05 p0541 N88-13299
Propulsion-induced effects caused by out-of-ground effects
[NASA-TM-100032] 06 p0666 N88-14088
Evaluation of a research circulation control airfoil using Navier-Stokes methods 10 p1269 N88-17591
On the effect of leading edge blowing on circulation control airfoil aerodynamics 10 p1270 N88-17595
The impact of circulation control on rotary aircraft controls systems 10 p1271 N88-17601
Analysis of a fixed-pitch X-wing rotor employing lower surface blowing 10 p1271 N88-17602
An aerodynamic comparison of blown and mechanical high lift airfoils 10 p1272 N88-17606
Fixed wing CCW aerodynamics with and without supplementary thrust deflection
10 p1272 N88-17607
Circulation control STOL aircraft design aspects
10 p1272 N88-17610
An application of active surface heating for augmenting lift and reducing drag of an airfoil
[NASA-TM-100563] 11 p1436 N88-18570
Performance optimization of a cruise missile using dynamic-stall induced lift augmentation
[AD-A190497] 15 p2017 N88-22027
Analysis of a fixed-pitch X-wing rotor employing lower surface blowing
[AD-A187379] 24 p3321 N88-29779

LIFT COEFFICIENTS
U AERODYNAMIC COEFFICIENTS
U LIFT

LIFT DEVICES
Aircraft dynamic response calculation based on discrete-continual model 04 p0424 N88-12624
Studies of unsteadiness in boundary layers
[AD-A185662] 06 p0703 N88-14315
On the Kutta condition for flows around lifting airfoils and wings
[DFVLR-FB-87-40] 13 p1717 N88-20268
A panel method based on velocity potential to compute harmonically oscillating lift surface systems
[ETN-88-91886] 15 p2061 N88-22290
High-flaps for natural laminar flow airfoils
17 p2296 N88-23739
The identification of the direct lift control flap system of the research aircraft ATTAS
20 p2786 N88-26527

LIFT DISTRIBUTION
U FORCE DISTRIBUTION
U LIFT

LIFT DRAG RATIO
Conical wing with maximum lift-to-drag ratio in supersonic gas flow 04 p0425 N88-12633
Airframe/store compatibility 05 p0545 N88-13323
Study of descent of probes with high lift-drag ratio into the atmosphere of Jupiter 08 p1006 N88-16101
Investigation into the effects of flap end modifications on the performance of a wing with a single slotted flap
[BU-357] 14 p1866 N88-21148

LIFT FANS
Airborne remote operated device
[DE88-010324] 21 p2895 N88-27188

LIFT FORCES
U LIFT

LIFTING BODIES
NT LIFTING REENTRY VEHICLES
Aerodynamics of Hypersonic Lifting Vehicles
[AGARD-CP-428] 05 p0529 N88-13219
Numerical experiments with hypersonic flows beneath a cone-delta-wing combination 05 p0532 N88-13238
Numerical optimization of conical flow waveriders including detailed viscous effects
05 p0533 N88-13245
Dynamic stability of hypersonic conical lifting vehicles according to Newton-Busemann theory
05 p0534 N88-13247
Lifting bodies: An attractive aerodynamic configuration choice for hypervelocity vehicles
05 p0534 N88-13248
Aerodynamics of lifting bodies with combined transverse and longitudinal curvature 19 p2598 N88-25436
Aerodynamics of Hypersonic Lifting Vehicles: Fluid Dynamics Panel AGARD Symposium
[AGARD-AR-246] 21 p2943 N88-27480
VSAERO analysis of tip planforms for the free-tip rotor
[NASA-CR-177487] 22 p3038 N88-28036
Fellowships in hypersonic aerodynamics
[AD-A194265] 23 p3172 N88-28885

LIFTING REENTRY VEHICLES
European hypersonic wind tunnels
05 p0530 N88-13221
Shock tunnels for real gas hypersonics
05 p0530 N88-13223
Low Reynolds number influence on aerodynamic performance of hypersonic lifting vehicles
05 p0531 N88-13230

LIFTING ROTORS
NT BEARINGLESS ROTORS

LIFTING SURFACES
U LIFT DEVICES
U LIFTING BODIES
U SURFACES

LIGANDS
The formation and thermochemical properties of multiligand complexes
[AD-A184935] 05 p0561 N88-13416
Intramolecular energy transfer reactions as a method for metal complex assisted production of hydrogen
[DE88-001621] 05 p0562 N88-13425
Soluble metal chelate polymers of coordination numbers six, seven and eight
[AD-A185094] 05 p0568 N88-13459
The role of electronic structure calculation in mechanistic analysis of electron transfer reactions in the liquid phase
[DE87-014395] 05 p0647 N88-13963
Feasibility of a complex compound heat pump
[PB88-113022] 07 p0853 N88-15183
Coupling of vibrational modes of adsorbates: Application to field induced shifts for CO and CN on Cu(100)
[AD-A187891] 11 p1453 N88-18659
An investigation of metal complexes of some 2-substituted and 2,6-disubstituted pyridine N-oxides
11 p1460 N88-18701
Molecular and electronic mechanism in the control of Na+ and K+ permeability of excitable cell membrane by ligand binding on receptor sites
[AD-A188725] 13 p1808 N88-20805

LIGHT (VISIBLE RADIATION)
NT AIRGLOW
NT COHERENT LIGHT
NT DAYGLOW
NT GEOCORONAL EMISSIONS
NT NIGHTGLOW
NT POLARIZED LIGHT
NT SKY RADIATION
NT SUNLIGHT
NT ZODIACAL LIGHT

The largest white light flare ever observed: 25 April 1984, 0001 UT 01 p0111 N88-10714
New physical explanation of phase-conjugate waves produced in backward stimulated scattering 03 p0302 N88-11900
Solitons in stimulated Raman scattering: Generation and control of ultrashort optical pulses [AD-A185141] 05 p0650 N88-13983
Airborne Visible/Infrared Imaging Spectrometer (AVIRIS). A description of the sensor, ground data processing facility, laboratory calibration, and first results [NASA-CR-182365] 06 p0705 N88-14325
A system overview of the Airborne Visible/Infrared Imaging Spectrometer (AVIRIS) 06 p0705 N88-14326
Airborne Visible/Infrared Imaging Spectrometer (AVIRIS) spectrometer design and performance 06 p0706 N88-14327
AVIRIS foreoptics, fiber optics and on-board calibrator 06 p0706 N88-14328
Visible and infrared linear detector arrays for the Airborne Visible/Infrared Imaging Spectrometer (AVIRIS) 06 p0706 N88-14329
AVIRIS scan drive design and performance 06 p0706 N88-14330
Signal chain for the Airborne Visible/Infrared Imaging Spectrometer (AVIRIS) 06 p0706 N88-14331
AVIRIS onboard data handling and control 06 p0706 N88-14332
AVIRIS ground data-processing system 06 p0707 N88-14333
Spectral and radiometric calibration of the Airborne Visible/Infrared Imaging Spectrometer 06 p0707 N88-14334
First results from the Airborne Visible/Infrared Imaging Spectrometer (AVIRIS) 06 p0707 N88-14335
New description of Lau effect based on theory of raster image forming process 06 p0772 N88-14744
Parametric and resonance interaction of ultrashort light pulses in nonlinear multilevel medium 06 p0773 N88-14746
Total light flux and colour of solar corona [PB87-143335] 07 p0946 N88-15754
Joint services electronics program [AD-A188173] 11 p1478 N88-18822
Solid-state ring laser with acoustooptical phase nonreciprocity of opposing waves 14 p1970 N88-21761
Squeezed states of light 14 p1976 N88-21791
Pulsed squeezed light 14 p1976 N88-21792
Nonclassical lights 14 p1979 N88-21810
Open questions in closed-loop photodetection 14 p1979 N88-21812
Relationship between optical transfer function and natural light field in sea or atmosphere 15 p2054 N88-22247
Infrared-sensitive spatial light modulator [AD-A190391] 15 p2134 N88-22729
Experimental research on skin reflection, transmission, absorption of light rays 16 p2187 N88-23039
Nonlinear wave and diffusion equations [AD-A191421] 16 p2265 N88-23544
Research investigation directed toward extending the useful range of the electromagnetic spectrum [AD-A190198] 17 p2332 N88-23920
Light propagation through gravitationally perturbed Friedmann universes 18 p2577 N88-25307
A twin-mirrored galvanometer laser light sheet generator [NASA-TM-100587] 19 p2674 N88-25901
Precision measurement of the Fresnel drag coefficient using a ring laser [AD-A196025] 24 p3366 N88-30043

LIGHT ABSORPTION
U ELECTROMAGNETIC ABSORPTION

LIGHT ADAPTATION
Electroencephalographic changes during equilibrium test in the presence of rhythmic photic interference 19 p2703 N88-26075

LIGHT AIRCRAFT
NT DO-28 AIRCRAFT
NT OH-58 HELICOPTER
Modern materials for light constructions — aircraft [MBB-Z-136/86] 10 p1312 N88-17839
Determination of canopy loads for a light aircraft by wind tunnel testing and computer modelling [BU-353] 14 p1869 N88-21167
It's time to reinvent the general aviation airplane 17 p2294 N88-23726
An interim comparison of operational CG records in turbulence on small and large civil aircraft 24 p3313 N88-29729

LIGHT ALLOYS
NT ALUMINUM ALLOYS
NT BERYLLIUM ALLOYS
NT MAGNESIUM ALLOYS
Materials for fighter aircraft 05 p0546 N88-13325
Application of the ONERA model to the life estimation under fatigue cracking of a Al-Li alloy. Parameter identification and test-experiment comparison under FALSTAFF loading [ONERA-RT-32/7169-RY-063-R] 16 p2222 N88-23264
Crack retardation under load spectra. Experimental study and numerical simulation using the simplified K constant model --- light alloys, aircraft construction materials [ONERA-RT-30/7169-RY-054-R] 16 p2222 N88-23266

LIGHT AMPLIFIERS
An experimental study of CW HF chemical laser amplifier performance and zero power gain [AD-A185241] 05 p0588 N88-13584
Periodically pulsed excimer master oscillator-regenerative amplifier laser set 06 p0772 N88-14741
Phase phenomena in parametric generators and amplifiers of ultrashort light pulses 07 p0918 N88-15576
TEA-TE: Powerful nitrogen-based laser system 07 p0919 N88-15583
Generation of coherent soft X-rays using a single-pass free-electron laser amplifier [DE88-009137] 19 p2675 N88-25907
Optical guiding in the separable beam limit [AD-A192452] 21 p2952 N88-27534
Nonlinear optical phase conjugation techniques to reduce the physical size of lasers [AD-A196170] 24 p3379 N88-30122

LIGHT BEAMS
NT LASER BEAMS
The deviation of light rays passing through a curved windscreen --- aircraft [BAE-MSC.115] 01 p0093 N88-10610
Optoelectronic measurement methods for ballistic experiments [PB87-110706] 05 p0583 N88-13554
Periodically pulsed excimer master oscillator-regenerative amplifier laser set 06 p0772 N88-14741
Energy transmission using coherent, quasimonochromatic light beams 09 p1241 N88-17436
Continuous collective molecule rotation of a nematic liquid crystal induced from light angular momentum [FUB-17-1986] 14 p1986 N88-21845
An optical technique for measuring divergence, beam profile, and aiming direction, of relativistic negative hydrogen ions [DE88-007049] 18 p2572 N88-25278

LIGHT BULBS
U LUMINAIRES

LIGHT COMMUNICATION
U OPTICAL COMMUNICATION

LIGHT CURVE
Basic properties and variability 02 p0252 N88-11593
The giant spot on II Peg in 1986 04 p0508 N88-13120
The short-period RS CVn stars: Starspots and fundamental properties 04 p0508 N88-13124
The X-ray orbital lightcurves of AR Lac and TY Pyx 04 p0509 N88-13129
Differential B and V light curves of the bright BY Draconis star HD80715 04 p0509 N88-13130
Light curve behaviour in the near IR of the CG Cyg system 04 p0513 N88-13156
Pre-main sequence activity: How far is magnetism involved 04 p0517 N88-13179
Stromgren photometry of RSCVn and HD108102 04 p0519 N88-13187
The type Ia supernova 1986G in NGC5128: Optical photometry and spectra [INPE-4426-PRE/1230] 12 p1710 N88-20231
The light curve of P/Halley and the rotation of its nucleus 14 p2009 N88-21984
To the opportunities of cluster analysis of light curves of supernovae [DE88-701642] 21 p3030 N88-27982
The ultrashort period dwarf nova SW Ursae Majoris 24 p3453 N88-30553

LIGHT DURATION
U PULSE DURATION

LIGHT EMISSION
NT BIOLUMINESCENCE
NT CHEMILUMINESCENCE
NT ELECTROLUMINESCENCE
NT FLUORESCENCE
NT LASER INDUCED FLUORESCENCE
NT LUMINESCENCE
NT OPTICAL RESONANCE
NT PHOSPHORESCENCE
NT PHOTOLUMINESCENCE
NT RESONANCE FLUORESCENCE
NT SPACECRAFT GLOW
NT X RAY FLUORESCENCE
The largest white light flare ever observed: 25 April 1984, 0001 UT 01 p0111 N88-10714
IUE/Optical/VLA flares on AD Leo 04 p0512 N88-13152
Laser thermal propulsion [AD-A186407] 07 p0933 N88-15666
Linear theory of generation of longitudinal sound waves in semiconductors upon interband absorption of optical radiation 09 p1234 N88-17397
Scattering of optical radiation by bursting water particles in fog 09 p1236 N88-17410
The analytical exponential decay coefficient of the submarine light field [AD-A187215] 11 p1548 N88-19261
Merit of Hadamard transform active absorption spectrometer described 15 p2053 N88-22232
Development of liquid metal field-emission sources for use in fast repetitive opening switches [AD-A192230] 20 p2795 N88-26583
Optical emission behavior and radiation resistance of epoxy resins [DE88-752629] 23 p3196 N88-29023
Optical emission from surface waves supported in thin metal films 23 p3282 N88-29540

LIGHT EMITTING DIODES
Development of an optical feedback based high accuracy beam transmissometer [AD-A189396] 12 p1692 N88-20122
Atmospheric attenuation of near infrared radiation propagating through fog 14 p1899 N88-21342
Excitation of single-mode glass fiber by partially coherent sources [ETN-88-92121] 20 p2854 N88-26951

LIGHT GAS GUNS
Ideal-viscoplastic extrusion model with application to deforming pistons in light-gas guns [UTIAS-TN-266] 04 p0429 N88-12657
An investigation of soft launch and instability breakup with a two-stage light gas gun [DE88-010371] 21 p2901 N88-27218

LIGHT INTENSITY
U LUMINOUS INTENSITY

LIGHT IONS
Studies on surface chemical states of some metals and ceramics bombarded with energetic light-ions [DE87-752975] 02 p0145 N88-10910
Energy dependence of ion-induced sputtering yields of monatomic solids in the low energy region [IPPJ-AM-52] 05 p0651 N88-13988
Two-dimensional focusing of self-magnetically insulated plasma focus diode 16 p2278 N88-23639
Time-resolved spectroscopic measurement of anode plasma in magnetically-insulated diode 16 p2279 N88-23641
Pulsed power driver technologies for inertial confinement fusion power reactors [DE88-009260] 19 p2731 N88-26221

LIGHT MODULATION
Development of optical modulators for measurements of solar magnetic fields [NASA-TM-100315] 04 p0490 N88-13016
Phase phenomena in parametric generators and amplifiers of ultrashort light pulses 07 p0918 N88-15576
Joint services electronics program [AD-A188173] 11 p1478 N88-18822
A numerical analysis of the dynamics of PRIZ operation [AD-A188853] 12 p1678 N88-20035
Study of photochromic materials for use in optical signal processing [AD-A189068] 13 p1839 N88-21006
Infrared-sensitive spatial light modulator [AD-A190391] 15 p2134 N88-22729
Research on materials and components for opto-electronic signal processing and computing [AD-A190130] 15 p2143 N88-22788
Research investigation directed toward extending the useful range of the electromagnetic spectrum, appendix [AD-A190199] 17 p2332 N88-23921
Optical modulation above 20 GHz using a waveguide electrooptic switch 19 p2660 N88-25819
Use of depletion edge translation for high-speed modulation and switching of lightwaves [AD-A195611] 24 p3430 N88-30417

LIGHT PRESSURE
U ILLUMINANCE

LIGHT PROBES
U LIGHT BEAMS

LIGHT SCATTERING
NT HALOS

Light scattering by oriented and randomly dispersed chiral particles
[DE87-014758] 03 p0376 N88-12368
All-optical beam control by forced Rayleigh scattering
[AD-A184315] 04 p0490 N88-13018
Extinction by dielectric particles at optical and infrared wavelength
[AD-A184818] 05 p0650 N88-13981
Measurement of particle size distribution in a solid propellant rocket motor using light scattering
[AD-A184875] 06 p0673 N88-14124
Observing effect of laser radiation of low-frequency Raman scattering of light 06 p0772 N88-14742
Research on acoustical scattering, diffraction catastrophes, optics of bubbles, photoacoustics, and acoustical phase conjugation
[AD-A185785] 06 p0776 N88-14761
Chemical reactions in turbulent mixing flows
[AD-A186141] 07 p0849 N88-15153
Monte Carlo method calculation of spectral brightness coefficient of vegetation cover as function of illumination conditions 08 p1006 N88-16113
Stimulated Mandelstam-Brillouin scattering during forward scattering of light 08 p1078 N88-16499
A review of some flow visualization experiments carried out at the Institut Franco-Allemand de Recherches (ISL) shock tubes
[ISL-CO-243/86] 09 p1163 N88-16974
Digital imaging techniques for single- and multi-phase reacting flowfields 10 p1327 N88-17933
Advances in calculating macroionic solution structure
[DE88-003799] 10 p1409 N88-18406
Diagnostics for research in atomization and turbulent two-phase flows
[AD-A187338] 11 p1482 N88-18843
Depolarized infrared reflectance from dry and wetted surfaces
[AD-A188213] 11 p1492 N88-18903
Optical characterization of tropospheric aerosols
[AD-A187839] 11 p1511 N88-19029
Vibrational, mechanical and thermal properties of 3-5 semiconductors
[AD-A187569] 11 p1556 N88-19316
Thermodynamic theory of fluctuations and Rayleigh light scattering in solutions 13 p1785 N88-20681
Multiple scattering of polarized light in cirrus clouds 13 p1801 N88-20768
Additional peak of light scattering by sound under conditions of acoustic instability 14 p1968 N88-21752
A new class of multiple dispersion grating spectrometers
[PREPRINT-569] 14 p1983 N88-21830
Linear and circular polarization of Comet Halley light 14 p2009 N88-21982
Research on certain aspects of laser diffraction particle sizing relevant to autonomous self-diagnosing instrumentation
[AD-A190220] 15 p2071 N88-22348
The interaction of small particles with laser beams
[AD-A190716] 15 p2072 N88-22354
Multiple scattering from nonspherical targets
[AD-A189939] 15 p2133 N88-22723
Light scattering of intracellular gas vacuoles: Anomalous behavior of forward and perpendicular light scattering of a cyanobacterium due to intracellular gas vacuoles
[BCRS-87-08] 16 p2228 N88-23308
Enhanced backscattering from rough surfaces
[AD-A191089] 16 p2274 N88-23610
Analysis of dust grain properties in two star forming regions through comparison of theoretical models to observations 17 p2451 N88-24559
Molecular characterization of structure and bonding in thin film materials
[DE88-006811] 18 p2584 N88-25351
Effects of atmospheric model layering on LOWTRAN 6 calculations of 8-12 micrometers near-horizon sky radiances
[AD-A192969] 20 p2791 N88-26559
Light scattering by charged spheres
[AD-A193753] 22 p3153 N88-28759
Beam combining by phase transition nonlinear media
[AD-A194116] 23 p3283 N88-29547
Particle sizing in combustion systems, using scattered laser light
[AD-A196231] 24 p3352 N88-29953

LIGHT SCATTERING METERS
Study of the properties of a new detector class for liquid chromatography
[DE88-001666] 05 p0563 N88-13426

LIGHT SOURCES
National Synchrotron Light Source users manual: Guide to the VUV and X-ray beam lines
[DE88-001464] 04 p0490 N88-13020
Anti-Stokes generation of 226 nm light
[DE88-001612] 05 p0589 N88-13590
Soliton mode of propagation of light pulses through single-mode optical fibers and problems of its experimental realization 07 p0920 N88-15592
Pulsed laser stereophotography of plasmas and dynamically moving surfaces
[DE88-003170] 09 p1173 N88-17031
Signal processing studies program optical signal amplification, volume 2
[AD-A188054] 10 p1320 N88-17896
The light pulse generator 869 for high speed investigations
[MPIS-9/1987] 11 p1491 N88-18898
Coherent VUV source at 130 nm: Theory and modeling
[DE88-003874] 11 p1549 N88-19269
Rainbow holographic image reconstructed by spatially extended white light source 15 p2055 N88-22249
Tracking a monochromatic light source
[DE88-011260] 20 p2807 N88-26653
Fiber optic sensing systems using high frequency resonant sensing heads with intensity sensors
[NASA-TM-101318] 22 p3080 N88-28293
Eye movements and spatial pattern vision
[AD-A195496] 24 p3408 N88-30290

LIGHT SPEED
Superluminal velocities within relativity theory
[ETN-87-90958] 02 p0247 N88-11563
Theory of relativity and super-light-speeds-I: Kinematical part
[DE88-701832] 20 p2880 N88-27100

LIGHT TRANSMISSION
NT HALOS
NT LIGHT SCATTERING
Radiation-induced transient attenuation of optical fibers at 800 and 1300 nm
[DE87-013165] 02 p0235 N88-11485
Optical probe
[EP-PATENT-0-210-869-A1] 05 p0650 N88-13984
Effect of clarifying the atmosphere in relation to quasi-monochromatic CO2 laser radiation 06 p0709 N88-14348
Photoinduced low-temperature changes in optical losses in fiber optics based on chalcogenide glasses 06 p0770 N88-14731
Determination of cloud base height and emissivity from downwelling angular radiances
[AD-A185985] 07 p0879 N88-15331
Soliton mode of propagation of light pulses through single-mode optical fibers and problems of its experimental realization 07 p0920 N88-15592
Characterization of transparent insulation materials — solar energy absorbers
[ETN-88-91052] 09 p1163 N88-16970
Signal processing for an optical wide band data transmission system
[DE88-003854] 10 p1319 N88-17888
The analytical exponential decay coefficient of the submarine light field
[AD-A187215] 11 p1548 N88-19261
Remote sensing of atmospheric optical thickness and sea-water attenuation when submerged: Wavelength selection and anticipated errors
[AD-A187609] 11 p1548 N88-19262
Analysis of the inter-layer independence of stellar scintillometer profiles of Cn2
[AD-A189372] 12 p1645 N88-19654
Development of an optical feedback based high accuracy beam transmissometer
[AD-A189396] 12 p1692 N88-20122
Influence of nonlinear spectroscopic effects on atmospheric propagation of intense laser radiation at 10.6 microns wavelength 13 p1789 N88-20705
Coherence effects in optical physics with special reference to spectroscopy
[AD-A189520] 13 p1840 N88-21007
Atmospheric attenuation of near infrared radiation propagating through fog 14 p1899 N88-21342
Advanced programming and control techniques for complex mechanical systems
[AD-A190238] 15 p2071 N88-22349
Atmospheric propagation of laser beams
[AD-A191447] 18 p2520 N88-24952
Study of light transmission methods from scintillators to optical fiber with wave length shifter
[DE88-701587] 18 p2574 N88-25292
Low-loss, high-isolation, fiber-optic isolator
[NASA-CASE-NPO-17207-1-CU] 18 p2576 N88-25304
Stress-related phenomena in transient radiation-induced absorption in optical fibers
[DE88-010956] 20 p2854 N88-26949
Multichannel data transmission through a fiber optic cable
[AD-A193842] 22 p3070 N88-28221
Metal halide optical glasses
[AD-A193794] 23 p3198 N88-29032

LIGHT WATER REACTORS
A model for stationary and dynamic impression of undercooled boiling in coupled thermohydraulic and neutron physics calculations of nuclear reactors
[IKE-6-171] 09 p1247 N88-17472
Development of fast breeder reactors in China 16 p2186 N88-23032
Statistical evaluation of light water reactor piping damping data for use in PRA (Probabilistic Risk Assessment) analyses
[DE88-007708] 19 p2661 N88-25828

LIGHTING
U ILLUMINATING

LIGHTING EQUIPMENT
NT ARC LAMPS
NT FLASH LAMPS
NT LUMINAIRES
NT QUARTZ LAMPS
Failure of filament lamps subjected to vibration with special reference to the 26 volt 5 Watt tank lamp
[EL-135] 09 p1158 N88-16938

LIGHTNING
The physics of charge separation preceding lightning strokes in thunderclouds
[NASA-CR-178371] 01 p0071 N88-10452
Production of NO by galactic cosmic rays and lightning
[DE87-014613] 02 p0197 N88-11230
Short-term forecasting of lightning based on the surface wind field at Kennedy Space Center 02 p0208 N88-11306
Experimental and analytic studies of the triggered lightning environment of the F106B
[NASA-CR-4104] 04 p0469 N88-12897
Lightning discharge protection rod
[NASA-CASE-LAR-13470-1] 06 p0666 N88-14083
Atmospheric electricity
[NASA-CR-179239] 06 p0744 N88-14575
Radar observations of changes in precipitation size spectra associated with lightning 06 p0744 N88-14576
Lightning spectra in the near infrared
[DE88-002218] 07 p0880 N88-15341
Astrophysics and the solar nebula 07 p0883 N88-15355
Applicability of extremely low frequency global resonances for study of Venusian storm activity 08 p1005 N88-16093
Return stroke velocities and currents using a solid state silicon detector system 11 p1515 N88-19050
Validation of GEMACS (General Electromagnetic Model for the Analysis of Complex Systems) for modeling lightning-induced electromagnetic fields
[AD-A188822] 12 p1620 N88-19687
Atmospheric electrical modeling in support of the NASA F-106 storm hazards project
[NASA-CR-181639] 13 p1799 N88-20758
Characteristics of the positive lighting flash
[DE88-005854] 13 p1800 N88-20760
Upward propagating electric fields from thunderstorms and VLF transmitters 13 p1801 N88-20767
Activities report of the Physics Department
[ETN-88-91985] 13 p1833 N88-20964
Equipment test methods for externally produced electromagnetic transients
[RAE-TM-FS(F)-457] 14 p1865 N88-21140
Distribution of summertime lightning as a function of low-level wind flow in central Florida
[PB88-160759] 14 p1948 N88-21619
Experimental comparison of lightning simulation techniques to CV-580 airborne lightning strike measurements
[AD-A190576] 15 p2098 N88-22496
Study of lightning and lightning protection (selected pages)
[AD-A190623] 15 p2098 N88-22498
Proceedings of the Lightning Threat Warning Workshop
[DE88-006607] 15 p2098 N88-22499
Atmospheric Science and Remote Sensing Laboratory
[NASA-CR-179290] 16 p2236 N88-23355
Finite element simulation of the atmosphere's electromagnetic response to charge perturbations associated with lightning 17 p2375 N88-24124
Theoretical basis for an experimental test with regard to the origin of VHF (Very High Frequency) radiation from natural lightning
[DE88-007535] 18 p2544 N88-25102
Analysis of lightning field changes during active thunderstorms in Florida 18 p2545 N88-25103
Lightning detection and locating systems 18 p2546 N88-25112
Voltages induced by lightning on electric power distribution lines: Field data and analysis results for the period July 1984-1986
[DE88-007841] 19 p2693 N88-26006

Computer controlled data acquisition system for the NASA 1986 Rocket Triggered Lightning Program
[DE88-008335] 20 p2826 N88-26766
A radar study of the interaction between lightning and precipitation
[DE88-009120] 20 p2827 N88-26770
Investigations into the triggered lightning response of the F106B thunderstorm research aircraft
[NASA-CR-3902] 23 p3236 N88-29258
The 1983 direct strike lightning data, part 1
[NASA-TM-86426-PT-1] 23 p3237 N88-29259
The 1983 direct strike lightning data, part 2
[NASA-TM-86426-PT-2] 23 p3237 N88-29260
The 1983 direct strike lightning data, part 3
[NASA-TM-86426-PT-3] 23 p3237 N88-29261

LIGHTNING SUPPRESSION
Fuel containment, lightning protection and damage tolerance in large composite primary aircraft structures
[NASA-CR-3875] 17 p2317 N88-23839
An interagency working group on lightning threat warning
[DE88-009828] 20 p2826 N88-26767
The first synthesis of chem-prep varistor LAC (Lightning Arrestor Connector) granules
[DE88-008005] 21 p2936 N88-27438

LIGHTS
U LUMINAIRES

LIKELIHOOD RATIO
A note on extended quasi-likelihood
[AD-A186318] 07 p0915 N88-15555
A likelihood based grouping method for multidimensional observations. An interactive method used on large transportation data bases
[REPT-87-74] 16 p2286 N88-23685

LIMB DARKENING
Asymmetry and variations of solar limb darkening along the diameter defined by diurnal motion in April 1981
04 p0506 N88-13111
Calibration of the Ca II K line-core density and the magnetic flux density in stars using solar data
04 p0507 N88-13116

LIMBS (ANATOMY)
NT ARM (ANATOMY)
NT FINGERS
NT HAND (ANATOMY)
NT LEG (ANATOMY)
Dynamics and stability of bipedal locomotion robots
03 p0333 N88-12096
Limb regeneration in amphibians, a suitable model for investigations of the effects of weightlessness as regards evolution and modifications 07 p0885 N88-15369

LIME
U CALCIUM OXIDES

LIMITATIONS
U CONSTRAINTS

LIMITERS (FUSION REACTORS)
Technical evaluation of major candidate blanket systems for fusion power reactor
[DE87-752989] 02 p0239 N88-11512
Modular pump limiter systems for large tokamaks
[DE88-001487] 04 p0494 N88-13045
ALT-1 pump limiter experiments
[DE88-000822] 05 p0651 N88-13989
Pump limiter experiments and analysis in the TEXTOR tokamak 09 p1252 N88-17506
Stability of an RFP (Reversed-Field Pinch) with resistive and distant boundaries
[DE88-004155] 10 p1413 N88-18431
Analyses and experiments on the integrity and lifetime predictions of plasma-facing components in fusion reactors
[DE87-702957] 15 p2135 N88-22735
Erosion/redeposition modeling and calculations for carbon
[DE88-010382] 22 p3057 N88-28139
Tokamak plasma interaction with limiters
[UTIAS-325] 23 p3286 N88-29566

LIMITS (MATHEMATICS)
Stochastic filtering solutions for ill-posed linear problems and their extension to measurable transformations
[AD-A186016] 07 p0909 N88-15506
Mathematical foundations of signal processing. 2: The role of group theory
[AD-A188482] 12 p1620 N88-19685
The partially observed stochastic minimum principle
[AD-A189787] 15 p2124 N88-22658
A central limit theorem for M-estimators by the von Mises method
[CWI-MS-R8713] 16 p2262 N88-23525
Computation of filters by sampling and quantization
[AD-A192839] 21 p3005 N88-27826
Approximations and implementations of nonlinear filtering schemes
[AD-A194685] 23 p3271 N88-29462

LIMNOLOGY
The effect of wind and currents on gas exchange in an estuarine system
[NASA-CR-181424] 01 p0073 N88-10468

LINE CURRENT
Optical power line voltage and current measurement systems. Volume 1: Limits to the precision of electro-optic and magneto-optic sensors
[DE87-014558] 02 p0175 N88-11092
On the potential role of concentrated field-aligned currents in solar physics 08 p1099 N88-16614
Complex space monofilar approximation of diffraction currents on a conducting half plane
[NASA-CR-182883] 16 p2273 N88-23605

LINE OF SIGHT
Adaptive line of sight algorithms
[DE87-014275] 01 p0081 N88-10523

LINE OF SIGHT COMMUNICATION
Identification of microwave line-of-sight multipath components 12 p1616 N88-19665
Refractive index, meteorology and fading in line-of-sight transmission paths 12 p1616 N88-19666
Radio and radar holes and multipath zones: The global and local influences on atmospheric refractive structure and resulting adverse radio and radar performance
12 p1617 N88-19667
Space-diversity effects on line-of-sight propagation paths 12 p1617 N88-19670
An EHF telecommunication system engineering model
12 p1618 N88-19674

LINE SHAPE
Calculation of the line shapes of radiators immersed in plasma 19 p2729 N88-26210
Molecular line shape effects on atmospheric window absorption
[AD-A196316] 24 p3342 N88-29894

LINE SPECTRA
NT BALMER SERIES
NT ELECTRONIC SPECTRA
NT FRAUNHOFER LINES
NT H ALPHA LINE
NT H BETA LINE
NT H LINES
NT K LINES
NT LYMAN SPECTRA
NT RYDBERG SERIES
Evidence of a new spectral line intensity formula for optical emission
[KGI-PREPRINT-098] 01 p0090 N88-10585
Spectrograms of the visible region in the JT-60 tokamak (wavelength range from 2210 A to 5250 A)
[DE87-753002] 02 p0240 N88-11513
Relaxation effect of stark split levels for two-level system interacting with symmetrical strong resonant bichromatic field 03 p0299 N88-11882
Comparison of global and nuclear properties of starburst and Seyfert 1 galaxies 03 p0388 N88-12438
Investigations of extragalactic hydroxyl
03 p0389 N88-12441
Active phases on II Peg 04 p0507 N88-13119
H alpha and Ca II emission line variability of FK comae 04 p0509 N88-13128
Magnetic fields on K and M stars
04 p0510 N88-13137
Broadband linear polarization and chromospheric CaII H and K line emission in late-type main sequence stars
04 p0511 N88-13140
An analysis of the photospheric line profiles in F, G, and K supergiants 04 p0513 N88-13157
The Wilson-Bappu relationship: A barometric effect
04 p0516 N88-13170
Synthetic spectra for the N-type carbon star TX Psc
04 p0516 N88-13173
Infrared excesses of barium stars
04 p0516 N88-13174
The delta upsilon = 1 fundamental bands of carbon monoxide in late-type stars 04 p0517 N88-13177
A helium flare on the active G5 dwarf Kappa Ceti
04 p0519 N88-13189
A computer code to calculate line by line atmospheric transmission spectra on a microcomputer
[NASA-TM-100686] 05 p0554 N88-13372
Narrow linewidth gain measurements in a KrF excimer amplifier pumped longitudinally by a high-power electron beam
[DE88-001365] 05 p0586 N88-13575
An adaptive lattice algorithm for spectral line estimation
[AD-A184970] 05 p0634 N88-13876
Main results of atmospheric fine structure parameter observation in the lower thermosphere
06 p0735 N88-14518
Optical electronics for meteor observations
06 p0741 N88-14559
Justification and prospects of observations of interstellar, far-infrared emission lines, using a small-sized balloon-borne telescope 08 p1032 N88-16254
Gamma-ray imaging observations of the Crab and Cygnus regions 10 p1427 N88-18522
An analysis of longitude variations in the equatorial spectrum of Saturn 10 p1430 N88-18539
Spectral line-broadening codes for hydrogen-, helium- and lithium-like ions in plasmas
[DE88-005238] 11 p1552 N88-19289
An interpretation of the ethylenic, carbidic, and graphite auger lineshapes of chemisorbed carbon species
[AD-A189092] 13 p1736 N88-20379
The astrophysics of nebulae and active galactic nuclear emission-line regions: New methods and applications
13 p1858 N88-21111
Effect of Mg impurity on local vibrations of U-centers in LiF lattice 14 p1969 N88-21753
The observability of carbon monoxide in planetary nebulae
[ETN-88-91498] 14 p2011 N88-21994
Statistical fine structure in inhomogeneously broadened absorption lines in solids
[AD-A190341] 16 p2174 N88-22957
Implications of the trapping-desorption and direct inelastic scattering channels on Dicke-narrowed lineshapes
[AD-A191410] 16 p2270 N88-23581
Total photoionization cross sections of atomic oxygen from threshold to 44.3A
[NASA-CR-182992] 17 p2397 N88-24252
Helium-like titanium spectra from tokamak plasmas
17 p2440 N88-24516
Forbidden transitions as ion-temperature sensitive lines 17 p2441 N88-24520
Tokamak studies of density sensitive line ratios
17 p2441 N88-24521
Intensity calibration of a VUV system by branching line pairs 17 p2443 N88-24533
The gamma 1 and gamma 3 bands of (16)O3: Line positions and intensities
[NASA-TM-101162] 17 p2445 N88-24541
Line positions and intensities for the gamma 1 + gamma 2 and gamma 2 + gamma 3 bands of (16)O3
[NASA-TM-101161] 17 p2446 N88-24542
An optical preamplifier for detection of CO2 laser radiation
[AD-A190790] 18 p2520 N88-24949
Observations of wave number dependent spectral line ratio fluctuations in the atmospheric emissions
[IRF-PREPRINT-101] 18 p2542 N88-25085
Studies of spectral line ratio fluctuations using Inductively Coupled Plasma (ICP) light
[IRF-PREPRINT-100] 18 p2578 N88-25311
Recent data on Si:As impurity band conduction multiplexed arrays
[AD-A191752] 18 p2582 N88-25340
Inner-shell X-ray line spectra of highly ionized titanium, chromium, iron and nickel and their appliation to laboratory plasmas
[PB87-225181] 19 p2730 N88-26212
Detection of absorption lines in the spectra of X-ray bursts from X1608-52
[ISAS-RN-360] 20 p2887 N88-27143
Spectral line shapes from highly ionized sodium plasmas
[AD-A193401] 21 p3017 N88-27907
Paramagnetic point defects in boron-implanted HgO.7CdO.3Te
[AD-A193276] 21 p3021 N88-27934
The electromagnetic spectrum: The information mine
[AD-A194316] 22 p3069 N88-28215
First detection of HCN J=9 to 8 (797 GHz) line emission: Very high densities in the Orion core
[MPE-PREPRINT-110] 22 p3165 N88-28847
On selection rules and inelastic electron scattering at intermediate energies
[DE88-701833] 23 p3280 N88-29526
The optical spectroscopy of copper-blue luminescence in zinc sulfide crystals. Zero-phonon line spectra under the influence of magnetic field, temperature and excitation intensity
[ETN-88-93122] 24 p3344 N88-29903

LINEAMENT
U STRUCTURAL PROPERTIES (GEOLOGY)

LINEAR ACCELERATORS
Visible free electron laser oscillator
[AD-A183871] 01 p0051 N88-10324
Induction linac-driven free-electron lasers: Status and future prospects
[DE87-012914] 01 p0051 N88-10329
Open accelerating structures
[DE87-010540] 01 p0092 N88-10603
Transverse focussing using plasma wake fields
[DE87-011503] 01 p0099 N88-10652

Status of inertial fusion
[DE87-010966] 01 p0099 N88-10654
A simple self-breaking 2 MV gas switch
[DE87-014346] 02 p0166 N88-11047
A high-power RF linear accelerator for FELs (Free-Electron Lasers)
[DE87-011795] 02 p0177 N88-11104
The nature of beamstrahlung
[DE87-012637] 02 p0234 N88-11474
A conceptual design of Final Focus Systems for linear colliders
[DE87-012640] 02 p0234 N88-11475
Interactive Design of Accelerators (IDA)
[DE87-013298] 02 p0234 N88-11476
Simulation of tokamak runaway-electron events. Study of the response of materials by use of an electron linear accelerator
[IPPJ-841] 02 p0242 N88-11528
Proceedings: SDIO/DARPA Workshop on Laser Propulsion. Volume 3: Viewgraphs
[DE88-000964] 04 p0450 N88-12790
Development of a laced electromagnetic wiggler
[DE88-000972] 05 p0646 N88-13953
Heavy-ion accelerator research for inertial fusion
[DE88-000541] 05 p0653 N88-14001
A qualitative study of wake fields for very short bunches
[DE88-002565] 09 p1164 N88-16980
CEBAF design overview and project status
[CEBAF-PR-88-001] 09 p1246 N88-17470
Preliminary injector, accelerator, and beamline design for rf-linac-driven XUV free-electron lasers
[DE88-003185] 10 p1336 N88-17983
Medium high energy physics at Syracuse University
[DE88-003670] 11 p1545 N88-19235
The injector for the CEBAF CW superconducting linac
[CEBAF-PR-87-011] 11 p1546 N88-19241
Perturbation effects in the CEBAF beam transport system
[CEBAF-PR-87-010] 11 p1546 N88-19242
Investigation of multiple particle final states at CEBAF (Continuous Electron Beam Accelerator Facility)
[CEBAF-PR-87-026] 11 p1547 N88-19250
RF steering in the CEBAF CW superconducting linac
[CEBAF-PR-87-013] 11 p1547 N88-19251
The CEBAF project and its few-body research program
[CEBAF-PR-87-014] 11 p1547 N88-19253
Two dimensional simulations of multipass beam breakup
[CEBAF-PR-87-008] 11 p1547 N88-19254
Induction linacs: A technology come of age for international cooperation
[DE88-003953] 11 p1548 N88-19258
Big Bang Nucleosynthesis: Accelerator tests and can (UC OMEGA)(sub B) really be large
[DE88-003405] 11 p1570 N88-19396
Application of radio frequency superconductivity to recirculating linacs
[CEBAF-PR-88-002] 12 p1690 N88-20107
On (e,e'N) reactions
[CEBAF-PR-87-028] 12 p1690 N88-20109
Optics of the CEBAF CW superconducting accelerator
[CEBAF-PR-87-012] 12 p1690 N88-20110
Multipass beam breakup in recirculating linacs
[CEBAF-PR-87-007] 12 p1690 N88-20111
Projected performance of RF-linac-driven free-electron lasers in the VUV and soft X-ray regions
[DE88-004294] 13 p1776 N88-20625
The continuous electron beam accelerator facility
[CEBAF-PR-87-017] 13 p1838 N88-20996
Status of RF superconductivity at Argonne National Laboratory
[DE88-005913] 15 p2144 N88-22796
Heavy ion fusion system assessment: Final focus and transport model
[LBL-23040] 19 p2725 N88-26183
Accelerator research studies
[DE88-006236] 19 p2726 N88-26187
Results from the SLAC lasertron
[DE88-007816] 20 p2806 N88-26647
Research opportunities below 300 nm at the NBS Free-Electron Laser Facility
[AD-A193100] 21 p2953 N88-27538

LINEAR ARRAYS
Spectrometric test of a linear array sensor
[NASA-TM-100676] 01 p0064 N88-10414
Ground-based interferometry with the European Very Large Telescope (VLT) 01 p0096 N88-10632
Visible and infrared linear detector arrays for the Airborne Visible/Infrared Imaging Spectrometer (AVIRIS) 06 p0706 N88-14329
High bit rate serial input multipliers
[REPT-87-012] 11 p1530 N88-19140
On serial-input multipliers for two-complement numbers
[REPT-86-035] 11 p1536 N88-19181
Optimal and conventional space-time processing in flow noise
[AD-A189104] 13 p1833 N88-20965
Mid infrared multichannel focal plane breadboard --- pushbroom sensors
[RT-87/014] 14 p1982 N88-21827
Space time processing, environmental-acoustic effects
[AD-A190764] 15 p2130 N88-22708
Software development for the reconstruction of source parameters using research and development arrays
[REPT-840445-TW] 15 p2246 N88-23417
Flexible tactile sensing arrays for robotics: Architectural robustness and yield considerations 19 p2671 N88-25878

LINEAR CIRCUITS
Piecewise linear approach for timing simulation of VLSI (Very-Large-Scale-Integrated) circuits on serial and parallel computers
[AD-A191328] 16 p2252 N88-23462

LINEAR EQUATIONS
NT RICCATI EQUATION
Solution methods for bidiagonal and tridiagonal linear systems for parallel and vector computers
[REPT-87-04] 01 p0085 N88-10552
Nonequilibrium fluctuations and transport in sheared fluids 03 p0316 N88-11999
Polynomial compensation, inversion, and approximation of discrete time linear systems
[NASA-TM-100027] 03 p0372 N88-12344
Eigenvalue projection theory for linear operator equations of electromagnetics
[AD-A185434] 05 p0575 N88-13504
Stability analysis of finite difference schemes for hyperbolic systems, and problems in applied and computational linear algebra
[AD-A185824] 07 p0908 N88-15499
Techniques in linear and nonlinear partial differential equations
[AD-A187109] 09 p1227 N88-17347
Advances in reliable numerical computation: A summary --- conference
[NPL-DITC-102/87] 09 p1229 N88-17367
PSolve: A concurrent algorithm for solving sparse systems of linear equations
[DE88-003584] 10 p1386 N88-18275
Quasigroup approach to solution of linear algebraic equation systems
[DE88-700595] 10 p1398 N88-18330
Leapfrog variants of iterative methods for linear algebra equations
[NASA-CR-181616] 10 p1398 N88-18332
Schwarz splitting and template operators
[AD-A187956] 10 p1404 N88-18370
Method of reduction of polynomially nonlinear equations to linear equations
[DE88-700922] 12 p1683 N88-20064
Conservative finite volume solutions of a linear hyperbolic transport equation in two and three dimensions using multiple grids
[NASA-CR-182715] 13 p1828 N88-20934
Pointwise stabilization for coupled quasilinear and linear wave equations
[AD-A190031] 15 p2120 N88-22632
Iterative finite element solver on transputer networks 16 p2218 N88-23235
A new block solver for large, full, unsymmetric, complex systems of linear algebraic equations
[AD-A190590] 16 p2256 N88-23483
Solving bidiagonal systems of linear equations on the CDC CYBER 205
[CWI-NM-R8725] 18 p2558 N88-25187
Model reduction methods for control design
[NASA-CR-179434] 19 p2719 N88-26144
Parallel quasi-Newton methods for unconstrained optimization
[AD-A193250] 21 p3003 N88-27812
A review of parallel methods for solving sets of linear equations and their application within optimisation algorithms
[AD-A193137] 21 p3006 N88-27830
The computation of stationary distributions on Markov chains through perturbations
[AD-A193191] 21 p3009 N88-27855
Rational Newton algorithms to compute formal solutions of linear differential equations in an irregular singular point
[RR-704-M] 22 p3140 N88-28670
Second order differential equations in the complex domain
[RR-674-M] 22 p3144 N88-28695

LINEAR FILTERS
NT KALMAN FILTERS
Passage from two-parameters to infinite dimension
[ENST-87C002] 01 p0088 N88-10577
A generalization of order statistic filters: The alpha-trimmed linear filter
[AD-A186125] 07 p0842 N88-15107
Optical correlation using the magneto-optic device
[AD-A192342] 20 p2854 N88-26950
Analytical methods in stochastic control and nonlinear filtering
[AD-A194272] 24 p3426 N88-30388

LINEAR INTEGRATED CIRCUITS
Description, analysis and simulation of a new realization of digital filters
[AD-A187763] 11 p1477 N88-18614

LINEAR OPERATORS
Coordinate-momentum probability operator for point particles in a stationary electromagnetic field
[DE88-701165] 16 p2188 N88-23044
Multicontinuations method and strong regular perturbations of linear operators
[DE88-701375] 16 p2263 N88-23533
Recursive mass matrix factorization and inversion: An operator approach to open- and closed-chain multibody dynamics
[NASA-CR-182516] 23 p3247 N88-29328

LINEAR POLARIZATION
Spectroscopy and nonthermal processes 02 p0252 N88-11594
Observation of instabilities in time during dynamic self-diffraction of light in anisotropic nonhomogeneous medium 06 p0769 N88-14730
Polarization properties of SiO masers 13 p1858 N88-21113
Polarization of molecular fluorescence bands in comets: Recent observations and interpretation 14 p1998 N88-21907
Linear and circular polarization of Comet Halley light 14 p2009 N88-21982

LINEAR PREDICTION
On rate of convergence of equivariation linear prediction estimates of the number of signals and frequencies of multiple sinusoids
[AD-A186034] 07 p0914 N88-15549
Large-aperture sparse array antenna systems of moderate bandwidth for multiple emitter location
[AD-A188409] 12 p1619 N88-19683
Evaluating the performance of the LPC (Linear Predictive Coding) 2.4 kbps (kilobits per second) processor with bit errors using a sentence verification task
[AD-A188573] 12 p1620 N88-19686
Spire based speaker-independent continuous speech recognition using mixed feature sets
[AD-A188834] 12 p1620 N88-19688
Multichannel 2-D power spectral estimation and applications
[AD-A191273] 16 p2191 N88-23068
Analysis and improvement of the vector quantization in SELP (Stochastically Excited Linear Prediction) 19 p2653 N88-25756
An analysis of the efficiency and directivity of the sound generated by a moving laser source
[AD-A192220] 20 p2849 N88-26914
Two biased estimation techniques in linear regression: Application to aircraft
[NASA-TM-100649] 23 p3274 N88-29489

LINEAR PROGRAMMING
A new pivoting rule for the dual network simplex method
[REPT-87-17] 01 p0080 N88-10511
The box method for linear programming. Part 1: Basic theory
[DE87-011029] 01 p0080 N88-10515
A look at the evolution of mathematical software for dense matrix problems over the past fifteen years
[DE87-011485] 01 p0081 N88-10517
Report outline of a programming variable and application through example
[INPE-4211-PRE/1092] 01 p0081 N88-10521
S-step iterative methods for symmetric linear systems
[DE87-010819] 01 p0086 N88-10559
Parallel computation of a domain decomposition method
[DE87-011444] 01 p0086 N88-10560
An analysis of an available set of linear programming test problems
[DE87-014578] 02 p0221 N88-11392
Methods for design and evaluation of integrated hardware/software systems for concurrent computation
[NASA-CR-181522] 04 p0479 N88-12953
Parallel superconvergent multigrid
[DE87-013153] 04 p0480 N88-12960
Computing block-angular Karmarker projections with applications to stochastic programming, revision
[AD-A185647] 06 p0759 N88-14656
Progress in mathematical programming
[AD-A185729] 06 p0759 N88-14658

A multicut algorithm for two-stage stochastic linear programs
[AD-A186148] 07 p0903 N88-15466
Parallel LU-factorization algorithms for dense matrices
[DE88-002179] 07 p0904 N88-15478
Explicit construction and analysis of some efficient empirical production functions in data envelopment analysis
[AD-A185907] 07 p0908 N88-15502
A modal control based limiting performance formulation for shock excited systems 08 p0998 N88-16046
Analytical study of the effect of early warning on optimal shock isolation 08 p0998 N88-16047
Task allocation in a distributed computing system 09 p1206 N88-17230
The impact of hierarchical memory systems on linear algebra algorithm design
[DE88-003574] 10 p1385 N88-18274
Eliminating columns in the simplex method for linear programming
[DE88-004191] 10 p1386 N88-18277
Performance studies of a parallel processor for large linear programming problems
[PB88-121611] 10 p1393 N88-18310
Primal-dual parallel solution of very large sparse linear programs
[AD-A188500] 12 p1680 N88-20045
Linear programming along the trajectory of the problem
[REPT-87-41] 14 p1956 N88-21662
On the trajectory of a linear programming problem
[REPT-87-53] 16 p2250 N88-23442
A mixed-integer linear programming problem which is efficiently solvable
[AD-A191028] 18 p2556 N88-25168
Decomposition of linear programs using parallel computation
[AD-A191718] 18 p2556 N88-25173
A centered projective algorithm for linear programming
[AD-A192100] 18 p2557 N88-25178
A new trajectory following polynomial-time algorithm for the linear programming problem
[REPT-87-87] 20 p2840 N88-26848
A linear-programming method inspired by the neural networks framework
[DE88-008688] 20 p2842 N88-26862
Linear programming in R sup 3 and the skeleton and largest incircle of a convex polygon
[PB88-124664] 20 p2846 N88-26892
Linear programming for Air Force decision aiding 21 p2928 N88-27378
Maximum entropy signal restoration with linear programming
[DE88-011740] 21 p2999 N88-27787
Linear goal programming as a military decision aid
[AD-A194276] 22 p3137 N88-28652

LINEAR QUADRATIC GAUSSIAN CONTROL

A linear quadratic Gaussian with loop transfer recovery proximity operations autopilot for spacecraft
[NASA-CR-172028] 02 p0227 N88-11433
New feedback design methodologies for large space structures: A multi-criterion optimization approach 04 p0408 N88-12535
Closed-loop system analysis using Lyapunov stability theory 04 p0483 N88-12978
Design of low order controllers for robust disturbance rejection in large space structures
[AD-A185202] 05 p0555 N88-13376
Feedback in LQCP (Linear Quadratic Control Problem) with a terminal inequality constraint
[PB87-220034] 06 p0762 N88-14676
Large-angle slewing maneuvers for flexible spacecraft
[NASA-CR-4123] 08 p1000 N88-16060
Attitude control of an artificial satellite through the extension of the linear quadratic regulator theory
[INPE-4407-TDL/304] 12 p1600 N88-19577
Analysis and design of gain scheduled control systems
[NASA-CR-182867] 16 p2163 N88-22904
State covariance assignment of discrete systems: Development and applications 17 p2393 N88-24225
Experiments in adaptive control of a very flexible one link manipulator 20 p2842 N88-26865
Robust finite-dimensional LQG (Linear Quadric Gaussian)-based controllers for a class of distributed parameter systems
[AD-A194872] 24 p3425 N88-30382

LINEAR QUADRATIC REGULATOR

NT LINEAR QUADRATIC GAUSSIAN CONTROL

The design of a turboshaft speed governor using modern control techniques
[NASA-CR-175046] 01 p0053 N88-10339
A LQG regulator for the angular motion of the rotor at a tuned gyroscope
[INPE-4280-PRE/1152] 12 p1631 N88-19759
Optimal discrete-time LQR problems for parabolic systems with unbounded input: Approximation and convergence
[NASA-CR-181673] 18 p2567 N88-25247

LINEAR REGULATOR

U LINEAR QUADRATIC REGULATOR

LINEAR SYSTEMS

Maximum likelihood estimates of parameters in linear systems with process and measurement noise
[DFVLR-FB-87-20] 01 p0083 N88-10532
Extraction and evaluation of Boolean relations for the solution of linear programs in 0-1 variables, volume 1
[ENST-86E023-VOL-1] 02 p0227 N88-11430
Polynomial compensation, inversion, and approximation of discrete time linear systems
[NASA-TM-100027] 03 p0372 N88-12344
A new state space model for the NASA/JPL 70-meter antenna servo controls 04 p0436 N88-12702
Parallel superconvergent multigrid
[DE87-013153] 04 p0480 N88-12960
Closed-loop system analysis using Lyapunov stability theory 04 p0483 N88-12978
Oscillation theory for linear second-order differential systems
[DE87-011393] 04 p0484 N88-12983
The linear characteristic method in XYZ geometry
[DE87-011668] 04 p0484 N88-12984
Tridiagonal approximate factorization method: A preconditioning technique for solving nonsymmetric linear systems suitable to supercomputers 05 p0537 N88-13271
Equivalence of input-output stability and exponential stability for infinite dimensional systems
[TW-276] 05 p0638 N88-13903
Robustness of linear systems
[PB87-220042] 05 p0639 N88-13909
Development of a technique for estimating noise covariances using multiple observers
[NASA-TM-4020] 06 p0669 N88-14098
The solution of large linear inverse problems 06 p0691 N88-14238
Strong consistency of M-estimates for the linear model
[AD-A185487] 06 p0764 N88-14696
Asymptotic normality of poly-t densities with Bayesian applications
[AD-A185718] 06 p0768 N88-14719
The design and implementation of surface acoustic wave devices for linear FM and a new non-linear FM pulse compression technique for radar applications
[AD-A186741] 08 p0980 N88-15922
A direct approach to almost disturbance and almost input-output decoupling
[MEMO-641] 08 p1072 N88-16471
Tensorial calibration. Part 1: First order tensorial calibration
[AD-A186708] 09 p1167 N88-16995
System characterization in nonlinear random vibration 09 p1180 N88-17071
Multicolor numbering of irregular triangular meshes
[AD-A186559] 09 p1217 N88-17298
A method for designing robust multivariable feedback systems
[NASA-CR-182459] 09 p1225 N88-17341
Applications of nonlinear systems theory to control design
[NASA-CR-182485] 09 p1231 N88-17377
Linear theory of generation of longitudinal sound waves in semiconductors upon interband absorption of optical radiation 09 p1234 N88-17397
Dynamic observers as asymptotic limits of recursive filters: Special cases
[AD-A187578] 10 p1397 N88-18324
Linear prediction of stationary vector sequences
[NASA-TM-100069] 10 p1403 N88-18386
Innovative design of composite structures: Further studies in the use of a curvilinear fiber format to improve structural efficiency
[NASA-CR-182576] 11 p1450 N88-18641
A semianalytical technique for sensitivity analysis of unsteady aerodynamic computations
[NASA-TM-100810] 11 p1503 N88-18976
Deterministic equivalent for a continuous linear-convex stochastic control problem
[AD-A187818] 11 p1540 N88-19206
Recursive inversion of externally defined linear systems
[NASA-TM-100070] 11 p1541 N88-19215
A hybrid-stress finite element approach for stress and vibration analysis in linear anisotropic elasticity
[NASA-CR-179311] 12 p1634 N88-19784
Efficient parallel architecture for highly coupled real-time linear system applications
[NASA-CR-182649] 12 p1675 N88-20015
Analysis, estimation, and control for perturbed and singular systems and for systems subject to discrete events
[AD-A188496] 12 p1677 N88-20026
Preconditioned conjugate gradient algorithms and software for solving large sparse linear systems
[DE88-002180] 13 p1816 N88-20849
Further results on the McMillan degree and the Kronecker indices of ARMA models --- input-output relations of linear systems
[EUT-87-E-175] 13 p1827 N88-20925
Regional Conference on the Analysis of the Unbalanced Mixed Model
[AD-A188747] 13 p1830 N88-20943
A new approach to almost decoupling problems for linear and nonlinear systems
[MEMO-680] 14 p1962 N88-21700
Bilinear systems in the frequency domain and an application to optimal control
[RR-320] 14 p1962 N88-21704
Boundary stabilization of the reaction-diffusion equation with unilateral conditions
[RR-315] 14 p1964 N88-21720
Parametric methods of analysing linear and nonlinear systems
[RR-318] 14 p1967 N88-21741
The theory of flotation
[NASA-TT-20278] 16 p2207 N88-23172
Feedback decoupling and stabilization for linear systems with multiple exogenous variables
[ETN-88-92245] 16 p2255 N88-23474
Optimal control, estimation compensation of linear discrete-time systems with stochastic parameters
[REPT-87-56] 16 p2255 N88-23478
Formal solution of differential linear systems in the proximity of a singularity
[ETN-88-92190] 16 p2258 N88-23495
Derivative arrays, geometric control theory and realizations of linear descriptor systems
[AD-A190882] 16 p2260 N88-23513
The LDCM actuator for vibration suppression
[NASA-CR-182898] 17 p2335 N88-23940
State covariance assignment of discrete systems: Development and applications 17 p2393 N88-24225
Robust adaptive regulation without persistent excitation
[NASA-TM-100571] 18 p2561 N88-25204
Linear and nonlinear acoustic wave propagation in the atmosphere
[NASA-CR-4157] 18 p2571 N88-25268
Structural properties of multivariable linear systems
[PB88-181375] 19 p2717 N88-26134
Characterization of accelerating pipe flow
[AD-A193065] 21 p2943 N88-27481
Approximation problems of the Hilbert transform to identify minimum phase linear systems
[FUB-42-1986] 21 p2999 N88-27790
Asymptotic orders of reachability in perturbed linear systems
[AD-A192718] 22 p3143 N88-28688
Linear thyratron
[AD-A194111] 23 p3208 N88-29094
Improved finite strip Mindlin plate bending element using assumed shear strain distributions
[NASA-TM-100928] 23 p3225 N88-29195
Robust control of multivariable and large scale systems
[AD-A194250] 23 p3266 N88-29441
Topics in adaptive control and inference
[AD-A194718] 23 p3266 N88-29443
Linearized model matching for single-imput nonlinear systems
[AD-A193642] 23 p3266 N88-29445
Feedback stabilization of du/dt=Au + bf in Hilbert space when the normalization function is less than or equal to r
[AD-A193510] 23 p3277 N88-29506
Performance of DS/SSMA communications in impulsive channels. Part 1: Correlation receivers
[AD-A195712] 24 p3362 N88-30021
Increasing accuracy in evaluating vector of state under conditions of incomplete observability of expanded system 24 p3446 N88-30511

LINEAR TRANSFORMATIONS

Stochastic filtering solutions for ill-posed linear problems and their extension to measurable transformations
[AD-A186016] 07 p0909 N88-15506
Study of microcomputer-based real-time programmable optical signal processor and application
[AD-A190076] 15 p2133 N88-22726

LINEAR VIBRATION

Vibration and buckling of geometrically imperfect laminated cylindrical shells 04 p0456 N88-12822
Theoretical investigations of chaotic dynamics
[AD-A186404] 07 p0867 N88-15261

Parametric and experimental analysis using a power flow approach
[NASA-CR-182460] 09 p1116 N88-16693
Method for finding principal modes of nonlinear vibration systems and their stabilities 14 p1899 N88-21340

LINEARITY
NT COLLINEARITY
Linear emittance damper with megagauss fields
[DE87-013562] 01 p0093 N88-10606
Total linearisation method for solving viscous free boundary flow problems by the finite element method
[PB87-222337] 04 p0441 N88-12737
Numerical methods for reaction-diffusion problems with non-differentiable kinetics
[AD-A185405] 05 p0641 N88-13923
Comments on the theory of absolute and convective instabilities
[PB87-124624] 06 p0783 N88-14808
Estimation and testing in truncated and nontruncated linear median-regression models
[AD-A186317] 07 p0911 N88-15522
Conditionally unbiased bounded influence robust regression with applications to generalized linear models
[AD-A186319] 07 p0915 N88-15556
Test of linearity in general regression models
[AD-A186036] 08 p1073 N88-16477
Consistent linearization of the element-independent corotational formulation for the structural analysis of general shells
[NASA-CR-178418] 09 p1181 N88-17078
Application of empirical and linear methods to VSTOL powered-lift aerodynamics
[NASA-TM-100048] 10 p1267 N88-17581
Parametric study of choke flutter with a linear theory 10 p1283 N88-17673
On the stability of the supersonic boundary layer 11 p1435 N88-18561
Estimation in linear models with censored data
[AD-A187209] 11 p1540 N88-19203
Linear state space modeling of a turbofan engine
[AD-A190110] 15 p2019 N88-22035
An integral equation for the linearized supersonic flow over a wing
[AD-A191408] 16 p2158 N88-22875
The application of linear maximum likelihood estimation of aerodynamic derivatives for the Bell-205 and Bell-206
[AD-A191279] 16 p2161 N88-22894
Automated cartographic generalization for linear map features 18 p2532 N88-25021
Linear spaces, absolute retracts and the compact extension property
[PB88-181110] 18 p2564 N88-25225
A full but elementary treatment of systems of homogeneous ordinary linear differential equations with constant coefficients
[REPT-87-82] 20 p2845 N88-26887
On linear relationship between shock velocity and particle velocity
[DE88-701827] 20 p2880 N88-27099
On solvability of an equation arising in the theory of M-estimates
[AD-A193059] 21 p3006 N88-27828
An integral equation for the linearized unsteady supersonic flow over a wing
[AD-A193773] 23 p3172 N88-28887
Automatic classification of digitally modulated signals
[AD-A194623] 23 p3203 N88-29064
A linear-time algorithm for finding a minimum spanning pseudoforest
[AD-A194029] 23 p3250 N88-29346
Wigner distribution function: Relation to short-term spectral estimation, smoothing and performance in noise
[AD-A193865] 23 p3275 N88-29492
Formulation and solution of economic equilibrium problems
[AD-A196034] 24 p3439 N88-30470

LINEARIZATION
Linearized aeroelastic analysis of a wind turbine with a two-bladed rotor
[ETN-87-90600] 03 p0347 N88-12192
Numerical analysis of supersonic flows using panel method 05 p0537 N88-13266
Prediction of the response and optimal control of stochastic parametrically and externally excited nonlinear systems 11 p1496 N88-18930
Nonlinear input-output systems
[NASA-CR-182484] 11 p1535 N88-19171
Method of reduction of polynomially nonlinear equations to linear equations
[DE88-700922] 12 p1683 N88-20064
Transport and stability properties of free shear flows 13 p1768 N88-20577
User's manual for LINEAR, a FORTRAN program to derive linear aircraft models
[NASA-TP-2768] 14 p1967 N88-21740
Some numerical methods for the computation of capillary free boundaries governed by the Navier-Stokes equations
[REPT-87-69] 16 p2206 N88-23167
Linearization along invariant manifolds and a generalization of the Hartman-Grobman theorems for degenerate singularities of vector fields in R cubed
[REPT-87-80] 20 p2845 N88-26886
On the pseudo-linearization problem for nonlinear systems
[AD-A194021] 22 p3142 N88-28683
An approach to CMG steering using feedback linearization
[NASA-CR-183172] 24 p3422 N88-30369

LINERS
U LININGS

LINES (GEOMETRY)
NT GEODESIC LINES
Development of a line-drawing algorithm
[CS-8701] 01 p0082 N88-10530
Computing the bounded region determined by finitely many lines in the plane
[CS-8703] 01 p0086 N88-10558

LINES OF FORCE
Acceleration of auroral particles by magnetic field-aligned electric fields 08 p1031 N88-16246
Acceleration/heating processes on auroral field lines as observed by the Viking spacecraft 08 p1096 N88-16596
Simultaneous observation of upward moving field aligned energetic electrons and ions on auroral zone field lines
[IRF-PREPRINT-102] 16 p2231 N88-23326

LINGUISTICS
NT MACHINE TRANSLATION
NT SEMANTICS
NT SYLLABLES
NT SYNTAX
NT WORDS (LANGUAGE)
Antithesis: A study in clause combining and discourse structure
[AD-A184789] 03 p0368 N88-12313
Space languages 08 p1063 N88-16420
Quantitative and qualitative assessments of the impact of linguistic theory on information science 10 p1424 N88-18507
Linguistic and cultural barriers to the transfer of information 24 p3437 N88-30459
Linguistic-technical aspects of machine translation 24 p3438 N88-30461
Linguistic barriers: Translation problems 24 p3438 N88-30465

LININGS
Turbine Engine Hot Section Technology, 1985
[NASA-CP-2405] 02 p0184 N88-11140
An analysis of sound absorbing linings for the interior of the NASA Ames 80 x 120-foot wind tunnel
[NASA-CR-177396] 04 p0488 N88-13006
Fabric space radiators
[DE88-005569] 14 p1880 N88-21237
High-temperature combustor liner tests in structural component response test facility 15 p2077 N88-22383
Life assessment of combustor liner using unified constitutive models 15 p2077 N88-22384
Compositional redistribution during casting of Hg sub 0.8 Cd sub 0.2 Te alloys
[NASA-TM-101151] 17 p2326 N88-23893
Basic mechanisms of diesel lubrication correlation of bench and engine tests
[AD-A193360] 21 p2956 N88-27561

LINKAGES
Assessment of the COFSI/MAST I project
[NASA-CR-181366] 01 p0053 N88-10340
Kinematic optimization of mechanisms, a finite element approach
[ISBN-90-370-0012-6] 09 p1175 N88-17039
Dynamic response of a geared train of rotors subjected to random support excitations 09 p1181 N88-17073
The dynamics of an oscillating four-bar linkage 09 p1181 N88-17074
Adaptive control of a manipulator with a flexible link
[NASA-CR-181637] 11 p1476 N88-18807
Improvement in robot positioning accuracy by a kinematic identification model 11 p1496 N88-18931
Dynamics of high-speed mechanisms with elastic members 13 p1779 N88-20643
A three dimensional non-singular modelling of rigid manipulators
[AD-A189707] 15 p2116 N88-22604
Payload deployment method and system
[NASA-CASE-MSC-21330-1] 18 p2470 N88-24660
Skin friction balance
[NASA-CASE-LAR-13710-1] 23 p3216 N88-29145

LINKING
U JOINING

LIOUVILLE THEOREM
Systems near the onset and in the well-developed regimes of turbulence
[DE88-005365] 13 p1766 N88-20565

LIPIDS
NT ALDOSTERONE
NT CORTICOSTEROIDS
Development of microencapsulation techniques
[AD-A185019] 05 p0567 N88-13457
Effects of extreme hypoxia on phospholipid metabolism in subcellular structures of rat brain 08 p1046 N88-16323
Factors governing light driven electron and proton translocation in proteins across membranes
[DE88-002716] 08 p1082 N88-16519
Lipid peroxidation in rat tissues with exposure to antiorthostatic hypokinesia, exercise and immobilization stress 10 p1365 N88-18159
Studies of model ion channels in defect-free multibilayers of phospholipids
[AD-A188740] 16 p2238 N88-23365
Significance of nutrition to change in human carbohydrate and lipid metabolism under emotional stress 19 p2703 N88-26073

LIPSCHITZ CONDITION
Convergence of Runge-Kutta methods on classes of stiff initial value problems
[CWI-NM-R8717] 13 p1827 N88-20924
The global convergence of partitioned BFGS on problems with convex decompositions and Lipschitzian gradients
[DE88-006249] 14 p1968 N88-21744
Detection of the number, locations and magnitudes of jumps
[AD-A190328] 15 p2125 N88-22671
Incomplete Lipschitz-Hankel integrals of MacDonald functions
[AD-A191034] 16 p2261 N88-23515
Perturbation theory for dual semigroups. Part 3: Nonlinear Lipschitz continuous perturbations in the Sun-reflexive case
[CWI-AM-R8706-PT-3] 16 p2263 N88-23535

LIQUEFACTION
NT COAL LIQUEFACTION
Proceedings of the 1987 Biomass Thermochemical Conversion Contractors' Review Meeting
[DE88-006730] 18 p2535 N88-25041
An advanced extruder-feeder biomass liquefaction reactor system 18 p2535 N88-25042

LIQUEFIED GASES
NT LIQUEFIED NATURAL GAS
NT LIQUID AMMONIA
NT LIQUID HELIUM
NT LIQUID HELIUM 2
NT LIQUID HYDROGEN
NT LIQUID NITROGEN
NT LIQUID OXYGEN

LIQUEFIED NATURAL GAS
An investigation of high pressure/late cycle injection of CNG (Compressed Natural Gas) as a fuel for rail applications
[DE88-009000] 19 p2677 N88-25917

LIQUID AIR CYCLE ENGINES
Auxiliary propulsion technology for advanced Earth-to-orbit vehicles
[NASA-TM-100237] 06 p0674 N88-14127

LIQUID ALLOYS
Liquid alloys: New perspectives and challenges
[DE88-005935] 13 p1750 N88-20463
Fluid flow modeling in casting processes and its implications
[DE88-010009] 20 p2810 N88-26671

LIQUID AMMONIA
Ammonia transfer across rotating joints in space 14 p1927 N88-21492
Ammonia cleanup of lithium containing components 17 p2403 N88-24287
Ammonia boiling in long tubes. Heat transfer and charge loss in vertical and horizontal tubes
[NASA-TT-20313] 19 p2667 N88-25858

LIQUID ATOMIZATION
Stability relationship for water droplet crystallization with the NASA Lewis icing spray
[NASA-TM-100220] 02 p0125 N88-10790
Droplet formation for liquid monopropellant jets
[AD-A187172] 10 p1331 N88-17956
Dense-spray structure and phenomena. Part 2: Pressure-atomized sprays
[AD-A190312] 15 p2064 N88-22307
Effect of mass-velocity on liquid jet atomization in Mach 1 gasflow
[NASA-TM-100813] 16 p2211 N88-23194
Atomization of alternative fuels 24 p3345 N88-29913
Turbulence effects on the droplet distribution behind airblast atomizers 24 p3348 N88-29915

Influence of operating conditions on the atomization and distribution of fuel by air blast atomizers
24 p3346 N88-29918
Spray performance of a vaporizing fuel injector
24 p3346 N88-29919
The characterizatin of combustion by fuel composition: Measurements in a small conventional combustor
24 p3346 N88-29920
The performance of a surrogate blend in simulating JP-4 in a spray-fueled combustor 24 p3347 N88-29926

LIQUID CHROMATOGRAPHY
Application of high performance liquid chromatography to the fast determination of bitumen generic composition
[PC-2] 02 p0145 N88-10911
Study of the properties of a new detector class for liquid chromatography
[DE88-001666] 05 p0563 N88-13426
Chromatographic and related reactors
[AD-A188452] 12 p1605 N88-19599
Electrosorptive detection of simple organic compounds in liquid chromatography
[AD-A188757] 13 p1736 N88-20376
Fuels combustion research
[AD-A189114] 13 p1736 N88-20381
Determination of the partition coefficients of organophosphorus compounds using high-performance liquid chromatography
[AD-A189276] 13 p1737 N88-20385
Development and evaluation of supercritical fluid chromatography-mass spectrometry
[DE88-005122] 13 p1738 N88-20394
Instrumental aspects of capillary supercritical fluid chromatography
[ETN-88-92242] 16 p2174 N88-22960
Determination of low molecular weight thiols using monobromobimane fluorescent labeling and high-performance liquid chromatography
[NASA-CR-182932] 19 p2608 N88-25478

LIQUID COOLED REACTORS
NT BOILING WATER REACTORS
NT EXPERIMENTAL BREEDER REACTOR 2
NT LIGHT WATER REACTORS
NT LIQUID METAL COOLED REACTORS
NT PRESSURIZED WATER REACTORS
NT ZERO POWER REACTORS
Gas-cooled reactor power systems for space
17 p2413 N88-24350

LIQUID COOLING
NT FILM COOLING
Water source heat pump: How to get home heating and cooling from your own back yard
[DE88-900180] 07 p0875 N88-15306
Single phase liquid immersion cooling of discrete heat sources in a vertical channel
[AD-A191224] 17 p2337 N88-23944
The liquid droplet radiator in space: A parametric approach 17 p2427 N88-24437
Forced-convection, liquid-cooled, microchannel heat sinks
[AD-A193337] 21 p2937 N88-27444

LIQUID CRYSTALS
The development of a new and novel Hadamard transform infrared spectrometer for analytical chemistry
[DE87-014804] 02 p0175 N88-11094
Near-infrared dichroism of a mesogenic transition metal complex and its solubility in nematic hosts
[DE87-014471] 03 p0287 N88-11805
New theory for competing interactions and microstructures in partially-ordered (liquid-crystalline) phases
[DE87-014739] 03 p0380 N88-12389
Boundary effects on the drag of an oscillating sphere: Applications to the magnetic sphere rheometer. Attenuation and dispersion of acoustic waves in nematic liquid crystals 04 p0488 N88-13007
Guest-host interactions in thermotropic and lyotropic liquid crystals
[AD-A184402] 04 p0496 N88-13057
Observation of instabilities in time during dynamic self-diffraction of light in anisotropic nonhomogeneous medium 06 p0769 N88-14730
Thermoplastic elastomers as LOVA binders
[AD-A185865] 07 p0835 N88-15068
X-ray diffraction study of thermotropic liquid crystalline polyesters and diester model compounds
[AD-A186788] 09 p1255 N88-17521
Brightness contrast and character height of five flat panel computer displays
[AD-A187743] 11 p1524 N88-19096
Continuous collective molecule rotation of a nematic liquid crystal induced from light angular momentum
[FUB-17-1986] 14 p1986 N88-21845
Electronic and ionic transport in polymers
[AD-A190434] 15 p2045 N88-22185
Collective rotation of molecules driven by the angular momentum of light in a nematic film
[FUB-6-1986] 15 p2131 N88-22714
Basic design studies for the realization of liquid crystal display systems in aircraft
[VA-87-001] 16 p2163 N88-22900
Electrochemistry in liquid crystals
[AD-A191554] 18 p2481 N88-24719
Liquid crystal optics for laser systems
[DE88-008475] 20 p2854 N88-26948
Liquid crystals for unsteady surface shear stress visualization
[DE88-010570] 21 p2951 N88-27527
Interactions in miscible polymer blends
[AD-A193824] 22 p3058 N88-28144
Quasi-liquid crystalline materials with special electro-optic properties
[AD-A194579] 23 p3282 N88-29544
Thermodynamical, optical and X-rays studies of some thermotropic liquid crystals
[DE88-702301] 23 p3290 N88-29590

LIQUID DROPS
U DROPS (LIQUIDS)

LIQUID FILLED SHELLS
Internal fluid dynamics within a nonspinning partially liquid-filled shell due to burster rupture
[AD-A191055] 18 p2507 N88-24874
Theoretical investigation of the development of the normal fluid and superfluid velocity distributions during spin-up for a He2-filled cylinder
[MPIS-6/1987] 18 p2510 N88-24892
Liquid motions in partially filled containers: Preliminary results of the D-1 mission — Spacelab
[NLR-MP-86042-U] 20 p2802 N88-26629
Nonlinear oscillations of a nonviscous cylindrical liquid system in weightlessness condition
[LRT-WE-9-FB-14(1987)] 22 p3063 N88-28175
Nonlinear liquid motion in conical containers
[LRT-WE-9-FB-10(1987)] 22 p3077 N88-28270
Nonlinear hydroelastic vibrations in rectangular containers
[LRT-WE-9-FB-7(1987)] 22 p3088 N88-28340
Computational fluid dynamics methods for low Reynolds number precessing/spinning incompressible flows
[AD-A193891] 23 p3212 N88-29119
Numerical calculations of the response of a spinning spheroidal payload to coning motion
[AD-A195890] 24 p3368 N88-30059

LIQUID FLOW
NT OPEN CHANNEL FLOW
NT WATER FLOW
Gas diffusion studies in steady and nonsteady cavities
[AD-A185795] 06 p0704 N88-14318
An investigation into flow regimes for two-phase helium flow
[DE86-002834] 07 p0853 N88-15181
Experimental and numerical study of liquid distribution in dispersive-annular flow
[DE88-700844] 14 p1909 N88-21406
Dense-spray structure and phenomena. Part 1. Turbulence/dispersed-phase interactions
[AD-A190606] 15 p2065 N88-22315
Fluid motion in a spinning, coning cylinder via spatial eigenfunction expansion
[AD-A190758] 15 p2066 N88-22319
Development of a liquid-fed water resistojet
[NASA-TM-100927] 18 p2523 N88-24968

LIQUID FUELS
NT AIRCRAFT FUELS
NT ANTIMISTING FUELS
NT AUTOMOBILE FUELS
NT DIESEL FUELS
NT GASOLINE
NT HYDROGEN FUELS
NT JET ENGINE FUELS
NT JP-4 JET FUEL
NT JP-5 JET FUEL
NT JP-8 JET FUEL
NT KEROSENE
Droplet formation for liquid monopropellant jets
[AD-A187172] 10 p1331 N88-17956
Dense-spray structure and phenomena. Part 2: Pressure-atomized sprays
[AD-A190312] 15 p2064 N88-22307
The burning of HAN-based (hydroxylammonium nitrate) liquid propellants
[DE88-006863] 18 p2494 N88-24800
Electrical ignition of HAN-based liquid propellants
[AD-A191349] 18 p2495 N88-24801
Low pressure entrained flow pyrolysis of biomass to produce liquid fuels 18 p2535 N88-25043
Low-temperature thermochemical conversion of high moisture biomass feedstocks 18 p2536 N88-25047
Chemical/hydrogen energy systems
[DE88-007013] 19 p2687 N88-25969
An outdoor test facility for the large-scale production of microalgae
[DE88-001146] 21 p2984 N88-27723
Combustion studies of acoustically suspended liquid droplets
[AD-A193892] 23 p3192 N88-28998

LIQUID HELIUM
NT LIQUID HELIUM 2
Components for cryostat — spaceborne
[MBB/ISO-TN-CD00.003-REV-A] 01 p0032 N88-10207
Study of helium transfer technology for STICCR: Fluid management
[NASA-CR-177463] 10 p1291 N88-17720
Development of a motorized cryovalve for the control of superfluid liquid helium 14 p1925 N88-21477
Calorimetric technique for measuring liquid helium flow rate
[DE88-701308] 16 p2200 N88-23123
Peculiarities of non-stationary heat transfer to superfluid helium
[DE88-701174] 16 p2200 N88-23124
Preliminary study of niobium alloy contamination by transport through helium 17 p2402 N88-24279
Superfluid turbulence in counterflowing helium II 19 p2665 N88-25849
Superfluid Helium On-Orbit Transfer (SHOOT) operatons
[NASA-TM-101009] 22 p3048 N88-28084
An experimental setup for the study of polarized He3 and dilute He3-He4 mixtures
[B8705589] 23 p3193 N88-29001

LIQUID HELIUM 2
Theoretical investigation of the development of the normal fluid and superfluid velocity distributions during spin-up for a He2-filled cylinder
[MPIS-6/1987] 18 p2510 N88-24892

LIQUID HYDROGEN
Advanced fabrication techniques for hydrogen-cooled engine structures
[NASA-CR-3949] 06 p0723 N88-14447
Development of on-orbit fluid gaging techniques 08 p0982 N88-15936
Some problems of the theory of bubble growth and condensation in bubble chambers
[NASA-TT-20232] 13 p1771 N88-20593
Theory of Muon method for study of solid and liquid hydrogen 14 p1972 N88-21770
Rotor self-lubricating axial stop
[NASA-CASE-MFS-28273-1] 17 p2344 N88-23974

LIQUID INJECTION
NT WATER INJECTION

LIQUID LASERS
Bibliography of Soviet laser developments, number 88, March - April 1987
[AD-A195978] 24 p3378 N88-30116

LIQUID LITHIUM
Corrosion of ferritic steels by molten lithium: Influence of competing thermal gradient mass transfer and surface product reactions
[DE88-000334] 04 p0417 N88-12585
Ammonia cleanup of lithium containing components 17 p2403 N88-24287
Transient analysis of Li and LiH thermal storage spheres 17 p2411 N88-24334
Fabrication of a niobium 1 percent zirconium containment for SP-100 primary lithium system materials mass transfer studies 17 p2417 N88-24373
Liquid metal testing at ETEC for the SP-100 program 17 p2428 N88-24446
An evaluation of some thermodynamic and transport properties of solid and liquid lithium over the temperature range 200 to 1700 K
[DE88-008947] 19 p2614 N88-25512

LIQUID MERCURY
U MERCURY (METAL)

LIQUID METAL COOLED REACTORS
NT EXPERIMENTAL BREEDER REACTOR 2
Fast critical experiment data for space reactors
[DE87-007005] 01 p0093 N88-10605
Detecting the gas bubbles in a liquid metal coolant by means of magnetic flowmeters
[DE88-701427] 15 p2062 N88-22294
Status of CEA design and simulation studies of a 200 KWe turboelectric space power system 17 p2400 N88-24268
Conceptual design of the SP-100 GES test site 17 p2402 N88-24284
Selection of a handling and maintenance option for the SP-100 ground engineering system test 17 p2402 N88-24285
Fast critical experiment data for space reactors 17 p2403 N88-24286
A review of diffusion barrier technology for application in SP-100 fuel pins 17 p2410 N88-24328

Liquid-metal MHD power conversion for space electric systems 17 p2411 N88-24338
Studies for the definition of a Faraday converter for space nuclear systems 17 p2411 N88-24339
A liquid metal MHD concept for multimegawatt space power application 17 p2413 N88-24348
Nuclear Rankine/flywheel MMW space power concept 17 p2413 N88-24349
A dynamic model for the aft accumulator in the TE SP-100 system 17 p2414 N88-24354
Parametric analyses of the TE SP-100 system performance 17 p2415 N88-24358
Advanced LMMHD space power generation concept 17 p2415 N88-24364
Transient analyses of multimegawatt space reactors 17 p2430 N88-24458

LIQUID METAL FAST BREEDER REACTORS
Computation of failure probability of fatigue loaded cracked structures
[ETN-88-92360] 21 p2964 N88-27607

LIQUID METALS
NT LIQUID LITHIUM
NT LIQUID POTASSIUM
NT LIQUID SODIUM
NT MERCURY (METAL)
NT MERCURY VAPOR
Formation of amorphous alloys by solid state reactions
[DE87-013175] 02 p0146 N88-10918
Thermodynamics of interaction between nitrogen and molten nickel alloys
[BLL-M-37309-(5828.4)] 02 p0149 N88-10934
Relationships governing change in density in liquid ferrous alloys
[BLL-M-37305-(5828.4)] 02 p0149 N88-10935
Birch's law and the properties of high temperature fluid metals
[DE87-014744] 03 p0288 N88-11807
Cast iron freezing mechanisms 03 p0298 N88-11870
Corrosion strength of niobium and its alloys
[DE87-703693] 04 p0416 N88-12578
Inertial confinement fusion reactor cavity analysis
[DE88-000788] 04 p0492 N88-13028
The use of alloy 117 as a liquid metal current collector
[AD-A185740] 06 p0698 N88-14281
Spray deposition: A fundamental study of droplet impingement, spreading and consolidation
[AD-A186627] 08 p0970 N88-15869
The application of liquid-metal MHD (magnetohydrodynamics) to renewable energy sources
[DE88-003083] 09 p1251 N88-17495
Thermodynamics of wetting by liquid metals
[DE88-003634] 11 p1563 N88-19360
Liquid alloys: New perspectives and challenges
[DE88-005935] 13 p1750 N88-20463
Hydrodynamical regimes in molten metals under a horizontal temperature gradient 14 p1988 N88-21859
Electrical resistivities of some compound forming liquid metal alloys
[PB88-145172] 15 p2037 N88-22137
Angular resolved energy analysis of (69)Ga+ ions from a gallium liquid metal ion source
[AERE-R-12649] 15 p2139 N88-22760
A theoretical and experimental study of the thermophysical properties of lithium hydride
[NASA-TT-20179] 16 p2175 N88-22965
Detailed transient model of a liquid-metal heat pipe 17 p2412 N88-24345
A transient model for liquid metal heat pipes 17 p2421 N88-24398
The THROHPUT code: Thermohydraulic heat pipe modeling 17 p2421 N88-24399
Possible creep studies of lithium with a compact device 17 p2422 N88-24404
Review of alkali metal and refractory alloy compatibility for Rankine cycle applications 17 p2428 N88-24447
Nucleate pool boiling: High gravity to reduced gravity; liquid metals to cryogens 17 p2431 N88-24464
Liquid metal thermal electric converter theoretical and experimental studies
[DE88-008606] 19 p2688 N88-25974
MHD (magnetohydrodynamic) thermal hydraulic analysis of three-dimensional liquid metal flows in fusion blanket ducts
[DE88-009929] 19 p2731 N88-26219
Blanket technology experiments at Argonne National Laboratory
[DE88-010006] 19 p2731 N88-26220
Development of liquid metal field-emission sources for use in fast repetitive opening switches
[AD-A192230] 20 p2795 N88-26583
A method for determining the solubility of hydrogen in molten aluminum-lithium alloys
[DE88-009807] 21 p2910 N88-27270
Liquid metal thermal-electric converter electrode development
[DE88-009252] 23 p3230 N88-29221
Some theoretical considerations of the surface tension of liquid metals for metal matrix composites
[AD-A195999] 24 p3340 N88-29882

LIQUID NITROGEN
Chemical equilibrium calculations for the high pressure and temperature dissociation of liquid nitrogen
[DE87-013788] 01 p0021 N88-10135
The dissociation of dense liquid nitrogen and shock cooling
[DE87-013490] 01 p0022 N88-10136
Vibrational spectroscopy of shock-compressed fluid N2 and O2
[DE87-013138] 03 p0313 N88-11979
Hot carrier effects in CMOS field effect transistors at cryogenic temperatures 19 p2662 N88-25829

LIQUID OXIDIZERS
Bipropellant combustion in a liquid rocket combustion chamber 13 p1733 N88-20359

LIQUID OXYGEN
Vibrational spectroscopy of shock-compressed fluid N2 and O2
[DE87-013138] 03 p0313 N88-11979
Seal technology for liquid oxygen (LOX) turbopumps
[NASA-CR-174866] 05 p0591 N88-13603
Fluid mass and thermal loading effects on the modal characteristics of space shuttle main engine liquid oxygen inlet splitter vanes 05 p0594 N88-13628
Oxygen chemisorption cryogenic refrigerator
[NASA-CASE-NPO-16734-1-CU] 06 p0689 N88-14223
The determination of equivalent bearing loading for the BSMT that simulate SSME high pressure oxidizer turbopump conditions using the SHABERTH/SINDA computer programs 07 p0925 N88-15623
Development of on-orbit fluid gaging techniques 08 p0982 N88-15936
A lunar transportation system
[NASA-CR-182561] 11 p1567 N88-19379
Rotor self-lubricating axial stop
[NASA-CASE-MFS-28273-1] 17 p2344 N88-23974
Carbon deposition model for oxygen-hydrocarbon combustion, volume 2
[NASA-CR-179376] 21 p2908 N88-27255

LIQUID PHASE EPITAXY
Growth of HgZnTe layers by LPE technique
[AD-A186723] 09 p1255 N88-17520
Investigation of defect and electronic interactions associated with GaAs device processing
[AD-A188021] 11 p1556 N88-19313
Growth of Pb/sub 1-x/Eu/sub x/Te epitaxial layers by the liquid phase epitaxy technique
[DE88-701022] 15 p2139 N88-22763
Electrical and optical properties of Hg/sub 1-x/Cd/sub x/Te doped layers grown by Liquid Phase Epitaxy (LPE)
[DE88-701023] 16 p2281 N88-23653
Lattice-matched HgZnTe epitaxy development
[AD-A193677] 23 p3292 N88-29600

LIQUID PHASES
Physical properties of immiscible polymers 03 p0297 N88-11868
The role of electronic structure calculation in mechanistic analysis of electron transfer reactions in the liquid phase
[DE87-014395] 05 p0647 N88-13963
Visible InGaAsP/GaAsP lasers produced by epitaxial growth from liquid phase 09 p1237 N88-17416
Progress in the computer modeling of the liquid phase behavior of a liquid metal heat pipe 17 p2412 N88-24342
Microgravity thaw experiment (MITEX) 17 p2427 N88-24439
Liquid-phase oxidation of acetone with hydrogen peroxide on oxide catalysts 19 p2706 N88-26091
Electronic states of the Xe(sub n)HCl systems in gas and condensed phases
[AD-A193881] 23 p3192 N88-28997

LIQUID POTASSIUM
Design of a high-power-density Ljungstroem turbine using potassium as a working fluid 17 p2409 N88-24323
Nuclear Rankine/flywheel MMW space power concept 17 p2413 N88-24349

LIQUID PROPELLANT ROCKET ENGINES
NT HYDRAZINE ENGINES
NT HYDROGEN OXYGEN ENGINES
NT LIQUID AIR CYCLE ENGINES
NT SPACE SHUTTLE MAIN ENGINE
Space station resistojet system requirements and interface definition study
[NASA-CR-180832] 04 p0409 N88-12541
Zero-G thermodynamic vent system for shuttle/Centaur 08 p0983 N88-15943
Durability testing of an iridium-plated storable rocket engine injector
[AD-A190707] 15 p2027 N88-22078
The 24th JANNAF Combustion Meeting, volume 2
[AD-A190164] 19 p2622 N88-25554
Development of a generic combustion stability code for liquid propellant rocket engines 19 p2626 N88-25576
Breadboard RL10-2B low-thrust operating mode (second iteration) test report
[NASA-CR-182160] 24 p3338 N88-29867
Oxidizer heat exchanger component test
[NASA-CR-182159] 24 p3339 N88-29876

LIQUID ROCKET PROPELLANTS
NT CRYOGENIC ROCKET PROPELLANTS
NT GELLED ROCKET PROPELLANTS
NT MONOPROPELLANTS
NT RP-1 ROCKET PROPELLANTS
NT SLURRY PROPELLANTS
Performance analysis of advanced spacecraft TPS
[NASA-CR-181532] 04 p0399 N88-12484
Space station resistojet system requirements and interface definition study
[NASA-CR-180832] 04 p0409 N88-12541
Dynamics of propellant feedline systems
[AD-A184865] 05 p0580 N88-13537
Computational prediction of propellant reorientation 08 p0982 N88-15940
Low gravity liquid motions in spacecraft 08 p0982 N88-15941
Peacekeeper tank slosh model 08 p0983 N88-15942
An infra-red investigation of HAN (Hydroxylammonium Nitrate)-based liquid propellants
[AD-A187226] 10 p1307 N88-17815
Bipropellant combustion in a liquid rocket combustion chamber 13 p1733 N88-20359
Performance of a hydrogen pulsed electrothermal thruster. Strategic defense initiative organization innovative science and technology. SBIR, phase 1
[AD-A191999] 18 p2475 N88-24679
A dynamic model of liquid propellant combustion 19 p2622 N88-25556
Dynamical properties of a collapsing spherical cavity 19 p2623 N88-25562
Pressure/temperature sensitive inorganic phosphors 19 p2627 N88-25583
Liquid Engine Jet Atomization Workshop report 19 p2627 N88-25584

LIQUID ROTATION
U ROTATING LIQUIDS

LIQUID SLOSHING
Calculation of the eigenvibrations of axisymmetric fluid configurations with a singularity method, taking into account surface tension effects under reduced gravity
[ETN-87-90438] 01 p0048 N88-10304
Computational prediction of propellant reorientation 08 p0982 N88-15940
Low gravity liquid motions in spacecraft 08 p0982 N88-15941
Peacekeeper tank slosh model 08 p0983 N88-15942
Spatial pressure variations and three-dimensional effects on liquid sloshing loads
[PB88-120134] 10 p1326 N88-17926
The nonlinear dynamics of a spacecraft coupled to the vibration of a contained fluid
[DE88-007035] 16 p2168 N88-22925
Axisymmetric liquid sloshing under low-g conditions: Numerical simulation method (reference manual)
[NLR-TR-86057-U] 20 p2802 N88-26627
Liquid oscillations in a prolate spheroidal container
[LRT-WE-9-FB-4(1988)] 22 p3078 N88-28276

LIQUID SODIUM
Sodium heat engine/AMTEC system experiments 17 p2409 N88-24325

LIQUID SURFACES
New equilibrium forms of free surface of confined magnetic fluid 06 p0770 N88-14734
Liquid motions in partially filled containers: Preliminary results of the D-1 mission --- Spacelab
[NLR-MP-86042-U] 20 p2802 N88-26629
Development of computer-controlled thermogravimetric instrumentation for measurement of environmental and high temperature volatilization and desorption of contaminants from polymeric materials
[AD-A195934] 24 p3343 N88-29900
Effect of interfacial phenomena on contact line heat Transfer-3
[AD-A194941] 24 p3343 N88-29901

LIQUID WASTES
NT URINE
NT WASTE WATER
Space station resistojet system requirements and interface definition study
[NASA-CR-180832] 04 p0409 N88-12541

LIQUID-GAS MIXTURES
NT AEROSOLS
NT FOG
Thermodynamic properties for natural gas binaries
[PB87-226833] 04 p0500 N88-13074
Theoretical and experimental investigation of swirl flow phase separators for microgravity applications
17 p2411 N88-24335
Experimental investigation of a microgravity separator for two phase mixtures containing small volumes of gas/vapor 17 p2432 N88-24468
LIQUID-LIQUID INTERFACES
Natural frequencies and stability of immiscible spherical liquid systems
[LRT-WE-9-FB-2(1987)] 22 p3053 N88-28113
Natural frequencies and stability of circular cylindrical immiscible liquid systems
[LRT-WE-9-FB-3(1987)] 22 p3062 N88-28172
Nonlinear oscillations of axially independent liquid column under zero-gravity environment
[LRT-WE-9-FB-12(1987)] 22 p3063 N88-28174
LIQUID-SOLID INTERFACES
An advanced microcomputer design for processing of semiconductor materials 10 p1288 N88-17703
Effect of density change on rapid liquid-solid interface kinetics and heat flow
[DE88-004286] 11 p1487 N88-18878
Variable-energy positron studies on liquids and liquid-solid interfaces
[DE88-006356] 15 p2033 N88-22109
Arctic ice attenuation model study
[AD-A193382] 22 p3146 N88-28715
Attenuated total reflectance FT-IR spectroscopy to measure interfacial reaction kinetics at silica surfaces
[AD-A196330] 24 p3344 N88-29908
LIQUID-VAPOR EQUILIBRIUM
Study of the vapor-liquid equilibria used in the fabrication process of hydrogen by thermochemistry
[DE88-900239] 07 p0830 N88-15035
Feasibility of a complex compound heat pump
[PB88-113022] 07 p0853 N88-15183
Phase equilibria and density calculations in the critical region: A phenomenological correction for a classical equation of state
[PB88-185335] 19 p2723 N88-26167
LIQUID-VAPOR INTERFACES
Review of nucleation and incipient boiling under pool and forced convection conditions
08 p0982 N88-15938
Vapor condensation on a turbulent liquid interface
08 p0982 N88-15939
Investigation of real-time two-dimensional visualization of fuel spray liquid/vapor distribution via exciplex fluorescence
[AD-A188268] 10 p1307 N88-17816
An experiment to investigate Rankine cycle two-phase microgravity issues 17 p2409 N88-24322
The combustion of hydroxylammonium nitrate based liquid propellants 19 p2622 N88-25555
LIQUIDS
NT CRYOGENIC FLUIDS
NT FERMI LIQUIDS
NT HYDRAULIC FLUIDS
NT LIQUEFIED NATURAL GAS
NT LIQUID AMMONIA
NT LIQUID HELIUM
NT LIQUID HELIUM 2
NT LIQUID HYDROGEN
NT LIQUID LITHIUM
NT LIQUID METALS
NT LIQUID NITROGEN
NT LIQUID OXIDIZERS
NT LIQUID OXYGEN
NT LIQUID POTASSIUM
NT LIQUID SODIUM
NT MERCURY (METAL)
NT MERCURY ISOTOPES
NT MERCURY VAPOR
NT ORGANIC LIQUIDS
NT POTABLE WATER
NT ROTATING LIQUIDS
Theoretical approaches to chemical dynamics in highly compressed fluids
[DE87-012242] 01 p0046 N88-10296
Application of new conformal solution of theories
[PB87-214557] 01 p0105 N88-10684
Electrical conductivity and equation of state measurements on planetary fluids at high pressures and temperatures
[DE87-013787] 01 p0110 N88-10708
Application of new conformal solution theories
[PB87-211934] 02 p0247 N88-11558
Vacuum ultraviolet electronic properties of liquids
[DE88-000165] 03 p0282 N88-11772
Wear of iron and nickel in corrosive liquid environments
[NASA-TM-100246] 03 p0289 N88-11817
Novel macrocyclic carriers for proton-coupled liquid membrane transport
[DE88-000636] 04 p0413 N88-12560
Experimental study of thermocapillary flows in a thin liquid layer with heat fluxes imposed on the free surface
[NASA-TM-100252] 04 p0445 N88-12763
Some new ideas in liquid detectors
[DE88-000732] 04 p0446 N88-12768
Statistical process control applied to the liquid-fed ceramic melter process
[DE88-000271] 05 p0569 N88-13471
Molecular dynamics studies of aromatic hydrocarbon liquids
[DE88-001473] 05 p0648 N88-13973
Experimental and theoretical studies of dense fluid mixtures
[DE88-002710] 07 p0831 N88-15039
The generalized van der Waals theory of pure fluids and mixtures
[DE88-002380] 07 p0855 N88-15192
The properties of sound propagation in liquid constrained viscoelastic and polymeric structures
[AD-A185944] 07 p0929 N88-15640
Equation of state of condensed materials physical principles and applications
[NASA-TT-20007] 08 p0968 N88-15855
Liquid spring design methodology for shock isolation system applications 08 p0998 N88-16043
DSC (Differential Scanning Calorimeter) stability test for liquid propellants: A preliminary report
[AD-A187115] 09 p1150 N88-16888
Study of pattern formation at liquid interfaces
[DE88-001399] 09 p1160 N88-16954
Design and characteristics of a liquid aerosol generator
[AD-A186942] 09 p1174 N88-17034
Attenuation of ultrasonic waves in nonmagnetized magnetic fluids 09 p1234 N88-17398
Pulsed laser photothermal spectroscopy of liquids and solids
[DE88-003839] 11 p1455 N88-18675
Liquid ventilation: New data and possible use in space medicine 12 p1654 N88-19908
Contrasting conductance/viscosity relations in liquid states of vitreous and polymer solid electrolytes
[AD-A189378] 13 p1748 N88-20452
Mathematical models of sound waves in fluids
[AD-A189270] 13 p1834 N88-20968
Techniques for studying fast reactions in liquids
[DE88-005917] 14 p1888 N88-21285
Variable-energy positron studies on liquids and liquid-solid interfaces
[DE88-006356] 15 p2033 N88-22109
Density measurements on solids and liquids
[PB88-164934] 15 p2036 N88-22129
Nucleation in super-saturated products
[NASA-TT-20275] 15 p2037 N88-22134
The effect of internal relaxation on optoacoustic conversion in liquids
[AD-A191307] 16 p2176 N88-22970
Noncondensing round turbulent gas jets in liquids
[AD-A191191] 16 p2208 N88-23179
Direct emissivity measurements on liquids and corrections to multi-color pyrometers
17 p2329 N88-23906
Liquid carbon
[AD-A191707] 18 p2491 N88-24776
Kinetics of homogeneous nucleation in superheated F-11 and F-21 liquid freons
[NASA-TT-20286] 19 p2613 N88-25503
Observation of metallic conductivity in liquid carbon
[AD-A191723] 19 p2618 N88-25533
The use of liquid films for spacecraft survivability to laser radiation
[AD-A192954] 20 p2765 N88-26395
Extension of Boltzmann's theory to a liquid
[DE88-009153] 20 p2880 N88-27097
Natural frequencies and stability of immiscible cylindrical z-independent liquid systems
[LRT-WE-9-FB-1(1987)] 22 p3053 N88-28112
Natural convection immersion cooling of an array of simulated chips in an enclosure filled with dielectric liquid
[AD-A193594] 23 p3207 N88-29088
Liquid thickness gauge
[NASA-CASE-LAR-13826-1] 23 p3217 N88-29150
The dc power control for a liquid-fed resistojet
[NASA-TM-101326] 24 p3338 N88-29869
Design criteria for extraction with chemical reaction and liquid membrane permeation
[NASA-TT-20352] 24 p3343 N88-29899
Titrimetric analysis of HAN-based liquid propellants
[AD-A196225] 24 p3357 N88-29990
LISP (PROGRAMMING LANGUAGE)
LISP as a rapid prototyping environment: The chinese tutor
[AD-A184328] 03 p0369 N88-12319
The desktop interface in intelligent tutoring systems
09 p1205 N88-17225
A rule-based Lisp dialect translator using paramodulation 10 p1380 N88-18238
SimPL: A simulator for parallel LISP
[AD-A189831] 15 p2109 N88-22566
CK-LOG system conversion (user's manual and user interface)
[AD-A190273] 15 p2111 N88-22577
Simulating futures in extended common LISP
[NASA-TM-101000] 18 p2559 N88-25192
The concurrent common Lisp development environment 23 p3263 N88-29422
Scheme86: A system for interpreting SCHEME
[AD-A195931] 24 p3413 N88-30319
Lisp Object State Saver (LOSS): A facility used to save partial schedules of the Hubble Space Telescope
24 p3421 N88-30360
LISTS
Source header list. Volume 2: L through Z
[AD-A184001] 03 p0385 N88-12419
Source hierarchy list. Volume 1: A through D
[AD-A185900] 07 p0941 N88-15722
Source hierarchy list. Volume 2: E through O
[AD-A185901] 07 p0941 N88-15723
Source hierarchy list. Volume 3: P through Z
[AD-A185902] 07 p0942 N88-15724
On the productivity of recursive list definitions
[CS-8707] 14 p1960 N88-21692
LITERATURE
NT BIOGRAPHY
NT DOCUMENTATION
Translations of scientific and technical literature: A guide to their location 16 p2286 N88-23686
Publications of the Jet Propulsion Laboratory 1987
[NASA-CR-181198] 24 p3436 N88-30453
LITHIUM
NT LIQUID LITHIUM
NT LITHIUM ISOTOPES
Corrosion susceptibility study of candidate pin materials for ALTC (Active Lithium/Thionyl Chloride) batteries
[DE88-001449] 04 p0440 N88-12734
Technical evaluation of a solar-powered absorption cooling system (LiBr-H2O)
[PB87-108254] 04 p0463 N88-12867
Far-infrared spectra of lithium deposited on a gold electrode: Interpretation using a cluster model
[AD-A184231] 04 p0495 N88-13050
Survey state of the art: Electrical load management techniques and equipment
[AD-A184083] 05 p0577 N88-13517
A fluid simulation of the AMPTE lithium gas releases in the solar wind
[TRITA-EPP-87-06] 05 p0661 N88-14056
Interfacial effects in thin Li/PEO cells at room temperature
[AD-A186974] 09 p1157 N88-16931
Environment assisted degradation mechanisms in aluminum-lithium alloys
[NASA-CR-182482] 10 p1301 N88-17782
Polymeric electrolytes for ambient temperature lithium batteries
[DE88-004896] 13 p1763 N88-20547
Wavelength scaling of lithium-like recombination scheme for X-UV gain production — X-ray lasers
[ETN-88-92002] 13 p1778 N88-20634
Magnetic cavity formation at Comet Halley and at the AMPTE Li release 14 p1996 N88-21898
A transient model for liquid metal heat pipes
17 p2421 N88-24398
The THROHPUT code: Thermohydraulic heat pipe modeling 17 p2421 N88-24399
Possible creep studies of lithium with a compact device 17 p2422 N88-24404
A low divergence, high brightness lithium ion source for plasma diagnostics
[DE88-008063] 19 p2729 N88-26203
Optimizing superplastic response in lithium containing aluminum-magnesium alloys
[AD-A192217] 20 p2774 N88-26451
Ambient temperature secondary lithium batteries using LiAl lithium insertion anodes
[DE88-008394] 20 p2793 N88-26574
Molten salt electrolytes for high-temperature lithium cells
[DE88-010058] 20 p2794 N88-26581
Field-enhanced lithium ion sources for PBFA 2
[DE88-007195] 20 p2856 N88-26960
Poloidal field measurements using laser enhanced attenuation of an energetic lithium beam
[DE88-008360] 20 p2856 N88-26963

Generation of Adlam-Allen waves by plasma release experiments in the solar wind
[PB88-106000] 20 p2886 N88-27140
Morphological changes in polymer electrolyte cells
[AD-A195821] 24 p3388 N88-30054

LITHIUM ALLOYS
On the role of crack tip shielding in influencing the behavior of long and small fatigue cracks in aluminum-lithium alloy 2090 05 p0600 N88-13671
Variable amplitude fatigue crack growth in aluminum alloys 2090-T8E41 and 7075-T651 05 p0602 N88-13687
The age hardening response of thermomechanically processed Al-Mg-Li alloys
[AD-A189870] 15 p2039 N88-22147
Stress corrosion cracking properties of Al-Li alloys 17 p2320 N88-23853
Aluminum alloy
[NASA-CASE-LAR-13924-1-CU] 18 p2487 N88-24753
Nondestructive evaluation methods for determination of thermal history and mechanical properties of aluminum-lithium alloys
[DE88-007352] 19 p2615 N88-25516
Inelastic ion-surface collisions
[AFGL-TR-87-0206] 19 p2724 N88-26174
Fatigue of lithium-aluminum alloys: An example of localization of the plastic deformation
[ETN-88-92309] 20 p2775 N88-26456
A method for determining the solubility of hydrogen in molten aluminum-lithium alloys
[DE88-009807] 21 p2910 N88-27270
Structural relationship between icosahedral and Frank-Kasper phases of Al-Li-Cu
[AD-A193768] 23 p3195 N88-29011

LITHIUM CHLORIDES
Optimization of reserve lithium thionyl chloride battery electrochemical design parameters
[DE88-007109] 18 p2506 N88-24868

LITHIUM COMPOUNDS
NT LITHIUM CHLORIDES
NT LITHIUM FLUORIDES
NT LITHIUM HYDRIDES
NT LITHIUM HYDROXIDES
NT LITHIUM IODATES
NT LITHIUM NIOBATES
NT LITHIUM OXIDES
NT LITHIUM PERCHLORATES
NT ORGANIC LITHIUM COMPOUNDS
Study of the micromechanical behavior of a SiO2-Al2O3-Li2O glass ceramic and its relation to the microstructure
[ISAL-ITC1-87-01] 02 p0153 N88-10960
Steady-state deformation of some lithium ceramics
[DE88-003116] 08 p0972 N88-15882
Lithium fast-ion conductors: Polymer based materials
[AD-A187879] 11 p1481 N88-18712
The synthesis, characterization and structural studies of In(C5H4Me) by X-ray diffraction and electron diffraction techniques and a reinvestigation of the crystalline state of In(C5H5) by X-ray diffraction studies
[AD-A189110] 13 p1844 N88-21038
Structure and dynamics of solutions of lithium salts relevant to battery construction
[AD-A195399] 24 p3366 N88-30044

LITHIUM FLUORIDES
Growth and characteristics of materials for tunable lasers in the near infrared spectral region
[NASA-CR-182501] 11 p1491 N88-18901
Effect of Mg impurity on local vibrations of U-centers in LiF lattice 14 p1969 N88-21753

LITHIUM HYDRIDES
Development of encapsulated lithium hydride thermal energy storage for space power systems
[DE88-004762] 11 p1507 N88-19001
A theoretical and experimental study of the thermophysical properties of lithium hydride
[NASA-TT-20179] 16 p2175 N88-22965
Fabrication of lithium hydride shields for space nuclear power systems 17 p2402 N88-24282
Fabrication of reactor shields at the Y-12 plant 17 p2402 N88-24283
Transient analysis of Li and LiH thermal storage spheres 17 p2411 N88-24334
Energy storage for nuclear burst power systems 17 p2426 N88-24431

LITHIUM HYDROXIDES
DC conductivity studies in Li5AlO4 at intermediate temperatures and its possible application for the electrolysis of water
[AD-A185489] 06 p0697 N88-14276
Phase behavior in the Li-Al-O-H system at intermediate temperatures
[AD-A185732] 06 p0697 N88-14280
Hydroxide ion conductors as possible electrolytes in intermediate temperature fuel cells
[AD-A185508] 06 p0731 N88-14495

LITHIUM IODATES
High ionic conductivity in PEO.PPG block polymer and salt solutions
[AD-A183502] 01 p0026 N88-10168

LITHIUM ISOTOPES
Development and applications of new technical advances to problems of fluid/electrolyte/mineral imbalance in military personnel
[AD-A186437] 07 p0889 N88-15388

LITHIUM NIOBATES
Optical frequency doubling in Ti:LiMbO3 waveguide resonators
[ETN-88-91486] 11 p1550 N88-19271

LITHIUM OXIDES
Growth and characteristics of materials for tunable lasers in the near infrared spectral region
[NASA-CR-182501] 11 p1491 N88-18901
Single-crystal structural study of La2Cu/sub 0.95/Li/sub 0.05/O4
[DE88-003482] 11 p1554 N88-19302

LITHIUM PERCHLORATES
Lithium/polymer electrolyte interfacial instability
[AD-A187164] 09 p1147 N88-16874

LITHIUM SULFUR BATTERIES
Lithium/iron sulfide batteries: Development and demonstration
[DE87-014222] 01 p0042 N88-10265
The 1986 Goddard Space Flight Center Battery Workshop
[NASA-CP-2486] 02 p0163 N88-11021
Computer simulation of thermal modeling of primary lithium cells 02 p0163 N88-11022
The 250AH/90A active lithium-thionyl chloride cell for Centaur-G application 02 p0163 N88-11023
The MOLICEL(R) rechargeable lithium system: Multicell battery aspects 02 p0163 N88-11024
Fault tree safety analysis of a large Li/SOCl(sub)2 spacecraft battery 02 p0163 N88-11025
Chemical analysis of charged Li/SO(sub)2 cells 02 p0163 N88-11026
Impedance of passive lithium anodes in SOCl2 solutions under low-field polarization
[DE88-000922] 04 p0439 N88-12728
Reliability of Li/SO2 cells for long-life applications
[DE88-001360] 04 p0440 N88-12735
Ionically conducting polymers: Principles and properties of solid electrolytes
[DE88-001552] 06 p0684 N88-14190
Lithium/disulfide battery R and D
[DE88-003032] 11 p1481 N88-18839
All inorganic ambient temperature rechargeable lithium battery
[DE88-008425] 19 p2662 N88-25834
The kinetics of charge-transfer reactions on passive lithium electrodes
[DE88-009256] 21 p2939 N88-27454

LITHIUM 4
U LITHIUM ISOTOPES

LITHIUM 6
U LITHIUM ISOTOPES

LITHOGRAPHY
NT PHOTOLITHOGRAPHY
Basic research in ceramic and semiconductor science at selected Japanese laboratories, based on a September 1986 visit: Highlights, summary and overview and detailed notes from selected Japanese laboratories
[DOE/ER-0314] 12 p1696 N88-20150
Electronic properties of semiconductor inversion layers in sub-micron structures
[AD-A188635] 12 p1698 N88-20161
Content of natural radioactive elements in Venusian rocks determined using data from Vega-1 and Vega-2 stations 13 p1726 N88-20323
Practical constraints on sources for pulsed beam lithographies
[DE88-006594] 13 p1776 N88-20623
High-speed electron beam lithography devices discussed 16 p2185 N88-23023
Microelectronics the next fifteen years 17 p2305 N88-23792
Department of Defense statement on the X-ray Lithography Program to the Research and Development Subcommittee of the House Armed Services Committee of 100th Congress, second session
[AD-A191854] 18 p2582 N88-25341
Excitonic properties of GaAs-AlGaAs nanostructures 20 p2867 N88-27023
Precise rotational alignment of X-ray transmission diffraction gratings
[DE88-010599] 21 p2911 N88-27273
High-speed, precision processing using an electron beam 21 p2929 N88-27391
Equipment for an advanced electron beam lithography system
[AD-A192956] 21 p2936 N88-27435
The Kerala Khondalite Belt (KKB) of Southern India: An ensialic mobile belt 24 p3393 N88-30208
The timing and mechanism of depletion in Lewisian granulites 24 p3394 N88-30209

LITHOLOGY
Nature and origin of mineral coatings on volcanic rocks of the Black Mountain, Stonewall Mountain, and Kane Springs Wash volcanic centers, Southern Nevada
[NASA-CR-181437] 09 p1191 N88-17140
Geological evolution and analysis of confirmed or suspected gas hydrate localities. Volume 10: Basin analysis, formation and stability of gas hydrates of the Aleutian Trench and the Bering Sea
[DE88-001008] 10 p1346 N88-18048
Geological evolution and analysis of confirmed or suspected gas hydrate localities. Volume 9: Formation and stability of gas hydrates of the Middle America Trench
[DE88-001007] 10 p1347 N88-18050
Data-base of Antarctic pre-Pleistocene sediment cores
[PB88-124151] 10 p1354 N88-18094
Martian geomorphology and its relation to subsurface volatiles
[NASA-CR-182428] 12 p1711 N88-20237
Analysis and interpretation of image lithostructure: An application of the multiconcept in the metamorphic belt of Sul de Santana da Boa Vista (RS) 17 p2359 N88-24051
Some geological aspects of the Pirapemas Lineament Belt 17 p2368 N88-24099
Lithostructural interpretation of Chapda do Cachimbo (Pa-Am-Mt), based on radar and LANDSAT imagery 17 p2368 N88-24100
A sedimentological and mineralogical study of the Koogah Formation, New South Wales 18 p2542 N88-25087
Analysis of the multispectral content and of SPOT subscenes in two regions of Burundi. Lithologic and tectonic interpretations 22 p3105 N88-28439

LITHOSPHERE
NT EARTH CORE
NT EARTH CRUST
NT EARTH MANTLE
NT EARTH SURFACE
Ocean floor magmatism and problems of lithosphere formation 08 p1009 N88-16121
Thematic mapper study of Alaskan ophiolites
[NASA-CR-182554] 11 p1504 N88-18984
Synthesis of finite displacements and displacements in continental margins
[NASA-CR-182616] 12 p1642 N88-19832
Effects of a temperature-dependent rheology on large scale continental extension
[NASA-CR-183117] 20 p2825 N88-26759
Intraplate deformation, stress in the lithosphere and the driving mechanism for plate motions
[NASA-CR-183121] 23 p3231 N88-29231
Lithospheric evolution of the Northern Arabian Shield: Chemical and isotopic evidence from basalts, xenoliths and granites 24 p3399 N88-30242

LITTORAL CURRENTS
U COASTAL CURRENTS

LITTORAL TRANSPORT
Nearshore wave transformation study of sites near Port Canaveral Inlet, Florida
[AD-A185965] 09 p1195 N88-17159

LIVER
Effect of weightlessness on replicative function of rat hepatocyte DNA 10 p1360 N88-18129
RNA-synthesizing activity in rat liver following flight aboard Cosmos-1667 10 p1360 N88-18130

LIVERWORTS
U BRYOPHYTES

LMCR (REACTORS)
U LIQUID METAL COOLED REACTORS

LMFBR
U LIQUID METAL FAST BREEDER REACTORS

LNG
U LIQUEFIED NATURAL GAS

LOAD DISTRIBUTION (FORCES)
Physiological determinants of load bearing capacity
[AD-A184977] 05 p0629 N88-13848
Behavior of a steel cylinder under the influence of a local load in the elastic and elasto-plastic area
[PB87-154787] 07 p0869 N88-15272
Cubic spline solution of symmetric buckling problems of clamped shallow spherical shells 15 p2053 N88-22239
Development of a lightweight structure with load bearing capability and high thermal conductance 17 p2420 N88-24393

Wind tunnel investigation of wing and control panel loads at transonic and supersonic speeds on some schematic cruciform missile configurations
[FFA-TN-1986-43-SUPPL-1] 22 p3039 N88-28044
Tripping of stiffened plates using a refined beam theory
[AD-A193989] 22 p3087 N88-28333

LOAD FACTORS
U LOADS (FORCES)

LOAD TESTING MACHINES
Device for measuring hole elongation in a bolted joint
[NASA-CASE-LAR-13453-1] 06 p0712 N88-14361
User's guide: Lower neck transducer for the Hybrid 3 dummy
[PB88-133319] 12 p1628 N88-19743
Evaluation tests of lower neck transducer for the Hybrid 3 Dummy
[PB88-133327] 12 p1628 N88-19745
Bearing-bypass material system test
[NASA-CASE-LAR-13458-1] 17 p2342 N88-23967
Automated measurement of crack length and load line displacement at elevated temperature
[NLR-MP-87049-U] 20 p2816 N88-26706

LOAD TESTS
Requirements for a test stand for plastic rollers for the verification of nonequilibrium force laws
[ILR-MITT-176] 01 p0008 N88-10040
Cumulative fatigue and life prediction of fibre composites. Part 2: Experimental techniques and results
[BR101014] 02 p0142 N88-10894
A study of the crack tip parameters that govern environmentally assisted cracking by use of the rising displacement test 04 p0427 N88-12649
Durability of powdered aluminum structures 04 p0429 N88-12655
Control of a flexible one-link manipulator
[AD-A185035] 05 p0590 N88-13598
An optical interferometry technique to evaluate closure along a crack front 05 p0607 N88-13726
Deformation, fatigue and fracture behavior of two cast anisotropic superalloys 05 p0608 N88-13732
A summary of experimental results on square plates and stiffened panels subjected to air-blast loading 09 p1178 N88-17057
To determine the stress distribution in the vicinity of GRP end pads where the specimen is held and loaded (CFC coupon specimens) --- glass reinforced plastic (GRP) carbon fiber composite (CFC)
[BAE-WST-R-RES-CFC-12023] 09 p1182 N88-17080
Further tests to determine the stress distribution in the vicinity of GRP end pads where the specimen is held and loaded (CFC coupon specimens) --- glass reinforced plastic (GRP) carbon fiber composite (CFC)
[BAE-WST-R-RES-CFC-12023-ADD-1] 09 p1182 N88-17081
Application of ISRM testing methods to fracture toughness testing of graphite 13 p1747 N88-20446
European approaches in standard spectrum development --- aircraft load spectra
[NLR-MP-87007-U] 13 p1782 N88-20661
Determination of canopy loads for a light aircraft by wind tunnel testing and computer modelling
[BU-353] 14 p1869 N88-21167
Some structural aspects of crack propagation in heat-resistant steels under cyclic thermal and mechanical load 14 p1896 N88-21317
Controlled-strain rate tests at very low strain rates of 2618 aluminum at 200 C 14 p1931 N88-21513
Some implications for cyclic plastic and viscoplastic equations based on nonproportional loading experiments 14 p1931 N88-21515
A unified creep-plasticity model suitable for thermo-mechanical loading 14 p1932 N88-21518
Constitutive response of Rene 80 under thermal mechanical loads 14 p1932 N88-21524
Experiments investigating advanced materials under thermomechanical loading 15 p2077 N88-22385
MHOST: An efficient finite element program for inelastic analysis of solids and structures 15 p2079 N88-22394
Characterization of Mode 1 and Mode 2 delamination growth and thresholds in graphite/peek composites
[NASA-TM-100577] 16 p2172 N88-22947
Development of a biaxial test system for thin-walled metal tubes using tensile-compressive axial load and internal-external pressure
[DE88-011279] 21 p2962 N88-27592
Modal testing in the design evaluation of wind turbines
[DE88-010374] 21 p2968 N88-27632
Wind tunnel investigation of wing and control panel loads at transonic and supersonic speeds on some schematic cruciform missile configurations
[FFA-TN-1986-43-SUPPL-1] 22 p3039 N88-28044
Stress corrosion evaluation of powder metallurgy aluminum alloy 7091 with the breaking load test method 22 p3053 N88-28115
Calibration of quartz load cells: An in-situ procedure for instrumented falling weight impact machines
[NPL-DMA(A)-155] 22 p3081 N88-28297

LOADING FORCES
U LOADS (FORCES)

LOADING MOMENTS
Kinematic support using elastic elements 14 p1926 N88-21481

LOADING OPERATIONS
The composition of the gas in the loading inlet of the Space Shuttle Orbiter
[ETN-87-90430] 01 p0012 N88-10069
Modification of integrated partial payload lifting assembly
[NASA-CR-182573] 11 p1443 N88-18607

LOADING RATE
Composite materials applications program at the US Army Ballistic Research Laboratory: Work in progress 04 p0428 N88-12651
Loading rate sensitivity of open hole composites in compression
[NASA-TM-100634] 19 p2610 N88-25490
Cold worked reinforcing bars in tensile test under high loading rate and low temperatures
[DE88-752993] 21 p2964 N88-27610
An investigation of constitutive models for predicting viscoplastic response during cyclic loading
[AD-A194875] 24 p3385 N88-30163

LOADING WAVES
U ELASTIC WAVES
U LOADS (FORCES)

LOADS (FORCES)
NT AERODYNAMIC LOADS
NT AXIAL COMPRESSION LOADS
NT AXIAL LOADS
NT BLAST LOADS
NT COMPRESSION LOADS
NT CONTACT LOADS
NT CRITICAL LOADING
NT CYCLIC LOADS
NT DYNAMIC LOADS
NT EDGE LOADING
NT GUST LOADS
NT IMPACT LOADS
NT LANDING LOADS
NT RANDOM LOADS
NT ROLLING CONTACT LOADS
NT SHOCK LOADS
NT STATIC LOADS
NT TRANSIENT LOADS
NT VIBRATORY LOADS
NT WING LOADING
Calculation of the damage of highly loaded gas turbine disks under real flight conditions
[ETN-87-90416] 01 p0007 N88-10036
Assessment of the COFSI/MAST I project
[NASA-CR-181366] 01 p0053 N88-10340
Analysis of shell-type structures subjected to time-dependent mechanical and thermal loading
[NASA-CR-181409] 01 p0060 N88-10388
Nonsteady-state vibrations in acoustic medium of elastic elliptical shell subjected to instantaneously applied uniform pressure 02 p0160 N88-11000
Frozen-field, rigid-beam, uniform-conductivity-channel tracking force calculation
[DE87-012510] 02 p0190 N88-11190
Operational load measurements on service helicopters 03 p0263 N88-11658
Pump assisted heat pipe 03 p0319 N88-12018
Bearing loads in slider crank mechanisms
[PB87-216495] 03 p0332 N88-12089
Computational methods and results for dynamic fracture 03 p0337 N88-12123
Kinetics of crack growth: Thermal/mechanical interaction 03 p0337 N88-12124
Ideal-viscoplastic extrusion model with application to deforming pistons in light-gas guns
[UTIAS-TN-266] 04 p0429 N88-12657
The effect of mass, wind angle and erection technique on the aeroelastic behaviour of a cable-stayed bridge model
[NAE-AN-46] 04 p0455 N88-12819
A comparison of structural frequency response functions measured with forces from 500 to 250,000 lb
[DE88-000668] 04 p0457 N88-12829
Static aeroelastic considerations in the definition of design loads for fighter airplanes 05 p0550 N88-13351
An analytical study of the effects of transverse shear deformation and anisotropy on buckling loads of laminated cylinders
[NASA-TM-100508] 05 p0557 N88-13387
The simulation of the viscous flow around a cylinder by the random vortex method 05 p0579 N88-13534
A dislocation model for fatigue crack propagation under variable amplitude loading 05 p0602 N88-13683
Observations on the effect of overloads on fatigue crack growth 05 p0602 N88-13684
Variable amplitude fatigue crack growth in aluminum alloys 2090-T8E41 and 7075-T651 05 p0602 N88-13687
Fatigue of 30CrMnSiNi2A notched specimens under spectrum loading 05 p0602 N88-13689
Damping analysis of flexural waves in fluid-loaded single and constrained plates
[AD-A185116] 05 p0609 N88-13739
Fluctuating pressure loads under high speed boundary layers
[NASA-TM-100517] 05 p0647 N88-13962
Behavior of bolted joints in composite laminates 06 p0677 N88-14148
The effects of loading history on fatigue crack growth threshold 06 p0718 N88-14406
Beam and column buckling under directed loading
[PB87-124004] 06 p0722 N88-14436
A loading system for creep testing under constant compressive stress
[NASA-TT-20119] 06 p0722 N88-14441
Wave propagation experiments on 22-bay lattice
[AD-A186140] 07 p0824 N88-15002
Load carriage induced alterations of pulmonary function
[AD-A186227] 07 p0889 N88-15386
Integral equation method for the analysis of plates and shells
[PB87-144788] 08 p0996 N88-16030
TECOM's research efforts in the dynamic environments 08 p0999 N88-16048
Evaluation of vibration specifications for acoustic environments 08 p0999 N88-16053
Design procedures for fiber composite box beams
[NASA-TM-100296] 09 p1139 N88-16828
A research program on the aerodynamics of a highly loaded turbine stage 10 p1280 N88-17655
Tactile sensing and inverse problems
[AD-A187464] 10 p1340 N88-18011
Study of the mechanical behavior of a 2-D carbon-carbon composite
[NASA-CR-182594] 11 p1451 N88-18649
Fracture characteristics of a viscoelastic polymer under constant load: Experiments and analysis 11 p1501 N88-18963
Dynamic analysis of plane frames by microcomputer 11 p1531 N88-19143
Determination of design loads for modern combat aircraft 12 p1580 N88-19457
Mechanical response of unidirectional boron/aluminum under combined loading
[NASA-CR-182595] 12 p1604 N88-19591
Ply-level failure analysis of a graphite/epoxy laminate under bearing-bypass loading
[NASA-TM-100578] 13 p1735 N88-20372
Dynamic modelling of flexible rotor shafts mounted on hydrodynamic bearings 13 p1779 N88-20641
Component mode synthesis using experimental modes enhanced by mass loading
[DE88-006097] 13 p1781 N88-20657
Analysis of shell-type structures subjected to time-dependent mechanical and thermal loading
[NASA-CR-182705] 13 p1783 N88-20668
Quick actuating closure and handling system 14 p1925 N88-21476
Effects of state recovery on creep buckling under variable loading 14 p1933 N88-21527
Practical considerations for structural control: System uncertainty, system time delay and truncation of small control forces
[PB88-163738] 14 p1933 N88-21528
Determination of the commutation and angle and load response for a continuous-current, single phase controlled rectifier
[AD-A190602] 15 p2060 N88-22285
Fatigue crack growth behavior of a single crystal alloy as observed through an in situ fatigue loading stage
[NASA-TM-100863] 16 p2179 N88-22986
Crack retardation under load spectra. Experimental study and numerical simulation using the simplified K constant model --- light alloys, aircraft construction materials
[ONERA-RT-30/7169-RY-054-R] 16 p2222 N88-23266
Calculation of root-mean-square loads
[BLL-M-37776-(5828.4)] 18 p2531 N88-25015
Vertical ship motions and sea loads considering nonlinear effects
[TAE-592] 20 p2784 N88-26515

Instrumentation for the measurement of penetrator dynamic response to permit force estimation
[DE88-010608] 20 p2809 N88-26666
A comparison of the various helicopter mathematical models used in the methodology assessment
21 p2889 N88-27149
Wind tunnel tests of the influence of airfoil-thickness on normal force and pitching moment of two slender wings at transonic and supersonic Mach numbers
[DFVLR-FB-88-17] 21 p2893 N88-27171
Thermo-viscoelastic analysis of composite materials, volume 1
[NASA-CR-183048-VOL-1] 21 p2904 N88-27230
Analysis of crack arrest toughness
[AD-A193340] 21 p2913 N88-27286
A study of fluid-structure problems
21 p2941 N88-27468
The influence of weld metal properties, weld geometry and applied load on weld system performance
[AD-A193403] 21 p2961 N88-27588
Method to predict external store carriage characteristics at transonic speeds
[NASA-CR-4170] 22 p3037 N88-28034
Wave propagation and vibration of fibre reinforced laminates
[AD-A194144] 22 p3051 N88-28101
Estimation forces acting on an underwater vehicle with G.P.S. (Global Positioning System) and Kalman filtering
[AD-A194339] 23 p3175 N88-28901
Plastic flow and failure modeling under high strain rate loading
[AD-A194223] 23 p3226 N88-29199

LOCAL AREA NETWORKS
Space lab system analysis
[NASA-CR-179207] 02 p0138 N88-10869
Lewis Information Network (LINK): Background and overview
[NASA-TM-100162] 03 p0305 N88-11925
Applications of the hybrid automated reliability predictor
[NASA-TP-2780] 04 p0475 N88-12928
Introduction to local area network design on Ariane 5 and future launchers
[SNIAS-872-422-102] 05 p0635 N88-13886
On real-time systems using local area networks
[AD-A185475] 06 p0694 N88-14256
A new library of CAMAC routines for the control of the system CRATE by a microVAX in the VAXELN environment
[NOTA-INTERNA-893] 06 p0761 N88-14667
Facility design validation of the information systems laboratory
[AD-A186309] 07 p0906 N88-15488
Media independent interface
[NASA-CR-172033] 08 p1066 N88-16446
Media independent interface. Interface control document
[NASA-CR-172032] 08 p1067 N88-16447
MPAD MCC workstation system: ADDAM and EEVE
09 p1203 N88-17209
A classified bibliography on publications relevant to data security in LANs — local area networks (LANS)
[NPL-DITC-99/87] 09 p1223 N88-17331
The design of load balancing strategies for distributed systems 10 p1376 N88-18216
Experiments with parallel program execution on a network of workstations 10 p1377 N88-18217
An Ethernet local area network controller with supporting operating system software
[DE88-003534] 10 p1392 N88-18304
Air Force Institute of Technology (AFIT) Local Area Network (LAN) performance evaluation model: An analytic model for assessing the impact of changing LAN hardware and software configurations
[AD-A187191] 11 p1469 N88-18764
Performance analysis of slotted ring protocols in High Speed Local Area Networks (HSLANS)
[INF-87-31] 14 p1955 N88-21652
Passive coupler, network adapter, and network acquisition procedure for optical local networks
[ETN-88-92130] 14 p1961 N88-21695
Exact analyses of slotted ring protocols for local area networks with one transmitting station
[MEMO-650] 14 p1967 N88-21737
DATAC bus monitor 17 p2294 N88-23721
Development of a generic architecture
17 p2303 N88-23774
Interconnection of high-speed local area networks
17 p2390 N88-24205
An investigation of a distributed clock for local area networks with ring topology 18 p2516 N88-24924
The high speed local area network
19 p2717 N88-26133
A state-of-the-art survey of low-cost security in local area networks
[NPL-DITC-113/88] 22 p3141 N88-28678
Intelligent resource management for local area networks: Approach and evolution
23 p3256 N88-29385

LOCAL GROUP (ASTRONOMY)
NT MILKY WAY GALAXY
Duplicity in the solar neighborhood. Part 3: New spectroscopic elements for nine solar-type binary stars
[SER-C-PREPUBL-FASC-18-PT-3]
18 p2592 N88-25405
Duplicity in the solar neighborhood: Part 4: Spectroscopic orbits for four dwarf M stars
[SER-C-PREPUBL-FASC-21] 24 p3454 N88-30561
Duplicity in the solar neighborhood: Part 5: Spectroscopic orbit for the nearby double-lined solar-type star HR 8581
[SER-C-PREPUBL-FASC-23] 24 p3455 N88-30562

LOCALIZATION
U POSITION (LOCATION)

LOCATION
U POSITION (LOCATION)

LOCKHEED AIRCRAFT
NT C-130 AIRCRAFT
NT P-3 AIRCRAFT
NT T-33 AIRCRAFT
NT U-2 AIRCRAFT

LOCKHEED U-2 AIRCRAFT
U U-2 AIRCRAFT

LOCKING
NT LASER MODE LOCKING
Frequency locking of two lasers
[FOA-C-30458-3.1] 08 p0992 N88-16000
Locking hinge
[NASA-CASE-MSC-21056-1] 17 p2312 N88-23827
Mode locking of semiconductor laser with external cavity
[AD-A196018] 24 p3378 N88-30117

LOCKS (FASTENERS)
Modification and development of the external tank hydrogen vent umbilical system for the space shuttle vehicle 14 p1928 N88-21496
Collet lock joint for space station truss
[NASA-CASE-MSC-21207-1] 23 p3222 N88-29180

LOCOMOTION
NT ASTRONAUT LOCOMOTION
NT WALKING
Dynamics and stability of bipedal locomotion robots
03 p0333 N88-12096
Some remarks on gravitational biology
07 p0884 N88-15366
Investigations of Paramecium cells analyzed under microgravity conditions 07 p0884 N88-15367
Questions on the evolution of the development program of the vertebrate inner ear under long term zero-g conditions 07 p0886 N88-15379

LOCOMOTIVES
Application of Kalker's rolling contact theory to the simulation of rail vehicles
[DFVLR-FB-87-07] 01 p0057 N88-10363

LOG PERIODIC ANTENNAS
The use of coaxial transmission line elements in log-periodic dipole arrays
[AD-A184864] 05 p0574 N88-13499
A computer model investigation of a half square log-periodic array
[AD-A190955] 16 p2190 N88-23062

LOGARITHMS
Freidlin-Wentzell type estimates and the law of the iterated logarithm for a class of stochastic processes related to symmetric statistics
[AD-A185366] 05 p0644 N88-13944
On selecting the best of k lognormal distributions
[AD-A185628] 07 p0916 N88-15567
High speed transcendental elementary function architecture in support of the Vector Wave Equation (VWE)
[AD-A189746] 15 p2119 N88-22627
Research on algebraic manipulation
[AD-A190149] 15 p2120 N88-22634

LOGGING (INDUSTRY)
Applicability of SPOT for forest inventory, mapping and change monitoring 03 p0344 N88-12174

LOGIC
Induction instrument for logic conclusion
[LRT-WE-9-FB-5(1987)] 22 p3144 N88-28697

LOGIC CIRCUITS
Programmable Logic Arrays (PLA's) design for testability
[PB87-102935] 04 p0438 N88-12718
Mental models in expert physics reasoning
[AD-A184106] 04 p0500 N88-13075
An exact analysis and performance of framed ALOHA with capture
[AD-A185008] 05 p0574 N88-13500
New breakthrough in Chinese integrated circuits: Successful development of high-speed CMOS circuits
[AD-A185381] 05 p0578 N88-13525
Implementation of an FIR band pass filter using a bit-slice processor
[AD-A184895] 05 p0634 N88-13875
Interfacing slave designs to Fastbus: Practical experience
[DE88-002807] 09 p1215 N88-17286
Vertical charge transport in junction charge-coupled devices
[ETN-88-91613] 09 p1255 N88-17523
Signal processing studies program VLSI designs for unary functions
[AD-A188053] 10 p1325 N88-17922
New mode switching algorithm for the JPL 70-meter antenna servo controller 11 p1474 N88-18791
Modules of nanosecond logic electronics system with computer control
[DE88-700190] 11 p1479 N88-18828
Fast serial input-serial output pipelined inner product units
[REPT-87-031] 11 p1530 N88-19142
A methodology for hardware verification based on logic simulation
[AD-A188553] 12 p1622 N88-19704
A digital circuit design environment
[AD-A188831] 12 p1623 N88-19709
MOBICALC: An integrated and interactive system for development of administrative models
[INPE-4335-TDL/291] 12 p1679 N88-20038
Ultra-high speed integrated optical waveguide devices for optical computing
[AD-A188470] 12 p1691 N88-20118
Describing constraints on a digital circuit's behavior
[AD-A189200] 13 p1761 N88-20531
A fault injection experiment using the AIRLAB Diagnostic Emulation Facility
[NASA-CR-178390] 13 p1823 N88-20895
An expert system for discrete component digital circuit design
[AD-A189680] 15 p2059 N88-22274
Applications of optical computing to problems with symbolic computations
[AD-A189772] 15 p2106 N88-22548
Joint services electronics program research in electronics
[AD-A192206] 18 p2504 N88-24857
SYMBL: A new Boolean compiler
18 p2554 N88-25160
High-speed optical logic using GaAs
19 p2656 N88-25773
The design of a digital Eprom oscillator for electrical impedance tomography
[DE88-012243] 21 p2940 N88-27462
STAR: Sandia Timing Analyzer Routine
[DE88-012412] 21 p2940 N88-27463
Nanosequencer digital logic controller
[NASA-CASE-NPO-16116-2] 23 p3245 N88-29310
Use of depletion edge translation for high-speed modulation and switching of lightwaves
[AD-A195611] 24 p3430 N88-30417

LOGIC DESIGN
Mental models in expert physics reasoning
[AD-A184106] 04 p0500 N88-13075
Software program validity: A survey
[PB87-170593] 09 p1219 N88-17315
A framework for evaluating computer architectures to support systems with security requirements, with applications
[AD-A187082] 10 p1392 N88-18303
Fast serial input-serial output pipelined inner product units
[REPT-87-031] 11 p1530 N88-19142
A logical structuration for an administration of space projects
[INPE-4435-TDL/310] 12 p1585 N88-19482
A new approach on test generation for array structures using the behavior of the system — VLSI chips
[INF-87-27] 14 p1907 N88-21397
An optimal CMOS structure for the design of a cell library
[EUT-87-E-166] 14 p1985 N88-21841
HIFI: A design method for implementing signal processing algorithms on VLSI processor arrays
[ETN-88-92238] 16 p2247 N88-23421
Identification of control structures — expert systems
[REPT-87-66] 16 p2255 N88-23479
SYMBL: A new Boolean compiler
18 p2554 N88-25160
Knowledge elicitation for an operator assistant system in process control tasks 23 p3253 N88-29366

LOGIC NETWORKS
U LOGIC CIRCUITS

LOGIC PROGRAMMING
Improvements to the adaptive maneuvering logic program
[NASA-CR-3985] 03 p0262 N88-11648

Programmable Logic Arrays (PLA's) design for testability
[PB87-102935] 04 p0438 N88-12718
PROVER: A first-order logic system in Ada
[DE88-000220] 04 p0479 N88-12951
Near-horn prolog
[AD-A185172] 05 p0634 N88-13880
Parallel logic programming and ZMOB and parallel systems software and hardware
[AD-A186300] 07 p0903 N88-15470
Methodology for testing and validating knowledge bases 08 p1055 N88-16364
DOD Gateway Information System (DGIS) common command language: Prolog knowledge base profile. Common command language report no. 3
[AD-A186150] 08 p1092 N88-16574
An investigation of parallelism in rule based systems 10 p1377 N88-18223
Experimenting with parallel programing in logic 10 p1380 N88-18240
Parallel architectures for logic programming 10 p1380 N88-18241
Implementing logical variables on a graph reduction architecture 10 p1382 N88-18252
Deriving abstractions from a software object network
[AD-A187472] 10 p1389 N88-18294
A digital logic simulator with concurrent programming considerations
[AD-A188823] 12 p1678 N88-20032
MOBICALC: An integrated and interactive system for development of administrative models
[INPE-4335-TDL/291] 12 p1679 N88-20038
Northeast Artificial Intelligence Consortium (NAIC) administrative matters and ancillary functions, volume 1
[AD-A189466] 12 p1682 N88-20055
Towards a solution to the proper integration of a logic programming system and a large knowledge based management system
[AD-A188949] 12 p1705 N88-20207
Semantics for Prolog via term rewrite systems
[CWI-CS-R8739] 16 p2247 N88-23428
Semantics for logic programs without occur check
[CWI-CS-R8740] 16 p2248 N88-23429
Introduction to logic programming
[CWI-CS-R8741] 16 p2248 N88-23430
Towards fully abstract semantics for local variables: Preliminary report
[AD-A191065] 16 p2251 N88-23456
Subset-logic programming: Application and implementation
[AD-A193647] 22 p3138 N88-28655
Combined and-or parallel execution of logic programs
[AD-A193648] 22 p3138 N88-28656
Unification and set-valued functions for functional and logic programming
[AD-A193643] 23 p3250 N88-29341
Practical higher-order functional and logic programming based on lambda-calculus and set-abstraction
[AD-A193645] 23 p3271 N88-29466

LOGICAL ELEMENTS
Logical input devices and interaction --- computer graphics
[CWI-CS-R8738] 13 p1814 N88-20836

LOGISTICS
NT LUNAR LOGISTICS
NT SPACE LOGISTICS
Naval Aviation Integrated Logistics: Technical users guide version 1.0
[DE87-013368] 01 p0001 N88-10001
A functional interpretation of the logistic equation
[REPT-87-037] 05 p0645 N88-13946
A space transportation system operations model
[NASA-TM-100481] 07 p0823 N88-14999
Variable selection in logistic regression
[AD-A186032] 07 p0914 N88-15547
An elimination type two-stage procedure for selecting the population with the largest mean from k logistic populations
[AD-A185614] 07 p0916 N88-15586
Prototype resupply scheduler 08 p1064 N88-16428
Replication and reconfiguration in a distributed mail repository
[AD-A186967] 09 p1151 N88-16897
First Annual Workshop on Space Operations Automation and Robotics (SOAR 87)
[NASA-CP-2491] 09 p1203 N88-17206
Preliminary analysis of an integrated logistics system for OSSA payloads
[NASA-CR-4114] 12 p1584 N88-19477
Preliminary analysis of an integrated logistics system for OSSA payloads. Volume 1: Executive summary 12 p1584 N88-19478
Preliminary analysis of an integrated logistics system for OSSA payloads. Volume 2: OSSA integrated logistics support strategy 12 p1584 N88-19479
Preliminary analysis of an integrated logistics system for OSSA payloads. Volume 3: OSSA integrated logistics support planning document 12 p1584 N88-19480
Preliminary analysis of an integrated logistics system for OSSA payloads. Volume 4: Supportability analysis of the 1.8m centrifuge 12 p1584 N88-19481
Space station heavy lift launch vehicle utilization
[NASA-TM-100604] 14 p1873 N88-21188
A model of intrazonal trip distribution considering centrality index 16 p2257 N88-23486
Lunar base surface mission operations. Lunar Base Systems Study (LBSS) task 4.1
[NASA-CR-172050] 18 p2594 N88-25415
The assessment of human/computer performance using human productivity measures: MIPS and BIPS are MEGAFLOPS
[DE87-013491] 21 p2993 N88-27750
Introduction to artificial intelligence and expert systems
[SNIAS-881-320-101] 21 p3004 N88-27814
Expert system contribution to logistics improvement
[SNIAS-881-320-102] 21 p3004 N88-27815
An evaluation of SPOT imagery for Earth science studies in the Antarctic. Preliminary Evaluation Program (PEPS) 289 for SPOT 22 p3103 N88-28430
Inflight rearming
[AD-A193564] 23 p3176 N88-28909
Dirichlet prior in Bayesian estimation of item response curves
[AD-A195311] 24 p3426 N88-30392

LOGISTICS MANAGEMENT
NT INVENTORY CONTROLS
NT INVENTORY MANAGEMENT
Optimum dimensioning of field service centers: Analysis of the problem and solutions thereof 01 p0012 N88-10068
Introduction to artificial intelligence and expert systems
[SNIAS-881-320-101] 21 p3004 N88-27814
Expert system contribution to logistics improvement
[SNIAS-881-320-102] 21 p3004 N88-27815
Reliability and Maintainability (R and M)
[AD-A193857] 23 p3224 N88-29187

LOMONOSOV CURRENT
Propagation of subsurface salinity maximum in tropical Atlantic 13 p1786 N88-20686

LONG DURATION SPACE FLIGHT
Use of bifidumbacterin for correction of intestinal dysbacteriosis 07 p0895 N88-15427
Air Force cryocooler development for spacecraft 08 p0983 N88-15945
Zero gravity and living organism 08 p1046 N88-16320
Analysis of water recovered after being used for washing by men and women 10 p1361 N88-18135
Present stage of space medicine 10 p1364 N88-18151
Effect of spaceflight factors on biological material flown aboard Cosmos-1514 biosatellite 10 p1364 N88-18154
Basic results of medical studies during prolonged manned flights on-board the Salyut-7/Soyuz-T orbital complex
[NASA-TT-20217] 10 p1369 N88-18182
Hemolysis in runners as evidenced by low serum haptoglobin: Implications for preflight monitoring of astronauts
[NASA-TM-100304] 11 p1518 N88-19067
Results of medical research conducted in 1985 during long-term spaceflights 19 p2702 N88-26070
Studies of HZE particle interactions and transport for space radiation protection purposes
[NASA-TM-101159] 20 p2886 N88-27142

LONG PERIOD VARIABLES
U MIRA VARIABLES

LONG RANGE WEATHER FORECASTING
Sea ice observations and models 14 p1939 N88-21572

LONG TERM EFFECTS
Space technology to meet future needs
[NASA-CR-181473] 02 p0130 N88-10819
Effects of long term storage on aerospace nickel cadmium cell performance 02 p0165 N88-11035
Effect of long-term thermal aging on coated Celion/LARC-160 composites
[NASA-TM-100495] 04 p0410 N88-12544
Influence of creep on the precipitate structure under conditions of long-term creep. 4: Experiments on 10 CrMo 9 10 steel
[BLL-CE-TRANS-8256-(9022.09)] 04 p0417 N88-12589
Lifting bodies: An attractive aerodynamic configuration choice for hypervelocity vehicles 05 p0534 N88-13248
A study of charged particles/radiation damage to VLSI device materials
[NASA-CR-172036] 05 p0577 N88-13518
Contributions of lidar measurements to the study of long term variations of the middle atmosphere
[ETN-88-91237] 05 p0625 N88-13824
Carbon Dioxide observational platform system (CO-OPS) Feasibility Study
[NASA-CR-179225] 06 p0671 N88-14113
Morphometric analysis of rat aorta endothelium during long-term hypokinesia 07 p0894 N88-15417
Changes in functional parameters of animals during long-term inhalation of acetic acid 07 p0895 N88-15423
Long-term variation of total ozone
[INPE-4307-PRE/1173] 08 p1023 N88-16192
Long-term aging of cast stainless steels: Mechanisms and resulting properties
[DE88-002888] 09 p1145 N88-16864
Short- and long-term effects of nonlethal levels of fast high-energy helium ions on retention of developed and formation of new behavioral patterns in rats 10 p1362 N88-18140
Results of long-term electrocardiographic monitoring of cosmonauts 10 p1364 N88-18152
Research briefing on high-temperature superconductivity
[PB88-133004] 11 p1561 N88-19344
Conceptualization and design of a variable-gravity research facility
[NASA-CR-182574] 12 p1595 N88-19550
Sea ice observations and models 14 p1939 N88-21572
Fractographic and microstructural evaluation of 3500-hour durability specimens 17 p2325 N88-23887
Environment assisted degradation mechanisms in advanced light metals
[NASA-CR-182907] 18 p2486 N88-24746
Effect of long-term inhalation of acetic acid vapor on some functional parameters of man 19 p2705 N88-26084
Aging of CFRP due to longterm storage in heated air
[DFVLR-FB-88-05] 21 p2922 N88-27345
Physiology of prolonged bed rest
[NASA-TM-101010] 22 p3130 N88-28607
Long-term behavior of energy production systems with the example of HELIOS and SYMPHONIE
[ETN-88-92988] 23 p3230 N88-29223

LONG WAVE RADIATION
Numerical modeling of radiation fog 08 p1017 N88-16166
Application of satellite data in observational and theoretical studies of the evolving structure of baroclinic waves
[NASA-CR-179277] 10 p1354 N88-18091
Radiation balance components above the tropical evergreen Amazon forests (3rd campaign of data collection)
[INPE-4195-PRE/1079] 11 p1513 N88-19039
Tropical circulations and the associated rainfall anomalies during two contrasting years
[INPE-4506-PRE/1261-REV] 15 p2098 N88-22502
Estimation of total Outgoing Longwave Radiation (OLR) flux from geostationary meteorological satellite infrared window radiance 17 p2351 N88-24006
Nonlinear waves
[AD-A192148] 18 p2510 N88-24889
On the impact of low-latitude anomalous forcing on local and remote circulation: Winters(DJF) 1978/79 to 1986/87 22 p3123 N88-28560
An observational study of interaction between large scale tropical cumulus convection and the equatorial circulation anomalies 22 p3124 N88-28564
Proof of the feasibility of coherent and incoherent schemes for pumping a gamma-ray laser
[AD-A193856] 23 p3220 N88-29165

LONG WAVES (METEOROLOGY)
U PLANETARY WAVES

LONGERONS
The X-beam as a deployable boom for the space station 14 p1925 N88-21473

LONGITUDE
Navigation system from AVHRR data from NOAA series satellites 17 p2359 N88-24054
Vertical directionality of ambient noise at 32 deg N as a function of longitude: Tape number 86180
[AD-A193228] 21 p3012 N88-27872

LONGITUDINAL CONTROL
Lateral and longitudinal stability and control parameters for the space shuttle discovery as determined from flight test data
[NASA-TM-100555] 13 p1724 N88-20309
Investigations on higher harmonic blade pitch control at helicopters
[DFVLR-FB-87-36] 14 p1868 N88-21165

Steady and unsteady transonic pressure measurements on a clipped delta wing for pitching and control-surface oscillations
[NASA-TP-2594] 23 p3173 N88-28895
Low-speed longitudinal flying qualities of modern transport aircraft 24 p3314 N88-29738

LONGITUDINAL STABILITY
Effects of the installation and operation of jet-exhaust yaw vanes on the longitudinal and lateral-directional characteristics of the F-14 airplane
[NASA-TP-2769] 04 p0393 N88-12455
Natural laminar flow and airplane stability and control 17 p2298 N88-23747
Experiment investigation on longitudinal characteristics of the forward swept wing
[AD-A191553] 18 p2456 N88-24582
Calculation of aerodynamic characteristics of airplane configurations at high angles of attack
[NASA-CR-4182] 23 p3172 N88-28891

LONGITUDINAL WAVES
NT PLANE WAVES
High-frequency limit of the longitudinal impedance
[CEBAF-PR-87-030] 02 p0234 N88-11479
Plane longitudinal waves in solutions of Maxwell equations
[DE88-700347] 07 p0846 N88-15135
An analysis of longitude variations in the equatorial spectrum of Saturn 10 p1430 N88-18539
Generation of flux tube waves in stellar convection zones. 1: Longitudinal tube waves
[NASA-TM-101152] 17 p2451 N88-24561
Experimental proof of quasilongitudinal propagation of low-frequency waves in middle latitudes in upper ionosphere 24 p3447 N88-30516

LONGSHORE CURRENTS
U COASTAL CURRENTS

LOOP ANTENNAS
A MININEC model of the miniloop antenna
[AD-A191759] 18 p2500 N88-24830
MSAT-X phased array antenna adaptions to airborne applications 19 p2647 N88-25713
Research in electromagnetic shielding theory. Part 2: EMP (electromagnetic pulse) simulation using small loops
[AD-A192882] 20 p2791 N88-26558

LOOPS
Timing variation in dual loop benchmarks
[AD-A185697] 06 p0707 N88-14338
Performance evaluation of a loop interconnection structure 10 p1378 N88-18229
Loop coalescing: A compiler transformation for parallel machines
[DE88-003571] 10 p1392 N88-18307
Deadlock prevention in processor self-scheduling for parallel nested loops
[DE88-003573] 10 p1393 N88-18313
Effects of toroidal forces in current loops embedded in a background plasma
[AD-A188878] 12 p1695 N88-20143
Tactical Rubidium Frequency Standard (TRFS)
[AD-A191049] 16 p2193 N88-23078
Phase length optical phase-locked-loop sensor
[NASA-CASE-LAR-13387-1] 18 p2576 N88-25302
Polymeric heat pipe wick
[NASA-CASE-GSC-13019-1] 23 p3214 N88-29133

LORAN
NT LORAN C

LORAN C
Alaska Loran C probe test results
[AD-A189131] 13 p1720 N88-20284
Investigation of air transportation technology at Massachusetts Institute of Technology, 1986 17 p2293 N88-23716
Investigation of air transportation technology at Ohio University, 1986 17 p2293 N88-23719
Loran-C monitor correlation over a 92-mile baseline in Ohio 17 p2293 N88-23720
Integrated multisensor navigation systems 17 p2294 N88-23722
Descriptions of HF and VHF Loran-C buoys and evaluations as potential datum marker buoys
[AD-A192069] 18 p2462 N88-24618
Research project Loran-C of the Geometric Service of the Ministry of Public Works
[B8735055] 20 p2757 N88-26356

LORENTZ CONTRACTION
Analysis of absolute space-time Lorentz theories
[DE87-703371] 04 p0500 N88-13076

LORENTZ FORCE
Covariant Lorentz anomalies in higher dimensional space
[DE87-753021] 02 p0230 N88-11448
Difficulties with interpretation of underground muons from Cygnus X-3
[DE88-701645] 23 p3309 N88-29710

LORENTZ TRANSFORMATIONS
The entropy of the Lorentz model 08 p1015 N88-16153
Spin precession in stationary gravitational fields
[DE88-701107] 15 p2093 N88-22470
Recent developments in the path integral approach to anomalies
[DE87-703032] 15 p2118 N88-22616
Local time displacement as a symmetry of nature in flat space-time
[NASA-TM-100610] 16 p2264 N88-23542

LOS ALAMOS TURRET REACTOR
U HIGH TEMPERATURE NUCLEAR REACTORS

LOSS OF COOLANT
Development of a rotary fluid transfer coupling and support mechanism for space station 14 p1928 N88-21493
Inherently safe space reactors 17 p2415 N88-24363

LOSSES
Blade loss transient dynamics analysis, volume 1. Task 2: TETRA 2 theoretical development
[NASA-CR-179632] 02 p0125 N88-10791
Blade loss transient dynamics analysis, volume 2. Task 2: TETRA 2 user's manual
[NASA-CR-179633] 02 p0126 N88-10792
Static magnetization and microwave loss in shock-modified ferrites
[DE87-012362] 02 p0146 N88-10916
Mass loss 02 p0253 N88-11597
Circumstellar chemistry 02 p0253 N88-11598
A new method for measuring waveguide propagation losses
[DE87-011305] 03 p0307 N88-11938
Empirical relations between photospheric magnetic fields and atmospheric radiative losses for cool dwarf stars 04 p0511 N88-13145
IRAS and cool stellar mass loss 04 p0515 N88-13166
Improved understanding of the loss-of-symmetry phenomenon in the conventional Kalman filter
[NASA-TM-100041] 06 p0766 N88-14709
Status of microcirculation in high-altitude blood loss 12 p1663 N88-19973
Eddy current losses induced by rotation of magnetisation
[BLL-M-37634-(5828.4)] 14 p1890 N88-21298
The loss parameters for very short bunches
[CEBAF-PR-88-005] 18 p2574 N88-25291
Characteristics of shielded microstrip lines on GaAs-Si at millimeter-wave frequencies 19 p2657 N88-25787
Loss evaluation of self-commutated power conditioner for battery energy storage system
[DE88-752075] 20 p2794 N88-26575
The effects of moisture loss and elevated temperature upon the material damping of fibre reinforced polymer matrix composites
[UTIAS-324] 23 p3188 N88-28970
Conductor loss in superconducting power transmission cables
[DE88-011414] 23 p3290 N88-29586
Behaviour and hysteresis losses of irreversible type-2 superconducting cylindrical shell
[DE88-702708] 24 p3433 N88-30434

LOSSY MEDIA
Measurement of the properties of lossy materials inside a finite conducting cylinder
[NASA-CR-182664] 13 p1832 N88-20962
Born-type reconstruction of material parameters of an inhomogeneous, lossy dielectric slab from reflected-field data
[PB88-188958] 18 p2569 N88-25261

LOST WAX PROCESS
U INVESTMENT CASTING

LOUVERS
The acoustic source created by turbulent flow over orifices and louvers
[REPT-97674] 06 p0776 N88-14764
Describing the source created by turbulent flow over orifices and louvers
[AD-A190254] 15 p2130 N88-22706

LOW ALLOY STEELS
U HIGH STRENGTH STEELS

LOW ALTITUDE
Dispersion in the wake of aircraft: An investigation of the effects of a ground plane on trailing vortices. Literature survey
[IC-AERO-REP-86-04] 01 p0003 N88-10014
Evaluation of a mesoscale prediction system with surface weather observations and comparison with a large-scale prediction system 02 p0210 N88-11319
Development, testing and evaluation of a night vision goggle compatible BO-105 for night low level operation 03 p0265 N88-11668
Development of an acoustic echosounder for detection of lower level atmospheric turbulence
[AD-A184877] 05 p0626 N88-13831
State-of-the-art technologies for construction in space: A review
[AD-A188412] 12 p1585 N88-19483
The low-latitude auroral boundary: Steady-state and time-dependent representations
[AD-A193200] 21 p2972 N88-27656
Low altitude: A new dimension in air refueling
[AD-A193819] 23 p3176 N88-28910
Integration of LANTIRN (Low Altitude Navigation and Targeting Infrared for Night) into operational fighter training
[AD-A194906] 24 p3325 N88-29799

LOW ASPECT RATIO
Periodic natural convection in a rectangular enclosure of low aspect ratio 10 p1329 N88-17941
Computational design of low aspect ratio wing-winglet configurations for transonic wind-tunnel tests
[NASA-CR-183021] 18 p2464 N88-24630
Design studies of low aspect-ratio torsatrons
[DE88-007562] 18 p2579 N88-25320
Symmetrized magnetic field configuration of low aspect ratio helical system
[IPPJ-869] 20 p2855 N88-26956

LOW ASPECT RATIO WINGS
NT DELTA WINGS
Theoretical-numerical study of feasibility of use of winglets on low aspect ration wings at subsonic and transonic Mach numbers at reduce drag
[NASA-CR-4174] 21 p2892 N88-27168

LOW CARBON STEELS
Wear of hard steel in rolling lubricated contact
[RP-699] 03 p0332 N88-12094
The growth behavior of small fatigue cracks; the effect of microstructure and crack closure 05 p0600 N88-13673
A study of fatigue crack growth life under random stresses 05 p0602 N88-13685
Influence of cleavage on fatigue propagation rates in a low carbon steel 06 p0716 N88-14389
Notch-geometry effect on propagation threshold of short fatigue cracks in notched components 06 p0716 N88-14393
Sulfur-induced ductility-dip cracking in weld metal of low-carbon steel
[PB87-143814] 07 p0833 N88-15051
Investigation of the auto-tempering of low-carbon martensite
[PB87-143970] 07 p0833 N88-15053
New mechanism of the high temperature (reversible) temper brittleness of alloy steels
[PB87-143954] 07 p0833 N88-15056
An investigation of the influence of dislocation substructures on the deformation behavior of AK, DQ steel sheets
[DE88-006337] 14 p1889 N88-21289
Studies on hot-dip zinc-aluminum coated sheet steels
[ETN-88-92217] 15 p2042 N88-22166

LOW COST
Development of an innovative, low-cost solar collector
[PB87-206819] 02 p0194 N88-11210
Configuration evaluation and criteria plan. Volume 2: Evaluation criteria plan (update). Space Transportation Main Engine (STME) configuration study
[NASA-CR-181429] 03 p0270 N88-11699
Lightsats and their attraction to budget oriented Federal agencies 10 p1289 N88-17711
Low cost telemetry and telecommand system for remote measurement of magnitude character
[INPE-4273-PRE/1145] 12 p1598 N88-19564
Alternative program approaches for the advanced satellite technology program
[AD-A188917] 12 p1600 N88-19576
Low cost mobile robot
[AD-A188507] 12 p1633 N88-19778
Principles of a low-cost laser gyro for rotating vehicles and platforms
[DFVLR-MITT-87-15] 14 p1912 N88-21425
Laser-heated CVD process for depositing thin films for low-cost solar-cell applications
[DE88-001162] 21 p2967 N88-27623
Finding minimum-cost circulations by successive approximation
[AD-A192724] 21 p3005 N88-27824
Finding minimum-cost circulations by canceling negative cycles
[AD-A192727] 21 p3005 N88-27825
LO-CO-GRAF (low cost graphics): Generating maps to support command and control/crisis management using small computers
[AD-A193964] 22 p3139 N88-28661
Finding minimum-cost circulations by canceling negative cycles
[AD-A194027] 23 p3271 N88-29468

Finding minimum-cost circulations by successive approximation
[AD-A194026] 23 p3272 N88-29469
A multiprocessor avionics system for an unmanned research vehicle
[AD-A194806] 24 p3325 N88-29800
Low cost satellite
[ESA-CR(P)-2560] 24 p3334 N88-29844
Interim Flight Opportunity (IFO). Volume 1: Executive summary — space platform
[SE/LS/AP-36-818/CN-VOL-1] 24 p3334 N88-29849
Space systems cost study
[AD-A196024] 24 p3439 N88-30469

LOW CURRENTS
Low-current behavior and current chopping of vacuum arcs
[ISBN-90-9001649-X] 05 p0578 N88-13529

LOW DENSITY GASES
U RAREFIED GASES

LOW EARTH ORBITAL ENVIRONMENTS
U EARTH ORBITAL ENVIRONMENTS

LOW FREQUENCIES
NT VERY LOW FREQUENCIES
ELF/VLF/LF propagation and system design
[AD-A183261] 01 p0033 N88-10212
Compilation of 1986 annual reports of the Navy ELF (Extremely Low Frequency) communications system ecological monitoring program, volume 1
[AD-A184561] 03 p0306 N88-11930
Application of ray theory to propagation of low frequency noise from wind turbines
[NASA-CR-178367] 03 p0373 N88-12349
Low-frequency VLBI in space and interstellar refraction
[PB87-127643] 06 p0696 N88-14267
Observing effect of laser radiation of low-frequency Raman scattering of light 06 p0772 N88-14742
Low-frequency oscillations in nonideal plasma 06 p0774 N88-14751
Low frequency VLBI in space using GAS-Can satellites: Report on the May 1987 JPL Workshop
[NASA-CR-182362] 06 p0801 N88-14904
Acoustic scattering from composite wind-wave surfaces 3: Forward scatter intensities and spatial coherence at low and high frequencies and small grazing angles for Bubble-free regimes
[AD-A185908] 07 p0881 N88-15345
A proposed metric for assessing the potential of community annoyance from wind turbine low-frequency noise emissions
[DE88-001113] 08 p1022 N88-16187
Low frequency electrostatic waves observed on board the Coordinated Auroral Experiment using Scatter And Rockets (CAESAR) 2 payload 08 p1032 N88-16253
Low frequency waves and small scale solitary structures observed by Viking — Swedish satellite; auroras 08 p1099 N88-16611
Ray tracing of Jovian low frequency radiation
[NASA-CR-179262] 08 p1101 N88-16620
Subharmonic aliasing and its effects on the AFTI/F-16 digital flight control system
[AD-A190614] 15 p2020 N88-22042
Low frequency ocean ambient noise: Measurements and theory
[AD-A191188] 16 p2237 N88-23362
Practical VLF/LF radio test system
[AD-A191768] 18 p2500 N88-24831
Aircraft interior noise reduction by alternate resonance tuning
[NASA-CR-182540] 20 p2849 N88-26909
The polarization of radio galaxies: Its structure at low frequencies
[B8681611] 20 p2884 N88-27123
Airborne measurement of low frequency atmospheric noise ALFAN 1
[AD-A193056] 21 p2931 N88-27405
The observed dynamical structure of low frequency variabilities 22 p3120 N88-28541
Physiological effects of extremely low frequency electric and magnetic fields
[DE88-752814] 22 p3132 N88-28620

LOW FREQUENCY BANDS
NT VERY LOW FREQUENCIES

LOW GRAVITY
U REDUCED GRAVITY

LOW GRAVITY MANUFACTURING
Center for the Space Processing of Engineering Materials 07 p0838 N88-15083
Analysis of low gravity tolerance of model experiments for space station: Preliminary results for directional solidification
[NASA-CR-182657] 12 p1614 N88-19648
Preparation for microgravity: The role of the microgravity materials science laboratory
[NASA-TM-100906] 18 p2497 N88-24811
Optimization of low gravity materials processing experiments using expert systems 23 p3252 N88-29361

LOW LATITUDES
U TROPICAL REGIONS

LOW LEVEL TURBULENCE
Numerical calculation of appendage, flat plate junction flow
[AD-A186371] 07 p0850 N88-15158
Turbulence structure during high wind 08 p1014 N88-16149
Utilization of dense packed planar acoustic echosounders to identify turbulence structure in the lowest levels of the atmosphere
[AD-A191006] 16 p2233 N88-23335
Measurement and analysis of low altitude atmospheric turbulence obtained using a specially instrumented Gnat aircraft 24 p3313 N88-29728

LOW MASS
U MASS

LOW NOISE
Low noise-low power monolithic multiplexing readout electronics for silicon strip detectors
[MPI-PAE/EXP.EL.178] 02 p0168 N88-11057
Research in monolithic signal-processing circuits
[AD-A184680] 03 p0311 N88-11962
Low-noise cryogenic transmission line 04 p0434 N88-12688
The 8.4-GHz low-noise maser pump source assembly 04 p0436 N88-12705
Development of a low noise 10 K J-T refrigeration system
[AD-A186004] 07 p0838 N88-15085
Low noise cryogenic dielectric resonator oscillator
[NASA-CASE-NPO-17157-1-CU] 20 p2797 N88-26596

LOW PASS FILTERS
A digital low pass filter for the reduction of large quantities of data
[ESA-TT-1058] 03 p0363 N88-12281
On a circular correlation technique for filtering randomly noisy data
[AD-A184317] 04 p0431 N88-12669
Error reduction in two-dimensional pulse-area modulation, with application to computer-generated transparencies — optical field synthesis
[EUT-87-E-172] 14 p1982 N88-21825
High speed, bandpass sampling of digital communications waveforms
[AD-A189842] 15 p2056 N88-22254
A notch filter instrument for measuring ELF (Extremely Low Frequency) MSK (Minimum Shift Keying) signals
[AD-A193324] 21 p2933 N88-27414
Anti-aliasing filters for dynamics and control experiments
[AD-A193758] 23 p3226 N88-29203

LOW PRESSURE
An illustrative example of the nowcasting challenge 02 p0199 N88-11243
Forecasting polar lows using a numerical mesoscale model 02 p0210 N88-11321
Typhoon structural evolution
[AD-A186090] 07 p0879 N88-15333
Low pressure gas flow analysis through an effusive inlet using mass spectrometry
[NASA-CR-182712] 14 p1910 N88-21413
Study of surface discharges
[ONERA-12/7236-PY] 15 p2026 N88-22073
Low pressure entrained flow pyrolysis of biomass to produce liquid fuels 18 p2535 N88-25043
Microlaminate composite structures by low pressure plasma spray deposition
[DE88-006453] 19 p2610 N88-25488
Genesis of Atlantic lows experiment NASA electra boundary layer flights data report
[NASA-TM-100703] 22 p3128 N88-28597
Simulation of Vulcain engine operation at low inlet pressure
[ETN-88-93083] 24 p3339 N88-29875

LOW PRESSURE CHAMBERS
U VACUUM CHAMBERS

LOW REYNOLDS NUMBER
International Conference on the Aerodynamics at Low Reynolds Numbers between 10(4) and 10(6)
[ONRL-7-023-C] 01 p0002 N88-10010
Low Reynolds number influence on aerodynamic performance of hypersonic lifting vehicles 05 p0531 N88-13230
Two-equation low-Reynolds-number turbulence modeling of transitional boundary layer flows characteristic of gas turbine blades
[NASA-CR-4145] 16 p2209 N88-23185
Computational fluid dynamics methods for low Reynolds number precessing/spinning incompressible flows
[AD-A193891] 23 p3212 N88-29119
A study of the effect of random input motion on low Reynolds number flows
[AD-A195559] 24 p3316 N88-29747

LOW SPEED
On the prospects for increasing dynamic lift
[RAE-TM-AERO-2068] 01 p0003 N88-10018
Investigation of low-speed turbulent separated flow around airfoils
[NASA-CR-177450] 04 p0396 N88-12471
A swept wing panel in a low speed flexible walled test section
[NASA-CR-4106] 05 p0540 N88-13282
Advanced natural laminar flow airfoil with high lift to drag ratio 07 p0812 N88-14947
Preliminary airworthiness evaluation of a UH-1 equipped with a terrain mapping receiver antenna
[AD-A186274] 07 p0819 N88-14980
Planetary science 07 p0883 N88-15356
Investigation of low velocity impact damage on filamentary composite materials 07 p0923 N88-15607
Effect of low velocity impact on compression strength of a quasi-isotropic laminate
[FFA-TN-1987-38] 09 p1138 N88-16822
A review of technologies applicable to low-speed flight of high-performance aircraft investigated in the Langley 14- x 22-foot subsonic tunnel
[NASA-TP-2796] 13 p1717 N88-20264
The effect of sting interference at low speeds on the drag coefficient of an ellipsoidal body using a magnetic suspension and balance system
[NASA-CR-181611] 13 p1718 N88-20274

LOW SPEED STABILITY
Low-speed longitudinal flying qualities of modern transport aircraft 24 p3314 N88-29738

LOW SPEED WIND TUNNELS
NT SUBSONIC WIND TUNNELS
The 5.5 m low speed wind tunnel. Introduction to the facilities
[ARG-205] 14 p1870 N88-21172
Main features of Warton (United Kingdom) 2.7 x 2.1 m low speed wind tunnel
[AXM-124] 14 p1870 N88-21173
Details of low speed intake test facility at the Warton (United Kingdom) 2.7m x 2.1m wind tunnel
[AXM-127] 14 p1870 N88-21174
Contraction design for small low-speed wind tunnels
[NASA-CR-182747] 15 p2021 N88-22045
Summary of low-speed wind tunnel results of several high-speed counterrotation propeller configurations
[NASA-TM-100945] 18 p2458 N88-24597
A low speed wind tunnel investigation of Reynolds number effects on a 60-deg swept wing configuration with leading and trailing edge flaps
[NASA-CR-181684] 19 p2598 N88-25441
Effects of independent variation of Mach and Reynolds numbers on the low-speed aerodynamic characteristics of the NACA 0012 airfoil section
[NASA-TM-4074] 23 p3170 N88-28879

LOW TEMPERATURE
NT CRYOGENIC TEMPERATURE
Low temperature deposition by laser induced breakdown in the vapor phase
[DE87-007509] 01 p0024 N88-10151
The development of a friction model predicting the sliding behavior of materials pairs, especially at low temperatures: Progress report and renewal proposal
[DE87-013941] 01 p0055 N88-10354
Direct formation of thin films and epitaxial overlayers at low temperatures using a low-energy (10-500 eV) ion beam deposition system
[DE87-012291] 01 p0103 N88-10675
Near-threshold fatigue crack growth behavior at cryogenic temperature 06 p0718 N88-14409
The effect of non-metallic inclusions on fatigue and fatigue thresholds of 25Mn-5Cr-1Ni steel 06 p0718 N88-14410
Photoinduced low-temperature changes in optical losses in fiber optics based on chalcogenide glasses 06 p0770 N88-14731
The role of low temperature chemistry in the autoignition of n-butane
[DE88-002385] 07 p0829 N88-15031
Prediction of human thermoregulatory responses and endurance time in water at 20 and 24C
[AD-A186223] 08 p1048 N88-16326
Effect of low-temperature aging on the mechanical properties of cast stainless steels
[DE88-002872] 10 p1300 N88-17774
The Shubnikov de Haas effect in narrow-gap semimagnetic semiconductors
[ETN-88-92249] 14 p1988 N88-21861
Cellular thermosetting fluoropolymers and process for making them
[NASA-CASE-GSC-13008-1] 17 p2326 N88-23894

Update of low temperature catalyst development
[DE88-007032] 18 p2480 N88-24715
Antimisting kerosene: Low temperature degradation and blending
[NASA-CR-182725] 20 p2781 N88-26495
Superconducting electronic film structures
[AD-A192907] 20 p2879 N88-27091
Preparation and development of advanced battery catalysts
[AD-A193208] 21 p2937 N88-27441
Cold worked reinforcing bars in tensile test under high loading rate and low temperatures
[DE88-752993] 21 p2964 N88-27610
Low temperature film growth of the oxides of zinc, aluminum and vanadium (and related systems, oxides of gold and germanium, nitrides of aluminum and tungsten) by reactive sputter deposition
[AD-A193497] 23 p3191 N88-28986
Muon-spin rotation experiment (micro + SR) on aluminum and indium after low temperature electron irradiation
[ETN-88-92985] 23 p3294 N88-29617
Discovery of a low temperature form of TAGN (Triaminoguanidinium Nitrate)
[AD-A196059] 24 p3357 N88-29989

LOW TEMPERATURE ENVIRONMENTS
The initiation and growth of small fatigue cracks in copper at room and cryogenic temperatures
05 p0600 N88-13668
Polar worker adaptability to Antarctic high altitudes
10 p1366 N88-18165
The CRREL (Cold Regions Research and Engineering Laboratory) Hopkinson bar apparatus
[AD-A190599] 15 p2077 N88-22380
Hydraulic pumps and hydraulic equipment at low temperatures
[DE88-752871] 21 p2958 N88-27570
Accidental hypothermia
[AD-A194967] 24 p3406 N88-30278

LOW TEMPERATURE PHYSICS
Interactions between superconductivity and Kondo-grid properties in CeCu2Si2. Measurement results of specific heat under high pressure
[ETN-88-92377] 21 p3025 N88-27958

LOW TEMPERATURE PLASMAS
U COLD PLASMAS

LOW TEMPERATURE TESTS
Instrument for radiation testing/screening electronic devices over an extended temperature range
[AD-A184245] 03 p0326 N88-12060
A test facility for the in-vacuo assessment of dry lubricants and small mechanisms at cryogenic temperatures 14 p1878 N88-21224
Cryogenic test facilities for an optical cryomechanism qualification 14 p1879 N88-21228
Materials testing at cryogenic temperatures
[BU-359] 14 p1923 N88-21462
The CRREL (Cold Regions Research and Engineering Laboratory) Hopkinson bar apparatus
[AD-A190599] 15 p2077 N88-22380

LOW THRUST
Breadboard RL10-2B low-thrust operating mode (second iteration) test report
[NASA-CR-182160] 24 p3338 N88-29867

LOW THRUST PROPULSION
NT ELECTROMAGNETIC PROPULSION
NT ELECTROSTATIC PROPULSION
NT ION PROPULSION
NT PLASMA PROPULSION
NT SOLAR THERMAL PROPULSION
A technique for capture analysis of low thrust missions in a planetary system
[AD-A188934] 12 p1594 N88-19544
Recent advances in low-thrust propulsion technology
[NASA-TM-100959] 18 p2569 N88-25260

LOW VACUUM
Low jitter laser-triggered high-voltage vacuum switch using low laser energies
[DE88-001922] 05 p0587 N88-13576

LOW VELOCITY
U LOW SPEED

LOW VISIBILITY
Flight simulator experiments concerning take-off visibility minima
[NLR-TR-86050-U] 13 p1719 N88-20281

LOW VOLTAGE
High density CMOS technology
11 p1561 N88-19342
Extinction behavior of low voltage switching arc under consideration of cathodic coatings and dynamic arc column
[ETN-88-92384] 20 p2796 N88-26591

LOWER ATMOSPHERE
NT TROPOPAUSE
NT TROPOSPHERE
Experimental study of the propagation of an acoustic wave in the low atmosphere
[ISL-R-111/86] 02 p0231 N88-11454
Geochemistry of the middle and lower atmosphere: Environmental impact through the deterioration of the ozone layer
[INPE-4477-PRE/1241] 16 p2230 N88-23321

LOWER BODY NEGATIVE PRESSURE
Blood redistribution in man with lower body negative pressure 07 p0891 N88-15397
Leg volume change under Lower Body Negative Pressure (LBNP) in dependence on stratification
[DFVLR-FB-87-47] 16 p2238 N88-23367

LOWER IONOSPHERE
NT D REGION
Ionospheric research in Antarctica
[INPE-4521-PRE/1273] 16 p2232 N88-23331

LOX (OXYGEN)
U LIQUID OXYGEN

LOX-HYDROGEN ENGINES
U HYDROGEN OXYGEN ENGINES

LQG CONTROL
U LINEAR QUADRATIC GAUSSIAN CONTROL

LQR
U LINEAR QUADRATIC REGULATOR

LSI
U LARGE SCALE INTEGRATION

LST
U HUBBLE SPACE TELESCOPE

LUBRICANT TESTS
Activities report in tribology
[ESA-ESTL-79] 09 p1174 N88-17037
Standardization of lubricity test
[AD-A187776] 11 p1465 N88-18736
The SPOT solar array. Box opening mechanisms physical vapor deposition (PVD)-MoS2: Lubricated slides. Functional evaluation 14 p1876 N88-21211
A test facility for the in-vacuo assessment of dry lubricants and small mechanisms at cryogenic temperatures 14 p1878 N88-21224
Characterization of lubricants in terms of transition diagram data
[AD-A194264] 23 p3197 N88-29025
The lubricating properties of magnetron sputtered MoS2
[ESA-ESTL-76] 24 p3381 N88-30136

LUBRICANTS
NT GAS LUBRICANTS
NT HIGH TEMPERATURE LUBRICANTS
NT LUBRICATING OILS
NT SOLID LUBRICANTS
Boundary lubrication. Experiments with boundary lubrication and plain bearings at +60...-60 deg C temperatures
[DE87-752869] 02 p0180 N88-11124
Analysis of wear metals in engine oils using the atomic absorption spectrophotometric method
[NAL-TM-MT-8704] 05 p0564 N88-13435
Film thicknesses in circular elastohydrodynamic contacts
[PB87-123725] 06 p0710 N88-14354
Research study for materials/properties test results database
[NASA-CR-178923] 07 p0861 N88-15222
Evaluation of load tracks and wear of two sets of bearings from space shuttle main engine high pressure oxygen turbopumps
[NASA-CR-178969] 07 p0861 N88-15223
Improved perfluoroalkylether fluid development
[NASA-CR-180872] 08 p0967 N88-15851
On the performance of finite journal bearings lubricated with micropolar fluids
[NASA-TM-100293] 08 p0988 N88-15983
Technology developments for a compound cycle engine 09 p1107 N88-16637
Activities report in tribology
[ESA-ESTL-79] 09 p1174 N88-17037
An evaluation of effectiveness of PTFE (polytetrafluoroethylene) type friction reducers on reducing friction and wear
[AD-A187440] 10 p1340 N88-18010
Tribological properties of alumina-boria-silicate fabric from 25 to 850 C
[NASA-TM-100806] 11 p1464 N88-18726
Evaluation of centrifugal barrel tumbling process for impregnation of molybdenum disulfide powder lubricant
[BDX-613-3698] 11 p1464 N88-18727
Carbon residue studies of polyphenyl ethers and ester-based lubricants using a microcarbon residue tester
[AD-A188585] 12 p1611 N88-19632
Lubricating properties of molybdenum disulfide. Part 3: Performance of molybdenum disulfide-containing oils in fluid lubrication
[NASA-TT-20156] 13 p1752 N88-20480
A new approach to highly fluorinated lubricants
[AD-A190523] 15 p2045 N88-22188
Studies of dynamic contact of ceramics and alloys for advanced heat engines
[DE88-008996] 21 p2919 N88-27324
Perfluoropolyalkylether lubricants under boundary conditions: Iron catalysis of lubricant degradation
[AD-A193241] 21 p2956 N88-27560
The 000 stage equipment bearing performance with a lower viscosity lubricant
[DE88-011827] 21 p2957 N88-27566
Development of high temperature, high pressure rotating shaft seals
[DE88-001029] 23 p3221 N88-29172

LUBRICATING OILS
Piston ring friction and vehicle fuel economy
[DE87-014536] 02 p0181 N88-11127
High shear rate rheometry of low-viscosity liquids
[AD-A188447] 12 p1627 N88-19733
Corrosion-wear process under rolling-sliding motion
[AD-A189603] 13 p1778 N88-20635
A new method of measuring multigrade oil shear elasticity and viscosity at high shear rates
[AD-A190145] 15 p2064 N88-22304
Calibration of the portable wear metal analyzer
[AD-A192971] 21 p2950 N88-27524
Reaction-theoretical aspects of the thermal behavior of lubricating oils and working fluids
[NASA-TT-20304] 23 p3199 N88-29041

LUBRICATION
NT BOUNDARY LUBRICATION
NT SELF LUBRICATION
NT SPACECRAFT LUBRICATION
Boundary lubrication. Experiments with boundary lubrication and plain bearings at +60...-60 deg C temperatures
[DE87-752869] 02 p0180 N88-11124
Piston ring friction and vehicle fuel economy
[DE87-014536] 02 p0181 N88-11127
Improved oil-off survivability of tapered roller bearings
[NASA-CR-180804] 02 p0182 N88-11135
Film thicknesses in circular elastohydrodynamic contacts
[PB87-123725] 06 p0710 N88-14354
The numerical solution of the elastohydrodynamically lubricated line and point contact problem, using multigrid techniques
[ISBN-90-9001583-3] 06 p0714 N88-14377
Investigation of instability, dynamic forces, and effect of dynamic loading on strength of cages for the bearings in the high pressure oxygen turbopumps for the space shuttle main engine
[NASA-CR-178970] 06 p0714 N88-14378
A variational formulation of a hydrodynamic lubrication problem
[MEMO-642] 08 p0987 N88-15979
Activities report in tribology
[ESA-ESTL-79] 09 p1174 N88-17037
A comparison of measurements from the A/E35U-3 and PWMA (Portable Wear Metal Analyzer) spectrometers
[AD-A186855] 09 p1177 N88-17047
Characteristics and use of lubricating greases
[DE88-751103] 11 p1463 N88-18723
Standardization of lubricity test
[AD-A187776] 11 p1465 N88-18736
A hydrodynamic analysis of fluid flow between meshing spur gear teeth
[AD-A187671] 11 p1482 N88-18844
Overview of the DOE-ECUT Tribology Program
[DE88-002878] 13 p1778 N88-20637
Experience with duplex bearings in narrow angle oscillating applications 14 p1926 N88-21484
A new method of measuring multigrade oil shear elasticity and viscosity at high shear rates
[AD-A190145] 15 p2064 N88-22304
Traction model development
[AD-A188450] 15 p2073 N88-22359
High temperature solid lubrication by catalytically generated carbon
[AD-A190804] 16 p2182 N88-23004
Basic mechanisms of diesel lubrication correlation of bench and engine tests
[AD-A193360] 21 p2956 N88-27561
The 000 stage equipment bearing performance with a lower viscosity lubricant
[DE88-011827] 21 p2957 N88-27566
A lubrication study of engine bearings
21 p2958 N88-27574
Status and directions of modified tribological surfaces by ion processes
[NASA-TM-101304] 22 p3063 N88-28176

LUBRICATION SYSTEMS
Literature review of solid lubrication mechanisms
[AD-A185010] 05 p0567 N88-13456
Traction model development
[AD-A188450] 15 p2073 N88-22359

LUCITE (TRADEMARK)
U POLYMETHYL METHACRYLATE
LUDER BANDS
U PLASTIC DEFORMATION
U YIELD POINT
LUMBERING AREAS
U FORESTS
LUMINAIRES
NT ARC LAMPS
NT FLASH LAMPS
NT QUARTZ LAMPS
Evidence of a new spectral line intensity formula for optical emission
[KGI-PREPRINT-098] 01 p0090 N88-10585
Design concepts to improve high performance solar simulator 02 p0136 N88-10852
A defect investigation of Thunderflash MK N5 (Navy)
[MRL-TN-522] 13 p1754 N88-20488
Laser induced ignition of propellants
[AD-A191099] 16 p2213 N88-23206
Spectroradiometry in the industrial test laboratory
16 p2272 N88-23598
LUMINANCE
Target size and luminance effects on accommodation and vergence
[AD-A185861] 08 p1051 N88-16343
Pursuit tracking performance decrements associated with decreasing ambient illumination
[AD-A189336] 13 p1809 N88-20809
Design and testing of a luminance and chrominance stabilization system for a computer-controlled color display
[AD-A191922] 18 p2554 N88-25159
LUMINESCENCE
NT BIOLUMINESCENCE
NT CHEMILUMINESCENCE
NT ELECTROLUMINESCENCE
NT FLUORESCENCE
NT LASER INDUCED FLUORESCENCE
NT OPTICAL RESONANCE
NT PHOSPHORESCENCE
NT PHOTOLUMINESCENCE
NT RESONANCE FLUORESCENCE
NT SPACECRAFT GLOW
NT X RAY FLUORESCENCE
The influence of polymer structure on triplet luminescence
[DE87-014431] 02 p0152 N88-10952
A physico-chemical study of some areas of fundamental significance to biophysics
[DE87-013457] 02 p0217 N88-11365
Performance characteristics of magnesium-sodium nitrate flares in oxygen-nitrogen atmospheres
[AD-A185274] 05 p0570 N88-13476
Multicomponent analysis using synchronous-excitation phase-resolved fluorescence spectroscopy
[AD-A188883] 12 p1606 N88-19604
Electronic and ionic transport in polymers
[AD-A190434] 15 p2045 N88-22185
Superthermal electron processes in the upper atmosphere of Uranus: Aurora and electroglow
[NASA-TM-101150] 18 p2594 N88-25417
Laser spectroscopy of quantum well and superlattice structures
[AD-A193336] 21 p3022 N88-27937
The optical spectroscopy of copper-blue luminescence in zinc sulfide crystals. Zero-phonon line spectra under the influence of magnetic field, temperature and excitation intensity
[ETN-88-93122] 24 p3344 N88-29903
LUMINESCENT INTENSITY
U LUMINOUS INTENSITY
LUMINOSITY
NT STELLAR LUMINOSITY
Modes, masses, metallicities, and magnitudes of RR Lyrae variables
[DE87-013149] 01 p0109 N88-10703
Neutrinos in supernovae
[DE87-014295] 03 p0387 N88-12434
Comparison of global and nuclear properties of starburst and Seyfert 1 galaxies 03 p0388 N88-12438
Stellar cycle variability of solar-like stars: A sneak preview 04 p0510 N88-13136
A search for X-ray luminous late type stars in NIPSS data 04 p0511 N88-13143
Solar Dynamics and G-modes
[NASA-CR-180737] 06 p0805 N88-14911
Global properties of star formation in spiral galaxies
14 p1994 N88-21883
Hydrodynamical models of supernova SN 1987 A in the LMC
[DE88-701123] 15 p2151 N88-22837
Cosmological parameters and evolution of the galaxy luminosity function
[NASA-CR-183081] 21 p3030 N88-27986
The stability of disk galaxies and constraints on their mass-luminosity ratio
[SER-C-PREPUBL-FASC-27] 24 p3455 N88-30565
LUMINOUS FLUX DENSITY
U LUMINOUS INTENSITY
LUMINOUS INTENSITY
NT ILLUMINANCE
NT LUMINANCE
Trickle water and feeding system in plant culture and light-dark cycle effects on plant growth
03 p0361 N88-12273
Analysis of dust grain properties in two star forming regions through comparison of theoretical models to observations 17 p2451 N88-24559
Fiber optic sensors 19 p2670 N88-25870
Fiber optic sensing systems using high frequency resonant sensing heads with intensity sensors
[NASA-TM-101318] 22 p3080 N88-28293
LUMPING
Determination of lumped-mass thermal properties associated with autoclave curing of graphite/epoxy composites 21 p2925 N88-27364
LUNAR BASES
Space station accommodations for lunar base elements: A study
[NASA-TM-100501] 06 p0804 N88-14907
Advantages of manned lunar base
08 p1009 N88-16118
Critical issues for establishment of a permanently-occupied lunar base
[AD-A187128] 09 p1263 N88-17567
Lunar fiberglass: Properties and process design
[NASA-CR-182580] 11 p1466 N88-18740
Multimegawatt nuclear power system for lunar base applications 17 p2416 N88-24367
Applications of nuclear power to lunar and Mars missions 17 p2417 N88-24377
Electromagnetic powered vehicles (EMPV) for Mars exploration 17 p2419 N88-24388
Lunar base surface mission operations. Lunar Base Systems Study (LBSS) task 4.1
[NASA-CR-172050] 18 p2594 N88-25415
Advanced photovoltaic power system technology for lunar base applications
[NASA-TM-100965] 20 p2766 N88-26402
Lunar base launch and landing facility conceptual design, 2nd edition
[NASA-CR-172049] 20 p2885 N88-27135
Steps toward lunar settlement
[DE88-009141] 21 p2900 N88-27213
Space transportation nodes assumptions and requirements: Lunar base systems study task 2.1
[NASA-CR-172052] 23 p3183 N88-28944
Maintenance and supply options
[NASA-CR-172062] 24 p3332 N88-29837
LUNAR CRATERS
Conditions for geomagnetically trapping sub-micron lunar ejecta between L = 1.2 and L = 3.1
04 p0521 N88-13203
LUNAR CRUST
Chronology of early lunar crust
24 p3394 N88-30212
The complexity, depth, and rapidity of processes that formed the lunar crust 24 p3398 N88-30237
LUNAR EFFECTS
Orbital evolution of distant artificial earth satellites
24 p3445 N88-30506
LUNAR EVOLUTION
Chronology of early lunar crust
24 p3394 N88-30212
Nineteenth Lunar and Planetary Science Conference. Press abstracts
[NASA-CR-183037] 24 p3440 N88-30473
The origin of the moon: Further studies of the giant impact 24 p3440 N88-30474
LUNAR GRAVITATION
Resonance effects accompanying motion with low thrust in earth-moon system 24 p3446 N88-30510
LUNAR LANDING MODULES
A lunar transportation system
[NASA-CR-182561] 11 p1567 N88-19379
Lunar lander conceptual design: Lunar base systems study task 2.2
[NASA-CR-172051] 24 p3335 N88-29854
LUNAR LOGISTICS
Maintenance and supply options
[NASA-CR-172062] 24 p3332 N88-29837
LUNAR OCCULTATION
NT SOLAR ECLIPSES
LUNAR PERTURBATION
U LUNAR EFFECTS
LUNAR ROCKS
Chronology of early lunar crust
24 p3394 N88-30212
LUNAR SCATTERING
U DIFFUSE RADIATION
LUNAR SOIL
Photochemical conversion of nucleic acid components catalyzed by lunar soil 06 p0750 N88-14604
Uses of lunar sulfur
[DE88-009119] 21 p3031 N88-27990
LUNAR SPACECRAFT
NT LUNAR LANDING MODULES
Possibilities of economical improvements for Moon based rocket propulsion using lunar propellants
[ILR-MITT-196] 24 p3338 N88-29871
LUNAR SURFACE
Space station accommodations for lunar base elements: A study
[NASA-TM-100501] 06 p0804 N88-14907
Lunar fiberglass: Properties and process design
[NASA-CR-182580] 11 p1466 N88-18740
Energy requirements for HE-3 mining operations on the Moon 17 p2420 N88-24390
Lunar base launch and landing facility conceptual design, 2nd edition
[NASA-CR-172049] 20 p2885 N88-27135
Growth of planetary crusts 24 p3400 N88-30247
High-resolution (30 m) lunar radar images
24 p3442 N88-30486
LUNEBERG LENSES
U RADAR CORNER REFLECTORS
LUNG MORPHOLOGY
Lung function in simulated microgravity
12 p1654 N88-19907
LUNGS
NT ALVEOLI
Effect of exogenous cardiosynchronized counterpulsation on human regional and central hemodynamics 10 p1366 N88-18163
Liquid ventilation: New data and possible use in space medicine 12 p1654 N88-19908
Methods of measurement for the evaluation of monolayer properties. Development and applications --- lung surfactants
[ETN-88-92229] 15 p2104 N88-22532
LUTETIUM COMPOUNDS
Electrochromic cells with lutetium diphthalocyanine and semisolid polymer electrolytes
[AD-A188031] 10 p1352 N88-18078
LYAPUNOV FUNCTIONS
U LIAPUNOV FUNCTIONS
LYMAN ALPHA RADIATION
Lyman alpha SMM/UVSP absolute calibration and geocoronal correction
[NASA-TM-100314] 03 p0389 N88-12446
Hydrogen and deuterium in the local interstellar medium 04 p0521 N88-13204
Lyman-alfa/OH-resonance-absorbtion measurements and simulation calculations for the investigation of the induction behavior of methane/ethane/oxygen mixtures in reflected shock waves
[ETN-88-90806] 07 p0831 N88-15042
IUE program SUGSD: Varability time scale of H Ly-alpha from Uranus
[NASA-CR-182706] 13 p1856 N88-21107
The role of hydrogen thermalization in shaping the Lyman-alpha coma --- comets 14 p2007 N88-21971
Long duration coherent Lyman-alpha sources
16 p2268 N88-23571
A theoretical determination of the density at a traveling source that emitts particles
[ISAS-RN-351] 21 p3013 N88-27883
LYMAN SPECTRA
Experimental study of the role of plasma polarization on line shape in dense laboratory plasmas
[ETN-88-92001] 13 p1844 N88-21033
LYMPHOCYTES
Spleen lymphocyte nucleic acids in pregnant rats flown in space and their offspring 07 p0892 N88-15403
White blood cells in space: An experiment for the first Spacelab mission 09 p1127 N88-16757
Effects of pulsed and CW (Continuous Wave) 2450 MHz radiation on transformation and chromosomes of human lymphocytes in vitro
[AD-A193104] 21 p2987 N88-27736
Effect of microgravity on lymphocyte activation --- Spacelab D1 mission 22 p3061 N88-28163
LYOPHILIZATION
U COLLOIDING
LYOPHILS
U COLLOIDS
LYRA CONSTELLATION
Modes, masses, metallicities, and magnitudes of RR Lyrae variables
[DE87-013149] 01 p0109 N88-10703
The distances and absolute magnitudes of RR Lyrae variable stars 11 p1568 N88-19386

M

M STARS
The M-type stars
[NASA-SP-492] 02 p0252 N88-11592
Basic properties and variability
02 p0252 N88-11593
Spectroscopy and nonthermal processes
02 p0252 N88-11594
Mass loss 02 p0253 N88-11597
Circumstellar chemistry 02 p0253 N88-11598
Thermal atmospheric models
02 p0253 N88-11599
Quasi-thermal models 02 p0253 N88-11600
The atmospheres of M dwarfs: Observations
02 p0253 N88-11601
M dwarfs: Theoretical work 02 p0253 N88-11602
Evidence for an additional source of opacity during the impulsive phase of stellar flares
04 p0510 N88-13133
Magnetic fields on K and M stars
04 p0510 N88-13137
Carbon abundances and C12/C13 ratios in M giants
04 p0515 N88-13167
M dwarfs from the Einstein medium sensitivity survey
04 p0519 N88-13188
Asymptotic giant branch populations in composite stellar systems 13 p1854 N88-21098
Analysis of emission features in IRAS LRS spectra
21 p2928 N88-27380
Duplicity in the solar neighborhood: Part 4: Spectroscopic orbits for four dwarf M stars
[SER-C-PREPUBL-FASC-21] 24 p3454 N88-30561

M WINGS
U VARIABLE SWEEP WINGS

MAARS
U CRATERS

MACH NUMBER
Fundamentals of fighter aircraft design: Engine intake and afterbody 05 p0545 N88-13322
Static force and moment test of the Holloman narrow-gage rocket sled at Mach numbers from 3.5 to 5.5
[AD-A186291] 07 p0822 N88-14995
Shock structure and noise of supersonic jets in simulated flight to Mach 0.4
[NASA-TP-2785] 08 p1080 N88-16510
Mach number effects on transonic aeroelastic forces and flutter characteristics
[NASA-TM-100547] 09 p1113 N88-16675
Influence of base modifications on in-flight base drag in the presence of jet exhaust for Mach numbers from 0.7 to 1.5
[NASA-TP-2802] 11 p1488 N88-18881
Galileo probe parachute test program: Wake properties of the Galileo probe at Mach numbers from 0.25 to 0.95
[NASA-RP-1130] 11 p1488 N88-18884
Nonaxisymmetric body supersonic, aerodynamic prediction
[AD-A189338] 13 p1716 N88-20259
The influence of Mach number and heat transfer on the turbulent flow wall law
[NASA-TT-20230] 13 p1771 N88-20594
Preliminary in-flight boundary layer transition measurements on a 45 deg swept wing at Mach Numbers between 0.9 and 1.8
[NASA-TM-100412] 13 p1772 N88-20598
Measurement and analysis of the noise radiated by low Mach numbers centrifugal blowers
[AD-A189226] 13 p1833 N88-20966
The turbulent heat flux in low Mach number flows with large density variations
[DE88-006445] 14 p1911 N88-21419
High Reynolds number, low Mach number, steady flow field calculations over a NACA 0012 airfoil using Navier-Stokes and interactive boundary layer theory
[AD-A189871] 15 p2013 N88-22005
Flow quality of NAL two-dimensional transonic wind tunnel. Part 1: Mach number distributions, flow angularities and preliminary study of side wall boundary layer suction
[NASA-TT-20209] 16 p2165 N88-22911
Aeropropulsive characteristics of isolated combined turbojet/ramjet nozzles at Mach numbers from 0 to 1.20
[NASA-TP-2814] 17 p2290 N88-23757
Spatial stability of a compressible mixing layer
[NASA-CR-181671] 18 p2514 N88-24916
Effects of Mach number on acoustic-vortex interactions in a ramjet 19 p2625 N88-25573
The effects of RCS jet firing on the isolated Orbiter and mated coast phases of the glide return to launch site maneuver at Mach number 6 (IA302B)
[NASA-CR-180223] 20 p2766 N88-26403
Analysis of experimental data for cast 10-2/DOA2 supercritical airfoil at high Reynolds numbers
[AD-A192827] 21 p2892 N88-27166
Theoretical-numerical study of feasibility of use of winglets on low aspect ration wings at subsonic and transonic Mach numbers at reduce drag
[NASA-CR-4174] 21 p2892 N88-27168
Wind tunnel tests of elliptical missile body configurations at Mach numbers 0.4 to 5.0
[AD-A193525] 22 p3038 N88-28040

MACH REFLECTION
Analytical investigation of reflection of a regular or mach reflection over a secondary wedge
[AD-A185690] 06 p0703 N88-14316
The effect of collision angle on mach reflection
[AD-A185798] 06 p0704 N88-14319

MACH-ZEHNDER INTERFEROMETERS
Fiber optic single mode sensors
[FOA-C-30453-3.1] 06 p0780 N88-14790

MACHINE LEARNING
U LEARNING MACHINES

MACHINE LIFE
U SERVICE LIFE

MACHINE RECOGNITION
U ARTIFICIAL INTELLIGENCE

MACHINE STORAGE
U COMPUTER STORAGE DEVICES

MACHINE TOOLS
NT GRINDING MACHINES
NT LATHES
NT MILLING MACHINES
A passive vibration-cancelling isolation mount
05 p0595 N88-13636
Selected aspects of microelectronics technology and applications: Numerically controlled machine tools. Technology trends series no. 2
[PB87-132973] 06 p0696 N88-14266
Alignment and assembly tool for very large diameter cylinders
[NASA-CASE-MFS-28001-2] 06 p0711 N88-14360
Identification and feedback control of machine tool vibrations
[PB88-109715] 08 p0976 N88-15902
A problem of machine repair with a variable number of heterogeneous servers
[INPE-4245-PRE/1118] 08 p1074 N88-16482
Fiber-reinforced plastic composites. Possibilities and limitations of applications as machine-construction materials
[NASA-TT-20159] 15 p2031 N88-22102
Contribution to the study of modern materials for cutting tools
[ISAL-IDI1-87-17] 16 p2185 N88-23029
Determination of settings of a tilted head-cutter for generation of hypoid and spiral bevel gears
[NASA-CR-182138] 18 p2524 N88-24976

MACHINE TRANSLATION
Program translation via abstraction and reimplementation
[AD-A185845] 07 p0901 N88-15459
The Ada compiler: On the design and implementation of an Ada compiler
[ETN-88-91594] 09 p1215 N88-17284
Linguistic-technical aspects of machine translation
24 p3438 N88-30461
Linguistic barriers: Translation problems
24 p3438 N88-30465

MACHINERY
Optimization of a controlled two-server maintenance system
[INPE-4202-PRE/1083] 01 p0107 N88-10694

MACHINING
NT MILLING (MACHINING)
NT SPARK MACHINING
Components for measuring robots
[KFK-PFT-126] 03 p0332 N88-12092
Interactions between science and precision engineering
[DE87-010873] 04 p0426 N88-12643
Diamond turning of silicon for optics applications
[DE88-002501] 07 p0840 N88-15095
The mechanism of anisotropic silicon etching and its relevance for micromachinings
[MBB-UA-1013/86] 10 p1311 N88-17838
Government research on ceramics coating technology
16 p2184 N88-23019
Spur gears: Optimal geometry, methods for generation and Tooth Contact Analysis (TCA) program
[NASA-CR-4135] 16 p2215 N88-23216
Frequency Analysis of Acoustic Emission - Application to machining and welding
[DE88-701478] 18 p2570 N88-25262
The use of micromachined structures for the management of mechanical properties and adhesion of thin films 19 p2674 N88-25899
Ductile-brittle transition of cutting behavior in diamond turning of single crystal Si
[DE88-008890] 20 p2809 N88-26664
The knowledge based automatic extraction of the machinable surfaces for automatic CAD-CAM system
[INPE-4542-PRE/1288] 20 p2836 N88-26824
Surface properties in electric discharge machining
[NASA-TT-20243] 23 p3223 N88-29182
Evaluation of the potential health hazards associated with the machining of carbon fiber composites
[AD-A194835] 24 p3408 N88-30286

MACROCLIMATE
U CLIMATE

MACROMOLECULES
U MOLECULES

MACULAR VISION
U VISION

MAGAZINES (SUPPLY CHAMBERS)
Organic coatings to improve the storageability and safety of pyrotechnic compositions
[AD-A187158] 09 p1150 N88-16889

MAGELLANIC CLOUDS
Data recorded by the Rome room temperature gravitational wave antenna, during the supernova SN 1987 A in the Large Magellanic Cloud
[NOTA-INTERNA-879] 06 p0806 N88-14922
Color-magnitude diagrams of star clusters in the Magellanic clouds from wide-field electronography. Part 3: NGC 1841
[PUBL-SER-C-FASC-14] 07 p0944 N88-15740
Investigation of nuclei of active galaxies as well as sources in the Large Magellanic Cloud using the X-ray astronomy satellite EXOSAT
[ETN-88-91494] 11 p1570 N88-19399
Astron observations of supernova 1987A in large magellanic cloud 24 p3445 N88-30504
Gamma radiation expected from supernova 1987A in large magellanic cloud 24 p3445 N88-30505

MAGMA
Recent progress in magma energy extraction
[DE87-013083] 01 p0066 N88-10424
Petrogenesis of basalts from the Archean Matachewan Dike Swarm Superior Province of Canada
06 p0796 N88-14878
Upper mantle heterogeneity and composition of primary ocean island magmas 08 p1009 N88-16120
Ocean floor magmatism and problems of lithosphere formation 08 p1009 N88-16121
Status of the Magma Energy Project
[DE88-002413] 13 p1792 N88-20719
Advanced geothermal technologies
[DE88-004307] 15 p2091 N88-22463
Carbon analysis in natural olivine crystals of deep origin
[NASA-TT-20311] 19 p2734 N88-26239
Fine-scale traverses in cumulate rocks, Stillwater Complex: A lunar analogue study
[NASA-CR-183066] 20 p2823 N88-26747
Geothermal energy technology: Issues, R and D (Research and Development) and cooperative arrangements
[PB88-193107] 21 p2967 N88-27626
Time-dependent thermal convection of Earth mantle and double diffusive convection in magma chambers
[MITT-52] 21 p2974 N88-27663
What SNC meteorites tell us about Martian magmatism 23 p3303 N88-29679
Growth of continental crust: Clues from Nd isotopes and Nb-Th relationships in mantle-derived magmas
24 p3393 N88-30205
Pluton emplacement and magmatic arc construction: A model from the Patagonian batholith
24 p3393 N88-30206
Does subduction zone magmatism produce average continental crust 24 p3394 N88-30214
Evidence for crustal recycling during the Archean: The parental magmas of the stillwater complex
24 p3396 N88-30226
Mid to late proterozoic magmatism within Northeastern North America and its iplications for the growth of the continental crust 24 p3397 N88-30229
Late-Archaean crustal growth in the Lewisian Complex of Northwest Scotland: Diachroneity in magmatic accretion and implications for models of crustal growth
24 p3401 N88-30253
Volcanic contribution to crustal growth in the Central Andes: A new estimate and a discussion of uncertainties
24 p3401 N88-30255

MAGNESIUM
NT MAGNESIUM ISOTOPES
Investigation by differential scanning calorimetry of microstructure in a superplastic Al-Mg-Zr alloy
[AD-A184902] 05 p0564 N88-13439
The influence of slip mechanism on fatigue of Mg and Mg-2.3Li 05 p0600 N88-13672
Effect of Mg impurity on local vibrations of U-centers in LiF lattice 14 p1969 N88-21753

Microplasticity phenomena in graphite/magnesium metal matrix composites
[DE88-006772] 15 p2029 N88-22086

MAGNESIUM ALLOYS
Cyclic deformation of an extruded AlMgSi alloy 05 p0598 N88-13654
The influence of microstructure and residual stresses on the initiation and propagation of short surface cracks on AlMgSi1 05 p0601 N88-13674
Characterization of the microstructures of various materials
[AD-A184961] 05 p0655 N88-14017
A fundamental understanding of the effect of alloying elements on the corrosion resistance of rapidly solidified Mg alloys
[AD-A189385] 13 p1741 N88-20413
Diffusion welding of aluminomagnesium alloys to ceramics 14 p1898 N88-21333
The age hardening response of thermomechanically processed Al-Mg-Li alloys
[AD-A189870] 15 p2039 N88-22147
Corrosion and electrochemical behavior of binary magnesium alloys
[AD-A190624] 15 p2040 N88-22154
Laser cladding of Ni, Nb and Mg alloys for improved environmental resistance at high temperature
[AD-A191274] 16 p2213 N88-23208
Strain hardening at large strains in aluminum alloys
[DE88-007415] 18 p2484 N88-24737
Effect of Zr or Cr content on the fracture toughness of the high purity Al-Zn-Mg alloys
[NASA-TT-20294] 19 p2616 N88-25518
Optimizing superplastic response in lithium containing aluminum-magnesium alloys
[AD-A192217] 20 p2774 N88-26451
Analysis of grain refinement and superplasticity in aluminum-magnesium alloys
[AD-A193029] 21 p2912 N88-27283

MAGNESIUM CHLORIDES
Influence of some parameters on the stress corrosion of a ABNT 304 stainless steel in MgCl/sub 2/
[DE87-703707] 04 p0416 N88-12580

MAGNESIUM COMPOUNDS
NT CHLOROPHYLLS
NT MAGNESIUM CHLORIDES
NT MAGNESIUM OXIDES
Performance characteristics of magnesium-sodium nitrate flares in oxygen-nitrogen atmospheres
[AD-A185274] 05 p0570 N88-13476

MAGNESIUM ISOTOPES
Prospects for large dynamic range isotope analysis using photon burst mass spectrometry
[DE88-009110] 19 p2613 N88-25505

MAGNESIUM OXIDES
Brittle to ductile transition to cleavage fracture
[DE88-004074] 10 p1420 N88-18481
Sintering of the heterogeneous MgO compacts
[DE88-010357] 20 p2767 N88-26408

MAGNESYN (TRADEMARK)
U SERVOMOTORS

MAGNET COILS
Development of a strong electromagnet wiggler
[DE88-000971] 05 p0645 N88-13952
The TITAN magnet configuration
[DE88-001826] 06 p0782 N88-14800
Proceedings of the International Workshop on Engineering Design of Next Step Reversed Field Pinch Devices
[DE88-001915] 09 p1251 N88-17494
Plasma physics design and major specifications of candidate reactors for FER design studies. Conceptual design study of FY86 FER
[DE88-751066] 10 p1411 N88-18416
Electromechanical timing measurement technique
[DE88-005098] 11 p1489 N88-18889
Development activities for a 21-T superconducting magnet and cryostat
[DE88-004370] 11 p1558 N88-19327
Quench detection by fluid dynamic means in cable-in-conduit superconductors
[DE88-007269] 18 p2585 N88-25359

MAGNETIC ABSORPTION
U ELECTROMAGNETIC ABSORPTION

MAGNETIC ANOMALIES
Area of reduced electron concentration in terrestrial plasmasphere 08 p1003 N88-16078

MAGNETIC BEARINGS
Model adaptation and imbalance compensation in rotors with active magnetic bearings
[ETN-87-90440] 01 p0056 N88-10361
Design feasibility report on investigation of magnetic bearings for the ocean colour monitor radiometer scanner
[BAE-TP-7849] 09 p1174 N88-17036
Modelling and control of an annular momentum control device
[NASA-CR-4138] 13 p1754 N88-20491
An advanced low-cost 2-axis active magnetic bearing flywheel --- satellite attitude control 14 p1877 N88-21213
Vibration and control of flexible rotor supported by magnetic bearings
[NASA-TM-100888] 17 p2345 N88-23977

MAGNETIC CIRCUITS
Test results on dual resonant power supply with flat top and flat bottom current
[DE87-007506] 09 p1157 N88-16933
Electromechanical timing measurement technique
[DE88-005098] 11 p1489 N88-18889
Influence of magnetic material on the transient of a controle electrovalve
[INPE-4418-PRE/1223] 12 p1624 N88-19713

MAGNETIC CLOUDS
Solar activity, magnetic clouds, and geomagnetic storms 01 p0115 N88-10735
Dynamics of magnetic clouds in interplanetary space 01 p0115 N88-10736
The expansion of magnetic clouds 01 p0115 N88-10737

MAGNETIC COILS
NT MAGNET COILS
Design and testing of electrical insulation for superconducting coils
[DE87-012256] 01 p0039 N88-10246
XeCl excimer laser with magnetic compressor 03 p0299 N88-11879
Scaling the electromagnetically driven explosive shock simulator 05 p0592 N88-13612

MAGNETIC COMPRESSION
Proceedings of the Energy Independence Conference: Fusion Energy and Plasma Physics
[DE88-700657] 09 p1253 N88-17507

MAGNETIC CONTROL
Magnetic control of low pressure discharges
[AD-A186794] 10 p1322 N88-17900

MAGNETIC COOLING
Magnetic anomalies in the rare earth oxide superconductors GdBa2Cu3O(7-x) and YbBa2Cu3O(7-x)
[AD-A190713] 15 p2144 N88-22793
Study of a magnetic refrigerator for space applications for temperatures under 20 K
[NASA-TT-20283] 19 p2641 N88-25668

MAGNETIC DIFFUSION
Influence of a magnetic field on the diffusion of small particles in a turbulent flow
[DE87-702877] 01 p0046 N88-10291
Vortex dynamics and transport to the wall in a crossed-field plasma sheath
[DE87-013286] 01 p0100 N88-10657

MAGNETIC DIPOLES
Modeling of proximity coupling between superconducting filaments in superconducting dipole magnets
[DE87-014684] 03 p0382 N88-12403
Rotation of magnetized particle in electrically conducting viscous medium 06 p0770 N88-14733
Properties of a magnetic dipole
[AD-A186128] 07 p0922 N88-15600
Magnetic field of planet Uranus: Predictions, measurements, interpretations 08 p1005 N88-16094
Investigation of a new magnetic dipole mode in the heavy, deformed nuclei 154 Sm, 156 Gd, 158 Gd, 164 Dy, 168 Er, and 174 Yb with high resolution electron scattering
[ETN-88-91084] 09 p1245 N88-17460
Modeling the behavior of oriented permanent magnet material using current double theory
[DE88-004446] 13 p1833 N88-20963
SSC (Superconducting Super Collider) magnet technology
[DE88-007386] 19 p2733 N88-26230
Far- and mid-infrared properties of metal-insulator composite materials
[AD-A193227] 21 p2905 N88-27236
Passage of relativistic magnetic dipole moments through magnetic fields
[DE88-702640] 23 p3295 N88-29624

MAGNETIC DISKS
High density ion implanted contiguous disk bubble technology
[AD-A190169] 15 p2143 N88-22789
Corrosion problems associated with computer disk packs 22 p3054 N88-28121

MAGNETIC DISPERSION
Time-domain reciprocity theorems for electromagnetic fields in dispersive media
[PB88-126925] 10 p1319 N88-17886

MAGNETIC DISTURBANCES
NT MAGNETIC STORMS
The large Type 4 radio burst event of 24 April 1985 interpreted by dynamic spectral recordings and associated recordings 01 p0112 N88-10717
New results from high angular resolution observations of alpha Ori 04 p0514 N88-13161
Characteristics of atmospheric disturbances with a quasi-two day period 06 p0734 N88-14515
A compilation of Sudden Storm Commencements (SSCs), associated interplanetary disturbances, and cosmic ray variations
[IFSI-86-11] 06 p0807 N88-14923
Flare doublet: Interplanetary and geomagnetic effects 08 p1001 N88-16066
Unusually strong density decrease in near-Earth interplanetary plasma and magnetically quiet day as effects of isolated solar flare 08 p1002 N88-16072
Relationship between characteristics of low-energy electrons and geomagnetic disturbance in geostationary orbit 24 p3444 N88-30501

MAGNETIC EFFECTS
Electrodynamic tether system study
[NASA-CR-172024] 03 p0275 N88-11737
Magnetic field dependence of the specific heat of some high-T/sub c/ superconductors
[DE87-014078] 04 p0497 N88-13063
Study of some superconducting and magnetic materials on high T sub c oxide superconductors
[NASA-CR-182330] 06 p0785 N88-14813
Criteria of interplanetary parameters causing intense magnetic storms (Dst less than -100nT)
[NASA-CR-182423] 08 p1024 N88-16200
The Shubnikov de Haas effect in narrow-gap semimagnetic semiconductors
[ETN-88-92249] 14 p1988 N88-21861
Embryonic development of the newt Cynops pyrrhogaster in very weak magnetic fields
[ISAS-RN-357] 19 p2702 N88-26068
Effect of a weak magnetic field on high temperature superconductivity in Y-Ba-Cu-O ceramics
[DE88-702192] 19 p2733 N88-26235
Energy levels and magneto-electric effects in some quasi uni-dimensional semiconductor heterostructures 20 p2864 N88-27009

MAGNETIC FIELD CONFIGURATIONS
On tokamak equilibrium
[DE87-014811] 02 p0239 N88-11507
Magnetic field morphology in the upper layers 02 p0255 N88-11610
Laser induced fluorescent study of relativistic electron beams
[AD-A184456] 04 p0447 N88-12774
Large scale solar and stellar magnetic fields 04 p0507 N88-13117
Model of solar-wind magnetosphere coupling 04 p0525 N88-13211
Reversed field pinch plasmas with various boundary conditions
[DE88-000832] 05 p0653 N88-14004
A fluid simulation of the AMPTE lithium gas releases in the solar wind
[TRITA-EPP-87-06] 05 p0661 N88-14056
Magnetic field draping about coronal mass ejecta
[DE88-001805] 05 p0661 N88-14057
Observations of field-aligned current structures during the Coordinated Auroral Experiment using Scatter And Radar (CAESAR) flight 2 08 p1031 N88-16250
Experimental model of halo plasma observed in small-aspect FRC plasma
[INPE-4159-PRE/1061] 08 p1085 N88-16534
Design, construction and operation of a small RFP for turbulent plasma studies
[INPE-4241-PRE/1116] 08 p1087 N88-16545
Magnetic reconnection and solar flare loops 08 p1094 N88-16583
The effects of viscosity on resistive ballooning modes in line-tied coronal magnetic fields 08 p1097 N88-16599
Influence of viscosity on the structure of a magnetic neutral layer 08 p1098 N88-16605
D-3He fuels in a field-reversed configuration
[IPPJ-855] 10 p1411 N88-18419
Applications of Lie group methods to the equations of magnetohydrodynamics 10 p1411 N88-18422
Evaluation of magnetic coordinates in finite-beta, asymmetric plasmas
[DE88-003665] 10 p1412 N88-18424
Magnetic and inertial fusion status and development plans
[DE88-004405] 11 p1552 N88-19288
Fully implicit three-dimensional MHD (magnetohydrodynamics) stability and evolution in toroidal geometry
[DE88-000624] 13 p1842 N88-21023
Magnetic cavity formation at Comet Halley and at the AMPTE Li release 14 p1996 N88-21898

Plasmapause formation
[AERONOMICA-ACTA-A-319-1987] 15 p2138 N88-22759
A mode-transforming polarization-rotatable launcher for the ATF (Advanced Toroidal Facility) fusion experiment
[DE88-005070] 19 p2730 N88-26213
Parallel gradient effects on ICRH (Ion Cyclotron Resonance Heating) in tokamaks
[DE88-009038] 19 p2730 N88-26216
MACH2: A two-dimensional magnetohydrodynamic simulation code for complex experimental configurations
[AD-A192285] 20 p2860 N88-26988
Global and local magnetohydrodynamic relaxations
[DE88-752602] 21 p3018 N88-27913
Millimeter wave generation by relativistic electron beams
[AD-A195683] 24 p3362 N88-30016

MAGNETIC FIELD INTENSITY
U MAGNETIC FLUX

MAGNETIC FIELD RECONNECTION
Numerical modeling of slow shocks
[DE87-014768] 04 p0454 N88-12808
Model of solar-wind magnetosphere coupling 04 p0525 N88-13211
Magnetic reconnection and solar flare loops 06 p1094 N88-16583
Coupling of microscopic and macroscopic processes in the Earth's magnetotail 06 p1095 N88-16586
Emerging flux, magnetic reconnection, plasma turbulence and waves in the transition zone of the solar atmosphere 08 p1096 N88-16597
Evidence of small-scale reconnection in the magnetosphere 08 p1097 N88-16601
An unusual magnetopause encounter by AMPTE-UKS 08 p1097 N88-16602

MAGNETIC FIELDS
NT BIOMAGNETISM
NT FORCE-FREE MAGNETIC FIELDS
NT GEOMAGNETISM
NT INTERPLANETARY MAGNETIC FIELDS
NT MAGNETIC CLOUDS
NT MAGNETOSTATIC FIELDS
NT PALEOMAGNETISM
NT PLANETARY MAGNETIC FIELDS
NT SOLAR MAGNETIC FIELD
NT STELLAR MAGNETIC FIELDS
NT TRAPPED MAGNETIC FIELDS
Recovery of vacuum gaps after arcing
[DE87-013852] 01 p0039 N88-10250
Influence of a magnetic field on the diffusion of small particles in a turbulent flow
[DE87-702877] 01 p0046 N88-10291
Visible free electron laser oscillator
[AD-A183871] 01 p0051 N88-10324
Plasma properties
[DE87-013662] 01 p0101 N88-10663
Electrical conductivity and equation of state measurements on planetary fluids at high pressures and temperatures
[DE87-013787] 01 p0110 N88-10708
Magnetic field twist driven by remote convective motions: Characteristics and twist rates 01 p0113 N88-10724
Study of pickup of cometary ions in turbulent solar winds 01 p0113 N88-10725
Dynamics of magnetic clouds in interplanetary space 01 p0115 N88-10736
The expansion of magnetic clouds 01 p0115 N88-10737
Equilibrium and tearing stability of thin current layers in magnetic arcades 01 p0118 N88-10754
Solar-geophysical data number 513, May 1987. Part 1: (Prompt reports). Data for April, March 1987 and late data
[PB87-204939] 01 p0119 N88-10760
Complex scattering dynamics and the integer quantum Hall effect
[DE87-011790] 02 p0243 N88-11536
Method estimating integral mean value of enhancement factor and path latitude for whistlers below magnetic latitude 10 deg 03 p0300 N88-11885
Excimer laser cell with longitudinal electron-beam excitation 03 p0302 N88-11903
Experimental study of stabilizing He-Ne laser output power with transverse magnetic field 03 p0303 N88-11906
Analysis of undulator field errors for XUV FELs (Extreme Ultraviolet Free Electron Laser)
[DE87-014734] 03 p0328 N88-12073
A tapered poloidal gap for the reduction of field errors
[DE87-014750] 03 p0377 N88-12375
Specific heat of the high T/sub c superconductors (La,M)2CuO4 and YBa2Cu3O7 in magnetic fields
[DE87-014680] 03 p0380 N88-12388
The impact of varves on solar physics
[NASA-CR-181519] 03 p0390 N88-12448
Relativistic electron precipitations in a pulsating aurora 04 p0468 N88-12894
Magnetic field dependence of the specific heat of some high-T/sub c/ superconductors
[DE87-014078] 04 p0497 N88-13063
Resistivity of EuBa2(Cu/sub 1-y/Zn/sub y/)3O/sub x/ as a function of temperature, magnetic field, pressure and Zn concentration
[DE87-014740] 04 p0499 N88-13069
The dynamics of solar magnetic flux tubes subjected to resonant foot point shaking 04 p0507 N88-13118
Completely magnetically contained electrothermal thrusters
[AD-A185674] 06 p0674 N88-14129
Ferromagnetic mitigation of electromagnetic pulse effects
[AD-A185685] 06 p0694 N88-14258
The TITAN oscillating-field current-drive system
[DE88-001823] 06 p0782 N88-14798
Nature and the nonlinear evolution of electrostatic waves associated with the AMPTE (Active Magnetosphere Particle Tracer Explorers) solar wind releases
[AD-A185471] 06 p0806 N88-14920
Metallurgical processes in multi-component rare earth-transition metal permanent magnet alloys
[AD-A186401] 07 p0832 N88-15045
Harmonic expansion for the magnetic field of the helical solenoid
[DE88-700100] 07 p0928 N88-15638
Poloidal magnetics of compact ignition tokamaks
[DE88-001774] 07 p0934 N88-15672
Study on the model of a toroidal magnet for a tokamak with a strong field
[DE88-700346] 07 p0935 N88-15681
Simulation an experiment on plasma instability investigation in a tokamak with a divertor
[DE88-700352] 07 p0935 N88-15683
Possibility of calculation of magnetic surface function gradient and related quantities
[DE88-700561] 07 p0936 N88-15686
FTE like variations in the geomagnetic field at ground based conjugate stations in the cusp regions
[INPE-4345-PRE/1182] 08 p1024 N88-16199
Magnetic investigations of superconductive, polycrystalline (RE)1Ba2Cu3O(7-x) compounds (RE = Y, Gd, Ho, Dy)
[DE88-002537] 08 p1090 N88-16558
Acceleration of auroral particles by magnetic field-aligned electric fields
[TRITA-EPP-87-08] 09 p1190 N88-17131
Mechanism of change of vortex structure orientation in type-2 superconductors 09 p1239 N88-17425
Suppression of the mass enhancement in CeB6 in high magnetic fields
[DE88-002946] 09 p1241 N88-17439
Magneto-Inertia Confinement Approach (MICA) to fusion in dynamic Z-pinch formed from a frozen deuterium-tritium tube
[IPPJ-856] 09 p1252 N88-17504
X-ray diffraction study of thermotropic liquid crystalline polyesters and diester model compounds
[AD-A186788] 09 p1255 N88-17521
Realistic conductivity geometry model of the human head for interpretation of neuromagnetic data
[PB88-112230] 10 p1369 N88-18179
Evaluation of magnetic coordinates in finite-beta, asymmetric plasmas
[DE88-003665] 10 p1412 N88-18424
The relation of solar wind structure to hydromagnetic discontinuities
[DE88-004304] 10 p1431 N88-18546
Computer-aided modeling and prediction of performance of the modified Lundell class of alternators in space station solar dynamic power systems
[NASA-CR-182538] 11 p1507 N88-19000
Potential benefits of a broad magnetic fusion R and D program
[DE88-003288] 11 p1553 N88-19297
Toward a comprehensive theory for the sweeping of trapped radiation by inert orbiting matter
[NASA-CR-182584] 11 p1569 N88-19395
The effects of a dc electric field on the current driven ion cyclotron instability
[AD-A188877] 12 p1695 N88-20142
Effects of toroidal forces in current loops embedded in a background plasma
[AD-A188878] 12 p1695 N88-20143
Solar flares and magnetic topology
[AD-A188692] 12 p1712 N88-20244
Wiggler taper optimization for free-electron-laser amplifiers with moderate space-charge effects
[DE88-003758] 13 p1775 N88-20618
Experience with and ways to upgrade accuracy of hydromagnetic surveys in ocean 13 p1787 N88-20692
The Magnetically Insulated Inertial Confinement Fusion (MICF): A novel approach
[DE88-005480] 13 p1842 N88-21026
Helical ripple transport in stellarators at low collision frequency
[DE88-006431] 13 p1843 N88-21031
Increasing the rate at which ceramic castings undergo preliminary heat-treatment in an ultra-high frequency magnetic field 14 p1886 N88-21275
Eddy current losses induced by rotation of magnetisation
[BLL-M-37634-(5828.4)] 14 p1890 N88-21298
Research on variable-period wiggler type free electron lasers 14 p1902 N88-21360
Pulsed magnet fields for free-electron lasers 14 p1903 N88-21367
Analysis of induction motors based on the numerical solution of the magnetic field and circuit equations
[EL-59] 14 p1907 N88-21398
Statistical analysis of feasibility of non-destructive inspection of mechanical properties of hot worked pipes of alloy steels
[BLL-M-37598-(5828.4)] 14 p1922 N88-21455
Chaotic diffusion across magnetic field in a model of electrostatic turbulent plasma
[PREPRINT-566] 14 p1985 N88-21839
Analysis of anomalous resistivity during the conduction phase of the plasma erosion opening switch
[DE88-006382] 15 p2061 N88-22286
On the acceleration of electrons and positive ions in the same direction along magnetic field lines by parallel electric fields
[IRF-PREPRINT-103] 15 p2096 N88-22488
Electrical circuit modeling of reversed field pinches
[DE88-006942] 15 p2136 N88-22745
Parametric instabilities of inhomogeneous plasma near the lower-hybrid resonance
[DE88-701201] 15 p2137 N88-22748
Quantization of axial electrodynamics
[DE88-701498] 15 p2147 N88-22813
Application of magnetic barrier for increasing the efficiency of laser ion source
[DE88-701669] 16 p2212 N88-23200
Magnetic traps for an anti-hydrogen gas 16 p2269 N88-23572
Numerical research of dispersion properties of plasma cylindrical waveguides located in magnetic field
[DE87-703009] 16 p2275 N88-23615
Corpuscular plasma diagnostics complex on a tokamak with a strong field
[DE88-701576] 16 p2279 N88-23646
Solar-geophysical data number 520, December 1987. Part 1: (Prompt reports). Data for November 1987, October 1987 and late data
[PB88-164199] 16 p2290 N88-23712
Magnetic drive coupling
[NASA-CASE-MSC-21171-1] 17 p2344 N88-23973
Systematic variation of magnetic-field penetration depth in high-T(c) superconductors studied by muon spin relaxation 17 p2396 N88-24243
Electromagnetic penetration into a conducting circular cylinder through a narrow slot, TE case
[AD-A191602] 18 p2500 N88-24828
Application of particle simulations to the NRL laser experiment
[AD-A191641] 18 p2520 N88-24953
Solving time-dependent two-dimensional eddy current problems
[NASA-TM-100875] 18 p2566 N88-25239
Propagation of neutralized ion beams
[AD-A191599] 18 p2574 N88-25289
Basic processes of plasma propulsion
[AD-A192117] 18 p2577 N88-25310
Design studies of low aspect-ratio torsatrons
[DE88-007562] 18 p2579 N88-25320
Influence of alternating magnetic fields on Zn-67 Moessbauer resonance in ZnO
[PB88-186432] 18 p2584 N88-25352
Space station induced electromagnetic effects 18 p2591 N88-25394
Anomalous temperature-dependent negative magnetoresistance in pregraphitic carbons
[AD-A191725] 19 p2619 N88-25535
Theoretical study of the folded waveguide
[DE88-007877] 19 p2654 N88-25759
Optical sensing of magnetic fields 19 p2670 N88-25871
Experiments on insulation of relativistic electron flows in oblique and tapered magnetic fields
[DE88-007199] 19 p2724 N88-26176
Rutherford magnetic spectrograph for intense ion beam measurements on PBFA 2
[DE88-007261] 19 p2725 N88-26181
ECRH current drive in tokamak plasmas
[IPPJ-864] 19 p2729 N88-26209

The effects of magnetic nozzle configurations on plasma thrusters
[NASA-CR-183096] 19 p2732 N88-26223
Superconductive analogue of spin glasses
[DE88-702059] 19 p2733 N88-26233
Effect of a weak magnetic field on high temperature superconductivity in Y-Ba-Cu-O ceramics
[DE88-702192] 19 p2733 N88-26235
Application of superconducting technology to earth-to-orbit electromagnetic launch systems
[NASA-TM-101134] 20 p2763 N88-26385
Magnetic heat pump design
[DE88-007730] 20 p2798 N88-26605
Magnetohydrodynamic squeeze film
[DE88-701876] 20 p2810 N88-26669
Interaction of biological systems with static and ELF electric and magnetic fields
[DE88-007951] 20 p2831 N88-26792
Sources of polarized ions and atoms
[DE88-010910] 20 p2852 N88-26931
Symmetrized magnetic field configuration of low aspect ratio helical system
[IPPJ-869] 20 p2855 N88-26956
Thermal inhibition by megagauss field due to variation of electron temperature in laser plasma
[DE88-701887] 20 p2859 N88-26977
Megagauss field variation along axis of wire target in laser produced plasma
[DE88-701895] 20 p2859 N88-26979
An interferometric measurement technique for railgun structures
[AD-A192851] 21 p2901 N88-27217
Magnetic excitations in transition metal systems
[DE88-011022] 21 p2912 N88-27279
Electric and Magnetic Activity of the Central Nervous System: Research and Clinical Applications in Aerospace Medicine
[AGARD-CP-432] 21 p2977 N88-27683
Studies of the intact human brain: Implications for performance 21 p2977 N88-27684
Squid instrumentation for neuromagnetic study of complex brain activity 21 p2978 N88-27691
Electric and magnetic brain activity related to cognitive performance 21 p2979 N88-27692
Neuromagnetic evidence of place mechanisms for frequency and intensity coding in the human auditory cortex 21 p2979 N88-27693
Staggered-grid finite element solution technique for the Maxwell's equations in the time domain
[DE88-011731] 21 p3007 N88-27838
Tokamak magnetic turbulence over the safety factor range 0.6 less than q less than 3
[DE88-008421] 21 p3017 N88-27904
TE/TM (Transverse Electric/Transverse Magnetic) height profile measurements of transpolar VLF (Very Low Frequency) signals
[AD-A194503] 22 p3069 N88-28216
The far field from a hybrid electromagnetic pulse (HPD) simulator
[FOA-C-30480-4.2] 22 p3071 N88-28231
Physiological effects of extremely low frequency electric and magnetic fields
[DE88-752814] 22 p3132 N88-28620
CryoSQUID: A SQUID-based magnetic field sensor
[AD-A194237] 23 p3239 N88-29275
Waves and instabilities in an electron-positron plasma in an ultra-strong magnetic field 23 p3283 N88-29551
High-T(sub c) superconductor and its use in superconducting magnets
[DE88-008403] 23 p3289 N88-29581
Activity-rotation relations for lower main sequence stars 23 p3298 N88-29640
Resonant spin-flavor precession of solar and supernova neutrinos
[DE88-752604] 23 p3308 N88-29707
More than a solar cycle of synoptic solar and coronal data: A video presentation
[NASA-CR-181459] 23 p3308 N88-29708
NASA Marshall Space Flight Center solar observatory
[NASA-TM-100339] 24 p3332 N88-29832
Relationships among earth's gravity field, magnetic field, crustal structure and the magnetic character of crustal rocks
[AD-A195539] 24 p3392 N88-30198
Structuring processes in expanding laser-produced plasmas
[AD-A195249] 24 p3431 N88-30424
Stability of Venusian ionopause 24 p3448 N88-30523

MAGNETIC FLUX

The method of rigid armature flux orientation for the field-oriented control of highly dynamic drives with synchronous machines
[ETN-87-90405] 01 p0042 N88-10269
Theoretical Problems in High Resolution Solar Physics, 2
[NASA-CP-2483] 02 p0254 N88-11609
Magnetic field morphology in the upper layers 02 p0255 N88-11610
Magnetic fields in the overshoot zone: The great escape 02 p0256 N88-11616
Theoretical modelling of the fine structures in sunspots 02 p0256 N88-11617
Observational constraints and evidence for saturation 04 p0503 N88-13097
Magnetic flux tubes as sources of wave generation 04 p0505 N88-13108
Calibration of the Ca II K line-core density and the magnetic flux density in stars using solar data 04 p0507 N88-13116
The dynamics of solar magnetic flux tubes subjected to resonant foot point shaking 04 p0507 N88-13118
Reversed field pinch plasmas with various boundary conditions
[DE88-000832] 05 p0653 N88-14004
The appearance and disappearance of magnetic flux on the quiet sun
[AD-A185432] 05 p0661 N88-14055
Electrodynamics of midnight sector of auroral oval in period of slight disturbance 08 p1003 N88-16077
Flux tubes and loops in the solar chromosphere and corona 08 p1095 N88-16591
Emerging flux, magnetic reconnection, plasma turbulence and waves in the transition zone of the solar atmosphere 08 p1096 N88-16597
Evidence of small-scale reconnection in the magnetosphere 08 p1097 N88-16601
Ion flows in magnetospheric flux transfer events 08 p1098 N88-16607
Observations of small scale structures using data from the wave experiment on the AMPTE-UKS spacecraft 08 p1099 N88-16612
Magnetic emissions testing of the space station engineering model resistojet
[NASA-TM-100788] 10 p1292 N88-17728
Magnetic control of low pressure discharges
[AD-A186794] 10 p1322 N88-17900
Research on variable-period wiggler type free electron lasers 14 p1902 N88-21360
Properties of superconductors with strong electron-phonon interaction 14 p1974 N88-21779
Generation of flux tube waves in stellar convection zones. 1: Longitudinal tube waves
[NASA-TM-101152] 17 p2451 N88-24561
Permanent magnet excitation of axial flow synchronous machines with high rotation moment
[ETN-88-92385] 20 p2796 N88-26592

MAGNETIC INDUCTION

Electromagnetic induction in spherical earth containing oceans and continents in electrical contact with underlying section: Theory, method, example 08 p1011 N88-16127
Theoretical and experimental investigations on a linear, permanently excited stepping motor
[ETN-88-91061] 09 p1158 N88-16939
Evaluation of the magnetic induction conductivity method for detecting frazil ice deposits
[AD-A186940] 09 p1194 N88-17157
Magnetic drive coupling
[NASA-CASE-MSC-21171-1] 17 p2344 N88-23973
Integrated magnetic field sensor using high magnetotransistors
[ETN-88-92356] 21 p2941 N88-27465

MAGNETIC INDUCTION PROBES

U MAGNETIC PROBES

MAGNETIC LENSES

Bevalac external beamline optics
[LBL-23240] 19 p2727 N88-26194

MAGNETIC LEVITATION VEHICLES

Repulsive force support system feasibility study
[NASA-CR-178400] 04 p0402 N88-12497
The MBB propulsion concepts for magnetic suspension railways: Retrospective view and prospects
[MBB-Z-141/87] 10 p1316 N88-17865

MAGNETIC MATERIALS

NT FERROMAGNETIC MATERIALS
Magnetic diffuse scattering
[DE87-013539] 04 p0489 N88-13014
Rotation of magnetized particle in electrically conducting viscous medium 06 p0770 N88-14733
New equilibrium forms of free surface of confined magnetic fluid 06 p0770 N88-14734
Application of high temperature ceramic superconductors (CSC) to commercial tokamak reactors
[DE88-003973] 09 p1257 N88-17538
CdTe(110)-Mn interface reaction and the formation of non-equilibrium ternary semimagnetic semiconductor alloys
[AD-A187593] 10 p1422 N88-18491
Study of the production of some superconducting and magnetic materials by solidification in the drop tube and drop tower
[NASA-CR-182494] 11 p1461 N88-18708
Influence of magnetic material on the transient of a controle electrovalve
[INPE-4418-PRE/1223] 12 p1624 N88-19713
Exact image theory for the problem of dielectric/magnetic slab
[NASA-CR-182865] 16 p2189 N88-23055
Magnetic superlattices
[AD-A191450] 18 p2581 N88-25334
Use of magnetic materials in excimer laser circuits
[DE88-006449] 19 p2674 N88-25903
Novel magnetic materials research using free electron lasers
[DE88-009989] 20 p2807 N88-26652
An undulator radiation source for spin-polarized photoemission studies of novel magnetic materials
[AD-A193756] 22 p3083 N88-28307
Investigation of magnetic anisotropy and spin wave modes in transition metal multilayers
[DE88-009007] 22 p3154 N88-28765
DARPA-URI consortium meetings on submicron heterostructures of diluted magnetic semiconductors
[AD-A193499] 23 p3206 N88-29081
Mathematical theory and calculations of magnetic hysteresis curves
[DE88-011055] 23 p3277 N88-29510

MAGNETIC MEASUREMENT

Narsarsuaq (Greenland) Geophysical Observatory. Magnetic results, 1984
[ISBN-87-7478-281-9] 02 p0198 N88-11235
Measurements of stellar magnetic fields 04 p0503 N88-13093
The photospheric magnetic fields of cool stars: Recent results of survey and time-variability programs 04 p0503 N88-13094
Hitachi develops ceramic superconducting device 06 p0688 N88-14214
Viking quick look plots: A short description --- Swedish satellite 06 p0692 N88-14243
Effective methods of gravimetric and magnetometric data processing 06 p0728 N88-14479
Study of the technique of stress determination by measuring magnetism
[PB87-143905] 08 p0996 N88-16028
Magnetic field of planet Uranus: Predictions, measurements, interpretations 08 p1005 N88-16094
Report on ground-based activity at Andoya (Norway) in relation to the Aureid-VIP high rocket and to the Viking satellite --- Swedish satellite 08 p1026 N88-16212
Observations of field-aligned current structures during the Coordinated Auroral Experiment using Scatter And Radar (CAESAR) flight 2 08 p1031 N88-16250
Spaceborne magnetometry 12 p1644 N88-19846
Magnetic results, 1985
[ISBN-8-77-478282-7] 14 p1944 N88-21600
Excitations in magnetic low-dimensional systems: A spectroscopic study
[ETN-88-92230] 15 p2129 N88-22697
The SAMEX vector magnetograph: A design study for a space-based solar vector magnetograph
[NASA-TM-4048] 18 p2596 N88-25424
Rutherford magnetic spectrograph for intense ion beam measurements on PBFA 2
[DE88-007281] 19 p2725 N88-26181
Tokamak magnetic turbulence over the safety factor range 0.6 less than q less than 3
[DE88-008421] 21 p3017 N88-27904

MAGNETIC METALS

U MAGNETIC MATERIALS
U METALS

MAGNETIC MIRRORS

NT TANDEM MIRRORS
Fusion reactor physics and technology studies
[DE87-013691] 01 p0101 N88-10664
MHD stability and control for mirror machines 04 p0493 N88-13038
Curvature driven drift mirror instability in the magnetosphere
[IFSI-86-14] 06 p0742 N88-14568
Mirror theory applied to toroidal systems
[DE88-003832] 07 p0933 N88-15669
New methods of confinement and heating of plasma in magnetic fields
[DE88-701021] 15 p2135 N88-22738

MAGNETIC MOMENTS

Rotation of magnetized particle in electrically conducting viscous medium 06 p0770 N88-14733
TRISTAN research on neutron rich nuclei: Magnetic moments and nuclear structure
[DE88-002122] 06 p0783 N88-14807
Superconductivity in La/sub 1.85-x/Nd/sub x/Sr/sub .15/CuO
[DE88-003014] 09 p1258 N88-17540

High temperature processing of superconducting Y1Ba2Cu3O6.9
[DE88-003002] 10 p1416 N88-18449
Neutrino magnetic moment and time variation of solar neutrino flux
[DE88-700687] 10 p1430 N88-18542
Passage of relativistic magnetic dipole moments through magnetic fields
[DE88-702640] 23 p3295 N88-29624

MAGNETIC PERMEABILITY
The effect of magnetic impurities and barriers on the magnetization and critical current of fine filament NbTi composites
[DE88-004443] 10 p1419 N88-18472

MAGNETIC POLES
Theoretical investigations of drift waves in a magnetic quadrupole 18 p2578 N88-25312

MAGNETIC PROBES
Thin superconducting film characterization by surface acoustic waves
[AD-A190417] 15 p2143 N88-22791

MAGNETIC PROPERTIES
NT ANTIFERROMAGNETISM
NT BIOMAGNETISM
NT CURIE TEMPERATURE
NT DIAMAGNETISM
NT FERROMAGNETISM
NT GEOMAGNETISM
NT GYROFREQUENCY
NT MAGNETIC EFFECTS
NT MAGNETIC FIELD RECONNECTION
NT MAGNETIC INDUCTION
NT MAGNETIC MOMENTS
NT MAGNETIC PERMEABILITY
NT MAGNETIC SUSPENSION
NT MAGNETOACOUSTICS
NT MAGNETORESISTIVITY
NT MAGNETOSTRICTION
NT PALEOMAGNETISM
NT PARAMAGNETISM
NT POLARIZATION CHARACTERISTICS
NT SPIN-LATTICE RELAXATION
Application of spin-sensitive electron spectroscopies to investigations of electronic and magnetic properties of solid surfaces and epitaxial systems
[DE87-014235] 02 p0245 N88-11550
Temperature hysteresis and magnetic transitions in amorphous Fe-Ni-Zr alloys
[DE88-000228] 03 p0294 N88-11848
Effect of rapid solidification on short-range order: A magnetic study
[AD-A185216] 05 p0565 N88-13444
Integrated systems with applications to the multi-phases of the ephemerides, physics and methematics of the upper atmosphere
[AD-A185748] 06 p0743 N88-14570
Study of some superconducting and magnetic materials on high T sub c oxide superconductors
[NASA-CR-182330] 06 p0785 N88-14813
The consequences of intergrain Josephson coupling in ceramic high-temperature superconductors
[DE87-013713] 06 p0785 N88-14816
Microstructure and magnetic properties of cobalt-chromium alloys
[DE88-002762] 07 p0835 N88-15064
. Properties of a magnetic dipole
[AD-A186128] 07 p0922 N88-15600
Low field characterization of YBa2Cu3O sub 7-delta single crystals
[DE88-002895] 07 p0938 N88-15700
Magnetic investigations of superconductive, polycrystalline (RE)1Ba2Cu3O(7-x) compounds (RE = Y, Gd, Ho, Dy)
[DE88-002537] 08 p1090 N88-16558
Attenuation of ultrasonic waves in nonmagnetized magnetic fluids 09 p1234 N88-17398
Magnetic investigations of the one-dimensional Heisenberg magnet Gd2Cl3
[ETN-88-91083] 09 p1241 N88-17438
Magnetic properties of heavy fermion superconductors
[ETN-88-91078] 09 p1255 N88-17524
Superconducting and magnetic properties of Fe-doped oxide superconductors
[DE88-003024] 10 p1416 N88-18451
The physics of metallic superlattices: An experimental point of view
[DE88-003060] 10 p1416 N88-18452
Magnetic rare earth superlattices
[DE88-003483] 10 p1418 N88-18465
Brillouin scattering from collective spin waves in magnetic superlattices
[DE88-005347] 12 p1697 N88-20154
Theoretical studies on the electronic structure and properties of complex ceramic crystals and glasses
[DE88-005837] 13 p1846 N88-21049
A qualitative approach to electricity
[AD-A189854] 15 p2128 N88-22693
Magnetic anomalies in the rare earth oxide superconductors GdBa2Cu3O(7-x) and YbBa2Cu3O(7-x)
[AD-A190713] 15 p2144 N88-22793
Magnetic studies of iron-rare-earth-metalloid alloys
[DE88-006801] 16 p2282 N88-23660
Coexisting static magnetic ordering and superconductivity in CeCu2.1Si2 found by muon spin relaxation 17 p2396 N88-24245
Static magnetic ordering of CeCu2.1Si2 found by muon spin relaxation 17 p2396 N88-24246
Electromagnetic damping and vibration isolation of space structures
[AD-A191492] 18 p2471 N88-24665
The theory of random alloys
[DE88-006408] 18 p2487 N88-24756
Physical properties of f electron systems
[DE88-006886] 18 p2581 N88-25331
Magnetic superlattices
[AD-A191450] 18 p2581 N88-25334
Epitaxial iron films
[AD-A191815] 19 p2732 N88-26225
Structural and magnetic properties of Fe impurities in YBa2Cu3O(sub 7-delta)
[DE88-009961] 19 p2735 N88-26247
Magneto-optical studies of GaInAs-InP quantum wells 20 p2870 N88-27039
Influence of interfaces on electronic and magnetic properties of MnSe/ZnSe superlattices near monolayer limit 20 p2872 N88-27050
Characterization of structural and magnetic order of Er/Y superlattices 20 p2873 N88-27056
Investigation of magnetic anisotropy and spin wave modes in transition metal multilayers
[DE88-009007] 22 p3154 N88-28765
CryoSQUID: A SQUID-based magnetic field sensor
[AD-A194237] 23 p3239 N88-29275
Particle trajectories and potentials in a plane sheath moving in a magnetoplasma
[AD-A196228] 24 p3390 N88-30190

MAGNETIC RECORDING
Simulation of the perpendicular magnetic recording process
[B8713537] 05 p0586 N88-13570

MAGNETIC RELAXATION
NT SPIN-LATTICE RELAXATION

MAGNETIC RESONANCE
NT ELECTRON PARAMAGNETIC RESONANCE
NT NUCLEAR MAGNETIC RESONANCE
NT PARAMAGNETIC RESONANCE
Nuclear magnetic resonance studies of ion motion in solid electrolytes
[DE87-014547] 02 p0232 N88-11464

MAGNETIC SHIELDING
Magnet shielding analysis for SOAR: A space fusion reactor 17 p2400 N88-24269

MAGNETIC SIGNALS
SQUID (superconducting quantum interference device) arrays for simultaneous magnetic measurements: Calibration and source localization performance
[AD-A193815] 23 p3216 N88-29143

MAGNETIC SIGNATURES
Narssarssuaq Geophysical Observatory: Magnetic results, 1980-83. Instrumentation and formulas
[ISBN-87-7478-280-0] 03 p0350 N88-12209

MAGNETIC SPECTROSCOPY
Excitations in magnetic low-dimensional systems: A spectroscopic study
[ETN-88-92230] 15 p2129 N88-22697

MAGNETIC STARS
Ultraviolet spectra of two magnetic white dwarfs and ultraviolet spectra of subluminous objects found in the Kiso Schmidt survey
[NASA-CR-183051] 18 p2593 N88-25408

MAGNETIC STORAGE
NT BUBBLE MEMORY DEVICES
NT MAGNETIC DISKS

MAGNETIC STORMS
Solar activity, magnetic clouds, and geomagnetic storms 01 p0115 N88-10735
Magnetospheric storms 03 p0272 N88-11711
Modeling of environmentally-induced effects within satellites. Part 1: NASCAP modeling of satellites 03 p0273 N88-11721
Configurations of the quiet polar cap and its response to a sudden increase of the energy input rate epsilon
[DMI-GEOPHYS-PAPERS-R-74] 03 p0350 N88-12210
A compilation of Sudden Storm Commencements (SSCs), associated interplanetary disturbances, and cosmic ray variations
[IFSI-86-11] 06 p0807 N88-14933
Multispectral optical observations of ionospheric F-region storm effects at low latitude
[INPE-4231-PRE/1105] 08 p1024 N88-16198
Criteria of interplanetary parameters causing intense magnetic storms (Dst less than -100nT)
[NASA-CR-182423] 08 p1024 N88-16200
Balloon measurement of magnetic field during substorms in auroral zone 08 p1026 N88-16213
Interplanetary Magnetic Field (IMF) influence on the magnetic configuration and particle fluxes at geostationary orbit and on the substorm onset 08 p1031 N88-16247
A possible role for ionospheric ions in triggering a geomagnetic substorm onset 08 p1096 N88-16594
Field-aligned fluxes of energetic electrons related to the onset of magnetospheric substorms 08 p1096 N88-16595
The effects of a geomagnetic storm on thermospheric circulation
[AD-A186638] 09 p1190 N88-17128
Dynamics of small and large scale irregularities at sub-auroral latitudes
[AD-A189052] 12 p1645 N88-19853
Dynamics Explorer-2 measurements during an isolated auroral substorm
[AD-A191202] 18 p2543 N88-25091
Field-aligned structure of the storm time Pc 5 wave of November 14-15, 1979
[AD-A193022] 21 p2972 N88-27653
On the dynamics of the auroral ionosphere during the breakup of a substorm
[AD-A193368] 21 p2972 N88-27657
Corona-solar wind coupling review
[AFGL-TR-87-0203] 24 p3458 N88-30575

MAGNETIC SUBSTORMS
U MAGNETIC STORMS

MAGNETIC SURVEYS
Experience with and ways to upgrade accuracy of hydromagnetic surveys in ocean 13 p1787 N88-20692
Resolution of the magnetotelluric method for determining local inhomogeneities in the sedimentary cover 13 p1789 N88-20701

MAGNETIC SUSCEPTIBILITY
U MAGNETIC PERMEABILITY

MAGNETIC SUSPENSION
Repulsive force support system feasibility study
[NASA-CR-178400] 04 p0402 N88-12497
Status of magnetic suspension technology 07 p0811 N88-14939
The effect of sting interference at low speeds on the drag coefficient of an ellipsoidal body using a magnetic suspension and balance system
[NASA-CR-181611] 13 p1718 N88-20274
The 22nd Aerospace Mechanisms Symposium
[NASA-CP-2506] 14 p1924 N88-21468
Development of a magnetically suspended, tetrahedron-shaped antenna pointing system 14 p1926 N88-21478
Drag measurements on a laminar flow body of revolution in Langley's 13 inch magnetic suspension and balance system
[NASA-CR-182909] 19 p2597 N88-25432
Nutational stability of a satellite equipped with an active magnetic momentum wheel 20 p2784 N88-26513

MAGNETIC SWITCHING
Investigations into the design of multi-terawatt magnetic switches
[DE87-012014] 01 p0040 N88-10254
Magnetically switched power supply system for lasers
[NASA-CASE-NPO-16402-2] 18 p2505 N88-24862

MAGNETIC TAPE RECORDERS
U MAGNETIC RECORDING
U TAPE RECORDERS

MAGNETIC TAPES
Specification for IBM/IBM compatible 3480 tape cartridge
[NASA-TM-100702] 17 p2384 N88-24168
A guide to good magnetic tape management practice for MODAS users --- modular airborne data acquisition system (MODAS)
[RAE-TM-IT-212] 22 p3162 N88-28834

MAGNETIC TRANSDUCERS
Comparison of five readout techniques for an integrated magnetometer 19 p2671 N88-25876

MAGNETIC VARIATIONS
NT GEOMAGNETIC MICROPULSATIONS
NT GEOMAGNETIC PULSATIONS
NT NOCTURNAL VARIATIONS
Narssarssuaq Geophysical Observatory: Magnetic results, 1980-83. Instrumentation and formulas
[ISBN-87-7478-280-0] 03 p0350 N88-12209
Development of high stability fiber optic spectrophotometric systems for study of solar/stellar magnetic activity
[AD-A189327] 13 p1852 N88-21088
Magnetic field hourly averages from the Rome-GSFC experiment aboard Helios 1 and Helio 2
[NASA-TM-89782] 14 p2011 N88-21995

DOD 1985 world magnetic model: Charts and grid values
[AD-A191484] 18 p2541 N88-25080
MAGNETICALLY TRAPPED PARTICLES
NT INNER RADIATION BELT
NT RADIATION BELTS
Conditions for geomagnetically trapping sub-micron lunar ejecta between L = 1.2 and L = 3.1 04 p0521 N88-13203
Magnetic trapping of neutral atoms
[AD-A188473] 12 p1689 N88-20103
Helical ripple transport in stellarators at low collision frequency
[DE88-006431] 13 p1843 N88-21031
Magnetic traps for an anti-hydrogen gas 16 p2269 N88-23572
On the self-trapping of an electromagnetic wave in magnetized plasma
[DE88-701872] 20 p2858 N88-26974
MAGNETIZATION
Static magnetization and microwave loss in shock-modified ferrites
[DE87-012362] 02 p0146 N88-10916
Bulk superconductivity in La2CuO4
[DE88-002509] 09 p1254 N88-17516
Improved magnetization for YBa2Cu3O/sub 7-delta annealed in oxygen above 1000 C
[DE88-003934] 10 p1418 N88-18469
The effect of magnetic impurities and barriers on the magnetization and critical current of fine filament NbTi composites
[DE88-004443] 10 p1419 N88-18472
Magnetization studies of multifilamentary Nb3Sn wires
[DE88-009103] 19 p2735 N88-26243
Superconducting properties of oxygen deficient YBa2Cu3O(sub 7-delta)
[DE88-009969] 22 p3155 N88-28774
Effect of neutron irradiation on critical magnetization current in single crystal YBa2Cu3O(sub 7-delta)
[DE88-009970] 22 p3156 N88-28775
MAGNETO-OPTICS
Limits to the precision of electro-optic and magneto-optic sensors
[PB87-212536] 03 p0323 N88-12040
Optical correlation using the magneto-optic device
[AD-A192342] 20 p2854 N88-26950
MAGNETOACOUSTIC WAVES
Method and apparatus for non-destructive testing of temper embrittlement in steels
[NASA-CASE-LAR-13817-1] 23 p3195 N88-29012
MAGNETOACOUSTICS
The measurement of stress in steels of varying microstructure by Barkhausen and magneto-acoustic emission
[AERE-R-12387] 10 p1343 N88-18027
MAGNETOACTIVITY
NT MAGNETIC FIELD RECONNECTION
NT MAGNETORESISTIVITY
MAGNETOCARDIOGRAPHY
Methods and instrumentation for biomagnetism
[AD-A193811] 23 p3239 N88-29278
MAGNETOELASTIC WAVES
NT MAGNETOACOUSTIC WAVES
MAGNETOELASTICITY
U MAGNETOSTRICTION
MAGNETOGASDYNAMICS
U MAGNETOHYDRODYNAMICS
MAGNETOGRAMS
U MAGNETIC SIGNATURES
MAGNETOHYDRODYNAMIC ACCELERATION
U PLASMA ACCELERATION
MAGNETOHYDRODYNAMIC FLOW
Evolution of the solar wind structure in the outer heliosphere 01 p0112 N88-10721
Comparative plasma tails of Venus and comets 01 p0116 N88-10742
Solar transition region and coronal response to heating rate perturbations 02 p0256 N88-11620
Large-scale horizontal flows from SOUP observations of solar granulation 02 p0256 N88-11621
Sunspot observations from the SOUP instrument on Spacelab 2 02 p0257 N88-11623
The effect of object potentials on the wake of a flowing plasma
[AD-A184038] 03 p0379 N88-12385
Flux tube dynamics and solar/stellar redshift measurements 04 p0503 N88-13095
Subcommittee for MHD theory
[DE88-000596] 05 p0653 N88-14003
Numerical models for high beta magnetohydrodynamic flow
[DE88-001850] 05 p0654 N88-14008
Ultraviolet rocket-spectra of a sunspot 08 p1032 N88-16257
Experimental model of halo plasma observed in small-aspect FRC plasma
[INPE-4159-PRE/1061] 08 p1085 N88-16534
The formation of boundary layers by the entry of low-energy electrons and energetic ions into the Earth's magnetosphere 08 p1095 N88-16590
Evidence of small-scale reconnection in the magnetosphere 08 p1097 N88-16601
Influence of viscosity on the structure of a magnetic neutral layer 08 p1098 N88-16605
A study of single and binary ion plasma expansion into laboratory-generated plasma wakes
[NASA-CR-4125] 10 p1412 N88-18427
An adaptive grid finite difference method for time-dependent Magnetohydrodynamic (MHD) flows and its astrogeophysical applications 11 p1553 N88-19294
Investigation of low energy space plasma
[NASA-CR-182611] 12 p1694 N88-20138
Calculation of the shape of the contact surface at Comet Halley 14 p1995 N88-21892
Advanced diagnostics for reacting flows
[AD-A190485] 15 p2035 N88-22122
MPD (magnetoplasmadynamic) thrust chamber flow dynamics
[AD-A189940] 15 p2137 N88-22751
Basic processes of plasma propulsion
[AD-A192117] 18 p2577 N88-25310
Full-wave calculations in flux coordinates for toroidal geometry
[DE88-010131] 20 p2860 N88-26985
MAGNETOHYDRODYNAMIC GENERATORS
MHD (magnetohydrodynamics) channel development
[DE87-014126] 02 p0237 N88-11498
Gasdynamic effects in linear MHD generators
[ETN-88-91372] 06 p0784 N88-14810
Pulsed power sources based on MHD generators (a state-of-art review)
[DE88-700296] 07 p0935 N88-15677
Laser production and heating of plasma for MHD application
[NASA-TP-2798] 10 p1415 N88-18443
Arcs in cesium seeded noble gases resulting from a magnetically induced electric field
[EUT-87-E-177] 13 p1843 N88-21028
A general 2D electrical model for diagonally connected MHD generators
[DE88-004283] 14 p1984 N88-21835
Acoustical gas core reactor with MHD power generation for burst power in a bimodal system 17 p2403 N88-24290
Fluid dynamics of spherical cavity reactors 17 p2403 N88-24291
Nuclear reactor magnetohydrodynamic power generator for directed energy weapons 17 p2411 N88-24336
Fundamental analysis of space nuclear-MHD generator for gigawatt-level power 17 p2411 N88-24337
Liquid-metal MHD power conversion for space electric systems 17 p2411 N88-24338
Studies for the definition of a Faraday converter for space nuclear systems 17 p2411 N88-24339
A liquid metal MHD concept for multimegawatt space power application 17 p2413 N88-24348
Advanced LMMHD space power generation concept 17 p2415 N88-24364
A multimegawatt space power source radiator design 17 p2427 N88-24436
A nuclear powered space based multimegawatt MHD disc power system 17 p2432 N88-24471
Burst power gas core reactor with MHD power generation 17 p2433 N88-24472
Unified study of plasma/surface interactions for space power and propulsion
[AD-A195971] 24 p3338 N88-29870
MAGNETOHYDRODYNAMIC STABILITY
Equilibrium and tearing stability of thin current layers in magnetic arcades 01 p0118 N88-10754
Numerical simulation of Tokamaks: Ideal MHD equilibrium and stability
[DE87-013452] 02 p0218 N88-11373
Compact torus studies
[DE87-014254] 02 p0237 N88-11496
New directions in Vlasov plasma turbulence and anomalous transport
[DE87-014425] 02 p0238 N88-11500
Field-reversing electron and ion rings for the confinement and heating of plasmas
[DE87-014669] 02 p0238 N88-11505
Vectorization of MHD equilibrium and stability codes
[DE87-753013] 02 p0240 N88-11516
Stability of spheroidal spheromak plasma by use of force-free approximation
[IPPJ-846] 02 p0241 N88-11523
Magnetohydrodynamic stability of spheromak plasma in toroidal flux conserver with rectangular cross section 3. Stability for symmetric modes
[IPPJ-845] 02 p0241 N88-11524
Long wavelength vortices of low frequency interchange modes
[IPPJ-844] 02 p0241 N88-11525
Wavepacket propagation and current startup near the lower hybrid frequency in the torus
[IPPJ-840] 02 p0242 N88-11529
Limit of possible operation of crescent and bean shaped Tokamaks
[IPPJ-837] 02 p0242 N88-11532
Current-filamentation instability in railgun arcs
[AD-A184618] 03 p0269 N88-11693
Stability of low-shear Tokamaks
[DE88-000305] 03 p0379 N88-12383
The role of stellarators in the advanced toroidal program
[DE87-014815] 04 p0491 N88-13025
Transport simulations of the oscillating field current drive experiment in the ZT-40M reversed field pinch
[DE88-000538] 04 p0491 N88-13027
Magnetic fluctuation behaviour of current termination in reversed field pinch
[IPPJ-849] 04 p0492 N88-13034
MHD stability and control for mirror machines 04 p0493 N88-13038
A review of the experimental and theoretical status of the reversed-field pinch
[DE88-000529] 05 p0652 N88-14000
Reversed field pinch plasmas with various boundary conditions
[DE88-000832] 05 p0653 N88-14004
Curvature driven drift mirror instability in the magnetosphere
[IFSI-86-14] 06 p0742 N88-14568
Comments on the theory of absolute and convective instabilities
[PB87-124624] 06 p0783 N88-14808
Experimental research of electron beam instability on the Doppler anomalous effect
[DE88-700565] 07 p0932 N88-15658
Studies on parametric instabilities in high-frequency wave heating of fusion plasmas
[PH-156] 07 p0933 N88-15667
Free-boundary equilibrium problem for helically symmetric plasmas
[DE88-700101] 07 p0934 N88-15674
Simulation an experiment on plasma instability investigation in a tokamak with a divertor
[DE88-700352] 07 p0935 N88-15683
Experimental evaluation for efficiency of excitation slow plasma and cyclotron waves in collective accelerators
[DE88-700566] 07 p0936 N88-15687
The rocket and scatter experiment ROSE: Presentation of the scientific payload 08 p1034 N88-16269
A generalized description of the anomalous Doppler resonance and the stabilizing role of ion dynamics
[INPE-4384-PRE/1204] 08 p1081 N88-16513
Experimental model of halo plasma observed in small-aspect FRC plasma
[INPE-4159-PRE/1061] 08 p1085 N88-16534
Design, construction and operation of a small RFP for turbulent plasma studies
[INPE-4241-PRE/1116] 08 p1087 N88-16545
The effects of viscosity on resistive ballooning modes in line-tied coronal magnetic fields 08 p1097 N88-16599
Conditional sampling in plasma turbulence 08 p1097 N88-16603
Data reduction and analysis of HELIOS plasma wave data
[NASA-CR-182466] 09 p1264 N88-17572
Tokamak with highly elongated cross-section of a plasma
[DE88-700356] 10 p1410 N88-18412
Plasma confinement calculations for TIBER-2
[DE88-004044] 10 p1412 N88-18425
Stability of an RFP (Reversed-Field Pinch) with resistive and distant boundaries
[DE88-004155] 10 p1413 N88-18431
The stability of free-electron lasers against filamentation
[DE88-004712] 10 p1414 N88-18435
Formation of high-Beta plasmas in various modes of operation in TPE-2 12 p1693 N88-20132
The stability of a screw-pinch plasma to global MHD modes 12 p1694 N88-20133
Improved confinement of screw pinch plasmas in SPICA 2 12 p1694 N88-20137
Large scale plasma irregularities observed in the nighttime ionosphere over Natal using a rocket-borne Langmuir probe
[INPE-4422-PRE/1226] 12 p1694 N88-20139

The effects of a dc electric field on the current driven ion cyclotron instability
[AD-A188877] 12 p1695 N88-20142
Effects of toroidal forces in current loops embedded in a background plasma
[AD-A188878] 12 p1695 N88-20143
Fully implicit three-dimensional MHD (magnetohydrodynamics) stability and evolution in toroidal geometry
[DE88-000624] 13 p1842 N88-21023
Magnetohydrodynamic (MHD) simulation of solar prominence formation 13 p1858 N88-21109
Particle simulation research by plasma parametric heating caused by strong laser
14 p1903 N88-21368
Ionization equilibrium and radiative energy losses in a stationary plasma
[DE88-700856] 14 p1984 N88-21832
Preliminary analysis on plasma equilibrium control. Conceptual design study of FY86 FER
[DE88-751441] 14 p1984 N88-21834
Analyses and experiments on the integrity and lifetime predictions of plasma-facing components in fusion reactors
[DE87-702957] 15 p2135 N88-22735
A proposal for the establishment of a center of excellence in theoretical geoplasma research
[AD-A189742] 16 p2231 N88-23327
Proceedings of Symposium on Physics of Target Implosion and Pulsed Power Techniques
[IPPJ-859] 16 p2276 N88-23619
The 2-D magnetohydrostatic configurations leading to flares or quiescent filament eruptions
[NASA-TM-101147] 18 p2595 N88-25423
Electron-acoustic waves in a beam-plasma system
[DE88-702053] 19 p2729 N88-26207
Stability of spheromak against current driven modes: Effects of flux hole on stability
[IPPJ-868] 19 p2730 N88-26211
Modulational instability of electric helicons in a magnetized collisional plasma
[DE88-701885] 20 p2858 N88-26976
Kinetic modulational instability of electron cyclotron waves in plasmas
[DE88-701893] 20 p2859 N88-26978
Reminimization of energy integral and stability limit for non-ideal MHD (magnetohydrodynamic) plasma
[DE88-008422] 21 p3018 N88-27911
On plasma stability under anisotropic random electric field influence
[DE88-702422] 21 p3019 N88-27918
Density fluctuations in currentless high beta plasmas in Heliotron E
[DE88-752310] 23 p3283 N88-29550
A survey of the current experimental database for lower hybrid current-drive and heating
[DE88-009830] 23 p3283 N88-29552
Numerical simulations of resistive magnetohydrodynamic instabilities in a poloidal divertor tokamak
[DE88-010768] 23 p3285 N88-29559

MAGNETOHYDRODYNAMIC TURBULENCE
NT PLASMA TURBULENCE
Evolution of mean square magnetic vector potential in compressible, two-dimensional, magnetofluid turbulence
[AD-A184985] 05 p0651 N88-13990
Coronal heating by means of helical magnetohydrodynamic turbulence
[AD-A187084] 10 p1410 N88-18413
Study of resistive pressure-gradient-driven turbulence
[DE88-005062] 10 p1414 N88-18441

MAGNETOHYDRODYNAMIC WAVES
NT ELECTROSTATIC WAVES
NT PLASMA WAVES
Interactions of oblique interplanetary discontinuities and their manifestations during STIP intervals 15-19
01 p0119 N88-10758
The acceleration of winds by MHD waves in open magnetic structures 04 p0506 N88-13109
MHD energy fluxes for late type dwarfs
04 p0512 N88-13148
Solar corona and solar wind 08 p1094 N88-16584
Small scale MHD wave processes in the solar atmosphere and solar wind 08 p1098 N88-16608
MHD waves in the solar atmosphere
08 p1098 N88-16609
Hydromagnetic cavity eigenmodes in a non-uniform plasma 08 p1098 N88-16610
Observation of a hydromagnetic wave in the earth's magnetosphere
[AD-A188942] 12 p1644 N88-19841
Shear Alfven spectrum of analytic high-Beta equilibria
12 p1694 N88-20136
Resonant Alfven wave instabilities driven by streaming fast particles 13 p1855 N88-21104
Alfven waves in plasma with finite ion temperatures
14 p1972 N88-21769
MHD bending waves in a current sheet
[NASA-TM-101149] 18 p2579 N88-25323
Magnetohydrodynamic wave propagation in the solar wind
[DE88-702411] 21 p3032 N88-27995
The study of hydromagnetic waves and RF heating using the TORTUS tokamak, the development of diagnostic techniques based on submillimeter lasers and the gyrotron, and gas discharge 24 p3431 N88-30419

MAGNETOHYDRODYNAMICS
Fundamentals of numerical magnetohydrodynamics
[DE87-011769] 01 p0100 N88-10656
Plasma properties
[DE87-013662] 01 p0101 N88-10663
Comparison of MHD simulation for the February 1986 events with interplanetary observations by the spacecraft Sakigake 01 p0113 N88-10722
A simulation of the IPS variations from a magnetohydrodynamical simulation
01 p0118 N88-10755
Compact torus studies
[DE87-014254] 02 p0237 N88-11496
Computational study of three-dimensional magnetohydrodynamic equilibria in toroidal helical systems
[DE87-753007] 02 p0240 N88-11514
Numerical modeling of slow shocks
[DE87-014768] 04 p0454 N88-12808
Implementation of a 3-D nonlinear MHD calculation on the Intel hypercube
[DE87-014637] 04 p0479 N88-12949
Numerical simulation of the Reversed Field Pinch
[AD-A184353] 04 p0491 N88-13023
Rotation of magnetized particle in electrically conducting viscous medium 06 p0770 N88-14733
Coupling of microscopic and macroscopic processes in the Earth's magnetotail 08 p1095 N88-16588
The application of liquid-metal MHD (magnetohydrodynamics) to renewable energy sources
[DE88-003083] 09 p1251 N88-17495
Two-dimensional analysis for a scrapeoff and divertor regions with an MHD model. Conceptual design study of FY86 FER
[DE88-751059] 09 p1251 N88-17497
Applications of Lie group methods to the equations of magnetohydrodynamics 10 p1411 N88-18422
Self-similar solutions of MHD equations of plasma filament in the case of complete degenerated ultrarelativistic electron gas
[DE88-700684] 10 p1412 N88-18426
The relation of solar wind structure to hydromagnetic discontinuities
[DE88-004304] 10 p1431 N88-18546
Plasma rotation in a tokamak
[DE88-700855] 12 p1693 N88-20128
Experience with and ways to upgrade accuracy of hydromagnetic surveys in ocean
13 p1787 N88-20692
Implementation of a 3-D nonlinear MHD (magnetohydrodynamics) calculation on the Intel hypercube
[DE88-000625] 13 p1816 N88-20848
Time dependent MHD models for the cometary magnetosphere 14 p1997 N88-21900
Cometary MHD and chemistry: Application to Halley
14 p2000 N88-21922
ALEX results: A comparison of measurements from a round and a rectangular duct with 3-D code predictions
[DE88-005947] 15 p2135 N88-22741
Gigawatt, closed cycle, vapor core-MHD space power system conceptual design study
17 p2433 N88-24473
Generation of flux tube waves in stellar convection zones. 1: Longitudinal tube waves
[NASA-TM-101152] 17 p2451 N88-24561
MHD (magnetohydrodynamic) thermal hydraulic analysis of three-dimensional liquid metal flows in fusion blanket ducts
[DE88-009929] 19 p2731 N88-26219
Blanket technology experiments at Argonne National Laboratory
[DE88-010006] 19 p2731 N88-26220
Magnetohydrodynamic squeeze film
[DE88-701876] 20 p2810 N88-26669
Proceedings of the 2nd US-Japan Workshop on Advanced Plasma Modeling, volume 3
[IPPJ-867] 20 p2855 N88-26957
MACH2: A two-dimensional magnetohydrodynamic simulation code for complex experimental configurations
[AD-A192285] 20 p2860 N88-26988
Global and local magnetohydrodynamic relaxations
[DE88-752602] 21 p3018 N88-27913
Piecewise-parabolic methods for systems of hyperbolic conservation laws in multiprocessing environments
[DE88-010202] 23 p3248 N88-29329
The interaction of Io with the plasma torus
23 p3308 N88-29704
Theoretical modeling of accelerating arc plasmas
[AD-A195606] 24 p3432 N88-30426

MAGNETOIONIC PLASMA
U PLASMAS (PHYSICS)

MAGNETOMETERS
NT VARIOMETERS
Interplanetary magnetic field effects on the interaction of the solar wind with Venus 06 p0805 N88-14910
Comparison of five readout techniques for an integrated magnetometer 19 p2671 N88-25876
Carrier transport in semiconductor magnetic sensors under nonuniform fields 19 p2672 N88-25888
Studies of the intact human brain: Implications for performance 21 p2977 N88-27684

MAGNETOMETRY
U MAGNETIC MEASUREMENT

MAGNETOPAUSE
The formation of boundary layers by the entry of low-energy electrons and energetic ions into the Earth's magnetosphere 08 p1095 N88-16590
Evidence of small-scale reconnection in the magnetosphere 08 p1097 N88-16601
An unusual magnetopause encounter by AMPTE-UKS
08 p1097 N88-16602
Experimental evidence of micro-nonequilibrium on the magnetopause and further predictions
08 p1098 N88-16606
A study of the magnetic field annihilation process in the magnetosphere and some geotechnical applications
[DE88-004165] 10 p1355 N88-18096

MAGNETOPLASMADYNAMICS
Plasma thruster development
[AD-A184173] 04 p0408 N88-12536
MPD (magnetoplasmadynamic) thrust chamber flow dynamics
[AD-A189940] 15 p2137 N88-22751
Fundamental studies on MPD thrusters
[AD-A190307] 15 p2137 N88-22753
Physical fluid mechanics in MPD thrusters
[AD-A190309] 15 p2138 N88-22754
MPD (magnetoplasmadynamic) thruster advanced pumping system concepts
[AD-A190513] 15 p2138 N88-22756
Basic processes of plasma propulsion
[AD-A192117] 18 p2577 N88-25310
The effects of magnetic nozzle configurations on plasma thrusters
[NASA-CR-183096] 19 p2732 N88-26223
Performance and lifetime assessment of MPD arc thruster technology
[NASA-TM-101293] 24 p3336 N88-29860

MAGNETOPLASMAS
U PLASMAS (PHYSICS)

MAGNETORESISTIVITY
Nature of gigantic resistance fluctuations in metal-oxide-semiconductor wires
[DE88-002905] 09 p1256 N88-17533
Spin disorder resistivity and bare Curie temperature in the ferromagnetic superconductor ErRh4B4
[DE88-003016] 10 p1415 N88-18445
Normal and superconducting state properties of La2-xSr/sub x/CuO4
[DE88-003013] 10 p1416 N88-18450
Magnetic impurities in superconductors
[DE88-006917] 14 p1986 N88-21846
The Shubnikov de Haas effect in narrow-gap semimagnetic semiconductors
[ETN-88-92249] 14 p1988 N88-21861
Electrical conduction in thin film carbons
[AD-A191726] 18 p2491 N88-24780
Electron-Rayleigh wave interaction in thin film carbons
[AD-A191727] 18 p2492 N88-24781
Anomalous temperature-dependent negative magnetoresistance in pregraphitic carbons
[AD-A191725] 19 p2619 N88-25535
Anomalous RF magnetoresistance in copper at 4 K
[DE88-010232] 19 p2722 N88-26162

MAGNETOSPHERE-IONOSPHERE COUPLING
Model of solar-wind magnetosphere coupling
04 p0525 N88-13211
Studies of ionosphere/magnetosphere dynamics using SABRE and HILAT
[AD-A190947] 16 p2232 N88-23333
Investigations of magnetosphere-ionosphere coupling relevant to operational systems
[AD-A195972] 24 p3391 N88-30195
Corona-solar wind coupling review
[AFGL-TR-87-0203] 24 p3458 N88-30575

MAGNETOSPHERES
MAXIE 1
[AD-A189688] 14 p1882 N88-21247

Characteristics of solitary waves and weak double layers in the magnetospheric plasma
[IRF-PREPRINT-105] 24 p3431 N88-30418

MAGNETOSPHERIC ELECTRON DENSITY
Electrostatic VLF emission determined from rocket and satellite experiments 08 p1002 N88-16068
Field-aligned fluxes of energetic electrons related to the onset of magnetospheric substorms 08 p1096 N88-16595
Approximate analytical formulae for electron density and collision frequency in the natural and nuclear-disturbed ionosphere and inner magnetosphere
[AD-A193129] 21 p2972 N88-27654

MAGNETOSPHERIC ION DENSITY
The polar ionosphere and interplanetary field
[AD-A185386] 05 p0624 N88-13822

MAGNETOSTATIC FIELDS
Boundary element method for three-dimensional magnetostatic fields in terms of vector variables
[EL-61] 15 p2122 N88-22649

MAGNETOSTATICS
Boundary element method for three-dimensional magnetostatic fields in terms of vector variables
[EL-61] 15 p2122 N88-22649
Algorithm for accounting the conditions in infinity for two-dimensional magnetostatics problems
[DE88-701673] 16 p2264 N88-23541

MAGNETOSTRICTION
Static magnetization and microwave loss in shock-modified ferrites
[DE87-012362] 02 p0146 N88-10916
Ferromagnetic mitigation of electromagnetic pulse effects
[AD-A185685] 06 p0694 N88-14258
High density ion implanted contiguous disk bubble technology
[AD-A190169] 15 p2143 N88-22789
Research work completed at the Naval Surface Warfare Center Solid State Group of the Radiation Division
[AD-A191627] 18 p2582 N88-25339

MAGNETOTELLURIC PROFILING
U MAGNETIC SURVEYS

MAGNETOVARIOGRAPHS
U VARIOMETERS

MAGNETRON SPUTTERING
Method of producing high T(subc) superconducting NBN films
[NASA-CASE-NPO-16681-1-CU] 17 p2446 N88-24543
Equipment for building and testing superconductive flux flow electronic devices
[AD-A192959] 21 p2936 N88-27436
Preparation of superconducting YBa2Cu3O(sub 7-x) films by magnetron sputtering
[DE88-009977] 23 p3289 N88-29583
The lubricating properties of magnetron sputtered MoS2
[ESA-ESTL-76] 24 p3381 N88-30136

MAGNETRONS
Initial operation of a high-power whispering-gallery-mode gyrotron
[DE88-002500] 07 p0857 N88-15207

MAGNETS
NT ELECTROMAGNETS
NT FERRIMAGNETS
NT PERMANENT MAGNETS
NT SUPERCONDUCTING MAGNETS
NT WIGGLER MAGNETS
Present status of the high resolution spectrometers
[CEBAF-PR-87-029] 02 p0234 N88-11478

MAGNIFICATION
Taper sectioning to magnify the interface thickness of a dissimilar metal joint
[RFP-3890-REV] 03 p0333 N88-12099
Application of magnification xeroradiography to advanced ceramics
[DE88-009965] 20 p2778 N88-26473

MAGNIFIERS
U MAGNIFICATION

MAGNITUDE
NT STELLAR MAGNITUDE
The absolute total magnitudes of periodic comets and their variations 14 p1994 N88-21887
Cometary magnitude distribution: The tabulated data 14 p1995 N88-21888
Comet P/Halley: Visual magnitude estimates and gas production 14 p2007 N88-21968

MAGNONS
Non-lattice matched metallic superlattices
[DE87-011512] 04 p0497 N88-13062
Brillouin scattering from collective spin waves in magnetic superlattices
[DE88-005347] 12 p1697 N88-20154

MAGSAT SATELLITES
Spaceborne magnetometry 12 p1644 N88-19846

MAIN SEQUENCE STARS
NT DWARF NOVAE
NT DWARF STARS
NT FLARE STARS
NT RED DWARF STARS
NT SUN
PG 0308 + 096: A short-period white dwarf + dM binary with strongly modulated H-alpha emission 04 p0509 N88-13132
Stellar cycle variability of solar-like stars: A sneak preview 04 p0510 N88-13136
Relations between chromospheric and coronal structure, flux-flux correlations and convective zone properties 04 p0510 N88-13138
Broadband linear polarization and chromospheric CaII H and K line emission in late-type main sequence stars 04 p0511 N88-13140
Activity in warm stars 04 p0511 N88-13142
Emission features in IRAS LRS spectra of MS, S and CS stars 04 p0514 N88-13163
Spin-up and spin-down on the way to the main sequence 04 p0518 N88-13181
Mass loss from evolved stars 11 p1569 N88-19394
Activity-rotation relations for lower main sequence stars 23 p3298 N88-29640

MAINE
Revised Uniform Summary of Surface Weather Observations, Loring AFB, Maine, Parts A - F
[AD-A188201] 14 p1947 N88-21610

MAINTAINABILITY
Improving repairability of gears 02 p0158 N88-10989
An independent evaluation of the CH-46 Safety Reliability and Maintainability Program (SR and M)
[AD-A186310] 07 p0817 N88-14971
Supportability in aircraft systems through technology and acquisition strategy applications
[AD-A186465] 08 p0949 N88-15759
Preliminary analysis of an integrated logistics system for OSSA payloads. Volume 4: Supportability analysis of the 1.8m centrifuge 12 p1584 N88-19481
Statistical aspects of reliability, maintainability and availability
[AD-A188491] 12 p1634 N88-19783
Determining system maintainability as a probability
[DE88-007722] 19 p2679 N88-25927
Behavioral, psychological and demographic predictors of physical fitness
[AD-A192697] 21 p2986 N88-27733
Reliability and Maintainability (R and M)
[AD-A193857] 23 p3224 N88-29187

MAINTENANCE
NT AIRCRAFT MAINTENANCE
NT FILE MAINTENANCE (COMPUTERS)
NT SPACE MAINTENANCE
NT SPACECRAFT MAINTENANCE
Naval Aviation Integrated Logistics: Technical users guide version 1.0
[DE87-013368] 01 p0001 N88-10001
Rivista Tecnica Selenia, volume 10, number 2
[ETN-87-90763] 01 p0011 N88-10064
Optimum dimensioning of field service centers: Analysis of the problem and solutions thereof 01 p0012 N88-10066
Space Assembly, Maintenance, and Servicing Study (SAMSS) 01 p0015 N88-10089
Spacecraft Systems Working Group report 01 p0015 N88-10091
Space station assembly/servicing capabilities 01 p0016 N88-10100
Wet deposition and snowpack monitoring operations and quality assurance manual
[PB87-212817] 01 p0064 N88-10413
Optimization of a controlled two-server maintenance system
[INPE-4202-PRE/1083] 01 p0107 N88-10694
DEDALE: An expert system for analog circuit maintenance 02 p0128 N88-10809
Airworthiness of long-life jet transport structures 03 p0265 N88-11674
Diagnostics aid for mass spectrometer trouble-shooting
[DE88-000350] 03 p0324 N88-12049
Software maintenance in scientific and engineering environments: An introduction and guide
[NASA-CR-177409] 04 p0479 N88-12954
Avionic corrosion 05 p0547 N88-13332
US Naval Air Force avionic and electrical system corrosion prevention and control maintenance 05 p0547 N88-13334
Turbine engine supportability study for Army Aviation Systems Command (AVSCOM)
[DE88-002339] 07 p0820 N88-14984
Documentation in a software maintenance environment
[AD-A185892] 07 p0901 N88-15459
Rotorcraft transmission 08 p0956 N88-15802
Embedded expert system for space shuttle main engine maintenance 08 p1058 N88-16382
Expert systems relations in space applications 08 p1059 N88-16391
Verification of a micro-thrusting model to maintain satellites in low orbit
[AD-A186874] 09 p1133 N88-16793
The knowledge-based software assistant 09 p1204 N88-17213
Concept of a programmable maintenance processor applicable to multiprocessing systems
[NASA-TM-100406] 09 p1223 N88-17333
Micro PAVER concept and development airport pavement management system
[AD-A187360] 11 p1441 N88-18598
Profilometer for bomb-damage-repaired airfield pavements and measurement of pavement upheaval. Report 1: Technology evaluation
[AD-A187985] 11 p1442 N88-18601
Long term measurement network for FIFE
[NASA-CR-182491] 12 p1646 N88-19857
Turnaround operations analysis for OTV. Volume 1: Executive summary
[NASA-CR-179316] 13 p1729 N88-20340
Turnaround operations analysis for OTV. Volume 3: Technology development plan
[NASA-CR-179318] 13 p1729 N88-20342
Remote maintenance design activities and research and development accomplishments for the compact ignition tokamak
[DE88-006980] 16 p2279 N88-23645
Costs and benefits of AC propulsion
[PB88-173380] 16 p2287 N88-23691
The Environment for Application Software Integration and Execution (EASIE) version 1.0. Volume 4: System installation and maintenance guide
[NASA-TM-100576] 17 p2386 N88-24185
Aerospace energy systems laboratory: Requirements and design approach
[NASA-TM-100423] 17 p2390 N88-24206
Selection of a handling and maintenance option for the SP-100 ground engineering system test 17 p2402 N88-24285
Predictive corrosion modeling, volume 1
[AD-A191229] 18 p2485 N88-24739
A perspective of PC-based probabilistic risk assessment
[DE88-006715] 18 p2568 N88-25251
Mutually exclusive alternatives by clustering
[DE88-007707] 20 p2882 N88-27115
Evaluation of explosive bonding for patching aluminum with aluminum
[AD-A193303] 21 p2913 N88-27285
Avionic and electrical system corrosion prevention and control maintenance 22 p3054 N88-28119
Maintenance of vision-related components 23 p3242 N88-29296
Maintenance and supply options
[NASA-CR-172062] 24 p3332 N88-29837
Fuel effects on flame radiation and hot-section durability 24 p3347 N88-29925

MAINTENANCE TRAINING
Field evaluation of interactive simulation for maintenance training: SH-3 helicopter electro-mechanical bladefold system
[AD-A185923] 07 p0821 N88-14991
Air Force Human Resources Laboratory technical reports and technical papers
[AD-A186830] 09 p1201 N88-17200

MALDIVE ISLANDS
Application of SPOT data to renewable resources in the Maldives 22 p3109 N88-28469

MALES
Meta-analysis of leadership differences between males and females and the effect on performance
[AD-A187769] 11 p1564 N88-19361
Human factor in engineering work 12 p1663 N88-19970
Individual functional typology of sympathoadrenal system as indicator of physiological status in adverse environments 12 p1665 N88-19979

MALFUNCTIONS
A research on pilot performance in the case of aircraft malfunction
[ETN-87-90652] 02 p0217 N88-11369
A framework for real-time distributed expert systems: On-orbit spacecraft fault diagnosis, monitoring and control 08 p1066 N88-16440
TES: A modular systems approach to expert system development for real time space applications 08 p1066 N88-16441

Long term measurement network for FIFE
[NASA-CR-182491] 12 p1646 N88-19857
TALOS: A distributed architecture for intelligent monitoring and anomaly diagnosis of the Hubble Space Telescope 17 p2388 N88-24193

MALI
SPOT images and geochemical mapping of lateritic covers in southern Mali 22 p3105 N88-28438

MAMMALS
NT CATS
NT DOGS
NT HUMAN BEINGS
NT MICE
NT MONKEYS
NT PRIMATES
NT RATS
General biological character of adaptive capacity of mammalian metabolism in response to diverse and extreme environmental factors 08 p1047 N88-16324
Some process control/design considerations in the development of a microgravity mammalian cell bioreactor 09 p1197 N88-17174
Physiological and ecological implications of coupled heat- and water-transport mechanisms of endotherms and vegetation
[DE88-004170] 10 p1352 N88-18081

MAN
U HUMAN BEINGS

MAN ENVIRONMENT INTERACTIONS
Desertification in the Sahelian and Sudanian Zones of West Africa
[PB87-217063] 03 p0345 N88-12183
Disturbance and recovery of Arctic Alaskan tundra terrain. A review of recent investigations
[AD-A184442] 04 p0467 N88-12887
International geosphere-biosphere program: A study of global change
[PB88-142393] 11 p1510 N88-19021
System-wide medium-term environment programme for the period 1990-1995: Strategies of the United Nations system for the environment
[UNEP/GCSS.I/2] 12 p1641 N88-19826
An efficient model for changes of global climate and composition of the atmosphere due to human activities
[ETN-88-92359] 20 p2827 N88-26775

MAN MACHINE SYSTEMS
NT MAN-COMPUTER INTERFACE
A methodology for dynamic task allocation in a man-machine system
[DE87-007373] 01 p0077 N88-10492
System adaptivity and the modelling of stereotypes --- human-computer interaction
[NPL-DITC-91/87] 01 p0077 N88-10494
Input devices for tasks using interactive video
[NPL-DITC-87/87] 01 p0080 N88-10510
A rule-based system for arrival sequencing and scheduling in air traffic control 02 p0129 N88-10815
Nowcasting microbursts using Doppler radar in a forecaster-computer environment 02 p0200 N88-11246
A research on pilot performance in the case of aircraft malfunction
[ETN-87-90652] 02 p0217 N88-11389
A review of computer-assisted photo interpretation research at USAETL (US Army Engineer Topographic Laboratories)
[AD-A184034] 03 p0348 N88-12186
Architecture for dynamic task allocation in a man-robot symbiotic system
[DE87-013872] 03 p0362 N88-12277
A scientific workstation operator-interface for accelerator control
[DE87-014689] 03 p0362 N88-12278
Ground vehicle convoying
[DE88-000360] 04 p0502 N88-13088
A general architecture for intelligent training systems 06 p0796 N88-14875
Tools and technologies for expert systems: A human factors perspective 06 p0797 N88-14882
FAA air traffic control operations concepts. Volume 1: ATC background and analysis methodology
[AD-A185979] 07 p0818 N88-14973
Measurement and modification of sensorimotor system function during visual-motor performance
[AD-A186351] 07 p0889 N88-15387
Development and testing of an interactive procedure for the improvement of objective analyses
[AD-A186595] 08 p1040 N88-16290
Third Conference on Artificial Intelligence for Space Applications, part 1
[NASA-CP-2492-Pt-1] 08 p1055 N88-16360
Intelligent man/machine interfaces on the space station 08 p1063 N88-16418
Interfacing the expert: Characteristics and requirements for the user interface in expert systems 08 p1063 N88-16419
Space languages 08 p1063 N88-16420
Case-based reasoning for space applications: Utilization of prior experience in knowledge-based systems 08 p1065 N88-16433
A framework for real-time distributed expert systems: On-orbit spacecraft fault diagnosis, monitoring and control 08 p1066 N88-16440
Helicopter human factors research 09 p1109 N88-16644
Rotorcraft handling-qualities design criteria development 09 p1109 N88-16645
A piloted simulation investigating handling qualities and performance requirements of a single-pilot helicopter in air combat employing a helmet-driven turreted gun
[AD-A186878] 09 p1116 N88-16689
Analysis of tasks for dynamic man/machine load balancing in advanced helicopters
[DE88-003735] 09 p1117 N88-16696
Dynamic function allocation in fighter cockpits
[AD-A185397] 09 p1201 N88-17199
Comparison of alphanumeric data entry methods for advanced helicopter cockpits
[AD-A186934] 09 p1201 N88-17201
First Annual Workshop on Space Operations Automation and Robotics (SOAR 87)
[NASA-CP-2491] 09 p1203 N88-17206
Development of a comprehensive software engineering environment 09 p1203 N88-17211
An intelligent training system for payload-assist module deploys 09 p1204 N88-17214
Development and experimentation of an eye/brain/task testbed 09 p1205 N88-17219
Crew interface with a telerobotic control station 09 p1213 N88-17273
Crew interface with windshear systems 10 p1275 N88-17631
Medical and psychological problems of assuring flight safety under present conditions 10 p1359 N88-18123
Motion planning and control of robot manipulators via application of a computer graphics animated display 11 p1496 N88-18932
A worked example of an application of the SAINT simulation program
[AD-A186198] 11 p1524 N88-19097
Realtime pilot model parameter identification
[AD-A188873] 12 p1584 N88-19476
The ESA/Fokker service end-effector subsystem. A robotic/man-compatible servicing approach 12 p1587 N88-19502
Ground based supervisory and programming system for automatic experiment execution in orbit 12 p1590 N88-19519
Man-tended options for European space robotics 12 p1593 N88-19538
OMV man/system simulation integration: A preliminary analysis and recommendation
[NASA-CR-182602] 12 p1671 N88-20005
NAVLAB: An autonomous navigation testbed
[AD-A189049] 13 p1720 N88-20283
A personalized and prescriptive decision aid for choice from a database of options
[AD-A186726] 13 p1811 N88-20820
Mental models of mechanical systems: Individual differences in qualitative and quantitative reasoning
[AD-A189035] 13 p1812 N88-20823
Human problem solving in dynamic environments. Understanding and supporting operators in large-scale, complex systems
[AD-A189539] 13 p1812 N88-20826
F-16 simulator for man-in-the-loop testing of aircraft control systems (SIMTACS)
[AD-A189675] 14 p1870 N88-21178
Construction of a multidimensional questionnaire to determine interindividual differences in controlling attention
[DFVLR-FB-87-45] 14 p1952 N88-21637
Improving the man-machine interface to robotic systems
[NPL-DITC-100/87] 14 p1953 N88-21641
Human interfaces in remote driving
[DE88-006843] 14 p1953 N88-21643
Conflict resolution in cooperative systems
[AD-A190351] 15 p2104 N88-22535
Toward a mathematical formalism of performance, task difficulty, and activation 16 p2239 N88-23372
Capitalizing on failure through case-based inference
[AD-A190927] 16 p2255 N88-23480
Development and testing of a predictive methodology for optimization of man-machine interface in future avionics systems 17 p2304 N88-23780
Crewstation Information and Development System (CIDS) 17 p2304 N88-23781
A change in system design emphasis: From machine to man 17 p2304 N88-23782
Psychosensory cockpit ergonomics, advantages of intelligent information systems 17 p2304 N88-23784
Experience in the integration of human engineering effort with avionics systems development 17 p2305 N88-23793
A look toward the future of complex avionics systems development using the USAF Test Pilot School's avionics systems test training aircraft 17 p2306 N88-23797
Teleoperator human factors study
[NASA-CR-178930] 17 p2382 N88-24162
Dialog design: General requirements and analysis of an Ada system --- user interface design
[FOA-C-20691-2.7] 17 p2385 N88-24177
Human problem solving in complex dynamic environments
[AD-A190788] 18 p2551 N88-25142
Eye and head response to an attention cue in a dual task paradigm
[AD-A191052] 18 p2551 N88-25143
An advanced prototyping tool for human factors design
[AD-A187290] 18 p2552 N88-25149
A graphical, intelligent interface for discrete-event simulations
[DE88-000522] 18 p2557 N88-25181
Man versus machine: The role of astronauts in extravehicular activity 19 p2699 N88-26045
Introduction to human factors
[DE88-009021] 19 p2711 N88-26103
Preliminary study within a project for the development of intelligent assistance to piloting: Formal description of combat pilot expertise and implementation of an interactive system to represent operations
[CERMA-87-31] 20 p2833 N88-26806
Interaction management in CAD systems with a history mechanism
[CWI-CS-R8756] 20 p2840 N88-26851
Review of past and current trials and uses of unmanned vehicles
[AD-A194527] 22 p3084 N88-28311
General operational and training visual concerns 23 p3242 N88-29295
Artificial intelligence applied to process signal analysis 23 p3252 N88-29359
Prediction and measurement of human pilot dynamic characteristics in a manned rotorcraft simulation
[NASA-CR-183246] 24 p3410 N88-30297
Haptic exploration in humans and machines: Attribute integration and machine recognition/implementation
[AD-A193692] 24 p3410 N88-30299
Artificial intelligence in a mission operations and satellite test environment 24 p3416 N88-30334
Integrated resource scheduling in a distributed scheduling environment 24 p3417 N88-30342
Barriers to Information Transfer and Approaches Toward Their Reduction
[AGARD-CP-430] 24 p3437 N88-30458

MAN-COMPUTER INTERFACE
Gender and cognitive style differences at the human-computer interface
[NPL-DITC-90/87] 01 p0077 N88-10493
System adaptivity and the modelling of stereotypes --- human-computer interaction
[NPL-DITC-91/87] 01 p0077 N88-10494
Concepts and techniques for support of real time distributed operating systems
[AD-A184491] 03 p0367 N88-12307
Advanced Information Processing System (AIPS) proof-of-concept system functional requirements I/O network system services
[NASA-CR-181481] 03 p0384 N88-12412
SDVS (State Delta Verification System) 5 users' manual
[AD-A184339] 04 p0478 N88-12943
The ISI (Information Sciences Institute) grapher: A portable tool for displaying graphs pictorially
[AD-A184354] 04 p0478 N88-12944
User interface for a partially incompatible system software environment with non-ADP users
[DE88-001518] 04 p0482 N88-12968
Window system: A toolbox for interactive computer graphics
[PB87-234282] 06 p0756 N88-14637
Communications for the DTroll distributed database system
[AD-A185579] 06 p0791 N88-14853
A review of hypertext in a NASA project management context 06 p0793 N88-14859
A general architecture for intelligent training systems 06 p0796 N88-14875
Using multiple dialog modes in a user-system interface to accomodate different levels of user experience: An experimental study
[AD-A186115] 07 p0899 N88-15444

The crustal dynamics intelligent user interface anthology
[NASA-TM-100693] 08 p1067 N88-16448
User engineering: A new look at system engineering 09 p1206 N88-17231
Crew interface with a telerobotic control station 09 p1213 N88-17273
Methods of eliciting information from experts
[AD-A187468] 10 p1372 N88-18189
A digital circuit design environment
[AD-A188831] 12 p1623 N88-19709
Online aiding for human-computer interfaces
[AD-A189239] 13 p1815 N88-20842
A model for graphical interaction --- computer graphics
[CWI-CS-R8718] 13 p1818 N88-20866
Parallel graphical output from dialogue cells
[CWI-CS-R8719] 13 p1818 N88-20867
Application of expert systems in project management decision aiding
[NASA-CR-180762] 13 p1850 N88-21074
Applicability of nonlinear programming in decision support systems: Realization of user-friendly software
[REPT-87-42] 14 p1957 N88-21663
DataViews: A personalizable, interactive, data display system for the decisionmaker
[AD-A188509] 14 p1991 N88-21868
Investigation into the development of computer aided design software for space based sensors
[NASA-CR-180772] 15 p2107 N88-22552
Extension of computer based algorithms by operator analysts
[NASA-CR-182798] 15 p2111 N88-22575
The Scientific and Technical Information Network (STINET). Foundation for evolution
[AD-A189750] 15 p2148 N88-22822
Toward a mathematical formalism of performance, task difficulty, and activation 16 p2239 N88-23372
Resource management in dialog cell specification (DICE) method
[CWI-CS-R8746] 16 p2248 N88-23433
Virtual interface environment 17 p2381 N88-24153
An advanced prototyping tool for human factors design
[AD-A187290] 18 p2552 N88-25149
Knowledge acquisition tool implementation
[AD-A190415] 18 p2555 N88-25164
Development of training implying man-machine interface: From the aircraft to the spacecraft 19 p2700 N88-26052
Introduction to human factors
[DE88-009021] 19 p2711 N88-26103
The relationship between system response time, working memory, and task complexity: An empirical investigation
[DE88-000976] 19 p2711 N88-26105
SIMS: Single Interface to Multiple Systems
[AD-A192264] 20 p2837 N88-26832
The assessment of human/computer performance using human productivity measures: MIPS and BIPS are MEGAFLOPS
[DE87-013491] 21 p2993 N88-27750
The effect of input device on user performance with a menu-based natural language interface
[AD-A193095] 21 p2996 N88-27772
Image processing using a parallel architecture
[AD-A192833] 21 p3002 N88-27803
What's on the menu? Friendlier computers
[AD-A194393] 22 p3135 N88-28637
Knowledge elicitation for an operator assistant system in process control tasks 23 p3253 N88-29366
Intelligent interfaces for expert systems 23 p3258 N88-29397
A space station onboard scheduling assistant 23 p3259 N88-29402
Intelligent interface design and evaluation 23 p3260 N88-29405
MANIP --- spacecraft modeling program
[MANIP-217A] 24 p3335 N88-29855
Contributions to engineering models of human-computer interaction, volume 1
[AD-A195590] 24 p3409 N88-30295

MANAGEMENT
NT CONFIGURATION MANAGEMENT
NT CONTRACT MANAGEMENT
NT DATA MANAGEMENT
NT ENGINEERING MANAGEMENT
NT ENVIRONMENT MANAGEMENT
NT FINANCIAL MANAGEMENT
NT FOREST MANAGEMENT
NT INDUSTRIAL MANAGEMENT
NT INFORMATION MANAGEMENT
NT INVENTORY CONTROLS
NT INVENTORY MANAGEMENT
NT LAND MANAGEMENT
NT LOGISTICS MANAGEMENT
NT PERSONNEL MANAGEMENT
NT PROJECT MANAGEMENT
NT RESEARCH MANAGEMENT
NT RESOURCES MANAGEMENT
NT SAFETY MANAGEMENT
NT SYSTEMS MANAGEMENT
NT WATER MANAGEMENT
NT WEAPON SYSTEM MANAGEMENT
Issues in air transport and airport management
[PB87-204509] 02 p0124 N88-10782
Evaluating software testing methods to reduce testing duplication in US Army communications equipment acquisition
[AD-A186961] 09 p1216 N88-17292
Report of the Defense Science Board Summer Study on Technology Base Management
[AD-A188560] 13 p1851 N88-21078
Management: A bibliography for NASA managers
[NASA-SP-7500(22)] 14 p1991 N88-21867
Napping and human functioning during prolonged work
[AD-A190228] 15 p2102 N88-22525
Models and metrics for software management and engineering
[NASA-CR-182953] 17 p2389 N88-24200
Management and the executive
[AD-A190778] 18 p2587 N88-25374
Department of Defense Statement on the Balanced Technology Initiative to the Committee on Armed Services, United States Senate, 100th Congress, second session
[AD-A191841] 18 p2588 N88-25378
Idea processing for creativity and management
[DE88-006110] 19 p2714 N88-26113
Anatomy of an organizational change effort at the Lewis Research Center
[NASA-CR-4146] 19 p2739 N88-26264

MANAGEMENT ANALYSIS
FAA air traffic control operations concepts. Volume 1: ATC background and analysis methodology
[AD-A185979] 07 p0818 N88-14973
Field dependence-independence and its relationship to flight training performance
[AD-A188888] 12 p1670 N88-20003

MANAGEMENT INFORMATION SYSTEMS
CNET (Chief of Naval Education and Training) Program Automated Tracking System (CPATS): A comprehensive study
[AD-A184694] 03 p0385 N88-12418
University research initiative research program summaries
[AD-A184876] 05 p0658 N88-14035
Information needs analysis for the Aeronautical Systems Division Executive Information System
[AD-A186912] 09 p1261 N88-17556
Management Information and Downloader Interface System (MIDIS)
[AD-A186978] 09 p1261 N88-17557
Management information systems design implications: The effect of cognitive style and information presentation on problem solving
[AD-A188850] 12 p1705 N88-20205
Report of the Defense Science Board Summer Study on Technology Base Management
[AD-A188560] 13 p1851 N88-21078
Management and the executive
[AD-A190778] 18 p2587 N88-25374
IEMIS (Integrated Emergency Management Information System) floodplain mapping based on a LIDAR derived data set
[AD-A193071] 21 p2966 N88-27616
Database design and management in engineering optimization
[AD-A193325] 21 p3003 N88-27813
Developing a connector selection DBMS (database management system) using NIAM (Nijssen's Information Analysis Methodology)
[DE88-008110] 21 p3028 N88-27972
Reliability and Maintainability (R and M)
[AD-A193857] 23 p3224 N88-29187
The P-3 Scheduling Support System (P-3 S3)
[AD-A194824] 24 p3436 N88-30450

MANAGEMENT METHODS
NT DELPHI METHOD (FORECASTING)
Cost savings possible with Air Force conversion to JP-8 as its primary fuel
[AD-A183784] 01 p0030 N88-10192
A study of the Department of Defense configuration management policies and procedures as applied to the FA-18 Strike/Fighter program
[AD-A184872] 05 p0657 N88-14034
Design and management of research projects
[PB88-106380] 07 p0941 N88-15721
Operations research in management?
[MBB-Z-138/87] 10 p1311 N88-17835
Using SIR (Scientific Information Retrival) system for data management during a field program
[DE88-001555] 10 p1424 N88-18508
Distributed transaction processing and the Camelot system
[AD-A188614] 13 p1821 N88-20885
Application of expert systems in project management decision aiding
[NASA-CR-180762] 13 p1850 N88-21074
Management: A bibliography for NASA managers
[NASA-SP-7500(22)] 14 p1991 N88-21867
Propagation management for no-acknowledge HF communications links 18 p2502 N88-24843
Management and the executive
[AD-A190778] 18 p2587 N88-25374
Weight savings in aerospace vehicles through propellant scavenging
[NASA-TM-100900] 19 p2605 N88-25470
Engineering research centers and their evaluation
[PB88-180054] 19 p2739 N88-26262
Overview of the TITAN-2 reversed-field pinch aqueous fusion power core design
[DE88-008170] 20 p2857 N88-26966
Integration of SPOT data into a geocoded information system 22 p3098 N88-28400
Carrying out space projects 22 p3160 N88-28811
The Ariane line 22 p3161 N88-28828
Advanced information processing system: Input/output network management software
[NASA-CR-181678] 23 p3264 N88-29431
SDI (Strategic Defense Initiative) battle management/C3 (Command, Control and Communications) algorithms technology program plan
[AD-A194357] 23 p3275 N88-29495
Technical change needs organizational change 24 p3438 N88-30466

MANAGEMENT PLANNING
NT PRODUCTION PLANNING
NT PROJECT PLANNING
Documentation as a management strategy for reaching goals in high-risk research-oriented projects
[DE87-012394] 01 p0105 N88-10685
Space Construction
[NASA-CP-2490] 02 p0138 N88-10870
Marshall Space Flight Center's role in EASE/ACCESS mission management 02 p0139 N88-10875
An allotment planning concept and related computer software for planning the fixed satellite service at the 1988 space WARC
[NASA-TM-100244] 03 p0308 N88-11944
Comparison of pascal and the dBASE 3 PLUS language in programming an inventory management system
[AD-A184027] 03 p0365 N88-12300
Experimental use of artificial intelligence for (future) ATC systems
[PB87-106449] 04 p0482 N88-12970
Strategic management of research and development: A literature search
[NASA-CR-182337] 06 p0790 N88-14847
An evaluation of project scheduling techniques in a dynamic environment
[AD-A187057] 09 p1260 N88-17554
Information needs analysis for the Aeronautical Systems Division Executive Information System
[AD-A186912] 09 p1261 N88-17556
State of the art of natural language processing
[AD-A188112] 11 p1530 N88-19136
Science and technology in India
[PB88-134747] 11 p1564 N88-19362
District information system of National Information Centre
[PB88-134739] 11 p1565 N88-19373
A logical structuration for an administration of space projects
[INPE-4435-TDL/310] 12 p1585 N88-19482
Prototype manufacturing techniques for reducing cost, schedule, and technical risk 12 p1702 N88-20189
Minimizing development flight test time and cost in the US Air Force 12 p1703 N88-20192
Implementing information systems/office automation in an Air Force environment
[AD-A188956] 12 p1707 N88-20218
Management: A bibliography for NASA managers
[NASA-SP-7500(22)] 14 p1991 N88-21867
The challenges and opportunities of supersonic transport propulsion technology
[NASA-TM-100921] 17 p2307 N88-23806
Anatomy of an organizational change effort at the Lewis Research Center
[NASA-CR-4146] 19 p2739 N88-26264
Engine component retirement for cause. Volume 1: Executive summary
[AD-A192730] 20 p2760 N88-26371
Managing microcomputer applications: A primer and guide to good practice
[AD-A192992] 20 p2835 N88-26817
Large space projects --- management 22 p3159 N88-28805

Development and demonstration of an on-board mission planner for helicopters
[NASA-CR-177482] 24 p3328 N88-29817
Reduced flexibility in processing Titan 4 space launch vehicles at Cape Canaveral Air Force Station
[AD-A194908] 24 p3332 N88-29834

MANAGEMENT SYSTEMS
NT FLIGHT MANAGEMENT SYSTEMS
NT MANAGEMENT INFORMATION SYSTEMS
Comparison of pascal and the dBASE 3 PLUS language in programming an inventory management system
[AD-A184027] 03 p0365 N88-12300
Chicago's O'Hare Runway Configuration Management System (RCMS). Volume 1: Description of the operational software
[AD-A185886] 07 p0821 N88-14990
Chicago's O'Hare Runway Configuration Management System (RCMS). Volume 2: Users guide
[AD-A186222] 08 p0953 N88-15783
Using SIR (Scientific Information Retrival) system for data management during a field program
[DE88-001555] 10 p1424 N88-18508
Micro PAVER concept and development airport pavement management system
[AD-A187360] 11 p1441 N88-18598
RIAR automated research and management systems
[DE88-700934] 12 p1706 N88-20209
GTE battery management system: State of charge indicator evaluation
[DE88-006800] 15 p2052 N88-22272
A timestamp ordering mechanism with dynamic selection of rollback objects 16 p2257 N88-23489
Background to the UK military requirements for engine usage, condition and maintenance management systems 22 p3033 N88-28004

MANDELSTAM REPRESENTATION
Stimulated Mandelstam-Brillouin scattering during forward scattering of light 08 p1078 N88-16499
Secondary gauge conditions in field theory
[DE88-701499] 15 p2147 N88-22814

MANEUVERABILITY
Airframe/store compatibility 05 p0545 N88-13323
Future fighter maneuverability for air combat
[MBB/LKE-1/S/PUB/120] 10 p1312 N88-17843
On the maneuvering of vehicles
[AD-A187632] 10 p1427 N88-18521
Assessments of maneuverability with the TeleOperated Vehicle (TOV)
[AD-A191584] 21 p2993 N88-27751
Passive multipath target tracking in an inhomogeneous acoustic medium
[AD-A193284] 21 p3012 N88-27873
A second look at MIL prime flying qualities requirements 24 p3314 N88-29740

MANEUVERABLE REENTRY BODIES
NT LIFTING REENTRY VEHICLES
Maneuverable reentry vehicle trajectory footprints: Calculation and properties
[DE88-004726] 10 p1292 N88-17726

MANEUVERABLE SPACECRAFT
NT AEROSPACE PLANES
NT HOTOL LAUNCH VEHICLE
NT X-30 VEHICLE
National aero-space plane: A technology development and demonstration program to build the X-30
[GAO/NSIAD-88-122] 17 p2301 N88-23764

MANEUVERS
NT AIRCRAFT MANEUVERS
NT EVASIVE ACTIONS
NT HOVERING
NT ORBITAL MANEUVERS
NT ORBITAL RENDEZVOUS
NT SIDESLIP
NT SPACECRAFT DOCKING
NT SPACECRAFT MANEUVERS
Dynamics of spacecraft control laboratory experiment (SCOLE) slew maneuvers
[NASA-CR-4098] 01 p0014 N88-10082
Approach trajectory planning system for maximum concealment
[NASA-TM-88258] 02 p0227 N88-11435
How space, the fourth operational medium, supports operational maneuver
[AD-A184742] 03 p0373 N88-12346
Analytical investigation of the dynamics of tethered constellations in Earth orbit (phase 2)
[NASA-CR-179218] 04 p0408 N88-12533
Combined problem of slew maneuver control and vibration suppression
[NASA-CR-181537] 04 p0455 N88-12817
Aircraft flight test trajectory control
[NASA-CR-179428] 09 p1120 N88-16707
ADAM (Acquisition Deployment and Maneuvering): The space game
[AD-A189512] 12 p1685 N88-20078
Nonlinear flying quality parameters based on dynamic inversion
[AD-A192146] 18 p2464 N88-24627
Large planar maneuvers for articulated flexible manipulators
[NASA-CR-183079] 19 p2711 N88-26104
The effects of RCS jet firing on the isolated Orbiter and mated coast phases of the glide return to launch site maneuver at Mach number 6 (IA302B)
[NASA-CR-180223] 20 p2766 N88-26403
Performance of GPS-aided INS during high-dynamic maneuvers
[AD-A194624] 23 p3175 N88-28903
The principles of mass and maneuver applied to space operations
[AD-A194037] 23 p3276 N88-29500

MANGANESE
Sintered steels of high resistance alloyed to Nb, Mo, Mn and Si
[DE87-703546] 04 p0415 N88-12573
Effects of MN dispersoids on near threshold fatigue crack growth in 2134 type alloys 05 p0603 N88-13692
Concentration coefficients of elements in ferromanganese nodules relative to ocean sediments 06 p0726 N88-14464
Remote acoustic sounding of ferromanganese nodules 06 p0727 N88-14471
Ferromanganese nodules of Antarctic sector in Pacific Ocean 06 p0727 N88-14472
CdTe(110)-Mn interface reaction and the formation of non-equilibrium ternary semimagnetic semiconductor alloys
[AD-A187593] 10 p1422 N88-18491
Preparation and characterization of Cu2Zn1-xMnxGeS4
[AD-A188113] 11 p1556 N88-19315
Electron paramagnetic resonance studies of Mn(2+) in 2-6 semiconductor alloys 11 p1560 N88-19340
An experimental method for species concentration measurements in a welding arc using laser-induced fluorescence
[DE88-005638] 13 p1778 N88-20636
Kinetic of oxidation to air of a Fe-Al-Mn alloy system at 600-800(sup 0)C temperature range
[DE88-702309] 21 p2920 N88-27330

MANGANESE ALLOYS
Development of ultrafine grains and related properties in Hadfield manganese steels
[DE87-011884] 01 p0024 N88-10154
A comparison of high damping shape memory alloys with Cu-Mn-based and Fe-Cr-based alloys
[AD-A184110] 04 p0414 N88-12566
X-ray measurements of phason distortion in ion-implanted Al-Mn
[DE87-014566] 07 p0937 N88-15694
Influence of non-metallic elements in the mechanical properties of 20 Mn Mo Ni 55 steel
[DE88-700412] 10 p1300 N88-17775
Response of Fe-Cr-Mn austenitic alloys to thermal aging neutron irradiation
[DE88-003415] 10 p1302 N88-17785
The role of composition and microstructure gradients on weld metal properties and behavior
[DE88-004956] 10 p1303 N88-17791
Evaporation characteristics of elements during vacuum arc remelting of alloy A-286 15 p2055 N88-22248
Strain hardening at large strains in aluminum alloys
[DE88-007415] 18 p2484 N88-24737
Development of fine-grained carbide-particle hardened Hadfield manganese steels
[DE88-006919] 19 p2617 N88-25523
Reduced-activation austenitic stainless steels: The Fe-Cr-C system
[DE88-006091] 20 p2773 N88-26442

MANGANESE COMPOUNDS
NT MANGANESE OXIDES
Structure and function of the manganese complex involved in photosynthetic oxygen evolution determined by X-ray adsorption spectroscopy and electron paramagnetic resonance spectroscopy
[DE88-010360] 21 p2985 N88-27725

MANGANESE OXIDES
An investigation of the rechargability of certain modified forms of MnO2
[AD-A185919] 07 p0847 N88-15140

MANIFOLDS (MATHEMATICS)
NT RIEMANN MANIFOLD
Direction dependent connections of complex manifolds and their submanifolds
[DE87-703073] 02 p0225 N88-11419
A theory for the articulation of robot manipulators 03 p0333 N88-12097
Phenomenological implications of the blown-up orbifolds
[DE87-014608] 03 p0373 N88-12347
Transient periodic behavior related to a saddle-node bifurcation
[ETN-88-91321] 05 p0642 N88-13928
There exists a C sup infinity symbol Kupka-Smale diffeomorphism of S sup 2 with neither sinks nor sources
[PB87-225967] 06 p0769 N88-14725
Error questions in the computation of solution manifolds of parametrized equations
[AD-A188648] 12 p1684 N88-20068
Multicontinuations method and strong regular perturbations of linear operators
[DE88-701375] 16 p2263 N88-23533
Linearization along invariant manifolds and a generalization of the Hartman-Grobman theorems for degenerate singularities of vector fields in R cubed
[REPT-87-80] 20 p2845 N88-26886
Geometry of superconformai manifolds, part 1
[DE88-702405] 21 p3011 N88-27863
Geometry of superconformal manifolds, part 2
[DE88-702406] 21 p3011 N88-27864

MANIPULATION
U MANIPULATORS

MANIPULATORS
NT REMOTE MANIPULATOR SYSTEM
Telepresence work station system definition study, part 2
[NASA-CR-172006] 01 p0013 N88-10071
Telerobotics 01 p0015 N88-10090
Traction-drive seven degrees-of-freedom telerobot arm: A concept for manipulation in space
[DE87-010895] 01 p0054 N88-10346
Exact solution of the inverse problem for a six-link manipulator with a mechanical offset
[DE87-702646] 01 p0054 N88-10349
Augmenting the control of a flexible manipulator with passive mechanical damping 01 p0055 N88-10350
A methodology for dynamic task allocation in a man-machine system
[DE87-007373] 01 p0077 N88-10492
Human factors in robotic system design discussed 02 p0158 N88-10988
Robotics and Intelligent Systems Program
[DE87-014561] 02 p0223 N88-11404
Structure-dependent matrix representation of manipulator kinematics and its inverse solution
[DE87-752966] 02 p0229 N88-11447
A theory for the articulation of robot manipulators 03 p0333 N88-12097
Architecture for dynamic task allocation in a man-robot symbiotic system
[DE87-013872] 03 p0362 N88-12277
Modeling and control of large flexible vehicles in the atmosphere and space
[AD-A185368] 05 p0555 N88-13377
Control of a flexible one-link manipulator
[AD-A185035] 05 p0590 N88-13598
Trajectory control of robot manipulators with closed-kinematic chain mechanism
[NASA-TM-89305] 05 p0591 N88-13605
Cartesian path control of a two-degree-of-freedom robot manipulator
[NASA-CR-182331] 05 p0639 N88-13908
Heuristic control of the Utah/MIT dextrous robot hand 06 p0793 N88-14858
Dynamics, control and sensor issues pertinent to robotic hands for the EVA retriever system 06 p0796 N88-14876
Goal driven kinematic simulation of flexible arm robot for space station missions 08 p1059 N88-16388
Solid modelling for the manipulative robot arm (power) and adaptive vision control for space station missions 08 p1061 N88-16409
Control system simulation for a single-link flexible arm
[AD-A187037] 09 p1174 N88-17035
Robotic planner expert system (RPLANES) 09 p1209 N88-17246
An optimal resolved rate law for kinematically redundant manipulators 09 p1212 N88-17268
Telerobotic research at NASA Langley Research Center 09 p1213 N88-17269
Manipulator arm design for the Extravehicular Teleoperator Assist Robot (ETAR): Applications on the space station 09 p1213 N88-17270
Telerobotic truss assembly 09 p1213 N88-17272
Design conditions and workspace for the generally-proportioned 3-hinge spherical wrist for robots 10 p1339 N88-18003
Recursive forward dynamics for multiple robot arms moving a common task object
[NASA-CR-182526] 10 p1340 N88-18008
Tactile sensing and inverse problems
[AD-A187464] 10 p1340 N88-18011
Parameter identification and sensitivity analysis for a robotic manipulator arm
[NASA-CR-181608] 10 p1385 N88-18272

Adaptive control of a manipulator with a flexible link
[NASA-CR-181637] 11 p1476 N88-18807
Changes in the turbulent boundary layer structure associated with net drag reduction by outer layer manipulators
[NASA-CR-178152] 11 p1483 N88-18853
Time varying controller design for robot manipulator control
[AD-A188094] 11 p1494 N88-18919
Kinematic and dynamic analyses of the Stanford/JPL robot hand
[DE88-004637] 11 p1495 N88-18923
Real-time kinematic and dynamic analysis and adaptive model following control of manipulator arms
11 p1495 N88-18927
Motion planning and control of robot manipulators via application of a computer graphics animated display
11 p1496 N88-18932
Free boundary problems arising in the control of a flexible robot arm
[AD-A189124] 12 p1634 N88-19781
Intelligent control of robot manipulators in hazardous environments
[DE88-003305] 13 p1778 N88-20638
Modelling and simulation of a rate controlled manipulator arm --- Hermes
[NLR-TR-87010-U] 13 p1778 N88-20639
Force distribution and trajectory control for closed kinematic chains with applications to walking machines
13 p1779 N88-20642
Dynamics of high-speed mechanisms with elastic members 13 p1779 N88-20643
The dynamic control of robotic manipulators in space
[NASA-CR-182710] 13 p1779 N88-20646
New representation for kinematics of manipulator
[DE88-751446] 14 p1917 N88-21445
An efficient gradient projection optimization scheme for a seven-degree-of-freedom redundant robot with spherical wrist
[DE88-005440] 14 p1919 N88-21453
Telerobotic operation of conventional robot manipulators
[DE88-005718] 15 p2073 N88-22363
Design, development and evaluation of Stanford/Ames EVA prehensors
[NASA-CR-182688] 15 p2105 N88-22540
A three dimensional non-singular modelling of rigid manipulators
[AD-A189707] 15 p2116 N88-22604
Path following robot
[AD-A190960] 16 p2215 N88-23217
Microgravity mechanisms and robotics program
16 p2219 N88-23237
Base reaction optimization of manipulators with redundant kinematics 16 p2219 N88-23238
Microgravity manipulator demonstration
16 p2219 N88-23242
Accurate positioning of long, flexible ARM's (Articulated Robotic Manipulator) 16 p2219 N88-23243
Contribution to the adaptive dynamic control of a robot manipulator
[LAAS-87-350] 16 p2255 N88-23475
Remote maintenance design activities and research and development accomplishments for the compact ignition tokamak
[DE88-006980] 16 p2279 N88-23645
Space spider crane
[NASA-CASE-LAR-13411-1-SB]
17 p2312 N88-23828
A design analysis for an automated robotic workpiece manipulator 17 p2344 N88-23975
Point accessibility and primary workspace of simple six-link robots 17 p2345 N88-23976
Precise computer controlled positioning of robot end effectors using force sensors
[NASA-CR-182887] 17 p2391 N88-24213
Energy optimal trajectory planning for robot manipulators and autonomous vehicles 17 p2437 N88-24497
The coordination of multiple robotic manipulators
[AD-A190869] 18 p2522 N88-24963
Kinematics, dynamics and control of a closed chain mechanism manipulator 18 p2523 N88-24967
Real-time implementation of a kinematic optimization scheme for seven-degree-of-freedom redundant robots with spherical wrists
[DE88-006785] 18 p2524 N88-24974
A computational model of motor behavior
[AD-A191179] 18 p2553 N88-25152
The efficacy of using human myoelectric signals to control the limbs of robots in space
[NASA-CR-182901] 18 p2553 N88-25155
Introduction to compliance in programming of robots
[ETN-88-92189] 18 p2561 N88-25201
Analysis of a closed-kinematic chain robot manipulator
[NASA-CR-183031] 18 p2561 N88-25206
Flexible tactile sensing arrays for robotics: Architectural robustness and yield considerations
19 p2671 N88-25878
Automatic calibration of space based manipulators and mechanisms
[NASA-CR-182804] 19 p2676 N88-25912
Underwater simulation for space teleoperation
19 p2698 N88-26040
Man versus machine: The role of astronauts in extravehicular activity 19 p2699 N88-26045
Underwater robotics in the service of oil field exploitation: The Running and Interconnecting Tool (RIT) in the East Frigg field (North Sea) 19 p2699 N88-26049
Large planar maneuvers for articulated flexible manipulators
[NASA-CR-183079] 19 p2711 N88-26104
Mobile remote manipulator system for a tetrahedral truss
[NASA-CASE-MSC-20985-1] 20 p2765 N88-26398
Design of a controller to reduce residual vibration in the positioning control of flexible robotic manipulators
20 p2808 N88-26658
Optimization of performance criteria with bounded joint velocities for robots with one degree of redundancy
[DE88-003915] 20 p2810 N88-26670
An introduction to robot joint control methods
[NLR-TR-86080-U] 20 p2811 N88-26677
Simulation of space manipulator operations (EUROSIM)
[NLR-MP-87017-U] 20 p2811 N88-26678
Experiments in adaptive control of a very flexible one link manipulator 20 p2842 N88-26865
Development of a hybrid simulator for robotic manipulators
[AD-A193119] 21 p2956 N88-27557
Control of free-flying space robot manipulator systems
[NASA-CR-183017] 21 p2956 N88-27562
Control of free-flying space robot manipulator systems
[NASA-CR-183104] 21 p2957 N88-27563
General expression of manipulator kinematics
[DE88-753430] 21 p2957 N88-27567
Dexterous hands: Optimizing grasp by design and planning 21 p2958 N88-27572
The VITE model: A neutral command circuit for a generating arm and articulator trajectories
[AD-A192715] 21 p2987 N88-27734
The analysis and control of robotic manipulators operating at or near kinematically singular configurations
22 p3084 N88-28315
Motion planning with obstacles and dynamic constraints 23 p3222 N88-29175
Study on design and control of torque-controlled manipulators
[NASA-TT-20197] 23 p3223 N88-29183
Implementation of a flexible link model in a designed robot system, using the finite element method
[ETN-88-92902] 23 p3243 N88-29303
A robotic system for automation of logistics functions on the Space Station 23 p3260 N88-29407
Next-generation space manipulator
23 p3263 N88-29428
Low-speed longitudinal flying qualities of modern transport aircraft 24 p3314 N88-29738
Modeling robot flexibility for endpoint force control
[AD-A195923] 24 p3380 N88-30132
Adaptive control in positioning a rigid-flexible robot arm
[AD-A195194] 24 p3422 N88-30367
Simulation of a two link robot manipulator with elastic members
[AD-A196014] 24 p3422 N88-30368
A standard architecture for controlling robots
[AD-A195929] 24 p3423 N88-30371

MANNED MANEUVERING UNITS
Personnel occupied woven envelope robot power
[NASA-CR-182367] 07 p0856 N88-15196
Personnel occupied woven envelope robot
23 p3260 N88-29408

MANNED MARS MISSIONS
Aeroassisted-vehicle design studies for a manned Mars mission
[NASA-TM-100031] 03 p0271 N88-11700
Aeroassisted manned transfer vehicle (TAXI) for advanced Mars Transportation: NASA/USRA 1987 Senior Design Project
[NASA-CR-181478] 03 p0275 N88-11736
Manned Mars mission accommodation: Sprint mission
[NASA-TM-100598] 16 p2290 N88-23711
Applications of nuclear power to lunar and Mars missions 17 p2417 N88-24377

MANNED ORBITAL LABORATORIES
NT SPACELAB
Metallurgy laboratory for Columbus, executive summary
[SNIAS-813-CA/TS] 02 p0157 N88-10980
Thermophysical Properties Measurement Facility (TPMF) --- Columbus space station
[ESA-CR(P)-2417] 02 p0157 N88-10981
A preliminary study of a fluid science laboratory for space station (Columbus). Part 4: Executive summary
[NLR-TR-87023-L-PT-4] 02 p0170 N88-11072
Man-Tended Free Flyer operational design features
12 p1585 N88-19485
Mission profiles of the MTFF co-orbiting with the US Space Station 12 p1585 N88-19487
Analysis of RVD operations in manned space missions
12 p1586 N88-19494
On a knowledge based assisted system for highly autonomous control of experiment-manipulators in the Man-Tended Free Flyer 12 p1588 N88-19505
Microgravity User Support Center (MUSC) for EURECA, Spacelab and Columbus missions
12 p1660 N88-19947
Arguments for manned or unmanned spacecraft activities
[REPT-46/87] 17 p2309 N88-23813

MANNED ORBITAL SPACE STATIONS
U SPACE STATIONS

MANNED SPACE FLIGHT
NT SPACE SHUTTLE MISSION 31-A
NT SPACE SHUTTLE MISSION 31-B
NT SPACE SHUTTLE MISSION 41-C
NT SPACE SHUTTLE MISSION 51-L
NT SPACE SHUTTLE MISSION 61-B
NT SPACE SHUTTLE MISSIONS
USSR report: Space
[JPRS-USP-87-003] 01 p0009 N88-10050
A matter-antimatter propulsion system for manned interstellar flight
[DE87-013311] 02 p0141 N88-10885
Progress in European CELSS activities
03 p0358 N88-12252
National Aeronautics and Space Administration space station proposal, fiscal year 1988
[S-HRG-100-328] 05 p0659 N88-14043
Preliminary estimates of galactic cosmic ray exposures for manned interplanetary missions
[NASA-TM-100519] 05 p0661 N88-14058
JPRS report: Science and technology. USSR: Space Biology and Aerospace Medicine, volume 21, no. 4, July - August 1987
[JPRS-USB-88-002] 07 p0893 N88-15412
Bibliography of space biology and medicine
07 p0897 N88-15435
Safety philosophy, policy, and requirements for manned spaceflight. Volume 1: Executive summary
[HEG-0886/1036-VOL-1] 08 p0962 N88-15826
Electrochemical processing of solid waste
[NASA-CR-182413] 08 p0967 N88-15852
JPRS report: Science and technology. USSR: Space
[JPRS-USP-87-006] 08 p1001 N88-16063
Integrity control of carbon fiber reinforced plastics (CFRP) structural elements. Conclusion with respect to the control methodology of CFRP primary structures in manned space flight and the implications to the design, analysis and testing of CFRP structural elements, executive summary
[MBB-TR-RB517-014/85] 09 p1139 N88-16824
Study on long term evolution towards European manned space flight. Volume 1: Executive summary
[MBB-RA3-004/87-VOL-1] 10 p1286 N88-17689
Present stage of space medicine
10 p1364 N88-18151
Certain aspects of human metabolism during spaceflights of varying duration
[NASA-TT-20215] 10 p1369 N88-18181
Basic results of medical studies during prolonged manned flights on-board the Salyut-7/Soyuz-T orbital complex
[NASA-TT-20217] 10 p1369 N88-18182
Liquid ventilation: New data and possible use in space medicine 12 p1654 N88-19908
Fluid volume changes in astronauts: How they fit our understanding of physiology 12 p1655 N88-19919
Radiation problems in manned space flight with a view to the Space Station 12 p1658 N88-19934
The influence of space flight on water-salt homeostasis in man and animals 12 p1659 N88-19943
JPRS report: Science and technology. USSR: Space
[JPRS-USP-88-002] 13 p1724 N88-20312
Study on long term evolution Towards European Autonomous Manned Spaceflight (STEAMS)
[SNIAS-SE/LS/AP-35-073] 13 p1727 N88-20330
Aeronautics and space report of the President: 1986 activities 13 p1852 N88-21087
International manned flight, USSR-SAR
[NASA-TT-20260] 16 p2166 N88-22914
Human performance issues arising from manned space station missions
[NASA-CR-3942] 18 p2553 N88-25156

Preliminary estimates of radiation exposures for manned interplanetary missions from anomalously large solar flare events
[NASA-TM-100620] 18 p2596 N88-25427
Proceedings of the Colloquium on Space and Sea
[ESA-SP-280] 19 p2695 N88-26016
Similarities between diving operations and space missions 19 p2697 N88-26027
Contribution of ultrasonic Doppler detection of circulating bubbles to human interventions under the sea and in space 19 p2697 N88-26029
History of manned spaceflight
[CNES-NT-121] 21 p3032 N88-28000
Study of biological effects and radiation protection to future European manned space flights
[DGT-33061] 23 p3281 N88-29535
Study on long-term evolution towards European manned spaceflight. Volume 1: Executive summary
[ERNO-OX1-002/88-VOL-1] 24 p3330 N88-29827
JPRS report: Science and technology. USSR: Space
[JPRS-USP-88-001] 24 p3444 N88-30498

MANNED SPACECRAFT
NT AEROSPACE PLANES
NT CHALLENGER (ORBITER)
NT COLUMBUS SPACE STATION
NT DISCOVERY (ORBITER)
NT HERMES MANNED SPACEPLANE
NT HOTOL LAUNCH VEHICLE
NT MANNED ORBITAL LABORATORIES
NT MIR SPACE STATION
NT SALYUT SPACE STATION
NT SOYUZ SPACECRAFT
NT SPACE SHUTTLE ORBITERS
NT SPACE SHUTTLES
NT SPACELAB
NT X-30 VEHICLE
Design study for asteroidal exploitation
03 p0389 N88-12445
Techniques for fire detection
04 p0406 N88-12521
Space station accommodations for lunar base elements: A study
[NASA-TM-100501] 06 p0804 N88-14907
A systems analysis of fire suppression alternatives for the US space station
[AD-A189847] 15 p2025 N88-22064
Arguments for manned or unmanned spacecraft activities
[REPT-46/87] 17 p2309 N88-23813
Hatch cover
[NASA-CASE-MSC-21356-1] 18 p2472 N88-24671
The human element in space: Lessons from Antarctica
[AD-A193440] 21 p2988 N88-27741

MANPOWER
NT SCIENTISTS
MANPRINT handbook for RFP (Request For Proposal) development
[AD-A188321] 13 p1850 N88-21075

MANTLE (EARTH STRUCTURE)
U EARTH MANTLE

MANUAL CONTROL
The optimal control pilot model and applications
24 p3315 N88-29741

MANUALS
NT USER MANUALS (COMPUTER PROGRAMS)
Naval Aviation Integrated Logistics: Technical users guide version 1.0
[DE87-013368] 01 p0001 N88-10001
Wet deposition and snowpack monitoring operations and quality assurance manual
[PB87-212817] 01 p0064 N88-10413
DOE explosives safety manual
[DE88-000831] 04 p0422 N88-12616
A portable hypercube simulator
[DE87-013369] 04 p0478 N88-12947
National Synchrotron Light Source users manual: Guide to the VUV and X-ray beam lines
[DE88-001464] 04 p0490 N88-13020
US Naval Air Force avionic and electrical system corrosion prevention and control maintenance
05 p0547 N88-13334
Development of a prototype H-46 helicopter diagnostic expert system
[AD-A186077] 07 p0809 N88-14924
Standardization of software development
[INPE-4330-NTE/272] 08 p1068 N88-16455
Temperament Structure Scales (TSS). Test manual
[ESA-TT-1069] 09 p1201 N88-17197
ZAP user's manual
[LBL-21270] 11 p1546 N88-19248
User's manual for EULER3DS
[AD-A191048] 16 p2208 N88-23177
Users guide to CAESAR
[BCRS-87-04] 16 p2228 N88-23306
Concurrency efficiency user's manual
[AD-A190884] 16 p2251 N88-23450
Advisory circular: Noise certification handbook
[FAA-AC-36-4B] 17 p2394 N88-24234
Defense Technical Information Center cataloging guidelines
[AD-A192200] 18 p2589 N88-25382
MVS (Multiple Virtual Storage) batch computing and data management at ANL
[DE88-007342] 19 p2718 N88-26137
Technical instructions for a control operating system of the gas flow installation for the solid fuel combustion chamber
[LR-507] 20 p2788 N88-26537
Engineering data compendium. Human perception and performance. User's guide
[LC-87-19560] 21 p2993 N88-27749
SERI standard broadband format: A solar and meteorological data archival format
[DE88-001145] 21 p3028 N88-27975
Avionic and electrical system corrosion prevention and control maintenance 22 p3054 N88-28119
Engineering data compendium. Human perception and performance, volume 1
[LC-87-19560] 22 p3134 N88-28630
Engineering data compendium. Human perception and performance, volume 2
[LC-87-19560] 22 p3134 N88-28631
Engineering data compendium. Human perception and performance, volume 3
[LC-87-19560] 22 p3134 N88-28632

MANUFACTURING
NT COMPUTER AIDED MANUFACTURING
NT LOW GRAVITY MANUFACTURING
NT SPACE MANUFACTURING
Spacecraft Systems Working Group report
01 p0015 N88-10091
NBS (National Bureau of Standards) research reports (April 1987)
[PB87-210258] 01 p0018 N88-10111
Statistically determined nickel cadmium performance relationships 02 p0165 N88-11039
Improved cathode life testing
[REPT-3189-T] 02 p0168 N88-11056
A 1987 progress report of manufacturing techniques for Gravity Probe B gyroscope rotors
[NASA-TM-100312] 02 p0176 N88-11101
Silicon oxidation photoassisted with a continuous wave CO2 laser beam and contribution to the study of silica layers obtained
[LAAS-87-158] 02 p0179 N88-11115
Elevated temperature strain gages
02 p0184 N88-11144
Precision metrology comparing ultrasonic and other techniques for the determination of steel thickness
[DE87-011051] 02 p0230 N88-11452
Study and optimization of a technological process for the fabrication of heterojunction bipolar transistors. Applications to high speed devices
[LAAS-87-134] 02 p0246 N88-11555
Spinoff, 1987
[NASA-TM-89652] 02 p0250 N88-11577
Airworthiness of long-life jet transport structures
03 p0265 N88-11674
Status of titanium alloys R and D described
03 p0298 N88-11876
Requirements for the calibration of mechanical shock transducers
[PB87-227591] 03 p0325 N88-12054
Activities at government research laboratories reported 04 p0403 N88-12503
Research and development on high strength ceramic heaters discussed 04 p0404 N88-12508
Thixotropic surface composition for phenolaldehyde resin laminates
[GB-PATENT-2-180-251-A] 04 p0410 N88-12545
Avionics and corrosion 05 p0547 N88-13336
Development of strength in cements
[PB87-232971] 06 p0684 N88-14189
Design, fabrication and delivery of a miniature Cassegrainian concentrator solar array system
[NASA-CR-179237] 06 p0730 N88-14493
Selection of polymer materials for manufacturing optical parts
[AD-A185898] 07 p0836 N88-15069
Activities report in metal manufacturing
[ISSN-0524-7705] 07 p0839 N88-15086
Powder metallurgical preparation of A15 superconductors
[ETN-88-91072] 09 p1144 N88-16858
Contribution to the design of flexible manufacturing systems: Modeling, simulation, and evaluation of parameters
[ISAL-IDI1-87-04] 09 p1151 N88-16894
Systems integrated human engineering on the Navy's rapid acquisition of manufactured parts/test and integration facility 09 p1206 N88-17226
Software for integrated manufacturing systems, part 1
09 p1211 N88-17261
Software for integrated manufacturing systems, part 2
09 p1211 N88-17262
Communication and control in an integrated manufacturing system 09 p1212 N88-17263
Development of Moire machine vision
09 p1212 N88-17264
Automated Composites, First International Conference, September 10-12, 1986, University of Nottingham, England
[PB87-126199] 10 p1294 N88-17734
Ion chromatography in the manufacture of multilayer circuit boards
[DE88-002428] 10 p1322 N88-17902
Measurements as a process
[DE88-005275] 11 p1497 N88-18938
JPRS report. Science and technology: Europe and Latin America
[JPRS-ELS-87-054] 12 p1573 N88-19406
Presentation of structural component designs for the family of commuter airplanes
[NASA-CR-182568] 12 p1581 N88-19463
JPRS report. Science and technology: Europe and Latin America
[JPRS-ELS-87-055] 12 p1686 N88-20086
Basic research in ceramic and semiconductor science at selected Japanese laboratories, based on a September 1986 visit: Highlights, summary and overview and detailed notes from selected Japanese laboratories
[DOE/ER-0314] 12 p1696 N88-20150
Reducing rotary wing aircraft development time/cost through the use of simulation 12 p1702 N88-20186
The design of aircraft using the decision support problem technique
[NASA-CR-4134] 13 p1721 N88-20291
Development of a manufacturing unit for selective coating of solar absorbers made out of aluminum
[BMFT-FB-T-86-204] 14 p1942 N88-21590
Manufacturing of ultrasonic focused probes
[VTT-RR-487] 15 p2074 N88-22368
Insertions using geometric analysis and hybrid force-position control: Method and analysis
[DE87-013652] 15 p2117 N88-22611
Multivariate analysis and its application
[AD-A189983] 15 p2124 N88-22661
Computer aided design tools for integrated silicon system structures
[ETN-88-92186] 16 p2247 N88-23424
Manufacturing requirements 17 p2297 N88-23745
Preliminary aerodynamic design considerations for advanced laminar flow aircraft configurations
17 p2297 N88-23746
Manufacturing of a ceramic-ceramic composite matrix using the sol-gel procedure
[ETN-88-92157] 20 p2768 N88-26414
Preparation technology for thin film solid electrolyte fuel cells
[PB88-131925] 20 p2821 N88-26735
Application of sol-gel procedures to ceramic composites
[ETN-88-92741] 21 p2921 N88-27338
A small annular combustor of high power density, wide operating range and low manufacturing cost
24 p3351 N88-29951
Advanced planar array development for space station
[NASA-CR-179373] 24 p3389 N88-30181

MANURES
Evaluation of manure as a feedstock for gas turbines
18 p2536 N88-25050

MANY BODY PROBLEM
FDM-FEM zonal method for viscous flow computations over multiple-bodies
[NAL-TR-925T] 02 p0170 N88-11069
Development of many-body methods for flame chemistry and large molecule applications
[AD-A184451] 03 p0284 N88-11789
A periodic small-cluster approach to many-body problems
[DE88-002235] 06 p0763 N88-14683
Whither many-body theory. A summary of the Oulu Conference
[DE88-003095] 11 p1563 N88-19358
Very large vortex calculations in two dimensions
[DE88-005748] 13 p1770 N88-20587
Numerical solution of multibody systems in space applications 14 p1875 N88-21200
Monte Carlo modified method for Green function. Algorithm and computer code for calculations in equal mass many-body system
[DE88-701114] 14 p1957 N88-21667
Corrosion Research Center, University of Minnesota
[DE88-006681] 15 p2041 N88-22160

On new solvable many-body dynamical systems with velocity dependent forces
[PREPRINT-581] 15 p2127 N88-22683
An electron-scattering study of N-15
[ETN-88-92479] 16 p2266 N88-23552
Spatial dynamics of deformable multibody systems with variable kinematic structure 20 p2813 N88-26687
Atomistic simulation of stability, metastability and growth of strained layer structures 20 p2873 N88-27053
Dynamics of interacting galaxies
23 p3299 N88-29647

MANY PARTICLE THEORY
U MANY BODY PROBLEM

MAP MATCHING GUIDANCE
The integration of digital maps in vehicle navigation systems 16 p2225 N88-23286

MAPPING
NT CADASTRAL MAPPING
NT COMPUTER AIDED MAPPING
NT ICE MAPPING
NT PHOTOMAPPING
NT PLANETARY MAPPING
NT SOIL MAPPING
NT THEMATIC MAPPING
NT THERMAL MAPPING
Study of Earth from space and strengthening of economy 01 p0010 N88-10055
NBS (National Bureau of Standards) research reports (April 1987)
[PB87-210258] 01 p0018 N88-10111
Smooth dynamics on the interval (with an emphasis on unimodal maps)
[REPT-87-09] 01 p0086 N88-10555
Correlation between aircraft MSS and LIDAR remotely sensed data on a forested wetland in South Carolina
[NASA-TM-89643] 02 p0193 N88-11204
Components and cycles of a random function
[DE87-014155] 02 p0228 N88-11437
Illustrations of a density-equalizing map projection technique
[DE87-013992] 03 p0339 N88-12130
SPOT 1: First In-Flight Results — conferences
[ISBN-2-85428-177-2] 03 p0340 N88-12143
A review of computer-assisted photo interpretation research at USAETL (US Army Engineer Topographic Laboratories)
[AD-A184034] 03 p0346 N88-12186
East coast gravity validation study
[AD-A184292] 03 p0351 N88-12217
Mapping a battlefield simulation onto message-passing parallel architectures
[NASA-CR-178396] 03 p0363 N88-12287
Phase transition of multifractals
[DE87-014344] 03 p0383 N88-12409
Principles for problem aggregation and assignment in medium scale multiprocessors
[NASA-CR-178379] 04 p0476 N88-12935
Foundations of O-theory 2: Measurements and relation to fuzzy set theory
[DE88-000013] 04 p0485 N88-12986
Scientific and Operational Requirements for TOMS Data
[NASA-CP-2497] 05 p0615 N88-13774
Observation guidelines for a Total Ozone Mapping Spectrometer (TOMS) in geosynchronous orbit
05 p0619 N88-13801
Research needs for hydrocarbon fuels
[DE87-014555] 06 p0687 N88-14209
Mathematical-cartographic modeling of economic utilization of Atlantic Ocean 06 p0726 N88-14469
Fast, colour displays of digital terrain elevation data
[AD-A185596] 06 p0729 N88-14485
Description of data on the Nimbus 7 LIMS map archive tape: Water vapor and nitrogen dioxide
[NASA-TP-2761] 06 p0744 N88-14572
Optimal pre-scheduling of problem remappings
[NASA-CR-178378] 06 p0756 N88-14633
There exists a C sup infinity symbol Kupka-Smale diffeomorphism of S sup 2 with neither sinks nor sources
[PB87-225967] 06 p0769 N88-14725
Preliminary airworthiness evaluation of a UH-1 equipped with a terrain mapping receiver antenna
[AD-A186274] 07 p0819 N88-14980
Determination of network attributes from a high resolution terrain data base
[AD-A186078] 07 p0870 N88-15279
An experimental mapping of the flow field behind a glaze ice shape on a NACA 0012 airfoil
[NASA-CR-180847] 08 p0950 N88-15766
Photogrammetric principles for combining remote sounding and three-dimensional mapping
08 p1012 N88-16135
Laser system for automating topographic terrain survey 08 p1012 N88-16136
Construction of airborne radars for remote sensing
[PB88-113063] 09 p1154 N88-16916
An automatic finite element mesh generator
[AD-A186939] 09 p1216 N88-17291
Navigation planning using quadtrees
[DE88-003706] 09 p1225 N88-17343
A smart, mapping, charting and geodesy control generator, phase 1
[AD-A188184] 10 p1347 N88-18055
An overview of the transactional interpretation of quantum mechanics
[DE88-004236] 10 p1423 N88-18497
Chaos, mappings and spatial complexity in fluids
11 p1484 N88-18860
Contour-to-grid interpolation with nonlinear finite elements: A feasibility study
[AD-A188108] 11 p1503 N88-18980
A digital terrain system for microcomputers
[INPE-4170-PRE/1067] 11 p1505 N88-18987
Reports on cartography and geodesy. Series 1, report 98
[ISSN-0469-4236] 11 p1506 N88-18993
A sky temperature survey at 19.2 GHz using a balloon borne Dicke radiometer for anisotropy tests of the cosmic microwave background 11 p1571 N88-19403
Department of Defense World Geodetic System 1984: Its definition and relationships with local geodetic systems
[AD-A188815] 12 p1639 N88-19811
Comparison of simulation modeling and satellite techniques for monitoring ecological processes
[NASA-CR-182592] 12 p1641 N88-19825
Proceedings of US-Japan Heliotron-Stellarator Workshop, volume 4
[DE88-004787] 12 p1693 N88-20126
Development of an interactive real-time graphics system for the display of vehicle space positioning
[NASA-TM-100429] 13 p1730 N88-20344
The 1987 Airborne Antarctic Ozone Experiment: The Nimbus-7 TOMS data atlas
[NASA-RP-1201] 13 p1791 N88-20714
Bathymetric hazard survey test
[AD-A189150] 13 p1803 N88-20775
Retinotopic mapping of the human visual system with magnetoencephalography
[AD-A189557] 13 p1810 N88-20811
Vegetation mapping using high resolution MSS (multispectral scanner) data: Canopy reflectance and shadow problems encountered and possible solutions
[DE88-004273] 14 p1939 N88-21574
Parallel algorithms for mapping pipelined and parallel computations
[NASA-CR-181655] 14 p1960 N88-21687
Enhanced viscous flow drag reduction using acoustic excitation
[NASA-CR-182734] 15 p2062 N88-22295
Fatigue damage mapping 15 p2084 N88-22423
Geometric restoration of satellite image data
[AD-A190462] 15 p2089 N88-22450
Matched index laser anemometry systems for flow studies in complex geometries 16 p2203 N88-23145
Contributions to geodesy, photogrammetry and cartography. Series 1, number 46 — conference
[ISSN-0469-4244] 16 p2225 N88-23279
Report on the cartographic activities of the Federal Republic of Germany in the period 1984 - 1987
16 p2225 N88-23280
Do we need a new cartography?
16 p2225 N88-23283
Down-to-Earth approach for final projects in Karlsruhe (Federal Republic of Germany)
16 p2226 N88-23292
Urban cartography: A book review
16 p2227 N88-23297
Near-real-time TOMS, telecommunications and meteorological support for the 1987 Airborne Antarctic Ozone Experiment
[NASA-CR-4133] 16 p2233 N88-23338
Updating land-use of the Sao Jose dos Campos municipality through remote sensing data
[INPE-4479-RPE/562] 16 p2287 N88-23693
A proposal for a project entitled assessment of forest resources in Uruguay submitted to the United Nations Industrial Development Organization (UNIDO)
17 p2352 N88-24016
The geometric workstation, a new approach for geometric corrections of remotely sensed data
17 p2352 N88-24017
Mapping from LANDSAT and SPOT satellite imagery
17 p2352 N88-24018
Airborne and spaceborne radar images for geologic and environmental mapping in the Amazon rain forest, Brazil
17 p2353 N88-24021
Mapping soil and rock variation from satellite images in the Sahel 17 p2354 N88-24023
Remote sensing and data integration: Practical solutions for resource managers 17 p2356 N88-24034
Utilization of TM/LANDSAT images in the implanted forests mapping in the Mogi-Guacu Region (SP-Brazil)
17 p2357 N88-24042
CANASATE: Sugar cane mapping by satellite
17 p2358 N88-24046
Structure and dynamics of vegetation in the middle semi-arid tropics. Quixaba's Caatinga (PE): Terrain analysis of MSS/LANDSAT data 17 p2358 N88-24049
Study of fracturing for groundwater research in the Sergipe state with remote sensing products
17 p2359 N88-24052
Implantation of a geo-cartographical information system through microcomputers 17 p2361 N88-24064
Detection of biomass burning and smoke plumes in the Amazon region through NOAA satellite imagery
17 p2365 N88-24085
The 35 mm vertical aerial photographs for mapping stands of bracatinga in different age classes
17 p2366 N88-24087
The breaked anticlines, cuesta and crest homoclines, ortoclinal valleys, and other forms of relief outcrops delineated with the help of remote sensing imagery
17 p2366 N88-24089
Current stage of remote sensing system for cartographic application 17 p2366 N88-24090
Mapping of plant associations and the variation of surface water in the Pantanal Mato-Grossense National Park, through remote sensing techniques
17 p2366 N88-24092
Characteristics of drainage determinations in aerial photographs and relief determination on different scales planialtimetric charts for three soils in the state of Sao Paulo 17 p2367 N88-24095
Criteria for planimetric and altimetric correction of maps restituted from aerial photographs in 1:100,000 scale
17 p2367 N88-24097
Geomorphologic sector maps of Niquizanga-Mayares, province of San Juan, Argentina
17 p2368 N88-24098
Research on enhancing the utilization of digital multispectral data and geographic information systems in global habitability studies
[NASA-CR-182799] 17 p2368 N88-24101
Automated cartographic generalization for linear map features 18 p2532 N88-25021
Drilling investigation of a young magmatic intrusion beneath the Inyo Domes, Long Valley, California: Structural and textural studies
[DE88-006613] 18 p2541 N88-25078
A framework for a theory of mapping
[AD-A191071] 18 p2551 N88-25144
Territorial management program
19 p2682 N88-25942
The impact of hemp production on the development of the municipalities of Araras, Leme, Santa Cruz da Conceicao and Pirassununga 19 p2683 N88-25948
Remote sensing technique applied to vegetation as an aid to municipal planning 19 p2683 N88-25951
Application of 35mm EM aerial reconnaissance photographic format of the municipality of Ubatuba (SP)
19 p2684 N88-25953
Aerial photography as an instrument of atmospheric analysis: Maps of the middle atmosphere and its dynamics, Baixada Santista (SP) 19 p2684 N88-25955
Remote sensing applied to integrated regional development programs 19 p2685 N88-25958
Generalization and the backward propagation neural network
[AD-A191634] 19 p2710 N88-26100
Solar microwave radiation maps measured at Metsaehovi Radio Research Station in 1980-1981
[PB88-193453] 19 p2741 N88-26276
The Viking landing sites: A cartographic perspective
[NASA-CR-177486] 19 p2742 N88-26282
Efficient bit-level, word-level and block-level systolic arrays for matrix-matrix multiplication
[DE88-011331] 20 p2841 N88-26856
IEMIS (Integrated Emergency Management Information System) floodplain mapping based on a LIDAR derived data set
[AD-A193071] 21 p2966 N88-27616
Review of geographic processing techniques applicable to regional analysis
[DE88-010759] 21 p2970 N88-27643
CEEG dynamic brain mapping: A new method to evaluate brain function in different psychological and drug conditions 21 p2977 N88-27685
Geologic applications of SPOT-1, TM, and NOAA-7 data: Finding and defining unmapped structural features
22 p3104 N88-28434
The use of SPOT imagery for topographic mapping
22 p3110 N88-28473

Topographic mapping with SPOT 1 data. A practical approach by the Ordnance Survey
22 p3111 N88-28479
Mapping and urban multi-experimental assessment of SPOT: Mapping results
22 p3112 N88-28483
Production of satellite image maps based on SPOT data
22 p3113 N88-28491
SPOT: A data capture and data updating tool for the French National Geographic Institute's (IGN's) cartographic data base
22 p3114 N88-28497
Some remarks on geodesics in gauge groups and harmonic maps
[DE88-702685] 22 p3115 N88-28510
On the computation of finite invariant sets of mappings
[AD-A193670] 22 p3143 N88-28690
Monotone recurrence relations, their Birkhoff orbits and topological entropy
[AD-A193481] 23 p3276 N88-29504
Mapping of volcanic units at Alba Patera, Mars
23 p3301 N88-29663
Sub-kilometer rampart craters in the equatorial region of Mars: Possible implications for the state and distribution of regolith H2O
23 p3302 N88-29666
Chemical and spectroscopic characterization of a suite of Mars soil analogs
23 p3302 N88-29667
The Martian sedimentary record
23 p3302 N88-29669
Progress in determining the thickness and distribution of volcanic materials on Mars
23 p3302 N88-29670
Geology of six possible Martian landing sites
23 p3304 N88-29682
Spectral reflectance of SNC meteorites: Relationships to Martian surface composition
23 p3304 N88-29683
Evaluation of LANDSAT-TM data for geomorphological mapping
[INPE-4593-PRE/1324] 24 p3386 N88-30168
The use of orbital remote sensing data for low cost ground-water survey
[INPE-4587-PRE/1318] 24 p3386 N88-30170
Use of digital images as a mineral prospecting tool in the tin province of Goias, Brazil
[INPE-4537-PRE/1284] 24 p3387 N88-30173
Implementation of the NCAR (National Centre for Atmospheric Research) graphics package at ARL (Aeronautical Research Laboratory)
[AD-A195163] 24 p3391 N88-30193
Structure of Southwestern Michipicoten Greenstone Belt, Ontario: Evidence for Archean accretion
24 p3397 N88-30228
Supermap for Cray FORTRAN: A user's guide
[NASA-CR-177410] 24 p3412 N88-30308
A digital terrain model system for a microcomputer
[INPE-4610-PRE/1333] 24 p3413 N88-30316
Faulting and its relation to volcanism: Mars western equatorial region
24 p3443 N88-30489

MAPS

NT ASTRONOMICAL MAPS
NT METEOROLOGICAL CHARTS
NT RADAR CLUTTER MAPS
NT RADAR MAPS
NT RELIEF MAPS
X-rays, color, and the Vaughan-Preston gap
04 p0510 N88-13135
Fatigue damage maps
06 p0715 N88-14382
Mathematical-cartographic modeling of economic utilization of Atlantic Ocean
06 p0726 N88-14469
Fast, colour displays of digital terrain elevation data
[AD-A185596] 06 p0729 N88-14485
Protected areas with enhanced bird-aircraft collision risk in the Federal Republic of Germany
[GEOPHYSBDBW-FM-209] 11 p1437 N88-18576
Terrain Analyst Work Station (TAWS) demonstrations
[AD-A188139] 11 p1504 N88-18981
A digital terrain system for microcomputers
[INPE-4170-PRE/1067] 11 p1505 N88-18987
The US Army Electronic Map Data (EMD) initiative
[AD-A188209] 11 p1565 N88-19372
Development of a ground-conductivity map for the area of the Federal Republic of Germany from measured field-strength contours
12 p1615 N88-19656
Mono- and bistatic radar coverage diagrams including diffractive wave propagation
12 p1616 N88-19660
An application of digital cartography updating middle and small scale thematic maps using orbital data
[INPE-4460-TDL/317] 12 p1637 N88-19805
Digital Topographic Support System (DTSS)
[AD-A188304] 12 p1638 N88-19808
Soft maps for US Army electronic map background applications
[AD-A188427] 12 p1638 N88-19809
Relative orientation
[AD-A190385] 15 p2089 N88-22449
PLOT3D (version-5): A computer code for drawing three dimensional graphs, maps and histograms, in single or multiple colours, for mono or stereoscopic viewing
[DE88-701410] 15 p2108 N88-22558
Regularity of the Albanese map for nonoriented surfaces
[DE88-006428] 15 p2126 N88-22679
Contributions to geodesy, photogrammetry and cartography. Series 1, number 46 --- conference
[ISSN-0469-4244] 16 p2225 N88-23279
Report on the cartographic activities of the Federal Republic of Germany in the period 1984 - 1987
16 p2225 N88-23280
Developments in the design of topographic maps in the Federal Republic of Germany: Activities and suggestions
16 p2226 N88-23290
The atlas of regional development
16 p2226 N88-23291
Thailand in maps. Application of the mapping system THEMAK2 for specific purpose atlas preparation
16 p2226 N88-23295
Maps for tourists. A systematic approach to tourist cartography
16 p2227 N88-23296
Urban cartography: A book review
16 p2227 N88-23297
Maps for the blind and methods of their production
16 p2227 N88-23298
Research in enumeration and graph theory with applications to computer science
[AD-A191567] 18 p2556 N88-25171
LO-CO-GRAF (low cost graphics): Generating maps to support command and control/crisis management using small computers
[AD-A193964] 22 p3139 N88-28661
Distortion estimates for negative Schwarzian maps
[AD-A193172] 23 p3228 N88-29209
Polynomial definition of discrete field points of map of diffusion equation, part 1
[AD-A193697] 23 p3271 N88-29467

MARAGING STEELS

Metallography of maraging 350 steel
[DE87-013746] 04 p0418 N88-12591

MARANGONI CONVECTION

Numerical analysis of Marangoni convection in Bridgman method
03 p0319 N88-12014
Flight results of the ESA experiment modules in Materials Science Experiment Rocket (MASER) 1
08 p1033 N88-16261
Marangoni convection in finite cylindrical liquid bridges
[LRT-WE-9-FB-5(1988)] 22 p3078 N88-28277

MARECS MARITIME SATELLITES

A conformal aircraft phased array antenna for airplane-satellite communication in the L band
[ESA-TT-1057] 03 p0305 N88-11926

MARINE BIOLOGY

Compilation of 1986 annual reports of the Navy ELF (Extremely Low Frequency) communications system ecological monitoring program, volume 3
[AD-A184563] 03 p0306 N88-11932
Varifront 3 expedition data report (USNS DE STEIGUER CRUISE 1202-82). Bioluminescence, hydrographic, nutrient, and satellite data from the Gulf of California (November-December 1981)
[AD-A185011] 05 p0620 N88-13805
Remote sensing of ocean colour for studies of biological productivity and biochemical cycles
08 p1042 N88-16296
Relationships between remotely-sensed surface properties and subsurface structure in the ocean
[AD-A189317] 12 p1650 N88-19881
Remote determination of chlorophyll concentration in the ocean using an optical pulse radar
[NASA-TT-20301] 19 p2694 N88-26014

MARINE CHEMISTRY

Satellite and synoptic studies of chemical fronts in the California current and coastal upwelling zone
[AD-A183909] 01 p0073 N88-10466
Remote sensing of ocean colour for studies of biological productivity and biochemical cycles
08 p1042 N88-16296
The use of chlorophyll fluorescence measurements from space for separating constituents of sea water
08 p1043 N88-16307
Physical oceanography and tracer chemistry of the southern ocean
[DE88-006852] 20 p2828 N88-26779

MARINE ENVIRONMENTS

Modelling of crack-tip deformation and transient electrochemical processes in relation to corrosion fatigue of steels cathodically protected in marine environments
[NPL-DMA(A)-145] 01 p0059 N88-10379
NOAA's (National Oceanic and Atmospheric Administration's) Northeast Monitoring Program (NEMP): A report on progress of the first five years (1979-84) and a plan for the future
[PB87-210100] 02 p0196 N88-11225
Properties of the atmospheric boundary layer above a subtropical oceanic front
[AD-A184006] 03 p0351 N88-12215
Estimation of marine boundary layer depth and relative humidity with multispectral satellite measurements
[AD-A184881] 05 p0620 N88-13804
The ocean heat budget
[AD-A186130] 07 p0881 N88-15346
Formation of sediments in fuels containing added sulphonic acids --- marine diesel fuels
[RAE-TM-NAV-ENG-1163] 09 p1150 N88-16891
Corrosion performance of high damping alloys in 3.5 percent sodium chloride environment
[AD-A188048] 11 p1457 N88-18687
A propagation campaign in a marine environment utilizing a digital system at 36 GHz
12 p1618 N88-19675
The effects of atmospheric and thermohaline variability on the validation of the GEOSAT altimeter oceanographic signal between Scotland and Iceland
[AD-A189324] 12 p1650 N88-19882
Cavitation inception
[AD-A189220] 13 p1785 N88-20557
The corrosion resistance of an aluminum alloy coated with polysilazane derived ceramics
[AD-A190703] 15 p2046 N88-22189
Derivation of consistent surface fixed fields for use in a global NWP model
[AD-A190131] 15 p2093 N88-22475
Real-time environmental Arctic monitoring (R-TEAM)
[AD-A189948] 15 p2099 N88-22508
Corrosion of tungsten alloys in marine environments
17 p2320 N88-23854
The effects of better environmental inputs in estimating sea clutter
[AD-A192058] 19 p2643 N88-25678
Doppler radar analysis of coastal marine atmospheric boundary layer structure during a cold air outbreak
[AD-A196023] 24 p3403 N88-30261

MARINE METEOROLOGY

A proposal of the nowcasting system for sea fog
02 p0202 N88-11264
A one-dimensional model of thermally-driven coastal front evolution
02 p0204 N88-11274
Australian East Coast cyclones 3: Case study of the storm of August 1986
02 p0204 N88-11276
A short-range forecasting experiment conducted during the Canadian Atlantic storms program
02 p0205 N88-11285
An hourly analysis, updating and short-range forecasting system --- numerical weather forecasting
02 p0206 N88-11288
Statistical relationships between the mesoscale organization of convection and the large-scale wind profiles during GATE --- GARP Atlantic Tropical Experiment (GATE)
02 p0208 N88-11302
Mesoscale analysis and forecasting for the 1987 America's Cup, Fremantle, Western Australia
02 p0214 N88-11350
Properties of the atmospheric boundary layer above a subtropical oceanic front
[AD-A184006] 03 p0351 N88-12215
New precipitation map of world ocean
04 p0458 N88-12834
Review of the potential of satellite remote sensing for marine flood protection
[IOS-237] 07 p0870 N88-15280
Annual data summary and climatological evaluation, CERC (Coastal Engineering Research Center) field research facility, 1985, volume 2, append‹ C
[AD-A185894] 07 p0881 N88-15344
Mariners Weather Log, Volume 31, Number 3, Summer 1987
[PB87-234894] 08 p1039 N88-16284
North Pacific Ocean. Tradewind region east of Hawaii, R/V Thomas G Thompson: 25 September - 1 November 1972. STD data report
[AD-A186586] 08 p1044 N88-16311
US Navy climatic study of the Mediterranean Sea
[AD-A188264] 10 p1356 N88-18107
Study of cations in the precipation of Estacao Antartica Comandante Ferraz
[INPE-4377-PRE/1197] 12 p1644 N88-19843
Worldwide distributions of shipboard surface meteorological observations for EM propagation analysis
[AD-A188771] 12 p1648 N88-19871
Dynamical modeling of marine boundary layer convection
13 p1797 N88-20750
Predictions and studies with a one-dimensional ice/ocean model
[AD-A189158] 13 p1803 N88-20778
Mariners weather log, volume 32, number 1, Winter 1988
[PB88-173869] 18 p2544 N88-25097
Mariners weather log, volume 31, number 4, Fall 1987
[PB88-173851] 20 p2825 N88-26761

Stability of a coastal upwelling front over topography
[AD-A192354] 20 p2829 N88-26784
Genesis of Atlantic lows experiment NASA electra boundary layer flights data report
[NASA-TM-100703] 22 p3128 N88-28597
Meteorological features during the marginal ice zone experiment from 20 March to 10 April 1987
[AD-A193960] 23 p3235 N88-29251

MARINE NAVIGATION
U SURFACE NAVIGATION

MARINE PROPULSION
Calculations of the turbulent wake behind a slender self-propelled double-body and comparisons with experiment
[AD-A185661] 06 p0703 N88-14314
Formation of sediments in fuels containing added sulphonic acids --- marine diesel fuels
[RAE-TM-NAV-ENG-1163] 09 p1150 N88-16891
A comparative study of various electric propulsion systems and their impact on a nominal ship design
[AD-A187800] 11 p1477 N88-18816
Design features of small Brayton cycles for autonomous underwater vehicles
[AD-A187799] 11 p1506 N88-18999
Cavitation inception
[AD-A189220] 13 p1765 N88-20557

MARINE RESOURCES
Remote sensing of ocean colour for studies of biological productivity and biochemical cycles
08 p1042 N88-16296

MARINE TECHNOLOGY
Marine gas turbines - engine health monitoring, new approaches
[PNR90369] 02 p0182 N88-11132
Integrating syntax, semantics, and discourse DARPA (Defense Advanced Research Projects Agency) Natural Language Understanding Program
[AD-A184505] 03 p0364 N88-12289
JPRS report: Science and technology. Japan
[JPRS-JST-87-023] 06 p0684 N88-14191
Trends in research and development in the Netherlands. The influence of national science policy between 1973 and 1986
[B8701588] 08 p1094 N88-16580
Analysis of wind turbines on offshore support structures excited by random wind and random waves
[DE88-004772] 10 p1351 N88-18074
Digital correlator for the portable channel prober measurement instrument
[AD-A189065] 14 p1904 N88-21377
Naval research reviews, volume 39, number 3
[AD-A191392] 16 p2264 N88-23543
Marine techniques: R and D axes, identification of areas of common interest with space techniques
19 p2699 N88-26047
Materials qualification in oceanology and the offshore industry 19 p2700 N88-26050

MARISAT SATELLITES
The JPL mechanically steered antenna
19 p2647 N88-25715

MARITIME SATELLITES
NT ERS-1 (ESA SATELLITE)
NT MARECS MARITIME SATELLITES
NROSS (Navy Remote Ocean Sensing System): A force multiplier
[AD-A186853] 10 p1346 N88-18045
Proceedings of the Colloquium on Space and Sea
[ESA-SP-280] 19 p2695 N88-26016
Satellites at sea --- INMARSAT
19 p2700 N88-26054
The contribution of space to maritime activities
19 p2700 N88-26055

MARKERS
Descriptions of HF and VHF Loran-C buoys and evaluations as potential datum marker buoys
[AD-A192069] 18 p2462 N88-24618

MARKET RESEARCH
Study of the feasibility of a satellite communication system for road transportation home office to vehicle communication. Volume 2: Market study
[SC/87-E/6-VOL-2] 05 p0575 N88-13506
National Point Of Contact (NPOC)-SPOT inquiry 1986
[NLR-MP-86055-U] 05 p0620 N88-13807
Data base management in CAD/CAM systems: Requirements for CAD/CAM data bases, actual market offer, advice for an efficient data base management, development tendencies
[MBB/LWD-11/S/PUB/254] 16 p2285 N88-23683

MARKETING
JPRS report: Science and technology. China
[JPRS-CST-87-026] 03 p0269 N88-11688
Production of jet fuels from coal derived liquids. Volume 1: Market assessment for liquid by-products from the Great Plains gasification plant
[AD-A184846] 05 p0570 N88-13475
Research briefing on high-temperature superconductivity
[PB88-133004] 11 p1561 N88-19344
Selling to NASA
[NASA-TM-89724] 12 p1705 N88-20208
High temperature materials: What's available
[AERE-R-12632] 15 p2028 N88-22081
Preliminary market analysis for large zeolite crystals
[NASA-CR-182882] 15 p2049 N88-22207
Function of Japan Fine Ceramics Center described
15 p2052 N88-22227
Commercialization and export --- aerospace industry
22 p3161 N88-28824

MARKING
NT ISOTOPIC LABELING
A labeling procedure for linear finite-state codes
11 p1472 N88-18781
Study of flow tracer behavior models and experimental validation with multiple exposure holographic velocimetry
[IMFL-87/30] 20 p2801 N88-26622
Velocity measurements and flow visualization in turbulent three-dimensional supersonic flows using oxygen flow tagging
[AD-A192551] 21 p2892 N88-27165
Development of automatic names placement software
[AD-A192786] 21 p2996 N88-27770

MARKOV CHAINS
Contribution to the study of circuit switched networks: Modeling and numerical solutions
[LAAS-87-174] 02 p0162 N88-11017
On the approximation of the output process of multi-user random access communication networks
[AD-A186197] 07 p0842 N88-15108
Power series for stationary distributions of coupled processor models
[REPT-87-70] 16 p2254 N88-23470
Colored stochastic Petri nets. Application to real time distributed systems
[ENST-87E017] 20 p2839 N88-26843
Asymptotically efficient adaptive allocation schemes for controlled Markov chains: Finite parameter space
[AD-A192228] 20 p2846 N88-26893
Markov chain computations to a solution of the mutual-exclusion problem in concurrency
[REPT-87-89] 20 p2847 N88-26896

MARKOV PROCESSES
NT MARKOV CHAINS
Passage from two-parameters to infinite dimension
[ENST-87C002] 01 p0088 N88-10577
White noise calculus for two-parameter filtering
[ENST-87C003] 01 p0088 N88-10578
Optimization of a controlled two-server maintenance system
[INPE-4202-PRE/1083] 01 p0107 N88-10694
Real-time expert systems: A status report
02 p0129 N88-10817
Electronic system reliability and effectiveness
[AD-A184522] 03 p0311 N88-11961
Overlooked potential of systems with Markovian coefficients
[NLR-MP-86049-U] 05 p0552 N88-13366
Stationary regenerative sets and subordinators
[AD-A186298] 07 p0918 N88-15573
Formal grammars and Markov models
[RSRE-MEMO-4051] 09 p1219 N88-17311
Experiments with the back propagation algorithm: A systematic look at a small problem
[RSRE-MEMO-4049] 09 p1224 N88-17340
SURE reliability analysis: Program and mathematics
[NASA-TP-2764] 09 p1231 N88-17380
Random truncation models and Markov processes
[CWI-MS-R8702] 09 p1232 N88-17389
A queueing system with independent Markov input streams
[AD-A187601] 10 p1402 N88-18363
Estimation of the probability of a long time to the first entrance to a state in a semi-Markov model
[AD-A188960] 12 p1685 N88-20074
An optimal branch-and-bound procedure for the constrained path, moving target search problem
[AD-A188962] 12 p1685 N88-20075
The acoustic-modeling problem in automatic speech recognition
[AD-A188529] 13 p1757 N88-20510
On relaxation algorithms based on Markov random fields
[AD-A189043] 13 p1814 N88-20840
Nonstationary solution in random vibration theory
[PB88-163746] 14 p1933 N88-21529
Analysis and testing of the SURE program
[NASA-TP-2817] 15 p2123 N88-22653
Filtering of jump processes
[AD-A189701] 15 p2123 N88-22656
Structural decomposition of multiple time scale Markov processes
[AD-A189739] 15 p2123 N88-22657
The partially observed stochastic minimum principle
[AD-A189787] 15 p2124 N88-22658
Markov processes applied to control, replacement and signal analysis
[AD-A190563] 15 p2126 N88-22674
EDQNM closure: A homogeneous simulation to support it. A quasi-homogeneous simulation to disprove it
16 p2195 N88-23091
Validation of EDQNM for subgrid and supergrid models 16 p2195 N88-23092
Angular distribution of turbulence in wave space
16 p2195 N88-23093
Experimental evaluation of algorithms for connected speech recognition using hidden Markov models
[RSRE-MEMO-4099] 17 p2333 N88-23928
Poisson functionals of Markov processes and queueing networks
[AD-A191217] 18 p2568 N88-25252
Semi-Markov adjunction to the Computer-Aided Markov Evaluator (CAME)
[NASA-CR-181645] 19 p2678 N88-25924
Distributed algorithms for probabilistic solution of computational vision problems
[AD-A193150] 21 p2997 N88-27773
Performability analysis: Measures, an algorithm and a case study
[AD-A192477] 21 p3001 N88-27800
Free boundary control of the Markov process
[AD-A192401] 21 p3008 N88-27846
The computation of stationary distributions on Markov chains through perturbations
[AD-A193191] 21 p3009 N88-27855
Importance sampling for stochastic simulations
[AD-A193585] 22 p3138 N88-28654
Poisson functionals of Markov processes and queueing networks
[AD-A194289] 22 p3145 N88-28705
Use of Markov probability and reliability model generation methods in the analysis of reliability of a fault tolerant hardware and software based system with flexible repair policies
[PNR90467] 22 p3145 N88-28706
Approximate evaluation of semi-Markov chain reliability models
[AD-A194669] 23 p3223 N88-29185
Dynamic analysis of computer and communications sytems: Semi-Markov approach
23 p3244 N88-29305
Hidden Markov models for automatic speech recognition: Theory and application
[RSRE-MEMO-4135] 23 p3251 N88-29350
Approximations and implementations of nonlinear filtering schemes
[AD-A194685] 23 p3271 N88-29462
On stable Markov processes
[AD-A192892] 23 p3273 N88-29482
Range data description based on multiple characteristics 24 p3419 N88-30351

MARS
Interplanetary mission design handbook. Volume 1, Part 5: Mars-to-Earth ballistic mission opportunities, 1992-2007
[NASA-CR-182525] 10 p1430 N88-18538

MARS (PLANET)
Possible dynamical mechanisms for the Martian polar warming phenomenon
[NASA-CR-181454] 02 p0254 N88-11605
A near-earth optical communications terminal with a corevolving planetary sun shield
04 p0434 N88-12693
An evolutionary communications scenario for Mars exploration
[NASA-TM-100263] 05 p0576 N88-13515
Mars: High resolution VLA observations at wavelengths of 2 and 6 cm and derived properties
06 p0804 N88-14909
Frozen orbit analysis in the Martian system
[AD-A189574] 13 p1856 N88-21106
Periodic orbits around a satellite modelled as a triaxial ellipsoid
[AD-A190592] 15 p2022 N88-22051
Engineering planetary lasers for interstellar communication
[NASA-CR-180780] 17 p2311 N88-23825
Electromagnetic powered vehicles (EMPV) for Mars exploration 17 p2419 N88-24388
Power requirements for mining and microwave processing of extraterrestrial resources
17 p2420 N88-24389
A design study of onboard navigation and guidance during aerocapture at Mars
[NASA-CR-172053] 18 p2469 N88-24654
The Viking landing sites: A cartographic perspective
[NASA-CR-177486] 19 p2742 N88-26282
A bibliography of dunes: Earth, Mars, and Venus
[NASA-CR-4149] 20 p2885 N88-27134

Mars: Near-infrared comparative spectroscopy during the 1986 opposition 23 p3301 N88-29658
An introduction to the historical records of China about Mars 23 p3301 N88-29664
How dirty is Mars' North Polar cap, and why isn't it black 23 p3303 N88-29677
Preliminary analysis of recent 2.2-4.2 micrometers telescopic observations of Elysium, Mars: Implications for crystallinity and hydration state of surface materials 23 p3306 N88-29692
Mars earth-based radar: 1986 results and 1988-1990 opportunities 23 p3306 N88-29697
Nineteenth Lunar and Planetary Science Conference. Press abstracts
[NASA-CR-183037] 24 p3440 N88-30473

MARS ATMOSPHERE
Possible dynamical mechanisms for the Martian polar warming phenomenon
[NASA-CR-181454] 02 p0254 N88-11605
The atmosphere of Mars and optical communications 04 p0434 N88-12692
Particle-gas temperature differentials resulting from time-dependent radiative-conductive heat flux divergences in the tenuous dust-laden atmosphere of mars
[AD-A185888] 07 p0945 N88-15747
Aerosols in Martian Atmosphere and Natural Dust Observation (AMANDO). Proposal for the Mars orbiter balloon and rover to study the Martian atmosphere, its thermal content, and its interaction with the soil
[IFSI-87-9] 08 p1100 N88-16619
Development of an engineering model atmosphere for Mars
[NASA-CR-182462] 09 p1263 N88-17568
Mars Lander/Rover vehicle development: An advanced space design project for USRA and NASA/OAST
[NASA-CR-182571] 12 p1709 N88-20227
Martian Clouds Data Workshop
[NASA-CR-182431] 12 p1711 N88-20238
Diurnal variations in optical depth at Mars: Observations and interpretations
[NASA-TM-100057] 18 p2595 N88-25420
Chemical interactions between the present-day Martian atmosphere and surface minerals 23 p3305 N88-29689
Volatiles on Mars
[NASA-CR-183113] 24 p3456 N88-30571

MARS ENVIRONMENT
NT MARS ATMOSPHERE
Mars Lander/Rover vehicle development: An advanced space design project for USRA and NASA/OAST
[NASA-CR-182562] 12 p1709 N88-20226

MARS GEOSCIENCE CLIMATOLOGY ORBITER
U MARS OBSERVER

MARS LANDING
Mars Lander/Rover vehicle development: An advanced space design project for USRA and NASA/OAST
[NASA-CR-182562] 12 p1709 N88-20226
Energy storage considerations for a robotic Mars surface sampler
[NASA-TM-100969] 22 p3166 N88-28853

MARS OBSERVER
Mars Lander/Rover vehicle development: An advanced space design project for USRA and NASA/OAST
[NASA-CR-182562] 12 p1709 N88-20226

MARS PROBES
NT MARS OBSERVER
Mars Lander/Rover vehicle development: An advanced space design project for USRA and NASA/OAST
[NASA-CR-182570] 11 p1567 N88-19380
Mars rover/sample return mission requirements affecting space station
[NASA-CR-172048] 18 p2594 N88-25414

MARS SATELLITES
NT DEIMOS
NT PHOBOS

MARS SURFACE
An evolutionary communications scenario for Mars exploration
[NASA-TM-100263] 05 p0576 N88-13515
Gamma-ray and neutron spectroscopy of planetary surfaces and atmospheres
[DE88-004287] 10 p1430 N88-18541
Martian geomorphology and its relation to subsurface volatiles
[NASA-CR-182428] 12 p1711 N88-20237
Groundwater sapping valleys: Experimental studies, geological controls and implications to the interpretation of valley networks on Mars
[NASA-CR-182718] 15 p2152 N88-22847
The Viking landing sites: A cartographic perspective
[NASA-CR-177486] 19 p2742 N88-26282
MEVTV Workshop on Nature and Composition of Surface Units on Mars
[NASA-CR-183075] 23 p3300 N88-29654
Surface composition of Mars: A Viking multispectral view 23 p3300 N88-29655
A review: Quantitative models for lava flows on Mars 23 p3301 N88-29656
Mars: Spectral signatures seen and unseen 23 p3301 N88-29659
Selective weathering of shocked minerals and chondritic enrichment of the Martian fines 23 p3301 N88-29660
Intercrater plains deposits and the origin of Martian valleys 23 p3301 N88-29661
Weathering of sulfides on Mars 23 p3301 N88-29662
Elemental composition of the Martian surface 23 p3302 N88-29665
Sub-kilometer rampart craters in the equatorial region of Mars: Possible implications for the state and distribution of regolith H2O 23 p3302 N88-29666
Chemical and spectroscopic characterization of a suite of Mars soil analogs 23 p3302 N88-29667
The Martian sedimentary record 23 p3302 N88-29669
Gamma-ray/neutron spectroscopy from the Mars observer 23 p3302 N88-29671
Aqueous alteration in S-N-C meteorites and implications for weathering products on Mars 23 p3303 N88-29673
Distribution and timing of thick transient air-fall deposits in Electris: Implications for the nature of the upland plains 23 p3303 N88-29674
Photogeological inferences of Martian surface composition 23 p3303 N88-29675
Some probable characteristics of the Martian regolith 23 p3303 N88-29676
Surface units on Mars: The assemblage in the Valles Marineris 23 p3304 N88-29680
Morphologic contrasts between Nirgal and Auqakuh Valles, Mars: Evidence of different crustal properties 23 p3304 N88-29681
Geology of six possible Martian landing sites 23 p3304 N88-29682
Spectral reflectance of SNC meteorites: Relationships to Martian surface composition 23 p3304 N88-29683
Constraints on the origin of fractured terrane, Northern Martian plains 23 p3304 N88-29684
Viking Landers and remote sensing 23 p3304 N88-29685
Origin of northern lowland plains: Constraints from boundary morphology 23 p3305 N88-29687
Episodic vs. epochal release of SO2 on Mars 23 p3305 N88-29688
Chemical interactions between the present-day Martian atmosphere and surface minerals 23 p3305 N88-29689
Stratigraphy of the Kasei Valles region, Mars 23 p3305 N88-29690
Topography of large craters on Mars: Implications for the highlands resurfacing history 23 p3306 N88-29691
Early cratering rates and the nature of the Martian cratered uplands 23 p3306 N88-29694
Documenting volcano-tectonic episodes in Mars' stratigraphic record 23 p3306 N88-29695
The surface composition of Mars from earthbased observations 23 p3306 N88-29696
Crystal fractionation in the SNC meteorites: Implications for surface units on Mars 23 p3307 N88-29698
Martian surface analogs: Laboratory spectral studies in the mid infrared 23 p3307 N88-29699
Ridged and gullied terrains in the Martian uplands 23 p3307 N88-29700
Variation in the thickness of ejecta cover on Mars with increasing crater density 23 p3307 N88-29701
Coadsorption of H2O and CO2 on the Martian surface 23 p3307 N88-29702
High resolution Viking Orbiter images: A useful data source for testing the viability of geomorphic processes attributed to Martian landforms 23 p3307 N88-29703
Debris flows of the Simud-Tiu outflow system of Mars 24 p3442 N88-30485
Faulting and its relation to volcanism: Mars western equatorial region 24 p3443 N88-30489
Physical properties of surface materials on Martian volcanoes: Dust-covered lava and ash 24 p3443 N88-30493
Simulations of lava flows on Mars 24 p3443 N88-30495
Volatiles on Mars
[NASA-CR-183113] 24 p3456 N88-30571

MARS VOLCANOES
MEVTV Workshop on Nature and Composition of Surface Units on Mars
[NASA-CR-183075] 23 p3300 N88-29654
The history of Martian volcanism determined from a revised relative chronology 23 p3301 N88-29657
Weathering of sulfides on Mars 23 p3301 N88-29662
Mapping of volcanic units at Alba Patera, Mars 23 p3301 N88-29663
Small Martian valcanoes 23 p3302 N88-29668
The Martian sedimentary record 23 p3302 N88-29669
Progress in determining the thickness and distribution of volcanic materials on Mars 23 p3302 N88-29670
Variability in spectral signatures of terrestrial volcanic rocks and implications for volcanology on Mars 23 p3303 N88-29672
What SNC meteorites tell us about Martian magmatism 23 p3303 N88-29679
Volcano evolution on Mars 23 p3305 N88-29686
Episodic vs. epochal release of SO2 on Mars 23 p3305 N88-29688
Documenting volcano-tectonic episodes in Mars' stratigraphic record 23 p3306 N88-29695
NASA MEVTV Program Working Group Meeting: Volcanism on Mars
[NASA-CR-183074] 24 p3442 N88-30487
Mars: Volcanism in the Valles Marineris overlooked 24 p3443 N88-30491
The Martian highland paterae: Evidence for explosive volcanism on Mars 24 p3443 N88-30492
Physical properties of surface materials on Martian volcanoes: Dust-covered lava and ash 24 p3443 N88-30493
Rifts of deeply eroded Hawaiian basaltic shields: A structural analog for large Martian volcanoes 24 p3443 N88-30494
Simulations of lava flows on Mars 24 p3443 N88-30495
Small-scale volcanic landforms indicative of distributary tube systems 24 p3444 N88-30496
Volcanic styles at Alba Patera, Mars: Implications of lava flow morphology to the volcanic history 24 p3444 N88-30497

MARSHES
U MARSHLANDS

MARSHLANDS
Seasonal cycling of sulfur and iron in porewaters of a Delaware salt marsh
[NASA-CR-182385] 07 p0876 N88-15311
Relevance of a thematic map (SPOT data) with regards to the real flora and structure of the vegetation covering of salt marshes (Mont Saint Michel Bay, France) 22 p3109 N88-28468

MARTENSITE
Low activation ferritic alloys for nuclear fusion reactors
[DE87-010711] 03 p0286 N88-11801
A comparison of high damping shape memory alloys with Cu-Mn-based and Fe-Cr-based alloys
[AD-A184110] 04 p0414 N88-12566
Fracture analysis of drawn composite dual-phase steel wire
[DE88-001396] 06 p0681 N88-14173
Fatigue, fracture and strain hardening of high carbon hardened alloy steel
[AD-A186101] 07 p0831 N88-15043
Investigation of the auto-tempering of low-carbon martensite
[PB87-143970] 07 p0833 N88-15053
Propagation of fatigue crack in the medium-carbon steel containg both martensite and ferrite
[PB87-143962] 07 p0869 N88-15273
Studies of transverse phonon modes in premartensitic indium-thallium alloys
[DE88-003481] 13 p1744 N88-20428
Irradiation effects on tungsten stabilized martensitic steels
[DE88-007074] 18 p2486 N88-24748
Twin boundaries and heterophase interfaces in ferroelastic martensites
[DE88-011894] 21 p2916 N88-27304

MARTENSITIC STAINLESS STEELS
Microstructural evolution and response to double-loop reactivation testing of heat-treated pH 13-8 Mo martensitic stainless steel
[DE87-009058] 02 p0146 N88-10915
Swelling behavior of ferritic/martensitic steels
[DE88-001757] 06 p0682 N88-14177
Data requirements to model creep in 9Cr-1Mo-V steel 14 p1931 N88-21512

MARTENSITIC TRANSFORMATION
Soliton twin boundaries of the cubic-tetragonal martensitic transformations in ferroelastic materials
[DE87-014741] 04 p0495 N88-13047
Martensitic transformation and microstructures in sintered NiAl alloys
[NASA-TT-20178] 18 p2488 N88-24761
Martensitic transformation and microstructures in sintered NiAl alloys
[NASA-TT-20192] 19 p2616 N88-25519

Kinetic of martensitic transformations induced by hydrogen in the austenite
[DE88-701623] 23 p3194 N88-29007

MARTIN AIRCRAFT
NT B-57 AIRCRAFT

MARTINGALES
Stochastic integration for operator valued processes on Hilbert spaces and on nuclear spaces
[ENST-87D002] 01 p0089 N88-10580
On the relations between increasing functions associated with two-parameter continuous martingales
[AD-A185572] 06 p0765 N88-14699
Point processes in the plane
[AD-A186017] 07 p0913 N88-15542
Martingale representation and the Malliavin calculus
[AD-A189721] 15 p2119 N88-22626
Stochastic evolution equations driven by nuclear space valued martingales
[AD-A189342] 15 p2126 N88-22677
A Wong-Zakai type theorem for certain discontinuous semimartingales
[AD-A192713] 21 p3005 N88-27822

MASER RESONATORS
U MASERS

MASERS
NT HYDROGEN MASERS
NT INTERSTELLAR MASERS
NT TRAVELING WAVE MASERS
NT WATER MASERS
The 8.4-GHz low-noise maser pump source assembly 04 p0436 N88-12705
Traveling-wave maser closed-cycle refrigerator data acquisition and display system 04 p0437 N88-12708
Two-watt, 4-Kelvin closed cycle refrigerator performance 04 p0437 N88-12709
Nonthermal phenomena in stellar coronae: Evidence from radio observations 04 p0503 N88-13096
Higher harmonic generation in the induced resonance electron cyclotron maser
[AD-A186236] 07 p0858 N88-15210
VLBI research on OH-maser IN W33 08 p1001 N88-16064
Physics modeling support contract
[DE88-004039] 10 p1335 N88-17980
Polarization properties of SiO masers 13 p1858 N88-21113

MASKS
NT OXYGEN MASKS
Optical Fourier transformation by lensless method with perforated mask and with modified Talbot interferometer for analysis of interferograms 09 p1236 N88-17408
Smoke hoods: Net safety benefit analysis --- aircraft accidents
[CAA-PAPER-87017] 23 p3174 N88-28898

MASS
NT CENTER OF MASS
NT CRITICAL MASS
NT GALACTIC MASS
NT MISSING MASS (ASTROPHYSICS)
NT PARTICLE MASS
NT PLANETARY MASS
NT STELLAR MASS
Aqueous-phase reactions in clouds
[DE86-005249] 01 p0069 N88-10445
Modes, masses, metallicities, and magnitudes of RR Lyrae variables
[DE87-013149] 01 p0109 N88-10703
Phase 3 study of selected tether applications in space. Volume 2: Study results
[NASA-CR-179186] 02 p0132 N88-10828
Physics of few-body lambda hypernuclei
[DE87-014746] 03 p0375 N88-12357
Gravitational accretion of hot dark matter 03 p0388 N88-12439
Effect of permissible variations of center-of-gravity locations of cargo airplane on its mass 04 p0424 N88-12625
A search for very low mass (brown dwarf) stars as wide binaries using a seven element infrared camera-photometer 04 p0512 N88-13150
The effect of maximum-allowable payload temperature on the mass of a multimegawatt space-based platform
[DE88-001921] 05 p0555 N88-13381
Fluid mass and thermal loading effects on the modal characteristics of space shuttle main engine liquid oxygen inlet splitter vanes 05 p0594 N88-13628
Pressure and mass velocity measurements in solids subjected to dynamic loadings 07 p0921 N88-15595
Finite element method with continuous mass elements
[PB87-143384] 08 p0995 N88-16019
Dynamic finite element with diagonalized consistent mass matrix and elastic-plastic impact calculation
[PB87-143376] 08 p0995 N88-16020
Suppression of the mass enhancement in CeB6 in high magnetic fields
[DE88-002946] 09 p1241 N88-17439
Renormalization group analysis of the temperature dependent coupling constant in massless theory
[DE88-751059] 09 p1259 N88-17552
Spacecraft telecommunications system mass estimates 11 p1473 N88-18784
The rate of adaptation to altered g in the human centrifuge: Implications for simulations of mass-discrimination in space flight 12 p1659 N88-19941
Optimal placement of tuning masses for vibration reduction in helicopter rotor blades
[NASA-TM-100562] 13 p1782 N88-20665
To the field theory with a fundamental mass
[DE88-701159] 15 p2146 N88-22807
Effect of mass-velocity on liquid jet atomization in Mach 1 gasflow
[NASA-TM-100813] 16 p2211 N88-23194
The effect of maximum allowable payload temperature on the mass of a multimegawatt space based platform 17 p2424 N88-24416
MACRAD: A mass analysis code for radiators 17 p2424 N88-24418
Energy storage for nuclear burst power systems 17 p2426 N88-24431
Hydrogen turbines for space power systems: A simplified axial flow gas turbine model
[DE88-009585] 19 p2677 N88-25920
A Vlasov ion zero mass electron model for plasma simulations 20 p2855 N88-26958
Electromagnetic theory of the gravitation 22 p3158 N88-28793
The principles of mass and maneuver applied to space operations
[AD-A194037] 23 p3276 N88-29500
Spacecraft mass estimation, relationships and engine data: Task 1.1 of the lunar base systems study
[NASA-CR-172061] 24 p3332 N88-29836
The stability of disk galaxies and constraints on their mass-luminosity ratio
[SER-C-PREPUBL-FASC-27] 24 p3455 N88-30565

MASS DISTRIBUTION
Aerosol sensor: Real time determination of aerosol mass size distributors using filtering quartz oscillators
[ETN-87-90397] 01 p0049 N88-10311
Identification of linear structural models 03 p0337 N88-12121
The role of fragmentation in interaction of meteoroids with the Earth's atmosphere 06 p0737 N88-14532
A method of long-term radar shower data analysis 06 p0738 N88-14541
Incident meteoroid flux density 06 p0739 N88-14542
Analysis of the mass formula dependence of spallation product distribution
[DE88-750297] 07 p0864 N88-15243
Evidence for human adaptive response to dehydration: Increase of circulating protein mass
[AD-A186225] 08 p1048 N88-16328
On the time delay of the ultrahigh-energy radiation signal from the source Cygnus X-3
[DE88-700649] 10 p1431 N88-18547
The evolution of the mass distribution of cometary particles 14 p2004 N88-21946
Estimates of masses, volumes and densities of short-period comet nuclei 14 p2004 N88-21950
Angular resolved energy analysis of (69)Ga+ ions from a gallium liquid metal ion source
[AERE-R-12649] 15 p2139 N88-22760
A review of the Initial Mass Function (IMF) --- stellar mass
[MPE-PREPRINT-112] 22 p3165 N88-28848
Laser sensing for identification and control of distributed parameter systems
[AD-A195886] 24 p3379 N88-30124

MASS DRIVERS (PAYLOAD DELIVERY)
Design study for asteroidal exploitation 03 p0389 N88-12445

MASS FILTERS
U FLUID FILTERS

MASS FLOW
Studies of transport processes in porous and ion exchange membranes
[ISBN-951-99847-0-4] 01 p0021 N88-10133
IRAS and cool stellar mass loss 04 p0515 N88-13166
Combustion characteristics of gas turbine alternative fuels
[NASA-TM-100247] 05 p0548 N88-13338
Speed control of a missile with throttleable ducted rocket propulsion 12 p1597 N88-19561
Mass transport in flow of sources
[LRT-WE-9-FB-4(1987)] 22 p3077 N88-28268
Mass transfer instabilities due to angular momentum flows in close binaries --- stars
[MPE-PREPRINT-113] 22 p3165 N88-28849

MASS FLOW FACTORS
Mass transport in flow of sources
[LRT-WE-9-FB-4(1987)] 22 p3077 N88-28268
Mass transport in annular spherical system
[LRT-WE-9-FB-11(1987)] 22 p3077 N88-28271
Analysis of a feed device for the pneumatic transport of noncohesive particles
[VKI-TM-44] 24 p3369 N88-30062

MASS FLOW RATE
Equipment for mass flow measurements in the low-speed wind tunnel at DFVLR in Brunswick, West Germany
[DFVLR-MITT-88-02] 21 p2900 N88-27212
Turbulence structure of mixing swirling flows
[AD-A193063] 21 p2943 N88-27478
Mass flow rate influence on void fraction of two-phase helium flow
[DE88-702456] 21 p2945 N88-27495
Mass transport in flow of sources
[LRT-WE-9-FB-4(1987)] 22 p3077 N88-28268

MASS RATIOS
NT PAYLOAD MASS RATIO
NT PROPELLANT MASS RATIO
A review of the Initial Mass Function (IMF) --- stellar mass
[MPE-PREPRINT-112] 22 p3165 N88-28848

MASS SPECTRA
Real time analysis of detonation products
[DE87-007453] 01 p0031 N88-10195
Trace analysis by MS/MS on a double focussing mass spectrometer
[AD-A187954] 10 p1334 N88-17973
Accuracy of analytic energy level formulas applied to hadronic spectroscopy of heavy mesons
[NASA-TM-4042] 19 p2725 N88-26185

MASS SPECTROMETERS
Ion composition measurements in the upper stratosphere --- parachute-borne mass spectrometer
[ETN-87-90423] 01 p0069 N88-10442
Research relative to an advanced rod control system for quadrupole mass spectrometry applications
[NASA-CR-181458] 02 p0167 N88-11050
Mass spectroscopic facility 03 p0296 N88-11861
Diagnostics aid for mass spectrometer trouble-shooting
[DE88-000350] 03 p0324 N88-12049
The tail lobe ion spectrometer: Theory and observations
[IFSI-86-12] 05 p0585 N88-13589
Trace analysis by MS/MS on a double focussing mass spectrometer
[AD-A187954] 10 p1334 N88-17973
Energy spectra of pick-up ions recorded during the encounter of Giotto with Comet Halley 14 p1997 N88-21901
Evidence for first polymer in Comet Halley: Polyoxymethylene 14 p1997 N88-21906
High-voltage inverse-square function generator
[DE88-701109] 15 p2058 N88-22270
Stratospheric positive ion composition measurements and acetonitrile detection: A consistent picture
[AERONOMICA-ACTA-A-326-1987] 18 p2542 N88-25084
A mass spectrometer for the analysis of thermally labile compounds 19 p2668 N88-25859
Evaluation of the ion trap mass spectrometer for potential application in the space station
[DE88-008940] 19 p2674 N88-25902
Synopsis of a computer program designed to interface a personal computer with the fast data acquisition system of a time-of-flight mass spectrometer
[NASA-CR-177474] 21 p3001 N88-27798

MASS SPECTROMETRY
U MASS SPECTROSCOPY

MASS SPECTROSCOPY
Simultaneous TG/DSC (thermogravimetry/Differential Scanning Calorimetry) and TG/MS (thermogravimetry/Mass Spectrometry) analyses of polymeric and energetic materials
[DE88-000727] 04 p0413 N88-12561
Supersonic beam observations of semiconductor clusters
[AD-A184991] 05 p0655 N88-14018
Atomic-level studies of superconducting YBa2Cu3O sub 7-x
[DE88-002522] 06 p0788 N88-14831
Development of FTMS methods for the detection of trace chemical species and development of FTMS methods for the analysis of various chemical species
[AD-A185857] 07 p0828 N88-15023
Monitoring of space station life support systems with miniature mass spectrometry and artificial intelligence 08 p1057 N88-16376
Laser post-ionization secondary neutral mass spectroscopy
[DE88-002979] 09 p1172 N88-17027

A chemical precursor to optical damage. Studies by laser ionization mass spectrometry
[DE88-004321] 10 p1409 N88-18408
Determining chemical composition of aerosol in Venusian cloud layer on Vega-1 automatic interplanetary station using Malakhit mass spectrum analyzer
13 p1726 N88-20321
Development and evaluation of supercritical fluid chromatography-mass spectrometry
[DE88-005122] 13 p1738 N88-20394
A mass spectrometer evolved gas analysis experiment for in-situ analysis of cometary dust volatiles
13 p1854 N88-21097
Low pressure gas flow analysis through an effusive inlet using mass spectrometry
[NASA-CR-182712] 14 p1910 N88-21413
Chromatographic and mass spectrometric separation and analysis
[AD-A190113] 16 p2174 N88-22958
Molecular-beam, mass-spectrometric studies of wood vapor and model compounds over HZSM-5 catalyst
18 p2535 N88-25044
Mass spectrometric high temperature measurements of the barium oxide-zirconium dioxide system and the determination of thermodynamic data for barium zirconate. Clarification of the counter-stopping capacity of coated particles for solid fission products by zirconium dioxide addition
[NASA-TT-20187] 19 p2611 N88-25496
Prospects for large dynamic range isotope analysis using photon burst mass spectrometry
[DE88-009110] 19 p2613 N88-25505
High-fidelity in isotope ratio measurements for resonance ionization mass spectrometry
[DE88-009129] 19 p2613 N88-25506
Simultaneous thermogravimetric modulated beam mass spectrometry and time-of-flight velocity spectra measurements: Thermal decomposition mechanisms of RDX and HMX 19 p2632 N88-25612
Laser desorption/ablation studies by resonance ionization mass spectrometry
[DE88-009124] 20 p2807 N88-26650
Recent advances in atom-probe field ion microscopy
[DE88-008799] 20 p2876 N88-27070
Measurement of Beta-decay energies of short-lived neutron-rich nuclei in the vicinity of mass number between 101 and 106, and A = 109
[ETN-88-92376] 21 p3014 N88-27890
Impurity analysis in SIMOX samples by high-efficiency resonance ionization time-of-flight mass spectrometry
[DE88-012061] 24 p3367 N88-30051
Ion kinetics in silane plasmas
[AD-A196202] 24 p3431 N88-30423

MASS TRANSFER
Flow and heat transfer with impinging jets and rough surfaces
[DE87-014162] 02 p0169 N88-11065
On the surging potential of polar ice streams. Antarctic surges: A clear and present danger
[DE87-013980] 02 p0216 N88-11363
Mass transport by diffusion 03 p0297 N88-11864
Heat transfer in laminar flow for mass inlet into an annular channel
[DE87-702890] 03 p0314 N88-11983
Local heat/mass transfer and pressure drop in a two-pass rib-roughened channel for turbine airfoil cooling
[NASA-CR-179635] 03 p0322 N88-12039
Novel macrocyclic carriers for proton-coupled liquid membrane transport
[DE88-000636] 04 p0413 N88-12560
Corrosion of ferritic steels by molten lithium: Influence of competing thermal gradient mass transfer and surface product reactions
[DE88-000334] 04 p0417 N88-12585
Heat and moisture transport in the atmospheric boundary layer
[AD-A184222] 04 p0470 N88-12904
Study of the effect of mass transfer on a transonic boundary layer. Application to flow relaminarization
[ETN-88-91169] 05 p0541 N88-13296
Systematic stratospheric-tropospheric exchange viewed from isentropic coordinates 05 p0615 N88-13777
Modern concept concerning transport of bottom sediments in abyssal regions of world ocean
06 p0728 N88-14478
The adaption and use of research codes for performance assessment
[DE88-000552] 06 p0756 N88-14639
EXOSAT guest observer program. Binary parameters of the X-ray Pulsar 4U1626-67
[NASA-CR-182374] 06 p0802 N88-14905
Examination of the development of a compressible turbulent boundary layer on a rough and porous wall
[PB87-148266] 07 p0815 N88-14964
A numerical study of transient heat and mass transfer in crystal growth 07 p0925 N88-15619
The paradoxical asymptotic status of massless springs
[AD-A185625] 07 p0928 N88-15637
Investigations in field of surface forces in metallurgy
[BLL-M-47406-(5828.4)] 08 p0969 N88-15860
Determination of the effect of walking on the forced convective heat transfer coefficient using an articulated mannikin
[AD-A186452] 08 p1049 N88-16335
Application of Hoffman modulation contrast microscopy coupled with three-wavelength two-beam interferometry to the in situ direct observation of the growth process of a crystal in microgravity 10 p1288 N88-17704
Experimental studies of heat and mass exchange in parallel-passage rotary desiccant dehumidifiers for solar cooling applications
[DE88-001119] 10 p1350 N88-18069
Physiological and ecological implications of coupled heat- and water-transport mechanisms of endotherms and vegetation
[DE88-004170] 10 p1352 N88-18081
Mass transport phenomena between bubbles and dissolved gases in liquids under reduced gravity conditions
[NASA-TM-100273] 11 p1455 N88-18672
Effect of density change on rapid liquid-solid interface kinetics and heat flow
[DE88-004286] 11 p1487 N88-18878
Mass transport and chemical demixing of Y-Ba-Cu-O compounds during sintering in temperature gradients
[DE88-004887] 12 p1696 N88-20151
Mass, heat and nutrient fluxes in the Atlantic Ocean determined by inverse methods
[NASA-CR-180535] 14 p1950 N88-21626
The mass loss rates of periodic comets
14 p2010 N88-21991
Mass transfer mechanisms for water adsorbed on silica gel
[DE88-005993] 15 p2032 N88-22107
The numerical simulation of viscous flows with change of phase and chemical reaction
[DE88-003204] 15 p2062 N88-22292
Studies of heat and mass transfer during chemical vapor deposition 17 p2338 N88-23953
Thermochemical analysis of mass transfer in a NB-1ZR-potassium heat pipe 17 p2412 N88-24346
Fabrication of a niobium 1 percent zirconium containment for SP-100 primary lithium system materials mass transfer studies 17 p2417 N88-24373
Irreversible dissolution of solid solutions: A kinetic and stoichiometric model
[DE88-009194] 19 p2614 N88-25513
Parametric methodologies of cloud vertical transport for acid deposition models
[PB88-191374] 20 p2825 N88-26762
Development of an experimental system for studying fast transient ignition phenomena
[DE88-011917] 21 p2911 N88-27276
Heat and mass transfer in a transport channel
[DE88-701968] 21 p2945 N88-27493
Heat and mass transfer in laminar wavy film absorption with the presence of non-absorbable gases
21 p2947 N88-27502
Mass transport in flow of sources
[LRT-WE-9-FB-4(1987)] 22 p3077 N88-28268
Mass transport in sector and annular sector tubes
[LRT-WE-9-FB-9(1987)] 22 p3077 N88-28269
Mass transport in annular spherical system
[LRT-WE-9-FB-11(1987)] 22 p3077 N88-28271
Mass transport in a parabolic conduit
[LRT-WE-9-FB-1(1988)] 22 p3077 N88-28273
Mass transfer instabilities due to angular momentum flows in close binaries --- stars
[MPE-PREPRINT-113] 22 p3165 N88-28849
The evolution of low-mass X-ray binaries
[MPE-PREPRINT-118] 22 p3165 N88-28851
Global vertical mass transport by clouds: A two-dimensional model study
[CM-74] 24 p3391 N88-30192

MASSACHUSETTS
Tide- and wind-forced currents in Buzzards Bay, Massachusetts
[PB88-110580] 07 p0882 N88-15350

MATCHED FILTERS
Detection of signals by the digital integrate-and-dump filter with offset sampling 04 p0435 N88-12695
Detection of signals by weighted integrate-and-dump filter 04 p0435 N88-12696
On the design of suboptimal matched filters for three-dimensional moving target detection
[AD-A188384] 12 p1619 N88-19682
Computation of LMS (Least-Mean-Square) and matched digital filters for optical clutter suppression
[AD-A188885] 12 p1687 N88-20093
Synthetic-aperture radars viewed as interferometers with matched filter processing of the collected data
[AD-A190608] 15 p2057 N88-22262
Spatial matched processing for multipath propagation
[AD-A189790] 15 p2129 N88-22701
A numerically efficient digital matched filter for periodic and windowed periodic radar waveforms
[AD-A193132] 21 p2932 N88-27410
Maximum dynamic responses using matched filter theory and random process theory
[NASA-TM-100653] 22 p3042 N88-28059

MATCHING
Multiple-object motion estimation by maximal matching of 3-D point and line features 09 p1220 N88-17322
Digital SPOT stereoplotting: An original approach to the formation of epipolar images and matching
22 p3113 N88-28493
Cleanability of aircraft polyurethane topcoats
[AD-A193456] 23 p3170 N88-28878
On broadband matching of multiport electrical networks with applications
[AD-A194224] 23 p3207 N88-29086
Linearized model matching for single-imput nonlinear systems
[AD-A193642] 23 p3266 N88-29445

MATERIAL ABSORPTION
Microwave dispersion and absorption in tissues: Molecular mechanisms
[AD-A190118] 15 p2100 N88-22512
Bimolecular reactions and energy-transfer processes of highly vibrationally excited molecules related to energetic materials
[AD-A189013] 18 p2571 N88-25270

MATERIAL BALANCE
NT WATER BALANCE
Design of an elemental analysis system for CELSS research 03 p0360 N88-12266
Mass balances for a biological life support system simulation model 03 p0361 N88-12272
Problems appearing at interface balances --- flames
14 p1987 N88-21855

MATERIAL REMOVAL (MACHINING)
U MACHINING

MATERIAL STRENGTH
U MECHANICAL PROPERTIES

MATERIALS HANDLING
NT GROUND HANDLING
NT PROPELLANT TRANSFER
NT REMOTE HANDLING
The development of a friction model predicting the sliding behavior of materials pairs, especially at low temperatures: Progress report and renewal proposal
[DE87-013941] 01 p0055 N88-10354
Experimental molecular spectroscopy in shock-compressed materials
[DE87-013139] 02 p0144 N88-10903
DOE explosives safety manual
[DE88-000831] 04 p0422 N88-12616
Nuclear techniques in studies of condensed matter
[NASA-RP-1195] 04 p0489 N88-13015
To determine the stress distribution in the vicinity of GRP end pads where the specimen is held and loaded (CFC coupon specimens) --- glass reinforced plastic (GRP) carbon fiber composite (CFC)
[BAE-WST-R-RES-CFC-12023]
09 p1182 N88-17080
Non-proprietary research projects of the Center for the Space Processing of Engineering Materials
[AR-2] 10 p1426 N88-18516
Selection of a handling and maintenance option for the SP-100 ground engineering system test
17 p2402 N88-24285
Proposed quality assurance/quality control plan
[AD-A191490] 18 p2525 N88-24978
RRSAS (Robotic Radiation Survey and Analysis System) Project: A real time sensor driven robotic system
[DE88-006825] 20 p2808 N88-26661
Expert system application education project
[NASA-CR-183089] 20 p2843 N88-26867
Aircraft refueling demonstrator using a microbot alpha 2 robot 21 p2926 N88-27367
Mobile robotics R and D at the Savannah River Laboratory
[DE88-011665] 22 p3083 N88-28310
A guide to good magnetic tape management practice for MODAS users --- modular airborne data acquisition system (MODAS)
[RAE-TM-IT-212] 22 p3162 N88-28834
A robotic system for automation of logistics functions on the Space Station 23 p3260 N88-29407
Vanderbilt free electron laser project in biomedical and materials research
[AD-A195961] 24 p3378 N88-30121
Applications of synchrotron radiation to materials science: Diffraction imaging (topography) and microradiography
[NASA-CR-183265] 24 p3434 N88-30440

MATERIALS RECOVERY
NT SOLVOLYSIS
NT WATER RECLAMATION
Separation of anionic from nonionic alkoxy compounds using silica gel
[GB-PATENT-2-140-415-A] 01 p0020 N88-10122
A large-scale perspective on ecosystems
03 p0360 N88-12265
An overview of Japanese CELSS research activities
03 p0360 N88-12267
Design study for asteroidal exploitation
03 p0389 N88-12445
STS propellant scavenging systems study. Part 2, volume 1: Executive summary and study results
[NASA-CR-179275] 10 p1290 N88-17716
Evaluation of bituminous materials used in pavement recycling projects at Tyndall, MacDill, and Hurlburt Air Force Bases
[AD-A188068] 10 p1317 N88-17871
MATERIALS SCIENCE
JPRS report: Science and technology. USSR: Materials science
[JPRS-UMS-87-006] 03 p0285 N88-11791
The contribution of electron microscopy of materials science to society
[DE88-006341] 15 p2028 N88-22082
MATERIALS TESTING REACTORS
U NUCLEAR RESEARCH AND TEST REACTORS
MATERIALS TESTS
Spectroradiometry in materials testing
16 p2273 N88-23601
MATHEMATICAL ANALYSIS
U APPLICATIONS OF MATHEMATICS
MATHEMATICAL LOGIC
NT ALGORITHMS
NT AXIOMS
NT BOOLEAN ALGEBRA
NT BOOLEAN FUNCTIONS
NT BOREL SETS
NT EQUIVALENCE
NT FORMULAS (MATHEMATICS)
NT LATTICES (MATHEMATICS)
NT PARSING ALGORITHMS
NT SET THEORY
NT SIMPLEX METHOD
Extraction and evaluation of Boolean relations for the solution of linear programs in 0-1 variables, volume 1
[ENST-86E023-VOL-1] 02 p0227 N88-11430
Extraction and evaluation of Boolean relations for the solution of linear programs in 0-1 variables, volume 2
[ENST-86E023-VOL-2] 02 p0227 N88-11431
Maintaining state constraints in relational databases: A proof theoretic basis
[DE87-014329] 02 p0248 N88-11569
An exact penalization viewpoint of constrained optimization
[DE88-001477] 04 p0486 N88-12995
The implementation of artificial intelligence in control systems
[DE88-003497] 10 p1396 N88-18318
The representation of knowledge within model-based control systems
[DE88-004863] 10 p1396 N88-18319
Measures of similarity between fuzzy concepts: A comparative analysis
[AD-A189430] 13 p1825 N88-20910
Abstraction and empty process in process algebra
[CWI-CS-R8721] 13 p1826 N88-20919
ONTIC: A knowledge representation system for mathematics
[AD-A190553] 15 p2121 N88-22643
Improving the performance of AI algorithms
[AD-A192848] 21 p3003 N88-27809
MATHEMATICAL MODELS
NT ANALOG SIMULATION
NT BIOLOGICAL MODELS (MATHEMATICS)
NT DIGITAL SIMULATION
NT K-EPSILON TURBULENCE MODEL
NT MANDELSTAM REPRESENTATION
NT PETRI NETS
NT THOMAS-FERMI MODEL
NT TURBULENCE MODELS
The numerical simulation of an idealised one-dimensional, steady monopropellant rocket
[PDR/CFDU/IC/31] 01 p0018 N88-10107
The dissociation of dense liquid nitrogen and shock cooling
[DE87-013490] 01 p0022 N88-10136
A quantitative statistical model for cleavage fracture initiation in carbide strengthened steels
[ETN-87-90735] 01 p0025 N88-10157
Current experimental and theoretical understanding of detonation waves in heterogeneous solid explosives
[DE87-012177] 01 p0032 N88-10201
Performance of rotary regenerative heat exchanger: A numerical simulation 01 p0046 N88-10292
Cooling effect of a single evaporating droplet on a hot semi-infinite metal body
[PB87-201802] 01 p0046 N88-10294
Experimental and theoretical studies of vertical annular liquid jets
[DE87-013907] 01 p0047 N88-10299
Problem specifications and collated solutions of the two-phase numerical-benchmark exercise 1986-7 --- two phase flow
[CFDU/87/1] 01 p0047 N88-10300
Phase dynamics: A review and a perspective
[DE87-013173] 01 p0048 N88-10306
Development of response models for the Earth Radiation Budget Experiment (ERBE) sensors. Part 4: Preliminary nonscanner models and count conversion algorithms
[NASA-CR-178295] 01 p0050 N88-10317
The development of a friction model predicting the sliding behavior of materials pairs, especially at low temperatures: Progress report and renewal proposal
[DE87-013941] 01 p0055 N88-10354
Analysis of shell-type structures subjected to time-dependent mechanical and thermal loading
[NASA-CR-181409] 01 p0060 N88-10388
High-efficiency silicon solar cells: Numerical modeling, transient measurements, efficiency goals, and v-shaped grooves
[DE87-012842] 01 p0066 N88-10423
Status of the solar and infrared radiation submodels in the LLNL 1-D and 2-D chemical-transport models
[DE87-014320] 01 p0069 N88-10441
Experimental study and modeling of the physical mechanisms of the gliding spark
[ESA-TT-1029] 01 p0070 N88-10447
Conception and discussion of a model describing ice formation on various obstacles
[ONERA-NT-1986-6] 01 p0072 N88-10460
Contributions to the modeling of wind shear for danger studies
[ETN-87-90442] 01 p0072 N88-10463
The box method for linear programming. Part 1: Basic theory
[DE87-011029] 01 p0080 N88-10515
Language modelling for automatic speech recognition: A review
[RSRE-MEMO-4038] 01 p0084 N88-10544
The use of splines in the modelling of a photodiode response
[NPL-DITC-88/87] 01 p0085 N88-10550
Data Model of Objects and Relations (DAMOR): A data model for knowledge representation
[REPT-87-05] 01 p0085 N88-10553
Steady state theta pinch concept for slow formation of FRC
[ISSN-0469-4732] 01 p0098 N88-10648
Optimization of SIS mixer elements
[NASA-CR-180710] 01 p0104 N88-10680
Spontaneous symmetry breaking in N=2 supergravity
[DE87-702749] 01 p0109 N88-10704
Spontaneous symmetry breaking in N=3 supergravity
[DE87-702753] 01 p0109 N88-10705
Real-time expert systems: A status report
02 p0129 N88-10817
Mathematical modelling of solar ultraviolet radiation induced optical degradation in anodized aluminum
02 p0135 N88-10846
Structural Assembly Demonstration Experiment (SADE)
[NASA-CR-179205] 02 p0138 N88-10868
Numerical simulation of a supersonic chemically reacting mixing layer 02 p0143 N88-10900
Computer modeling of metal forming
[DE87-013804] 02 p0157 N88-10984
Modeling and performance evaluation of the DPS25 packet switching multiprocessor system --- communication networks
[ENST-87E009] 02 p0162 N88-11016
Contribution to the study of circuit switched networks: Modeling and numerical solutions
[LAAS-87-174] 02 p0162 N88-11017
On the modelling of non-reactive and reactive turbulent combustor flows 02 p0169 N88-11061
An approximate solution to the problem of heating massive bodies by both radiation and convection
[BLL-M-37315-(5828.4)] 02 p0170 N88-11068
Impact of turbulence modeling on numerical accuracy and efficiency of compressible flow simulations
[NASA-TM-88333] 02 p0173 N88-11088
Turbine Engine Hot Section Technology, 1985
[NASA-CP-2405] 02 p0184 N88-11140
Aerothermal modeling program, phase 2
02 p0185 N88-11149
Constitutive modeling for single crystal superalloys
02 p0187 N88-11168
Life prediction and constitutive models for engine hot section anisotropic materials program
02 p0188 N88-11175
Coating life prediction 02 p0189 N88-11181
Thermal barrier coating life prediction model development 02 p0190 N88-11184
Thermal barrier coating life prediction model development 02 p0190 N88-11185
Estimating scattered and absorbed radiation in plant canopies by remote sensing
[NASA-CR-181390] 02 p0193 N88-11205
A real-data numerical study and four-dimensional data assimilation application for mesobeta-scale flow in complex terrain 02 p0212 N88-11329
On the surging potential of polar ice streams. Antarctic surges: A clear and present danger
[DE87-013980] 02 p0216 N88-11363
Numerical simulation of Tokamaks: Ideal MHD equilibrium and stability
[DE87-013452] 02 p0218 N88-11373
Software reliability models for fault-tolerant avionics computers and related topics
[NASA-CR-181440] 02 p0220 N88-11382
Projection-space iterative interpolation for limited-angle tomography in parallel- and fan-beam geometry, part 1
[DE87-013965] 02 p0221 N88-11391
A treatment of jw-axis model-matching transformation zeros in the optimal H squared and H infinity control designs
[OUEL-1673/87] 02 p0223 N88-11407
On the relational modeling of discrete PDE problems
[DE87-013336] 02 p0224 N88-11409
An adaptive pseudo-spectral method for reaction diffusion problems
[NASA-CR-178394] 02 p0224 N88-11414
Parallel methods for ordinary differential equations
[DE87-014667] 02 p0226 N88-11425
An empirical investigation of the use of ranks in pips sampling
[DE87-010609] 02 p0228 N88-11438
Measures of diversity based on fuzzy multinomial distributions
[DE87-010617] 02 p0228 N88-11439
Evaluation of a scale-model experiment to investigate long-range acoustic propagation
[NASA-TP-2748] 02 p0230 N88-11450
Pinhole occulter experiment
[NASA-CR-179206] 02 p0235 N88-11481
Computer models for kinetic equations of magnetically confined plasmas
[DE87-011571] 02 p0236 N88-11492
Thin film microstructures: Simulation and theory
[DE87-014732] 02 p0246 N88-11553
The Shock and Vibration Digest, Volume 19, No. 11
03 p0265 N88-11673
Analytical average model of studies on orbital resonance 03 p0269 N88-11689
Stability of mechanical joints in launching vehicles: Local and global stationary values of energy density
03 p0270 N88-11696
Three-dimensional finite element based, interative approach for analysis of laminated composites
03 p0280 N88-11763
Combustion in turbulent jets and buoyant flames
[PB87-232674] 03 p0283 N88-11779
Ignition and flame propagation in sprays
[AD-A184679] 03 p0283 N88-11781
Numerical simulation of turbulent premixed combustion and decay of turbulent swirling flow
[DE87-014253] 03 p0284 N88-11787
Crevice corrosion of stainless steels and related alloys. Part 2: Summary of experimental test data for input to mathematical model
[BR99871-PT-2] 03 p0289 N88-11816
Generalized coupled-mode equations, applications to fiber couplers 03 p0298 N88-11875
Generalized hybrid variational principle, corresponding finite element model 03 p0301 N88-11895
Compactness of quasi-conforming element spaces, convergence of quasi-conforming element method
03 p0301 N88-11896
Numerical modeling: Integral equation method
03 p0304 N88-11919
Hollow cathode plasma coupling study, 1986
[NASA-CR-171985] 03 p0309 N88-11949
Computation of turbulent flows using an extended k-epsilon turbulence closure model
[NASA-CR-179204] 03 p0312 N88-11969
Special Course on Modern Theoretical and Experimental Approaches to Turbulent Flow Structure and its Modelling
[AGARD-R-755] 03 p0312 N88-11970
Turbulence modelling through one point closures-applications-enlightening by large eddy simulation 03 p0312 N88-11972
Transition to turbulence via spatio-temporal intermittency 03 p0313 N88-11976
Lattice gas hydrodynamics 03 p0313 N88-11978

A transient model for thermal detonation
[IKE-2-75] 03 p0314 N88-11984
Stochastic model of the motion of suspended particles in turbulent flow
[HSBW-MITT-21/1987] 03 p0315 N88-11990
Conjugated heat transfer from a radiating fluid in a rectangular channel 03 p0317 N88-12003
Thrust and specific impulse of repetitively-pulsed-laser propulsion rocket 03 p0318 N88-12012
Heat transfer performance of axially grooved heat pipes 03 p0319 N88-12016
Heat transfer characteristics of arterial heat pipe with axial grooves 03 p0319 N88-12017
On the root locus method applied to flexural vibration control systems 03 p0320 N88-12022
Unsteady flow about cambered plates
[AD-A184725] 03 p0320 N88-12025
A study of chaos and mixing in Rayleigh-Taylor and Richtmyer-Meshkov unstable interfaces
[AD-A184751] 03 p0320 N88-12026
The dynamics of bubble growth for Rayleigh-Taylor unstable interfaces
[AD-A184752] 03 p0321 N88-12027
Continued research on direct contact heat exchangers: Effects of crystallization
[DE87-014931] 03 p0322 N88-12035
Multidimensional modeling of convective heat transfer with application to I.C. engines
[DE87-014983] 03 p0322 N88-12036
Bearing loads in slider crank mechanisms
[PB87-216495] 03 p0332 N88-12089
Models for conducting economic analysis of alternative fuel vehicles
[AD-A184028] 03 p0334 N88-12103
Teleoperator and robotics system analysis
[NASA-CR-179220] 03 p0334 N88-12105
Effects of state recovery on creep buckling induced by thermomechanical loading 03 p0336 N88-12116
Dynamic response of a 330 KW horizontal axis wind turbine generator
[DE87-014867] 03 p0347 N88-12195
Heats of mixing for thermal energy storage systems. Phase 1: Selection of suitable liquid-liquid mixtures
[DE87-014971] 03 p0347 N88-12196
An algorithmic approach to crustal deformation analysis
[NASA-CR-181497] 03 p0349 N88-12203
Earthquake source mechanisms and transform fault tectonics in the Gulf of California 03 p0349 N88-12206
Kinds of bootstraps and kinds of jackknives, discussed in terms of a year of weather-related data
[AD-A184495] 03 p0353 N88-12227
A simulation study of a speed control system for autonomous on-road operation of automotive vehicles
[AD-A184030] 03 p0362 N88-12279
Nonlinear parametric least-squares adjustment
[AD-A184039] 03 p0371 N88-12336
Stochastic model of the NASA/MSFC ground facility for large space structures with uncertain parameters: The maximum entropy approach
[NASA-CR-181489] 03 p0372 N88-12343
Mathematical models for the S.D.I.
[AD-A184667] 03 p0373 N88-12345
Applications of a theory of ferromagnetic hysteresis
[DE87-014725] 03 p0373 N88-12348
A hybrid numerical technique for predicting the aerodynamic and acoustic fields of advanced turboprops
[NASA-CR-174926] 03 p0374 N88-12352
Monte Carlo simulation of primitive atom-transfer reactions in solution
[AD-A183977] 03 p0375 N88-12360
Mathematical models of plasma discharge control in a tokamak
[DE87-702891] 03 p0378 N88-12377
Stability of low-shear Tokamaks
[DE88-000305] 03 p0379 N88-12383
The itinerant resonating-valence-bond model for superconductivity
[DE87-014794] 03 p0380 N88-12391
Modeling of proximity coupling between superconducting filaments in superconducting dipole magnets
[DE87-014684] 03 p0382 N88-12403
Hovering helicopter flight dynamics: A study of vertical motion
[AR-004-526] 04 p0399 N88-12485
An integrated study of structures, aerodynamics and controls on the forward swept wing X-29A and the oblique wing research aircraft
[NASA-CR-181548] 04 p0399 N88-12486
Aircraft engine exhaust plume dynamics
[AD-A184238] 04 p0400 N88-12488
Efficiency aspects of short, low velocity railguns
[AR-004-847] 04 p0405 N88-12517
Analytical investigation of the dynamics of tethered constellations in Earth orbit (phase 2)
[NASA-CR-179218] 04 p0408 N88-12533
A study of mechanisms of hydrogen diffusion in separation devices
[DE88-000328] 04 p0416 N88-12584
Microgravity nucleation and particle coagulation experiments support
[NASA-CR-181540] 04 p0423 N88-12618
Microgravity nucleation and particle coagulation experiments support
[NASA-CR-181541] 04 p0423 N88-12619
Aircraft dynamic response calculation based on discrete-continual model 04 p0424 N88-12624
A direct method to obtain constitutive model constants from cylinder impact test results 04 p0427 N88-12647
Ideal-viscoplastic extrusion model with application to deforming pistons in light-gas guns
[UTIAS-TN-266] 04 p0429 N88-12657
Heterogeneous multi-trunking queueing systems
[AD-A184255] 04 p0431 N88-12668
Programmable Logic Arrays (PLA's) design for testability
[PB87-102935] 04 p0438 N88-12718
An analytical and experimental study of injection-locked two-port oscillators
[NASA-TM-100119] 04 p0439 N88-12727
The Pierce diode with an external circuit. Part 1: Simulations in the linear regime
[DE88-000413] 04 p0440 N88-12731
Fully developed turbulence via Feigenbaum's period-doubling bifurcations
[DE88-000242] 04 p0441 N88-12739
Numerical simulation of unsteady separated flows
[AD-A184132] 04 p0442 N88-12741
Tracking through turbulence at the Tonopah Test Range
[DE88-001448] 04 p0446 N88-12766
Analysis of sideband spectra from untapered undulator using analytical technique
[DE87-014763] 04 p0448 N88-12778
The modelling of orientation in planar polymer welding flows
[AD-A184404] 04 p0451 N88-12793
Nonlinear axial stiffness characteristics of axisymmetric bolted joints 04 p0452 N88-12799
Creep life prediction based on stochastic model of microstructurally short crack growth
[NASA-TM-100245] 04 p0456 N88-12825
Two-layer stratified flow analysis of gravity currents and turbidity currents in lakes, reservoirs and the ocean 04 p0463 N88-12864
Statistics of the geomagnetic secular variation for the past 5Ma
[NASA-CR-181558] 04 p0467 N88-12890
An algorithmic approach to crustal deformation analysis 04 p0468 N88-12891
The effects of minor trace gases on the transfer of thermal infrared radiation through the Earth's atmosphere 04 p0468 N88-12893
Experimental and analytic studies of the triggered lightning environment of the F106B
[NASA-CR-4104] 04 p0469 N88-12897
Estimation of a multivariate continuous variable panel model
[AD-A184472] 04 p0484 N88-12982
The shifted Adams method for ordinary differential equations
[DE88-000810] 04 p0486 N88-12994
Radiation induced collapse of the crystalline structure
[DE87-014407] 04 p0498 N88-13064
Subjective probability, combination of expert opinion and probabilistic approaches to information retrieval 04 p0501 N88-13085
The acceleration of winds by MHD waves in open magnetic structures 04 p0506 N88-13109
Cosmological applications of singular hypersurfaces in general relativity 04 p0521 N88-13202
Gamma ray lines from novae 04 p0526 N88-13214
Computation of rime ice accretion on airfoils
[FFA-TN-1987-08] 05 p0542 N88-13301
Non-linear maximum likelihood estimation of stability derivatives from range data
[NAL-TM-SE-8608] 05 p0552 N88-13365
Development of an integrated BEM approach for hot fluid structure interaction
[NASA-CR-181577] 05 p0556 N88-13384
OH(A-X) fluorescence from photodissociative excitation of HO2 at 157.5 nm
[NASA-CR-181580] 05 p0563 N88-13429
A mathematical model of high alloy nickel base high temperature alloys
[BLL-M-37381-(5828.4)] 05 p0564 N88-13436
Noise modelling in the time domain with the aid of Spice
[PB87-221941] 05 p0573 N88-13492
Large bandwidth ground scattering model --- radar scattering
[FOA-C-30458-3.2] 05 p0576 N88-13511
Conditional second order closure for turbulent shear flows
[AD-A185369] 05 p0581 N88-13542
Active and passive plume distribution models in the convective boundary layer using a large eddy simulation model
[KNMI-TR-90] 05 p0581 N88-13546
Model-based motion estimation and its application to restoration and interpolation of motion pictures
[AD-A185054] 05 p0584 N88-13558
Simulation of the perpendicular magnetic recording process
[B8713537] 05 p0586 N88-13570
Theoretical studies of solar lasers and converters
[NASA-CR-181569] 05 p0587 N88-13577
Control of a flexible one-link manipulator
[AD-A185035] 05 p0590 N88-13598
Non-linear shipboard shock analysis of the Tomahawk missile shock isolation system 05 p0592 N88-13614
Analysis of photopole data reduction models 05 p0593 N88-13616
Initial dynamic load estimates during configuration design 05 p0593 N88-13621
Significance of fatigue crack closure under spectrum loading 05 p0599 N88-13662
Low cycle fatigue life predictions of a 1CrMoV steel in terms of a J-controlled short crack growth model 05 p0599 N88-13665
A unified model for fatigue crack initiation, short crack growth, long crack propagation, and closure effects 05 p0601 N88-13680
A dislocation model for fatigue crack propagation under variable amplitude loading 05 p0602 N88-13683
Observations on the effect of overloads on fatigue crack growth 05 p0602 N88-13684
Computer aided modeling and fatigue failure forecast under stochastic loading 05 p0607 N88-13720
Fatigue under nonnormal random stresses using Monte Carlo method 05 p0607 N88-13723
Applications of fatigue analyses: Transportation 05 p0608 N88-13733
The application of doubly-truncated hydrometeor distributions to numerical cloud models
[AD-A185273] 05 p0627 N88-13836
Modeling cloudy and clear interval length probabilities using space shuttle imagery
[AD-A185290] 05 p0627 N88-13837
Human thermoregulatory model for whole body immersion in water at 20 and 28 C
[AD-A185052] 05 p0629 N88-13849
Optimal control of large space structures via generalized inverse matrix
[NASA-CR-182336] 05 p0639 N88-13907
Multidimensional least squares fitting of fuzzy models
[AD-A185148] 05 p0640 N88-13916
The estimation of basic matrices using travel intensity theorems
[REPT-87-13] 05 p0642 N88-13926
SHARP simulation of discontinuities in highly convective steady flow
[NASA-TM-100240] 05 p0642 N88-13931
Sample reuse in statistical remodeling
[AD-A184916] 05 p0643 N88-13938
Presentation of a computer program permitting the exploitation of tests designed to determine the sensitivity of one shot devices to a parameter. Application to a degenerate one shot sequence
[SNIAS-872-430-117] 05 p0644 N88-13945
The interaction of DC plasma jet with a melting metal: Experimental measurements and mathematical description
[AD-A185173] 05 p0651 N88-13993
Numerical models for high beta magnetohydrodynamic flow
[DE88-001850] 05 p0654 N88-14008
A numerical model of unsteady, subsonic aeroelastic behavior
[NASA-TM-100487] 06 p0663 N88-14064
Integration of a supersonic unsteady aerodynamic code into the NASA FASTEX system
[NASA-CR-182329] 06 p0663 N88-14068
Post stall behavior in axial-flow compressors
[AD-A185712] 06 p0665 N88-14081
Performance-limiting factors in MPD thrusters
[AD-A185605] 06 p0674 N88-14128
An overview of metal plasticity
[DE88-001658] 06 p0681 N88-14175
The effective elastic properties of low-density foams
[DE87-014629] 06 p0684 N88-14194

Theory of displaced phase center antenna for space based radar applications
[PB87-229837] 06 p0690 N88-14227
Advanced numerical modeling of microwave penetration and coupling for complex structures
[DE88-001873] 06 p0690 N88-14231
A model for ultra-low fatigue crack growth
06 p0717 N88-14404
Crack closure phenomena in modes 1 and 2 interactions 06 p0719 N88-14417
Fatigue life prediction modeling for turbine hot section materials
[NASA-TM-100291] 06 p0724 N88-14453
Mathematical-cartographic modeling of economic utilization of Atlantic Ocean 06 p0726 N88-14469
Numerical modeling of troposphere-induced gravity wave propagation 06 p0735 N88-14522
Meteor velocity distribution and an optimum monitoring mathematical model 06 p0739 N88-14546
Monte Carlo modeling and meteor showers
06 p0740 N88-14549
Some models of the Geminids meteor stream formation 06 p0740 N88-14551
Estimation of rainfall rates in tropical cyclones by passive microwave radiometry 06 p0744 N88-14577
Interim review of the possibilities and opportunities for the ONR tropical cyclone motion research initiative
[AD-A185679] 06 p0746 N88-14592
Forecast of current patterns for an eddy tracking experiment in the Norwegian coastal current
[PB87-224853] 06 p0747 N88-14595
Dimensional analysis of nonlinear oscillations in brain, heart and muscle
[DE87-014749] 06 p0751 N88-14614
Model based monitoring of human sleep stages
[ISBN-90-9001448-9] 06 p0752 N88-14618
A taxonomy of analytical computer performance models for computer design
[AD-A185561] 06 p0755 N88-14632
The adaption and use of research codes for performance assessment
[DE88-000552] 06 p0756 N88-14639
Diffusion first passage times: Approximations and related differential equations
[AD-A185592] 06 p0765 N88-14700
A unified mathematical approach to image analysis
[AD-A185719] 06 p0765 N88-14703
Characteristic trajectories of generalized Lanchester equations
[AD-A185762] 06 p0766 N88-14705
Asymptotic normality of poly-t densities with Bayesian applications
[AD-A185718] 06 p0768 N88-14719
Sound propagation over uneven ground and irregular topography
[NASA-CR-182352] 06 p0776 N88-14763
A long term radiological risk model for plutonium-fueled and fission reactor space nuclear system
[DE87-010466] 06 p0779 N88-14782
Mathematical model for the dc-ac inverter for the Space Shuttle 06 p0793 N88-14860
Prediction of physical workload in reduced gravity environments 06 p0794 N88-14867
Inventory behavior at remote sites
06 p0796 N88-14873
Modeling the growth dynamics of four candidate crops for Controlled Ecological Life Support Systems (CELSS)
06 p0799 N88-14889
Consistent spherical Nonlocal Thermal Equilibrium (NLTE) models for objects with B-star-like luminosities
[ETN-88-90601] 06 p0800 N88-14897
Observation and interpretation of solar S-component radiation at millimetre waves
[PB87-225207] 06 p0805 N88-14916
A theory for the core flow of leading-edge vortices
07 p0810 N88-14935
Microwave Landing System (MLS) mathematical model installation manual
[AD-A185612] 07 p0819 N88-14978
Mathematical models of continuous flow electrophoresis: Electrophoresis technology
[NASA-CR-179241] 07 p0828 N88-15021
SRB combustion dynamics analysis computer program (CDA-1)
[NASA-CR-182404] 07 p0830 N88-15032
Catalog of compartment fire model algorithms and associated computer subroutines
[PB88-110861] 07 p0839 N88-15087
Channel access protocols for multihop packet radio networks
[AD-A186074] 07 p0842 N88-15105
Chemical reactions in turbulent mixing flows
[AD-A186141] 07 p0849 N88-15153
Microcomputer controlled arc welding power source: Its steady state and transient performance
[PB87-143921] 07 p0863 N88-15233
Behavior of a steel cylinder under the influence of a local load in the elastic and elasto-plastic area
[PB87-154787] 07 p0869 N88-15272
Hurricane Danny storm surge data, report 4
[AD-A186373] 07 p0879 N88-15334
Hurricane Kate storm surge data, report 5
[AD-A186374] 07 p0880 N88-15335
The ocean heat budget
[AD-A186130] 07 p0881 N88-15346
New methods for numerical solution of one class of strongly nonlinear partial differential equations with applications
[AD-A186166] 07 p0899 N88-15445
Modelling of clustering effects in point processes: An application to failures in SPC-systems (stored program control-systems)
[PB87-149241] 07 p0904 N88-15480
On two methods of identifying influential sets of observations
[AD-A186270] 07 p0910 N88-15518
The information metric for univariate linear elliptic models
[AD-A186385] 07 p0911 N88-15527
Maximum likelihood principle and model selection when the true model is unspecified
[AD-A186027] 07 p0914 N88-15544
A simplified model of elementary particles
[NOTA-INTERNA-890] 07 p0930 N88-15647
Model for plasma equilibrium configuration evolution in a tokamak with adiabatic compression
[DE88-700354] 07 p0936 N88-15684
Simple model for hot ion plasmas
[DE88-750045] 07 p0936 N88-15688
Numerical modelling of the classical nova outburst
[NASA-TM-89707] 07 p0945 N88-15746
Energetics and dynamics of simple impulsive solar flares
[NASA-TM-87816] 07 p0947 N88-15755
Rotorcraft transmission 08 p0956 N88-15802
The dynamics and control of large-flexible space structures, part 10
[NASA-CR-182426] 08 p0963 N88-15830
Contribution to modeling flexion fatigue damage in unidirectional composite materials
[ECL-87-12] 08 p0965 N88-15843
Velocity and density measurements in a turbulent nonpremixed flame with comparison to numerical model predictions
[DE87-014695] 08 p0967 N88-15854
A continuous oxidizer regression model for the combustion of composite solid propellants
[AD-A186742] 08 p0974 N88-15894
Peacekeeper tank slosh model
08 p0983 N88-15942
A computationally efficient modelling of laminar separation bubbles
[NASA-CR-182417] 08 p0984 N88-15949
Time accurate techniques using characteristic flux averaging with application to unsteady aerodynamics
08 p0985 N88-15957
Nonequilibrium reacting flows
08 p0985 N88-15959
Introduction to the Modeling of Turbulence
[VKI-LS-81-06] 08 p0986 N88-15972
Examples of turbulence-model applications
08 p0987 N88-15975
Turbulence modeling for compressible flows
08 p0987 N88-15978
Modeling the unsteady flow found in axial turbomachinery
[ECL-87-07] 08 p0987 N88-15980
Dynamic analysis of a structure with sliding base
08 p0998 N88-16045
Summary of HSST wide-plate crack-arrest tests and analyses
[DE88-002601] 08 p1000 N88-16061
Theory of deformation. Part 1: Kinematics
[DE88-003007] 08 p1001 N88-16062
Gyrostabilizer system of Kvant module
08 p1006 N88-16099
Selection of efficient correcting motor for an artificial Earth satellite 08 p1007 N88-16102
Statistical model of interaction of electromagnetic waves with natural objects being sensed
08 p1008 N88-16112
Modeling of architecture of a problem-oriented on-board processor 08 p1008 N88-16114
Geomechanical model of seismofocal zone of active continental margin 08 p1011 N88-16128
The entropy of the Lorentz model
08 p1015 N88-16153
Model calculations of the behavior of orographically influenced cold fronts 08 p1015 N88-16155
The iterative radiance model of the Meteorological Institute of the University of Munich (West Germany)
08 p1019 N88-16178
Nonlinear, relativistic Langmuir waves in astrophysical magnetospheres
[NASA-CR-182422] 08 p1024 N88-16197
Wave acceleration of auroral electrons
08 p1031 N88-16245
Prediction of human thermoregulatory responses and endurance time in water at 20 and 24C
[AD-A186223] 08 p1048 N88-16326
Short pseudorandom test sequences
[AD-A185883] 08 p1054 N88-16357
Automatic mathematical modeling for space application 08 p1060 N88-16402
LISP based simulation generators for modeling complex space processes 08 p1061 N88-16403
Rapid prototyping and AI programming environments applied to payload modeling 08 p1061 N88-16405
Qualitative models for planning: A gentle introduction
08 p1062 N88-16414
Development of a computer model for missile simulation, or simulation of a kinetic coverage area for a target detection missile
[FOA-C-20666-2.5] 08 p1067 N88-16449
Development of a computer model for missile simulation, or simulation of a kinetic coverage area for a collimation guided missile
[FOA-C-20667-2.5] 08 p1067 N88-16450
Effects of uniform target density on random search
[AD-A186468] 08 p1073 N88-16473
Test of linearity in general regression models
[AD-A186036] 08 p1073 N88-16477
Estimation and comparison of changes in the presence of information right censoring by modeling the censoring process
[AD-A186320] 08 p1074 N88-16478
Numerical analysis of motion of solid bodies in atmosphere 08 p1079 N88-16505
Digital image processing
[INPE-4131-TDL/264] 08 p1083 N88-16527
Interpretation of the temperature dependence of conductivity in superconducting oxides
[DE88-003028] 08 p1091 N88-16565
Comprehensive rotorcraft analysis methods
09 p1106 N88-16630
Rotorcraft aeroelastic stability
09 p1106 N88-16631
Helicopter mathematical models and control law development for handling qualities research
09 p1108 N88-16642
An initial investigation into methods of computing transonic aerodynamics sensitivity coefficients
[NASA-CR-182444] 09 p1112 N88-16663
Verification of obstacle accountability areas using a simple mathematical model. Part 1: Description of general model and application for a specific case --- engine failure at takeoff
[NLR-TR-85069-U] 09 p1115 N88-16683
Communications satellite systems operations with the space station. Volume 3: Supplementary technical report
[NASA-CR-180875] 09 p1133 N88-16794
Kinetic isolation tether experiment
[NASA-CR-182458] 09 p1135 N88-16810
Helium-ion-induced release of hydrogen from graphite
[DE88-002599] 09 p1142 N88-16846
The effects of fuel composition on ignition delay in homogeneous charge and direct injection compression ignition engines
[DE88-003691] 09 p1143 N88-16849
Dynamical characteristics of weak turbulence
[AD-A186724] 09 p1161 N88-16957
Numerical modeling of multidimensional flow in seals and bearings used in rotating machinery
[NASA-TM-100779] 09 p1165 N88-16988
Modeling of pulsed gas flow lasers
[DFVLR-FB-87-19] 09 p1171 N88-17021
New model to estimate the perforation power of kinetic energy projectiles
[PB87-166757] 09 p1175 N88-17040
Maximum likelihood estimates for the discrete application of the AMSAA growth model
[AD-A186921] 09 p1177 N88-17048
Mechanical impact: Theoretical simulation and correlation 09 p1179 N88-17060
Dynamic stress at critical locations of a structure as a criterion for mathematical model modification
09 p1180 N88-17066
Statistics of two-dimensional structure elements of mountainous ranges (mosaic model) for calculating three-dimensional reflection functions
[DFVLR-FB-87-33] 09 p1185 N88-17099
VAWT (Vertical-Axis Wind Turbine) stochastic loads produced by atmospheric turbulence
[DE88-001355] 09 p1187 N88-17110
A comparison of different module configurations for multibandgap solar cells
[DE88-002718] 09 p1187 N88-17113

Simulation of global wet and dry deposition of nitric acid in a three-dimensional chemistry-transport model
[DE87-009847] 09 p1188 N88-17116

Numerical investigation of orographically enhanced instability
[AD-A186841] 09 p1189 N88-17125

Induced turbulence in aerosol-loaded atmospheres, Jun. 1987
[DE87-014724] 09 p1192 N88-17141

Application of satellite data in variational analysis for global cyclonic systems
[NASA-CR-182468] 09 p1193 N88-17152

Development of a physically-based general circulation model parameterization of clouds and their radiative interactions
[DE88-004060] 09 p1194 N88-17154

GAVID and ACQUIR, two Operations-Research (OR) models for visual detection
[FEL-1985-72] 09 p1200 N88-17194

A situation-response model for intelligent pilot aiding
09 p1208 N88-17241

A human performance modelling approach to intelligent decision support systems 09 p1208 N88-17242

Autonomous control procedures for shuttle rendezvous proximity operations 09 p1208 N88-17244

Artificial Intelligence (AI), Operations Research (OR), and Decision Support Systems (DSS): A conceptual framework 09 p1209 N88-17245

Methodological and structural principles for flexible geometric modeling in computer aided design
[MA-48] 09 p1218 N88-17306

Modification of a successive corrections objective analysis for improved higher order calculations
[NASA-CR-182467] 09 p1230 N88-17370

SURE reliability analysis: Program and mathematics
[NASA-TP-2764] 09 p1231 N88-17380

Prediction of polytomous events: Model description, algorithm development and methodological aspects, with an application
[AD-A186549] 09 p1232 N88-17384

Numerical fluid mechanics 09 p1240 N88-17434

A model for stationary and dynamic impression of undercooled boiling in coupled thermohydraulic and neutron physics calculations of nuclear reactors
[IKE-6-171] 09 p1247 N88-17472

Modeling considerations for selected rf-plasma edge effects
[DE88-003285] 09 p1252 N88-17500

Optimization of volume produced H(-) ions in a low-pressure hydrogen plasma
[IPPJ-853] 09 p1252 N88-17505

Effect of the subgap conductance on the metastable states in a Josephson tunnel junction
[DE88-003102] 09 p1258 N88-17543

Oscillations of solar models with internal element diffusion
[DE88-003156] 09 p1264 N88-17573

Navier-Stokes calculations and turbulence modeling in the trailing edge region of a circulation control airfoil
10 p1268 N88-17587

Wall jet analysis for circulation control aerodynamics. Part 1: Fundamental CFD and turbulence modeling concepts 10 p1269 N88-17588

A theory for turbulent curved wall jets
10 p1269 N88-17590

Wall jet analysis for circulation control aerodynamics. Part 2: Zonal modeling concepts for wall jet/potential flow coupling 10 p1269 N88-17593

Frequency-response identification of XV-15 tilt-rotor aircraft dynamics 10 p1277 N88-17643

Maneuverable reentry vehicle trajectory footprints: Calculation and properties
[DE88-004726] 10 p1292 N88-17726

Insights into the mechanisms of chemical reactions: Reaction paths for chemical reactions
[DE88-003041] 10 p1297 N88-17755

Gas hydrate model development and validation
[DE88-001004] 10 p1298 N88-17762

A large strain thermomechanical forming model for elastic-viscoplastic behavior in metals
10 p1301 N88-17780

The mathematization of the military sciences
[MBB-Z-139/87] 10 p1311 N88-17834

Radar reflectivity and attenuation of radio waves in the melting layer of precipitation
[PB88-121553] 10 p1318 N88-17882

Pulsed current transformer for low inductive loads
[AD-A187224] 10 p1324 N88-17913

Leeside crossflow modeling in Euler space-marching computations
[NASA-TM-89710] 10 p1325 N88-17924

Centerplane source distribution for slender bodies
10 p1328 N88-17940

Periodic natural convection in a rectangular enclosure of low aspect ratio 10 p1329 N88-17941

Three-dimensional incompressible flowfield analysis for establishing rotor designs which optimize power extraction 10 p1329 N88-17943

A review of flow-induced vibration in two-phase flow
[DE88-002873] 10 p1329 N88-17946

Capacitive charge division in centroid finding cathode readouts in MWPCs
[DE88-003545] 10 p1333 N88-17969

Physics modeling support contract
[DE88-004039] 10 p1335 N88-17980

Analysis and application of the constant tensile load test for polyethylene gas pipe materials
[DE88-002868] 10 p1345 N88-18037

Turbulence loads on the Howden 26-m-diameter wind turbine
[DE88-001118] 10 p1351 N88-18075

Evaluation of regional-scale air quality models: Chairmen reports from four workshops
[DE88-001397] 10 p1352 N88-18080

Simulation and modeling of whistler mode wave growth through cyclotron resonance with energetic electrons in the magnetosphere 10 p1353 N88-18089

Analysis of gases in the earth's crust
[PB88-141619] 10 p1354 N88-18093

Systematic errors of the FSU global spectral model
10 p1356 N88-18103

Membrane model of cupula or vestibular semicircular canals 10 p1361 N88-18132

Two-dimensional static otolith model
10 p1367 N88-18167

Scaling physiological pharmacokinetic models by physiological time
[DE88-000335] 10 p1368 N88-18173

Modeling of the non-auditory response to blast overpressure
[AD-A187397] 10 p1369 N88-18184

Parameter identification and sensitivity analysis for a robotic manipulator arm
[NASA-CR-181608] 10 p1385 N88-18272

Identifiability of multivariate ARMA models
[AD-A187394] 10 p1400 N88-18350

Well-posedness and spectral estimation for infinite dimensional systems
[AD-A187821] 10 p1401 N88-18354

A component synthesis method using Lanczos vectors
[DE88-002263] 10 p1403 N88-18368

Applied mathematics of transport theory
[DE88-004098] 10 p1404 N88-18369

Semiempirical studies of atomic structure
[DE88-004096] 10 p1407 N88-18392

Advances in calculating macroionic solution structure
[DE88-003799] 10 p1409 N88-18406

Coronal heating by means of helical magnetohydrodynamic turbulence
[AD-A187084] 10 p1410 N88-18413

Positron-annihilation 2D-ACAR studies of disordered and defected alloys
[DE88-003118] 10 p1416 N88-18454

An experimental investigation of straight and curved annular wall jets
[NASA-CR-182546] 11 p1434 N88-18557

Matrix-fiber stress transfer in composite materials: Elasto-plastic model with an interphase layer
[PB88-136635] 11 p1450 N88-18643

Finite element analysis of adhesively bonded composite joints including geometric nonlinearity, nonlinear viscoelasticity, moisture diffusion and delayed failure
[PB88-147822] 11 p1451 N88-18648

Reactions of some thiol collectors at noble-metal and pyrite electrodes
[PB88-138318] 11 p1455 N88-18674

Experimental set-up and mathematical modeling of H-shaped beam type structure
[AD-A187196] 11 p1466 N88-18743

Investigation of a ray-mode representation of the Green's function in a rectangular cavity
[PB88-131677] 11 p1469 N88-18763

Air Force Institute of Technology (AFIT) Local Area Network (LAN) performance evaluation model: An analytic model for assessing the impact of changing LAN hardware and software configurations
[AD-A187191] 11 p1469 N88-18764

The coaxial colinear antenna: Theoretical and experimental models 11 p1475 N88-18803

Numerical and analytical study of fluid dynamic forces in seals and bearings
[NASA-TM-100268] 11 p1485 N88-18867

Further development of a finite element model of orthogonal metal cutting
[DE88-004048] 11 p1494 N88-18921

Improvement in robot positioning accuracy by a kinematic identification model 11 p1496 N88-18931

Mathematical modeling of the postbuckling behavior of structural elements 11 p1500 N88-18960

A nonlinear computational model for the strength and failure of composite plates and shells
11 p1501 N88-18964

Numerical fracture mechanics using finite element method 11 p1501 N88-18966

Multisource context classification methods in remote sensing 11 p1504 N88-18985

Status of the special-purpose airfoil families
[DE88-001124] 11 p1506 N88-18998

Computer-aided modeling and prediction of performance of the modified Lundell class of alternators in space station solar dynamic power systems
[NASA-CR-182538] 11 p1507 N88-19000

Energetic particle drift motions in the outer dayside magnetosphere
[DE88-005097] 11 p1512 N88-19034

Five New South Wales barrier lagoons: Their macrobenthic fauna and seagrass communities
11 p1517 N88-19059

Center for nonlinear dynamics of the brain
[AD-A187245] 11 p1518 N88-19068

Center for the study of rhythmic processes
[AD-A188204] 11 p1520 N88-19078

Two attentional models of classical conditioning: Variations in CS effectiveness revisited
[AD-A187697] 11 p1522 N88-19088

Integration of finite element modeling with solid modeling through a dynamic interface 11 p1526 N88-19112

Integration of geometric modeling and advanced finite element preprocessing 11 p1526 N88-19114

Finite element meshing of ANSYS (trademark) solid models 11 p1526 N88-19115

Solid/FEM integration at SNLA
[SAND-87-0882A] 11 p1526 N88-19116

Geometrical and topological issues in octree based automatic meshing 11 p1527 N88-19118

Finite octree meshing through topologically driven geometric operators 11 p1527 N88-19121

Design modeling for shape optimization
11 p1527 N88-19122

Postprocessing techniques for 3D non-linear structures 11 p1528 N88-19124

Geometric versus finite element modeling current and future trends at Northrop 11 p1528 N88-19125

Estimation in linear models with censored data
[AD-A187209] 11 p1540 N88-19203

Irreducible tensor operators and multiple-quantum NMR 11 p1542 N88-19217

Theory of two-photon emission from atomic inner shells
[AD-A187742] 11 p1543 N88-19223

Problems in modeling TF ripple loss of fast alphas from a tokamak reactor
[DE88-000612] 11 p1553 N88-19296

Thermodynamics of wetting by liquid metals
[DE88-003634] 11 p1563 N88-19360

A comparative survey of mathematical models for dynamic simulation of in-orbit manipulation operations
12 p1592 N88-19533

Dynamics modeling, simulation, and control of a spacecraft/manipulator system
12 p1592 N88-19534

Modeling of a nutation damper for satellite stabilization through rotation
[INPE-4275-PRE/1147] 12 p1601 N88-19584

Linear and nonlinear acoustics with nonuniform entropy in combustion chambers 12 p1607 N88-19609

Analysis of low gravity tolerance of model experiments for space station: Preliminary results for directional solidification
[NASA-CR-182657] 12 p1614 N88-19648

Reliability analyses of a surface mounted package using finite element simulation
[AD-A189488] 12 p1624 N88-19717

Accelerating the computation of steady state solutions for non-equilibrium, chemically reacting flow fields
12 p1625 N88-19724

Compressible friction coefficients in a simulated heat pipe
[AD-A188818] 12 p1627 N88-19735

A simulation of void lining during ductile fracture
[AD-A188404] 12 p1635 N88-19792

Report on phase 1 of the project estimate development of a model for yield estimation of sugar cane based on LANDSAT and agromet data
[INPE-4466-RPE/560] 12 p1638 N88-19807

Department of Defense World Geodetic System 1984: Its definition and relationships with local geodetic systems
[AD-A188815] 12 p1639 N88-19811

Measuring and modeling near surface reflected and emitted radiation fluxes at the FIFE site
[NASA-CR-182660] 12 p1640 N88-19818

Systems approach to energy quality and efficiency
[PB88-139506] 12 p1640 N88-19823

Numerical simulation of near-surface environments and particulate clouds generated by large-area fires
[AD-A188375] 12 p1641 N88-19828
Estimating the solar irradiance of an intermountain region using GOES (Geostationary Operational Environmental Satellite) satellite data: A test of two statistical models
[AD-A188414] 12 p1642 N88-19834
Mesoscale monitoring of the soil freeze/thaw boundary from orbital microwave radiometry
[NASA-CR-182659] 12 p1645 N88-19855
Human factor in engineering work
12 p1663 N88-19970
A neuronal model of classical conditioning
[AD-A188378] 12 p1670 N88-19999
Regenerative life support system research
[NASA-CR-182606] 12 p1671 N88-20006
An experiment in software reliability: Additional analyses using data from automated replications
[NASA-CR-178395] 12 p1676 N88-20017
Procedure for initial data input and checkup in the system for film data mathematical processing
[DE88-700926] 12 p1676 N88-20022
Image segmentation via fractal dimension
[AD-A188825] 12 p1678 N88-20033
A numerical analysis of the dynamics of PRIZ operation
[AD-A188853] 12 p1678 N88-20035
Further refinement and applications of the mixed computational algorithm for plane elastic contact problems
[AD-A188308] 12 p1683 N88-20065
Structural-acoustic interior noise modeling and analysis from experimental data
[PB88-141775] 12 p1687 N88-20088
A study of methods to predict and measure the transmission of sound through the walls of light aircraft
[NASA-CR-182656] 12 p1687 N88-20090
Pion absorption in nuclei: The pion(+ or -),proton reactions
[LA-10997-T] 12 p1688 N88-20098
Multipass beam breakup in recirculating linacs
[CEBAF-PR-87-007] 12 p1690 N88-20111
Improved zero dimensional model of a reversed field pinch fusion device
[DE88-005212] 12 p1693 N88-20127
Phase transitions in two-dimensional superconducting arrays in a transverse magnetic field
[INPE-4457-RPE/559] 12 p1697 N88-20157
Task allocation for efficient performance of a decentralized organization
[AD-A188699] 12 p1705 N88-20204
The TempIS Project: Performance analysis of temporal queries
[AD-A188354] 12 p1706 N88-20213
HNC: A detector to study ultraheavy cosmic rays
12 p1713 N88-20252
Fully-coupled analysis of jet mixing problems. Three-dimensional PNS model, SCIP3D
[NASA-CR-4139] 13 p1715 N88-20256
A study of combustion and flow behaviour in solid-propellant rocket motors
[UTIAS-280] 13 p1732 N88-20357
Bipropellant combustion in a liquid rocket combustion chamber 13 p1733 N88-20359
Numerical model of the time independent mean flow in a rotating rocket motor 13 p1733 N88-20360
Erosion in dual-phase microstructures
[DE88-004507] 13 p1743 N88-20421
PNL-1 improved ceramic composites through controlled fiber matrix interaction
[DE88-005680] 13 p1750 N88-20462
Molecular dynamics of laser ablation of a polymer coating
[DE88-004337] 13 p1750 N88-20486
Computer-aided transformation of descriptive mode of mathematical models of a control system
13 p1756 N88-20503
Theoretical investigation of EM wave generation and radiation in the ULF, ELF and VLF bands by the electrodynamic orbiting tether
[NASA-CR-182720] 13 p1760 N88-20529
Aluminum-air battery development
[DE88-006617] 13 p1762 N88-20542
Development, manufacturing and testing of a gas-loaded variable conductance methanol heat pipe
[NLR-MP-87010-U] 13 p1767 N88-20571
Transport and stability properties of free shear flows
13 p1768 N88-20577
Calculations of viscous flows with a multigrid method
13 p1769 N88-20580
Direct solar-pumped iodine laser amplifier
[NASA-CR-182674] 13 p1777 N88-20630
Modelling and simulation of a rate controlled manipulator arm --- Hermes
[NLR-TR-87010-U] 13 p1778 N88-20639
Dynamic modelling of flexible rotor shafts mounted on hydrodynamic bearings 13 p1779 N88-20641
Finite element methods for quasi-prismatic bodies with application to gears 13 p1779 N88-20644
Numerical modeling of wave migration of seismic data
13 p1786 N88-20684
Numerical model of Rayleigh instability and spin-off eddies on fronts 13 p1788 N88-20696
Model of hydrodynamic adjustment of temperature, salinity and current fields 13 p1789 N88-20700
Performance and cost benefits associated with nonimaging secondary concentrators used in point-focus dish solar thermal applications
[DE88-001104] 13 p1792 N88-20718
Correlation of data on strain accumulation adjacent to the San Andreas Fault with available models
[NASA-CR-180757] 13 p1796 N88-20742
Ultrasonic physical modeling of seismic wave propagation from graben-like structures
[AD-A189066] 13 p1796 N88-20744
The pressure drag and momentum flux during a cold frontal passage over the Alps 13 p1800 N88-20763
Planetary scale barotropic spectral model
13 p1801 N88-20766
The use of a barotropic finite element model for the study of circulation on the continental shelf of the southeast coast of Brazil
[INPE-4401-PRE/1218] 13 p1802 N88-20774
Studies toward observing and modelling large energetic ocean regions
[AD-A189267] 13 p1803 N88-20778
Evaluation of wave calculations using GONO in the period October 1985 - April 1986
[KNMI-TR-96] 13 p1807 N88-20804
A model for graphical interaction --- computer graphics
[CWI-CS-R8718] 13 p1818 N88-20866
Interpolation algorithms for digital terrain models
[INPE-4373-PRE/1196] 13 p1820 N88-20877
Mathematic modeling of visual perception problems
[INPE-4355-PRE/1186] 13 p1823 N88-20897
A Darwinian approach to artificial neural systems
[DE87-013184] 13 p1824 N88-20900
Further results on the McMillan degree and the Kronecker indices of ARMA models --- input-output relations of linear systems
[EUT-87-E-175] 13 p1827 N88-20925
Model structure selection for multivariable systems by cross-validation methods
[EUT-87-E-176] 13 p1827 N88-20926
Regional Conference on the Analysis of the Unbalanced Mixed Model
[AD-A188747] 13 p1830 N88-20943
The automated symbolic derivation of state equations for dynamic systems
[DE88-000968] 13 p1830 N88-20945
Double layer polarization of nonconducting spheroidal particles and its application to Kerr effect
[ISSN-0208-5658] 13 p1832 N88-20960
Modeling the behavior of oriented permanent magnet material using current double theory
[DE88-004446] 13 p1833 N88-20963
Mathematical models of sound waves in fluids
[AD-A189270] 13 p1834 N88-20968
Modeling of laser ultrasound generation in a weld pool
[DE88-005546] 13 p1834 N88-20971
Optics for large telescope 13 p1840 N88-21014
Electrical characteristics of MBE (Molecular Beam Epitaxyl)-grown GaAs/sub 1-x/Sb/sub x on InP and correlation with film microstructure
[DE88-003841] 13 p1847 N88-21053
The thermodynamic properties of organic oxygen compounds
[DE88-001208] 13 p1849 N88-21065
Review of selenium thermodynamic data
[DE88-006194] 13 p1849 N88-21068
On the role of complete reducibility in general competitive equilibrium models
[DE88-005693] 13 p1851 N88-21083
Magnetohydrodynamic (MHD) simulation of solar prominence formation 13 p1858 N88-21109
Comparison of methods for the calculation of thermal contact resistance of the first Brazilian satellite
[NASA-TT-20180] 14 p1880 N88-21239
Spacecraft dielectric surface charging property determination
[NASA-CR-180879] 14 p1881 N88-21243
Finite area combustor theoretical rocket performance
[NASA-TM-100785] 14 p1883 N88-21252
Numerical modeling of divergent detonation wave
14 p1903 N88-21373
Potential applications of computational fluid dynamics to biofluid analysis
[NASA-TM-100089] 14 p1911 N88-21422
Accuracy requirements and benchmark experiments for CFD validation
[NASA-TM-100087] 14 p1911 N88-21423
Nonlinear Constitutive Relations for High Temperature Applications, 1986
[NASA-CP-10010] 14 p1928 N88-21498
Development of a unified constitutive model for an isotropic nickel base superalloy Rene 80
14 p1929 N88-21501
Modeling the viscoplastic behavior of Inconel 718 at 1200 F 14 p1929 N88-21502
An internal variable constitutive model for the large deformation of metals at high temperatures
14 p1929 N88-21503
Constitutive modeling and thermoviscoplasticity
14 p1930 N88-21506
A theory of viscoplasticity accounting for internal damage 14 p1930 N88-21508
A constitutive model with damage for high temperature superalloys 14 p1930 N88-21510
An automated procedure for material parameter evaluation for viscoplastic constitutive models
14 p1932 N88-21520
A constitutive material model for nonlinear finite element structural analysis using an iterative matrix approach
14 p1932 N88-21521
Nonlinear structural analysis of a turbine airfoil using the Walker viscoplastic material model for B1900 + Hf
14 p1932 N88-21522
Unified constitutive models for high-temperature structural applications 14 p1932 N88-21523
A constitutive model for an overlay coating
14 p1933 N88-21525
Non-isothermal elastoviscoplastic analysis of planar curved beams 14 p1933 N88-21526
Simulation of thermo-mechanical forming processes: A mixed Eulerian-Langrangian finite element method
[PB88-155247] 14 p1933 N88-21530
Large-scale ocean dynamics
14 p1938 N88-21562
The 25 m horizontal-axis turbine as a test case for standard Dutch aerodynamic calculation methods for high-speed rotors
[R-762-D] 14 p1942 N88-21589
Thermal modeling of solar central receiver cavities
[DE88-004940] 14 p1943 N88-21594
Report of Atmospheric-Canopy Exchange Panel
[DE88-004478] 14 p1944 N88-21597
Masking of motion cues by random motion: Comparison of human performance with a signal detection model
[UTIAS-313] 14 p1953 N88-21639
On a bound of the modeling errors of black-box transfer function estimates
[EUT-87-E-173] 14 p1963 N88-21708
Procedures for updating dynamic mathematical models
[EMSB-23/86] 14 p1964 N88-21716
Application of the NARMAX method to nonlinear frequency response estimation
[RR-319] 14 p1964 N88-21721
Additional peak of light scattering by sound under conditions of acoustic instability
14 p1968 N88-21752
Thermal model describing development of normal region in superconductor film carrying electric current
14 p1973 N88-21776
Comprehensive model for laser instability in a CO2 laser with gaseous saturable absorber
14 p1979 N88-21808
Analysis of hadron production in deep inelastic muon-proton collisions through the fire-string model
[PREPRINT-578] 14 p1981 N88-21822
A general 2D electrical model for diagonally connected MHD generators
[DE88-004283] 14 p1984 N88-21835
Linear state space modeling of a turbofan engine
[AD-A190110] 15 p2019 N88-22035
Baseline estimation from simultaneous satellite laser tracking
[NASA-CR-182750] 15 p2022 N88-22052
Moving-bank multiple model adaptive estimation applied to flexible spacestructure control
[AD-A190761] 15 p2026 N88-22071
Numerical simulation of turbulent flames using vortex methods
[AD-A189813] 15 p2034 N88-22116
Duct flow nonuniformities: Effect of struts in SSME HGM III(+)
[NASA-CR-179285] 15 p2062 N88-22296
On the prediction of highly vortical flows using an Euler equation model, part 2
[AD-A190245] 15 p2064 N88-22305
Numerical modelling specific energy charcteristics of excimer KrF lasers with electron beam excitation
[DE88-701525] 15 p2070 N88-22344
Life assessment of combustor liner using unified constitutive models 15 p2077 N88-22384

Biaxial experiments supporting the development of constitutive theories for advanced high-temperature materials 15 p2078 N88-22386
Unified constitutive model development for metal matrix composites at high temperature 15 p2078 N88-22387
Unified constitutive model for single crystal deformation behavior with applications 15 p2078 N88-22388
Finite element (MARC) solution technologies for viscoplastic analyses 15 p2078 N88-22389
Continuous fiber ceramic matrix composites for heat engine components 15 p2082 N88-22411
Cumulative fatigue damage models 15 p2084 N88-22422
Life prediction modeling based on strainrange partitioning 15 p2084 N88-22425
Fatigue damage modeling for coated single crystal superalloys 15 p2085 N88-22427
Review and assessment of the HOST turbine heat transfer program 15 p2086 N88-22431
Atmospheric carbon dioxide and the global carbon cycle: The key uncertainties [DE88-005059] 15 p2092 N88-22465
A survey of denser-than-air atmospheric dispersion models [DE88-006626] 15 p2092 N88-22467
Description of ground motion data processing codes, volume 2 [DE88-007137] 15 p2095 N88-22481
Proceedings of the Lightning Threat Warning Workshop [DE88-006607] 15 p2098 N88-22499
SEARCH: An interactive computer program for optimizing two-variable, unconstrained experiments or simulation [AD-A190593] 15 p2112 N88-22583
Artificial neural networks: An introduction with an annotated bibliography [DE88-007003] 15 p2116 N88-22603
Higher order crossings [AD-A190489] 15 p2121 N88-22641
Analysis and testing of the SURE program [NASA-TP-2817] 15 p2123 N88-22653
Statistical inference for stochastic processes [AD-A190491] 15 p2126 N88-22673
Lumped model generation and evaluation: Sensitivity and Lie algebraic techniques with applications to combustion [AD-A190402] 15 p2127 N88-22689
Model-scale sound propagation experiment [NASA-TM-100602] 15 p2130 N88-22709
Electrical circuit modeling of reversed field pinches [DE88-006942] 15 p2136 N88-22745
Plasma-gas interaction studies in a hybrid plume plasma rocket [AD-A190310] 15 p2138 N88-22755
A method for estimating and controlling the cost of extending technology [AD-A190717] 15 p2150 N88-22831
Design method for laminar flow control of two-dimensional airfoils in incompressible flow. Numerical study of LFC design concepts [DE88-751809] 16 p2155 N88-22659
A numerical model of unsteady, subsonic aeroelastic behavior [NASA-TM-101126] 16 p2156 N88-22862
Development of a digital sun sensor for a spin-stabilized satellite [INPE-4506-TDL/327] 16 p2169 N88-22929
Dynamic fracture toughness evaluation by measurement of CTOD [WNS/ASD-88-02] 16 p2178 N88-22982
Finite elements for the computation of three-dimensional electromagnetic fields in inhomogeneous media (revised) [PB88-173471] 16 p2190 N88-23057
Studying Turbulence Using Numerical Simulation Databases. Proceedings of the 1987 Summer Program [NASA-CR-182692] 16 p2194 N88-23086
A low dimensional dynamical system for the wall layer 16 p2194 N88-23088
Self similarity of two point correlations in wall bounded turbulent flows 16 p2195 N88-23089
EDQNM closure: A homogeneous simulation to support it. A quasi-homogeneous simulation to disprove it 16 p2195 N88-23091
Validation of EDQNM for subgrid and supergrid models 16 p2195 N88-23092
Angular distribution of turbulence in wave space 16 p2195 N88-23093
Modeling scalar flux and the energy and dissipation equations 16 p2196 N88-23096
Premixed turbulent flame calculation 16 p2196 N88-23098
Modeling of turbulent transport as a volume process 16 p2196 N88-23099
Analysis of non-premixed turbulent reacting flows 16 p2196 N88-23100
A statistical investigation of the single-point pdf of velocity and vorticity based on direct numerical simulations 16 p2196 N88-23101
On local approximations of the pressure-strain term in turbulence models 16 p2197 N88-23102
Local structure of intercomponent energy transfer in homogeneous turbulent shear flow 16 p2197 N88-23103
Test code for the assessment and improvement of Reynolds stress models 16 p2197 N88-23105
Reynolds stress models of homogeneous turbulence 16 p2197 N88-23106
The decay of isotropic turbulence in a rapidly rotating frame 16 p2197 N88-23107
Evaluation of a theory for pressure-strain rate 16 p2198 N88-23108
Relations between two-point correlations and pressure strain terms 16 p2198 N88-23109
Shear-layer structures in near-wall turbulence 16 p2198 N88-23110
Inflectional instabilities in the wall region of bounded turbulent shear flows 16 p2199 N88-23114
Active layer model for wall-bounded turbulence 16 p2199 N88-23115
Wave-growth associated with turbulent spot in plane Poiseuille flow 16 p2199 N88-23116
Coherent structures and modeling: Some background comments 16 p2199 N88-23120
Fast algorithms for Euler and Navier-Stokes simulations [AD-A190897] 16 p2208 N88-23175
Investigation of subgrid models in homogeneous incompressible turbulence [ONERA-RSF-13/3419-AY-106-A] 16 p2209 N88-23183
Two-equation low-Reynolds-number turbulence modeling of transitional boundary layer flows characteristic of gas turbine blades [NASA-CR-4145] 16 p2209 N88-23185
Pump rod forces due to hydrodynamic effects in piston pumps [PB88-164850] 16 p2214 N88-23212
Automatic control of robot motion [AD-A191012] 16 p2215 N88-23218
Periodic response of nonlinear systems 16 p2217 N88-23228
Multigrid for structures analysis 16 p2218 N88-23232
Aeroelastic forced response analysis of turbomachinery 16 p2220 N88-23247
Stall flutter analysis of propfans 16 p2221 N88-23256
Models in nonlinear thermomechanics. Finite element models and constitutive models for large deformation elastoplasticity [ETN-88-92240] 16 p2222 N88-23262
Application of the ONERA model to the life estimation under fatigue cracking of a Al-Li alloy. Parameter identification and test-experiment comparison under FALSTAFF loading [ONERA-RT-32/7169-RY-063-R] 16 p2222 N88-23264
Effects of axial load on elastomeric isolation bearings [PB88-179015] 16 p2223 N88-23269
Method and models for R-curve instability calculations [NASA-TM-100935] 16 p2224 N88-23278
Computer assisted generalization of buildings for digital landscape models by classification methods 16 p2226 N88-23294
The spreading and mixing of dense gas clouds in still air [KNMI-WR-87-12] 16 p2230 N88-23320
A three-dimensional gravity model of the geologic structure of Long Valley caldera [DE88-006331] 16 p2231 N88-23324
A proposal for the establishment of a center of excellence in theoretical geoplasma research [AD-A189742] 16 p2231 N88-23327
Modeling and estimation of a low degree geopotential model from terrestrial gravity data [NASA-CR-182808] 16 p2232 N88-23330
Towards fully abstract semantics for local variables: Preliminary report [AD-A191065] 16 p2251 N88-23456
Algorithms and intuition [NASA-CR-182900] 16 p2252 N88-23459
A model of intrazonal trip distribution considering centrality index 16 p2257 N88-23486
Inference for a nonlinear semimartingale regression model [AD-A190857] 16 p2262 N88-23527
Proceedings of Symposium on Physics of Target Implosion and Pulsed Power Techniques [IPPJ-859] 16 p2276 N88-23619
Development of Electromagnetic PIC code for LIB diode 16 p2276 N88-23622
Simulation code for ICF including radiative energy transfer 16 p2277 N88-23627
Efficient shell implosion and target design 16 p2277 N88-23630
Some aspects of the unified model of non-ideal high-parameter plasmas: Electron EOS and conduction coefficients 16 p2277 N88-23632
Coronal fluid-dynamics in laser fusion 16 p2278 N88-23634
Finite ion-relaxation and nonequilibrium radiation effects on laser-driven implosions 16 p2278 N88-23636
High pressure operation of beam diodes for generating relativistic electron beams 16 p2279 N88-23643
Propulsive performance of a lifting flapping wing 17 p2295 N88-23733
Travelling wave concepts for the modeling and control of space structures [AD-A191235] 17 p2310 N88-23819
Preventing aircraft corrosion by predictive corrosion modeling 17 p2321 N88-23863
Modeling, filtering and control of stochastic processes --- communication networks [ENST-87E021] 17 p2333 N88-23925
Numerical modelling of flows using phoenics 17 p2339 N88-23955
Theory of neutron moisture probes and interpretation of measurements in complex soil and water systems 17 p2342 N88-23965
Theoretical studies of solar-pumped lasers [NASA-CR-182929] 17 p2344 N88-23971
Parameter identification methods for improving structural dynamic models [NASA-TM-100812] 17 p2349 N88-23994
Three-dimensional curved shell and solid-shell transition finite elements with temperature and temperature gradients as primary variables for steady state heat conduction 17 p2349 N88-23997
Navigation system from AVHRR data from NOAA series satellites 17 p2359 N88-24054
Low altitude remote sensing data in the implementation of a mathematical model for the planning of urban equipment networks 17 p2363 N88-24074
Visualization of digital terrain models 17 p2364 N88-24081
Digital monoplotting, part 1 [B8735122-PT-1] 17 p2369 N88-24106
Digital monoplotting, part 2 [B8735122-PT-2] 17 p2369 N88-24107
An update on remote measurement of soil moisture over vegetation using infrared temperature measurements: A FIFE perspective [NASA-CR-182926] 17 p2370 N88-24109
Evaluation of a model of the Earth's gravity field [EPSHOM-003/87] 17 p2373 N88-24116
A theoretical model of the washout of trace gases by raindrops in the atmosphere 17 p2375 N88-24125
Mathematical modelling of the heat and water vapour transport in the human respiratory tract 17 p2382 N88-24160
Separability and security models --- software [RSRE-87020] 17 p2386 N88-24180
Adjusting a finite element model using vibration type experimental data. Concept and error detection [ONERA-RT-7/3313-RY-060-R] 17 p2392 N88-24220
A recursive prediction error parameter estimator for nonlinear models [RR-326] 17 p2392 N88-24222
On Hotelling's approach to testing for a nonlinear parameter in regression [AD-A191189] 17 p2393 N88-24229
A thermal equilibrium model for multi-megawatt space platforms 17 p2410 N88-24332
Progress in the computer modeling of the liquid phase behavior of a liquid metal heat pipe 17 p2412 N88-24342
A compressible vapor flux model for transient heat pipe analysis 17 p2412 N88-24343
ATHENA heat pipe transient model 17 p2412 N88-24344
Detailed transient model of a liquid-metal heat pipe 17 p2412 N88-24345
Transient thermohydraulic heat pipe modeling 17 p2413 N88-24347
RSMASS: A simple model for estimating reactor/shield masses 17 p2414 N88-24355
SP-100 control system modeling 17 p2414 N88-24356
Expert systems approach to modeling systems with the ATHENA thermal-hydraulics code 17 p2416 N88-24365
A generalized method for optimizing the mass of space power systems 17 p2416 N88-24369

Modeling of radiation dose dependence of MOSFETs
17 p2416 N88-24370
SP-100 system modeling: SNPSAM update
17 p2417 N88-24372
Microgravity two-phase fluid flow pattern modeling
17 p2432 N88-24467
Experimental evaluation of the MIT-SNL period-generated minimum time control laws for the rapid adjustment of reactor power 17 p2436 N88-24494
Consistent transport coefficients in astrophysics
[NASA-TM-101154] 17 p2451 N88-24560
A model for the X-ray binary 4U1820-30
[NASA-TM-101143] 17 p2451 N88-24562
The Jovian aurora: Electron or ion precipitation
[NASA-TM-101153] 17 p2452 N88-24566
A benchmark for galactic cosmic ray transport codes
[NASA-TM-101157] 17 p2453 N88-24571
An analytic model for aerodynamic shapes
[AD-A191573] 18 p2456 N88-24583
Compressible flow in a pie-shaped cylinder rotating about the vertex 18 p2460 N88-24604
Microwave landing system mathematical modeling study for Midway Airport Runway 22L, Chicago, Illinois
[AD-A191721] 18 p2462 N88-24616
Nonlinear flying quality parameters based on dynamic inversion
[AD-A192146] 18 p2464 N88-24627
Particle-laden weakly swirling free jets: Measurements and predictions
[NASA-TM-100920] 18 p2466 N88-24639
An enumeration of research to determine the optimal design and use of Army flight training simulators
[AD-A191242] 18 p2468 N88-24649
Analytic and numerical modeling of heat and material transport in electrical hypervelocity guns
[AD-A192178] 18 p2469 N88-24655
Fundamental limits to the velocity of solid armatures in railguns 18 p2469 N88-24656
Thermodynamic modeling of the no-vent fill methodology for transferring cryogens in low gravity
[NASA-TM-100932] 18 p2476 N88-24686
Interaction of ultrasonic waves with composite plates
[AD-A191879] 18 p2478 N88-24702
Shape stability in composites
18 p2479 N88-24706
The influence of cathodic protection on erosion-corrosion of metals and model alloys
[AD-A191613] 18 p2485 N88-24742
Delay-doppler radar imaging
[AD-A191509] 18 p2499 N88-24826
Internal fluid dynamics within a nonspinning partially liquid-filled shell due to burster rupture
[AD-A191055] 18 p2507 N88-24874
Transient particle deposition in a boundary layer of impulsive flow over a flat plate
[AD-A191537] 18 p2508 N88-24880
Research in nonlinear wave motion
[AD-A191686] 18 p2509 N88-24884
Gas diffusion studies in steady and nonsteady cavities
18 p2512 N88-24902
Numerical solutions of the complete Navier-Stokes equations
[NASA-CR-183023] 18 p2514 N88-24914
Experimental study of active vibration control
[AD-A191454] 18 p2526 N88-24989
Self-consistent model for the brittle response of solids
18 p2528 N88-24999
Reduced order modelling and analytical model modification for structural dynamics and control
18 p2529 N88-25006
Theory of viscoplasticity based on overstress with applications 18 p2529 N88-25007
Multishaker modal testing
[NASA-CR-179355] 18 p2530 N88-25010
Fatigue crack growth due to random loading
18 p2531 N88-25017
Yaw dynamics of horizontal axis wind turbines
[DE88-001137] 18 p2537 N88-25055
Photovoltaic Advanced Research and Development Project, solar radiation research
[DE88-001143] 18 p2537 N88-25056
Drilling investigation of a young magmatic intrusion beneath the Inyo Domes, Long Valley, California: Structural and textural studies
[DE88-006613] 18 p2541 N88-25078
DOD 1985 world magnetic model: Charts and grid values
[AD-A191484] 18 p2541 N88-25080
Report on project WIND: Preliminary experiments w ith the UK Meteorological Office mesoscale model, September 1987
[AD-A191621] 18 p2544 N88-25099
Analysis of lightning field changes during active thunderstorms in Florida 18 p2545 N88-25103
A computational model of motor behavior
[AD-A191179] 18 p2553 N88-25152
A concurrent neural network algorithm for the traveling salesman problem
[DE88-006981] 18 p2562 N88-25208
Mathematical models for VLSI device simulation
[AD-A191125] 18 p2562 N88-25212
Theoretical investigation of optical computing based on neural network models
[AD-A191668] 18 p2563 N88-25214
Direct numerical simulations of the PDF's (Probability Density Functions) of a passive scalar in a forced mixing layer
[AD-A192134] 18 p2568 N88-25256
Transmitting boundary for finite-difference calculations with finite modeling of an infinite medium
[AD-A191441] 18 p2570 N88-25264
Computer simulation of uphill diffusion in ternary ionic system
[NASA-TT-20194] 18 p2573 N88-25285
Para-ortho abundance ratio of molecular hydrogen in NGC2023
[ISAS-RN-352] 18 p2573 N88-25286
Modelling of thermal plasma systems
18 p2578 N88-25314
Study of data distributions and functions for the development of thermodynamic equations of state
[PB88-196365] 18 p2587 N88-25370
Superthermal electron processes in the upper atmosphere of Uranus: Aurora and electroglow
[NASA-TM-101150] 18 p2594 N88-25417
Cluster analysis of multiple planetary flow regimes
[NASA-CR-182931] 18 p2594 N88-25418
Diurnal variations in optical depth at Mars: Observations and interpretations
[NASA-TM-100057] 18 p2595 N88-25420
Development of a computerized analysis for solid propellant combustion instability with turbulence
[NASA-CR-182351] 19 p2611 N88-25497
Coal particle behaviour in a counter-current combustor
[TAE-606] 19 p2612 N88-25498
An assessment of the state of the art in predicting the failure of ceramics
[DE88-008998] 19 p2621 N88-25551
Droplet formation for liquid monopropellant jets
19 p2623 N88-25557
Comparison of calculated and measured ignition times for boron agglomerates 19 p2624 N88-25563
Liquid phase decomposition in slurry fuels
19 p2624 N88-25564
Effects of Mach number on acoustic-vortex interactions in a ramjet 19 p2625 N88-25573
Development of a generic combustion stability code for liquid propellant rocket engines
19 p2626 N88-25576
Numerical grid generation and flow simulation in SSME thrust chamber 19 p2626 N88-25577
Fuel droplet vaporization and temperature distributions of axisymmetric unsteady sprays
19 p2626 N88-25579
Boundary layer simulator (BLIMPJ) improvement
19 p2627 N88-25582
Liquid Engine Jet Atomization Workshop report
19 p2627 N88-25584
One person's view of velocity-coupled instability
19 p2629 N88-25595
The scaling of the threshold conditions for solid propellant erosive burning 19 p2630 N88-25601
Effect of burn-path tortuosity on the burn rate of composite propellants 19 p2630 N88-25602
Solid rocket motor performance: A workshop report
19 p2631 N88-25607
How much do edges affect the ignition of a homogeneous reactive solid: Summary to date
19 p2631 N88-25608
Minimum ignition energy measurements using laser induced spark initiation 19 p2632 N88-25610
Chemical kinetics modeling of HMX combustion
19 p2633 N88-25617
A multiple chamber volume-filling model for prediction of transient solid rocket motor ballistic performance
19 p2633 N88-25618
Numerical simulation of turbulent flow using the exponential expression of k-Epsilon equation
19 p2640 N88-25662
Color charge motion in non-Abelian fields
[DE88-701306] 19 p2642 N88-25672
System capacity and economic modeling computer tool for satellite mobile communications systems
19 p2644 N88-25686
Mobile satellite propagation measurements and modeling: A review of results for systems engineers
19 p2645 N88-25696
Quantum transport calculation of resonant-tunneling response time 19 p2659 N88-25810
Photocurrent modeling of modern microcircuit PN junctions
[DE88-007037] 19 p2662 N88-25832
The propagation of pressure perturbations in bubbly air/water flows 19 p2664 N88-25843
Thermal management of integrated microsensors
19 p2670 N88-25875
Automatic calibration of space based manipulators and mechanisms
[NASA-CR-182804] 19 p2676 N88-25912
Energy dissipation in a rolling aircraft tire
[NASA-CR-182978] 19 p2676 N88-25913
Semi-Markov adjunction to the Computer-Aided Markov Evaluator (CAME)
[NASA-CR-181645] 19 p2678 N88-25924
Determining system maintainability as a probability
[DE88-007722] 19 p2679 N88-25927
Study of probabilistic fatigue crack growth and associated scatter under constant-and-variable amplitude loading spectrum
[AD-A192027] 19 p2679 N88-25929
Timing regulations to prevent stratospheric-ozone depletion
[R-3495-JMO/RC] 19 p2690 N88-25987
Sulfur dioxide-hydrogen peroxide relationships in clean air, clouds, and precipitation
[DE88-006352] 19 p2690 N88-25990
Theory on conductivity measurement technique for Langmuir probes in the stratosphere
[INPE-4514-PRE/1268] 19 p2692 N88-25999
Voltages induced by lightning on electric power distribution lines: Field data and analysis results for the period July 1984-1986
[DE88-007841] 19 p2693 N88-26006
Bathymetry estimation by analyzing swell on SPOT images 19 p2701 N88-26062
Method of assessing changes in biorhythmological structure of human physiological functions
19 p2706 N88-26088
Adaptive residual mode filter control of distributed parameter systems for large space structure applications
19 p2719 N88-26143
Model reduction methods for control design
[NASA-CR-179434] 19 p2719 N88-26144
The Potts model in a random field
19 p2721 N88-26158
Acoustic wave dispersion in a viscous, compressible, liquid-filled cylindrical elastic tube
19 p2722 N88-26164
Phase equilibria and density calculations in the critical region: A phenomenological correction for a classical equation of state
[PB88-185335] 19 p2723 N88-26167
Primer on coupling collective electronic oscillations to nuclei
[LA-10878] 19 p2723 N88-26170
Heavy ion fusion system assessment: Final focus and transport model
[LBL-23040] 19 p2725 N88-26183
REFLEX: An energy deposition code that models the effects of electron reflection during electron beam heating tests
[DE88-009789] 19 p2726 N88-26186
Superstrings
[DE87-702982] 19 p2737 N88-26249
Quantum gravity and new forces
[DE88-007829] 19 p2737 N88-26250
Multidimensional modeling of convective heat transfer with application to I.C. engines
[DE88-007446] 19 p2738 N88-26257
The solar flare of 18 August 1979: Incoherent scatter radar data and photochemical model comparisons
[DE88-007616] 19 p2743 N88-26286
Finite element approximation to a model problem of transonic flow
[DE88-701835] 20 p2752 N88-26333
Stiffness degradation of composite laminates
20 p2767 N88-26405
Experimental and theoretical analysis of the radiative transfer within a sooty pool fire
[DE88-007099] 20 p2769 N88-26419
A constitutive model with damage for high-temperature superalloys 20 p2771 N88-26434
A numerical study of Rayleigh-Taylor instability in aluminum and steel plates
[DE88-010475] 20 p2774 N88-26449
Numerical modeling of the effect of particle size of explosives on shock initiation properties
[DE88-010479] 20 p2780 N88-26491
Dynamics of satellites with radial wire antennas
20 p2784 N88-26514
Vertical ship motions and sea loads considering nonlinear effects
[TAE-592] 20 p2784 N88-26515
Modeling and parameter identification of motor vehicles 20 p2785 N88-26521
A two-point aerodynamic model for identification
20 p2786 N88-26526

Utilization of identification methods in the time and frequency domain for the determination of the XV-15 (tilt-rotor) dynamics for lateral motion in hover flight
20 p2787 N88-26532

A random access algorithm for environments with capture and limited feedback capabilities
[AD-A192233] 20 p2790 N88-26552

Modeling and thermal management of advanced batteries
[DE88-010023] 20 p2794 N88-26580

Microwave amplifiers
[AD-A192974] 20 p2795 N88-26585

The Oak Ridge Heat Pump Design Model: Mark 3 version program documentationon
[DE88-007863] 20 p2799 N88-26607

Nonlinear equation of state effects and the momentum-dilution trade-off in a turbulent buoyant jet
[DE88-701839] 20 p2799 N88-26610

Axisymmetric liquid sloshing under low-g conditions: Numerical simulation method (reference manual)
[NLR-TR-86057-U] 20 p2802 N88-26627

Vibration frequencies of tapered bars with nonclassical boundary conditions
[NASA-CR-183059] 20 p2813 N88-26688

Microstructural effects in static and dynamic numerical experiments
[DE88-004289] 20 p2813 N88-26690

Random vibration analysis of rattling structures
[DE88-007196] 20 p2813 N88-26691

An assessment of modelling techniques for the finite element analysis of reinforced concrete plate and shell structures
[AD-A192263] 20 p2814 N88-26697

Interpreting forest biome productivity and cover utilizing nested scales of image resolution and biogeographical analysis
[NASA-CR-183036] 20 p2817 N88-26711

Surface hydrology, sediment transport dynamics and remote sensing of disturbed watersheds in a humid temperate region
[DE88-008719] 20 p2817 N88-26715

Development of a model procedure for the determination of volume diffusion lengths by transient measurements on monocrystal silicon solar cells
[ETN-88-92119] 20 p2821 N88-26733

Development of an atmospheric diffusion evaluation method incorporating topographical effects. Part 1: Literature review of atmospheric diffusion models incorporating terrain effects
[DE88-753104] 20 p2822 N88-26742

Effects of a temperature-dependent rheology on large scale continental extension
[NASA-CR-183117] 20 p2825 N88-26759

Parametric methodologies of cloud vertical transport for acid deposition models
[PB88-191374] 20 p2825 N88-26762

Synoptic patterns related to tropical cyclone recurvature
[AD-A192338] 20 p2827 N88-26771

Evaluation of surface energy and radiation balance systems for FIFE
[NASA-CR-183118] 20 p2828 N88-26778

Prediction of continental shelf sediment transport using a theoretical model of the wave-current boundary layer
[AD-A192272] 20 p2829 N88-26783

Stability of a coastal upwelling front over topography
[AD-A192354] 20 p2829 N88-26784

Aircraft interior noise reduction by alternate resonance tuning
[NASA-CR-182540] 20 p2849 N88-26909

A modal approach to Arctic noise modelling with implied vertical coherence
[AD-A192966] 20 p2850 N88-26916

Proceedings of the 2nd US-Japan Workshop on Advanced Plasma Modeling, volume 3
[IPPJ-867] 20 p2855 N88-26957

A Vlasov ion zero mass electron model for plasma simulations 20 p2855 N88-26958

Modeling of subtle kinetic processes in plasma simulation 20 p2856 N88-26959

Atomistic simulation of stability, metastability and growth of strained layer structures 20 p2873 N88-27053

Superconductivity of Cr/V superlattices
20 p2874 N88-27057

Integrated Technology Rotor Methodology Assessment Workshop
[NASA-CP-10007] 21 p2889 N88-27148

A comparison of the various helicopter mathematical models used in the methodology assessment
21 p2889 N88-27149

A comparison of theory and experiment for coupled rotor-body stability of a hingeless rotor model in hover under simulated vacuum conditions
21 p2889 N88-27151

A comparison of theory and experiment for coupled rotor-body stability of a hingeless rotor model in hover
21 p2889 N88-27152

A comparison of theory and experiment for the aeroelastic stability of a bearingless model rotor in hover
21 p2890 N88-27153

The importance of steady and dynamic inflow on the stability of rotor-body systems 21 p2890 N88-27156

Effects of static equilibrium and higher-order nonlinearities on rotor blade stability in hover
21 p2890 N88-27157

Aeroelastic modeling of rotor blades with spanwise variable elastic axis offset: Classic issues revisited and new formulations 21 p2890 N88-27158

Comparison of experimental coupled helicopter rotor/body stability results with a simple analytical model
21 p2891 N88-27160

Aeromechanical stability analysis of COPTER
21 p2891 N88-27161

Improved procedure for impact probability computation of aircraft crash based on Balfanz model
[JUEL-SPEZ-425] 21 p2894 N88-27176

Contribution to the numerical solution of airplane spin motion
[ETN-88-92368] 21 p2896 N88-27190

In-flight motor torque estimates for the second-stage Strypi 9 launch vehicle
[DE88-010833] 21 p2902 N88-27222

Evaluation and improvement of liquid propellant rocket chugging analysis techniques. Part 2: A study of low frequency combustion instability in rocket engine preburners using a heterogeneous stirred tank reactor model
[NASA-CR-182724] 21 p2903 N88-27225

Probabilistic anisotropic failure criteria for composite materials
[AD-A193046] 21 p2904 N88-27232

Analysis of transverse strength of composites using percolation theory
[AD-A193204] 21 p2904 N88-27234

The structure and stability of nonpremixed gas jet flames 21 p2908 N88-27257

Laser probes and numerical modeling as process diagnostics in chemical vapor deposition
[DE88-011622] 21 p2911 N88-27275

Computer modeling for surface properties of carbon fibers 21 p2928 N88-27383

Basic research on optical neural computers
21 p2929 N88-27389

Model for dynamically structured communicating systems
[PB88-105263] 21 p2931 N88-27402

Dependence effects in unique signal transmission
[DE88-010331] 21 p2933 N88-27419

Numerical experiments on turbulent mixing
[AD-A192572] 21 p2942 N88-27473

User's manual for C-HEMP: A two-dimensional wave propagation code. Volume 1: Description and derivations of the code
[AD-A193197] 21 p2944 N88-27486

A comparison of analytical techniques for modeling the Rayleigh-Taylor response of elastic-plastic solids
[DE88-010372] 21 p2962 N88-27596

Reduced order modeling of grid-connected photovoltaic inverter systems
[DE88-010603] 21 p2969 N88-27635

Prediction of regional pollutant dispersion using a nested-grid, three-dimensional numerical model
21 p2971 N88-27649

An empirical surface temperature model
[AD-A192737] 21 p2974 N88-27665

Angular radiation models for Earth-atmosphere system. Volume 1: Shortwave radiation
[NASA-RP-1184] 21 p2976 N88-27677

Dissecting the visual and auditory pathways by means of the two-input technique 21 p2978 N88-27690

Contribution to almost realistic picture processing by a computer graphics procedure
[ETN-88-92372] 21 p2999 N88-27789

Benefits of an object approach in a computer aided design environment
[SNIAS-881-440-102] 21 p3000 N88-27791

Modeling and approximate performance analysis of multiuser computer systems
[ETN-88-92137] 21 p3002 N88-27806

Feedback control of a hyperbolic partial-differential equation with viscoelastic damping
[AD-A192896] 21 p3003 N88-27810

A zoomable and adaptable hidden fine-mesh approach to solving advection-dispersion equations
[DE88-006174] 21 p3004 N88-27816

Parallel solutions to geometric problems on the scan model of computation
[AD-A192321] 21 p3004 N88-27819

Measuring dispersion effects of factors in factorial experiments
[AD-A193216] 21 p3006 N88-27831

Asymptotic normality of minimum L1-norm estimates in linear models
[AD-A193399] 21 p3006 N88-27835

Matrix substructuring, domain decomposition and particle methods: Current trends for solving PDEs in parallel
[DE88-009826] 21 p3007 N88-27836

Reminimization of energy integral and stability limit for non-ideal MHD (magnetohydrodynamic) plasma
[DE88-008422] 21 p3018 N88-27911

Cascade model of gamma-ray bursts: Power-law and annihilation-line components
[NASA-TM-101176] 21 p3032 N88-27998

Literal dynamic modeling
[REPT-881-440-114] 22 p3048 N88-28083

Interactions between coherent structures and premixed flame fronts
[ETN-88-92685] 22 p3053 N88-28111

A review of solid particle erosion of engineering materials
[DE88-010065] 22 p3054 N88-28124

Thermal barrier coating life-prediction model development
[NASA-CR-179507] 22 p3058 N88-28142

Non-Gaussian models for surface clutter
22 p3068 N88-28212

Large-signal modeling of gallium arsenide field-effect transistors 22 p3073 N88-28242

The calculation of the flow through a two-dimensional faired diffuser
[PNR90433] 22 p3076 N88-28259

Modeling of spray combustion in direct injection diesel engine
[AD-A193787] 22 p3084 N88-28314

Modeling discrete bathtub and upside down bathtub mean residual life functions
[AD-A192000] 22 p3085 N88-28320

Determination of the residual stresses in welded structures using the elastoplastodynamic method
[ETN-88-92745] 22 p3087 N88-28330

Parametric identification of mechanical structures
[ETN-88-92861] 22 p3088 N88-28339

Aspects of the 30-60 day oscillation in a GCM simulation 22 p3121 N88-28545

Systematic behavior of NMC medium range forecasts and the effect of model changes 1985-87
22 p3125 N88-28575

The impact of the El Nino event on the ECMWF model performance 22 p3125 N88-28576

Application of Dynamic Extended Range Forecasting (DERF) to the monthly forecast problem
22 p3125 N88-28578

Analysis of the dynamic extended range forecast experiment 22 p3126 N88-28581

Experimental 30-day forecasts from several spectral general circulation models 22 p3126 N88-28582

Correction of systematic errors in NMC medium range forecasts 22 p3126 N88-28584

Theoretical and practical limits of predictability of the NMC medium-range model 22 p3127 N88-28586

The predictability of low frequency patterns in the NMC MRF 22 p3127 N88-28587

Reduce uncertainty in projection of future sea-level changes due to ice wastage
[DE88-009883] 22 p3129 N88-28601

A probabilistic model of the apparent radiance of a rough sea
[AD-A193867] 22 p3129 N88-28602

Models for motion perception
22 p3133 N88-28629

VAXGAP: A code for the routine analysis of gamma-ray pulse-height spectra on a VAX computer
[DE88-011702] 22 p3137 N88-28648

Connectionist models and artificial intelligence
[RR-684-I-IMAG-66-LIFIA] 22 p3142 N88-28684

Refining finite element models. Numerical application to a lattice structure. Study of a macroelement of Timoshenko beam type
[ONERA-RT-8/3313-RY-070-R]
22 p3144 N88-28696

An introduction to the nested sequence of tuples data model and algebra
[REPT-87-049] 22 p3145 N88-28702

Numerical modeling results for mode propagation in a wedge
[AD-A193998] 22 p3147 N88-28718

Sound propagation at low altitude
22 p3148 N88-28725

Customizing Space Nuclear Power System Analysis Model (SNPSAM): Introducing a secondary coolant loop
[AD-A194620] 22 p3151 N88-28750

Development and analysis of turbulent non-equilibrium boundary layers 23 p3169 N88-28872

Vortex flows 23 p3170 N88-28875
Environmental effects on transition and boundary layer characteristics 23 p3170 N88-28876
Contributions to the modeling of wind shear for danger studies
[NASA-TT-20293] 23 p3174 N88-28900
Structural dynamics of maneuvering aircraft
[AD-A192376] 23 p3176 N88-28908
Progress on a Monte Carlo shuttle contamination model
[AD-A193694] 23 p3183 N88-28945
SRB/SLEEC (Solid Rocket Booster/Shingle Lap Extendible Exit Cone) feasibility study, volume 2. Appendix A: Design study for a SLEEC actuation system
[NASA-CR-178974] 23 p3187 N88-28965
Phenomena of the ionic transport in the stress corrosion of metals
[DE88-702502] 23 p3195 N88-29013
Thin film-residual stress assessment
[AD-A193205] 23 p3196 N88-29018
Development of creep fracture modelling in ceramics
[PB88-202825] 23 p3196 N88-29021
Open bosonic string in background electromagnetic field
[DE88-702140] 23 p3201 N88-29053
Development and experimental verification of a two-dimensional numerical model of piezoelectrically induced threshold voltage shifts in GaAs MESFETs
[AD-A193462] 23 p3206 N88-29080
Numerical investigations in three-dimensional internal flows
[NASA-CR-183108] 23 p3210 N88-29106
Stability control of leakage flow channels
[DE88-009995] 23 p3210 N88-29107
Modeling of large stall in axial compressors
[VKI-TN-164] 23 p3213 N88-29124
Modeling of momentum transport of axially parallel turbulent flows in rod cascades
[ETN-88-92978] 23 p3214 N88-29131
Solid-state laser research report: Energy transfer in non-uniform codoped crystals
[AD-A194358] 23 p3219 N88-29161
Modeling of pulsed gas flow lasers
[ESA-TT-1090] 23 p3220 N88-29169
Development of the Simplified Compressor Model (SCM) for performance analysis of gaseous diffusion compressors
[DE88-009066] 23 p3221 N88-29173
Approximate evaluation of semi-Markov chain reliability models
[AD-A194669] 23 p3223 N88-29185
Nonlinear dynamic analysis and optimal control of shallow shells 23 p3224 N88-29191
Mechanics of thrust fault formation 23 p3231 N88-29229
Intraplate deformation, stress in the lithosphere and the driving mechanism for plate motions
[NASA-CR-183121] 23 p3231 N88-29231
Analysis of the hopfield neural networks and their application to pattern recognition
[AD-A193827] 23 p3239 N88-29279
Optimization-driven machine-oriented motion measurement 23 p3245 N88-29312
Piecewise-parabolic methods for systems of hyperbolic conservation laws in multiprocessing environments
[DE88-010202] 23 p3248 N88-29329
Hidden Markov models for automatic speech recognition: Theory and application
[RSRE-MEMO-4135] 23 p3251 N88-29350
AI and simulation: What can they learn from each other 23 p3257 N88-29391
Large-grain pipelining on distributed-memory multiprocessors
[DE88-009974] 23 p3264 N88-29432
Computer-Aided-Control Engineering (CACE) primitives for robust and adaptive control systems, phase 1
[AD-A192446] 23 p3265 N88-29439
Easy Bayes estimation for Rasch-type models
[AD-A193628] 23 p3274 N88-29491
Mathematical theory and calculations of magnetic hysteresis curves
[DE88-011055] 23 p3277 N88-29510
Fusion product spectra
[DE88-010912] 23 p3284 N88-29554
Electrical conductivity of GaAs layers implanted on semi-insulator nondoped substrates
[CERT-422000/RF] 23 p3294 N88-29614
A review: Quantitative models for lava flows on Mars 23 p3301 N88-29656
Origin of northern lowland plains: Constraints from boundary morphology 23 p3305 N88-29687
Coadsorption of H2O and CO2 on the Martian surface 23 p3307 N88-29702
Status review of atmosphere turbulence and aircraft response 24 p3312 N88-29726
Extreme gusts distribution 24 p3314 N88-29734
Advances in Flying Qualities
[AGARD-LS-157] 24 p3314 N88-29735
Pilot modeling 24 p3314 N88-29736
Pilot modeling applications 24 p3314 N88-29737
Advances in flying qualities: Concepts and criteria for a mission oriented flying qualities specification 24 p3314 N88-29739
The optimal control pilot model and applications 24 p3315 N88-29741
Prediction of dynamic derivatives 24 p3318 N88-29761
Prediction of base-flows 24 p3319 N88-29765
Computational methods for the problems of the tip vortex
[NASA-CR-181438] 24 p3320 N88-29775
Minimum-complexity helicopter simulation math model
[NASA-CR-177476] 24 p3328 N88-29819
Procedures for updating dynamic mathematical models, test phase --- spacecraft hardware
[MEBS-38/87] 24 p3335 N88-29852
Some theoretical considerations of the surface tension of liquid metals for metal matrix composites
[AD-A195999] 24 p3340 N88-29882
Combustion and fuels in gas turbine engines
[AGARD-CP-422] 24 p3345 N88-29910
Flamelet chemistry modelling of soot formation for radiation 24 p3348 N88-29928
Numerical models for analytical predictions of combustor aerothermal performance characteristics 24 p3349 N88-29935
Gas turbine combustion modeling 24 p3349 N88-29936
Three-dimensional gas turbine combustor modelling 24 p3349 N88-29937
Flamelet modeling of turbulent premixed flames 24 p3350 N88-29942
Numerical modelling of premixed flames in gaseous media 24 p3350 N88-29944
Modelling of CO oxidation in dilution jet flows 24 p3351 N88-29947
Influence of the convection on evaporation and combustion of a fuel droplet 24 p3351 N88-29948
Numerical field model simulation of full scale fire tests in a closed spherical/cylindrical vessel
[AD-A195067] 24 p3359 N88-29998
The use of upwind schemes at high Reynolds number: A cautionary note
[AD-A196227] 24 p3371 N88-30074
Transition mixing study empirical model report
[NASA-CR-182139] 24 p3371 N88-30076
Numerical simulation of the function of scientific instrumentation for measuring the speed of electron devices
[AD-A194969] 24 p3376 N88-30103
Fatigue crack propagation: Probabilistic modeling and statistical analysis
[AD-A195885] 24 p3384 N88-30155
Relief effect correction on LANDSAT imagery for forest applications using digital terrain models
[INPE-4611-PRE/1334] 24 p3388 N88-30179
LANDSAT TM and agrometeorological data for wheat yield estimation at the farm level
[INPE-4591-PRE/1321] 24 p3388 N88-30180
Nd isotopes and crustal growth rate 24 p3392 N88-30203
Construction of mass-age curves for the continental crust: An empirical model and an example from the western US 24 p3394 N88-30213
Temperature profile construction methods: An evaluation
[AD-A195919] 24 p3403 N88-30262
Some results from the Amazon Forest micrometeorological experiment
[INPE-4631-PRE/1346] 24 p3403 N88-30263
Cloud/mesoscale model development and application studies
[AFGL-TR-87-0219] 24 p3404 N88-30269
A digital terrain model system for a microcomputer
[INPE-4610-PRE/1333] 24 p3413 N88-30316
Range data description based on multiple characteristics 24 p3419 N88-30351
Automatic mathematical modeling for real time simulation system 24 p3420 N88-30356
Adaptive control in positioning a rigid-flexible robot arm
[AD-A195194] 24 p3422 N88-30367
Nested neural networks
[NASA-TM-101032] 24 p3423 N88-30373
Generation of surface grids through elliptic partial differential equations for aircraft and missile configurations
[AD-A195639] 24 p3424 N88-30378
Dirichlet prior in Bayesian estimation of item response curves
[AD-A195311] 24 p3426 N88-30392
Theoretical modeling of accelerating arc plasmas
[AD-A195606] 24 p3432 N88-30426
The origin of the moon: Further studies of the giant impact 24 p3440 N88-30474
Volatiles on Mars
[NASA-CR-183113] 24 p3456 N88-30571

MATHEMATICAL PROGRAMMING
NT DYNAMIC PROGRAMMING
NT LINEAR PROGRAMMING
NT NONLINEAR PROGRAMMING
NT QUADRATIC PROGRAMMING
On the exact solution of large-scale simple plant location problems
[FI-032-TB-22E] 02 p0229 N88-11441
Computing block-angular Karmarker projections with applications to stochastic programming, revision
[AD-A185647] 06 p0759 N88-14656
Progress in mathematical programming
[AD-A185729] 06 p0759 N88-14658
Local and global techniques for the tracking of periodic solutions of parameter-dependent functional differential equations
[AD-A185756] 06 p0766 N88-14704
Bounding the expectation of convex functions with limited distribution information
[AD-A186147] 07 p0910 N88-15512
Sublinear upper bounds for stochastic programs with recourse, revision
[AD-A186436] 07 p0916 N88-15564
Tutorial on GAMS (Generalized Algebraic Modeling System): A modeling language for optimization
[AD-A189867] 15 p2109 N88-22568
Discrete generalized networks: Application to integer constrained flow problems
[AD-A190823] 16 p2190 N88-23060
Towards fully abstract semantics for local variables: Preliminary report
[AD-A191065] 16 p2251 N88-23456
Experimental design and structural optimization
[ETN-88-92232] 16 p2257 N88-23492
Optimal design of viscoelastic structures 21 p2959 N88-27579
Motion planning with obstacles and dynamic constraints 23 p3222 N88-29175
Multicriteria integer programming for problems involving linear and nonlinear utility functions
[AD-A194530] 23 p3249 N88-29336
Computer systems for the representation and manipulation of mathematical knowledge
[AD-A193547] 23 p3249 N88-29340

MATHEMATICS
Interdisciplinary research in mathematics, science and technology education
[PB88-131446] 10 p1398 N88-18333
JPRS report: Science and technology. USSR: Physics and mathematics
[JPRS-UPM-88-001] 14 p1968 N88-21751

MATRICES (CIRCUITS)
Photodiode matrix for the analysis of two-beam interferences
[PTB-OPT-23] 01 p0048 N88-10310
Reducing the parallel solution time of sparse circuit matrices using reordered Gaussian elimination and relaxation
[AD-A195152] 24 p3366 N88-30045

MATRICES (MATHEMATICS)
NT ADJOINTS
NT CANONICAL FORMS
NT EIGENVALUES
NT EIGENVECTORS
NT HESSIAN MATRICES
NT STIFFNESS MATRIX
Implementation of a digital optical matrix-vector multiplier using a holographic look-up table and residue arithmetic
[NASA-CR-180431] 01 p0078 N88-10496
The box method for linear programming. Part 1: Basic theory
[DE87-011029] 01 p0080 N88-10515
Finite-dimensional matrix representation of the differential operator, determinental form and zeros of special functions
[DE87-703091] 02 p0225 N88-11421
Structure-dependent matrix representation of manipulator kinematics and its inverse solution
[DE87-752966] 02 p0229 N88-11447
QR factorization of a dense matrix on a shared-memory multiprocessor
[DE88-001506] 04 p0480 N88-12956
Two classes of preconditioners computed using block matrix factorization techniques
[DE88-001313] 04 p0485 N88-12988
Reduced order optimal command applied to longitudinal automatic pilots
[SNIAS-872-111-114] 05 p0552 N88-13362

Mechanics of anisotropic media. Study of the boundary conditions — stratified composites
[SNIAS-872-430-112] 05 p0559 N88-13404
The matrix exponential in transient structural analysis
05 p0593 N88-13619
Simultaneous structural and control optimization via linear quadratic regulator eigenstructure assignment
05 p0594 N88-13622
Illustrative examples of principal component analysis using BMDP/4M
[AD-A185179] 05 p0635 N88-13881
Structuring data for concurrent vectorized processing in a transient dynamics finite element program
[DE87-013082] 05 p0636 N88-13890
Optimal control of large space structures via generalized inverse matrix
[NASA-CR-182336] 05 p0639 N88-13907
Eigenvectors of distance-regular graphs
[AD-A185375] 05 p0641 N88-13919
Computation of natural frequencies of planar lattice structure
[AD-A185387] 05 p0641 N88-13920
The estimation of basic matrices using travel intensity theorems
[REPT-87-13] 05 p0642 N88-13926
Illustrative examples of principal component analysis using SYSTAT/FACTOR
[AD-A184920] 05 p0644 N88-13939
On the work needed to factor a symmetric positive definite matrix
[AD-A185781] 06 p0759 N88-14660
Parallel pivoting combined with parallel reduction
[NASA-CR-178422] 06 p0760 N88-14662
Analysis of a parallel solution method for tridiagonal systems
[PB87-230536] 06 p0762 N88-14678
Parallel LU-factorization algorithms for dense matrices
[DE88-002179] 07 p0904 N88-15478
Parallel LU-factorization algorithms for dense matrices
[DE88-002179] 07 p0904 N88-15478
A Schur-complement method for sparse quadratic programming
[DE88-002520] 07 p0904 N88-15479
The effect of response scaling on the detection of singularities in multiresponse estimation
[AD-A185964] 07 p0908 N88-15503
Strong laws of large numbers for arrays of orthogonal random variables
[AD-A186159] 07 p0910 N88-15513
On the asymptotic joint distributions of the eigenvalues of random matrices which arise under components of covariance model
[AD-A186387] 07 p0915 N88-15558
Method for joint adjustment of satellite and surface geodetic networks 08 p1007 N88-16105
A parallel algorithm for the general LU-factorization
[DE88-002177] 08 p1066 N88-16444
Matrix functions in the stability of higher-order numerical schemes
[INPE-4245-PRE/1119] 08 p1073 N88-16472
An efficient method for computing leading Eigenvalues and Eigenvectors of large asymmetric matrices
09 p1159 N88-16949
Mesospheric dynamics and chemistry from SME data
[NASA-CR-182465] 09 p1191 N88-17139
Multicolor numbering of irregular triangular meshes
[AD-A186559] 09 p1217 N88-17298
An applicative programmer's approach to matrix algebra, lessons for hardware and software
10 p1382 N88-18251
A multigrid preconditioner applied to a two-dimensional convection-diffusion problem
[DE88-004765] 10 p1397 N88-18329
Identifiability of multivariate ARMA models
[AD-A187394] 10 p1400 N88-18350
Status of the electroweak theory
[DE88-002342] 10 p1422 N88-18494
Multipass beam breakup in recirculating linacs
[CEBAF-PR-87-007] 12 p1690 N88-20111
Further results on the McMillan degree and the Kronecker indices of ARMA models — input-output relations of linear systems
[EUT-87-E-175] 13 p1827 N88-20925
The parameterization of orthogonal matrices: A review mainly for statisticians
[AD-A189144] 13 p1829 N88-20936
Optimization of the real level 2 BLAS on the Cyber 205
[CWI-NM-R8715] 14 p1956 N88-21657
A parallel algorithm for computing the singular value decomposition of a matrix
[DE88-007059] 14 p1958 N88-21673
Split-coefficient matrix solution and experimental study of axisymmetric underexpanded exhaust plumes
15 p2054 N88-22242
Sufficient matrices and the linear complementarity problem
[AD-A190429] 15 p2128 N88-22690
Homogenization study of matrix behavior in a composite material
[ONERA-RT-1/7256-RY-060-R]
16 p2172 N88-22943
Systolic algorithm for matrix-vector multiplication
[PB88-165394] 16 p2256 N88-23484
Minimal parameter solution of the orthogonal matrix differential equation
[NASA-TM-4043] 17 p2383 N88-24165
Nonequilibrium phonons and disorder in Al sub x Ga sub 1-x As 19 p2657 N88-25788
QR factorization of a dense matrix on a hypercube multiprocessor
[DE88-009187] 19 p2716 N88-26129
A diagonally inverted LU implicit multigrid scheme
[NASA-TM-100911] 20 p2753 N88-26340
Eigenmatrix representations of radiance distributions in layered natural waters with wind-roughened surfaces
[PB88-188701] 20 p2828 N88-26780
Computing small singular values of bidiagonal matrices with guaranteed high relative accuracy: LAPACK working note number 3
[DE88-008465] 20 p2837 N88-26829
A matroid algorithm and its application to the efficient solution of two optimization problems on graphs, revision
[AD-A192709] 20 p2838 N88-26838
Derivation of space groups in mm2, 222 and mmm crystal classes
[DE88-701881] 20 p2876 N88-27076
Sidelobe level of an adaptive array using the SMI (Sampled Matrix Inversion) algorithm
[AD-A193131] 21 p2932 N88-27409
A programmable systolic array for factorial analysis. Part 2: The symmetric eigenvalue problem
[AD-A192396] 21 p2995 N88-27762
A unified approach to estimation in linear models with fixed and mixed effects
[AD-A193060] 21 p3006 N88-27829
On matrix pencil equivalents of a general polynomial matrix
[MATH-REPT-207] 23 p3273 N88-29479
On Wiener-Masani's algorithm for finding the generating function of multivariate stochastic processes
[NASA-CR-182905] 23 p3273 N88-29481
Invariant ideals of multiplicity free algebraic group actions
[B8803517] 23 p3277 N88-29509

MATRIX ANALYSIS
U MATRICES (MATHEMATICS)

MATRIX MATERIALS
Calculation methods of atomic number density for various nuclear materials
[DE87-753006] 02 p0233 N88-11467
Ion-matrix coupling in polymer electrolytes from relaxation time studies
[AD-A184632] 03 p0293 N88-11841
Carbon fiber reinforced glass matrix composites for space based applications
[AD-A184355] 04 p0410 N88-12546
Composite materials with glass matrix
[SGR/PR-4305/86-SV/JC] 05 p0558 N88-13394
Fabrication of composites by chemical vapor deposition
[DE87-014565] 05 p0559 N88-13408
Development of an impact- and solvent-resistant thermoplastic composite matrix, phase 4
[NASA-CR-178413] 06 p0677 N88-14145
Sintering and densification of particulate composites: Inclusion size and clustering
[DE88-002230] 06 p0685 N88-14199
Characterization of mechanical damage mechanisms in ceramic composite materials
[AD-A185549] 06 p0686 N88-14205
Dynamic finite element with diagonalized consistent mass matrix and elastic-plastic impact calculation
[PB87-143376] 08 p0995 N88-16020
Analysis of composite laminates with matrix cracks
[CCMS-88-03] 11 p1451 N88-18645
Effect of rigid inclusions on sintering
[DE88-005745] 12 p1609 N88-19623
Interface structure and properties of alumina/glass ceramic composites
[DE88-006219] 14 p1892 N88-21302
Physical-mechanical properties of matrices on the comet nuclei surface models 14 p2010 N88-21967
Cement paste matrix composite materials center
[AD-A188657] 15 p2028 N88-22083
Microplasticity phenomena in graphite/magnesium metal matrix composites
[DE88-006772] 15 p2029 N88-22086
Singlet oxygen behavior in solid polymer matrices
[DE88-005171] 15 p2043 N88-22171
Donor acceptor polymerization chemistry as a vehicle to low energy cure matrix resins
[AD-A190119] 15 p2044 N88-22179
A test for interfacial effects and stress transfer in ceramic matrix composites
[NASA-CR-182758] 15 p2046 N88-22194
Investigation of non-linear optical behavior of semiconductors for optical switching, volume 1
[AD-A191297] 16 p2274 N88-23611
Carbon matrix composites prospective roles for biotechnology 18 p2477 N88-24694
Sol/gel processing techniques for glass matrix composites
[AD-A191748] 18 p2478 N88-24701
Effects of electron beam irradiation on mechanical properties at low and high temperature of fiber reinforced composites using PEEK as matrix material
[DE88-753134] 21 p2905 N88-27239
Fabrication of SiC fiber reinforced glass matrix by extrusion process and investigation of its mechanical properties
[ETN-88-92367] 21 p2906 N88-27244
Programs for preliminary design of composite materials which were developed by the design group of Aerospatiale Aquitaine
[REPT-881-430-112] 21 p2907 N88-27251
Determination of impurities in silicon carbide by ICP AES (inductively coupled plasma atomic emission spectrometry) after coprecipitation with lanthanum hydroxide
[NASA-TT-20332] 23 p3193 N88-29003
Creep of carbon yarn and carbon-carbon composites at high temperatures and high stresses
[AD-A195224] 24 p3340 N88-29878
Criteria for matrix dominated failure
[AD-A196263] 24 p3341 N88-29887

MATRIX METHODS
A DMAP for updating dynamic mathematical models with measured data
[NLR-MP-86027-U] 01 p0060 N88-10387
Relaxation effect of stark split levels for two-level system interacting with symmetrical strong resonant bichromatic field 03 p0299 N88-11882
Structural optimization in the design process — aircraft
[SNIAS-872-111-115] 05 p0635 N88-13885
An efficient sparse matrix multiplication scheme for the CYBER 205 computer
[NASA-TM-4028] 10 p1390 N88-18302
A constitutive material model for nonlinear finite element structural analysis using an iterative matrix approach
14 p1932 N88-21521
Coupled bending-torsion steady-state response of pretwisted, nonuniform rotating beams using a transfer-matrix method
[NASA-TM-100596] 15 p2086 N88-22435
Efficient bit-level, word-level and block-level systolic arrays for matrix-matrix multiplication
[DE88-011331] 20 p2841 N88-26856
Effective buffering schemes for performing matrix operations for numerical databases
21 p3027 N88-27968

MATRIX STRESS CALCULATION
U MATRIX METHODS

MATRIX THEORY
REDUCE-aided study of a problem in Hermitian matrix theory
[DE87-014331] 02 p0229 N88-11445
Graph partitioning by eigenvectors
[AD-A184430] 03 p0372 N88-12338
The matrix exponential in transient structural analysis
05 p0593 N88-13619
Strong representation of weak convergence
[AD-A186433] 07 p0916 N88-15563
Relativistic corrections for one- and two-photon matrix elements of weakly-bound systems
[NOTA-INTERNA-884] 07 p0929 N88-15645
Predicting oscillatory finite difference solutions to the heat equation: A comparative study of the coefficient and matrix methods
[AD-A189591] 13 p1825 N88-20911
Sufficient matrices and the linear complementarity problem
[AD-A190429] 15 p2128 N88-22690
Computing partial correlations from the data matrix
[AD-A193904] 22 p3138 N88-28659

MATTER (PHYSICS)
NT DARK MATTER
Gravitational accretion of hot dark matter
03 p0388 N88-12439
Beta limitation of matter-antimatter boundary layers
[TRITA-EPP-87-11] 09 p1250 N88-17490
The origin of the diffuse X-ray background and the formation of galaxies and voids
10 p1428 N88-18527
Quark matter in astrophysics and cosmology
[DE88-003406] 10 p1429 N88-18534

Atomic processes in matter-antimatter interactions
[DE88-008911] 19 p2723 N88-26172
N=2 supergravity in superspace: different versions and matter couplings
[DE88-702137] 19 p2741 N88-26274
Inelastic mean free paths of electrons and positrons in matter
[DE88-008086] 20 p2851 N88-26929

MATURING
U GROWTH

MAXIMA
Additional peak of light scattering by sound under conditions of acoustic instability
14 p1968 N88-21752
Structural dynamics of high-latitude magnetosphere determined from solar electron data
24 p3444 N88-30500

MAXIMUM ENTROPY METHOD
Stochastic model of the NASA/MSFC ground facility for large space structures with uncertain parameters: The maximum entropy approach
[NASA-CR-181489] 03 p0372 N88-12343
Restoration of particle pitch angle distribution functions by a maximum entropy algorithm
[ATR-86(7098)-3] 05 p0648 N88-13969
The maximum entropy method for the analysis of radar echoes from hovering helicopters in clutter
[FB-2-87] 11 p1475 N88-18799
Electron density profile reconstruction by maximum entropy method with multichannel HCN laser interferometer system on SPAC 7
[IPPJ-858] 11 p1553 N88-19295
A maximum entropy solution for the underdetermined electromagnetic field within a volume
[DE88-007020] 20 p2790 N88-26550
Maximum entropy signal restoration with linear programming
[DE88-011740] 21 p2999 N88-27787
The maximum entropy method for the analysis of short-time radar echoes from hovering helicopters
22 p3149 N88-28737

MAXIMUM LIKELIHOOD ESTIMATES
Maximum likelihood estimates of parameters in linear systems with process and measurement noise
[DFVLR-FB-87-20] 01 p0083 N88-10532
Exploiting auxiliary information about items in the estimation of Rasch item difficulty parameters
[AD-A184383] 03 p0372 N88-12341
Tau ranging revisited 04 p0437 N88-12710
Estimation of a multivariate continuous variable panel model
[AD-A184472] 04 p0484 N88-12982
An urn model for the multi-sample capture/recapture sequential tagging process
[AD-A184470] 04 p0486 N88-12998
Non-linear maximum likelihood estimation of stability derivatives from range data
[NAL-TM-SE-8608] 05 p0552 N88-13365
Approximating multivariate normal orthant probabilities using the Clark algorithm
[AD-A184855] 05 p0634 N88-13873
The maximum likelihood estimator method of image reconstruction: Its fundamental characteristics and their origin
[DE88-000462] 05 p0636 N88-13892
Presentation of a computer program permitting the exploitation of tests designed to determine the sensitivity of one shot devices to a parameter. Application to a degenerate one shot sequence
[SNIAS-872-430-117] 05 p0644 N88-13945
A three-parameter generalisation of the beta-binomial distribution with applications
[AD-A185733] 06 p0768 N88-14720
Discrete reliability growth models using failure discounting
[AD-A186380] 07 p0866 N88-15252
Strong consistency of maximum likelihood parameter estimation of superimposed exponential signals in noise
[AD-A186384] 07 p0911 N88-15526
Maximum likelihood principle and model selection when the true model is unspecified
[AD-A186027] 07 p0914 N88-15544
A simultaneous M-ary channel hypothesis test with least-mean-square signal amplitude estimation
[AD-A186526] 08 p0978 N88-15913
Short data length effects in an asymptotically efficient ARMA (AutoRegressive Moving Average) spectral estimator
[AD-A186561] 08 p1068 N88-16458
Estimation and comparison of changes in the presence of information right censoring by modeling the censoring process
[AD-A186320] 08 p1074 N88-16478
Lateral stability and control derivatives extracted from space shuttle Challenger flight data
[NASA-TM-100520] 09 p1132 N88-16788
Maximum likelihood estimates for the discrete application of the AMSAA growth model
[AD-A186921] 09 p1177 N88-17048
Random truncation models and Markov processes
[CWI-MS-R8702] 09 p1232 N88-17389
A maximum likelihood parameter estimation program for general non-linear systems
[ARL-AERO-TM-392] 11 p1532 N88-19154
Optimal recursive maximum likelihood estimation
[AD-A187980] 11 p1536 N88-19176
Statistical signal processing using a class of iterative estimation algorithms
[AD-A189050] 13 p1757 N88-20511
Estimating system and component reliabilities under partial information on cause of failure
[AD-A189107] 13 p1780 N88-20653
Non- and semi-parametric maximum likelihood estimators and the von Misis Method, part 1
[CWI-MS-R8709] 13 p1829 N88-20941
The application of linear maximum likelihood estimation of aerodynamic derivatives for the Bell-205 and Bell-206
[AD-A191279] 16 p2161 N88-22894
Maximum likelihood parameter identification of flexible spacecraft
[LR-508] 16 p2168 N88-22924
Multichannel 2-D power spectral estimation and applications
[AD-A191273] 16 p2191 N88-23068
Partial likelihood analysis of time series models with application to rainfall-runoff data
[AD-A191157] 16 p2261 N88-23516
Leave-K-Out diagnostics for time series
[AD-A191343] 16 p2261 N88-23518
A central limit theorem for M-estimators by the von Mises method
[CWI-MS-R8713] 16 p2262 N88-23525
A comparison of supervised maximum likelihood and decision tree classification for crop cover estimation from multitemporal LANDSAT MSS data
17 p2352 N88-24014
Generation of thematic maps for updating aeronautical pilot charts utilizing LANDSAT-TM images
17 p2361 N88-24062
Adaptive time series analysis using predictive inference and entropy
[AD-A191858] 18 p2560 N88-25199
Recursive maximum likelihood identification of a nonlinear output-affine model
[RR-322] 18 p2569 N88-25257
System identification in vehicle dynamics
[DFVLR-MITT-87-22] 20 p2785 N88-26518
Parameter estimation of dynamical systems
20 p2785 N88-26519
Parametric estimation of aerodynamic nonlinearities in rolling moment due to sideslip using maximum likelihood method
20 p2786 N88-26528
Tuning a major part of a clustering algorithm
[AD-A191446] 20 p2836 N88-26821
Spectral estimation of received phase in the presence of amplitude scintillation 22 p3064 N88-28180
Easy Bayes estimation for Rasch-type models
[AD-A193628] 23 p3274 N88-29491
Maximum-likelihood multichannel deconvolution of P waves at seismic arrays
[AD-A194990] 24 p3391 N88-30191
Advancement of latent trait theory
[AD-A194302] 24 p3408 N88-30289

MAXIMUM PRINCIPLE
Conference on Maximum Principles and Eigenvalue Problems in Partial Differential Equations
[AD-A187870] 11 p1536 N88-19175

MAXIMUM USABLE FREQUENCY
HF (High Frequency) Maximum Usable Frequency (MUF) model uncertainty assessment
[AD-A189132] 13 p1757 N88-20513
The MUF (Maximum Usable Frequency) (3000) as an indicator for F-region variations
[AD-A191655] 19 p2690 N88-25991

MAXWELL EQUATION
Trajectory versus PIC methods in diode design
[DE87-012135] 02 p0166 N88-11043
On the collective variables description of a high gain free electron laser
[DE87-013315] 02 p0178 N88-11108
Spectral evolution equation for the sideband instability in a free-electron laser oscillator
[DE88-000510] 04 p0447 N88-12771
Plane longitudinal waves in solutions of Maxwell equations
[DE88-700347] 07 p0846 N88-15135
A moment approach to modeling negative ion sources
[AD-A188858] 12 p1691 N88-20114
Study of inhomogeneously filled cylindrical resonant cavities by the finite integration technique
[PB88-133707] 12 p1697 N88-20156
Chronometrically invariant formulation of electrodynamics equation
[DE88-701030] 13 p1849 N88-21071
Topics in curved and flat space electromagnetism
13 p1854 N88-21100
Galilei relativity principle in classical electrodynamics
[DE87-703203] 14 p1904 N88-21376
A general 2D electrical model for diagonally connected MHD generators
[DE88-004283] 14 p1984 N88-21835
Wave energy flow conservation for propagation in inhomogeneous Vlasov-Maxwell equilibria
[DE88-006705] 15 p2055 N88-22251
High speed transcendental elementary function architecture in support of the Vector Wave Equation (VWE)
[AD-A189746] 15 p2119 N88-22627
Microinstabilities in ion beam propagation
16 p2277 N88-23631
Coronal fluid-dynamics in laser fusion
16 p2278 N88-23634
The MAFIA approach to solving Maxwell's equations in three dimensions
[DE88-007826] 19 p2720 N88-26155
Stochastic modeling of EM scattering from foliage
[AD-A192258] 20 p2790 N88-26553
SARLAC: A relativistic electron beam code
[AD-A193134] 21 p2932 N88-27411
Kinetic theory for plane flows of rough, inelastic, circular disks 21 p2946 N88-27499
Wave equations for pulse propagation
[DE88-011760] 21 p2954 N88-27548
Staggered-grid finite element solution technique for the Maxwell's equations in the time domain
[DE88-011731] 21 p3007 N88-27838
On the self-consistent equation for the microscopic local electric field in dielectric systems
[PREPRINT-589] 22 p3074 N88-28247
Research on a two-stage free electron laser oscillator
[AD-A195991] 24 p3377 N88-30115

MAXWELL-BOLTZMANN DENSITY FUNCTION
Effects of low reflection on the collector and source sheaths of a finite ion temperature plasma
[DE88-008929] 21 p3017 N88-27908

MAXWELLIAN DISTRIBUTION (DENSITY)
U MAXWELL-BOLTZMANN DENSITY FUNCTION

MAZE LEARNING
Path planning and path following for the Amsterdam autonomous cart
[FVI-86-22] 24 p3380 N88-30133

MCDONNELL AIRCRAFT
NT F-4 AIRCRAFT
NT RF-4 AIRCRAFT

MCDONNELL DOUGLAS AIRCRAFT
NT DC 9 AIRCRAFT
NT F-4 AIRCRAFT
NT F-18 AIRCRAFT
NT RF-4 AIRCRAFT
McDonnell Douglas Helicopter Company independent research and development: Preparing for the future
09 p1111 N88-16660

MEADOWLANDS
U GRASSLANDS

MEAN
Testing and interval estimation in a change-point model allowing at most one change
[AD-A185525] 06 p0767 N88-14716
On detection of change points using mean vectors
[AD-A185581] 06 p0767 N88-14717
An elimination type two-stage procedure for selecting the population with the largest mean from k logistic populations
[AD-A185614] 07 p0916 N88-15566
Modeling discrete bathtub and upside down bathtub mean residual life functions
[AD-A192000] 22 p3085 N88-28320

MEAN FREE PATH
Study of mean free path effects on growth of ultrafine metallic aerosols
[AD-A190206] 15 p2039 N88-22149
Inelastic mean free paths of electrons and positrons in matter
[DE88-008086] 20 p2851 N88-26929

MEAN SQUARE VALUES
Evolution of mean square magnetic vector potential in compressible, two-dimensional, magnetofluid turbulence
[AD-A184985] 05 p0651 N88-13990
A simultaneous M-ary channel hypothesis test with least-mean-square signal amplitude estimation
[AD-A186526] 08 p0978 N88-15913

MEAN TIME BETWEEN FAILURES
U MTBF

MEASURE AND INTEGRATION
NT BINARY INTEGRATION
NT BOREL SETS
NT INTEGRAL CALCULUS

NT J INTEGRAL
NT LEBESGUE THEOREM
NT NUMERICAL INTEGRATION
NT RUNGE-KUTTA METHOD
NT WEIGHTING FUNCTIONS
The precision of limits on bodily fluids when using beta-expectation inner tolerance limits
[AD-A187966] 10 p1369 N88-18185
Path integration on the upper half-plane
[DE88-751050] 12 p1682 N88-20057
Remarks on the time transformation of path-integral measures
[DE87-703040] 15 p2118 N88-22617
Why are certain nonlinear Partial Differential Equations (PDE) both widely applicable and integrable
[PREPRINT-582] 22 p3144 N88-28698

MEASURE THEORY
U MEASURE AND INTEGRATION

MEASUREMENT
Group quantization of constrained systems
[PREPRINT-564] 06 p0790 N88-14844

MEASURING
U MEASUREMENT

MEASURING INSTRUMENTS
NT ACCELEROMETERS
NT ADVANCED VERY HIGH RESOLUTION RADIOMETER
NT ALTIMETERS
NT ANALYZERS
NT ANEMOMETERS
NT ATOMIC CLOCKS
NT ATTITUDE INDICATORS
NT BALLOON-BORNE INSTRUMENTS
NT BAROMETERS
NT BATHYMETERS
NT BATHYTHERMOGRAPHS
NT BOLOMETERS
NT BOMB CALORIMETERS
NT CALORIMETERS
NT CERENKOV COUNTERS
NT CLOCKS
NT CLOUD HEIGHT INDICATORS
NT COMPARATORS
NT COUNTERS
NT DENSIMETERS
NT DENSITOMETERS
NT DICKE RADIOMETERS
NT DIFFRACTOMETERS
NT DISTANCE MEASURING EQUIPMENT
NT DOSIMETERS
NT DYNAMOMETERS
NT EBERT SPECTROMETERS
NT ELECTRICAL CONDUCTIVITY METERS
NT ELECTRON COUNTERS
NT ELECTRON PROBES
NT ELECTROPHOTOMETERS
NT ELECTROSTATIC PROBES
NT ELLIPSOMETERS
NT ENGINE ANALYZERS
NT ENGINE MONITORING INSTRUMENTS
NT ERGOMETERS
NT ETALONS
NT EXTENSOMETERS
NT FABRY-PEROT INTERFEROMETERS
NT FABRY-PEROT SPECTROMETERS
NT FLAME PROBES
NT FLIGHT RECORDERS
NT FLIR DETECTORS
NT FLOWMETERS
NT GALVANOMETERS
NT GAMMA RAY SPECTROMETERS
NT GONIOMETERS
NT GRAVIMETERS
NT GRAVITY GRADIOMETERS
NT HOT-FILM ANEMOMETERS
NT HOT-WIRE ANEMOMETERS
NT HOT-WIRE FLOWMETERS
NT IMAGING SPECTROMETERS
NT IMPEDANCE PROBES
NT INDICATING INSTRUMENTS
NT INFRARED DETECTORS
NT INFRARED INSTRUMENTS
NT INFRARED INTERFEROMETERS
NT INFRARED RADIOMETERS
NT INFRARED SCANNERS
NT INFRARED SPECTROMETERS
NT INFRARED SPECTROPHOTOMETERS
NT INTERFEROMETERS
NT ION PROBES
NT ION TRAPS (INSTRUMENTATION)
NT IONIZATION GAGES
NT IONOSONDES
NT LASER ALTIMETERS
NT LASER ANEMOMETERS
NT LASER DOPPLER VELOCIMETERS
NT LASER RANGE FINDERS
NT LASER SPECTROMETERS
NT LIGHT SCATTERING METERS
NT MACH-ZEHNDER INTERFEROMETERS
NT MAGNETIC PROBES
NT MAGNETOMETERS
NT MASS SPECTROMETERS
NT METEOROLOGICAL INSTRUMENTS
NT MICHELSON INTERFEROMETERS
NT MICRODENSITOMETERS
NT MICROMETERS
NT MICROWAVE INTERFEROMETERS
NT MICROWAVE RADIOMETERS
NT MICROWAVE SENSORS
NT MICROWAVE SPECTROMETERS
NT MOISTURE METERS
NT MONOCHROMATORS
NT NEUTRON COUNTERS
NT NEUTRON SPECTROMETERS
NT OCULOMETERS
NT OMEGA NAVIGATION SYSTEM
NT OPTICAL MEASURING INSTRUMENTS
NT OPTICAL PYROMETERS
NT OXYGEN ANALYZERS
NT PARTICLE TELESCOPES
NT PHASE SWITCHING INTERFEROMETERS
NT PHOTOMETERS
NT PIEZOELECTRIC GAGES
NT PLASMA PROBES
NT PNEUMATIC PROBES
NT POLARIMETERS
NT POSITION INDICATORS
NT PRESSURE GAGES
NT PROFILOMETERS
NT PROPORTIONAL COUNTERS
NT PYROMETERS
NT RADIATION COUNTERS
NT RADIATION DETECTORS
NT RADIATION MEASURING INSTRUMENTS
NT RADIATION PYROMETERS
NT RADIO ALTIMETERS
NT RADIO INTERFEROMETERS
NT RADIOMETERS
NT RADIOSONDES
NT RAIN GAGES
NT RANGE FINDERS
NT RAWINSONDES
NT REFRACTOMETERS
NT RESISTANCE THERMOMETERS
NT SATELLITE-BORNE INSTRUMENTS
NT SCATTEROMETERS
NT SCINTILLATION COUNTERS
NT SEISMOGRAPHS
NT SIGNAL ANALYZERS
NT SILICON RADIATION DETECTORS
NT SOLAR BACKSCATTER UV SPECTROMETER
NT SOLAR SPECTROMETERS
NT SONDES
NT SPARK CHAMBERS
NT SPECTROHELIOGRAPHS
NT SPECTROMETERS
NT SPECTROPHOTOMETERS
NT SPECTRORADIOMETERS
NT STRAIN GAGE ACCELEROMETERS
NT STRAIN GAGES
NT TACHOMETERS
NT TEMPERATURE MEASURING INSTRUMENTS
NT THEODOLITES
NT THERMOMETERS
NT THRESHOLD DETECTORS (DOSIMETERS)
NT TILTMETERS
NT TIME OF FLIGHT SPECTROMETERS
NT TIMING DEVICES
NT TORQUEMETERS
NT TOTAL OZONE MAPPING SPECTROMETER
NT TRANSMISSOMETERS
NT TURBULENCE METERS
NT ULTRAVIOLET SPECTROMETERS
NT ULTRAVIOLET SPECTROPHOTOMETERS
NT VACUUM GAGES
NT VARIOMETERS
NT VIBRATION METERS
NT VISCOMETERS
NT VOLTMETERS
NT WATTMETERS
NT WEIGHT INDICATORS
Nonintrusive ultrasonic flow measurement techniques and their applications to BTU metering
[DE87-011390] 01 p0045 N88-10286
NBS (National Bureau of Standards) calibration services users guide: Fee schedule
[PB87-210654] 01 p0090 N88-10586
The use of fiber optics in the determination of temperature and extent of reaction in detonating explosives
[DE87-012632] 01 p0094 N88-10612
Simple instrumentation for testing of ceramic superconductors
[DE87-013849] 01 p0103 N88-10672
Further development of the dynamic gas temperature measurement system 02 p0184 N88-11141
Description of a multiframe optical probing system
[DE87-014255] 02 p0236 N88-11487
Combustion control with smart sensors
[DE87-013688] 03 p0261 N88-11768
Particle velocity and stress gage measurements in spherical diverging flow
[DE87-007333] 03 p0321 N88-12033
Components for measuring robots
[KFK-PFT-126] 03 p0332 N88-12092
Proceedings of the Fifth Symposium on Energy Engineering Sciences: Instrumentation, Diagnostics, and Material Behavior
[DE88-001479] 04 p0429 N88-12660
Non-linearity in measurement systems: Evaluation method and application to microwave radiometers 04 p0433 N88-12684
Evaluation of the sensidyne toxic gas sensor for HF (Hydrogen Fluoride) vapor
[DE88-000647] 04 p0446 N88-12767
Optimization of dilatometer test procedures
[DE87-014998] 04 p0447 N88-12769
Use of electron beam instruments to determine fluctuations in vertical refraction partial angle 04 p0461 N88-12853
Computerized certification of digital ultrasonic instrumentation
[DE88-000820] 04 p0488 N88-13008
New approach to telemetry development will significantly increase productivity of Joint Test Assembly (JTA) teams
[DE88-001676] 05 p0554 N88-13373
Research for electric energy systems
[DE88-001733] 06 p0695 N88-14265
Recent advances in high temperature instrumentation for hot section applications
[NASA-TM-100282] 06 p0707 N88-14339
Quick measurement of individual stress reaction level: Development of the Emotional Stress Reaction Questionnaire (ESRQ)
[FOA-C-50050-5.3] 06 p0752 N88-14617
Investigation of the performance of a novel double crystal X-ray monochromator measurements
[PB87-125167] 06 p0788 N88-14834
Survey of electronic measurement needs below 10 MHz
[PB88-110366] 07 p0844 N88-15121
Scientific research in the field of measurement and control technology
[SMBT-322] 07 p0907 N88-15493
Fiber optics refractometer for absorption machines
[DE88-002296] 07 p0932 N88-15662
Aeropropulsion '87. Session 4: Instrumentation and Controls Research
[NASA-CP-10003-SESS-4] 08 p0955 N88-15794
Research sensors 08 p0955 N88-15795
Development of on-orbit fluid gaging techniques 08 p0982 N88-15936
Effectiveness of oceanographic method in earthquake prediction 08 p1010 N88-16124
Surface acoustic wave deposition sensor
[DE87-006527] 09 p1243 N88-17452
A technique for low level, wide range CW microwave power meter calibrations
[DE88-004147] 10 p1333 N88-17966
Into the thermosphere: The atmosphere explorers
[NASA-SP-490] 10 p1353 N88-18084
Developments in National Weather Service meteorological data collection programs as related to EPA (Environmetal Protection Agency) air pollution models
[PB88-130240] 10 p1356 N88-18104
Cleanliness tests with the Omega Meter: A comparative study for solder flux removal
[DE88-004634] 11 p1480 N88-18704
LiNbO3:Ti directional-coupler modulators for high-bandwidth, single-shot instrumentation systems operating at 800 nm
[DE88-003830] 11 p1479 N88-18823
Measurement of velocity and temperature profiles in low-speed, turbulent non-isothermal flows
[PB88-155833] 11 p1486 N88-18872
Measurements as a process
[DE88-005275] 11 p1497 N88-18938
Ultrasonic testing of heat exchanger tubes
[DE88-751172] 11 p1497 N88-18939
Applications of lower cost computers to dimensional gaging
[BDX-613-3606] 11 p1525 N88-19108
Long term measurement network for FIFE
[NASA-CR-182491] 12 p1646 N88-19857

The Joint NASA/Goddard-University of Maryland Research Program in Charged Particle and High Energy Photon Detector Technology
[NASA-CR-182612] 12 p1712 N88-20247
Development of a torsion balance for adhesion measurements
[NASA-TM-100799] 13 p1748 N88-20454
Digital correlator for the portable channel prober measurement instrument
[AD-A189065] 14 p1904 N88-21377
Density measurements on solids and liquids
[PB88-164934] 15 p2036 N88-22129
A 150,000 pounds per square inch dynamic pressure calibrator
[AD-A190659] 15 p2069 N88-22335
Research sensors 15 p2085 N88-22430
Proceedings of the Lightning Threat Warning Workshop
[DE88-006607] 15 p2098 N88-22499
Development of a digital sun sensor for a spin-stabilized satellite
[INPE-4508-TDL/327] 16 p2169 N88-22929
French evaluation of Japanese biosensors 16 p2184 N88-23020
A compact high resolution piezoresistive digital tactile sensor
[DE88-000430] 16 p2210 N88-23188
Cylindrical surface profile and diameter measuring tool and method
[NASA-CASE-MFS-28287-1] 17 p2341 N88-23959
Apparatus for the measurement of resistivity of glasses and ceramics 17 p2431 N88-24460
Electrostatic discharge test apparatus
[NASA-CASE-MSC-21094-1] 18 p2518 N88-24941
Universal precision sine bar attachment
[NASA-CASE-MFS-28253-1] 18 p2523 N88-24971
A non-contact picosecond prober for integrated circuit testing 19 p2655 N88-25766
Fast GaAs photoconductive detectors with high sensitivity integrated in coplanar systems onto GaAs substrates 19 p2658 N88-25790
A technique for wing suppressed IR sampling 19 p2658 N88-25794
MESFET compatible IMSM detectors 19 p2659 N88-25801
Surface temperature thermal fluxmeters for shock tubes
[NASA-TT-20319] 20 p2762 N88-26381
Instrumentation for the measurement of penetrator dynamic response to permit force estimation
[DE88-010608] 20 p2809 N88-26666
Acoustic emission calibration instrumentation
[DE88-010817] 21 p2951 N88-27528
Components of an atmospheric lidar system
[AD-A193366] 21 p2953 N88-27539
Direct measurement of solids: High temperature sensing. Experimental development and testing of high temperature pulsed EMATs
[DE88-009859] 21 p2954 N88-27546
Atmospheric nitrogen oxides: Their detection and chemistry
[PB88-193057] 21 p2970 N88-27642
Apparent brightness of stars and lasers 22 p3065 N88-28188
A wideband, high-resolution spectrum analyzer 22 p3066 N88-28194
Langley Research Center Metrology Program status for fiscal year 1987
[NASA-TM-100651] 22 p3086 N88-28324
Aerodynamics of seeing on large transport aircraft
[NASA-CR-183122] 23 p3174 N88-28896
Skin friction balance
[NASA-CASE-LAR-13710-1] 23 p3216 N88-29145
Ice detector
[NASA-CASE-LAR-13776-1] 23 p3217 N88-29149
Liquid thickness gauge
[NASA-CASE-LAR-13826-1] 23 p3217 N88-29150

MECHANICAL DEVICES
Tape wrapping apparatus and method
[EP-PATENT-0-181-747-A2] 01 p0053 N88-10336
Mechanical design of the ac bracket package for the RETE experiment
[IFSI-87-4] 05 p0555 N88-13379
Utilization of FEP energetics
[NASA-CR-182373] 06 p0714 N88-14379
ESA Bulletin No. 10
[ETN-87-90514] 09 p1123 N88-16728
Why mechanisms are critical to spacecraft performance 09 p1125 N88-16737
Seven year thermal vacuum real life test of a medium speed (despin) mechanism manufactured by Dornier System
[ESA-ESTL-64] 09 p1175 N88-17038
A substructure method for dynamic simulation of flexible mechanical systems with geometric nonlinearities 09 p1176 N88-17044
Tactile sensing and inverse problems
[AD-A187464] 10 p1340 N88-18011
Understanding machines from text and diagrams
[AD-A189034] 13 p1755 N88-20493
Mental models of mechanical systems: Individual differences in qualitative and quantitative reasoning
[AD-A189035] 13 p1812 N88-20823
The SPOT solar array. Box opening mechanisms physical vapor deposition (PVD)-MoS2: Lubricated slides. Functional evaluation 14 p1876 N88-21211
Nonlinear analysis and optimal design of dynamic mechanical systems for spacecraft application
[AD-A190644] 15 p2026 N88-22070
A technique for measuring area under a curve
[AD-A193559] 23 p3271 N88-29463

MECHANICAL DRAWINGS
U ENGINEERING DRAWINGS

MECHANICAL DRIVES
NT PROPELLER DRIVE
NT TRANSMISSIONS (MACHINE ELEMENTS)
Improvements to the precision pan and tilt head
[RSRE-MEMO-3996] 01 p0057 N88-10365
Adaptive control of hydraulic devices
[FB-1/85] 01 p0084 N88-10543
Pulse width modulator controller design for a brushless DC motor position servo
[AD-A186618] 08 p0980 N88-15921
Why mechanisms are critical to spacecraft performance 09 p1125 N88-16737
Theoretical and experimental investigations on a linear, permanently excited stepping motor
[ETN-88-91061] 09 p1158 N88-16939
Analysis of possible transmission arrangements applicable for driving single or twin counterrotating fans on propfan engines 10 p1282 N88-17670
Hemispherical pointing mechanism drive unit — satellite payloads antennas 14 p1874 N88-21193
Development of a cryogenic stepping drive for ISO/LWS 14 p1878 N88-21220
Qualification testing of the EUROSTAR Solar Array Drive Mechanism (SADM) 14 p1879 N88-21229
Advanced transmission studies
[NASA-TM-100867] 14 p1919 N88-21454
The 22nd Aerospace Mechanisms Symposium
[NASA-CP-2506] 14 p1924 N88-21468
Development of drive mechanism for an oscillating airfoil 14 p1926 N88-21482
A high performance inverter-fed drive system of an interior permanent magnet synchronous machine
[DE88-006753] 15 p2061 N88-22288
Evaluation of a high-torque backlash-free roller actuator 16 p2219 N88-23239
Roller drive materials performance 16 p2219 N88-23241
A microcomputer-based control and simulation of an advanced IPM (Interior Permanent Magnet) synchronous machine drive system for electric vehicle propulsion
[DE88-006735] 18 p2505 N88-24859
Optimization of planetary gears
[ETN-88-92375] 21 p2958 N88-27573

MECHANICAL ENGINEERING
National Science Foundation
[PB87-228375] 03 p0384 N88-12410
Interactions between science and precision engineering
[DE87-010873] 04 p0426 N88-12643
COLA2: A computer program for the structural synthesis of two components using general modal coordinates
[DE88-001457] 04 p0481 N88-12963
Bulletin of the Yamagata University (Engineering), Volume 20, No. 1, January 1988
[ISSN-0085-834X] 07 p0839 N88-15091
Why mechanisms are critical to spacecraft performance 09 p1125 N88-16737
Kinematic optimization of mechanisms, a finite element approach
[ISBN-90-370-0012-6] 09 p1175 N88-17039
Mechanical design and construction of a 200 mA, 100 keV, dc, negative ion accelerator
[DE88-003855] 11 p1548 N88-19257
DARM: A new deployment and retraction mechanism which does not need electric power 14 p1876 N88-21206

MECHANICAL FINGERS
U END EFFECTORS

MECHANICAL HANDS
U END EFFECTORS

MECHANICAL IMPEDANCE
Analyses by equivalent mechanical circuits of bending vibration bars with load-impedance at one end 07 p0840 N88-15093
Dynamic response of plates to moving loads: Structural impedance and finite element methods 18 p2528 N88-25000

MECHANICAL MEASUREMENT
NT DISPLACEMENT MEASUREMENT
NT DRAG MEASUREMENT
NT FLOW MEASUREMENT
NT FRICTION MEASUREMENT
NT PRESSURE MEASUREMENT
NT STRESS MEASUREMENT
NT THRUST MEASUREMENT
NT VELOCITY MEASUREMENT
NT VIBRATION MEASUREMENT
NT WIND MEASUREMENT
NT WIND VELOCITY MEASUREMENT
In-service measurements of SAAB SF-340 landing gear loads
[FFA-TN-1987-48] 15 p2018 N88-22032

MECHANICAL OSCILLATORS
NT PENDULUMS
Equivalent circuit consideration on the rotation of resonant modes of double resonant vibrators 07 p0839 N88-15092
Analyses by equivalent mechanical circuits of bending vibration bars with load-impedance at one end 07 p0840 N88-15093

MECHANICAL PROPERTIES
NT ABRASION RESISTANCE
NT AEROELASTICITY
NT ANELASTICITY
NT BRITTLENESS
NT BULK MODULUS
NT COMPRESSIBILITY
NT COMPRESSIVE STRENGTH
NT CREEP PROPERTIES
NT CREEP RUPTURE STRENGTH
NT CREEP STRENGTH
NT DIMENSIONAL STABILITY
NT DUCTILITY
NT ELASTIC PROPERTIES
NT ELASTOPLASTICITY
NT ELECTROSTRICTION
NT FATIGUE LIFE
NT FIBER STRENGTH
NT FLEXIBILITY
NT FRACTURE STRENGTH
NT HARDNESS
NT HIGH STRENGTH
NT HYDROELASTICITY
NT IMPACT STRENGTH
NT MAGNETOSTRICTION
NT MICROHARDNESS
NT MODULUS OF ELASTICITY
NT NOTCH SENSITIVITY
NT NOTCH STRENGTH
NT PHOTOELASTICITY
NT PIEZOELECTRICITY
NT PLASTIC PROPERTIES
NT POISSON RATIO
NT PROPORTIONAL LIMIT
NT SHEAR CREEP
NT SHEAR PROPERTIES
NT SHEAR STRENGTH
NT SHELL STABILITY
NT STIFFNESS
NT STRESS CYCLES
NT STRESS RELAXATION
NT STRUCTURAL STABILITY
NT SUPERPLASTICITY
NT TENSILE PROPERTIES
NT TENSILE STRENGTH
NT THERMAL RESISTANCE
NT THERMOELASTICITY
NT THERMOPLASTICITY
NT THERMOVISCOELASTICITY
NT TOUGHNESS
NT VISCOELASTICITY
NT VISCOPLASTICITY
NT WEAR RESISTANCE
NT WELD STRENGTH
NT YIELD POINT
NT YIELD STRENGTH
Structural reliability and damage tolerance of ceramic composites for high-temperature applications
[PB87-208310] 01 p0019 N88-10119
Mechanical properties characterization of composite sandwich materials intended for space antenna applications
[NASA-TM-88883] 01 p0020 N88-10121
Development of ultrafine grains and related properties in Hadfield manganese steels
[DE87-011884] 01 p0024 N88-10154
Evaluation of mechanical and technological parameters of different steel states by nondestructive micro- and macromagnetic measuring quantities as well as ultrasonic techniques
[MPA-810-079] 01 p0057 N88-10366

An experimental and theoretical study of the bending behavior of Kevlar 49/epoxy beams and rings
[DE87-010430] 01 p0061 N88-10394
Measurement of agglomerate strength distributions in agglomerated powders
[DE87-013605] 01 p0090 N88-10591
Colloidal structure of bitumens. Relationship between composition-structure behavior
[PC-4] 02 p0146 N88-10912
Needs assessment for nondestructive testing and materials characterization for improved reliability in structural ceramics for heat engines
[DE88-000040] 02 p0153 N88-10957
Study of the micromechanical behavior of a SiO2-Al2O3-Li2O glass ceramic and its relation to the microstructure
[ISAL-ITC1-87-01] 02 p0153 N88-10960
Elevated temperature strain gages 02 p0184 N88-11144
Effect of irradiation on the tensile properties of niobium-base alloys
[DE87-002409] 03 p0285 N88-11790
Development and application of composites 03 p0286 N88-11795
Low activation ferritic alloys for nuclear fusion reactors
[DE87-010711] 03 p0286 N88-11801
Birch's law and the properties of high temperature fluid metals
[DE87-014744] 03 p0288 N88-11807
Modified 14Cr-16Ni stainless steels with improved creep resistance at 700 C due to tailored precipitate microstructures
[DE87-014788] 03 p0290 N88-11825
Microstructural characterization of irradiated PWR steels using the atom probe field-ion microscope
[DE88-000341] 03 p0291 N88-11828
High temperature characterization of ceramic materials
[REPT-NT-3403] 03 p0292 N88-11837
Indentation damage in ceramics
[AD-A184686] 03 p0294 N88-11844
Joining of silicon carbide reinforced ceramics
[DE87-014881] 03 p0294 N88-11847
Wittig synthesis of conductive segmented block polymer compositions
[AD-A184018] 03 p0295 N88-11850
Effects of cure pressure on resin flow, voids, and mechanical properties
[AD-A184267] 03 p0295 N88-11853
Status of titanium alloys R and D described 03 p0298 N88-11876
Gas tungsten arc welding of Al-10Fe-5Ce
[AD-A184202] 03 p0334 N88-12104
Investigation of reliability of strength values measured on CFRP test bars by statistical methods. Part 1: Probability distributions for strength analysis
[ESA-TT-1036] 03 p0336 N88-12115
Scaling of size/time/temperature associated with dilatation and distortion in uniaxial specimens 03 p0336 N88-12117
Materials studies for magnetic fusion energy applications at low temperatures-X
[PB87-232575] 03 p0381 N88-12395
Research and development on high strength ceramic heaters discussed 04 p0404 N88-12508
Parachute materials
[DE87-014845] 04 p0411 N88-12550
Mechanical properties of a microalloyed steel with high niobium content
[DE87-703545] 04 p0415 N88-12572
Mechanical properties of an acicular ferrite steel microalloyed to niobium and vanadium
[DE87-703547] 04 p0415 N88-12574
Mechanical strength and niobium and niobium-base alloys substructures
[DE87-703692] 04 p0415 N88-12577
Effects of stress-relieving on the mechanical properties and the structure of specimens of high-temperature fine-grained structural steels heat-treated to simulate welding
[BLL-CE-TRANS-8258-(9022.09)] 04 p0417 N88-12586
The aging behavior of types 308 and 308CRE stainless steels and its effect on mechanical properties
[DE87-012541] 04 p0417 N88-12590
Development of advanced fiber reinforced ceramics
[DE88-000779] 04 p0420 N88-12604
Thermomechanical cracking in coated media due to high speed asperity excitation
[AD-A184176] 04 p0454 N88-12809
Micromechanics of the degradation of composite materials
[SNIAS-872-430-113] 05 p0559 N88-13405
Mechanical property evaluation of a series of commercial tungsten alloys
[AD-A185440] 05 p0565 N88-13446
The evolution of local mechanical properties of Al 2219-T851 during fatigue 05 p0598 N88-13653
An investigation of physical properties of thermoplastic polyimides
[NASA-TM-100530] 06 p0678 N88-14151
Study of surface treatment before bonding of light alloys
[DCQ/L-48-287/F] 06 p0682 N88-14181
Development of strength in cements
[PB87-232971] 06 p0684 N88-14189
The effective elastic properties of low-density foams
[DE87-014629] 06 p0684 N88-14194
Characterization of mechanical damage mechanisms in ceramic composite materials
[AD-A185549] 06 p0686 N88-14205
Waves and vibrations in elastic superlattice composites 06 p0776 N88-14765
Precipitation in alumina-rich spinel: A transformation-toughened ceramic single crystal
[DE87-012380] 06 p0785 N88-14815
Natural frequencies and structural integrity assessment of large space structures
[AD-A186139] 07 p0824 N88-15001
Interface effects on the mechanical properties of ceramic composites
[AD-A185899] 07 p0826 N88-15009
Composite reliability enhancement via preloading
[AD-A185938] 07 p0826 N88-15010
Characterization of current steels. The 35 NCD 16 alloy in 30 mm diam laminated bars made by Aubert and Duval
[CEAT-41/N/76] 07 p0832 N88-15046
Microstructural observations of the Sn-Pb solder/Cu system and thermal fatigue of the solder joint
[DE88-001392] 07 p0832 N88-15048
Study on substructures of martensite in steels containing rare earth metals
[PB87-143996] 07 p0833 N88-15050
Method of obtaining of fire resistant polyacrylonitrile fiber or cloth from it
[AD-A185941] 07 p0836 N88-15071
Center for the Space Processing of Engineering Materials 07 p0838 N88-15083
Weldability of a leaded carbon steel
[PB88-110341] 07 p0861 N88-15225
Computer-aided analysis for the Mechanics of Granular Materials (MGM) experiment, part 2 07 p0926 N88-15626
Effects of aviation fluids on fiber composite material
[FOA-C-20674-2.6] 08 p0965 N88-15840
Interface characteristics and the mechanical properties of metal matrix composites
[AD-A186441] 08 p0966 N88-15845
Methods of improving compacting quality of intricately shaped powder components
[BLL-M-37412-(5828.4)] 08 p0968 N88-15859
Kinetics and mechanism of thermal aging embrittlement of duplex stainless steels
[DE88-002987] 08 p0969 N88-15866
Mechanical properties of steel-to-steel adhesive bonds
[PB88-111299] 08 p0971 N88-15877
Laser transformation hardening of precision V-slide way
[PB87-144028] 08 p0991 N88-15999
Solid mechanics research for quantitative non-destructive evaluation
[AD-A186599] 08 p0993 N88-16010
Group 2A metastable collision complexes: Spectroscopy and behavior in intense radiation fields
[AD-A186737] 08 p1082 N88-16524
High temperature polymer matrix composites 09 p1119 N88-16700
Sublaminate damage mechanisms in composite structures
[AD-A186807] 09 p1137 N88-16815
Study of the temperature dependence of the mechanical characteristics of the steels GX 5 CrNi 13 4 and GGG 40 in tensile and bending tests
[DE88-001469] 09 p1143 N88-16850
Correlations of norbornenyl crosslinked polyimide resin structures with resin thermo-oxidative stability, resin glass transition temperature and composite initial mechanical properties
[NASA-TM-100791] 09 p1147 N88-16877
Residual stiffness and strength of Kevlar/epoxy laminated impulsively loaded to 7.9 ktaps
[DE88-003724] 09 p1149 N88-16886
Detection of hydrogen-assisted-cracking in U-0.8Ti alloy weldments by acoustic emission monitoring
[DE88-003221] 09 p1184 N88-17093
Effect of post-cure heat-treatment on static and fatigue behaviour of XAS-914C carbon fibre composite
[AD-A186943] 10 p1294 N88-17735
Mechanics of composite materials: Past, present and future
[NASA-TM-100793] 10 p1295 N88-17744
Influence of non-metallic elements in the mechanical properties of 20 Mn Mo Ni 55 steel
[DE88-700412] 10 p1300 N88-17775
Effects of the neutron spectrum on mechanical property changes in low dose irradiations
[DE88-003429] 10 p1302 N88-17786
The role of composition and microstructure gradients on weld metal properties and behavior
[DE88-004956] 10 p1303 N88-17791
Bias, internal stress and substrate effects on the microstructure and properties of PVD-wear resistant coatings
[AERE-R-12360] 10 p1304 N88-17798
Adhesion, friction and micromechanical properties of ceramics
[NASA-TM-100782] 10 p1305 N88-17801
Mechanisms of wear in single- and two-phase materials
[DE88-003846] 10 p1305 N88-17806
Physical and structural characteristics of Weddell Sea pack ice
[AD-A188189] 10 p1358 N88-18119
Study of the mechanical behavior of a 2-D carbon-carbon composite
[NASA-CR-182594] 11 p1451 N88-18649
Fracture mechanisms and strengthening of slab lasers
[DE88-004002] 11 p1493 N88-18914
The place for thermoplastic composites in structural components
[AD-A189149] 12 p1604 N88-19596
An interdisciplinary approach to predictive modeling of structural adhesive bonding: Factors affecting the durability of titanium/epoxy bonds
[AD-A189503] 12 p1611 N88-19636
Advanced durability analysis. Volume 1: Analytical methods
[AD-A188341] 12 p1635 N88-19789
Nonaxisymmetric body supersonic, aerodynamic prediction
[AD-A189338] 13 p1716 N88-20259
Viscoelastic behavior of a polyetheretherketone (PEEK) composite
[AD-A189545] 13 p1734 N88-20368
The influence of the fiber-matrix bond on the mechanical behavior of NICALON/SiC composites
[DE88-006155] 13 p1734 N88-20369
A fundamental understanding of the effect of alloying elements on the corrosion resistance of rapidly solidified Mg alloys
[AD-A189385] 13 p1741 N88-20413
Gordon Conference on Intermetallic Compounds held at Tilton, New Hampshire on 20-24 July 1987
[AD-A188502] 13 p1745 N88-20435
PNL-1 improved ceramic composites through controlled fiber matrix interaction
[DE88-005680] 13 p1750 N88-20462
Analysis of shell-type structures subjected to time-dependent mechanical and thermal loading
[NASA-CR-182705] 13 p1783 N88-20668
Mechanical properties of sea ice and sea ice deformation in the near-shore zone
[PB88-147889] 13 p1804 N88-20782
On the structure of pulsed plasma jets 13 p1843 N88-21030
Exploring the relation between interface structure and mechanical properties in multilayer structures
[DE88-005428] 13 p1848 N88-21060
Static mechanical properties of 30 x 11.5 - 14.5, type 8 aircraft tires of bias-ply and radial-belted design
[NASA-TP-2810] 14 p1867 N88-21157
Influence of heat treatment on the properties of boroaluminum 14 p1886 N88-21270
Processing, texture and mechanical properties of sintered silicon carbide
[NASA-TT-20253] 14 p1893 N88-21305
Effect of oxidation on strength and thermal stability of material based on Si3N4 14 p1896 N88-21319
Statistical analysis of feasibility of non-destructive inspection of mechanical properties of hot worked pipes of alloy steels
[BLL-M-37596-(5828.4)] 14 p1922 N88-21455
Applications of elastic-viscoplastic constitutive models in dynamic analyses of crack run-arrest events 14 p1930 N88-21507
High temperature materials: What's available
[AERE-R-12632] 15 p2028 N88-22081
Galvanic corrosion initiatives
[AD-A190658] 15 p2040 N88-22155
Transformation toughening of ceramics
[AD-A190399] 15 p2045 N88-22183
Mechanical behaviour of particle filled thermoplastics
[PB88-169297] 15 p2047 N88-22196

Hafnia-rich mixed oxide ceramics of the system HfO2-ZrO2-TiO2 for heaters and heat exchangers in electrothermal thrusters: The effects of titania on selected electrical and mechanical properties of Hafnia-rich mixed oxides in the system Hafnia-Zirconia-Titania, volume 1
[NASA-CR-182800-VOL-1] 15 p2047 N88-22197
Developments in ceramic superconducting materials 15 p2052 N88-22229
Features and applications of the integrated composites analyzer (ICAN) code 15 p2078 N88-22391
Structural decomposition of multiple time scale Markov processes
[AD-A189739] 15 p2123 N88-22657
Experimental studies on electronic properties of HgTe/CdTe and Hg sub 1-z Cd sub x Te/CdTe heterostructures and superlattices
[AD-A189826] 15 p2142 N88-22783
Fundamental studies of the mechanical behavior of microelectronic thin film materials
[AD-A190038] 15 p2143 N88-22786
Delamination analysis in crossed layer composites
[REPT-48-447/F] 16 p2171 N88-22942
Test procedures and standards for mechanical property measurements on metal matrix composites
[NPL-DMA(A)-153] 16 p2172 N88-22944
Thermoviscoelastic characterization and predictions of Kevlar/epoxy composite laminates
[NASA-CR-182878] 16 p2172 N88-22946
Strength and failure rate of composite materials with carbon in ceramic matrix 16 p2180 N88-22995
Small-scale cleavage test of polymer products
[PB88-165360] 16 p2181 N88-23001
Seasonal variation for structural strength value
[PB88-169248] 16 p2222 N88-23260
Technology Reports of Kyushu University, volume 61, no. 2
[ISSN-0023-2718] 16 p2256 N88-23485
Travelling wave concepts for the modeling and control of space structures
[AD-A191235] 17 p2310 N88-23819
Structural ceramics research 17 p2324 N88-23878
Improved silicon carbide for advanced heat engines 17 p2324 N88-23879
Improved silicon nitride for advanced heat engines 17 p2324 N88-23881
Improved processing of Si3N4 17 p2325 N88-23882
Colloidal characterization of silicon nitride and silicon carbide 17 p2325 N88-23883
SiC fiber analysis 17 p2326 N88-23891
Improved GaP doped SiGe thermoelectric material 17 p2437 N88-24503
Carbon matrix composites prospective roles for biotechnology 18 p2477 N88-24694
Interaction of ultrasonic waves with composite plates
[AD-A191879] 18 p2478 N88-24702
Fundamental studies of beta phase decomposition modes in titanium alloys
[AD-A191495] 18 p2485 N88-24740
Environment assisted degradation mechanisms in advanced light metals
[NASA-CR-182907] 18 p2486 N88-24746
Characterization of 7090 and 7091 profiles made with Cegedur powder --- powder metallurgy, aircraft construction materials
[REPT-48-441/F] 18 p2487 N88-24752
Effect of size of precipitates on recrystallization temperatures in Cu-Cr, Cu-Zr, and Cu-Zr-Cr alloys
[NASA-TT-20166] 18 p2489 N88-24763
Stress measurements in graphite fibers by laser raman spectroscopy
[AD-A191710] 18 p2491 N88-24779
The influence of the chemical nature of resins on their reticulation kinetics and the consequences for their nonelastic mechanical properties
[ETN-88-92539] 18 p2493 N88-24788
Characterization of aluminum/RP-1 gel propellant properties
[NASA-TM-100951] 18 p2496 N88-24808
Microlaminate composite structures by low pressure plasma spray deposition
[DE88-006453] 19 p2610 N88-25488
Nondestructive evaluation methods for determination of thermal history and mechanical properties of aluminum-lithium alloys
[DE88-007352] 19 p2615 N88-25516
Optimization of mechanical/corrosion properties of TI-CODE 12 plate and sheet. Part 2: Thermomechanical processing effects
[DE88-007493] 19 p2616 N88-25517
Extended ductility of Al and alpha-Fe alloys through dynamic recovery mechanisms
[DE88-008679] 19 p2616 N88-25522
Development of fine-grained carbide-particle hardened Hadfield manganese steels
[DE88-008919] 19 p2617 N88-25523
Dimensional analysis and experimental observation of the coupling phenomena between combustion and fracture of damaged propellant samples 19 p2630 N88-25603
Interface modification in Nicalon (trademark)/SiC composites
[DE88-009708] 20 p2767 N88-26409
A constitutive model with damage for high-temperature superalloys 20 p2771 N88-26434
Phase stability and alloy design of ordered intermetallics
[DE88-007479] 20 p2772 N88-26435
Investigation of structure and surface state effect on hydrogen embrittlement of steels, under consideration of acoustic emission analysis
[ETN-88-92350] 20 p2775 N88-26457
Application of electron microscopy for the analysis of the mechanical behavior of advanced ceramics
[DE88-005049] 20 p2777 N88-26469
Resistance of polyamide-6 against long time effects of various media at various temperatures
[NASA-TT-20297] 20 p2779 N88-26484
Polymerization of epoxy matrix composites using pulsed microwaves
[CERT-3/1324-MO] 20 p2780 N88-26487
A finite element analysis for the hydroforming of aluminum
[DE88-008050] 20 p2784 N88-26516
Electrodynamic driver for the space thermoacoustic refrigerator (STAR)
[AD-A192337] 20 p2785 N88-26517
Research on the kinetics of phase changes in solids
[AD-A192222] 20 p2814 N88-26696
Analysis of transverse strength of composites using percolation theory
[AD-A193204] 21 p2904 N88-27234
Fabrication of SiC fiber reinforced glass matrix by extrusion process and investigation of its mechanical properties
[ETN-88-92367] 21 p2906 N88-27244
Rocket motor case materials. An evaluation of new fibers for composites
[FOA-C-20696-2.1] 21 p2906 N88-27245
Factors affecting strength in composite materials used for aircraft
[DT-212/87] 21 p2907 N88-27248
Development of high strength and toughness microcomposite HSLA Fe/Cr/Mn/C steel with and without Nb
[DE88-009813] 21 p2913 N88-27290
Thin film and near-surface characterization using a mechanical properties microprobe
[DE88-011399] 21 p2915 N88-27302
Superconducting oxides with high critical temperatures 21 p2930 N88-27392
FEB (Multifilter Electronics Box) lifting device analysis, revision A
[AD-A192313] 21 p2935 N88-27427
The influence of weld metal properties, weld geometry and applied load on weld system performance
[AD-A193403] 21 p2961 N88-27588
Corrosion fatigue of small cracks: Mechanics and chemistry
[DE88-012121] 21 p2964 N88-27605
Durability of continuous fiber reinforced metal matrix composites
[AD-A193868] 22 p3050 N88-28097
An endochronic rate-sensitive constitutive equation for metals, application to generalized creep and large deformations
[AD-A194167] 22 p3055 N88-28125
An investigation into the metallurgical aspects of joining rapidly-solidified aluminum alloys
[AD-A194677] 23 p3194 N88-29009
Relation between strength, creep and relaxation behavior in Cu and Al at room temperature
[ETN-88-92982] 23 p3195 N88-29015
Thin film-residual stress assessment
[AD-A193205] 23 p3196 N88-29018
The mechanical behavior of surface modified ceramics
[DE88-010564] 23 p3196 N88-29022
Experimental investigation of the effects of underwater exposure on the damping characteristics of bolted structural connections for plates and shells
[AD-A194486] 23 p3226 N88-29200
Fatigue crack growth characteristics of ARALL (trademark)-1
[AD-A196185] 24 p3341 N88-29889
Attenuated total reflectance FT-IR spectroscopy to measure interfacial reaction kinetics at silica surfaces
[AD-A196330] 24 p3344 N88-29908
Additional fracture and strength test results for A723 steel and 38644 titanium
[AD-A196329] 24 p3353 N88-29960
Initial value problems in viscoelasticity
[AD-A196052] 24 p3382 N88-30145

MECHANICAL RESONANCE
U RESONANT VIBRATION

MECHANICAL SHOCK
Requirements for the calibration of mechanical shock transducers
[PB87-227591] 03 p0325 N88-12054
Mechanical shock test specification using nonstationary random excitation models
[DE87-013650] 04 p0454 N88-12812
The 58th Shock and Vibration Symposium, volume 1
[NASA-CP-2488-VOL-1] 05 p0592 N88-13609
Conservatism implications of shock test tailoring for multiple design environments 05 p0592 N88-13611
Scaling the electromagnetically driven explosive shock simulator 05 p0592 N88-13612
Initial dynamic load estimates during configuration design 05 p0593 N88-13621
Optimal shock isolation with minimum settling time 05 p0595 N88-13633
The Shock and Vibration Digest, Volume 20, No. 1 08 p0975 N88-15897
The Shock and Vibration Bulletin. Part 4: Structural Dynamics and Modal Test and Analysis
[AD-A186751] 09 p1179 N88-17062
The Shock and Vibration Digest, volume 20, no. 2 10 p1417 N88-18459
Design and dynamic testing of an instrumented spacecraft component 11 p1499 N88-18952
The Shock and Vibration Digest, volume 20, no. 4 17 p2391 N88-24214
Peak Acceleration Device (PAD)
[AD-A191639] 18 p2461 N88-24611
Selective weathering of shocked minerals and chondritic enrichment of the Martian fines 23 p3301 N88-29660

MECHANIZATION
Ultrasonic mechanized checking of weld joints of nuclear power plant equipment 02 p0158 N88-10987

MEDIA
NT ANISOTROPIC FLUIDS
NT ANISOTROPIC MEDIA
NT ELASTIC MEDIA
NT INTERGALACTIC MEDIA
NT INTERPLANETARY DUST
NT INTERPLANETARY GAS
NT INTERPLANETARY MEDIUM
NT ZODIACAL DUST
Mathematical problems of nonlinear wave propagation and of waves in heterogeneous media
[AD-A195970] 24 p3368 N88-30057

MEDIAN (STATISTICS)
PROGRESS: A program for robust regression analysis on the IBM PC
[REPT-85-14] 01 p0088 N88-10576
Embedding topological median algebras in products of dendrons
[PB88-100888] 06 p0767 N88-14713
Contour interactive extraction using image numerical treatment
[ISL-R-114/86] 15 p2113 N88-22587

MEDICAL EQUIPMENT
NT ENDOSCOPES
NT PROSTHETIC DEVICES
NT X RAY APPARATUS
NT X RAY TUBES
Spinoff, 1987
[NASA-TM-89652] 02 p0250 N88-11577
Photonic temperature and pressure sensors for biosystems/pulsed microwave. Part 1: Interaction studies
[AD-A188887] 12 p1629 N88-19751
Low altitude remote sensing data in the implementation of a mathematical model for the planning of urban equipment networks 17 p2363 N88-24074
Analysis of annular microstrip antennas for hyperthermic applicators
[PB88-181508] 19 p2643 N88-25679
Miniature radiation dosimeter for in vivo radiation measurements 19 p2672 N88-25889

MEDICAL PERSONNEL
Satellite communications experiment for the Ontario air ambulance service 19 p2646 N88-25705
Central serous chorioretinopathy in USAF aviators: A review
[AD-A195697] 24 p3407 N88-30280

MEDICAL PHENOMENA
Experience in occupational medicine, derived from 16 operational deep saturation trimix 5 dives in GUSI from 150 to 600 m 19 p2695 N88-26018

MEDICAL SCIENCE
NT CARDIOLOGY
NT CLINICAL MEDICINE
NT ENDOCRINOLOGY
NT EPIDEMIOLOGY
NT HISTOLOGY
NT HUMAN PATHOLOGY
NT IMMUNOLOGY
NT NEUROLOGY
NT NEUROPSYCHIATRY
NT NUCLEAR MEDICINE
NT OPHTHALMOLOGY
NT PATHOLOGY
NT PSYCHIATRY
NT RADIOBIOLOGY
USSR report: Life sciences. Biomedical and behavioral sciences
[JPRS-UBB-86-022] 08 p1046 N88-16318
Using IMSL mathematical and statistical computer subroutines in physiological and biomechanical research
[AD-A192594] 21 p2995 N88-27765
The NBS/NRL (National Bureau of Standards/Naval Research Laboratory) free electron laser facility
[AD-A194214] 23 p3219 N88-29159
Vanderbilt free electron laser project in biomedical and materials research
[AD-A195961] 24 p3378 N88-30121

MEDICAL SERVICES
Safety study: Commercial emergency medical service helicopter operation
[PB88-917001] 12 p1575 N88-19422
Satellite communications experiment for the Ontario air ambulance service 19 p2646 N88-25705
Activities report in aerospace medicine
[ETN-88-92906] 23 p3240 N88-29283

MEDITERRANEAN SEA
NT ADRIATIC SEA
Accuracy of GPS surveying technique and its possible application to the Wegener project --- Mediterranean tectonics
[REPT-85.3] 01 p0063 N88-10407
Large balloon development and trans-Mediterranean flights 08 p1030 N88-16239
Italian activities in ocean colour remote sensing 08 p1043 N88-16304
US Navy climatic study of the Mediterranean Sea
[AD-A188264] 10 p1356 N88-18107
The physical oceanography of the Alboran Sea
[AD-A189027] 12 p1650 N88-19880
Deep water mass circulation in the Alboran Basin. Measurements - January to April 1982: ALBORAN 2
[AD-A189205] 13 p1803 N88-20777
The interpretation of crustal dynamics data in terms of plate interactions and active tectonics of the Anatolian Plate and surrounding regions in the Middle East
[NASA-CR-183024] 18 p2543 N88-25092

MEETINGS
U CONFERENCES

MEGALOPOLISES
Spread of large tropical conurbations 22 p3098 N88-28398

MEISSNER EFFECT
U DIAMAGNETISM
U SUPERCONDUCTIVITY

MELLIN TRANSFORMS
Theory of the generalized Abel integral equations
[ETN-88-91086] 09 p1229 N88-17382

MELT SPINNING
Development of metastable processing paths for high temperature alloys
[AD-A188682] 12 p1608 N88-19617
Hydrodynamic simulation of forced convection in the Czochralski process
[INPE-4471-TDL/323] 12 p1697 N88-20158

MELTING
NT ARC MELTING
NT FUSION (MELTING)
NT VACUUM MELTING
Formation of amorphous alloys by solid state reactions
[DE87-013175] 02 p0146 N88-10918
Thermodynamics of interaction between nitrogen and molten nickel alloys
[BLL-M-37309-(5826.4)] 02 p0149 N88-10934
Shock-induced melting and rapid solidification
[DE88-000226] 03 p0288 N88-11810
Data base on the high heat flux behaviour of metals and carbon materials for plasma facing components: Experiments at the 10 MW neutral beam injection test stand of the IPP Nagoya
[IPPJ-AM-53] 04 p0492 N88-13031
Advances in processing techniques for nickel aluminides
[DE87-014571] 05 p0566 N88-13449
Statistical process control applied to the liquid-fed ceramic melter process
[DE88-000271] 05 p0569 N88-13471
Results from the melting of tungsten composites under microgravity (TEXUS 10 flight)
[FOA-C-20676-2.1] 05 p0571 N88-13482
Exploitation of the sol-gel route in processing of ceramics and composites
[AD-A185482] 06 p0686 N88-14204
Radar reflectivity and attenuation of radio waves in the melting layer of precipitation
[PB88-121553] 10 p1318 N88-17882
Mesoscale monitoring of the soil freeze/thaw boundary from orbital microwave radiometry
[NASA-CR-182659] 12 p1645 N88-19855
Integral equation theory of homopolymer melts
[DE88-005304] 13 p1751 N88-20470
Rapid e-beam heating for measuring thermodynamics of metastable materials
[DE88-003565] 13 p1849 N88-21066
Laser surface melting
[BMFT-FB-T-86-072] 14 p1914 N88-21435
Brillouin scattering and transmission electron microscopy studies of radiation-induced elastic softening, disordering and amorphization of intermetallic compounds
[DE88-005927] 14 p1987 N88-21850
On rotating sphere-on-a-plate experiments and the questions of whether high angle grain boundaries melt below bulk melting temperatures
[DE88-006627] 15 p2038 N88-22142
Directed-energy electron-beam processing of a hypoeutectic Cr90Ta10 alloy
[DE88-005621] 15 p2040 N88-22157
Melt processing ceramic YBa2Cu3O(sub 6.9)
[DE88-007039] 15 p2047 N88-22199
Microgravity thaw experiment (MITEX) 17 p2427 N88-24439
The viscosity of molten TNT
[MRL-R-1100] 19 p2622 N88-25553
Component stress during freeze/thaw cycling
[DE88-011204] 21 p2938 N88-27449
Effect of thermal cycling on CSPL (Chloride Silent Power Ltd.) sodium/sulfur cells
[DE88-011205] 21 p2939 N88-27455
Theory of surface melting and non-melting
[DE88-702652] 22 p3157 N88-28785
Initiation of explosive molten aluminum-water interactions at wet or underwater surfaces
[DE88-004686] 23 p3194 N88-29006
Evidence of the in situ decay of Al-26 in a Semarkona chondrule 24 p3441 N88-30479

MELTING POINTS
The use of alloy 117 as a liquid metal current collector
[AD-A185740] 06 p0698 N88-14281
Determination of the melting and decomposition points of different materials in an oxygen stream
[INFORME-I-158/86] 09 p1142 N88-16844
Research and development to acquire and reduce melting layer cloud physics and evaluate a prototype M-meter
[AD-A188390] 12 p1648 N88-19873
Processing of glass to aluminum (low melting metals) seals via an injection molding technique
[DE88-004689] 13 p1751 N88-20468
The crystallization of tough thermoplastic resins in the presence of carbon fibers
[NASA-CR-182984] 20 p2776 N88-26464

MELTS (CRYSTAL GROWTH)
NT CONTAINERLESS MELTS
NT IMPACT MELTS
NT MELT SPINNING
Raman spectroscopic investigations of Hg-Cd-Te melts 07 p0926 N88-15625
Investigation of defect and electronic interactions associated with GaAs device processing
[AD-A188021] 11 p1556 N88-19313
Real time thermal imaging of high temperature semiconductor melts 17 p2330 N88-23914
A review of melt and vapor growth techniques for polydiacetylene thin films for nonlinear optical applications
[NASA-TM-100340] 24 p3430 N88-30412

MEMBRANE ANALOGY
U MEMBRANE STRUCTURES
U STRUCTURAL ANALYSIS

MEMBRANE STRUCTURES
NT SKIN (STRUCTURAL MEMBER)
Large change-of-curvature effects in quadratic finite elements for CAD of membrane structures 04 p0480 N88-12958
Optimization of the southern electrophoretic transfer method
[DE88-004527] 10 p1299 N88-17765
Use of nonporous metals membranes for the separation of hydrogen from gas mixtures
[BMFT-FB-T-86-206] 14 p1888 N88-21280

MEMBRANE THEORY
U STRUCTURAL ANALYSIS

MEMBRANES
NT ION EXCHANGE MEMBRANE ELECTROLYTES
NT MEMBRANE STRUCTURES
NT SKIN (STRUCTURAL MEMBER)
Membrane heat pipe development for space radiator applications
[DE86-006015] 01 p0045 N88-10285
Rheological behaviors of an elastomeric membrane
[DE87-013105] 01 p0061 N88-10392
Photocatalytic electrochemistry at a biological-membrane metal-colloid interface
[DE87-009122] 02 p0166 N88-11041
Investigation of structure-permeability relationships of silicone polymer membranes
[PB87-230181] 03 p0293 N88-11839
Vapor compression distiller and membrane technology for water revitalization 03 p0359 N88-12262
The formation of optical membrane reflector surfaces using uniform pressure loading
[DE87-012275] 03 p0376 N88-12367
Novel macrocyclic carriers for proton-coupled liquid membrane transport
[DE88-000636] 04 p0413 N88-12560
Photochemical solar energy conversion utilizing semiconductors localized in membrane mimetic systems
[DE88-002887] 10 p1349 N88-18065
Critical phenomena and electromagnetic effects in biological membranes
[AD-A188156] 11 p1518 N88-19064
Molecular and electronic mechanism in the control of Na+ and K+ permeability of excitable cell membrane by ligand binding on receptor sites
[AD-A188725] 13 p1808 N88-20805
Enzyme-based fiber optic sensors
[DE88-005674] 13 p1840 N88-21013
Synthesis and analysis of novel polymers with potential for providing both high permselectivity and permeability in gas separation applications
[DE88-006533] 15 p2043 N88-22174
Mechanisms of gas permeation through polymer membranes: Renewal proposal for period December 1, 1986 - November 30, 1989
[DE88-007436] 18 p2494 N88-24796
The flying characteristics of the membrane slider bearing 18 p2522 N88-24965
Employment of porous polytetrafluoroethylene Membrane with a hydrophilic and hydrophobic stratal structure for construction of an enzyme electrode
[NASA-TT-20296] 19 p2620 N88-25543
Chemical multisensors with selective encapsulation of ion-selective membranes 19 p2670 N88-25869
Air loading effects on a capacitively sensed membrane supported silicon accelerometer 19 p2672 N88-25886
Optical evaluation of prototype stretched-membrane mirror modules for solar central receivers
[DE88-011884] 21 p2969 N88-27637
Factors governing light driven electron and proton translocation in proteins across membranes
[DE88-011120] 21 p2984 N88-27724
Hyperthermia: New thoughts on an old problem
[AD-A192602] 21 p2986 N88-27731
Method of forming dynamic membrane on stainless steel support
[NASA-CASE-MSC-18172-3] 23 p3201 N88-29052
Hydrogen concentration cells as converters of heat into electricity
[DE88-009662] 23 p3229 N88-29216
Design criteria for extraction with chemical reaction and liquid membrane permeation
[NASA-TT-20352] 24 p3343 N88-29899

MEMORY
A learning model as a basis for investigations of the effects of gravity on the learning processes and memory formulation 07 p0886 N88-15374
Stability, reliability and cross-mode correlations of tests in a recommended 8-minute performance assessment battery
[NASA-CR-172039] 08 p1052 N88-16351
Relationship of encoding speed and memory tests to flight training performance
[AD-A190670] 15 p2105 N88-22539
On categorizing sounds
[AD-A189784] 15 p2129 N88-22700
Short-term memory load and pronunciation rate 16 p2241 N88-23386
Processing deficits in monitoring analog and digital displays: Implications for attentional theory and mental-state estimation research 16 p2241 N88-23389

Information processing deficits in psychiatric populations: Implications for normal workload assessment 16 p2241 N88-23390
Working memory capacity: An individual differences approach
[AD-A192359] 20 p2833 N88-26803
Cognitive and neural bases of skilled performance
[AD-A193392] 21 p2992 N88-27747
Skilled memory and expertise: Mechanisms of exceptional performance
[AD-A193829] 22 p3133 N88-28628
Thermocouple for heating and cooling of memory metal actuators
[NASA-CASE-NPO-17068-1-CU] 23 p3217 N88-29151
Analysis of the hopfield neural networks and their application to pattern recognition
[AD-A193827] 23 p3239 N88-29279
Transformations of short-term visual memory
[AD-A193873] 23 p3241 N88-29290
Nested neural networks
[NASA-TM-101032] 24 p3423 N88-30373

MEMORY (COMPUTERS)
Memory systems for single bus multiprocessor architecture. Application to the SCOM system
[ENST-86E022] 02 p0219 N88-11379
Hardware-assisted multiprocessor performance measurements
[PB87-226908] 03 p0363 N88-12282
General potential surfaces and neural networks
[AD-A184484] 03 p0367 N88-12311
Least squares linear lags and limited memory filters
[NASA-CR-178381] 03 p0372 N88-12339
An approach to implementing state space searches on heterogeneous systems of multiprocessors
[DE88-001321] 04 p0482 N88-12967
A rudimentary database for three-dimensional objects using structural representation
[CSE-87-00004] 05 p0590 N88-13597
Storing and retrieving data in a parallel distributed memory system
[AD-A185177] 05 p0637 N88-13897
Recording materials for optical disk memory discussed 06 p0684 N88-14193
A comparison of the Cray-2 performance before and after the installation of memory pseudo-banking
[NASA-CR-177462] 09 p1215 N88-17287
The effectiveness of caches and data prefetch buffers in large-scale shared memory multiprocessors
[DE88-003594] 09 p1223 N88-17334
Research and development trends for memory hierarchies --- cache memories 10 p1374 N88-18198
Vector performance of register-to-register vector computers
[DE88-004013] 10 p1384 N88-18265
The impact of hierarchical memory systems on linear algebra algorithm design
[DE88-003574] 10 p1385 N88-18274
Debugging FORTRAN on a shared memory machine
[DE88-003589] 10 p1386 N88-18276
Using program structure to achieve prefetching for cache memories
[DE88-003599] 10 p1387 N88-18282
The performance of software-managed multiprocessor caches on parallel numerical programs
[DE88-003590] 10 p1393 N88-18308
Data prefetching in shared memory multiprocessors
[DE88-003576] 10 p1394 N88-18314
Measurement and analysis of memory conflicts on vector multiprocessors
[AD-A188206] 11 p1525 N88-19104
A shared memory algorithm and proof for the alternative construct in CSP (Communicating Sequential Processes)
[AD-A187820] 11 p1533 N88-19156
Gaussian techniques on shared memory multiprocessor computers
[DE88-005426] 13 p1817 N88-20855
Implementation and evaluation of a combined test-error correction procedure for memories with defects
[EUT-87-E-169] 14 p1955 N88-21651
Characteristics of LSI-wiring expert system discussed 15 p2052 N88-22226
Application of static memory for data acquisition and transmission into a computer
[DE88-701491] 15 p2106 N88-22544
Coding for write-unidirectional memories and conflict resolution
[ENST-87C005] 16 p2245 N88-23408
Effective use of shared memory multiprocessors
[DE88-007019] 18 p2560 N88-25195
On the implementation of applicative on shared-memory, MIMD multiprocessors
[DE88-005367] 19 p2718 N88-26136
Content-addressable memory storage by neural networks: A general model and global Liapunov method
[AD-A192716] 21 p3002 N88-27807
Large-grain pipelining on distributed-memory multiprocessors
[DE88-009974] 23 p3264 N88-29432

MENSTRUATION
Temperature regulation at rest and exercise during the human menstrual cycle
[AD-A186461] 08 p1050 N88-16341

MENTAL PERFORMANCE
Computer-controlled testing of visual-spatial ability
[AD-A183971] 03 p0357 N88-12249
Analogical inference and analogical access
[AD-A184345] 03 p0369 N88-12321
Mental models in expert physics reasoning
[AD-A184106] 04 p0500 N88-13075
Taskomat, a task battery for information processing
[IZF-1987-2] 05 p0630 N88-13851
Cirrus: An automated protocol analysis tool
[AD-A186646] 08 p1052 N88-16348
Measuring mental workload: A performance battery
[AD-A187118] 09 p1200 N88-17192
Intelligent tutoring systems as tools for investigating individual differences in learning 09 p1204 N88-17216
Cardiovascular and subjective measures of task demand in a low workload monitoring task
[REPT-8804] 10 p1368 N88-18176
Center for nonlinear dynamics of the brain
[AD-A187245] 11 p1518 N88-19068
Electromagnetic metrics of mental workload
[AD-A188205] 11 p1523 N88-19093
When decision aids fail
[AD-A187531] 11 p1523 N88-19095
Effects of intense, time-constrained mental effort on hemodynamics and cardiovascular function 12 p1664 N88-19975
Neurocognitive predictions of performance
[AD-A188323] 12 p1669 N88-19998
A comparison of the Army's Project A: Cognitive and psychomotor tests to analogous Air Force and Navy tests
[AD-A188636] 12 p1670 N88-20002
Understanding machines from text and diagrams
[AD-A189034] 13 p1755 N88-20493
A comparison of terrain association and resection as methods of position location
[AD-A189480] 13 p1790 N88-20710
Distraction and inhibition in continuous CRT performance: A replication and some new findings
[PB88-150941] 13 p1811 N88-20821
Identification of visual evoked response parameters sensitive to pilot mental state
[NASA-CR-4140] 13 p1811 N88-20822
Mental models of mechanical systems: Individual differences in qualitative and quantitative reasoning
[AD-A189035] 13 p1812 N88-20823
Knowledge retrieval as specialized inference
[AD-A189042] 13 p1823 N88-20899
Relationship of encoding speed and memory tests to flight training performance
[AD-A190670] 15 p2105 N88-22539
Mental-State Estimation, 1987
[NASA-CP-2504] 16 p2239 N88-23370
Vagal tone as an index of mental state 16 p2239 N88-23373
Primary task event-related potentials related to different aspects of information processing 16 p2240 N88-23382
Defining and measuring pilot mental workload 16 p2240 N88-23383
Estimating the cost of mental loading in a bimodal divided-attention task: Combining reaction time, heart-rate variability and signal-detection theory 16 p2241 N88-23385
Short-term memory load and pronunciation rate 16 p2241 N88-23386
Processing deficits in monitoring analog and digital displays: Implications for attentional theory and mental-state estimation research 16 p2241 N88-23389
Information processing deficits in psychiatric populations: Implications for normal workload assessment 16 p2241 N88-23390
Neurophysiological predictors of quality of performance 16 p2242 N88-23391
Brainstem response and state-trait variables 16 p2242 N88-23394
The event-related brain potential as an index of information processing and cognitive activity: A program of basic research
[AD-A191244] 16 p2243 N88-23400
The representational code of the internal model of dynamic systems: An individual differences and dual task approach
[AD-A190876] 16 p2244 N88-23403
A framework for a theory of mapping
[AD-A191071] 18 p2551 N88-25144
Proceedings of the Workshop on the Assessment of Crew Workload Measurement Methods, Techniques and Procedures. Volume 2: Library references
[AD-A191209] 19 p2710 N88-26101
Method for observing changes in functional state of human operator 20 p2830 N88-26789
The effects of increased cognitive demands on autonomic self-regulation: An indicator of parallel processing in the brain 21 p2925 N88-27362
Thermal stress and its effects on fine motor skill and decoding tasks 21 p2926 N88-27369
Event-related brain potentials as indices of mental workload and attentional allocation 21 p2979 N88-27696
Cognitive and neural bases of skilled performance
[AD-A193392] 21 p2992 N88-27747
WORDNET: An electronic lexical reference system based on theories of lexical memory
[AD-A193086] 21 p3027 N88-27970
Human performance and acute hypoxia, chapter 12
[AD-A192604] 23 p3238 N88-29270
Visual motion perception and visual attentive processes
[AD-A193640] 23 p3241 N88-29288
Pilot modeling applications 24 p3314 N88-29737
Central adrenergic receptors as mediators of central response to stress: Study with Positron Emission Tomography (PET)
[AD-A194947] 24 p3407 N88-30284
Venture theory: A model of decision weights
[AD-A194809] 24 p3426 N88-30391

MENTAL STRESS
U STRESS (PSYCHOLOGY)

MERCAPTAN
U THIOLS

MERCAPTO COMPOUNDS
U THIOLS

MERCURY (METAL)
NT MERCURY ISOTOPES
NT MERCURY VAPOR
The JPL trapped mercury ion frequency standard 11 p1471 N88-18776
Lattice-matched HgZnTe epitaxy development
[AD-A193677] 23 p3292 N88-29600

MERCURY CADMIUM TELLURIDES
Growth of solid solution single crystals
[NASA-TP-2787] 06 p0688 N88-14212
Raman spectroscopic investigations of Hg-Cd-Te melts 07 p0926 N88-15625
Growth of HgZnTe layers by LPE technique
[AD-A186723] 09 p1255 N88-17520
Ytterbium monolayer diffusion barriers at Hg(1-x)Cd(x)Te/Al junctions
[AD-A188013] 10 p1299 N88-17768
MBE growth, characterization and electronic device processing of HgCdTe, HgZnTe related heterojunctions and HgCdTe-CdTe superlattices
[AD-A187456] 10 p1421 N88-18486
Local stoichiometry and atomic interdiffusion during reactive metal/mercury-cadmium-telluride junction formation
[AD-A187554] 10 p1421 N88-18488
Nonmonotonic evolution and thermodynamic trends at metal/(Hg,Cd)Te interfaces: Yb/Hg0.78Cd0.22Te
[AD-A187591] 10 p1422 N88-18490
MBE (Molecular Beam Epitaxial) growth characterization and electronic device processing of HgCdTe, HgZnTe related heterojunctions and HgCdTe-CdTe superlattices
[AD-A187416] 11 p1555 N88-19307
Optical absorption in doped CdxHg1-xTe
[AD-A187434] 11 p1560 N88-19338
HP-41CX programs for HgCdTe detectors and IR systems
[AD-A188935] 12 p1692 N88-20120
Research on mercury cadmium telluride
[AD-A189155] 13 p1845 N88-21039
Study for the determination of general and specific properties of wide energy-band gap HgHdTe in the 1-2 micrometer wavelength range
[AD-A189177] 13 p1845 N88-21041
Experimental studies on electronic properties of HgTe/CdTe and Hg sub 1-z Cd sub x Te/CdTe heterostructures and superlattices
[AD-A189826] 15 p2142 N88-22783
Hybrid PV HgCdTe IR detectors technology reliability and failure program: Environmental stress testing plan
[AD-A191165] 16 p2211 N88-23195
MBE of HgCdTe
[AD-A191423] 16 p2283 N88-23671

Compositional redistribution during casting of Hg sub 0.8 Cd sub 0.2 Te alloys
[NASA-TM-101151] 17 p2326 N88-23893
Study for the determination of general and specific properties of wide energy-band gap HgCdTe in the 1 to 2 micrometer wavelength range
[AD-A191091] 17 p2334 N88-23934
Studies of boron implantation through photochemically deposited SiO2 films on Hg(sub 1-x)Cd(sub x)Te
[SD-TR-87-26] 19 p2621 N88-25548
Paramagnetic point defects in boron-implanted HgO.7CdO.3Te
[AD-A193276] 21 p3021 N88-27934
Migration and stability of HgCdTe lattice defects
[AD-A193293] 21 p3021 N88-27935
New method for preparation of (Cd, Hg)Te thin films
[DE88-702727] 23 p3293 N88-29608

MERCURY COMPOUNDS
NT MERCURY TELLURIDES
Grace DAKASEP alkaline battery separator 02 p0164 N88-11031
Organic metal (ET)4Hg3Br8A quasi-two-dimensional superconductor 14 p1974 N88-21778

MERCURY ION ENGINES
The design and development of mercury vaporisers for use with electron-bombardment ion engines
[RAE-TR-70042] 01 p0018 N88-10108
An experimental comparison of two designs of mercury propellant tank for use with an electric propulsion engine
[RAE-TR-75109] 01 p0018 N88-10109
Auxiliary propulsion system flight package
[NASA-CR-180828] 02 p0141 N88-10886
Successful completion of a cyclic ground test of a mercury ion auxiliary propulsion system
[NASA-TM-101351] 24 p3339 N88-29873

MERCURY ISOTOPES
Shape isomers as candidates for the gamma ray laser storage state
[DE88-005228] 11 p1492 N88-18909

MERCURY TELLURIDES
Electrical and optical properties of Hg/sub 1-x/Cd/sub x/Te doped layers grown by Liquid Phase Epitaxy (LPE)
[DE88-701023] 16 p2281 N88-23653
MBE growth of HgTe/CdTe superlattices on Si(100) substrates 20 p2869 N88-27033
Type 3 - type 1 transition and strain effect in Hg(1-x)Cd(x)Te-CdTe and Hg(1-x)Zn(x)Te-CdTe superlattices 20 p2872 N88-27052
Tunnelling currents in reverse biased CMT photodiodes
[RSRE-MEMO-4137] 23 p3209 N88-29097

MERCURY VAPOR
High efficiency generation of 130-nm radiation from sum-frequency mixing in Hg
[DE87-013714] 04 p0431 N88-12674
Coherent VUV source at 130 nm: Theory and modeling
[DE88-003874] 11 p1549 N88-19269

MERGING ROUTINES
Merge and termination in process algebra
[CWI-CS-R8716] 13 p1826 N88-20918

MERIDIONAL FLOW
Systematic stratospheric-tropospheric exchange viewed from isentropic coordinates 05 p0615 N88-13777
The lower thermosphere wind regime from simultaneous observations over Eurasia (Collm, Dushanbe, Frunze) 06 p0733 N88-14510
Wind regime peculiarities in the lower thermosphere in the winter of 1983/84 06 p0733 N88-14511
Longitudinal peculiarities of meridional circulation in lower thermosphere and mesosphere 06 p0736 N88-14525
Lower thermosphere wind regime according to radiometeor measurements in Kazan 06 p0736 N88-14526
Atmosphere dynamic processes structure at 80-105 km altitude 06 p0736 N88-14527
Large-scale dynamics of the mean flow breakdown in the stratosphere and mesosphere during the winter 1983/84 08 p1028 N88-16228
Numerical simulation of the ocean front response to the mesoscale atmospheric forcing
[INPE-4473-TDL/324] 12 p1648 N88-19868
Seasonal variations and excitation mechanisms of the equatorially trapped waves 13 p1798 N88-20751
JPRS report: Science and technology. China
[JPRS-CST-87-042] 14 p1899 N88-21338
Physical processes for maintaining mean meridional and zonal circulation of atmosphere in middle latitudes, volume 1 14 p1900 N88-21343
Numerical simulation of generation of mesoscale convective systems in large-scale environment 14 p1900 N88-21344
Physical process for maintenance of mean meridional and zonal circulation of atmosphere in middle latitudes, volume 2 14 p1900 N88-21345

MEROMORPHIC FUNCTIONS
NT ELLIPTIC FUNCTIONS
Systems near the onset and in the well-developed regimes of turbulence
[DE88-005365] 13 p1766 N88-20565

MESFETS
U FIELD EFFECT TRANSISTORS

MESH
The generation of nearly isotropic turbulence by means of grids
[PNR90411] 02 p0172 N88-11084
The integration of a mesh reflector to a 15-foot box truss structure. Task 3: Box truss analysis and technology development
[NASA-CR-178228] 11 p1497 N88-18941
Fatigue failure of regenerator screens in a high frequency Stirling engine 17 p2436 N88-24491
Accurate, productive aerodynamic simulation on patched mesh systems
[AD-A192040] 19 p2714 N88-26110

MESH (MATHEMATICS)
U COMPUTATIONAL GRIDS

MESH GENERATION (MATHEMATICS)
U GRID GENERATION (MATHEMATICS)

MESOMETEOROLOGY
Research work at the Meteorological Institute of the University of Munich (Federal Republic of Germany)
[MITT-56] 08 p1013 N88-16141
Results of the experiment MERKUR: Structural change of a weak cold front in the sphere of influence of the Alps --- mesoscale experiment 08 p1014 N88-16146
Numerical simulation of thermally generated mountain-foreland circulation
[DFVLR-FB-87-30] 09 p1190 N88-17132
The accuracy of the radiation parameterization in mesoscale models
[DFVLR-IB-553-85/11] 09 p1190 N88-17133

MESON RESONANCE
Search for bound states of the eta-meson in light nuclei 17 p2397 N88-24248

MESONS
NT KAONS
NT MESON RESONANCE
NT MUONS
NT PIONS
Two-photon exclusive meson production at large angles
[NIKHEF-H/87-4] 08 p1081 N88-16515
Basic physics program for a low energy antiproton source in North America
[DE88-003148] 08 p1082 N88-16522
Search for bound states of the eta-meson in light nuclei 17 p2397 N88-24248
Accuracy of analytic energy level formulas applied to hadronic spectroscopy of heavy mesons
[NASA-TM-4042] 19 p2725 N88-26185

MESOPAUSE
Long-period variations of wind parameters in the mesopause region and the solar cycle dependence 06 p0733 N88-14509
Rocket experiments and payloads for Super CAMP --- Cold Arctic Mesopause Project (CAMP) 08 p1034 N88-16271

MESOSCALE PHENOMENA
NT JET STREAMS (METEOROLOGY)
Mesoscale Analysis and Forecasting: Incorporating Nowcasting
[ESA-SP-282] 02 p0199 N88-11239
Applications and benefits of short period weather forecasts 02 p0199 N88-11240
Mesoscale forecasting today and tomorrow: Problems and opportunities. A position paper 02 p0199 N88-11244
The use of advanced data sets in the short-range forecasting of the development of a tornadic thunderstorm along a mesoscale convergence zone 02 p0200 N88-11250
Improved geostationary satellite soundings for the mesoscale weather analysis/forecast operation 02 p0200 N88-11252
The combined use of diagnosed mesoscale frontogenesis and satellite imagery in forecasting squall line formation 02 p0201 N88-11258
Observation of the development of mesoscale systems by operational meteorological satellites 02 p0201 N88-11259
Use of simulated satellite radiances from a mesoscale numerical model to understand kinematic and dynamic processes 02 p0202 N88-11261
The numerical simulation of the mesoscale characteristics associated with Baiu front. Part 1: Structure, low-level jet and radiation characteristics 02 p0203 N88-11272
The importance of mesoscale waves in the upper troposphere for formation of cloud and precipitation areas 02 p0203 N88-11273
On the interaction between radar and satellite image nowcasting systems and mesoscale numerical models 02 p0204 N88-11277
Satellite imagery and conceptual models in mesoscale forecasting 02 p0205 N88-11282
The use of McIDAS as a Mesoscale forecasting tool during the Canadian Atlantic storms programs --- Man-computer Interactive Data Access System (McIDAS) 02 p0205 N88-11284
A short-range forecasting experiment conducted during the Canadian Atlantic storms program 02 p0205 N88-11285
Simplified models for use in an operational short range forecasting system 02 p0206 N88-11289
Statistical remote sensing algorithm development: A complementary process to mesoscale numerical models 02 p0206 N88-11292
Mesoscale thunderstorm forecasting using RAOB data, surface mesonet observations, and an expert system 02 p0206 N88-11293
Analysis of squall line based on conventional data 02 p0207 N88-11295
Detailed analysis of a mesoscale convective complex situation in the Carpathian Basin (Europe) 02 p0207 N88-11296
Effects of the large scale motion and horizontal inhomogeneity of the moist static instability on development of the mesoscale convective systems in the midlatitudes 02 p0207 N88-11297
Statistical relationships between the mesoscale organization of convection and the large-scale wind profiles during GATE --- GARP Atlantic Tropical Experiment (GATE) 02 p0208 N88-11302
Toward operational forecasting and detection of weather-producing gravity waves 02 p0208 N88-11303
Two-dimensional numerical modeling of the life cycle of fog 02 p0209 N88-11311
Mesoscale MOS forecast support for 1988 winter Olympics ski events --- model output statistics (MOS) 02 p0209 N88-11312
Mesoscale surface field analysis from routine observations --- pressure, wind fields 02 p0209 N88-11315
Evaluation of a mesoscale prediction system with surface weather observations and comparison with a large-scale prediction system 02 p0210 N88-11319
The Norwegian mesoscale Numerical Weather Prediction (NWP) system 02 p0210 N88-11320
Forecasting polar lows using a numerical mesoscale model 02 p0210 N88-11321
Preliminary results from real data experiments with the NRL mesoscale numerical model 02 p0211 N88-11323
Short range forecasting of sea breeze generated thunderstorms at the Kennedy Space Center: A real-time experiment using a primitive equation mesoscale numerical model 02 p0211 N88-11324
Validation of a three dimensional numerical model of the sea breeze in complex terrain 02 p0211 N88-11325
The mesoscale numerical model for heavy rainfall forecasting in Yangtze River Valley, China 02 p0211 N88-11326
The impact on short-term precipitation forecast skill of time-dependent lateral and lower boundary conditions within a meso-beta numerical cloud prediction model 02 p0211 N88-11327
Mesoscale analysis and nowcasting via a numerical model coupled with satellite sounder data 02 p0211 N88-11328
A real-data numerical study and four-dimensional data assimilation application for mesobeta-scale flow in complex terrain 02 p0212 N88-11329
Opportunities and problems in mesoscale objective analysis 02 p0212 N88-11331
An isentropic mesoscale analysis system 02 p0212 N88-11332
An isentropic coordinate model used in a mesoscale data assimilation system 02 p0212 N88-11333
Strategies for using mesoscale data in an operational mesoscale model 02 p0212 N88-11335
Methods of incorporating satellite data into mesoscale numerical forecast models 02 p0212 N88-11336
Toward optimizing the use of data for operational mesoscale forecasting at the National Meteorological Center 02 p0213 N88-11337
Assimilation of high resolution TOVS data into a mesoscale NWP model --- numerical weather prediction (NWP) 02 p0213 N88-11338
Use of four-dimensional data assimilation to improve a mesoscale-model precipitation forecast: A case study 02 p0213 N88-11340
Mesoscale very short-range numerical prediction with dynamical initialization including condensation heating 02 p0213 N88-11341

The future of data in mesoscale numerical models
02 p0214 N88-11344
Simulation of mesoscale satellite sounder data from a mesoscale numerical model 02 p0214 N88-11345
The challenge of using mesoscale data in mesoscale numerical models 02 p0214 N88-11346
The challenge of using mesoscale data in mesoscale numerical models: A position paper
02 p0214 N88-11347
Comments on the challenge of using mesoscale data in mesoscale numerical models
02 p0214 N88-11348
Four-dimensional initialization of mesoscale models
02 p0214 N88-11349
Mesoscale analysis and forecasting for the 1987 America's Cup, Fremantle, Western Australia
02 p0214 N88-11350
Windfield simulations from a hierarchy of nested meso- and micrometeorological models
02 p0215 N88-11351
Mesoscale forecasting with satellite data: Challanges and opportunities for today and tomorrow
02 p0215 N88-11353
Documentation of the regional climate model based on FITNAH
[DFVLR-MITT-87-07] 02 p0216 N88-11358
Mesoscale eddy dynamics by the method of point vortices 04 p0463 N88-12863
Mesoscale applications of high resolution imagery
[AD-A185039] 05 p0627 N88-13833
Mesoscale aerosol clouds 08 p1013 N88-16140
Spectral analysis of an orographically structured area in the forefield of mesoscale flow simulations
08 p1016 N88-16160
Numerical simulation of thermally generated mountain-foreland circulation
[DFVLR-FB-87-30] 09 p1190 N88-17132
Simulations of thermally induced winds and cross flow situations
[MITT-57] 09 p1193 N88-17148
The retardation of cold fronts at high mesoscale mountains 09 p1241 N88-17437
Analysis of quasi-geostrophic forcing during the AIMCS (Airborne Investigations of Mesoscale Convective Systems) Project. Volume 2: Results for June 14 through July 16, 1984
[PB88-123807] 10 p1354 N88-18092
Mesoscale coastal ocean dynamics
11 p1517 N88-19060
Analysis of quasi-geostrophic forcing during the AIMCS (Airborne Investigations of Mesoscale Convective System) Project. Volume 1: Discussion
[PB88-133095] 12 p1646 N88-19860
National Severe Storms Laboratory, fiscal year 1987
[PB88-140108] 12 p1647 N88-19863
Numerical simulation of the ocean front response to the mesoscale atmospheric forcing
[INPE-4473-TDL/324] 12 p1648 N88-19868
Phenomenological description of eddy registered in Gulf Stream 13 p1787 N88-20694
JPRS report: Science and technology. China
[JPRS-CST-87-042] 14 p1899 N88-21338
Numerical simulation of generation of mesoscale convective systems in large-scale environment
14 p1900 N88-21344
Numerical simulation of medium scale disturbance on meiyu front 14 p1900 N88-21346
Ocean eddies 14 p1938 N88-21566
Taiwan area mesoscale experiment: Daily operations summary
[PB88-169081] 16 p2235 N88-23348
Taiwan area mesoscale experiment: P-3 aircraft operations summary
[PB88-169073] 18 p2544 N88-25098
Report on project WIND: Preliminary experiments w ith the UK Meteorological Office mesoscale model, September 1987
[AD-A191621] 18 p2544 N88-25099
Determination of mesoscale variability of sea surface temperature and attenuation in the North Atlantic from satellite measurement
[REPT-162] 18 p2548 N88-25127
MM4 (Penn State/NCAR (National Center for Atmospheric Research)) mesoscale model version 4 documentation
[PB88-173232] 19 p2688 N88-25979
Composite, meso-gamma scale diagnostic modeling
[DE88-008189] 19 p2689 N88-25983
Satellite observed Mesoscale Convective System (MCS) propagation characteristics and a 3-12 hour heavy precipitation forecast index
[PB88-180161] 19 p2692 N88-26004
Modelling and forecasting deep ocean and near surface mesoscale eddies: Hindcasting and forecasting with, and coupling a surface boundary layer model to, the Harvard quasigeostrophic model 19 p2694 N88-26013
Beaufort sea mesoscale circulation study: Hydrography helicopter operations, April 1987
[PB88-203658] 21 p2976 N88-27681

MESOSPHERE
NT MESOPAUSE
Theoretical and lidar studies of the seasonal and nocturnal variations of the mesospheric sodium layer at Urbana, Illinois 01 p0068 N88-10435
Circulation in the mesosphere and lower thermosphere during the MAP (Middle Atmosphere Program)/WINE (Winter in the Northern Europe) period
06 p0734 N88-14514
Longitudinal peculiarities of meridional circulation in lower thermosphere and mesosphere
06 p0736 N88-14525
Mesoscale density variability in the mesosphere and thermosphere: Effects of vertical flow accelerations
06 p0736 N88-14529
Some aspects of metallic ion chemistry and dynamics in the mesosphere and thermosphere
06 p0737 N88-14534
Lidar investigations of M-zone
06 p0741 N88-14558
Observations of inertial period waves and vertical velocities in the tropical middle atmosphere using the MST radar technique 06 p0742 N88-14562
Radar observations of high-latitude lower-thermospheric and upper-mesospheric winds and their response to geomagnetic activity 06 p0742 N88-14563
Middle atmospheric wind measurements using a medium frequency radar
[AD-A185931] 07 p0879 N88-15330
Comparison of simultaneous MST radar and electron density probe measurements in the polar mesosphere --- Mesospheric, Stratospheric, Tropospheric (MST)
08 p1028 N88-16226
Large-scale dynamics of the mean flow breakdown in the stratosphere and mesosphere during the winter 1983/84 08 p1028 N88-16228
Observational evidence for saturation of gravity waves and the production of turbulence in the mesosphere
08 p1028 N88-16229
TOTAL: A new instrument to study turbulent parameters in the mesosphere and lower thermosphere
08 p1029 N88-16234
Rayleigh lidar observations of gravity wave activity in the stratosphere and lower mesosphere
[NASA-CR-182384] 09 p1189 N88-17123
Mesospheric dynamics and chemistry from SME data
[NASA-CR-182465] 09 p1191 N88-17139
Polar mesospheric cloud experiment
[AD-A188936] 12 p1648 N88-19872

MESSAGE PROCESSING
Token execution strategies for distributed algorithms: Simulation studies
[AD-A184792] 03 p0365 N88-12294
An interactive computer graphics network monitor for a tactical communications network
[AD-A184131] 04 p0477 N88-12938
On real-time systems using local area networks
[AD-A185475] 06 p0694 N88-14256
Voice technology using personal computers
[AD-A186743] 09 p1218 N88-17300
Optical symbolic processor for expert system execution
[AD-A187494] 10 p1385 N88-18268
Theory and practice of fault tolerance in distributed systems
[AD-A187559] 11 p1540 N88-19204
Experience with Berkeley UNIX interprocess communications
[AD-A188353] 12 p1680 N88-20041
A simulation study of a parallel processor with unbalanced loads
[AD-A189573] 13 p1822 N88-20887
Deadlock-free message routing in processor networks
[CS-8706] 14 p1960 N88-21691
Performance of data compression codes in channels with errors
[AD-A189667] 15 p2055 N88-22253
Implementation of a distributed adaptive routing algorithm on the Intel iPSC (Intel Personal Super-Computer)
[AD-A189849] 15 p2109 N88-22567
Alpha structure based B-HIVE multicomputer
[AD-A188708] 16 p2244 N88-23405
Motor theory of auditory perception
[AD-A192095] 18 p2550 N88-25136
Automatic discovery of optimal classes
[NASA-TM-101174] 18 p2566 N88-25238
Narrative compression coding for a channel with errors
[AD-A191577] 19 p2642 N88-25673
A cockpit natural language study - selected transcripts
[AD-A192972] 20 p2834 N88-26808
Relay approach message routing in hypercube multiprocessors
[DE88-009973] 20 p2835 N88-26814
Method for Veterbi decoding of large constraint length convolutional codes
[NASA-CASE-NPO-17310-1-CU]
23 p3183 N88-28946
Coding for meteor-burst communications channel and side information for channels with block-interference
23 p3202 N88-29054
An overview of technology for spoken interaction with machines
[AD-A194153] 23 p3202 N88-29058
A performance study of the hypercube architecture
[AD-A194361] 23 p3264 N88-29433
Performance analysis of k-ary n-cube interconnection networks
[AD-A195542] 24 p3361 N88-30010
Integrated resource scheduling in a distributed scheduling environment 24 p3417 N88-30342
Integrating information systems in a major decentralized international organization, volume 7
[AD-A195856] 24 p3439 N88-30468

MESSAGES
Technical characteristics of the OmniTRACS: The first operation mobile Ku-band satellite communications system 19 p2647 N88-25709

METABOLIC WASTES
NT HUMAN WASTES
NT URINE

METABOLISM
NT CALCIUM METABOLISM
NT CARBOHYDRATE METABOLISM
NT CATABOLISM
NT ELECTROLYTE METABOLISM
NT ENZYME ACTIVITY
NT FERMENTATION
NT HORMONE METABOLISMS
NT HYPOGLYCEMIA
NT NITROGEN METABOLISM
NT OXYGEN METABOLISM
NT PHOSPHORUS METABOLISM
Long term investigations of the growth, metabolism, and reproduction of fish under conditions close to weightlessness 01 p0074 N88-10473
The influence of weightlessness on the metabolism of the Biomphalaria glabrata 01 p0074 N88-10475
Fundamental study on gas monitoring in CELSS
03 p0359 N88-12263
The toxicology and metabolism of nickel compounds
[DE87-014801] 04 p0474 N88-12921
Human thermoregulatory model for whole body immersion in water at 20 and 28 C
[AD-A185052] 05 p0629 N88-13849
Trace-element metabolism in man and animals in the presence of hypoxic states of diverse etiology
07 p0889 N88-15390
Human metabolism and peripheral circulation during antiorthostatic hypokinesia 07 p0891 N88-15398
Investigation of energy metabolism of biological systems in weightlessness 07 p0893 N88-15409
Third Soviet-French Symposium on Space Cytology
07 p0893 N88-15411
Experiments with rats flown aboard Cosmos-1667 biosatellite (main objectives, conditions and results)
07 p0893 N88-15414
Regulation of energy metabolism during parachute jumps 07 p0896 N88-15428
Rational considerations for modelling human thermoregulation during cold water immersion
[AD-A186226] 08 p1048 N88-16329
Temperature regulation at rest and exercise during the human menstrual cycle
[AD-A186461] 08 p1050 N88-16341
Some process control/design considerations in the development of a microgravity mammalian cell bioreactor 09 p1197 N88-17174
Role of body fat in the prediction of the metabolic response for immersion in cold water
[AD-A186914] 09 p1198 N88-17182
Human blood glutamic acid level with exposure to high ambient concentrations of ammonia
10 p1361 N88-18134
New book on metabolic aspects of spaceflight stress
10 p1367 N88-18172
Certain aspects of human metabolism during spaceflights of varying duration
[NASA-TT-20215] 10 p1369 N88-18181
The evolution of glutathione metabolism in phototrophic microorganisms
[NASA-CR-182902] 19 p2695 N88-26015
The US space programme spacewalk/extravehicular activity experience: Past, present and future
19 p2697 N88-26031

Human erykthrocyte metabolism in the presence of hyperoxygenation during antiorthostatic hypokinesia
19 p2706 N88-26092
Regulatory biochemical and metabolic responses in photoreceptors
[AD-A192898] 20 p2831 N88-26794
Metabolic and cardiorespiratory parameters during three consecutive days of exhaustive running
[AD-A192598] 21 p2985 N88-27728
Software modifications to total data reporting accessory for metabolic measurement cart
[AD-A193641] 22 p3132 N88-28623

METABOLITES
Specific organic compounds in excreta
07 p0895 N88-15422
Effect of low-frequency whole-body vertical vibration on the serotoninergic system of the brain and spinal cord
19 p2704 N88-26081

METAGALAXY
U UNIVERSE

METAL AIR BATTERIES
NT ZINC-OXYGEN BATTERIES
Extended abstracts: Eighth Battery and Electrochemical Contractors' Conference
[DE88-000960] 06 p0730 N88-14489
Aluminum-air battery development
[DE88-006617] 13 p1762 N88-20542
Aluminum-air battery development
[DE88-006618] 13 p1762 N88-20543
Technology base research on zinc/air battery systems
[DE88-004893] 13 p1763 N88-20546
Aluminum-air battery development
[DE88-006620] 15 p2061 N88-22287
Crystallization of aluminum hydroxide in the aluminum-air battery: Literature review, crystallizer design and results of integrated system tests
[DE88-010510] 20 p2797 N88-26594
Metal-air battery assessment
[DE88-011361] 21 p2940 N88-27459

METAL BONDING
NT METAL-METAL BONDING
Bonding and coupling of C sub 1 fragments on metal surfaces
[AD-A184186] 03 p0295 N88-11852
Valence bond cluster studies of alkali metal/semiconductor bonding
[AD-A184276] 04 p0496 N88-13054
Analysis of end stresses in glass-metal bimaterial strips
[DE87-007848] 05 p0610 N88-13750
Behavior of metal ceramic interfaces
[PB87-147500] 07 p0837 N88-15076
Improved glass-ceramic to metal seals in actuator and detonator applications with an aluminum-containing austenitic stainless steel
[DE88-004691] 13 p1749 N88-20458
The relationship of the chemical bonding topology of high critical temperature copper oxide superconductors to that of the chevrel phases and the ternary lanthanide rhodium borides
[AD-A189255] 13 p1845 N88-21042
Composite piston
[NASA-CASE-LAR-13435-1] 17 p2346 N88-23981
Composite repair of cracked aluminum alloy aircraft structure
[AD-A190514] 18 p2455 N88-24573
A scientific basis for an alternate cathode architecture
[AD-A191498] 18 p2481 N88-24717
Environmental integrity of coating/metal interface
[AD-A192184] 18 p2492 N88-24786

METAL COATINGS
NT ALUMINUM COATINGS
NT NICKEL COATINGS
NT ZINC COATINGS
Corrosion-resistant amorphous metallic coatings: Engineering development
[NASA-CR-181487] 03 p0287 N88-11802
Bond character at a silicon/copper surface
[AD-A184167] 03 p0295 N88-11851
Investigation of the fabrication parameters of laser mirrors with hard oxide interference coatings
[ESA-TT-1064] 03 p0329 N88-12077
Deformation mechanisms of thermostructural materials
[AD-A184070] 03 p0338 N88-12128
The analysis of metal finishing solutions by ion chromatography
[AD-A184812] 05 p0561 N88-13414
Ion plating for corrosion control
[AD-A185061] 05 p0565 N88-13442
Development of methods for low temperature diffusion bonding
[AD-A186875] 09 p1174 N88-17033
Reaction mechanism of sulfur dioxide with single crystal cobalt and chromium and CoCrAlY coatings
[AD-A185989] 09 p1253 N88-17509
Study of adherent oxide scales
[AD-A187368] 11 p1456 N88-18680
Adhesion of PVD titanium coatings to beryllium substrates
[DE88-005147] 11 p1463 N88-18721
Technical applications of solar energy. Project: Selective coatings
[BMFT-FB-T-86-213] 14 p1943 N88-21591
Corrosion of electroless nickel-coated steel
[AD-A191045] 16 p2179 N88-22985
Dependence of structure of stabilized ZrO2 coatings on condensation rate 16 p2180 N88-22990
Recent advances in metallic/ceramic coatings for corrosion control in military applications
17 p2320 N88-23858
Vanadic hot corrosion of gas turbine blade coating materials 17 p2321 N88-23864
Development of reliable fuel pins for space reactor applications 17 p2409 N88-24326
Corrosion control through a better understanding of the metallic substrate/organic coating/interface
[AD-A193981] 22 p3056 N88-28132
Zinc filled coatings 24 p3355 N88-29978

METAL COMBUSTION
Measurement of combustion aerosol size distributions with multistage inertial impactors
[DE88-751101] 11 p1454 N88-18669

METAL CORROSION
U CORROSION

METAL CRYSTALS
Computer simulations of knock-on processes in bcc Ta crystal
[DE87-752960] 02 p0246 N88-11554
Production of metallic monocrystals described
03 p0286 N88-11796
Progress toward a crystal streak camera using tungsten bronze crystals for the electrooptic material
[DE87-013110] 03 p0323 N88-12044
Measurements of the scintillation time constants of inorganic crystals for the development of a triple-Phoswich detector for high-energy X-ray quanta
[ETN-88-91501] 14 p1983 N88-21875

METAL CUTTING
Analysis of free cutting brass by A.C. polarography
[PD-MT-8728] 04 p0417 N88-12587
Identification and feedback control of machine tool vibrations
[PB88-109715] 08 p0976 N88-15902
Further development of a finite element model of orthogonal metal cutting
[DE88-004048] 11 p1494 N88-18921
Optimization of oxygen cutting process for titanium alloys 14 p1897 N88-21323
Friction welding: Advanced method of producing end cutting tool 14 p1897 N88-21327
The technical feasibility of using spiked-radiation lasers to cut out and weld metals 14 p1898 N88-21332

METAL FATIGUE
The effect of fretting corrosion on the fatigue strength of steel and cast iron under sinusoidal and random loading
[LBF-FB-177] 01 p0023 N88-10142
Modelling of crack-tip deformation and transient electrochemical processes in relation to corrosion fatigue of steels cathodically protected in marine environments
[NPL-DMA(A)-145] 01 p0059 N88-10379
Fatigue crack propagation of low-alloy steel in a vacuum environment
[DE87-013770] 01 p0061 N88-10393
Turbine Engine Hot Section Technology, 1985
[NASA-CP-2405] 02 p0184 N88-11140
Constitutive modeling for single crystal superalloys
02 p0187 N88-11168
Microstructural effects on the fatigue behavior of Fe-C-X alloys
[DE88-000155] 03 p0288 N88-11809
Fatigue failure of thin porous strips
04 p0426 N88-12640
Welded joint fatigue of a AISI 304 L type stainless steel
[DE87-703530] 05 p0592 N88-13607
Fatigue 87, volume 1
[AD-A184045] 05 p0597 N88-13645
Cyclic deformation and crack initiation
05 p0597 N88-13646
Effect of grain orientation on the origination and the initial growth of fatigue cracks in pure iron
05 p0597 N88-13647
The growth of persistent slip bands
05 p0597 N88-13648
The mechanics of fatigue-crack nucleation in a low-alloy steel under fretting conditions 05 p0597 N88-13649
Surface deformation and fatigue crack initiation of alpha-iron 05 p0598 N88-13651
The effect of ion beam mixed Ni-Al surface layers on PSB extrusion morphology in fatigued nickel
05 p0598 N88-13652
The evolution of local mechanical properties of Al 2219-T851 during fatigue 05 p0598 N88-13653
Cyclic deformation of an extruded AlMgSi alloy
05 p0598 N88-13654
Closure behavior under constant effective stress intensity loading conditions 05 p0598 N88-13656
Growth of short fatigue cracks in a squeeze formed aluminum alloy 05 p0598 N88-13658
Influence of microstructure and aging condition on the fatigue crack propagation in age hardened aluminium alloys 05 p0599 N88-13659
Fatigue crack growth behavior of A356-T6 cast aluminum alloy 05 p0599 N88-13660
Striations and the fatigue growth mechanism in a micro-alloyed steel 05 p0599 N88-13661
Significance of fatigue crack closure under spectrum loading 05 p0599 N88-13662
Near-threshold short crack growth behavior in Nimonic 105 05 p0599 N88-13663
Fatigue crack propagation of short and long cracks: Phys. basis, prediction methods and engineering significance 05 p0599 N88-13664
Low cycle fatigue life predictions of a 1CrMoV steel in terms of a J-controlled short crack growth model
05 p0599 N88-13665
The statistics of the shape of small fatigue cracks
05 p0599 N88-13666
The effect of alpha platelet morphology and beta-grain size on the initiation and growth of short fatigue cracks in Ti65S 05 p0600 N88-13667
The initiation and growth of small fatigue cracks in copper at room and cryogenic temperatures
05 p0600 N88-13668
On the role of crack tip shielding in influencing the behavior of long and small fatigue cracks in aluminum-lithium alloy 2090 05 p0600 N88-13671
The influence of slip mechanism on fatigue of Mg and Mg-2.3Li 05 p0600 N88-13672
The growth behavior of small fatigue cracks; the effect of microstructure and crack closure
05 p0600 N88-13673
The influence of microstructure and residual stresses on the initiation and propagation of short surface cracks on AlMgSi1 05 p0601 N88-13674
Threshold stress for fatigue crack initiation from a small crack 05 p0601 N88-13675
An experimental study of closure behavior of naturally initiated small cracks 05 p0601 N88-13676
Behavior of long and short fatigue cracks in a powder metallurgy superalloy at room and at high temperature
05 p0601 N88-13677
Propagation of small fatigue cracks in 2024-T3 aluminum alloy 05 p0601 N88-13678
Closure and propagation behavior of short fatigue cracks at different R-ratios 05 p0601 N88-13679
A unified model for fatigue crack initiation, short crack growth, long crack propagation, and closure effects
05 p0601 N88-13680
Fatigue crack retardation in aluminium alloys
05 p0602 N88-13681
Fatigue crack growth under random overloads
05 p0602 N88-13682
A dislocation model for fatigue crack propagation under variable amplitude loading 05 p0602 N88-13683
Observations on the effect of overloads on fatigue crack growth 05 p0602 N88-13684
A study of fatigue crack growth life under random stresses 05 p0602 N88-13685
Crack growth in contrasting titanium alloys under the conjoint action of high and low cycle fatigue
05 p0602 N88-13686
Variable amplitude fatigue crack growth in aluminum alloys 2090-T8E41 and 7075-T651
05 p0602 N88-13687
Fatigue of 30CrMnSiNi2A notched specimens under spectrum loading 05 p0602 N88-13689
The how and why of variable amplitude testing
05 p0603 N88-13690
Near-threshold growth of defects in engineering materials 05 p0603 N88-13691
Interaction of microstructure and fatigue in tool steels
05 p0603 N88-13693
Tensile mean stress effects on uniaxial fatigue behavior of 1045 HR steel 05 p0603 N88-13694
Fatigue strength of alloy A286 at cryogenic temperature 05 p0603 N88-13695
The initiation and growth of fatigue cracks in carburised 9Cr1Mo steel 05 p0603 N88-13696
Fretting wear and fretting fatigue damage
05 p0603 N88-13697
The role of inclusions in corrosion fatigue crack initiation in Q1N 05 p0604 N88-13699

A study of corrosion fatigue crack initiation, growth and the threshold condition under variable amplitude loading
05 p0604 N88-13701
The influence of crack conditions on hydrogen uptake by steels 05 p0604 N88-13702
Occurance and growth of fatigue cracks in corrosion environment 05 p0604 N88-13704
The effect of environment on low cycle fatigue properties in HSLA steel 05 p0605 N88-13705
Coupling effects between the ferrite and austenite phases during corrosion fatigue of a ferrite/austenite duplex stainless steel 05 p0605 N88-13706
Development of research on fatigue of spot-weld in automobile structures in Japan
05 p0608 N88-13728
Environmentally assisted fatigue crack growth
05 p0608 N88-13731
Deformation, fatigue and fracture behavior of two cast anisotropic superalloys 05 p0608 N88-13732
Fatigue crack growth 05 p0608 N88-13734
Temperature dependent mechanical properties of an alumina fiber reinforced aluminum composite
06 p0677 N88-14147
Fatigue damage maps 06 p0715 N88-14382
An investigation of fatigue crack growth in a ductile material at high growth rates 06 p0715 N88-14383
Cyclic deformation behaviour of cast irons with various graphite shapes in the temperature range 20 C less than or = T less than or = 500 C 06 p0715 N88-14384
Life prediction of steel cords
06 p0715 N88-14386
Effect of hold time on fatigue of lead rich PbSn solder
06 p0715 N88-14387
On cleavage in fatigue for rail steels
06 p0716 N88-14388
Influence of cleavage on fatigue propagation rates in a low carbon steel 06 p0716 N88-14389
Effect of metal surface properties on the fatigue crack growth behavior 06 p0716 N88-14390
Fatigue crack growth behavior in hydrogen gas environment 06 p0716 N88-14391
Near-threshold fatigue 06 p0716 N88-14392
Notch-geometry effect on propagation threshold of short fatigue cracks in notched components
06 p0716 N88-14393
Influence of crack closure on fatigue crack propagation and threshold 06 p0716 N88-14394
An explanation of the fractography of near-threshold fatigue in FCC metals 06 p0716 N88-14395
The relationship between microstructural size and fatigue threshold in iron and steel
06 p0716 N88-14396
Threshold behaviour of semi-elliptic hydrogen-induced and fatigue-induced cracks 06 p0717 N88-14397
Effect of compressive portion of loading cycles on the near threshold fatigue closure behavior
06 p0717 N88-14398
Absolute fatigue thresholds in metallic materials
06 p0717 N88-14399
Thermometrical investigations on the near threshold fatigue crack propagation behavior
06 p0717 N88-14400
A re-evaluation of fatigue threshold test methods
06 p0717 N88-14401
The factors which govern the acceleration of corrosion fatigue crack growth rate of a ferritic stainless steel
06 p0717 N88-14402
Fatigue thresholds of C.Mn steels in saline environments 06 p0717 N88-14403
Influence of stress ratio R on fatigue threshold delta K(th) for 40Cr steel 06 p0718 N88-14405
The effects of loading history on fatigue crack growth threshold 06 p0718 N88-14406
Threshold stress intensity for stable crack growth in high strength steel at ambient temperature and below
06 p0718 N88-14407
The effect of shear lips on fatigue crack growth in Al-2024 sheet material 06 p0718 N88-14408
Near-threshold fatigue crack growth behavior at cryogenic temperature 06 p0718 N88-14409
The effect of non-metallic inclusions on fatigue and fatigue thresholds of 25Mn-5Cr-1Ni steel
06 p0718 N88-14410
Role of interstitials and precipitates in initiation and propagation of L.C.F. cracks in austenitic stainless steels
06 p0718 N88-14411
Threshold and crack-growth tests on pre-cracked specimens produced in cyclic compression
06 p0718 N88-14412
Micromechanics of fatigue crack initiation under axial and torsional loadings 06 p0719 N88-14413
Study of the characteristic curve of hardening and softening during low-cycle fatigue process
06 p0719 N88-14414
The effect of prestraining on fatigue crack growth in nickel-base alloys 06 p0719 N88-14415
Mixed mode fatigue crack growth using the Brasilian disc 06 p0719 N88-14416
Crack closure phenomena in modes 1 and 2 interactions 06 p0719 N88-14417
Multiaxial fatigue failure criterion: A new approach
06 p0719 N88-14418
Profiles of self stress and of load stress at notches
06 p0719 N88-14419
Fatigue oxidation interaction in low cycle fatigue
06 p0719 N88-14420
Effect of temperature exposure on fatigue crack propagation 06 p0720 N88-14421
High temperature low cycle fatigue of oxide dispersion strengthened and single crystal nickel base superalloys
06 p0720 N88-14422
Orientation effects in copper single crystals fatigued at elevated temperatures 06 p0720 N88-14423
Elevated temperature fatigue crack propagation
06 p0720 N88-14424
High temperature low cycle fatigue behavior and creep-fatigue interation of MA 6000 ODS alloy
06 p0720 N88-14425
Creep-fatigue cracking in high temperature turbine rotors 06 p0720 N88-14426
The effect of temperature on fatigue crack initiation from aluminosilicate inclusions 06 p0720 N88-14427
Dependence of strainrange partitioned fatigue life at elevated temperature on monotonic stress-strain properties 06 p0721 N88-14428
Thermal mechanical low cycle fatigue of 25CDV4-10 steel 06 p0721 N88-14429
Axial creep-fatigue damage assessment in type 316 SS material 06 p0721 N88-14430
An analysis of temperature effect on LCF crack growth rates in superalloy GH36 06 p0721 N88-14431
Thermomechanical fatigue of lead-base low tin solder
06 p0721 N88-14432
Fatigue life prediction modeling for turbine hot section materials
[NASA-TM-100291] 06 p0724 N88-14453
Transients in elevated temperature crack growth
[DE87-013189] 06 p0724 N88-14454
Fatigue, fracture and strain hardening of high carbon hardened alloy steel
[AD-A186101] 07 p0831 N88-15043
Effect of overload ratios on fatigue crack growth behavior in Ti-6Al-4V alloy
[PB87-147062] 07 p0833 N88-15055
Propagation of fatigue crack in the medium-carbon steel contaiing both martensite and ferrite
[PB87-143962] 07 p0869 N88-15273
Review of fatigue and fracture research at NASA Langley Research Center 09 p1106 N88-16633
Fatigue crack growth due to random loading
[DE88-004641] 10 p1345 N88-18038
Thermal fatigue of stainless steel
[DE88-004146] 11 p1458 N88-18694
Thermal-mechanical fatigue testing of a titanium-aluminide alloy
[AD-A189555] 12 p1609 N88-19620
Advanced durability analysis. Volume 1: Analytical methods
[AD-A188341] 12 p1635 N88-19789
A simulation of void lining during ductile fracture
[AD-A188404] 12 p1635 N88-19792
Non-destructive evaluation techniques applied to the study of fatigue microcrack growth in steel alloys
[DE88-004090] 13 p1742 N88-20420
The fatigue behavior of ferritic and austenitic steels at elevated temperatures
[DE88-006304] 13 p1744 N88-20431
Investigation of the use of horizontally polarised shear waves for TOFD studies on austenitic steel
[AERE-R-12145] 13 p1780 N88-20649
JPRS report: Science and technology. USSR: Materials science
[JPRS-UMS-87-007] 14 p1895 N88-21312
Some structural aspects of crack propagation in heat-resistant steels under cyclic thermal and mechanical load 14 p1896 N88-21317
The growth of corner cracks under the conjoint action of high and low cycle fatigue
[AD-A190510] 15 p2076 N88-22379
Lewis Structures Technology, 1988. Volume 3: Structural Integrity Fatigue and Fracture Wind Turbines HOST
[NASA-CP-3003-VOL-3] 15 p2081 N88-22408
Life prediction modeling based on cyclic damage accumulation 15 p2085 N88-22426
Fatigue damage modeling for coated single crystal superalloys 15 p2085 N88-22427
Development of a flexible and economic helicopter engine monitoring system
[PB88-165147] 16 p2160 N88-22887
Fatigue crack growth under full-scale cyclic plasticity
[DFVLR-FB-87-48] 16 p2222 N88-23263
Study of mechanisms of time-dependent crack growth at elevated temperature
[DE88-006918] 16 p2223 N88-23271
AC impedance analysis of corrosion fatigue in naval aircraft alloys
[AD-A190822] 17 p2322 N88-23865
The application of high-rate biaxial testing to the design of containment vessels for radioisotope heat sources
17 p2426 N88-24428
Environment assisted degradation mechanisms in advanced light metals
[NASA-CR-182907] 18 p2486 N88-24746
Isothermal and bithermal thermomechanical fatigue behavior of a NiCoCrAlY-coated single crystal superalloy
[NASA-TM-100907] 18 p2489 N88-24766
Cyclic fatigue damage characteristics observed for simple loadings extended to multiaxial life prediction
[NASA-CR-182126] 18 p2531 N88-25016
Characterization of fatigue crack initiation and propagation in Ti-6Al-4V with electrical potential drop technique
[NASA-TM-100877] 19 p2681 N88-25937
Analyses and correlations of environment assisted fatigue crack propagation for attachment lugs
22 p3053 N88-28116
Load interaction effects on compression fatigue crack growth in ductile solids
[FFA-TN-1988-12] 22 p3089 N88-28342
AGARD engine disc cooperative test programme
[AGARD-R-766] 23 p3179 N88-28926

METAL FIBERS

Magnetization studies of multifilamentary Nb3Sn wires
[DE88-009103] 19 p2735 N88-26243

METAL FILMS

Simulation of the layer-growth dynamics in silver films: Dynamics of adatom clusters and vacancy clusters on Ag(100)
[DE87-014764] 03 p0380 N88-12390
Superconducting switch program
[AD-A185682] 07 p0848 N88-15144
Optical measurements of surface oxide layer formation on metal films
[DE88-003163] 10 p1409 N88-18405
Characterization of redox states of nickel hydroxide film electrodes by in-situ Raman spectroscopy
[AD-A189288] 13 p1741 N88-20411
Properties of reactively sputtered WNx films Zhao, X. -A.
[AD-A188711] 13 p1835 N88-20976
Laser enhanced adhesion of copper films to sapphire substrates
[DE88-006802] 15 p2038 N88-22144
Vapor phase deposition and growth of polyimide films on copper
[AD-A189969] 15 p2044 N88-22178
Ion-beam mixing and amorphization in Au/Zr bilayers
[DE88-005999] 15 p2140 N88-22767
Femtosecond nonequilibrium electronic heat transport in thin gold films 19 p2659 N88-25807
Epitaxial iron films
[AD-A191815] 19 p2732 N88-26225
Aharonov-Bohm effects in disordered metals
20 p2864 N88-27008
PECVD of amorphous nickel–phosphorus films
[DE88-011088] 21 p2915 N88-27299
Status and directions of modified tribological surfaces by ion processes
[NASA-TM-101304] 22 p3063 N88-28176
Optical emission from surface waves supported in thin metal films 23 p3282 N88-29540
Temperature dependence of conductivity and of Hall coefficients for noble metal films
[ETN-88-92981] 23 p3294 N88-29616
The lubricating properties of magnetron sputtered MoS2
[ESA-ESTL-76] 24 p3381 N88-30136

METAL FINISHING

The analysis of metal finishing solutions by ion chromatography
[AD-A184812] 05 p0561 N88-13414

METAL FLUORIDES

NT ALUMINUM FLUORIDES
NT CALCIUM FLUORIDES
NT LITHIUM FLUORIDES
NT SODIUM FLUORIDES
NT URANIUM FLUORIDES

METAL FOILS

High-temperature properties of ceramic fibers and insulations for thermal protection of atmospheric entry and hypersonic cruise vehicles
[NASA-TM-100059] 10 p1295 N88-17743
Composition and thickness of multilayer foils using MeV ion-beam techniques
[DE88-004360] 11 p1448 N88-18629
Erosion of metals exposed to hot, dense gases
[AD-A193708] 22 p3056 N88-28131

Hydrogen permeation through metallic foils
[DE88-702600] 23 p3193 N88-29000

METAL FORGING
U FORGING

METAL FORMING
U FORMING TECHNIQUES
U METAL WORKING

METAL HALIDES
NT ALUMINUM FLUORIDES
NT CALCIUM FLUORIDES
NT CESIUM IODIDES
NT COPPER CHLORIDES
NT LITHIUM CHLORIDES
NT LITHIUM FLUORIDES
NT POTASSIUM BROMIDES
NT SILVER CHLORIDES
NT SILVER IODIDES
NT SODIUM CHLORIDES
NT SODIUM FLUORIDES
NT URANIUM FLUORIDES

An investigation of metal complexes of some 2-substituted and 2,6-disubstituted pyridine N-oxides
11 p1460 N88-18701

Metal halide optical glasses
[AD-A193794] 23 p3198 N88-29032

METAL HARDENING
U HARDENING (MATERIALS)

METAL HYDRIDES
NT LITHIUM HYDRIDES
NT SODIUM HYDRIDES

Performance analysis of advanced spacecraft TPS
[NASA-CR-181532] 04 p0399 N88-12484

Method for preparing hydride configurations and reactive metal surfaces
[DE88-000845] 06 p0679 N88-14161

Electronic structure calculations and binding analyses for selected binary and ternary metal hydrides
[ETN-88-91087] 09 p1256 N88-17527

Metal hydrides
[DE88-005083] 10 p1299 N88-17766

Chemical activation of molecules by metals: Experimental studies of electron distributions and bonding
[DE88-004485] 10 p1407 N88-18393

Materials science with muon spin rotation
[NASA-CR-182891] 17 p2396 N88-24242

Muon motion in titanium hydride
17 p2396 N88-24247

Super hydrides
[AD-A193710] 23 p3192 N88-28995

METAL INSULATOR SEMICONDUCTORS
U MIS (SEMICONDUCTORS)

METAL IONS
NT FERRIC IONS

Segmented hollow cathode discharges for copper ion lasers
[ETN-87-90403] 01 p0052 N88-10333

Some aspects of metallic ion chemistry and dynamics in the mesosphere and thermosphere
06 p0737 N88-14534

Meteor matter interaction with the Earth's atmosphere and the ionospheric E-region structure
06 p0738 N88-14537

Development of FTMS methods for the detection of trace chemical species and development of FTMS methods for the analysis of various chemical species
[AD-A185857] 07 p0828 N88-15023

Electrosorptive detection based on double-layer capacitance for selective anion monitoring in ion chromatography. Part 1: Mercury electrodes
[AD-A186780] 12 p1606 N88-19603

Transition metal cluster chemistry
[AD-A186731] 13 p1740 N88-20405

Wavelength scaling of lithium-like recombination scheme for X-UV gain production --- X-ray lasers
[ETN-88-92002] 13 p1778 N88-20634

Determination of aquo-complexes of chromium and iron in chromium plating and polishing solutions by ion chromatography
[AD-A190168] 15 p2039 N88-22148

Ion beam alloying of aluminum for corrosion resistance
17 p2321 N88-23860

Complexation and hydrolysis reactions of iron(III)
17 p2322 N88-23867

Self shielding of surfaces irradiated by intense energy fluxes
[DE88-007094] 18 p2579 N88-25318

Field-enhanced lithium ion sources for PBFA 2
[DE88-007195] 20 p2856 N88-26960

Storing bits on a DNA polymer chain
[AD-A195701] 24 p3356 N88-29981

METAL JOINTS
NT SOLDERED JOINTS
NT SPOT WELDS
NT WELDED JOINTS

Taper sectioning to magnify the interface thickness of a dissimilar metal joint
[RFP-3890-REV] 03 p0333 N88-12099

Investigation of Super*Zip separation joint
[NASA-TM-4031] 15 p2026 N88-22072

Stress relaxation of a titanium (Ti-6Al-4V) threaded joint
[DE88-010102] 21 p2961 N88-27590

Shielding effectiveness of metallic joints versus corrosion prevention
22 p3054 N88-28120

METAL MATRIX COMPOSITES
NT ALUMINUM BORON COMPOSITES
NT ALUMINUM GRAPHITE COMPOSITES
NT EUTECTIC COMPOSITES

An investigation of the high strain rate deformation of SiCw/2124 Al composite
[OUEL-1675/87] 02 p0142 N88-10895

High temperature metal matrix composites for future aerospace systems
[NASA-TM-100212] 02 p0149 N88-10938

Composite structural materials
[NASA-CR-181416] 02 p0190 N88-11186

Plasticity of fibrous composites
[AD-A184637] 03 p0280 N88-11765

Corrosion resistance of silver-plated carbon-aluminum composite
03 p0285 N88-11793

Corrosion-electrochemical and mechanical properties of composite graphite-carbide metal materials based on titanium and its alloys
03 p0285 N88-11794

The infiltration kinetics of aluminum in silicon carbide compacts
[AD-A184682] 03 p0290 N88-11823

Damping characteristics of a composite-reinforced stainless-steel plate
[DE88-000303] 04 p0457 N88-12828

Plasma joining of metal matrix composites
[AD-A184828] 05 p0557 N88-13390

Micromechanisms of fatigue crack growth and fracture toughness in metal matrix composites
[AD-A185200] 05 p0558 N88-13392

Time-temperature-stress capabilities of composite materials for advanced supersonic technology application
[NASA-CR-178272] 06 p0677 N88-14144

Thermo-mechanical behavior of high temperature fiber composites
06 p0678 N88-14149

Bending properties of aluminum base composite with CVD-fiber
[PB87-130878] 06 p0678 N88-14156

Interface characteristics and the mechanical properties of metal matrix composites
[AD-A186441] 08 p0966 N88-15845

Aeropropulsion '87. Session 1: Aeropropulsion Materials Research
[NASA-CP-10003-SESS-1] 09 p1118 N88-16697

Development of a new generation of high-temperature composite materials
09 p1119 N88-16702

Micromechanisms of fatigue crack growth and fracture toughness in metal matrix composites
[AD-A186941] 09 p1137 N88-16816

Micro-mechanisms of deformation in SiC/Al composites
[AD-A186282] 10 p1296 N88-17749

Creep behavior of tungsten/niobium and tungsten/niobium-1 percent zirconium composites
[NASA-TM-100804] 11 p1460 N88-18707

Mechanical response of unidirectional boron/aluminum under combined loading
[NASA-CR-182595] 12 p1604 N88-19591

Plasma joining of metal matrix composites
[AD-A188559] 12 p1604 N88-19593

Composites strengthening
[AD-A189258] 13 p1734 N88-20364

High-temperature metal matrix composites
[AD-A189516] 13 p1734 N88-20367

Processing, structure and properties of heavily deformed in situ composites
[AD-A189611] 13 p1742 N88-20416

Fracture criteria for discontinuously reinforced metal matrix composites
[NASA-CR-182665] 13 p1782 N88-20662

Structure and strength of boron-aluminum composites
14 p1885 N88-21264

A viscoplastic constitutive theory for metal matrix composites at high temperature
14 p1929 N88-21500

Microplasticity phenomena in graphite/magnesium metal matrix composites
[DE88-006772] 15 p2029 N88-22086

Drilling metal matrix composites
[AD-A190480] 15 p2029 N88-22091

Interfacial structure-property relationships at the fiber-matrix interphase in advanced composites
[AD-A190649] 15 p2030 N88-22093

Specimen preparation techniques for the examination of ceramic and metal-matrix composites
[DE88-005157] 15 p2030 N88-22094

Thermal expansion behavior of randomly oriented short carbon fiber reinforced copper composites
[NASA-TT-20175] 15 p2031 N88-22099

Reciprocating sliding wear characteristics of copper-carbon fiber composites
[NASA-TT-20176] 15 p2031 N88-22100

Application of copper-carbon fiber composites to power semiconductor devices
[NASA-TT-20171] 15 p2031 N88-22101

Joints in fiber-reinforced aluminum alloys
[NASA-TT-20160] 15 p2031 N88-22104

Processing, microstructure, and mechanical properties of silicon carbide particulate reinforced aluminum alloys
[AD-A188981] 15 p2037 N88-22136

Investigation and synthesis of high temperature and increased stiffness RSP aluminum alloys
[AD-A190407] 15 p2039 N88-22151

Growth and deformation mechanisms of refractory alloy hybrid materials
[AD-A190492] 15 p2039 N88-22152

Unified constitutive model development for metal matrix composites at high temperature
15 p2078 N88-22387

METCAN: The metal matrix composite analyzer
15 p2079 N88-22395

Test procedures and standards for mechanical property measurements on metal matrix composites
[NPL-DMA(A)-153] 16 p2172 N88-22944

Thermal conductivity, electrical conductivity and specific heat of copper-carbon fiber composite
[NASA-TT-20172] 16 p2172 N88-22948

Structure and mechanical properties of metal matrix composites made using semi-solid processes: The case of the system Al-Si/SiC
[ETN-88-92299] 17 p2316 N88-23836

Strain intensity factor approach for predicting the strength of continuously reinforced metal matrix composites
[NASA-TM-100617] 17 p2317 N88-23838

Analysis of notched metal matrix composites under tension loading
[NASA-TM-100629] 18 p2480 N88-24713

Research work completed at the Naval Surface Warfare Center Solid State Group of the Radiation Division
[AD-A191627] 18 p2582 N88-25339

Fatigue testing and damage development in continuous fiber reinforced metal matrix composites
[NASA-TM-100628] 19 p2610 N88-25489

Fracture resistance of a TiB2 particle/SiC matrix composite at elevated temperature
[NASA-TM-100967] 20 p2779 N88-26482

Damping characteristics of metal matrix composites
[AD-A193144] 21 p2904 N88-27233

Analysis of transverse strength of composites using percolation theory
[AD-A193204] 21 p2904 N88-27234

Refractory metal alloys and composites for space power systems
[NASA-TM-100946] 21 p2916 N88-27310

The composite aeroengine
[PNR90451] 22 p3045 N88-28070

Durability of continuous fiber reinforced metal matrix composites
[AD-A193868] 22 p3050 N88-28097

Plasma joining of metal matrix composites
[AD-A193939] 22 p3051 N88-28100

Investigation of a SiC/Ti-24Al-11Nb composite
[NASA-TM-100956] 23 p3190 N88-28980

A fundamental study of P/M processed elevated temperature aluminum alloys
[AD-A192958] 23 p3194 N88-29005

Some theoretical considerations of the surface tension of liquid metals for metal matrix composites
[AD-A195999] 24 p3340 N88-29882

METAL NITRIDES
NT ALUMINUM NITRIDES
NT GALLIUM NITRIDES
NT TITANIUM NITRIDES
NT ZIRCONIUM NITRIDES

Process for preparing transition metal nitrides and transition metal carbonitrides and their reaction intermediates
[DE88-000849] 06 p0679 N88-14162

METAL OXIDE SEMICONDUCTORS
NT CMOS
NT SOS (SEMICONDUCTORS)

Hydrogen annealing of P(sub) b and E prime defect centers in oxidized silicon wafers
[DE87-014293] 02 p0152 N88-10951

A review of the semiconductor storage of television signals. Part 2: Applications 1975-1986
[BBC-RD-1987/6] 02 p0161 N88-11009

Development of standard cells in NMOS technology for the design of digital integrated circuits
[FI-62-TB-6] 03 p0310 N88-11953
Research in monolithic signal-processing circuits
[AD-A184680] 03 p0311 N88-11962
Reevaluating the worst-case radiation response of MOS transistors
[DE87-014157] 04 p0497 N88-13059
A study of charged particles/radiation damage to VLSI device materials
[NASA-CR-172036] 05 p0577 N88-13518
Integrated photo-responsive metal oxide semiconductor circuit
[NASA-CASE-GSC-12782-1] 06 p0696 N88-14271
The role of hydrogen in radiation-induced defect formation in polysilicon gate MOS devices
[DE87-012374] 06 p0785 N88-14814
Further study of inversion layer MOS solar cells
07 p0925 N88-15621
Extraction of MOS VLSI (Very-Large-Scale-Integrated) circuit models including critical interconnect parasitics
[AD-A185847] 08 p0979 N88-15914
Impurity bands in quantum wells
[INPE-4250-PRE/1123] 08 p1089 N88-16552
Dispersive hole transport in SiO2
[AD-A187077] 09 p1254 N88-17513
Nature of gigantic resistance fluctuations in metal-oxide-semiconductor wires
[DE88-002905] 09 p1256 N88-17533
Formal multilevel hierarchical verification of synchronous MOS VLSI circuits
[AD-A187532] 10 p1324 N88-17918
RELIC: A reliability simulator for integrated circuits
[AD-A187493] 11 p1477 N88-18811
Radiation response of thin oxides grown by rapid thermal oxidation and rapid thermal annealing techniques
[DE88-003632] 11 p1561 N88-19347
Metal oxide varistor polarization from an initial transient
[AD-A189012] 12 p1623 N88-19711
Response characteristics of dual MOSFET gamma-ray sensors produced by Mitel Corporation
[AD-A189026] 12 p1630 N88-19755
Fundamental studies and device development in beta silicon carbide
[AD-A189540] 12 p1699 N88-20165
GM: A gate matrix layout generator
[EUT-87-E-179] 13 p1820 N88-20875
Two papers on a symbolic analyzer for MOS (Metal-Oxide Semiconductors) circuits
[AD-A188617] 15 p2139 N88-22761
Modeling the effects of heavy charged particles on MOSFETs (Metal-Oxide-Semiconductor Field Effect Transistors)
[AD-A190575] 15 p2143 N88-22792
The effect of elevated temperature on irradiated MOS devices 17 p2406 N88-24308
Development of the field-induced electron injection and impact ionization (F4I) technique for radiation hardness testing of MOS (Metal-Oxide-Semiconductor) gate insulators
[AD-A192114] 18 p2583 N88-25345
The response of ultrathin palladium gate sensors to hydrogen and carbon monoxide
19 p2672 N88-25885
Zinc-oxide thin films for integrated-sensor applications
19 p2673 N88-25896
Extended and local plasmons in a lateral superlattice
20 p2870 N88-27041
Dose-enhancement effects in TaSi/Al- and Al-gate MOS devices
[DE88-005483] 21 p3020 N88-27926
Sol-gel processing of metal-oxide-semiconductor structures
[DE88-009853] 22 p3156 N88-28778
Electrical properties of metal-oxide-silicon structures with sol-gel oxides
[DE88-011791] 22 p3156 N88-28779
Evaluation of silicon-on-insulator MOS (Metal-Oxide-Semiconductor) transistor response to 10-keV X-ray and cobalt-60 irradiation
[DE88-006102] 23 p3206 N88-29082
Waveform relaxation applied to transient device simulation
[AD-A194992] 24 p3432 N88-30429
Joint services electronics program
[AD-A195731] 24 p3434 N88-30439

METAL OXIDES
NT ALKALINE EARTH OXIDES
NT ALUMINUM OXIDES
NT BARIUM OXIDES
NT BERYLLIUM OXIDES
NT BISMUTH OXIDES
NT CALCIUM OXIDES
NT CERIUM OXIDES
NT CHROMIUM OXIDES
NT COBALT OXIDES
NT COPPER OXIDES
NT HAFNIUM OXIDES
NT HEMATITE
NT IRON OXIDES
NT LANTHANUM OXIDES
NT LEAD OXIDES
NT LITHIUM OXIDES
NT MAGNESIUM OXIDES
NT MANGANESE OXIDES
NT MOLYBDENUM OXIDES
NT NICKEL OXIDES
NT NIOBIUM OXIDES
NT RUTILE
NT SAPPHIRE
NT TANTALUM OXIDES
NT TIN OXIDES
NT TITANIUM OXIDES
NT VANADIUM OXIDES
NT YTTRIUM OXIDES
NT ZINC OXIDES
NT ZIRCONIUM OXIDES
Slip casting and extruding shapes of rhenium with metal oxide additives. Part 2: Development of grain stabilized rhenium parts for resistojets
[NASA-CR-180851] 03 p0278 N88-11749
Shock-induced chemical synthesis of phases similar to the high temperature superconductor oxides
[DE87-013725] 03 p0380 N88-12387
Activated metal oxide surfaces as highly basic and reducing environments
[AD-A184958] 05 p0561 N88-13417
Effect of the gate oxide thickness on the speed of MOS integrated circuits
[PB88-155783] 10 p1323 N88-17910
Gas-phase photoelectron spectroscopy of metals and metal oxides of importance in the upper atmosphere
[AD-A187771] 11 p1511 N88-19027
Composite ceramic superconducting filaments for superconducting cable
[AD-A187833] 11 p1556 N88-19312
Metal oxide varistor polarization from an initial transient
[AD-A189012] 12 p1623 N88-19711
Compound ceramic processing
15 p2050 N88-22212
The structure and properties of RF reactive sputtered IrO2 films 19 p2672 N88-25884
Surface phases and their influence on metal-oxide interfaces
[DE88-007938] 20 p2769 N88-26420
Defect characterization of the redox behavior and stability of conducting oxides
[DE88-010799] 20 p2878 N88-27088

METAL PARTICLES
NT METAL POWDER
NT POWDERED ALUMINUM
NT SINTERED ALUMINUM POWDER
Rotation of magnetized particle in electrically conducting viscous medium 06 p0770 N88-14733
Characterization of the arc/spark excitation sources used in the spectrometric oil analysis program
[AD-A187131] 10 p1297 N88-17758
Suspension of small metallic plates: A versatile sensor
[PB88-130901] 11 p1487 N88-18874
The percolation approach as a basis for experimental research on the mechanical properties of composite materials 14 p1886 N88-21271
Study of mean free path effects on growth of ultrafine metallic aerosols
[AD-A190206] 15 p2039 N88-22149
Far- and mid-infrared properties of metal-insulator composite materials
[AD-A193227] 21 p2905 N88-27236
Calibration of the portable wear metal analyzer
[AD-A192971] 21 p2950 N88-27524

METAL PLATES
Evaluation of mechanical and technological parameters of different steel states by nondestructive micro- and macromagnetic measuring quantities as well as ultrasonic techniques
[MPA-810-079] 01 p0057 N88-10366
Experiments: Test range facilities, part 2
03 p0305 N88-11921
Fatigue failure of thin porous strips
04 p0426 N88-12640
Water disbondment characterization of organic Coating/metal substrate systems
[AD-A184847] 05 p0567 N88-13454
Numerical simulations of impact tests on a rigid wall --- armor steel
[SNIAS-872-320-102] 05 p0610 N88-13744
A summary of experimental results on square plates and stiffened panels subjected to air-blast loading
09 p1178 N88-17057
A detailed microstructural examination of the cause of HAZ cracking in type 316 steel
[AERE-R-12428] 10 p1301 N88-17777
Effects of commercial cladding on the fracture behavior of pressure vessel steel plates
[DE88-004333] 10 p1303 N88-17790
Removal of out-of-plane distortion in mild steel panels using flame heating, volume 1
[AD-A187802] 11 p1457 N88-18684
Removal of out-of-plane distortion in mild steel panels using flame heating, volume 2
[AD-A187803] 11 p1457 N88-18685
Mechanisms in thermal mechanical forming of plates
[AD-A187797] 11 p1466 N88-18744
Performance evaluation of plate-fin heat exchangers
[AD-A187798] 11 p1482 N88-18845
Investigation of constrained-layer technique using exact elasticity theory
[AD-A188664] 12 p1636 N88-19795
Mechanical design of a ultrahigh gravity UHV facility to launch and recover a low-speed projectile tested on board KC 135 14 p1877 N88-21216
Impact shock generator from explosively driven plates
[DE88-003596] 14 p1918 N88-21452
The effective fracture toughness of aluminum at rapid heating rates
[AD-A189745] 15 p2038 N88-22146
Finite element simulation of perforation of aluminum plates
[DE88-002092] 15 p2073 N88-22362
Processing defects and strength of alumina substrates
[W-10/87] 15 p2087 N88-22441
Plate response analysis using shock tube
[AD-A190828] 18 p2526 N88-24987
Optimization of mechanical/corrosion properties of TI-CODE 12 plate and sheet. Part 2: Thermomechanical processing effects
[DE88-007493] 19 p2616 N88-25517
A numerical study of Rayleigh-Taylor instability in aluminum and steel plates
[DE88-010475] 20 p2774 N88-26449
Analysis of the perforation of monolithic and simple laminate aluminium targets as a test of analytical deformation models
[MRL-R-1111] 20 p2813 N88-26686
Vibration response of constrained viscoelastically damped plates: Analyses and experiments
[AD-A192329] 20 p2815 N88-26699
Finite element method for plate structures with inclined angles
[ILR-MITT-182] 21 p3008 N88-27842
High effectiveness contour matching contact heat exchanger
[NASA-CASE-MSC-20840-1] 23 p3214 N88-29132

METAL POWDER
NT POWDERED ALUMINUM
NT SINTERED ALUMINUM POWDER
Development and production of new and modified powders for sprayed coatings and components for saving important raw materials
[BMFT-FB-T-86-129] 01 p0025 N88-10159
GSSR powder metallurgy research, production expanding 03 p0286 N88-11797
Cast iron freezing mechanisms
03 p0298 N88-11870
Fatigue failure of thin porous strips
04 p0426 N88-12640
Improved silicon nitride for advanced heat engines
[NASA-CR-175006] 08 p0973 N88-15886
A case study of the development of a military specification - zirconium powder for thermal batteries
[AD-A188751] 13 p1792 N88-20717
Microprobe examination of composite materials produced by burning of Ti, Cr, C powders with powder of any one Fe-group metal 14 p1886 N88-21269
Grain growth behavior of extrusion consolidated centrifugally atomized Type 304 stainless steel powder
[DE88-006788] 15 p2038 N88-22143
Laboratory scale inert gas atomizer for producing rapidly solidified powders
[DE88-006734] 18 p2497 N88-24812
Hot isostatic pressing of nickel aluminide powders
[DE88-009677] 19 p2617 N88-25525
Assessment of opportunities for gas-fired sintering in the advanced ceramics and powdered metals industries
[PB88-197157] 19 p2620 N88-25545
Plasma joining of metal matrix composites
[AD-A193939] 22 p3051 N88-28100

METAL PROPELLANTS
Metal containing polymers as fuel cell catalysts
[AD-A184505] 03 p0347 N88-12194
A holographic investigation of particulates in metallized solid fuel ramjet combustion
[AD-A186887] 09 p1140 N88-16831

Holographic investigation of metallized solid propellant combustion in two-dimensional and three-dimensional rocket motors
[AD-A187000] 09 p1140 N88-16832
Characterization of aluminum/RP-1 gel propellant properties
[NASA-TM-100951] 18 p2496 N88-24808
Possibilities of economical improvements for Moon based rocket propulsion using lunar propellants
[ILR-MITT-196] 24 p3338 N88-29871

METAL SHEETS
Superplastic deformation and post forming tensile properties of Ti-6Al-4V sheet
[RAE-TR-86015] 01 p0023 N88-10144
Fatigue failure of thin porous strips 04 p0426 N88-12640
Behavior of short cracks in a 2024 aluminum alloy sheet tested at several stress ratios 05 p0600 N88-13669
The effect of shear lips on fatigue crack growth in Al-2024 sheet material 06 p0718 N88-14408
An investigation of the influence of dislocation substructures on the deformation behavior of AK, DQ steel sheets
[DE88-006337] 14 p1889 N88-21289
Studies on hot-dip zinc-aluminum coated sheet steels
[ETN-88-92217] 15 p2042 N88-22166
Weldability of general purpose heat source iridium capsules 17 p2426 N88-24429
Optimization of mechanical/corrosion properties of TI-CODE 12 plate and sheet. Part 2: Thermomechanical processing effects
[DE88-007493] 19 p2616 N88-25517
Constant amplitude fatigue life data for notched and unnotched annealed Ti-6Al-4V sheet
[AD-A193420] 21 p2913 N88-27287
Ultrasonic detection of diffusion and adhesion loss 24 p3354 N88-29967

METAL SHELLS
Vibration-absorbing characteristics of metal-polymer shells 02 p0158 N88-10991

METAL STRIPS
Method for maintaining precise suction strip porosities
[NASA-CASE-LAR-13638-1] 23 p3201 N88-29051

METAL SURFACES
A surface science investigation of potential intermediates, catalysts, and promoters in the synthesis of higher alcohols by metals
[DE87-014188] 02 p0144 N88-10906
Studies on surface chemical states of some metals and ceramics bombarded with energetic light-ions
[DE87-752975] 02 p0145 N88-10910
Studies on temporal field emission from stainless steel surfaces
[DE87-014237] 02 p0147 N88-10919
On the interaction of a planar metal surface with a charge and with a molecule
[DE87-703083] 02 p0147 N88-10920
Thermal resistance of contacting metal surfaces at helium temperatures
[BLL-RISLEY-TR-5500-(9091.9F)] 02 p0148 N88-10929
Experimental determination of flow potential surfaces supporting a multiaxial formulation of viscoplasticity 02 p0187 N88-11167
A theoretical analysis of the deactivation of metal surfaces upon carburization
[AD-A184556] 03 p0290 N88-11821
Bonding and coupling of C sub 1 fragments on metal surfaces
[AD-A184186] 03 p0295 N88-11852
Study of field adsorption using pulsed-laser field ion microscopy
[DE88-000310] 03 p0330 N88-12085
The structure of adsorbed sulfur and carbon on molybdenum and rhenium single crystal surfaces, and their influence on carbon monoxide and hydrocarbon chemisorption
[DE88-001393] 04 p0499 N88-13073
Master plots for predicting the case-depth in laser surface treatments
[PB87-221875] 05 p0586 N88-13574
The effect of ion beam mixed Ni-Al surface layers on PSB extrusion morphology in fatigued nickel 05 p0598 N88-13652
The influence of the topography of fracture surfaces on crack closure 05 p0598 N88-13657
Atomic beam studies of the interaction of hydrogen with transition metal surfaces
[DE88-000208] 05 p0648 N88-13970
Method for preparing hydride configurations and reactive metal surfaces
[DE88-000845] 06 p0679 N88-14161
Surface gouging by hypervelocity sliding contact between metallic materials
[DE88-001937] 06 p0682 N88-14178
Ion-beam nitriding of steels
[NASA-CASE-LEW-14104-2] 06 p0682 N88-14179
Profiles of self stress and of load stress at notches 06 p0719 N88-14419
Partial analysis of experiment LDEF A-0114
[NASA-CR-179236] 06 p0780 N88-14787
Ion mixing and surface modification in metal-semiconductor systems
[DE88-001702] 06 p0786 N88-14823
Wind tunnel model surface gauge for measuring roughness
[NASA-CR-182392] 07 p0822 N88-14996
Processing and interfacial analysis of glass-ceramic to metal seals
[DE88-002999] 08 p0971 N88-15873
Review of nucleation and incipient boiling under pool and forced convection conditions 06 p0982 N88-15938
Geometric structure, pseudoband gaps, and surface vibrational resonances on metal surfaces
[AD-A187001] 09 p1143 N88-16851
Local stoichiometry and atomic interdiffusion during reactive metal/mercury-cadmium-telluride junction formation
[AD-A187554] 10 p1421 N88-18488
Laser measurements of state-resolved Ga and in atom sticking and desorption on metal and semiconductor surfaces
[AD-A187644] 11 p1555 N88-19310
Thermodynamics of wetting by liquid metals
[DE88-003634] 11 p1563 N88-19360
Chemical cleaning of metal surfaces in vacuum systems by exposure to reactive gases
[AD-A188588] 12 p1608 N88-19616
Correlations between photons in resonance fluorescence emitted by an atom near a metal surface
[AD-A188365] 12 p1689 N88-20102
A study of the interaction of light with sub-micron metallic surfaces
[DE88-003138] 13 p1776 N88-20624
Spontaneous decay and atomic fluorescence near a metal surface of an absorbing dielectric
[AD-A187508] 13 p1835 N88-20975
Recent progress in structure determination by LEED (Low-Energy Electron Diffraction) measure the properties of the deep donors (DX-cent)
[DE88-003851] 13 p1846 N88-21048
Development of a laboratory test for multiport injector deposits: Approaches 1 and 2
[AD-A190697] 15 p2048 N88-22203
Theory of the dissociation dynamics of small molecules on metal surfaces: Finite temperature studies
[DE88-006495] 15 p2132 N88-22716
Auger electron spectroscopy of contrast-forming layers on metals
[NASA-TT-20182] 16 p2178 N88-22980
Enhanced emittance of oxidized 304 stainless steel 17 p2423 N88-24408
Specular steel surfaces for solar mirror substrates
[DE88-001153] 21 p2968 N88-27630
Theory of the dissociation dynamics of small molecules on metal surfaces: Finite temperature studies
[DE88-007763] 21 p3013 N88-27682
Dynamics of a plasma produced under effect of the XeCl-laser radiation on metallic surface
[DE88-701983] 21 p3017 N88-27902
Reaction dynamics on semiconductor surfaces
[AD-A194305] 22 p3156 N88-28781
Influence of local volume forces on surface relaxation of pure metals and alloys: Applications to Ni, Al, Ni3Al
[DE88-702718] 23 p3195 N88-29014
Storing bits on a DNA polymer chain
[AD-A195701] 24 p3356 N88-29981

METAL VAPOR LASERS
Ignition and high speed photography of energetic materials with a copper vapor laser
[DE88-004831] 12 p1631 N88-19765
Electronic energy transfer processes in the alkali/alkaline earth metal vapors
[AD-A190035] 15 p2034 N88-22119
Alkali metal diffuse band lasers
[AD-A190244] 15 p2071 N88-22350

METAL VAPORS
NT MERCURY VAPOR
NT SODIUM VAPOR
Generation of IR stimulated radiation, UV visible violet coherent radiation by two-photon resonance pumping in K vapor 03 p0301 N88-11892
Microgravity nucleation and particle coagulation experiments support
[NASA-CR-181541] 04 p0423 N88-12619
Behavior and structure of metal vapor arc plasma between molten electrodes
[DE88-001854] 06 p0782 N88-14801
TiN coatings on M2 steel produced by plasma assisted chemical vapor deposition
[DE88-003189] 08 p0970 N88-15867
The band systems of alkali vapors
[NASA-TT-20206] 10 p1417 N88-18462
Multiply stripped ion generation in the metal vapor vacuum arc
[DE88-008418] 19 p2725 N88-26179

METAL WHISKER REINFORCEMENT
U WHISKER COMPOSITES

METAL WORKING
NT CLADDING
NT EXPLOSIVE FORMING
NT FORGING
NT HYDROFORMING
NT SIZING (SHAPING)
Superplastic deformation and post forming tensile properties of Ti-6Al-4V sheet
[RAE-TR-86015] 01 p0023 N88-10144
Hardening of metal during production of bent shapes
[BLL-M-37250-(5828.4)] 02 p0148 N88-10928
Activities report in metal manufacturing
[ISSN-0524-7705] 07 p0839 N88-15086
Contribution to the study of wrinkling in metal stamping
[ISAL-IDI1-87-08] 08 p0976 N88-15900
Modification of properties of metals by high-power ion beams 08 p1079 N88-16507
Metals. Preliminary study for an Innovation-Oriented research Program (IOP)
[ETN-88-91317] 14 p1889 N88-21290
Innovation-Oriented research Program (IOP) metals. Annexes
[ETN-88-91318] 14 p1889 N88-21291
Simulation of thermo-mechanical forming processes: A mixed Eulerian-Langrangian finite element method
[PB88-155247] 14 p1933 N88-21530

METAL-GAS SYSTEMS
Studies for the definition of a Faraday converter for space nuclear systems 17 p2411 N88-24339
Evaluation of a diffusion/trapping model for hydrogen ingress in high-strength alloys
[AD-A194301] 23 p3194 N88-29008

METAL-INSULATOR-METAL DIODES
U MIM DIODES

METAL-INSULATOR-METAL SEMICONDUCTORS
U MIM (SEMICONDUCTORS)

METAL-METAL BONDING
Investigation on diffusion reaction brazing of aluminium
[PB87-143368] 08 p0992 N88-16001
Composite/metal jointing technology for vehicle weight reduction
[DE88-900228] 08 p0992 N88-16005
Evaluation of high temperature structural adhesives for extended service, phase 5
[NASA-CR-178176] 09 p1149 N88-16884
New scientific findings on the morphology of aluminum oxide layers, serving as an adhesive basis
[MBB-Z-137/86] 10 p1312 N88-17840
Surface free energy of laser-produced bond percolators
[PB88-130885] 11 p1493 N88-18913
The relationship of the chemical bonding topology of high critical temperature copper oxide superconductors to that of the chevrel phases and the ternary lanthanide rhodium borides
[AD-A189255] 13 p1845 N88-21042
Optimum duration of steady-state stage in friction welding of metals without artificial braking 14 p1898 N88-21330
Interface characterization of Cu-Cu and Cu-Ag-Cu low temperature solid state bonds
[AD-A191015] 16 p2283 N88-23667
Evaluation of explosive bonding for patching aluminum with aluminum
[AD-A193303] 21 p2913 N88-27285
Shielding effectiveness of metallic joints versus corrosion prevention 22 p3054 N88-28120
Static and dynamic metal-metal friction at plastic stress levels
[DE88-011281] 23 p3222 N88-29176

METAL-SEMICONDUCTOR-METAL SEMICONDUCTORS
U MSM (SEMICONDUCTORS)

METAL-WATER REACTIONS
Corrosion problems associated with computer disk packs 22 p3054 N88-28121

METALLIC GLASSES
Studies on some Ge-Se-Te glasses
[PD-MT-8721] 04 p0420 N88-12607
Structural investigations of some metallic glasses
[ECN-198] 06 p0686 N88-14203
Neutron- and X-ray-small angle scattering with Fe-base metallic glasses
[DE88-002538] 09 p1147 N88-16876

Anodic behavior of Ni-P and Ni-Cr-P metallic glasses
[DE88-005334] 11 p1463 N88-18722
Metastable materials by laser irradiation
[PB88-130364] 11 p1493 N88-18912
Corrosion and fatique properties of FeCrB/Si metallic glass wires in aqueous environments
17 p2320 N88-23855
Oxidation behavior and microstructural studies of melt-spun glassy Fe-Al-Zr metal
[DE88-009964] 19 p2617 N88-25526

METALLIC PLASMAS
NT CESIUM PLASMA
Behavior and structure of metal vapor arc plasma between molten electrodes
[DE88-001854] 06 p0782 N88-14801
X-ray source model for Z-pinch aluminum plasmas
[AD-A189509] 12 p1696 N88-20148
Ultraviolet-visible spectroscopy of laser-produced aluminum plasmas
[AD-A193004] 20 p2860 N88-26990
Spectral line shapes from highly ionized sodium plasmas
[AD-A193401] 21 p3017 N88-27907

METALLICITY
Modes, masses, metallicities, and magnitudes of RR Lyrae variables
[DE87-013149] 01 p0109 N88-10703
A geometrical model for determining the physicochemical properties of ternary metallic systems
[BLL-M-37303-(5828.4)] 02 p0149 N88-10931
Molecular hydrogen in galaxies
23 p3299 N88-29645

METALLIZING
Microscopic control of metallization stability
[AD-A187553] 10 p1421 N88-18487
UV-Laser reactions of molecular adsorbates
[AD-A190796] 16 p2212 N88-23201
Microscopic control of semiconductor interface reactivity
[AD-A191193] 16 p2283 N88-23668
Shock wave compression and metallization of simple molecules
[DE88-008031] 20 p2851 N88-26925
Laser and electrochemical studies of metallizations in electronic devices
[AD-A193786] 23 p3208 N88-29090
Stress related failures causing open metallization
[AD-A195061] 24 p3383 N88-30150

METALLOGRAPHY
Evaluation of cracking in aluminum cylinders
[PB87-201398] 01 p0024 N88-10149
Precision metrology comparing ultrasonic and other techniques for the determination of steel thickness
[DE87-011051] 02 p0230 N88-11452
Study of stainless steel time-temperature sensitization diagrams, part 1
[ETN-87-90762] 03 p0289 N88-11815
International Conference on Microstructology held in Gainesville, Florida on 7-9 May 1986
[AD-A184604] 03 p0290 N88-11822
Calibration standard for metallographic microscopes
[RFP-3956-REV] 03 p0326 N88-12057
Metallography of maraging 350 steel
[DE87-013746] 04 p0418 N88-12591
A detailed microstructural examination of the cause of HAZ cracking in type 316 steel
[AERE-R-12428] 10 p1301 N88-17777
Metallurgical analysis of fractured F-27 aircraft landing gear
[DE88-005885] 11 p1460 N88-18705
Processing, structure and properties of heavily deformed in situ composites
[AD-A189611] 13 p1742 N88-20416
Auger electron spectroscopy of contrast-forming layers on metals
[NASA-TT-20182] 16 p2178 N88-22980
The adherence of nickel oxide on nickel during high temperature oxidation
[DE88-011194] 20 p2774 N88-26450
As-received microstructure of a SiC/Ti-15-3 composite
[NASA-TM-100938] 22 p3050 N88-28095

METALLOIDS
NT AMORPHOUS SILICON
NT ARSENIC
NT BORON
NT BORON ISOTOPES
NT GERMANIUM
NT SILICON
NT TELLURIUM

METALLORGANIC COMPOUNDS
U ORGANOMETALLIC COMPOUNDS

METALLURGY
Metallurgy laboratory for Columbus, executive summary
[SNIAS-813-CA/TS] 02 p0157 N88-10980
Investigations in field of surface forces in metallurgy
[BLL-M-47406-(5828.4)] 08 p0969 N88-15860

METALS
NT ALKALI METALS
NT ALKALINE EARTH METALS
NT ALUMINUM
NT BARIUM
NT BERYLLIUM
NT BISMUTH
NT CADMIUM
NT CALCIUM
NT CALCIUM ISOTOPES
NT CERIUM
NT CESIUM
NT CHROMIUM
NT COBALT
NT COBALT 60
NT DYSPROSIUM
NT ERBIUM
NT EUROPIUM
NT FERROUS METALS
NT GADOLINIUM
NT GALLIUM
NT GOLD
NT HAFNIUM
NT HOLMIUM
NT INDIUM
NT IRIDIUM
NT IRIDIUM ISOTOPES
NT IRON
NT IRON ISOTOPES
NT IRON 57
NT LANTHANUM
NT LAWRENCIUM
NT LEAD (METAL)
NT LEAD ISOTOPES
NT LIQUID LITHIUM
NT LIQUID METALS
NT LIQUID POTASSIUM
NT LIQUID SODIUM
NT LITHIUM
NT LITHIUM ISOTOPES
NT MAGNESIUM
NT MAGNESIUM ISOTOPES
NT MANGANESE
NT MERCURY (METAL)
NT MERCURY ISOTOPES
NT MERCURY VAPOR
NT METAL VAPORS
NT MOLYBDENUM
NT NEODYMIUM
NT NEODYMIUM ISOTOPES
NT NEPTUNIUM
NT NICKEL
NT NIOBIUM
NT NIOBIUM ISOTOPES
NT NOBLE METALS
NT OSMIUM
NT PALLADIUM
NT PLATINUM
NT PLATINUM ISOTOPES
NT PLUTONIUM ISOTOPES
NT PLUTONIUM 238
NT POTASSIUM
NT RARE EARTH ELEMENTS
NT REFRACTORY METALS
NT RHENIUM
NT RHENIUM ISOTOPES
NT RHODIUM
NT RUBIDIUM
NT RUBIDIUM ISOTOPES
NT RUTHENIUM
NT SAMARIUM ISOTOPES
NT SILVER
NT SODIUM
NT SODIUM VAPOR
NT STRONTIUM
NT TANTALUM
NT THORIUM
NT TIN
NT TITANIUM
NT TRANSITION METALS
NT TUNGSTEN
NT ULTRAPURE METALS
NT URANIUM
NT URANIUM ISOTOPES
NT URANIUM 238
NT VANADIUM
NT YTTERBIUM
NT YTTRIUM
NT ZINC
NT ZIRCONIUM
Transient absorption behavior of metals at the onset of the laser welding process
[DFVLR-FB-87-12] 01 p0025 N88-10160
Electrical heating method --- pipelines, metal tanks
[GB-PATENT-2-137-059-A] 01 p0043 N88-10274
Analysis of shell-type structures subjected to time-dependent mechanical and thermal loading
[NASA-CR-181409] 01 p0060 N88-10388
Channeled particle acceleration by plasma waves in metals
[DE87-010541] 01 p0093 N88-10604
Metal-sensing layer-semiconductor and metal-sensing layer-metal heterostructure gas sensors
[DE87-011293] 01 p0103 N88-10674
Grain boundary phase equilibria in metallic systems
[DE87-014123] 01 p0104 N88-10679
Reduction of CO2 to methanol and methane by photo and dark reactions on semiconductor and metal electrodes
[PB87-226825] 02 p0156 N88-10975
Computer modeling of metal forming
[DE87-013804] 02 p0157 N88-10984
Photocatalytic electrochemistry at a biological-membrane metal-colloid interface
[DE87-009122] 02 p0166 N88-11041
Electron capture from solids by positrons
[DE87-014355] 02 p0232 N88-11463
Birch's law and the properties of high temperature fluid metals
[DE87-014744] 03 p0288 N88-11807
Shock-induced melting and rapid solidification
[DE88-000226] 03 p0288 N88-11810
Surface coatings and catalyst production by electrodeposition 03 p0297 N88-11863
Gas tungsten arc welding of Al-10Fe-5Ce
[AD-A184202] 03 p0334 N88-12104
Activities at government research laboratories reported 04 p0403 N88-12503
Ignition and combustion of metals in oxygen
04 p0407 N88-12530
Topological aspects of infinite metal clusters and superconductors
[AD-A184104] 04 p0495 N88-13049
Analysis of wear metals in engine oils using the atomic absorption spectrophotometric method
[NAL-TM-MT-8704] 05 p0564 N88-13435
Molecular-level synthesis and characterization of metal-polymer interfaces
[AD-A184956] 05 p0567 N88-13455
Photocurrent generation from basic metals, utilizing a short pulsed ArF excimer laser
[AD-A184928] 05 p0587 N88-13579
The orientations of dipolar walls produced by cyclic deformation 05 p0598 N88-13655
The interaction of DC plasma jet with a melting metal: Experimental measurements and mathematical description
[AD-A185173] 05 p0651 N88-13993
Singularities in X-ray spectra of metals
[DE88-001440] 06 p0681 N88-14174
An overview of metal plasticity
[DE88-001658] 06 p0681 N88-14175
Characterization of microstructure in metallic and composite materials
[AD-A186193] 07 p0826 N88-15012
Studies of metal/carbon surface chemistry
[DE87-009545] 07 p0829 N88-15029
Studies of supported metal catalysts
[DE88-002546] 07 p0831 N88-15038
Computer simulation of impurities and interfaces in body centered cubic metals
[PB88-108162] 07 p0832 N88-15047
Computer simulation of pencil glide in B.C.C. metals
[DE88-001802] 07 p0834 N88-15062
Study of the embedded atom method of atomistic calculations for metals and alloys
[DE88-002798] 07 p0835 N88-15065
Life prediction of thermomechanical fatigue using total strain version of strainrange partitioning (SRP): A proposal
[NASA-TP-2779] 07 p0867 N88-15263
Phonon dispersion for several surfaces with ordered overlayers: A lattice dynamical study
07 p0876 N88-15315
Atomic oxygen effects on metals
07 p0924 N88-15617
Interrelation and measurement of formability, strengthening, and thermomechanical processing under metalworking conditions
[DE88-002485] 08 p0967 N88-15850
Critical analysis of the dynamic behavior laws for metallic materials --- ballistics
[ISL-NB-401/86] 08 p0969 N88-15862
Submerged arc flux welding with CaF2-CaO-SiO2 fluxes: Possible electrochemical effects on weld metal
[DE88-003107] 08 p0992 N88-16004
Characteristics of thermooptical sound excitation in metals 08 p1076 N88-16486

A comparison of measurements from the A/E35U-3 and PWMA (Portable Wear Metal Analyzer) spectrometers
[AD-A186855] 09 p1177 N88-17047
Electronic and chemical structure of 3-5/metal and Si/metal interfaces
[AD-A186579] 09 p1254 N88-17518
A large strain thermomechanical forming model for elastic-viscoplastic behavior in metals
10 p1301 N88-17780
Irradiation effects in metals
[DE88-004272] 10 p1303 N88-17789
Metal modification for improved glass-ceramic to metal seals: 1. Auger results on ion implantation and vapor deposition films
[DE88-005244] 10 p1339 N88-18006
Chemical activation of molecules by metals: Experimental studies of electron distributions and bonding
[DE88-004465] 10 p1407 N88-18393
Non-proprietary research projects of the Center for the Space Processing of Engineering Materials
[AR-2] 10 p1426 N88-18516
Deactivation of alumina based catalysts
11 p1455 N88-18673
Reference standards for nondestructive tests
[AD-A187766] 11 p1497 N88-18936
Gas-phase photoelectron spectroscopy of metals and metal oxides of importance in the upper atmosphere
[AD-A187771] 11 p1511 N88-19027
Atomistic studies of the structure and properties of grain boundaries with substitutional impurities
[DE88-004161] 11 p1545 N88-19237
An experimental measurement of metal multilayer X-ray reflectivity degradation due to intense X-ray flux
[LA-10989-T] 11 p1547 N88-19255
Microstructure characterization with a pulsed laser ultrasonic source
[DE88-005207] 12 p1632 N88-19766
Photochemistry at structured surfaces: A classical electromagnetic approach
[AD-A189519] 13 p1737 N88-20387
Material instabilities in solids
[AD-A189525] 13 p1738 N88-20388
The coordination cluster theory for metallic solutions
[DE88-005934] 13 p1738 N88-20389
Formation of nuclei during precipitation in metallic mixed crystals
[NASA-TT-20248] 13 p1745 N88-20437
Spontaneous decay and atomic fluorescence near a metal surface of an absorbing dielectric
[AD-A187508] 13 p1835 N88-20975
Image charge, coherent scattering, and symmetry effects in electron stimulated desorption: O(-) from O sub 2 condensed on metals
[AD-A189093] 13 p1835 N88-20979
Annihilation momentum density of positrons trapped at vacancy-type defects in metals and alloys
[DE88-005936] 15 p2144 N88-22797
Surface enhanced Raman scattering applied to surface chemical kinetics
[AD-A191275] 16 p2176 N88-22969
Question on the measurement of the metal work function in an electron spectrometer by the secondary-electron emission threshold method
[NASA-TT-20190] 16 p2178 N88-22979
Friction and wear of ceramics
17 p2323 N88-23874
Noncontact temperature measurement: Requirements and applications for metals and alloys research
17 p2328 N88-23899
The influence of cathodic protection on erosion-corrosion of metals and model alloys
[AD-A191613] 18 p2485 N88-24742
Arc-textured metal surfaces for high thermal emittance space radiators
[NASA-TM-100894] 18 p2487 N88-24754
The stress analysis of ceramic, polymeric, and metallic composite systems by the finite element method
18 p2529 N88-25004
Metals and Ceramics Division
[DE88-008955] 19 p2618 N88-25530
Observation of metallic conductivity in liquid carbon
[AD-A191723] 19 p2618 N88-25533
Plastic deformation and roughness of free metal surfaces
[PB88-196621] 20 p2772 N88-26439
Abnormal diffusion of vacancies in metals
[DE88-701880] 20 p2773 N88-26441
Shock wave compression and metallization of simple molecules
[DE88-008031] 20 p2851 N88-26925
Metallic superlattices 20 p2864 N88-27012
Pure metallic bridge and point-contact tunneling into single- and polycrystal YBa2CuO(sub 7-y)
[DE88-010030] 20 p2878 N88-27084
On the systematics of phase transformation in metallic alloys
[DE88-008041] 21 p2913 N88-27288
Oxidation-erosion of metals and alloys: Models, verification, and prediction
[DE88-010016] 21 p2915 N88-27300
Soluble metal chelate polymers of coordination numbers six, seven and eight
[AD-A192485] 21 p2917 N88-27314
Effects of near interfacial microstructure on toughness and subcritical crack growth in ceramic/metal systems
[DE88-009842] 21 p2919 N88-27325
The influence of weld metal properties, weld geometry and applied load on weld system performance
[AD-A193403] 21 p2961 N88-27588
Amorphous silicon solar cells using a metal substrate
[PB88-131941] 21 p2968 N88-27628
An endochronic rate-sensitive constitutive equation for metals, application to generalized creep and large deformations
[AD-A194167] 22 p3055 N88-28125
Equipment for the pressure welding of metals and alloys utilising the effects of superplasticity
[RAE-TRANS-2162] 22 p3055 N88-28129
Chemistry of adhesion at the polyimide-metal interface
[AD-A194647] 22 p3058 N88-28143
Stress intensity factors for cracked metallic structures under rapid thermal loading
[AD-A191219] 23 p3193 N88-29004
Phenomena of the ionic transport in the stress corrosion of metals
[DE88-702502] 23 p3195 N88-29013
Thermocouple for heating and cooling of memory metal actuators
[NASA-CASE-NPO-17068-1-CU]
23 p3217 N88-29151
System suitable for observing surface plasmon in a semi-infinite semiconductor superlattice
[DE88-702686] 23 p3293 N88-29606

METAMORPHISM (GEOLOGY)
Isotopic and chemical studies of early crustal metasedimentary rocks
[NASA-CR-182711] 14 p1944 N88-21601
The timing and mechanism of depletion in Lewisian granulites 24 p3394 N88-30209
Decoupled Rb-Sr and Sm-Nd isotopic evolution of the continental crust 24 p3395 N88-30216
Metamorphic P-T paths and Precambrian crustal growth in East Antarctica 24 p3395 N88-30218
The early archaean crustal history of West Greenland as recorded by detrital zircons 24 p3395 N88-30221
Reappraisal of the geology of Kangimut Sammisoq, Ameralik Fjord, Southern West Greenland: Crustal structure and interpretation of isotopic data
24 p3398 N88-30234
Growth of the lower continental crust
24 p3398 N88-30236
Late-Archaean crustal growth in the Lewisian Complex of Northwest Scotland: Diachroneity in magmatic accretion and implications for models of crustal growth
24 p3401 N88-30253

METASTABILITY
U METASTABLE STATE

METASTABLE ATOMS
Group 2A metastable collision complexes: Spectroscopy and behavior in intense radiation fields
[AD-A186737] 08 p1082 N88-16524

METASTABLE STATE
Application of spin-sensitive electron spectroscopies to investigations of electronic and magnetic properties of solid surfaces and epitaxial systems
[DE87-014235] 02 p0245 N88-11550
The gamma-ray laser project
[AD-A184824] 05 p0587 N88-13578
Structural relaxation in strained-layer heterostructures
[DE88-002326] 07 p0868 N88-15264
Group 2A metastable collision complexes: Spectroscopy and behavior in intense radiation fields
[AD-A186737] 08 p1082 N88-16524
Relaxation of metastable semiconductor strained-layer structures by plastic flow
[DE88-002729] 08 p1090 N88-16560
Effect of the subgap conductance on the metastable states in a Josephson tunnel junction
[DE88-003102] 09 p1258 N88-17543
Stability and metastability in semiconductor strained-layer structures
[DE88-003308] 09 p1258 N88-17544
Metastable materials by laser irradiation
[PB88-130364] 11 p1493 N88-18912
Development of metastable processing paths for high temperature alloys
[AD-A188682] 12 p1608 N88-19617
Quantum Monte Carlo study of the MIES associated with H2 (X 1 sigma sub g (+)) and H2 (B 1 sigma sub u (+))
[AD-A189063] 13 p1835 N88-20977
Investigations of the origins of metastable, light-induced changes in hydrogenated amorphous silicon
[DE88-001117] 13 p1846 N88-21051
Laser cooling of neon metastable states
14 p1975 N88-21785
Stability limits in the monoclinic-tetragonal transformations of zirconia
[DE88-005924] 14 p1986 N88-21849
Effect of vibrational excitation on rate parameters of atmospheric reactions
[AD-A190464] 15 p2094 N88-22477
Synthesis of metastable superconductors by high dynamic pressure
[DE88-005620] 15 p2139 N88-22764
Magnetic anomalies in the rare earth oxide superconductors GdBa2Cu3O(7-x) and YbBa2Cu3O(7-x)
[AD-A190713] 15 p2144 N88-22793
Metastability in SiGe/Si strained-layer structures
[DE88-007603] 18 p2585 N88-25361
Formation of metastable structures and amorphous phases in Cu-W alloys using the triod sputtering technique
[DE88-009051] 21 p2915 N88-27298
Proof of the feasibility of coherent and incoherent schemes for pumping a gamma-ray laser
[AD-A193856] 23 p3220 N88-29165

METAZOA
U ANIMALS

METEOR BURSTS
U METEOROID SHOWERS

METEOR CRATERS
U CRATERS

METEOR HAZARDS
U METEOROID HAZARDS

METEOR TRAILS
Meteor-burst communications: Is this what the Navy needs?
[AD-A184433] 04 p0431 N88-12672
Middle Atmosphere Program. Handbook for MAP, volume 25
[NASA-CR-181571] 06 p0732 N88-14502
Elementary process and meteor train spectra
06 p0732 N88-14504
Atmosphere dynamic processes structure at 80-105 km altitude 06 p0736 N88-14527
Internal gravity waves in the meteor zone in the Tbilisi Region 06 p0736 N88-14528
On the wave excitation in the turbulent meteor trace
06 p0737 N88-14530
Methods and first results of plasma non-isothermal parameters measurements in meteor trails
06 p0737 N88-14531
On the meteor trail spectra 06 p0737 N88-14533
Ozone formation due to interaction of meteoroids with Earth's atmosphere 06 p0738 N88-14536
Meteor matter interaction with the Earth's atmosphere and the ionospheric E-region structure
06 p0738 N88-14537
Incident meteoroid flux density
06 p0739 N88-14542
On meteor stream spatial structure theory
06 p0739 N88-14544
Meteor velocity distribution and an optimum monitoring mathematical model 06 p0739 N88-14546
Optical electronics for meteor observations
06 p0741 N88-14559

METEORITE COLLISIONS
Measurements of iridium and the meteoric impact hypothesis at cretaceous end
[DE87-703765] 04 p0521 N88-13200
Conditions for geomagnetically trapping sub-micron lunar ejecta between L = 1.2 and L = 3.1
04 p0521 N88-13203

METEORITE COMPRESSION TESTS
U COMPRESSION TESTS
U MECHANICAL PROPERTIES
U METEORITES

METEORITE CRATERS
Early intense cratering: Effects on growth of earth's crust 24 p3395 N88-30219
A compilation of information and data on the Manson impact structure
[NASA-CR-183169] 24 p3401 N88-30258

METEORITES
NT ACHONDRITES
NT CARBONACEOUS CHONDRITES
NT CARBONACEOUS METEORITES
NT CHONDRITES
NT IRON METEORITES
Moessbauer study of shock induced effects in the Fe-Ni 50/50 ordered alloy in meteorites
[DE87-703364] 04 p0521 N88-13199

The archiving of meteor research information
06 p0732 N88-14505
The nonlinear thermodynamics of meteors, noctilucent clouds, enhanced airglow and global atmospheric circulation 06 p0738 N88-14538
The distribution of evaporitic weathering products on Antarctic meteorites 06 p0798 N88-14888
Products from cosmic-ray interactions in extraterrestrial matter: What they tell us about radiation backgrounds in space
[DE88-009143] 19 p2743 N88-26288
MEVTV Workshop on Nature and Composition of Surface Units on Mars
[NASA-CR-183075] 23 p3300 N88-29654
Selective weathering of shocked minerals and chondritic enrichment of the Martian fines
23 p3301 N88-29660
Aqueous alteration in S-N-C meteorites and implications for weathering products on Mars
23 p3303 N88-29673
What SNC meteorites tell us about Martian magmatism 23 p3303 N88-29679
Spectral reflectance of SNC meteorites: Relationships to Martian surface composition
23 p3304 N88-29683
Origin of SNC kaersutitic amphibole: Experimental data 23 p3306 N88-29693
Crystal fractionation in the SNC meteorites: Implications for surface units on Mars 23 p3307 N88-29698
Nineteenth Lunar and Planetary Science Conference. Press abstracts
[NASA-CR-183037] 24 p3440 N88-30473
Exotic minerals in 3,500 million year old rocks: Evidence for large meteorite impacts 24 p3440 N88-30475
Evidence of the in situ decay of Al-26 in a Semarkona chondrule 24 p3441 N88-30479
LSU scientists discover evidence of large meteorite impacts on the early earth 24 p3441 N88-30480
Lewis Cliff 86010, a unique Antarctic meteorite: Possible new clues to the early history of the solar system
24 p3442 N88-30482
Did the greenhouse effect kill the dinosaurs
24 p3442 N88-30484
Antarctic Meteorite Newsletter, Volume 11, Number 2, August 1988
[NASA-TM-89801] 24 p3457 N88-30573

METEORITIC COMPOSITION
The end height of fireball as a function of their residual kinetic energy 06 p0737 N88-14535
Meteor matter interaction with the Earth's atmosphere and the ionospheric E-region structure
06 p0738 N88-14537
A processing method and results of meteor shower radar observations 06 p0738 N88-14539
Optical electronics for meteor observations
06 p0741 N88-14559
Nineteenth Lunar and Planetary Science Conference. Press abstracts
[NASA-CR-183037] 24 p3440 N88-30473
Ureilites are not igneous differentiates
24 p3441 N88-30477
New type of primitive meteorite found in Antarcitca
24 p3441 N88-30478
Physical processes and timescales in planet and small-body accretion 24 p3451 N88-30540
Nebular processes recorded in chondritic meteorites
24 p3451 N88-30541

METEORITIC DAMAGE
Space environmental considerations for a long-term cryogenic storage vessel 08 p0981 N88-15933
A review of impact design criteria for space power heat rejection systems 17 p2410 N88-24333
The effect of the near earth micrometeoroid environment on a highly reflective mirror surface
[NASA-TM-101307] 24 p3332 N88-29833

METEORITIC DUST
U MICROMETEOROIDS

METEORITIC IONIZATION
U ATMOSPHERIC IONIZATION
U METEOR TRAILS

METEOROID CONCENTRATION
A method of long-term radar shower data analysis
06 p0738 N88-14541
Models of sporadic meteor body distributions
06 p0739 N88-14543
Density variations of meteor flux along the Earth's orbit 06 p0739 N88-14545

METEOROID CRATERS
U METEORITE CRATERS

METEOROID DUST CLOUDS
NT ZODIACAL DUST

METEOROID HAZARDS
Space environmental considerations for a long-term cryogenic storage vessel 08 p0981 N88-15933
Assessment of the effects of space debris and meteoroids environment on the space station solar array assembly
[NASA-TM-101315] 23 p3185 N88-28959

METEOROID PROTECTION
Optimization techniques applied to passive measures for in-orbit spacecraft survivability
[NASA-CR-179216] 04 p0408 N88-12532
Space suit extravehicular hazards protection development
[NASA-TM-100458] 04 p0475 N88-12927
Space environmental considerations for a long-term cryogenic storage vessel 08 p0981 N88-15933
Space station integrated wall damage and penetration damage control. Task 5: Space debris measurement, mapping and characterization system
[NASA-CR-179281] 10 p1285 N88-17688
An analysis of penetration and ricochet phenomena in oblique hypervelocity impact
[NASA-TM-100319] 10 p1339 N88-18004
A review of impact design criteria for space power heat rejection systems 17 p2410 N88-24333

METEOROID SHOWERS
NT AQUARID METEOROIDS
NT GEMINID METEOROIDS
NT ORIONID METEOROIDS
NT PERSEID METEOROIDS
NT QUADRANTID METEOROIDS
NT TAURID METEOROIDS
Meteor-burst communications: Is this what the Navy needs?
[AD-A184433] 04 p0431 N88-12672
Middle Atmosphere Program. Handbook for MAP, volume 25
[NASA-CR-181571] 06 p0732 N88-14502
Dynamics of meteor streams
06 p0732 N88-14503
Elementary process and meteor train spectra
06 p0732 N88-14504
Main results of atmospheric fine structure parameter observation in the lower thermosphere
06 p0735 N88-14518
On connection between evolution of troposphere fronts and changes of circulation regime in meteor zone
06 p0735 N88-14519
Study of internal gravity waves in the meteor zone
06 p0735 N88-14521
The role of fragmentation in interaction of meteoroids with the Earth's atmosphere 06 p0737 N88-14532
On the meteor trail spectra 06 p0737 N88-14533
A processing method and results of meteor shower radar observations 06 p0738 N88-14539
Photographic fireball networks
06 p0738 N88-14540
On meteor stream spatial structure theory
06 p0739 N88-14544
The Valec fireball and predicted meteorite fall
06 p0739 N88-14547
Results of observations of the Eta Aquarid and Orionid meteor showers in 1980-1984 06 p0740 N88-14548
Monte Carlo modeling and meteor showers
06 p0740 N88-14549
On the spatial structure of the Perseids meteor stream
06 p0740 N88-14550
Some models of the Geminids meteor stream formation 06 p0740 N88-14551
Structural peculiarities of the Quadrantid meteor shower 06 p0740 N88-14552
On the possible origin of meteoroid generating asteroid orbits 06 p0740 N88-14553
New approaches to some methodological problems of meteor science 06 p0741 N88-14557
Hard- and software problems of spaced meteor observations by optical electronics
06 p0741 N88-14560
The evolution of the mass distribution of cometary particles 14 p2004 N88-21946
Communications using channels formed by meteor bursts
[AD-A192088] 18 p2501 N88-24834
A study of a meteor burst communication system
21 p2934 N88-27421

METEOROIDS
NT AQUARID METEOROIDS
NT BOLIDES
NT GEMINID METEOROIDS
NT MICROMETEOROIDS
NT ORIONID METEOROIDS
NT PERSEID METEOROIDS
NT QUADRANTID METEOROIDS
NT SPORADIC METEOROIDS
NT TAURID METEOROIDS
NT ZODIACAL DUST
Ozone formation due to interaction of meteoroids with Earth's atmosphere 06 p0738 N88-14536
Meteor detection on ST (MST) radars
06 p0740 N88-14554
The Cyclone meteor radar system for routine wind measurements in the lower thermosphere
06 p0741 N88-14555
Optical electronics for meteor observations
06 p0741 N88-14559
Effects of meteoroids and space debris on the particulate environment for space station 18 p2591 N88-25399

METEOROLOGICAL BALLOONS
NT JIMSPHERE BALLOONS

METEOROLOGICAL CHARTS
New precipitation map of world ocean
04 p0458 N88-12834
Mariners weather log, volume 31, number 4, Fall 1987
[PB88-173851] 20 p2825 N88-26761
Meteorological atlas of the Southern Hemisphere lower stratosphere for August and September 1987
[NASA-TM-4049] 20 p2825 N88-26763
The 1985 Meteorological Yearbook of Ispra (27th)
[PB88-125729] 20 p2828 N88-26777
Intercomparison of NMC (National Meteorological Center) and ECMWF (European Centre for Medium Range Weather Forecasts) global analyses: 1980-1986
[PB88-196548] 21 p2974 N88-27668

METEOROLOGICAL FLIGHT
Definition and use of sensors for measuring electrical conductivity in thunderclouds
[ESA-TT-1047] 03 p0352 N88-12222

METEOROLOGICAL INSTRUMENTS
NT BAROMETERS
NT CLOUD HEIGHT INDICATORS
NT IONOSONDES
NT RADIOSONDES
NT RAIN GAGES
NT RAWINSONDES
BARS-1M meteorological complex carried on IL-18 airplane 06 p0725 N88-14458
On-site meteorological program guidance for regulatory modeling applications
[PB87-227542] 06 p0731 N88-14498
Air temperature shield tests
[AD-A187459] 11 p1514 N88-19043
MRS-3000 meteorological rocket probe for the MMR-06 dart integrated meteorological rocket system
[NASA-TT-20303] 19 p2693 N88-26010
The pneumatic wind shear sensor: A tool for meteorological investigations and flight management
22 p3036 N88-28024

METEOROLOGICAL PARAMETERS
Effects on electromagnetic wave propagation at frequencies over 10 GHz due to inhomogeneities of the complex refraction index
[REPT-86-025] 01 p0036 N88-10228
Conception and discussion of a model describing ice formation on various obstacles
[ONERA-NT-1986-6] 01 p0072 N88-10460
A mini system for nowcasting
02 p0204 N88-11278
Use of time changes of surface data parameters in short range forecasting 02 p0206 N88-11291
An isentropic mesoscale analysis system
02 p0212 N88-11332
Experimental study of the propagation of an acoustic wave in the low atmosphere
[ISL-R-111/86] 02 p0231 N88-11454
The CNR/PSN Advanced Microwave Imaging Radiometer (AMIR) --- satellite-borne
03 p0340 N88-12141
Application of multitemporal SPOT data for crop monitoring: Effects of frost and drought
03 p0344 N88-12171
Documentation of NCAR (National Center for Atmospheric Research) CCM1 program modules
[PB87-213567] 03 p0352 N88-12220
Global atmospheric circulation statistics: Four year averages
[NASA-TM-100690] 05 p0628 N88-13842
Results on the low elevation angle propagation experiment, part 1
[TUD-R-328] 06 p0693 N88-14250
Middle Atmosphere Program. Handbook for MAP, volume 25
[NASA-CR-181571] 06 p0732 N88-14502
The climatic wind regime in the lower thermosphere from meteor radar observations 06 p0733 N88-14506
Report of the second session of the CAS/JSC working group on numerical experimentation --- weather forecasting
[WMO/TD-168] 06 p0745 N88-14579
Eighth Session of the Commission for Aeronautical Meteorology (abridged)
[WMO-673] 06 p0745 N88-14585

Facilities for research and weather observations on the 213 m tower at Cabauw (Netherlands) and at remote locations
[KNMI-WR-87-5] 06 p0746 N88-14587
Three dimensional display of meteorological scientific data
[DE88-000776] 07 p0880 N88-15339
Influence of Environmental Factors on Aircraft Wing Performance
[VKI-LS-1987-03] 08 p0951 N88-15771
Characterization of meteorological phenomena influencing aircraft operations 08 p0951 N88-15772
The influence of wind shear, downdraft, and turbulence in aircraft performance 08 p0952 N88-15773
The potential influence of rain on airfoil performance 08 p0952 N88-15774
Revised uniform summary of surface weather observations. Parts A-F: Carswell AFB, Texas
[AD-A186820] 09 p1192 N88-17144
Modification of a successive corrections objective analysis for improved higher order calculations
[NASA-CR-182467] 09 p1230 N88-17370
Development of an engineering model atmosphere for Mars
[NASA-CR-182462] 09 p1263 N88-17568
NASA Oceanic Processes Program
[NASA-TM-4025] 10 p1357 N88-18109
Long term measurement network for FIFE
[NASA-CR-182491] 12 p1646 N88-19857
Calibration of the solar radiation estimation method by satellites
[INPE-4349-PRE/1185] 12 p1646 N88-19861
Quality control of upper air conventional data (TEMP and PILOT)
[INPE-4223-RPE/546] 12 p1647 N88-19862
Remote sensing of meteorological parameters with the aid of a clear-air Doppler radar
[PB88-142518] 12 p1647 N88-19864
Worldwide distributions of shipboard surface meteorological observations for EM propagation analysis
[AD-A188771] 12 p1648 N88-19871
Climatology and space observations
[ISBN-2-85-428179-9] 14 p1935 N88-21536
Global meteorological data facility for real-time field experiments support and guidance
[NASA-TM-4023] 14 p1947 N88-21608
Local meteorological processes and air mass origin during a cloud chemical field experiment on Areskutan, Sweden, in summer 1986
[AP-28] 14 p1948 N88-21615
Analysis of meteorological conditions and haze distribution for the Second Arctic Gas and Aerosol Sampling Program (AGASP 2), March-April 1986
[PB88-164140] 14 p1948 N88-21618
Tropic heat MR (Meteorological Recorder) meteorological data (April 1984 - June 1985)
[PB88-161286] 14 p1948 N88-21620
A study on electric fields and conductivity associated with electrified clouds in the region of South America
[INPE-4487-TDL/325] 15 p2096 N88-22486
A multivariate variational objective analysis-assimilation method. Part 1: Development of the basic model
[NASA-CR-182651] 15 p2097 N88-22491
Acoustic propagation in the low atmosphere. Experimental study and modeling by the radius method
[ISL-CO-247/86] 15 p2131 N88-22713
Use of energy emission for detecting the necessity of irrigation in wheat in field conditions
[INPE-4461-TDL/318] 16 p2229 N88-23315
Spectroradiometry in meteorology 16 p2272 N88-23599
Ice formation on aircraft
[ETN-88-92154] 18 p2545 N88-25104
Effects of atmospheric model layering on LOWTRAN 6 calculations of 8-12 micrometers near-horizon sky radiances
[AD-A192969] 20 p2791 N88-26559
The 1985 Meteorological Yearbook of Ispra (27th)
[PB88-125729] 20 p2828 N88-26777
Intercomparison of NMC (National Meteorological Center) and ECMWF (European Centre for Medium Range Weather Forecasts) global analyses: 1980-1986
[PB88-196548] 21 p2974 N88-27668
The Hanford meteorological data collection system and data base
[DE88-008632] 21 p2975 N88-27672
Space shuttle natural environment analysis
[NASA-CR-179337] 21 p2976 N88-27676
SERI standard broadband format: A solar and meteorological data archival format
[DE88-001145] 21 p3028 N88-27975
The effects of changes in observation and data assimilation systems on CAC climate data sets 22 p3124 N88-28568
Evaluation of global data sets for climate studies 22 p3124 N88-28569
A method to adjust climatological time series for discontinuous inhomogeneities 22 p3124 N88-28570
A comparison of typical meteorological year solar radiation information with the SOLMET data base
[DE88-009242] 23 p3234 N88-29247
Microwave remote sensing at INPE (Institute for Space Research) Brazil: Concepts and future prospects of soil moisture studies
[INPE-4569-PRE/1310] 24 p3388 N88-30178

METEOROLOGICAL PROBES
U SONDES

METEOROLOGICAL RADAR
COST-73 and its application in very short range forecasting 02 p0199 N88-11242
New nowcasting opportunities using modern meteorological radar 02 p0199 N88-11245
Nowcasting microbursts using Doppler radar in a forecaster-computer environment 02 p0200 N88-11246
Use of a 5 cm Doppler radar to detect and forecast severe thunderstorms in a real time forecast operation 02 p0200 N88-11247
Thunderstorm nowcasting using Doppler radar and soundings 02 p0200 N88-11248
A real-time system for automatic single-Doppler wind field analysis 02 p0200 N88-11249
Diagnosing short term changes in temperature and moisture profiles from single Doppler radar 02 p0200 N88-11251
On the interaction between radar and satellite image nowcasting systems and mesoscale numerical models 02 p0204 N88-11277
Evaluation of the Rainsat precipitation analysis system in real-time use 02 p0205 N88-11283
The Pacific Weather Center Satellite Facility: An overview 02 p0205 N88-11286
Specification of predictors necessary for the determination of over or underestimation of radar derived total rainfall
[AD-A185363] 05 p0628 N88-13838
Waveform for short-dwell-time meteorological Doppler radars
[PB88-102199] 07 p0845 N88-15126
Development of a Doppler wind lidar system for atmospheric wind measurements 08 p1027 N88-16217
Improved resolution atmospheric density measurements based on simulations 08 p1027 N88-16221
Meteorological radar and its usage in the Navy
[AD-A186650] 09 p1152 N88-16902
Airborne Doppler radar technology for wind shear detection 10 p1274 N88-17622
Status of FAA terminal Doppler weather radar programs 10 p1275 N88-17632
Information transfer in the National Airspace System 10 p1275 N88-17634
Research and development to acquire and reduce melting layer cloud physics and evaluate a prototype M-meter
[AD-A188390] 12 p1648 N88-19873
A polarization diversity meteorological radar system
[AD-A189291] 13 p1758 N88-20515
TDWR (Terminal Doppler Weather Radar) clutter residue map generation and usage
[AD-A191148] 16 p2235 N88-23352
Observation of stratiform rain with 94 GHz and s-b and Doppler radar
[AD-A192013] 18 p2544 N88-25100
Remote sensing of temperature profiles. Performance test of PASS
[DE88-753108] 20 p2826 N88-26768
A radar study of the interaction between lightning and precipitation
[DE88-009120] 20 p2827 N88-26770
TDWR (Terminal Doppler Weather Radar) PRF (Pulse Repetition Frequency) selection criteria
[AD-A193089] 21 p2932 N88-27407
Utilization of a single clear-air Doppler radar beam to measure vertical divergence
[AD-A195543] 24 p3405 N88-30271

METEOROLOGICAL ROCKETS
U SOUNDING ROCKETS

METEOROLOGICAL SATELLITES
NT DMSP SATELLITES
NT METEOSAT SATELLITE
NT NIMBUS 7 SATELLITE
NT NOAA SATELLITES
NT NOAA 7 SATELLITE
NT TIROS N SERIES SATELLITES
NT TIROS SATELLITES
Improved geostationary satellite soundings for the mesoscale weather analysis/forecast operation 02 p0200 N88-11252
Impact of a direct assimilation of satellite-inferred precipitation rates into a regional meteorological model 02 p0213 N88-11342
Fabricate, calibrate and test a dosimeter for integration into the CRRES (Combined Release and Radiation Effects Satellite) satellite
[AD-A185439] 05 p0585 N88-13564
Estimation of marine boundary layer depth and relative humidity with multispectral satellite measurements
[AD-A184881] 05 p0620 N88-13804
Country plans three-axis weather satellite 06 p0688 N88-14218
Regional weather satellite data processing center opens in Tashkent 06 p0725 N88-14457
Suggested severe local storm operational scenario for GOES I-M
[NASA-TM-100688] 11 p1515 N88-19052
Space projects for the 90's relevant to climatology 14 p1935 N88-21539
Satellite rainfall retrieval by logistic regression
[NASA-CR-180485] 14 p1946 N88-21607
Global meteorological data facility for real-time field experiments support and guidance
[NASA-TM-4023] 14 p1947 N88-21608
Baseline observing system experiments using the AFGL global data assimilation system
[AD-A188861] 15 p2024 N88-22062
A multivariate variational objective analysis-assimilation method. Part 2: Case study results with and without satellite data
[NASA-CR-182653] 15 p2097 N88-22492
Meteorological Satellite Center Technical Note No. 16
[ISSN-0388-9653] 17 p2350 N88-24003
Prospects of satellite wind sensing systems in the years 1995-2000 17 p2350 N88-24004
Outline of the GPCP strategy 17 p2351 N88-24007
VISSR line number monitoring system 17 p2351 N88-24008
Contribution of space to marine activities 19 p2700 N88-26057
Meteorological satellite product support and research for project GALE
[NASA-CR-180989] 19 p2727 N88-26193
Satellite remote sensing of the wet bulb globe temperature heat stress index, phase 2
[AD-A192798] 20 p2818 N88-26717
The effects of changes in observation and data assimilation systems on CAC climate data sets 22 p3124 N88-28568
Global-scale temperature changes to August 1987 and a comparison of satellite and conventional data 22 p3125 N88-28572
Investigations of magnetosphere-ionosphere coupling relevant to operational systems
[AD-A195972] 24 p3391 N88-30195
Passive microwave measurements of water vapor fields and rain for locating fronts in cyclonic storms
[AD-A195632] 24 p3404 N88-30267
Analytical method for approximate geodetic referencing of scanner images of meteorological artificial earth satellites using control points 24 p3449 N88-30527

METEOROLOGICAL SERVICES
Applications and benefits of short period weather forecasts 02 p0199 N88-11240
Mesoscale forecasting today and tomorrow: Problems and opportunities. A position paper 02 p0199 N88-11244
Meteorological systems support to critical shuttle requirements on the Eastern Test Range — STS 02 p0205 N88-11281
The Pacific Weather Center Satellite Facility: An overview 02 p0205 N88-11286
Mesoscale analysis and forecasting for the 1987 America's Cup, Fremantle, Western Australia 02 p0214 N88-11350
Regional weather satellite data processing center opens in Tashkent 06 p0725 N88-14457
Current status of world weather service 06 p0725 N88-14459
Wave and wind data sources, environmental conditions committee report, International Ship and Offshore Structures Congress
[PB87-234902] 06 p0746 N88-14588
Federal plan for meteorological services and supporting research, fiscal year 1988
[PB88-118716] 07 p0880 N88-15336
WMO Region 2/Region 5 Training Seminar on Climate Data Management and User Services
[WCP-133] 16 p2234 N88-23344
A drought watch system
[WCP-134] 16 p2234 N88-23345

METEOROLOGICAL STATIONS
U WEATHER STATIONS

METEOROLOGY
NT AEROLOGY
NT AGROMETEOROLOGY
NT ALPINE METEOROLOGY
NT AVIATION METEOROLOGY
NT HYDROMETEOROLOGY
NT LONG RANGE WEATHER FORECASTING
NT MARINE METEOROLOGY
NT MESOMETEOROLOGY
NT MICROBURSTS (METEOROLOGY)
NT MICROMETEOROLOGY
NT NOWCASTING
NT NUCLEAR METEOROLOGY
NT NUMERICAL WEATHER FORECASTING
NT POLAR METEOROLOGY
NT RADIO METEOROLOGY
NT STATISTICAL WEATHER FORECASTING
NT SYNOPTIC METEOROLOGY
NT TROPICAL METEOROLOGY
NT WEATHER FORECASTING
Diagnostics of atmospheric chemistry through ozone measurement
[INPE-4230-PRE/1105] 01 p0068 N88-10437
Solar Energy Meteorological Research and Training Site, Alaska
[DE87-013706] 01 p0069 N88-10440
Hanford Meteorological Station computer codes. Volume 1: The GEN computer code
[DE87-012816] 01 p0071 N88-10456
Hanford Meteorological Station computer codes. Volume 2: The PROD computer code
[DE87-014807] 02 p0215 N88-11355
Convective cross section analysis
[PB87-204566] 02 p0216 N88-11361
Publications and final reports on contracts and grants, 1986 (National Environmental Satellite, Data and Information Service)
[PB87-220810] 03 p0352 N88-12218
Short reference year
[PB87-107470] 03 p0352 N88-12221
Study of an airborne Doppler radar: Project Asterix
[BLL-MO-TRANS-1667-(9022.552)] 04 p0432 N88-12675
USSR report: Earth sciences
[JPRS-UES-86-006] 04 p0458 N88-12831
Application of TOMS data to weather analysis models 05 p0617 N88-13787
USSR report: Earth sciences
[JPRS-UES-87-004] 06 p0725 N88-14455
AN-30M cloud-seeding airplane in international exhibition 06 p0725 N88-14456
Current status of world weather service 06 p0725 N88-14459
CTD/02 measurements during 1984 and 1985 as part of the Equatorial Pacific Ocean Climate Studies (EPOCS)
[PB88-102082] 06 p0748 N88-14600
USSR report: Earth sciences
[JPRS-UES-87-003] 08 p1009 N88-16119
Application of satellite data in variational analysis for global cyclonic systems
[NASA-CR-182468] 09 p1193 N88-17152
NASA wind shear model: Summary of model analyses 10 p1273 N88-17617
Cape Blanco wind farm feasibility study
[DE88-003748] 10 p1348 N88-18059
Wake effects in a Fayette 95-IIS wind turbine array
[DE88-001103] 10 p1349 N88-18063
The structure and dynamics of monsoon depressions 10 p1355 N88-18102
Developments in National Weather Service meteorological data collection programs as related to EPA (Environmetal Protection Agency) air pollution models
[PB88-130240] 10 p1356 N88-18104
Refractive index, meteorology and fading in line-of-sight transmission paths 12 p1616 N88-19666
The correlation between methodological and low-level angle-of-arrival measurements 12 p1617 N88-19668
Historical electromagnetic propagation condition database description
[AD-A189157] 12 p1621 N88-19695
A study of satellite emission computed tomography
[AD-A189567] 13 p1797 N88-20745
A multivariate variational objective analysis-assimilation method. Part 2: Case study results with and without satellite data
[NASA-CR-182653] 15 p2097 N88-22492
The collection of statistics on the frequency of cloud cover over North America
[AD-A190456] 15 p2097 N88-22495
Evaluation of NMC (National Meteorological Center) global analyses: 1979-1987
[PB88-178157] 18 p2544 N88-25096
Taiwan area mesoscale experiment: P-3 aircraft operations summary
[PB88-169073] 18 p2544 N88-25098
NOAA (National Oceanic and Atmospheric Administration) Meteorology Division support to the Environmental Protection Agency
[PB88-179866] 19 p2689 N88-25980
Meteorological satellite product support and research for project GALE
[NASA-CR-180989] 19 p2727 N88-26193
Our climate in danger
[DE88-701824] 20 p2822 N88-26743
An evaluation of two millimeter wave propagation models for horizontal atmospheric attenuation at 70-115 GHZ
[AD-A192699] 21 p2931 N88-27403
Update on the meso-microscale meteorological hierarchy
[DE88-009133] 21 p2975 N88-27670
A comparison of typical meteorological year solar radiation information with the SOLMET data base
[DE88-009242] 23 p3234 N88-29247
Activities report of the World Meteorological Organization
[WMO-689] 24 p3404 N88-30265
METEORS
U METEOROIDS
METEOSAT SATELLITE
Study on data compression systems for operational remote sensing --- meteosat imagery
[NLR-TR-86029-L] 05 p0620 N88-13808
The Meteosat operational program 09 p1127 N88-16759
Meteorological Information Extraction Center (MIEC) processing --- Meteosat imagery
[ESA-STR-224] 09 p1192 N88-17143
Introduction to the Meteosat system
[ESA-SP-1041] 09 p1193 N88-17146
La Recherche Aerospatiale, bimonthly bulletin, number 1987-2, 237/March-April
[ESA-TT-1074] 11 p1433 N88-18550
Presentation of the METEOSAT system and the roles of EUMETSAT within the meteorological community 17 p2357 N88-24039
METERS
U MEASURING INSTRUMENTS
METHACRYLATE RESINS
U ACRYLIC RESINS
METHANE
Reduction of CO2 to methanol and methane by photo and dark reactions on semiconductor and metal electrodes
[PB87-226825] 02 p0156 N88-10975
Pulsed plasma jet igniters: Species measurements in methane combustion
[DE88-001389] 05 p0562 N88-13422
A process study of the biothermal conversion of water hyacinths to methane
[DE88-000554] 06 p0730 N88-14488
Catalytic combustion of methane
[PB88-123112] 07 p0829 N88-15028
Gas hydrate model development and validation
[DE88-001004] 10 p1298 N88-17762
Geological evolution and analysis of confirmed or suspected gas hydrate localities. Volume 9: Formation and stability of gas hydrates of the Middle America Trench
[DE88-001007] 10 p1347 N88-18050
Novel catalysts for methane activation
[DE88-003637] 13 p1738 N88-20390
Oxide-bound transition metal complexes for methane activation
[PB88-169719] 14 p1887 N88-21277
Basic research on natural gas combustion phenomena
[PB88-168380] 14 p1887 N88-21278
Evaluation of direct methane conversion to higher hydrocarbons and oxygenates
[DE88-003812] 15 p2049 N88-22204
A theoretical model of the washout of trace gases by raindrops in the atmosphere 17 p2375 N88-24125
Probing the possibility of a (12)C/(13)C abundance gradient from observations of interstellar CH+
[DE88-008908] 20 p2884 N88-27125
On the bond distance in methane
[NASA-CR-181436] 22 p3150 N88-28741
Molecular composites processing and properties, 1
[AD-A194113] 23 p3189 N88-28974
The design of methane activation catalysts
[DE88-002265] 23 p3199 N88-29043
Ultraviolet absorption cross sections of chloro- and chlorofluoromethanes at stratospheric temperatures
[AERONOMICA-ACTA-A-324-1988] 23 p3231 N88-29228
METHANOL
U METHYL ALCOHOL
METHOD OF CHARACTERISTICS
The linear characteristic method in XYZ geometry
[DE87-011668] 04 p0484 N88-12984
Analysis and optimization of truncated scarf nozzles subject to external flow conditions
[NASA-TM-100955] 24 p3316 N88-29746
METHOD OF MOMENTS
Treatment of small wire loops in the method of moments code NEC (Numerical Electromagnetics Code)
[DE88-002995] 07 p0846 N88-15136
Electromagnetic scattering from and natural resonances of the circular strip 13 p1759 N88-20523
The new MININEC (version 3): A mini-numerical electromagnetic code
[AD-A191778] 19 p2642 N88-25675
METHODOLOGY
A design methodology for the utilization of metrics within various phases of software lifecycle models
[DE87-010519] 02 p0220 N88-11385
A flight-test methodology for identification of an aerodynamic model for a V/STOL aircraft
[NASA-TM-100067] 09 p1117 N88-16694
Approaches to the verification of rule-based expert systems 09 p1206 N88-17232
A methodology for the synthesis of robust feedback systems
[NASA-CR-182455] 09 p1225 N88-17342
Space station operating system study
[NASA-CR-179308] 11 p1446 N88-18619
Structural analysis methods development for turbine hot section components
[NASA-TM-100298] 11 p1501 N88-18967
The formal specification of computer systems
[AD-A188947] 12 p1675 N88-20013
Design of feedback control systems for stable plants with saturating actuators
[NASA-CR-182613] 12 p1681 N88-20050
Avionics acquisition, trends and future approaches 12 p1702 N88-20184
A comparison of information system development methodologies
[AD-A188957] 12 p1707 N88-20219
Active cooling design for scramjet engines using optimization methods
[NASA-TM-100581] 13 p1783 N88-20669
METHODS
U METHODOLOGY
U PROCEDURES
METHYL ALCOHOL
Reduction of CO2 to methanol and methane by photo and dark reactions on semiconductor and metal electrodes
[PB87-226825] 02 p0156 N88-10975
Alternative fuels: Information on DOD's (Department of Defense's) methanol vehicle program
[PB87-213328] 02 p0156 N88-10976
Application of electronic fuel injection to the optimum engine for methanol utilization
[PB87-201950] 02 p0180 N88-11120
Model Cu/ZnO catalysts for methanol synthesis: The role of surface structure
[DE88-002354] 07 p0830 N88-15037
Fuel cell/battery hybrid vehicle assessment
[DE88-005087] 10 p1427 N88-18520
Practical system for the use of alcohol in diesel engines
[PB88-147863] 12 p1612 N88-19638
Alternative fuels: Information on DOE's (Department of Energy's) methanol vehicle demonstration program
[PB88-118203] 13 p1753 N88-20481
Combustion and performance characteristics of methanol plus higher alcohols in a spark ignition engine
[PB88-147962] 14 p1918 N88-21451
Technical highlights of the Alternative Fuels Utilization Program
[DE88-005064] 15 p2049 N88-22205
Improvements to Raney copper zinc methanol synthesis catalysts 17 p2318 N88-23844
Update of low temperature catalyst development
[DE88-007032] 18 p2480 N88-24715
METHYL COMPOUNDS
NT ACETONITRILE
Thermally stable aromatic structures from acyclic precursors. 1. Para polyphenylene model compounds from 3-Dimethyl amino hex-5-EN-1-YNES
[AD-A185300] 05 p0568 N88-13462
Heterogeneous isotope exchange between solid cesium iodide and gaseous methyl iodide
[ETN-88-91085] 09 p1141 N88-16840
Ultraviolet absorption cross sections of methylbromide at stratospheric temperatures
[AERONOMICA-ACTA-A-320-1987] 15 p2036 N88-22132
Corrosion and corrosion inhibition of metals/alloys in methyphosphonic difluoride 17 p2319 N88-23850
Modification of polymers by photografting processes 17 p2323 N88-23871
Preferential surface adsorption in miscible blends of polystyrene and poly(vinyl methyl ether)
[AD-A191451] 18 p2490 N88-24769

Stratospheric positive ion composition measurements and acetonitrile detection: A consistent picture
[AERONOMICA-ACTA-A-326-1987] 18 p2542 N88-25084
Dissolution rates of polymers and copolymers based on methyl, ethyl and butyl methacrylate
[AD-A194713] 23 p3197 N88-29027

METHYL CYANIDE
U ACETONITRILE

METHYLENE
Evidence for first polymer in Comet Halley: Polyoxymethylene 14 p1997 N88-21906

METRIC CONVERSION
U METRICATION

METRIC PHOTOGRAPHY
Accuracy potential of non-metric cameras in close-range photogrammetry 04 p0463 N88-12862
Investigations on the application of space photographs (Spacelab metric camera) for routine inventories of extensively managed forest areas
[DFVLR-FB-87-22] 09 p1185 N88-17098

METRIC SPACE
NT HILBERT SPACE
Nonsymmetric metrics in nonlinear field theory
[DE88-700509] 07 p0913 N88-15537
Heuristic search in robot configuration space using variable metric 08 p1059 N88-16389
Solving reflexive domain equations in a category of complete metric spaces
[CWI-CS-R8709] 13 p1832 N88-20956
On the Fefferman class of metrics associated with a 3-dimensional Cauchy-Riemann (CR)-space
[PREPRINT-579] 14 p1991 N88-21865
Einstein metrics and Brans-Dicke superfields
[DE88-006992] 15 p2146 N88-22809
Pairwise complete regularity as a separation axiom
[REPT-87-57] 16 p2264 N88-23539

METRIC SYSTEM
U INTERNATIONAL SYSTEM OF UNITS

METRICATION
ADAMEASURE: An implementation of the Halstead and Henry metrics
[AD-A184005] 03 p0365 N88-12299

METROLOGY
Precision metrology comparing ultrasonic and other techniques for the determination of steel thickness
[DE87-011051] 02 p0230 N88-11452
Metrology and calibrating laboratories
[ETN-88-90761] 06 p0670 N88-14104
Temperature Metrology '86
[DE88-700236] 08 p0989 N88-15990
Results from a questionnaire on particulate metrology in the UK
[NPL-MOM-81] 09 p1141 N88-16841
Evaluation of a miniature horizontal pendulum tilt transducer 12 p1577 N88-19435
The effects of humidity on the profile of photographic plates
[NPL-DMOM-88] 14 p1913 N88-21429
Development and applications of optical interferometric micrometrology in the angstrom and subangstrom range
[NASA-TM-100299] 16 p2211 N88-23196
Calibration technique and study on metrological characteristics of a high-voltage inverse square-law function generator
[DE88-702101] 22 p3072 N88-28236
Langley Research Center Metrology Program status for fiscal year 1987
[NASA-TM-100651] 22 p3086 N88-28324
Metrology in France: Industrial aspects and its status in the world
[SNIAS-881-430-109] 22 p3146 N88-28713
Electromagnetic metrology 24 p3363 N88-30024

METROPOLITAN AREAS
U CITIES

MEXICO
Varifront 3 expedition data report (USNS DE STEIGUER CRUISE 1202-82). Bioluminescence, hydrographic, nutrient, and satellite data from the Gulf of California (November-December 1981)
[AD-A185011] 05 p0620 N88-13805
Land use systems and rural landscapes in the center of Veracruz State (Mexico): First results
22 p3092 N88-28364

MGCO
U MARS OBSERVER

MICA
NT BIOTITE

MICE
A learning model as a basis for investigations of the effects of gravity on the learning processes and memory formulation 07 p0886 N88-15374
Changes in functional parameters of animals during long-term inhalation of acetic acid
07 p0895 N88-15423
Effect of pyrocetam on mouse resistance to hypoxic hypoxia 2-3 months after exposure to X-radiation
07 p0895 N88-15425
Scaling physiological pharmacokinetic models by physiological time
[DE88-000335] 10 p1368 N88-18173
Life sciences research in space: The requirement for animal models 12 p1654 N88-19909
The effect of microgravity on mammalian cell polarization at the ultrastructural level --- Spacelab D1 mission
22 p3061 N88-28164

MICHELSON INTERFEROMETERS
Photodiode matrix for the analysis of two-beam interferences
[PTB-OPT-23] 01 p0048 N88-10310
Milliarcsecond ground-based imaging with single telescopes 01 p0097 N88-10637
A test-bed for space interferometry: Space Platform Interferometer (SPI) 01 p0097 N88-10640
Performances of an Actively Stabilized Stellar Interferometer (ASSI): Faint magnitudes, low fringe contrast measurements and operationality
01 p0097 N88-10641
Optical fiber interferometric sensor to measure temperature in gas flow
[ENST-87E006] 02 p0170 N88-11071
On the theory of the Michelson-Morley experiment in the Earth's gravitational field
[DE87-703077] 02 p0198 N88-11233
Optical determination of the virial coefficients of the gases C2H4, C2H6 and SF6
[ETN-87-90610] 03 p0282 N88-11776
Phase-coherent astrometric interferometry
[AD-A184428] 04 p0439 N88-12725
Fiber optic single mode sensors
[FOA-C-30453-3.1] 06 p0780 N88-14790
Telescope design for Michelson interferometer for Passive Atmospheric Sounding (MIPAS) B
08 p1017 N88-16167
Computerized evaluation of interferograms of the Michelson Interferometer for Passive Atmospheric Sounding (MIPAS) Laboratory Model (LM)
08 p1019 N88-16177
Modern pulsed wavemeters
[DE88-003875] 10 p1335 N88-17978
Investigations in electro-optical multistability for signal processing 18 p2518 N88-24938
An interferometric measurement technique for railgun structures
[AD-A192851] 21 p2901 N88-27217
Investigations on Mie and Rayleigh scattering as basis for the development of Rayleigh temperature lidars with aid of Michelson interferometry
[GKSS-87/E/62] 21 p2976 N88-27675
Piezoelectric and electrostrictive materials for transducer applications, volume 2
[AD-A194956] 24 p3376 N88-30104

MICHIGAN
Aircraft accident report: Northwest Airlines, Inc., McDonnell Douglas DC-9-82, N312RC, Detroit Metropolitan Wayne County Airport, Romulus, Michigan, August 16, 1987
[PB88-910406] 19 p2601 N88-25449

MICROANALYSIS
Electron sputtering in the analytical electron microscope: Calculations and experimental data
[DE87-011457] 01 p0049 N88-10312
Multidimensional elemental analysis with the Sandia nuclear microprobe
[DE87-014158] 02 p0183 N88-11136
Development of an X-ray fluorescence microprobe at the National Synchrotron Light Source, Brookhaven National Laboratory: Early results: Comparison with data from other techniques
[NASA-CR-181468] 02 p0236 N88-11486
Quantitative electron probe microanalysis investigation of the oxidation of high temperature alloys at low oxygen partial pressures
[JUEL-2120] 03 p0288 N88-11811
X-ray microfluorescence analysis of thin- and thick-sectioned geologic materials
[DE87-009803] 09 p1189 N88-17126
Atom probe microanalysis of superconducting YBa2Cu3O(sub 7-x)
[DE88-003203] 11 p1557 N88-19322
Development, high temperature properties, and microanalysis of nonoxide ceramics
[ETN-88-92103] 14 p1893 N88-21304
Advances in geochemistry and cosmochemistry: Trace element microdistributions with the synchrotron X-ray fluorescence microprobe
[DE88-006355] 15 p2032 N88-22108
Microchemical analysis of polycrystalline Ni3Al and other ordered alloys using the field-ion microscope atom probe
[DE88-011519] 21 p2914 N88-27294
Thin film and near-surface characterization using a mechanical properties microprobe
[DE88-011399] 21 p2915 N88-27302
Superconducting oxides with high critical temperatures
21 p2930 N88-27392

MICROBE
U MICROORGANISMS

MICROBIOLOGY
NT BACTERIOLOGY
JPRS report: Science and technology. USSR: Life sciences
[JPRS-ULS-87-009] 04 p0473 N88-12915
Review of cytoskeleton research in cell differentiation and development
[AD-A185832] 07 p0882 N88-15353
Safety guidelines and procedures for bioscience-based industry and other applied microbiology
[PB87-140521] 08 p1045 N88-16316
USSR report: Life sciences. Biomedical and behavioral sciences
[JPRS-UBB-87-010] 12 p1651 N88-19889
JPRS report: Science and technology. USSR: Life sciences
[JPRS-ULS-88-002] 12 p1665 N88-19982
Digital image processing from speckle interferograms by correlation methods: Application in atmospheric optics, astronomy, and biology
[ETN-88-92125] 20 p2855 N88-26953
Quality control in microbiology: CDC lab manual
[PB88-179890] 23 p3237 N88-29263

MICROBURSTS (METEOROLOGY)
Study of microburst detection performance during 1985 in Memphis, Tennessee
[AD-A184013] 03 p0354 N88-12231
Power spectral density analysis of wind-shear turbulence for related flight simulations
[NASA-CR-182721] 13 p1802 N88-20773
Flight penetration of wind shear: Control strategies
17 p2294 N88-23727
The Federal Aviation Administration/Massachusetts Institute of Technology (FAA/MIT) Lincoln Laboratory Doppler weather radar program
18 p2547 N88-25118
Flight-management strategies for escape from microburst encounters
[NASA-TM-4057] 19 p2603 N88-25461
Influence of wind shear on the aerodynamic characteristics of airplanes
[NASA-TP-2827] 20 p2755 N88-26344
Control of flight through microburst wind shear using deterministic trajectory optimization
20 p2761 N88-26375

MICROCALORIMETERS
U CALORIMETERS

MICROCHANNEL PLATES
A neutron detector based on microchannel plates
[DE87-014703] 02 p0232 N88-11466
A high-speed, eight-frame image intensified electro-optic camera with 200-800mm zoom objective capability
[DE88-000229] 03 p0326 N88-12059
Performance of a photon counting microchannel plate intensifier with wedge and strip image readout
[DE88-003831] 10 p1334 N88-17970
Conception and realization of components for a microchannel-plate detector, and testing of the detector system in the laboratory and in astronomical use
[ETN-88-91495] 11 p1491 N88-18899
The off-axis channel macroplate
[NASA-CR-182938] 18 p2505 N88-24861
An elliptical spectrograph/gated microchannel plate detector for time-resolved spectral measurements in the X-ray region
[DE88-007590] 20 p2856 N88-26961

MICROCHANNELS
A focussed MCP (microchannel plate) image intensifier type for high speed gating
[DE88-000480] 05 p0583 N88-13555
Forced-convection, liquid-cooled, microchannel heat sinks
[AD-A193337] 21 p2937 N88-27444

MICROCIRCUITS
U MICROELECTRONICS

MICROCLIMATOLOGY
Portable, ambient air microclimate cooling in simulated desert and tropic conditions
[AD-A186457] 08 p1050 N88-16338
Perspectives in microclimate cooling involving protective clothing in hot environments
[AD-A188370] 12 p1671 N88-20007
The effects of different combinations of inlet air conditions used for cooling as measured on a heated manikin
[AD-A191116] 18 p2552 N88-25151

MICROCOMPUTERS
NT PERSONAL COMPUTERS

The microcomputer as an engineering management tool
[DE87-014882] 02 p0219 N88-11378
Microcomputer control of spectroscopic instruments
[ATR-86(8431)-4] 03 p0326 N88-12058
The MicroVAX-based data acquisition system for D0
[DE87-014475] 03 p0366 N88-12303
A computer code to calculate line by line atmospheric transmission spectra on a microcomputer
[NASA-TM-100686] 05 p0554 N88-13372
An extension to the multilevel logic simulator for microcomputers
[AD-A185032] 05 p0634 N88-13879
Data analysis at the Oulu (Finland) EISCAT laboratory 06 p0691 N88-14241
MINIX: A UNIX clone with source code
[PB88-100862] 06 p0760 N88-14664
Life sciences flight experiments microcomputer 06 p0792 N88-14857
Microcomputer controlled arc welding power source: Its steady state and transient performance
[PB87-143921] 07 p0863 N88-15233
Study on automatic detection and identification of defects in weld by microcomputer
[PB87-143897] 07 p0863 N88-15237
Data acquisition, reduction and analysis of shock and vibration testing using a super microcomputer
[AD-A186123] 07 p0867 N88-15260
Version description document for the Ada compiler validation capability (version 1.9) (for microcomputer)
[AD-A186390] 07 p0903 N88-15471
Preliminary evaluation of a micro-based repeated measures testing system
[NASA-CR-172038] 08 p1048 N88-16331
Stability, reliability and cross-mode correlations of tests in a recommended 8-minute performance assessment battery
[NASA-CR-172039] 08 p1052 N88-16351
Development of a menu of performance tests self-administered on a portable microcomputer
[NASA-CR-172040] 08 p1067 N88-16452
Measuring mental workload: A performance battery
[AD-A187118] 09 p1200 N88-17192
Design of a neural network simulator on a transputer array 09 p1205 N88-17221
The desktop interface in intelligent tutoring systems 09 p1205 N88-17225
An advanced microcomputer design for processing of semiconductor materials 10 p1288 N88-17703
Microcomputer analysis of regenerative heat exchangers for oscillating flow
[DE88-001773] 10 p1329 N88-17945
Parallelism at the microlevel: Cooperative microcontrollers with real time considerations 10 p1381 N88-18246
Applications of lower cost computers to dimensional gaging
[BDX-613-3606] 11 p1525 N88-19108
Interfacing of a microcomputer with a simultaneous atomic-emission spectrometer
[PB88-139571] 11 p1526 N88-19109
Report on desktop publishing
[AD-A187698] 11 p1528 N88-19128
Computer aided tactics for air combat 12 p1597 N88-19559
Development of a digital terrain modeling system for microcomputers
[INPE-4406-TDL/303] 12 p1639 N88-19816
Automatic data acquisition system utilizing microcomputers: Automatic Meteorological Stations (AMS)
[INPE-4215-PRE/1096] 12 p1646 N88-19859
A simplified computer code for reduction to burning rates of closed bomb pressure-time data (MINICB)
[AD-A189112] 13 p1736 N88-20380
Interactive automated system for testing analog units of digital seismic stations 13 p1789 N88-20702
Study of microcomputer-based real-time programmable optical signal processor and application
[AD-A190076] 15 p2133 N88-22726
Fundamentals of microprocessor-based design: A tutorial, second edition
[DE88-006761] 16 p2244 N88-23406
DATAC bus monitor 17 p2294 N88-23721
Implantation of a geo-cartographical information system through microcomputers 17 p2361 N88-24064
Effective communication between a microVAX and a specialized high-speed subprocessor
[DE88-007967] 19 p2714 N88-26115
On-line measurement of heat of combustion
[NASA-CR-183076] 19 p2738 N88-26255
A microcomputer based frequency-domain processor for laser Doppler anemometry
[NASA-TM-100998] 20 p2803 N88-26634
Managing microcomputer applications: A primer and guide to good practice
[AD-A192992] 20 p2835 N88-26817
Design of high performance microcomputers for numerical data processing
[ETN-88-92371] 20 p2835 N88-26818
A multiprocess operating system for 16 bit microcomputers or porting Unix (trademark) to a NS32016 with enhancements 20 p2836 N88-26822
What's on the menu? Friendlier computers
[AD-A194393] 22 p3135 N88-28637
Microsupercomputers: Design and implementation
[AD-A194712] 22 p3135 N88-28638
LO-CO-GRAF (low cost graphics): Generating maps to support command and control/crisis management using small computers
[AD-A193964] 22 p3139 N88-28661
Finite Element Composite Analysis Program (FECAP) for a microcomputer
[NASA-TM-100670] 23 p3190 N88-28982
A computer program package for introductory one-dimensional digital signal processing applications
[AD-A194656] 23 p3249 N88-29338
A standard library for modeling satellite orbits on a microcomputer
[AD-A195759] 24 p3331 N88-29830

MICROCRACKS

Transply crack density detection by acousto-ultrasonics
[NASA-TM-100224] 03 p0279 N88-11758
Environmentally assisted cracking: Overview of evidence for an adsorption-induced localised-slip process
[AD-A185175] 05 p0565 N88-13443
The orientations of dipolar walls produced by cyclic deformation 05 p0598 N88-13655
Crack propagation properties of sintered steel 05 p0604 N88-13698
The effect of environment on low cycle fatigue properties in HSLA steel 05 p0605 N88-13705
X-ray fatigue failure prediction based on plasticity response to microcracks 05 p0607 N88-13725
Development of crack under periodically pulsed laser radiation 06 p0774 N88-14754
Deformation induced cracking in steel girder bridges and retrofit guidelines
[PB88-102710] 07 p0868 N88-15265
Study on the correlation of polystyrene (PS) film craze to its fracture behaviour by TEM (Transmission Electron Microscopy)
[PB87-143343] 08 p0970 N88-15870
La Recherche Aerospatiale, bimonthly bulletin, number 1987-2, 237/March-April
[ESA-TT-1074] 11 p1433 N88-18550
Study of the effects of metallurgical factors on the growth of fatigue microcracks
[AD-A188475] 12 p1608 N88-19615
Stress analysis in elastic solids with many cracks
[AD-A189015] 12 p1636 N88-19799
Non-destructive evaluation techniques applied to the study of fatigue microcrack growth in steel alloys
[DE88-004090] 13 p1742 N88-20420
Bimodular behavior and crack closure in compression in a brittle material
[AD-A191267] 16 p2224 N88-23275
Time-domain boundary element analysis of dynamic near-tip fields for impact-loaded collinear cracks
[AD-A192930] 20 p2815 N88-26700
Kinetic of martensitic transformations induced by hydrogen in the austenite
[DE88-701623] 23 p3194 N88-29007
The use of a surface acoustic wave technique to study the growth behavior of small cracks in a high strength steel alloy 23 p3225 N88-29193

MICROCRYSTALS

Amorphous or microcrystalline semiconductor memory device
[EP-PATENT-0-162-529-A1] 01 p0026 N88-10167
Gigantic optical nonlinearity in low dimensional systems 14 p1975 N88-21786
Enhanced excitonic optical nonlinearity and exciton dynamics in semiconductor microstructures 14 p1977 N88-21795
Optical characterization of microcrystals
[DE88-006622] 15 p2141 N88-22775
Dispersion measurements of microcrystals in the near ultraviolet and infrared
[DE88-006234] 15 p2145 N88-22800
Semiconductor microcrystallites in porous glass and their applications in optics 20 p2863 N88-27005

MICROCYSTIS

Light scattering of intracellular gas vacuoles: Anomalous behavior of forward and perpendicular light scattering of a cyanobacterium due to intracellular gas vacuoles
[BCRS-87-08] 16 p2228 N88-23308

MICRODENSITOMETERS

Method of digital surface photometry of galaxies and its application to the edge-on galaxy NGC 5907 16 p2287 N88-23695

MICROELECTRONICS

NT LARGE SCALE INTEGRATION
NT VERY LARGE SCALE INTEGRATION
Use of sol-gels in the application of ceramic oxide thin films
[DE87-013610] 01 p0028 N88-10176
Wire interconnection reliability and moisture levels in hybrid microcircuits with epoxy-attached components
[DE87-012987] 01 p0039 N88-10247
Physics and device design of vacuum integrated circuits 01 p0039 N88-10251
Applications of heat pipes to cool PWBS and hybrid microcircuits 02 p0136 N88-10858
Study and realization of Schottky diodes for forthcoming integrated hyperfrequency devices
[LAAS-87-062] 02 p0167 N88-11054
Silicon oxidation photoassisted with a continuous wave CO2 laser beam and contribution to the study of silica layers obtained
[LAAS-87-158] 02 p0179 N88-11115
Study and optimization of a technological process for the fabrication of heterojunction bipolar transistors. Applications to high speed devices
[LAAS-87-134] 02 p0246 N88-11555
Molecular beam heteroepitaxy: (Ca,Sr)F2-GaAs system
[LAAS-87-168] 02 p0246 N88-11556
RADC/NBS (Rome Air Development Center/National Bureau of Standards) Workshop. Moisture Measurement and Control for Microelectronics (4)
[PB87-224614] 03 p0309 N88-11947
Research in monolithic signal-processing circuits
[AD-A184680] 03 p0311 N88-11962
Chemically modified microelectrode arrays. New kinds of electronic devices
[AD-A184389] 04 p0439 N88-12724
Electromagnetics and electrothermal approach to evaluate failures in microelectronic devices caused by electrostatic discharges: Stochastical aspects of the device reliability
[AD-A184906] 05 p0577 N88-13522
Developments in electronics ceramics reported 06 p0684 N88-14192
Selected aspects of microelectronics technology and applications: Numerically controlled machine tools. Technology trends series no. 2
[PB87-132973] 06 p0696 N88-14268
Generic specifications for hybrid microcircuits
[ESA-PSS-01-608-ISSUE-2] 06 p0696 N88-14273
An analysis of simplified feed architectures for MMIC (Monolithic Microwave Integrated Circuit) T/R (Transmit/Receive) module arrays
[AD-A185474] 06 p0697 N88-14275
Assessment of electroceramics research in Europe and the Middle East
[AD-A186377] 07 p0836 N88-15074
Properties of superconducting tunnel structures in microwave radiation field 09 p1239 N88-17424
Solid state research
[AD-A185987] 09 p1253 N88-17508
Superlattice photodetectors
[AD-A186956] 09 p1253 N88-17511
Random vibration (stress screening) of printed wiring assemblies 11 p1499 N88-18953
Microelectronic applications of the conductor-thin insulator-semiconductor (CIS) structure 11 p1560 N88-19341
JPRS report. Science and technology: Europe and Latin America
[JPRS-ELS-87-054] 12 p1573 N88-19406
JPRS report: Science and technology. Europe and Latin America
[JPRS-ELS-88-001] 12 p1614 N88-19649
Emerging technologies program 3-5: Microelectronics Panel report
[AD-A189463] 12 p1624 N88-19716
JPRS report. Science and technology: Europe and Latin America
[JPRS-ELS-87-055] 12 p1686 N88-20086
Solid state research
[AD-A188388] 12 p1699 N88-20166
Advanced packaging for VLSI/VHSIC (Very Large Scale Integrated Circuits/Very High Speed Integrated Circuits) applications: Electrical, thermal and mechanical considerations, an IR and D report
[AD-A189666] 14 p1965 N88-21724
JPRS report: Science and technology. Japan
[JPRS-JST-88-001] 15 p2051 N88-22218
Nondestructive moisture measurement in microelectronics
[AD-A190515] 15 p2060 N88-22281

The Department of Defense Superconductivity Research and Development (DSRD) options. A study of possible directions for exploitation of superconductivity in military applications
[AD-A189747] 15 p2142 N88-22780
Fundamental studies of the mechanical behavior of microelectronic thin film materials
[AD-A190038] 15 p2143 N88-22786
JPRS report: Science and technology. Japan
[JPRS-JST-87-026] 16 p2184 N88-23018
Local density of states in double-barrier resonant tunneling structures
[AD-A190673] 16 p2281 N88-23656
Microelectronics the next fifteen years
17 p2305 N88-23792
Photocurrent modeling of modern microcircuit PN junctions
[DE88-007037] 19 p2662 N88-25832
Anomalous emissivity from periodic micro-machined silicon surfaces 19 p2670 N88-25872
Thermal management of integrated microsensors
19 p2670 N88-25875
Application-specific packaging for custom micromechanical structures 19 p2671 N88-25879
An integrated on-chip pressure sensor for accurate control applications 19 p2671 N88-25880
Silver multi-layers for planar Ag/AgCl reference electrodes 19 p2672 N88-25883
Solid state research
[AD-A192837] 21 p3020 N88-27929
Electronic and optical devices and applications
24 p3363 N88-30027
Microcircuit trace cutting with focused ion beams
[AD-A196030] 24 p3367 N88-30050
A system study with an infrared sensitive microelectronic image sensor
[FOA-C-30481-3.1] 24 p3429 N88-30407

MICROGRAPHY
U PHOTOMICROGRAPHY

MICROGRAVITY
U REDUCED GRAVITY

MICROHARDNESS
Welding and weldability of ductile intermetallic alloys
[DE87-014061] 04 p0416 N88-12582
Tribological studies on high speed steel cutting tools
[DE88-002550] 07 p0864 N88-15246
Effects of cold working on precipitation in age hardenable alloys: On the copper alloys
[NASA-TT-20164] 16 p2177 N88-22973
Microstructural characterization and properties of 3Cr-1.5Mo-0.1V thick section electron beam welds
[DE88-004330] 18 p2486 N88-24747
Characterization of coating wear phenomena in nitride and carbide coated tool inserts
[DE88-011196] 20 p2779 N88-26478

MICROINDENTATION
U MICROHARDNESS

MICROINSTRUMENTATION
A monolithic gas flow sensor with polyimide as thermal insulator 19 p2669 N88-25864

MICROMECHANICS
A quantitative statistical model for cleavage fracture initiation in carbide strengthened steels
[ETN-87-90735] 01 p0025 N88-10157
Pin joints, gears, springs, cranks and other novel micromechanical structures
[DE88-002504] 07 p0864 N88-15245
Micromechanisms of fatigue crack growth and fracture toughness in metal matrix composites
[AD-A186941] 09 p1137 N88-16816
A fiber-resin micromechanics analysis of the delamination front in a DCB specimen
[NASA-TM-100540] 10 p1294 N88-17737
Mechanics of composite materials: Past, present and future
[NASA-TM-100793] 10 p1295 N88-17744
Adhesion, friction and micromechanical properties of ceramics
[NASA-TM-100782] 10 p1305 N88-17801
The mechanism of anisotropic silicon etching and its relevance for micromachinings
[MBB-UA-1013/86] 10 p1311 N88-17838
Mechanical response of unidirectional boron/aluminum under combined loading
[NASA-CR-182595] 12 p1604 N88-19591
Micromechanical and microstructural studies of ceramic superplasticity
[DE88-005793] 13 p1751 N88-20472
Microplasticity phenomena in graphite/magnesium metal matrix composites
[DE88-006772] 15 p2029 N88-22086
Whisker-reinforced ceramic composites for heat engine components 15 p2082 N88-22410
A micromechanics model of the stiffness and strength of laminates with fiber waviness
[NASA-CR-181670] 20 p2768 N88-26413
Micromechanics of composite laminate compression failures
[NASA-CR-183179] 22 p3050 N88-28098
Modeling of micromechanisms of fatigue and fracture in hybrid materials
[AD-A195604] 24 p3382 N88-30142

MICROMETEOROIDS
NT ZODIACAL DUST
Atmospheric entry heating of cosmic dust
06 p0794 N88-14865
Assessment of the effects of space debris and meteoroids environment on the space station solar array assembly
[NASA-TM-101315] 23 p3185 N88-28959
The effect of the near earth micrometeoroid environment on a highly reflective mirror surface
[NASA-TM-101307] 24 p3332 N88-29833

MICROMETEOROLOGY
NT MICROBURSTS (METEOROLOGY)
An update on remote measurement of soil moisture over vegetation using infrared temperature measurements: A FIFE perspective
[NASA-CR-182926] 17 p2370 N88-24109
Some results from the Amazon Forest micrometeorological experiment
[INPE-4631-PRE/1346] 24 p3403 N88-30263
Microphysical processes in cloud layers of Venus
24 p3448 N88-30522

MICROMETEORS
U MICROMETEOROIDS

MICROMETERS
Study for the determination of general and specific properties of wide energy-band gap HgHdTe in the 1-2 micrometer wavelength range
[AD-A189177] 13 p1845 N88-21041

MICROMINIATURIZATION
Development of a low noise 10 K J-T refrigeration system
[AD-A186004] 07 p0838 N88-15085
The 1986 IEEE Solid-State Sensor Workshop
[AD-A190922] 19 p2668 N88-25860
Microminiature fluidic amplifier
19 p2669 N88-25865
Electrical and chemical sensors for biological cell research 19 p2669 N88-25866
Resonant structures for integrated sensors
19 p2673 N88-25893
Tin oxide microsensors on thin silicon membranes
19 p2673 N88-25897

MICROMINIATURIZED ELECTRONIC DEVICES
Study and realization of Schottky diodes for forthcoming integrated hyperfrequency devices
[LAAS-87-062] 02 p0167 N88-11054

MICROORGANISMS
NT AMOEBA
NT BACILLUS
NT BACTERIA
NT ESCHERICHIA
NT PARAMECIA
NT PSEUDOMONAS
NT STAPHYLOCOCCUS
Exobiology and life science 07 p0883 N88-15358
Physiological and immunological aspects of human adaptation to temperature elevation in a closed environment 07 p0895 N88-15424
Design concepts for bioreactors in space
09 p1198 N88-17179
Degradation of jet and missile fuels by aquatic microbial communities
[AD-A188065] 11 p1465 N88-18737
Ecological risk factors related to environmental uses of genetically engineered organisms
[DE88-006674] 18 p2549 N88-25132
Biodegradation of JP-5 aviation fuel by subsurface microbial communities
[AD-A192743] 20 p2781 N88-26493
An outdoor test facility for the large-scale production of microalgae
[DE88-001146] 21 p2984 N88-27723

MICROPARTICLES
The effect of Ca(OH)2-treated ceramic microspheres on the mechanical properties of high-temperature lightweight cement composites
[DE88-004590] 13 p1749 N88-20457
A chemical method for achieving acceleration of macroparticles to ultrahigh velocities
[DE88-006377] 15 p2128 N88-22695
Distribution of chain ends inside the polybutadiene microspheres of SB diblock copolymers
[AD-A191257] 16 p2182 N88-23007

MICROPHONES
Vital signs rate meter
[AD-A187015] 09 p1198 N88-17183
Experimental study on the influence of wind on acoustic pressure sensors
[ISL-R-121/86] 15 p2131 N88-22712
Outdoor sound propagation, its implications for unattended ground sensors
[FEL-1986-64] 20 p2850 N88-26917
Detection of helicopters using ground-controlled microphones 22 p3148 N88-28730
Noise levels from a jet-engined aircraft measured at ground level and at 1.2 m above the ground
[NPL-AC-114] 23 p3279 N88-29524

MICROPHOTOGRAPHS
Method for measuring absolute linear parameters of chromosomes 19 p2707 N88-26095

MICROPHOTOMETERS
U PHOTOMETERS

MICROPOLAR FLUIDS
On the performance of finite journal bearings lubricated with micropolar fluids
[NASA-TM-100293] 08 p0988 N88-15983

MICROPOROSITY
Ultrasonic characterization of non-uniform porosity distributions in SiC ceramic
[DE88-004814] 13 p1749 N88-20459

MICROPROCESSORS
The impact of new computer technology on accelerator control
[DE87-014021] 02 p0219 N88-11376
The pros and cons of using a CAI package on a central computer as opposed to a microprocessor: What's your CAI MO, mainframe or micro
[DE87-011123] 04 p0475 N88-12929
Test and evaluation of the transputer in a multi-transputer system
[AD-A184969] 05 p0631 N88-13859
Reserach on microprocessor controller for spot welding
[PB87-143913] 07 p0863 N88-15240
Microprocessor emulating the intermediate code for FORTRAN compiler
[DE88-700540] 07 p0900 N88-15452
High performance data buses: Progress and evolution
[DE88-002570] 09 p1215 N88-17285
Multitasking and microtasking experience on the NA S Cray-2 and ACF Cray X-MP
[NASA-CR-177464] 09 p1221 N88-17325
Microcomputer analysis of regenerative heat exchangers for oscillating flow
[DE88-001773] 10 p1329 N88-17945
High-performance CPU implementation of the nebula instruction set architecture 10 p1373 N88-18194
The design of ultra high-speed numeric intensive systems (having fault tolerant and load balancing capabilities) 10 p1374 N88-18196
Hardware implementation for special functions. An application for combat simulation
10 p1374 N88-18197
MICRO system for control, acquisition and processing of experimental data
[DE88-700724] 10 p1386 N88-18278
Implementation of encoders and decoders for Reed-Solomon codes
[PB88-126628] 10 p1387 N88-18286
Modular CAMAC system, 2
[DE88-700237] 11 p1525 N88-19106
Efficient instruction level simulation of computers
[AD-A187821] 11 p1529 N88-19130
A microprocessor-based real-time simulator of a turbofan engine
[NASA-TM-100889] 14 p1868 N88-21163
Microprocessors in space instrumentation
[RR-321] 14 p1955 N88-21655
MIG-1 on-line measuring holographic microscope
[DE88-701103] 15 p2068 N88-22332
Fundamentals of microprocessor-based design: A tutorial, second edition
[DE88-006761] 16 p2244 N88-23406
Design of high yield microprocessors
[ETN-88-92184] 16 p2245 N88-23410
Automatic layout generation of data processing sections of VLSI microprocessor-like circuits
[ETN-88-92185] 16 p2245 N88-23411
SP-100 ground engineering systems test facility control systems 17 p2436 N88-24496
Sensors for process control requirements for design and test 19 p2671 N88-25877
The relationship between system response time, working memory, and task complexity: An empirical investigation
[DE88-000976] 19 p2711 N88-26105
Idea processing for creativity and management
[DE88-006110] 19 p2714 N88-26113
FASTRUN phase sequencer descriptor language (PDL)
[DE88-007966] 20 p2837 N88-26828
Mutually exclusive alternatives by clustering
[DE88-007707] 20 p2882 N88-27115
SP-100 Ground Engineering Systems: Test facility control systems
[DE88-009195] 21 p3015 N88-27895

DSS 13 microprocessor antenna controller
22 p3066 N88-28192
Multichannel data transmission through a fiber optic cable
[AD-A193842] 22 p3070 N88-28221
The VIPER microprocessor
[RSRE-87014] 22 p3135 N88-28640
Feasibility study of a microprocessor controlled actuator test mechanism
[AD-A194654] 23 p3249 N88-29337
Heavy ion and proton tests for subsystem upset
[AD-A195267] 24 p3434 N88-30442

MICROPROGRAMMING
The UMAC simulator 20 p2834 N88-26811

MICROPULSATIONS
NT GEOMAGNETIC MICROPULSATIONS

MICROSCOPES
NT ACOUSTIC MICROSCOPES
NT ELECTRON MICROSCOPES
NT ION MICROSCOPES
NT OPTICAL MICROSCOPES
Calibration standard for metallographic microscopes
[RFP-3956-REV] 03 p0326 N88-12057

MICROSCOPY
NT ELECTRON MICROSCOPY
NT LASER MICROSCOPY
NT PHOTOACOUSTIC MICROSCOPY
Structural characterization of undoped and doped GaAs: A comparative study of four techniques
[DE88-004552] 11 p1555 N88-19304
Scanning tunneling microscopy of silver, gold, and aluminium monomers and small clusters on graphite
[DE88-003871] 11 p1562 N88-19349
Computer software for the computation of the scattered field and the optical microscope image of line objects patterned in thick layers
[PB88-153705] 13 p1814 N88-20838
Microprobe examination of composite materials produced by burning of Ti, Cr, C powders with powder of any one Fe-group metal 14 p1886 N88-21269
Recent advances in atom-probe field ion microscopy
[DE88-008799] 20 p2876 N88-27070
Progress in diagnostic techniques for SC (superconducting) cavities
[DE88-008600] 20 p2876 N88-27077
Scanning tunneling microscopy as a surface chemical probe
[AD-A192710] 21 p2909 N88-27263

MICROSPORES
Ultraviolet (180 to 300 nm) action spectra for inactivation and DNA photoproduct formation of Bacillus subtilis spores under ultrahigh vacuum 12 p1657 N88-19931

MICROSTRIP ANTENNAS
Investigation of surface wave blindness in microstrip phased array antennas
[AD-A189326] 12 p1621 N88-19696
Conformal microstrip slot antenna and antenna array
[AD-A189623] 15 p2055 N88-22252
Investigation of radiating and guiding structures in microstrip patch antennas
[AD-A191445] 16 p2193 N88-23082
Analysis of annular microstrip antennas for hyperthermic applicators
[PB88-181508] 19 p2643 N88-25679
A microstrip array feed for MSAT spacecraft reflector antenna 19 p2652 N88-25747
Array trade-off study using multilayer parasitic subarrays
[NASA-TM-101321] 22 p3070 N88-26222

MICROSTRIP DEVICES
NT MICROSTRIP ANTENNAS
NT MICROSTRIP TRANSMISSION LINES
The silicon microstrip detector --- particle position measurement
[ETN-88-92235] 16 p2210 N88-23189
Investigation of photoconductive picosecond microstripline switches on self-implanted Silicon On Sapphire (SOS) 19 p2657 N88-25789

MICROSTRIP TRANSMISSION LINES
Simple, low-profile, circularly polarized arrays
19 p2647 N88-25716
An optically strobed sample and hold circuit
19 p2656 N88-25772
Characteristics of shielded microstrip lines on GaAs-Si at millimeter-wave frequencies 19 p2657 N88-25787
Picosecond optoelectronic study of a thin film transmission line structure 19 p2661 N88-25823

MICROSTRUCTURE
NBS (National Bureau of Standards) research reports (April 1987)
[PB87-210258] 01 p0018 N88-10111
Isothermal forging and its effect on the microstructure of powder route nickel alloy AP1
[RAE-TM-P-1094] 01 p0022 N88-10138
Development of creep resistant austenitic stainless steels for advanced steam cycle superheater application
[DE87-012929] 01 p0023 N88-10147
Fatigue and thermal fatigue of Pb-Sn solder joints
[DE87-012881] 01 p0024 N88-10150
Laser chemically vapor deposited silicon-carbide: Growth features, topography, microstructure, and composition
[DE87-013767] 01 p0029 N88-10184
Effect of high-temperature annealing on the microstructure and thermoelectric properties of GaP doped SiGe
[NASA-TM-100164] 01 p0029 N88-10188
Microstructural effects in shock initiation of granular explosives
[DE87-011282] 01 p0031 N88-10200
Fabrication of microstructures with extreme structural heights by vacuum reaction injection molding and electroforming
[KFK-4267] 01 p0033 N88-10210
Analytical electron microscopy characterization of boron in sintered alpha-SiC
[DE87-012532] 02 p0142 N88-10889
Microstructural evolution and response to double-loop reactivation testing of heat-treated pH 13-8 Mo martensitic stainless steel
[DE87-009058] 02 p0146 N88-10915
Investigation of the structure of coatings of self fluxing alloys fused by laser energy
[BLL-M-37301-(5828.4)] 02 p0148 N88-10930
Analysis of phase equilibria in NiTi-C system in high nickel regions
[BLL-M-37304-(5828.4)] 02 p0149 N88-10932
Study of the microscopic mechanisms of cyclic deformation. Development of a new approach: The case of aluminum
[ISAL-87-0003] 02 p0149 N88-10936
A microstructural lattice model for strain oriented problems: A combined Monte Carlo finite element technique
[NASA-TM-100215] 02 p0150 N88-10939
Study of the micromechanical behavior of a SiO2-Al2O3-Li2O glass ceramic and its relation to the microstructure
[ISAL-ITC1-87-01] 02 p0153 N88-10960
Need for composites, new materials discussed
02 p0160 N88-11001
Thin film microstructures: Simulation and theory
[DE87-014732] 02 p0246 N88-11553
Resistance of welded joints in high temperature Hastelloy N-type nickel alloy to hot crack formation
03 p0286 N88-11798
Microstructural effects on the fatigue behavior of Fe-C-X alloys
[DE88-000155] 03 p0288 N88-11809
Stress corrosion cracking of high-strength steels in aqueous environments 03 p0289 N88-11818
A fundamental study of the mechanical and microstructural response of elevated temperature PM aluminum-titanium alloys 03 p0289 N88-11819
Ultra-fine grained alloy material
[AD-A184500] 03 p0290 N88-11820
International Conference on Microstructology held in Gainesville, Florida on 7-9 May 1986
[AD-A184604] 03 p0290 N88-11822
Modified 14Cr-16Ni stainless steels with improved creep resistance at 700 C due to tailored precipitate microstructures
[DE87-014788] 03 p0290 N88-11825
Reduced-activation ferritic steels: A comparison with Cr-Mo steels
[DE88-000332] 03 p0290 N88-11826
Microstructural characterization of irradiated PWR steels using the atom probe field-ion microscope
[DE88-000341] 03 p0291 N88-11828
The correlation between microstructure and thermomechanical properties of two-phase materials and porous sintered materials
[KFK-4205] 03 p0292 N88-11835
Indentation damage in ceramics
[AD-A184686] 03 p0294 N88-11844
Flaw imaging and ultrasonic techniques for characterizing sintered silicon carbide
[NASA-TM-100177] 03 p0334 N88-12106
Monte Carlo simulation of modulated phases
[NASA-TM-89654] 03 p0369 N88-12323
New theory for competing interactions and microstructures in partially-ordered (liquid-crystalline) phases
[DE87-014739] 03 p0380 N88-12389
Corrosion behavior of P/M mechanically alloyed IN-9052.1: An electro-chemical investigation
[AD-A184191] 04 p0414 N88-12567
The nature of metallurgical reactions in underwater welding
[AD-A184464] 04 p0414 N88-12568
Mechanical properties of a microalloyed steel with high niobium content
[DE87-703545] 04 p0415 N88-12572
Mechanical strength and niobium and niobium-base alloys substructures
[DE87-703692] 04 p0415 N88-12577
Welding and weldability of ductile intermetallic alloys
[DE87-014061] 04 p0416 N88-12582
The accommodation of precipitate plates modelled as a tensile test
[DE88-000207] 04 p0454 N88-12814
Characterization of thin layers for optics
[PB87-217949] 04 p0490 N88-13017
Microstructural change of Al on H implantation
[IPPJ-847] 04 p0493 N88-13036
Theory and simulations of Zone 2 microstructures in thin films
[DE87-014752] 04 p0499 N88-13071
Study of the influence of mechanical - thermal treatments on the creep behavior of a niobium stainless steel
[DE87-703506] 05 p0563 N88-13431
Investigation by differential scanning calorimetry of microstructure in a superplastic Al-Mg-Zr alloy
[AD-A184902] 05 p0564 N88-13439
Ion plating for corrosion control
[AD-A185061] 05 p0565 N88-13442
Effect of rapid solidification on short-range order: A magnetic study
[AD-A185216] 05 p0565 N88-13444
Effect of rapid solidification on stainless steel weld metal microstructures and its implications on the Schaeffler diagram
[DE88-001489] 05 p0566 N88-13451
United States - Japan Workshop on Dielectric and Piezoelectric Ceramics (3rd) held in Toyama, Japan on November 9-12, 1986
[AD-A185113] 05 p0568 N88-13460
Fatigue 87, volume 1
[AD-A184045] 05 p0597 N88-13645
The influence of the topography of fracture surfaces on crack closure 05 p0598 N88-13657
Influence of microstructure and aging condition on the fatigue crack propagation in age hardened aluminium alloys 05 p0599 N88-13659
The effect of microstructure on the surface crack length: Crack depth relationship for short cracks
05 p0600 N88-13670
The growth behavior of small fatigue cracks; the effect of microstructure and crack closure
05 p0600 N88-13673
The influence of microstructure and residual stresses on the initiation and propagation of short surface cracks on AlMgSi1 05 p0601 N88-13674
Propagation of small fatigue cracks in 2024-T3 aluminum alloy 05 p0601 N88-13678
Interaction of microstructure and fatigue in tool steels
05 p0603 N88-13693
Deformation mechanisms and crack initiation in fatigue 05 p0608 N88-13730
Environmentally assisted fatigue crack growth
05 p0608 N88-13731
Fatigue crack growth 05 p0608 N88-13734
Characterization of the microstructures of various materials
[AD-A184961] 05 p0655 N88-14017
Basic energy sciences research in the Metals and Ceramics Division of Oak Ridge National Laboratory
[DE87-013538] 06 p0681 N88-14171
Fractographic and microstructural aspects of fracture toughness testing in irradiated 304 stainless steel
[DE88-000795] 06 p0681 N88-14172
Fracture analysis of drawn composite dual-phase steel wire
[DE88-001396] 06 p0681 N88-14173
The effect of neutron irradiation on the tensile properties and microstructure of several vanadium alloys
[DE88-001755] 06 p0682 N88-14176
Electron microscopy studies of tensile cyclic fatigue-tested silicon nitride ceramics
[DE88-001438] 06 p0685 N88-14196
Characterization of mechanical damage mechanisms in ceramic composite materials
[AD-A185549] 06 p0686 N88-14205
The relationship between microstructural size and fatigue threshold in iron and steel
06 p0716 N88-14396
Crack closure phenomena in modes 1 and 2 interactions 06 p0719 N88-14417
The microstructure and texture of torsion-reverse torsion experiments
[DE88-001801] 06 p0721 N88-14434
Dynamic high pressure process for fabricating superconducting and permanent magnetic materials
[DE88-000848] 06 p0785 N88-14817

Interface effects on the mechanical properties of ceramic composites
[AD-A185899] 07 p0826 N88-15009
Characterization of microstructure in metallic and composite materials
[AD-A186193] 07 p0826 N88-15012
Fatigue, fracture and strain hardening of high carbon hardened alloy steel
[AD-A186101] 07 p0831 N88-15043
Metallurgical processes in multi-component rare earth-transition metal permanent magnet alloys
[AD-A186401] 07 p0832 N88-15045
Characterization of current steels. The 35 NCD 16 alloy in 30 mm diam laminated bars made by Aubert and Duval
[CEAT-41/N/76] 07 p0832 N88-15046
Microstructural observations of the Sn-Pb solder/Cu system and thermal fatigue of the solder joint
[DE88-001392] 07 p0832 N88-15048
The influence of grain boundary chemistry and structure on the intergranular attack and intergranular stress corrosion cracking of austenitic alloys
[DE88-002436] 07 p0835 N88-15063
Microstructure and magnetic properties of cobalt-chromium alloys
[DE88-002762] 07 p0835 N88-15064
Imaging subtle microstructural variations in ceramics with precision ultrasonic velocity and attenuation measurements
[NASA-TM-100129] 07 p0867 N88-15257
Processing and interfacial analysis of glass-ceramic to metal seals
[DE88-002999] 08 p0971 N88-15873
The mechanism of stereo regulation during anionic polymerization of polar monomers
[AD-A186530] 08 p0973 N88-15888
Experimental aspects of high-T/sub c/ superconductors
[DE88-003019] 08 p1090 N88-16564
Microstructure modifications of micron thick NbN films to improve J/sub c/ and H/sub c2/
[DE88-003078] 08 p1091 N88-16567
Monolayer films prepared by the spontaneous self-assembly of symmetrical and unsymmetrical dialkyl sulfides from solution onto gold substrates: Structure, properties, and reactivity of constituent functional groups
[AD-A186717] 09 p1137 N88-16814
Investigation of microstructural factors that cause low fracture toughness in silicon carbide whisker/Al alloy composites
[AD-A186443] 09 p1137 N88-16817
Microstructures and properties of SiC whisker-reinforced mullite composites
[DE88-002611] 09 p1139 N88-16826
Microstructural modification during laser welding
[DE88-002344] 09 p1144 N88-16860
Long-term-aging embrittlement of cast duplex stainless steels: Mechanism and kinetics
[DE88-002929] 09 p1145 N88-16861
Study of molecular mobility of noncrystaline polymer alloys of different compatibility using mechanical spectrometry
[ISAL-87-0032] 09 p1149 N88-16883
The effect of varying sputtering parameters on the microstructure and mechanical properties of 10 percent Ni + TiB2 thin films
[DE88-002600] 09 p1254 N88-17517
Micro-mechanisms of deformation in SiC/Al composites
[AD-A186282] 10 p1296 N88-17749
A detailed microstructural examination of the cause of HAZ cracking in type 316 steel
[AERE-R-12428] 10 p1301 N88-17777
Influence of convection on microstructure
[NASA-CR-182489] 10 p1302 N88-17784
Response of Fe-Cr-Mn austenitic alloys to thermal aging neutron irradiation
[DE88-003415] 10 p1302 N88-17785
Irradiation effects in metals
[DE88-004272] 10 p1303 N88-17789
The role of composition and microstructure gradients on weld metal properties and behavior
[DE88-004956] 10 p1303 N88-17791
Bias, internal stress and substrate effects on the microstructure and properties of PVD-wear resistant coatings
[AERE-R-12360] 10 p1304 N88-17798
Mechanisms of wear in single- and two-phase materials
[DE88-003846] 10 p1305 N88-17806
Durability and damage tolerance of aluminum castings
[AD-A186444] 10 p1341 N88-18013
Acoustic emission-microstructural relations in ferritic steels. Part 3: The effect of inclusion content
[AERE-R-12041] 10 p1341 N88-18015
The measurement of stress in steels of varying microstructure by Barkhausen and magneto-acoustic emission
[AERE-R-12387] 10 p1343 N88-18027
Relationship between fatigue life in the creep-fatigue region and stress-strain response
[NASA-TM-100796] 10 p1345 N88-18040
Optical characterization of GaAs/sub 1-x/Sb/sub x/ and GaAs/sub 1-x/Sb/sub x/GaAs strained layer superlattices
[DE88-003393] 10 p1418 N88-18464
The structure and properties of twin boundaries in superconducting YBa2Cu3O7
[DE88-003864] 10 p1418 N88-18468
Freestanding films of YBa2Cu3O/sub 6.9/
[DE88-003995] 10 p1419 N88-18471
Simulation and processing of high resolution images of defects and interfaces in superconducting YBa2Cu3O7
[DE88-003856] 10 p1420 N88-18480
High-resolution X-ray microstructural study of single crystals of YBa2Cu3O/sub 7-y/
[DE88-004856] 10 p1421 N88-18484
The metallurgical database of Aladin: An alloy de sign system
[AD-A187724] 11 p1457 N88-18682
Microstructural characterization of HSLA-100 GMA-weldments
[AD-A187782] 11 p1457 N88-18683
Microstructural characterization of the heat affected zone of HSLA (High Strength Low Alloy)-100 steel GMA (Gas Metal Arc)-weldment
[AD-A187825] 11 p1457 N88-18688
Thermal fatigue of stainless steel
[DE88-004146] 11 p1458 N88-18694
Institute for Materials Science and Engineering, Metallurgy: Technical activities 1987
[PB88-157722] 11 p1460 N88-18702
Photoacoustic studies of surface plasmons in metallic microstructures
[DE88-004423] 11 p1460 N88-18703
Crystallization and glass formation in electron and laser beam irradiated Cu-Zr alloys
[DE88-003390] 11 p1464 N88-18729
In situ ultrahigh vacuum friction measurement and wear track analysis of ion implanted 304 stainless steel
[DE88-004537] 11 p1494 N88-18922
Novel analytical X-ray Non-Destructive Evaluation (NDE) tool for quality control of energetic materials
[AD-A187737] 11 p1497 N88-18935
Plasma joining of metal matrix composites
[AD-A188559] 12 p1604 N88-19593
Ultrasonic-velocity studies of composite and heterogeneous materials
[AD-A189000] 12 p1604 N88-19595
Study of the effects of metallurgical factors on the growth of fatigue microcracks
[AD-A188475] 12 p1608 N88-19615
Microdesigning of lightweight/high strength ceramic materials
[AD-A188526] 12 p1610 N88-19631
Microstructure characterization with a pulsed laser ultrasonic source
[DE88-005207] 12 p1632 N88-19786
The effect of microstructure on the fatigue crack growth resistance of nickel base superalloys
[AD-A189526] 13 p1741 N88-20414
Processing, structure and properties of heavily deformed in situ composites
[AD-A189611] 13 p1742 N88-20416
Use of the LLNL 40 kV electric gun to study the shock response of 21-6-9 stainless steel
[DE87-014550] 13 p1742 N88-20418
Non-destructive evaluation techniques applied to the study of fatigue microcrack growth in steel alloys
[DE88-004090] 13 p1742 N88-20420
Erosion in dual-phase microstructures
[DE88-004507] 13 p1743 N88-20421
Grain refinement during primary breakdown of alloy 718
[DE88-005193] 13 p1743 N88-20423
Advances in X-ray line profile analysis to determine microstructure information about ceramics
[DE88-003938] 13 p1750 N88-20465
Micromechanical and microstructural studies of ceramic superplasticity
[DE88-005793] 13 p1751 N88-20472
Mixing of viscous fluids: Behavior of microstructures and chaos
[DE88-006287] 13 p1766 N88-20566
Ductile failure
[AD-A189429] 13 p1781 N88-20654
Anisotropy of microstructural eddy motion in surface layer during calm 13 p1784 N88-20677
Electrical characteristics of MBE (Molecular Beam Epitaxyl)-grown GaAs/sub 1-x/Sb/sub x on InP and correlation with film microstructure
[DE88-003841] 13 p1847 N88-21053
Microprobe examination of composite materials produced by burning of Ti, Cr, C powders with powder of any one Fe-group metal 14 p1886 N88-21269
The unique characteristics of the structure of composite materials made on a base of sphalerite-analogous boron nitride 14 p1886 N88-21273
Development, high temperature properties, and microanalysis of nonoxide ceramics
[ETN-88-92103] 14 p1893 N88-21304
Processing, texture and mechanical properties of sintered silicon carbide
[NASA-TT-20253] 14 p1893 N88-21305
New method of examining microninhomogeneity of local centers in high-resistivity semiconductor materials under scanning electron microscope 14 p1969 N88-21754
Dynamic and spectral properties of semiconductor lasers with quantum well, quantum wire, and quantum box structures 14 p1975 N88-21788
Enhanced excitonic optical nonlinearity and exciton dynamics in semiconductor microstructures 14 p1977 N88-21795
The contribution of electron microscopy of materials science to society
[DE88-006341] 15 p2028 N88-22082
Processing, microstructure, and mechanical properties of silicon carbide particulate reinforced aluminum alloys
[AD-A188981] 15 p2037 N88-22136
Segregation effects in welded stainless steels
[DE88-701224] 15 p2037 N88-22139
The age hardening response of thermomechanically processed Al-Mg-Li alloys
[AD-A189870] 15 p2039 N88-22147
Directed-energy electron-beam processing of a hypoeutectic Cr90Ta10 alloy
[DE88-005621] 15 p2040 N88-22157
Transformation toughening of ceramics
[AD-A190399] 15 p2045 N88-22183
Strength and microstructure of ceramics
[AD-A190712] 15 p2046 N88-22191
A three-dimensional model for the elastic properties of a foam
[DE88-006197] 15 p2046 N88-22192
High temperature corrosion of ceramics
[DE88-006567] 15 p2046 N88-22193
The growth of corner cracks under the conjoint action of high and low cycle fatigue
[AD-A190510] 15 p2076 N88-22379
Evolution of hardening and damage during viscoplastic deformation
[AD-A190714] 15 p2077 N88-22381
Characterization of sintered SiC by using NDE 15 p2082 N88-22413
The weldability of consolidated rapidly solidified Type 304 SS powders
[DE88-006738] 16 p2178 N88-22978
Deformation of rapidly solidified dispersion strengthened titanium alloys
[AD-A190793] 16 p2179 N88-22984
Dependence of structure of stabilized ZrO2 coatings on condensation rate 16 p2180 N88-22990
Applications research studies of microtubules
[AD-A190855] 16 p2182 N88-23005
Laser cladding of Ni, Nb and Mg alloys for improved environmental resistance at high temperature
[AD-A191274] 16 p2213 N88-23208
Investigation of non-linear optical behavior of semiconductors for optical switching, volume 1
[AD-A191297] 16 p2274 N88-23611
Radiation effects in silicon
[DE88-006642] 16 p2282 N88-23659
Magnetic studies of iron-rare-earth-metalloid alloys
[DE88-006801] 16 p2282 N88-23660
Structure and mechanical properties of metal matrix composites made using semi-solid processes: The case of the system Al-Si/SiC
[ETN-88-92299] 17 p2316 N88-23836
Improved processing of Si3N4 17 p2325 N88-23882
Fractographic and microstructural evaluation of 3500-hour durability specimens 17 p2325 N88-23887
The role of oxygen on the mechanical behavior of molybdenum alloys 17 p2401 N88-24278
Chemical compatibility between silicon carbide and a nickel aluminide
[DE88-006188] 18 p2479 N88-24708
Superplasticity: A fundamental investigation on deformation mechanism and cavitation phenomena
[AD-A191548] 18 p2485 N88-24741
Dynamic consolidation of metal powders
[AD-A192126] 18 p2485 N88-24744

Microstructural characterization and properties of 3Cr-1.5Mo-O.1V thick section electron beam welds
[DE88-004330] 18 p2486 N88-24747
High temperature embrittleness of Cu-Cr alloy
[NASA-TT-20184] 18 p2488 N88-24759
An investigation of 2-6 superlattice deposition by laser photochemical techniques
[AD-A191547] 18 p2581 N88-25336
Electronic and structural studies of carbon/carbon composites
[AD-A191729] 19 p2609 N88-25481
Microlaminate composite structures by low pressure plasma spray deposition
[DE88-006453] 19 p2610 N88-25488
The postirradiation tensile properties and microstructure of several vanadium alloys
[DE88-007140] 19 p2615 N88-25515
Influence of strain rate on the substructure evolution and yield behavior of Ti-6Al-4V
[DE88-006457] 19 p2616 N88-25520
Development of fine-grained carbide-particle hardened Hadfield manganese steels
[DE88-008919] 19 p2617 N88-25523
Low-chromium reduced-activation ferritic steels
[DE88-009060] 19 p2617 N88-25524
Hot isostatic pressing of nickel aluminide powders
[DE88-009677] 19 p2617 N88-25525
Oxidation behavior and microstructural studies of melt-spun glassy Fe-Al-Zr metal
[DE88-009964] 19 p2617 N88-25526
Mechanical testing and microscopic analysis of structure of extruded powder aluminum
[DE88-007193] 19 p2617 N88-25528
Microstructure of thin intercalated benezene derived graphite fibers
[AD-A191724] 19 p2618 N88-25534
The structure and properties of RF reactive sputtered IrO2 films 19 p2672 N88-25884
Initial development of high-temperature titanium silicide alloys
[DE88-007860] 20 p2772 N88-26437
Helium induced degradation in the weldability of an austenitic stainless steel
[DE88-009062] 20 p2773 N88-26443
The structure and properties of grain boundaries in B2 ordered alloys
[DE88-009890] 20 p2773 N88-26447
Application of electron microscopy for the analysis of the mechanical behavior of advanced ceramics
[DE88-005049] 20 p2777 N88-26469
Microstructural effects in static and dynamic numerical experiments
[DE88-004289] 20 p2813 N88-26690
Third International Conference on Superlattices, Microstructures and Microdevices
[AD-A191416] 20 p2861 N88-26995
Hot electron transistors grown by MOCVD 20 p2861 N88-26996
Spectroscopy of one-dimensional subbands on InSb 20 p2864 N88-27007
Metallic superlattices 20 p2864 N88-27012
Quantum interference and transport in microstructures 20 p2866 N88-27022
EXAFS studies of the microstructure of semiconductor alloys, defects and semiconductor-metal interfaces 20 p2868 N88-27031
The theory of electron-polar phonon scattering rates in semiconductor micro-structures 20 p2871 N88-27043
Influence of interfaces on electronic and magnetic properties of MnSe/ZnSe superlattices near monolayer limit 20 p2872 N88-27050
Type 3 - type 1 transition and strain effect in Hg(1-x)Cd(x)Te-CdTe and Hg(1-x)Zn(x)Te-CdTe superlattices 20 p2872 N88-27052
Damping characteristics of metal matrix composites
[AD-A193144] 21 p2904 N88-27233
Gaseous tracer techniques for pore structure characterization of granular materials
[DE88-011542] 21 p2911 N88-27274
Thermomechanical processing of Al alloy 2090 for grain refinement and superplasticity
[AD-A192333] 21 p2912 N88-27281
Processing and properties of advanced aluminum alloys
[AD-A193224] 21 p2912 N88-27284
On the systematics of phase transformation in metallic alloys
[DE88-008041] 21 p2913 N88-27288
Development of high strength and toughness microcomposite HSLA Fe/Cr/Mn/C steel with and without Nb
[DE88-009813] 21 p2913 N88-27290
Controlling phase formation and stability to improve the high temperature creep resistance of austenitic stainless steels
[DE88-011401] 21 p2914 N88-27293
Processing and additive effects of ZrO2 on microstructure and dielectric porperties of BaTiO3 ceramics
[AD-A193126] 21 p2917 N88-27316
Preparation and properties of high Q microwave dielectrics in the (CA, SR, BA) zirconate system
[AD-A193127] 21 p2918 N88-27317
Effects of near interfacial microstructure on toughness and subcritical crack growth in ceramic/metal systems
[DE88-009842] 21 p2919 N88-27325
Influence of microstructure and microdamage processes on fracture at high loading rates
[AD-A192957] 21 p2960 N88-27583
Ultrafast physics in semiconductor microstructures
[AD-A193300] 21 p3022 N88-27936
X-ray studies of strain, interface and impurities in semiconductors
[DE88-012460] 21 p3025 N88-27954
As-received microstructure of a SiC/Ti-15-3 composite
[NASA-TM-100938] 22 p3050 N88-28095
Study of fatigue cracks in aluminum alloys. Influence of microstructure
[REPT-48-553] 22 p3056 N88-28134
High temperature electric arc furnace
[NASA-CASE-MFS-28281-1] 23 p3181 N88-28938
Ultrafine microstructure composites prepared by chemical vapor deposition
[AD-A193849] 23 p3189 N88-28973
Low temperature film growth of the oxides of zinc, aluminum and vanadium (and related systems, oxides of gold and germanium, nitrides of aluminum and tungsten) by reactive sputter deposition
[AD-A193497] 23 p3191 N88-28986
An investigation into the metallurgical aspects of joining rapidly-solidified aluminum alloys
[AD-A194677] 23 p3194 N88-29009
Effects of metal substitutions (Fe and Ga) in YBa2Cu3O7 on its superconducting properties and microstructures
[DE88-007393] 23 p3287 N88-29572
An HVEM study of displacement cascade damage in Nb3Sn at 13 K
[DE88-009997] 23 p3289 N88-29584
Creep of carbon yarn and carbon-carbon composites at high temperatures and high stresses
[AD-A195224] 24 p3340 N88-29878
Modeling of micromechanisms of fatigue and fracture in hybrid materials
[AD-A195604] 24 p3382 N88-30142

MICROTRONS

Analysis of free electron laser performance utilizing the National Bureau of Standards CW microtron
[AD-A194217] 23 p3219 N88-29160

MICROWAVE AMPLIFIERS

NT CYCLOTRON RESONANCE DEVICES
Initial operation of a high-power whispering-gallery-mode gyrotron
[DE88-002500] 07 p0857 N88-15207
GaAs MMIC yield evaluation --- monolithic microwave integrated circuits (MMIC)
[ESA-CR(P)-2470] 08 p0979 N88-15916
Low-noise cryogenically cooled broad-band microwave preamplifiers
[DE88-004561] 10 p1324 N88-17912
Wiggler taper optimization for free-electron-laser amplifiers with moderate space-charge effects
[DE88-003758] 13 p1775 N88-20618
Construction of a 60 GHz Traveling Wave Tube (TWT) for intersatellite link on geostationary orbit (ISL/TWT)
[BMFT-FB-W-86-015] 16 p2192 N88-23076
Monolithic GaAs Ku-band one watt constant phase variable power amplifier
[DE88-006272] 18 p2506 N88-24866
Microwave amplifiers
[AD-A192974] 20 p2795 N88-26585
Recent advances in high-power microwave amplifiers
[DE88-007820] 23 p3206 N88-29083
Space-charge-wave solid state microwave amplifier
[AD-A193792] 23 p3208 N88-29091

MICROWAVE ANTENNAS

The 8.4-GHz low-noise maser pump source assembly 04 p0436 N88-12705
An evaluation of equivalent models for design of rectangular microstrip antennas
[FOA-C-30451-3.2] 08 p0977 N88-15905

MICROWAVE ATTENUATION

Numerical simulation of the propagation and absorption due to air breakdown of long microwave pulses
[DE88-005227] 11 p1475 N88-18798
Research and development to acquire and reduce melting layer cloud physics and evaluate a prototype M-meter
[AD-A188390] 12 p1648 N88-19873
Microwave dispersion and absorption in tissues: Molecular mechanisms
[AD-A190118] 15 p2100 N88-22512
An evaluation of two millimeter wave propagation models for horizontal atmospheric attenuation at 70-115 GHZ
[AD-A192699] 21 p2931 N88-27403
Rain attenuation at 35 GHz over an 18 km path
[AD-A194504] 22 p3069 N88-28217

MICROWAVE CIRCUITS

An analysis of simplified feed architectures for MMIC (Monolithic Microwave Integrated Circuit) T/R (Transmit/Receive) module arrays
[AD-A185474] 06 p0697 N88-14275
GaAs varactor diode MMIC fabrication technology --- monolithic microwave integrated circuit (MMIC)
[RSRE-MEMO-4022] 09 p1158 N88-16943
Optical RF distribution links for MMIC phased array antennas
[NASA-TM-100841] 13 p1764 N88-20555
Monolithic microwave integrated circuit technology for advanced space communication
[NASA-TM-100829] 14 p1906 N88-21389
Instrumentation for ultrafast electronics
[AD-A191379] 16 p2193 N88-23080
A 30 GHz monolithic receive module technology assessment
[NASA-CR-180825] 16 p2194 N88-23084
Identification of cascaded microwave circuits with moderate reflections using reflections and transmission measurements
[PB88-171921] 18 p2503 N88-24849
Computer aided design of monolithic microwave and millimeter wave integrated circuits and subsystems
[AD-A191593] 18 p2503 N88-24852
Active feed array compensation for reflector antenna surface distortions
[NASA-TM-100826] 19 p2654 N88-25762
Analysis of networks with parameters S: Generalization of junction matrix
[INPE-4535-PRE/1282] 20 p2793 N88-26570
Guided wave interactions in millimeter-wave integrated circuits
[AD-A193017] 21 p2936 N88-27437
Array trade-off study using multilayer parasitic subarrays
[NASA-TM-101321] 22 p3070 N88-28222
Electronic and optical devices and applications 24 p3363 N88-30027

MICROWAVE COUPLING

Advanced numerical modeling of microwave penetration and coupling for complex structures
[DE88-001873] 06 p0690 N88-14231
Microwave polymerization of composite structures
[REPT-881-430-116] 21 p2922 N88-27343
Nonlinear dynamics of coupled oscillator arrays
[AD-A194888] 24 p3367 N88-30053

MICROWAVE EMISSION

Meterwave observations of a coronal hole 01 p0114 N88-10730
VLA observations of the X-ray bright Hyades M-dwarfs 04 p0512 N88-13147
Microwave observations of red dwarf flare stars 04 p0513 N88-13153
Current status of high power microwave effects and simulation
[DE87-004112] 06 p0751 N88-14615
Techniques for ceramic sintering using microwave energy
[DE88-001416] 07 p0837 N88-15080
Phase control of the microwave radiation in free electron laser two-beam accelerator
[DE88-001460] 07 p0859 N88-15219
Dynamic evolution of the source volumes of gradual and impulsive solar flare emissions
[NASA-TM-87815] 08 p1102 N88-16621
Research relative to angular distribution of snow reflectance/snow cover characterization and microwave emission
[NASA-CR-182733] 14 p1941 N88-21582
High power, high frequency radiation from beam-plasma interactions
[AD-A190207] 15 p2137 N88-22752

MICROWAVE EQUIPMENT

NT CYCLOTRON RESONANCE DEVICES
NT KLYSTRONS
NT MAGNETRONS
NT MICROWAVE AMPLIFIERS
NT MICROWAVE ANTENNAS
NT MICROWAVE FILTERS
NT MICROWAVE INTERFEROMETERS
NT MICROWAVE OSCILLATORS
NT MICROWAVE RADIOMETERS
NT MICROWAVE TUBES
NT THYRATRONS
NT TRAVELING WAVE TUBES

Anechoic Chamber test of the Electromagnetic Measurement System ground test unit
[DE87-012998] 01 p0035 N88-10226
Microwave refractive index structure function profiles (Cn2) measured from a small aircraft
[AD-A184343] 04 p0431 N88-12670
The lasertron RF generator for FEL (Free-Electron Laser) applications
[DE88-000515] 04 p0448 N88-12776
Evaluation of device figure of merit in microwave switching circuit design
[AD-A184896] 05 p0577 N88-13520
Observation guidelines for a Total Ozone Mapping Spectrometer (TOMS) in geosynchronous orbit
05 p0619 N88-13801
An analysis of simplified feed architectures for MMIC (Monolithic Microwave Integrated Circuit) T/R (Transmit/Receive) module arrays
[AD-A185474] 06 p0697 N88-14275
Microwave system for the microwave Tokamak experiment (MTX)
[DE88-002391] 09 p1250 N88-17487
Thermal analysis of transistor packages, part 2
[DE88-005091] 10 p1323 N88-17909
The bit-error rate performance of a satellite microwave matrix switch
[NASA-TM-100285] 16 p2167 N88-22920
The off-axis channel macroplate
[NASA-CR-182938] 18 p2505 N88-24861
The effects of better environmental inputs in estimating sea clutter
[AD-A192058] 19 p2643 N88-25678
Study and implementation of ultrahigh frequency coupling devices using the fin line technology --- millimeter waves
[ETN-88-92307] 20 p2796 N88-26588
Microwave polymerization of composite structures
[REPT-881-430-116] 21 p2922 N88-27343
Use of microwave measuring systems for the nondestructive control of resins and composites
[REPT-881-430-123] 21 p2959 N88-27576
Solid state research
[AD-A192837] 21 p3020 N88-27929
SSVCO feed characteristics
[DE88-011322] 22 p3068 N88-28208
HPM (High Power Microwave) simulation fidelity studies
[DE88-012229] 22 p3068 N88-28209
HPM (High-Power Microwave) coupling into realistic targets
[DE88-011788] 23 p3207 N88-29084
Millimeter wave generation by relativistic electron beams
[AD-A195683] 24 p3362 N88-30016
Growth of GaAs crystals by the Heat Exchanger Method for microwave device applications
[AD-A196028] 24 p3433 N88-30435
Estimation of soil temperature profile from remote microwave and IR measurements
24 p3450 N88-30532
The Deep Space Network: An instrument for radio astronomy research
[NASA-CR-183219] 24 p3453 N88-30554

MICROWAVE FILTERS
Band pass with cavity resonators by use of three oscillation types
[ETN-88-92984] 23 p3209 N88-29096

MICROWAVE FREQUENCIES
NT EXTREMELY HIGH FREQUENCIES
NT SUPERHIGH FREQUENCIES
Study and realization of Schottky diodes for forthcoming integrated hyperfrequency devices
[LAAS-87-062] 02 p0167 N88-11054
Deformation effects on microwave reflectivity
[AD-A185664] 07 p0844 N88-15120
Microwave response of an HEMT photoconductor
[NASA-TM-100819] 11 p1480 N88-18835
Polymerization of epoxy matrix composites using pulsed microwaves
[CERT-3/1324-MO] 20 p2780 N88-26487
Microwave frequency nondestructive control
[CERT-2/1355-MO] 23 p3189 N88-28976
Coupling between radiation and gas dynamics
[AD-A194593] 23 p3211 N88-29113
Microwave remote sensing in the French industries
[ETN-88-93081] 24 p3387 N88-30171

MICROWAVE IMAGERY
Validate algorithms for the determination of rainfall rates from SSM/I microwave satellite imagery
[AD-A188769] 16 p2233 N88-23337
Validate algorithms for the determination of rainfall rates from SSM/I microwave satellite imagery
[AD-A191337] 16 p2236 N88-23353
Microwave image understanding and its application to radar cross section management
20 p2788 N88-26542
Validate algorithms for the determination of rainfall rates from SSM/I microwave satellite imagery
[AD-A192299] 21 p2974 N88-27664
Validate algorithms for the determination of rainfall rates from SSM/I microwave satellite imagery
[AD-A195428] 24 p3404 N88-30270

MICROWAVE INTERFEROMETERS
Testing a very good microwave interferometer
[TRITA-EPP-86-09] 09 p1167 N88-16996
Geodesy by radio interferometry: Optimization of wet path delay algorithms using microwave radiometer data
[PB88-167739] 18 p2498 N88-24820

MICROWAVE LANDING SYSTEMS
Effect of motion cues during complex curved approach and landing tasks: A piloted simulation study
[NASA-TP-2773] 04 p0398 N88-12480
Boeing 727 MLS (Microwave Landing System) terminal instrument procedures (TERPS) approach data collection and processing, data report
[AD-A185523] 06 p0667 N88-14090
Microwave Landing System (MLS) mathematical model installation manual
[AD-A185612] 07 p0819 N88-14978
Crew procedures for microwave landing system operations
[NASA-CR-178359] 09 p1116 N88-16688
Flight simulations of MLS interception procedures applicable to laterally segmented approach paths
[NLR-MP-86037-U] 13 p1721 N88-20288
Analysis of a range estimator which uses MLS angle measurements
[NASA-CR-182896] 16 p2160 N88-22884
Development of an airborne facility for advanced avionics research 17 p2307 N88-23801
Cessna 172 MLS (Microwave Landing System) terminal instrument procedures (TERPS) approach data collection and processing data report
[AD-A191241] 18 p2461 N88-24613
Microwave landing system mathematical modeling study for Midway Airport Runway 22L, Chicago, Illinois
[AD-A191721] 18 p2462 N88-24616
Development of an airborne facility for advanced avionics research
[NLR-MP-87012-U] 20 p2760 N88-26388

MICROWAVE OSCILLATORS
NT MAGNETRONS
Optically tuned MM-wave IMPATT source
[AD-A185250] 05 p0577 N88-13523
High peak power ka-band gyrotron oscillator experiment
[AD-A185424] 05 p0585 N88-13563
High peak power Ka-band gyrotron oscillator experiments with slotted and unslotted cavities
[AD-A188109] 11 p1478 N88-18819
Low noise cryogenic dielectric resonator oscillator
[NASA-CASE-NPO-17157-1-CU] 20 p2797 N88-26596

MICROWAVE RADIATION
U MICROWAVES

MICROWAVE RADIOMETERS
Study of a payload for Columbus Polar Platform Earth observation demonstration mission, executive summary
[ESA-CR(P)-2412] 01 p0014 N88-10079
The CNR/PSN Advanced Microwave Imaging Radiometer (AMIR) --- satellite-borne
03 p0340 N88-12141
Non-linearity in measurement systems: Evaluation method and application to microwave radiometers
04 p0433 N88-12684
A multibody dynamic analysis of the N-ROSS (Navy Remote Ocean Sensing System) satellite rotating flexible reflector using Kane's method
[AD-A184452] 04 p0462 N88-12860
Cloud cover determination in polar regions from satellite imagery
[NASA-CR-181544] 04 p0471 N88-12908
In-orbit calibration adjustment of the Nimbus-7 SMMR
[NASA-TM-100678] 05 p0614 N88-13773
Estimation of rainfall rates in tropical cyclones by passive microwave radiometry 06 p0744 N88-14577
Characterization of 6 soils in the X-band, through measurements of complex permittivity
[INPE-4376-TDL/302] 12 p1639 N88-19814
Contribution of spaceborne high resolution radiometers to mapping of precoastal depths
19 p2701 N88-26063
Passive microwave measurements of water vapor fields and rain for locating fronts in cyclonic storms
[AD-A195632] 24 p3404 N88-30267

MICROWAVE SCATTERING
Active and passive remote sensing of ice
[AD-A186685] 09 p1195 N88-17162
Characteristics of coherent and incoherent waves in snow at microwave and millimeter wave frequencies
[AD-A188990] 12 p1620 N88-19692
Almond test body --- for microwave anechoic chambers
[NASA-CASE-LAR-13747-1] 18 p2502 N88-24845
Microwave amplifiers
[AD-A192974] 20 p2795 N88-26585
Transient interaction of electromagnetic pulses in dielectrics and microwave biophysics
[AD-A195687] 24 p3360 N88-30008

MICROWAVE SENSORS
Fundamental aspects of the physics of remote sensing
[ESA-TT-1045] 09 p1185 N88-17100
Principal space programs in the area of microwaves
[INPE-4164-PRE/1064] 12 p1618 N88-19677
Microwave calibration system 2
[AD-A192976] 20 p2805 N88-26639
Active and passive remote sensing of ice
[AD-A193307] 21 p2966 N88-27617
Microwave instrument for planetary mission (Titan/CASSINI mission orbiter spacecraft)
[BAE-CS/TP-8359] 24 p3375 N88-30102

MICROWAVE SOUNDING
Determination of total ozone from HIRS2/MSU sounding data 05 p0619 N88-13799
Multifilter spectrometer (FEB) for microwave atmospheric sounder
[AD-A192312] 21 p2935 N88-27426

MICROWAVE SPECTRA
Microwave observations of nonthermal phenomena in pre-main sequence stars 04 p0505 N88-13107
Microwave dielectric spectrum of rocks
[NASA-TM-89719] 12 p1642 N88-19831
Microwave spectroscopy and gravitational collapse
18 p2594 N88-25413
Mode locking of semiconductor laser with external cavity
[AD-A196018] 24 p3378 N88-30117

MICROWAVE SPECTROMETERS
Precise measurement of refractive index and absorption coefficient of near millimeter wave and far infrared materials
[AD-A184538] 03 p0293 N88-11840

MICROWAVE SWITCHING
Loss measurement of 3-port ferrite switches in the 90 GHz range
[ESA-TT-1054] 03 p0310 N88-11958
Evaluation of device figure of merit in microwave switching circuit design
[AD-A184896] 05 p0577 N88-13520
RF-switches: Application and design --- satellite communication 14 p1877 N88-21215

MICROWAVE TRANSMISSION
Operation of the TEMPO machine
[DE87-011285] 01 p0038 N88-10241
An evaluation of equivalent models for design of rectangular microstrip antennas
[FOA-C-30451-3.2] 08 p0977 N88-15905
A review of the role of surface reflection in multipath propagation over terrestrial microwave links
12 p1615 N88-19655
Identification of cascaded microwave circuits with moderate reflections using reflections and transmission measurements
[PB88-171921] 18 p2503 N88-24849

MICROWAVE TUBES
NT CYCLOTRON RESONANCE DEVICES
NT KLYSTRONS
NT MAGNETRONS
NT TRAVELING WAVE TUBES
Microwave tubes: Literature study no. 8 comprising the year 1986
[FOA-C-30467-3] 09 p1159 N88-16944
A crude scaling law for lasertrons
[DE88-003880] 09 p1173 N88-17032

MICROWAVES
NT CENTIMETER WAVES
NT DECIMETER WAVES
NT MICROWAVE EMISSION
NT MILLIMETER WAVES
Static magnetization and microwave loss in shock-modified ferrites
[DE87-012362] 02 p0146 N88-10916
Laboratory evaluation and application of microwave absorption properties under simulated conditions for planetary atmospheres
[NASA-CR-181466] 02 p0254 N88-11606
Measurement of solid propellant combustion velocity by means of microwaves
[CERT-1/1316-MO] 03 p0283 N88-11778
Automated microwave dielectric constant measurement
[AD-A184182] 04 p0431 N88-12667
United States - Japan Workshop on Dielectric and Piezoelectric Ceramics (3rd) held in Toyama, Japan on November 9-12, 1986
[AD-A185113] 05 p0568 N88-13460

Microwave challenges to the thermoregulatory system
[AD-A185391] 05 p0629 N88-13847
Microwave superheaters for fusion
[DE88-001656] 05 p0653 N88-14007
Propagation effects on satellite systems at frequencies below 10 GHz: A handbook for satellite systems design
[NASA-RP-1108/2] 06 p0690 N88-14226
Time-domain robotic vision application
06 p0798 N88-14886
Modulation of an intense beam by an external microwave source: Theory and simulation
[AD-A185683] 07 p0848 N88-15145
Combined effect of microwaves and ionizing radiation
07 p0893 N88-15413
Construction of airborne radars for remote sensing
[PB88-113063] 09 p1154 N88-16916
Properties of superconducting tunnel structures in microwave radiation field 09 p1239 N88-17424
Fundamental cyclotron frequency generation from a cusptron oscillator
[AD-A188187] 10 p1321 N88-17898
A technique for low level, wide range CW microwave power meter calibrations
[DE88-004147] 10 p1333 N88-17966
Numerical simulation of the propagation and absorption due to air breakdown of long microwave pulses
[DE88-005227] 11 p1475 N88-18798
Microwave radiation from rotating, annular electron beams 11 p1475 N88-18801
Experimental results of a high-gain microwave FEL operating at 140 GHz
[DE88-004358] 11 p1492 N88-18907
A sky temperature survey at 19.2 GHz using a balloon borne Dicke radiometer for anisotropy tests of the cosmic microwave background 11 p1571 N88-19403
Two-dimensional electron fluid computer calculations of nanosecond pulse, low pressure microwave air breakdown in a rectangular waveguide and their verification by experimental measurement
[DE88-004407] 12 p1618 N88-19678
Microwave generation from a cusptron oscillator with a six-vane circuit
[AD-A188377] 12 p1619 N88-19680
Solid-state travelling wave amplifiers based on multi-stream instability
[AD-A189566] 12 p1624 N88-19718
Photonic temperature and pressure sensors for biosystems/pulsed microwave. Part 1: Interaction studies
[AD-A188887] 12 p1629 N88-19751
Effects of whole-body irradiation with low-intensity microwaves on morphological, functional and cytochemical characteristics of leukocytes 12 p1663 N88-19971
Microwave and structural properties of saline ice
[AD-A189307] 13 p1803 N88-20779
Design of electron beam accelerator for microwave application
[DE88-005252] 13 p1838 N88-20999
Solar microwave radiation maps measured at Metsaehovi Radio Research Station in 1978-1979
[PB88-127543] 13 p1857 N88-21108
Tabulation of Mie scattering calculation results for microwave radiative transfer modeling
[NASA-CR-4130] 14 p1947 N88-21612
Generating squeezed microwave radiation with a Josephson parametric amplifier
14 p1978 N88-21805
Microwave sintering of alumina-SiC composites at 2.45 and 60 GHz
[DE88-006455] 15 p2030 N88-22095
Preparing the Alcator C bolometer system for use on MTX (Microwave Tokamak Experiment)
[DE88-006724] 15 p2134 N88-22733
Validate algorithms for the determination of rainfall rates from SSM/I microwave satellite imagery
[AD-A188769] 16 p2233 N88-23337
Power requirements for mining and microwave processing of extraterrestrial resources
17 p2420 N88-24389
The radar cross section of some simple reflectors at short wavelengths
[FOA-C-30472-3.3] 18 p2501 N88-24839
Behavioral response of rats exposed to high-power microwave radiation
[AD-A192199] 18 p2548 N88-25128
Analysis of microwave burner measurement system using a microwave network analysis computer program
19 p2631 N88-25604
A simple technique to generate or gate microwave pulses with picosecond speeds 19 p2657 N88-25784
Radar and EW applications of multi-gigahertz optical components and systems 19 p2660 N88-25816
The ratio of microwaves to X-rays in solar flares: The case for the thick target model
[NASA-CR-183102] 19 p2743 N88-26287
Antenna heights for the optimum utilization of the oceanic evaporation duct. Part 3: Results from the Mediterranean measurements, volume 2
[AD-A192311] 20 p2791 N88-26554
MTX (Microwave Tokamak Experiment) plasma diagnostic system
[DE88-011326] 20 p2861 N88-26993
Preparation and properties of high Q microwave dielectrics in the (CA, SR, BA) zirconate system
[AD-A193127] 21 p2918 N88-27317
A method for estimating the susceptibility of electronic systems to HPM (High Power Microwave)
[DE88-012246] 21 p2934 N88-27422
Genetic effects of low level microwave radiation
[AD-A192687] 21 p2984 N88-27722
Effects of pulsed and CW (Continuous Wave) 2450 MHz radiation on transformation and chromosomes of human lymphocytes in vitro
[AD-A193104] 21 p2987 N88-27736
Assessment of cochlear damage after microwave irradiation
[AD-A193237] 21 p2987 N88-27737
Behavioral effects of exposure to the tempo high-power microwave system
[AD-A193305] 21 p2987 N88-27738
Experiments applications guide: Advanced Communications Technology Satellite (ACTS)
[NASA-TM-100265] 22 p3048 N88-28082
Improvements in techniques of microwave thermography
[AD-A194613] 23 p3203 N88-29062
Improvements in techniques of microwave thermography
[AD-A193620] 23 p3239 N88-29276
The surface evaporative duct height product: An evaluation
[AD-A195918] 24 p3392 N88-30199

MICROWEIGHING
U WEIGHT MEASUREMENT

MIDAIR COLLISIONS
NT BIRD-AIRCRAFT COLLISIONS
UK airmiss statistics
[CAP-530] 03 p0261 N88-11642
Aircraft accident report: Midair collision of Cessna-340A, N8716K, and North American SNJ-4N, N711SQ, Orlando, Florida, May 1, 1987
[PB88-910402] 13 p1720 N88-20282
UK airmiss statistics
[REPT-3/87] 14 p1865 N88-21141
Aircraft accident report: Midair collision of US Army U-21A, Army 18061 and Sachs Electric Company Piper PA-31-350, N60SE, Independence, Missouri, January 20, 1987
[PB88-910401] 16 p2159 N88-22877
UK airmiss statistics
[CAA-1/87] 17 p2300 N88-23761
Aircraft accident report: Midair collision of SkyWest Airlines Swearingen METRO 2, N163SW, and Mooney M20, N6485U, Kearns, Utah, January 15, 1987
[PB88-910404] 20 p2755 N88-26346
UK airmisses involving commercial air transport
[CAA-1/88] 23 p3176 N88-28907

MIDCOURSE GUIDANCE
Report to congress on the strategic defense system architecture
[AD-A195476] 24 p3426 N88-30393

MIDDLE ATMOSPHERE
NT MESOPAUSE
NT MESOSPHERE
NT OZONOSPHERE
NT STRATOPAUSE
NT STRATOSPHERE
Contributions of lidar measurements to the study of long term variations of the middle atmosphere
[ETN-88-91237] 05 p0625 N88-13824
Latitude coverage of observations of the middle atmosphere by solar absorption spectrometry from a heliosynchronous orbit
[AERONOMICA-ACTA-A-316-1987] 06 p0742 N88-14566
New techniques for rocket and balloon-borne instrumentation for investigations of the structure, dynamics and electrodynamics of the middle atmosphere 08 p1027 N88-16220
Electrodynamics of the high latitude middle atmosphere 08 p1028 N88-16225
Dynamic modeling of the middle atmosphere 08 p1028 N88-16227
Project CONDOR: Middle atmosphere wind structure obtained with lightweight inflatable spheres near the equatorial electrojet 08 p1028 N88-16230
ROCOZ-A (improved rocket launched ozone sensor) for middle atmosphere ozone measurements 08 p1029 N88-16233
The Cryogenic Infrared Spectrometer and Telescope for the Atmosphere (CRISTA) experiment on Astro-SPAS 08 p1034 N88-16270
Geochemistry of the middle and lower atmosphere: Environmental impact through the deterioration of the ozone layer
[INPE-4477-PRE/1241] 16 p2230 N88-23321
Finite element simulation of the atmosphere's electromagnetic response to charge perturbations associated with lightning 17 p2375 N88-24124
Aerial photography as an instrument of atmospheric analysis: Maps of the middle atmosphere and its dynamics, Baixada Santista (SP) 19 p2684 N88-25955
Diffusion of slight solar induced disturbances in the middle atmosphere
[MITT-53] 20 p2825 N88-26758

MIDDLE EAR
Novel nonlinear signal processing principles
[AD-A191644] 19 p2707 N88-26097

MIDLATITUDE ATMOSPHERE
Physical processes for maintaining mean meridional and zonal circulation of atmosphere in middle latitudes, volume 1 14 p1900 N88-21343
Physical process for maintenance of mean meridional and zonal circulation of atmosphere in middle latitudes, volume 2 14 p1900 N88-21345
Experimental proof of quasilongitudinal propagation of low-frequency waves in middle latitudes in upper ionosphere 24 p3447 N88-30516

MIDLATITUDES
U TEMPERATE REGIONS

MIE SCATTERING
NT RAYLEIGH SCATTERING
Extinction by dielectric particles at optical and infrared wavelength
[AD-A184818] 05 p0650 N88-13981
Tabulation of Mie scattering calculation results for microwave radiative transfer modeling
[NASA-CR-4130] 14 p1947 N88-21612
Advanced diagnostics for reacting flows
[AD-A190485] 15 p2035 N88-22122
Investigations on Mie and Rayleigh scattering as basis for the development of Rayleigh temperature lidars with aid of Michelson interferometry
[GKSS-87/E/62] 21 p2976 N88-27675

MIE THEORY
U MIE SCATTERING

MIG AIRCRAFT
Proposal for a new aggressor aircraft
[AD-A194311] 22 p3041 N88-28056

MIGRATION
Migration and transfer of triplet energy in selected polymer systems
[DE87-014432] 02 p0152 N88-10953
The migration of grain boundaries in ceramic materials with particular reference to the sintering process
[DE88-004085] 10 p1306 N88-17808
Electrohydrodynamic migration of charged droplets in an insulating fluid
[NASA-TM-100849] 14 p1912 N88-21424
Energy migration, motion and order in synthetic polymers
[AD-A193334] 21 p2918 N88-27320
Migration and stability of HgCdTe lattice defects
[AD-A193293] 21 p3021 N88-27935

MILANKOVITCH THEORY
U CLIMATOLOGY

MILITARY AIR FACILITIES
ZEUS: A knowledge-based expert system that assists in predicting visibility at airbases
[AD-A184197] 05 p0626 N88-13829
Evaluation of bituminous materials used in pavement recycling projects at Tyndall, MacDill, and Hurlburt Air Force Bases
[AD-A188068] 10 p1317 N88-17871
Revised Uniform Summary of Surface Weather Observations, Loring AFB, Maine, Parts A - F
[AD-A188201] 14 p1947 N88-21610
Vegetation studies on Vandenberg Air Force Base, California
[NASA-TM-100985] 20 p2831 N88-26795
Reduced flexibility in processing Titan 4 space launch vehicles at Cape Canaveral Air Force Station
[AD-A194908] 24 p3332 N88-29834
EMPTAC (Electromagnetic Pulse Test Aircraft) user's guide
[AD-A195072] 24 p3360 N88-30006

MILITARY AIRCRAFT
The EH-101 integrated project: A naval, utility and commercial helicopter system 03 p0265 N88-11672
Aircraft field degradation and electromagnetic compatibility
[PB88-183975] 19 p2602 N88-25456
Background to the UK military requirements for engine usage, condition and maintenance management systems 22 p3033 N88-28004

MILITARY HELICOPTERS
NT AH-64 HELICOPTER
NT CH-46 HELICOPTER
NT HEAVY LIFT HELICOPTERS
NT OH-58 HELICOPTER
NT UH-1 HELICOPTER
NT UH-60A HELICOPTER
The influence of operational requirements on LHX concept formulation 03 p0262 N88-11650
Investigation of vertical axis handling qualities for helicopter hover and NOE flight 03 p0263 N88-11653
MBB simulation facilities applied for rotorcraft research 03 p0263 N88-11655
Impacts of rotor hub design criteria on the operational capabilities of rotorcraft systems 03 p0264 N88-11663
Helicopter (performance) management 03 p0264 N88-11666
Helicopter fire control: Advantages of an automatic target tracker 03 p0264 N88-11667
Development, testing and evaluation of a night vision goggle compatible BO-105 for night low level operation 03 p0265 N88-11668
A129 advanced solutions for meeting today's combat helicopter requirement 03 p0265 N88-11669
Advanced helicopter cockpit and control configurations for helicopter combat missions
[NASA-TM-100017] 07 p0821 N88-14988
A piloted simulation investigating handling qualities and performance requirements of a single-pilot helicopter in air combat employing a helmet-driven turreted gun
[AD-A186878] 09 p1116 N88-16689
Helicopter activities in Germany
[MBB-UD-487/86] 10 p1314 N88-17853
Artificial and natural icing tests of AH-64, phase 2
[AD-A188231] 11 p1439 N88-18585
User perceptions of side-arm flight control in rotary-wing aircraft
[AD-A188519] 12 p1672 N88-20009
AVSCOM'S modifications to Teledyne Systems Company's air-to-air fire control system simulation model
[AD-A189136] 13 p1722 N88-20294
An investigation of the ability to recover from transients following failures for single-pilot rotorcraft
[NASA-TM-100078] 16 p2164 N88-22905
Test philosophy of the EH101 integrated avionic 17 p2303 N88-23775
Operation and performance of an integrated helicopter communication system 17 p2305 N88-23787
Operational noise data for CH-47D and AH-64 army helicopters
[AD-A191059] 18 p2570 N88-25263
Helicopter transmission research at NASA Lewis Research Center
[NASA-TM-100962] 24 p3379 N88-30128
MILITARY OPERATIONS
NT COMBAT
NT ELECTRONIC WARFARE
Automation strategy and results for an airbase command and control information system
[NLR-MP-86031-U] 01 p0035 N88-10223
How space, the fourth operational medium, supports operational maneuver
[AD-A184742] 03 p0373 N88-12346
High resolution satellite imagery simulation --- treaty verification
[FOA-C-30462-3.3,9.3] 05 p0620 N88-13810
Assessment of physical activity intensity by heart rate during sleep limited military operations
[AD-A185913] 07 p0888 N88-15382
Analysis of the reliability of Royal Australian Air force non-destructive inspection
[AD-A186979] 09 p1177 N88-17049
Computer assisted instruction: Two decades in perspective
[AD-A186813] 09 p1216 N88-17289
The evolution of naval warfare technology and the impact of space systems
[AD-A186900] 09 p1233 N88-17392
The mathematization of the military sciences
[MBB-Z-139/87] 10 p1311 N88-17834
Development of a graphics based two-attribute utility assessment program with application to mission planning
[AD-A187276] 10 p1388 N88-18292
State-of-the-art technologies for construction in space: A review
[AD-A188412] 12 p1585 N88-19483
Alternative program approaches for the advanced satellite technology program
[AD-A188917] 12 p1600 N88-19576
Emerging technologies program 3-5: Microelectronics Panel report
[AD-A189463] 12 p1624 N88-19716
Selected aspects of triazolam in relation to aviator performance in naval flight operations
[AD-A189322] 12 p1667 N88-19996
Knowledge-based system analysis and control
[AD-A188163] 12 p1681 N88-20049
Expert systems for decision support in military aircraft mission preparation
[NLR-MP-87013-U] 13 p1830 N88-20946
MANPRINT handbook for RFP (Request For Proposal) development
[AD-A188321] 13 p1850 N88-21075
Soviet military power, 1987 13 p1858 N88-21114
Application of hybrid laminar flow control to global range military transport aircraft
[NASA-CR-181638] 14 p1862 N88-21124
An overview of the army GIS (Geographic Information Systems) Research Program
[AD-A189711] 14 p1992 N88-21871
Department of Defense statement on the X-ray Lithography Program to the Research and Development Subcommittee of the House Armed Services Committee of 100th Congress, second session
[AD-A191854] 18 p2582 N88-25341
Real time data base management
[AD-A191758] 19 p2739 N88-26265
NAVSTAR global positioning system
[AD-A192609] 20 p2757 N88-26354
The strategic defense initiative: Strategic implications
[AD-A192341] 20 p2847 N88-26902
Launch operations to support future space forces
[AD-A192679] 20 p2881 N88-27107
Aerospace applications studies, 1971-1987
[AGARD-R-759] 21 p2889 N88-27147
Army space systems for terrestrial applications
[AD-A192735] 21 p2965 N88-27613
Analysis of ATCRBS (Air Traffic Control Radar Beacon System), mode select (Mode S) in combat operations
[AD-A193140] 22 p3040 N88-28050
Biomedical aspects of military operations at high altitude
[AD-A192677] 22 p3132 N88-28619
Tactical air force night/adverse weather training
[AD-A194243] 22 p3133 N88-28625
Linear goal programming as a military decision aid
[AD-A194276] 22 p3137 N88-28652
Inflight rearming
[AD-A193564] 23 p3176 N88-28909
Low altitude: A new dimension in air refueling
[AD-A193819] 23 p3176 N88-28910
Defensive platform size and survivability
[DE88-011634] 23 p3184 N88-28948
Remotely Operated Vehicle (ROV) reliability study, phase 1
[AD-A194367] 23 p3222 N88-29177
SDI (Strategic Defense Initiative): A policy analysis
[AD-A194240] 23 p3275 N88-29493
The problem of space in Soviet operational art
[AD-A194150] 23 p3276 N88-29502
Centralized class A flight mishap investigation
[AD-A194397] 24 p3322 N88-29786
Integration of LANTIRN (Low Altitude Navigation and Targeting Infrared for Night) into operational fighter training
[AD-A194906] 24 p3325 N88-29799
Long haul communications in the HF spectrum utilizing high speed modems
[AD-A194683] 24 p3360 N88-30003
Looking beyond the strategic defense initiative
[AD-A195079] 24 p3427 N88-30394
Antisatellite weapons and satellite deployment strategies
[AD-A195014] 24 p3427 N88-30396
MILITARY PSYCHIATRY
U MILITARY PSYCHOLOGY
MILITARY PSYCHOLOGY
New US book on aviation psychology reviewed 07 p0896 N88-15433
MILITARY SPACECRAFT
NT DMSP SATELLITES
NT RECONNAISSANCE SPACECRAFT
An introduction to military satellite communications
[RSRE-MEMO-3976] 09 p1153 N88-16911
NROSS (Navy Remote Ocean Sensing System): A force multiplier
[AD-A186853] 10 p1346 N88-18045
Alternative program approaches for the advanced satellite technology program
[AD-A188917] 12 p1600 N88-19576
Alternative force structuring strategies for military satellite communication systems
[AD-A189492] 13 p1758 N88-20516
Air Force space power requirements and nuclear power assessment methodology 17 p2418 N88-24378
Comparison of a direct thrust nuclear engine, nuclear electric engine and a chemical engine for future space missions 17 p2418 N88-24379
The Army's role in space: Support for the battlefield commander
[RAND-P-7396] 19 p2721 N88-26159
Launch operations to support future space forces
[AD-A192679] 20 p2881 N88-27107
The principles of mass and maneuver applied to space operations
[AD-A194037] 23 p3276 N88-29500
The problem of space in Soviet operational art
[AD-A194150] 23 p3276 N88-29502
Antisatellite weapons and satellite deployment strategies
[AD-A195014] 24 p3427 N88-30396
MILITARY TECHNOLOGY
Soviet aviation technology's state of the art SU-27 fighter
[AD-A184121] 03 p0259 N88-11628
Fuel cells --- military applications
[PML-1986-43] 05 p0622 N88-13813
University research initiative research program summaries
[AD-A184876] 05 p0658 N88-14035
Investigation of design concepts for large space structures to support military applications
[AD-A186098] 07 p0824 N88-15000
A summary of the Naval Postgraduate School research program
[AD-A186362] 07 p0942 N88-15727
AGARD reports: A quarterly listing, 1 July through September 30, 1987
[AD-A186572] 08 p1093 N88-16579
Advanced composite airframe program: Today's technology 09 p1107 N88-16636
Cooperative analysis expert situation assessment research 09 p1206 N88-17228
The evolution of naval warfare technology and the impact of space systems
[AD-A186900] 09 p1233 N88-17392
The military techniques of tomorrow. A contribution to active peace assurance
[MBB-UA-1049/87] 10 p1315 N88-17860
Optical memory cards: A comparison with other current technologies and potential military applications
[AD-A187287] 10 p1425 N88-18512
Soviet high-technology restructuring drive: the MNTK network
[AD-A188138] 11 p1565 N88-19370
Soviet military power, 1987 13 p1858 N88-21114
JPRS report: Science and technology. Japan
[JPRS-JST-87-029] 15 p2052 N88-22228
Laser comparison study of Nd:BEL and Nd:YAG
[AD-A191084] 16 p2213 N88-23205
Development of a C3 generic workstation: System overview 16 p2242 N88-23396
C3 generic workstation: Performance metrics and applications 16 p2242 N88-23397
Department of Defense statement on defense agency research and development to the Subcommittee on Defense of the Committee on Appropriations, United States House of Representatives, 100th Congress, second session
[AD-A191840] 18 p2588 N88-25377
The FY 1989 Department of Defense statement on the Science and Technology Program to 100th Congress, second session
[AD-A191843] 18 p2588 N88-25380
Radar and EW applications of multi-gigahertz optical components and systems 19 p2660 N88-25816
On 3-5 transistors for MM-wave applications
[AD-A191580] 19 p2661 N88-25825
The Army's role in space: Support for the battlefield commander
[RAND-P-7396] 19 p2721 N88-26159
Air Force technical objective document, FY89
[AD-A193110] 21 p2896 N88-27194
Intelligent Mobile Autonomous System (IMAS)
[AD-A193181] 21 p3003 N88-27811
Dynamically reconfigurable distributed database systems
[AD-A194716] 23 p3297 N88-29636
MILKY WAY GALAXY
The astrophysics of nebulae and active galactic nuclear emission-line regions: New methods and applications 13 p1858 N88-21111
Royal Observatory, Edinburgh: Research and Facilities
[ISSN-0267-6281] 14 p1993 N88-21881
The galactic nucleus at mm-, sub-mm and far-infrared wavelengths
[MPE-PREPRINT-102] 16 p2288 N88-23700
The distance to the center of the galaxy: H2O maser proper motions in Sgr B2(N)
[MPE-PREPRINT-104] 16 p2288 N88-23702
The velocity field of the outer galaxy
[B8681472] 20 p2885 N88-27132

Gamma radiation from center of the galaxy of the order of MeV values
[MPE-207] 21 p3032 N88-27999
Distribution of hydroxyl clouds in the galaxy
[DE88-702415] 22 p3164 N88-28844
The kinematics of Milky Way halo gas
23 p3299 N88-29648

MILLIMETER WAVES
Millimeter wave tokamak heating and current drive with a high power free electron laser
[DE87-011324] 01 p0099 N88-10651
The impact of environmental factors on the performance of millimeter wave seekers in smart munitions
[DE87-014277] 03 p0270 N88-11697
Precise measurement of refractive index and absorption coefficient of near millimeter wave and far infrared materials
[AD-A184538] 03 p0293 N88-11840
Millimeter-wave studies of moist air
[AD-A184681] 03 p0306 N88-11935
Investigation of hexagonal ferrite film growth techniques for millimeter-wave systems applications
[AD-A184335] 03 p0383 N88-12406
An investigation of millimeter wave propagation in the atmosphere: Measurement program
[AD-A184837] 05 p0574 N88-13498
Optically tuned MM-wave IMPATT source
[AD-A185250] 05 p0577 N88-13523
Observation and interpretation of solar S-component radiation at millimetre waves
[PB87-225207] 06 p0805 N88-14916
Horn design equations for the NBS (National Bureau of Standards) horn-type noise standards
[PB88-110226] 07 p0844 N88-15122
An adiabatic demagnetization cooled bolometer system for millimeter continuum astronomy
07 p0943 N88-15735
Finnish-Soviet Symposium on Radio Astronomy (1st) held at Otanlemi on August 26-27, 1985
[PB87-140661] 07 p0944 N88-15736
ESA Bulletin No. 10
[ETN-87-90514] 09 p1123 N88-16728
Technology developments to meet tomorrow's need for higher satellite frequencies 09 p1124 N88-16732
Fabrication and packaging of discontinuous MIM (Metal-Insulator-Metal) film arrays for efficient MM wave and IR detection and mixing
[AD-A186809] 09 p1146 N88-16869
MM-wave propagation and application in military communication systems 12 p1617 N88-19669
Millimeter and submillimeter wave research: Spectroscopy, energy transfer, and techniques
[AD-A188952] 12 p1620 N88-19691
Characteristics of coherent and incoherent waves in snow at microwave and millimeter wave frequencies
[AD-A188990] 12 p1620 N88-19692
Development of a high speed InGaAs/InP Schottky barrier photodetector for millimeter-wave fiber optical links
[AD-A188594] 12 p1629 N88-19750
Observations of the large scale anisotropy in the cosmic background radiation at 3 mm
[INPE-4425-PRE/1229] 12 p1712 N88-20249
Millimeter-wave properties of the atmosphere: Laboratory studies and propagation modeling
[PB88-164215] 14 p1905 N88-21387
Millimeter-wave pulse distortion by a single adsorption line simulating the terrestrial atmosphere
[PB88-161237] 14 p1906 N88-21388
Calculation of the efficiency of a resonant cyclotronic electron maser (gyrotrons)
[INPE-4387-PRE/1207] 14 p1915 N88-21444
Some models for rain and cloud attenuation of millimeter waves
[PB88-160809] 14 p1948 N88-21616
Instrumentation for the characterization and development of millimeter wave components compatible with monolithic integration
[AD-A189724] 15 p2059 N88-22275
The superconducting phase shifter in the development of a terahertz imaging radar system
[AD-A190666] 16 p2188 N88-23046
UV-Laser reactions of molecular adsorbates
[AD-A190796] 16 p2212 N88-23201
The galactic nucleus at mm-, sub-mm and far-infrared wavelengths
[MPE-PREPRINT-102] 16 p2288 N88-23700
Submillimeter and far infrared line observations of M17 SW: A clumpy molecular cloud penetrated by UV radiation
[NASA-CR-182866] 16 p2288 N88-23701
Operation and performance of an integrated helicopter communication system 17 p2305 N88-23787
Optical constants of minerals and other materials from the millimeter to the ultraviolet
[AD-A192210] 18 p2482 N88-24724
Millimeter and submillimeter waves and frequency selective surfaces
[AD-A191511] 18 p2500 N88-24827
Computer aided design of monolithic microwave and millimeter wave integrated circuits and subsystems
[AD-A191593] 18 p2503 N88-24852
Millimeter-wave integrated circuits
19 p2656 N88-25774
Characteristics of shielded microstrip lines on GaAs-Si at millimeter-wave frequencies 19 p2657 N88-25787
Picosecond response of an optically controlled millimeter wave phase shifter 19 p2660 N88-25820
On 3-5 transistors for MM-wave applications
[AD-A191580] 19 p2661 N88-25825
Study and implementation of ultrahigh frequency coupling devices using the fin line technology --- millimeter waves
[ETN-88-92307] 20 p2796 N88-26588
An evaluation of two millimeter wave propagation models for horizontal atmospheric attenuation at 70-115 GHZ
[AD-A192699] 21 p2931 N88-27403
Multifilter spectrometer (FEB) for microwave atmospheric sounder
[AD-A192312] 21 p2935 N88-27426
A planar IC-compatible transferred electron device for millimeter-wave operation
[AD-A192692] 21 p2936 N88-27433
Guided wave interactions in millimeter-wave integrated circuits
[AD-A193017] 21 p2936 N88-27437
Rapid-scanning Fourier transform spectrometer for studies of propagation of near-millimeter-wave radiation through clear air and fog
[AD-A193752] 22 p3070 N88-28219
A millimeter-wave tunneLadder TWT
[NASA-CR-182184] 22 p3072 N88-28239
Multi-sensory tracking mount control
[AD-A194675] 23 p3249 N88-29339
Laboratory evaluation and application of microwave absorption properties under simulated conditions for planetary atmospheres
[NASA-CR-182443] 23 p3300 N88-29653
Millimeter wave generation by relativistic electron beams
[AD-A195683] 24 p3362 N88-30016
Dielectric millimeter waveguides: A feasibility study for a novel dielectric millimeter waveguide
[AD-A195104] 24 p3366 N88-30042
Light-millimeter wave interactions in semiconductor devices
[AD-A195898] 24 p3432 N88-30428

MILLING (MACHINING)
Size-reduction and sorting behavior in sieve hammer mills
[ETN-88-91480] 11 p1467 N88-18749
An automatic system for extraction of information from a Computer Aided Design (CAD), selection, sequencing, and execution of turning processes
[INPE-4350-TDL/294] 12 p1676 N88-20020
Improvements in end point detection --- semiconductor fabrication
[RSRE-MEMO-4035/A] 14 p1899 N88-21336

MILLING MACHINES
Structure and properties of titanium nitride and zirconium nitride thin films prepared by reactive ion plating --- cutting tools
[ETN-88-92218] 15 p2042 N88-22167

MIM (SEMICONDUCTORS)
Fabrication and packaging of discontinuous MIM (Metal-Insulator-Metal) film arrays for efficient MM wave and IR detection and mixing
[AD-A186809] 09 p1146 N88-16869

MIM DIODES
Studies of tunneling in metals under high pressure
06 p0775 N88-14757

MIMD (COMPUTERS)
Performance of a multigrid method on parallel architecture 11 p1539 N88-19200
An analysis of multiple grain CHiP architectures
[AD-A189942] 15 p2110 N88-22570
Transformations of concurrent algorithms for highly parallel systems: A one year project summary report
[AD-A190236] 15 p2111 N88-22576
Multidimensional nodal transport methods for multiple-instruction multiple-data distributed memory machines
[DE88-004732] 19 p2713 N88-26108
Basic database operations on the butterfly parallel processor: Experiment results
[AD-A193199] 21 p3002 N88-27804
What have we learnt from using real parallel machines to solve real problems
[DE88-011227] 22 p3135 N88-28636

MINERAL DEPOSITS
A mineral reconnaissance sampling manual for Costa Rica: Central American energy and resource project
[DE87-014997] 04 p0462 N88-12859
Proceedings of the Third Airborne Imaging Spectrometer Data Analysis Workshop
[NASA-CR-181552] 05 p0611 N88-13755
Preliminary results from an investigation of AIS-1 data over an area of epithermal alteration: Plateau, Northern Queensland, Australia 05 p0613 N88-13768
Space photographs of the Onega-Ladoga isthmus and prediction of useful minerals 08 p1008 N88-16108
Study of relief of ore regions using space images (on the example of Eastern Yakutia)
08 p1008 N88-16111
Character of five selected LANDSAT lineaments in southwestern Pennsylvania: Report of investigations, 1987
[PB88-133517] 11 p1505 N88-18988

MINERAL EXPLORATION
Study of Earth from space and strengthening of economy 01 p0010 N88-10055
Marine minerals: Exploring our new ocean frontier
[PB87-217725] 02 p0216 N88-11364
Application of SPOT-1 data to mineral exploration in Nevada 03 p0343 N88-12163
Evolution of remote sensing utilization in geological mapping and ore exploration: Example in Zimbabwe
03 p0343 N88-12165
A mineral reconnaissance sampling manual for Costa Rica: Central American energy and resource project
[DE87-014997] 04 p0462 N88-12859
Remote sensing in mineral exploration
[PB87-138558] 06 p0729 N88-14484
Study of relief of ore regions using space images (on the example of Eastern Yakutia)
08 p1008 N88-16111
International role of US geoscience
[NASA-CR-182407] 08 p1035 N88-16281
Three-dimensional transient electromagnetic modeling for exploration geophysics 10 p1346 N88-18047
An integrated study of the Alto Paranaiba Kimberlite Province, Minas Gerais, Brazil: A possible tool for diamond exploration 17 p2355 N88-24031
Lithostructural interpretation of Chapda do Cachimbo (Pa-Am-Mt), based on radar and LANDSAT imagery
17 p2368 N88-24100
Remote sensing applied to the monitoring of mineral extraction in the proximity of urban areas: Pros and cons
19 p2684 N88-25954
First results of international investigations of the applications of SPOT-1 data to geologic problems, mineral and energy exploration 22 p3101 N88-28419
Results of the Geosat program to evaluate SPOT data for petroleum and mineral exploration
22 p3102 N88-28422
Evaluation of SPOT imagery for discriminating vegetation communities associated with surficial and bedbrock geology and identifying anomalous and stressed vegetation associated with mineralization
22 p3103 N88-28426
Use of digital images as a mineral prospecting tool in the tin province of Goias, Brazil
[INPE-4537-PRE/1284] 24 p3387 N88-30173
Obligue metallogenic zones recognized by interpreting space photographs of southern Tien Shan
24 p3450 N88-30529

MINERAL OILS
The wear process during the RUNNING-IN of steel in lubricated sliding
[NAL-TR-922T] 02 p0181 N88-11130
Lubricating properties of molybdenum disulfide. Part 3: Performance of molybdenum disulfide-containing oils in fluid lubrication
[NASA-TT-20156] 13 p1752 N88-20480
A study relating to the fog oil replacement program
[AD-A192536] 21 p2923 N88-27347

MINERALOGY
The distribution of evaporitic weathering products on Antarctic meteorites 06 p0798 N88-14888
A sedimentological and mineralogical study of the Koogah Formation, New South Wales
18 p2542 N88-25087
Analyzing the stratigraphy, tectonism, and mineralization at the Spanish side of the pyrite belt, Huelva province, Spain, using SPOT imagery 22 p3104 N88-28433
Volcano evolution on Mars 23 p3305 N88-29686
Nineteenth Lunar and Planetary Science Conference. Press abstracts
[NASA-CR-183037] 24 p3440 N88-30473
Exotic minerals in 3,500 million year old rocks: Evidence for large meteorite impacts 24 p3440 N88-30475

MINERALS
NT AMPHIBOLES
NT ASBESTOS
NT BIOTITE

NT CALCITE
NT GARNETS
NT GRAPHITE
NT HEMATITE
NT OLIVINE
NT PEROVSKITES
NT PYRITES
NT PYROLYTIC GRAPHITE
NT QUARTZ
NT SERPENTINE
NT SPINEL
NT VERMICULITE
NT YTTRIUM-ALUMINUM GARNET
Determination of thermodynamic function of minerals at high temperatures
[DE88-001911] 07 p0940 N88-15713
Determination of thermodynamic function of minerals at high temperatures
[DE88-002311] 07 p0940 N88-15714
Characteristics and climatic relevance of the atmospheric aerosol components
08 p1017 N88-16164
X-ray microfluorescence analysis of thin- and thick-sectioned geologic materials
[DE87-009803] 09 p1189 N88-17126
Experimental and theoretical constraints on the origin of mid-ocean ridge geothermal fluids
13 p1804 N88-20784
An investigation of the crystalchemistry and thermochemistry of selected mineral systems
[AD-A189758] 15 p2142 N88-22781
Optical constants of minerals and other materials from the millimeter to the ultraviolet
[AD-A192210] 18 p2482 N88-24724
Selective weathering of shocked minerals and chondritic enrichment of the Martian fines
23 p3301 N88-29660
Mineralization through geologic time: Evolution of continental crust 24 p3400 N88-30250

MINES
Criteria for planimetric and altimetric correction of maps restituted from aerial photographs in 1:100,000 scale
17 p2367 N88-24097

MINES (EXCAVATIONS)
Mining volume measurement system
[NASA-CASE-LAR-13519-1] 17 p2342 N88-23963
Remote sensing applied to the monitoring of mineral extraction in the proximity of urban areas: Pros and cons
19 p2684 N88-25954

MINES (ORDNANCE)
Application of the analysis phase of the instructional system development to the MK-105 magnetic minesweeping mission of the MH-53E helicopter
[AD-A186282] 07 p0822 N88-14994
Preliminary airworthiness evaluation of the UH-60A equipped with the XM-139 VOLCANO mine dispensing system
[AD-A190604] 15 p2018 N88-22029

MINIATURE ELECTRONIC EQUIPMENT
Development of the field-induced electron injection and impact ionization (F4I) technique for radiation hardness testing of MOS (Metal-Oxide-Semiconductor) gate insulators
[AD-A192114] 18 p2583 N88-25345
Miniature radiation dosimeter for in vivo radiation measurements 19 p2672 N88-25889
The effects of incoming boundary layer thickness on unsteady shock-induced turbulent separations induced by cylinders
[AD-A196190] 24 p3368 N88-30060

MINIATURIZATION
NT MICROMINIATURIZATION
NT SUBMINIATURIZATION
TABLET: The personal computer of the year 2000
[NASA-CR-182528] 10 p1384 N88-18267
Concentrating photovoltaic collectors: Fabrication design
[PB88-148051] 12 p1640 N88-19821
French evaluation of Japanese biosensors
16 p2184 N88-23020
Miniature traveling wave tube and method of making
[NASA-CASE-LEW-14520-1] 17 p2335 N88-23936
Tactical Rubidium Frequency Standard (TRFS), volume 2
[AD-A191190] 18 p2503 N88-24850
Tactical Rubidium Frequency Standard (TRFS), volume 1
[AD-A192981] 20 p2805 N88-26640

MINICOMPUTERS
A data analysis environment for HP (Hewlett-Packard) 1000 computers
[DE87-010511] 04 p0477 N88-12936
Error propagation in a digital avionic mini processor
[NASA-CR-181565] 05 p0633 N88-13872
SAHAYOG: A testbed for load sharing under failure
[AD-A186615] 08 p1069 N88-16460
Rocketdyne automated dynamics data analysis and management system 11 p1499 N88-18954
The PC/AT compatible computer as a mission control center display processor at Ames-Dryden Flight Research Facility
[NASA-TM-100426] 14 p1955 N88-21654
Introduction to the VMS (DEC) operating system
[ENST-87D006] 16 p2245 N88-23409

MINIMA
The partially observed stochastic minimum principle
[AD-A189787] 15 p2124 N88-22658
A linear-time algorithm for finding a minimum spanning pseudoforest
[AD-A194029] 23 p3250 N88-29346
Faster algorithms for the shortest path problem
[AD-A194031] 23 p3250 N88-29347

MINIMAL SURFACES
Computer graphics tools for the study of minimal surfaces
[DE88-006421] 15 p2108 N88-22557
Complete minimal surfaces in R^3 of low total curvature
[DE88-006425] 15 p2118 N88-22619
Embedded minimal sufaces with an infinite number of ends
[DE88-006429] 15 p2126 N88-22680

MINIMAX TECHNIQUE
Control of an unstable launcher in atmospheric flight using minimax optimal control laws
[SNIAS-872-422-107] 05 p0638 N88-13901
Min-max bias robust regression
[AD-A191345] 16 p2263 N88-23529
A mixed min-max control problem governed by integral equations 18 p2564 N88-25228
Mixed min-max optimization problem with restrictions
18 p2565 N88-25232
A minimax method for a class of Hamiltonian systems with singular potentials
[AD-A193478] 23 p3270 N88-29453

MINIMIZATION
U OPTIMIZATION

MINING
Marine minerals: Exploring our new ocean frontier
[PB87-217725] 02 p0216 N88-11364
Character of five selected LANDSAT lineaments in southwestern Pennsylvania: Report of investigations, 1987
[PB88-133517] 11 p1505 N88-18988
Power requirements for mining and microwave processing of extraterrestrial resources
17 p2420 N88-24389
Energy requirements for HE-3 mining operations on the Moon 17 p2420 N88-24390
Lunar base surface mission operations. Lunar Base Systems Study (LBSS) task 4.1
[NASA-CR-172050] 18 p2594 N88-25415
Application SPOT-1 data to mining activity: Example of the Imiter Silver Mine, Morocco
22 p3102 N88-28424

MINKOWSKI SPACE
To the field theory with a fundamental mass
[DE88-701159] 15 p2146 N88-22807
Finite width corrections to the Nambu action for the Nielsen-Olesen string
[DE88-006996] 15 p2147 N88-22812
Using Clifford algebras for the geometry of a tube domain (and its corresponding bounded domain) in the complexified Minkowski space of arbitrary dimension
[REPT-87-64] 16 p2264 N88-23540
On the GKP and BS constructions of C-boundary
[DE88-702643] 22 p3159 N88-28799

MINORITIES
A national model at Howard University demonstrating private sector interrelationships that facilitate research in predominantly Black colleges and universities
[DE88-000160] 04 p0502 N88-13089
A study of the minority college programs at the NASA Johnson Space Center 06 p0798 N88-14887

MINORITY CARRIERS
Picosecond carrier transport in GaAs quantum wells
19 p2660 N88-25813

MIR SPACE STATION
USSR report: Space
[JPRS-USP-87-003] 01 p0009 N88-10050
Blagov commentary on Mir station, first manning
01 p0009 N88-10051
X-ray astronomy instruments to operate on Mir station
01 p0009 N88-10052
Gyrostabilizer system of Kvant module
08 p1006 N88-16099
Medilab: A project of a medical laboratory in space
12 p1660 N88-19946
The Soviet MIR space station
[AD-A194040] 23 p3184 N88-28951

MIRA VARIABLES
Basic properties and variability
02 p0252 N88-11593
Spectroscopy and nonthermal processes
02 p0252 N88-11594
Mass loss 02 p0253 N88-11597
Quasi-thermal models 02 p0253 N88-11600
Application of dynamic atmosphere models to the analysis of angular diameter observations of Mira variables 04 p0515 N88-13168

MIRAGE AIRCRAFT
Airplane load drop and missile firing: Experimental methods for predicting trajectories
[PB87-170494] 09 p1117 N88-16695
Testing complex avionics software: A practical experience 17 p2306 N88-23794
Development of complex avionics systems: Experience from French military programs 17 p2307 N88-23804
Supplements to the study of the wake of a Mirage G8 model at F2 — wind tunnel
[CERT-RT-OA-20/5025-AYD] 18 p2458 N88-24596

MIRROR FUSION
Mirror theory applied to toroidal systems
[DE88-003832] 07 p0933 N88-15669
SOAR: Space orbiting advanced fusion power reactor
17 p2416 N88-24366

MIRRORS
NT ETALONS
NT MAGNETIC MIRRORS
NT TANDEM MIRRORS
ESA technological research activities on lightweight mirrors — spaceborne interferometry
01 p0096 N88-10629
Multilayer monochromators for neutron spectrometers
[DE87-014291] 02 p0175 N88-11093
Investigation of the fabrication parameters of laser mirrors with hard oxide interference coatings
[ESA-TT-1064] 03 p0329 N88-12077
Solar converging method 04 p0403 N88-12504
Long-range pulselength scaling of 351nm laser damage thresholds
[DE87-014754] 04 p0448 N88-12777
USSR report: Physics and mathematics
[JPRS-UPM-87-006] 06 p0708 N88-14344
Lasers with wavefront-reversing mirrors (review article)
06 p0709 N88-14349
Performance of highly concentrating mirror collectors and collector systems
[DFVLR-FB-87-29] 09 p1186 N88-17107
Mirrors for high-power continuous-wave Ar-lasers
09 p1235 N88-17404
Polymer reflectors research during FY86
[DE88-001101] 11 p1508 N88-19009
Soft X-ray beamsplitters and highly dispersive multilayer mirrors for use as soft X-ray laser cavity components
[DE88-004003] 11 p1549 N88-19270
Multilayer-coated mirrors as power filters in synchrotron radiation beamlines
[DE88-003872] 11 p1550 N88-19276
Optics for large telescope 13 p1840 N88-21014
Chemical vapor deposited silica coatings for solar mirror protection
[NASA-TM-100834] 14 p1893 N88-21306
Constellation sizing for modest directed energy platforms
[DE88-007033] 15 p2070 N88-22343
Optimization of metal-dielectric laser mirrors of TiO2/SiO2 and silver
[ESA-TT-1068] 16 p2212 N88-23199
Development of mirrors for high-precision laser gyroscopes 18 p2517 N88-24931
A twin-mirrored galvanometer laser light sheet generator
[NASA-TM-100587] 19 p2674 N88-25901
X-ray and optical analysis of surface properties of metal optics
[DE88-004033] 19 p2727 N88-26195
Specular steel surfaces for solar mirror substrates
[DE88-001153] 21 p2968 N88-27630
Performance evaluation of large-area glass-mirror heliostats
[DE88-011883] 21 p2969 N88-27636
Planarization of metal substrates for solar mirrors
[DE88-011492] 23 p3229 N88-29214
The effect of the near earth micrometeoroid environment on a highly reflective mirror surface
[NASA-TM-101307] 24 p3332 N88-29833

MIS (SEMICONDUCTORS)
Analysis of the voltage-current characteristics of metal-isolator-tin-telluride sandwich structures
[ETN-88-91089] 09 p1256 N88-17528
Steady state and transient behavior of the Pd-SnO(sub x) MIS oxygen sensors 19 p2672 N88-25890

MISCIBILITY
U SOLUBILITY

MISFETS
U FIELD EFFECT TRANSISTORS

MISMATCH (ELECTRICAL)
Information and coding capacities of mismatched Gaussian channels
[AD-A190321] 15 p2124 N88-22665
Coding capacity of generalized additive channels
[AD-A190315] 15 p2127 N88-22685
Atomistic simulation of stability, metastability and growth of strained layer structures 20 p2873 N88-27053
MISSILE BODIES
Empirical formulas for the base pressure of missile bodies with a central propulsive jet
[ESA-TT-1046] 03 p0270 N88-11694
Base pressure measurements on a missile body with cruciform tail
[ESA-TT-1062] 03 p0270 N88-11695
Flow visualization on an ogive-nosed circular cylinder body at high incidence using the laser light sheet method
[ESA-TT-1066] 03 p0315 N88-11993
Wind tunnel tests of elliptical missile body configurations at Mach numbers 0.4 to 5.0
[AD-A193525] 22 p3038 N88-28040
MISSILE CASES
U MISSILE BODIES
MISSILE COMPONENTS
NT MISSILE BODIES
Nonaxisymmetric body supersonic, aerodynamic prediction
[AD-A189338] 13 p1716 N88-20259
MISSILE CONFIGURATIONS
Utilization of dynamic characteristics of materials to optimize military explosive charges. Application to antiship devices
[SNIAS-872-320-101] 05 p0610 N88-13743
Generation of surface grids through elliptic partial differential equations for aircraft and missile configurations
[AD-A186631] 11 p1535 N88-19169
Zero-lift drag predictions in supersonic flow for complex configurations 15 p2054 N88-22246
Submunitions simulations, volume 2
[TR-CR-RD-SS-87-7-VOL-2] 19 p2641 N88-25669
Wind tunnel investigation of wing and control panel loads at transonic and supersonic speeds on some schematic cruciform missile configurations
[FFA-TN-1986-43-SUPPL-1] 22 p3039 N88-28044
Prediction of dynamic derivatives
24 p3318 N88-29761
Semiempirical methods for airbreathing missiles
24 p3318 N88-29763
Aerodynamic heating of missiles
24 p3319 N88-29764
Next generation missile design
24 p3319 N88-29766
Generation of surface grids through elliptic partial differential equations for aircraft and missile configurations
[AD-A195639] 24 p3424 N88-30378
MISSILE CONTROL
A study into the effects and viability of applying lateral force control to an air to ground rocket
[ETN-87-90925] 02 p0131 N88-10821
Empirical formulas for the base pressure of missile bodies with a central propulsive jet
[ESA-TT-1046] 03 p0270 N88-11694
Optimal guidance of homing missiles
06 p0671 N88-14111
An inexpensive real-time interactive three dimensional flight simulation system
[AD-A184868] 07 p0821 N88-14989
POLYPHEM, a universal defensive missile with optical waveguides guidance
[MBB-UA-1045/87] 10 p1315 N88-17862
Covariance analysis and post-processing of gravity compensation effects for aided multi-state navigation systems
[PAPER-87-13] 12 p1577 N88-19430
Advances in Air-Launched Weapon Guidance and Control
[AGARD-CP-431] 12 p1596 N88-19553
A prototype fibre optic gyroscope for missile guidance applications 12 p1596 N88-19554
Effects of closing speed uncertainty on optimal guidance 12 p1597 N88-19556
Guidance and control of air-launched armaments: An aeroengineer's perspective 12 p1597 N88-19557
A fiber optic gyro strapdown reference system for guided weapons 12 p1597 N88-19560
The use of hardware-in-the-loop-techniques in the development of a modern air-to-surface missile system
12 p1597 N88-19562
Advanced guidance algorithms for homing missiles with bearings-only measurements
[AD-A190435] 15 p2017 N88-22026
Memory efficient evaluations of nonlinear stochastic equations and C3 applications
[AD-A189872] 15 p2110 N88-22569
IREPS (Integrated Refractive Effects Prediction System) 3.0, user's manual
[AD-A190398] 16 p2188 N88-23045
Optical data processing
[AD-A193024] 20 p2839 N88-26841
Feasibility study of a microprocessor controlled actuator test mechanism
[AD-A194654] 23 p3249 N88-29337
Special Course on Missile Aerodynamics
[AGARD-R-754] 24 p3317 N88-29755
The present status and the future of missile aerodynamics
[NASA-TM-100063] 24 p3320 N88-29773
MISSILE DEFENSE
Where directed energy stands in strategic defense
[DE88-005092] 10 p1403 N88-18365
SEAT: A strategic engagement analysis tool
[DE88-000498] 13 p1830 N88-20944
Free electron lasers in strategic defense
[DE88-007024] 17 p2394 N88-24231
A simulation of post boost vehicle deployment of multiple reentry vehicles
[DE88-009537] 20 p2764 N88-26391
SDI: Myth or reality
[DE88-009121] 20 p2847 N88-26901
An overview of the development of a linear broadband analog fiber-optic link
[DE88-008668] 20 p2854 N88-26945
MISSILE DESIGN
Determination of the drag of missiles with variable lateral acceleration possibility
[REPT-FM15] 10 p1310 N88-17831
Calculation and design of a ramjet missile
[REPT-TR-500] 10 p1311 N88-17832
Guidance and control of air-launched armaments: An aeroengineer's perspective 12 p1597 N88-19557
Special Course on Missile Aerodynamics
[AGARD-R-754] 24 p3317 N88-29755
Accuracy criteria for evaluating supersonic aerodynamic coefficient predictions 24 p3317 N88-29756
Survey on nonlinear effects 24 p3317 N88-29757
Semi-empirical methods for conventional and unconventional missiles 24 p3318 N88-29758
Space marching Euler solvers
24 p3318 N88-29759
Numerical methods: Euler time dependent solver
24 p3318 N88-29760
Semiempirical methods for airbreathing missiles
24 p3318 N88-29763
Aerodynamic heating of missiles
24 p3319 N88-29764
Next generation missile design
24 p3319 N88-29766
MISSILE DETECTION
NT RADAR DETECTION
A cockpit natural language study - selected transcripts
[AD-A192972] 20 p2834 N88-26808
MISSILE ENGINE CASES
U ROCKET ENGINE CASES
MISSILE GUIDANCE
U MISSILE CONTROL
MISSILE LAUNCHERS
Store separation and missile firing from aircraft: Experimental methods for trajectory projection
[NASA-TT-20214] 11 p1439 N88-18589
Expert system contribution to logistics improvement
[SNIAS-881-320-102] 21 p3004 N88-27815
Preliminary airworthiness evaluation of the UH-60A/ESSS (External Stores Support System) with HELLFIRE launcher installed
[AD-A196187] 24 p3323 N88-29793
MISSILE STABILIZATION
U MISSILE CONTROL
U STABILIZATION
MISSILE SYSTEMS
Aircraft avionics and missile system installation cost study. Volume 1: Technical report and appendices A through E
[AD-A194605] 23 p3178 N88-28923
Aircraft avionics and missile system installation cost study. Volume 2: Appendices F and G
[AD-A195372] 24 p3325 N88-29801
MISSILE TRACKING
Use of the global positioning system for trajectory determination of SRAM 2 missiles at the Eastern Test Range
[AD-A185266] 05 p0544 N88-13314
Strategic Defense Initiative Program: Status of space surveillance and tracking system
[PB88-150438] 14 p1967 N88-21739
MISSILE TRAJECTORIES
Use of the global positioning system for trajectory determination of SRAM 2 missiles at the Eastern Test Range
[AD-A185266] 05 p0544 N88-13314
Airplane load drop and missile firing: Experimental methods for predicting trajectories
[PB87-170494] 09 p1117 N88-16695
Store separation and missile firing from aircraft: Experimental methods for trajectory projection
[NASA-TT-20214] 11 p1439 N88-18589
Effect of rotation on the lateral stability of a free-flying column subjected to an axial thrust with directional control
[AD-A188690] 13 p1728 N88-20338
Advanced guidance algorithms for homing missiles with bearings-only measurements
[AD-A190435] 15 p2017 N88-22026
MISSILES
NT AIR TO AIR MISSILES
NT AIR TO SURFACE MISSILES
NT ANTIAIRCRAFT MISSILES
NT ANTIMISSILE MISSILES
NT ANTISHIP MISSILES
NT ANTITANK MISSILES
NT BALLISTIC MISSILES
NT CRUISE MISSILES
NT MX MISSILE
NT RAMJET MISSILES
NT SURFACE TO AIR MISSILES
NT SURFACE TO SURFACE MISSILES
NT TOMAHAWK MISSILES
High resolution ultraviolet filter development
[AD-A184183] 05 p0649 N88-13979
Peacekeeper tank slosh model
08 p0983 N88-15942
Leeside crossflow modeling in Euler space-marching computations
[NASA-TM-89710] 10 p1325 N88-17924
A prototype fibre optic gyroscope for missile guidance applications 12 p1596 N88-19554
A fiber optic gyro strapdown reference system for guided weapons 12 p1597 N88-19560
Speed control of a missile with throttleable ducted rocket propulsion 12 p1597 N88-19561
Advanced guidance algorithms for homing missiles with bearings-only measurements
[AD-A190435] 15 p2017 N88-22026
Efficient, high resolution computations of projectile and missile flow fields
[AD-A191086] 16 p2158 N88-22873
Description of a water tank facility: Study of a missile at high incidence 16 p2201 N88-23133
Wind tunnel investigation of wing and control panel loads at transonic and supersonic speeds on some schematic cruciform missile configurations
[FFA-TN-1986-43] 18 p2457 N88-24585
Launch operations to support future space forces
[AD-A192679] 20 p2881 N88-27107
Missiles, fuselage and similar bodies
23 p3167 N88-28858
Missiles, fuselages and similar bodies
23 p3169 N88-28869
Air intake aerodynamics 24 p3318 N88-29762
Prediction of base-flows 24 p3319 N88-29765
MISSING MASS (ASTROPHYSICS)
Comments on H. Arp The persistent problem of spiral galaxies
[TRITA-EPP-87-05] 05 p0660 N88-14052
Finnish-Soviet Symposium on Radio Astronomy (1st) held at Otaniemi on August 26-27, 1985
[PB87-140661] 07 p0944 N88-15736
MISSION PLANNING
Space Station Mission Planning System (MPS) development study. Volume 2
[NASA-CR-179200] 01 p0009 N88-10048
Space Station Mission Planning Study (MPS) development study. Volume 3: Software development plan
[NASA-CR-179203] 01 p0009 N88-10049
Planning and execution of the NAVEX experiment in the Spacelab Mission D1
[DFVLR-FB-87-03] 01 p0010 N88-10056
Columbus preparatory program. Payload element study on a technology demonstration mission, executive summary
[CS-RP-AI-016] 01 p0014 N88-10080
Military needs and forecast, 2
01 p0015 N88-10087
Automation strategy and results for an airbase command and control information system
[NLR-MP-86031-U] 01 p0035 N88-10223
Space technology to meet future needs
[NASA-CR-181473] 02 p0130 N88-10819
Space Construction
[NASA-CP-2490] 02 p0138 N88-10870

The flight demonstration program and selection process 02 p0138 N88-10871
Mission Peculiar Equipment Support Structure: A platform for space construction 02 p0139 N88-10874
Marshall Space Flight Center's role in EASE/ACCESS mission management 02 p0139 N88-10875
Helicopter (performance) management 03 p0264 N88-11666
High power ion thruster performance [NASA-TM-100127] 04 p0409 N88-12542
Mission requirements and aircraft sizing 05 p0545 N88-13317
Space station systems: A bibliography with indexes [NASA-SP-7056(05)] 05 p0556 N88-13382
Impact of flying qualities on mission effectiveness for helicopter air combat, volume 1 [NASA-CR-166568] 06 p0669 N88-14100
Simulation and analysis of a geopotential research mission [NASA-CR-182354] 06 p0670 N88-14109
Rendezvous and Docking Verification (RVDV) and in-orbit demonstration, executive summary [RVD-RVDV-FR-AS-01] 06 p0673 N88-14120
Tethers in space handbook [NASA-CR-181371] 06 p0673 N88-14123
Controlled Ecological Life Support Systems (CELSS) conceptual design option study [NASA-CR-177421] 06 p0754 N88-14625
Max '91: Flare research at the next solar maximum [NASA-TM-89700] 06 p0806 N88-14919
A space transportation system operations model [NASA-TM-100481] 07 p0823 N88-14999
Advancing automation and robotics technology for the space station and for the US economy: Submitted to the United States Congress May 15, 1987 [NASA-TM-89811] 08 p0959 N88-15817
Studies for future scientific projects 09 p1123 N88-16720
Numerical arc segmentation algorithm for a radio conference-NASARC, version 2.0: User's manual [NASA-TM-100161] 09 p1156 N88-16928
Expert system verification concerns in an operations environment 09 p1207 N88-17234
Expert mission planning and replanning scheduling system for NASA KSC payload operations 09 p1209 N88-17247
Management of complex information in support of evolving autonomous expert systems [AD-A186680] 09 p1224 N88-17337
POCC capabilities document. Payload support capabilities description: MCC, JSC POCC, remote POCC interface [NASA-TM-89708] 09 p1260 N88-17555
The 1987 Get Away Special Experimenter's Symposium [NASA-CP-2500] 10 p1286 N88-17691
Planet X probe: A fresh new look at an old familiar place 10 p1287 N88-17699
America plans for space [AD-A187465] 10 p1289 N88-17713
Rendezvous and docking verification and demonstration in orbit, executive summary [MBB-303-16/86] 10 p1291 N88-17719
Development of a graphics based two-attribute utility assessment program with application to mission planning [AD-A187276] 10 p1388 N88-18292
Interplanetary mission design handbook. Volume 1, Part 5: Mars-to-Earth ballistic mission opportunities, 1992-2007 [NASA-CR-182525] 10 p1430 N88-18538
A two stage launch vehicle for use as an advanced space transportation system for logistics support of the space station [NASA-CR-182572] 11 p1443 N88-18606
Search problems in mission planning and navigation of autonomous aircraft [NASA-CR-182666] 12 p1579 N88-19448
Rendezvous and docking (RVD) verification and demonstration in-orbit 12 p1592 N88-19531
Conceptual design and programmatics studies of space station accommodations for Life Sciences Research Facilities (LSRF) [NASA-CR-179270] 12 p1598 N88-19567
The integration of artificial intelligence techniques to improve the effectiveness of electronic countermeasure strategies in a tactical environment [AD-A189483] 12 p1682 N88-20056
Mars Lander/Rover vehicle development: An advanced space design project for USRA and NASA/OAST [NASA-CR-182562] 12 p1709 N88-20226
Mars Lander/Rover vehicle development: An advanced space design project for USRA and NASA/OAST [NASA-CR-182571] 12 p1709 N88-20227
Orbital transfer vehicle concept definition and system analysis study. Volume 2: OTV concept definition and evaluation. Book 1: Mission and system requirements [NASA-CR-179321] 13 p1729 N88-20339
Turnaround operations analysis for OTV. Volume 1: Executive summary [NASA-CR-179316] 13 p1729 N88-20340
Turnaround operations analysis for OTV. Volume 2: Detailed technical report [NASA-CR-179317] 13 p1729 N88-20341
Turnaround operations analysis for OTV. Volume 3: Technology development plan [NASA-CR-179318] 13 p1729 N88-20342
Development of an interactive real-time graphics system for the display of vehicle space positioning [NASA-TM-100429] 13 p1730 N88-20344
Expert systems for decision support in military aircraft mission preparation [NLR-MP-87013-U] 13 p1830 N88-20946
Johnson Space Center's strategic game plan: Charting a course to the year 2000 and beyond [NASA-TM-89733] 13 p1850 N88-21076
The German Spacelab mission D1: Payload integration [ETN-88-91507] 14 p1871 N88-21179
Satellite acquisition: Global positioning system acquisition changes after Challenger's accident [PB88-155536] 14 p1880 N88-21236
The PC/AT compatible computer as a mission control center display processor at Ames-Dryden Flight Research Facility [NASA-TM-100426] 14 p1955 N88-21654
The comet rendezvous asteroid flyby mission 14 p2005 N88-21956
The Giotto extended mission 14 p2005 N88-21957
Rosetta: A mission to sample the nucleus of a comet 14 p2005 N88-21958
Retrieving samples from comet nuclei 14 p2006 N88-21959
Alternative cometary targets for the Giotto extended mission 14 p2010 N88-21990
Orbital transfer vehicle: Concept definition and system analysis study [NASA-CR-179315] 15 p2024 N88-22060
Space utilization plans 15 p2051 N88-22219
External tank gamma ray imaging telescope study. Final review, phase 2 [NASA-CR-179320] 15 p2150 N88-22834
The NAVEX experiment in the Spacelab D1 mission: Planning and execution [ESA-TT-1078] 16 p2166 N88-22913
Manned Mars mission accommodation: Sprint mission [NASA-TM-100598] 16 p2290 N88-23711
Civil missions applications study 17 p2417 N88-24376
Human performance issues arising from manned space station missions [NASA-CR-3942] 18 p2553 N88-25156
Modeling and evaluation of variable structure organizations [AD-A191947] 18 p2588 N88-25381
Mars rover/sample return mission requirements affecting space station [NASA-CR-172048] 18 p2594 N88-25414
Lunar base surface mission operations. Lunar Base Systems Study (LBSS) task 4.1 [NASA-CR-172050] 18 p2594 N88-25415
Flight Mechanics Panel Symposium on Rotorcraft Design for Operations: Technical evaluation report [AGARD-AR-243] 20 p2758 N88-26362
The Telecommunications and Data Acquisition Report [NASA-CR-183131] 22 p3063 N88-28178
Mark IV-85 mission support planning and future mission set 22 p3067 N88-28202
Inflight rearming [AD-A193564] 23 p3176 N88-28909
Analyst-centered models for systems design, analysis, and development 23 p3253 N88-29364
A plan for time-phased incorporation of automation and robotics on the US space station 23 p3255 N88-29377
A scheduling and resource management system for space applications 23 p3256 N88-29383
Two implementations of the Expert System for the Flight Analysis System (ESFAS) project 23 p3259 N88-29400
Experiment scheduling for Spacelab missions 23 p3259 N88-29404
Blackboard architectures and their relationship to autonomous space systems 23 p3261 N88-29414
Development and demonstration of an on-board mission planner for helicopters [NASA-CR-177482] 24 p3328 N88-29817
Definition of common support equipment and space station interface requirements for IOC model technology experiments [NASA-TM-100656] 24 p3336 N88-29856
The 1988 Goddard Conference on Space Applications of Artificial Intelligence [NASA-CP-3009] 24 p3415 N88-30330
Contingency rescheduling of spacecraft operations 24 p3416 N88-30337
Knowledge based tools for Hubble Space Telescope planning and scheduling: Constraints and strategies 24 p3417 N88-30338
Candidate functions for advanced technology implementation in the Columbus mission planning environment 24 p3417 N88-30340
A rule-based systems approach to spacecraft communications configuration optimization 24 p3417 N88-30341
Integrated resource scheduling in a distributed scheduling environment 24 p3417 N88-30342

MISSISSIPPI
Hypocenters (1977-1984) around the Richton Dome and the Melvin, Alabama, 1978 earthquake [DE87-014336] 03 p0351 N88-12214

MIST
Investigation of the nature and concentration of vapor and mist during the cleaning of aircraft [PML-1985-29] 05 p0623 N88-13817

MITOSIS
Zero gravity and living organism 08 p1046 N88-16320

MIXED CRYSTALS
Calibration constants for the 1986 BGO crystals matrix [NOTA-INTERNA-886] 07 p0856 N88-15197
Formation of nuclei during precipitation in metallic mixed crystals [NASA-TT-20248] 13 p1745 N88-20437
Statistical fine structure in the inhomogeneously broadened electronic origin of pentacene in p-terphenyl [AD-A191211] 16 p2176 N88-22968

MIXED FLOW
U MULTIPHASE FLOW

MIXERS
A GaAs MESFET balanced mixer with very low intermodulation [AD-A184848] 05 p0655 N88-14015
Dual-fuel, dual-mode rocket engine [NASA-CASE-LAR-13773-1] 18 p2475 N88-24685
SIS (Superconductor-Insulator-Superconductor) mixer research [AD-A192908] 20 p2879 N88-27092

MIXING
NT COLLOIDING
NT DISSOLVING
NT HOMOGENIZING
NT PREMIXING
NT SIGNAL MIXING
NT SUSPENDING (MIXING)
NT TURBULENT MIXING
Numerical simulation of a supersonic chemically reacting mixing layer 02 p0143 N88-10900
Combustion in turbulent jets and buoyant flames [PB87-232674] 03 p0283 N88-11779
Generation of IR stimulated radiation, UV visible violet coherent radiation by two-photon resonance pumping in K vapor 03 p0301 N88-11892
A study of chaos and mixing in Rayleigh-Taylor and Richtmyer-Meshkov unstable interfaces [AD-A184751] 03 p0320 N88-12026
Heats of mixing for thermal energy storage systems. Phase 1: Selection of suitable liquid-liquid mixtures [DE87-014971] 03 p0347 N88-12196
Activities at government research laboratories reported 04 p0403 N88-12503
Atomic and electronic structure of surfaces and chemisorbed layers [DE87-014987] 04 p0498 N88-13065
The effect of ion beam mixed Ni-Al surface layers on PSB extrusion morphology in fatigued nickel 05 p0598 N88-13652
Mixing and combustion of pulsed gas jets [PB88-112834] 06 p0680 N88-14169
Mixing and combustion of pulsed gas jets [PB88-108014] 06 p0680 N88-14170
Ion mixing and surface modification in metal-semiconductor systems [DE88-001702] 06 p0786 N88-14823
Structural study of the impregnating resins of the type TGMDA/DDS --- expoxy resins [ETN-88-91616] 08 p0965 N88-15842
O2-I laser (Oxygen-iodine) mixing studies using LIF (Laser Induced Fluorescence) [AD-A186667] 09 p1171 N88-17018
A computational study of thrust augmenting ejectors based on a viscous-inviscid approach 10 p1326 N88-17929

Radial mixing in turbomachines
[AD-A188028] 11 p1482 N88-18847
Investigations into shock-induced enhancement of mixing and combustion in supersonic burners
[AD-A189609] 12 p1607 N88-19608
Mass transport and chemical demixing of Y-Ba-Cu-O compounds during sintering in temperature gradients
[DE88-004887] 12 p1696 N88-20151
Mixing of viscous fluids: Behavior of microstructures and chaos
[DE88-006287] 13 p1766 N88-20566
Structures and fluxes in a deep convecting mixed layer 13 p1804 N88-20786
Equatorial turbulence: Mixed layer and thermocline 13 p1804 N88-20787
The mixed layer of the western equatorial Pacific Ocean
[HIG-1861] 13 p1805 N88-20789
Squeezing via travelling-wave forward four-wave mixing in atomic vapors: Comparison with nondegenerate theory 14 p1978 N88-21804
Experimental investigation of a spanwise forced mixing layer
[AD-A190136] 15 p2013 N88-22007
Effect of moisture level in PBXW-109(E) (plastic-bonded explosive) mixes on the aging of the cured explosive
[AD-A190200] 15 p2048 N88-22202
Mixing: Stretching, breakup and chaos
[DE88-006699] 15 p2067 N88-22327
Optical switching and control techniques using nonlinear optical wave mixing
[AD-A190467] 15 p2134 N88-22730
Ion-beam mixing and amorphization in Au/Zr bilayers
[DE88-005999] 15 p2140 N88-22767
Analysis of molecular mixing and chemical reaction in mixing layer
[AD-A191600] 18 p2482 N88-24721
Signal processing with degenerate four-wave mixing
[AD-A191496] 18 p2499 N88-24825
Spatial stability of a compressible mixing layer
[NASA-CR-181671] 18 p2514 N88-24916
Direct numerical simulations of the PDF's (Probability Density Functions) of a passive scalar in a forced mixing layer
[AD-A192134] 18 p2568 N88-25256
Turbulence structure of mixing swirling flows
[AD-A193063] 21 p2943 N88-27478
Burn-in with mixed populations
[AD-A194651] 22 p3085 N88-28321
Soot and radiation in a gas turbine combustor
[AD-A191991] 23 p3179 N88-28924
Strong law for mixing sequence
[AD-A193615] 23 p3274 N88-29490

MIXING CIRCUITS
Comparative investigation of heterodyne mixers at 1000 GHz
[FTL-068627] 09 p1158 N88-16940
Supercomputer-aided generalized mixer analysis and optimization
[FUB-15-1986] 14 p1957 N88-21668
Heterodyne spectrometer for the very high frequency range between 300 and 3000 GHz (1 mm to 0.1 mm) using a mixer in open structure 16 p2271 N88-23589

MIXING LENGTH FLOW THEORY
Velocity and density measurements in a turbulent nonpremixed flame with comparison to numerical model predictions
[DE87-014695] 08 p0967 N88-15854
Turbulent reacting flows and supersonic combustion
[AD-A189690] 15 p2034 N88-22115
An investigation of flow structure, mixing and chemical reaction in combusting turbulent flows
[AD-A189980] 15 p2034 N88-22117
Numerical predictions for the flow induced by an enclosed rotating disc
[PNR90463] 22 p3078 N88-28281

MIXTURES
NT ADMIXTURES
NT AEROSOLS
NT AIR
NT ALVEOLAR AIR
NT AQUEOUS SOLUTIONS
NT BINARY MIXTURES
NT COLLOIDS
NT DETONABLE GAS MIXTURES
NT DISPERSIONS
NT EMULSIONS
NT EUTECTIC ALLOYS
NT EUTECTICS
NT FOG
NT GAS MIXTURES
NT HIGH TEMPERATURE AIR
NT LIQUID-GAS MIXTURES
NT SIALON
NT SLURRIES
NT SMOKE
NT SOLID SOLUTIONS
NT SOLID SUSPENSIONS
NT SOLUTIONS
Application of new conformal solution theories
[PB87-211934] 02 p0247 N88-11558
Annotated computer output for illustrative examples of clustering using the mixture method and two comparable methods from SAS
[AD-A184687] 03 p0364 N88-12292
Thermodynamic properties of supercritical mixtures
[DE88-000809] 04 p0413 N88-12562
A laboratory study of asphalt concrete mix designs for high-contact pressure aircraft traffic
[AD-A185753] 06 p0670 N88-14106
Experimental and theoretical study of condensation in multicomponent mixtures
[DE88-002715] 07 p0830 N88-15033
Experimental and theoretical studies of dense fluid mixtures
[DE88-002710] 07 p0831 N88-15039
Theoretical studies of multicomponent mixtures: Phase equilibrium and transport
[DE88-002717] 07 p0831 N88-15040
The generalized van der Waals theory of pure fluids and mixtures
[DE88-002380] 07 p0855 N88-15192
Realization of an instrument to measure temperature and concentration gradients in fluids --- microgravity
[CISE-3128] 09 p1168 N88-17003
Predicting transforms of stable noise and other Gaussian mixtures
[AD-A189280] 12 p1684 N88-20071
Prediction of high-temperature thermodynamic properties of mixed electrolyte solutions including solubility equilibria, vapor pressure depression and boiling point elevation
[DE88-006344] 13 p1849 N88-21069
Noise generation by air bubbles in water: An experimental study of creation and splitting
[AD-A192063] 19 p2664 N88-25839
Interactions in miscible polymer blends
[AD-A193824] 22 p3058 N88-28144
Blends of crystallizable polybutadienes
[AD-A194536] 23 p3197 N88-29026

MNEMONICS
Long term synaptic plasticity and learning in neuronal networks
[AD-A186834] 09 p1199 N88-17188

MOBILE COMMUNICATION SYSTEMS
NT LAND MOBILE SATELLITE SERVICE
Measured characteristics of 800/900 MHz mobile radio channels with high-angle propagation through moderately dense foliage
[CRC-1398] 05 p0573 N88-13493
Two-signal cross modulation effects, half-IF effects and interference criteria in land mobile sharing with UHF (Ultra High Frequency) television
[PB87-228037] 05 p0576 N88-13514
A multi user random access communication system for users with different priorities
[AD-A186041] 07 p0841 N88-15102
Spread spectrum mobile radio communications
[AD-A187487] 11 p1470 N88-18765
Spatial distribution of traffic in a cellular mobile data network
[EUT-87-E-168] 14 p1904 N88-21378
Development of a mobile research flight test support capability
[NASA-TM-100428] 16 p2159 N88-22883
MSAT-X: A technical introduction and status report
[NASA-CR-182921] 17 p2334 N88-23933
Proceedings of the Mobile Satellite Conference
[NASA-CR-182964] 19 p2643 N88-25680
The AMSC mobile satellite system 19 p2643 N88-25681
NASA's mobile satellite development program 19 p2643 N88-25682
Mobile satellite service for Canada 19 p2643 N88-25683
AUSSAT mobile satellite services 19 p2643 N88-25684
A satellite system for land-mobile communications in Europe 19 p2643 N88-25685
System capacity and economic modeling computer tool for satellite mobile communications systems 19 p2644 N88-25686
World-wide aeronautical satellite communications 19 p2644 N88-25688
An overview of the OmniTRACS: The first operational mobile Ku-band satellite communications 19 p2644 N88-25689
International and domestic mobile satellite regulatory proceedings: A comparison of outcomes and discussion of implications 19 p2644 N88-25690
Mobile satellite services: International co-ordination, co-operation and competition 19 p2644 N88-25691
International and domestic regulator issues facing the Canadian MSAT system 19 p2644 N88-25692
Propagation effects by roadside trees measured at UHF and L-band for mobile satellite systems 19 p2644 N88-25693
Propagation modeling for land mobile satellite systems 19 p2645 N88-25694
Attenuated direct and scattered wave propagation on simulated land mobile satellite service paths in the presence of trees 19 p2645 N88-25695
Mobile satellite propagation measurements and modeling: A review of results for systems engineers 19 p2645 N88-25696
Propagation measurements for an Australian land mobile satellite system 19 p2645 N88-25697
Land mobile satellite propagation results 19 p2645 N88-25698
Propagation effects on spread-spectrum mobile satellite systems 19 p2645 N88-25699
Miltipath measurements for land mobile satellite service using global positioning system signals 19 p2645 N88-25700
Development of a mobile satellite communication unit 19 p2646 N88-25701
Development of the network architecture of the Canadian MSAT system 19 p2646 N88-25702
System architecture for the Canadian interim mobile satellite system 19 p2646 N88-25703
Satellite communications experiment for the Ontario air ambulance service 19 p2646 N88-25705
Land mobile satellite demonstration system 19 p2646 N88-25706
Mobilestar field test program 19 p2646 N88-25707
The JPL MSAT mobile laboratory and the pilot field experiments 19 p2646 N88-25708
Technical characteristics of the OmniTRACS: The first operation mobile Ku-band satellite communications system 19 p2647 N88-25709
An adaptive array antenna for mobile satellite communications 19 p2647 N88-25710
MSAT mobile electronically steered phased array antenna development 19 p2647 N88-25711
MSAT-X electronically steered phased array antenna system 19 p2647 N88-25712
MSAT-X phased array antenna adaptions to airborne applications 19 p2647 N88-25713
Adaptive interference techniques for mobile antennas 19 p2647 N88-25714
The JPL mechanically steered antenna 19 p2647 N88-25715
Simple, low-profile, circularly polarized arrays 19 p2647 N88-25716
Omni-directional L-band antenna for mobile communications 19 p2648 N88-25717
Trellis-coded CPM for satellite-based mobile communications 19 p2648 N88-25718
Interleaver design for trellis-coded differential 8-PSK modulation with non-coherent detection 19 p2648 N88-25719
Codes for QPSK modulation with invariance under 90 degrees rotation 19 p2648 N88-25720
Trellis-coded MPSK modulation techniques for MSAT-X(sup)1 19 p2648 N88-25721
Modulation and coding for fast fading mobile satellite communication channels 19 p2648 N88-25722
Comparison of CDMA and FDMA for the MobileStar(sm) system 19 p2649 N88-25724
An 8-DPSK TCM modem for MSAT-X 19 p2649 N88-25725
Modem for the land mobile satellite channel 19 p2649 N88-25727
Pilot-aided modulation for narrow-band satellite communications 19 p2649 N88-25728
A study on the co- and adjacent channel protection requirements for mobile satellite ACSSB modulation 19 p2650 N88-25732
A framework for implementing data services in multi-service mobile satellite systems 19 p2650 N88-25733
L-band and SHF multiple access schemes for the MSAT system 19 p2650 N88-25734
Rearrangement procedures in regenerative multibeammobile communications satellites with frequency reuse 19 p2650 N88-25735
Design mobile satellite system architecture as an integral part of the cellular access digital network 19 p2650 N88-25736
An access alternative for mobile satellite networks 19 p2651 N88-25737
An operational open-end file transfer protocol for mobile satellite communications 19 p2651 N88-25738
Integrated voice/data protocols for satellite channels 19 p2651 N88-25739

Evaluation of CDMA system capacity for mobile satellite system applications 19 p2651 N88-25740
Considerations for spacecraft design for MSAT 19 p2651 N88-25741
Antenna system for MSAT mission 19 p2651 N88-25742
Antenna technology for advanced mobile communication systems 19 p2651 N88-25743
Frequency addressable beams for land mobile communications 19 p2652 N88-25744
Speech coding at 4800 bps for mobile satellite communications 19 p2652 N88-25749
Real-time speech encoding based on Code-Excited Linear Prediction (CELP) 19 p2653 N88-25751
Development of an 8000 bps voice codec for AvSat 19 p2653 N88-25755
Mobile satellite communications in the Forest Service 19 p2654 N88-25757
Mobile satellite service in the United States 19 p2654 N88-25758
Random-access algorithms for environments with capture
[AD-A194303] 23 p3203 N88-29060

MOBILITY
NT CARRIER MOBILITY
NT ELECTRON MOBILITY
NT HOLE MOBILITY
NT IONIC MOBILITY
Influence of thermocyclic treatment on mobility of grain boundaries
[BLL-M-37329-(5828.4)] 02 p0149 N88-10933
Dealing with unanticipated events in autonomous navigation
[DE88-000590] 05 p0590 N88-13602
An investigation of classical dynamic scaling techniques applied to an oleo-pneumatic landing gear strut
[AD-A187664] 13 p1721 N88-20292
Examples of ice pack rigidity and mobility characteristics determined from ice motion
[AD-A191163] 17 p2377 N88-24129

MODAL RESPONSE
Mode purity measurements on gyrotrons for plasma heating at the stellarator W 7-AS
[IPF-87-3] 01 p0101 N88-10660
Modal survey of the space shuttle solid rocket motor using multiple input methods 05 p0593 N88-13617
A new method to real-normalize measured complex modes 05 p0593 N88-13618
Improvement of modal scaling factors using mass additive technique 05 p0593 N88-13620
Viscous damped space structure for reduced jitter 05 p0594 N88-13623
On the glitches in the force transmitted by an electrodynamic exciter to a structure 05 p0594 N88-13624
Modal analyses of the Kernville diagnostic canister
[DE88-003268] 07 p0870 N88-15277
Modal analysis using frequency response measurement data 08 p0976 N88-15899
Finite element method with continuous mass elements
[PB87-143384] 08 p0995 N88-16019
Centaur G Prime modal test 09 p1161 N88-17075
An adaptive filtering technique for removing periodic noise from modal response data
[DE88-002347] 10 p1322 N88-17903
A component synthesis method using Lanczos vectors
[DE88-002263] 10 p1403 N88-18368
Overview of multi-input frequency domain modal testing methods with an emphasis on sine testing 11 p1499 N88-18949
Modal forced response of propfans in yawed flow 16 p2221 N88-23253
Dynamic characteristics of a vibrating beam with periodic variation in bending stiffness
[NASA-TP-2697] 17 p2348 N88-23988
Reduced order modelling and analytical model modification for structural dynamics and control 18 p2529 N88-25006
Multishaker modal testing
[NASA-CR-179355] 18 p2530 N88-25010
Modal synthesis by use of substructures with fixed or free coupling points
[ILR-MITT-191] 22 p3089 N88-28341
Asymptotic modal analysis and statistical energy analysis
[NASA-CR-183077] 23 p3278 N88-29514

MODE (STATISTICS)
The bimodality of large scale averaged flow parameters --- statistical weather forecasting 08 p1016 N88-16159

MODE COUPLING
U COUPLED MODES

MODE OF VIBRATION
U VIBRATION MODE

MODE SHAPES
U MODAL RESPONSE

MODE TRANSFORMERS
Optimization of mode converters for generating the fundamental TE(06) gyrotron output at 140 GHz
[IPF-87-1] 01 p0043 N88-10273
Harmonic and rectangular pulse reproduction through current transformers
[EUT-86-E-159] 14 p1907 N88-21395

MODEL REFERENCE ADAPTIVE CONTROL
Adaptive control of scientific balloon-borne gondola attitude 13 p1755 N88-20497

MODELS
NT AIRCRAFT MODELS
NT ANALOG SIMULATION
NT ASTRONOMICAL MODELS
NT ATMOSPHERIC MODELS
NT BIOLOGICAL MODELS (MATHEMATICS)
NT BREADBOARD MODELS
NT DENSITY WAVE MODEL
NT DIGITAL SIMULATION
NT DYNAMIC MODELS
NT ENVIRONMENT MODELS
NT HYDROLOGY MODELS
NT K-EPSILON TURBULENCE MODEL
NT MANDELSTAM REPRESENTATION
NT MATHEMATICAL MODELS
NT NUCLEAR MODELS
NT OCEAN MODELS
NT PETRI NETS
NT QUARK MODELS
NT REFERENCE ATMOSPHERES
NT SCALE MODELS
NT SEMISPAN MODELS
NT SPACECRAFT MODELS
NT STATIC MODELS
NT STELLAR MODELS
NT THOMAS-FERMI MODEL
NT THREE DIMENSIONAL MODELS
NT TURBULENCE MODELS
NT TWO DIMENSIONAL MODELS
NT WIND TUNNEL MODELS
Modeling and measurement of heat transfer on turbine blade tips 01 p0006 N88-10032
HF (High Frequency) broadcasting planning model: A comparison of two versions
[PB87-210282] 01 p0036 N88-10230
Two-phase non-Newtonian hydrodynamic modeling of slurries
[DE87-011519] 01 p0047 N88-10298
Multidimensional modeling of convective heat transfer with application to IC engines
[DE87-011046] 01 p0055 N88-10353
Thermal stress analysis of space shuttle orbiter subjected to reentry aerodynamic heating
[NASA-TM-88286] 01 p0061 N88-10389
Self-consistent modification of a fast tail distribution by resonant fields in nonuniform plasmas
[AD-A183790] 01 p0099 N88-10650
A simulation of the IPS variations from a magnetohydrodynamical simulation 01 p0118 N88-10755
Reliability modeling of fault-tolerant computer based systems 02 p0127 N88-10801
A stochastic delamination growth model for fatigue loaded laminated composite materials 02 p0141 N88-10888
Models of degradation of stratified composite structures
[ONERA-RT-13/3542-RY-061-R] 02 p0142 N88-10892
A numerical method for the treatment of kinked cracks in finite bodies 02 p0190 N88-11189
A design methodology for the utilization of metrics within various phases of software lifecycle models
[DE87-010519] 02 p0220 N88-11385
Application of new conformal solution theories
[PB87-211934] 02 p0247 N88-11558
A heat transfer model for a heated helium airship
[AD-A183786] 03 p0259 N88-11629
The effects of corona on current surges induced on conducting lines by EMP: A comparison of experiment data with results of analytic corona models
[DE87-014970] 03 p0305 N88-11924
Visualization of the flow field around a generic destroyer model in a simulated turbulent atmospheric boundary layer
[AD-A184658] 03 p0320 N88-12023
Conservation and transport properties of turbulence with large density variations
[LA-10911-MS] 03 p0321 N88-12032
Interseismic deformation for normal fault earthquakes 03 p0349 N88-12207
Transform fault earthquakes in the North Atlantic: Source mechanisms and depth of faulting 03 p0350 N88-12208
Microcomputer control of a hydraulically actuated piston
[AD-A184130] 03 p0368 N88-12317
Number count-redshift relation in universe models with nonzero cosmological constant
[DE87-703043] 03 p0388 N88-12435
Reduced complexity structural modeling for automated airframe synthesis
[NASA-CR-177440] 04 p0393 N88-12453
Experimental evidence for modifying the current physical model for ice accretion on aircraft surfaces
[NASA-TM-87184] 04 p0397 N88-12473
A multiple-time-scale turbulence model based on variable partitioning of turbulent kinetic energy spectrum
[NASA-CR-179222] 04 p0444 N88-12754
On dynamic loads in parallel shaft transmissions. 1: Modeling and analysis
[NASA-TM-100180] 04 p0451 N88-12797
On dynamic loads in parallel shaft transmissions. 2: Parameter study
[NASA-TM-100181] 04 p0452 N88-12798
User's guide to NCAR (National Center for Atmospheric Research) CCM1
[PB87-224366] 04 p0469 N88-12899
A tight upper bound for the speed-up of parallel best-first branch-and-bound algorithms
[AD-A184246] 04 p0477 N88-12939
Mental models in expert physics reasoning
[AD-A184106] 04 p0500 N88-13075
Full-envelope aerodynamic modeling of the Harrier aircraft
[NASA-TM-88376] 05 p0552 N88-13363
Model helicopter rotor rig and associated strain gauge balance for performance studies
[NAL-TM-AE-8704] 05 p0552 N88-13364
Damping analysis of flexural waves in fluid-loaded single and constrained plates
[AD-A185116] 05 p0609 N88-13739
Performability modeling based on real data: A casestudy
[NASA-CR-181563] 05 p0633 N88-13870
Example of correlation between space and spin coordinates
[DE87-703366] 05 p0657 N88-14030
Approaches and possible improvements in the area of multibody dynamics modeling
[NASA-CR-179227] 06 p0663 N88-14067
Balanced realizations: Canonical form, parametrization, model reduction
[PB87-123360] 06 p0757 N88-14642
Model of earlier stage of universe's evolution 06 p0775 N88-14758
Unsteady stall penetration experiments at high Reynolds number
[AD-A186120] 07 p0814 N88-14958
A space transportation system operations model
[NASA-TM-100481] 07 p0823 N88-14999
Treatment of small wire loops in the method of moments code NEC (Numerical Electromagnetics Code)
[DE88-002995] 07 p0846 N88-15136
User manual for ATILA, a finite-element code for modeling piezoelectric transducers
[AD-A185948] 07 p0847 N88-15141
Reynolds-stress and dissipation rate budgets in a turbulent channel flow
[NASA-TM-89451] 07 p0852 N88-15174
Numerical solution of turbulent flow past a backward facing step using a nonlinear K-epsilon model
[NASA-CR-178421] 07 p0854 N88-15189
A software planning and development methodology with resource allocation capability
[AD-A186088] 07 p0902 N88-15462
Estimation and testing in truncated and nontruncated linear median-regression models
[AD-A186317] 07 p0911 N88-15522
Development of an emulation-simulation thermal control model for space station application
[NASA-CR-182409] 08 p0962 N88-15823
Nonlinear line-spring model for surface crack analysis with particular reference to work hardening materials
[PB87-144838] 08 p0994 N88-16016
Expert systems relations in space applications 08 p1059 N88-16391
Emulating a flexible space structure: Modeling
[NASA-TM-100320] 09 p1135 N88-16812
Experimental identification of nonlinear structural models
[DE88-001795] 09 p1184 N88-17094
Solid modelling with faceted primitives
[ETN-88-91593] 09 p1218 N88-17305
Phenomenological model of superconductivity of heavy fermions in U(sub 1-x)ThsubxBesub13 09 p1238 N88-17423
Theory of the tetragonal-to-orthorhombic structural phase transition in La2CuO4
[AD-A187141] 09 p1254 N88-17514

Research in theoretical physics
[DE88-003201] 09 p1259 N88-17548
Overview of heat transfer and fluid flow problem areas encountered in Stirling engine modeling
[NASA-TM-100131] 09 p1262 N88-17561
Modeling of some coplanar waveguide discontinuities
[NASA-TM-100808] 10 p1318 N88-17880
Improved canopy reflectance modeling and scene inference through improved understanding of scene pattern
[NASA-CR-182488] 10 p1347 N88-18049
A paradigm for concurrency control performance evaluation 10 p1377 N88-18220
Machine models and simulations
[PB88-118690] 10 p1386 N88-18280
Analysis and synthesis of adaptive neural elements
[AD-A187047] 10 p1395 N88-18316
Hierachical object recognition using libraries of parameterized model sub-parts
[AD-A187476] 10 p1396 N88-18322
Zero-dimensional model of a reversed field pinch fusion reactor
[DE88-005213] 10 p1414 N88-18442
Procedures for quantitative sensitivity and performance validation studies of a deterministic fire safety model
[NBS/GCR-88/544] 11 p1469 N88-18762
Turbulence modeling in non-inertial frames of reference
[NASA-CR-181646] 11 p1488 N88-18880
Characterization of damped structural connections for multi-component systems
[NASA-TM-100801] 11 p1502 N88-18974
A digital terrain system for microcomputers
[INPE-4170-PRE/1067] 11 p1505 N88-18987
Target-reflectivity models for various terrain types
[DE88-005510] 11 p1505 N88-18992
Concepts and nomenclature in the world modeling system (a lesson in applied metaphysics)
[AD-A188246] 11 p1534 N88-19166
MCT crystal growth
[NASA-CR-179297] 11 p1557 N88-19318
Notes on a class of homogeneous space-times
[DE88-700138] 11 p1562 N88-19353
The early years of string theory: The dual resonance model
[DE88-003521] 11 p1563 N88-19359
A modeling analysis program for the JPL table mountain lo sodium cloud data
[NASA-CR-182555] 11 p1570 N88-19400
Modeling of limit cycle stall flutter oscillations 12 p1583 N88-19472
Mathematical foundations of signal processing. 2: The role of group theory
[AD-A188482] 12 p1620 N88-19685
Validation of GEMACS (General Electromagnetic Model for the Analysis of Complex Systems) for modeling lightning-induced electromagnetic fields
[AD-A188822] 12 p1620 N88-19687
Electromagnetic modeling of a control valve
[INPE-4140-PRE/1048] 12 p1622 N88-19700
KREME (Knowledge Representation, Editing and Modeling Environment): A user's introduction, phase 1
[AD-A188906] 12 p1681 N88-20052
Motion in a random gyrotropic environment in D dimensions
[PB87-170650] 12 p1685 N88-20079
A moment approach to modeling negative ion sources
[AD-A188858] 12 p1691 N88-20114
Development savings through parametric modeling of program costs 12 p1700 N88-20175
Nonaxisymmetric body supersonic, aerodynamic prediction
[AD-A189338] 13 p1716 N88-20259
Understanding machines from text and diagrams
[AD-A189034] 13 p1755 N88-20493
Estimation-correlation, modeling, and identification in adaptive array processors
[AD-A189130] 13 p1757 N88-20512
Numerical methods in the resolution of control electrovalve model
[INPE-4154-RPE/540] 13 p1764 N88-20554
Improvement of the Reynolds-stress model by a new pressure-strain correlation
[NASA-CR-182699] 13 p1783 N88-20667
Atmospheric electrical modeling in support of the NASA F-106 storm hazards project
[NASA-CR-181639] 13 p1799 N88-20758
Broadband correlation analysis
[AD-A188732] 13 p1814 N88-20839
Relativistic jet models for the BL Lacertae object Mrk 421 during three epochs of observation
[NASA-TM-89727] 13 p1853 N88-21090
Modeling surface exchanges: The soil-vegetation-atmosphere continuum 14 p1937 N88-21553
Hydrological models 14 p1937 N88-21559
Tabulation of Mie scattering calculation results for microwave radiative transfer modeling
[NASA-CR-4130] 14 p1947 N88-21612
Some models for rain and cloud attenuation of millimeter waves
[PB88-160809] 14 p1948 N88-21616
Aero/structural tailoring of engine blades (AERO/STAEBL)
[NASA-CR-180805] 14 p1959 N88-21682
Strings in four dimensions
[DE88-006435] 14 p1990 N88-21864
Geometric modeling of flight information for graphical cockpit display
[AD-A190484] 15 p2021 N88-22043
A model for nitrogen atom recombination on a silicon dioxide surface
[AD-A189843] 15 p2142 N88-22784
Georelational data model
[INPE-4490-PRE/1254] 15 p2149 N88-22829
Inflow measurements made with a laser velocimeter on a helicopter model in forward flight. Volume 4: Tapered planform blades at an advance ratio of 0.15
[NASA-TM-100544] 16 p2156 N88-22863
On the validation of a code and a turbulence model appropriate to circulation control airfoils
[NASA-TM-100090] 16 p2156 N88-22864
Measurements of the time dependent velocity field surrounding a model propeller in uniform water flow 16 p2205 N88-23155
On the prediction of equilibrium states in homogeneous turbulence
[NASA-CR-181659] 16 p2207 N88-23174
User's manual for EULER3DS
[AD-A191048] 16 p2208 N88-23177
Computerized life and reliability modelling for turboprop transmissions
[NASA-TM-100918] 16 p2215 N88-23220
Characterization of structural connections for multicomponent systems 16 p2220 N88-23251
Computer based modeling of thematic mapping 16 p2225 N88-23285
The event-related brain potential as an index of information processing and cognitive activity: A program of basic research
[AD-A191244] 16 p2243 N88-23400
On 2-D versus 3-D: Sine of squared angular error and weighted perpendicular fixing
[NASA-CR-182899] 16 p2252 N88-23458
Flight testing a V/STOL aircraft to identify a full-envelope aerodynamic model
[NASA-TM-100996] 17 p2301 N88-23762
The Systeme d'Analyse Geographique (SAGE) geographic analysis system 17 p2353 N88-24019
A proposal of adaptation of a knowledge-based scene analysis model to some remote sensing problems 17 p2354 N88-24026
Three-dimensional models of conventional and vertical junction laser-photovoltaic energy converters
[NASA-TM-4039] 17 p2370 N88-24111
Models and metrics for software management and engineering
[NASA-CR-182953] 17 p2389 N88-24200
Induction of models under uncertainty
[NASA-TM-101173] 17 p2394 N88-24230
Analytical modeling of the structureborne noise path on a small twin-engine aircraft
[NASA-CR-4136] 17 p2394 N88-24233
Hydrogen turbines for space power systems: A simplified axial flow gas turbine model 17 p2419 N88-24385
A transient model for liquid metal heat pipes 17 p2421 N88-24398
Analysis of dust grain properties in two star forming regions through comparison of theoretical models to observations 17 p2451 N88-24559
Dynamic consolidation of metal powders
[AD-A192126] 18 p2485 N88-24744
Computational Fluid Mechanics
[NASA-CR-183022] 18 p2514 N88-24915
An investigation of a distributed clock for local area networks with ring topology 18 p2516 N88-24924
The Effect of the Ionosphere on Communication, Navigation and Surveillance Systems Based on Ionospheric Effects Symposium held on 5-7 May 1987 in Springfield, Virginia
[AD-A191855] 18 p2541 N88-25081
Energy measurements in oxygen-induced reactions at 60 A GeV and 200 A GeV
[DE88-006420] 18 p2573 N88-25283
Modeling and evaluation of variable structure organizations
[AD-A191947] 18 p2588 N88-25381
F-14 modeling study
[NASA-CR-4164] 19 p2603 N88-25462
Next-generation fire extinguishing agent. Phase 1: Suppression concepts
[AD-A192279] 19 p2614 N88-25514
Structure and refinement of ordered aromatic heterocyclic polymers by diffraction methods: Application of results to electro-optic phenomena
[AD-A191859] 19 p2619 N88-25537
Entrance and exit region friction factor models for annular seal analysis
[NASA-CR-183084] 19 p2678 N88-25921
Improved description of base dynamics in the modeling of bipolar transistors
[PB88-181516] 19 p2732 N88-26229
Development of a GaAs solid state device model for high power applications
[DE88-009048] 19 p2734 N88-26242
Analysis and synthesis of decision-making organizations
[AD-A191948] 19 p2738 N88-26258
Voyager imaging photometry and radiative transfer modeling of the spoke-like features in Saturn's outer B-ring 19 p2742 N88-26278
Stochastic modeling of EM scattering from foliage
[AD-A192258] 20 p2790 N88-26553
Modeling and optimum time performance for concurrent processing
[NASA-CR-4167] 20 p2797 N88-26595
Numerical model for the computation of radiance distributions in natural waters with wind-roughened surfaces
[PB88-192703] 20 p2826 N88-26765
Prediction of continental shelf sediment transport using a theoretical model of the wave-current boundary layer
[AD-A192272] 20 p2829 N88-26783
Experimental study of planetary gases with applications to planetary interior models
[NASA-CR-183098] 20 p2886 N88-27137
Carbon deposition model for oxygen-hydrocarbon combustion, volume 1
[NASA-CR-179375] 21 p2908 N88-27254
Carbon deposition model for oxygen-hydrocarbon combustion, volume 2
[NASA-CR-179376] 21 p2908 N88-27255
Surface-wave model uncertainty assessment
[AD-A193094] 21 p2932 N88-27408
Evaluation of fracture models through pressurized-thermal-shock testing
[DE88-011834] 21 p2963 N88-27603
The relationship between observed fatigue damage and life estimation models
[NASA-CR-182191] 21 p2965 N88-27611
Solar cell modeling and simulation
[AD-A193249] 21 p2966 N88-27620
Enhancement of modeling and image generation techniques for high-resolution 3-dimensional imagery
[DE88-008923] 21 p2998 N88-27782
Some stability criteria in fluid and solid mechanics 21 p3027 N88-27966
Modeling, designing and simulating a pointing control system for balloon-borne solar experiments
[NASA-TM-100337] 22 p3082 N88-28300
An overview of technology for spoken interaction with machines
[AD-A194153] 23 p3202 N88-29058
A statistical rain attenuation prediction model with application to the advanced communication technology satellite project. 1: Theoretical development and application to yearly predictions for selected cities in the United States
[NASA-CR-179498] 23 p3205 N88-29077
Regional intercomparisons of General Circulation Model predictions and historical climate data: CO2
[DE88-010416] 23 p3235 N88-29248
Conjunctive measurement theory: Cognitive research prospects
[AD-A193627] 23 p3239 N88-29277
A model of information growth 23 p3265 N88-29440
Linearized model matching for single-imput nonlinear systems
[AD-A193642] 23 p3266 N88-29445
An analysis of heat transfer after loss of primary coolant in the SP-100 reactor system
[AD-A194619] 23 p3281 N88-29539
Can we calculate the fundamental dimensionless constants of physics
[DE88-702641] 23 p3295 N88-29625
Constitutive modeling for isotropic materials
[NASA-CR-182132] 24 p3327 N88-29811
Gas phase combustion chemistry of nitramine propellants
[AD-A195082] 24 p3344 N88-29902
Attenuated total reflectance FT-IR spectroscopy to measure interfacial reaction kinetics at silica surfaces
[AD-A196330] 24 p3344 N88-29908
Synchronous response modelling and control of an annular momentum control device
[NASA-CR-4166] 24 p3358 N88-29995

Track performance considerations for monopulse radars
[AD-A196232] 24 p3360 N88-30007
Measurement and interpretation of North Atlantic Ocean marine radar sea scatter
[AD-A196239] 24 p3364 N88-30036
An improvement in the numerical integration procedure used in the NASA Marshall engineering thermosphere model
[NASA-CR-179389] 24 p3392 N88-30200
Thermal models pertaining to continental growth 24 p3397 N88-30230
Continental crustal formation and recycling: Evidence from oceanic basalts 24 p3398 N88-30236
Physical processes in the growth of the continental crust 24 p3398 N88-30240
Trace element differences between Archean, Proterozoic and Phanerozoic crustal components: Implications for crustal growth processes 24 p3399 N88-30243
The growth of the continental crust: Constraints from radiogenic isotope geochemistry 24 p3399 N88-30245
Crustal growth in the Archean: The geochemical evidence 24 p3400 N88-30246
Growth of the continental crust: A planetary-mantle perspective 24 p3400 N88-30251
Late-Archaean crustal growth in the Lewisian Complex of Northwest Scotland: Diachroneity in magmatic accretion and implications for models of crustal growth 24 p3401 N88-30253
The effect of thicker oceanic crust in the Archaean on the growth of continental crust through time 24 p3401 N88-30254
An analysis of results of a high-resolution world ocean circulation model
[AD-A195760] 24 p3405 N88-30272
Contributions to engineering models of human-computer interaction, volume 1
[AD-A195590] 24 p3409 N88-30295
A model for architectural comparison
[AD-A195993] 24 p3411 N88-30302
A shared-world conceptual model for integrating space station life sciences telescience operations 24 p3416 N88-30333
Automatic qualitative analysis of ordinary differential equations using piecewise linear approximations
[AD-A196310] 24 p3424 N88-30379
Orbital evolution of distant artificial earth satellites 24 p3445 N88-30506

MODEMS
Digital receiver structures and methods for the determination of the scanning frequency in modems for fast data transmission via telephone channels
[ETN-87-90429] 01 p0037 N88-10235
High data rate modem simulation for the space station multiple-access communications system 06 p0795 N88-14870
Modem for digital phase modulation: Results and summary
[PB87-149233] 07 p0845 N88-15129
Compilation and development of K-6 aerospace materials for implementation in NASA spacelink electronic information system 07 p0922 N88-15605
An 8-DPSK TCM modem for MSAT-X 19 p2649 N88-25725
Development of a coded 16-ary CPFSK coherent demodulator 19 p2649 N88-25726
Modem for the land mobile satellite channel 19 p2649 N88-25727
A mixed-modem solution for sensitive data segregation on a broadband network
[DE88-001765] 19 p2718 N88-26139
Performance of a rapid carrier acquisition circuit for satellite ground terminal modems
[RSRE-TEST-REPORT-87/CC3/2] 22 p3071 N88-28227
An OKQPSK/modem incorporating numerically controlled carrier synthesis
[DE88-009536] 23 p3244 N88-29304

MODERATION (ENERGY ABSORPTION)
NT THERMALIZATION (ENERGY ABSORPTION)
Particle bed reactor scaling relationships 17 p2400 N88-24267

MODES
NT AXIAL MODES
NT BALLOONING MODES
NT COUPLED MODES
NT FAILURE MODES
NT LASER MODES
NT PROPAGATION MODES
NT PUSHBROOM SENSOR MODES
NT VIBRATION MODE
Fully plastic analysis of mixed mode plane-strain crack problems
[PB87-144929] 08 p0994 N88-16015
New mode conversion process and overdense plasma heating in the electron cyclotron range of frequencies
[IPPJ-854] 10 p1411 N88-18420

MODFETS
Enhanced performance ultrabroadband distributed amplifiers 19 p2656 N88-25775
High performance quarter-micron-gate MODFETs 19 p2656 N88-25776
Progress and challenges in HEMT LSI technology 19 p2656 N88-25779
Modulation efficiency limited high frequency performance of the MODFET 19 p2657 N88-25786
Non-stationary transport in MODFET's and heterojunction devices 19 p2659 N88-25804

MODIFICATION
U REVISIONS

MODULARITY
Modular CAMAC system, 2
[DE88-700237] 11 p1525 N88-19106
Multimission Modular Spacecraft (MMS). A serviceable design spacecraft 12 p1587 N88-19501
Status of modular RTG technology 17 p2422 N88-24403
Loading and linking in a modular language, an exercise in verification by unification
[INF-87-30] 22 p3136 N88-28642
Modularity in the PASCAL model compiler
[NPL-DITC-111/88] 22 p3139 N88-28664
The SMITE modular compilation system
[RSRE-MEMO-4145] 23 p3244 N88-29307

MODULATED CONTINUOUS RADIATION
Discussion on the modelling and processing of signals from an acousto-optic spectrum analyzer
[AD-A185639] 06 p0694 N88-14257

MODULATION
NT AMPLITUDE MODULATION
NT DELTA MODULATION
NT DIFFERENTIAL PULSE CODE MODULATION
NT FREQUENCY MODULATION
NT FREQUENCY SHIFT KEYING
NT INTERMODULATION
NT LIGHT MODULATION
NT PHASE MODULATION
NT PHASE SHIFT KEYING
NT PULSE AMPLITUDE MODULATION
NT PULSE CODE MODULATION
NT PULSE DURATION MODULATION
NT PULSE MODULATION
NT PULSE POSITION MODULATION
NT TRAVELING WAVE MODULATION
Metallic superlattices with monolayer modulation
[DE87-012724] 01 p0023 N88-10145
Reception of pseudo noise-modulated signals using digital correlators for satellite navigation tasks
[ETN-87-90426] 01 p0037 N88-10234
Phase dynamics: A review and a perspective
[DE87-013173] 01 p0048 N88-10306
Solar modulation of the cosmic radiation in the heliosphere 01 p0112 N88-10720
A digital audio link to the Channel Islands in the UHF television band: Protection of television signals from digitally modulated interference
[BBC-RD-1987/7] 02 p0161 N88-11010
Study of a coding and modulation system for the V32 call of the CCITT
[ENST-87E007] 02 p0162 N88-11015
High-power RF-pulsed modulators for the Los Alamos free-electron laser
[DE88-000514] 04 p0448 N88-12775
Study of electrostatic modulation of fuel sprays to enhance combustion performance in an aviation gas turbine
[AD-A184967] 05 p0548 N88-13341
Two-signal cross modulation effects, half-IF effects and interference criteria in land mobile sharing with UHF (Ultra High Frequency) television
[PB87-228037] 05 p0576 N88-13514
Evaluation of a satellite laser ranging technique using pseudonoise code modulated laser diodes
[NASA-CR-182347] 06 p0708 N88-14343
Response of a sequential damper to shock inputs 08 p0998 N88-16042
LiNbO3:Ti directional-coupler modulators for high-bandwidth, single-shot instrumentation systems operating at 800 nm
[DE88-003830] 11 p1479 N88-18823
Atomic monolayer metallic superlattices
[DE88-005348] 12 p1607 N88-19612
A concatenated coded modulation scheme for error control
[NASA-CR-182639] 12 p1621 N88-19697
Signal-filler design and system performance for polarimetric radar
[AD-A189257] 13 p1758 N88-20514
Efficiency characteristics of speed modulated drives at predicted torque conditions for air-to-air heat pumps
[DE88-005846] 13 p1770 N88-20588
Nonlinear dynamics of interaction between charged particles modulated beam and bounded plasma regular oscillations
[DE88-701681] 16 p2280 N88-23648
Doppler radar with multiphase modulation of transmitted and reflected signal
[NASA-CASE-MSC-18808-1] 17 p2332 N88-23923
Dynamic characteristics of a vibrating beam with periodic variation in bending stiffness
[NASA-TP-2697] 17 p2348 N88-23988
Interleaver design for trellis-coded differential 8-PSK modulation with non-coherent detection 19 p2648 N88-25719
Pilot-aided modulation for narrow-band satellite communications 19 p2649 N88-25728
ACSB: A minimum performance assessment 19 p2649 N88-25731
Kinetic modulational instability of electron cyclotron waves in plasmas
[DE88-701893] 20 p2859 N88-26978
Modulated-splitting-ratio fiber-optic temperature sensor
[NASA-TM-101332] 22 p3042 N88-28062
Direct bit detection receiver performance analyses for 8-DPSK (Differential Phase Shift Keyed) modulated signals operating with improper carrier phase synchronization
[AD-A193839] 22 p3070 N88-28220
Automatic classification of digitally modulated signals
[AD-A194623] 23 p3203 N88-29064
Long haul communications in the HF spectrum utilizing high speed modems
[AD-A194683] 24 p3360 N88-30003

MODULATION DOPED FETS
U MODFETS

MODULATION TRANSFER FUNCTION
Modulation transfer function --- SPOT 03 p0341 N88-12153
High-energy laser-assisted imaging through vaporizing aerosols
[DE88-007911] 18 p2521 N88-24957

MODULATORS
NT MODEMS
The 8.4-GHz low-noise maser pump source assembly 04 p0436 N88-12705
Pulse width modulator controller design for a brushless DC motor position servo
[AD-A186618] 08 p0980 N88-15921
LiNbO3:Ti directional-coupler modulators for high-bandwidth, single-shot instrumentation systems operating at 800 nm
[DE88-003830] 11 p1479 N88-18823
Analysis of pre-flight modulator voltage calibration data for the Voyager plasma science experiment
[NASA-CR-182577] 12 p1710 N88-20236
Characteristics and application of wideband guided-wave devices 19 p2660 N88-25817
Error performance of voice band data signals with an overloaded delta modulator
[FEL-1987-05] 20 p2792 N88-26562
A high frequency GaAlAs travelling wave electro-optic modulator at 0.82 micrometers
[NASA-TM-100970] 22 p3073 N88-28240
High frequency GaAlAs modulator and photodetector for phased array antenna applications
[NASA-TM-101328] 24 p3367 N88-30048

MODULATORS-DEMODULATORS
U MODEMS

MODULES
NT CHEMICAL RELEASE MODULES
NT COMMAND MODULES
NT ELECTRONIC MODULES
NT LANDING MODULES
NT LUNAR LANDING MODULES
NT PAYLOAD ASSIST MODULE
NT POWER MODULES (STS)
NT SPACECRAFT MODULES
Columbus pressurized module verification 02 p0134 N88-10842
Documentation of NCAR (National Center for Atmospheric Research) CCM1 program modules
[PB87-213567] 03 p0352 N88-12220
A modular BLSS simulation model 03 p0359 N88-12260
Modular pump limiter systems for large tokamaks
[DE88-001487] 04 p0494 N88-13045
An analysis of simplified feed architectures for MMIC (Monolithic Microwave Integrated Circuit) T/R (Transmit/Receive) module arrays
[AD-A185474] 06 p0697 N88-14275
Interaction of different modules in depth perception: Stereo and shading
[AD-A185607] 06 p0759 N88-14655

Evaluate the application of modal test and analysis processes to structural fault detection in MSFC - STS project elements 07 p0927 N88-15630
The German Honeywell ring laser gyro: Development and test results 12 p1578 N88-19440
Parts-R-Us
[AD-A188621] 12 p1622 N88-19705
Optics of the CEBAF CW superconducting accelerator
[CEBAF-PR-87-012] 12 p1690 N88-20110
Component mode synthesis using experimental modes enhanced by mass loading
[DE88-006097] 13 p1781 N88-20657
Advanced avionics system analysis. Modular avionics cost benefit study formulation
[AD-A189019] 14 p1867 N88-21158
Thermophotovoltaic space power system, phase 3
[NASA-CR-179327] 14 p1942 N88-21585
Japanese space station module 15 p2052 N88-22224
Solar cell cover glasses for satellites 15 p2052 N88-22225
Investigation into the development of computer aided design software for space based sensors
[NASA-CR-180772] 15 p2107 N88-22552
Complexity of some problems in module algebra
[PB88-165386] 15 p2122 N88-22648
A 30 GHz monolithic receive module technology assessment
[NASA-CR-180825] 16 p2194 N88-23084
IPC for modular software requires a third party connect
[AD-A189199] 16 p2246 N88-23414
Systems for the 21st century 17 p2302 N88-23769
Design for interoperability (interchangeability) 17 p2305 N88-23789
EMPTAC (Electromagnetic Pulse Test Aircraft) user's guide
[AD-A195072] 24 p3360 N88-30006
Advanced planar array development for space station
[NASA-CR-179373] 24 p3389 N88-30181
The design of an intelligent multidisk control module for VME bus based systems
[AD-A195587] 24 p3411 N88-30303

MODULUS OF ELASTICITY
Elastic moduli of copper under compression
[DE87-013137] 02 p0147 N88-10922
Anelastic behaviour of materials under multiaxial strains. Part 3: Order-disorder transition, Shoek effect and Poisson's ratio in AISI-1080 steel
[DE87-703087] 02 p0191 N88-11193
Ion-matrix coupling in polymer electrolytes from relaxation time studies
[AD-A184632] 03 p0293 N88-11841
Effects of cure pressure on resin flow, voids, and mechanical properties
[AD-A184267] 03 p0295 N88-11853
Carbon fiber reinforced glass matrix composites for space based applications
[AD-A184355] 04 p0410 N88-12546
Determination of through-plane shear moduli for glass-reinforced plastics
[PB87-106274] 04 p0418 N88-12592
High temperature low cycle fatigue of oxide dispersion strengthened and single crystal nickel base superalloys 06 p0720 N88-14422
Structural relaxation and mechanical properties of amorphous Fe-Zr alloys 07 p0840 N88-15094
Investigation of low velocity impact damage on filamentary composite materials 07 p0923 N88-15607
Applications and limitations of the spectral-analysis-of-surface-waves method
[PB88-136619] 11 p1513 N88-19038
A continuum damage model for viscoelastic materials
[AD-A189426] 12 p1637 N88-19800
High temperature Young's modulus of IG-110 graphite 13 p1746 N88-20443
Effects of high temperature neutron irradiation on the physical, chemical and mechanical properties of fine-grained isotropic graphite 13 p1747 N88-20444
Determination of the modulus of elasticity of structural silicone sealants
[PB88-157458] 14 p1893 N88-21307
The age hardening response of thermomechanically processed Al-Mg-Li alloys
[AD-A189870] 15 p2039 N88-22147
The sensitivity of boundary layer instability growth rates to compliant wall properties
[AD-A190433] 15 p2064 N88-22309
The mechanical behavior of particle filled thermoplastics
[ETN-88-92234] 16 p2181 N88-22999
The use of micromachined structures for the management of mechanical properties and adhesion of thin films 19 p2674 N88-25899

MOHAWK AIRCRAFT
U OV-1 AIRCRAFT

MOHR CIRCLES
U FRACTURE MECHANICS

MOIRE EFFECTS
The mechanical properties of card measured by photographic Moire
[NPL-DMOM-87] 14 p1923 N88-21463

MOIRE FRINGES
Optical deformation measurement on shells following the raster principle
[ETN-88-90608] 05 p0609 N88-13741
Transient welding strain measurement by Moire technique: A comparison between experimental measurement and numerical analysis for strain-stress cycles during GTA spot-welding
[PB87-143871] 07 p0868 N88-15269

MOIRE INTERFEROMETRY
Diffraction moire: The dynamic regime
[DE87-014883] 03 p0335 N88-12111
A composite grating for moire interferometry
[AD-A186330] 07 p0832 N88-15044
J-estimation procedure based on moire interferometry data
[AD-A185965] 07 p0867 N88-15258
Development of Moire machine vision 09 p1212 N88-17264
The magic of carrier patterns in moire interferometry
[AD-A187582] 10 p1296 N88-17748
The analysis of deformations and strains in composites by moire interferometry
[AD-A187482] 10 p1345 N88-18043
Interfacial shear phenomena in graphite epoxy composites under impact loading using dynamic moire interferometry
[DE88-006773] 18 p2479 N88-24709
Experimental investigation of ductile fracture by white light moire interferometry 22 p3087 N88-28329
J-integral measurement using moire interferometry
[AD-A193751] 23 p3226 N88-29202

MOISTURE
NT ATMOSPHERIC MOISTURE
NT SOIL MOISTURE
RADC/NBS (Rome Air Development Center/National Bureau of Standards) Workshop. Moisture Measurement and Control for Microelectronics (4)
[PB87-224614] 03 p0309 N88-11947
Theory of heat and moisture exchange between finely disperse storm-generated spray and turbulent air flow 04 p0461 N88-12851
A finite element analysis of adhesively bonded composite joints including geometric nonlinearity, nonlinear viscoelasticity moisture diffusion and delayed failure
[AD-A187455] 10 p1296 N88-17747
Suggested severe local storm operational scenario for GOES I-M
[NASA-TM-100688] 11 p1515 N88-19052
Effects of moisture, elevated temperature, and fatigue loading on the behavior of graphite/epoxy buffer strip panels with center cracks
[NASA-TM-100558] 12 p1603 N88-19590
Temperature, moisture and strain rate effects on the compressive mechanical behavior of Nylon 6/6
[DE88-010734] 21 p2961 N88-27591
The effects of moisture loss and elevated temperature upon the material damping of fibre reinforced polymer matrix composites
[UTIAS-324] 23 p3188 N88-28970

MOISTURE CONTENT
NT ATMOSPHERIC MOISTURE
Moisture determinations in and under vegetation canopies. Part 2: Results after parameterization of the CLOUD model
[FEL-1986-63] 01 p0064 N88-10410
A method for remote sensing of precipitable water vapor and liquid in the atmosphere using a 22-ghz radiometer
[AD-A184204] 03 p0354 N88-12232
Lidar-radiometric method for determining liquid-water content of cirrus clouds 04 p0461 N88-12854
Variations of tropical circulation and associated rainfall anomalies, during 2 years of contrast
[INPE-4359-TDL/300] 08 p1039 N88-16286
Moisture plotting of carbon fiber composite in flight operations
[MBB-UT-119/87] 09 p1138 N88-16823
Detection of soil erosion with Thematic Mapper (TM) satellite data within Pinyon-Juniper woodlands
[NASA-CR-182476] 09 p1185 N88-17103
Measuring and modeling near surface reflected and emitted radiation fluxes at the FIFE site
[NASA-CR-182660] 12 p1640 N88-19818
Ion content and infrared absorption of moist atmospheric air
[AD-A188839] 12 p1643 N88-19838
Environmental effects on the post-impact compressive strength of CFC
[RAE-TM-MAT-STR-1088] 14 p1884 N88-21258
Effect of moisture level in PBXW-109(E) (plastic-bonded explosive) mixes on the aging of the cured explosive
[AD-A190200] 15 p2048 N88-22202
Use of energy emission for detecting the necessity of irrigation in wheat in field conditions
[INPE-4461-TDL/318] 16 p2229 N88-23315
Low-temperature thermochemical conversion of high moisture biomass feedstocks 18 p2536 N88-25047
Studies of the mechanisms and rates with which nitrogen species are incorporated into cloud water and precipitation
[PB88-193065] 20 p2826 N88-26764
Simulation of moisture diffusion of fiber reinforced components of aircraft for general air transportation
[IFL-IB-87-05] 21 p2907 N88-27253
On experiences with two hot-wire instruments for measuring the liquid water content in clouds
[ESA-TT-1085] 23 p3236 N88-29255

MOISTURE DETECTORS
U MOISTURE METERS

MOISTURE METERS
High polymer sensor materials discussed 06 p0676 N88-14140
Nondestructive moisture measurement in microelectronics
[AD-A190515] 15 p2060 N88-22281

MOISTURE RESISTANCE
The analysis of moisture absorption in multi-layered media
[NPL-DMA(A)-147] 01 p0019 N88-10115
The water absorption of model epoxy resin networks cured with aromatic diamines
[BR100722] 01 p0027 N88-10169
Stability of uncapsulated weight cells with thin film elongation measurement bands under influence of humidity, temperature and operation voltage
[ETN-88-92383] 21 p2951 N88-27531

MOL (ORBITAL LABORATORIES)
U MANNED ORBITAL LABORATORIES

MOLDING MATERIALS
High explosive moulding powders from RDX and aqueous polyurethane dispersions
[AD-A185026] 05 p0568 N88-13458
Intelligent process development of foam molding for the Thermal Protection System (TPS) of the space shuttle external tank 08 p1060 N88-16397
Development of a shell system for DS moulds at RR precision casting facility --- directional solidification (DS)
[PNR90400] 09 p1151 N88-16893

MOLDS
Process for producing sandwich mouldings
[EP-PATENT-0-191-623-A2] 04 p0426 N88-12642
Intelligent process development of foam molding for the Thermal Protection System (TPS) of the space shuttle external tank 08 p1060 N88-16397
Development of a shell system for DS moulds at RR precision casting facility --- directional solidification (DS)
[PNR90400] 09 p1151 N88-16893
Injection compression for short fiber reinforced plastics
[SNIAS-881-430-118] 21 p2922 N88-27344

MOLECULAR ABSORPTION
MODTRAN: A moderate resolution model for LOWTRAN
[AD-A185384] 05 p0574 N88-13503
Statistical fine structure in inhomogeneously broadened absorption lines in solids
[AD-A190341] 16 p2174 N88-22957
Molecular line shape effects on atmospheric window absorption
[AD-A196316] 24 p3342 N88-29894

MOLECULAR BEAM EPITAXY
Quantum well laser diodes: Modeling and realization of GaAs/GaAlAs
[LAAS-87-165] 02 p0179 N88-11116
Molecular beam heteroepitaxy: (Ca,Sr)F2-GaAs system
[LAAS-87-168] 02 p0246 N88-11556
JPRS report: Science and technology. China
[JPRS-CST-87-026] 03 p0269 N88-11688
Raman scattering spectrum along a bevel etched GaAs on Si, TEM (Transmission Electron Microscope) study and GaAs P-I-N photodetector on Si
[DE88-000210] 04 p0498 N88-13066
MBE growth of InAsSb strained-layer superlattices
[DE88-000365] 05 p0654 N88-14011
Molecular beam epitaxial growth and characterization of 3-5 compound semiconductor single and multiple interface structures
[AD-A185400] 05 p0656 N88-14021

Some investigations of molecular beam epitaxial growth of 3-5 semiconductor films via Monte-Carlo computer simulations, carrier tunnelling and spectroscopic ellipsometry
[AD-A185520] 06 p0789 N88-14839
Molecular beam epitaxy for research on quantum well structures
[AD-A186791] 09 p1255 N88-17522
Epitaxial growth and new phase of single crystal Dy by molecular beam epitaxy
[DE88-002850] 09 p1256 N88-17531
Microwave semiconductor research-materials, devices and circuits
[AD-A187121] 10 p1415 N88-18444
Grazing incidence X-ray scattering study of defect structures in MBE GaAs/Si using synchrotron radiation
[DE88-004556] 10 p1420 N88-18483
MBE growth, characterization and electronic device processing of HgCdTe, HgZnTe related heterojunctions and HgCdTe-CdTe superlattices
[AD-A187456] 10 p1421 N88-18486
Theoretical studies of the interface electronic properties of tetrahedrally coordinated semiconductors
[AD-A187216] 11 p1555 N88-19306
MBE (Molecular Beam Epitaxial) growth characterization and electronic device processing of HgCdTe, HgZnTe related heterojunctions and HgCdTe-CdTe superlattices
[AD-A187416] 11 p1555 N88-19307
Comparison of low temperature photoluminescence of bulk MBE (Molecular Beam Epitaxy) grown AlGaAs and GaAs using a graphite generated dimer versus a standard tetramer arsenic group-V source
[DE88-004939] 11 p1558 N88-19329
Characterization of enhanced Schottky-barrier InGaAs/Al(1-x)As strained channel modulation-doped field-effect transistors
[AD-A188820] 12 p1698 N88-20162
Research on multibandgap solar cells
[DE87-012261] 13 p1792 N88-20721
Development of Si/SiGe heterostructures
[AD-A189527] 13 p1845 N88-21044
Electrical characteristics of MBE (Molecular Beam Epitaxyl)-grown GaAs/sub 1-x/Sb/sub x on InP and correlation with film microstructure
[DE88-003841] 13 p1847 N88-21053
Gas source MBE (Molecular Beam Epitaxy)
[AD-A189763] 15 p2142 N88-22782
Beam assisted fabrication of 3-5/Si monolithic devices
[AD-A189979] 15 p2142 N88-22785
Microelectronics the next fifteen years
17 p2305 N88-23792
Molecular Beam Epitaxy (MBE) for high speed devices
19 p2656 N88-25770
Epitaxial iron films
[AD-A191815] 19 p2732 N88-26225
Center for thin film studies
[AD-A191996] 19 p2732 N88-26226
Analysis of the performance of the space ultravacuum research facility in attached and free-flyer mode
[NASA-TM-100325] 20 p2763 N88-26387
Integrated optoelectronic circuits utilizing InGaAsP grown by molecular beam epitaxy (erbium doping of MBE GaAs)
[AD-A192269] 20 p2795 N88-26584
MBE growth of HgTe/CdTe superlattices on Si(100) substrates 20 p2869 N88-27033
Preparation of high-T(sub)c Y1Ba2Cu3O(sub 7-Delta) superconducting thin films by MBE (Molecular-Beam-Epitaxy) techniques
[DE88-009999] 20 p2877 N88-27082
Molecular beam epitaxy of GaP films on Si substrates
[PB88-131974] 21 p3020 N88-27923
Investigations on the MBE (Molecular Beam Epitaxy) growth and properties of Al(sub y)Ga(sub y)In(sub 1-x-y)AsInP and InGaAs-InAlAs superlattices
[DE88-009105] 21 p3022 N88-27941
Spectroscopic studies with multiple quantum well materials with applications to optical signal processing at room temperature
[AD-A194171] 24 p3429 N88-30409
Electronic materials and devices prepared by molecular beam epitaxy
[AD-A195694] 24 p3433 N88-30433

MOLECULAR BEAMS
Direct infrared absorption of clusters in pulsed molecular beams
[DE87-014802] 02 p0236 N88-11490
Materials preparation and longevity in hyperthermal atomic oxygen 03 p0297 N88-11862
Ceramics thin film 04 p0403 N88-12505
Reactive sticking coefficients of silane on silicon
[DE88-000601] 05 p0570 N88-13473
Supersonic beam observations of semiconductor clusters
[AD-A184991] 05 p0655 N88-14018
Determination of molecular-ion structures through the use of accelerated beams
[DE88-002960] 09 p1246 N88-17467
Apparatus for the study of silicon film deposition and silicon etching
[AD-A187616] 10 p1334 N88-17972
Self-pumped phase conjugation in a supersonically flowing medium
[AD-A188281] 10 p1338 N88-17998
Development of a planar heterojunction bipolar transistor for very high speed logic
[AD-A188137] 11 p1478 N88-18820
A study of the interaction of light with sub-micron metallic surfaces
[DE88-003138] 13 p1776 N88-20624
Crossed molecular beam studies of substitution and exchange reactions
[DE88-006322] 14 p1980 N88-21814
Molecular-beam, mass-spectrometric studies of wood vapor and model compounds over HZSM-5 catalyst
18 p2535 N88-25044
Interactions of molecules with surfaces
[DE88-007950] 19 p2723 N88-26169
Electron-impact-ionization and electron-attachment cross sections of radicals important in transient gaseous discharges
[AD-A192248] 20 p2770 N88-26424
Reaction dynamics on semiconductor surfaces
[AD-A194305] 22 p3156 N88-28781

MOLECULAR BIOLOGY
Molecular mechanisms of neuronal responsivity
[AD-A187061] 09 p1199 N88-17185
Biology and Medicine Division
[DE87-009280] 14 p1952 N88-21632
Studies of molecular biology
[DE88-005906] 15 p2101 N88-22514
ECUT (Energy Conversion and Utilization Technologies) program: Biocatalysis Project
[NASA-CR-182917] 17 p2370 N88-24110

MOLECULAR BONDS
U CHEMICAL BONDS

MOLECULAR CHAINS
Applications and limitations of deuterium labeling methods to neutron scattering studies of polymers
[DE87-012936] 02 p0151 N88-10945
Estimations of gravitational effects on thermal denaturation process in a biopolymer
03 p0318 N88-12013
Feasibility of chemical lasers based on chain reaction involving hydrogen fluorination with thermal branching mechanism 09 p1238 N88-17420
Basic research on macromolecular dynamics
[PB88-141643] 10 p1305 N88-17805
Storing bits on a DNA polymer chain
[AD-A195701] 24 p3356 N88-29981
Novel ladder polymers for use as high temperature stable resins or coatings
[NASA-CASE-LEW-14203-1] 24 p3356 N88-29984

MOLECULAR CLOUDS
Soft X-ray observations of pre-main sequence stars in the chamaeleon dark cloud
[NASA-CR-181457] 02 p0250 N88-11579
Composition, structure and chemistry of interstellar dust
[NASA-TM-88350] 02 p0253 N88-11603
Molecular clouds at high galactic latitudes
11 p1569 N88-19392
Submillimeter and far infrared line observations of M17 SW: A clumpy molecular cloud penetrated by UV radiation
[NASA-CR-182866] 16 p2288 N88-23701
Optical and infrared observations of high latitude dust clouds --- interstellar matter
[B8621135] 16 p2289 N88-23709
Analysis of dust grain properties in two star forming regions through comparison of theoretical models to observations 17 p2451 N88-24559
Microwave spectroscopy and gravitational collapse
18 p2594 N88-25413
High spatial resolution observations of neutral atomic carbon in the molecular clouds M17 and W51
[MPE-PREPRINT-109] 22 p3164 N88-28846
First detection of HCN J=9 to 8 (797 GHz) line emission: Very high densities in the Orion core
[MPE-PREPRINT-110] 22 p3165 N88-28847
Star formation and molecular clouds
24 p3451 N88-30537
Observations of star formation
24 p3451 N88-30538
Comparisons of solar nebula models
24 p3451 N88-30539

MOLECULAR COLLISIONS
Ab initio methods for electron-molecule collisions
[DE87-011728] 01 p0092 N88-10598
The Conference on the Dynamics of Molecular Collisions held in Oglebay Park, Wheeling, West Virginia on 12-17 July 1987
[AD-A184690] 03 p0374 N88-12354
Theoretical atomic and molecular physics
[DE88-001625] 05 p0649 N88-13974
Molecular collision processes in gases and at surfaces
[AD-A189518] 13 p1836 N88-20982
Excimer laser photolysis studies of T-V (Translation-to-Vibration) energy transfer
[AD-A189613] 13 p1837 N88-20989
Molecular reaction and energy transfer rate estimation for chemical-laser analysis
[AD-A190664] 15 p2035 N88-22126
Energy transfer processes in free radicals: A collaborative experimental and theoretical investigation
[AD-A191264] 16 p2269 N88-23578
Theoretical calculations of XeF ground state kinetics
[AD-A191398] 16 p2270 N88-23580
Bimolecular reactions and energy-transfer processes of highly vibrationally excited molecules related to energetic materials
[AD-A189013] 18 p2571 N88-25270
Energy-transfer properties and mechanisms
[DE88-007107] 18 p2571 N88-25272
Theoretical studies of dynamics combustion
[DE88-007565] 19 p2611 N88-25495
Interactions of molecules with surfaces
[DE88-007950] 19 p2723 N88-26169
Low energy molecular collisions
[ISAS-RN-366] 20 p2850 N88-26919

MOLECULAR DIFFUSION
The modelling of orientation in planar polymer welding flows
[AD-A184404] 04 p0451 N88-12793
Does the pipe diffusion of self-interstitials in crystals under stresses exist
[DE88-701027] 15 p2139 N88-22762
Mechanisms of gas permeation through polymer membranes: Renewal proposal for period December 1, 1986 - November 30, 1989
[DE88-007436] 18 p2494 N88-24796
Study of mixing and reaction in the field of a vortex
[AD-A191489] 18 p2508 N88-24878
Molecular composites processing and properties, 1
[AD-A194113] 23 p3189 N88-28974

MOLECULAR DISSOCIATION
U DISSOCIATION

MOLECULAR ELECTRONICS
A strategy to determine the transition state of an electron transfer reaction
[AD-A183976] 03 p0382 N88-12404

MOLECULAR ENERGY LEVELS
Intramolecular energy transfer reactions as a method for metal complex assisted production of hydrogen
[DE88-001621] 05 p0562 N88-13425
Molecular-level synthesis and characterization of metal-polymer interfaces
[AD-A184956] 05 p0567 N88-13455
Sequential excitation preparation of molecular energy levels with special structural and chemical properties
[AD-A190041] 15 p2132 N88-22718
Energy-transfer properties and mechanisms
[DE88-007107] 18 p2571 N88-25272
Study of energy levels and decay mechanisms for singlet Rydberg states of molecular nitrogen
[AD-A192505] 21 p3014 N88-27886

MOLECULAR EXCITATION
Picosecond CO2 laser interactions with polyatomic molecules
[DE87-012072] 01 p0051 N88-10327
Ro-vibrational laser spectroscopy of ESD neutrals from chemisorbed species
[DE87-013011] 04 p0447 N88-12770
Intramolecular energy transfer reactions as a method for metal complex assisted production of hydrogen
[DE88-001621] 05 p0562 N88-13425
Pure dephasing of a vibrational adbond
[AD-A185222] 05 p0609 N88-13740
Explosive absorption of laser beam of finite diameter
07 p0921 N88-15597
Molecular and electronic mechanism in the control of Na+ and K+ permeability of excitable cell membrane by ligand binding on receptor sites
[AD-A188725] 13 p1808 N88-20805
Quantum Monte Carlo study of the MIES associated with H2 (X 1 sigma sub g (+)) and H2 (B 1 sigma sub u (+))
[AD-A189063] 13 p1835 N88-20977
Excimer laser photolysis studies of T-V (Translation-to-Vibration) energy transfer
[AD-A189613] 13 p1837 N88-20989
Molecular reaction and energy transfer rate estimation for chemical-laser analysis
[AD-A190664] 15 p2035 N88-22126

Reactions of N2(A sup 3 sigma sup + sub u) candidates for short wavelength lasers
[DE88-007018] 15 p2070 N88-22342
Experiments on reactions of the electronically excited molecule nitron NH (a sup 1 delta) and carbon CH2 (a bar sup 1 A(1)) in gas phase
[MPIS-3/1987] 17 p2397 N88-24249
Steady-state approximations in Raman excitation equations
[DE88-011759] 21 p3014 N88-27889
Molecular fluorescence measurements with a charge-coupled device detector
[AD-A194221] 22 p3080 N88-28291
Charge storage and switching phenomena in metal complexes
[AD-A193778] 23 p3192 N88-28996
Molecular fluorescence measurements with a charge-coupled device detector
[AD-A194437] 23 p3216 N88-29141
Intramolecular dynamics: A study of molecules at high levels of vibrational excitation
[AD-A195285] 24 p3428 N88-30400

MOLECULAR FLOW
NT SLIP FLOW
NT TRANSITION FLOW
Three dimensional Monte Carlo simulation of molecular movement and heat radiation in vacuum devices: Computer code MOVAK3D --- fusion reactors
[KFK-4292] 09 p1246 N88-17471
Analysis of molecular mixing and chemical reaction in mixing layer
[AD-A191600] 18 p2462 N88-24721

MOLECULAR GASES
NT DIATOMIC GASES
Atomic and molecular gas phase spectrometry
[AD-A187562] 11 p1452 N88-18655
Molecular collision processes in gases and at surfaces
[AD-A189518] 13 p1836 N88-20982
Solar generation and storage of O2 (a 1 delta g)
[NASA-CR-4127] 14 p1913 N88-21431
Kinetics of electrons and molecules at plasma-beam discharge in molecular gases
[DE88-701196] 16 p2275 N88-23616
Molecular gas in Virgo cluster spiral galaxies
17 p2450 N88-24557
Thermostatistical estimations of vapor-state molecules affected by gravity in a heat pipe
20 p2783 N88-26505
Molecular hydrogen in galaxies
23 p3299 N88-29645

MOLECULAR INTERACTIONS
NT MOLECULAR COLLISIONS
On the interaction of a planar metal surface with a charge and with a molecule
[DE87-703083] 02 p0147 N88-10920
Modeling shockwave deformation via molecular dynamics
[DE87-013157] 02 p0169 N88-11063
Systematic studies of molecular vibrational anharmonicity and vibration-rotation interaction by self-consistent-field higher derivative methods: Applications to asymmetric and symmetric top and linear polyatomic molecules
[DE87-014691] 02 p0232 N88-11465
New theory for competing interactions and microstructures in partially-ordered (liquid-crystalline) phases
[DE87-014739] 03 p0380 N88-12389
Soluble metal chelate polymers of coordination numbers six, seven and eight
[AD-A185094] 05 p0568 N88-13459
Investigation of impurity defects in alpha-iron by molecular dynamics method
[DE88-700355] 07 p0834 N88-15058
Van der Waals clusters of aromatic molecules studied using supersonic molecular jet spectroscopy
[AD-A186087] 07 p0929 N88-15644
Energy disposal in ion-molecule reactions
[AD-A186772] 09 p1171 N88-17019
Free energy calculation via MD (molecular dynamics): Methodology and application to bicrystals
[DE88-002902] 09 p1256 N88-17532
Rovibrational spectroscopy of ArCO van der Waals complex
[DE88-004291] 10 p1406 N88-18387
Soluble polysilane derivatives: Chemistry and spectroscopy
[AD-A187889] 11 p1461 N88-18713
Photochemistry at structured surfaces: A classical electromagnetic approach
[AD-A189519] 13 p1737 N88-20387
Molecular reaction and energy transfer rate estimation for chemical-laser analysis
[AD-A190664] 15 p2035 N88-22126
Fast atom bombardment study on interaction of anticodonic nucleotides and their cognate amino acid
[ISAS-RN-355] 20 p2850 N88-26918
Low energy molecular collisions
[ISAS-RN-366] 20 p2850 N88-26919
Precise ultraviolet absorbance study of the interaction of amino acids and mononucleosides in aqueous solution
[ISAS-RN-356] 21 p2908 N88-27256
Corrosion control through a better understanding of the metallic substrate/organic coating/interface
[AD-A193981] 22 p3056 N88-28132
Interactions in miscible polymer blends
[AD-A193824] 22 p3058 N88-28144
Cytochrome electron transfer and biomolecular electronics
[AD-A195482] 24 p3406 N88-30277

MOLECULAR IONS
NT HYDRONIUM IONS
Ionic mechanisms of soot formation in flames
[AD-A186195] 08 p0966 N88-15848
Efficiency of ionic noble gas and alkali metal molecules as ultraviolet and far-ultraviolet lasers
09 p1238 N88-17419
Determination of molecular-ion structures through the use of accelerated beams
[DE88-002960] 09 p1246 N88-17467
The role of electron-ion recombination in bulk antimatter production
16 p2268 N88-23567

MOLECULAR ORBITALS
Accurate ab initio calculations which demonstrate a 3 Pi u ground state for Al2
[NASA-TM-89302] 01 p0102 N88-10666
Clusters: Link between molecules and solids
[AD-A188170] 11 p1543 N88-19224
Molecular orbital studies of the bonding in heavy element organometallics: Progress report
[DE88-007765] 19 p2723 N88-26168

MOLECULAR OSCILLATIONS
Pure dephasing of a vibrational adbond
[AD-A185222] 05 p0609 N88-13740
The 1,2,3-triaminoguanidinium nitrate: An alternate explanation of the nitrate anion disorder
[AD-A188386] 12 p1612 N88-19640
Instrumentation for collisional energy transfer studies
[AD-A188495] 12 p1689 N88-20105

MOLECULAR RELAXATION
Relaxation effect of stark split levels for two-level system interacting with symmetrical strong resonant bichromatic field
03 p0299 N88-11882
Study of vibration relaxation in active medium of CO2-laser using phase-absorption method
07 p0919 N88-15582
Exciton relaxation phenomena in a disordered system
14 p1978 N88-21802
Reactions of N2(A sup 3 sigma sup + sub u) candidates for short wavelength lasers
[DE88-007018] 15 p2070 N88-22342
Monte Carlo investigation of hot photoexcited electron relaxation in GaAs
19 p2659 N88-25805
Monte Carlo simulations of femtosecond relaxation of photoexcited electrons in AlGaAs/GaAs quantum wells
20 p2869 N88-27036
Reaction dynamics on semiconductor surfaces
[AD-A194305] 22 p3156 N88-28781

MOLECULAR ROTATION
Ro-vibrational laser spectroscopy of ESD neutrals from chemisorbed species
[DE87-013011] 04 p0447 N88-12770
Dynamical analysis of molecular decay at spherical surfaces
[AD-A184908] 05 p0647 N88-13964
Rovibrational spectroscopy of ArCO van der Waals complex
[DE88-004291] 10 p1406 N88-18387
The 1,2,3-triaminoguanidinium nitrate: An alternate explanation of the nitrate anion disorder
[AD-A188386] 12 p1612 N88-19640
Continuous collective molecule rotation of a nematic liquid crystal induced from light angular momentum
[FUB-17-1986] 14 p1986 N88-21845
Rotational structure and absorption cross sections from 300 to 190 K of the Schumann-Runge bands
[AERONOMICA-ACTA-A-318-1987]
15 p2036 N88-22131
Collective rotation of molecules driven by the angular momentum of light in a nematic film
[FUB-6-1986] 15 p2131 N88-22714
Sequential excitation preparation of molecular energy levels with special structural and chemical properties
[AD-A190041] 15 p2132 N88-22718
Time-resolved studies of free radicals and laser-initiated chain reactions
[DE88-006569] 16 p2266 N88-23553
Low energy molecular collisions
[ISAS-RN-366] 20 p2850 N88-26919

MOLECULAR SPECTRA
NT ELECTRONIC SPECTRA
NT RAMAN SPECTRA
NT VIBRATIONAL SPECTRA
CARS measurements of combustion. 2: Gas species concentration measurements
[NAL-TR-940] 11 p1453 N88-18663

MOLECULAR SPECTROSCOPY
NT RAMAN SPECTROSCOPY
Experimental molecular spectroscopy in shock-compressed materials
[DE87-013139] 02 p0144 N88-10903
Supersonic beam observations of semiconductor clusters
[AD-A184991] 05 p0655 N88-14018
On the signal strength dependency on pressure in laser sub-Doppler saturation spectroscopy with special attention to gaseous diatonic molecules
[USIP-87-13] 09 p1171 N88-17023
Polarization of molecular fluorescence bands in comets: Recent observations and interpretation
14 p1998 N88-21907
Reaction dynamics on semiconductor surfaces
[AD-A194305] 22 p3156 N88-28781
Molecular fluorescence measurements with a charge-coupled device detector
[AD-A194437] 23 p3216 N88-29141

MOLECULAR STRUCTURE
The influence of polymer structure on triplet luminescence
[DE87-014431] 02 p0152 N88-10952
The Conference on the Dynamics of Molecular Collisions held in Oglebay Park, Wheeling, West Virginia on 12-17 July 1987
[AD-A184690] 03 p0374 N88-12354
Improper ferroelectricity: A theoretical and experimental study
[AD-A184614] 03 p0381 N88-12397
Molecular engineering of ceramics
[DE88-000174] 04 p0420 N88-12603
Advances in inherently conducting polymers
[DE88-000501] 04 p0421 N88-12610
The Moessbauer effect of SnI4 at high pressure
[DE87-014771] 04 p0495 N88-13048
Molecular and supramolecular orientation in conducting polymers
[DE88-000533] 05 p0569 N88-13472
Pressure induced phase transitions, superconductivity of phosphorus described
06 p0675 N88-14134
Observing effect of laser radiation of low-frequency Raman scattering of light
06 p0772 N88-14742
X-ray structure analyses and molecular mechanics analyses of dense energetic materials
[AD-A185462] 06 p0779 N88-14781
Structure-property relationships in thermoplastic elastomers 4. Dynamic mechanical relaxations in poly(dioxolane), poly(butyltrioxocane) and poly(propylene oxide) polyurethanes
[AD-A186278] 07 p0836 N88-15073
The Coupled Cluster Single and Double excitation (CCSD) method in quantum chemistry: An efficient formulation of the theory and application to closed shell molecular systems
[DE88-000475] 07 p0930 N88-15650
Determination of molecular-ion structures through the use of accelerated beams
[DE88-002960] 09 p1246 N88-17467
Electronic and chemical structure of 3-5/metal and Si/metal interfaces
[AD-A186579] 09 p1254 N88-17518
Copper oxidation states, vacancy ordering and their effect on high temperature superconductivity
[DE88-003079] 09 p1258 N88-17542
Application of inverse gas chromatography to fluidity studies
[DE88-002896] 10 p1296 N88-17750
Investigations on the usefulness of the Massively Parallel Processor for study of electronic properties of atomic and condensed matter systems
[NASA-CR-182514] 10 p1383 N88-18259
Energy-related atomic and molecular structure and scattering studies
[DE88-004246] 10 p1406 N88-18386
Absolute rate measurements of two-photon process of gases, liquids, and solids
[DE88-003800] 10 p1407 N88-18391
Effect of density change on rapid liquid-solid interface kinetics and heat flow
[DE88-004286] 11 p1487 N88-18878
Clusters: Link between molecules and solids
[AD-A188170] 11 p1543 N88-19224
Raman enhancement methods for molecular structure characterization of optical thin films
[DE88-003421] 11 p1558 N88-19324

The 1,2,3-triaminoguanidinium nitrate: An alternate explanation of the nitrate anion disorder
[AD-A188386] 12 p1612 N88-19640
A procedure for estimating the crystal densities of organic explosives
[AD-A189023] 12 p1613 N88-19646
Novel catalysts for methane activation
[DE88-003637] 13 p1738 N88-20390
Properties of molecular solids and fluids at high pressure and temperature
[DE88-004195] 13 p1738 N88-20391
Gordon Conference on Intermetallic Compounds held at Tilton, New Hampshire on 20-24 July 1987
[AD-A188502] 13 p1745 N88-20435
Thermodynamic theory of fluctuations and Rayleigh light scattering in solutions 13 p1785 N88-20681
Sequential excitation preparation of molecular energy levels with special structural and chemical properties
[AD-A190041] 15 p2132 N88-22718
Chromatographic and mass spectrometric separation and analysis
[AD-A190113] 16 p2174 N88-22958
Synthesis and properties of novel cluster phases
[DE88-006816] 16 p2175 N88-22964
Correlation between dielectric and structural properties during epoxy cure
[AD-A190696] 16 p2181 N88-22997
Distribution of chain ends inside the polybutadiene microspheres of SB diblock copolymers
[AD-A191257] 16 p2182 N88-23007
Studies of model ion channels in defect-free multibilayers of phospholipids
[AD-A188740] 16 p2238 N88-23365
Disclination structures in carbon and graphite
[AD-A191056] 17 p2322 N88-23868
Topological stereochemistry
[AD-A191867] 18 p2477 N88-24891
Structural study of the TGMDA-DDS system --- epoxy system
[ONERA-RT-4/3346-M] 18 p2493 N88-24792
A compatible encapsulant for explosives
[DE88-007212] 18 p2495 N88-24806
A constraint algorithm for maintaining rigid bonds in molecular dynamics simulations of large molecules
[AD-A191663] 18 p2572 N88-25277
Neutron diffraction refinement of CsHSO4 superionic phase structure
[DE88-701496] 18 p2580 N88-25326
Molecular characterization of structure and bonding in thin film materials
[DE88-006811] 18 p2584 N88-25351
Structure and refinement of ordered aromatic heterocyclic polymers by diffraction methods: Application of results to electro-optic phenomena
[AD-A191859] 19 p2619 N88-25537
High resolution spectroscopy of dissociating molecules
[DE88-007959] 20 p2851 N88-26924
Spatial organization of homopolymer chains inside spherical polybutadiene domains of SB diblock copolymers
[AD-A193390] 21 p2918 N88-27321
Experiments in microgravity environment: Protein crystallization
[REPT-881-430-101] 21 p2924 N88-27354
Chemistry of adhesion at the polyimide-metal interface
[AD-A194647] 22 p3058 N88-28143
Raman spectroscopy on simple molecular systems at very high density
[DE88-010947] 23 p3191 N88-28987
Hydrogen storage by molecular polyhydrides
[AD-A194207] 23 p3191 N88-28989
Blends of crystallizable polybutadienes
[AD-A194536] 23 p3197 N88-29026
Nonlinear optical processes in molecular systems
[AD-A193871] 23 p3282 N88-29546
Localized excitations in one-dimensional molecular crystal with structural defect
[DE88-702691] 23 p3293 N88-29607
Discovery of a low temperature form of TAGN (Triaminoguanidinium Nitrate)
[AD-A196059] 24 p3357 N88-29989

MOLECULAR TRAJECTORIES
Theoretical calculations of XeF ground state kinetics
[AD-A191398] 16 p2270 N88-23580

MOLECULAR WEIGHT
Synthesis of high molecular weight peptide polymers and copolymers containing L-dope residues
[AD-A186462] 08 p0973 N88-15887
Ordered polymers for space applications
[AD-A188460] 12 p1610 N88-19630
North Carolina Biomolecular Engineering and Materials Applications Center (NC-BEMAC)
[AD-A190923] 16 p2237 N88-23364
Interfacial tension of immiscible polymer blends: Temperature and molecular weight dependence
[AD-A192463] 21 p2917 N88-27312

MOLECULES
NT DIATOMIC MOLECULES
NT MONATOMIC MOLECULES
NT POLYATOMIC MOLECULES
Polyitaconic acid macromolecule primer for adhesive bonding and corrosion control of aluminum
[DE87-013306] 01 p0027 N88-10173
An investigation of the behavior of outgassed molecules in thermal vacuums 02 p0133 N88-10836
IR laser excitation in molecules: Chaos and diffusive energy growth
[DE87-013147] 02 p0178 N88-11105
Quantum-mechanical aspects of classically chaotic driven systems
[DE87-013152] 02 p0178 N88-11106
Development of many-body methods for flame chemistry and large molecule applications
[AD-A184451] 03 p0284 N88-11789
Theory of atomic additivity in molecular hyperpolizabilities 03 p0297 N88-11867
Wake shield 03 p0298 N88-11871
JPRS report: Science and technology. China
[JPRS-CST-87-031] 03 p0299 N88-11880
XeCl excimer laser induced multiphoton ionization of ammonia molecule 03 p0299 N88-11883
Study of IR laser photoacoustic spectra of organic molecules adsorbed on metal surface
03 p0301 N88-11891
Tetrahedral carbon and interstitial electrons in Li cluster: CLi4 and (LiCH3)4
[AD-A184277] 04 p0496 N88-13055
The formation and thermochemical properties of multiligand complexes
[AD-A184935] 05 p0561 N88-13416
High energy molecules of high symmetry
[AD-A185385] 05 p0647 N88-13965
First flight of the ATMOS instrument during the Spacelab 3 Mission, April 29 through May 6, 1985
[NASA-CR-182360] 06 p0728 N88-14482
Photoabsorption and phototdissociation of molecules important in the interstellar medium
[NASA-CR-182435] 08 p1100 N88-16617
Photoionization dynamics of excited molecular states
[DE88-002982] 09 p1246 N88-17468
Molecular dynamics study of high-temperature grain-boundary stability in a (100) sigma = 29 bicrystal model
[DE88-002955] 09 p1258 N88-17546
Clusters: Link between molecules and solids
[AD-A188170] 11 p1543 N88-19224
Mass loss from evolved stars
11 p1569 N88-19394
Resonance energy transfer between carbon monoxide and oxygen molecules using dye laser intracavity absorption spectroscopy
[AD-A188488] 12 p1689 N88-20104
Results of infrared spectrometer experiment. 1: Infrared radiation of parent molecules in Halley's Comet
13 p1726 N88-20325
MOPAC manual: A general molecular orbital package, fourth edition
[AD-A188623] 13 p1733 N88-20362
New polyisoimides: An approach to in situ rigid-rod polyimide formation
[AD-A191665] 18 p2490 N88-24773
Bimolecular reactions and energy-transfer processes of highly vibrationally excited molecules related to energetic materials
[AD-A189013] 18 p2571 N88-25270
Modeling the primary events of photosynthesis using chlorophyll containing fixed distance donor-acceptor molecules
[DE88-010033] 20 p2831 N88-26793
Shock wave compression and metallization of simple molecules
[DE88-008031] 20 p2851 N88-26925
Equilibrium distribution functions for limited plasma-molecular systems
[DE88-702412] 21 p3018 N88-27916
Semi-microdroplet assay for cell adhesion molecules
[NASA-CR-183139] 24 p3406 N88-30274

MOLIERE FORMULA
U COSMIC RAY SHOWERS
U SPATIAL DISTRIBUTION

MOLLUSKS
NT SNAILS
Synthesis of high molecular weight peptide polymers and copolymers containing L-dope residues
[AD-A186462] 08 p0973 N88-15887

MOLTEN SALT ELECTROLYTES
Determination of optimum electrolyte composition for molten carbonate fuel cells literature review
[DE88-001015] 10 p1348 N88-18058
Molten salt electrolytes for high-temperature lithium cells
[DE88-010058] 20 p2794 N88-26581

MOLTEN SALTS
Electronic conduction in molten sodium chloride
[DE87-010063] 02 p0144 N88-10901
Direct Absorption Receiver (DAR) systems assessment
[DE87-012277] 02 p0196 N88-11222
Quantitative determination of a hydrogen impurity in a sodium coolant by hydride thermal dissociation
[NASA-TT-20239] 13 p1740 N88-20402
Thermal modeling of solar central receiver cavities
[DE88-004940] 14 p1943 N88-21594
Fast ion conducting glasses
[AD-A191412] 16 p2183 N88-23010
Production of powdered sodium hydride with large specific surface by the catalyzed reaction of molten sodium with hydrogen-1
[NASA-TT-20185] 20 p2776 N88-26462
Nuclear magnetic resonance spectrometer
[AD-A192928] 21 p2950 N88-27523

MOLYBDENUM
Metallic superlattices with monolayer modulation
[DE87-012724] 01 p0023 N88-10145
Superconducting properties of metallic superlattices
[DE87-012725] 01 p0023 N88-10146
Sintered steels of high resistance alloyed to Nb, Mo, Mn and Si
[DE87-703546] 04 p0415 N88-12573
Data base on the high heat flux behaviour of metals and carbon materials for plasma facing components: Experiments at the 10 MW neutral beam injection test stand of the IPP Nagoya
[IPPJ-AM-53] 04 p0492 N88-13031
Development of encapsulated lithium hydride thermal energy storage for space power systems
[DE88-004762] 11 p1507 N88-19001
The effect of microstructure on the fatigue crack growth resistance of nickel base superalloys
[AD-A189526] 13 p1741 N88-20414
The relationship of the chemical bonding topology of high critical temperature copper oxide superconductors to that of the chevrel phases and the ternary lanthanide rhodium borides
[AD-A189255] 13 p1845 N88-21042
AMTEC electrode development
17 p2409 N88-24324
An experimental study of biaxial yield in modified 9Cr-1Mo steel at room temperature
[NASA-CR-175012] 24 p3385 N88-30164

MOLYBDENUM ALLOYS
Investigation of creep crack growth in heat resistant tube steels
[ETN-87-90606] 03 p0288 N88-11813
Effect of low-temperature aging on the mechanical properties of cast stainless steels
[DE88-002872] 10 p1300 N88-17774
The role of oxygen on the mechanical behavior of molybdenum alloys 17 p2401 N88-24278

MOLYBDENUM COMPOUNDS
NT MOLYBDENUM DISULFIDES
NT MOLYBDENUM OXIDES
Surface modification by metal deposition and laser irradiation 01 p0023 N88-10148

MOLYBDENUM DISULFIDES
Evaluation of centrifugal barrel tumbling process for impregnation of molybdenum disulfide powder lubricant
[BDX-613-3698] 11 p1464 N88-18727
Lubricating properties of molybdenum disulfide. Part 3: Performance of molybdenum disulfide-containing oils in fluid lubrication
[NASA-TT-20156] 13 p1752 N88-20480
The SPOT solar array. Box opening mechanisms physical vapor deposition (PVD)-MoS2: Lubricated slides. Functional evaluation 14 p1876 N88-21211
The effects of Hertzian stress and test ambient on the friction coefficient of MsS2 coatings
[DE88-008118] 20 p2777 N88-26467
The lubricating properties of magnetron sputtered MoS2
[ESA-ESTL-76] 24 p3381 N88-30136

MOLYBDENUM OXIDES
The tribological properties of MoS2 coatings in vacuum, low relative humidity and high relative humidity environments
[DE88-001611] 06 p0711 N88-14356

MOLYBDENUM SULFIDES
NT MOLYBDENUM DISULFIDES
The tribological properties of MoS2 coatings in vacuum, low relative humidity and high relative humidity environments
[DE88-001611] 06 p0711 N88-14356
Electron tunneling microscopy
[AD-A187426] 11 p1452 N88-18652

Schottky-barrier formation on a covalent semiconductor without Fermi-level pinning: The Metal-MoS2(0001) interface
[AD-A193044] 21 p3021 N88-27931

MOMENT DISTRIBUTION
An introduction to single point closure methodology
08 p0986 N88-15973

MOMENTS
NT BENDING MOMENTS
NT DIPOLE MOMENTS
NT DISTRIBUTION MOMENTS
NT ELECTRIC MOMENTS
NT LOADING MOMENTS
NT MAGNETIC MOMENTS
NT MEAN
NT MOMENTS OF INERTIA
NT ORTHOGONALITY
NT PITCHING MOMENTS
NT ROLLING MOMENTS
NT STABILITY DERIVATIVES
NT STANDARD DEVIATION
NT TORQUE
NT YAWING MOMENTS
Semiempirical method for prediction of aerodynamic forces and moments on a steadily spinning light airplane
[NASA-TM-4009] 04 p0393 N88-12456
Measurement of forces and moments on, and velocity about a body of revolution with an attached fin at angles of attack
[AD-A187796] 11 p1433 N88-18554
Regional wave attenuation and seismic moment from the inversion of NORESS spectra
[AD-A187399] 11 p1510 N88-19023
Joint moments of the maximum in a critical branching process
[AD-A188157] 11 p1541 N88-19209
A moment approach to modeling negative ion sources
[AD-A188858] 12 p1691 N88-20114
Application of Moment Iteration Method (MIM) to electromagnetic field computation
[PB88-194139] 20 p2789 N88-26546
Moment invariants for particle beams
[DE88-011052] 23 p3281 N88-29537

MOMENTS OF INERTIA
What is the maximum length of a spin stabilized projectile
[PB88-130919] 13 p1728 N88-20336
A new method for the estimation of aircraft inertia characteristics 20 p2787 N88-26530

MOMENTUM
NT ANGULAR MOMENTUM
Predictive momentum management for a space station measurement and computation requirements
[NASA-CR-172026] 02 p0138 N88-10866
Efficient numerical techniques for complex fluid flows
02 p0185 N88-11151
Momentum transport and particle dynamics in turbulent shear flows 03 p0317 N88-12002
Lagrangian procedures for higher order field equations
[DE87-703365] 05 p0640 N88-13911
Theory of neutron scattering experiments on momentum distributions in quantum fluids
[DE87-01369] 05 p0648 N88-13968
The pressure drag and momentum flux during a cold frontal passage over the Alps 13 p1800 N88-20763
Energy and momentum fluxes through the sea surface
13 p1806 N88-20798
Large momentum pairing in one-dimensional systems
[AD-A189228] 13 p1835 N88-20981
Inflation in Einstein-Cartan theory with energy-momentum tensor with spin
[NASA-TM-101164] 17 p2447 N88-24547
Symmetry problem of energy-momentum tensor and the creation of gravitational field
[DE88-702442] 21 p3026 N88-27964

MOMENTUM ENERGY
U KINETIC ENERGY

MOMENTUM THEORY
Parametric dependence in the equilibrium dynamics of rotating structures
[AD-A187817] 11 p1498 N88-18945

MOMENTUM TRANSFER
Variable collision frequency effects on hose and sausage instabilities in relativistic electron beams
[AD-A184206] 04 p0490 N88-13021
Spin-up and spin-down on the way to the main sequence 04 p0518 N88-13181
Statistical theory of turbulent incompressible multimaterial flow
[DE88-000435] 05 p0579 N88-13535
Approximate solutions for the momentum transport in turbulent flows in narrow rod array bundles using the finite element method
[ETN-88-90810] 06 p0701 N88-14306
The effect of eddy distribution on momentum and heat transfer near the wall in turbulent pipe flow
[NASA-TM-100257] 08 p0988 N88-15984
Design issues for a laboratory high gain fusion facility
[DE88-004406] 10 p1413 N88-18434
Studies in finite time thermodynamics
[DE88-004531] 10 p1423 N88-18500
On (p,n) systematics and the cosmological connection
[DE88-005031] 12 p1712 N88-20245
Turbulent transfer of momentum and heat in boundary layer of fluid beyond an obstacle. 1: Hydrodynamic characteristics 13 p1787 N88-20690
On the zonal momentum balance at the equator
13 p1805 N88-20788
Energy and momentum fluxes through the sea surface
13 p1806 N88-20798
Fragmentation and flow in central collisions
[DE88-005386] 13 p1837 N88-20991
Continuum theories for fluid-particle flows: Some aspects of lift forces and turbulence
[DE88-007038] 18 p2511 N88-24898
Comparison of exclusive reactions at large momentum transfer
[DE88-007544] 20 p2851 N88-26922
Modeling of momentum transport of axially parallel turbulent flows in rod cascades
[ETN-88-92978] 23 p3214 N88-29131
Development of a more general Reynolds stress closure for swirling flow
[AD-A195121] 24 p3374 N88-30092

MONATOMIC GASES
Mechanisms of polymer degradation using an oxygen plasma generator
[NASA-TM-100681] 01 p0018 N88-10110
Atomic oxygen effects on metals
07 p0924 N88-15617
Atomic and molecular gas phase spectrometry
[AD-A187562] 11 p1452 N88-18655
Solar generation and storage of O2 (a 1 delta g)
[NASA-CR-4127] 14 p1913 N88-21431
Total photoionization cross sections of atomic oxygen from threshold to 44.3A
[NASA-CR-182992] 17 p2397 N88-24252
Design and demonstration of a system for the deposition of atomic-oxygen durable coatings for reflective solar dynamic power system concentrators
[NASA-CR-4158] 19 p2606 N88-25474
Breakdown of molecular oxygen by brief pulses of laser radiation
[DE88-702687] 23 p3220 N88-29168
Theoretical investigation of image states of the hydrogen covered Cu (100)
[DE88-702662] 23 p3292 N88-29604

MONATOMIC MOLECULES
Breakdown of molecular oxygen by brief pulses of laser radiation
[DE88-702687] 23 p3220 N88-29168

MONITORS
Rapid toxicity detection in water quality control utilizing automated multispecies biomonitoring for permanent space stations 02 p0135 N88-10848
Development of an acoustic emission monitor and monitoring techniques for long-term monitoring of U-0.8Ti electron-beam weldments for postweld cracking
[DE88-000819] 04 p0453 N88-12804
An interactive computer graphics network monitor for a tactical communications network
[AD-A184131] 04 p0477 N88-12938
Plant Growth Module (PGM) conceptual design
05 p0631 N88-13855
Monitoring corrosion and process physical-chemical parameters in electric power plants
[CISE-3708] 06 p0682 N88-14182
Welding monitoring system
[NASA-CASE-MFS-29177-1] 06 p0712 N88-14362
Online monitoring of laserpulses using the GPIB-interface of a Tektronix 2430 Digital Storage Oscilloscope
[DE88-002836] 07 p0856 N88-15201
On line instrument systems for monitoring steam turbogenerators
[CISE-3860] 08 p0990 N88-15995
Monitoring of space station life support systems with miniature mass spectrometry and artificial intelligence
08 p1057 N88-16376
Knowledge-based monitoring of the pointing control system on the Hubble space telescope
08 p1057 N88-16378
A distributed architecture for intelligent monitoring and anomaly diagnosis of the Hubble Space Telescope
08 p1057 N88-16379
A knowledge-based system for monitoring the electrical power system of the Hubble Space Telescope
08 p1058 N88-16380
Qualitative and temporal reasoning in engine behavior analysis 08 p1058 N88-16383
A multiprocessing architecture for real-time monitoring
08 p1059 N88-16390
Space shuttle main engine anomaly data and inductive knowledge based systems: Automated corporate expertise 08 p1060 N88-16398
Space shuttle onboard navigation console expert/trainer system 09 p1203 N88-17208
Knowledge based jet engine diagnostics
09 p1203 N88-17210
Pattern-recognition software detecting the onset of failures in complex systems
[DE88-002861] 09 p1220 N88-17318
Results of long-term electrocardiographic monitoring of cosmonauts 10 p1364 N88-18152
Acoustic wave electroless deposition monitor
[DE88-004023] 11 p1489 N88-18887
Calibration of beam power monitors for laser welding
[DE88-004687] 11 p1492 N88-18908
Real-time environmental Arctic monitoring (R-TEAM)
[AD-A189948] 15 p2099 N88-22508
DATAC bus monitor 17 p2294 N88-23721
Television monitor field shifter and an opto-electronic method for obtaining a stereo image of optimal depth resolution and reduced depth distrotion on a single screen
[NASA-CASE-NPO-17249-1-CU]
17 p2332 N88-23924
TES: A modular systems approach to expert system development for real-time space applications
17 p2388 N88-24197
Airplane runway performance monitoring system
[NASA-CASE-LAR-13854-1-CU]
18 p2462 N88-24621
Aircraft emissions characterization: TF41-A2, TF30-P103 and TF30-P109 engines
[AD-A192053] 18 p2466 N88-24638
Automated test device for FASR (Fixed Array Surveillance Radar) beam steering componentry
[AD-A191650] 18 p2500 N88-24829
Radio Frequency (RF) strain monitor
[NASA-CASE-LAR-13705-1] 18 p2530 N88-25011
Monitoring of divers/astronauts during missions
19 p2698 N88-26036
Performance evaluation for multiprocessors programmed using monitors
[DE88-010056] 19 p2718 N88-26138
Low cost corrosion sensors 22 p3054 N88-28123

MONKEYS
Microwave challenges to the thermoregulatory system
[AD-A185391] 05 p0629 N88-13847
Effect of spaceflight factors on primate's blood circulation 10 p1359 N88-18124
Inflight simian circadian rhythms and temperature homeostasis aboard Cosmos-1514 biosatellite
10 p1359 N88-18125
Effect of spaceflight factors on primate hydration homeostasis 10 p1360 N88-18126
Motor control in man and monkey
11 p1518 N88-19065
Life sciences research in space: The requirement for animal models 12 p1654 N88-19909
Biological patterns of growth in postnatal ontogenesis of lower primates 19 p2705 N88-26087
Evoked potential analysis of impact acceleration experiments 21 p2981 N88-27708

MONOCHROMATIC RADIATION
Effect of clarifying the atmosphere in relation to quasi-monochromatic CO2 laser radiation
06 p0709 N88-14348
Energy transmission using coherent, quasimonochromatic light beams
09 p1241 N88-17436
Comparison of Halley's monochromatic comae with others 14 p2006 N88-21965
Diffraction imaging (topography) with monochromatic synchrotron radiation
[NASA-CR-183264] 24 p3433 N88-30431
Streaking images that appear only in the plane of diffraction in undoped GaAs single crystals: Diffraction imaging (topography) by monochromatic synchrotron radiation
[NASA-CR-183267] 24 p3433 N88-30437

MONOCHROMATORS
Multilayer monochromators for neutron spectrometers
[DE87-014291] 02 p0175 N88-11093
Use of spherical optics in high resolution soft X-ray grating monochromators
[PB87-125191] 06 p0780 N88-14788
Investigation of the performance of a novel double crystal X-ray monochromator measurements
[PB87-125167] 06 p0788 N88-14834
Thermal stress analysis of a cooled monochromator crystal .
[DE88-002116] 07 p0937 N88-15696

Application of a simple rotational spherical grating mounting to high resolution soft X-ray spectroscopy
[PB87-164836] 09 p1142 N88-16845
Characteristics of an Ebert monochromator for an infrared spectrometer in the wavelength range 1 micrometer to 15 micrometers
[AD-A186945] 09 p1166 N88-16991
UHV (Ultra-High Vacuum) double crystal monochromator design
[DE88-003904] 11 p1456 N88-18676
Multilayer-coated mirrors as power filters in synchrotron radiation beamlines
[DE88-003872] 11 p1550 N88-19276
A new class of multiple dispersion grating spectrometers
[PREPRINT-569] 14 p1983 N88-21830
Intensity calibration of a VUV system by branching line pairs 17 p2443 N88-24533
Instrumentation for turbulent reacting flows
[AD-A191671] 18 p2515 N88-24923
The detection and interpretation of long-term changes in ozone from space
[NASA-TM-101135] 21 p2971 N88-27650

MONOCRYSTALS
U SINGLE CRYSTALS

MONOCULAR VISION
Biorhythms of binocular vision 20 p2830 N88-26788
A new approach to machine-based perception of monocular images
[DE88-002418] 20 p2853 N88-26942

MONOLITHIC CIRCUITS
U INTEGRATED CIRCUITS

MONOMERS
Ion-matrix coupling in polymer electrolytes from relaxation time studies
[AD-A184632] 03 p0293 N88-11841
The mechanism of stereo regulation during anionic polymerization of polar monomers
[AD-A186530] 08 p0973 N88-15888
Pressure induced ageing of polymers 14 p1929 N88-21504
Synthesis and characterization of new phosphazene polymers
[AD-A191508] 18 p2490 N88-24771
Substituted 1,1,1-Triaryl-2,2,2-Trifluoroethanes and processes for their synthesis
[NASA-CASE-LEW-14345-1] 20 p2767 N88-26404
Synthesis of model polymers and related structures in support of vinyl monomer grafting studies
[DE88-010245] 20 p2778 N88-26476
Charge storage and switching phenomena in metal complexes
[AD-A193778] 23 p3192 N88-28996
Polymerization of azaethylenes (imines) and aza-1,3-dienes: Potential reactive monomers
[AD-A194717] 23 p3197 N88-29028

MONOMOLECULAR FILMS
Ceramics thin film 04 p0403 N88-12505
Methods of measurement for the evaluation of monolayer properties. Development and applications — lung surfactants
[ETN-88-92229] 15 p2104 N88-22532

MONOPLANES
NT B-57 AIRCRAFT
NT B-70 AIRCRAFT
NT BOEING 737 AIRCRAFT
NT C-130 AIRCRAFT
NT C-135 AIRCRAFT
NT DO-28 AIRCRAFT
NT F-4 AIRCRAFT
NT F-27 AIRCRAFT
NT F-106 AIRCRAFT
NT MIRAGE AIRCRAFT
NT OV-1 AIRCRAFT
NT P-3 AIRCRAFT
NT RF-4 AIRCRAFT
NT T-33 AIRCRAFT
NT U-2 AIRCRAFT
NT VC-10 AIRCRAFT

MONOPOLE ANTENNAS
Land mobile satellite propagation results 19 p2645 N88-25698
An adaptive array antenna for mobile satellite communications 19 p2647 N88-25710
Evaluation of vertical monopole antennas with elevated radials
[DE88-008339] 19 p2654 N88-25760
Performance study of a unipole antenna with conventional and elevated radial wire ground screens
[AD-A193283] 21 p2933 N88-27413

MONOPOLES
Electronics for the External Muon Detector (EMD) of ICARUS
[NOTA-INTERNA-880] 07 p0647 N88-15143

MONOPROPELLANTS
The numerical simulation of an idealised one-dimensional, steady monopropellant rocket
[PDR/CFDU/IC/31] 01 p0018 N88-10107
Orbital Spacecraft Consumables Resupply System (OSCRS): Monopropellant application to space station and OMV automatic refueling impacts of an ELV launch, volume 4
[NASA-CR-172029] 03 p0276 N88-11741
Droplet formation for liquid monopropellant jets
[AD-A187172] 10 p1331 N88-17956
Electrical ignition of HAN-based liquid propellants
[AD-A191349] 18 p2495 N88-24801
The combustion of hydroxylammonium nitrate based liquid propellants 19 p2622 N88-25555
Droplet formation for liquid monopropellant jets 19 p2623 N88-25557
Mixing and thermodynamic critical phenomena of combusting monopropellant sprays 19 p2623 N88-25558

MONOPULSE RADAR
Track performance considerations for monopulse radars
[AD-A196232] 24 p3360 N88-30007

MONOSACCHARIDES
NT GLUCOSE

MONOTECTIC ALLOYS
Cellular solidification in a monotectic system
[NASA-TM-100317] 07 p0829 N88-15027
Transparent metal model study of the use of a cellular growth front to form aligned monotectic composite materials
[NASA-CR-182414] 08 p0969 N88-15861
A study of surface tension driven segregation in monotectic alloy systems
[NASA-CR-182894] 16 p2178 N88-22983

MONOTONE FUNCTIONS
Software reliability models for fault-tolerant avionics computers and related topics
[NASA-CR-181440] 02 p0220 N88-11382
Efficient monotone sequential design
[CWI-MS-R8705] 14 p1962 N88-21707
Periodic solutions of perturbed superquadratic Hamiltonian systems
[AD-A194292] 23 p3270 N88-29457
Monotone recurrence relations, their Birkhoff orbits and topological entropy
[AD-A193481] 23 p3276 N88-29504

MONSOONS
Observational analysis of the interaction between fronts and the orography in Taiwan during the late winter monsoon season 02 p0203 N88-11270
The mesoscale numerical model for heavy rainfall forecasting in Yangtze River Valley, China 02 p0211 N88-11326
Interactions between the Asian monsoons, the tropical Pacific and the southern hemisphere extratropics 04 p0470 N88-12907
The structure and dynamics of monsoon depressions 10 p1355 N88-18102
Study of passages of cross-equatorial current during southern monsoon 14 p1900 N88-21347
Tropical and monsoonal studies
[AD-A186367] 14 p1947 N88-21611
Indian monsoon rainfall, 1986-1987 22 p3120 N88-28536
Differences in radiation budget parameters over Asia in relation to contrasting Indian monsoons 22 p3125 N88-28574
On climate prediction for India 22 p3127 N88-28580

MONTE CARLO METHOD
The importance sampling and its application to radar simulation 01 p0012 N88-10065
Feature selection applied to radar target identification
[AD-A183880] 01 p0034 N88-10215
Monte Carlo calculations for the simulation of channeling experiments on irradiated aluminum alloys. Calculation of angle-dependent efficiency curves
[HMI-B-433] 01 p0092 N88-10597
A microstructural lattice model for strain oriented problems: A combined Monte Carlo finite element technique
[NASA-TM-100215] 02 p0150 N88-10939
A relativistic Monte Carlo binary collision model for use in plasma particle simulation codes
[DE87-013287] 02 p0237 N88-11494
Two dimensional neutral transport analysis in tokamak plasma
[DE87-752984] 02 p0239 N88-11510
Solute segregation to phase interfaces and grain boundaries: Studies by analytical electron microscopy and profile deconvolution
[DE87-012129] 02 p0243 N88-11537
Wake shield 03 p0298 N88-11871
Monte Carlo simulation of modulated phases
[NASA-TM-89654] 03 p0369 N88-12323
A computational examination of orthogonal distance regression
[AD-A184374] 03 p0371 N88-12337
Development and evaluation of a Monte Carlo code system for analysis of ionization chamber responses
[AD-A183970] 03 p0375 N88-12359
Monte Carlo simulation of primitive atom-transfer reactions in solution
[AD-A183977] 03 p0375 N88-12360
Gravitational accretion of hot dark matter 03 p0388 N88-12439
Creep life prediction based on stochastic model of microstructurally short crack growth
[NASA-TM-100245] 04 p0456 N88-12825
Final (n,l) state-resolved electron capture by multiply charged ions from neutral atoms
[IPPJ-AM-54] 04 p0492 N88-13030
Monte Carlo analysis of neoclassical transport for a compact helical system
[IPPJ-850] 04 p0492 N88-13033
The statistics of the shape of small fatigue cracks 05 p0599 N88-13666
Fatigue under nonnormal random stresses using Monte Carlo method 05 p0607 N88-13723
Approximating multivariate normal orthant probabilities using the Clark algorithm
[AD-A184855] 05 p0634 N88-13873
Monte Carlo modeling and meteor showers 06 p0740 N88-14549
The adaption and use of research codes for performance assessment
[DE88-000552] 06 p0756 N88-14639
Some investigations of molecular beam epitaxial growth of 3-5 semiconductor films via Monte-Carlo computer simulations, carrier tunnelling and spectroscopic ellipsometry
[AD-A185520] 06 p0789 N88-14839
Estimating system reliability: Monte Carlo methods, sensitivity and errors in input parameters
[AD-A186182] 07 p0865 N88-15248
Discrete reliability growth models using failure discounting
[AD-A186380] 07 p0866 N88-15252
Monte Carlo photon transport on vector and parallel supercomputers
[DE88-002503] 07 p0905 N88-15486
Monte Carlo simulation of triangulated random surfaces in grand canonical ensemble
[DE88-700378] 07 p0941 N88-15718
Frequency response functions of a nonlinear system 09 p1180 N88-17070
Three dimensional Monte Carlo simulation of molecular movement and heat radiation in vacuum devices: Computer code MOVAK3D — fusion reactors
[KFK-4292] 09 p1246 N88-17471
Plasma theory and simulation
[AD-A187100] 09 p1249 N88-17486
Two-dimensional analysis for a scrapeoff and divertor regions with an MHD model. Conceptual design study of FY86 FER
[DE88-751069] 09 p1251 N88-17497
Unidimensional Rasch model and multidimensional data: An analytic approach
[PB88-105861] 10 p1372 N88-18187
The hybrid Monte Carlo Algorithm and the chiral transition
[DE88-004305] 10 p1399 N88-18341
An analytic model for ionization distributions produced in nanometer sites by protons
[DE88-003943] 10 p1406 N88-18385
Algorithmic alternatives
[DE88-003905] 11 p1531 N88-19149
Robustness in cost performance models
[AD-A187183] 11 p1566 N88-19374
Analysis of simulated annealing type algorithms
[AD-A189382] 12 p1679 N88-20037
Estimating system and component reliabilities under partial information on cause of failure
[AD-A189107] 13 p1780 N88-20653
Performance and cost benefits associated with nonimaging secondary concentrators used in point-focus dish solar thermal applications
[DE88-001104] 13 p1792 N88-20718
Biophysical applications of solid state and tritium NMR
[DE88-005328] 13 p1808 N88-20806
The physical structure of concurrent problems and concurrent computers
[DE88-005812] 13 p1814 N88-20835
A simulation study of a parallel processor with unbalanced loads
[AD-A189573] 13 p1822 N88-20887

Quantum Monte Carlo study of the MIES associated with H2 (X 1 sigma sub g (+)) and H2 (B 1 sigma sub u (+))
[AD-A189063] 13 p1835 N88-20977
Modeling and transport in semiconductor devices
[AD-A188760] 13 p1844 N88-21037
Monte Carlo modified method for Green function. Algorithm and computer code for calculations in equal mass many-body system
[DE88-701114] 14 p1957 N88-21667
Monte Carlo reliability analysis
[AD-A189972] 15 p2074 N88-22366
Quantum Monte Carlo study of the MIES associated with H2(X 1 sigma g +) and H2(B 1 sigma u +)
16 p2268 N88-23564
Computational quantum field theory
[DE88-700918] 16 p2284 N88-23672
Monte Carlo analysis of lateral collection diode arrays
[RSRE-MEMO-4080] 17 p2335 N88-23938
Multiple scattering of waves in discrete random media
[AD-A191068] 18 p2499 N88-24823
Sensitivity analysis for the system reliability function
[AD-A191648] 18 p2525 N88-24979
The development of KENO and the calculation of differential parameters with KENO
[DE88-006176] 18 p2555 N88-25166
A fast and efficient procedure for generalized cross-validation with large data sets. Application to image reconstruction
[RR-669-M] 18 p2563 N88-25220
Introduction to lattice gauge theory
[DE88-006073] 18 p2584 N88-25349
Non-stationary transport in MODFET's and heterojunction devices 19 p2659 N88-25804
Monte Carlo investigation of hot photoexcited electron relaxation in GaAs 19 p2659 N88-25805
Statistical mechanics of polymer systems
[DE88-011172] 20 p2778 N88-26477
Theoretical studies in elementary particle physics
[DE88-006929] 20 p2851 N88-26926
Monte Carlo simulations of femtosecond relaxation of photoexcited electrons in AlGaAs/GaAs quantum wells
20 p2869 N88-27036
Hot electrons in silicon dioxide: Ballistic to steady-state transport 20 p2871 N88-27042
Recent applications of Monte Carlo methods for semiconductor microdevice simulation
20 p2871 N88-27046
Atomistic simulation of stability, metastability and growth of strained layer structures 20 p2873 N88-27053
Sampling strategies for Monte-Carlo forecasting methods 22 p3126 N88-28583
Importance sampling for stochastic simulations
[AD-A193585] 22 p3138 N88-28654
Progress on a Monte Carlo shuttle contamination model
[AD-A193694] 23 p3183 N88-28945
Variation in the thickness of ejecta cover on Mars with increasing crater density 23 p3307 N88-29701
Monte-Carlo estimation of the influence of plant architecture parameters on spectral brightness
24 p3450 N88-30533

MOODS
Computer response time measurements of mood, fatigue and symptom scale items: Implications for scale response time uses
[AD-A186093] 07 p0888 N88-15384

MOON
Computing basic solar and lunar data from the Air Almanac
[AD-A190777] 16 p2290 N88-23710
A basis of settlement: Economic foundations of permanent pioneer communities
[DE88-010907] 20 p2762 N88-26382
Steps toward lunar settlement
[DE88-009141] 21 p2900 N88-27213

MOORING
SEQUAL (seasonal Equatorial Atlantic) meteorological data from Moorings S2, S5 and S6 (March 1983 - March 1985)
[PB88-108048] 07 p0880 N88-15337
Moored current meter data from the Canary Basin near 32 deg N, 24 W (84-1986), volume 40
[PB88-108105] 07 p0882 N88-15351
Real-time environmental Arctic monitoring (R-TEAM)
[AD-A189948] 15 p2099 N88-22508
An FSK (Frequency Shift Keying) telemetry module for vector measuring current meters
[AD-A192142] 18 p2470 N88-24661

MOORINGS
U MOORING

MORAINES
U GLACIAL DRIFT

MORALE
A comparison of the effects of group dynamics on individuals assigned to integral and non-integral aircrews
[AD-A186467] 08 p1051 N88-16345

MORL
U MANNED ORBITAL LABORATORIES

MORPHINE
Protection from stress 12 p1664 N88-19978

MORPHOLOGY
NT GEOMORPHOLOGY
NT ISOMORPHISM
NT LUNG MORPHOLOGY
Experimental assembly of structures in EVA: Hardware morphology and development issues
02 p0139 N88-10872
Magnetic field morphology in the upper layers
02 p0255 N88-11610
Morphology of the Earth's environment
03 p0272 N88-11706
Factors determining the morphology of precipitation in aluminum-germanium and aluminum-silicon alloys
[DE87-014682] 03 p0287 N88-11806
Cure and properties of thermosetting polymers
[AD-A184669] 03 p0293 N88-11843
Wittig synthesis of conductive segmented block polymer compositions
[AD-A184018] 03 p0295 N88-11850
Corrosion behavior of P/M mechanically alloyed IN-9052.1: An electro-chemical investigation
[AD-A184191] 04 p0414 N88-12567
Steady shearing in a viscoplastic solid
[AD-A184341] 04 p0454 N88-12810
Banded ion morphology 04 p0468 N88-12892
Study of certain biological characteristics of bacteria during the French-Soviet CYTOS-2 space experiment
04 p0473 N88-12917
Molecular and supramolecular orientation in conducting polymers
[DE88-000533] 05 p0569 N88-13472
The effect of alpha platelet morphology and beta-grain size on the initiation and growth of short fatigue cracks in Ti65S 05 p0600 N88-13667
Characterization of the microstructures of various materials
[AD-A184961] 05 p0655 N88-14017
Comparative anatomic analysis of seedling organs of pisum sativum (fabaceae) cultivated under space flight conditions 06 p0749 N88-14603
High spatial resolution observations of dust and gas in NGC 7027 and the M8 Hourglass
06 p0801 N88-14903
Study on substructures of martensite in steels containing rare earth metals
[PB87-143996] 07 p0833 N88-15050
Experiments with rats flown aboard Cosmbs-1667 biosatellite (main objectives, conditions and results)
07 p0893 N88-15414
Brain morphogenesis in rats developing in weightlessness 07 p0894 N88-15415
Morphometric analysis of rat aorta endothelium during long-term hypokinesia 07 p0894 N88-15417
Examination of the physical processes associated with the keyhole region of variable polarity plasma arc welds in aluminum alloy 2219 07 p0927 N88-15634
The morphology of emulsion polymerized latex particles
[DE88-002672] 08 p0972 N88-15879
A new technique for rocket and space-borne investigations of time-dependant auroral morphology
08 p1030 N88-16241
Morphology control and reinforcing mechanisms using an elastomer in an epoxy network based on diamine menthane
[ISAL-IDI1-87-09] 09 p1148 N88-16881
Bias, internal stress and substrate effects on the microstructure and properties of PVD-wear resistant coatings
[AERE-R-12360] 10 p1304 N88-17798
New scientific findings on the morphology of aluminum oxide layers, serving as an adhesive basis
[MBB-Z-137/86] 10 p1312 N88-17840
Collaborative studies of polar cap ionospheric dynamics
[AD-A187888] 10 p1355 N88-18098
Histomorphometric analysis of rat bones after spaceflight aboard Cosmos-1667 biosatellite
10 p1360 N88-18128
JPRS Report: Science and Technology. USSR: Space Biology and Aerospace Medicine, volume 21, no. 6, November - December 1987
[JPRS-USB-88-004] 10 p1364 N88-18150
Morphological and functional state of the hypothalamo-hypophyseal neurosecretory system of rats flown aboard Cosmos-1667 10 p1365 N88-18156
Investigation of rat skeletal muscles following short-term spaceflight aboard Cosmos-1667 biosatellite
10 p1365 N88-18157
Morphological study of early changes in rat bones in simulated weightlessness 10 p1365 N88-18158
Morphological manifestations of primate adaptation to orthograde statics and walking erect
10 p1366 N88-18162
Local stoichiometry and atomic interdiffusion during reactive metal/mercury-cadmium-telluride junction formation
[AD-A187554] 10 p1421 N88-18488
Synthesis and structure property studies of toughened epoxy resins via functionalized polysiloxanes
[AD-A187984] 11 p1462 N88-18715
A unified approach for digital image processing problems: Mathematical morphology
[INPE-4311-TDL/278] 11 p1537 N88-19183
Electron microscopy study of morphology and composition of a ferrisilicate catalyst
[DE88-005754] 11 p1562 N88-19352
Elevated temperature crack growth studies of advanced titanium aluminides
[AD-A189025] 12 p1608 N88-19618
Morphological studies of conductive polymers
[AD-A188456] 12 p1610 N88-19629
Applications of mathematical morphology to range imagery
[AD-A189316] 12 p1684 N88-20072
Dependence of hydrogen embrittlement of austenitic stainless steels on structural state of grain boundaries
14 p1896 N88-21316
Dust coma morphology of Comet Halley during the Giotto encounter 14 p2000 N88-21921
Reconstruction of the orientation and shape of the nucleus of Comet Halley 14 p2004 N88-21949
Laser enhanced adhesion of copper films to sapphire substrates
[DE88-006802] 15 p2038 N88-22144
Fracture morphologies of carbon-black-loaded SBR (Styrene-Butadiene Rubber) subjected to low-cycle, high-stress fatigue
[DE88-006808] 16 p2181 N88-23002
Mathematical morphology: An algebraic approach
[CWI-AM-R8707] 16 p2258 N88-23497
Study of fracturing for groundwater research in the Sergipe state with remote sensing products
17 p2359 N88-24052
Dune fields in central Western Argentina
17 p2366 N88-24088
Molecular gas in Virgo cluster spiral galaxies
17 p2450 N88-24557
Dynamic consolidation of metal powders
[AD-A192126] 18 p2485 N88-24744
Mathematical morphology for structures without translation symmetry
[CWI-AM-R8803] 18 p2566 N88-25241
NASA research Program: The roles of fluid motion and other transport phenomena in the morphology of materials
[NASA-CR-182801] 18 p2580 N88-25327
The morphological stability of continuous interganular phases: Thermodynamic considerations
[DE88-006328] 18 p2584 N88-25350
The Io sulfur torus in 1981
[NASA-TM-101139] 18 p2595 N88-25419
Method for measuring absolute linear parameters of chromosomes 19 p2707 N88-26095
Damping characteristics of metal matrix composites
[AD-A193144] 21 p2904 N88-27233
Rubber-modified epoxies: Interfacial tension and morphology
[AD-A192464] 21 p2917 N88-27313
Plasma treatment of polymers for improved adhesion
[DE88-011623] 21 p2921 N88-27334
Analysis of remotely sensed imagery using digital morphology
[AD-A192738] 21 p2965 N88-27614
Mechanics of thrust fault formation
23 p3231 N88-29229
Mars: Near-infrared comparative spectroscopy during the 1986 opposition 23 p3301 N88-29658
Sub-kilometer rampart craters in the equatorial region of Mars: Possible implications for the state and distribution of regolith H2O 23 p3302 N88-29666
Small Martian valcanoes 23 p3302 N88-29668
Distribution and timing of thick transient air-fall deposits in Electris: Implications for the nature of the upland plains 23 p3303 N88-29674
Lava flow-field morphology: A case study from Mount Etna, Sicily 23 p3303 N88-29676
Constraints on the origin of fractured terrane, Northern Martian plains 23 p3304 N88-29684
Volcano evolution on Mars 23 p3305 N88-29686
Origin of northern lowland plains: Constraints from boundary morphology 23 p3305 N88-29687

Ridged and gullied terrains in the Martian uplands
23 p3307 N88-29700
Morphological changes in polymer electrolyte cells
[AD-A195821] 24 p3368 N88-30054
Volcanic styles at Alba Patera, Mars: Implications of lava flow morphology to the volcanic history
24 p3444 N88-30497

MORPHOTROPISM
U ISOMORPHISM
MOS (JAPANESE SPACECRAFT)
U JAPANESE SPACECRAFT
MOS (SEMICONDUCTORS)
U METAL OXIDE SEMICONDUCTORS
MOSAICS
Implementation of nonsquare tilings on an image processing system
[FOA-C-30487-3.3] 22 p3140 N88-28669
MOSFET
U FIELD EFFECT TRANSISTORS
MOSS (SPACE STATIONS)
U SPACE STATIONS
MOSSBAUER EFFECT
Temperature hysteresis and magnetic transitions in amorphous Fe-Ni-Zr alloys
[DE88-000228] 03 p0294 N88-11848
The Moessbauer effect of SnI4 at high pressure
[DE87-014771] 04 p0495 N88-13048
Moessbauer study of shock induced effects in the Fe-Ni 50/50 ordered alloy in meteorites
[DE87-703364] 04 p0521 N88-13199
SDIO/IST ultrashort wavelength laser: Novel experimental schemes for observing the Mossbauer effect in long-lived nuclear levels
[AD-A190275] 15 p2072 N88-22351
SDIO/IST ultrashort wavelength laser. Mossbauer effect in gamma-ray lasers
[AD-A190306] 15 p2072 N88-22352
A sup 57 Fe Mossbauer study of the superconductor YBa sub 2 (Fe sub x Cu sub 1-x) sub 3 O sub y
[DE88-701543] 16 p2282 N88-23661
A scientific basis for an alternate cathode architecture
[AD-A191498] 18 p2481 N88-24717
Influence of alternating magnetic fields on Zn-67 Moessbauer resonance in ZnO
[PB88-186432] 18 p2584 N88-25352
Structural and magnetic properties of Fe impurities in YBa2Cu3O(sub 7-delta)
[DE88-009961] 19 p2735 N88-26247
Phase modulation of recoilless gamma radiation in Mossbauer spectroscopy
[ETN-88-92648] 24 p3428 N88-30403
MOSSES
U BRYOPHYTES
MOTILITY
U LOCOMOTION
MOTION
Effect of motion cues during complex curved approach and landing tasks: A piloted simulation study
[NASA-TP-2773] 04 p0398 N88-12480
Computing 3-D structure of rigid objects using stereo and motion 08 p1061 N88-16407
Motion planning for legged locomotion systems on uneven terrain 23 p3221 N88-29170
Motion planning with obstacles and dynamic constraints 23 p3222 N88-29175
Passive damping concepts for free and forced member and grillage vibration
[NASA-CR-183114] 23 p3225 N88-29196
Optimization-driven machine-oriented motion measurement 23 p3245 N88-29312
MOTION EQUATIONS
U EQUATIONS OF MOTION
MOTION PERCEPTION
Television motion measurement for DATV and other applications
[BBC-RD-1987/11] 05 p0573 N88-13496
Massively parallel implementations of theories for apparent motion
[AD-A185841] 07 p0901 N88-15455
Perception and control of simulated self motion
[AD-A187444] 10 p1372 N88-18188
A method to detect and digitize small plant movements 12 p1654 N88-19912
Computerised measurement of human horizontal smooth pursuit eye movements
13 p1811 N88-20819
Masking of motion cues by random motion: Comparison of human performance with a signal detection model
[UTIAS-313] 14 p1953 N88-21639
Designing for design effectiveness of complex avionics systems 17 p2305 N88-23788
Visual information processing in the perception of features and objects
[AD-A192026] 18 p2552 N88-25148
Image pyramid motion detection applied to sea ice
20 p2817 N88-26713
Influence of moving visual environment on saccadic eye movements and fixation 21 p2926 N88-27368
Perception of motion in statistically-defined displays
[AD-A193076] 21 p2991 N88-27745
Models for motion perception
22 p3133 N88-28629
Determining vehicle motion from stereo image sequences
[AD-A194371] 23 p3216 N88-29140
Visual motion perception and visual attentive processes
[AD-A193640] 23 p3241 N88-29288
Dynamical systems and motion vision
[AD-A195932] 24 p3422 N88-30366
MOTION PICTURES
Cineradiography
[DE87-013158] 03 p0324 N88-12045
Model-based motion estimation and its application to restoration and interpolation of motion pictures
[AD-A185054] 05 p0584 N88-13558
MOTION SICKNESS
Motion and space sickness 04 p0404 N88-12510
Change in functional activity of cortical brain structures and their blood supply in alert rabbits in response to rocking 04 p0473 N88-12916
Long-term adaptation of the otolith organs
07 p0886 N88-15375
Development of methods for the study of space motion sickness 07 p0892 N88-15408
Discrete adaptation to sensory conflict
10 p1363 N88-18146
Summary of Payload Integration Plan (PIP) for Starlab-1 flight experiment, enclosure 3
[NASA-TM-89713] 11 p1522 N88-19086
Gastric emptying assessment by echography after a stress (rotating chair) 12 p1661 N88-19955
Studies of the vestibulo-ocular reflex on STS 4, 5 and 6
[NASA-TM-100461] 12 p1666 N88-19987
Motion sickness: A study of its effects on human physiology
[AD-A188821] 12 p1667 N88-19995
An analysis of physiological data related to motion sickness for use in a real-time motion sickness indicator
[AD-A189589] 13 p1810 N88-20812
Motion sickness: Quantitative, algorithmic malaise indication in real time
[AD-A189674] 15 p2101 N88-22516
The relationship between preflight underwater training and space motion sickness 19 p2696 N88-26025
Significance of sensory signal phase mismatch in mechanisms of motion sickness development
20 p2830 N88-26787
Simulator sickness in the AH-64 Apache combat mission simulator
[AD-A193419] 21 p2988 N88-27739
MOTION SIMULATION
Application of Kalker's rolling contact theory to the simulation of rail vehicles
[DFVLR-FB-87-07] 01 p0057 N88-10363
Determination of the effect of walking on the forced convective heat transfer coefficient using an articulated mannikin
[AD-A186452] 08 p1049 N88-16335
Motion simulation for in-orbit operations
12 p1589 N88-19514
Dynamics of high-speed mechanisms with elastic members 13 p1779 N88-20643
Effects of update and refresh rates on flight simulation visual displays
[NASA-TM-100415] 15 p2018 N88-22033
Fast algorithm development for large-eddy simulation of circular-jet turbulence
[AD-A192044] 18 p2509 N88-24887
Parameter identification of the passenger simulation model MADYMO: Methods and experience
20 p2788 N88-26536
Motion evoked vestibular potentials
21 p2982 N88-27712
Interactive, networked moving platform simulators
[AD-A192374] 23 p3182 N88-28940
MOTION SIMULATORS
Measurement and effects of transport delays in a state-of-the-art F-16C flight simulator
[AD-A187367] 11 p1441 N88-18599
EPOS: European Proximity Operations Simulation
12 p1589 N88-19515
Dynamic testing of a docking system --- ground-based simulator 12 p1589 N88-19516
MOTION STABILITY
NT AERODYNAMIC STABILITY
NT AIRCRAFT STABILITY
NT BOUNDARY LAYER STABILITY
NT DIRECTIONAL STABILITY
NT FLAME STABILITY
NT FLOW STABILITY
NT GYROSCOPIC STABILITY
NT LATERAL STABILITY
NT LONGITUDINAL STABILITY
NT LOW SPEED STABILITY
NT MAGNETOHYDRODYNAMIC STABILITY
NT ROTARY STABILITY
NT SPACECRAFT STABILITY
Stability of a coastal upwelling front over topography
[AD-A192354] 20 p2829 N88-26784
An efficient patched grid Navier-Stokes solution for multiple bodies, phase 1
[AD-A194166] 23 p3211 N88-29110
Utilizing dynamic stability of orient parts
[AD-A195730] 24 p3427 N88-30397
Orbital stability in rotating triaxial stellar systems
[SER-C-PREPUBL-FASC-24] 24 p3455 N88-30569
MOTIVATION
A comparison of the effects of group dynamics on individuals assigned to integral and non-integral aircrews
[AD-A186467] 09 p1051 N88-16345
MOTOR SYSTEMS (BIOLOGY)
U EFFERENT NERVOUS SYSTEMS
MOTOR VEHICLES
NT AUTOMOBILES
NT ELECTRIC AUTOMOBILES
NT ELECTRIC MOTOR VEHICLES
NT TRACKED VEHICLES
NT TRUCKS
Evaluation of vision systems for teleoperated land vehicles
[DE87-013086] 03 p0333 N88-12100
Ground vehicle convoying
[DE88-000360] 04 p0502 N88-13088
Experiences in teleoperation of land vehicles
[DE88-000429] 06 p0711 N88-14355
Pollution from motor vehicles and aircraft at Stapleton International Airport (abbreviated report), revision 2
[AD-A185916] 07 p0875 N88-15307
Creating title blocks for vehicle animations
[AD-A185620] 07 p0904 N88-15473
TECOM's research efforts in the dynamic environments 08 p0999 N88-16048
The development of laboratory vibration test schedules: Philosophies and techniques 08 p0999 N88-16049
Laboratory vibration test schedules development beyond MIL-STD-810D 08 p0999 N88-16050
Aircraft and ground vehicle friction correlation test results obtained under winter runway conditions during joint FAA/NASA Runway Friction Program
[NASA-TM-100506] 11 p1438 N88-18582
Alternative fuels: Information on DOE's (Department of Energy's) methanol vehicle demonstration program
[PB88-118203] 13 p1753 N88-20481
Human interfaces in remote driving
[DE88-006843] 14 p1953 N88-21643
Propagation effects by roadside trees measured at UHF and L-band for mobile satellite systems
19 p2644 N88-25693
Propagation modeling for land mobile satellite systems
19 p2645 N88-25694
Propagation measurements for an Australian land mobile satellite system 19 p2645 N88-25697
The JPL MSAT mobile laboratory and the pilot field experiments 19 p2646 N88-25708
System identification in vehicle dynamics
[DFVLR-MITT-87-22] 20 p2785 N88-26518
Modeling and parameter identification of motor vehicles 20 p2785 N88-26521
Identification methods for transport dynamical investigations 20 p2787 N88-26531
Parameter identification of the passenger simulation model MADYMO: Methods and experience
20 p2788 N88-26536
MOTORS
NT ASYNCHRONOUS MOTORS
NT ELECTRIC MOTORS
NT INDUCTION MOTORS
NT SERVOMOTORS
NT STEPPING MOTORS
NT SYNCHRONOUS MOTORS
NT TORQUE MOTORS
Design verification tests for an axial gap permanent magnet compressor motor
[DE87-014360] 02 p0167 N88-11049
Dynamics of high-speed mechanisms with elastic members 13 p1779 N88-20643
Performance test results: AXIAL-GAP, permanent magnet compressor motor
[DE88-006857] 15 p2061 N88-22289
A universal computer control system for motors
[NASA-CASE-NPO-17134-1-CU]
18 p2506 N88-24864

MOUNTAINS
NT ALPS MOUNTAINS (EUROPE)
NT ANDES MOUNTAINS (SOUTH AMERICA)
NT CARPATHIAN MOUNTAINS (EUROPE)
NT SIERRA NEVADA MOUNTAINS (CA)
Description of the Mountain Cloud Chemistry Program version of the PLUVIUS MOD 5.0 reactive storm simulation model
[DE87-012846] 01 p0070 N88-10450
Mesoscale MOS forecast support for 1988 winter Olympics ski events --- model output statistics (MOS)
02 p0209 N88-11312
Measurements of vapor flux, liquid water contents, precipitation rates and riming in a Utah mountain cloud system
[PB87-224945] 04 p0469 N88-12900
Wind and temperature structure on the slopes of a mountain valley
[DE88-000080] 07 p0880 N88-15338
Density flows at the mountain edge
08 p1016 N88-16156
Operation Everest 2: Nutrition and body composition
[AD-A186449] 08 p1049 N88-16333
Numerical investigation of orographically enhanced instability
[AD-A186841] 09 p1189 N88-17125
Numerical simulation of thermally generated mountain-foreland circulation
[DFVLR-FB-87-30] 09 p1190 N88-17132
Surface ozone measurements at a Swedish mountain site
[CM-72] 09 p1191 N88-17138
The retardation of cold fronts at high mesoscale mountains 09 p1241 N88-17437
Thematic mapper study of Alaskan ophiolites
[NASA-CR-182554] 11 p1504 N88-18984
Local meteorological processes and air mass origin during a cloud chemical field experiment on Areskutan, Sweden, in summer 1986
[AP-28] 14 p1948 N88-21615
Geometric modeling of flight information for graphical cockpit display
[AD-A190484] 15 p2021 N88-22043
Photointerpretation with instrumentation for evaluation of environmental impact: Mata Atlantica in Cubatao
19 p2683 N88-25946
Study of evolution of vegetal cover and slide scars in the Cubatao municipality-Sao Paulo
19 p2683 N88-25947
Structure of eastern Turkestan Ridge based on space photographs 24 p3450 N88-30530

MOUNTING
Dynamic analysis of a structure with sliding base
08 p0998 N88-16045
A study of the TCAS 2 collision avoidance system mounted on a Boeing 737 aircraft
[NASA-CR-182457] 09 p1116 N88-16687
Application of a simple rotational spherical grating mounting to high resolution soft X-ray spectroscopy
[PB87-164836] 09 p1142 N88-16845
To determine the stress distribution in the vicinity of GRP end pads where the specimen is held and loaded (CFC coupon specimens) --- glass reinforced plastic (GRP) carbon fiber composite (CFC)
[BAE-WST-R-RES-CFC-12023]
09 p1182 N88-17080
Further tests to determine the stress distribution in the vicinity of GRP end pads where the specimen is held and loaded (CFC coupon specimens) --- glass reinforced plastic (GRP) carbon fiber composite (CFC)
[BAE-WST-R-RES-CFC-12023-ADD-1]
09 p1182 N88-17081
Microgravity isolation mount
[ESA-CR(P)-2480] 11 p1443 N88-18604
Structural analysis of the space shuttle solid rocket booster/external tank attach ring
[NASA-TM-100510] 11 p1446 N88-18618
Almond test body --- for microwave anechoic chambers
[NASA-CASE-LAR-13747-1] 18 p2502 N88-24845
Thermal compensating mount
[NASA-CASE-LAR-13794-1] 18 p2519 N88-24942

MOUNTS
U SUPPORTS

MOVEMENT
U MOTION

MOVING TARGET INDICATORS
Investigation and implementation of an algorithm for computing optimal search paths
[AD-A185927] 07 p0902 N88-15461
Moving Target Indicator (MTI) interface for simple radar
[FOA-C-30463-3.2] 09 p1154 N88-16914
Experiments for the high resolution detection of moving targets using a CO2 laser radar
[MBB-UA-1044/87] 10 p1316 N88-17864
An optimal branch-and-bound procedure for the constrained path, moving target search problem
[AD-A188962] 12 p1685 N88-20075
Passive multipath target tracking in an inhomogeneous acoustic medium
[AD-A193284] 21 p3012 N88-27873
Autoregressive moving average modeling of radar target signatures
[AD-A194612] 22 p3069 N88-28218

MRAC (SYSTEMS)
U MODEL REFERENCE ADAPTIVE CONTROL

MRCA AIRCRAFT
German Air Force requirements for the on-board life monitoring system (OLMOS) on Tornado
22 p3033 N88-28007
Event monitoring functions introduced by the Onboard Life Monitoring System (OLMOS) into a German aircraft
22 p3034 N88-28008
Onboard Life Monitoring System (OLMOS), hardware equipment onboard and on ground
22 p3034 N88-28009
Onboard Life Monitoring System (OLMOS): Engine life cycle calculation and trending 22 p3034 N88-28010
Tornado: Airframe fatigue life monitoring
22 p3034 N88-28011

MSM (SEMICONDUCTORS)
MESFET compatible IMSM detectors
19 p2659 N88-25801

MTBF
Explicit formulate for the distributions of stopping variables under Wald's truncated SPRT (Sequential Probability Radio Tests) for a poisson process
[AD-A185053] 05 p0640 N88-13914
Rivista Tecnica Selenia, volume 10, no. 3, 1987
[ETN-88-92717] 22 p3068 N88-28210
An application of the Bayesian method to the estimation and forecast of system hardware components MTBF
22 p3068 N88-28211

MTF
U MODULATION TRANSFER FUNCTION

MTI RADAR
U MOVING TARGET INDICATORS

MULLITES
Microstructures and properties of SiC whisker-reinforced mullite composites
[DE88-002611] 09 p1139 N88-16826
Superplastic flow of mullite-zirconia composites
[DE88-005905] 15 p2028 N88-22085

MULTI-ROLE COMBAT AIRCRAFT
U MRCA AIRCRAFT

MULTIBEAM ANTENNAS
Multiple-beam ground station reflector antenna system: A preliminary study
[EUT-87-E-171] 14 p1904 N88-21379
Rearrangement procedures in regenerative multibeammobile communications satellites with frequency reuse 19 p2650 N88-25735
Antenna system for MSAT mission
19 p2651 N88-25742
Antenna technology for advanced mobile communication systems 19 p2651 N88-25743
Frequency addressable beams for land mobile communications 19 p2652 N88-25744

MULTICHANNEL COMMUNICATION
Multi-channel communications system analyzer
[AD-A184756] 03 p0307 N88-11937
In-orbit calibration adjustment of the Nimbus-7 SMMR
[NASA-TM-100678] 05 p0614 N88-13773
Multicarrier demodulator design, volume 1 --- communication satellites
[ESA-CR(P)-2468-VOL-1] 09 p1158 N88-16941
Multicarrier demodulator design. Volume 2: Executive summary --- communication satellites
[ESA-CR(P)-2468-VOL-2] 09 p1158 N88-16942
Code division multiple access applied to fiber optic data transmission
[AD-A186873] 09 p1247 N88-17477
Multichannel data transmission through a fiber optic cable
[AD-A193842] 22 p3070 N88-28221

MULTICHANNEL PLATES
U MICROCHANNEL PLATES

MULTILAYER INSULATION
Radiative heat transfer solutions in plane-parallel participating media: Application to multilayer insulations for space vehicles
[INPE-4221-PRE/1101] 08 p0962 N88-15824
High-temperature properties of ceramic fibers and insulations for thermal protection of atmospheric entry and hypersonic cruise vehicles
[NASA-TM-100059] 10 p1295 N88-17743

MULTILAYER STRUCTURES
U LAMINATES

MULTILOOP SYSTEMS
U CASCADE CONTROL

MULTIPATH TRANSMISSION
Multipath time-delay estimation via the EM algorithm
[PB88-106851] 07 p0845 N88-15124
Wideband HF (High Frequency) modeling and simulation
[PB88-116116] 10 p1317 N88-17874
Terrestrial Propagation Characteristics in Modern Systems of Communications, Surveillance, Guidance and Control
[AGARD-CP-407] 12 p1614 N88-19653
An investigation of terrain related variables for predicting the multipath fade depth distribution on terrestrial microwave lines 12 p1615 N88-19654
A review of the role of surface reflection in multipath propagation over terrestrial microwave links
12 p1615 N88-19655
Identification of microwave line-of-sight multipath components 12 p1616 N88-19665
Radio and radar holes and multipath zones: The global and local influences on atmospheric refractive structure and resulting adverse radio and radar performance
12 p1617 N88-19667
The 6 GHz propagation measurements over a 51 km path in the UK 12 p1617 N88-19673
Spatial matched processing for multipath propagation
[AD-A189790] 15 p2129 N88-22701
Miltipath measurements for land mobile satellite service using global positioning system signals
19 p2645 N88-25700
A random access algorithm for environments with capture and limited feedback capabilities
[AD-A192233] 20 p2790 N88-26552
Description of the MPTR system: Multi Path Transmissometer Radiometer
[FEL-1987-14] 20 p2855 N88-26954
Passive multipath target tracking in an inhomogeneous acoustic medium
[AD-A193284] 21 p3012 N88-27873
Random-access algorithms for environments with capture
[AD-A194303] 23 p3203 N88-29060

MULTIPHASE FLOW
NT TWO PHASE FLOW
A guide to the transient three phase porous flow model implemented in the two-dimensional CRAY-TENSOR code: Physics, numerics, and code description
[DE88-003709] 09 p1165 N88-16983
Turbulence interactions in single- and multi-phase turbulent mixing and combustion processes
[AD-A187505] 10 p1332 N88-17960
Laser velocimeter measurements of solids in multiphase flow
[DE88-000196] 11 p1487 N88-18876
Noncondensing round turbulent gas jets in liquids
[AD-A191191] 16 p2208 N88-23179
Study of a water-steam two phase flow in a T-branch
[ETN-88-92306] 20 p2801 N88-26624

MULTIPHOTON ABSORPTION
Third-harmonic generation and multiphoton ionization spectroscopy
[DE87-013545] 03 p0281 N88-11769
Interaction of intense electromagnetic fields with SF/sub 6/ molecules and clusters in supersonic expansion
[DE88-700310] 07 p0846 N88-15132
Photoionization dynamics of excited molecular states
[DE88-002982] 09 p1246 N88-17468
Memory effects on infrared adsorbate spectra
[AD-A186976] 09 p1253 N88-17512
High-order multiphoton ionization of the noble gases
[DE88-007489] 18 p2571 N88-25273
Multiphoton transitions in semiconductors in the non-perturbative approach
[DE88-702664] 22 p3157 N88-28786

MULTIPLE ACCESS
NT ALOHA SYSTEM
NT CODE DIVISION MULTIPLE ACCESS
NT DEMAND ASSIGNMENT MULTIPLE ACCESS
NT FREQUENCY DIVISION MULTIPLE ACCESS
NT TIME DIVISION MULTIPLE ACCESS
High data rate modem simulation for the space station multiple-access communications system
06 p0795 N88-14870
Channel access protocols for multihop packet radio networks
[AD-A186074] 07 p0842 N88-15105
On the approximation of the output process of multi-user random access communication networks
[AD-A186197] 07 p0842 N88-15108
Measured noise performance of a direct-sequence spread-spectrum system and a comparison of single vice dual-channel delay-lock loops
[AD-A186288] 07 p0843 N88-15110
Coding for spread-spectrum communications networks
[AD-A185667] 07 p0844 N88-15119

Accessing hierarchical databases via SQL transactions in a multi-model database system
[AD-A187878] 11 p1565 N88-19369
An access alternative for mobile satellite networks 19 p2651 N88-25737
Integrated voice/data protocols for satellite channels 19 p2651 N88-25739
The emergence of multi-user expert systems 23 p3260 N88-29406
Optical multiple access intersatellite links
[BAE-TP-8502] 24 p3361 N88-30013
Performance of DS/SSMA communications in impulsive channels. Part 1: Correlation receivers
[AD-A195712] 24 p3362 N88-30021

MULTIPLE INSTRUCTION MULTIPLE DATA STREAM
U MIMD (COMPUTERS)

MULTIPLETS
U FINE STRUCTURE

MULTIPLEX TRANSMISSION
U MULTIPLEXING

MULTIPLEXERS
U MULTIPLEXING

MULTIPLEXING
NT FREQUENCY DIVISION MULTIPLEXING
NT TIME DIVISION MULTIPLEXING
NT WAVELENGTH DIVISION MULTIPLEXING
Low noise-low power monolithic multiplexing readout electronics for silicon strip detectors
[MPI-PAE/EXP.EL.178] 02 p0168 N88-11057
A129 advanced solutions for meeting today's combat helicopter requirement 03 p0265 N88-11669
Development of a multiplexer module for use in a spaceborne cryogenic environment based on GaAs MESFET technology
[RPT/CRY/62463/BOP] 11 p1559 N88-19335
Applications of optical computing to problems with symbolic computations
[AD-A189772] 15 p2106 N88-22548
Multiplex methods in infrared spectrometry 16 p2271 N88-23586
Adaptive data acquisition multiplexing system and method
[NASA-CASE-MSC-21170-1] 18 p2471 N88-24662
The MELMUX MX-7100 series high-speed digital multiplexers 21 p2930 N88-27396
Multichannel data transmission through a fiber optic cable
[AD-A193842] 22 p3070 N88-28221
Development of 30 micrometers extrinsic silicon multiplexed infrared detector array
[NASA-CR-177446] 22 p3082 N88-28301
On broadband matching of multiport electrical networks with applications
[AD-A194224] 23 p3207 N88-29086

MULTIPLICATION
Efficient multiplication algorithms over the finite fields GF(q sup m), where q equals 3,5 22 p3066 N88-28191
Sequential approach to Colombeau's theory of generalized functions
[DE88-701869] 23 p3276 N88-29503

MULTIPLIER PHOTOTUBES
U PHOTOMULTIPLIER TUBES

MULTIPLIERS
Implementation of a digital optical matrix-vector multiplier using a holographic look-up table and residue arithmetic
[NASA-CR-180431] 01 p0078 N88-10496
High bit rate serial input multipliers
[REPT-87-012] 11 p1530 N88-19140
A serial input pipelined multiplier
[REPT-87-030] 11 p1530 N88-19141
On serial-input multipliers for two-complement numbers
[REPT-86-035] 11 p1536 N88-19181

MULTIPOLES
Solar oscillations, gravitational multipole field of the Sun and the solar neutrino paradox
[DE88-002100] 07 p0946 N88-15752
Application of state-multipole Heisenberg equations to Raman excitation dynamics
[DE88-003828] 10 p1335 N88-17977
On the efficient implementation of the fast multipole algorithm
[AD-A191167] 17 p2385 N88-24173

MULTIPROCESSING (COMPUTERS)
Memory systems for single bus multiprocessor architecture. Application to the SCOM system
[ENST-86E022] 02 p0219 N88-11379
Multi-processor architectures for artificial intelligence processing
[OUEL-1671/87] 02 p0219 N88-11380
Concurrent algorithms for transient nonlinear FE analysis
[NASA-CR-181455] 02 p0221 N88-11389
Semantic network processing systems --- artificial intelligence
[OUEL-1677/87] 02 p0223 N88-11401
QUICKSILVER: A 3D, electromagnetic, PIC code
[DE87-013013] 02 p0245 N88-11547
On the control of a compliant robot arm 03 p0332 N88-12095
Hardware-assisted multiprocessor performance measurements
[PB87-226908] 03 p0363 N88-12282
Delft parallel processor 84/16
[PB87-226254] 03 p0366 N88-12305
Comparing barrier algorithms
[NASA-CR-178377] 04 p0476 N88-12934
Principles for problem aggregation and assignment in medium scale multiprocessors
[NASA-CR-178379] 04 p0476 N88-12935
An approach to implementing state space searches on heterogeneous systems of multiprocessors
[DE88-001321] 04 p0482 N88-12967
Contribution to optimal flow in networks. A experimental multiprocessor for asynchronous iteration implementation
[LAAS-87-269] 05 p0576 N88-13510
Set of multi-process primitives for stack based machines
[PB87-234381] 06 p0756 N88-14636
Life sciences flight experiments microcomputer 06 p0792 N88-14857
A multiprocessing architecture for real-time monitoring 08 p1059 N88-16390
Numerical experiments with a parallel conjugate gradient method
[DE88-002178] 08 p1066 N88-16445
Communications patterns in a symbolic multiprocessor
[AD-A186896] 09 p1215 N88-17282
Types and effects towards the integration of functional and imperative programming
[AD-A186930] 09 p1216 N88-17290
Algorithm design for scientific computation for highly parallel multiprocessor systems
[AD-A186713] 09 p1217 N88-17299
Twisted cube
[PB87-162814] 09 p1220 N88-17316
Multitasking and microtasking experience on the NA S Cray-2 and ACF Cray X-MP
[NASA-CR-177464] 09 p1221 N88-17325
Concept of a programmable maintenance processor applicable to multiprocessing systems
[NASA-TM-100406] 09 p1223 N88-17333
Role of broadcasting in multiprocessor systems 10 p1374 N88-18201
Multiple-bus interconnection for future multiprocessor systems 10 p1375 N88-18203
Implementation of a buddy failure recovery concept in the NOVAC system 10 p1375 N88-18205
The case for a shared address space 10 p1378 N88-18225
Performance evaluation of a loop interconnection structure 10 p1378 N88-18229
Aspects of a multiprocessor architecture 10 p1379 N88-18232
Parallelism at the microlevel: Cooperative microcontrollers with real time considerations 10 p1381 N88-18246
A VLSI implementable block oriented data driven multiprocessor 10 p1381 N88-18249
Multi-processor reduction machines 10 p1382 N88-18253
A measurement-based study of concurrency in a multiprocessor
[DE88-003536] 10 p1383 N88-18260
A performance analysis of architectural scalability
[DE88-003537] 10 p1383 N88-18261
A multiprocessor scheme for the singular value decomposition
[DE88-003591] 10 p1388 N88-18288
Data prefetching in shared memory multiprocessors
[DE88-003576] 10 p1394 N88-18314
Measurement and analysis of memory conflicts on vector multiprocessors
[AD-A188206] 11 p1525 N88-19104
Implementing dynamic arrays: A challenge for high-performance machines
[AD-A188142] 11 p1533 N88-19157
Accessing hierarchical databases via SQL transactions in a multi-model database system
[AD-A187878] 11 p1565 N88-19369
Evaluation of network communication multiprocessor fault tolerance
[INPE-4305-PRE/1171] 12 p1674 N88-20011
Architecture with parallel processing for incremental computation
[INPE-4326-PRE/1178] 12 p1675 N88-20012
An emulation tool for simulating matrix operations on an SIMD (Single Instruction Multiple Data stream) multiprocessor
[AD-A188654] 12 p1678 N88-20030
A laboratory facility for research in parallel computation
[AD-A188499] 12 p1680 N88-20044
Primal-dual parallel solution of very large sparse linear programs
[AD-A188500] 12 p1680 N88-20045
NAVLAB: An autonomous navigation testbed
[AD-A189049] 13 p1720 N88-20283
Very large vortex calculations in two dimensions
[DE88-005748] 13 p1770 N88-20587
Data traffic reduction schemes for sparse Cholesky factorizations
[NASA-CR-181626] 13 p1813 N88-20831
Gaussian techniques on shared memory multiprocessor computers
[DE88-005426] 13 p1817 N88-20855
Locality, communication and interconnect length in multicomputers
[CWI-CS-R8708] 13 p1822 N88-20890
Evaluation of a parallel chart parser
[AD-A189172] 14 p1959 N88-21685
Distributed operating systems: An overview
[INF-87-29] 14 p1960 N88-21688
Parallel memory addressing using coincident optical pulses
[AD-A189767] 15 p2106 N88-22547
An analysis of multiple grain CHiP architectures
[AD-A189942] 15 p2110 N88-22570
Comparative analysis of multistage interconnection networks
[AD-A190436] 15 p2115 N88-22598
A methodolgy, based on analytical modeling, for the design of parallel and distributed architectures for relational database query processors
[AD-A189844] 15 p2149 N88-22825
New generation knowledge processing, volume 1
[AD-A190165] 15 p2149 N88-22826
Fast algorithms for Euler and Navier-Stokes simulations
[AD-A190897] 16 p2208 N88-23175
Multiprocessor graphics computation and display using transputers 16 p2218 N88-23236
Program profiling in Cedar
[AD-A190883] 16 p2250 N88-23449
VPC: A proposal for a vector parallel C programming language
[AD-A190885] 16 p2251 N88-23451
Supercomputer programming environments
[AD-A190887] 16 p2251 N88-23452
Locality, communication and interconnect length in multicomputers
[CWI-CS-R8743] 16 p2254 N88-23466
New generation knowledge processing, volume 2
[AD-A190166] 16 p2285 N88-23681
New generation knowledge processing, volume 3
[AD-A190167] 16 p2285 N88-23682
A multiprocessor data flow accelerator module
[DE88-007587] 18 p2554 N88-25161
Decomposition of linear programs using parallel computation
[AD-A191718] 18 p2556 N88-25173
Effective use of shared memory multiprocessors
[DE88-007019] 18 p2560 N88-25195
Gaussian techniques on shared-memory multiprocessors
[DE88-010594] 19 p2716 N88-26126
On the implementation of applicative on shared-memory, MIMD multiprocessors
[DE88-005367] 19 p2718 N88-26136
Performance evaluation for multiprocessors programmed using monitors
[DE88-010056] 19 p2718 N88-26138
SLAPP: A special multiprocessor array for signal processing and linear algebra
[AD-A191587] 19 p2719 N88-26146
A multiprocess operating system for 16 bit microcomputers or porting Unix (trademark) to a NS32016 with enhancements 20 p2836 N88-26822
Definition of an auxiliary processor dedicated to real-time operating system kernels
[NASA-CR-183070] 20 p2841 N88-26860
An evaluation methodology for dependable multiprocessors
[AD-A192799] 20 p2842 N88-26863
Dynamic modelling and estimation of the error due to asynchronism in a redundant asynchronous multiprocessor system
[NASA-CR-177427] 21 p2898 N88-27205
FTMP data acquisition environment
[NASA-TM-100636] 21 p2938 N88-27447
MINIAC: A small embedded computer
[DE88-008142] 21 p2994 N88-27757

The sub-implicit method: New multiprocessor algorithms for old implicit codes
[DE88-011345] 21 p2999 N88-27785
Performability analysis: Measures, an algorithm and a case study
[AD-A192477] 21 p3001 N88-27800
Constructing a highly-available location service for a distributed environment
[AD-A192723] 21 p3001 N88-27801
Modeling and approximate performance analysis of multiuser computer systems
[ETN-88-92137] 21 p3002 N88-27806
Dynamic resource allocation in a hierarchical multiprocessor system: A preliminary study
[NASA-CR-183177] 22 p3141 N88-28675
Partitioning of regular computation on multiprocessor systems
[NASA-CR-183176] 22 p3141 N88-28676
Piecewise-parabolic methods for systems of hyperbolic conservation laws in multiprocessing environments
[DE88-010202] 23 p3248 N88-29329
The FORCE
[AD-A193463] 23 p3264 N88-29429
Programming language concepts for multiprocessors
[AD-A193465] 23 p3264 N88-29430
Large-grain pipelining on distributed-memory multiprocessors
[DE88-009974] 23 p3264 N88-29432
Parallel real-time expert systems
[AD-A193673] 23 p3264 N88-29434
Compression and decompression of imaging sensor signals (CADISS): A multiprocessor system for image compression/decompression on board scientific satellites
[NLR-TR-87076-L] 24 p3414 N88-30323
The triangle: A multiprocessor architecture for fast curve and surface generation
[AD-A195882] 24 p3414 N88-30324
Reification without evaluation
[AD-A195928] 24 p3414 N88-30326

MULTIPROPELLANTS
U ROCKET PROPELLANTS

MULTIRADAR TRACKING
U RADAR NETWORKS

MULTISENSOR APPLICATIONS
From pattern to process: The strategy of the Earth Observing System: Volume 2: EOS Science Steering Committee report
[NASA-TM-89702] 07 p0871 N88-15283
Development of subminiature multi-sensor hot-wire probes
[NASA-TM-100052] 15 p2069 N88-22336
Multi-sensor integration on the NCUBE hypercube computer
[DE88-007472] 18 p2554 N88-25162
Path planning and path following for the Amsterdam autonomous cart
[FVI-86-22] 24 p3380 N88-30133

MULTISPECTRAL BAND CAMERAS
Land cover/use classification of Cairns, Queensland, Australia: A remote sensing study involving the conjunctive use of the airborne imaging spectrometer, the large format camera and the thematic mapper simulator
05 p0612 N88-13759
Development of a CCD characterization system
[INPE-4361-TDL/301] 12 p1623 N88-19712

MULTISPECTRAL BAND SCANNERS
NT THEMATIC MAPPERS (LANDSAT)
Study, design, and evaluation of data reduction by encoding or information extraction. Part 1: Data generation analysis --- multispectral satellite imagery
[NLR-TR-85094-L-PT-1] 01 p0078 N88-10501
Study, design and evaluation of data reduction by encoding or information extraction. Part 2: Operational considerations --- multispectral satellite imagery
[NLR-TR-85094-L-PT-2] 01 p0079 N88-10502
Study, design and evaluation of data reduction by encoding or information extraction. Part 3: Algorithm design --- multispectral satellite imagery
[NLR-TR-85094-L-PT-3] 01 p0079 N88-10503
Study, design and evaluation of data reduction by encoding or information extraction. Part 4: Performance demonstration --- multispectral satellite imagery
[NLR-TR-85094-L-PT-4] 01 p0079 N88-10504
Study, design and evaluation of data reduction by encoding or information extraction. Part 5: Algorithm implementation aspects --- multispectral satellite imagery
[NLR-TR-85094-L-PT-5] 01 p0079 N88-10505
MBB-ERNO view of remote sensing commercialization
03 p0340 N88-12140
Development of a method for forest damage inventory using multispectral scanner data
[KFK-PEF-25] 03 p0345 N88-12182
Cloud cover determination in polar regions from satellite imagery
[NASA-CR-181544] 04 p0471 N88-12908
Commercial applications and scientific research requirements for thermal-infrared observations of terrestrial surfaces
[NASA-TM-89704] 08 p1019 N88-16179
Autocorrelation of control points on 11-band multispectral imagery
[AD-A188185] 10 p1348 N88-18056
NIMBUS-7 CZCS. Coastal Zone Color Scanner imagery for selected coastal regions. North America - Europe. South America - Africa - Antarctica. Level 2 photographic product
[NASA-CR-180755] 15 p2089 N88-22447
Turbidity patterns in the delta waters of southwest Netherlands on Thematic Mapper (TM) and multispectral scanner (MSS) satellite images
[BCRS-86-06] 16 p2227 N88-23303
Applications of multitemporal compositions obtained from LANDSAT data in the study of urban growth
[INPE-4480-PRE/1246] 16 p2287 N88-23692

MULTISPECTRAL PHOTOGRAPHY
NT INFRARED PHOTOGRAPHY
NT RADAR PHOTOGRAPHY
Vegetation classification, land systems and mapping using SPOT multispectral data: Preliminary results
03 p0342 N88-12160
Coastal dynamics of the mouth of the Saloum (Senegal) --- SPOT imagery 03 p0345 N88-12177
Development of a method for forest damage inventory using multispectral scanner data
[KFK-PEF-25] 03 p0345 N88-12182
Multistep component analysis of correlations
08 p1009 N88-16115
Commercial applications and scientific research requirements for thermal-infrared observations of terrestrial surfaces
[NASA-TM-89704] 08 p1019 N88-16179
A variant of the ISODATA algorithm for application to agricultural targets
[INPE-4436-PRE/1235] 12 p1676 N88-20023
Study of methods of post-processing applied to a problem of standard classification
17 p2362 N88-24067
Remote sensing of wetlands: Applications overview
[DE88-010895] 21 p2966 N88-27618
Comparative study of crop and soil mapping using multitemporal and multispectral SPOT and LANDSAT data 22 p3091 N88-28354
Pilot study of rice culture in sub-tropical high population density region (Madagascar) with SPOT 1 multispectral data 22 p3097 N88-28392
Utilization of SPOT-1 multispectral data for mapping land cover and phytohygiene monitoring in the central zone of the Mercantour National Park (France)
22 p3100 N88-28413

MULTISTAGE COMPRESSORS
U TURBOCOMPRESSORS

MULTISTAGE ROCKET VEHICLES
NT ARIANE LAUNCH VEHICLE
NT SKYLARK ROCKET VEHICLE
NT TITAN LAUNCH VEHICLES
Multi-stage plasma thruster
[AD-A183635] 01 p0017 N88-10105

MULTISTATIC RADAR
Airborne bistatic radar applications
[ETN-87-90930] 02 p0163 N88-11020
Mono- and bistatic radar coverage diagrams including diffractive wave propagation 12 p1616 N88-19660
DSS 14 antenna calibrations for GSSR/VLA Saturn radar experiments 22 p3068 N88-28207

MULTITEMPORAL ANALYSIS
U TEMPORAL RESOLUTION

MULTIVARIATE STATISTICAL ANALYSIS
NT BIVARIATE ANALYSIS
NT COVARIANCE
NT ORTHOGONALITY
NT REGRESSION ANALYSIS
Breakdown points of affine equivariant estimators of multivariate location and covariance matrices
[REPT-87-14] 01 p0088 N88-10574
Horizontal shape matching applied to VAS data --- Visible and Infrared Spin Scan Radiometer Atmospheric Sounder (VAS) 02 p0201 N88-11254
Estimation of a multivariate continuous variable panel model
[AD-A184472] 04 p0484 N88-12982
Approximating multivariate normal orthant probabilities using the Clark algorithm
[AD-A184855] 05 p0634 N88-13873
Illustrative examples of principal component analysis using BMDP/4M
[AD-A185179] 05 p0635 N88-13881
Illustrative examples of principal component analysis using SYSTAT/FACTOR
[AD-A184920] 05 p0644 N88-13939
Illustrative examples of principal component analysis using GENSTAT/PCP
[AD-A185085] 05 p0644 N88-13941
Modeling and generating input processes
[DE87-013162] 05 p0645 N88-13948
Asymptotic normality of poly-t densities with Bayesian applications
[AD-A185718] 06 p0768 N88-14719
Control charts when the observations are correlated
[AD-A186388] 07 p0866 N88-15253
On the least squares estimator in moving average models of order one
[AD-A186028] 07 p0909 N88-15508
A new method of estimation in a moving average model of order one
[AD-A186039] 07 p0909 N88-15510
On the extreme points of the set of all 2xn bivariate positive quadrant dependent distributions with fixed marginals and some applications
[AD-A186316] 07 p0911 N88-15521
The information metric for univariate linear elliptic models
[AD-A186385] 07 p0911 N88-15527
Estimation of multivariate binary density using orthonormal functions
[AD-A186386] 07 p0912 N88-15528
Strategies of data analysis
[AD-A186033] 07 p0914 N88-15548
Some new approaches to multivariate probability distributions
[AD-A186038] 07 p0914 N88-15551
A weighting sequence approach to the analysis and design of multivariable control systems
[AD-A186086] 07 p0917 N88-15570
Test of linearity in general regression models
[AD-A186036] 08 p1073 N88-16477
New directions for multivariate statistical computation and data analysis
[AD-A186523] 08 p1074 N88-16480
Tensorial calibration. 2. Second order tensorial calibration
[AD-A186614] 09 p1167 N88-16994
Tensorial calibration. Part 1: First order tensorial calibration
[AD-A186708] 09 p1167 N88-16995
Modification of a successive corrections objective analysis for improved higher order calculations
[NASA-CR-182467] 09 p1230 N88-17370
The linear dependency structure of covariance nonstationary time series
[AD-A186548] 09 p1232 N88-17383
Strong consistency of certain information theoretic criteria for model selection in calibration, discriminant analysis and canonical correlation analysis
[AD-A186584] 09 p1232 N88-17385
Identifiability of multivariate ARMA models
[AD-A187394] 10 p1400 N88-18350
Statistical aspects of reliability, maintainability and availability
[AD-A188491] 12 p1634 N88-19783
Visual display representation of multidimensional systems: The effect of information correlation and display integrality
[AD-A188655] 12 p1672 N88-20010
A variant of the ISODATA algorithm for application to agricultural targets
[INPE-4436-PRE/1235] 12 p1676 N88-20023
Force distribution and trajectory control for closed kinematic chains with applications to walking machines
13 p1779 N88-20642
A multivariate variational objective analysis-assimilation method. Part 1: Development of the basic model
[NASA-CR-182651] 15 p2097 N88-22491
A multivariate variational objective analysis-assimilation method. Part 2: Case study results with and without satellite data
[NASA-CR-182653] 15 p2097 N88-22492
Some comments on quadrant dependence in higher dimensions
[AD-A190329] 15 p2121 N88-22639
Multivariate analysis and its application
[AD-A189983] 15 p2124 N88-22661
Detection of the number, locations and magnitudes of jumps
[AD-A190328] 15 p2125 N88-22671
Very short range statistical forecasting of automated weather observations
[AD-A190803] 16 p2235 N88-23349
The display of multivariate information: The effects of auto- and cross-correlation, reliability and heterogeneity
[AD-A191070] 16 p2243 N88-23398
An innovation approach to goodness of fit tests in R sup m
[CWI-MS-R8712] 16 p2259 N88-23501

Improved estimators in simultaneous estimation of scale parameters
[AD-A191108] 17 p2392 N88-24216
Almost sure L(gamma)-norm convergence for data-based histogram density estimates
[AD-A189944] 17 p2393 N88-24228
Parameter-adaptive model-following for in-flight simulation
[AD-A190567] 18 p2467 N88-24645
Poisson functionals of Markov processes and queueing networks
[AD-A191217] 18 p2568 N88-25252
Structural properties of multivariable linear systems
[PB88-181375] 19 p2717 N88-26134
On solvability of an equation arising in the theory of M-estimates
[AD-A193059] 21 p3006 N88-27828
Further extensions of the choquet-deny and deny theorems with applications in characterization theory
[AD-A193358] 21 p3006 N88-27834
Asymptotic normality of minimum L1-norm estimates in linear models
[AD-A193399] 21 p3006 N88-27835
Joint asymptotic distribution of marginal quantiles and quantile functions in samples from a multivariate population
[AD-A193385] 21 p3010 N88-27856
Poisson functionals of Markov processes and queueing networks
[AD-A194289] 22 p3145 N88-28705
An expert system for reliability modeling
23 p3252 N88-29355
Robust control of multivariable and large scale systems
[AD-A194250] 23 p3266 N88-29441
Reconstruction of multidimensional signals from multiple level threshold crossings
[AD-A195561] 24 p3425 N88-30383

MUON SPIN ROTATION
Wrong helicity events induced by the CERN-SPS wide band muonic (anti)neutrino beam
[NIKHEF-H/87-2] 06 p0779 N88-14779
Materials science with muon spin rotation
[NASA-CR-182891] 17 p2396 N88-24242
Systematic variation of magnetic-field penetration depth in high-T(c) superconductors studied by muon spin relaxation 17 p2396 N88-24243
Comparison between muon spin rotation and neutron scattering studies on the 3-dimensional magnetic ordering of La2CuO(4-y) 17 p2396 N88-24244
Coexisting static magnetic ordering and superconductivity in CeCu2.1Si2 found by muon spin relaxation 17 p2396 N88-24245
Static magnetic ordering of CeCu2.1Si2 found by muon spin relaxation 17 p2396 N88-24246
Muon motion in titanium hydride
17 p2396 N88-24247
Muon-spin rotation experiment (micro + SR) on aluminum and indium after low temperature electron irradiation
[ETN-88-92985] 23 p3294 N88-29617

MUONS
Electronics for the External Muon Detector (EMD) of ICARUS
[NOTA-INTERNA-880] 07 p0847 N88-15143
Characteristics of multimuon events from fourth generation quarks at the SSC (Superconducting Super Collider)
[DE88-002954] 09 p1257 N88-17535
A combined cosmic ray muon spectrometer and high energy air shower array
[DE88-003057] 09 p1264 N88-17574
Theory of Muon method for study of solid and liquid hydrogen 14 p1972 N88-21770
Analysis of hadron production in deep inelastic muon-proton collisions through the fire-string model
[PREPRINT-578] 14 p1981 N88-21822
High energy cosmic muons and the calibration of the L3 electromagnetic calorimeter
[NOTA-INTERNA-895] 14 p2011 N88-21999
Muon motion in titanium hydride
17 p2396 N88-24247
Difficulties with interpretation of underground muons from Cygnus X-3
[DE88-701645] 23 p3309 N88-29710

MUSCLES
NT MYOCARDIUM
Motion and space sickness 04 p0404 N88-12510
Dimensional analysis of nonlinear oscillations in brain, heart and muscle
[DE87-014749] 06 p0751 N88-14614
Model based monitoring of human sleep stages
[ISBN-90-9001448-9] 06 p0752 N88-14618
Nucleic acid content of skeletal muscles during hypokinesia and in the recovery period
07 p0894 N88-15418
Muscle preservation in the study of bioenergetic effects of hypokinesia 10 p1362 N88-18139
Investigation of rat skeletal muscles following short-term spaceflight aboard Cosmos-1667 biosatellite
10 p1365 N88-18157
Morphological manifestations of primate adaptation to orthograde statics and walking erect
10 p1366 N88-18162
P-31 Magnetic Resonance Spectroscopy (MRS) of limb muscles during bedrest with exercise countermeasures
12 p1656 N88-19925
Endocrine responses to resistance exercise
[AD-A188681] 12 p1667 N88-19993
A program for the study of skeletal muscle catabolism following physical trauma
[AD-A189771] 15 p2102 N88-22521
Activation, strength and endurance of human respiratory and limb muscles 17 p2381 N88-24158
Dexamethasone regulates glutamine synthetase expression in rat skeletal muscles
[NASA-CR-182935] 18 p2549 N88-25129

MUSCULAR FATIGUE
Activation, strength and endurance of human respiratory and limb muscles 17 p2381 N88-24158

MUSCULAR FUNCTION
Investigation of interactions between limb-manipulator dynamics and effective vehicle roll control characteristics
[NASA-CR-3983] 01 p0007 N88-10039
Results of research with biological satellites
08 p1006 N88-16097
Models describing muscle behavior and control
[LR-522] 16 p2238 N88-23368
Activation, strength and endurance of human respiratory and limb muscles 17 p2381 N88-24158
Motor theory of auditory perception
[AD-A192095] 18 p2550 N88-25136

MUSCULAR STRENGTH
Ergonomics of car controls for disabled people, phase 1. Part 1: Chapters 1-7. Part 2: Appendices. Part 3: References
[ISBN-0-947767-82-7] 09 p1202 N88-17204
Activation, strength and endurance of human respiratory and limb muscles 17 p2381 N88-24158
The effects of acute cold exposure on exercise performance
[AD-A192650] 22 p3130 N88-28610

MUSCULAR TONUS
Oxidative enzyme activity in healthy subjects and individuals with neurocirculatory dystonia during graded exercise 10 p1367 N88-18170
Hemostasis parameters of individuals with neurocirculatory dystonia submitted to dry immersion
19 p2703 N88-26072

MUSCULOSKELETAL SYSTEM
NT BONE MARROW
NT BONES
NT COLLAGENS
NT JOINTS (ANATOMY)
NT MUSCLES
NT SKULL
NT TIBIA
NT WRIST
Physiological determinants of load bearing capacity
[AD-A184977] 05 p0629 N88-13848
The origin of the spicule skeleton of fresh water sponges (Spongillides) 07 p0885 N88-15368
Xiphophorus: A system to recognize radiation-induced mutations and to study the effects of zero-gravity environment on embryo development
07 p0885 N88-15372
Functional development of gravity receptors in insects and amphibians 07 p0886 N88-15376
Influence of skeletal muscle glycogen on passive rewarming after hypothermia
[AD-A186451] 08 p1049 N88-16334
A program for the study of skeletal muscle catabolism following physical trauma
[AD-A189771] 15 p2102 N88-22521

MUTAGENS
Genetic effects of low level microwave radiation
[AD-A192687] 21 p2984 N88-27722

MUTATIONS
Xiphophorus as an experimental system for genetic and biological development studies under microgravity conditions 01 p0074 N88-10472
Xiphophorus: A system to recognize radiation-induced mutations and to study the effects of zero-gravity environment on embryo development
07 p0885 N88-15372
Investigation of genetic structures of rat germ cells following flight aboard Cosmos-1514 biosatellite during their prenatal development 10 p1364 N88-18155

MX MISSILE
Convective heat transfer and its effect on inertial measurement units 12 p1578 N88-19442

MYOCARDIAL INFARCTION
Aircraft accident report: Joe Foster Excavating, Inc., Bell 206B, N49606, in-flight collision with trees, Alamo, California, August 3, 1986
[PB88-910405] 20 p2755 N88-26345

MYOCARDIUM
Myosin Ca sup (2+), Mg sup (2+)-adenosine triphosphatase activity in ray myocardium following 30-day expose to 1.1 and 2.0 G 10 p1362 N88-18141
Effect of cardioactive compounds on rat myocardium actomyosin following exposure to accelerations
10 p1365 N88-18161

MYOELECTRICITY
The efficacy of using human myoelectric signals to control the limbs of robots in space
[NASA-CR-182901] 18 p2553 N88-25155

MYOPIA
Does the knife open perspectives for the myopic pilot?
[ETN-87-90166] 09 p1199 N88-17187

N

N-BODY PROBLEM
U MANY BODY PROBLEM

N-P JUNCTIONS
U P-N JUNCTIONS

N-P-N JUNCTIONS
Vertical charge transport in junction charge-coupled devices
[ETN-88-91613] 09 p1255 N88-17523
Neutron effects on the electrical and switching characteristics of NPN bipolar power transistors
17 p2431 N88-24463

N-TYPE SEMICONDUCTORS
Integrated fiber-optic coupler
[AD-A184494] 03 p0377 N88-12369
Point defect structure of Cr2O3
[AD-A187620] 11 p1556 N88-19317
Fundamental studies and device development in beta silicon carbide
[AD-A189540] 12 p1699 N88-20165
Calculating depletion region carrier concentrations with capacitance-voltage measurements and etching
[AD-A189630] 15 p2141 N88-22777
Electrical anisotropy of layered semiconductor ZrSe2
16 p2257 N88-23488
Photovoltaic cells with n-silicon and conductive polymers
[ETN-88-92133] 20 p2821 N88-26734
Electrical properties of p-type and n-type ZnSe-ZnTe strained-layer superlattices 20 p2868 N88-27029
Growth and characterization of CuGaS2, CuAlS2 and CuGa0.9Al0.1S2 single crystals
[AD-A192963] 21 p3021 N88-27930

NACELLES
Numerical computation of transonic potential flow about 3-dimensional inlets
[NAL-TR-924] 02 p0122 N88-10770
Computation of transonic flows with nacelle simulation
[SNIAS-872-111-117] 05 p0542 N88-13300
Low speed wind tunnel investigation of propeller slipstream aerodynamic effects on different nacelle/wing combinations. Part 1: Total forces and moments and pressure distributions on nacelle/wing at different angles of attack and yaw and at different thrust coefficients
[FFA-TN-1987-22] 05 p0542 N88-13302
Aerodynamic and propeller performance characteristics of a propfan-powered, semispan model
[NASA-TM-86705] 06 p0667 N88-14092
Natural laminar flow nacelle for transport aircraft
07 p0813 N88-14949
Flight research on natural laminar flow
07 p0813 N88-14950
Roughness and waviness requirements for laminar flow surfaces 07 p0813 N88-14953
Testing of the engine compartment fire extinguishing system in the F/EF-111 aircraft
[AD-A188801] 12 p1576 N88-19423

NAMIBIA
Evolution of thermal structure of Benguela upswelling system according to satellite and shipboard data
24 p3449 N88-30525

NAMING
NT NORMS
Contributions to geodesy, photogrammetry, and cartography. Series 2, number 45
[ISSN-0469-4244] 01 p0065 N88-10416
Digital Name Data Base Antarctic as a component of a landscape data base of the Antarctic
01 p0065 N88-10419
Inventory of topographic mapping and standardization of geographic names as the basis of a Geographic Information System (GIS) 16 p2225 N88-23281

NAP-OF-THE-EARTH NAVIGATION
Investigation of vertical axis handling qualities for helicopter hover and NOE flight
03 p0263 N88-11653
Handling qualities criterion for very low visibility rotorcraft
03 p0263 N88-11654
Some data processing requirements for precision Nap-Of-the-Earth (NOE) guidance and control of rotorcraft
[NASA-CR-177453] 04 p0401 N88-12493
Low altitude: A new dimension in air refueling
[AD-A193819] 23 p3176 N88-28910
LANTIRN simulator training in the F-16C
[AD-A195201] 24 p3330 N88-29826
NAPHTHALENE
Transport and relaxation processes in supercritical fluids
[DE88-004804] 10 p1419 N88-18474
NAPHTHENES
Availability and cost estimate of a high naphthene, modified aviation turbine fuel
[NASA-TM-100823] 13 p1749 N88-20455
NARCOTICS
NT MORPHINE
NARROWBAND
Improving the method of calculating electronic properties of narrow bandgap semiconductors
07 p0926 N88-15627
Estimation of broadband planetary albedo from operational narrowband satellite measurements
[PB88-107644] 07 p0945 N88-15748
Simulated performance of an order statistic threshold strategy for detection of narrowband signals
11 p1474 N88-18796
Optimal and conventional space-time processing in flow noise
[AD-A189104] 13 p1833 N88-20965
A study on the co- and adjacent channel protection requirements for mobile satellite ACSSB modulation
19 p2650 N88-25732
NASA PROGRAMS
NT ACEE PROGRAM
NT EARTH RESOURCES PROGRAM
NT GALILEO PROJECT
NT NASA SPACE PROGRAMS
NT NATIONAL AEROSPACE PLANE PROGRAM
NT PROJECT SETI
NT QUIET ENGINE PROGRAM
NT ROVER PROJECT
NT SKYLAB PROGRAM
NT SUPERSONIC CRUISE AIRCRAFT RESEARCH
NT TILT ROTOR RESEARCH AIRCRAFT PROGRAM
Middle Atmosphere Program: Handbook for MAP, volume 24
[NASA-CR-181451] 01 p0069 N88-10444
Budget reimbursements: The National Aeronautics and Space Administration's reimbursable work
[PB87-207296] 01 p0107 N88-10696
Space technology to meet future needs
[NASA-CR-181473] 02 p0130 N88-10819
Report from the MPP Working Group to the NASA Associate Administrator for Space Science and Applications
[NASA-TM-87819] 02 p0223 N88-11402
Spinoff, 1987
[NASA-TM-89952] 02 p0250 N88-11577
Materials processing in space program support
[NASA-CR-179217] 03 p0298 N88-11872
National Aeronautics and Space Administration Authorization Act, 1988
[PUB-LAW-100-147] 03 p0385 N88-12422
Department of Housing and Urban Development, and Certain Independent Agencies Appropriations, 1988, Part 2
[S-HRG-100-106-PT-2] 03 p0385 N88-12423
Department of Housing and Urban Development-Independent Agencies Appropriations for fiscal year 1988, Thursday, 9 April 1987: National Aeronautics and Space Administration
03 p0386 N88-12424
Department of Housing and Urban Development-Independent Agencies Appropriations for fiscal year 1988, Friday, 10 April 1987: National Aeronautics and Space Administration
03 p0386 N88-12425
Spinoff
[NASA-TM-89651] 03 p0386 N88-12426
FY 1985 scientific and technical reports, articles, papers and presentations
[NASA-TM-86521] 04 p0501 N88-13083
National Aeronautics and Space Administration space station proposal, fiscal year 1988
[S-HRG-100-328] 05 p0659 N88-14043
The 1988 NASA (National Aeronautics and Space Administration) authorization
[GPO-80-245] 05 p0659 N88-14044
University program management information system, fiscal year 1985
[NASA-TM-88381] 06 p0790 N88-14846
The 1988 National Aeronautics and Space Administration (NASA) authorization
[GPO-76-600] 06 p0792 N88-14854
National Aeronautics and Space Administration (NASA)/American Society for Engineering Education (ASEE) Summer Faculty Fellowship Program, 1987. Volume 1
[NASA-CR-172009-VOL-1] 06 p0792 N88-14855
A study of the minority college programs at the NASA Johnson Space Center 06 p0798 N88-14887
Research reports: 1987 NASA/ASEE Summer Faculty Fellowship Program
[NASA-CR-179219] 07 p0922 N88-15601
Risk analysis methodology survey
07 p0922 N88-15604
Compilation and development of K-6 aerospace materials for implementation in NASA spacelink electronic information system 07 p0922 N88-15605
NASA patent abstracts bibliography: A continuing bibliography. Section 1: Abstracts (supplement 32)
[NASA-SP-7039(32)-SECT-1-ABST]
07 p0943 N88-15732
Future plans for the NASA suborbital program
08 p1034 N88-16267
NASA thesaurus supplement: A four part cumulative supplement to the 1985 edition of the NASA Thesaurus
[NASA-SP-7053(SUPP-4)] 08 p1093 N88-16575
Research and technology 1987
[NASA-TM-4021] 09 p1265 N88-17577
Report of the Committee on the Space Station of the National Research Council
[NASA-CR-181602] 10 p1292 N88-17727
Into the thermosphere: The atmosphere explorers
[NASA-SP-490] 10 p1353 N88-18084
NASA patent abstracts bibliography: A continuing bibliography. Section 2: Indexes (supplement 32)
[NASA-SP-7039(32)-SECT-2] 10 p1425 N88-18511
Preliminary analysis of an integrated logistics system for OSSA payloads. Volume 1: Executive summary
12 p1584 N88-19478
Preliminary analysis of an integrated logistics system for OSSA payloads. Volume 2: OSSA integrated logistics support strategy 12 p1584 N88-19479
Communication satellites: Guidelines for a strategic plan
[NASA-TM-89306] 12 p1599 N88-19569
Selling to NASA
[NASA-TM-89724] 12 p1705 N88-20208
NASA/UK TAP
[NASA-CR-180350] 12 p1708 N88-20223
A project to transfer technology from NASA centers in support of industrial innovation in the midwest
[NASA-CR-180360] 12 p1708 N88-20224
Development of a nationwide network for technology transfer
[NASA-CR-181058] 12 p1709 N88-20225
The Joint NASA/Goddard-University of Maryland Research Program in Charged Particle and High Energy Photon Detector Technology
[NASA-CR-182612] 12 p1712 N88-20247
Research and technology, 1987
[NASA-TM-100323] 12 p1713 N88-20253
The Deep Space Network
[NASA-CR-182700] 13 p1759 N88-20524
Application of expert systems in project management decision aiding
[NASA-CR-180762] 13 p1850 N88-21074
Johnson Space Center's strategic game plan: Charting a course to the year 2000 and beyond
[NASA-TM-89733] 13 p1850 N88-21076
NASA advanced turboprop research and concept validation program
[NASA-TM-100891] 16 p2163 N88-22902
Department of Housing and Urban Development independent agencies appropriations for 1989. Part 7: National Aeronautics and Space Administration
[GPO-85-166] 16 p2286 N88-23689
PAN AIR analysis of the NASA/MCAIR 279-3: An advanced supersonic V/STOL fighter/attack aircraft
[NASA-TM-86838] 17 p2298 N88-23750
Structural ceramics research
17 p2324 N88-23878
Structures and Dynamics Division research and technology plans for FY 1988 and accomplishments for FY 1987
[NASA-TM-100585] 17 p2350 N88-24000
NAS: The first year
[NASA-TM-101006] 18 p2560 N88-25196
Financial reporting: NASA (National Aeronautics and Space Administration) can improve compliance with GAO (General Accounting Office) standards and treasury requirements
[PB88-172523] 18 p2587 N88-25373
NASA combined file postings statistics based on NASA thesaurus, Jan. 1968 - July 1988
[NASA-CR-182985] 18 p2589 N88-25384
NASA patent abstracts bibliography: A continuing bibliography. Section 1: Abstracts
[NASA-SP-7039(33)] 18 p2590 N88-25388
NASA history data book. Volume 1: NASA resources 1958-1968
[NASA-SP-4012-VOL-1] 18 p2596 N88-25428
NASA historical data book. Volume 2: Programs and projects 1958-1968
[NASA-SP-4012-VOL-2] 18 p2596 N88-25429
NASA historical data book. Volume 3: Programs and projects 1969-1978
[NASA-SP-4012-VOL-3] 18 p2596 N88-25430
Overview of NASA research in fiber optics for aircraft controls
[NASA-TM-100919] 19 p2603 N88-25458
Resources: NASA for entrepreneurs
[NASA-CR-182152] 20 p2883 N88-27119
Bibliography of Lewis Research Center technical publications announced in 1987
[NASA-TM-100910] 22 p3162 N88-28832
SR-7A aeroelastic model design report
[NASA-CR-174791] 23 p3179 N88-28928
Development and verification of NASA Standard Initiator-2 (NSI-2)
[NASA-CR-172069] 23 p3200 N88-29044
Development and verification of NASA Standard Initiator-2 (NSI-2): Appendix
[NASA-CR-172070] 23 p3200 N88-29045
NASA SPACE PROGRAMS
NT EARTH RESOURCES PROGRAM
NT GALILEO PROJECT
NT PROJECT SETI
NT ROVER PROJECT
NT SKYLAB PROGRAM
Columbus preparatory program. Payload element study on a technology demonstration mission, executive summary
[CS-RP-AI-016] 01 p0014 N88-10080
NASA/JPL study on optical imaging interferometry in space 01 p0096 N88-10630
Space station: National Aeronautics and Space Administration's 1987 cost estimate
[PB87-220760] 02 p0140 N88-10883
The Telecommunications and Data Acquisition Report
[NASA-CR-181546] 04 p0432 N88-12679
Expert system development for commonality analysis in space programs 07 p0928 N88-15635
NASA (National Aeronautics and Space Administration) ADP (Automated Data Processing) system: Information on the automated mission and the payload tracking system
[PB88-104989] 07 p0942 N88-15730
Update of NASA's ocean colour activities
08 p1042 N88-16295
The European space physics analysis network
08 p1099 N88-16613
An overview of the current Earth observation programs (Europe, USA, and Japan) 09 p1129 N88-16778
America plans for space
[AD-A187465] 10 p1289 N88-17713
Relationships between coronary heart disease risk factors and serum ionized calcium in Kennedy Space Center Cohort
[NASA-TM-100979] 10 p1368 N88-18177
Research and technology 1987 annual report of the Kennedy Space Center
[NASA-TM-100303] 10 p1431 N88-18548
Columbus feasibility studies. Volume 4: Integration, test, and operations
[ETN-88-90576] 11 p1445 N88-18614
NASA (National Aeronautics and Space Administration) procurement: The 1973 space shuttle solid rocket motor contractor selection
[PB88-135264] 11 p1447 N88-18623
NASA Office of Space Flight (OSF) in-orbit servicing program 12 p1587 N88-19498
NASA's geodynamics program
12 p1644 N88-19845
Aeronautics and space report of the President: 1986 activities 13 p1852 N88-21087
Chronology of KSC and KSC related events for 1987
[NASA-CR-182754] 14 p2012 N88-22002
Science at NASA field centers: Findings and recommendations on the scope, strength and interactions of science and science-related technology programs
[NASA-TM-101188] 24 p3459 N88-30581
Research and technology of the Lyndon B. Johnson Space Center
[NASA-TM-100463] 24 p3460 N88-30583
NASA STRUCTURAL ANALYSIS PROGRAM
U NASTRAN
NASTRAN
Qualification by analysis of IUS plume deflectors
09 p1179 N88-17063

Optimized structure design using reanalysis techniques 09 p1180 N88-17067
Dynamic substructuring for shock spectrum analysis using component mode synthesis 11 p1499 N88-18950
Sixteenth NASTRAN (trademark) Users' Colloquium [NASA-CP-2505] 13 p1780 N88-20652
A preliminary investigation of finite-element modeling for composite rotor blades [NASA-TM-100559] 13 p1781 N88-20656
Thermostructural analysis of simulated cowl lips 15 p2080 N88-22403
Lewis Structures Technology, 1988. Volume 1: Structural Dynamics [NASA-CP-3003-VOL-1] 16 p2217 N88-23226
Analysis of rotating flexible blades using MSC/NASTRAN 16 p2222 N88-23259
Interactive plotting of NASTRAN aerodynamic models using NPLOT and DISSPLA [AD-A194115] 23 p3226 N88-29204
Computer programs for generation of NASTRAN and VIBRA-6 aircraft models [AD-A195467] 24 p3323 N88-29792

NATIONAL AEROSPACE PLANE PROGRAM
Hypersonic propulsion research 08 p0958 N88-15812
Numerical investigations in three-dimensional internal flows [NASA-CR-183108] 23 p3210 N88-29106

NATIONAL AIRSPACE SYSTEM
FAA (Federal Aviation Administration) technical center: Mission and role in natinal airspace system plan implementation [PB88-169818] 18 p2460 N88-24609

NATIONAL SEVERE STORMS PROJECT
Verification of severe local storm forecasts issued by the National Severe Storms Forecast Center, 1986 [PB88-101407] 06 p0747 N88-14594

NATIONS
NT ALABAMA
NT ALASKA
NT ARIZONA
NT AUSTRALIA
NT BELGIUM
NT BRAZIL
NT BRITISH COLUMBIA
NT BURKINA
NT BURUNDI
NT CALIFORNIA
NT CANADA
NT CHAD
NT CHINA
NT COLOMBIA
NT CONNECTICUT
NT CZECHOSLOVAKIA
NT DELAWARE
NT EGYPT
NT ENGLAND
NT FINLAND
NT FLORIDA
NT FRANCE
NT HAWAII
NT HUNGARY
NT ICELAND
NT ILLINOIS
NT INDIA
NT INDONESIA
NT ISRAEL
NT ITALY
NT JAPAN
NT KANSAS
NT KENTUCKY
NT KENYA
NT LAOS
NT MAINE
NT MALDIVE ISLANDS
NT MALI
NT MASSACHUSETTS
NT MEXICO
NT MICHIGAN
NT MISSISSIPPI
NT NEPAL
NT NETHERLANDS
NT NEVADA
NT NEW MEXICO
NT NEW YORK
NT NEW ZEALAND
NT NORTH CAROLINA
NT NORTH DAKOTA
NT NORWAY
NT SCOTLAND
NT SIERRA LEONE
NT SPAIN
NT SRI LANKA
NT SWEDEN
NT SWITZERLAND
NT SYRIA
NT TAIWAN
NT TEXAS
NT THAILAND
NT TIBET
NT TUNISIA
NT TURKEY
NT U.S.S.R.
NT UNITED KINGDOM
NT UNITED STATES
NT WEST GERMANY
NT WISCONSIN
NT WYOMING
NT YEMEN
NT ZIMBABWE

NATURAL FREQUENCIES
U RESONANT FREQUENCIES

NATURAL GAS
Laser probes of natural gas ignition chemistry [PB87-209599] 01 p0021 N88-10129
Endurance testing of a natural gas-fueled rotary engine [PB87-215703] 01 p0055 N88-10356
Development of a light duty gas engine for cogeneration service [PB87-221297] 02 p0180 N88-11119
Use of natural gas diesel engines in mechanical pulp production: A preliminary study [DE87-753065] 02 p0181 N88-11129
High pressure autoignition of natural gas/air mixtures and the problem of engine knock [DE87-013799] 03 p0284 N88-11784
Advanced natural gas fueled engine development. Part 1: Design and analyses [PB87-224804] 03 p0331 N88-12087
Advanced natural gas fueled engine development. Part 2: Materials investigation [PB87-223160] 03 p0331 N88-12088
Thermodynamic properties for natural gas binaries [PB87-226833] 04 p0500 N88-13074
Projects within the Center for Advanced Materials [PB88-123054] 06 p0677 N88-14143
Advanced communication systems: A report on fiber optic technology and its possible applications in the gas industry [PB88-112792] 07 p0845 N88-15125
Geological evolution and analysis of confirmed or suspected gas hydrate localities. Volume 9: Formation and stability of gas hydrates of the Middle America Trench [DE88-001007] 10 p1347 N88-18050
Basic research on natural gas combustion phenomena [PB88-168380] 14 p1887 N88-21278
Assessment of opportunities for gas-fired sintering in the advanced ceramics and powdered metals industries [PB88-197157] 19 p2620 N88-25545
Direct gas injection with glow plug ignition [PB88-187323] 19 p2676 N88-25911
Advanced energy system program [PB88-183025] 19 p2686 N88-25965
Development of an equation of state for computation of supercompressibility factors, critical flow factors and other properties for wet, sour natural gases, synthetic gases and admixtures [PB88-202676] 20 p2798 N88-26602
Laser probes of natural gas ignition chemistry [PB88-212568] 21 p2910 N88-27271
Absorption heat pumps [DE88-752820] 23 p3229 N88-29218

NATURAL LANGUAGE (COMPUTERS)
Intelligent man/machine interfaces on the space station 08 p1063 N88-16418
SWAN: An expert system with natural language interface for tactical air capability assessment 09 p1210 N88-17253
Voice/natural language interfacing for robotic control [AD-A187765] 11 p1494 N88-18917
Research in knowledge representation for natural language communication and planning assistance [AD-A187355] 11 p1522 N88-19087
State of the art of natural language processing [AD-A188112] 11 p1530 N88-19136
Realization of natural language style robot task instruction by using the object oriented concept 16 p2257 N88-23487
A cockpit natural language study - selected transcripts [AD-A192972] 20 p2834 N88-26808
The effect of input device on user performance with a menu-based natural language interface [AD-A193095] 21 p2996 N88-27772
An expert system for natural language processing 23 p3263 N88-29426
Exploiting lexical regularities in designing natural language systems [AD-A195922] 24 p3423 N88-30375

NATURAL LASERS
U LASERS

NATURAL SATELLITES
NT DEIMOS
NT IO
NT JUPITER SATELLITES
NT MOON
NT PHOBOS
NT SATURN SATELLITES
NT TITAN
NT TITANIA
NT URANUS SATELLITES
A technique for capture analysis of low thrust missions in a planetary system [AD-A188934] 12 p1594 N88-19544
Extended atmospheres of outer planet satellites and comets [NASA-CR-183157] 24 p3457 N88-30572

NAUTICAL CHARTS
Generation of thematic maps for updating aeronautical pilot charts utilizing LANDSAT-TM images 17 p2361 N88-24062
Contribution of spaceborne high resolution radiometers to mapping of precoastal depths 19 p2701 N88-26063

NAVIER-STOKES EQUATION
Accurate, stable, explicit solution of the parabolized Navier-Stokes equations 01 p0043 N88-10276
Laminar flow over a spinning projectile at an angle of attack 02 p0121 N88-10766
Navier-Stokes cascade analysis with a stiff Kappa-Epsilon turbulence solver [NASA-TM-100218] 02 p0123 N88-10778
Characteristics and boundary elements for three dimensional nonstationary Navier Stokes flows [PREPRINT-1051] 02 p0172 N88-11086
Personal Computer (PC) based image processing applied to fluid mechanics [NASA-TM-100024] 02 p0172 N88-11087
Computation of transonic separated wing flows using an Euler/Navier-Stokes zonal approach [NASA-TM-88311] 02 p0173 N88-11089
Flow in a model turbine stator 02 p0187 N88-11163
Efficient numerical approaches for predicting supersonic flows with viscous/inviscid interaction 03 p0260 N88-11637
Application of an upwind algorithm to the parabolized Navier-Stokes equations 03 p0316 N88-12000
The diffusion-convection vortex method for solving two-dimensional incompressible Navier-Stokes equation 03 p0317 N88-12001
Development and application of computational aerothermodynamics flowfield computer codes [NASA-CR-181534] 04 p0395 N88-12465
Blowup for a nonlinear evolution equation and self-reproducing strained shear layers 04 p0444 N88-12755
Cauchy problem for linearized system of Navier-Stokes equations considering compressibility 04 p0459 N88-12837
Asymptotic form of stationary solutions of the Navier-Stokes equations for large Reynolds numbers 04 p0459 N88-12838
On operator splitting for unsteady boundary value problems [AD-A184281] 04 p0484 N88-12981
INS3D: An incompressible Navier-Stokes code in generalized three-dimensional coordinates [NASA-TM-100012] 04 p0485 N88-12991
Numerical analysis of flow through scramjet engine inlets 05 p0532 N88-13233
Numerical simulation of the hypersonic flow around lifting vehicles 05 p0532 N88-13234
Solution of some 3-D viscous and inviscid supersonic flow problems by finite-volume space-marching schemes 05 p0532 N88-13235
Numerical experiments with hypersonic flows beneath a cone-delta-wing combination 05 p0532 N88-13238
Numerical analysis of cascade flow solving Navier-Stokes equations 05 p0536 N88-13262
Relaxation method for the compressible Navier-Stokes equations using upwind schemes 05 p0539 N88-13283
Navier-Stokes analysis of laminar flow control of a two-dimensional airfoil 05 p0540 N88-13286
Navier-Stokes simulation of transonic transportation aircraft configurations. 1: Flow-field simulation over wing-fuselage combinations 05 p0540 N88-13288
Numerical simulation of transonic aircraft in comparison to wind tunnel test 05 p0540 N88-13289
Calculation of helicopter rotor blade/vortex interaction by Navier-Stokes procedures [NASA-CR-177441] 05 p0540 N88-13291
Solution procedure for the Navier-Stokes equations applied to rotors 05 p0579 N88-13533

Physical analysis and numerical simulation of coherent turbulent structures in mixed layers, jets, and wakes
[ETN-88-91183] 05 p0581 N88-13548
Low thrust viscous nozzle flow fields prediction
[NASA-CR-182334] 05 p0582 N88-13551
The interaction of DC plasma jet with a melting metal: Experimental measurements and mathematical description
[AD-A185173] 05 p0651 N88-13993
Transonic Navier-Stokes computations of strake-generated vortex interactions for a fighter-like configuration 06 p0664 N88-14073
Post stall behavior in axial-flow compressors
[AD-A185712] 06 p0665 N88-14081
Vectorization of a multigrid method for the compressible Navier-Stokes equations
[PB87-230496] 06 p0698 N88-14284
Computational fluid dynamics overview 07 p0809 N88-14927
Upwind relaxation algorithms for Euler/Navier-Stokes equations 07 p0810 N88-14931
A multistage time-stepping scheme for the thin-layer Navier-Stokes equations 07 p0810 N88-14932
Numerical simulation of a controlled boundary layer 07 p0810 N88-14933
Viscous vortex flows 07 p0810 N88-14934
Analysis and performance prediction of scramjet inlets utilizing a three-dimensional Navier-Stokes code 07 p0811 N88-14936
Boundary layer transition 07 p0811 N88-14942
The numerical and analytical study of bifurcation and multicellular flow instability due to natural convection between narrow horizontal isothermal cylindrical annuli at high Rayleigh numbers
[AD-A186113] 07 p0849 N88-15151
On the parabolized Navier-Stokes equations without sublayer assumptions
[AD-A186127] 07 p0849 N88-15152
Analysis of three-dimensional viscous internal flows
[AD-A186254] 07 p0849 N88-15155
Multitasked embedded multigrid for three-dimensional flow simulation
[NASA-CR-182398] 07 p0852 N88-15173
Consistent boundary conditions for Reduced Navier-Stokes (RNS) scheme applied to 3-dimensional internal viscous flows
[NASA-CR-180874] 08 p0950 N88-15762
The simulation of three-dimensional viscous supersonic flow past blunt bodies with a hybrid implicit/explicit finite difference method
[DFVLR-FB-87-32] 08 p0950 N88-15765
Inlets, ducts and nozzles 08 p0955 N88-15791
Turbomachinery 08 p0955 N88-15792
Integration of Navier-Stokes equations in finite volume formulation 08 p0984 N88-15954
Viscous flows. Part 3: Formulation of the Navier-Stokes equations by stream function vorticity methods 08 p0986 N88-15969
Navier-Stokes solutions for laminar incompressible flow over a NACA 0012 airfoil and a backward facing step
[FFA-TN-1987-50] 09 p1162 N88-16966
A project to experimentally and theoretically examine fluid interfacial wave phenomena in a rotating cylindrical geometry: Current results and future plans
[DE88-003738] 09 p1165 N88-16984
Numerical modeling of multidimensional flow in seals and bearings used in rotating machinery
[NASA-TM-100779] 09 p1165 N88-16988
Numerical solutions of three-dimensional Navier-Stokes equations for closed-bluff bodies
[NASA-CR-182359] 09 p1166 N88-16990
Solution of the three-dimensional Navier-Stokes equations for transonic flow using a multigrid method 10 p1267 N88-17579
Navier-Stokes simulation of wind-tunnel flow using LU-ADI factorization algorithm
[NASA-TM-100042] 10 p1268 N88-17584
Navier-Stokes calculations and turbulence modeling in the trailing edge region of a circulation control airfoil 10 p1268 N88-17587
Evaluation of a research circulation control airfoil using Navier-Stokes methods 10 p1269 N88-17591
Navier-Stokes computations for circulation control airfoils 10 p1269 N88-17592
Implicit solution of the incompressible Navier-Stokes equations in primitive variables on non-staggered grids 10 p1326 N88-17930
A numerical study of unsteady two-dimensional subsonic compressible base flow 10 p1327 N88-17931
The numerical and analytical study of bifurcation and multicellular flow instability due to natural convection between narrow horizontal isothermal cylindrical annuli at high Rayleigh numbers 10 p1328 N88-17937
Instability and transition in curved channel flow 10 p1328 N88-17938
Three-dimensional incompressible flowfield analysis for establishing rotor designs which optimize power extraction 10 p1329 N88-17943
Free-surface flow phenomena ahead of a two-dimensional body in a viscous fluid 10 p1329 N88-17944
A visual programming environment for the Navier-Stokes computer
[NASA-CR-181615] 10 p1390 N88-18299
Implementation and analysis of a Navier-Stokes algorithm on parallel computers
[NASA-CR-181614] 10 p1390 N88-18301
On the smallest scale for the incompressible Navier-Stokes equations
[NASA-CR-181628] 11 p1434 N88-18558
Fluctuations and massive separation in three-dimensional shock-wave/boundary-layer interactions
[NASA-TM-89224] 11 p1434 N88-18559
Comparisons of Monte-Carlo and PNS (Parabolized Navier-Stokes) calculations for rarefied flow over reentry vehicle configurations
[DE88-004937] 11 p1435 N88-18560
High performance Solid Rocket Motor (SRM) submerged nozzle/combustion cavity flowfield assessment
[NASA-CR-179307] 11 p1446 N88-18622
A code development system for computational fluid dynamics
[AD-A188050] 11 p1482 N88-18848
A new computational technique for generating algorithms, with application to the solution of the time-dependent incompressible Navier-Stokes equations 11 p1485 N88-18864
Numerical and analytical study of fluid dynamic forces in seals and bearings
[NASA-TM-100268] 11 p1485 N88-18867
A velocity-pressure integrated, mixed interpolation, Galerkin finite element method for high Reynolds number laminar flows
[NASA-CR-179264] 11 p1486 N88-18868
Estimates of green tensors for certain boundary value problems
[NASA-TT-20203] 11 p1535 N88-19172
Solution of a rotating Navier-Stokes problem by a nonlinear multigrid algorithm 11 p1538 N88-19194
Applications of a multigrid finite volume method with Runge-Kutta time integrations for solving the Euler and Navier-Stokes equations 11 p1539 N88-19201
Three-dimensional incompressible Navier-Stokes computations of internal flows
[NASA-TM-100076] 12 p1576 N88-19425
A new parabolized Navier-Stokes code for chemically reacting flow fields 12 p1625 N88-19721
Time-accurate simulations of a shear layer forced at a single frequency
[NASA-TM-100836] 12 p1628 N88-19740
Fully-coupled analysis of jet mixing problems. Three-dimensional PNS model, SCIP3D
[NASA-CR-4139] 13 p1715 N88-20256
The construction of a three-dimensional finite volume grid generator for a wing in a wind tunnel with application to Navier-Stokes flow solvers
[FFA-TN-1987-58] 13 p1719 N88-20277
Numerical model of the time independent mean flow in a rotating rocket motor 13 p1733 N88-20360
Calculations of viscous flows with a multigrid method 13 p1769 N88-20580
Numerical experiments on the stability of controlled boundary layers
[NASA-CR-181649] 13 p1771 N88-20591
Numerical analysis of three-dimensional viscous internal flows
[NASA-TM-100878] 14 p1861 N88-21116
High-speed flow calculations past 3-D configurations based on the Reynolds averaged Navier-Stokes equations
[NASA-TM-100082] 14 p1911 N88-21421
Choice of implicit and explicit operators for the upwind differencing method
[NASA-TM-100857] 14 p1964 N88-21718
High Reynolds number, low Mach number, steady flow field calculations over a NACA 0012 airfoil using Navier-Stokes and interactive boundary layer theory
[AD-A189871] 15 p2013 N88-22005
Transonic Navier-Stokes computations of strake-generated vortex interactions for a fighter-like configuration
[NASA-TM-100009] 15 p2014 N88-22010
Random processes, turbulence and disordering fields
[AD-A190123] 15 p2063 N88-22303
Review and assessment of the HOST turbine heat transfer program 15 p2086 N88-22431
Numerical study of unsteady viscous hypersonic blunt body flows with an impinging shock
[NASA-TM-100096] 15 p2122 N88-22650
High-resolution shock-capturing schemes for inviscid and viscous hypersonic flows
[NASA-TM-100097] 15 p2122 N88-22651
A low dimensional dynamical system for the wall layer 16 p2194 N88-23088
Test code for the assessment and improvement of Reynolds stress models 16 p2197 N88-23105
Numerical treatment of Navier-Stokes equations
[REPT-87-22] 16 p2206 N88-23162
Application of a multigrid method for solving the Navier-Stokes equation in two-dimensional flow problems
[KU-SFB-210/T/32] 16 p2206 N88-23164
Some numerical methods for the computation of capillary free boundaries governed by the Navier-Stokes equations
[REPT-87-69] 16 p2206 N88-23167
Fast algorithms for Euler and Navier-Stokes simulations
[AD-A190897] 16 p2208 N88-23175
Solution of the compressible Navier-Stokes equations of motion by Chebyshev polynomials for laminar shock-boundary layer flow
[AD-A191033] 16 p2208 N88-23176
Reduced order models for nonlinear aerodynamics 16 p2220 N88-23248
Application of Navier-Stokes analysis to stall flutter 16 p2220 N88-23249
Research in nonlinear partial differential equations and bifurcation theory
[AD-A190986] 16 p2260 N88-23514
Numerical simulation of scramjet inlet flow fields
[NASA-TP-2517] 17 p2296 N88-23735
An efficient parallel algorithm for the simulation of three-dimensional compressible transition on a 20 processor Flex/32 multicomputer
[NASA-CR-178340] 17 p2337 N88-23943
Prediction of laminar and turbulent flows past single and twin airfoils 18 p2457 N88-24589
Some rotorcraft applications of computational fluid dynamics
[NASA-TM-100066] 18 p2459 N88-24601
Applications of the Navier-Stokes equations to wings and complex configurations using a zonal approach
[NASA-TM-100080] 18 p2459 N88-24602
Computation and characteristics of pulsatile multi-bifurcation flow 18 p2483 N88-24729
Composite reduced Navier-Stokes procedures for flow problems with strong pressure interactions
[AD-A191127] 18 p2508 N88-24875
Two dimensional hyperbolic grid generation
[VKI-TN-162] 18 p2511 N88-24897
Finite element solution of 3-D turbulent Navier-Stokes equations for propeller-driven slender bodies 18 p2515 N88-24919
Characteristic time correlations to liquid fuel ramjet combustion efficiency 19 p2624 N88-25566
Numerical investigation of acoustic energy exchange through flow turning 19 p2629 N88-25593
Aerodynamic analysis of natural laminar flow airfoil 19 p2634 N88-25624
Numerical calculation of supersonic flow by the PNS equations 19 p2636 N88-25636
Navier-Stokes analysis of transonic transport aircraft empennage 19 p2636 N88-25637
Numerical simulation of the shock tube flows by TVD scheme 19 p2638 N88-25648
Numerical calculation of three dimensional flow by TVD scheme 19 p2638 N88-25649
Numerical analysis of three dimensional cascade flow by solving Navier-Stokes equations 19 p2638 N88-25650
Numerical analysis of duct flow using three-dimensional parabolized Navier-Stokes equation 19 p2638 N88-25652
The role of computational fluid dynamics in aeronautical engineering (5). Improvements and applications of implicit TVD finite volume code 19 p2638 N88-25653
Scaling laws for homogeneous turbulent shear flows in a rotating frame
[NASA-CR-181672] 19 p2665 N88-25847
Numerical simulation studies of laminar-turbulent transition in the plan channel 19 p2665 N88-25850
Navier-Stokes code NS3D for blunt bodies. Part 1: Analysis, results and verification
[DE88-010105] 19 p2666 N88-25855
A Navier-Stokes solver for cascade flows
[NASA-CR-181682] 19 p2666 N88-25856
Vortex methods for separated flows
[NASA-TM-100068] 20 p2753 N88-26342
Numerical analysis of reconnection of vortex rings 20 p2782 N88-26500
Navier-Stokes simulation of shock-tube flows over a wedge-type step by finite volume method
[ISAS-RN-628] 20 p2797 N88-26599

Spectral resolution of the Navier-Stokes equations in multi-domain curved complex geometries
[ONERA-NT-1987-2] 20 p2802 N88-26631
An h-p adaptive finite element method for steady compressible flow 21 p2941 N88-27467
A Navier-Stokes study of cascade flow fields including inlet distortion and rotating stall
[AD-A193109] 21 p2943 N88-27483
Computational boundary conditions for the incompressible Navier-Stokes equations in channels and pipes
[AD-A193356] 21 p2944 N88-27487
Numerical treatment of the pressure singularity at a re-entrant corner
[AD-A193357] 21 p2944 N88-27488
Stream function-vorticity finite elements and the resolution of the Navier-Stokes equations
[DE88-702318] 21 p2945 N88-27494
Determination of the local heat-transfer characteristics on glaze ice accretions on a cylinder and a NACA 0012 airfoil 21 p2946 N88-27500
Distributive iteration for indefinite systems as smoothing method in multigrid process on example of Stokes and Navier-Stokes equations with emphasis on incomplete decompositions
[ETN-88-92127] 21 p2948 N88-27509
Numerical integration of Navier-Stokes equations by application of multigrid concept
[ETN-88-92365] 21 p2949 N88-27513
The three-dimensional stress field around a cylindrical inclusion in a plate of arbitrary thickness
21 p2963 N88-27602
Runge-Kutta finite-volume simulation of laminar transonic flow over the ONERA M6 wing using the Navier-Stokes equations
[FFA-TN-1987-06] 22 p3039 N88-28045
Numerical computation of space shuttle orbiter flow field
[NASA-CR-183193] 22 p3040 N88-28048
A study of the vortex sheet method for solving the Prandtl boundary layer equations
[DE88-011346] 22 p3074 N88-28249
Solution to the compressible Navier-Stokes equations of motion by Chebyshev polynomials with implicit time stepping
[AD-A194119] 22 p3075 N88-28257
Steady and unsteady internal flow computations via the solution of the compressible Navier Stokes equations for low Mach numbers 23 p3209 N88-29100
Three-dimensional laser Doppler velocimeter studies of flow in a 90 deg curved duct having a square cross-section 23 p3209 N88-29101
Computation of the eigenvalues for perturbations of Poiseuille flow using a two-point boundary value method
[AD-A193479] 23 p3210 N88-29104
An exponential decay estimate for the stationary perturbation of Poiseuille flow
[AD-A193480] 23 p3210 N88-29105
An efficient patched grid Navier-Stokes solution for multiple bodies, phase 1
[AD-A194166] 23 p3211 N88-29110
Navier-Stokes calculations of transonic flows past cavities
[NASA-CR-180484] 23 p3212 N88-29116
Computational fluid dynamics methods for low Reynolds number precessing/spinning incompressible flows
[AD-A193891] 23 p3212 N88-29119
Lessons learned in the mesh generation for PN/S calculations 23 p3245 N88-29314
Mesh generation for industrial application of Euler and Navier Stokes solvers 23 p3247 N88-29323
Experience with three dimensional composite grids
23 p3247 N88-29324
Three-dimensional Navier-Stokes simulations of turbine rotor-stator interaction
[NASA-TM-100081] 24 p3316 N88-29750
A streamwise upwind algorithm for the Euler and Navier-Stokes equations applied to transonic flows
[NASA-TM-101019] 24 p3316 N88-29751
Application of unsteady aerodynamic methods for transonic aeroelastic analysis
[NASA-TM-100665] 24 p3317 N88-29754
Aerodynamic heating of missiles
24 p3319 N88-29764
Computational aerodynamic analysis for a range-limited 25mm training round
[AD-A185270] 24 p3320 N88-29772
The computation of flow past an oblique wing using the thin-layer Navier-Stokes equations
[NASA-TM-88317] 24 p3320 N88-29774
On the application of finite-difference techniques for the computation of the flow field in gas turbine combustors with complex geometries 24 p3349 N88-29938
Modeling the stability of a turbulent premixed flame, downstream from a step by a Lagrangian method
24 p3350 N88-29943
Numerical simulation of unsteady incompressible viscous flows in generalized coordinate systems
[NASA-TM-101016] 24 p3373 N88-30085

NAVIGATION
NT AIR NAVIGATION
NT ALL-WEATHER AIR NAVIGATION
NT AREA NAVIGATION
NT DEAD RECKONING
NT DIGITAL NAVIGATION
NT INERTIAL NAVIGATION
NT LORAN C
NT NAP-OF-THE-EARTH NAVIGATION
NT OMEGA NAVIGATION SYSTEM
NT RADIO NAVIGATION
NT SPACE NAVIGATION
NT SURFACE NAVIGATION
Calendar of selected aeronautical and space meetings
[AGARD-CAL-87/1] 05 p0657 N88-14033
The power of neural nets 08 p1064 N88-16430
Navigation planning using quadtrees
[DE88-003706] 09 p1225 N88-17343
An overview of vision-based navigation for autonomous land vehicles 1986
[AD-A188186] 10 p1276 N88-17640
Search problems in mission planning and navigation of autonomous aircraft
[NASA-CR-182666] 12 p1579 N88-19448
Alaska Loran C probe test results
[AD-A189131] 13 p1720 N88-20284
The visit problem: Visibility graph-based solution
[DE88-000343] 15 p2108 N88-22556
A design study of onboard navigation and guidance during aerocapture at Mars
[NASA-CR-172053] 18 p2469 N88-24654
Ice conditions along the Ohio River as observed on LANDSAT images, 1972-1985
[AD-A191172] 18 p2531 N88-25018
Robot navigation using simple sensor fusion
[DE88-006184] 18 p2561 N88-25203
Aircraft accident report: Midair collision of SkyWest Airlines Swearingen METRO 2, N163SW, and Mooney M20, N6485U, Kearns, Utah, January 15, 1987
[PB88-910404] 20 p2755 N88-26346
Treatment of systematic errors in the processing of wide angle sonar sensor data for robotic navigation
[DE88-008961] 20 p2756 N88-26352
Spacecraft applications of advanced global positioning system technology
[NASA-CR-172063] 20 p2757 N88-26359
Sensor fusion for robot navigation
[DE88-008383] 20 p2809 N88-26663
Kalman filter-based algorithms for estimating depth from image sequences
[AD-A195818] 24 p3424 N88-30380

NAVIGATION AIDS
NT ATTITUDE INDICATORS
NT BEACONS
NT NAVIGATION INSTRUMENTS
NT RADAR BEACONS
NT RADIO BEACONS
Advanced dead reckoning navigation for mobile robots
03 p0262 N88-11646
Comparison of alphanumeric data entry methods for advanced helicopter cockpits
[AD-A186934] 09 p1201 N88-17201
Navigation recovery block design description
[NASA-CR-182473] 10 p1342 N88-18022
Optimal selection of global positioning system set to minimize emitter location errors
[AD-A189559] 12 p1579 N88-19447
Assessment of the differential technique for land navigation within 1000 km of Omega Australia
[AD-A191036] 16 p2160 N88-22885
The integration of digital maps in vehicle navigation systems 16 p2225 N88-23286
Refraction in underwater acoustics --- navigation systems
[B8735053] 17 p2395 N88-24236
Search and rescue satellite system (SERES), phase A0
[ETN-88-92335] 18 p2472 N88-24669
Digital maps for an electronic traffic guide
18 p2534 N88-25033
Geographical information for design purposes
[NLR-MP-87014-U] 20 p2818 N88-26719
Accuracy of satellite data navigation
[AD-A195877] 24 p3322 N88-29787
The guide star catalog
[NASA-CR-183253] 24 p3452 N88-30547

NAVIGATION INSTRUMENTS
NT ATTITUDE INDICATORS
Simple 2-D navigation for wheeled vehicles
[DE88-007115] 20 p2756 N88-26351
Observed track-keeping performance of DC10 aircraft equipped with the Collins AINS-70 area navigation system: Karlsruhe and Maastricht UACs (Upper Area Control centres)
[EEC-202] 24 p3323 N88-29788

NAVIGATION SATELLITES
NT NAVSTAR SATELLITES
Accurate position measuring spacecraft package
[ESA-CR(P)-2398-VOL-1] 01 p0004 N88-10022
Accurate position measuring spacecraft package, executive summary
[ESA-CR(P)-2398-VOL-2] 01 p0004 N88-10023
Implications of a simplified signal structure for Navsat
[REPT-63/1439] 01 p0005 N88-10024
Planning and execution of the NAVEX experiment in the Spacelab Mission D1
[DFVLR-FB-87-03] 01 p0010 N88-10056
Dynamic positioning at sea using the global positioning system
[AD-A184453] 04 p0397 N88-12476
Use of the global positioning system for trajectory determination of SRAM 2 missiles at the Eastern Test Range
[AD-A185266] 05 p0544 N88-13314
Determination of TRANET (tracking station coordinates for tracking network) and SMTP (Special Mission Tracking Program) tracking station coordinates for use in the WGS (World Geodetic System) 84
[AD-A185863] 07 p0817 N88-14972
NAVARES: A prototype expert system for NAVSTAR anomaly resolution
[AD-A189491] 12 p1600 N88-19579
The NAVEX experiment in the Spacelab D1 mission: Planning and execution
[ESA-TT-1078] 16 p2166 N88-22913

NAVIGATORS
US civil airmen statistics, 1987
[AD-A191714] 18 p2455 N88-24577

NAVSTAR SATELLITES
Mobile test fixture system for use in a thermal vacuum facility 02 p0134 N88-10843
On-orbit frequency stability analysis of the GPS NAVSTAR 8 rubidium clock and NAVSTARs 9 and 10 cesium clocks
[AD-A184984] 05 p0544 N88-13312
NAVARES: A prototype expert system for NAVSTAR anomaly resolution
[AD-A189491] 12 p1600 N88-19579
Satellite acquisition: Global positioning system acquisition changes after Challenger's accident
[PB88-155536] 14 p1880 N88-21236
Global Positioning System (GPS) exploitation by ODOT (Ohio Department of Transportation)
[PB88-172796] 16 p2159 N88-22882
NAVSTAR global positioning system
[AD-A192609] 20 p2757 N88-26354

NAVY
Naval Aviation Integrated Logistics: Technical users guide version 1.0
[DE87-013368] 01 p0001 N88-10001
CNET (Chief of Naval Education and Training) Program Automated Tracking System (CPATS): A comprehensive study
[AD-A184694] 03 p0385 N88-12418
Avionic corrosion 05 p0547 N88-13332
A summary of the Naval Postgraduate School research program
[AD-A186362] 07 p0942 N88-15727
Meteorological radar and its usage in the Navy
[AD-A186650] 09 p1152 N88-16902
The evolution of naval warfare technology and the impact of space systems
[AD-A186900] 09 p1233 N88-17392
NROSS (Navy Remote Ocean Sensing System): A force multiplier
[AD-A186853] 10 p1346 N88-18045
US Navy climatic study of the Mediterranean Sea
[AD-A188264] 10 p1356 N88-18107
The accommodative status in the dark of US Navy fighter pilots
[AD-A188188] 10 p1370 N88-18186
Worldwide distributions of shipboard surface meteorological observations for EM propagation analysis
[AD-A188771] 12 p1648 N88-19871
A review of the NATO special group of experts on Naval hydromechanics and related problems
16 p2205 N88-23157
Challenges of physiological monitoring in a Navy operational setting 16 p2239 N88-23374
Naval research reviews, volume 39, number 3
[AD-A191392] 16 p2264 N88-23543
Analysis of gas turbine test cell number 1, Lemoore Naval Air Station, California
[AD-A192870] 20 p2762 N88-26380

Multiple-Purpose Subsonic Naval Aircraft (MPSNA): Multiple Application Propfan Study (MAPS)
[NASA-CR-175104] 23 p3177 N88-28917
The spatial and temporal variability of the arctic atmospheric boundary layer and its effect on electromagnetic (EM) propagation
[AD-A193958] 23 p3204 N88-29068

NC-130 AIRCRAFT
U C-130 AIRCRAFT

NEAR FIELDS
The effect of object potentials on the wake of a flowing plasma
[AD-A184038] 03 p0379 N88-12385
Power density measurements in the near field of the DSS 13 26-meter antenna 04 p0437 N88-12711
Regional wave attenuation and seismic moment from the inversion of NORESS spectra
[AD-A187399] 11 p1510 N88-19023
State-of-the-art for assessing earthquake hazards in the US. Parameters for specifying intensity-related earthquake ground motions
[AD-A188230] 11 p1512 N88-19032
Fast algorithm development for large-eddy simulation of circular-jet turbulence
[AD-A192044] 18 p2509 N88-24887
Effects of tectonic release on broadband regional distance bodywaves
[AD-A194247] 22 p3119 N88-28529
Application of sampling techniques to near-field far-field transformation
[ESA-CR(P)-2546] 24 p3359 N88-30002

NEAR INFRARED RADIATION
Near-infrared dichroism of a mesogenic transition metal complex and its solubility in nematic hosts
[DE87-014471] 03 p0287 N88-11805
Precise measurement of refractive index and absorption coefficient of near millimeter wave and far infrared materials
[AD-A184538] 03 p0293 N88-11840
A search for X-ray luminous late type stars in NIPSS data 04 p0511 N88-13143
Light curve behaviour in the near IR of the CG Cyg system 04 p0513 N88-13156
The angular diameter of alpha Scorpii in the near-infrared Ca II triplet 04 p0514 N88-13162
Measuring near infrared spectral reflectance changes from water stressed conifer stands with AIS-2 05 p0613 N88-13765
Lightning spectra in the near infrared
[DE88-002218] 07 p0880 N88-15341
Method of determining atmospheric moisture content by measurement of upward radiation intensity in near IR 08 p1007 N88-16106
Signal and data processing for IR sensors 10 p1374 N88-18199
Growth and characteristics of materials for tunable lasers in the near infrared spectral region
[NASA-CR-182501] 11 p1491 N88-18901
Global solar oscillations observed in the visible to near infrared continuum 13 p1858 N88-21110
Effect of atmospheric turbulence on the bit error probability of a space to ground near infrared laser communications link using binary pulse position modulation and an avalanche photodiode detector
[NASA-TM-100699] 14 p1873 N88-21189
Atmospheric attenuation of near infrared radiation propagating through fog 14 p1899 N88-21342
Near-infrared imaging of Comet Halley: Discovery of a color gradient in the inner coma 14 p2009 N88-21980
Near-infrared observations of cepheids: The distance to M33 15 p2152 N88-22846
A disposable liquid microcell for near-infrared reflectance analysis
[AD-A192190] 18 p2575 N88-25298
Infrared astronomy at extremely faint light levels in support of the LAIRTS program
[AD-A191497] 18 p2592 N88-25404
A new near-infrared tunable-room temperature solid state laser La3Ga5SiO14:Cr(3+)
[DE88-011341] 21 p2953 N88-27543
Growth and characterization of materials for tunable lasers in the near infrared spectral region
[NASA-CR-183132] 24 p3377 N88-30113

NEAR ULTRAVIOLET RADIATION
Literature survey relating to the absorption properties of ozone in the near ultraviolet
[ESRO-SM-81] 09 p1190 N88-17129
Spectroscopic studies of a laser-produced carbon plasma in the near and extreme ultraviolet 11 p1553 N88-19292
Dispersion measurements of microcrystals in the near ultraviolet and infrared
[DE88-006234] 15 p2145 N88-22800

NEAR WAKES
Investigation of large-scale structures in the near wake of a parallel flat plate
[DFVLR-FB-87-31] 09 p1162 N88-16967
Mean flow structure in the near wake of a turbulent junction vortex
[PB88-150115] 14 p1910 N88-21416
Influence of rear body geometry on the velocity characteristics of the near wake
[ISL-R-113/87] 20 p2753 N88-26339
Investigation of large-scale structures in the near wake of a parallel flat plate
[ESA-TT-1100] 24 p3372 N88-30080

NEARSHORE WATER
NT COASTAL WATER

NEBULAE
NT CRAB NEBULA
NT H II REGIONS
NT HERBIG-HARO OBJECTS
NT ORION NEBULA
NT PLANETARY NEBULAE
The astrophysics of nebulae and active galactic nuclear emission-line regions: New methods and applications 13 p1858 N88-21111
Far-infrared (120-300 micron) observations of the Carina Nebula 14 p1993 N88-21876
Para-ortho abundance ratio of molecular hydrogen in NGC2023
[ISAS-RN-352] 18 p2573 N88-25286
Cometary nucleus as aggregate of planetesimals
[ISAS-RN-364] 19 p2741 N88-26275
Comparisons of solar nebula models 24 p3451 N88-30539
Physical processes and timescales in planet and small-body accretion 24 p3451 N88-30540
Nebular processes recorded in chondritic meteorites 24 p3451 N88-30541
Cosmochemical trends of volatile elements in the solar system 24 p3451 N88-30542
Terrestrial versus giant planet formation 24 p3451 N88-30543

NECK (ANATOMY)
Motion and space sickness 04 p0404 N88-12510
Neck receptor stimulation in 0 and 1 g 12 p1658 N88-19938
Basic research on flame radiation
[PB88-168372] 15 p2032 N88-22105
Analysis of head response to torso acceleration. Volume 2: Description of data retrieval, analysis and display software
[PB88-156765] 15 p2104 N88-22536

NEEDLES
Selective growth velocity in needle crystals 14 p1988 N88-21858

NEGATIVE IONS
NT ANIONS
Negative ion beams for heating and current-drive in NET
[AD-A184390] 04 p0489 N88-13012
Theoretical studies of kinetic mechanisms of negative ion formation in plasmas
[AD-A185735] 06 p0784 N88-14812
Experiments on ion-acoustic rarefactive solitons in a multi-component plasma with negative ions
[INPE-4393-PRE/1213] 08 p1086 N88-16542
Gas phase reactions of electrons, negative ions and free-radicals with transition metal complexes 11 p1560 N88-19339
A moment approach to modeling negative ion sources
[AD-A188858] 12 p1691 N88-20114
Photoenhanced attachment for optical control of diffuse discharges
[AD-A188989] 12 p1696 N88-20147
Studies of compound states of negative ions using laser beams
[DE88-004708] 13 p1777 N88-20627
A new approach to generating negative ion beams
[AD-A191119] 18 p2572 N88-25276
An optical technique for measuring divergence, beam profile, and aiming direction, of relativistic negative hydrogen ions
[DE88-007049] 18 p2572 N88-25278
Plasma neutralizer work at BNL (Brookhaven National Laboratory)
[DE88-007046] 18 p2579 N88-25317
Development of high current and high brightness negative hydrogen ion sources
[DE88-010882] 20 p2852 N88-26934

NEGATIVE RESISTANCE DEVICES
Quantum transport theory of resonant-tunneling heterostructure devices 20 p2865 N88-27017
Resonant tunneling transistors and resonant tunneling hot electron spectroscopy 20 p2866 N88-27018
Excellent negative differential resistance of InGaAs/InAlAs resonant tunneling barrier structures and applications to a new functional device, RHET 20 p2872 N88-27048

NEMESIS (STAR)
An astrometric search for a stellar companion to the sun 04 p0520 N88-13195

NEODYMIUM
Effects of galactic chemical evolution on thorium/neodymium cosmochronology
[DE88-003829] 11 p1570 N88-19397
Design, development, fabrication and launch support for a high altitude release of neodymium vapor
[AD-A194196] 22 p3118 N88-28527
Absorption spectra and energy levels of Gd(3+), Nd(3+) and Cr(3+) in the garnet Gd3Sc2Ga3O12
[AD-A193634] 23 p3292 N88-29599

NEODYMIUM COMPOUNDS
Superconductivity in La/sub 1.85-x/Nd/sub x/Sr/sub .15/CuO
[DE88-003014] 09 p1258 N88-17540

NEODYMIUM ISOTOPES
Nd isotopes and crustal growth rate 24 p3392 N88-30203
Growth of continental crust: Clues from Nd isotopes and Nb-Th relationships in mantle-derived magmas 24 p3393 N88-30205
Changing styles of crustal growth in Southern Africa: Constraints from geochemical and Sr-Nd isotope studies in Archaean to Pan African terrains 24 p3396 N88-30227

NEODYMIUM LASERS
Large-scale stimulated rotational Raman scattering experiments using the LLNL Nova laser
[DE87-012661] 01 p0051 N88-10328
Saturable absorbers for colliding pulse-locked Nd:YAG lasers 03 p0302 N88-11902
Physical design of parameters of Nd:YAG disk laser 03 p0302 N88-11904
Status, development of laser devices in China 03 p0303 N88-11907
An investigation of unipolar arcing at atmospheric pressure in aluminum 2024 and aluminum coated glass slides
[AD-A184903] 05 p0577 N88-13521
Super-short yttrium aluminate pulse generator with controlled resonator Q-factor 06 p0772 N88-14740
Investigations of solid state slab lasers
[ETN-88-91055] 09 p1171 N88-17022
Mode locking in Nd-laser by means of Gd-Sc-Ga-garnet shutter 09 p1237 N88-17412
Polarization effects in laser-pumped Nd:YAG lasers
[DE88-004019] 11 p1492 N88-18904
Burst mode Nd:YLF laser oscillator
[DE88-004040] 11 p1492 N88-18905
Magnetic and inertial fusion status and development plans
[DE88-004405] 11 p1552 N88-19288
Phosphorus oxynitride glass for laser applications
[DE88-005413] 12 p1632 N88-19768
Radiation absorption in neodymium glasses during passage of strong laser pulse 14 p1969 N88-21757
Solid-state ring laser with acoustooptical phase nonreciprocity of opposing waves 14 p1970 N88-21761
Nonlinear stage of ultrashort-pulse formation in solid-state laser 14 p1971 N88-21765
A preliminary comparison of the transient effects of single versus multiple q-switched doubled-neodymium laser pulses
[AD-A189855] 15 p2071 N88-22347
Observation of synchronously transient pumped mode-locking dye laser under negative cavity detuning 16 p2187 N88-23041
Graphite as a picosecond laser activated opening switch 19 p2657 N88-25783
Coupling of a spark source mass spectrograph and a ND-YAG laser
[DE88-012116] 21 p2951 N88-27530
Radial compression of picosecond electrical pulses
[DE88-008440] 21 p2953 N88-27544
Process control improvements in pulsed Nd:YAG laser closure welding of electromechanical relays
[DE88-006275] 21 p2957 N88-27564
Short pulse X-ray diffraction studies of shocked and annealed crystals using the JANUS research laser
[DE88-011329] 23 p3288 N88-29579

NEON
Experimental study of stabilizing He-Ne laser output power with transverse magnetic field 03 p0303 N88-11906
Extreme ultraviolet beam-foil spectroscopy of highly ionized neon and argon
[AD-A185197] 05 p0561 N88-13418

Equation of state of solid neon from X-ray diffraction measurements to 110 GPa
[DE88-008723] 19 p2734 N88-26241

NEOPLASMS
NT CANCER
Radon Research Program, FY-1987
[DE88-002633] 09 p1188 N88-17120

NEPAL
SPOT for slope instability survey in Nepal
22 p3105 N88-28441

NEPHANALYSIS
Cloud climatology derived from the AFGWC (Air Force Global Weather Central) 3D-nephanalysis for January and July 1979
[AD-A183686] 01 p0070 N88-10446

NEPTUNE (PLANET)
Electrical conductivity and equation of state measurements on planetary fluids at high pressures and temperatures
[DE87-013787] 01 p0110 N88-10708
A noise-adding radiometer for the Parkes antenna
11 p1473 N88-18788

NEPTUNE ATMOSPHERE
The solar radiation incident at the top of the atmosphere of Uranus and Neptune
[AERONOMICA-ACTA-A-317-1987]
07 p0878 N88-15323

NEPTUNIUM
Atlas of atomic spectral lines of neptunium emitted by an inductively coupled plasma
[DE88-000640] 06 p0782 N88-14796

NERVA (ENGINE)
U NUCLEAR ENGINE FOR ROCKET VEHICLES

NERVES
NT OCULOMOTOR NERVES
Motion and space sickness 04 p0404 N88-12510
Relation between VEP and visual function in lesions of the optic nerve and visual pathway
21 p2983 N88-27718

NERVOUS SYSTEM
NT AUTONOMIC NERVOUS SYSTEM
NT BRAIN
NT CENTRAL NERVOUS SYSTEM
NT CEREBELLUM
NT CEREBRAL CORTEX
NT CEREBRUM
NT EFFERENT NERVOUS SYSTEMS
NT HIPPOCAMPUS
NT HYPOTHALAMUS
NT NERVES
NT OCULOMOTOR NERVES
NT SPINAL CORD
NT SYMPATHETIC NERVOUS SYSTEM
NT THALAMUS
Function-dependent plasticity in the nervous system
07 p0886 N88-15377
Analysis and synthesis of adaptive neural elements
[AD-A187047] 10 p1395 N88-18316
A neuronal model of classical conditioning
[AD-A188378] 12 p1670 N88-19999
A program for the study of skeletal muscle catabolism following physical trauma
[AD-A189771] 15 p2102 N88-22521
Hemostasis parameters of individuals with neurocirculatory dystonia submitted to dry immersion
19 p2703 N88-26072
Interplanetary travel: Is gravity needed to close the loop
[NASA-TM-101013] 22 p3132 N88-28622
New method for the study of spontaneous brain activity
[AD-A193613] 22 p3132 N88-28624

NETHERLANDS
Civil aeronautics
[ETN-88-90616] 05 p0543 N88-13309
Inventory of weather stations. Climatological data from Dutch stations, no. 26
[KNMI-150-26] 05 p0628 N88-13841
National Remote Sensing Program (NRSP) of the Netherlands 08 p1043 N88-16305
Trends in research and development in the Netherlands. The influence of national science policy between 1973 and 1986
[B8701586] 08 p1094 N88-16580
Activities report in civil aeronautics
[ETN-88-91344] 13 p1715 N88-20255
Study of the plan for a national data center for the European Remote Sensing Satellite ERS-1
[BCRS-87-11] 16 p2228 N88-23309
Advice for astronomical research
[ISBN-9-03-460977-4] 16 p2289 N88-23703

NETS
NT NEURAL NETS
NT PETRI NETS
The significance of orientation unknowns in station and net adjustments 11 p1506 N88-18994

NETWORK ANALYSIS
Development of methods for the analysis of the frequency and voltage statics of electricity users and electrical networks
[ETN-87-90412] 01 p0043 N88-10271
Study into a data relay satellite mission analysis tool
[ESA-CR(P)-2422] 02 p0220 N88-11384
Network reconstitution protocol
[AD-A184755] 03 p0367 N88-12309
On real-time systems using local area networks
[AD-A185475] 06 p0694 N88-14256
A note on the partitioning shortest path algorithm
[CWI-OS-R8703] 08 p1067 N88-16451
Approximating the size of a dynamically growing asynchronous distributed network
[AD-A187011] 09 p1152 N88-16899
Calibration of neural networks using genetic algorithms, with application to optimal path planning
09 p1214 N88-17277
Experiments with the back propagation algorithm: A systematic look at a small problem
[RSRE-MEMO-4049] 09 p1224 N88-17340
Air Force Institute of Technology (AFIT) Local Area Network (LAN) performance evaluation model: An analytic model for assessing the impact of changing LAN hardware and software configurations
[AD-A187191] 11 p1469 N88-18764
Photoconductor switch and circuit analysis
[AD-A188168] 11 p1478 N88-18821
Stochastic heuristics in network design: Parameter tuning and performance evaluation
[REPT-87-017] 11 p1541 N88-19210
A computer code for the solution of large scale network reliability analysis problems
[AD-A188455] 12 p1680 N88-20042
An extension of the MS pivoting rule to capacitated network flow problems
[REPT-87-33] 14 p1963 N88-21711
Exact analyses of slotted ring protocols for local area networks with one transmitting station
[MEMO-650] 14 p1967 N88-21737
Instrumentation for the characterization and development of millimeter wave components compatible with monolithic integration
[AD-A189724] 15 p2059 N88-22275
ECP (Electrical Circuitry Program): A proposed program for electrical circuitry analysis
[AD-A190494] 15 p2060 N88-22280
Analysis of microwave burner measurement system using a microwave network analysis computer program
19 p2631 N88-25604
Fault diagnosis in distributed computer networks
[AD-A192406] 19 p2718 N88-26140
Analysis of networks with parameters S: Generalization of junction matrix
[INPE-4535-PRE/1282] 20 p2793 N88-26570
A network approach to the certainty factor model — expert systems
[CWI-CS-R8757] 20 p2840 N88-26852
Some equivalent circuit models for AC impedance analysis of pyrite/solution interface
[DE88-010574] 21 p2939 N88-27452
Automatic line network extraction from aerial imagery of urban areas through knowledge based image analysis
[AD-A193067] 21 p2965 N88-27615
Automatic line network extraction from aerial imagery of urban areas through knowledge-based image analysis
[AD-A192399] 23 p3227 N88-29208
An analysis of heat transfer after loss of primary coolant in the SP-100 reactor system
[AD-A194619] 23 p3281 N88-29539
Performance analysis of k-ary n-cube interconnection networks
[AD-A195542] 24 p3361 N88-30010

NETWORK CONTROL
Design, manufacture and testing of an elegant breadboard model communications processor
[D/2244] 01 p0034 N88-10217
Advanced Information Processing System (AIPS) proof-of-concept system functional requirements I/O network system services
[NASA-CR-181481] 03 p0384 N88-12412
Advanced Information Processing System (AIPS) proof-of-concept system functional design I/O network system services
[NASA-CR-181488] 03 p0384 N88-12413
Multicast gateway design considerations
[PB87-219960] 04 p0430 N88-12663
Survey on large scale system control methods
[NASA-CR-181556] 05 p0554 N88-13374
An analysis of simplified feed architectures for MMIC (Monolithic Microwave Integrated Circuit) T/R (Transmit/Receive) module arrays
[AD-A185474] 06 p0697 N88-14275
A new library of CAMAC routines for the control of the system CRATE by a microVAX in the VAXELN environment
[NOTA-INTERNA-893] 06 p0761 N88-14667
Channel access protocols for multihop packet radio networks
[AD-A186074] 07 p0842 N88-15105
Throughput analysis of a flow-contoured communication network with buffer space limitations
[CWI-OS-R8702] 08 p0977 N88-15908
Waiting times in discrete-time cyclic-service systems — communication networks
[CWI-OS-R8707] 08 p0977 N88-15909
Knowledge-based system analysis and control
[AD-A188163] 12 p1681 N88-20049
Sojourn times in feedback queues
[CWI-OS-R8710] 13 p1830 N88-20947
Two queues with alternating service and switching times
[CWI-OS-R8712] 13 p1831 N88-20949
Deadlock-free message routing in processor networks
[CS-8706] 14 p1960 N88-21691
Impact of blocking policies in closed, exponential and symmetrical ring networks
[FUB-8-1986] 14 p1960 N88-21693
Passive coupler, network adapter, and network acquisition procedure for optical local networks
[ETN-88-92130] 14 p1961 N88-21695
Exact analyses of slotted ring protocols for local area networks with one transmitting station
[MEMO-650] 14 p1967 N88-21737
Implementation of a distributed adaptive routing algorithm on the Intel iPSC (Intel Personal Super-Computer)
[AD-A189849] 15 p2109 N88-22567
Software structuring principles for VLSI CAD
[AD-A190386] 15 p2112 N88-22579
Problems in integrated networks
[AD-A191391] 16 p2191 N88-23069
Reasoning about networks with many identical finite-state processes
[AD-A188743] 16 p2245 N88-23413
Distributed matchmaking
[CWI-CS-R8750] 16 p2254 N88-23467
Modeling, filtering and control of stochastic processes — communication networks
[ENST-87E021] 17 p2333 N88-23925
The MELMUX MX-7100 series high-speed digital multiplexers 21 p2930 N88-27396
Optimum-Path-to-Go guidance of command adjusted trajectory projectiles
[AD-A193377] 22 p3040 N88-28051
Experiments applications guide: Advanced Communications Technology Satellite (ACTS)
[NASA-TM-100265] 22 p3048 N88-28082
Design of a self-timed VLSI multicomputer communication controller
[AD-A194567] 24 p3361 N88-30014

NETWORK SYNTHESIS
Synthesizing controllers for uncertain systems by a quantitative pole-placement
[PB87-195590] 02 p0223 N88-11403

NEUMANN PROBLEM
IMPSOR: A fully vectorized FORTRAN code for three dimensional moving boundary problems with Dirichlet or Neumann boundary conditions
[DE87-014964] 02 p0226 N88-11427
Diffraction of sound at junction of two waveguides
08 p1076 N88-16491
On an overdetermined Neumann problem
[AD-A187451] 10 p1401 N88-18352
A note on the analyticity of the Neumann Kernel and an associated quadrature problem in two-dimensional boundary element methods
[ETN-88-92054] 14 p1964 N88-21719
On a class of functionals invariant under a Z(sup n) action
[AD-A193474] 23 p3269 N88-29451

NEURAL NETS
General potential surfaces and neural networks
[AD-A184484] 03 p0367 N88-12311
A survey of artificial neural systems
[AD-A184759] 03 p0368 N88-12312
Large-scale neuronal circuits for selective storage and recognition of complex stimuli, a pilot study
[AD-A184134] 04 p0474 N88-12920
Dynamics, control and sensor issues pertinent to robotic hands for the EVA retriever system
06 p0796 N88-14876
Improved input representation for enhancement of neural network performance
[DE88-001830] 07 p0907 N88-15496
Neural network based speech synthesizer: A preliminary report 08 p1064 N88-16429
The power of neural nets 08 p1064 N88-16430

Neural networks as a possible architecture for the distributed control of space systems
08 p1064 N88-16431
Long term synaptic plasticity and learning in neuronal networks
[AD-A186834] 09 p1199 N88-17188
Probabilistic neural networks: In or out of equilibrium
[DE88-002907] 09 p1201 N88-17198
First Annual Workshop on Space Operations Automation and Robotics (SOAR 87)
[NASA-CP-2491] 09 p1203 N88-17206
Neural network based architectures for aerospace applications 09 p1204 N88-17218
NASA JSC neural network survey results
09 p1205 N88-17220
Design of a neural network simulator on a transputer array 09 p1205 N88-17221
Teaching artificial neural systems to drive: Manual training techniques for autonomous systems
09 p1207 N88-17238
Calibration of neural networks using genetic algorithms, with application to optimal path planning
09 p1214 N88-17277
Experiments with the back propagation algorithm: A systematic look at a small problem
[RSRE-MEMO-4049] 09 p1224 N88-17340
Introduction to a system for implementing neural net connections on SIMD architectures
[NASA-CR-181612] 10 p1386 N88-18279
Orthogonal patterns in binary neural networks
[NASA-TM-100060] 10 p1396 N88-18320
Automated radar target recognition based on models of neural nets 11 p1476 N88-18804
Center for the study of rhythmic processes
[AD-A188204] 11 p1520 N88-19078
Optical computing research
[AD-A187862] 11 p1549 N88-19264
Neurocognitive predictions of performance
[AD-A188323] 12 p1669 N88-19998
A neuronal model of classical conditioning
[AD-A188378] 12 p1670 N88-19999
A Darwinian approach to artificial neural systems
[DE87-013184] 13 p1824 N88-20900
Adaptive neural network architecture
[AD-A190114] 15 p2104 N88-22533
Instrumentation for scientific computing in neural networks, information science, artificial intelligence and applied mathematics
[AD-A189981] 15 p2106 N88-22549
Optical Conceptual Computing and Associative Memory (OCCAM)
[AD-A190030] 15 p2107 N88-22550
Rapid feature extraction via the radon transform
[AD-A190032] 15 p2110 N88-22573
Artificial neural networks: An introduction with an annotated bibliography
[DE88-007003] 15 p2116 N88-22603
Nonlinear signal processing using neural networks: Prediction and system modelling
[DE88-006479] 15 p2118 N88-22621
Genetic algorithms for adaptive real-time control in space systems 17 p2388 N88-24195
The efficacy of using human myoelectric signals to control the limbs of robots in space
[NASA-CR-182901] 18 p2553 N88-25155
A concurrent neural network algorithm for the traveling salesman problem
[DE88-006981] 18 p2562 N88-25208
Theoretical investigation of optical computing based on neural network models
[AD-A191668] 18 p2563 N88-25214
Optical computing based on neuronal models
[AD-A191481] 18 p2575 N88-25293
Generalization and the backward propagation neural network
[AD-A191634] 19 p2710 N88-26100
An extension of the Hopfield-Tank model for solution of the multiple traveling salesmen problem
[DE88-008377] 19 p2715 N88-26122
A linear-programming method inspired by the neural networks framework
[DE88-008688] 20 p2842 N88-26862
Basic research on optical neural computers
21 p2929 N88-27389
Content-addressable memory storage by neural networks: A general model and global Liapunov method
[AD-A192716] 21 p3002 N88-27807
Neural network research: A personal perspective
[AD-A192717] 21 p3003 N88-27808
A virtual statistical mechanical neural computer
[AD-A193962] 22 p3139 N88-28660
Survey of neural net paradigms for specification of discrete networks
[AD-A192682] 22 p3141 N88-28674
Analysis of the hopfield neural networks and their application to pattern recognition
[AD-A193827] 23 p3239 N88-29279
Design of a feeling-thinking machine
[AD-A194107] 23 p3267 N88-29448
Circuit design criteria for stable lateral inhibition neural networks
[AD-A195066] 24 p3366 N88-30046
Autonomous image data reduction by analysis and interpretation 24 p3418 N88-30347
Parallel and distributed computation for fault-tolerant object recognition 24 p3419 N88-30350
Nested neural networks
[NASA-TM-101032] 24 p3423 N88-30373

NEUROLOGY
Neurochemical changes in hibernation
08 p1046 N88-16322
Molecular mechanisms of neuronal responsivity
[AD-A187061] 09 p1199 N88-17185
Three-dimensional computer graphics brain-mapping project
[AD-A187202] 11 p1528 N88-19126
Direct interaction between autonomic nerves and the immune system
[AD-A188576] 12 p1667 N88-19991
Neurocognitive predictions of performance
[AD-A188323] 12 p1669 N88-19998
Computing with structured connections networks
[AD-A189244] 13 p1821 N88-20886
Normative developmental equations for the EEG and their sensitivity to neurological and psychiatric disorders
21 p2977 N88-27687
Models of cerebral-body perfusion and cerebral chemical transport
[AD-A194945] 24 p3407 N88-30283
Central adrenergic receptors as mediators of central response to stress: Study with Positron Emission Tomography (PET)
[AD-A194947] 24 p3407 N88-30284

NEUROMUSCULAR TRANSMISSION
Biophysical and biochemical mechanisms in synaptic transmitter release
[AD-A187059] 09 p1199 N88-17184
Long term synaptic plasticity and learning in neuronal networks
[AD-A186834] 09 p1199 N88-17188
Facilitory effects of voluntary movements on vestibulomotor reaction 12 p1664 N88-19976
Evaluation of the endogenous glucocorticoid hypothesis of denervation atrophy
[NASA-CR-182848] 17 p2381 N88-24157
A systems engineering based methodology for analyzing human electrocortical responses
[AD-A190809] 18 p2550 N88-25135
The VITE model: A neutral command circuit for a generating arm and articulator trajectories
[AD-A192715] 21 p2987 N88-27734

NEURON TRANSMISSION
U BIOELECTRICITY

NEURONS
Function-dependent plasticity in the nervous system
07 p0886 N88-15377
Karyometric evaluation of neuronal reactions of rat cerebral cortex to the combined effect of ionizing radiation, longitudinal accelerations and vibration
07 p0890 N88-15396
Molecular mechanisms of neuronal responsivity
[AD-A187061] 09 p1199 N88-17185
Analysis and synthesis of adaptive neural elements
[AD-A187047] 10 p1395 N88-18316
Center for nonlinear dynamics of the brain
[AD-A187245] 11 p1518 N88-19068
Synapses that compute motion
[AD-A190389] 15 p2116 N88-22607

NEUROPHYSIOLOGY
Functional plasticity of the nervous system of vertebrates 01 p0074 N88-10474
Visual evoked responses to sinusoidal gratings presented in central and right visual fields: 1
[DE87-014731] 04 p0473 N88-12919
Large-scale neuronal circuits for selective storage and recognition of complex stimuli, a pilot study
[AD-A184134] 04 p0474 N88-12920
Neurophysiological analysis of hypothalamic regulation mechanisms of primary sleep and hypobiosis
06 p0751 N88-14611
Functional development of gravity receptors in insects and amphibians 07 p0886 N88-15376
The filtering problem for infinite dimensional stochastic processes
[AD-A186431] 07 p0916 N88-15562
Molecular mechanisms of neuronal responsivity
[AD-A187061] 09 p1199 N88-17185
Long term synaptic plasticity and learning in neuronal networks
[AD-A186834] 09 p1199 N88-17188
Neuro-reflex mechanisms of circulation regulation in simulated microgravity 12 p1656 N88-19923
Vestibular integrated function and microgravity
12 p1658 N88-19937
Synopsis of the Spacelab D-1 frog statolith experiment STATEX 12 p1659 N88-19940
A neuronal model of classical conditioning
[AD-A188378] 12 p1670 N88-19999
Complex sound processing: An interdisciplinary approach
[AD-A189782] 15 p2102 N88-22523
Neurophysiological predictors of quality of performance 16 p2242 N88-23391
Electric and Magnetic Activity of the Central Nervous System: Research and Clinical Applications in Aerospace Medicine
[AGARD-CP-432] 21 p2977 N88-27683
Fourth generation neurocognitive pattern analysis system 21 p2977 N88-27686
Neurophysiological patterns of operational fatigue: Preliminary results 21 p2981 N88-27703
Neurophysiological precursors of accurate visuomotor performance 21 p2981 N88-27706
The neuroelectric selection of Naval aviation personnel: An evaluation 21 p2981 N88-27707
Electroencephalographic correlates of pilot performance: Simulation and in-flight studies
21 p2982 N88-27711
Spontaneous cerebral electrical activity during prolonged hypoglycemia: A quantitative study in humans
21 p2983 N88-27717
Relation between VEP and visual function in lesions of the optic nerve and visual pathway
21 p2983 N88-27718
Models for motion perception
22 p3133 N88-28629
Comparative aspects of multiple processes of attention
[AD-A195805] 24 p3408 N88-30291

NEUROPSYCHIATRY
Attention, effort, and fatigue: Neuropsychological perspectives 16 p2241 N88-23387

NEUROSCIENCE
U NEUROLOGY

NEUROTRANSMITTERS
Large-scale neuronal circuits for selective storage and recognition of complex stimuli, a pilot study
[AD-A184134] 04 p0474 N88-12920
Neurohumoral aspects of sleep
[AD-A188653] 12 p1667 N88-19992

NEUTRAL ATOMS
Improvement of energy confinement of neutral beam heated plasma by lower hybrid current drive in JT-60
[DE87-752983] 02 p0239 N88-11509
Ro-vibrational laser spectroscopy of ESD neutrals from chemisorbed species
[DE87-013011] 04 p0447 N88-12770
Forces on neutral atoms due to electromagnetic fields
[AD-A187461] 10 p1408 N88-18396
Magnetic trapping of neutral atoms
[AD-A188473] 12 p1689 N88-20103
Optical trapping of neutral atoms and dielectric particles by radiation pressure 14 p1974 N88-21783
Electromagnetic manipulation of atomic hydrogen
16 p2268 N88-23568
Corpuscular plasma diagnostics complex on a tokamak with a strong field
[DE88-701576] 16 p2279 N88-23646
Flux density measurements of neutral iron in TEXTOR with laser induced fluorescence
17 p2442 N88-24528

NEUTRAL BEAMS
NT MOLECULAR BEAMS
NT NEUTRON BEAMS
Improvement of energy confinement of neutral beam heated plasma by lower hybrid current drive in JT-60
[DE87-752983] 02 p0239 N88-11509
Applications of neutral beam and rf technologies
[DE87-014936] 03 p0379 N88-12382
TIBER 2 (Tokamak Ignition/Burn Experimental Reactor) parameters with neutral beams at high energies
[DE88-001891] 06 p0783 N88-14803
A calorimeter for measuring the neutral beam power reaching the plasma
[DE88-001412] 07 p0937 N88-15691
Design considerations for a negative ion source for DC operation of high-power, multi-megaelectron-volt neutral beams
[DE88-002692] 08 p1083 N88-16525
Benchmarks of neutral beam injection codes for stellarators
[DE88-003786] 10 p1412 N88-18428
Neutral beam propagation through the atmosphere
[AD-A188984] 12 p1691 N88-20115

A segmented calorimeter for low-energy particle beams in space
[DE88-001806] 13 p1838 N88-20997
Power source selection for neutral particle beam systems 17 p2407 N88-24314
Ion temperature profile measurement using charge exchange recombination spectroscopy on JIPP T-IIU 17 p2440 N88-24518
Spectroscopic measurements of ion temperature, rotation speed and beam deposition profile on DIII-D 17 p2440 N88-24519
Arcing and rf signal generation during target irradiation by a high-energy, pulsed neutral particle beam
[DE88-007169] 18 p2471 N88-24664
Propagation of neutralized ion beams
[AD-A191599] 18 p2574 N88-25289
Requirements for neutral beam current drive in tokamaks
[DE88-006180] 20 p2859 N88-26980

NEUTRAL BUOYANCY SIMULATION
Structural Assembly Demonstration Experiment (SADE)
[NASA-CR-179205] 02 p0138 N88-10868
Research and development at the Marshall Space Flight Center Neutral Buoyancy Simulator 02 p0139 N88-10878
EASE (Experimental Assembly of Structures in EVA) overview of selected results 02 p0140 N88-10881

NEUTRAL CURRENTS
Determination of the neutral current chiral coupling constants u sub1sq, u subrsq, d sub1sq and d subrsq from an (anti)neutrino-deuterium experiment
[B8715857] 06 p0779 N88-14780

NEUTRAL GASES
Design study for measurement of neutral hydrogen atom density by laser induced fluorescence method
[DE87-752964] 02 p0179 N88-11114
Kinematics and dynamics of barred spiral galaxies 03 p0388 N88-12440
Upper-thermospheric observations and neutral-gas dynamics at high latitudes during solar maximum
[AD-A188058] 11 p1512 N88-19031
Distribution of neutral gas molecules at large distances from Halley's comet 14 p1999 N88-21914
A model of the anisotropic structure of the neutral gas coma of a comet 14 p1999 N88-21918

NEUTRAL PARTICLES
NT FAST NEUTRONS
NT NEUTRONS
NT SOLAR NEUTRONS
NT THERMAL NEUTRONS
Neutral environment for space station 18 p2590 N88-25391
Space station neutral external environment 18 p2590 N88-25392

NEUTRAL SHEETS
The solar wind 03 p0271 N88-11705
Hot plasmas in the Earth's magnetosphere 03 p0272 N88-11710
Influence of viscosity on the structure of a magnetic neutral layer 06 p1098 N88-16605
A quadratic-form analysis of the collisionless tearing mode
[AD-A188886] 12 p1695 N88-20144

NEUTRALIZERS
Products of the neutralization of hydrazine fuels with hypochlorite, 2
[DE87-011454] 01 p0030 N88-10193
Photodetachment neutralizer development: Laser window design study. Volume 2: Window design details
[DE88-000783] 09 p1170 N88-17014
Plasma neutralizer work at BNL (Brookhaven National Laboratory)
[DE88-007046] 18 p2579 N88-25317

NEUTRINO BEAMS
Wrong helicity events induced by the CERN-SPS wide band muonic (anti)neutrino beam
[NIKHEF-H/87-2] 06 p0779 N88-14779
Determination of the neutral current chiral coupling constants u sub1sq, u subrsq, d sub1sq and d subrsq from an (anti)neutrino-deuterium experiment
[B8715857] 06 p0779 N88-14780

NEUTRINOS
NT SOLAR NEUTRINOS
Summary and conclusions of the 6th Moriond workshop — standard electroweak model
[USIP-87-11] 01 p0092 N88-10602
Quantification of the background signal to solar neutrino detection from cosmogenic activation of the atmosphere
[DE87-013830] 01 p0119 N88-10762
Neutrinos in supernovae
[DE87-014295] 03 p0387 N88-12434
A theoretical model for neutrino masses and mixing
[PREPRINT-553] 06 p0778 N88-14777
Event classification in (anti)neutrino experiments using an Internal Picket Fence-External Muon Identifier (IPF-EMI) detector system
[NIKHEF-H/87-6] 09 p1245 N88-17457
Oscillations of solar models with internal element diffusion
[DE88-003156] 09 p1264 N88-17573
A research program in neutrino physics, cosmic rays and elementary particles
[DE88-003507] 09 p1264 N88-17575
A look at Supernova 1987A
[DE88-003411] 10 p1429 N88-18531
Neutrino magnetic moment and time variation of solar neutrino flux
[DE88-700687] 10 p1430 N88-18542
Intermediate energy neutrino physics
[DE88-005378] 13 p1836 N88-20984
Strange, quark and metastable neutron stars
[DE88-702404] 21 p3030 N88-27984
Neutrino detection primer
[AD-A193805] 23 p3280 N88-29529
On neutrino fields in Einstein-Cartan theory
[MATH-REPT-208] 23 p3295 N88-29629

NEUTRON ABSORBERS
Fabrication of lithium hydride shields for space nuclear power systems 17 p2402 N88-24282

NEUTRON ACTIVATION ANALYSIS
Cryogenic cell — neutron borehole logging
[GB-PATENT-2-139-745-A] 01 p0048 N88-10308
Characterization of yttrium aluminum garnet/YAG/using 14 MeV neutron activation
[AD-A191925] 18 p2582 N88-25342

NEUTRON BEAMS
A layered scintillation detector for solar neutron observations
[DE87-011354] 01 p0049 N88-10314
Multilayer monochromators for neutron spectrometers
[DE87-014291] 02 p0175 N88-11093
Interaction of slow neutrons with Ge74 single crystals
[DE87-703010] 17 p2445 N88-24536
Tracking a monochromatic light source
[DE88-011260] 20 p2807 N88-26853

NEUTRON COUNTERS
NT NEUTRON SPECTROMETERS
A layered scintillation detector for solar neutron observations
[DE87-011354] 01 p0049 N88-10314
Probable detection of solar neutrons by ground-level neutron monitors during STIP interval 16 01 p0111 N88-10715
A neutron detector based on microchannel plates
[DE87-014703] 02 p0232 N88-11466
Cosmic ray NM-64 neutron monitor data 14, Rome, Italy, January - December 1985
[IFSI-87-8] 05 p0661 N88-14060
Rome Neutron Monitor (NM) - 64 data for 5 solar particle ground-level events
[IFSI-86-7] 06 p0806 N88-14918
Properties of nuclei and elementary particles at low and intermediate energies
[DE88-001913] 09 p1244 N88-17456
A combined cosmic ray muon spectrometer and high energy air shower array
[DE88-003057] 09 p1264 N88-17574

NEUTRON CROSS SECTIONS
Computer programs for calculating group cross-section covariances from uncertainty parameters in the ENDF/B-V format. UNC 32/33 — neutron physics
[ECN-202] 13 p1837 N88-20995
Systematics on neutron-induced isomeric cross-section ratios at 14.5 MeV
[ECN-200] 14 p1980 N88-21815
Effects of space-dependent cross sections on core physics parameters for compact fast spectrum space power reactors 17 p2399 N88-24263
Nucleon-nucleus interaction data base: Total nuclear and absorption cross sections
[NASA-TM-4053] 20 p2852 N88-26935

NEUTRON DECAY
Measurement of Beta-decay energies of short-lived neutron-rich nuclei in the vicinity of mass number between 101 and 106, and A = 109
[ETN-88-92376] 21 p3014 N88-27890

NEUTRON DETECTORS
U NEUTRON COUNTERS

NEUTRON DIFFRACTION
Characterization of the dimensions of colloidal calcium carbonate dispersions in toluene with neutron small-angle scattering
[ECN-197] 06 p0680 N88-14167
Nondestructive characterization of ceramic composite whiskers with neutron diffraction and ultrasonic techniques
[DE88-003075] 08 p0965 N88-15844
High-temperature charge-density studies of CeO/sub 2-x/ using X-ray and neutron diffraction techniques
[DE88-002988] 09 p1257 N88-17536
Magnetic rare earth superlattices
[DE88-003483] 10 p1418 N88-18465
Single-crystal structural study of La2Cu/sub 0.95/Li/sub 0.05/O4
[DE88-003482] 11 p1554 N88-19302
The structural analysis of some crystalline and semi-crystalline substances using X-ray and neutron diffraction 17 p2445 N88-24540
Neutron diffraction refinement of CsHSO4 superionic phase structure
[DE88-701496] 18 p2580 N88-25326
Structural studies on La/sub 2/CuO/sub 4+delta/
[DE88-006828] 18 p2581 N88-25330
Structural and magnetic properties of Fe impurities in YBa2Cu3O(sub 7-delta)
[DE88-009961] 19 p2735 N88-26247
Observations on residual stresses in ceramic composites by neutron diffraction techniques
[DE88-009937] 20 p2778 N88-26472

NEUTRON EMISSION
Probable detection of solar neutrons by ground-level neutron monitors during STIP interval 16 01 p0111 N88-10715
Solar-geophysical data number 514, June 1987. Part 1: (Prompt reports). Data for May 1987, April 1987 and late data
[PB87-217261] 02 p0257 N88-11626
Properties of hydrogen/helium accretion plasmas
[DE88-006831] 19 p2728 N88-26197

NEUTRON FLUX
U FLUX (RATE)

NEUTRON FLUX DENSITY
Application of the reactivity constraint approach to the transient control of spacecraft reactors 17 p2406 N88-24305

NEUTRON IRRADIATION
Computed neutron tomography and coded aperture holography from real time neutron images 04 p0427 N88-12645
The effect of neutron irradiation on the tensile properties and microstructure of several vanadium alloys
[DE88-001755] 06 p0682 N88-14176
Experimental method for investigating helium effects in irradiated vanadium
[DE88-002891] 08 p0969 N88-15865
A report on the effects of neutron irradiation of GaAs semiconductors
[AD-A186816] 09 p1253 N88-17510
Response of Fe-Cr-Mn austenitic alloys to thermal aging neutron irradiation
[DE88-003415] 10 p1302 N88-17785
Influence of neutron irradiation on the Charpy impact properties of V-15Cr-5Ti
[DE88-003430] 11 p1458 N88-18692
Effects of high temperature neutron irradiation on the physical, chemical and mechanical properties of fine-grained isotropic graphite 13 p1747 N88-20444
Degradations of thermal shock resistance and the fracture toughness of reactor graphite subjected to neutron irradiation 13 p1747 N88-20445
Anthropomorphic phantom radiation dosimetry at the NATO standard reference point at Aberdeen Proving Ground
[AD-A190508] 15 p2103 N88-22528
Material tradeoffs to minimize flooding reactivity 17 p2399 N88-24265
Neutron radiation tolerance of Au-activated silicon 17 p2408 N88-24316
Defects in cubic silicon carbide on silicon 17 p2408 N88-24317
Point defects in irradiated silicates 17 p2408 N88-24319
MMW shielding design and analysis 17 p2430 N88-24457
Neutron effects on the electrical and switching characteristics of NPN bipolar power transistors 17 p2431 N88-24463
Development of refractory thermocouples for space nuclear power tests 17 p2434 N88-24478
Effect of neutron irradiation on critical magnetization current in single crystal YBa2Cu3O(sub 7-delta)
[DE88-009970] 22 p3156 N88-28775

NEUTRON PHYSICS
A model for stationary and dynamic impression of undercooled boiling in coupled thermohydraulic and neutron physics calculations of nuclear reactors
[IKE-6-171] 09 p1247 N88-17472
Systematics on neutron-induced isomeric cross-section ratios at 14.5 MeV
[ECN-200] 14 p1980 N88-21815

NEUTRON RADIOGRAPHY
Computed neutron tomography and coded aperture holography from real time neutron images
04 p0427 N88-12645

NEUTRON SCATTERING
Applications and limitations of deuterium labeling methods to neutron scattering studies of polymers
[DE87-012936] 02 p0151 N88-10945
Small-Angle Neutron Scattering (SANS) from polymers and colloids
[DE87-013548] 02 p0151 N88-10946
Applied nuclear science research and development
[LA-10915-PR] 03 p0374 N88-12355
Theory of neutron scattering experiments on momentum distributions in quantum fluids
[DE87-01369] 05 p0648 N88-13968
Characterization of the dimensions of colloidal calcium carbonate dispersions in toluene with neutron small-angle scattering
[ECN-197] 06 p0680 N88-14167
Characterization of duplex stainless steel by TEM (Transmission Electron Microscopy), SANS (Small-Angle Neutron Scattering) and APFIM (Atom-Probe Field Ion Microscopy) techniques
[DE88-002916] 09 p1145 N88-16865
Neutron- and X-ray-small angle scattering with Fe-base metallic glasses
[DE88-002538] 09 p1147 N88-16876
Neutron and X-ray scattering studies of layered solids
09 p1246 N88-17469
Structural analysis using X-ray scattering and neutron scattering on binary amorphous (Co,Cu)Ti alloys
[ETN-88-91487] 11 p1459 N88-18699
Determination of the equilibrium concentration of characteristic defects by the measurement of thermal expansion using neutron scattering and laser interferometry
[ETN-88-91489] 11 p1490 N88-18890
Theory of neutron moisture probes and interpretation of measurements in complex soil and water systems
17 p2342 N88-23965
Comparison between muon spin rotation and neutron scattering studies on the 3-dimensional magnetic ordering of La2CuO(4-y)
17 p2396 N88-24244
Calculation of far infrared absorption in B poly(dA).poly(dT)
[AD-A193128] 21 p2918 N88-27318

NEUTRON SPECTRA
Effects of the neutron spectrum on mechanical property changes in low dose irradiations
[DE88-003429] 10 p1302 N88-17786
Computer programs for calculating group cross-section covariances from uncertainty parameters in the ENDF/B-V format. UNC 32/33 --- neutron physics
[ECN-202] 13 p1837 N88-20995
Systematics on neutron-induced isomeric cross-section ratios at 14.5 MeV
[ECN-200] 14 p1980 N88-21815
The development of KENO and the calculation of differential parameters with KENO
[DE88-006176] 18 p2555 N88-25166

NEUTRON SPECTROMETERS
Multilayer monochromators for neutron spectrometers
[DE87-014291] 02 p0175 N88-11093
Investigation of the evolution of the fusion processes in the plasma focus using time-resolved neutron spectroscopy
[IPF-87-4] 09 p1251 N88-17493
Gamma-ray/neutron spectroscopy from the Mars observer
23 p3302 N88-29671

NEUTRON STARS
NT PULSARS
Neutrinos in supernovae
[DE87-014295] 03 p0387 N88-12434
Core bounce supernovae
[DE87-014910] 04 p0520 N88-13197
Neutron stars observations as astrophysical probes
06 p0800 N88-14896
EXOSAT guest observer program. Binary parameters of the X-ray Pulsar 4U1626-67
[NASA-CR-182374] 06 p0802 N88-14905
HEAO-1 observations of gamma-ray bursts
07 p0947 N88-15756
Stellar energy loss and anomalous contributions to the (photon photon) (neutrino antineutrino) interaction
[DE88-700618] 10 p1428 N88-18529
Hadron-quark phase transition in dense stars
[DE88-003412] 10 p1429 N88-18532
Photohydrodynamical processes near compact objects
11 p1569 N88-19390
Thermal radiation from neutron stars
[MPE-203] 11 p1571 N88-19404
Generation and propagation of sound waves in a collapsing or anti-collapsing star with uniform density
[DE87-703034] 15 p2151 N88-22839
Quark core stars, quark stars and strange stars
[DE88-006991] 17 p2450 N88-24555
A model for the X-ray binary 4U1820-30
[NASA-TM-101143] 17 p2451 N88-24562
Spectral modelling of the soft gamma ray repeater
[DE88-007027] 17 p2453 N88-24570
Nuclear and astrophysical evidence on the equation of state
[DE88-007397] 18 p2572 N88-25279
Heavy ion collisions with A = 10(sup 57): Aspects of nuclear stability and the nuclear equation of state in coalescing neutron-star binary systems
[DE88-008029] 19 p2741 N88-26277
Detection of absorption lines in the spectra of X-ray bursts from X1608-52
[ISAS-RN-360] 20 p2887 N88-27143
Strange, quark and metastable neutron stars
[DE88-702404] 21 p3030 N88-27984
EXOSAT observations of Hercules X-1
[MPE-PREPRINT-119] 22 p3164 N88-28841
On the origin of gamma ray bursts
[MPE-PREPRINT-120] 22 p3166 N88-28855

NEUTRON TRANSMUTATION
U NUCLEAR REACTIONS

NEUTRONS
NT FAST NEUTRONS
NT SOLAR NEUTRONS
NT THERMAL NEUTRONS
TRISTAN research on neutron rich nuclei: Magnetic moments and nuclear structure
[DE88-002122] 06 p0783 N88-14807
New nuclear structure calculations and the astrophysical r-process
[DE88-000979] 08 p1082 N88-16518
Two-dimensional analysis for a scrapeoff and divertor regions with an MHD model. Conceptual design study of FY86 FER
[DE88-751069] 09 p1251 N88-17497
The effects of low doses of 14 MeV neutrons on the tensile properties of three binary copper alloys
[DE88-003400] 11 p1458 N88-18691
Emission of gamma rays from various materials pulsed with 14-MeV neutrons
[DE88-003837] 11 p1544 N88-19227
Symmetry problems in particle physics
[DE88-004927] 12 p1688 N88-20099
Reference nuclear data for space applications
[DE88-007041] 16 p2270 N88-23583
Stability requirement FOT ignition and high gain implosion = 2-D simulation for high neutron yield experiment =
16 p2278 N88-23633
Observation of ferromagnetism in ultrathin f.c.c. films by spin polarised neutron reflection
20 p2865 N88-27015

NEVADA
Delineation of ephemeral fluvial networks on low-relief Piedmont surfaces, Plutonium Valley, Nevada, USA
22 p3093 N88-28367
The application of SPOT data to the structural geology of western Nevada
22 p3102 N88-28423
The dynamics of transuranics and other radionuclides in natural environments, December 1985
[DE87-014456] 24 p3390 N88-30189

NEW ENGLAND (US)
NOAA's (National Oceanic and Atmospheric Administration's) Northeast Monitoring Program (NEMP): A report on progress of the first five years (1979-84) and a plan for the future
[PB87-210100] 02 p0196 N88-11225

NEW MEXICO
Transactions of the Fifth Symposium on Space Nuclear Power Systems
[DE88-006165] 17 p2417 N88-24374

NEW YORK
New York TRACON demonstration of program recoding requirements analysis document
[DOT/FAA/CT-87/34] 18 p2462 N88-24622

NEW ZEALAND
Numerical simulation of the flow about New Zealand
08 p1017 N88-16163
Wind energy resource survey of New Zealand: National resource assessment
[PB88-139365] 12 p1640 N88-19822
Systems approach to energy quality and efficiency
[PB88-139506] 12 p1640 N88-19823
Ozonesonde observations at Lauder, New Zealand during the Spring and early Summer of 1986
[PB88-173273] 16 p2232 N88-23328

NEWTON METHODS
NT NEWTON-RAPHSON METHOD
Computational behavior of Gauss-Newton methods
[DE87-014486] 02 p0224 N88-11413
A tool for the analysis of quasi-Newton methods with application to unconstrained minimization
[DE88-005783] 11 p1532 N88-19153
Some numerical methods for the computation of capillary free boundaries governed by the Navier-Stokes equations
[REPT-87-69] 16 p2206 N88-23167
High degree interpolation polynomial in Newton form
[NASA-CR-181677] 18 p2567 N88-25249
Parallel quasi-Newton methods for unconstrained optimization
[AD-A193250] 21 p3003 N88-27812
Optimisation algorithms for highly parallel computer architectures. The performance of the truncated Newton, conjugate gradient algorithm in FORTRAN and Ada
[AD-A193940] 23 p3265 N88-29435
Generating semi-Gaussian two dimensional quadrature rules
[REPT-205] 23 p3272 N88-29476

NEWTON SECOND LAW
A comparative survey of mathematical models for dynamic simulation of in-orbit manipulation operations
12 p1592 N88-19533

NEWTON THEORY
Some considerations on measuring the Newtonian gravitational constant G in an orbiting laboratory
07 p0922 N88-15603
Post-Newtonian equations of motion in an expanding universe
[DE88-750303] 07 p0945 N88-15744
Non-Newtonian gravity or gravity anomalies?
[NASA-TM-4030] 17 p2374 N88-24118
Transcending Newton's legacy
[DE88-010784] 19 p2738 N88-26254

NEWTON-RAPHSON METHOD
Efficient numerical techniques for complex fluid flows
02 p0185 N88-11151
Computational behavior of Gauss-Newton methods
[DE87-014486] 02 p0224 N88-11413
Numerical methods in the resolution of control electrovalve model
[INPE-4154-RPE/540] 13 p1764 N88-20554
An analytical investigation of geared system dynamics containing spur and helical gears
22 p3085 N88-28317
Rational Newton algorithms to compute formal solutions of linear differential equations in an irregular singular point
[RR-704-M] 22 p3140 N88-28670

NEWTONIAN FLUIDS
Review of the equations of fluid mechanics and heat transfer
08 p0986 N88-15970
Boundary effects on the drag of a cylinder in axial motion at low Reynolds number
13 p1768 N88-20578
Extrema principles of entrophy production and energy dissipation in fluid mechanics
[NASA-TM-100992] 18 p2519 N88-24946
A computer model for the flow of a molten polymer in a narrow cavity
[NPL-DMA(A)-157] 22 p3058 N88-28146

NICKEL
A simulation study of interfaces in Ni, Al and Ni3Al with and without boron
[DE87-013156] 01 p0102 N88-10667
The water permeability of multi-layer coatings
[BLL-M-37252-(5828.4)] 02 p0148 N88-10927
Low-pressure eutectic bonding of depleted uranium to copper
[DE87-014625] 02 p0181 N88-11128
Constitutive modeling for isotropic materials
02 p0188 N88-11171
Kinetics of CO adsorption on nickel using time resolved vibration spectroscopy
[ETN-87-90615] 03 p0289 N88-11814
Wear of iron and nickel in corrosive liquid environments
[NASA-TM-100246] 03 p0289 N88-11817
Studies on estimation of nickel in zinc base die casting by D.C. polarography
[PD-MT-8729] 04 p0417 N88-12588
Moessbauer study of shock induced effects in the Fe-Ni 50/50 ordered alloy in meteorites
[DE87-703364] 04 p0521 N88-13199
The mechanism by which sigma-phase forms in Fe-Cr-Ni system alloys
[BLL-M-37380-(5828.4)] 05 p0564 N88-13437
Advances in processing techniques for nickel aluminides
[DE87-014571] 05 p0566 N88-13449
Contrast between the chemical, structural and electronic properties of thin films of Cu and Ni on the Ru(0001) surface
[DE88-002360] 07 p0938 N88-15698
TiN coatings on M2 steel produced by plasma assisted chemical vapor deposition
[DE88-003189] 08 p0970 N88-15867
Study on the fracture behavior of 9 percent Ni steel welded joint
[PB87-143863] 08 p0995 N88-16023

Dynamic recrystallization during high temperature low cycle fatigue of nickel
[DE88-003224] 10 p1302 N88-17788
Effects of ion implantation on cavitation erosion of a cobalt based metal/carbide alloy
[AD-A187239] 10 p1303 N88-17793
Growth and electronic properties of strained metal overlayers
[DE87-010956] 10 p1417 N88-18463
Studies of the electron spectrum with reference to the clean surfaces of iron, cobalt and nickel and their subsequent exposure to oxygen
11 p1459 N88-18700
The effect of microstructure on the fatigue crack growth resistance of nickel base superalloys
[AD-A189526] 13 p1741 N88-20414
Temperature dependence of Kr precipitation in Ni
[DE88-005953] 13 p1744 N88-20429
The unique characteristics of the structure of composite materials made on a base of sphalerite-analogous boron nitride 14 p1886 N88-21273
Bithermal fatigue of a nickel-base superalloy single crystal
[NASA-TM-100885] 15 p2042 N88-22168
Performance of lightweight nickel electrodes
[NASA-TM-100958] 20 p2771 N88-26430
Grain boundary structure in Ni3Al
[DE88-009164] 20 p2773 N88-26444
The adherence of nickel oxide on nickel during high temperature oxidation
[DE88-011194] 20 p2774 N88-26450
A fundamental understanding of the interfacial compatibility in hybrid material systems
[AD-A192921] 21 p2909 N88-27264
Inelastic electron scattering and electron-hole excitations in iron and nickel
[DE88-011843] 21 p2915 N88-27303

NICKEL ALLOYS
NT ASTROLOY (TRADEMARK)
NT HASTELLOY (TRADEMARK)
NT INCONEL (TRADEMARK)
NT NITINOL ALLOYS
Isothermal forging and its effect on the microstructure of powder route nickel alloy AP1
[RAE-TM-P-1094] 01 p0022 N88-10138
Structure of rapidly solidified Ni-Ti
[DE87-012252] 02 p0147 N88-10921
Thermodynamics of interaction between nitrogen and molten nickel alloys
[BLL-M-37309-(5828.4)] 02 p0149 N88-10934
The effect of sulfur and zirconium Co-doping on the oxidation of NiCrAl
[NASA-TM-100209] 02 p0150 N88-10940
Influence of boron on porosity in nickel-base superalloy castings 03 p0299 N88-11877
A mathematical model of high alloy nickel base high temperature alloys
[BLL-M-37381-(5828.4)] 05 p0564 N88-13436
The effect of ion beam mixed Ni-Al surface layers on PSB extrusion morphology in fatigued nickel
05 p0598 N88-13652
Low cycle fatigue behaviour of notched specimens of nickel based superalloy single crystal
05 p0605 N88-13712
An overview of fatigue 05 p0608 N88-13729
Basic energy sciences research in the Metals and Ceramics Division of Oak Ridge National Laboratory
[DE87-013538] 06 p0681 N88-14171
Undercooling and nucleation in iron nickel alloys
[AD-A185500] 06 p0683 N88-14184
The effect of prestraining on fatigue crack growth in nickel-base alloys 06 p0719 N88-14415
High temperature low cycle fatigue of oxide dispersion strengthened and single crystal nickel base superalloys
06 p0720 N88-14422
High temperature low cycle fatigue behavior and creep-fatigue interation of MA 6000 ODS alloy
06 p0720 N88-14425
The effect of temperature on fatigue crack initiation from aluminosilicate inclusions 06 p0720 N88-14427
Dependence of strainrange partitioned fatigue life at elevated temperature on monotonic stress-strain properties 06 p0721 N88-14428
The effect of varying sputtering parameters on the microstructure and mechanical properties of 10 percent Ni + TiB2 thin films
[DE88-002600] 09 p1254 N88-17517
Diffusion studies in amorphous NiZr alloys
[DE88-003009] 10 p1301 N88-17781
The role of composition and microstructure gradients on weld metal properties and behavior
[DE88-004956] 10 p1303 N88-17791
Friction and wear of monolithic and fiber reinforced silicon-ceramics sliding against IN-718 alloy at 25 to 800 C in atmospheric air at ambient pressure
[NASA-TM-100294] 10 p1304 N88-17796
Study of adherent oxide scales
[AD-A187368] 11 p1456 N88-18680
High temperature oxidation studies on alloys containing dispersed phase particles and clarification of the mechanism of growth of SiO2
[AD-A188158] 11 p1457 N88-18688
Effects of thermal and thermo-mechanical treatments on the mechanical properties of centrifugally cast alloy 718
[AD-A188195] 11 p1458 N88-18690
Corrosion resistance of electrodeposited amorphous Ni-Cr-P alloys
[DE88-005116] 11 p1459 N88-18695
Anodic behavior of Ni-P and Ni-Cr-P metallic glasses
[DE88-005334] 11 p1463 N88-18722
The cyclic stress-strain behavior of a single crystal nickel-base superalloy
[NASA-TM-100269] 12 p1607 N88-19610
The effect of microstructure on the fatigue crack growth resistance of nickel base superalloys
[AD-A189526] 13 p1741 N88-20414
Processing, physical metallurgy and creep of NiAl + Ta and NiAl + Nb alloys
[NASA-CR-182113] 14 p1880 N88-21295
Electron diffraction evidence for the ordering of excess nickel atoms by relation to stoichiometry in nickel-rich beta'-NiAl formation of a nickel-aluminum (Ni2Al) superlattices
[NASA-TT-20177] 14 p1890 N88-21297
Effect of nonuniform state of thermal stress on resistance of EI826 alloy to thermal fatigue
14 p1895 N88-21313
Growth of fatigue cracks in nickel alloys at high temperatures 14 p1896 N88-21318
The viscoplasticity theory based on overstress applied to the modeling of a nickel base superalloy at 815 C
14 p1928 N88-21499
Development of a unified constitutive model for an isotropic nickel base superalloy Rene 80
14 p1929 N88-21501
Constitutive response of Rene 80 under thermal mechanical loads 14 p1932 N88-21524
Characterization of an explosively consolidated rapidly solidified Fe-16Ni-9Cr-5Mo-2Cu alloy powder
[DE88-006733] 15 p2041 N88-22162
Atomic beam study of crystalline order and precipitation in nickel based alloys
[ETN-88-91994] 16 p2177 N88-22975
Laser cladding of Ni, Nb and Mg alloys for improved environmental resistance at high temperature
[AD-A191274] 16 p2213 N88-23208
Martensitic transformation and microstructures in sintered NiAl alloys
[NASA-TT-20178] 18 p2488 N88-24761
Rapidly solidified lightweight durable disk material
[AD-A191697] 18 p2491 N88-24775
Martensitic transformation and microstructures in sintered NiAl alloys
[NASA-TT-20192] 19 p2616 N88-25519
Electrodeposition of amorphous Ni-Cr-P alloys
[DE88-006868] 19 p2616 N88-25521
Hot isostatic pressing of nickel aluminide powders
[DE88-009677] 19 p2617 N88-25525
New super alloys used in turbochargers
19 p2634 N88-25628
Glass forming ranges of amorphous alloys
[DE88-007897] 20 p2772 N88-26438
Precipitation study by electrical resistivity measurement in Ni-Al alloys
[DE88-701877] 20 p2773 N88-26440
Shape memory alloys: New materials for future engineering
[NASA-TT-20193] 20 p2775 N88-26455
The preparation of mechanically alloyed powders for TEM (Transmission Electron Microscopy) examination
[DE88-008043] 20 p2775 N88-26460
Nickel aluminides: A new family of nickel + aluminum alloys featuring simple composition, low density, excellent oxidation resistance and high yield strength that increases with temperature
[DE88-010692] 20 p2776 N88-26461
PECVD of amorphous nickel--phosphorus films
[DE88-011088] 21 p2915 N88-27299
Hot isostatic pressing of tungsten-nickel-iron composites
[FOA-C-20698-2.1] 22 p3056 N88-28135
Development of Nb-Ti multifilamentar superconducting wires
[DE88-702324] 23 p3290 N88-29592
Hydrogen embrittlement of iron-nickel alloys
[AD-A195909] 24 p3353 N88-29958
Anisotropic constitutive modeling for nickel-base single crystal superalloys
[NASA-CR-182157] 24 p3353 N88-29961

NICKEL CADMIUM BATTERIES
The 1986 Goddard Space Flight Center Battery Workshop
[NASA-CP-2486] 02 p0163 N88-11021
Battery development and testing at ESA
02 p0164 N88-11027
BRASILSAT A2: Ground and in-orbit anomalies
02 p0164 N88-11032
International Ultraviolet Explorer (IUE) spacecraft battery performance update 02 p0164 N88-11033
Effects of long term storage on aerospace nickel cadmium cell performance 02 p0165 N88-11035
Qualification testing of General Electric 50 Ah nickel-cadmium cells with Pellon 2536 separator and passivated positive plates 02 p0165 N88-11036
Flight experience of solar mesosphere explorer's power system over high temperatures ranges
02 p0165 N88-11037
Real time charge efficiency monitoring for nickel electrodes in NiCD and NiH2 cells
02 p0165 N88-11038
Statistically determined nickel cadmium performance relationships 02 p0165 N88-11039
Test summary for advanced H2 cycle NI-CD cell
02 p0165 N88-11040
High energy density rechargeable batteries for aerospace power requirements
[AD-A184883] 05 p0577 N88-13519
Investigation of self-discharge characteristics of spacecraft nickel-cadmium cells at elevated temperatures
[AD-A186497] 08 p0979 N88-15919
ESL batteries and multi-segment applications --- ESA Simulation Language (ESL)
[CS-1029/00-QFIN4] 10 p1322 N88-17901
Effects of cadmium electrode properties on nickel-cadmium cell performance
[AD-A191394] 16 p2193 N88-23081
Aerospace energy systems laboratory: Requirements and design approach
[NASA-TM-100423] 17 p2390 N88-24206
Results from life test in progress on eagle-picher nickel cadmium cells
[AD-A192816] 21 p2936 N88-27434
Aircraft battery state of charge and charge control system
[AD-A194979] 24 p3367 N88-30052

NICKEL COATINGS
Corrosion of electroless nickel-coated steel
[AD-A191045] 16 p2179 N88-22985

NICKEL COMPOUNDS
NT NICKEL OXIDES
Analysis of phase equilibria in NiTi-C system in high nickel regions
[BLL-M-37304-(5828.4)] 02 p0149 N88-10932
The toxicology and metabolism of nickel compounds
[DE87-014801] 04 p0474 N88-12921
Phase purity of NiCo2O4, a catalyst candidate for electrolysis of water
[NASA-TM-100239] 05 p0556 N88-13385
An investigation of metal complexes of some 2-substituted and 2,6-disubstituted pyridine N-oxides
11 p1460 N88-18701
Characterization of redox states of nickel hydroxide film electrodes by in-situ Raman spectroscopy
[AD-A189288] 13 p1741 N88-20411

NICKEL HYDROGEN BATTERIES
Effect of NASA advanced designs on thermal behavior of Ni-H2 cells
[NASA-TM-100197] 01 p0021 N88-10132
The 1986 Goddard Space Flight Center Battery Workshop
[NASA-CP-2486] 02 p0163 N88-11021
Battery development and testing at ESA
02 p0164 N88-11027
Nickel hydrogen low Earth orbit test program update and status 02 p0164 N88-11028
Advances in nickel hydrogen technology at Yardney Battery Division 02 p0164 N88-11029
Failure analysis of a 3.5 inch, 50 ampere-hour nickel-hydrogen cell 02 p0164 N88-11030
Real time charge efficiency monitoring for nickel electrodes in NICD and NIH2 cells
02 p0165 N88-11038
Effects of pressure fluctuations on nickel electrodes
[AD-A184293] 03 p0311 N88-11967
Making space nickel/hydrogen batteries lighter and less expensive
[DE88-000168] 05 p0578 N88-13530
Nickel hydrogen low earth orbit life testing
[AD-A191946] 18 p2504 N88-24855
Small scale bipolar nickel-hydrogen testing
[NASA-TM-100936] 18 p2538 N88-25059
Effect of LEO cycling at shallow depths of discharge on MANTECH IPV nickel-hydrogen cells
[NASA-TM-101300] 19 p2688 N88-25978

Performance of lightweight nickel electrodes
[NASA-TM-100958] 20 p2771 N88-26430
Nickel hydrogen cell positive-electrode studies: Cobalt segregation in reducing environments
[AD-A193025] 20 p2796 N88-26587
Recent developments in nickel hydrogen technology
[DE88-011248] 21 p2939 N88-27456
The effect of compression on individual pressure vessel nickel/hydrogen components
[NASA-TM-101312] 22 p3052 N88-28109

NICKEL IRON BATTERIES
Post-test analyses of aqueous batteries developed for electric propulsion
[DE88-000655] 03 p0311 N88-11965

NICKEL OXIDES
A hydrogen/nickel oxide battery for remote applications
[DE87-009048] 04 p0464 N88-12872
The migration of grain boundaries in ceramic materials with particular reference to the sintering process
[DE88-004085] 10 p1306 N88-17808
The adherence of nickel oxide on nickel during high temperature oxidation
[DE88-011194] 20 p2774 N88-26450

NICKEL PLATE
Analysis of nickel sulphamate bath using charging current compensated D.C. polarography
[NAL-TM-MT-8705] 05 p0564 N88-13433

NICKEL STEELS
Modified 14Cr-16Ni stainless steels with improved creep resistance at 700 C due to tailored precipitate microstructures
[DE87-014788] 03 p0290 N88-11825
Impact behavior of 9-Cr and 12-Cr ferritic steels after low-temperature irradiation
[DE88-000333] 03 p0291 N88-11827
Texture profile in thermomechanically processed 2-inch-thick 5 Ni-steel armor plate
[AD-A189275] 13 p1741 N88-20410

NICKEL ZINC BATTERIES
Grace DAKASEP alkaline battery separator
02 p0164 N88-11031

NICOTINIC ACID
Rapid hypothermia subsequent to oral nicotinic acid and immersion in warm (30C) water
[AD-A186458] 08 p1050 N88-16339

NIGHT
Pyroelectric line scanner for remote IR imaging of vehicles
[DE87-012127] 02 p0235 N88-11484
Distribution of electron concentration in nighttime atmosphere of Venus based on radio transmission data
08 p1005 N88-16092
Biorhythmic aspects of intercontinental Antarctic adaptation 08 p1046 N88-16321
Tactical air force night/adverse weather training
[AD-A194243] 22 p3133 N88-28625

NIGHT AIRGLOW
U NIGHTGLOW

NIGHT E LAYER
U E REGION
U NIGHT SKY

NIGHT F LAYER
U F REGION
U NIGHT SKY

NIGHT FLIGHTS (AIRCRAFT)
The accommodative status in the dark of US Navy fighter pilots
[AD-A188188] 10 p1370 N88-18186
Simulator evaluation of lineup visual landing aids for night carrier landing
[AD-A191212] 18 p2468 N88-24648
Integration of LANTIRN (Low Altitude Navigation and Targeting Infrared for Night) into operational fighter training
[AD-A194906] 24 p3325 N88-29799
LANTIRN simulator training in the F-16C
[AD-A195201] 24 p3330 N88-29826

NIGHT SKY
Ionospheric convection and structure using ground-based digital ionosondes
[AD-A194246] 23 p3233 N88-29237
One equatorial anomaly in nighttime ionospheric F region 24 p3447 N88-30517

NIGHT VISION
Development, testing and evaluation of a night vision goggle compatible BO-105 for night low level operation
03 p0265 N88-11668
Scotopic sensitivity with 10 percent oxygen
[AD-A183973] 03 p0356 N88-12243
Management Information and Downloader Interface System (MIDIS)
[AD-A186978] 09 p1261 N88-17557
The accommodative status in the dark of US Navy fighter pilots
[AD-A188188] 10 p1370 N88-18186
Night Vision: Current Research and Future Directions, symposium proceedings
[PB88-132006] 11 p1550 N88-19274
Mechanisms of early light and dark adaptations
12 p1663 N88-19972
Fast Algorithm Simulation and Test (FAST) facility
[AD-A191183] 16 p2252 N88-23457
Night lighting and night vision goggle compatibility
23 p3242 N88-29297
Visual sensitivities under reduced oxygen
[AD-A195628] 24 p3406 N88-30279
Common modules: A success story
[AD-A195937] 24 p3430 N88-30415

NIGHTGLOW
Electrodynamics of midnight sector of auroral oval in period of slight disturbance 08 p1003 N88-16077
Multispectral optical observations of ionospheric F-region storm effects at low latitude
[INPE-4231-PRE/1105] 08 p1024 N88-16198
The photons payload, G-494: A learning experience
10 p1288 N88-17701

NIMBUS SATELLITES
NT NIMBUS 7 SATELLITE

NIMBUS 7 SATELLITE
In-orbit calibration adjustment of the Nimbus-7 SMMR
[NASA-TM-100678] 05 p0614 N88-13773
Volcanic eruption detection with TOMS
05 p0618 N88-13793
Selection of optimum wavelengths for ozone mapping from satellites 05 p0619 N88-13798
Determination of total ozone from HIRS2/MSU sounding data 05 p0619 N88-13799
Description of data on the Nimbus 7 LIMS map archive tape: Water vapor and nitrogen dioxide
[NASA-TP-2761] 06 p0744 N88-14572
Nimbus 7 Solar Backscatter Ultraviolet (SBUV) spectral scan solar irradiance and Earth radiance product user's guide
[NASA-RP-1199] 09 p1184 N88-17096
The 1987 Airborne Antarctic Ozone Experiment: The Nimbus-7 TOMS data atlas
[NASA-RP-1201] 13 p1791 N88-20714
NIMBUS-7 CZCS. Coastal Zone Color Scanner imagery for selected coastal regions. North America - Europe. South America - Africa - Antarctica. Level 2 photographic product
[NASA-CR-180755] 15 p2089 N88-22447

NIMONIC ALLOYS
Near-threshold short crack growth behavior in Nimonic 105 05 p0599 N88-13663

NIMPHE (ENGINE)
U HYDRAZINE ENGINES

NIOBATES
NT LITHIUM NIOBATES
The role of point defects on structural phase transitions
[DE88-005209] 12 p1696 N88-20152

NIOBIUM
NT NIOBIUM ISOTOPES
Mechanical properties of a microalloyed steel with high niobium content
[DE87-703545] 04 p0415 N88-12572
Sintered steels of high resistance alloyed to Nb, Mo, Mn and Si
[DE87-703546] 04 p0415 N88-12573
Mechanical properties of an acicular ferrite steel microalloyed to niobium and vanadium
[DE87-703547] 04 p0415 N88-12574
Partial substitution of vanadium by niobium in AISI H13 steel
[DE87-703548] 04 p0415 N88-12575
Progress in the development of niobium alloyed high speed steel
[DE87-703549] 04 p0415 N88-12576
Hadfield steels with Nb and Ti carbides
[DE87-703706] 04 p0416 N88-12579
Study of the influence of mechanical - thermal treatments on the creep behavior of a niobium stainless steel
[DE87-703506] 05 p0563 N88-13431
Nb3Al formation in sputter-deposited Nb/Al multi-layer samples
[DE88-003192] 08 p0970 N88-15868
Creep behavior of tungsten/niobium and tungsten/niobium-1 percent zirconium composites
[NASA-TM-100804] 11 p1460 N88-18707
The effects of various conductor components on Nb3Sn filament prestrain in cable-in-conduit conductors
[DE88-003956] 11 p1479 N88-18824
Use of nonporous metals membranes for the separation of hydrogen from gas mixtures
[BMFT-FB-T-86-206] 14 p1888 N88-21280
Structure and properties of welded joints produced between niobium parts in controllable helium atmosphere 14 p1897 N88-21326
Superconducting transition temperature of Cu-Nb microcomposites 14 p1973 N88-21775
Thermal model describing development of normal region in superconductor film carrying electric current
14 p1973 N88-21776
Creep behavior of tungsten/niobium and tungsten/niobium-1 percent zirconium composites
17 p2425 N88-24427
Effect of alloying, rapid solidification, and surface kinetics on the high temperature environmental resistance of niobium
[AD-A192093] 18 p2485 N88-24743
Magnetization studies of multifilamentary Nb3Sn wires
[DE88-009103] 19 p2735 N88-26243
Rocket-propellant burn tests of silicide-coated niobium and tantalum
[DE88-010729] 20 p2781 N88-26496
Investigation of a SiC/Ti-24Al-11Nb composite
[NASA-TM-100956] 23 p3190 N88-28980

NIOBIUM ALLOYS
Strain rate effects in fast-gas-cooled uranium-titanium and uranium-niobium alloys
[OUEL-1683/87] 02 p0149 N88-10937
Effect of irradiation on the tensile properties of niobium-base alloys
[DE87-002409] 03 p0285 N88-11790
Mechanical strength and niobium and niobium-base alloys substructures
[DE87-703692] 04 p0415 N88-12577
Corrosion strength of niobium and its alloys
[DE87-703693] 04 p0416 N88-12578
Characteristics of joint formation during friction welding of Ti alloys to Nb alloys 14 p1898 N88-21329
Superconducting transition temperature of Cu-Nb microcomposites 14 p1973 N88-21775
Growth and deformation mechanisms of refractory alloy hybrid materials
[AD-A190492] 15 p2039 N88-22152
Characterization of precipitates in a niobium-zirconium-carbon alloy
[NASA-TM-100848] 16 p2178 N88-22981
Laser cladding of Ni, Nb and Mg alloys for improved environmental resistance at high temperature
[AD-A191274] 16 p2213 N88-23208
Preliminary study of niobium alloy contamination by transport through helium 17 p2402 N88-24279
Fabrication of a niobium 1 percent zirconium containment for SP-100 primary lithium system materials mass transfer studies 17 p2417 N88-24373
The preparation of mechanically alloyed powders for TEM (Transmission Electron Microscopy) examination
[DE88-008043] 20 p2775 N88-26460
An HVEM study of displacement cascade damage in Nb3Sn at 13 K
[DE88-009997] 23 p3289 N88-29584

NIOBIUM CARBIDES
Contributions to the investigation of mechanical behavior of gamma/gamma NbC Cotac composites at medium and at high temperature
[ESA-TT-1031] 03 p0280 N88-11760

NIOBIUM COMPOUNDS
NT LITHIUM NIOBATES
NT NIOBATES
NT NIOBIUM CARBIDES
NT NIOBIUM OXIDES
NT NIOBIUM STANNIDES
Microstructure modifications of micron thick NbN films to improve J/sub c/ and H/sub c2/
[DE88-003078] 08 p1091 N88-16567
Hydrogen in niobium-tantalum superlattices
09 p1148 N88-16867
Method of producing high T(subc) superconducting NBN films
[NASA-CASE-NPO-16681-1-CU]
17 p2446 N88-24543

NIOBIUM ISOTOPES
Bulk plasmon enhanced photoemission from Nb(100) surface resonances
[AD-A192711] 22 p3154 N88-28767

NIOBIUM OXIDES
Growth and characteristics of materials for tunable lasers in the near infrared spectral region
[NASA-CR-182501] 11 p1491 N88-18901

NIOBIUM STANNIDES
Properties of Nb3Sn superconductor wires with composite cores
[KFK-4263] 02 p0246 N88-11557
Powder-metallurgical preparation of A15 superconductors
[ETN-87-90584] 03 p0380 N88-12392
Powder metallurgical preparation of A15 superconductors
[ETN-88-91072] 09 p1144 N88-16858

NITINOL ALLOYS
On the stressing of annealed NITINOL: The electrical resistance and calorimetric effects
[AD-A184465] 04 p0414 N88-12569

NITRAMINE PROPELLANTS
High pressure strand burn rate tests of polyvinylnitrate/nitramine propellants
[AD-A184178] 04 p0422 N88-12615
Laser ignition of nitramine composite propellants and crack propagation and branching in burning solid propellants
[AD-A189260] 13 p1753 N88-20483
Structure/property/reactivity relations among nitramine and other energetic materials
[AD-A190878] 18 p2481 N88-24716
Chemical kinetics of nitramine propellant combustion
[AD-A191556] 18 p2495 N88-24802
The 24th JANNAF Combustion Meeting, volume 1
[AD-A190163] 19 p2627 N88-25585
Deuterium isotope effects in the combustion of formulated nitramine propellants
19 p2632 N88-25611
Discovery of a low temperature form of TAGN (Triaminoguanidinium Nitrate)
[AD-A196059] 24 p3357 N88-29989
NITRATES
NT AMMONIUM NITRATES
NT HYDRAZINE NITRATE
NT PETN
NT SODIUM NITRATES
Comparison of three aerosol sampling techniques and the differences in the nitrate determined by each
[DE87-011456] 03 p0348 N88-12200
High pressure strand burn rate tests of polyvinylnitrate/nitramine propellants
[AD-A184178] 04 p0422 N88-12615
The 1,2,3-triaminoguanidinium nitrate: An alternate explanation of the nitrate anion disorder
[AD-A188386] 12 p1612 N88-19640
The unique characteristics of the structure of composite materials made on a base of sphalerite-analogous boron nitride 14 p1886 N88-21273
Meteorological aspects of wet deposition in Southern Finland
[FMI-3] 19 p2693 N88-26007
Studies of the mechanisms and rates with which nitrogen species are incorporated into cloud water and precipitation
[PB88-193065] 20 p2826 N88-26764
Foliar nitrate reductase: A marker for assimilation of atmospheric nitrogen oxides
[DE88-010453] 21 p2971 N88-27648
Atmospheric deposition of nitrate to the ocean surface
23 p3231 N88-29227
Some effects of nitrates on the tensile properties of Al 7075-T7351
[AD-A195118] 24 p3354 N88-29965
Discovery of a low temperature form of TAGN (Triaminoguanidinium Nitrate)
[AD-A196059] 24 p3357 N88-29989
NITRATION
Research in energetic compounds
[AD-A192953] 20 p2781 N88-26494
NITRIC ACID
Simulation of global wet and dry deposition of nitric acid in a three-dimensional chemistry-transport model
[DE87-009847] 09 p1188 N88-17116
Mechanism of the nitric oxide-carbon monoxide-oxygen reaction over a single crystal rhodium catalyst
[DE88-006274] 21 p2910 N88-27268
NITRIDES
NT ALUMINUM NITRIDES
NT BORON NITRIDES
NT GALLIUM NITRIDES
NT METAL NITRIDES
NT OXYNITRIDES
NT SILICON NITRIDES
NT TITANIUM NITRIDES
NT ZIRCONIUM NITRIDES
High temperature oxidation studies on alloys containing dispersed phase particles and clarification of the mechanism of growth of SiO2
[AD-A188158] 11 p1457 N88-18688
Formation of buried nitride layers in (110) silicon
[DE88-003255] 11 p1557 N88-19323
Properties of reactively sputtered WNx films Zhao, X. -A.
[AD-A188711] 13 p1835 N88-20976
Uranium nitride fuel swelling and thermal conductivity correlations 17 p2409 N88-24327
An irradiation performance data base for nitride fuels
17 p2427 N88-24438
Material property and irradiation performance correlations for nitride fuels 17 p2434 N88-24483
A comparison of uranium nitride and mixed carbide fuels swelling 17 p2435 N88-24485
Method of producing high T(subc) superconducting NBN films
[NASA-CASE-NPO-16681-1-CU]
17 p2446 N88-24543
NITRIDING
Fatigue characteristics of ion treated surfaces
05 p0606 N88-13713
Ion-beam nitriding of steels
[NASA-CASE-LEW-14104-2] 06 p0682 N88-14179
Analysis of load-bearing capacity of nitrided layer
[PB87-144176] 08 p0968 N88-15857
Antistokes coherent Raman diffusion of a nitriding plasma
[ONERA-RF-6/3644-PY] 16 p2175 N88-22962
SiC fiber reinforced reaction-bonded Si3N4 composites 17 p2326 N88-23892
NITRILES
NT ACETONITRILE
NT ACRYLONITRILES
Transparent metal model study of the use of a cellular growth front to form aligned monotectic composite materials
[NASA-CR-182414] 08 p0969 N88-15861
Development of a nitrile rubber for dynamic damping
[AD-A194060] 22 p3058 N88-28145
NITRO COMPOUNDS
NT NITROMETHANE
NT TETRYL
NT TRINITROTOLUENE
Theoretical investigations of nitrocubane decomposition
[AD-A194556] 23 p3200 N88-29047
NITROBENZENES
NT TRINITROTOLUENE
NITROGEN
NT LIQUID NITROGEN
NT NITROGEN ISOTOPES
Nitrogen at high pressure
[DE87-013797] 01 p0021 N88-10130
Nitrogen at very high pressure
[DE87-013800] 01 p0021 N88-10131
Rocket nozzle thermal shock tests in an arc heater facility 02 p0133 N88-10832
Thermodynamics of interaction between nitrogen and molten nickel alloys
[BLL-M-37309-(5828.4)] 02 p0149 N88-10934
Shock-induced cooling in dense fluids
[DE87-014343] 02 p0170 N88-11067
Absorption of far IR-radiation by H2O-N2 complexes under atmospheric conditions 04 p0462 N88-12855
Nitrogen energy transfer study
[AD-A184457] 04 p0464 N88-12869
Development of a low noise 10 K J-T refrigeration system
[AD-A185258] 05 p0571 N88-13484
Fuel nitrogen conversion in a supercharged spark ignition engine
[DE88-003739] 08 p0974 N88-15893
CARS measurements of combustion. 1: Precision of thermometry
[NAL-TR-939] 10 p1299 N88-17769
Effects of ion implantation on cavitation erosion of a cobalt based metal/carbide alloy
[AD-A187239] 10 p1303 N88-17793
Investigations of surface coatings based on silicon and nitrogen: From amorphous Si to silicon nitride
[DE88-004995] 12 p1609 N88-19622
Nitrogen's biological effect on oxygen transport through hematoparenchymal barrier 12 p1662 N88-19967
Spectrographic detection of nitrogen impurity in helium
[DE88-752301] 15 p2033 N88-22111
Reactions of N2(A sup 3 sigma sup + sub u) candidates for short wavelength lasers
[DE88-007018] 15 p2070 N88-22342
Thermal conductivity of selected foams and systems from 100 to 300 K
[PB88-201553] 20 p2777 N88-26466
A shock-tube experiment on gases mixing processes associated with CO2/N2 mixing gasdynamic laser
[ISAS-RN-350] 20 p2797 N88-26598
Study of energy levels and decay mechanisms for singlet Rydberg states of molecular nitrogen
[AD-A192505] 21 p3014 N88-27886
Chemically-produced N2(A) to NO(X) energy transfer in a supersonic flow
[AD-A192501] 22 p3082 N88-28302
NF (a 1 delta) production in a supersonic flow using N2F4 + H2 in a BCL-16 nozzle
[AD-A194478] 22 p3082 N88-28304
Computed potential energy surfaces for chemical reactions
[NASA-CR-183168] 24 p3342 N88-29893
NITROGEN ATOMS
A model for nitrogen atom recombination on a silicon dioxide surface
[AD-A189843] 15 p2142 N88-22784
NITROGEN COMPOUNDS
NT ALUMINUM NITRIDES
NT AMIDES
NT AMMONIA
NT AMMONIUM NITRATES
NT ATROPINE
NT AZIDES (INORGANIC)
NT AZIDES (ORGANIC)
NT BORON NITRIDES
NT CAFFEINE
NT CYANO COMPOUNDS
NT ERGOTAMINE
NT GALLIUM NITRIDES
NT HMX
NT HYDRAZINE NITRATE
NT HYDRAZINIUM COMPOUNDS
NT IMIDES
NT IMINES
NT ISOCYANATES
NT LIQUID AMMONIA
NT METAL NITRIDES
NT MORPHINE
NT NITRATES
NT NITRIC ACID
NT NITRIDES
NT NITRO COMPOUNDS
NT NITROGEN DIOXIDE
NT NITROGEN FLUORIDES
NT NITROGEN HYDRIDES
NT NITROGEN OXIDES
NT NITROGEN POLYMERS
NT NITROMETHANE
NT NITROUS OXIDES
NT OXYNITRIDES
NT PETN
NT POLYIMIDES
NT QUINOLINE
NT RDX
NT SILICON NITRIDES
NT SODIUM NITRATES
NT TETRYL
NT THYMINE
NT TITANIUM NITRIDES
NT TRINITROTOLUENE
NT URACIL
NT UREAS
NT XANTHINES
NT ZIRCONIUM NITRIDES
Investigations of the influence of chemical reactions of the vertical flow of gaseous and particulate compounds
08 p1017 N88-16165
NITROGEN DIOXIDE
NO2 heterodyne frequency measurements with a tunable diode laser, a CO laser transfer oscillator and CO2 laser standards
[NASA-CR-182393] 06 p0710 N88-14353
Effect of nitrogen dioxide release on thermosphere
13 p1789 N88-20704
Pyrolyzed organic polymer nitrogen dioxide sensor
19 p2669 N88-25868
NITROGEN FIXATION
U NITROGENATION
NITROGEN FLUORIDES
N2(A3epsilon u+) by reaction of N2F4+H2 in a supersonic flow
[AD-A194493] 23 p3219 N88-29163
NITROGEN HYDRIDES
Experiments on reactions of the electronically excited molecule nitron NH (a sup 1 delta) and carbon CH2 (a bar sup 1 A(1)) in gas phase
[MPIS-3/1987] 17 p2397 N88-24249
NITROGEN IONS
The effect of object potentials on the wake of a flowing plasma
[AD-A184038] 03 p0379 N88-12385
The magnitude of secondary electron contributions in photon stimulated desorption
[AD-A189094] 13 p1835 N88-20980
NITROGEN ISOTOPES
The atomic weight and isotopic composition of nitrogen and their variation in nature
[DE87-012867] 02 p0144 N88-10902
NITROGEN LASERS
TEA-TE: Powerful nitrogen-based laser system
07 p0919 N88-15583
NITROGEN METABOLISM
Comparison of morning with afternoon nitrogen elimination in resting subjects breathing 100 percent oxygen
[AD-A196191] 24 p3407 N88-30282
NITROGEN OXIDES
NT NITROGEN DIOXIDE
NT NITROUS OXIDES
Production of NO by galactic cosmic rays and lightning
[DE87-014613] 02 p0197 N88-11230
Study of polyatomic dynamics in the atmosphere
[AD-A190964] 16 p2233 N88-23334

Atmospheric nitrogen oxides: Their detection and chemistry
[PB88-193057] 21 p2970 N88-27642
Chemically-produced N2(A) to NO(X) energy transfer in a supersonic flow
[AD-A192501] 22 p3082 N88-28302
A study of the interaction of NO2 with carbon particles
[DE88-010778] 22 p3118 N88-28524
Photochemistry of ionospheric D-region with injection of nitrogen oxides 24 p3444 N88-30499

NITROGEN PLASMA
Nonequilibrium characteristics of nitrogen plasmas appropriate to an AOTV flight 03 p0319 N88-12019
The effect of object potentials on the wake of a flowing plasma
[AD-A184038] 03 p0379 N88-12385

NITROGEN POLYMERS
Interfacial shear strength of pitch and high strain pan fibers in an epoxy matrix
[AD-A185966] 07 p0826 N88-15011
Electronic and ionic transport in polymers
[AD-A187253] 11 p1452 N88-18651
MOPAC manual: A general molecular orbital package, fourth edition
[AD-A188623] 13 p1733 N88-20362

NITROGENATION
Application of photosynthetic N(2)-fixing cyanobacteria to the CELSS program 03 p0358 N88-12257

NITROMETHANE
Kinetic measurements of thermal decomposition of energetic materials at high pressures
[AD-A191612] 19 p2622 N88-25552

NITROUS OXIDES
Formation and destruction of nitrous oxide in lean, premixed combustion
[DE88-001390] 05 p0562 N88-13423

NMR
U NUCLEAR MAGNETIC RESONANCE

NOAA SATELLITES
NT NOAA 7 SATELLITE
Observation of the development of mesoscale systems by operational meteorological satellites 02 p0201 N88-11259
TOMS and the NOAA/FAA volcano support plan 05 p0618 N88-13796
An overview of the current Earth observation programs (Europe, USA, and Japan) 09 p1129 N88-16778
Processing of HRPT data from the NOAA series satellites 17 p2359 N88-24053

NOAA 7 SATELLITE
Analysis of thickness fields retrieved from NOAA-7 observations through the 3I (Improved Initialization Inversion) method. Interest for weather forecasting 02 p0201 N88-11255

NOBLE GASES
U RARE GASES

NOBLE METALS
NT GOLD
NT RUTHENIUM
NT SILVER
Reactions of some thiol collectors at noble-metal and pyrite electrodes
[PB88-138318] 11 p1455 N88-18674
Temperature dependence of conductivity and of Hall coefficients for noble metal films
[ETN-88-92981] 23 p3294 N88-29616

NOCTILUCENCE
U LUMINESCENCE

NOCTILUCENT CLOUDS
The nonlinear thermodynamics of meteors, noctilucent clouds, enhanced airglow and global atmospheric circulation 06 p0738 N88-14538

NOCTURNAL VARIATIONS
Theoretical and lidar studies of the seasonal and nocturnal variations of the mesospheric sodium layer at Urbana, Illinois 01 p0068 N88-10435
Effect of neutral wind on the latitudinal variation of nighttime F-layer vertical movements 08 p1030 N88-16244
Is ANF implied in the night attenuated renal response to central hypervolemia? 12 p1659 N88-19945
Computer simulation of tropospheric chemistry
[JUEL-2144] 13 p1798 N88-20756

NODES (STANDING WAVES)
Five-point form of the nodal diffusion method and comparison with finite-difference
[DE88-004141] 19 p2720 N88-26154
A nodal method for time-dependent transport equation
[DE88-004285] 20 p2844 N88-26876

NODULES
Concentration coefficients of elements in ferromanganese nodules relative to ocean sediments 06 p0726 N88-14464
Remote acoustic sounding of ferromanganese nodules 06 p0727 N88-14471
Ferromanganese nodules of Antarctic sector in Pacific Ocean 06 p0727 N88-14472

NOE NAVIGATION
U NAP-OF-THE-EARTH NAVIGATION

NOISE
Application of ray theory to propagation of low frequency noise from wind turbines
[NASA-CR-178367] 03 p0373 N88-12349
Development of a technique for estimating noise covariances using multiple observers
[NASA-TM-4020] 06 p0669 N88-14098
A new method of boundary parameter estimation for a two-dimensional diffusion system under noisy observations
[NASA-CR-178405] 06 p0767 N88-14714
IRAC test report. Gallium doped silicon band 2: Read noise and dark current
[NASA-TM-87813] 09 p1159 N88-16945
Research in applied mathematics ralated to identification of noisy systems
[AD-A189355] 13 p1825 N88-20908
Fundamental noise processes in a laser excited optical filter
[DE88-006460] 15 p2070 N88-22340

NOISE (SOUND)
NT AERODYNAMIC NOISE
NT AIRCRAFT NOISE
NT BLADE SLAP NOISE
NT ENGINE NOISE
NT JET AIRCRAFT NOISE
NT SONIC BOOMS
NT THERMAL NOISE
Activities report of the Institute of Sound and Vibration Research
[ETN-87-90685] 01 p0090 N88-10589
Noise modelling in the time domain with the aid of Spice
[PB87-221941] 05 p0573 N88-13492
A study of rotor broadband noise mechanisms and helicopter tail rotor noise 06 p0777 N88-14766
Brain potentials and personality: A new look at stress susceptibility
[AD-A186931] 09 p1199 N88-17189
Structural-acoustic interior noise modeling and analysis from experimental data
[PB88-141775] 12 p1687 N88-20088
Auditory perception of complex sounds
[AD-A190528] 15 p2103 N88-22529
Low frequency ocean ambient noise: Measurements and theory
[AD-A191188] 16 p2237 N88-23362
Overground Excess Sound Attenuation (ESA). Volume 1: Experimental study for flat grassy terrains
[AD-A191289] 16 p2265 N88-23549
Higher frequency ambient noise in the arctic ocean
[AD-A192203] 18 p2547 N88-25122
Noise and chaos in driven Josephson junctions 19 p2734 N88-26238
A modal approach to Arctic noise modelling with implied vertical coherence
[AD-A192966] 20 p2850 N88-26916
Vertical directionality of ambient noise at 32 deg N as a function of longitude: Tape number 86180
[AD-A193228] 21 p3012 N88-27872
Signal, noise, and reverberation in bistatic sonar systems
[FOA-C-20703-2.7] 22 p3147 N88-28721
CryoSQUID: A SQUID-based magnetic field sensor
[AD-A194237] 23 p3239 N88-29275
An investigation of acoustic cavitation produced by pulsed ultrasound
[AD-A193523] 23 p3278 N88-29516

NOISE ATTENUATION
U NOISE REDUCTION

NOISE ELIMINATION
U NOISE REDUCTION

NOISE GENERATORS
Noise emission of civil and military aero-engines. Sources of generation and measures for attenuation
[ETN-87-91021] 01 p0091 N88-10595
A digital control system for high level acoustic noise generation 02 p0138 N88-10865
An experimental investigation of noise generation and noise reduction in a pipe flow downstream of a discontinuous area enlargement
[ESA-TT-1027] 03 p0374 N88-12351
Higher frequency ambient noise in the arctic ocean
[AD-A192203] 18 p2547 N88-25122
Noise generation by air bubbles in water: An experimental study of creation and splitting
[AD-A192063] 19 p2664 N88-25839
Noise generation and boundary layer effects in vortex-airfoil interaction and methods of digital hologram analysis for these flow fields
[AD-A194191] 23 p3171 N88-28883

NOISE HAZARDS
U HAZARDS
U NOISE (SOUND)

NOISE INJURIES
Further investigation of tests for susceptibility to noise-induced hearing loss
[ISVR-TR-149] 14 p1952 N88-21633

NOISE INTENSITY
First article test noise survey of the A/F32T-9 large turbo fan engine enclosed noise suppressor system, Sky Harbor IAP (International Airport), Phoenix, Arizona
[AD-A183799] 01 p0090 N88-10588
Helicopter main-rotor speed effects on far-field acoustic levels
[NASA-TM-100512] 02 p0230 N88-11451
AFAR (Azores Fixed Acoustic Range) measurements of intensity and intensity moments
[AD-A184431] 03 p0355 N88-12237
Development of rotorcraft interior noise control concepts. Phase 2: Full scale testing, revision 1
[NASA-CR-172594-REV-1] 06 p0777 N88-14769
Measuring the annoyance of aircraft noise
[AD-A185494] 06 p0777 N88-14770
Annoyance caused by advanced turboprop aircraft flyover noise: Single-rotating propeller configuration
[NASA-TP-2782] 09 p1242 N88-17441
Wideband HF (High Frequency) modeling and simulation
[PB88-116116] 10 p1317 N88-17874
Operational noise data for CH-47D and AH-64 army helicopters
[AD-A191059] 18 p2570 N88-25263
Sound power measurements in situ using a reference sound source
[PB88-182571] 20 p2849 N88-26910
Discrimination studies using short-period P waves at upper mantle distances
[AD-A195468] 24 p3401 N88-30257

NOISE MEASUREMENT
Noise levels from propeller-driven aircraft measured at ground level and at 1.2 m above the ground
[NPL-AC-110] 01 p0091 N88-10594
An experimental investigation of noise generation and noise reduction in a pipe flow downstream of a discontinuous area enlargement
[ESA-TT-1027] 03 p0374 N88-12351
Overview of NASA PTA propfan flight test program 08 p0957 N88-15805
Advanced propeller research 08 p0957 N88-15806
Identification and proposed control of helicopter transmission noise at the source 09 p1109 N88-16647
Wind turbine acoustics research bibliography with selected annotation
[NASA-TM-100528] 09 p1243 N88-17450
Analysis of in-flight acoustic data for a twin-engined turboprop airplane
[NASA-CR-178389] 11 p1543 N88-19220
Experimental study on the influence of wind on acoustic pressure sensors
[ISL-R-121/86] 15 p2131 N88-22712
Advisory circular: Noise certification handbook
[FAA-AC-36-4B] 17 p2394 N88-24234
Sound power measurements in situ using a reference sound source
[PB88-182571] 20 p2849 N88-26910
Aeroacoustic investigation on the noise from ultralight aircraft
[DFVLR-FB-88-03] 21 p3013 N88-27879
Minimizing escape probabilities: A large deviations approach
[AD-A194534] 23 p3275 N88-29496
Noise levels from a jet-engined aircraft measured at ground level and at 1.2 m above the ground
[NPL-AC-114] 23 p3279 N88-29524

NOISE POLLUTION
A proposed metric for assessing the potential of community annoyance from wind turbine low-frequency noise emissions
[DE88-001113] 08 p1022 N88-16187
Cape Blanco wind farm feasibility study
[DE88-003749] 10 p1349 N88-18060
Supersonic and subsonic aircraft noise effects on animals: A literature survey
[AD-A186922] 10 p1404 N88-18373
Noise assessment of unsuppressed TF-34-GE-100A engine at Warfield ANG, Baltimore, Maryland
[AD-A189966] 15 p2129 N88-22702
The MOD-2 wind turbine: Aeroacoustical noise sources, emissions, and potential impact
[DE88-001132] 19 p2687 N88-25971
Aircraft noise: A review
[PNR90450] 22 p3147 N88-28719

NOISE PREDICTION
Surface effects and low frequency noises in GaAs field effect transistors
[LAAS-87-179] 02 p0168 N88-11055
High speed propeller performance and noise predictions at takeoff/landing conditions
[NASA-TM-100267] 05 p0646 N88-13960
Comparison of two transonic noise prediction formulations using the aircraft noise prediction program
[NASA-CR-181609] 12 p1688 N88-20095
Aircraft noise prediction program propeller analysis system IBM-PC version user's manual version 2.0
[NASA-CR-181689] 24 p3428 N88-30399
NOISE PREDICTION (AIRCRAFT)
Compressor large bandwidth noise emission mechanisms
[ETN-88-91177] 05 p0646 N88-13959
Development of rotorcraft interior noise control concepts. Phase 3: Development of noise control concepts
[NASA-CR-178172] 06 p0776 N88-14762
A comparison of simple analytical models for representing propeller aircraft structural and acoustic responses
[ISVR-TR-153] 23 p3279 N88-29523
NOISE PROPAGATION
A new method for determining acoustic properties of the seabed from the ambient noise field in the ocean
[RAE-TR-86035] 01 p0090 N88-10590
Noise emission of civil and military aero-engines. Sources of generation and measures for attenuation
[ETN-87-91021] 01 p0091 N88-10595
Sound propagation over uneven ground and irregular topography
[NASA-CR-182956] 20 p2849 N88-26911
Investigation of helicopter rotor blade/wake interactive impulsive noise
[NASA-CR-177435] 23 p3171 N88-28882
NOISE REDUCTION
Masking effects of fine and coarse grain pictorial noise
[IZF-1985-21] 01 p0076 N88-10485
First article test noise survey of the A/F32T-9 large turbo fan engine enclosed noise suppressor system, Sky Harbor IAP (International Airport), Phoenix, Arizona
[AD-A183799] 01 p0090 N88-10588
Active minimisation of acoustic fields. A review of research into the active control of sound undertaken at ISVR from 1983 to 1986
[ISVR-TR-146] 01 p0091 N88-10593
Noise emission of civil and military aero-engines. Sources of generation and measures for attenuation
[ETN-87-91021] 01 p0091 N88-10595
An experimental investigation of noise generation and noise reduction in a pipe flow downstream of a discontinuous area enlargement
[ESA-TT-1027] 03 p0374 N88-12351
On a circular correlation technique for filtering randomly noisy data
[AD-A184317] 04 p0431 N88-12669
Design of source coders and joint source/channel coders for noisy channels
[NASA-CR-181547] 04 p0432 N88-12678
Aircraft interior noise reduction by alternate resonance tuning
[NASA-CR-181530] 04 p0488 N88-13005
Noise of a model counterrotation propeller with reduced aft rotor diameter at simulated takeoff/approach conditions (F7/A3)
[NASA-TM-100254] 05 p0647 N88-13961
A computer decision-making process for the elimination of noise from data
[AD-A185746] 06 p0759 N88-14659
Development of rotorcraft interior noise control concepts. Phase 3: Development of noise control concepts
[NASA-CR-178172] 06 p0776 N88-14762
Propulsion challenges and opportunities for high-speed transport aircraft 08 p0958 N88-15809
Recent Langley helicopter acoustics contributions 09 p1109 N88-16646
Identification and proposed control of helicopter transmission noise at the source 09 p1109 N88-16647
A decade of aeroacoustic research at NASA Ames Research Center 09 p1109 N88-16648
Rotorcraft technology at Boeing Vertol: Recent advances 09 p1111 N88-16658
Optimal application of Morrison's iterative noise removal for deconvolution. Appendices
[NASA-CR-182477] 09 p1231 N88-17376
Measured and calculated acoustic attenuation rates of tuned resonator arrays for two surface impedance distribution models with flow
[NASA-TP-2766] 09 p1241 N88-17440
Silencium resonators (Silators) for the attenuation and elimination of sound
[MBB-Z-546/83] 10 p1312 N88-17841
The assessment of the sound insulation requirements for a large broadcasting studio, using a scale model: Practical details
[BBC-RD-1987/21] 10 p1318 N88-17878
An adaptive filtering technique for removing periodic noise from modal response data
[DE88-002347] 10 p1322 N88-17903
Advanced propfan analysis for the family of commuter airplanes
[NASA-CR-182566] 12 p1582 N88-19468
A study of methods to predict and measure the transmission of sound through the walls of light aircraft
[NASA-CR-182656] 12 p1687 N88-20090
Evaluation of chemical and atmospheric sciences research
[AD-A188468] 12 p1687 N88-20091
Design, optimization and construction of a dc-SQUID with complete flux transformer circuits
[PB88-160742] 14 p1907 N88-21399
Ultrahigh coherent semiconductor lasers and their applications to Rb atomic clock 14 p1976 N88-21789
Generation of number-phase minimum uncertainty states 14 p1978 N88-21803
Investigation of aeroacoustic mechanisms by remote thermal imaging
[DE88-002612] 15 p2021 N88-22046
Noise assessment of unsuppressed TF-34-GE-100A engine at Warfield ANG, Baltimore, Maryland
[AD-A189966] 15 p2129 N88-22702
Experimental study on the influence of wind on acoustic pressure sensors
[ISL-R-121/86] 15 p2131 N88-22712
The calculation of casually constrained optima in the active control of sound
[ISVR-TR-147] 17 p2395 N88-24237
Evaluation of the US Army fitting program for the integrated helmet unit of the integrated helmet and display sighting system
[AD-A191616] 18 p2465 N88-24635
First article noise survey of the A/F32T-9 large turbo fan engine enclosed noise suppressor system, far-field noise, Ellsworth AFB, South Dakota
[AD-A191938] 19 p2602 N88-25457
Signal processing in digital speech transmission systems
[ETN-88-92122] 20 p2792 N88-26561
A review of gear housing dynamics and acoustics literature
[NASA-CR-183110] 20 p2811 N88-26675
Aircraft interior noise reduction by alternate resonance tuning
[NASA-CR-182540] 20 p2849 N88-26909
Electromagnetic compatibility. View of the near future
[SNIAS-881-422-104] 22 p3071 N88-28229
Aircraft noise: A review
[PNR90450] 22 p3147 N88-28719
A comparison of simple analytical models for representing propeller aircraft structural and acoustic responses
[ISVR-TR-153] 23 p3279 N88-29523
NOISE SPECTRA
Compressor large bandwidth noise emission mechanisms
[ETN-88-91177] 05 p0646 N88-13959
HOC spectral analysis of an almost periodic random sequence in noise
[AD-A185528] 06 p0765 N88-14697
The acoustic source created by turbulent flow over orifices and louvers
[REPT-97674] 06 p0776 N88-14764
Universal power spectra for wave turbulence: Applications to wind waves, flicker noise, solar wind spectrum and classical second sound 10 p1318 N88-17879
Determination of distributed resistance of base of bipolar transistors measuring noise spectral densities
[DE88-700197] 11 p1479 N88-18829
Regional wave attenuation and seismic moment from the inversion of NORESS spectra
[AD-A187399] 11 p1510 N88-19023
Optimal and conventional space-time processing in flow noise
[AD-A189104] 13 p1833 N88-20965
Describing the source created by turbulent flow over orifices and louvers
[AD-A190254] 15 p2130 N88-22706
Sound power measurements in situ using a reference sound source
[PB88-182571] 20 p2849 N88-26910
Application of pattern recognition techniques to the identification of aerospace acoustic sources
[NASA-CR-183116] 21 p3013 N88-27877
Aeroacoustic investigation on the noise from ultralight aircraft
[DFVLR-FB-88-03] 21 p3013 N88-27879
High performance charge transfer device detectors
[AD-A194409] 23 p3192 N88-28993
NOISE SUPPRESSORS
U NOISE REDUCTION
NOISE TEMPERATURE
Capacitive resonant transducer for the Frascati gravitational antenna
[IFSI-86-9] 05 p0578 N88-13528
DSS 14 64-meter antenna S- and X-band efficiency and system noise temperature calibrations, September 1987 11 p1473 N88-18790
A study of satellite emission computed tomography
[AD-A189567] 13 p1797 N88-20745
Generating squeezed microwave radiation with a Josephson parametric amplifier 14 p1978 N88-21805
The kinetics of contact noise in NaBeta alumina
[AD-A190651] 15 p2130 N88-22707
Fluxons and order in long Josephson junctions
[AD-A190879] 16 p2282 N88-23665
X-band noise temperature near the Sun at a 34-meter high efficiency antenna 22 p3067 N88-28200
NOISE TOLERANCE
Annoyance caused by advanced turboprop aircraft flyover noise: Single-rotating propeller configuration
[NASA-TP-2782] 09 p1242 N88-17441
Electroencephalographic changes during equilibrium test in the presence of rhythmic photic interference 19 p2703 N88-26075
NOMENCLATURES
Abregrams or deleweds: A forty-year view of acronyms
[DE87-010808] 01 p0106 N88-10690
NOMINAL VALUES
U APPROXIMATION
NONADIABATIC PROCESSES
U HEAT TRANSFER
NONAQUEOUS ELECTROLYTES
Metal intercalation characteristics of n-HfS2 photoelectrodes in non-aqueous electrolytes
[AD-A184381] 03 p0383 N88-12407
Re-usable thin-layer spectroelectrochemical cell for non-aqueous solvent systems
[AD-A186951] 09 p1248 N88-17478
NONCONDUCTORS
U ELECTRICAL INSULATION
NONCONSERVATIVE FORCES
Contribution to the dynamical analysis of rheolinear nonconservative, gyroscopic systems using finite element methods
[ETN-87-90410] 01 p0050 N88-10320
Examples of nonconservatism in the CARE 3 program
[NASA-TM-100524] 09 p1233 N88-17390
NONDESTRUCTIVE TESTS
NT NEUTRON RADIOGRAPHY
Compendium of post-failure analysis techniques for composite materials
[AD-A183783] 01 p0018 N88-10113
X-ray tomography and nuclear magnetic resonance imaging applications for advanced ceramic materials
[DE87-011534] 01 p0027 N88-10171
Evaluation of mechanical and technological parameters of different steel states by nondestructive micro- and macromagnetic measuring quantities as well as ultrasonic techniques
[MPA-810-079] 01 p0057 N88-10366
Nondestructive inspection of the pressure vessel in Stuttgart. ALOK part. Phase 1: ALOK combined with conventional probes
[REPT-860113-TW] 01 p0057 N88-10367
Model-based ultrasonic tomography
[DE87-013786] 01 p0058 N88-10369
Needs assessment for NDT and characterization of ceramics: Assessment of inspection technology for green state and sintered ceramics
[DE87-013550] 02 p0151 N88-10947
Needs assessment for nondestructive testing and materials characterization for improved reliability in structural ceramics for heat engines
[DE88-000040] 02 p0153 N88-10957
Ultrafast holography using optical fibers
[ISL-R-101/86] 02 p0176 N88-11096
Development of an X-ray fluorescence microprobe at the National Synchrotron Light Source, Brookhaven National Laboratory: Early results: Comparison with data from other techniques
[NASA-CR-181468] 02 p0236 N88-11486
Transply crack density detection by acousto-ultrasonics
[NASA-TM-100224] 03 p0279 N88-11758
Ultrasonic characterization of the nonlinear elastic properties of unidirectional graphite/epoxy composites
[NASA-CR-4100] 03 p0281 N88-11767

NDE (Nondestructive Evaluation) of advanced structural ceramics
[DE87-014417] 03 p0292 N88-11832
Flaw imaging and ultrasonic techniques for characterizing sintered silicon carbide
[NASA-TM-100177] 03 p0334 N88-12106
Real time analysis of the results from mechanized ultrasonic testing
[DE87-752511] 03 p0334 N88-12107
Elastodynamic ray theory and asymptotic methods for direct and inverse scattering problems
03 p0335 N88-12108
Failure analysis of composite structure materials
[AD-A184468] 04 p0410 N88-12548
Detection of defects on structures
[EP-PATENT-0-210-794-A2] 04 p0453 N88-12807
Philosophy and practice of nondestructive tests of composite material structures at Aerospatiale Aquitaine
[SNIAS-872-430-105] 05 p0559 N88-13400
Utilization of microwave measuring systems for nondestructive control of composite materials
[SNIAS-872-430-109] 05 p0559 N88-13402
Measurement and control of damage in composite materials: Nondestructive controls by thermography, holography, and radiography
[SNIAS-872-430-110] 05 p0559 N88-13403
Contribution of acoustic analysis to assess damage in fluid storage tanks under high pressure --- composite materials, filament winding
[SNIAS-872-430-119] 05 p0559 N88-13407
Water disbondment characterization of organic Coating/metal substrate systems
[AD-A184847] 05 p0567 N88-13454
First International Week of Adhesive Bonding and Assembling
[SNIAS-872-430-106] 05 p0569 N88-13468
Investigation of the exposure to harmful compounds in the workshop of nondestructive materials testing at Gilze-Rijen (Netherlands)
[PML-1985-42] 05 p0623 N88-13816
Comparative study of nondestructive pavement testing, MacDill Air Force Base, Florida
[AD-A186082] 07 p0822 N88-14993
Natural frequencies and structural integrity assessment of large space structures
[AD-A186139] 07 p0824 N88-15001
Macroscopic distribution of fiber finish
[DCQ/L-48-283/F] 07 p0827 N88-15013
Improvement of deep resolution in ultrasonic echographic nondestructive evaluation using signal processing methods
[PB87-147658] 07 p0866 N88-15256
Through-transmission/pulse-echo ultrasonic equipment evaluation
[AD-A186340] 07 p0929 N88-15641
Determining structural performance
08 p0954 N88-15787
Nondestructive characterization of ceramic composite whiskers with neutron diffraction and ultrasonic techniques
[DE88-003075] 08 p0965 N88-15844
Nondestructive control: Modeling of electromagnetic phenomena, defect characterization, and sensor optimization
[ECL-86-14] 08 p0993 N88-16008
Solid mechanics research for quantitative non-destructive evaluation
[AD-A186599] 08 p0993 N88-16010
Study of the technique of stress determination by measuring magnetism
[PB87-143905] 08 p0996 N88-16028
Nondestructive magnetic testing of laser hardening parameters (hardening depth, hardness profile, retained austenite)
[ETN-88-91070] 09 p1144 N88-16857
Nondestructive evaluation of structural ceramics by photoacoustic microscopy
[NASA-CR-180858] 09 p1146 N88-16868
Image correlation on an IBM-PC for characterization of advanced ceramics
[DE88-002829] 09 p1149 N88-16885
Thermal wave imaging
[AD-A186810] 09 p1177 N88-17046
Analysis of the reliability of Royal Australian Air force non-destructive inspection
[AD-A186979] 09 p1177 N88-17049
Experience of developing an integrated nondestructive assay system
[DE88-003149] 09 p1184 N88-17092
Durability and damage tolerance of aluminum castings
[AD-A186444] 10 p1341 N88-18013
The development of emission tomography for the nuclear industry
[AERE-R-12319] 10 p1341 N88-18014
Training guidelines in non-destructive testing techniques
[DE88-700613] 10 p1342 N88-18019
Institute for Materials Science and Engineering, nondestructive evaluation: Technical activities 1987
[PB88-153655] 10 p1342 N88-18020
Application of nondestructive testing techniques to materials testing
[AD-A187645] 10 p1342 N88-18021
Institute for Materials Science and Engineering, Fracture and Deformation Division: Technical activities, 1987
[PB88-153622] 10 p1345 N88-18039
Ultrasonic characterization of layered composite systems 10 p1404 N88-18374
Scattering of impulsive acoustic waves by a semi-infinite crack in the plane interface of a half-space and a layer
[PB88-126396] 10 p1405 N88-18377
Quantitative non-destructive evaluation of porous composite materials based on ultrasonic wave propagation
[NASA-CR-182544] 11 p1447 N88-18627
Quality assurance of ceramic materials and gas turbine components
[IZFP-850303-TW] 11 p1465 N88-18735
Novel analytical X-ray Non-Destructive Evaluation (NDE) tool for quality control of energetic materials
[AD-A187737] 11 p1497 N88-18935
Reference standards for nondestructive tests
[AD-A187766] 11 p1497 N88-18936
STA-2A NDT testing
[NASA-CR-179301] 11 p1497 N88-18937
Imaging methods for nondestructive materials testing
[ETN-88-91477] 11 p1497 N88-18940
Non-destructive evaluation techniques applied to the study of fatigue microcrack growth in steel alloys
[DE88-004090] 13 p1742 N88-20420
High temperature Young's modulus of IG-110 graphite
13 p1746 N88-20443
Nondestructive testings of HTGR graphites
13 p1747 N88-20448
Nondestructive evaluation of carbon-carbon coatings
[AD-A189524] 13 p1748 N88-20453
Recent developments in nondestructive evaluation for structural ceramics
[DE88-005889] 13 p1751 N88-20473
X-ray computed tomography for structural ceramic applications: Beam hardening corrections
[DE88-005891] 13 p1752 N88-20474
Noncontact thermometry via laser pumped, thermographic phosphors: Characterization of systematic errors and industrial applications
[DE88-005599] 13 p1777 N88-20628
Thermionic Technology Program. A: Insulator test and evaluation
[DE88-004707] 13 p1795 N88-20735
Statistical analysis of feasibility of non-destructive inspection of mechanical properties of hot worked pipes of alloy steels
[BLL-M-37598-(5828.4)] 14 p1922 N88-21455
A system to measure damage in composite materials by the ultrasonic method
[ONERA-RT-2/7256-RY-061-R]
15 p2031 N88-22103
Electromagnetic sensor arrays for nondestructive evaluation and robot control
[AD-A190210] 15 p2056 N88-22260
Nondestructive moisture measurement in microelectronics
[AD-A190515] 15 p2060 N88-22281
An evaluation of nondestructive methods for ceramic heat exchanger applications
[DE88-006731] 15 p2068 N88-22328
Eddy current nondestructive inspection of graphite epoxy using ferrite cup core probes
[AD-A189823] 15 p2074 N88-22365
Manufacturing of ultrasonic focused probes
[VTT-RR-487] 15 p2074 N88-22368
A 3-D solid rendering of NDT data
[DE88-006199] 15 p2076 N88-22373
Impact damage in composite laminates
15 p2080 N88-22402
Lewis Structures Technology, 1988. Volume 3: Structural Integrity Fatigue and Fracture Wind Turbines HOST
[NASA-CP-3003-VOL-3] 15 p2081 N88-22408
Nondestructive evaluation by acousto-ultrasonics
15 p2082 N88-22412
Characterization of sintered SiC by using NDE
15 p2082 N88-22413
Nondestructive evaluation of sintered ceramics
15 p2083 N88-22416
Nondestructive evaluation of large scale composite components
[AD-A190998] 16 p2173 N88-22954
Detection sensitivity in thick assemblies --- eddy currents, light alloys, aircraft construction materials
[REPT-48-912/F] 16 p2216 N88-23221
Utility NDE personnel qualification/certification: Enhanced personnel qualification requirements for ASME (American Society for Mechanical Engineers) Code Section 11 examinations
[DE88-006748] 16 p2216 N88-23222
Acousto-ultrasonic input-output characterization of unidirectional fiber composite plate by SV waves
[NASA-CR-4152] 16 p2217 N88-23224
Structural Ceramics
[NASA-CP-2427] 17 p2323 N88-23872
Nondestructive evaluation of structural ceramics
17 p2324 N88-23876
Nondestructive Evaluation (NDE) of structural ceramics by photoacoustic microscopy 17 p2325 N88-23884
Acoustic emission frequency discrimination
[NASA-CASE-MSC-20467-1] 17 p2342 N88-23966
Method of radiographic inspection of wooden members
[NASA-CASE-LAR-13724-1] 17 p2346 N88-23983
Input-output characterization of fiber composites by SH waves
[NASA-CR-4153] 17 p2347 N88-23986
Characterization of noncontact piezoelectric transducer with conically shaped piezoelement
[NASA-CR-4151] 17 p2347 N88-23987
Stress measurements in graphite fibers by laser raman spectroscopy
[AD-A191710] 18 p2491 N88-24779
Defect detection and classification in VLSI pattern inspection 18 p2507 N88-24871
Knowledge based systems in nondestructive evaluation
[DE88-006653] 18 p2525 N88-24981
Nondestructive testing using ultrahigh frequencies
[CERT-5/1333-MO] 18 p2526 N88-24984
Nondestructive evaluation methods for determination of thermal history and mechanical properties of aluminum-lithium alloys
[DE88-007352] 19 p2615 N88-25516
Model-based computed tomography for nondestructive evaluation: An overview and proposal
[DE88-010600] 19 p2679 N88-25926
Sensitivity to crack initiation in thick assemblies. Test report 48-444
[REPT-48-444] 20 p2758 N88-26365
Microfocus X-ray techniques for flaw location
[DE88-008636] 20 p2812 N88-26680
Development of an automated X-ray gauge for nondestructive quantitative analysis
[DE88-008633] 20 p2812 N88-26681
Methods and techniques of NDA (nondestructive assay)
[DE88-009145] 20 p2812 N88-26682
Principles of a nondestructive evaluation process for damage location, damage profile, and damage extension in welded joints by radiometric measurements
[MPA-86-02] 20 p2812 N88-26683
Stress analysis using infrared thermography
[ETN-88-92169] 20 p2816 N88-26705
Assembly Test Article (ATA)
[NASA-CR-179361] 21 p2903 N88-27226
Design and implementation of contact ultrasonic sensors to assess internal damage
[I-177/87] 21 p2906 N88-27247
Balance of X-ray radioscopy application to nondestructive tests of composite materials
[SNIAS-881-430-110] 21 p2907 N88-27250
NDE performance in predicting failure strength of spherical composite specimens with implanted flaws
[DE88-008223] 21 p2959 N88-27575
Interface control using low frequency (3 to 20 MHz) acoustic microscopy
[REPT-48-411/F] 21 p2959 N88-27577
Genetic effects of low level microwave radiation
[AD-A192687] 21 p2984 N88-27722
Use of penetrating radiations for the dynamic examination of aero gas turbines
[PNR90470] 22 p3045 N88-28073
Optimization of nondestructive control of ceramic pieces for aeronautical turbines
[ETN-88-92884] 22 p3059 N88-28149
Direct and inverse diffraction problems for QNDE (Quantitative Non-Destructive Evaluation) applications
[AD-A194721] 22 p3085 N88-28322
New acousto-ultrasonic techniques applied to aerospace materials
[NASA-TM-101299] 22 p3086 N88-28323
Comparison of 2-D Fourier and spatial techniques for removing noise in real-time X-ray radiography
[AD-A193700] 23 p3187 N88-28962
Nondestructive tests and high performance composite structures
[SNIAS-881-430-119] 23 p3188 N88-28969
Microwave frequency nondestructive control
[CERT-2/1355-MO] 23 p3189 N88-28976

Contribution to the study of materials behavior in space environment
[SNIAS-881-430-104] 23 p3189 N88-28977
Method and apparatus for non-destructive testing of temper embrittlement in steels
[NASA-CASE-LAR-13817-1] 23 p3195 N88-29012
Radioactivity as a means of nondestructive testing
[DE88-702778] 23 p3224 N88-29188
Nondestructive investigations for space use
[SNIAS-881-430-105] 23 p3224 N88-29189
A generic expert system for materials processing in space 23 p3255 N88-29376
Evaluation of bond testing equipment for inspection of Army advanced composite airframe structures
[AD-A195795] 24 p3341 N88-29885
In situ fault detection by the hybrid ray mode method
[AD-A195226] 24 p3381 N88-30137
Application of nondestructive testing techniques to materials testing
[AD-A195716] 24 p3381 N88-30138
Automated early fatigue damage sensing system
[AD-A195717] 24 p3382 N88-30143
Report on an overseas visit to USA relating to the thermoelastic measurement of stresses, 16-21 August 1987
[AD-A195313] 24 p3385 N88-30161

NONEQUILIBRIUM CONDITIONS
Requirements for a test stand for plastic rollers for the verification of nonequilibrium force laws
[ILR-MITT-176] 01 p0008 N88-10040
Development of the non-equilibrium reactive chemical transport code CHMTRNS
[DE88-000682] 04 p0481 N88-12964
Studies in finite time thermodynamics
[DE88-004531] 10 p1423 N88-18500
Nonequilibrium phonons and disorder in Al sub x Ga sub 1-x As 19 p2657 N88-25788
Femtosecond nonequilibrium electronic heat transport in thin gold films 19 p2659 N88-25807
Non-equilibrium phases and phase diagrams
[DE88-006896] 20 p2880 N88-27098

NONEQUILIBRIUM DRAG
U FRICTION DRAG

NONEQUILIBRIUM FLOW
Interface characteristics and the mechanical properties of metal matrix composites
[AD-A186441] 08 p0966 N88-15845
Nonequilibrium reacting flows 08 p0985 N88-15959
Experimental evidence of micro-nonequilibrium on the magnetopause and further predictions 08 p1098 N88-16606
A study of numerical methods for hyperbolic conservation laws with stiff source terms
[NASA-TM-100075] 10 p1399 N88-18343
Accelerating the computation of steady state solutions for non-equilibrium, chemically reacting flow fields 12 p1625 N88-19724
Low density real gas flows about hypersonic vehicles
[AD-A194251] 22 p3075 N88-28253
Development and analysis of turbulent non-equilibrium boundary layers 23 p3169 N88-28872
Nonequilibrium flow of a radiating gas in a vertical channel with axial temperature variation
[DE88-702535] 23 p3212 N88-29120
Beam combining by phase transition nonlinear media
[AD-A194116] 23 p3283 N88-29547
Nonequilibrium flow of a dissociating gas in a horizontal channel with axial temperature variation
[DE88-702536] 24 p3373 N88-30089
Nonequilibrium flow computations. 1: An analysis of numerical formulations of conservation laws
[NASA-CR-177489] 24 p3425 N88-30384

NONEQUILIBRIUM IONIZATION
Nonequilibrium ionization of pregalactic plasma and lessening of relic radiation anisotropy 08 p1002 N88-16071
Nonequilibrium superconductivity for particle detectors
[DE88-002876] 09 p1257 N88-17539

NONEQUILIBRIUM PLASMAS
Nonequilibrium ionization of pregalactic plasma and lessening of relic radiation anisotropy 08 p1002 N88-16071
Experimental evidence of micro-nonequilibrium on the magnetopause and further predictions 08 p1098 N88-16606
Ionization equilibrium and radiative energy losses in a stationary plasma
[DE88-700856] 14 p1984 N88-21832

NONEQUILIBRIUM RADIATION
Consistent spherical Nonlocal Thermal Equilibrium (NLTE) models for objects with B-star-like luminosities
[ETN-88-90601] 06 p0800 N88-14897

NONEQUILIBRIUM THERMODYNAMICS
Nonequilibrium characteristics of nitrogen plasmas appropriate to an AOTV flight 03 p0319 N88-12019

NONEUCLIDIAN GEOMETRY
U DIFFERENTIAL GEOMETRY

NONHOMOGENEITY
U INHOMOGENEITY

NONISOTHERMAL PROCESSES
Methods and first results of plasma non-isothermal parameters measurements in meteor trails 06 p0737 N88-14531
Bithermal fatigue: A simplified alternative to thermomechanical fatigue 15 p2084 N88-22424

NONISOTROPIC PLATES
U ANISOTROPIC PLATES

NONISOTROPY
U ANISOTROPY

NONLINEAR EQUATIONS
NT CUBIC EQUATIONS
NT NONLINEAR EVOLUTION EQUATIONS
NT QUADRATIC EQUATIONS
An asymptotic theory for a class of initial-boundary value problems for weakly nonlinear wave equations with an application to a model of the galloping oscillations of overhead transmission lines
[REPT-87-12] 01 p0086 N88-10556
Nonlinear fluid equations for a low collisionality toroidal plasma
[DE87-013006] 01 p0100 N88-10655
Extending Green's function formalism to general nonlinear equations
[DE87-013541] 02 p0224 N88-11411
Long wavelength vortices of low frequency interchange modes
[IPPJ-844] 02 p0241 N88-11525
New physical explanation of phase-conjugate waves produced in backward stimulated scattering 03 p0302 N88-11900
Blowup for a nonlinear evolution equation and self-reproducing strained shear layers 04 p0444 N88-12755
Solution of three-dimensional inverse problem of gravimetry in contact surfaces class by local corrections method 04 p0460 N88-12848
Steady waves in a nonlinear theory of viscoelasticity
[AD-A185548] 06 p0723 N88-14448
Development of symbolic computation methods for nonlinear dynamics
[AD-A185562] 06 p0758 N88-14653
Characteristic trajectories of generalized Lanchester equations
[AD-A185762] 06 p0766 N88-14705
Nonlinear reflection of sound wave in gas mixture 06 p0769 N88-14728
New methods for numerical solution of one class of strongly nonlinear partial differential equations with applications
[AD-A186166] 07 p0899 N88-15445
Nonlinear diffusion in the presence of a time-dependent external electric field
[INPE-4378-PRE/1198] 08 p1085 N88-16533
Techniques in linear and nonlinear partial differential equations
[AD-A187109] 09 p1227 N88-17347
Straightening and the Stanley decomposition for the (2;n)-nilpotent vectorfield
[PB88-126685] 10 p1398 N88-18336
Method of reduction of polynomially nonlinear equations to linear equations
[DE88-700922] 12 p1683 N88-20064
Nonlinear differential equations
[DE88-006047] 13 p1828 N88-20933
The biHamiltonian formulations of integrable evolution equations in multidimensions
[PREPRINT-568] 14 p1968 N88-21745
Memory efficient evaluations of nonlinear stochastic equations and C3 applications
[AD-A189872] 15 p2110 N88-22569
Almost-periodic solutions of nonlinear parabolic equations
[DE88-006423] 15 p2118 N88-22618
Numerical solution of nonlinear algebraic equations in stiff ODE solving
[DE88-006634] 15 p2118 N88-22622
New methods for numerical solution of one class of strongly nonlinear partial differential equations with applications
[AD-A189945] 15 p2119 N88-22630
Research in nonlinear partial differential equations and bifurcation theory
[AD-A190986] 16 p2260 N88-23514
On a generalization of renormalization group equations to quantum field theories of an arbitrary type
[DE88-701143] 16 p2263 N88-23531
Similarity solutions of nonlinear partial differential equations invariant to a family of affine groups
[DE88-003404] 18 p2567 N88-25245
Semi-discrete approximations to nonlinear systems of conservation laws; consistency and L(infinity)-stability imply convergence
[NASA-CR-181683] 19 p2721 N88-26157
Initial value problems for nonlinear heat equations
[DE88-702021] 19 p2737 N88-26251
Nonlinear equation of state effects and the momentum-dilution trade-off in a turbulent buoyant jet
[DE88-701839] 20 p2799 N88-26610
Numerical optimization
[AD-A193032] 21 p3005 N88-27827
Cauchy problem for the nonlinear Schroedinger equation
[DE88-702454] 21 p3011 N88-27867
Initial boundary value problems of nonlinear wave equations in an exterior domain
[DE88-701883] 21 p3026 N88-27962
The construction of implicit and explicit solitary wave solutions of nonlinear partial differential equations
[AD-A193475] 23 p3269 N88-29452
MACSYMA program for the painleve test of nonlinear ordinary and partial differential equations
[AD-A194293] 23 p3270 N88-29458
On nonlinear equations admitting soliton solutions with a deBroglie phase
[DE88-702694] 23 p3277 N88-29508
New methods for nonlinear optimization
[AD-A195982] 24 p3412 N88-30313
Convergence acceleration for vector sequences and applications to computational fluid dynamics
[NASA-TM-101327] 24 p3424 N88-30377
Convergence of Galerkin approximations for operator Riccati equations: A nonlinear evolution equation approach
[NASA-CR-181706] 24 p3425 N88-30386

NONLINEAR EVOLUTION EQUATIONS
The Eckhaus Partial Differential Equation (PDE) I psi t + psi xx + 2(psi/sq)x psi +2(/psi/) to the 4th power psi = 0
[PREPRINT-546] 06 p0763 N88-14686
Equations of nonlinear Schroedinger type in 1 + 1 and 2 + 1 dimensions, obtained from integrable Partial Differential Equations (PDEs)
[PREPRINT-548] 06 p0764 N88-14687
Recursion operator and bihamiltonian structure for integrable multi-dimensional lattices
[PREPRINT-552] 06 p0764 N88-14688
Nonlinear evolution equations, rescalings, model partial differential equations (PDES) and their integrability, 2
[PREPRINT-560] 06 p0764 N88-14691
Algebraic structure of linear and nonlinear models of open quantum systems
[PREPRINT-573] 14 p1968 N88-21747
Perturbation theory for dual semigroups. Part 3: Nonlinear Lipschitz continuous perturbations in the Sun-reflexive case
[CWI-AM-R8706-PT-3] 16 p2263 N88-23535
Nonlinear wave propagation
[AD-A192104] 18 p2501 N88-24835
Nonlinear waves
[AD-A192148] 18 p2510 N88-24889
Why are certain nonlinear Partial Differential Equations (PDE) both widely applicable and integrable
[PREPRINT-582] 22 p3144 N88-28698

NONLINEAR FEEDBACK
Approximation methods for the identification and control of distributed parameter systems
[AD-A190201] 15 p2124 N88-22662
Problems in nonlinear continuum dynamics
[AD-A190538] 15 p2128 N88-22691
A feedback linearization approach to spacecraft control using momentum exchange devices
[NASA-CR-172057] 18 p2472 N88-24668
Robust control of multivariable and large scale systems
[AD-A194250] 23 p3266 N88-29441
Feedback stabilization of du/dt=Au + bf in Hilbert space when the normalization function is less than or equal to r
[AD-A193510] 23 p3277 N88-29506

NONLINEAR FILTERS
White noise calculus for two-parameter filtering
[ENST-87C003] 01 p0088 N88-10578
Nonlinear techniques for detection and filtering of discrete-time signals 02 p0160 N88-11004
Statistical techniques for signal processing
[AD-A185774] 06 p0694 N88-14259
The filtering problem for infinite dimensional stochastic processes
[AD-A186431] 07 p0916 N88-15562
Lie algebraic method in filtering and identification
[CWI-PM-R8606] 08 p1072 N88-16467
Nonlinear filtering and large deviations: A PDE-Control theoretic approach
[AD-A187436] 10 p1396 N88-18321

Dynamic observers as asymptotic limits of recursive filters: Special cases
[AD-A187578] 10 p1397 N88-18324
Advanced guidance algorithms for homing missiles with bearings-only measurements
[AD-A190435] 15 p2017 N88-22026
Introduction to nilpotent approximation filtering
[CWI-PM-R8709] 16 p2262 N88-23524
Investigation of non-linear optical behavior of semiconductors for optical switching, volume 1
[AD-A191297] 16 p2274 N88-23611
A nonlinear filtering process diagnostic system for the Space Station 23 p3262 N88-29417
Approximations and implementations of nonlinear filtering schemes
[AD-A194685] 23 p3271 N88-29462
Analytical methods in stochastic control and nonlinear filtering
[AD-A194272] 24 p3426 N88-30388

NONLINEAR OPTICS

Phase equilibrium and crystal growth studies on AgGaSe2 and related nonlinear optical materials
[AD-A184768] 03 p0382 N88-12400
Anti-Stokes generation of 226 nm light
[DE88-001612] 05 p0589 N88-13590
Parametric and resonance interaction of ultrashort light pulses in nonlinear multilevel medium
06 p0773 N88-14746
Nonlinear optics with broad-band lasers
[DE88-005026] 10 p1337 N88-17992
Subpicosecond optical digital computation using phase conjugate parametric generators
[AD-A188279] 10 p1410 N88-18411
Optical signal processing using nonlinear optics
[AD-A188461] 12 p1691 N88-20117
Solid state research
[AD-A188388] 12 p1699 N88-20166
Influence of nonlinear spectroscopic effects on atmospheric propagation of intense laser radiation at 10.6 microns wavelength 13 p1789 N88-20705
United States - Japan Seminar on Quantum Mechanical Aspects of Quantum Electronics
[AD-A186938] 14 p1974 N88-21781
Gigantic optical nonlinearity in low dimensional systems 14 p1975 N88-21786
Quantum nondemolition detection and squeezing in optical fibers 14 p1976 N88-21793
Optical properties of quantum well structures with electric field: Life time free switching of luminescence intensity and virtual charge-induced ultrafast optical nonlinearity 14 p1978 N88-21794
Enhanced excitonic optical nonlinearity and exciton dynamics in semiconductor microstructures
14 p1977 N88-21795
Free carrier nonlinear optics 14 p1977 N88-21796
Collective rotation of molecules driven by the angular momentum of light in a nematic film
[FUB-6-1986] 15 p2131 N88-22714
Studies of surfaces using optical sum-frequency generation
[DE88-006334] 15 p2131 N88-22715
Theory of interactions of intense light with nonlinear, inhomogeneous and periodic structures and its applications to optical bistability, optic gyroscopes, nonlinear spectroscopy, radiation protection, X-ray emission and related fields
[AD-A190040] 15 p2133 N88-22725
Optical switching and control techniques using nonlinear optical wave mixing
[AD-A190467] 15 p2134 N88-22730
Unstable behavior of lasers and other optical systems
[AD-A190875] 16 p2213 N88-23204
Enhancement of second harmonic generation on silver gratings by resonant excitation of surface plasmon
[ETN-88-92304] 17 p2439 N88-24509
Nonlinear surface polaritons
[AD-A191046] 18 p2499 N88-24822
Nonlinear waves
[AD-A192148] 18 p2510 N88-24889
Research in the optical sciences
[AD-A192175] 18 p2575 N88-25297
Liquid crystal optics for laser systems
[DE88-008475] 20 p2854 N88-26948
Solid state research
[AD-A192837] 21 p3020 N88-27929
High energy and high intensity laser effects on aerosols: Changes in droplet morphology, surrounding temperature and vapor concentration
[AD-A193825] 23 p3220 N88-29164
Nonlinear optical processes in molecular systems
[AD-A193871] 23 p3282 N88-29546
Nonlinear optical phase conjugation techniques to reduce the physical size of lasers
[AD-A196170] 24 p3379 N88-30122
A review of melt and vapor growth techniques for polydiacetylene thin films for nonlinear optical applications
[NASA-TM-100340] 24 p3430 N88-30412

NONLINEAR PROGRAMMING

Using MINOS (Modular In-core Nonlinear Optimization System) as a subroutine for decomposition
[DE87-013086] 02 p0221 N88-11390
Performance analysis of coded frequency-hopped spread-spectrum systems with unknown interference
[AD-A186069] 07 p0841 N88-15103
A Schur-complement method for sparse quadratic programming
[DE88-002520] 07 p0904 N88-15479
Search rearrangement backtracking often requires exponential time to verify unsatisfiability
[AD-A186121] 07 p0909 N88-15511
Research on algorithms for nonlinear programming
[AD-A188326] 12 p1677 N88-20024
Constrained nonlinear programming
[DE88-005695] 13 p1817 N88-20860
Applicability of nonlinear programming in decision support systems: Realization of user-friendly software
[REPT-87-42] 14 p1957 N88-21663
Efficient method for structural optimization
15 p2054 N88-22240
On the capacity of channels with unknown interference
[AD-A191160] 16 p2191 N88-23067
Nonlinear programming extensions to rational function approximation methods for unsteady aerodynamic forces
[NASA-TP-2776] 18 p2463 N88-24623
The Sizing and Optimization Language, (SOL): Computer language for design problems
[NASA-TM-100565] 18 p2559 N88-25190
Conditions for finite convergence of algorithms for nonlinear programs and variational inequalities
[AD-A192355] 20 p2838 N88-26834

NONLINEAR SYSTEMS

Geometrically nonlinear rod mechanism analogy of axisymmetrically loaded spherical shells based on a comprehensive approach to the stability of circular arches
[ETN-87-90419] 01 p0062 N88-10398
Dimension densities for turbulent systems with spatially decaying correlation functions
[DE87-010119] 02 p0169 N88-11066
Iterative solution of a nonlinear system arising in phase change problems
[DE87-014672] 02 p0226 N88-11426
Solution of nonlinear least-squares problems
[AD-A184010] 03 p0371 N88-12335
A refined nonlinear analysis of laminated composite plates and shells
[AD-A184436] 04 p0454 N88-12811
Nonlinear acoustics
[AD-A184271] 04 p0488 N88-13004
Supertracks: The building blocks of chaos
[DE88-001513] 04 p0522 N88-13207
On the correlation free forms for nonlinear stochastic systems
[DE87-011169] 05 p0645 N88-13947
Nonlinear aerodynamic wing design
[NASA-CR-3950] 06 p0665 N88-14079
Steady waves in a nonlinear theory of viscoelasticity
[AD-A185548] 06 p0723 N88-14448
Nature and the nonlinear evolution of electrostatic waves associated with the AMPTE (Active Magnetosphere Particle Tracer Explorers) solar wind releases
[AD-A185471] 06 p0806 N88-14920
Numerical solution of turbulent flow past a backward facing step using a nonlinear K-epsilon model
[NASA-CR-178421] 07 p0854 N88-15189
Theoretical investigations of chaotic dynamics
[AD-A186404] 07 p0867 N88-15261
The design and implementation of surface acoustic wave devices for linear FM and a new non-linear FM pulse compression technique for radar applications
[AD-A186741] 08 p0980 N88-15922
Some aspects of control for semilinear distributed parameter systems
[INPE-4147-PRE/1054] 08 p1075 N88-16484
Studies on nonlinear mechanisms of excimer laser propagation in fused silica fibers
[AD-A186822] 09 p1156 N88-16929
Reliability of structures with stiffness and strength degradation 09 p1180 N88-17068
Frequency response functions of a nonlinear system
09 p1180 N88-17070
Regulation of nonlinear and generalized linear systems
[AD-A186706] 09 p1224 N88-17338
Applications of nonlinear systems theory to control design
[NASA-CR-182485] 09 p1231 N88-17377
Numerical fluid mechanics 09 p1240 N88-17434
The role of photodetectors in optical signal processing
[AD-A186804] 09 p1247 N88-17476
A finite element analysis of adhesively bonded composite joints including geometric nonlinearity, nonlinear viscoelasticity moisture diffusion and delayed failure
[AD-A187455] 10 p1296 N88-17747
Design sensitivity analysis of nonlinear structural systems and numerical implementation with established finite element codes 10 p1344 N88-18032
Nonlinear dynamic maximum power theorem
[AD-A187491] 11 p1477 N88-18810
Symmetries in nonlinear control systems and their applications 11 p1496 N88-18929
Prediction of the response and optimal control of stochastic parametrically and externally excited nonlinear systems 11 p1496 N88-18930
Optimal control theory of load-following and parameter-tracking of nonlinear systems: An application of Pontryagin Maximum Principle to reactor dynamics
[DE88-004770] 11 p1532 N88-19152
A maximum likelihood parameter estimation program for general non-linear systems
[ARL-AERO-TM-392] 11 p1532 N88-19154
Nonlinear input-output systems
[NASA-CR-182464] 11 p1535 N88-19171
Optimal recursive maximum likelihood estimation
[AD-A187980] 11 p1536 N88-19176
Advanced nonlinear theory: Long-term stability at the SSC
[CEBAF-PR-87-027] 11 p1548 N88-19248
Non-linear materials (TAS)
[AD-A189197] 12 p1633 N88-19775
A numerical study of automated dynamic relaxation for nonlinear static tensioned structures
[AD-A188372] 12 p1635 N88-19790
On analysis of viscoelastic structures
[AD-A188445] 12 p1636 N88-19793
NFEARS (Nonlinear Finite Element Adaptive Research Solver): A nonlinear adaptive finite element solver. Part 2: User's manual
[AD-A189009] 12 p1684 N88-20070
Nonlinear optical principles and the photorefractive effect applied to optical phase conjugation
[AD-A188856] 12 p1691 N88-20119
Nonlinear resonance of two-dimensional ion layers
[AD-A188890] 12 p1695 N88-20145
Stability and uniqueness in nonlinear continuum mechanics
[AD-A189616] 12 p1699 N88-20172
Robustifying the Kalman filter
[AD-A189240] 13 p1825 N88-20907
Stochasticity in nonlinear Hamiltonian systems
[DE88-005499] 13 p1826 N88-20915
Period-doubling universality in multidimensional dissipative and conservative systems
[PB88-148812] 13 p1832 N88-20961
Method for finding principal modes of nonlinear vibration systems and their stabilities 14 p1899 N88-21340
Identification of nonlinear output-affine systems using an orthogonal least squares algorithm
[RR-313] 14 p1958 N88-21678
A prediction-error estimation algorithm for nonlinear output-affine systems
[RR-314] 14 p1959 N88-21679
Identification of nonlinear rational systems using a prediction-error estimation algorithm
[RR-317] 14 p1959 N88-21680
A new approach to almost decoupling problems for linear and nonlinear systems
[MEMO-660] 14 p1962 N88-21700
Some maximum norm estimates for the finite element method applied to nonlinear two dimensional boundary value problems
[ETN-88-91505] 14 p1964 N88-21715
An orthogonal parameter estimation algorithm for nonlinear stochastic systems
[RR-307] 14 p1966 N88-21736
Parametric methods of analysing linear and nonlinear systems
[RR-318] 14 p1967 N88-21741
Three-wave parametric resonance in plasma of relativistic electron flux 14 p1972 N88-21772
Nonlinear analysis and optimal design of dynamic mechanical systems for spacecraft application
[AD-A190644] 15 p2026 N88-22070
Random processes, turbulence and disordering fields
[AD-A190123] 15 p2063 N88-22303
Buckling of blast loaded cylinder
[AD-A190124] 15 p2076 N88-22376
The analysis of non-linear dynamic behavior (including snap-through) of postbuckled plates by simple analytical solution
[NASA-TM-89165] 15 p2087 N88-22439

Memory efficient evaluations of nonlinear stochastic equations and C3 applications
[AD-A189872] 15 p2110 N88-22569
Nonlinear signal processing using neural networks: Prediction and system modelling
[DE88-006479] 15 p2118 N88-22621
Numerical methods for linear and nonlinear optimization
[AD-A190029] 15 p2120 N88-22631
Symmetry and global bifurcation in nonlinear solid mechanics
[AD-A190521] 15 p2121 N88-22642
Applications research studies of microtubules
[AD-A190855] 16 p2182 N88-23005
On the computation of stationary deterministic behavior of nonlinear dynamic systems with applications to rotor-bearing structures
[ETN-88-92241] 16 p2214 N88-23213
Periodic response of nonlinear systems 16 p2217 N88-23228
A multigrid approach for the solution of a nonlinear diffusion equation in a time-dependent area using Cartesian coordinates
[GMD-STUDIEN-122] 16 p2257 N88-23491
An approximation theory for the identification of nonlinear distributed parameter systems
[NASA-CR-181658] 16 p2260 N88-23510
Inference for a nonlinear semimartingale regression model
[AD-A190857] 16 p2262 N88-23527
Nonlinear wave and diffusion equations
[AD-A191421] 16 p2265 N88-23544
Time-domain frequency-selective optical memories: A study of the basic mechanisms and potential systems
[AD-A190854] 16 p2274 N88-23607
Observation of nonlinear wave decay processes in the solar wind by the AMPTE IRM plasma wave experiment
[AD-A191409] 16 p2290 N88-23713
Parallel processors and nonlinear structural dynamics algorithms and software
[NASA-CR-182925] 17 p2387 N88-24187
A recursive prediction error parameter estimator for nonlinear models
[RR-326] 17 p2392 N88-24222
User's guide to the Fault Inferring Nonlinear Detection System (FINDS) computer program
[NASA-CR-178410] 18 p2462 N88-24619
Signal processing with degenerate four-wave mixing
[AD-A191496] 18 p2499 N88-24825
Research in nonlinear wave motion
[AD-A191686] 18 p2509 N88-24884
Calculation of root-mean-square loads
[BLL-M-37776-(5828.4)] 18 p2531 N88-25015
On frequency response for nonlinear systems
[RR-323] 18 p2563 N88-25221
Galerkin approximation for inverse problems for nonautonomous nonlinear distributed systems
[NASA-CR-181676] 18 p2567 N88-25246
Linear and nonlinear acoustic wave propagation in the atmosphere
[NASA-CR-4157] 18 p2571 N88-25268
Parametric estimation of aerodynamic nonlinearities in rolling moment due to sideslip using maximum likelihood method 20 p2786 N88-26528
Identification of lateral operation dynamics of rail vehicles using roll test stand tests 20 p2787 N88-26534
Nonlinear identification of an aircraft for the direct calculation of an anticipatory control 20 p2787 N88-26535
Studying materials using acoustic waves
[AD-A192234] 20 p2850 N88-26915
Determination of Tafel constants in nonlinear polarization curves
[AD-A192335] 21 p2912 N88-27282
Nonlinear vibrations of periodically stiffened plates 21 p2963 N88-27598
Periodic oscillations in nonlinear mechanical systems 21 p2963 N88-27599
The robust tracking control of nonlinear systems with uncertain dynamics 21 p2999 N88-27788
Effects of applied stress and temperature on the nonlinear elastic properties of graphite fibers
[AD-A194469] 22 p3050 N88-28093
Studies of coherent beam processing concepts, phase 1
[AD-A194749] 22 p3083 N88-28306
A computer-aided approach to nonlinear control systhesis
[NASA-CR-179391] 22 p3140 N88-28673
Nonlinear dynamic analysis and optimal control of shallow shells 23 p3224 N88-29191
Linearized model matching for single-imput nonlinear systems
[AD-A193642] 23 p3266 N88-29445
Approximations and implementations of nonlinear filtering schemes
[AD-A194685] 23 p3271 N88-29462
Finite element analysis of steady and transiently moving/rolling nonlinear viscoelastic structure. Part 1: Theory
[NASA-CR-179886] 23 p3273 N88-29480
Limiting distributions of non-linear vector functions of stationary Gaussian processes
[AD-A194569] 23 p3274 N88-29488
Beam combining by phase transition nonlinear media
[AD-A194116] 23 p3283 N88-29547
Nonlinear analysis of non-neutral plasmas
[AD-A192506] 23 p3284 N88-29556
The construction of the thermoelasticity equations on the basis of contemporary notions of nonlinear continua mechanics
[NASA-TT-20307] 23 p3296 N88-29631
Resonance excitation of linear and non-linear spiral density waves in a gaseous disk 23 p3299 N88-29643
Nonlinear Tollmien-Schlichting/vortex interaction in boundary layers
[NASA-CR-181698] 24 p3311 N88-29715
The strong nonlinear interaction of Tollmien-Schlichting waves and Taylor-Goertler vortices in curved channel flow
[NASA-CR-181697] 24 p3311 N88-29716
Nonlinear dynamics of coupled oscillator arrays
[AD-A194888] 24 p3367 N88-30053
Mathematical problems of nonlinear wave propagation and of waves in heterogeneous media
[AD-A195970] 24 p3368 N88-30057
Initial value problems in viscoelasticity
[AD-A196052] 24 p3382 N88-30145
Algorithms for nonlinear least-squares problems
[AD-A196071] 24 p3411 N88-30305
K(sup th)-order extended linearization
[AD-A194786] 24 p3421 N88-30363
Automatic qualitative analysis of ordinary differential equations using piecewise linear approximations
[AD-A196310] 24 p3424 N88-30379
Multiple solutions and bifurcation for a class of nonlinear Sturm-Liouville eigenvalue problems on an unbounded domain
[AD-A195954] 24 p3426 N88-30389

NONLINEARITY

Concurrent algorithms for transient nonlinear FE analysis
[NASA-CR-181455] 02 p0221 N88-11389
Using MINOS (Modular In-core Nonlinear Optimization System) as a subroutine for decomposition
[DE87-013086] 02 p0221 N88-11390
Ultrasonic characterization of the nonlinear elastic properties of unidirectional graphite/epoxy composites
[NASA-CR-4100] 03 p0281 N88-11767
Highly Non-Linear Optical (NLO) organic crystals 03 p0297 N88-11865
Highly Non-Linear Optical (NLO) organic crystals and films. Electrooptical organic materials 03 p0297 N88-11866
Perturbation and characterization of nonlinear processes
[DE87-014580] 03 p0369 N88-12322
Nonlinear parametric least-squares adjustment
[AD-A184039] 03 p0371 N88-12336
Non-linearity in measurement systems: Evaluation method and application to microwave radiometers 04 p0433 N88-12684
Implementation of a 3-D nonlinear MHD calculation on the Intel hypercube
[DE87-014637] 04 p0479 N88-12949
Non-linear maximum likelihood estimation of stability derivatives from range data
[NAL-TM-SE-8606] 05 p0552 N88-13365
HF sidebands in the ionosphere 05 p0574 N88-13497
Nonlinear hyperbolic conservation laws
[AD-A184963] 05 p0580 N88-13538
Applications of nonlinear hole burning spectroscopy
[AD-A184943] 05 p0587 N88-13580
Dynamics of cables and chains 05 p0610 N88-13747
Geometrically nonlinear analysis of stiffened panels 06 p0722 N88-14440
Development of symbolic computation methods for nonlinear dynamics
[AD-A185562] 06 p0758 N88-14653
The history and development of nonlinear stellar pulsation codes
[DE88-001828] 06 p0801 N88-14899
Nonsymmetric metrics in nonlinear field theory
[DE88-700509] 07 p0913 N88-15537
The design and implementation of surface acoustic wave devices for linear FM and a new non-linear FM pulse compression technique for radar applications
[AD-A186741] 08 p0980 N88-15922
Nonlinear line-spring model for surface crack analysis with particular reference to work hardening materials
[PB87-144838] 08 p0994 N88-16016
Steady ship waves at low Froude numbers, part 2
[AD-A176805] 09 p1160 N88-16953
A substructure method for dynamic simulation of flexible mechanical systems with geometric nonlinearities 09 p1176 N88-17044
Experimental identification of nonlinear structural models
[DE88-001795] 09 p1184 N88-17094
Nonlinear and diffraction effects in sound beams with random transverse structure 09 p1235 N88-17402
Explicit approximations for strictly nonlinear oscillators with slowly varying parameters with applications to free electron lasers
[DE88-004116] 10 p1336 N88-17984
Nonlinear dynamic maximum power theorem
[AD-A187491] 11 p1477 N88-18810
Nonlinear absorption of CO2 laser radiation in p-type InSb
[DE88-004055] 11 p1492 N88-18906
Numerical-experimental investigation of singularity at a crack in nonlinear rubber elasticity 11 p1500 N88-18961
Contour-to-grid interpolation with nonlinear finite elements: A feasibility study
[AD-A188108] 11 p1503 N88-18980
Postprocessing techniques for 3D non-linear structures 11 p1528 N88-19124
Design for performance enhancement in feedback control systems with multiple saturating nonlinearities
[NASA-CR-182614] 11 p1535 N88-19168
An improved data reduction procedure for accelerometer centrifuge data 12 p1577 N88-19436
The lattice nonlinearities and the long term stability of the SSC
[CEBAF-PR-87-009] 12 p1690 N88-20108
Finite element methodology for nonlinear free and harmonic forced vibrations of beam and plate structures 13 p1782 N88-20663
Algorithms with conic termination for nonlinear optimization
[DE88-005893] 13 p1816 N88-20851
Nonlinear refractive index measurements of glasses and crystals
[DE88-005673] 13 p1840 N88-21009
Energy transfer and non-linear optical properties at near ultraviolet wavelengths: Rare earth 4f yields 5d transitions in crystals and glasses
[DE88-005403] 13 p1840 N88-21012
Two studies of nonlinear processes in irreversible thermodynamics
[DE88-005794] 13 p1849 N88-21067
Nonlinear acoustic parameter and its application in ultrasonic imaging 14 p1902 N88-21364
Nonlinear stage of ultrashort-pulse formation in solid-state laser 14 p1971 N88-21765
Numerical methods for linear and nonlinear optimization
[AD-A190029] 15 p2120 N88-22631
Symmetry and global bifurcation in nonlinear solid mechanics
[AD-A190521] 15 p2121 N88-22642
Nonlinear effects in plasma wake field acceleration
[DE88-700972] 15 p2134 N88-22734
Nonlinear wave interactions in swept wing flows
[NASA-CR-4142] 16 p2206 N88-23160
Multigrid for structures analysis 16 p2218 N88-23232
Reduced order models for nonlinear aerodynamics 16 p2220 N88-23248
The 1 and 2D symmetric Helmert transformation: An exact nonlinear least squares solution
[REPT-87-1] 16 p2259 N88-23503
Investigation of non-linear optical behavior of semiconductors for optical switching, volume 1
[AD-A191297] 16 p2274 N88-23611
Nonlinear dynamics of interaction between charged particles modulated beam and bounded plasma regular oscillations
[DE88-701681] 16 p2280 N88-23648
Electromagnetic scattering from nonlinear anisotropic cylinders 17 p2333 N88-23930
On Hotelling's approach to testing for a nonlinear parameter in regression
[AD-A191189] 17 p2393 N88-24229
Electronic structure of Zintl phase compounds by nonlinear optimization
[DE88-009998] 19 p2613 N88-25508
Nonlinear mechanisms of solid propellant combustion instability 19 p2628 N88-25588

Electron tunneling in junctions doped with semiconductors and metals 19 p2734 N88-26236
Finite element welding computations using general purpose nonlinear analysis codes
[DE88-005398] 20 p2808 N88-26659
Comparison theorems and their use in the analysis of some nonlinear diffusion problems
[DE88-010032] 20 p2845 N88-26884
Ultrafast optical nonlinearity in quantum well structures with electric field 20 p2863 N88-27003
Nonlinear materials for frequency conversion
[DE88-008343] 20 p2875 N88-27067
Effects of static equilibrium and higher-order nonlinearities on rotor blade stability in hover 21 p2890 N88-27157
Nonlinear dynamics of the electron self-field interaction
[DE88-010597] 21 p2934 N88-27420
Nonlinear interaction between overall and local buckling of stiffened panels with symmetric cross-sections
[PB88-104054] 21 p2960 N88-27580
Nonlinear liquid motion in conical containers
[LRT-WE-9-FB-10(1987)] 22 p3077 N88-28270
Regularity of solutions for nonlinear degenerate elliptic boundary value problems
[DE88-702646] 22 p3146 N88-28710
A singular perturbation analysis of the weakly nonlinear evolution of long and short water waves and waves in boundary layers 23 p3209 N88-29102
Nonlinear vibrations of imperfect thin walled cylindrical shells
[ETN-88-92904] 23 p3227 N88-29205
On the periodic nonlinearity and the multiplicity of solutions
[AD-A194295] 23 p3270 N88-29459
Investigation of non-classical effects in two-photon interference processes 23 p3282 N88-29541
Non-linear scale invariance in a cold-dark-matter universe
[DE88-011725] 23 p3299 N88-29644
Survey on nonlinear effects 24 p3317 N88-29757
Nonlinear optical phase conjugation techniques to reduce the physical size of lasers
[AD-A196170] 24 p3379 N88-30122
Geometric and material nonlinear analysis of structures comprising rectangular hollow sections
[CE-79] 24 p3382 N88-30141

NONNEWTONIAN FLOW
Theoretical and experimental analysis of pressure pulse transmission in non-Newtonian pipe flow 11 p1485 N88-18863

NONNEWTONIAN FLUIDS
Two-phase non-Newtonian hydrodynamic modeling of slurries
[DE87-011519] 01 p0047 N88-10298
A review of approaches to the study of turbulence modification by means of non-Newtonian additives
[AD-A188799] 12 p1627 N88-19734
Approximation of viscoelastic stresses from Newtonian turbulent kinematics
[AD-A194317] 24 p3371 N88-30077

NONOSCILLATORY ACTION
Non-oscillatory spectral Fourier methods for shock wave calculations
[NASA-CR-181675] 19 p2720 N88-26148

NONPARAMETRIC STATISTICS
Feature selection applied to radar target identification
[AD-A183880] 01 p0034 N88-10215
An APL workspace for conducting nonparametric statistical inference
[AD-A184971] 05 p0634 N88-13877
Further studies in estimation of life distribution characteristics from censored data
[AD-A184862] 05 p0643 N88-13937
Sample reuse in statistical remodeling
[AD-A184916] 05 p0643 N88-13938
Quantile statistical data analysis
[AD-A185181] 05 p0644 N88-13943
A unified mathematical approach to image analysis
[AD-A185719] 06 p0765 N88-14703
Robust prediction and interpolation for vector stationary processes, 2d enriched version
[AD-A185875] 07 p0865 N88-15247
Nonparametric estimation of the generalized variance
[AD-A186029] 07 p0914 N88-15545
A smooth nonparametric quantile estimator from right-censored data
[AD-A186180] 07 p0915 N88-15552
On determining the weight for obtaining a large number of items
[AD-A186181] 07 p0915 N88-15553
Practical applicability of exact and approximate forms of the randomization test for two independent samples
[AD-A186815] 09 p1231 N88-17381
A generalized quantile estimator under censoring
[AD-A188280] 10 p1402 N88-18364
Analysis of learning curve fitting techniques
[AD-A187680] 11 p1535 N88-19173
Nonparametric discriminant analysis applied to the extraction and selection of radar target signature features
[AD-A191849] 18 p2501 N88-24833
Symmetrized nearest neighbor regression estimates
[AD-A191998] 18 p2568 N88-25254
Joint asymptotic distribution of marginal quantiles and quantile functions in samples from a multivariate population
[AD-A193385] 21 p3010 N88-27856
A nonparametric multidimensional IRT approach with applications to ability estimation and test bias
[AD-A194212] 23 p3273 N88-29483

NONREFLECTION
U ENERGY ABSORPTION

NONRELATIVISTIC ELECTRONS
U ELECTRONS

NONRIGIDITY
U FLEXIBILITY

NONTHERMAL EMISSION
U NONTHERMAL RADIATION

NONTHERMAL RADIATION
NT CYCLOTRON RADIATION
NT ION CYCLOTRON RADIATION
NT SYNCHROTRON RADIATION
Microwave observations of nonthermal phenomena in pre-main sequence stars 04 p0505 N88-13107
Spherical models of QSO/AGN emission line clouds 06 p0806 N88-14921
High density femtosecond excitation of nonthermal carrier distributions in intrinsic and modulation doped GaAs quantum wells 14 p1977 N88-21798
Experimental and theoretical studies of coherent and nonthermal processes in semiconductors probed by femtosecond laser techniques 14 p1977 N88-21800

NONUNIFORM FLOW
The spatially nonuniform convergence of the numerical solution of flows
[NASA-TM-100037] 02 p0226 N88-11429
Turbulence modelling of flows with non-uniform density 22 p3075 N88-28256
Gaseous premixed flames in non-uniform flows 24 p3351 N88-29945

NONUNIFORM PLASMAS
Self-consistent modification of a fast tail distribution by resonant fields in nonuniform plasmas
[AD-A183790] 01 p0099 N88-10650
Electron acceleration by wave processes in the earth's ionosphere
[AD-A186110] 07 p0877 N88-15320

NONUNIFORMITY
Interaction of interplanetary shocks with nonuniform ambient solar wind 01 p0116 N88-10740
Programs for calculating transient Darcian flow through non-uniform materials
[DE88-001924] 07 p0852 N88-15177

NONVISCOUS FLOW
U INVISCID FLOW

NOREPINEPHRINE
Distinctions and mechanisms of effects of epinephrine and norepinephrine on cardiac pumping function under hypokinetic conditions 07 p0891 N88-15399
Individual functional typology of sympathoadrenal system as indicator of physiological status in adverse environments 12 p1665 N88-19979
Direct interaction between autonomic nerves and the immune system
[AD-A188576] 12 p1667 N88-19991

NORMAL DENSITY FUNCTIONS
Statistics of the geomagnetic secular variation for the past 5Ma
[NASA-CR-181558] 04 p0467 N88-12890
Local likelihood method in the problems related to change points
[AD-A185604] 06 p0768 N88-14718
Asymptotic normality of poly-t densities with Bayesian applications
[AD-A185718] 06 p0768 N88-14719
The information metric for univariate linear elliptic models
[AD-A186385] 07 p0911 N88-15527
On selecting the best of k lognormal distributions
[AD-A185628] 07 p0916 N88-15567
An APL function for bivariate normal probabilities
[AD-A186535] 09 p1232 N88-17382
On two-stage allocation procedures for selection problems
[AD-A190766] 15 p2126 N88-22675
Analysis of means in some nonstandard situations
[ETN-88-92247] 16 p2262 N88-23522
Weak solution of the Langevin equation on a generalized functional space
[AD-A194290] 23 p3270 N88-29456

NORMAL DISTRIBUTIONS
U NORMAL DENSITY FUNCTIONS

NORMAL FORCE DISTRIBUTION
U FORCE DISTRIBUTION

NORMALITY
Asymptotic normality of minimum L1-norm estimates in linear models
[AD-A193399] 21 p3006 N88-27835

NORMALIZING (STATISTICS)
Detector normalization --- SPOT remote sensors 03 p0341 N88-12151
Consistency question in the renormalization group analysis of deep inelastic scattering
[DE87-703372] 04 p0487 N88-12999
On the extreme order statistics for a stationary sequence
[AD-A186428] 07 p0916 N88-15561
A small concentration expansion for the effective heat conductivity of a random disperse two-component material; an assessment of Batchelor's renormalization method
[REPT-87-71] 16 p2207 N88-23168
Feedback stabilization of du/dt=Au + bf in Hilbert space when the normalization function is less than or equal to r
[AD-A193510] 23 p3277 N88-29506

NORMS
Norm inequalities for derivatives and differences
[DE88-002920] 09 p1230 N88-17371
On the norm equivalence of singularly perturbed elliptic difference operators
[DE88-006353] 13 p1826 N88-20913
Contribution to the study of modern materials for cutting tools
[ISAL-IDI1-87-17] 16 p2185 N88-23029
Asymptotic of Peanokerns of finite fixed order
[ETN-88-92381] 21 p3008 N88-27843

NORTH AMERICA
Theory and methods for design of pulse shapes for broadcast teletext
[CRC-1405] 02 p0162 N88-11013
A survey of existing hypersonic ground test facilities: North America 05 p0529 N88-13220
Mid-tertiary volcano-tectonic development of the Southwestern Cordillera of North America 06 p0797 N88-14879
Biogeochemical cycling in the ocean. Part 1: Introduction to the effects of upwelling along the west coast of North America
[NASA-TM-88230] 07 p0882 N88-15349
Meteorological and aerosol measurements from the NOAA WP-3D aircraft during WATOX-86, January 4-9, 1986
[PB88-120860] 10 p1352 N88-18079
Synthesis of finite displacements and displacements in continental margins
[NASA-CR-182616] 12 p1642 N88-19832
Northern Hemisphere circulation and the principal components of subsequent summer patterns in North America and West Africa 13 p1801 N88-20765
The collection of statistics on the frequency of cloud cover over North America
[AD-A190456] 15 p2097 N88-22495
DATATRAN: Datum transformation software
[AD-A195723] 24 p3387 N88-30175
Gravity anomalies, plate tectonics and the lateral growth of Precambrian North America 24 p3400 N88-30248

NORTH AMERICAN AIRCRAFT
NT B-1 AIRCRAFT
NT B-70 AIRCRAFT

NORTH ATLANTIC TREATY ORGANIZATION (NATO)
Special Course on Fundamentals of Fighter Aircraft Design
[AGARD-R-740] 05 p0544 N88-13315
Calendar of selected aeronautical and space meetings
[AGARD-CAL-88/1] 05 p0658 N88-14037
AGARD reports: A quarterly listing, 1 July through September 30, 1987
[AD-A186572] 08 p1093 N88-16579
Anthropomorphic phantom radiation dosimetry at the NATO standard reference point at Aberdeen Proving Ground
[AD-A190508] 15 p2103 N88-22528
A review of the NATO special group of experts on Naval hydromechanics and related problems 16 p2205 N88-23157

NORTH CAROLINA
Annual data summary and climatological evaluation CERC (Coastal Engineering Research Center) field research facility, 1985. Volume 1. Main text and appendixes A and B
[AD-A186442] 08 p1039 N88-16289

NORTH DAKOTA
Feasibility of producing jet fuel from GPGP (Great Plains Gasification Plant) by-products
[DE88-010233] 20 p2781 N88-26492

NORTH SEA
An hourly analysis, updating and short-range forecasting system — numerical weather forecasting
02 p0206 N88-11288
Forecast of current patterns for an eddy tracking experiment in the Norwegian coastal current
[PB87-224853] 06 p0747 N88-14595
Climatological data of the Netherlands lightvessels over the period 1949-1980 — North Sea
[KNMI-WR-87-9] 14 p1947 N88-21613

NORTHERN HEMISPHERE
NT ARCTIC REGIONS
Mean pressure distribution and geostrophic circulation in the meteor zone 06 p0734 N88-14513
Objective prediction of monthly mean surface temperature and climatological relationships to mid-tropospheric heights
[DE88-000908] 07 p0880 N88-15340
Upper-thermospheric observations and neutral-gas dynamics at high latitudes during solar maximum
[AD-A188058] 11 p1512 N88-19031
Northern Hemisphere circulation and the principal components of subsequent summer patterns in North America and West Africa 13 p1801 N88-20765
Health and environmental consequences of the Chernobyl nuclear power plant accident
[DOE/ER-0332] 19 p2689 N88-25985
Some evidence for a Northern Hemispheric extratropic trigger mechanism of ENSO events
22 p3123 N88-28558
Persistence of North Pacific Sea surface temperature and atmospheric flow patterns 22 p3123 N88-28559
Northern Hemisphere 700 mb teleconnections based on half-monthly mean anomaly data stratified by season and by sign 22 p3123 N88-28561
Interannual variability of 850 mb temperatures during the Northern Hemisphere winter
22 p3123 N88-28562
Dependence of medium range forecast errors upon the large-scale initial state 22 p3126 N88-28585

NORTHROP AIRCRAFT
NT F-18 AIRCRAFT

NORWAY
The Norwegian scientific balloon and sounding rocket program 1987-1990 08 p1025 N88-16204
Facilities and plans for improvements at Andoya (Norway) rocket range 08 p1029 N88-16236

NOSE CAPS
U NOSE CONES

NOSE CONES
NT ABLATIVE NOSE CONES
NT ROCKET NOSE CONES
Numerical study of supersonic flow around blunt bodies with extended needle nose 04 p0425 N88-12635
A spatial marching technique for the inviscid blunt body problem 05 p0533 N88-13239
A simplified streamline swallowing procedure for the windward meridian of axisymmetric blunt bodies
[AD-A188413] 12 p1626 N88-19732

NOSES (FOREBODIES)
NT ABLATIVE NOSE CONES
NT NOSE CONES
NT ROCKET NOSE CONES
An experimental investigation of appendage-flat plate junction flow. Volume 2: Elliptical nose appendage data base
[AD-A184074] 05 p0580 N88-13539

NOTATION
U CODING

NOTCH SENSITIVITY
Fatigue strength of alloy A286 at cryogenic temperature 05 p0603 N88-13695
An experimental and numerical study of notch sensitivity of ARALL laminates
[CCMS-88-04] 11 p1450 N88-18644
Notch sensitivity of graphite materials for VHTR
13 p1747 N88-20447
Cyclic crack growth emanating at a round notch considering viscoplasticity
[AD-A189577] 13 p1781 N88-20655

NOTCH STRENGTH
Estimation multiaxial elastic-plastic notch stresses and strains in combined loading
[FB-2/1986] 01 p0060 N88-10382
The use of Hencky's equations for the estimation of multiaxial elastic-plastic notch stresses and strains
[FB-3/1986] 01 p0060 N88-10383
Crack initiation life estimations for notched specimens with residual stresses based on local strains
[FF-17/1986] 01 p0060 N88-10385
Laminated ferrous composites based on ultrahigh carbon (UHC) steels
[AD-A184617] 03 p0280 N88-11764
Influence of strain rate and notch depth on tensile properties of HITCO 6250
[DE88-001324] 04 p0455 N88-12816
Low cycle fatigue behaviour of notched specimens of nickel based superalloy single crystal
05 p0605 N88-13712
Profiles of self stress and of load stress at notches
06 p0719 N88-14419
Hybrid FEM (Finite Element Method) approach to stress distribution in the vicinity of a notch in non-homogeneous materials
[PB87-143392] 07 p0868 N88-15268
A comprehensive study on damage tolerance properties of notched composite laminates
[AD-A192952] 23 p3188 N88-28968
The effect of notch root radius on the determination of toughness in ultrahigh strength steel friction welds
[AD-A195952] 24 p3384 N88-30156

NOTCH TESTS
NT CHARPY IMPACT TEST
The effect of size and surface on the lifetime prediction of StE 460 notched bars
[FD-6/1986] 01 p0058 N88-10374
Closure and propagation behavior of short fatigue cracks at different R-ratios 05 p0601 N88-13679
Crack growth in contrasting titanium alloys under the conjoint action of high and low cycle fatigue
05 p0602 N88-13686
Fatigue of 30CrMnSiNi2A notched specimens under spectrum loading 05 p0602 N88-13689
Initiation and propagation of damage in notched unidirectional and multidirectional CFRE resin laminates
11 p1449 N88-18633
Application of ISRM testing methods to fracture toughness testing of graphite 13 p1747 N88-20446
Notch sensitivity of graphite materials for VHTR
13 p1747 N88-20447
An investigation of the mechanical properties of improved carbon fibre composite materials
[RAE-TR-86021] 14 p1884 N88-21259
Analysis of notched metal matrix composites under tension loading
[NASA-TM-100629] 18 p2480 N88-24713

NOTCHED METALS
U NOTCH TESTS

NOTCHES
Spread of plastic deformation in notched and cracked plates 03 p0337 N88-12122
Influence of strain rate and notch depth on tensile properties of HITCO 6250
[DE88-001324] 04 p0455 N88-12816
Notch-geometry effect on propagation threshold of short fatigue cracks in notched components
06 p0716 N88-14393
Profiles of self stress and of load stress at notches
06 p0719 N88-14419
Cyclic crack growth emanating at a round notch considering viscoplasticity
[AD-A189577] 13 p1781 N88-20655

NOVA LASER SYSTEM
Large-scale stimulated rotational Raman scattering experiments using the LLNL Nova laser
[DE87-012661] 01 p0051 N88-10328
Thermal stress in the edge cladding of Nova glass laser disks
[DE88-000425] 04 p0448 N88-12780
Design of the Backscatter Spectroscopy System for the Nova Laser Facility
[DE88-001880] 07 p0859 N88-15214
High Z interaction physics on Nova
[DE88-004397] 10 p1413 N88-18433

NOVAE
NT DWARF NOVAE
NT HERCULES NOVA
Gamma ray lines from novae
04 p0526 N88-13214
The classical nova outburst
[DE88-009138] 21 p3030 N88-27987

NOWCASTING
Mesoscale Analysis and Forecasting: Incorporating Nowcasting
[ESA-SP-282] 02 p0199 N88-11239
Nowcasting for the national economy needs
02 p0199 N88-11241
An illustrative example of the nowcasting challenge
02 p0199 N88-11243
New nowcasting opportunities using modern meteorological radar 02 p0199 N88-11245
Nowcasting microbursts using Doppler radar in a forecaster-computer environment
02 p0200 N88-11246
Thunderstorm nowcasting using Doppler radar and soundings 02 p0200 N88-11248
The use of advanced data sets in the short-range forecasting of the development of a tornadic thunderstorm along a mesoscale convergence zone
02 p0200 N88-11250
The use of satellite IR data in the enhancement of surface thermal fields 02 p0202 N88-11260
Forecasting and nowcasting cumulus convection with soundings released from a storm-intercept vehicle
02 p0202 N88-11262
Structure and modification of winter mountain clouds in the Sierra Nevada: Nowcasting/forecasting the onset of supercooled liquid water 02 p0202 N88-11263
A proposal of the nowcasting system for sea fog
02 p0202 N88-11264
Nowcasting rain/snow transitions and freezing rain
02 p0202 N88-11265
On the interaction between radar and satellite image nowcasting systems and mesoscale numerical models
02 p0204 N88-11277
A mini system for nowcasting
02 p0204 N88-11278
FRONTIERS: An operational system for nowcasting precipitation 02 p0204 N88-11279
Operational experiment in very short range forecast of precipitation 02 p0204 N88-11280
Satellite imagery and conceptual models in mesoscale forecasting 02 p0205 N88-11282
The studies of physical models on hailstorms and their applications in nowcasting 02 p0207 N88-11300
Toward operational forecasting and detection of weather-producing gravity waves
02 p0208 N88-11303
Opportunities for nowcasting air pollution episodes and accidental toxic and radioactive releases
02 p0210 N88-11317
Mesoscale analysis and nowcasting via a numerical model coupled with satellite sounder data
02 p0211 N88-11328
Opportunities and problems in mesoscale objective analysis 02 p0212 N88-11331
Mesoscale forecasting with satellite data: Challanges and opportunities for today and tomorrow
02 p0215 N88-11353

NOXIOUS MATERIALS
U CONTAMINANTS

NOZZLE COEFFICIENT
U NOZZLE FLOW

NOZZLE DESIGN
The aerodynamic design of hypersonic contoured axisymmetric nozzles including real gas effects
[VKI-TM-43] 06 p0665 N88-14076
Investigation of the need for in-use dispensing rate limits and fuel nozzle geometry standardization
[PB88-102611] 07 p0839 N88-15089
Design of supersonic Coanda jet nozzles
10 p1270 N88-17599
Analysis for high compressible supersonic flow in converging nozzle
[IPPJ-860] 16 p2157 N88-22869
The effects of magnetic nozzle configurations on plasma thrusters
[NASA-CR-183096] 19 p2732 N88-26223
Variable Mach number wall jets for control/propulsion on hypervelocity projectiles/interceptors: Tests with an existing model
[AD-A192845] 21 p2892 N88-27167
Numerical investigations in three-dimensional internal flows
[NASA-CR-183108] 23 p3210 N88-29106
Analysis and optimization of truncated scarf nozzles subject to external flow conditions
[NASA-TM-100955] 24 p3316 N88-29746
Stresses in cylindrical shells with tangential nozzles submitted to external loads and internal pressure
[CRIF-MT-172] 24 p3382 N88-30146

NOZZLE EFFICIENCY
Aeropropulsive characteristics of isolated combined turbojet/ramjet nozzles at Mach numbers from 0 to 1.20
[NASA-TP-2814] 17 p2299 N88-23757
Analysis and optimization of truncated scarf nozzles subject to external flow conditions
[NASA-TM-100955] 24 p3316 N88-29746

NOZZLE FLOW
Rayleigh scattering measurements of a freejet with homogeneous condensation 03 p0319 N88-12020
Numerical simulation and visualization of a flowfield by interaction of two parallel two-dimensional freejets
03 p0320 N88-12021
Method of calculations for flow of ideal gas through plane and axisymmetric nozzles with broken-line contour
06 p0771 N88-14737
Experimental evaluation of a translating nozzle sidewall radial turbine 10 p1280 N88-17656
Laval nozzle flow of a binary, retrograde mixture
[MPIS-1/1987] 11 p1488 N88-18882
J85-21 fuel nozzle atomization tests
[AD-A189394] 12 p1613 N88-19647
Application of a flux vector splitting methodology towards the solution of unsteady transonic flows, with future emphasis on the blade flutter problem
[AD-A189500] 13 p1716 N88-20260

An adaptive grid technique for solution of the Euler equations 13 p1768 N88-20579
Effect of flow convergence on turbulence level in stream 14 p1973 N88-21773
Tests on oscillating flows in a pipe nozzle with an abrupt diameter variation
[MPIS-2/1987] 17 p2337 N88-23947
Fast algorithm development for large-eddy simulation of circular-jet turbulence
[AD-A192044] 18 p2509 N88-24887
Nozzle lip effects on gas expansion into the plume backflow region
[AD-A192806] 21 p2942 N88-27475
Aerodynamics in ground effect and predicted landing ground roll of a fighter configuration with a secondary-nozzle thrust reverser
[NASA-TP-2834] 24 p3317 N88-29752
Nozzle airflow influences on fuel patternation 24 p3346 N88-29916
Numerical simulation of nozzle flows
[AD-A195144] 24 p3369 N88-30064

NOZZLE GEOMETRY
Development and application of computational aerothermodynamics flowfield computer codes
[NASA-CR-181534] 04 p0395 N88-12465
Combustion related shear-flow dynamics in elliptic supersonic jets 05 p0531 N88-13232
An experimental and numerical investigation of swirling flows in a rectangular nozzle 06 p0700 N88-14295
Investigation of the need for in-use dispensing rate limits and fuel nozzle geometry standardization
[PB88-102611] 07 p0839 N88-15089
Experimental evaluation of a translating nozzle sidewall radial turbine 10 p1280 N88-17656
High performance Solid Rocket Motor (SRM) submerged nozzle/combustion cavity flowfield assessment
[NASA-CR-179307] 11 p1446 N88-18622
Aeropropulsive characteristics of isolated combined turbojet/ramjet nozzles at Mach numbers from 0 to 1.20
[NASA-TP-2814] 17 p2299 N88-23757
Nozzle fabrication technique
[NASA-CASE-MSC-21299-1] 18 p2475 N88-24684
A detailed description of the uncertainty analysis for high area ratio rocket nozzle tests at the NASA Lewis Research Center 19 p2626 N88-25580
Extensive verification of blade-to-blade flow code based on Denton scheme 19 p2638 N88-25654

NOZZLE THRUST COEFFICIENTS
Comparison of wind tunnel and flight test afterbody and nozzle pressures for a twin-jet fighter aircraft at transonic speeds
[NASA-TP-2588] 02 p0121 N88-10765

NOZZLE WALLS
Experimental evaluation of a translating nozzle sidewall radial turbine 10 p1280 N88-17656

NOZZLELESS ROCKET ENGINES
Evaluation of techniques for direct measurement of burning rates in nozzleless motors 19 p2631 N88-25609

NOZZLES
Effect of empennage arrangement on single-engine nozzle/afterbody static pressures at transonic speeds
[NASA-TP-2753] 02 p0122 N88-10771
Verification of FANTASTIC integrated code 07 p0924 N88-15613
Equilibrium retention in the nozzle of oxygen hydrogen propulsion systems 07 p0924 N88-15616
Aeropropulsion '87. Session 3: Internal Fluid Mechanics Research
[NASA-CP-10003-SESS-3] 08 p0954 N88-15790
Inlets, ducts and nozzles 08 p0955 N88-15791
Comparison of UNL laser imaging and sizing system and a phase/Doppler system for analyzing sprays from a NASA nozzle
[NASA-CR-182437] 09 p1161 N88-16956
SRB/SLEEC (Solid Rocket Booster/Shingle Lap Extendible Exit Cone) feasibility study, volume 1
[NASA-CR-178973] 23 p3187 N88-28964

NUCLEAR ASTROPHYSICS
Influences of the astrophysical environment on nuclear decay rates
[DE88-001461] 04 p0522 N88-13208
New nuclear structure calculations and the astrophysical r-process
[DE88-000979] 08 p1082 N88-16518
An introduction to nuclear astrophysics
[DE88-002761] 08 p1100 N88-16618

NUCLEAR AUXILIARY POWER UNITS
NT FISSION ELECTRIC CELLS
NT SNAP
NT SNAP 19
NT SPACE POWER REACTORS
Creep behavior of tungsten/niobium and tungsten/niobium-1 percent zirconium composites
[NASA-TM-100804] 11 p1460 N88-18707

NUCLEAR BINDING ENERGY
Schottky-barrier formation on a covalent semiconductor without Fermi-level pinning: The Metal-MoS2(0001) interface
[AD-A193044] 21 p3021 N88-27931

NUCLEAR CAPTURE
NT ELECTRON CAPTURE
Neutron capture nucleosynthesis in low mass AGB stars 04 p0517 N88-13178
First capture of antiprotons in an ion trap and the possibility of antihydrogen 16 p2268 N88-23569

NUCLEAR ELECTRIC POWER GENERATION
NT FISSION ELECTRIC CELLS
NT NUCLEAR AUXILIARY POWER UNITS
NT NUCLEAR POWER PLANTS
NT NUCLEAR POWER REACTORS
NT SNAP
NT SNAP 19
NT SPACE POWER REACTORS
NT THERMONUCLEAR POWER GENERATION
Procedure and program used for data processing in a poll on nuclear energy utilization
[IFSI-87-3] 05 p0649 N88-13977
Starpower: The US and the international quest for fusion energy
[PB88-128731] 11 p1551 N88-19283
Benefits of 20 kHz PMAD in a nuclear space station 17 p2398 N88-24256
Nuclear electric power for multimegawatt orbit transfer vehicles 17 p2399 N88-24261

NUCLEAR ELECTRIC PROPULSION
Nuclear electric propulsion system: Nuclear plant and thermomechanical conversion system 17 p2405 N88-24298
Comparison of a direct thrust nuclear engine, nuclear electric engine and a chemical engine for future space missions 17 p2418 N88-24379

NUCLEAR ENERGY
USSR report: Engineering and equipment
[JPRS-UEQ-87-008] 04 p0423 N88-12621
Power systems for production, construction, life support and operations in space
[NASA-TM-100838] 14 p1883 N88-21254
Analytical Chemistry Division
[DE88-701236] 16 p2174 N88-22956

NUCLEAR ENGINE FOR ROCKET VEHICLES
History of some direct nuclear propulsion developments since 1946 17 p2400 N88-24270
A critique of NERVA based nuclear reactor design and performance for MMW space propulsion applications 17 p2404 N88-24297
Nuclear propulsion: Past, present and future 17 p2427 N88-24441
The NERVA derivative reactor and a systematic approach to multiple space power requirements 17 p2430 N88-24458

NUCLEAR EXPLOSION EFFECT
Buckling of blast loaded cylinder
[AD-A190124] 15 p2076 N88-22376
Effects of tectonic release on broadband regional distance bodywaves
[AD-A194247] 22 p3119 N88-28529

NUCLEAR EXPLOSIONS
Historical catalog of Southern Great Basin earthquakes, 1868-1978
[DE87-014340] 02 p0198 N88-11232
The development of low level coastal flow fields when solar radiation is blocked by smoke
[DE87-014348] 03 p0354 N88-12230
NORSAR detection processing system
[AD-A185968] 07 p0877 N88-15318
A methodology to assess the effects of high altitude electromagnetic pulse (HEMP) on electric power systems
[DE88-000338] 11 p1476 N88-18808
Announced United States nuclear tests: July 1945 through December 1986
[NVO-209-REV-7] 11 p1546 N88-19247
Characteristics of seismic sources of some Asian earthquakes and Soviet underground explosions from Gauribidanur array records
[DE88-701233] 15 p2093 N88-22472
An approximation technique for solving a system of Fredholm integral equations for asymmetric detector response functions
[AD-A190577] 15 p2121 N88-22645
Research and development activities of the Seismology Section
[DE88-701235] 16 p2231 N88-23323
Acute radiation syndrones and their management
[DE88-009839] 20 p2831 N88-26797
Approximate analytical formulae for electron density and collision frequency in the natural and nuclear-disturbed ionosphere and inner magnetosphere
[AD-A193129] 21 p2972 N88-27654
Effects of tectonic release on broadband regional distance bodywaves
[AD-A194247] 22 p3119 N88-28529
Maximum-likelihood multichannel deconvolution of P waves at seismic arrays
[AD-A194990] 24 p3391 N88-30191

NUCLEAR FISSION
Space based nuclear-pumped laser/reactor concepts 17 p2403 N88-24289
Influence of pairing correlations on the probability and dynamics of tunneling through the barrier in fission and fusion of complex nuclei
[DE88-701500] 23 p3286 N88-29570

NUCLEAR FUEL BURNUP
Effect of fuel burnup and cross sections on modular HTGR (High-Temperature Gas-cooled Reactor) reactivity coefficients
[DE88-006656] 22 p3151 N88-28748

NUCLEAR FUEL ELEMENTS
Review of diffusion barrier technology for application in SP-100 fuel pins
[DE88-000021] 02 p0234 N88-11480
Material tradeoffs to minimize flooding reactivity 17 p2399 N88-24265
Particle bed reactor scaling relationships 17 p2400 N88-24267
Irradiation test results on thermionic fuel element sheath insulators 17 p2402 N88-24280
Development of reliable fuel pins for space reactor applications 17 p2409 N88-24326
A review of diffusion barrier technology for application in SP-100 fuel pins 17 p2410 N88-24328
Evaluation of UN fuel pin failure modes and motion of fuel during severe accidents for reactors in space 17 p2425 N88-24424
Research and development of electrical insulators for thermionic applications 17 p2429 N88-24449
SNAP fuel performance 17 p2435 N88-24484
Methods and techniques of NDA (nondestructive assay)
[DE88-009145] 20 p2812 N88-26682
Effect of fuel burnup and cross sections on modular HTGR (High-Temperature Gas-cooled Reactor) reactivity coefficients
[DE88-006656] 22 p3151 N88-28748

NUCLEAR FUELS
NT CERAMIC NUCLEAR FUELS
NT SPENT FUELS
Experience of developing an integrated nondestructive assay system
[DE88-003149] 09 p1184 N88-17092
Fusion, and advanced fuel, reaction bibliography: Particle reactions from H1 to B11
[AD-A187420] 11 p1552 N88-19286
Studies in solid state ionics
[DE88-700830] 11 p1559 N88-19333
CIT (Compact Ignition Tokamak) fueling
[DE88-002709] 12 p1692 N88-20125
Compatibility in space reactor fuel systems
[DE88-005698] 13 p1839 N88-21004
Analysis for high compressible supersonic flow in converging nozzle
[IPPJ-860] 16 p2157 N88-22869
Analysis for fuel implosion in ICF target and pellet gain 16 p2276 N88-23620
Pusherless implosion, pulse tailoring and ignition scaling law for laser fusion 16 p2277 N88-23629
Fully passive space reactor conceptual design 17 p2403 N88-24288
Uranium nitride fuel swelling and thermal conductivity correlations 17 p2409 N88-24327
Helium-3 fusion fuel resources for space power 17 p2410 N88-24330
Fabrication of SP-100 fuel barrier structures by chemical vapor deposition 17 p2416 N88-24371
Critical nuclear launch issues: A perspective from the State of Florida 17 p2423 N88-24412
A novel plant protection strategy for transient reactors 17 p2425 N88-24423
Evaluation of UN fuel pin failure modes and motion of fuel during severe accidents for reactors in space 17 p2425 N88-24424
Weldability of general purpose heat source iridium capsules 17 p2426 N88-24429
An irradiation performance data base for nitride fuels 17 p2427 N88-24438
A high power density radial-in-flow reactor split core design for space power systems 17 p2430 N88-24455
Molybdenum-base cermet fuel development 17 p2434 N88-24481
Test plan and facilities for qualifying nuclear rocket fuel elements 17 p2434 N88-24482
Material property and irradiation performance correlations for nitride fuels 17 p2434 N88-24483
SNAP fuel performance 17 p2435 N88-24484

A comparison of uranium nitride and mixed carbide fuels swelling
17 p2435 N88-24485
The JET (Joint European Torus) multipellet launcher and fueling of JET plasmas by multipellet injection
[DE88-008367] 19 p2729 N88-26206
The hole of a blanket tritium system on the fusion fuel cycle
[DE88-010007] 20 p2859 N88-26983

NUCLEAR FUSION
NT CONTROLLED FUSION
System studies of compact ignition tokamaks
[DE87-014976] 02 p0239 N88-11508
Feasibility of alpha particle measurement in a magnetically confined plasma by CO2 laser Thomson scattering
[DE88-000039] 02 p0241 N88-11522
Volume produced H(-),D(-) ion source for proton accelerator and thermo-nuclear fusion research by sheet plasma (III)
[IPPJ-838] 02 p0242 N88-11531
Measurement of parallel ion energy distribution function in PISCES plasma
[DE88-000108] 03 p0378 N88-12380
Interchange stability of noncircular reversed field pinches
[DE88-000177] 03 p0378 N88-12381
The attitudes of science policy, environmental, and utility leaders on US energy issues and fusion
[DE88-000784] 04 p0494 N88-13041
Neutron capture nucleosynthesis in low mass AGB stars
04 p0517 N88-13178
A review of the experimental and theoretical status of the reversed-field pinch
[DE88-000529] 05 p0652 N88-14000
Mirror theory applied to toroidal systems
[DE88-003832] 07 p0933 N88-15669
Summary of the report of the Senior Committee on Environmental, Safety and Economic Aspects of Magnetic Fusion Energy
[DE88-003270] 07 p0937 N88-15692
Primordial nucleosynthesis during the keV era
[DE88-002233] 08 p1104 N88-16623
Investigation of the evolution of the fusion processes in the plasma focus using time-resolved neutron spectroscopy
[IPF-87-4] 09 p1251 N88-17493
Understanding and accepting fusion as an alternative energy source
[DE88-004356] 10 p1413 N88-18432
Starpower: The US and the international quest for fusion energy
[PB88-128731] 11 p1551 N88-19283
Low aspect ratio torsatrons
[DE88-004173] 11 p1552 N88-19284
Fusion, and advanced fuel, reaction bibliography: Particle reactions from H1 to B11
[AD-A187420] 11 p1552 N88-19286
Intermixing processes in massive stars and their influence on stellar evolution and nucleosynthesis
[ETN-88-91484] 11 p1568 N88-19388
Big Bang Nucleosynthesis: Accelerator tests and can (UC OMEGA)(sub B) really be large
[DE88-003405] 11 p1570 N88-19396
Application of railgun principle to high-velocity hydrogen pellet injection for magnetic fusion reactor refueling
[DE88-005830] 13 p1728 N88-20334
SOAR: Space orbiting advanced fusion power reactor
[AD-A189234] 13 p1732 N88-20356
JPRS report: Science and technology. China
[JPRS-CST-87-043] 15 p2053 N88-22233
Smoothing technique to resolve X-ray spectra in laser nuclear fusion
15 p2053 N88-22235
Magnetic fusion energy plasma interactive and high heat flux components. Volume 5: Technical assessment of critical issues in the steady state operation of fusion confinement devices
[DE88-006920] 15 p2136 N88-22744
Soviet magnetic confinement fusion research
[PB88-182316] 16 p2279 N88-23644
Helium-3 fusion fuel resources for space power
17 p2410 N88-24330
Intense ion beam diagnostics for particle beam fusion experiments on PBFA 2
[DE88-007279] 18 p2577 N88-25308
A mode-transforming polarization-rotatable launcher for the ATF (Advanced Toroidal Facility) fusion experiment
[DE88-005070] 19 p2730 N88-26213
Heavy ion collisions with A = 10(sup 57): Aspects of nuclear stability and the nuclear equation of state in coalescing neutron-star binary systems
[DE88-008029] 19 p2741 N88-26277
Fusion programs in applied plasma physics and development and technology at GA Technologies, Inc.
[DE88-008406] 20 p2856 N88-26964
Overview of the TITAN-2 reversed-field pinch aqueous fusion power core design
[DE88-008170] 20 p2857 N88-26966
Influence of pairing correlations on the probability and dynamics of tunneling through the barrier in fission and fusion of complex nuclei
[DE88-701500] 23 p3286 N88-29570

NUCLEAR HEAT
Basic characteristics of heat-exchanger-type steam reformer heated by high-temperature helium gas (2). Analysis by simulation model (2)
[DE87-702962] 15 p2061 N88-22291

NUCLEAR INTERACTIONS
NT ELECTRON CAPTURE
NT NUCLEAR CAPTURE
NT WEAK INTERACTIONS (FIELD THEORY)
Cosmic-ray nuclear event with an anomalously strong concentration of energy and particles in the central region
[DE87-703376] 04 p0526 N88-13213
Nucleon-nucleus interaction data base: Total nuclear and absorption cross sections
[NASA-TM-4053] 20 p2852 N88-26935

NUCLEAR MAGNETIC RESONANCE
X-ray tomography and nuclear magnetic resonance imaging applications for advanced ceramic materials
[DE87-011534] 01 p0027 N88-10171
Nuclear magnetic resonance studies of ion motion in solid electrolytes
[DE87-014547] 02 p0232 N88-11464
Evaluation of one-sided nuclear magnetic resonance for remote detection of explosives
[AD-A184490] 03 p0296 N88-11857
Synthesis, NMR characterization and electrical properties of siloxane-based polymer electrolytes
[AD-A184184] 04 p0418 N88-12596
Solid state C-13 NMR characterization of textiles: Qualitative and quantitative analysis
[AD-A184349] 04 p0419 N88-12598
A low volume insert for solid state magic angle spinning NMR of small samples
[AD-A184359] 04 p0419 N88-12601
Alternating current circuit theory and pulsed NMR (Nuclear Magnetic Resonance)
[DE88-000641] 04 p0440 N88-12732
The use of NMR imaging to measure porosity and binder distributions in green-state and partially sintered ceramics
[DE88-003099] 08 p0972 N88-15881
A 13C and 15N solid state NMR characterization of aramid-containing nylon-6 polymers synthesized by in situ polymerization of caprolactam with benzoyl caprolactam derivatives
[AD-A187067] 09 p1147 N88-16872
NMR (Nuclear Magnetic Resonance) imaging for detecting binder/plasticizers in green-state structural ceramics
[DE88-003111] 10 p1304 N88-17800
Instrumentation and quantitative methods of evaluation
[DE87-013639] 10 p1342 N88-18017
Irreducible tensor operators and multiple-quantum NMR
11 p1542 N88-19217
FTIR (Fourier Transform Infrared) and FTNMR (Fourier Transform Nuclear Magnetic Resonance) study of organophosphorus surface reactions
[AD-A188337] 12 p1609 N88-19625
Recent developments in nondestructive evaluation for structural ceramics
[DE88-005689] 13 p1751 N88-20473
Velocity and concentration measurements in flowing suspensions by nuclear magnetic resonance
[DE88-006225] 13 p1770 N88-20589
Biophysical applications of solid state and tritium NMR
[DE88-005328] 13 p1808 N88-20806
Biology and Medicine Division
[DE87-009280] 14 p1952 N88-21632
Structure of sol-gel silica
[DE88-006870] 15 p2033 N88-22114
Fluids, gels and glasses under extreme conditions of pressure and temperature
[AD-A190655] 15 p2035 N88-22125
NMR analysis of a fluorocarbon copolymer
[DE88-002364] 15 p2043 N88-22170
Chromatographic and mass spectrometric separation and analysis
[AD-A190113] 16 p2174 N88-22958
Structural study of the TGMDA-DDS system — epoxy system
[ONERA-RT-4/3346-M] 18 p2493 N88-24792
An instrument control and data analysis program for NMR imaging and spectroscopy
[DE88-007377] 19 p2717 N88-26132
Determination of binder distributions in green-state ceramics by NMR imaging
[DE88-009990] 20 p2778 N88-26474
Nuclear magnetic resonance spectrometer
[AD-A192928] 21 p2950 N88-27523
Sol-gel kinetics: Si(sup)29 NMR and a statistical reaction model
[DE88-011545] 23 p3191 N88-28988
Static and dynamic behavior of a quasi one-dimensional Heisenberg antiferromagnet in the long-range ordered state. A nuclear magnetic resonance study performed with a He3-He4 dilution refrigerator
[B8705564] 23 p3281 N88-29533

NUCLEAR MEDICINE
NT RADIOBIOLOGY
South African Association of Physicists in Medicine and Biology: 26th Annual Congress
[DE88-700824] 11 p1521 N88-19082
Nuclear health and safety: Radiation exposures for some cloud-sampling personnel need to be reexamined
[PB88-130497] 12 p1662 N88-19965
JPRS report: Science and technology. USSR: Life sciences
[JPRS-ULS-88-002] 12 p1665 N88-19982
Technology '87: Research and Development Laboratory Technology Transfer Program
[DE88-003142] 13 p1852 N88-21084
Biology and Medicine Division
[DE87-009280] 14 p1952 N88-21632

NUCLEAR METEOROLOGY
Opportunities for nowcasting air pollution episodes and accidental toxic and radioactive releases
02 p0210 N88-11317
Nuclear health and safety: Radiation exposures for some cloud-sampling personnel need to be reexamined
[PB88-130497] 12 p1662 N88-19965
Health and environmental consequences of the Chernobyl nuclear power plant accident
[DOE/ER-0332] 19 p2689 N88-25985

NUCLEAR MODELS
Development and evaluation of a Monte Carlo code system for analysis of ionization chamber responses
[AD-A183970] 03 p0375 N88-12359
New nuclear structure calculations and the astrophysical r-process
[DE88-000979] 08 p1082 N88-16518
Simulation of nuclear collisions at high energies in the frames of quark-gluon string model
[DE88-700914] 12 p1690 N88-20113
Development of nuclear models for higher energy calculations
[DE88-010919] 20 p2852 N88-26932

NUCLEAR PARTICLES
NT ALPHA PARTICLES
NT ANTINEUTRINOS
NT ANTINUCLEONS
NT ANTIPARTICLES
NT ANTIPROTONS
NT BETA PARTICLES
NT BOSONS
NT KAONS
NT MESON RESONANCE
NT MESONS
NT MUONS
NT NUCLEONS
NT PHOTOELECTRONS
NT PHOTONS
NT PIONS
NT POSITRONS
Theory of double beta decay
[DE88-002285] 07 p0931 N88-15653
Large area nuclear particle detectors using ET materials
[NASA-CR-180777] 23 p3215 N88-29136

NUCLEAR PHYSICS
NT NUCLEAR ASTROPHYSICS
NT REACTOR PHYSICS
Mathematics applied to nuclear geophysics
[INPE-4234-PRE/1109] 01 p0086 N88-10561
Experimental nuclear physics
[DE87-014586] 02 p0231 N88-11459
Electron interactions with nuclei
[DE87-014587] 02 p0232 N88-11460
Future directions in interplays between particle and nuclear physics: Summary session
[DE87-011791] 04 p0489 N88-13013
Nuclear techniques in studies of condensed matter
[NASA-RP-1195] 04 p0489 N88-13015
Research in elementary particle physics
[DE88-002130] 06 p0777 N88-14771
USSR report: Physics and mathematics
[JPRS-UPM-87-002] 07 p0918 N88-15575
Theoretical nuclear physics
[DE87-004504] 09 p1244 N88-17455
Activities report in nuclear physics
[ETN-88-91609] 09 p1245 N88-17458
Semiclassical theory of the nuclear response function. Quasielastic electron scattering
[ETN-88-91082] 09 p1245 N88-17459

Technical activities 1987, Center for Radiation Research
[PB88-129325] 09 p1245 N88-17464
The development of emission tomography for the nuclear industry
[AERE-R-12319] 10 p1341 N88-18014
Research in experimental nuclear physics
[DE88-004100] 10 p1408 N88-18397
Experimental elementary particle physics at the University of Pittsburgh
[DE88-003542] 11 p1545 N88-19234
Experimental aspects of hypernuclear physics at CEBAF
[CEBAF-R-86-013] 11 p1546 N88-19245
Channeling and dechanneling at high energy
[DE88-003989] 11 p1548 N88-19259
Reports and contributions of the Max-Planck Institute of Chemistry (Otto Hahn Institute)
[REPT-1/87] 11 p1570 N88-19398
Intermediate energy neutrino physics
[DE88-005378] 13 p1836 N88-20984
Research in high energy elementary particle physics
[DE88-006065] 13 p1837 N88-20994
Particle physics and cosmology
[DE88-004944] 13 p1854 N88-21096
Experimental elementary particle physics
[DE88-007510] 18 p2572 N88-25274

NUCLEAR POWER GENERATION
U NUCLEAR ELECTRIC POWER GENERATION

NUCLEAR POWER PLANTS
Reinforced flexural elements for TEMP-STRESS Program
[DE87-012961] 01 p0061 N88-10391
USSR Report: Engineering and Equipment
[JPRS-UEQ-87-007] 02 p0157 N88-10985
Ultrasonic mechanized checking of weld joints of nuclear power plant equipment 02 p0158 N88-10987
Real-time evaluation and prediction of coastal dispersion near the SW tip of Africa --- effluents 02 p0210 N88-11318
Expert robots in nuclear plants
[DE87-014839] 04 p0452 N88-12800
Ultrasonic method of imspecting austenitic weld joints in nuclear power station equipment
[BLL-CE-TRANS-8281-(9022.09)] 04 p0453 N88-12806
Computer code simulations of explosions in flow networks and comparison with experiments
[DE88-001946] 05 p0573 N88-13491
Effects of commercial cladding on the fracture behavior of pressure vessel steel plates
[DE88-004333] 10 p1303 N88-17790
Understanding and accepting fusion as an alternative energy source
[DE88-004356] 10 p1413 N88-18432
Proceedings of the 19th DOE/NRC Airborne Waste Management and Air Cleaning Conference
[NUREG/CP-0086-VOL-1] 11 p1509 N88-19018
Proceedings of the 19th DOE/NRC Airborne Waste Management and Air Cleaning Conference
[NUREG/CP-0086-VOL-2] 11 p1509 N88-19019
Uncertainties in hydrogen combustion
[DE88-005354] 13 p1739 N88-20395
Small and medium power reactors 1987
[DE88-701435] 15 p2132 N88-22720
JPRS report: Science and technology. Japan
[JPRS-JST-87-030] 16 p2185 N88-23026
Design of nuclear heat, power co-generation plant detailed 16 p2186 N88-23033
Nuclear electric propulsion system: Nuclear plant and thermomechanical conversion system 17 p2405 N88-24298
Thermal management for multi-modal nuclear power plants 17 p2410 N88-24331
Knowledge based systems in nondestructive evaluation
[DE88-006653] 18 p2525 N88-24981
Health and environmental consequences of the Chernobyl nuclear power plant accident
[DOE/ER-0332] 19 p2689 N88-25985
Qualification of expansion and welding procedures of tube-to-tubesheet joints for heat exchangers in nuclear power plants
[DE88-701621] 23 p3221 N88-29174

NUCLEAR POWER REACTORS
NT FISSION ELECTRIC CELLS
NT SPACE POWER REACTORS
Small reactor power systems for manned planetary surface bases
[NASA-TM-100223] 04 p0524 N88-13209
Small and medium power reactors 1987
[DE88-701435] 15 p2132 N88-22720
Development of fast breeder reactors in China 16 p2186 N88-23032
Operational concerns involving a shadow-shielded nuclear reactor for space station applications 17 p2398 N88-24257
Nuclear electric power for multimegawatt orbit transfer vehicles 17 p2399 N88-24261
Gigawatt, closed cycle, vapor core-MHD space power system conceptual design study 17 p2433 N88-24473
Critical issues for SOAR: The space orbiting advanced fusion power reactor 17 p2433 N88-24474
Comparison of 20-kWe space nuclear power systems: Impact of reactor temperature and technology upon system design and performances 17 p2433 N88-24475
Potassium Rankine power system for space power 17 p2433 N88-24476
Low cross-section Mo-Nb thermocouples for nuclear application: The state-of-the-art 17 p2433 N88-24477
Material property and irradiation performance correlations for nitride fuels 17 p2434 N88-24483
Health and environmental consequences of the Chernobyl nuclear power plant accident
[DOE/ER-0332] 19 p2689 N88-25985
Pulsed power driver technologies for inertial confinement fusion power reactors
[DE88-009260] 19 p2731 N88-26221

NUCLEAR PROPULSION
NT NUCLEAR ELECTRIC PROPULSION
Fusion, and advanced fuel, reaction bibliography: Particle reactions from H1 to B11
[AD-A187420] 11 p1552 N88-19286
Nuclear electric power for multimegawatt orbit transfer vehicles 17 p2399 N88-24261
History of some direct nuclear propulsion developments since 1946 17 p2400 N88-24270
Direct nuclear propulsion for Earth-to-orbit vehicles 17 p2400 N88-24271
Nuclear propulsion systems for orbit transfer based on the particle bed reactor 17 p2401 N88-24272
Ultra high temperature direct propulsion 17 p2401 N88-24275
Safety constraints and considerations in the development of nuclear powered propulsion 17 p2401 N88-24276
Comparison of a direct thrust nuclear engine, nuclear electric engine and a chemical engine for future space missions 17 p2418 N88-24379
Nuclear propulsion: Past, present and future 17 p2427 N88-24441
Gas core reactors for direct nuclear propulsion 17 p2428 N88-24442
Noncryogenic propellants for a nuclear orbit transfer vehicle 17 p2428 N88-24444

NUCLEAR PUMPED LASERS
Refractive index gradients in nuclear-reactor-pumped lasers: Gasdynamic effects
[DE88-006099] 13 p1776 N88-20621

NUCLEAR RADIATION
NT BETA PARTICLES
NT FAST NEUTRONS
NT GAMMA RAY BURSTS
NT GAMMA RAYS
NT NEUTRON BEAMS
NT SPALLATION
NT THERMAL NEUTRONS

NUCLEAR RADIATION SPECTROSCOPY
Phase modulation of recoiless gamma radiation in Mossbauer spectroscopy
[ETN-88-92648] 24 p3428 N88-30403

NUCLEAR REACTIONS
NT ALPHA DECAY
NT CONTROLLED FUSION
NT ELECTRON CAPTURE
NT NEUTRON EMISSION
NT NEUTRON SCATTERING
NT NUCLEAR CAPTURE
NT NUCLEAR FISSION
NT NUCLEAR FUSION
NT NUCLEAR INTERACTIONS
NT NUCLEAR SCATTERING
NT NUCLEAR TRANSFORMATIONS
NT PHOTONUCLEAR REACTIONS
NT PROTON SCATTERING
NT PROTON-PROTON REACTIONS
NT RADIOACTIVE DECAY
NT RESONANCE SCATTERING
NT SPALLATION
NT THERMONUCLEAR REACTIONS
NT TRANSMUTATION
NT WEAK INTERACTIONS (FIELD THEORY)
Experimental nuclear physics
[DE87-014586] 02 p0231 N88-11459
The development of diagnostic fuses
[SAND-86-0395] 03 p0311 N88-11963
Applied nuclear science research and development
[LA-10915-PR] 03 p0374 N88-12355
Computer simulations of fragmentation
[DE87-900985] 03 p0375 N88-12358
Anomalous phonon behavior of superconductor Y-Ba-Cu-O
[DE87-703401] 05 p0854 N88-14010
Analysis of the mass formula dependence of spallation product distribution
[DE88-750297] 07 p0864 N88-15243
An introduction to nuclear astrophysics
[DE88-002761] 08 p1100 N88-16618
Theoretical nuclear physics
[DE87-004504] 09 p1244 N88-17455
Measurements of astrophysical reaction rates for radioactive samples
[DE88-004309] 10 p1429 N88-18537
Gamma-ray and neutron spectroscopy of planetary surfaces and atmospheres
[DE88-004287] 10 p1430 N88-18541
Ion energy diagnostics for voltage determinations in plasma-erosion-opening-switch experiments
[DE88-004822] 11 p1479 N88-18827
Emission of gamma rays from various materials pulsed with 14-MeV neutrons
[DE88-003837] 11 p1544 N88-19227
Fusion, and advanced fuel, reaction bibliography: Particle reactions from H1 to B11
[AD-A187420] 11 p1552 N88-19286
On (p,n) systematics and the cosmological connection
[DE88-005031] 12 p1712 N88-20245
Theory of Muon method for study of solid and liquid hydrogen 14 p1972 N88-21770
Reference nuclear data for space applications
[DE88-007041] 16 p2270 N88-23583
Search for bound states of the eta-meson in light nuclei 17 p2397 N88-24248
Nuclear and astrophysical evidence on the equation of state
[DE88-007397] 18 p2572 N88-25279
Automated system for mathematical processing of the data from a hybrid spectrometer
[DE87-702995] 20 p2836 N88-26820
Development of nuclear models for higher energy calculations
[DE88-010919] 20 p2852 N88-26932
Measure of hydrogen concentration profile in materials by resonant nuclear reactions
[DE88-702599] 23 p3193 N88-28999
Hadrons produced in atmospheric interactions
[DE88-702492] 23 p3309 N88-29712

NUCLEAR REACTOR CONTROL
Application of the reactivity constraint approach to the transient control of spacecraft reactors 17 p2406 N88-24305
Reactor instrumentation and control design and performance simulation for SP-100 17 p2406 N88-24306
An adaptive load-following control system for a space nuclear power system 17 p2406 N88-24307
Benchmark physics experiments for SP-100 17 p2429 N88-24453
A high power density radial-in-flow reactor split core design for space power systems 17 p2430 N88-24455
Transient analyses of multimegawatt space reactors 17 p2430 N88-24456
Silicon-on-insulator electronics for a space nuclear power system 17 p2431 N88-24461

NUCLEAR REACTORS
NT BOILING WATER REACTORS
NT BREEDER REACTORS
NT EXPERIMENTAL BREEDER REACTOR 2
NT FAST NUCLEAR REACTORS
NT FISSION ELECTRIC CELLS
NT FUSION REACTORS
NT FUSION-FISSION HYBRID REACTORS
NT GAS COOLED REACTORS
NT GASEOUS FISSION REACTORS
NT HIGH TEMPERATURE GAS COOLED REACTORS
NT HIGH TEMPERATURE NUCLEAR REACTORS
NT JOINT EUROPEAN TORUS
NT LIGHT WATER REACTORS
NT LIQUID COOLED REACTORS
NT LIQUID METAL COOLED REACTORS
NT LIQUID METAL FAST BREEDER REACTORS
NT NUCLEAR POWER REACTORS
NT NUCLEAR RESEARCH AND TEST REACTORS
NT PEBBLE BED REACTORS
NT PLASMA CORE REACTORS
NT PRESSURIZED WATER REACTORS
NT SPACE POWER REACTORS
NT SPHEROMAKS
NT STELLARATORS
NT THERMAL REACTORS
NT TOKAMAK DEVICES
NT ZERO POWER REACTORS

Oxidation of TSX graphite over the temperature range 450 to 1200°C
[DE87-012230] 01 p0020 N88-10127
Transient modeling of the thermohydraulic behavior of high temperature heat pipes for space reactor applications 02 p0136 N88-10857
Assessment of the impacts of transferring certain nuclear reactor technologies to the Soviet Union and Eastern Europe
[DE87-014388] 02 p0249 N88-11576
Computerized system for studies on creep of irradiated materials in the BR-10 reactor. Control system for electric motor
[DE87-702888] 03 p0310 N88-11952
Shielding analysis of a small compact space nuclear reactor
[AD-A185566] 06 p0779 N88-14784
Effects of the neutron spectrum on mechanical property changes in low dose irradiations
[DE88-003429] 10 p1302 N88-17786
Ballistic deficits in pulse shaping amplifiers
[DE88-003908] 11 p1451 N88-18840
Optimal control theory of load-following and parameter-tracking of nonlinear systems: An application of Pontryagin Maximum Principle to reactor dynamics
[DE88-004770] 11 p1532 N88-19152
The use of least squares in undetermined problems
[DE88-004473] 12 p1682 N88-20059
Requirements and cost considerations for a combined space nuclear reactor test facility 17 p2401 N88-24277
The role of integral experiments and nuclear cross section evaluations in space nuclear reactor design 17 p2404 N88-24293
Nuclear reactor magnetohydrodynamic power generator for directed energy weapons 17 p2411 N88-24336
EETAP (End-to-End Transient Analysis Program) for space nuclear power system simulation 17 p2418 N88-24381
Relating design and environmental variables to reliability 17 p2418 N88-24383
Theoretical prediction of single phase turbulent flow distribution in particulate bed reactors 17 p2419 N88-24386
Monolithic fuel cell based power source for burst power generation 17 p2429 N88-24450
High power density alkaline fuel cell technology for MMW space burst power 17 p2429 N88-24451
Computer aided remote control: A general concept for intervention in the nuclear, underwater, and space domains 19 p2699 N88-26046
The safety designs for the TITAN reversed-field pinch reactor study
[DE88-008169] 19 p2729 N88-26205
Principles of a nondestructive evaluation process for damage location, damage profile, and damage extension in welded joints by radiometric measurements
[MPA-86-02] 20 p2812 N88-26683
Fusion programs in applied plasma physics and development and technology at GA Technologies, Inc.
[DE88-008406] 20 p2856 N88-26964
TIBER (Tokamak Ignition/Burn Experimental Reactor) 2 as a precursor to an international thermonuclear experimental reactor
[DE88-008906] 20 p2858 N88-26970

NUCLEAR RELAXATION
A review of the experimental and theoretical status of the reversed-field pinch
[DE88-000529] 05 p0652 N88-14000

NUCLEAR RESEARCH
Applied nuclear science research and development
[LA-10915-PR] 03 p0374 N88-12355
The birth of big science: Nuclear physics as advanced technology source
[NOTA-INTERNA-861] 05 p0648 N88-13967
Technology security, volume 1
[DE88-008612] 21 p3029 N88-27978

NUCLEAR RESEARCH AND TEST REACTORS
NT EXPERIMENTAL BREEDER REACTOR 2
NT HIGH TEMPERATURE NUCLEAR REACTORS
Radiation effects testing capabilities of the Texas A and M Nuclear Science Center 17 p2416 N88-24368

NUCLEAR ROCKET ENGINES
TRICE design, evaluation and feasibility tests 17 p2437 N88-24498
Advanced nuclear rocket engine mission analysis
[DE88-006797] 18 p2475 N88-24681

NUCLEAR SCATTERING
NT NEUTRON SCATTERING
NT RESONANCE SCATTERING
Status of cross section data for photon scattering by atoms
[DE87-011281] 08 p1081 N88-16517
Pion elastic and inelastic scattering near N = 28
[LA-10968-T] 11 p1544 N88-19232
Eikonal solutions to optical model coupled-channel equations
[NASA-TP-2830] 24 p3428 N88-30402

NUCLEAR SHIELDING
U RADIATION SHIELDING

NUCLEAR SPIN
Theory of Muon method for study of solid and liquid hydrogen 14 p1972 N88-21770

NUCLEAR STRUCTURE
Electron interactions with nuclei
[DE87-014587] 02 p0232 N88-11460
TRISTAN research on neutron rich nuclei: Magnetic moments and nuclear structure
[DE88-002122] 06 p0783 N88-14807
Double beta decay and nuclear structure
[DE88-001966] 07 p0931 N88-15652
New nuclear structure calculations and the astrophysical r-process
[DE88-000979] 08 p1082 N88-16518
Theoretical nuclear physics
[DE87-004504] 09 p1244 N88-17455
Extension of nuclear structure data base searches for gamma-ray laser candidates
[DE88-004288] 10 p1336 N88-17985
A nuclear structure study of the proposed gamma-ray laser candidate nucleus Re-186
[DE88-004299] 10 p1336 N88-17986
Nuclear structure at intermediate energies
[DE88-002796] 10 p1407 N88-18390
Nuclear structure studies by the scattering of medium-energy electrons
[DE88-003803] 11 p1545 N88-19236
Presentations to the SuperHILAC Program Advisory Committee
[DE88-003853] 11 p1547 N88-19256
Ground-state correlations in C12 and the mechanism of the (e,e'p) reaction
[B8729349] 14 p1980 N88-21816
Nuclear structure studies at intermediate energies
[DE88-006683] 18 p2571 N88-25271
Tagging of gamma yields qq bar events and direct measurement of the gluon structure function at HERA
[NOTA-INTERNA-910] 22 p3151 N88-28745
Nuclear magnetic ordering and paramagnetic relaxation of diatomic molecules in Ca (OH)2
[B8681469] 23 p3281 N88-29532
Fluctuation and relaxation phenomena studied by means of nuclear orientation
[B8679671] 23 p3281 N88-29534

NUCLEAR TEST REACTORS
U NUCLEAR RESEARCH AND TEST REACTORS

NUCLEAR TRANSFORMATIONS
NT TRANSMUTATION
Nuclear transitions induced by atomic excitations
[DE88-004311] 11 p1545 N88-19239

NUCLEAR VULNERABILITY
The strategic defense initiative: Strategic implications
[AD-A192341] 20 p2847 N88-26902

NUCLEAR WARFARE
SDI (Strategic Defense Initiative). Where do we go from here
[AD-A194544] 23 p3275 N88-29497

NUCLEAR WASTES
U RADIOACTIVE WASTES

NUCLEAR WEAPONS
Anechoic Chamber test of the Electromagnetic Measurement System ground test unit
[DE87-012998] 01 p0035 N88-10226
Store separation of nuclear weapons
[DE87-010778] 02 p0124 N88-10785
The effects of corona on current surges induced on conducting lines by EMP: A comparison of experiment data with results of analytic corona models
[DE87-014970] 03 p0305 N88-11924
An excitation-term modification for a certain class of electromagnetic aperture-coupling problems
[DE88-000260] 04 p0437 N88-12713
New approach to telemetry development will significantly increase productivity of Joint Test Assembly (JTA) teams
[DE88-001676] 05 p0554 N88-13373
Announced United States nuclear tests: July 1945 through December 1986
[NVO-209-REV-7] 11 p1546 N88-19247
Characteristics of the positive lighting flash
[DE88-005854] 13 p1800 N88-20760
An agenda for the strategic defense initiative
[RAND-P-7404] 20 p2847 N88-26898
Monitoring space weaponry: Detection and verification issues
[DE88-008726] 20 p2847 N88-26900
SDI and/or arms control
[RAND-P-7357] 20 p2848 N88-26903
Technology security, volume 1
[DE88-008612] 21 p3029 N88-27978
Looking beyond the strategic defense initiative
[AD-A195079] 24 p3427 N88-30394

NUCLEATE BOILING
An experiment to investigate Rankine cycle two-phase microgravity issues
[DE88-004197] 10 p1308 N88-17818
Nucleate pool boiling: High gravity to reduced gravity; liquid metals to cryogens 17 p2431 N88-24464
Heating and evaporation of turbulent liquid films: Measurement of film thickness and the onset of nucleate boiling
[DE88-006388] 18 p2512 N88-24905
Forced-convective boiling in small diameter tube 20 p2783 N88-26510

NUCLEATION
NT CLOUD SEEDING
Abrikosov vortex motion and elementary pinning force in a SNS Josephson junction
[DE87-013607] 01 p0105 N88-10683
Experimental and theoretical study of condensation in multicomponent vapors
[DE87-013663] 02 p0145 N88-10907
Continued research on direct contact heat exchangers: Effects of crystallization
[DE87-014931] 03 p0322 N88-12035
Experimental and theoretical study of condensation in multicomponent mixtures
[DE88-000897] 04 p0413 N88-12563
Microgravity nucleation and particle coagulation experiments support
[NASA-CR-181540] 04 p0423 N88-12618
Microgravity nucleation and particle coagulation experiments support
[NASA-CR-181541] 04 p0423 N88-12619
Plume mechanics and aerosol growth processes
[AD-A184467] 04 p0442 N88-12742
The mechanics of fatigue-crack nucleation in a low-alloy steel under fretting conditions 05 p0597 N88-13649
Undercooling and nucleation in iron nickel alloys
[AD-A185500] 06 p0683 N88-14184
Astrophysics and the solar nebula 07 p0883 N88-15355
Atmospheric science 07 p0883 N88-15357
Ionic mechanisms of soot formation in flames
[AD-A186195] 08 p0966 N88-15848
Kinetics and mechanism of thermal aging embrittlement of duplex stainless steels
[DE88-002987] 08 p0969 N88-15866
TiN coatings on M2 steel produced by plasma assisted chemical vapor deposition
[DE88-003189] 08 p0970 N88-15867
Review of nucleation and incipient boiling under pool and forced convection conditions 08 p0982 N88-15938
Mechanistic model for void distribution in flashing flow
[DE88-002948] 10 p1326 N88-17928
Deactivation of alumina based catalysts 11 p1455 N88-18673
Crystallization and glass formation in electron and laser beam irradiated Cu-Zr alloys
[DE88-003390] 11 p1464 N88-18729
Nucleation and growth of calcium carbonate crystals on surface-modified polyethylene and polystyrene
[DE88-005126] 11 p1465 N88-18733
Cavitation inception
[AD-A189220] 13 p1765 N88-20557
Ductile failure
[AD-A189429] 13 p1781 N88-20654
Stability limits in the monoclinic-tetragonal transformations of zirconia
[DE88-005924] 14 p1986 N88-21849
Nucleation in super-saturated products
[NASA-TT-20275] 15 p2037 N88-22134
Optical monitoring of protein crystal growth
[NASA-CR-182869] 18 p2484 N88-24738
Kinetics of homogeneous nucleation in superheated F-11 and F-21 liquid freons
[NASA-TT-20286] 19 p2613 N88-25503
Studies of metal-silicon, silicon-metal and silicide based interfaces: Synchrotron radiation photo emission and inverse photoemission investigations of interface formation and compound nucleation
[AD-A191808] 19 p2619 N88-25536
Center for thin film studies
[AD-A191996] 19 p2732 N88-26226
Cloud simulation warm cloud experiments: Droplet growth and aerosol scavenging
[AD-A192944] 21 p2974 N88-27666
Atomic layer epitaxy of ZnS and ZnSe
[AD-A192307] 21 p3020 N88-27928
Finite-rate water condensation in combustion-heated wind tunnels
[NASA-TP-2833] 22 p3046 N88-28075

NUCLEI (NUCLEAR PHYSICS)
NT ALPHA PARTICLES
NT DEUTERONS
NT EVEN-EVEN NUCLEI
NT HEAVY NUCLEI
NT HYPERNUCLEI
NT ODD-ODD NUCLEI
NT TRITONS
Experimental nuclear physics
[DE87-014586] 02 p0231 N88-11459
TRISTAN research on neutron rich nuclei: Magnetic moments and nuclear structure
[DE88-002122] 06 p0783 N88-14807
Pion nucleus single charge exchange reactions above the delta(1232) resonance
[LA-11004-T] 11 p1544 N88-19231
Nucleon resonances and nuclei: Experimental aspects
[CEBAF-PR-87-025] 11 p1545 N88-19233
Nucleation in super-saturated products
[NASA-TT-20275] 15 p2037 N88-22134
Search for bound states of the eta-meson in light nuclei 17 p2397 N88-24248

NUCLEIC ACID DENATURATION
U BIOPOLYMER DENATURATION

NUCLEIC ACIDS
NT DEOXYRIBONUCLEIC ACID
NT RIBONUCLEIC ACIDS
Photochemical conversion of nucleic acid components catalyzed by lunar soil 06 p0750 N88-14604
Biopolymers: Protein and nucleic acids
[AD-A185837] 07 p0835 N88-15066
Nucleic acid content of skeletal muscles during hypokinesia and in the recovery period 07 p0894 N88-15418

NUCLEON-NUCLEON INTERACTIONS
An electron-scattering study of N-15
[ETN-88-92479] 16 p2266 N88-23552
Computer program for parameterization of nucleus-nucleus electromagnetic dissociation cross sections
[NASA-TM-4038] 16 p2270 N88-23584
Nuclear structure studies at intermediate energies
[DE88-006683] 18 p2571 N88-25271
Energy measurements in oxygen-induced reactions at 60 A GeV and 200 A GeV
[DE88-006420] 18 p2573 N88-25283

NUCLEONS
Dynamics of coupled electron-nucleon motion in a laser field
[DE88-005063] 10 p1337 N88-17994
Nucleon resonances and nuclei: Experimental aspects
[CEBAF-PR-87-025] 11 p1545 N88-19233
Single nucleon coincidence cross sections in a relativistic mean field theory
[CEBAF-PR-87-016] 11 p1546 N88-19243
Theoretical studies in few-body intermediate energy physics
[DE88-004101] 12 p1689 N88-20106
On (e,e'N) reactions
[CEBAF-PR-87-028] 12 p1690 N88-20109
Production of pi(0) mesons and charged hadrons in nu bar neon and nu neon charges current interactions
[MPI-PAE/EXP.EL.188] 22 p3150 N88-28743

NUCLEOSIDES
Precise ultraviolet absorbance study of the interaction of amino acids and mononucleosides in aqueous solution
[ISAS-RN-356] 21 p2908 N88-27256

NUCLEOSYNTHESIS
U NUCLEAR FUSION

NUCLEOTIDES
NT ADENOSINE TRIPHOSPHATE
NT ADENOSINES
Fed-batch control based upon the measurement of intracellular NADH 09 p1197 N88-17175
Fast atom bombardment study on interaction of anticodonic nucleotides and their cognate amino acid
[ISAS-RN-355] 20 p2850 N88-26918

NUCLIDES
NT ARGON ISOTOPES
NT BORON ISOTOPES
NT BROMINE ISOTOPES
NT CALCIUM ISOTOPES
NT CARBON 12
NT CARBON 13
NT COBALT 60
NT DEUTERIUM
NT HELIUM ISOTOPES
NT HYDROGEN ISOTOPES
NT IODINE ISOTOPES
NT IRIDIUM ISOTOPES
NT IRON ISOTOPES
NT IRON 57
NT ISOTOPES
NT KRYPTON ISOTOPES
NT LAWRENCIUM
NT LEAD ISOTOPES
NT LITHIUM ISOTOPES
NT MERCURY ISOTOPES
NT NEODYMIUM ISOTOPES
NT NEPTUNIUM
NT NIOBIUM ISOTOPES
NT NITROGEN ISOTOPES
NT OXYGEN ISOTOPES
NT PLATINUM ISOTOPES
NT PLUTONIUM ISOTOPES
NT PLUTONIUM 238
NT RADIOACTIVE ISOTOPES
NT RADON ISOTOPES
NT RUBIDIUM ISOTOPES
NT TELLURIUM
NT TRITIUM
NT URANIUM ISOTOPES
NT URANIUM 238
Calculation methods of atomic number density for various nuclear materials
[DE87-753006] 02 p0233 N88-11467

NULL ZONES
Null steering applications of polynomials with unimodular coefficients
[AD-A191087] 18 p2562 N88-25211
Polynomials with restricted coefficients and their applications
[AD-A192589] 23 p3202 N88-29055

NUMBER THEORY
NT ARITHMETIC
NT DIVIDING (MATHEMATICS)
NT EXPONENTS
NT FLOATING POINT ARITHMETIC
NT INDUCTION (MATHEMATICS)
NT INTEGERS
NT MULTIPLICATION
The design of ultra high-speed numeric intensive systems (having fault tolerant and load balancing capabilities) 10 p1374 N88-18196
On a classification of problems on sets of bilinear forms by formal polynomials
[RR-642-I-IMAG-53-LIFIA] 17 p2392 N88-24219
Some properties of modular equations and the partition function 18 p2564 N88-25224

NUMERICAL ANALYSIS
NT APPROXIMATION
NT BORN APPROXIMATION
NT BORN-OPPENHEIMER APPROXIMATION
NT BOUNDARY INTEGRAL METHOD
NT CHEBYSHEV APPROXIMATION
NT COMPUTATIONAL CHEMISTRY
NT COMPUTATIONAL FLUID DYNAMICS
NT CONJUGATE GRADIENT METHOD
NT DIFFERENCE EQUATIONS
NT ERROR ANALYSIS
NT FINITE DIFFERENCE THEORY
NT FINITE ELEMENT METHOD
NT FINITE VOLUME METHOD
NT FLUX VECTOR SPLITTING
NT HARTREE APPROXIMATION
NT INTERPOLATION
NT ITERATION
NT ITERATIVE SOLUTION
NT LEAST SQUARES METHOD
NT MEAN SQUARE VALUES
NT MONTE CARLO METHOD
NT NEWTON METHODS
NT NEWTON-RAPHSON METHOD
NT NUMERICAL INTEGRATION
NT PADE APPROXIMATION
NT PARTICLE IN CELL TECHNIQUE
NT RAYLEIGH-RITZ METHOD
NT RELAXATION METHOD (MATHEMATICS)
NT RITZ AVERAGING METHOD
NT RUNGE-KUTTA METHOD
NT TRUNCATION ERRORS
Laser probes of natural gas ignition chemistry
[PB87-209599] 01 p0021 N88-10129
Transactions of the 4th Army Conference on Applied Mathematics and Computing
[AD-A183544] 01 p0085 N88-10547
Finite difference solution of a generic differential equation
[PB87-205878] 01 p0087 N88-10568
Fundamentals of numerical magnetohydrodynamics
[DE87-011769] 01 p0100 N88-10656
A numerical study of transient, thermally-conductive solar wind 01 p0115 N88-10738
Numerical simulation of a supersonic chemically reacting mixing layer 02 p0143 N88-10900
Impact of turbulence modeling on numerical accuracy and efficiency of compressible flow simulations
[NASA-TM-88333] 02 p0173 N88-11088
A numerical method for the treatment of kinked cracks in finite bodies 02 p0190 N88-11189
Numerical simulation of Tokamaks: Ideal MHD equilibrium and stability
[DE87-013452] 02 p0218 N88-11373
The spatially nonuniform convergence of the numerical solution of flows
[NASA-TM-100037] 02 p0226 N88-11429
Analytic investigation of helicopter rotor blade appended aeroelastic devices
[NASA-CR-166525] 03 p0266 N88-11676
Electromagnetic scattering by a thick strip on a half-space
[PB87-227096] 03 p0306 N88-11928
Performance evaluation of a half-wave resonant slot antenna over perfect ground using NEC (Numerical Electromagnetic Code)
[AD-A184004] 03 p0308 N88-11942
Computation of turbulent flows using an extended k-epsilon turbulence closure model
[NASA-CR-179204] 03 p0312 N88-11969
Momentum transport and particle dynamics in turbulent shear flows 03 p0317 N88-12002
Numerical study of the entrance flow and its transition in a circular pipe (2) 03 p0318 N88-12011
Numerical analysis of Marangoni convection in Bridgman method 03 p0319 N88-12014
Numerical simulation and visualization of a flowfield by interaction of two parallel two-dimensional freejets 03 p0320 N88-12021
On the root locus method applied to flexural vibration control systems 03 p0320 N88-12022
The dynamics of bubble growth for Rayleigh-Taylor unstable interfaces
[AD-A184752] 03 p0321 N88-12027
Some aspects of high resolution numerical methods for hyperbolic systems of conservation laws, with applications to gas dynamics
[DMS-86-7] 03 p0321 N88-12031
Adaptation of numerical SPOT data to an urban environment 03 p0342 N88-12158
Numerical solution of partial differential equations on irregular grids
[DE87-014760] 03 p0369 N88-12324
The development of ODE methods: A symbiosis between hardware and numerical analysis
[DE87-014925] 03 p0370 N88-12325
Institute for Computational Mechanics in Propulsion (ICOMP) first year summary
[NASA-TM-100225] 03 p0370 N88-12330
Numerical experiments with a symmetric high-resolution shock-capturing scheme
[NASA-TM-88325] 03 p0370 N88-12332
Numerical solution of bound constrained problems
[DE88-000653] 03 p0371 N88-12334
Concepts for radically increasing the numerical convergence rate of the Euler equations
[NASA-CR-177456] 04 p0395 N88-12463
Natural control of flexible space structures 04 p0408 N88-12534
An analytical and experimental study of injection-locked two-port oscillators
[NASA-TM-100119] 04 p0439 N88-12727
Numerical simulation of unsteady separated flows
[AD-A184132] 04 p0442 N88-12741
Methods for design and evaluation of integrated hardware/software systems for concurrent computation
[NASA-CR-181522] 04 p0479 N88-12953
Flux tube dynamics and solar/stellar redshift measurements 04 p0503 N88-13095
Numerical analysis of flow through scramjet engine inlets 05 p0532 N88-13233
Eigenvalue projection theory for linear operator equations of electromagnetics
[AD-A185434] 05 p0575 N88-13504
Numerical analysis, computing and fundamental studies in fluid mechanics
[DE88-001912] 05 p0582 N88-13550
The numerical and analytic of implicit differential equations and their application to control and circuit problems
[AD-A185404] 05 p0641 N88-13922
Numerical methods for reaction-diffusion problems with non-differentiable kinetics
[AD-A185405] 05 p0641 N88-13923
Numerical simulation of boundary layers. Part 3: Turbulence and relaminarization in sink flows
[NASA-TM-88220] 06 p0698 N88-14283
Theoretical and numerical analysis of shock wave propagation through different dusty-gas mixture layers 06 p0699 N88-14292
Development of symbolic computation methods for nonlinear dynamics
[AD-A185562] 06 p0758 N88-14653
Local and global techniques for the tracking of periodic solutions of parameter-dependent functional differential equations
[AD-A185756] 06 p0766 N88-14704

Characteristic trajectories of generalized Lanchester equations
[AD-A185762] 06 p0766 N88-14705
Analytical investigations of bulk wave resonators in the piezoelectric thin film on gallium-arsenide configuration
[AD-A185716] 06 p0789 N88-14840
Numerical simulation of a controlled boundary layer
07 p0810 N88-14933
Boundary layer transition 07 p0811 N88-14942
Packet error probabilities in frequency-hopped spread spectrum packet radio networks. Markov frequency hopping patterns considered
[AD-A186071] 07 p0841 N88-15104
User manual for ATILA, a finite-element code for modeling piezoelectric transducers
[AD-A185948] 07 p0847 N88-15141
On the parabolized Navier-Stokes equations without sublayer assumptions
[AD-A186127] 07 p0849 N88-15152
Numerical calculation of appendage, flat plate junction flow
[AD-A186371] 07 p0850 N88-15158
Numerical solution of turbulent flow past a backward facing step using a nonlinear K-epsilon model
[NASA-CR-178421] 07 p0854 N88-15189
Numerical methods for fluid flow problems
[DE88-000156] 07 p0854 N88-15190
Transient welding strain measurement by Moire technique: A comparison between experimental measurement and numerical analysis for strain-stress cycles during GTA spot-welding
[PB87-143871] 07 p0868 N88-15269
Bending analysis of thin plates with openings
[PB87-143400] 07 p0869 N88-15274
Recent developments in the numerical solution of differential/algebraic systems
[DE88-001885] 07 p0912 N88-15535
A numerical study of transient heat and mass transfer in crystal growth 07 p0925 N88-15619
Simple model for hot ion plasmas
[DE88-750045] 07 p0936 N88-15688
Acta Aerodynamica Sinica (selected articles)
[AD-A185723] 08 p0949 N88-15757
A multistage mesh generator for solving the average-passage equation system
[NASA-CR-179539] 08 p0951 N88-15769
Numerical solution methods for viscoelastic orthotropic materials
[NASA-CR-182381] 08 p0971 N88-15874
The single particle and collective descriptions of the anomalous Doppler resonance and the role of ion dynamics
[INPE-4390-PRE/1210] 08 p0976 N88-15904
Scanning finite element calculation method
[PB87-143442] 08 p0995 N88-16017
Mixed method of finite strip and finite element
[PB87-143467] 08 p0996 N88-16027
Integral equation method for the analysis of plates and shells
[PB87-144788] 08 p0996 N88-16030
A study of finite difference and finite element vertical discretization schemes for baroclinic prediction equations
[AD-A186617] 08 p1040 N88-16291
Research in progress at the Institute for Computer Applications in Science and Engineering
[NASA-CR-181607] 08 p1053 N88-16354
Matrix functions in the stability of higher-order numerical schemes
[INPE-4246-PRE/1119] 08 p1073 N88-16472
FOR3D: A computer model for solving the LSS (Lee-Saad-Schultz) three-dimensional, wide angle wave equation
[AD-A186649] 08 p1080 N88-16511
Comprehensive rotorcraft analysis methods
09 p1106 N88-16630
Computational analysis of propagation properties of integrated-optical waveguides using a domain integral equation
[PB87-163358] 09 p1154 N88-16917
Numerical simulation of heat transfer turbulence, volume 4
[AD-A185132] 09 p1159 N88-16947
Steady ship waves at low Froude numbers, part 2
[AD-A176805] 09 p1160 N88-16953
A guide to the transient three phase porous flow model implemented in the two-dimensional CRAY-TENSOR code: Physics, numerics, and code description
[DE88-003709] 09 p1165 N88-16983
Numerical solutions of three-dimensional Navier-Stokes equations for closed-bluff bodies
[NASA-CR-182359] 09 p1166 N88-16990
Numerical investigation of orographically enhanced instability
[AD-A186841] 09 p1189 N88-17125
Numerical simulation of axisymmetric turbulent flow in combustors and diffusors
[NASA-CR-4115] 10 p1268 N88-17582
A finite element analysis of adhesively bonded composite joints including geometric nonlinearity, nonlinear viscoelasticity moisture diffusion and delayed failure
[AD-A187455] 10 p1296 N88-17747
Flame propagation in the approximation of straight-line trajectories of burning products
[DE88-700675] 10 p1297 N88-17756
A numerical study of unsteady two-dimensional subsonic compressible base flow 10 p1327 N88-17931
The numerical and analytical study of bifurcation and multicellular flow instability due to natural convection between narrow horizontal isothermal cylindrical annuli at high Rayleigh numbers 10 p1328 N88-17937
Instability and transition in curved channel flow
10 p1328 N88-17938
Periodic natural convection in a rectangular enclosure of low aspect ratio 10 p1329 N88-17941
Recent progress in the p and h-p version on the finite element method
[AD-A187254] 10 p1400 N88-18347
Eigenvalue problems
[AD-A188069] 10 p1401 N88-18356
Coronal heating by means of helical magnetohydrodynamic turbulence
[AD-A187084] 10 p1410 N88-18413
An experimental investigation of straight and curved annular wall jets
[NASA-CR-182546] 11 p1434 N88-18557
Analysis of shear-layer probe data for holes in hypersonic configurations
[DE88-003992] 11 p1435 N88-18564
Backscattering from three dimensional conducting bodies
[AD-A187570] 11 p1470 N88-18766
Analytical and numerical analysis of finite amplitude Rayleigh-Taylor instability
[DE88-004056] 11 p1474 N88-18797
Two and three dimensional elliptic flows
11 p1485 N88-18886
A posteriori error estimates in computational fluid mechanics 11 p1486 N88-18869
Transient radiative energy transfer in incompressible laminar flows
[NASA-CR-182605] 11 p1488 N88-18883
Multisource context classification methods in remote sensing 11 p1504 N88-18985
Cumulative reports and publications through December 31, 1987
[NASA-CR-181624] 11 p1524 N88-19099
Compact high order schemes for the Euler equations
[NASA-CR-181625] 11 p1530 N88-19138
Generation of surface grids through elliptic partial differential equations for aircraft and missile configurations
[AD-A186631] 11 p1535 N88-19169
Simulation of the plasma interaction with thin dust clouds 11 p1552 N88-19291
Numerical analysis, computing and fundamental studies in fluid mechanics
[DE88-005343] 12 p1625 N88-19725
Compressible friction coefficients in a simulated heat pipe
[AD-A186818] 12 p1627 N88-19735
Reynold stress closure in jet flows using wave models
[NASA-CR-182662] 12 p1628 N88-19741
Sub-scaling of projectile/target system damaged by hypervelocity
[AD-A188683] 12 p1634 N88-19779
A numerical study of automated dynamic relaxation for nonlinear static tensioned structures
[AD-A186372] 12 p1635 N88-19790
Numerical simulation of near-surface environments and particulate clouds generated by large-area fires
[AD-A188375] 12 p1641 N88-19828
Geophysical study of the structure and processes of the continental convergence zones: Alpine-Himalayan Belt
[NASA-CR-182647] 12 p1644 N88-19842
Gradiometer mission spectral analysis and simulation studies: Past and future 12 p1645 N88-19851
A numerical analysis of the dynamics of PRIZ operation
[AD-A188853] 12 p1678 N88-20035
Object-oriented design in numerical linear algebra
[AD-A189427] 12 p1685 N88-20073
Three-dimensional scattering of impulsive acoustic waves by a semi-infinite crack in the plane interface of a half space and a layer
[PB88-146998] 12 p1687 N88-20089
Numerical simulation of subsonic and transonic propeller flow
[NASA-TM-100163] 13 p1716 N88-20262
Detection and angle estimation of coherent plane waves 13 p1759 N88-20522
Numerical methods in the resolution of control electrovalve model
[INPE-4154-RPE/540] 13 p1764 N88-20554
Control of structure in turbulent flows: Bifurcating and blooming jets
[AD-A189607] 13 p1766 N88-20562
Center for Turbulence Research 1987 activities
[NASA-CR-182693] 13 p1769 N88-20583
Numerical experiments on the stability of controlled boundary layers
[NASA-CR-181649] 13 p1771 N88-20591
Structural clearances and internal friction: Simulation by Eigen distortions
[ISSN-0208-5658] 13 p1779 N88-20640
Dynamical modeling of marine boundary layer convection 13 p1797 N88-20750
Multiple scattering of polarized light in cirrus clouds
13 p1801 N88-20768
Computer aided surface representation
[DE88-005408] 13 p1817 N88-20854
Numerical solution of ill posed problems in partial differential equations
[AD-A189383] 13 p1825 N88-20909
Elimination of quantifiers of linear variables and corresponding transfer principles
[DE88-005692] 13 p1826 N88-20912
Numerical simulations of multiphoton processes in many electron atoms
[DE88-003293] 13 p1837 N88-20990
Silicon-germanium heterostructures
13 p1844 N88-21034
Numerical analysis of three-dimensional viscous internal flows
[NASA-TM-100878] 14 p1861 N88-21116
Numerical solution of multibody systems in space applications 14 p1875 N88-21200
Practical considerations for structural control: System uncertainty, system time delay and truncation of small control forces
[PB88-163738] 14 p1933 N88-21528
Estimation of geopotential from satellite-to-satellite range rate data: Numerical results
[NASA-CR-180771] 14 p1941 N88-21583
Numerical orbit propagation methods for earth artificial satellites
[INPE-4405-RPE/556] 15 p2023 N88-22053
Nonlinear analysis and optimal design of dynamic mechanical systems for spacecraft application
[AD-A190644] 15 p2026 N88-22070
Numerical simulation of turbulent flames using vortex methods
[AD-A189813] 15 p2034 N88-22116
Mode 2 fracture mechanics 15 p2083 N88-22418
Numerical solution of nonlinear algebraic equations in stiff ODE solving
[DE88-006634] 15 p2118 N88-22622
Numerical methods for singularly perturbed differential equations with applications
[AD-A189786] 15 p2119 N88-22628
New methods for numerical solution of one class of strongly nonlinear partial differential equations with applications
[AD-A189945] 15 p2119 N88-22630
Numerical methods for linear and nonlinear optimization
[AD-A190029] 15 p2120 N88-22631
Expressing mathematical subroutines constructively
[AD-A190559] 15 p2121 N88-22644
Numerical study of unsteady viscous hypersonic blunt body flows with an impinging shock
[NASA-TM-100096] 15 p2122 N88-22650
Approximation methods for the identification and control of distributed parameter systems
[AD-A190201] 15 p2124 N88-22662
Design method for laminar flow control of two-dimensional airfoils in incompressible flow. Numerical study of LFC design concepts
[DE88-751809] 16 p2155 N88-22859
Thermoviscoelastic characterization and predictions of Kevlar/epoxy composite laminates
[NASA-CR-182878] 16 p2172 N88-22946
Theoretical and numerical solution of the forward-scattering problem in a circularly cylindrical configuration
[PB88-173489] 16 p2189 N88-23056
A computer model investigation of a half square log-periodic array
[AD-A190955] 16 p2190 N88-23062
Calculation of displacement, constraints and eigenmodes of rotating blades
[ETN-88-92296] 16 p2224 N88-23277

Numerical simulation of coastal upwelling phenomena in Cabo Frio (RJ) through a two layer finite element model
[INPE-4502-RPE/561] 16 p2237 N88-23361
Supercomputer programming environments
[AD-A190887] 16 p2251 N88-23452
Research in nonlinear partial differential equations and bifurcation theory
[AD-A190986] 16 p2260 N88-23514
Analysis for fuel implosion in ICF target and pellet gain 16 p2276 N88-23620
Numerical analysis for effects of irradiation nonuniformities on target implosion 16 p2276 N88-23621
Numerical analysis of target implosion in LIB ICF 16 p2277 N88-23628
Unsteady flow about cambered plates
[AD-A191226] 17 p2337 N88-23945
Activities of the Institute for Computer Applications in Science and Engineering (ICASE)
[NASA-CR-181666] 17 p2384 N88-24166
Scientific computing environments
[AD-A191239] 17 p2385 N88-24175
Consistent transport coefficients in astrophysics
[NASA-TM-101154] 17 p2451 N88-24560
Dynamics of a flexible orbiting platform with MRMS
[ISSN-0285-6808] 18 p2473 N88-24673
Internal fluid dynamics within a nonspinning partially liquid-filled shell due to burster rupture
[AD-A191055] 18 p2507 N88-24874
SOLA-DM: A numerical solution algorithm for transient three-dimensional flows
[DE88-007159] 18 p2514 N88-24913
NAS: The first year
[NASA-TM-101006] 18 p2560 N88-25196
Mathematical models for VLSI device simulation
[AD-A191125] 18 p2562 N88-25212
Computational sciences
[AD-A190826] 18 p2564 N88-25226
Numerical solution of a system of random Volterra integral equations. 1: Successive approximation method 18 p2564 N88-25227
Numerical solutions to stochastic difference equations 18 p2564 N88-25229
Numerical solution to a system of random Volterra integral equations 18 p2565 N88-25230
A method for the numerical solution of random Cauchy singular integral equation 18 p2565 N88-25234
Numerical solution of random Love's integral equation 18 p2565 N88-25235
High degree interpolation polynomial in Newton form
[NASA-CR-181677] 18 p2567 N88-25249
The 2-D magnetohydrostatic configurations leading to flares or quiescent filament eruptions
[NASA-TM-101147] 18 p2595 N88-25423
Improved numerical methods for turbulent viscous recirculating flows
[NASA-CR-180852] 19 p2599 N88-25445
Comparison of calculated and measured ignition times for boron agglomerates 19 p2624 N88-25563
Proceedings of the 5th NAL Symposium on Aircraft Computational Aerodynamics
[NAL-SP-8] 19 p2635 N88-25630
Numerical simulations of aerodynamic contribution of flows about a space-plane-type configuration 19 p2635 N88-25632
Numerical simulations of astrophysical jets 19 p2636 N88-25635
A numerical analysis of flow characteristics in laser propulsion system 19 p2637 N88-25645
Numerical calculation of three dimensional flow by TVD scheme 19 p2638 N88-25649
Numerical analysis of three dimensional cascade flow by solving Navier-Stokes equations 19 p2638 N88-25650
Numerical analysis of duct flow using three-dimensional parabolized Navier-Stokes equation 19 p2638 N88-25652
Picosecond response of an optically controlled millimeter wave phase shifter 19 p2660 N88-25820
Study of the structure of turbulence in accelerating transitional boundary layers
[AD-A191698] 19 p2663 N88-25837
A Navier-Stokes solver for cascade flows
[NASA-CR-181682] 19 p2666 N88-25856
Static analysis of thin plates using the finite strip-element method 19 p2679 N88-25931
Changes in seismic velocity and apparent attenuation due to isotropic and anisotropic scattering: Results from physical modeling 19 p2691 N88-25997
Scaling laws for geomagnetic tail current sheet acceleration
[AD-A193379] 19 p2691 N88-25998
Solution of Faddeev-Yakubovsky differential equations by the finite-dimensional approximation method for four spinless particles in the 1+3 scattering problem
[DE87-702983] 19 p2719 N88-26145
Analysis of gas turbine test cell number 1, Lemoore Naval Air Station, California
[AD-A192870] 20 p2762 N88-26380
Numerical analysis of reconnection of vortex rings 20 p2782 N88-26500
Numerical solution of weak forms of conservation laws on optimal unstructured triangular grids 20 p2797 N88-26597
Navier-Stokes simulation of shock-tube flows over a wedge-type step by finite volume method
[ISAS-RN-628] 20 p2797 N88-26599
A numerical simulation of two-dimensional transient shear flow
[ISAS-RN-627] 20 p2797 N88-26600
Off-boundary approach to the boundary element method
[AD-A192931] 20 p2815 N88-26701
Numerical model for the computation of radiance distributions in natural waters with wind-roughened surfaces
[PB88-192703] 20 p2826 N88-26765
Prediction of continental shelf sediment transport using a theoretical model of the wave-current boundary layer
[AD-A192272] 20 p2829 N88-26783
Superconductivity of Cr/V superlattices 20 p2874 N88-27057
A computational analysis of under-expanded jets in the hypersonic regime
[NASA-TM-101319] 21 p2893 N88-27174
Evaluation and improvement of liquid propellant rocket chugging analysis techniques. Part 1: A one-dimensional analysis of low frequency combustion instability in the fuel preburner of the space shuttle main engine
[NASA-CR-183106] 21 p2903 N88-27224
The structure and stability of nonpremixed gas jet flames 21 p2908 N88-27257
Analytical approximation of a distorted reflector surface defined by a discrete set of points
[NASA-TM-101323] 21 p2934 N88-27424
Numerical simulation of fuel droplet interactions and breakup
[AD-A192431] 21 p2941 N88-27470
Numerical experiments on turbulent mixing
[AD-A192572] 21 p2942 N88-27473
Effects of numerical dissipation on finite-volume solutions of compressible flow problems
[AD-A193173] 21 p2944 N88-27485
Numerical treatment of the pressure singularity at a re-entrant corner
[AD-A193357] 21 p2944 N88-27488
Numerical methods for incompressible viscous flows with engineering applications
[NASA-CR-183143] 21 p2948 N88-27508
Three-dimensional aspects of fatigue crack closure
[AD-A192296] 21 p2960 N88-27581
A zoomable and adaptable hidden fine-mesh approach to solving advection-dispersion equations
[DE88-006174] 21 p3004 N88-27816
Research in applied mathematics
[AD-A192385] 21 p3004 N88-27820
A numerical treatment of the fluid/elastic interface under range-dependent environments
[AD-A192476] 21 p3005 N88-27821
Numerical optimization
[AD-A193032] 21 p3005 N88-27827
On the estimation of a variance ratio
[AD-A193190] 21 p3009 N88-27854
VSAERO analysis of tip planforms for the free-tip rotor
[NASA-CR-177487] 22 p3038 N88-28036
Theoretical study and numerical simulation of flame fronts
[PB88-122932] 22 p3051 N88-28104
Time domain wave propagation in multilayered integrated circuits
[AD-A193821] 22 p3073 N88-28241
Observational/numerical study of the upper ocean response to hurricanes
[AD-A193592] 22 p3128 N88-28598
A method for determining absolute velocities from hydrographic data: The numerical code
[AD-A193997] 22 p3129 N88-28603
A fast algorithm for the numerical evaluation of conformal mappings
[AD-A193903] 22 p3138 N88-28658
Ill-posed problems and integral equations
[AD-A193709] 22 p3143 N88-28691
A numerical study of the test time in a hypersonic shock tunnel
[AD-A194057] 23 p3172 N88-28888
Random-access algorithms for environments with capture
[AD-A194303] 23 p3203 N88-29060
Stability and drag reduction in a boundary layer with microbubbles
[AD-A191975] 23 p3209 N88-29099
Steady and unsteady internal flow computations via the solution of the compressible Navier Stokes equations for low Mach numbers 23 p3209 N88-29100
Computational fluid dynamics methods for low Reynolds number precessing/spinning incompressible flows
[AD-A193891] 23 p3212 N88-29119
Thickness effects on the stability of shell like structures 23 p3224 N88-29192
Wigner distribution function: Relation to short-term spectral estimation, smoothing and performance in noise
[AD-A193865] 23 p3275 N88-29492
Numerical simulations of resistive magnetohydrodynamic instabilities in a poloidal divertor tokamak
[DE88-010768] 23 p3285 N88-29559
Numerical solutions of unsteady inviscid transonic turbine cascade flows
[AD-A196111] 24 p3316 N88-29748
Space marching Euler solvers 24 p3318 N88-29759
Simulation of Vulcain engine operation at low inlet pressure
[ETN-88-93083] 24 p3339 N88-29875
Analysis of the flow through double swirl airblast atomizers 24 p3351 N88-29949
Numerical field model simulation of full scale fire tests in a closed spherical/cylindrical vessel
[AD-A195067] 24 p3359 N88-29998
Transition at hypersonic speeds
[NASA-CR-178315] 24 p3368 N88-30058
Transition mixing study empirical model report
[NASA-CR-182139] 24 p3371 N88-30076
Numerical simulation of the function of scientific instrumentation for measuring the speed of electron devices
[AD-A194969] 24 p3376 N88-30103
A detection theory analysis of visual display performance
[AD-A196291] 24 p3409 N88-30292
Nonequilibrium flow computations. 1: An analysis of numerical formulations of conservation laws
[NASA-CR-177489] 24 p3425 N88-30384
Regularity and numerical solution of eigenvalue problems with piecewise analytic data
[AD-A194993] 24 p3425 N88-30387
Orbital evolution of distant artificial earth satellites 24 p3445 N88-30506
The atmospheres of the earth and the other planets: Origin, evolution and composition 24 p3452 N88-30544
Study of modern instrumentation and methods for astronomic positioning in the field
[AD-A196173] 24 p3452 N88-30548
Numerical evidence that the motion of Pluto is chaotic
[AD-A195920] 24 p3455 N88-30568

NUMERICAL CONTROL

Telerobotics 01 p0015 N88-10090
Microcomputer control of a hydraulically actuated piston
[AD-A184130] 03 p0368 N88-12317
Digital control of a direct current converter for a hybrid vehicle
[LAAS-87-266] 05 p0578 N88-13527
The numerical and analytic of implicit differential equations and their application to control and circuit problems
[AD-A185404] 05 p0641 N88-13922
Selected aspects of microelectronics technology and applications: Numerically controlled machine tools. Technology trends series no. 2
[PB87-132973] 06 p0696 N88-14268
Microcomputer controlled arc welding power source: Its steady state and transient performance
[PB87-143921] 07 p0863 N88-15233
Reserach on microprocessor controller for spot welding
[PB87-143913] 07 p0863 N88-15240
Intelligent controllers
[DE88-001862] 07 p0904 N88-15475
Regulation of nonlinear and generalized linear systems
[AD-A186706] 09 p1224 N88-17338
Instrumentation and quantitative methods of evaluation
[DE87-013639] 10 p1342 N88-18017
Automatic riveting machine for spherically-formed airframe structures
[ETN-88-91024] 11 p1495 N88-18924
Control test and validation for a large diameter high stability centrifuge 12 p1577 N88-19437
Intelligent control of robot manipulators in hazardous environments
[DE88-003305] 13 p1778 N88-20638

A novel method for sputter-deposition of high T(sub c) superconductor films via a computer-controlled mass analyzed ion beam
[DE88-006001] 13 p1848 N88-21064
On the use of nonstaggered pressure-velocity arrangement for the numerical solution of incompressible flows
[KU-SFB-210/T/35] 16 p2206 N88-23165
A timing evaluator for C programs generated by the model system
[AD-A191204] 17 p2385 N88-24174
A universal computer control system for motors
[NASA-CASE-NPO-17134-1-CU] 18 p2506 N88-24864
Design and testing of a luminance and chrominance stabilization system for a computer-controlled color display
[AD-A191922] 18 p2554 N88-25159
Ultrasonic and video computerized data acquisition for automated welding
[DE88-006741] 19 p2677 N88-25918
Compliant robotic structures, part 3
[AD-A192426] 21 p2955 N88-27556
IEMIS (Integrated Emergency Management Information System) floodplain mapping based on a LIDAR derived data set
[AD-A193071] 21 p2966 N88-27616

NUMERICAL DATA BASES
Stochastic estimation of conditional eddies in turbulent channel flow 16 p2194 N88-23087
Theory of numerical information environment and its applications 19 p2640 N88-25666
Effective buffering schemes for performing matrix operations for numerical databases 21 p3027 N88-27968

NUMERICAL FLOW VISUALIZATION
Efficient implementation of essentially non-oscillatory shock capturing schemes, 2
[NASA-CR-181656] 17 p2392 N88-24217

NUMERICAL INTEGRATION
NT RUNGE-KUTTA METHOD
Stochastic integration for operator valued processes on Hilbert spaces and on nuclear spaces
[ENST-87D002] 01 p0089 N88-10580
Preliminary results from real data experiments with the NRL mesoscale numerical model 02 p0211 N88-11323
Propagation of random initial conditions in time 04 p0486 N88-12903
VHF/UHF propagation by diffraction: Calculation by numerical integration 12 p1615 N88-19659
Vibration protection of inelastic structures by means of active and passive control 18 p2528 N88-25001
Analysis of gas turbine test cell number 1, Lemoore Naval Air Station, California
[AD-A192870] 20 p2762 N88-26380
Numerical integration of Navier-Stokes equations by application of multigrid concept
[ETN-88-92365] 21 p2949 N88-27513
Multiple integration with respect to Poisson and Levy processes
[AD-A192895] 21 p3009 N88-27851
Approximate and numerical methods in acousto-optics. Part 1: Normal incidence of the light
[AD-A194294] 22 p3152 N88-28755
An improvement in the numerical integration procedure used in the NASA Marshall engineering thermosphere model
[NASA-CR-179389] 24 p3392 N88-30200

NUMERICAL STABILITY
Numerical and analytical methods in nonlinear partial differential equations
[AD-A185210] 05 p0641 N88-13918
The numerical and analytical study of bifurcation and multicellular flow instability due to natural convection between narrow horizontal isothermal cylindrical annuli at high Rayleigh numbers
[AD-A186113] 07 p0849 N88-15151
Some stability results for the hopscotch difference method when applied to convection-diffusion equations
[CWI-NM-R8711] 08 p1072 N88-16465
Improving the stability of predictor-corrector methods by residue smoothing
[CWI-NM-R8707] 09 p1228 N88-17359
Stability results for theta methods applied to a class of stiff differential-algebraic equations
[CWI-NM-R8706] 09 p1228 N88-17360
Boundary layer calculation using digital computers
[REPT-MM-4] 10 p1309 N88-17821
Transport and stability properties of free shear flows 13 p1768 N88-20577
Stabilization of explicit difference schemes by smoothing techniques
[CWI-NM-R8714] 13 p1827 N88-20923
Nonlinear differential equations
[DE88-006047] 13 p1828 N88-20933
Boundary stabilization of the reaction-diffusion equation with unilateral conditions
[RR-315] 14 p1964 N88-21720
Global spatial periodic solutions to the Ginzburg-Landau equations
[DE88-006424] 15 p2119 N88-22623
Continuity of symmetric stable processes
[AD-A190324] 15 p2125 N88-22667
Stability and convergence of the Peaceman-Rachford ADI method for initial-boundary value problems
[CWI-NM-R8724] 18 p2566 N88-25243
New mixed finite element methods 18 p2567 N88-25248
QN3D: A 3-dimensional quasi-neutral hybrid particle-in-cell code with applications to the tilt mode instability in field reversed configurations 18 p2580 N88-25325
Semi-discrete approximations to nonlinear systems of conservation laws; consistency and L(infinity)-stability imply convergence
[NASA-CR-181683] 19 p2721 N88-26157
Semilinear elliptic problems on domains with corners
[REPT-87-83] 20 p2846 N88-26888
Two classes of self-similar stable processes with stationary increments
[AD-A192842] 20 p2846 N88-26894
A study on Lebesgue decomposition of measures induced by stable processes
[AD-A192893] 21 p3009 N88-27850
Method to predict external store carriage characteristics at transonic speeds
[NASA-CR-4170] 22 p3037 N88-28034
Stability and convergence in the numerical solution of stiff initial value problems
[B8681480] 23 p3272 N88-29474
On stable Markov processes
[AD-A192892] 23 p3273 N88-29482
Stability, stochastic stationarity and generalized Lyapunov equations for two-point boundary-value descriptor systems
[AD-A195645] 24 p3425 N88-30385

NUMERICAL WEATHER FORECASTING
Mesoscale Analysis and Forecasting: Incorporating Nowcasting
[ESA-SP-282] 02 p0199 N88-11239
Use of simulated satellite radiances from a mesoscale numerical model to understand kinematic and dynamic processes 02 p0202 N88-11261
An hourly analysis, updating and short-range forecasting system --- numerical weather forecasting 02 p0206 N88-11288
Statistical remote sensing algorithm development: A complementary process to mesoscale numerical models 02 p0206 N88-11292
The application of divergence equation in the analysis of heavy rainfall 02 p0207 N88-11299
Forecasting boundary layer clouds and fog: A review of operational numerical models 02 p0208 N88-11307
Operational practice of an air mass transformation model 02 p0208 N88-11308
Two-dimensional numerical modeling of the life cycle of fog 02 p0209 N88-11311
Evaluation of a mesoscale prediction system with surface weather observations and comparison with a large-scale prediction system 02 p0210 N88-11319
The Norwegian mesoscale Numerical Weather Prediction (NWP) system 02 p0210 N88-11320
Forecasting polar lows using a numerical mesoscale model 02 p0210 N88-11321
Development and testing of a vertically-nested regional prediction system --- weather forecasting 02 p0210 N88-11322
Preliminary results from real data experiments with the NRL mesoscale numerical model 02 p0211 N88-11323
Short range forecasting of sea breeze generated thunderstorms at the Kennedy Space Center: A real-time experiment using a primitive equation mesoscale numerical model 02 p0211 N88-11324
Validation of a three dimensional numerical model of the sea breeze in complex terrain 02 p0211 N88-11325
The mesoscale numerical model for heavy rainfall forecasting in Yangtze River Valley, China 02 p0211 N88-11326
The impact on short-term precipitation forecast skill of time-dependent lateral and lower boundary conditions within a meso-beta numerical cloud prediction model 02 p0211 N88-11327
Mesoscale analysis and nowcasting via a numerical model coupled with satellite sounder data 02 p0211 N88-11328
A preliminary demonstration of the use of boundary-layer models of flow in complex terrain for high resolution surface wind forecasting 02 p0212 N88-11330
Opportunities and problems in mesoscale objective analysis 02 p0212 N88-11331
An isentropic coordinate model used in a mesoscale data assimilation system 02 p0212 N88-11333
Strategies for using mesoscale data in an operational mesoscale model 02 p0212 N88-11335
Methods of incorporating satellite data into mesoscale numerical forecast models 02 p0212 N88-11336
Toward optimizing the use of data for operational mesoscale forecasting at the National Meteorological Center 02 p0213 N88-11337
Assimilation of high resolution TOVS data into a mesoscale NWP model --- numerical weather prediction (NWP) 02 p0213 N88-11338
A VAS-numerical model impact study using the Gal-Chen variational approach --- Visible Infrared Spin-Scan Radiometer Atmospheric Sounder (VAS) 02 p0213 N88-11339
Use of four-dimensional data assimilation to improve a mesoscale-model precipitation forecast: A case study 02 p0213 N88-11340
Mesoscale very short-range numerical prediction with dynamical initialization including condensation heating 02 p0213 N88-11341
Impact of a direct assimilation of satellite-inferred precipitation rates into a regional meteorological model 02 p0213 N88-11342
Initialization experiments with the NMC nested grid model --- National Meteorological Center (NMC) 02 p0213 N88-11343
The future of data in mesoscale numerical models 02 p0214 N88-11344
Simulation of mesoscale satellite sounder data from a mesoscale numerical model 02 p0214 N88-11345
The challenge of using mesoscale data in mesoscale numerical models 02 p0214 N88-11346
The challenge of using mesoscale data in mesoscale numerical models: A position paper 02 p0214 N88-11347
Comments on the challenge of using mesoscale data in mesoscale numerical models 02 p0214 N88-11348
Four-dimensional initialization of mesoscale models 02 p0214 N88-11349
Study of isolated convective clouds in the lower Alps in summer 1984, using radar and a simple Weinstein numerical model
[ESA-TT-1061] 03 p0353 N88-12224
Report of the second session of the CAS/JSC working group on numerical experimentation --- weather forecasting
[WMO/TD-168] 08 p0745 N88-14579
Prognosis using spectral embedding --- weather forecasting 08 p1016 N88-16157
On the dynamic estimation of relative weights for observation and forecast in numerical weather prediction
[NASA-CR-182531] 10 p1356 N88-18106
Quality control of upper air conventional data (TEMP and PILOT)
[INPE-4223-RPE/546] 12 p1647 N88-19862
Assimilation of meteorological observations 14 p1936 N88-21544
Nonlinear normal mode initialization of a limited area model using nonstationary Rossby modes --- numerical weather forecasting
[KNMI-WR-87-10] 14 p1947 N88-21614
Analysis of a six-component barotropic spectral model: Chaotic motion, predictability and vacillation --- atmospheric circulation
[CWI-AM-R8710] 18 p2542 N88-25090
Adaptive grid refinement for numerical weather prediction
[AD-A192172] 18 p2544 N88-25101
Bracknell Meteorological Office 18 p2545 N88-25107
Applications products of aviation forecast models 18 p2546 N88-25109
Computer and model changes at National Meteorological Center (NWC) 18 p2547 N88-25116
The Federal Aviation Administration/Massachusetts Institute of Technology (FAA/MIT) Lincoln Laboratory Doppler weather radar program 18 p2547 N88-25118
Proceedings of the Twelfth Annual Climate Diagnostics Workshop
[PB88-191747] 22 p3119 N88-28534
Extratropical response to tropical heating as a function of period of model integrations 22 p3125 N88-28577
Application of Dynamic Extended Range Forecasting (DERF) to the monthly forecast problem 22 p3125 N88-28578
Another approach for forecasting forecast skill 22 p3126 N88-28580
Experimental 30-day forecasts from several spectral general circulation models 22 p3126 N88-28582

Sampling strategies for Monte-Carlo forecasting methods 22 p3126 N88-28583
Correction of systematic errors in NMC medium range forecasts 22 p3126 N88-28584
Dependence of medium range forecast errors upon the large-scale initial state 22 p3126 N88-28585
Theoretical and practical limits of predictability of the NMC medium-range model 22 p3127 N88-28586
The predictability of low frequency patterns in the NMC MRF 22 p3127 N88-28587
The relative utility of persistence and medium-range dynamical forecasts of monthly mean 700 mb heights 22 p3127 N88-28588
Some screening experiments in objective prediction of monthly mean temperature over the United States during the winter season 22 p3127 N88-28589
On climate prediction for India 22 p3127 N88-28590
Characteristics of regression equations for specifying monthly precipitation amounts over the United States from the field of concurrent mean 700 mb heights 22 p3127 N88-28591
Operational multifield analog forecasting of US seasonal temperatures for non-winter seasons 22 p3127 N88-28592
Determination of most probable predicted 50 kPa pattern by empirical orthogonal functions 22 p3128 N88-28593

NUSSELT NUMBER
Experimental study of local natural convection heat transfer in inclined and rotating enclosures 09 p1165 N88-16986

NUTATION
Preliminary design of the ORION attitude control system [AD-A187179] 10 p1292 N88-17729
Observation model and parameter partials for the JPL VLBI parameter estimation software MASTERFIT-1987 [NASA-CR-182524] 10 p1427 N88-18523
Separation dynamics for the last stage of a launch vehicle and satellite [INPE-4281-PRE/1153] 12 p1601 N88-19582
Rotational evolution of dynamically symmetric gyrostat with internal friction 24 p3446 N88-30509

NUTATION DAMPERS
Effect of void gas lying between fluid slugs in nutation dampers 03 p0319 N88-12015
Modeling of a nutation damper for satellite stabilization through rotation [INPE-4275-PRE/1147] 12 p1601 N88-19584
Nutational stability of a satellite equipped with an active magnetic momentum wheel 20 p2784 N88-26513

NUTATIONAL OSCILLATION
U NUTATION

NUTRITION
Study of the relationship between photosynthesis, respiration, transpiration, and mineral nutrition in wheat 03 p0360 N88-12268
Controlled ecological life support systems: Development of a plant growth module 05 p0630 N88-13854
Plant Growth Module (PGM) conceptual design 05 p0631 N88-13855
Trace-element metabolism in man and animals in the presence of hypoxic states of diverse etiology 07 p0889 N88-15390
Operation Everest 2: Nutrition and body composition [AD-A186449] 08 p1049 N88-16333
Dietary factors related to physical fitness [AD-A190272] 15 p2103 N88-22527
Significance of nutrition to change in human carbohydrate and lipid metabolism under emotional stress 19 p2703 N88-26073

NUTRITIONAL REQUIREMENTS
NT CALORIC REQUIREMENTS
Design of an elemental analysis system for CELSS research 03 p0360 N88-12266
The determination of nutritional requirements for Safe Haven Food Supply System (emergency/survival foods) 06 p0792 N88-14856
Fed-batch control based upon the measurement of intracellular NADH 09 p1197 N88-17175
Nutrient requirements and other factors involved in the culture of human kidney cells on microcarrier beads 09 p1197 N88-17176
Botany Facility: Problems of water supply, plant nutrients and soil in the Botany Facility [SIRA-A/7373/WP220/RJS/003] 17 p2379 N88-24141
Supply and distribution of plant nutrients in the Botany Facility [SIRA-A/7373/WP220/RJS/004] 17 p2379 N88-24142
Nutrient requirements for high stress environments [AD-A194595] 23 p3243 N88-29301

NYLON (TRADEMARK)
Optimization of the southern electrophoretic transfer method [DE88-004527] 10 p1299 N88-17765
Temperature, moisture and strain rate effects on the compressive mechanical behavior of Nylon 6/6 [DE88-010734] 21 p2961 N88-27591

NYLON RESINS
U POLYAMIDE RESINS

NYSTAGMUS
NT VESTIBULAR NYSTAGMUS
Nystagmometric distinctions of individuals regularly exposed to vibration 07 p0891 N88-15401

O

O RING SEALS
Results of the development motor 8 test firing [GPO-78-692] 03 p0278 N88-11751
Design and test of a spacecraft instrument shock isolator 08 p0998 N88-16044

O STARS
The effects of rotation on the winds from hot stars 11 p1569 N88-19393

OBESITY
Prediction of physical fitness: Estimated percent body fat using body circumferences versus weight-height measures [AD-A190233] 15 p2103 N88-22526

OBJECT PROGRAMS
ERIC: An object-oriented simulation language [AD-A184757] 03 p0364 N88-12293
Realization of natural language style robot task instruction by using the object oriented concept 16 p2257 N88-23487
Mentat: An object-oriented macro data flow system [NASA-TM-101165] 17 p2388 N88-24199
Towards knowledge bases-semantics, rules and object-oriented programming [PB88-108154] 20 p2882 N88-27110

OBLATE SPHEROIDS
Investigation of the feasibility of an analytical method of accounting for the effects of atmospheric drag on satellite motion 07 p0923 N88-15608

OBLIQUE SHOCK WAVES
Experimental and numerical investigation of the effect of distributed suction on oblique shock wave/turbulent boundary layer interaction [NASA-TM-101334] 24 p3372 N88-30084

OBLIQUE WINGS
An integrated study of structures, aerodynamics and controls on the forward swept wing X-29A and the oblique wing research aircraft [NASA-CR-181548] 04 p0399 N88-12486
Conceptual final paper on the preliminary design of an oblique flying wing SST [NASA-CR-182879] 16 p2161 N88-22891
The computation of flow past an oblique wing using the thin-layer Navier-Stokes equations [NASA-TM-88317] 24 p3320 N88-29774

OBLIQUENESS
An investigation of oblique hypervelocity impact 07 p0927 N88-15629
An analysis of penetration and ricochet phenomena in oblique hypervelocity impact [NASA-TM-100319] 10 p1339 N88-18004

OBSCURATION
U OCCULTATION

OBSERVABILITY (SYSTEMS)
Optimal detection of sensor failures in flight control systems using deterministic observers 02 p0128 N88-10803
Closed-loop system analysis using Lyapunov stability theory 04 p0483 N88-12978
Development of a technique for estimating noise covariances using multiple observers [NASA-TM-4020] 06 p0669 N88-14098
Optimal observers for ARMA models [OUEL-1659/86] 07 p0907 N88-15495
Increasing accuracy in evaluating vector of state under conditions of incomplete observability of expanded system 24 p3446 N88-30511

OBSERVATION
NT EARTH OBSERVATIONS (FROM SPACE)
NT SATELLITE OBSERVATION
NT SKY SURVEYS (ASTRONOMY)
NT SPACE OBSERVATIONS (FROM EARTH)
NT SPOT (FRENCH SATELLITE)
NT VISUAL OBSERVATION
Method for investigating the formation of crystals in a transparent material [NASA-CASE-MFS-26008-1-CU] 06 p0788 N88-14835
On observer problems for systems governed by partial differential equations [AD-A187430] 10 p1400 N88-18351
A two-stage isolated-word recognition system using discriminant analysis [AD-A187425] 10 p1402 N88-18360
Editing master oceanographic observation data set 4 [AD-A188405] 12 p1649 N88-19876
Revised Uniform Summary of Surface Weather Observations, Loring AFB, Maine, Parts A - F [AD-A188201] 14 p1947 N88-21610
Observation of nonlinear wave decay processes in the solar wind by the AMPTE IRM plasma wave experiment [AD-A191409] 16 p2290 N88-23713

OBSERVATION AIRCRAFT
NT MIRAGE AIRCRAFT
NT OV-1 AIRCRAFT
NT RF-4 AIRCRAFT
NT U-2 AIRCRAFT

OBSERVATORIES
NT ASTRONOMICAL OBSERVATORIES
NT ASTRONOMICAL SATELLITES
NT GAMMA RAY OBSERVATORY
NT GEOPHYSICAL OBSERVATORIES
NT HEAO 2
NT HUBBLE SPACE TELESCOPE
NT INFRARED ASTRONOMY SATELLITE
NT INFRARED SPACE OBSERVATORY (ISO)
NT IUE
NT PINHOLE OCCULTER FACILITY
NT ROSAT MISSION
NT SAS
NT SOLAR OBSERVATORIES
NT SPACE INFRARED TELESCOPE FACILITY
NT X RAY ASTROPHYSICS FACILITY
Astrophysics observatory in Byurakan [AD-A185144] 05 p0660 N88-14050

OBSTACLES
U BARRIERS

OBSTRUCTING
U BLOCKING

OCCLUSION
Local versus global minima in visual pattern completion [PB87-234803] 07 p0897 N88-15439
Shape from shading, occlusion and texture [AD-A184840] 18 p2571 N88-25269

OCCULTATION
NT RADIO OCCULTATION
NT SOLAR ECLIPSES
Balloon-based infrared solar occultation measurements of stratospheric O3, H2O, HNO3 and CFC-12 [NOAA-TR-NESDIS-34] 01 p0068 N88-10438
Occultation of compact radio sources by the ion tail of Halley's Comet 01 p0118 N88-10753
Manual for obscuration code with space station applications [NASA-CR-178099] 17 p2334 N88-23931
A study relating to the fog oil replacement program [AD-A192536] 21 p2923 N88-27347

OCCUPATIONAL DISEASES
Radon Research Program, FY-1987 [DE88-002633] 09 p1188 N88-17120

OCEAN BOTTOM
Geoacoustic models of the Hudson Canyon area [AD-A183535] 01 p0073 N88-10465
A new method for determining acoustic properties of the seabed from the ambient noise field in the ocean [RAE-TR-86035] 01 p0090 N88-10590
Marine minerals: Exploring our new ocean frontier [PB87-217725] 02 p0216 N88-11364
RRS DISCOVERY cruise 160, 30 June-25 July, 1986. Geochemical sampling over the Madeira and Porcupine Abyssal Plains [PB87-222030] 04 p0471 N88-12910
USSR report: Earth sciences [JPRS-UES-87-004] 06 p0725 N88-14455
Tectonics of the Caroline Oceanic Step (southwestern Pacific Ocean) 06 p0725 N88-14462
Tectonics and magmatism of Walvis Ridge and Discovery Rise (Atlantic Ocean) 06 p0726 N88-14463
Tectonics of sedimentary cover and basement of Labrador Sea 06 p0726 N88-14468
Remote acoustic sounding of ferromanganese nodules 06 p0727 N88-14471
Modern concept concerning transport of bottom sediments in abyssal regions of world ocean 06 p0728 N88-14478
RRS DISCOVERY Cruise 161, 15 August (227)-19 September (262) 1986. Portuguese Ocean-continent boundary, plate boundaries west of Iberia and seismic structure of sediments off Madeira [PB87-222006] 06 p0747 N88-14596
Ocean floor magmatism and problems of lithosphere formation 08 p1009 N88-16121

Acoustic backscattering from bottom sediment at normal incidence in the laboratory
[AD-A186905] 09 p1242 N88-17443
A deep-water OBS (Ocean Bottom Seismometer) array with real-time telemetry
[AD-A187404] 10 p1357 N88-18112
Rapid underway sediment classification by electrical methods
[AD-A187477] 10 p1357 N88-18114
On the barotropic model of the ocean circulation
[AD-A188148] 10 p1358 N88-18118
Thematic mapper study of Alaskan ophiolites
[NASA-CR-182554] 11 p1504 N88-18984
Sea duct: A deep-sea computer-controlled recirculating flume for the study of sea floor stability
[AD-A187734] 11 p1516 N88-19056
Relationship between oceanic geological formations and tectonic structures 13 p1785 N88-20683
Experience with and ways to upgrade accuracy of hydromagnetic surveys in ocean 13 p1787 N88-20692
Research on turbulence in bottom boundary layer in ocean 13 p1788 N88-20697
Bathymetric hazard survey test
[AD-A189150] 13 p1803 N88-20775
Experimental and theoretical constraints on the origin of mid-ocean ridge geothermal fluids 13 p1804 N88-20784
A computerized investigation using the method of images to predict the sound field in a fluid wedge overlying a slow fluid half-space
[AD-A190013] 15 p2130 N88-22704
The representation of the sea-bottom in deep sea areas by the Digital Terrain Model (DTM) program TASH 16 p2226 N88-23293
To relate measurements of gravity and geoid anomalies over the oceans to near surface density distributions
[AD-A192168] 18 p2547 N88-25120
Evaluation of the biot coefficients
[AD-A191643] 18 p2570 N88-25265
Remote sensing of acoustic properties of shallow water sediments: A review
[AD-A192107] 18 p2570 N88-25267
Evaluation of the contribution of SPOT in the framework of the mineral exploration program of the Aitutaki Atoll (Cook Islands). Preliminary study of the impact of the passage of Hurricane Sally 22 p3109 N88-28483
Acoustic pressure distribution on the bottom of a wedge-shaped ocean
[AD-A193961] 23 p3278 N89-29518
The growth of continents and some consequences since 1.5 Ga 24 p3395 N88-30220
The tectonic setting of the Seychelles, Mascarene and Amirante Plateaus in the Western Equatorial Indian Ocean 24 p3396 N88-30225
The petrogenesis of oceanic kimberlites and included mantle megacrysts: The Malaitan alnoite 24 p3397 N88-30232
Continental crustal formation and recycling: Evidence from oceanic basalts 24 p3398 N88-30238
Solid earth as a recycling systems and the lateral growth of Precambrian North America 24 p3400 N88-30249
The effect of thicker oceanic crust in the Archaean on the growth of continental crust through time 24 p3401 N88-30254

OCEAN COLOR SCANNER
The distinction between different water masses using optical remote sensing applied to data from the Alboran Sea Experiment 1982
[DFVLR-FB-86-48] 03 p0345 N88-12181
Design feasibility report on investigation of magnetic bearings for the ocean colour monitor radiometer scanner
[BAE-TP-7649] 09 p1174 N88-17036

OCEAN CURRENTS
NT COASTAL CURRENTS
NT EL NINO
NT GULF STREAM
NT LOMONOSOV CURRENT
Satellite and synoptic studies of chemical fronts in the California current and coastal upwelling zone
[AD-A183909] 01 p0073 N88-10466
Vertical profiles of wind-induced current --- North Sea
[IOS-238] 02 p0193 N88-11207
Experimental study of turbulent diffusion parameters in ocean 04 p0459 N88-12840
Intensive synoptic eddies and quasigeostrophic approximation 04 p0460 N88-12844
Dynamics of isolated intrathermocline eddy 04 p0460 N88-12845
Influence of secondary eddy currents on scattering of admixture in zonal flow 04 p0460 N88-12846
Two-layer model of circulation in world ocean with detailed description of seasonal evolution of upper quasihomogeneous layer 06 p0727 N88-14470
Role of anomalous currents in formation of ocean surface temperature field 06 p0727 N88-14474
Modern concept concerning transport of bottom sediments in abyssal regions of world ocean 06 p0728 N88-14478
Forecast of current patterns for an eddy tracking experiment in the Norwegian coastal current
[PB87-224853] 06 p0747 N88-14595
Preliminary report of hydrological measurements carried out in the southern Adriatic Sea: Palma 86 campaign
[PREPRINT-555] 06 p0748 N88-14597
Statistical analyses of measured directional wave and current data
[PB87-144523] 07 p0853 N88-15185
An investigation of offshore circulation using satellite data and feature tracking techniques
[AD-A186271] 07 p0881 N88-15347
Moored current meter data from the Canary Basin near 32 deg N, 24 W (84-1986), volume 40
[PB88-108105] 07 p0882 N88-15351
On estimating the basin-scale ocean circulation from satellite altimetry. Part 1: Straightforward spherical harmonic expansion
[NASA-CR-182387] 07 p0882 N88-15352
North Pacific Ocean. Tradewind region east of Hawaii, R/V Thomas G Thompson: 25 September - 1 November 1972. STD data report
[AD-A186566] 08 p1044 N88-16311
North Pacific Ocean. Gulf of Alaska, R/V Thomas G. Thompson: 1 February - 8 March 1967. STD data report
[AD-A186569] 08 p1045 N88-16314
Sea surface current estimates off central California as derived from enhanced AVHRR (Advanced Very High Resolution Radiometer) infrared images
[AD-A186867] 09 p1194 N88-17155
Oceanographic features of the east and southeast Indian Ocean for June 1983
[AD-A186948] 09 p1195 N88-17158
North Pacific Ocean. Northeast Pacific Transition Zone, R/V Thomas G. Thompson: 1 November - 6 December 1969. STD data report
[AD-A186574] 09 p1195 N88-17161
Hydrographic and current measurements in the North-East Atlantic Ocean. Data report on F.S. Meteor cruises 69/5 and 69/6, October to November 1984
[REPT-166] 09 p1196 N88-17164
Analysis of low frequency current fluctuations in the North-East Atlantic Ocean
[REPT-170] 09 p1196 N88-17165
Numerical simulations of the California current: Filament formation as related to baroclinic instability
[AD-A187573] 10 p1358 N88-18115
Energy transfers for multilayer hydrodynamic ocean models: General formulation and specific examples
[AD-A187604] 10 p1358 N88-18116
On the barotropic model of the ocean circulation
[AD-A188148] 10 p1358 N88-18118
Sea duct: A deep-sea computer-controlled recirculating flume for the study of sea floor stability
[AD-A187734] 11 p1516 N88-19056
Mesoscale coastal ocean dynamics 11 p1517 N88-19060
Current velocity and hydrographic observations in the Straits of Florida, the Caribbean Sea and offshore of the Antillean Archipelago: Subtropical Atlantic climate studies (STACS) 1984 and 1985
[PB88-149299] 12 p1649 N88-19874
Research on the physical oceanography of the Gulf Stream
[AD-A188512] 12 p1649 N88-19877
The physical oceanography of the Alboran Sea
[AD-A189027] 12 p1650 N88-19880
Relationships between remotely-sensed surface properties and subsurface structure in the ocean
[AD-A189317] 12 p1650 N88-19881
Anisotropy of microstructural eddy motion in surface layer during calm 13 p1784 N88-20677
Mushroom-shaped currents (eddy dipoles) under rotation and stratification conditions 13 p1784 N88-20678
Determining Langmuir circulation parameters on basis of similarity theory 13 p1785 N88-20680
Space-time analysis of oceanographic fields by modified empirical orthogonal functions method 13 p1786 N88-20687
Intrathermocline lens of Mediterranean water in tropical North Atlantic 13 p1786 N88-20688
Dynamics of synoptic ocean eddies 13 p1786 N88-20689
Contribution to theory of quasigeostrophic motions of finite amplitude in viscous stratified ocean 13 p1788 N88-20695
Research on turbulence in bottom boundary layer in ocean 13 p1788 N88-20697
Study of spectra of sea waves on horizontally nonuniform current in rip zone 13 p1788 N88-20699
Model validation research: Comparison of simulated and observed climate patterns for the past 18,000 years
[DE88-004945] 13 p1800 N88-20759
Deep water mass circulation in the Alboran Basin. Measurements - January to April 1982: ALBORAN 2
[AD-A189205] 13 p1803 N88-20777
Survey of acoustic techniques for monitoring El Nino
[PB88-157615] 13 p1804 N88-20783
Dynamics of the Oceanic Surface Mixed Layer
[AD-A188348] 13 p1804 N88-20785
Equatorial turbulence: Mixed layer and thermocline 13 p1804 N88-20787
On the zonal momentum balance at the equator 13 p1805 N88-20788
The mixed layer of the western equatorial Pacific Ocean
[HIG-1861] 13 p1805 N88-20789
Observations of waves and Langmuir circulation with Doppler sonars 13 p1805 N88-20790
Some effects of heating on the wind-driven velocity in the upper ocean 13 p1805 N88-20792
Mixed-layer shear related to wind stress in the central equatorial Pacific 13 p1805 N88-20793
Mixed-layer fronts in the California current 13 p1805 N88-20794
Horizontal scales of wind forced inertial motions 13 p1806 N88-20795
Subduction 13 p1806 N88-20796
Wind forcing and observed oceanic wavenumber spectra 13 p1806 N88-20797
Hamiltonian description of the interaction of surface waves with mixed-layer currents 13 p1806 N88-20799
Large-scale ocean dynamics 14 p1938 N88-21562
Wind and buoyancy driven ocean circulation 14 p1938 N88-21564
Climatological data of the Netherlands lightvessels over the period 1949-1980 --- North Sea
[KNMI-WR-87-9] 14 p1947 N88-21613
Current velocity and hydrographic observations in the Straits of Florida, the Caribbean Sea and offshore of the Antillean Archipelago: Subtropical Atlantic Climate Studies (STACS) 1986
[PB88-160767] 14 p1951 N88-21628
Ocean general circulation models: Report on proceedings of a meeting of ocean and climate modelers
[DE88-005530] 15 p2099 N88-22504
Hydrographic data from the OPTOMA (Ocean Prediction Through Observation, Modeling and Analysis) program: OPTOMA 23, 9-19 November 1986
[AD-A189868] 15 p2099 N88-22506
The physical oceanography of the northern Baffin Bay-Nares Strait region
[AD-A190015] 15 p2100 N88-22509
Changes in the California current system observed off northern California during July-August 1986
[AD-A190027] 15 p2100 N88-22510
The effects of time-dependent winds and ocean eddies on ice motion in a marginal ice zone
[AD-A190105] 15 p2100 N88-22511
The WOCE Core Project Planning Meeting on the Gyre Dynamics Experiment --- ocean dynamics
[WCP-139] 16 p2236 N88-23358
Near surface current determined from INPE's satellite-tracked buoy, during 6-26 November, 1985 17 p2360 N88-24058
Determination of the ocean circulation by spaceborne radar altimeter 19 p2701 N88-26060
Image processing applied to quantitative numerical cartography of ocean circulation 19 p2702 N88-26065
Survey on utility technology of a tidal and ocean current energy
[DE88-770148] 20 p2819 N88-26722
The 1986-87 Pacific warm episode: Oceanic and Atmospheric features 22 p3120 N88-28535
Interannual variability in the Atlantic and Indian Oceans and its relationship to the southern oscillation 22 p3121 N88-28548
Atlantic SST variability and high latitude climate fluctuations 22 p3122 N88-28551
Low frequency variability of SST and its relationship to atmospheric forcing 22 p3122 N88-28554
Observational/numerical study of the upper ocean response to hurricanes
[AD-A193592] 22 p3128 N88-28598
Application of acoustic-Doppler current profiler and expendable bathythermograph measurements to the study of the velocity structure and transport of the Gulf Stream
[NASA-CR-183188] 22 p3129 N88-28605
An analysis of results of a high-resolution world ocean circulation model
[AD-A195760] 24 p3405 N88-30272

KOSPAS-SARSAT satellites used for ocean current study 24 p3450 N88-30534

OCEAN DATA ACQUISITIONS SYSTEMS

Complex for ocean study from space and hydroacoustic stations 04 p0458 N88-12836

A multibody dynamic analysis of the N-ROSS (Navy Remote Ocean Sensing System) satellite rotating flexible reflector using Kane's method [AD-A184452] 04 p0462 N88-12860

Status and prospects of the Joint Research Commitee (JRC) work on the application of ocean colour monitoring from space 08 p1043 N88-16299

NROSS (Navy Remote Ocean Sensing System): A force multiplier [AD-A186853] 10 p1346 N88-18045

Basic networks of TOGA: Determination of thermal profiles by XBT and of sea level by tide gage 14 p1939 N88-21568

From satellite altimetry to ocean topography, a survey of data processing techniques [ETN-88-91841] 14 p1939 N88-21575

Hydrographic data from the OPTOMA (Ocean Prediction Through Observation, Modeling and Analysis) program: OPTOMA 23, 9-19 November 1986 [AD-A189868] 15 p2099 N88-22506

Overview of space missions and techniques for ocean monitoring 19 p2700 N88-26053

Sensors in spaceborne oceanography 19 p2700 N88-26056

The French spaceborne oceanography program 19 p2701 N88-26058

SPOT: A satellite for oceanography 22 p3108 N88-28462

OCEAN DATA PLATFORMS

U OCEAN DATA ACQUISITIONS SYSTEMS

OCEAN DATA STATIONS

U OCEAN DATA ACQUISITIONS SYSTEMS

OCEAN DYNAMICS

The distinction between different water masses using optical remote sensing applied to data from the Alboran Sea Experiment 1982 [DFVLR-FB-86-48] 03 p0345 N88-12181

Dynamics of isolated intrathermocline eddy 04 p0460 N88-12845

Influence of secondary eddy currents on scattering of admixture in zonal flow 04 p0460 N88-12846

Studies of thin surface films aim at seeing deep ocean processes 04 p0460 N88-12847

Ocean colour applications in ocean dynamics and coastal processes 08 p1042 N88-16297

Interpretation of equatorial current meter data as internal waves [PB88-108113] 08 p1044 N88-16309

The physical oceanography of the Alboran Sea [AD-A189027] 12 p1650 N88-19880

Negative viscosity in global circulations 13 p1786 N88-20685

Propagation of subsurface salinity maximum in tropical Atlantic 13 p1786 N88-20686

Intrathermocline lens of Mediterranean water in tropical North Atlantic 13 p1786 N88-20688

Dynamics of synoptic ocean eddies 13 p1786 N88-20689

Structures and fluxes in a deep convecting mixed layer 13 p1804 N88-20786

Equatorial turbulence: Mixed layer and thermocline 13 p1804 N88-20787

On the zonal momentum balance at the equator 13 p1805 N88-20788

The mixed layer of the western equatorial Pacific Ocean [HIG-1861] 13 p1805 N88-20789

Some effects of heating on the wind-driven velocity in the upper ocean 13 p1805 N88-20792

Subduction 13 p1806 N88-20796

Introduction to the dynamics of the ocean and the atmosphere 14 p1935 N88-21537

Ocean eddies 14 p1938 N88-21566

Study of the dynamic topography of oceans by means of satellite altimetry 14 p1938 N88-21567

Hydrographic data from the OPTOMA (Ocean Prediction Through Observation, Modeling and Analysis) program: OPTOMA 23, 9-19 November 1986 [AD-A189868] 15 p2099 N88-22506

The physical oceanography of the northern Baffin Bay-Nares Strait region [AD-A190015] 15 p2100 N88-22509

The WOCE Core Project Planning Meeting on the Gyre Dynamics Experiment --- ocean dynamics [WCP-139] 16 p2236 N88-23358

Physical oceanography and tracer chemistry of the southern ocean [DE88-006852] 20 p2828 N88-26779

OCEAN MODELS

Ocean model processor for climate studies [PB87-224713] 03 p0353 N88-12226

Intensive synoptic eddies and quasigeostrophic approximation 04 p0460 N88-12844

Coupled acoustic and ocean thermodynamic model [AD-A184357] 04 p0472 N88-12911

Influence of gas exchange between ocean and atmosphere on formation of atmospheric pressure field 06 p0726 N88-14467

Two-layer model of circulation in world ocean with detailed description of seasonal evolution of upper quasihomogeneous layer 06 p0727 N88-14470

NASA Oceanic Processes Program [NASA-TM-4025] 10 p1357 N88-18109

Numerical simulations of the California current: Filament formation as related to baroclinic instability [AD-A187573] 10 p1358 N88-18115

Energy transfers for multilayer hydrodynamic ocean models: General formulation and specific examples [AD-A187604] 10 p1358 N88-18116

On the barotropic model of the ocean circulation [AD-A188148] 10 p1358 N88-18118

Spatial-temporal variability of North Pacific sea surface temperature anomaly patterns 11 p1516 N88-19058

Model validation research: Comparison of simulated and observed climate patterns for the past 18,000 years [DE88-004945] 13 p1800 N88-20759

Predictions and studies with a one-dimensional ice/ocean model [AD-A189158] 13 p1803 N88-20776

Wind forcing and observed oceanic wavenumber spectra 13 p1806 N88-20797

Evaluation of wave calculations using GONO in the period October 1985 - April 1986 [KNMI-TR-96] 13 p1807 N88-20804

The main ocean thermocline 14 p1938 N88-21563

Wind and buoyancy driven ocean circulation 14 p1938 N88-21564

Sea ice observations and models 14 p1939 N88-21572

An improved wind input source term for third generation ocean wave modeling [KNMI-WR-87-8] 14 p1950 N88-21624

Ocean general circulation models: Report on proceedings of a meeting of ocean and climate modelers [DE88-005530] 15 p2099 N88-22504

A study of the dynamics of the Intertropical Convergence Zone (ITCZ) in a symmetric atmosphere-ocean model [NASA-TM-86220] 19 p2693 N88-26005

Modelling and forecasting deep ocean and near surface mesoscale eddies: Hindcasting and forecasting with, and coupling a surface boundary layer model to, the Harvard quasigeostrophic model 19 p2694 N88-26013

Air-sea interaction in the vicinity of a land-sea boundary in the presence of upwelling 21 p2973 N88-27661

Research on ocean forecasting and nonlinear wave propagation and numerical hydrodynamics in the ocean [AD-A193363] 21 p2976 N88-27680

On the energy source of 1982-83 ENSO episode simulated by the NCAR community climate model 22 p3122 N88-28556

The active layer of the upper Atlantic Ocean 22 p3124 N88-28566

Observational/numerical study of the upper ocean response to hurricanes [AD-A193592] 22 p3128 N88-28598

A method for determining absolute velocities from hydrographic data: The numerical code [AD-A193997] 22 p3129 N88-28603

An analysis of results of a high-resolution world ocean circulation model [AD-A195760] 24 p3405 N88-30272

OCEAN SURFACE

Study on propagation and inverse scattering --- sea studies [ESA-CR(P)-2394] 01 p0063 N88-10405

Precise orbit computation, gravity model adjustment and altimeter data processing for the ERS-1 altimetry mission [ESA-CR(P)-2436] 02 p0130 N88-10820

High resolution determination of true surface winds at sea from wind and pressure data 02 p0210 N88-11316

Spherical harmonic expansion of the Levitus Sea surface topography [NASA-CR-181448] 02 p0216 N88-11362

GEOSAT altimeter geophysical data record user handbook [PB87-213336] 03 p0276 N88-11743

Studies of thin surface films aim at seeing deep ocean processes 04 p0460 N88-12847

Theory of heat and moisture exchange between finely disperse storm-generated spray and turbulent air flow 04 p0461 N88-12851

Radial orbit error reduction and sea surface topography determination using satellite altimetry 04 p0462 N88-12861

Sea level changes [DE87-014357] 04 p0472 N88-12913

Varifront 3 expedition data report (USNS DE STEIGUER CRUISE 1202-82). Bioluminescence, hydrographic, nutrient, and satellite data from the Gulf of California (November-December 1981) [AD-A185011] 05 p0620 N88-13805

Correlation between refraction over sea and nature of radar reflections from sea surface 06 p0728 N88-14477

Texture study of Synthetic Aperture Radar (SAR) images of ocean surfaces [AD-A186021] 07 p0841 N88-15101

Foam generation and air entrainment near a free surface [AD-A185986] 07 p0848 N88-15149

Acoustic scattering from composite wind-wave surfaces 3: Forward scatter intensities and spatial coherence at low and high frequencies and small grazing angles for Bubble-free regimes [AD-A185908] 07 p0881 N88-15345

The ocean heat budget [AD-A186130] 07 p0881 N88-15346

Interaction of a vortex pair with a free surface [AD-A186619] 08 p0988 N88-15988

Limiting accuracy of scatterometer determination of wind speed over ocean from satellite 08 p1007 N88-16107

Sea surface current estimates off central California as derived from enhanced AVHRR (Advanced Very High Resolution Radiometer) infrared images [AD-A186867] 09 p1194 N88-17155

Investigation of the quantitative determination of two dimensional sea surface wave spectra from shipborne radar measurements [GKSS-87/E/10] 09 p1195 N88-17163

Radar returns from ground clutter in vicinity of airports 10 p1274 N88-17624

Numerical simulations of the California current: Filament formation as related to baroclinic instability [AD-A187573] 10 p1358 N88-18115

Estimation of sea surface wave spectra using acoustic tomography [AD-A187837] 11 p1516 N88-19057

Observations of the upper ocean using a multi-beam Doppler sonar [AD-A188896] 12 p1649 N88-19878

Relationships between remotely-sensed surface properties and subsurface structure in the ocean [AD-A189317] 12 p1650 N88-19881

The effects of atmospheric and thermohaline variability on the validation of the GEOSAT altimeter oceanographic signal between Scotland and Iceland [AD-A189324] 12 p1650 N88-19882

Spectral reflective characteristics of sea surface 13 p1784 N88-20676

Anisotropy of microstructural eddy motion in surface layer during calm 13 p1784 N88-20677

Vertical turbulent transfer of matter in thin ocean surface layer during daytime heating 13 p1787 N88-20693

Dynamics of the Oceanic Surface Mixed Layer [AD-A188348] 13 p1804 N88-20785

Structures and fluxes in a deep convecting mixed layer 13 p1804 N88-20786

Equatorial turbulence: Mixed layer and thermocline 13 p1804 N88-20787

Observations of waves and Langmuir circulation with Doppler sonars 13 p1805 N88-20790

Unsteady shallowing mixed layer 13 p1805 N88-20791

Some effects of heating on the wind-driven velocity in the upper ocean 13 p1805 N88-20792

Mixed-layer shear related to wind stress in the central equatorial Pacific 13 p1805 N88-20793

Mixed-layer fronts in the California current 13 p1805 N88-20794

Horizontal scales of wind forced inertial motions 13 p1806 N88-20795

Energy and momentum fluxes through the sea surface 13 p1806 N88-20798

Monitoring ocean surface layer processes 13 p1806 N88-20801

Global mixed-layer natural and anthropogenic fluxes 13 p1807 N88-20803

From satellite altimetry to ocean topography, a survey of data processing techniques [ETN-88-91841] 14 p1939 N88-21575

Climatic summaries of ocean weather stations [PB88-162920] 14 p1948 N88-21617

Relationship between optical transfer function and natural light field in sea or atmosphere 15 p2054 N88-22247

Models for electromagnetic scattering from the sea at extremely low grazing angles
[AD-A190472] 15 p2057 N88-22261
NIMBUS-7 CZCS. Coastal Zone Color Scanner imagery for selected coastal regions. North America - Europe. South America - Africa - Antarctica. Level 2 photographic product
[NASA-CR-180755] 15 p2089 N88-22447
Derivation of consistent surface fixed fields for use in a global NWP model
[AD-A190131] 15 p2093 N88-22475
The effects of better environmental inputs in estimating sea clutter
[AD-A192058] 19 p2643 N88-25678
Bathymetry estimation by analyzing swell on SPOT images 19 p2701 N88-26062
Image processing applied to quantitative numerical cartography of ocean circulation
19 p2702 N88-26065
Definition of long ocean wave slope for radar applications
[AD-A193196] 21 p2933 N88-27412
Research on ocean forecasting and nonlinear wave propagation and numerical hydrodynamics in the ocean
[AD-A193363] 21 p2976 N88-27680
Non-Gaussian models for surface clutter
22 p3068 N88-28212
IR (infrared) sky radiance distributions in the marine boundary layer
[AD-A193683] 22 p3119 N88-28531
Interannual variability in the Atlantic and Indian Oceans and its relationship to the southern oscillation
22 p3121 N88-28548
ENSO, sea-surface temperatures and African rainfall
22 p3122 N88-28550
Atlantic SST variability and high latitude climate fluctuations 22 p3122 N88-28551
Sub-Saharan rainfall anomalies and global sea-surface temperature relationships for the recent fifteen year (1970-1984) period 22 p3122 N88-28552
Simulation studies of the influence of sea-surface temperature anomalies on the Sahelian circulation and rainfall 22 p3122 N88-28553
Low frequency variability of SST and its relationship to atmospheric forcing 22 p3122 N88-28554
On the energy source of 1982-83 ENSO episode simulated by the NCAR community climate model
22 p3122 N88-28556
Persistence of North Pacific Sea surface temperature and atmospheric flow patterns 22 p3123 N88-28559
The active layer of the upper Atlantic Ocean
22 p3124 N88-28566
A probabilistic model of the apparent radiance of a rough sea
[AD-A193867] 22 p3129 N88-28602
Atmospheric deposition of nitrate to the ocean surface
23 p3231 N88-29227
Measurement and interpretation of North Atlantic Ocean marine radar sea scatter
[AD-A196239] 24 p3364 N88-30036
Analysis of environmental parameters from the Panama City tower radar experiment
[AD-A194994] 24 p3404 N88-30264
Determining near-water wind speed using radar data from Cosmos-1500 artificial earth satellite
24 p3449 N88-30524

OCEAN TEMPERATURE
NT SEA SURFACE TEMPERATURE
Detection of CO2-induced climate change
[DE87-013127] 01 p0071 N88-10457
Role of anomalous currents in formation of ocean surface temperature field 06 p0727 N88-14474
Moored current meter data from the Canary Basin near 32 deg N, 24 W (84-1986), volume 40
[PB88-108105] 07 p0882 N88-15351
Editing master oceanographic observation data set 4
[AD-A188405] 12 p1649 N88-19876
Determination of mean thermohaline characteristics of the ocean 13 p1784 N88-20675
Estimates of ocean-atmosphere thermal interaction in Gulf Stream energy-active test range in winter of 1984
13 p1785 N88-20679
Propagation of subsurface salinity maximum in tropical Atlantic 13 p1786 N88-20686
Space-time analysis of oceanographic fields by modified empirical orthogonal functions method
13 p1786 N88-20687
Intrathermocline lens of Mediterranean water in tropical North Atlantic 13 p1786 N88-20688
Model of hydrodynamic adjustment of temperature, salinity and current fields 13 p1789 N88-20700
Dynamics of the Oceanic Surface Mixed Layer
[AD-A188348] 13 p1804 N88-20785
Structures and fluxes in a deep convecting mixed layer 13 p1804 N88-20786
Equatorial turbulence: Mixed layer and thermocline
13 p1804 N88-20787
The mixed layer of the western equatorial Pacific Ocean
[HIG-1861] 13 p1805 N88-20789
Mixed-layer fronts in the California current
13 p1805 N88-20794
Wind forcing and observed oceanic wavenumber spectra 13 p1806 N88-20797
Radiative processes affecting ocean mixed-layer heat content and their monitoring from satellite
13 p1806 N88-20800
Monitoring ocean surface layer processes
13 p1806 N88-20801
Sea surface temperatures of winter 1982-83 and their effect on atmospheric circulation
14 p1936 N88-21546
Climatological data of the Netherlands lightvessels over the period 1949-1980 — North Sea
[KNMI-WR-87-9] 14 p1947 N88-21613
The physical oceanography of the northern Baffin Bay-Nares Strait region
[AD-A190015] 15 p2100 N88-22509
Evaluating evaporation with satellite thermal data
[AD-A192042] 18 p2531 N88-25019
The 1986-87 Pacific warm episode: Oceanic and Atmospheric features 22 p3120 N88-28535
Interannual variability in the Atlantic and Indian Oceans and its relationship to the southern oscillation
22 p3121 N88-28548
ENSO, sea-surface temperatures and African rainfall
22 p3122 N88-28550
Atlantic SST variability and high latitude climate fluctuations 22 p3122 N88-28551
Sub-Saharan rainfall anomalies and global sea-surface temperature relationships for the recent fifteen year (1970-1984) period 22 p3122 N88-28552
Simulation studies of the influence of sea-surface temperature anomalies on the Sahelian circulation and rainfall 22 p3122 N88-28553
Low frequency variability of SST and its relationship to atmospheric forcing 22 p3122 N88-28554
On the energy source of 1982-83 ENSO episode simulated by the NCAR community climate model
22 p3122 N88-28556
Persistence of North Pacific Sea surface temperature and atmospheric flow patterns 22 p3123 N88-28559

OCEAN THERMAL ENERGY CONVERSION
Federal Ocean Energy Technology
[DE87-012279] 13 p1792 N88-20722
Ocean, Wave, and Tidal Energy Systems: Current abstracts
[DE88-008299] 19 p2687 N88-25973

OCEANOGRAPHIC PARAMETERS
NT OCEAN TEMPERATURE
NT SEA SURFACE TEMPERATURE
Regime dependent analysis experiments — sea level pressure field 02 p0209 N88-11314
The CNR/PSN Advanced Microwave Imaging Radiometer (AMIR) — satellite-borne
03 p0340 N88-12141
Eastern - western Arctic Sea ice analysis 1986
[AD-A184016] 03 p0355 N88-12235
The influence of yellow substances on remote sensing of sea water constituents from space. Volume 1: Summary
[ESA-CR(P)-2443-VOL-1] 07 p0872 N88-15292
The influence of yellow substances on remote sensing of sea water constituents from space. Volume 2: Appendices
[ESA-CR(P)-2443-VOL-2] 07 p0873 N88-15293
SEQUAL (seasonal Equatorial Atlantic) meteorological data from Moorings S2, S5 and S6 (March 1983 - March 1985)
[PB88-108048] 07 p0880 N88-15337
Annual data summary and climatological evaluation, CERC (Coastal Engineering Research Center) field research facility, 1985, volume 2, appendix C
[AD-A185894] 07 p0881 N88-15344
An investigation of offshore circulation using satellite data and feature tracking techniques
[AD-A186271] 07 p0881 N88-15347
Mariners Weather Log, Volume 31, Number 3, Summer 1987
[PB87-234894] 08 p1039 N88-16284
Annual data summary and climatological evaluation CERC (Coastal Engineering Research Center) field research facility, 1985. Volume 1. Main text and appendixes A and B
[AD-A186442] 08 p1039 N88-16289
Ocean Colour Workshop — conference
[ESA-SP-1083] 08 p1042 N88-16292
Europe's position concerning ocean colour activities
08 p1042 N88-16293
Overview of ESA's activities in ocean colour remote sensing 08 p1042 N88-16294
Update of NASA's ocean colour activities
08 p1042 N88-16295
Remote sensing of ocean colour for studies of biological productivity and biochemical cycles
08 p1042 N88-16296
Ocean colour applications in ocean dynamics and coastal processes 08 p1042 N88-16297
Technical aspects of future ocean colour remote sensing 08 p1042 N88-16298
Status and prospects of the Joint Research Commitee (JRC) work on the application of ocean colour monitoring from space 08 p1043 N88-16299
Canadian activities and goals in remote sensing of ocean colour and fluorescence from space
08 p1043 N88-16300
Federal Republic of Germany's interests, activities and goals in remote sensing of ocean colour/fluorescence from space 08 p1043 N88-16302
French activities in ocean colour observations
08 p1043 N88-16303
Developments in ocean colour research in the United Kingdom 08 p1043 N88-16306
North Pacific Ocean. Subtropical front north of Hawaii, R/V Thomas G. Thompson: 7 January - 10 February 1974. CTD data report
[AD-A186565] 08 p1044 N88-16310
North Pacific Ocean. Tradewind region east of Hawaii, R/V Thomas G Thompson: 25 September - 1 November 1972. STD data report
[AD-A186566] 08 p1044 N88-16311
North Pacific Ocean. Subarctic front central Pacific, R/V Thomas G. Thompson: 8 September - 9 October 1975. CTD data report
[AD-A186567] 08 p1044 N88-16312
North Pacific Ocean. Northwest Pacific Transition Zone, R/V Thomas G. Thompson: 19 March - 1 May 1971. STD data report
[AD-A186568] 08 p1044 N88-16313
Oceanographic features of the east and southeast Indian Ocean for June 1983
[AD-A186948] 09 p1195 N88-17158
North Pacific Ocean. Central Pacific Transition Zone, R/V Thomas G. Thompson: 25 March - 3 May 1968. STD data report
[AD-A186570] 09 p1195 N88-17160
North Pacific Ocean. Northeast Pacific Transition Zone, R/V Thomas G. Thompson: 1 November - 6 December 1969. STD data report
[AD-A186574] 09 p1195 N88-17161
NROSS (Navy Remote Ocean Sensing System): A force multiplier
[AD-A186853] 10 p1346 N88-18045
CTD observations in the coastal transition zone off northern California, 16-25 February 1987
[AD-A187283] 10 p1357 N88-18111
Editing master oceanographic observation data set 4
[AD-A188405] 12 p1649 N88-19876
The effects of atmospheric and thermohaline variability on the validation of the GEOSAT altimeter oceanographic signal between Scotland and Iceland
[AD-A189324] 12 p1650 N88-19882
Predictions and studies with a one-dimensional ice/ocean model
[AD-A189158] 13 p1803 N88-20776
Oceanographic export system development, year 1
[AD-A189134] 14 p1950 N88-21623
Hydrographic data from the OPTOMA (Ocean Prediction Through Observation, Modeling and Analysis) program: OPTOMA 23, 9-19 November 1986
[AD-A189868] 15 p2099 N88-22506
The physical oceanography of the northern Baffin Bay-Nares Strait region
[AD-A190015] 15 p2100 N88-22509
ERS-1 data products and services and their value for tropical countries 17 p2357 N88-24040
SeaSoar profiles in the Iceland-Scotland area, May 1987
[IOS-253] 18 p2548 N88-25124
Overview of space missions and techniques for ocean monitoring 19 p2700 N88-26053
MIZPAC (marginal ice zone Pacific) 84-86 CTD (Conductivity, Temperature, Depth) data report
[AD-A192478] 21 p2976 N88-27679
A method for determining absolute velocities from hydrographic data: The numerical code
[AD-A193997] 22 p3129 N88-28603
A study of the feasibility of using sea and wind information from the ERS-1 satellite. Part 1: Wind scatterometer data
[NASA-CR-182833] 24 p3386 N88-30167
A study of the feasibility of using sea and wind information from the ERS-1 satellite. Part 2: Use of scatterometer and altimeter data in wave modeling and assimilation
[ESA-CR(P)-2604-PT-2] 24 p3387 N88-30176

OCEANOGRAPHY
The effect of wind and currents on gas exchange in an estuarine system
[NASA-CR-181424] 01 p0073 N88-10468
Publications and final reports on contracts and grants, 1986 (National Environmental Satellite, Data and Information Service)
[PB87-220810] 03 p0352 N88-12218
USSR report: Earth sciences
[JPRS-UES-86-006] 04 p0458 N88-12831
Experimental study of turbulent diffusion parameters in ocean 04 p0459 N88-12840
Effects of rainfall on the seasonal thermocline
[AD-A184432] 04 p0472 N88-12912
USSR report: Earth sciences
[JPRS-UES-87-004] 06 p0725 N88-14455
Tectonics of the Caroline Oceanic Step (southwestern Pacific Ocean) 06 p0725 N88-14462
Tectonics and magmatism of Walvis Ridge and Discovery Rise (Atlantic Ocean) 06 p0726 N88-14463
Study of evolution of Gulf Stream cyclinic eddy 06 p0727 N88-14473
Wave and wind data sources, environmental conditions committee report, International Ship and Offshore Structures Congress
[PB87-234902] 06 p0746 N88-14588
Preliminary report of hydrological measurements carried out in the southern Adriatic Sea: Palma 86 campaign
[PREPRINT-555] 06 p0748 N88-14597
WOCE Core Project 2 Planning Meeting: The Southern Ocean
[WCP-138] 07 p0882 N88-15348
USSR report: Earth sciences
[JPRS-UES-87-003] 08 p1009 N88-16119
Sea surface current estimates off central California as derived from enhanced AVHRR (Advanced Very High Resolution Radiometer) infrared images
[AD-A186867] 09 p1194 N88-17155
Oceanographic features of the east and southeast Indian Ocean for June 1983
[AD-A186948] 09 p1195 N88-17158
Continental shelf processes affecting the oceanography of the South Atlantic Bight
[DE88-004102] 09 p1196 N88-17166
NASA Oceanic Processes Program
[NASA-TM-4025] 10 p1357 N88-18109
Coordination: Southeast continental shelf studies
[DE88-003680] 10 p1357 N88-18110
Mesoscale coastal ocean dynamics 11 p1517 N88-19060
Current velocity and hydrographic observations in the Straits of Florida, the Caribbean Sea and offshore of the Antillean Archipelago: Subtropical Atlantic climate studies (STACS) 1984 and 1985
[PB88-149299] 12 p1649 N88-19874
JEDA (Joint Environmental Data Analysis) Center report on tropical Pacific subsurface thermal data management, 1986
[PB88-140090] 12 p1649 N88-19875
Editing master oceanographic observation data set 4
[AD-A188405] 12 p1649 N88-19876
Research on the physical oceanography of the Gulf Stream
[AD-A188512] 12 p1649 N88-19877
The physical oceanography of the Alboran Sea
[AD-A189027] 12 p1650 N88-19880
The effects of atmospheric and thermohaline variability on the validation of the GEOSAT altimeter oceanographic signal between Scotland and Iceland
[AD-A189324] 12 p1650 N88-19882
JPRS report: Science and technology. USSR: Earth sciences
[JPRS-UES-88-001] 13 p1784 N88-20674
Studies toward observing and modelling large energetic ocean regions
[AD-A189267] 13 p1803 N88-20778
Dynamics of the Oceanic Surface Mixed Layer
[AD-A188348] 13 p1804 N88-20785
Inversion algorithms for geophysical problems
[AD-A189252] 13 p1815 N88-20845
ONR Far East Scientific Bulletin, volume 12, number 3, July-September 1987
[AD-A188554] 13 p1851 N88-21081
Introduction to the dynamics of the ocean and the atmosphere 14 p1935 N88-21537
Large-scale ocean dynamics 14 p1938 N88-21562
The main ocean thermocline 14 p1938 N88-21563
Basic networks of TOGA: Determination of thermal profiles by XBT and of sea level by tide gage 14 p1939 N88-21568
Oceanographic export system development, year 1
[AD-A189134] 14 p1950 N88-21623
Biological processes in the water column of the South Atlantic bight: Zooplankton responses
[DE88-004811] 14 p1951 N88-21630
Definition and implementation study for the Varan-S radar
[CNES-CT/DRT/TIT/RL-143-T] 15 p2058 N88-22267
Instruments for use in experimental studies of complex turbulent shear flow: Three component LDVs
[AD-A190526] 15 p2065 N88-22312
Ocean general circulation models: Report on proceedings of a meeting of ocean and climate modelers
[DE88-005530] 15 p2099 N88-22504
Hydrographic data from the OPTOMA (Ocean Prediction Through Observation, Modeling and Analysis) program: OPTOMA 23, 9-19 November 1986
[AD-A189868] 15 p2099 N88-22506
Two decades of achievement in the ocean, 1968-1988
[PB88-167077] 16 p2236 N88-23356
Investigation of the imaging of ocean surface waves using a synthetic aperture radar
[SER-A-WISS-ABHANDL-84] 16 p2236 N88-23357
The WOCE Core Project Planning Meeting on the Gyre Dynamics Experiment --- ocean dynamics
[WCP-139] 16 p2236 N88-23358
Research and Technology, 1987, Goddard Space Flight Center
[NAS 1.15:101097] 17 p2453 N88-24572
Mariners weather log, volume 32, number 1, Winter 1988
[PB88-173869] 18 p2544 N88-25097
Sensors in spaceborne oceanography 19 p2700 N88-26056
The French spaceborne oceanography program 19 p2701 N88-26058
Mariners weather log, volume 31, number 4, Fall 1987
[PB88-173851] 20 p2825 N88-26761
Physical oceanography and tracer chemistry of the southern ocean
[DE88-006852] 20 p2828 N88-26779
An analysis of horizontal temperature gradients and heat content in the mixed layer and the surface forcing during PATCHEX
[AD-A192330] 21 p2976 N88-27678
Beaufort sea mesoscale circulation study: Hydrography helicopter operations, April 1987
[PB88-203658] 21 p2976 N88-27681
ERS-1: A satellite with an oceanographic mission
[NLR-MP-86072-U] 24 p3333 N88-29838

OCEANS
NT ANTARCTIC OCEAN
NT ARCTIC OCEAN
NT ATLANTIC OCEAN
NT INDIAN OCEAN
NT PACIFIC OCEAN
The effect of ocean fluctuations on sound transmission in the ocean
[AD-A184382] 03 p0355 N88-12236
New method of estimating continentality of climate on global scale 06 p0725 N88-14460
Uses of airborne laser Chayka-1 for probing water, land surfaces 06 p0725 N88-14461
Concentration coefficients of elements in ferromanganese nodules relative to ocean sediments 06 p0726 N88-14464
Two-layer model of circulation in world ocean with detailed description of seasonal evolution of upper quasihomogeneous layer 06 p0727 N88-14470
Modern concept concerning transport of bottom sediments in abyssal regions of world ocean 06 p0728 N88-14478
Wave and wind data sources, environmental conditions committee report, International Ship and Offshore Structures Congress
[PB87-234902] 06 p0746 N88-14588
Cavitation inception scale effects. 1. Nuclei distributions in natural waters. 2. Cavitation inception in a turbulent shear flow
[AD-A186553] 08 p0988 N88-15987
Sea resonance vibrational source of seismic waves 08 p1010 N88-16126
Numerical studies of propagation of Lg waves across ocean continent boundaries using the Representation Theorem (RT) 10 p1353 N88-18085
Review of recent developments in evaporation ducting assessment 12 p1616 N88-19664
Determination of mean thermohaline characteristics of the ocean 13 p1784 N88-20675
Structures and fluxes in a deep convecting mixed layer 13 p1804 N88-20786
On the zonal momentum balance at the equator 13 p1805 N88-20788
Subduction 13 p1806 N88-20796
Wind forcing and observed oceanic wavenumber spectra 13 p1806 N88-20797
Energy and momentum fluxes through the sea surface 13 p1806 N88-20798
Global mixed-layer natural and anthropogenic fluxes 13 p1807 N88-20803
Low frequency ocean ambient noise: Measurements and theory
[AD-A191188] 16 p2237 N88-23362
Identification and acoustic characterization of seamounts
[AD-A192204] 18 p2548 N88-25123
Construction of approximations to acoustic Green's functions for nonhomogeneous oceans using transmutation
[PB88-185384] 18 p2548 N88-25126
The distribution of some chemical elements between dissolved and particulate phases in the ocean
[DE88-010181] 21 p2977 N88-27682
Simulation studies of the influence of sea-surface temperature anomalies on the Sahelian circulation and rainfall 22 p3122 N88-28553
MIZEX (marginal ice zone experiment) 1987 SAR (Synthetic Aperture Radar) data summary
[AD-A195560] 24 p3364 N88-30035
Rossby waves in mid-latitude oceans 24 p3405 N88-30273

OCTANE NUMBER
The effect of weathering on octane quality for winter-grade and summer-grade gasolines
[AD-A190640] 16 p2183 N88-23012

OCULOMETERS
A human factors evaluation of the Advanced Visual Technology System (AVTS) eye tracking oculometer 21 p2925 N88-27361

OCULOMOTOR NERVES
Research on visual information processing with special reference to oculomotor behavior in the areas of exploration, recognition and search
[AD-A186598] 08 p1051 N88-16346

ODAS
U OCEAN DATA ACQUISITIONS SYSTEMS

ODD-ODD NUCLEI
Influence of pairing correlations on the probability and dynamics of tunneling through the barrier in fission and fusion of complex nuclei
[DE88-701500] 23 p3286 N88-29570

OFF-ON CONTROL
Control design challenges of large space systems and spacecraft control laboratory experiment (SCOLE)
[NASA-CR-178392] 03 p0275 N88-11735

OFFSHORE PLATFORMS
High performance composite tubes for offshore applications
[SNIAS-872-430-116] 05 p0572 N88-13488
A system identification technique based on the random decrement signatures. Part 2: Experimental results 05 p0594 N88-13626
Experimental studies on acoustic emission monitoring of crack propagation in offshore structures: A literature survey 05 p0610 N88-13748
Hurricane Danny storm surge data, report 4
[AD-A186373] 07 p0879 N88-15334
Geological evolution and analysis of confirmed or suspected gas hydrate localities. Volume 9: Formation and stability of gas hydrates of the Middle America Trench
[DE88-001007] 10 p1347 N88-18050
Analysis of wind turbines on offshore support structures excited by random wind and random waves
[DE88-004772] 10 p1351 N88-18074
The effect of H2S concentration and pH on hydrogen permeation in AISI 410 stainless steel in 5 percent NaCl
[NPL-DMA(A)-148] 14 p1890 N88-21293
The effect of H2S concentration and pH on the cracking resistance of AISI 410 stainless steel in 5 percent brine
[NPL-DMA(A)-149] 14 p1890 N88-21294
Underwater robotics in the service of oil field exploitation: The Running and Interconnecting Tool (RIT) in the East Frigg field (North Sea) 19 p2699 N88-26049

OFT 4
U SPACE TRANSPORTATION SYSTEM 4 FLIGHT

OGEE WINGS
U VARIABLE SWEEP WINGS

OGIVES
Flow visualization on an ogive-nosed circular cylinder body at high incidence using the laser light sheet method
[ESA-TT-1066] 03 p0315 N88-11993
Calculation of symmetric and asymmetric vortex seperation on cones and tangent ogives based on discrete vortex models
[NASA-CR-4122] 08 p0950 N88-15768

OH-58 HELICOPTER
Identification and proposed control of helicopter transmission noise at the source 09 p1109 N88-16647

OHIO RIVER (US)
Ice conditions along the Ohio River as observed on LANDSAT images, 1972-1985
[AD-A191172] 18 p2531 N88-25018
OHMIC DISSIPATION
Use of polarimetry to measure the current profile in MTX
[DE87-013835] 02 p0237 N88-11495
Helicity dissipation in the plasma edge
[DE87-014762] 03 p0378 N88-12376
On the potential role of concentrated field-aligned currents in solar physics 08 p1099 N88-16614
Transport simulations of ohmic ignition experiment: IGNITEX
[DE88-006055] 15 p2138 N88-22757
Dissipative relativistic radiation hydrodynamics
[DE88-702092] 19 p2665 N88-25846
OHMS LAW
Aging behavior of Au-based ohmic contacts to GaAs
[NASA-CR-182146] 19 p2662 N88-25831
OIL ADDITIVES
The performance of perfluoropolyalkylether oils under boundary lubrication conditions
[AD-A191057] 17 p2323 N88-23869
OIL EXPLORATION
Research needs for hydrocarbon fuels
[DE87-014555] 06 p0687 N88-14209
Three-dimensional transient electromagnetic modeling for exploration geophysics 10 p1346 N88-18047
Utilizing SPOT data for seismic shot-line mapping and environmental monitoring in oil and gas exploration 22 p3098 N88-28401
First results of international investigations of the applications of SPOT-1 data to geologic problems, mineral and energy exploration 22 p3101 N88-28419
Results of the Geosat program to evaluate SPOT data for petroleum and mineral exploration 22 p3102 N88-28422
Evaluation of SPOT imagery contribution to petroleum exploration: The Suez Rift (Egypt) 22 p3102 N88-28425
Structural analysis of the Jura mountains-Rhine Graben intersection (Switzerland) for petroleum exploration using SPOT stereoscopic data 22 p3103 N88-28431
Methodology for the use of SPOT imagery in petroleum exploration. Example of the Bas-Languedoc area (France) 22 p3104 N88-28432
OIL FIELDS
Underwater robotics in the service of oil field exploitation: The Running and Interconnecting Tool (RIT) in the East Frigg field (North Sea) 19 p2699 N88-26049
OIL POLLUTION
Application of SPOT imagery for oil spill contingency planning 22 p3108 N88-28460
OILS
NT CRUDE OIL
NT LUBRICATING OILS
NT MINERAL OILS
Low extractable wipers for cleaning space flight hardware 02 p0137 N88-10863
Boundary lubrication. Experiments with boundary lubrication and plain bearings at +60...-50 deg C temperatures
[DE87-752869] 02 p0180 N88-11124
Analysis of wear metals in engine oils using the atomic absorption spectrophotometric method
[NAL-TM-MT-8704] 05 p0564 N88-13435
A comparison of measurements from the A/E35U-3 and PWMA (Portable Wear Metal Analyzer) spectrometers
[AD-A186655] 09 p1177 N88-17047
Characterization of the arc/spark excitation sources used in the spectrometric oil analysis program
[AD-A187131] 10 p1297 N88-17758
Oil flow patterns on a series of capsule-type re-entry vehicles at hypersonic speeds
[DE88-751805] 16 p2155 N88-22858
Boundary layer flow visualization for flight testing 17 p2297 N88-23742
Low pressure entrained flow pyrolysis of biomass to produce liquid fuels 18 p2535 N88-25043
Research on hydrotreating catalysts to hydrodeoxygenate biocrude oils 18 p2536 N88-25046
Measurement of the radiative properties of gas and oil flames
[NASA-TT-20299] 19 p2612 N88-25502
Study of experimental technique of oil flow with emphasis on quantitative determination of the flow position parameters on the surface
[NASA-TT-20341] 23 p3215 N88-29135
OLEFINS
U ALKENES
OLIVINE
Carbon analysis in natural olivine crystals of deep origin
[NASA-TT-20311] 19 p2734 N88-26239
OMEGA NAVIGATION SYSTEM
Assessment of the differential technique for land navigation within 1000 km of Omega Australia
[AD-A191036] 16 p2160 N88-22885
Western Pacific Omega validation: Project description
[AD-A191753] 18 p2462 N88-24617
Automatic omega station and LOP (Line Of Position) selection
[AD-A193302] 21 p2894 N88-27179
Indian Ocean validation
[AD-A194458] 23 p3175 N88-28902
OMNIDIRECTIONAL ANTENNAS
NT MONOPOLE ANTENNAS
The AMSC mobile satellite system 19 p2643 N88-25681
Omni-directional L-band antenna for mobile communications 19 p2648 N88-25717
ON-LINE SYSTEMS
The VAXONLINE software system at Fermilab
[DE87-013565] 02 p0220 N88-11387
Towards automated consulting: Design feedback from the performance of online documentation
[DE87-012243] 04 p0501 N88-13082
Online monitoring of laserpulses using the GPIB-interface of a Tektronix 2430 Digital Storage Oscilloscope
[DE88-002836] 07 p0856 N88-15201
DoD Gateway Information System (DGIS): Common command language mapping
[AD-A185951] 07 p0942 N88-15726
MICRO system for control, acquisition and processing of experimental data
[DE88-700724] 10 p1386 N88-18278
Modules of nanosecond logic electronics system with computer control
[DE88-700190] 11 p1479 N88-18828
Neurocognitive predictions of performance
[AD-A188323] 12 p1669 N88-19998
Improved flight test productivity using advanced on line data systems 12 p1703 N88-20193
Parallel image compression
[NASA-CR-180758] 13 p1814 N88-20837
Online aiding for human-computer interfaces
[AD-A189239] 13 p1815 N88-20842
MIG-1 on-line measuring holographic microscope
[DE88-701103] 15 p2066 N88-22332
Argus reference manual
[AD-A190382] 15 p2111 N88-22578
IPC for modular software requires a third party connect
[AD-A189199] 16 p2246 N88-23414
On-line measurement of heat of combustion
[NASA-CR-183076] 19 p2738 N88-26255
WORDNET: An electronic lexical reference system based on theories of lexical memory
[AD-A193086] 21 p3027 N88-27970
Geometric modeling for computer aided design
[NASA-CR-183161] 24 p3413 N88-30320
ONBOARD COMPUTERS
U AIRBORNE/SPACEBORNE COMPUTERS
ONBOARD DATA PROCESSING
Design, manufacture and testing of an elegant breadboard model communications processor
[D/2244] 01 p0034 N88-10217
Study, design and evaluation of data reduction by encoding or information extraction. Part 2: Operational considerations --- multispectral satellite imagery
[NLR-TR-85094-L-PT-2] 01 p0079 N88-10502
Digital bus unit engineering model: Design, manufacture and test
[MRM/TREP/1003/SAAB] 01 p0083 N88-10537
Study and design of a communication processor unit
[RIDU/TREP/1002/SAAB] 01 p0083 N88-10538
Calibration of attitude control sensors 02 p0159 N88-10995
Prototype Rendezvous Onboard Software (PROBS)
[MATRA-EPT-DT-PRB-2A-00068] 02 p0222 N88-11396
Study of fault tolerant techniques for satellite data handling
[FTT/REP/0001/SAAB] 05 p0632 N88-13860
Data processing of the JPA instrument. Part 1: Data management
[IFSI-86-15-PT-1] 06 p0757 N88-14645
Expert system study for spacecraft management
[TL-2699-ISS-1] 07 p0824 N88-15004
Packet telecommand. System performance assessment study --- onboard data handling
[PTC/TNOT/0015/SAAB] 07 p0843 N88-15113
Study of communication options in a distributed data handling system and survey of advanced man machine communications schemes. Work package 1: Interprocess communication
[ESA-CR(P)-2447] 07 p0843 N88-15114
ESA Bulletin No. 10
[ETN-87-90514] 09 p1123 N88-16728
Introducing new technology into onboard handling systems 09 p1124 N88-16733
An expert system to support the verification/validation of flight-critical software
[MBB-UT-102/87] 10 p1314 N88-17852
The RVD mission: The on-board data processing requirements 12 p1586 N88-19495
Prototype on-board software for rendezvous and docking 12 p1586 N88-19496
On-board processing for mobile satellite communications
[ESA-CR(P)-2519] 14 p1905 N88-21382
Development of a flexible and economic helicopter engine monitoring system
[PB88-165147] 16 p2160 N88-22887
On-board data processing of navigation data at high latitudes in Antarctica 22 p3036 N88-28027
Study of standard generic approach for spacecraft (S/C) autonomy and automation (phase 3). Book A: Autonomy concept description
[ESA-CR(P)-2555-VOL-1] 23 p3185 N88-28955
Study of standard generic approach for spacecraft (S/C) autonomy and automation (phase 3). Book B: Autonomy concept application example
[ESA-CR(P)-2555-VOL-2] 23 p3185 N88-28956
Study of standard generic approach for spacecraft (S/C) autonomy and automation (phase 3). Book C: Autonomy concept summary
[ESA-CR(P)-2555-VOL-3] 23 p3185 N88-28957
Investigation of the use of High Order Languages (HOLs) for on-board software
[CRI/FR/HOL-C/1/87] 23 p3251 N88-29349
An expert systems application to space base data processing 23 p3256 N88-29384
Compression and decompression of imaging sensor signals (CADISS): A multiprocessor system for image compression/decompression on board scientific satellites
[NLR-TR-87076-L] 24 p3414 N88-30323
ONBOARD EQUIPMENT
NT AIRBORNE EQUIPMENT
NT AIRBORNE LASERS
NT AIRBORNE/SPACEBORNE COMPUTERS
NT AIRCRAFT EQUIPMENT
NT SPACECRAFT ELECTRONIC EQUIPMENT
NT SPACECRAFT EQUIPMENT
An assessment of clinical chemical sensing technology for potential use in space station health maintenance facility
[NASA-CR-172013] 04 p0475 N88-12926
A project of an intelligent system to help on-line trouble shooting --- aircraft maintenance
[SNIAS-872-111-106] 05 p0529 N88-13216
Definition and implementation study for the Varan-S radar
[CNES-CT/DRT/TIT/RL-143-T] 15 p2058 N88-22267
Systems for the 21st century 17 p2302 N88-23769
On-orbit technology experiment facility definition
[NASA-TM-100614] 17 p2311 N88-23824
Digital maps for an electronic traffic guide 18 p2534 N88-25033
Generic supervisor: A knowledge-based tool for control of space station on-board systems 23 p3257 N88-29389
A space station onboard scheduling assistant 23 p3259 N88-29402
Flight test equipment for the on-board measurement of wind turbulence 24 p3311 N88-29719
ONE DIMENSIONAL FLOW
Relaxation method for the compressible Navier-Stokes equations using upwind schemes 05 p0539 N88-13283
TOPP: A post-processor for TOPAZ, the one dimensional pipe flow analysis code
[DE88-003711] 09 p1164 N88-16981
One dimensional calculation model for laser produced plasmas expanding in vacuum
[ISL-R-128/86] 14 p1984 N88-21836
ONE-PHASE FLOW
U SINGLE-PHASE FLOW
ONISOTROPY
U ANISOTROPY
ONSAGER RELATIONSHIP
Application of Onsager's reciprocity relations to interface motion
[DE88-003286] 10 p1397 N88-18327
ONTOGENESIS
U ONTOGENY
ONTOGENY
Some remarks on gravitational biology 07 p0884 N88-15366
Biological patterns of growth in postnatal ontogenesis of lower primates 19 p2705 N88-26087

OPACITY
Evidence for an additional source of opacity during the impulsive phase of stellar flares
04 p0510 N88-13133
Computer program in BASIC language for computation of spectrochemical analytical data
[DE88-701229] 15 p2032 N88-22106
Survey of material for an infrared-opaque coating
[NASA-TM-88204] 22 p3153 N88-28757
OPEN CHANNEL FLOW
Open channel flow near the resonance speed
18 p2514 N88-24918
Recent insights into instability and transition to turbulence in open-flow systems
[NASA-CR-181693] 24 p3372 N88-30079
OPENINGS
NT APERTURES
NT PORTS (OPENINGS)
NT SLITS
NT SYNTHETIC APERTURES
Superconducting switch program
[AD-A185682] 07 p0848 N88-15144
Theoretical and observational problems with Holes in the far UV dayglow
[AD-A188190] 10 p1355 N88-18100
Strength and failure analysis of composite laminate containing a circular hole with reinforcement
[AD-A189629] 14 p1884 N88-21260
OPERATING COSTS
Requirements and cost considerations for a Combined Space Nuclear Reactor Test Facility
[DE88-006763] 15 p2132 N88-22719
Costs and benefits of AC propulsion
[PB88-173380] 16 p2287 N88-23691
A contribution to the quantitative analysis of the influence of design parameters on the optimal design of passenger aircraft
[ETN-88-92979] 23 p3176 N88-28912
OPERATING SYSTEMS (COMPUTERS)
UNIX benchmark system
[AD-A184492] 03 p0367 N88-12308
Connecting RPC (Remote Procedure Call)-based distributed systems using wide-area networks
[PB87-234423] 05 p0658 N88-14041
MINIX: A UNIX clone with source code
[PB88-100862] 06 p0760 N88-14664
Clouds: A support architecture for fault tolerant, distributed systems 10 p1375 N88-18206
The mapping of parallel algorithms to reconfigurable parallel architectures 10 p1376 N88-18209
Performance and evaluation at the Center for Supercomputing Research and Development
[DE88-003563] 10 p1417 N88-18456
Space station operating system study
[NASA-CR-179308] 11 p1446 N88-18619
Applicability of Ada (trademark) tasking for avionics executives
[AD-A188827] 12 p1578 N88-19445
A production-quality UNIX Very High Speed Integrated Circuit (VHSIC) Hardware Description Language (VHDL) subset analyzer
[AD-A188832] 12 p1623 N88-19710
Experience with Berkeley UNIX interprocess communications
[AD-A188353] 12 p1680 N88-20041
MultiRPC: A parallel remote procedure call mechanism
[AD-A188613] 12 p1680 N88-20045
An interface between object-oriented systems
[AD-A189245] 13 p1815 N88-20844
An amoeba replicated service organisation --- Amoeba operating system
[CWI-CS-R8723] 13 p1822 N88-20892
Distributed operating systems: An overview
[INF-87-29] 14 p1960 N88-21688
Sigma system: Overview, prospects
15 p2052 N88-22230
Introduction to the VMS (DEC) operating system
[ENST-87D006] 16 p2245 N88-23409
Concurrency efficiency user's manual
[AD-A190884] 16 p2251 N88-23450
Design, implementation and evaluation of an operating system for a network of transputers
[AD-A186593] 18 p2559 N88-25193
The MELCOM PSI 2 AI workstation
21 p2930 N88-27395
Process migration in UNIX environments
[NASA-CR-182951] 23 p3245 N88-29311
A rule-based systems approach to spacecraft communications configuration optimization
24 p3417 N88-30341
OPERATING TEMPERATURE
Evaluating and testing thermographic phosphors for turbine-engine temperature measurements
[DE87-011772] 02 p0174 N88-11090
Blade excitation criteria developed for aero derived engines in Arctic Alaska
[PNR90368] 02 p0182 N88-11131
The effect of operating temperature on open, multimegawatt space power systems
17 p2414 N88-24352
The effect of operating temperature and turbine blade cooling on Brayton cycle space power systems
17 p2435 N88-24489
OPERATIONS RESEARCH
Workshop on AI (Artificial Intelligence) and Simulation (2nd) held in Seattle, Washington on 14 July 1987
[AD-A183736] 01 p0084 N88-10542
Extraction and evaluation of Boolean relations for the solution of linear programs in 0-1 variables, volume 1
[ENST-86E023-VOL-1] 02 p0227 N88-11430
Extraction and evaluation of Boolean relations for the solution of linear programs in 0-1 variables, volume 2
[ENST-86E023-VOL-2] 02 p0227 N88-11431
Potential applications of expert systems and operations research to space station logistics functions
[NASA-CR-180473] 03 p0372 N88-12342
Inventory behavior at remote sites
06 p0796 N88-14873
Estimating system reliability: Monte Carlo methods, sensitivity and errors in input parameters
[AD-A186182] 07 p0865 N88-15248
A multicut algorithm for two-stage stochastic linear programs
[AD-A186148] 07 p0903 N88-15466
Explicit construction and analysis of some efficient empirical production functions in data envelopment analysis
[AD-A185907] 07 p0908 N88-15502
GAVID and ACQUIR, two Operations-Research (OR) models for visual detection
[FEL-1985-72] 09 p1200 N88-17194
Artificial Intelligence (AI), Operations Research (OR), and Decision Support Systems (DSS): A conceptual framework 09 p1209 N88-17245
Range and mission scheduling automation using combined AI and operations research techniques
09 p1209 N88-17249
Operations research in management?
[MBB-Z-138/87] 10 p1311 N88-17835
Perspectives on parallel computing
[CWI-OS-R8709] 13 p1822 N88-20889
SEARCH: An interactive computer program for optimizing two-variable, unconstrained experiments or simulation
[AD-A190593] 15 p2112 N88-22583
Optical symbolic processor for expert system execution
[AD-A192005] 18 p2575 N88-25296
Realistic planning scenarios
[AD-A191640] 19 p2740 N88-26267
A fast parametric maximum flow algorithm, revision
[AD-A194026] 23 p3250 N88-29345
Faster scaling algorithms for network problems
[AD-A194032] 23 p3251 N88-29348
Finding minimum-cost circulations by canceling negative cycles
[AD-A194027] 23 p3271 N88-29468
Finding minimum-cost circulations by successive approximation
[AD-A194028] 23 p3272 N88-29469
Improved time bounds for the maximum flow problem
[AD-A194034] 23 p3272 N88-29471
OPERATOR PERFORMANCE
Report of safety survey: Human integration of approach charts
[DOT/FAA/PM-87/15] 01 p0076 N88-10488
Gender and cognitive style differences at the human-computer interface
[NPL-DITC-90/87] 01 p0077 N88-10493
Input devices for tasks using interactive video
[NPL-DITC-87/87] 01 p0080 N88-10510
Assessment of fatigue in aviation crews
[AD-A184129] 03 p0356 N88-12245
Proceedings of the DOD Workload Assessment Workshop on Workload Assessment Techniques and Tools held in Dayton, Ohio on 27-28 September 1986
[AD-A185650] 08 p1052 N88-16352
Crew procedures for microwave landing system operations
[NASA-CR-178359] 09 p1116 N88-16688
A human performance modelling approach to intelligent decision support systems 09 p1208 N88-17242
Investigation of effects of short-term exposure to high concentrations of carbon monoxide on operator's psychophysiological functions 10 p1361 N88-18133
Risk of hypertension and functional cerebral laterality in oil expedition works in far north
12 p1665 N88-19980
OMV man/system simulation integration: A preliminary analysis and recommendation
[NASA-CR-182602] 12 p1671 N88-20005
Human problem solving in dynamic environments. Understanding and supporting operators in large-scale, complex systems
[AD-A189539] 13 p1812 N88-20826
Mental-State Estimation, 1987
[NASA-CP-2504] 16 p2239 N88-23370
An overview of current approaches and future challenges in physiological monitoring
16 p2239 N88-23371
Toward a mathematical formalism of performance, task difficulty, and activation 16 p2239 N88-23372
Challenges of physiological monitoring in a Navy operational setting 16 p2239 N88-23374
Predicting operator workload during system design
16 p2239 N88-23375
POPEYE: A production rule-based model of multitask supervisory control (POPCORN)
16 p2240 N88-23384
A correlational approach to predicting operator status
16 p2242 N88-23393
Development of a C3 generic workstation: System overview 16 p2242 N88-23396
C3 generic workstation: Performance metrics and applications 16 p2242 N88-23397
The biomorphic model of the human operator controlling a single or a double integrator
[LR-505] 16 p2243 N88-23402
The representational code of the internal model of dynamic systems: An individual differences and dual task approach
[AD-A190876] 16 p2244 N88-23403
Spatial cognition 17 p2380 N88-24152
Teleoperator human factors study
[NASA-CR-178930] 17 p2382 N88-24162
An advanced prototyping tool for human factors design
[AD-A187290] 18 p2552 N88-25149
Method for observing changes in functional state of human operator 20 p2830 N88-26789
Neurophysiological patterns of operational fatigue: Preliminary results 21 p2981 N88-27703
Display system image quality
23 p3242 N88-29298
OPERATORS (MATHEMATICS)
NT LINEAR OPERATORS
Semidiscrete Galerkin method for semilinear evolution equations with a differential operator of third order
[BONNER-MATHE-SCHR-181]
01 p0087 N88-10570
Processing of fractal functions by linear and nonlinear operators
[RAE-TR-85079] 01 p0088 N88-10571
Spectral and structural properties of nonnegative reducible operators in Banach relations
[ETN-87-90402] 01 p0089 N88-10581
Finite-dimensional matrix representation of the differential operator, determinental form and zeros of special functions
[DE87-703091] 02 p0225 N88-11421
On operator splitting for unsteady boundary value problems
[AD-A184281] 04 p0484 N88-12981
Eigenvalue projection theory for linear operator equations of electromagnetics
[AD-A185434] 05 p0575 N88-13504
On a boundary data operator and generalized exterior Robin problems for the Helmholtz equation
[AD-A185124] 05 p0640 N88-13915
Introduction to string field theory
[DE87-014583] 05 p0657 N88-14032
Pseudodifferential operators on the circle and finite differences
[PB87-222352] 06 p0763 N88-14681
Recursion operator and bihamiltonian structure for integrable multi-dimensional lattices
[PREPRINT-552] 06 p0764 N88-14688
Nonisospectral deformations and Darboux transformations for the 3rd order spectral problem
[PREPRINT-558] 06 p0764 N88-14690
Embedding topological median algebras in products of dendrons
[PB88-100888] 06 p0767 N88-14713
Operator foundation of functional integral in non-Abelian gauge theory
[DE88-700508] 07 p0941 N88-15719
A learning apprentice for software parts composition
08 p1065 N88-16436
Developments related to scattering eigen elements in Schroedinger operators for particles with spin
[ETN-88-91077] 09 p1229 N88-17361
Application of state-multipole Heisenberg equations to Raman excitation dynamics
[DE88-003828] 10 p1335 N88-17977

Schwarz splitting and template operators
[AD-A187956] 10 p1404 N88-18370
Canonical coordinates for partial differential equations
[NASA-CR-182486] 11 p1535 N88-19170
Irreducible tensor operators and multiple-quantum NMR 11 p1542 N88-19217
On the norm equivalence of singularly perturbed elliptic difference operators
[DE88-006353] 13 p1826 N88-20913
Choice of implicit and explicit operators for the upwind differencing method
[NASA-TM-100857] 14 p1964 N88-21718
Peetre's Theorem and generalized functions
[MEMO-661] 14 p1967 N88-21742
The two-dimensional Toda-lattice and its recursion operators
[PREPRINT-571] 14 p1968 N88-21746
Algebraic structure of linear and nonlinear models of open quantum systems
[PREPRINT-573] 14 p1968 N88-21747
Mixing coefficients of the lattice weak Hamiltonian with dimension five operators
[PREPRINT-576] 14 p1968 N88-21749
Recursion operator and Backlund Transformation for the Ruijsenaars-Toda lattice
[PREPRINT-577] 14 p1968 N88-21750
Coding capacity of generalized additive channels
[AD-A190315] 15 p2127 N88-22685
Systolic algorithm for matrix-vector multiplication
[PB86-165394] 16 p2256 N88-23484
On the efficient implementation of the fast multipole algorithm
[AD-A191167] 17 p2385 N88-24173
Canonical construction of differential operators intertwining representations of real semisimple Lie groups
[DE88-701852] 20 p2845 N88-26882
Theory of pseudo-differential operators over C*-algebras
[DE88-701860] 20 p2845 N88-26883

OPERATORS (PERSONNEL)
NT AIRCRAFT PILOTS
NT PILOTS (PERSONNEL)
Measurement of suspension and ride characteristics of the M1 main battle tank 05 p0596 N88-13637
Using multiple dialog modes in a user-system interface to accomodate different levels of user experience: An experimental study
[AD-A186115] 07 p0899 N88-15444
Interfacing the expert: Characteristics and requirements for the user interface in expert systems 08 p1063 N88-16419
Space languages 08 p1063 N88-16420
Human problem solving in dynamic environments. Understanding and supporting operators in large-scale, complex systems
[AD-A189539] 13 p1812 N88-20826
Extension of computer based algorithms by operator analysts
[NASA-CR-182796] 15 p2111 N88-22575

OPHTHALMOLOGY
Does the knife open perspectives for the myopic pilot?
[ETN-87-90166] 09 p1199 N88-17187
Microesotropia patients performa well as military jet pilots 21 p2925 N88-27363

OPTICAL ABSORPTION
U ELECTROMAGNETIC ABSORPTION
U LIGHT TRANSMISSION

OPTICAL ACTIVITY
Image processing for optical engineering applications
[PB87-210035] 03 p0376 N88-12364

OPTICAL AMPLIFIERS
U LIGHT AMPLIFIERS

OPTICAL BISTABILITY
Ultrafast intrinsic bistable devices
[PB87-109310] 05 p0649 N88-13978
Dependence of formation of radiative color centers in optical glass fibers on technological factors 14 p1896 N88-21321
Theory of interactions of intense light with nonlinear, inhomogeneous and periodic structures and its applications to optical bistability, optic gyroscopes, nonlinear spectroscopy, radiation protection, X-ray emission and related fields
[AD-A190040] 15 p2133 N88-22725
Cooperative effects and intrinsic optical bistability in collections of atoms
[AD-A193993] 23 p3280 N88-29530

OPTICAL COMMUNICATION
Coherent infrared detection, volume B --- CO2 laser intersatellite data link
[ESA-CR(P)-2392-VOL-1] 01 p0034 N88-10218
Coherent infrared detection, volume D --- CO2 laser intersatellite data link
[ESA-CR(P)-2392-VOL-2] 01 p0034 N88-10219
The design and testing of an analog optical communication link capable of the simultaneous transmission of four frequency division multiplexed audio signals
[AD-A184695] 03 p0307 N88-11936
Frequency doubling conversion efficiencies for deep space optical communications 04 p0434 N88-12691
The atmosphere of Mars and optical communications 04 p0434 N88-12692
A near-earth optical communications terminal with a corevolving planetary sun shield 04 p0434 N88-12693
Electro-optical studies of semiconductor compounds for electroluminescent and laser devices
[PH-155] 07 p0937 N88-15693
Optical communication with semiconductor laser diodes
[NASA-CR-182464] 09 p1154 N88-16918
Signal processing studies program optical signal amplification, volume 1
[AD-A188055] 10 p1321 N88-17897
Design and implementation of a fiber optic RS232 link
[AD-A187319] 10 p1409 N88-18409
Microwave semiconductor research-materials, devices and circuits
[AD-A187121] 10 p1415 N88-18444
A laser communication experiment utilizing the ACT satellite and an airborne laser transceiver
[NASA-TM-100792] 11 p1492 N88-18910
Computation of LMS (Least-Mean-Square) and matched digital filters for optical clutter suppression
[AD-A188885] 12 p1687 N88-20093
Effect of atmospheric turbulence on the bit error probability of a space to ground near infrared laser communications link using binary pulse position modulation and an avalanche photodiode detector
[NASA-TM-100699] 14 p1873 N88-21189
Continued design of a Pointing, Acquisition, and Tracking (PAT) subsystem for InterSatellite Laser links (ISL2)
[TELDIX-15-093-178] 14 p1905 N88-21384
Characteristics of disiributed feedback lasers discussed 16 p2185 N88-23028
Design and evaluation of single-lobed far-field pattern laser arrays: AlGaAs/GaAs and InGaAsP/InP systems --- optical communication
[LAAS-88-023] 16 p2214 N88-23211
Engineering planetary lasers for interstellar communication
[NASA-CR-180780] 17 p2311 N88-23825
Interaction of solitons in single model optical fibres 17 p2439 N88-24511
Assessment of optical communications systems for Data Relay Satellite. Volume 1: Executive summary
[ESA-CR(P)-2488-VOL-1] 18 p2502 N88-24841
Assessment of optical communications systems for the Data Relay Satellite
[ESA-CR(P)-2488-VOL-2] 18 p2502 N88-24842
Activities report of the Division of Optical Technology
[FOA-C-30477-3] 18 p2576 N88-25299
New semiconductor laser structure for an optical communication system
[ETN-88-92353] 20 p2807 N88-26654
Use of fiber optic equipment for security
[DE88-007898] 20 p2853 N88-26943
Strawman Optical Reception Development Antenna (SORDA) 22 p3065 N88-28187
Effect of detector dead time on the performance of optical direct-detection communication links 22 p3065 N88-28190
Multichannel data transmission through a fiber optic cable
[AD-A193842] 22 p3070 N88-28221
Optical multiple access intersatellite links
[BAE-TP-8502] 24 p3361 N88-30013

OPTICAL COMPUTERS
Optical symbolic processor for expert system execution
[AD-A187494] 10 p1385 N88-18268
Integrated optical synthetic aperture radar processor
[AD-A188019] 11 p1471 N88-18772
Optical symbolic processor for expert system execution
[AD-A187882] 11 p1525 N88-19103
Optical computing research
[AD-A187862] 11 p1549 N88-19264
Ultra-high speed integrated optical waveguide devices for optical computing
[AD-A188470] 12 p1691 N88-20118
Applications of optical computing to problems with symbolic computations
[AD-A189772] 15 p2106 N88-22548
Optical Conceptual Computing and Associative Memory (OCCAM)
[AD-A190030] 15 p2107 N88-22550
Optical computer and optical methods for data processing 18 p2518 N88-24939
Theoretical investigation of optical computing based on neural network models
[AD-A191668] 18 p2563 N88-25214
Optical computing based on neuronal models
[AD-A191481] 18 p2575 N88-25293
Optical symbolic processor for expert system execution
[AD-A192005] 18 p2575 N88-25296
Mitsubishi Electric Advance (R and D Edition), Volume 41
[PB88-194162] 21 p2929 N88-27388
Basic research on optical neural computers 21 p2929 N88-27389
Architecture for optical digital computers
[AD-A195477] 24 p3430 N88-30416

OPTICAL CORRECTION PROCEDURE
Corrections for differential scattering by aerosols in the measurement of ozone by DIAL --- differential absorption lidar (DIAL)
[NPL-QU-78] 14 p1945 N88-21603

OPTICAL COUNTERMEASURES
MIDIR (Mid-Infrared) laser, phase 1
[AD-A193935] 23 p3220 N88-29166

OPTICAL COUPLING
Research on acoustical scattering, diffraction catastrophes, optics of bubbles, photoacoustics, and acoustical phase conjugation
[AD-A185785] 06 p0776 N88-14761
Passive coupler, network adapter, and network acquisition procedure for optical local networks
[ETN-88-92130] 14 p1961 N88-21695
Discussion of two-mode two-photon CW laser oscillation 16 p2187 N88-23042

OPTICAL DATA PROCESSING
NT SCENE ANALYSIS
Implementation of a digital optical matrix-vector multiplier using a holographic look-up table and residue arithmetic
[NASA-CR-180431] 01 p0078 N88-10496
Nonconventional optical techniques for optical wavefront processing
[AD-A185099] 05 p0650 N88-13982
The role of photodetectors in optical signal processing
[AD-A186804] 09 p1247 N88-17476
Image texture classification with an optical crossbar interconnected processor 10 p1375 N88-18202
Integrated optical synthetic aperture radar processor
[AD-A188019] 11 p1471 N88-18772
Optical symbolic processor for expert system execution
[AD-A187882] 11 p1525 N88-19103
Optical computing research
[AD-A187862] 11 p1549 N88-19264
Optical signal processing using nonlinear optics
[AD-A188461] 12 p1691 N88-20117
Ultra-high speed integrated optical waveguide devices for optical computing
[AD-A188470] 12 p1691 N88-20118
Study of photochromic materials for use in optical signal processing
[AD-A189068] 13 p1839 N88-21006
Gigantic optical nonlinearity in low dimensional systems 14 p1975 N88-21786
Error reduction in two-dimensional pulse-area modulation, with application to computer-generated transparencies --- optical field synthesis
[EUT-87-E-172] 14 p1982 N88-21825
Applications of optical computing to problems with symbolic computations
[AD-A189772] 15 p2106 N88-22548
Optical Conceptual Computing and Associative Memory (OCCAM)
[AD-A190030] 15 p2107 N88-22550
Space-variant optical systems
[AD-A189967] 15 p2133 N88-22724
Sky radiance distributions for thermal imaging backgrounds
[AD-A191135] 17 p2373 N88-24115
Nonlinear surface polaritons
[AD-A191046] 18 p2499 N88-24822
Theoretical investigation of optical computing based on neural network models
[AD-A191668] 18 p2563 N88-25214
Optical computing based on neuronal models
[AD-A191481] 18 p2575 N88-25293
Activities report of the Division of Optical Technology
[FOA-C-30477-3] 18 p2576 N88-25299
Optical nonlinearities in GaAs/GaAlAs multiple quantum wells fabricated by metalorganic chemical vapor deposition for use in optical signal processing
[AD-A191558] 18 p2582 N88-25337
Optical data processing
[AD-A193024] 20 p2839 N88-26841
Investigation of the potential impact of new photonic materials on optical processing systems 21 p2924 N88-27359

Optical interconnections for digital image coding
21 p2928 N88-27381
An optical 2-dimensional correlator for pattern recognition in embedded computing
[DE88-007198] 21 p2998 N88-27780
Optical symbolic computing
[AD-A195690] 24 p3429 N88-30406
Spectroscopic studies with multiple quantum well materials with applications to optical signal processing at room temperature
[AD-A194171] 24 p3429 N88-30409
Use of depletion edge translation for high-speed modulation and switching of lightwaves
[AD-A195611] 24 p3430 N88-30417

OPTICAL DATA STORAGE MATERIALS
Holographic disk for data storage
14 p1972 N88-21771
Evaluation of multi-focus holographic lenses
[AD-A196167] 24 p3377 N88-30110

OPTICAL DENSITY
Study of kinetics of intracavity absorption in pulsed dye lasers 07 p0919 N88-15585
Perception and control of simulated self motion
[AD-A187444] 10 p1372 N88-18188
Characteristics of coherent and incoherent waves in snow at microwave and millimeter wave frequencies
[AD-A188990] 12 p1620 N88-19692
The visioceilometer and its tactical applications
[AD-A188216] 12 p1647 N88-19866

OPTICAL DEPTH
U OPTICAL THICKNESS

OPTICAL DISKS
Storing photomicrographs on optical laser disks
[DE87-013747] 04 p0449 N88-12785
Recording materials for optical disk memory discussed
06 p0684 N88-14193
Holographic disk for data storage
14 p1972 N88-21771
Use of optical disk technology at the Air Command and Staff College
[AD-A192424] 21 p3027 N88-27969

OPTICAL EMISSION
U LIGHT EMISSION

OPTICAL EMISSION SPECTROSCOPY
NT LASER SPECTROSCOPY
Evidence of a new spectral line intensity formula for optical emission
[KGI-PREPRINT-098] 01 p0090 N88-10585
Optical spectroscopy of IRAS sources with infrared emission bands. 1: IRAS 21282+5050 and the diffuse interstellar bands
[NASA-CR-181387] 01 p0094 N88-10611
On the signal strength dependency on pressure in laser sub-Doppler saturation spectroscopy with special attention to gaseous diatonic molecules
[USIP-87-13] 09 p1171 N88-17023
The relationship between low activity comets and more active comets 14 p1997 N88-21904
The optical spectroscopy of copper-blue luminescence in zinc sulfide crystals. Zero-phonon line spectra under the influence of magnetic field, temperature and excitation intensity
[ETN-88-93122] 24 p3344 N88-29903

OPTICAL EQUIPMENT
NT CAMERAS
NT COLLIMATORS
NT DIFFRACTION LIMITED CAMERAS
NT DIFFRACTOMETERS
NT EBERT SPECTROMETERS
NT ELECTROPHOTOMETERS
NT ELLIPSOMETERS
NT ENDOSCOPES
NT ETALONS
NT FAINT OBJECT CAMERA
NT FRAMING CAMERAS
NT HIGH SPEED CAMERAS
NT IMAGE CONVERTERS
NT IMAGE TUBES
NT INFRARED SPECTROMETERS
NT INFRARED SPECTROPHOTOMETERS
NT LASER DOPPLER VELOCIMETERS
NT LASER RANGE FINDERS
NT LIGHT SCATTERING METERS
NT MICRODENSITOMETERS
NT MULTISPECTRAL BAND CAMERAS
NT MULTISPECTRAL BAND SCANNERS
NT OCULOMETERS
NT OPTICAL GYROSCOPES
NT OPTICAL MEASURING INSTRUMENTS
NT OPTICAL MICROSCOPES
NT OPTICAL PYROMETERS
NT OPTICAL RADAR
NT OPTICAL SCANNERS
NT PERISCOPES
NT PHOTOMETERS
NT PINHOLE CAMERAS
NT POLARIMETERS
NT PRISMS
NT REFRACTOMETERS
NT SPECTROHELIOGRAPHS
NT SPECTROPHOTOMETERS
NT STREAK CAMERAS
NT TELEVISION CAMERAS
NT THEMATIC MAPPERS (LANDSAT)
NT THEODOLITES
NT TOTAL OZONE MAPPING SPECTROMETER
NT TRANSMISSOMETERS
NT ULTRAVIOLET SPECTROMETERS
NT ULTRAVIOLET SPECTROPHOTOMETERS
NT WIDE ANGLE LENSES
Optically time-resolved detonation break out
[DE87-010340] 01 p0031 N88-10199
Test of the Hipparcos payload in the Liege vacuum facility focal 02 p0135 N88-10850
Fundamentals and techniques of nonimaging optics research
[DE87-014544] 02 p0236 N88-11488
Storing photomicrographs on optical laser disks
[DE87-013747] 04 p0449 N88-12785
Development of optical modulators for measurements of solar magnetic fields
[NASA-TM-100315] 04 p0490 N88-13016
Airborne Visible/Infrared Imaging Spectrometer (AVIRIS) spectrometer design and performance
06 p0706 N88-14327
Optical electronics for meteor observations
06 p0741 N88-14559
Hard- and software problems of spaced meteor observations by optical electronics
06 p0741 N88-14560
Use of spherical optics in high resolution soft X-ray grating monochromators
[PB87-125191] 06 p0780 N88-14788
Investigation of the performance of a novel double crystal X-ray monochromator measurements
[PB87-125167] 06 p0788 N88-14834
Laser Program
[DE87-011009] 07 p0858 N88-15212
Design of the Backscatter Spectroscopy System for the Nova Laser Facility
[DE88-001880] 07 p0859 N88-15214
The magic of carrier patterns in moire interferometry
[AD-A187582] 10 p1296 N88-17748
Remote sensing of atmospheric crosswinds by utilizing speckle-turbulence interaction and optical heterodyne detection
[AD-A187580] 10 p1347 N88-18052
Fabrication and evaluation of transmissive multilayer optics for 8 keV X-rays
[DE88-003999] 10 p1409 N88-18402
A chemical precursor to optical damage. Studies by laser ionization mass spectrometry
[DE88-004321] 10 p1409 N88-18406
Subpicosecond optical digital computation using phase conjugate parametric generators
[AD-A188279] 10 p1410 N88-18411
Microwave semiconductor research-materials, devices and circuits
[AD-A187121] 10 p1415 N88-18444
Optical memory cards: A comparison with other current technologies and potential military applications
[AD-A187287] 10 p1425 N88-18512
Multiaperture optical system research
[AD-A188211] 11 p1549 N88-19267
Radiation effects on gallium arsenide integrated optical devices
[DE88-004107] 11 p1551 N88-19277
Optical waveguide formation by ion implantation of Ti or Ag
[DE88-004595] 11 p1551 N88-19278
Holographically correcting synthetic aperture aberrations
[AD-A189510] 12 p1692 N88-20123
Laser gyro attitude control system feasibility
[AD-A189368] 13 p1720 N88-20285
Aberrations: Their effect on off-axis beam steering
[AD-A189601] 13 p1840 N88-21008
Applications of the lateral shearing interferometer in measurement of synchrotron radiation optical elements
[DE88-005184] 13 p1840 N88-21011
Cryogenic test facilities for an optical cryomechanism qualification 14 p1879 N88-21228
Laser technology: CO2 lasers and laser optics
[ETN-88-91469] 14 p1915 N88-21441
Preliminary airworthiness evaluation of the UH-60A with Advanced Digital Optical Control System (ADOCS)
[AD-A190674] 15 p2018 N88-22030
Applications of optical computing to problems with symbolic computations
[AD-A189772] 15 p2106 N88-22548
Computer tomography and hybrid optical/digital methods for aerodynamic measurements
[AD-A190909] 16 p2157 N88-22872
Applications research studies of microtubules
[AD-A190855] 16 p2182 N88-23005
Tunable optical sources/growth and characterization of nonlinear optical materials
[AD-A190874] 16 p2274 N88-23608
Joint services electronics program
[AD-A192076] 18 p2504 N88-24856
Optical symbolic processor for expert system execution
[AD-A192005] 18 p2575 N88-25296
Research in the optical sciences
[AD-A192175] 18 p2575 N88-25297
Investigation of the Sun-aligned F-region walls and related phenomena in the auroral latitude range
[AFGL-TR-87-0248] 19 p2692 N88-26000
Use of fiber optic equipment for security
[DE88-007898] 20 p2853 N88-26943
In-situ reactive of X-ray optics by glow discharge
[DE88-009840] 20 p2854 N88-26947
Fabrication technology
[DE88-010598] 20 p2855 N88-26955
Novel quantum well optical devices
20 p2868 N88-27028
An optical 2-dimensional correlator for pattern recognition in embedded computing
[DE88-007198] 21 p2998 N88-27780
Four-frame gated optical imager with 120-ps resolution
[DE88-011735] 22 p3080 N88-28288
Beam optics test stand
[AD-A193901] 23 p3216 N88-29144
Center for opto-electronic systems research instrumentation grant
[AD-A193711] 23 p3282 N88-29545
A fiber optic collective flight control system for helicopters
[AD-A195406] 24 p3328 N88-29818
Optoelectronic gain control of a microwave single stage GaAs MESFET amplifier
[NASA-CR-182201] 24 p3368 N88-30055
Application of nondestructive testing techniques to materials testing
[AD-A195716] 24 p3381 N88-30138

OPTICAL FIBERS
Ultrafast holography using optical fibers
[ISL-R-101/86] 02 p0176 N88-11096
Effects of radiation damage in optical fibers: A tutorial
[PB87-210308] 02 p0235 N88-11482
Radiation-induced transient attenuation of optical fibers at 800 and 1300 nm
[DE87-013165] 02 p0235 N88-11485
Photoinduced low-temperature changes in optical losses in fiber optics based on chalcogenide glasses
06 p0770 N88-14731
Synchronous multi-image high speed photography of welding arc by optical fibers
[PB87-143939] 07 p0857 N88-15202
Transversely anisotropic curved optical fibres: Variational analysis of a nonstandard Eigenproblem
[PB88-112966] 08 p1083 N88-16526
Studies on nonlinear mechanisms of excimer laser propagation in fused silica fibers
[AD-A186822] 09 p1156 N88-16929
Turbine flow meter with optical fiber pick-up
[NAL-TR-923] 09 p1169 N88-17009
Wide band data transmission system using optical fibers
[DE88-004555] 10 p1319 N88-17889
The use of optical fibers for shock pressure and timing measurements at high pressures
[DE88-004012] 10 p1334 N88-17971
Optically controlled phased-array antenna technology for space communication systems
[NASA-TM-100852] 11 p1476 N88-18809
New monostatic balanced Doppler velocimeter using a polarization preserving fiber
[PB88-130869] 11 p1490 N88-18895
Diode pumped fiber laser
[AD-A187694] 11 p1491 N88-18902
Quantum nondemolition detection and squeezing in optical fibers 14 p1976 N88-21793
Berry's phase in fiber optics 14 p1977 N88-21797
Hermetic coating of optical fibers
[AD-A189886] 15 p2044 N88-22177
Clinical measurements using fiber optic sensors
[DE88-005624] 15 p2134 N88-22731
Lifetime of pristine optical fibers
[ETN-88-92246] 16 p2273 N88-23602
Interaction of solitons in single model optical fibres
17 p2439 N88-24511
Study of light transmission methods from scintillators to optical fiber with wave length shifter
[DE88-701587] 18 p2574 N88-25292

Novel fiber preforms: Rare earth doping
[AD-A191549] 18 p2575 N88-25294
Optical sensing of magnetic fields
19 p2670 N88-25871
Perturbational analysis of the curved anisotropic optical fiber for the birefringence due to the geometry
[PB88-171848] 19 p2726 N88-26189
Stress-related phenomena in transient radiation-induced absorption in optical fibers
[DE88-010956] 20 p2854 N88-26949
Multi-mode optical fibers for simultaneous 13-position measurements Thomson scattering apparatus in the JFT-2M tokamak
[DE88-753133] 21 p3015 N88-27897
Fiber optic sensing systems using high frequency resonant sensing heads with intensity sensors
[NASA-TM-101318] 22 p3080 N88-28293

OPTICAL FILTERS
Improving coherent visualization by means of film optical filtering — projectile visualization
[ISL-R-116/86] 02 p0176 N88-11097
Reduction of temperature rise in high-speed photography
[NASA-TM-100222] 02 p0176 N88-11100
Sideband suppression by an intracavity optical filter in the Los Alamos free-electron laser oscillator
[DE87-011740] 02 p0177 N88-11103
Multilayer-coated mirrors as power filters in synchrotron radiation beamlines
[DE88-003872] 11 p1550 N88-19276
Raman enhancement methods for molecular structure characterization of optical thin films
[DE88-003421] 11 p1558 N88-19324
Photographic filters
[INPE-4448-RPE/558] 12 p1692 N88-20124
Study of photochromic materials for use in optical signal processing
[AD-A189068] 13 p1839 N88-21006
Fundamental noise processes in a laser excited optical filter
[DE88-006460] 15 p2070 N88-22340
Advanced programming and control techniques for complex mechanical systems
[AD-A190238] 15 p2071 N88-22349
Fabry-Perot etalons as prefilters for astronomical far infrared Fourier transform spectroscopy
[MPE-205] 16 p2273 N88-23603
Analysis of binarized Hartley phase-only filter performance with respect to stochastic noise
[DE88-007604] 18 p2519 N88-24945
Optical correlation using the magneto-optic device
[AD-A192342] 20 p2854 N88-26950

OPTICAL GENERATORS
U LASER CAVITIES

OPTICAL GYROSCOPES
Navigation using the Teldix fiber-optic gyroscope
18 p2517 N88-24933

OPTICAL HETERODYNING
Methods for a coherent CO2 laser heterodyne radar system
[ESA-TT-1035] 03 p0328 N88-12076
Remote sensing of atmospheric crosswinds by utilizing speckle-turbulence interaction and optical heterodyne detection
[AD-A187580] 10 p1347 N88-18052

OPTICAL IMAGES
U IMAGES

OPTICAL MASER MODULATION
U LIGHT MODULATION

OPTICAL MASERS
U LASERS

OPTICAL MATERIALS
Phase equilibrium and crystal growth studies on AgGaSe2 and related nonlinear optical materials
[AD-A193763] 22 p3157 N88-28783

OPTICAL MEASUREMENT
NT ASTRONOMICAL PHOTOMETRY
NT COLORIMETRY
NT ELECTROPHOTOMETRY
NT INFRARED PHOTOMETRY
NT PHOTOMETRY
NT POLARIMETRY
NT SPECTROPHOTOMETRY
NT STELLAR SPECTROPHOTOMETRY
NT ULTRAVIOLET PHOTOMETRY
NT VISUAL PHOTOMETRY
An instrument for the quasi-continuous determination of atmospheric soot content
[DFVLR-FB-87-04] 01 p0068 N88-10433
Optical power line voltage and current measurement systems. Volume 1: Limits to the precision of electro-optic and magneto-optic sensors
[DE87-014556] 02 p0175 N88-11092
Description of a multiframe optical probing system
[DE87-014255] 02 p0236 N88-11487
Microcomputer control of spectroscopic instruments
[ATR-86(8431)-4] 03 p0326 N88-12058
Lidar-radiometric method for determining liquid-water content of cirrus clouds 04 p0461 N88-12854
Optical deformation measurement on shells following the raster principle
[ETN-88-90608] 05 p0609 N88-13741
Optical measurement systems
08 p0955 N88-15796
Evaluation of a temperature remote sensing technique
[AD-A187885] 10 p1347 N88-18053
Diagnostics for research in atomization and turbulent two-phase flows
[AD-A187338] 11 p1482 N88-18843
Ion content and infrared absorption of moist atmospheric air
[AD-A188839] 12 p1643 N88-19838
Computer software for the computation of the scattered field and the optical microscope image of line objects patterned in thick layers
[PB88-153705] 13 p1814 N88-20838
Technical applications of solar energy. Project: Selective coatings
[BMFT-FB-T-86-213] 14 p1943 N88-21591
Ray tracing optical analysis of offset solar collector for space station solar dynamic system
[NASA-TM-100853] 15 p2027 N88-22080
Development and applications of optical interferometric micrometrology in the angstrom and subangstrom range
[NASA-TM-100299] 16 p2211 N88-23196
Air Force ultrafast optical electronics center
[AD-A191491] 17 p2438 N88-24507
Measurements of Z(sub eff) profile with a visible bremsstrahlung continuum detector array
17 p2443 N88-24529
Optical monitoring of protein crystal growth
[NASA-CR-182669] 18 p2484 N88-24738
Instrumentation for turbulent reacting flows
[AD-A191671] 18 p2515 N88-24923
An optical preamplifier for detection of CO2 laser radiation
[AD-A190790] 18 p2520 N88-24949
An optical technique for measuring divergence, beam profile, and aiming direction, of relativistic negative hydrogen ions
[DE88-007049] 18 p2572 N88-25278
Fiber optic sensors 19 p2670 N88-25870
Optical sensing of magnetic fields
19 p2670 N88-25871
Optical measurement of propeller blade deflections
[NASA-TP-2841] 22 p3079 N88-28286
Metal halide optical glasses
[AD-A193794] 23 p3198 N88-29032
Optical measurement of unducted fan blade deflections
[NASA-TM-100966] 23 p3216 N88-29142
Volumetric measurement of vorticity vectors by optical probe
[AD-A195997] 24 p3389 N88-30061
Optical measurements of soot in premixed flames
[NASA-TM-101305] 24 p3373 N88-30090

OPTICAL MEASURING INSTRUMENTS
NT DIFFRACTOMETERS
NT EBERT SPECTROMETERS
NT ELECTROPHOTOMETERS
NT ELLIPSOMETERS
NT ETALONS
NT INFRARED SPECTROMETERS
NT INFRARED SPECTROPHOTOMETERS
NT LASER RANGE FINDERS
NT LIGHT SCATTERING METERS
NT MICRODENSITOMETERS
NT OCULOMETERS
NT OPTICAL PYROMETERS
NT PHOTOMETERS
NT POLARIMETERS
NT REFRACTOMETERS
NT SPECTROPHOTOMETERS
NT THEODOLITES
NT TOTAL OZONE MAPPING SPECTROMETER
NT TRANSMISSOMETERS
NT ULTRAVIOLET SPECTROMETERS
NT ULTRAVIOLET SPECTROPHOTOMETERS
Surface scattering characteristics and the measurement of particulate contamination 02 p0137 N88-10862
Optical instrumentation and study of gas-solid suspension flows
[DE88-000147] 04 p0442 N88-12744
Determination of the fiber ratio in carbon fiber/resin composites by means of image analysis
[SNIAS-872-422-101] 05 p0558 N88-13398
Developments in optical sensor technologies described 06 p0689 N88-14220
Optical seam tracking in robotic arc welding
[VTT-RR-463] 06 p0713 N88-14376
Integrated systems with applications to the multi-phases of the ephemerides, physics and mathematics of the upper atmosphere
[AD-A185748] 06 p0743 N88-14570
Wind tunnel model surface gauge for measuring roughness
[NASA-CR-182392] 07 p0822 N88-14996
Fundamental aspects of the physics of remote sensing
[ESA-TT-1045] 09 p1185 N88-17100
Multichannel anisotropic single-mode fiber optics for transducers 09 p1240 N88-17429
Computer modeling for optical waveguide sensors
[AD-A187702] 11 p1549 N88-19263
Cramer-Rao bounds on the accuracy of location and velocity estimations using CCD optical sensors
[AD-A188481] 12 p1629 N88-19748
Activities report of the Physics Department
[ETN-88-91985] 13 p1833 N88-20964
Research on certain aspects of laser diffraction particle sizing relevant to autonomous self-diagnosing instrumentation
[AD-A190220] 15 p2071 N88-22348
Optical sensors for the measurement of electric current and voltage
[PB88-172945] 16 p2193 N88-23077
Low-cost optical data acquisition system for blade vibration measurement 16 p2219 N88-23240
Phase length optical phase-locked-loop sensor
[NASA-CASE-LAR-13387-1] 18 p2576 N88-25302
IPS guidestar selection for stellar mode (ASTRO)
[NASA-TM-100336] 21 p2894 N88-27181
Diffraction by a simple deep phase object — integrated circuit measurement
[RSRE-MEMO-4039] 22 p3070 N88-28224
Optical method to measure the deformations of structures loaded by hydraulic pressure
[SNIAS-881-430-111] 22 p3088 N88-28338
Research and development objectives: Installation, startup, and test operation of a remote and program controlled measuring table for the calibration of EGRET experiment
[ETN-88-92105] 22 p3152 N88-28752
Investigations on periodically perturbed optical waveguides
[B8712725] 23 p3283 N88-29548

OPTICAL MEMORY (DATA STORAGE)
Optical laser technology, specifically CD-ROM (Compact Disc - Read Only Memory) and its application to the storage and retrieval of information
[AD-A184111] 03 p0330 N88-12086
Optical memory cards: A comparison with other current technologies and potential military applications
[AD-A187287] 10 p1425 N88-18512
Rapid feature extraction via the radon transform
[AD-A190032] 15 p2110 N88-22573
Time-domain frequency-selective optical memories: A study of the basic mechanisms and potential systems
[AD-A190854] 16 p2274 N88-23607
Optical computing based on neuronal models
[AD-A191481] 18 p2575 N88-25293
Evaluation of multi-focus holographic lenses
[AD-A196167] 24 p3377 N88-30110

OPTICAL METHODS
U OPTICS

OPTICAL MICROSCOPES
Three dimensional reconstruction of optical microscope pictures using the three dimensional microscopic inverse point spread function
[ETN-87-90420] 01 p0098 N88-10646
Computer software for the computation of the scattered field and the optical microscope image of line objects patterned in thick layers
[PB88-153705] 13 p1814 N88-20838
MIG-1 on-line measuring holographic microscope
[DE88-701103] 15 p2068 N88-22332

OPTICAL MODULATION
U LIGHT MODULATION

OPTICAL PATHS
Uniform geometrical theory of diffraction
03 p0303 N88-11911
All-optical beam control by forced Rayleigh scattering
[AD-A184315] 04 p0490 N88-13018
Program to development an optical transistor and switch
[AD-A185666] 06 p0697 N88-14278
Navigation planning using quadtrees
[DE88-003706] 09 p1225 N88-17343
Applications of optical computing to problems with symbolic computations
[AD-A189772] 15 p2106 N88-22548
Phase length optical phase-locked-loop sensor
[NASA-CASE-LAR-13387-1] 18 p2576 N88-25302

OPTICAL POLARIZATION

Determination of the origin of self-pumped phase conjugation in barium titanate
[AD-A184697] 03 p0377 N88-12372

Research on acoustical scattering, diffraction catastrophes, optics of bubbles, photoacoustics, and acoustical phase conjugation
[AD-A185785] 06 p0776 N88-14761

New monostatic balanced Doppler velocimeter using a polarization preserving fiber
[PB88-130869] 11 p1490 N88-18895

Optical characterization of tropospheric aerosols
[AD-A187839] 11 p1511 N88-19029

Nonlinear optical principles and the photorefractive effect applied to optical phase conjugation
[AD-A188856] 12 p1691 N88-20119

Spontaneous decay and atomic fluorescence near a metal surface of an absorbing dielectric
[AD-A187508] 13 p1835 N88-20975

Real-time image difference detection using a polarization rotation spacial light modulator
[NASA-CASE-NPO-17144-1-CU] 18 p2576 N88-25305

OPTICAL PROPERTIES

NT ABSORPTIVITY
NT BIDIRECTIONAL REFLECTANCE
NT BIREFRINGENCE
NT BRIGHTNESS
NT BRIGHTNESS DISTRIBUTION
NT COLOR
NT DICHROISM
NT KERR ELECTROOPTICAL EFFECT
NT LUMINOSITY
NT OPACITY
NT OPTICAL BISTABILITY
NT OPTICAL REFLECTION
NT PHOSPHORESCENCE
NT PHOTOCONDUCTIVITY
NT RADIANCE
NT REFLECTANCE
NT REFRACTIVITY
NT SKY BRIGHTNESS
NT SPECTRAL REFLECTANCE
NT STELLAR LUMINOSITY
NT STIGMATISM
NT TRANSLUCENCE
NT TRANSMISSIVITY
NT TRANSMITTANCE
NT TRANSPARENCE
NT TURBIDITY
NT WATER COLOR

Optical sizing of soot in gas turbine combustors and exhaust augmentor tubes
[AD-A183785] 01 p0006 N88-10034

Calorimetric Absorption Spectroscopy (CAS): A new method for the characterization of the optical properties of semiconductor systems
[ETN-87-90407] 01 p0098 N88-10645

Direct detection of optical radiation through a sampling orifice for inductively coupled plasma atomic emission spectroscopy
[DE87-013609] 01 p0101 N88-10662

An evaluation of the LEC-460 solar collector
[DE88-000052] 02 p0196 N88-11224

Composition, structure and chemistry of interstellar dust
[NASA-TM-88350] 02 p0253 N88-11603

Near-infrared dichroism of a mesogenic transition metal complex and its solubility in nematic hosts
[DE87-014471] 03 p0287 N88-11805

Highly Non-Linear Optical (NLO) organic crystals 03 p0297 N88-11865

Theory of atomic additivity in molecular hyperpolizabilities 03 p0297 N88-11867

Advances in inherently conducting polymers
[DE88-000501] 04 p0421 N88-12610

Conducting hybrid polymeric systems
[DE88-000527] 04 p0421 N88-12611

Measurement of cirrus cloud optical properties by high spectral resolution lidar 04 p0470 N88-12906

Characterization of thin layers for optics
[PB87-217949] 04 p0490 N88-13017

Fundamental studies in the OM-CVD growth of Ga-in-As-Sb
[AD-A184822] 05 p0655 N88-14014

Material design of high performance glasses discussed 06 p0688 N88-14216

Coherence, propagation and fluctuations of light: A generalized ray approach
[DE88-001669] 06 p0780 N88-14786

Selection of polymer materials for manufacturing optical parts
[AD-A185898] 07 p0836 N88-15069

Astrophysics and the solar nebula 07 p0883 N88-15355

Development of a physically-based general circulation model parameterization of clouds and their radiative interactions
[DE88-004060] 09 p1194 N88-17154

Optical Fourier transformation by lensless method with perforated mask and with modified Talbot interferometer for analysis of interferograms 09 p1236 N88-17408

Molecular beam epitaxy for research on quantum well structures
[AD-A186791] 09 p1255 N88-17522

Relaxing the brightness constancy assumption in computing optical flow
[AD-A187437] 10 p1410 N88-18410

Optical characterization of GaAs/sub 1-x/Sb/sub x/ and GaAs/sub 1-x/Sb/sub x/GaAs strained layer superlattices
[DE88-003393] 10 p1418 N88-18464

Photoconductor switch and circuit analysis
[AD-A188168] 11 p1478 N88-18821

Nonlinear optical waveguides containing a transition metal-based dye molecule
[DE88-003257] 11 p1550 N88-19275

Raman enhancement methods for molecular structure characterization of optical thin films
[DE88-003421] 11 p1558 N88-19324

Spatial distribution of carbon and native defects in large-diameter bulk grown GaAs
[DE88-003870] 11 p1562 N88-19348

Investigations of surface coatings based on silicon and nitrogen: From amorphous Si to silicon nitride
[DE88-004995] 12 p1609 N88-19622

Experimental and analytical investigation on a proposed embedded fiber optic displacement sensor
[AD-A189030] 12 p1630 N88-19756

Optical properties of compressible inhomogeneous shear layers relevant to high power lasers
[AD-A189299] 12 p1633 N88-19774

A continued study of optical sound generation and amplification
[AD-A188362] 12 p1691 N88-20116

Development of an optical feedback based high accuracy beam transmissometer
[AD-A189396] 12 p1692 N88-20122

Tungsten-carbon multilayer system studied with X-ray scattering
[DE88-005749] 13 p1735 N88-20373

Materials Research Laboratory at Brown University
[AD-A188006] 13 p1739 N88-20396

Optical studies of dynamical processes in disordered system
[DE88-005965] 13 p1837 N88-20993

Energy transfer and non-linear optical properties at near ultraviolet wavelengths: Rare earth 4f yields 5d transitions in crystals and glasses
[DE88-005403] 13 p1840 N88-21012

Optical properties of quantum well structures with electric field: Life time free switching of luminescence intensity and virtual charge-induced ultrafast optical nonlinearity 14 p1976 N88-21794

High density femtosecond excitation of nonthermal carrier distributions in intrinsic and modulation doped GaAs quantum wells 14 p1977 N88-21798

Recent progress in optical bistability and tristability 14 p1979 N88-21809

Oxide optical coatings prepared by metal-organic vapor deposition
[DE88-006809] 15 p2043 N88-22175

Research on stable processible conducting polymers for electronic applications
[AD-A190246] 15 p2044 N88-22180

A 104-km unrepeatered bidirectional fiber optic demonstration link
[AD-A190282] 15 p2134 N88-22728

Optical characterization of microcrystals
[DE88-008622] 15 p2141 N88-22775

The effect of internal relaxation on optoacoustic conversion in liquids
[AD-A191307] 16 p2176 N88-22970

The optical properties of aerosols
[AD-A191420] 16 p2176 N88-22972

Nonlinear wave and diffusion equations
[AD-A191421] 16 p2265 N88-23544

Tunable optical sources/growth and characterization of nonlinear optical materials
[AD-A190874] 16 p2274 N88-23608

Investigation of non-linear optical behavior of semiconductors for optical switching, volume 1
[AD-A191297] 16 p2274 N88-23611

Air Force ultrafast optical electronics center
[AD-A191491] 17 p2438 N88-24507

Time resolved spectroscopy facility for the study of nonlinear optical properties of semiconducting polymers
[AD-A191221] 18 p2490 N88-24766

Stress measurements in graphite fibers by laser raman spectroscopy
[AD-A191710] 18 p2491 N88-24779

Studies of optical matrix multiplication and reconfigurable optical interconnect concepts
[AD-A191635] 18 p2575 N88-25295

Research in the optical sciences
[AD-A192175] 18 p2575 N88-25297

Electronic structure, elementary excitations, optical and transport properties of semiconductor superlattices
[AD-A190795] 18 p2581 N88-25333

Optical properties of heterostructures and superlattices
[AD-A191542] 18 p2581 N88-25335

Dual Stokes cars measurements in supersonic combusting flow 19 p2625 N88-25589

Selective radiation absorption in aluminized composite propellant combustion 19 p2630 N88-25598

X-ray and optical analysis of surface properties of metal optics
[DE88-004033] 19 p2727 N88-26195

Nonlinear optical properties and subpicosecond dynamics of excitons and electron-hole plasmas in multiple quantum well structures
[AD-A191926] 19 p2727 N88-26196

Development of liquid metal field-emission sources for use in fast repetitive opening switches
[AD-A192230] 20 p2795 N88-26583

Interferometric recording of holographic optical elements using partially coherent light 20 p2805 N88-26636

Optical coatings for high average power XeF lasers
[DE88-011356] 20 p2807 N88-26656

Determination and application of bidirectional solar-optical properties of fenestration systems
[DE88-010364] 20 p2820 N88-26727

Stress-related phenomena in transient radiation-induced absorption in optical fibers
[DE88-010956] 20 p2854 N88-26949

Ultrafast optical nonlinearity in quantum well structures with electric field 20 p2863 N88-27003

Semiconductor microcrystallites in porous glass and their applications in optics 20 p2863 N88-27005

Properties of multilayers for soft X-ray optics 20 p2867 N88-27025

Magneto-optical studies of GaInAs-InP quantum wells 20 p2870 N88-27039

On a-SiH/a-SiN(x):H superlattices: Confinement or contamination 20 p2870 N88-27040

Performance evaluation of large-area glass-mirror heliostats
[DE88-011883] 21 p2969 N88-27636

The collection of statistics on the frequency of cloud cover over North America
[AD-A193093] 21 p2974 N88-27667

Atomic layer epitaxy of ZnS and ZnSe
[AD-A192307] 21 p3020 N88-27928

Studies of coherent beam processing concepts, phase 1
[AD-A194749] 22 p3083 N88-28306

Recent advances in optical spectroscopy using high performance array detectors
[AD-A194219] 22 p3152 N88-28753

Optical bistable behavior of a planar quasi-waveguide interferometer made with a conjugated organic polymer film
[AD-A194349] 22 p3152 N88-28756

Phase equilibrium and crystal growth studies on AgGaSe2 and related nonlinear optical materials
[AD-A193763] 22 p3157 N88-28783

Aerodynamics of seeing on large transport aircraft
[NASA-CR-183122] 23 p3174 N88-28896

Optical emission behavior and radiation resistance of epoxy resins
[DE88-752629] 23 p3196 N88-29023

Metal halide optical glasses
[AD-A193794] 23 p3198 N88-29032

LLE (Laboratory for Laser Energetics) review
[DE88-008065] 23 p3219 N88-29158

Proof of the feasibility of coherent and incoherent schemes for pumping a gamma-ray laser
[AD-A193856] 23 p3220 N88-29165

Planarization of metal substrates for solar mirrors
[DE88-011492] 23 p3229 N88-29214

Vision through aircraft transparencies 23 p3242 N88-29294

Quasi-liquid crystalline materials with special electro-optic properties
[AD-A194579] 23 p3282 N88-29544

Nonlinear optical processes in molecular systems
[AD-A193871] 23 p3282 N88-29546

Growth and characterization of materials for tunable lasers in the near infrared spectral region
[NASA-CR-183132] 24 p3377 N88-30113

Spontaneous force optical traps
[AD-A196103] 24 p3377 N88-30114

Bibliography of Soviet laser developments, number 88, March - April 1987
[AD-A195978] 24 p3378 N88-30116

Atmospheric corrections for in-flight satellite radiometric calibration
[AD-A196124] 24 p3391 N88-30194
An organometallic route to micron-sized whiskers of zinc sulfide
[AD-A195889] 24 p3430 N88-30414
On 3-5 heterojunction structures and high speed devices
[AD-A195464] 24 p3433 N88-30438

OPTICAL PUMPING
NT LASER PUMPING
Thermo-optical modeling of flashlamp-pumped zig-zag slabs
[DE87-011878] 01 p0051 N88-10326
Nonconventional optical techniques for optical wavefront processing
[AD-A185099] 05 p0650 N88-13982
Solitons in stimulated Raman scattering: Generation and control of ultrashort optical pulses
[AD-A185141] 05 p0650 N88-13983
Lasers with wavefront-reversing mirrors (review article)
06 p0709 N88-14349
Population inversion in gapless semiconductors as result of interband pumping 06 p0770 N88-14732
Time characteristics of travelling wave lasing with two-photon picosecond optical pumping
07 p0918 N88-15578
Atomic clocks research: An overview
[AD-A185567] 07 p0930 N88-15648
Tunable Al2O3:Ti3+-laser with optical pumping
09 p1237 N88-17415
High power, high efficiency, 2D laser diode arrays for pumping solid state lasers
[DE88-004042] 13 p1777 N88-20632
Squeezing via travelling-wave forward four-wave mixing in atomic vapors: Comparison with nondegenerate theory 14 p1978 N88-21804
Generation of tunable coherent radiation in 3 micrometers-5 micrometers region using semiconductor lasers in external cavities
[AD-A190860] 16 p2212 N88-23202
High-speed phenomena in GaAs multiple-quantum-wells 19 p2680 N88-25812
Sources of polarized ions and atoms
[DE88-010910] 20 p2852 N88-26931
Far-infrared studies of doped AlGaAs/GaAs multiple-quantum-well structures
20 p2862 N88-26998

OPTICAL PYROMETERS
Noncontact Temperature Measurement
[NASA-CP-2503] 17 p2327 N88-23895
Direct emissivity measurements on liquids and corrections to multi-color pyrometers
17 p2329 N88-23906
Common but unappreciated sources of error in one, two, and multiple-color pyrometry 17 p2329 N88-23907
Fast optical pyrometry 17 p2329 N88-23908

OPTICAL RADAR
Investigation of lidar backscatter including depolarization and higher scattering orders
[ETN-87-90431] 01 p0052 N88-10334
Theoretical and lidar studies of the seasonal and nocturnal variations of the mesospheric sodium layer at Urbana, Illinois 01 p0066 N88-10435
Airborne lidar studies of Arctic polar stratospheric clouds 01 p0069 N88-10443
A study of the performance of airborne laser radar systems and techniques
[ETN-87-90928] 02 p0179 N88-11117
Correlation between aircraft MSS and LIDAR remotely sensed data on a forested wetland in South Carolina
[NASA-TM-89643] 02 p0193 N88-11204
Airborne lidar experiments at the Savannah River Plant
[NASA-TM-4007] 02 p0194 N88-11209
The Avionics Flight Evaluation System (AFES) of the DFVLR
[ESA-TT-1037] 03 p0266 N88-11677
Methods for a coherent CO2 laser heterodyne radar system
[ESA-TT-1035] 03 p0328 N88-12076
Review of inversion techniques for spaceborne lidar systems
[AD-A184164] 04 p0447 N88-12772
Multiwave laser soundings of atmospheric aerosol: Experimental research (review)
04 p0461 N88-12852
Lidar-radiometric method for determining liquid-water content of cirrus clouds 04 p0461 N88-12854
Measurement of cirrus cloud optical properties by high spectral resolution lidar 04 p0470 N88-12906
Italy's Institute of Research on Electromagnetic Waves--the Istituto di Ricerca sulle Onde Elettromagnetiche
[AD-A185020] 05 p0574 N88-13501
Contributions of lidar measurements to the study of long term variations of the middle atmosphere
[ETN-88-91237] 05 p0625 N88-13824
Lidar investigations of M-zone
06 p0741 N88-14558
Problems and possible solutions involved in hard target calibration of coherent Doppler lidar
07 p0922 N88-15602
Inversion of simulated satellite signals
08 p1017 N88-16168
A backscatter lidar proposed for the second German Spacelab mission 08 p1018 N88-16173
Development of a Doppler wind lidar system for atmospheric wind measurements
08 p1027 N88-16217
The sodium layer at 69 N latitude in wintertime
08 p1027 N88-16218
Lidar metal density measurements in the upper atmosphere 08 p1027 N88-16219
Rayleigh lidar observations of gravity wave activity in the stratosphere and lower mesosphere
[NASA-CR-182384] 09 p1189 N88-17123
Concept, construction, and experimental testing of a polychromator for a Raman lidar for the simultaneous telemetering of carbon dioxide and water vapor, relative to oxygen
[GKSS-87/E/20] 09 p1191 N88-17134
Airborne Wind Shear Detection and Warning Systems: First Combined Manufacturers' and Technologists' Conference
[NASA-CP-10006] 10 p1273 N88-17616
Lidar windshear detection and avoidance: Performance and technical assessment 10 p1274 N88-17626
Airborne Doppler lidar detection of wind shear. Results of performance analysis 10 p1275 N88-17627
Experiments for the high resolution detection of moving targets using a CO2 laser radar
[MBB-UA-1044/87] 10 p1316 N88-17864
Integrated optical synthetic aperture radar processor
[AD-A188019] 11 p1471 N88-18772
Atmospheric backscatter at 10.6 microns; a compendium of measurements made outside the United Kingdom by the airborne LATAS coherent laser radar velocimeter
[RSRE-87002] 12 p1631 N88-19763
Distortion of wideband carbon dioxide laser radar waveforms due to atmospheric dispersion and absorption
[AD-A188687] 12 p1632 N88-19771
Position, scale, and rotation invariant target recognition using range imagery
[AD-A188828] 12 p1633 N88-19772
Coherent laser radar system theory
[AD-A188759] 13 p1774 N88-20612
Lidar active remote sensing. Applications to the atmosphere 14 p1935 N88-21547
Corrections for differential scattering by aerosols in the measurement of ozone by DIAL --- differential absorption lidar (DIAL)
[NPL-QU-78] 14 p1945 N88-21603
Optical properties of Southern Hemisphere aerosols: Report of the joint CSIRO/NASA study
[NASA-CR-179287] 14 p1945 N88-21605
Aerosol lidar for environment protection and meteorology
[DFVLR-FB-87-43] 14 p1982 N88-21828
Infrared differential absorption lidar for vapor detection
[AD-A190600] 15 p2098 N88-22497
Optics: Perspectives for Measurement Techniques and Signal Processing for Flight Guidance --- conference
[DFVLR-MITT-87-21] 18 p2516 N88-24928
Limits of accuracy and range of laser radars
18 p2517 N88-24934
Aircraft/lidar turbulence comparison
18 p2546 N88-25111
High speed opto-isolator for radar applications
19 p2658 N88-25795
Remote determination of chlorophyll concentration in the ocean using an optical pulse radar
[NASA-TT-20301] 19 p2694 N88-26014
Components of an atmospheric lidar system
[AD-A193366] 21 p2953 N88-27539
IEMIS (Integrated Emergency Management Information System) floodplain mapping based on a LIDAR derived data set
[AD-A19307*] 21 p2966 N88-27616
Investigations on Mie and Rayleigh scattering as basis for the development of Rayleigh temperature lidars with aid of Michelson interferometry
[GKSS-87/E/62] 21 p2976 N88-27675
South Pole lidar: Brief description of the instrument
[NOTA-INTERNA-907] 22 p3083 N88-28308
Atmospheric Lidar Experiment In Space (ALEXIS)
[DFVLR-MITT-88-10] 22 p3118 N88-28526
Genesis of Atlantic lows experiment NASA electra boundary layer flights data report
[NASA-TM-100703] 22 p3128 N88-28597
Helicopter recognition using laser radars
22 p3149 N88-28736
Program to increase the measurement capabilities of the AFGL (Air Force Geophysics Laboratory) fixed and mobile high altitude lidar systems
[AD-A194614] 23 p3203 N88-29063
Large aperture multi-dimensional laser radar testbed
[AD-A193447] 23 p3218 N88-29155
Forty-eight-inch lidar aerosol measurements taken at the Langley Research Center, May 1974 to December 1987
[NASA-RP-1209] 23 p3232 N88-29234
Spaceborne lidar: Development of a laboratory test system
[BF-R-66.090-1] 24 p3378 N88-30118

OPTICAL RANGE FINDERS
NT LASER RANGE FINDERS

OPTICAL REFLECTION
Space-time structure of ultrashort light pulses formed during stimulated backscattering of laser beam
14 p1972 N88-21767
Phase length optical phase-locked-loop sensor
[NASA-CASE-LAR-13387-1] 18 p2576 N88-25302

OPTICAL RELAY SYSTEMS
Coherent infrared detection, volume B --- CO2 laser intersatellite data link
[ESA-CR(P)-2392-VOL-1] 01 p0034 N88-10218
Coherent infrared detection, volume D --- CO2 laser intersatellite data link
[ESA-CR(P)-2392-VOL-2] 01 p0034 N88-10219

OPTICAL RESONANCE
Ultrafast intrinsic bistable devices
[PB87-109310] 05 p0649 N88-13978
Experimental observation of photoresonance of electrons localized above surface of solid hydrogen
06 p0774 N88-14755
Enhancement of second harmonic generation on silver gratings by resonant excitation of surface plasmon
[ETN-88-92304] 17 p2439 N88-24509
Laser desorption/ablation studies by resonance ionization mass spectrometry
[DE88-009124] 20 p2807 N88-26650

OPTICAL RESONATORS
Computer simulation of cw HF chemical laser unstable resonator performance
[AD-A185059] 05 p0587 N88-13581
Effect of optical inhomogeneities on space coherence of radiation emitted by laser with unstable resonator
06 p0771 N88-14738
Super-short yttrium aluminate pulse generator with controlled resonator Q-factor 06 p0772 N88-14740
High-power periodic-pulse YAG:Nd3+-laser system with telescopic unstable resonator and two-stage amplifier
09 p1237 N88-17414
The 80 fsec soliton-like pulses from an optical-nonlinear fiber resonator
[PB88-127303] 10 p1409 N88-18403
Optical frequency doubling in Ti:LiNbO3 waveguide resonators
[ETN-88-91486] 11 p1550 N88-19271
Squeezed states of light 14 p1976 N88-21791
Beam quality of stable and unstable resonators: A theoretical approach
[DFVLR-FB-87-35] 14 p1982 N88-21826
High power axial flow CO2 laser
[ETN-88-91951] 18 p2521 N88-24959
Analytical description of noise in phase-conjugate resonators
[PB88-171947] 19 p2726 N88-26188
Spectral properties of semiconductor lasers with external resonators
[ETN-88-93119] 24 p3379 N88-30125

OPTICAL SCANNERS
NT MULTISPECTRAL BAND SCANNERS
NT THEMATIC MAPPERS (LANDSAT)
Applications of nonlinear hole burning spectroscopy
[AD-A184943] 05 p0587 N88-13580
Range imagery algorithms for the detection of obstacles by autonomous vehicles
[AD-A185421] 05 p0659 N88-14045
Joint services electronics program
[AD-A188173] 11 p1478 N88-18822
Application of new technologies to DTIC document processing
[AD-A189778] 15 p2148 N88-22823
Users guide to CAESAR
[BCRS-87-04] 16 p2228 N88-23306
Development of an automated X-ray gauge for nondestructive quantitative analysis
[DE88-008633] 20 p2812 N88-26681
Five channel auroral photometer
[REPT-112] 24 p3375 N88-30101

Application of nondestructive testing techniques to materials testing
[AD-A195716] 24 p3381 N88-30138

OPTICAL SENSORS
U OPTICAL MEASURING INSTRUMENTS

OPTICAL SIGNALS
U OPTICAL COMMUNICATION

OPTICAL SPECTRUM
U LIGHT (VISIBLE RADIATION)
U SPECTRA

OPTICAL SWITCHING
The design and construction of a thermally controlled single mode fiber switch
[ETN-87-90929] 02 p0236 N88-11491
Theory of interactions of intense light with nonlinear, inhomogeneous and periodic structures and its applications to optical bistability, optic gyroscopes, nonlinear spectroscopy, radiation protection, X-ray emission and related fields
[AD-A190040] 15 p2133 N88-22725
Optical switching and control techniques using nonlinear optical wave mixing
[AD-A190467] 15 p2134 N88-22730
Investigation of non-linear optical behavior of semiconductors for optical switching, volume 1
[AD-A191297] 16 p2274 N88-23611

OPTICAL THICKNESS
Aerosol optical depth and ratios of diffuse-sky to total solar irradiance measured from aircraft following the eruption of El Chichon
[PB88-100789] 07 p0878 N88-15326
Remote sensing of atmospheric optical thickness and sea-water attenuation when submerged: Wavelength selection and anticipated errors
[AD-A187609] 11 p1548 N88-19262
Diurnal variations in optical depth at Mars: Observations and interpretations
[NASA-TM-100057] 18 p2595 N88-25420

OPTICAL TRACKING
Resources, confusions and compatibility in dual axis tracking: Displays, controls and dynamics
[AD-A185871] 07 p0898 N88-15440
Intelligent robotic tracker 09 p1214 N88-17276
Multiaperture optical system research
[AD-A188211] 11 p1549 N88-19267
Pursuit tracking performance decrements associated with decreasing ambient illumination
[AD-A189336] 13 p1809 N88-20809
Real-time optical multiple object recognition and tracking system and method
[NASA-CASE-NPO-17139-1-CU] 18 p2576 N88-25301
Tracking a monochromatic light source
[DE88-011260] 20 p2807 N88-26653

OPTICAL TRANSFER FUNCTION
Imaging interferometry with non-redundant arrays 02 p0257 N88-11624
Relationship between optical transfer function and natural light field in sea or atmosphere 15 p2054 N88-22247

OPTICAL TRANSITION
Program to development an optical transistor and switch
[AD-A185666] 06 p0697 N88-14278
Effect of extraneous factors on optical one-phonon transitions in impurity centers with cubic symmetry 08 p1077 N88-16496
Infrared devices using semiconductor quantum wells
[RSRE-MEMO-4018] 22 p3157 N88-28788

OPTICAL WAVEGUIDES
NT OPTICAL FIBERS
Coupling and absorption phenomena in semiconductor-clad dielectric optical waveguides
[DE87-013446] 03 p0307 N88-11939
Ultrafast intrinsic bistable devices
[PB87-109310] 05 p0649 N88-13978
Design, production, and characterization of broadband optical waveguides
[DFVLR-FB-85-52] 06 p0780 N88-14791
A surface plasmon waveguide sensor: A new type of chemical transducer based on optical phenomena
[ETN-88-91322] 06 p0780 N88-14792
Surface modification using ion beams: Recent developments at ORNL
[DE88-000951] 06 p0786 N88-14819
Pressure and tension dependence of phase shift of polarization modes in birefringent single-mode fiber-optic waveguide 08 p1078 N88-16501
Computational analysis of propagation properties of integrated-optical waveguides using a domain integral equation
[PB87-163358] 09 p1154 N88-16917
Semiconductor laser with electron-beam pumping and fiber-optic output waveguide 09 p1235 N88-17405
Multichannel anisotropic single-mode fiber optics for transducers 09 p1240 N88-17429
Light Electronic Control System (LECOS): A proposal for a interconnected error-tolerant, optoelectronic control system
[MBB-UT-004/87] 10 p1311 N88-17836
POLYPHEM, a universal defensive missile with optical waveguides guidance
[MBB-UA-1045/87] 10 p1315 N88-17862
Formation of optical waveguides by ion implantation
[DE88-003894] 10 p1409 N88-18407
Computer modeling for optical waveguide sensors
[AD-A187702] 11 p1549 N88-19263
Optical frequency doubling in Ti:LiMbO3 waveguide resonators
[ETN-88-91486] 11 p1550 N88-19271
Nonlinear optical waveguides containing a transition metal-based dye molecule
[DE88-003257] 11 p1550 N88-19275
Optical waveguide formation by ion implantation of Ti or Ag
[DE88-004595] 11 p1551 N88-19278
Ultra-high speed integrated optical waveguide devices for optical computing
[AD-A188470] 12 p1691 N88-20118
Coupled high power waveguide laser research
[AD-A189800] 15 p2071 N88-22345
Monolithic integration on a GaAs substrate of a quarter ring laser and an optical guide coupled by an evanescent wave
[ETN-88-92308] 17 p2344 N88-23969
Silicon-sapphire waveguides
[AD-A191754] 18 p2504 N88-24854
A high frequency GaAlAs travelling wave electro-optic modulator at 0.82 micrometers
[NASA-TM-100970] 22 p3073 N88-28240
Investigations on periodically perturbed optical waveguides
[B8712725] 23 p3283 N88-29548
Ion exchange processes for fabrication of integrated optical waveguide structures into glass substrates
[VTT-46] 24 p3429 N88-30405
Use of depletion edge translation for high-speed modulation and switching of lightwaves
[AD-A195611] 24 p3430 N88-30417

OPTICS
JPRS report: Science and technology. USSR: Physics and mathematics
[JPRS-UPM-87-008] 06 p0769 N88-14727
JPRS report: Science and technology. USSR: Physics and mathematics
[JPRS-UPM-87-009] 09 p1233 N88-17395
Optically interconnected phased arrays
[NASA-TM-100855] 14 p1908 N88-21400
Computing X-ray effects in optics
[DE88-006722] 15 p2134 N88-22732
Flow velocity measurements by image processing of optically modulated traces 16 p2203 N88-23147
Optics and symbolic computing
[AD-A195119] 24 p3360 N88-30004

OPTIMAL CONTROL
NT LINEAR QUADRATIC GAUSSIAN CONTROL
NT LINEAR QUADRATIC REGULATOR
NT TIME OPTIMAL CONTROL
A treatment of jw-axis model-matching transformation zeros in the optimal H squared and H infinity control designs
[OUEL-1673/87] 02 p0223 N88-11407
Stochastic model of the NASA/MSFC ground facility for large space structures with uncertain parameters: The maximum entropy approach
[NASA-CR-181489] 03 p0372 N88-12343
Local-optimal control in systems with delay 04 p0424 N88-12627
Investigation, development, and application of optimal output feedback theory. Volume 3: The relationship between dynamic compensators and observers and Kalman filters
[NASA-CR-4107] 05 p0638 N88-13900
Control of an unstable launcher in atmospheric flight using minimax optimal control laws
[SNIAS-872-422-107] 05 p0638 N88-13901
Guidance and control strategies for aerospace vehicles
[NASA-CR-181579] 05 p0643 N88-13935
Optimal guidance of homing missiles 06 p0671 N88-14111
Feedback in LQCP (Linear Quadratic Control Problem) with a terminal inequality constraint
[PB87-220034] 06 p0762 N88-14676
Optimal repeated measurements designs for comparing test treatments with a control
[AD-A185999] 07 p0917 N88-15569
Analytical study of the effect of early warning on optimal shock isolation 08 p0998 N88-16047
Optimal control of windpowered plants
[FOA-C-20610-2.7] 08 p1022 N88-16188
Control variate selection for multiresponse simulation
[AD-A186637] 08 p1069 N88-16463
Nonlinear filtering and large deviations: A PDE-Control theoretic approach
[AD-A187436] 10 p1396 N88-18321
Viscosity methods in optimal control of distributed systems
[AD-A188086] 10 p1401 N88-18357
Symmetries in nonlinear control systems and their applications 11 p1496 N88-18929
Prediction of the response and optimal control of stochastic parametrically and externally excited nonlinear systems 11 p1496 N88-18930
Optimal control theory of load-following and parameter-tracking of nonlinear systems: An application of Pontryagin Maximum Principle to reactor dynamics
[DE88-004770] 11 p1532 N88-19152
Deterministic equivalent for a continuous linear-convex stochastic control problem
[AD-A187818] 11 p1540 N88-19206
Effects of closing speed uncertainty on optimal guidance 12 p1597 N88-19556
Bilinear systems in the frequency domain and an application to optimal control
[RR-320] 14 p1962 N88-21704
Advanced guidance algorithms for homing missiles with bearings-only measurements
[AD-A190435] 15 p2017 N88-22026
Optimal control and identification of space structures
[AD-A190033] 15 p2025 N88-22065
The adjoint process in stochastic optimal control
[AD-A189720] 15 p2116 N88-22605
An algorithm for super-optimal H sup inf design: The 2-block case
[OUEL-1711/87] 17 p2391 N88-24210
A state-space approach to discrete-time super-optimal H sup inf control problems
[OUEL-1712/87] 17 p2391 N88-24211
Energy optimal trajectory planning for robot manipulators and autonomous vehicles 17 p2437 N88-24497
Estimation and control of distributed models for certain elastic systems arising in large space structures
[AD-A192120] 18 p2472 N88-24666
Low authority control of large space structures using a constrained threshold control formulation 18 p2472 N88-24667
Optimal processes governed by integral equations with unilateral constraint 18 p2565 N88-25231
Optimal control of the wing rock phenomenon 21 p2927 N88-27373
Computer aided design for linear control State Variable System (SVS)
[AD-A193282] 21 p2997 N88-27775
Free boundary control of the Markov process
[AD-A192401] 21 p3008 N88-27846
Approximations and optimal control for the pathwise average cost per unit time and discounted problems for wideband noise driven systems
[AD-A192712] 21 p3008 N88-27847
Motion planning with obstacles and dynamic constraints 23 p3222 N88-29175
Nonlinear dynamic analysis and optimal control of shallow shells 23 p3224 N88-29191
Convex duality approach to the optimal control or diffusions
[AD-A194535] 23 p3266 N88-29442
The optimal control pilot model and applications 24 p3315 N88-29741
Sensor and actuator selection for large space structure control
[AD-A194912] 24 p3333 N88-29842
Theory of filtering and control with application to control of large space structures
[AD-A195500] 24 p3335 N88-29851
Analytical methods in stochastic control and nonlinear filtering
[AD-A194272] 24 p3426 N88-30388
Increasing accuracy in evaluating vector of state under conditions of incomplete observability of expanded system 24 p3446 N88-30511

OPTIMIZATION
NT DYNAMIC PROGRAMMING
NT FLIGHT OPTIMIZATION
NT LINEAR PROGRAMMING
NT LINEAR QUADRATIC GAUSSIAN CONTROL
NT LINEAR QUADRATIC REGULATOR
NT MATHEMATICAL PROGRAMMING
NT NONLINEAR PROGRAMMING
NT OPERATIONS RESEARCH
NT OPTIMAL CONTROL
NT QUADRATIC PROGRAMMING
NT SIMPLEX METHOD
NT TIME OPTIMAL CONTROL
NT TRAJECTORY OPTIMIZATION
Shape optimization of linear antennas
[ETN-87-90413] 01 p0036 N88-10233

Optimum size of staged flux compression generators
[DE87-011741] 01 p0038 N88-10244
An interactive optimization procedure for the computer aided dimensioning of integrated circuits
[ETN-87-90414] 01 p0082 N88-10531
Spectral and structural properties of nonnegative reducible operators in Banach relations
[ETN-87-90402] 01 p0089 N88-10581
Optimization of a controlled two-server maintenance system
[INPE-4202-PRE/1083] 01 p0107 N88-10694
Using MINOS (Modular in-core Nonlinear Optimization System) as a subroutine for decomposition
[DE87-013086] 02 p0221 N88-11390
A treatment of jw-axis model-matching transformation zeros in the optimal H squared and H infinity control designs
[OUEL-1673/87] 02 p0223 N88-11407
Irreducible *-representations of the Lie superalgebra osp(1,4) with finite-degenerated vacuum
[DE87-703089] 02 p0225 N88-11420
Numerical solution of bound constrained problems
[DE88-000653] 03 p0371 N88-12334
Mathematical models of plasma discharge control in a tokamak
[DE87-702891] 03 p0378 N88-12377
Reduced complexity structural modeling for automated airframe synthesis
[NASA-CR-177440] 04 p0393 N88-12453
New feedback design methodologies for large space structures: A multi-criterion optimization approach
04 p0408 N88-12535
Performance optimization of electronic networks in the frequency domain
[PB87-123873] 04 p0438 N88-12720
Optimization of explicit time-stepping algorithms and Stream-Function-Coordinate (SFC) concept for fluid dynamics problems 04 p0445 N88-12762
Optimization of dilatometer test procedures
[DE87-014996] 04 p0447 N88-12769
Parallel superconvergent multigrid
[DE87-013153] 04 p0480 N88-12960
Investigation, development and application of optimal output feedback theory. Vol. 4: Measures of eigenvalue/eigenvector sensitivity to system parameters and unmodeled dynamics
[NASA-CR-4108] 04 p0482 N88-12969
An exact penalization viewpoint of constrained optimization
[DE88-001477] 04 p0486 N88-12995
Techniques for performance optimisation in cruise and manoeuverability 05 p0545 N88-13321
Aeroelasticity and optimization in fighter aircraft design
05 p0546 N88-13324
Reduced order optimal command applied to longitudinal automatic pilots
[SNIAS-872-111-114] 05 p0552 N88-13362
Design of low order controllers for robust disturbance rejection in large space structures
[AD-A185202] 05 p0555 N88-13376
Digital video bit-rate reduction: DPCM for sub-Nyquist PAL
[BBC-RD-1987/16] 05 p0573 N88-13494
Contribution to optimal flow in networks. A experimental multiprocessor for asynchronous iteration implementation
[LAAS-87-269] 05 p0576 N88-13510
Establishment of complete minimum test sets for digital circuits with safety engineering significance
[ETN-88-90599] 05 p0578 N88-13526
Finite-element grid improvement by minimization of stiffness matrix trace
[NASA-TM-100255] 05 p0591 N88-13604
Simultaneous structural and control optimization via linear quadratic regulator eigenstructure assignment
05 p0594 N88-13622
Shape optimization of damping layers
05 p0595 N88-13635
STAEBL/general composites with hygrothermal effects (STAEBL/GENCOM)
[NASA-TM-100266] 05 p0611 N88-13754
Structural optimization in the design process --- aircraft
[SNIAS-872-111-115] 05 p0635 N88-13885
Aerodynamic design and test performance of supersonic turbines for the Vulcain rocket engine
06 p0713 N88-14373
Fast algorithms for structural optimization and least squares
[AD-A185766] 06 p0724 N88-14452
Meteor velocity distribution and an optimum monitoring mathematical model 06 p0739 N88-14546
Parallel algorithms for unconstrained and constrained nonlinear optimization
[PB87-230454] 06 p0756 N88-14634
Stress effects and the optimum format of a scrolling seven-line VDT text window
[AD-A185559] 06 p0758 N88-14651
Composite reliability enhancement via preloading
[AD-A185938] 07 p0826 N88-15010
Investigation of fuel additive effects on sooting flames
[AD-A186403] 07 p0829 N88-15026
Optimization of charged particle acceleration rate over wave parameters in the scheme with acceleration by surface electromagnetic waves
[DE88-700320] 07 p0846 N88-15134
Optimization of photogrammetric image adjustment
[SER-C-323] 07 p0872 N88-15289
Image processing language development
[AD-A186251] 07 p0903 N88-15467
On stochastic optimality of policies in first passage problems
[AD-A186293] 07 p0915 N88-15554
Integrated analysis and applications
08 p0954 N88-15789
A study to evaluate STS heads-up ascent trajectory performance employing a minimum-Hamiltonian optimization strategy
[NASA-TP-2793] 08 p0960 N88-15820
A modal control based limiting performance formulation for shock excited systems 08 p0998 N88-16046
Method of iterative coupling between periodic aerodynamic and dynamic fields
[PB87-169934] 09 p1113 N88-16669
Effect of an optimized fiber orientation on transonic flutter characteristics of a high-aspect-ratio composite wing
[NAL-TR-930] 09 p1120 N88-16709
Contribution to the design of flexible manufacturing systems: Modeling, simulation, and evaluation of parameters
[ISAL-IDI1-87-04] 09 p1151 N88-16894
A project to experimentally and theoretically examine fluid interfacial wave phenomena in a rotating cylindrical geometry: Current results and future plans
[DE88-003738] 09 p1165 N88-16984
High-resolution Real-Time Radiography (RTR) system design
[AD-A187107] 09 p1166 N88-16992
Resolution limitations and optimization of the ITT F4157 streak tube focus for fast (10 ps) operation
[DE88-003727] 09 p1169 N88-17007
Kinematic optimization of mechanisms, a finite element approach
[ISBN-90-370-0012-6] 09 p1175 N88-17039
The Shock and Vibration Bulletin. Part 4: Structural Dynamics and Modal Test and Analysis
[AD-A186751] 09 p1179 N88-17062
Optimized structure design using reanalysis techniques 09 p1180 N88-17067
Algorithms for transitive reduction of an acyclic graph
[PB87-162822] 09 p1220 N88-17317
On line search termination criteria for and convergence of conic algorithms for minimization
[DE88-002844] 09 p1227 N88-17351
Optimal application of Morrison's iterative noise removal for deconvolution. Appendices
[NASA-CR-182477] 09 p1231 N88-17376
Optimization of imaging energy filters for analytical electron microscopy
[ETN-88-91079] 09 p1248 N88-17483
Optimisation of military compressors for weight and volume 10 p1279 N88-17649
Specification of an engine and its components starting from a consideration of aircraft missions
10 p1279 N88-17651
The design of impedance- matching networks for broadband antennas
[AD-A187600] 10 p1320 N88-17895
Optimal design and parameter identification of flexible rotor-bearing systems 10 p1339 N88-18002
Applications of energy density theory in cyclic plasticity
[AD-A186947] 10 p1342 N88-18023
Continuous deformation algorithm on the product space of unit simplices, revised version
[PB88-114210] 10 p1387 N88-18281
Graph transformation algorithms for array memory optimization in applicative languages
[DE88-004727] 10 p1387 N88-18283
Experiences with serial and parallel algorithms for channel routing using simulated annealing
[NASA-CR-182530] 10 p1388 N88-18289
A parallel quasi-Newton method for partially separable large scale minimization
[DE88-003592] 10 p1393 N88-18309
Strongly sequential term rewriting systems
[PB88-126693] 10 p1398 N88-18334
Viscosity methods in optimal control of distributed systems
[AD-A188086] 10 p1401 N88-18357
Optimization of outlet channel of plasma ion source
[DE88-700471] 10 p1410 N88-18415
On the maneuvering of vehicles
[AD-A187632] 10 p1427 N88-18521
The aerodynamic design optimisation of a forward swept wing fighter aircraft
[CAR-87-18] 11 p1433 N88-18553
Improving battery reliability by using regression trees
[DE88-004539] 11 p1481 N88-18841
Design modeling for shape optimization
11 p1527 N88-19122
Shape optimization of three-dimensional stamped and solid automotive components
[GMR-5168] 11 p1528 N88-19123
EqL: The language and its implementation
[AD-A188161] 11 p1530 N88-19137
Data flow graph optimization in IF1
[DE88-004396] 11 p1532 N88-19151
A tool for the analysis of quasi-Newton methods with application to unconstrained minimization
[DE88-005783] 11 p1532 N88-19153
Parallel processing in nonlinear programming
[INPE-4298-PRE/1169] 11 p1533 N88-19158
Research on output feedback control
[NASA-CR-182543] 11 p1534 N88-19167
Optimal recursive maximum likelihood estimation
[AD-A187980] 11 p1536 N88-19176
Multigrid methods in convex optimization
11 p1538 N88-19190
Deterministic equivalent for a continuous linear-convex stochastic control problem
[AD-A187818] 11 p1540 N88-19206
Solution of the Lloyd-Max quantizer parameters by the method of successive substitution
[AD-A187829] 11 p1540 N88-19207
Optimal arrangement of components via pairwise rearrangements
[AD-A187633] 11 p1541 N88-19213
Structural shape optimization in multidisciplinary system synthesis
[NASA-TM-100538] 12 p1614 N88-19650
Optimum filters and smoothers design for carrier phase and frequency tracking
[NASA-CR-182654] 12 p1618 N88-19679
On the design of suboptimal matched filters for three-dimensional moving target detection
[AD-A188384] 12 p1619 N88-19682
A technique for local refinement of the stress field by finite element method
[INPE-4219-PRE/1099] 12 p1683 N88-20061
Method of reduction of polynomially nonlinear equations to linear equations
[DE88-700922] 12 p1683 N88-20064
A view of unconstrained optimization
[AD-A188327] 12 p1684 N88-20066
Optimizing powerplant design and development cycles
12 p1701 N88-20183
Control augmented structural synthesis
[NASA-CR-4132] 13 p1721 N88-20290
The design of aircraft using the decision support problem technique
[NASA-CR-4134] 13 p1721 N88-20291
Optimization of binary pigment coatings
[AD-A189103] 13 p1748 N88-20450
Optimal placement of tuning masses for vibration reduction in helicopter rotor blades
[NASA-TM-100562] 13 p1782 N88-20665
Active cooling design for scramjet engines using optimization methods
[NASA-TM-100581] 13 p1783 N88-20669
On the sensitivity of complex, internally coupled systems
[NASA-TM-100537] 13 p1813 N88-20829
A new algorithm for general multiobjective optimization
[NASA-TM-100536] 13 p1813 N88-20830
Conic algorithms for unconstrained minimization with special consideration of problems with large sparse Hessians: A summary of research performed
[DE88-002549] 13 p1816 N88-20850
Algorithms with conic termination for nonlinear optimization
[DE88-005893] 13 p1816 N88-20851
Constrained nonlinear programming
[DE88-005695] 13 p1817 N88-20860
Deterministic uncertainty analysis
[DE88-006139] 13 p1829 N88-20942
Optimal and conventional space-time processing in flow noise
[AD-A189104] 13 p1833 N88-20965
Design, optimization and construction of a dc-SQUID with complete flux transformer circuits
[PB88-160742] 14 p1907 N88-21399
An efficient gradient projection optimization scheme for a seven-degree-of-freedom redundant robot with spherical wrist
[DE88-005440] 14 p1919 N88-21453

Sensitivity of control-augmented structure obtained by a system decomposition method
[NASA-TM-100535] 14 p1954 N88-21647
Optimization of the real level 2 BLAS on the Cyber 205
[CWI-NM-R8715] 14 p1956 N88-21657
Multiextremal optimization via adaptive partition algorithms
[REPT-87-44] 14 p1957 N88-21664
Aero/structural tailoring of engine blades (AERO/STAEBL)
[NASA-CR-180805] 14 p1959 N88-21682
Unsteady aerodynamics of a Wortmann FX-63-137 wing in a fluctuating wind field
[AD-A190128] 15 p2013 N88-22006
Nonlinear analysis and optimal design of dynamic mechanical systems for spacecraft application
[AD-A190644] 15 p2026 N88-22070
Efficient method for structural optimization
15 p2054 N88-22240
Optimum signal processing in distributed sensor systems
[AD-A189443] 15 p2055 N88-22250
Structural tailoring of high-speed turbine blades (SSME/STAEBL) 15 p2080 N88-22398
Structural tailoring of advanced turboprops
15 p2080 N88-22400
Experimental design and structural optimization
[PB88-169255] 15 p2087 N88-22436
SEARCH: An interactive computer program for optimizing two-variable, unconstrained experiments or simulation
[AD-A190593] 15 p2112 N88-22583
Numerical methods for linear and nonlinear optimization
[AD-A190029] 15 p2120 N88-22631
Lumped model generation and evaluation: Sensitivity and Lie algebraic techniques with applications to combustion
[AD-A190402] 15 p2127 N88-22689
Dynamical optimization techniques for the calculation of electronic structure in solids
[DE88-006010] 15 p2140 N88-22768
Minimum weight design of rotorcraft blades with multiple frequency and stress constraints
[NASA-TM-100569] 16 p2161 N88-22892
Vibration control of large structures
[AD-A191358] 16 p2168 N88-22928
On the capacity of channels with unknown interference
[AD-A191160] 16 p2191 N88-23067
Problems in integrated networks
[AD-A191391] 16 p2191 N88-23069
Spur gears: Optimal geometry, methods for generation and Tooth Contact Analysis (TCA) program
[NASA-CR-4135] 16 p2215 N88-23216
Mixed finite element formulation applied to shape optimization 16 p2221 N88-23252
Variable speed optimal control of a wind turbine generator
[LAAS-87-358] 16 p2229 N88-23316
STRUTEX: A prototype knowledge-based system for initially configuring a structure to support point loads in two dimensions
[NASA-TM-100613] 16 p2250 N88-23448
Parallel computing in combinatorial optimization
[CWI-OS-R8720] 16 p2254 N88-23468
Convergence qualification of partition algorithms in global optimization
[REPT-87-61] 16 p2259 N88-23505
Sensitivity analysis and multidisciplinary optimization for aircraft design: Recent advances and results
[NASA-TM-100630] 17 p2302 N88-23766
A generalized method for optimizing the mass of space power systems 17 p2416 N88-24369
Optimization of SP-100 thermoelectric electromagnetic pump 17 p2418 N88-24382
Optimization of organic Rankine cycles for space station applications 17 p2423 N88-24407
Small particle bed reactors: Sensitivity to Brayton cycle parameters 17 p2435 N88-24487
Energy conversion system optimization study for multimegawatt space nuclear power application
17 p2436 N88-24492
Superconducting thin film vertex detector for SSC (Superconducting Super Collider) applications
[DE88-005951] 17 p2445 N88-24535
Nonlinear programming extensions to rational function approximation methods for unsteady aerodynamic forces
[NASA-TP-2776] 18 p2463 N88-24623
Guidance and control strategies for aerospace vehicles
[NASA-CR-183032] 18 p2467 N88-24644
A feedback linearization approach to spacecraft control using momentum exchange devices
[NASA-CR-172057] 18 p2472 N88-24668
Optimization of reserve lithium thionyl chloride battery electrochemical design parameters
[DE88-007109] 18 p2506 N88-24868
Applications of fault tree analysis to the design process
[DE88-007048] 18 p2525 N88-24982
A mixed-integer linear programming problem which is efficiently solvable
[AD-A191028] 18 p2556 N88-25168
Solving bidiagonal systems of linear equations on the CDC CYBER 205
[CWI-NM-R8725] 18 p2558 N88-25187
The Sizing and Optimization Language, (SOL): Computer language for design problems
[NASA-TM-100565] 18 p2559 N88-25190
Gram-Schmidt implementation of a linearly constrained adaptive array
[AD-A191651] 18 p2560 N88-25198
Mixed min-max optimization problem with restrictions
18 p2565 N88-25232
The use of Lagrange multipliers and Kuhn-Tucker's theory in optimization problems
18 p2565 N88-25236
Optimal discrete-time LQR problems for parabolic systems with unbounded input: Approximation and convergence
[NASA-CR-181673] 18 p2567 N88-25247
Electronic structure of Zintl phase compounds by nonlinear optimization
[DE88-009998] 19 p2613 N88-25508
Fluid dynamics of high performance turbomachines
[AD-A192073] 19 p2664 N88-25840
An extension of the Hopfield-Tank model for solution of the multiple traveling salesmen problem
[DE88-008377] 19 p2715 N88-26122
Model reduction methods for control design
[NASA-CR-179434] 19 p2719 N88-26144
The Oak Ridge National Laboratory strategic defense initiative shield optimization program
[DE88-006946] 19 p2721 N88-26160
Structural optimization of fiber composite turbomachine blades
[ETN-88-92351] 20 p2760 N88-26372
Modeling and optimum time performance for concurrent processing
[NASA-CR-4167] 20 p2797 N88-26595
Optimization of performance criteria with bounded joint velocities for robots with one degree of redundancy
[DE88-003915] 20 p2810 N88-26870
A matroid algorithm and its application to the efficient solution of two optimization problems on graphs, revision
[AD-A192709] 20 p2838 N88-26838
Using common subexpressions to optimize multiple queries
[DE88-008210] 20 p2844 N88-26877
Combining expert opinions: An optimization framework
[REPT-87-84] 20 p2846 N88-26895
Visible tunable source
[DE88-006442] 20 p2854 N88-26944
A feasibility study in path planning using optimization techniques
[AD-A193030] 21 p2894 N88-27177
Numerical optimization, system theoretic and software tools for the integrated design of flexible structures and their control systems
[AD-A192927] 21 p2895 N88-27183
Optimal rheological characteristics in dynamic stability of polymer flow through porous media
[DE88-001225] 21 p2918 N88-27322
An aspect graph-based control strategy for 3-D object recognition 21 p2927 N88-27377
Efficiency optimization for FEL oscillators
[AD-A192541] 21 p2952 N88-27536
Dexterous hands: Optimizing grasp by design and planning 21 p2958 N88-27572
An investigation of techniques for determination of optimum/self-optimizing systems
21 p2963 N88-27600
Parallel quasi-Newton methods for unconstrained optimization
[AD-A193250] 21 p3003 N88-27812
Database design and management in engineering optimization
[AD-A193325] 21 p3003 N88-27813
Finding minimum-cost circulations by successive approximation
[AD-A192724] 21 p3005 N88-27824
Finding minimum-cost circulations by canceling negative cycles
[AD-A192727] 21 p3005 N88-27825
Numerical optimization
[AD-A193032] 21 p3005 N88-27827
Optimization of fatigue and friction properties of titanium by means of surface treatments
[ECL-87-22] 22 p3056 N88-28133
Optimization and scale-up performance of polymer electrolyte batteries
[AD-A193987] 22 p3073 N88-28243
Optimization techniques for relational database systems 22 p3137 N88-28650
Design of multirate control systems via parameter optimization
[REPT-87-013] 22 p3142 N88-28686
Refining finite element models. Numerical application to a lattice structure. Study of a macroelement of Timoshenko beam type
[ONERA-RT-8/3313-RY-070-R]
22 p3144 N88-28696
A contribution to the quantitative analysis of the influence of design parameters on the optimal design of passenger aircraft
[ETN-88-92979] 23 p3176 N88-28912
Small scale mixing in the initial region of a jet
[AD-A193500] 23 p3192 N88-28994
Free electron lasers with small period wigglers
[DE88-011627] 23 p3218 N88-29156
Optimization-driven machine-oriented motion measurement 23 p3245 N88-29312
Faster scaling algorithms for network problems
[AD-A194032] 23 p3251 N88-29348
Optimization of low gravity materials processing experiments using expert systems
23 p3252 N88-29361
Design consideration in constructing high performance embedded Knowledge-Based Systems (KBS)
23 p3261 N88-29415
Optimisation algorithms for highly parallel computer architectures. The performance of the truncated Newton, conjugate gradient algorithm in FORTRAN and Ada
[AD-A193940] 23 p3265 N88-29435
Analysis and optimization of truncated scarf nozzles subject to external flow conditions
[NASA-TM-100955] 24 p3316 N88-29746
New methods for nonlinear optimization
[AD-A195982] 24 p3412 N88-30313
A rule-based systems approach to spacecraft communications configuration optimization
24 p3417 N88-30341
Formulation and solution of economic equilibrium problems
[AD-A196034] 24 p3439 N88-30470

OPTIMUM CONTROL
U OPTIMAL CONTROL

OPTIMUM THRUST PROGRAMMING
U THRUST PROGRAMMING

OPTOELECTRONIC DEVICES
NT PHOTODIODES
Optoelectronic measurement methods for ballistic experiments
[PB87-110706] 05 p0583 N88-13554
Light Electronic Control System (LECOS): A proposal for a interconnected error-tolerant, optoelectronic control system
[MBB-UT-004/87] 10 p1311 N88-17836
A laser communication experiment utilizing the ACT satellite and an airborne laser transceiver
[NASA-TM-100792] 11 p1492 N88-18910
Concept of an Opto-electronic Accelerometer System (OAS) 12 p1645 N88-19852
Mid infrared multichannel focal plane breadboard --- pushbroom sensors
[RT-87/014] 14 p1982 N88-21827
Television monitor field shifter and an opto-electronic method for obtaining a stereo image of optimal depth resolution and reduced depth distrotion on a single screen
[NASA-CASE-NPO-17249-1-CU]
17 p2332 N88-23924
Electronic and optical devices and applications
24 p3363 N88-30027
Optoelectronic gain control of a microwave single stage GaAs MESFET amplifier
[NASA-CR-182201] 24 p3368 N88-30055

OPTOELECTRONIC SWITCHING
U OPTICAL SWITCHING

OR-GATES
U GATES (CIRCUITS)

ORBIT CALCULATION
Satellite orbits: Plot routines
[UIO-SR-87-02] 01 p0011 N88-10060
Precise orbit computation, gravity model adjustment and altimeter data processing for the ERS-1 altimetry mission
[ESA-CR(P)-2436] 02 p0130 N88-10820
A demonstration of high precision GPS orbit determination for geodetic applications
04 p0432 N88-12680

Determination of TRANET (tracking station coordinates for tracking network) and SMTP (Special Mission Tracking Program) tracking station coordinates for use in the WGS (World Geodetic System) 84
[AD-A185863] 07 p0817 N88-14972
An orbit simulation study of a geopotential research mission including satellite-to-satellite tracking and disturbance compensation systems
[NASA-CR-182353] 07 p0823 N88-14997
Error assessments of widely-used orbit error approximations in satellite altimetry
[NASA-CR-182390] 07 p0823 N88-14998
Limitation of spacecraft orbit near colinear libration center of limited elliptical three body problem
08 p1003 N88-16075
Selection of efficient correcting motor for an artificial Earth satellite 08 p1007 N88-16102
Mission profiles of the MTFF co-orbiting with the US Space Station 12 p1585 N88-19487
Preliminary orbit determination algorithms: Application to the Brazilian satellite
[INPE-4411-NTE/276] 12 p1594 N88-19546
Orbit correction requirements for a natural resources satellite
[INPE-4286-PRE/1158] 12 p1594 N88-19548
Analysis of orbital geometry and orbit maintenance of an Earth observation satellite
[INPE-4276-PRE/1148] 12 p1594 N88-19549
Orbit correction strategy for an Earth observation satellite
[INPE-4287-PRE/1159] 13 p1727 N88-20331
Orbit accuracy requirement of GPS for precise positioning and orbit determination within local area
13 p1756 N88-20499
Seasat orbit determination experiments in preparation for the ERS-1 altimetry mission
[ETN-88-91842] 14 p1871 N88-21182
Analysis of the orbit of Cosmos 1335 (1982-07A) at 3:12 resonance
[RAE-TR-87041] 14 p1872 N88-21185
Numerical orbit propagation methods for earth artificial satellites
[INPE-4405-RPE/556] 15 p2023 N88-22053
Analytical orbit propagation of artificial satellites
[INPE-4454-TDL/315] 16 p2166 N88-22915
Orbit determination of 1965-09A for analysis of the eccentricity at 15th-order resonance
[RAE-TR-87059] 22 p3047 N88-28081

ORBIT DECAY
The contraction of satellite orbits under the influence of air drag. Part 8: Orbital lifetime in an oblate atmosphere, when perigee distance is perturbed by odd zonal harmonics in the geopotential
[RAE-TR-86069-PT-8] 01 p0010 N88-10058
Verification of a micro-thrusting model to maintain satellites in low orbit
[AD-A186674] 09 p1133 N88-16793
Mission profiles of the MTFF co-orbiting with the US Space Station 12 p1585 N88-19487
Orbit correction requirements for a natural resources satellite
[INPE-4286-PRE/1158] 12 p1594 N88-19548
Analysis of the orbit of Cosmos 1335 (1982-07A) at 3:12 resonance
[RAE-TR-87041] 14 p1872 N88-21185
The prediction of satellite lifetimes
[RAE-TR-87030] 17 p2310 N88-23818

ORBIT EQUATIONS
U ORBITAL MECHANICS

ORBIT PERTURBATION
NT SATELLITE PERTURBATION
Electrodynamic tether system study
[NASA-CR-172024] 03 p0275 N88-11737
Orbit correction strategy for an Earth observation satellite
[INPE-4287-PRE/1159] 13 p1727 N88-20331
How typical is Halley's Comet?
14 p1994 N88-21886

ORBIT TRANSFER VEHICLES
Aeroassisted-vehicle design studies for a manned Mars mission
[NASA-TM-100031] 03 p0271 N88-11700
Aeroassisted manned transfer vehicle (TAXI) for advanced Mars Transportation: NASA/USRA 1987 Senior Design Project
[NASA-CR-181478] 03 p0275 N88-11736
Nonequilibrium characteristics of nitrogen plasmas appropriate to an AOTV flight 03 p0319 N88-12019
Study of fault tolerant techniques for satellite data handling
[FTT/REP/0001/SAAB] 05 p0632 N88-13860
An analysis of the effect of aeroassist maneuvers on orbital transfer vehicle performance
[NASA-TM-89117] 06 p0672 N88-14116
AF cryogenic and fluid management spacecraft technology program 08 p0981 N88-15925
SAMSS: An in-progress review of the Spacecraft Assembly, Maintenance, and Servicing Study
08 p0981 N88-15930
Orbital transfer vehicle studies overview
08 p0981 N88-15931
Large capacity cryopropellant orbital storage facility
08 p0981 N88-15932
Orbiter transfer vehicle concept definition and system analysis study. Volume 4: Space station accommodations. Revision 1
[NASA-CR-179293] 11 p1444 N88-18609
Orbital transfer vehicle concept definition and system analysis study. Volume 4, Appendix A: Space station accommodations. Revision 1
[NASA-CR-179294] 11 p1444 N88-18610
A lunar transportation system
[NASA-CR-182561] 11 p1567 N88-19379
Automatic in-orbit payload deployment mechanisms, logistic operations and transport vehicle design compatibilities 12 p1586 N88-19493
Aeroassisted orbit transfer vehicle trajectory analysis
[NASA-TM-89138] 12 p1599 N88-19575
Orbital transfer vehicle concept definition and system analysis study. Volume 2: OTV concept definition and evaluation. Book 1: Mission and system requirements
[NASA-CR-179321] 13 p1729 N88-20339
Turnaround operations analysis for OTV. Volume 1: Executive summary
[NASA-CR-179316] 13 p1729 N88-20340
Turnaround operations analysis for OTV. Volume 2: Detailed technical report
[NASA-CR-179317] 13 p1729 N88-20341
Turnaround operations analysis for OTV. Volume 3: Technology development plan
[NASA-CR-179318] 13 p1729 N88-20342
Turnaround operations analysis for OTV. Volume 4: WBS and dictionary and cost methodology
[NASA-CR-179319] 13 p1729 N88-20343
Space station mobile transporter
14 p1927 N88-21488
Space station full-scale docking/berthing mechanisms development 14 p1927 N88-21491
Orbital transfer vehicle: Concept definition and system analysis study
[NASA-CR-179315] 15 p2024 N88-22060
Nuclear electric power for multimegawatt orbit transfer vehicles 17 p2399 N88-24261
Analysis of a nuclear orbital transfer vehicle reentry accident 17 p2425 N88-24426
Noncryogenic propellants for a nuclear orbit transfer vehicle 17 p2428 N88-24444
Solar thermal propulsion for orbit transfer vehicles
17 p2428 N88-24445
Advanced nuclear rocket engine mission analysis
[DE88-006797] 18 p2475 N88-24681
Centaur operations at the space station
[NASA-CR-179593] 19 p2606 N88-25473
Centaur operations at the space station: Cost and transportation analysis
[NASA-CR-182128] 24 p3332 N88-29835
Orbital transfer vehicle 3000 LBF thrust chamber assembly hot fire test program
[NASA-CR-182145] 24 p3336 N88-29858

ORBITAL ASSEMBLY
Potential for on-orbit manufacture of large space structures using the pultrusion process
[NASA-TM-4016] 05 p0557 N88-13388
Definition and economic evaluation of Space Solar Power Systems (SSPS), part 2
[ILR-MITT-184-2(1987)] 08 p1022 N88-16190
Planning and scheduling for robotic assembly
08 p1062 N88-16416
ESA Bulletin No. 25
[ISSN-0376-4265] 09 p1128 N88-16767
Satellite assembly in geostationary orbit: A plug-and-socket concept 09 p1128 N88-16769
Space station structures development
[NASA-CR-179261] 09 p1133 N88-16792
Telerobotic truss assembly 09 p1213 N88-17272
Assessment of mixed fleet potential for space station launch and assembly
[NASA-TM-100550] 11 p1443 N88-18608
Orbital transfer vehicle concept definition and system analysis study. Volume 4, Appendix A: Space station accommodations. Revision 1
[NASA-CR-179294] 11 p1444 N88-18610
State-of-the-art technologies for construction in space: A review
[AD-A188412] 12 p1585 N88-19483
Proceedings of the 1st European In-Orbit Operations Technology Symposium
[ESA-SP-272] 12 p1585 N88-19484
Assembly of user systems at Space Station
12 p1586 N88-19490
In-orbit automatic assembly of reticular structures
12 p1586 N88-19491
Assembly and servicing of a European Space Station
12 p1586 N88-19492
A knowledge-based approach for sensory-controlled assembly operations 12 p1588 N88-19506
Remote manipulation in orbital construction, servicing and repair missions: Is one arm enough? A comparative evaluation of the performance features of robots with one or more arms 12 p1588 N88-19509
Utilization of robotics and teleoperation for future in-orbit operations 12 p1591 N88-19527
External payload servicing: Operational requirements and technology 12 p1593 N88-19541
Space station heavy lift launch vehicle utilization
[NASA-TM-100604] 14 p1873 N88-21188
A 60-meter erectable assembly concept for a control of flexible structures flight experiment
[NASA-TM-100497] 14 p1873 N88-21190
Structural latches for modular assembly of spacecraft and space mechanisms 14 p1925 N88-21471
Space spider crane
[NASA-CASE-LAR-13411-1-SB]
17 p2312 N88-23828
Bi-stem gripping apparatus
[NASA-CASE-MFS-28185-1] 17 p2345 N88-23979
Design guidelines for robotically serviceable hardware
[NASA-TM-100700] 19 p2606 N88-25472
Mobile remote manipulator system for a tetrahedral truss
[NASA-CASE-MSC-20985-1] 20 p2765 N88-26398
Centaur operations at the space station: Cost and transportation analysis
[NASA-CR-182128] 24 p3332 N88-29835
Study of robotics spacecraft servicing and assembly in space. Volume 1: Executive summary
[ESA-CR(P)-2612-VOL-1] 24 p3333 N88-29839

ORBITAL ELEMENTS
Numerical arc segmentation algorithm for a radio conference-NASARC (version 2.0) technical manual
[NASA-TM-100160] 08 p0977 N88-15910
Numerical arc segmentation algorithm for a radio conference-NASARC, version 2.0: User's manual
[NASA-TM-100161] 09 p1156 N88-16928
Universal procedures for conversion of orbital elements to and from position and velocity (unperturbed orbits)
[RAE-TR-87043] 14 p1872 N88-21184
On orbits and association of meteor streams with Comets P/Halley and P/Encke
14 p2003 N88-21945
Duplicity in the solar neighborhood: Part 4: Spectroscopic orbits for four dwarf M stars
[SER-C-PREPUBL-FASC-21] 24 p3454 N88-30561

ORBITAL FLIGHT TEST 4 (SHUTTLE)
U SPACE TRANSPORTATION SYSTEM 4 FLIGHT

ORBITAL LAUNCHING
Department of Housing and Urban Development-Independent Agencies Appropriations for fiscal year 1988, Thursday, 9 April 1987: National Aeronautics and Space Administration
03 p0386 N88-12424
The determination of exhaust cloud dimensions from films of space shuttle launches
[NASA-CR-4103] 06 p0732 N88-14500
Alternative program approaches for the advanced satellite technology program
[AD-A188917] 12 p1600 N88-19576
Interplanetary propulsion using inertial fusion
17 p2401 N88-24273
Centaur operations at the space station
[NASA-CR-179593] 19 p2606 N88-25473
LRS-2: A specialized knowledge system for launch resource scheduling
[AD-A194625] 23 p3182 N88-28941

ORBITAL LIFETIME
The contraction of satellite orbits under the influence of air drag. Part 8: Orbital lifetime in an oblate atmosphere, when perigee distance is perturbed by odd zonal harmonics in the geopotential
[RAE-TR-86069-PT-8] 01 p0010 N88-10058
Electric propulsion: A controversial must for long-lived applications satellites 09 p1124 N88-16735
The prediction of satellite lifetimes
[RAE-TR-87030] 17 p2310 N88-23818
An extended life and performance test of a low-power arcjet
[NASA-TM-100942] 18 p2476 N88-24687
Attitude and orbit control for the AMPTE-UKS (Active Magnetospheric Particle Tracer Explores-UK Subsatellite): Evaluation of the in-flight performance
[PB87-225199] 19 p2604 N88-25467

ORBITAL MANEUVERING VEHICLES
Telepresence work station system definition study, part 2
[NASA-CR-172006] 01 p0013 N88-10071

Orbital Spacecraft Consumables Resupply System (OSCRS). Volume 4: Extended study results Part 1: Executive Summary
[NASA-CR-172012] 03 p0268 N88-11686
Orbital Spacecraft Consumables Resupply System (OSCRS): Monopropellant application to space station and OMV automatic refueling impacts of an ELV launch, volume 4
[NASA-CR-172029] 03 p0276 N88-11741
Teleoperator and robotics system analysis
[NASA-CR-179220] 03 p0334 N88-12105
Orbital Spacecraft Consumables Resupply System (OSCRS). Volume 1: Executive summary
[NASA-CR-172010] 05 p0553 N88-13368
Servicer system demonstration plan and capability development
[NASA-CR-179246] 08 p0975 N88-15895
OMV man/system simulation integration: A preliminary analysis and recommendation
[NASA-CR-182602] 12 p1671 N88-20005
Space station mobile transporter 14 p1927 N88-21488
OMV docking simulator 23 p3255 N88-29379

ORBITAL MANEUVERS
Study of Plasma Motor Generator (PMG) tether system for orbit reboost
[NASA-CR-172016] 04 p0403 N88-12501
Orbit correction strategy for an Earth observation satellite
[INPE-4287-PRE/1159] 13 p1727 N88-20331
Optimal thrust vector control of coplanar orbital evasive maneuvers
[AD-A189544] 13 p1730 N88-20346
Docking/berthing subsystem: Design and breadboard test 14 p1879 N88-21233
Study of Plasma Motor Generator (PMG) tether system for orbit reboost
[NASA-CR-172074] 23 p3184 N88-28949
Machine vision for real time orbital operations 23 p3253 N88-29367
Automated generation of spacecraft activity plans 23 p3258 N88-29396
The eivaN: A forward-looking interactive orbital trajectory plotting tool for use with proximity operations (PROX OPS) and other maneuvers: Description and user's manual
[NASA-CR-177490] 24 p3414 N88-30327

ORBITAL MECHANICS
NT KEPLER LAWS
A study of a satellite-to-satellite tracking configuration by application of linear perturbation theory
[REPT-86.3] 01 p0011 N88-10059
Estimability of potential coefficients from orbit perturbations --- satellite geodesy
[REPT-86.1] 01 p0064 N88-10408
Analytical average model of studies on orbital resonance 03 p0269 N88-11689
Computational method for orbit improvement for short arc observations of artificial satellites 03 p0269 N88-11690
On air-drag perturbation of transit satellite and selection of parameters in orbit improvement 03 p0269 N88-11691
Adaptive control of Large Space Structure (LSS)
[ISAS-R-621] 03 p0276 N88-11740
Phenomenological implications of the blown-up orbifolds
[DE87-014608] 03 p0373 N88-12347
Radial orbit error reduction and sea surface topography determination using satellite altimetry 04 p0462 N88-12861
Engineering calculations for the Delta S method of solving the orbital allotment problem
[NASA-CR-182372] 06 p0671 N88-14110
An analysis of the effect of aeroassist maneuvers on orbital transfer vehicle performance
[NASA-TM-89117] 06 p0672 N88-14116
Geosat crossover analysis in the tropical Pacific. Part 1: Constrained sinusoidal crossover adjustment
[NASA-CR-182391] 07 p0871 N88-15285
Study on orbits near the triangular libration points in the perturbed restricted three body problem
[ESA-CR(P)-2440] 07 p0944 N88-15741
Selection of efficient correcting motor for an artificial Earth satellite 08 p1007 N88-16102
Application of artificial intelligence to impulsive orbital transfers 08 p1066 N88-16439
Verification of a micro-thrusting model to maintain satellites in low orbit
[AD-A186874] 09 p1133 N88-16793
Numerical arc segmentation algorithm for a radio conference-NASARC, version 2.0: User's manual
[NASA-TM-100161] 09 p1156 N88-16926
An intelligent tutor for the space domain 09 p1204 N88-17217
Orbit correction requirements for a natural resources satellite
[INPE-4286-PRE/1158] 12 p1594 N88-19548
Analysis of orbital geometry and orbit maintenance of an Earth observation satellite
[INPE-4276-PRE/1148] 12 p1594 N88-19549
Simulation and tests of a satellite attitude and orbit control system. General considerations concerning an example case (INPE) and design of a servo rate table
[INPE-4282-PRE/1154] 12 p1599 N88-19572
Orbit correction strategy for an Earth observation satellite
[INPE-4287-PRE/1159] 13 p1727 N88-20331
Study of the optimization of satellite system design for transfer orbit
[MBB-URV-135] 13 p1727 N88-20332
Frozen orbit analysis in the Martian system
[AD-A189574] 13 p1856 N88-21106
Universal procedures for conversion of orbital elements to and from position and velocity (unperturbed orbits)
[RAE-TR-87043] 14 p1872 N88-21184
Estimation of geopotential from satellite-to-satellite range rate data: Numerical results
[NASA-CR-180771] 14 p1941 N88-21583
How typical is Halley's Comet? 14 p1994 N88-21886
The structure of the Halley meteor stream and the orbital history of the comet 14 p2008 N88-21975
Three approaches to the modeling of Comet Halley's motion over long periods of time 14 p2010 N88-21992
A model of the nongravitational motion of Comet P/Encke 14 p2010 N88-21993
Numerical orbit propagation methods for earth artificial satellites
[INPE-4405-RPE/556] 15 p2023 N88-22053
Spacecraft trajectories
[ISBN-2-85-428166-7] 15 p2023 N88-22054
A generic multibody simulation
[NASA-CR-182949] 17 p2388 N88-24198
Stochasticity in elliptical galaxies
[SER-C-PREPUBL-FASC-20] 17 p2450 N88-24556
The limits of direct satellite tracking with the Global Positioning System (GPS) 22 p3064 N88-28179
Study of Plasma Motor Generator (PMG) tether system for orbit reboost
[NASA-CR-172074] 23 p3184 N88-28949
Investigation of the validity of the non-rotating planet assumption for three-dimensional earth atmospheric entry
[AD-A194877] 24 p3331 N88-29829
Orbital evolution of distant artificial earth satellites 24 p3445 N88-30506
Plane periodic satellite motions relative to center of mass in neighborhood of collinear libration point 24 p3445 N88-30507
Orbital stability in rotating triaxial stellar systems
[SER-C-PREPUBL-FASC-24] 24 p3455 N88-30569

ORBITAL MOTION
U ORBITS

ORBITAL POSITION ESTIMATION
Precise near-earth navigation with GPS: A survey of techniques 04 p0433 N88-12682
Short baseline phase delay interferometry 04 p0433 N88-12683
Long range sensor for rendezvous and docking missions 12 p1587 N88-19497
Geodetic positioning by employment of the GPS-NAVSTAR satellites applying the techniques of VLBI and sequential recursive optimal estimation
[INPE-4438-TDL/311] 12 p1594 N88-19547
Seasat orbit determination experiments in preparation for the ERS-1 altimetry mission
[ETN-88-91842] 14 p1871 N88-21182
Universal procedures for conversion of orbital elements to and from position and velocity (unperturbed orbits)
[RAE-TR-87043] 14 p1872 N88-21184
Baseline estimation from simultaneous satellite laser tracking
[NASA-CR-182750] 15 p2022 N88-22052
Approximation of atmospheric density by Chebyshev polynomials in predicting motion of low artificial earth satellites 24 p3445 N88-30503

ORBITAL RENDEZVOUS
Proceedings of the 1st European In-Orbit Operations Technology Symposium
[ESA-SP-272] 12 p1585 N88-19484
Safe rendezvous approach to a space station by impulsive transfers and continuous thrust arcs 12 p1585 N88-19486
Safe and fuel minimum reference trajectories for closed loop controlled approaches --- space stations 12 p1585 N88-19488
Analysis of RVD operations in manned space missions 12 p1586 N88-19494
Rendezvous and docking (RVD) verification and demonstration in-orbit 12 p1592 N88-19531
Space transportation nodes assumptions and requirements: Lunar base systems study task 2.1
[NASA-CR-172052] 23 p3183 N88-28944

ORBITAL RESONANCES (CELESTIAL MECHANICS)
Analytical average model of studies on orbital resonance 03 p0269 N88-11689

ORBITAL SERVICING
Telepresence work station system definition study, part 2
[NASA-CR-172006] 01 p0013 N88-10071
Robotic sensors and actuators for a service manipulator system. Volume 1: Executive summary
[MATRA-EPT/DT/VT187/120] 01 p0053 N88-10341
Robotic sensors and actuators for a service manipulator system. Volume 2: Service Manipulator System (SMS) handbook
[MATRA-EPT/DT/VT187/227] 01 p0053 N88-10342
Robotic sensors and actuators for a service manipulator system. Volume 3, phase A report and program plan
[MATRA-EPT/DT/VT187/228] 01 p0054 N88-10343
Teleoperation and control study --- orbital servicing
[BAE-TP-8268] 01 p0076 N88-10489
Orbital Spacecraft Consumables Resupply System (OSCRS). Volume 4: Extended study results Part 1: Executive Summary
[NASA-CR-172012] 03 p0268 N88-11686
Orbital Spacecraft Consumables Resupply System (OSCRS): Monopropellant application to space station and OMV automatic refueling impacts of an ELV launch, volume 4
[NASA-CR-172029] 03 p0276 N88-11741
Payload configurations and serviceability --- Columbus Polar Platforms 03 p0339 N88-12133
Space station resistojet system requirements and interface definition study
[NASA-CR-180832] 04 p0409 N88-12541
Orbital Spacecraft Consumables Resupply System (OSCRS). Volume 1: Executive summary
[NASA-CR-172010] 05 p0553 N88-13368
In-orbit calibration adjustment of the Nimbus-7 SMMR
[NASA-TM-100678] 05 p0614 N88-13773
Servicer system demonstration plan and capability development
[NASA-CR-179246] 08 p0975 N88-15895
Proceedings of the 1st European In-Orbit Operations Technology Symposium
[ESA-SP-272] 12 p1585 N88-19484
Man-Tended Free Flyer operational design features 12 p1585 N88-19485
Cost-effective orbit transfer modes for satellite retrieval and servicing --- Space Station 12 p1586 N88-19489
Assembly of user systems at Space Station 12 p1586 N88-19490
Assembly and servicing of a European Space Station 12 p1586 N88-19492
NASA Office of Space Flight (OSF) in-orbit servicing program 12 p1587 N88-19498
In-orbit and laboratory exchange of ORUs designed/not designed for servicing 12 p1587 N88-19499
Utilization of SMS and EVA for the servicing of European Space Station 12 p1587 N88-19500
Multimission Modular Spacecraft (MMS). A serviceable design spacecraft 12 p1587 N88-19501
The ESA/Fokker service end-effector subsystem. A robotic/man-compatible servicing approach 12 p1587 N88-19502
Customer concerns regarding satellite servicing 12 p1587 N88-19503
Remote manipulation in orbital construction, servicing and repair missions: Is one arm enough? A comparative evaluation of the performance features of robots with one or more arms 12 p1588 N88-19509
Remote repair demonstration of Solar Maximum main electronics box 12 p1588 N88-19510
Treatment of unforeseen situations by online knowledge-based diagnostic systems --- spacecraft maintenance 12 p1589 N88-19511
EPOS: European Proximity Operations Simulation 12 p1589 N88-19515
EUROSIM: A design concept for an in-orbit operations simulator 12 p1589 N88-19517
Explorer Platform on-orbit servicing operations 12 p1591 N88-19526
Utilization of robotics and teleoperation for future in-orbit operations 12 p1591 N88-19527
Review of commercial spacecraft: Recovery and repair experiences. Implications for future spacecraft designs and operations 12 p1591 N88-19528
Robotics servicing experiment --- European space programs 12 p1591 N88-19529

Technology requirements for telerobotic satellite servicing in space 12 p1592 N88-19536
A teleoperated manipulator system concept for unmanned platforms — Columbus 12 p1593 N88-19537
External payload servicing: Operational requirements and technology 12 p1593 N88-19541
Turnaround operations analysis for OTV. Volume 1: Executive summary [NASA-CR-179316] 13 p1729 N88-20340
Turnaround operations analysis for OTV. Volume 3: Technology development plan [NASA-CR-179318] 13 p1729 N88-20342
Turnaround operations analysis for OTV. Volume 4: WBS and dictionary and cost methodology [NASA-CR-179319] 13 p1729 N88-20343
Space station heavy lift launch vehicle utilization [NASA-TM-100604] 14 p1873 N88-21188
Space station mobile transporter 14 p1927 N88-21488
Operational experience and design recommendations for teleoperated flight hardware 14 p1927 N88-21489
Design guidelines for robotically serviceable hardware [NASA-TM-100700] 19 p2606 N88-25472
Man versus machine: The role of astronauts in extravehicular activity 19 p2699 N88-26045
Temperature rise in superfluid helium pumps [NASA-TM-100997] 21 p2948 N88-27507
Ariane 5, HERMES and European vehicles for space station servicing [SNIAS-881-422-102] 23 p3183 N88-28943
Remote servicing of space systems 23 p3260 N88-29409
A teleoperated robotic manipulator system for materials processing experiment servicing 23 p3260 N88-29410
Centaur operations at the space station: Cost and transportation analysis [NASA-CR-182128] 24 p3332 N88-29835
Study of robotics spacecraft servicing and assembly in space. Volume 1: Executive summary [ESA-CR(P)-2612-VOL-1] 24 p3333 N88-29839
Technology requirements for an orbiting fuel depot: A necessary element of a space infrastructure [NASA-TM-101370] 24 p3334 N88-29845
Design and development of a refueling test bed [FTMS-RP-ER-011] 24 p3357 N88-29986

ORBITAL SIMULATORS
U SPACE SIMULATORS

ORBITAL TRANSFER
U TRANSFER ORBITS

ORBITAL VELOCITY
Universal procedures for conversion of orbital elements to and from position and velocity (unperturbed orbits) [RAE-TR-87043] 14 p1872 N88-21184

ORBITAL WORKERS
Implications of shiftwork in space for human physiology experiments 12 p1659 N88-19942

ORBITALS
NT ELECTRON ORBITALS
NT MOLECULAR ORBITALS
Symmetry and equivalence restrictions in electronic structure calculations [NASA-TM-89252] 11 p1557 N88-19320

ORBITS
NT CIRCULAR ORBITS
NT EARTH ORBITS
NT ECCENTRIC ORBITS
NT ELLIPTICAL ORBITS
NT GEOSYNCHRONOUS ORBITS
NT PLANETARY ORBITS
NT POLAR ORBITS
NT SATELLITE ORBITS
NT SOLAR ORBITS
NT SPACECRAFT ORBITS
NT STATIONARY ORBITS
NT STELLAR ORBITS
NT TRANSFER ORBITS
Local and global techniques for the tracking of periodic solutions of parameter-dependent functional differential equations [AD-A185756] 06 p0766 N88-14704
A quadratic-form analysis of the collisionless tearing mode [AD-A188886] 12 p1695 N88-20144
Periodic orbits around a satellite modelled as a triaxial ellipsoid [AD-A190592] 15 p2022 N88-22051
Distortion functions [DE88-752634] 21 p3015 N88-27896
A limiting viscosity approach to the Riemann problem for materials exhibiting change of phase [AD-A193477] 23 p3210 N88-29103
Monotone recurrence relations, their Birkhoff orbits and topological entropy [AD-A193481] 23 p3276 N88-29504

ORCHARDS
Preliminary study on the application of digital processing of TM-LANDSAT data in the mapping of apple orchards in Fraiburgo (SC) 17 p2367 N88-24093

ORDER-DISORDER TRANSFORMATIONS
Vibrational properties of disordered solids. Far infrared studies: Performance report [DE88-001474] 06 p0786 N88-14821
Dispersive hole transport in SiO2 [AD-A187077] 09 p1254 N88-17513
Positron-annihilation 2D-ACAR studies of disordered and defected alloys [DE88-003118] 10 p1416 N88-18454
Theoretical studies of the interface electronic properties of tetrahedrally coordinated semiconductors [AD-A187216] 11 p1555 N88-19306
Morphological studies of conductive polymers [AD-A188456] 12 p1610 N88-19629
Ordered polymers for space applications [AD-A188460] 12 p1610 N88-19630
Fast protonic conducting solid electrolytes [AD-A188524] 12 p1698 N88-20160
A calorimetric determination of the enthalpy of formation and a description of the defect structure of the ordered beta-phase /Ni, Cu/ /1-x/ Al/x/ [NASA-TT-20157] 13 p1745 N88-20434
Optical studies of dynamical processes in disordered system [DE88-005965] 13 p1837 N88-20993
Ordered structures in YBa2Cu3O/sub 7-y/, La2CuO/sub 7-y/, La/sub 2-x/Sr/sub x/CuO/sub 4-par. delta/ and related perovskites [DE88-006461] 14 p1987 N88-21851
Renormalized Fermi liquid theory for disordered electron systems and the metal-insulator transition [NOTA-INTERNA-900] 14 p1988 N88-21862
The theory of random alloys [DE88-006408] 18 p2487 N88-24756
Structure and refinement of ordered aromatic heterocyclic polymers by diffraction methods: Application of results to electro-optic phenomena [AD-A191859] 19 p2619 N88-25537
The structure and properties of grain boundaries in B2 ordered alloys [DE88-009890] 20 p2773 N88-26447
Ordering transitions of ternary alloys A(1-x)B(x)C 20 p2873 N88-27054
Defects and disorder in amorphous and damaged silicon [AD-A192277] 20 p2879 N88-27089

ORDNANCE
Compatibility of explosives: A data base system [PB87-234464] 06 p0687 N88-14208
Texture profile in thermomechanically processed 2-inch-thick 5 Ni-steel armor plate [AD-A189275] 13 p1741 N88-20410
Timing control system [NASA-CASE-NPO-16882-1-CU] 18 p2506 N88-24863

ORES
U MINERALS

ORGANIC CHARGE TRANSFER SALTS
Organic metal (ET)4Hg3Br8A quasi-two-dimensional superconductor 14 p1974 N88-21778

ORGANIC CHEMISTRY
Super hydrides [AD-A193710] 23 p3192 N88-28995

ORGANIC COMPOUNDS
NT ACETIC ACID
NT ACETYL COMPOUNDS
NT ACETYLENE
NT ACRYLIC ACID
NT ADENOSINE TRIPHOSPHATE
NT ADENOSINES
NT ALDOSTERONE
NT ALKANES
NT ALKENES
NT AMINO ACIDS
NT ANTHRACENE
NT ATROPINE
NT AZOLES
NT AZULENE
NT BENZENE
NT BUTADIENE
NT BUTANES
NT BUTENES
NT CAFFEINE
NT CARBAZOLES
NT CARBOHYDRATES
NT CARBONIC ANHYDRASE
NT CARBOXYLIC ACIDS
NT CAROTENE
NT CATALASE
NT CELLULOSE
NT CETANE
NT CHOLINESTERASE
NT CORTICOSTEROIDS
NT CUBANE
NT CYCLIC COMPOUNDS
NT CYCLIC HYDROCARBONS
NT CYCLOBUTANE
NT CYCLOHEXANE
NT CYTOCHROMES
NT DEOXYRIBONUCLEIC ACID
NT DICARBOXYLIC ACIDS
NT ENZYMES
NT ERGOTAMINE
NT ETHANE
NT ETHYLENE
NT FIBRINOGEN
NT FLUORINE ORGANIC COMPOUNDS
NT FLUOROCARBONS
NT FLUOROHYDROCARBONS
NT FLUOROPOLYMERS
NT FURANS
NT GLUCOSE
NT GLUTAMIC ACID
NT GLUTAMINE
NT GLUTATHIONE
NT GLYCOGENS
NT HEMOGLOBIN
NT HETEROCYCLIC COMPOUNDS
NT HMX
NT HYDROCARBONS
NT LIPIDS
NT LIQUEFIED NATURAL GAS
NT METHANE
NT METHYLENE
NT MORPHINE
NT NAPHTHALENE
NT NAPHTHENES
NT NATURAL GAS
NT NICOTINIC ACID
NT NUCLEIC ACIDS
NT NUCLEOSIDES
NT NUCLEOTIDES
NT ORGANIC CHARGE TRANSFER SALTS
NT ORGANIC LIQUIDS
NT ORGANIC LITHIUM COMPOUNDS
NT ORGANIC PHOSPHORUS COMPOUNDS
NT ORGANIC SILICON COMPOUNDS
NT OXYACETYLENE
NT PARAFFINS
NT PEPTIDES
NT PHOSPHAZENE
NT PHTHALOCYANIN
NT POLYBUTADIENE
NT POLYPEPTIDES
NT POLYTETRAFLUOROETHYLENE
NT POLYVINYL FLUORIDE
NT PROPANE
NT PROPYLENE
NT PROTEINS
NT PYRENES
NT PYRIDINES
NT PYRROLES
NT QUINOLINE
NT RDX
NT RIBONUCLEIC ACIDS
NT SEROTONIN
NT STARCHES
NT TEFLON (TRADEMARK)
NT THYMINE
NT TOLUENE
NT URACIL
NT VINYLIDENE
NT XANTHINES
Surface chemistry of transition metal carbides: A theoretical analysis [AD-A184237] 03 p0291 N88-11829
Specific organic compounds in excreta 07 p0895 N88-15422
The Coupled Cluster Single and Double excitation (CCSD) method in quantum chemistry: An efficient formulation of the theory and application to closed shell molecular systems [DE88-000475] 07 p0930 N88-15650
Estimation of aerial deposition and foliar uptake of xenobiotics: Assessment of current models [DE88-000993] 09 p1188 N88-17117
Supercritical fluid extraction-gas chromatography of Volatile Organic Compounds (VOC) from tenax devices [PB88-124300] 10 p1298 N88-17759
Evaluation and prediction of Henry's law constants and aqueous solubilities for solvents and hydrocarbon fuel components. Volume 1: Technical discussion [AD-A188571] 12 p1613 N88-19643

Electrosorptive detection of simple organic compounds in liquid chromatography
[AD-A188757] 13 p1736 N88-20376
Mechanisms of photoinduced electron transfer
[DE88-004917] 13 p1836 N88-20983
The thermodynamic properties of organic oxygen compounds
[DE88-001208] 13 p1849 N88-21065
Properties of superconductors with strong electron-phonon interaction 14 p1974 N88-21779
Direct determination of part-per-billion levels of volatile organics in water and soil samples using glow discharge mass spectrometry
[DE88-011389] 21 p2910 N88-27272
National ambient Volatile Organic Compounds (VOCs) data base update, documentation
[PB88-195631] 21 p2971 N88-27646
Electron impact ionization cross-section of some organic compounds
[DE88-702044] 23 p3280 N88-29525
Band electronic structures and crystal packing forces
[DE88-010247] 23 p3289 N88-29585

ORGANIC FLUORINE COMPOUNDS
U FLUORINE ORGANIC COMPOUNDS

ORGANIC LASERS
NT DYE LASERS

ORGANIC LIQUIDS
Detection of vapors of flammable liquids in air by atmospheric sampling mass spectrometry/mass spectrometry
[DE88-000030] 02 p0196 N88-11227

ORGANIC LITHIUM COMPOUNDS
Tetrahedral carbon and interstitial electrons in Li cluster: CLi4 and (LiCH3)4
[AD-A184277] 04 p0496 N88-13055

ORGANIC MATERIALS
Consortium for Materials Development in Space. Technical section
[NASA-CR-181508] 03 p0296 N88-11859
Highly Non-Linear Optical (NLO) organic crystals 03 p0297 N88-11865
Highly Non-Linear Optical (NLO) organic crystals and films. Electrooptical organic materials 03 p0297 N88-11866
Theory of atomic additivity in molecular hyperpolizabilities 03 p0297 N88-11867
Proton abstraction as a route to conductive polymers
[AD-A184019] 04 p0421 N88-12612
Cellular solidification in a monotectic system
[NASA-TM-100317] 07 p0829 N88-15027
Exobiology and life science 07 p0883 N88-15358
Effects of energy, distance and orientation on electron transfer rates studied by pulse radiolysis in organic media
[DE88-002906] 08 p1082 N88-16521
Trace analysis by MS/MS on a double focussing mass spectrometer
[AD-A187954] 10 p1334 N88-17973
North Carolina Biomolecular Engineering and Materials Applications Center (NC-BEMAC)
[AD-A190923] 16 p2237 N88-23364
The evolution of cometary activity 18 p2594 N88-25416
Corrosion control through a better understanding of the metallic substrate/organic coating/interface
[AD-A193981] 22 p3056 N88-28132
Hydrogen storage by molecular polyhydrides
[AD-A194207] 23 p3191 N88-28989
Transport of organic vapors in multiphase polymer system
[AD-A194097] 23 p3198 N88-29033
Evaluation of organic coating deterioration and substrate corrosion in seawater using electrochemical impedance measurements 24 p3355 N88-29976

ORGANIC NITRATES
NT PETN

ORGANIC PHOSPHORUS COMPOUNDS
NT PHOSPHAZENE
FTIR (Fourier Transform Infrared) and FTNMR (Fourier Transform Nuclear Magnetic Resonance) study of organophosphorus surface reactions
[AD-A188337] 12 p1609 N88-19625
Determination of the partition coefficients of organophosphorus compounds using high-performance liquid chromatography
[AD-A189276] 13 p1737 N88-20385

ORGANIC SEMICONDUCTORS
Pyrolyzed organic polymer nitrogen dioxide sensor 19 p2669 N88-25868

ORGANIC SILICON COMPOUNDS
Boron-containing organosilane polymers and ceramic materials thereof
[NASA-CASE-ARC-11649-1-SB] 23 p3199 N88-29040

ORGANIZATIONS
NT EUROPEAN SPACE AGENCY
NT NORTH ATLANTIC TREATY ORGANIZATION (NATO)
NT WORLD METEOROLOGICAL ORGANIZATION
Source header list. Volume 2: L through Z
[AD-A184001] 03 p0385 N88-12419
National Center for Atmospheric Research
[PB87-228391] 04 p0470 N88-12901
Source header list. Volume 1: A through K
[AD-A184000] 04 p0501 N88-13086
Organizations of intermediation in technology transfer: Its role in technological innovation
[INPE-4354-TDL/297] 08 p1094 N88-16581
Hydrogen Energy Coordinating Committee: Summary of DOE hydrogen programs for FY 1987
[DE88-003960] 10 p1306 N88-17811
Soviet high-technology restructuring drive: the MNTK network
[AD-A188138] 11 p1565 N88-19370
Conditions and mechanisms of the process of technological innovation in Brazil: The role of research institutes
[INPE-4175-TDL/274] 11 p1567 N88-19383
Task allocation for efficient performance of a decentralized organization
[AD-A188699] 12 p1705 N88-20204
Implementing information systems/office automation in an Air Force environment
[AD-A188956] 12 p1707 N88-20218
NASA and the challenge of ISDN: The role of satellites in an ISDN world
[NASA-CR-182749] 15 p2126 N88-22676
Analysis and synthesis of decision-making organizations
[AD-A191948] 19 p2738 N88-26258
Decision aiding and coordination in decision-making organizations
[AD-A191950] 19 p2738 N88-26259
Modeling and evaluation of expert systems in decisionmaking organizations
[AD-A191951] 19 p2739 N88-26260
Coordination in decision-making organizations
[AD-A191952] 19 p2739 N88-26261
Anatomy of an organizational change effort at the Lewis Research Center
[NASA-CR-4146] 19 p2739 N88-26264
Strategic, organizational and standardization aspects of integrated information systems, volume 6
[AD-A195855] 24 p3437 N88-30457
Technical change needs organizational change 24 p3438 N88-30466

ORGANOMETALLIC COMPOUNDS
NT CHLOROPHYLLS
NT FERROCENES
NT HEMOGLOBIN
NT ORGANIC LITHIUM COMPOUNDS
United States - Japan Workshop on Dielectric and Piezoelectric Ceramics (3rd) held in Toyama, Japan on November 9-12, 1986
[AD-A185113] 05 p0568 N88-13460
Effects of hydrolysis on metallo-organic solution deposition of PZT films
[ATR-86(8443)-1] 06 p0679 N88-14160
Heteroepitaxial growth of 3-5 semiconductor compounds by metal-organic chemical vapor deposition for device applications
[NASA-CR-182346] 06 p0788 N88-14832
Superlattice photodetectors
[AD-A186956] 09 p1253 N88-17511
Molecular beam epitaxy for research on quantum well structures
[AD-A186791] 09 p1255 N88-17522
Chemical activation of molecules by metals: Experimental studies of electron distributions and bonding
[DE88-004465] 10 p1407 N88-18393
Feasibility studies of the growth of 3-5 compounds of boron by MOCVD
[NASA-CR-181622] 11 p1561 N88-19343
Preparation and characterization of thin films of alumina by metalorganic chemical vapor deposition
[AD-A188366] 12 p1608 N88-19614
The spectroscopy and reaction kinetics of coordinatively unsaturated metal carbonyls
[AD-A190533] 15 p2035 N88-22124
Molecular orbital studies of the bonding in heavy element organometallics: Progress report
[DE88-007765] 19 p2723 N88-26168
Metal grid base heterojunction transistor operating at 60 and 94 GHz
[AD-A194763] 23 p3207 N88-29087

ORGANOMETALLIC POLYMERS
Soluble metal chelate polymers of coordination numbers six, seven and eight
[AD-A185094] 05 p0568 N88-13459
Silicon containing photoresists
[AD-A188666] 12 p1605 N88-19601
Ceramic materials from preceramic organometallic copolymers
[DE88-006087] 14 p1892 N88-21301

ORIFICES
Dilution jet mixing program, phase 3 02 p0185 N88-11153
Drop formation from an orifice in an electric field
[DE87-014405] 03 p0322 N88-12034
The acoustic source created by turbulent flow over orifices and louvers
[REPT-97674] 06 p0776 N88-14764
Describing the source created by turbulent flow over orifices and louvers
[AD-A190254] 15 p2130 N88-22706

ORIGINS
Statistical fine structure in the inhomogeneously broadened electronic origin of pentacene in p-terphenyl
[AD-A191211] 16 p2176 N88-22968

ORION AIRCRAFT
U P-3 AIRCRAFT

ORION NEBULA
The Einstein survey of the young stars in the Orion Nebula 04 p0518 N88-13182
The velocity structure and turbulence at the center of the Orion Nebula 04 p0521 N88-13201
Models of recombination lines in radio H2 regions
[INPE-4302-TDL/277] 12 p1710 N88-20232
First detection of HCN J = 9 to 8 (797 GHz) line emission: Very high densities in the Orion core
[MPE-PREPRINT-110] 22 p3165 N88-28847

ORIONID METEOROIDS
Results of observations of the Eta Aquarid and Orionid meteor showers in 1980-1984 06 p0740 N88-14548
The structure of the Halley meteor stream and the orbital history of the comet 14 p2008 N88-21975

ORNITHOPTER AIRCRAFT
U RESEARCH AIRCRAFT

OROGRAPHY
The air flow on hills from models and experiments
[BMFT-FB-T-86-175] 02 p0198 N88-11236
The 54-hours continuous post-frontal precipitation north of the Alpine mountain barrier, 22-25 August 1975 02 p0203 N88-11268
Longer-duration post-frontal precipitation at Vancouver International Airport, 1953-1983 02 p0203 N88-11269
Observational analysis of the interaction between fronts and the orography in Taiwan during the late winter monsoon season 02 p0203 N88-11270
Detailed analysis of a mesoscale convective complex situation in the Carpathian Basin (Europe) 02 p0207 N88-11296
Cumulus and thunderstorm initiation by mountains 02 p0207 N88-11301
A real-data numerical study and four-dimensional data assimilation application for mesobeta-scale flow in complex terrain 02 p0212 N88-11329
Research work at the Meteorological Institute of the University of Munich (Federal Republic of Germany)
[MITT-56] 08 p1013 N88-16141
Model calculations of the behavior of orographically influenced cold fronts 08 p1015 N88-16155
Spectral analysis of an orographically structured area in the forefield of mesoscale flow simulations 08 p1016 N88-16160
Orographically influenced cold fronts in a spectral approach 08 p1016 N88-16161
Statistics of two-dimensional structure elements of mountainous ranges (mosaic model) for calculating three-dimensional reflection functions
[DFVLR-FB-87-33] 09 p1185 N88-17099
Numerical simulation of thermally generated mountain-foreland circulation
[DFVLR-FB-87-30] 09 p1190 N88-17132
The retardation of cold fronts at high mesoscale mountains 09 p1241 N88-17437
Systematic errors of the FSU global spectral model 10 p1356 N88-18103
Cloud physics studies in SCPP (Sierra Cooperative Pilot Project) from 1977-87
[PB88-136924] 11 p1516 N88-19054
The German Front Experiment 1987: Experimental design
[DFVLR-MITT-87-24] 16 p2234 N88-23343

ORR-SOMMERFELD EQUATIONS
Solution of the Orr-Sommerfeld equation for the Blausius boundary-layer documentation of program ORRBL and a test case
[NASA-CR-4169] 20 p2841 N88-26858

ORRERIES
U ASTRONOMICAL MODELS

ORTHOGONAL FUNCTIONS
NT WALSH FUNCTION

Errors in retrieving hydrological fields and fields of their differential characteristics by method of approximation by orthogonal functions 06 p0727 N88-14475
Spectral iterative technique with Gram-Schmidt orthogonalization
[PB88-127451] 10 p1399 N88-18338
The inverse problem and the pseudo-empirical orthogonal function method of solution. Part 1: Theory; Part 2: Application
[AD-A188894] 12 p1684 N88-20069
Space-time analysis of oceanographic fields by modified empirical orthogonal functions method
13 p1786 N88-20687
Group theoretic interpretations of Askey's scheme of hypergeometric orthogonal polynomials
[CWI-PM-R8703] 13 p1831 N88-20954
Identification of nonlinear output-affine systems using an orthogonal least squares algorithm
[RR-313] 14 p1958 N88-21678
A Gram-Schmidt space-time adaptive canceller using adaptive lattice filters
[AD-A189684] 14 p1959 N88-21684
New stable, vectorisable Kalman filter algorithms based on orthogonal transformations
[DFVLR-FB-87-52] 16 p2258 N88-23494
Orthogonal polynomials with respect to a symmetric inner product involving derivates
[REPT-87-59] 16 p2259 N88-23504
Solving singular systems using orthogonal functions
[AD-A190881] 16 p2260 N88-23512
Minimal parameter solution of the orthogonal matrix differential equation
[NASA-TM-4043] 17 p2383 N88-24165
Optimal a priori covariance selection for the solution of ill-conditioned nonlinear inverse problems
18 p2564 N88-25222
On a biorthogonal system associated with uniform asymptotic expansions
[CWI-AM-R8709] 18 p2586 N88-25240
Numerical simulations of flow around shuttle orbiter
19 p2635 N88-25633
Nonlinear conformal transformations and Clifford algebras
[PB87-225942] 19 p2719 N88-26147
Coherent structures in the axisymmetric turbulent jet mixing layer 21 p2947 N88-27504
Complex EOF analysis of intraseasonal tropical wind fluctuations 22 p3121 N88-28544
Sub-Saharan rainfall anomalies and global sea-surface temperature relationships for the recent fifteen year (1970-1984) period 22 p3122 N88-28552
The predictability of low frequency patterns in the NMC MRF 22 p3127 N88-28587
Determination of most probable predicted 50 kPa pattern by empirical orthogonal functions
22 p3128 N88-28593
Determining the spatial structure of fields of precipitation from space radar images in two orthogonal polarizations
24 p3450 N88-30531

ORTHOGONALITY
A computational examination of orthogonal distance regression
[AD-A184374] 03 p0371 N88-12337
Eigenvectors of distance-regular graphs
[AD-A185375] 05 p0641 N88-13919
Separable orthogonal coordinates and particle creation for an accelerating observer
[DE87-703358] 05 p0657 N88-14029
An orthogonal oriented quadrature hexagonal image pyramid
[NASA-TM-100054] 06 p0755 N88-14630
Optimal repeated measurements designs for comparing test treatments with a control
[AD-A185999] 07 p0917 N88-15569
Mechanism of change of vortex structure orientation in type-2 superconductors 09 p1239 N88-17425
Orthogonal patterns in binary neural networks
[NASA-TM-100060] 10 p1396 N88-18320
The parameterization of orthogonal matrices: A review mainly for statisticians
[AD-A189144] 13 p1829 N88-20936
An orthogonal parameter estimation algorithm for nonlinear stochastic systems
[RR-307] 14 p1966 N88-21736
Solving singular systems using orthogonal functions
[AD-A190881] 16 p2260 N88-23512
Development of adaptive grid schemes based on Poisson grid generators
[AD-A190953] 16 p2262 N88-23526

ORTHONORMAL FUNCTIONS
Estimation of multivariate binary density using orthonormal functions
[AD-A186386] 07 p0912 N88-15528

ORTHOPHOTOGRAPHY
Automatic production of orthophoto using SPOT images 22 p3112 N88-28487
High resolution orthoimage quadrangle maps using SPOT satellite data 22 p3112 N88-28488

ORTHOSTATIC TOLERANCE
Daily dynamics of some physiological indicators of man under desert condition 06 p0750 N88-14605
Human metabolism and peripheral circulation during antiorthostatic hypokinesia 07 p0891 N88-15398
Biorhythmological analysis of dynamics of pulmonary ventilation parameters during orthostatic tests
07 p0891 N88-15400
Circulatory response of males 45-52 years of age to antiorthostatic hypokinesia 07 p0894 N88-15416
Comparative evaluation of orthostatic stability following immersion in horizontal and vertical positions
10 p1363 N88-18143
Effect of antiorthostatic position and different illumination on sensitivity of skin in upper half of the body to ultraviolet radiation 10 p1363 N88-18145
Effect of exogenous cardiosynchronized counterpulsation on human regional and central hemodynamics 10 p1366 N88-18163
Changes in the status of the human tibia during antiorthostatic hypokinesia
[NASA-TT-20221] 13 p1810 N88-20813
Propranolol and the compensatory circulatory responses to orthostasis at high altitude
[AD-A192675] 22 p3131 N88-28618

ORTHOTROPIC PLATES
Spatial strength variation and statistical size effect of laminated orthotropic composite materials
04 p0427 N88-12646
A generalized variational method for solving stress intensity factors at cracks on the edge of holes in orthotropic plates
[IC-AERO-87-02] 17 p2348 N88-23992
The surface crack problem in an orthotropic plate under bending and tension
[NASA-CR-178281] 18 p2531 N88-25014

ORTHOTROPIC SHELLS
Nonsteady-state vibrations in acoustic medium of elastic elliptical shell subjected to instantaneously applied uniform pressure 02 p0160 N88-11000

ORTHOTROPISM
Numerical solution methods for viscoelastic orthotropic materials
[NASA-CR-182381] 08 p0971 N88-15874
An analytical study of the effects of transverse shear deformation and anisotropy on natural vibration frequencies of laminated cylinders
[NASA-TM-100554] 10 p1295 N88-17739
A simplified orthotropic formulation of the viscoplasticity theory based on overstress 14 p1929 N88-21505

OSCILLATING CYLINDERS
Experimental comparison of lightning simulation techniques to CV-580 airborne lightning strike measurements
[AD-A190576] 15 p2098 N88-22496

OSCILLATING FLOW
The phenomenology of Karman vortex streets via sound in oscillatory flow
[MPIS-MITT-84-1987] 02 p0122 N88-10775
A supersonic potential gradient method for the calculation of unsteady aerodynamic pressures on harmonically oscillating wings
[ESA-TT-930] 03 p0259 N88-11631
Unsteady aerodynamics of an oscillating cascade in a compressible flow field
[NASA-TM-100219] 05 p0549 N88-13346
Microcomputer analysis of regenerative heat exchangers for oscillating flow
[DE88-001773] 10 p1329 N88-17945
Oscillating airfoils: Achievements and conjectures
[AD-A190490] 15 p2014 N88-22008
A survey of oscillating flow in Stirling engine heat exchangers
[NASA-CR-182108] 15 p2067 N88-22322
Description of an oscillating flow pressure drop test rig
[NASA-TM-100905] 16 p2170 N88-22933
Oscillating flow over bluff bodies in a U-shaped water tunnel 16 p2201 N88-23131
Tests on oscillating flows in a pipe nozzle with an abrupt diameter variation
[MPIS-2/1987] 17 p2337 N88-23947
Surface tension and viscosity with Lagrangian hydrodynamics on a triangular mesh
[AD-A194120] 22 p3075 N88-28258

OSCILLATION DAMPERS
Variation of wave action: Modulations of the phase shift for strongly nonlinear dispersive waves with weak dissipation. A new adiabatic invariant involving the modulated phase shift for strongly nonlinear, slowly varying, and weakly damped oscillators. The modulated phase shift for weakly dissipated nonlinear oscillatory waves of the Korteweg-de vries type
[AD-A185630] 06 p0765 N88-14702
Characterizing particle combustion in a Rijke burner
[AD-A186157] 08 p0966 N88-15847
Response of a sequential damper to shock inputs
08 p0998 N88-16042
Survey of impact damper performance
16 p2217 N88-23227
Experimental study of unsteady separating turbulent boundary layers
[AD-A192997] 21 p2943 N88-27477

OSCILLATIONS
NT AIRFOIL OSCILLATIONS
NT ELECTRON OSCILLATIONS
NT H WAVES
NT HARMONIC OSCILLATION
NT MOLECULAR OSCILLATIONS
NT NONOSCILLATORY ACTION
NT PLASMA OSCILLATIONS
NT PRESSURE OSCILLATIONS
NT SOLAR OSCILLATIONS
NT SOUTHERN OSCILLATION
NT STABLE OSCILLATIONS
NT STELLAR OSCILLATIONS
NT TRANSIENT OSCILLATIONS
NT WING OSCILLATIONS
On oscillation of a kind of integro-differential equation with delay
[DE87-703059] 02 p0225 N88-11417
Oscillatory and nonoscillatory properties of first order differential equations with piecewise constant deviating arguments
[DE87-703061] 02 p0225 N88-11418
Theory of interstitial solutions
[BLL-M-37314-(5828.4)] 02 p0233 N88-11469
Physical design of parameters of Nd:YAG disk laser
03 p0302 N88-11904
Excitation of natural oscillations of a boundary layer by an external acoustic field 04 p0425 N88-12634
Dynamics of reverse flows at pump inlet
04 p0425 N88-12636
Oscillation theory for linear second-order differential systems
[DE87-011393] 04 p0484 N88-12983
Boundary effects on the drag of an oscillating sphere: Applications to the magnetic sphere rheometer. Attenuation and dispersion of acoustic waves in nematic liquid crystals 04 p0488 N88-13007
The dynamics of solar magnetic flux tubes subjected to resonant foot point shaking 04 p0507 N88-13118
An experimental investigation of the aerodynamics of a NACA 64A010 airfoil-flap combination with and without flap oscillations. Part 1: Steady-state characteristics
[NASA-TM-88217] 05 p0542 N88-13305
Interpretation of our present terrestrial climatic record
[DE88-000223] 06 p0744 N88-14573
Dimensional analysis of nonlinear oscillations in brain, heart and muscle
[DE87-014749] 06 p0751 N88-14614
Observation of instabilities in time during dynamic self-diffraction of light in anisotropic nonhomogeneous medium 06 p0769 N88-14730
A possible accelerator experiment to solve the solar neutrino puzzle
[PREPRINT-556] 06 p0778 N88-14778
The TITAN oscillating-field current-drive system
[DE88-001823] 06 p0782 N88-14798
Solar Dynamics and G-modes
[NASA-CR-180737] 06 p0805 N88-14911
Sliding charge density waves and related problems
[AD-A186720] 09 p1157 N88-16934
The dynamics of an oscillating four-bar linkage
09 p1181 N88-17074
Lifting-surface theory of oscillating propellers in compressible flow
[NAL-TR-943] 10 p1273 N88-17613
Betatron oscillations in a free electron laser
[DE88-004859] 10 p1337 N88-17990
Modal testing the EOLE
[DE88-003795] 10 p1350 N88-18066
Modal testing of a very flexible 110 m wind turbine structure
[DE88-003796] 10 p1351 N88-18072
Statistical studies of low frequency oscillations in satellite-observed stratospheric temperatures
10 p1353 N88-18086
Probability bounds for M-Skorohod oscillations
[AD-A187981] 10 p1404 N88-18371
Conditions at infinity for theories of oscillating wings and propellers in subsonic flow
[NAL-TR-937] 11 p1434 N88-18556
Modeling of limit cycle stall flutter oscillations
12 p1583 N88-19472
Predicting oscillatory finite difference solutions to the heat equation: A comparative study of the coefficient and matrix methods
[AD-A189591] 13 p1825 N88-20911

Stochastic and chaotic oscillations
[CWI-AM-R8704] 13 p1829 N88-20940
Bloch oscillations in small Josephson junctions: Their manifestation in switching effects
14 p1969 N88-21756
Hydrodynamical regimes in molten metals under a horizontal temperature gradient
14 p1988 N88-21859
Oscillation damped movement of suspended objects
[DE88-005715] 15 p2086 N88-22433
Discussion of two-mode two-photon CW laser oscillation 16 p2187 N88-23042
Low frequency ocean ambient noise: Measurements and theory
[AD-A191188] 16 p2237 N88-23362
Efficient implementation of essentially non-oscillatory shock capturing schemes, 2
[NASA-CR-181656] 17 p2392 N88-24217
Development of a computerized analysis for solid propellant combustion instability with turbulence
[NASA-CR-182351] 19 p2611 N88-25497
Control of combustion instabilities in ramjet motors
19 p2625 N88-25574
One person's view of velocity-coupled instability
19 p2629 N88-25595
The importance of steady and dynamic inflow on the stability of rotor-body systems 21 p2890 N88-27156
Periodic oscillations in nonlinear mechanical systems
21 p2963 N88-27599
Investigation of oscillating cascade aerodynamics by an experimental influence coefficient technique
[NASA-TM-101313] 22 p3039 N88-28041
Nonlinear oscillations of an inviscid liquid column under zero-gravity
[LRT-WE-9-FB-8(1987)] 22 p3063 N88-28173
Nonlinear oscillations of axially independent liquid column under zero-gravity environment
[LRT-WE-9-FB-12(1987)] 22 p3063 N88-28174
Nonlinear oscillations in paraboloidal containers
[LRT-WE-9-FB-3(1988)] 22 p3078 N88-28275
Steady and unsteady transonic pressure measurements on a clipped delta wing for pitching and control-surface oscillations
[NASA-TP-2594] 23 p3173 N88-28895
Prediction of dynamic derivatives
24 p3318 N88-29761
Theories of comparative analysis
[AD-A196328] 24 p3427 N88-30395
Intermediate polars observed in Brazil in the last eight years
[INPE-4567-PRE/1308] 24 p3454 N88-30559

OSCILLATOR STRENGTHS
The 2D Rydberg series in Al I
[NASA-TM-101189] 22 p3150 N88-28740
On selection rules and inelastic electron scattering at intermediate energies
[DE88-701833] 23 p3280 N88-29526

OSCILLATORS
NT CRYSTAL OSCILLATORS
NT HARMONIC OSCILLATORS
NT MAGNETRONS
NT MECHANICAL OSCILLATORS
NT MICROWAVE OSCILLATORS
NT PENDULUMS
NT PIEZOELECTRIC CRYSTALS
NT SYNCHRONIZED OSCILLATORS
NT VOLTAGE CONTROLLED OSCILLATORS
Induction linac-driven free-electron lasers: Status and future prospects
[DE87-012914] 01 p0051 N88-10329
Diode pumped solid-state laser oscillators for spectroscopic applications
[NASA-CR-180576] 01 p0052 N88-10331
Sideband suppression by an intracavity optical filter in the Los Alamos free-electron laser oscillator
[DE87-011740] 02 p0177 N88-11103
Dynamics and routes to chaos from quasiperiodicity
03 p0312 N88-11974
The impact of varves on solar physics
[NASA-CR-181519] 03 p0390 N88-12448
Measurement and analysis of cryogenic sapphire dielectric resonators and DROs
04 p0433 N88-12686
The 8.4-GHz low-noise maser pump source assembly
04 p0436 N88-12705
An analytical and experimental study of injection-locked two-port oscillators
[NASA-TM-100119] 04 p0439 N88-12727
Spectral evolution equation for the sideband instability in a free-electron laser oscillator
[DE88-000510] 04 p0447 N88-12771
Development of symbolic computation methods for nonlinear dynamics
[AD-A185562] 06 p0758 N88-14653
Production-process CO2 laser with amplified pulse-repetition operation 06 p0771 N88-14739
Periodically pulsed excimer master oscillator-regenerative amplifier laser set
06 p0772 N88-14741
Fundamental cyclotron frequency generation from a cusptron oscillator
[AD-A188187] 10 p1321 N88-17898
Conceptual designs of a 50 NM FEL (Free-Electron Laser) oscillator and a 20-40 NM SASE (Self-Amplified Spontaneous Emission) amplifier
[DE88-003150] 10 p1334 N88-17974
Explicit approximations for strictly nonlinear oscillators with slowly varying parameters with applications to free electron lasers
[DE88-004116] 10 p1336 N88-17984
Tapered wiggler analysis of high gain free electron laser oscillators
[AD-A187997] 10 p1338 N88-17997
Research and development of surface skimming bulk wave devices for sensor applications
[AD-A187504] 11 p1470 N88-18766
Polarization effects in laser-pumped Nd:YAG lasers
[DE88-004019] 11 p1492 N88-18904
Quenched-laser operation of a Littman dye oscillator
[DE88-004020] 11 p1493 N88-18915
Solid-state travelling wave amplifiers based on multi-stream instability
[AD-A189566] 12 p1624 N88-19718
Time-dependent Slow-Time-Scale theory of free-running and phase-locked gyrotron oscillators
[AD-A188910] 12 p1629 N88-19752
Quartz oscillator analysis
[DE88-005886] 13 p1764 N88-20550
Direct solar-pumped iodine laser amplifier
[NASA-CR-182674] 13 p1777 N88-20630
Quantum statistics of parametric oscillators above threshold 14 p1979 N88-21811
Survey of impact damper performance
16 p2217 N88-23227
Periodic response of nonlinear systems
16 p2217 N88-23228
Integral equation for the laser field: Multimode description of a free-electron laser oscillator
[DE88-007050] 18 p2521 N88-24956
Microwave and millimeter-wave resonant tunneling diodes 19 p2659 N88-25809
Thin-membrane Lamb-mode acoustic oscillators for chemical detection 19 p2673 N88-25895
Focused ion beam fabrication of graded channel FETs in GaAs and Si
[AD-A193098] 21 p2936 N88-27439
Long-pulse, high-power vircator experiments
[DE88-011787] 21 p2940 N88-27458
The design of a digital Eprom oscillator for electrical impedance tomography
[DE88-012243] 21 p2940 N88-27462
Efficiency optimization for FEL oscillators
[AD-A192541] 21 p2952 N88-27536
An electronically tuned, stable 8415-MHz dielectric resonator FET oscillator for space applications
22 p3068 N88-28205
Liquid oscillations in a prolate spheroidal container
[LRT-WE-9-FB-4(1988)] 22 p3078 N88-28276
Distortions in processed signals and their application in electronic design. Part 2: A new variable signal generator
[DE88-702732] 23 p3205 N88-29071
An OKQPSK modem incorporating numerically controlled carrier synthesis
[DE88-009536] 23 p3244 N88-29304
Nonlinear dynamics of coupled oscillator arrays
[AD-A194888] 24 p3367 N88-30053
Research on a two-stage free electron laser oscillator
[AD-A195991] 24 p3377 N88-30115

OSCILLOSCOPES
Online monitoring of laserpulses using the GPIB-interface of a Tektronix 2430 Digital Storage Oscilloscope
[DE88-002836] 07 p0856 N88-15201
Comparison of sampling oscilloscopes with less than 35 ps transition durations 19 p2658 N88-25793

OSMIUM
Johnson noise thermometer for high radiation and high temperature environments
[DE88-003770] 10 p1323 N88-17911
Johnson noise thermometer for high-radiation and high-temperature environments
17 p2434 N88-24480

OSMIUM COMPOUNDS
Improved cathode life testing
[REPT-3189-T] 02 p0168 N88-11056

OSMOSIS
NT REVERSE OSMOSIS
Investigations of Paramecium cells analyzed under microgravity conditions 07 p0884 N88-15367
Use of hydrophilic polymer coatings for control of electroosmosis and protein adsorption
07 p0925 N88-15620

OSMOTIC PRESSURE
U OSMOSIS

OSTEOPOROSIS
Prevention of disuse osteoporosis: Effect of sodium fluoride during five weeks of bed rest
[NASA-CR-172018] 01 p0075 N88-10483
Disuse condition stimulates bone resorption in organ culture 12 p1656 N88-19926
Effect of different doses of alpha-hydroxydimethyl-gamma-aminopropylidene phonate on rat bones 19 p2704 N88-26078

OTF
U OPTICAL TRANSFER FUNCTION

OTOLITH ORGANS
Long-term adaptation of the otolith organs
07 p0886 N88-15375
Morphology and development of the inner ear of Anurans 07 p0886 N88-15378
Two-dimensional static otolith model
10 p1367 N88-18167

OTV
U ORBIT TRANSFER VEHICLES

OUTCROPS
A comparison between SPOT and LANDSAT TM for mapping of vegetation and bedrock outcrops
22 p3100 N88-28409

OUTGASSING
Outgassing data for selecting spacecraft materials
[NASA-RP-1124] 01 p0019 N88-10117
An investigation of the behavior of outgassed molecules in thermal vacuums 02 p0133 N88-10836
Mass spectroscopic facility 03 p0296 N88-11861
Gas coma of Comet Giacobini-Zinner: Emission from grains 14 p2000 N88-21923
Anisotropic emission from comets: Fans versus jets. 1: Concept and modeling 14 p2001 N88-21927
Comet P/Halley: Visual magnitude estimates and gas production 14 p2007 N88-21968
Neutral environment for space station
18 p2590 N88-25391
Space station neutral external environment
18 p2590 N88-25392
The evolution of cometary activity
18 p2594 N88-25416

OUTLETS
NT VENTS
Optimization of outlet channel of plasma ion source
[DE88-700471] 10 p1410 N88-18415

OUTLETS (GEOLOGY)
U ESTUARIES

OUTLIERS (STATISTICS)
Identification of multivariate outliers and leverage points by means of robust covariance matrices
[REPT-87-15] 01 p0088 N88-10575
PROGRESS: A program for robust regression analysis on the IBM PC
[REPT-85-14] 01 p0088 N88-10576
Robust statistical methods for automated outlier detection 04 p0433 N88-12681
Robust prediction operations for stationary processes
[AD-A185408] 05 p0641 N88-13924
Simulated performance of an order statistic threshold strategy for detection of narrowband signals
11 p1474 N88-18796
Outliner resistant filtering and smoothing: 2D version
[AD-A193319] 21 p3012 N88-27874

OUTPUT
NT LASER OUTPUTS
Output power enhancement of AC Raman free-electron laser
[DE88-000503] 04 p0449 N88-12786
Equivalence of input-output stability and exponential stability for infinite dimensional systems
[TW-276] 05 p0638 N88-13903
Outlier resistant predictive source encoding for a Gaussian stationary nominal source
[AD-A186725] 09 p1232 N88-17387
Research on output feedback control
[NASA-CR-182543] 11 p1534 N88-19167
Output formatting in Apple-soft BASIC
[DE88-701413] 15 p2108 N88-22559
Near optimal blind deconvolution
[REPT-87-016] 15 p2123 N88-22655
Electrochemical hydrogen concentrator for phosphoric acid fuel cells
[AD-A191355] 16 p2229 N88-23917
Simulation methodology
[AD-A192548] 21 p2995 N88-27764
Linearized model matching for single-input nonlinear systems
[AD-A193642] 23 p3266 N88-29445

OV-1 AIRCRAFT
Flaps-up takoff performance of the OV-1D aircraft with YT53-L-704 engine installed
[AD-A185960] 07 p0819 N88-14979
OVER-THE-HORIZON RADAR
The effect of equatorial ionospheric irregularities on the performance of a south-looking OTH-B (Over-The-Horizon-Backscatter) radar
[AD-A195090] 24 p3362 N88-30018
Modeling and performance of HF/OTH (High-Frequency/Over-the-Horizon) radar target identification systems
[AD-A196287] 24 p3365 N88-30038
OVERCAST
U CLOUD COVER
OVERPRESSURE
Modeling of the non-auditory response to blast overpressure
[AD-A187397] 10 p1369 N88-18184
OVERTONES
U HARMONICS
OVERVOLTAGE
The influence of current stressing on the structure of Ag contacts to GaAs
[DE88-005988] 15 p2140 N88-22771
OXALATES
Manufacturing of a barium titanate with high dielectric coefficient by decomposition of precipitates of double oxalates
[ISAL-IDI1-88-02] 21 p2911 N88-27278
OXIDATION
NT ELECTROCHEMICAL OXIDATION
NT PHOTOOXIDATION
NT RUSTING
Oxidation of TSX graphite over the temperature range 450 to 1200°C
[DE87-012230] 01 p0020 N88-10127
Si - SiO2 interfaces: A High Resolution Transmission Electron Microscopy (HRTEM) study
[DE87-012255] 01 p0028 N88-10181
The effect of sulfur and zirconium Co-doping on the oxidation of NiCrAl
[NASA-TM-100209] 02 p0150 N88-10940
Silicon oxidation photoassisted with a continuous wave CO2 laser beam and contribution to the study of silica layers obtained
[LAAS-87-158] 02 p0179 N88-11115
Thermal expansion mismatch and oxidation in thermal barrier coatings 02 p0189 N88-11182
Detailed mechanism of benzene oxidation
[NASA-TM-100202] 03 p0282 N88-11775
Detailed kinetic modeling of autoignition chemistry
[DE87-013226] 03 p0283 N88-11782
Quantitative electron probe microanalysis investigation of the oxidation of high temperature alloys at low oxygen partial pressures
[JUEL-2120] 03 p0288 N88-11811
The applicability of the catalytic wet-oxidation to CELSS 03 p0360 N88-12264
The effect of organic inhibitors on the atmospheric corrosion and solderability of copper
[DE88-000261] 04 p0414 N88-12585
Detailed mechanism of toluene oxidation and comparison with benzene
[NASA-TM-100261] 05 p0563 N88-13428
Occurance and growth of fatigue cracks in corrosion environment 05 p0604 N88-13704
High energy molecules of high symmetry
[AD-A185385] 05 p0647 N88-13965
Fatigue oxidation interaction in low cycle fatigue 06 p0719 N88-14420
Partial analysis of experiment LDEF A-0114
[NASA-CR-179236] 06 p0780 N88-14787
Investigation of fuel additive effects on sooting flames
[AD-A186403] 07 p0829 N88-15026
Sliding-wear properties of retained austenite in carburized layer
[PB87-149092] 07 p0833 N88-15054
Atomic oxygen effects on metals 07 p0924 N88-15617
Low temperature reactivity of chars towards oxygen, appendix E2
[DE88-004088] 10 p1298 N88-17760
The influence of the heating procedure on the oxidation behaviour of NiAl studied by XPS
[AERE-R-12498] 10 p1300 N88-17776
Lipid peroxidation in rat tissues with exposure to antiorthostatic hypokinesia, exercise and immobilization stress 10 p1365 N88-18159
Oxidative enzyme activity in healthy subjects and individuals with neurocirculatory dystonia during graded exercise 10 p1367 N88-18170
Optical measurements of surface oxide layer formation on metal films
[DE88-003163] 10 p1409 N88-18405
Formation of optical waveguides by ion implantation
[DE88-003894] 10 p1409 N88-18407
Effects of X irradiation and high field electron injection on the electrical properties of rapid thermal oxides
[DE88-002642] 10 p1417 N88-18461
A viscoelastic BEM (Boundary Element Method) for modeling oxidation
[AD-A187490] 11 p1452 N88-18653
Fuels combustion research
[AD-A187688] 11 p1453 N88-18657
Cost 501 Project U.K.10. Part 4: The oxidation of fecralloy steel co-extruded onto strong steel substrates
[AERE-R-12432-PT-4] 11 p1456 N88-18679
High temperature oxidation studies on alloys containing dispersed phase particles and clarification of the mechanism of growth of SiO2
[AD-A188158] 11 p1457 N88-18688
Studies of the electron spectrum with reference to the clean surfaces of iron, cobalt and nickel and their subsequent exposure to oxygen 11 p1459 N88-18700
Oxidation and protection of fiberglass-epoxy composite masts for photovoltaic arrays in the low Earth orbital environment
[NASA-TM-100839] 11 p1465 N88-18734
Dynamics of production and oxidation of boranes
[AD-A188988] 12 p1606 N88-19605
Thermal oxide growth on silicon: Intrinsic stress and silicon cleaning effects
[AD-A188790] 13 p1736 N88-20377
Novel catalysts for methane activation
[DE88-003637] 13 p1738 N88-20390
High-temperature thermosets derived from the Diels-Alder polymerization of bisbenzocyclobutenes and bimaleimides
[AD-A188800] 13 p1747 N88-20449
Oxidation/sulfidation of materials in an SO3/SO2/O2 thermochemical-transport, distributed-receiver, solar-energy system
[DE88-005875] 13 p1795 N88-20739
Oxide-bound transition metal complexes for methane activation
[PB88-169719] 14 p1887 N88-21277
Copper peroxide
[NASA-TT-20245] 14 p1888 N88-21282
Corrosion Research Center, University of Minnesota
[DE88-006681] 15 p2041 N88-22160
High temperature corrosion of ceramics
[DE88-006567] 15 p2046 N88-22193
Evaluation of direct methane conversion to higher hydrocarbons and oxygenates
[DE88-003812] 15 p2049 N88-22204
The analysis of fatigue crack growth mechanism and oxidation and fatigue life at elevated temperatures
[NASA-CR-182129] 16 p2179 N88-22987
Development of a laboratory test for multiport fuel injector deposits - evaluation of the Jet Fuel Thermal Oxidation Test apparatus (JFTOT)
[AD-A191313] 16 p2183 N88-23015
Enhanced emittance of oxidized 304 stainless steel 17 p2423 N88-24408
Surface composition-reactivity relationships in heterogeneous catalysis
[DE88-006679] 18 p2480 N88-24714
Calculation of oxidation rates for iron in CO-CO2
[DE88-007313] 18 p2487 N88-24757
Effect of carbohydrate oxidation on the tropospheric HOx-system 18 p2539 N88-25067
Kinetics of CO oxidation over a deactivated Rh(111) single crystal catalyst
[DE88-003000] 19 p2613 N88-25504
Oxidation behavior and microstructural studies of melt-spun glassy Fe-Al-Zr metal
[DE88-009964] 19 p2617 N88-25526
Liquid-phase oxidation of acetone with hydrogen peroxide on oxide catalysts 19 p2706 N88-26091
The adherence of nickel oxide on nickel during high temperature oxidation
[DE88-011194] 20 p2774 N88-26450
Research in energetic compounds
[AD-A192953] 20 p2781 N88-26494
Oxidation-erosion of metals and alloys: Models, verification, and prediction
[DE88-010016] 21 p2915 N88-27300
Kinetic of oxidation to air of a Fe-Al-Mn alloy system at 600-800(sup 0)C temperature range
[DE88-702309] 21 p2920 N88-27330
Methods of quantifying and enhancing reactive oxygen species production 21 p2924 N88-27357
Silicon oxidation studies: A review of recent studies on thin film silicon dioxide formation in the physics and chemistry of SiO2 and the Si-SiO2 interface
[AD-A193176] 21 p3021 N88-27932
Study of the erosion corrosion of alloys and coatings
[AD-A194337] 22 p3055 N88-28128
Development of a test method to determine potential peroxide content in turbine fuels. Part 2
[AD-A192244] 23 p3199 N88-29042
Preparation and testing of Nb-Zr and Nb-ZrO2 single crystals for deformation studies
[DE88-702798] 23 p3293 N88-29613
Modelling of CO oxidation in dilution jet flows 24 p3351 N88-29947
OXIDATION RESISTANCE
Research and development on high strength ceramic heaters discussed 04 p0404 N88-12508
Improved perfluoroalkylether fluid development
[NASA-CR-180872] 08 p0967 N88-15851
Oxidation resistance of CVD coatings
[AD-A178337] 09 p1147 N88-16875
Correlations of norbornenyl crosslinked polyimide resin structures with resin thermo-oxidative stability, resin glass transition temperature and composite initial mechanical properties
[NASA-TM-100791] 09 p1147 N88-16877
Reaction mechanism of sulfur dioxide with single crystal cobalt and chromium and CoCrAlY coatings
[AD-A185989] 09 p1253 N88-17509
Beneficial and detrimental effects of silica in the high temperature oxidation of 20Cr/25Ni/Nb stainless steel
[AERE-R-12667] 10 p1301 N88-17779
Study of adherent oxide scales
[AD-A187368] 11 p1456 N88-18680
High temperature oxidation studies on alloys containing dispersed phase particles and clarification of the mechanism of growth of SiO2
[AD-A188158] 11 p1457 N88-18688
Nondestructive evaluation of carbon-carbon coatings
[AD-A189524] 13 p1748 N88-20453
Effect of oxidation on strength and thermal stability of material based on Si3N4 14 p1896 N88-21319
Secondary electron emission characteristics improved by ion implantation 14 p1903 N88-21370
Strength and failure rate of composite materials with carbon in ceramic matrix 16 p2180 N88-22995
Recent advances in metallic/ceramic coatings for corrosion control in military applications 17 p2320 N88-23858
Design and demonstration of a system for the deposition of atomic-oxygen durable coatings for reflective solar dynamic power system concentrators
[NASA-CR-4158] 19 p2606 N88-25474
A thermally modified polymer matrix composite material with structural integrity to 371 C
[NASA-TM-100922] 19 p2609 N88-25483
Studies in support of oxidation-resistant composite materials
[AD-A193320] 21 p2905 N88-27238
Processing technology research in composites
[AD-A195693] 24 p3341 N88-29890
OXIDATION-REDUCTION REACTIONS
Electronic and ionic transport in polymers
[AD-A187253] 11 p1452 N88-18651
Dynamics of production and oxidation of boranes
[AD-A188988] 12 p1606 N88-19605
The redox chemistry of some peroxo and superoxo metal ion complexes
[AD-A189159] 12 p1606 N88-19606
Advanced B and Al combustion kinetics over wide temperature ranges
[AD-A190752] 15 p2036 N88-22128
Electronic and ionic transport in polymers
[AD-A190434] 15 p2045 N88-22185
Oxidation and reduction rates for organic carbon in the Amazon mainstream tributary and floodplain, inferred from distributions of dissolved gases
[NASA-CR-182943] 18 p2538 N88-25062
Photochemical and thermal modeling in the early atmosphere of the earth
[NASA-CR-183029] 18 p2543 N88-25093
Carbon analysis in natural olivine crystals of deep origin
[NASA-TT-20311] 19 p2734 N88-26239
Oxygen reduction in fuel cell electrolytes
[DE88-008240] 20 p2819 N88-26723
Defect characterization of the redox behavior and stability of conducting oxides
[DE88-010799] 20 p2878 N88-27088
High power storage system based on thin film solid ionics
[AD-A193623] 23 p3291 N88-29598
Electrocatalytic reduction of oxygen on modified oxide surfaces
[NASA-TM-101333] 24 p3352 N88-29952
OXIDE FILMS
Use of sol-gels in the application of ceramic oxide thin films
[DE87-013610] 01 p0026 N88-10176
Progress toward a superconducting opening switch
[DE87-014170] 02 p0167 N88-11051

The effects of thin anodic films on the cyclic microstrain/macrostrain behavior of tungsten
05 p0597 N88-13650
On 1064 nm and 350 nm laser damage thresholds of high index oxide films deposited from organic solutions and sols
[DE88-001636] 07 p0859 N88-15217
Fabrication and packaging of discontinuous MIM (Metal-Insulator-Metal) film arrays for efficient MM wave and IR detection and mixing
[AD-A186809] 09 p1146 N88-16869
New scientific findings on the morphology of aluminum oxide layers, serving as an adhesive basis
[MBB-Z-137/86] 10 p1312 N88-17840
Effect of the gate oxide thickness on the speed of MOS integrated circuits
[PB88-155783] 10 p1323 N88-17910
Optical measurements of surface oxide layer formation on metal films
[DE88-003163] 10 p1409 N88-18405
Effects of X irradiation and high field electron injection on the electrical properties of rapid thermal oxides
[DE88-002642] 10 p1417 N88-18461
Freestanding films of YBa2Cu3O/sub 6.9/
[DE88-003995] 10 p1419 N88-18471
SiO2 film stress distribution during thermal oxidation of Si
[AD-A189552] 12 p1612 N88-19637
Thermal oxide growth on silicon: Intrinsic stress and silicon cleaning effects
[AD-A188790] 13 p1736 N88-20377
Superconducting electronic film structures
[AD-A192907] 20 p2879 N88-27091
Low temperature film growth of the oxides of zinc, aluminum and vanadium (and related systems, oxides of gold and germanium, nitrides of aluminum and tungsten) by reactive sputter deposition
[AD-A193497] 23 p3191 N88-28986

OXIDES
NT ALKALINE EARTH OXIDES
NT ALUMINUM OXIDES
NT ANHYDRIDES
NT BARIUM OXIDES
NT BERYLLIUM OXIDES
NT BISMUTH OXIDES
NT BORON OXIDES
NT CALCIUM OXIDES
NT CARBON DIOXIDE
NT CARBON MONOXIDE
NT CERIUM OXIDES
NT CHROMIUM OXIDES
NT COBALT OXIDES
NT COPPER OXIDES
NT DIOXIDES
NT HAFNIUM OXIDES
NT HEMATITE
NT HYDROGEN PEROXIDE
NT IRON OXIDES
NT LANTHANUM OXIDES
NT LEAD OXIDES
NT LITHIUM OXIDES
NT MAGNESIUM OXIDES
NT MANGANESE OXIDES
NT METAL OXIDES
NT MOLYBDENUM OXIDES
NT NICKEL OXIDES
NT NIOBIUM OXIDES
NT NITROGEN DIOXIDE
NT NITROGEN OXIDES
NT NITROUS OXIDES
NT PEROXIDES
NT QUARTZ
NT RUTILE
NT SAPPHIRE
NT SILICON DIOXIDE
NT SILICON OXIDES
NT SULFUR DIOXIDES
NT TANTALUM OXIDES
NT TIN OXIDES
NT TITANIUM OXIDES
NT VANADIUM OXIDES
NT YTTRIUM OXIDES
NT ZINC OXIDES
NT ZIRCONIUM OXIDES

Preparation of oxide glasses from metal alkoxides by sol-gel method
[NASA-TT-20124] 02 p0154 N88-10965
The wear process during the RUNNING-IN of steel in lubricated sliding
[NAL-TR-922T] 02 p0181 N88-11130
Theory of the one- and two-dimensional electron gas
[DE87-012864] 02 p0244 N88-11540
High temperature low cycle fatigue of oxide dispersion strengthened and single crystal nickel base superalloys
06 p0720 N88-14422
High temperature low cycle fatigue behavior and creep-fatigue interation of MA 6000 ODS alloy
06 p0720 N88-14425
Non-phonon mechanisms of superconductivity in high T/sub c/ superconducting oxides and other materials and their manifestation
[DE88-002708] 07 p0939 N88-15709
Properties of lanthanide oxides as supports for transition metal catalysts
[DE88-004520] 11 p1456 N88-18678
High temperature oxidation studies on alloys containing dispersed phase particles and clarification of the mechanism of growth of SiO2
[AD-A188158] 11 p1457 N88-18688
An investigation of metal complexes of some 2-substituted and 2,6-disubstituted pyridine N-oxides
11 p1460 N88-18701
An electron spectroscopic investigation of high-temperature superconducting oxides
[DE88-003807] 11 p1558 N88-19325
An overview of recent developments in high-temperature superconductivity
[DE88-005477] 12 p1697 N88-20155
Discussion of radiation effects and high-temperature oxide superconductors
[DE88-001427] 13 p1846 N88-21046
Thermal conductivity of oxide ceramics
[DE88-005842] 15 p2042 N88-22169
Effects of 67.5 MeV electron irradiation on Y-Ba-Cu-O and Gd-Ba-Cu-O high-temperature superconductors
[AD-A191271] 16 p2283 N88-23669
Thermal and power availability transient responses for the Argonne monolithic solid oxide fuel cell
17 p2419 N88-24384
Development of protective coatings for ceramic tubular components
[PB88-197165] 20 p2776 N88-26463
Preparation of oxide superconductors
[DE88-009136] 20 p2875 N88-27063
Phenomenological approach to high T/sub c/ oxide superconductors
[DE88-701868] 20 p2876 N88-27074
Preparation and properties of new inorganic glasses and gel-derived solids
[AD-A192922] 21 p2917 N88-27315
Monolithic fuel cells
[DE88-012004] 21 p2969 N88-27638
Development of planar geometry solid oxide fuel cell technology, phase 1
[PB88-210356] 23 p3229 N88-29215

OXIDIZERS
NT LIQUID OXIDIZERS
NT LIQUID OXYGEN
NT ROCKET OXIDIZERS

Physiological and biochemical aspects of toxic effects of oxidants in man's environment (air, water)
07 p0890 N88-15391
A continuous oxidizer regression model for the combustion of composite solid propellants
[AD-A186742] 08 p0974 N88-15894
Thermal oxide growth on silicon: Intrinsic stress and silicon cleaning effects
[AD-A188790] 13 p1736 N88-20377
Basic research in supersonic combustion
19 p2634 N88-25623
Oxidizer heat exchanger component test
[NASA-CR-182159] 24 p3339 N88-29876

OXYACETYLENE
Blast waves generated by planar detonations
[DE88-002219] 09 p1164 N88-16979

OXYALKYLATION
U ALKYLATION

OXYGEN
NT LIQUID OXYGEN
NT OXYGEN ISOTOPES

Mechanisms of polymer degradation using an oxygen plasma generator
[NASA-TM-100681] 01 p0018 N88-10110
High intensity 5 eV O-atom exposure facility for material degradation studies 02 p0135 N88-10847
Spacecraft surface exposure to atomic oxygen in low Earth orbit 03 p0273 N88-11715
Scotopic sensitivity with 10 percent oxygen
[AD-A183973] 03 p0356 N88-12243
Inerting and atmospheres 04 p0406 N88-12524
Fire-related medical science 04 p0406 N88-12525
Ignition and combustion of metals in oxygen
04 p0407 N88-12530
High efficiency generation of 130-nm radiation from sum-frequency mixing in Hg
[DE87-013714] 04 p0431 N88-12674
Oxygen enriched combustion system performance study
[DE88-001500] 05 p0562 N88-13424
Anti-Stokes generation of 226 nm light
[DE88-001612] 05 p0589 N88-13590
Controlled ecological life support systems: Development of a plant growth module 05 p0630 N88-13854
Progress in the measurement of salinity and oxygen at the Woods Hole Oceanographic Institution
[PB88-108089] 06 p0748 N88-14598
High temperature stability of superconducting YBa2Cu3O subx as characterized by X-ray diffraction
[DE88-001856] 06 p0787 N88-14824
L2,3 XANES of the high T sub c superconductor YBa2Cu3O7 with variable oxygen content
[NOTA-INTERNA-888] 06 p0788 N88-14837
The carbon dioxide chaperon efficiency for the reaction H + O2 + M yields HO2 + M from ignition delay times behind reflected shock waves
[NASA-TM-100125] 07 p0830 N88-15036
Atomic oxygen effects on metals
07 p0924 N88-15617
Coulomb interactions and effective strong coupling Hamiltonians in Cu-O superconductors
[DE88-002942] 08 p1090 N88-16561
Oxygen diffusion in high T/sub c/-superconductors
[DE88-002965] 08 p1090 N88-16562
Determination of the melting and decomposition points of different materials in an oxygen stream
[INFORME-I-158/86] 09 p1142 N88-16844
The photons payload, G-494: A learning experience
10 p1288 N88-17701
Development and application of oxygen flow tagging for velocity measurements and flow visualization in turbulent three-dimensional supersonic flows
[AD-A187982] 10 p1289 N88-17714
Materials development for JPL oxygen plant
[DE88-003067] 10 p1297 N88-17752
Low temperature reactivity of chars towards oxygen, appendix E2
[DE88-004088] 10 p1298 N88-17760
Theoretical and observational problems with Holes in the far UV dayglow
[AD-A188190] 10 p1355 N88-18100
Effect of oxygen inhalation on respiratory function during exercise and exposure to added resistance to respiration
10 p1366 N88-18164
Study of the vibrational modes of subsurface oxygen on Al (111) using diode laser infrared reflection-absorption spectroscopy
[AD-A188322] 12 p1632 N88-19769
Closed system physiology: Role of oxygen in the development of wheat 12 p1655 N88-19916
Nitrogen's biological effect on oxygen transport through hematoparenchymal barrier 12 p1662 N88-19967
Resonance energy transfer between carbon monoxide and oxygen molecules using dye laser intracavity absorption spectroscopy
[AD-A188488] 12 p1689 N88-20104
Optimization of oxygen cutting process for titanium alloys 14 p1897 N88-21323
Solar generation and storage of O2 (a 1 delta g)
[NASA-CR-4127] 14 p1913 N88-21431
Spatial distribution of O(supra 1D) from Comet Halley
14 p1999 N88-21913
Total photoionization cross sections of atomic oxygen from threshold to 44.3A
[NASA-CR-182992] 17 p2397 N88-24252
The role of oxygen on the mechanical behavior of molybdenum alloys 17 p2401 N88-24278
Catalytic ignition of hydrogen and oxygen propellants
[NASA-TM-100957] 18 p2476 N88-24689
Effect of hydrogen, deuterium and oxygen on the anelastic properties of refractory alloys
[DE88-007349] 18 p2484 N88-24736
Design and demonstration of a system for the deposition of atomic-oxygen durable coatings for reflective solar dynamic power system concentrators
[NASA-CR-4158] 19 p2606 N88-25474
Paramagnetic spins in oxygen-loaded ceramic La2CuO4/sub 4+delta/
[DE88-007114] 19 p2619 N88-25539
Theory of oxygen content, atomic ordering and oxygen diffusion in 1,2,3 superconducting oxides as a function of temperature and oxygen pressure
[DE88-007961] 19 p2735 N88-26248
In situ spectroscopic studies of transition metal macrocycles as catalysts for the electrochemical reduction of oxygen
[PB88-203195] 20 p2769 N88-26416
Electrocatalysts for oxygen electrodes
[DE88-008397] 20 p2819 N88-26724
The superconducting transition in oxygen deficient YBa2Cu3O(sub 7-Delta)
[DE88-009957] 20 p2877 N88-27079
Oxygen vacancy ordering and superconductivity in YBa2Cu3O(sub 7-x)
[DE88-010005] 20 p2877 N88-27083
Carbon deposition model for oxygen-hydrocarbon combustion, volume 1
[NASA-CR-179375] 21 p2908 N88-27254

Mechanism of the nitric oxide-carbon monoxide-oxygen reaction over a single crystal rhodium catalyst
[DE88-006274] 21 p2910 N88-27268

Breakdown of molecular oxygen by brief pulses of laser radiation
[DE88-702687] 23 p3220 N88-29168

Aeronomic problems of the molecular oxygen photodissociation. Part 3: Solar spectral irradiances in the region of the O2 Herzberg continuum, Schumann-Runge bands and continuum
[AERONOMICA-ACTA-A-332-1988] 24 p3343 N88-29897

Aeronomic problems of molecular oxygen photodissociation. Part 2: Theoretical absorption cross sections of the Schumann-Runge bands at 79 K
[AERONOMICA-ACTA-A-331-1988] 24 p3344 N88-29907

Aeronomic problems of molecular oxygen photodissociation. Part 4: The various parameters for the Herzberg continuum
[AERONOMICA-ACTA-A-333-1988] 24 p3352 N88-29955

OXYGEN ANALYZERS

The study of excited oxygen molecule gas species production and quenching on thermal protection system materials
[NASA-CR-172027] 02 p0233 N88-11470

A simplified CARS measurement system for rapid determination of temperature and oxygen concentration
[NASA-TM-100496] 03 p0374 N88-12353

Ultrasonic oxygen sensor
[AD-A189723] 15 p2105 N88-22537

Steady state and transient behavior of the Pd-SnO(sub x) MIS oxygen sensors 19 p2672 N88-25890

OXYGEN ATOMS

Degradation mechanisms of materials for large space systems in low Earth orbit
[NASA-CR-181472] 02 p0143 N88-10896

Partial analysis of experiment LDEF A-0114
[NASA-CR-179236] 06 p0780 N88-14787

Mast material test program (MAMATEP)
[NASA-TM-100821] 12 p1604 N88-19592

Measurement of rate constants of elementary gas reactions of importance to upper atmosphere and combustion systems
[AD-A189432] 13 p1737 N88-20386

Laboratory experiments of relevance to the space station environment 18 p2592 N88-25402

OXYGEN BREATHING

Scotopic sensitivity with 10 percent oxygen
[AD-A183973] 03 p0358 N88-12243

Man rating the b-1B molecular sieve oxygen generation system
[AD-A186275] 07 p0899 N88-15447

Experimental study of protective effect of antioxidant enzymes-superoxide dismutase and catalase-when using intermittent toxic modes of hyperbaric oxygenation 19 p2707 N88-26094

Human performance and acute hypoxia, chapter 12
[AD-A192604] 23 p3238 N88-29270

OXYGEN CONSUMPTION

Detection of hyperventilation of parachutists
[DFVLR-FB-87-11] 01 p0075 N88-10482

A device and methodology for measuring repetitive lifting VO2max (oxygen consumption rate)
[AD-A185195] 05 p0630 N88-13850

Oxygen transport during exercise at extreme simulated altitude: Operation Everest 2
[AD-A185720] 06 p0752 N88-14620

Maximal cardiorespiratory responses to one- and two-legged cycling during acute and long-term exposure to 4300m
[AD-A185730] 06 p0752 N88-14621

Role of hemoglobin affinity for oxygen in efficiency of blood respiratory function 07 p0892 N88-15406

Respiratory and cardiovascular responses to cold stress following repeated cold water immersion
[AD-A186460] 08 p1050 N88-16340

Increase in influence of oxygen on the body in the presence of helium 13 p1810 N88-20816

Hypothalamic-pituitary-adrenal responses to short duration high intensity cycle exercise
[AD-A192597] 21 p2985 N88-27727

Human acclimatization and physical performance at high altitude
[AD-A192651] 22 p3130 N88-28611

Alterations in upper extremity motor function in soldiers during acute high altitude exposure
[AD-A192676] 23 p3238 N88-29272

Effect of hypoxia on speech recognition in noise
[AD-A193943] 23 p3240 N88-29280

OXYGEN DEFICIENCY

U HYPOXIA

OXYGEN DETECTORS

U OXYGEN ANALYZERS

OXYGEN IONS

The tail lobe ion spectrometer: Theory and observations
[IFSI-86-12] 05 p0585 N88-13569

Total and partial cross sections for electron capture for C(q+) (q=6-2) and O(q+) (q=8-2) ions in collisions with H, H2 and He atoms
[IPPJ-AM-56] 09 p1252 N88-17501

Determination of the content of CO(+) and H2O(+) ions in the tail of Comet Giacobini-Zinner and Comet Halley 14 p2006 N88-21964

Polymeric electrolytes
[AD-A193766] 23 p3198 N88-29031

La2CuO(sub 4 + delta): A superconducting superoxide
[DE88-010325] 23 p3288 N88-29578

OXYGEN ISOTOPES

Relativisitic heavy ion collisions
[DE87-014292] 02 p0232 N88-11462

The atomic weight and isotopic composition of oxygen and their variation in nature
[DE87-014397] 04 p0413 N88-12558

Preparation and characterization of isotopic oxygen-enriched yttrium barium copper oxide
[DE88-010939] 22 p3154 N88-28766

OXYGEN MASKS

Miniature respiratory sensor
[AD-A193430] 23 p3243 N88-29300

OXYGEN METABOLISM

Operation Everest 2: Comparison of four instruments for measuring blood oxygen saturation
[AD-A186456] 08 p1049 N88-16337

Nitrogen's biological effect on oxygen transport through hematoparenchymal barrier 12 p1662 N88-19967

Increase in influence of oxygen on the body in the presence of helium 13 p1810 N88-20816

OXYGEN PLASMA

Photochemical ignition studies. 3: Ignition by efficient and resonant multiphoton photochemical formation of microplasmas
[AD-A184644] 03 p0283 N88-11780

Silicon containing photoresists
[AD-A188666] 12 p1605 N88-19601

Advanced diagnostics for reacting flows
[AD-A190485] 15 p2035 N88-22122

OXYGEN PRODUCTION

A review of recent activities in the NASA CELSS program 03 p0359 N88-12259

Man rating the b-1B molecular sieve oxygen generation system
[AD-A186275] 07 p0899 N88-15447

Photosynthetic water splitting
[DE88-007809] 20 p2830 N88-26791

Advancements in oxygen generation and humidity control by water vapor electrolysis
[NASA-CR-172073] 22 p3134 N88-28633

OXYGEN RECOMBINATION

The study of excited oxygen molecule gas species production and quenching on thermal protection system materials
[NASA-CR-172027] 02 p0233 N88-11470

Molecular sources of ionospheric holes
[AD-A191857] 18 p2541 N88-25082

OXYGEN SPECTRA

On the forbidden red lines of oxygen in comets 14 p2006 N88-21963

Rotational structure and absorption cross sections from 300 to 190 K of the Schumann-Runge bands
[AERONOMICA-ACTA-A-318-1987] 15 p2036 N88-22131

Structural studies on La/sub 2/CuO/sub 4+delta/
[DE88-006826] 18 p2581 N88-25330

OXYGEN SUPPLY EQUIPMENT

NT OXYGEN MASKS

OXYGEN TENSION

Quantitative electron probe microanalysis investigation of the oxidation of high temperature alloys at low oxygen partial pressures
[JUEL-2120] 03 p0288 N88-11811

Respiration and oxygen tension in the blood of animals exposed to high pressures 20 p2830 N88-26790

OXYGEN TOXICITY

U HYPEROXIA

OXYGENATION

Acid-base equilibrium and some rat blood parameters following exposure to hyperbaric oxygenation 07 p0894 N88-15420

OXYNITRIDES

Aluminum oxynitride spinel (ALON): A review
[AD-A184753] 03 p0294 N88-11845

Phosphorus oxynitride glass for laser applications
[DE88-005413] 12 p1632 N88-19768

Fracture toughness of silicon nitride-silicon nitride joints bonded with oxynitride glass
[DE88-005548] 15 p2043 N88-22172

OZONE

Diagnostics of atmospheric chemistry through ozone measurement
[INPE-4230-PRE/1105] 01 p0068 N88-10437

ECC (Electrochemical Concentration Cell) ozonesonde observations at South Pole, Antarctica during 1986
[PB87-207502] 02 p0197 N88-11228

The study of excited oxygen molecule gas species production and quenching on thermal protection system materials
[NASA-CR-172027] 02 p0233 N88-11470

Global environmental change research
[S-HRG-100-301] 03 p0348 N88-12199

Photochemical ozone overburden correction 05 p0615 N88-13778

Analysis of the breakdown of the Antarctic circumpolar vortex using TOMS ozone data 05 p0615 N88-13779

Insights into the general circulation of the lower stratosphere from TOMS 05 p0616 N88-13780

Ozone, jet streaks and severe weather 05 p0616 N88-13781

Lower-stratospheric/upper-tropospheric exchange processes associated with tropical cyclones as observed by TOMS 05 p0616 N88-13782

Tropical easterly jet located using TOMS data 05 p0616 N88-13783

The use of TOMS data for tropospheric ozone studies 05 p0616 N88-13784

Northwest Airlines flight experiments 05 p0617 N88-13786

An analysis of tropopause pressure and total ozone correlations 05 p0617 N88-13789

TOMS ozone data compared at mesoscale resolution to tropopause heights from the AVE radiosonde network and to VAS radiances over the south-central United States 05 p0617 N88-13790

Dobson-stations performance assessment using TOMS data 05 p0618 N88-13792

Comparison of ground based and TOMS measurements of SO2 from volcanic emissions 05 p0618 N88-13795

Selection of optimum wavelengths for ozone mapping from satellites 05 p0619 N88-13798

Determination of total ozone from HIRS2/MSU sounding data 05 p0619 N88-13799

Complementary information between UV and IR for remote sensing of total ozone 05 p0619 N88-13800

Observation guidelines for a Total Ozone Mapping Spectrometer (TOMS) in geosynchronous orbit 05 p0619 N88-13801

A geostationary imaging spectrometer TOMS instrument 05 p0619 N88-13802

A review of atmospheric ozone and current thinking on the Antarctic ozone hole
[AD-A185608] 06 p0732 N88-14501

Long-term variation of total ozone
[INPE-4307-PRE/1173] 08 p1023 N88-16192

Literature survey relating to the absorption properties of ozone in the near ultraviolet
[ESRO-SM-81] 09 p1190 N88-17129

Tropospheric ultraviolet radiation: Assessment of existing data and effect on ozone formation
[PB88-130133] 10 p1354 N88-18095

Experimental measurements of the uptake of ozone in rats and human subjects
[PB88-125422] 10 p1364 N88-18149

Ozone sonde and Dobson spectrometer data obtained during the MAP/GLOBUS 1983 campaign over Western Europe
[BPT-5/87] 13 p1802 N88-20771

Assessment of crop loss from air pollutants: Meteorology-atmospheric chemistry and long range transport
[PB88-146857] 15 p2089 N88-22448

Surface ozone and ozonesounding results from the ABLE-2B expedition to Amazonia
[INPE-4523-PRE/1275] 15 p2095 N88-22484

Ozonesonde observations at Lauder, New Zealand during the Spring and early Summer of 1986
[PB88-173273] 16 p2232 N88-23328

Study of polyatomic dynamics in the atmosphere
[AD-A190964] 16 p2233 N88-23334

Near-real-time TOMS, telecommunications and meteorological support for the 1987 Airborne Antarctic Ozone Experiment
[NASA-CR-4133] 16 p2233 N88-23338

The gamma 1 and gamma 3 bands of (16)O3: Line positions and intensities
[NASA-TM-101162] 17 p2445 N88-24541

Line positions and intensities for the gamma 1 + gamma 2 and gamma 2 + gamma 3 bands of (16)O3
[NASA-TM-101161] 17 p2446 N88-24542

Air pollution: Ozone attainment requires long-term solutions to solve complex problems
[PB88-167275] 18 p2538 N88-25060

Workshop on Atmospheric OH
[BPT-7/87] 18 p2538 N88-25063
Ozone in the atmosphere 18 p2539 N88-25064
Ultraviolet measurements: Measurements of photolysis rates 18 p2539 N88-25065
Motor vehicles as sources of compounds important to tropospheric and stratospheric ozone
[PB88-195219] 18 p2540 N88-25076
ECC (Electrochemical Concentration Cell) ozonesonde observations at South Pole, Antarctica during 1987
[PB88-202015] 21 p2970 N88-27644
Photochemical oxidant formation: Overview of current knowledge and emerging issues
[PB88-195235] 21 p2971 N88-27647
The detection and interpretation of long-term changes in ozone from space
[NASA-TM-101135] 21 p2971 N88-27650
Filling of the atmospheric transmission window due to emission from very high rotational levels of NO and O3
[AD-A194670] 23 p3233 N88-29239
European validation of SAGE-2 aerosol profiles
[AERONOMICA-ACTA-A-327-1988] 23 p3234 N88-29243
Recent measurements of ozone in the Amazon forests
[INPE-4494-PRE/1258] 24 p3389 N88-30185
Changes in stratospheric ozone: Observations and theories
[AERONOMICA-ACTA-A-334-1988] 24 p3390 N88-30188

OZONE DEPLETION
Scientific and Operational Requirements for TOMS Data
[NASA-CP-2497] 05 p0615 N88-13774
TOMS: The Antarctic ozone hole and ozone trends 05 p0615 N88-13775
October lower stratospheric Antarctic temperature and total ozone from 1979-1985 05 p0615 N88-13776
A review of atmospheric ozone and current thinking on the Antarctic ozone hole
[AD-A185608] 06 p0732 N88-14501
Ozone formation due to interaction of meteoroids with Earth's atmosphere 06 p0738 N88-14536
The 1987 Airborne Antarctic Ozone Experiment: The Nimbus-7 TOMS data atlas
[NASA-RP-1201] 13 p1791 N88-20714
An automated ozone photometer
[NASA-TM-100064] 14 p1908 N88-21404
Geochemistry of the middle and lower atmosphere: Environmental impact through the deterioration of the ozone layer
[INPE-4477-PRE/1241] 16 p2230 N88-23321
The potential impact on atmospheric ozone and temperature of increasing trace gas concentrations
[NASA-CR-182965] 17 p2373 N88-24112
Changes in the Antarctic atmosphere due to the reduction of stratospheric ozone
[ETN-88-92565] 18 p2540 N88-25074
Timing regulations to prevent stratospheric-ozone depletion
[R-3495-JMO/RC] 19 p2690 N88-25987
Impact on ozone attainment of CFC (chlorofluorocarbon) controls used to prevent future depletion of stratospheric ozone
[PB88-195177] 19 p2690 N88-25989
Meteorological atlas of the Southern Hemisphere lower stratosphere for August and September 1987
[NASA-TM-4049] 20 p2825 N88-26763
Radiative heat transfer to chemically reacting flow between concentric rotating spheres
[DE88-702538] 22 p3118 N88-28525
Present state of knowledge of the upper atmosphere 1988: An assessment report
[NASA-RP-1208] 23 p3232 N88-29233
Changes in stratospheric ozone: Observations and theories
[AERONOMICA-ACTA-A-334-1988] 24 p3390 N88-30188

OZONE HOLE
U OZONE DEPLETION

OZONE LAYER
U OZONOSPHERE

OZONOMETRY
Scientific and Operational Requirements for TOMS Data
[NASA-CP-2497] 05 p0615 N88-13774
TOMS: The Antarctic ozone hole and ozone trends 05 p0615 N88-13775
Analysis of the breakdown of the Antarctic circumpolar vortex using TOMS ozone data 05 p0615 N88-13779
The use of TOMS data for tropospheric ozone studies 05 p0616 N88-13784
Laboratory measurements of the ozone absorption coefficient in the wavelength region 339 to 362 nm at different temperatures
[NOTA-INTERNA-882] 07 p0878 N88-15324
ROCOZ-A (improved rocket launched ozone sensor) for middle atmosphere ozone measurements 08 p1029 N88-16233
Surface ozone measurements at a Swedish mountain site
[CM-72] 09 p1191 N88-17138
Ozone sonde and Dobson spectrometer data obtained during the MAP/GLOBUS 1983 campaign over Western Europe
[BPT-5/87] 13 p1802 N88-20771
Corrections for differential scattering by aerosols in the measurement of ozone by DIAL --- differential absorption lidar (DIAL)
[NPL-QU-78] 14 p1945 N88-21603
Workshop on Atmospheric OH
[BPT-7/87] 18 p2538 N88-25063
Ozone in the atmosphere 18 p2539 N88-25064
Ultraviolet measurements: Measurements of photolysis rates 18 p2539 N88-25065
Changes in the Antarctic atmosphere due to the reduction of stratospheric ozone
[ETN-88-92565] 18 p2540 N88-25074
Changes in stratospheric ozone: Observations and theories
[AERONOMICA-ACTA-A-334-1988] 24 p3390 N88-30188

OZONOSPHERE
The potential impact on atmospheric ozone and temperature of increasing trace gas concentrations
[NASA-CR-182965] 17 p2373 N88-24112

P

P WAVES
Multichannel deconvolution of P waves at seismic arrays and three component stations
[AD-A184450] 04 p0467 N88-12888
Earthquakes from peninsular India: Data from the Gauribidanur seismic array
[DE88-701232] 15 p2093 N88-22471
Acousto-ultrasonic input-output characterization of unidirectional fiber composite plate by P waves
[NASA-CR-4162] 19 p2678 N88-25923
Maximum-likelihood multichannel deconvolution of P waves at seismic arrays
[AD-A194990] 24 p3391 N88-30191
Discrimination studies using short-period P waves at upper mantle distances
[AD-A195468] 24 p3401 N88-30257

P-I-N DIODES
U DIODES
U P-I-N JUNCTIONS

P-I-N JUNCTIONS
Computer calculations of PIN diode limiter characteristics
[AD-A185563] 06 p0697 N88-14277
The qualitative determination of high injection effects in flux-loaded P-I-N diodes using the recombination radiation measuring method
[ETN-88-91475] 11 p1560 N88-19336
Research on high-efficiency, stacked, multijunction, amorphous silicon alloy thin-film solar cells
[DE88-001108] 13 p1793 N88-20723
Development program for 1.93-micron lasers
[NASA-CR-4148] 16 p2212 N88-23198
InP/GaInAs/InP PIN photodiode with FWHM less than 18 ps 19 p2658 N88-25799
Study of Staebler-Wronsky degradation effect in a Si:H based P-I-N solar cells
[NASA-CR-182564] 19 p2687 N88-25970
Silicon-on-insulator pin diodes
[AD-A193359] 21 p2937 N88-27445

P-N JUNCTIONS
An investigation of the equivalent circuit and carrier lifetimes of Si/SiGe heterostructure p-n diodes for frequencies between 0.5 and 18.5 MHz
[FOA-C-30469-3.2] 09 p1256 N88-17529
Photocurrent modeling of modern microcircuit PN junctions
[DE88-007037] 19 p2662 N88-25832

P-N-P JUNCTIONS
Joint services electronics program research in electronics
[AD-A192206] 18 p2504 N88-24857

P-N-P-N JUNCTIONS
Electric design rules related to latch-up and radiation --- simulation
[FOA-E-30006-3.1] 08 p0979 N88-15917
High density CMOS technology 11 p1561 N88-19342

P-TYPE SEMICONDUCTORS
Integrated fiber-optic coupler
[AD-A184494] 03 p0377 N88-12369
Preparation and characterization of Cu2Zn1-xMnxGeS4
[AD-A188113] 11 p1556 N88-19315
Point defect structure of Cr2O3
[AD-A187620] 11 p1556 N88-19317
Characterization of enhanced Schottky-barrier InGaAs/Al(1-x)As strained channel modulation-doped field-effect transistors
[AD-A188820] 12 p1698 N88-20162
Fundamental studies and device development in beta silicon carbide
[AD-A189540] 12 p1699 N88-20165
Electrical properties of p-type and n-type ZnSe-ZnTe strained-layer superlattices 20 p2868 N88-27029

P-3 AIRCRAFT
Taiwan area mesoscale experiment: P-3 aircraft operations summary
[PB88-169073] 18 p2544 N88-25098

PACE
U PHYSICS AND CHEMISTRY EXPERIMENT IN SPACE

PACIFIC ISLANDS
NT JAPAN
NT NEW ZEALAND

PACIFIC OCEAN
V/STOL aircraft configurations and opportunities in the Pacific Basin
[NASA-TM-100005] 03 p0261 N88-11644
Tropical cyclone intensity prediction based on empirical orthogonal function representation of wind and shear fields
[AD-A184699] 03 p0353 N88-12229
On the interannual variability of South American climate and the Southern Oscillation 04 p0470 N88-12905
Interactions between the Asian monsoons, the tropical Pacific and the southern hemisphere extratropics 04 p0470 N88-12907
Tectonics of the Caroline Oceanic Step (southwestern Pacific Ocean) 06 p0725 N88-14462
Statistical structure of temperature field over South Pacific Ocean 06 p0726 N88-14485
Ferromanganese nodules of Antarctic sector in Pacific Ocean 06 p0727 N88-14472
Modes of surface circulation and climate over the tropical Atlantic, Eastern Pacific, and Indian Oceans 06 p0742 N88-14564
CTD/02 measurements during 1984 and 1985 as part of the Equatorial Pacific Ocean Climate Studies (EPOCS)
[PB88-102082] 06 p0748 N88-14600
Geosat crossover analysis in the tropical Pacific. Part 1: Constrained sinusoidal crossover adjustment
[NASA-CR-182391] 07 p0871 N88-15285
Biogeochemical cycling in the ocean. Part 1: Introduction to the effects of upwelling along the west coast of North America
[NASA-TM-88230] 07 p0882 N88-15349
Nature of Western Pacific transition zone 08 p1010 N88-16122
Neogene paleoclimate in Pacific Ocean subarctic region determined from study of diatoms 08 p1010 N88-16125
North Pacific Ocean. Subtropical front north of Hawaii, R/V Thomas G. Thompson: 7 January - 10 February 1974. CTD data report
[AD-A186565] 08 p1044 N88-16310
North Pacific Ocean. Tradewind region east of Hawaii, R/V Thomas G Thompson: 25 September - 1 November 1972. STD data report
[AD-A186566] 08 p1044 N88-16311
North Pacific Ocean. Subarctic front central Pacific, R/V Thomas G. Thompson: 8 September - 9 October 1975. CTD data report
[AD-A186567] 08 p1044 N88-16312
North Pacific Ocean. Northwest Pacific Transition Zone, R/V Thomas G. Thompson: 19 March - 1 May 1971. STD data report
[AD-A186568] 08 p1044 N88-16313
North Pacific Ocean. Gulf of Alaska, R/V Thomas G. Thompson: 1 February - 8 March 1967. STD data report
[AD-A186569] 08 p1045 N88-16314
North Pacific Ocean. Central Pacific Transition Zone, R/V Thomas G. Thompson: 25 March - 3 May 1968. STD data report
[AD-A186570] 09 p1195 N88-17160
North Pacific Ocean. Northeast Pacific Transition Zone, R/V Thomas G. Thompson: 1 November - 6 December 1969. STD data report
[AD-A186574] 09 p1195 N88-17161
Materials of the World Data Center B. Deep Seismic Sounding (DSS): Pacific data 09 p1196 N88-17167

Geological evolution and analysis of confirmed or suspected gas hydrate localities. Volume 9: Formation and stability of gas hydrates of the Middle America Trench
[DE88-001007] 10 p1347 N88-18050
CTD observations in the coastal transition zone off northern California, 16-25 February 1987
[AD-A187283] 10 p1357 N88-18111
JEDA (Joint Environmental Data Analysis) Center report on tropical Pacific subsurface thermal data management, 1986
[PB88-140090] 12 p1649 N88-19875
Tidal estimation in the Pacific with application to SEASAT altimetry
[NASA-TM-100694] 13 p1803 N88-20780
Dynamics of the Oceanic Surface Mixed Layer
[AD-A188348] 13 p1804 N88-20785
Equatorial turbulence: Mixed layer and thermocline
13 p1804 N88-20787
The mixed layer of the western equatorial Pacific Ocean
[HIG-1661] 13 p1805 N88-20789
Mixed-layer shear related to wind stress in the central equatorial Pacific 13 p1805 N88-20793
Monitoring ocean surface layer processes
13 p1806 N88-20801
CTD/O2 data collected in 1985 and 1986 for EPOCS (Equatorial Pacific Ocean Climate Studies)
[PB88-160775] 14 p1951 N88-21629
Physical, chemical and CTD (Conductivity/Temperature/Depth) data from the Marathon 2 expedition
[AD-A189930] 15 p2099 N88-22507
Diagnostic studies of the HxOy-NzOy-O3 photochemical system using data from NASA GTE field expeditions
[NASA-CR-183038] 19 p2689 N88-25984
MIZPAC (marginal ice zone Pacific) 84-86 CTD (Conductivity, Temperature, Depth) data report
[AD-A192478] 21 p2976 N88-27679
RB211 developments
[PNR90444] 22 p3045 N88-28069
The 1986-87 Pacific warm episode: Oceanic and Atmospheric features 22 p3120 N88-28535
Zonal wind observations at Christmas Island (2 deg N, 157 deg W) during the 1986-1987 El-Nino
22 p3120 N88-28539
Climatology of various synoptic systems over the tropical North Pacific 22 p3121 N88-28542
Some evidence for a Northern Hemispheric extratropic trigger mechanism of ENSO events
22 p3123 N88-28558
Persistence of North Pacific Sea surface temperature and atmospheric flow patterns 22 p3123 N88-28559
The impact of the El Nino event on the ECMWF model performance 22 p3125 N88-28576

PACKAGES
NT EREP
NT INSTRUMENT PACKAGES

PACKAGING
NT ELECTRONIC PACKAGING
The effect of different packagings on the vibration behavior and the coupling factors of steam turbine blading
[ETN-87-90425] 01 p0056 N88-10357
RADC/NBS (Rome Air Development Center/National Bureau of Standards) Workshop. Moisture Measurement and Control for Microelectronics (4)
[PB87-224614] 03 p0309 N88-11947
Fabrication and packaging of discontinuous MIM (Metal-Insulator-Metal) film arrays for efficient MM wave and IR detection and mixing
[AD-A186809] 09 p1146 N88-16869
Electrophoretically deposited styrene-acrylate coatings for suppression of internal electromagnetic pulse effects
[DE88-003820] 12 p1609 N88-19621
Response characteristics of dual MOSFET gamma-ray sensors produced by Mitel Corporation
[AD-A189026] 12 p1630 N88-19755
Utilization of dense packed planar acoustic echosounders to identify turbulence structure in the lowest levels of the atmosphere
[AD-A191006] 16 p2233 N88-23335
Procedures for identification and handling of Printed Circuit Boards (PCBs)
[AD-A191177] 23 p3206 N88-29078

PACKET SWITCHING
Modeling and performance evaluation of the DPS25 packet switching multiprocessor system --- communication networks
[ENST-87E009] 02 p0162 N88-11016
A packet-switched wide-area communication network simulator
[FUB-3-1986] 14 p1905 N88-21381
Alpha structure based B-HIVE multicomputer
[AD-A188708] 16 p2244 N88-23405

PACKET TRANSMISSION
NT ALOHA SYSTEM
The role of spread spectrum in packet radio networks
[AD-A184511] 03 p0306 N88-11929
Packet error probabilities in frequency-hopped spread spectrum packet radio networks. Markov frequency hopping patterns considered
[AD-A186071] 07 p0841 N88-15104
On the approximation of the output process of multi-user random access communication networks
[AD-A186197] 07 p0842 N88-15108
Adaptive spread spectrum networks
[AD-A187154] 09 p1152 N88-16900
The high speed local area network
19 p2717 N88-26133

PACKETS (COMMUNICATION)
Packet error probabilities in frequency-hopped spread spectrum packet radio networks. Markov frequency hopping patterns considered
[AD-A186071] 07 p0841 N88-15104
Channel access protocols for multihop packet radio networks
[AD-A186074] 07 p0842 N88-15105
Packet telecommand. System performance assessment study --- onboard data handling
[PTC/TNOT/0015/SAAB] 07 p0843 N88-15113
Exact analyses of slotted ring protocols for local area networks with one transmitting station
[MEMO-650] 14 p1967 N88-21737
Multiple address facility for packet radio: An investigation of performance/complexity trade off
[AD-A191043] 16 p2190 N88-23064

PACKINGS (SEALS)
Study on shaft seals for potassium turbine
[EL-891] 15 p2074 N88-22364

PADE APPROXIMATION
The matrix exponential in transient structural analysis
05 p0593 N88-13619

PAINTS
Paints required for aeronautical construction
[SNIAS-872-551-102] 05 p0569 N88-13470
Development of microencapsulated DNBM quaternary ammonium inhibitors for paints
17 p2319 N88-23851
Predictive corrosion modeling, volume 1
[AD-A191229] 18 p2485 N88-24739
Cleanability of aircraft polyurethane topcoats
[AD-A193456] 23 p3170 N88-28878
Prediction of degradation of polymeric coating materials 24 p3354 N88-29970
Electrochemical evaluation of the long term corrosion resistance of polymer coated steel
24 p3355 N88-29974
Reduced time frame for predicting coating performance 24 p3356 N88-29979

PAIR PRODUCTION
Single leptons from heavy quark production
[DE87-014917] 04 p0488 N88-13009
Vector boson pair production in e(+)e(-) collisions
[PREPRINT-549] 06 p0778 N88-14774
Study of tau pairs and search for new particles
[B8680488] 07 p0931 N88-15655
Two-photon exclusive meson production at large angles
[NIKHEF-H/87-4] 08 p1081 N88-16515
Electronic factors for K-shell-electron conversion probability and electron-positron pair formation probability in electric monopole transitions
[DE87-753040] 08 p1089 N88-16551
Characteristics of multimuon events from fourth generation quarks at the SSC (Superconducting Super Collider)
[DE88-002954] 09 p1257 N88-17535
Diffraction theory in QCD and beyond
[DE88-005958] 13 p1837 N88-20992
Model-independent requirements to the source of positrons in the galactic centre
[DE88-700968] 14 p1992 N88-21874
A new approach to generating negative ion beams
[AD-A191119] 18 p2572 N88-25276
Gamma rays from Cygnus X-1: Modeling and nonthermal pair production
[DE88-006830] 18 p2596 N88-25426
Cascade model of gamma-ray bursts: Power-law and annihilation-line components
[NASA-TM-101178] 21 p3032 N88-27998
Influence of pairing correlations on the probability and dynamics of tunneling through the barrier in fission and fusion of complex nuclei
[DE88-701500] 23 p3286 N88-29570

PALEOCLIMATOLOGY
Neogene paleoclimate in Pacific Ocean subarctic region determined from study of diatoms
08 p1010 N88-16125
Model validation research: Comparison of simulated and observed climate patterns for the past 18,000 years
[DE88-004945] 13 p1800 N88-20759

PALEOMAGNETISM
Statistics of the geomagnetic secular variation for the past 5Ma
[NASA-CR-181558] 04 p0467 N88-12890

PALEONTOLOGY
Use of space photographs for paleoseismogeological studies (on the example of Mongolian Altay)
08 p1008 N88-16110

PALLADIUM
A surface science investigation of potential intermediates, catalysts, and promoters in the synthesis of higher alcohols by metals
[DE87-014188] 02 p0144 N88-10906
The effect of additives on the reactivity of palladium surfaces for the chemisorption and hydrogenation of carbon monoxide: A surface science and catalytic study
[DE87-014685] 02 p0145 N88-10909
Characterization of catalysts with metal-support effects and of the species adsorbed on their surfaces
[DE87-014636] 04 p0414 N88-12564
Determination, by X-ray fluorescence, of platinum, palladium, ruthenium, iron and chromium in special steels
[PB87-132114] 06 p0683 N88-14183
Electron scattering off palladium isotopes. An investigation of the equivalence of the anharmonic vibrator model and the interacting boson model
[B8671274] 07 p0931 N88-15654
The response of ultrathin palladium gate sensors to hydrogen and carbon monoxide
19 p2672 N88-25885
Electronic and geometric structure of silver and palladium on aluminum (111) in monoatomic surface layers
[ETN-88-92120] 20 p2879 N88-27093

PALLADIUM COMPOUNDS
Steady state and transient behavior of the Pd-SnO(sub x) MIS oxygen sensors 19 p2672 N88-25890
The catalytic reactivity of thin film crystal surfaces
[DE88-006387] 19 p2732 N88-26228

PAM (MODULATION)
U PULSE AMPLITUDE MODULATION

PANEL METHOD (FLUID DYNAMICS)
ARSPNS: A method to calculate steady and unsteady potential flow about fixed and rotational lifting and nonlifting bodies
[NLR-TR-85114-U] 01 p0044 N88-10282
Integration of a supersonic unsteady aerodynamic code into the NASA FASTEX system
[NASA-CR-182329] 06 p0663 N88-14068
A direct calculation method for perturbation fields of moving bodies in compressible media at subsonic Mach numbers
[ETN-88-90808] 06 p0701 N88-14305
ARSPNSC: A method to calculate subsonic steady and unsteady potential flow about complex configurations
[NLR-TR-86122-U] 13 p1717 N88-20265
A panel method based on velocity potential to compute harmonically oscillating lift surface systems
[ETN-88-91886] 15 p2061 N88-22290
On the dynamic behavior of balloon during its launch; application of panel method and extension to unsteady problem
[ISAS-RN-622] 20 p2751 N88-26330
VSAERO analysis of tip planforms for the free-tip rotor
[NASA-CR-177487] 22 p3038 N88-28036

PANELS
NT CURVED PANELS
NT RECTANGULAR PANELS
NT WING PANELS
Interactive buckling effects in stiffened FRP panels
[ARE-TM(UMS)-87204] 01 p0059 N88-10378
Fabrication and testing of fire resistant graphite composite panels
[NASA-CR-177397] 04 p0397 N88-12472
Theoretical and practical aspects of the functional absorber method of arranging sound absorbing panels
[BBC-RD-1987/15] 05 p0646 N88-13955
Postbuckling of laminated anisotropic panels
[NASA-TM-100509] 08 p0994 N88-16011
Excimer plasma displays
[AD-A186731] 09 p1250 N88-17489
Detecting serial correlation in the error structure of a cross-lagged panel model
[AD-A189070] 12 p1685 N88-20077
Postbuckling delamination of a stiffened composite panel using finite element methods
[NASA-CR-182803] 15 p2030 N88-22098
The effective fracture toughness of aluminum at rapid heating rates
[AD-A189745] 15 p2038 N88-22146
Operational considerations for laminar flow aircraft
17 p2298 N88-23748
Stiffened titanium panels
[NASA-CASE-LAR-13814-1] 18 p2497 N88-24816

Nonlinear interaction between overall and local buckling of stiffened panels with symmetric cross-sections
[PB88-104054] 21 p2960 N88-27580
Two-dimensional sequential and concurrent finite element analysis of unstiffened and stiffened aluminum and composite panels with hole
[NASA-CR-183083] 22 p3086 N88-28325

PANORAMIC SCANNING
System for detecting objects that represent a threat
[NASA-TT-20244] 13 p1760 N88-20528
Atmospheric autorotating imaging device
[NASA-CASE-NPO-17390-1-CU] 18 p2519 N88-24944

PAPER (MATERIAL)
Fiber-reinforced composite hot-gas filters
[DE87-012257] 01 p0033 N88-10208
Observations on electrostatic effects in a filter test system
[AD-A188797] 13 p1736 N88-20378
Reference filters for electrostatic charging tendency measurements of fuels
[AD-A191717] 18 p2495 N88-24803
Effect of thickness on downward flame spread over paper
[NASA-TT-20282] 19 p2612 N88-25501
New duplicating paper with high resolution for aerial photography
[PB87-228706] 19 p2685 N88-25962
Absorption heat pumps
[DE88-752820] 23 p3229 N88-29218

PAPERS
FY 1985 scientific and technical reports, articles, papers and presentations
[NASA-TM-86521] 04 p0501 N88-13083

PARABOLAS
Spectral methods: Analysis and applications to flow problems
[AD-A186265] 07 p0850 N88-15156
Adaptive finite element methods for parabolic systems in one- and two-space dimensions
[AD-A186534] 08 p1073 N88-16475
Fitting a generalized parabola to data
[NPL-DITC-96/87] 09 p1229 N88-17364
Inversion of parabolic and paraboloidal projections
[AD-A187538] 10 p1405 N88-18380
An adaptive overlapping local grid refinement method for two-dimensional parabolic systems
[AD-A193560] 23 p3271 N88-29464
Reflection and scattering of acoustic rays computed for parabolic ice keel models
[AD-A193898] 23 p3278 N88-29517
Large displacement and rotational formulation for laminated cylindrical shells including parabolic transverse shear
[AD-A194871] 24 p3384 N88-30158

PARABOLIC ANTENNAS
New main reflector, subreflector and dual chamber concepts for compact range applications
[NASA-CR-181506] 04 p0402 N88-12498
Modification of parabolic dish antenna pattern using two symmetrically placed circular flat plates
[AD-A189543] 13 p1758 N88-20517
An improved method for calculating power density in the Fresnel region of circular parabolic reflector antennas
[AD-A190569] 15 p2060 N88-22284
The focal plane reception pattern calculation for a paraboloidal antenna with a nearby fence
[NASA-TM-100691] 24 p3365 N88-30039

PARABOLIC BODIES
Fundamentals and techniques of nonimaging optics research
[DE87-014544] 02 p0236 N88-11488
Mass transport in a parabolic conduit
[LRT-WE-9-FB-1(1988)] 22 p3077 N88-28273
Heat transport in a parabolic tube of circular cross-section
[LRT-WE-9-FB-2(1988)] 22 p3078 N88-28274
Nonlinear oscillations in paraboloidal containers
[LRT-WE-9-FB-3(1988)] 22 p3078 N88-28275

PARABOLIC DIFFERENTIAL EQUATIONS
Accurate, stable, explicit solution of the parabolized Navier-Stokes equations 01 p0043 N88-10276
Error estimates for finite element approximations of parabolic variational equations
[BONNER-MATHE-SCHR-179] 01 p0087 N88-10569
Computation of free boundaries
[PB87-226023] 06 p0763 N88-14680
Propagation of radiation along a constricting optical waveguide 07 p0920 N88-15590
Comparisons of Monte-Carlo and PNS (Parabolized Navier-Stokes) calculations for rarefied flow over reentry vehicle configurations
[DE88-004937] 11 p1435 N88-18560
A signal processing approach to the numerical solution of parabolic differential equations 11 p1539 N88-19197
A new parabolized Navier-Stokes code for chemically reacting flow fields 12 p1625 N88-19721
Boundary stabilization of the reaction-diffusion equation with unilateral conditions
[RR-315] 14 p1964 N88-21720
Almost-periodic solutions of nonlinear parabolic equations
[DE88-006423] 15 p2118 N88-22618
A posterior error estimation in a finite element method for parabolic partial differential equations
[AD-A190296] 15 p2120 N88-22636
Optimal discrete-time LQR problems for parabolic systems with unbounded input: Approximation and convergence
[NASA-CR-181673] 18 p2567 N88-25247
Accurate solution of parabolic equations by expansion in ultraspherical polynomials
[DE88-701829] 20 p2845 N88-26880
Numerical computation of space shuttle orbiter flow field
[NASA-CR-183193] 22 p3040 N88-28048
Numerical modeling results for mode propagation in a wedge
[AD-A193998] 22 p3147 N88-28718
Lessons learned in the mesh generation for PN/S calculations 23 p3245 N88-29314

PARABOLIC FLIGHT
Access to microgravity: A technical description of the NAE T-33 microgravity facility
[NAE-AN-47] 04 p0405 N88-12518
Respiratory parameters aboard an aircraft performing parabolic flights 12 p1653 N88-19902
The Marshall Space Flight Center KC-135 microgravity test program for FY84-86
[NASA-TM-4059] 22 p3056 N88-28136

PARABOLIC REFLECTORS
Wavefront error sensing
[NASA-CR-181504] 03 p0321 N88-12030
The formation of optical membrane reflector surfaces using uniform pressure loading
[DE87-012275] 03 p0376 N88-12367
New main reflector, subreflector and dual chamber concepts for compact range applications
[NASA-CR-181506] 04 p0402 N88-12498
MBA payload testing by Compact Antenna Test Range (CATR)
[ESA-CR(P)-2473] 08 p0977 N88-15906
The integration of a mesh reflector to a 15-foot box truss structure. Task 3: Box truss analysis and technology development
[NASA-CR-178228] 11 p1497 N88-18941
Modification of parabolic dish antenna pattern using two symmetrically placed circular flat plates
[AD-A189543] 13 p1758 N88-20517
Point-focus concentrator reflector assembly, phase 1
[DE88-003616] 13 p1792 N88-20720
Thermophotovoltaic space power system, phase 3
[NASA-CR-179327] 14 p1942 N88-21585
Reflux heat-pipe solar receivers for dish-electric systems
[DE88-008671] 21 p2968 N88-27631

PARABOLOIDS
U PARABOLIC BODIES

PARACHUTE DESCENT
Detection of hyperventilation of parachutists
[DFVLR-FB-87-11] 01 p0075 N88-10482
Parachute characteristics of Titan descent modules — planetary probe
[BF-3/86-B] 02 p0122 N88-10774
Regulation of energy metabolism during parachute jumps 07 p0896 N88-15428
Galileo probe parachute test program: Wake properties of the Galileo probe at Mach numbers from 0.25 to 0.95
[NASA-RP-1130] 11 p1488 N88-18884
Parachute for in-flight training on parachute ejection
[REPT-87-11] 18 p2458 N88-24593

PARACHUTE FABRICS
Parachute materials
[DE87-014845] 04 p0411 N88-12550

PARACHUTES
NT DRAG CHUTES
NT RIBBON PARACHUTES
Developmental airdrop testing techniques and devices
[AGARD-AG-300-VOL-6] 04 p0398 N88-12481
Parachute materials
[DE87-014845] 04 p0411 N88-12550
An investigation of cruciform parachutes and towed targets
[BU-360] 14 p1862 N88-21122
Measurements of aerodynamic forces on unsteadily moving bluff parachute canopies 16 p2202 N88-23137
Parachute for in-flight training on parachute ejection
[REPT-87-11] 18 p2458 N88-24593

PARACHUTING
U PARACHUTE DESCENT

PARADOXES
Solar oscillations, gravitational multipole field of the Sun and the solar neutrino paradox
[DE88-002100] 07 p0946 N88-15752

PARAFFINS
High output paraffin actuators: Utilization in aerospace mechanisms 14 p1924 N88-21470

PARALLEL COMPUTERS
NT MIMD (COMPUTERS)
NT SIMD (COMPUTERS)
Report from the MPP Working Group to the NASA Associate Administrator for Space Science and Applications
[NASA-TM-87819] 02 p0223 N88-11402
Parallel algorithms for computer vision on the connection machine
[AD-A185842] 07 p0901 N88-15456
Research in progress at the Institute for Computer Applications in Science and Engineering
[NASA-CR-181607] 08 p1053 N88-16354
Implementing clips on a parallel computer 09 p1211 N88-17259
Massive fine-grain parallelism in array computation: A data flow solution 10 p1382 N88-18254
Finely grained parallelism in an applicative architecture 10 p1383 N88-18256
Implementation and analysis of a Navier-Stokes algorithm on parallel computers
[NASA-CR-181614] 10 p1390 N88-18301
The roll back chip: Hardware support for distributed simulation using time warp
[AD-A187823] 11 p1529 N88-19132
An analysis of multiple grain CHiP architectures
[AD-A189942] 15 p2110 N88-22570
Implementation and performance analysis of parallel assignment algorithms on a hypercube computer
[AD-A190678] 15 p2115 N88-22600
Design and implementation of a parallel computer for expert system applications
[DE88-005288] 15 p2115 N88-22601
Piecewise linear approach for timing simulation of VLSI (Very-Large-Scale-Integrated) circuits on serial and parallel computers
[AD-A191328] 16 p2252 N88-23462
Factorization of large integers on a massively parallel computer
[DE88-011625] 21 p2999 N88-27786
Optimisation algorithms for highly parallel computer architectures. The performance of the truncated Newton, conjugate gradient algorithm in FORTRAN and Ada
[AD-A193940] 23 p3265 N88-29435

PARALLEL FLOW
NT PIPE FLOW
NT THREE DIMENSIONAL FLOW
Some asymptotic modes of transonic vortex flow 04 p0425 N88-12632

PARALLEL PLATES
Quantum electrodynamics based on self-energy: Spontaneous emission in cavities
[DE87-703071] 02 p0232 N88-11461
A note on the aerodynamic design of thin parallel-sided aerofoil sections
[ARL-AERO-TM-388] 09 p1114 N88-16677
Changes in the turbulent boundary layer structure associated with net drag reduction by outer layer manipulators
[NASA-CR-178152] 11 p1483 N88-18853

PARALLEL PROCESSING (COMPUTERS)
NBS (National Bureau of Standards) research reports (April 1987)
[PB87-210258] 01 p0018 N88-10111
A graphical tool for observing the behavior of parallel logic programs
[DE87-011467] 01 p0080 N88-10516
A look at the evolution of mathematical software for dense matrix problems over the past fifteen years
[DE87-011485] 01 p0081 N88-10517
Measurement of fault-tolerant parallel processors
[PB87-208328] 01 p0084 N88-10539
A unified approach to parallel computation: Performance evaluation and architecturally independent parallel programming
[DE87-012519] 01 p0084 N88-10540
Solution methods for bidiagonal and tridiagonal linear systems for parallel and vector computers
[REPT-87-04] 01 p0085 N88-10552
Parallel computation of a domain decomposition method
[DE87-011444] 01 p0086 N88-10560
Locating parallel numerical tasks in the solution of viscous fluid flows
[DE87-013510] 02 p0169 N88-11064

Benchmarking the Connection Machine
[DE87-013500] 02 p0218 N88-11374
Implementation of preconditioned s-step conjugate gradient methods on a multiprocessor system with memory hierarchy
[DE87-014401] 02 p0222 N88-11400
Hardware-assisted multiprocessor performance measurements
[PB87-226908] 03 p0363 N88-12282
Mapping a battlefield simulation onto message-passing parallel architectures
[NASA-CR-178396] 03 p0363 N88-12287
Algorithms and hardware for efficient image smoothing
[TR-149] 03 p0365 N88-12296
Delft parallel processor 84/16
[PB87-226254] 03 p0366 N88-12305
Implementation of the Runge-Kutta-Fehlberg method for solution of ordinary differential equations on a parallel processor
[AD-A184660] 03 p0370 N88-12331
Programmable real-time digital video image processing
[PB87-104162] 04 p0430 N88-12661
Center for Supercomputing Research and Development (CEDAR)
[DE88-000807] 04 p0475 N88-12930
Principles for problem aggregation and assignment in medium scale multiprocessors
[NASA-CR-178379] 04 p0476 N88-12935
A tight upper bound for the speed-up of parallel best-first branch-and-bound algorithms
[AD-A184246] 04 p0477 N88-12939
Methods for design and evaluation of integrated hardware/software systems for concurrent computation
[NASA-CR-181522] 04 p0479 N88-12953
A review and analysis of Fortran 8x
[DE88-001320] 04 p0479 N88-12955
QR factorization of a dense matrix on a shared-memory multiprocessor
[DE88-001506] 04 p0480 N88-12956
Parallel superconvergent multigrid
[DE87-013153] 04 p0480 N88-12960
An approach to implementing state space searches on heterogeneous systems of multiprocessors
[DE88-001321] 04 p0482 N88-12967
Computational methods for problems in aerodynamics and large space structure using parallel and vector architectures
[AD-A185401] 05 p0541 N88-13294
Arrays for discrete Fourier transform
[REPT-87-019] 05 p0632 N88-13861
Storing and retrieving data in a parallel distributed memory system
[AD-A185177] 05 p0637 N88-13897
Research and development of finite elements and iterative algorithms for elliptic partial differential equations
[DE88-001381] 05 p0643 N88-13934
A zonal approach for the solution of coupled Euler and potential solutions of flows with complex geometries
[AD-A185465] 06 p0702 N88-14310
Methods for reducing computational costs of typical finite element unsteady hydrodynamic models
[AD-A185499] 06 p0702 N88-14312
Fast algorithms for structural optimization and least squares
[AD-A185786] 06 p0724 N88-14452
Optimal pre-scheduling of problem remappings
[NASA-CR-178378] 06 p0756 N88-14633
Parallel algorithms for polynomials
[PB87-226304] 06 p0756 N88-14635
Set of multi-process primitives for stack based machines
[PB87-234381] 06 p0756 N88-14636
Algorithms and programming tools for image processing on the MPP:3
[NASA-CR-182349] 06 p0757 N88-14641
Parallel pyrdting combined with parallel reduction
[NASA-CR-178422] 06 p0760 N88-14662
Fault-tolerant computer architecture based on INMOS transputer processor 06 p0797 N88-14880
Reliability modelling for fault-tolerant parallel processor
[AD-A185867] 07 p0900 N88-15451
Massively parallel implementations of theories for apparent motion
[AD-A185841] 07 p0901 N88-15455
Monte Carlo photon transport on vector and parallel supercomputers
[DE88-002503] 07 p0905 N88-15488
AFL-1: A programming language for massively concurrent computers
[AD-A186422] 07 p0906 N88-15489
Local uniform mesh refinement for partial differential equations
[AD-A186312] 07 p0910 N88-15519
Application of parallel distributed processing to space based systems 08 p1059 N88-16393
Neural network based speech synthesizer: A preliminary report 08 p1064 N88-16429
A parallel algorithm for the general LU-factorization
[DE88-002177] 08 p1066 N88-16444
Numerical experiments with a parallel conjugate gradient method
[DE88-002178] 08 p1066 N88-16445
Media independent interface
[NASA-CR-172033] 08 p1066 N88-16446
Applicative parallelism: Potential and challenge
[DE87-011885] 08 p1068 N88-16459
ESA Bulletin No. 25
[ISSN-0376-4265] 09 p1128 N88-16767
Parallel-processing computer systems and their possible applications in the agency 09 p1128 N88-16774
Image chunking: Defining spatial building blocks for scene analysis
[AD-A187072] 09 p1200 N88-17191
First Annual Workshop on Space Operations Automation and Robotics (SOAR 87)
[NASA-CP-2491] 09 p1203 N88-17206
Performance analysis of parallel branch and bound search with the hypercube architecture
09 p1206 N88-17229
Algorithm design for scientific computation for highly parallel multiprocessor systems
[AD-A186713] 09 p1217 N88-17299
Occam/Ada parallel programming system
[ISAL-IDI1-87-11] 09 p1219 N88-17312
A parallel block cyclic reduction algorithm for the fast solution of elliptic equations
[DE88-003595] 09 p1221 N88-17324
A multithreaded processor architecture for parallel symbolic computation
[AD-A187034] 09 p1222 N88-17327
The effectiveness of caches and data prefetch buffers in large-scale shared memory multiprocessors
[DE88-003594] 09 p1223 N88-17334
Nonpreemptive run-time scheduling issues on a multitasked, multiprogrammed multiprocessor with dependencies, bidimensional tasks, folding and dynamic graphs
[DE88-003598] 09 p1223 N88-17335
The design of ultra high-speed numeric intensive systems (having fault tolerant and load balancing capabilities) 10 p1374 N88-18196
Hardware implementation for special functions. An application for combat simulation
10 p1374 N88-18197
On parallelism in software/hardware design tools
10 p1374 N88-18200
Role of broadcasting in multiprocessor systems
10 p1374 N88-18201
Image texture classification with an optical crossbar interconnected processor 10 p1375 N88-18202
A large-grain dataflow architecture
10 p1375 N88-18207
The mapping of parallel algorithms to reconfigurable parallel architectures 10 p1376 N88-18209
A distributed system architecture based on macro dataflow model 10 p1376 N88-18210
Distributed control of large parallel computers
10 p1376 N88-18215
Experiments with parallel program execution on a network of workstations 10 p1377 N88-18217
Predicate analysis for parallel program generation
10 p1377 N88-18222
An investigation of parallelism in rule based systems
10 p1377 N88-18223
The next generation of hypercube computers
10 p1378 N88-18226
A parallel computer based on cube connected cycles
10 p1378 N88-18227
Investigations on the usefulness of the Massively Parallel Processor for study of electronic properties of atomic and condensed matter systems
[NASA-CR-182514] 10 p1383 N88-18259
A measurement-based study of concurrency in a multiprocessor
[DE88-003536] 10 p1383 N88-18260
Features of a TeraFlop supercomputer
[DE88-003540] 10 p1384 N88-18263
The impact of hierarchical memory systems on linear algebra algorithm design
[DE88-003574] 10 p1385 N88-18274
PSolve: A concurrent algorithm for solving sparse systems of linear equations
[DE88-003584] 10 p1386 N88-18275
Introduction to a system for implementing neural net connections on SIMD architectures
[NASA-CR-181612] 10 p1386 N88-18279
Programming methodology and performance issues for advanced computer architectures
[DE88-003098] 10 p1387 N88-18287
A multiprocessor scheme for the singular value decomposition
[DE88-003591] 10 p1388 N88-18288
Parallel access to synchronization variables
[DE88-003570] 10 p1392 N88-18306
Loop coalescing: A compiler transformation for parallel machines
[DE88-003571] 10 p1392 N88-18307
The performance of software-managed multiprocessor caches on parallel numerical programs
[DE88-003590] 10 p1393 N88-18308
A parallel quasi-Newton method for partially separable large scale minimization
[DE88-003592] 10 p1393 N88-18309
Performance studies of a parallel processor for large linear programming problems
[PB88-121611] 10 p1393 N88-18310
Dynamic processor self-scheduling for general parallel nested loops
[DE88-003572] 10 p1393 N88-18311
Parallel discrete event simulation: A shared memory approach
[NASA-CR-182521] 10 p1393 N88-18312
Deadlock prevention in processor self-scheduling for parallel nested loops
[DE88-003573] 10 p1393 N88-18313
Parallel garbage collection on a virtual memory system
[DE88-003567] 10 p1396 N88-18317
Fast and practical parallel polynomial interpolation
[DE88-003530] 10 p1397 N88-18328
Center for Supercomputing Research and Development
[DE88-003564] 10 p1418 N88-18466
Automated radar target recognition based on models of neural nets 11 p1476 N88-18804
Optimal performance of distributed simulation programs
[AD-A187822] 11 p1529 N88-19131
Performance measurements of distributed simulation strategies
[AD-A187824] 11 p1529 N88-19133
Distributed computation of graphics primitives on a transputer network
[NASA-TM-100814] 11 p1531 N88-19147
A shared memory algorithm and proof for the alternative construct in CSP (Communicating Sequential Processes)
[AD-A187820] 11 p1533 N88-19156
Implementing dynamic arrays: A challenge for high-performance machines
[AD-A188142] 11 p1533 N88-19157
Parallel processing in nonlinear programming
[INPE-4298-PRE/1169] 11 p1533 N88-19158
Object recognition on a systolic array
[AD-A187726] 11 p1534 N88-19164
Performance of a multigrid method on parallel architecture 11 p1539 N88-19200
Allocation of database files across parallel stores for efficient processing of partial-match queries
[AD-A188196] 11 p1565 N88-19371
Architecture with parallel processing for incremental computation
[INPE-4326-PRE/1178] 12 p1675 N88-20012
An intelligent allocation algorithm for parallel processing
[NASA-CR-182648] 12 p1675 N88-20014
Efficient parallel architecture for highly coupled real-time linear system applications
[NASA-CR-182649] 12 p1675 N88-20015
Computer architecture for efficient algorithmic executions in real-time systems: New technology for avionics systems and advanced space vehicles
[NASA-CR-182650] 12 p1675 N88-20016
Automatic restructuring of FORTRAN programs for parallel execution
[DE88-003585] 12 p1676 N88-20018
BLITZ: Blitzen's micron-code assembly language design document, version 1.0
[TR88-14] 12 p1676 N88-20019
A laboratory facility for research in parallel computation
[AD-A188499] 12 p1680 N88-20044
Primal-dual parallel solution of very large sparse linear programs
[AD-A188500] 12 p1680 N88-20045
MultiRPC: A parallel remote procedure call mechanism
[AD-A188613] 12 p1680 N88-20046
ARCTIC: Programmer's manual and tutorial
[AD-A188619] 12 p1680 N88-20047
Analysis for architecture for image processing
[INPE-4294-PRE/1165] 13 p1791 N88-20715
The physical structure of concurrent problems and concurrent computers
[DE88-005812] 13 p1814 N88-20835
Parallel image compression
[NASA-CR-180758] 13 p1814 N88-20837

Implementation of a 3-D nonlinear MHD (magnetohydrodynamics) calculation on the Intel hypercube
[DE88-000625] 13 p1816 N88-20848
Gaussian techniques on shared memory multiprocessor computers
[DE88-005426] 13 p1817 N88-20855
Approximation algorithms for scheduling unrelated parallel machines
[CWI-OS-R8714] 13 p1817 N88-20861
Computing with structured connections networks
[AD-A189244] 13 p1821 N88-20886
A simulation study of a parallel processor with unbalanced loads
[AD-A189573] 13 p1822 N88-20887
On the design of parallel numerical methods in message passing and shared memory environments
[DE88-003566] 13 p1822 N88-20888
Perspectives on parallel computing
[CWI-OS-R8709] 13 p1822 N88-20889
Locality, communication and interconnect length in multicomputers
[CWI-CS-R8708] 13 p1822 N88-20890
Utilization of parallel processing in solving the inviscid form of the average-passage equation system for multistage turbomachinery
[NASA-TM-89845] 14 p1868 N88-21160
A parallel algorithm for computing the singular value decomposition of a matrix
[DE88-007059] 14 p1958 N88-21673
Evaluation of a parallel chart parser
[AD-A189172] 14 p1959 N88-21685
Parallel algorithms for mapping pipelined and parallel computations
[NASA-CR-181655] 14 p1960 N88-21687
Parallel processes in the knowledge based system HYDRA
[REPT-87-38] 14 p1960 N88-21689
Using a parallel computer system for statistical resampling methods
[REPT-87-47] 14 p1960 N88-21690
Proposal for a parallel system with image processing applications
[INPE-4293-PRE/1164] 14 p1961 N88-21696
Lewis Structures Technology, 1988. Volume 3: Structural Integrity Fatigue and Fracture Wind Turbines HOST
[NASA-CP-3003-VOL-3] 15 p2081 N88-22408
Parallel memory addressing using coincident optical pulses
[AD-A189767] 15 p2106 N88-22547
Applications of optical computing to problems with symbolic computations
[AD-A189772] 15 p2106 N88-22548
SimPL: A simulator for parallel LISP
[AD-A189831] 15 p2109 N88-22566
Transformations of concurrent algorithms for highly parallel systems: A one year project summary report
[AD-A190236] 15 p2111 N88-22576
Two-dimensional graphics tools for a transputer based display board
[NASA-TM-100820] 15 p2113 N88-22591
Logarithmically connected, repetitive computer networks and numerical applications
[DE88-006632] 15 p2114 N88-22592
Modeling a parallel architecture for image processing
[RR-646-I] 15 p2114 N88-22593
Simulation of fault tolerance in a hypercube arrangement of discrete processors
[AD-A189682] 15 p2114 N88-22594
The modeling, simulation and comparison of interconnection networks for parallel processing
[AD-A190571] 15 p2115 N88-22599
Implementation and performance analysis of parallel assignment algorithms on a hypercube computer
[AD-A190678] 15 p2115 N88-22600
Design and implementation of a parallel computer for expert system applications
[DE88-005288] 15 p2115 N88-22601
A direct-execution parallel architecture for the Advanced Continuous Simulation Language (ACSL)
[NASA-CR-182809] 15 p2115 N88-22602
Synapses that compute motion
[AD-A190389] 15 p2116 N88-22607
Study of microcomputer-based real-time programmable optical signal processor and application
[AD-A190076] 15 p2133 N88-22726
A methodolgy, based on analytical modeling, for the design of parallel and distributed architectures for relational database query processors
[AD-A189844] 15 p2149 N88-22825
Fast algorithms for Euler and Navier-Stokes simulations
[AD-A190897] 16 p2208 N88-23175
Lewis Structures Technology, 1988. Volume 1: Structural Dynamics
[NASA-CP-3003-VOL-1] 16 p2217 N88-23226
Parallel computer methods for eigenvalue extraction
16 p2218 N88-23233
Adapting high-level language programs for parallel processing using data flow 16 p2218 N88-23234
Iterative finite element solver on transputer networks
16 p2218 N88-23235
Multiprocessor graphics computation and display using transputers 16 p2218 N88-23236
Parafrase restructuring of FORTRAN code for parallel processing 16 p2221 N88-23258
Synthesis and simulation of systolic algorithms
[ETN-88-92183] 16 p2247 N88-23423
The PROMISE simulation system: Software for the simulation of parallel processes
[NLR-MP-86077-U] 16 p2247 N88-23427
A queueing network model for analyzing a class of branch and bound algorithms on a master-slave architecture
[CWI-OS-R8717] 16 p2249 N88-23441
VPC: A proposal for a vector parallel C programming language
[AD-A190885] 16 p2251 N88-23451
Simulation of FELIN logics. Polynomials roots simultaneous computation algorithms
[ETN-88-92182] 16 p2253 N88-23464
Locality, communication and interconnect length in multicomputers
[CWI-CS-R8743] 16 p2254 N88-23466
Parallel computing in combinatorial optimization
[CWI-OS-R8720] 16 p2254 N88-23468
Domain decomposition in parallel reservoir simulation
[REPT-87-63] 16 p2254 N88-23469
Power series for stationary distributions of coupled processor models
[REPT-87-70] 16 p2254 N88-23470
Parallelization of Gauss-Seidel algorithms as an example of parallel iterative equation solving
[REPT-87-76] 16 p2254 N88-23471
Parallel artificial intelligence search techniques for real time applications
[AD-A190683] 16 p2255 N88-23473
Parallelism in a Prolog knowledge base machine
[ETN-88-92187] 16 p2255 N88-23477
An efficient parallel algorithm for the simulation of three-dimensional compressible transition on a 20 processor Flex/32 multicomputer
[NASA-CR-178340] 17 p2337 N88-23943
Evolution of a family of image processing systems at INPE 17 p2361 N88-24065
Parallel processors and nonlinear structural dynamics algorithms and software
[NASA-CR-182925] 17 p2387 N88-24187
Parallel discrete-event simulation of FCFS stochastic queueing networks
[NASA-CR-181669] 17 p2389 N88-24203
Decomposition of linear programs using parallel computation
[AD-A191718] 18 p2556 N88-25173
An improved simulated annealing algorithm for standard cell placement
[NASA-CR-182952] 18 p2558 N88-25183
Algorithms and software for solving finite element equations on serial and parallel architectures
[NASA-CR-183027] 18 p2559 N88-25191
Network architecture for OPS5
[DE88-002802] 18 p2560 N88-25194
Cellular Array Processor (CAP) and its application to computer graphics 19 p2641 N88-25667
Signal processing computational needs
[AD-A191756] 19 p2642 N88-25674
Multidimensional nodal transport methods for multiple-instruction multiple-data distributed memory machines
[DE88-004732] 19 p2713 N88-26108
Intermediate level computer vision processing algorithm development for the content addressable array parallel processor
[AD-A192086] 19 p2714 N88-26111
Graphical Multiprocessing Analysis Tool (GMAT)
[DE88-008019] 19 p2715 N88-26116
Efficient parallel algorithm for the connected component problem and its implementation on the DPP84 (Delft Parallel Processor)
[PB87-225959] 19 p2715 N88-26118
On the implementation of applicative on shared-memory, MIMD multiprocessors
[DE88-005367] 19 p2718 N88-26136
SLAPP: A special multiprocessor array for signal processing and linear algebra
[AD-A191587] 19 p2719 N88-26146
Parallelization on a multiprocessor system of a solution method for the unsteady Navier-Stokes equations at high Reynolds numbers
[ONERA-NT-1987-8] 20 p2803 N88-26632
Computer science research, 1987: Computation Directorate
[DE88-008637] 20 p2834 N88-26812
The performance of the NEC SX-2 and Cray X-MP supercomputers
[DE88-009177] 20 p2835 N88-26813
Efficient bit-level, word-level and block-level systolic arrays for matrix-matrix multiplication
[DE88-011331] 20 p2841 N88-26856
Extensible networks. Part 1: Principles and constructions
[REPT-87-91-PT-1] 20 p2842 N88-26864
The scaled-sized model: A revision of Amdahl's law
[DE88-008114] 20 p2844 N88-26875
Computational fluid dynamics on parallel processors
[AD-A192397] 21 p2941 N88-27469
Supercomputer for parallel data analysis
[DE88-702148] 21 p2995 N88-27759
Linguistic semantics for parallel computation
[PB88-105960] 21 p2995 N88-27761
Bisimulation can't be traced
[AD-A192725] 21 p2996 N88-27766
Research into the architecture of CAD based robot vision systems
[AD-A193330] 21 p2997 N88-27776
The sub-implicit method: New multiprocessor algorithms for old implicit codes
[DE88-011345] 21 p2999 N88-27785
Implementing direct, spatially isolated problems on transputer networks
[NASA-TM-101297] 21 p3000 N88-27796
User's manual for the two-dimensional transputer graphics toolkit
[NASA-TM-100974] 21 p3001 N88-27799
Image processing using a parallel architecture
[AD-A192833] 21 p3002 N88-27803
Basic database operations on the butterfly parallel processor: Experiment results
[AD-A193199] 21 p3002 N88-27804
Parallel solutions to geometric problems on the scan model of computation
[AD-A192321] 21 p3004 N88-27819
A review of parallel methods for solving sets of linear equations and their application within optimisation algorithms
[AD-A193137] 21 p3006 N88-27830
Matrix substructuring, domain decomposition and particle methods: Current trends for solving PDEs in parallel
[DE88-009826] 21 p3007 N88-27836
Parallel implementation of the boundary element method
[DE88-011846] 21 p3007 N88-27839
Two-dimensional sequential and concurrent finite element analysis of unstiffened and stiffened aluminum and composite panels with hole
[NASA-CR-183083] 22 p3086 N88-28325
What have we learnt from using real parallel machines to solve real problems
[DE88-011227] 22 p3135 N88-28636
Partitioning of regular computation on multiprocessor systems
[NASA-CR-183176] 22 p3141 N88-28676
Queueing network models for parallel processing of task systems: An operational approach
[NASA-CR-183174] 22 p3141 N88-28677
Using Petri nets for real-time development environments
[REPT-88-005] 22 p3141 N88-28679
Parallel real-time expert systems
[AD-A193673] 23 p3264 N88-29434
Adaptive identification by systolic arrays
[AD-A193532] 23 p3266 N88-29444
Performance analysis of k-ary n-cube interconnection networks
[AD-A195542] 24 p3361 N88-30010
Reducing the parallel solution time of sparse circuit matrices using reordered Gaussian elimination and relaxation
[AD-A195152] 24 p3366 N88-30045
Performance prediction of concurrent systems
[NASA-CR-183175] 24 p3412 N88-30312
Parallel and distributed computation for fault-tolerant object recognition 24 p3419 N88-30350

PARALLEL PROGRAMMING

Report from the MPP Working Group to the NASA Associate Administrator for Space Science and Applications
[NASA-TM-87819] 02 p0223 N88-11402
Parallel algorithms for unconstrained and constrained nonlinear optimization
[PB87-230454] 06 p0756 N88-14634
Algorithms and programming tools for image processing on the MPP:3
[NASA-CR-182349] 06 p0757 N88-14641

Parallel logic programming and ZMOB and parallel systems software and hardware
[AD-A186300] 07 p0903 N88-15470
UNITY: A framework for study of parallel programming problem-solving
[AD-A185616] 07 p0906 N88-15490
Teaching artificial neural systems to drive: Manual training techniques for autonomous systems
09 p1207 N88-17238
Implementing clips on a parallel computer
09 p1211 N88-17259
Communications patterns in a symbolic multiprocessor
[AD-A186896] 09 p1215 N88-17282
Preconditioned iterative methods for partial differential equations
[DE88-003071] 09 p1230 N88-17372
Experimenting with parallel programing in logic
10 p1380 N88-18240
Parallel architectures for logic programming
10 p1380 N88-18241
Programming language translation for multicomputers
10 p1381 N88-18244
Parallelism at the microlevel: Cooperative microcontrollers with real time considerations
10 p1381 N88-18246
FX-87 reference manual, edition 1.0
[AD-A187031] 10 p1385 N88-18273
Experiences with serial and parallel algorithms for channel routing using simulated annealing
[NASA-CR-182530] 10 p1388 N88-18289
Theory and practice of fault tolerance in distributed systems
[AD-A187559] 11 p1540 N88-19204
Automatic restructuring of FORTRAN programs for parallel execution
[DE88-003585] 12 p1676 N88-20018
Design of the CONSUL programming language
[AD-A189202] 13 p1815 N88-20841
An interface between object-oriented systems
[AD-A189245] 13 p1815 N88-20844
Designing equivalent semantic models for process creation
[CWI-CS-R8732] 13 p1819 N88-20872
Activities and operations of the Advanced Computing Research Facility, October 1986-October 1987
[DE88-006223] 14 p1955 N88-21653
On the productivity of recursive list definitions
[CS-8707] 14 p1960 N88-21692
Supercomputer environment
[AD-A190633] 15 p2107 N88-22551
MultiScheme: A parallel processing system based on MIT (Massachusetts Institute of Technology) scheme
[AD-A190383] 15 p2114 N88-22597
VPC: A proposal for a vector parallel C programming language
[AD-A190885] 16 p2251 N88-23451
Beyond Ada: Generating Ada code from equational specifications
[AD-A191866] 18 p2557 N88-25176
The FORCE
[AD-A193463] 23 p3264 N88-29429

PARALLEL STRIP LINES
U MICROSTRIP TRANSMISSION LINES

PARALLELOGRAMS
NT RHOMBOIDS

PARAMAGNETIC AMPLIFIERS
U MASERS

PARAMAGNETIC RESONANCE
NT ELECTRON PARAMAGNETIC RESONANCE
Paramagnetic spins in oxygen-loaded ceramic La2CuO4/sub 4+delta/
[DE88-007114] 19 p2619 N88-25539
Paramagnetic point defects in boron-implanted HgO.7CdO.3Te
[AD-A193276] 21 p3021 N88-27934

PARAMAGNETISM
Electron Spin Resonance (ESR) measurements on intermediate-valence Cer compounds doped with paramagnetic ions: CeOs2:Gd ion and CePd3:Mn-ion
[ETN-88-91081] 09 p1256 N88-17526
Superconducting and magnetic properties of Fe-doped oxide superconductors
[DE88-003024] 10 p1416 N88-18451
Nuclear magnetic ordering and paramagnetic relaxation of diatomic molecules in Ca (OH)2
[B8681469] 23 p3281 N88-29532

PARAMECIA
Investigations of Paramecium cells analyzed under microgravity conditions 07 p0884 N88-15367
Experiments concerning gravisensitivity of protozoa
12 p1660 N88-19949
The Paramecium experiment --- Spacelab D1 mission
22 p3060 N88-28161

PARAMETER IDENTIFICATION
Maximum likelihood estimates of parameters in linear systems with process and measurement noise
[DFVLR-FB-87-20] 01 p0083 N88-10532
Breakdown points of affine equivariant estimators of multivariate location and covariance matrices
[REPT-87-14] 01 p0088 N88-10574
Modeling XV-15 tilt-rotor aircraft dynamics by frequency and time-domain identification techniques
03 p0263 N88-11657
Integrated 3-parameter diagram for determining thermodynamic properties of fluids
03 p0298 N88-11874
Full-envelope aerodynamic modeling of the Harrier aircraft
[NASA-TM-88376] 05 p0552 N88-13363
Non-linear maximum likelihood estimation of stability derivatives from range data
[NAL-TM-SE-8608] 05 p0552 N88-13365
Robot accuracy improvement through kinematic parameter identification 06 p0712 N88-14363
A new method of boundary parameter estimation for a two-dimensional diffusion system under noisy observations
[NASA-CR-178405] 06 p0767 N88-14714
Lie algebraic method in filtering and identification
[CWI-PM-R8606] 08 p1072 N88-16487
Contribution to the design of flexible manufacturing systems: Modeling, simulation, and evaluation of parameters
[ISAL-IDI1-87-04] 09 p1151 N88-16894
Parameter identification and sensitivity analysis for a robotic manipulator arm
[NASA-CR-181608] 10 p1385 N88-18272
The estimation of target trajectory parameters from Closest Point of Approach (CPA) time measurements in a field of acoustic sensors
[FB-3-87] 11 p1439 N88-18586
Fixed and adaptive interframe image prediction for remote piloting application
[AD-A187987] 11 p1471 N88-18771
Using ridge regression in systematic pointing error corrections 11 p1472 N88-18777
Overview of multi-input frequency domain modal testing methods with an emphasis on sine testing
11 p1499 N88-18949
Application of the estimation method to parameter performance date of solar water heating systems
[INPE-4268-PRE/1141] 11 p1508 N88-19007
A maximum likelihood parameter estimation program for general non-linear systems
[ARL-AERO-TM-392] 11 p1532 N88-19154
Realtime pilot model parameter identification
[AD-A188873] 12 p1584 N88-19476
Aircraft flight flutter testing at the NASA Ames-Dryden Flight Research Facility
[NASA-TM-100417] 13 p1723 N88-20301
Material parameter measurements at high temperatures
[NASA-CR-182707] 13 p1739 N88-20397
On error equations for determining Earth rotation parameters with VLBI network 13 p1756 N88-20500
An automated procedure for material parameter evaluation for viscoplastic constitutive models
14 p1932 N88-21520
Identification of nonlinear rational systems using a prediction-error estimation algorithm
[RR-317] 14 p1959 N88-21680
Application of the NARMAX method to nonlinear frequency response estimation
[RR-319] 14 p1964 N88-21721
Deterministic approximations of probability inequalities
[REPT-87-43] 14 p1966 N88-21732
An orthogonal parameter estimation algorithm for nonlinear stochastic systems
[RR-307] 14 p1966 N88-21736
Parametric methods of analysing linear and nonlinear systems
[RR-318] 14 p1967 N88-21741
Optimal control and identification of space structures
[AD-A190033] 15 p2025 N88-22065
A survey of oscillating flow in Stirling engine heat exchangers
[NASA-CR-182108] 15 p2067 N88-22322
Boundary shape identification problems in two-dimensional domains related to thermal testing of materials
[NASA-CR-181654] 15 p2105 N88-22541
Consistent estimates of autoregressive parameters for autoregressive moving average models
[RR-663-I] 15 p2109 N88-22564
Parametric study of supersonic STOVL flight characteristics
[NASA-CR-177330] 16 p2161 N88-22893
Analysis and design of gain scheduled control systems
[NASA-CR-182867] 16 p2163 N88-22904
Maximum likelihood parameter identification of flexible spacecraft
[LR-508] 16 p2168 N88-22924
Studies in reliability and inference
[AD-A191389] 16 p2217 N88-23223
Optimal control, estimation compensation of linear discrete-time systems with stochastic parameters
[REPT-87-56] 16 p2255 N88-23478
An algebraic construction of a class of one-dependent processes
[REPT-87-65] 16 p2259 N88-23507
Control law parameterization for an aeroelastic wind-tunnel model equipped with an active roll control system and comparison with experiment
[NASA-TM-100593] 17 p2308 N88-23807
Parameter estimation for boundary value problems by integral equations of the second kind
[NASA-CR-181660] 17 p2332 N88-23918
Parameter identification methods for improving structural dynamic models
[NASA-TM-100812] 17 p2349 N88-23994
Estimation of time- and state-dependent delays and other parameters in functional differential equations
[NASA-CR-181663] 17 p2383 N88-24164
Minimal parameter solution of the orthogonal matrix differential equation
[NASA-TM-4043] 17 p2383 N88-24165
Application of spline functions to digital image processing
[ETN-88-92194] 17 p2392 N88-24218
A recursive prediction error parameter estimator for nonlinear models
[RR-326] 17 p2392 N88-24222
TVC (Thrust Vector Control) jet vane thermal modeling using parametric system identification
[AD-A191518] 18 p2474 N88-24678
A fast and efficient procedure for generalized cross-validation with large data sets. Application to image reconstruction
[RR-669-M] 18 p2563 N88-25220
Single-mode projection filters for modal parameter identification for flexible structures
[NASA-CR-182680] 18 p2566 N88-25244
Recursive maximum likelihood identification of a nonlinear output-affine model
[RR-322] 18 p2569 N88-25257
System identification in vehicle dynamics
[DFVLR-MITT-87-22] 20 p2785 N88-26518
Parameter estimation of dynamical systems
20 p2785 N88-26519
Flight vehicle system identification: Status and prospects 20 p2785 N88-26520
Modeling and parameter identification of motor vehicles 20 p2785 N88-26521
Parametric estimation of aerodynamic nonlinearities in rolling moment due to sideslip using maximum likelihood method 20 p2786 N88-26528
Flight test preparation and measuring data validation for parameter identification 20 p2786 N88-26529
Application of complementary parameter identification techniques to flight test data of a transport aircraft
20 p2787 N88-26533
Parameter identification of the passenger simulation model MADYMO: Methods and experience
20 p2788 N88-26536
Parameter identification of material constants in a composite shell structure
[DE88-008115] 22 p3086 N88-28326
Parametric identification of mechanical structures
[ETN-88-92881] 22 p3088 N88-28339
Estimation of aircraft parameters using filter error methods and extended Kalman filter
[DFVLR-FB-88-15] 23 p3176 N88-28911
Identification and control of time-varying flexible structures: An artificial intelligence approach
23 p3265 N88-29437
Procedures for updating dynamic mathematical models, test phase --- spacecraft hardware
[MEBS-38/87] 24 p3335 N88-29852

PARAMETERIZATION
NT PARAMETER IDENTIFICATION
Moisture determinations in and under vegetation canopies. Part 2: Results after parameterization of the CLOUD model
[FEL-1986-63] 01 p0064 N88-10410
Description of NCAR (National Center for Atmospheric Research) Community Climate Model (CCM1)
[PB87-203782] 01 p0072 N88-10462
Statistically determined nickel cadmium performance relationships 02 p0165 N88-11039
Parametrization in scattering models
03 p0304 N88-11916

Nonlinear parametric least-squares adjustment
[AD-A184039] 03 p0371 N88-12336
Simulation studies for surfaces and materials strength
[NASA-CR-181535] 04 p0412 N88-12557
Local-optimal control in systems with delay
04 p0424 N88-12627
A review of parameterizations of microphysical processes in clouds for application in models of regional atmospheric deposition
[DE88-000451] 04 p0471 N88-12909
Estimation of a multivariate continuous variable panel model
[AD-A184472] 04 p0484 N88-12982
A system identification technique based on the random decrement signatures. Part 1: Theory and simulation
05 p0594 N88-13625
Fatigue crack growth: Statistical considerations
05 p0606 N88-13718
Nitrogen scale-up
[AD-A185702] 06 p0709 N88-14351
Report of the second session of the CAS/JSC working group on numerical experimentation — weather forecasting
[WMO/TD-168] 06 p0745 N88-14579
Balanced realizations: Canonical form, parametrization, model reduction
[PB87-123360] 06 p0757 N88-14642
Development of symbolic computation methods for nonlinear dynamics
[AD-A185562] 06 p0758 N88-14653
Asymptotically stable all-pass transfer functions: Canonical form, parametrization and realization
[PB87-123972] 06 p0763 N88-14684
A three-parameter generalisation of the beta-binomial distribution with applications
[AD-A185733] 06 p0768 N88-14720
Plasma parameters for alternate operating modes of TIBER-2
[DE88-001890] 06 p0783 N88-14802
TIBER 2 (Tokamak Ignition/Burn Experimental Reactor) parameters with neutral beams at high energies
[DE88-001891] 06 p0783 N88-14803
Parameter estimation for the Dirichlet-Multinomial Distribution (DMD) using supplementary beta-binomial data
[AD-A186335] 07 p0911 N88-15524
Energetics and dynamics of simple impulsive solar flares
[NASA-TM-87816] 07 p0947 N88-15755
Effect of extraneous factors on optical one-phonon transitions in impurity centers with cubic symmetry
08 p1077 N88-16496
Relativistic Calogero-Moser systems and solutions
[CWI-PM-R8702] 08 p1092 N88-16570
The accuracy of the radiation parameterization in mesoscale models
[DFVLR-IB-553-85/11] 09 p1190 N88-17133
Development of a physically-based general circulation model parameterization of clouds and their radiative interactions
[DE88-004060] 09 p1194 N88-17154
Fitting a generalized parabola to data
[NPL-DITC-96/87] 09 p1229 N88-17364
The TITAN Reversed-Field Pinch Reactor: Design-point determination and parametric studies
[DE88-001824] 09 p1251 N88-17498
Parametric study of choke flutter with a linear theory
10 p1283 N88-17673
Parameterization of radiative transfer in the Earth's atmosphere with specific applications to clouds
10 p1353 N88-18087
Effect of hypercapnic-hypoxic test on cariorespiratory parameters of individuals with neurocirculatory dystonia
10 p1367 N88-18169
Unidimensional Rasch model and multidimensional data: An analytic approach
[PB88-105861] 10 p1372 N88-18187
Hierachical object recognition using libraries of parameterized model sub-parts
[AD-A187476] 10 p1396 N88-18322
Semiempirical studies of atomic structure
[DE88-004096] 10 p1407 N88-18392
Analysis of learning curve fitting techniques
[AD-A187680] 11 p1535 N88-19173
Stochastic heuristics in network design: Parameter tuning and performance evaluation
[REPT-87-017] 11 p1541 N88-19210
Development savings through parametric modeling of program costs 12 p1700 N88-20175
Picking winners: Parametric cost estimating and project management 12 p1700 N88-20176
Parametric study of acceleration-induced stresses and frequency changes in doubly-rotated crystal resonators
[AD-A189261] 13 p1761 N88-20532
Generalized expression for radio navigation parameter error 13 p1787 N88-20691
Algebraic specifications for parameterized data types: The case of minimal computable algebras and parameters with equality
[CWI-CS-R8714] 13 p1826 N88-20916
Model structure selection for multivariable systems by cross-validation methods
[EUT-87-E-176] 13 p1827 N88-20926
The parameterization of orthogonal matrices: A review mainly for statisticians
[AD-A189144] 13 p1829 N88-20936
Non- and semi-parametric maximum likelihood estimators and the von Misis Method, part 1
[CWI-MS-R8709] 13 p1829 N88-20941
Representation of physical processes in global atmospheric models 14 p1935 N88-21542
Parameterization of radiation in a general circulation model 14 p1935 N88-21543
The role of radiation transfer in climate modification
14 p1936 N88-21549
An introduction to the parameterization of land-surface processes 14 p1937 N88-21554
Concentration inequalities for Gauss Markov estimators
[CWI-MS-R8706] 14 p1965 N88-21726
On a consistent estimate of the index of an extreme value distribution
[CWI-MS-R8710] 14 p1966 N88-21729
A robust scale estimator based on the shortest half
[REPT-87-36] 14 p1966 N88-21731
Modeling failures of intermittently used machines
[AD-A190298] 15 p2074 N88-22367
Parameterization of horizontal wind velocity variability
[AD-A190107] 15 p2097 N88-22493
Computer program for parameterization of nucleus-nucleus electromagnetic dissociation cross sections
[NASA-TM-4038] 16 p2270 N88-23584
Digital monoplotting, part 2
[B8735122-PT-2] 17 p2369 N88-24107
The liquid droplet radiator in space: A parametric approach 17 p2427 N88-24437
Analysis of lightning field changes during active thunderstorms in Florida 18 p2545 N88-25103
Making progress during a stall in the simplex algorithm
[DE88-007120] 18 p2558 N88-25182
Fast parametrization procedure for solar cells
[PB88-186416] 19 p2686 N88-25966
Scaling laws for geomagnetic tail current sheet acceleration
[AD-A193379] 19 p2691 N88-25998
Structural properties of multivariable linear systems
[PB88-181375] 19 p2717 N88-26134
Calculating the self-intersections of Bezier curves
[AD-A192371] 19 p2721 N88-26156
The Potts model in a random field
19 p2721 N88-26158
Parametric methodologies of cloud vertical transport for acid deposition models
[PB88-191374] 20 p2825 N88-26762
Lattice strain in heteroepitaxial films
20 p2868 N88-27032
An aspect graph-based control strategy for 3-D object recognition 21 p2927 N88-27377
Development of radiation and cloud parameterization programs for AFGL (Air Force Geophysics Laboratory) global models
[AD-A193369] 21 p2973 N88-27658
Design of multirate control systems via parameter optimization
[REPT-87-013] 22 p3142 N88-28686
Boundary layer manipulation 23 p3170 N88-28877
Human auditory and visual continuous evoked potentials 23 p3238 N88-29269
A fast parametric maximum flow algorithm, revision
[AD-A194026] 23 p3250 N88-29345
Properties of strong coupled superconductors
[DE88-702050] 23 p3287 N88-29574

PARAMETERS
U INDEPENDENT VARIABLES

PARAMETRIC AMPLIFIERS
Phase phenomena in parametric generators and amplifiers of ultrashort light pulses
07 p0918 N88-15576

PARAMETRIC OSCILLATORS
U PARAMETRIC AMPLIFIERS

PARASITIC DISEASES
TOMS as a monitor of the ultraviolet radiation environment: Applications to photobiology
05 p0617 N88-13785

PARITY
Coupled even-parity superconducting states: Square lattice
[AD-A193432] 21 p3022 N88-27938

PARKS
Comparative utilization of analog and digital processes in the treatment of MSS-LANDSAT data for studying the national parks of Brazil
[INPE-4011-TDL/240] 15 p2090 N88-22456
Temporal analysis of the changes in Parque Estadual de Jacupiranga vegetation through digital treatment of LANDSAT imagery 17 p2367 N88-24094

PARSING ALGORITHMS
Automated program recognition
[AD-A186421] 07 p0903 N88-15472
Semi-applicative programming
10 p1380 N88-18239
A parser generator for finitely ambiguous context-free grammars
[CWI-CS-R8712] 13 p1818 N88-20864
Evaluation of a parallel chart parser
[AD-A189172] 14 p1959 N88-21685
Programmer-friendly LL(1) parser generator
[PB88-126933] 20 p2841 N88-26857
A cockpit natural language study: Vocabulary and grammar analyses
[AD-A193289] 21 p2993 N88-27753

PARTIAL DIFFERENTIAL EQUATIONS
NT BIHARMONIC EQUATIONS
NT BURGER EQUATION
NT CAUCHY-RIEMANN EQUATIONS
NT ELLIPTIC DIFFERENTIAL EQUATIONS
NT EULER-CAUCHY EQUATIONS
NT FOKKER-PLANCK EQUATION
NT GAUSS EQUATION
NT HELMHOLTZ VORTICITY EQUATION
NT PARABOLIC DIFFERENTIAL EQUATIONS
NT POISSON EQUATION
NT VLASOV EQUATIONS
On the relational modeling of discrete PDE problems
[DE87-013336] 02 p0224 N88-11409
Determination of fractal dimension, connection of space and temporal chaos and application to experimental results 03 p0313 N88-11977
Numerical solution of partial differential equations on irregular grids
[DE87-014760] 03 p0369 N88-12324
Application of the finite difference method to the solution of mixed partial differential equations for the case of transonic flow
[ETN-87-90760] 03 p0370 N88-12327
Optimization of explicit time-stepping algorithms and Stream-Function-Coordinate (SFC) concept for fluid dynamics problems 04 p0445 N88-12762
A comparison of adaptive refinement techniques for elliptic problems
[DE88-000805] 04 p0485 N88-12987
Two classes of preconditioners computed using block matrix factorization techniques
[DE88-001313] 04 p0485 N88-12988
Numerical and analytical methods in nonlinear partial differential equations
[AD-A185210] 05 p0641 N88-13918
The Eckhaus Partial Differential Equation (PDE) I psi t + psi xx + 2(psi/sq)x psi +2(/psi/) to the 4th power psi = 0
[PREPRINT-546] 06 p0763 N88-14686
Equations of nonlinear Schroedinger type in 1 + 1 and 2 + 1 dimensions, obtained from integrable Partial Differential Equations (PDEs)
[PREPRINT-548] 06 p0764 N88-14687
Nonisospectral deformations and Darboux transformations for the 3rd order spectral problem
[PREPRINT-558] 06 p0764 N88-14690
Nonlinear evolution equations, rescalings, model partial differential equations (PDES) and their integrability, 2
[PREPRINT-560] 06 p0764 N88-14691
New methods for numerical solution of one class of strongly nonlinear partial differential equations with applications
[AD-A186166] 07 p0899 N88-15445
Local uniform mesh refinement for partial differential equations
[AD-A186312] 07 p0910 N88-15519
The paradoxical asymptotic status of massless springs
[AD-A185625] 07 p0928 N88-15637
Numerical experiments with a parallel conjugate gradient method
[DE88-002178] 08 p1066 N88-16445
Some stability results for the hopscotch difference method when applied to convection-diffusion equations
[CWI-NM-R8711] 08 p1072 N88-16465
Supercomputers for solving PDE (Partial Differential Equations) problems
[AD-A186583] 09 p1215 N88-17283
Feedback stabilization of distributed systems
[AD-A187111] 09 p1222 N88-17328
Techniques in linear and nonlinear partial differential equations
[AD-A187109] 09 p1227 N88-17347

Explicit-implicit methods for time-dependent partial differential equations
[CWI-NM-R8703] 09 p1228 N88-17355
Preconditioned iterative methods for partial differential equations
[DE88-003071] 09 p1230 N88-17372
Programming methodology and performance issues for advanced computer architectures
[DE88-003098] 10 p1387 N88-18287
Nonlinear filtering and large deviations: A PDE-Control theoretic approach
[AD-A187436] 10 p1396 N88-18321
A multigrid preconditioner applied to a two-dimensional convection-diffusion problem
[DE88-004765] 10 p1397 N88-18329
Parallels between control PDE's (Partial Differential Equations) and systems of ODE's (Ordinary Differential Equations)
[NASA-CR-182487] 10 p1398 N88-18331
On observer problems for systems governed by partial differential equations
[AD-A187430] 10 p1400 N88-18351
Applications of Lie group methods to the equations of magnetohydrodynamics 10 p1411 N88-18422
Canonical coordinates for partial differential equations
[NASA-CR-182486] 11 p1535 N88-19170
Conference on Maximum Principles and Eigenvalue Problems in Partial Differential Equations
[AD-A187870] 11 p1536 N88-19175
Multigrid methods in convex optimization 11 p1538 N88-19190
The Euler-Bernoulli beam equation with boundary energy dissipation
[AD-A189517] 13 p1765 N88-20560
Propagator solutions of partial differential equations applied to plasma transport
[DE88-006432] 13 p1816 N88-20852
Spectral element methods: Algorithms and architectures
[NASA-CR-182701] 13 p1820 N88-20878
Numerical solution of ill posed problems in partial differential equations
[AD-A189383] 13 p1825 N88-20909
A Lagrangian moving grid scheme for one-dimensional evolutionary partial differential equations
[CWI-NM-R8713] 13 p1827 N88-20922
Stabilization of explicit difference schemes by smoothing techniques
[CWI-NM-R8714] 13 p1827 N88-20923
Nonlinear differential equations
[DE88-006047] 13 p1828 N88-20933
Lie groups in prolongation theory
[B8721781] 14 p1967 N88-21743
New methods for numerical solution of one class of strongly nonlinear partial differential equations with applications
[AD-A189945] 15 p2119 N88-22630
Research in nonlinear partial differential equations and bifurcation theory
[AD-A190986] 16 p2260 N88-23514
Similarity solutions of nonlinear partial differential equations invariant to a family of affine groups
[DE88-003404] 18 p2567 N88-25245
Computer science research, 1987: Computation Directorate
[DE88-006637] 20 p2834 N88-26812
Nontrivial critical points for asymptotically quadratic function
[DE88-101851] 20 p2845 N88-26881
Feedback control of a hyperbolic partial-differential equation with viscoelastic damping
[AD-A192896] 21 p3003 N88-27810
Numerical optimization
[AD-A193032] 21 p3005 N88-27827
Unified multilevel adaptive finite element methods for elliptic problems
[DE88-011938] 21 p3007 N88-27840
Application of differential quadrature to the analysis of structural components 22 p3087 N88-28331
Why are certain nonlinear Partial Differential Equations (PDE) both widely applicable and integrable
[PREPRINT-582] 22 p3144 N88-28698
The construction of implicit and explicit solitary wave solutions of nonlinear partial differential equations
[AD-A193475] 23 p3269 N88-29452
MACSYMA program for the painleve test of nonlinear ordinary and partial differential equations
[AD-A194293] 23 p3270 N88-29458
Laser sensing for identification and control of distributed parameter systems
[AD-A195886] 24 p3379 N88-30124
Multiple solutions and bifurcation for a class of nonlinear Sturm-Liouville eigenvalue problems on an unbounded domain
[AD-A195954] 24 p3426 N88-30389

PARTIAL PRESSURE
NT OXYGEN TENSION
Inerting and atmospheres 04 p0406 N88-12524
Nitrogen's biological effect on oxygen transport through hematoparenchymal barrier 12 p1662 N88-19967
Phase transformations and thermodynamic behavior of the YBa2Cu3O(sub)x system via EMF measurements
[DE88-010054] 20 p2878 N88-27086

PARTICLE ACCELERATION
Channeled particle acceleration by plasma waves in metals
[DE87-010541] 01 p0093 N88-10604
Particle injection and cosmic ray acceleration at collisionless parallel shocks
[DE88-000507] 04 p0430 N88-12665
Prompt simultaneous acceleration of protons and electrons to relativistic energies by shock waves in solar flares
[IPPJ-851] 04 p0493 N88-13037
Optimization of charged particle acceleration rate over wave parameters in the scheme with acceleration by surface electromagnetic waves
[DE88-700320] 07 p0846 N88-15134
Experimental evaluation for efficiency of excitation slow plasma and cyclotron waves in collective accelerators
[DE88-700566] 07 p0936 N88-15687
Solar event of 27 April 1981 08 p1004 N88-16084
Characteristics of particle acceleration at high latitude 08 p1026 N88-16210
First results from the Viking associated Aureld-VIP rocket and EISCAT campaign --- auroras; Swedish satellite 08 p1026 N88-16211
Acceleration of auroral particles by magnetic field-aligned electric fields 08 p1031 N88-16246
Low frequency waves and small scale solitary structures observed by Viking --- Swedish satellite; auroras 08 p1099 N88-16611
On the potential role of concentrated field-aligned currents in solar physics 08 p1099 N88-16614
Acceleration of auroral particles by magnetic field-aligned electric fields
[TRITA-EPP-87-08] 09 p1190 N88-17131
Determination of molecular-ion structures through the use of accelerated beams
[DE88-002960] 09 p1246 N88-17467
Advanced nonlinear theory: Long-term stability at the SSC
[CEBAF-PR-87-027] 11 p1546 N88-19246
Waves and static electric fields in the auroral acceleration region 12 p1646 N88-19856
The lattice nonlinearities and the long term stability of the SSC
[CEBAF-PR-87-009] 12 p1690 N88-20108
On the acceleration of electrons and positive ions in the same direction along magnetic field lines by parallel electric fields
[IRF-PREPRINT-103] 15 p2096 N88-22488
A chemical method for achieving acceleration of macroparticles to ultrahigh velocities
[DE88-006377] 15 p2128 N88-22695
Particle acceleration to high energies and amplification of coherent radiation by electromagnetic interactions in plasmas
[DE88-701020] 15 p2135 N88-22737
Simultaneous observation of upward moving field aligned energetic electrons and ions on auroral zone field lines
[IRF-PREPRINT-102] 16 p2231 N88-23326
Numerical simulation for particle acceleration and trapping by an electromagnetic wave 16 p2277 N88-23626
Scaling laws for geomagnetic tail current sheet acceleration
[AD-A193379] 19 p2691 N88-25998
Mechanisms for particle acceleration: Possibilities and constraints
[PB88-102538] 19 p2725 N88-26184
Accelerator research studies
[DE88-008236] 19 p2726 N88-26187

PARTICLE ACCELERATOR TARGETS
Development of nuclear models for higher energy calculations
[DE88-010919] 20 p2852 N88-26932

PARTICLE ACCELERATORS
NT BETATRONS
NT CYCLIC ACCELERATORS
NT ELECTRON ACCELERATORS
NT ION ACCELERATORS
NT LINEAR ACCELERATORS
NT MICROTRONS
NT STORAGE RINGS (PARTICLE ACCELERATORS)
NT SUPERCONDUCTING SUPER COLLIDER
NT SYNCHROTRONS
NT VAN DE GRAAFF ACCELERATORS
Investigations into the design of multi-terawatt magnetic switches
[DE87-012014] 01 p0040 N88-10254
Recording multiple signals on a single waveform recorder
[DE87-011632] 01 p0049 N88-10313
Open accelerating structures
[DE87-010540] 01 p0092 N88-10603
Current experiments in elementary particle physics
[DE87-013961] 02 p0231 N88-11456
Experimental nuclear physics
[DE87-014586] 02 p0231 N88-11459
Electron interactions with nuclei
[DE87-014587] 02 p0232 N88-11460
Saturn: A large area X-ray simulation accelerator
[DE87-012021] 02 p0233 N88-11472
Volume produced H(-),D(-) ion source for proton accelerator and thermo-nuclear fusion research by sheet plasma (III)
[IPPJ-838] 02 p0242 N88-11531
The LPX (Long Pulse Experiment) facility
[DE87-010493] 03 p0311 N88-11964
A scientific workstation operator-interface for accelerator control
[DE87-014689] 03 p0362 N88-12278
Energy cascading in the beat-wave accelerator
[DE87-014727] 03 p0377 N88-12374
The role of basic research in society
[DE88-000459] 04 p0502 N88-13090
Experimental studies of elementary particle interactions at high energies
[DE88-000804] 05 p0648 N88-13971
The standard theory group: Summary and conclusions
[PREPRINT-551] 06 p0778 N88-14776
A possible accelerator experiment to solve the solar neutrino puzzle
[PREPRINT-556] 06 p0778 N88-14778
Collider constraints in the choices for wavelength and gradient scaling
[PB87-123691] 06 p0779 N88-14783
Simulation of effect on biological systems of impact wave from heavy charged particle track 07 p0896 N88-15429
Accelerators and Superconductivity: A Marriage of Convenience. Second John Adams Memorial Lecture
[DE88-700005] 07 p0931 N88-15656
High midplane accessibility stellarator windings for high current toroidal accelerators
[AD-A186235] 07 p0933 N88-15665
Design considerations for a negative ion source for DC operation of high-power, multi-megaelectron-volt neutral beams
[DE88-002692] 08 p1083 N88-16525
Solid antimatter
[PB87-166146] 09 p1259 N88-17549
The implementation of artificial intelligence in control systems
[DE88-003497] 10 p1396 N88-18318
The numerical simulation of accelerator components
[DE87-011597] 10 p1412 N88-18423
Incorporation of multigrid in accelerator software --- particle accelerators 11 p1539 N88-19199
Theory of elementary particle studies in weak iteration and grand unification and studies in accelerator design
[DE88-004261] 11 p1545 N88-19238
ZAP user's manual
[LBL-21270] 11 p1546 N88-19248
Initial operation of the Tevatron collider
[FNAL-TM-1449] 11 p1547 N88-19252
The CEBAF project and its few-body research program
[CEBAF-PR-87-014] 11 p1547 N88-19253
Mechanical design and construction of a 200 mA, 100 keV, dc, negative ion accelerator
[DE88-003855] 11 p1548 N88-19257
A practical guide to modern high energy particle accelerators
[DE88-004035] 11 p1548 N88-19260
Time-dependent Slow-Time-Scale theory of free-running and phase-locked gyrotron oscillators
[AD-A188910] 12 p1629 N88-19752
Development of electrostatic-accelerator free-electron lasers
[AD-A189507] 13 p1774 N88-20614
Collective acceleration of electrons and ions in a high relativistic electron beam
[DE88-005261] 13 p1838 N88-20998
Space experiments with particle accelerators (SEPAC): Description of instrumentation
[NASA-TM-89728] 14 p1945 N88-21606
Tutorial on computer control
[DE88-006185] 18 p2554 N88-25157
Computer programs for high-current beam transport in accelerators
[AD-A192356] 20 p2838 N88-26835

Superconducting rf and beam-cavity interactions
[DE88-008598] 20 p2852 N88-26936
Activities report of the Werner-Heisenberg Institute of Physics
[ETN-88-92946] 21 p3015 N88-27893

PARTICLE BEAMS
NT ATOMIC BEAMS
NT ELECTRON BEAMS
NT ION BEAMS
NT MOLECULAR BEAMS
NT NEUTRAL BEAMS
NT NEUTRINO BEAMS
NT NEUTRON BEAMS
NT PROTON BEAMS
NT RELATIVISTIC ELECTRON BEAMS
Status of inertial fusion
[DE87-010988] 01 p0099 N88-10654
Frozen-field, rigid-beam, uniform-conductivity-channel tracking force calculation
[DE87-012510] 02 p0190 N88-11190
Saturn: A large area X-ray simulation accelerator
[DE87-012021] 02 p0233 N88-11472
The LPX (Long Pulse Experiment) facility
[DE87-010493] 03 p0311 N88-11964
Single wire drift chamber design
[DE87-011002] 07 p0857 N88-15205
Physics and chemistry 07 p0883 N88-15359
Determination of beam orientation of optical diagnostics of excited 200-MeV hydrogen atoms resulting from photodetachment of H(-)ions
[AD-A189976] 14 p1981 N88-21823
Particle beam alignment system for single event upset-Van de Graaf experiments
[AD-A189695] 15 p2132 N88-22721
Utilization of dense packed planar acoustic echosounders to identify turbulence structure in the lowest levels of the atmosphere
[AD-A191006] 16 p2233 N88-23335
Bevalac external beamline optics
[LBL-23240] 19 p2727 N88-26194
Electron-impact-ionization and electron-attachment cross sections of radicals important in transient gaseous discharges
[AD-A192248] 20 p2770 N88-26424
Computer programs for high-current beam transport in accelerators
[AD-A192356] 20 p2838 N88-26835
Propagation of charged particle beams in the atmosphere
[AD-A193185] 21 p3014 N88-27887
Effects of charge distribution within a particle beam on the sub-Cerenkov radiation
[AD-A193992] 22 p3150 N88-28742
Beam optics test stand
[AD-A193901] 23 p3216 N88-29144
Moment invariants for particle beams
[DE88-011052] 23 p3281 N88-29537
Nonlinear analysis of non-neutral plasmas
[AD-A192506] 23 p3284 N88-29556
Cluster beam studies
[AD-A195182] 24 p3434 N88-30443

PARTICLE CHARGING
Combined aerodynamic size, charge-to-mass, and velocity measurements of aerosol particles
[ST-REPT-VOL-5-NO-4] 14 p1944 N88-21599

PARTICLE COLLISIONS
Relativisitic heavy ion collisions
[DE87-014292] 02 p0232 N88-11462
A conceptual design of Final Focus Systems for linear colliders
[DE87-012840] 02 p0234 N88-11475
A relativistic Monte Carlo binary collision model for use in plasma particle simulation codes
[DE87-013287] 02 p0237 N88-11494
Nonequilibrium characteristics of nitrogen plasmas appropriate to an AOTV flight 03 p0319 N88-12019
Light scattering by oriented and randomly dispersed chiral particles
[DE87-014758] 03 p0376 N88-12368
W decays
[NOTA-INTERNA-877] 05 p0648 N88-13966
The kinetics and dynamics of iodine monofluoride formation in gas-phase collisions
[AD-A185715] 06 p0709 N88-14352
On the meteor trail spectra 06 p0737 N88-14533
Vector boson pair production in e(+)e(-) collisions
[PREPRINT-549] 06 p0778 N88-14774
Single weak gauge boson production at CLIC
[PREPRINT-550] 06 p0778 N88-14775
The standard theory group: Summary and conclusions
[PREPRINT-551] 06 p0778 N88-14776
Collider constraints in the choices for wavelength and gradient scaling
[PB87-123691] 06 p0779 N88-14783
Interaction of intense electromagnetic fields with SF/sub 6/ molecules and clusters in supersonic expansion
[DE88-700310] 07 p0846 N88-15132
Planetary science 07 p0883 N88-15356
Analysis of relativistic nucleus-nucleus interactions in emulsion chambers 07 p0926 N88-15624
Parton densities from deep inelastic scattering to hadronic processes at super collider energies
[NOTA-INTERNA-885] 07 p0930 N88-15646
Correlation effects on double electron capture in highly-charged, low-energy ion-atom collisions
[DE87-013179] 07 p0930 N88-15651
Study of tau pairs and search for new particles
[B8680488] 07 p0931 N88-15655
Resonance excitation in gamma gamma collisions at LEP200
[NIKHEF-H/87-3] 08 p1081 N88-16514
Status of cross section data for photon scattering by atoms
[DE87-011281] 08 p1081 N88-16517
Event classification in (anti)neutrino experiments using an Internal Picket Fence-External Muon Identifier (IPF-EMI) detector system
[NIKHEF-H/87-6] 09 p1245 N88-17457
Initial operation of the Tevatron collider
[FNAL-TM-1449] 11 p1547 N88-19252
Simulation of nuclear collisions at high energies in the frames of quark-gluon string model
[DE88-700914] 12 p1690 N88-20113
Fragmentation and flow in central collisions
[DE88-005386] 13 p1837 N88-20991
Hadronic overlap and total multiplicity distributions in high energy physics collisions
[NIKHEF-H/87-10] 13 p1838 N88-21001
The astrophysics of nebulae and active galactic nuclear emission-line regions: New methods and applications
13 p1858 N88-21111
Ground-state correlations in C12 and the mechanism of the (e,e'p) reaction
[B8729349] 14 p1980 N88-21816
Summary of supersymmetric particle search with the CELLO detector at Petra (Italy)
[NOTA-INTERNA-898] 14 p1980 N88-21818
Analysis of hadron production in deep inelastic muon-proton collisions through the fire-string model
[PREPRINT-578] 14 p1981 N88-21822
The silicon microstrip detector --- particle position measurement
[ETN-88-92235] 16 p2210 N88-23189
Ion generator and ion application system
[NASA-CASE-MFS-28122-1] 17 p2397 N88-24253
A new approach to generating negative ion beams
[AD-A191119] 18 p2572 N88-25276
Calorimetry applied to nucleus-nucleus collisions at ultrarelativistic energies
[DE88-006173] 18 p2573 N88-25282
Theoretical investigations of drift waves in a magnetic quadrupole 18 p2578 N88-25312
Heavy ion collisions with A = 10(sup 57): Aspects of nuclear stability and the nuclear equation of state in coalescing neutron-star binary systems
[DE88-008029] 19 p2741 N88-26277
Charged pion production and projectile breakup in 85A MeV(sup)12C induced heavy ion reactions
[LUIP-8802] 20 p2850 N88-26920

PARTICLE COUNTERS
U RADIATION COUNTERS

PARTICLE DECAY
U RADIOACTIVE DECAY

PARTICLE DENSITY (CONCENTRATION)
NT CARRIER DENSITY (SOLID STATE)
NT ELECTRON DENSITY (CONCENTRATION)
NT ELECTRON DENSITY PROFILES
NT ELECTRON DISTRIBUTION
NT ION DENSITY (CONCENTRATION)
NT IONOSPHERIC ELECTRON DENSITY
NT IONOSPHERIC ION DENSITY
NT MAGNETOSPHERIC ELECTRON DENSITY
NT MAGNETOSPHERIC ION DENSITY
NT PLASMA DENSITY
NT PROTON DENSITY (CONCENTRATION)
Design study for measurement of neutral hydrogen atom density by laser induced fluorescence method
[DE87-752964] 02 p0179 N88-11114
Performance and operating envelope of imaging and scattering particle sizing instruments
[NASA-CR-180859] 03 p0323 N88-12042
Restoration of particle pitch angle distribution functions by a maximum entropy algorithm
[ATR-86(7098)-3] 05 p0648 N88-13969
Parton densities from deep inelastic scattering to hadronic processes at super collider energies
[NOTA-INTERNA-885] 07 p0930 N88-15646
CAESAR investigations — Coordinated Auroral Experiment using Scatter And Rockets (CAESAR)
08 p1031 N88-16249
Fluidization mechanisms in slurry flows
[DE88-005191] 13 p1766 N88-20563
Velocity and concentration measurements in flowing suspensions by nuclear magnetic resonance
[DE88-006225] 13 p1770 N88-20589
Dense-spray structure and phenomena. Part 1. Turbulence/dispersed-phase interactions
[AD-A190606] 15 p2065 N88-22315
Quantitative particle characterization by scattered ultrasound 20 p2848 N88-26908
The influence of ionization within a plasma opening switch
[AD-A193147] 21 p3017 N88-27906
Optical measurements of soot in premixed flames
[NASA-TM-101305] 24 p3373 N88-30090

PARTICLE DETECTORS
U RADIATION COUNTERS

PARTICLE DIFFUSION
NT IONIC DIFFUSION
Influence of a magnetic field on the diffusion of small particles in a turbulent flow
[DE87-702877] 01 p0046 N88-10291
Solar cosmic ray propagation in high-velocity solar wind stream 08 p1002 N88-16073
Investigations of the influence of chemical reactions of the vertical flow of gaseous and particulate compounds
08 p1017 N88-16165
Observation of injected silicon in heliotron E
17 p2441 N88-24524

PARTICLE EMISSION
NT ELECTRON EMISSION
NT FIELD EMISSION
NT ION EMISSION
NT NEUTRON EMISSION
NT PHOTOELECTRIC EMISSION
NT SECONDARY EMISSION
NT THERMIONIC EMISSION
Research in particles and fields
[NASA-CR-180412] 01 p0119 N88-10763
Single leptons from heavy quark production
[DE87-014917] 04 p0488 N88-13009
On the spatial structure of the Perseids meteor stream
06 p0740 N88-14550
WIPP (Wave Induced Particle Precipitation) experiment logistic support
[AD-A191184] 18 p2499 N88-24824
A theoretical determination of the density at a traveling source that emitts particles
[ISAS-RN-351] 21 p3013 N88-27883
Positron emission tomography: A new technique for observing fluid behavior in engineering systems
[PNR90471] 24 p3374 N88-30091

PARTICLE ENERGY
NT ELECTRON ENERGY
NT ELECTRON STATES
NT PROTON ENERGY
Cosmic-ray nuclear event with an anomalously strong concentration of energy and particles in the central region
[DE87-703376] 04 p0526 N88-13213
Inelastic two composite particle systems scattering at high energy
[DE88-701841] 20 p2851 N88-26928
The low-latitude auroral boundary: Steady-state and time-dependent representations
[AD-A193200] 21 p2972 N88-27656
Solar flares and magnetospheric particles: Investigations based upon the ONR-602 and ONR-604 experiments
[AD-A193396] 21 p3031 N88-27994

PARTICLE FLUX
U FLUX (RATE)

PARTICLE FLUX DENSITY
NT ELECTRON FLUX DENSITY
NT NEUTRON FLUX DENSITY
A processing method and results of meteor shower radar observations 06 p0738 N88-14539
Photographic fireball networks
06 p0738 N88-14540
A method of long-term radar shower data analysis
06 p0738 N88-14541
Incident meteoroid flux density
06 p0739 N88-14542
Models of sporadic meteor body distributions
06 p0739 N88-14543
On meteor stream spatial structure theory
06 p0739 N88-14544
Results of observations of the Eta Aquarid and Orionid meteor showers in 1980-1984 06 p0740 N88-14548
Structural peculiarities of the Quadrantid meteor shower 06 p0740 N88-14552

PARTICLE IN CELL TECHNIQUE
Trajectory versus PIC methods in diode design
[DE87-012135] 02 p0166 N88-11043
Numerical simulation of Tollmien-Schlichting waves by use of a modified vortex particle-in-cell method
[IC-AERO-85-02] 02 p0171 N88-11079

QUICKSILVER: A 3D, electromagnetic, PIC code
[DE87-013013] 02 p0245 N88-11547
FLIP (Fluid-Implicit-Particle): A low-dissipation, particle-in-cell method for fluid flow
[DE87-014745] 03 p0313 N88-11981
Performance and optimization of direct implicit time integration schemes for use in electrostatic particle simulation codes
[DE88-003254] 10 p1406 N88-18381
Development of Electromagnetic PIC code for LIB diode 16 p2276 N88-23622
Numerical simulation for particle acceleration and trapping by an electromagnetic wave 16 p2277 N88-23626
Two-dimensional focusing of self-magnetically insulated plasma focus diode 16 p2278 N88-23639
QN3D: A 3-dimensional quasi-neutral hybrid particle-in-cell code with applications to the tilt mode instability in field reversed configurations 18 p2580 N88-25325
Hybrid simulations
[DE88-009125] 19 p2715 N88-26123
Computer programs for high-current beam transport in accelerators
[AD-A192356] 20 p2838 N88-26835

PARTICLE INTERACTIONS
NT ELECTRON CAPTURE
NT ELEMENTARY PARTICLE INTERACTIONS
NT HIGH ENERGY INTERACTIONS
NT MOLECULAR COLLISIONS
NT MOLECULAR INTERACTIONS
NT NUCLEAR CAPTURE
NT NUCLEAR INTERACTIONS
NT NUCLEON-NUCLEON INTERACTIONS
NT PLASMA-PARTICLE INTERACTIONS
NT STRONG INTERACTIONS (FIELD THEORY)
NT WEAK ENERGY INTERACTIONS
NT WEAK INTERACTIONS (FIELD THEORY)
Relativisitic heavy ion collisions
[DE87-014292] 02 p0232 N88-11462
Superfluid He4 as a solar neutrino detector
[DE87-014477] 02 p0257 N88-11625
Momentum transport and particle dynamics in turbulent shear flows 03 p0317 N88-12002
On charm decays: Present status and future goals
[DE87-013586] 03 p0375 N88-12356
Particle physics and cosmology
[DE87-005400] 03 p0387 N88-12432
Future directions in interplays between particle and nuclear physics: Summary session
[DE87-011791] 04 p0489 N88-13013
The formation and thermochemical properties of multiligand complexes
[AD-A184935] 05 p0561 N88-13416
Feasibility study for gas-grain simulation facility
[NASA-CR-177468] 05 p0646 N88-13954
Mechanistic studies of polymeric samples exposed aboard STS 8
[NASA-CR-182364] 06 p0686 N88-14202
Analysis of relativistic nucleus-nucleus interactions in emulsion chambers 07 p0926 N88-15624
Nuclear structure at intermediate energies
[DE88-002796] 10 p1407 N88-18390
Kinetic and turbulence models for granular and two-phase flows 11 p1484 N88-18862
Channeling and dechanneling at high energy
[DE88-003989] 11 p1548 N88-19259
Big Bang Nucleosynthesis: Accelerator tests and can (UC OMEGA)(sub B) really be large
[DE88-003405] 11 p1570 N88-19396
Theoretical studies in few-body intermediate energy physics
[DE88-004101] 12 p1689 N88-20106
On (e,e'N) reactions
[CEBAF-PR-87-028] 12 p1690 N88-20109
Research in high energy elementary particle physics
[DE88-006065] 13 p1837 N88-20994
Quark core stars, quark stars and strange stars
[DE88-006991] 17 p2450 N88-24555
Calorimetry applied to nucleus-nucleus collisions at ultrarelativistic energies
[DE88-006173] 18 p2573 N88-25282
Atomic processes in matter-antimatter interactions
[DE88-008911] 19 p2723 N88-26172
Electron-positron physics at 1 TeV
[DE88-009019] 19 p2725 N88-26180
Mechanisms for particle acceleration: Possibilities and constraints
[PB88-102538] 19 p2725 N88-26184
Ion and electron interactions of atmospheric importance
[AD-A192255] 20 p2824 N88-26751
Charged pion production and projectile breakup in 85A MeV(sup)12C induced heavy ion reactions
[LUIP-8802] 20 p2850 N88-26920
Comparison of exclusive reactions at large momentum transfer
[DE88-007544] 20 p2851 N88-26922
Inelastic two composite particle systems scattering at high energy
[DE88-701841] 20 p2851 N88-26928
Recoil saturation of the self-energy in atomic systems
[DE88-010450] 20 p2851 N88-26930
Self-energies and the interactions of particles with surfaces
[DE88-010451] 21 p3014 N88-27885
Quark nuclear model: Classification groups and two and three body correlations
[NOTA-INTERNA-896] 21 p3014 N88-27891
Study of the production of Ko mesons in proton antiproton interactions at 630 GeV
[NOTA-INTERNA-908] 21 p3015 N88-27892
Study of superconducting properties in some many valley semiconductors
[DE88-702325] 23 p3291 N88-29593

PARTICLE LADEN JETS
On the periodic southward jets of Comet Halley before perihelion passage 14 p2008 N88-21978

PARTICLE MASS
Performance and operating envelope of imaging and scattering particle sizing instruments
[NASA-CR-180859] 03 p0323 N88-12042
On the spatial structure of the Perseids meteor stream 06 p0740 N88-14550
Scalar densities and baryon mass differences in lattice QCD with Wilson fermions
[PREPRINT-544] 06 p0778 N88-14773
A theoretical model for neutrino masses and mixing
[PREPRINT-553] 06 p0778 N88-14777
The paradoxical asymptotic status of massless springs
[AD-A185625] 07 p0928 N88-15637
Properties of nuclei and elementary particles at low and intermediate energies
[DE88-001913] 09 p1244 N88-17456
Measurements of gas turbine combustor and engine augmentor tube sooting characteristics
[AD-A187831] 11 p1440 N88-18592
The origin of low mass particles within and beyond the dust coma envelopes of Comet Halley 14 p2002 N88-21938
Theory of quark mixing matrix and invariant functions of mass matrices
[USIP-87-14] 22 p3159 N88-28800

PARTICLE MOTION
New directions in Vlasov plasma turbulence and anomalous transport
[DE87-014425] 02 p0238 N88-11500
Elements of plasma physics 03 p0271 N88-11703
A simplified approach to the dynamics of charged particles in the magnetosphere 03 p0273 N88-11718
Stochastic model of the motion of suspended particles in turbulent flow
[HSBW-MITT-21/1987] 03 p0315 N88-11990
Wave functions for bound states of relativistic electrons in a crystal at electron movement along crystallographic planes
[DE88-700563] 07 p0939 N88-15708
Nonlinear diffusion in the presence of a time-dependent external electric field
[INPE-4378-PRE/1198] 08 p1085 N88-16533
Introductory review: Physics of electron slowing-down processes
[DE88-002918] 09 p1246 N88-17466
Dynamics of coupled electron-nucleon motion in a laser field
[DE88-005063] 10 p1337 N88-17994
Energetic particle drift motions in the outer dayside magnetosphere
[DE88-005097] 11 p1512 N88-19034
Theory of laser cooling and spectroscopy of harmonically trapped single atoms
[AD-A189576] 13 p1775 N88-20617
Fragmentation and flow in central collisions
[DE88-005386] 13 p1837 N88-20991
Comparison of analytic and full guiding center behavior at a trapped-passing interface in stellarators
[DE88-004174] 13 p1842 N88-21025
Free Laplacian with attractive boundary conditions
[DE87-702971] 16 p2256 N88-23482
Electrical resistivity as quantum chaos
[DE88-007026] 16 p2284 N88-23675
Muon motion in titanium hydride 17 p2396 N88-24247
Optical guiding in the separable beam limit
[AD-A192452] 21 p2952 N88-27534
Regular and chaotic motion of fluid particles in a two dimensional fluid
[PREPRINT-591] 22 p3078 N88-28278
Application of optical correlation techniques to particle imaging velocimetry
[NASA-TM-101306] 23 p3218 N88-29152

PARTICLE PRECIPITATION
NT ELECTRON PRECIPITATION
Electrodynamics of midnight sector of auroral oval in period of slight disturbance 08 p1003 N88-16077
Formation of nuclei during precipitation in metallic mixed crystals
[NASA-TT-20248] 13 p1745 N88-20437
Stimulated Emission of Energetic Particles (SEEP)
[AD-A188724] 13 p1853 N88-21094
The precipitation of energetic heavy ions into the upper atmosphere of Jupiter
[NASA-TM-101155] 17 p2452 N88-24565
WIPP (Wave Induced Particle Precipitation) experiment logistic support
[AD-A191184] 18 p2499 N88-24824
The low-latitude auroral boundary: Steady-state and time-dependent representations
[AD-A193200] 21 p2972 N88-27656
Solar flares and magnetospheric particles: Investigations based upon the ONR-602 and ONR-604 experiments
[AD-A193396] 21 p3031 N88-27994

PARTICLE PRODUCTION
NT PAIR PRODUCTION
Single weak gauge boson production at CLIC
[PREPRINT-550] 06 p0778 N88-14775
The standard theory group: Summary and conclusions
[PREPRINT-551] 06 p0778 N88-14776
Production by pyrolysis of diffusion particles for velocimetry in shock tubes
[ISL-R-119/86] 11 p1455 N88-18671
Theoretical studies in few-body intermediate energy physics
[DE88-004101] 12 p1689 N88-20106
Simulation of nuclear collisions at high energies in the frames of quark-gluon string model
[DE88-700914] 12 p1690 N88-20113
Physics at large transverse momenta
[DE88-005758] 13 p1836 N88-20986
New limits on charged Higgs boson mass with CELLO at Petra (Italy) and status of the neutral Higgs boson search
[NOTA-INTERNA-897] 14 p1980 N88-21817
Analysis of hadron production in deep inelastic muon-proton collisions through the fire-string model
[PREPRINT-578] 14 p1981 N88-21822
The dust tail of Comet Halley 14 p2008 N88-21974
The role of electron-ion recombination in bulk antimatter production 16 p2268 N88-23567
Electromagnetic manipulation of atomic hydrogen 16 p2268 N88-23568
Production of heavy antinuclei: Review of experimental results 16 p2269 N88-23574
Subthreshold pion production in proton induced reactions at 180 to 201 MeV and He3 at 283 MeV
[ETN-88-92303] 17 p2397 N88-24250
Experimental elementary particle physics
[DE88-007510] 18 p2572 N88-25274
Charged pion production and projectile breakup in 85A MeV(sup)12C induced heavy ion reactions
[LUIP-8802] 20 p2850 N88-26920
Hadrons produced in atmospheric interactions
[DE88-702492] 23 p3309 N88-29712

PARTICLE SIZE DISTRIBUTION
Optical sizing of soot in gas turbine combustors and exhaust augmentor tubes
[AD-A183785] 01 p0006 N88-10034
The effect of RDX particle size on the shock sensitivity of cast PBX formulations. 2: Bimodal compositions
[DE87-009581] 01 p0031 N88-10198
Performance and operating envelope of imaging and scattering particle sizing instruments
[NASA-CR-180859] 03 p0323 N88-12042
Experimental and theoretical study of condensation in multicomponent mixtures
[DE88-000897] 04 p0413 N88-12563
Experiments on densely-loaded non-Newtonian slurries in laminar and turbulent pipe flows
[DE88-000719] 04 p0442 N88-12746
Operating envelopes of particle sizing instrumentation used for icing research
[NASA-CR-180870] 05 p0586 N88-13573
The application of doubly-truncated hydrometeor distributions to numerical cloud models
[AD-A185273] 05 p0627 N88-13836
Measurement of particle size distribution in a solid propellant rocket motor using light scattering
[AD-A184875] 06 p0673 N88-14124
An analysis of the effect of system variables on the quality of thin films and powders produced by laser-breakdown chemical vapor deposition
[DE88-001793] 06 p0708 N88-14342

Results of observations of the Eta Aquarid and Orionid meteor showers in 1980-1984 06 p0740 N88-14548
Radar observations of changes in precipitation size spectra associated with lightning 06 p0744 N88-14576
An aureolar radiometer for the determination of aerosol size distribution 08 p1018 N88-16174
Aerosol size distribution from measurements of the radiance in the solar aureole 08 p1019 N88-16176
Mechanisms of wear in single- and two-phase materials [DE88-003846] 10 p1305 N88-17806
Turbulence interactions in single- and multi-phase turbulent mixing and combustion processes [AD-A187505] 10 p1332 N88-17960
Measurements of gas turbine combustor and engine augmentor tube sooting characteristics [AD-A187831] 11 p1440 N88-18592
Measurements of particulates in solid propellant rocket motors [AD-A187777] 11 p1446 N88-18621
Measurement of combustion aerosol size distributions with multistage inertial impactors [DE88-751101] 11 p1454 N88-18669
Diagnostics for research in atomization and turbulent two-phase flows [AD-A187338] 11 p1482 N88-18843
Vertical structure of Venusian cloud layer at landing sites of Vega-1 and Vega-2 vehicles 13 p1725 N88-20317
Erosion in dual-phase microstructures [DE88-004507] 13 p1743 N88-20421
Characterization and fundamental studies on CuO sorbent materials to determine attrition mechanisms on substrate gamma alumina [DE88-003674] 13 p1749 N88-20456
Processing of nanophase ceramics [DE88-005985] 13 p1752 N88-20475
Combined aerodynamic size, charge-to-mass, and velocity measurements of aerosol particles [ST-REPT-VOL-5-NO-4] 14 p1944 N88-21599
Optical and hydrodynamic implications of Comet Halley dust size distribution 14 p2003 N88-21939
The evolution of the mass distribution of cometary particles 14 p2004 N88-21946
Transient compressible flow in porous materials [DE88-006685] 15 p2067 N88-22324
Research on certain aspects of laser diffraction particle sizing relevant to autonomous self-diagnosing instrumentation [AD-A190220] 15 p2071 N88-22348
The interaction of small particles with laser beams [AD-A190716] 15 p2072 N88-22354
Obtaining information on cloud particles by a commercial miniature camera [DFVLR-MITT-87-19] 16 p2234 N88-23342
Fog, rain and aerosol attenuation in the atmosphere [AD-A190867] 16 p2235 N88-23350
Method of evaporation [NASA-CASE-NPO-15609-2] 17 p2318 N88-23846
Transient particle deposition in a boundary layer of impulsive flow over a flat plate [AD-A191537] 18 p2508 N88-24880
The 24th JANNAF Combustion Meeting, volume 1 [AD-A190163] 19 p2627 N88-25585
A review of particle sizing methods in rocket propulsion 19 p2630 N88-25597
Measurement of particulate size in solid propellant rocket motors 19 p2630 N88-25599
Instantaneous two-dimensional multiple particle sizing diagnostic 19 p2630 N88-25600
The preparation of mechanically alloyed powders for TEM (Transmission Electron Microscopy) examination [DE88-008043] 20 p2775 N88-26460
Numerical modeling of the effect of particle size of explosives on shock initiation properties [DE88-010479] 20 p2780 N88-26491
Preparation and properties of high Q microwave dielectrics in the (CA, SR, BA) zirconate system [AD-A193127] 21 p2918 N88-27317
Real-time measurements of the size fractionation of ambient black carbon aerosols at elevated humidities [DE88-010870] 23 p3215 N88-29138
Automatic data retrieval from rocket motor holograms [AD-A195586] 24 p3337 N88-29864
Simulation study of spraying, streaming and vaporization phenomena associated with fuel injection 24 p3345 N88-29914
Turbulence effects on the droplet distribution behind airblast atomizers 24 p3346 N88-29915
Multiple scattering effects in drop sizing of dense fuel sprays by laser diffraction 24 p3346 N88-29917
Influence of operating conditions on the atomization and distribution of fuel by air blast atomizers 24 p3346 N88-29918
Particle size measurements in sooting combustion systems 24 p3348 N88-29931
Particle sizing in combustion systems, using scattered laser light [AD-A196231] 24 p3352 N88-29953
Optical measurements of soot and temperature profiles in premixed propane-oxygen flames [NASA-TM-101343] 24 p3358 N88-29997
Optical measurements of soot in premixed flames [NASA-TM-101305] 24 p3373 N88-30090
Evaluation of the potential health hazards associated with the machining of carbon fiber composites [AD-A194835] 24 p3408 N88-30286

PARTICLE SPIN
NT ISOTOPIC SPIN
NT NUCLEAR SPIN
Developments related to scattering eigen elements in Schroedinger operators for particles with spin [ETN-88-91077] 09 p1229 N88-17361

PARTICLE TELESCOPES
Design, fabricate, calibrate, test and deliver two satellite electron flux detectors [AD-A190799] 16 p2169 N88-22930

PARTICLE THEORY
Research program in elementary particle theory [DE88-000159] 02 p0233 N88-11468
On charm decays: Present status and future goals [DE87-013586] 03 p0375 N88-12356
Plasma theory and simulation [AD-A187100] 09 p1249 N88-17486
Laser fluorescence velocimeter [AD-A189010] 12 p1630 N88-19753
Theory of laser cooling and spectroscopy of harmonically trapped single atoms [AD-A189576] 13 p1775 N88-20617
Particle physics and cosmology [DE88-004944] 13 p1854 N88-21096
Summary of supersymmetric particle search with the CELLO detector at Petra (Italy) [NOTA-INTERNA-898] 14 p1980 N88-21818
Renormalized Fermi liquid theory for disordered electron systems and the metal-insulator transition [NOTA-INTERNA-900] 14 p1988 N88-21862
Particle cosmology comes of age [DE88-006998] 15 p2151 N88-22844
Material void opening computation using particle method [DE88-010950] 19 p2680 N88-25936
Analysis of transverse strength of composites using percolation theory [AD-A193204] 21 p2904 N88-27234
Quark nuclear model: Classification groups and two and three body correlations [NOTA-INTERNA-896] 21 p3014 N88-27891

PARTICLE TRACKS
Some new ideas in liquid detectors [DE88-000732] 04 p0446 N88-12768
Dynamics of meteor streams 06 p0732 N88-14503
Scanning and measuring peculiarities with high-space resolution objects recorded at the Gabor holograms [DE88-700373] 07 p0857 N88-15203
Algorithm and program for recognition of compactly positioned vertices of events for the HPD minimum guidance system [DE88-700542] 07 p0905 N88-15482
An analytic model for ionization distributions produced in nanometer sites by protons [DE88-003943] 10 p1406 N88-18385
Measuring accuracy of 3-dimensional bodies by the GOMER-1 device [DE87-703230] 12 p1628 N88-19744
HNC: A detector to study ultraheavy cosmic rays 12 p1713 N88-20252
MIG-1 on-line measuring holographic microscope [DE88-701103] 15 p2068 N88-22332
Flow velocity measurements by image processing of optically modulated traces 16 p2203 N88-23147
Optical system of laser illuminated streamer chamber [DE88-702127] 18 p2577 N88-25306
Application of optical correlation techniques to particle imaging velocimetry [NASA-TM-101306] 23 p3218 N88-29152

PARTICLE TRAJECTORIES
NT ELECTRON TRAJECTORIES
Influence of a magnetic field on the diffusion of small particles in a turbulent flow [DE87-702877] 01 p0046 N88-10291
Use of back air trajectories in interpreting atmospheric chemistry data: A review and bibliography [PB88-102108] 07 p0876 N88-15312
Particle transport in microdetonations — inertial confinement fusion pellets [OEFZS-4402] 09 p1164 N88-16976
Particle-dynamics calculations of gravity flow of inelastic, frictional spheres [DE88-005224] 13 p1770 N88-20586
Studies of heat and mass transfer during chemical vapor deposition 17 p2338 N88-23953
Centrifugal acceleration of ions in the polar magnetosphere [NASA-TM-101148] 17 p2374 N88-24120
Gone with the solar wind: A study of protons accelerated by interplanetary shocks 19 p2743 N88-26283
Particle trajectories and potentials in a plane sheath moving in a magnetoplasma [AD-A196228] 24 p3390 N88-30190

PARTICLES
NT AEROSOLS
NT ALPHA PARTICLES
NT ANTINEUTRINOS
NT ANTINUCLEONS
NT ANTIPARTICLES
NT ANTIPROTONS
NT ARGON PLASMA
NT BARYONS
NT BETA PARTICLES
NT BOSONS
NT BOUNDARY LAYER PLASMAS
NT CESIUM PLASMA
NT CHARGED PARTICLES
NT COLD PLASMAS
NT COLLISIONAL PLASMAS
NT COLLISIONLESS PLASMAS
NT CONDUCTION ELECTRONS
NT CORPUSCULAR RADIATION
NT COSMIC DUST
NT COSMIC PLASMA
NT CYLINDRICAL PLASMAS
NT DENSE PLASMAS
NT DEUTERIUM PLASMA
NT DEUTERONS
NT DROPS (LIQUIDS)
NT DUST
NT ELECTRON BEAMS
NT ELECTRON PLASMA
NT ELECTRON PRECIPITATION
NT ELECTRON-POSITRON PAIRS
NT ELECTRONS
NT ELEMENTARY PARTICLES
NT ENERGETIC PARTICLES
NT EVEN-EVEN NUCLEI
NT FAST NEUTRONS
NT FERMIONS
NT FINES
NT FOG
NT FREE ELECTRONS
NT GLUONS
NT GRAVITONS
NT HADRONS
NT HEAVY NUCLEI
NT HELIUM PLASMA
NT HIGH ENERGY ELECTRONS
NT HIGH TEMPERATURE PLASMAS
NT HOT ELECTRONS
NT HYDROGEN PLASMA
NT HYPERNUCLEI
NT INNER RADIATION BELT
NT INTERPLANETARY DUST
NT IONIZED GASES
NT KAONS
NT LASER PLASMAS
NT LEPTONS
NT MAGNETIC CLOUDS
NT MAGNETICALLY TRAPPED PARTICLES
NT MESON RESONANCE
NT MESONS
NT METAL PARTICLES
NT METAL POWDER
NT METALLIC PLASMAS
NT MICROPARTICLES
NT MIST
NT MUONS
NT NEUTRAL PARTICLES
NT NEUTRINOS
NT NEUTRONS
NT NITROGEN PLASMA
NT NONEQUILIBRIUM PLASMAS
NT NONUNIFORM PLASMAS
NT NUCLEAR PARTICLES
NT NUCLEI (NUCLEAR PHYSICS)
NT NUCLEONS
NT ODD-ODD NUCLEI
NT OXYGEN PLASMA
NT PARTICULATES
NT PARTONS
NT PHOTOELECTRONS
NT PHOTONS
NT PIONS
NT PLASMA CLOUDS

NT PLASMA FOCUS
NT PLASMA JETS
NT PLASMA LAYERS
NT PLASMA SHEATHS
NT PLASMAS (PHYSICS)
NT POLARONS
NT POLLEN
NT POSITRONS
NT POWDER (PARTICLES)
NT POWDERED ALUMINUM
NT PRIMARY COSMIC RAYS
NT PROTONS
NT QUARKS
NT RADIATION BELTS
NT RADIO JETS (ASTRONOMY)
NT RAINDROPS
NT RELATIVISTIC ELECTRON BEAMS
NT RELATIVISTIC PARTICLES
NT RELATIVISTIC PLASMAS
NT ROTATING PLASMAS
NT SEMICONDUCTOR PLASMAS
NT SINTERED ALUMINUM POWDER
NT SOLAR COSMIC RAYS
NT SOLAR ELECTRONS
NT SOLAR NEUTRINOS
NT SOLAR NEUTRONS
NT SOLAR PROTONS
NT SOLAR WIND
NT SOOT
NT SPACE PLASMAS
NT SPHERICAL PLASMAS
NT STELLAR WINDS
NT STRONGLY COUPLED PLASMAS
NT TERRESTHIAL DUST BELT
NT THERMAL NEUTRONS
NT THERMAL PLASMAS
NT TOROIDAL PLASMAS
NT TRAPPED PARTICLES
NT TRITONS
NT ZODIACAL DUST

Redistribution of particulates in shuttle bay during launch 02 p0133 N88-10837
Shear stress cleaning for surface departiculation 02 p0134 N88-10838
Particle velocity and stress gage measurements in spherical diverging flow
[DE87-007333] 03 p0321 N88-12033
Particle physics and cosmology
[DE87-005400] 03 p0387 N88-12432
Activities at government research laboratories reported 04 p0403 N88-12503
Use of a thermodynamic analog for pneumatic transport in horizontal pipes
[AD-A184076] 04 p0441 N88-12740
Plume mechanics and aerosol growth processes
[AD-A184467] 04 p0442 N88-12742
Experimental and analytic studies of the triggered lightning environment of the F106B
[NASA-CR-4104] 04 p0469 N88-12897
Separable orthogonal coordinates and particle creation for an accelerating observer
[DE87-703358] 05 p0657 N88-14029
Theoretical and numerical analysis of shock wave propagation through different dusty-gas mixture layers 06 p0699 N88-14292
Nature and the nonlinear evolution of electrostatic waves associated with the AMPTE (Active Magnetosphere Particle Tracer Explorers) solar wind releases
[AD-A185471] 06 p0806 N88-14920
Microgravity Particle Research on the Space Station
[NASA-CP-2496] 07 p0883 N88-15354
Astrophysics and the solar nebula 07 p0883 N88-15355
Planetary science 07 p0883 N88-15356
Physics and chemistry 07 p0883 N88-15359
Characterizing particle combustion in a Rijke burner
[AD-A186157] 08 p0966 N88-15847
Spray deposition: A fundamental study of droplet impingement, spreading and consolidation
[AD-A186627] 08 p0970 N88-15869
The morphology of emulsion polymerized latex particles
[DE88-002672] 08 p0972 N88-15879
Christiansen effect in infrared spectra of soil-derived atmospheric dusts
[AD-A187071] 09 p1248 N88-17479
Optimization of volume produced H(-) ions in a low-pressure hydrogen plasma
[IPPJ-853] 09 p1252 N88-17505
Ice-shelf response to ice-stream discharge fluctuation. Part 1: Unconfined ice tongues
[AD-A188147] 10 p1358 N88-18117
Dynamical and photometric studies of Saturn's rings 12 p1711 N88-20241
Global mixed-layer natural and anthropogenic fluxes 13 p1807 N88-20803
Double layer polarization of nonconducting spheroidal particles and its application to Kerr effect
[ISSN-0208-5658] 13 p1832 N88-20960
Mechanical behaviour of particle filled thermoplastics
[PB88-169297] 15 p2047 N88-22196
The interaction of small particles with laser beams
[AD-A190716] 15 p2072 N88-22354
Hybrid particle simulation for focusing of rotating and propagating LIB 16 p2276 N88-23624
On the efficient implementation of the fast multipole algorithm
[AD-A191167] 17 p2385 N88-24173
Particle-laden weakly swirling free jets: Measurements and predictions
[NASA-TM-100920] 18 p2466 N88-24639
Application of particle simulations to the NRL laser experiment
[AD-A191641] 18 p2520 N88-24953
Modelling of thermal plasma systems 18 p2578 N88-25314
Aerodynamic focusing of particles and heavy molecules
[DE88-007145] 19 p2598 N88-25440
Laser measurement of particle velocities in vacuum plasma spray deposition
[DE88-007111] 19 p2728 N88-26198
The influence of foreign particles on bearing metals
[NASA-TT-20155] 20 p2775 N88-26454
Reducing adhesion and agglomeration within a cloud of combustible particles
[NASA-TM-100902] 20 p2788 N88-26539
Research in theoretical particle physics
[DE88-008230] 20 p2851 N88-26927
On linear relationship between shock velocity and particle velocity
[DE88-701827] 20 p2880 N88-27099
Matrix substructuring, domain decomposition and particle methods: Current trends for solving PDEs in parallel
[DE88-009826] 21 p3007 N88-27836
Theoretical and experimental investigations on the structure of stationary shock waves in gas particle dispersions
[ETN-88-92983] 23 p3213 N88-29122
Theoretical particle physics
[DE88-011499] 23 p3295 N88-29621

PARTICULATE FILTERS
U FLUID FILTERS

PARTICULATE SAMPLING
Comparison of three aerosol sampling techniques and the differences in the nitrate determined by each
[DE87-011456] 03 p0348 N88-12200
Results from a questionnaire on particulate metrology in the UK
[NPL-MOM-81] 09 p1141 N88-16841
Measurement of combustion aerosol size distributions with multistage inertial impactors
[DE88-751101] 11 p1454 N88-18669

PARTICULATES
NT SOOT
Thermoplastic elastomers as LOVA binders
[AD-A185864] 07 p0835 N88-15067
Non-steady group combustion of a cloud of char particles
[DE87-010773] 08 p0966 N88-15849
A holographic investigation of particulates in metallized solid fuel ramjet combustion
[AD-A186887] 09 p1140 N88-16831
Surface acoustic wave deposition sensor
[DE87-006527] 09 p1243 N88-17452
Numerical simulation of near-surface environments and particulate clouds generated by large-area fires
[AD-A186375] 12 p1641 N88-19828
Interaction of particulate and transformation toughening
[AD-A189321] 13 p1741 N88-20412
Cavitation inception
[AD-A189220] 13 p1765 N88-20557
Production and turnover of suspended organic detritus in the coastal water of the southeastern continental shelf
[DE88-005118] 14 p1951 N88-21631
Theoretical prediction of single phase turbulent flow distribution in particulate bed reactors 17 p2419 N88-24386
Space station particulate contamination environment 18 p2591 N88-25397
The particulate environment surrounding the space station: Estimates from the PACS data 18 p2591 N88-25398
Effects of meteoroids and space debris on the particulate environment for space station 18 p2591 N88-25399
Analysis of debris from accelerated life test of the Hughes five-year Vuilleumier cryocooler
[AD-A193101] 21 p2931 N88-27400
The distribution of some chemical elements between dissolved and particulate phases in the ocean
[DE88-010181] 21 p2977 N88-27682

PARTITIONS (MATHEMATICS)
A multiple-time-scale turbulence model based on variable partitioning of turbulent kinetic energy spectrum
[NASA-CR-179222] 04 p0444 N88-12754
An emulation tool for simulating matrix operations on an SIMD (Single Instruction Multiple Data stream) multiprocessor
[AD-A188654] 12 p1678 N88-20030
Multiextremal optimization via adaptive partition algorithms
[REPT-87-44] 14 p1957 N88-21664
Graph labelings
[AD-A189649] 14 p1964 N88-21722
The global convergence of partitioned BFGS on problems with convex decompositions and Lipschitzian gradients
[DE88-006249] 14 p1968 N88-21744
Life prediction modeling based on strainrange partitioning 15 p2084 N88-22425
Some properties of modular equations and the partition function 18 p2564 N88-25224
Partitioning of regular computation on multiprocessor systems
[NASA-CR-183176] 22 p3141 N88-28676

PARTONS
Parton densities from deep inelastic scattering to hadronic processes at super collider energies
[NOTA-INTERNA-885] 07 p0930 N88-15646

PARTS
U COMPONENTS

PASCAL (PROGRAMMING LANGUAGE)
Comparison of pascal and the dBASE 3 PLUS language in programming an inventory management system
[AD-A184027] 03 p0365 N88-12300
Validation tests for standard PASCAL and extented PASCAL
[NPL-DITC-108/88] 22 p3139 N88-28663
Modularity in the PASCAL model compiler
[NPL-DITC-111/88] 22 p3139 N88-28664
Appraisal of prototype PASCAL program validation suite
[NPL-DITC-112/88] 22 p3139 N88-28665

PASSAGEWAYS
NT TRANSFER TUNNELS
Personnel occupied woven envelope robot power
[NASA-CR-182367] 07 p0856 N88-15196

PASSENGER AIRCRAFT
NT A-300 AIRCRAFT
NT A-320 AIRCRAFT
NT BO-105 HELICOPTER
NT BOEING 737 AIRCRAFT
NT BOEING 747 AIRCRAFT
NT CH-46 HELICOPTER
NT DO-28 AIRCRAFT
NT EUROPEAN AIRBUS
NT F-27 AIRCRAFT
NT VC-10 AIRCRAFT
Summary report of the history and events pertinent to the Civil Aeromedical Institute's evaluation of providing smoke/fume protective breathing equipment for airline passenger use
[AD-A184499] 03 p0261 N88-11645
Contribution to the improvement of the guidance accuracy of automatic pilots
[ETN-88-90607] 05 p0551 N88-13360
The intelligent wing. Aerodynamic development direction for future passenger aircraft
[MBB-UT-006/87] 10 p1313 N88-17848
Presentation of Class 1 designs for a family of commuter airplanes
[NASA-CR-182563] 11 p1439 N88-18587
Presentation of structural component designs for the family of commuter airplanes
[NASA-CR-182568] 12 p1581 N88-19463
A class 2 weight assessment for the implementation of commonality and preliminary structural designs for the family of commuter airplanes
[NASA-CR-182565] 12 p1581 N88-19464
Advanced propfan analysis for the family of commuter airplanes
[NASA-CR-182566] 12 p1582 N88-19468
Presentation of flight control design and handling quality commonality by separate surface stability augmentation for the family of commuter airplanes
[NASA-CR-182567] 12 p1583 N88-19471
A cost analysis for the implementation of commonality in the family of commuter airplanes, revised
[NASA-CR-182569] 12 p1708 N88-20221
In-service measurements of SAAB SF-340 landing gear loads
[FFA-TN-1987-48] 15 p2018 N88-22032

Class 2 design update for the family of commuter airplanes
[NASA-CR-182681] 18 p2464 N88-24629
Enhanced emergency smoke venting
[DOT/FAA/CT-88/22] 20 p2756 N88-26350
A contribution to the quantitative analysis of the influence of design parameters on the optimal design of passenger aircraft
[ETN-88-92979] 23 p3176 N88-28912

PASSENGERS

Aviation security: FAA (Federal Aviation Administration) needs preboard passenger screening performance standards
[PB87-216800] 02 p0124 N88-10783
Summary report of the history and events pertinent to the Civil Aeromedical Institute's evaluation of providing smoke/fume protective breathing equipment for airline passenger use
[AD-A184499] 03 p0261 N88-11645
Design, development and trials of an airline passenger telephone system 19 p2646 N88-25704

PASSIVATION

U PASSIVITY

PASSIVE SATELLITES

NT LAGEOS (SATELLITE)
Comparative analysis of passive communications satellites employing the SHF and HF spectrum for use in a strategic role
[AD-A194682] 24 p3362 N88-30019

PASSIVITY

Wide bandgap passivation layers on silicon
[DE87-014307] 02 p0244 N88-11543
A review of pitting corrosion in high temperature aqueous solutions
[DE88-003547] 10 p1302 N88-17787
Corrosion, passivity and breakdown of alloys used in high energy density batteries
[DE88-004891] 13 p1743 N88-20422
Experimental and theoretical investigation of passive damping concepts for member forced and free vibration
[NASA-CR-183082] 20 p2814 N88-26693

PASTES

Cement paste matrix composite materials center
[AD-A188657] 15 p2028 N88-22083

PATENT APPLICATIONS

Navigation system for land vehicles
[NASA-CASE-LAR-13322-1] 18 p2462 N88-24620
Airplane runway performance monitoring system
[NASA-CASE-LAR-13854-1-CU] 18 p2462 N88-24621
Nozzle fabrication technique
[NASA-CASE-MSC-21299-1] 18 p2475 N88-24684
Dual-fuel, dual-mode rocket engine
[NASA-CASE-LAR-13773-1] 18 p2475 N88-24685
Energy efficient continuous flow ash lockhopper
[NASA-CASE-NPO-16985-1-CU] 18 p2497 N88-24814
Low temperature storage container for transporting perishables to space station
[NASA-CASE-MFS-28248-1] 18 p2498 N88-24817
Noncontact temperature pattern measuring device
[NASA-CASE-NPO-17024-1-CU] 18 p2519 N88-24943
Atmospheric autorotating imaging device
[NASA-CASE-NPO-17390-1-CU] 18 p2519 N88-24944
Universal precision sine bar attachment
[NASA-CASE-MFS-28253-1] 18 p2523 N88-24971
Trailer shield assembly for a welding torch
[NASA-CASE-MFS-29260-1] 18 p2524 N88-24972
Radio Frequency (RF) strain monitor
[NASA-CASE-LAR-13705-1] 18 p2530 N88-25011
Optical pressure sealing couping (light joint)
[NASA-CASE-MFS-29348-1] 18 p2576 N88-25303
Crystal growth apparatus
[NASA-CASE-MFS-28182-1] 18 p2585 N88-25357
Ultrasonic method and apparatus for determining crack opening load
[NASA-CASE-LAR-13889-1] 24 p3385 N88-30160

PATENT POLICY

Identifying areas of leading edge Japanese science and technology: Activity analysis using SIC (Standard Industrial Classes) categories and scientific subfields
[PB87-204087] 02 p0249 N88-11574
Identifying areas of leading edge Japanese science and technology: Patent activity and citation analysis using US POC (Patent Office Classification) classification
[PB87-204095] 02 p0249 N88-11575
Thixotropic surface composition for phenolaldehyde resin laminates
[GB-PATENT-2-180-251-A] 04 p0410 N88-12545
Thermoplastic elastomer compositions — cable jackets
[EP-PATENT-0-204-453-A1] 04 p0418 N88-12593
Detection of defects on structures
[EP-PATENT-0-210-794-A2] 04 p0453 N88-12807
Core material — honeycombs
[EP-PATENT-0-196-926-A2] 05 p0558 N88-13393
Antistatic coating compositions
[GB-PATENT-2-177-413-A] 05 p0568 N88-13463
Flame retardant phenolic foams
[EP-PATENT-0-223-489-A2] 05 p0568 N88-13464
Process for the production of a thermoplastic elastomer composition
[EP-PATENT-0-202-782-A2] 05 p0569 N88-13465
Optical probe
[EP-PATENT-0-210-869-A1] 05 p0650 N88-13984
Preparation of amorphous silicon semiconductors
[GB-PATENT-2-176-054-A] 05 p0656 N88-14022
NASA patent abstracts bibliography: A continuing bibliography. Section 1: Abstracts (supplement 32)
[NASA-SP-7039(32)-SECT-1-ABST] 07 p0943 N88-15732
NASA patent abstracts bibliography: A continuing bibliography. Section 2: Indexes (supplement 32)
[NASA-SP-7039(32)-SECT-2] 10 p1425 N88-18511
NASA patent abstracts bibliography: A continuing bibliography. Section 1: Abstracts
[NASA-SP-7039(33)] 18 p2590 N88-25388
Argonne National Laboratory technology transfer report, FY87
[DE88-010091] 23 p3298 N88-29639

PATENTS

Identifying areas of leading edge Japanese science and technology: Activity analysis using SIC (Standard Industrial Classes) categories and scientific subfields
[PB87-204087] 02 p0249 N88-11574
Identifying areas of leading edge Japanese science and technology: Patent activity and citation analysis using US POC (Patent Office Classification) classification
[PB87-204095] 02 p0249 N88-11575
Magnetically switched power supply system for lasers
[NASA-CASE-NPO-16402-2] 18 p2505 N88-24862
Linear force device
[NASA-CASE-MSC-20549-2] 18 p2516 N88-24927
Range and range rate system
[NASA-CASE-MSC-20867-1] 18 p2521 N88-24958

PATHOGENESIS

Development of methods for the study of space motion sickness 07 p0892 N88-15408

PATHOLOGICAL EFFECTS

Questions on the evolution of the development program of the vertebrate inner ear under long term zero-g conditions 07 p0886 N88-15379
Neuropeptides in experimental head injury
[AD-A188067] 11 p1520 N88-19077

PATHOLOGY

NT HUMAN PATHOLOGY
Diagnostic value of some load tests in evaluation of nonspecific electrocardiographic changes 07 p0895 N88-15426
Squid instrumentation for neuromagnetic study of complex brain activity 21 p2978 N88-27691

PATHS

Two dimensional path planning with obstacles and shadows
[AD-A184075] 04 p0397 N88-12474
Task path planning, scheduling and learning for free-ranging robot systems 08 p1058 N88-16386

PATTERN DISTRIBUTION

U DISTRIBUTION (PROPERTY)

PATTERN RECOGNITION

NT CHARACTER RECOGNITION
Estimation of the position and orientation of objects using associative memories
[ESA-TT-1034] 01 p0079 N88-10507
Recognizing rigid objects by aligning them with an image
[AD-A184253] 03 p0368 N88-12318
On the recognition of curved objects
[AD-A184441] 04 p0478 N88-12945
An approach to object recognition: Aligning pictorial descriptions
[AD-A184462] 04 p0482 N88-12972
Intelligent signal analysis and recognition
[NASA-CR-181531] 04 p0501 N88-13084
Towards building a team of intelligent robots
[NASA-CR-181538] 05 p0589 N88-13595
A rudimentary database for three-dimensional objects using structural representation
[CSE-87-00004] 05 p0590 N88-13597
Supercomputing at Florida State University (FSU)
[DE87-013900] 05 p0654 N88-14009
Artificial intelligence systems 06 p0761 N88-14670
Transient classifier systems and man-machine interface research
[AD-A186213] 07 p0899 N88-15446
Automated program recognition
[AD-A186421] 07 p0903 N88-15472
Algorithm and program for recognition of compactly positioned vertices of events for the HPD minimum guidance system
[DE88-700542] 07 p0905 N88-15482
Pattern recognition techniques for failure trend detection in SSME ground tests 07 p0924 N88-15614
Recognition of polyhedral objects under structured illumination
[PB88-106703] 07 p0932 N88-15661
A knowledge-based object recognition system for applications in the space station
[NASA-CR-182411] 08 p0989 N88-15991
Research on visual information processing with special reference to oculomotor behavior in the areas of exploration, recognition and search
[AD-A186598] 08 p1051 N88-16346
Stability, reliability and cross-mode correlations of tests in a recommended 8-minute performance assessment battery
[NASA-CR-172039] 08 p1052 N88-16351
Embedded expert system for space shuttle main engine maintenance 08 p1058 N88-16382
Pattern-recognition software detecting the onset of failures in complex systems
[DE88-002861] 09 p1220 N88-17318
A comparison of algorithms for the analysis of images generated by two-dimensional electrophoresis
[DE88-003730] 09 p1220 N88-17319
Hierachical object recognition using libraries of parameterized model sub-parts
[AD-A187476] 10 p1396 N88-18322
Visual evoked potentials
[AD-A187942] 11 p1519 N88-19071
Learning functions from examples
[AD-A187725] 11 p1534 N88-19163
Object recognition on a systolic array
[AD-A187726] 11 p1534 N88-19164
Multiaperture optical system research
[AD-A188211] 11 p1549 N88-19267
Automated stereophotogrammetry
[AD-A189617] 12 p1630 N88-19757
An automatic system for extraction of information from a Computer Aided Design (CAD), selection, sequencing, and execution of turning processes
[INPE-4350-TDL/294] 12 p1676 N88-20020
A procedure for automatic classification of crop areas
[INPE-4467-PRE/1240] 13 p1780 N88-20708
Measures of similarity between fuzzy concepts: A comparative analysis
[AD-A189430] 13 p1825 N88-20910
Generalised threshold selection for edge detection
[RAE-TR-87035] 14 p1941 N88-21581
Range image segmentation and surface parameter extraction for a mobile robot
[DE87-013877] 15 p2073 N88-22360
Motion sickness: Quantitative, algorithmic malaise indication in real time
[AD-A189674] 15 p2101 N88-22518
Perception of complex auditory patterns
[AD-A190218] 15 p2102 N88-22524
Auditory perception of complex sounds
[AD-A190528] 15 p2103 N88-22529
Auditory pattern memory: Mechanisms of tonal sequence discrimination by human observers
[AD-A190337] 15 p2104 N88-22534
Rapid feature extraction via the radon transform
[AD-A190032] 15 p2110 N88-22573
Multi-disciplinary techniques for understanding time-varying space-based imagery
[AD-A190711] 15 p2117 N88-22610
Concurrent algorithms for a mobile robot vision system
[DE88-005850] 15 p2117 N88-22614
Multivariate analysis and its application
[AD-A189983] 15 p2124 N88-22661
Method and device for the detection and identification of a helicopter
[NASA-TT-20251] 15 p2129 N88-22698
Study of microcomputer-based real-time programmable optical signal processor and application
[AD-A190076] 15 p2133 N88-22726
OCR vision system, an alternative to bar code
[DE88-003761] 15 p2149 N88-22828
Activities report of the Department of Systems and Communications
[ENST-87D004] 16 p2189 N88-23053
Extraction of texts and symbols from unstructured vector data — mapping 16 p2225 N88-23287
Generic cueing in image understanding
[RSRE-MEMO-4109] 17 p2386 N88-24181
Nonparametric discriminant analysis applied to the extraction and selection of radar target signature features
[AD-A191849] 18 p2501 N88-24833
Tests for the automatic pattern recognition of building surfaces by the TK 50 18 p2533 N88-25030

Feature extraction using the Hough transform
[AD-A190679] 18 p2555 N88-25165
Real-time optical multiple object recognition and tracking system and method
[NASA-CASE-NPO-17139-1-CU] 18 p2576 N88-25301
Cluster analysis of multiple planetary flow regimes
[NASA-CR-182931] 18 p2594 N88-25418
A high dynamic range acousto-optic image correlator for real-time pattern recognition
[DE88-007933] 19 p2726 N88-26191
Treatment of systematic errors in the processing of wide angle sonar sensor data for robotic navigation
[DE88-008961] 20 p2756 N88-26352
Synoptic patterns related to tropical cyclone recurvature
[AD-A192338] 20 p2827 N88-26771
Optical data processing
[AD-A193024] 20 p2839 N88-26841
Optical correlation using the magneto-optic device
[AD-A192342] 20 p2854 N88-26950
Applications of differential geometry to the shape analysis of gray-value images 21 p2924 N88-27358
An aspect graph-based control strategy for 3-D object recognition 21 p2927 N88-27377
Creating aspect graphs for use in object recognition 21 p2928 N88-27379
Linear feature extraction from radar imagery. Phase 2: Base contract report
[AD-A192828] 21 p2931 N88-27404
Analysis of remotely sensed imagery using digital morphology
[AD-A192738] 21 p2965 N88-27614
Fourth generation neurocognitive pattern analysis system 21 p2977 N88-27686
Texture perception and shape from texture
[AD-A192923] 21 p2996 N88-27771
Simulation of real time problem solving
[AD-A193436] 21 p2997 N88-27778
An optical 2-dimensional correlator for pattern recognition in embedded computing
[DE88-007198] 21 p2998 N88-27780
Application of pattern recognition techniques to the identification of aerospace acoustic sources
[NASA-CR-183116] 21 p3013 N88-27877
Pattern information processing and multimedia database system: Current research on multimedia information system
[PB88-131917] 21 p3026 N88-27973
Research for reducing the labor intensive nature of high-resolution terrain analysis feature extraction
[AD-A192661] 22 p3089 N88-28345
Natural object categorization
[AD-A194103] 22 p3139 N88-28662
Survey of neural net paradigms for specification of discrete networks
[AD-A192682] 22 p3141 N88-28674
Determining vehicle motion from stereo image sequences
[AD-A194371] 23 p3216 N88-29140
Automatic line network extraction from aerial imagery of urban areas through knowledge-based image analysis
[AD-A192399] 23 p3227 N88-29208
Limits of pattern discrimination in human vision
[AD-A193449] 23 p3239 N88-29273
Analysis of the hopfield neural networks and their application to pattern recognition
[AD-A193827] 23 p3239 N88-29279
Automatic object recognition 23 p3254 N88-29368
Two dimensional convolute integers for machine vision and image recognition 23 p3254 N88-29369
A generic expert system for materials processing in space 23 p3255 N88-29376
Corner extraction from radar images
[AD-A194857] 24 p3362 N88-30020
Path planning and path following for the Amsterdam autonomous cart
[FVI-88-22] 24 p3380 N88-30133
Eye movements and spatial pattern vision
[AD-A195406] 24 p3408 N88-30290
An interactive testbed for development of expert tools for pattern recognition 24 p3419 N88-30349
Parallel and distributed computation for fault-tolerant object recognition 24 p3419 N88-30350
Nested neural networks
[NASA-TM-101032] 24 p3423 N88-30373

PATTERN REGISTRATION
A smart, mapping, charting and geodesy control generator, phase 1
[AD-A188184] 10 p1347 N88-18055
Autocorrelation of control points on 11-band multispectral imagery
[AD-A188185] 10 p1348 N88-18056
The modeling of error budget analysis and tolerance specifications for BRESEX multiband linear array CCD camera 17 p2355 N88-24029
Automatic registration of satellite imagery 17 p2364 N88-24080
Application of dynamic programming to image registration
[ENST-87E022] 18 p2557 N88-25180
Method for combined image interpolation-restoration through a fir filter design technique
[INPE-4561-PRE/1302] 24 p3413 N88-30315

PATTERNS
Orthogonal patterns in binary neural networks
[NASA-TM-100060] 10 p1396 N88-18320

PAULI EXCLUSION PRINCIPLE
Theory of two-photon emission from atomic inner shells
[AD-A187742] 11 p1543 N88-19223

PAVEMENTS
Polymer modified binders for bituminous or asphaltic paving layers
[PC-5] 02 p0153 N88-10958
The ability of modified pavement quality concrete to resist ground erosion caused by VTOL aircraft
[BAE-ARG-238] 03 p0267 N88-11683
Open-graded bases for airfield pavements
[AD-A184461] 04 p0402 N88-12500
A laboratory study of asphalt concrete mix designs for high-contact pressure aircraft traffic
[AD-A185753] 06 p0670 N88-14106
Comparative study of nondestructive pavement testing, MacDill Air Force Base, Florida
[AD-A186082] 07 p0822 N88-14993
Evaluation of bituminous materials used in pavement recycling projects at Tyndall, MacDill, and Hurlburt Air Force Bases
[AD-A188068] 10 p1317 N88-17871
Micro PAVER concept and development airport pavement management system
[AD-A187360] 11 p1441 N88-18598
Probabilistic and reliability design procedures for flexible airfield pavements: Elastic layered method
[AD-A187533] 11 p1442 N88-18600
Profilometer for bomb-damage-repaired airfield pavements and measurement of pavement upheaval. Report 1: Technology evaluation
[AD-A187985] 11 p1442 N88-18601
Applications and limitations of the spectral-analysis-of-surface-waves method
[PB88-136619] 11 p1513 N88-19038
Investigation of the inter-relationship between base pavement stiffness and asphalt overlay compaction
[DOT/FAA/ES-88/1] 14 p1869 N88-21170
Design of overlays for rigid airport pavements
[DOT/FAA/PM-87/19] 18 p2468 N88-24652

PAYLOAD ASSIST MODULE
An intelligent training system for payload-assist module deploys 09 p1204 N88-17214

PAYLOAD CONTROL
Test of the Hipparcos payload in the Liege vacuum facility focal 02 p0135 N88-10850
Hemispherical pointing mechanism drive unit — satellite payloads antennas 14 p1874 N88-21193
Deployment, hold down and release mechanisms for Wind Scatterometer Antenna (WSA) — ERS-1 wind scatterometer antenna (WSA) 14 p1876 N88-21207
A spin and deployment mechanism 14 p1926 N88-21479
Aerospace payload support systems
[AFGL-TR-87-0241] 24 p3334 N88-29843

PAYLOAD DELIVERY (STS)
Payload deployment system — STS 14 p1875 N88-21199
Noncryogenic propellants for a nuclear orbit transfer vehicle 17 p2428 N88-24444

PAYLOAD DEPLOYMENT & RETRIEVAL SYSTEM
NT REMOTE MANIPULATOR SYSTEM
Payload deployment method and system
[NASA-CASE-MSC-21330-1] 18 p2470 N88-24660

PAYLOAD INTEGRATION
A monograph of the National Space Transportation System Office (NSTSO) integration activities conducted at the NASA Lyndon B. Johnson Space Center for the EASE/ACCESS payload flown on STS 61-B 02 p0139 N88-10876
EASE/ACCESS ground processing at Kennedy Space Center 02 p0139 N88-10877
RETE experiment Assembly, Integration, and Verification (AIV) activities
[IFSI-87-6] 05 p0555 N88-13380
An AI approach for scheduling space-station payloads at Kennedy Space Center 08 p1064 N88-16425
Scheduling spacecraft operations 08 p1064 N88-16426
SYLDA: A dual-launch system for Ariane 09 p1125 N88-16745
Coorbiting Platform Utilization Study (CPLUS), executive summary — Columbus
[SN-WP-4000-DOC-8609/85/F] 09 p1133 N88-16798
Expert mission planning and replanning scheduling system for NASA KSC payload operations 09 p1209 N88-17247
Laser investigations for payload G-652 prior to filing pre-flight accommodation requirements 10 p1286 N88-17694
Modification of integrated partial payload lifting assembly
[NASA-CR-182573] 11 p1443 N88-18607
The German Spacelab mission D1: Payload integration
[ETN-88-91507] 14 p1871 N88-21179
Space nuclear reactor shielding optimization studies 17 p2408 N88-24320
Turbomachinery in space 17 p2408 N88-24321

PAYLOAD MASS RATIO
Ariane launch performance 09 p1125 N88-16743
Increased performance for Ariane 09 p1125 N88-16744

PAYLOAD RETRIEVAL (STS)
Cost-effective orbit transfer modes for satellite retrieval and servicing — Space Station 12 p1586 N88-19489
Review of commercial spacecraft: Recovery and repair experiences. Implications for future spacecraft designs and operations 12 p1591 N88-19528

PAYLOAD TRANSFER
A spin and deployment mechanism 14 p1926 N88-21479

PAYLOADS
NT ASTRO MISSIONS (STS)
NT EARTH RADIATION BUDGET EXPERIMENT
NT GET AWAY SPECIALS (STS)
NT PHYSICS AND CHEMISTRY EXPERIMENT IN SPACE
NT SEPAC (PAYLOAD)
NT SHUTTLE IMAGING RADAR
NT SPACE SHUTTLE PAYLOADS
NT SPACE STATION PAYLOADS
NT SPACELAB
NT SPACELAB PAYLOADS
NT X RAY ASTROPHYSICS FACILITY
Redistribution of particulates in shuttle bay during launch 02 p0133 N88-10837
Test of the Hipparcos payload in the Liege vacuum facility focal 02 p0135 N88-10850
Estimating payload internal temperatures and radiator size for multimegawatt space platforms
[DE88-000244] 03 p0275 N88-11738
The effect of maximum-allowable payload temperature on the mass of a multimegawatt space-based platform
[DE88-001921] 05 p0555 N88-13381
Carbon Dioxide observational platform system (CO-OPS) Feasibility Study
[NASA-CR-179225] 06 p0671 N88-14113
Performance considerations for the astrometric telescope facility on the phase 1 space station
[NASA-TM-100040] 06 p0800 N88-14898
Orbital Replaceable Unit (ORU)/cold plate thermal interface study. Volume 1: Executive Summary
[BAE-TP-8430] 07 p0855 N88-15195
Evaluate the application of modal test and analysis processes to structural fault detection in MSFC - STS project elements 07 p0927 N88-15630
Rapid prototyping and AI programming environments applied to payload modeling 08 p1061 N88-16405
Mechanical in-flight environment of Ariane payloads 09 p1126 N88-16748
Coorbiting Platform Utilization Study (CPLUS), executive summary — Columbus
[SN-WP-4000-DOC-8609/85/F] 09 p1133 N88-16798
Apollo Lightcraft project
[NASA-CR-182575] 11 p1445 N88-18615
A lunar transportation system
[NASA-CR-182561] 11 p1567 N88-19379
Mars Lander/Rover vehicle development: An advanced space design project for USRA and NASA/OAST
[NASA-CR-182570] 11 p1567 N88-19380
Preliminary analysis of an integrated logistics system for OSSA payloads
[NASA-CR-4114] 12 p1584 N88-19477
Preliminary analysis of an integrated logistics system for OSSA payloads. Volume 1: Executive summary 12 p1584 N88-19478
Preliminary analysis of an integrated logistics system for OSSA payloads. Volume 2: OSSA integrated logistics support strategy 12 p1584 N88-19479
Preliminary analysis of an integrated logistics system for OSSA payloads. Volume 3: OSSA integrated logistics support planning document 12 p1584 N88-19480

Automatic in-orbit payload deployment mechanisms, logistic operations and transport vehicle design compatibilities 12 p1586 N88-19493
Vehicle glow observed on the SONDA 3
[INPE-4297-PRE/1168] 12 p1600 N88-19581
Mars Lander/Rover vehicle development: An advanced space design project for USRA and NASA/OAST
[NASA-CR-182562] 12 p1709 N88-20226
Mars Lander/Rover vehicle development: An advanced space design project for USRA and NASA/OAST
[NASA-CR-182571] 12 p1709 N88-20227
The Joint NASA/Goddard-University of Maryland Research Program in Charged Particle and High Energy Photon Detector Technology
[NASA-CR-182612] 12 p1712 N88-20247
Expected value analysis for an unmanned expendable launch vehicle payload escape system
[AD-A189494] 13 p1728 N88-20337
Orbital transfer vehicle concept definition and system analysis study. Volume 2: OTV concept definition and evaluation. Book 1: Mission and system requirements
[NASA-CR-179321] 13 p1729 N88-20339
ERS-1 data products and services and their value for tropical countries 17 p2357 N88-24040
The effect of maximum allowable payload temperature on the mass of a multimegawatt space based platform 17 p2424 N88-24416
Lunar base surface mission operations. Lunar Base Systems Study (LBSS) task 4.1
[NASA-CR-172050] 18 p2594 N88-25415

PBRE (REACTORS)
U PEBBLE BED REACTORS

PCM (MATERIALS)
U PHASE CHANGE MATERIALS

PCM (MODULATION)
U PULSE CODE MODULATION

PCM TELEMETRY
Rivista Tecnica Selenia, volume 10, number 2
[ETN-87-90763] 01 p0011 N88-10064
Telemetry conditioning units for the European launcher Ariane 01 p0012 N88-10068
PCM telemetry standard
[ESA-PSS-46(TTC.A.02)ISSUE-1] 09 p1132 N88-16790

PDM (MODULATION)
U PULSE DURATION MODULATION

PEACETIME
The military techniques of tomorrow. A contribution to active peace assurance
[MBB-UA-1049/87] 10 p1315 N88-17860

PEBBLE BED REACTORS
Thermal-hydraulic considerations for particle bed reactors 17 p2400 N88-24266
Particle bed reactor scaling relationships 17 p2400 N88-24267
Direct nuclear propulsion for Earth-to-orbit vehicles 17 p2400 N88-24271
Nuclear propulsion systems for orbit transfer based on the particle bed reactor 17 p2401 N88-24272
Ultra high temperature direct propulsion 17 p2401 N88-24275
Small particle bed reactors: Sensitivity to Brayton cycle parameters 17 p2435 N88-24487
The closed Brayton cycle: An energy conversion system for near-term military space missions 17 p2435 N88-24488
Energy conversion system optimization study for multimegawatt space nuclear power application 17 p2436 N88-24492

PECLET NUMBER
Review of numerical methods for radionuclide transport in three-dimensional porous media, at high Peclet numbers
[CFDU/87/10] 18 p2538 N88-25061

PEDIMENTS
U PIEDMONTS

PEDIPLAINS
U PIEDMONTS

PEDOLOGY
U SOIL SCIENCE

PEEK
Electron beam irradiation effects on carbon fiber reinforced PEEK composite
[DE87-753001] 02 p0142 N88-10890
Effects of solvent exposures on poly(etheretherketone) (PEEK) and PEEK-fiberglass composites
[MLM-3405] 03 p0281 N88-11766
Molecular composites: Processing, post-treatment and mechanics
[AD-A184458] 04 p0410 N88-12547
Characterization of Mode 1 and Mode 2 delamination growth and thresholds in graphite/peek composites
[NASA-TM-100577] 16 p2172 N88-22947
The crystallization of tough thermoplastic resins in the presence of carbon fibers
[NASA-CR-182984] 20 p2776 N88-26464
Compression creep of filamentary composites
[NASA-CR-182550] 20 p2798 N88-26601

PEELING
Effect of peel angle on peel force
[AD-A186117] 08 p0972 N88-15878
Effect of post-cure heat-treatment on static and fatigue behaviour of XAS-914C carbon fibre composite
[AD-A186943] 10 p1294 N88-17735

PEGASUS SATELLITES
Orbit determination of 1965-09A for analysis of the eccentricity at 15th-order resonance
[RAE-TR-87059] 22 p3047 N88-28081

PELLETS
Microstructural effects in shock initiation of granular explosives
[DE87-011282] 01 p0031 N88-10200
CIT (Compact Ignition Tokamak) fueling
[DE88-002709] 12 p1692 N88-20125
Application of railgun principle to high-velocity hydrogen pellet injection for magnetic fusion reactor refueling
[DE88-005830] 13 p1728 N88-20334
Improvements to Raney copper zinc methanol synthesis catalysts 17 p2318 N88-23844
The JET (Joint European Torus) multipellet launcher and fueling of JET plasmas by multipellet injection
[DE88-008367] 19 p2729 N88-26206

PENALTY FUNCTION
An exact penalization viewpoint of constrained optimization
[DE88-001477] 04 p0486 N88-12995
Velocity-pressure integrated versus penalty finite element methods for high Reynolds number flows
[NASA-CR-179357] 20 p2803 N88-26635

PENDULUMS
Allowance for influence of gravity field nonuniformity 08 p1012 N88-16137
Evaluation of a miniature horizontal pendulum tilt transducer 12 p1577 N88-19435

PENETRATING PARTICLES
U CORPUSCULAR RADIATION

PENETRATION
Space station integrated wall design and penetration damage control
[NASA-CR-179169] 01 p0013 N88-10070
Analysis of compressible flow on high-velocity jet penetration 03 p0302 N88-11898
Models for penetration of thin plates
[DE87-013727] 03 p0332 N88-12090
Mechanical property evaluation of a series of commercial tungsten alloys
[AD-A185440] 05 p0565 N88-13446
Structural frequency functions for an impulsive, distributed forcing function 05 p0594 N88-13627
Study of extended least-square iterative techniques in electromagnetic scattering by penetrable objects
[PB88-105879] 06 p0694 N88-14262
Unsteady stall penetration experiments at high Reynolds number
[AD-A186120] 07 p0814 N88-14958
Earth penetrator strain gage applications
[DE88-002260] 09 p1166 N88-16993
New model to estimate the perforation power of kinetic energy projectiles
[PB87-166757] 09 p1175 N88-17040
Mechanism of change of vortex structure orientation in type-2 superconductors 09 p1239 N88-17425
Space station integrated wall damage and penetration damage control. Task 5: Space debris measurement, mapping and characterization system
[NASA-CR-179281] 10 p1285 N88-17688
Penetration theory for inclined and moving shaped charges
[MBB-UA-940/86] 10 p1315 N88-17861
An analysis of penetration and ricochet phenomena in oblique hypervelocity impact
[NASA-TM-100319] 10 p1339 N88-18004
Penetration depth measurements of YBa2Cu3O/sub 7-delta/ at 4 MHz
[DE88-003493] 10 p1420 N88-18478
Fracture toughness of steel weldments containing lack of penetration defects 11 p1501 N88-18965
Observations on electrostatic effects in a filter test system
[AD-A188797] 13 p1736 N88-20378
A direct correlation of strength with impact velocity
[AD-A189251] 13 p1741 N88-20409
Numerical analysis of critical penetration velocity for jet perpendicular penetration 16 p2186 N88-23037
Subsurface morphology and geoarchaeology revealed by spaceborne and airborne radar 17 p2353 N88-24022
Ballistic evaluation of applique armours: Presentation and interpretation of ballistic data
[MRL-TN-527] 19 p2635 N88-25629
Instrumentation for the measurement of penetrator dynamic response to permit force estimation
[DE88-010608] 20 p2809 N88-26666
GTAW characterization for weld penetration on 304L stainless steel
[DE88-010611] 20 p2810 N88-26672
Study of comet nucleus gamma-ray spectrometer penetration system
[NASA-CR-177393] 20 p2883 N88-27120
Investigation of hydrogen isotope penetration through stainless steels Kh18N10T and Kh3M2BFR
[DE88-702189] 21 p2915 N88-27297
Signal processing software for ground penetrating radar, user's manual
[AD-A194286] 23 p3203 N88-29059

PENETRATION BALLISTICS
U TERMINAL BALLISTICS

PENNING EFFECT
Ion traps for large storage capacity 16 p2268 N88-23570
Examination of the termalization of confined ions
[PB87-227815] 19 p2723 N88-26171
Theoretical atomic and molecular physics
[DE88-007122] 19 p2724 N88-26175

PENTACHLORIDES
U CHLORIDES

PENTAERYTHRITOL TETRANITRATE
U PETN

PENUMBRAS
Exploiting the IR: Solar and stellar spectroscopy in the IR 04 p0504 N88-13102

PEPTIDES
NT GLUTATHIONE
NT POLYPEPTIDES
Synthesis of high molecular weight peptide polymers and copolymers containing L-dope residues
[AD-A186462] 08 p0973 N88-15887
Neuropeptides in experimental head injury
[AD-A188067] 11 p1520 N88-19077
Protection from stress 12 p1664 N88-19978
Development of polymeric films with piezoelectrical properties from polypeptides; low, odd nylons; or polyureas
[AD-A190301] 15 p2044 N88-22181
Studies of model ion channels in defect-free multibilayers of phospholipids
[AD-A188740] 16 p2238 N88-23365
Role of opioid peptides in pathogenesis of vestibulovegetative disorders 19 p2704 N88-26079

PERCENTAGE
U RATIOS

PERCEPTION
NT AUDITORY PERCEPTION
NT CONSCIOUSNESS
NT MOTION PERCEPTION
NT PROPRIOCEPTION
NT SENSORY PERCEPTION
NT SOUND LOCALIZATION
NT SPACE PERCEPTION
NT TACTILE DISCRIMINATION
NT TOUCH
NT VISUAL DISCRIMINATION
NT VISUAL PERCEPTION
Studies of the processing of single words using positron tomographic measures of cerebral blood flow change
[AD-A184058] 03 p0356 N88-12244
An evaluation of perceptions of form, fit, function (F3) standardization on the Standard Inertial Navigation Unit (STD INU) program
[AD-A188955] 12 p1579 N88-19446
Relationship of encoding speed and memory tests to flight training performance
[AD-A190670] 15 p2105 N88-22539
The N2-P3 complex of the evoked potential and human performance 16 p2241 N88-23388
Problem solving in a natural task as a function of experience
[AD-A191180] 16 p2243 N88-23399
The interaction of sensory and perceptual variables: Spatial, temporal and orientation response to figure and ground
[AD-A192897] 20 p2832 N88-26798
Cognitive and neural bases of skilled performance
[AD-A193392] 21 p2992 N88-27747
Texture perception and shape from texture
[AD-A192923] 21 p2996 N88-27771
Issues in computer-assisted interpretation of graphs and quantitative information
[PB88-116280] 21 p2998 N88-27783
Advancement of latent trait theory
[AD-A194302] 24 p3408 N88-30289

PERCEPTRONS
U SELF ORGANIZING SYSTEMS

PERCEPTUAL ERRORS
Ejection situations in the U-2/TR-1: An analysis of emotions and events
[AD-A192672] 21 p2893 N88-27175
PERCHLORATES
NT AMMONIUM PERCHLORATES
NT LITHIUM PERCHLORATES
PERCOLATION
De-alloying
[DE87-012488] 01 p0022 N88-10139
Surface free energy of laser-produced bond percolators
[PB88-130885] 11 p1493 N88-18913
The percolation approach as a basis for experimental research on the mechanical properties of composite materials 14 p1886 N88-21271
Analysis of transverse strength of composites using percolation theory
[AD-A193204] 21 p2904 N88-27234
PERFECT GAS
U IDEAL GAS
PERFLUORO COMPOUNDS
Polyvinyl esters of omega-H-perfluoroacids and polyvinyl alcohol obtained from them
[AD-A184633] 03 p0279 N88-11755
Surface catalytic degradation study of two linear perfluoropolyalkylethers at 345 C
[NASA-TP-2774] 04 p0410 N88-12543
Electrochemical characteristics of acid electrolytes for fuel cells
[PB88-104641] 06 p0731 N88-14497
Improved perfluoroalkylether fluid development
[NASA-CR-180872] 08 p0967 N88-15851
The performance of perfluoropolyalkylether oils under boundary lubrication conditions
[AD-A191057] 17 p2323 N88-23869
Theoretical studies of solar lasers and converters
[NASA-CR-182927] 17 p2344 N88-23972
PERFORATED PLATES
Computational studies of wave-shaping in a blast simulator by perforated plates in the driver
[AD-A188200] 11 p1483 N88-18850
Stress-strain behaviour of a bolt hole in carbon fibre composite plates
[BU-354] 14 p1923 N88-21460
Finite element simulation of perforation of aluminum plates
[DE88-002092] 15 p2073 N88-22362
Operational considerations for laminar flow aircraft 17 p2298 N88-23748
Dynamical stress concentration problems, from every side, bordered and perforated plates
[ETN-88-92128] 20 p2815 N88-26703
PERFORATING
New model to estimate the perforation power of kinetic energy projectiles
[PB87-166757] 09 p1175 N88-17040
Optical Fourier transformation by lensless method with perforated mask and with modified Talbot interferometer for analysis of interferograms 09 p1236 N88-17408
Numerical simulation of the perforation of thin plates
[ISL-R-122/86] 11 p1495 N88-18926
PERFORATION
Analysis of the perforation of monolithic and simple laminate aluminium targets as a test of analytical deformation models
[MRL-R-1111] 20 p2813 N88-26686
PERFORMANCE
Post-test analyses of aqueous batteries developed for electric propulsion
[DE88-000655] 03 p0311 N88-11965
Nonconformity testing for the Graphical Kernel System (GKS)
[GMD/VAL-86-104] 06 p0757 N88-14644
Preliminary analysis of helium generation and its effects on the SP-100 system performance 17 p2422 N88-24406
PERFORMANCE PREDICTION
Propulsion Working Group report 01 p0016 N88-10098
Endurance testing of a natural gas-fueled rotary engine
[PB87-215703] 01 p0055 N88-10356
Global positioning satellite-based automatic landing system and wind estimated feedback for the AH-64 helicopter 02 p0124 N88-10784
Modeling and performance evaluation of the DPS25 packet switching multiprocessor system — communication networks
[ENST-87E009] 02 p0162 N88-11016
Flight experience of solar mesosphere explorer's power system over high temperatures ranges 02 p0165 N88-11037
Real time charge efficiency monitoring for nickel electrodes in NICD and NIH2 cells 02 p0165 N88-11038
Methodology of performance evaluation of real time distributed systems
[ENST-87D003] 02 p0228 N88-11440
Stability of mechanical joints in launching vehicles: Local and global stationary values of energy density 03 p0270 N88-11696
The impact of environmental factors on the performance of millimeter wave seekers in smart munitions
[DE87-014277] 03 p0270 N88-11697
A hybrid numerical technique for predicting the aerodynamic and acoustic fields of advanced turboprops
[NASA-CR-174926] 03 p0374 N88-12352
Numerical prediction of propeller performance by vortex lattice method
[UTIAS-TN-265] 04 p0400 N88-12489
Applications of the hybrid automated reliability predictor
[NASA-TP-2760] 04 p0475 N88-12928
Predictions of F-111 TACT aircraft buffet response and correlations of fluctuating pressures measured on aluminum and steel models and the aircraft
[NASA-CR-4069] 05 p0529 N88-13218
The off-design performance of hypersonic waveriders 05 p0533 N88-13244
Numerical optimization of conical flow waveriders including detailed viscous effects 05 p0533 N88-13245
Dynamic stability of hypersonic conical lifting vehicles according to Newton-Busemann theory 05 p0534 N88-13247
Experiences using the Mark IV supersonic hypersonic arbitrary body program 05 p0534 N88-13249
The RAE experimental data-base for missiles at high Mach number and its use in assessing CFD methods 05 p0534 N88-13250
Damage considerations in sizing aircraft cells. Life predictions
[SNIAS-872-111-116] 05 p0546 N88-13330
Model helicopter rotor rig and associated strain gauge balance for performance studies
[NAL-TM-AE-8704] 05 p0552 N88-13364
Performability modeling based on real data: A casestudy
[NASA-CR-181563] 05 p0633 N88-13870
Mainline performance prediction for radial inflow turbines 06 p0712 N88-14366
Analysis and performance prediction of scramjet inlets utilizing a three-dimensional Navier-Stokes code 07 p0811 N88-14936
Flow in Centrifugal Compressors — conference
[VKI-LS-1987-01] 07 p0850 N88-15160
Overview of NASA PTA propfan flight test program 08 p0957 N88-15805
Failure modes of laminate structures
[DE88-002579] 08 p0996 N88-16033
A validity study of a selection procedure for student airline pilots
[DFVLR-FB-87-34] 09 p1201 N88-17196
Method for predicting performance limits of centrifugal compressors 10 p1283 N88-17677
A strategy for failure prediction 10 p1380 N88-18243
Damage mechanisms and fatigue life prediction of graphite/epoxy laminates 11 p1449 N88-18637
Seventy-meter antenna performance predictions: GTD analysis compared with traditional ray-tracing methods 11 p1474 N88-18793
Test results of a 40-kW Stirling engine and comparison with the NASA Lewis computer code predictions
[NASA-TM-87050] 11 p1508 N88-19013
OMV man/system simulation integration: A preliminary analysis and recommendation
[NASA-CR-182602] 12 p1671 N88-20005
Robustifying the Kalman filter
[AD-A189240] 13 p1825 N88-20907
Analysis of induction motors based on the numerical solution of the magnetic field and circuit equations
[EL-59] 14 p1907 N88-21398
Stall flutter analysis of propfans 16 p2221 N88-23256
A correlational approach to predicting operator status 16 p2242 N88-23393
The performance of the VKI longshot hypersonic wind tunnel
[VKI-TN-161] 18 p2468 N88-24650
Propagation management for no-acknowledge HF communications links 18 p2502 N88-24843
Performance estimates for operations conducted while wearing individual protective equipment: User manual
[AD-A191871] 18 p2553 N88-25154
Armoured vehicle track elastomers: Research and development at MRL
[MRL-GD-0012] 19 p2620 N88-25541
A computer program for performance prediction of tripropellant rocket engines with tangential slot injection 19 p2627 N88-25581
Boundary layer simulator (BLIMPJ) improvement 19 p2627 N88-25582
Motor test data comparisons with laboratory data and stability predictions 19 p2629 N88-25594
A multiple chamber volume-filling model for prediction of transient solid rocket motor ballistic performance 19 p2633 N88-25618
Failure rate prediction of electronic components
[PB87-228953] 19 p2678 N88-25925
Predicting Air Combat Maneuvering (ACM) performance: Fleet fighter ACM readiness program grades as performance criteria
[AD-A191605] 19 p2710 N88-26099
Prediction of fatigue growth
[NLR-MP-87052-U] 20 p2816 N88-26707
A comparison of the various helicopter mathematical models used in the methodology assessment 21 p2889 N88-27149
A comparison of theory and experiment for aeroelastic stability of a hingeless rotor model in hover 21 p2889 N88-27150
A comparison of theory and flight test of the BO 105/BMR in hover and forward flight 21 p2890 N88-27155
Failure analysis of laminated composite angles 21 p2959 N88-27578
Recent advances in engine health management 22 p3033 N88-28005
Onboard Life Monitoring System (OLMOS): Engine life cycle calculation and trending 22 p3034 N88-28010
Goldstone solar system radar performance analysis 22 p3068 N88-28206
High-aspect-ratio wings 23 p3167 N88-28859
Measured and predicted responses of the Nord 260 aircraft to the low altitude atmospheric turbulence 24 p3312 N88-29723
Semi-empirical methods for conventional and unconventional missiles 24 p3318 N88-29758
Space marching Euler solvers 24 p3318 N88-29759
Numerical models for analytical predictions of combustor aerothermal performance characteristics 24 p3349 N88-29935
Three-dimensional gas turbine combustor modelling 24 p3349 N88-29937
Numerical modeling of combustion processes in gas turbines 24 p3350 N88-29939
Performance Prediction for Coatings. Proceedings of a Workshop
[AD-A188973] 24 p3354 N88-29966
Ultrasonic detection of diffusion and adhesion loss 24 p3354 N88-29967
Performance prediction of concurrent systems
[NASA-CR-183175] 24 p3412 N88-30312
Theories of comparative analysis
[AD-A196328] 24 p3427 N88-30395
PERFORMANCE TESTS
Numerical predictions of EML system performance
[DE87-011727] 01 p0011 N88-10061
Space station propulsion technology: Space station propulsion system test bed test plan
[NASA-CR-179201] 01 p0017 N88-10104
Fiber-reinforced composite hot-gas filters
[DE87-012257] 01 p0033 N88-10208
Test results and predictions for the response of near-ceiling sprinkler links in a full-scale compartment fire
[NBSIR-87/3633] 01 p0033 N88-10209
Analysis of the electromagnetic performance characteristics of stripline transformers
[DE87-012515] 01 p0042 N88-10264
Endurance testing of a natural gas-fueled rotary engine
[PB87-215703] 01 p0055 N88-10356
Hardware fault insertion and instrumentation system: Mechanization and validation
[NASA-CR-181445] 01 p0078 N88-10497
Analysis and synthesis of abstract data types through generalization from examples
[NASA-CR-178369] 01 p0081 N88-10519
Infra-red lamp panel study and assessment application to thermal vacuum testing of sigma telescope 02 p0132 N88-10830
Rocket nozzle thermal shock tests in an arc heater facility 02 p0133 N88-10832
Surveillance systems test and evaluation facilities 02 p0134 N88-10845
Characteristics and performance of the ESTEC large space simulator cryogenic system 02 p0135 N88-10849
Design, construction, activation, and operation of a high intensity acoustic test chamber 02 p0137 N88-10864
Operating experiences and test results of six cold helium compressors
[DE87-012115] 02 p0157 N88-10982

Battery development and testing at ESA
02 p0164 N88-11027
Nickel hydrogen low Earth orbit test program update and status 02 p0164 N88-11028
Grace DAKASEP alkaline battery separator
02 p0164 N88-11031
BRASILSAT A2: Ground and in-orbit anomalies
02 p0164 N88-11032
Qualification testing of General Electric 50 Ah nickel-cadmium cells with Pellon 2536 separator and passivated positive plates 02 p0165 N88-11036
Statistically determined nickel cadmium performance relationships 02 p0165 N88-11039
Test summary for advanced H2 cycle NI-CD cell
02 p0165 N88-11040
Performance of high power S-band klystrons focused with permanent magnet
[DE87-753024] 02 p0167 N88-11053
The four spot time-of-flight laser anemometer
02 p0184 N88-11145
Constitutive modeling for isotropic materials
02 p0188 N88-11172
Lewis' enhanced laboratory for research into the fatigue and constitutive behavior of high temperature materials
02 p0189 N88-11177
Performance evaluation of a half-wave resonant slot antenna over perfect ground using NEC (Numerical Electromagnetic Code)
[AD-A184004] 03 p0308 N88-11942
Study of aeropropulsion laboratory pressure drop rig and recommended test procedure
[AD-A184333] 03 p0322 N88-12038
Advanced natural gas fueled engine development. Part 1: Design and analyses
[PB87-224804] 03 p0331 N88-12087
Performance evaluation of artificial intelligence systems
[AD-A184054] 03 p0368 N88-12316
General-Purpose Heat Source Safety Verification Test Program: Edge-on flyer plate tests
[DE87-006309] 03 p0376 N88-12362
The aerodynamics of supersonic parachutes
[DE87-014846] 04 p0395 N88-12464
Performance and combustion characteristics of direct-injection stratified-charge rotary engines
[NASA-TM-100134] 04 p0400 N88-12490
Programmable Logic Arrays (PLA's) design for testability
[PB87-102935] 04 p0438 N88-12718
Long-range pulselength scaling of 351nm laser damage thresholds
[DE87-014754] 04 p0448 N88-12777
Calculation of the tribological properties of surfaces by semi-empirical methods
[AD-A184283] 04 p0450 N88-12791
Performance analysis of solar thermal power systems
[DE88-000563] 04 p0465 N88-12874
Performance monitoring and analysis of electric van fleet vehicles
[DE88-900066] 04 p0502 N88-13091
Application of modified loss and deviation correlations to transonic axial compressors
[AGARD-R-745] 05 p0549 N88-13344
Error control techniques for satellite and space communications
[NASA-CR-181581] 05 p0576 N88-13516
Establishment of complete minimum test sets for digital circuits with safety engineering significance
[ETN-88-90599] 05 p0578 N88-13526
Seal technology for liquid oxygen (LOX) turbopumps
[NASA-CR-174866] 05 p0591 N88-13603
Trajectory control of robot manipulators with closed-kinematic chain mechanism
[NASA-TM-89305] 05 p0591 N88-13605
Test and evaluation of the transputer in a multi-transputer system
[AD-A184969] 05 p0631 N88-13859
High speed propeller performance and noise predictions at takeoff/landing conditions
[NASA-TM-100267] 05 p0646 N88-13960
Performance measurements of the Kolibrie and FACT rotor blades without tip vanes on the full-scale experimental wind turbine
[IW-R518] 06 p0665 N88-14077
Rendezvous and Docking Verification (RVDV) and in-orbit demonstration, executive summary
[RVD-RVDV-FR-AS-01] 06 p0673 N88-14120
Aerodynamic testing of small turbines
06 p0713 N88-14371
Aerodynamic design and test performance of supersonic turbines for the Vulcain rocket engine
06 p0713 N88-14373
Development of a supersonic steam turbine with a single stage pressure ratio of 200 for generator and mechanical drive 06 p0713 N88-14374
A 1,000-watt solar power unit for Far North
06 p0728 N88-14481
ATF (Advanced Toroidal Facility) ECH (Electron Cyclotron Heating) waveguide component development and testing
[DE88-001432] 06 p0782 N88-14797
Data acquisition, reduction and analysis of shock and vibration testing using a super microcomputer
[AD-A186123] 07 p0867 N88-15260
Realization and demonstration of a wind turbine of 200 kW demonstration project
[DE88-900207] 07 p0874 N88-15302
Feasibility of software built-in test for SDI (Strategic Defense Initiative) applications
[AD-A185750] 07 p0917 N88-15572
Pattern recognition techniques for failure trend detection in SSME ground tests 07 p0924 N88-15614
The development of test methodology for testing glassy materials 07 p0927 N88-15633
Determining structural performance
08 p0954 N88-15787
Analysis, design, construction and testing of a reaction wheel model for space applications
[INPE-4358-TDL/299] 08 p0963 N88-15834
The ESTEC Mini Compact Antenna Test Range
[ESA-CR(P)-2475] 08 p0977 N88-15907
Comparison of a thermoelectric cooling system and a groundwater heat pump
[DE88-001753] 08 p0984 N88-15950
Solid mechanics research for quantitative non-destructive evaluation
[AD-A186599] 08 p0993 N88-16010
Preliminary evaluation of a micro-based repeated measures testing system
[NASA-CR-172038] 08 p1048 N88-16331
Ada (trade name) compiler validation summary report. Systems designers' PLC SD Ada-plus VAX/VMS x MC68020. Version 2B.00. Host: VAX 8600. Target: Motorola MC68020. Completion of on-site testing
[AD-A186571] 08 p1053 N88-16356
Short pseudorandom test sequences
[AD-A185883] 08 p1054 N88-16357
Development of a menu of performance tests self-administered on a portable microcomputer
[NASA-CR-172040] 08 p1067 N88-16452
Helicopters as test carriers for avionics systems (HETAS)
[DFVLR-IB-112-85/18] 09 p1116 N88-16692
Integration testing of the propulsion system of Ariane's first stage 09 p1126 N88-16751
Testing a very good microwave interferometer
[TRITA-EPP-86-09] 09 p1167 N88-16996
The 5-GHz operation of the ITT and RCA streak tubes with a 7.5-ns time window
[DE88-003342] 09 p1169 N88-17008
An integration test for accelerometer evaluation
09 p1178 N88-17054
Development of a facility using robotics for testing automation of inertial instruments
09 p1213 N88-17271
A performance comparison of the Cray-2 and the Cray X-MP
[NASA-CR-177461] 09 p1216 N88-17288
Design and test of a high blade speed, high work capacity transonic turbine 10 p1281 N88-17658
Design and testing of a front stage for an advanced high pressure compressor 10 p1283 N88-17679
Simulation test beds for the space station electrical power system
[NASA-TM-100786] 10 p1290 N88-17715
Development of vertical takeoff aircraft with turbojet engines in Germany 10 p1309 N88-17822
Flight testing of fighter aircraft
[MBB/LKE-62/S/PUB/292] 10 p1312 N88-17844
Testing of a tail rotor system in a fiber composite type of construction
[MBB-UD-472/86] 10 p1314 N88-17854
Solid-state voltage standard performance and design guidelines
[PB88-123757] 10 p1322 N88-17905
Analysis of the performance of an air-water heat pump: Regulation of intrinsic performances
[DE88-900241] 10 p1349 N88-18061
Wake effects in a Fayette 95-IIS wind turbine array
[DE88-001103] 10 p1349 N88-18063
Modal testing the EOLE
[DE88-003795] 10 p1350 N88-18066
Preliminary results from the dynamic response testing of the Westinghouse 600-kW wind turbine
[DE88-001123] 10 p1350 N88-18070
Signal and data processing for IR sensors
10 p1374 N88-18199
A performance analysis of architectural scalability
[DE88-003537] 10 p1383 N88-18261
Factors causing unexpected variations in Ada benchmarks
[AD-A187231] 10 p1388 N88-18291
On the maneuvering of vehicles
[AD-A187632] 10 p1427 N88-18521
A performance index approach to aerodynamic design with the use of analysis codes only
[NASA-TP-2805] 11 p1433 N88-18552
Performance survey of airfoil profiles
[ETN-88-91093] 11 p1436 N88-18568
Columbus feasibility studies. Volume 4: Integration, test, and operations
[ETN-88-90576] 11 p1445 N88-18614
UHV (Ultra-High Vacuum) double crystal monochromator design
[DE88-003904] 11 p1456 N88-18676
Procedures for quantitative sensitivity and performance validation studies of a deterministic fire safety model
[NBS/GCR-88/544] 11 p1469 N88-18762
Conception and realization of components for a microchannel-plate detector, and testing of the detector system in the laboratory and in astronomical use
[ETN-88-91495] 11 p1491 N88-18899
Testing of a one-bladed 30-meter-diameter rotor on the DOE/NASA Mod-O wind turbine
[NASA-TM-100274] 11 p1509 N88-19014
Results of the 1987 NASA/JPL balloon flight solar cell calibration program
[NASA-CR-182617] 12 p1574 N88-19413
Simultaneous estimation and detection of bias shifts for inertial navigation systems 12 p1576 N88-19429
Reference position vector 12 p1577 N88-19432
Control test and validation for a large diameter high stability centrifuge 12 p1577 N88-19437
Rate and dynamic tests on the Canadian Strapdown Gyroscope (CSG-2) 12 p1578 N88-19439
The German Honeywell ring laser gyro: Development and test results 12 p1578 N88-19440
Simulation and tests of a satellite attitude and orbit control system. General considerations concerning an example case (INPE) and design of a servo rate table
[INPE-4282-PRE/1154] 12 p1599 N88-19572
Performance test results for the Eaton dc development power train in an electric test bed vehicle
[DE88-005458] 12 p1622 N88-19699
Planning, construction, and commissioning of a vacuum apparatus with a cold surface for the measurement of transistor functions at 20 K
[JUEL-SPEZ-397] 12 p1622 N88-19703
The effects of two Carlucci initiatives concurrency and streamlining, on the test and evaluation phase of system acquisitions 12 p1704 N88-20198
An investigation of classical dynamic scaling techniques applied to an oleo-pneumatic landing gear strut
[AD-A187664] 13 p1721 N88-20292
Combustion theory and related questions
[AD-A189160] 13 p1737 N88-20382
Materials Research Laboratory at Brown University
[AD-A188006] 13 p1739 N88-20396
Optimization of binary pigment coatings
[AD-A189103] 13 p1748 N88-20450
Improve the lifetime of the hollow fiber sodium sulfur cell
[DE88-004881] 13 p1751 N88-20469
Aluminum-air battery development
[DE88-006618] 13 p1762 N88-20543
Testing and development of electric vehicle batteries for EPRI Electric Transportation Program
[DE88-005894] 13 p1764 N88-20551
The evaluation of automatic barometers, illustrated by the Nakaasa barometer
[KNMI-TR-95] 13 p1774 N88-20610
Stable, high-efficiency, CuInSe2-based, polycrystalline, thin-film tandem solar cells
[DE88-001116] 13 p1793 N88-20726
Cadmium sulfide/copper ternary heterojunction cell research
[DE88-001122] 13 p1793 N88-20727
Pursuit tracking performance decrements associated with decreasing ambient illumination
[AD-A189336] 13 p1809 N88-20809
Electron emission from conductors subjected to intense, short-pulse electric fields
[DE88-005412] 13 p1836 N88-20985
Space infrared telescope facility wide field and diffraction limited array camera (IRAC)
[NASA-CR-182704] 13 p1853 N88-21092
Equipment test methods for externally produced electromagnetic transients
[RAE-TM-FS(F)-457] 14 p1865 N88-21140
Recommended test specification for the electromagnetic compatibility of aircraft equipment
[RAE-TM-FS(F)-510] 14 p1867 N88-21155
Qualification of the OLYMPUS reaction wheel
14 p1878 N88-21226

Qualification testing of the EUROSTAR Solar Array Drive Mechanism (SADM) 14 p1879 N88-21229
Determination of the modulus of elasticity of structural silicone sealants
[PB88-157458] 14 p1893 N88-21307
Industrial electric motors and controllers
[PB88-139589] 14 p1907 N88-21394
Performance of elastomeric bearings
[PB88-159470] 14 p1918 N88-21450
Combustion and performance characteristics of methanol plus higher alcohols in a spark ignition engine
[PB88-147962] 14 p1918 N88-21451
Space station full-scale docking/berthing mechanisms development 14 p1927 N88-21491
Development of a laboratory test for multiport injector deposits: Approaches 1 and 2
[AD-A190697] 15 p2048 N88-22203
Performance of single and multiple system AM stereo decoder receivers
[PB88-168307] 15 p2057 N88-22265
Performance test results: AXIAL-GAP, permanent magnet compressor motor
[DE88-006857] 15 p2061 N88-22289
UARS spacecraft recorder
[NASA-CR-180768] 15 p2068 N88-22331
Performance evaluation of molten salt thermal storage systems
[DE87-014645] 15 p2091 N88-22461
Prediction of physical fitness: Estimated percent body fat using body circumferences versus weight-height measures
[AD-A190233] 15 p2103 N88-22526
Exhaustive and pseudo-exhaustive testing
[AD-A190140] 15 p2111 N88-22574
Model-scale sound propagation experiment
[NASA-TM-100602] 15 p2130 N88-22709
Design and test of a new coaxial air joints
[DE88-751808] 16 p2164 N88-22908
Small-scale cleavage test of polymer products
[PB88-165360] 16 p2181 N88-23001
Development of a laboratory test for multiport fuel injector deposits - evaluation of the Jet Fuel Thermal Oxidation Test apparatus (JFTOT)
[AD-A191313] 16 p2183 N88-23015
Instrumentation for ultrafast electronics
[AD-A191379] 16 p2193 N88-23080
Use of water towing tanks for aerodynamics and hydrodynamics 16 p2204 N88-23149
The new UCSB (University of California, Santa Barbara) compact far-infrared FEL
[AD-A190864] 16 p2212 N88-23203
Roller drive materials performance 16 p2219 N88-23241
Microgravity manipulator demonstration 16 p2219 N88-23242
Spectroradiometry in the industrial test laboratory 16 p2272 N88-23596
Method of digital surface photometry of galaxies and its application to the edge-on galaxy NGC 5907 16 p2287 N88-23695
Test philosophy of the EH101 integrated avionic 17 p2303 N88-23775
Testing complex avionics software: A practical experience 17 p2306 N88-23794
Error contrpl techniques for satellite and space communications
[NASA-CR-182886] 17 p2332 N88-23922
Botany Facility. Thermal Control (TC) subsystem test report on experiment container of laboratory model and breadboard centrifuge
[BF-TN-ER-061/86] 17 p2378 N88-24135
Botany Facility: Test report on breadboard tests for the determination of the heat transfer at the glass disk and of the temperature distribution in the fluorescent tube
[BF-TN-ER-053] 17 p2378 N88-24136
SP-100 GES test site 17 p2417 N88-24375
Development of refractory thermocouples for space nuclear power tests 17 p2434 N88-24478
SNAP fuel performance. 17 p2435 N88-24484
Performance and long duration test of a 30 kw thermal arcjet engine
[AD-A190962] 18 p2474 N88-24677
An extended life and performance test of a low-power arcjet
[NASA-TM-100942] 18 p2476 N88-24687
Laboratory tests of laser gyroscopes for future utilization in multifunction systems for precision navigation and flight guidance 18 p2517 N88-24932
SRM propellant and polymer materials structural test program
[NASA-TP-2821] 18 p2530 N88-25013
Small scale bipolar nickel-hydrogen testing
[NASA-TM-100936] 18 p2538 N88-25059
The scaling of the threshold conditions for solid propellant erosive burning 19 p2630 N88-25601
Propagation effects by roadside trees measured at UHF and L-band for mobile satellite systems 19 p2644 N88-25693
Land mobile satellite propagation results 19 p2645 N88-25698
System architecture for the Canadian interim mobile satellite system 19 p2646 N88-25703
Design, development and trials of an airline passenger telephone system 19 p2646 N88-25704
Land mobile satellite demonstration system 19 p2646 N88-25706
Mobilestar field test program 19 p2646 N88-25707
Test results of the Electric Vehicle Field-Laboratory Correspondence Program, phase 1 report
[DE88-007706] 19 p2661 N88-25827
Pulsatile fluidic pump performance at elevated temperatures
[DE88-008046] 19 p2677 N88-25919
Solar assisted absorption or motor driven heat pump with earth seasonal storage. Part 2: Tables and figures
[DE88-900226] 19 p2686 N88-25964
Performance evaluation for multiprocessors programmed using monitors
[DE88-010056] 19 p2718 N88-26138
X-ray and optical analysis of surface properties of metal optics
[DE88-004033] 19 p2727 N88-26195
Hover performance tests of baseline metal and Advanced Technology Blade (ATB) rotor systems for the XV-15 tilt rotor aircraft
[NASA-CR-177436] 20 p2759 N88-26367
Digital communication transmitter and receiver test procedures
[AD-A191218] 20 p2788 N88-26540
Computer controlled procedures for traction battery power performance tests
[ETN-88-92352] 20 p2796 N88-26589
Evaluation of thermophosphor temperature technique
[DE88-007654] 20 p2805 N88-26638
Testing of a gravimeter LCR G 785
[B8735061] 20 p2806 N88-26643
Automated system for mathematical processing of the data from a hybrid spectrometer
[DE87-702995] 20 p2836 N88-26820
The evaluation of a deformable diffraction grating for a stigmatic EUV spectroheliometer
[NASA-CR-183064] 20 p2853 N88-26941
Plasma armature formation in high-pressure, high-velocity hydrogen
[DE88-008347] 20 p2857 N88-26967
A comparison of theory and experiment for aeroelastic stability of a hingeless rotor model in hover 21 p2889 N88-27150
A comparison of theory and experiment for coupled rotor-body stability of a hingeless rotor model in hover under simulated vacuum conditions 21 p2889 N88-27151
A comparison of theory and experiment for the aeroelastic stability of a bearingless model rotor in hover 21 p2890 N88-27153
Assembly Test Article (ATA)
[NASA-CR-179361] 21 p2903 N88-27226
Alkaline fuel cell performance investigation
[NASA-TM-100937] 21 p2909 N88-27267
Thermomechanical processing of Al alloy 2090 for grain refinement and superplasticity
[AD-A192333] 21 p2912 N88-27281
Sodium/sulfur cell evaluation results
[DE88-011488] 21 p2938 N88-27451
Post-test observations on CSPL (Chloride Silent Power Limited) cells
[DE88-011975] 21 p2940 N88-27461
The 210-HP diesel engine endurance and performance testing with fire resistant diesel fuel
[AD-A193153] 21 p2956 N88-27558
Basic mechanisms of diesel lubrication correlation of bench and engine tests
[AD-A193360] 21 p2956 N88-27561
Performance sensitivities for point-focus dish systems with secondary concentrators
[DE88-001152] 21 p2968 N88-27629
Photovoltaic Measurements and Performance Branch
[DE88-001142] 21 p2968 N88-27633
Performance evaluation of large-area glass-mirror heliostats
[DE88-011883] 21 p2969 N88-27636
Vapor Compression Distillation Subsystem (VCDS) component enhancement, testing and expert fault diagnostics development, volume 2
[NASA-CR-172076] 21 p2994 N88-27755
On-board data processing of navigation data at high latitudes in Antarctica 22 p3036 N88-28027
Performance of 10-kW class xenon ion thrusters
[NASA-TM-101292] 22 p3049 N88-28088
X-band resonant ring operation at 450 kW 22 p3064 N88-28181
Performance analysis of a noncoherently combined large aperture optical heterodyne receiver 22 p3065 N88-28189
An electronically tuned, stable 8415-MHz dielectric resonator FET oscillator for space applications 22 p3068 N88-28205
Goldstone solar system radar performance analysis 22 p3068 N88-28206
Development of 30 micrometers extrinsic silicon multiplexed infrared deterctor array
[NASA-CR-177448] 22 p3082 N88-28301
Acoustic detection of helicopters: Experiments 22 p3148 N88-28727
Performance of the Los Alamos expanding telescope
[DE88-010924] 22 p3151 N88-28751
Verification and tests --- space projects 22 p3160 N88-28814
Reliability assessment of Surface Mount Technology (SMT)
[AD-A193759] 23 p3208 N88-29089
Construction of a laser Doppler anemometer and its use for the testing of a novel probe for the measurement of the variations of the lateral component of the vortex vector
[MPIS-13/1987] 23 p3217 N88-29147
Two phase flow in a rotating screw tube (screw tube pump). Investigation of the function and efficiency of the screw tube pump
[MPIS-16/1987] 23 p3222 N88-29178
Effects of precipitation on wind turbine performance
[DE88-001144] 23 p3228 N88-29211
Systolic array fault tolerance performance analysis
[AD-A193521] 23 p3244 N88-29306
A performance study of the hypercube architecture
[AD-A194361] 23 p3264 N88-29433
On the design and optimization of distributed signal detection and parameter estimation systems
[AD-A193934] 23 p3266 N88-29446
SSTS (Space Surveillance and Tracking System): The importance of early test and evaluation organizational participation
[AD-A193745] 23 p3276 N88-29499
Controlled degradation of resolution of high-quality flight simulator images for training effectiveness evaluation
[AD-A196189] 24 p3330 N88-29823
Performance and lifetime assessment of MPD arc thruster technology
[NASA-TM-101293] 24 p3336 N88-29860
A small annular combustor of high power density, wide operating range and low manufacturing cost 24 p3351 N88-29951
Additional fracture and strength test results for A723 steel and 38644 titanium
[AD-A196329] 24 p3353 N88-29960
EMPTAC (Electromagnetic Pulse Test Aircraft) user's guide
[AD-A195072] 24 p3360 N88-30006
Qualification test levels for units to be derived from mechanical test data analysis --- ESA
[REPT-87-158-EI/ET/AG] 24 p3381 N88-30139

PERFUSION
U DIFFUSION

PERIDOTITE
An integrated study of the Alto Paranaiba Kimberlite Province, Minas Gerais, Brazil: A possible tool for diamond exploration 17 p2355 N88-24031
The petrogenesis of oceanic kimberlites and included mantle megacrysts: The Malaitan alnoite 24 p3397 N88-30232

PERIGEES
Study of a safe attitude for the Infrared Space Observatory (ISO) during perigee pass
[SNIAS-881-440-113] 23 p3185 N88-28954

PERIHELIONS
On the possible origin of meteoroid generating asteroid orbits 06 p0740 N88-14553
Comparative analysis of ultraviolet observations of Halley's comet on ASTRON astrophysical station before and after perihelion 08 p1004 N88-16086
Mars earth-based radar: 1986 results and 1988-1990 opportunities 23 p3306 N88-29697

PERIOD DOUBLING
Fully developed turbulence via Feigenbaum's period-doubling bifurcations
[DE88-000242] 04 p0441 N88-12739
Period-doubling universality in multidimensional dissipative and conservative systems
[PB88-148812] 13 p1832 N88-20961

PERIOD EQUATIONS
U PERIODIC FUNCTIONS

PERIODIC FUNCTIONS
NT COSINE SERIES
NT TANGENTS
NT TRIGONOMETRIC FUNCTIONS

Efficient computation of periodic Green's functions with application to grating structures
[AD-A184853] 05 p0640 N88-13912
Global bifurcation of periodic solutions with symmetry
[AD-A185881] 07 p0908 N88-15501
Almost-periodic solutions of nonlinear parabolic equations
[DE88-006423] 15 p2118 N88-22618
Periodically correlated processes and their stationary dilations
[NASA-CR-182904] 16 p2263 N88-23530
On a class of functionals invariant under a Z(sup n) action
[AD-A193474] 23 p3269 N88-29451
Periodic solutions of perturbed superquadratic Hamiltonian systems
[AD-A194292] 23 p3270 N88-29457
On the periodic nonlinearity and the multiplicity of solutions
[AD-A194295] 23 p3270 N88-29459

PERIODIC ORBITS
U ORBITS

PERIODIC PROCESSES
U CYCLES

PERIODIC VARIATIONS
NT ANNUAL VARIATIONS
NT DIURNAL VARIATIONS
NT NOCTURNAL VARIATIONS
NT SECULAR VARIATIONS
Basic properties and variability
02 p0252 N88-11593
On the interannual variability of South American climate and the Southern Oscillation 04 p0470 N88-12905
Long-period variations of wind parameters in the mesopause region and the solar cycle dependence
06 p0733 N88-14509
Short-term temporal variations of Nimbus-7 measurements of the solar UV spectral irradiance
[PB88-102132] 07 p0946 N88-15753
Quasiperiodic variations in manifestations of solar activity 08 p1004 N88-16083
Analysis of low frequency current fluctuations in the North-East Atlantic Ocean
[REPT-170] 09 p1196 N88-17165
A note on a diagonally implicit Runge-Kutta-Nystrom method
[CWI-NM-R8706] 09 p1228 N88-17358
Analysis of the spectral vanishing viscosity method for periodic conservation laws
[NASA-CR-181613] 09 p1231 N88-17378
An adaptive filtering technique for removing periodic noise from modal response data
[DE88-002347] 10 p1322 N88-17903
The absolute total magnitudes of periodic comets and their variations 14 p1994 N88-21887
The comet flux and the 15 Myr galactic cycle
14 p1995 N88-21889
Recent observations of the OH radio lines in comets
14 p1999 N88-21917
Color fluctuations in the inner coma of Comet Halley as measured from VEGA-2 14 p2000 N88-21925
Variation of grain properties at the dust outbursts --- Halley's comet 14 p2003 N88-21943
Dynamic characteristics of a vibrating beam with periodic variation in bending stiffness
[NASA-TP-2697] 17 p2348 N88-23988
Nonlinear vibrations of periodically stiffened plates
21 p2963 N88-27598
Periodic oscillations in nonlinear mechanical systems
21 p2963 N88-27599
Asymptotic giant branch stars in the Infrared Astronomical Satellite (IRAS) catalogs: Selection and analysis of the population characteristics
[MPE-PREPRINT-116] 22 p3163 N88-28840
Regular orbital variations in the ultraviolet resonance lines of YZ Cnc
[MPE-PREPRINT-117] 22 p3165 N88-28850
Time periodic control of a multi-blade helicopter
[AD-A194435] 23 p3180 N88-28931
Plane periodic satellite motions relative to center of mass in neighborhood of collinear libration point
24 p3445 N88-30507

PERIODICALS
Solar-geophysical data number 515, July 1987. Supplement (explanation of data reports)
[PB87-233169] 06 p0805 N88-14914
Wind Energy Technology: Generating power from the wind, a current awareness bulletin
[DE88-008292] 20 p2820 N88-26729

PERIODICITY
U PERIODIC VARIATIONS

PERIODICITY (BIOLOGY)
U RHYTHM (BIOLOGY)

PERIPHERAL CIRCULATION
Cardiac and peripheral circulation assessment by ultrasound on 3 astronauts during two 7-day space flights (1982 Salyut-7 - 1985 STS 51G)
12 p1656 N88-19921
Leg volume change under Lower Body Negative Pressure (LBNP) in dependence on stratification
[DFVLR-FB-87-47] 16 p2238 N88-23367
Physiological responses to acute exercise-heat stress
[AD-A192606] 21 p2986 N88-27732
The effects of acute cold exposure on exercise performance
[AD-A192650] 22 p3130 N88-28610
Alterations in cutaneous vasomotor regulation during acute and chronic hypoxia
[AD-A192653] 22 p3131 N88-28612

PERIPHERAL EQUIPMENT (COMPUTERS)
NT PRINTERS (DATA PROCESSING)
NT REMOTE CONSOLES
Computer architecture for research in meteorology and atmospheric chemistry
[PB88-145313] 11 p1510 N88-19020
Microvax networked computer system
[AD-A190308] 15 p2114 N88-22596
Definition of an auxiliary processor dedicated to real-time operating system kernels
[NASA-CR-183070] 20 p2841 N88-26860

PERIPHERIES
U BOUNDARIES

PERISCOPES
Welding monitoring system
[NASA-CASE-MFS-29177-1] 06 p0712 N88-14362

PERMANENT MAGNETS
Study of free-piston Stirling engine driven linear alternators
[NASA-CR-181425] 01 p0055 N88-10355
Process support compressor motor electromagnetic design summary
[DE87-014359] 02 p0167 N88-11048
Design verification tests for an axial gap permanent magnet compressor motor
[DE87-014360] 02 p0167 N88-11049
Performance of high power S-band klystrons focused with permanent magnet
[DE87-753024] 02 p0167 N88-11053
A long electromagnetic wiggler for the paladin free-electron laser experiments
[DE88-000970] 05 p0588 N88-13589
Development of a laced electromagnetic wiggler
[DE88-000972] 05 p0646 N88-13953
Dynamic high pressure process for fabricating superconducting and permanent magnetic materials
[DE88-000848] 06 p0785 N88-14817
Metallurgical processes in multi-component rare earth-transition metal permanent magnet alloys
[AD-A186401] 07 p0832 N88-15045
Modeling the behavior of oriented permanent magnet material using current double theory
[DE88-004446] 13 p1833 N88-20963
ONR Far East Scientific Bulletin, volume 12, number 3, July-September 1987
[AD-A188554] 13 p1851 N88-21081
A high performance inverter-fed drive system of an interior permanent magnet synchronous machine
[DE88-006753] 15 p2061 N88-22288
Performance test results: AXIAL-GAP, permanent magnet compressor motor
[DE88-006857] 15 p2061 N88-22289
A microcomputer-based control and simulation of an advanced IPM (Interior Permanent Magnet) synchronous machine drive system for electric vehicle propulsion
[DE88-006735] 18 p2505 N88-24859

PERMEABILITY
The water permeability of multi-layer coatings
[BLL-M-37252-(5828.4)] 02 p0148 N88-10927
Investigation of structure-permeability relationships of silicone polymer membranes
[PB87-230181] 03 p0293 N88-11839
Geological characterization and statistical comparison of outcrop and subsurface facies: Shannon Shelf sand ridges
[DE87-001243] 03 p0348 N88-12202
Novel macrocyclic carriers for proton-coupled liquid membrane transport
[DE88-000636] 04 p0413 N88-12560
A study of mechanisms of hydrogen diffusion in separation devices
[DE88-000328] 04 p0416 N88-12584
Programs for calculating transient Darcian flow through non-uniform materials
[DE88-001924] 07 p0852 N88-15177
Physics of immiscible flow in porous media
[PB88-131008] 11 p1487 N88-18873
The effect of Ca(OH)2-treated ceramic microspheres on the mechanical properties of high-temperature lightweight cement composites
[DE88-004590] 13 p1749 N88-20457
Molecular and electronic mechanism in the control of Na+ and K+ permeability of excitable cell membrane by ligand binding on receptor sites
[AD-A188725] 13 p1808 N88-20805
Use of nonporous metals membranes for the separation of hydrogen from gas mixtures
[BMFT-FB-T-86-206] 14 p1888 N88-21280
Synthesis and analysis of novel polymers with potential for providing both high permselectivity and permeability in gas separation applications
[DE88-006533] 15 p2043 N88-22174
Study of fracturing for groundwater research in the Sergipe state with remote sensing products
17 p2359 N88-24052
Interaction of vinylidene fluoride: Tetrafluoroethylene copolymer with ammonia
[NASA-TT-20292] 19 p2620 N88-25542
Characteristics of pressure loss during filtration using a porous ceramic filter
[DE88-752547] 20 p2798 N88-26604
Investigation of hydrogen isotope penetration through stainless steels Kh18N10T and Kh3M2BFR
[DE88-702189] 21 p2915 N88-27297
Optimal rheological characteristics in dynamic stability of polymer flow through porous media
[DE88-001225] 21 p2918 N88-27322
Hyperthermia: New thoughts on an old problem
[AD-A192602] 21 p2986 N88-27731

PERMEATING
Physics of immiscible flow in porous media
[PB88-131008] 11 p1487 N88-18873
The effect of H2S concentration and pH on hydrogen permeation in AISI 410 stainless steel in 5 percent NaCl
[NPL-DMA(A)-148] 14 p1890 N88-21293
Mechanisms of gas permeation through polymer membranes: Renewal proposal for period December 1, 1986 - November 30, 1989
[DE88-007436] 18 p2494 N88-24796
Hydrogen permeation through metallic foils
[DE88-702600] 23 p3193 N88-29000
Design criteria for extraction with chemical reaction and liquid membrane permeation
[NASA-TT-20352] 24 p3343 N88-29899

PERMITTIVITY
Automated microwave dielectric constant measurement
[AD-A184182] 04 p0431 N88-12667
Electromagnetic wave probing of Earth's environment
[NASA-CR-182358] 06 p0690 N88-14232
Mars: High resolution VLA observations at wavelengths of 2 and 6 cm and derived properties
06 p0804 N88-14909
Investigation of surface wave blindness in microstrip phased array antennas
[AD-A189326] 12 p1621 N88-19696
Characterization of 6 soils in the X-band, through measurements of complex permittivity
[INPE-4376-TDL/302] 12 p1639 N88-19814
Method for characterizing end-plate surface resistance of dielectric resonator 14 p1903 N88-21371
Processing and additive effects of ZrO2 on microstructure and dielectric porperties of BaTiO3 ceramics
[AD-A193126] 21 p2917 N88-27316
Active and passive remote sensing of ice
[AD-A193307] 21 p2966 N88-27617
Viking Landers and remote sensing
23 p3304 N88-29685

PERMUTATIONS
The Lambda network: A new permutation network
[DE88-003568] 10 p1392 N88-18305
Graphs related to Held's simple group
[CWI-PM-28707] 16 p2264 N88-23536

PEROVSKITES
Structural relationships in high temperature superconductors
[DE88-002924] 09 p1257 N88-17534
Ordered structures in YBa2Cu3O/sub 7-y/, La2Cu3O/sub 7-y/, La/sub 2-x/Sr/sub x/CuO/sub 4-par. delta/ and related perovskites
[DE88-006461] 14 p1987 N88-21851
Probing the electronic and defect structure of perovskite superconductors
[DE88-008349] 21 p3022 N88-27939

PEROXIDES
NT HYDROGEN PEROXIDE
The redox chemistry of some peroxo and superoxo metal ion complexes
[AD-A189159] 12 p1606 N88-19606
Copper peroxide
[NASA-TT-20245] 14 p1888 N88-21282

Solar generation and storage of O2 (a 1 delta g)
[NASA-CR-4127] 14 p1913 N88-21431
Development of a test method to determine potential peroxide content in turbine fuels. Part 2
[AD-A192244] 23 p3199 N88-29042
Electrocatalytic reduction of oxygen on modified oxide surfaces
[NASA-TM-101333] 24 p3352 N88-29952
Determination of the hydroperoxide potential of jet fuels
[AD-A195975] 24 p3357 N88-29991

PERSEID METEOROIDS
On the spatial structure of the Perseids meteor stream 06 p0740 N88-14550

PERSONAL COMPUTERS
A work station for EXELFS data acquisition and analysis
[USIP-87-10] 01 p0078 N88-10498
A CAMAC system controlled by an IBM AT computer for time-resolved spectroscopy
[DE87-010111] 01 p0080 N88-10514
An evaluation of WPS-Plus word processing software for the IBM PC and compatibles
[DE87-011972] 01 p0081 N88-10518
Personal Computer (PC) based image processing applied to fluid mechanics
[NASA-TM-100024] 02 p0172 N88-11087
A mini system for nowcasting 02 p0204 N88-11278
Personal computers: A powerful tool for project management
[DE87-013381] 02 p0219 N88-11377
Electronic authoring tools
[DE87-011797] 02 p0248 N88-11567
The Macintosh computer as a tool for rapid data analysis and for producing camera ready viewgraphs/publications
[DE87-014350] 03 p0362 N88-12280
FORTRAN compiler performance benchmarks for the IBM personal computer
[LA-10883-MS] 03 p0363 N88-12284
BASIC desk-top computer program for the three-dimensional static configuration of an extensible flexible cable in a uniform stream
[AD-A184852] 05 p0609 N88-13737
Mixing Microsoft C and Microsoft FORTRAN program modules on the IBM Personal Computer
[DE88-001947] 05 p0637 N88-13895
Compilation and development of K-6 aerospace materials for implementation in NASA spacelink electronic information system 07 p0922 N88-15605
Satellite interference analysis and simulation using personal computers
[NASA-CR-182522] 10 p1319 N88-17890
Personal computers and All-In-1: Document transfer and translation
[DE88-003760] 10 p1384 N88-18264
TABLET: The personal computer of the year 2000
[NASA-CR-182528] 10 p1384 N88-18267
An IBM PC version of ASENT
[DE88-004244] 11 p1532 N88-19150
The global positioning system as an aid to the testing of inertial navigation units (volume 1, addendum 1)
[AD-A185783] 12 p1578 N88-19443
Output formatting in Apple-soft BASIC
[DE88-701413] 15 p2106 N88-22559
Implementation of a distributed adaptive routing algorithm on the Intel iPSC (Intel Personal Super-Computer)
[AD-A189849] 15 p2109 N88-22567
Measurement data processing system based on personal computer: For scramjet combustion test
[DE88-751807] 16 p2174 N88-22959
Practical image analysis using personal computers: The Canadian experience 17 p2356 N88-24037
Personal computer as a workstation in a cartographic automation system? 18 p2535 N88-25039
Advances in personal computers for scientific applications
[DE88-009824] 19 p2713 N88-26107
Synopsis of a computer program designed to interface a personal computer with the fast data acquisition system of a time-of-flight mass spectrometer
[NASA-CR-177474] 21 p3001 N88-27796
Waveform analysis on the IBM PC
[AD-A194249] 23 p3248 N88-29330
Aircraft noise prediction program propeller analysis system IBM-PC version user's manual version 2.0
[NASA-CR-181689] 24 p3428 N88-30399

PERSONALITY
Brain potentials and personality: A new look at stress susceptibility
[AD-A186931] 09 p1199 N88-17189
Brainstem response and state-trait variables 16 p2242 N88-23394
Research on piloting under conditions of breakdown in flight
[PB87-217980] 19 p2710 N88-26102

PERSONALITY TESTS
Computer response time measurements of mood, fatigue and symptom scale items: Implications for scale response time uses
[AD-A186093] 07 p0888 N88-15384
Temperament Structure Scales (TSS). Test manual
[ESA-TT-1069] 09 p1201 N88-17197

PERSONNEL
NT AIR TRAFFIC CONTROLLERS (PERSONNEL)
NT AIRCRAFT PILOTS
NT ASTRONAUTS
NT COSMONAUTS
NT CREWS
NT FLIGHT CREWS
NT GROUND CREWS
NT INSTRUCTORS
NT MEDICAL PERSONNEL
NT NAVIGATORS
NT OPERATORS (PERSONNEL)
NT ORBITAL WORKERS
NT PILOTS (PERSONNEL)
NT PROGRAMMERS
NT SCIENTISTS
NT SPACECREWS
Antarctic field tests of SARSAT personal locater beacons
[NASA-TM-4008] 01 p0063 N88-10403
A review of computer-assisted photo interpretation research at USAETL (US Army Engineer Topographic Laboratories)
[AD-A184034] 03 p0346 N88-12186
On computing environments in data analysis
[DE88-000078] 04 p0480 N88-12961
Group adaptation and individual adjustment in antarctica: A summary of recent research
[AD-A186605] 08 p1051 N88-16347
Lewis materials research and technology: An overview 09 p1119 N88-16699
Brain potentials and personality: A new look at stress susceptibility
[AD-A186931] 09 p1199 N88-17189
Information needs analysis for the Aeronautical Systems Division Executive Information System
[AD-A186912] 09 p1261 N88-17556
Relationships between coronary heart disease risk factors and serum ionized calcium in Kennedy Space Center Cohort
[NASA-TM-100979] 10 p1368 N88-18177
The accommodative status in the dark of US Navy fighter pilots
[AD-A188188] 10 p1370 N88-18186
Report of the participation in the International Training Course: Remote Sensing in Village Forestry
[INPE-4476-NTE/278] 12 p1637 N88-19802
A comparison of terrain association and resection as methods of position location
[AD-A189480] 13 p1790 N88-20710
Napping and human functioning during prolonged work
[AD-A190228] 15 p2102 N88-22525
Prediction of physical fitness: Estimated percent body fat using body circumferences versus weight-height measures
[AD-A190233] 15 p2103 N88-22526
An evaluation of the effects of high visual taskload on the separate behaviors involved in complex monitoring performance
[AD-A190641] 15 p2105 N88-22538
Relationship of encoding speed and memory tests to flight training performance
[AD-A190670] 15 p2105 N88-22539
Problem solving in a natural task as a function of experience
[AD-A191180] 16 p2243 N88-23399
US civil airmen statistics, 1987
[AD-A191714] 18 p2455 N88-24577
Development of inductive storage pulsed power generators
[AD-A193878] 22 p3117 N88-28521
Computer-aided decision making
[AD-A194210] 22 p3137 N88-28651
Flight information publication (FLIP) feedback
[AD-A194462] 23 p3174 N88-28897
Reliability and construct validity of reaction time, inspection time and machine-paced tests of cognitive speed
[AD-A193779] 23 p3241 N88-29289

PERSONNEL DEVELOPMENT
Field evaluation of interactive simulation for maintenance training: SH-3 helicopter electro-mechanical bladefold system
[AD-A185923] 07 p0821 N88-14991
Tutoring electronic troubleshooting in a simulated maintenance work environment 09 p1204 N88-17215
Anatomy of an organizational change effort at the Lewis Research Center
[NASA-CR-4146] 19 p2739 N88-26264

PERSONNEL MANAGEMENT
Development of a prototype H-46 helicopter diagnostic expert system
[AD-A186077] 07 p0809 N88-14924
Meta-analysis of leadership differences between males and females and the effect on performance
[AD-A187769] 11 p1564 N88-19361
People, procedures, performance: The keys to improving the development environment 12 p1704 N88-20197
Management and the executive
[AD-A190778] 18 p2587 N88-25374
The time of leaders 22 p3160 N88-28809

PERSONNEL PROPULSION SYSTEMS
U SELF MANEUVERING UNITS

PERSONNEL SELECTION
NT PILOT SELECTION
Antarctica as a model for the human exploration of Mars
[AD-A185835] 08 p1051 N88-16342
Temperament Structure Scales (TSS). Test manual
[ESA-TT-1069] 09 p1201 N88-17197
Human factor in engineering work 12 p1663 N88-19970
Field dependence-independence and its relationship to flight training performance
[AD-A188888] 12 p1670 N88-20003
The program Kennedy Approach as an experimental design of a dynamic computerized air traffic control test
[DFVLR-FB-87-50] 16 p2159 N88-22881
Utility NDE personnel qualification/certification: Enhanced personnel qualification requirements for ASME (American Society for Mechanical Engineers) Code Section 11 examinations
[DE88-006748] 16 p2216 N88-23222
Stress in relation to the physical and social environment 19 p2695 N88-26020
Selecting the right crew for future space stations: An analysis of selection research on offshore divers, aviation pilots and other high risk groups in Scandinavia 19 p2696 N88-26021
Selection and training of subjects to live and work in hostile and unusual environments 19 p2696 N88-26026
Selection of isolated space crews 19 p2697 N88-26028
USAF flying screening: First step on the road to wings
[AD-A192613] 20 p2833 N88-26804
Proposed improvements to the USAF flight screening program
[AD-A194506] 23 p3240 N88-29285
Validity of the academic aptitude composite of the Air Force Officer Qualifying Test (AFOQT)
[AD-A194753] 23 p3240 N88-29286
Literature review: Validity and potential usefulness of psychomotor ability tests for personnel selection and classification
[AD-A193558] 23 p3241 N88-29287

PERSPIRATION
Physiological and hematological responses of matched older and younger men during dry-heat acclimation
[AD-A186450] 18 p2550 N88-25139
Physiological responses to acute exercise-heat stress
[AD-A192606] 21 p2986 N88-27732
The role of textile material in clothing on thermoregulatory responses to intermittent exercise
[AD-A192599] 22 p3130 N88-28608
Depressed sweating during exercise at altitude
[AD-A192603] 22 p3130 N88-28609

PERT
Project Monitoring Package (PMP): A package for project activity monitoring
[DE88-701234] 15 p2107 N88-22554

PERTURBATION
NT ORBIT PERTURBATION
NT SATELLITE PERTURBATION
On the role of snow in the redistribution of precipitation by small scale topography 02 p0203 N88-11267
Magnetohydrodynamic stability of spheromak plasma in toroidal flux conserver with rectangular cross section 3. Stability for symmetric modes
[IPPJ-845] 02 p0241 N88-11524
Long wavelength vortices of low frequency interchange modes
[IPPJ-844] 02 p0241 N88-11525
Numerical study of the entrance flow and its transition in a circular pipe (2) 03 p0318 N88-12011
Hardware-assisted multiprocessor performance measurements
[PB87-226908] 03 p0363 N88-12282

Perturbation and characterization of nonlinear processes
[DE87-014580] 03 p0369 N88-12322
Identification of perturbations in turbomachines by the analysis of pressure signals, vibrations and wavelike motions
[ETN-88-90602] 05 p0590 N88-13600
Improvement of modal scaling factors using mass additive technique 05 p0593 N88-13620
Development of a data analysis system for the detection of lower level atmospheric turbulence with an acoustic sounder
[AD-A184972] 05 p0624 N88-13821
A direct calculation method for perturbation fields of moving bodies in compressible media at subsonic Mach numbers
[ETN-88-90808] 06 p0701 N88-14305
Evolution of perturbations in expanding universe 06 p0775 N88-14759
Analytical investigations of bulk wave resonators in the piezoelectric thin film on gallium-arsenide configuration
[AD-A185716] 06 p0789 N88-14840
Analysis and interpretation of satellite fragmentation data 06 p0798 N88-14885
Low-disturbance wind tunnels 07 p0811 N88-14937
An additional study and implementation of tone calibrated technique of modulation
[NASA-CR-182377] 07 p0844 N88-15117
Infrared emission and tidal interactions of spiral galaxies 07 p0923 N88-15611
Perturbations of the Sun's gravitational field due to solar oscillations
[DE88-002099] 07 p0946 N88-15751
Large-angle slewing maneuvers for flexible spacecraft
[NASA-CR-4123] 08 p1000 N88-16060
Dynamic modeling of the middle atmosphere 08 p1028 N88-16227
Adaptive proximate time-optimal servomechanisms 09 p1175 N88-17043
Convective wind fields as investigated with doppler lidar
[PB88-115472] 09 p1193 N88-17151
Perturbation theory for dual semigroups 2. Time-dependent perturbations in the sun-reflexive case
[PB88-113097] 09 p1230 N88-17369
Microgravity experiments in space: Compatibility with dynamic perturbing effects 09 p1241 N88-17435
Waves and static electric fields in the auroral acceleration region 12 p1646 N88-19856
On the theory of electromagnetic scattering from a raindrop splash
[AD-A188720] 14 p1906 N88-21393
Solutions for direct and indirect problems in free surface flows
[REPT-87-35] 14 p1909 N88-21409
Spacecraft trajectories
[ISBN-2-85-428166-7] 15 p2023 N88-22054
Comparative analysis
[AD-A190556] 15 p2065 N88-22313
Effect of vibrational excitation on rate parameters of atmospheric reactions
[AD-A190464] 15 p2094 N88-22477
Numerical methods for singularly perturbed differential equations with applications
[AD-A189786] 15 p2119 N88-22628
Density perturbations in a rotating universe
[DE87-703036] 15 p2151 N88-22840
Development and improvement of a code to calculate small, three dimensional, unsteady transonic perturbations
[ONERA-RTS-31/3064-RY-062-R] 17 p2338 N88-23951
Finite element simulation of the atmosphere's electromagnetic response to charge perturbations associated with lightning 17 p2375 N88-24124
On the propagating speed in difference approximations for conservation laws 19 p2639 N88-25658
The propagation of pressure perturbations in bubbly air/water flows 19 p2664 N88-25843
Peturbational analysis of the curved anisotropic optical fiber for the birefringence due to the geometry
[PB88-171848] 19 p2726 N88-26189
An initial investigation into methods of computing transonic aerodynamic sensitivity coefficients
[NASA-CR-183061] 20 p2752 N88-26332
The feasibility of the disturbance accommodating controller for precision antenna pointing 22 p3064 N88-28182
Asymptotic orders of reachability in perturbed linear systems
[AD-A192718] 22 p3143 N88-28688
A singular perturbation analysis of the weakly nonlinear evolution of long and short water waves and waves in boundary layers 23 p3209 N88-29102
Computation of the eigenvalues for perturbations of Poiseuille flow using a two-point boundary value method
[AD-A193479] 23 p3210 N88-29104
An exponential decay estimate for the stationary perturbation of Poiseuille flow
[AD-A193480] 23 p3210 N88-29105
Periodic solutions of perturbed superquadratic Hamiltonian systems
[AD-A194292] 23 p3270 N88-29457
Chaotic behaviour in quantum dynamics
[AD-A193936] 23 p3295 N88-29623
Theories of comparative analysis
[AD-A196328] 24 p3427 N88-30395

PERTURBATION THEORY
A study of a satellite-to-satellite tracking configuration by application of linear perturbation theory
[REPT-86.3] 01 p0011 N88-10059
Estimability of potential coefficients from orbit perturbations --- satellite geodesy
[REPT-86.1] 01 p0064 N88-10408
Development of many-body methods for flame chemistry and large molecule applications
[AD-A184451] 03 p0284 N88-11789
Theory of atomic additivity in molecular hyperpolizabilities 03 p0297 N88-11867
Analytical studies of axially symmetric motion of an incompressible viscous fluid between two concentric rotating spheres 04 p0444 N88-12757
The free electron laser sideband instability reconsidered
[AD-A184269] 04 p0447 N88-12773
Vibration and parametric excitation in rotating asymmetric circular plates 04 p0456 N88-12823
Model of solar-wind magnetosphere coupling 04 p0525 N88-13211
Design of low order controllers for robust disturbance rejection in large space structures
[AD-A185202] 05 p0555 N88-13376
Robustness of linear systems
[PB87-220042] 05 p0639 N88-13909
Molecular dynamics studies of aromatic hydrocarbon liquids
[DE88-001473] 05 p0648 N88-13973
Dynamics of meteor streams 06 p0732 N88-14503
Perturbative coherence in field theory
[DE88-700366] 07 p0941 N88-15717
Study on orbits near the triangular libration points in the perturbed restricted three body problem
[ESA-CR(P)-2440] 07 p0944 N88-15741
Synoptic perturbations and climate 08 p1016 N88-16158
Effect of extraneous factors on optical one-phonon transitions in impurity centers with cubic symmetry 08 p1077 N88-16496
An initial investigation into methods of computing transonic aerodynamics sensitivity coefficients
[NASA-CR-182444] 09 p1112 N88-16663
A dynamical system/coherent structure approach to the fully developed turbulent wall layer 10 p1267 N88-17578
Application of state-multipole Heisenberg equations to Raman excitation dynamics
[DE88-003828] 10 p1335 N88-17977
Theoretical studies of atomic transitions
[DE88-004719] 10 p1407 N88-18389
Nuclear structure at intermediate energies
[DE88-002796] 10 p1407 N88-18390
Theoretical and experimental analysis of pressure pulse transmission in non-Newtonian pipe flow 11 p1485 N88-18863
Domain perturbation method in the static equilibrium of masses in rotation
[INPE-4217-PRE/1098] 12 p1686 N88-20085
Horizontal scales of wind forced inertial motions 13 p1806 N88-20795
Unfoldings of quasi-periodic tori
[ZW-8706] 13 p1828 N88-20928
Finite width corrections to the Nambu action for the Nielsen-Olesen string
[DE88-006996] 15 p2147 N88-22812
Multicontinuations method and strong regular perturbations of linear operators
[DE88-701375] 16 p2263 N88-23533
Perturbation theory for dual semigroups. Part 3: Nonlinear Lipschitz continuous perturbations in the Sun-reflexive case
[CWI-AM-R8706-PT-3] 16 p2263 N88-23535
Stark effect in intense field. Perturbation theory and 1/n-expansion
[DE87-702947] 16 p2266 N88-23550
Electromagnetic scattering from nonlinear anisotropic cylinders 17 p2333 N88-23930
An experimental study of the coherent under-ice reflectivity of sound in the Greenland Sea Marginal Ice Zone 18 p2548 N88-25125
Perturbation theory for dual semigroups. Part 4: The intertwining formula and the canonical pairing
[CWI-AM-R8802-PT-4] 18 p2569 N88-25258
Magnetohydrodynamic squeeze film
[DE88-701876] 20 p2810 N88-26669
Recoil saturation of the self-energy in atomic systems
[DE88-010450] 20 p2851 N88-26930
Perturbation expansions generated by an approximate propagator
[DE88-702435] 21 p3011 N88-27886
Reminimization of energy integral and stability limit for non-ideal MHD (magnetohydrodynamic) plasma
[DE88-008422] 21 p3018 N88-27911
Self energy corrections to the ab initio band structures: Chromium
[DE88-701825] 21 p3020 N88-27927
Vortices on the world sheet and string's critical dynamics
[DE88-702116] 21 p3026 N88-27961
Multiphoton transitions in semiconductors in the non-perturbative approach
[DE88-702664] 22 p3157 N88-28786
Calculations in perturbative string field theory
[DE88-011616] 22 p3158 N88-28798
Unfoldings of quasi-periodic tori
[B8811118] 23 p3278 N88-29513
On the meaning of perturbation expansions in quantum field theory
[DE88-702138] 23 p3294 N88-29620
Free vibration of rectangular plates with a small initial curvature
[NASA-CR-179370] 24 p3383 N88-30148

PETN
Shock measurements on explosives in the supra compressive region
[DE87-008423] 01 p0031 N88-10196
The equation of state of PETN detonation products
[DE87-013796] 02 p0155 N88-10971
Thermal decomposition studies of explosives for component applications
[DE88-007201] 18 p2495 N88-24805
Freely expanding detonation products: Scaling of rate processes
[DE88-007827] 20 p2799 N88-26606

PETRI NETS
Strategies for concurrent processing of complex algorithms in data driven architectures
[NASA-CR-181435] 01 p0082 N88-10527
Petri nets as a support to symbolic execution of concurrent Ada programs
[REPT-87-007] 01 p0082 N88-10529
Methodology of performance evaluation of real time distributed systems
[ENST-87D003] 02 p0228 N88-11440
Computer aided design for Petri Nets
[AD-A186109] 07 p0902 N88-15465
Strategies for concurrent processing of complex algorithms 10 p1379 N88-18236
Conception of a knowledge-based system for designing distributed systems
[DFVLR-MITT-87-16] 14 p1961 N88-21694
Using Colored Stochastic Petri Net (CS-PN) software for protocol specification, validation, and evaluation
[ENST-87C004] 15 p2113 N88-22588
The Colored Stochastic Petri Net (CS-PN) software: Application to the validation and the performance evaluation of distributed systems
[ENST-87D005] 15 p2113 N88-22589
Simultaneous use of artificial intelligence and Petri nets: Application to the monitoring of a fabrication plan
[LAAS-87-354] 17 p2390 N88-24207
Some unsolved problems in modelling self-timed circuits using Petri Nets, series B, number 2
[PB88-181466] 18 p2507 N88-24872
Colored stochastic Petri nets. Application to real time distributed systems
[ENST-87E017] 20 p2839 N88-26843
On eclecticism in specifications: A case study centered around Petri nets --- software engineering
[REPT-87-008] 22 p3140 N88-28671
Using Petri nets for real-time development environments
[REPT-88-005] 22 p3141 N88-28679

PETROGRAPHY
A sedimentological and mineralogical study of the Koogah Formation, New South Wales 18 p2542 N88-25087

PETROLEUM
U CRUDE OIL

PETROLEUM PRODUCTS
NT ASPHALT
NT DIESEL FUELS
NT GASOLINE
Evaluation of the acute toxicity of a synthetic polyalphaolefin-based hydraulic fluid
[AD-A190412] 15 p2045 N88-22184

PETROLOGY
NT PETROGRAPHY
Geological characterization and statistical comparison of outcrop and subsurface facies: Shannon Shelf sand ridges
[DE87-001243] 03 p0348 N88-12202
Petrogenesis of basalts from the Archean Matachewan Dike Swarm Superior Province of Canada
06 p0796 N88-14878
Nature and origin of mineral coatings on volcanic rocks of the Black Mountain, Stonewall Mountain, and Kane Springs Wash volcanic centers, Southern Nevada
[NASA-CR-181437] 09 p1191 N88-17140
Aqueous alteration in S-N-C meteorites and implications for weathering products on Mars
23 p3303 N88-29673
Evidence for crustal recycling during the Archean: The parental magmas of the stillwater complex
24 p3396 N88-30226
The tectonic setting of Archean anorthosites
24 p3397 N88-30231
The petrogenesis of oceanic kimberlites and included mantle megacrysts: The Malaitan alnoite
24 p3397 N88-30232
Growth of the continental crust: A planetary-mantle perspective 24 p3400 N88-30251
Crustal underplating in the North American Craton: Evidence from the Petrogenesis of anorthositic rocks in the Middle Proterozoic Midcontinent Rift System
24 p3400 N88-30252

PH
Microstructural evolution and response to double-loop reactivation testing of heat-treated pH 13-8 Mo martensitic stainless steel
[DE87-009058] 02 p0146 N88-10915
The effect of H2S concentration and pH on hydrogen permeation in AISI 410 stainless steel in 5 percent NaCl
[NPL-DMA(A)-148] 14 p1890 N88-21293
The effect of H2S concentration and pH on the cracking resistance of AISI 410 stainless steel in 5 percent brine
[NPL-DMA(A)-149] 14 p1890 N88-21294
Complexation and hydrolysis reactions of iron(III)
17 p2322 N88-23867
Effect of process conditions on aluminum oxide thin film used in pH ISFET 19 p2673 N88-25892

PH FACTOR
Monitoring corrosion and process physical-chemical parameters in electric power plants
[CISE-3708] 06 p0682 N88-14182

PHANTOM AIRCRAFT
NT F-4 AIRCRAFT

PHARMACOLOGY
JPRS report: Science and technology. USSR: Life sciences
[JPRS-ULS-87-012] 03 p0355 N88-12238
JPRS report: Science and technology. USSR: Life sciences
[JPRS-ULS-87-009] 04 p0473 N88-12915
JPRS report: Science and technology. USSR: Life sciences
[JPRS-ULS-87-013] 06 p0750 N88-14608
Pharmacological resetting of the Circadian sleep-wake cycle
[AD-A186194] 07 p0889 N88-15385
Scaling physiological pharmacokinetic models by physiological time
[DE88-000335] 10 p1368 N88-18173
Changes in hemostasis system of animals under conditions of granulocytopoiesis inhibition under effect of decreased barometric pressure
12 p1651 N88-19890
JPRS report: Science and technology. USSR: Life sciences
[JPRS-ULS-88-002] 12 p1665 N88-19982
Changes in the status of the human tibia during antiorthostatic hypokinesia
[NASA-TT-20221] 13 p1810 N88-20813
Development of a C3 generic workstation: System overview 18 p2242 N88-23396
JPRS report: Science and technology. USSR: Life sciences
[JPRS-ULS-88-009] 20 p2829 N88-26785
Does dihydroergotamine used in therapeutical doses influence the physical and psychomotor performance of young pilots or other traffic drivers subjected to hypotonia?
[ETN-88-92136] 20 p2832 N88-26799

PHASE ANGLE
U PHASE SHIFT

PHASE CHANGE MATERIALS
Performance analysis of advanced spacecraft TPS
[NASA-CR-181532] 04 p0399 N88-12484
A study of the optimal transition temperatue of PCM (Phase Change Material) wallboard for solar energy storage
[DE88-001522] 04 p0466 N88-12682
Nickel hydroxide active material densities
[AD-A191411] 16 p2230 N88-23319
Magnetic studies of iron-rare-earth-metalloid alloys
[DE88-006801] 16 p2282 N88-23660
The morphological stability of continuous intergranular phases: Thermodynamic considerations
[DE88-006328] 18 p2584 N88-25350
Beam combining by phase transition nonlinear media
[AD-A194116] 23 p3283 N88-29547

PHASE COHERENCE
Optimized tracking of RF carriers with phase noise, including Pioneer 10 results 04 p0434 N88-12694
Coherent vortex structures in the wake of a stationary disk and of a disk excited to vibration
[ESA-TT-994] 09 p1163 N88-16968
Holographic phase correction
[RSRE-MEMO-4036] 09 p1167 N88-17000
Reduced tolerance imaging 2, volume 2
[AD-A189604] 13 p1829 N88-20939
Use of a coherent square wave reference to demodulate BPSK (Binary Phase Shift Keying) carriers and a visual indicator of the quality of received QPSK (Quadrature Phase Shift Keying) carriers
[AD-A193528] 23 p3204 N88-29065
Cooperative effects and intrinsic optical bistability in collections of atoms
[AD-A193993] 23 p3280 N88-29530

PHASE CONJUGATION
New physical explanation of phase-conjugate waves produced in backward stimulated scattering
03 p0302 N88-11900
Determination of the origin of self-pumped phase conjugation in barium titanate
[AD-A184697] 03 p0377 N88-12372
Research on acoustical scattering, diffraction catastrophes, optics of bubbles, photoacoustics, and acoustical phase conjugation
[AD-A185785] 06 p0776 N88-14761
Acoustical phase conjugation
[PREPRINT-561] 06 p0777 N88-14768
Self-pumped phase conjugation in a supersonically flowing medium
[AD-A188281] 10 p1338 N88-17998
Subpicosecond optical digital computation using phase conjugate parametric generators
[AD-A188279] 10 p1410 N88-18411
Nonlinear optical principles and the photorefractive effect applied to optical phase conjugation
[AD-A188856] 12 p1691 N88-20119
Analytical description of noise in phase-conjugate resonators
[PB88-171947] 19 p2726 N88-26188
Laser CO2/TEA frequency-stabilized by phase conjugation 22 p3082 N88-28303
Beam combining by phase transition nonlinear media
[AD-A194116] 23 p3283 N88-29547
Nonlinear optical phase conjugation techniques to reduce the physical size of lasers
[AD-A196170] 24 p3379 N88-30122

PHASE CONTROL
Phase control of the microwave radiation in free electron laser two-beam accelerator
[DE88-001460] 07 p0859 N88-15219
Determination of the commutation and angle and load response for a continuous-current, single phase controlled rectifier
[AD-A190602] 15 p2060 N88-22285
Active phase compensation system for fiber optic holography
[NASA-TM-101295] 20 p2805 N88-26641

PHASE DEMODULATORS
Use of a coherent square wave reference to demodulate BPSK (Binary Phase Shift Keying) carriers and a visual indicator of the quality of received QPSK (Quadrature Phase Shift Keying) carriers
[AD-A193528] 23 p3204 N88-29065

PHASE DETECTORS
Optimum filters and smoothers design for carrier phase and frequency tracking
[NASA-CR-182654] 12 p1618 N88-19679

PHASE DIAGRAMS
Contribution to the study of the Ti-Al phase diagram by conventional and high resolution electron microscopy
[ESA-TT-1021] 01 p0023 N88-10143
Theory of the carbon phase diagram at high pressures and temperatures
[DE87-012245] 01 p0028 N88-10180
Analysis of phase equilibria in NiTi-C system in high nickel regions
[BLL-M-37304-(5828.4)] 02 p0149 N88-10932
DTA/DSC studies of phase equilibria in binary mixtures of barium carbonate with alkali carbonates
[DE87-001195] 02 p0194 N88-11213
On the search for experimentally observed grain boundary phase transitions
[DE87-012747] 02 p0244 N88-11539
The mechanism by which sigma-phase forms in Fe-Cr-Ni system alloys
[BLL-M-37380-(5828.4)] 05 p0564 N88-13437
Phase diagram and thermochemical properties of the Al-Cu system
[ETN-88-91015] 05 p0566 N88-13447
Phase behavior in the Li-Al-O-H system at intermediate temperatures
[AD-A185732] 06 p0697 N88-14280
Theoretical studies of multicomponent mixtures: Phase equilibrium and transport
[DE88-002717] 07 p0831 N88-15040
Microstructural observations of the Sn-Pb solder/Cu system and thermal fatigue of the solder joint
[DE88-001392] 07 p0832 N88-15048
The generalized van der Waals theory of pure fluids and mixtures
[DE88-002380] 07 p0855 N88-15192
Determination of thermodynamic function of minerals at high temperatures
[DE88-001911] 07 p0940 N88-15713
Determination of thermodynamic function of minerals at high temperatures
[DE88-002311] 07 p0940 N88-15714
Copper oxidation states, vacancy ordering and their effect on high temperature superconductivity
[DE88-003079] 09 p1258 N88-17542
Metal hydrides
[DE88-005083] 10 p1299 N88-17766
Electronic structure of random alloys and the theory of ordering processes
[DE88-004476] 10 p1407 N88-18394
Transport and relaxation processes in supercritical fluids
[DE88-004804] 10 p1419 N88-18474
Joining of dissimilar materials with the pulsed Nd-YAG laser
[DE88-003757] 11 p1458 N88-18693
Electronic structure and phase stability of alloys
[DE88-004574] 11 p1562 N88-19350
Transformation, metallurgical response and behavior of the weld fusion zone and heat affected zone in Cr-Mo steels for fossil energy application
[DE88-006037] 13 p1744 N88-20430
Titanium powder frit made during the transformation alpha-beta
[ETN-88-91999] 16 p2177 N88-22976
The Time-Temperature-Transformation (TTT) diagram as a basis for relating the formation and properties of reactive coatings
[AD-A190872] 16 p2182 N88-23006
Vacancy ordering in the basal plane of YBa2Cu3O(sub)z
[DE88-004572] 18 p2583 N88-25348
Non-equilibrium phases and phase diagrams
[DE88-008896] 20 p2880 N88-27098
Migration and stability of HgCdTe lattice defects
[AD-A193293] 21 p3021 N88-27935
Raman spectroscopy on simple molecular systems at very high density
[DE88-010947] 23 p3191 N88-28987

PHASE ERROR
Effects on electromagnetic wave propagation at frequencies over 10 GHz due to inhomogeneities of the complex refraction index
[REPT-86-025] 01 p0036 N88-10228
Digital method for correction of the phase error in the discrete generation of periodic signals in real time
[INPE-4327-RPE/552] 12 p1618 N88-19676
Reduced tolerance imaging 2, volume 2
[AD-A189604] 13 p1829 N88-20939
Coherent RF error statistics
[AD-A193002] 20 p2792 N88-26560
Approximation problems of the Hilbert transform to identify minimum phase linear systems
[FUB-42-1986] 21 p2999 N88-27790
Direct bit detection receiver performance analyses for 8-DPSK (Differential Phase Shift Keyed) modulated signals operating with improper carrier phase synchronization
[AD-A193839] 22 p3070 N88-28220
Effect of phase errors in stepped-frequency radar systems
[AD-A194476] 23 p3203 N88-29061

PHASE LOCKED SYSTEMS
A compact digital communications system. Part 3: Generalising the phase locked loop
[RSRE-MEMO-4027-PT-3] 01 p0035 N88-10222
Detection of signals by weighted integrate-and-dump filter 04 p0435 N88-12696
Phase-locked semiconductor quantum well laser arrays
[AD-A185155] 05 p0588 N88-13583
Time-dependent Slow-Time-Scale theory of free-running and phase-locked gyrotron oscillators
[AD-A188910] 12 p1629 N88-19752

Resonator coupling of two ring cavity, argon-ion lasers
[AD-A189558] 13 p1775 N88-20616
An investigation of a distributed clock for local area networks with ring topology 18 p2516 N88-24924
Phase length optical phase-locked-loop sensor
[NASA-CASE-LAR-13387-1] 18 p2576 N88-25302
Contribution to speed regulation of small motors with phase-locked loops
[ETN-88-92373] 20 p2796 N88-26590
Spectral estimation of received phase in the presence of amplitude scintillation 22 p3064 N88-28180
Telemetry SNR improvement using the DSN Advanced Receiver with results for Pioneer 10 22 p3064 N88-28184
A digitally implemented phase-locked loop detection scheme for analysis of the phase and power stability of a calibration tone 22 p3066 N88-28196
Digital phase-lock loop having an estimator and predictor of error
[NASA-CASE-NPO-17196-1-CU] 23 p3205 N88-29076
Human auditory and visual continuous evoked potentials 23 p3238 N88-29269
Tolerances for phase locking of semiconductor laser arrays
[AD-A195974] 24 p3378 N88-30120

PHASE MATCHING
Frequency doubling conversion efficiencies for deep space optical communications 04 p0434 N88-12691
Significance of sensory signal phase mismatch in mechanisms of motion sickness development 20 p2830 N88-26787

PHASE MODULATION
NT PHASE SHIFT KEYING
HF sidebands in the ionosphere 05 p0574 N88-13497
Error control techniques for satellite and space communications
[NASA-CR-181581] 05 p0576 N88-13516
Adaptive digital phase modulation
[PB87-134607] 06 p0693 N88-14253
Variation of wave action: Modulations of the phase shift for strongly nonlinear dispersive waves with weak dissipation. A new adiabatic invariant involving the modulated phase shift for strongly nonlinear, slowly varying, and weakly damped oscillators. The modulated phase shift for weakly dissipated nonlinear oscillatory waves of the Korteweg-de vries type
[AD-A185630] 06 p0765 N88-14702
Modem for digital phase modulation: Results and summary
[PB87-149233] 07 p0845 N88-15129
Modulation of an intense beam by an external microwave source: Theory and simulation
[AD-A185683] 07 p0848 N88-15145
A fiber optic gyro strapdown reference system for guided weapons 12 p1597 N88-19560
Magnet strength fluctuations in the SSC (Superconducting Super Collider) lattice. Part 2: Frequency modulation
[DE88-006491] 15 p2141 N88-22774
Influence of alternating magnetic fields on Zn-67 Moessbauer resonance in ZnO
[PB88-186432] 18 p2584 N88-25352
Trellis-coded CPM for satellite-based mobile communications 19 p2648 N88-25718
Fiber optic sensors 19 p2670 N88-25870
Phase modulation of recoiless gamma radiation in Mossbauer spectroscopy
[ETN-88-92648] 24 p3428 N88-30403

PHASE RESPONSE
U FREQUENCY RESPONSE
U PHASE SHIFT

PHASE SHIFT
A compact digital communications system. Part 3: Generalising the phase locked loop
[RSRE-MEMO-4027-PT-3] 01 p0035 N88-10222
Basic properties and variability 02 p0252 N88-11593
Measurement of solid propellant combustion velocity by means of microwaves
[CERT-1/1316-MO] 03 p0283 N88-11778
Short baseline phase delay interferometry 04 p0433 N88-12683
Compensation of small-scale phase distortions by means of a Fourier phase corrector 06 p0708 N88-14345
Variation of wave action: Modulations of the phase shift for strongly nonlinear dispersive waves with weak dissipation. A new adiabatic invariant involving the modulated phase shift for strongly nonlinear, slowly varying, and weakly damped oscillators. The modulated phase shift for weakly dissipated nonlinear oscillatory waves of the Korteweg-de vries type
[AD-A185630] 06 p0765 N88-14702
Study of vibration relaxation in active medium of CO2-laser using phase-absorption method 07 p0919 N88-15582
Pressure and tension dependence of phase shift of polarization modes in birefringent single-mode fiber-optic waveguide 08 p1078 N88-16501
Magnetic rare earth superlattices
[DE88-003483] 10 p1418 N88-18465
Optics for large telescope 13 p1840 N88-21014
Considerations in GaAs standard cell design
[DE88-003310] 14 p1985 N88-21840
Determination of the commutation and angle and load response for a continuous-current, single phase controlled rectifier
[AD-A190602] 15 p2060 N88-22285
Near optimal blind deconvolution
[REPT-87-016] 15 p2123 N88-22655
A new fiber-optic-based phase-resolved phosphorescence spectrometer
[AD-A191325] 16 p2275 N88-23613
Doppler radar with multiphase modulation of transmitted and reflected signal
[NASA-CASE-MSC-18808-1] 17 p2332 N88-23923
Picosecond response of an optically controlled millimeter wave phase shifter 19 p2660 N88-25820
Phase comparator for range imaging laser radar
[DE88-008109] 21 p2954 N88-27545
Direct bit detection receiver performance analyses for 8-DPSK (Differential Phase Shift Keyed) modulated signals operating with improper carrier phase synchronization
[AD-A193839] 22 p3070 N88-28220
Experimental investigations for the generation of phase modes for adaptive antennas
[REPT-10-87] 23 p3205 N88-29074

PHASE SHIFT CIRCUITS
RELIC: A reliability simulator for integrated circuits
[AD-A187493] 11 p1477 N88-18811
Intergrated circuit design, phase 2
[AD-A189060] 13 p1760 N88-20530
Monolithic phase shifter study
[AD-A190213] 15 p2059 N88-22278
The superconducting phase shifter in the development of a terahertz imaging radar system
[AD-A190666] 16 p2188 N88-23046
Development of 20 GHz monolithic transmit modules
[NASA-CR-182134] 17 p2445 N88-24539

PHASE SHIFT KEYING
Bandwidth efficient block codes for M-ary PSK modulation
[NASA-CR-181543] 04 p0437 N88-12712
High data rate modem simulation for the space station multiple-access communications system 06 p0795 N88-14870
Envelope and phase statistics for non-Gaussian noise and resulting error probabilities for digital communications systems 12 p1617 N88-19672
Direct bit detection receiver noise performance analysis for 32-PSK and 64-PSK modulated signals
[AD-A190009] 15 p2056 N88-22256
The 2 FSK/QPSK (Frequency Shift Keying/Quadrature Phase Shift Keying) transmitter and receiver: Design and performance
[AD-A190028] 15 p2056 N88-22258
A Differential Phase Shift Keying (DPSK) modulator for a frequency hopping short wave system
[FOA-C-30460-3.3] 18 p2501 N88-24840
Codes for QPSK modulation with invariance under 90 degrees rotation 19 p2648 N88-25720
Trellis-coded MPSK modulation techniques for MSAT-X(sup)1 19 p2648 N88-25721
Modulation and coding for fast fading mobile satellite communication channels 19 p2648 N88-25722
Performance of the ICAO standard core service modulation and coding techniques 19 p2648 N88-25723
An 8-DPSK TCM modem for MSAT-X 19 p2649 N88-25725
Development of a coded 16-ary CPFSK coherent demodulator 19 p2649 N88-25726
Modem for the land mobile satellite channel 19 p2649 N88-25727
Error performance of voice band data signals with an overloaded delta modulator
[FEL-1987-05] 20 p2792 N88-26562
Digital carrier demodulation for the DSN Advanced Receiver 22 p3064 N88-28183
Automatic classification of digitally modulated signals
[AD-A194623] 23 p3203 N88-29064
Use of a coherent square wave reference to demodulate BPSK (Binary Phase Shift Keying) carriers and a visual indicator of the quality of received QPSK (Quadrature Phase Shift Keying) carriers
[AD-A193528] 23 p3204 N88-29065
Doppler-corrected differential detection system
[NASA-CASE-NPO-16987-1-CU] 24 p3359 N88-30001

PHASE SWITCHING INTERFEROMETERS
Imaging interferometry with non-redundant arrays 02 p0257 N88-11624

PHASE TRANSFORMATIONS
NT ARC MELTING
NT BOILING
NT COAL LIQUEFACTION
NT EVAPORATION
NT EVAPOTRANSPIRATION
NT FILM BOILING
NT FLASHING (VAPORIZING)
NT FREEZING
NT FUSION (MELTING)
NT LIQUEFACTION
NT MARTENSITIC TRANSFORMATION
NT MELTING
NT NUCLEATE BOILING
NT SUBLIMATION
NT TRANSPIRATION
NT VACUUM MELTING
NT VAPORIZING
NT ZONE MELTING
Nitrogen at high pressure
[DE87-013797] 01 p0021 N88-10130
Structure of rapidly solidified Ni-Ti
[DE87-012252] 02 p0147 N88-10921
Analysis of phase equilibria in NiTi-C system in high nickel regions
[BLL-M-37304-(5828.4)] 02 p0149 N88-10932
Shock-induced cooling in dense fluids
[DE87-014343] 02 p0170 N88-11067
Anelastic behaviour of materials under multiaxial strains. Part 3: Order-disorder transition, Shoek effect and Poisson's ratio in AISI-1080 steel
[DE87-703087] 02 p0191 N88-11193
Iterative solution of a nonlinear system arising in phase change problems
[DE87-014672] 02 p0226 N88-11426
Solute segregation to phase interfaces and grain boundaries: Studies by analytical electron microscopy and profile deconvolution
[DE87-012129] 02 p0243 N88-11537
On the search for experimentally observed grain boundary phase transitions
[DE87-012747] 02 p0244 N88-11539
Cure and properties of thermosetting polymers
[AD-A184669] 03 p0293 N88-11843
Wittig synthesis of conductive segmented block polymer compositions
[AD-A184018] 03 p0295 N88-11850
Determination of the origin of self-pumped phase conjugation in barium titanate
[AD-A184697] 03 p0377 N88-12372
Improper ferroelectricity: A theoretical and experimental study
[AD-A184614] 03 p0381 N88-12397
Phase equilibrium and crystal growth studies on AgGaSe2 and related nonlinear optical materials
[AD-A184768] 03 p0382 N88-12400
Phase transition of multifractals
[DE87-014344] 03 p0383 N88-12409
Experimental perspectives on heavy electron metals
[DE87-014766] 04 p0416 N88-12583
Synthesis of the monoclinic yttria by thermal plasma processing
[DE88-000496] 04 p0421 N88-12608
Nonlinear acoustics
[AD-A184271] 04 p0488 N88-13004
The Moessbauer effect of SnI4 at high pressure
[DE87-014771] 04 p0495 N88-13048
Guest-host interactions in thermotropic and lyotropic liquid crystals
[AD-A184402] 04 p0496 N88-13057
Radiation induced collapse of the crystalline structure
[DE87-014407] 04 p0498 N88-13064
The mechanism by which sigma-phase forms in Fe-Cr-Ni system alloys
[BLL-M-37380-(5828.4)] 05 p0564 N88-13437
Coupling effects between the ferrite and austenite phases during corrosion fatigue of a ferrite/austenite duplex stainless steel 05 p0605 N88-13706
Pressure induced phase transitions, superconductivity of phosphorus described 06 p0675 N88-14134
Precipitation in alumina-rich spinel: A transformation-toughened ceramic single crystal
[DE87-012380] 06 p0785 N88-14815
Atmospheric science 07 p0883 N88-15357
Embedded cluster models for electronic structure and energetics of complex oxides
[DE88-003097] 07 p0938 N88-15702
Change of europium crystallographic symmetry at helicoidal magnetic ordering
[DE88-700559] 07 p0939 N88-15707
Evolution from pure states into mixed states in de Sitter space
[DE88-750316] 07 p0945 N88-15745

Metal-oxide superconductor BaPbsub1-xBisubxO3: Unusual properties and new applications
08 p1077 N88-16494

Characterization of duplex stainless steel by TEM (Transmission Electron Microscopy), SANS (Small-Angle Neutron Scattering) and APFIM (Atom-Probe Field Ion Microscopy) techniques
[DE88-002916] 09 p1145 N88-16865

Superconductivity and crystal structure of high-pressure phases in V-Ru-H system 09 p1239 N88-17426

Theory of the tetragonal-to-orthorhombic structural phase transition in La2CuO4
[AD-A187141] 09 p1254 N88-17514

High temperature superconductivity research at Argonne National Laboratory
[DE88-003055] 09 p1258 N88-17541

Copper oxidation states, vacancy ordering and their effect on high temperature superconductivity
[DE88-003079] 09 p1258 N88-17542

Application of inverse gas chromatography to fluidity studies
[DE88-002896] 10 p1296 N88-17750

Influence of convection on microstructure
[NASA-CR-182489] 10 p1302 N88-17784

Irradiation effects in metals
[DE88-004272] 10 p1303 N88-17789

The role of composition and microstructure gradients on weld metal properties and behavior
[DE88-004956] 10 p1303 N88-17791

Fabrication, phase transformation studies and characterization of SiC-AlN-Al2OC ceramics
[DE88-004053] 10 p1306 N88-17807

Advanced materials for solid oxide fuel cells
[DE88-002338] 10 p1350 N88-18071

Application of Onsager's reciprocity relations to interface motion
[DE88-003286] 10 p1397 N88-18327

Electronic structure of random alloys and the theory of ordering processes
[DE88-004476] 10 p1407 N88-18394

High temperature processing of superconducting Y1Ba2Cu3O6.9
[DE88-003002] 10 p1416 N88-18449

Magnetic rare earth superlattices
[DE88-003483] 10 p1418 N88-18465

Order-disorder transition of Au and Pt (110) surfaces: The significance of relaxations and vibrations
[DE88-004651] 10 p1419 N88-18473

Superconductivity and phase stability in the heavy rare earth quaternary compounds RBa2Cu3O7 (R = Ho, Er, Tm, Yb, Lu)
[DE88-003478] 10 p1419 N88-18476

Superconducting properties and structural characterization of high T/sub c/ oxides
[DE88-003479] 10 p1420 N88-18477

Hadron-quark phase transition in dense stars
[DE88-003412] 10 p1429 N88-18532

Deactivation of alumina based catalysts
11 p1455 N88-18673

Crystallization and glass formation in electron and laser beam irradiated Cu-Zr alloys
[DE88-003390] 11 p1464 N88-18729

Perturbed angular correlations in zirconia ceramics
[DE88-004117] 11 p1464 N88-18731

Development of encapsulated lithium hydride thermal energy storage for space power systems
[DE88-004762] 11 p1507 N88-19001

An interdisciplinary approach to predictive modeling of structural adhesive bonding: Factors affecting the durability of titanium/epoxy bonds
[AD-A189503] 12 p1611 N88-19636

The role of point defects on structural phase transitions
[DE88-005209] 12 p1696 N88-20152

Phase transitions in two-dimensional superconducting arrays in a transverse magnetic field
[INPE-4457-RPE/559] 12 p1697 N88-20157

Interaction of particulate and transformation toughening
[AD-A189321] 13 p1741 N88-20412

Transformation, metallurgical response and behavior of the weld fusion zone and heat affected zone in Cr-Mo steels for fossil energy application
[DE88-006037] 13 p1744 N88-20430

Diffraction theory in QCD and beyond
[DE88-005958] 13 p1837 N88-20992

Rapid e-beam heating for measuring thermodynamics of metastable materials
[DE88-003565] 13 p1849 N88-21066

Experimental studies of elastic properties of crystals by Brillouin scattering
[DE88-005923] 14 p1986 N88-21848

Stability limits in the monoclinic-tetragonal transformations of zirconia
[DE88-005924] 14 p1986 N88-21849

Thermal analysis of heat storage canisters for a solar dynamic, space power system
[DE88-004199] 15 p2027 N88-22075

Directed-energy electron-beam processing of a hypoeutectic Cr90Ta10 alloy
[DE88-005621] 15 p2040 N88-22157

Transformation toughening of ceramics
[AD-A190399] 15 p2045 N88-22183

Synthesis of metastable superconductors by high dynamic pressure
[DE88-005620] 15 p2139 N88-22764

Superconductivity and the tailcring of lattice parameters of the compound YBa2Cu3O(sub x)
[DE88-005904] 15 p2140 N88-22769

An investigation of the crystalchemistry and thermochemistry of selected mineral systems
[AD-A189758] 15 p2142 N88-22781

Remarks on solid state amorphizing transformations
[DE88-006452] 15 p2145 N88-22803

Peculiarities of non-stationary heat transfer to superfluid helium
[DE88-701174] 16 p2200 N88-23124

The thermodynamic properties of quinoline and isoquinoline
[DE88-001218] 18 p2484 N88-24735

Dynamic consolidation of metal powders
[AD-A192126] 18 p2485 N88-24744

On the abnormal phenomena observed in the electrical resistivity measurement during the decomposition process of saturated Cu-Fe alloys
[NASA-TT-20183] 18 p2507 N88-24869

The Potts model in a random field
19 p2721 N88-26158

Refractory Materials of Zirconate. Part 2: Synthesis and some properties of strontium, zirconate, calcium zirconate and barium zirconate
[NASA-TT-20186] 20 p2779 N88-26483

Fluid dynamical model of ultrarelativistic heavy ion collisions
[DE88-007905] 20 p2850 N88-26921

The electronic structure of condensed molecular systems
[DE88-007823] 20 p2851 N88-26923

Shock wave compression and metallization of simple molecules
[DE88-008031] 20 p2851 N88-26925

Phase transformations and thermodynamic behavior of the YBa2Cu3O(sub)x system via EMF measurements
[DE88-010054] 20 p2878 N88-27086

Survey of the literature on fractals with possible applications to phase change processes
[DE88-012240] 21 p2911 N88-27277

On the systematics of phase transformation in metallic alloys
[DE88-008041] 21 p2913 N88-27288

Twin boundaries and heterophase interfaces in ferroelastic martensites
[DE88-011894] 21 p2916 N88-27304

Energy migration, motion and order in synthetic polymers
[AD-A193334] 21 p2918 N88-27320

Component stress during freeze/thaw cycling
[DE88-011204] 21 p2938 N88-27449

New synthetic approaches to boron hydride transformations
[AD-A193872] 22 p3052 N88-28108

Superconducting properties of oxygen deficient YBa2Cu3O(sub 7-delta)
[DE88-009969] 22 p3155 N88-28774

Band electronic structures and crystal packing forces
[DE88-010247] 23 p3289 N88-29585

Magnetic phase transitions in 90-K superconductors Ho1Ba2Cu3O(7-delta) and Gd1Ba2Cu3O(7-delta) observed by ZF-muon(+)SR
[DE88-752611] 23 p3290 N88-29588

Thermodynamical, optical and X-rays studies of some thermotropic liquid crystals
[DE88-702301] 23 p3290 N88-29590

Crustal evolution and the eclogite to granulite phase transition in xenoliths from the West African Craton
24 p3395 N88-30217

A method for the quantitative determination of crystalline phases by X-ray
[NASA-TT-20324] 24 p3434 N88-30444

PHASE VELOCITY

A spectral method for computing complete synthetic seismograms
[AD-A187663] 11 p1510 N88-19024

Phase velocity and attenuation of plane elastic waves in a particle-reinforced composite medium
[AD-A189414] 13 p1734 N88-20366

Two-phase flows in the wake of in-cylinder projectiles
[AD-A189422] 13 p1765 N88-20559

The superconducting phase shifter in the development of a terahertz imaging radar system
[AD-A190666] 16 p2188 N88-23046

PHASE-SPACE INTEGRAL

Fundamentals and techniques of nonimaging optics research
[DE87-014544] 02 p0236 N88-11488

Introduction to classical mechanics of systems with constraints, part 3
[DE88-701057] 13 p1850 N88-21073

PHASED ARRAYS

COSMIC --- Coherent Optical System of Modular Image Collectors (COSMIC); spaceborne telescope
01 p0095 N88-10623

A conformal aircraft phased array antenna for airplane-satellite communication in the L band
[ESA-TT-1057] 03 p0305 N88-11926

High power phased array and tailored gain semiconductor lasers 03 p0329 N88-12078

Multichannel deconvolution of P waves at seismic arrays and three component stations
[AD-A184450] 04 p0467 N88-12888

Theory of displaced phase center antenna for space based radar applications
[PB87-229837] 06 p0690 N88-14227

An analysis of simplified feed architectures for MMIC (Monolithic Microwave Integrated Circuit) T/R (Transmit/Receive) module arrays
[AD-A185474] 06 p0697 N88-14275

NORSAR detection processing system
[AD-A185968] 07 p0877 N88-15318

Optically controlled phased-array antenna technology for space communication systems
[NASA-TM-100852] 11 p1476 N88-18809

Investigation of surface wave blindness in microstrip phased array antennas
[AD-A189326] 12 p1621 N88-19696

Optical RF distribution links for MMIC phased array antennas
[NASA-TM-100841] 13 p1764 N88-20555

Optically interconnected phased arrays
[NASA-TM-100855] 14 p1908 N88-21400

Automated test device for FASR (Fixed Array Surveillance Radar) beam steering componentry
[AD-A191650] 18 p2500 N88-24829

MSAT mobile electronically steered phased array antenna development 19 p2647 N88-25711

MSAT-X electronically steered phased array antenna system 19 p2647 N88-25712

Proceedings of the Array Signal Processing Symposium: Treaty Verification Program
[DE88-008346] 20 p2790 N88-26548

A novel method to correct radiation pattern distortion of conformal antennas
[AD-A193675] 23 p3204 N88-29066

High frequency GaAlAs modulator and photodetector for phased array antenna applications
[NASA-TM-101328] 24 p3367 N88-30048

Maximum-likelihood multichannel deconvolution of P waves at seismic arrays
[AD-A194990] 24 p3391 N88-30191

PHENOL FORMALDEHYDE

A process for producing phenolic foams
[EP-PATENT-0-170-357-A1] 01 p0026 N88-10162

PHENOLIC RESINS

Thixotropic surface composition for phenolaldehyde resin laminates
[GB-PATENT-2-180-251-A] 04 p0410 N88-12545

PHENOLOGY

Pilot study of rice culture in sub-tropical high population density region (Madagascar) with SPOT 1 multispectral data 22 p3097 N88-28392

PHENOLS

Flame retardant phenolic foams
[EP-PATENT-0-223-489-A2] 05 p0568 N88-13464

Production of jet fuels from coal derived liquids. Volume 1: Market assessment for liquid by-products from the Great Plains gasification plant
[AD-A184846] 05 p0570 N88-13475

PHENOMENOLOGY

Phenomenological implications of the blown-up orbifolds
[DE87-014608] 03 p0373 N88-12347

Breaking of supersymmetry degeneracy and phenomenological conditions
[PREPRINT-559] 06 p0790 N88-14843

Phenomenological model of superconductivity of heavy fermions in U(sub 1-x)ThsubxBesub13
09 p1238 N88-17423

A viscoplastic theory applied to copper
[NASA-TM-100831] 14 p1928 N88-21497

State variable approach to deformation phenomena in Face Centered Cubic (FCC) metals
[VTT-44] 24 p3354 N88-29964

PHENYLS

NT POLYPHENYLS

Thermally stable aromatic structures from acyclic precursors. 1. Para polyphenylene model compounds from 3-Dimethyl amino hex-5-EN-1-YNES
[AD-A185300] 05 p0568 N88-13462
Boundary layer flow visualization for flight testing
17 p2297 N88-23742

PHILOSOPHY
NT PARADOXES
Resonance, information, and the primacy of process: Ancient light on modern information and communication theory and technology 10 p1424 N88-18506
Induction instrument for logic conclusion
[LRT-WE-9-FB-5(1987)] 22 p3144 N88-28697

PHOBOS
Periodic orbits around a satellite modelled as a triaxial ellipsoid
[AD-A190592] 15 p2022 N88-22051
Power requirements for mining and microwave processing of extraterrestrial resources
17 p2420 N88-24389

PHONETICS
Speech recognition: Acoustic-phonetic knowledge acquisition and representation
[AD-A185897] 07 p0840 N88-15097
Speech recognition: Acoustic-phonetic knowledge acquisition and representation
[AD-A187293] 10 p1320 N88-17893
Time-frequency representations for speech signals
[AD-A188661] 18 p2498 N88-24819

PHONOCARDIOGRAPHY
NT ECHOCARDIOGRAPHY

PHONON BEAMS
Effect of extraneous factors on optical one-phonon transitions in impurity centers with cubic symmetry
08 p1077 N88-16496

PHONONS
NT PHONON BEAMS
Anomalous phonon behavior of superconductor Y-Ba-Cu-O
[DE87-703401] 05 p0654 N88-14010
Phonon dispersion for several surfaces with ordered overlayers: A lattice dynamical study
07 p0876 N88-15315
On the coexistence of phonon and non-phonon (plasmon) mechanisms in new high T/sub c/ superconductors
[DE88-003188] 07 p0938 N88-15703
Non-phonon mechanisms of superconductivity in high T/sub c/ superconducting oxides and other materials and their manifestation
[DE88-002708] 07 p0939 N88-15709
Memory effects on infrared adsorbate spectra
[AD-A186976] 09 p1253 N88-17512
Dynamical properties of aluminium from experimental dispersion relations
[DE88-700240] 11 p1459 N88-18697
Raman scattering in mixed crystal semiconductors
12 p1696 N88-20149
Acoustic phonons, surface plasmons and surface acoustic plasmons in a superlattice and their nonreciprocal device applications
[AD-A188918] 12 p1698 N88-20163
Studies of transverse phonon modes in premartensitic indium-thallium alloys
[DE88-003481] 13 p1744 N88-20428
Nonequilibrium phonons and disorder in Al sub x Ga sub 1-x As 19 p2657 N88-25788
Phonons in semiconductor superlattices
20 p2869 N88-27035
Monte Carlo simulations of femtosecond relaxation of photoexcited electrons in AlGaAs/GaAs quantum wells
20 p2869 N88-27036

PHOSPHATES
NT ADENOSINE TRIPHOSPHATE
NT DIPHOSPHATES
NT INDIUM PHOSPHATES
Adhesion properties of polyelectrolyte-chemisorbed zinc phosphate conversion coatings
[DE87-012489] 01 p0029 N88-10186
Recent advances in metallic/ceramic coatings for corrosion control in military applications
17 p2320 N88-23858
Growth and characterization of thin films of ZnSnP(sub)2
[DE88-001164] 20 p2874 N88-27060

PHOSPHAZENE
Effect of sidechain length and crosslinking on ionic conductivity in polyphosphazene solid electrolytes
[AD-A184419] 04 p0497 N88-13058
Aromatic cyclotriphosphazenes
[NASA-CASE-ARC-11428-3] 18 p2477 N88-24692
Synthesis and characterization of new phosphazene polymers
[AD-A191508] 18 p2490 N88-24771

PHOSPHIDES
NT BORON PHOSPHIDES
NT GALLIUM PHOSPHIDES
NT INDIUM PHOSPHIDES
Cohesive energies of transition metal silicides and phosphides --- Knudsen effusion
[AD-A186691] 09 p1254 N88-17519

PHOSPHONIUM COMPOUNDS
Use of diphosphonates to correct disorders in calcium metabolism and mineral composition of bone tissue with 60-day hypokinesia in rats
[NASA-TT-20220] 13 p1809 N88-20807
Corrosion and corrosion inhibition of metals/alloys in methyphosphonic difluoride 17 p2319 N88-23850

PHOSPHORESCENCE
Canadian activities and goals in remote sensing of ocean colour and fluorescence from space
08 p1043 N88-16300
Federal Republic of Germany's interests, activities and goals in remote sensing of ocean colour/fluorescence from space 08 p1043 N88-16302
A new fiber-optic-based phase-resolved phosphorescence spectrometer
[AD-A191325] 16 p2275 N88-23613

PHOSPHORIC ACID
Electrochemical characteristics of acid electrolytes for fuel cells
[PB88-104641] 06 p0731 N88-14497
Factors governing light driven electron and proton translocation in proteins across membranes
[DE88-002716] 08 p1082 N88-16519
The effect on initial bond strength and durability of a Phosphoric Acid Dip (PAD) following chromic acid anodising of aluminum
[ARE-TM(UMM)-87402] 10 p1300 N88-17772
Studies of model ion channels in defect-free multibilayers of phospholipids
[AD-A188740] 16 p2238 N88-23365
Characterization of proton conducting polymer blends
19 p2669 N88-25867

PHOSPHORIC ACID FUEL CELLS
Synthesis of novel acid electrolytes for phosphoric acid fuel cells
[PB87-221305] 01 p0066 N88-10426
Electrochemical hydrogen concentrator for phosphoric acid fuel cells
[AD-A191355] 16 p2229 N88-23317
Compact regenerable sulfur scrubber for phosphoric acid fuel cells
[AD-A191356] 16 p2230 N88-23318
Phosphoric acid electric utility fuel cell technology development
[DE88-010187] 20 p2795 N88-26582

PHOSPHORS
Evaluating and testing thermographic phosphors for turbine-engine temperature measurements
[DE87-011772] 02 p0174 N88-11090
Calibration of a laser-pumped, thermographic phosphor remote thermometry system
[DE88-000452] 04 p0449 N88-12781
Performance and preference with various VDT (Video Display Terminal) phosphors
[AD-A184085] 04 p0475 N88-12925
Generation of specific chromaticities on CRT monitors
[AD-A187739] 11 p1440 N88-18590
Noncontact thermometry via laser pumped, thermographic phosphors: Characterization of systematic errors and industrial applications
[DE88-005599] 13 p1777 N88-20628
Remote temperature-measurement instrumentation for a heated rotating turbine disk
[DE88-006456] 18 p2516 N88-24925

PHOSPHORUS
Pressure induced phase transitions, superconductivity of phosphorus described 06 p0675 N88-14134
The influence of phosphorus on the solid state reaction between copper and silicon or germanium
[ETN-88-91361] 06 p0789 N88-14838
Influence of grain boundary phosphorus segregation on hydrogen embrittlement in steel
[DE88-700176] 11 p1459 N88-18696
Phosphorus oxynitride glass for laser applications
[DE88-005413] 12 p1632 N88-19768
Evaluation of thermophosphor temperature technique
[DE88-007654] 20 p2805 N88-26638
PECVD of amorphous nickel--phosphorus films
[DE88-011088] 21 p2915 N88-27299

PHOSPHORUS COMPOUNDS
NT ADENOSINE TRIPHOSPHATE
NT BORON PHOSPHIDES
NT DIPHOSPHATES
NT GALLIUM PHOSPHIDES
NT INDIUM PHOSPHATES
NT INDIUM PHOSPHIDES
NT ORGANIC PHOSPHORUS COMPOUNDS
NT PHOSPHATES
NT PHOSPHAZENE
NT PHOSPHIDES
NT PHOSPHONIUM COMPOUNDS
NT PHOSPHORIC ACID
NT PHOSPHORUS POLYMERS
Electrodeposition of amorphous Ni-Cr-P alloys
[DE88-006868] 19 p2616 N88-25521

PHOSPHORUS METABOLISM
Effects of extreme hypoxia on phospholipid metabolism in subcellular structures of rat brain
08 p1046 N88-16323
Effect of different doses of alpha-hydroxydimethyl-gamma-aminopropylidene phonate on rat bones 19 p2704 N88-26078

PHOSPHORUS POLYMERS
High-molecular compounds (selected articles)
[AD-A184668] 03 p0293 N88-11842
Effects of extreme hypoxia on phospholipid metabolism in subcellular structures of rat brain
08 p1046 N88-16323
New phosphorus based polymer systems
[AD-A190457] 15 p2045 N88-22186

PHOSPHORYLATION
Muscle preservation in the study of bioenergetic effects of hypokinesia 10 p1362 N88-18139

PHOTOABSORPTION
Intramolecular energy transfer reactions as a method for metal complex assisted production of hydrogen
[DE88-001621] 05 p0562 N88-13425
Nonuniformity of electromagnetic field at Lambda = 10.6 micron wavelength inside atmospheric aerosol particles
06 p0772 N88-14743
Experimental observation of photoresonance of electrons localized above surface of solid hydrogen
06 p0774 N88-14755
Photoabsorption and phototdissociation of molecules important in the interstellar medium
[NASA-CR-182435] 08 p1100 N88-16617
Memory effects on infrared adsorbate spectra
[AD-A186976] 09 p1253 N88-17512
Light absorption by an atom moving inside a spherical box
[AD-A187241] 10 p1407 N88-18395
Optical absorption in doped CdxHg1-xTe
[AD-A187434] 11 p1560 N88-19338

PHOTOACOUSTIC MICROSCOPY
Nondestructive evaluation of structural ceramics by photoacoustic microscopy
[NASA-CR-180858] 09 p1146 N88-16868
Nondestructive Evaluation (NDE) of structural ceramics by photoacoustic microscopy 17 p2325 N88-23884

PHOTOACOUSTIC SPECTROSCOPY
DSA RuO2/TiO2 electrode modeled by ion implantation: An in situ characterization by photoacoustic and photocurrent spectroscopy
[DE87-009129] 02 p0245 N88-11545
Study of IR laser photoacoustic spectra of organic molecules adsorbed on metal surface
03 p0301 N88-11891
A critical review of measurements of water vapor absorption in the 840 to 1100 cm(-1) spectral region
[NASA-CR-182361] 06 p0742 N88-14585
Photoacoustic infrared laser spectroscopy for analyzing gaseous contaminants
[ETN-88-90805] 07 p0831 N88-15041
Photoacoustic measurements of atmospheric aerosol absorption coefficients at ultraviolet, visible and infrared wavelengths 11 p1512 N88-19036
A laser-based photoacoustic spectrometer for direct breath C-13O2/C-12O2 measurement
[DE88-004915] 15 p2101 N88-22516
Photoacoustic Fourier transform infrared spectroscopy. An early detection technique for coatings degradation
24 p3354 N88-29968

PHOTOCATHODES
A focussed MCP (microchannel plate) image intensifier type for high speed gating
[DE88-000480] 05 p0583 N88-13555
Streak camera dynamic range optimization
[DE88-001632] 05 p0586 N88-13571
Stellar scintillometer atmospheric optical turbulence profiling experiment. A qualitative comparison of two identical instruments at AMOS (Air Force Maui Optical Station), 1985
[AD-A190589] 15 p2094 N88-22479

PHOTOCELLS
U PHOTOELECTRIC CELLS

PHOTOCHEMICAL REACTIONS
NT PHOTOCHROMISM
NT PHOTODECOMPOSITION
NT PHOTOLYSIS
NT PHOTOSYNTHESIS
NT RADIOLYSIS
The photophysics and chemistry of PAH (Polycyclic Aromatic Hydrocarbons) compounds
[DE87-014455] 02 p0153 N88-10954

Photochemical ignition studies. 3: Ignition by efficient and resonant multiphoton photochemical formation of microplasmas
[AD-A184644] 03 p0283 N88-11780
Proceedings of the Eleventh DOE Solar Photochemistry Research Conference
[DE88-000678] 04 p0486 N88-12883
Intramolecular energy transfer reactions as a method for metal complex assisted production of hydrogen
[DE88-001621] 05 p0562 N88-13425
Scientific and Operational Requirements for TOMS Data
[NASA-CP-2497] 05 p0615 N88-13774
Photochemical ozone overburden correction
05 p0615 N88-13778
Practical photochemistry: General considerations
[PB87-123386] 06 p0730 N88-14491
Laser action from syn-(methyl,methyl) bimane
[AD-A188314] 07 p0858 N88-15211
Effect of the band-gap characteristics on laser-induced dry etching of semiconductors
[DE88-001853] 07 p0937 N88-15695
Short-term temporal variations of Nimbus-7 measurements of the solar UV spectral irradiance
[PB88-102132] 07 p0946 N88-15753
Mechanisms of cloud layer formation in Venusian atmosphere 08 p1004 N88-16087
Variable band gap materials for thermophotovoltaic generators
[AD-A186858] 09 p1186 N88-17104
Control of solid-excitation-based photochemical dry etching of semiconductors by ion-bombardment-induced damage
[DE88-003214] 09 p1257 N88-17537
Energy transfer and photochemistry in biomimetic solar conversion
[PB88-130026] 10 p1348 N88-18057
Photochemical solar energy conversion utilizing semiconductors localized in membrane mimetic systems
[DE88-002887] 10 p1349 N88-18065
Photophysics and photochemistry of poly(di-n-hexylsilane) in room temperature solution
[AD-A187890] 11 p1462 N88-18714
Photochemical energy storage: Studies of inorganic photoassistance agents
[DE88-002596] 11 p1508 N88-19010
Initial results with the LLNL 2-D chemical-radiative-transport model of the troposphere and stratosphere
[DE88-004355] 11 p1512 N88-19033
The influence of atmospheric thermal tides on diurnal variations in chemical constituents in the mesosphere
11 p1512 N88-19035
Surface mediated photocatalysis
[AD-A188882] 12 p1603 N88-19589
Ultraviolet (180 to 300 nm) action spectra for inactivation and DNA photoproduct formation of Bacillus subtilis spores under ultrahigh vacuum 12 p1657 N88-19931
Photochemistry at structured surfaces: A classical electromagnetic approach
[AD-A189519] 13 p1737 N88-20387
Mechanisms of photoinduced electron transfer
[DE88-004917] 13 p1836 N88-20983
The photochemistry of some possible cometary CN parent species 14 p1997 N88-21905
The role of hydrogen thermalization in shaping the Lyman-alpha borna --- comets 14 p2007 N88-21971
Hard ceramic film by laser PVD
15 p2051 N88-22216
UV-Laser reactions of molecular adsorbates
[AD-A190796] 16 p2212 N88-23201
Nanosecond laser photolysis of opaque heterogeneous photosensitizers
[AD-A191424] 16 p2213 N88-23209
Time-resolved studies of free radicals and laser-initiated chain reactions
[DE88-006569] 16 p2266 N88-23553
Modification of polymers by photografting processes
17 p2323 N88-23871
Chemical kinetics and photochemical data for use in stratospheric modeling evaluation Number 8
[NASA-CR-182919] 17 p2351 N88-24012
Photochemical and thermal modeling in the early atmosphere of the earth
[NASA-CR-183029] 18 p2543 N88-25093
Recent advances in photochemical techniques for ignition and combustion enhancement
19 p2625 N88-25570
The solar flare of 18 August 1979: Incoherent scatter radar data and photochemical model comparisons
[DE88-007616] 19 p2743 N88-26286
Ultraviolet geometric albedo of Uranus
[NASA-CR-183099] 20 p2885 N88-27136
Photochemical oxidant formation: Overview of current knowledge and emerging issues
[PB88-195235] 21 p2971 N88-27647
Low-band-gap, amorphous-silicon-based alloys by photochemical vapor deposition
[DE88-001165] 21 p3023 N88-27944
Chemical interactions between the present-day Martian atmosphere and surface minerals
23 p3305 N88-29689
Photochemistry of ionospheric D-region with injection of nitrogen oxides 24 p3444 N88-30499

PHOTOCHEMISTRY
U PHOTOCHEMICAL REACTIONS

PHOTOCHROMISM
Anisotropy of light absorption by color centers in waveguides produced on photochromic glasses by diffusion 14 p1896 N88-21320
Quasi-liquid crystalline materials with special electro-optic properties
[AD-A194579] 23 p3282 N88-29644

PHOTOCLINOMETRY
U PHOTOGRAMMETRY

PHOTOCONDUCTIVITY
Construction and characterization of amorphous-silicon test structures
[DE87-013595] 01 p0029 N88-10182
Toward pulsed power uses for photoconductive semiconductor switches: Closing switches
[DE87-012020] 01 p0041 N88-10262
Recent developments in opening photoconductive semiconductor switches
[DE87-012130] 01 p0041 N88-10263
The application of photoconductive detectors to the measurement of X-ray production in laser produced plasmas
[DE88-001630] 07 p0934 N88-15671
Dispersive hole transport in SiO2
[AD-A187077] 09 p1254 N88-17513
High density CMOS technology
11 p1561 N88-19342
Pressure-dependent DLTS (Deep Level Transient Spectroscopy) experiments on Si-doped AlGaAs
[DE88-003842] 13 p1846 N88-21047
Liquid carbon
[AD-A191707] 18 p2491 N88-24776
Photoconductivity in carbon fibers
[AD-A191728] 18 p2492 N88-24782
Picosecond electrical pulses for VLSI electronics characterization 19 p2655 N88-25768
Picosecond photoconductive transceivers
19 p2656 N88-25777
Photoconductive generation of sub-picosecond electrical pulses and their measurement applications
19 p2656 N88-25778
Generation and forming of ultrashort high voltage pulses 19 p2657 N88-25782
Investigation of photoconductive picosecond microstripline switches on self-implanted Silicon On Sapphire (SOS) 19 p2657 N88-25789
Fast GaAs photoconductive detectors with high sensitivity integrated in coplanar systems onto GaAs substrates 19 p2658 N88-25790
Characteristics, packaging and physics of ultra high speed diode lasers and detectors
19 p2658 N88-25797
Picosecond optoelectronic study of a thin film transmission line structure 19 p2661 N88-25823
Photoconducting X-ray detectors for Z-pinch experiments
[DE88-007118] 19 p2728 N88-26199
Control of carrier lifetime in PbTe nipi superlattices by external photoinjection 20 p2863 N88-27006
Pressure-dependent measurement on n+GaAs (Si, Sn): The effect of deep donor (DX) states on the electrical properties and presistent photoconductivity effects
20 p2866 N88-27020
Magneto-optical studies of GaInAs-InP quantum wells
20 p2870 N88-27039

PHOTOCONDUCTORS
An optically strobed sample and hold circuit
[DE87-011877] 01 p0038 N88-10245
Ultrafast photoconductor detector-laser-diode transmitter
[DE87-013803] 03 p0329 N88-12082
Photoconductor switch and circuit analysis
[AD-A188168] 11 p1478 N88-18821
Microwave response of an HEMT photoconductor
[NASA-TM-100819] 11 p1480 N88-18835
Optical absorption in doped CdxHg1-xTe
[AD-A187434] 11 p1560 N88-19338
Silicon containing photoresists
[AD-A188666] 12 p1605 N88-19601
Infrared-sensitive spatial light modulator
[AD-A190391] 15 p2134 N88-22729
An optically strobed sample and hold circuit
19 p2656 N88-25772
High speed, high repetition rate, high voltage photoconductive switching 19 p2657 N88-25781
Graphite as a picosecond laser activated opening switch 19 p2657 N88-25783
A new optoelectronic CW microwave source
19 p2660 N88-25818
Electrical pulse compression by traveling-wave photoconductivity 19 p2661 N88-25822
Characterization of new FPS (Focus Projection and Scale) vidicons for scientific imaging applications
[DE88-011213] 22 p3080 N88-28290

PHOTOCURRENTS
U ELECTRIC CURRENT
U PHOTOELECTRIC EMISSION

PHOTODECOMPOSITION
Vectorial electron transfer on designed surfaces
[PB87-232229] 03 p0381 N88-12394
Theoretical bases of polymer photodegradation and photooxidation
[AD-A186533] 08 p0974 N88-15889
Instrumentation for collisional energy transfer studies
[AD-A188495] 12 p1689 N88-20105

PHOTODETACHMENT
Photodetachment neutralizer development: Laser window design study. Volume 2: Window design details
[DE88-000783] 09 p1170 N88-17014
Determination of beam orientation of optical diagnostics of excited 200-MeV hydrogen atoms resulting from photodetachment of H(-)ions
[AD-A189976] 14 p1981 N88-21823

PHOTODETECTORS
U PHOTOMETERS

PHOTODIODES
Photodiode matrix for the analysis of two-beam interferences
[PTB-OPT-23] 01 p0048 N88-10310
The use of splines in the modelling of a photodiode response
[NPL-DITC-88/87] 01 p0085 N88-10550
Optical communication with semiconductor laser diodes
[NASA-CR-182464] 09 p1154 N88-16918
Superlattice photodetectors
[AD-A186956] 09 p1253 N88-17511
Measurement of the gamma-ray response of some commercial silicon detectors
[AD-A187431] 11 p1543 N88-19221
Development of integrated detectors for attitude sensors
[INPE-4409-PRE/1222] 12 p1602 N88-19586
Characterization of integrated photovoltaic detectors for MECB solar sensors
[INPE-4408-PRE/1221] 12 p1630 N88-19754
A method to detect and digitize small plant movements 12 p1654 N88-19912
A 104-km unrepeatered bidirectional fiber optic demonstration link
[AD-A190282] 15 p2134 N88-22728
Hybrid PV HgCdTe IR detectors technology reliability and failure program: Environmental stress testing plan
[AD-A191165] 16 p2211 N88-23195
Spectral radiation measurement using a photodiode array as receiver 16 p2271 N88-23591
Application of chaos theory to 1/f noise
[AD-A191150] 17 p2334 N88-23935
Studies of boron implantation through photochemically deposited SiO2 films on Hg(sub 1-x)Cd(sub x)Te
[SD-TR-87-26] 19 p2621 N88-25548
High speed opto-isolator for radar applications
19 p2658 N88-25795
InP/GaInAs/InP PIN photodiode with FWHM less than 18 ps 19 p2658 N88-25799
MESFET compatible IMSM detectors
19 p2659 N88-25801
X-ray response of GaAlAs/GaAs radiation hardened double: Heterostructure photodiode compared to Si:PIN photodiodes
[DE88-007425] 19 p2733 N88-26231
Photodiodes for optical communication in the near infrared
[ETN-88-92379] 21 p3016 N88-27900
Array detectors for plasma spectrochemistry
[AD-A194220] 22 p3052 N88-28105
Effect of detector dead time on the performance of optical direct-detection communication links
22 p3065 N88-28190
Tunnelling currents in reverse biased CMT photodiodes
[RSRE-MEMO-4137] 23 p3209 N88-29097

PHOTODISSOCIATION
OH(A-X) fluorescence from photodissociative excitation of HO2 at 157.5 nm
[NASA-CR-181580] 05 p0563 N88-13429
Photoabsorption and photodissociation of molecules important in the interstellar medium
[NASA-CR-182435] 08 p1100 N88-16617
Energy disposal in ion-molecule reactions
[AD-A186772] 09 p1171 N88-17019

The photochemistry of some possible cometary CN parent species 14 p1997 N88-21905
Photodissociation lifetimes of CH and CD radicals in comets 14 p1998 N88-21908
Aeronomic problems of the molecular oxygen photodissociation. Part 3: Solar spectral irradiances in the region of the O2 Herzberg continuum, Schumann-Runge bands and continuum
[AERONOMICA-ACTA-A-332-1988] 24 p3343 N88-29897
Aeronomic problems of molecular oxygen photodissociation. Part 2: Theoretical absorption cross sections of the Schumann-Runge bands at 79 K
[AERONOMICA-ACTA-A-331-1988] 24 p3344 N88-29907
Aeronomic problems of molecular oxygen photodissociation. Part 4: The various parameters for the Herzberg continuum
[AERONOMICA-ACTA-A-333-1988] 24 p3352 N88-29955

PHOTOELASTIC ANALYSIS
Optical analysis of stress and strain in photoelastic particle assemblies
[ETN-88-91591] 09 p1182 N88-17082
Photoelastic model tests of the Dornier linear actuator --- far IR telescope 14 p1877 N88-21218
The use of photoelastic methods to study the stressed states of spot-welded joints 14 p1898 N88-21335
The mechanical properties of card measured by photographic Moire
[NPL-DMOM-87] 14 p1923 N88-21463

PHOTOELASTIC MATERIALS
Optical analysis of stress and strain in photoelastic particle assemblies
[ETN-88-91591] 09 p1182 N88-17082

PHOTOELASTIC STRESS MEASUREMENT
U PHOTOELASTIC ANALYSIS

PHOTOELASTICITY
Vibrational, mechanical and thermal properties of 3-5 semiconductors
[AD-A187569] 11 p1556 N88-19316

PHOTOELECTRIC CELLS
NT PHOTOVOLTAIC CELLS
NT SOLAR CELLS
NT VERTICAL JUNCTION SOLAR CELLS
Photovoltaic cells with n-silicon and conductive polymers
[ETN-88-92133] 20 p2821 N88-26734
Space photovoltaic generators. State of the art, trends
[REPT-881-440-106] 21 p2970 N88-27640

PHOTOELECTRIC EFFECT
NT PHOTOCONDUCTIVITY
NT PHOTOELECTRIC EMISSION
NT PHOTOIONIZATION
NT PHOTOVOLTAIC EFFECT
Metal intercalation characteristics of n-HfS2 photoelectrodes in non-aqueous electrolytes
[AD-A184381] 03 p0383 N88-12407
An experimental and theoretical investigation of optogalvanic effects
[AD-A189618] 12 p1625 N88-19720
NBS (National Bureau of Standards) measurement services: The NBS photodetector spectral response calibration transfer program
[PB88-201595] 24 p3376 N88-30109

PHOTOELECTRIC EMISSION
The photophysics and chemistry of PAH (Polycyclic Aromatic Hydrocarbons) compounds
[DE87-014455] 02 p0153 N88-10954
DSA RuO2/TiO2 electrode modeled by ion implantation: An in situ characterization by photoacoustic and photocurrent spectroscopy
[DE87-009129] 02 p0245 N88-11545
Short-pulse high-current-density photoemission in high electric fields
[DE87-014909] 03 p0310 N88-11951
Atomic and electronic structure of surfaces and chemisorbed layers
[DE87-014987] 04 p0498 N88-13065
Photocurrent generation from basic metals, utilizing a short pulsed ArF excimer laser
[AD-A184928] 05 p0587 N88-13579
Electronic band structure and photoemission: A review and projection
[DE88-002236] 06 p0787 N88-14829
Differential spectral radiometry 16 p2272 N88-23594
Physical properties of f electron systems
[DE88-006886] 18 p2581 N88-25331
Studies of metal-silicon, silicon-metal and silicide based interfaces: Synchrotron radiation photo emission and inverse photoemission investigations of interface formation and compound nucleation
[AD-A191808] 19 p2619 N88-25536
Photocurrent modeling of modern microcircuit PN junctions
[DE88-007037] 19 p2662 N88-25832
Investigation of electronic band structure of semiconductors by photoemission
[ETN-88-92370] 21 p3025 N88-27957
An undulator radiation source for spin-polarized photoemission studies of novel magnetic materials
[AD-A193756] 22 p3083 N88-28307
Bulk plasmon enhanced photoemission from Nb(100) surface resonances
[AD-A192711] 22 p3154 N88-28767

PHOTOELECTRIC GENERATORS
NT PHOTOVOLTAIC CELLS
NT SOLAR CELLS
NT VERTICAL JUNCTION SOLAR CELLS
Application of pulse compression and shaping to the FEL photoelectric injector
[DE88-007908] 19 p2675 N88-25910

PHOTOELECTRIC PHOTOMETERS
U ELECTROPHOTOMETERS

PHOTOELECTRICITY
NT PHOTOCONDUCTIVITY
NT PHOTOELECTRIC EFFECT
NT PHOTOELECTRIC EMISSION
NT PHOTOIONIZATION
NT PHOTOVOLTAIC EFFECT
Detective quantum efficiency and design of a parallel data recording system for EXELFS-measurements --- electron microscopy
[USIP-87-06] 01 p0050 N88-10318
New method of examining micrononhomogeneity of local centers in high-resistivity semiconductor materials under scanning electron microscope 14 p1969 N88-21754
Defects in high-mobility semiconductor systems
[AD-A192298] 20 p2879 N88-27090

PHOTOELECTROCHEMISTRY
Corrosion Research Center, University of Minnesota
[DE88-006681] 15 p2041 N88-22160

PHOTOELECTROMAGNETIC DETECTORS
U RADIATION MEASURING INSTRUMENTS

PHOTOELECTRON SPECTROSCOPY
Localization of Cu 3d levels in the high Tc superconductor YBa2Cu3O approximately 7 by Cu2p X-ray photoelectron spectroscopy
[NOTA-INTERNA-887] 07 p0939 N88-15710
High-temperature photoelectron spectroscopy. An increased sensitivity spectrometer for studying vapor-phase species produced at furnace temperatures greater than 2000K
[AD-A186542] 09 p1140 N88-16835
Gas-phase photoelectron spectroscopy of metals and metal oxides of importance in the upper atmosphere
[AD-A187771] 11 p1511 N88-19027
Laser photoelectron spectroscopy of ions
[DE88-006860] 15 p2033 N88-22113
Differential spectral radiometry 16 p2272 N88-23594
Electronic and geometric structure of silver and palladium on aluminum (111) in monoatomic surface layers
[ETN-88-92120] 20 p2879 N88-27093

PHOTOELECTRONICS
U ELECTRONICS
U PHOTOELECTRICITY

PHOTOELECTRONS
Near threshold behavior of photoelectron satellite intensities
[DE88-002231] 08 p1081 N88-16512
A simple interpretation of the Fe2(-) photoelectron spectrum
[NASA-CR-182553] 11 p1543 N88-19225
Photoenhanced attachment for optical control of diffuse discharges
[AD-A188989] 12 p1696 N88-20147

PHOTOEMISSION
U PHOTOELECTRIC EMISSION

PHOTOEMISSIVITY
U EMISSIVITY
U PHOTOELECTRIC EMISSION

PHOTOGEOLOGY
MEVTV Workshop on Nature and Composition of Surface Units on Mars
[NASA-CR-183075] 23 p3300 N88-29654
Surface composition of Mars: A Viking multispectral view 23 p3300 N88-29655
Mapping of volcanic units at Alba Patera, Mars 23 p3301 N88-29663
Small Martian valcanoes 23 p3302 N88-29668
Photogeological inferences of Martian surface composition 23 p3303 N88-29675

PHOTOGRAMMETRY
The program DSMME: Digital Situation Model, Measurement --- mapping 01 p0065 N88-10418
A review of computer-assisted photo interpretation research at USAETL (US Army Engineer Topographic Laboratories)
[AD-A184034] 03 p0346 N88-12186
Accuracy potential of non-metric cameras in close-range photogrammetry 04 p0463 N88-12862
The determination of exhaust cloud dimensions from films of space shuttle launches
[NASA-CR-4103] 06 p0732 N88-14500
The aerophotogrammetric determination of Earth surface deformations
[SER-C-321] 07 p0872 N88-15288
Optimization of photogrammetric image adjustment
[SER-C-323] 07 p0872 N88-15289
Theory and research on the disjunction of cross passage errors and systematic image errors in photogrammetric point determination
[SER-C-324] 07 p0872 N88-15290
Photogrammetric principles for combining remote sounding and three-dimensional mapping 08 p1012 N88-16135
Earth resources: A continuing bibliography with indexes (supplement 56)
[NASA-SP-7041(56)] 10 p1347 N88-18051
Dynamics of high-speed mechanisms with elastic members 13 p1779 N88-20643
Classification of small image areas by digital correlation for the connection of different images in photogrammetry and long-range reconnaissance
[ETN-88-91506] 14 p1940 N88-21578
Relative orientation
[AD-A190385] 15 p2089 N88-22449
Stereoscopic photographs, ground and aerial, of trees used in the arborization of Curitiba (PR) 17 p2366 N88-24091
Adjustment in photogrammetry: Methods, programs and applications
[B8735130] 17 p2369 N88-24105
Development in data structures in PHOCUS for digital mapping 18 p2534 N88-25034
The use of SPOT imagery on analytical photogrammetric instruments 22 p3110 N88-28471
Evaluation of SPOT cartographic capabilities over the Aix Marseille area (France) 22 p3110 N88-28476
Rigorous stereophotogrammetric treatment of SPOT images 22 p3111 N88-28482

PHOTOGRAPH INTERPRETATION
U PHOTOINTERPRETATION

PHOTOGRAPHIC DEVELOPERS
The calibration of photographic and spectroscopic films: Reciprocity failure and thermal responses of IIaO film at liquid nitrogen temperatures
[NASA-CR-181094] 13 p1773 N88-20606

PHOTOGRAPHIC EQUIPMENT
NT CAMERAS
NT DIFFRACTION LIMITED CAMERAS
NT FAINT OBJECT CAMERA
NT FRAMING CAMERAS
NT HIGH SPEED CAMERAS
NT MULTISPECTRAL BAND CAMERAS
NT PINHOLE CAMERAS
NT STREAK CAMERAS
NT TELEVISION CAMERAS
Trajectory measurement of the Fokker 100 aircraft during autoland testing
[NLR-MP-86010-U] 20 p2758 N88-26366

PHOTOGRAPHIC FILM
Use of a 35mm camera for remote surface cleanliness verification 02 p0133 N88-10835
The calibration of photographic and spectroscopic films: Reciprocity failure and thermal responses of IIaO film at liquid nitrogen temperatures
[NASA-CR-181094] 13 p1773 N88-20606
The calibration of photographic and spectroscopic films: The response of 2aO film to small dosages of alpha particles from 3/10th's rad to 8 rads at energy levels 153 MeV, 79 MeV and 47 MeV
[NASA-CR-177830] 13 p1773 N88-20608
New duplicating paper with high resolution for aerial photography
[PB87-228706] 19 p2685 N88-25962

PHOTOGRAPHIC MEASUREMENT
NT PHOTOGRAMMETRY

PHOTOGRAPHIC PLATES
The effects of humidity on the profile of photographic plates
[NPL-DMOM-88] 14 p1913 N88-21429
Method of digital surface photometry of galaxies and its application to the edge-on galaxy NGC 5907 16 p2287 N88-23695

PHOTOGRAPHIC PROCESSING
Improving coherent visualization by means of film optical filtering --- projectile visualization
[ISL-R-116/86] 02 p0176 N88-11097
Digital enhancement of flow field images
[NASA-TP-2770] 13 p1813 N88-20833

PHOTOGRAPHS
NT MICROPHOTOGRAPHS
NT MOTION PICTURES
NT PHOTOMICROGRAPHS
Academic course Space Methods for Studying Modern Landscapes of Continents 08 p1012 N88-16133
Automated stereophotogrammetry
[AD-A189617] 12 p1630 N88-19757
PLZT (Lead-Lathanium-Zirconium-Titanium) electro-optic photographic system
[AD-A193473] 23 p3215 N88-29137

PHOTOGRAPHY
NT AERIAL PHOTOGRAPHY
NT ASTRONOMICAL PHOTOGRAPHY
NT AUTORADIOGRAPHY
NT BLACK AND WHITE PHOTOGRAPHY
NT CINEMATOGRAPHY
NT CLOUD PHOTOGRAPHY
NT COLOR PHOTOGRAPHY
NT ELECTRO-OPTICAL PHOTOGRAPHY
NT FRACTOGRAPHY
NT HIGH SPEED PHOTOGRAPHY
NT HOLOGRAPHY
NT INFRARED IMAGERY
NT INFRARED PHOTOGRAPHY
NT METRIC PHOTOGRAPHY
NT MULTISPECTRAL PHOTOGRAPHY
NT ORTHOPHOTOGRAPHY
NT PHOTOMICROGRAPHY
NT RADAR PHOTOGRAPHY
NT SATELLITE-BORNE PHOTOGRAPHY
NT SCHLIEREN PHOTOGRAPHY
NT SHADOWGRAPH PHOTOGRAPHY
NT SPACEBORNE PHOTOGRAPHY
NT SPECKLE HOLOGRAPHY
NT SPECTROPHOTOGRAPHY
NT STEREOPHOTOGRAPHY
NT STEREOSCOPY
NT STREAK PHOTOGRAPHY
NT ULTRAVIOLET PHOTOGRAPHY
NT ULTRAVIOLET PHOTOMETRY
NT WHITE LIGHT HOLOGRAPHY
Use of a 35mm camera for remote surface cleanliness verification 02 p0133 N88-10835
Identifying areas of leading edge Japanese science and technology: Patent activity and citation analysis using US POC (Patent Office Classification) classification
[PB87-204095] 02 p0249 N88-11575
Tracking through turbulence at the Tonopah Test Range
[DE88-001448] 04 p0446 N88-12766
MAXIE 1 (Magnetospheric Atmospheric X-ray Imaging Experiment) Program
[AD-A185878] 07 p0877 N88-15317
A directed method for locating the focus of expansion
[AD-A185640] 07 p0906 N88-15491
Study on cineradiography
[ISL-R-120/86] 08 p0990 N88-15994
Pulsed laser stereophotography of plasmas and dynamically moving surfaces
[DE88-003170] 09 p1173 N88-17031
Description of MSFC engineering photographic analysis
[NASA-TM-4035] 11 p1491 N88-18900
Photographic filters
[INPE-4448-RPE/558] 12 p1692 N88-20124
The use of a water towing tank for aerodynamic testing and methods for quantitative evaluation of photographs 16 p2202 N88-23140
The USSR space systems for remote sensing of earth resources and the environment (sensor systems, processing techniques, applications) 17 p2356 N88-24035

PHOTOINTERPRETATION
Vegetation studies in the national Park of Comoe (Ivory Coast) using SPOT 1 satellite data 03 p0343 N88-12166
A review of computer-assisted photo interpretation research at USAETL (US Army Engineer Topographic Laboratories)
[AD-A184034] 03 p0346 N88-12186
Model-based building verification in aerial photographs
[AD-A186010] 07 p0670 N88-15278
Study of relief of ore regions using space images (on the example of Eastern Yakutia) 08 p1008 N88-16111
Automatic knowledge acquisition for aerial image interpretation
[AD-A188616] 12 p1638 N88-19810
Northeast Artificial Intelligence Consortium (NAIC) administrative matters and ancillary functions, volume 1
[AD-A189486] 12 p1682 N88-20055
Utilization of space color transformation, linear contrast and filtration for enhancement of colored digital images
[INPE-4310-PRE/1176] 14 p1983 N88-21831
Comparative utilization of analog and digital processes in the treatment of MSS-LANDSAT data for studying the national parks of Brazil
[INPE-4011-TDL/240] 15 p2090 N88-22456
Updating land-use of the Sao Jose dos Campos municipality through remote sensing data
[INPE-4479-RPE/562] 16 p2287 N88-23693
An integrated study of the Alto Paranaiba Kimberlite Province, Minas Gerais, Brazil: A possible tool for diamond exploration 17 p2355 N88-24031
Anomalies in the vegetation in the Alto Xingu - MT 17 p2357 N88-24043
Remote sensing and structural rupture: Application examples in the study of tectonics 17 p2359 N88-24050
Analysis and interpretation of image lithostructure: An application of the multiconcept in the metamorphic belt of Sul de Santana da Boa Vista (RS) 17 p2359 N88-24051
Application of its transformation in color enhancement of LANDSAT imagery 17 p2365 N88-24082
The 35 mm vertical aerial photographs for mapping stands of bracatinga in different age classes 17 p2366 N88-24087
Stereoscopic photographs, ground and aerial, of trees used in the arborization of Curitiba (PR) 17 p2366 N88-24091
Characteristics of drainage determinations in aerial photographs and relief determination on different scales planialtimetric charts for three soils in the state of Sao Paulo 17 p2367 N88-24095
Lithostructural interpretation of Chapda do Cachimbo (Pa-Am-Mt), based on radar and LANDSAT imagery 17 p2368 N88-24100
National Meeting on Remote Sensing Applied to Municipal Planning 19 p2681 N88-25939
Photointerpretation with instrumentation for evaluation of environmental impact: Mata Atlantica in Cubatao 19 p2683 N88-25946
Application of interactive graphic system (CAD/CAM) in the determination of process evolution in land use in the Ribeirao Preto municipality 19 p2684 N88-25956
PHOTODIGITIZE: A software/hardware system
[DE88-009575] 19 p2716 N88-26125
Methods of determining playa surface conditions using remote sensing
[AD-A192663] 21 p2965 N88-27612
An objective technique for Arctic cloud analysis using multispectral AVHRR (Advanced Very High Resolution Radiometer) satellite imagery
[AD-A194732] 23 p3235 N88-29250
High resolution Viking Orbiter images: A useful data source for testing the viability of geomorphic processes attributed to Martian landforms 23 p3307 N88-29703
The use of orbital remote sensing data for low cost ground-water survey
[INPE-4587-PRE/1318] 24 p3386 N88-30170
Reflectance pattern and the physical and chemical characteristics of three Brazilian Oxisols
[INPE-4590-PRE/1320] 24 p3387 N88-30172

PHOTOIONIZATION
A physico-chemical study of some areas of fundamental significance to biophysics
[DE87-013457] 02 p0217 N88-11365
Third-harmonic generation and multiphoton ionization spectroscopy
[DE87-013545] 03 p0281 N88-11769
Two-laser resonance enhanced photoionization spectrum of gas phase benzene 03 p0300 N88-11889
Theory of multiphoton ionization of atoms by strong, short pulsed lasers
[DE88-000963] 05 p0588 N88-13588
Photoinduced charge separation by polymer-bound chromophores
[DE88-002101] 06 p0685 N88-14198
Photoionization of atoms and ions: Application of time-dependent response method within the density functional theory
[AD-A185686] 07 p0930 N88-15649
Laser post-ionization secondary neutral mass spectroscopy
[DE88-002979] 09 p1172 N88-17027
Photoionization dynamics of excited molecular states
[DE88-002982] 09 p1246 N88-17468
Two-photon (VUV and visible) resonant ionization spectroscopy of atoms and molecules
[DE88-004332] 10 p1407 N88-18388
Theoretical studies of atomic transitions
[DE88-004719] 10 p1407 N88-18389
Resonantly-enhanced, four-photon ionization of krypton at laser intensities exceeding 10(12) W/sq cm
[DE88-005038] 11 p1544 N88-19229
Fast switching of far infrared radiation by refractive index change in semiconductors using photoionization
[ETN-88-91490] 11 p1551 N88-19279
A global model for planetary nebulae, taking into account central stellar evolution and influence on halo ionization
[ETN-88-91491] 11 p1568 N88-19389
Photoenhanced attachment for optical control of diffuse discharges
[AD-A188989] 12 p1696 N88-20147
To what extent is mass loading responsible for the Venus bowshock precursor?
[NASA-TM-89307] 12 p1711 N88-20239
The astrophysics of nebulae and active galactic nuclear emission-line regions: New methods and applications 13 p1858 N88-21111
Measurement of species concentrations in flames by laser-induced fluorescence
[DE88-007096] 14 p1889 N88-21286
Total photoionization cross sections of atomic oxygen from threshold to 44.3A
[NASA-CR-182992] 17 p2397 N88-24252
Selective detection in gas chromatography
[AD-A191499] 18 p2481 N88-24718
Photoionization dynamics and abundance patterns in laser vaporized tin and lead clusters
[AD-A191604] 18 p2482 N88-24722
High-order multiphoton ionization of the noble gases
[DE88-007489] 18 p2571 N88-25273
XUV source for ultra-high resolution photoionization spectroscopy
[DE88-007531] 19 p2614 N88-25510
Target designs for plasma-implosion-driven, photoionization-pumped soft X-ray lasers
[DE88-011278] 21 p2954 N88-27547
Multiphoton ionization of alkaline earth atoms in an intense laser field
[DE88-008078] 21 p3014 N88-27884

PHOTOLITHOGRAPHY
The production of ultrasmall and superfine holographic diffraction gratings using synchrotron radiation and lithographic techniques
[AD-A185395] 05 p0585 N88-13562
X-ray lithographic research: A collection of NRL contributions
[AD-A188313] 12 p1695 N88-20140

PHOTOLUMINESCENCE
NT X RAY FLUORESCENCE
Blue-green laser diode research program
[AD-A183517] 01 p0051 N88-10323
Photoluminescence studies of GaAs/AlAs superlattices
[DE87-013617] 02 p0245 N88-11548
400-nm photoluminescence of a color center in undoped YAG grown under reducing atmosphere
[DE88-001760] 07 p0858 N88-15213
Photoluminescence study of InP surfaces and InP-insulator interfaces
[ECL-87-13] 08 p1089 N88-16555
Optical characterization of GaAs/sub 1-x/Sb/sub x/ and GaAs/sub 1-x/Sb/sub x/GaAs strained layer superlattices
[DE88-003393] 10 p1418 N88-18464
Pulsed laser photothermal spectroscopy of liquids and solids
[DE88-003839] 11 p1455 N88-18675
Structural characterization of undoped and doped GaAs: A comparative study of four techniques
[DE88-004552] 11 p1555 N88-19304
Optical study of germanium, germanium plus arsenic, and germanium plus gallium implants in gallium arsenide
[AD-A189600] 13 p1845 N88-21045
Optical properties of quantum well structures with electric field: Life time free switching of luminescence intensity and virtual charge-induced ultrafast optical nonlinearity 14 p1976 N88-21794
Singlet oxygen behavior in solid polymer matrices
[DE88-005171] 15 p2043 N88-22171
Raman, photoluminescence and modulation spectroscopy of semiconductor heterostructures 20 p2861 N88-26997
Magneto-optical studies of GaInAs-InP quantum wells 20 p2870 N88-27039
Photoluminescence studies of InGaAlAs quaternary alloys
[DE88-007197] 20 p2874 N88-27062
Picosecond transient reflectivity of unpinned gallium arsenide (100) surfaces
[AD-A193242] 21 p3021 N88-27933
Ultrafast physics in semiconductor microstructures
[AD-A193300] 21 p3022 N88-27936
Intrinsic and extrinsic energy states of semiconductors and heterostructures using novel techniques
[DE88-008560] 23 p3289 N88-29582

PHOTOLYSIS
Photolytic processes for measurement of combustion heats of formation and reaction rates
[DE87-014047] 02 p0144 N88-10905
Energy transformation in molecular electronic systems
[DE87-013916] 03 p0282 N88-11771
Photochemical conversion of nucleic acid components catalyzed by lunar soil 06 p0750 N88-14604
Low-power photolytically pumped lasers
[DE88-002448] 08 p0991 N88-15998
Investigation of OH reaction products. Excimer laser photolysis/slab laser fluorescence under tropospheric conditions
[REPT-8] 09 p1191 N88-17137
Laser studies of the dynamics of free radical reactions
[DE88-004431] 10 p1337 N88-17989
Photolytic formation of free radicals and their effect on hydrocarbon pyrolysis chemistry in a concentrated solar environment
[DE88-004129] 13 p1794 N88-20730
Excimer laser photolysis studies of T-V (Translation-to-Vibration) energy transfer
[AD-A189613] 13 p1837 N88-20989
Photon-controlled growth of multilayered structures
[DE88-005061] 13 p1847 N88-21054
Techniques for studying fast reactions in liquids
[DE88-005917] 14 p1888 N88-21285
Nanosecond laser photolysis of opaque heterogeneous photosensitizers
[AD-A191424] 16 p2213 N88-23209
Ultraviolet measurements: Measurements of photolysis rates 18 p2539 N88-25065
An investigation of 2-6 superlattice deposition by laser photochemical techniques
[AD-A191547] 18 p2581 N88-25336
Photosynthetic water splitting
[DE88-007809] 20 p2830 N88-26791
Studies of photochemically and electrochemically driven electron transport in zeolites
[DE88-008644] 22 p3155 N88-28769

PHOTOMAGNETIC EFFECTS
Recording materials for optical disk memory discussed 06 p0684 N88-14193

PHOTOMAPPING
Evaluation of SPOT stereoscopic possibilities for cartography 03 p0342 N88-12156
Cartography and topography with SPOT 03 p0342 N88-12159
Use of SPOT panchromatic imagery to update forest maps of northern Quebec, Canada 03 p0344 N88-12172
Use of space photographs for geomorphological studies in southwestern Tajikistan 08 p1008 N88-16109
The use of LANDSAT-TM pictures for the detection of space-limiting elements for the benefit of landscape photomapping
[BCRS-87-02] 16 p2228 N88-23305
Cartographic applications of SPOT imagery 22 p3110 N88-28472
Larger scale image mapping with SPOT 22 p3111 N88-28481
High resolution orthoimage quadrangle maps using SPOT satellite data 22 p3112 N88-28488
Integrating multispectral imagery and ground level hyperspectral signature data
[AD-A195976] 24 p3386 N88-30166

PHOTOMETERS
NT ELECTROPHOTOMETERS
NT TOTAL OZONE MAPPING SPECTROMETER
NT ULTRAVIOLET SPECTROMETERS
NT ULTRAVIOLET SPECTROPHOTOMETERS
Direct detection of optical radiation through a sampling orifice for inductively coupled plasma atomic emission spectroscopy
[DE87-013609] 01 p0101 N88-10662
Comet West: A view from the HELIOS zodiacal light photometers 01 p0117 N88-10749
Optical probe
[EP-PATENT-0-210-869-A1] 05 p0650 N88-13984
Optical photometer for the Tirgo telescope
[IFSI-87-5] 05 p0650 N88-13985
Optical communication with semiconductor laser diodes
[NASA-CR-182464] 09 p1154 N88-16918
Growth of HgZnTe layers by LPE technique
[AD-A186723] 09 p1255 N88-17520
The photons payload, G-494: A learning experience 10 p1288 N88-17701
Remote sensing of atmospheric optical thickness and sea-water attenuation when submerged: Wavelength selection and anticipated errors
[AD-A187609] 11 p1548 N88-19262
Development of a high speed InGaAs/InP Schottky barrier photodetector for millimeter-wave fiber optical links
[AD-A188594] 12 p1629 N88-19750
Analysis of contamination data recorded by the IECM camera/photometer
[NASA-TM-100324] 14 p1882 N88-21246
An automated ozone photometer
[NASA-TM-100064] 14 p1908 N88-21404
Open questions in closed-loop photodetection 14 p1979 N88-21812
Thomson scattering for determining electron concentrations and temperatures in an inductively coupled plasma. 2: Description and evaluation of a multichannel instrument
[AD-A191324] 16 p2280 N88-23652
Characteristics, packaging and physics of ultra high speed diode lasers and detectors 19 p2658 N88-25797
Picosecond optical autocorrelation experiments on fast photodetectors 19 p2659 N88-25802
A survey of the Ap stars for rapid variability 20 p2884 N88-27127
Effect of interfacial phenomena on contact line heat Transfer-3
[AD-A194941] 24 p3343 N88-29901
High frequency GaAlAs modulator and photodetector for phased array antenna applications
[NASA-TM-101328] 24 p3367 N88-30048

PHOTOMETRY
NT ASTRONOMICAL PHOTOMETRY
NT ELECTROPHOTOMETRY
NT INFRARED PHOTOMETRY
NT SPECTROPHOTOMETRY
NT STELLAR SPECTROPHOTOMETRY
NT ULTRAVIOLET PHOTOMETRY
NT VISUAL PHOTOMETRY
Spectral analysis of APT RS CVn binary light curves 04 p0508 N88-13122
Starspots on the short-period RS CVn system SV Cam: 45 years of activity 04 p0508 N88-13123
The short-period RS CVn stars: Starspots and fundamental properties 04 p0508 N88-13124
Doppler snapshots 04 p0508 N88-13125
Titanium oxide absorption and spot sizes in II Peg, HR 1099 and UX Ari 04 p0508 N88-13126
Stellar cycle variability of solar-like stars: A sneak preview 04 p0510 N88-13136
Contemporaneous B,V,R,I photometry and H alpha spectroscopy of YY Gem 04 p0513 N88-13155
Brightness contrast and character height of five flat panel computer displays
[AD-A187743] 11 p1524 N88-19096
Zoom versus full-field sensitivity at the ETS (Experimental Test System)
[AD-A188162] 12 p1628 N88-19742
Photometry of P/Halley (1982): Is what we have learned useful for other comets? 14 p1998 N88-21909
Narrow-band photometry of Comet P/Giacobini-Zinner at the time of ICE encounter 14 p1998 N88-21911
Dust photometry in the near nucleus region of Comet Halley from VEGA-2 observations 14 p2001 N88-21930
Speckle interferometry of asteroids
[NASA-CR-180438] 15 p2151 N88-22843

PHOTOMICROGRAPHS
Storing photomicrographs on optical laser disks
[DE87-013747] 04 p0449 N88-12785

PHOTOMICROGRAPHY
Study of stainless steel time-temperature sensitization diagrams, part 1
[ETN-87-90762] 03 p0289 N88-11815
Improving knowledge of the corrosion behavior of aluminum alloys of the 7XXX series
[REPT-48-451/F] 18 p2486 N88-24750
Microstructural effects in static and dynamic numerical experiments
[DE88-004289] 20 p2813 N88-26690

PHOTOMULTIPLIER TUBES
Study of solid state photomultiplier
[NASA-CR-177465] 05 p0583 N88-13556
Streak camera dynamic range optimization
[DE88-001632] 05 p0586 N88-13571
Signal processing studies program optical signal amplification, volume 1
[AD-A188055] 10 p1321 N88-17897
The off-axis channel macroplate
[NASA-CR-182938] 18 p2505 N88-24861
Array detectors for plasma spectrochemistry
[AD-A194220] 22 p3052 N88-28105

PHOTON BEAMS
National Synchrotron Light Source users manual: Guide to the VUV and X-ray beam lines
[DE88-001464] 04 p0490 N88-13020
Theory of two-photon emission from atomic inner shells
[AD-A187742] 11 p1543 N88-19223
Experimental set-up for measurements of Compton scattering cross section on light nuclei
[DE88-700161] 12 p1688 N88-20097
Correlations between photons in resonance fluorescence emitted by an atom near a metal surface
[AD-A188365] 12 p1689 N88-20102
Synchronous measurements of effective photon path length in visible and near-IR spectral regions in real cloud systems 13 p1790 N88-20706

PHOTONIC PROPULSION
NT LASER PROPULSION

PHOTONIC SWITCHING
U OPTICAL SWITCHING

PHOTONICS
Image sharpening observations of active galactic nuclei 01 p0098 N88-10643
A new technique for rocket and space-borne investigations of time-dependant auroral morphology 08 p1030 N88-16241
Multichannel anisotropic single-mode fiber optics for transducers 09 p1240 N88-17429

PHOTONS
Theoretical atomic and molecular photophysics
[DE87-014249] 02 p0231 N88-11458
Families of Bose rays in quantum optics
[DE87-014584] 02 p0236 N88-11489
XeCl excimer laser induced multiphoton ionization of ammonia molecule 03 p0299 N88-11883
High energy experimental physics
[DE87-013516] 03 p0376 N88-12363
Gamma ray lines from novae 04 p0526 N88-13214
Study of solid state photomultiplier
[NASA-CR-177465] 05 p0583 N88-13556
Photon counting image sensor development for astronomical applications
[NASA-CR-181507] 05 p0660 N88-14049
Photon stimulated desorption from oxidized Al(110)
[DE88-002209] 06 p0787 N88-14828
Monte Carlo photon transport on vector and parallel supercomputers
[DE88-002503] 07 p0905 N88-15486
Time characteristics of travelling wave lasing with two-photon picosecond optical pumping 07 p0918 N88-15578
Relativistic corrections for one- and two-photon matrix elements of weakly-bound systems
[NOTA-INTERNA-884] 07 p0929 N88-15645
Two-photon exclusive meson production at large angles
[NIKHEF-H/87-4] 08 p1081 N88-16515
Status of cross section data for photon scattering by atoms
[DE87-011281] 08 p1081 N88-16517
Memory effects on infrared adsorbate spectra
[AD-A186976] 09 p1253 N88-17512
Performance of a photon counting microchannel plate intensifier with wedge and strip image readout
[DE88-003831] 10 p1334 N88-17970
Application of state-multipole Heisenberg equations to Raman excitation dynamics
[DE88-003828] 10 p1335 N88-17977
The development of emission tomography for the nuclear industry
[AERE-R-12319] 10 p1341 N88-18014
Photonic temperature and pressure sensors for biosystems/pulsed microwave. Part 1: Interaction studies
[AD-A188887] 12 p1629 N88-19751
Proof of the feasibility of coherent and incoherent schemes for pumping a gamma-ray laser
[AD-A189238] 13 p1774 N88-20613
The use of four-photon Raman spectroscopy for the remote sensing of natural objects
[NASA-TT-20257] 13 p1791 N88-20716
The magnitude of secondary electron contributions in photon stimulated desorption
[AD-A189094] 13 p1835 N88-20980
Diffraction theory in QCD and beyond
[DE88-005958] 13 p1837 N88-20992
The response of a small liquid scintillation counter for low energy (gamma, p) experiments
[NOTA-INTERNA-901] 14 p1980 N88-21819
Measurement of the sup 4He(gamma, p)sup 3H total cross section and charge symmetry
[NOTA-INTERNA-902] 14 p1981 N88-21820
Cosmology for high energy physicists
[DE88-005705] 15 p2151 N88-22842
The position-sensitive counting of photons 16 p2271 N88-23590
Bimolecular reactions and energy-transfer processes of highly vibrationally excited molecules related to energetic materials
[AD-A189013] 18 p2571 N88-25270
Prospects for large dynamic range isotope analysis using photon burst mass spectrometry
[DE88-009110] 19 p2613 N88-25505

Third International Conference on Superlattices, Microstructures and Microdevices
[AD-A191416] 20 p2861 N88-26995
Infrared detectors based on the photon drag effect and intersubband absorption by a two-dimensional electron gas 20 p2867 N88-27024
Investigation of non-classical effects in two-photon interference processes 23 p3282 N88-29541
Intramolecular dynamics: A study of molecules at high levels of vibrational excitation
[AD-A195285] 24 p3428 N88-30400

PHOTONUCLEAR REACTIONS
Photon-assisted formation and cooling of molecular hydrogen
[MP-87-102] 16 p2267 N88-23563

PHOTOOXIDATION
Theoretical bases of polymer photodegradation and photooxidation
[AD-A186533] 08 p0974 N88-15889
Structure and function of the manganese complex involved in photosynthetic oxygen evolution determined by X-ray adsorption spectroscopy and electron paramagnetic resonance spectroscopy
[DE88-010360] 21 p2985 N88-27725

PHOTORECEPTORS
Laboratory equipment update
[AD-A189781] 15 p2102 N88-22522
Regulatory biochemical and metabolic responses in photoreceptors
[AD-A192898] 20 p2831 N88-26794
Limits of pattern discrimination in human vision
[AD-A193449] 23 p3239 N88-29273

PHOTORECONNAISSANCE
A review of computer-assisted photo interpretation research at USAETL (US Army Engineer Topographic Laboratories)
[AD-A184034] 03 p0346 N88-12186
Space applications in geography
08 p1007 N88-16104
Classification of small image areas by digital correlation for the connection of different images in photogrammetry and long-range reconnaissance
[ETN-88-91506] 14 p1940 N88-21578

PHOTOREDUCTION
U PHOTOCHEMICAL REACTIONS

PHOTORESISTIVITY
U PHOTOCONDUCTIVITY

PHOTORESISTORS
U PHOTOCONDUCTORS

PHOTOSENSITIVITY
NT LIGHT ADAPTATION
NT PHOTOTROPISM
Develop techniques for ion implantation of (lead-lanthanum-zirconate-titanate) for adaptive optics
[DE88-000642] 05 p0650 N88-13986
Nanosecond laser photolysis of opaque heterogeneous photosensitizers
[AD-A191424] 16 p2213 N88-23209
Dynamic range compression/expansion of light beams by photorefractive crystals
[NASA-CASE-NPO-17140-1-CU]
17 p2438 N88-24508

PHOTOSENSORS
U PHOTOELECTRICITY
U RADIATION MEASURING INSTRUMENTS

PHOTOSPHERE
NT SOLAR GRANULATION
Magnetic field twist driven by remote convective motions: Characteristics and twist rates 01 p0113 N88-10724
Spectroscopy and nonthermal processes
02 p0252 N88-11594
Thermal atmospheric models
02 p0253 N88-11599
Quasi-thermal models 02 p0253 N88-11600
Active region flows 02 p0255 N88-11611
Coronal magnetic fields produced by photospheric shear
[NASA-CR-181514] 03 p0390 N88-12447
Empirical relations between photospheric magnetic fields and atmospheric radiative losses for cool dwarf stars 04 p0511 N88-13145
An analysis of the photospheric line profiles in F, G, and K supergiants 04 p0513 N88-13157
New results from high angular resolution observations of alpha Ori 04 p0514 N88-13161
Emission features in IRAS LRS spectra of MS, S and CS stars 04 p0514 N88-13163
IUE observations of the hybrid K3 II star Iota Aurigae and constraints on the outer atmospheric structure
04 p0516 N88-13171
Solar flares and magnetic topology
[AD-A188692] 12 p1712 N88-20244
More than a solar cycle of synoptic solar and coronal data: A video presentation
[NASA-CR-181459] 23 p3308 N88-29708

PHOTOSYNTHESIS
Photocatalytic electrochemistry at a biological-membrane metal-colloid interface
[DE87-009122] 02 p0166 N88-11041
Operation of an experimental algal gas exchanger for use in a CELSS 03 p0358 N88-12255
Application of photosynthetic N(2)-fixing cyanobacteria to the CELSS program 03 p0358 N88-12257
A review of recent activities in the NASA CELSS program 03 p0359 N88-12259
Fundamental study on gas monitoring in CELSS
03 p0359 N88-12263
Study of the relationship between photosynthesis, respiration, transpiration, and mineral nutrition in wheat
03 p0360 N88-12268
Utilization of potatoes in bioregenerative life support systems 03 p0360 N88-12269
Wheat production in controlled environments
[UAES-PAPER-3324] 03 p0361 N88-12270
Artificial photosynthesis using chlorophyll based carotenoid-quinone triads
[DE88-001660] 07 p0884 N88-15362
Factors governing light driven electron and proton translocation in proteins across membranes
[DE88-002716] 08 p1082 N88-16519
Picosecond laser spectroscopy of charge-separation in photosynthetic model systems
[DE88-003122] 09 p1172 N88-17028
Energy transfer and photochemistry in biomimetic solar conversion
[PB88-130026] 10 p1348 N88-18057
Research on a solar biotechnology based on the culture of photosynthetic cells
[DE88-900129] 10 p1359 N88-18120
Spectroscopic studies of energy transfer in photosynthetic reaction centers of higher plants
[DE88-003850] 10 p1359 N88-18121
The evolution of glutathione metabolism in phototrophic microorganisms
[NASA-CR-182902] 19 p2695 N88-26015
Mechanisms of photochemical energy conversion by chlorophyll
[DE88-008763] 20 p2819 N88-26725
Photosynthetic water splitting
[DE88-007809] 20 p2830 N88-26791
Modeling the primary events of photosynthesis using chlorophyll containing fixed distance donor-acceptor molecules
[DE88-010033] 20 p2831 N88-26793
Factors governing light driven electron and proton translocation in proteins across membranes
[DE88-011120] 21 p2984 N88-27724
Structure and function of the manganese complex involved in photosynthetic oxygen evolution determined by X-ray adsorption spectroscopy and electron paramagnetic resonance spectroscopy
[DE88-010360] 21 p2985 N88-27725
Electrochemical and optical studies of model photosynthetic systems
[DE88-009291] 23 p3237 N88-29264

PHOTOTHERMAL CONVERSION
Pulsed laser photothermal spectroscopy of liquids and solids
[DE88-003839] 11 p1455 N88-18675
Thermophotovoltaic space power system, phase 3
[NASA-CR-179327] 14 p1942 N88-21585
Photochemical and thermal modeling in the early atmosphere of the earth
[NASA-CR-183029] 18 p2543 N88-25093
Noncontact photo-thermal sensing
[AD-A195450] 24 p3344 N88-29905

PHOTOTHERMOTROPISM
U ANISOTROPY
U PHOTOTROPISM
U TEMPERATURE EFFECTS

PHOTOTROPISM
The evolution of glutathione metabolism in phototrophic microorganisms
[NASA-CR-182902] 19 p2695 N88-26015

PHOTOTUBES
NT PHOTOMULTIPLIER TUBES

PHOTOVOLTAIC CELLS
NT SOLAR CELLS
NT VERTICAL JUNCTION SOLAR CELLS
The fundamentals of photovoltaic system electrical design
[DE87-009061] 02 p0194 N88-11214
Photovoltaic power modules for NASA's manned space station
[NASA-TM-100229] 03 p0277 N88-11745
Polymers in solar technologies
[DE88-001102] 03 p0294 N88-11849
Recent progress in space photovoltaic systems
[NASA-TM-100208] 03 p0311 N88-11966
Electricity from photovoltaic solar cells. Flat-Plate Solar Array Project of the US Department of Energy's National Photovoltaics Program: 10 years of progress
[NASA-TM-89653] 03 p0346 N88-12188
Low Earth orbit environmental effects on the space station photovoltaic power generation systems
[NASA-TM-100230] 03 p0387 N88-12429
Light funnel concentrator panel for solar power
[NASA-CR-179223] 04 p0464 N88-12870
Design description report for a photovoltaic power system for a remote satellite earth terminal
[NASA-CR-179586] 04 p0465 N88-12875
Radiation performance of AlGaAs concentrator cells and expected performance of cascade structures
[NASA-TM-100145] 04 p0465 N88-12878
Oxidation and protection of fiberglass-epoxy composite masts for photovoltaic arrays in the low Earth orbital environment
[NASA-TM-100839] 11 p1465 N88-18734
PbSnTe photovoltaic detectors for operation in the 2-14 micron band
[INPE-4252-PRE/1125] 11 p1508 N88-19008
Proceedings of the 1987 High-Efficiency Photovoltaic Subcontractors' Review Meeting
[DE88-003354] 11 p1508 N88-19011
Development of integrated detectors for attitude sensors
[INPE-4409-PRE/1222] 12 p1602 N88-19586
Mast material test program (MAMATEP)
[NASA-TM-100821] 12 p1604 N88-19592
Characterization of integrated photovoltaic detectors for MECB solar sensors
[INPE-4408-PRE/1221] 12 p1630 N88-19754
Concentrating photovoltaic collectors: Fabrication design
[PB88-148051] 12 p1640 N88-19821
SERI's Photovoltaic R and D Project: Recent progress and future directions
[DE88-001129] 13 p1794 N88-20728
Control strategies and hardware used in solar thermal applications
[DE88-004631] 13 p1794 N88-20731
Progress of amorphous silicon based solar cells and modules
[DE88-004666] 13 p1794 N88-20733
Crystalline photovoltaic cell technology: Present and future
[DE88-004684] 13 p1795 N88-20734
Power systems for production, construction, life support and operations in space
[NASA-TM-100838] 14 p1883 N88-21254
Recent advances in photovoltaic concentrator technology
[DE88-003948] 15 p2091 N88-22462
An integrated and modular digital modeling approach for the space station electrical power system development
[NASA-TM-100904] 16 p2170 N88-22935
Power source selection for neutral particle beam systems 17 p2407 N88-24314
Photovoltaic Advanced Research and Development Project, solar radiation research
[DE88-001143] 18 p2537 N88-25056
Advanced photovoltaic power system technology for lunar base applications
[NASA-TM-100965] 20 p2766 N88-26402
Photovoltaic concentrator technology: Recent results
[DE88-009588] 20 p2819 N88-26726
Photovoltaic cells with n-silicon and conductive polymers
[ETN-88-92133] 20 p2821 N88-26734
Growth and characterization of thin films of ZnSnP(sub)2
[DE88-001164] 20 p2874 N88-27060
Photovoltaic Energy. Electricity from Sunlight: A current awareness bulletin
[DE88-008289] 21 p2969 N88-27634
Reduced order modeling of grid-connected photovoltaic inverter systems
[DE88-010603] 21 p2969 N88-27635
SERI's photovoltaic research project: A foundation for tomorrow's utility-scale electricity
[DE88-001161] 23 p3230 N88-29220
Solar dynamic power systems
[ETN-88-92969] 23 p3230 N88-29224

PHOTOVOLTAIC CONVERSION
The preparation of thin films for photovoltaic conversion by novel MOCVD techniques
[DE87-001185] 02 p0194 N88-11212
SERI's Photovoltaic R and D Project: Recent progress and future directions
[DE88-001129] 13 p1794 N88-20728
Progress of amorphous silicon based solar cells and modules
[DE88-004666] 13 p1794 N88-20733

Thermophotovoltaic space power system, phase 3
[NASA-CR-179327] 14 p1942 N88-21585
Today's photovoltaic systems: An evaluation of their performance
[DE88-006926] 15 p2090 N88-22457
Three-dimensional models of conventional and vertical junction laser-photovoltaic energy converters
[NASA-TM-4039] 17 p2370 N88-24111
Photovoltaic Measurements and Performance Branch
[DE88-001142] 21 p2968 N88-27633

PHOTOVOLTAIC EFFECT
Photovoltaic energy systems
[DE88-007504] 19 p2687 N88-25968

PHTHALOCYANIN
Electrochromic cells with lutetium diphthalocyanine and semisolid polymer electrolytes
[AD-A188031] 10 p1352 N88-18078

PHUGOID OSCILLATIONS
U OSCILLATIONS
U OSCILLATORS
U PITCH (INCLINATION)

PHYSICAL CHEMISTRY
NT QUANTUM CHEMISTRY
A physico-chemical study of some areas of fundamental significance to biophysics
[DE87-013457] 02 p0217 N88-11365
Physico-chemical studies on copper sulfide behavior in the CdS-Cu2S solar cell
[ETN-88-91068] 09 p1187 N88-17109
Dry adhesive friction of elastomers: A study of the fundamental mechanical aspects
[ETN-88-92903] 23 p3198 N88-29036

PHYSICAL CONSTANTS TESTING REACTOR
U NUCLEAR RESEARCH AND TEST REACTORS

PHYSICAL ENDURANCE
U PHYSICAL FITNESS

PHYSICAL EXAMINATIONS
US civil airmen statistics, 1987
[AD-A191714] 18 p2455 N88-24577

PHYSICAL EXERCISE
Oxygen transport during exercise at extreme simulated altitude: Operation Everest 2
[AD-A185720] 06 p0752 N88-14620
Exercise in the heat: Effects of dinitrophenol administration
[AD-A185731] 06 p0752 N88-14622
Exercise thermoregulation after prolonged wakefulness
[AD-A186224] 08 p1048 N88-16327
Temperature regulation at rest and exercise during the human menstrual cycle
[AD-A186461] 08 p1050 N88-16341
Lipid peroxidation in rat tissues with exposure to antiorthostatic hypokinesia, exercise and immobilization stress 10 p1365 N88-18159
Effect of oxygen inhalation on respiratory function during exercise and exposure to added resistance to respiration 10 p1366 N88-18164
Oxidative enzyme activity in healthy subjects and individuals with neurocirculatory dystonia during graded exercise 10 p1367 N88-18170
Carbamates, atropine, and diazepam: Effects on performance in the running rat
[AD-A188009] 11 p1517 N88-19062
Manipulation of muscle glycogen concentrations using high and low carbohydrate diets and exercise
[AD-A187732] 11 p1519 N88-19069
Gastric emptying during exercise: Effects of acute heat stress, acclimation and hypohydration
[AD-A188008] 11 p1519 N88-19073
Heat acclimatization under controlled hyperthermia 12 p1665 N88-19981
Endocrine responses to resistance exercise
[AD-A188681] 12 p1667 N88-19993
Hypothalamic-pituitary-adrenal responses to short duration high intensity cycle exercise
[AD-A192597] 21 p2985 N88-27727
Metabolic and cardiorespiratory parameters during three consecutive days of exhaustive running
[AD-A192598] 21 p2985 N88-27728
Validation of a modified one-step rebreathing technique for measuring exercise cardiac output
[AD-A192600] 21 p2986 N88-27729
A resistive-film based force transducer for the study of exercise
[AD-A192601] 21 p2986 N88-27730
The role of textile material in clothing on thermoregulatory responses to intermittent exercise
[AD-A192599] 22 p3130 N88-28608
Depressed sweating during exercise at altitude
[AD-A192603] 22 p3130 N88-28609
The effects of acute cold exposure on exercise performance
[AD-A192650] 22 p3130 N88-28610
Influence of altitude and caffeine during rest and exercise on plasma levels of proenkephalin peptide F
[AD-A192659] 22 p3131 N88-28616
Effects of air polution on human exercise performance
[AD-A192660] 22 p3131 N88-28617

PHYSICAL FITNESS
Physiological determinants of load bearing capacity
[AD-A184977] 05 p0629 N88-13848
The use of heart rate in the prescription and evaluation of exercise programs
[AD-A186454] 08 p1049 N88-16336
Development of a coping strategies questionnaire to assess endurance performance
[AD-A188010] 11 p1520 N88-19074
Fish as a tool for testing fitness in space 12 p1662 N88-19963
Lifting and carrying capacities relative to physical fitness measures
[AD-A189305] 13 p1809 N88-20808
Prediction of physical fitness: Estimated percent body fat using body circumferences versus weight-height measures
[AD-A190233] 15 p2103 N88-22526
Dietary factors related to physical fitness
[AD-A190272] 15 p2103 N88-22527
Behavioral, psychological and demographic predictors of physical fitness
[AD-A192697] 21 p2986 N88-27733

PHYSICAL OPTICS
Theoretical Aspects of Target Classification
[AGARD-LS-152] 03 p0303 N88-11909
Physical optics method: Prediction of radar signatures 03 p0304 N88-11914
Theoretical aspects of target classification: Physical optics and radon transform methods 03 p0304 N88-11915
Large bandwidth ground scattering model --- radar scattering
[FOA-C-30458-3.2] 05 p0576 N88-13511
Scattering and depolarization by random rough terrain and vegetation covered terrain-unified full wave approach 12 p1615 N88-19657
Coherence effects in optical physics with special reference to spectroscopy
[AD-A189520] 13 p1840 N88-21007
Curvature of blended rolled edge reflectors at the shadow boundary contour
[NASA-CR-182974] 18 p2576 N88-25300

PHYSICAL WORK
Nystagmometric distinctions of individuals regularly exposed to vibration 07 p0891 N88-15401
Lifting and carrying capacities relative to physical fitness measures
[AD-A189305] 13 p1809 N88-20808
Simultaneous multiple control force exertion capabilities of males and females versus helicopter control force design limits
[AD-A191653] 18 p2553 N88-25153

PHYSICS
JPRS report: Science and technology. China
[JPRS-CST-88-003] 13 p1755 N88-20495
JPRS report: Science and technology. USSR: Physics and mathematics
[JPRS-UPM-88-001] 14 p1968 N88-21751

PHYSICS AND CHEMISTRY EXPERIMENT IN SPACE
The challenge of G-376 10 p1288 N88-17705

PHYSIOCHEMISTRY
A geometrical model for determining the physicochemical properties of ternary metallic systems
[BLL-M-37303-(5828.4)] 02 p0149 N88-10931
Physicochemical correlates of human adaptation to extreme environments 06 p0750 N88-14607
Controlled Ecological Life Support Systems (CELSS) physiochemical waste management systems evaluation
[NASA-CR-177422] 06 p0754 N88-14626

PHYSIOGRAPHY
U GEOMORPHOLOGY

PHYSIOLOGICAL DEFENSES
NT IMMUNE SYSTEMS

PHYSIOLOGICAL EFFECTS
NT HEMODYNAMIC RESPONSES
NT PHYSIOLOGICAL RESPONSES
Eyesight trainer for pilots 03 p0355 N88-12239
Human adaptation to isolated and confined environments
[NASA-CR-181502] 03 p0357 N88-12248
Change in functional activity of cortical brain structures and their blood supply in alert rabbits in response to rocking 04 p0473 N88-12916
Human respiratory responses during high performance flight
[AGARD-AG-312] 04 p0474 N88-12923
Effect of night watches and intermittent sleep on state of circadian rhythms of physiological functions of fishermen 06 p0750 N88-14610
Exercise in the heat: Effects of dinitrophenol administration
[AD-A185731] 06 p0752 N88-14622
Proceedings and program draft in Gravitational Biology in the Federal Republic of Germany --- Effects of Weightlessness on the Human Organism
[ESA-TT-988] 07 p0884 N88-15363
JPRS report: Science and technology. USSR: Space Biology and Aerospace Medicine, volume 21, no. 4, July - August 1987
[JPRS-USB-88-002] 07 p0893 N88-15412
Morphometric analysis of rat aorta endothelium during long-term hypokinesia 07 p0894 N88-15417
Changes in functional parameters of animals during long-term inhalation of acetic acid 07 p0895 N88-15423
Physiological and immunological aspects of human adaptation to temperature elevation in a closed environment 07 p0895 N88-15424
Results of research with biological satellites 08 p1006 N88-16097
Research on cotton plants grown in space 08 p1006 N88-16098
Scientific objectives and functional requirements of life sciences in the Space Station 08 p1033 N88-16264
Operation Everest 2: Comparison of four instruments for measuring blood oxygen saturation
[AD-A186456] 08 p1049 N88-16337
Ultra-low frequency vibration data acquisition concerns in operating flight simulators
[DE88-004795] 10 p1285 N88-17687
JPRS Report: Science and Technology. USSR: Space Biology and Aerospace Medicine, volume 21, no. 5, September - October 1987
[JPRS-USB-88-003] 10 p1359 N88-18122
Effect of spaceflight factors on primate's blood circulation 10 p1359 N88-18124
Inflight simian circadian rhythms and temperature homeostasis aboard Cosmos-1514 biosatellite 10 p1359 N88-18125
Effect of spaceflight factors on primate hydration homeostasis 10 p1360 N88-18126
Investigation of effects of short-term exposure to high concentrations of carbon monoxide on operator's psychophysiological functions 10 p1361 N88-18133
Results of long-term electrocardiographic monitoring of cosmonauts 10 p1364 N88-18152
Effect of spaceflight factors on biological material flown aboard Cosmos-1514 biosatellite 10 p1364 N88-18154
Lipid peroxidation in rat tissues with exposure to antiorthostatic hypokinesia, exercise and immobilization stress 10 p1365 N88-18159
Certain aspects of human metabolism during spaceflights of varying duration
[NASA-TT-20215] 10 p1369 N88-18181
Basic results of medical studies during prolonged manned flights on-board the Salyut-7/Soyuz-T orbital complex
[NASA-TT-20217] 10 p1369 N88-18182
Modeling of the non-auditory response to blast overpressure
[AD-A187397] 10 p1369 N88-18184
Effects of breathing air containing contaminants such as CO2, CO and hydrocarbons at 1 and 5 atmospheres
[PB88-132915] 11 p1521 N88-19084
Implications of shiftwork in space for human physiology experiments 12 p1659 N88-19942
Renal effects of anti-gravity suit inflation in man in relation to cardiovascular and hormonal changes 12 p1661 N88-19959
The suspended Japanese quail as an animal model for experiments related to microgravity 12 p1662 N88-19960
Facilitory effects of voluntary movements on vestibulomotor reaction 12 p1664 N88-19976
Air quality and human performance, chapter 16
[AD-A188335] 12 p1666 N88-19988
Medical problems related to altitude in: Human performance physiology and environmental medicine at terrestrial extremes, chapter 14
[AD-A188340] 12 p1666 N88-19989
Motion sickness: A study of its effects on human physiology
[AD-A188821] 12 p1667 N88-19995
Protection against laser damage to human body reviewed 15 p2053 N88-22237
A comparison of visual evoked potential and behavioral measures of flashblindness in humans
[AD-A189757] 15 p2101 N88-22519
Age, alcohol, and simulated altitude: Effects on performance and breathalyzer scores
[AD-A190642] 15 p2103 N88-22531
Behavior, physiology and energy deposition in rats chronically exposed to 2450 MHz radiation
[PB88-171418] 16 p2237 N88-23363

Effects of moderate cold and heat stress on the potential work performance of industrial workers. Part 6: The effects of increasing vapour pressure at four air temperatures on the performance and physiology of white females
[PB88-124854] 18 p2550 N88-25137
Physiological and hematological responses of matched older and younger men during dry-heat acclimation
[AD-A186450] 18 p2550 N88-25139
Physiological effects on man of long duration confinement in a carbon dioxide enriched environment
19 p2695 N88-26017
Experience in occupational medicine, derived from 16 operational deep saturation trimix 5 dives in GUSI from 150 to 600 m 19 p2695 N88-26018
Effect of low-frequency whole-body vertical vibration on the serotoninergic system of the brain and spinal cord
19 p2704 N88-26081
Effect of long-term inhalation of acetic acid vapor on some functional parameters of man
19 p2705 N88-26084
Physiological monitoring methodology in the USAFSAM centrifuge 21 p2924 N88-27356
Hyperthermia: New thoughts on an old problem
[AD-A192602] 21 p2986 N88-27731
Simulator sickness in the AH-64 Apache combat mission simulator
[AD-A193419] 21 p2988 N88-27739
Human acclimatization and physical performance at high altitude
[AD-A192651] 22 p3130 N88-28611
Physiological effects of extremely low frequency electric and magnetic fields
[DE88-752814] 22 p3132 N88-28620
USAF hyperbaric animal transfer chamber system
[AD-A193633] 23 p3237 N88-29265
Effect of hypoxia on speech recognition in noise
[AD-A193943] 23 p3240 N88-29280
Nutrient requirements for high stress environments
[AD-A194595] 23 p3243 N88-29301

PHYSIOLOGICAL RESPONSES
NT HEMODYNAMIC RESPONSES
Determination of the individual state of acclimatization
[IZF-1986-27] 01 p0075 N88-10478
Human thermoregulatory model for whole body immersion in water at 20 and 28 C
[AD-A185052] 05 p0629 N88-13849
Maximal cardiorespiratory responses to one- and two-legged cycling during acute and long-term exposure to 4300m
[AD-A185730] 06 p0752 N88-14621
Measurement and modification of sensorimotor system function during visual-motor performance
[AD-A186351] 07 p0889 N88-15387
Mother-fetus system as object for investigation of mechanisms of physiological effect of weightlessness
07 p0891 N88-15402
Combined effect of microwaves and ionizing radiation
07 p0893 N88-15413
Circulatory response of males 45-52 years of age to antiorthostatic hypokinesia 07 p0894 N88-15416
Nucleic acid content of skeletal muscles during hypokinesia and in the recovery period
07 p0894 N88-15418
Changes in regional and central hemodynamics during seven-day water immersion 07 p0895 N88-15421
Effect of intermittent hypercapnia on visual analyzer function 07 p0896 N88-15431
Mononuclear phagocytes during adaptation of essentially healthy people to high altitudes
07 p0896 N88-15432
Prediction of human thermoregulatory responses and endurance time in water at 20 and 24C
[AD-A186223] 08 p1048 N88-16326
Exercise thermoregulation after prolonged wakefulness
[AD-A186224] 08 p1048 N88-16327
Influence of skeletal muscle glycogen on passive rewarming after hypothermia
[AD-A186451] 08 p1049 N88-16334
Determination of the effect of walking on the forced convective heat transfer coefficient using an articulated mannikin
[AD-A186452] 08 p1049 N88-16335
The use of heart rate in the prescription and evaluation of exercise programs
[AD-A186454] 08 p1049 N88-16336
Portable, ambient air microclimate cooling in simulated desert and tropic conditions
[AD-A186457] 08 p1050 N88-16338
Rapid hypothermia subsequent to oral nicotinic acid and immersion in warm (30C) water
[AD-A186458] 08 p1050 N88-16339
Respiratory and cardiovascular responses to cold stress following repeated cold water immersion
[AD-A186460] 08 p1050 N88-16340
Temperature regulation at rest and exercise during the human menstrual cycle
[AD-A186461] 08 p1050 N88-16341
A-scan ultrasound measurement of ocular changes during accommodation
[AD-A186818] 09 p1198 N88-17181
Role of body fat in the prediction of the metabolic response for immersion in cold water
[AD-A186914] 09 p1198 N88-17182
Physiological and ecological implications of coupled heat- and water-transport mechanisms of endotherms and vegetation
[DE88-004170] 10 p1352 N88-18081
Membrane model of cupula or vestibular semicircular canals 10 p1361 N88-18132
Comparative evaluation of stress repsonse of rats to different methods of simulating some effects of weightlessness 10 p1363 N88-18144
Second All-Union Conference on Physiology of Extreme States and Individual Protection of Man
10 p1363 N88-18147
JPRS Report: Science and Technology. USSR: Space Biology and Aerospace Medicine, volume 21, no. 6, November - December 1987
[JPRS-USB-88-004] 10 p1364 N88-18150
Polar worker adaptability to Antarctic high altitudes
10 p1366 N88-18165
Effect of hypercapnic-hypoxic test on cariorespiratory parameters of individuals with neurocirculatory dystonia
10 p1367 N88-18169
Hemodynamic effects of beta-adrenergic blocking with obsidan in clinostatic and orthostatic positions
10 p1367 N88-18171
Supersonic and subsonic aircraft noise effects on animals: A literature survey
[AD-A186922] 10 p1404 N88-18373
Role of adenosine analogs and growth hormone in waking and sleep
[AD-A187897] 11 p1519 N88-19070
Operation Everest 2: Alterations in the immune system at high altitude
[AD-A188011] 11 p1520 N88-19075
Regulation of calcium metabolism during prolonged antiorthostatic hypokinesia
[NASA-TT-20219] 11 p1521 N88-19085
Changes in hemostasis system of animals under conditions of granulocytopoiesis inhibition under effect of decreased barometric pressure
12 p1651 N88-19890
Acute mountain sickness at 4500 m is not altered by repeated eight-hour exposures to 3200-3550 m normobaric hypoxic equivalent
[AD-A188358] 12 p1666 N88-19990
Neurohumoral aspects of sleep
[AD-A188853] 12 p1667 N88-19992
Endocrine responses to resistance exercise
[AD-A188581] 12 p1667 N88-19993
Plasma cortisol, renin and aldosterone during an intense heat acclimation program
[AD-A189387] 13 p1809 N88-20810
A program for the study of skeletal muscle catabolism following physical trauma
[AD-A189771] 15 p2102 N88-22521
Complex sound processing: An interdisciplinary approach
[AD-A189782] 15 p2102 N88-22523
Behavioral response of rats exposed to high-power microwave radiation
[AD-A192199] 18 p2548 N88-25128
A systems engineering based methodology for analyzing human electrocortical responses
[AD-A190809] 18 p2550 N88-25135
Extremely Low Frequency (ELF) communications program: Non-ionizing electromagnetic radiation literature evaluation and assessment, 1986-1987 literature review
[AD-A192024] 19 p2642 N88-25677
Method of assessing changes in biorhythmological structure of human physiological functions
19 p2706 N88-26088
Contra- and ipsilateral auditory stimuli produce different activation patterns at the human auditory cortex: A neuromagnetic study
[PB88-181490] 19 p2708 N88-26098
Regulatory biochemical and metabolic responses in photoreceptors
[AD-A192898] 20 p2831 N88-26794
Human response to prolonged motionless suspension in four types of full body harnesses
21 p2929 N88-27387
Electric and Magnetic Activity of the Central Nervous System: Research and Clinical Applications in Aerospace Medicine
[AGARD-CP-432] 21 p2977 N88-27683
The interaction of thalamo-cortical systems in the 40 Hz following response 21 p2979 N88-27694
A study of sources in the human brain associated with stereopsis 21 p2979 N88-27695
Cognitive task demands as reflected in physiological measures 21 p2980 N88-27699
Hypothalamic-pituitary-adrenal responses to short duration high intensity cycle exercise
[AD-A192597] 21 p2985 N88-27727
Physiological responses to acute exercise-heat stress
[AD-A192606] 21 p2986 N88-27732
Behavioral effects of exposure to the tempo high-power microwave system
[AD-A193305] 21 p2987 N88-27738
Plasma volume expansion in rats: Effects on thermoregulation and exercise
[AD-A192658] 22 p3130 N88-28606
Physiology of prolonged bed rest
[NASA-TM-101010] 22 p3130 N88-28607
The role of textile material in clothing on thermoregulatory responses to intermittent exercise
[AD-A192599] 22 p3130 N88-28608
Hierarchical structure in polymeric solids and its influence on properties
[AD-A194720] 23 p3197 N88-29029
Low doses of atropine sulfate impair retention of a well-learned spatial task
[AD-A194065] 23 p3237 N88-29266
Central adrenergic receptors as mediators of central response to stress: Study with Positron Emission Tomography (PET)
[AD-A194947] 24 p3407 N88-30284

PHYSIOLOGICAL TELEMETRY
U BIOTELEMETRY

PHYSIOLOGICAL TESTS
NT BODY SWAY TEST
NT VESTIBULAR TESTS
Determination of the individual state of acclimatization
[IZF-1986-27] 01 p0075 N88-10478
Measuring functional feasibility of human visual system 12 p1665 N88-19983
Literature review: Validity and potential usefulness of psychomotor ability tests for personnel selection and classification
[AD-A193558] 23 p3241 N88-29287

PHYSIOLOGY
NT AUDIOLOGY
NT ELECTROPHYSIOLOGY
NT EXERCISE PHYSIOLOGY
NT GRAVITATIONAL PHYSIOLOGY
NT MENSTRUATION
NT NEUROPHYSIOLOGY
NT PSYCHOPHYSIOLOGY
NT RESPIRATORY PHYSIOLOGY
NT UNDERWATER PHYSIOLOGY
NT WORKLOADS (PSYCHOPHYSIOLOGY)
JPRS report: Science and technology. USSR: Life sciences
[JPRS-ULS-87-012] 03 p0355 N88-12238
JPRS report: Science and technology. USSR: Life sciences
[JPRS-ULS-87-009] 04 p0473 N88-12915
JPRS report: Science and technology. USSR: Life sciences
[JPRS-ULS-87-011] 06 p0749 N88-14601
JPRS report: Science and technology. USSR: Life sciences
[JPRS-ULS-87-013] 06 p0750 N88-14608
USSR report: Life sciences. Biomedical and behavioral sciences
[JPRS-UBB-86-022] 08 p1046 N88-16318
Ultra-low frequency vibration data acquisition concerns in operating flight simulators
[DE88-004795] 10 p1285 N88-17687
Evaluation of spare room in cerebrospinal system using noninvasive methods 10 p1361 N88-18137
Scaling physiological pharmacokinetic models by physiological time
[DE88-000335] 10 p1368 N88-18173
USSR report: Life sciences. Biomedical and behavioral sciences
[JPRS-UBB-87-008] 12 p1662 N88-19966
JPRS report: Science and technology. USSR: Life sciences
[JPRS-ULS-88-009] 20 p2829 N88-26785
Squid instrumentation for neuromagnetic study of complex brain activity 21 p2978 N88-27691
Using IMSL mathematical and statistical computer subroutines in physiological and biomechanical research
[AD-A192594] 21 p2995 N88-27765
Vision and visual protection in fast jet aircraft
23 p3241 N88-29292
Comparison of morning with afternoon nitrogen elimination in resting subjects breathing 100 percent oxygen
[AD-A196191] 24 p3407 N88-30282

PHYTOPLANKTON
Thematic mapper research in the earth sciences: Small scale patches of suspended matter and phytoplankton in the Elbe River Estuary, German Bight and Tidal Flats
[NASA-CR-182378] 08 p1019 N88-16180
Research on influence of individual sea water components on spectral brightness coefficient of outgoing radiation 13 p1785 N88-20682
Biological processes in the water column of the South Atlantic bight: Zooplankton responses
[DE88-004811] 14 p1951 N88-21630
PICKOFFS
U SENSORS
PICKUPS
U SENSORS
PICOSECOND PULSES
Powerful picosecond ultraviolet laser output at 354.7 nanometers 03 p0327 N88-12063
Phase phenomena in parametric generators and amplifiers of ultrashort light pulses 07 p0918 N88-15576
Time characteristics of travelling wave lasing with two-photon picosecond optical pumping 07 p0918 N88-15578
Increasing time resolution of picosecond absorption spectrometer by selection of length of laser light pulses 07 p0919 N88-15579
Stimulated Raman scattering of picosecond light pulses in long dispersive medium 08 p1078 N88-16498
Kinetics and spectrum of light pulse used in picosecond holography 09 p1236 N88-17409
Subpicosecond optical digital computation using phase conjugate parametric generators
[AD-A188279] 10 p1410 N88-18411
Time characteristics of ultrashort light pulses from dye lasers with distributed feedback 14 p1970 N88-21759
Nonlinear stage of ultrashort-pulse formation in solid-state laser 14 p1971 N88-21765
Investigation of ultrashort traveling-wave amplified spontaneous emission 16 p2187 N88-23040
Picosecond sampling of integrated circuits 19 p2655 N88-25767
Picosecond electrical pulses for VLSI electronics characterization 19 p2655 N88-25768
Picosecond photoconductive transceivers 19 p2656 N88-25777
Photoconductive generation of sub-picosecond electrical pulses and their measurement applications 19 p2656 N88-25778
Picosecond switching in Josephson tunnel junctions 19 p2657 N88-25780
High speed, high repetition rate, high voltage photoconductive switching 19 p2657 N88-25781
Generation and forming of ultrashort high voltage pulses 19 p2657 N88-25782
A simple technique to generate or gate microwave pulses with picosecond speeds 19 p2657 N88-25784
Investigation of photoconductive picosecond microstripline switches on self-implanted Silicon On Sapphire (SOS) 19 p2657 N88-25789
Picosecond optoelectronic switches using composite electronic materials 19 p2658 N88-25792
Comparison of sampling oscilloscopes with less than 35 ps transition durations 19 p2658 N88-25793
A technique for wing suppressed IR sampling 19 p2658 N88-25794
Picosecond measurements of gain-switching in a semiconductor laser driven by ultrashort electrical pulses 19 p2658 N88-25800
Picosecond optical autocorrelation experiments on fast photodetectors 19 p2659 N88-25802
Picosecond carrier transport in GaAs quantum wells 19 p2660 N88-25813
A new optoelectronic CW microwave source 19 p2660 N88-25818
Picosecond response of an optically controlled millimeter wave phase shifter 19 p2660 N88-25820
Electron device probing in the femtosecond time scale 19 p2660 N88-25821
Electrical pulse compression by traveling-wave photoconductivity 19 p2661 N88-25822
Picosecond optoelectronic study of a thin film transmission line structure 19 p2661 N88-25823
Radial compression of picosecond electrical pulses
[DE88-008440] 21 p2953 N88-27544
A deconvolution technique using least-squares model-fitting and its application to optical pulse measurement
[NPL-DES-87] 22 p3144 N88-28694
PICTURE ELEMENTS
U PIXELS
PIEDMONTS
Delineation of ephemeral fluvial networks on low-relief Piedmont surfaces, Plutonium Valley, Nevada, USA 22 p3093 N88-28367
PIERCING
Numerical simulation of the perforation of thin plates
[ISL-R-122/86] 11 p1495 N88-18926
Phenomenological piercing characteristics of composite materials 14 p1895 N88-21315
PIERS
U WHARVES
PIEZOELECTRIC CERAMICS
NT LEAD ZIRCONATE TITANATES
United States - Japan Workshop on Dielectric and Piezoelectric Ceramics (3rd) held in Toyama, Japan on November 9-12, 1986
[AD-A185113] 05 p0568 N88-13460
Waves and vibrations in elastic superlattice composites 06 p0776 N88-14765
Contemporary ceramics and the new technological revolution 14 p1902 N88-21363
Effect of uniaxial compression on physical and mechanical properties of ferroelectric ceramic material 16 p2180 N88-22993
Piezoelectric and electrostrictive materials for transducer applications, volume 3
[AD-A194949] 24 p3377 N88-30112
PIEZOELECTRIC CRYSTALS
Defect characterization in quartz and related materials
[AD-A184754] 03 p0294 N88-11846
A dynamic analysis of piezoelectric strained elements
[AD-A191478] 18 p2503 N88-24851
A dynamic analysis of piezoelectric strained elements
[AD-A196079] 24 p3432 N88-30430
PIEZOELECTRIC GAGES
Polymer materials for pressure sensors 06 p0676 N88-14141
Zeroshift of piezoelectric accelerometers in pyroshock measurements 08 p0997 N88-16039
PIEZOELECTRIC TRANSDUCERS
NT PIEZOELECTRIC GAGES
Active control of flexural vibrations in beams 06 p0794 N88-14866
User manual for ATILA, a finite-element code for modeling piezoelectric transducers
[AD-A185948] 07 p0847 N88-15141
Ferroelectric properties and impact behavior of the PVF2 polymer and the VF2/C2F3H polarized copolymers --- vinylidene polyfluorides
[ISL-CO-245/86] 08 p0971 N88-15876
New wide-band transducer developed 14 p1901 N88-21353
PIEZOELECTRICITY
Fabrication of standardized piezoelectric polymer shock gauges by the Bauer method
[DE87-012738] 01 p0049 N88-10315
Developments in electronics ceramics reported 06 p0684 N88-14192
Analytical investigations of bulk wave resonators in the piezoelectric thin film on gallium-arsenide configuration
[AD-A185716] 06 p0789 N88-14840
Piezoelectric laminates for torsional and bending model control: Theory and experiment 10 p1343 N88-18029
Recent progress in the dynamic applications of piezoelectric crystals 10 p1417 N88-18460
Piezoelectric polymer tactile sensor arrays for robotics
[AD-A188852] 12 p1634 N88-19780
Development of polymeric films with piezoelectrical properties from polypeptides; low, odd nylons; or polyureas
[AD-A190301] 15 p2044 N88-22181
A compact high resolution piezoresistive digital tactile sensor
[DE88-000430] 16 p2210 N88-23188
Piezoelectric pushers for active vibration control of rotating machinery 16 p2218 N88-23229
Characterization of noncontact piezoelectric transducer with conically shaped piezoelement
[NASA-CR-4151] 17 p2347 N88-23987
Dynamic consolidation of metal powders
[AD-A192126] 18 p2485 N88-24744
Zinc-oxide thin films for integrated-sensor applications 19 p2673 N88-25896
Piezoelectric effects in strained layer superlattices 20 p2863 N88-27002
Piezoelectric and electrostrictive materials for transducer applications, volume 1
[AD-A194957] 24 p3374 N88-30096
Piezoelectric and electrostrictive materials for transducer applications, volume 2
[AD-A194956] 24 p3376 N88-30104
Piezoelectric and electrostrictive materials for transducer applications, volume 3
[AD-A194949] 24 p3377 N88-30112
PIEZORESISTIVE TRANSDUCERS
NT PIEZOELECTRIC GAGES
Characteristics of polysilicon layers and their application in sensors 19 p2669 N88-25861
Design and construction techniques for planar polysilicon pressure transducers with piezoresistive read-out 19 p2669 N88-25862
Integrated polysilicon tactile sensor 19 p2669 N88-25863
Noise in piezoresistive and capacitive sensors 19 p2670 N88-25874
Simulation of diaphragm-type IC pressure sensors 19 p2672 N88-25887
PIGMENTS
NT CAROTENE
NT CHLOROPHYLLS
NT CYTOCHROMES
Artificial photosynthesis using chlorophyll based carotenoid-quinone triads
[DE88-001660] 07 p0884 N88-15362
Optimization of binary pigment coatings
[AD-A189103] 13 p1748 N88-20450
PILE FOUNDATIONS
Breaking wave forces on vertical cylinders
[RR-CE71] 03 p0338 N88-12126
PILOT ERROR
Brain activity during tactical decision-making. Part 2: Probe-evoked potentials and workload
[AD-A188688] 12 p1667 N88-19994
Aircraft accident report: Northwest Airlines, Inc., McDonnell Douglas DC-9-82, N312RC, Detroit Metropolitan Wayne County Airport, Romulus, Michigan, August 16, 1987
[PB88-910406] 19 p2601 N88-25449
Research on piloting under conditions of breakdown in flight
[PB87-217980] 19 p2710 N88-26102
PILOT PERFORMANCE
Investigation of interactions between limb-manipulator dynamics and effective vehicle roll control characteristics
[NASA-CR-3983] 01 p0007 N88-10039
Report of safety survey: Human integration of approach charts
[DOT/FAA/PM-87/15] 01 p0076 N88-10488
A research on pilot performance in the case of aircraft malfunction
[ETN-87-90652] 02 p0217 N88-11369
A research on pilot performance in a flight incident situation
[ETN-87-90653] 02 p0217 N88-11370
An aerodynamic performance evaluation of the NASA/Ames Research Center advanced concepts flight simulator
[NASA-TM-89659] 03 p0268 N88-11685
Eyesight trainer for pilots 03 p0355 N88-12239
Investigation of pilot behavior in a training program for assessing handling qualities using a ground simulator
[ESA-TT-999] 03 p0357 N88-12247
Effect of motion cues during complex curved approach and landing tasks: A piloted simulation study
[NASA-TP-2773] 04 p0398 N88-12480
Some data processing requirements for precision Nap-Of-the-Earth (NOE) guidance and control of rotorcraft
[NASA-CR-177453] 04 p0401 N88-12493
CGI delay compensation
[NASA-TM-86703] 04 p0476 N88-12932
New US book on aviation psychology reviewed 07 p0896 N88-15433
Rotorcraft flight-propulsion control integration 09 p1108 N88-16643
Helicopter human factors research 09 p1109 N88-16644
Status of NASA/Army rotorcraft research and development piloted flight simulation 09 p1110 N88-16651
An integrated approach to rotorcraft human factors research 09 p1110 N88-16653
Refinement of eye-point-of-regard measurement with helicopter pilots in a flight experiment
[ESA-TT-1073] 09 p1200 N88-17195
A validity study of a selection procedure for student airline pilots
[DFVLR-FB-87-34] 09 p1201 N88-17196
A situation-response model for intelligent pilot aiding 09 p1208 N88-17241
Autonomous control procedures for shuttle rendezvous proximity operations 09 p1208 N88-17244
Are windshear training aid recommendations appropriate for other than large jet transports? Pilot procedures: Shear models 10 p1275 N88-17635
Trends in the distribution of tasks between commercial pilots and flight control systems
[MBB-UT-008/87] 10 p1314 N88-17851
Cardiovascular and subjective measures of task demand in a low workload monitoring task
[REPT-8804] 10 p1368 N88-18176
Cockpit data management
[NASA-CR-178407] 11 p1438 N88-18579

Selected aspects of triazolam in relation to aviator performance in naval flight operations
[AD-A189322] 12 p1667 N88-19996
Field dependence-independence and its relationship to flight training performance
[AD-A188888] 12 p1670 N88-20003
The integration of artificial intelligence techniques to improve the effectiveness of electronic countermeasure strategies in a tactical environment
[AD-A189483] 12 p1682 N88-20056
Flight simulator experiments concerning take-off visibility minima
[NLR-TR-86050-U] 13 p1719 N88-20281
Psychophysical load of glider pilots on long-duration flights
[DFVLR-FB-87-38] 14 p1953 N88-21642
Aircraft accident report: North Star Aviation, Inc., PA-32 RT-300, N39614 and Alameda Aero Club Cessna 172, N75584, Oakland, California, March 31, 1987
[PB87-910412] 15 p2016 N88-22021
Relationship of encoding speed and memory tests to flight training performance
[AD-A190670] 15 p2105 N88-22539
Challenges of physiological monitoring in a Navy operational setting 16 p2239 N88-23374
Predicting operator workload during system design 16 p2239 N88-23375
Chronic stress as a factor in aircraft mishaps 16 p2239 N88-23376
Acute stress 16 p2239 N88-23377
Probe-evoked event-related potential techniques for evaluating aspects of attention and information processing 16 p2240 N88-23379
Defining and measuring pilot mental workload 16 p2240 N88-23383
Neurophysiological predictors of quality of performance 16 p2242 N88-23391
A correlational approach to predicting operator status 16 p2242 N88-23393
Aircraft accident/incident, Copperhill, Tennessee, February 22, 1986
[PB88-910407] 18 p2461 N88-24612
Analysis procedures and subjective flight results of a simulator validation and cue fidelity experiment
[NASA-TM-88270] 18 p2465 N88-24634
An evaluation of three linear scale radar altimeter displays
[AD-A192173] 18 p2465 N88-24636
Predicting Air Combat Maneuvering (ACM) performance: Fleet fighter ACM readiness program grades as performance criteria
[AD-A191605] 19 p2710 N88-26099
Research on piloting under conditions of breakdown in flight
[PB87-217980] 19 p2710 N88-26102
Aircraft accident report: Joe Foster Excavating, Inc., Bell 206B, N49606, in-flight collision with trees, Alamo, California, August 3, 1986
[PB88-910405] 20 p2755 N88-26345
Aircraft accident report: Midair collision of SkyWest Airlines Swearingen METRO 2, N163SW, and Mooney M20, N6485U, Kearns, Utah, January 15, 1987
[PB88-910404] 20 p2755 N88-26346
Checklist interruption and resumption: A linguistic study
[NASA-CR-177460] 20 p2756 N88-26348
Control of flight through microburst wind shear using deterministic trajectory optimization 20 p2761 N88-26375
Computer simulation of a single pilot flying a modern high-performance helicopter
[NASA-TM-100182] 20 p2761 N88-26376
Computer simulation of multiple pilots flying a modern high performance helicopter
[NASA-TM-100183] 20 p2761 N88-26377
Flight simulator: Field of view utilized in performing tactical maneuvers
[AD-A192412] 20 p2762 N88-26379
Does dihydroergotamine used in therapeutical doses influence the physical and psychomotor performance of young pilots or other traffic drivers subjected to hypotonia?
[ETN-88-92136] 20 p2832 N88-26799
Preliminary study within a project for the development of intelligent assistance to piloting: Formal description of combat pilot expertise and implementation of an interactive system to represent operations
[CERMA-87-31] 20 p2833 N88-26806
Microesotropia patients performa well as military jet pilots 21 p2925 N88-27363
Event-related brain potentials as indices of mental workload and attentional allocation 21 p2979 N88-27696
Fighter pilot performance during airborne and simulator missions: Physiological comparisons 21 p2981 N88-27704
The neuroelectric selection of Naval aviation personnel: An evaluation 21 p2981 N88-27707
Electroencephalographic correlates of pilot performance: Simulation and in-flight studies 21 p2982 N88-27711
Correlation between EEG abnormal activity and aircraft accidents: A long term observation 21 p2984 N88-27719
The auditory evoked response in military pilots 21 p2984 N88-27721
Personality, attitudes, and pilot training performance: Preliminary analysis
[AD-A193102] 21 p2991 N88-27746
Stress and the military pilot
[AD-A194313] 22 p3133 N88-28626
Proposed improvements to the USAF flight screening program
[AD-A194506] 23 p3240 N88-29285
Visual Effects in the High Performance Aircraft Cockpit
[AGARD-LS-156] 23 p3241 N88-29291
Vision and visual protection in fast jet aircraft 23 p3241 N88-29292
Visual related accidents/incidents 23 p3242 N88-29293
Advances in Flying Qualities
[AGARD-LS-157] 24 p3314 N88-29735
Pilot modeling 24 p3314 N88-29736
Pilot modeling applications 24 p3314 N88-29737
Low-speed longitudinal flying qualities of modern transport aircraft 24 p3314 N88-29738
The optimal control pilot model and applications 24 p3315 N88-29741
Threat expert system technology advisor
[NASA-CR-177479] 24 p3328 N88-29816
Prediction and measurement of human pilot dynamic characteristics in a manned rotorcraft simulation
[NASA-CR-183246] 24 p3410 N88-30297

PILOT PLANTS
Development of a pilot plant for the production of rapidly solidified aluminum alloy powders
[BMFT-FB-T-86-153] 02 p0146 N88-10914
Aviation turbine fuels from tar sands bitumen and heavy oils. Part 3: Laboratory sample production
[AD-A189278] 13 p1753 N88-20484
Turbine fuels from tar sands bitumen and heavy oil. Volume 2, phase 3: Process design specifications for a turbine fuel refinery charging San Ardo heavy crude oil
[AD-A190120] 16 p2183 N88-23011
An outdoor test facility for the large-scale production of microalgae
[DE88-001146] 21 p2984 N88-27723

PILOT SELECTION
Some aspects of sociopsychological screening of flying school applicants 07 p0890 N88-15392
A validity study of a selection procedure for student airline pilots
[DFVLR-FB-87-34] 09 p1201 N88-17196
The accommodative status in the dark of US Navy fighter pilots
[AD-A188188] 10 p1370 N88-18186
Personality, attitudes, and pilot training performance: Preliminary analysis
[AD-A193102] 21 p2991 N88-27746

PILOT TRAINING
A research on pilot performance in a flight incident situation
[ETN-87-90653] 02 p0217 N88-11370
New US book on aviation psychology reviewed 07 p0896 N88-15433
A prototype of pilot knowledge evaluation by an intelligent CAI (Computer-Aided Instruction) system using a Bayesian diagnostic model
[AD-A186080] 08 p1054 N88-16358
Are windshear training aid recommendations appropriate for other than large jet transports? Pilot procedures: Shear models 10 p1275 N88-17635
Windshear training aid. Volume 1: Overview, pilot guide, training program
[PB88-127196] 10 p1276 N88-17637
The accommodative status in the dark of US Navy fighter pilots
[AD-A188188] 10 p1370 N88-18186
MOAOPS and BOOM-MAP computer programs for sonic boom research, volume 1
[AD-A189548] 12 p1574 N88-19414
Field dependence-independence and its relationship to flight training performance
[AD-A188888] 12 p1670 N88-20003
Relationship of encoding speed and memory tests to flight training performance
[AD-A190670] 15 p2105 N88-22539
Task listing: Visually assisted and visually dependent tasks for fighter aircraft
[AD-A191041] 16 p2244 N88-23404
A look toward the future of complex avionics systems development using the USAF Test Pilot School's avionics systems test training aircraft 17 p2306 N88-23797
An enumeration of research to determine the optimal design and use of Army flight training simulators
[AD-A191242] 18 p2468 N88-24649
Development of training implying man-machine interface: From the aircraft to the spacecraft 19 p2700 N88-26052
Intelligent guidance and control for wind shear encounter
[NASA-CR-183060] 20 p2755 N88-26347
USAF flying screening: First step on the road to wings
[AD-A192613] 20 p2833 N88-26804
Preliminary study within a project for the development of intelligent assistance to piloting: Formal description of combat pilot expertise and implementation of an interactive system to represent operations
[CERMA-87-31] 20 p2833 N88-26806
Personality, attitudes, and pilot training performance: Preliminary analysis
[AD-A193102] 21 p2991 N88-27746
Cockpit and cabin crew coordination
[AD-A192445] 21 p2993 N88-27752
Flight information publication (FLIP) feedback
[AD-A194462] 23 p3174 N88-28897
Future air-to-air training for the RF-4
[AD-A194363] 23 p3240 N88-29284
General operational and training visual concerns 23 p3242 N88-29295
Controlled degradation of resolution of high-quality flight simulator images for training effectiveness evaluation
[AD-A196189] 24 p3330 N88-29823

PILOTED CENTRIFUGES
U HUMAN CENTRIFUGES

PILOTLESS AIRCRAFT
NT DRONE AIRCRAFT
The aerodynamic performance of propellers suitable for unmanned aircraft (UMAs)
[RAE-TM-AERO-2094] 09 p1112 N88-16667
Robotic air vehicle. Blending artificial intelligence with conventional software 09 p1210 N88-17252

PILOTS
Pilot-aided modulation for narrow-band satellite communications 19 p2649 N88-25728
An error floor in tone calibrated transmission 19 p2649 N88-25729

PILOTS (PERSONNEL)
NT AIRCRAFT PILOTS
Aircraft accident report: Grand Canyon Airlines, Inc., and Helitech, Inc., midair collision over Grand Canyon National Park, June 18, 1986
[PB87-910403] 06 p0666 N88-14087
US civil airmen statistics, 1987
[AD-A191714] 18 p2455 N88-24577
USAF flying screening: First step on the road to wings
[AD-A192613] 20 p2833 N88-26804

PINCH EFFECT
NT PLASMA PINCH
NT REVERSE FIELD PINCH
NT SCREW PINCH
NT THETA PINCH
NT ZETA PINCH
Transverse focussing using plasma wake fields
[DE87-011503] 01 p0099 N88-10652
Improvement of plasma confinement due to electron Landau damping in tokamaks
[DE88-752339] 15 p2136 N88-22747
Kinetic theoretical analysis for propagation of rotating ion beam in ICF 16 p2276 N88-23623
On selfsimilar thermonuclear ignition of a plasma in necks of zeta devices
[DE88-701640] 16 p2280 N88-23647

PINHOLE CAMERAS
A multi-frame ion pinhole camera for intense ion beam transport and focusing experiments
[DE88-007283] 18 p2516 N88-24926
Intense ion beam diagnostics for particle beam fusion experiments on PBFA 2
[DE88-007279] 18 p2577 N88-25308

PINHOLE OCCULTER FACILITY
Pinhole occulter experiment
[NASA-CR-179206] 02 p0235 N88-11481

PINHOLES
Particle beam alignment system for single event upset-Van de Graaf experiments
[AD-A189695] 15 p2132 N88-22721

PINNING
NT FLUX PINNING
Schottky-barrier formation on a covalent semiconductor without Fermi-level pinning: The Metal-MoS2(0001) interface
[AD-A193044] 21 p3021 N88-27931
Picosecond transient reflectivity of unpinned gallium arsenide (100) surfaces
[AD-A193242] 21 p3021 N88-27933

PINS
Review of diffusion barrier technology for application in SP-100 fuel pins
[DE88-000021] 02 p0234 N88-11480
Pin joints, gears, springs, cranks and other novel micromechanical structures
[DE88-002504] 07 p0864 N88-15245
Computed stress and strain distributions under interference fit and after coldworking
[AD-A186950] 10 p1342 N88-18024
PIONEER VENUS SPACECRAFT
Vertical structure of Venusian cloud layer at landing sites of Vega-1 and Vega-2 vehicles
13 p1725 N88-20317
PIONEER 12 SPACE PROBE
U PIONEER VENUS SPACECRAFT
PIONS
Electrical behavior of layers implanted with low energy pions in Si
[INPE-4199-PRE/1051] 01 p0102 N88-10670
Conceptual design of a high-resolution pion (0) spectrometer
[DE87-014757] 03 p0324 N88-12047
Experimental studies of elementary particle interactions at high energies
[DE88-000804] 05 p0648 N88-13971
Research in experimental nuclear physics
[DE88-004100] 10 p1408 N88-18397
Pion nucleus single charge exchange reactions above the delta(1232) resonance
[LA-11004-T] 11 p1544 N88-19231
Pion elastic and inelastic scattering near N=28
[LA-10968-T] 11 p1544 N88-19232
Pion absorption in nuclei: The pion(+ or -),proton reactions
[LA-10997-T] 12 p1688 N88-20098
Theoretical studies in few-body intermediate energy physics
[DE88-004101] 12 p1689 N88-20106
Subthreshold pion production in proton induced reactions at 180 to 201 MeV and He3 at 283 MeV
[ETN-88-92303] 17 p2397 N88-24250
Charged pion production and projectile breakup in 85A MeV(sup)12C induced heavy ion reactions
[LUIP-8802] 20 p2850 N88-26920
PIPE FLOW
Large scale structures in turbulent pipe flow
[MPIS-MITT-83-1987] 02 p0172 N88-11085
Carbon dioxide treatment for scale removal and control in potable water systems
[AD-A184346] 04 p0412 N88-12556
Dynamics of reverse flows at pump inlet
04 p0425 N88-12636
Use of a thermodynamic analog for pneumatic transport in horizontal pipes
[AD-A184076] 04 p0441 N88-12740
Experiments on densely-loaded non-Newtonian slurries in laminar and turbulent pipe flows
[DE88-000719] 04 p0442 N88-12746
Flow induced pulsations in pipe systems
[ETN-88-91367] 06 p0702 N88-14307
The effect of eddy distribution on momentum and heat transfer near the wall in turbulent pipe flow
[NASA-TM-100257] 08 p0988 N88-15984
Investigation of critical heating in narrow flow channels with R12 refrigerant as model fluid
[GKSS-87/E/25] 09 p1163 N88-16972
The dynamics of heat transfer at a turbulent pipe flow
[OEFZS-4400] 09 p1164 N88-16975
On some asymptotics of laminar flow in a coiled pipe
10 p1328 N88-17936
Operating loading of piping systems
[ETN-88-91057] 11 p1484 N88-18856
Theoretical and experimental analysis of pressure pulse transmission in non-Newtonian pipe flow
11 p1485 N88-18863
Experiments on densely-loaded non-Newtonian slurries in laminar and turbulent pipe flows
[DE88-006209] 15 p2067 N88-22323
Piston-driven, unsteady separation at a sudden expansion in a tube: Flow visualization and Laser Doppler Anemometer (LDA) measurements
[ETN-88-92104] 15 p2068 N88-22329
Tests on oscillating flows in a pipe nozzle with an abrupt diameter variation
[MPIS-2/1987] 17 p2337 N88-23947
Modeling of cavitation phenomena in homogeneous flow in transitory regimes in pipes
[ISAL-IDI1-87-15] 17 p2337 N88-23948
Energy efficient continuous flow ash lockhopper
[NASA-CASE-NPO-16985-1-CU]
18 p2497 N88-24814
Hydroacoustic pulsating jet generator
[MPIS-7/1987] 18 p2510 N88-24891
Turbulent heat transfer and fluid flow measurements downstream of abrupt expansions and in a cavity of a circular tube at a uniform wall temperature
18 p2515 N88-24920
Pressure drop and heat transfer in turbulent non-Newtonian pipe flow of advanced energy transmission fluids
[DE88-010021] 19 p2666 N88-25853
Ammonia boiling in long tubes. Heat transfer and charge loss in vertical and horizontal tubes
[NASA-TT-20313] 19 p2667 N88-25858
Turbulence transition in a circular pipe
20 p2782 N88-26503
Characteristics of long size thermosyphons made of corrugated tube 20 p2784 N88-26511
Experiments on densely-loaded non-Newtonian slurries in laminar and turbulent pipe flows
[DE88-010579] 20 p2800 N88-26612
Investigation on refrigerant R12 critical boiling point in narrow flow pipes considered as model fluid
[ETN-88-92374] 20 p2802 N88-26626
Characterization of accelerating pipe flow
[AD-A193065] 21 p2943 N88-27481
Computational boundary conditions for the incompressible Navier-Stokes equations in channels and pipes
[AD-A193356] 21 p2944 N88-27487
Numerical computation of three-dimensional turbulent flow in tightly curved ducts and spiral turbine casings
[ETN-88-92362] 21 p2948 N88-27511
Investigations on drag reduction in turbulent pipe flows by addition of ionic and nonionic high polymers
[ETN-88-92380] 21 p2949 N88-27515
Investigations of rough surface effects on friction factors in turbulent pipe flow
[AD-A193774] 22 p3075 N88-28255
Application of rectangular co-ordinates to the problem of laminar combined convection in a straight horizontal tube whose circumference is heated nonuniformly
[PDR/CFDU/IC/33] 22 p3076 N88-28263
Mass transport in sector and annular sector tubes
[LRT-WE-9-FB-9(1987)] 22 p3077 N88-28269
Mass transport in a parabolic conduit
[LRT-WE-9-FB-1(1988)] 22 p3077 N88-28273
Heat transport in a parabolic tube of circular cross-section
[LRT-WE-9-FB-2(1988)] 22 p3078 N88-28274
Development of a hot-wire measurement technique for moderate intensity three-dimensional flows
22 p3080 N88-28289
Rotation symmetric inside flow with diametric expansion resolution
[ILR-MITT-193] 23 p3213 N88-29123
Laser Doppler Velocimeter (LDV) and pressure measurements of gas particle flows in bends
[VKI-TN-163] 24 p3372 N88-30083
PIPELINES
Electrical heating method — pipelines, metal tanks
[GB-PATENT-2-137-059-A] 01 p0043 N88-10274
Investigation on ductile fracture behavior of 3-inch diameter Type 304 stainless steel pipe with a circumferential through-wall crack
[DE87-753016] 02 p0191 N88-11196
Dynamics of propellant feedline systems
[AD-A184865] 05 p0580 N88-13537
Dynamic modelling by finite element method of an elasto-acoustic beam with due consideration of flow and viscosity
[PB87-178166] 09 p1164 N88-16978
Chemical/hydrogen energy systems
[DE88-007013] 19 p2687 N88-25969
PIPELINING (COMPUTERS)
On the VLSI design of a pipeline Reed-Solomon decoder using systolic arrays 04 p0436 N88-12700
Arrays for discrete Fourier transform
[REPT-87-019] 05 p0632 N88-13861
Parallel algorithms for polynomials
[PB87-226304] 06 p0756 N88-14635
A multithreaded processor architecture for parallel symbolic computation
[AD-A187034] 09 p1222 N88-17327
Massive fine-grain parallelism in array computation: A data flow solution 10 p1382 N88-18254
A serial input pipelined multiplier
[REPT-87-030] 11 p1530 N88-19141
Parallel algorithms for mapping pipelined and parallel computations
[NASA-CR-181655] 14 p1960 N88-21687
Multiple-transform pipelines for image coding
[REPT-87-038] 15 p2108 N88-22561
Real time pipelined system for forming the sum of products in the processing of video data
[NASA-CASE-NPO-16462-1-CU]
17 p2384 N88-24169
The performance of the NEC SX-2 and Cray X-MP supercomputers
[DE88-009177] 20 p2835 N88-26813
Large-grain pipelining on distributed-memory multiprocessors
[DE88-009974] 23 p3264 N88-29432
PIPES (TUBES)
NT GAS PIPES
NT U BENDS
Blowdown of two-component gas mixtures in branching systems
[DE87-011392] 01 p0045 N88-10287
Damping characteristics of a composite-reinforced stainless-steel tube
[DE87-012455] 02 p0191 N88-11192
Numerical study of the entrance flow and its transition in a circular pipe (2) 03 p0318 N88-12011
Dynamics of reverse flows at pump inlet
04 p0425 N88-12636
Pipe and bend erosion by pneumatic transport of solids at high temperature
[DE88-001345] 04 p0429 N88-12658
Pulsed eddy-current inspection of thin-walled stainless steel tubing
[DE88-001492] 04 p0457 N88-12830
Development on thin wall tubes of dispersion type
[DE87-703384] 05 p0571 N88-13483
Design and test of high performance composite tubes for use in deep water drilling and production systems
[SNIAS-872-430-107] 05 p0572 N88-13487
High performance composite tubes for offshore applications
[SNIAS-872-430-116] 05 p0572 N88-13488
Qualification of expansion and joint welding procedures of tube-to-tubesheet joints for heat exchangers in nuclear power plants
[DE87-703526] 05 p0589 N88-13592
Finite element model for the stress and flexibility analysis of curved pipes
[DE87-703632] 05 p0592 N88-13608
Analysis of photopole data reduction models
05 p0593 N88-13616
Computation of turbulent flow of air through smooth and rough pipes using a two-equation turbulence model
06 p0700 N88-14298
Flow induced pulsations in pipe systems
[ETN-88-91367] 06 p0702 N88-14307
Tool and process for miniature explosive joining of tubes
[NASA-CASE-LAR-13662-1] 06 p0711 N88-14359
Creep test of Hastelloy X for use as the components of OGL-1 in helium environment
[DE88-750289] 07 p0834 N88-15059
The effect of asymmetric heating on flow stability and heat transfer for flow in a vertical tube
[DE88-003242] 07 p0855 N88-15193
A pulsed eddy current method for examining thin-walled stainless steel tubing
[DE88-002294] 07 p0866 N88-15255
Fully turbulent internal flow excitation of pipe systems
08 p1000 N88-16056
Indirect measurement of local condensing heat-transfer coefficient around horizontal finned tubes
[AD-A186929] 09 p1160 N88-16950
TOPP: A post-processor for TOPAZ, the one dimensional pipe flow analysis code
[DE88-003711] 09 p1164 N88-16981
Accuracies of southwell and force/stiffness methods in the prediction of buckling strength of hypersonic aircraft wing tubular panels
[NASA-TM-88295] 09 p1183 N88-17090
The dishomogeneity of the degree of sensitization in large recirculation pipes in Boiling Water Reactor (BWR) power plants
[CISE-3955] 09 p1247 N88-17473
Magneto-Inertia Confinement Approach (MICA) to fusion in dynamic Z-pinch formed from a frozen deuterium-tritium tube
[IPPJ-856] 09 p1252 N88-17504
Cost 501 Project UK10 part 3: Thermal fatigue damage of Fecralloy steel-sprayed and co-extruded tubing
[AERE-R-12230] 10 p1343 N88-18026
An experimental investigation of the hydrodynamic and heat-transfer behavior of aqueous foam in laminar tube flow
[DE88-004954] 11 p1483 N88-18855
Reduction of erosion in elbows due to flow modifications, phase 1
[DE88-001028] 13 p1769 N88-20584
The CTM program of masts and the CTM engineering model — spacecraft mechanism
14 p1874 N88-21196
Statistical analysis of feasibility of non-destructive inspection of mechanical properties of hot worked pipes of alloy steels
[BLL-M-37598-(5828.4)] 14 p1922 N88-21455

Experiments on the creep behavior of semifinished X10NiCrAlTi 32 20 (Nicrofer 32 20) tubes under multiaxial loading — nuclear reactors
[JUEL-2127] 14 p1923 N88-21484
Applications research studies of microtubules
[AD-A190855] 16 p2182 N88-23005
A reflux tube fabric radiator 17 p2421 N88-24394
Theoretical and experimental damping values of piping systems at high ductilities
[DE88-006717] 18 p2526 N88-24986
Numerical analysis of duct flow using three-dimensional parabolized Navier-Stokes equation
19 p2638 N88-25652
Statistical evaluation of light water reactor piping damping data for use in PRA (Probabilistic Risk Assessment) analyses
[DE88-007708] 19 p2661 N88-25828
Acoustic wave dispersion in a viscous, compressible, liquid-filled cylindrical elastic tube
19 p2722 N88-26164
Forced-convective boiling in small diameter tube
20 p2783 N88-26510
Evaluation of engineering leak before break assessment methods by piping tests
[PB88-126982] 20 p2788 N88-26538
Experimental investigation of turbulent flow in smooth and longitudinal grooved tubes
[NASA-TM-77480] 20 p2800 N88-26615
Cross flow induced vibrations in tube bundle by displaced and misaligned tube configurations
[ETN-88-92132] 20 p2801 N88-26621
Thermal and mechanical analysis of the Faraday shield for the compact ignition tokamak
[DE88-007855] 20 p2856 N88-26962
Characterization of accelerating pipe flow
[AD-A193065] 21 p2943 N88-27481
Distribution of weld quality in thin section stainless steel tube attachment welds
[PB88-109632] 21 p2955 N88-27555
Computation of failure probability of fatigue loaded cracked structures
[ETN-88-92360] 21 p2964 N88-27607
Mass transport in sector and annular sector tubes
[LRT-WE-9-FB-9(1987)] 22 p3077 N88-28269
Passive damping concepts for free and forced member and grillage vibration
[NASA-CR-183114] 23 p3225 N88-29196
Elastic-plastic analysis of part-through crack propagation in piping and pressure vessels
[DE88-701619] 23 p3225 N88-29198
Analytical study of graphite-epoxy tube response to thermal loads
[NASA-CR-183215] 24 p3341 N88-29884

PISTON ENGINES
NT DIESEL ENGINES
NT FREE-PISTON ENGINES
NT STIRLING ENGINES
Free-piston Stirling engine diaphragm-coupled heat-actuated heat pump component technology program, phase 1C
[DE88-003654] 10 p1330 N88-17949
Comparison between computed and measured swirl and turbulence in reciprocating engines
[PDR/CFDU/IC/32] 13 p1779 N88-20647
Investigation of the misfueling of reciprocating piston aircraft engines
[NASA-TP-2803] 14 p1865 N88-21144
Two-fluid turbulence models and reciprocating engines
[CFD/87/6] 14 p1918 N88-21449
Computer simulation of turbulent combustion in reciprocating engines
[CFDU/87/11] 18 p2482 N88-24725
Analytical and experimental investigation of ringless piston concept
[AD-A193213] 21 p2956 N88-27559
The application of the two-fluid model of turbulence to the 3-D simulation of turbulent combustion in reciprocating engines
[PDR/CFDU/IC/37] 22 p3052 N88-28110

PISTON THEORY
The performance of the VKI longshot hypersonic wind tunnel
[VKI-TN-161] 18 p2468 N88-24650

PISTONS
Piston ring friction and vehicle fuel economy
[DE87-014536] 02 p0181 N88-11127
Microcomputer control of a hydraulically actuated piston
[AD-A184130] 03 p0388 N88-12317
Overview of free-piston Stirling engine technology for space power application
[NASA-TM-88886] 03 p0396 N88-12427
Ideal-viscoplastic extrusion model with application to deforming pistons in light-gas guns
[UTIAS-TN-266] 04 p0429 N88-12657
Hot piston ring tests
[NASA-TM-100256] 06 p0729 N88-14486
Hot piston ring/cylinder liner materials: Selection and evaluation
[NASA-TM-100276] 08 p0971 N88-15872
Free-piston Stirling engine diaphragm-coupled heat-actuated heat pump component technology program, phase 1C
[DE88-003654] 10 p1330 N88-17949
Calibration of a Harwood DWT-1000 controlled-clearance piston gauge
[DE88-004496] 11 p1489 N88-18888
Piston-driven, unsteady separation at a sudden expansion in a tube: Flow visualization and Laser Doppler Anemometer (LDA) measurements
[ETN-88-92104] 15 p2068 N88-22329
Pump rod forces due to hydrodynamic effects in piston pumps
[PB88-164850] 16 p2214 N88-23212
Composite piston
[NASA-CASE-LAR-13435-1] 17 p2346 N88-23981
Analytical and experimental investigation of ringless piston concept
[AD-A192835] 20 p2810 N88-26673
Variable-compression-ratio pistons for high power output diesel engines 22 p3084 N88-28316
Static and dynamic metal-metal friction at plastic stress levels
[DE88-011261] 23 p3222 N88-29176

PITCH
Pilot-aided modulation for narrow-band satellite communications 19 p2649 N88-25728
An error floor in tone calibrated transmission
19 p2649 N88-25729

PITCH (INCLINATION)
Measurement of velocity and vorticity fields in the wake of an airfoil in periodic pitching motion
[NASA-TP-2780] 04 p0487 N88-13002
Restoration of particle pitch angle distribution functions by a maximum entropy algorithm
[ATR-86(7098)-3] 05 p0648 N88-13969
Handling qualities of a wide-body transport airplane utilizing Pitch Active Control Systems (PACS) for relaxed static stability application
[NASA-TP-2482] 07 p0821 N88-14987
Degradation of downlink distance measurement indexes by the addition of a third tone — tone ranging
[CNES-CT/DRT/TIT/TR-122-T]
15 p2058 N88-22268
Hybrid procedure for dynamic measurements in transonic wind tunnels: Demonstrated by pitch oscillation
[DFVLR-FB-88-19] 21 p2900 N88-27211
Time periodic control of a multi-blade helicopter
[AD-A194435] 23 p3180 N88-28931

PITCH (MATERIAL)
Interfacial shear strength of pitch and high strain pan fibers in an epoxy matrix
[AD-A185966] 07 p0826 N88-15011
Electrical dc conductivity of pitch
[AD-A191266] 16 p2182 N88-23008
Electronic and structural studies of carbon/carbon composites
[AD-A191729] 19 p2609 N88-25481

PITCH ANGLES
U PITCH (INCLINATION)

PITCH ATTITUDE CONTROL
U LONGITUDINAL CONTROL

PITCHING MOMENTS
An experimental evaluation of advanced rotorcraft airfoils in the NASA Ames eleven-foot transonic wind tunnel
[NASA-CR-166587] 03 p0261 N88-11640
Dynamic stability of hypersonic conical lifting vehicles according to Newton-Busemann theory
05 p0534 N88-13247
Prediction of wing aeroelastic effects on aircraft life and pitching moment characteristics
05 p0551 N88-13356
Unsteady stall penetration experiments at high Reynolds number
[AD-A186120] 07 p0814 N88-14958
An experimental study of the effect of pitch rate on delta wing aerodynamics and stability
[NASA-CR-183159] 21 p2893 N88-27173
Control and use of unsteady flows: Insect use of various wing kinematics and related pressure measurements using a pitching airfoil 21 p2926 N88-27366
Forces and moments on a slender, cavitating body
[DE88-007208] 21 p2945 N88-27491

PITOT TUBES
Heterogeneous diffusion flame stabilization
[AD-A193014] 20 p2771 N88-26429

PITTING
Evaluation of load tracks and wear of two sets of bearings from space shuttle main engine high pressure oxygen turbopumps
[NASA-CR-178969] 07 p0861 N88-15223
Studies of the initiation of pitting corrosion on stainless steels
[AERE-M-3615] 10 p1301 N88-17778
A review of pitting corrosion in high temperature aqueous solutions
[DE88-003547] 10 p1302 N88-17787
Corrosion behavior of sputter-deposited aluminum-based alloys exposed to chloride solutions
[AD-A187262] 10 p1303 N88-17794
Significance of the local electrode potential within pits, crevices and cracks
[AD-A192482] 21 p2935 N88-27432
Corrosion problems associated with computer disk packs 22 p3054 N88-28121

PITUITARY GLAND
Morphological and functional state of the hypothalamo-hypophyseal neurosecretory system of rats flown aboard Cosmos-1667 10 p1365 N88-18156
Hypothalamic-pituitary-adrenal responses to short duration high intensity cycle exercise
[AD-A192597] 21 p2985 N88-27727

PITUITARY HORMONES
Role of adenosine analogs and growth hormone in waking and sleep
[AD-A187897] 11 p1519 N88-19070

PIVOTS
A new pivoting rule for the dual network simplex method
[REPT-87-17] 01 p0080 N88-10511
An examination of coating failure on wing pivot fittings of f111 aircraft
[AD-A185028] 05 p0548 N88-13328
Parallel pivoting combined with parallel reduction
[NASA-CR-178422] 06 p0760 N88-14662
Balloon-borne three-meter telescope for far-infrared and submillimeter astronomy
[NASA-CR-182310] 09 p1262 N88-17565
An extension of the MS pivoting rule to capacitated network flow problems
[REPT-87-33] 14 p1963 N88-21711

PIXELS
Textural features for image classification in remote sensing
[INPE-4169-PRE/1066] 08 p1020 N88-16181
Textural features for image classification in remote sensing 17 p2354 N88-24027
Study of methods of post-processing applied to a problem of standard classification
17 p2362 N88-24067
SEGMERGE: A scanline visible surface algorithm with adaptive span selection and inexpensive antialiasing
[DE88-009186] 20 p2836 N88-26826
Image focusing in space and time
[AD-A195839] 24 p3429 N88-30410

PLAGES (FACULAE)
U FACULAE

PLAINS
NT COASTAL PLAINS
NT FLOOD PLAINS
NT PLAYAS
NT TUNDRA
Analysis of winter season precipitation bands over the Southern Plains 14 p1947 N88-21609
Intercrater plains deposits and the origin of Martian valleys 23 p3301 N88-29661
Distribution and timing of thick transient air-fall deposits in Electris: Implications for the nature of the upland plains 23 p3303 N88-29674
Constraints on the origin of fractured terrane, Northern Martian plains 23 p3304 N88-29684
Origin of northern lowland plains: Constraints from boundary morphology 23 p3305 N88-29687
Early cratering rates and the nature of the Martian cratered uplands 23 p3306 N88-29694

PLANAR STRUCTURES
A study of scattering from E-plane circuit elements
[AD-A184473] 04 p0431 N88-12673
An adaptive subdivision method with crack prevention for rendering beta-spline objects
[AD-A184249] 04 p0477 N88-12940
Computation of natural frequencies of planar lattice structure
[AD-A185387] 05 p0641 N88-13920
The effect of collision angle on mach reflection
[AD-A185798] 06 p0704 N88-14319
The dynamics of coupled planar rigid bodies. Part 1: Reduction, equilibria and stability
[AD-A187467] 10 p1345 N88-18042
Technology development of a planar BiPolar transistor
[AD-A188761] 12 p1623 N88-19708

Nonaxisymmetric body supersonic, aerodynamic prediction
[AD-A189338] 13 p1716 N88-20259
On effectively labeling planar projections of polyhedra
[CWI-CS-R8715] 13 p1826 N88-20917
Quantitative use of exciplex-based vapor/liquid visualization systems, users' manual
[AD-A191649] 19 p2610 N88-25491
Large planar maneuvers for articulated flexible manipulators
[NASA-CR-183079] 19 p2711 N88-26104
Radiative heat transfer and selective emission in planar slab coatings on hot emissive substrates
[AD-A193133] 21 p2918 N88-27319
Guided wave interactions in millimeter-wave integrated circuits
[AD-A193017] 21 p2936 N88-27437
Development of planar geometry solid oxide fuel cell technology, phase 1
[PB88-210356] 23 p3229 N88-29215
Development of a general software package for the analysis and synthesis of planar antenna arrays for space applications
[S-247-02] 24 p3359 N88-30000
Advanced planar array development for space station
[NASA-CR-179373] 24 p3389 N88-30181
Particle trajectories and potentials in a plane sheath moving in a magnetoplasma
[AD-A196228] 24 p3390 N88-30190
Computer-Aided Structural Engineering (CASE) project. Computer program for analysis of planar grid structures (CGRID), user's guide
[AD-A195977] 24 p3413 N88-30317

PLANE STRAIN

Theoretical investigation of stress concentrations in damaged carbon fibre reinforced plastic plate structures. Volume 2: Tables, figures and plates
[BR99873-VOL-2] 03 p0280 N88-11762
Closure and propagation behavior of short fatigue cracks at different R-ratios 05 p0601 N88-13679
Analysis of crack closure under plane strain conditions
[NASA-CR-182369] 06 p0722 N88-14439
Fully plastic analysis of mixed mode plane-strain crack problems
[PB87-144929] 08 p0994 N88-16015
Fracture mechanics 17 p2324 N88-23877
Dynamic shear band development in plane strain
[AD-A190915] 18 p2526 N88-24988

PLANE STRESS

Theoretical investigation of stress concentrations in damaged carbon fibre reinforced plastic plate structures. Volume 2: Tables, figures and plates
[BR99873-VOL-2] 03 p0280 N88-11762
Analysis of crack closure under plane strain conditions
[NASA-CR-182369] 06 p0722 N88-14439
Elastic-plastic fracture investigation on stable crack growth for plane stress
[PB87-144820] 08 p0995 N88-16022
Static analysis of thin plates using the finite strip-element method 19 p2679 N88-25931

PLANE WAVES

New main reflector, subreflector and dual chamber concepts for compact range applications
[NASA-CR-181506] 04 p0402 N88-12498
Pulse-mode expansions and refractive indices in plane-wave propagation
[DE88-001328] 04 p0437 N88-12714
Dispersion equation for plane capillary-gravity wave on free surface of viscous incompressible fluid 04 p0459 N88-12842
Boundary effects on the drag of an oscillating sphere: Applications to the magnetic sphere rheometer. Attenuation and dispersion of acoustic waves in nematic liquid crystals 04 p0488 N88-13007
Plane longitudinal waves in solutions of Maxwell equations
[DE88-700347] 07 p0846 N88-15135
Interior impedance wedge diffraction with surface waves
[NASA-CR-182405] 07 p0854 N88-15186
Plane wave diffraction by a thin dielectric wedge
[RSRE-MEMO-4045] 09 p1153 N88-16912
Wave curves for simple isotropic elastic solids
[AD-A188865] 12 p1636 N88-19798
Phase velocity and attenuation of plane elastic waves in a particle-reinforced composite medium
[AD-A189414] 13 p1734 N88-20366
Detection and angle estimation of coherent plane waves 13 p1759 N88-20522
Research in nonlinear partial differential equations and bifurcation theory
[AD-A190986] 16 p2260 N88-23514
Saturation and the limit of jet mixing enhancement by single frequency plane wave excitation: Experiment and theory
[NASA-TM-100882] 17 p2295 N88-23732
Electromagnetic scattering from nonlinear anisotropic cylinders 17 p2333 N88-23930
Experimental investigation of the reflection of a planar shock wave over a double wedge
[AD-A193078] 21 p2943 N88-27482
On the degenerate Ferrari-Ibanez solution for colliding plane gravitational waves
[MATH-REPT-209] 23 p3296 N88-29630
Time-domain far-field scattering of plane electromagnetic waves by a penetrable object in the Born approximation
[PB87-176129] 24 p3365 N88-30040
Mathematical problems of nonlinear wave propagation and of waves in heterogeneous media
[AD-A195970] 24 p3368 N88-30057

PLANET ORIGINS

U PLANETARY EVOLUTION

PLANETARY ATMOSPHERES

NT JUPITER ATMOSPHERE
NT MARS ATMOSPHERE
NT NEPTUNE ATMOSPHERE
NT PLANETARY IONOSPHERES
NT SATURN ATMOSPHERE
NT URANUS ATMOSPHERE
NT VENUS ATMOSPHERE
NT VENUS CLOUDS

Laboratory evaluation and application of microwave absorption properties under simulated conditions for planetary atmospheres
[NASA-CR-181466] 02 p0254 N88-11606
Planetary science 07 p0883 N88-15356
Atmospheric science 07 p0883 N88-15357
Extended atmospheres of outer planet satellites and comets
[NASA-CR-181449] 10 p1430 N88-18540
Gamma-ray and neutron spectroscopy of planetary surfaces and atmospheres
[DE88-004287] 10 p1430 N88-18541
A modeling analysis program for the JPL table mountain Io sodium cloud data
[NASA-CR-182555] 11 p1570 N88-19400
Negative viscosity in global circulations 13 p1786 N88-20685
A design study of onboard navigation and guidance during aerocapture at Mars
[NASA-CR-172053] 18 p2469 N88-24654
Investigation of Rossby-number similarity in the neutral boundary layer using large-eddy simulation
[DE88-008910] 19 p2666 N88-25851
The rate of volcanism on Venus
[NASA-CR-183039] 19 p2742 N88-26281
Experimental study of planetary gases with applications to planetary interior models
[NASA-CR-183098] 20 p2886 N88-27137
Interpretation of the polarimetric observations of Jupiter
[DE88-702414] 21 p3031 N88-27991
Polarization of light reflected by vertically inhomogeneous planetary atmosphere
[DE88-702416] 21 p3031 N88-27992
Workshop on the Origins of Solar Systems
[NASA-CR-183025] 24 p3451 N88-30536
The atmospheres of the earth and the other planets: Origin, evolution and composition 24 p3452 N88-30544

PLANETARY BOUNDARY LAYER

Effects of rainfall on the seasonal thermocline
[AD-A184432] 04 p0472 N88-12912
A bulk model for the unstable planetary boundary layer over the sea. A sensitivity investigation
[DM-51] 22 p3129 N88-28600

PLANETARY COMPOSITION

Growth of continental crust: Clues from Nd isotopes and Nb-Th relationships in mantle-derived magmas 24 p3393 N88-30205
The Kerala Khondalite Belt (KKB) of Southern India: An ensialic mobile belt 24 p3393 N88-30208
Does subduction zone magmatism produce average continental crust 24 p3394 N88-30214

PLANETARY CORES

NT EARTH CORE

PLANETARY CRUSTS

NT EARTH CRUST

Kinetics of thermochemical gas-solid reactions important in the Venus sulfur cycle
[NASA-CR-182963] 19 p2742 N88-26280
Morphologic contrasts between Nirgal and Auqakuh Valles, Mars: Evidence of different crustal properties 23 p3304 N88-29681
Stratigraphy of the Kasei Valles region, Mars 23 p3305 N88-29690
Growth of planetary crusts 24 p3400 N88-30247
Debris flows of the Simud-Tiu outflow system of Mars 24 p3442 N88-30485

PLANETARY ENTRY

U ATMOSPHERIC ENTRY

PLANETARY ENVIRONMENTS

NT JUPITER ATMOSPHERE
NT MARS ATMOSPHERE
NT MARS ENVIRONMENT
NT NEPTUNE ATMOSPHERE
NT PLANETARY ATMOSPHERES
NT PLANETARY IONOSPHERES
NT SATURN ATMOSPHERE
NT URANUS ATMOSPHERE
NT VENUS ATMOSPHERE
NT VENUS CLOUDS

Model of Jovian F region ionosphere
[NASA-CR-182587] 13 p1855 N88-21105

PLANETARY EVOLUTION

Remote sensing of planets and cartographic results
[HSBW-HEFT-14] 03 p0389 N88-12444
Studies in Aeolian geology
[NASA-CR-182328] 05 p0625 N88-13828
Impact-induced devolatilization and hydrogen isotopic fractionation of serpentine: Implications for planetary accretion
[NASA-CR-182877] 16 p2175 N88-22966
Reports of planetary geology and geophysics program, 1987
[NASA-TM-4041] 20 p2885 N88-27133
Mars: Spectral signatures seen and unseen 23 p3301 N88-29659
Workshop on the Growth of Continental Crust
[NASA-CR-183073] 24 p3392 N88-30201
Nd isotopes and crustal growth rate 24 p3392 N88-30203
An illustration of the complexity of continent formation 24 p3393 N88-30207
The Kerala Khondalite Belt (KKB) of Southern India: An ensialic mobile belt 24 p3393 N88-30208
The timing and mechanism of depletion in Lewisian granulites 24 p3394 N88-30209
Construction of mass-age curves for the continental crust: An empirical model and an example from the western US 24 p3394 N88-30213
Pb isotope constaints on the extent of crustal recycling into a steady state mantle 24 p3394 N88-30215
Decoupled Rb-Sr and Sm-Nd isotopic evolution of the continental crust 24 p3395 N88-30216
Early intense cratering: Effects on growth of earth's crust 24 p3395 N88-30219
The growth of continents and some consequences since 1.5 Ga 24 p3395 N88-30220
Growth of early archaean crust in the ancient Gneiss complex of Swaziland and adjacent Barberton Greenstone Belt, Southern Africa 24 p3396 N88-30223
Diapirs of the Mediterranean ridge: The tectonic regime of an incipient accreted terrane 24 p3396 N88-30224
Changing styles of crustal growth in Southern Africa: Constraints from geochemical and Sr-Nd isotope studies in Archaean to Pan African terrains 24 p3396 N88-30227
Growth of the continental crust: A planetary-mantle perspective 24 p3400 N88-30251
Exotic minerals in 3,500 million year old rocks: Evidence for large meteorite impacts 24 p3440 N88-30475
Lewis Cliff 86010, a unique Antarctic meteorite: Possible new clues to the early history of the solar system 24 p3442 N88-30482
Workshop on the Origins of Solar Systems
[NASA-CR-183025] 24 p3451 N88-30536
Physical processes and timescales in planet and small-body accretion 24 p3451 N88-30540
Terrestrial versus giant planet formation 24 p3451 N88-30543
The atmospheres of the earth and the other planets: Origin, evolution and composition 24 p3452 N88-30544

PLANETARY EXPLORATION

U SPACE EXPLORATION

PLANETARY GEOLOGY

NT MARS VOLCANOES

Remote sensing of planets and cartographic results
[HSBW-HEFT-14] 03 p0389 N88-12444
Planetary Geology: Goals, Future Directions, and Recommendations
[NASA-CP-3005] 19 p2742 N88-26279
Reports of planetary geology and geophysics program, 1987
[NASA-TM-4041] 20 p2885 N88-27133

PLANETARY GRAVITATION

Simulation and analysis of a geopotential research mission
[NASA-CR-182354] 06 p0670 N88-14109

PLANETARY IONOSPHERES

Relativistic electron precipitations in a pulsating aurora 04 p0468 N88-12894
Peculiarities of daytime ionosphere of Venus during years of low and high solar activity 08 p1005 N88-16091

Distribution of electron concentration in nightime atmosphere of Venus based on radio transmission data
08 p1005 N88-16092
Applicability of extremely low frequency global resonances for study of Venusian storm activity
08 p1005 N88-16093
Model of Jovian F region ionosphere
[NASA-CR-182587] 13 p1855 N88-21105
Tethered diagnostic package for use from the space station
[DE88-006264] 16 p2167 N88-22921

PLANETARY LANDING
Lunar base launch and landing facility conceptual design, 2nd edition
[NASA-CR-172049] 20 p2885 N88-27135

PLANETARY MAGNETIC FIELDS
Interplanetary magnetic field effects on the interaction of the solar wind with Venus 06 p0805 N88-14910
Magnetic field of planet Uranus: Predictions, measurements, interpretations 08 p1005 N88-16094

PLANETARY MANTLES
NT EARTH MANTLE
Astrophysics and the solar nebula
07 p0883 N88-15355

PLANETARY MAPPING
Remote sensing of planets and cartographic results
[HSBW-HEFT-14] 03 p0389 N88-12444

PLANETARY MASS
Construction of mass-age curves for the continental crust: An empirical model and an example from the western US 24 p3394 N88-30213
The growth of continents and some consequences since 1.5 Ga 24 p3395 N88-30220

PLANETARY MOTION
U SOLAR ORBITS

PLANETARY NEBULAE
The nucleus of LT-5: An unusual triple system? — planetary nebula
[PUBL-SER-C-FASC-11] 03 p0388 N88-12436
Winds and shells around low-mass supergiants
04 p0514 N88-13164
High spatial resolution observations of dust and gas in NGC 7027 and the M8 Hourglass
06 p0801 N88-14903
A global model for planetary nebulae, taking into account central stellar evolution and influence on halo ionization
[ETN-88-91491] 11 p1568 N88-19389
Radiation transport in planetary nebulae
[ETN-88-91500] 14 p1993 N88-21880
The observability of carbon monoxide in planetary nebulae
[ETN-88-91498] 14 p2011 N88-21994
International ultraviolet explorer spectral atlas of planetary nebulae, central stars, and related objects
[NASA-RP-1203] 22 p3164 N88-28843

PLANETARY ORBITS
Discovery by Voyager-2 of predicted satellites which determine resonance nature of Uranian rings
08 p1006 N88-16095
The 1985 mutual phenomena of Jupiter's satellites observed in Brazil
[INPE-4526-PRE/1276] 15 p2152 N88-22848

PLANETARY RADIATION
Ray tracing of Jovian low frequency radiation
[NASA-CR-179262] 08 p1101 N88-16620
Research in particle and gamma-ray astrophysics
[NASA-CR-183111] 20 p2887 N88-27146

PLANETARY RINGS
NT SATURN RINGS
NT URANUS RINGS
Toward a comprehensive theory for the sweeping of trapped radiation by inert orbiting matter
[NASA-CR-182584] 11 p1569 N88-19395

PLANETARY SATELLITES
U NATURAL SATELLITES

PLANETARY SPACE FLIGHT
U INTERPLANETARY FLIGHT

PLANETARY SPACECRAFT
U INTERPLANETARY SPACECRAFT

PLANETARY STRUCTURE
Experimental study of planetary gases with applications to planetary interior models
[NASA-CR-183098] 20 p2886 N88-27137

PLANETARY SURFACES
NT MARS SURFACE
NT VENUS SURFACE
Shock-chemistry in natural materials and evolution of planetary surfaces
[DE87-012737] 02 p0254 N88-11604
Small reactor power systems for manned planetary surface bases
[NASA-TM-100223] 04 p0524 N88-13209
Studies in Aeolian geology
[NASA-CR-182328] 05 p0625 N88-13828
Running head: What color is it
[NASA-CR-182600] 11 p1551 N88-19280
Electromagnetic powered vehicles (EMPV) for Mars exploration 17 p2419 N88-24388

PLANETARY SYSTEMS
NT SOLAR SYSTEM
Reports of planetary astronomy, 1988
[NASA-TM-4063] 22 p3163 N88-28835

PLANETARY WAVES
A baroclinic wavy basic state model: Description and preliminary experiments
[KNMI-WR-87-1] 01 p0068 N88-10436
Dynamics of isolated intrathermocline eddy
04 p0460 N88-12845
Dynamic modeling of the middle atmosphere
08 p1028 N88-16227
Seasonal variations and excitation mechanisms of the equatorially trapped waves 13 p1798 N88-20751
Nonlinear normal mode initialization of a limited area model using nonstationary Rossby modes — numerical weather forecasting
[KNMI-WR-87-10] 14 p1947 N88-21614
Interactions between synoptic and planetary scales of motion
[AD-A192328] 23 p3234 N88-29246
Rossby waves in mid-latitude oceans
24 p3405 N88-30273

PLANETESIMALS
U PROTOPLANETS

PLANETOLOGY
Laser simulation of light and plasma action on comets and planets 09 p1237 N88-17413
Reflectance spectroscopy in planetary science: Review and strategy for the future
[NASA-SP-493] 17 p2451 N88-24564
Research and Technology, 1987, Goddard Space Flight Center
[NAS 1.15:101097] 17 p2453 N88-24572
Planetary Geology: Goals, Future Directions, and Recommendations
[NASA-CP-3005] 19 p2742 N88-26279

PLANETS
NT EARTH (PLANET)
NT GAS GIANT PLANETS
NT JUPITER (PLANET)
NT MARS (PLANET)
NT NEPTUNE (PLANET)
NT TERRESTRIAL PLANETS
NT URANUS (PLANET)
NT VENUS (PLANET)

PLANFORMS
NT ARROW WINGS
NT DELTA WINGS
NT RECTANGULAR PANELS
NT RECTANGULAR PLANFORMS
NT RECTANGULAR PLATES
NT SWEPT FORWARD WINGS
NT SWEPTBACK WINGS
NT VARIABLE SWEEP WINGS
NT WING PLANFORMS
Planform effects on the supersonic aerodynamics of multibody configurations
[NASA-TP-2762] 04 p0393 N88-12454
Inflow measurements made with a laser velocimeter on a helicopter model in forward flight. Volume 4: Tapered planform blades at an advance ratio of 0.15
[NASA-TM-100544] 16 p2156 N88-22863

PLANIGRAPHY
U TOMOGRAPHY

PLANKTON
NT PHYTOPLANKTON
Varifront 3 expedition data report (USNS DE STEIGUER CRUISE 1202-82). Bioluminescence, hydrographic, nutrient, and satellite data from the Gulf of California (November-December 1981)
[AD-A185011] 05 p0620 N88-13805
The use of chlorophyll fluorescence measurements from space for separating constituents of sea water. Volume 2: Appendices
[ESA-CR(P)-2444-VOL-2] 07 p0873 N88-15295
Biological processes in the water column of the South Atlantic bight: Zooplankton responses
[DE88-004811] 14 p1951 N88-21630

PLANKTON BLOOM
U PLANKTON

PLANNING
NT AIRPORT PLANNING
NT MANAGEMENT PLANNING
NT MISSION PLANNING
NT PRODUCTION PLANNING
NT PROJECT PLANNING
NT REGIONAL PLANNING
NT URBAN PLANNING
CNET (Chief of Naval Education and Training) Program Automated Tracking System (CPATS): A comprehensive study
[AD-A184694] 03 p0385 N88-12418
Federal plan for meteorological services and supporting research, fiscal year 1988
[PB88-118716] 07 p0880 N88-15336
Task path planning, scheduling and learning for free-ranging robot systems 08 p1058 N88-16386
Qualitative models for planning: A gentle introduction
08 p1062 N88-16414
Operational aspects of a spacecraft planning/scheduling expert system
08 p1062 N88-16415
Prototype resupply scheduler
08 p1064 N88-16428
Loads and aeroelasticity division research and technology accomplishments for FY 1987 and plans for FY 1988
[NASA-TM-100534] 09 p1114 N88-16680
Trimodal interpretation of constraints for planning
09 p1209 N88-17248
Computer assisted instruction: Two decades in perspective
[AD-A186813] 09 p1216 N88-17289
Motion planning and control of robot manipulators via application of a computer graphics animated display
11 p1496 N88-18932
Preliminary analysis of an integrated logistics system for OSSA payloads
[NASA-CR-4114] 12 p1584 N88-19477
Preliminary analysis of an integrated logistics system for OSSA payloads. Volume 3: OSSA integrated logistics support planning document 12 p1584 N88-19480
Preliminary analysis on plasma equilibrium control. Conceptual design study of FY86 FER
[DE88-751441] 14 p1984 N88-21834
Hybrid PV HgCdTe IR detectors technology reliability and failure program: Environmental stress testing plan
[AD-A191165] 16 p2211 N88-23195
Identification of areas cultivated with soybeans in the cerrados regions, through digital processingof satellite images: A methodological approach
17 p2358 N88-24048
Sensitivity analysis for the system reliability function
[AD-A191648] 18 p2525 N88-24979
Management and the executive
[AD-A190778] 18 p2587 N88-25374
Department of Defense statement on defense agency research and development to the Subcommittee on Defense of the Committee on Appropriations, United States House of Representatives, 100th Congress, second session
[AD-A191840] 18 p2588 N88-25377
Department of Defense Statement on the Balanced Technology Initiative to the Committee on Armed Services, United States Senate, 100th Congress, second session
[AD-A191841] 18 p2588 N88-25378
Centre for International Co-Operation and Appropriate Technology (CICAT)
[PB88-165501] 18 p2590 N88-25389
Plans for discourse
[AD-A192242] 20 p2832 N88-26802
Vision research. A national plan: 1983-1987, 1987 evaluation and update
[PB88-192604] 21 p2985 N88-27726
Motion planning for legged locomotion systems on uneven terrain 23 p3221 N88-29170
Motion planning with obstacles and dynamic constraints 23 p3222 N88-29175
Lisp Object State Saver (LOSS): A facility used to save partial schedules of the Hubble Space Telescope
24 p3421 N88-30360
Research on problem-solving systems
[AD-A195154] 24 p3423 N88-30370

PLANT DESIGN
Facility design validation of the information systems laboratory
[AD-A186309] 07 p0906 N88-15488
Lunar fiberglass: Properties and process design
[NASA-CR-182580] 11 p1466 N88-18740
Design of nuclear heat, power co-generation plant detailed 16 p2186 N88-23033
More on exact state reconstruction in deterministic digital control systems
[NASA-TP-2847] 22 p3063 N88-28177

PLANT ROOTS
Cytomorphology and ultrastructure of corn root meristem in weightlessness 12 p1651 N88-19891
Gravisensing in lentil seedling roots grown in space (Spacelab D-1 mission) 12 p1654 N88-19911
Graviperception of lentil seedling roots grown in space
22 p3061 N88-28165

PLANT STRESS
Overview of Austrian Airborne Imaging Spectrometer (AIS) programme and first results
05 p0612 N88-13762
Measuring near infrared spectral reflectance changes from water stressed conifer stands with AIS-2
05 p0613 N88-13765

PLANTING
Controlled ecological life support systems: Development of a plant growth module 05 p0630 N88-13854
PLANTS (BOTANY)
NT ALGAE
NT BLUE GREEN ALGAE
NT BRYOPHYTES
NT CHLORELLA
NT CONIFERS
NT CORN
NT COTTON
NT GRASSES
NT LEGUMINOUS PLANTS
NT MICROCYSTIS
NT PHYTOPLANKTON
NT POTATOES
NT RICE
NT SEA GRASSES
NT SOYBEANS
NT SUGAR CANE
NT TRADESCANTIA
NT TREES (PLANTS)
NT YEAST
Compilation of 1986 annual reports of the Navy ELF (Extremely Low Frequency) communications system ecological monitoring program, volume 1
[AD-A184561] 03 p0306 N88-11930
Controlled Ecological Life Support System. Design, Development, and Use of a Ground-Based Plant Growth Module
[NASA-CP-2479] 05 p0630 N88-13852
Uses of airborne laser Chayka-1 for probing water, land surfaces 06 p0725 N88-14461
A process study of the biothermal conversion of water hyacinths to methane
[DE88-000554] 06 p0730 N88-14488
Comparative anatomic analysis of seedling organs of pisum sativum (fabaceae) cultivated under space flight conditions 06 p0749 N88-14603
Investigation of effect of silver compounds on microflora in water reclaimed from atmospheric moisture condensate in a closed environment 07 p0892 N88-15407
Space station accommodations for life sciences research facilities. Phase 1: Conceptual design and programmatics studies for Missions SAAX0307, SAAX0302 and the transition from SAAX0307 to SAAX0302. Volume 2: Study results
[NASA-CR-179244] 08 p0962 N88-15829
Neogene paleoclimate in Pacific Ocean subarctic region determined from study of diatoms 08 p1010 N88-16125
Plant cell technologies in space: Background, strategies and prospects 09 p1198 N88-17177
Spectroscopic studies of energy transfer in photosynthetic reaction centers of higher plants
[DE88-003850] 10 p1359 N88-18121
Species biology and potential for controlling four exotic plants (Ammophila arenaria, Carpobrotus edulis, Cortaderia jubata and Gasoul crystallinum) on Vandenberg Air Force Base, California
[NASA-TM-100980] 10 p1363 N88-18148
Five New South Wales barrier lagoons: Their macrobenthic fauna and seagrass communities 11 p1517 N88-19059
Space station accommodations for life sciences research facilities: Phase A conceptual design and programmatics studies for Missions SAAX0307, SAAX0302 and the transition from SAAX0307 to SAAX0302. Volume 1: Executive summary
[NASA-CR-179267] 12 p1599 N88-19571
Plant biology in space 12 p1654 N88-19910
A method to detect and digitize small plant movements 12 p1654 N88-19912
Plant cell cultures in space biology studies 12 p1654 N88-19913
The use of plant protoplasts in biotechnological space research 12 p1655 N88-19914
Effects of cosmic heavy ion radiation and space microgravity on plant systems 12 p1658 N88-19936
The 35 mm vertical aerial photographs for mapping stands of bracatinga in different age classes 17 p2366 N88-24087
Mapping of plant associations and the variation of surface water in the Pantanal Mato-Grossense National Park, through remote sensing techniques 17 p2366 N88-24092
Botany Facility: The problems of plant fixation
[SIRA-A/7373/WP220/RJS/001] 17 p2379 N88-24140
Botany Facility: Problems of water supply, plant nutrients and soil in the Botany Facility
[SIRA-A/7373/WP220/RJS/003] 17 p2379 N88-24141
Supply and distribution of plant nutrients in the Botany Facility
[SIRA-A/7373/WP220/RJS/004] 17 p2379 N88-24142
Photochrome from green plants: Assay, purification and characterization
[DE88-007511] 19 p2702 N88-26067
PLANTS (INDUSTRIES)
U INDUSTRIAL PLANTS
PLASMA ACCELERATION
Hot plasmas in the Earth's magnetosphere 03 p0272 N88-11710
Particle injection and cosmic ray acceleration at collisionless parallel shocks
[DE88-000507] 04 p0430 N88-12665
Microphysics of the auroral acceleration region of other regions of the magnetosphere 08 p1096 N88-16592
Acceleration/heating processes on auroral field lines as observed by the Viking spacecraft 08 p1096 N88-16596
Stochastic acceleration of cometary ions: The effects of composition and source strength distributions 14 p1997 N88-21902
Nonlinear effects in plasma wake field acceleration
[DE88-700972] 15 p2134 N88-22734
PLASMA ANTENNAS
Analysis of plasma coupling with the prototype DIII-D ICRF antenna
[DE88-008085] 19 p2729 N88-26204
PLASMA ARC SPRAYING
U ARC SPRAYING
PLASMA ARC WELDING
Plasma joining of metal matrix composites
[AD-A184828] 05 p0557 N88-13390
The interaction of DC plasma jet with a melting metal: Experimental measurements and mathematical description
[AD-A185173] 05 p0651 N88-13993
Pulsed plasma arc welding process with double closed-loop adaptive penetration control system
[PB87-143780] 07 p0863 N88-15236
Study on arc sound in TIG and plasma welding processes and the possibility of its application in practice
[PB87-143947] 07 p0863 N88-15238
Study on the square wave alternating plasma arc welding for aluminum alloys
[PB87-143772] 07 p0863 N88-15239
Examination of the physical processes associated with the keyhole region of variable polarity plasma arc welds in aluminum alloy 2219 07 p0927 N88-15634
Plasma joining of metal matrix composites
[AD-A188559] 12 p1604 N88-19593
Plasma joining of metal matrix composites
[AD-A193939] 22 p3051 N88-28100
ARC length control for plasma welding
[NASA-CASE-MSC-20900-1] 24 p3380 N88-30131
PLASMA ARCS
U PLASMA JETS
PLASMA BUBBLES
In-situ plasma bubble observations associated with equatorial spread-F over Natal
[INPE-4488-PRE/1252] 15 p2095 N88-22482
PLASMA CHEMISTRY
Plasma deposition of silicon carbide thin films
[AD-A188093] 11 p1556 N88-19314
PLASMA CLOUDS
NT MAGNETIC CLOUDS
The expansion of magnetic clouds 01 p0115 N88-10737
CRRES chemical release mechanisms 14 p1874 N88-21192
A plasma wave instrument on the AMPTE/IRM (Active Magnetospheric Particle Tracing Explorers/Ion Release Module) spacecraft
[AD-A191216] 16 p2233 N88-23336
Application of particle simulations to the NRL laser experiment
[AD-A191641] 18 p2520 N88-24953
PLASMA COMPRESSION
System studies of compact ignition tokamaks
[DE87-014976] 02 p0239 N88-11508
Factors which affect operation of a plasma focus in various gases
[DE88-701882] 20 p2858 N88-26975
PLASMA CONDUCTIVITY
Current generation and induced conductivity of a plasma under common action of constant electric field and lower-hybrid or ECR waves
[DE88-700345] 07 p0935 N88-15680
Transport properties of conductive polymers
[AD-A188411] 12 p1610 N88-19628
Characterization of PEOS (Plasma Erosion Opening Switch) plasma parameters and conduction phase properties
[AD-A189024] 12 p1624 N88-19714
PLASMA CONFINEMENT
U PLASMA CONTROL
PLASMA CONTROL
Steady state theta pinch concept for slow formation of FRC
[ISSN-0469-4732] 01 p0098 N88-10648
Massachusetts Institute of Technology Plasma Fusion Center: 1986-1987 Report to the President
[DE87-013518] 01 p0101 N88-10661
Numerical simulation of laser filamentation experiments
[ETN-87-90959] 02 p0179 N88-11118
Computer models for kinetic equations of magnetically confined plasmas
[DE87-011571] 02 p0236 N88-11492
Field-reversing electron and ion rings for the confinement and heating of plasmas
[DE87-014869] 02 p0238 N88-11505
Improvement of energy confinement of neutral beam heated plasma by lower hybrid current drive in JT-60
[DE87-752983] 02 p0239 N88-11509
Two dimensional neutral transport analysis in tokamak plasma
[DE87-752984] 02 p0239 N88-11510
Analysis of energy confinement of slideaway discharges
[DE87-753008] 02 p0240 N88-11515
Reactivity for DT plasma with beam-induced tail in magnetic confinement system
[DE87-753017] 02 p0240 N88-11517
Feasibility of alpha particle measurement in a magnetically confined plasma by CO2 laser Thomson scattering
[DE88-000039] 02 p0241 N88-11522
Potential formation in the plasma confinement region of a radio-frequency plugged linear device
[IPPJ-843] 02 p0242 N88-11526
Application of a two fluid theoretical plasma transport model on current Tokamak reactor designs
[DE87-013511] 03 p0377 N88-12373
Measurement of parallel ion energy distribution function in PISCES plasma
[DE88-000108] 03 p0378 N88-12380
Interchange stability of noncircular reversed field pinches
[DE88-000177] 03 p0378 N88-12381
The role of stellarators in the advanced toroidal program
[DE87-014815] 04 p0491 N88-13025
Data base on the high heat flux behaviour of metals and carbon materials for plasma facing components: Experiments at the 10 MW neutral beam injection test stand of the IPP Nagoya
[IPPJ-AM-53] 04 p0492 N88-13031
Confinement time of electrons and H(-)/D(-) ions in the Uramoto type sheet plasma
[IPPJ-852] 04 p0492 N88-13032
Monte Carlo analysis of neoclassical transport for a compact helical system
[IPPJ-850] 04 p0492 N88-13033
MHD stability and control for mirror machines 04 p0493 N88-13038
ALT-1 pump limiter experiments
[DE88-000822] 05 p0651 N88-13989
A review of the experimental and theoretical status of the reversed-field pinch
[DE88-000529] 05 p0652 N88-14000
Confinement of energy in tokamak-10 plasma during electron-cyclotron-resonance heating 06 p0773 N88-14750
Reversed field pinch experiments: Summary of progress report
[DE88-002367] 07 p0934 N88-15673
Recent results of plasma research activities at the Instituto de Pesquisas Espaciais
[INPE-4383-PRE/1203] 08 p1085 N88-16538
Particle transport in microdetonations — inertial confinement fusion pellets
[OEFZS-4402] 09 p1164 N88-16976
Experimental study of the initial plasma formation stage in a linear theta pinch of inverted field
[DE88-700010] 09 p1249 N88-17485
Plasma theory and simulation
[AD-A187100] 09 p1249 N88-17486
Influence of fast alpha diffusion and thermal alpha buildup on Tokamak reactor performance
[DE88-003661] 09 p1251 N88-17496
Observation of enhanced electric field in an RF-plugged sheet plasma in the RFC-XX-M open-ended machine
[IPPJ-857] 09 p1252 N88-17503
Pump limiter experiments and analysis in the TEXTOR tokamak 09 p1252 N88-17506
D-3He fuels in a field-reversed configuration
[IPPJ-855] 10 p1411 N88-18419
Plasma confinement calculations for TIBER-2
[DE88-004044] 10 p1412 N88-18425

First and second harmonic ECRH experience at gyrotron frequencies at LLNL
[DE88-003998] 10 p1413 N88-18430
Stability of an RFP (Reversed-Field Pinch) with resistive and distant boundaries
[DE88-004155] 10 p1413 N88-18431
Toroidal confinement research concepts evaluation and tradeoff studies
[DE88-004277] 11 p1551 N88-19282
Toroidal confinement research concepts evaluation and tradeoff studies
[DE88-004841] 11 p1552 N88-19285
Diagnostics for intelligent control of MPD (Magneto-Plasma Dynamic) engines
[AD-A189619] 12 p1603 N88-19587
CIT (Compact Ignition Tokamak) fueling
[DE88-002709] 12 p1692 N88-20125
FOM contributions to the 14th European Conference on Controlled Fusion and Plasma Physics
[REPT-87-174] 12 p1693 N88-20129
Simulation of electron cyclotron heating in TFR
12 p1693 N88-20130
Formation of high-Beta plasmas in various modes of operation in TPE-2 12 p1693 N88-20132
SOAR: Space orbiting advanced fusion power reactor
[AD-A189234] 13 p1732 N88-20356
Reversed field pinch operation with a thin shell
[DE88-005521] 13 p1843 N88-21027
Preliminary analysis on plasma equilibrium control. Conceptual design study of FY86 FER
[DE88-751441] 14 p1984 N88-21834
New methods of confinement and heating of plasma in magnetic fields
[DE88-701021] 15 p2135 N88-22738
Long-time impurity confinement as a precursor to disruptions in ohmically heated tokamaks
[DE88-006183] 15 p2136 N88-22742
Improvement of plasma confinement due to electron Landau damping in tokamaks
[DE88-752339] 15 p2136 N88-22747
Transport simulations of ohmic ignition experiment: IGNITEX
[DE88-006055] 15 p2138 N88-22757
Ion traps for large storage capacity
16 p2268 N88-23570
A fusion based plasma propulsion system
17 p2401 N88-24274
Fluid dynamics of spherical cavity reactors
17 p2403 N88-24291
Stability of spheromak against current driven modes: Effects of flux hole on stability
[IPPJ-868] 19 p2730 N88-26211
Zero-dimensional calculation for ZT-H
[DE88-009175] 19 p2731 N88-26217
Symmetrized magnetic field configuration of low aspect ratio helical system
[IPPJ-869] 20 p2855 N88-26956
Neoclassical diffusion due to trapping/detrapping orbits in stellarators
[DE88-008566] 20 p2857 N88-26968
The effect of ICRF on the Alcator C Scrape-Off Layer plasma
[DE88-009821] 20 p2858 N88-26972
Tokamak magnetic turbulence over the safety factor range 0.6 less than q less than 3
[DE88-008421] 21 p3017 N88-27904
Optical imaging diagnostics for fusion plasmas
[DE88-997572] 21 p3018 N88-27910
A survey of the current experimental database for lower hybrid current-drive and heating
[DE88-009830] 23 p3283 N88-29552
Vortex formation and particle transport in a cross-field plasma sheath
[DE88-008931] 23 p3284 N88-29553

PLASMA COOLING
Methods and first results of plasma non-isothermal parameters measurements in meteor trails
06 p0737 N88-14531
Modeling and transport in semiconductor devices
[AD-A188760] 13 p1844 N88-21037

PLASMA CORE REACTORS
Fluid dynamics of spherical cavity reactors
17 p2403 N88-24291

PLASMA CURRENTS
Fast wave injection into high temperature tokamak plasmas in the lower-hybrid-density regime of JIPP T-IIU
[ISSN-0469-4732] 01 p0099 N88-10649
Use of polarimetry to measure the current profile in MTX
[DE87-013835] 02 p0237 N88-11495
Stability of spheroidal spheromak plasma by use of force-free approximation
[IPPJ-846] 02 p0241 N88-11523
Current-driven lower hybrid waves at the inner edge of the ring current --- magnetosphere
[MPE-PREPRINT-94] 02 p0243 N88-11534
Application of a two fluid theoretical plasma transport model on current Tokamak reactor designs
[DE87-013511] 03 p0377 N88-12373
Magnetic fluctuation behaviour of current termination in reversed field pinch
[IPPJ-849] 04 p0492 N88-13034
Observations of propagating double layers in a high current discharge
[TRITA-EPP-87-10] 05 p0652 N88-13997
Conceptual design of a radio-frequency driven compact tokamak
[INPE-4364-PRE/1190] 08 p1085 N88-16535
Shape of the plasma boundary in TBR
[INPE-4388-PRE/1208] 08 p1086 N88-16540
Tokamak with highly elongated cross-section of a plasma
[DE88-700356] 10 p1410 N88-18412
Structural consequences of railgun augmentation
[DE88-007036] 15 p2023 N88-22058
Interpretation of the northward B sub z (NBZ) Birkeland current system and polar cap convection patterns in terms of the impulsive penetration model
[AERONOMICA-ACTA-A-321-1987]
18 p2595 N88-25422
ECRH current drive in tokamak plasmas
[IPPJ-864] 19 p2729 N88-26209
Cosmic electric currents and the generalized Bennett pinch
[TRITA-EPP-87-14] 22 p3154 N88-28764
The interaction of Io with the plasma torus
23 p3308 N88-29704
RFP (Revised Field Pinch) plasma experiment at INPE
[INPE-4613-PRE/1336] 24 p3431 N88-30420

PLASMA CYLINDERS
NT CYLINDRICAL PLASMAS

PLASMA DECAY
Observation of nonlinear wave decay processes in the solar wind by the AMPTE IRM plasma wave experiment
[AD-A191409] 16 p2290 N88-23713

PLASMA DENSITY
Study of ionization equilibrium of high temperature and low density plasma
[DE87-703070] 02 p0238 N88-11502
X-ray pulsars: Accretion flow deceleration
03 p0390 N88-12451
ALT-1 pump limiter experiments
[DE88-000822] 05 p0651 N88-13989
State parameters of pulse-discharge plasma in xenon-filled closed tube 06 p0773 N88-14747
Unusually strong density decrease in near-Earth interplanetary plasma and magnetically quiet day as effects of isolated solar flare 08 p1002 N88-16072
Small scale plasma density structures observed by the Viking double probe instrument --- Swedish satellite
08 p1098 N88-16604
Pump limiter experiments and analysis in the TEXTOR tokamak 09 p1252 N88-17506
A study of single and binary ion plasma expansion into laboratory-generated plasma wakes
[NASA-CR-4125] 10 p1412 N88-18427
Large scale plasma irregularities observed in the nighttime ionosphere over Natal using a rocket-borne Langmuir probe
[INPE-4422-PRE/1226] 12 p1694 N88-20139
Ionization equilibrium and radiative energy losses in a stationary plasma
[DE88-700856] 14 p1984 N88-21832
Correlation between magnetic and electric field fluctuations observed during flyby near Halley's comet
14 p1996 N88-21897
Magnetic cavity formation at Comet Halley and at the AMPTE Li release 14 p1996 N88-21898
Long-time impurity confinement as a precursor to disruptions in ohmically heated tokamaks
[DE88-006183] 15 p2136 N88-22742
Application of magnetic barrier for increasing the efficiency of laser ion source
[DE88-701669] 16 p2212 N88-23200
Summary report on the Japan-US Workshop on the Assessment of Spectroscopic Data for Temperature and Density Measurements --- plasma diagnostics
[IPPJ-861] 17 p2439 N88-24512
Tokamak studies of density sensitive line ratios
17 p2441 N88-24521
Density diagnostics by hydrogen line intensity ratios: Excitation cross section between excited states
17 p2441 N88-24522
Spectral diagnostics for temperature and density measurements on ATF 17 p2442 N88-24525
Measurements of Z(sub eff) profile with a visible bremsstrahlung continuum detector array
17 p2443 N88-24529
Low frequency electrostatic turbulence in the polar cap E-region
[DRI-3-88] 18 p2540 N88-25077
Plasma neutralizer work at BNL (Brookhaven National Laboratory)
[DE88-007046] 18 p2579 N88-25317
Infrared and far-infrared laser development for plasma diagnostics at Oak Ridge National Laboratory
[DE88-007262] 19 p2674 N88-25904
Calculation of the line shapes of radiators immersed in plasma 19 p2729 N88-26210
Poloidal field measurements using laser enhanced attenuation of an energetic lithium beam
[DE88-008360] 20 p2856 N88-26963
A plasma ultraviolet source for short wavelength lasers
[AD-A192844] 21 p2952 N88-27537
Heating efficiency of beat wave excitation in a density gradient
[AD-A193086] 21 p3017 N88-27905
Density fluctuations in currentless high beta plasmas in Heliotron E
[DE88-752310] 23 p3283 N88-29550
Consideration of plasma opening switches from a wave propagation perspective
[AD-A195681] 24 p3431 N88-30421

PLASMA DIAGNOSTICS
Diagnostic technique for monitoring high temperature plasma dynamics
[DE87-011786] 01 p0099 N88-10653
Nonlinear fluid equations for a low collisionality toroidal plasma
[DE87-013006] 01 p0100 N88-10655
Direct detection of optical radiation through a sampling orifice for inductively coupled plasma atomic emission spectroscopy
[DE87-013609] 01 p0101 N88-10662
Use of polarimetry to measure the current profile in MTX
[DE87-013835] 02 p0237 N88-11495
Thermally driven convective cells and tokamak edge turbulence
[DE87-014424] 02 p0238 N88-11499
Spectrograms of the visible region in the JT-60 tokamak (wavelength range from 2210 A to 5250 A)
[DE87-753002] 02 p0240 N88-11513
Laser blow-off experiments on ASDEX --- tokamak
[IPP-III/119] 02 p0243 N88-11535
Production of atom flows at materials evaporation by laser radiation
[DE87-703327] 03 p0328 N88-12074
Review of X-ray spectroscopy from laser-produced plasmas
[DE88-000755] 04 p0494 N88-13043
Proceedings of the 17th International Conference on Phenomena in Ionized Gases held in Budapest, Hungary, July 8-12, 1985: Invited papers
[DE87-703562] 05 p0651 N88-13987
Intracavity spectrum analyzer with NaF:F2(+):F3(-) crystal laser for long-wave IR wave band
07 p0919 N88-15584
Activities report of the Institute of Plasma Physics
[ETN-88-91020] 07 p0933 N88-15668
Method of plasma diagnostics by a heavy ion beam for the T-15 tokamak
[DE88-700342] 07 p0935 N88-15678
Relativistic plasma concentration measuring by Bremsstrahlung
[DE88-700560] 07 p0936 N88-15685
Diagnostic concept of the resonance cone technique and its application in ground and space experiments
08 p1027 N88-16222
Resonance cones in nonthermal plasmas: Laboratory experiments 08 p1027 N88-16223
MAIMIK: A high current electron beam experiment on a sounding rocket from Andoya rocket range (Norway)
08 p1030 N88-16243
Effect of neutral wind on the latitudinal variation of nighttime F-layer vertical movements
08 p1030 N88-16244
Remote and in-situ plasma measurements during the Coordinated Auroral Experiment using Scatter And Rockets (CAESAR) flight 08 p1032 N88-16252
Shape of the plasma boundary in TBR
[INPE-4388-PRE/1208] 08 p1086 N88-16540
Tangential Thomson scattering --- plasma diagnostics
[REPT-87-173] 08 p1087 N88-16548
Conditional sampling in plasma turbulence
08 p1097 N88-16603
Testing a very good microwave interferometer
[TRITA-EPP-86-09] 09 p1167 N88-16996
Microwave system for the microwave Tokamak experiment (MTX)
[DE88-002391] 09 p1250 N88-17487
Investigation of the evolution of the fusion processes in the plasma focus using time-resolved neutron spectroscopy
[IPF-87-4] 09 p1251 N88-17493

Overview of applications of Laser-Induced Breakdown Spectroscopy (LIBS)
[DE88-004314] 10 p1336 N88-17987
Diagnostics for ATF
[DE88-004175] 10 p1414 N88-18438
Ion energy diagnostics for voltage determinations in plasma-erosion-opening-switch experiments
[DE88-004822] 11 p1479 N88-18827
ICF research at Los Alamos
[DE88-005394] 11 p1493 N88-18916
Summaries of FY86 research in the Applied Plasma Physics Fusion Theory Program
[DE88-004242] 11 p1554 N88-19298
A neutral-beam diagnostic for fast confined alpha particles in a burning plasma: Applicatoin on CIT (Compact Ignition Tokamak)
[DE88-004890] 11 p1554 N88-19301
Diagnostics for intelligent control of MPD (Magneto-Plasma Dynamic) engines
[AD-A189619] 12 p1603 N88-19587
An experimental and theoretical investigation of optogalvanic effects
[AD-A189618] 12 p1625 N88-19720
Measurements of optically thin electron cyclotron emission from relativistic electrons
[DE88-004713] 12 p1688 N88-20096
FOM contributions to the 14th European Conference on Controlled Fusion and Plasma Physics
[REPT-87-174] 12 p1693 N88-20129
X-ray source model for Z-pinch aluminum plasmas
[AD-A189509] 12 p1696 N88-20148
Laser pulse detection with infrared range semiconductor detectors
[DE88-700857] 14 p1914 N88-21432
Variability of Comet Halley's coma: VEGA-1 and VEGA-2 magnetic field observations 14 p1995 N88-21891
Physical processes in the vicinity of the cometopause interpreted on the basis of plasma, magnetic field and plasma wave data measured on board VEGA-2 spacecraft --- Halley's comet 14 p1996 N88-21894
Some new features of plasma wave phenomena at Halley: APV-N observations --- VEGA 14 p1996 N88-21895
Plasma phenomena in the vicinity of the closest approach of VEGA-1, 2 spacecraft to the Comet Halley nucleus 14 p1996 N88-21899
Halley's environments by the Japanese Suisei spacecraft 14 p1999 N88-21915
Plasma tail of Comet Halley in January 1986 14 p2006 N88-21960
Advanced diagnostics for reacting flows
[AD-A190485] 15 p2035 N88-22122
High-voltage inverse-square function generator
[DE88-701109] 15 p2058 N88-22270
The development of high power KrF laser systems for plasma research by the application of stimulated Raman scattering
[ETN-88-92220] 15 p2073 N88-22358
Corpuscular plasma diagnostics complex on a tokamak with a strong field
[DE88-701576] 16 p2279 N88-23646
Measurement of time evolution of plasma electron component parameters on the Ogra-4 device by the Thomson scattering method
[DE88-701575] 16 p2282 N88-23662
Summary report on the Japan-US Workshop on the Assessment of Spectroscopic Data for Temperature and Density Measurements --- plasma diagnostics
[IPPJ-861] 17 p2439 N88-24512
Ion temperature measurement with spectroscopy in JT-60 17 p2439 N88-24513
X-ray emission from tokamaks 17 p2439 N88-24514
X-ray spectroscopic diagnostics on JIPPT-IIU and HELIOTRON-E 17 p2440 N88-24515
Helium-like titanium spectra from tokamak plasmas 17 p2440 N88-24516
Spectroscopic results from JET: Some examples of data comparison and data needs 17 p2440 N88-24517
Ion temperature profile measurement using charge exchange recombination spectroscopy on JIPP T-IIU 17 p2440 N88-24518
Spectroscopic measurements of ion temperature, rotation speed and beam deposition profile on DIII-D 17 p2440 N88-24519
Forbidden transitions as ion-temperature sensitive lines 17 p2441 N88-24520
Tokamak studies of density sensitive line ratios 17 p2441 N88-24521
Density diagnostics by hydrogen line intensity ratios: Excitation cross section between excited states 17 p2441 N88-24522
Spectroscopic study of heliotron E plasmas: Stark profile, CXR, poloidal rotation and carbon coating 17 p2441 N88-24523
Observation of injected silicon in heliotron E 17 p2441 N88-24524
Spectral diagnostics for temperature and density measurements on ATF 17 p2442 N88-24525
Cascade fluorescences from laser-excited lithium atom for plasma diagnostics 17 p2442 N88-24526
Spectroscopic data relevant to alpha particle diagnostics 17 p2442 N88-24527
Flux density measurements of neutral iron in TEXTOR with laser induced fluorescence 17 p2442 N88-24528
Measurements of Z(sub eff) profile with a visible bremsstrahlung continuum detector array 17 p2443 N88-24529
Hot electron diagnostics using X-ray imaging on GAMMA10 17 p2443 N88-24530
Polarization spectroscopy: Prospect and data needs 17 p2443 N88-24531
Intensity calibration of a VUV system by branching line pairs 17 p2443 N88-24533
Availability and quality of spectroscopic data and standards for tokamak studies 17 p2443 N88-24534
Trochoidal analysis of scattered electrons in a merged electron-ion beam
[NASA-CASE-NPO-16789-1-CU] 18 p2573 N88-25281
Intense ion beam diagnostics for particle beam fusion experiments on PBFA 2
[DE88-007279] 18 p2577 N88-25308
A two-wavelength infrared interferometer/polarimeter system for CIT (Compact Ignition Tokamak)
[DE88-007681] 18 p2579 N88-25321
Optical diagnostics for a high power, rf-inductively coupled plasma
[DE88-007822] 18 p2579 N88-25322
Activities report in plasma physics
[ETN-88-92221] 18 p2580 N88-25324
Infrared and far-infrared laser development for plasma diagnostics at Oak Ridge National Laboratory
[DE88-007262] 19 p2674 N88-25904
The XRD (X-Ray Diode) array, the grazing incidence spectrometer and the X-ray imaging camera on PBFA 2
[DE88-007282] 19 p2728 N88-26200
Design and calibration of a two-channel low-noise heterodyne receiver for use in a CO2 laser Thomson scattering alpha particle diagnostic
[DE88-007866] 19 p2728 N88-26201
Simultaneously time- and space-resolved spectroscopic characterization of laser-produced plasmas
[DE88-008038] 19 p2728 N88-26202
A low divergence, high brightness lithium ion source for plasma diagnostics
[DE88-008063] 19 p2729 N88-26203
Calculation of the line shapes of radiators immersed in plasma 19 p2729 N88-26210
An elliptical spectrograph/gated microchannel plate detector for time-resolved spectral measurements in the X-ray region
[DE88-007590] 20 p2856 N88-26961
Poloidal field measurements using laser enhanced attenuation of an energetic lithium beam
[DE88-008360] 20 p2856 N88-26963
Fusion programs in applied plasma physics and development and technology at GA Technologies, Inc.
[DE88-008406] 20 p2856 N88-26964
A CO2 laser Thomson scattering diagnostic for fusion product alpha particle measurement
[DE88-007683] 20 p2857 N88-26965
Multipoint Thomson scattering diagnostic for DIII-D
[DE88-008737] 20 p2857 N88-26969
Developing diagnostic methods for plasma-particle interaction
[DE88-007726] 20 p2858 N88-26973
Vertical viewing ECE diagnostic for the D3-D tokamak
[DE88-010586] 20 p2860 N88-26987
MTX (Microwave Tokamak Experiment) plasma diagnostic system
[DE88-011326] 20 p2861 N88-26993
Dynamics of a plasma produced under effect of the XeCl-laser radiation on metallic surface
[DE88-701983] 21 p3017 N88-27902
Optical imaging diagnostics for fusion plasmas
[DE88-997572] 21 p3018 N88-27910
Four-frame gated optical imager with 120-ps resolution
[DE88-011735] 22 p3080 N88-28288
Introduction to laser plasma diagnostics
[DE88-011056] 23 p3285 N88-29560
Apparatus for submillimeter laser diagnostics of high-temperature plasma
[DE88-702464] 23 p3285 N88-29563
Ionospheric radio and propagation: Waves in plasmas 24 p3364 N88-30030

PLASMA DIFFUSION
Relation of wave energy and momentum with the plasma dispersion relation in an inhomogeneous plasma
[DE88-002305] 08 p1084 N88-16530
Nonlinear diffusion in the presence of a time-dependent external electric field
[INPE-4378-PRE/1198] 08 p1085 N88-16533
Chaotic diffusion across magnetic field in a model of electrostatic turbulent plasma
[PREPRINT-586] 14 p1985 N88-21839
Consideration of plasma opening switches from a wave propagation perspective
[AD-A195681] 24 p3431 N88-30421

PLASMA DIODES
Electron temperature measurements in an argon/cesium plasma diode
[AD-A188835] 12 p1695 N88-20141
Development of inductive storage pulsed power generators
[AD-A193878] 22 p3117 N88-28521

PLASMA DISCHARGES
U PLASMA JETS

PLASMA DISPERSION
U PLASMA DIFFUSION

PLASMA DISPLAY DEVICES
Excimer plasma displays
[AD-A186731] 09 p1250 N88-17489
Brightness contrast and character height of five flat panel computer displays
[AD-A187743] 11 p1524 N88-19096

PLASMA DRIFT
Curvature driven drift mirror instability in the magnetosphere
[IFSI-86-14] 06 p0742 N88-14568
Effect of neutral wind on the latitudinal variation of nighttime F-layer vertical movements 08 p1030 N88-16244
A study of single and binary ion plasma expansion into laboratory-generated plasma wakes
[NASA-CR-4125] 10 p1412 N88-18427
Plasma rotation in a tokamak
[DE88-700855] 12 p1693 N88-20128
Large scale plasma irregularities observed in the nighttime ionosphere over Natal using a rocket-borne Langmuir probe
[INPE-4422-PRE/1226] 12 p1694 N88-20139
The effects of a dc electric field on the current driven ion cyclotron instability
[AD-A188877] 12 p1695 N88-20142
Improvement of plasma confinement due to electron Landau damping in tokamaks
[DE88-752339] 15 p2136 N88-22747
Application of particle simulations to the NRL laser experiment
[AD-A191641] 18 p2520 N88-24953
Plasma theory and simulation
[AD-A194674] 23 p3286 N88-29565
Vortex formation and particle transport in a cross-field plasma sheath
[AD-A194838] 24 p3432 N88-30425

PLASMA DYNAMICS
Diagnostic technique for monitoring high temperature plasma dynamics
[DE87-011786] 01 p0099 N88-10653
Study of the mechanism for solar wind formation 01 p0118 N88-10756
A high-power RF linear accelerator for FELs (Free-Electron Lasers)
[DE87-011795] 02 p0177 N88-11104
Laboratory and near-earth space plasma as a key to the plasma universe
[TRITA-EPP-87-09] 05 p0652 N88-13996
Numerical models for high beta magnetohydrodynamic flow
[DE88-001850] 05 p0654 N88-14008
A fluid simulation of the AMPTE lithium gas releases in the solar wind
[TRITA-EPP-87-06] 05 p0661 N88-14056
State parameters of pulse-discharge plasma in xenon-filled closed tube 06 p0773 N88-14747
Experimental evidence of micro-nonequilibrium on the magnetopause and further predictions 08 p1098 N88-16606
Dynamical aspects of electrostatic double layers
[TRITA-EPP-87-13] 09 p1250 N88-17492
Diagnostics for intelligent control of MPD (Magneto-Plasma Dynamic) engines
[AD-A189619] 12 p1603 N88-19587
Electric fields in Earth orbital space. Magnetospheric structural dynamic response to external variables
[AD-A188592] 12 p1643 N88-19836
Waves and static electric fields in the auroral acceleration region 12 p1646 N88-19856
Effects of toroidal forces in current loops embedded in a background plasma
[AD-A188878] 12 p1695 N88-20143
Studies of ionosphere/magnetosphere dynamics using SABRE and HILAT
[AD-A190947] 16 p2232 N88-23333

Spectroscopic measurements of ion temperature, rotation speed and beam deposition profile on DIII-D
17 p2440 N88-24519
Finite element methodology for integrated flow-thermal-structural analysis
[NASA-CR-183144] 21 p2964 N88-27606
Plasma theory and simulation
[AD-A194674] 23 p3286 N88-29565
Characteristics of solitary waves and weak double layers in the magnetospheric plasma
[IRF-PREPRINT-105] 24 p3431 N88-30418
Consideration of plasma opening switches from a wave propagation perspective
[AD-A195681] 24 p3431 N88-30421

PLASMA ELECTRODES
Behavior and structure of metal vapor arc plasma between molten electrodes
[DE88-001854] 06 p0782 N88-14801
Continuously frequency-tunable high-pressure CO2-laser with plasmatic cathode
09 p1238 N88-17418
Fundamental studies on MPD thrusters
[AD-A190307] 15 p2137 N88-22753
Basic processes of plasma propulsion
[AD-A192117] 18 p2577 N88-25310
Pierce diode with external circuit. Part 3: Chaotic behavior
[AD-A194837] 24 p3365 N88-30041

PLASMA ENGINES
Multi-stage plasma thruster
[AD-A183635] 01 p0017 N88-10105
Study of Plasma Motor Generator (PMG) tether system for orbit reboost
[NASA-CR-172016] 04 p0403 N88-12501
Completely magnetically contained electrothermal thrusters
[AD-A185674] 06 p0674 N88-14129
Diagnostics for intelligent control of MPD (Magneto-Plasma Dynamic) engines
[AD-A189619] 12 p1603 N88-19587
Fundamental studies on MPD thrusters
[AD-A190307] 15 p2137 N88-22753
Physical fluid mechanics in MPD thrusters
[AD-A190309] 15 p2138 N88-22754
Plasma-gas interaction studies in a hybrid plume plasma rocket
[AD-A190310] 15 p2138 N88-22755
MPD (magnetoplasmadynamic) thruster advanced pumping system concepts
[AD-A190513] 15 p2138 N88-22756
Megawatt level electric propulsion perspectives
17 p2404 N88-24294
Unified study of plasma/surface interactions for space power and propulsion
[AD-A195971] 24 p3338 N88-29870

PLASMA EQUILIBRIUM
On tokamak equilibrium
[DE87-014811] 02 p0239 N88-11507
Computational study of three-dimensional magnetohydrodynamic equilibria in toroidal helical systems
[DE87-753007] 02 p0240 N88-11514
Elements of plasma physics 03 p0271 N88-11703
Simulation an experiment on plasma instability investigation in a tokamak with a divertor
[DE88-700352] 07 p0935 N88-15683
Model for plasma equilibrium configuration evolution in a tokamak with adiabatic compression
[DE88-700354] 07 p0936 N88-15684
Possibility of calculation of magnetic surface function gradient and related quantities
[DE88-700561] 07 p0936 N88-15686
Beta limitation of matter-antimatter boundary layers
[TRITA-EPP-87-11] 09 p1250 N88-17490
Tokamak with highly elongated cross-section of a plasma
[DE88-700356] 10 p1410 N88-18412
The Pierce diode with an external circuit. 2: Non-uniform equilibria
[AD-A188027] 11 p1478 N88-18818
Diagnostics for intelligent control of MPD (Magneto-Plasma Dynamic) engines
[AD-A189619] 12 p1603 N88-19587
Shear Alfven spectrum of analytic high-Beta equilibria
12 p1694 N88-20136
Effects of toroidal forces in current loops embedded in a background plasma
[AD-A188878] 12 p1695 N88-20143
Nonlinear resonance of two-dimensional ion layers
[AD-A188890] 12 p1695 N88-20145
Fully implicit three-dimensional MHD (magnetohydrodynamics) stability and evolution in toroidal geometry
[DE88-000624] 13 p1842 N88-21023
Nonlinear effects in plasma wake field acceleration
[DE88-700972] 15 p2134 N88-22734
Moment approach to neoclassical flows, currents and transport in auxiliary heated tokamaks
[DE88-008024] 21 p3016 N88-27901
ITER plasma equilibrium and poloidal field system design
[DE88-011005] 21 p3018 N88-27912
Theory and simulation of relaxed plasmoids
[AD-A192884] 21 p3032 N88-27997
Vortex formation and particle transport in a cross-field plasma sheath
[DE88-008931] 23 p3284 N88-29553
Plasmoid propagation
[AD-A192378] 23 p3284 N88-29555

PLASMA ETCHING
Silicon containing photoresists
[AD-A188666] 12 p1605 N88-19601
Fundamental studies and device development in beta silicon carbide
[AD-A189540] 12 p1699 N88-20165

PLASMA FLOW
U MAGNETOHYDRODYNAMIC FLOW

PLASMA FLUX MEASUREMENT
MHD energy fluxes for late type dwarfs
04 p0512 N88-13148
Array detectors for plasma spectrochemistry
[AD-A194220] 22 p3052 N88-28105

PLASMA FOCUS
Activities report of the Institute of Plasma Physics
[ETN-88-91020] 07 p0933 N88-15668
Investigation of the evolution of the fusion processes in the plasma focus using time-resolved neutron spectroscopy
[IPF-87-4] 09 p1251 N88-17493
The effects of optical smoothing techniques on filamentation in laser plasmas
[AD-A188719] 16 p2275 N88-23614
On the self-focusing of electric helicons
[DE88-701870] 20 p2848 N88-26905
Factors which affect operation of a plasma focus in various gases
[DE88-701882] 20 p2858 N88-26975
A plasma ultraviolet source for short wavelength lasers
[AD-A192844] 21 p2952 N88-27537

PLASMA FREQUENCIES
Elements of plasma physics 03 p0271 N88-11703
Laser thermal propulsion
[AD-A186407] 07 p0933 N88-15666
Microwave radiation from rotating, annular electron beams 11 p1475 N88-18801
The effects of a dc electric field on the current driven ion cyclotron instability
[AD-A188877] 12 p1695 N88-20142

PLASMA GENERATION
U PLASMA GENERATORS

PLASMA GENERATORS
NT JOINT EUROPEAN TORUS
NT PLASMA GUNS
NT TOKAMAK DEVICES
Mechanisms of polymer degradation using an oxygen plasma generator
[NASA-TM-100681] 01 p0018 N88-10110
Analysis of a series of electromagnetic launcher firings
[AR-005-131] 04 p0405 N88-12516
ICRF launcher studies
[DE88-001710] 04 p0495 N88-13046
Preparation of qualification tests of a plasma generator for the feeding of a hypersonic wind tunnel
05 p0530 N88-13222
High peak power ka-band gyrotron oscillator experiment
[AD-A185424] 05 p0585 N88-13563
A synthetic plasma source
[TRITA-EPP-86-15] 05 p0652 N88-13995
Plasma contactors for use with electodynamic tethers for power generation
[NASA-CR-182424] 08 p1087 N88-16547
Vacuum-arc plasma centrifuge experiment
[INPE-4509-PRE/1263] 15 p2138 N88-22758
Multiply stripped ion generation in the metal vapor vacuum arc
[DE88-008418] 19 p2725 N88-26179
Study of Plasma Motor Generator (PMG) tether system for orbit reboost
[NASA-CR-172074] 23 p3184 N88-28949
Bibliography of Soviet laser developments, number 88, March - April 1987
[AD-A195978] 24 p3378 N88-30116

PLASMA GUNS
Analytical solution of the equations for a coaxial plasma gun operating in the snowplow mode. 1. Weak coupling limit
[AD-A185370] 05 p0652 N88-13994
Antistokes coherent Raman diffusion of a nitriding plasma
[ONERA-RF-6/3644-PY] 16 p2175 N88-22962
Evaluation of the chromium oxide arc spraying treatment on solar energy collectors
[ETN-88-92564] 18 p2537 N88-25053
Refractory fibers surface treatment
[REPT-47-803/F] 21 p2922 N88-27339

PLASMA HEATING
NT ELECTRON CYCLOTRON HEATING
Mode purity measurements on gyrotrons for plasma heating at the stellarator W 7-AS
[IPF-87-3] 01 p0101 N88-10660
Massachusetts Institute of Technology Plasma Fusion Center: 1986-1987 Report to the President
[DE87-013518] 01 p0101 N88-10661
Field-reversing electron and ion rings for the confinement and heating of plasmas
[DE87-014669] 02 p0238 N88-11505
Transport analysis of OH and NBI heated discharges in JT-60
[DE87-752985] 02 p0239 N88-11511
Spectrograms of the visible region in the JT-60 tokamak (wavelength range from 2210 A to 5250 A)
[DE87-753002] 02 p0240 N88-11513
Reactivity for DT plasma with beam-induced tail in magnetic confinement system
[DE87-753017] 02 p0240 N88-11517
Fusion reactivity enhancement due to ion tail formation by beam and ion cyclotron heating
[DE87-753018] 02 p0240 N88-11518
Effect of electrostatic field on behaviour of peripheric plasma at high-frequency heating
[DE87-703328] 03 p0378 N88-12378
Negative ion beams for heating and current-drive in NET
[AD-A184390] 04 p0489 N88-13012
ALT-1 pump limiter experiments
[DE88-000822] 05 p0651 N88-13989
Atlas of atomic spectral lines of neptunium emitted by an inductively coupled plasma
[DE88-000640] 06 p0782 N88-14796
Techniques for ceramic sintering using microwave energy
[DE88-001416] 07 p0837 N88-15080
Electron acceleration by wave processes in the earth's ionosphere
[AD-A186110] 07 p0877 N88-15320
Studies on parametric instabilities in high-frequency wave heating of fusion plasmas
[PH-156] 07 p0933 N88-15667
Gyrotron development at the Instituto de Pesquisas Espaciais
[INPE-4240-PRE/1115] 08 p0990 N88-15992
A ray-tracing study of electron cyclotron resonance heating in tokamak plasmas with a superthermal electron tail
[INPE-4381-PRE/1201] 08 p1085 N88-16536
Absorption of electron cyclotron radiation in tokamak plasmas with a superthermal tail in the electron velocity distribution
[INPE-4391-PRE/1211] 08 p1086 N88-16541
Acceleration/heating processes on auroral field lines as observed by the Viking spacecraft
08 p1096 N88-16596
Theoretical studies of mass loss and shock phenomena in cool star envelopes
[NASA-CR-182433] 08 p1099 N88-16616
Experimental study of the initial plasma formation stage in a linear theta pinch of inverted field
[DE88-700010] 09 p1249 N88-17485
Microwave system for the microwave Tokamak experiment (MTX)
[DE88-002391] 09 p1250 N88-17487
D-3He fuels in a field-reversed configuration
[IPPJ-855] 10 p1411 N88-18419
New mode conversion process and overdense plasma heating in the electron cyclotron range of frequencies
[IPPJ-854] 10 p1411 N88-18420
ATF experimental plans
[DE88-004177] 10 p1414 N88-18439
Laser production and heating of plasma for MHD application
[NASA-TP-2798] 10 p1415 N88-18443
Induction linacs: A technology come of age for international cooperation
[DE88-003953] 11 p1548 N88-19258
Magnetic and inertial fusion status and development plans
[DE88-004405] 11 p1552 N88-19288
Microturbulent fluctuations in the TORTUR tokamak
12 p1693 N88-20131
The stability of a screw-pinch plasma to global MHD modes 12 p1694 N88-20133
Effects of toroidal forces in current loops embedded in a background plasma
[AD-A188878] 12 p1695 N88-20143

Experimental studies of plasma heating due to the parametric decay of a large amplitude pump into lower hybrid waves 13 p1841 N88-21017
Particle simulation research by plasma parametric heating caused by strong laser 14 p1903 N88-21368
Consistency between current ramp-up/recharging scenario by non-inductive current drive and dense and cold divertor plasma. Conceptual design study of FY86 FER
[DE88-751438] 14 p1984 N88-21833
Preliminary analysis on plasma equilibrium control. Conceptual design study of FY86 FER
[DE88-751441] 14 p1984 N88-21834
New methods of confinement and heating of plasma in magnetic fields
[DE88-701021] 15 p2135 N88-22738
Heating and confinement studies of electron cyclotron resonance heated plasmas in Heliotron E
[DE88-752312] 15 p2136 N88-22746
Theoretical studies of the heating of toroidal plasmas with radiofrequency electromagnetic radiation
[DE88-006913] 15 p2137 N88-22749
Plasma-gas interaction studies in a hybrid plume plasma rocket
[AD-A190310] 15 p2138 N88-22755
Measurements of Z(sub eff) profile with a visible bremsstrahlung continuum detector array 17 p2443 N88-24529
Activities report in plasma physics
[ETN-88-92221] 18 p2580 N88-25324
A mode-transforming polarization-rotatable launcher for the ATF (Advanced Toroidal Facility) fusion experiment
[DE88-005070] 19 p2730 N88-26213
Parallel gradient effects on ICRH (Ion Cyclotron Resonance Heating) in tokamaks
[DE88-009038] 19 p2730 N88-26216
The effect of ICRF on the Alcator C Scrape-Off Layer plasma
[DE88-009821] 20 p2858 N88-26972
Moment approach to neoclassical flows, currents and transport in auxiliary heated tokamaks
[DE88-008024] 21 p3016 N88-27901
Heating efficiency of beat wave excitation in a density gradient
[AD-A193066] 21 p3017 N88-27905
Plasma technology: Preliminary studies 2
[DE88-752815] 22 p3154 N88-28763
Initial operation and edge plasma studies in ATF (Advanced Toroidal Facility)
[DE88-011400] 23 p3285 N88-29562
Apparatus for submillimeter laser diagnostics of high-temperature plasma
[DE88-702464] 23 p3285 N88-29563
Theoretical modeling of accelerating arc plasmas
[AD-A195606] 24 p3432 N88-30426

PLASMA INSTABILITY
U MAGNETOHYDRODYNAMIC STABILITY

PLASMA INTERACTIONS
NT LASER PLASMA INTERACTIONS
NT PLASMA-ELECTROMAGNETIC INTERACTION
NT PLASMA-PARTICLE INTERACTIONS
Evolution of the solar wind structure in the outer heliosphere 01 p0112 N88-10721
Solar wind-cometary interaction at the ionopause and associated phenomena 01 p0117 N88-10748
The solar wind interaction with comets: A post encounter view 01 p0118 N88-10751
Plasma-tail activity and the interplanetary medium at Halley's Comet during Armada Week: 6-14 March 1986 01 p0118 N88-10752
Coherent emission from relativistic beam-plasma interactions 04 p0493 N88-13039
Analysis of geophysical data bases and models for spacecraft interactions
[AD-A184809] 05 p0555 N88-13375
Laboratory and near-earth space plasma as a key to the plasma universe
[TRITA-EPP-87-09] 05 p0652 N88-13996
Unified study of plasma-surface interactions for space power and propulsion
[AD-A186211] 07 p0825 N88-15007
Plasma theory and simulation
[DE88-000412] 07 p0934 N88-15670
CAESAR investigations — Coordinated Auroral Experiment using Scatter And Rockets (CAESAR) 08 p1031 N88-16249
Field-aligned fluxes of energetic electrons related to the onset of magnetospheric substorms 08 p1096 N88-16595
Critical Ionization Velocity (CIV) interaction: Some unsolved questions
[TRITA-EPP-87-12] 09 p1250 N88-17491
On the role of the ionization frequency to gyrofrequency ratio in the critical ionization velocity interaction
[TRITA-EPP-86-10] 10 p1410 N88-18414
A study of single and binary ion plasma expansion into laboratory-generated plasma wakes
[NASA-CR-4125] 10 p1412 N88-18427
USU (Utah State University) Center of Excellence in Theory and Analysis of the Geo-Plasma Environment
[AD-A187687] 11 p1511 N88-19026
Simulation of the plasma interaction with thin dust clouds 11 p1552 N88-19291
Improved confinement of screw pinch plasmas in SPICA 2 12 p1694 N88-20137
Hydrogen pumping and release by graphite under high flux plasma bombardment
[DE88-005880] 13 p1842 N88-21021
Reversed field pinch operation with a thin shell
[DE88-005521] 13 p1843 N88-21027
Modeling and transport in semiconductor devices
[AD-A188760] 13 p1844 N88-21037
A comparison between wave observations performed in the environments of Comets Halley and Giacobini-Zinner 14 p1996 N88-21896
High power, high frequency radiation from beam-plasma interactions
[AD-A190207] 15 p2137 N88-22752
Fundamental studies on MPD thrusters
[AD-A190307] 15 p2137 N88-22753
A plasma wave instrument on the AMPTE/IRM (Active Magnetospheric Particle Tracing Explorers/Ion Release Module) spacecraft
[AD-A191216] 16 p2233 N88-23336
The effects of optical smoothing techniques on filamentation in laser plasmas
[AD-A188719] 16 p2275 N88-23614
Theoretical plasma physics research of active space experiments
[AD-A192075] 18 p2577 N88-25309
Fluid dynamical model of ultrarelativistic heavy ion collisions
[DE88-007905] 20 p2850 N88-26921
The effect of ICRF on the Alcator C Scrape-Off Layer plasma
[DE88-009821] 20 p2858 N88-26972
Coupling between radiation and gas dynamics
[AD-A194593] 23 p3211 N88-29113
Tokamak plasma interaction with limiters
[UTIAS-325] 23 p3286 N88-29566

PLASMA JETS
NT RADIO JETS (ASTRONOMY)
NBS (National Bureau of Standards) measurement services: Radiometric standards in the vacuum ultraviolet
[PB87-227625] 03 p0325 N88-12055
Mathematical models of plasma discharge control in a tokamak
[DE87-702891] 03 p0378 N88-12377
Design study for asteroidal exploitation 03 p0389 N88-12445
Pulsed plasma jet igniters: Species measurements in methane combustion
[DE88-001389] 05 p0562 N88-13422
The interaction of DC plasma jet with a melting metal: Experimental measurements and mathematical description
[AD-A185173] 05 p0651 N88-13993
Observations of propagating double layers in a high current discharge
[TRITA-EPP-87-10] 05 p0652 N88-13997
The effect of propane on atomic spectrometric signals in the direct current plasma
[DE88-002457] 07 p0934 N88-15676
Analysis of the decomposition of transparent polymer materials (blocks) under the action of laser beams in free generation mode
[AD-A187090] 09 p1147 N88-16873
Simulation of electron cyclotron heating in TFR 12 p1693 N88-20130
Improved confinement of screw pinch plasmas in SPICA 2 12 p1694 N88-20137
On the structure of pulsed plasma jets 13 p1843 N88-21030
Relativistic jet models for the BL Lacertae object Mrk 421 during three epochs of observation
[NASA-TM-89727] 13 p1853 N88-21090
Structural consequences of railgun augmentation
[DE88-007036] 15 p2023 N88-22058
Vacuum-arc plasma centrifuge experiment
[INPE-4509-PRE/1263] 15 p2138 N88-22758
The thermal evolution of the jets in SS433 — galactic object
[MPE-PREPRINT-107] 16 p2289 N88-23705
Optical investigations of the thermal boundary layer in arc plasmas 18 p2578 N88-25313
Modelling of thermal plasma systems 18 p2578 N88-25314
Plasma neutralizer work at BNL (Brookhaven National Laboratory)
[DE88-007046] 18 p2579 N88-25317
STARFIRE: Hypervelocity railgun development for high-pressure research
[DE88-008348] 19 p2605 N88-25469
Plasma deposition: Investigations on a new approach
[ETN-88-92619] 20 p2861 N88-26992
A study of mechanisms producing astrophysical jets
[AD-A194100] 23 p3300 N88-29649
Theoretical modeling of accelerating arc plasmas
[AD-A195606] 24 p3432 N88-30426

PLASMA LAYERS
NT PLASMA SHEATHS
Observations of propagating double layers in a high current discharge
[TRITA-EPP-87-10] 05 p0652 N88-13997
Double layer formed by beam driven ion-acoustic turbulence
[INPE-4292-PRE/1163] 08 p1086 N88-16543
Experimental investigation of double layers formed by ion-acoustic turbulence
[INPE-4296-PRE/1167] 08 p1086 N88-16544
Plasma theory and simulation
[AD-A187100] 09 p1249 N88-17486
Dynamical aspects of electrostatic double layers
[TRITA-EPP-87-13] 09 p1250 N88-17492
Silicon containing photoresists
[AD-A188666] 12 p1605 N88-19601
The effects of a dc electric field on the current driven ion cyclotron instability
[AD-A188877] 12 p1695 N88-20142
Nonlinear resonance of two-dimensional ion layers
[AD-A188890] 12 p1695 N88-20145
A proposal for the establishment of a center of excellence in theoretical geoplasma research
[AD-A189742] 16 p2231 N88-23327
Absorption characteristics of Si3N4 ablation layer plasma 20 p2783 N88-26504
The effect of ICRF on the Alcator C Scrape-Off Layer plasma
[DE88-009821] 20 p2858 N88-26972
The influence of ionization within a plasma opening switch
[AD-A193147] 21 p3017 N88-27906
Characteristics of solitary waves and weak double layers in the magnetospheric plasma
[IRF-PREPRINT-105] 24 p3431 N88-30418

PLASMA LOSS
Analysis of energy confinement of slideaway discharges
[DE87-753008] 02 p0240 N88-11515
Potential formation in the plasma confinement region of a radio-frequency plugged linear device
[IPPJ-843] 02 p0242 N88-11526
Characteristics of laser-plasma X-radiation source (review) 09 p1239 N88-17428

PLASMA OSCILLATIONS
Low-frequency oscillations in nonideal plasma 06 p0774 N88-14751
Particle simulation research by plasma parametric heating caused by strong laser 14 p1903 N88-21368
Nonlinear dynamics of interaction between charged particles modulated beam and bounded plasma regular oscillations
[DE88-701681] 16 p2280 N88-23648

PLASMA PERTURBATION
U PLASMA OSCILLATIONS

PLASMA PHYSICS
Compact torus studies
[DE87-014254] 02 p0237 N88-11496
Pressure structure of solar coronal loops 02 p0256 N88-11618
Space Environment Technology — conference
[ISBN-2-85428-170-5] 03 p0271 N88-11702
Elements of plasma physics 03 p0271 N88-11703
The solar wind 03 p0271 N88-11705
Ionosphere and plasmasphere 03 p0272 N88-11709
Three-dimensional charging effects — spacecraft 03 p0273 N88-11720
Theoretical plasma physics
[DE88-001475] 04 p0492 N88-13029
Activities report of the Ionospheric Observatory
[UIO-SR-87-01] 05 p0625 N88-13827
Energy dependence of ion-induced sputtering yields of monatomic solids in the low energy region
[IPPJ-AM-52] 05 p0651 N88-13988
Laboratory and near-earth space plasma as a key to the plasma universe
[TRITA-EPP-87-09] 05 p0652 N88-13996
Comments on H. Arp The persistent problem of spiral galaxies
[TRITA-EPP-87-05] 05 p0660 N88-14052
Cosmology in the plasma universe
[TRITA-EPP-87-07] 05 p0660 N88-14053

JPRS report: Science and technology. USSR: Physics and mathematics
[JPRS-UPM-87-008] 06 p0769 N88-14727
Theoretical studies of kinetic mechanisms of negative ion formation in plasmas
[AD-A185735] 06 p0784 N88-14812
USSR report: Physics and mathematics
[JPRS-UPM-87-002] 07 p0918 N88-15575
Activities report of the Institute of Plasma Physics
[ETN-88-91020] 07 p0933 N88-15668
Plasma theory and simulation
[DE88-000412] 07 p0934 N88-15670
Electrodynamics of midnight sector of auroral oval in period of slight disturbance 06 p1003 N88-16077
JPRS report: Science and technology. USSR: Physics and mathematics
[JPRS-UPM-87-010] 08 p1075 N88-16485
Recent results of plasma research activities at the Instituto de Pesquisas Espaciais
[INPE-4383-PRE/1203] 08 p1085 N88-16538
Plasma centrifuge development at INPE
[INPE-4243-PRE/1117] 08 p1087 N88-16546
Solar corona and solar wind 08 p1094 N88-16584
Plasma theory and simulation
[AD-A187100] 09 p1249 N88-17486
Critical Ionization Velocity (CIV) interaction: Some unsolved questions
[TRITA-EPP-87-12] 09 p1250 N88-17491
Proceedings of the Energy Independence Conference: Fusion Energy and Plasma Physics
[DE88-700657] 09 p1253 N88-17507
Physics modeling support contract
[DE88-004039] 10 p1335 N88-17980
Plasma physics design and major specifications of candidate reactors for FER design studies. Conceptual design study of FY86 FER
[DE88-751066] 10 p1411 N88-18416
New mode conversion process and overdense plasma heating in the electron cyclotron range of frequencies
[IPPJ-854] 10 p1411 N88-18420
Plasma theory and simulation
[DE88-003620] 10 p1414 N88-18437
Toroidal confinement research concepts evaluation and tradeoff studies
[DE88-004841] 11 p1552 N88-19285
Sixteenth AINSE Plasma Physics Conference. Conference handbook
[DE88-700625] 11 p1552 N88-19290
Summaries of FY86 research in the Applied Plasma Physics Fusion Theory Program
[DE88-004242] 11 p1554 N88-19298
Basic physics of laser-plasma interactions
[ETN-88-92055] 14 p1984 N88-21838
Magic light high-power laser passes state certification
15 p2053 N88-22236
Theoretical model of the cathode spot on a unipolar arc
[AD-A190109] 15 p2059 N88-22277
Plasmapause formation
[AERONOMICA-ACTA-A-319-1987]
15 p2138 N88-22759
A proposal for the establishment of a center of excellence in theoretical geoplasma research
[AD-A189742] 16 p2231 N88-23327
Soviet magnetic confinement fusion research
[PB88-182316] 16 p2279 N88-23644
Theoretical plasma physics research of active space experiments
[AD-A192075] 18 p2577 N88-25309
Activities report in plasma physics
[ETN-88-92221] 18 p2580 N88-25324
Fusion programs in applied plasma physics and development and technology at GA Technologies, Inc.
[DE88-008406] 20 p2856 N88-26964
Plasma technology: Preliminary studies 2
[DE88-752815] 22 p3154 N88-28763
Plasma theory and simulation
[AD-A194674] 23 p3286 N88-29565
Pierce diode with external circuit. Part 3: Chaotic behavior
[AD-A194837] 24 p3365 N88-30041
Bibliography of Soviet laser developments, number 88, March - April 1987
[AD-A195978] 24 p3378 N88-30116

PLASMA PINCH
NT SCREW PINCH
NT THETA PINCH
NT ZETA PINCH
Transverse focussing using plasma wake fields
[DE87-011503] 01 p0099 N88-10652
Numerical simulation of the Reversed Field Pinch
[AD-A184353] 04 p0491 N88-13023
Advanced concepts theory annual report 1986
[AD-A184986] 05 p0651 N88-13991
Potential benefits of a broad magnetic fusion R and D program
[DE88-003288] 11 p1553 N88-19297
X-rays from z-pinches
[AD-A188911] 12 p1696 N88-20146
X-ray source model for Z-pinch aluminum plasmas
[AD-A189509] 12 p1696 N88-20148
Activities report in plasma physics
[ETN-88-92221] 18 p2580 N88-25324
Photoconducting X-ray detectors for Z-pinch experiments
[DE88-007118] 19 p2728 N88-26199
Factors which affect operation of a plasma focus in various gases
[DE88-701882] 20 p2858 N88-26975
Theory and simulation of relaxed plasmoids
[AD-A192884] 21 p3032 N88-27997
Cosmic electric currents and the generalized Bennett pinch
[TRITA-EPP-87-14] 22 p3154 N88-28764

PLASMA POTENTIALS
Potential formation in the plasma confinement region of a radio-frequency plugged linear device
[IPPJ-843] 02 p0242 N88-11526
Confinement time of electrons and H(-)/D(-) ions in the Uramoto type sheet plasma
[IPPJ-852] 04 p0492 N88-13032
Experimental investigation of double layers formed by ion-acoustic turbulence
[INPE-4296-PRE/1167] 08 p1086 N88-16544

PLASMA POWER SOURCES
NT PLASMA ENGINES
Advanced electric propulsion and space plasma contactor research
[NASA-CR-180862] 06 p0674 N88-14126

PLASMA PROBES
NT ELECTROSTATIC PROBES
Preparation of qualification tests of a plasma generator for the feeding of a hypersonic wind tunnel
05 p0530 N88-13222
Diagnostic concept of the resonance cone technique and its application in ground and space experiments
08 p1027 N88-16222
Resonance cones in nonthermal plasmas: Laboratory experiments 08 p1027 N88-16223

PLASMA PROPULSION
Study of Plasma Motor Generator (PMG) tether system for orbit reboost
[NASA-CR-172016] 04 p0403 N88-12501
Plasma thruster development
[AD-A184173] 04 p0408 N88-12536
Interplanetary propulsion using inertial fusion
[NASA-TM-89661] 04 p0409 N88-12540
Unified study of plasma-surface interactions for space power and propulsion
[AD-A186211] 07 p0825 N88-15007
Fundamental studies on MPD thrusters
[AD-A190307] 15 p2137 N88-22753
Physical fluid mechanics in MPD thrusters
[AD-A190309] 15 p2138 N88-22754
Plasma-gas interaction studies in a hybrid plume plasma rocket
[AD-A190310] 15 p2138 N88-22755
Interplanetary propulsion using inertial fusion
17 p2401 N88-24273
A fusion based plasma propulsion system
17 p2401 N88-24274
Basic processes of plasma propulsion
[AD-A192117] 18 p2577 N88-25310
The effects of magnetic nozzle configurations on plasma thrusters
[NASA-CR-183096] 19 p2732 N88-26223
Performance and lifetime assessment of MPD arc thruster technology
[NASA-TM-101293] 24 p3336 N88-29660

PLASMA PUMPING
Pump limiter experiments and analysis in the TEXTOR tokamak 09 p1252 N88-17506
A plasma ultraviolet source for short wavelength lasers
[AD-A192844] 21 p2952 N88-27537

PLASMA RADIATION
Direct detection of optical radiation through a sampling orifice for inductively coupled plasma atomic emission spectroscopy
[DE87-013609] 01 p0101 N88-10662
Radio studies of large scale structures of the Sun's corona and transient activity 01 p0114 N88-10728
Advanced concepts theory annual report 1986
[AD-A184986] 05 p0651 N88-13991
Electrostatic VLF emission determined from rocket and satellite experiments 08 p1002 N88-16068
X-rays from z-pinches
[AD-A188911] 12 p1696 N88-20146
X-ray source model for Z-pinch aluminum plasmas
[AD-A189509] 12 p1696 N88-20148
High power, high frequency radiation from beam-plasma interactions
[AD-A190207] 15 p2137 N88-22752
X-ray emission from tokamaks
17 p2439 N88-24514
Polarization spectroscopy: Prospect and data needs
17 p2443 N88-24531
Studies of spectral line ratio fluctuations using Inductively Coupled Plasma (ICP) light
[IRF-PREPRINT-100] 18 p2578 N88-25311
Dynamics of a plasma produced under effect of the XeCl-laser radiation on metallic surface
[DE88-701983] 21 p3017 N88-27902

PLASMA RENIN ACTIVITY
U IMMUNOASSAY

PLASMA RESONANCE
Self-consistent modification of a fast tail distribution by resonant fields in nonuniform plasmas
[AD-A183790] 01 p0099 N88-10650
Effect of plasma resonance on properties of surface waves 06 p0773 N88-14749
Electron acceleration by wave processes in the earth's ionosphere
[AD-A186110] 07 p0877 N88-15320
Diagnostic concept of the resonance cone technique and its application in ground and space experiments
08 p1027 N88-16222
A generalized description of the anomalous Doppler resonance and the stabilizing role of ion dynamics
[INPE-4384-PRE/1204] 08 p1081 N88-16513
Nonlinear resonance of two-dimensional ion layers
[AD-A188890] 12 p1695 N88-20145
Parametric instabilities of inhomogeneous plasma near the lower-hybrid resonance
[DE88-701201] 15 p2137 N88-22748
Electrostatic whistler mode conversion at plasma resonance
[AD-A192951] 20 p2860 N88-26989
Role of ordinary to extraordinary mode wave coupling in ionospheric heating experiments
[AD-A195335] 24 p3362 N88-30017

PLASMA RINGS
U TOROIDAL PLASMAS

PLASMA SHEATHS
Vortex dynamics and transport to the wall in a crossed-field plasma sheath
[DE87-013286] 01 p0100 N88-10657
Three-dimensional charging effects — spacecraft
03 p0273 N88-11720
Analytical solution of the equations for a coaxial plasma gun operating in the snowplow mode. 1. Weak coupling limit
[AD-A185370] 05 p0652 N88-13994
Observations of an ion acoustic oscillation near a pulsed sheath
[INPE-4386-PRE/1206] 08 p0979 N88-15915
Plasma theory and simulation
[DE88-003620] 10 p1414 N88-18437
Effects of secondary electron emission on the collector and source sheaths of a finite ion temperature plasma
[DE88-008930] 20 p2858 N88-26971
The influence of ionization within a plasma opening switch
[AD-A193147] 21 p3017 N88-27906
Vortex formation and particle transport in a cross-field plasma sheath
[DE88-008931] 23 p3284 N88-29553
Plasma theory and simulation
[AD-A194674] 23 p3286 N88-29565
Vortex formation and particle transport in a cross-field plasma sheath
[AD-A194838] 24 p3432 N88-30425

PLASMA SOUND WAVES
U MAGNETOHYDRODYNAMIC WAVES
U PLASMA WAVES

PLASMA SPECTRA
Transport properties of conductive polymers
[AD-A188411] 12 p1610 N88-19628
Flux coordinate studies of elongated plasmas at high Beta 12 p1694 N88-20134
Shear Alfven spectrum of analytic high-Beta equilibria
12 p1694 N88-20136
Experimental study of the role of plasma polarization on line shape in dense laboratory plasmas
[ETN-88-92001] 13 p1844 N88-21033
Stimulated Emission of Energetic Particles (SEEP)
[AD-A188724] 13 p1853 N88-21094
Some new features of plasma wave phenomena at Halley: APV-N observations — VEGA
14 p1996 N88-21895
Energy spectra of pick-up ions recorded during the encounter of Giotto with Comet Halley
14 p1997 N88-21901

Thomson scattering for determining electron concentrations and temperatures in an inductively coupled plasma. 2: Description and evaluation of a multichannel instrument
[AD-A191324] 16 p2280 N88-23652
Ion temperature measurement with spectroscopy in JT-60 17 p2439 N88-24513
X-ray emission from tokamaks 17 p2439 N88-24514
X-ray spectroscopic diagnostics on JIPPT-IIU and HELIOTRON-E 17 p2440 N88-24515
Helium-like titanium spectra from tokamak plasmas 17 p2440 N88-24516
Spectroscopic results from JET: Some examples of data comparison and data needs 17 p2440 N88-24517
Ion temperature profile measurement using charge exchange recombination spectroscopy on JIPP T-IIU 17 p2440 N88-24518
Spectroscopic measurements of ion temperature, rotation speed and beam deposition profile on DIII-D 17 p2440 N88-24519
Forbidden transitions as ion-temperature sensitive lines 17 p2441 N88-24520
Tokamak studies of density sensitive line ratios 17 p2441 N88-24521
Density diagnostics by hydrogen line intensity ratios: Excitation cross section between excited states 17 p2441 N88-24522
Observation of injected silicon in heliotron E 17 p2441 N88-24524
Spectral diagnostics for temperature and density measurements on ATF 17 p2442 N88-24525
Intensity calibration of a VUV system by branching line pairs 17 p2443 N88-24533
Availability and quality of spectroscopic data and standards for tokamak studies 17 p2443 N88-24534
Time-resolved doubly bent crystal X-ray spectrometer
[DE88-007899] 20 p2805 N88-26637

PLASMA SPRAYING
Thermal expansion mismatch and oxidation in thermal barrier coatings 02 p0189 N88-11182
Thermal barrier coating life prediction model development 02 p0190 N88-11183
Thermal barrier coating life prediction model development 02 p0190 N88-11184
Self-lubricating coatings for high-temperature applications 09 p1119 N88-16703
Corrosion Research Center, University of Minnesota
[DE88-006681] 15 p2041 N88-22160
Protective coatings on metals, volume 10
[PB88-174461] 16 p2181 N88-23000
Government research on ceramics coating technology 16 p2184 N88-23019
Microlaminate composite structures by low pressure plasma spray deposition
[DE88-006453] 19 p2610 N88-25488
Plasma deposition: Investigations on a new approach
[ETN-88-92619] 20 p2861 N88-26992
Thermal barrier coating life-prediction model development
[NASA-CR-179507] 22 p3058 N88-28142

PLASMA STABILITY
U MAGNETOHYDRODYNAMIC STABILITY

PLASMA TEMPERATURE
State parameters of pulse-discharge plasma in xenon-filled closed tube 06 p0773 N88-14747
Laser thermal propulsion
[AD-A186407] 07 p0933 N88-15666
Asymmetric double Langmuir probe for fast and automatic measurements of plasma temperature
[DE88-004773] 10 p1414 N88-18436
Electron temperature measurements in an argon/cesium plasma diode
[AD-A188835] 12 p1695 N88-20141
Temperature estimates for a free flowing railgun plasma
[MRL-R-1054] 13 p1843 N88-21032
Summary report on the Japan-US Workshop on the Assessment of Spectroscopic Data for Temperature and Density Measurements --- plasma diagnostics
[IPPJ-861] 17 p2439 N88-24512
Spectroscopic study of heliotron E plasmas: Stark profile, CXR, poloidal rotation and carbon coating 17 p2441 N88-24523
Spectral diagnostics for temperature and density measurements on ATF 17 p2442 N88-24525
Calculation of the line shapes of radiators immersed in plasma 19 p2729 N88-26210
Energy conversion measurements in laser-sustained argon plasmas for application to rocket propulsion
[AD-A194931] 24 p3337 N88-29861

PLASMA THEORY
U PLASMA PHYSICS

PLASMA TORCHES
Plasma and ion etching for failure analysis. Part 2. The etching of plastic encapsulant and other semiconductor device materials, using the Technics Giga Etch 100-E plasma etch system
[AERE-R-12212] 09 p1177 N88-17050
Waste destruction by plasma
[SNIAS-881-430-113] 21 p2971 N88-27651
Plasma torch design codes package
[SNIAS-881-430-115] 23 p3286 N88-29569

PLASMA TURBULENCE
New directions in Vlasov plasma turbulence and anomalous transport
[DE87-014425] 02 p0238 N88-11500
Theoretical plasma physics
[DE88-001475] 04 p0492 N88-13029
Observations of turbulence and fluctuations in the solar wind 04 p0525 N88-13212
Evolution of mean square magnetic vector potential in compressible, two-dimensional, magnetofluid turbulence
[AD-A184985] 05 p0651 N88-13990
Fluctuations in frequency of coherent radio signals in solar plasma according to Venera-15 and Venera-16 data 08 p1003 N88-16079
Dynamics and turbulence of solar wind in area of its formation based on radio transmission data measured with Venera-15 and Venera-16 spacecraft 08 p1003 N88-16080
Recent results of plasma research activities at the Instituto de Pesquisas Espaciais
[INPE-4383-PRE/1203] 08 p1085 N88-16538
Double layer formed by beam driven ion-acoustic turbulence
[INPE-4292-PRE/1163] 08 p1086 N88-16543
Experimental investigation of double layers formed by ion-acoustic turbulence
[INPE-4296-PRE/1167] 08 p1086 N88-16544
Design, construction and operation of a small RFP for turbulent plasma studies
[INPE-4241-PRE/1116] 08 p1087 N88-16545
Emerging flux, magnetic reconnection, plasma turbulence and waves in the transition zone of the solar atmosphere 08 p1096 N88-16597
Conditional sampling in plasma turbulence 08 p1097 N88-16603
Microturbulent fluctuations in the TORTUR tokamak 12 p1693 N88-20131
Chaotic diffusion across magnetic field in a model of electrostatic turbulent plasma
[PREPRINT-586] 14 p1985 N88-21839

PLASMA WAVES
NT ELECTROSTATIC WAVES
Channeled particle acceleration by plasma waves in metals
[DE87-010541] 01 p0093 N88-10604
Local spectra and wave distribution functions --- space plasma
[KGI-PREPRINT-099] 01 p0100 N88-10659
The duskside plasmapause/ring current interface: Convection and plasma wave observations
[MPE-PREPRINT-93] 02 p0243 N88-11533
Current-driven lower hybrid waves at the inner edge of the ring current --- magnetosphere
[MPE-PREPRINT-94] 02 p0243 N88-11534
Energy cascading in the beat-wave accelerator
[DE87-014727] 03 p0377 N88-12374
Output power enhancement of AC Raman free-electron laser
[DE88-000503] 04 p0449 N88-12786
Ballooning modes or Fourier modes in a toroidal plasma?
[AD-A184299] 04 p0491 N88-13022
Nature and the nonlinear evolution of electrostatic waves associated with the AMPTE (Active Magnetosphere Particle Tracer Explorers) solar wind releases
[AD-A185471] 06 p0806 N88-14920
Experimental research of electron beam instability on the Doppler anomalous effect
[DE88-700565] 07 p0932 N88-15658
Current generation and induced conductivity of a plasma under common action of constant electric field and lower-hybrid or ECR waves
[DE88-700345] 07 p0935 N88-15680
Experimental evaluation for efficiency of excitation slow plasma and cyclotron waves in collective accelerators
[DE88-700566] 07 p0936 N88-15687
Observations of an ion acoustic oscillation near a pulsed sheath
[INPE-4386-PRE/1206] 08 p0979 N88-15915
Wave acceleration of auroral electrons 08 p1031 N88-16245
Experiments on ion-acoustic rarefactive solitons in a multi-component plasma with negative ions
[INPE-4393-PRE/1213] 08 p1086 N88-16542
AMPTE-UKS ion observations at a quasi-parallel bow shock 08 p1095 N88-16589
Emerging flux, magnetic reconnection, plasma turbulence and waves in the transition zone of the solar atmosphere 08 p1096 N88-16597
Small scale MHD wave processes in the solar atmosphere and solar wind 08 p1098 N88-16608
An analysis of whistler-mode radiation from the Spacelab-2 electron beam, revision
[AD-A188228] 11 p1552 N88-19287
Experimental study of scattered waves and cylindrical antenna sheaths in a microwave driven plasma 11 p1553 N88-19293
Basic physics of laser-plasma interactions
[ETN-88-92055] 14 p1984 N88-21838
The foreshock region upstream from the Comet Halley bow shock 14 p1995 N88-21893
Physical processes in the vicinity of the cometopause interpreted on the basis of plasma, magnetic field and plasma wave data measured on board VEGA-2 spacecraft --- Halley's comet 14 p1996 N88-21894
Some new features of plasma wave phenomena at Halley: APV-N observations --- VEGA 14 p1996 N88-21895
A comparison between wave observations performed in the environments of Comets Halley and Giacobini-Zinner 14 p1996 N88-21896
Wave energy flow conservation for propagation in inhomogeneous Vlasov-Maxwell equilibria
[DE88-006705] 15 p2055 N88-22251
Nonlinear effects in plasma wake field acceleration
[DE88-700972] 15 p2134 N88-22734
Plasma wave radiative damping of a new type in a relativistic one-dimensional plasma
[DE88-701191] 15 p2135 N88-22739
Parametric instabilities of inhomogeneous plasma near the lower-hybrid resonance
[DE88-701201] 15 p2137 N88-22748
Survey of the Air Force P78-2 (SCATHA) satellite plasma wave data during electron gun operations
[AD-A191014] 16 p2168 N88-22926
A plasma wave instrument on the AMPTE/IRM (Active Magnetospheric Particle Tracing Explorers/Ion Release Module) spacecraft
[AD-A191216] 16 p2233 N88-23336
Numerical research of dispersion properties of plasma cylindrical waveguides located in magnetic field
[DE87-703009] 16 p2275 N88-23615
Observation of nonlinear wave decay processes in the solar wind by the AMPTE IRM plasma wave experiment
[AD-A191409] 16 p2290 N88-23713
Activities report in plasma physics
[ETN-88-92221] 18 p2580 N88-25324
Contaminant ions and waves in the space station environment 18 p2590 N88-25393
Observations of electron cyclotron harmonic emissions associated with field-aligned electron beams
[SD-TR-87-33] 19 p2724 N88-26173
Alternative analysis of CO2-laser-produced plasma waves
[DE88-008434] 19 p2730 N88-26215
On the self-focusing of electric helicons
[DE88-701870] 20 p2848 N88-26905
Kinetic modulational instability of electron cyclotron waves in plasmas
[DE88-701893] 20 p2859 N88-26978
Drift wave vortices and anomalous transport
[DE88-009562] 20 p2859 N88-26982
Generation of Adlam-Allen waves by plasma release experiments in the solar wind
[PB88-106000] 20 p2886 N88-27140
Plasmoid propagation
[AD-A192378] 23 p3284 N88-29555
Ionospheric radio and propagation: Waves in plasmas 24 p3364 N88-30030
Characteristics of solitary waves and weak double layers in the magnetospheric plasma
[IRF-PREPRINT-105] 24 p3431 N88-30418
Reconstruction of wave distribution functions in warm plasmas
[IRF-PREPRINT-104] 24 p3431 N88-30422

PLASMA-ELECTROMAGNETIC INTERACTION
NT LASER PLASMA INTERACTIONS
Environmental interactions of solar generators in space 03 p0274 N88-11730
Laboratory simulation of the electrodynamic interactions of a tethered satellite with an ionospheric plasma
[IFSI-86-3] 08 p0961 N88-15822
Absorption of cyclotron radiation in skin layer in Araks experiment 08 p1003 N88-16076
Fluctuations in frequency of coherent radio signals in solar plasma according to Venera-15 and Venera-16 data 08 p1003 N88-16079
MAIMIK: A high current electron beam experiment on a sounding rocket from Andoya rocket range (Norway) 08 p1030 N88-16243
Wave acceleration of auroral electrons 08 p1031 N88-16245

Absorption of electron cyclotron radiation in tokamak plasmas with a superthermal tail in the electron velocity distribution
[INPE-4391-PRE/1211] 08 p1086 N88-16541
Coordinated Auroral Experiments using Scatter And Rocket investigations (CAESAR investigations)
[MPAE-W-47-87-13] 15 p2096 N88-22487
Influence of plasma parameters on VLF radiation in near-rocket region 24 p3448 N88-30518

PLASMA-PARTICLE INTERACTIONS
Planetary science 07 p0883 N88-15356
Electrostatic VLF emission determined from rocket and satellite experiments 08 p1002 N88-16068
Analytically modeling the carbothermic reduction of alumina in a thermal plasma
[DE88-005535] 13 p1841 N88-21020
Kinetics of electrons and molecules at plasma-beam discharge in molecular gases
[DE88-701196] 16 p2275 N88-23616
Developing diagnostic methods for plasma-particle interaction
[DE88-007726] 20 p2858 N88-26973
Equilibrium distribution functions for limited plasma-molecular systems
[DE88-702412] 21 p3018 N88-27916

PLASMAGUIDES
Numerical research of disperaion properties of plasma cylindrical waveguides located in magnetic field
[DE87-703009] 16 p2275 N88-23615

PLASMAPAUSE
The duskside plasmapause/ring current interface: Convection and plasma wave observations
[MPE-PREPRINT-93] 02 p0243 N88-11533
Plasmapause formation
[AERONOMICA-ACTA-A-319-1987] 15 p2138 N88-22759

PLASMAS (PHYSICS)
NT ARGON PLASMA
NT BETA PARTICLES
NT BOUNDARY LAYER PLASMAS
NT CESIUM PLASMA
NT COLD PLASMAS
NT COLLISIONAL PLASMAS
NT COLLISIONLESS PLASMAS
NT COSMIC PLASMA
NT CYLINDRICAL PLASMAS
NT DENSE PLASMAS
NT DEUTERIUM PLASMA
NT ELECTRON PLASMA
NT HELIUM PLASMA
NT HIGH TEMPERATURE PLASMAS
NT HYDROGEN PLASMA
NT LASER PLASMAS
NT METALLIC PLASMAS
NT NITROGEN PLASMA
NT NONEQUILIBRIUM PLASMAS
NT NONUNIFORM PLASMAS
NT OXYGEN PLASMA
NT PLASMA FOCUS
NT RELATIVISTIC PLASMAS
NT ROTATING PLASMAS
NT SEMICONDUCTOR PLASMAS
NT SOLAR WIND
NT SPACE PLASMAS
NT SPHERICAL PLASMAS
NT STELLAR WINDS
NT STRONGLY COUPLED PLASMAS
NT THERMAL PLASMAS
NT TOROIDAL PLASMAS
Exact solutions to the governing dynamic equations of plasma armature electromagnetic railguns
[DE87-014442] 01 p0011 N88-10063
Plasma properties
[DE87-013662] 01 p0101 N88-10663
Heavy-particle collisions in the plasma edge
[DE87-012926] 02 p0237 N88-11493
Time-resolved temperature and density measurements in ionizing, uniformly irradiated UV-laser-produced plasmas
[DE87-014649] 02 p0238 N88-11504
Two dimensional neutral transport analysis in tokamak plasma
[DE87-752984] 02 p0239 N88-11510
Progress in stellarator/heliotron research, 1981-1986: Executive summary
[DE88-000017] 02 p0241 N88-11519
Wavepacket propagation and current startup near the lower hybrid frequency in the torus
[IPPJ-840] 02 p0242 N88-11529
Volume produced H(-),D(-) ion source for proton accelerator and thermo-nuclear fusion research by sheet plasma (III)
[IPPJ-838] 02 p0242 N88-11531
Hollow cathode plasma coupling study, 1986
[NASA-CR-171985] 03 p0309 N88-11949
Helicity dissipation in the plasma edge
[DE87-014762] 03 p0378 N88-12376
Analytic model of an imploding Z-pinch plasma colliding inelastically with a thin-shelled cylindrical target
[DE88-000051] 03 p0378 N88-12379
Confinement time of electrons and H(-)/D(-) ions in the Uramoto type sheet plasma
[IPPJ-852] 04 p0492 N88-13032
Monte Carlo analysis of neoclassical transport for a compact helical system
[IPPJ-850] 04 p0492 N88-13033
Proceedings of the Japan-US Workshop P-92 on Plasma Material Interaction/High Heat Flux Data Needs for the Next Step Ignition and Steady State Devices
[DE87-013568] 04 p0494 N88-13042
Review of X-ray spectroscopy from laser-produced plasmas
[DE88-000755] 04 p0494 N88-13043
PISCES: Plasma-surface interactions and materials research
[DE88-001323] 04 p0494 N88-13044
Radio continuum emission from the ionized stellar winds of the cool supergiants in zeta Aurigae-like systems 04 p0514 N88-13160
Theoretical atomic and molecular physics
[DE88-001625] 05 p0649 N88-13974
Reversed field pinch plasmas with various boundary conditions
[DE88-000832] 05 p0653 N88-14004
Flight model discharge system
[AD-A185657] 06 p0673 N88-14122
Global convection patterns in the high latitude
[AD-A185794] 06 p0743 N88-14571
State parameters of pulse-discharge plasma in xenon-filled closed tube 06 p0773 N88-14747
Self-alignment of ions drifting in plasma 06 p0774 N88-14752
Atlas of atomic spectral lines of neptunium emitted by an inductively coupled plasma
[DE88-000640] 06 p0782 N88-14796
Edge plasmas and plasma/wall interactions in an ignition-class reversed field pinch
[DE88-001825] 06 p0782 N88-14799
Plasma parameters for alternate operating modes of TIBER-2
[DE88-001890] 06 p0783 N88-14802
Modeling of thermal effects on TIBER 2 (Thermal Ignition/Burn Experimental Reactor) divertor during plasma disruptions
[DE88-001893] 06 p0783 N88-14805
Comments on the theory of absolute and convective instabilities
[PB87-124624] 06 p0783 N88-14808
Free-boundary equilibrium problem for helically symmetric plasmas
[DE88-700101] 07 p0934 N88-15674
Interaction between a module cluster and a plasma in a magnetic field
[PB87-148276] 07 p0934 N88-15675
The effect of propane on atomic spectrometric signals in the direct current plasma
[DE88-002457] 07 p0934 N88-15676
TiN coatings on M2 steel produced by plasma assisted chemical vapor deposition
[DE88-003189] 08 p0970 N88-15867
Relation of wave energy and momentum with the plasma dispersion relation in an inhomogeneous plasma
[DE88-002305] 08 p1084 N88-16530
Magnetically insulated ion diode with a gas-breakdown plasma anode
[INPE-4382-PRE/1202] 08 p1085 N88-16537
Advanced studies of integrable systems
[AD-A186792] 09 p1151 N88-16895
Two-dimensional analysis for a scrapeoff and divertor regions with an MHD model. Conceptual design study of FY86 FER
[DE88-751069] 09 p1251 N88-17497
The approach to equilibrium in a quark-gluon plasma
[DE88-002117] 09 p1251 N88-17499
Total and partial cross sections for electron capture for C(q+) (q=6-2) and O(q+) (q=8-2) ions in collisions with H, H2 and He atoms
[IPPJ-AM-56] 09 p1252 N88-17501
Optimization of volume produced H(-) ions in a low-pressure hydrogen plasma
[IPPJ-853] 09 p1252 N88-17505
Optimization of outlet channel of plasma ion source
[DE88-700471] 10 p1410 N88-18415
Investigations of stimulated Raman scattering from high density underdense plasmas irradiated by a 0.35 micron laser 10 p1411 N88-18421
The numerical simulation of accelerator components
[DE87-011597] 10 p1412 N88-18423
The deposition rate dependence of plasma polymerization on the radius of curvature of the substrate
[DE88-003811] 10 p1412 N88-18429
Zero temperature quark matter equation of state
[DE88-003408] 10 p1422 N88-18496
Spectral line-broadening codes for hydrogen-, helium- and lithium-like ions in plasmas
[DE88-005238] 11 p1552 N88-19289
Plasma deposition of silicon carbide thin films
[AD-A188093] 11 p1556 N88-19314
Gas phase reactions of electrons, negative ions and free-radicals with transition metal complexes 11 p1560 N88-19339
Characterization of PEOS (Plasma Erosion Opening Switch) plasma parameters and conduction phase properties
[AD-A189024] 12 p1624 N88-19714
Proceedings of US-Japan Heliotron-Stellarator Workshop, volume 4
[DE88-004787] 12 p1693 N88-20126
Plasma rotation in a tokamak
[DE88-700855] 12 p1693 N88-20128
Acoustic phonons, surface plasmons and surface acoustic plasmons in a superlattice and their nonreciprocal device applications
[AD-A188918] 12 p1698 N88-20163
Propagator solutions of partial differential equations applied to plasma transport
[DE88-006432] 13 p1816 N88-20852
Interaction of a strong vortex with decaying turbulence
[DE88-007102] 14 p1911 N88-21420
Alfven waves in plasma with finite ion temperatures 14 p1972 N88-21769
Three-wave parametric resonance in plasma of relativistic electron flux 14 p1972 N88-21772
Pulse duration control of XeCl*-laser by means of plasma shutter 14 p1973 N88-21774
Analytic solutions to dynamic equations of plasma armature railguns
[DE88-006842] 15 p2023 N88-22057
Analysis of anomalous resistivity during the conduction phase of the plasma erosion opening switch
[DE88-006382] 15 p2061 N88-22286
Magnetic fusion energy plasma interactive and high heat flux components. Volume 5: Technical assessment of critical issues in the steady state operation of fusion confinement devices
[DE88-006920] 15 p2136 N88-22744
Measurements of edge turbulence with Langmuir probes in currentless Heliotron E plasmas
[DE88-752313] 16 p2275 N88-23617
Some aspects of the unified model of non-ideal high-parameter plasmas: Electron EOS and conduction coefficients 16 p2277 N88-23632
Coronal fluid-dynamics in laser fusion 16 p2278 N88-23634
Self-similar expansions in ion beam fusion 16 p2278 N88-23635
Finite ion-relaxation and nonequilibrium radiation effects on laser-driven implosions 16 p2278 N88-23636
Research on anode plasma behavior of flashover pulsed ion sources 16 p2279 N88-23640
Time-resolved spectroscopic measurement of anode plasma in magnetically-insulated diode 16 p2279 N88-23641
On selfsimilar thermonuclear ignition of a plasma in necks of zeta devices
[DE88-701640] 16 p2280 N88-23647
Space plasma contactor research, 1987
[NASA-CR-182148] 16 p2280 N88-23649
Thomson scattering for determining electron concentrations and temperatures in an inductively coupled plasma. 1: Assessment of the technique for a low-flow, low-power plasma
[AD-A191323] 16 p2280 N88-23651
Thomson scattering for determining electron concentrations and temperatures in an inductively coupled plasma. 2: Description and evaluation of a multichannel instrument
[AD-A191324] 16 p2280 N88-23652
On the magnetic structure and energy balance of EUV-emitting plasma in the quiet Sun 17 p2452 N88-24567
Theoretical plasma physics research of active space experiments
[AD-A192075] 18 p2577 N88-25309
Theoretical investigations of drift waves in a magnetic quadrupole 18 p2578 N88-25312
Stochasticity in a Q-machine plasma 18 p2578 N88-25315
Plasma neutralizer work at BNL (Brookhaven National Laboratory)
[DE88-007046] 18 p2579 N88-25317

Self shielding of surfaces irradiated by intense energy fluxes
[DE88-007094] 18 p2579 N88-25318
Optical diagnostics for a high power, rf-inductively coupled plasma
[DE88-007822] 18 p2579 N88-25322
Microlaminate composite structures by low pressure plasma spray deposition
[DE88-006453] 19 p2610 N88-25488
Accelerator research studies
[DE88-008236] 19 p2726 N88-26187
Simultaneously time- and space-resolved spectroscopic characterization of laser-produced plasmas
[DE88-008038] 19 p2728 N88-26202
Electron-acoustic waves in a beam-plasma system
[DE88-702053] 19 p2729 N88-26207
Inner-shell X-ray line spectra of highly ionized titanium, chromium, iron and nickel and their appliation to laboratory plasmas
[PB87-225181] 19 p2730 N88-26212
Vaporization studies of plasma interactive materials in simulated plasma disruption events
[DE88-010100] 19 p2731 N88-26222
Why plasma armature railguns don't work (and what can be done about it)
[DE88-007900] 20 p2763 N88-26384
Proceedings of the 2nd US-Japan Workshop on Advanced Plasma Modeling, volume 3
[IPPJ-867] 20 p2855 N88-26957
A Vlasov ion zero mass electron model for plasma simulations 20 p2855 N88-26958
Modeling of subtle kinetic processes in plasma simulation 20 p2856 N88-26959
Effects of secondary electron emission on the collector and source sheaths of a finite ion temperature plasma
[DE88-008930] 20 p2858 N88-26971
On the self-trapping of an electromagnetic wave in magnetized plasma
[DE88-701872] 20 p2858 N88-26974
Plasma separation process. Betacell (BCELL) code, user's manual
[DE88-006955] 20 p2859 N88-26981
Impurity transport calculations for a drift-dependent tokamak scrape-off plasma
[DE88-010053] 20 p2859 N88-26984
MACH2: A two-dimensional magnetohydrodynamic simulation code for complex experimental configurations
[AD-A192285] 20 p2860 N88-26988
Electrostatic whistler mode conversion at plasma resonance
[AD-A192951] 20 p2860 N88-26989
Plasma treatment of polymers for improved adhesion
[DE88-011623] 21 p2921 N88-27334
Ion Bernstein modes in current-carrying plasmas 21 p3017 N88-27903
Tokamak magnetic turbulence over the safety factor range 0.6 less than q less than 3
[DE88-008421] 21 p3017 N88-27904
The influence of ionization within a plasma opening switch
[AD-A193147] 21 p3017 N88-27906
Effects of low reflection on the collector and source sheaths of a finite ion temperature plasma
[DE88-008929] 21 p3017 N88-27908
Reminimization of energy integral and stability limit for non-ideal MHD (magnetohydrodynamic) plasma
[DE88-008422] 21 p3018 N88-27911
Global and local magnetohydrodynamic relaxations
[DE88-752602] 21 p3018 N88-27913
Design of divertor plate and measurements of double-null open divertor plasma in the JFT-2M tokamak
[DE88-753130] 21 p3018 N88-27914
Design of divertor plate and measurements of double-null open divertor plasma in the JFT-2M tokamak
[DE88-753130] 21 p3018 N88-27914
Analysis of lower hybrid current drive and rampup experiments on the JT-60 tokamak
[DE88-753136] 21 p3018 N88-27915
Electromagnetic wave incoherent reflection by a half-space of weakly-ionized plasma with an absorbing boundary
[DE88-702413] 21 p3019 N88-27917
Energy distribution and transfer in flowing hydrogen microwave plasmas 21 p3019 N88-27919
Activities report of the Institute for Extraterrestrial Physics
[MPE-206] 21 p3029 N88-27981
Measurement of macroscopic electric fields in solar plasma structures
[AD-A193291] 21 p3031 N88-27993
Theory and simulation of relaxed plasmoids
[AD-A192884] 21 p3032 N88-27997
Effect of a laser field in the electron inelastic scattering into plasma fields
[DE88-702295] 23 p3218 N88-29157
Waves and instabilities in an electron-positron plasma in an ultra-strong magnetic field 23 p3283 N88-29551
Fusion product spectra
[DE88-010912] 23 p3284 N88-29554
Nonlinear analysis of non-neutral plasmas
[AD-A192506] 23 p3284 N88-29556
Bootstrap currents in radio-frequency-driven tokamak equilibria
[DE88-011136] 23 p3285 N88-29561
Collector and source sheaths of a finite ion temperature plasma
[DE88-008934] 23 p3286 N88-29564
Millimeter wave generation by relativistic electron beams
[AD-A195683] 24 p3362 N88-30016
Autoionization for lower level detrapping in X-ray lasers
[AD-A195845] 24 p3379 N88-30123
Particle trajectories and potentials in a plane sheath moving in a magnetoplasma
[AD-A196228] 24 p3390 N88-30190
Ion kinetics in silane plasmas
[AD-A196202] 24 p3431 N88-30423
Ring current role in dynamics of fluctuating electron and ion fluxes in low-latitude magnetosphere 24 p3447 N88-30514
Plasma of earth's magnetosphere ring currents. Model compared with results of AMPTE/CCE experiment 24 p3447 N88-30515

PLASMASPHERE
Ionosphere and plasmasphere 03 p0272 N88-11709
Area of reduced electron concentration in terrestrial plasmasphere 08 p1003 N88-16078
Application of correlation method of reception of direct and reflected cosmic radiation to study of plasmaspheres of planet and distribution of radiation brightness 08 p1004 N88-16085
USU (Utah State University) Center of Excellence in Theory and Analysis of the Geo-Plasma Environment
[AD-A187687] 11 p1511 N88-19026
Observation of nonlinear wave decay processes in the solar wind by the AMPTE IRM plasma wave experiment
[AD-A191409] 16 p2290 N88-23713
Field-aligned structure of the storm time Pc 5 wave of November 14-15, 1979
[AD-A193022] 21 p2972 N88-27653

PLASMOIDS
U PLASMAS (PHYSICS)

PLASMONS
Plasmon resonance absorption in layered structures of silver with periodic corrugation
[DE87-013183] 02 p0231 N88-11453
A theoretical study of enhanced Smith-Purcell radiation from a bigrating
[AD-A184530] 03 p0329 N88-12080
A surface plasmon waveguide sensor: A new type of chemical transducer based on optical phenomena
[ETN-88-91322] 06 p0780 N88-14792
On the coexistence of phonon and non-phonon (plasmon) mechanisms in new high T/sub c/ superconductors
[DE88-003188] 07 p0938 N88-15703
Photoacoustic studies of surface plasmons in metallic microstructures
[DE88-004423] 11 p1460 N88-18703
Acoustic phonons, surface plasmons and surface acoustic plasmons in a superlattice and their nonreciprocal device applications
[AD-A188918] 12 p1698 N88-20163
Enhancement of second harmonic generation on silver gratings by resonant excitation of surface plasmon
[ETN-88-92304] 17 p2439 N88-24509
Extended and local plasmons in a lateral superlattice 20 p2870 N88-27041
Fundamental optical studies of competitive adsorption and thin film phenomena
[DE88-008780] 20 p2875 N88-27068
Solar energy conversion through the interaction of plasmons with tunnel junctions. Part A: Solar cell analysis. Part B: Photoconductor analysis
[NASA-CR-183044] 21 p2967 N88-27621
Bulk plasmon enhanced photoemission from Nb(100) surface resonances
[AD-A192711] 22 p3154 N88-28767
Optical emission from surface waves supported in thin metal films 23 p3282 N88-29540
System suitable for observing surface plasmon in a semi-infinite semiconductor superlattice
[DE88-702686] 23 p3293 N88-29606

PLASTIC AIRCRAFT STRUCTURES
Advanced organic composite materials for aircraft structures: Future program
[NASA-CR-181467] 06 p0678 N88-14155
Investigations on the modification of structural reliability by substitution of aluminum by carbon fiber reinforced plastics in aircraft construction
[ILR-MITT-195] 24 p3339 N88-29877

PLASTIC ANISOTROPY
NT ELASTIC ANISOTROPY

PLASTIC COATINGS
Vibration-absorbing characteristics of metal-polymer shells 02 p0158 N88-10991
Water disbondment characterization of organic Coating/metal substrate systems
[AD-A184847] 05 p0567 N88-13454
Plasma and ion etching for failure analysis. Part 2. The etching of plastic encapsulant and other semiconductor device materials, using the Technics Giga Etch 100-E plasma etch system
[AERE-R-12212] 09 p1177 N88-17050
Cleanability of aircraft polyurethane topcoats
[AD-A193456] 23 p3170 N88-28878

PLASTIC DEFORMATION
Superplastic deformation and post forming tensile properties of Ti-6Al-4V sheet
[RAE-TR-86015] 01 p0023 N88-10144
Large-strain softening of aluminum at elevated temperature
[DE87-011559] 01 p0024 N88-10153
Applications of dislocation theory to crack growth problems 02 p0190 N88-11188
Spread of plastic deformation in notched and cracked plates 03 p0337 N88-12122
Plastic strain localization between voids in shear deformation fields 04 p0427 N88-12648
Plasticity of aluminum and iron at high shear strain rate and high pressure 05 p0563 N88-13430
Tribology of thin film systems
[ETN-88-91365] 05 p0590 N88-13601
Surface deformation and fatigue crack initiation of alpha-iron 05 p0598 N88-13651
X-ray fatigue failure prediction based on plasticity response to microcracks 05 p0607 N88-13725
Thermometrical investigations on the near threshold fatigue crack propagation behavior 06 p0717 N88-14400
A critical review of the development of several viscoplastic constitutive theories
[AD-A185652] 07 p0867 N88-15262
On the relations between cyclic contraction ratio flowstress and deformation mechanisms in bainitic CrMoV steels
[DE87-753043] 08 p0968 N88-15856
The relationship of tensile specimen size and geometry effects to unique constitutive parameters for ductile materials
[AD-A186020] 08 p0994 N88-16012
Stability and metastability in semiconductor strained-layer structures
[DE88-003308] 09 p1258 N88-17544
Institute for Materials Science and Engineering, Fracture and Deformation Division: Technical activities, 1987
[PB88-153622] 10 p1345 N88-18039
Stress corrosion cracking and metal-induced embrittlement: Comparative studies of local chemistries
[DE88-003235] 13 p1742 N88-20419
Influence of hydrogen on crack formation tendency in heat-affected zone with stress concentrator 14 p1687 N88-21276
An internal variable constitutive model for the large deformation of metals at high temperatures 14 p1929 N88-21503
On the global/local time incrementing for viscoplastic analysis 14 p1932 N88-21519
Finite element (MARC) solution technologies for viscoplastic analyses 15 p2078 N88-22389
Phenomenological modelling of rate-dependent plasticity for high strain rate problems
[DE88-006647] 15 p2087 N88-22440
The mechanical behavior of particle filled thermoplastics
[ETN-88-92234] 16 p2181 N88-22999
The influence of the chemical nature of resins on their reticulation kinetics and the consequences for their nonelastic mechanical properties
[ETN-88-92539] 18 p2493 N88-24788
On the abnormal phenomena observed in the electrical resistivity measurement during the decomposition process of saturated Cu-Fe alloys
[NASA-TT-20183] 18 p2507 N88-24869
Dynamic shear band development in plane strain
[AD-A190915] 18 p2526 N88-24988
Plastic deformation and roughness of free metal surfaces
[PB88-196621] 20 p2772 N88-26439
Shape memory alloys: New materials for future engineering
[NASA-TT-20193] 20 p2775 N88-26455

Fatigue of lithium-aluminum alloys: An example of localization of the plastic deformation
[ETN-88-92309] 20 p2775 N88-26456
On the possibility of the soliton description of acoustic emission during plastic deformation of crystals
[DE88-701878] 20 p2876 N88-27075
Ultrasonic studies of stresses and plastic deformation in steel during tension and compression
[AD-A192308] 21 p2912 N88-27280
Analysis of grain refinement and superplasticity in aluminum-magnesium alloys
[AD-A193029] 21 p2912 N88-27283
Plastic yielding at crack tips
[AD-A192549] 21 p2960 N88-27582
Results on the influence of crack tip plasticity during dynamic crack growth
[AD-A193460] 23 p3225 N88-29194
Anisotropic constitutive modeling for nickel-base single crystal superalloys
[NASA-CR-182157] 24 p3353 N88-29961
State variable approach to deformation phenomena in Face Centered Cubic (FCC) metals
[VTT-44] 24 p3354 N88-29964
Response of SMA (Shielded Metal Arc) and narrow gap HY80 weldments to explosive shock loading
[AD-A195994] 24 p3385 N88-30162

PLASTIC FILMS
U POLYMERIC FILMS

PLASTIC FLOW
Relaxation of metastable semiconductor strained-layer structures by plastic flow
[DE88-002729] 08 p1090 N88-16560
On stress collapse in adiabatic shear bands
[AD-A187185] 11 p1498 N88-18942
Elasto-plastic analysis using a stress-based finite element method and an endochronic theory of plasticity
[DE88-003001] 15 p2075 N88-22372
Plastic flow and failure modeling under high strain rate loading
[AD-A194223] 23 p3226 N88-29199

PLASTIC MEMORY
Shape memory alloys: New materials for future engineering
[NASA-TT-20193] 20 p2775 N88-26455

PLASTIC PLATES
The nonlinear dynamic response of an elastic-plastic thin plate under impulse loading
[AD-A182147] 08 p0994 N88-16013

PLASTIC PROPELLANTS
Effect of moisture level in PBXW-109(E) (plastic-bonded explosive) mixes on the aging of the cured explosive
[AD-A190200] 15 p2048 N88-22202

PLASTIC PROPERTIES
NT ELASTOPLASTICITY
NT SUPERPLASTICITY
NT THERMOPLASTICITY
NT VISCOPLASTICITY
NT YIELD POINT
Relation between shock strength and strain-rate plasticity at maximum deviatoric stress
[DE87-011736] 01 p0061 N88-10390
Functional plasticity of the nervous system of vertebrates 01 p0074 N88-10474
3D inelastic analysis methods for hot section components 02 p0187 N88-11164
Plasticity of fibrous composites
[AD-A184637] 03 p0280 N88-11765
The behavior of plastic, ceramic masses in compression tests
[ETN-87-90603] 03 p0292 N88-11836
Surface deformation and fatigue crack initiation of alpha-iron 05 p0598 N88-13651
Embrittling effect of the plastic zone 05 p0607 N88-13721
A comparison of plastic work energy and external input for fatigue crack propagation 05 p0607 N88-13722
An overview of metal plasticity
[DE88-001658] 06 p0681 N88-14175
Absolute fatigue thresholds in metallic materials 06 p0717 N88-14399
The effects of loading history on fatigue crack growth threshold 06 p0718 N88-14406
Crack closure phenomena in modes 1 and 2 interactions 06 p0719 N88-14417
Dependence of strainrange partitioned fatigue life at elevated temperature on monotonic stress-strain properties 06 p0721 N88-14428
Axial creep-fatigue damage assessment in type 316 SS material 06 p0721 N88-14430
Function-dependent plasticity in the nervous system 07 p0886 N88-15377
Interrelation and measurement of formability, strengthening, and thermomechanical processing under metalworking conditions
[DE88-002485] 08 p0967 N88-15850
Fully plastic analysis of mixed mode plane-strain crack problems
[PB87-144929] 08 p0994 N88-16015
Application of inverse gas chromatography to fluidity studies
[DE88-002896] 10 p1296 N88-17750
Applications of energy density theory in cyclic plasticity
[AD-A186947] 10 p1342 N88-18023
Computed stress and strain distributions under interference fit and after coldworking
[AD-A186950] 10 p1342 N88-18024
Materials Research Laboratory at Brown University
[AD-A188006] 13 p1739 N88-20396
Microplasticity phenomena in graphite/magnesium metal matrix composites
[DE88-006772] 15 p2029 N88-22086
Elasto-plastic analysis using a stress-based finite element method and an endochronic theory of plasticity
[DE88-003001] 15 p2075 N88-22372
Measurement of the elastic-plastic surface flaw back surface topology and its relation to constraint
[DE88-006765] 15 p2087 N88-22437
Fatigue crack growth under full-scale cyclic plasticity
[DFVLR-FB-87-48] 16 p2222 N88-23263
Characterization of elastic-plastic properties of AS4/APC-2 thermoplastic composite
[NASA-CR-183145] 21 p2906 N88-27242
Thermomechanical processing of Al alloy 2090 for grain refinement and superplasticity
[AD-A192333] 21 p2912 N88-27281
An endochronic rate-sensitive constitutive equation for metals, application to generalized creep and large deformations
[AD-A194167] 22 p3055 N88-28125
Theory of acoustoplasticity and ultrasonic measurements of residual stresses 22 p3087 N88-28328

PLASTIC YIELDING
U PLASTIC DEFORMATION

PLASTICITY
U PLASTIC PROPERTIES

PLASTICIZERS
NMR (Nuclear Magnetic Resonance) imaging for detecting binder/plasticizers in green-state structural ceramics
[DE88-003111] 10 p1304 N88-17800
Reactive plasticizers in negative E-beam resists
[AD-A195161] 24 p3368 N88-30056

PLASTICS
NT ACRYLIC RESINS
NT CARBON FIBER REINFORCED PLASTICS
NT EPOXY RESINS
NT GLASS FIBER REINFORCED PLASTICS
NT KEVLAR (TRADEMARK)
NT NYLON (TRADEMARK)
NT PEEK
NT PHENOLIC RESINS
NT POLYAMIDE RESINS
NT POLYBUTADIENE
NT POLYETHER RESINS
NT POLYETHYLENES
NT POLYMETHYL METHACRYLATE
NT POLYPROPYLENE
NT POLYSTYRENE
NT POLYTETRAFLUOROETHYLENE
NT POLYVINYL ALCOHOL
NT POLYVINYL CHLORIDE
NT POLYVINYL FLUORIDE
NT REINFORCED PLASTICS
NT SYNTHETIC RESINS
NT TEFLON (TRADEMARK)
NT THERMOPLASTIC FILMS
NT THERMOPLASTIC RESINS
NT THERMOSETTING RESINS
NT VINYL COPOLYMERS
Requirements for a test stand for plastic rollers for the verification of nonequilibrium force laws
[ILR-MITT-176] 01 p0008 N88-10040
Anti-abrasion protection with highly organized materials
[DE87-014238] 01 p0029 N88-10187
Cure and properties of thermosetting polymers
[AD-A184669] 03 p0293 N88-11843
Polymer material for heat sensors 06 p0676 N88-14142
TMA-microrheological testing of polymers (thermomechanical analysis)
[PB87-228805] 06 p0683 N88-14187
Waves and vibrations in elastic superlattice composites 06 p0776 N88-14765
Selection of polymer materials for manufacturing optical parts
[AD-A185898] 07 p0836 N88-15069
Correlation between flammability and heat of combustion of polymers
[NASA-TT-20116] 08 p0973 N88-15884
Lithium/polymer electrolyte interfacial instability
[AD-A187164] 09 p1147 N88-16874
Flame retardants
[NASA-TT-20250] 13 p1739 N88-20400
Kinetics of polymer decomposition
[DE88-005500] 13 p1749 N88-20460
Solid hosts for dye laser rods. Part 1: Criteria for choosing a host material
[DE88-006478] 15 p2072 N88-22355
Soft-ground aircraft arresting systems
[AD-A190838] 16 p2165 N88-22912
Small-scale cleavage test of polymer products
[PB88-165360] 16 p2181 N88-23001
Differential technology in plastics industries differentiation in combination technology nonflammability technology
[NASA-TT-20256] 18 p2494 N88-24797
Statistical mechanics of polymer systems
[DE88-011172] 20 p2778 N88-26477

PLASTISOLS
NT SMOKE

PLATE (METAL)
U METAL PLATES

PLATE THEORY
An exact theory of elastic plates
[ETN-87-90675] 01 p0062 N88-10396
Correction to a single higher order theory of elastic plates
[ETN-87-90676] 01 p0062 N88-10397
The nonlinear dynamic response of an elastic-plastic thin plate under impulse loading
[AD-A182147] 08 p0994 N88-16013
Transient sound radiation from infinite thin plate
[ARE-TM(UHA)-87508] 09 p1243 N88-17449
An efficient Mindlin finite strip plate element based on assumed strain distribution 15 p2081 N88-22407
A generalized variational method for solving stress intensity factors at cracks on the edge of holes in orthotropic plates
[IC-AERO-87-02] 17 p2348 N88-23992
Improved finite strip Mindlin plate bending element using assumed shear strain distributions
[NASA-TM-100928] 23 p3225 N88-29195

PLATEAUS
NT GREAT BASIN (US)
NT PIEDMONTS
The tectonic setting of the Seychelles, Mascarene and Amirante Plateaus in the Western Equatorial Indian Ocean 24 p3396 N88-30225

PLATES
Analysis of compressible flow on high-velocity jet penetration 03 p0302 N88-11898
Spread of plastic deformation in notched and cracked plates 03 p0337 N88-12122
Damping characteristics of a composite-reinforced stainless-steel plate
[DE88-000303] 04 p0457 N88-12828
Fracture-resistant characteristics of medium-strength plates with regard to the initiation, stable and unstable propagation of surface cracks
[PB87-144804] 08 p0996 N88-16025
Optimum design of geodesically stiffened composite plates
[NASA-CR-182499] 10 p1344 N88-18035
Transient dynamics of fibre reinforced composite plates
[IIT-B/CE/RR/87-1] 13 p1734 N88-20370
An experimental investigation of decelerating flow about two-dimensional cambered plates
[DE88-006598] 13 p1766 N88-20567
Finite element methodology for nonlinear free and harmonic forced vibrations of beam and plate structures 13 p1782 N88-20663
The analysis of non-linear dynamic behavior (including snap-through) of postbuckled plates by simple analytical solution
[NASA-TM-89165] 15 p2087 N88-22439
Stress-intensity factors for small surface and corner cracks in plates
[NASA-TM-100599] 15 p2088 N88-22445
Nonlinear vibrations of periodically stiffened plates 21 p2963 N88-27598

PLATES (STRUCTURAL MEMBERS)
NT ANISOTROPIC PLATES
NT ANNULAR PLATES
NT CIRCULAR PLATES
NT CORRUGATED PLATES
NT ELASTIC PLATES
NT END PLATES
NT METAL PLATES
NT ORTHOTROPIC PLATES
NT PERFORATED PLATES
NT PLASTIC PLATES

NT POROUS PLATES
NT RECTANGULAR PLATES
NT REINFORCED PLATES
Theoretical investigation of stress concentrations in damaged carbon fibre reinforced plastic plate structures. Volume 1: Main text
[BR99872-VOL-1] 03 p0280 N88-11761
Compactness of quasi-conforming element spaces, convergence of quasi-conforming element method
03 p0301 N88-11896
Damping analysis of flexural waves in fluid-loaded single and constrained plates
[AD-A185116] 05 p0609 N88-13739
Viscous drag reduction of horizontal plates
[VKI-TN-159] 07 p0851 N88-15171
A method for the approximate calculation of the skin friction coefficient of horizontal wavy plates
[VKI-TN-160] 07 p0851 N88-15172
Experimental investigation of damping characteristics of bolted structural connections for plates and shells
[AD-A186075] 07 p0867 N88-15259
Numerical solution methods for viscoelastic orthotropic materials
[NASA-CR-182381] 08 p0971 N88-15874
Stress strain fields at crack tip and stress intensity factors in Reissner's plate
[PB87-144945] 08 p0994 N88-16014
A nonlinear computational model for the strength and failure of composite plates and shells
11 p1501 N88-18964
Discrete vortex analysis of unsteady flow about two-dimensional cambered plates
[DE88-006597] 14 p1909 N88-21407
Transient analysis of a plate on an elastic foundation under a moving load 19 p2680 N88-25933
Hole diameters in plates impacted by projectiles
21 p2929 N88-27386
Power flow analysis of two coupled plates with arbitrary characteristics
[NASA-CR-183165] 22 p3075 N88-28251
Tripping of stiffened plates using a refined beam theory
[AD-A193989] 22 p3087 N88-28333

PLATES (TECTONICS)
The interpretation of crustal dynamics data in terms of plate motions and regional deformation near plate boundaries
[NASA-CR-181475] 03 p0349 N88-12205
Earthquake source mechanisms and transform fault tectonics in the Gulf of California
03 p0349 N88-12206
RRS DISCOVERY Cruise 161, 15 August (227)-19 September (262) 1986. Portuguese Ocean-continent boundary, plate boundaries west of Iberia and seismic structure of sediments off Madeira
[PB87-222006] 06 p0747 N88-14596
State-of-the-art for assessing earthquake hazards in the United States. Report 26: Parameters for specifying magnitude-related earthquake ground motions
[AD-A185997] 07 p0877 N88-15319
Relationship between oceanic geological formations and tectonic structures 13 p1785 N88-20683
The interpretation of crustal dynamics data in terms of plate interactions and active tectonics of the Anatolian Plate and surrounding regions in the Middle East
[NASA-CR-183024] 18 p2543 N88-25092
Geologic results obtained from the use of SPOT imagery along plate boundaries: Examples in the East African rift and of the northern-Caribbean collision
22 p3105 N88-28437
Intraplate deformation, stress in the lithosphere and the driving mechanism for plate motions
[NASA-CR-183121] 23 p3231 N88-29231
The tectonic setting of the Seychelles, Mascarene and Amirante Plateaus in the Western Equatorial Indian Ocean 24 p3396 N88-30225
Ridge-trench collision in Archean and Post-Archean crustal growth: Evidence from southern Chile
24 p3397 N88-30233
Continental growth through time by underplating of subducted oceanic crust: Evidence from kimberlites in South Africa and SW Pacific 24 p3399 N88-30244
Gravity anomalies, plate tectonics and the lateral growth of Precambrian North America 24 p3400 N88-30248
Solid earth as a recycling systems and the lateral growth of Precambrian North America 24 p3400 N88-30249
Crustal underplating in the North American Craton: Evidence from the Petrogenesis of anorthositic rocks in the Middle Proterozoic Midcontinent Rift System
24 p3400 N88-30252

PLATING
NT ELECTROPLATING
NT ION PLATING
NT NICKEL PLATE
Equations for determining CVD tungsten-rhenium alloy composition and plating rate
[DE87-008831] 01 p0024 N88-10152
Corrosion resistance of silver-plated carbon-aluminum composite 03 p0285 N88-11793
The analysis of metal finishing solutions by ion chromatography
[AD-A184812] 05 p0561 N88-13414
Analysis of nickel sulphamate bath using charging current compensated D.C. polarography
[NAL-TM-MT-8705] 05 p0564 N88-13433
Hydrogen embrittlement of gun steel
[AD-A188972] 13 p1740 N88-20407
Durability testing of an iridium-plated storable rocket engine injector
[AD-A190707] 15 p2027 N88-22078
Determination of aquo-complexes of chromium and iron in chromium plating and polishing solutions by ion chromatography
[AD-A190168] 15 p2039 N88-22148
Technical feasibility study of applying auto-control methods to plating process solutions
[DE88-008014] 19 p2641 N88-25670
Fabrication of a flexible conductor by vapor deposition
[DE88-007500] 19 p2661 N88-25826
A rapid electrochemical technique for determining the current efficiency for cadmium plating
[AD-A193679] 22 p3056 N88-28130

PLATINUM
NT PLATINUM ISOTOPES
Compatability of dispersion-strengthened platinum with resistojet propellants
[NASA-TP-2765] 04 p0409 N88-12538
Characterization of catalysts with metal-support effects and of the species adsorbed on their surfaces
[DE87-014636] 04 p0414 N88-12564
Determination, by X-ray fluorescence, of platinum, palladium, ruthenium, iron and chromium in special steels
[PB87-132114] 06 p0683 N88-14183
NBS (National Bureau of Standards) measurement services: Platinum resistance thermometer calibrations
[PB88-138367] 10 p1333 N88-17967
Order-disorder transition of Au and Pt (110) surfaces: The significance of relaxations and vibrations
[DE88-004651] 10 p1419 N88-18473
The effect of oriented defects on long-range ordering of hydrocarbon films: Azulene on Pt(111)
[AD-A196089] 24 p3344 N88-29904

PLATINUM ISOTOPES
Experimental and theoretical investigations of isotope shift and hyperfine structure on 5d elements (especially platinum, iridium and rhenium)
[ETN-88-93121] 24 p3353 N88-29957

PLAYAS
Methods of determining playa surface conditions using remote sensing
[AD-A192663] 21 p2965 N88-27612

PLENUM CHAMBERS
Advanced Technology for Aero Gas Turbine Components
[AGARD-CP-421] 10 p1279 N88-17647
Development of a plenum chamber burner system for an advanced VTOL engine 10 p1281 N88-17664

PLETHYSMOGRAPHY
A plethysmograph for measuring pulmonary ventilation in small animals
[AD-A184978] 05 p0629 N88-13846

PLEXIGLASS (TRADEMARK)
U POLYMETHYL METHACRYLATE

PLIES
U LAYERS

PLOTTERS
Use of modern scanner techniques in cartography
18 p2535 N88-25040

PLOTTING
Satellite orbits: Plot routines
[UIO-SR-87-02] 01 p0011 N88-10060
A computer code to process and plot laser altimetry data interactively on a microcomputer
[NASA-TM-100687] 05 p0554 N88-13371
Boeing 727 MLS (Microwave Landing System) terminal instrument procedures (TERPS) approach data collection and processing, data report
[AD-A185523] 06 p0667 N88-14090
On the influence of false plots on tracking reliability: Simulations and preliminary analyses
[FOA-C-30443-3.2] 06 p0692 N88-14245
The effects of data structure on total time on test plots
[AD-A187628] 10 p1389 N88-18296
Physical, chemical and CTD (Conductivity/Temperature/Depth) data from the Marathon 2 expedition
[AD-A189930] 15 p2099 N88-22507
PLOT300: A Tektronics PLOT10 emulator for HP 9000 series 200/300 computers
[NASA-TM-100606] 16 p2250 N88-23447
Digital SPOT stereoplotting: An original approach to the formation of epipolar images and matching
22 p3113 N88-28493
Interactive plotting of NASTRAN aerodynamic models using NPLOT and DISSPLA
[AD-A194115] 23 p3226 N88-29204
A computer program package for introductory one-dimensional digital signal processing applications
[AD-A194656] 23 p3249 N88-29338
Implementation of the NCAR (National Centre for Atmospheric Research) graphics package at ARL (Aeronautical Research Laboratory)
[AD-A195163] 24 p3391 N88-30193

PLOTTING INSTRUMENTS
U PLOTTERS

PLOWED FIELDS
U FARMLANDS

PLUGS
Rotor self-lubricating axial stop
[NASA-CASE-MFS-28273-1] 17 p2344 N88-23974

PLUMBANE
U METAL HYDRIDES

PLUMES
NT ROCKET EXHAUST
Development and application of computational aerothermodynamics flowfield computer codes
[NASA-CR-181534] 04 p0395 N88-12465
Aircraft engine exhaust plume dynamics
[AD-A184238] 04 p0400 N88-12488
Plume mechanics and aerosol growth processes
[AD-A184467] 04 p0442 N88-12742
Active and passive plume distribution models in the convective boundary layer using a large eddy simulation model
[KNMI-TR-90] 05 p0581 N88-13546
High resolution ultraviolet filter development
[AD-A184183] 05 p0649 N88-13979
On the correlation of plume centerline velocity decay of turbulent acoustically excited jets
[NASA-TM-100193] 09 p1114 N88-16681
Measurement of velocity and temperature profiles in low-speed, turbulent non-isothermal flows
[PB88-155833] 11 p1486 N88-18872
Numerical simulation of near-surface environments and particulate clouds generated by large-area fires
[AD-A188375] 12 p1641 N88-19828
Kinetic mechanisms for ionization and afterburning suppression
[AD-A189219] 13 p1737 N88-20383
Split-coefficient matrix solution and experimental study of axisymmetric underexpanded exhaust plumes
15 p2054 N88-22242
Plasma-gas interaction studies in a hybrid plume plasma rocket
[AD-A190310] 15 p2138 N88-22755
Detection of biomass burning and smoke plumes in the Amazon region through NOAA satellite imagery
17 p2365 N88-24085
Research study: Space shuttle main engine plume flowfield model
[NASA-CR-179336] 18 p2474 N88-24676
Evaluation of the communications impact of a low power arcjet thruster
[NASA-TM-100926] 18 p2475 N88-24682
Variable Mach number wall jets for control/propulsion on hypervelocity projectiles/interceptors: Tests with an existing model
[AD-A192845] 21 p2892 N88-27167
A computational analysis of under-expanded jets in the hypersonic regime
[NASA-TM-101319] 21 p2893 N88-27174
Nozzle lip effects on gas expansion into the plume backflow region
[AD-A192806] 21 p2942 N88-27475
Application of laser diffraction techniques to particle sizing in solid propellant rocket motors
[AD-A193841] 22 p3049 N88-28089
Project wind, phase 4 (smoke test), Meadow Brook Valley, Red Bluff, California
[AD-A194742] 22 p3128 N88-28596
Automatic data retrieval from rocket motor holograms
[AD-A195586] 24 p3337 N88-29864
Experimental evaluation of resistojet thruster plume shields
[NASA-TM-101363] 24 p3338 N88-29868

PLUNGERS
Influence of shock wave and gas pressure on the behavior of a pyrotechnical device
[SNIAS-872-430-111] 05 p0570 N88-13477
Advantages of internal thermal protection in a pyrotechnical plunger
[SNIAS-872-430-114] 05 p0571 N88-13478

Numerical simulation applied to the development of a pyrotechnical system
[SNIAS-872-430-115] 05 p0571 N88-13479

PLUTONIUM
NT PLUTONIUM ISOTOPES
NT PLUTONIUM 238

PLUTONIUM ISOTOPES
NT PLUTONIUM 238
A long term radiological risk model for plutonium-fueled and fission reactor space nuclear system
[DE87-010466] 06 p0779 N88-14782
Milliwatt generator project
[DE88-011261] 20 p2853 N88-26939

PLUTONIUM 238
BIFOLD: A dual-mode nuclear space power system
17 p2404 N88-24292

PLUVIOGRAPHS
U RAIN GAGES
U RECORDING INSTRUMENTS

PLY ORIENTATION
Investigation of instability, dynamic forces, and effect of dynamic loading on strength of cages for the bearings in the high pressure oxygen turbopumps for the space shuttle main engine
[NASA-CR-178970] 06 p0714 N88-14378
A study of the mechanical behavior of a 2-D carbon-carbon composite 11 p1449 N88-18638
Ply-level failure analysis of a graphite/epoxy laminate under bearing-bypass loading
[NASA-TM-100578] 13 p1735 N88-20372
A preliminary investigation of finite-element modeling for composite rotor blades
[NASA-TM-100559] 13 p1781 N88-20656
Delamination analysis in crossed layer composites
[REPT-48-447/F] 16 p2171 N88-22942
Harmfulness of defects: Behaviour in service of a delamination in a composite containing many differently oriented layers
[PB88-124714] 18 p2479 N88-24705

PNEUMATIC CONTROL
Space station resistojet system requirements and interface definition study
[NASA-CR-180832] 04 p0409 N88-12541
Use of a thermodynamic analog for pneumatic transport in horizontal pipes
[AD-A184076] 04 p0441 N88-12740

PNEUMATIC EQUIPMENT
A three-barrel repeating pneumatic pellet injector for plasma fueling of the Joint European Torus
[DE88-000330] 04 p0491 N88-13026
A device and methodology for measuring repetitive lifting VO2max (oxygen consumption rate)
[AD-A185195] 05 p0630 N88-13850
Electrical/pneudraulic design considerations
[AD-A188097] 12 p1581 N88-19462
Reduction of erosion in elbows due to flow modifications, phase 1
[DE88-001028] 13 p1769 N88-20584
The pneumatic wind shear sensor: A tool for meteorological investigations and flight management
22 p3036 N88-28024
JUH-1H redesigned pneumatic boot deicing system flight test evaluation
[AD-A194918] 24 p3322 N88-29785
Analysis of a feed device for the pneumatic transport of noncohesive particles
[VKI-TM-44] 24 p3369 N88-30062

PNEUMATIC PROBES
Formulation of a general technique for predicting pneumatic attenuation errors in airborne pressure sensing devices
[NASA-TM-100430] 13 p1723 N88-20302

PNEUMATIC RESET
U PNEUMATIC CONTROL

PNEUMATICS
Pipe and bend erosion by pneumatic transport of solids at high temperature
[DE88-001345] 04 p0429 N88-12658
Analysis of a feed device for the pneumatic transport of noncohesive particles
[VKI-TM-44] 24 p3369 N88-30062
Laser Doppler Velocimeter (LDV) and pressure measurements of gas particle flows in bends
[VKI-TN-163] 24 p3372 N88-30083

POCKELS EFFECT
U BIREFRINGENCE

POGO EFFECTS
ESA Bulletin No. 8
[ETN-87-90513] 09 p1122 N88-16718
Launch vehicle vibration: Measures taken to avoid pogo on ESA's Ariane launch vehicle
09 p1123 N88-16727

POINCARE PROBLEM
Compactness of quasi-conforming element spaces, convergence of quasi-conforming element method
03 p0301 N88-11896

POINT DEFECTS
NT VACANCIES (CRYSTAL DEFECTS)
Hot spots: Subnanometer femtosecond energy localization
[DE87-010276] 02 p0155 N88-10968
Effect of point defects on graphite lattice parameters
[DE88-700340] 07 p0827 N88-15019
Effect of extraneous factors on optical one-phonon transitions in impurity centers with cubic symmetry
08 p1077 N88-16496
Diffusion studies in amorphous NiZr alloys
[DE88-003009] 10 p1301 N88-17781
Silicon and indium doping of GaAs: Measurements of the effect of doping on mechanical behavior and relation with dislocation formation
[DE88-003862] 11 p1554 N88-19303
Point defect structure of Cr2O3
[AD-A187620] 11 p1556 N88-19317
The role of point defects on structural phase transitions
[DE88-005209] 12 p1696 N88-20152
Study of activationless reactions of point defects with impurities and impurity-defect complexes in alpha-iron
[DE88-701028] 13 p1745 N88-20433
Point defects in irradiated silicates
17 p2408 N88-24319
A general qualitative study of point and extended defects and their interactions in non-metallic systems
[AD-A191687] 19 p2618 N88-25532
Paramagnetic point defects in boron-implanted HgO.7CdO.3Te
[AD-A193276] 21 p3021 N88-27934
Prediction of deep levels and equilibrium concentrations of defects in semiconductors 21 p3023 N88-27945

POINT IMPACT
The numerical solution of the elastohydrodynamically lubricated line and point contact problem, using multigrid techniques
[ISBN-90-9001583-3] 06 p0714 N88-14377

POINT MATCHING METHOD (MATHEMATICS)
U BOUNDARY VALUE PROBLEMS

POINT SOURCES
Multipath time-delay estimation via the EM algorithm
[PB88-106851] 07 p0845 N88-15124
Bistable cellular flames
[DE88-003074] 09 p1142 N88-16848
Space-time processing of field produced by moving source 09 p1234 N88-17399
Bearing detection in the presence of two sources of varying coherence using the complex cepstrum
[NASA-CR-181605] 09 p1243 N88-17451
Observation of a point source in Cygnus constellation with the underground detector at Frejus (France)
[PITHA-87/02] 20 p2884 N88-27122

POINT SPREAD FUNCTIONS
Three dimensional reconstruction of optical microscope pictures using the three dimensional microscopic inverse point spread function
[ETN-87-90420] 01 p0098 N88-10648
Vision of details in space and time
[B8711402] 06 p0753 N88-14624

POINTING CONTROL SYSTEMS
NT ANNULAR SUSPENSION AND POINTING SYSTEM
An autonomous, closed-loop pointing system for use with satellite optics
[DE87-012011] 02 p0235 N88-11483
Wavefront error sensing
[NASA-CR-181504] 03 p0321 N88-12030
A new state space model for the NASA/JPL 70-meter antenna servo controls 04 p0436 N88-12702
A modern control theory based algorithm for control of the NASA/JPL 70-meter antenna axis servos
04 p0436 N88-12706
Knowledge-based monitoring of the pointing control system on the Hubble space telescope
08 p1057 N88-16378
Balloon-borne three-meter telescope for far-infrared and submillimeter astronomy
[NASA-CR-182310] 09 p1262 N88-17565
Using ridge regression in systematic pointing error corrections 11 p1472 N88-18777
Optical links in the angle-data assembly of the 70-meter antennas 11 p1474 N88-18792
Progress toward a cosmic dust collection facility on space station
[NASA-CR-182427] 12 p1598 N88-19566
Continued design of a Pointing, Acquisition, and Tracking (PAT) subsystem for InterSatellite Laser links (ISL2)
[TELDIX-15-093-178] 14 p1905 N88-21384
Development of a magnetically suspended, tetrahedron-shaped antenna pointing system
14 p1926 N88-21478
Utilization of the IR telescope gimbaling system as a stabilized pointing platform for balloon payloads. Volume 1: Technical results
[NASA-CR-179339] 18 p2522 N88-24962
Time-Optimal Adaptive Shaped Torque (TOAST) technical note
[AD-A192719] 20 p2843 N88-26869
IPS guidestar selection for stellar mode (ASTRO)
[NASA-TM-100336] 21 p2894 N88-27181
Slew-induced deformations in a space-based electromagnetic rail gun 21 p2929 N88-27385
The feasibility of the disturbance accommodating controller for precision antenna pointing
22 p3064 N88-28182
DSS 14 antenna calibrations for GSSR/VLA Saturn radar experiments 22 p3068 N88-28207
Modeling, designing and simulating a pointing control system for balloon-borne solar experiments
[NASA-TM-100337] 22 p3082 N88-28300

POINTS (MATHEMATICS)
NT FIXED POINTS (MATHEMATICS)
NT INFLECTION POINTS
Point vortex dynamics: Recent results and open problems
[DE87-014759] 03 p0314 N88-11982
Point processes
[AD-A185398] 05 p0641 N88-13921
Errors in retrieving hydrological fields and fields of their differential characteristics by method of approximation by orthogonal functions 06 p0727 N88-14475
Testing and interval estimation in a change-point model allowing at most one change
[AD-A185525] 06 p0767 N88-14716
Local likelihood method in the problems related to change points
[AD-A185604] 06 p0768 N88-14718
Point processes in the plane
[AD-A186017] 07 p0913 N88-15542
On the characterization of certain point processes
[AD-A186427] 07 p0916 N88-15560
Automatic registration of satellite imagery
17 p2364 N88-24080
Procedure for converting a Wilson-Fowler spline to a cubic B-spline with double knots
[DE88-008971] 20 p2844 N88-26878
Evaluation of a multi-point method for determining acoustic impedance
[NASA-TM-100637] 20 p2849 N88-26913
An algorithm for determining the location of points in computer simulations
[AD-A193713] 23 p3250 N88-29343
On the Nash point equilibria in the calculus of variations
[AD-A194959] 24 p3424 N88-30381

POISEUILLE FLOW
U LAMINAR FLOW

POISONS
NT CARBAMATES (TRADENAME)
NT URETHANES

POISSON DENSITY FUNCTIONS
Explicit formulate for the distributions of stopping variables under Wald's truncated SPRT (Sequential Probability Radio Tests) for a poisson process
[AD-A185053] 05 p0640 N88-13914
Decoupling identities and predictable transformations in exchangeability
[AD-A186013] 07 p0913 N88-15540
A Prohorov bound for a Poisson process and a Bernoulli process
[CWI-MS-R8701] 09 p1232 N88-17388
A code development system for computational fluid dynamics
[AD-A188050] 11 p1482 N88-18848
Tests for uniformity arising from a series of events
[AD-A189069] 13 p1828 N88-20935
Bias reduction when there is no unbiased estimate
[AD-A189407] 13 p1829 N88-20937
Open questions in closed-loop photodetection
14 p1979 N88-21812
Extreme value for dependent sequences via the Stein-Chen method of poisson approximation
[AD-A190325] 15 p2125 N88-22668
Development of adaptive grid schemes based on Poisson grid generators
[AD-A190953] 16 p2262 N88-23528
Poisson functionals of Markov processes and queueing networks
[AD-A191217] 18 p2568 N88-25252
On path properties of certain infinitely divisible processes
[AD-A192016] 18 p2568 N88-25255
Full analysis of a powerful window random access algorithm
[AD-A192437] 21 p2995 N88-27763

Multiple integration with respect to Poisson and Levy processes
[AD-A192895] 21 p3009 N88-27851
Poisson functionals of Markov processes and queueing networks
[AD-A194289] 22 p3145 N88-28705

POISSON EQUATION
Generation of body-fitted grids for two dimensional interior domains by the solution of a system of Poisson equations using multigrid techniques
[GMD-246] 01 p0044 N88-10281
The finite element method for electronic structure
[DE88-001708] 04 p0485 N88-12989
Point processes in the plane
[AD-A186017] 07 p0913 N88-15542
A vectorized Poisson solver over a spherical shell and its application to the quasi-geostrophic omega-equation
[NASA-CR-4116] 08 p1039 N88-16285
Fast Poisson solver on irregular regions by boundary integral-based domain decomposition methods
[DE88-003583] 10 p1399 N88-18340
Propagator solutions of partial differential equations applied to plasma transport
[DE88-006432] 13 p1816 N88-20852
Heating efficiency of beat wave excitation in a density gradient
[AD-A193066] 21 p3017 N88-27905
Three-dimensional zonal grids about arbitrary shapes by Poisson's equation
[NASA-TM-101018] 22 p3039 N88-28042
Poisson functionals of Markov processes and queueing networks
[AD-A194289] 22 p3145 N88-28705
An asymptotic evaluation of the tail of a multiple symmetric alpha-stable integral
[AD-A194570] 23 p3270 N88-29460

POISSON PROCESS
U POISSON DENSITY FUNCTIONS
U STOCHASTIC PROCESSES

POISSON RATIO
Anelastic behaviour of materials under multiaxial strains. Part 3: Order-disorder transition, Shoek effect and Poisson's ratio in AISI-1080 steel
[DE87-703087] 02 p0191 N88-11193

POLAR AURORAS
U AURORAS

POLAR CAPS
Configurations of the quiet polar cap and its response to a sudden increase of the energy input rate epsilon
[DMI-GEOPHYS-PAPERS-R-74] 03 p0350 N88-12210
Characteristics of particle acceleration at high latitude 08 p1026 N88-16210
F-layer polar cap arcs
[AD-A186592] 09 p1190 N88-17127
Collaborative studies of polar cap ionospheric dynamics
[AD-A187888] 10 p1355 N88-18098
The role of remote sensing in the study of polar ice sheets 14 p1939 N88-21570
Elements of sea ice dynamics and thermodynamics 14 p1939 N88-21571
High latitude ionospheric radio studies
[AD-A192270] 20 p2824 N88-26753
Rocket measurements within a polar cap arc: Ionospheric modelling
[AD-A192381] 20 p2824 N88-26754
On the conjugacy of the aurora: High and low latitudes
[AD-A193008] 20 p2824 N88-26755
Ionospheric convection and structure using ground-based digital ionosondes
[AD-A194246] 23 p3233 N88-29237
How dirty is Mars' North Polar cap, and why isn't it black 23 p3303 N88-29677

POLAR CUSPS
Polar cusp electrodynamics 08 p1030 N88-16242

POLAR METEOROLOGY
Large ice masses: Characteristics, behaviour and relation to climate 14 p1939 N88-21569

POLAR ORBITS
Study of mobile communications payload for Columbus Polar Platforms
[ITS-TR-056A/86] 01 p0034 N88-10220
Satellite environment: Polar orbits 03 p0272 N88-11713
Planning for future operational sensors and other priorities
[PB87-220802] 03 p0325 N88-12056
Viking quick look plots: A short description --- Swedish satellite 06 p0692 N88-14243
Polar platform element of Space Station: Mission objectives, European priorities, candidate instrumentation and selection procedure 09 p1129 N88-16779
Frozen orbit analysis in the Martian system
[AD-A189574] 13 p1856 N88-21106

POLAR PLATFORMS (SPACE STATIONS)
U SPACE STATION POLAR PLATFORMS

POLAR REGIONS
NT ANTARCTIC REGIONS
NT ARCTIC REGIONS
NT ROSS ICE SHELF
Forecasting polar lows using a numerical mesoscale model 02 p0210 N88-11321
Possible dynamical mechanisms for the Martian polar warming phenomenon
[NASA-CR-181454] 02 p0254 N88-11605
High latituoe problems to be studied by incoherent scatter radars
[DMI-GEOPHYS-PAPERS-R-77] 03 p0350 N88-12211
Eastern - western Arctic Sea ice analysis 1986
[AD-A184016] 03 p0355 N88-12235
USSR report: Earth sciences
[JPRS-UES-86-006] 04 p0458 N88-12831
Huurre expedition to the North Pole in 1984
[PB87-220935] 04 p0462 N88-12858
Cloud cover determination in polar regions from satellite imagery
[NASA-CR-181544] 04 p0471 N88-12908
The polar ionosphere and interplanetary field
[AD-A185386] 05 p0624 N88-13822
Electric field measurements on Viking: First results
[TRITA-EPP-87-04] 05 p0625 N88-13826
Activities report of the Ionospheric Observatory
[UIO-SR-87-01] 05 p0625 N88-13827
Axial anisotropy of the intensity of the cosmic ray nuclear component
[IFSI-87-7] 05 p0662 N88-14061
Global convection patterns in the high latitude
[AD-A185794] 06 p0743 N88-14571
Atmosphere of Venus in southern polar area 08 p1005 N88-16088
Atmosphere of Venus in south polar area based on radio transmission data 08 p1005 N88-16089
Atmosphere of Venus in north polar area based on radio transmission data from Venera-15 and Venera-16 spacecraft 08 p1005 N88-16090
Instantaneous pictures of the high-latitude electrodynamics using Viking and DMSP/F7 observations --- Swedish satellite 08 p1025 N88-16209
Characteristics of particle acceleration at high latitude 08 p1026 N88-16210
The sodium layer at 69 N latitude in wintertime 08 p1027 N88-16218
Electrodynamics of the high latitude middle atmosphere 08 p1028 N88-16225
Comparison of simultaneous MST radar and electron density probe measurements in the polar mesosphere --- Mesospheric, Stratospheric, Tropospheric (MST) 08 p1028 N88-16226
Predictability of ice concentration in the high-latitude North Atlantic from statistical analysis of SST (Sea Surface Temperature) and ice concentration data
[AD-A186621] 08 p1045 N88-16315
Collaborative studies of polar cap ionospheric dynamics
[AD-A187888] 10 p1355 N88-18098
Upper-thermospheric observations and neutral-gas dynamics at high latitudes during solar maximum
[AD-A188058] 11 p1512 N88-19031
Polar mesospheric cloud experiment
[AD-A188936] 12 p1648 N88-19872
The 1987 Airborne Antarctic Ozone Experiment: The Nimbus-7 TOMS data atlas
[NASA-RP-1201] 13 p1791 N88-20714
Sea ice observations and models 14 p1939 N88-21572
The Greenland Sea Project: The Arctemiz project 14 p1939 N88-21573
Centrifugal acceleration of ions in the polar magnetosphere
[NASA-TM-101148] 17 p2374 N88-24120
Cloud cover determination in polar regions from satellite imagery
[NASA-CR-182906] 17 p2375 N88-24123
Low frequency electrostatic turbulence in the polar cap E-region
[DRI-3-88] 18 p2540 N88-25077
SAM 2 data user's guide
[NASA-RP-1200] 18 p2543 N88-25094
TE/TM (Transverse Electric/Transverse Magnetic) height profile measurements of transpolar VLF (Very Low Frequency) signals
[AD-A194503] 22 p3069 N88-28216
The influence of conductivities consistent with field-aligned currents on high-latitude convection patterns
[TRITA-EPP-88-02] 22 p3119 N88-28533
Intraseasonal variability in atmospheric surface pressure and relationship to polar motion 22 p3120 N88-28540
Variations in the atmosphere associated with the 11-year solar cycle 22 p3122 N88-28557
The relationship between polar sea ice and the position of the near equatorial convergence zone 22 p3123 N88-28563
Sea ice processes
[AD-A193980] 23 p3237 N88-29262
The effect of equatorial ionospheric irregularities on the performance of a south-looking OTH-B (Over-The-Horizon-Backscatter) radar
[AD-A195090] 24 p3362 N88-30018
MIZEX (marginal ice zone experiment) 1987 SAR (Synthetic Aperture Radar) data summary
[AD-A195560] 24 p3364 N88-30035

POLARIMETERS
Lyman alpha SMM/UVSP absolute calibration and geocoronal correction
[NASA-TM-100314] 03 p0389 N88-12446
A polarimetric rain backscatter model developed for coherent polarization diversity radar applications 13 p1759 N88-20520
A two-wavelength infrared interferometer/polarimeter system for CIT (Compact Ignition Tokamak)
[DE88-007681] 18 p2579 N88-25321
Investigations on multiport antennas for polarimetric and modal field scanning
[REPT-5-87] 23 p3205 N88-29073
Development of a multiport-hybrid-mode exciter for use in antennas for polarimetric field measurements
[REPT-12-87] 23 p3205 N88-29075

POLARIMETRY
Use of polarimetry to measure the current profile in MTX
[DE87-013835] 02 p0237 N88-11495
Signal-filter design and system performance for polarimetric radar
[AD-A189257] 13 p1758 N88-20514
Similarity and diversity of the polarization of comets 14 p2003 N88-21940
Cometary grains and interplanetary dust: A polarimetric sensing --- Halley 14 p2003 N88-21941
The dust around the nucleus of Comet Halley 14 p2003 N88-21942
Data volume reduction for imaging radar polarimetry
[NASA-CASE-NPO-17184-1-CU] 20 p2788 N88-26541
Interpretation of the polarimetric observations of Jupiter
[DE88-702414] 21 p3031 N88-27991

POLARITONS
NT PLASMONS
Surface polariton resonances and reflectance on a bigrating
[AD-A184663] 03 p0377 N88-12370
Nonlinear surface polaritons
[AD-A191046] 18 p2499 N88-24822

POLARITY
Examination of the physical processes associated with the keyhole region of variable polarity plasma arc welds in aluminum alloy 2219 07 p0927 N88-15634
The mechanism of stereo regulation during anionic polymerization of polar monomers
[AD-A186530] 08 p0973 N88-15888

POLARIZATION
Broadband linear polarization and chromospheric CaII H and K line emission in late-type main sequence stars 04 p0511 N88-13140
The effect of microgravity on mammalian cell polarization at the ultrastructural level --- Spacelab D1 mission 22 p3061 N88-28164
Determining the spatial structure of fields of precipitation from space radar images in two orthogonal polarizations 24 p3450 N88-30531

POLARIZATION (CHARGE SEPARATION)
NT DIELECTRIC POLARIZATION
The physics of charge separation preceding lightning strokes in thunderclouds
[NASA-CR-178371] 01 p0071 N88-10452
Photoinduced charge separation by polymer-bound chromophores
[DE88-002101] 06 p0685 N88-14198
Atmospheric science 07 p0883 N88-15357
Ferroelectric properties and impact behavior of the PVF2 polymer and the VF2/C2F3H polarized copolymers --- vinylidene polyfluorides
[ISL-CO-245/86] 08 p0971 N88-15876
Picosecond laser spectroscopy of charge-separation in photosynthetic model systems
[DE88-003122] 09 p1172 N88-17028
Preparation of thin film polyvinylidene fluoride shock wave pressure transducers
[PB88-156070] 11 p1490 N88-18893

Spontaneous decay and atomic fluorescence near a metal surface of an absorbing dielectric
[AD-A187508] 13 p1835 N88-20975
Determination of Tafel constants in nonlinear polarization curves
[AD-A192335] 21 p2912 N88-27282
Techniques and instrumentation for transient characterization of metal-insulator-semiconductor diodes. Applications to metal-insulator InP system
[ECL-87-17] 21 p3025 N88-27959
Electron impact ionization cross-section of some organic compounds
[DE88-702044] 23 p3280 N88-29525
An electrochemical impedance spectroscopy study of reactions at the metal/coating interface
24 p3355 N88-29975

POLARIZATION (SPIN ALIGNMENT)
Application of spin-sensitive electron spectroscopies to investigations of electronic and magnetic properties of solid surfaces and epitaxial systems
[DE87-014235] 02 p0245 N88-11550
High energy polarized electron beams
[CEBAF-R-87-002] 11 p1546 N88-19244
Recent progress in optical bistability and tristability
14 p1979 N88-21809
Magnetic traps for an anti-hydrogen gas
16 p2269 N88-23572
Observation of ferromagnetism in ultrathin f.c.c. films by spin polarised neutron reflection
20 p2865 N88-27015
An undulator radiation source for spin-polarized photoemission studies of novel magnetic materials
[AD-A193756] 22 p3083 N88-28307
Fluctuation and relaxation phenomena studied by means of nuclear orientation
[B8679671] 23 p3281 N88-29534

POLARIZATION (WAVES)
NT CIRCULAR POLARIZATION
NT ELLIPTICAL POLARIZATION
NT LINEAR POLARIZATION
Study of advanced satellite concept using a multifeed reconfigurable antenna. Detailed report on Polarization Sensitive Reflector (PSR) and offset parabolic antennas, Appendix 1
[ESA-CR(P)-2406-VOL-3] 01 p0013 N88-10075
Theory of atomic additivity in molecular hyperpolizabilities 03 p0297 N88-11867
Development of optical modulators for measurements of solar magnetic fields
[NASA-TM-100315] 04 p0490 N88-13016
A polarization diversity meteorological radar system
[AD-A189291] 13 p1758 N88-20515
Polarization spectroscopy: Prospect and data needs
17 p2443 N88-24531

POLARIZATION CHARACTERISTICS
Polarization effects in laser-pumped Nd:YAG lasers
[DE88-004019] 11 p1492 N88-18904
Effect of double layer structure on the determination of corroion rates from polarization measurements
[DE88-010097] 20 p2774 N88-26448

POLARIZATION CHARTS
U GRAPHS (CHARTS)
U POLARIZATION (WAVES)

POLARIZED ELASTIC WAVES
Anomalies in electromagnetic absorption of circularly polarized ultrasonic waves by tungsten within Doppler-shifted cyclotron resonance range
06 p0775 N88-14756

POLARIZED ELECTROMAGNETIC RADIATION
NT POLARIZED LIGHT
NT SYNCHROTRON RADIATION
Optimization of charged particle acceleration rate over wave parameters in the scheme with acceleration by surface electromagnetic waves
[DE88-700320] 07 p0846 N88-15134
Polarization of electrons in an electromagnetic wave field in the presence of magnetic field
[DE88-700169] 13 p1757 N88-20509
Mode priming in an overmoded gyrotron oscillator
[AD-A189151] 13 p1772 N88-20602

POLARIZED LIGHT
Use of a 35mm camera for remote surface cleanliness verification 02 p0133 N88-10835
Multiple scattering of polarized light in cirrus clouds
13 p1801 N88-20768
Continuous collective molecule rotation of a nematic liquid crystal induced ! om light angular momentum
[FUB-17-1986] 14 p1986 N88-21845
Polarization of light reflected by vertically inhomogeneous planetary atmosphere
[DE88-702416] 21 p3031 N88-27992

POLARIZED RADIATION
NT POLARIZED ELASTIC WAVES
NT POLARIZED ELECTROMAGNETIC RADIATION
NT POLARIZED LIGHT
NT SYNCHROTRON RADIATION

POLAROGRAPHS
U POLAROGRAPHY

POLAROGRAPHY
Analysis of nickel sulphamate bath using charging current compensated D.C. polarography
[NAL-TM-MT-8705] 05 p0564 N88-13433
Water tunnel measurements by an electrochemical method 16 p2203 N88-23146

POLARONS
Soliton and polaron dynamics in conducting polymers
[DE88-702539] 23 p3198 N88-29035

POLICIES
NT ENERGY POLICY
NT PATENT POLICY
NT PROCUREMENT POLICY
Global environmental change research
[S-HRG-100-301] 03 p0348 N88-12199
National Science Foundation
[PB87-228375] 03 p0384 N88-12410
The attitudes of science policy, environmental, and utility leaders on US energy issues and fusion
[DE88-000784] 04 p0494 N88-13041
A study of the Department of Defense configuration management policies and procedures as applied to the FA-18 Strike/Fighter program
[AD-A184872] 05 p0657 N88-14034
National Aeronautics and Space Administration space station proposal, fiscal year 1988
[S-HRG-100-328] 05 p0659 N88-14043
On stochastic optimality of policies in first passage problems
[AD-A186293] 07 p0915 N88-15554
Relating service doctrine to space system requirements
[AD-A186620] 08 p1074 N88-16483
Organizations of intermediation in technology transfer: Its role in technological innovation
[INPE-4354-TDL/297] 08 p1094 N88-16581
Committee on Interagency Radiation Research and Policy Coordination
[DE88-003358] 09 p1188 N88-17121
Alternative Energy in the Midwest: Research and Applications. Conference Proceedings, Rosemont, Illinois, March 19-20, 1987
[PB88-142278] 11 p1509 N88-19015
Science and technology in India
[PB88-134747] 11 p1564 N88-19362
Conditions and mechanisms of the process of technological innovation in Brazil: The role of research institutes
[INPE-4175-TDL/274] 11 p1567 N88-19383
JPRS report. Science and technology: Europe and Latin America
[JPRS-ELS-87-054] 12 p1573 N88-19406
Communication satellites: Guidelines for a strategic plan
[NASA-TM-89306] 12 p1599 N88-19569
JPRS report: Science and technology. Europe and Latin America
[JPRS-ELS-88-001] 12 p1614 N88-19649
Systems approach to energy quality and efficiency
[PB88-139506] 12 p1640 N88-19823
JPRS report. Science and technology: Europe and Latin America
[JPRS-ELS-87-055] 12 p1686 N88-20086
Selling to NASA
[NASA-TM-89724] 12 p1705 N88-20208
Defending secrets, sharing data: New locks and keys for electronic information
[PB88-143185] 12 p1706 N88-20210
Implementing information systems/office automation in an Air Force environment
[AD-A188956] 12 p1707 N88-20218
Science, technology and the Constitution: Background paper
[PB88-142534] 12 p1708 N88-20222
JPRS report: Science and technology. Japan
[JPRS-JST-87-029] 15 p2052 N88-22228
A proposed national policy concerning the reentry of space reactors 17 p2415 N88-24359
Sensitivity analysis for the system reliability function
[AD-A191648] 18 p2525 N88-24979
Centre for International Co-Operation and Approriate Technology (CICAT)
[PB88-165501] 18 p2590 N88-25389
Timing regulations to prevent stratospheric-ozone depletion
[R-3495-JMO/RC] 19 p2690 N88-25987
An agenda for the strategic defense initiative
[RAND-P-7404] 20 p2847 N88-26898
SDI and/or arms control
[RAND-P-7357] 20 p2848 N88-26903
Space policy of common sense and moderation
[REPT-49/87] 20 p2883 N88-27118
Stress/fatigue and the ARNG (Army National Guard) aviator
[AD-A194184] 22 p3132 N88-28621
Quality control in microbiology: CDC lab manual
[PB88-179890] 23 p3237 N88-29263
SDI (Strategic Defense Initiative): A policy analysis
[AD-A194240] 23 p3275 N88-29493
The principles of mass and maneuver applied to space operations
[AD-A194037] 23 p3276 N88-29500
The problem of space in Soviet operational art
[AD-A194150] 23 p3276 N88-29502

POLISHING
Some speculations on the mechanisms of abrasive grinding and polishing
[DE87-014242] 02 p0181 N88-11126
A rapid polishing method for KBr and NaCl infrared windows
[DE88-002480] 07 p0862 N88-15229
Determination of aquo-complexes of chromium and iron in chromium plating and polishing solutions by ion chromatography
[AD-A190168] 15 p2039 N88-22148
Center for thin film studies
[AD-A191996] 19 p2732 N88-26226

POLITICS
Technology transfer to China
[PB87-223418] 04 p0502 N88-13087
German space policy on the threshold of the century. Analysis and proposals for the future
[ETN-88-90573] 07 p0943 N88-15734
Book analysis. Challenger: A major malfunction
[AD-A192458] 20 p2764 N88-26388
Political and economic barriers to information transfer
24 p3437 N88-30460

POLLEN
Examination of methods for pollen storage and dispersal
[TN-RB524-097/86] 17 p2378 N88-24134

POLLUTANTS
U CONTAMINANTS

POLLUTION
NT AIR POLLUTION
NT ENVIRONMENT POLLUTION
NT GLOBAL AIR POLLUTION
NT INDOOR AIR POLLUTION
NT NOISE POLLUTION
NT OIL POLLUTION
NT WATER POLLUTION
Withstand voltage of slightly polluted insulator chains in humid weather conditions
[DE88-752818] 22 p3072 N88-28237

POLLUTION CONTROL
Contamination control concepts for space station customer servicing 02 p0137 N88-10860
Emerging environmental constraints on the use of gasoline and diesel fuel and tradeoffs associated with the use of alternative fuels
[DE87-011504] 04 p0422 N88-12614
Innovative and alternative technology projects
[PB87-230165] 05 p0623 N88-13818
AN-30M cloud-seeding airplane in international exhibition 06 p0725 N88-14456
Integrated Global Background Monitoring Network
[DE88-001503] 06 p0731 N88-14499
The role of repowering in America's power generation future
[DOE/FE-0096] 10 p1351 N88-18076
Acid Precipitation: A current awareness bulletin
[DE88-007987] 20 p2821 N88-26738

POLLUTION MONITORING
Remote sensing of environmental pollution
[DFVLR-MITT-87-04] 01 p0067 N88-10428
An instrument for the quasi-continuous determination of atmospheric soot content
[DFVLR-FB-87-04] 01 p0068 N88-10433
Influence of surfactants on damping of gravity-capillary waves. 1: Frequency dependence
04 p0459 N88-12843
Hydrogen chloride measurements in launch-vehicle exhaust clouds
[DE87-011552] 08 p0964 N88-15837
Feasibility study for a 2nd generation system for airborne maritime pollution surveillance
[ETN-88-92108] 15 p2092 N88-22466
Application of SPOT imagery for oil spill contingency planning 22 p3108 N88-28460

POLLUTION TRANSPORT
Investigations of the dispersion of spontaneously released heavy gases
[WA-81] 01 p0066 N88-10427
A study of carbon monoxide distribution determinations for a global transport model
[NASA-CR-181423] 01 p0067 N88-10432

Opportunities for nowcasting air pollution episodes and accidental toxic and radioactive releases
02 p0210 N88-11317
Real-time evaluation and prediction of coastal dispersion near the SW tip of Africa --- effluents
02 p0210 N88-11318
Use of back air trajectories in interpreting atmospheric chemistry data: A review and bibliography
[PB88-102108] 07 p0876 N88-15312
Simulation of a typical flow in a broad valley
08 p1015 N88-16154
Simulation of global wet and dry deposition of nitric acid in a three-dimensional chemistry-transport model
[DE87-009847] 09 p1188 N88-17116
A comparison of multi-layer meso-alpha MLAM model results with surface and aircraft observations from CAPTEX
[DE88-000549] 09 p1188 N88-17118
Assessment of crop loss from air pollutants: Meteorology-atmospheric chemistry and long range transport
[PB88-146857] 15 p2089 N88-22448
Detection, monitoring and analysis of some environmental effects of fires in the Amazon region through utilization of NOAA and LANDSAT satellite imagery and aircraft data
[INPE-4503-TDL/326] 16 p2230 N88-23322
Review of numerical methods for radionuclide transport in three-dimensional porous media, at high Peclet numbers
[CFDU/87/10] 18 p2538 N88-25061
Prediction of regional pollutant dispersion using a nested-grid, three-dimensional numerical model
21 p2971 N88-27649
Development of an adjustable buoyancy balloon tracer of atmospheric motion. Phase 3: Refinement of the operational prototype system
[PB88-190764] 23 p3231 N88-29230

POLOIDAL FLUX
On tokamak equilibrium
[DE87-014811] 02 p0239 N88-11507
Poloidal magnetics of compact ignition tokamaks
[DE88-001774] 07 p0934 N88-15672
Evolution of poloidal variation of impurity density and ambipolar potential in rotating tokamak plasma, part 1
[DE88-006263] 13 p1842 N88-21022
An introduction to poloidal and toroidal fields
[MITT-54] 17 p2394 N88-24232
The 2-D magnetohydrostatic configurations leading to flares or quiescent filament eruptions
[NASA-TM-101147] 18 p2595 N88-25423
Toroidal and poloidal soft X-ray imaging system on the D3-D tokamak
[DE88-010585] 20 p2860 N88-26986
ITER plasma equilibrium and poloidal field system design
[DE88-011005] 21 p3018 N88-27912
Density fluctuations in currentless high beta plasmas in Heliotron E
[DE88-752310] 23 p3283 N88-29550

POLYACETYLENE
Novel polymers and copolymers and production of poly(acetylene)
[EP-PATENT-0-173-473-A2] 01 p0026 N88-10161
Ionically conductive polymers: Application to solid state batteries
[AD-A183733] 01 p0037 N88-10239
Molecular and supramolecular orientation in conducting polymers
[DE88-000533] 05 p0569 N88-13472
Time resolved spectroscopy facility for the study of nonlinear optical properties of semiconducting polymers
[AD-A191221] 18 p2490 N88-24768

POLYACRYLATES
U ACRYLIC RESINS

POLYAMIDE RESINS
NT KEVLAR (TRADEMARK)
NT NYLON (TRADEMARK)
Determination of the melting and decomposition points of different materials in an oxygen stream
[INFORME-I-158/86] 09 p1142 N88-16844
Development of polymeric films with piezoelectrical properties from polypeptides; low, odd nylons; or polyureas
[AD-A190301] 15 p2044 N88-22181
The adhesive bonding of thermoplastic composites
[AD-A190994] 16 p2173 N88-22953
Initial adhesive screening of novel polyamide-imides and their copolymers
[NASA-TM-100641] 20 p2779 N88-26481
Resistance of polyamide-6 against long time effects of various media at various temperatures
[NASA-TT-20297] 20 p2779 N88-26484

POLYATOMIC GASES
NT DIATOMIC GASES

POLYATOMIC MOLECULES
NT DIATOMIC MOLECULES
Picosecond CO2 laser interactions with polyatomic molecules
[DE87-012072] 01 p0051 N88-10327
A physico-chemical study of some areas of fundamental significance to biophysics
[DE87-013457] 02 p0217 N88-11365
Systematic studies of molecular vibrational anharmonicity and vibration-rotation interaction by self-consistent-field higher derivative methods: Applications to asymmetric and symmetric top and linear polyatomic molecules
[DE87-014691] 02 p0232 N88-11465
Study of polyatomic dynamics in the atmosphere
[AD-A190964] 16 p2233 N88-23334
Time-resolved studies of free radicals and laser-initiated chain reactions
[DE88-006569] 16 p2266 N88-23553
Proceedings of the Cooling, Condensation, and Storage of Hydrogen Cluster Ions Workshop
[AD-A189857] 16 p2266 N88-23555
Overview of hydrogen clusters
16 p2267 N88-23557
Large hydrogen cluster ions 16 p2267 N88-23558
Formation and reactivity of small hydrogen cluster ions 16 p2267 N88-23560
Electronic structure and stability of small cation and anion hydrogen clusters 16 p2267 N88-23562
Photon-assisted formation and cooling of molecular hydrogen
[MP-87-102] 16 p2267 N88-23563
Infrared spectroscopy of H3(+)
16 p2268 N88-23565
Vibrational spectroscopy of the hydrogen and hydrated hydronium cluster ions 16 p2268 N88-23566
The role of electron-ion recombination in bulk antimatter production 16 p2268 N88-23567
Electromagnetic manipulation of atomic hydrogen
16 p2268 N88-23568
Key problems and hydrogen atom formation
16 p2269 N88-23573
Production of heavy antinuclei: Review of experimental results 16 p2269 N88-23574
The cluster ion approach to the condensation and storage of antihydrogen 16 p2269 N88-23575
Analysis of containerless condensation of polyatomic hydrogen ions, with emphasis on H3(+,-) association channels and a future workshop to study related topics
16 p2269 N88-23576
Small molecule and small cluster ion formation in a low-density containerless mixture of electrons, protons and hydrogen atoms 16 p2269 N88-23577

POLYBENZIMIDAZOLE
Improved structural polymer alloys and composites
[AD-A192092] 19 p2619 N88-25538

POLYBUTADIENE
Distribution of chain ends inside the polybutadiene microspheres of SB diblock copolymers
[AD-A191257] 16 p2182 N88-23007
Environmental integrity of coating/metal interface
[AD-A192184] 18 p2492 N88-24786
Spatial organization of homopolymer chains inside spherical polybutadiene domains of SB diblock copolymers
[AD-A193390] 21 p2918 N88-27321
Blends of crystallizable polybutadienes
[AD-A194536] 23 p3197 N88-29026

POLYCARBONATES
The effect of heat treatment on fatigue crack growth in polycarbonate 05 p0606 N88-13714
Reinforcing of thermoplastic polycarbonate and polysulfone with carbon fibers: Production and characteristics of UD-compound objects
[NASA-TT-20158] 13 p1735 N88-20374
Interactions in miscible polymer blends
[AD-A193824] 22 p3058 N88-28144

POLYCRYSTALS
Understanding the transport properties of silicon grain boundaries and how they relate to I.C. applications of polysilicon
[DE87-013809] 01 p0104 N88-10677
Electrical properties of high T/sub c/ superconductors under high pressures
[DE87-012818] 02 p0245 N88-11548
Surface chemistry of transition metal carbides: A theoretical analysis
[AD-A184237] 03 p0291 N88-11829
X-ray analysis of polycrystalline aluminium subjected to fatigue cycling
[NAL-TM-MT-8706] 05 p0564 N88-13434
An overview of metal plasticity
[DE88-001658] 06 p0681 N88-14175
Observing effect of laser radiation of low-frequency Raman scattering of light 06 p0772 N88-14742
Magnetic investigations of superconductive, polycrystalline (RE)1Ba2Cu3O(7-x) compounds (RE = Y, Gd, Ho, Dy)
[DE88-002537] 08 p1090 N88-16558
X-ray diffraction study of thermotropic liquid crystalline polyesters and diester model compounds
[AD-A186788] 09 p1255 N88-17521
Adhesion of vapour phase deposited ultra-thin polyimide films on polycrystalline silver
[AD-A187930] 10 p1306 N88-17810
Proceedings of the Polycrystalline Thin Film Program Meeting
[DE87-001169] 11 p1557 N88-19321
Recommendations on developing polycrystalline alumina fiber 13 p1756 N88-20502
Photon-controlled growth of multilayered structures
[DE88-005061] 13 p1847 N88-21054
Strength and microstructure of ceramics
[AD-A190712] 15 p2046 N88-22191
Role of cracks in the creep of structural polycrystalline ceramics
[AD-A191485] 18 p2490 N88-24770
Characteristics of polysilicon layers and their application in sensors 19 p2689 N88-25861
The effects of thin compressive films on indentation fracture toughness measurements
[AD-A192243] 20 p2779 N88-26480
Pure metallic bridge and point-contact tunneling into single- and polycrystal YBa2Cu3O(sub 7-y)
[DE88-010030] 20 p2878 N88-27084
Microchemical analysis of polycrystalline Ni3Al and other ordered alloys using the field-ion microscope atom probe
[DE88-011519] 21 p2914 N88-27294
Superconducting thin films, composites and junctions
[AD-A193123] 21 p2937 N88-27440

POLYCYTHEMIA
Polycythemia and hydration status: Effects on blood volume and thermoregulation during exercise-heat stress
[AD-A185946] 07 p0888 N88-15383

POLYESTERS
Structure of thermotropic polyesters with large substituents
[AD-A184086] 04 p0418 N88-12595
X-ray diffraction study of thermotropic liquid crystalline polyesters and diester model compounds
[AD-A186788] 09 p1255 N88-17521
Polyether-polyester graft copolymer
[NASA-CASE-LAR-13447-1] 11 p1463 N88-18725
Combustion of PMMA, PE and PS in a ramjet
[VTH-LR-514] 18 p2484 N88-24733
Polyacrylic acid electrolyte-modified zinc phosphate conversion coatings for corrosion protection of steel
[DE88-004878] 19 p2617 N88-25527

POLYETHER RESINS
NT PEEK
NT POLYMETHYL METHACRYLATE
Polyether-polyester graft copolymer
[NASA-CASE-LAR-13447-1] 11 p1463 N88-18725

POLYETHERETHERKETONES
U PEEK

POLYETHYLENES
High ionic conductivity in PEO.PPG block polymer and salt solutions
[AD-A183502] 01 p0026 N88-10168
Ionically conductive polymers: Application to solid state batteries
[AD-A183733] 01 p0037 N88-10239
Physical properties of immiscible polymers
03 p0297 N88-11868
Polymer composition --- cable insulation
[EP-PATENT-0-199-444-A1] 04 p0418 N88-12594
Effects of additives on fire properties of polyethylene
[AD-A187064] 09 p1146 N88-16871
Nucleation and growth of calcium carbonate crystals on surface-modified polyethylene and polystyrene
[DE88-005126] 11 p1465 N88-18733
Fracture characteristics of a viscoelastic polymer under constant load: Experiments and analysis
11 p1501 N88-18963
Partial discharges and the electrical aging of cross linked polyethene (XLPE) cable insulation
[EUT-88-E-160] 14 p1892 N88-21300
Combustion of PMMA, PE and PS in a ramjet
[VTH-LR-514] 18 p2484 N88-24733
Combustion of PMMA (polymethylmethacrylate), PE (polyethylene) and PS (polystyrene) in a ramjet
[PB88-186572] 20 p2769 N88-26417
Morphological changes in polymer electrolyte cells
[AD-A195821] 24 p3368 N88-30054

POLYGONS
NT RECTANGLES
NT RHOMBOIDS
NT TRIANGLES
Two low-order mixed methods for the elasticity problem
[PB87-225272] 05 p0610 N88-13749

An application of digital cartography updating middle and small scale thematic maps using orbital data
[INPE-4460-TDL/317] 12 p1637 N88-19805
Investigation into the use of texturing for real-time computer animation
[AD-A191008] 16 p2251 N88-23454
Linear programming in R sup 3 and the skeleton and largest incircle of a convex polygon
[PB88-124664] 20 p2846 N88-26892

POLYHEDRONS
NT CUBES (MATHEMATICS)
NT ICOSAHEDRONS
NT PYRAMIDS
Two low-order mixed methods for the elasticity problem
[PB87-225272] 05 p0610 N88-13749
Adaptive grid for polyhedral visibility in object space: An implementation
[PB88-100938] 06 p0760 N88-14663
Recognition of polyhedral objects under structured illumination
[PB88-106703] 07 p0932 N88-15661
Polyhedral combinatorics
[CWI-OS-R8701] 08 p1072 N88-16466
On effectively labeling planar projections of polyhedra
[CWI-CS-R8715] 13 p1826 N88-20917

POLYIMIDE RESINS
Development of a polyimide matrix for filament winding with improved extensibility and fracture toughness for permanent use at 200 C
[BMFT-FB-T-86-118] 01 p0030 N88-10190
Addition polyimide composition
[EP-PATENT-0-167-304-A1] 01 p0053 N88-10337
Synthesis and characterization of block copolymers
[AD-A184406] 03 p0296 N88-11856
In-situ characterization of the interface of glass reinforced composites
[AD-A185136] 05 p0557 N88-13391
High temperature adhesive
[PB87-109229] 06 p0683 N88-14186
Correlations of norbornenyl crosslinked polyimide resin structures with resin thermo-oxidative stability, resin glass transition temperature and composite initial mechanical properties
[NASA-TM-100791] 09 p1147 N88-16877
Fabrication and electrical characterization of multilevel aluminum interconnects used to achieve silicon-hybrid wafer-scale integration
[AD-A190519] 15 p2060 N88-22282
New polyisoimides: An approach to in situ rigid-rod polyimide formation
[AD-A191665] 18 p2490 N88-24773
High temperature resins for injection. High temperature pre-impregnated
[RC-648676] 20 p2780 N88-26486

POLYIMIDES
Synthesis and characterization of processable polyimides with enhanced thermal stability
[NASA-CR-181447] 01 p0030 N88-10191
A quantum theoretical study of polyimides
[NASA-CR-181495] 03 p0292 N88-11831
Flexibilized copolyimide adhesives
[NASA-TM-89303] 05 p0570 N88-13474
Development of an impact- and solvent-resistant thermoplastic composite matrix, phase 4
[NASA-CR-178413] 06 p0677 N88-14145
An investigation of physical properties of thermoplastic polyimides
[NASA-TM-100530] 06 p0678 N88-14151
Space environmental effects on polymeric materials
[NASA-CR-182454] 09 p1148 N88-16879
Adhesion of vapour phase deposited ultra-thin polyimide films on polycrystalline silver
[AD-A187930] 10 p1306 N88-17810
Vapor phase deposition and growth of polyimide films on copper
[AD-A189969] 15 p2044 N88-22178
Evaluation of a thermoplastic polyimide (422) for bonding GR/PI composite
[NASA-TM-100584] 16 p2182 N88-23003
Carboxylate formation at the interface between a polyimide coating and cobalt 17 p2320 N88-23859
Improved structural polymer alloys and composites
[AD-A192092] 19 p2619 N88-25538
A monolithic gas flow sensor with polyimide as thermal insulator 19 p2669 N88-25864
Substituted 1,1,1-Triaryl-2,2,2-Trifluoroethanes and processes for their synthesis
[NASA-CASE-LEW-14345-1] 20 p2767 N88-26404
Initial adhesive screening of novel polyamide-imides and their copolymers
[NASA-TM-100641] 20 p2779 N88-26481

POLYMER CHEMISTRY
Novel polymers and copolymers and production of poly(acetylene)
[EP-PATENT-0-173-473-A2] 01 p0026 N88-10161
Novel conductive polymers
[EP-PATENT-0-182-548-A2] 01 p0026 N88-10163
Crosslinkable elastomeric materials
[EP-PATENT-0-181-735-A1] 01 p0026 N88-10165
Boronium complexes as polymer catalysts
[GB-PATENT-2-161-475-A] 01 p0026 N88-10166
Adhesion properties of polyelectrolyte-chemisorbed zinc phosphate conversion coatings
[DE87-012489] 01 p0029 N88-10186
Preparation of polymer polyols
[EP-PATENT-0-162-589-A1] 01 p0102 N88-10665
Experiments of the selection of a method evaluating the fire resistance of some materials based on macromolecular compounds
[NASA-TT-20129] 02 p0154 N88-10966
Physical properties of immiscible polymers
03 p0297 N88-11868
Estimations of gravitational effects on thermal denaturation process in a biopolymer
03 p0318 N88-12013
Simultaneous TG/DSC (thermogravimetry/Differential Scanning Calorimetry) and TG/MS (thermogravimetry/Mass Spectrometry) analyses of polymeric and energetic materials
[DE88-000727] 04 p0413 N88-12561
Effect of sidechain length and crosslinking on ionic conductivity in polyphosphazene solid electrolytes
[AD-A184419] 04 p0497 N88-13058
Characterization of the microstructures of various materials
[AD-A184961] 05 p0655 N88-14017
Correlation between flammability and heat of combustion of polymers
[NASA-TT-20116] 06 p0973 N88-15884
Theoretical bases of polymer photodegradation and photooxidation
[AD-A186533] 08 p0974 N88-15889
Contrasting conductance/viscosity relations in liquid states of vitreous and polymer solid electrolytes
[AD-A189378] 13 p1748 N88-20452
Examination of polysulfide sealants by scanning electron microscopy
[MRL-R-1096] 13 p1752 N88-20478
Aging properties of cable polmers (2)
[NASA-TT-2022B] 13 p1752 N88-20479
Evidence for first polymer in Comet Halley: Polyoxymethylene 14 p1997 N88-21906
Molecular dynamics of materials possessing high energy content
[AD-A190034] 15 p2034 N88-22118
Donor acceptor polymerization chemistry as a vehicle to low energy cure matrix resins
[AD-A190119] 15 p2044 N88-22179
Research on stable processible conducting polymers for electronic applications
[AD-A190246] 15 p2044 N88-22180
Structural Ceramics
[NASA-CP-2427] 17 p2323 N88-23872
Synthesis and characterization of new phosphazene polymers
[AD-A191508] 18 p2490 N88-24771
Electronic and ionic transport in polymers
[AD-A191642] 18 p2490 N88-24772
Next-generation fire extinguishing agent. Phase 1: Suppression concepts
[AD-A192279] 19 p2614 N88-25514
Substituted 1,1,1-Triaryl-2,2,2-Trifluoroethanes and processes for their synthesis
[NASA-CASE-LEW-14345-1] 20 p2767 N88-26404
Fundamental studies of elastomers
[DE88-009879] 20 p2778 N88-26471
Statistical mechanics of polymer systems
[DE88-011172] 20 p2778 N88-26477
Initial adhesive screening of novel polyamide-imides and their copolymers
[NASA-TM-100641] 20 p2779 N88-26481
Energy migration, motion and order in synthetic polymers
[AD-A193334] 21 p2918 N88-27320
Optimization and scale-up performance of polymer electrolyte batteries
[AD-A193987] 22 p3073 N88-28243
The overcharge behavior of polymer electrolyte cells
[AD-A193984] 22 p3117 N88-28522
Polyazidoesters as energetic polymers and copolymer components with fluoro derivatives
[AD-A194236] 23 p3199 N88-29039
Prediction of degradation of polymeric coating materials 24 p3354 N88-29970
Novel ladder polymers for use as high temperature stable resins or coatings
[NASA-CASE-LEW-14203-1] 24 p3356 N88-29984

POLYMER MATRIX COMPOSITES
NT BORON-EPOXY COMPOSITES
NT CARBON FIBER REINFORCED PLASTICS
NT EPOXY MATRIX COMPOSITES
NT GLASS FIBER REINFORCED PLASTICS
NT GRAPHITE-POLYIMIDE COMPOSITES
NT REINFORCED PLASTICS
Ultrasonic examination of high performance polymer composites
[DRIC-T-7862] 01 p0027 N88-10170
Development and application of composites
03 p0286 N88-11795
Time-temperature-stress capabilities of composite materials for advanced supersonic technology application
[NASA-CR-178272] 06 p0677 N88-14144
Space environmental effects on polymeric materials
[NASA-CR-182418] 07 p0838 N88-15082
Aeropropulsion '87. Session 1: Aeropropulsion Materials Research
[NASA-CP-10003-SESS-1] 09 p1118 N88-16897
High temperature polymer matrix composites
09 p1119 N88-16700
Thermal deformation and strength of composite materials at high temperatures 14 p1885 N88-21263
Singlet oxygen behavior in solid polymer matrices
[DE88-005171] 15 p2043 N88-22171
Nondestructive evaluation by acousto-ultrasonics
15 p2082 N88-22412
Homogenization study of matrix behavior in a composite material
[ONERA-RT-1/7256-RY-060-R]
16 p2172 N88-22943
A thermally modified polymer matrix composite material with structural integrity to 371 C
[NASA-TM-100922] 19 p2609 N88-25483
Thermoplastic coating of carbon fibers
[NASA-CR-183067] 20 p2787 N88-26407
Irreversible deformations during fracture in polymers
[W-7/86] 20 p2780 N88-26485
Microwave polymerization of composite structures
[REPT-881-430-116] 21 p2922 N88-27343
The effects of moisture loss and elevated temperature upon the material damping of fibre reinforced polymer matrix composites
[UTIAS-324] 23 p3188 N88-28970

POLYMER PHYSICS
Mechanisms of polymer degradation using an oxygen plasma generator
[NASA-TM-100681] 01 p0018 N88-10110
Fluid mechanical issues in polymer processing
[DE88-002767] 08 p0972 N88-15880
Study of molecular mobility of noncrystaline polymer alloys of different compatibility using mechanical spectrometry
[ISAL-87-0032] 09 p1149 N88-16883
Integral equation theory of homopolymer melts
[DE88-005304] 13 p1751 N88-20470
Integral equation theory of polymer blends
[DE88-005305] 13 p1751 N88-20471
Next-generation fire extinguishing agent. Phase 1: Suppression concepts
[AD-A192279] 19 p2614 N88-25514
Storing bits on a DNA polymer chain
[AD-A195701] 24 p3356 N88-29981

POLYMERIC FILMS
Optical damage in polymers by millisecond light pulses
[DE87-013106] 02 p0151 N88-10943
Molecular composites: Processing, post-treatment and mechanics
[AD-A184458] 04 p0410 N88-12547
Elementary fluorination of polymers
[ETN-88-90812] 07 p0836 N88-15075
Use of hydrophilic polymer coatings for control of electroosmosis and protein adsorption
07 p0925 N88-15620
Interfacial effects in thin Li/PEO cells at room temperature
[AD-A186974] 09 p1157 N88-16931
Electrically conducting polymer-copper sulphide composite films, preparation by treatment of polymer-copper (2) acetate composites with hydrogen sulfide
[NASA-TT-20204] 10 p1305 N88-17803
Interactions of cultured human endothelial cells with polymeric surfaces
[PB88-112255] 10 p1369 N88-18178
Electronic and ionic transport in polymers
[AD-A187253] 11 p1452 N88-18651
Polymer reflectors research during FY86
[DE88-001101] 11 p1508 N88-19009
Transport properties of conductive polymers
[AD-A188411] 12 p1610 N88-19628
Morphological studies of conductive polymers
[AD-A188456] 12 p1610 N88-19629
The effects of thin polymeric surface films in reducing fretting corrosion and wear
[AD-A188633] 12 p1611 N88-19634

Molecular dynamics of laser ablation of a polymer coating
[DE88-004337] 13 p1750 N88-20466
Safety research of insulating materials of cable for nuclear power generating station
[NASA-TT-20202] 13 p1752 N88-20477
Measuring thin film properties using SAW (Surface Acoustic Wave) devices: Diffusivity and surface area
[DE88-002216] 13 p1834 N88-20970
Research on stable processible conducting polymers for electronic applications
[AD-A190246] 15 p2044 N88-22180
Development of polymeric films with piezoelectrical properties from polypeptides; low, odd nylons; or polyureas
[AD-A190301] 15 p2044 N88-22181
Polymer fuel cell as an energy storage component for space power applications 17 p2429 N88-24452
Mechanisms of gas permeation through polymer membranes: Renewal proposal for period December 1, 1986 - November 30, 1989
[DE88-007436] 18 p2494 N88-24796
Fabrication of a flexible conductor by vapor deposition
[DE88-007500] 19 p2661 N88-25826
Characterization of proton conducting polymer blends 19 p2669 N88-25867
Pyrolyzed organic polymer nitrogen dioxide sensor 19 p2669 N88-25868
Thermodynamic study of hygroscopic polymers using surface acoustic waves 19 p2672 N88-25882
Thin-membrane Lamb-mode acoustic oscillators for chemical detection 19 p2673 N88-25895
Refractory films from spin-cast carbon
[DE88-011251] 21 p2919 N88-27327
A resistive-film based force transducer for the study of exercise
[AD-A192601] 21 p2986 N88-27730
Chemistry of adhesion at the polyimide-metal interface
[AD-A194647] 22 p3058 N88-28143
SRM (Solid Rocket Motor) propellant and polymer materials structural modeling
[NASA-TP-2824] 22 p3089 N88-28343
Optical bistable behavior of a planar quasi-waveguide interferometer made with a conjugated organic polymer film
[AD-A194349] 22 p3152 N88-28756
The radiation sensitivity of select metal chelate polymers: Mechanistic changes at higher energies
[AD-A193467] 23 p3196 N88-29019
Polymeric heat pipe wick
[NASA-CASE-GSC-13019-1] 23 p3214 N88-29133
Performance Prediction for Coatings. Proceedings of a Workshop
[AD-A188973] 24 p3354 N88-29966
Electrochemical evaluation of the long term corrosion resistance of polymer coated steel 24 p3355 N88-29974
An electrochemical impedance spectroscopy study of reactions at the metal/coating interface 24 p3355 N88-29975
A review of melt and vapor growth techniques for polydiacetylene thin films for nonlinear optical applications
[NASA-TM-100340] 24 p3430 N88-30412

POLYMERIZATION
NT COPOLYMERIZATION
NT DIMERIZATION
Synthesis and characterization of processable polyimides with enhanced thermal stability
[NASA-CR-181447] 01 p0030 N88-10191
Applications and limitations of deuterium labeling methods to neutron scattering studies of polymers
[DE87-012936] 02 p0151 N88-10945
The influence of polymer structure on triplet luminescence
[DE87-014431] 02 p0152 N88-10952
Migration and transfer of triplet energy in selected polymer systems
[DE87-014432] 02 p0152 N88-10953
Polyvinyl esters of omega-H-perfluoroacids and polyvinyl alcohol obtained from them
[AD-A184633] 03 p0279 N88-11755
High-molecular compounds (selected articles)
[AD-A184668] 03 p0293 N88-11842
Cure and properties of thermosetting polymers
[AD-A184669] 03 p0293 N88-11843
Polymers in solar technologies
[DE88-001102] 03 p0294 N88-11849
Wittig synthesis of conductive segmented block polymer compositions
[AD-A184018] 03 p0295 N88-11850
Highly Non-Linear Optical (NLO) organic crystals and films. Electrooptical organic materials 03 p0297 N88-11866
Conductive polymers via reactive oligomer
[AD-A184270] 04 p0419 N88-12597
Conducting hybrid polymeric systems
[DE88-000527] 04 p0421 N88-12611
Proton abstraction as a route to conductive polymers
[AD-A184019] 04 p0421 N88-12612
Molecular-level synthesis and characterization of metal-polymer interfaces
[AD-A184956] 05 p0567 N88-13455
Molecular and supramolecular orientation in conducting polymers
[DE88-000533] 05 p0569 N88-13472
Effects of hydrolysis on metallo-organic solution deposition of PZT films
[ATR-86(8443)-1] 06 p0679 N88-14160
TMA-microrheological testing of polymers (thermomechanical analysis)
[PB87-228805] 06 p0683 N88-14187
Ionically conducting polymers: Principles and properties of solid electrolytes
[DE88-001552] 06 p0684 N88-14190
The morphology of emulsion polymerized latex particles
[DE88-002672] 08 p0972 N88-15879
Processing, fabrication, applications and limitations of inherently conducting polymers
[DE88-003210] 08 p0973 N88-15883
Synthesis of high molecular weight peptide polymers and copolymers containing L-dope residues
[AD-A186462] 08 p0973 N88-15887
The mechanism of stereo regulation during anionic polymerization of polar monomers
[AD-A186530] 08 p0973 N88-15888
A 13C and 15N solid state NMR characterization of aramid-containing nylon-6 polymers synthesized by in situ polymerization of caprolactam with benzoyl caprolactam derivatives
[AD-A187067] 09 p1147 N88-16872
Thermogravimetric analysis of polymeric materials for an intermediate temperature solid electrolyte
[DE88-004854] 10 p1306 N88-17809
The deposition rate dependence of plasma polymerization on the radius of curvature of the substrate
[DE88-003811] 10 p1412 N88-18429
Polymerization of fluorinated diacetylenes
[AD-A188051] 11 p1462 N88-18716
Polymeric materials for electro-optic testing
[AD-A188382] 12 p1610 N88-19627
Reinforcing of thermoplastic polycarbonate and polysulfone with carbon fibers: Production and characteristics of UD-compound objects
[NASA-TT-20158] 13 p1735 N88-20374
High-temperature thermosets derived from the Diels-Alder polymerization of bisbenzocyclobutenes and bimaleimides
[AD-A188800] 13 p1747 N88-20449
Donor acceptor polymerization chemistry as a vehicle to low energy cure matrix resins
[AD-A190119] 15 p2044 N88-22179
High-performance polymeric materials
[AD-A190708] 15 p2046 N88-22190
Elementary characterization of Fibredux 913 CTS 5 34 percent preimpregnated carbon-epoxy from Ciba Geigy
[M-484300] 16 p2171 N88-22941
Electrochemistry in near-critical and supercritical fluids. 5: The dimerization of quinoline and acridine radical anions and dianions in ammonia from -70 C to 150 C
[AD-A190858] 16 p2175 N88-22967
Complexation and hydrolysis reactions of iron(III) 17 p2322 N88-23867
Polymer precursors for SiC ceramic materials 17 p2326 N88-23889
Polymer precursors for ceramic composites 17 p2326 N88-23890
Aromatic cyclotriphosphazenes
[NASA-CASE-ARC-11428-3] 18 p2477 N88-24692
Current and future molecular structures of aerospace organic matrix resins 18 p2477 N88-24695
Synthesis and characterization of new phosphazene polymers
[AD-A191508] 18 p2490 N88-24771
Electronic and ionic transport in polymers
[AD-A191642] 18 p2490 N88-24772
Demixing of aqueous polymer two-phase systems in low gravity
[NASA-TM-101141] 18 p2496 N88-24809
Fundamental studies of elastomers
[DE88-009679] 20 p2778 N88-26471
Polymerization of epoxy matrix composites using pulsed microwaves
[CERT-3/1324-MO] 20 p2780 N88-26487
Structural study of impregnating resins of TGMDA/DDS type
[ETN-88-92167] 20 p2780 N88-26488
The electronic structure of condensed molecular systems
[DE88-007823] 20 p2851 N88-26923
Soluble metal chelate polymers of coordination numbers six, seven and eight
[AD-A192485] 21 p2917 N88-27314
Precursor chemistry and the structure of silica aerogels
[DE88-011253] 21 p2920 N88-27328
Study of crosslinking and nonelastic mechanical properties of epoxy and PSP networks --- epoxy resins; polystyrylpyridine resins (psp)
[ETN-88-92740] 21 p2921 N88-27337
Microwave polymerization of composite structures
[REPT-881-430-116] 21 p2922 N88-27343
Polymerization of azaethylenes (imines) and aza-1,3-dienes: Potential reactive monomers
[AD-A194717] 23 p3197 N88-29028
Novel ladder polymers for use as high temperature stable resins or coatings
[NASA-CASE-LEW-14203-1] 24 p3356 N88-29984
A review of melt and vapor growth techniques for polydiacetylene thin films for nonlinear optical applications
[NASA-TM-100340] 24 p3430 N88-30412

POLYMERS
Structure of sol-gel-derived inorganic polymers. 2: Silicates and borates
[DE87-013068] 01 p0027 N88-10172
Space environmental effects on polymeric materials
[NASA-CR-182454] 09 p1148 N88-16879
Modification of polymers by photografting processes 17 p2323 N88-23871
A computer model for the flow of a molten polymer in a narrow cavity
[NPL-DMA(A)-157] 22 p3058 N88-28146
Design analysis in polymeric materials
[NPL-DMA(A)-159] 22 p3058 N88-28147

POLYMETHYL METHACRYLATE
High-molecular compounds (selected articles)
[AD-A184668] 03 p0293 N88-11842
Development of crack under periodically pulsed laser radiation 06 p0774 N88-14754
Some aspects of the mechanics and mechanisms of dynamic brittle fracture 10 p1343 N88-18028
Combustion of PMMA, PE and PS in a ramjet
[VTH-LR-514] 18 p2484 N88-24733
Adhesion between polystyrene and polymethylmethacrylate
[AD-A192050] 18 p2492 N88-24785
Flame spread mechanisms over PMMA surfaces
[NASA-TT-20284] 19 p2612 N88-25500
Combustion of PMMA (polymethylmethacrylate), PE (polyethylene) and PS (polystyrene) in a ramjet
[PB88-186572] 20 p2769 N88-26417
Ignition and flame spread of PMMA
[NASA-TT-20290] 20 p2771 N88-26431
Irreversible deformations during fracture in polymers
[W-7/86] 20 p2780 N88-26485
Interactions in miscible polymer blends
[AD-A193824] 22 p3058 N88-28144

POLYNOMIALS
NT BINOMIALS
NT DYADICS
NT HERMITIAN POLYNOMIAL
Approximate polynomial preconditioning applied to biharmonic equations on vector supercomputers
[NASA-TM-100217] 01 p0087 N88-10563
Polynomial compensation, inversion, and approximation of discrete time linear systems
[NASA-TM-100027] 03 p0372 N88-12344
A simplified procedure for correcting both errors and erasures of a Reed-Solomon code using the Euclidean algorithm 04 p0435 N88-12898
On color polynomials of Fibonacci graphs
[AD-A184133] 04 p0486 N88-12996
Parallel algorithms for polynomials
[PB87-226304] 06 p0756 N88-14635
Progress in mathematical programming
[AD-A195729] 06 p0759 N88-14658
Diagonalisation methods in polynomial setting
[PB87-138616] 06 p0769 N88-14726
An O(n3L) interior point algorithm for convex quadratic programming
[AD-A186001] 07 p0909 N88-15504
Single-layer wire routing
[AD-A186990] 09 p1157 N88-16932
Acceleration techniques for decoupling algorithms in semiconductor simulation
[DE88-003593] 09 p1221 N88-17323
On exact solutions of multidimensional Schroedinger equation with polynomial potentials
[DE88-700460] 09 p1230 N88-17373
Fast and practical parallel polynomial interpolation
[DE88-003530] 10 p1397 N88-18326
Polynomial preconditioning for conjugate gradient methods
[DE88-005214] 10 p1399 N88-18342

Small degree solutions for the polynomial Bezout equation
[AD-A187630] 10 p1401 N88-18355
An exact pseudo polynomial algorithm for the 0-1 linear diophantine equation
[INPE-4289-PRE/1160] 11 p1531 N88-19148
Elimination of quantifiers of linear variables and corresponding transfer principles
[DE88-005692] 13 p1826 N88-20912
Group theoretic interpretations of Askey's scheme of hypergeometric orthogonal polynomials
[CWI-PM-R8703] 13 p1831 N88-20954
A polynomial approach to the H sub infinity control design method
[MEMO-662] 14 p1962 N88-21701
Generalizations of Laguerre (type) polynomials
[REPT-87-58] 14 p1963 N88-21714
Solution of the compressible Navier-Stokes equations of motion by Chebyshev polynomials for laminar shock-boundary layer flow
[AD-A191033] 16 p2208 N88-23176
Simulation of FELIN logics. Polynomials roots simultaneous computation algorithms
[ETN-88-92182] 16 p2253 N88-23464
Jacobi polynomials as generalized Faber polynomials
[CWI-PM-R8706] 16 p2258 N88-23498
Orthogonal polynomials with respect to a symmetric inner product involving derivates
[REPT-87-59] 16 p2259 N88-23504
On a classification of problems on sets of bilinear forms by formal polynomials
[RR-642-I-IMAG-53-LIFIA] 17 p2392 N88-24219
Sensitivity analysis for the system reliability function
[AD-A191648] 18 p2525 N88-24979
Null steering applications of polynomials with unimodular coefficients
[AD-A191087] 18 p2562 N88-25211
On a biorthogonal system associated with uniform asymptotic expansions
[CWI-AM-R8709] 18 p2566 N88-25240
High degree interpolation polynomial in Newton form
[NASA-CR-181677] 18 p2567 N88-25249
A new trajectory following polynomial-time algorithm for the linear programming problem
[REPT-87-87] 20 p2840 N88-26848
Accurate solution of parabolic equations by expansion in ultraspherical polynomials
[DE88-701829] 20 p2845 N88-26880
Finding minimum-cost circulations by canceling negative cycles
[AD-A192727] 21 p3005 N88-27825
Structure of bound states in polynomial potentials
[DE88-702437] 21 p3007 N88-27837
Evaluation of quantum mechanics path integrals by the approximations exact on a class of polynomial functionals
[DE88-702434] 21 p3011 N88-27865
Optimum-Path-to-Go guidance of command adjusted trajectory projectiles
[AD-A193377] 22 p3040 N88-28051
Solution to the compressible Navier-Stokes equations of motion by Chebyshev polynomials with implicit time stepping
[AD-A194119] 22 p3075 N88-28257
Random pseudo-polynomial algorithms and exact problems
[REPT-87-014] 22 p3140 N88-28672
Polynomials with restricted coefficients and their applications
[AD-A192589] 23 p3202 N88-29055
Polynomial definition of discrete field points of map of diffusion equation, part 1
[AD-A193697] 23 p3271 N88-29467
On matrix pencil equivalents of a general polynomial matrix
[MATH-REPT-207] 23 p3273 N88-29479

POLYPEPTIDES
NT GLUTATHIONE
Estimations of gravitational effects on thermal denaturation process in a biopolymer
03 p0318 N88-12013
Development of polymeric films with piezoelectrical properties from polypeptides; low, odd nylons; or polyureas
[AD-A190301] 15 p2044 N88-22181
Influence of altitude and caffeine during rest and exercise on plasma levels of proenkephalin peptide F
[AD-A192659] 22 p3131 N88-28616

POLYPHENYLS
Carbon residue studies of polyphenyl ethers and ester-based lubricants using a microcarbon residue tester
[AD-A186585] 12 p1611 N88-19632
The synthesis of polyphenylene from a CIS-dihydrocatechol biologically produced monomer
18 p2478 N88-24699
The crystallization of tough thermoplastic resins in the presence of carbon fibers
[NASA-CR-182984] 20 p2776 N88-26464

POLYPROPYLENE
High ionic conductivity in PEO.PPG block polymer and salt solutions
[AD-A183502] 01 p0026 N88-10168
Prediction of long-term creep in polypropylene from short-term tests
[NPL-DMA(A)-156] 22 p3088 N88-28337

POLYSACCHARIDES
NT CELLULOSE
NT GLYCOGENS
NT STARCHES

POLYSTATION DOPPLER TRACKING SYSTEM
A preliminary assessment of thunderstorm outflow wind measurement with airport surveillance radars
[AD-A189064] 13 p1799 N88-20757

POLYSTYRENE
Polymer chain segment orientation during stress relaxation
[DE87-013392] 01 p0027 N88-10174
Metal containing polymers as fuel cell catalysts
[AD-A184605] 03 p0347 N88-12194
Group contribution analysis of the damping behavior of homopolymers, statistical copolymers and interpenetrating polymer networks based on acrylic, vinyl and styrenic mers
[AD-A185904] 07 p0836 N88-15070
Study on the correlation of polystyrene (PS) film craze to its fracture behaviour by TEM (Transmission Electron Microscopy)
[PB87-143343] 08 p0970 N88-15870
Nucleation and growth of calcium carbonate crystals on surface-modified polyethylene and polystyrene
[DE88-005126] 11 p1465 N88-18733
A new polymer-based hydrogen getter
[DE88-004538] 13 p1751 N88-20467
Preferential surface adsorption in miscible blends of polystyrene and poly(vinyl methyl ether)
[AD-A191451] 18 p2490 N88-24769
Adhesion between polystyrene and polymethylmethacrylate
[AD-A192050] 18 p2492 N88-24785
Diffusion of homopolymers into nonequilibrum diblock copolymer structures
[DE88-005306] 18 p2494 N88-24794
Combustion of PMMA (polymethylmethacrylate), PE (polyethylene) and PS (polystyrene) in a ramjet
[PB88-186572] 20 p2769 N88-26417

POLYSULFIDES
Examination of polysulfide sealants by scanning electron microscopy
[MRL-R-1096] 13 p1752 N88-20478

POLYTETRAFLUOROETHYLENE
NT TEFLON (TRADEMARK)
An evaluation of effectiveness of PTFE (polytetrafluoroethylene) type friction reducers on reducing friction and wear
[AD-A187440] 10 p1340 N88-18010
Evaluation of transfer films of Salox M on 440C for HPOTP bearing cage applications, task 119
[NASA-CR-179020] 23 p3223 N88-29184

POLYTOPES
The perfectly matchable subgraph polytope of an arbitrary graph
[AD-A185993] 07 p0913 N88-15539
The clique polytope of a graph
[MEMO-663] 14 p1963 N88-21710

POLYURETHANE FOAM
Evaluation of the thermal effectiveness of urethane foam and fiberglass as insulation systems for tank cars
[PB88-100797] 06 p0686 N88-14207
Investigations of the stability of the cell opening of soft polyurethane foams
[ETN-88-91481] 11 p1463 N88-18724
Thermal conductivity of selected foams and systems from 100 to 300 K
[PB88-201553] 20 p2777 N88-26466

POLYURETHANE RESINS
Urea-polyurethane and polydimethylsiloxane mixtures. Morphology control using a block copolymer
[ISAL-IDI1-87-05] 02 p0153 N88-10959
Synthesis and characterization of block copolymers
[AD-A184405] 03 p0295 N88-11855
Study of aeropropulsion laboratory pressure drop rig and recommended test procedure
[AD-A184333] 03 p0322 N88-12038
High explosive moulding powders from RDX and aqueous polyurethane dispersions
[AD-A185026] 05 p0568 N88-13458
Structure-property relationships in thermoplastic elastomers 4. Dynamic mechanical relaxations in poly(dioxolane), poly(butyltrioxocane) and poly(propylene oxide) polyurethanes
[AD-A186278] 07 p0836 N88-15073
Optimization of binary pigment coatings
[AD-A189103] 13 p1748 N88-20450
Polyacrylic acid electrolyte-modified zinc phosphate conversion coatings for corrosion protection of steel
[DE88-004878] 19 p2617 N88-25527
Cleanability of aircraft polyurethane topcoats
[AD-A193456] 23 p3170 N88-28878

POLYVINYL ALCOHOL
Polyvinyl esters of omega-H-perfluoroacids and polyvinyl alcohol obtained from them
[AD-A184633] 03 p0279 N88-11755
High-molecular compounds (selected articles)
[AD-A184668] 03 p0293 N88-11842
Characterization of proton conducting polymer blends
19 p2669 N88-25867

POLYVINYL CHLORIDE
Effect of test temperature and frequency on fatigue crack propagation in PVC 05 p0606 N88-13715
Evaluation of flammability for cable-like polymers
[NASA-TT-20225] 13 p1752 N88-20476
Burning characteristics and flammability of PVC cables in groups
[NASA-TT-20226] 14 p1893 N88-21303

POLYVINYL FLUORIDE
Polymer materials for pressure sensors
06 p0676 N88-14141
Polymer material for heat sensors
06 p0676 N88-14142
Piezoelectric laminates for torsional and bending model control: Theory and experiment
10 p1343 N88-18029
Statistical-mechanical study of polyvinylidene fluoride
[AD-A188310] 12 p1609 N88-19624
Piezoelectric polymer tactile sensor arrays for robotics
[AD-A188852] 12 p1634 N88-19780

PONDEROMOTIVE FORCES
Numerical simulation of laser filamentation experiments
[ETN-87-90959] 02 p0179 N88-11118
HF sidebands in the ionosphere
05 p0574 N88-13497

PONTRYAGIN PRINCIPLE
Optimal control theory of load-following and parameter-tracking of nonlinear systems: An application of Pontryagin Maximum Principle to reactor dynamics
[DE88-004770] 11 p1532 N88-19152

POPULATION INVERSION
Active medium formation in lasers using mixtures of inert gases and optical breakdown pumping
06 p0709 N88-14347
Population inversion in gapless semiconductors as result of interband pumping 06 p0770 N88-14732
Further study of inversion layer MOS solar cells
07 p0925 N88-15621

POPULATION THEORY
A tight upper bound for the speed-up of parallel best-first branch-and-bound algorithms
[AD-A184246] 04 p0477 N88-12939
An urn model for the multi-sample capture/recapture sequential tagging process
[AD-A184470] 04 p0486 N88-12998
A comparison of the basket method and the stratified random sampling for contract change order negotiations
[AD-A184170] 04 p0500 N88-13080
A functional interpretation of the logistic equation
[REPT-87-037] 05 p0645 N88-13946
An elimination type two-stage procedure for selecting the population with the largest mean from k logistic populations
[AD-A185614] 07 p0916 N88-15566
On selecting the best of k lognormal distributions
[AD-A185628] 07 p0916 N88-15567
Perturbation theory for dual semigroups 2. Time-dependent perturbations in the sun-reflexive case
[PB88-113097] 09 p1230 N88-17369
Empirical and hierarchical Bayes competitors of preliminary test estimators in two sample problems
[AD-A190327] 15 p2125 N88-22670
Selecting the best binomial population: Parametric empirical Bayes approach
[AD-A193341] 23 p3269 N88-29450

POPULATIONS
Galaxy evolution in dense clusters
13 p1855 N88-21101
On two-stage allocation procedures for selection problems
[AD-A190766] 15 p2126 N88-22675
Thailand in maps. Application of the mapping system THEMAK2 for specific purpose atlas preparation
16 p2226 N88-23295
Burn-in with mixed populations
[AD-A194651] 22 p3085 N88-28321

PORES
U POROSITY

POROSITY
NT MICROPOROSITY

Influence of boron on porosity in nickel-base superalloy castings
03 p0299 N88-11877
Geological characterization and statistical comparison of outcrop and subsurface facies: Shannon Shelf sand ridges
[DE87-001243] 03 p0348 N88-12202
Porosity influence on the strength and elasticity of first-year sea ice
[AD-A184493] 03 p0354 N88-12233
Crack propagation properties of sintered steel
05 p0604 N88-13698
The use of NMR imaging to measure porosity and binder distributions in green-state and partially sintered ceramics
[DE88-003099] 08 p0972 N88-15881
Quantitative non-destructive evaluation of porous composite materials based on ultrasonic wave propagation
[NASA-CR-182544] 11 p1447 N88-18627
Porosity and fractality of a cometary nucleus
14 p2004 N88-21951
Effects of irradiation on thermal coalescence of pores in real crystals
[DE88-701683] 16 p2282 N88-23663
Krypton based adsorption type cryogenic refrigerator
[NASA-CASE-NPO-17334-1-CU]
17 p2331 N88-23917
Electrode films of porous agarose: The effects of physical structure on electron transport processes
[DE88-007366] 19 p2611 N88-25493
Employment of porous polytetrafluoroethylene Membrane with a hydrophilic and hydrophobic stratal structure for construction of an enzyme electrode
[NASA-TT-20296] 19 p2620 N88-25543
A model for insulated wires in the method of moments code NEC (Numerical Electromagnetics Code)
[DE88-008920] 20 p2794 N88-26577
Characterization of the surface area and porosity of sol-gel films using saw devices
[DE88-008794] 20 p2875 N88-27069
Gaseous tracer techniques for pore structure characterization of granular materials
[DE88-011542] 21 p2911 N88-27274
Application of controlled interfacial pore structures to kinetic studies in alumina
[DE88-010884] 21 p2919 N88-27326
Computer modeling for surface properties of carbon fibers
21 p2928 N88-27383
Method for maintaining precise suction strip porosities
[NASA-CASE-LAR-13638-1] 23 p3201 N88-29051

POROUS MATERIALS
Studies of transport processes in porous and ion exchange membranes
[ISBN-951-99847-0-4] 01 p0021 N88-10133
Optical characterization of silica aerogel glass
[DE87-014617] 02 p0153 N88-10956
Voltammetric investigation of porous silicon for integrated circuit applications
[DE87-009287] 02 p0166 N88-11042
The correlation between microstructure and thermomechanical properties of two-phase materials and porous sintered materials
[KFK-4205] 03 p0292 N88-11835
Development of a new method of measuring the characteristic impedance and complex wave number of a porous acoustic material
[AD-A185038] 05 p0646 N88-13957
Fundamental studies of surfaces processes and trace analysis using solid electrodes
[AD-A186156] 07 p0828 N88-15024
Programs for calculating transient Darcian flow through non-uniform materials
[DE88-001924] 07 p0852 N88-15177
Physics of immiscible flow in porous media
[PB88-131008] 11 p1487 N88-18873
Development, manufacturing and testing of a gas-loaded variable conductance methanol heat pipe
[NLR-MP-87010-U] 13 p1767 N88-20571
Abrasion resistant porous silica antireflective coatings
[DE88-006230] 14 p1894 N88-21308
Molecular dynamics of materials possessing high energy content
[AD-A190034] 15 p2034 N88-22118
Transient compressible flow in porous materials
[DE88-006685] 15 p2067 N88-22324
Review of numerical methods for radionuclide transport in three-dimensional porous media, at high Peclet numbers
[CFDU/87/10] 18 p2538 N88-25061

POROUS PLATES
Fatigue failure of thin porous strips
04 p0426 N88-12640

POROUS WALLS
Heterogeneous diffusion flame stabilization
[AD-A193014] 20 p2771 N88-26429
Radiative heat transfer to steady flow of a chemically reacting fluid in a horizontal porous channel with variable wall temperature
[DE88-702704] 24 p3372 N88-30081

PORPHYRINS
NT CHLOROPHYLLS
Reactions of porphyrins in surfactant assemblies, microemulsions and in solutions
[AD-A184797] 05 p0560 N88-13412
Artificial photosynthesis using chlorophyll based carotenoid-quinone triads
[DE88-001660] 07 p0884 N88-15362
Novel catalysts for methane activation
[DE88-003637] 13 p1738 N88-20390
The design of methane activation catalysts
[DE88-002265] 23 p3199 N88-29043

PORTABLE EQUIPMENT
Loss of performance due to military clothing and equipment
[IZF-1986-13] 01 p0077 N88-10490
A portable hypercube simulator
[DE87-013369] 04 p0478 N88-12947
The Portable Instant Display and Analysis Spectrometer (PIDAS)
05 p0611 N88-13756
A comparison of measurements from the A/E35U-3 and PWMA (Portable Wear Metal Analyzer) spectrometers
[AD-A186855] 09 p1177 N88-17047
TABLET: The personal computer of the year 2000
[NASA-CR-182528] 10 p1384 N88-18267
A hybrid transform/DPCM encoder for data compression
[DE87-014852] 13 p1758 N88-20518
Ultrasonic inspection of irregular surfaces
[AERE-R-12465] 13 p1780 N88-20648
Portability of software. The use of software in the hardware mixture
[MBB/LWD-11/S/PUB/253] 16 p2246 N88-23416
An investigation of conformable antennas for the astronaut backpack communication system
[NASA-CR-182908] 17 p2333 N88-23929

PORTS (OPENINGS)
An analytical and experimental study of injection-locked two-port oscillators
[NASA-TM-100119] 04 p0439 N88-12727
Dimensions of ignition zones in blow-outs of combustible gases from rectangular and circular ports
07 p0918 N88-15577

POSITION (LOCATION)
NT SOLAR POSITION
Accurate position measuring spacecraft package
[ESA-CR(P)-2398-VOL-1] 01 p0004 N88-10022
Accurate position measuring spacecraft package, executive summary
[ESA-CR(P)-2398-VOL-2] 01 p0004 N88-10023
Antarctic field tests of SARSAT personal locater beacons
[NASA-TM-4008] 01 p0063 N88-10403
Energy-selected electron diffraction experiments using the rocking-crystal method in the raster microscope for the investigation of localization effects in single crystals
[ETN-87-90409] 01 p0104 N88-10682
Quantum mechanics with spontaneous localization and the quantum theory of measurement
[DE87-703072] 02 p0247 N88-11559
GPS vertical axis performance enhancement for helicopter precision landing approach
[NASA-CR-177443] 04 p0397 N88-12477
Effect of permissible variations of center-of-gravity locations of cargo airplane on its mass
04 p0424 N88-12625
Knot selection for least squares thin plate splines
[AD-A185681] 06 p0759 N88-14657
Recursive m-estimators of location and scale for dependent sequences
[AD-A186292] 07 p0903 N88-15469
A directed method for locating the focus of expansion
[AD-A185840] 07 p0906 N88-15491
Localization of Cu 3d levels in the high Tc superconductor YBa2Cu3O approximately 7 by Cu2p X-ray photoelectron spectroscopy
[NOTA-INTERNA-887] 07 p0939 N88-15710
Ariane localization technique by Data Relay Satellite (DRS)
[SES/ENG/TN-548/86] 08 p0961 N88-15821
Effects of uniform target density on random search
[AD-A186468] 08 p1073 N88-16473
Dynamic stress at critical locations of a structure as a criterion for mathematical model modification
09 p1180 N88-17066
Strategic placement of accelerometers to measure forces by the sum of weighted accelerations
[DE88-002262] 10 p1333 N88-17968
Reference position vector 12 p1577 N88-19432
Optimal selection of global positioning system set to minimize emitter location errors
[AD-A189559] 12 p1579 N88-19447
Cramer-Rao bounds on the accuracy of location and velocity estimations using CCD optical sensors
[AD-A188481] 12 p1629 N88-19748
The evaluation and selection of a 5th ground antenna site for the global positioning system
[AD-A189495] 13 p1720 N88-20286
A comparison of terrain association and resection as methods of position location
[AD-A189480] 13 p1790 N88-20710
Method for determining artillery position
[NASA-TT-20236] 14 p1979 N88-21813
Real-time environmental Arctic monitoring (R-TEAM)
[AD-A189948] 15 p2099 N88-22508
Target localization in an inhomogeneous medium
[AD-A190008] 15 p2130 N88-22703
Path following robot
[AD-A190960] 16 p2215 N88-23217
Algorithms and intuition
[NASA-CR-182900] 16 p2252 N88-23459
Point accessibility and primary workspace of simple six-link robots
17 p2345 N88-23976
Angular position measurements at high temperatures and high radiation environments
17 p2434 N88-24479
Search and rescue satellite system (SERES), phase A0
[ETN-88-92335] 18 p2472 N88-24669
Geometric rectangular data file (GERD): An aid to the rapid access to position data
18 p2534 N88-25037
Estimation of balloon position from wind data
[DE88-008968] 19 p2597 N88-25434
Tropical cyclone report
[AD-A191883] 19 p2693 N88-26009
NAVSTAR global positioning system
[AD-A192609] 20 p2757 N88-26354
Automatic omega station and LOP (Line Of Position) selection
[AD-A193302] 21 p2894 N88-27179
Radar information from the partial derivatives of the echo signal phase from a point scatterer
[AD-A193402] 21 p2933 N88-27415
Constructing a highly-available location service for a distributed environment
[AD-A192723] 21 p3001 N88-27801
An algorithm for determining the location of points in computer simulations
[AD-A193713] 23 p3250 N88-29343
DATATRAN: Datum transformation software
[AD-A195723] 24 p3387 N88-30175
Passive microwave measurements of water vapor fields and rain for locating fronts in cyclonic storms
[AD-A195632] 24 p3404 N88-30267
Adaptive control in positioning a rigid-flexible robot arm
[AD-A195194] 24 p3422 N88-30367
Utilizing dynamic stability of orient parts
[AD-A195730] 24 p3427 N88-30397
Study of modern instrumentation and methods for astronomic positioning in the field
[AD-A196173] 24 p3452 N88-30548

POSITION ERRORS
Effect of installation and calibration errors of sensors on system identification results of an aircraft
[ESA-TT-1059] 03 p0266 N88-11678
Determination of TRANET (tracking station coordinates for tracking network) and SMTP (Special Mission Tracking Program) tracking station coordinates for use in the WGS (World Geodetic System) 84
[AD-A185863] 07 p0817 N88-14972
A method and measures to evaluate trackers for air traffic control
[NLR-TR-86072-U] 13 p1720 N88-20287
A comparison of terrain association and resection as methods of position location
[AD-A189480] 13 p1790 N88-20710
A positioning system based on NAVSAT
[NLR-MP-87018-U] 20 p2757 N88-26358
Implementation of a flexible link model in a designed robot system, using the finite element method
[ETN-88-92902] 23 p3243 N88-29303

POSITION INDICATORS
Calibration of attitude control sensors
02 p0159 N88-10995
Effects of combining vertical and horizontal information into a primary flight display
[NASA-TP-2783] 04 p0399 N88-12487
Procedure for detection and identification of a helicopter
[NASA-TT-20234] 13 p1722 N88-20297
Development of an interactive real-time graphics system for the display of vehicle space positioning
[NASA-TM-100429] 13 p1730 N88-20344
Electronics and communications in air traffic control: The Presidential Address
[ETN-88-92057] 14 p1865 N88-21146

Accurate positioning of long, flexible ARM's (Articulated Robotic Manipulator) 16 p2219 N88-23243
Integrated multisensor navigation systems 17 p2294 N88-23722
Technical characteristics of the OmniTRACS: The first operation mobile Ku-band satellite communications system 19 p2647 N88-25709

POSITION SENSING
Error detection and recovery for robot motion planning with uncertainty [AD-A187746] 11 p1534 N88-19165
Long range sensor for rendezvous and docking missions 12 p1587 N88-19497
Procedure for detection and identification of a helicopter [NASA-TT-20234] 13 p1722 N88-20297
The silicon microstrip detector --- particle position measurement [ETN-88-92235] 16 p2210 N88-23189
Accurate positioning of long, flexible ARM's (Articulated Robotic Manipulator) 16 p2219 N88-23243
The position-sensitive counting of photons 16 p2271 N88-23590
Motion planning for a free-flying robot 23 p3255 N88-29378
Path planning and path following for the Amsterdam autonomous cart [FVI-86-22] 24 p3380 N88-30133

POSITIONING
Theoretical and practical aspects of the functional absorber method of arranging sound absorbing panels [BBC-RD-1987/15] 05 p0646 N88-13955
Errors in retrieving hydrological fields and fields of their differential characteristics by method of approximation by orthogonal functions 06 p0727 N88-14475
Improvement in robot positioning accuracy by a kinematic identification model 11 p1496 N88-18931
Geodetic positioning by employment of the GPS-NAVSTAR satellites applying the techniques of VLBI and sequential recursive optimal estimation [INPE-4438-TDL/311] 12 p1594 N88-19547
Method for determining artillery position [NASA-TT-20237] 13 p1834 N88-20974
A control technique for improved robot performance 17 p2391 N88-24212
Position and velocity determination using a Global Positioning System: An outline [B8735052] 20 p2757 N88-26355
Research project Loran-C of the Geometric Service of the Ministry of Public Works [B8735055] 20 p2757 N88-26356
The Sercel TR5S Global Positioning System (GPS) receiver [ETN-88-92473] 20 p2757 N88-26357
Acoustic helicopter positioning 22 p3148 N88-28726
Implementation of a flexible link model in a designed robot system, using the finite element method [ETN-88-92902] 23 p3243 N88-29303
Study of modern instrumentation and methods for astronomic positioning in the field [AD-A196173] 24 p3452 N88-30548

POSITIONING DEVICES (MACHINERY)
NT BOOMS (EQUIPMENT)
NT CAMS
Contributions to fast-reacting and high-precision three-phase positioning systems --- machinery [ETN-87-90427] 01 p0056 N88-10358
AVIRIS scan drive design and performance 06 p0706 N88-14330
Hemispherical pointing mechanism drive unit --- satellite payloads antennas 14 p1874 N88-21193
A pointing mechanism for intersatellite link system 14 p1874 N88-21194
Deployment, hold down and release mechanisms for Wind Scatterometer Antenna (WSA) --- ERS-1 wind scatterometer antenna (WSA) 14 p1876 N88-21207
Development and qualification of the OLYMPUS antenna pointing mechanism 14 p1879 N88-21227

POSITIVE IONS
NT CATIONS
NT HYDRONIUM IONS
On the acceleration of electrons and positive ions in the same direction along magnetic field lines by parallel electric fields [IRF-PREPRINT-103] 15 p2096 N88-22488
Stratospheric positive ion composition measurements and acetonitrile detection: A consistent picture [AERONOMICA-ACTA-A-326-1987] 18 p2542 N88-25084

POSITRON ANNIHILATION
Vector boson pair production in e(+)e(-) collisions [PREPRINT-549] 06 p0778 N88-14774
Single weak gauge boson production at CLIC [PREPRINT-550] 06 p0778 N88-14775
Positron annihilation spectroscopy of AlGaAs/GaAs interfaces in MOCVD-grown GaAs heterojunction solar cells [DE88-003903] 11 p1508 N88-19012
Study of defects in metals by positron annihilation [DE88-701042] 13 p1745 N88-20432
Cascade model of gamma-ray bursts: Power-law and annihilation-line components [NASA-TM-101176] 21 p3032 N88-27998

POSITRONIUM
Electron capture from solids by positrons [DE87-014355] 02 p0232 N88-11463

POSITRONS
Electron capture from solids by positrons [DE87-014355] 02 p0232 N88-11463
Studies of the processing of single words using positron tomographic measures of cerebral blood flow change [AD-A184058] 03 p0356 N88-12244
Gamma radiation at the 970 MeV plane positron channeling in diamond crystals [DE88-700557] 07 p0939 N88-15705
Three-dimensional image reconstruction in object space [DE88-900279] 12 p1712 N88-20246
Model-independent requirements to the source of positrons in the galactic centre [DE88-700958] 14 p1992 N88-21874
Variable-energy positron studies on liquids and liquid-solid interfaces [DE88-006356] 15 p2033 N88-22109
Annihilation momentum density of positrons trapped at vacancy-type defects in metals and alloys [DE88-005936] 15 p2144 N88-22797
The cluster ion approach to the condensation and storage of antihydrogen 16 p2269 N88-23575
Electron-positron physics at 1 TeV [DE88-009019] 19 p2725 N88-26180
Inelastic mean free paths of electrons and positrons in matter [DE88-008086] 20 p2851 N88-26929
Positron emission tomography: A new technique for observing fluid behavior in engineering systems [PNR90471] 24 p3374 N88-30091

POSTFLIGHT ANALYSIS
Propulsion estimation techniques 07 p0927 N88-15632
GAS 450: A space payload for the People Central Coast Student Experimenters 10 p1289 N88-17709
Space shuttle natural environment analysis [NASA-CR-179337] 21 p2978 N88-27676

POSTULATES
U AXIOMS

POSTURE
Sitting posture of helicopter pilots of the Royal Netherlands Air Force; preliminary recommendations [IZF-1986-16] 05 p0631 N88-13857
Sitting posture of pilots in the Boelkow 105c helicopter [IZF-1986-22] 09 p1202 N88-17202
Effect of antiorthostatic position and different illumination on sensitivity of skin in upper half of the body to ultraviolet radiation 10 p1363 N88-18145
Morphological manifestations of primate adaptation to orthograde statics and walking erect 10 p1366 N88-18162
The effect of orthostatic changes in central blood volume on the heart rate response to graded Valsalva maneuvers 12 p1653 N88-19904
Estimation of body fluid shift by electrical impedance in various postures 12 p1661 N88-19956
Ergonomy and interior furnishing of the cabins of deep diving manned submarines: The Nautile example --- couch 19 p2697 N88-26032

POTABLE LIQUIDS
NT POTABLE WATER

POTABLE WATER
Carbon dioxide treatment for scale removal and control in potable water systems [AD-A184346] 04 p0412 N88-12556
Cardiac rhythm of animals consuming reclaimed water differing in concentration of sodium and potassium ions 19 p2705 N88-26085
Validation of maximum permissible concentration of urea in reclaimed potable water and evaluation of its biological effect 19 p2705 N88-26086

POTASSIUM
NT LIQUID POTASSIUM
K-CO on transition metals: A local ionic interaction [AD-A184342] 04 p0496 N88-13056
Alkali metal diffuse band lasers [AD-A190244] 15 p2071 N88-22350
Study on shaft seals for potassium turbine [EL-891] 15 p2074 N88-22364
Cardiac rhythm of animals consuming reclaimed water differing in concentration of sodium and potassium ions 19 p2705 N88-26085

POTASSIUM BROMIDES
A rapid polishing method for KBr and NaCl infrared windows [DE88-002480] 07 p0862 N88-15229

POTASSIUM COMPOUNDS
NT POTASSIUM BROMIDES
Potassium cuprate (3) [NASA-TT-20246] 13 p1739 N88-20401

POTATOES
Utilization of potatoes in bioregenerative life support systems 03 p0360 N88-12269
Food Irradiation Newsletter, Vol. 11, No. 1 [DE88-700808] 12 p1671 N88-20004

POTENTIAL ENERGY
NT BIOELECTRIC POTENTIAL
NT COULOMB POTENTIAL
NT ELECTRIC POTENTIAL
NT GEOPOTENTIAL HEIGHT
NT IONIZATION POTENTIALS
NT LOW VOLTAGE
NT PLASMA POTENTIALS
NT QUANTUM WELLS
NT THRESHOLD VOLTAGE
Variational and nonvariational theory of frictionless adhesive contact between bodies [REPT-87-11] 01 p0054 N88-10345
Monte Carlo simulation of primitive atom-transfer reactions in solution [AD-A183977] 03 p0375 N88-12360
Simulation studies for surfaces and materials strength [NASA-CR-181535] 04 p0412 N88-12557
Coupling of vibrational modes of adsorbates: Application to field induced shifts for CO and CN on Cu(100) [AD-A187891] 11 p1453 N88-18659
Theoretical studies of the potential surface for the F - H2 greater than HF + H reaction [NASA-CR-182551] 11 p1557 N88-19319
Quantum Monte Carlo study of the MIES associated with H2 (X 1 sigma sub g (+)) and H2 (B 1 sigma sub u (+)) [AD-A189063] 13 p1835 N88-20977
Molecular reaction and energy transfer rate estimation for chemical-laser analysis [AD-A190664] 15 p2035 N88-22126
The H5(+) potential energy hypersurface: Characterization of ten distinct energetically low-lying stationary points 16 p2267 N88-23561
Theoretical calculations of XeF ground state kinetics [AD-A191398] 16 p2270 N88-23580
Computed potential energy surfaces for chemical reactions [NASA-CR-183168] 24 p3342 N88-29893

POTENTIAL FIELDS
Equation of gravitational-gyroscopic waves: Angular potential and its applications 08 p1079 N88-16504
Realistic conductivity geometry model of the human head for interpretation of neuromagnetic data [PB88-112230] 10 p1369 N88-18179
Motion planning for a free-flying robot 23 p3255 N88-29378

POTENTIAL FLOW
ARSPNS: A method to calculate steady and unsteady potential flow about fixed and rotational lifting and nonlifting bodies [NLR-TR-85114-U] 01 p0044 N88-10282
Perfine: Personal finite elements on a microcomputer [ETN-87-90678] 01 p0082 N88-10528
A full potential flow analysis with realistic wake influence for helicopter rotor airload prediction [NASA-CR-4007] 04 p0393 N88-12452
Calculation of aerodynamic characteristics of three-dimensional finite span wings in potential incompressible flow 04 p0425 N88-12631
Numerical analysis of supersonic flows using panel method 05 p0537 N88-13266
Computation of transonic flows with nacelle simulation [SNIAS-872-111-117] 05 p0542 N88-13300
Potential flow around two-dimensional airfoils using a singular integral method [NASA-CR-182345] 06 p0664 N88-14070
Finite-volume scheme for transonic potential flow about airfoils and bodies in an arbitrarily shaped channel 07 p0809 N88-14928
Breakdown of the conservative potential equation 07 p0809 N88-14929
Application of a full potential method for analysis of complex aircraft geometries 07 p0809 N88-14930
Finite element fundamentals, part 2 08 p0985 N88-15962
Inviscid flows, part 2 08 p0985 N88-15968
Wall jet analysis for circulation control aerodynamics. Part 2: Zonal modeling concepts for wall jet/potential flow coupling 10 p1269 N88-17593

A numerical procedure for conformal mapping of the exterior of a circle onto the exterior of a wing profile with a spoiler
[ISL-R-110/86] 11 p1536 N88-19180
A multigrid solver for two-dimensional transonic full potential flow calculations 11 p1538 N88-19189
A multigrid full potential transonic code for arbitrary configurations — aircraft 11 p1539 N88-19195
A discretization of the integral equation for the time dependent linearized subsonic potential flow over a wing
[AD-A188534] 12 p1574 N88-19411
ARSPNSC: A method to calculate subsonic steady and unsteady potential flow about complex configurations
[NLR-TR-86122-U] 13 p1717 N88-20265
A physically consistent model for artificial dissipation in transonic potential flow computations
[NASA-TM-100846] 15 p2122 N88-22652
La Recherche Aerospatiale, bimonthly bulletin, number 1987-3, 238/May-June
[ESA-TT-1075] 16 p2206 N88-23161
The 2-D and 3-D time marching transonic potential flow method for propfans 16 p2220 N88-23245
Reduced order models for nonlinear aerodynamics 16 p2220 N88-23248
Improved potential flow computational methods with Euler corrections for airfoil and wing/body design
[AD-A192303] 20 p2752 N88-26334
Calculation of 2-D unsteady transonic full potential flow about oscillating airfoils by two complementary approaches
[PB88-127519] 20 p2753 N88-26341
An improved version of NCOREL: A computer program for 3-D nonlinear supersonic potential flow computations
[NASA-CR-4165] 22 p3038 N88-28039
Accurate solutions, parameter studies and comparisons for the Euler and potential flow equations
[NASA-TM-100664] 23 p3173 N88-28892

POTENTIAL GRADIENTS
A supersonic potential gradient method for the calculation of unsteady aerodynamic pressures on harmonically oscillating wings
[ESA-TT-930] 03 p0259 N88-11631

POTENTIAL THEORY
Resonant level lifetime in GaAs/ AlGaAs double-barrier structures
[AD-A185376] 05 p0655 N88-14020
Nacelle-wing interactions (studies 1986) development of a finite element code in a multi-domain version
[ONERA-RTS-10/3417-AY-308A] 08 p0950 N88-15764
Application of a nonisentropic full potential method to AGARD standard airfoils
[NASA-TM-100560] 13 p1716 N88-20263
Numerical solution of ill posed problems in partial differential equations
[AD-A189383] 13 p1825 N88-20909
A note on the analyticity of the Neumann Kernel and an associated quadrature problem in two-dimensional boundary element methods
[ETN-88-92054] 14 p1964 N88-21719
Use of long-distance pair potentials in calculations of defect characteristics in metals
[DE88-701039] 15 p2037 N88-22138
A panel method based on velocity potential to compute harmonically oscillating lift surface systems
[ETN-88-91886] 15 p2061 N88-22290
Full potential methods for analysis/design of complex aerospace configurations
[NASA-CR-3982] 17 p2296 N88-23736
On the efficient implementation of the fast multipole algorithm
[AD-A191167] 17 p2385 N88-24173

POTENTIOMETERS (RESISTORS)
Low cost corrosion sensors 22 p3054 N88-28123

POTENTIOMETRIC ANALYSIS
High energy molecules of high symmetry
[AD-A185385] 05 p0647 N88-13965
Shelf life degradation of selected anaerobic threadlocking adhesives at various storage temperatures
[AD-A187712] 11 p1461 N88-18711

POTENTIOMETRY
U POTENTIOMETRIC ANALYSIS

POWDER (PARTICLES)
NT FINES
NT METAL POWDER
NT POWDERED ALUMINUM
NT SINTERED ALUMINUM POWDER
Physics and chemistry of packing fine ceramic powders
[DE87-013709] 01 p0029 N88-10183
Measurement of agglomerate strength distributions in agglomerated powders
[DE87-013605] 01 p0090 N88-10591
Colloidal stability of oxidized silicon particles in ethanolic and aqueous media
[DE87-014783] 05 p0562 N88-13421
High explosive moulding powders from RDX and aqueous polyurethane dispersions
[AD-A185026] 05 p0568 N88-13458
Extinguishing diffusion flames with dry powder and halon at low Froude numbers
[PB87-111365] 06 p0679 N88-14159
An analysis of the effect of system variables on the quality of thin films and powders produced by laser-breakdown chemical vapor deposition
[DE88-001793] 06 p0708 N88-14342
Composite ceramic superconducting filaments for superconducting cable
[AD-A187833] 11 p1556 N88-19312
Effect of rigid inclusions on sintering
[DE88-005745] 12 p1609 N88-19623
Creep behavior of consolidated rapidly solidified Type 304 stainless steel powder containing helium
[DE88-005536] 13 p1743 N88-20424
A new process for synthesis of silicon nitride powders for advanced ceramics
[AD-A189354] 13 p1748 N88-20451
Processing of nanophase ceramics
[DE88-005985] 13 p1752 N88-20475
Scale-up of a batch-type chemical powder preparation process for high field varistor fabrication
[DE88-006601] 13 p1762 N88-20541
A hydroxycarbonate route to superconductor precursor powders
[DE88-003638] 13 p1846 N88-21052
Analysis of explosives. 1: Computer programs for processing of X-ray powder deffraction data
[PB88-156898] 14 p1894 N88-21309
The weldability of consolidated rapidly solidified Type 304 SS powders
[DE88-006738] 16 p2178 N88-22978
Colloidal characterization of silicon nitride and silicon carbide 17 p2325 N88-23883
Production of powdered sodium hydride with large specific surface by the catalyzed reaction of molten sodium with hydrogen-1
[NASA-TT-20185] 20 p2776 N88-26462
A study of solvent effects on the synthesis of pure component and composite ceramic powders by metal alkoxide hydrolysis
[DE88-008381] 20 p2777 N88-26470
Ceramic processing of high-T(sub)c superconductors
[DE88-010090] 20 p2878 N88-27087
Preparation and properties of high Q microwave dielectrics in the (CA, SR, BA) zirconate system
[AD-A193127] 21 p2918 N88-27317
Relative flow rates of explosive powders
[DE88-010767] 21 p2923 N88-27350
The first synthesis of chem-prep varistor LAC (Lightning Arrestor Connector) granules
[DE88-008005] 21 p2936 N88-27438
Sinterable ceramic powders from laser-heated gases
[AD-A194162] 23 p3197 N88-29024

POWDER METALLURGY
Isothermal forging and its effect on the microstructure of powder route nickel alloy AP1
[RAE-TM-P-1094] 01 p0022 N88-10138
Development and production of new and modified powders for sprayed coatings and components for saving important raw materials
[BMFT-FB-T-86-129] 01 p0025 N88-10159
GSSR powder metallurgy research, production expanding 03 p0286 N88-11797
Powder-metallurgical preparation of A15 superconductors
[ETN-87-90584] 03 p0380 N88-12392
Durability of powdered aluminum structures 04 p0429 N88-12655
A fundamental study of P/M processed elevated temperature aluminum alloys
[AD-A185393] 05 p0565 N88-13445
Tensile properties of extrusion consolidated Type 304 SS rapidly solidified powders
[DE87-014875] 05 p0566 N88-13450
Development on thin wall tubes of dispersion type
[DE87-703384] 05 p0571 N88-13483
Behavior of long and short fatigue cracks in a powder metallurgy superalloy at room and at high temperature 05 p0601 N88-13677
Undercooling and nucleation in iron nickel alloys
[AD-A185500] 06 p0683 N88-14184
Dynamic high pressure process for fabricating superconducting and permanent magnetic materials
[DE88-000848] 06 p0785 N88-14817
Methods of improving compacting quality of intricately shaped powder components
[BLL-M-37412-(5828.4)] 08 p0968 N88-15859
Powder metallurgical preparation of A15 superconductors
[ETN-88-91072] 09 p1144 N88-16858
Materials development for JPL oxygen plant
[DE88-003067] 10 p1297 N88-17752
Evaluation of centrifugal barrel tumbling process for impregnation of molybdenum disulfide powder lubricant
[BDX-613-3698] 11 p1464 N88-18727
Microdesigning of lightweight/high strength ceramic materials
[AD-A188526] 12 p1610 N88-19631
Activities report of the Materials Department
[ETN-88-91984] 13 p1745 N88-20436
A case study of the development of a military specification - zirconium powder for thermal batteries
[AD-A188751] 13 p1792 N88-20717
Processing, physical metallurgy and creep of NiAl + Ta and NiAl + Nb alloys
[NASA-CR-182113] 14 p1890 N88-21295
Processing, microstructure, and mechanical properties of silicon carbide particulate reinforced aluminum alloys
[AD-A188981] 15 p2037 N88-22136
Characterization of an explosively consolidated rapidly solidified Fe-16Ni-9Cr-5Mo-2Cu alloy powder
[DE88-006733] 15 p2041 N88-22162
Gamma-ray densitometry: Nondestructive analysis of density evolution during ceramic powder processing
[DE88-006671] 15 p2047 N88-22198
Titanium powder frit made during the transformation alpha-beta
[ETN-88-91999] 16 p2177 N88-22976
Fabrication of reactor shields at the Y-12 plant 17 p2402 N88-24283
Characterization of 7090 and 7091 profiles made with Cegedur powder — powder metallurgy, aircraft construction materials
[REPT-48-441/F] 18 p2487 N88-24752
Laboratory scale inert gas atomizer for producing rapidly solidified powders
[DE88-006734] 18 p2497 N88-24812
Hot isostatic pressing of nickel aluminide powders
[DE88-009677] 19 p2617 N88-25525
The preparation of mechanically alloyed powders for TEM (Transmission Electron Microscopy) examination
[DE88-008043] 20 p2775 N88-26460
Stress corrosion evaluation of powder metallurgy aluminum alloy 7091 with the breaking load test method 22 p3053 N88-28115
Hot isostatic pressing of tungsten-nickel-iron composites
[FOA-C-20698-2.1] 22 p3056 N88-28135
An investigation into the metallurgical aspects of joining rapidly-solidified aluminum alloys
[AD-A194677] 23 p3194 N88-29009

POWDERED ALUMINUM
NT SINTERED ALUMINUM POWDER
Development of a pilot plant for the production of rapidly solidified aluminum alloy powders
[BMFT-FB-T-86-153] 02 p0146 N88-10914
Durability of powdered aluminum structures 04 p0429 N88-12655
Organic coatings to improve the storageability and safety of pyrotechnic compositions
[AD-A187158] 09 p1150 N88-16889
Plasma joining of metal matrix composites
[AD-A188559] 12 p1604 N88-19593
Advanced B and Al combustion kinetics over wide temperature ranges
[AD-A190752] 15 p2036 N88-22128
Dynamic consolidation of metal powders
[AD-A192126] 18 p2485 N88-24744
Mechanical testing and microscopic analysis of structure of extruded powder aluminum
[DE88-007193] 19 p2617 N88-25526

POWDERED METALS
U METAL POWDER

POWER AMPLIFIERS
V-band IMPATT power amplifier
[NASA-CR-180711] 01 p0042 N88-10267
Theoretical and experimental investigation of electron beam acceleration and sub-millimeter wave generation in cyclotron resonant cavities
[AD-A184806] 05 p0649 N88-13975
Design of a velocity and position control laboratory servo system
[AD-A186596] 08 p0990 N88-15997
RF pulse compression development
[DE88-004818] 11 p1479 N88-18826
Application of copper-carbon fiber composites to power semiconductor devices
[NASA-TT-20171] 15 p2031 N88-22101
Development of 20 GHz monolithic transmit modules
[NASA-CR-182134] 17 p2445 N88-24539

POWER CONDITIONING
Evaluation of stand-alone inverters for remote applications
[DE87-010957] 01 p0040 N88-10257
Estimating payload internal temperatures and radiator size for multimegawatt space platforms
[DE88-000244] 03 p0275 N88-11738

High average power solid state laser power conditioning system
[DE87-013558] 03 p0328 N88-12071
High energy density rechargeable batteries for aerospace power requirements
[AD-A184863] 05 p0577 N88-13519
Solar pumped, alkali vapor laser
[AD-A187156] 09 p1170 N88-17016
Laboratory evaluation and analysis of advanced lead-acid load-leveling batteries
[DE88-002851] 10 p1349 N88-18064
Microwave semiconductor research-materials, devices and circuits
[AD-A187121] 10 p1415 N88-18444
Lead-acid load-leveling battery testing at Argonne National Laboratory
[DE88-002853] 11 p1480 N88-18837
Evaluation of advanced lead-acid batteries developed for load-leveling applications
[DE88-002871] 11 p1481 N88-18838
Power systems for production, construction, life support and operations in space
[NASA-TM-100838] 14 p1883 N88-21254
Test results of high-voltage, high-power, solid-state remote power controllers
[NASA-TM-100322] 16 p2194 N88-23085
Application of the reactivity constraint approach to the transient control of spacecraft reactors
17 p2406 N88-24305
Reactor instrumentation and control design and performance simulation for SP-100
17 p2406 N88-24306
Nuclear reactor magnetohydrodynamic power generator for directed energy weapons 17 p2411 N88-24336
Parametric analyses of the TE SP-100 system performance 17 p2415 N88-24358
Energy storage evaluation for burst power applications
17 p2426 N88-24430
Multimegawatt power conditioning requirements study
17 p2438 N88-24504
A role for high frequency superconducting devices in free space power transmission systems
[NASA-TM-100971] 19 p2662 N88-25830
Determination of satcom access power levels within the ground segment
[RSRE-MEMO-4097] 22 p3070 N88-28226
Development of inductive storage pulsed power generators
[AD-A193878] 22 p3117 N88-28521
Power supply conditioning circuit
[NASA-CASE-NPO-17233-1-CU]
23 p3208 N88-29095
Utilization of artificial intelligence techniques for the Space Station power system 23 p3261 N88-29412
The dc power control for a liquid-fed resistojet
[NASA-TM-101326] 24 p3338 N88-29869

POWER CONVERTERS
Overview of free-piston Stirling engine technology for space power application
[NASA-TM-88886] 03 p0386 N88-12427
A comparative study of various electric propulsion systems and their impact on a nominal ship design
[AD-A187800] 11 p1477 N88-18816
SNAP-DYN: Concepts for multikilowatt space power applications 17 p2435 N88-24486
Alkali metal thermoelectric converter design for space power systems applications 17 p2437 N88-24499

POWER DENSITY (ELECTROMAGNETIC)
U RADIANT FLUX DENSITY

POWER EFFICIENCY
Development of a light duty gas engine for cogeneration service
[PB87-221297] 02 p0180 N88-11119
A new method for measuring waveguide propagation losses
[DE87-011305] 03 p0307 N88-11938
Adiabatic diesel engine component development: Reference engine for on-highway applications
[NASA-CR-179531] 03 p0386 N88-12428
Efficiency testing of a helicopter transmission planetary reduction stage
[NASA-TP-2795] 07 p0861 N88-15224
Solar pumped, alkali vapor laser
[AD-A187156] 09 p1170 N88-17016
High-efficiency GaAs semiconductor laser with longitudinal excitation by scanning electron beam
09 p1238 N88-17421
A comparative study of various electric propulsion systems and their impact on a nominal ship design
[AD-A187800] 11 p1477 N88-18816
Microwave generation from a cuaptron oscillator with a six-vane circuit
[AD-A188377] 12 p1619 N88-19680
Hercules: A power analyzer for MOS VLSI circuits
[AD-A188702] 12 p1623 N88-19706
High power, high efficiency 770 nm laser diode array
[DE88-004043] 12 p1631 N88-19762
Low power consumption current transducer
[NASA-CASE-NPO-16888-1-CU]
17 p2335 N88-23937
High performance quarter-micron-gate MODFETs
19 p2656 N88-25776
Computer controlled procedures for traction battery power performance tests
[ETN-88-92352] 20 p2796 N88-26589

POWER GAIN
An experimental study of CW HF chemical laser amplifier performance and zero power gain
[AD-A185241] 05 p0588 N88-13584
Effect of electron beam divergence on the gain of free electron lasers 14 p1902 N88-21358

POWER GENERATORS
U ELECTRIC GENERATORS

POWER LINES
An asymptotic theory for a class of initial-boundary value problems for weakly nonlinear wave equations with an application to a model of the galloping oscillations of overhead transmission lines
[REPT-87-12] 01 p0086 N88-10556
Optical power line voltage and current measurement systems. Volume 1: Limits to the precision of electro-optic and magneto-optic sensors
[DE87-014558] 02 p0175 N88-11092
Thermoplastic elastomer compositions — cable jackets
[EP-PATENT-0-204-453-A1] 04 p0418 N88-12593
Cape Blanco wind farm feasibility study
[DE88-003749] 10 p1349 N88-18060
Derivation of strength factors related to the coordination of the strength of transmission line components — electric power lines
[S/T-REPT-VOL-5-NO-2] 11 p1500 N88-18959
Safety research of insulating materials of cable for nuclear power generating station
[NASA-TT-20202] 13 p1752 N88-20477
Partial discharges and the electrical aging of cross linked polyethene (XLPE) cable insulation
[EUT-88-E-160] 14 p1892 N88-21300
Asymptotics for a system of nonlinearly coupled wave equations with an application to the galloping oscillations of overhead transmission lines
[REPT-87-78] 17 p2348 N88-23991
Technologies applicable to space tethers
[NASA-CR-183055] 19 p2606 N88-25471
Voltages induced by lightning on electric power distribution lines: Field data and analysis results for the period July 1984-1986
[DE88-007841] 19 p2693 N88-26006
Development of external cooling cryo-resistive cable systems. Part 2: Insulation characteristics on 66 kV rated cryo-resistive testing cable
[DE88-770191] 20 p2793 N88-26571
Current induced by high-altitude electromagnetic pulse (HEMP) on wire above ground
[FOA-C-30485-4.2] 22 p3072 N88-28235

POWER MODULES (STS)
Photovoltaic power modules for NASA's manned space station
[NASA-TM-100229] 03 p0277 N88-11745

POWER PROCESSING SYSTEMS
U POWER CONDITIONING

POWER REACTORS
Low power consumption current transducer
[NASA-CASE-NPO-16888-1-CU]
17 p2335 N88-23937

POWER SERIES
NT TAYLOR SERIES
Power series for stationary distributions of coupled processor models
[REPT-87-70] 16 p2254 N88-23470
An improved spherical earth diffraction algorithm for SEKE
[AD-A195847] 24 p3360 N88-30005

POWER SPECTRA
Local spectra and wave distribution functions — space plasma
[KGI-PREPRINT-099] 01 p0100 N88-10659
Multichannel deconvolution of P waves at seismic arrays and three component stations
[AD-A184450] 04 p0467 N88-12888
An examination of chaotic motion for the buckled beam 05 p0597 N88-13644
The acoustic source created by turbulent flow over orifices and louvers
[REPT-97674] 06 p0776 N88-14764
Evolution of spectral densities in weakly inhomogeneous plasmas
[PB87-137402] 06 p0784 N88-14811
Parametric and experimental analysis using a power flow approach
[NASA-CR-182460] 09 p1116 N88-16693
Spectral density estimates of coarsely quantized random vibration data 09 p1178 N88-17055
Universal power spectra for wave turbulence: Applications to wind waves, flicker noise, solar wind spectrum and classical second sound
10 p1318 N88-17879
How to generate equal probability design load conditions — aircraft design
[NLR-TR-86060-U] 13 p1722 N88-20295
European approaches in standard spectrum development — aircraft load spectra
[NLR-MP-87007-U] 13 p1782 N88-20661
Power spectral density analysis of wind-shear turbulence for related flight simulations
[NASA-CR-182721] 13 p1802 N88-20773
Analysis, suppression of land clutter characteristics reported 14 p1903 N88-21369
Spectral estimation of received phase in the presence of amplitude scintillation 22 p3064 N88-28180
Matching P.S.D.: Design loads
24 p3312 N88-29720
Performance of DS/SSMA communications in impulsive channels. Part 1: Correlation receivers
[AD-A195712] 24 p3362 N88-30021
Vibrational power flow analysis of rods and beams
[NASA-CR-183166] 24 p3383 N88-30151

POWER SUPPLIES
Pulsed current transformer for low inductive loads
[AD-A187224] 10 p1324 N88-17913

POWER SUPPLY CIRCUITS
Evaluation of high-voltage, high-power, solid-state remote power controllers for amps
07 p0924 N88-15612
A technique for low level, wide range CW microwave power meter calibrations
[DE88-004147] 10 p1333 N88-17966
Multi-hundred kilowatt roll ring assembly evaluation results
[NASA-TM-100865] 14 p1904 N88-21375
Arc lamp power supply using a voltage multiplier
[NASA-CASE-LAR-13202-1] 17 p2335 N88-23942

POWER TRANSMISSION
Power flow in terms of Poynting vector for Extremely Low Frequency (ELF) dipole sources in seawater
[ARE-TM(UTM)-87102] 01 p0035 N88-10221
Power systems for production, construction, life support and operations in space
[NASA-TM-100838] 14 p1883 N88-21254
Power components for the space station 20-kHz power distribution system
[NASA-TM-100866] 14 p1904 N88-21374
A role for high frequency superconducting devices in free space power transmission systems
[NASA-TM-100971] 19 p2662 N88-25830
HPM (High Power Microwave) simulation fidelity studies
[DE88-012229] 22 p3068 N88-28209

POWER TRANSMISSION (LASERS)
Thrust and specific impulse of repetitively-pulsed-laser propulsion rocket 03 p0318 N88-12012
Overview and future direction for blackbody solar-pumped lasers
[NASA-TM-100621] 21 p2955 N88-27553

POWERED LIFT AIRCRAFT
Civil applications of high-speed rotorcraft and powered-lift aircraft configurations
[NASA-TM-100035] 03 p0261 N88-11643
Application of empirical and linear methods to VSTOL powered-lift aerodynamics
[NASA-TM-100048] 10 p1267 N88-17581
Development of circulation control technology for powered-lift STOL aircraft 10 p1272 N88-17608
A potential flight evaluation of an upper-surface-blowing/circulation-control-wing concept
10 p1272 N88-17609
A perspective on 15 years of proof-of-concept aircraft development and flight research at Ames-Moffett by the Rotorcraft and Powered-Lift Flight Projects Division, 1970-1985
[NASA-RP-1187] 12 p1582 N88-19467
Takeoff predictions for powered-lift aircraft
[NASA-CR-177491] 19 p2597 N88-25431

POYNTING THEOREM
Power flow in terms of Poynting vector for Extremely Low Frequency (ELF) dipole sources in seawater
[ARE-TM(UTM)-87102] 01 p0035 N88-10221
SSVCO feed characteristics
[DE88-011322] 22 p3068 N88-28208

PPM (MODULATION)
U PULSE POSITION MODULATION

PRACTICES
U PROCEDURES

PRAIRIES
U GRASSLANDS

PRANDTL NUMBER
Ludwig Prandtl collected treatises on applied mechanics, hydro- and aerodynamics, part 1
[NASA-TT-20316] 20 p2752 N88-26337
Ludwig Prandtl collected treatises on applied mechanics, hydro- and aerodynamics, part 2, IV interfaces and resistance
[NASA-TT-20315] 20 p2752 N88-26338
PRE-MAIN SEQUENCE STARS
NT T TAURI STARS
Soft X-ray observations of pre-main sequence stars in the chamaeleon dark cloud
[NASA-CR-181457] 02 p0250 N88-11579
Fifth Cambridge Workshop on Cool Stars, Stellar Systems and the Sun 04 p0502 N88-13092
Disk accretion during the early stages of stellar evolution 04 p0505 N88-13106
Microwave observations of nonthermal phenomena in pre-main sequence stars 04 p0505 N88-13107
Pre-main sequence activity: How far is magnetism involved 04 p0517 N88-13179
Chromospheric variability mechanisms affecting pre-main sequence stars 04 p0517 N88-13180
A spherical, non-LTE, blanketed model stellar atmosphere for Phi Cas (FOIa) 10 p1428 N88-18528
Radio and infrared properties of young stars
[NASA-CR-183252] 24 p3459 N88-30579
PREAMPLIFIERS
On the choice of a element low-noise preamplifier on bipolar transistors
[DE88-700639] 10 p1322 N88-17904
Design of a charge sensitive preamplifier on high resistivity silicon
[DE88-003491] 10 p1323 N88-17907
Low-noise cryogenically cooled broad-band microwave preamplifiers
[DE88-004561] 10 p1324 N88-17912
An optical preamplifier for detection of CO2 laser radiation
[AD-A190790] 18 p2520 N88-24949
PREBURNERS
Duct flow nonuniformities for Space Shuttle Main Engine (SSME)
[NASA-CR-179338] 18 p2511 N88-24899
Evaluation and improvement of liquid propellant rocket chugging analysis techniques. Part 2: A study of low frequency combustion instability in rocket engine preburners using a heterogeneous stirred tank reactor model
[NASA-CR-182724] 21 p2903 N88-27225
PRECAMBRIAN PERIOD
Metamorphic P-T paths and Precambrian crustal growth in East Antarctica 24 p3395 N88-30218
PRECAUTIONS
U ACCIDENT PREVENTION
PRECESSION
NT QUENCHING (ATOMIC PHYSICS)
Spin precession in stationary gravitational fields
[DE88-701107] 15 p2093 N88-22470
Resonant spin-flavor precession of solar and supernova neutrinos
[DE88-752604] 23 p3308 N88-29707
PRECIOUS METALS
U NOBLE METALS
PRECIPITATES
Modified 14Cr-16Ni stainless steels with improved creep resistance at 700 C due to tailored precipitate microstructures
[DE87-014788] 03 p0290 N88-11825
Microstructural characterization of irradiated PWR steels using the atom probe field-ion microscope
[DE88-000341] 03 p0291 N88-11826
The accommodation of precipitate plates modelled as a tensile test
[DE88-000207] 04 p0454 N88-12814
Characterization of precipitates in a niobium-zirconium-carbon alloy
[NASA-TM-100848] 16 p2178 N88-22981
Theoretical predictions of precipitate shapes in cubic alloys
[DE88-010856] 21 p2914 N88-27291
PRECIPITATION
Digital processing of infrared and visible images from the GOES satellite and its integration with meteorological radar data 17 p2360 N88-24057
PRECIPITATION (CHEMISTRY)
Factors determining the morphology of precipitation in aluminum-germanium and aluminum-silicon alloys
[DE87-014682] 03 p0287 N88-11806
Influence of creep on the precipitate structure under conditions of long-term creep. 4: Experiments on 10 CrMo 9 10 steel
[BLL-CE-TRANS-8256-(9022.09)] 04 p0417 N88-12589
Precipitation of surfactants and surfactant mixtures in aqueous solutions
[DE88-003333] 10 p1298 N88-17763
Temperature dependence of Kr precipitation in Ni
[DE88-005953] 13 p1744 N88-20429
A hydroxycarbonate route to superconductor precursor powders
[DE88-003638] 13 p1846 N88-21052
Effect of size of precipitates on recrystallization temperatures in Cu-Cr, Cu-Zr, and Cu-Zr-Cr alloys
[NASA-TT-20166] 18 p2489 N88-24763
A study on the precipitation and reversion behaviors of Cu-0.3 percent Cr alloy by the step annealing method
[NASA-TT-20169] 18 p2489 N88-24764
Dual mechanism bifunctional polymers: Design, synthesis and application of a new category of metal ion complexing agents
[DE88-008233] 20 p2777 N88-26468
PRECIPITATION (METEOROLOGY)
NT ACID RAIN
NT RAIN
NT SNOW
NT SNOW COVER
Aqueous-phase reactions in clouds
[DE86-005249] 01 p0069 N88-10445
Enhancement of surface-atmosphere fluxes by desert-fringe vegetation through reduction of surface albedo and of soil heat flux
[NASA-CR-181442] 02 p0197 N88-11231
Forecasting the kind of precipitation in winter 02 p0202 N88-11266
Longer-duration post-frontal precipitation at Vancouver International Airport, 1953-1983 02 p0203 N88-11269
The importance of mesoscale waves in the upper troposphere for formation of cloud and precipitation areas 02 p0203 N88-11273
FRONTIERS: An operational system for nowcasting precipitation 02 p0204 N88-11279
Operational experiment in very short range forecast of precipitation 02 p0204 N88-11280
The impact on short-term precipitation forecast skill of time-dependent lateral and lower boundary conditions within a meso-beta numerical cloud prediction model 02 p0211 N88-11327
Use of four-dimensional data assimilation to improve a mesoscale-model precipitation forecast: A case study 02 p0213 N88-11340
Impact of a direct assimilation of satellite-inferred precipitation rates into a regional meteorological model 02 p0213 N88-11342
Initialization experiments with the NMC nested grid model — National Meteorological Center (NMC) 02 p0213 N88-11343
The effect of enhanced conventional and VAS moisture analysis on RAFS short-range precipitation forecasts — Regional Analysis and Forecasting System (RAFS) 02 p0215 N88-11352
A method for remote sensing of precipitable water vapor and liquid in the atmosphere using a 22-ghz radiometer
[AD-A184204] 03 p0354 N88-12232
Computer modeling aids studies of precipitation formation 04 p0458 N88-12832
New precipitation map of world ocean 04 p0458 N88-12834
Measurements of vapor flux, liquid water contents, precipitation rates and riming in a Utah mountain cloud system
[PB87-224945] 04 p0469 N88-12900
Radar observations of changes in precipitation size spectra associated with lightning 06 p0744 N88-14576
Report of the first session of the International Working Group on Data Management for the Global Precipitation Climatology project
[WCP-132] 06 p0745 N88-14582
The global climate system: Autumn 1984 to spring 1986
[CSM-R84/86] 06 p0745 N88-14583
Moscow USSR. Limited surface observations climatic summary (LISOCS), parts A-F
[AD-A188080] 11 p1514 N88-19046
Determination of atmospheric moisture structure from high resolution MAMS radiance data 11 p1515 N88-19049
Research and development to acquire and reduce melting layer cloud physics and evaluate a prototype M-meter
[AD-A188390] 12 p1648 N88-19873
The mixed layer of the western equatorial Pacific Ocean
[HIG-1861] 13 p1805 N88-20789
Spatial and temporal distribution of precipitation chemistry across Maryland in 1984, volume 1
[PB88-148929] 14 p1943 N88-21595
Spatial and temporal distribution of precipitation chemistry across Maryland in 1984, volume 2
[PB88-148937] 14 p1944 N88-21596
Satellite rainfall retrieval by logistic regression
[NASA-CR-180485] 14 p1946 N88-21607
Analysis of winter season precipitation bands over the Southern Plains 14 p1947 N88-21609
Tropical circulations and the associated rainfall anomalies during two contrasting years
[INPE-4506-PRE/1261-REV] 15 p2098 N88-22502
A drought watch system
[WCP-134] 16 p2234 N88-23345
Taiwan area mesoscale experiment: Daily operations summary
[PB88-169081] 16 p2235 N88-23348
Satellite observed Mesoscale Convective System (MCS) propagation characteristics and a 3-12 hour heavy precipitation forecast index
[PB88-180161] 19 p2692 N88-26004
Meteorological aspects of wet deposition in Southern Finland
[FMI-3] 19 p2693 N88-26007
A radar study of the interaction between lightning and precipitation
[DE88-009120] 20 p2827 N88-26770
Factors influencing summer temperatures and precipitation in the southwest 22 p3124 N88-28565
On the modes of growing-season precipitation over central North America 22 p3124 N88-28567
On climate prediction for India 22 p3127 N88-28590
Characteristics of regression equations for specifying monthly precipitation amounts over the United States from the field of concurrent mean 700 mb heights 22 p3127 N88-28591
Determining the spatial structure of fields of precipitation from space radar images in two orthogonal polarizations 24 p3450 N88-30531
PRECIPITATION HARDENING
Investigation of rapidly-solidified dispersion strengthened titanium alloys
[AD-A183862] 01 p0022 N88-10140
Microstructural evolution and response to double-loop reactivation testing of heat-treated pH 13-8 Mo martensitic stainless steel
[DE87-009058] 02 p0146 N88-10915
Compatability of dispersion-strengthened platinum with resistojet propellants
[NASA-TP-2765] 04 p0409 N88-12538
Role of interstitials and precipitates in initiation and propagation of L.C.F. cracks in austenitic stainless steels 06 p0718 N88-14411
Precipitation in alumina-rich spinel: A transformation-toughened ceramic single crystal
[DE87-012380] 06 p0785 N88-14815
Long-term-aging embrittlement of cast duplex stainless steels: Mechanism and kinetics
[DE88-002929] 09 p1145 N88-16861
Characterization of duplex stainless steel by TEM (Transmission Electron Microscopy), SANS (Small-Angle Neutron Scattering) and APFIM (Atom-Probe Field Ion Microscopy) techniques
[DE88-002916] 09 p1145 N88-16865
Micro-mechanisms of deformation in SiC/Al composites
[AD-A188282] 10 p1296 N88-17749
Dependence of hydrogen embrittlement of austenitic stainless steels on structural state of grain boundaries 14 p1896 N88-21316
The age hardening response of thermomechanically processed Al-Mg-Li alloys
[AD-A189870] 15 p2039 N88-22147
Effects of cold working on precipitation in age hardenable alloys: On the copper alloys
[NASA-TT-20164] 16 p2177 N88-22973
Deformation of rapidly solidified dispersion strengthened titanium alloys
[AD-A190793] 16 p2179 N88-22984
The precipitation processes of Cu-Zr-Cr alloys
[NASA-TT-20168] 18 p2488 N88-24758
Critical cooling rates on solution treatment of Cu-Cr and Cu-Be alloys
[NASA-TT-20163] 18 p2488 N88-24760
Precipitation study by electrical resistivity measurement in Ni-Al alloys
[DE88-701877] 20 p2773 N88-26440
PRECISION
Contributions to fast-reacting and high-precision three-phase positioning systems — machinery
[ETN-87-90427] 01 p0056 N88-10358
Limits to the precision of electro-optic and magneto-optic sensors
[PB87-212536] 03 p0323 N88-12040
GPS vertical axis performance enhancement for helicopter precision landing approach
[NASA-CR-177443] 04 p0397 N88-12477

Interactions between science and precision engineering
[DE87-010873] 04 p0426 N88-12643
A demonstration of high precision GPS orbit determination for geodetic applications
04 p0432 N88-12680
Precise near-earth navigation with GPS: A survey of techniques 04 p0433 N88-12682
Short baseline phase delay interferometry
04 p0433 N88-12683
Precision analysis of regular networks
[B8709808] 05 p0620 N88-13806
Faraday cup characterization of electron beam welding parameters
[DE88-001896] 07 p0864 N88-15241
CARS measurements of combustion. 1: Precision of thermometry
[NAL-TR-939] 10 p1299 N88-17769
On precision and accuracy (bias) statements for measurement procedures
[DE88-004434] 10 p1402 N88-18359
Development of mirrors for high-precision laser gyroscopes 18 p2517 N88-24931
Fabrication technology
[DE88-010598] 20 p2855 N88-26955
Aerodynamic data accuracy and quality: Requirements and capabilities in wind tunnel testing
[AGARD-AR-254] 23 p3173 N88-28893
High definition television: Evaluation for remote task performance
[DE88-011573] 23 p3202 N88-29057

PRECONDITIONING

Approximate polynomial preconditioning applied to biharmonic equations on vector supercomputers
[NASA-TM-100217] 01 p0087 N88-10563
Preconditioned iterative methods for partial differential equations
[DE88-003071] 09 p1230 N88-17372
Polynomial preconditioning for conjugate gradient methods
[DE88-005214] 10 p1399 N88-18342
Domain decomposition preconditioners for the spectral collocation method
[NASA-CR-181620] 10 p1400 N88-18345

PREDICTION ANALYSIS TECHNIQUES

Modelling of crack-tip deformation and transient electrochemical processes in relation to corrosion fatigue of steels cathodically protected in marine environments
[NPL-DMA(A)-145] 01 p0059 N88-10379
Dugdale solutions for strain hardening materials
[FD-6/1985] 01 p0059 N88-10380
Fatigue life evaluation according to local strain concept
[FF-14/1985] 01 p0059 N88-10381
The use of Hencky's equations for the estimation of multiaxial elastic-plastic notch stresses and strains
[FB-3/1986] 01 p0060 N88-10383
Stress-strain analysis and life predictions of a notched shaft under multiaxial loading
[FB-5/1986] 01 p0060 N88-10384
Crack initiation life estimations for notched specimens with residual stresses based on local strains
[FF-17/1986] 01 p0060 N88-10385
Criteria for determination of significant load cycles in variable amplitude load sequences
[NLR-MP-86013-U] 01 p0060 N88-10386
Prediction and spectral decomposition of wide sense stationary processes on Z squared
[ENST-87C001] 01 p0087 N88-10564
Predictive momentum management for a space station measurement and computation requirements
[NASA-CR-172026] 02 p0138 N88-10866
Cumulative fatigue and life prediction of fibre composites. Part 1: Literature reviews
[BR101013] 02 p0142 N88-10893
Cumulative fatigue and life prediction of fibre composites. Part 2: Experimental techniques and results
[BR101014] 02 p0142 N88-10894
Personal Computer (PC) based image processing applied to fluid mechanics
[NASA-TM-100024] 02 p0172 N88-11087
Component specific modeling
02 p0187 N88-11166
Prediction of fatigue cracking and rupture of large structures
[ONERA-RT-31/7169-RY-055-R]
02 p0192 N88-11199
Combustion in turbulent jets and buoyant flames
[PB87-232674] 03 p0283 N88-11779
Advanced natural gas fueled engine development. Part 2: Materials investigation
[PB87-223160] 03 p0331 N88-12088
Bearing loads in slider crank mechanisms
[PB87-216495] 03 p0332 N88-12089
Investigation of reliability of strength values measured on CFRP test bars by statistical methods. Part 1: Probability distributions for strength analysis
[ESA-TT-1036] 03 p0336 N88-12115
An algorithmic approach to crustal deformation analysis
[NASA-CR-181497] 03 p0349 N88-12203
Kinds of bootstraps and kinds of jackknives, discussed in terms of a year of weather-related data
[AD-A184495] 03 p0353 N88-12227
Tropical cyclone intensity prediction based on empirical orthogonal function representation of wind and shear fields
[AD-A184699] 03 p0353 N88-12229
A heteroscedastic hierarchical model
[AD-A184256] 03 p0372 N88-12340
Numerical prediction of propeller performance by vortex lattice method
[UTIAS-TN-265] 04 p0400 N88-12489
A study of two-phase flow in a reduced gravity environment
[NASA-CR-172035] 04 p0422 N88-12617
Creep life prediction based on stochastic model of microstructurally short crack growth
[NASA-TM-100245] 04 p0456 N88-12825
Results of the 1986 NASA/FAA/DFVLR main rotor test entry in the German-Dutch wind tunnel (DNW)
[NASA-TM-100507] 04 p0487 N88-13003
Hypersonic static and dynamic stability of axisymmetric shapes: A comparison of prediction methods and experiment 05 p0534 N88-13246
Experiences using the Mark IV supersonic hypersonic arbitrary body program 05 p0534 N88-13249
Application of modified loss and deviation correlations to transonic axial compressors
[AGARD-R-745] 05 p0549 N88-13344
An analytical study of the effects of transverse shear deformation and anisotropy on buckling loads of laminated cylinders
[NASA-TM-100508] 05 p0557 N88-13387
The simulation of the viscous flow around a cylinder by the random vortex method 05 p0579 N88-13534
Low thrust viscous nozzle flow fields prediction
[NASA-CR-182334] 05 p0582 N88-13551
An examination of chaotic motion for the buckled beam 05 p0597 N88-13644
Fatigue crack growth: Statistical considerations
05 p0606 N88-13718
Comparing hard and soft prior bounds in geophysical inverse problems
[NASA-CR-181557] 05 p0624 N88-13820
Specification of predictors necessary for the determination of over or underestimation of radar derived total rainfall
[AD-A185363] 05 p0628 N88-13838
Post stall behavior in axial-flow compressors
[AD-A185712] 06 p0665 N88-14081
Measurement of mechanical parameters to define damage criteria in delamination of crossed stratified layers
[DCQ/L-47-361/F] 06 p0678 N88-14154
Fatigue life prediction modeling for turbine hot section materials
[NASA-TM-100291] 06 p0724 N88-14453
Sound propagation over uneven ground and irregular topography
[NASA-CR-182352] 06 p0776 N88-14763
Prediction of physical workload in reduced gravity environments 06 p0794 N88-14867
Fracture study of windshield glass panes
06 p0799 N88-14891
Spherical models of QSO/AGN emission line clouds
06 p0806 N88-14921
Aeropropulsion '87. Session 3: Internal Fluid Mechanics Research
[NASA-CP-10003-SESS-3] 08 p0954 N88-15790
The dynamics and control of large-flexible space structures, part 10
[NASA-CR-182426] 08 p0963 N88-15830
Validation of a stochastic model to determine failure rates for communication-electronic systems
[AD-A186536] 08 p0980 N88-15920
A computationally efficient modelling of laminar separation bubbles
[NASA-CR-182417] 08 p0984 N88-15949
On free decay damping tests
08 p0997 N88-16041
Comprehensive inflight vibration and acoustic testing
08 p0999 N88-16052
A study of finite difference and finite element vertical discretization schemes for baroclinic prediction equations
[AD-A186617] 08 p1040 N88-16291
FOR3D: A computer model for solving the LSS (Lee-Saad-Schultz) three-dimensional, wide angle wave equation
[AD-A186649] 08 p1080 N88-16511
A review of research in rotor loads
09 p1106 N88-16629
Comprehensive rotorcraft analysis methods
09 p1106 N88-16630
Helicopter crashworthiness research program
09 p1107 N88-16635
Recent Langley helicopter acoustics contributions
09 p1109 N88-16646
A decade of aeroacoustic research at NASA Ames Research Center 09 p1109 N88-16648
Aeroacoustic research programs at the Army Aviation Research and Technology Activity
09 p1109 N88-16649
Optimized approach to damage tolerance — spacecraft
[FOK-FSS-R-87-024] 09 p1134 N88-16806
Sublaminate damage mechanisms in composite structures
[AD-A186807] 09 p1137 N88-16815
A quasi-three-dimensional calculation procedure for the prediction of flow and heat transfer in heat exchanger passages 09 p1165 N88-16985
The failure and fracture analysis of adhesive bonds
[ETN-87-90713] 09 p1181 N88-17077
Fracture mechanics characterization of crack growth under creep and fatigue conditions
[W-2/87] 09 p1183 N88-17087
Improving the stability of predictor-corrector methods by residue smoothing
[CWI-NM-R8707] 09 p1228 N88-17359
Modification of a successive corrections objective analysis for improved higher order calculations
[NASA-CR-182467] 09 p1230 N88-17370
Prediction of polytomous events: Model description, algorithm development and methodological aspects, with an application
[AD-A186549] 09 p1232 N88-17384
An experimental investigation of pressure driven three-dimensional turbulent boundary layers
10 p1327 N88-17934
Forecasting complications of cardiovascular disease in flight personnel 10 p1361 N88-18136
Radial mixing in turbomachines
[AD-A188028] 11 p1482 N88-18847
Kinetic and turbulence models for granular and two-phase flows 11 p1484 N88-18862
A posteriori error estimates in computational fluid mechanics 11 p1486 N88-18869
Fracture characteristics of a viscoelastic polymer under constant load: Experiments and analysis
11 p1501 N88-18963
Stochastic heuristics in network design: Parameter tuning and performance evaluation
[REPT-87-017] 11 p1541 N88-19210
Predictive wall adjustment strategy for two-dimensional flexible walled adaptive wind tunnel: A detailed description of the first one-step method
[NASA-CR-181635] 12 p1573 N88-19409
An interdisciplinary approach to predictive modeling of structural adhesive bonding: Factors affecting the durability of titanium/epoxy bonds
[AD-A189503] 12 p1611 N88-19636
Active vibration control of a cantilevered beam with three elastic coordinates
[AD-A188824] 12 p1636 N88-19797
Comparison of simulation modeling and satellite techniques for monitoring ecological processes
[NASA-CR-182592] 12 p1641 N88-19825
A study of combustion and flow behaviour in solid-propellant rocket motors
[UTIAS-280] 13 p1732 N88-20357
Ply-level failure analysis of a graphite/epoxy laminate under bearing-bypass loading
[NASA-TM-100578] 13 p1735 N88-20372
Detection and angle estimation of coherent plane waves 13 p1759 N88-20522
Pseudo-stationary oblique-shock-wave reflections in low gamma gases: Isobutane and sulphur hexafluoride
[UTIAS-TN-267] 13 p1768 N88-20576
Predictions and studies with a one-dimensional ice/ocean model
[AD-A189158] 13 p1803 N88-20776
Aberrations: Their effect on off-axis beam steering
[AD-A189601] 13 p1840 N88-21008
Strength and failure analysis of composite laminate containing a circular hole with reinforcement
[AD-A189629] 14 p1884 N88-21260
On the theory of electromagnetic scattering from a raindrop splash
[AD-A188720] 14 p1906 N88-21393

Experiments on the creep behavior of semifinished X10NiCrAlTi 32 20 (Nicrofer 32 20) tubes under multiaxial loading — nuclear reactors
[JUEL-2127] 14 p1923 N88-21464
Probabilistic analysis of crack containing structures with the PARIS code
[KFK-4286] 14 p1924 N88-21465
Evaluation of structural analysis methods for life prediction 14 p1930 N88-21511
The 25 m horizontal-axis turbine as a test case for standard Dutch aerodynamic calculation methods for high-speed rotors
[R-762-D] 14 p1942 N88-21589
A prediction-error estimation algorithm for nonlinear output-affine systems
[RR-314] 14 p1959 N88-21679
Identification of nonlinear rational systems using a prediction-error estimation algorithm
[RR-317] 14 p1959 N88-21680
Admissibility in fair Bayes prediction problems. Part 1: General theory
[CWI-MS-R8703] 14 p1965 N88-21725
Large quantile estimation under extreme-value conditions
[CWI-MS-R8711] 14 p1966 N88-21730
Investigation of boundary layer disturbances caused by periodic heating of a thin ribbon
[AD-A190572] 15 p2065 N88-22314
Whisker-reinforced ceramic composites for heat engine components 15 p2082 N88-22410
Fracture technology for brittle materials 15 p2083 N88-22417
Grain boundary oxidation and low-cycle fatigue at elevated temperatures 15 p2083 N88-22420
Cumulative fatigue damage models 15 p2084 N88-22422
Life prediction modeling based on strainrange partitioning 15 p2084 N88-22425
Life prediction modeling based on cyclic damage accumulation 15 p2085 N88-22426
Fatigue damage modeling for coated single crystal superalloys 15 p2085 N88-22427
Life and reliability of rotating disks 15 p2085 N88-22428
Review and assessment of the HOST turbine heat transfer program 15 p2086 N88-22431
The existence of smooth densities for the prediction filtering and smoothing problems
[AD-A189865] 15 p2119 N88-22629
A numerical model of unsteady, subsonic aeroelastic behavior
[NASA-TM-101126] 16 p2156 N88-22862
Thermoviscoelastic characterization and predictions of Kevlar/epoxy composite laminates
[NASA-CR-182878] 16 p2172 N88-22948
Reynolds stress models of homogeneous turbulence 16 p2197 N88-23106
Application of the ONERA model to the life estimation under fatigue cracking of a Al-Li alloy. Parameter identification and test-experiment comparison under FALSTAFF loading
[ONERA-RT-32/7169-RY-063-R] 16 p2222 N88-23264
Modeling and estimation of a low degree geopotential model from terrestrial gravity data
[NASA-CR-182808] 16 p2232 N88-23330
Very short range statistical forecasting of automated weather observations
[AD-A190803] 16 p2235 N88-23349
Space plasma contactor research, 1987
[NASA-CR-182148] 16 p2280 N88-23649
PAN AIR analysis of the NASA/MCAIR 279-3: An advanced supersonic V/STOL fighter/attack aircraft
[NASA-TM-86838] 17 p2298 N88-23750
The prediction of satellite lifetimes
[RAE-TR-87030] 17 p2310 N88-23818
Ceramics for turbine engines 17 p2323 N88-23873
Some design considerations for ceramic components in heat engine applications 17 p2323 N88-23875
Generalized predictive control of multivariable systems
[OUEL-1640/86] 17 p2391 N88-24209
A recursive prediction error parameter estimator for nonlinear models
[RR-326] 17 p2392 N88-24222
Particle-laden weakly swirling free jets: Measurements and predictions
[NASA-TM-100920] 18 p2466 N88-24639
Design of overlays for rigid airport pavements
[DOT/FAA/PM-87/19] 18 p2468 N88-24652
Research study: Space shuttle main engine plume flowfield model
[NASA-CR-179336] 18 p2474 N88-24676
Predictive corrosion modeling, volume 1
[AD-A191229] 18 p2485 N88-24739
Environment assisted degradation mechanisms in advanced light metals
[NASA-CR-182907] 18 p2486 N88-24748
Investigation of the effect of minimum loads and compression of load spectra on the prediction capacities of the ONERA crack model — wings
[ONERA-RTS-33/7169-RY-064-R] 18 p2527 N88-24994
Some stress intensity factor equations
[FFA-TN-1987-07] 18 p2527 N88-24995
Automated analysis of crack growth rate for obtaining da/dN versus delta K relation
[FFA-TN-1987-70] 18 p2527 N88-24996
Adaptive grid refinement for numerical weather prediction
[AD-A192172] 18 p2544 N88-25101
Adaptive time series analysis using predictive inference and entropy
[AD-A191858] 18 p2560 N88-25199
A multiple chamber volume-filling model for prediction of transient solid rocket motor ballistic performance 19 p2633 N88-25618
Propagation modeling for land mobile satellite systems 19 p2645 N88-25694
Picosecond response of an optically controlled millimeter wave phase shifter 19 p2660 N88-25820
A simple unified method for predicting the deflections of reinforced concrete structures 19 p2679 N88-25930
Changes in seismic velocity and apparent attenuation due to isotropic and anisotropic scattering: Results from physical modeling 19 p2691 N88-25997
BOLETIM: An expert system for weather forecasting
[INPE-4538-TDL/329] 19 p2693 N88-26011
Experimental and theoretical analysis of the radiative transfer within a sooty pool fire
[DE88-007099] 20 p2769 N88-26419
Interpreting forest biome productivity and cover utilizing nested scales of image resolution and biogeographical analysis
[NASA-CR-183036] 20 p2817 N88-26711
Synoptic patterns related to tropical cyclone recurvature
[AD-A192338] 20 p2827 N88-26771
Computation of ECM (Electronic Counter-Measures) war reserve materiel spare requirements
[AD-A193301] 21 p2897 N88-27195
Approximations of stochastic equations driven by predictable processes
[AD-A192714] 21 p3005 N88-27823
Robust prediction for stationary processes: 2D enriched version
[AD-A193318] 21 p3006 N88-27833
Method to predict external store carriage characteristics at transonic speeds
[NASA-CR-4170] 22 p3037 N88-28034
Applications of fatigue analyses: Aircraft engines
[PNR90439] 22 p3044 N88-28066
Analyses and correlations of environment assisted fatigue crack propagation for attachment lugs 22 p3053 N88-28116
Thermal barrier coating life-prediction model development
[NASA-CR-179507] 22 p3058 N88-28142
An application of the Bayesian method to the estimation and forecast of system hardware components MTBF 22 p3068 N88-28211
Prediction of long-term creep in polypropylene from short-term tests
[NPL-DMA(A)-156] 22 p3088 N88-28337
The relative utility of persistence and medium-range dynamical forecasts of monthly mean 700 mb heights 22 p3127 N88-28588
Computational tools for simulation methodologies 23 p3168 N88-28865
Critical conditions for failure in materials subjected to high rates of loading
[AD-A194697] 23 p3226 N88-29201
Atmospheric deposition of nitrate to the ocean surface 23 p3231 N88-29227
On Wiener-Masani's algorithm for finding the generating function of multivariate stochastic processes
[NASA-CR-182905] 23 p3273 N88-29481
Investigation of non-classical effects in two-photon interference processes 23 p3282 N88-29541
Special Course on Missile Aerodynamics
[AGARD-R-754] 24 p3317 N88-29755
Accuracy criteria for evaluating supersonic aerodynamic coefficient predictions 24 p3317 N88-29756
Survey on nonlinear effects 24 p3317 N88-29757
Prediction of base-flows 24 p3319 N88-29765
Next generation missile design 24 p3319 N88-29766
A new computational capability for ramjet projectiles
[AD-A196061] 24 p3327 N88-29812
Three-dimensional combustor predictors: A comparison of equilibrium and laminar flamelet chemistry models 24 p3350 N88-29940
Preliminary investigation of flow modeling during solid propellant processing
[AD-A196168] 24 p3357 N88-29987

PREDICTIONS
NT FLOOD PREDICTIONS
NT IMPACT PREDICTION
NT LINEAR PREDICTION
NT NOISE PREDICTION
NT NOISE PREDICTION (AIRCRAFT)
NT PERFORMANCE PREDICTION
Structural reliability and damage tolerance of ceramic composites for high-temperature applications
[PB87-208310] 01 p0019 N88-10119
HF (High Frequency) broadcasting planning model: A comparison of two versions
[PB87-210282] 01 p0036 N88-10230
Cooling effect of a single evaporating droplet on a hot semi-infinite metal body
[PB87-201802] 01 p0046 N88-10294
The development of a friction model predicting the sliding behavior of materials pairs, especially at low temperatures: Progress report and renewal proposal
[DE87-013941] 01 p0055 N88-10354
Life prediction and constitutive models for engine hot section anisotropic materials program 02 p0188 N88-11175
Coating life prediction 02 p0189 N88-11181
Thermal barrier coating life prediction model development 02 p0190 N88-11184
Thermal barrier coating life prediction model development 02 p0190 N88-11185
Applications of dislocation theory to crack growth problems 02 p0190 N88-11188
Severe weather potential (SPOT) plotfile generator
[PB87-217717] 02 p0216 N88-11360
Software reliability models for fault-tolerant avionics computers and related topics
[NASA-CR-181440] 02 p0220 N88-11382
Physical optics method: Prediction of radar signatures 03 p0304 N88-11914
A statistical rain attenuation prediction model with application to the advanced communication technology satellite project. Part 2: Theoretical development of a dynamic model and application to rain fade durations and tolerable control delays for fade countermeasures
[NASA-TM-100242] 03 p0308 N88-11945
Application of prediction of equilibrium to servo-controlled calorimetry measurements
[DE87-013745] 03 p0324 N88-12046
Laser sources today and tomorrow
[DE87-014247] 03 p0330 N88-12083
Comparison of measured temperatures, thermal stresses and creep residues with predictions on a built-up titanium structure
[NASA-TM-86814] 03 p0337 N88-12125
Vibration and parametric excitation in rotating asymmetric circular plates 04 p0456 N88-12823
Reevaluating the worst-case radiation response of MOS transistors
[DE87-014157] 04 p0497 N88-13059
The velocity structure and turbulence at the center of the Orion Nebula 04 p0521 N88-13201
Numerical prediction of turbulent flows in dump diffusers 05 p0537 N88-13265
Prediction of wing aeroelastic effects on aircraft life and pitching moment characteristics 05 p0551 N88-13356
Fiber composite structural durability and damage tolerance: Simplified predictive methods
[NASA-TM-100179] 05 p0580 N88-13409
Master plots for predicting the case-depth in laser surface treatments
[PB87-221875] 05 p0586 N88-13574
Significance of fatigue crack closure under spectrum loading 05 p0599 N88-13662
Low cycle fatigue life predictions of a 1CrMoV steel in terms of a J-controlled short crack growth model 05 p0599 N88-13665
Crack growth prediction in 3D structures under aeronautical-type spectrum loadings 05 p0602 N88-13688
Accurate rotor loads prediction using the FLAP (Force and Loads Analysis Program) dynamics code
[DE88-001109] 05 p0623 N88-13815
File usage analysis and resource usage prediction: A measurement-based study
[NASA-CR-181553] 05 p0633 N88-13867
Predictability of process resource usage: A measurement-based study of UNIX
[NASA-CR-181562] 05 p0633 N88-13869
Robust prediction operations for stationary processes
[AD-A185408] 05 p0641 N88-13924

A numerical model of unsteady, subsonic aeroelastic behavior
[NASA-TM-100487] 06 p0663 N88-14064
Life prediction of steel cords
06 p0715 N88-14386
Verification of severe local storm forecasts issued by the National Severe Storms Forecast Center, 1986
[PB88-101407] 06 p0747 N88-14594
Investigations on the crack growth retardation behavior and fatigue life prediction in structural materials
[PB87-143756] 07 p0827 N88-15016
Life prediction of thermomechanical fatigue using total strain version of strainrange partitioning (SRP): A proposal
[NASA-TP-2779] 07 p0867 N88-15263
On two methods of identifying influential sets of observations
[AD-A186270] 07 p0910 N88-15518
On rate of convergence of equivariation linear prediction estimates of the number of signals and frequencies of multiple sinusoids
[AD-A186034] 07 p0914 N88-15549
Computational prediction of propellant reorientation
08 p0962 N88-15940
A comparison of experimental and theoretical results for labyrinth gas seals with honeycomb stators
[NASA-CR-182441] 08 p0993 N88-16006
Statistical measures of clipped random signals
08 p1000 N88-16055
The effects of rotor unbalance on the vertical response of a soft-mounted block 08 p1000 N88-16057
Satellite monitoring of earthquake precursor effects in magnetosphere 08 p1007 N88-16103
Effectiveness of oceanographic method in earthquake prediction 08 p1010 N88-16124
Prediction of the next solar activity cycle
08 p1035 N88-16276
Predictability of ice concentration in the high-latitude North Atlantic from statistical analysis of SST (Sea Surface Temperature) and ice concentration data
[AD-A186621] 08 p1045 N88-16315
Experimental evidence of micro-nonequilibrium on the magnetopause and further predictions
08 p1098 N88-16606
Primordial nucleosynthesis during the keV era
[DE88-002233] 08 p1104 N88-16623
Dynamic stress at critical locations of a structure as a criterion for mathematical model modification
09 p1180 N88-17066
Accuracies of southwell and force/stiffness methods in the prediction of buckling strength of hypersonic aircraft wing tubular panels
[NASA-TM-88295] 09 p1183 N88-17090
A comparison of the predicted and measured gravitational stresses in VAWT (Vertical Axis Wind Turbine) blades
[DE88-002113] 09 p1187 N88-17111
Outlier resistant predictive source encoding for a Gaussian stationary nominal source
[AD-A186725] 09 p1232 N88-17387
Studies of the initiation of pitting corrosion on stainless steels
[AERE-M-3615] 10 p1301 N88-17778
A three-dimensional dual potential procedure for rotational flows 10 p1329 N88-17942
On the dynamic estimation of relative weights for observation and forecast in numerical weather prediction
[NASA-CR-182531] 10 p1356 N88-18106
Future directions in computer architecture
10 p1383 N88-18257
Application of a multigrid method to a buoyancy-induced flow problem
[DE88-003961] 10 p1397 N88-18326
Linear prediction of stationary vector sequences
[NASA-TM-100069] 10 p1403 N88-18366
Wing flutter calculations with the CAP-TSD unsteady transonic small disturbance program
[NASA-TM-100580] 12 p1575 N88-19419
Validation of GEMACS (General Electromagnetic Model for the Analysis of Complex Systems) for modeling lightning-induced electromagnetic fields
[AD-A188822] 12 p1620 N88-19687
Crop forecasting in Brazil: A short history of productivity models
[INPE-4150-PRE/1056] 12 p1637 N88-19801
Avionics acquisition, trends and future approaches
12 p1702 N88-20184
Structural materials: The changing scene
12 p1703 N88-20190
Formulation of a general technique for predicting pneumatic attenuation errors in airborne pressure sensing devices
[NASA-TM-100430] 13 p1723 N88-20302
Predictive monitoring research: Summary of the PREMON system
[NASA-CR-182687] 13 p1824 N88-20905
MOSFET performance degradation due to hot carriers
13 p1848 N88-21063
Millimeter-wave properties of the atmosphere: Laboratory studies and propagation modeling
[PB88-164215] 14 p1905 N88-21387
The atmosphere as a component of the climate system: Structure and variability 14 p1935 N88-21540
Carbon dioxide and climate 14 p1936 N88-21545
Flexiwall 3 SO: A second order predictive strategy for rapid wall adjustment in two-dimensional compressible flow
[NASA-CR-181662] 15 p2015 N88-22018
Forecast of Atlantic seasonal hurricane activity for 1988 15 p2098 N88-22500
The existence of smooth densities for the prediction filtering and smoothing problems
[AD-A189865] 15 p2119 N88-22629
The analysis of fatigue crack growth mechanism and oxidation and fatigue life at elevated temperatures
[NASA-CR-182129] 16 p2179 N88-22987
On the prediction of equilibrium states in homogeneous turbulence
[NASA-CR-181659] 16 p2207 N88-23174
The 2-D and 3-D time marching transonic potential flow method for propfans 16 p2220 N88-23245
Aeroelastic forced response analysis of turbomachinery 16 p2220 N88-23247
Predicting operator workload during system design
16 p2239 N88-23375
Neurophysiological predictors of quality of performance 16 p2242 N88-23391
Development and testing of a predictive methodology for optimization of man-machine interface in future avionics systems 17 p2304 N88-23780
Progress and future directions in computational fluid dynamics
[NASA-TM-100091] 18 p2456 N88-24579
Prediction of laminar and turbulent flows past single and twin airfoils 18 p2457 N88-24589
Simulating futures in extended common LISP
[NASA-TM-101000] 18 p2559 N88-25192
Automatic discovery of optimal classes
[NASA-TM-101174] 18 p2566 N88-25238
Single-mode projection filters for modal parameter identification for flexible structures
[NASA-CR-182680] 18 p2566 N88-25244
Energy measurements in oxygen-induced reactions at 60 A GeV and 200 A GeV
[DE88-006420] 18 p2573 N88-25283
Takeoff predictions for powered-lift aircraft
[NASA-CR-177491] 19 p2597 N88-25431
An assessment of the state of the art in predicting the failure of ceramics
[DE88-008998] 19 p2621 N88-25551
Mixing and thermodynamic critical phenomena of combusting monopropellant sprays
19 p2623 N88-25558
Velocity coupling 19 p2629 N88-25596
Modeling and experimental measurements of solid propellant flame structure 19 p2631 N88-25605
Pressure differential scanning calorimetry (DSC) evaluation of solid rocket propellant burn rate mod
19 p2631 N88-25606
Numerical analysis of three dimensional cascade flow by solving Navier-Stokes equations
19 p2638 N88-25650
Prediction of fatigue life of notched specimens under aircraft loading and importance of the relative method in the case of local strain approach, part 2
[TAE-595-PT-2] 19 p2680 N88-25934
Canopy reflectance modeling in a tropical wooded grassland
[NASA-CR-182981] 19 p2685 N88-25961
Health and environmental consequences of the Chernobyl nuclear power plant accident
[DOE/ER-0332] 19 p2689 N88-25985
RCL model for the development of hysteresis in superconductors
[DE88-702061] 19 p2733 N88-26234
Intelligent guidance and control for wind shear encounter
[NASA-CR-183060] 20 p2755 N88-26347
Prediction of continental shelf sediment transport using a theoretical model of the wave-current boundary layer
[AD-A192272] 20 p2829 N88-26783
Hot electrons in silicon dioxide: Ballistic to steady-state transport 20 p2871 N88-27042
Oxidation-erosion of metals and alloys: Models, verification, and prediction
[DE88-010016] 21 p2915 N88-27300
Prediction of velocity and temperature profiles in thermally driven gravity currents applied to stratified thermal storage tanks
[DE88-004452] 21 p2946 N88-27496
NDE performance in predicting failure strength of spherical composite specimens with implanted flaws
[DE88-008223] 21 p2959 N88-27575
Size effects in linear elastic fracture mechanics
21 p2964 N88-27609
Behavioral, psychological and demographic predictors of physical fitness
[AD-A192697] 21 p2986 N88-27733
Empirical tools for simulation methodologies
23 p3168 N88-28866
Digital phase-lock loop having an estimator and predictor of error
[NASA-CASE-NPO-17196-1-CU]
23 p3205 N88-29076
A statistical rain attenuation prediction model with application to the advanced communication technology satellite project. 1: Theoretical development and application to yearly predictions for selected cities in the United States
[NASA-CR-179498] 23 p3205 N88-29077
Prediction of degradation of polymeric coating materials 24 p3354 N88-29970
A reliability-based program for predicting the service life of organic coating systems 24 p3355 N88-29971
Predicting the durability of adhesives and coatings by remote detection of hidden defects and coating-thickness irregularities: A theoretical and numerical study
24 p3355 N88-29972
Contributions to engineering models of human-computer interaction, volume 1
[AD-A195590] 24 p3409 N88-30295

PREDICTORS
U PREDICTIONS

PREFLIGHT ANALYSIS
Laser investigations for payload G-652 prior to filing pre-flight accommodation requirements
10 p1286 N88-17694
Two implementations of the Expert System for the Flight Analysis System (ESFAS) project
23 p3259 N88-29400

PREFLIGHT OPERATIONS
Aviation security: FAA (Federal Aviation Administration) needs preboard passenger screening performance standards
[PB87-216800] 02 p0124 N88-10783

PREFORMS
Novel fiber preforms: Rare earth doping
[AD-A191549] 18 p2575 N88-25294

PREGNANCY
Mother-fetus system as object for investigation of mechanisms of physiological effect of weightlessness
07 p0891 N88-15402
Spleen lymphocyte nucleic acids in pregnant rats flown in space and their offspring 07 p0892 N88-15403

PREHEATERS
U HEATING EQUIPMENT

PREHEATING
U HEATING

PREIMPREGNATION
Elementary characterization of Fibredux 913 CTS 5 34 percent preimpregnated carbon-epoxy from Ciba Geigy
[M-484300] 16 p2171 N88-22941
Elementary characterization of preimpregnated carbon epoxy T400H/DA0506 from STRUCTIL. Test report M6-577100
[CEAT-047426] 18 p2478 N88-24703

PRELAUNCH TESTS
NT STATIC FIRING
Altitude simulation testing of Ariane's second-stage engine 09 p1126 N88-16747
Stage separation testing of Ariane
09 p1126 N88-16752
Pre-launch calibration of channels 1 and 2 of the advanced very high resolution radiometer
[PB88-157169] 14 p1913 N88-21427

PRELOADING
U PRESTRESSING

PREMIXED FLAMES
Turbulence generation in combustion
[AD-A184810] 05 p0561 N88-13413
Analysis of a turbulent premixed V-flame (influence of flame-thickening)
[NAL-TR-941] 10 p1299 N88-17770
Premixed turbulent flame calculation
16 p2196 N88-23098
On the structure, propagation, extinction and stability of laminar premixed flames in dissociation equilibrium
18 p2483 N88-24728
Driving of axial acoustic fields by side-wall stabilized premixed flames 19 p2629 N88-25592
Structure of laminar, premixed flames of CH2O/NO2/O2 mixtures 19 p2632 N88-25613
Modelling of premixed combustion using a thin flame sheet and the effect of the hydrodynamic instability
[DE88-009467] 20 p2770 N88-26423

Premixed turbulent flame propagation
[AD-A192955] 21 p2909 N88-27265
Theoretical study and numerical simulation of flame fronts
[PB88-122932] 22 p3051 N88-28104
The influence of pressure on soot formation
24 p3349 N88-29934
Flamelet modeling of turbulent premixed flames
24 p3350 N88-29942
Modeling the stability of a turbulent premixed flame, downstream from a step by a Lagrangian method
24 p3350 N88-29943
Numerical modelling of premixed flames in gaseous media
24 p3350 N88-29944
Gaseous premixed flames in non-uniform flows
24 p3351 N88-29945
Optical measurements of soot and temperature profiles in premixed propane-oxygen flames
[NASA-TM-101343] 24 p3358 N88-29997
Optical measurements of soot in premixed flames
[NASA-TM-101305] 24 p3373 N88-30090

PREMIXING
Numerical simulation of turbulent premixed combustion and decay of turbulent swirling flow
[DE87-014253] 03 p0284 N88-11787
Formation and destruction of nitrous oxide in lean, premixed combustion
[DE88-001390] 05 p0562 N88-13423
Mixing fuel particles for space combustion research using acoustics
[NASA-TM-100295] 14 p1872 N88-21186
Numerical simulation of turbulent premixed combustion and decay of turbulent swirling flow
[DE88-006588] 14 p1888 N88-21284

PREPARATION
NT PRECONDITIONING
NT PRESTRESSING
NT PRETREATMENT
Specimen preparation techniques for the examination of ceramic and metal-matrix composites
[DE88-005157] 15 p2030 N88-22094
Preparation of the operational phase of the European Remote Sensing Satellite ERS-1
[BCRS-87-06] 16 p2228 N88-23307

PREPOLYMERS
NT DIMERS
Conductive polymers via reactive aligomer
[AD-A184270] 04 p0419 N88-12597

PREPREGS
Damage initiation and growth in sateen laminates under static and cyclic loading 11 p1449 N88-18634
Fatigue damage development of various CFRP-laminates
[NASA-TT-20247] 16 p2172 N88-22945

PREPROCESSING
Measurements in the functional mock up test of the NAL QSTOL aircraft control system
[NAL-TR-928] 02 p0126 N88-10793
Integration of geometric modeling and advanced finite element preprocessing 11 p1526 N88-19114

PRESELECTORS
U PREAMPLIFIERS

PRESERVING
A shape preserving interpolant which has tension controls
[DE87-014615] 02 p0229 N88-11443
Irradiation preservation of seafood: Literature review
[DE88-001691] 05 p0631 N88-13858

PRESIDENTIAL REPORTS
Space shuttle accident: NASA's actions to address the Presidential Commission report
[PB88-135306] 15 p2024 N88-22059

PRESINTERING
U SINTERING

PRESSING (FORMING)
NT STAMPING
Selection of polymer materials for manufacturing optical parts
[AD-A185898] 07 p0836 N88-15069
Fabrication of YBa2Cu3O7 superconducting ceramics
[DE88-003012] 07 p0938 N88-15701

PRESSURE
NT ATMOSPHERIC PRESSURE
NT BASE PRESSURE
NT BLOOD PRESSURE
NT DENSIFICATION
NT DYNAMIC PRESSURE
NT FLUID PRESSURE
NT GAS PRESSURE
NT GEOPRESSURE
NT HIGH PRESSURE
NT HIGH VACUUM
NT HYDROSTATIC PRESSURE
NT HYPERTENSION
NT ILLUMINANCE
NT INLET PRESSURE
NT INTERNAL PRESSURE
NT INTRACRANIAL PRESSURE
NT ISOSTATIC PRESSURE
NT LOW PRESSURE
NT LOW VACUUM
NT LOWER BODY NEGATIVE PRESSURE
NT LUMINANCE
NT LUMINOUS INTENSITY
NT OVERPRESSURE
NT OXYGEN TENSION
NT PARTIAL PRESSURE
NT RADIATION PRESSURE
NT SOUND PRESSURE
NT STAGNATION PRESSURE
NT STATIC PRESSURE
NT THRUST CHAMBER PRESSURE
NT ULTRAHIGH VACUUM
NT VACUUM
NT VAPOR PRESSURE
NT WALL PRESSURE
NT WIND PRESSURE
Effects of pressure fluctuations on nickel electrodes
[AD-A184293] 03 p0311 N88-11967
Studies of pressure-velocity coupling schemes for analysis of incompressible and compressible flows
[NASA-CR-181526] 04 p0443 N88-12748
Spectral methods: Analysis and applications to flow problems
[AD-A186265] 07 p0850 N88-15156
Pressure and mass velocity measurements in solids subjected to dynamic loadings 07 p0921 N88-15595
A simplified computer code for reduction to burning rates of closed bomb pressure-time data (MINICB)
[AD-A189112] 13 p1736 N88-20380
Lattice relaxation of the DX centers in Ga/sub 1-x/Al/sub x/As and of the pressure-induced deep donors in GaAs
[DE88-005452] 13 p1848 N88-21061
Calibration of a hot-wire/hot-film anemometer over a range of temperatures, velocities and pressures
[AD-A189717] 14 p1913 N88-21430
Monthly mean global climatology of temperature, wind, geopotential height, and pressure for 0 - 120 km
[NASA-TM-100697] 15 p2099 N88-22503
Absolute pressure derivatives of deep level defects in 3-5 semiconductors
[DE88-006318] 15 p2140 N88-22772
Theory of oxygen content, atomic ordering and oxygen diffusion in 1,2,3 superconducting oxides as a function of temperature and oxygen pressure
[DE88-007961] 19 p2735 N88-26248
The acoustic field scattered from some approximate pressure release materials
[AD-A194768] 23 p3278 N88-29515
Determination of the specific area of liquid gas and the velocity of weak pressure waves in aqueous foams
[NASA-TT-20347] 24 p3373 N88-30087

PRESSURE CABINS
U PRESSURIZED CABINS

PRESSURE CHAMBERS
NT HYPERBARIC CHAMBERS
NT VACUUM CHAMBERS
Columbus pressurized module verification
02 p0134 N88-10842
Cooling electronic equipment at simulated high altitude in hypobaric chambers
[AD-A185196] 05 p0584 N88-13560

PRESSURE DEPENDENCE
Nitrogen at very high pressure
[DE87-013800] 01 p0021 N88-10131
Ignition and combustion of metals in oxygen
04 p0407 N88-12530
Retention processes in supercritical fluid chromatography
[DE88-000079] 04 p0413 N88-12559
Experimental perspectives on heavy electron metals
[DE87-014766] 04 p0416 N88-12583
Pressure and tension dependence of phase shift of polarization modes in birefringent single-mode fiber-optic waveguide 08 p1078 N88-16501
Pressure-dependent DLTS (Deep Level Transient Spectroscopy) experiments on Si-doped AlGaAs
[DE88-003842] 13 p1846 N88-21047
Kinetic measurements of thermal decomposition of energetic materials at high pressures
[AD-A191612] 19 p2622 N88-25552

PRESSURE DISTRIBUTION
Advanced turboprop wing installation effects measured by unsteady blade pressure and noise
[NASA-TM-100200] 01 p0002 N88-10008
Transonic analysis and design of axisymmetric bodies in nonuniform flow
[NASA-CR-4101] 01 p0003 N88-10013
Time-resolved measurements of shock-induced vapor-pressure profiles
[DE87-012972] 01 p0045 N88-10289
Regime dependent analysis experiments --- sea level pressure field 02 p0209 N88-11314
Mesoscale surface field analysis from routine observations --- pressure, wind fields
02 p0209 N88-11315
High resolution determination of true surface winds at sea from wind and pressure data
02 p0210 N88-11316
An improved method of analyzing surface geostrophic winds and pressure 02 p0212 N88-11334
Investigations on a transonic airfoil with a 30 mm wide perforation/cavity arrangement
[ESA-TT-1072] 03 p0260 N88-11634
Mechanical and flow excited vibrations of elastic plates and cylindrical shells in dense fluids
03 p0316 N88-11996
An experimental investigation of unsteadiness in swept shock wave/turbulent boundary layer interactions
04 p0445 N88-12760
Application of discrete vortex method to analysis of separated flow around aerofoils
05 p0537 N88-13268
Low speed wind tunnel investigation of propeller slipstream aerodynamic effects on different nacelle/wing combinations. Part 1: Total forces and moments and pressure distributions on nacelle/wing at different angles of attack and yaw and at different thrust coefficients
[FFA-TN-1987-22] 05 p0542 N88-13302
Plasticity of aluminum and iron at high shear strain rate and high pressure 05 p0563 N88-13430
Identification of perturbations in turbomachines by the analysis of pressure signals, vibrations and wavelike motions
[ETN-88-90602] 05 p0590 N88-13600
Gas diffusion studies in steady and nonsteady cavities
[AD-A185795] 06 p0704 N88-14318
Influence of gas exchange between ocean and atmosphere on formation of atmospheric pressure field
06 p0726 N88-14467
Mean pressure distribution and geostrophic circulation in the meteor zone 06 p0734 N88-14513
Circulation in the mesosphere and lower thermosphere during the MAP (Middle Atmosphere Program)/WINE (Winter in the Northern Europe) period
06 p0734 N88-14514
A study of the mechanism of internal gravity wave generation by quasigeostrophic meteorological motions
06 p0735 N88-14520
Observations of a midlatitude squall line boundary layer wake
[AD-A185609] 06 p0746 N88-14589
Laminar flow control leading edge glove flight test article development
[NASA-CR-172137] 07 p0815 N88-14960
Numerical study of a centrifugal impeller response to a downstream static pressure perturbation
07 p0851 N88-15170
The global balance of dynamic vorticity in relation to heat sources and sinks 07 p0876 N88-15316
Sound pressure distribution in front of a serrated boundary: Standing wave suppression and diffusion
07 p0928 N88-15639
Full scale and wind tunnel surface pressure measurements on the T.R.R.L. spray dispersion programme vehicles
[REPT-8623] 09 p1114 N88-16676
Ariane 4, long version: Pressure distribution measurements on two models of different scale of the Ariane 4 nose fairings in the transonic tunnel of F+W Emmen (Switzerland) with varying tunnel configurations. Comparison with measurements taken at Modane (France) and with calculations after the Euler method
[F+W-TF-1878] 09 p1122 N88-16716
Beta limitation of matter-antimatter boundary layers
[TRITA-EPP-87-11] 09 p1250 N88-17490
The further development of circulation control airfoils
10 p1270 N88-17594
Pressure distributions and oil-flow patterns for a swept circulation-control wing 10 p1270 N88-17596
Leeside crossflow modeling in Euler space-marching computations
[NASA-TM-89710] 10 p1325 N88-17924
Spatial pressure variations and three-dimensional effects on liquid sloshing loads
[PB88-120134] 10 p1326 N88-17926
A component synthesis method using Lanczos vectors
[DE88-002263] 10 p1403 N88-18368
Pressure distributions from high Reynolds number transonic tests of an NACA 0012 airfoil in the Langley 0.3-meter transonic cryogenic tunnel
[NASA-TM-100526] 11 p1435 N88-18565
A velocity-pressure integrated, mixed interpolation, Galerkin finite element method for high Reynolds number laminar flows
[NASA-CR-179264] 11 p1486 N88-18868

Application of the multigrid technique to the pressure-correction equation for the SIMPLE algorithm — Semi-Implicit Method for Pressure Linked Equations (SIMPLE) 11 p1539 N88-19196
Compressible friction coefficients in a simulated heat pipe
[AD-A188818] 12 p1627 N88-19735
Pressure distributions and losses in a waterjet propulsion system
[AD-A188423] 12 p1633 N88-19777
Nonaxisymmetric body supersonic, aerodynamic prediction
[AD-A189338] 13 p1716 N88-20259
New definition of pressure-center coefficient of reentry craft with asymmetrical configuration 14 p1864 N88-21138
Comparison of pressure distributions on model and full-scale NACA 64-621 airfoils with ailerons for wind turbine application
[NASA-TM-100802] 14 p1943 N88-21593
High Reynolds number, low Mach number, steady flow field calculations over a NACA 0012 airfoil using Navier-Stokes and interactive boundary layer theory
[AD-A189871] 15 p2013 N88-22005
Contraction design for small low-speed wind tunnels
[NASA-CR-182747] 15 p2021 N88-22045
Structural consequences of railgun augmentation
[DE88-007036] 15 p2023 N88-22058
Investigation of side-wall effects in wind tunnel with supercritical airfoil testing 15 p2054 N88-22241
Aerothermal tests of quilted dome models on a flat plate at a Mach number of 6.5
[NASA-TP-2804] 15 p2067 N88-22325
Big whorls carry little whorls 16 p2195 N88-23094
Supersonic axial-flow fan flutter 16 p2221 N88-23255
Methodology for matching experimental and computational aerodynamic data
[NASA-TM-100592] 17 p2295 N88-23728
Pressure distributions from subsonic tests of an advanced laminar-flow-control wing with leading- and trailing-edge flaps
[NASA-TM-4040-PT-1] 17 p2300 N88-23758
Coal particle behaviour in a counter-current combustor
[TAE-606] 19 p2612 N88-25498
The pressure field generated in a cold-flow side-dump ramjet combustor 19 p2625 N88-25572
The propagation of pressure perturbations in bubbly air/water flows 19 p2664 N88-25843
Turbulence structure of mixing swirling flows
[AD-A193063] 21 p2943 N88-27478
Study of three-dimensional transonic flow separations
[AD-A193018] 22 p3037 N88-28032
Development of direct-inverse 3-D methods for applied transonic aerodynamic wing design and analysis
[NASA-CR-183127] 22 p3037 N88-28033
Prediction of the pressure distribution for radial inflow between co-rotating discs
[PNR90464] 22 p3076 N88-28261
Rotation symmetric inside flow with diametric expansion resolution
[ILR-MITT-193] 23 p3213 N88-29123
Acoustic pressure distribution on the bottom of a wedge-shaped ocean
[AD-A193961] 23 p3278 N88-29518
Pressure distributions from subsonic tests of an advanced laminar-flow-control wing with leading- and trailing-edge flaps
[NASA-TM-4040-PT-2] 24 p3321 N88-29776
An experimental study of an adaptive-wall wind tunnel
[NASA-CR-183152] 24 p3329 N88-29821
The effects of incoming boundary layer thickness on unsteady shock-induced turbulent separations induced by cylinders
[AD-A196190] 24 p3368 N88-30060
Studies on pressure response of gas bubbles contributions of condensed droplets in bubbles generated by a uniform nucleation
[NASA-TT-20343] 24 p3370 N88-30068

PRESSURE DRAG
NT INTERFERENCE DRAG
NT SUPERSONIC DRAG
The pressure drag and momentum flux during a cold frontal passage over the Alps 13 p1800 N88-20763
Multi-body aircraft with an all-movable center fuselage actively controlling fuselage pressure drag
[NASA-CASE-LAR-13511-1] 17 p2301 N88-23765

PRESSURE EFFECTS
Pressure effects on the thermal stability of SiC fibers
[NASA-TM-100146] 01 p0019 N88-10120
Apparatus for storing kinetic energy
[EP-PATENT-0-181-736-A1] 01 p0066 N88-10422
A numerical and analytical investigation of Rayleigh-Taylor instability in a solid tungsten plate
[DE87-013593] 01 p0087 N88-10562
Elastic moduli of copper under compression
[DE87-013137] 02 p0147 N88-10922
Nonsteady-state vibrations in acoustic medium of elastic elliptical shell subjected to instantaneously applied uniform pressure 02 p0160 N88-11000
Shock-induced cooling in dense fluids
[DE87-014343] 02 p0170 N88-11067
Pressure structure of solar coronal loops 02 p0256 N88-11618
Processing and properties of SiC/Nicalon composites
[DE87-013885] 03 p0279 N88-11757
Effects of cure pressure on resin flow, voids, and mechanical properties
[AD-A184267] 03 p0295 N88-11853
Millimeter-wave studies of moist air
[AD-A184681] 03 p0306 N88-11935
Effects of pressure fluctuations on nickel electrodes
[AD-A184293] 03 p0311 N88-11967
The Moessbauer effect of SnI4 at high pressure
[DE87-014771] 04 p0495 N88-13048
Fluid mass and thermal loading effects on the modal characteristics of space shuttle main engine liquid oxygen inlet splitter vanes 05 p0594 N88-13626
JPRS report: Science and technology. Japan
[JPRS-JST-87-028] 06 p0675 N88-14130
Pressure induced phase transitions, superconductivity of phosphorus described 06 p0675 N88-14134
Study of some superconducting and magnetic materials on high T sub c oxide superconductors
[NASA-CR-182330] 06 p0785 N88-14813
Effect of high pressure oxygen loading on the superconductivity of La2CuO4
[DE88-002108] 06 p0787 N88-14827
Model for plasma equilibrium configuration evolution in a tokamak with adiabatic compression
[DE88-700354] 07 p0936 N88-15684
Effects of commercial cladding on the fracture behavior of pressure vessel steel plates
[DE88-004333] 10 p1303 N88-17790
Evaluation of spare room in cerebrospinal system using noninvasive methods 10 p1361 N88-18137
Quick actuating closure and handling system 14 p1925 N88-21476
Pressure induced ageing of polymers 14 p1929 N88-21504
Modifications to the Langley 8-foot transonic pressure tunnel for the laminar flow control experiment
[NASA-TM-4032] 15 p2021 N88-22047
Oil flow patterns on a series of capsule-type re-entry vehicles at hypersonic speeds
[DE88-751805] 16 p2155 N88-22858
Electronic structure of matter at high compression: Isostructural transitions and approach of the Fermi-gas limit
[MPQ-124] 16 p2266 N88-23551
Unsteady flow in a supercritical supersonic inlet 18 p2460 N88-24605
Structure/property/reactivity relations among nitramine and other energetic materials
[AD-A190878] 18 p2481 N88-24716
Optical pressure sealing couping (light joint)
[NASA-CASE-MFS-29348-1] 18 p2576 N88-25303
Pressure/temperature sensitive inorganic phosphors 19 p2627 N88-25583
Nonlinear mechanisms of solid propellant combustion instability 19 p2628 N88-25588
Life in a hyperbaric environment. A new O2-H2 breathing mixture for industrial diving 19 p2695 N88-26019
Contribution of ultrasonic Doppler detection of circulating bubbles to human interventions under the sea and in space 19 p2697 N88-26029
Deep level defects in semiconductors: Stress and pressure studies
[DE88-010855] 21 p3024 N88-27948
Influence of peak pressure on the substructure evolution and shock wave profiles of Ti-6Al-4V
[DE88-006458] 23 p3225 N88-29197
Mechanics of thrust fault formation 23 p3231 N88-29229
Origin of SNC kaersutitic amphibole: Experimental data 23 p3306 N88-29693
Comparison of the performance of a reverse flow annular combustion chamber under low and high pressure conditions 24 p3347 N88-29923

PRESSURE FIELDS
U PRESSURE DISTRIBUTION

PRESSURE GAGES
NT BAROMETERS
NT IONIZATION GAGES
NT PIEZOELECTRIC GAGES
NT VACUUM GAGES
Calibration of a Harwood DWT-1000 controlled-clearance piston gauge
[DE88-004496] 11 p1489 N88-18888

PRESSURE GRADIENTS
Local heat/mass transfer and pressure drop in a two-pass rib-roughened channel for turbine airfoil cooling
[NASA-CR-179635] 03 p0322 N88-12039
The formation of optical membrane reflector surfaces using uniform pressure loading
[DE87-012275] 03 p0376 N88-12367
NCSU code: Validation and extension on NAL's UNIVAC 1100/60 system
[PD-FM-8716] 04 p0476 N88-12931
Statistical theory of turbulent incompressible multimaterial flow
[DE88-000435] 05 p0579 N88-13535
Asymptotic analysis of a turbulent boundary layer in a strong adverse pressure gradient
[AD-A185406] 05 p0581 N88-13543
Mean velocities and Reynolds stresses in the juncture flow and in the shear layer downstream of an appendage
[AD-A185819] 08 p0980 N88-15923
Study of resistive pressure-gradient-driven turbulence
[DE88-005062] 10 p1414 N88-18441
Shock wave/turbulent boundary layer interaction in high-Reynolds-number hypersonic flows
[AD-A188029] 11 p1434 N88-18555
Numerical model of the time independent mean flow in a rotating rocket motor 13 p1733 N88-20360
The turbulent heat flux in low Mach number flows with large density variations
[DE88-006445] 14 p1911 N88-21419
An experimental investigation of rocket ramjet nozzle assembly base pressures
[AD-A189714] 15 p2027 N88-22076
ALEX results: A comparison of measurements from a round and a rectangular duct with 3-D code predictions
[DE88-005947] 15 p2135 N88-22741
On local approximations of the pressure-strain term in turbulence models 16 p2197 N88-23102
Computational wing design studies relating to natural laminar flow 17 p2297 N88-23740
Surface curvature and pressure gradient effects on turbulent flow: An assessment based on numerical solution of the Reynolds equations 17 p2336 N88-23954
HeFlow: A program for calculating pressure and temperature of helium in forced-flow superconductors. Part 1: Numerical solutions. Part 2: HeFlow user's manual
[DE88-008941] 20 p2876 N88-27071
Experimental and analytical study of two-phase flow in zero gravity
[AD-A195223] 24 p3358 N88-29993

PRESSURE ICE
Underwater acoustic backscatter from a model of arctic ice open leads and pressure ridges
[AD-A184693] 03 p0354 N88-12234
Physical and structural characteristics of Weddell Sea pack ice
[AD-A188189] 10 p1358 N88-18119
MIZEX (marginal ice zone experiment) 1987 SAR (Synthetic Aperture Radar) data summary
[AD-A195560] 24 p3364 N88-30035

PRESSURE MEASUREMENT
Base pressure measurements on a missile body with cruciform tail
[ESA-TT-1062] 03 p0270 N88-11695
Study of aeropropulsion laboratory pressure drop rig and recommended test procedure
[AD-A184333] 03 p0322 N88-12038
Fluctuating pressure loads under high speed boundary layers
[NASA-TM-100517] 05 p0647 N88-13962
Performance of low upper-shelf material under pressurized-thermal-shock loading (PTSE-2)
[DE88-002297] 07 p0832 N88-15049
Multi-component stress history measurements and analysis
[DE88-000977] 09 p1168 N88-17004
A reliable data collection/control system 10 p1289 N88-17708
Development and application of oxygen flow tagging for velocity measurements and flow visualization in turbulent three-dimensional supersonic flows
[AD-A187982] 10 p1289 N88-17714
The use of optical fibers for shock pressure and timing measurements at high pressures
[DE88-004012] 10 p1334 N88-17971
Flash threshold of shocked aluminum silicofluoride
[DE88-003978] 10 p1339 N88-18005
Verification of the momemtum theory for rotors using measurements on a model helicopter
[R-840-S] 13 p1718 N88-20275
Formulation of a general technique for predicting pneumatic attenuation errors in airborne pressure sensing devices
[NASA-TM-100430] 13 p1723 N88-20302

Exhaust-gas pressure and temperature survey of F404-GE-400 turbofan engine
[NASA-TM-88273] 13 p1724 N88-20307
Remote fiber fluorimetry techniques for pressure measurements
[DE88-004486] 13 p1773 N88-20604
Evaluation of a theory for pressure-strain rate 16 p2198 N88-23108
Relations between two-point correlations and pressure strain terms 16 p2198 N88-23109
Initial condition effect on pressure waves in an axisymmetric jet
[NASA-TM-100915] 16 p2209 N88-23184
Unsteady pressure and structural response measurements of an elastic supercritical wing
[NASA-TM-100591] 17 p2299 N88-23756
Pressure measuring probe
[NASA-CASE-LAR-13853-1] 17 p2341 N88-23961
Calibration of averaging total pressure flight wake rake and natural-laminar-flow airfoil drag certification
[NASA-CR-181630] 19 p2599 N88-25443
Velocity-pressure integrated versus penalty finite element methods for high Reynolds number flows
[NASA-CR-179357] 20 p2803 N88-26635
Evaluation of a multi-point method for determining acoustic impedance
[NASA-TM-100637] 20 p2849 N88-26913
Shock initiation studies on heterogeneous explosives
[DE88-008681] 21 p2923 N88-27351
Control and use of unsteady flows: Insect use of various wing kinematics and related pressure measurements using a pitching airfoil 21 p2926 N88-27366
Measurement of pressure fluctuations in a resonant chamber with laser-induced iodine fluorescence
[DFVLR-FB-87-53] 21 p2955 N88-27551
A resistive-film based force transducer for the study of exercise
[AD-A192601] 21 p2986 N88-27730
Energy distribution and transfer in flowing hydrogen microwave plasmas 21 p3019 N88-27919
Steady and unsteady transonic pressure measurements on a clipped delta wing for pitching and control-surface oscillations
[NASA-TP-2594] 23 p3173 N88-28895
Intrinsic and extrinsic energy states of semiconductors and heterostructures using novel techniques
[DE88-008560] 23 p3289 N88-29582
Laser Doppler Velocimeter (LDV) and pressure measurements of gas particle flows in bends
[VKI-TN-163] 24 p3372 N88-30083

PRESSURE OSCILLATIONS
Predictions of F-111 TACT aircraft buffet response and correlations of fluctuating pressures measured on aluminum and steel models and the aircraft
[NASA-CR-4069] 05 p0529 N88-13218
Longitudinal mode combustion instabilities in air breathing engines 06 p0680 N88-14166
Gas diffusion studies in steady and nonsteady cavities
[AD-A185795] 06 p0704 N88-14318
Investigation of instability, dynamic forces, and effect of dynamic loading on strength of cages for the bearings in the high pressure oxygen turbopumps for the space shuttle main engine
[NASA-CR-178970] 06 p0714 N88-14378
Pressure measurements of impinging jet with asymmetric nozzle
[NASA-CR-182759] 15 p2014 N88-22011
Low frequency pressure oscillations in a model ramjet combustor 19 p2625 N88-25571
The pressure field generated in a cold-flow side-dump ramjet combustor 19 p2625 N88-25572
Dynamics and stability of combustion driven self oscillations in presence of various frequencies. Extensive stability criteria
[ETN-88-92123] 20 p2771 N88-26432
Observed normal mode structure of low frequency oscillations 22 p3128 N88-28595

PRESSURE PROBES
U PRESSURE SENSORS

PRESSURE PULSES
Operating loading of piping systems
[ETN-88-91057] 11 p1484 N88-18856
Theoretical and experimental analysis of pressure pulse transmission in non-Newtonian pipe flow 11 p1485 N88-18863
Transient interaction of electromagnetic pulses in dielectrics and microwave biophysics
[AD-A195687] 24 p3360 N88-30008

PRESSURE RATIO
Performance characteristics of magnesium-sodium nitrate flares in oxygen-nitrogen atmospheres
[AD-A185274] 05 p0570 N88-13476
Small High Pressure Ratio Turbines — conference
[VKI-LS-1987-07] 06 p0712 N88-14364
Development of a supersonic steam turbine with a single stage pressure ratio of 200 for generator and mechanical drive 06 p0713 N88-14374
Improvement of the Reynolds-stress model by a new pressure-strain correlation
[NASA-CR-182699] 13 p1783 N88-20667

PRESSURE RECORDERS
A resistive-film based force transducer for the study of exercise
[AD-A192601] 21 p2986 N88-27730

PRESSURE RECOVERY
Compressible friction coefficients in a simulated heat pipe
[AD-A188818] 12 p1627 N88-19735

PRESSURE REDUCTION
A study of two-phase flow in a reduced gravity environment
[NASA-CR-172035] 04 p0422 N88-12617
Two-phase flow forms and pressure drop in horizontal T tube joints with vertical branch
[GKSS-87/E/12] 09 p1163 N88-16969
Composite reduced Navier-Stokes procedures for flow problems with strong pressure interactions
[AD-A191127] 18 p2508 N88-24875
Pressure drop and heat transfer in turbulent non-Newtonian pipe flow of advanced energy transmission fluids
[DE88-010021] 19 p2666 N88-25853
Decompression procedures and accidents in space and sea 19 p2698 N88-26035
Characteristics of pressure loss during filtration using a porous ceramic filter
[DE88-752547] 20 p2798 N88-26604
The use of fins to reduce the pressure drop in a rotating cavity with a radial flow
[PNR90465] 22 p3079 N88-28282

PRESSURE REGULATORS
Zero-G thermodynamic vent system for shuttle/Centaur 08 p0983 N88-15943
A control system for maintaining high stability in gas pressure
[DE88-003712] 09 p1175 N88-17042

PRESSURE RIDGES
U PRESSURE ICE

PRESSURE SENSORS
Calibration of a five hole probe and testing of an evaluation method for flow field measurements
[ESA-TT-1051] 03 p0325 N88-12051
Polymer materials for pressure sensors 06 p0676 N88-14141
Thin film electret boundary layer transition detector: A feasibility study
[AD-A185675] 07 p0856 N88-15199
An integrated pressure sensor for in-vivo use 10 p1333 N88-17965
Preparation of thin film polyvinylidene fluoride shock wave pressure transducers
[PB88-156070] 11 p1490 N88-18893
Photonic temperature and pressure sensors for biosystems/pulsed microwave. Part 1: Interaction studies
[AD-A188887] 12 p1629 N88-19751
Formulation of a general technique for predicting pneumatic attenuation errors in airborne pressure sensing devices
[NASA-TM-100430] 13 p1723 N88-20302
High Reynolds number pump facility for cavitation research
[AD-A189310] 13 p1765 N88-20558
A 150,000 pounds per square inch dynamic pressure calibrator
[AD-A190659] 15 p2069 N88-22335
Boundary layer measurements using hot-film sensors 17 p2297 N88-23743
Pressure measuring probe
[NASA-CASE-LAR-13853-1] 17 p2341 N88-23961
The 1986 IEEE Solid-State Sensor Workshop
[AD-A190922] 19 p2668 N88-25860
Characteristics of polysilicon layers and their application in sensors 19 p2669 N88-25861
Design and construction techniques for planar polysilicon pressure transducers with piezoresistive read-out 19 p2669 N88-25862
Stress modeling of microdiaphragm pressure sensors 19 p2670 N88-25873
Noise in piezoresistive and capacitive sensors 19 p2670 N88-25874
An integrated on-chip pressure sensor for accurate control applications 19 p2671 N88-25880
Simulation of diaphragm-type IC pressure sensors 19 p2672 N88-25887
Resonant structures for integrated sensors 19 p2673 N88-25893
Deposition techniques and properties of strain compensated LPCVD silicon nitride films 19 p2673 N88-25898
A resistive-film based force transducer for the study of exercise
[AD-A192601] 21 p2986 N88-27730
The pneumatic wind shear sensor: A tool for meteorological investigations and flight management 22 p3036 N88-28024
Further improvements relating to the temperature compensation of semiconductor strain gauge pressure transducers
[RAE-TR-87061] 22 p3081 N88-28298

PRESSURE SUITS
NT EXTRAVEHICULAR MOBILITY UNITS
NT SPACE SUITS
Research and development of anti-G life support systems. Part 1: Development and evaluation of uniform-pressure anti-G suits
[AD-A185658] 06 p0754 N88-14628
Effects of anti-g suit inflation on renin and aldosterone response physical exercise 12 p1659 N88-19944
Renal effects of anti-gravity suit inflation in man in relation to cardiovascular and hormonal changes 12 p1661 N88-19959
Design, development and evaluation of Stanford/Ames EVA prehensors
[NASA-CR-182688] 15 p2105 N88-22540

PRESSURE TRANSDUCERS
U PRESSURE SENSORS

PRESSURE VESSEL DESIGN
The structures of large wound propulsion shells --- carbon fiber composites filament winding
[SNIAS-872-430-116] 05 p0559 N88-13406

PRESSURE VESSELS
NT PREBURNERS
Nondestructive inspection of the pressure vessel in Stuttgart. ALOK part. Phase 1: ALOK combined with conventional probes
[REPT-860113-TW] 01 p0057 N88-10367
Microstructural characterization of irradiated PWR steels using the atom probe field-ion microscope
[DE88-000341] 03 p0291 N88-11828
Making space nickel/hydrogen batteries lighter and less expensive
[DE88-000168] 05 p0578 N88-13530
Geometrically nonlinear analysis of stiffened panels 06 p0722 N88-14440
An automated flow calorimeter for heat capacity and enthalpy measurements at elevated temperatures and pressures
[DE88-002357] 07 p0857 N88-15206
Summary of HSST wide-plate crack-arrest tests and analyses
[DE88-002601] 08 p1000 N88-16061
Proceedings of the International Workshop on Engineering Design of Next Step Reversed Field Pinch Devices
[DE88-001915] 09 p1251 N88-17494
Effects of commercial cladding on the fracture behavior of pressure vessel steel plates
[DE88-004333] 10 p1303 N88-17790
Acoustic emission measurements of PWR weld materials with inserted defects
[AERE-R-12386] 10 p1341 N88-18016
Fracture mechanics and creep crack growth of 1 percent Cr 1/2 percent Mo steel with and without prior exposure to creep conditions
[NLR-TR-86051-U] 13 p1743 N88-20426
Fracture toughness characterization of SA508 and Sa533B RPB steels
[CISE-3908] 14 p1889 N88-21292
Remote maintenance design activities and research and development accomplishments for the compact ignition tokamak
[DE88-006980] 16 p2279 N88-23645
Cellular thermosetting fluoropolymers and process for making them
[NASA-CASE-GSC-13008-1] 17 p2326 N88-23894
Stress corrosion cracking of A723 steel pressure vessels: Two case studies
[AD-A191741] 18 p2527 N88-24990
Investigation of leaks in fiberglass-reinforced pressure vessels by direct observation of hollow fibers in glass cloth
[DE88-006936] 19 p2609 N88-25485
The effect of compression on individual pressure vessel nickel/hydrogen components
[NASA-TM-101312] 22 p3052 N88-28109
Elastic-plastic analysis of part-through crack propagation in piping and pressure vessels
[DE88-701619] 23 p3225 N88-29198

PRESSURE WAVES
U ELASTIC WAVES

PRESSURE WELDING
NT DIFFUSION WELDING
NT EXPLOSIVE WELDING
NT ULTRASONIC WELDING

Inertia welding with variable magnitude of impact load
14 p1897 N88-21328
Apparatus for pressure welding of titanium structures with a controlled rate of deformation
[RAE-TRANS-2161] 19 p2677 N88-25915
Equipment for the pressure welding of metals and alloys utilising the effects of superplasticity
[RAE-TRANS-2162] 22 p3055 N88-28129

PRESSURIZED CABINS
The SAGA highly autonomous assistance submarine
19 p2696 N88-26034

PRESSURIZED WATER REACTORS
Two-phase flow forms and pressure drop in horizontal T tube joints with vertical branch
[GKSS-87/E/12] 09 p1163 N88-16969

PRESSURIZING
Research and development of anti-G life support systems. Part 1: Development and evaluation of uniform-pressure anti-G suits
[AD-A185658] 06 p0754 N88-14628
Pressurizing systems and air conditioning systems
[MBB/LKE-312/S/PUB/246] 13 p1812 N88-20828
Evaluation of fracture models through pressurized-thermal-shock testing
[DE88-011834] 21 p2963 N88-27603
A study of flame spreading and combustion phenomena of stick propellants
[AD-A193598] 22 p3052 N88-28106

PRESTON TUBES
U PITOT TUBES

PRESTRAINING
U PRESTRESSING

PRESTRESSING
Reinforced flexural elements for TEMP-STRESS Program
[DE87-012961] 01 p0061 N88-10391
Buckling and breakdown problems in structural mechanics. Failure of prestressed double-walled containers or rings
[MBB-UR-E-956/87] 13 p1783 N88-20671
Forced motion of initially stressed shells and plates
18 p2529 N88-25005
A simple unified method for predicting the deflections of reinforced concrete structures
19 p2679 N88-25930
Preloaded brake disc
[NASA-CASE-MSC-21132-1] 23 p3223 N88-29181
Free vibration of rectangular plates with a small initial curvature
[NASA-CR-179370] 24 p3383 N88-30148

PRETESTS
U TESTS

PRETREATMENT
NT PRESTRESSING
Method for preparing hydride configurations and reactive metal surfaces
[DE88-000845] 06 p0679 N88-14161
Growth and characteristics of materials for tunable lasers in the near infrared spectral region
[NASA-CR-182501] 11 p1491 N88-18901
A modified sulphuric acid anodising process used as a pretreatment for the adhesive bonding of aluminum alloys
[ARE-TM(UMM)-87410] 16 p2177 N88-22974
Colloidal characterization of silicon nitride and silicon carbide 17 p2325 N88-23883

PRETWISTING
U PRESTRESSING
U TWISTING

PREVENTION
NT ACCIDENT PREVENTION
NT CORROSION PREVENTION
NT FIRE PREVENTION
NT ICE PREVENTION
An adaptive subdivision method with crack prevention for rendering beta-spline objects
[AD-A184249] 04 p0477 N88-12940
Summary of Payload Integration Plan (PIP) for Starlab-1 flight experiment, enclosure 3
[NASA-TM-89713] 11 p1522 N88-19086

PRIMARY BATTERIES
NT ALKALINE BATTERIES
NT METAL AIR BATTERIES
NT NICKEL ZINC BATTERIES
NT SODIUM SULFUR BATTERIES
NT THERMAL BATTERIES
NT ZINC-OXYGEN BATTERIES
Development of standard cells in NMOS technology for the design of digital integrated circuits
[FI-62-TB-6] 03 p0310 N88-11953
The kinetics of charge-transfer reactions on passive lithium electrodes
[DE88-009256] 21 p2939 N88-27454

PRIMARY COSMIC RAYS
NT SOLAR COSMIC RAYS
Heavy element compositions and energy spectra of galactic and solar cosmic rays 03 p0272 N88-11714
Multiply charged particles in primary cosmic rays with energy less than or equal to 2 TeV
07 p0921 N88-15596
Charge composition of primary cosmic ray nuclei with z greater than or equal to 2 in energy region greater than or equal to 2 TeV 24 p3448 N88-30519

PRIMATES
NT HUMAN BEINGS
NT MONKEYS
Morphological manifestations of primate adaptation to orthograde statics and walking erect
10 p1386 N88-18162
Psychophysical, biochemical and histological studies of spectrally selective photic damage to primate retina
[AD-A188115] 11 p1517 N88-19063

PRIMERS (COATINGS)
Polyitaconic acid macromolecule primer for adhesive bonding and corrosion control of aluminum
17 p2319 N88-23849
Water based primers for structural adhesive bonding of aircraft 17 p2321 N88-23862
Primerless RTV silicones
[BDX-613-3807] 24 p3356 N88-29980

PRIMERS (EXPLOSIVES)
Stability of the high-temperature G-16 primer composition
[DE88-006201] 15 p2049 N88-22206

PRIMITIVE EARTH ATMOSPHERE
Exobiology and life science 07 p0883 N88-15358
Photochemical and thermal modeling in the early atmosphere of the earth
[NASA-CR-183029] 18 p2543 N88-25093

PRIMITIVE EQUATIONS
Implicit solution of the incompressible Navier-Stokes equations in primitive variables on non-staggered grids
10 p1326 N88-17930

PRINCIPAL COMPONENTS ANALYSIS
Effective use of principal component analysis with high resolution remote sensing data to delineate hydrothermal alteration and carbonate rocks 05 p0612 N88-13758
Illustrative examples of principal component analysis using GENSTAT/PCP
[AD-A185085] 05 p0644 N88-13941
Multistep component analysis of correlations
08 p1009 N88-16115
Environmental gradient analysis, ordination, and classification in environmental impact assessments
[AD-A187294] 11 p1509 N88-19016
Use of principal component method for analysis of multidimensional quantitative data in biomedical investigations 19 p2706 N88-26089

PRINTED CIRCUITS
The 8.4-GHz low-noise maser pump source assembly
04 p0436 N88-12705
Single-layer wire routing
[AD-A186990] 09 p1157 N88-16932
Random vibration (stress screening) of printed wiring assemblies 11 p1499 N88-18953
VAXELN experimentation: Programming a real-time clock and interrupt handling using VAXELN Ada 1.1
[AD-A188100] 11 p1525 N88-19107
Fabrication and electrical characterization of multilevel aluminum interconnects used to achieve silicon-hybrid wafer-scale integration
[AD-A190519] 15 p2060 N88-22282
The use of rule induction to assist in the diagnosis of avionic circuit board defects
[ETN-88-92077] 16 p2162 N88-22899
The inspection of electronic metallurgical bonds
[AD-A192197] 18 p2486 N88-24745
Thermal cycling tests on surface-mount assemblies
[DE88-007695] 21 p2939 N88-27453
Procedures for identification and handling of Printed Circuit Boards (PCBs)
[AD-A191177] 23 p3206 N88-29078

PRINTERS
NT PRINTERS (DATA PROCESSING)
The Quick Response Multicolor Printer (QRMP) system
[AD-A188140] 11 p1504 N88-18982
Report on desktop publishing
[AD-A187698] 11 p1528 N88-19128

PRINTERS (DATA PROCESSING)
Microvax networked computer system
[AD-A190308] 15 p2114 N88-22596

PRINTING
NT LITHOGRAPHY
NT PHOTOLITHOGRAPHY
The Quick Response Multicolor Printer (QRMP) system
[AD-A188140] 11 p1504 N88-18982
Synthesis and characterization of high-T(sub c) screen-printed Y-Ba-Cu-O films on alumina
[NASA-TM-100860] 15 p2146 N88-22805
Maps for the blind and methods of their production
16 p2227 N88-23298

PRIORITIES
A multi user random access communication system for users with different priorities
[AD-A186041] 07 p0841 N88-15102
Physics rationale for the engineering specifications for ZTH
[DE88-000938] 07 p0936 N88-15690
A note on the effect of preemptive policies on the stability of a priority queue
[AD-A186871] 09 p1227 N88-17345

PRISMS
Optical alignment of Centaur's inertial guidance system
[NASA-TM-88844] 04 p0405 N88-12515

PRIVACY
Incorporation of privacy elements in space station design
[NASA-CR-182748] 14 p1881 N88-21242
Computer resource management technology program (PE 64740F). Task no. 9: Advanced user authentication
[PB88-183066] 18 p2555 N88-25163

PRIVATE AIRCRAFT
U GENERAL AVIATION AIRCRAFT

PROBABILITY
U PROBABILITY THEORY

PROBABILITY DENSITY FUNCTIONS
NT NORMAL DENSITY FUNCTIONS
NT RAYLEIGH DISTRIBUTION
NT WEIBULL DENSITY FUNCTIONS
Analyses and assessments of span wise gust gradient data from NASA B-57B aircraft
[NASA-CR-178288] 01 p0002 N88-10007
Conditional second order closure for turbulent shear flows
[AD-A185369] 05 p0581 N88-13542
Dual cylindrical wave Laser-Doppler method for measurement of skin friction in fluid flow
06 p0700 N88-14297
HOC spectral analysis of an almost periodic random sequence in noise
[AD-A185528] 06 p0765 N88-14697
Estimation of multivariate binary density using orthonormal functions
[AD-A186386] 07 p0912 N88-15528
Necessary and sufficient conditions for the convergence of integrated and mean-integrated r-th order error of histogram density estimates
[AD-A186037] 07 p0914 N88-15550
Photoionization of atoms and ions: Application of time-dependent response method within the density functional theory
[AD-A185686] 07 p0930 N88-15649
An APL function for bivariate normal probabilities
[AD-A186535] 09 p1232 N88-17382
Some majorization inequalities for functions of exchangeable random variables
[AD-A188207] 11 p1536 N88-19178
Envelope and phase statistics for non-Gaussian noise and resulting error probabilities for digital communications systems 12 p1617 N88-19672
Bragg-cell receiver study
[NASA-CR-182684] 13 p1781 N88-20535
Electromagnetic shadowing by an exponentially distributed rough surface
[AD-A189677] 14 p1906 N88-21391
Electromagnetic scattering by an exponentially distributed rough surface with the introduction of a rough surface generation technique
[AD-A189678] 14 p1906 N88-21392
Filtering of jump processes
[AD-A189701] 15 p2123 N88-22656
Almost sure L(gamma)-norm convergence for data-based histogram density estimates
[AD-A189944] 17 p2393 N88-24228
Probabilistic finite element methods
18 p2564 N88-25223
Direct numerical simulations of the PDF's (Probability Density Functions) of a passive scalar in a forced mixing layer
[AD-A192134] 18 p2568 N88-25256
Cluster analysis of multiple planetary flow regimes
[NASA-CR-182931] 18 p2594 N88-25418

PROBABILITY DISTRIBUTION FUNCTIONS
Analyses and assessments of span wise gust gradient data from NASA B-57B aircraft
[NASA-CR-178288] 01 p0002 N88-10007
Investigation of reliability of strength values measured on CFRP test bars by statistical methods. Part 1: Probability distributions for strength analysis
[ESA-TT-1036] 03 p0336 N88-12115
Propagation of random initial conditions in time
04 p0486 N88-12993

An urn model for the multi-sample capture/recapture sequential tagging process
[AD-A184470] 04 p0486 N88-12998
Comparing hard and soft prior bounds in geophysical inverse problems
[NASA-CR-181557] 05 p0624 N88-13820
Explicit formulate for the distributions of stopping variables under Wald's truncated SPRT (Sequential Probability Radio Tests) for a poisson process
[AD-A185053] 05 p0640 N88-13914
A three-parameter generalisation of the beta-binomial distribution with applications
[AD-A185733] 06 p0768 N88-14720
On the extreme points of the set of all 2xn bivariate positive quadrant dependent distributions with fixed marginals and some applications
[AD-A186316] 07 p0911 N88-15521
The information metric for univariate linear elliptic models
[AD-A186385] 07 p0911 N88-15527
Some new approaches to multivariate probability distributions
[AD-A186038] 07 p0914 N88-15551
Strong representation of weak convergence
[AD-A186433] 07 p0916 N88-15563
Contributions to selection and ranking theory with special reference to logistic populations
[AD-A185629] 07 p0917 N88-15568
Measuring the dependence between two point processes through confidence intervals for the second order distribution
[AD-A186735] 08 p1074 N88-16481
Dependence of the expectancy of hitting on the number of spread shots. Determination of the expectancy of hitting using a spread salvo
[REPT-FM6] 10 p1310 N88-17829
The convergence rate for the strong law of large numbers: General lattice distributions
[AD-A187560] 10 p1402 N88-18362
Extrema of Gaussian process by simulation
11 p1541 N88-19211
Bragg-cell receiver study
[NASA-CR-182684] 13 p1761 N88-20535
Hadronic overlap and total multiplicity distributions in high energy physics collisions
[NIKHEF-H/87-10] 13 p1838 N88-21001
Advanced probabilistic methods for quantifying the effects of various uncertainties in structural response
15 p2080 N88-22401
Memory efficient evaluations of nonlinear stochastic equations and C3 applications
[AD-A189872] 15 p2110 N88-22569
Some comments on quadrant dependence in higher dimensions
[AD-A190329] 15 p2121 N88-22639
Structural decomposition of multiple time scale Markov processes
[AD-A189739] 15 p2123 N88-22657
A note on phase-type, almost phase-type, generalized hyperexponential and Coxian distribution, revision
[AD-A191236] 16 p2261 N88-23517
On solvability of an equation arising in the theory of M-estimates
[AD-A193059] 21 p3006 N88-27828
Polynomial definition of discrete field points of map of diffusion equation, part 1
[AD-A193697] 23 p3271 N88-29467

PROBABILITY THEORY

A problem in quantum probability --- statistical invariants problem
[REPT-87-06] 01 p0088 N88-10573
Components and cycles of a random function
[DE87-014155] 02 p0228 N88-11437
An empirical investigation of the use of ranks in pips sampling
[DE87-010609] 02 p0228 N88-11438
A probabilistic model of brittle crack formation
[AD-A184423] 03 p0338 N88-12129
More on the decoder error probability for Reed-Solomon codes 04 p0435 N88-12699
Foundations of O-theory 2: Measurements and relation to fuzzy set theory
[DE88-000013] 04 p0485 N88-12986
Lower bounds on bearing accuracy for closely spaced sources
[AD-A184258] 04 p0486 N88-12997
Subjective probability, combination of expert opinion and probabilistic approaches to information retrieval
04 p0501 N88-13085
Approximating multivariate normal orthant probabilities using the Clark algorithm
[AD-A184855] 05 p0634 N88-13873
Point processes
[AD-A185398] 05 p0641 N88-13921
Isotropic probability measures in infinite dimensional spaces: Inverse problems/prior information/stochastic inversion
[NASA-CR-181555] 05 p0643 N88-13936
The adaption and use of research codes for performance assessment
[DE88-000552] 06 p0756 N88-14639
Subcritical branching processes in a two state random environment, and a percolation problem on trees
[PB87-230439] 06 p0762 N88-14677
Packet error probabilities in frequency-hopped spread spectrum packet radio networks. Markov frequency hopping patterns considered
[AD-A186071] 07 p0841 N88-15104
Reliability and survivability of communication networks
[AD-A186248] 07 p0842 N88-15109
An elementary approach to the Daniell-Kolmogorov theorem and some related results
[AD-A186011] 07 p0909 N88-15505
Spectral representation of infinitely divisible processes
[AD-A186210] 07 p0910 N88-15515
On determining the weight for obtaining a large number of items
[AD-A186181] 07 p0915 N88-15553
Monte Carlo simulation of triangulated random surfaces in grand canonical ensemble
[DE88-700378] 07 p0941 N88-15718
A flux analysis of the solar cells
[INPE-4247-PRE/1120] 08 p1022 N88-16186
Short pseudorandom test sequences
[AD-A185883] 08 p1054 N88-16357
Electronic factors for K-shell-electron conversion probability and electron-positron pair formation probability in electric monopole transitions
[DE87-753040] 08 p1089 N88-16551
Probabilistic neural networks: In or out of equilibrium
[DE88-002907] 09 p1201 N88-17198
An application of fuzzy set theory to statistical hypothesis testing
[AD-A186705] 09 p1232 N88-17386
The evolution of naval warfare technology and the impact of space systems
[AD-A186900] 09 p1233 N88-17392
The impact of deployment rates on the effectiveness of strategic defenses
[AD-A186907] 09 p1233 N88-17393
Response of wind shear warning systems to turbulence with implication of nuisance alerts
10 p1274 N88-17618
Development of a graphics based two-attribute utility assessment program with application to mission planning
[AD-A187276] 10 p1388 N88-18292
Explicit solutions of moment problems, 1
[AD-A186018] 10 p1397 N88-18325
Asymptotic expansions for large deviation probabilities in the strong law of large numbers
[AD-A187432] 10 p1402 N88-18361
Probabilistic and reliability design procedures for flexible airfield pavements: Elastic layered method
[AD-A187533] 11 p1442 N88-18600
A lower bound for the decoder error probability of the linear MDS code 11 p1472 N88-18780
Frame synchronization performance and analysis
11 p1473 N88-18787
Derivation of strength factors related to the coordination of the strength of transmission line components --- electric power lines
[S/T-REPT-VOL-5-NO-2] 11 p1500 N88-18959
Generating the states of a probabilistic system
[AD-A187896] 11 p1540 N88-19208
Joint moments of the maximum in a critical branching process
[AD-A188157] 11 p1541 N88-19209
A computer code for the solution of large scale network reliability analysis problems
[AD-A188455] 12 p1680 N88-20042
Estimation of the probability of a long time to the first entrance to a state in a semi-Markov model
[AD-A188960] 12 p1685 N88-20074
Uncertain knowledge in distributed systems
[AD-A189017] 12 p1685 N88-20076
Convolution metrics and rates of convergence in the CLT (Central Limit Theorem)
[AD-A189341] 12 p1686 N88-20084
Characteristics of the positive lighting flash
[DE88-005854] 13 p1800 N88-20760
On the theory of the conversion of metallic mixed phases. 5: Fluctuations and nucleation in sub-cooled phases
[NASA-TT-20249] 14 p1890 N88-21296
Deterministic approximations of probability inequalities
[REPT-87-43] 14 p1966 N88-21732
Macroscopic quantum jumps in a single atom
14 p1975 N88-21784
Multiple model parameter adaptive control for in-flight simulation
[AD-A190568] 15 p2021 N88-22044
Probabilistic structural analysis computer code (NESSUS) 15 p2079 N88-22397
A probabilistic approach to low-level vision
[AD-A189041] 15 p2107 N88-22553
Mathematics clinic probabilistic position-fixing
[NASA-CR-182753] 15 p2125 N88-22672
Coordinate-momentum probability operator for point particles in a stationary electromagnetic field
[DE88-701165] 16 p2188 N88-23044
Applicability and limitations of probability models in connection with the reliability of large-scale technical installations
[W-3/87] 16 p2261 N88-23520
Restrictions in activity monitoring through remote sensing 17 p2365 N88-24084
Induction of models under uncertainty
[NASA-TM-101173] 17 p2394 N88-24230
Additive prophet inequalities for transforms of uniformly bounded pairwise independent random variables
[PB88-173513] 18 p2568 N88-25250
A perspective of PC-based probabilistic risk assessment
[DE88-006715] 18 p2568 N88-25251
Transition probabilities in OH A 2 sigma + - X 2 pi i: Bands with v prime = 0 and 1, v double prime = 0 to 4
[NASA-CR-182946] 18 p2584 N88-25353
Narrative compression coding for a channel with errors
[AD-A191577] 19 p2642 N88-25673
Study of probabilistic fatigue crack growth and associated scatter under constant-and-variable amplitude loading spectrum
[AD-A192027] 19 p2679 N88-25929
Timing regulations to prevent stratospheric-ozone depletion
[R-3495-JMO/RC] 19 p2690 N88-25987
Antenna heights for the optimum utilization of the oceanic evaporation duct. Part 3: Results from the Mediterranean measurements, volume 2
[AD-A192311] 20 p2791 N88-26554
Improved procedure for impact probability computation of aircraft crash based on Balfanz model
[JUEL-SPEZ-425] 21 p2894 N88-27176
Probabilistic anisotropic failure criteria for composite materials
[AD-A193046] 21 p2904 N88-27232
Computation of failure probability of fatigue loaded cracked structures
[ETN-88-92360] 21 p2964 N88-27607
Distributed algorithms for probabilistic solution of computational vision problems
[AD-A193150] 21 p2997 N88-27773
The computation of stationary distributions on Markov chains through perturbations
[AD-A193191] 21 p3009 N88-27855
Comparison of results based on a deterministic versus a statistical uncertainty analysis
[DE88-010751] 21 p3010 N88-27858
Probabilistic structural analysis to quantify uncertainties associated with turbopump blades
[NASA-TM-100278] 22 p3050 N88-28094
A probabilistic model of the apparent radiance of a rough sea
[AD-A193867] 22 p3129 N88-28602
Extremal two-correlations of two-valued stationary one-dependent processes
[REPT-88-01] 22 p3145 N88-28704
Use of Markov probability and reliability model generation methods in the analysis of reliability of a fault tolerant hardware and software based system with flexible repair policies
[PNR90467] 22 p3145 N88-28706
Analysis of the effect of faulty spares on the performance of diagnostic algorithms in reliable systems
[AD-A193526] 23 p3223 N88-29186
Mathematical algorithms for approximate reasoning
23 p3262 N88-29418
Minimizing escape probabilities: A large deviations approach
[AD-A194534] 23 p3275 N88-29496
Sequential approach to Colombeau's theory of generalized functions
[DE88-701869] 23 p3276 N88-29503
Influence of pairing correlations on the probability and dynamics of tunneling through the barrier in fission and fusion of complex nuclei
[DE88-701500] 23 p3286 N88-29570
Fatigue crack propagation: Probabilistic modeling and statistical analysis
[AD-A195885] 24 p3384 N88-30155
Venture theory: A model of decision weights
[AD-A194809] 24 p3426 N88-30391

PROBLEM SOLVING
NT ALTERNATING DIRECTION IMPLICIT METHODS
NT ASYMPTOTIC METHODS
NT ITERATIVE SOLUTION
NT THEOREM PROVING

Problem specifications and collated solutions of the two-phase numerical-benchmark exercise 1986-7 — two phase flow
[CFDU/87/1] 01 p0047 N88-10300

A study of carbon monoxide distribution determinations for a global transport model
[NASA-CR-181423] 01 p0067 N88-10432

A look at the evolution of mathematical software for dense matrix problems over the past fifteen years
[DE87-011485] 01 p0081 N88-10517

The reliability of numerical solutions of ordinary differential equations, obtained by implicit calculation schemes
[PTB-W-30] 01 p0085 N88-10549

On the maximum of solutions for a semilinear elliptic problem
[REPT-87-08] 01 p0086 N88-10554

Synthesizing controllers for uncertain systems by a quantitative pole-placement
[PB87-195590] 02 p0223 N88-11403

Oscillatory and nonoscillatory properties of first order differential equations with piecewise constant deviating arguments
[DE87-703061] 02 p0225 N88-11418

Technology applications branch graphics projects
[AD-A184621] 03 p0364 N88-12291

Performance evaluation of artificial intelligence systems
[AD-A184054] 03 p0368 N88-12316

Analogical inference and analogical access
[AD-A184345] 03 p0369 N88-12321

Implementation of the Runge-Kutta-Fehlberg method for solution of ordinary differential equations on a parallel processor
[AD-A184660] 03 p0370 N88-12331

Numerical solution of bound constrained problems
[DE88-000653] 03 p0371 N88-12334

Solution of nonlinear least-squares problems
[AD-A184010] 03 p0371 N88-12335

Design of digital filters for electronic instrumentation
[PB87-100418] 04 p0438 N88-12716

Principles for problem aggregation and assignment in medium scale multiprocessors
[NASA-CR-178379] 04 p0476 N88-12935

A model of functional knowledge and insight
[AD-A184113] 04 p0483 N88-12975

Back-of-the-envelope problems
[AD-A184105] 04 p0484 N88-12980

A 3-D Euler solution for hypersonic Mach numbers
05 p0533 N88-13240

Two low-order mixed methods for the elasticity problem
[PB87-225272] 05 p0610 N88-13749

Indirect solution of static problems using concurrent vector processing computers
[DE87-012105] 05 p0636 N88-13889

Application of the Von Karman equation to the bifurcation theory
[NOTA-INTERNA-891] 05 p0642 N88-13927

The solution of large linear inverse problems
06 p0691 N88-14238

Artificial intelligence systems
06 p0761 N88-14670

Tools and technologies for expert systems: A human factors perspective 06 p0797 N88-14882

Development of a prototype H-46 helicopter diagnostic expert system
[AD-A186077] 07 p0809 N88-14924

New methods for numerical solution of one class of strongly nonlinear partial differential equations with applications
[AD-A186166] 07 p0899 N88-15445

Investigation and implementation of an algorithm for computing optimal search paths
[AD-A185927] 07 p0902 N88-15461

UNITY: A framework for study of parallel programming problem-solving
[AD-A185616] 07 p0906 N88-15490

Optimal repeated measurements designs for comparing test treatments with a control
[AD-A185999] 07 p0917 N88-15569

Finite element fundamentals, part 1
08 p0985 N88-15961

Comparative performance of the conjugate gradient and SOR (Successive Over Relaxation) methods for computational thermal hydraulics
[DE88-002553] 08 p0988 N88-15986

Solution in vibration problems of rectangular plates with spline function
[PB87-143459] 08 p0996 N88-16029

Cirrus: An automated protocol analysis tool
[AD-A186646] 08 p1052 N88-16348

Deriving descriptions of the mind
[AD-A186647] 08 p1052 N88-16349

Problem solving as intelligent retrieval from distributed knowledge sources 08 p1059 N88-16392

Discovery and problem solving: Triangulation as a weak heuristic 08 p1062 N88-16412

Commonality analysis as a knowledge acquisition problem 08 p1062 N88-16413

Qualitative models for planning: A gentle introduction
08 p1062 N88-16414

Interfacing the expert: Characteristics and requirements for the user interface in expert systems
08 p1063 N88-16419

Case-based reasoning for space applications: Utilization of prior experience in knowledge-based systems
08 p1065 N88-16433

Application of artificial intelligence to impulsive orbital transfers 08 p1066 N88-16439

FOR3D: A computer model for solving the LSS (Lee-Sead-Schultz) three-dimensional, wide angle wave equation
[AD-A186649] 08 p1080 N88-16511

An initial investigation into methods of computing transonic aerodynamics sensitivity coefficients
[NASA-CR-182444] 09 p1112 N88-16863

Team problem solving: Effects of communication and function overlap
[AD-A187010] 09 p1152 N88-16898

Tutoring electronic troubleshooting in a simulated maintenance work environment
09 p1204 N88-17215

Performance analysis of parallel branch and bound search with the hypercube architecture
09 p1206 N88-17229

The empirical accuracy of uncertain inference models
09 p1208 N88-17243

Trimodal interpretation of constraints for planning
09 p1209 N88-17248

Advanced decision aiding techniques applicable to space 09 p1209 N88-17250

Explicit-implicit methods for time-dependent partial differential equations
[CWI-NM-R8703] 09 p1228 N88-17355

On exact solutions of multidimensional Schroedinger equation with polynomial potentials
[DE88-700460] 09 p1230 N88-17373

A fast Riemann solver with constant covolume applied to the random choice method
[CAR-87-19] 09 p1231 N88-17375

Continuous deformation algorithm on the product space of unit simplices, revised version
[PB88-114210] 10 p1387 N88-18281

A visual programming environment for the Navier-Stokes computer
[NASA-CR-181615] 10 p1390 N88-18299

Knowledge base refinement by monitoring abstract control knowledge, revision 1
[AD-A187502] 10 p1397 N88-18323

Applications of Lie group methods to the equations of magnetohydrodynamics 10 p1411 N88-18422

Finite element methods of analysis for high speed viscous flows
[NASA-CR-182529] 11 p1483 N88-18852

Modeling incorrect responses to multiple-choice items with multilinear formula score theory
[AD-A187887] 11 p1522 N88-19090

Effects of stress on judgement and decision making in dynamic tasks
[AD-A188203] 11 p1523 N88-19092

EqL: The language and its implemantation
[AD-A188161] 11 p1530 N88-19137

Subroutines for solving the equation of diffusion in media with anisotropic properties
[DE88-700743] 11 p1536 N88-19179

A signal processing approach to the numerical solution of parabolic differential equations
11 p1539 N88-19197

Extrema of Gaussian process by simulation
11 p1541 N88-19211

The construction of a pedagogy to promote meaningful learning of strategies and tactics for solving problems of elementary combinatorics
[AD-A187928] 11 p1542 N88-19216

Learning by experimentation
[AD-A188912] 12 p1681 N88-20053

Northeast Artificial Intelligence Consortium (NAIC) administrative matters and ancillary functions, volume 1
[AD-A189466] 12 p1682 N88-20055

The inverse problem and the pseudo-empirical orthogonal function method of solution. Part 1: Theory; Part 2: Application
[AD-A188894] 12 p1684 N88-20069

Management information systems design implications: The effect of cognitive style and information presentation on problem solving
[AD-A188850] 12 p1705 N88-20205

Text organization and comprehensibility in technical writing
[AD-A188913] 12 p1707 N88-20217

NASA/UK TAP
[NASA-CR-180350] 12 p1708 N88-20223

Finite element methods for quasi-prismatic bodies with application to gears 13 p1779 N88-20644

A personalized and prescriptive decision aid for choice from a database of options
[AD-A188726] 13 p1811 N88-20820

An implementation of the OPS5 language for computers compatible with IBM-PC
[INPE-4291-PRE/1162] 13 p1821 N88-20882

New way to solve Volterra equations of the second kind
[PB88-148820] 13 p1828 N88-20931

Parallel algorithms for mapping pipelined and parallel computations
[NASA-CR-181655] 14 p1960 N88-21687

Comparative analysis
[AD-A190556] 15 p2065 N88-22313

A zonal approach for the solution of coupled Euler and potential solutions of flows with complex geometries
[AD-A189752] 15 p2114 N88-22595

Numerical solution of nonlinear algebraic equations in stiff ODE solving
[DE88-006634] 15 p2118 N88-22622

About disequations simplification
[RR-645-I-IMAG-55-LIFIA] 15 p2119 N88-22624

Admissible Bayes tests for structural relationship
[AD-A190326] 15 p2125 N88-22669

Water facilities in retrospect and prospect: An illuminating tool for vehicle design
16 p2200 N88-23126

Iterative finite element solver on transputer networks
16 p2218 N88-23235

Problem solving in a natural task as a function of experience
[AD-A191180] 16 p2243 N88-23399

Extending problem solver capabilities through case-based inference
[AD-A191332] 16 p2243 N88-23401

Vectorization of the odd-even hopscotch scheme and the alternating direction implicit scheme for the two-dimensional Burgers' equations
[CWI-NM-R8720] 16 p2249 N88-23440

On the trajectory of a linear programming problem
[REPT-87-53] 16 p2250 N88-23442

Capitalizing on failure through case-based inference
[AD-A190927] 16 p2255 N88-23480

Generalizing the structure of explanations in explanation-based learning
[AD-A191327] 16 p2256 N88-23481

A new block solver for large, full, unsymmetric, complex systems of linear algebraic equations
[AD-A190590] 16 p2256 N88-23483

Continuous decoupling transformations for linear boundary value problems
[ETN-88-92248] 16 p2258 N88-23493

Extracting information from problem solving experience
[AD-A191331] 16 p2286 N88-23688

Numerical modelling of flows using phoenics
17 p2339 N88-23955

A proposal of adaptation of a knowledge-based scene analysis model to some remote sensing problems
17 p2354 N88-24026

Navigation system from AVHRR data from NOAA series satellites 17 p2359 N88-24054

A proposal of adaptation of a knowledge-based scene analysis model to some remote sensing problems
17 p2362 N88-24068

Human problem solving in complex dynamic environments
[AD-A190788] 18 p2551 N88-25142

A mixed-integer linear programming problem which is efficiently solvable
[AD-A191028] 18 p2556 N88-25168

Algorithms and software for solving finite element equations on serial and parallel architectures
[NASA-CR-183027] 18 p2559 N88-25191

Optimal a priori covariance selection for the solution of ill-conditioned nonlinear inverse problems
18 p2564 N88-25222

Mixed min-max optimization problem with restrictions
18 p2565 N88-25232

Multigrid methods for elliptic Partial Differential Equations (PDEs)
[CWI-NM-R8722] 18 p2566 N88-25242

Similarity solutions of nonlinear partial differential equations invariant to a family of affine groups
[DE88-003404] 18 p2567 N88-25245

Numerical calculation of three dimensional flow by TVD scheme 19 p2638 N88-25649
La Recherche Aerospatiale, bimonthly bulletin, no. 1986-5, 234/September-October
[ESA-TT-1032] 19 p2641 N88-25671
Scaling laws for geomagnetic tail current sheet acceleration
[AD-A193379] 19 p2691 N88-25998
Accurate, productive aerodynamic simulation on patched mesh systems
[AD-A192040] 19 p2714 N88-26110
Accurate, productive aerodynamic simulation on patched mesh systems
[AD-A192040] 19 p2714 N88-26110
Engineering research centers and their evaluation
[PB88-180054] 19 p2739 N88-26262
An initial investigation into methods of computing transonic aerodynamic sensitivity coefficients
[NASA-CR-183061] 20 p2752 N88-26332
Use of direct solvers for multidimensional fluid flow computations
[DE88-010063] 20 p2799 N88-26611
Vibration frequencies of tapered bars with nonclassical boundary conditions
[NASA-CR-183059] 20 p2813 N88-26688
Inference and discovery in an exploratory laboratory
[AD-A192231] 20 p2832 N88-26801
Challenge problems focusing on equality and combinatory logic: Evaluating automated theorem-proving programs
[DE88-010057] 20 p2844 N88-26879
Combining expert opinions: An optimization framework
[REPT-87-84] 20 p2846 N88-26895
Boundary layer solutions for the free-edge problem in composite laminates 21 p2904 N88-27229
The integration of decision support problems into feature modeling based design 21 p2927 N88-27372
Effects of numerical dissipation on finite-volume solutions of compressible flow problems
[AD-A193173] 21 p2944 N88-27485
An investigation of techniques for determination of optimum/self-optimizing systems
21 p2963 N88-27600
Inspection methods in programming: Cliches and plans
[AD-A192782] 21 p2996 N88-27767
Simulation of real time problem solving
[AD-A193436] 21 p2997 N88-27778
Implementing direct, spatially isolated problems on transputer networks
[NASA-TM-101297] 21 p3000 N88-27796
Intelligent Mobile Autonomous System (IMAS)
[AD-A193181] 21 p3003 N88-27811
Transonic blade-vortex interactions
22 p3037 N88-28035
Heat exchanger demonstration expert system
22 p3066 N88-28193
On the pseudo-linearization problem for nonlinear systems
[AD-A194021] 22 p3142 N88-28683
General analytic solution of certain functional equations of addition type
[PREPRINT-583] 22 p3144 N88-28699
On recognizing ignorance 23 p3254 N88-29372
AI tools in computer based problem solving
23 p3263 N88-29424
Distributed knowledge base systems for diagnosis and information retrieval
[AD-A193107] 23 p3296 N88-29633
Resonance excitation of linear and non-linear spiral density waves in a gaseous disk
23 p3299 N88-29643
Reducing the parallel solution time of sparse circuit matrices using reordered Gaussian elimination and relaxation
[AD-A195152] 24 p3366 N88-30045
MOORE: A prototype expert system for diagnosing spacecraft problems 24 p3418 N88-30343
Research on problem-solving systems
[AD-A195154] 24 p3423 N88-30370
Multiple solutions and bifurcation for a class of nonlinear Sturm-Liouville eigenvalue problems on an unbounded domain
[AD-A195954] 24 p3426 N88-30389
Barriers to Information Transfer and Approaches Toward Their Reduction
[AGARD-CP-430] 24 p3437 N88-30458
Linguistic barriers: Translation problems
24 p3438 N88-30465
Formulation and solution of economic equilibrium problems
[AD-A196034] 24 p3439 N88-30470

PROCEDURES
NT BOUNDARY INTEGRAL METHOD
NT CREW PROCEDURES (INFLIGHT)
NT CREW PROCEDURES (PREFLIGHT)
NT FINITE ELEMENT METHOD
NT FINITE VOLUME METHOD
NT OPTICAL CORRECTION PROCEDURE
NT PANEL METHOD (FLUID DYNAMICS)
Study of aeropropulsion laboratory pressure drop rig and recommended test procedure
[AD-A184333] 03 p0322 N88-12038
Implementation of a new shock testing procedure using nonstationary random excitation
[DE87-014643] 04 p0456 N88-12827
The how and why of variable amplitude testing
05 p0603 N88-13690
The use of alloy 117 as a liquid metal current collector
[AD-A185740] 06 p0698 N88-14281
AVHRR/HIRS (Advanced Very High Resolution Radiometer/High Resolution Infra-Red Sounder) operational method for satellite based sea surface temperature determination
[PB88-107594] 06 p0708 N88-14340
A re-evaluation of fatigue threshold test methods
06 p0717 N88-14401
Practical photochemistry: General considerations
[PB87-123386] 06 p0730 N88-14491
Development and testing of an interactive procedure for the improvement of objective analyses
[AD-A186595] 08 p1040 N88-16290
Using output to evaluate and refine rules in rule-based expert systems 08 p1055 N88-16362
Are windshear training aid recommendations appropriate for other than large jet transports? Pilot procedures: Shear models 10 p1275 N88-17635
Supercritical fluid extraction-gas chromatography of Volatile Organic Compounds (VOC) from tenax devices
[PB88-124300] 10 p1298 N88-17759
Research on a solar biotechnology based on the culture of photosynthetic cells
[DE88-900129] 10 p1359 N88-18120
Air traffic control
[FAA-ORDER-7110.65E] 12 p1576 N88-19426
A procedure for estimating the crystal densities of organic explosives
[AD-A189023] 12 p1613 N88-19646
A simplified streamline swallowing procedure for the windward meridian of axisymmetric blunt bodies
[AD-A188413] 12 p1626 N88-19732
Selling to NASA
[NASA-TM-89724] 12 p1705 N88-20208
Software verification using partition analysis
[AD-A190570] 15 p2112 N88-22582
Test procedures and standards for mechanical property measurements on metal matrix composites
[NPL-DMA(A)-153] 16 p2172 N88-22944
Benefits of an object approach in a computer aided design environment
[SNIAS-881-440-102] 21 p3000 N88-27791

PROCEEDINGS
U CONFERENCES
U CONGRESSIONAL REPORTS

PROCESS CONTROL (INDUSTRY)
Optimization of a controlled two-server maintenance system
[INPE-4202-PRE/1083] 01 p0107 N88-10694
Needs assessment for NDT and characterization of ceramics: Assessment of inspection technology for green state and sintered ceramics
[DE87-013550] 02 p0151 N88-10947
A fundamental study of the mechanical and microstructural response of elevated temperature PM aluminum-titanium alloys 03 p0289 N88-11819
Avionics and corrosion 05 p0547 N88-13336
Advances in processing techniques for nickel aluminides
[DE87-014571] 05 p0566 N88-13449
Statistical process control applied to the liquid-fed ceramic melter process
[DE88-000271] 05 p0569 N88-13471
Master plots for predicting the case-depth in laser surface treatments
[PB87-221875] 05 p0586 N88-13574
Using hierarchically structured problem-solving knowledge in a rule-based process planning system
[DE87-011639] 05 p0639 N88-13906
A study of the Department of Defense configuration management policies and procedures as applied to the FA-18 Strike/Fighter program
[AD-A184872] 05 p0657 N88-14034
High temperature adhesive
[PB87-109229] 06 p0683 N88-14186
Glassy GeO2 obtained by the gel process
[NASA-TT-20125] 06 p0685 N88-14201
Knowledge acquisition for a simple expert controller
[NASA-TT-20118] 06 p0761 N88-14672
Fluid mechanical issues in polymer processing
[DE88-002767] 08 p0972 N88-15880
Improved silicon nitride for advanced heat engines
[NASA-CR-175006] 08 p0973 N88-15886
Innovating systems and techniques for the diagnosis of materials and industrial plants
[CISE-3856] 08 p0976 N88-15901
Intelligent process development of foam molding for the Thermal Protection System (TPS) of the space shuttle external tank 08 p1060 N88-16397
A problem of machine repair with a variable number of heterogeneous servers
[INPE-4245-PRE/1118] 08 p1074 N88-16482
Experience of developing an integrated nondestructive assay system
[DE88-003149] 09 p1184 N88-17092
Some process control/design considerations in the development of a microgravity mammalian cell bioreactor 09 p1197 N88-17174
Fabrication and materials evaluation of high performance aligned ceramic fibre reinforced glass matrix composite
[AERE-R-12517] 10 p1294 N88-17736
Measurements as a process
[DE88-005275] 11 p1497 N88-18938
The influence of processing variables on physical properties of sol-gel derived TiO2 films
[DE88-005155] 11 p1559 N88-19331
Development of metastable processing paths for high temperature alloys
[AD-A188682] 12 p1608 N88-19617
Reducing time required for the development of avionic systems 12 p1702 N88-20185
Prototype manufacturing techniques for reducing cost, schedule, and technical risk 12 p1702 N88-20189
Recommended replacements for tetryl in Australian production fuzes and related ordnance
[MRL-R-1089] 13 p1754 N88-20489
EDF's studies and first choices regarding the design of electrical equipment
[NASA-TT-20222] 13 p1764 N88-20553
Improvements in end point detection --- semiconductor fabrication
[RSRE-MEMO-4035/A] 14 p1899 N88-21336
Measurement of emissivity of industrial surfaces using a simple method
[NASA-TT-20165] 15 p2036 N88-22130
Application and technology requirements for heat pumps at the process industries
[DE88-006740] 15 p2062 N88-22293
A fault tolerant supervision system
[INPE-4419-TDL/307] 15 p2148 N88-22819
Information systems for quality. Experience at the Nerviano Aeritalia plant. Avionic systems and equipment group
[ETN-88-92274] 15 p2148 N88-22821
Automatic control of an industrial process and computer aided process control by means of an expert system
[LAAS-88-004] 16 p2255 N88-23476
Simultaneous use of artificial intelligence and Petri nets: Application to the monitoring of a fabrication plan
[LAAS-87-354] 17 p2390 N88-24207
Sensors for process control requirements for design and test 19 p2671 N88-25877
Effect of process conditions on aluminum oxide thin film used in pH ISFET 19 p2673 N88-25892
Granulation of pyrotechnic tracer composition R284T
[MRL-TN-528] 20 p2780 N88-26490
Industrial processes influenced by gravity
[NASA-CR-182140] 20 p2782 N88-26497
The knowledge based automatic extraction of the machinable surfaces for automatic CAD-CAM system
[INPE-4542-PRE/1288] 20 p2835 N88-26824
The hole of a blanket tritium system on the fusion fuel cycle
[DE88-010007] 20 p2859 N88-26983
Ceramic processing of high-T(sub)c superconductors
[DE88-010090] 20 p2878 N88-27087
Processing and properties of advanced aluminum alloys
[AD-A193224] 21 p2912 N88-27284
Optical diagnostics for metallurgical processes
[DE88-009255] 21 p2913 N88-27289
Use of microwave measuring systems for the nondestructive control of resins and composites
[REPT-881-430-123] 21 p2959 N88-27576
Nondestructive tests and high performance composite structures
[SNIAS-881-430-119] 23 p3188 N88-28969
Molecular composites processing and properties, 1
[AD-A194113] 23 p3189 N88-28974
Advanced processing and properties of high performance alloys
[AD-A193767] 23 p3194 N88-29010
Material and process selection and quality control for ESA space systems and associated equipment
[ESA-PSS-01-70-ISSUE-3] 23 p3224 N88-29190
Preliminary investigation of flow modeling during solid propellant processing
[AD-A196168] 24 p3357 N88-29987

PROCESSORS (COMPUTERS)
U CENTRAL PROCESSING UNITS
PROCUREMENT
NT GOVERNMENT PROCUREMENT
Specialized instrumentation for computational fluid dynamics research
[AD-A188160] 11 p1482 N88-18849
Electric vehicle demonstration project
[DE88-004078] 11 p1566 N88-19376
Commonality in the design and production of the H-423 (F3) and H-770 (F-15) RLG inertial navigation systems
12 p1577 N88-19431
Selling to NASA
[NASA-TM-89724] 12 p1705 N88-20208
Developing systems using state-of-the-art CAD/CAM technology 17 p2306 N88-23795
PROCUREMENT POLICY
Generic specifications for hybrid microcircuits
[ESA-PSS-01-608-ISSUE-2] 06 p0696 N88-14273
Promotion of European components for ESA projects
09 p1128 N88-16764
The technical reporting and approval procedure for materials and processes
[ESA-PSS-01-700-ISSUE-1] 22 p3162 N88-28833
The cost and performance implications of reliability improvements in the F-16A/B
[AD-A195096] 24 p3324 N88-29796
PRODUCT DEVELOPMENT
Development of a polyimide matrix for filament winding with improved extensibility and fracture toughness for permanent use at 200 C
[BMFT-FB-T-86-118] 01 p0030 N88-10190
Robotic sensors and actuators for a service manipulator system. Volume 3, phase A report and program plan
[MATRA-EPT/DT/VT187/228]
01 p0054 N88-10343
ESA technological research activities on lightweight mirrors — spaceborne interferometry
01 p0096 N88-10629
Development of a pilot plant for the production of rapidly solidified aluminum alloy powders
[BMFT-FB-T-86-153] 02 p0146 N88-10914
Development of highly porous calcium silicate hydrate materials with extremely low thermal conductivity
[BMFT-FB-T-86-164] 02 p0150 N88-10941
A 1987 progress report of manufacturing techniques for Gravity Probe B gyroscope rotors
[NASA-TM-100312] 02 p0176 N88-11101
Commercial perspective of an imaging spectrometer development program 03 p0340 N88-12138
Production of flows for aeroballistic investigation in the shock tubes of the Franco-German Research Institute (ISL), Saint-Louis (France)
[ISL-R-113/86] 05 p0541 N88-13295
Carbon-carbon composites and Aerospatiale. State of the art and prospects
[SNIAS-872-430-106] 05 p0559 N88-13401
A contribution to the realization of active filters for high frequency applications
[ETN-88-90811] 06 p0696 N88-14272
Design, production, and characterization of broadband optical waveguides
[DFVLR-FB-85-52] 06 p0780 N88-14791
Past, present and future role of Black Brant rocket systems to support international space science programs 08 p1034 N88-16272
The appropriate use of contract types in development contracts (a systems approach with emphasis on the European space sector)
[ESA-STR-222] 08 p1092 N88-16573
Specialist support for projects: Activities, methods and infrastructure 09 p1124 N88-16729
The objectives and methods of the technological research program 09 p1124 N88-16730
Technology developments to meet tomorrow's need for higher satellite frequencies 09 p1124 N88-16732
The Ariane launcher and its progress
09 p1125 N88-16742
The new approach to the definition of the ESA technological research program
09 p1127 N88-16763
The Ariane-3 program 09 p1128 N88-16771
Solid fuel combustion chamber
[VTH-LR-515] 09 p1141 N88-16842
Study for history of technology developments in European space projects
[REPT-8518-1] 10 p1286 N88-17690
The intelligent wing. Aerodynamic development direction for future passenger aircraft
[MBB-UT-006/87] 10 p1313 N88-17848
Trends in the development of space transportation systems
[MBB-UR-911/86] 10 p1315 N88-17857
Microgravity and Materials Processing Facility study (MMPF): Requirements and Analyses of Commercial Operations (RACO) preliminary data release
[NASA-CR-179309] 11 p1466 N88-18742
Splinter generator
[MBB-UA-1048/87] 11 p1491 N88-18897
The light pulse generator 869 for high speed investigations
[MPIS-9/1987] 11 p1491 N88-18898
Conception and realization of components for a microchannel-plate detector, and testing of the detector system in the laboratory and in astronomical use
[ETN-88-91495] 11 p1491 N88-18899
Automatic riveting machine for spherically-formed airframe structures
[ETN-88-91024] 11 p1495 N88-18924
Status of emerging technologies: An economic/technological assessment to the year 2000
[PB88-155775] 11 p1567 N88-19381
Assessment, development and application of combustor aerothermal models
[NASA-TM-100290] 12 p1582 N88-19469
EVA, the technological challenge
12 p1592 N88-19535
Multi-axis control of telemanipulators
12 p1593 N88-19539
Planning, construction, and commissioning of a vacuum apparatus with a cold surface for the measurement of transistor functions at 20 K
[JUEL-SPEZ-397] 12 p1622 N88-19703
Flight Vehicle Development Time and Cost Reduction
[AGARD-CP-424] 12 p1700 N88-20173
Risk reduction cost avoidance for full scale development begins with concept formulation
12 p1700 N88-20174
Picking winners: Parametric cost estimating and project management 12 p1700 N88-20176
Parametric study of the total cost of aircraft modernization in terms of development and equipment series costs 12 p1700 N88-20177
The increased time and cost of development: Causes and (some) remedies 12 p1701 N88-20178
Reasons for increasing development cost of rotary wing aircraft and ideas to reverse the trend
12 p1701 N88-20179
What can be done to face growing development costs
12 p1701 N88-20181
Optimizing powerplant design and development cycles
12 p1701 N88-20183
Reducing rotary wing aircraft development time/cost through the use of simulation 12 p1702 N88-20186
The use of simulation in the development of the Airbus 12 p1702 N88-20188
Use of demonstration/validation prototypes: Impact on total development costs and times
12 p1703 N88-20194
Engineering management for validation prototype phase 12 p1703 N88-20195
People, procedures, performance: The keys to improving the development environment 12 p1704 N88-20197
Organization of helicopter development activities with a view toward reduction of costs and cycles
12 p1704 N88-20200
Advanced Gas Turbine (AGT) technology development project
[NASA-CR-180891] 12 p1709 N88-20230
Pressurizing systems and air conditioning systems
[MBB/LKE-312/S/PUB/246] 13 p1812 N88-20828
Principles of a low-cost laser gyro for rotating vehicles and platforms
[DFVLR-MITT-87-15] 14 p1912 N88-21425
Further development of a stellar camera following the rotation-modulation-collimator principle for balloon-borne observations in the X-ray range
[ETN-88-91496] 14 p1913 N88-21428
French Multiproject Chip (MPC) activity report, 1986
[RR-650-I] 15 p2059 N88-22273
Development and qualification of an Augmented Electro-Thermal Hydrazine-Thruster (AEHT) with 0.1 to 0.2 N vacuum thrust
[BMFT-FB-W-86-012] 16 p2169 N88-22931
International commercialization of remote sensing
[BCRS-87-14] 16 p2228 N88-23310
Summary of the activities performed during the Botany Facility (BF) predevelopment phase for the Life Support S/S (LSS)
[TB-RB524-002/87] 17 p2376 N88-24133
P-Plus: Polar Platform utilization study, executive summary
[BAE-TP-8391] 18 p2469 N88-24653
Development of mirrors for high-precision laser gyroscopes 18 p2517 N88-24931
Navigation using the Teldix fiber-optic gyroscope
18 p2517 N88-24933
New semiconductor laser structure for an optical communication system
[ETN-88-92353] 20 p2807 N88-26654
Design of high performance microcomputers for numerical data processing
[ETN-88-92371] 20 p2835 N88-26818
Delfi-3 as a development environment for expert systems
[REPT-8767] 20 p2839 N88-26845
Investigation of expert system design approaches for electronic design environments
21 p2926 N88-27365
Planning for AIMS on the next generation 7J7 aircraft
22 p3035 N88-28017
Reaching for the skies: The Ariane family story and beyond. An introduction to Europe's successful series of space transportation systems
[ESA-BR-42] 22 p3048 N88-28078
Sensors adapted for acoustic detection
22 p3148 N88-28731
Starting point of a project: Decision mechanisms — space projects 22 p3159 N88-28806
The development phases of a project — space projects 22 p3159 N88-28807
Development of a glass fiber wing following the construction regulation FAR Part 23
[ETN-88-92966] 23 p3189 N88-28979
Development of a multiport-hybrid-mode exciter for use in antennas for polarimetric field measurements
[REPT-12-87] 23 p3205 N88-29075
Next-generation space manipulator
23 p3263 N88-29428
PRODUCTION COSTS
NT AIRCRAFT PRODUCTION COSTS
Making space nickel/hydrogen batteries lighter and less expensive
[DE88-000168] 05 p0578 N88-13530
A problem of machine repair with a variable number of heterogeneous servers
[INPE-4245-PRE/1118] 08 p1074 N88-16482
Production costs of hydrocarbon fuels from biomass
[DE88-006667] 18 p2495 N88-24804
PRODUCTION ENGINEERING
NT PRODUCTION PLANNING
Development and production of new and modified powders for sprayed coatings and components for saving important raw materials
[BMFT-FB-T-86-129] 01 p0025 N88-10159
Fabrication of microstructures with extreme structural heights by vacuum reaction injection molding and electroforming
[KFK-4267] 01 p0033 N88-10210
Development of a pilot plant for the production of rapidly solidified aluminum alloy powders
[BMFT-FB-T-86-153] 02 p0146 N88-10914
Selected aspects of microelectronics technology and applications: Numerically controlled machine tools. Technology trends series no. 2
[PB87-132973] 06 p0696 N88-14268
Effects of processing variables on the behavior of E-glass/913 and XAS carbon fibre/913 laminates subjected to hot/wet environmental conditions
[BR101940] 09 p1138 N88-16820
Advanced manufacturing management current and forthcoming technologies
[PNR90445] 22 p3159 N88-28802
PRODUCTION METHODS
U PRODUCTION ENGINEERING
PRODUCTION PLANNING
XCUT: A rule-based expert system for the automated process planning of machined parts
[DE87-011638] 05 p0639 N88-13905
Using hierarchically structured problem-solving knowledge in a rule-based process planning system
[DE87-011639] 05 p0639 N88-13906
An extended Cobb-Douglas form for use in production economics
[AD-A186372] 07 p0943 N88-15733
Product planning in civil aircraft construction
[MBB-UT-002/87] 10 p1313 N88-17849
Viscosity methods in optimal control of distributed systems
[AD-A188086] 10 p1401 N88-18357
PRODUCTIVITY
NBS (National Bureau of Standards) calibration services users guide: Fee schedule
[PB87-210654] 01 p0090 N88-10586
Implementing and managing change: A guide for assessing information technology
[DE88-000035] 02 p0249 N88-11571
Spinoff, 1987
[NASA-TM-89652] 02 p0250 N88-11577
The effect of radiation on the long term productivity of a plant based CELSS 03 p0361 N88-12271

Report on phase 1 of the project estimate development of a model for yield estimation of sugar cane based on LANDSAT and agromet data
[INPE-4466-RPE/560] 12 p1638 N88-19807
JPRS report: Science and technology. USSR: Life sciences
[JPRS-ULS-88-002] 12 p1665 N88-19982
Efficiency of human workers and means to increase it 12 p1666 N88-19986
Time and cost reduction through computer integrated manufacture 12 p1703 N88-20191
Improved flight test productivity using advanced on line data systems 12 p1703 N88-20193
People, procedures, performance: The keys to improving the development environment 12 p1704 N88-20197
Practical image analysis using personal computers: The Canadian experience 17 p2356 N88-24037
Interpretation of MSS/LANDSAT data for evaluation of physical distribution of mangroves in Cananeia-Iguape (SP) 17 p2363 N88-24072
Research on enhancing the utilization of digital multispectral data and geographic information systems in global habitability studies
[NASA-CR-182799] 17 p2368 N88-24101
Quality and productivity drive innovation and improvement at United Technologies Aerospace Operations, Inc.
[NASA-CR-182944] 18 p2525 N88-24983
The assessment of human/computer performance using human productivity measures: MIPS and BIPS are MEGAFLOPS
[DE87-013491] 21 p2993 N88-27750

PRODUCTS
NT ASPHALT
NT DIESEL FUELS
NT GASOLINE
NT GREASES
NT PETROLEUM PRODUCTS
NT REACTION PRODUCTS
An introduction to the GOES I-M imager and sounder instruments and the GVAR retransmission format
[NOAA-TR-NESDIS-33] 02 p0140 N88-10884
A note on compactifications of products of semigroups
[CWI-PM-R8701] 08 p1072 N88-16469
Fast serial input-serial output pipelined inner product units
[REPT-87-031] 11 p1530 N88-19142

PROFICIENCY
U ABILITIES

PROFILES
Possibilities of determining vertical profiles of microphysical characteristics of stratospheric aerosol using space measurements of transparency and solar halo 24 p3449 N88-30526
Estimation of soil temperature profile from remote microwave and IR measurements 24 p3450 N88-30532

PROFILOMETERS
Profilometer for bomb-damage-repaired airfield pavements and measurement of pavement upheaval. Report 1: Technology evaluation
[AD-A187985] 11 p1442 N88-18601
Space shuttle solid rocket motor Profile Measuring Device (PMD) 14 p1928 N88-21495

PROGNOZ SATELLITES
Intershock observations during STIP intervals 17 and 18 01 p0119 N88-10759
Measurement of galactic radio emission at frequency 37 GHz from aboard spacecraft 24 p3448 N88-30520

PROGRAM EVALUATION REVIEW TECHNIQUE
U PERT

PROGRAM MANAGEMENT
U PROJECT MANAGEMENT

PROGRAM VERIFICATION (COMPUTERS)
Design and implementation of a debugger for an abstract machine
[AD-A184691] 03 p0363 N88-12283
ADAMEASURE: An implementation of the Halstead and Henry metrics
[AD-A184005] 03 p0365 N88-12299
SDVS (State Delta Verification System): Program verification system development fiscal year 1986
[AD-A184338] 03 p0366 N88-12302
Experimental aerothermodynamic research of hypersonic aircraft
[NASA-CR-181533] 04 p0399 N88-12483
Digital-flight-control-system software written in automated-engineering-design language: A user's guide of verification and validation tools
[NASA-TM-88313] 04 p0401 N88-12494
SDVS (State Delta Verification System) 5 users' manual
[AD-A184339] 04 p0478 N88-12943
Aircraft interior noise reduction by alternate resonance tuning
[NASA-CR-181530] 04 p0488 N88-13005
Effectiveness of back-to-back testing
[TR-87-08] 05 p0632 N88-13865
RSDIMU acceptance testing system: Overview of acceptance software and procedures 05 p0632 N88-13866
An extension to the multilevel logic simulator for microcomputers
[AD-A185032] 05 p0634 N88-13879
The adaption and use of research codes for performance assessment
[DE88-000552] 06 p0756 N88-14639
Space station software reliability analysis based on failures observed during testing at the multisystem integration facility 06 p0798 N88-14884
Version description document for the Ada compiler validation capability (version 1.9) (for microcomputer)
[AD-A186390] 07 p0903 N88-15471
The NASA aircraft icing research program 08 p0957 N88-15803
An approach to the hierarchical specification, design and verification of software
[RSRE-MEMO-4063] 09 p1223 N88-17332
An expert system to support the verification/validation of flight-critical software
[MBB-UT-102/87] 10 p1314 N88-17852
A generalized method for automatic downhand and wirefeed control of a welding robot and positioner
[NASA-TP-2807] 10 p1316 N88-17869
AEV local verification for aviation, precipitation and temperature programs: AV, REL, TEM (September 1987 revision)
[PB88-115662] 10 p1355 N88-18101
Feasibility study of generating plans and strategies for software testing by knowledge based system
[AD-A187834] 11 p1529 N88-19134
A theory of program correctness, and algorithms for proofs
[ANL-87-4] 11 p1531 N88-19146
EqL's user's guide
[AD-A188351] 12 p1677 N88-20025
Research on automatic verification of finite-state concurrent systems
[AD-A188618] 12 p1677 N88-20029
Modification, implementation, and evaluation of a remote terminal emulator as a software validation and stress testing tool
[AD-A188833] 12 p1678 N88-20034
Dynamic run-time graphics
[DE87-008997] 13 p1820 N88-20879
Sensitivity of control-augmented structure obtained by a system decomposition method
[NASA-TM-100535] 14 p1954 N88-21647
Ada (Trademark) compiler validation summary report. ALSYS: AlsyCOMP-013, V2.0 HOST: IBM PC AT. Target: IBM 370 3084Q
[AD-A189640] 15 p2106 N88-22546
Software verification using partition analysis
[AD-A190570] 15 p2112 N88-22582
The Colored Stochastic Petri Net (CS-PN) software: Application to the validation and the performance evaluation of distributed systems
[ENST-87D005] 15 p2113 N88-22589
An approximation technique for solving a system of Fredholm integral equations for asymmetric detector response functions
[AD-A190577] 15 p2121 N88-22645
Program profiling in Cedar
[AD-A190883] 16 p2250 N88-23449
Supercomputer programming environments
[AD-A190887] 16 p2251 N88-23452
Testing complex avionics software: A practical experience 17 p2306 N88-23794
A benchmark for galactic cosmic ray transport codes
[NASA-TM-101157] 17 p2453 N88-24571
Automated test device for FASR (Fixed Array Surveillance Radar) beam steering componentry
[AD-A191650] 18 p2500 N88-24829
Advanced development of the boundary element method for elastic and inelastic thermal stress analysis 18 p2529 N88-25002
A general approach for automating source code verification
[AD-A191461] 18 p2556 N88-25170
Checkout system software for INPE satellites
[INPE-4554-PRE/1297] 19 p2715 N88-26120
Inspection methods in programming: Cliches and plans
[AD-A192782] 21 p2996 N88-27767
Verification of flight software written in C using ACSL
[DE88-006100] 21 p2998 N88-27779
A modular proof of correctness for a network synchronizer
[AD-A192726] 21 p3002 N88-27802
Loading and linking in a modular language, an exercise in verification by unification
[INF-87-30] 22 p3136 N88-28642
Air Force Systems Command software independent verification and validation implementation analysis and guidance
[AD-A194309] 22 p3137 N88-28653
Validation tests for standard PASCAL and extented PASCAL
[NPL-DITC-108/88] 22 p3139 N88-28663
Validation code for the Whetstone Benchmark
[NPL-DITC-107/88] 22 p3140 N88-28667
Validation of expert systems 23 p3262 N88-29416
Verification and validation of rulebased systems for Hubble Space Telescope ground support 24 p3421 N88-30361

PROGRAMMED INSTRUCTION
NT COMPUTER ASSISTED INSTRUCTION
KA-PROLOG. KAP-computer: Computer model and instructions set
[ETN-88-91948] 18 p2558 N88-25186

PROGRAMMERS
NOSTRADAMUS programmable translator user's manual and programmer's manual
[DE87-013414] 01 p0083 N88-10533
On computing environments in data analysis
[DE88-000078] 04 p0480 N88-12961
Programmer-friendly LL(1) parser generator
[PB88-126933] 20 p2841 N88-26857
The programmer's apprentice project: A research overview
[AD-A192784] 21 p2996 N88-27769

PROGRAMMING (SCHEDULING)
NT THRUST PROGRAMMING

PROGRAMMING LANGUAGES
NT ADA (PROGRAMMING LANGUAGE)
NT APL (PROGRAMMING LANGUAGE)
NT ASSEMBLY LANGUAGE
NT BASIC (PROGRAMMING LANGUAGE)
NT C (PROGRAMMING LANGUAGE)
NT COBOL
NT CONTEXT FREE LANGUAGES
NT FORTRAN
NT HIGH LEVEL LANGUAGES
NT LISP (PROGRAMMING LANGUAGE)
NT NATURAL LANGUAGE (COMPUTERS)
NT PASCAL (PROGRAMMING LANGUAGE)
NT PROLOG (PROGRAMMING LANGUAGE)
Naval Aviation Integrated Logistics: Technical users guide version 1.0
[DE87-013368] 01 p0001 N88-10001
EVA reference manual
[DE87-014073] 01 p0082 N88-10526
NOSTRADAMUS programmable translator user's manual and programmer's manual
[DE87-013414] 01 p0083 N88-10533
An embedded multiprocessor computer for proof-of-principle testing of exploratory systems concepts
[DE87-012735] 02 p0218 N88-11372
Praxis: The programming language: An advanced overview
[DE87-014319] 02 p0220 N88-11388
Integrating syntax, semantics, and discourse DARPA (Defense Advanced Research Projects Agency) Natural Language Understanding Program
[AD-A184505] 03 p0364 N88-12289
ERIC: An object-oriented simulation language
[AD-A184757] 03 p0364 N88-12293
Low-level vision on warp and the apply programming model
[AD-A184330] 03 p0369 N88-12320
A network definition and solution of simulation problems
[DE88-000675] 04 p0481 N88-12962
Mixing Microsoft C and Microsoft FORTRAN program modules on the IBM Personal Computer
[DE88-001947] 05 p0637 N88-13895
A requirements specification for a software design support system
[NASA-CR-182333] 05 p0637 N88-13896
Learning to program methodically. 3: The newly designed course of the elementary programming
[PB87-119871] 06 p0757 N88-14643
Benchmarking and evaluation of hardware description languages for design of VLSI systems
[PB87-134557] 06 p0758 N88-14648
Computer architectures for artificial intelligence
[PB87-123824] 06 p0761 N88-14671
Using multiple dialog modes in a user-system interface to accomodate different levels of user experience: An experimental study
[AD-A186115] 07 p0899 N88-15444
Formalizing reusable software components in the programmer's apprentice
[AD-A185843] 07 p0901 N88-15457

Image processing language development
[AD-A186251] 07 p0903 N88-15467
DoD Gateway Information System (DGIS) common command language: The first prototyping and the decision for artificial intelligence
[AD-A185950] 07 p0942 N88-15725
DoD Gateway Information System (DGIS): Common command language mapping
[AD-A185951] 07 p0942 N88-15726
Clips as a knowledge based language
08 p1055 N88-16365
CLIPS: An expert system tool for delivery and training
08 p1056 N88-16368
ESSAA: Embedded system safety analysis assistant
08 p1060 N88-16396
LISP based simulation generators for modeling complex space processes 08 p1061 N88-16403
Applicative parallelism: Potential and challenge
[DE87-011885] 08 p1068 N88-16459
Interchange of electronic design through VHDL and EIS 09 p1205 N88-17222
The IDEAL (Integrated Design and Engineering Analysis Languages) modeling methodology: Capabilities and Applications 09 p1206 N88-17227
Implementing clips on a parallel computer
09 p1211 N88-17259
ESL batteries and multi-segment applications — ESA Simulation Language (ESL)
[CS-1029/00-QFIN4] 10 p1322 N88-17901
SISAL: Initial MIMD performance results
10 p1375 N88-18208
Predicate analysis for parallel program generation
10 p1377 N88-18222
Software support for heterogeneous machines
10 p1378 N88-18224
Portable (and disposable) interpreters
10 p1380 N88-18237
Programming language translation for multicomputers
10 p1381 N88-18244
Finely grained parallelism in an applicative architecture
10 p1383 N88-18256
FX-87 reference manual, edition 1.0
[AD-A187031] 10 p1385 N88-18273
Graph transformation algorithms for array memory optimization in applicative languages
[DE88-004727] 10 p1387 N88-18283
Semantics of EqL
[AD-A188151] 10 p1389 N88-18297
A worked example of an application of the SAINT simulation program
[AD-A188198] 11 p1524 N88-19097
EqL: The language and its implemantation
[AD-A188161] 11 p1530 N88-19137
A theory of program correctness, and algorithms for proofs
[ANL-87-4] 11 p1531 N88-19146
The SAS (Statistical Analysis System) by forms: Putting statistical power into the hands of an end-user
[DE88-002217] 11 p1541 N88-19212
Accessing hierarchical databases via SQL transactions in a multi-model database system
[AD-A187878] 11 p1565 N88-19369
A production-quality UNIX Very High Speed Integrated Circuit (VHSIC) Hardware Description Language (VHDL) subset analyzer
[AD-A188832] 12 p1623 N88-19710
EqL's user's guide
[AD-A188351] 12 p1677 N88-20025
Building software systems economically with mechanized logic: Initial design proposal
[AD-A188791] 12 p1678 N88-20031
A prototype for remotely shared textual workspaces
[AD-A188352] 12 p1679 N88-20040
Experience with Berkeley UNIX interprocess communications
[AD-A188353] 12 p1680 N88-20041
MultiRPC: A parallel remote procedure call mechanism
[AD-A188613] 12 p1680 N88-20046
ARCTIC: Programmer's manual and tutorial
[AD-A188619] 12 p1680 N88-20047
Design of the CONSUL programming language
[AD-A189202] 13 p1815 N88-20841
An interface between object-oriented systems
[AD-A189245] 13 p1815 N88-20844
Algebra of Communicating Processes (ACP)tau: A universal axiom system for process specification
[CWI-CS-R8725] 13 p1819 N88-20869
Designing equivalent semantic models for process creation
[CWI-CS-R8732] 13 p1819 N88-20872
Two normal form theorems for Communicating Sequential Processes (CSP) program
[CWI-CS-R8735] 13 p1819 N88-20874
Predicate-transformer semantics of general recursion
[CS-8709] 13 p1820 N88-20876
An implementation of the OPS5 language for computers compatible with IBM-PC
[INPE-4291-PRE/1162] 13 p1821 N88-20882
A proof rule process creation
[CWI-CS-R8710] 13 p1822 N88-20891
Type-checking Mini-ML: An algebraic specification with user-defined syntax
[CWI-CS-R8737] 13 p1827 N88-20921
Activities and operations of the Advanced Computing Research Facility, October 1986-October 1987
[DE88-006223] 14 p1955 N88-21653
Geometric modeling of flight information for graphical cockpit display
[AD-A190484] 15 p2021 N88-22043
Output formatting in Apple-soft BASIC
[DE88-701413] 15 p2108 N88-22559
A UNIX-based interactive VHDL (hardware description language) simulator
[AD-A189749] 15 p2109 N88-22565
Tutorial on GAMS (Generalized Algebraic Modeling System): A modeling language for optimization
[AD-A189667] 15 p2109 N88-22568
Argus reference manual
[AD-A190382] 15 p2111 N88-22578
Software structuring principles for VLSI CAD
[AD-A190386] 15 p2112 N88-22579
A direct-execution parallel architecture for the Advanced Continuous Simulation Language (ACSL)
[NASA-CR-182809] 15 p2115 N88-22602
The synthesizer generator, a useful tool?
[REPT-87-77] 16 p2250 N88-23443
Data management and language enhancement for generalized set theory computer language for operation of large relational databases
[NASA-CR-182868] 16 p2250 N88-23446
Supercomputer programming environments
[AD-A190887] 16 p2251 N88-23452
Editfont an interactive font editing system
[AD-A191007] 16 p2251 N88-23453
Parallelism in a Prolog knowledge base machine
[ETN-88-92187] 16 p2255 N88-23477
Linguistic definition of generic models in computer vision
[RSRE-MEMO-4110] 17 p2386 N88-24182
KA-PROLOG. KAP-computer: Computer model and instructions set
[ETN-88-91948] 18 p2558 N88-25186
The Sizing and Optimization Language, (SOL): Computer language for design problems
[NASA-TM-100565] 18 p2559 N88-25190
Design, implementation and evaluation of an operating system for a network of transputers
[AD-A186593] 18 p2559 N88-25193
The new MININEC (version 3): A mini-numerical electromagnetic code
[AD-A191778] 19 p2642 N88-25675
MVS (Multiple Virtual Storage) batch computing and data management at ANL
[DE88-007342] 19 p2718 N88-26137
FASTRUN phase sequencer descriptor language (PDL)
[DE88-007966] 20 p2837 N88-26828
Why is it difficult to program in von Neumann languages
[AD-A192830] 20 p2838 N88-26839
Contractions in comparing concurrency semantics
[CWI-CS-R8755] 20 p2840 N88-26850
A semantic approach to fairness
[CWI-CS-R8759] 20 p2840 N88-26853
Implementation of an OPS5 derivative on the Novix RISC processor
[DE88-011392] 21 p2994 N88-27758
Linguistic semantics for parallel computation
[PB88-105960] 21 p2995 N88-27761
Bisimulation can't be traced
[AD-A192725] 21 p2996 N88-27766
The SAS System by forms: Putting statistical power into the hands of an end-user
[DE88-010512] 21 p3010 N88-27857
Software development without languages
23 p3257 N88-29392
Programming language concepts for multiprocessors
[AD-A193465] 23 p3264 N88-29430
Conversion of productions in OPS5 to their equivalent English
[ORNL/TM-10246] 24 p3411 N88-30306
Syntactic closures
[AD-A195921] 24 p3412 N88-30311
Schemo86: A system for interpreting SCHEME
[AD-A195931] 24 p3413 N88-30319
Reification without evaluation
[AD-A195928] 24 p3414 N88-30326

PROGRAMS
NT ACEE PROGRAM
NT AGRISTARS PROJECT
NT BRAZILIAN SPACE PROGRAM
NT CANADIAN SPACE PROGRAM
NT CHINESE SPACE PROGRAM
NT DEFENSE PROGRAM
NT EARTH RESOURCES PROGRAM
NT EUROPEAN SPACE PROGRAMS
NT FRENCH SPACE PROGRAMS
NT GALILEO PROJECT
NT GLOBAL ATMOSPHERIC RESEARCH PROGRAM
NT INTERNATIONAL GEOSPHERE-BIOSPHERE PROGRAM
NT JAPANESE SPACE PROGRAM
NT NASA PROGRAMS
NT NASA SPACE PROGRAMS
NT NATIONAL AEROSPACE PLANE PROGRAM
NT PROJECT SETI
NT PROJECTS
NT QUIET ENGINE PROGRAM
NT ROVER PROJECT
NT SKYLAB PROGRAM
NT SPACE PROGRAMS
NT SUPERSONIC CRUISE AIRCRAFT RESEARCH
NT SWEDISH SPACE PROGRAM
NT TILT ROTOR RESEARCH AIRCRAFT PROGRAM
NT U.S.S.R. SPACE PROGRAM
NT UK SPACE PROGRAM
NT UNIVERSITY PROGRAM
Alternative fuels: Information on DOE's (Department of Energy's) methanol vehicle demonstration program
[PB88-118203] 13 p1753 N88-20481
The World Climate Research Program
14 p1935 N88-21538
Acid rain: Delays and management changes in the Federal research program
[GAO/RCED-87-89] 19 p2690 N88-25988

PROGRESS
Progress in the development of niobium alloyed high speed steel
[DE87-703549] 04 p0415 N88-12576
Recent progress in the p and h-p version on the finite element method
[AD-A187254] 10 p1400 N88-18347
Progress and future directions in computational fluid dynamics
[NASA-TM-100091] 18 p2456 N88-24579

PROJECT MANAGEMENT
Middle Atmosphere Program: Handbook for MAP, volume 24
[NASA-CR-181451] 01 p0069 N88-10444
Analysis and synthesis of abstract data types through generalization from examples
[NASA-CR-178369] 01 p0081 N88-10519
The microcomputer as an engineering management tool
[DE87-014882] 02 p0219 N88-11378
A review of hypertext in a NASA project management context 06 p0793 N88-14859
Research and technology objectives and plans. Summary, Fiscal Year 1988
[NASA-TM-87504] 06 p0800 N88-14894
The role of the DFVLR project management life sciences in the space program of the Federal Republic of Germany 07 p0884 N88-15364
Program draft for a special field: Gravitational biology
07 p0887 N88-15381
Risk analysis methodology survey
07 p0922 N88-15604
Design and management of research projects
[PB88-106380] 07 p0941 N88-15721
Aeropropulsion structures 08 p0954 N88-15786
Realization of the immediate objectives of the Aero-Gas Dynamics and Vibration Laboratory (LAGG) at the National Center for Research, Science and Technology (PUSPIPTEK) at Serpong, Java (Indonesia), Project TTA-79
[GG/QPR-10] 08 p1092 N88-16572
The ESA centralized management system for satellite electronic test and checkout instrumentation
09 p1124 N88-16731
Columbus feasibility studies. Volume 5: Programmatics
[ETN-88-91076] 09 p1134 N88-16802
Recommendations for a US ice coring program
[PB88-115043] 09 p1185 N88-17102
Study for history of technology developments in European space projects
[REPT-8518-1] 10 p1286 N88-17690
System analysis study of space platform and station accommodations for life sciences research facilities. Volume 2: Study results. Appendix E: Work breakdown structure and dictionary
[NASA-CR-179274] 10 p1292 N88-17723
Project management in astronautics: From Spacelab to Columbus
[MBB-URE-943/87] 10 p1315 N88-17858
Coordination: Southeast continental shelf studies
[DE88-003680] 10 p1357 N88-18110

What can be done to face growing development costs
12 p1701 N88-20181
Post-Challenger evaluation of space shuttle risk assessment and management
[NASA-CR-182461] 12 p1705 N88-20202
Application of expert systems in project management decision aiding
[NASA-CR-180762] 13 p1850 N88-21074
Engineering support of space shuttle experiment integration
[AD-A190135] 15 p2024 N88-22061
Project Monitoring Package (PMP): A package for project activity monitoring
[DE88-701234] 15 p2107 N88-22554
The multiannual National Remote Sensing Program (NRSP)
[BCRS-87-16] 16 p2229 N88-23311
Two decades of achievement in the ocean, 1968-1988
[PB88-167077] 16 p2236 N88-23356
The integration, characterisation and trialling of a modern complex airborne radar 17 p2305 N88-23791
Outline of the GPCP strategy
17 p2351 N88-24007
Acid rain: Delays and management changes in the Federal research program
[GAO/RCED-87-89] 19 p2690 N88-25988
Procedures for peer review assessments
[DE88-007749] 19 p2739 N88-26263
Management of large space projects --- conference
[ISBN-2-85-428192-6] 22 p3159 N88-28803
Management 22 p3159 N88-28804
Large space projects --- management
22 p3159 N88-28805
Starting point of a project: Decision mechanisms --- space projects 22 p3159 N88-28806
The development phases of a project --- space projects 22 p3159 N88-28807
Human organization --- space projects
22 p3160 N88-28808
The time of leaders 22 p3160 N88-28809
Contracts 22 p3160 N88-28810
Carrying out space projects 22 p3160 N88-28811
System configuration management --- space systems
22 p3160 N88-28813
Timetable control in a management system (space program) 22 p3160 N88-28815
Costs --- space projects 22 p3160 N88-28816
Value engineering --- space projects
22 p3160 N88-28817
Value analysis 22 p3161 N88-28819
Decision making aids: Methods and risks
22 p3161 N88-28820
Project management software
22 p3161 N88-28821
Management of large space projects. Financial means. Part 1: Financing of constructors
22 p3161 N88-28822
The role and the place of insurance of large space projects 22 p3161 N88-28826
Organization of the TDF1/TDF2 program
22 p3161 N88-28827
The Ariane line 22 p3161 N88-28828
The Ariane 5 program management specifications
22 p3162 N88-28829
Management of large space projects. Case study: The Hermes program 22 p3162 N88-28830
Case study: The Hermes program product assurance
22 p3162 N88-28831
Activities report of the World Meteorological Organization
[WMO-689] 24 p3404 N88-30265

PROJECT PLANNING

NAL news updated: FY87 business plan, developments 06 p0675 N88-14135
Supersonic STOVL propulsion technology program: An overview 08 p0957 N88-15808
Knowledge-based simulation
08 p1061 N88-16404
Planning and scheduling for robotic assembly
08 p1062 N88-16416
Planning activities in space 08 p1063 N88-16417
An AI approach for scheduling space-station payloads at Kennedy Space Center 08 p1064 N88-16425
Basic physics program for a low energy antiproton source in North America
[DE88-003148] 08 p1082 N88-16522
Critical issues in NASA information systems
[NASA-CR-182380] 08 p1093 N88-16577
Columbus feasibility studies. Volume 5: Programmatics
[ETN-88-91076] 09 p1134 N88-15802
The 1987 Get Away Special Experimenter's Symposium
[NASA-CP-2500] 10 p1286 N88-17691
Planet X probe: A fresh new look at an old familiar place 10 p1287 N88-17699
GAS 450: A space payload for the People Central Coast Student Experimenters 10 p1289 N88-17709
The NORSTAR Program: Space shuttle to space station 10 p1289 N88-17710
System analysis study of space platform and station accommodations for life sciences research facilities. Volume 2: Study results. Appendix E: Work breakdown structure and dictionary
[NASA-CR-179274] 10 p1292 N88-17723
Coordination: Southeast continental shelf studies
[DE88-003680] 10 p1357 N88-18110
Development of a graphics based two-attribute utility assessment program with application to mission planning
[AD-A187276] 10 p1388 N88-18292
Alternative Energy in the Midwest: Research and Applications. Conference Proceedings, Rosemont, Illinois, March 19-20, 1987
[PB88-142278] 11 p1509 N88-19015
AFAL (Air Force Astronautics Laboratory) technical objective document FY89
[AD-A187861] 11 p1567 N88-19378
Communication satellites: Guidelines for a strategic plan
[NASA-TM-89306] 12 p1599 N88-19569
European Progress on Space (EPOS): Participation in the creation of long term European space programs
[ILR-MITT-189] 14 p1871 N88-21180
Engineering support of space shuttle experiment integration
[AD-A190135] 15 p2024 N88-22061
Proposals for the pre-operational use of data from the European Remote Sensing Satellite ERS-1
[BCRS-86-02] 16 p2227 N88-23300
Preparation of the operational phase of the European Remote Sensing Satellite ERS-1
[BCRS-87-06] 16 p2228 N88-23307
Study of the plan for a national data center for the European Remote Sensing Satellite ERS-1
[BCRS-87-11] 16 p2228 N88-23309
The Engineer Studies Center guide to research and data collection
[AD-A189971] 16 p2285 N88-23680
Fuel cell systems program plan: Fiscal year 1988
[DE88-011080] 20 p2820 N88-26731
European transonic wind tunnel project: Assistance to the design group
[ONERA-RSF-11/0694-GY-010-G]
21 p2900 N88-27208
Studies concerning the European transonic wind tunnel
[ONERA-RSF-10/0694-GY-010-G]
21 p2900 N88-27209
Linear goal programming as a military decision aid
[AD-A194276] 22 p3137 N88-28652
Management 22 p3159 N88-28804
SDI (Strategic Defense Initiative) battle management/C3 (Command, Control and Communications) algorithms technology program plan
[AD-A194357] 23 p3275 N88-29495

PROJECT SETI

Intelligent signal analysis and recognition
[NASA-CR-181531] 04 p0501 N88-13084
SETI data controllers 11 p1474 N88-18795
The Telecommunications and Data Acquisition Report
[NASA-CR-183131] 22 p3063 N88-28178
DSS 13 microprocessor antenna controller
22 p3066 N88-28192
New CCIR report on SETI 22 p3067 N88-28204

PROJECTILE CRATERING

Hole diameters in plates impacted by projectiles
21 p2929 N88-27386

PROJECTILE PENETRATION

U TERMINAL BALLISTICS

PROJECTILES

NT HYPERVELOCITY PROJECTILES
NT SABOT PROJECTILES
Shock-wave studies using plastic flyers driven by an electric gun for hypervelocity impact on selected materials
[DE87-012631] 01 p0008 N88-10046
Switching devices used in the Lethality Test System
[DE87-011734] 01 p0011 N88-10062
Exact solutions to the governing dynamic equations of plasma armature electromagnetic railguns
[DE87-014442] 01 p0011 N88-10063
Laminar flow over a spinning projectile at an angle of attack 02 p0121 N88-10766
Jet formation and characterization of a conical shaped charge
[DE87-012102] 02 p0155 N88-10969
Improving coherent visualization by means of film optical filtering --- projectile visualization
[ISL-R-116/86] 02 p0176 N88-11097
Fin gaps and body slots of guided projectiles: Effects, data correlation and modeling
[AD-A184440] 03 p0270 N88-11698
The LLNL 150-mm equation-of-state gun system
[DE88-000423] 04 p0405 N88-12519
Mechanical property evaluation of a series of commercial tungsten alloys
[AD-A185440] 05 p0565 N88-13446
Optoelectronic measurement methods for ballistic experiments
[PB87-110706] 05 p0583 N88-13554
Computer simulations of ballistic experiments
[DE87-005835] 07 p0862 N88-15226
An investigation of oblique hypervelocity impact
07 p0927 N88-15629
New model to estimate the perforation power of kinetic energy projectiles
[PB87-166757] 09 p1175 N88-17040
Investigation of several spread shot conditions
[REPT-TR-164] 10 p1310 N88-17830
Splinter generator
[MBB-UA-1048/87] 11 p1491 N88-18897
Sub-scaling of projectile/target system damaged by hypervelocity
[AD-A188683] 12 p1634 N88-19779
What is the maximum length of a spin stabilized projectile
[PB88-130919] 13 p1728 N88-20336
Simulated impact damage in a thick graphite/epoxy laminate using spherical indenters
[NASA-TM-100539] 13 p1733 N88-20363
Two-phase flows in the wake of in-cylinder projectiles
[AD-A189422] 13 p1765 N88-20559
Mechanical design of a ultrahigh gravity UHV facility to launch and recover a low-speed projectile tested on board KC 135 14 p1877 N88-21216
Continuous measurements of in-bore projectile velocity
[DE88-006841] 15 p2023 N88-22056
Fluid motion in a spinning, coning cylinder via spatial eigenfunction expansion
[AD-A190758] 15 p2066 N88-22319
Efficient, high resolution computations of projectile and missile flow fields
[AD-A191086] 16 p2158 N88-22873
Power and energy requirements for electromagnetic launchers 17 p2420 N88-24391
Use of a two-stage light-gas gun as an injector for electromagnetic railguns
[DE88-007200] 18 p2469 N88-24657
Contact force history and dynamic response due to the impact of a soft projectile
[NASA-TM-100961] 20 p2811 N88-26679
Analysis of the perforation of monolithic and simple laminate aluminium targets as a test of analytical deformation models
[MRL-R-1111] 20 p2813 N88-26686
Charged pion production and projectile breakup in 85A MeV(sup)12C induced heavy ion reactions
[LUIP-8802] 20 p2850 N88-26920
Optimum-Path-to-Go guidance of command adjusted trajectory projectiles
[AD-A193377] 22 p3040 N88-28051
Computational fluid dynamics methods for low Reynolds number precessing/spinning incompressible flows
[AD-A193891] 23 p3212 N88-29119
Computational aerodynamic analysis for a range-limited 25mm training round
[AD-A185270] 24 p3320 N88-29772
A new computational capability for ramjet projectiles
[AD-A196061] 24 p3327 N88-29812
Numerical calculations of the response of a spinning spheroidal payload to coning motion
[AD-A195890] 24 p3368 N88-30059

PROJECTIVE GEOMETRY

On effectively labeling planar projections of polyhedra
[CWI-CS-R8715] 13 p1826 N88-20917

PROJECTS

NT AGRISTARS PROJECT
NT GALILEO PROJECT
NT PROJECT SETI
NT ROVER PROJECT
The International Satellite Land-Surface Climatology Project (ISLSCP) 14 p1937 N88-21558
Defense Small Business Innovation Research Program (SBIR). Volume 3: Air Force abstracts of phase 1 awards, 1987 17 p2448 N88-24548

PROKARYOTES

Biorack experiments in Spacelab D-1 and TML-1: Further developments in gravitational biology
12 p1661 N88-19953

PROLATE SPHEROIDS

The application of the hybrid iterative method to scattering by perfectly conducting bodies of revolution
11 p1475 N88-18802

Steady conduction of heat in prolate spheroidal systems
[LRT-WE-9-FB-16(1987)] 22 p3077 N88-28272
Liquid oscillations in a prolate spheroidal container
[LRT-WE-9-FB-4(1988)] 22 p3078 N88-28276

PROLOG (PROGRAMMING LANGUAGE)
How to use PROLOG for expert system programming
02 p0129 N88-10816
Near-horn prolog
[AD-A185172] 05 p0634 N88-13880
Automatic program generation from specifications using Prolog 08 p1065 N88-16437
DOD Gateway Information System (DGIS) common command language: Prolog knowledge base profile. Common command language report no. 3
[AD-A186150] 08 p1092 N88-16574
Experimenting with parallel programing in logic
10 p1380 N88-18240
KA-Prolog: Language definition
[GMD-249] 11 p1532 N88-19155
Implementing embedded artificial intelligence rules within algorithmic programming languages
[NASA-CR-178393] 14 p1959 N88-21686
Conversion of productions in OPS5 to their equivalent English
[ORNL/TM-10246] 24 p3411 N88-30306

PROMINENCES
NT SOLAR PROMINENCES
On the association of erupting magnetic fields with eruptive prominences and coronal mass ejections
01 p0113 N88-10727
Solar-geophysical data number 521, January 1988. Part 2: (Comprehensive reports). Data for July 1987 and miscellanea
[PB88-179221] 19 p2743 N88-26285

PRONE POSITION
Ergonomy and interior furnishing of the cabins of deep diving manned submarines: The Nautile example --- couch
19 p2697 N88-26032

PROOFS
U PROVING

PROP-FAN TECHNOLOGY
Aerodynamic and propeller performance characteristics of a propfan-powered, semispan model
[NASA-TM-86705] 06 p0667 N88-14092
Analysis and test evaluation of the dynamic stability of three advanced turboprop models at zero forward speed
[NASA-CR-175025] 06 p0668 N88-14095
Analysis and test evaluation of the dynamic response and stability of three advanced turboprop models at low forward speed
[NASA-CR-175026] 06 p0668 N88-14096
Large-Scale Advanced Prop-Fan (LAP) blade design
[NASA-CR-174790] 06 p0668 N88-14097
Aeropropulsion '87. Session 5: Subsonic Propulsion Technology
[NASA-CP-10003-SESS-5] 08 p0956 N88-15800
Overview of NASA PTA propfan flight test program
08 p0957 N88-15805
Analysis of possible transmission arrangements applicable for driving single or twin counterrotating fans on propfan engines 10 p1282 N88-17670
Vibration and flutter characteristics of the SR7L large-scale propfan
[NASA-TM-100272] 10 p1344 N88-18036
Technical-economical evaluation of a novel propfan concept in comparison with the turbofan for the nineties
[ETN-88-91022] 11 p1441 N88-18596
Counter-Rotating Integrated Shrouded Propfan (CRISP): The MTU propfan program --- Motoren und Turbinen Union (MTU)
[ETN-88-91023] 11 p1441 N88-18597
Advanced propfan analysis for the family of commuter airplanes
[NASA-CR-182566] 12 p1582 N88-19468
Large-Scale Advanced Prop-Fan (LAP)
[NASA-CR-182112] 13 p1723 N88-20306
Development of aeroelastic analysis methods for turborotors and propfans, including mistuning
16 p2219 N88-23244
The 2-D and 3-D time marching transonic potential flow method for propfans 16 p2220 N88-23245
Propfan model wind tunnel aeroelastic research results 16 p2220 N88-23246
A computational procedure for automated flutter analysis 16 p2220 N88-23250
Modal forced response of propfans in yawed flow
16 p2221 N88-23253
Vibration and flutter analysis of the SR-7L large-scale propfan 16 p2221 N88-23254
Propfan test assessment testbed aircraft stability and control/performance 1/9-scale wind tunnel tests
[NASA-CR-182121] 20 p2757 N88-26360
Structural Tailoring of Advanced Turboprops (STAT)
[NASA-CR-180861] 22 p3045 N88-28074
Experimental investigation of propfan aeroelastic response in off-axis flow with mistuning
[NASA-TM-101320] 22 p3089 N88-28344
Multiple-Purpose Subsonic Naval Aircraft (MPSNA): Multiple Application Propfan Study (MAPS)
[NASA-CR-175104] 23 p3177 N88-28917
Test results at transonic speeds on a contoured over-the-wing propfan model
[NASA-TM-88206] 23 p3177 N88-28918
SR-7A aeroelastic model design report
[NASA-CR-174791] 23 p3179 N88-28928
Optical measurement of unducted fan blade deflections
[NASA-TM-100966] 23 p3216 N88-29142
Euler analysis of a swirl recovery vane design for use with an advanced single-rotation propfan
[NASA-TM-101357] 24 p3320 N88-29771

PROPAGATION
Propagation of random initial conditions in time
04 p0486 N88-12993
Space communication link propagation data for selected cities within the multiple beam and steerable antenna coverage areas of the advanced communications technology satellite
[NASA-TM-100861] 16 p2191 N88-23070
Kinetic theoretical analysis for propagation of rotating ion beam in ICF 16 p2276 N88-23623
The propagation of pressure perturbations in bubbly air/water flows 19 p2664 N88-25843
Satellite observed Mesoscale Convective System (MCS) propagation characteristics and a 3-12 hour heavy precipitation forecast index
[PB88-180161] 19 p2692 N88-26004
Perturbation expansions generated by an approximate propagator
[DE88-702435] 21 p3011 N88-27866

PROPAGATION (EXTENSION)
NT CRACK PROPAGATION
NT FLAME PROPAGATION
Error propagation in a digital avionic mini processor
[NASA-CR-181565] 05 p0633 N88-13872

PROPAGATION MODES
The wavenumber: An alternative to the directional coupler for multimode analysis in oversized waveguides
[IPF-87-2] 01 p0037 N88-10237
Optimization of mode converters for generating the fundamental TE(06) gyrotron output at 140 GHz
[IPF-87-1] 01 p0043 N88-10273

PROPAGATION VELOCITY
Coherent structure-reflective turbulent viscous flow modeling
[AD-A188339] 13 p1765 N88-20556
Detonation velocity of the hydrazinum nitrate-hydrazine water system
[NASA-TT-20213] 13 p1770 N88-20590
Numerical and experimental research on propagation of elastic stress waves in conical shell under axial impulsive loading 15 p2053 N88-22238
The determination of gravity and topography from seismic velocities, accounting for dynamic behavior of the Earth's mantle
[ETN-88-92420] 17 p2374 N88-24117
Determination of the specific area of liquid gas and the velocity of weak pressure waves in aqueous foams
[NASA-TT-20347] 24 p3373 N88-30087

PROPAGATORS
U PROPAGATION

PROPANE
Molecular dynamics studies of aromatic hydrocarbon liquids
[DE88-001473] 05 p0648 N88-13973
The effect of propane on atomic spectrometric signals in the direct current plasma
[DE88-002457] 07 p0934 N88-15676
Gas hydrate model development and validation
[DE88-001004] 10 p1298 N88-17762
Geological evolution and analysis of confirmed or suspected gas hydrate localities. Volume 9: Formation and stability of gas hydrates of the Middle America Trench
[DE88-001007] 10 p1347 N88-18050

PROPELLANT ADDITIVES
NT PROPELLANT BINDERS
NT SOLID ROCKET BINDERS
A holographic investigation of particulates in metallized solid fuel ramjet combustion
[AD-A186887] 09 p1140 N88-16831

PROPELLANT BINDERS
NT SOLID ROCKET BINDERS
High pressure strand burn rate tests of polyvinylnitrate/nitramine propellants
[AD-A184178] 04 p0422 N88-12615
Thermoplastic elastomers as LOVA binders
[AD-A185864] 07 p0835 N88-15067
Thermoplastic elastomers as LOVA binders
[AD-A185865] 07 p0835 N88-15068
Thermomechanical computations for GAP, a high energy binder for composite propellants
[FOA-C-20718-2.1] 24 p3357 N88-29988

PROPELLANT CHEMISTRY
Reaction products of solid propellants after burning at pressures up to 1000 MPa: Comparison between theoretical and experimental results
[ISL-CO-227/87] 22 p3059 N88-28153

PROPELLANT COMBUSTION
NT SOLID PROPELLANT COMBUSTION
NT SOLID PROPELLANT IGNITION
KR+ laser excitation of NH2 in atmospheric pressure flames
[AD-A183421] 01 p0050 N88-10322
High pressure strand burn rate tests of polyvinylnitrate/nitramine propellants
[AD-A184178] 04 p0422 N88-12615
Laser probes of propellant combustion chemistry
[AD-A184854] 05 p0561 N88-13415
Holographic investigation of metallized solid propellant combustion in two-dimensional and three-dimensional rocket motors
[AD-A187000] 09 p1140 N88-16832
Shuttle rocket booster computational fluid dynamics
[NASA-CR-182518] 10 p1293 N88-17733
Continued studies of programmed-splitting stick propellant
[AD-A188987] 12 p1613 N88-19644
On the possibility of high velocity deflagration front propagation by radiative energy transfer
[AD-A189022] 12 p1613 N88-19645
Bipropellant combustion in a liquid rocket combustion chamber 13 p1733 N88-20359
Mixing fuel particles for space combustion research using acoustics
[NASA-TM-100295] 14 p1872 N88-21186
Finite area combustor theoretical rocket performance
[NASA-TM-100785] 14 p1883 N88-21252
Catalytic ignition of hydrogen and oxygen propellants
[NASA-TM-100957] 18 p2476 N88-24689
The burning of HAN-based (hydroxylammonium nitrate) liquid propellants
[DE88-006863] 18 p2494 N88-24800
Electrical ignition of HAN-based liquid propellants
[AD-A191349] 18 p2495 N88-24801
Chemical kinetics of nitramine propellant combustion
[AD-A191556] 18 p2495 N88-24802
The 24th JANNAF Combustion Meeting, volume 2
[AD-A190164] 19 p2622 N88-25554
The combustion of hydroxylammonium nitrate based liquid propellants 19 p2622 N88-25555
A dynamic model of liquid propellant combustion
19 p2622 N88-25556
Droplet formation for liquid monopropellant jets
19 p2623 N88-25557
Mixing and thermodynamic critical phenomena of combusting monopropellant sprays
19 p2623 N88-25558
The development of a user friendly thermodynamic code for the personal computer 19 p2623 N88-25559
Measurement of burning rates of NOSOL-363 propellants under cross-flow and strand burner conditions using real-time X-ray radiography
19 p2623 N88-25560
Burning rate measurements of Non-Newtonian Liquid Propellant (NNLP) 19 p2623 N88-25561
Dynamical properties of a collapsing spherical cavity
19 p2623 N88-25562
Propellant combustion response to oscillatory radiant heat flux 19 p2628 N88-25589
Dynamics of propellant ignition
19 p2628 N88-25590
New instability phenomena in solid propellant combustion 19 p2628 N88-25591
Analysis of microwave burner measurement system using a microwave network analysis computer program
19 p2631 N88-25604
Modeling and experimental measurements of solid propellant flame structure 19 p2631 N88-25605
Solid rocket motor performance: A workshop report
19 p2631 N88-25607
How much do edges affect the ignition of a homogeneous reactive solid: Summary to date
19 p2631 N88-25608
Evaluation of techniques for direct measurement of burning rates in nozzleless motors
19 p2631 N88-25609
Deuterium isotope effects in the combustion of formulated nitramine propellants
19 p2632 N88-25611
Simultaneous thermogravimetric modulated beam mass spectrometry and time-of-flight velocity spectra measurements: Thermal decomposition mechanisms of RDX and HMX 19 p2632 N88-25612
Structure of laminar, premixed flames of CH2O/NO2/O2 mixtures 19 p2632 N88-25613

Temperature and species profiles in propellant ignition and combustion 19 p2633 N88-25616
Chemical kinetics modeling of HMX combustion 19 p2633 N88-25617
Rocket-propellant burn tests of silicide-coated niobium and tantalum
[DE88-010729] 20 p2781 N88-26496
Some properties of ignition gases. Review of measuring results in the years 1981-1986)
[PB88-106968] 21 p2908 N88-27259
Ignition and extinguishing of a Solid Fuel Ramjet (SOFRAM)
[FOA-C-20713-2.1] 24 p3337 N88-29865
Combustion diagnostics of propellant with new grain geometries
[AD-A194944] 24 p3342 N88-29895
Gas phase combustion chemistry of nitramine propellants
[AD-A195082] 24 p3344 N88-29902

PROPELLANT DECOMPOSITION
Free radical detection and reactions in the decomposition of energetic materials
[AD-A184677] 03 p0296 N88-11858
Test number 2 of propellant for rocket motor MK52
[PB87-226155] 05 p0571 N88-13480
The chemistry of the hypochlorite neutralization of hydrazine fuels
[DE88-002971] 10 p1307 N88-17812
Novel analytical X-ray Non-Destructive Evaluation (NDE) tool for quality control of energetic materials
[AD-A187737] 11 p1497 N88-18935
Chemical kinetics of nitramine propellant combustion
[AD-A191556] 18 p2495 N88-24802
Theoretical investigations of nitrocubane decomposition
[AD-A194556] 23 p3200 N88-29047
Gas phase combustion chemistry of nitramine propellants
[AD-A195082] 24 p3344 N88-29902

PROPELLANT EXPLOSIONS
Semiconductor bridge (SCB) igniter studies. 1: Comparison of SCB and hot-wire pyrotechnic actuators
[DE88-008802] 23 p3200 N88-29046

PROPELLANT GRAINS
Measurements of particulates in solid propellant rocket motors
[AD-A187777] 11 p1446 N88-18621
Mixing fuel particles for space combustion research using acoustics
[NASA-TM-100295] 14 p1872 N88-21186
Crack opening and extension in inert solid propellant. An experimental study
[AD-A189808] 15 p2048 N88-22201
Some properties of ignition gases. Review of measuring results in the years 1981-1986)
[PB88-106968] 21 p2908 N88-27259
A study of flame spreading and combustion phenomena of stick propellants
[AD-A193598] 22 p3052 N88-28106
Combustion diagnostics of propellant with new grain geometries
[AD-A194944] 24 p3342 N88-29895
Flamespreading processes in obliquely loaded stick propellant beds
[AD-A195081] 24 p3352 N88-29956
Descriptive characterization of propellant particles
[AD-A195176] 24 p3356 N88-29985

PROPELLANT MASS RATIO
The initial calculation of range and mission fuel during conceptual design --- aircraft design
[LR-525] 16 p2161 N88-22889

PROPELLANT OXIDIZERS
U ROCKET OXIDIZERS

PROPELLANT PROPERTIES
NT PROPELLANT SENSITIVITY
NT PROPELLANT STORABILITY
Modal survey of the space shuttle solid rocket motor using multiple input methods 05 p0593 N88-13617
Fuel property effects on the US Navy's TF30 engine 24 p3345 N88-29911
Alternative fuel spray behavior 24 p3345 N88-29912
The characterizatin of combustion by fuel composition: Measurements in a small conventional combustor 24 p3346 N88-29920

PROPELLANT SENSITIVITY
An infra-red investigation of HAN (Hydroxylammonium Nitrate)-based liquid propellants
[AD-A187226] 10 p1307 N88-17815
On the possibility of high velocity deflagration front propagation by radiative energy transfer
[AD-A189022] 12 p1613 N88-19645
Structure/property/reactivity relations among nitramine and other energetic materials
[AD-A190878] 18 p2481 N88-24716

PROPELLANT STORABILITY
Uranium nitride fuel swelling and thermal conductivity correlations 17 p2409 N88-24327

PROPELLANT STORAGE
Orbital Spacecraft Consumables Resupply System (OSCRS). Volume 2: Study results
[NASA-CR-172011] 03 p0268 N88-11687
DOE explosives safety manual
[DE88-000831] 04 p0422 N88-12616
Test number 2 of propellant for rocket motor MK52
[PB87-226155] 05 p0571 N88-13480
Turbomachinery in space 17 p2408 N88-24321
Weight savings in aerospace vehicles through propellant scavenging
[NASA-TM-100900] 19 p2605 N88-25470
Pressure/temperature sensitive inorganic phosphors 19 p2627 N88-25583

PROPELLANT TANKS
Orbital transfer vehicle studies overview 08 p0981 N88-15931
Low-g propellant gaging 08 p0982 N88-15937
Computational prediction of propellant reorientation 08 p0982 N88-15940
Low gravity liquid motions in spacecraft 08 p0982 N88-15941
Peacekeeper tank slosh model 08 p0983 N88-15942
Zero-G thermodynamic vent system for shuttle/Centaur 08 p0983 N88-15943
Orbital Propulsion Module (OPM). Study on coni-spherical surface tension tanks (COSTA)
[MBB-URV-170/87] 23 p3187 N88-28963

PROPELLANT TRANSFER
Orbital Spacecraft Consumables Resupply System (OSCRS). Volume 1: Executive summary
[NASA-CR-172010] 05 p0553 N88-13368
Servicer system demonstration plan and capability development
[NASA-CR-179246] 08 p0975 N88-15895
Design and development of a refueling test bed
[FTMS-RP-ER-011] 24 p3357 N88-29986

PROPELLANTS
NT COMPOSITE PROPELLANTS
NT CRYOGENIC ROCKET PROPELLANTS
NT DOUBLE BASE PROPELLANTS
NT DOUBLE BASE ROCKET PROPELLANTS
NT GELLED PROPELLANTS
NT GELLED ROCKET PROPELLANTS
NT GUN PROPELLANTS
NT HIGH TEMPERATURE PROPELLANTS
NT HMX
NT HTPB PROPELLANTS
NT LIQUID ROCKET PROPELLANTS
NT METAL PROPELLANTS
NT MONOPROPELLANTS
NT NITRAMINE PROPELLANTS
NT PLASTIC PROPELLANTS
NT RDX
NT ROCKET PROPELLANTS
NT RP-1 ROCKET PROPELLANTS
NT SLURRY PROPELLANTS
NT SOLID PROPELLANTS
NT SOLID ROCKET PROPELLANTS
NT TETRYL
Strategic Defense Initiative Organization/DARPA (Defense Advanced Research Projects Agency) workshop on laser propulsion. Volume 1: Executive summary
[DE87-003254] 06 p0768 N88-14722
SAMSS: An in-progress review of the Spacecraft Assembly, Maintenance, and Servicing Study 08 p0981 N88-15930
DSC (Differential Scanning Calorimeter) stability test for liquid propellants: A preliminary report
[AD-A187115] 09 p1150 N88-16888
Laser induced ignition of propellants
[AD-A191100] 16 p2168 N88-22927
Laser induced ignition of propellants
[AD-A191099] 16 p2213 N88-23206
An extinguisher to quench propellant fires
[AD-A190785] 18 p2497 N88-24813
SRM (Solid Rocket Motor) propellant and polymer materials structural modeling
[NASA-TP-2824] 22 p3089 N88-28343
Lunar lander conceptual design: Lunar base systems study task 2.2
[NASA-CR-172051] 24 p3335 N88-29854
Energy conversion measurements in laser-sustained argon plasmas for application to rocket propulsion
[AD-A194931] 24 p3337 N88-29861
Titrimetric analysis of HAN-based liquid propellants
[AD-A196225] 24 p3357 N88-29990

PROPELLER BLADES
Numerical prediction of propeller performance by vortex lattice method
[UTIAS-TN-265] 04 p0400 N88-12489
High speed propeller performance and noise predictions at takeoff/landing conditions
[NASA-TM-100267] 05 p0646 N88-13960
Large-Scale Advanced Prop-Fan (LAP) blade design
[NASA-CR-174790] 06 p0668 N88-14097
Aerodynamic and acoustic characteristics of an advanced propeller under take-off and landing conditions
[NAL-TR-935] 09 p1243 N88-17453
Numerical methods for propeller aerodynamics and acoustics at DFVLR 10 p1282 N88-17668
Numerical simulation of subsonic and transonic propeller flow
[NASA-TM-100163] 13 p1716 N88-20262
Calculation of the distributed loads on the blades of individual multiblade propellers in axial flow using linear and nonlinear lifting surface theories
[NASA-TT-20173] 13 p1719 N88-20278
Large-Scale Advanced Prop-Fan (LAP)
[NASA-CR-182112] 13 p1723 N88-20306
Development of aeroelastic analysis methods for turborotors and propfans, including mistuning 16 p2219 N88-23244
Modal forced response of propfans in yawed flow 16 p2221 N88-23253
Vibration and flutter analysis of the SR-7L large-scale propfan 16 p2221 N88-23254
Advanced turboprop aircraft flyover noise: Annoyance to counter-rotating-propeller configurations with an equal number of blades on each rotor, preliminary results
[NASA-TM-100612] 16 p2265 N88-23547
Optical measurement of propeller blade deflections
[NASA-TP-2841] 22 p3079 N88-28286

PROPELLER DRIVE
Noise levels from propeller-driven aircraft measured at ground level and at 1.2 m above the ground
[NPL-AC-110] 01 p0091 N88-10594

PROPELLER EFFICIENCY
The aerodynamic performance of propellers suitable for unmanned aircraft (UMAs)
[RAE-TM-AERO-2094] 09 p1112 N88-16667
Numerical methods for propeller aerodynamics and acoustics at DFVLR 10 p1282 N88-17668
Summary of low-speed wind tunnel results of several high-speed counterrotation propeller configurations
[NASA-TM-100945] 18 p2458 N88-24597
Finite element solution of 3-D turbulent Navier-Stokes equations for propeller-driven slender bodies 18 p2515 N88-24919
Aircraft noise prediction program propeller analysis system IBM-PC version user's manual version 2.0
[NASA-CR-181689] 24 p3428 N88-30399

PROPELLER FANS
Transonic analysis and design of axisymmetric bodies in nonuniform flow
[NASA-CR-4101] 01 p0003 N88-10013
Annoyance caused by advanced turboprop aircraft flyover noise: Single-rotating propeller configuration
[NASA-TP-2782] 09 p1242 N88-17441
Analysis of possible transmission arrangements applicable for driving single or twin counterrotating fans on propfan engines 10 p1282 N88-17670
The effects of rotational flow, viscosity, thickness, and shape on transonic flutter dip phenomena
[NASA-TM-100811] 11 p1502 N88-18969
Aeroelastic response of metallic and composite propfan models in yawed flow
[NASA-TM-100964] 24 p3326 N88-29807

PROPELLER SLIPSTREAMS
Low speed wind tunnel investigation of propeller slipstream aerodynamic effects on different nacelle/wing combinations. Part 1: Total forces and moments and pressure distributions on nacelle/wing at different angles of attack and yaw and at different thrust coefficients
[FFA-TN-1987-22] 05 p0542 N88-13302
Numerical simulation of subsonic and transonic propeller flow
[NASA-TM-100163] 13 p1716 N88-20262

PROPELLERS
NT CONTRAROTATING PROPELLERS
NT PROPELLER FANS
NT SHROUDED PROPELLERS
NT VARIABLE PITCH PROPELLERS
Advanced turboprop wing installation effects measured by unsteady blade pressure and noise
[NASA-TM-100200] 01 p0002 N88-10008
Numerical calculations of the flowfield around propellers 05 p0536 N88-13261
Aerodynamic and propeller performance characteristics of a propfan-powered, semispan model
[NASA-TM-86705] 06 p0667 N88-14092
An investigation of the effects of the propeller slipstream on a wing boundary layer 06 p0700 N88-14293
Advanced propeller research 08 p0957 N88-15806

The aerodynamic performance of propellers suitable for unmanned aircraft (UMAs)
[RAE-TM-AERO-2094] 09 p1112 N88-16667
Lifting-surface theory of oscillating propellers in compressible flow
[NAL-TR-943] 10 p1273 N88-17613
Aerodynamic performance of a scale-model, counter-rotating unducted fan 10 p1282 N88-17666
Numerical methods for propeller aerodynamics and acoustics at DFVLR 10 p1282 N88-17668
Analysis of highspeed propellers aerodynamics 10 p1282 N88-17669
Conditions at infinity for theories of oscillating wings and propellers in subsonic flow
[NAL-TR-937] 11 p1434 N88-18556
Analysis of in-flight acoustic data for a twin-engined turboprop airplane
[NASA-CR-178369] 11 p1543 N88-19220
Comparison of two transonic noise prediction formulations using the aircraft noise prediction program
[NASA-CR-181609] 12 p1688 N88-20095
Cavitation inception
[AD-A189220] 13 p1765 N88-20557
Porous wind tunnel corrections for counterrotation propeller testing
[NASA-TM-100873] 15 p2015 N88-22019
NASA advanced turboprop research and concept validation program
[NASA-TM-100891] 16 p2163 N88-22902
Measurements of the time dependent velocity field surrounding a model propeller in uniform water flow 16 p2205 N88-23155
NASA/industry advanced turboprop technology program
[NASA-TM-100929] 18 p2466 N88-24641
Numerical solutions of the Euler equations for the flow field around counter-rotating propellers 19 p2636 N88-25638
Optical measurement of unducted fan blade deflections
[NASA-TM-100966] 23 p3216 N88-29142
Analysis of the transmission of sound into the passenger compartment of a propeller aircraft using the finite element method
[FFA-TN-1988-15] 23 p3279 N88-29520
A comparison of simple analytical models for representing propeller aircraft structural and acoustic responses
[ISVR-TR-153] 23 p3279 N88-29523
Euler analysis of a swirl recovery vane design for use with an advanced single-rotation propfan
[NASA-TM-101357] 24 p3320 N88-29771

PROPORTIONAL COUNTERS
Electronics for the External Muon Detector (EMD) of ICARUS
[NOTA-INTERNA-880] 07 p0847 N88-15143
Single wire drift chamber design
[DE87-011002] 07 p0857 N88-15205
The position-sensitive counting of photons 16 p2271 N88-23590

PROPORTIONAL LIMIT
Carbon fiber reinforced glass matrix composites for space based applications
[AD-A184355] 04 p0410 N88-12546
Fastening high resistance bolts in real assemblies
[CRIF-MT-171] 07 p0861 N88-15221

PROPRIOCEPTION
Some remarks on gravitational biology 07 p0884 N88-15366
Perception and control of simulated self motion
[AD-A187444] 10 p1372 N88-18188
Covariant control of bilateral servos for in-orbit manipulation 12 p1590 N88-19520

PROPRIOCEPTORS
Functional development of gravity receptors in insects and amphibians 07 p0886 N88-15376
Role of optokinetic stimulation in vestibulospinal reflexes 10 p1360 N88-18131

PROPULSION
NT ASCENT PROPULSION SYSTEMS
NT AUXILIARY PROPULSION
NT CHEMICAL PROPULSION
NT ELECTRIC PROPULSION
NT ELECTROMAGNETIC PROPULSION
NT ELECTROSTATIC PROPULSION
NT HYBRID PROPULSION
NT ION PROPULSION
NT JET PROPULSION
NT LASER PROPULSION
NT LOW THRUST PROPULSION
NT MARINE PROPULSION
NT MASS DRIVERS (PAYLOAD DELIVERY)
NT NUCLEAR ELECTRIC PROPULSION
NT NUCLEAR PROPULSION
NT PLASMA PROPULSION
NT SOLAR THERMAL PROPULSION
NT SPACE STATION PROPULSION
NT SPACECRAFT PROPULSION
Calendar of selected aeronautical and space meetings
[AGARD-CAL-87/1] 05 p0657 N88-14033
Propulsion-induced effects caused by out-of-ground effects
[NASA-TM-100032] 06 p0666 N88-14088
Recent advances in high temperature instrumentation for hot section applications
[NASA-TM-100282] 06 p0707 N88-14339
Aeropropulsion '87. Session 3: Internal Fluid Mechanics Research
[NASA-CP-10003-SESS-3] 08 p0954 N88-15790
Chemical reacting flows 08 p0955 N88-15793
Aeropropulsion '87. Session 4: Instrumentation and Controls Research
[NASA-CP-10003-SESS-4] 08 p0955 N88-15794
Directions in propulsion control 08 p0956 N88-15799
Aeropropulsion '87. Session 5: Subsonic Propulsion Technology
[NASA-CP-10003-SESS-5] 08 p0956 N88-15800
Rotorcraft transmission 08 p0956 N88-15802
Rotorcraft flight-propulsion control integration 09 p1108 N88-16643
Impact and promise of NASA aeropropulsion technology 09 p1118 N88-16698
Institute for Computational Mechanics in Propulsion (ICOMP)
[NASA-TM-100790] 11 p1540 N88-19202
Activities report of the Energetics Department
[ETN-88-91981] 14 p1888 N88-21281
Research as part of the Air Force in aero propulsion technology (AFRAPT) program
[AD-A190336] 15 p2019 N88-22036
AFRAPT (Air Force Research in Aero Propulsion Technology) trainee program
[AD-A190525] 15 p2035 N88-22123
Costs and benefits of AC propulsion
[PB88-173380] 16 p2287 N88-23691
Gravitation electromagnetic theory 22 p3158 N88-28790
Special Course on Missile Aerodynamics
[AGARD-R-754] 24 p3317 N88-29755
Energy conversion measurements in laser-sustained argon plasmas for application to rocket propulsion
[AD-A194931] 24 p3337 N88-29861

PROPULSION SYSTEM CONFIGURATIONS
NT ASCENT PROPULSION SYSTEMS
Multi-stage plasma thruster
[AD-A183635] 01 p0017 N88-10105
An 8-cm ion thruster characterization
[NASA-CR-180819] 01 p0017 N88-10106
Flight propulsion control integration for V/STOL aircraft
[NASA-TM-100226] 03 p0267 N88-11680
Configuration evaluation and criteria plan. Volume 2: Evaluation criteria plan (update). Space Transportation Main Engine (STME) configuration study
[NASA-CR-181429] 03 p0270 N88-11699
Institute for Computational Mechanics in Propulsion (ICOMP) first year summary
[NASA-TM-100225] 03 p0370 N88-12330
Integrated control and display research for transition and vertical flight on the NASA V/STOL Research Aircraft (VSRA)
[NASA-TM-100029] 05 p0551 N88-13359
Hermes propulsion system
[SNIAS-872-422-109] 05 p0556 N88-13383
Space station onboard propulsion system: Technology study
[NASA-CR-179233] 07 p0825 N88-15006
Internal fluid mechanics research on supercomputers for aerospace propulsion systems
[NASA-TM-100289] 07 p0854 N88-15188
Equilibrium retention in the nozzle of oxygen hydrogen propulsion systems 07 p0924 N88-15616
Advanced fusion power: A preliminary assessment
[AD-A185903] 07 p0933 N88-15664
Aeropropulsion '87. Session 2: Aeropropulsion Structures Research
[NASA-CP-10003-SESS-2] 08 p0954 N88-15785
Aeropropulsion structures 08 p0954 N88-15786
Determining structural performance 08 p0954 N88-15787
Life prediction technologies for aeronautical propulsion systems 08 p0954 N88-15788
Integrated analysis and applications 08 p0954 N88-15789
Aeropropulsion '87. Session 6: High-Speed Propulsion Technology
[NASA-CP-10003-SESS-6] 08 p0957 N88-15807
Supersonic STOVL propulsion technology program: An overview 08 p0957 N88-15808
Propulsion challenges and opportunities for high-speed transport aircraft 08 p0958 N88-15809
Supersonic throughflow fans for high-speed aircraft 08 p0958 N88-15810
High-speed inlet research program and supporting analyses 08 p0958 N88-15811
Hypersonic propulsion research 08 p0958 N88-15812
CFD validation experiments for internal flows
[NASA-TM-100797] 09 p1114 N88-16679
Lewis materials research and technology: An overview 09 p1119 N88-16699
Calculation and design of a ramjet missile
[REPT-TR-500] 10 p1311 N88-17832
The MBB propulsion concepts for magnetic suspension railways: Retrospective view and prospects
[MBB-Z-141/87] 10 p1316 N88-17865
Technical-economical evaluation of a novel propfan concept in comparison with the turbofan for the nineties
[ETN-88-91022] 11 p1441 N88-18596
Counter-Rotating Integrated Shrouded Propfan (CRISP): The MTU propfan program — Motoren und Turbinen Union (MTU)
[ETN-88-91023] 11 p1441 N88-18597
A comparative study of various electric propulsion systems and their impact on a nominal ship design
[AD-A187800] 11 p1477 N88-18816
Application of advanced computational technology to propulsion CFD
[NASA-TM-100843] 11 p1525 N88-19102
Advanced propfan analysis for the family of commuter airplanes
[NASA-CR-182566] 12 p1582 N88-19468
Electromagnetic propagation in PEC and absorbing curved S-ducts
[NASA-TM-100833] 12 p1621 N88-19698
A comparison of propulsion systems for potential space mission applications
[DE88-005637] 14 p1882 N88-21248
Advanced transmission studies
[NASA-TM-100867] 14 p1919 N88-21454
Activities report in flight and space travel
[ISSN-0070-3966] 14 p2012 N88-22000
Research and technology
[NASA-TM-100172] 15 p2153 N88-22851
The challenges and opportunities of supersonic transport propulsion technology
[NASA-TM-100921] 17 p2307 N88-23806
Heat transfer in aerospace propulsion
[NASA-TM-100874] 17 p2339 N88-23957
Nuclear propulsion systems for orbit transfer based on the particle bed reactor 17 p2401 N88-24272
Recent advances in low-thrust propulsion technology
[NASA-TM-100959] 18 p2589 N88-25260
A reusable rocket engine intelligen control
[NASA-TM-100963] 20 p2766 N88-26401
Variable Mach number wall jets for control/propulsion on hypervelocity projectiles/interceptors: Tests with an existing model
[AD-A192845] 21 p2892 N88-27167
Development of sensors for ceramic components in advanced propulsion systems: Survey and evaluation of measurement techniques for temperature, strain and heat flux for ceramic components in advanced propulsion systems
[NASA-CR-182111] 22 p3081 N88-28299
Experimental and analytical evaluation of the effects of simulated engine inlets on the blade vibratory stresses of the SR-3 model prop-fan
[NASA-CR-174959] 23 p3179 N88-28927
Orbital Propulsion Module (OPM). Study on coni-spherical surface tension tanks (COSTA)
[MBB-URV-170/87] 23 p3187 N88-28963
Evaluation of the advanced air breathing propulsion concepts, executive summary
[ESA-CR(P)-2540] 24 p3325 N88-29802
Evaluation of advanced air breathing concepts. Volume 1: Executive summary
[ESA-CR(P)-2539] 24 p3326 N88-29806
Spacecraft mass estimation, relationships and engine data: Task 1.1 of the lunar base systems study
[NASA-CR-172061] 24 p3332 N88-29836
The NASA Electric Propulsion Program
[NASA-TM-101324] 24 p3336 N88-29859
Hermes: Study of propulsion system for reusable man-rated spacecraft
[PSRM-TN-0000-00-04A] 24 p3337 N88-29866
Unified study of plasma/surface interactions for space power and propulsion
[AD-A195971] 24 p3338 N88-29870

PROPULSION SYSTEM PERFORMANCE
Propulsion Working Group report 01 p0016 N88-10098
Multi-stage plasma thruster
[AD-A183635] 01 p0017 N88-10105

An 8-cm ion thruster characterization
[NASA-CR-180819] 01 p0017 N88-10106
Flight propulsion control integration for V/STOL aircraft
[NASA-TM-100226] 03 p0267 N88-11680
Configuration evaluation and criteria plan. Volume 2: Evaluation criteria plan (update). Space Transportation Main Engine (STME) configuration study
[NASA-CR-181429] 03 p0270 N88-11699
Space station propulsion
[NASA-TM-100216] 03 p0277 N88-11746
NASA supersonic STOVL propulsion technology program
[NASA-TM-100227] 06 p0668 N88-14093
Propulsion estimation techniques 07 p0927 N88-15632
An investigation into the feasibility of using a dual-combustion mode ramjet in a high Mach number tactical missile
[AD-A186906] 09 p1119 N88-16705
Integration testing of the propulsion system of Ariane's first stage 09 p1126 N88-16751
A comparison of propulsion systems for potential space mission applications
[DE88-005637] 14 p1882 N88-21248
Activities report of the Energetics Department
[ETN-88-91981] 14 p1888 N88-21281
Nuclear propulsion systems for orbit transfer based on the particle bed reactor 17 p2401 N88-24272
High power ion thruster performance 17 p2404 N88-24295
Gas core reactors for direct nuclear propulsion 17 p2428 N88-24442
Status of high power electric propulsion technology 17 p2428 N88-24443
Noncryogenic propellants for a nuclear orbit transfer vehicle 17 p2428 N88-24444
Propulsion analysis and application potential of air breathing combined propulsion for ballistic space transporter
[ETN-88-92369] 21 p2903 N88-27227
COMPASS ground based engine monitoring program for general application --- Condition Monitoring and Performance Analysis Software System (COMPASS)
[PNR90420] 22 p3044 N88-28064
Evaluation of the advanced air breathing propulsion concepts, executive summary
[ESA-CR(P)-2540] 24 p3325 N88-29802
Evaluation of advanced air breathing concepts. Volume 1: Executive summary
[ESA-CR(P)-2539] 24 p3326 N88-29806
Hermes: Study of propulsion system for reusable man-rated spacecraft
[PSRM-TN-0000-00-04A] 24 p3337 N88-29866
Unified study of plasma/surface interactions for space power and propulsion
[AD-A195971] 24 p3338 N88-29870
Simulation of Vulcain engine operation at low inlet pressure
[ETN-88-93083] 24 p3339 N88-29875

PROPULSIVE EFFICIENCY
NT PROPELLER EFFICIENCY
Propulsion challenges and opportunities for high-speed transport aircraft 08 p0958 N88-15809
Gear systems for advanced turboprops 10 p1282 N88-17667
Rotorcraft flight-propulsion control integration: An eclectic design concept
[NASA-TP-2815] 12 p1584 N88-19475
China constructing high-altitude test cell 14 p1901 N88-21351
The 1988 overview of free-piston Stirling technology for space power at the NASA Lewis Research Center
[NASA-TM-100795] 16 p2170 N88-22934
Propfan model wind tunnel aeroelastic research results 16 p2220 N88-23246
Propulsive performance of a lifting flapping wing 17 p2295 N88-23733
Benefits of 20 kHz PMAD in a nuclear space station 17 p2398 N88-24256
High power ion thruster performance 17 p2404 N88-24295
Analytical and experimental investigation of ringless piston concept
[AD-A193213] 21 p2956 N88-27559

PROPYL COMPOUNDS
Identification of hydroxypropyl starch hydrolysate components 17 p2315 N88-23832

PROPYLENE
Studies on the use of propylene carbonate as a high-voltage insulator
[DE88-011786] 22 p3057 N88-28141

PROPYLENE OXIDE
Performance of polymer electrolyte cells at +25 to +100 C
[AD-A193988] 22 p3073 N88-28244

PROSPECTING
U EXPLORATION

PROSTHETIC DEVICES
The stress analysis of ceramic, polymeric, and metallic composite systems by the finite element method 18 p2529 N88-25004

PROTECTION
NT CIRCUIT PROTECTION
NT CORROSION PREVENTION
NT ENVIRONMENT PROTECTION
NT EYE PROTECTION
NT METEOROID PROTECTION
NT RADIATION PROTECTION
NT RADIATION SHIELDING
NT SOLAR RADIATION SHIELDING
NT THERMAL PROTECTION
Anti-abrasion protection with highly organized materials
[DE87-014238] 01 p0029 N88-10187
Lightning discharge protection rod
[NASA-CASE-LAR-13470-1] 06 p0666 N88-14083
A paper about electromagnetic pulse and principles of EMP protection
[FOA-C-30455-4.2] 06 p0692 N88-14246
Insect contamination protection for laminar flow surfaces 07 p0814 N88-14954
Solar cell cover glasses for satellites 15 p2052 N88-22225
Study of lightning and lightning protection (selected pages)
[AD-A190623] 15 p2098 N88-22498
Proposed quality assurance/quality control plan
[AD-A191490] 18 p2525 N88-24978
Vibration protection of inelastic structures by means of active and passive control 18 p2528 N88-25001
The use of liquid films for spacecraft survivability to laser radiation
[AD-A192954] 20 p2765 N88-26395
Future visual environment and concerns 23 p3242 N88-29299

PROTECTIVE CLOTHING
NT EXTRAVEHICULAR MOBILITY UNITS
NT PRESSURE SUITS
NT SPACE SUITS
Research and development of anti-G life support systems. Part 1: Development and evaluation of uniform-pressure anti-G suits
[AD-A185658] 06 p0754 N88-14628
Improvement of the construction of protective clothing for better wearability and comfort --- rainwear
[IZF-1986-26] 07 p0899 N88-15448
Portable, ambient air microclimate cooling in simulated desert and tropic conditions
[AD-A186457] 08 p1050 N88-16338
Perspectives in microclimate cooling involving protective clothing in hot environments
[AD-A188370] 12 p1671 N88-20007
Fit evaluation of female body armor
[AD-A188721] 14 p1953 N88-21638
Further development of a mathematical model for the specification of immersion clothing insulation
[IAM-653] 14 p1954 N88-21644
Study of benefits of passenger protective breathing equipment from analysis of past accidents
[DOT/FAA/CT-88/03] 18 p2461 N88-24610
The effects of different combinations of inlet air conditions used for cooling as measured on a heated manikin
[AD-A191116] 18 p2552 N88-25151
Performance estimates for operations conducted while wearing individual protective equipment: User manual
[AD-A191871] 18 p2553 N88-25154
The role of textile material in clothing on thermoregulatory responses to intermittent exercise
[AD-A192599] 22 p3130 N88-28608
Four-axis side-arm flight control simulator investigation
[AD-A196026] 24 p3409 N88-30294

PROTECTIVE COATINGS
NT ANODIC COATINGS
NT CERAMIC COATINGS
NT PRIMERS (COATINGS)
NT REFRACTORY COATINGS
Optimizing the application of high temperature corrosion resistant aluminium-silicon-base coatings
[BLL-M-37222-(5828.4)] 01 p0018 N88-10112
Development and production of new and modified powders for sprayed coatings and components for saving important raw materials
[BMFT-FB-T-86-129] 01 p0025 N88-10159
The water permeability of multi-layer coatings
[BLL-M-37252-(5828.4)] 02 p0148 N88-10927
Investigation of the structure of coatings of self fluxing alloys fused by laser energy
[BLL-M-37301-(5828.4)] 02 p0148 N88-10930
Comparison of high purity fine grain graphites from different suppliers with regard to physical, mechanical, and thermal properties --- Joint European Torus wall protection
[JUEL-SPEZ-401] 02 p0154 N88-10963
Coatings for Advanced Heat Engines Workshop: Book of abstracts
[DE87-012623] 02 p0180 N88-11121
Life prediction and constitutive models for engine hot section anisotropic materials program 02 p0188 N88-11175
Creep-fatigue behavior of NiCoCrAlY coated PWA 1480 02 p0189 N88-11176
Coating life prediction 02 p0189 N88-11181
Corrosion-resistant amorphous metallic coatings: Engineering development
[NASA-CR-181487] 03 p0287 N88-11802
Ion plating: Fundamental processing studies and synthesis of high performance coatings
[AD-A184766] 03 p0303 N88-11908
Carbon-fiber reinforced aluminum 04 p0403 N88-12507
Effect of long-term thermal aging on coated Celion/LARC-160 composites
[NASA-TM-100495] 04 p0410 N88-12544
Ceramic technology for advanced heat engines project
[DE88-001520] 04 p0420 N88-12605
Tribological properties of rf-sputtered MoS2 coatings
[DE88-000266] 04 p0452 N88-12802
An examination of coating failure on wing pivot fittings of f111 aircraft
[AD-A185028] 05 p0546 N88-13328
Simulated service test behavior of various internal and external coatings applied on CF6-50 first stage turbine blades
[NLR-MP-86018-U] 05 p0549 N88-13343
Coatings for high-temperature bearings and seals
[NASA-TM-100249] 05 p0567 N88-13453
Water disbondment characterization of organic Coating/metal substrate systems
[AD-A184847] 05 p0567 N88-13454
Antistatic coating compositions
[GB-PATENT-2-177-413-A] 05 p0568 N88-13463
Stress rupture behavior of silicon carbide coated, low modulus carbon/carbon composites
[NASA-CR-180863] 06 p0678 N88-14150
Life modeling of thermal barrier coatings for aircraft gas turbine engines
[NASA-TM-100283] 07 p0834 N88-15060
Chromic acid anodizing of aluminum foil
[NASA-CR-178417] 07 p0837 N88-15077
Use of hydrophilic polymer coatings for control of electroosmosis and protein adsorption 07 p0925 N88-15620
Hot piston ring/cylinder liner materials: Selection and evaluation
[NASA-TM-100276] 08 p0971 N88-15872
Effects of additives on fire properties of polyethylene
[AD-A187064] 09 p1146 N88-16871
Oxidation resistance of CVD coatings
[AD-A178337] 09 p1147 N88-16875
The effect of varying sputtering parameters on the microstructure and mechanical properties of 10 percent Ni + TiB2 thin films
[DE88-002600] 09 p1254 N88-17517
Bias, internal stress and substrate effects on the microstructure and properties of PVD-wear resistant coatings
[AERE-R-12360] 10 p1304 N88-17798
The soft/hard wet anodization of aluminum oxide and its use in a thin film multilayered capacitor
[AD-A187575] 10 p1325 N88-17919
High temperature oxidation studies on alloys containing dispersed phase particles and clarification of the mechanism of growth of SiO2
[AD-A188158] 11 p1457 N88-18688
Adhesion of PVD titanium coatings to beryllium substrates
[DE88-005147] 11 p1463 N88-18721
Oxidation and protection of fiberglass-epoxy composite masts for photovoltaic arrays in the low Earth orbital environment
[NASA-TM-100839] 11 p1465 N88-18734
Ion beam modification of film stress and the effectiveness of thin film encapsulants on GaAs
[DE88-004458] 11 p1558 N88-19328
Factors affecting the sticking of insects on modified aircraft wings
[NASA-CR-182615] 12 p1575 N88-19421
Mast material test program (MAMATEP)
[NASA-TM-100821] 12 p1604 N88-19592
Nondestructive evaluation of carbon-carbon coatings
[AD-A189524] 13 p1748 N88-20453
Abrasion and impact resistant coatings
[DE88-003562] 13 p1750 N88-20464

Safety research of insulating materials of cable for nuclear power generating station
[NASA-TT-20202] 13 p1752 N88-20477
Aging properties of cable polmers (2)
[NASA-TT-20228] 13 p1752 N88-20479
Measurement of the properties of lossy materials inside a finite conducting cylinder
[NASA-CR-182664] 13 p1832 N88-20962
JPRS report: Science and technology. USSR: Materials science
[JPRS-UMS-87-009] 14 p1884 N88-21261
Chemical vapor deposited silica coatings for solar mirror protection
[NASA-TM-100834] 14 p1893 N88-21306
Effect of protective coatings on high-temperature fatigue of heat-resistant alloys 14 p1895 N88-21314
Secondary electron emission characteristics improved by ion implantation 14 p1903 N88-21370
Laser surface melting
[BMFT-FB-T-86-072] 14 p1914 N88-21435
A constitutive model for an overlay coating 14 p1933 N88-21525
Development of a manufacturing unit for selective coating of solar absorbers made out of aluminum
[BMFT-FB-T-86-204] 14 p1942 N88-21590
Structure and properties of titanium nitride and zirconium nitride thin films prepared by reactive ion plating --- cutting tools
[ETN-88-92218] 15 p2042 N88-22167
Investigation of laser diagnostics of PACVD processes for depositing hard face coatings
[DE88-007083] 15 p2043 N88-22176
The corrosion resistance of an aluminum alloy coated with polysilazane derived ceramics
[AD-A190703] 15 p2046 N88-22189
JPRS report: Science and technology. USSR: Materials science
[JPRS-UMS-88-006] 16 p2179 N88-22988
Model study of thermal stresses in gas-turbine blades with protective coating 16 p2179 N88-22989
Protective coatings on metals, volume 10
[PB88-174461] 16 p2181 N88-23000
Development of a high-temperature resistant (700 F), corrosion-preventive organic coating
[AD-A191407] 16 p2182 N88-23009
Government research on ceramics coating technology 16 p2184 N88-23019
Inadequacies of EMI-seal material: A corrosion study 17 p2319 N88-23852
Surface conditioning products as tools for corrosion removal and corrosion prevention 17 p2320 N88-23856
Carboxylate formation at the interface between a polyimide coating and cobalt 17 p2320 N88-23859
Thrust chamber thermal barrier coating techniques
[NASA-TM-100933] 16 p2476 N88-24690
Isothermal and bithermal thermomechanical fatigue behavior of a NiCoCrAlY-coated single crystal superalloy
[NASA-TM-100907] 18 p2489 N88-24766
An investigation of ceramic coatings for protection of SiC from high-temperature corrosion
[DE88-007873] 18 p2493 N88-24790
A thermally modified polymer matrix composite material with structural integrity to 371 C
[NASA-TM-100922] 19 p2609 N88-25483
Corrosion prevention in gas turbines
[NLR-MP-87029-U] 20 p2760 N88-26373
Electrophoretic coatings. Part 1: Sandia applications
[DE88-008666] 20 p2776 N88-26465
The effects of thin compressive films on indentation fracture toughness measurements
[AD-A192243] 20 p2779 N88-26480
Rocket-propellant burn tests of silicide-coated niobium and tantalum
[DE88-010729] 20 p2781 N88-26496
Studies in support of oxidation-resistant composite materials
[AD-A193320] 21 p2905 N88-27238
Refractory fibers surface treatment
[REPT-47-603/F] 21 p2922 N88-27339
Proceedings of the 1987 Tri-Service Conference on Corrosion, volume 1
[AD-A191295] 22 p3053 N88-28114
Corrosion and stress corrosion of metals in decontamination solutions 22 p3054 N88-28118
Design guidelines for prevention of corrosion in combat and tactical vehicles
[AD-A194172] 22 p3055 N88-28126
Study of the erosion corrosion of alloys and coatings
[AD-A194337] 22 p3055 N88-28128
Corrosion control through a better understanding of the metallic substrate/organic coating/interface
[AD-A193981] 22 p3056 N88-28132
Optimization of fatigue and friction properties of titanium by means of surface treatments
[ECL-87-22] 22 p3056 N88-28133
Thermal barrier coating life-prediction model development
[NASA-CR-179507] 22 p3058 N88-28142
The effect of coatings on fatigue in aerospace materials --- gas turbine engines
[PNR90460] 22 p3059 N88-28150
Ultrafine microstructure composites prepared by chemical vapor deposition
[AD-A193849] 23 p3189 N88-28973
Processing technology research in composites
[AD-A195693] 24 p3341 N88-29890
Performance Prediction for Coatings. Proceedings of a Workshop
[AD-A188973] 24 p3354 N88-29966
Degradation of protective coatings on steel in corrosive environments 24 p3354 N88-29969
Prediction of degradation of polymeric coating materials 24 p3354 N88-29970
A reliability-based program for predicting the service life of organic coating systems 24 p3355 N88-29971
Electrical detection of coating deterioration 24 p3355 N88-29973
Electrochemical evaluation of the long term corrosion resistance of polymer coated steel 24 p3355 N88-29974
Evaluation of organic coating deterioration and substrate corrosion in seawater using electrochemical impedance measurements 24 p3355 N88-29976
Alternative immersion accelerated testing of coating systems for Naval shoreline facilities 24 p3355 N88-29977
Stressed fabric abrasion test procedure for urethane coated fabric fuel tanks
[AD-A196327] 24 p3356 N88-29982

PROTECTORS
Performance estimates for operations conducted while wearing individual protective equipment: User manual
[AD-A191871] 18 p2553 N88-25154

PROTEIN DENATURATION
U BIOPOLYMER DENATURATION

PROTEINS
NT CARBONIC ANHYDRASE
NT CATALASE
NT CHOLINESTERASE
NT CYTOCHROMES
NT ENZYMES
NT FIBRINOGEN
NT HEMOGLOBIN
Non-conventional approaches to food processing in CELSS, 1. Algal proteins: Characterization and process optimization 03 p0358 N88-12256
Biopolymers: Protein and nucleic acids
[AD-A185837] 07 p0835 N88-15066
Use of hydrophilic polymer coatings for control of electroosmosis and protein adsorption 07 p0925 N88-15620
Synthesis of high molecular weight peptide polymers and copolymers containing L-dope residues
[AD-A186462] 08 p0973 N88-15887
Evidence for human adaptive response to dehydration: Increase of circulating protein mass
[AD-A186225] 08 p1048 N88-16328
A comparison of algorithms for the analysis of images generated by two-dimensional electrophoresis
[DE88-003730] 09 p1220 N88-17319
Protein-crystal growth experiment (planned) 10 p1287 N88-17700
Response of coronary blood flow to step changes in plasma protein concentration in the isolated rat heart 12 p1651 N88-19892
Studies of molecular biology
[DE88-005906] 15 p2101 N88-22514
North Carolina Biomolecular Engineering and Materials Applications Center (NC-BEMAC)
[AD-A190923] 16 p2237 N88-23364
Optical monitoring of protein crystal growth
[NASA-CR-182869] 18 p2484 N88-24738
The electrokinetic behavior of calcium oxalate monohydrate in macromolecular solutions
[NASA-TM-101144] 18 p2493 N88-24791
A cardiostimulant protein from the Australian Red Waratah Sea anemone, Actinia tenebrosa 18 p2550 N88-25138
Two puzzling aspects of protein crystal growth 18 p2580 N88-25329
Hanging drop crystal growth apparatus and method
[NASA-CASE-MFS-28206-1-SB] 18 p2585 N88-25356
Crystal growth apparatus
[NASA-CASE-MFS-28182-1] 18 p2585 N88-25357
Experiments in microgravity environment: Protein crystallization
[REPT-881-430-101] 21 p2924 N88-27354

PROTOCOL (COMPUTERS)
Data Management Working Group report 01 p0016 N88-10097
The varieties of capabilities in Flex
[RSRE-MEMO-4042] 01 p0078 N88-10500
Space lab system analysis
[NASA-CR-179207] 02 p0138 N88-10869
Network reconstitution protocol
[AD-A184755] 03 p0367 N88-12309
An evaluation plan of bus architectures and protocols using the NASA Ames intelligent redundant actuation system
[NASA-CR-177458] 04 p0398 N88-12482
Distribution of records on a ring of processors
[PB87-235784] 06 p0758 N88-14649
Study of communication options in a distributed data handling system and survey of advanced man machine communications schemes. Work package 1: Interprocess communication
[ESA-CR(P)-2447] 07 p0843 N88-15114
A software planning and development methodology with resource allocation capability
[AD-A186088] 07 p0902 N88-15482
Cirrus: An automated protocol analysis tool
[AD-A186648] 08 p1052 N88-16348
AITI Test Report 87-002: Pratt and Whitney technical order transfer tests
[DE88-004045] 11 p1564 N88-19363
AITI Report 87-003: Honeywell technical order transfer tests
[DE88-004046] 11 p1564 N88-19364
Performance analysis of slotted ring protocols in High Speed Local Area Networks (HSLANS)
[INF-87-31] 14 p1955 N88-21652
Exact analyses of slotted ring protocols for local area networks with one transmitting station
[MEMO-650] 14 p1967 N88-21737
Using Colored Stochastic Petri Net (CS-PN) software for protocol specification, validation, and evaluation
[ENST-87C004] 15 p2113 N88-22588
A very simple construction for atomic multiwriter register
[CWI-CS-R8751] 16 p2249 N88-23436
A five-layer Open Systems Interconnection (OSI) implementation 17 p2390 N88-24204
An operational open-end file transfer protocol for mobile satellite communications 19 p2651 N88-25738
Integrated voice/data protocols for satellite channels 19 p2651 N88-25739
Minimum disclosure proofs of knowledge
[CWI-PM-R8710] 20 p2840 N88-26854
Markov chain computations to a solution of the mutual-exclusion problem in concurrency
[REPT-87-89] 20 p2847 N88-26896
A modular proof of correctness for a network synchronizer
[AD-A192726] 21 p3002 N88-27802
Performance analysis of FDDI
[NASA-CR-183206] 24 p3413 N88-30321

PROTON BEAMS
Performance of GaAs and silicon concentrator cells under 37 MeV proton irradiation
[NASA-TM-100144] 04 p0465 N88-12877
South African Association of Physicists in Medicine and Biology: 26th Annual Congress
[DE88-700824] 11 p1521 N88-19082
Initial operation of the Tevatron collider
[FNAL-TM-1449] 11 p1547 N88-19252
Microinstabilities in ion beam propagation 16 p2277 N88-23631
A multi-frame ion pinhole camera for intense ion beam transport and focusing experiments
[DE88-007283] 18 p2516 N88-24926
Intense ion beam diagnostics for particle beam fusion experiments on PBFA 2
[DE88-007279] 18 p2577 N88-25308
The XRD (X-Ray Diode) array, the grazing incidence spectrometer and the X-ray imaging camera on PBFA 2
[DE88-007282] 19 p2728 N88-26200

PROTON DENSITY (CONCENTRATION)
Calculation methods of atomic number density for various nuclear materials
[DE87-753006] 02 p0233 N88-11467

PROTON ENERGY
Study of the production of Ko mesons in proton antiproton interactions at 630 GeV
[NOTA-INTERNA-908] 21 p3015 N88-27892

PROTON IRRADIATION
Heavy ion and proton tests for subsystem upset
[AD-A195267] 24 p3434 N88-30442

PROTON SCATTERING
On the spin structure of the elastic ppbar scattering amplitude
[NOTA-INTERNA-892] 06 p0778 N88-14772

PROTON TELESCOPES
U PARTICLE TELESCOPES

PROTON-PROTON REACTIONS
Initial operation of the Tevatron collider
[FNAL-TM-1449] 11 p1547 N88-19252

PROTONS
NT SOLAR PROTONS
Effects of electron and proton irradiations on n/p and p/n GaAs cells grown by MOCVD
[NASA-TM-100199] 01 p0042 N88-10266
The elastic scattering of intermediate energy protons from (40)Ca and (208)Pb 01 p0092 N88-10599
Low altitude flux and dose measurements during two solar flare events 01 p0111 N88-10713
Volume produced H(-),D(-) ion source for proton accelerator and thermo-nuclear fusion research by sheet plasma (III)
[IPPJ-838] 02 p0242 N88-11531
Proton abstraction as a route to conductive polymers
[AD-A184019] 04 p0421 N88-12612
Prompt simultaneous acceleration of protons and electrons to relativistic energies by shock waves in solar flares
[IPPJ-851] 04 p0493 N88-13037
Experimental studies of elementary particle interactions at high energies
[DE88-000804] 05 p0648 N88-13971
An analytic model for ionization distributions produced in nanometer sites by protons
[DE88-003943] 10 p1406 N88-18385
Ion energy diagnostics for voltage determinations in plasma-erosion-opening-switch experiments
[DE88-004822] 11 p1479 N88-18827
Ground-state correlations in C12 and the mechanism of the (e,e'p) reaction
[B8729349] 14 p1980 N88-21816
The response of a small liquid scintillation counter for low energy (gamma, p) experiments
[NOTA-INTERNA-901] 14 p1980 N88-21819
Measurement of the sup 4He(gamma, p)sup 3H total cross section and charge symmetry
[NOTA-INTERNA-902] 14 p1981 N88-21820
Analysis of hadron production in deep inelastic muon-proton collisions through the fire-string model
[PREPRINT-578] 14 p1981 N88-21822
Photon-assisted formation and cooling of molecular hydrogen
[MP-87-102] 16 p2267 N88-23563
Small molecule and small cluster ion formation in a low-density containerless mixture of electrons, protons and hydrogen atoms 16 p2269 N88-23577
X-ray production in low energy proton stopping
[NASA-TM-100619] 16 p2270 N88-23582
Reference nuclear data for space applications
[DE88-007041] 16 p2270 N88-23583
Characterization of proton conducting polymer blends 19 p2669 N88-25867
Scaling laws for geomagnetic tail current sheet acceleration
[AD-A193379] 19 p2691 N88-25998
The protonic Beta double prime aluminas: Preparation, stability, conductivity and structure
[DE88-008442] 20 p2768 N88-26415
Rf cavity primer for cyclic proton accelerators
[DE88-010655] 20 p2853 N88-26938

PROTOPLANETS
Astrophysics and the solar nebula 07 p0883 N88-15355
Exobiology and life science 07 p0883 N88-15358
Cometary nucleus as aggregate of planetesimals
[ISAS-RN-364] 19 p2741 N88-26275

PROTOPLASTS
Plant cell cultures in space biology studies 12 p1654 N88-19913
The use of plant protoplasts in biotechnological space research 12 p1655 N88-19914

PROTOSTARS
NT PRE-MAIN SEQUENCE STARS
NT T TAURI STARS
Star formation and molecular clouds 24 p3451 N88-30537

PROTOTYPES
Double-effect absorption heat pump, phase 3
[PB87-232195] 03 p0317 N88-12005
A prototype expert system for separation science
[DE87-013542] 03 p0371 N88-12333
Renewed interest in airships for industry use discussed 04 p0424 N88-12628
Light funnel concentrator panel for solar power
[NASA-CR-179223] 04 p0464 N88-12870
A single-station weather forecasting expert system
[AD-A184889] 05 p0627 N88-13832
A prototype ray tracer
[AD-A184863] 05 p0634 N88-13874
A 1,000-watt solar power unit for Far North 06 p0728 N88-14481
Prototype space station automation system delivered and demonstrated at NASA 08 p1066 N88-16442
High-resolution Real-Time Radiography (RTR) system design
[AD-A187107] 09 p1166 N88-16992
Shared workspaces for real-time collaboration in distributed networks: Concepts, techniques, problems
[AD-A188150] 10 p1394 N88-18315
Prototype thin-film thermocouple/heat-flux sensor for a ceramic-insulated diesel engine
[NASA-TM-100798] 11 p1490 N88-18892
A new isodynamically-braked arm ergometer including the demonstration of a prototype 12 p1661 N88-19957
Reducing time required for the development of avionic systems 12 p1702 N88-20185
Prototype manufacturing techniques for reducing cost, schedule, and technical risk 12 p1702 N88-20189
Use of demonstration/validation prototypes: Impact on total development costs and times 12 p1703 N88-20194
Engineering management for validation prototype phase 12 p1703 N88-20195
Acceleration of prototype development and reduction of cost by multidisciplinary integration 12 p1704 N88-20199
The use of an automated flight test management system in the development of a rapid-prototyping flight research facility
[NASA-TM-100435] 13 p1823 N88-20896
Towards a tribology information system: The results of a Planning Workshop held at the National Bureau of Standards, July-August 1985
[PB88-168604] 14 p1918 N88-21448
STRUTEX: A prototype knowledge-based system for initially configuring a structure to support point loads in two dimensions
[NASA-TM-100613] 16 p2250 N88-23448
Rapid prototyping of complex avionic system architectures 17 p2302 N88-23771
The integration, characterisation and trialling of a modern complex airborne radar 17 p2305 N88-23791
Coherent functional development: Key to successful future system integration 17 p2307 N88-23803
SP-100 GES test site 17 p2417 N88-24375
Analysis of plasma coupling with the prototype DIII-D ICRF antenna
[DE88-008085] 19 p2729 N88-26204
Analytical and experimental investigation of ringless piston concept
[AD-A192835] 20 p2810 N88-26673
Expert system application education project
[NASA-CR-183089] 20 p2843 N88-26867
Optical evaluation of prototype stretched-membrane mirror modules for solar central receivers
[DE88-011884] 21 p2969 N88-27637
SP-100 Ground Engineering Systems: Test facility control systems
[DE88-009195] 21 p3015 N88-27895
Study of Plasma Motor Generator (PMG) tether system for orbit reboost
[NASA-CR-172074] 23 p3184 N88-28949
PLZT (Lead-Lathanium-Zirconium-Titanium) electro-optic photographic system
[AD-A193473] 23 p3215 N88-29137
ADP (Automated Data Processing) requirements definition and documentation through user-developed prototypes
[AD-A194407] 23 p3248 N88-29332
Contingency rescheduling of spacecraft operations 24 p3416 N88-30337
Achieving real-time performance in FIESTA 24 p3418 N88-30344

PROTOZOA
NT AMOEBA
NT PARAMECIA

PROVING
NT THEOREM PROVING
Generating diagnostic knowledge from a structural and functional description 02 p0129 N88-10813
Use of a 35mm camera for remote surface cleanliness verification 02 p0133 N88-10835
Columbus pressurized module verification 02 p0134 N88-10842
Fin gaps and body slots of guided projectiles: Effects, data correlation and modeling
[AD-A184440] 03 p0270 N88-11698
East coast gravity validation study
[AD-A184292] 03 p0351 N88-12217
SDVS (State Delta Verification System): Program verification system development fiscal year 1986
[AD-A184338] 03 p0366 N88-12302
High resolution satellite imagery simulation --- treaty verification
[FOA-C-30462-3.3,9.3] 05 p0620 N88-13810
Design verification and fabrication of active control systems for the DAST ARW-2 high aspect ratio wing, part 1
[NASA-CR-177959-PT-1] 06 p0669 N88-14101
Design verification and fabrication of active control systems for the DAST ARW-2 high aspect ratio wing. Part 2: Appendices
[NASA-CR-177959-PT-2] 06 p0669 N88-14102
A flow visualization study of the leading edge separation bubble on a NACA 0012 airfoil with simulated glaze ice
[NASA-CR-180846] 07 p0816 N88-14966
An approach to validation and verification of the communications load model with supporting user's guide
[AD-A185926] 07 p0840 N88-15098
Correctness proofs for systolic algorithms: Palindromes and sorting
[PB88-106075] 07 p0912 N88-15534
Feasibility of software built-in test for SDI (Strategic Defense Initiative) applications
[AD-A185750] 07 p0917 N88-15572
Verification of FANTASTIC integrated code 07 p0924 N88-15613
Verification issues for rule-based expert systems 08 p1055 N88-16361
Temporal and contextual knowledge in model-based expert systems 08 p1055 N88-16363
Methodology for testing and validating knowledge bases 08 p1055 N88-16364
KBS V and V as related to automation of space station subsystems: Rationale for a KBS lifecycle 08 p1057 N88-16375
CFD validation experiments for internal flows
[NASA-TM-100797] 09 p1114 N88-16679
Approaches to the verification of rule-based expert systems 09 p1206 N88-17232
A formal approach to validation and verification for knowledge-based control systems 09 p1207 N88-17233
Expert system verification concerns in an operations environment 09 p1207 N88-17234
Building validation tools for knowledge-based systems 09 p1207 N88-17235
Methods for evaluating the quality and reliability of aerodynamic software programs
[PB87-169793] 09 p1219 N88-17314
Software program validity: A survey
[PB87-170593] 09 p1219 N88-17315
Simulation test beds for the space station electrical power system
[NASA-TM-100786] 10 p1290 N88-17715
Formal multilevel hierarchical verification of synchronous MOS VLSI circuits
[AD-A187532] 10 p1324 N88-17918
Navigation recovery block design description
[NASA-CR-182473] 10 p1342 N88-18022
Benchmark computation and finite element performance evaluation for a rhombic plate bending problem
[AD-A187402] 10 p1345 N88-18041
Automated data flow diagram verification 10 p1382 N88-18255
Procedures for quantitative sensitivity and performance validation studies of a deterministic fire safety model
[NBS/GCR-88/544] 11 p1469 N88-18762
A perspective on 15 years of proof-of-concept aircraft development and flight research at Ames-Moffett by the Rotorcraft and Powered-Lift Flight Projects Division, 1970-1985
[NASA-RP-1187] 12 p1582 N88-19467
The Hermes robot arm, its design and verification 12 p1588 N88-19508
Robotics servicing experiment --- European space programs 12 p1591 N88-19529
Rendezvous and docking (RVD) verification and demonstration in-orbit 12 p1592 N88-19531
Use of demonstration/validation prototypes: Impact on total development costs and times 12 p1703 N88-20194
Engineering management for validation prototype phase 12 p1703 N88-20195
A correlation study of X-29A aircraft and associated analytical development
[NASA-CR-183103] 13 p1722 N88-20296
Experimental verification of a finite-difference time-domain thin slot algorithm
[DE88-005572] 13 p1817 N88-20859
Software verification using partition analysis
[AD-A190570] 15 p2112 N88-22582
On the validation of a code and a turbulence model appropriate to circulation control airfoils
[NASA-TM-100090] 16 p2156 N88-22864
Knowledge based system verification and validation as related to automation of space station subsystems: Rationale for a knowledge based system lifecycle 17 p2387 N88-24192
Analysis procedures and subjective flight results of a simulator validation and cue fidelity experiment
[NASA-TM-88270] 18 p2465 N88-24634
Structural margins assessment approach
[NASA-TM-100332] 18 p2473 N88-24672

Computer resource management technology program (PE 64740F). Task no. 9: Advanced user authentication
[PB88-183066] 18 p2555 N88-25163
Application of flight systems methodologies to the validation of knowledge-based systems
[NASA-TM-100442] 18 p2561 N88-25207
The experimental verification of wall movement influence coefficients for an adaptive walled test section
[NASA-CR-181681] 19 p2598 N88-25439
Verification of regional climates of GISS GCM. Part 1: Winter
[NASA-TM-100695] 19 p2694 N88-26012
Minimum disclosure proofs of knowledge
[CWI-PM-R8710] 20 p2840 N88-26854
Oxidation-erosion of metals and alloys: Models, verification, and prediction
[DE88-010016] 21 p2915 N88-27300
Ada (trade name) compiler validation summary report: Verdix Corporation VAda-010-03315, version 5.5 MicroVAX 2 host ISBC 386/20P Intel target
[AD-A193226] 21 p2997 N88-27774
Ada (trade name) compiler validation summary report: Verdix corporation VAda-010-13125, version 5.41 Sun Microsystems Sun-3/160 host microbar GPC68020 target
[AD-A193415] 21 p2997 N88-27777
Ada (trade name) compiler validation summary report: Verdix Corporation VAda-010-0101, version 5.41 VAX-11/750
[AD-A193414] 22 p3136 N88-28645
Air Force Systems Command software independent verification and validation implementation analysis and guidance
[AD-A194309] 22 p3137 N88-28653
LO-CO-GRAF (low cost graphics): Generating maps to support command and control/crisis management using small computers
[AD-A193964] 22 p3139 N88-28661
Induction instrument for logic conclusion
[LRT-WE-9-FB-5(1987)] 22 p3144 N88-28697
Verification and tests --- space projects
22 p3160 N88-28814
Validity of the academic aptitude composite of the Air Force Officer Qualifying Test (AFOQT)
[AD-A194753] 23 p3240 N88-29286
Ada (trade name) compiler validation summary report: Verdix Corporation VAda-010-03205, version 5.42 MicroVAX 2 host and national DB32000 (NS32032 target
[AD-A193485] 23 p3247 N88-29326
Confirmation of slow-waves in a crosstie overlay coplanar waveguide and its application to band-reject gratings and reflectors
[AD-A194961] 24 p3361 N88-30011

PROVISIONING
Inventory behavior at remote sites
06 p0796 N88-14873

PROXIMITY EFFECT (ELECTRICITY)
Modeling of proximity coupling between superconducting filaments in superconducting dipole magnets
[DE87-014684] 03 p0382 N88-12403
The effect of magnetic impurities and barriers on the magnetization and critical current of fine filament NbTi composites
[DE88-004443] 10 p1419 N88-18472

PSEUDOMONAS
Study of certain biological characteristics of bacteria during the French-Soviet CYTOS-2 space experiment
04 p0473 N88-12917

PSEUDOPOTENTIALS
The pseudopotential density functional method applied to semiconducting crystals
[ETN-88-91362] 05 p0656 N88-14024

PSEUDORANDOM SEQUENCES
Short pseudorandom test sequences
[AD-A185883] 08 p1054 N88-16357
A comparison of generators for pseudo-random normal deviates
[DE88-011711] 21 p3010 N88-27859
Random number generation
[USIP-87-15] 22 p3145 N88-28707

PSYCHIATRY
NT NEUROPSYCHIATRY
Normative developmental equations for the EEG and their sensitivity to neurological and psychiatric disorders
21 p2977 N88-27687

PSYCHOACOUSTICS
Transient classifier systems and man-machine interface research
[AD-A186213] 07 p0899 N88-15446
Mechanisms mediating perception of complex acoustic patterns
[AD-A189765] 15 p2102 N88-22520
On categorizing sounds
[AD-A189784] 15 p2129 N88-22700

PSYCHOLOGICAL EFFECTS
NT DESYNCHRONIZATION (BIOLOGY)
NT ILLUSIONS
NT JET LAG
Human adaptation to isolated and confined environments
[NASA-CR-181502] 03 p0357 N88-12248
JPRS report: Science and technology. USSR: Space Biology and Aerospace Medicine, volume 21, no. 4, July - August 1987
[JPRS-USB-88-002] 07 p0893 N88-15412
New US book on aviation psychology reviewed
07 p0896 N88-15433
Medical and psychological problems of assuring flight safety under present conditions
10 p1359 N88-18123
Investigation of effects of short-term exposure to high concentrations of carbon monoxide on operator's psychophysiological functions 10 p1361 N88-18133
Incorporation of privacy elements in space station design
[NASA-CR-182748] 14 p1881 N88-21242
Ejection situations in the U-2/TR-1: An analysis of emotions and events
[AD-A192872] 21 p2893 N88-27175
CEEG dynamic brain mapping: A new method to evaluate brain function in different psychological and drug conditions 21 p2977 N88-27685
Using ERPS to study human information processing
21 p2980 N88-27698
Behavioral, psychological and demographic predictors of physical fitness
[AD-A192697] 21 p2986 N88-27733
Attitudes towards the cold: Effects on psychological mood and subjective reports of illness during cold weather training
[AD-A194777] 23 p3239 N88-29274

PSYCHOLOGICAL FACTORS
Some aspects of sociopsychological screening of flying school applicants 07 p0890 N88-15392
Antarctica as a model for the human exploration of Mars
[AD-A185835] 08 p1051 N88-16342
Temperament Structure Scales (TSS). Test manual
[ESA-TT-1069] 09 p1201 N88-17197
Effects of stress on judgement and decision making in dynamic tasks
[AD-A188203] 11 p1523 N88-19092
Protection from stress 12 p1664 N88-19978
On categorizing sounds
[AD-A189784] 15 p2129 N88-22700
Chronic stress as a factor in aircraft mishaps
16 p2239 N88-23376
A framework for a theory of mapping
[AD-A191071] 18 p2551 N88-25144
Selection and training of subjects to live and work in hostile and unusual environments
19 p2696 N88-26026
Rules, schema and decision making
[AD-A193389] 21 p3027 N88-27967

PSYCHOLOGICAL INDEXES
U PSYCHOLOGICAL TESTS

PSYCHOLOGICAL TESTS
Exploiting auxiliary information about items in the estimation of Rasch item difficulty parameters
[AD-A184383] 03 p0372 N88-12341
Development of a menu of performance tests self-administered on a portable microcomputer
[NASA-CR-172040] 08 p1067 N88-16452
Temperament Structure Scales (TSS). Test manual
[ESA-TT-1069] 09 p1201 N88-17197
Surrogate measures: A proposed alternative in human factors assessment of operational measures of performance 09 p1215 N88-17281
Modeling incorrect responses to multiple-choice items with multilinear formula score theory
[AD-A187887] 11 p1522 N88-19090
Field dependence-independence and its relationship to flight training performance
[AD-A188888] 12 p1670 N88-20003
Quasi-loglinear models for test and item analysis --- psychometrics
[B8716249] 14 p1952 N88-21636
Construction of a multidimensional questionnaire to determine interindividual differences in controlling attention
[DFVLR-FB-87-45] 14 p1952 N88-21637
Properties of some Bayesian scoring procedures for computerized adaptive tests
[AD-A189925] 15 p2124 N88-22660
The program Kennedy Approach as an experimental design of a dynamic computerized air traffic control test
[DFVLR-FB-87-50] 16 p2159 N88-22881
NASA-Ames workload research program
17 p2380 N88-24151
Selecting the right crew for future space stations: An analysis of selection research on offshore divers, aviation pilots and other high risk groups in Scandinavia
19 p2696 N88-26021
Reliability and construct validity of reaction time, inspection time and machine-paced tests of cognitive speed
[AD-A193779] 23 p3241 N88-29289

PSYCHOLOGY
NT AVIATION PSYCHOLOGY
NT COGNITIVE PSYCHOLOGY
NT MILITARY PSYCHOLOGY
NT PSYCHOACOUSTICS
NT PSYCHOPHYSICS
NT SPACE PSYCHOLOGY
Assessment of fatigue in aviation crews
[AD-A184129] 03 p0356 N88-12245
The attitudes of science policy, environmental, and utility leaders on US energy issues and fusion
[DE88-000784] 04 p0494 N88-13041
JPRS report: Science and technology. USSR: Life sciences
[JPRS-ULS-87-013] 06 p0750 N88-14608
Innovation and creativity: A critical linkage
[DE88-003309] 10 p1426 N88-18515
USSR report: Life sciences. Biomedical and behavioral sciences
[JPRS-UBB-87-008] 12 p1662 N88-19966
Management information systems design implications: The effect of cognitive style and information presentation on problem solving
[AD-A188850] 12 p1705 N88-20205
Problem solving in a natural task as a function of experience
[AD-A191180] 16 p2243 N88-23399
The representational code of the internal model of dynamic systems: An individual differences and dual task approach
[AD-A190876] 16 p2244 N88-23403
Models of incremental concept formation
[AD-A191597] 18 p2552 N88-25147
Attitudes towards the cold: Effects on psychological mood and subjective reports of illness during cold weather training
[AD-A194777] 23 p3239 N88-29274
Transformations of short-term visual memory
[AD-A193873] 23 p3241 N88-29290
Comparison of morning with afternoon nitrogen elimination in resting subjects breathing 100 percent oxygen
[AD-A196191] 24 p3407 N88-30282
Advancement of latent trait theory
[AD-A194302] 24 p3408 N88-30289

PSYCHOMETRICS
Computer response time measurements of mood, fatigue and symptom scale items: Implications for scale response time uses
[AD-A186093] 07 p0888 N88-15384
Tutoring electronic troubleshooting in a simulated maintenance work environment
09 p1204 N88-17215
Intelligent tutoring systems as tools for investigating individual differences in learning
09 p1204 N88-17216
Modeling incorrect responses to multiple-choice items with multilinear formula score theory
[AD-A187887] 11 p1522 N88-19090
Quasi-loglinear models for test and item analysis --- psychometrics
[B8716249] 14 p1952 N88-21636
Construction of a multidimensional questionnaire to determine interindividual differences in controlling attention
[DFVLR-FB-87-45] 14 p1952 N88-21637
Conjunctive measurement theory: Cognitive research prospects
[AD-A193627] 23 p3239 N88-29277

PSYCHOMOTOR PERFORMANCE
A comparison of the Army's Project A: Cognitive and psychomotor tests to analogous Air Force and Navy tests
[AD-A188636] 12 p1670 N88-20002
Mental-State Estimation, 1987
[NASA-CP-2504] 16 p2239 N88-23370
The biomorphic model of the human operator controlling a single or a double integrator
[LR-505] 16 p2243 N88-23402
Teleoperator human factors study
[NASA-CR-178930] 17 p2382 N88-24162
Research on piloting under conditions of breakdown in flight
[PB87-217980] 19 p2710 N88-26102

Does dihydroergotamine used in therapeutical doses influence the physical and psychomotor performance of young pilots or other traffic drivers subjected to hypotonia?
[ETN-88-92136] 20 p2832 N88-26799
Cognitive and neural bases of skilled performance
[AD-A193392] 21 p2992 N88-27747
Determinants of dual-task interference and resource theories in cognitive psychology
[DFVLR-FB-88-14] 21 p2992 N88-27748
Literature review: Validity and potential usefulness of psychomotor ability tests for personnel selection and classification
[AD-A193558] 23 p3241 N88-29287

PSYCHOPHYSICS
NT PSYCHOACOUSTICS
Psychophysical considerations in measuring MRTD with staring arrays — minimum resolvable temperature difference (MRTD)
[RSRE-MEMO-4031] 01 p0076 N88-10487
Computing support for basic research in perception and cognition
[AD-A186192] 07 p0897 N88-15437
Vision algorithms and psychophysics
[AD-A186773] 09 p1200 N88-17193
Perception and control of simulated self motion
[AD-A187444] 10 p1372 N88-18188
Complex sound processing: An interdisciplinary approach
[AD-A189782] 15 p2102 N88-22523
Finding texture boundaries in images
[AD-A190554] 15 p2117 N88-22609
Does dihydroergotamine used in therapeutical doses influence the physical and psychomotor performance of young pilots or other traffic drivers subjected to hypotonia?
[ETN-88-92136] 20 p2832 N88-26799
Perception of motion in statistically-defined displays
[AD-A193076] 21 p2991 N88-27745
Models for motion perception
22 p3133 N88-28629
Effects of psychophysical lifting training on maximal repetitive lifting capacity
[AD-A192605] 23 p3238 N88-29271

PSYCHOPHYSIOLOGY
NT WORKLOADS (PSYCHOPHYSIOLOGY)
Evoked brain activity and personnel performance
[AD-A185922] 07 p0897 N88-15436
Considerations concerning the basic bandwidth reduction of high definition television systems (HDTV) component signals, based on psychophysiological properties of the eye
[IRT-B-83/87] 09 p1153 N88-16909
Neurocognitive predictions of performance
[AD-A188323] 12 p1669 N88-19998
An overview of current approaches and future challenges in physiological monitoring
16 p2239 N88-23371
Vagal tone as an index of mental state
16 p2239 N88-23373
Challenges of physiological monitoring in a Navy operational setting 16 p2239 N88-23374
Attention, effort, and fatigue: Neuropsychological perspectives 16 p2241 N88-23387
Physiological measures and mental-state assessment
16 p2242 N88-23392
Brainstem response and state-trait variables
16 p2242 N88-23394
The event-related brain potential as an index of information processing and cognitive activity: A program of basic research
[AD-A191244] 16 p2243 N88-23400
Psychophysiological measures of drowsiness as estimators of mental fatigue and performance degradation during sleep deprivation 21 p2980 N88-27702
Comparative aspects of multiple processes of attention
[AD-A195805] 24 p3408 N88-30291

PSYCHOSES
NT SCHIZOPHRENIA

PSYCHOTROPIC DRUGS
CEEG dynamic brain mapping: A new method to evaluate brain function in different psychological and drug conditions 21 p2977 N88-27685

PUBLIC HEALTH
JPRS report: Science and technology. USSR: Life sciences
[JPRS-ULS-87-012] 03 p0355 N88-12238
JPRS report: Science and technology. USSR: Life sciences
[JPRS-ULS-87-009] 04 p0473 N88-12915
JPRS report: Science and technology. USSR: Life sciences
[JPRS-ULS-87-013] 06 p0750 N88-14608
Food irradiation seminar: Asia and the Pacific
[DE88-700432] 09 p1202 N88-17203
USSR report: Life sciences. Biomedical and behavioral sciences
[JPRS-UBB-87-010] 12 p1651 N88-19889
Health and environmental consequences of the Chernobyl nuclear power plant accident
[DOE/ER-0332] 19 p2689 N88-25985

PUBLIC LAW
NT LEGAL LIABILITY

PUBLIC RELATIONS
Procedure and program used for data processing in a poll on nuclear energy utilization
[IFSI-87-3] 05 p0649 N88-13977
Datacast: The transmission system
[BBC-RD-1988/1] 14 p1905 N88-21385
Nuclear safety as applied to space power reactor systems 17 p2415 N88-24360

PUBLICATIONS
U DOCUMENTS

PULMONARY CIRCULATION
Validation of a modified one-step rebreathing technique for non-invasive measurement of submaximal cardiac output
[AD-A192852] 21 p2987 N88-27735

PULMONARY FUNCTIONS
A plethysmograph for measuring pulmonary ventilation in small animals
[AD-A184978] 05 p0629 N88-13846
Load carriage induced alterations of pulmonary function
[AD-A186227] 07 p0889 N88-15386
Biorhythmological analysis of dynamics of pulmonary ventilation parameters during orthostatic tests
07 p0891 N88-15400

PULSARS
On the (lack of) proper motion of the Vela pulsar
01 p0097 N88-10635
X-ray pulsars: Accretion flow deceleration
03 p0390 N88-12451
Neutron stars observations as astrophysical probes
06 p0800 N88-14896
Self-modulational formation of pulsar microstructures
[NASA-CR-182420] 08 p1104 N88-16622
The formation of single millisecond pulsars in globular clusters
[MPE-PREPRINT-97] 10 p1428 N88-18525
A search for medium energy gamma ray pulsars
11 p1568 N88-19385
Topics in curved and flat space electromagnetism
13 p1854 N88-21100
Range determination of pulsars, taking into account H2 regions
[ETN-88-91492] 14 p1993 N88-21877
A 23 hour EXOSAT observation of the X-ray pulsar 1E2259+586 and the associated supernova remnant G109.1-1.0
[MPE-PREPRINT-99] 14 p1994 N88-21882
Strange, quark and metastable neutron stars
[DE88-702404] 21 p3030 N88-27984
Cascade model of gamma-ray bursts: Power-law and annihilation-line components
[NASA-TM-101176] 21 p3032 N88-27998
Very high energy cosmic gamma rays from radio and X-ray pulsars 23 p3309 N88-29711

PULSATING FLOW
U UNSTEADY FLOW

PULSE (CARDIOVASCULAR)
U HEART RATE

PULSE AMPLITUDE
Four-wave mixing used in optical amplitude encoding
03 p0376 N88-12366
Flow induced pulsations in pipe systems
[ETN-88-91367] 06 p0702 N88-14307
VAXGAP: A code for the routine analysis of gamma-ray pulse-height spectra on a VAX computer
[DE88-011702] 22 p3137 N88-28648

PULSE AMPLITUDE MODULATION
Telemetry applications handbook
[AD-A186825] 09 p1132 N88-16789
Bragg-cell receiver study
[NASA-CR-182684] 13 p1761 N88-20535
Polymerization of epoxy matrix composites using pulsed microwaves
[CERT-3/1324-MO] 20 p2780 N88-26487
Currents induced in a human being for electromagnetic fields to 10 kHz-50 MHz
[AD-A191977] 23 p3238 N88-29268

PULSE CODE MODULATION
NT DELTA MODULATION
NT DIFFERENTIAL PULSE CODE MODULATION
Telemetry applications handbook
[AD-A186825] 09 p1132 N88-16789

PULSE COMMUNICATION
A compact digital communications system. Part 3: Generalising the phase locked loop
[RSRE-MEMO-4027-PT-3] 01 p0035 N88-10222
Digital receiver structures and methods for the determination of the scanning frequency in modems for fast data transmission via telephone channels
[ETN-87-90429] 01 p0037 N88-10235
A digital audio link to the Channel Islands in the UHF television band: Preliminary experimental results
[BBC-RD-1987/9] 02 p0161 N88-11011
Theory and methods for design of pulse shapes for broadcast teletext
[CRC-1405] 02 p0162 N88-11013
Ultra-low power digital filter
[AD-A184485] 03 p0310 N88-11959
Cross-correlation of uniform cyclic difference set sequences
[AD-A184879] 05 p0640 N88-13913
A generalization of order statistic filters: The alpha-trimmed linear filter
[AD-A186125] 07 p0842 N88-15107
Requirements and options for communications services in support of the Systems Autonomy Demonstration Project 08 p1057 N88-16374
Digital bit error rate estimator for telemetry links
[INPE-4351-TDL/295] 12 p1598 N88-19563
High speed, bandpass sampling of digital communications waveforms
[AD-A189842] 15 p2056 N88-22254
Design for interoperability (interchangeability)
17 p2305 N88-23789
Direct bit detection receiver performance analyses for 8-DPSK (Differential Phase Shift Keyed) modulated signals operating with improper carrier phase synchronization
[AD-A193839] 22 p3070 N88-28220
The 44/20 GHz ground terminal
[AD-A194002] 23 p3204 N88-29069
Signals and systems 24 p3363 N88-30026

PULSE COMPRESSION
Generation of light pulses in semiconductor laser upon excitation by several electron beams
07 p0920 N88-15589
The design and implementation of surface acoustic wave devices for linear FM and a new non-linear FM pulse compression technique for radar applications
[AD-A186741] 08 p0980 N88-15922
RF pulse compression development
[DE88-004818] 11 p1479 N88-18826
Space-time structure of ultrashort light pulses formed during stimulated backscattering of laser beam
14 p1972 N88-21767
Time-domain frequency-selective optical memories: A study of the basic mechanisms and potential systems
[AD-A190854] 16 p2274 N88-23607
Application of pulse compression and shaping to the FEL photoelectric injector
[DE88-007908] 19 p2675 N88-25910
Development of inductive storage pulsed power generators
[AD-A193878] 22 p3117 N88-28521

PULSE DIFFRACTION
Diffraction moire: The dynamic regime
[DE87-014883] 03 p0335 N88-12111
Short pulse X-ray diffraction studies of shocked and annealed crystals using the JANUS research laser
[DE88-011329] 23 p3288 N88-29579

PULSE DOPPLER RADAR
NT MONOPULSE RADAR

PULSE DURATION
Picosecond CO2 laser interactions with polyatomic molecules
[DE87-012072] 01 p0051 N88-10327
Saturable absorbers for colliding pulse-locked Nd:YAG lasers 03 p0302 N88-11902
Thrust and specific impulse of repetitively-pulsed-laser propulsion rocket 03 p0318 N88-12012
Long-range pulselength scaling of 351nm laser damage thresholds
[DE87-014754] 04 p0448 N88-12777
Optimization of field emission electron beam sources for high-power lasers
[PB87-218814] 06 p0708 N88-14341
Laser pulse width dependent surface ripples on silicon
[PB88-127311] 10 p1336 N88-17982
Efficiency of fusion during periodic-pulse laser-beam welding 14 p1897 N88-21324
The technical feasibility of using spiked-radiation lasers to cut out and weld metals 14 p1898 N88-21332
Folded long-pulse XeCl excimer laser described
14 p1901 N88-21357
XeCl laser-pumped nanosecond dye lasers
14 p1902 N88-21359
Theoretical study of colliding pulse mode-locking in dye lasers 14 p1903 N88-21366
Laser pulse detection with infrared range semiconductor detectors
[DE88-700857] 14 p1914 N88-21432

Time characteristics of ultrashort light pulses from dye lasers with distributed feedback
14 p1970 N88-21759
Nonlinear stage of ultrashort-pulse formation in solid-state laser 14 p1971 N88-21765
Pulse duration control of XeCl*-laser by means of plasma shutter 14 p1973 N88-21774
Timing for subnanosecond pulses
[DE88-701390] 16 p2192 N88-23074
Monolithic fuel cell based power source for sprint power generation 17 p2407 N88-24313
Fundamental analysis of space nuclear-MHD generator for gigawatt-level power 17 p2411 N88-24337
Burst power gas core reactor with MHD power generation 17 p2433 N88-24472

PULSE DURATION MODULATION
Digital to analog and analog to digital conversion using pulse duration modulation
[ETN-87-90415] 01 p0078 N88-10499
Digital control of a direct current converter for a hybrid vehicle
[LAAS-87-266] 05 p0578 N88-13527
Digital control of high frequency pulse-width modulated inverters
[ETN-87-90711] 09 p1157 N88-16936
The theory and implementation of a high quality pulse width modulated waveform synthesiser applicable to voltage FED inverters
[ETN-87-90712] 09 p1157 N88-16937

PULSE GENERATORS
Operation of the TEMPO machine
[DE87-011285] 01 p0038 N88-10241
Development of a repetitive 1-MV, 22-kJ Marx generator
[DE87-011286] 01 p0038 N88-10242
Response of helical structures to high speed pulses or when can a helix be called an inductor
[DE87-014347] 01 p0090 N88-10587
Progress toward a superconducting opening switch
[DE87-014170] 02 p0157 N88-11051
A tutorial on Rogowski coil theory and operation
[DE88-000006] 02 p0230 N88-11449
The LPX (Long Pulse Experiment) facility
[DE87-010493] 03 p0311 N88-11964
RIIM two-pulse injector experiments
[DE88-000926] 05 p0653 N88-14005
Super-short yttrium aluminate pulse generator with controlled resonator Q-factor 06 p0772 N88-14740
Pulsed power sources based on MHD generators (a state-of-art review)
[DE88-700296] 07 p0935 N88-15677
A unified model for the WTS and the generation on Pi 2 pulsations — Westward Traveling Surge (WTS)
08 p1096 N88-16593
The railgun and its power source
[MRL-R-1058] 09 p1130 N88-16786
Periodic-pulse semiconductor laser with electron-beam pumping 09 p1238 N88-17422
Proposal for construction of an Energetic Particle Injector (EPI)
[INPE-4242-RPE/548] 12 p1690 N88-20112
Optimum transformer design for a pulsed power system
[DE88-006054] 13 p1760 N88-20525
High-voltage inverse-square function generator
[DE88-701109] 15 p2058 N88-22270
Pulsed power simulation problems in magic
[AD-A191110] 16 p2191 N88-23065
Photoconductive generation of sub-picosecond electrical pulses and their measurement applications
19 p2656 N88-25778
Generation and forming of ultrashort high voltage pulses 19 p2657 N88-25782
A simple technique to generate or gate microwave pulses with picosecond speeds 19 p2657 N88-25784
Energy variations in optical pulses from gain-switched AlGaAs diode lasers 19 p2658 N88-25796
Research in electromagnetic shielding theory. Part 2: EMP (electromagnetic pulse) simulation using small loops
[AD-A192682] 20 p2791 N88-26558
Radial compression of picosecond electrical pulses
[DE88-008440] 21 p2953 N88-27544
Production of intensive electron beam impulsions by setup of pseudoglare discharges
[ISL-CO-210/87] 21 p3019 N88-27920
Electromagnetic characterization and acceptance test of the electromagnetic pulse (EMP) simulator SPERANS
[FOA-C-30476-4.2] 22 p3071 N88-28230
The far field from a hybrid electromagnetic pulse (HPD) simulator
[FOA-C-30480-4.2] 22 p3071 N88-28231
Development of inductive storage pulsed power generators
[AD-A193878] 22 p3117 N88-28521
Distortions in processed signals and their application in electronic design. Part 2: A new variable signal generator
[DE88-702732] 23 p3205 N88-29071
Distortions in processed signals and their application in electronic design. Part 3: An automated generator of communication jamming signals
[DE88-702733] 23 p3205 N88-29072

PULSE HEATING
Stress intensity factors for cracked metallic structures under rapid thermal loading
[AD-A191219] 23 p3193 N88-29004

PULSE HEIGHT
U PULSE AMPLITUDE

PULSE MODULATION
NT DELTA MODULATION
NT DIFFERENTIAL PULSE CODE MODULATION
NT PULSE AMPLITUDE MODULATION
NT PULSE CODE MODULATION
NT PULSE DURATION MODULATION
NT PULSE POSITION MODULATION
Collection and analysis of specific ELINT Signal Parameters
[NASA-CR-181419] 01 p0033 N88-10213
Correction method for Barker-coded modulation
06 p0691 N88-14240
Pulse width modulator controller design for a brushless DC motor position servo
[AD-A186618] 08 p0980 N88-15921
Self-modulational formation of pulsar microstructures
[NASA-CR-182420] 08 p1104 N88-16622
Modulatable thin film field emission space gun
[AD-A189279] 13 p1845 N88-21043
Laser pulse detection with infrared range semiconductor detectors
[DE88-700857] 14 p1914 N88-21432
Error reduction in two-dimensional pulse-area modulation, with application to computer-generated transparencies — optical field synthesis
[EUT-87-E-172] 14 p1982 N88-21825
Frequency chirping in pulse modulated gain and real index guided single quantum well lasers
19 p2658 N88-25798
Effect of detector dead time on the performance of optical direct-detection communication links
22 p3065 N88-28190

PULSE POSITION MODULATION
Optical communication with semiconductor laser diodes
[NASA-CR-182464] 09 p1154 N88-16918
Effect of atmospheric turbulence on the bit error probability of a space to ground near infrared laser communications link using binary pulse position modulation and an avalanche photodiode detector
[NASA-TM-100699] 14 p1873 N88-21189

PULSE RADAR
NT MONOPULSE RADAR
A very wide frequency band pulsed/IF radar system
[NASA-CR-182889] 16 p2190 N88-23059
TDWR (Terminal Doppler Weather Radar) PRF (Pulse Repetition Frequency) selection criteria
[AD-A193089] 21 p2932 N88-27407

PULSE RATE
NT PULSE REPETITION RATE

PULSE RECORDERS
U COUNTERS

PULSE REPETITION RATE
Operation of the TEMPO machine
[DE87-011285] 01 p0038 N88-10241
Development of a repetitive 1-MV, 22-kJ Marx generator
[DE87-011286] 01 p0038 N88-10242
An optically strobed sample and hold circuit
[DE87-011877] 01 p0038 N88-10245

PULSE TIME MODULATION
NT PULSE DURATION MODULATION
NT PULSE POSITION MODULATION

PULSE WIDTH
U PULSE DURATION

PULSE WIDTH MODULATION
U PULSE DURATION MODULATION

PULSED LASERS
NT Q SWITCHED LASERS
NT ULTRASHORT PULSED LASERS
NT ULTRAVIOLET LASERS
Saturable absorbers for colliding pulse-locked Nd:YAG lasers 03 p0302 N88-11902
Thrust and specific impulse of repetitively-pulsed-laser propulsion rocket 03 p0318 N88-12012
Distributed feedback effects in lasers and high gain laser instabilities in optically pumped CH3F
03 p0329 N88-12079
The generation and suppression of synchrotron sidebands
[DE88-000532] 04 p0449 N88-12787
All-optical beam control by forced Rayleigh scattering
[AD-A184315] 04 p0490 N88-13018
Determination of a flow velocity field using four-exposure laser holography
[IMFL-3114-85/32] 05 p0585 N88-13565
Transient processes in the interaction between pulsed laser radiation and matter
[ISL-R-115/86] 05 p0588 N88-13586
Raman microprobe characterization of dielectric films following high-energy pulsed laser irradiation
[DE88-000559] 05 p0588 N88-13587
Theory of multiphoton ionization of atoms by strong, short pulsed lasers
[DE88-000963] 05 p0588 N88-13588
Production-process CO2 laser with amplified pulse-repetition operation 06 p0771 N88-14739
Super-short yttrium aluminate pulse generator with controlled resonator Q-factor 06 p0772 N88-14740
Periodically pulsed excimer master oscillator-regenerative amplifier laser set
06 p0772 N88-14741
Development of crack under periodically pulsed laser radiation 06 p0774 N88-14754
Study of kinetics of intracavity absorption in pulsed dye lasers 07 p0919 N88-15585
Effect of multiplication of spectral components of multi-frequency lasing of pulsed tunable laser
07 p0920 N88-15586
Generation of light pulses in semiconductor laser upon excitation by several electron beams
07 p0920 N88-15589
Formation of high-coherence radiation in free-running mode ruby laser for pulse holography
08 p1077 N88-16497
High-power periodic-pulse YAG:Nd3+-laser system with telescopic unstable resonator and two-stage amplifier
09 p1237 N88-17414
Calculation of the spatial-temporal deformation of laser pulses in multiple scattering
[MBB-Z-111/87] 10 p1311 N88-17837
Monitoring interfacial dynamics by pulsed laser techniques
[DE88-003362] 10 p1335 N88-17976
Laser pulse width dependent surface ripples on silicon
[PB88-127311] 10 p1336 N88-17982
Overview of applications of Laser-Induced Breakdown Spectroscopy (LIBS)
[DE88-004314] 10 p1336 N88-17987
Optically controlled devices and ultrafast laser sources for signal processing
[AD-A187417] 10 p1338 N88-17995
Pulsed laser photothermal spectroscopy of liquids and solids
[DE88-003839] 11 p1455 N88-18675
Joining of dissimilar materials with the pulsed Nd-YAG laser
[DE88-003757] 11 p1458 N88-18693
Photoconductor switch and circuit analysis
[AD-A188168] 11 p1478 N88-18821
Picosecond laser studies of excited state processes
[AD-A189606] 12 p1607 N88-19607
Pulse-train amplification of subnanosecond near-transform-limited KrF laser pulses
[DE88-004460] 12 p1631 N88-19764
Microstructure characterization with a pulsed laser ultrasonic source
[DE88-005207] 12 p1632 N88-19766
Modeling and transport in semiconductor devices
[AD-A188760] 13 p1844 N88-21037
Efficiency of fusion during periodic-pulse laser-beam welding 14 p1897 N88-21324
The technical feasibility of using spiked-radiation lasers to cut out and weld metals 14 p1898 N88-21332
Folded long-pulse XeCl excimer laser described
14 p1901 N88-21357
XeCl laser-pumped nanosecond dye lasers
14 p1902 N88-21359
Laser pulse detection with infrared range semiconductor detectors
[DE88-700857] 14 p1914 N88-21432
Radiation absorption in neodymium glasses during passage of strong laser pulse 14 p1969 N88-21757
Time characteristics of ultrashort light pulses from dye lasers with distributed feedback
14 p1970 N88-21759
Effects of emission energy transient in periodic-pulse XeCl excimer laser of approximately 400 W average power 14 p1971 N88-21763
Nonlinear stage of ultrashort-pulse formation in solid-state laser 14 p1971 N88-21765
High-efficiency Y-Sc-Ga:Cr (sup)3+,Tu (sup)3+,Ho (sup)3+ garnet laser (gl= 2.088 gmm at room temperature 14 p1971 N88-21766
Space-time structure of ultrashort light pulses formed during stimulated backscattering of laser beam
14 p1972 N88-21767

Pulse duration control of XeCl*-laser by means of plasma shutter
14 p1973 N88-21774
A preliminary comparison of the transient effects of single versus multiple q-switched doubled-neodymium laser pulses
[AD-A189855] 15 p2071 N88-22347
Program to research laser-driven thermionic electron sources for free electron lasers
[AD-A190473] 15 p2072 N88-22353
Investigation of ultrashort traveling-wave amplified spontaneous emission 16 p2187 N88-23040
Observation of synchronously transient pumped mode-locking dye laser under negative cavity detuning
16 p2187 N88-23041
Time-resolved studies of free radicals and laser-initiated chain reactions
[DE88-006569] 16 p2266 N88-23553
Determination of tropospheric H concentrations by a double-pulsed UV laser method
18 p2539 N88-25070
The chirped-pulse free-electron laser
[DE88-009289] 20 p2807 N88-26651
Model for pulse amplification by a gaseous laser amplifier
[DE88-011729] 20 p2808 N88-26657
Process control improvements in pulsed Nd:YAG laser closure welding of electromechanical relays
[DE88-006275] 21 p2957 N88-27564
MIDIR (Mid-Infrared) laser, phase 1
[AD-A193935] 23 p3220 N88-29166
Breakdown of molecular oxygen by brief pulses of laser radiation
[DE88-702687] 23 p3220 N88-29168

PULSED RADIATION
NT ELECTROMAGNETIC PULSES
The Hermes-3 program
[DE87-012132] 02 p0234 N88-11473
The pulsation modes of CO Aur
[PUBL-SER-C-FASC-10] 03 p0387 N88-12430
Materials for acceleration by surface electromagnetic waves
[DE88-700312] 07 p0846 N88-15133
Advanced energy conversion concept for beamed-energy propulsion
[AD-A187336] 10 p1324 N88-17914
Emission of gamma rays from various materials pulsed with 14-MeV neutrons
[DE88-003837] 11 p1544 N88-19227
Response characteristics of dual MOSFET gamma-ray sensors produced by Mitel Corporation
[AD-A189026] 12 p1630 N88-19755
X-rays from z-pinches
[AD-A188911] 12 p1696 N88-20146
Practical constraints on sources for pulsed beam lithographies
[DE88-006594] 13 p1776 N88-20623
Fundamental analysis of space nuclear-MHD generator for gigawatt-level power 17 p2411 N88-24337

PULSES
NT ELECTRIC PULSES
NT ELECTROMAGNETIC PULSES
NT GEOMAGNETIC MICROPULSATIONS
NT GEOMAGNETIC PULSATIONS
NT PICOSECOND PULSES
NT PRESSURE PULSES
Toward pulsed power uses for photoconductive semiconductor switches: Closing switches
[DE87-012020] 01 p0041 N88-10262
Short-pulse high-current-density photoemission in high electric fields
[DE87-014909] 03 p0310 N88-11951
Alternating current circuit theory and pulsed NMR (Nuclear Magnetic Resonance)
[DE88-000641] 04 p0440 N88-12732
High-power RF-pulsed modulators for the Los Alamos free-electron laser
[DE88-000514] 04 p0448 N88-12775
Increased gain of channel intensifier tubes by pulsed biasing
[DE88-000512] 04 p0490 N88-13019
Cerenkov radiation field analysis due to a passing electron beam
[AD-A184870] 05 p0649 N88-13976
Mixing and combustion of pulsed gas jets
[PB88-112634] 06 p0680 N88-14169
Mixing and combustion of pulsed gas jets
[PB88-108014] 06 p0680 N88-14170
The history and development of nonlinear stellar pulsation codes
[DE88-001828] 06 p0801 N88-14899
Gas phase pulse radiolysis
[DE88-002981] 10 p1296 N88-17751
The 80 fsec soliton-like pulses from an optical-nonlinear fiber resonator
[PB88-127303] 10 p1409 N88-18403
Ballistic deficits in pulse shaping amplifiers
[DE88-003908] 11 p1481 N88-18840
The optimum solution to instrument quantization effects 12 p1577 N88-19434
Pulse-train amplification of subnanosecond near-transform-limited KrF laser pulses
[DE88-004460] 12 p1631 N88-19764
Millimeter-wave pulse distortion by a single adsorption line simulating the terrestrial atmosphere
[PB88-161237] 14 p1906 N88-21388
Laser-heterodyne interferometry with streak camera detection
[DE88-003292] 14 p1914 N88-21437
Timing for subnanosecond pulses
[DE88-701390] 16 p2192 N88-23074
Optical sensors for the measurement of electric current and voltage
[PB88-172945] 16 p2193 N88-23077
Rotating-hoop, pulsed-energy converter
17 p2426 N88-24433
Silicon pulse sharpening diodes-switching kilovolts in 10's of picoseconds 19 p2661 N88-25824
Long-pulse, high-power vircator experiments
[DE88-011787] 21 p2940 N88-27458
An investigation of acoustic cavitation produced by pulsed ultrasound
[AD-A193523] 23 p3278 N88-29516

PULTRUSION
Potential for on-orbit manufacture of large space structures using the pultrusion process
[NASA-TM-4016] 05 p0557 N88-13388

PUMP IMPELLERS
Rotor dynamic behavior of centrifugal pumps
08 p0975 N88-15898

PUMP SEALS
Disk pumping test
[AD-A187199] 11 p1440 N88-18591

PUMPING
An advanced extruder-feeder biomass liquefaction reactor system 18 p2535 N88-25042

PUMPS
NT AXIAL FLOW PUMPS
NT CENTRIFUGAL PUMPS
NT ELECTROMAGNETIC PUMPS
NT FUEL PUMPS
NT TURBINE PUMPS
NT VACUUM PUMPS
NT WINDPOWERED PUMPS
Stirling engines and irrigation pumping
[DE88-000020] 02 p0181 N88-11125
Build, install and demonstrate a variable stroke pump control and windmill system
[DE87-014656] 03 p0347 N88-12191
Dynamics of reverse flows at pump inlet
04 p0425 N88-12636
The 8.4-GHz low-noise maser pump source assembly
04 p0436 N88-12705
Modular pump limiter systems for large tokamaks
[DE88-001487] 04 p0494 N88-13045
Utilization of FEP energetics
[NASA-CR-182373] 06 p0714 N88-14379
Materials development for JPL oxygen plant
[DE88-003067] 10 p1297 N88-17752
Vibration characteristics of pumped fluid systems (VCPFS) --- microgravity payloads
[ESA-CR(P)-2499] 14 p1895 N88-21310
Computer simulation of a motor pump unit to aid in interpreting vibration data
[DE88-004481] 16 p2223 N88-23270
Pumped two-phase heat transfer loop
[NASA-CASE-MSC-20841-2] 17 p2339 N88-23958
Pulsatile fluidic pump performance at elevated temperatures
[DE88-008046] 19 p2677 N88-25919
Temperature rise in superfluid helium pumps
[NASA-TM-100997] 21 p2948 N88-27507
Hydraulic pumps and hydraulic equipment at low temperatures
[DE88-752871] 21 p2958 N88-27570
Polymeric heat pipe wick
[NASA-CASE-GSC-13019-1] 23 p3214 N88-29133
Preliminary studies of NF3+H2 production of N2(A3 sigma(+)u) in a supersonic flow
[AD-A194479] 23 p3219 N88-29162

PUNCTURING
U PIERCING

PUPIL SIZE
A human factors evaluation of the Advanced Visual Technology System (AVTS) eye tracking oculometer
21 p2925 N88-27361

PUPILS
Pupil measures of alertness and mental load
16 p2239 N88-23378
Probe-evoked event-related potential techniques for evaluating aspects of attention and information processing 16 p2240 N88-23379

PURGING
Evaluation and improvement of liquid propellant rocket chugging analysis techniques. Part 1: A one-dimensional analysis of low frequency combustion instability in the fuel preburner of the space shuttle main engine
[NASA-CR-183106] 21 p2903 N88-27224

PURIFICATION
NT AIR PURIFICATION
Gas separation using solid electrolytes described
06 p0675 N88-14131
Gas cleaning at high temperatures and pressures for gas turbines
[DE88-751171] 11 p1440 N88-18593
Growth and characteristics of materials for tunable lasers in the near infrared spectral region
[NASA-CR-182501] 11 p1491 N88-18901

PURIFIERS
U PURIFICATION

PURINES
NT CAFFEINE
NT XANTHINES

PURITY
Carbon monoxide (CO) concentration in the air as a purity parameter
[INPE-4232-PRE/1107] 01 p0067 N88-10429
Production of metallic monocrystals described
03 p0286 N88-11796
Conductive polymers via reactive oligomer
[AD-A184270] 04 p0419 N88-12597
Electrochemical hydrogen concentrator for phosphoric acid fuel cells
[AD-A191355] 16 p2229 N88-23317
The variation of torsional ductility of high-purity aluminum with temperature and strain rate
[DE88-005618] 18 p2487 N88-24755

PURSUIT TRACKING
Estimation filters with adaptive scanning time for flying target tracking
[ETN-87-90401] 01 p0036 N88-10232
The isotropic rocket: A surveillance evasion game
[REPT-87-21] 05 p0645 N88-13949
Pursuit tracking performance decrements associated with decreasing ambient illumination
[AD-A189336] 13 p1809 N88-20809
Eye and head response to an attention cue in a dual task paradigm
[AD-A191052] 18 p2551 N88-25143

PUSHBROOM SENSOR MODES
HIRIS (High-Resolution Imaging Spectrometer: Science opportunities for the 1990s. Earth observing system. Volume 2C: Instrument panel report
[NASA-TM-89703] 07 p0871 N88-15282
Mid infrared multichannel focal plane breadboard --- pushbroom sensors
[RT-87/014] 14 p1982 N88-21827
Imaging instrument of the vegetation payload (SPOT 4)
[SNIAS-881-440-107] 24 p3386 N88-30169

PUSHING
Pusherless implosion, pulse tailoring and ignition scaling law for laser fusion 16 p2277 N88-23629

PWM (MODULATION)
U PULSE DURATION MODULATION

PYLONS
Compression pylon
[NASA-CASE-LAR-13777-1] 24 p3323 N88-29789

PYRAMIDS
An orthogonal oriented quadrature hexagonal image pyramid
[NASA-TM-100054] 06 p0755 N88-14630

PYRENES
Measurement of species concentrations in flames by laser-induced fluorescence
[DE88-007096] 14 p1889 N88-21286

PYREX (TRADEMARK)
U BOROSILICATE GLASS

PYRIDINES
An investigation of metal complexes of some 2-substituted and 2,6-disubstituted pyridine N-oxides
11 p1460 N88-18701
Study of crosslinking and nonelastic mechanical properties of epoxy and PSP networks --- epoxy resins; polystyrylpyridine resins (psp)
[ETN-88-92740] 21 p2921 N88-27337

PYRIMIDINES
NT THYMINE
NT URACIL

PYRITES
Reactions of some thiol collectors at noble-metal and pyrite electrodes
[PB88-138318] 11 p1455 N88-18674
Some equivalent circuit models for AC impedance analysis of pyrite/solution interface
[DE88-010574] 21 p2939 N88-27452

PYROELECTRICITY
Polymer material for heat sensors
06 p0676 N88-14142
Statistical-mechanical study of polyvinylidene fluoride
[AD-A188310] 12 p1609 N88-19624
Fast acting optical beam detection and deflection system
[AD-A192161] 18 p2521 N88-24954
Zinc-oxide thin films for integrated-sensor applications
19 p2673 N88-25896

PYROGRAPHALLOY
U COMPOSITE MATERIALS
U PYROLYTIC GRAPHITE
U REFRACTORY MATERIALS

PYROHYDROLYSIS
Effect of process conditions on aluminum oxide thin film used in pH ISFET 19 p2673 N88-25892

PYROLYSIS
Laser probes of propellant combustion chemistry
[AD-A184854] 05 p0561 N88-13415
Detailed mechanism of toluene oxidation and comparison with benzene
[NASA-TM-100261] 05 p0563 N88-13428
A study of the interaction of laser light with liquid propellant drops
[AD-A185117] 05 p0587 N88-13582
Process for preparing transition metal nitrides and transition metal carbonitrides and their reaction intermediates
[DE88-000849] 06 p0679 N88-14162
Production by pyrolysis of diffusion particles for velocimetry in shock tubes
[ISL-R-119/86] 11 p1455 N88-18671
The preparation of titanium nitride and titanium carbonitride by the preceramic polymer route
[AD-A188357] 12 p1610 N88-19626
Photolytic formation of free radicals and their effect on hydrocarbon pyrolysis chemistry in a concentrated solar environment
[DE88-004129] 13 p1794 N88-20730
Proceedings of the 1987 Biomass Thermochemical Conversion Contractors' Review Meeting
[DE88-006730] 18 p2535 N88-25041
Low pressure entrained flow pyrolysis of biomass to produce liquid fuels 18 p2535 N88-25043
Molecular-beam, mass-spectrometric studies of wood vapor and model compounds over HZSM-5 catalyst
18 p2535 N88-25044
Upgrading pyrolysis vapors to aromatic gasoline with zeolite catalysis at atmospheric pressure
18 p2536 N88-25045
Technical and economic evaluation of emerging biomass pyrolysis processes for gasoline production
18 p2536 N88-25048
Bench-scale studies on fluid-bed pyrolysis of wood using different contact gases 18 p2536 N88-25049
Evaluation of the toxicity of products from the thermal degradation of materials
[ETN-88-91995] 18 p2549 N88-25130
Flame spread mechanisms over PMMA surfaces
[NASA-TT-20284] 19 p2612 N88-25500
New instability phenomena in solid propellant combustion 19 p2628 N88-25591
Simultaneous thermogravimetric modulated beam mass spectrometry and time-of-flight velocity spectra measurements: Thermal decomposition mechanisms of RDX and HMX 19 p2632 N88-25612
Laser-RDX aerosol pyrolysis with matrix isolation of unstable intermediates 19 p2632 N88-25614
Refractory films from spin-cast carbon
[DE88-011251] 21 p2919 N88-27327
Determination of relative flammability of materials by pyrolysis and gas-chromatographic light hydrocarbon analysis
[DE88-012449] 24 p3343 N88-29898
The influence of pressure on soot formation
24 p3349 N88-29934

PYROLYTIC GRAPHITE
Data base on the high heat flux behaviour of metals and carbon materials for plasma facing components: Experiments at the 10 MW neutral beam injection test stand of the IPP Nagoya
[IPPJ-AM-53] 04 p0492 N88-13031

PYROLYTIC MATERIALS
NT PYROLYTIC GRAPHITE
Disclination structures in carbon and graphite
[AD-A191056] 17 p2322 N88-23868
Pyrolyzed organic polymer nitrogen dioxide sensor
19 p2669 N88-25868

PYROMETALLURGY
The nature of metallurgical reactions in underwater welding
[AD-A184464] 04 p0414 N88-12568

PYROMETERS
NT RADIATION PYROMETERS
Noncontact temperature pattern measuring device
[NASA-CASE-NPO-17024-1-CU]
18 p2519 N88-24943
Principles of the optical differential thermal analysis
[AD-A195951] 24 p3429 N88-30408

PYROMETRY
U TEMPERATURE MEASUREMENT

PYROPHORIC MATERIALS
Chemical analysis of charged Li/SO(sub)2 cells
02 p0163 N88-11026

PYROTECHNICS
NT HMX
Pyrotechnic component development at Sandia National Laboratory
[DE87-006899] 02 p0154 N88-10967
A nondissipative Pyrotechnic Arming and Firing Unit (PAFU)
[CRA/REPO/8019] 02 p0155 N88-10974
Performance characteristics of magnesium-sodium nitrate flares in oxygen-nitrogen atmospheres
[AD-A185274] 05 p0570 N88-13476
Advantages of internal thermal protection in a pyrotechnical plunger
[SNIAS-872-430-114] 05 p0571 N88-13478
Numerical simulation applied to the development of a pyrotechnical system
[SNIAS-872-430-115] 05 p0571 N88-13479
The TV-SAT/TDF/TELE-X pyrotechnical system
[CNES-87/CT/DRT/TVE/IL/358]
08 p0974 N88-15891
The Shock and Vibration Bulletin. Part 1: Welcome, Keynote Address, Invited Papers, Nondevelopment Items Workshop and Pyrotechnic Shock Workshop
[AD-A186748] 08 p0997 N88-16034
Designing electronics for pyrotechnic shock
08 p0997 N88-16038
Zeroshift of piezoelectric accelerometers in pyroshock measurements 08 p0997 N88-16039
Organic coatings to improve the storageability and safety of pyrotechnic compositions
[AD-A187158] 09 p1150 N88-16889
Measurement, data analysis and prediction of pyrotechnic shock from pin-pullers and separation joints
09 p1179 N88-17061
A pyrotechnic delay ignition system for a submarine launched marine signal
[MRL-R-1079] 13 p1754 N88-20487
A defect investigation of Thunderflash MK N5 (Navy)
[MRL-TN-522] 13 p1754 N88-20488
Stability of the high-temperature G-16 primer composition
[DE88-006201] 15 p2049 N88-22206
A pyrotechnical opening valve
[SNIAS-MU/TYS-NT-2-06(0)] 16 p2167 N88-22922
Ariane 4 pyrotechnics system: Definition of the chains and pyrotechnic devices
[CNES-88/CT/DRT/TVE/IL/25]
17 p2310 N88-23816
Pyrotechnic system failures: Causes and prevention
[NASA-TM-100633] 20 p2765 N88-26394
Granulation of pyrotechnic tracer composition R284T
[MRL-TN-528] 20 p2780 N88-26490
Diode laser ignition of high explosives and pyrotechnics
[DE88-008771] 21 p2923 N88-27352
Development and verification of NASA Standard Initiator-2 (NSI-2)
[NASA-CR-172069] 23 p3200 N88-29044
Development and verification of NASA Standard Initiator-2 (NSI-2): Appendix
[NASA-CR-172070] 23 p3200 N88-29045
Semiconductor bridge (SCB) igniter studies. 1: Comparison of SCB and hot-wire pyrotechnic actuators
[DE88-008802] 23 p3200 N88-29046

PYRROLES
NT CARBAZOLES
Transport properties of conductive polymers
[AD-A188411] 12 p1610 N88-19628
Morphological studies of conductive polymers
[AD-A188456] 12 p1610 N88-19629

P3V AIRCRAFT
U P-3 AIRCRAFT

P78-2 SATELLITE
U SCATHA SATELLITE

Q

Q FACTORS
Super-short yttrium aluminate pulse generator with controlled resonator Q-factor 06 p0772 N88-14740

Q SWITCHED LASERS
An investigation of unipolar arcing at atmospheric pressure in aluminum 2024 and aluminum coated glass slides
[AD-A184903] 05 p0577 N88-13521
Diode pumped fiber laser
[AD-A187694] 11 p1491 N88-18902
Development of high efficiency q-switched glass laser via sol-gel processing
[AD-A192301] 23 p3218 N88-29154

QCD
U QUANTUM CHROMODYNAMICS

QSO (RADIO SOURCES)
U QUASARS

QUADRANTID METEOROIDS
Structural peculiarities of the Quadrantid meteor shower 06 p0740 N88-14552

QUADRANTS
On the extreme points of the set of all 2xn bivariate positive quadrant dependent distributions with fixed marginals and some applications
[AD-A186316] 07 p0911 N88-15521
Some comments on quadrant dependence in higher dimensions
[AD-A190329] 15 p2121 N88-22639

QUADRATIC EQUATIONS
Analytical treatment of the spatial trilateration problem (4, 6, 0, 0)
[SER-A-104] 01 p0085 N88-10548
Quantization of quadratic friction revisited
[DE88-700839] 12 p1686 N88-20081
Distributions of quadratic forms
[AD-A190224] 15 p2124 N88-22663
A piecewise quadratic strength tensor theory for composites
[AD-A190929] 16 p2173 N88-22952
A feasibility study in path planning using optimization techniques
[AD-A193030] 21 p2894 N88-27177
Application of differential quadrature to the analysis of structural components 22 p3087 N88-28331
Periodic solutions of perturbed superquadratic Hamiltonian systems
[AD-A194292] 23 p3270 N88-29457

QUADRATIC PROGRAMMING
A Schur-complement method for sparse quadratic programming
[DE88-002520] 07 p0904 N88-15479
An O(n3L) interior point algorithm for convex quadratic programming
[AD-A186001] 07 p0909 N88-15504
Active vibration control of a cantilevered beam with three elastic coordinates
[AD-A188824] 12 p1636 N88-19797
Sufficient matrices and the linear complementarity problem
[AD-A190429] 15 p2128 N88-22690

QUADRATURE APPROXIMATION
U QUADRATURES

QUADRATURES
A quadrature formula for a double-pole singular integral
[PD-FM-8725] 04 p0485 N88-12990
An orthogonal oriented quadrature hexagonal image pyramid
[NASA-TM-100054] 06 p0755 N88-14630
A quadratic-form analysis of the collisionless tearing mode
[AD-A188886] 12 p1695 N88-20144
A note on the analyticity of the Neumann Kernel and an associated quadrature problem in two-dimensional boundary element methods
[ETN-88-92054] 14 p1964 N88-21719
Asymptotic of Peanokerns of finite fixed order
[ETN-88-92381] 21 p3008 N88-27843
Application of differential quadrature to the analysis of structural components 22 p3087 N88-28331
Use of a coherent square wave reference to demodulate BPSK (Binary Phase Shift Keying) carriers and a visual indicator of the quality of received QPSK (Quadrature Phase Shift Keying) carriers
[AD-A193528] 23 p3204 N88-29065
Generating semi-Gaussian two dimensional quadrature rules
[REPT-205] 23 p3272 N88-29476

QUADRUPOLE LENSES
U MAGNETIC LENSES

QUADRUPOLES
Research relative to an advanced rod control system for quadrupole mass spectrometry applications
[NASA-CR-181458] 02 p0167 N88-11050
Present status of the high resolution spectrometers
[CEBAF-PR-87-029] 02 p0234 N88-11478
High gradient superconducting quadrupoles
[DE87-013590] 02 p0244 N88-11541
Modeling the behavior of oriented permanent magnet material using current double theory
[DE88-004446] 13 p1833 N88-20963
The exact calculation of quadrupole sources for some incompressible flows
[NASA-TM-100623] 17 p2395 N88-24240

Theoretical investigations of drift waves in a magnetic quadrupole 18 p2578 N88-25312

QUALIFICATIONS

Qualification by analysis of IUS plume deflectors 09 p1179 N88-17063

Qualification of frequency response functions using the rigid-body response [DE88-000745] 10 p1344 N88-18033

SP-100 flight qualification testing assessment 17 p2424 N88-24414

QUALITATIVE ANALYSIS

Solid state C-13 NMR characterization of textiles: Qualitative and quantitative analysis [AD-A184349] 04 p0419 N88-12598

A low volume insert for solid state magic angle spinning NMR of small samples [AD-A184359] 04 p0419 N88-12601

Predictive monitoring research: Summary of the PREMON system [NASA-CR-182687] 13 p1824 N88-20905

Qualitative reasoning for physicists [PB88-116298] 20 p2848 N88-26906

High hot-hardness gear lubricant evaluations, phase 2 [AD-A192309] 23 p3196 N88-29017

QUALITY

NT AIR QUALITY
NT ENVIRONMENTAL QUALITY
NT RIDING QUALITY
NT WATER QUALITY

Assessment of software quality for the AIRBUS A310 automatic pilot 02 p0128 N88-10804

The criterion of equal integrated quality: An improved method of planning DBS systems [BBC-RD-1987/10] 02 p0161 N88-11012

Software quality measurement demonstration project (1) [AD-A193429] 22 p3136 N88-28646

Aerodynamic data accuracy and quality: Requirements and capabilities in wind tunnel testing [AGARD-AR-254] 23 p3173 N88-28893

High definition television: Evaluation for remote task performance [DE88-011573] 23 p3202 N88-29057

An analysis of lateral-directional handling qualities and Eigenstructure of high performance aircraft [AD-A194874] 24 p3328 N88-29814

QUALITY CONTROL

Wet deposition and snowpack monitoring operations and quality assurance manual [PB87-212817] 01 p0064 N88-10413

Investment foundry melting stock. Rolls Royce requirements and demands in terms of quality and the relationship to end product performance [PNR90397] 02 p0160 N88-11003

Implementation of finite element quality assurance in a commercial industrial organisation [PNR90393] 02 p0183 N88-11137

Software reliability models for fault-tolerant avionics computers and related topics [NASA-CR-181440] 02 p0220 N88-11382

RADC/NBS (Rome Air Development Center/National Bureau of Standards) Workshop. Moisture Measurement and Control for Microelectronics (4) [PB87-224614] 03 p0309 N88-11947

NBS (National Bureau of Standards) measurement services: Radiometric standards in the vacuum ultraviolet [PB87-227625] 03 p0325 N88-12055

Software maintenance in scientific and engineering environments: An introduction and guide [NASA-CR-177409] 04 p0479 N88-12954

Avionics and corrosion 05 p0547 N88-13336

Philosophy and practice of nondestructive tests of composite material structures at Aerospatiale Aquitaine [SNIAS-872-430-105] 05 p0559 N88-13400

Chemical analysis for excimer laser systems [DE88-001941] 05 p0589 N88-13591

Sandia software guidelines: Software quality planning [DE88-001931] 05 p0636 N88-13894

Flammability, smoke and toxicity test on fire barrier fabric from the Porcher company --- Airbus aircraft [ETN-88-91168] 06 p0666 N88-14085

AVHRR/HIRS (Advanced Very High Resolution Radiometer/High Resolution Infra-Red Sounder) operational method for satellite based sea surface temperature determination [PB88-107594] 06 p0708 N88-14340

On-site meteorological program guidance for regulatory modeling applications [PB87-227542] 06 p0731 N88-14498

Reliability modelling for fault-tolerant parallel processor [AD-A185867] 07 p0900 N88-15451

Solid mechanics research for quantitative non-destructive evaluation [AD-A186599] 08 p0993 N88-16010

Spacelab Data Processing Facility (SLDPF) quality assurance expert systems development 08 p1059 N88-16394

Photoluminescence study of InP surfaces and InP-insulator interfaces [ECL-87-13] 08 p1089 N88-16555

ESTEC's product assurance activities 09 p1125 N88-16739

Training guidelines in non-destructive testing techniques [DE88-700613] 10 p1342 N88-18019

Analysis and application of the constant tensile load test for polyethylene gas pipe materials [DE88-002868] 10 p1345 N88-18037

A method for assessing the software engineering capability of contractors: Preliminary version [AD-A187230] 10 p1388 N88-18290

Quality assurance of ceramic materials and gas turbine components [IZFP-850303-TW] 11 p1465 N88-18735

Novel analytical X-ray Non-Destructive Evaluation (NDE) tool for quality control of energetic materials [AD-A187737] 11 p1497 N88-18935

Random vibration (stress screening) of printed wiring assemblies 11 p1499 N88-18953

Quality control of upper air conventional data (TEMP and PILOT) [INPE-4223-RPE/546] 12 p1647 N88-19862

Critical comparison of moving average and cumulative summation control charts for trace analysis data [AD-A188312] 12 p1705 N88-20203

Quality enhancement with machine intelligence [DE88-005639] 13 p1824 N88-20901

Electron beam sensitive devices for controllability [RR-658-I] 14 p1908 N88-21403

Software quality assurance workstation [P-1124/RT-14791] 14 p1957 N88-21670

Information systems for quality. Experience at the Nerviano Aeritalia plant. Avionic systems and equipment group [ETN-88-92274] 15 p2148 N88-22821

Systems engineering technique 17 p2303 N88-23776

A quality philosophy for research and development [DE88-006512] 18 p2524 N88-24977

Proposed quality assurance/quality control plan [AD-A191490] 18 p2525 N88-24978

Quality and productivity drive innovation and improvement at United Technologies Aerospace Operations, Inc. [NASA-CR-182944] 18 p2525 N88-24983

Study of Staebler-Wronsky degradation effect in a Si:H based P-I-N solar cells [NASA-CR-182564] 19 p2687 N88-25970

Analytical determination of critical crack size in solar cells [NASA-CR-183128] 20 p2821 N88-26736

Milliwatt generator project [DE88-011261] 20 p2853 N88-26939

Optical characterization of silica aerogel [DE88-008916] 20 p2854 N88-26946

Measuring dispersion effects of factors in factorial experiments [AD-A193216] 21 p3006 N88-27831

Direct and inverse diffraction problems for QNDE (Quantitative Non-Destructive Evaluation) applications [AD-A194721] 22 p3085 N88-28322

Quality of SPOT images 22 p3115 N88-28506

Effect of fiber diameter on the reliability of composites - automated laser diffraction implementation [AD-A193524] 23 p3188 N88-28972

Qualification of expansion and welding procedures of tube-to-tubesheet joints for heat exchangers in nuclear power plants [DE88-701621] 23 p3221 N88-29174

Material and process selection and quality control for ESA space systems and associated equipment [ESA-PSS-01-70-ISSUE-3] 23 p3224 N88-29190

Quality control in microbiology: CDC lab manual [PB88-179890] 23 p3237 N88-29263

Topics in adaptive control and inference [AD-A194718] 23 p3266 N88-29443

Quality measures and assurance for AI (Artificial Intelligence) software [NASA-CR-4187] 24 p3411 N88-30304

QUALITY FACTORS

U Q FACTORS

QUANTILES

Quantile based unified distribution of extreme values and order statistics [AD-A185171] 05 p0644 N88-13942

Quantile statistical data analysis [AD-A185181] 05 p0644 N88-13943

A modified kernel quantile estimator under censoring [AD-A186364] 07 p0911 N88-15525

A smooth nonparametric quantile estimator from right-censored data [AD-A186180] 07 p0915 N88-15552

A generalized quantile estimator under censoring [AD-A188260] 10 p1402 N88-18364

Large quantile estimation under extreme-value conditions [CWI-MS-R8711] 14 p1966 N88-21730

Use of principal component method for analysis of multidimensional quantitative data in biomedical investigations 19 p2706 N88-26089

Joint asymptotic distribution of marginal quantiles and quantile functions in samples from a multivariate population [AD-A193385] 21 p3010 N88-27856

QUANTITATIVE ANALYSIS

Auger electron spectroscopy of oxidized titanium overlayers: Speciation of homogeneous and heterogeneous samples [KFK-4221] 02 p0146 N88-10913

Cooperative analysis of zirconium and zirconium alloys by fluorescent X-ray method [DE87-753011] 02 p0148 N88-10926

Small-Angle Neutron Scattering (SANS) from polymers and colloids [DE87-013548] 02 p0151 N88-10946

Design of an elemental analysis system for CELSS research 03 p0360 N88-12266

Studies on estimation of nickel in zinc base die casting by D.C. polarography [PD-MT-8729] 04 p0417 N88-12588

Solid state C-13 NMR characterization of textiles: Qualitative and quantitative analysis [AD-A184349] 04 p0419 N88-12598

Abundance and distribution of ultramafic microbreccia in Moses Rock Dike: Quantitative application of AIS data 05 p0613 N88-13766

Characterization of microstructure in metallic and composite materials [AD-A186193] 07 p0826 N88-15012

Studies of supported metal catalysts [DE88-002546] 07 p0831 N88-15038

Quantitative non-destructive evaluation of porous composite materials based on ultrasonic wave propagation [NASA-CR-182544] 11 p1447 N88-18627

Procedures for quantitative sensitivity and performance validation studies of a deterministic fire safety model [NBS/GCR-88/544] 11 p1469 N88-18762

Multicomponent analysis using synchronous-excitation phase-resolved fluorescence spectroscopy [AD-A188883] 12 p1606 N88-19604

Quantitative determination of a hydrogen impurity in a sodium coolant by hydride thermal dissociation [NASA-TT-20239] 13 p1740 N88-20402

Computer program in BASIC language for computation of spectrochemical analytical data [DE88-701229] 15 p2032 N88-22106

Clinical measurements using fiber optic sensors [DE88-005624] 15 p2134 N88-22731

The use of a water towing tank for aerodynamic testing and methods for quantitative evaluation of photographs 16 p2202 N88-23140

Development of an automated X-ray gauge for nondestructive quantitative analysis [DE88-008633] 20 p2812 N88-26681

Direct determination of part-per-billion levels of volatile organics in water and soil samples using glow discharge mass spectrometry [DE88-011389] 21 p2910 N88-27272

The electromagnetic spectrum: The information mine [AD-A194316] 22 p3069 N88-28215

A method for the quantitative determination of crystalline phases by X-ray [NASA-TT-20324] 24 p3434 N88-30444

QUANTIZATION

U MEASUREMENT

QUANTIZER

U COUNTERS

QUANTUM CHEMISTRY

A quantum theoretical study of polyimides [NASA-CR-181495] 03 p0292 N88-11831

The Coupled Cluster Single and Double excitation (CCSD) method in quantum chemistry: An efficient formulation of the theory and application to closed shell molecular systems [DE88-000475] 07 p0930 N88-15650

Clusters: Link between molecules and solids [AD-A188170] 11 p1543 N88-19224

Quantum Monte Carlo study of the MIES associated with H2(X 1 sigma g +) and H2(B 1 sigma u +) 16 p2268 N88-23564

Gas phase combustion chemistry of nitramine propellants [AD-A195082] 24 p3344 N88-29902

QUANTUM CHROMODYNAMICS
NT INSTANTONS
An introduction to charm and heavy quark physics
[DE87-013589] 02 p0231 N88-11455
Research program in elementary particle theory
[DE88-000159] 02 p0233 N88-11468
Scalar densities and baryon mass differences in lattice QCD with Wilson fermions
[PREPRINT-544] 06 p0778 N88-14773
The approach to equilibrium in a quark-gluon plasma
[DE88-002117] 09 p1251 N88-17499
Status of the electroweak theory
[DE88-002342] 10 p1422 N88-18494
Negative-energy quanta
[DE88-700904] 12 p1689 N88-20101
Diffraction theory in QCD and beyond
[DE88-005958] 13 p1837 N88-20992
Lattice QCD calculation of K yields pi nonleptonic weak transition and other hadronic weak parameters
[PREPRINT-580] 15 p2132 N88-22717
Computational quantum field theory
[DE88-700918] 16 p2284 N88-23672
Color charge motion in non-Abelian fields
[DE88-701306] 19 p2642 N88-25672
Comparison of exclusive reactions at large momentum transfer
[DE88-007544] 20 p2851 N88-26922
Theoretical studies in elementary particle physics
[DE88-006929] 20 p2851 N88-26926
An overview of lattice QCD
[DE88-010867] 21 p3026 N88-27963
Theoretical studies in high energy physics
[DE88-011606] 23 p3281 N88-29538
Theoretical particle physics
[DE88-011499] 23 p3295 N88-29621
Resonant spin-flavor precession of solar and supernova neutrinos
[DE88-752604] 23 p3308 N88-29707

QUANTUM EFFICIENCY
Detective quantum efficiency and design of a parallel data recording system for EXELFS-measurements --- electron microscopy
[USIP-87-06] 01 p0050 N88-10318
Study of solid state photomultiplier
[NASA-CR-177465] 05 p0583 N88-13556
Area detectors for X-ray spectroscopy
[DE88-001429] 06 p0679 N88-14163
Performance of a photon counting microchannel plate intensifier with wedge and strip image readout
[DE88-003831] 10 p1334 N88-17970
Low threshold ridge waveguide single quantum well lasers 13 p1777 N88-20631
Quantum nondemolition detection and squeezing in optical fibers 14 p1976 N88-21793
Results from the SLAC lasertron
[DE88-007816] 20 p2806 N88-26647
High performance charge transfer device detectors
[AD-A194409] 23 p3192 N88-28993

QUANTUM ELECTRODYNAMICS
LLE review
[DE87-014468] 02 p0178 N88-11110
Proceedings of the Workshop on Opportunities for Atomic Physics Using Slow, Highly-Charged Ions
[DE87-013991] 02 p0231 N88-11457
Quantum electrodynamics based on self-energy: Spontaneous emission in cavities
[DE87-703071] 02 p0232 N88-11461
QED description of relativistic Coulomb excitation in heavy ion collisions
[DE88-700834] 12 p1689 N88-20100
Negative-energy quanta
[DE88-700904] 12 p1689 N88-20101
Solid state research
[AD-A188388] 12 p1699 N88-20166
Chiral symmetry breaking in finite quantum electrodynamics
[DE88-700860] 12 p1699 N88-20169
Quantization of axial electrodynamics
[DE88-701498] 15 p2147 N88-22813
Research in the optical sciences
[AD-A192175] 18 p2575 N88-25297
Nonlinear dynamics of the electron self-field interaction
[DE88-010597] 21 p2934 N88-27420
Infrared detection using Rydberg atoms
[AD-A194308] 23 p3191 N88-28990
Relativistic theory of the Lamb shift based on self energy
[DE88-702658] 23 p3295 N88-29626

QUANTUM ELECTRONICS
Numerical studies of the dual HEMT/algorithm development and numerical studies of Schrodinger's equation
[AD-A184471] 04 p0478 N88-12946
Development and study of fibre-optic link lines on the basis of the KEM-8-4PD, KEM-8-4PR quantum-electronic modules
[DE88-700372] 07 p0932 N88-15663
Nanoelectronics
[AD-A186969] 09 p1156 N88-16930
Solid state research
[AD-A185987] 09 p1253 N88-17508
Molecular beam epitaxy for research on quantum well structures
[AD-A186791] 09 p1255 N88-17522
Microwave semiconductor research-materials, devices and circuits
[AD-A187121] 10 p1415 N88-18444
Joint services electronics program
[AD-A189262] 13 p1761 N88-20533
Theory of interactions of intense light with nonlinear, inhomogeneous and periodic structures and its applications to optical bistability, optic gyroscopes, nonlinear spectroscopy, radiation protection, X-ray emission and related fields
[AD-A190040] 15 p2133 N88-22725
Fluxons and order in long Josephson junctions
[AD-A190879] 16 p2282 N88-23665
Joint services electronics program
[AD-A192076] 18 p2504 N88-24856
Joint services electronics program research in electronics
[AD-A192206] 18 p2504 N88-24857
Random quantum interference in microdevices 20 p2866 N88-27021
Defects and disorder in amorphous and damaged silicon
[AD-A192277] 20 p2879 N88-27089
Solid state research
[AD-A192837] 21 p3020 N88-27929
Spectroscopic studies with multiple quantum well materials with applications to optical signal processing at room temperature
[AD-A194171] 24 p3429 N88-30409

QUANTUM GENERATORS
U STIMULATED EMISSION DEVICES

QUANTUM MECHANICS
NT PAULI EXCLUSION PRINCIPLE
NT QUANTUM ELECTRODYNAMICS
Quantum-mechanical aspects of classically chaotic driven systems
[DE87-013152] 02 p0178 N88-11106
Quantum mechanics with spontaneous localization and the quantum theory of measurement
[DE87-703072] 02 p0247 N88-11559
A study of mechanisms of hydrogen diffusion in separation devices
[DE88-000328] 04 p0416 N88-12584
Final (n,l) state-resolved electron capture by multiply charged ions from neutral atoms
[IPPJ-AM-54] 04 p0492 N88-13030
Theory of neutron scattering experiments on momentum distributions in quantum fluids
[DE87-013691] 05 p0648 N88-13968
Resonant level lifetime in GaAs/ AlGaAs double-barrier structures
[AD-A185376] 05 p0655 N88-14020
Example of correlation between space and spin coordinates
[DE87-703366] 05 p0657 N88-14030
A mechanism for symmetry breaking in antiferromagnetic Heisenberg systems
[ETN-88-91320] 05 p0657 N88-14031
Macroscopic quantum effects in a Josephson tunnel junction
[DE88-002239] 06 p0787 N88-14830
Group quantization of constrained systems
[PREPRINT-564] 06 p0790 N88-14844
Modified quantum mechanics of small composite systems
[NIKHEF-H/87-1] 06 p0790 N88-14845
Coherent states for the damped harmonic oscillator
[AD-A186111] 07 p0922 N88-15599
Core spline method for solution of quantum-mechanical systems of differential equations for bound states
[DE88-700492] 09 p1259 N88-17551
An overview of the transactional interpretation of quantum mechanics
[DE88-004236] 10 p1423 N88-18497
Fundamental properties of spin-polarized quantum systems
[DE88-004425] 10 p1423 N88-18499
SUSY anomaly in quantum-mechanical systems
[DE88-700890] 12 p1699 N88-20170
Gordon Conference on Intermetallic Compounds held at Tilton, New Hampshire on 20-24 July 1987
[AD-A188502] 13 p1745 N88-20435
Algebraic structure of linear and nonlinear models of open quantum systems
[PREPRINT-573] 14 p1968 N88-21747
Optical cooling and trapping 14 p1974 N88-21782
Dynamic and spectral properties of semiconductor lasers with quantum well, quantum wire, and quantum box structures 14 p1975 N88-21788
Squeezed state in degenerate parametric amplification discussed by H. Takahasi in 1963 14 p1976 N88-21790
Quantum nondemolition detection and squeezing in optical fibers 14 p1976 N88-21793
Berry's phase in fiber optics 14 p1977 N88-21797
Generation of number-phase minimum uncertainty states 14 p1978 N88-21803
Singular Lagrangians. Classical dynamics and quantization. Lectures for young scientists
[DE88-701158] 15 p2146 N88-22806
On the Hilbert space of supersymmetric quantum systems
[DE88-701648] 16 p2284 N88-23677
Modulation efficiency limited high frequency performance of the MODFET 19 p2657 N88-25786
Electron device probing in the femtosecond time scale 19 p2660 N88-25821
High resolution spectroscopy of dissociating molecules
[DE88-007959] 20 p2851 N88-26924
Quantum transport theory of resonant-tunneling heterostructure devices 20 p2865 N88-27017
Quantum interference and transport in microstructures 20 p2866 N88-27022
Combining relativity and quantum mechanics: Schroedinger's interpretation of psi
[DE88-701899] 20 p2880 N88-27102
Determination of quantum corrections for electrical conductivity mechanism of three dimensional, perturbed copper coatings. Weak localization and electron-electron interaction
[ETN-88-92378] 21 p2941 N88-27466
Evaluation of quantum mechanics path integrals by the approximations exact on a class of polynomial functionals
[DE88-702434] 21 p3011 N88-27865
Wigner distribution function: Relation to short-term spectral estimation, smoothing and performance in noise
[AD-A193865] 23 p3275 N88-29492
Investigation of non-classical effects in two-photon interference processes 23 p3282 N88-29541

QUANTUM OPTICS
Families of Bose rays in quantum optics
[DE87-014584] 02 p0236 N88-11489
Experimental observation of photoresonance of electrons localized above surface of solid hydrogen 06 p0774 N88-14755
Activities report in quantum optics
[ISSN-0177-0101] 09 p1248 N88-17482

QUANTUM STATISTICS
A problem in quantum probability --- statistical invariants problem
[REPT-87-06] 01 p0088 N88-10573
Families of Bose rays in quantum optics
[DE87-014584] 02 p0236 N88-11489
Regular effective action of gauge field theory and quantum gravity
[DE87-703076] 02 p0247 N88-11560
Electronic structure and phase stability of alloys
[DE88-004574] 11 p1562 N88-19350
Macroscopic quantum jumps in a single atom 14 p1975 N88-21784
Quantum statistics of parametric oscillators above threshold 14 p1979 N88-21811

QUANTUM THEORY
NT BOHR THEORY
Inequivalent quantizations and fundamentally perfect spaces
[DE87-014225] 02 p0229 N88-11446
Quantum mechanics with spontaneous localization and the quantum theory of measurement
[DE87-703072] 02 p0247 N88-11559
Regular effective action of gauge field theory and quantum gravity
[DE87-703076] 02 p0247 N88-11560
Program to development an optical transistor and switch
[AD-A185666] 06 p0697 N88-14278
Theoretical studies of kinetic mechanisms of negative ion formation in plasmas
[AD-A185735] 06 p0784 N88-14812
A simplified model of elementary particles
[NOTA-INTERNA-890] 07 p0930 N88-15647
Superstrings on quantum spacetime
[DE88-700106] 07 p0940 N88-15715
Instanton in supersymmetric theory with static disorder
[DE88-700357] 07 p0940 N88-15716
Activities report in quantum optics
[ISSN-0177-0101] 09 p1248 N88-17482
Research in theoretical physics
[DE88-003201] 09 p1259 N88-17548

Study of quantum mechanical effects in deep submicron, grating-gate field effect transistors
[AD-A188283] 10 p1325 N88-17923
Antimatter: Its history and its properties
[DE88-004308] 10 p1423 N88-18498
Quantum limits of superconducting heterodyne receivers
[AD-A188014] 11 p1478 N88-18817
Semileptonic weak interactions in nuclei: A relativistic analysis
[CEBAF-PR-87-024] 11 p1547 N88-19249
Generalised scattering model for the quantum modulation of electrons 11 p1563 N88-19357
On exterior variational calculus
[DE88-700861] 12 p1683 N88-20062
Topics in string theory: Task D
[DE88-004532] 12 p1699 N88-20167
Generalized Levinson's theorem and quantum sticking coefficients at O K
[AD-A189371] 12 p1699 N88-20171
Spontaneous decay and atomic fluorescence near a metal surface of an absorbing dielectric
[AD-A187508] 13 p1835 N88-20975
Quantum Monte Carlo study of the MIES associated with H2 (X 1 sigma sub g (+)) and H2 (B 1 sigma sub u (+))
[AD-A189063] 13 p1835 N88-20977
Algebraic structure of linear and nonlinear models of open quantum systems
[PREPRINT-573] 14 p1968 N88-21747
Super Virasoro algebra and solvable supersymmetric quantum field theories
[DE88-752299] 15 p2127 N88-22681
To the field theory with a fundamental mass
[DE88-701159] 15 p2146 N88-22807
Free Laplacian with attractive boundary conditions
[DE87-702971] 16 p2256 N88-23482
On a generalization of renormalization group equations to quantum field theories of an arbitrary type
[DE88-701143] 16 p2263 N88-23531
Fluxons and order in long Josephson junctions
[AD-A190879] 16 p2282 N88-23665
Electrical resistivity as quantum chaos
[DE88-007026] 16 p2284 N88-23675
Joint services electronics program
[AD-A190239] 18 p2503 N88-24848
Quantum gravity and new forces
[DE88-007829] 19 p2737 N88-26250
Transcending Newton's legacy
[DE88-010784] 19 p2738 N88-26254
Cosmic wavefunction with induced gravity
[DE88-701873] 20 p2884 N88-27129
Superalgebras with Grassmann algebra-valued structure constants from superfields
[DE88-702239] 21 p3011 N88-27862
Quark nuclear model: Classification groups and two and three body correlations
[NOTA-INTERNA-896] 21 p3014 N88-27891
Gravitation and electromagnetism
22 p3158 N88-28792
Infrared detection using Rydberg atoms
[AD-A194308] 23 p3191 N88-28990
CryoSQUID: A SQUID-based magnetic field sensor
[AD-A194237] 23 p3239 N88-29275
On nonlinear equations admitting soliton solutions with a deBroglie phase
[DE88-702694] 23 p3277 N88-29508
Towards a finite quantum gravity
[DE88-701497] 23 p3294 N88-29619
On the meaning of perturbation expansions in quantum field theory
[DE88-702138] 23 p3294 N88-29620
Chaotic behaviour in quantum dynamics
[AD-A193936] 23 p3295 N88-29623

QUANTUM WELLS

Quantum well laser diodes: Modeling and realization of GaAs/GaAlAs
[LAAS-87-165] 02 p0179 N88-11116
Phase-locked semiconductor quantum well laser arrays
[AD-A185155] 05 p0588 N88-13583
Impurity bands in quantum wells
[INPE-4250-PRE/1123] 08 p1089 N88-16552
Diagonal and off-diagonal disorder in doped quantum wells
[INPE-4255-PRE/1128] 08 p1089 N88-16556
Density of states of electrons bound to impurities in quantum wells of GaAlAs/GaAs
[INPE-4257-PRE/1130] 08 p1089 N88-16557
Low threshold ridge waveguide single quantum well lasers 13 p1777 N88-20631
Energy loss rates for light holes in InGaAs/GaAs strained layer single quantum wells
[DE88-005744] 13 p1848 N88-21062
Measurements of optical nonlinearities in MOCVD-grown GaAs/GaAlAs multiple quantum wells
14 p1975 N88-21787
Dynamic and spectral properties of semiconductor lasers with quantum well, quantum wire, and quantum box structures 14 p1975 N88-21788
Optical properties of quantum well structures with electric field: Life time free switching of luminescence intensity and virtual charge-induced ultrafast optical nonlinearity 14 p1976 N88-21794
High density femtosecond excitation of nonthermal carrier distributions in intrinsic and modulation doped GaAs quantum wells 14 p1977 N88-21798
Research on materials and components for opto-electronic signal processing and computing
[AD-A190130] 15 p2143 N88-22788
Local density of states in double-barrier resonant tunneling structures
[AD-A190673] 16 p2281 N88-23656
Optical properties of heterostructures and superlattices
[AD-A191542] 18 p2581 N88-25335
Optical nonlinearities in GaAs/GaAlAs multiple quantum wells fabricated by metalorganic chemical vapor deposition for use in optical signal processing
[AD-A191558] 18 p2582 N88-25337
Molecular Beam Epitaxy (MBE) for high speed devices
19 p2656 N88-25770
A proposed Quantum Well Injection Transit Time device (QWITT) 19 p2657 N88-25785
Frequency chirping in pulse modulated gain and real index guided single quantum well lasers
19 p2658 N88-25798
High-speed phenomena in GaAs multiple-quantum-wells 19 p2660 N88-25812
Picosecond carrier transport in GaAs quantum wells
19 p2660 N88-25813
Quantum-confined stark effect in InGaAs/InP quantum wells grown by metal-organic chemical vapor deposition
19 p2660 N88-25814
Dynamics of below-gap photoexcitation in GaAs quantum wells 19 p2660 N88-25815
Nonlinear optical properties and subpicosecond dynamics of excitons and electron-hole plasmas in multiple quantum well structures
[AD-A191926] 19 p2727 N88-26196
Far-infrared studies of doped AlGaAs/GaAs multiple-quantum-well structures
20 p2862 N88-26998
Electro-optical studies of Al(x)Ga(1-x)As/GaAs coupled quantum wells 20 p2862 N88-26999
Quantum wells and bulk AlGaAs under hydrostatic pressure 20 p2862 N88-27000
Auger recombination in GaSb/AlSb-multi quantum well heterostructures 20 p2862 N88-27001
Ultrafast optical nonlinearity in quantum well structures with electric field 20 p2863 N88-27003
Strained layer and lattice matched transverse junction stripe quantum well lasers for continuous room temperature operation 20 p2863 N88-27004
Quantum transport theory of resonant-tunneling heterostructure devices 20 p2865 N88-27017
Superlattice doping interfaces
20 p2866 N88-27019
Excitonic properties of GaAs-AlGaAs nanostructures
20 p2867 N88-27023
A 10 microns photoexcited avalanche gain due to electron impact ionization from GaAs quantum well superlattices 20 p2867 N88-27026
Novel quantum well optical devices
20 p2868 N88-27028
Direct imaging of the columnar structure of GaAs quantum wells 20 p2868 N88-27030
Monte Carlo simulations of femtosecond relaxation of photoexcited electrons in AlGaAs/GaAs quantum wells
20 p2869 N88-27036
Electron-phonon interactions in In(0.53)Ga(0.47)As and in In(0.53)Ga(0.47)As/InP quantum wells
20 p2869 N88-27037
Electronic structure of quantum-well states revealed under high pressures 20 p2870 N88-27038
Magneto-optical studies of GaInAs-InP quantum wells
20 p2870 N88-27039
On a-Si:H/a-SiN(x):H superlattices: Confinement or contamination 20 p2870 N88-27040
Direct measurement of ultrafast electron-hole plasma expansion at high density at an asymmetric GaAs quantum well 20 p2871 N88-27044
Solar energy conversion through the interaction of plasmons with tunnel junctions. Part A: Solar cell analysis. Part B: Photoconductor analysis
[NASA-CR-183044] 21 p2967 N88-27621
Ultrafast physics in semiconductor microstructures
[AD-A193300] 21 p3022 N88-27936
Laser spectroscopy of quantum well and superlattice structures
[AD-A193336] 21 p3022 N88-27937
A study of tunneling phenomena in gallium arsenide-aluminum gallium arsenide heterostructures
21 p3023 N88-27946
Infrared devices using semiconductor quantum wells
[RSRE-MEMO-4018] 22 p3157 N88-28788
Studies on strained (In,Ga)As/GaAs semiconductors and optical devices 23 p3287 N88-29575
Spectroscopic studies with multiple quantum well materials with applications to optical signal processing at room temperature
[AD-A194171] 24 p3429 N88-30409

QUARK MODELS

Quark nuclear model: Classification groups and two and three body correlations
[NOTA-INTERNA-896] 21 p3014 N88-27891

QUARKS

An introduction to charm and heavy quark physics
[DE87-013589] 02 p0231 N88-11455
Single leptons from heavy quark production
[DE87-014917] 04 p0488 N88-13009
The approach to equilibrium in a quark-gluon plasma
[DE88-002117] 09 p1251 N88-17499
Zero temperature quark matter equation of state
[DE88-003408] 10 p1422 N88-18496
Hadron-quark phase transition in dense stars
[DE88-003412] 10 p1429 N88-18532
Quark matter in astrophysics and cosmology
[DE88-003406] 10 p1429 N88-18534
Proton/antiproton yields W(+/-)boson gamma X as a test of the quark charges
[NIKHEF-H/87-11] 13 p1836 N88-20987
Quark core stars, quark stars and strange stars
[DE88-006991] 17 p2450 N88-24555
Accuracy of analytic energy level formulas applied to hadronic spectroscopy of heavy mesons
[NASA-TM-4042] 19 p2725 N88-26185
Theoretical studies in elementary particle physics
[DE88-006929] 20 p2851 N88-26926
Strange, quark and metastable neutron stars
[DE88-702404] 21 p3030 N88-27984
Theory of quark mixing matrix and invariant functions of mass matrices
[USIP-87-14] 22 p3159 N88-28800

QUARRIES

U MINES (EXCAVATIONS)

QUARTZ

The use of optical fibers for shock pressure and timing measurements at high pressures
[DE88-004012] 10 p1334 N88-17971
Quartz oscillator analysis
[DE88-005886] 13 p1764 N88-20550

QUARTZ CRYSTALS

Aerosol sensor: Real time determination of aerosol mass size distributors using filtering quartz oscillators
[ETN-87-90397] 01 p0049 N88-10311
Defect characterization in quartz and related materials
[AD-A184754] 03 p0294 N88-11846
Quartz crystal resonators and oscillators for frequency control and timing applications
[AD-A193310] 21 p2937 N88-27443
Acoustic-optical detector of gravitational waves based on high-quality crystals
[DE88-702459] 23 p3232 N88-29232

QUARTZ LAMPS

Evaluation and certification of heater assemblies developed for thermal vacuum acceptance testing
02 p0136 N88-10853
A new type of lamp and reflector for I.R. simulation
02 p0136 N88-10855

QUARTZ TRANSDUCERS

Calibration of quartz load cells: An in-situ procedure for instrumented falling weight impact machines
[NPL-DMA(A)-155] 22 p3081 N88-28297

QUASARS

Extragalactic VLBI objects: Candidates for optical interferometry? 01 p0094 N88-10616
Galactic nuclei and quasars at high angular resolution
01 p0098 N88-10644
Spherical models of QSO/AGN emission line clouds
06 p0806 N88-14921
Finnish-Soviet Symposium on Radio Astronomy (1st) held at Otaniemi on August 26-27, 1985
[PB87-140661] 07 p0944 N88-15736
Prediction and analysis of basic gravitational microlensing phenomena 11 p1550 N88-19272
Data analysis of an observation of the quasar 3C 273 in the high-energy X-ray range, and the significance for astrophysical models
[ETN-88-91493] 14 p1993 N88-21878
Is the 3C273 quasar Mach nearer
[DE88-702235] 21 p3030 N88-27988
Detection of abundant molecular gas in the UV-excess quasar Mrk 1014 22 p3164 N88-28842

QUASI-PARTICLES
U ELEMENTARY EXCITATIONS
QUASI-STEADY STATES
Investigation of the quasi-steady approach used in transient two-phase flow analysis
[DE88-004303] 21 p2944 N88-27489
QUASI-STELLAR RADIO SOURCES
U QUASARS
QUASILINEARITY
U NONLINEARITY
QUATERNARY ALLOYS
Cadmium sulfide/copper ternary heterojunction cell research
[DE88-001122] 13 p1793 N88-20727
Development of microencapsulated DNBM quaternary ammonium inhibitors for paints
17 p2319 N88-23851
Photoluminescence studies of InGaAlAs quaternary alloys
[DE88-007197] 20 p2874 N88-27062
QUENCHING
On quench sensitivity of Cu-Cr alloys
[NASA-TT-20174] 18 p2489 N88-24765
QUENCHING (ATOMIC PHYSICS)
Quenched-laser operation of a Littman dye oscillator
[DE88-004020] 11 p1493 N88-18915
A new fiber-optic-based ion sensor
[AD-A191322] 16 p2274 N88-23612
QUENCHING (COOLING)
Investigation of rapidly-solidified dispersion strengthened titanium alloys
[AD-A183882] 01 p0022 N88-10140
Strain rate effects in fast-gas-cooled uranium-titanium and uranium-niobium alloys
[OUEL-1683/87] 02 p0149 N88-10937
Simulation of thermo-mechanical forming processes: A mixed Eulerian-Langrangian finite element method
[PB88-155247] 14 p1933 N88-21530
Critical cooling rates on solution treatment of Cu-Cr and Cu-Be alloys
[NASA-TT-20163] 18 p2488 N88-24760
The T-T-T curve in Cu-Cr alloy
[NASA-TT-20167] 20 p2774 N88-26453
Estimation of transient heat transfer coefficients in multidimensional problems by using inverse heat transfer methods 23 p3210 N88-29108
QUERY LANGUAGES
Distributed query processing: Present status and future direction 10 p1377 N88-18219
Reference model for DBMS (database management system) user facility
[PB88-169446] 13 p1851 N88-21080
The SAGE geographic analysis system
17 p2361 N88-24063
Using common subexpressions to optimize multiple queries
[DE88-008210] 20 p2844 N88-26877
Optimization techniques for relational database systems 22 p3137 N88-28650
Level 1 Ada/SQL (Structured Query Language) database language interface user's guide
[AD-A194480] 23 p3249 N88-29335
QUEUEING THEORY
Efficiency analysis of airborne Electronic CounterMeasures (ECM) systems
[AD-A184606] 03 p0306 N88-11934
The network queueing system
[NASA-CR-177433] 03 p0365 N88-12297
Heterogeneous multi-trunking queueing systems
[AD-A184255] 04 p0431 N88-12668
Waiting times in discrete-time cyclic-service systems --- communication networks
[CWI-OS-R8707] 08 p0977 N88-15909
Sojourn times in the M/G/1 queue with deterministic feedback
[CWI-OS-R8708] 08 p1074 N88-16479
A note on the effect of preemptive policies on the stability of a priority queue
[AD-A186871] 09 p1227 N88-17345
A queueing system with independent Markov input streams
[AD-A187601] 10 p1402 N88-18363
Sojourn times in feedback queues
[CWI-OS-R8710] 13 p1830 N88-20947
Two queues with alternating service and switching times
[CWI-OS-R8712] 13 p1831 N88-20949
Impact of blocking policies in closed, exponential and symmetrical ring networks
[FUB-8-1986] 14 p1960 N88-21693
Tape versus queue and stacks: The lower bounds
[CWI-CS-R8752] 16 p2249 N88-23437
A queueing network model for analyzing a class of branch and bound algorithms on a master-slave architecture
[CWI-OS-R8717] 16 p2249 N88-23441
Power series for stationary distributions of coupled processor models
[REPT-87-70] 16 p2254 N88-23470
Parallel discrete-event simulation of FCFS stochastic queueing networks
[NASA-CR-181669] 17 p2389 N88-24203
Poisson functionals of Markov processes and queueing networks
[AD-A191217] 18 p2568 N88-25252
Three-dimensional scene analysis using stero based imaging
[AD-A193120] 21 p2894 N88-27178
Queueing network models for parallel processing of task systems: An operational approach
[NASA-CR-183174] 22 p3141 N88-28677
Poisson functionals of Markov processes and queueing networks
[AD-A194289] 22 p3145 N88-28705
Relaxed heaps: An alternative to fibonacci heaps
[AD-A194030] 23 p3272 N88-29470
Performance prediction of concurrent systems
[NASA-CR-183175] 24 p3412 N88-30312
QUIET ENGINE PROGRAM
Flight research at NASA Ames Research Center: A test pilot's perspective
[NASA-TM-100025] 02 p0125 N88-10788
QUINOLINE
Electrochemistry in near-critical and supercritical fluids. 5: The dimerization of quinoline and acridine radical anions and dianions in ammonia from -70 C to 150 C
[AD-A190858] 16 p2175 N88-22967
The thermodynamic properties of quinoline and isoquinoline
[DE88-001218] 18 p2484 N88-24735

R

RACE FACTORS
A national model at Howard University demonstrating private sector interrelationships that facilitate research in predominantly Black colleges and universities
[DE88-000160] 04 p0502 N88-13089
RACON BEACONS
U RADAR BEACONS
RADAR
NT AIRBORNE SURVEILLANCE RADAR
NT COHERENT RADAR
NT CONTINUOUS WAVE RADAR
NT DOPPLER RADAR
NT EISCAT RADAR SYSTEM (EUROPE)
NT IMAGING RADAR
NT INCOHERENT SCATTER RADAR
NT INFRARED RADAR
NT METEOROLOGICAL RADAR
NT MONOPULSE RADAR
NT MOVING TARGET INDICATORS
NT MULTISTATIC RADAR
NT OPTICAL RADAR
NT OVER-THE-HORIZON RADAR
NT PULSE RADAR
NT RADAR MEASUREMENT
NT RANGE AND RANGE RATE TRACKING
NT SATELLITE-BORNE RADAR
NT SEARCH RADAR
NT SECONDARY RADAR
NT SIDE-LOOKING RADAR
NT SPACE BASED RADAR
NT SURVEILLANCE RADAR
NT SYNTHETIC APERTURE RADAR
Collection and analysis of specific ELINT Signal Parameters
[NASA-CR-181419] 01 p0033 N88-10213
JPRS report: Science and technology. China
[JPRS-CST-87-031] 03 p0299 N88-11880
Radar ECCM's new area: Anti-STEALTH and anti-ARM 03 p0299 N88-11881
On M-ARY sequential hypotheses testing for the classification of radar signals
[AD-A184094] 04 p0430 N88-12666
Correlation between refraction over sea and nature of radar reflections from sea surface
06 p0728 N88-14477
FAA air traffic control operations concepts. Volume 1: ATC background and analysis methodology
[AD-A185979] 07 p0818 N88-14973
TRACKER: A 3-D radio ray tracing code
[DE88-003267] 07 p0847 N88-15137
The design and implementation of surface acoustic wave devices for linear FM and a new non-linear FM pulse compression technique for radar applications
[AD-A186741] 08 p0980 N88-15922
Active and passive remote sensing of ice
[AD-A186685] 09 p1195 N88-17162
Wind shear radar simulation 10 p1274 N88-17625
Terrestrial Propagation Characteristics in Modern Systems of Communications, Surveillance, Guidance and Control
[AGARD-CP-407] 12 p1614 N88-19653
Radio and radar holes and multipath zones: The global and local influences on atmospheric refractive structure and resulting adverse radio and radar performance
12 p1617 N88-19667
Aircrew training devices: Utility and utilization of advanced instructional features, phase 4
[AD-A188418] 12 p1670 N88-20000
Simulation of effect of anti-radar stealth principle
13 p1755 N88-20496
Signal-filter design and system performance for polarimetric radar
[AD-A189257] 13 p1758 N88-20514
Modification of the BLUEMAX 2 terrain following model to incorporate radar detection
[AD-A190594] 15 p2017 N88-22026
High speed transcendental elementary function architecture in support of the Vector Wave Equation (VWE)
[AD-A189746] 15 p2119 N88-22627
The integration, characterisation and trialling of a modern complex airborne radar 17 p2305 N88-23791
High resolution radar techniques: Five contributions to MILINF 86
[PB88-172721] 18 p2498 N88-24821
Radio-wave scintillations and ionospheric irregularities at high latitudes
[AD-A192140] 18 p2501 N88-24837
The effects of better environmental inputs in estimating sea clutter
[AD-A192058] 19 p2643 N88-25678
Radar and EW applications of multi-gigahertz optical components and systems 19 p2660 N88-25816
Activities report of the Division of Reconnaissance and Seeker Systems
[FOA-C-30479-3.1/3.2/3.3/3.4]
22 p3116 N88-28513
Signal processing software for ground penetrating radar, user's manual
[AD-A194286] 23 p3203 N88-29059
Basic research in electronics (JSEP) Joint Services Electronics Program
[AD-A193072] 23 p3206 N88-29079
Scattering impulse response synthesis using random noise illumination: Initial concept evaluation
[AD-A195086] 24 p3364 N88-30034
Microwave remote sensing at INPE (Institute for Space Research) Brazil: Concepts and future prospects of soil moisture studies
[INPE-4569-PRE/1310] 24 p3388 N88-30178
The surface evaporative duct height product: An evaluation
[AD-A195918] 24 p3392 N88-30199
Validate algorithms for the determination of rainfall rates from SSM/I microwave satellite imagery
[AD-A195428] 24 p3404 N88-30270
RADAR ABSORBERS
NT ANTIRADAR COATINGS
The Soviet Stealth fighter: Check or checkmate
[AD-A195200] 24 p3323 N88-29791
RADAR ALTIMETERS
U RADIO ALTIMETERS
RADAR BEACONS
Analysis of ATCRBS (Air Traffic Control Radar Beacon System), mode select (Mode S) in combat operations
[AD-A193140] 22 p3040 N88-28050
RADAR BEAMS
Validate algorithms for the determination of rainfall rates from SSM/I microwave satellite imagery
[AD-A191337] 16 p2236 N88-23353
Automated test device for FASR (Fixed Array Surveillance Radar) beam steering componentry
[AD-A191650] 18 p2500 N88-24829
Utilization of a single clear-air Doppler radar beam to measure vertical divergence
[AD-A195543] 24 p3405 N88-30271
RADAR CLUTTER MAPS
TDWR (Terminal Doppler Weather Radar) clutter residue map generation and usage
[AD-A191148] 16 p2235 N88-23352
RADAR CORNER REFLECTORS
Scattering patterns of dihedral corner reflectors with impedance surface impedances
[NASA-CR-183078] 20 p2789 N88-26545
RADAR CROSS SECTIONS
Backscatter from a periodic rough surface at near grazing incidence
[NASA-CR-182397] 07 p0845 N88-15128
A study of Radar Cross Section (RCS) characteristics and their application in future weapon systems
[ETN-88-92081] 14 p1906 N88-21390

Modification of the BLUEMAX 2 terrain following model to incorporate radar detection
[AD-A190594] 15 p2017 N88-22028
High speed transcendental elementary function architecture in support of the Vector Wave Equation (VWE)
[AD-A189746] 15 p2119 N88-22627
The radar cross section of some simple reflectors at short wavelengths
[FOA-C-30472-3.3] 18 p2501 N88-24839
Almond test body — for microwave anechoic chambers
[NASA-CASE-LAR-13747-1] 18 p2502 N88-24845
Microwave image understanding and its application to radar cross section management
20 p2788 N88-26542
Scattering patterns of dihedral corner reflectors with impedance surface impedances
[NASA-CR-183078] 20 p2789 N88-26545
Radar cross section studies/compact range research
[NASA-CR-183124] 20 p2792 N88-26565
Definition of long ocean wave slope for radar applications
[AD-A193198] 21 p2933 N88-27412
Effect of phase errors in stepped-frequency radar systems
[AD-A194476] 23 p3203 N88-29061
Comparative analysis of passive communications satellites employing the SHF and HF spectrum for use in a strategic role
[AD-A194682] 24 p3362 N88-30019
Measurement and interpretation of North Atlantic Ocean marine radar sea scatter
[AD-A196239] 24 p3364 N88-30036
Analysis of environmental parameters from the Panama City tower radar experiment
[AD-A194994] 24 p3404 N88-30264

RADAR DATA
Data analysis at the Oulu (Finland) EISCAT laboratory
06 p0691 N88-14241
Study of synthetic aperture radar data compression and encoding. Part 3: Performance evaluation of speckle suppression and data compression algorithms
[NLR-TR-85085-L-PT-3] 06 p0692 N88-14248
Study of synthetic aperture radar data compression and encoding. Part 4: Algorithm implementation aspects
[NLR-TR-85085-L-PT-4] 06 p0692 N88-14249
Flightpath reconstruction and systematic radar error estimation from multiradar range-azimuth measurements
[NLR-MP-85064-U] 06 p0693 N88-14251
Study of synthetic aperture radar data compression and encoding. Part 1: SAR image data analysis
[NLR-TR-85085-L-PT-1] 07 p0843 N88-15115
Study of synthetic aperture radar data compression and encoding. Part 2: SAR image speckle suppression and data compression algorithms
[NLR-TR-85085-L-PT-2] 07 p0843 N88-15116
Improved resolution atmospheric density measurements based on simulations 08 p1027 N88-16221
Proposals for the pre-operational use of data from the European Remote Sensing Satellite ERS-1
[BCRS-86-02] 16 p2227 N88-23300
Preparation and execution of calibration measurements for handling of airborne SAR data (AGRISAR)
[ETN-88-92338] 17 p2333 N88-23926
The CERSAT archiving and processing center --- ERS-1 19 p2701 N88-26059
Ocean satellite data and the needs of designers and operators of marine units 19 p2701 N88-26061
Non-Gaussian models for surface clutter
22 p3068 N88-28212
Some characteristics in synthetic aperture radar (SAR) raw data and SAR images
[FOA-C-30483-3.2] 22 p3071 N88-28232
A study of the feasibility of using sea and wind information from the ERS-1 satellite. Part 1: Wind scatterometer data
[NASA-CR-182833] 24 p3386 N88-30167
A study of the feasibility of using sea and wind information from the ERS-1 satellite. Part 2: Use of scatterometer and altimeter data in wave modeling and assimilation
[ESA-CR(P)-2604-PT-2] 24 p3387 N88-30176

RADAR DETECTION
The importance sampling and its application to radar simulation 01 p0012 N88-10065
Meteor detection on ST (MST) radars
06 p0740 N88-14554
Backscattering signal analysis concerning a three-dimensional object configuration on the basis of object motion
[ESA-TT-1044] 09 p1154 N88-16915
Airborne Doppler radar technology for wind shear detection 10 p1274 N88-17622
Experiments for the high resolution detection of moving targets using a CO2 laser radar
[MBB-UA-1044/87] 10 p1316 N88-17864
Aircraft accident report: Midair collision of Cessna-340A, N8716K, and North American SNJ-4N, N711SQ, Orlando, Florida, May 1, 1987
[PB88-910402] 13 p1720 N88-20282
Influence of hydrometeorological factors on visibility of objects detected by radar 13 p1790 N88-20707
Modification of the BLUEMAX 2 terrain following model to incorporate radar detection
[AD-A190594] 15 p2017 N88-22028
Acta aeronautica et astronautica sinica (selected articles)
[AD-A191552] 18 p2455 N88-24575
The VHF experimental radar LARA. A long-wavelength radar for helicopter detection 22 p3149 N88-28738
The radar detection of hovering helicopters
22 p3150 N88-28739
On adaptive cell-averaging CFAR (Constant False-Alarm Rate) radar signal detection
[AD-A196286] 24 p3360 N88-30009
Modeling and performance of HF/OTH (High-Frequency/Over-the-Horizon) radar target identification systems
[AD-A196287] 24 p3365 N88-30038
The surface evaporative duct height product: An evaluation
[AD-A195918] 24 p3392 N88-30199

RADAR ECHOES
NT CLUTTER
NT VENUS RADAR ECHOES
The hybrid wavefront resonance method
03 p0303 N88-11913
Photographic fireball networks
06 p0738 N88-14540
Meteor detection on ST (MST) radars
06 p0740 N88-14554
The Newcastle meteor radar
06 p0741 N88-14556
Waveform for short-dwell-time meteorological Doppler radars
[PB88-102199] 07 p0845 N88-15126
Radar echo signatures versus relative precipitation
[AD-A186162] 08 p0976 N88-15903
SAR (Synthetic Aperture Radar) imaging of ship wakes in the Gulf of Alaska
[AD-A186554] 10 p1317 N88-17872
On the theory of electromagnetic scattering from a raindrop splash
[AD-A188720] 14 p1906 N88-21393
TDWR (Terminal Doppler Weather Radar) PRF (Pulse Repetition Frequency) selection criteria
[AD-A193069] 21 p2932 N88-27407
Definition of long ocean wave slope for radar applications
[AD-A193198] 21 p2933 N88-27412
Radar information from the partial derivatives of the echo signal phase from a point scatterer
[AD-A193402] 21 p2933 N88-27415
The maximum entropy method for the analysis of short-time radar echoes from hovering helicopters
22 p3149 N88-28737
Measurement and interpretation of North Atlantic Ocean marine radar sea scatter
[AD-A196239] 24 p3364 N88-30036

RADAR EQUIPMENT
NT RADAR BEACONS
NT RADAR CORNER REFLECTORS
NT RADAR FILTERS
NT RADAR RECEIVERS
NT RADAR TRANSMITTERS
A preliminary assessment of thunderstorm outflow wind measurement with airport surveillance radars
[AD-A189064] 13 p1799 N88-20757
Considerations in GaAs standard cell design
[DE88-003310] 14 p1985 N88-21840

RADAR FILTERS
Multi-sensory tracking mount control
[AD-A194675] 23 p3249 N88-29339

RADAR IMAGERY
Venusian surface and crust 01 p0010 N88-10054
Dike zones on Venus
[NASA-TT-20111] 02 p0254 N88-11607
Delay-Doppler radar imaging
[AD-A184165] 03 p0308 N88-11943
Correction of inertial navigation system drift errors for an autonomous land vehicle using optical radar terrain data
[AD-A184973] 05 p0544 N88-13311
Study of synthetic aperture radar data compression and encoding. Part 3: Performance evaluation of speckle suppression and data compression algorithms
[NLR-TR-85085-L-PT-3] 06 p0692 N88-14248
Study of synthetic aperture radar data compression and encoding. Part 4: Algorithm implementation aspects
[NLR-TR-85085-L-PT-4] 06 p0692 N88-14249
Texture study of Synthetic Aperture Radar (SAR) images of ocean surfaces
[AD-A186021] 07 p0841 N88-15101
Study of synthetic aperture radar data compression and encoding. Part 1: SAR image data analysis
[NLR-TR-85085-L-PT-1] 07 p0843 N88-15115
Study of synthetic aperture radar data compression and encoding. Part 2: SAR image speckle suppression and data compression algorithms
[NLR-TR-85085-L-PT-2] 07 p0843 N88-15116
Processing of radar images of Venus on the Magiscan-2 analyzer 08 p1009 N88-16117
Earthnet's experience with Seasat SAR image processing 09 p1127 N88-16760
SAR (Synthetic Aperture Radar) imaging of ship wakes in the Gulf of Alaska
[AD-A186554] 10 p1317 N88-17872
Radar reflectivity and attenuation of radio waves in the melting layer of precipitation
[PB88-121553] 10 p1318 N88-17882
Integrated optical synthetic aperture radar processor
[AD-A188019] 11 p1471 N88-18772
The complex point spread function of the RSRE SAR (Synthetic Aperture Radar)
[AD-A189011] 12 p1621 N88-19693
Position, scale, and rotation invariant target recognition using range imagery
[AD-A188828] 12 p1633 N88-19772
A polarimetric rain backscatter model developed for coherent polarization diversity radar applications
13 p1759 N88-20520
Results of the testing of the segmentation program on RESEDA
[BCRS-87-01] 16 p2228 N88-23304
Validate algorithms for the determination of rainfall rates from SSM/I microwave satellite imagery
[AD-A188769] 16 p2233 N88-23337
Investigation of the imaging of ocean surface waves using a synthetic aperture radar
[SER-A-WISS-ABHANDL-84] 16 p2236 N88-23357
Preparation and execution of calibration measurements for handling of airborne SAR data (AGRISAR)
[ETN-88-92338] 17 p2333 N88-23926
The Shuttle Imaging Radar B (SIR-B) experiment report
[NASA-CR-182923] 17 p2334 N88-23932
Radar penetration in the Amazonian rain forest
17 p2352 N88-24015
Airborne and spaceborne radar images for geologic and environmental mapping in the Amazon rain forest, Brazil
17 p2353 N88-24021
Subsurface morphology and geoarchaeology revealed by spaceborne and airborne radar
17 p2353 N88-24022
The use of SLAR and SIRA imagenes for the classification of forest typen in tropical rain forests
17 p2356 N88-24036
Radar penetration in the Amazonian rain forest
17 p2358 N88-24044
Analysis and interpretation of image lithostructure: An application of the multiconcept in the metamorphic belt of Sul de Santana da Boa Vista (RS)
17 p2359 N88-24051
Digital processing of infrared and visible images from the GOES satellite and its integration with meteorological radar data 17 p2360 N88-24057
Interpretation of MSS/LANDSAT data for evaluation of physical distribution of mangroves in Cananeia-Iguape (SP) 17 p2363 N88-24072
Some geological aspects of the Pirapemas Lineament Belt 17 p2368 N88-24099
Lithostructural interpretation of Chapda do Cachimbo (Pa-Am-Mt), based on radar and LANDSAT imagery
17 p2368 N88-24100
Delay-doppler radar imaging
[AD-A191509] 18 p2499 N88-24826
Observation of stratiform rain with 94 GHz and s-b and Doppler radar
[AD-A192013] 18 p2544 N88-25100
Sources of scattering in vegetarian and other surfaces and objects
[NASA-CR-182975] 20 p2816 N88-26710
Image pyramid motion detection applied to sea ice
20 p2817 N88-26713
Linear feature extraction from radar imagery. Phase 2: Base contract report
[AD-A192828] 21 p2931 N88-27404
Some characteristics in synthetic aperture radar (SAR) raw data and SAR images
[FOA-C-30483-3.2] 22 p3071 N88-28232
Mars earth-based radar: 1986 results and 1988-1990 opportunities 23 p3306 N88-29697
Acoustooptic processing of two-dimensional signals using temporal and spatial integration
[AD-A194803] 24 p3359 N88-29999

Corner extraction from radar images
[AD-A194857] 24 p3382 N88-30020
MIZEX (marginal ice zone experiment) 1987 SAR (Synthetic Aperture Radar) data summary
[AD-A195560] 24 p3364 N88-30035
Range data description based on multiple characteristics 24 p3419 N88-30351
High-resolution (30 m) lunar radar images 24 p3442 N88-30486
Determining the spatial structure of fields of precipitation from space radar images in two orthogonal polarizations 24 p3450 N88-30531

RADAR MAPS
Inverse scattering analysis of diffraction limited SAR
[FOA-C-30459-3.2] 05 p0576 N88-13512
Preliminary airworthiness evaluation of a UH-1 equipped with a terrain mapping receiver antenna
[AD-A188274] 07 p0819 N88-14980
Marginal Ice Zone Experiment (MIZEX) 1984 VARAN-S data set
[ETN-88-92032] 14 p1950 N88-21625
Geometric restoration of satellite image data
[AD-A190462] 15 p2089 N88-22450
Digital monoplotting, part 1
[B8735122-PT-1] 17 p2369 N88-24106
Digital monoplotting, part 2
[B8735122-PT-2] 17 p2369 N88-24107

RADAR MEASUREMENT
Collection and analysis of specific ELINT Signal Parameters
[NASA-CR-181419] 01 p0033 N88-10213
Moisture determinations in and under vegetation canopies. Part 2: Results after parameterization of the CLOUD model
[FEL-1986-63] 01 p0064 N88-10410
Theoretical and lidar studies of the seasonal and nocturnal variations of the mesospheric sodium layer at Urbana, Illinois 01 p0068 N88-10435
A real-time system for automatic single-Doppler wind field analysis 02 p0200 N88-11249
Radar measurement methods for the observation of convective clouds, and comparison of measurements and numerical simulation
[ESA-TT-1049] 03 p0352 N88-12223
Contributions of lidar measurements to the study of long term variations of the middle atmosphere
[ETN-88-91237] 05 p0625 N88-13824
Electromagnetic wave probing of Earth's environment
[NASA-CR-182358] 06 p0690 N88-14232
The Cyclone meteor radar system for routine wind measurements in the lower thermosphere 06 p0741 N88-14555
Middle atmospheric wind measurements using a medium frequency radar
[AD-A185931] 07 p0879 N88-15330
Development of a Doppler wind lidar system for atmospheric wind measurements 08 p1027 N88-16217
The sodium layer at 69 N latitude in wintertime 08 p1027 N88-16218
Lidar metal density measurements in the upper atmosphere 08 p1027 N88-16219
Improved resolution atmospheric density measurements based on simulations 08 p1027 N88-16221
Comparison of simultaneous MST radar and electron density probe measurements in the polar mesosphere --- Mesospheric, Stratospheric, Tropospheric (MST) 08 p1028 N88-16226
Project CONDOR: Middle atmosphere wind structure obtained with lightweight inflatable spheres near the equatorial electrojet 08 p1029 N88-16230
EISCAT measurements of ion velocities during Coordinated Auroral Experiment using Scatter And Rockets (CAESAR) campaign 08 p1031 N88-16251
Remote and in-situ plasma measurements during the Coordinated Auroral Experiment using Scatter And Rockets (CAESAR) flight 08 p1032 N88-16252
Future developments of auroral D-region research using the EISCAT VHF incoherent scatter radar 08 p1035 N88-16278
Investigation of the quantitative determination of two dimensional sea surface wave spectra from shipborne radar measurements
[GKSS-87/E/10] 09 p1195 N88-17163
Lower bounds on acceleration estimation accuracy
[AD-A188383] 12 p1619 N88-19681
Atmospheric backscatter at 10.6 microns; a compendium of measurements made outside the United Kingdom by the airborne LATAS coherent laser radar velocimeter
[RSRE-87002] 12 p1631 N88-19763
Applications of the differential reflectivity radar technique: Focus on estimation of rainfall parameters and microwave attenuation prediction 13 p1759 N88-20521
A preliminary assessment of thunderstorm outflow wind measurement with airport surveillance radars
[AD-A189064] 13 p1799 N88-20757
Inversion algorithms for geophysical problems
[AD-A189252] 13 p1815 N88-20845
Nonparametric discriminant analysis applied to the extraction and selection of radar target signature features
[AD-A191849] 18 p2501 N88-24833

RADAR NETWORKS
Study of microburst detection performance during 1985 in Memphis, Tennessee
[AD-A184013] 03 p0354 N88-12231
Description of data handling system installed December 11, 1986 --- EISCAT 06 p0692 N88-14242

RADAR OBSERVATION
U RADAR TRACKING

RADAR PHOTOGRAPHY
Inverse scattering analysis of diffraction limited SAR
[FOA-C-30459-3.2] 05 p0576 N88-13512

RADAR RANGE
TDWR (Terminal Doppler Weather Radar) PRF (Pulse Repetition Frequency) selection criteria
[AD-A193089] 21 p2932 N88-27407
Effect of phase errors in stepped-frequency radar systems
[AD-A194476] 23 p3203 N88-29061

RADAR RECEIVERS
Goldstone solar system radar performance analysis 22 p3068 N88-28206

RADAR REFLECTIONS
U RADAR ECHOES

RADAR REFLECTORS
NT RADAR CORNER REFLECTORS

RADAR RESOLUTION
Distortion of wideband carbon dioxide laser radar waveforms due to atmospheric dispersion and absorption
[AD-A186687] 12 p1632 N88-19771
Retrieval of three-dimensional wind and temperature fields from single-Doppler radar data 12 p1646 N88-19858
High resolution radar techniques: Five contributions to MILINF 86
[PB88-172721] 18 p2498 N88-24821
Sources of scattering in vegetarian and other surfaces and objects
[NASA-CR-182975] 20 p2816 N88-26710

RADAR SCANNING
Study on propagation and inverse scattering --- sea studies
[ESA-CR(P)-2394] 01 p0063 N88-10405
High latitude problems to be studied by incoherent scatter radars
[DMI-GEOPHYS-PAPERS-R-77] 03 p0350 N88-12211
Radar information from the partial derivatives of the echo signal phase from a point scatterer
[AD-A193402] 21 p2933 N88-27415

RADAR SCATTERING
Target strength: An overview of some recent theoretical developments 03 p0303 N88-11910
The hybrid wavefront resonance method 03 p0303 N88-11913
Physical optics method: Prediction of radar signatures 03 p0304 N88-11914
Input signal shaping: K-pulse 03 p0304 N88-11917
New main reflector, subreflector and dual chamber concepts for compact range applications
[NASA-CR-181506] 04 p0402 N88-12498
Large bandwidth ground scattering model --- radar scattering
[FOA-C-30458-3.2] 05 p0576 N88-13511
Inverse scattering analysis of diffraction limited SAR
[FOA-C-30459-3.2] 05 p0576 N88-13512
The rocket and scatter experiment ROSE: Presentation of the scientific payload 08 p1034 N88-16269
Radar returns from ground clutter in vicinity of airports 10 p1274 N88-17624
The radar scattering coefficient as a function of forest stand parameters and viewing angle. An empirical study of the Pinus sylvestris L. in the Kootwijk forest (The Netherlands), extended with observations in the Speulder and Sprielder forest (The Netherlands)
[ETN-88-91348] 13 p1780 N88-20527
Radial track of moving objects determined by HF backscatter technique 14 p1901 N88-21354
Scattering patterns of dihedral corner reflectors with impedance surface impedances
[NASA-CR-183078] 20 p2789 N88-26545
South Pole lidar: Brief description of the instrument
[NOTA-INTERNA-907] 22 p3083 N88-28308
Measurement and interpretation of North Atlantic Ocean marine radar sea scatter
[AD-A196239] 24 p3364 N88-30036

RADAR SIGNATURES
An investigation on Faraday rotators and quarter-wave plates of a 35 GHz radar signature system
[DFVLR-FB-87-14] 01 p0037 N88-10236
Physical optics method: Prediction of radar signatures 03 p0304 N88-11914
Numerical modeling: Integral equation method 03 p0304 N88-11919
Radar echo signatures versus relative precipitation
[AD-A186162] 08 p0976 N88-15903
Radar descriptors for the classification of terrain features
[AD-A188145] 11 p1504 N88-18983
A polarimetric rain backscatter model developed for coherent polarization diversity radar applications 13 p1759 N88-20520
A study of Radar Cross Section (RCS) characteristics and their application in future weapon systems
[ETN-88-92081] 14 p1908 N88-21390
Research on Faraday rotators and quarter-wave plates of a 35-GHz radar signature system
[ESA-TT-1081] 16 p2189 N88-23052
Nonparametric discriminant analysis applied to the extraction and selection of radar target signature features
[AD-A191849] 18 p2501 N88-24833
Autoregressive moving average modeling of radar target signatures
[AD-A194612] 22 p3069 N88-28218
Viking Landers and remote sensing 23 p3304 N88-29685
The Soviet Stealth fighter: Check or checkmate
[AD-A195200] 24 p3323 N88-29791

RADAR TARGETS
Feature selection applied to radar target identification
[AD-A183880] 01 p0034 N88-10215
Theoretical Aspects of Target Classification
[AGARD-LS-152] 03 p0303 N88-11909
Target strength: An overview of some recent theoretical developments 03 p0303 N88-11910
The hybrid wavefront resonance method 03 p0303 N88-11913
Theoretical aspects of target classification: Physical optics and radon transform methods 03 p0304 N88-11915
Parametrization in scattering models 03 p0304 N88-11916
Input signal shaping: K-pulse 03 p0304 N88-11917
Numerical modeling: Integral equation method 03 p0304 N88-11919
Experiments: Test range facilities, part 1 03 p0304 N88-11920
Delay-Doppler radar imaging
[AD-A184165] 03 p0308 N88-11943
New main reflector, subreflector and dual chamber concepts for compact range applications
[NASA-CR-181506] 04 p0402 N88-12498
Detection of signals in non-Gaussian correlated noise derived from Cauchy processes
[AD-A187488] 10 p1320 N88-17894
Mono- and bistatic radar coverage diagrams including diffractive wave propagation 12 p1616 N88-19660
A method for discrimination of radar targets using complex natural resonances
[AD-A191848] 18 p2500 N88-24832
Nonparametric discriminant analysis applied to the extraction and selection of radar target signature features
[AD-A191849] 18 p2501 N88-24833
Evaluation of LISBON TAR SSR radar
[EEC/NOTE-5/87] 24 p3362 N88-30015
Modeling and performance of HF/OTH (High-Frequency/Over-the-Horizon) radar target identification systems
[AD-A196287] 24 p3365 N88-30038

RADAR TRACKING
Balloon track data analysis
[AD-A184750] 03 p0350 N88-12213
Media calibrations of the Doppler signal for a gravitational wave experiment --- interplanetary medium
[IFSI-86-13] 05 p0625 N88-13825
Middle Atmosphere Program. Handbook for MAP, volume 25
[NASA-CR-181571] 06 p0732 N88-14502
The climatic wind regime in the lower thermosphere from meteor radar observations 06 p0733 N88-14506
Meteor observation by the Kyoto meteor radar 06 p0733 N88-14507
Hard- and software problems of spaced meteor observations by optical electronics 06 p0741 N88-14560
The correlation between methodological and low-level angle-of-arrival measurements 12 p1617 N88-19668

Aircraft accident report: Midair collision of Cessna-340A, N8716K, and North American SNJ-4N, N711SQ, Orlando, Florida, May 1, 1987
[PB88-910402] 13 p1720 N88-20282
A method and measures to evaluate trackers for air traffic control
[NLR-TR-86072-U] 13 p1720 N88-20287
Modification of the BLUEMAX 2 terrain following model to incorporate radar detection
[AD-A190594] 15 p2017 N88-22028
Polarimetric ISAR imaging using either measured or calculated transient signatures
[AD-A190077] 15 p2056 N88-22259
Studies of ionosphere/magnetosphere dynamics using SABRE and HILAT
[AD-A190947] 16 p2232 N88-23333
Space based radar application to air traffic control
17 p2399 N88-24262
A method for discrimination of radar targets using complex natural resonances
[AD-A191848] 18 p2500 N88-24832
Track performance considerations for monopulse radars
[AD-A196232] 24 p3360 N88-30007
MIZEX (marginal ice zone experiment) 1987 SAR (Synthetic Aperture Radar) data summary
[AD-A195560] 24 p3364 N88-30035
Modeling and performance of HF/OTH (High-Frequency/Over-the-Horizon) radar target identification systems
[AD-A196287] 24 p3365 N88-30038

RADAR TRANSMISSION
Inversion of simulated satellite signals
08 p1017 N88-16168
Electromagnetic interference to radar and radio link systems caused by large scale wind turbines
[FOA-C-30486-3.2] 22 p3071 N88-28234

RADAR TRANSMITTERS
Evaluation of LISBON TAR SSR radar
[EEC/NOTE-5/87] 24 p3362 N88-30015

RADIAL DISTRIBUTION
Fiber-optic accelerometer investigation
[AD-A185359] 05 p0584 N88-13561
Nonuniformity of electromagnetic field at Lambda = 10.6 micron wavelength inside atmospheric aerosol particles
06 p0772 N88-14743

RADIAL DRAINAGE PATTERNS
U DRAINAGE PATTERNS

RADIAL FLOW
Continuation finite element analysis of viscoelastic fluids 04 p0445 N88-12761
High pressure ratio turbine design constraints
[TRR-0279] 06 p0712 N88-14365
Mainline performance prediction for radial inflow turbines 06 p0712 N88-14366
Performance of supersonic impingement radial turbines 06 p0712 N88-14367
Conclusions from a research program on mixed flow gas generator turbines 06 p0713 N88-14368
Experimental and theoretical study of the dynamic operational behavior of a three stage radial compressor
[ETN-88-92129] 20 p2811 N88-26676
The use of fins to reduce the pressure drop in a rotating cavity with a radial flow
[PNR90465] 22 p3079 N88-28282

RADIAL VELOCITY
An application of L1 to astronomy --- stellar velocity
[REPT-87-10] 01 p0108 N88-10702
Retrieval of three-dimensional wind and temperature fields from single-Doppler radar data
12 p1646 N88-19858
A preliminary assessment of thunderstorm outflow wind measurement with airport surveillance radars
[AD-A189064] 13 p1799 N88-20757
New measurements of radial velocities in clusters of galaxies
[INPE-4527-PRE/1277] 15 p2152 N88-22845
Radial velocities monitoring of a sample of barium and S stars using CORAVEL: Towards an evolutionary link between barium and S stars?
[SER-C-PREPUBL-FASC-19] 18 p2593 N88-25410
Radial velocity measurements of a sample of northern metal-deficient stars
[SER-C-PREPUBL-FASC-25] 24 p3455 N88-30564

RADIANCE
The use of satellite IR data in the enhancement of surface thermal fields 02 p0202 N88-11260
Use of simulated satellite radiances from a mesoscale numerical model to understand kinematic and dynamic processes 02 p0202 N88-11261
Quantum electrodynamics based on self-energy: Spontaneous emission in cavities
[DE87-703071] 02 p0232 N88-11461
The absolute radiometric calibration of space-based sensors 03 p0277 N88-11744
Calibrating AIS images using the surface as a reference 05 p0612 N88-13760
The influence of yellow substances on remote sensing of sea water constituents from space. Volume 1: Summary
[ESA-CR(P)-2443-VOL-1] 07 p0872 N88-15292
The influence of yellow substances on remote sensing of sea water constituents from space. Volume 2: Appendices
[ESA-CR(P)-2443-VOL-2] 07 p0873 N88-15293
Determination of cloud base height and emissivity from downwelling angular radiances
[AD-A185985] 07 p0879 N88-15331
Monte Carlo method calculation of spectral brightness coefficient of vegetation cover as function of illumination conditions 08 p1008 N88-16113
Aerosol size distribution from measurements of the radiance in the solar aureole 08 p1019 N88-16176
The iterative radiance model of the Meteorological Institute of the University of Munich (West Germany)
08 p1019 N88-16178
Vertical atmospheric sounding
[INPE-4370-PRE/1195] 08 p1036 N88-16283
Depolarized infrared reflectance from dry and wetted surfaces
[AD-A188213] 11 p1492 N88-18903
Determination of atmospheric moisture structure from high resolution MAMS radiance data
11 p1515 N88-19049
Remote sensing of atmospheric optical thickness and sea-water attenuation when submerged: Wavelength selection and anticipated errors
[AD-A187609] 11 p1548 N88-19262
Enhancements to the atmospheric transmittance/radiance program FASCODE
[AD-A188863] 12 p1643 N88-19839
Progress in X-ray laser experiments
[ETN-88-92004] 14 p1915 N88-21442
Relationship between optical transfer function and natural light field in sea or atmosphere
15 p2054 N88-22247
Calibration and processing of AVHRR data for temperature estimation
[INPE-4493-PRE/1257] 15 p2095 N88-22485
The NBS scale of radiance temperature
17 p2328 N88-23897
Estimation of total Outgoing Longwave Radiation (OLR) flux from geostationary meteorological satellite infrared window radiance 17 p2351 N88-24006
Spectral measurements for correcting LANDSAT data for atmospheric effects 17 p2362 N88-24066
Sky radiance distributions for thermal imaging backgrounds
[AD-A191135] 17 p2373 N88-24115
Effects of atmospheric model layering on LOWTRAN 6 calculations of 8-12 micrometers near-horizon sky radiances
[AD-A192969] 20 p2791 N88-26559
Numerical model for the computation of radiance distributions in natural waters with wind-roughened surfaces
[PB88-192703] 20 p2826 N88-26765
Eigenmatrix representations of radiance distributions in layered natural waters with wind-roughened surfaces
[PB88-188701] 20 p2828 N88-26780
IR (infrared) sky radiance distributions in the marine boundary layer
[AD-A193683] 22 p3119 N88-28531
A probabilistic model of the apparent radiance of a rough sea
[AD-A193867] 22 p3129 N88-28602
Filling of the atmospheric transmission window due to emission from very high rotational levels of NO and O3
[AD-A194670] 23 p3233 N88-29239

RADIANT COOLING
Thermal radiation from neutron stars
[MPE-203] 11 p1571 N88-19404

RADIANT FLUX DENSITY
NT ELECTRON FLUX DENSITY
NT ILLUMINANCE
NT IRRADIANCE
NT LUMINANCE
NT LUMINOUS INTENSITY
NT NEUTRON FLUX DENSITY
NT PARTICLE FLUX DENSITY
NT RADIANCE
NT SOLAR CONSTANT
NT SOLAR FLUX DENSITY
Monitored background radiometer
02 p0133 N88-10831
Instrument for radiation testing/screening electronic devices over an extended temperature range
[AD-A184245] 03 p0326 N88-12060
Report of the Joint Scientific Commitee Ad Hoc Working Group on Radiative Flux Measurements --- Earth radiation budget
[WCP-136] 06 p0742 N88-14567
Nonuniformity of electromagnetic field at Lambda = 10.6 micron wavelength inside atmospheric aerosol particles
06 p0772 N88-14743
Overestimation of on-axis power density by the Fraunhofer (far-field) approximation
[AD-A186399] 07 p0843 N88-15111
The role of anisotropy in the long range reconnaissance of the albedo of land surfaces 08 p1017 N88-16169
High energy and high intensity laser effects on aerosols: Changes in droplet morphology, surrounding temperature and vapor concentration
[AD-A193825] 23 p3220 N88-29164

RADIANT HEATING
An approximate solution to the problem of heating massive bodies by both radiation and convection
[BLL-M-37315-(5828.4)] 02 p0170 N88-11068
Test methodology for infrared tubular heaters
[PB88-160916] 12 p1626 N88-19726

RADIANT INTENSITY
U RADIANT FLUX DENSITY

RADIATION ABSORPTION
NT ELECTROMAGNETIC ABSORPTION
NT GAMMA RAY ABSORPTION
NT INFRARED ABSORPTION
NT MOLECULAR ABSORPTION
NT MULTIPHOTON ABSORPTION
NT PHOTOABSORPTION
NT ULTRAVIOLET ABSORPTION
NT X RAY ABSORPTION
Transient absorption behavior of metals at the onset of the laser welding process
[DFVLR-FB-87-12] 01 p0025 N88-10160
Estimating scattered and absorbed radiation in plant canopies by remote sensing
[NASA-CR-181390] 02 p0193 N88-11205
Theoretical atomic and molecular photophysics
[DE87-014249] 02 p0231 N88-11458
Laboratory evaluation and application of microwave absorption properties under simulated conditions for planetary atmospheres
[NASA-CR-181466] 02 p0254 N88-11606
Millimeter-wave studies of moist air
[AD-A184681] 03 p0306 N88-11935
Study of kinetics of intracavity absorption in pulsed dye lasers 07 p0919 N88-15585
Explosive absorption of laser beam of finite diameter
07 p0921 N88-15597
The application of vector diffraction to the scalar anomalous diffraction approximation of Van de Hulst
[AD-A185930] 07 p0929 N88-15643
Absorption of cyclotron radiation in skin layer in Araks experiment 08 p1003 N88-16076
Nonlinear absorption of CO2 laser radiation in p-type InSb
[DE88-004055] 11 p1492 N88-18906
The YAlO(sub 3):Er laser
[PB88-130877] 11 p1493 N88-18911
Remote sensing of atmospheric optical thickness and sea-water attenuation when submerged: Wavelength selection and anticipated errors
[AD-A187609] 11 p1548 N88-19262
Laser fluorescence velocimeter
[AD-A189010] 12 p1630 N88-19753
Distortion of wideband carbon dioxide laser radar waveforms due to atmospheric dispersion and absorption
[AD-A188687] 12 p1632 N88-19771
Research on absorption of UV radiation in Venusian atmosphere from Vega-1 and Vega-2 landing modules
13 p1725 N88-20316
Spontaneous decay and atomic fluorescence near a metal surface of an absorbing dielectric
[AD-A187508] 13 p1835 N88-20975
Dependence of formation of radiative color centers in optical glass fibers on technological factors
14 p1896 N88-21321
Radiation absorption in neodymium glasses during passage of strong laser pulse 14 p1969 N88-21757
Dissipative relativistic radiation hydrodynamics
[DE88-702092] 19 p2665 N88-25846
Absorption characteristics of Si3N4 ablation layer plasma 20 p2783 N88-26504
Assessment of cochlear damage after microwave irradiation
[AD-A193237] 21 p2987 N88-27737
Differences in radiation budget parameters over Asia in relation to contrasting Indian monsoons
22 p3125 N88-28574
Coupling between radiation and gas dynamics
[AD-A194593] 23 p3211 N88-29113

RADIATION BELTS
NT INNER RADIATION BELT

Radiation effects in space
[DE87-012529] 01 p0075 N88-10479
Radiation belts 03 p0272 N88-11707
Analysis of geophysical data bases and models for spacecraft interactions
[AD-A184809] 05 p0555 N88-13375
Toward a comprehensive theory for the sweeping of trapped radiation by inert orbiting matter
[NASA-CR-182584] 11 p1589 N88-19395
Stimulated Emission of Energetic Particles (SEEP)
[AD-A188724] 13 p1853 N88-21094
Solar flares and magnetospheric particles: Investigations based upon the ONR-602 and ONR-604 experiments
[AD-A193396] 21 p3031 N88-27994

RADIATION CHEMISTRY
NT PHOTODECOMPOSITION
NT PHOTODISSOCIATION
NT PHOTOLYSIS
NT RADIOLYSIS
Astromag: A particle spectrometer for the Space Station
[PREPRINT-557] 06 p0707 N88-14336
Effects of energy, distance and orientation on electron transfer rates studied by pulse radiolysis in organic media
[DE88-002906] 08 p1082 N88-16521
Diversity of comets, synergic temperature effects and the stability of organic compounds in icy nuclei
14 p2005 N88-21955
The radiation sensitivity of select metal chelate polymers: Mechanistic changes at higher energies
[AD-A193467] 23 p3196 N88-29019

RADIATION COUNTERS
NT CERENKOV COUNTERS
NT ELECTRON COUNTERS
NT NEUTRON COUNTERS
NT NEUTRON SPECTROMETERS
NT PARTICLE TELESCOPES
NT PROPORTIONAL COUNTERS
NT SCINTILLATION COUNTERS
NT SPARK CHAMBERS
Calibration constants for the 1986 BGO crystals matrix
[NOTA-INTERNA-886] 07 p0856 N88-15197
Ionization losses in BGO
[NOTA-INTERNA-889] 07 p0856 N88-15198
Characteristics of multimuon events from fourth generation quarks at the SSC (Superconducting Super Collider)
[DE88-002954] 09 p1257 N88-17535
Nonequilibrium superconductivity for particle detectors
[DE88-002876] 09 p1257 N88-17539
High energy cosmic muons and the calibration of the L3 electromagnetic calorimeter
[NOTA-INTERNA-895] 14 p2011 N88-21999
Large area nuclear particle detectors using ET materials
[NASA-CR-180777] 23 p3215 N88-29136

RADIATION DAMAGE
NT LASER DAMAGE
Effects of electron and proton irradiations on n/p and p/n GaAs cells grown by MOCVD
[NASA-TM-100199] 01 p0042 N88-10266
Optical damage in polymers by millisecond light pulses
[DE87-013106] 02 p0151 N88-10943
Effects of radiation damage in optical fibers: A tutorial
[PB87-210308] 02 p0235 N88-11482
Prevention of radiation induced degradations and of electrostatic perturbations on the Arabsat spacecraft in flight results 03 p0275 N88-11734
DNA damage and repair in human skin in situ
[DE87-014288] 03 p0356 N88-12241
Performance of GaAs and silicon concentrator cells under 37 MeV proton irradiation
[NASA-TM-100144] 04 p0465 N88-12877
Radiation performance of AlGaAs concentrator cells and expected performance of cascade structures
[NASA-TM-100145] 04 p0465 N88-12878
Reevaluating the worst-case radiation response of MOS transistors
[DE87-014157] 04 p0497 N88-13059
Swelling behavior of ferritic/martensitic steels
[DE88-001757] 06 p0682 N88-14177
UV radiation: Human exposure to ultraviolet radiation
[PB87-137410] 06 p0752 N88-14619
Evolution of radiation-induced voids and dislocations at low temperature
[DE88-700350] 07 p0939 N88-15704
Space environmental considerations for a long-term cryogenic storage vessel 08 p0961 N88-15933
Forward-biased current annealing of radiation damaged gallium arsenide and silicon solar cells
[AD-A186904] 09 p1186 N88-17105
Irradiation effects in metals
[DE88-004272] 10 p1303 N88-17789
Suppression of X-rays generated by runaway electrons in ATF
[DE88-004179] 10 p1414 N88-18440
The effects of low doses of 14 MeV neutrons on the tensile properties of three binary copper alloys
[DE88-003400] 11 p1458 N88-18691
Measurement of the gamma-ray response of some commercial silicon detectors
[AD-A187431] 11 p1543 N88-19221
JPRS report: Science and technology. USSR: Life sciences
[JPRS-ULS-88-002] 12 p1665 N88-19982
Study of defects in metals by positron annihilation
[DE88-701042] 13 p1745 N88-20432
In situ TEM observations of heavy ion damage in gallium arsenide
[DE88-005984] 14 p1986 N88-21843
X-ray production in low energy proton stopping
[NASA-TM-100619] 16 p2270 N88-23582
Effects of 67.5 MeV electron irradiation on Y-Ba-Cu-O and Gd-Ba-Cu-O high-temperature superconductors
[AD-A191271] 16 p2283 N88-23669
Space nuclear reactor shielding optimization studies
17 p2408 N88-24320
Molecular characterization of structure and bonding in thin film materials
[DE88-006811] 18 p2584 N88-25351
An optically strobed sample and hold circuit
19 p2656 N88-25772
JFET/SOS (Junction Field-Effect Transistor/Silicon-on-Sapphire) devices: Gamma-radiation-induced effects
[AD-A193001] 20 p2795 N88-26586
Acute radiation syndromes and their management
[DE88-009839] 20 p2831 N88-26797
The Oak Ridge National Laboratory strategic defense initiative shield optimization program: Executive summary
[DE88-008016] 20 p2847 N88-26899
Electron irradiation effects in YBa2Cu3O7-Delta single crystals
[DE88-010050] 20 p2878 N88-27085
Data compilation for radiation damage on ceramic insulators. Revised with updated data and reviews
[DE88-753426] 21 p2920 N88-27329
Heavy ion and proton tests for subsystem upset
[AD-A195267] 24 p3434 N88-30442

RADIATION DETECTORS
NT DOSIMETERS
NT SILICON RADIATION DETECTORS
NT THRESHOLD DETECTORS (DOSIMETERS)
Construction and characterization of amorphous-silicon test structures
[DE87-013595] 01 p0029 N88-10182
Superfluid He4 as a solar neutrino detector
[DE87-014477] 02 p0257 N88-11625
Instrument for radiation testing/screening electronic devices over an extended temperature range
[AD-A184245] 03 p0326 N88-12060
Ultrafast photoconductor detector-laser-diode transmitter
[DE87-013803] 03 p0329 N88-12082
Design of source coders and joint source/channel coders for noisy channels
[NASA-CR-181547] 04 p0432 N88-12678
Low-cost teleoperator-controlled vehicle for damage assessment and dose measurement
[DE88-000713] 04 p0451 N88-12794
Study of solid state photomultiplier
[NASA-CR-177465] 05 p0583 N88-13556
Evaluation of surface energy and radiation balance systems on the Konza Prairie
[NASA-CR-182534] 10 p1355 N88-18097
PbSnTe photovoltaic detectors for operation in the 2-14 micron band
[INPE-4252-PRE/1125] 11 p1508 N88-19008
Advances in X-ray optics, 1987
[DE88-003298] 11 p1549 N88-19268
An attempt to measure the diffuse brightness of the sky at submillimeter wavelengths
12 p1710 N88-20233
HNC: A detector to study ultraheavy cosmic rays
12 p1713 N88-20252
An approximation technique for solving a system of Fredholm integral equations for asymmetric detector response functions
[AD-A190577] 15 p2121 N88-22645
A new fiber-optic-based phase-resolved phosphorescence spectrometer
[AD-A191325] 16 p2275 N88-23613
Superconducting thin film vertex detector for SSC (Superconducting Super Collider) applications
[DE88-005951] 17 p2445 N88-24535
Photoconducting X-ray detectors for Z-pinch experiments
[DE88-007118] 19 p2728 N88-26199

RADIATION DISTRIBUTION
NT ANTENNA RADIATION PATTERNS
NT DIFFRACTION PATTERNS
NT SIDELOBES
Radiation belts 03 p0272 N88-11707
Performance evaluation of a half-wave resonant slot antenna over perfect ground using NEC (Numerical Electromagnetic Code)
[AD-A184004] 03 p0308 N88-11942
Gamma-ray optics of multi-beam Borrmann modes with possible applications to nuclear lasing
04 p0449 N88-12784
Statistical distribution of solar radiation (hourly sums): Cumulative frequency curves preparation of a European data set and direction for use
[PB87-107454] 04 p0467 N88-12886
RADSPHERE: A computer program for calculating the steady-state, axially symmetric, forced response and radiation field of a submerged spherical shell
[AD-A185025] 05 p0609 N88-13738
Cerenkov radiation field analysis due to a passing electron beam
[AD-A184870] 05 p0649 N88-13976
Nonequilibrium ionization of pregalactic plasma and lessening of relic radiation anisotropy
08 p1002 N88-16071
The role of anisotropy in the long range reconnaissance of the albedo of land surfaces 08 p1017 N88-16169
The iterative radiance model of the Meteorological Institute of the University of Munich (West Germany)
08 p1019 N88-16178
Acoustic field in waveguide with sloping bed
08 p1076 N88-16490
Diffraction of sound at junction of two waveguides
08 p1076 N88-16491
Optimizing HF antenna systems on the Dolphin and Sea Hawk helicopters
[AD-A186552] 09 p1152 N88-16901
Time domain wave propagation in multilayered integrated circuits
[AD-A187462] 10 p1324 N88-17916
A computer model investigation of a half square log-periodic array
[AD-A190955] 16 p2190 N88-23062
A diagnostic technique used to obtain cross range radiation centers from antenna patterns
[NASA-CR-182903] 16 p2192 N88-23071
Sky radiance distributions for thermal imaging backgrounds
[AD-A191135] 17 p2373 N88-24115
The new MININEC (version 3): A mini-numerical electromagnetic code
[AD-A191778] 19 p2642 N88-25675
Automated spectrometric unit for the study of radiation characteristics of cosmic radiation aboard Prognoz-9 space stations 19 p2706 N88-26090
Development of radiation and cloud parameterization programs for AFGL (Air Force Geophysics Laboratory) global models
[AD-A193369] 21 p2973 N88-27658
Stratocumulus and cloud-free reflectance from multi-spectral satellite measurements
[AD-A193899] 22 p3128 N88-28599
A novel method to correct radiation pattern distortion of conformal antennas
[AD-A193675] 23 p3204 N88-29066

RADIATION DOSAGE
Effects of radiation damage in optical fibers: A tutorial
[PB87-210308] 02 p0235 N88-11482
Variations in semiconductor device response in a medium-energy x-ray dose-enhancing environment
[DE87-012400] 02 p0243 N88-11538
Irradiations. Accumulated doses. Heavy ions — space environment 03 p0272 N88-11708
The effect of radiation on the long term productivity of a plant based CELSS 03 p0361 N88-12271
Fabricate, calibrate and test a dosimeter for integration into the CRRES (Combined Release and Radiation Effects Satellite) satellite
[AD-A185439] 05 p0585 N88-13564
Research for electric energy systems
[DE88-001733] 06 p0695 N88-14265
UV radiation: Human exposure to ultraviolet radiation
[PB87-137410] 06 p0752 N88-14619
Effect of irradiation on the diffusion evolution of void ensemble in crystals
[DE88-700558] 07 p0939 N88-15706
Late radiation damage in bone, bone marrow and brain vasculature, with particular emphasis upon fractionation models
[DE87-753039] 08 p1048 N88-16330
The ISO narrow spectrum series of filtered X-radiations at NPL
[NPL-RS(EXT)-92] 09 p1245 N88-17462

Effects of the neutron spectrum on mechanical property changes in low dose irradiations
[DE88-003429] 10 p1302 N88-17786
International cooperative effort to establish ASTM (American Society for Testing and Materials) standards for the measurement of radiation dose for food processing
[DE88-002702] 10 p1372 N88-18190
South African Association of Physicists in Medicine and Biology: 26th Annual Congress
[DE88-700824] 11 p1521 N88-19082
Measurement of the gamma-ray response of some commercial silicon detectors
[AD-A187431] 11 p1543 N88-19221
Nuclear health and safety: Radiation exposures for some cloud-sampling personnel need to be reexamined
[PB88-130497] 12 p1662 N88-19965
Effects of whole-body irradiation with low-intensity microwaves on morphological, functional and cytochemical characteristics of leukocytes 12 p1663 N88-19971
The calibration of photographic and spectroscopic films: The response of 2aO film to small dosages of alpha particles from 3/10th's rad to 8 rads at energy levels 153 MeV, 79 MeV and 47 MeV
[NASA-CR-177830] 13 p1773 N88-20608
Anthropomorphic phantom radiation dosimetry at the NATO standard reference point at Aberdeen Proving Ground
[AD-A190508] 15 p2103 N88-22528
Modeling of radiation dose dependence of MOSFETs 17 p2416 N88-24370
Analysis of a nuclear orbital transfer vehicle reentry accident 17 p2425 N88-24426
Preliminary estimates of radiation exposures for manned interplanetary missions from anomalously large solar flare events
[NASA-TM-100620] 18 p2596 N88-25427
Radiation safety in commercial air traffic
[NASA-TM-101156] 19 p2600 N88-25447
Health and environmental consequences of the Chernobyl nuclear power plant accident
[DOE/ER-0332] 19 p2689 N88-25985
Hemorrhages and hemostasis in guinea pigs exposed to radiation at high altitude 19 p2705 N88-26083
Acute radiation syndromes and their management
[DE88-009639] 20 p2831 N88-26797
Behavioral effects of exposure to the tempo high-power microwave system
[AD-A193305] 21 p2987 N88-27738
Emetic mechanism in acute radiation sickness
[AD-A194102] 23 p3238 N88-29267
Study of biological effects and radiation protection to future European manned space flights
[DGT-33061] 23 p3281 N88-29535

RADIATION EFFECTS
NT LASER DAMAGE
NT RADIATION DAMAGE
NT RADIATION INJURIES
NT RADIOLYSIS
NT SINGLE EVENT UPSETS
An optically strobed sample and hold circuit
[DE87-011877] 01 p0038 N88-10245
Radiation effects in space
[DE87-012529] 01 p0075 N88-10479
The combined release and radiation effects satellite, a joint NASA/DOD program 02 p0135 N88-10851
Electron beam irradiation effects on carbon fiber reinforced PEEK composite
[DE87-753001] 02 p0142 N88-10890
Degradation mechanisms of materials for large space systems in low Earth orbit
[NASA-CR-181472] 02 p0143 N88-10896
The numerical simulation of the mesoscale characteristics associated with Baiu front. Part 1: Structure, low-level jet and radiation characteristics 02 p0203 N88-11272
Interaction between defects and the formation of dissipative structures in irradiated impure crystals
[DE87-703125] 02 p0246 N88-11552
Irradiation testing 03 p0274 N88-11727
Temperature hysteresis and magnetic transitions in amorphous Fe-Ni-Zr alloys
[DE88-000228] 03 p0294 # N88-11848
Compilation of 1986 annual reports of the Navy ELF (Extremely Low Frequency) communications system ecological monitoring program, volume 1
[AD-A184561] 03 p0306 N88-11930
Compilation of 1986 annual reports of the Navy ELF (Extremely Low Frequency) communications system ecological monitoring program, volume 2
[AD-A184562] 03 p0306 N88-11931
Compilation of 1986 annual reports of the Navy ELF (Extremely Low Frequency) communications system ecological monitoring program, volume 3
[AD-A184563] 03 p0306 N88-11932
Health hazards of video display terminals. A comprehensive, annotated bibliography on a critical issue of workplace health and safety with sources for obtaining items and list of terminal suppliers
[RSI-IAS-4] 03 p0355 N88-12240
The effect of radiation on the long term productivity of a plant based CELSS 03 p0361 N88-12271
Low Earth orbit environmental effects on the space station photovoltaic power generation systems
[NASA-TM-100230] 03 p0387 N88-12429
Microgravity nucleation and particle coagulation experiments support
[NASA-CR-181540] 04 p0423 N88-12618
JPRS report: Science and technology. USSR: Life sciences
[JPRS-ULS-87-009] 04 p0473 N88-12915
Radiation induced collapse of the crystalline structure
[DE87-014407] 04 p0498 N88-13064
A study of charged particles/radiation damage to VLSI device materials
[NASA-CR-172036] 05 p0577 N88-13518
Fabricate, calibrate and test a dosimeter for integration into the CRRES (Combined Release and Radiation Effects Satellite) satellite
[AD-A185439] 05 p0585 N88-13564
TOMS as a monitor of the ultraviolet radiation environment: Applications to photobiology 05 p0617 N88-13785
Irradiation preservation of seafood: Literature review
[DE88-001691] 05 p0831 N88-13858
Basic energy sciences research in the Metals and Ceramics Division of Oak Ridge National Laboratory
[DE87-013538] 06 p0681 N88-14171
Program description of FIBRAM: A radiation attenuation model for optical fibers
[PB87-230686] 06 p0890 N88-14229
Observing effect of laser radiation of low-frequency Raman scattering of light 06 p0772 N88-14742
The role of hydrogen in radiation-induced defect formation in polysilicon gate MOS devices
[DE87-012374] 06 p0785 N88-14814
Theoretical aspects of channeling, damage, and range distributions for low (keV) and high (MeV) energy implantation
[DE88-000949] 06 p0786 N88-14818
Effect of point defects on graphite lattice parameters
[DE88-700340] 07 p0827 N88-15019
Karyometric evaluation of neuronal reactions of rat cerebral cortex to the combined effect of ionizing radiation, longitudinal accelerations and vibration 07 p0890 N88-15396
JPRS report: Science and technology. USSR: Space Biology and Aerospace Medicine, volume 21, no. 4, July - August 1987
[JPRS-USB-88-002] 07 p0893 N88-15412
Combined effect of microwaves and ionizing radiation 07 p0893 N88-15413
Effect of pyrocetam on mouse resistance to hypoxic hypoxia 2-3 months after exposure to X-radiation 07 p0895 N88-15425
Effect of irradiation on the diffusion evolution of void ensemble in crystals
[DE88-700558] 07 p0939 N88-15706
Experimental method for investigating helium effects in irradiated vanadium
[DE88-002891] 08 p0969 N88-15865
Electric design rules related to latch-up and radiation — simulation
[FOA-E-30006-3.1] 08 p0979 N88-15917
Results of research with biological satellites 08 p1006 N88-16097
Life sciences experiments on stratospheric balloons and sounding rockets 08 p1033 N88-16262
Contribution of stratospheric balloon flights in space biology 08 p1033 N88-16266
Late radiation damage in bone, bone marrow and brain vasculature, with particular emphasis upon fractionation models
[DE87-753039] 08 p1048 N88-16330
Photoabsorption and photodissociation of molecules important in the interstellar medium
[NASA-CR-182435] 08 p1100 N88-16617
Radon Research Program, FY-1987
[DE88-002633] 09 p1188 N88-17120
Laser simulation of light and plasma action on comets and planets 09 p1237 N88-17413
Dispersive hole transport in SiO2
[AD-A187077] 09 p1254 N88-17513
JPRS Report: Science and Technology. USSR: Space Biology and Aerospace Medicine, volume 21, no. 5, September - October 1987
[JPRS-USB-88-003] 10 p1359 N88-18122
Short- and long-term effects of nonlethal levels of fast high-energy helium ions on retention of developed and formation of new behavioral patterns in rats 10 p1362 N88-18140
Effect of antiorthostatic position and different illumination on sensitivity of skin in upper half of the body to ultraviolet radiation 10 p1363 N88-18145
Effect of spaceflight factors on biological material flown aboard Cosmos-1514 biosatellite 10 p1364 N88-18154
Combined effect of ionizing radiation and altered gas atmosphere on central nervous system 10 p1367 N88-18168
Radiation and temperature effects on the time-dependent response of T300/934 graphite/epoxy
[NASA-CR-182603] 11 p1451 N88-18646
Soluble polysilane derivatives: Chemistry and spectroscopy
[AD-A187889] 11 p1461 N88-18713
Photophysics and photochemistry of poly(di-n-hexylsilane) in room temperature solution
[AD-A187890] 11 p1462 N88-18714
Ceramic decomposition under irradiation
[DE88-004327] 11 p1464 N88-18732
Laser flash effects on chromatic discrimination in monkeys
[AD-A187703] 11 p1517 N88-19061
Radiation effects on gallium arsenide integrated optical devices
[DE88-004107] 11 p1551 N88-19277
Simulation of the plasma interaction with thin dust clouds 11 p1552 N88-19291
Radiation response of thin oxides grown by rapid thermal oxidation and rapid thermal annealing techniques
[DE88-003632] 11 p1561 N88-19347
Photohydrodynamical processes near compact objects 11 p1569 N88-19390
Photonic temperature and pressure sensors for biosystems/pulsed microwave. Part 1: Interaction studies
[AD-A188887] 12 p1629 N88-19751
Ultraviolet (180 to 300 nm) action spectra for inactivation and DNA photoproduct formation of Bacillus subtilis spores under ultrahigh vacuum 12 p1657 N88-19931
Survival and mutation induction of dehydrated yeast cells after UV exposure 12 p1657 N88-19932
Cellular effects of heavy ions: Experimental results and theoretical approaches — space radiation 12 p1658 N88-19933
Radiation problems in manned space flight with a view to the Space Station 12 p1658 N88-19934
Effects of heavy ions on egg-developing systems 12 p1658 N88-19935
Effects of cosmic heavy ion radiation and space microgravity on plant systems 12 p1658 N88-19936
Antibiotic activity in space, results and hypothesis 12 p1660 N88-19952
Nuclear health and safety: Radiation exposures for some cloud-sampling personnel need to be reexamined
[PB88-130497] 12 p1662 N88-19965
Effects of whole-body irradiation with low-intensity microwaves on morphological, functional and cytochemical characteristics of leukocytes 12 p1663 N88-19971
Food Irradiation Newsletter, Vol. 11, No. 1
[DE88-700808] 12 p1671 N88-20004
Effects of high temperature neutron irradiation on the physical, chemical and mechanical properties of fine-grained isotropic graphite 13 p1747 N88-20444
Degradations of thermal shock resistance and the fracture toughness of reactor graphite subjected to neutron irradiation 13 p1747 N88-20445
Computer simulation of tropospheric chemistry
[JUEL-2144] 13 p1798 N88-20758
Discussion of radiation effects and high-temperature oxide superconductors
[DE88-001427] 13 p1846 N88-21046
Effect of off-axis radiation in amplified spontaneous emission
[DE88-007001] 14 p1915 N88-21440
Laser enhanced adhesion of copper films to sapphire substrates
[DE88-006802] 15 p2038 N88-22144
The effective fracture toughness of aluminum at rapid heating rates
[AD-A189745] 15 p2038 N88-22146
Oxide optical coatings prepared by metal-organic vapor deposition
[DE88-006809] 15 p2043 N88-22175
A preliminary comparison of the transient effects of single versus multiple q-switched doubled-neodymium laser pulses
[AD-A189655] 15 p2071 N88-22347
High-efficiency thin-film silicon-on-GaP solar cell for improved radiation resistance
[AD-A190268] 15 p2091 N88-22480
Characterization of space radiation environment in terms of the energy deposition in functionally important volumes
[DE88-005627] 15 p2100 N88-22513

A comparison of visual evoked potential and behavioral measures of flashblindness in humans
[AD-A189757] 15 p2101 N88-22519
Computing X-ray effects in optics
[DE88-006722] 15 p2134 N88-22732
Behavior, physiology and energy deposition in rats chronically exposed to 2450 MHz radiation
[PB88-171418] 16 p2237 N88-23363
Numerical analysis for effects of irradiation nonuniformities on target implosion
16 p2276 N88-23621
Radiation effects in silicon
[DE88-006642] 16 p2282 N88-23659
The response of a power MOSFET (N-channel) and a dielectric isolated operational amplifier to the combined environmental effects of high temperature and total dose gamma radiation 17 p2406 N88-24309
Radiation hardening design of nuclear powered spacecraft 17 p2407 N88-24315
Defects in cubic silicon carbide on silicon
17 p2408 N88-24317
Analysis of thermal and radiation effects in materials using the GEMAT process 17 p2408 N88-24318
Radiation effects testing capabilities of the Texas A and M Nuclear Science Center 17 p2416 N88-24368
Silicon-on-insulator electronics for a space nuclear power system 17 p2431 N88-24461
The response of selected semiconductor technologies to the combined environmental effects of high temperature and total dose gamma radiation
17 p2431 N88-24462
Neutron effects on the electrical and switching characteristics of NPN bipolar power transistors
17 p2431 N88-24463
Development of refractory thermocouples for space nuclear power tests 17 p2434 N88-24478
Irradiation effects on tungsten stabilized martensitic steels
[DE88-007074] 18 p2486 N88-24748
Behavioral response of rats exposed to high-power microwave radiation
[AD-A192159] 18 p2548 N88-25128
Selective radiation absorption in aluminized composite propellant combustion 19 p2630 N88-25598
Extremely Low Frequency (ELF) communications system ecological monitoring program: Summary of 1986 progress
[AD-A192014] 19 p2642 N88-25676
Health and environmental consequences of the Chernobyl nuclear power plant accident
[DOE/ER-0332] 19 p2689 N88-25985
Noise and chaos in driven Josephson junctions
19 p2734 N88-26238
Abnormal diffusion of vacancies in metals
[DE88-701880] 20 p2773 N88-26441
Helium induced degradation in the weldability of an austenitic stainless steel
[DE88-009062] 20 p2773 N88-26443
Effects of cosmic rays on single event upsets
[NASA-CR-183053] 20 p2793 N88-26569
A method for estimating the susceptibility of electronic systems to HPM (High Power Microwave)
[DE88-012246] 21 p2934 N88-27422
Genetic effects of low level microwave radiation
[AD-A192687] 21 p2984 N88-27722
Effects of pulsed and CW (Continuous Wave) 2450 MHz radiation on transformation and chromosomes of human lymphocytes in vitro
[AD-A193104] 21 p2987 N88-27736
Assessment of cochlear damage after microwave irradiation
[AD-A193237] 21 p2987 N88-27737
Behavioral effects of exposure to the tempo high-power microwave system
[AD-A193305] 21 p2987 N88-27738
Dynamics of a plasma produced under effect of the XeCl-laser radiation on metallic surface
[DE88-701963] 21 p3017 N88-27902
Dose-enhancement effects in TaSi/Al- and Al-gate MOS devices
[DE88-005483] 21 p3020 N88-27926
Embryogenesis and organogenesis of Carausius morosus under spaceflight conditions
22 p3061 N88-28167
Dosimetric mapping inside Biorack — Spacelab D1 mission 22 p3062 N88-28169
Avionics system design for high energy fields: A guide for the designer and airworthiness specialist
[NASA-CR-181590] 23 p3178 N88-28919
The radiation sensitivity of select metal chelate polymers: Mechanistic changes at higher energies
[AD-A193467] 23 p3196 N88-29019
Currents induced in a human being for electromagnetic fields to 10 kHz-50 MHz
[AD-A191977] 23 p3238 N88-29268
Vision and visual protection in fast jet aircraft
23 p3241 N88-29292
Study of biological effects and radiation protection to future European manned space flights
[DGT-33061] 23 p3281 N88-29535
An HVEM study of displacement cascade damage in Nb3Sn at 13 K
[DE88-009997] 23 p3289 N88-29584

RADIATION EXPOSURE
U RADIATION DOSAGE

RADIATION FIELDS
U RADIATION DISTRIBUTION

RADIATION HARDENING
Variations in semiconductor device response in a medium-energy x-ray dose-enhancing environment
[DE87-012400] 02 p0243 N88-11538
Effect of irradiation on the tensile properties of niobium-base alloys
[DE87-002409] 03 p0285 N88-11790
Dramatically improved radiation hardness for CMOS silicon gate integrated circuits even down to cryogenic temperatures
[AD-A184672] 03 p0381 N88-12398
Radiation hardness evaluation of thin film ferroelectric capacitors
[DE88-001357] 07 p0848 N88-15147
A report on the effects of neutron irradiation of GaAs semiconductors
[AD-A186818] 09 p1253 N88-17510
Dispersive hole transport in SiO2
[AD-A187077] 09 p1254 N88-17513
Radiation effects testing capabilities of the Texas A and M Nuclear Science Center 17 p2416 N88-24368
Development of the field-induced electron injection and impact ionization (F4I) technique for radiation hardness testing of MOS (Metal-Oxide-Semiconductor) gate insulators
[AD-A192114] 18 p2583 N88-25345
The postirradiation tensile properties and microstructure of several vanadium alloys
[DE88-007140] 19 p2615 N88-25515
Thermionic integrated circuit program
[DE88-010119] 19 p2662 N88-25833
X-ray response of GaAlAs/GaAs radiation hardened double: Heterostructure photodiode compared to Si:PIN photodiodes
[DE88-007425] 19 p2733 N88-26231
Electrophoretic coatings. Part 1: Sandia applications
[DE88-008666] 20 p2776 N88-26465
High bandwidth optoelectronic signal link for use in an EMP (electromagnetic pulse) plus radiation environment
[DE88-009254] 20 p2790 N88-26549
The p-well or n-well CMOS technology for advanced SEU-hard SRAMs
[DE88-006845] 22 p3156 N88-28777
EMPTAC (Electromagnetic Pulse Test Aircraft) user's guide
[AD-A195072] 24 p3360 N88-30006

RADIATION HAZARDS
Preliminary estimates of galactic cosmic ray exposures for manned interplanetary missions
[NASA-TM-100519] 05 p0661 N88-14058
South African Association of Physicists in Medicine and Biology: 26th Annual Congress
[DE88-700824] 11 p1521 N88-19082
Operational concerns involving a shadow-shielded nuclear reactor for space station applications
17 p2398 N88-24257
Radiation hardening design of nuclear powered spacecraft 17 p2407 N88-24315
Nuclear safety as applied to space power reactor systems 17 p2415 N88-24360
Radiation safety in commercial air traffic
[NASA-TM-101156] 19 p2600 N88-25447
Health and environmental consequences of the Chernobyl nuclear power plant accident
[DOE/ER-0332] 19 p2689 N88-25985
Products from cosmic-ray interactions in extraterrestrial matter: What they tell us about radiation backgrounds in space
[DE88-009143] 19 p2743 N88-26288
Studies of HZE particle interactions and transport for space radiation protection purposes
[NASA-TM-101159] 20 p2886 N88-27142

RADIATION HEATING
U RADIANT HEATING

RADIATION INJURIES
Assessment of cochlear damage after microwave irradiation
[AD-A193237] 21 p2987 N88-27737

RADIATION INTENSITY
U RADIANT FLUX DENSITY

RADIATION LAWS
NT KIRCHHOFF LAW OF RADIATION

RADIATION MEASUREMENT
Direct detection of optical radiation through a sampling orifice for inductively coupled plasma atomic emission spectroscopy
[DE87-013609] 01 p0101 N88-10662
Evaluation of the infrared test method for the olympus thermal balance tests 02 p0136 N88-10856
The development of diagnostic fuses
[SAND-86-0395] 03 p0311 N88-11963
Empirical relations between photospheric magnetic fields and atmospheric radiative losses for cool dwarf stars 04 p0511 N88-13145
Radio frequency electromagnetic interference fields. A study in Swedish industry
[FOA-E-30007-3.3] 06 p0692 N88-14247
NBS (National Bureau of Standards) measurement services: Fricke dosimetry in high-energy electron beams
[PB88-110374] 06 p0781 N88-14795
The use of the direct measurement of solar radiation for the determination of Pasquill Stability Parameter
[AD-A186084] 07 p0948 N88-15750
Method of determining atmospheric moisture content by measurement of upward radiation intensity in near IR
08 p1007 N88-16106
International cooperative effort to establish ASTM (American Society for Testing and Materials) standards for the measurement of radiation dose for food processing
[DE88-002702] 10 p1372 N88-18190
The inverse problem and the pseudo-empirical orthogonal function method of solution. Part 1: Theory; Part 2: Application
[AD-A188894] 12 p1684 N88-20069
Measurements of the cosmic background radiation
[NASA-CR-182637] 12 p1712 N88-20248
Global solar oscillations observed in the visible to near infrared continuum 13 p1858 N88-21110
A low-frequency measurement of the spectrum of the cosmic microwave background radiation
13 p1858 N88-21112
An approximation technique for solving a system of Fredholm integral equations for asymmetric detector response functions
[AD-A190577] 15 p2121 N88-22645
Radiation standards 16 p2272 N88-23592
Requirements for radiation receivers
16 p2272 N88-23593
Sky radiance distributions for thermal imaging backgrounds
[AD-A191135] 17 p2373 N88-24115
Results of radiation measurements in West Germany and from special measurement series in the Meteorological Observatory of Hamburg
[REPT-11] 18 p2542 N88-25088
Measurement of the radiative properties of gas and oil flames
[NASA-TT-20299] 19 p2612 N88-25502
Evaluation of surface energy and radiation balance systems for FIFE
[NASA-CR-183118] 20 p2828 N88-26778
Angular radiation models for Earth-atmosphere system. Volume 1: Shortwave radiation
[NASA-RP-1184] 21 p2976 N88-27677
Use of penetrating radiations for the dynamic examination of aero gas turbines
[PNR90470] 22 p3045 N88-28073
Stratocumulus and cloud-free reflectance from multi-spectral satellite measurements
[AD-A193899] 22 p3128 N88-28599

RADIATION MEASURING INSTRUMENTS
NT ADVANCED VERY HIGH RESOLUTION RADIOMETER
NT BOLOMETERS
NT CERENKOV COUNTERS
NT DICKE RADIOMETERS
NT DOSIMETERS
NT EBERT SPECTROMETERS
NT ELECTRON COUNTERS
NT ELECTROPHOTOMETERS
NT ELECTROSTATIC PROBES
NT FABRY-PEROT SPECTROMETERS
NT FLIR DETECTORS
NT INFRARED DETECTORS
NT INFRARED INSTRUMENTS
NT INFRARED RADIOMETERS
NT INFRARED SCANNERS
NT INFRARED SPECTROMETERS
NT INFRARED SPECTROPHOTOMETERS
NT MICROWAVE RADIOMETERS
NT NEUTRON COUNTERS
NT NEUTRON SPECTROMETERS
NT PARTICLE TELESCOPES
NT PHOTOMETERS
NT PROPORTIONAL COUNTERS
NT RADIATION COUNTERS
NT RADIATION DETECTORS

NT RADIOMETERS
NT SCINTILLATION COUNTERS
NT SILICON RADIATION DETECTORS
NT SOLAR SPECTROMETERS
NT SPARK CHAMBERS
NT SPECTROHELIOGRAPHS
NT SPECTROPHOTOMETERS
NT SPECTRORADIOMETERS
NT THRESHOLD DETECTORS (DOSIMETERS)
NT TOTAL OZONE MAPPING SPECTROMETER
NT ULTRAVIOLET SPECTROMETERS
NT ULTRAVIOLET SPECTROPHOTOMETERS
Development of response models for the Earth Radiation Budget Experiment (ERBE) sensors. Part 2: Analysis of the ERBE integrating sphere ground calibration
[NASA-CR-178293] 01 p0049 N88-10316
Ultraviolet measurements: Measurements of photolysis rates 18 p2539 N88-25065

RADIATION MEDICINE
U NUCLEAR MEDICINE

RADIATION METERS
U RADIATION MEASURING INSTRUMENTS

RADIATION NOISE
U ELECTROMAGNETIC NOISE

RADIATION PRESSURE
NT ILLUMINANCE
NT LUMINANCE
NT LUMINOUS INTENSITY
NT SOUND PRESSURE
Acoustic radiation from line- and point-loaded plates: Uniformly asymptotic solutions
[AD-A189367] 13 p1834 N88-20969
Optical trapping of neutral atoms and dielectric particles by radiation pressure 14 p1974 N88-21783
Doppler distortion of solar Fraunhofer lines in zodiacal light by reflection from interplanetary dust 19 p2740 N88-26270
Time-dependent mass loss from hot stars with and without radiative driving
[DE88-008899] 20 p2884 N88-27128

RADIATION PROTECTION
NT RADIATION SHIELDING
NT SOLAR RADIATION SHIELDING
Radiation effects in space
[DE87-012529] 01 p0075 N88-10479
Committee on Interagency Radiation Research and Policy Coordination
[DE88-003358] 09 p1188 N88-17121
Technical activities 1987, Center for Radiation Research
[PB88-129325] 09 p1245 N88-17464
South African Association of Physicists in Medicine and Biology: 26th Annual Congress
[DE88-700824] 11 p1521 N88-19082
Vega-1 and Vega-2 automatic stations: Functioning of flyby vehicles during encounter with Halley's comet 13 p1725 N88-20314
Theory of interactions of intense light with nonlinear, inhomogeneous and periodic structures and its applications to optical bistability, optic gyroscopes, nonlinear spectroscopy, radiation protection, X-ray emission and related fields
[AD-A190040] 15 p2133 N88-22725
Nuclear safety as applied to space power reactor systems 17 p2415 N88-24360
The use of liquid films for spacecraft survivability to laser radiation
[AD-A192954] 20 p2765 N88-26395
Mobile robot survival
[DE88-009108] 20 p2809 N88-26665
Studies of HZE particle interactions and transport for space radiation protection purposes
[NASA-TM-101159] 20 p2886 N88-27142
Study of biological effects and radiation protection to future European manned space flights
[DGT-33061] 23 p3281 N88-29535

RADIATION PYROMETERS
Noncontact Temperature Measurement
[NASA-CP-2503] 17 p2327 N88-23895
Radiation thermometry: The measurement problem 17 p2328 N88-23896
Noncontact temperature measurement in glass and other transparent materials 17 p2328 N88-23900
Multi-color pyrometer for materials processing in space 17 p2329 N88-23905
Direct emissivity measurements on liquids and corrections to multi-color pyrometers 17 p2329 N88-23906
Common but unappreciated sources of error in one, two, and multiple-color pyrometry 17 p2329 N88-23907
Fast optical pyrometry 17 p2329 N88-23908
The role of fiberoptics in remote temperature measurement 17 p2329 N88-23909
Laser pyrometry 17 p2330 N88-23910
Noncontact true temperature measurement, 2 17 p2330 N88-23911

RADIATION RESISTANCE
U RADIATION TOLERANCE

RADIATION SHIELDING
NT SOLAR RADIATION SHIELDING
A comparison of open and closed multimegawatt space power and weapon systems
[DE87-012975] 01 p0089 N88-10579
A paper about electromagnetic pulse and principles of EMP protection
[FOA-C-30455-4.2] 06 p0692 N88-14246
Shielding analysis of a small compact space nuclear reactor
[AD-A185566] 06 p0779 N88-14784
Suppression of X-rays generated by runaway electrons in ATF
[DE88-004179] 10 p1414 N88-18440
Project SKYLITE: A design exploration
[AD-A187906] 11 p1511 N88-19030
Radiation problems in manned space flight with a view to the Space Station 12 p1658 N88-19934
SOAR: Space orbiting advanced fusion power reactor
[AD-A189234] 13 p1732 N88-20356
Anthropomorphic phantom radiation dosimetry at the NATO standard reference point at Aberdeen Proving Ground
[AD-A190508] 15 p2103 N88-22528
X-ray production in low energy proton stopping
[NASA-TM-100619] 16 p2270 N88-23582
Operational concerns involving a shadow-shielded nuclear reactor for space station applications 17 p2398 N88-24257
Material tradeoffs to minimize flooding reactivity 17 p2399 N88-24265
Magnet shielding analysis for SOAR: A space fusion reactor 17 p2400 N88-24269
Fabrication of lithium hydride shields for space nuclear power systems 17 p2402 N88-24282
Fabrication of reactor shields at the Y-12 plant 17 p2402 N88-24283
Radiation hardening design of nuclear powered spacecraft 17 p2407 N88-24315
Space nuclear reactor shielding optimization studies 17 p2408 N88-24320
Comparison of open and closed multimegawatt space power systems 17 p2414 N88-24353
RSMASS: A simple model for estimating reactor/shield masses 17 p2414 N88-24355
MMW shielding design and analysis 17 p2430 N88-24457
Neutron effects on the electrical and switching characteristics of NPN bipolar power transistors 17 p2431 N88-24463
The Oak Ridge National Laboratory strategic defense initiative shield optimization program
[DE88-008946] 19 p2721 N88-26160
A method for estimating the susceptibility of electronic systems to HPM (High Power Microwave)
[DE88-012246] 21 p2934 N88-27422

RADIATION SICKNESS
Emetic mechanism in acute radiation sickness
[AD-A194102] 23 p3238 N88-29267

RADIATION SOURCES
NT MONOCHROMATORS
NT POINT SOURCES
The Hermes-3 program
[DE87-012132] 02 p0234 N88-11473
Center for X-Ray Optics, 1986
[DE88-000715] 04 p0449 N88-12783
Technical activities 1987, Center for Radiation Research
[PB88-129325] 09 p1245 N88-17464
On the time delay of the ultrahigh-energy radiation signal from the source Cygnus X-3
[DE88-700649] 10 p1431 N88-18547
Induction linacs: A technology come of age for international cooperation
[DE88-003953] 11 p1548 N88-19258
Coherent VUV source at 130 nm: Theory and modeling
[DE88-003874] 11 p1549 N88-19269
Microwave generation from a cuspitron oscillator with a six-vane circuit
[AD-A188377] 12 p1619 N88-19680
X-ray source model for Z-pinch aluminum plasmas
[AD-A189509] 12 p1696 N88-20148
Long duration coherent Lyman-alpha sources 16 p2268 N88-23571
Ultraviolet radiometry: Radiation sources and measuring methods 16 p2272 N88-23596
Spectroradiometry in the industrial test laboratory 16 p2272 N88-23598
SNAP-DYN: Proven technology for wear-term, higher power in space 17 p2425 N88-24422
A plasma ultraviolet source for short wavelength lasers
[AD-A192844] 21 p2952 N88-27537
Guided radiation beams in free electron lasers
[AD-A194525] 22 p3082 N88-28305
An undulator radiation source for spin-polarized photoemission studies of novel magnetic materials
[AD-A193756] 22 p3083 N88-28307

RADIATION SPECTRA
NT ABSORPTION SPECTRA
NT BALMER SERIES
NT ELECTROMAGNETIC SPECTRA
NT ELECTRONIC SPECTRA
NT EMISSION SPECTRA
NT FRAUNHOFER LINES
NT GAMMA RAY SPECTRA
NT H ALPHA LINE
NT H BETA LINE
NT H LINES
NT HERZBERG BANDS
NT INFRARED SPECTRA
NT K LINES
NT LINE SPECTRA
NT LYMAN SPECTRA
NT MICROWAVE SPECTRA
NT RADIO SPECTRA
NT RAMAN SPECTRA
NT RYDBERG SERIES
NT SOLAR SPECTRA
NT STELLAR SPECTRA
NT ULTRAVIOLET SPECTRA
NT VIBRATIONAL SPECTRA
NT VISIBLE SPECTRUM
NT X RAY SPECTRA
Mathematics applied to nuclear geophysics
[INPE-4234-PRE/1109] 01 p0086 N88-10561
Cloud cover determination in polar regions from satellite imagery
[NASA-CR-181544] 04 p0471 N88-12908
Elementary process and meteor train spectra 06 p0732 N88-14504
On the meteor trail spectra 06 p0737 N88-14533
Fog, rain and aerosol attenuation in the atmosphere
[AD-A190867] 16 p2235 N88-23350
Spectral radiation measurement using a photodiode array as receiver 16 p2271 N88-23591

RADIATION THERAPY
Biology and Medicine Division
[DE87-009280] 14 p1952 N88-21632

RADIATION TOLERANCE
Nuclear health and safety: Radiation exposures for some cloud-sampling personnel need to be reexamined
[PB88-130497] 12 p1662 N88-19965
High-efficiency thin-film silicon-on-GaP solar cell for improved radiation resistance
[AD-A190268] 15 p2091 N88-22480
Neutron radiation tolerance of Au-activated silicon 17 p2408 N88-24316
Development of a GaAs solid state device model for high power applications
[DE88-009048] 19 p2734 N88-26242
A comparison of the radiation tolerance characteristics of multijunction solar cells with series and voltage-matched configurations
[NASA-TM-101177] 21 p2967 N88-27624
The p-well or n-well CMOS technology for advanced SEU-hard SRAMs
[DE88-006845] 22 p3156 N88-28777
Optical emission behavior and radiation resistance of epoxy resins
[DE88-752629] 23 p3196 N88-29023
Emetic mechanism in acute radiation sickness
[AD-A194102] 23 p3238 N88-29267

RADIATION TRANSPORT
Status of the solar and infrared radiation submodels in the LLNL 1-D and 2-D chemical-transport models
[DE87-014320] 01 p0069 N88-10441
The iterative radiance model of the Meteorological Institute of the University of Munich (West Germany) 08 p1019 N88-16178
Radiation transport in planetary nebulae
[ETN-88-91500] 14 p1993 N88-21880
Multigroup flux-limited asymptotic diffusion Fokker-Planck equation
[DE88-700958] 15 p2118 N88-22615
High-energy laser-assisted imaging through vaporizing aerosols
[DE88-007911] 18 p2521 N88-24957

RADIATIVE HEAT TRANSFER
Radiative and free-convective heat transfer from a finite horizontal plate inside an enclosure 02 p0133 N88-10833
Conjugated heat transfer from a radiating fluid in a rectangular channel 03 p0317 N88-12003
Nonequilibrium characteristics of nitrogen plasmas appropriate to an AOTV flight 03 p0319 N88-12019
The effects of minor trace gases on the transfer of thermal infrared radiation through the Earth's atmosphere 04 p0468 N88-12893

Heating of stellar chromospheres and coronae: Evidence for non-magnetic basal heating
04 p0503 N88-13098
A hybrid fibreglass-CFRP cloth for new furnishings — aircraft cabins
[SNIAS-872-111-109] 05 p0558 N88-13396
The ocean heat budget
[AD-A186130] 07 p0881 N88-15346
Radiative heat transfer solutions in plane-parallel participating media: Application to multilayer insulations for space vehicles
[INPE-4221-PRE/1101] 08 p0962 N88-15824
Three dimensional Monte Carlo simulation of molecular movement and heat radiation in vacuum devices: Computer code MOVAK3D — fusion reactors
[KFK-4292] 09 p1246 N88-17471
Studies on homogeneous and heterogeneous reactive flows 11 p1484 N88-18861
Transient radiative energy transfer in incompressible laminar flows
[NASA-CR-182605] 11 p1488 N88-18883
Investigation of supersonic chemically reacting and radiating channel flow
[NASA-CR-182726] 14 p1862 N88-21125
Climatology and space observations
[ISBN-2-85-428179-9] 14 p1935 N88-21536
The role of radiation transfer in climate modification
14 p1936 N88-21549
Net radiative flux at the Earth surface: Estimation from satellite observations 14 p1936 N88-21550
The thermal radiative properties of metals at high temperature
[DE88-006625] 15 p2038 N88-22141
Liquid-metal MHD power conversion for space electric systems 17 p2411 N88-24338
Transient thermohydraulic heat pipe modeling
17 p2413 N88-24347
Development of materials for fabric radiators
17 p2429 N88-24448
Moving belt radiator development status
[NASA-TM-100909] 19 p2607 N88-25477
Anomalous emissivity from periodic micro-machined silicon surfaces 19 p2670 N88-25872
Experimental and theoretical analysis of the radiative transfer within a sooty pool fire
[DE88-007099] 20 p2769 N88-26419
Ignition and flame spread of PMMA
[NASA-TT-20290] 20 p2771 N88-26431
Radiative heat transfer and selective emission in planar slab coatings on hot emissive substrates
[AD-A193133] 21 p2918 N88-27319
Radiative heat transfer to chemically reacting flow between concentric rotating spheres
[DE88-702538] 22 p3118 N88-28525
Flamelet chemistry modelling of soot formation for radiation 24 p3348 N88-29928
Radiation transfer in gas turbine combustors
24 p3348 N88-29929
The effect of particle properties on radiative heat transfer 24 p3350 N88-29941
Radiative heat transfer to steady flow of a chemically reacting fluid in a horizontal porous channel with variable wall temperature
[DE88-702704] 24 p3372 N88-30061

RADIATIVE LIFETIME
Computed potential energy surfaces for chemical reactions
[NASA-CR-183168] 24 p3342 N88-29893

RADIATIVE RECOMBINATION
The qualitative determination of high injection effects in flux-loaded P-I-N diodes using the recombination radiation measuring method
[ETN-88-91475] 11 p1560 N88-19336
The role of electron-ion recombination in bulk antimatter production 18 p2268 N88-23567

RADIATIVE TRANSFER
NT RADIATIVE HEAT TRANSFER
Circumstellar radio molecular lines
02 p0252 N88-11595
Circumstellar shells, the formation of grains, and radiation transfer 02 p0252 N88-11596
Observations and analysis of the photospheric magnetic fields on dwarf G, K and M stars
04 p0520 N88-13196
MODTRAN: A moderate resolution model for LOWTRAN
[AD-A185384] 05 p0574 N88-13503
Automated satellite cloud analysis: A multispectral approach to the problem of snow/cloud discrimination
[AD-A185672] 06 p0746 N88-14591
Observation and interpretation of solar S-component radiation at millimetre waves
[PB87-225207] 06 p0805 N88-14916
Estimation of broadband planetary albedo from operational narrowband satellite measurements
[PB88-107644] 07 p0945 N88-15748
Thematic mapper research in the earth sciences: Small scale patches of suspended matter and phytoplankton in the Elbe River Estuary, German Bight and Tidal Flats
[NASA-CR-182378] 08 p1019 N88-16180
Application of satellite data in variational analysis for global cyclonic systems
[NASA-CR-182468] 09 p1193 N88-17152
Parameterization of radiative transfer in the Earth's atmosphere with specific applications to clouds
10 p1353 N88-18087
Light absorption by an atom moving inside a spherical box
[AD-A187241] 10 p1407 N88-18395
On the possibility of high velocity deflagration front propagation by radiative energy transfer
[AD-A189022] 12 p1613 N88-19645
Models of recombination lines in radio H2 regions
[INPE-4302-TDL/277] 12 p1710 N88-20232
Dynamical and photometric studies of Saturn's rings
12 p1711 N88-20241
Multiple scattering of polarized light in cirrus clouds
13 p1801 N88-20768
Tabulation of Mie scattering calculation results for microwave radiative transfer modeling
[NASA-CR-4130] 14 p1947 N88-21612
Analytic and numerical modeling of heat and material transport in electrical hypervelocity guns
[AD-A192178] 18 p2469 N88-24655
Voyager imaging photometry and radiative transfer modeling of the spoke-like features in Saturn's outer B-ring 19 p2742 N88-26278
Validate algorithms for the determination of rainfall rates from SSM/I microwave satellite imagery
[AD-A192299] 21 p2974 N88-27664
Infrared detection using Rydberg atoms
[AD-A194308] 23 p3191 N88-28990
An analysis of heat transfer after loss of primary coolant in the SP-100 reactor system
[AD-A194619] 23 p3281 N88-29539

RADICALS
NT FREE RADICALS
NT HYDROXYL RADICALS
Photoabsorption and phototdissociation of molecules important in the interstellar medium
[NASA-CR-182435] 08 p1100 N88-16617
On the interpretation of the CH cometary spectrum
14 p2007 N88-21969
Probing the possibility of a (12)C/(13)C abundance gradient from observations of interstellar CH+
[DE88-008906] 20 p2884 N88-27125

RADII
The deposition rate dependence of plasma polymerization on the radius of curvature of the substrate
[DE88-003811] 10 p1412 N88-18429
Fitting a circle to radially suppressed data
[NPL-DITC-103/87] 17 p2392 N88-24223

RADIO ALTIMETERS
An evaluation of three linear scale radar altimeter displays
[AD-A192173] 18 p2465 N88-24636
Determination of the ocean circulation by spaceborne radar altimeter 19 p2701 N88-26060
Ocean satellite data and the needs of designers and operators of marine units 19 p2701 N88-26061
Development of procedures for performing end-to-end tests on the ERS-1 radar altimeter and AMI using a compact antenna test range — Active Microwave Instrument (AMI)
[ESA-CR(P)-2558] 24 p3363 N88-30022

RADIO ANTENNAS
NT MICROWAVE ANTENNAS
A new state space model for the NASA/JPL 70-meter antenna servo controls 04 p0436 N88-12702
Analysis of the ICE combiner for multiple antenna arraying 04 p0436 N88-12704
A modern control theory based algorithm for control of the NASA/JPL 70-meter antenna axis servos
04 p0436 N88-12706
Power density measurements in the near field of the DSS 13 26-meter antenna 04 p0437 N88-12711
A dynamic simulation and feedback control scheme for the U.S. Marine Corps' Airborne Remotely Operated Device (AROD)
[AD-A186597] 08 p0953 N88-15784
Capacitor analysis for RF antennas
[DE88-004178] 10 p1318 N88-17883
Space-diversity effects on line-of-sight propagation paths 12 p1617 N88-19670
Some measurements of height gain at V.H.F.
12 p1617 N88-19671
Environmental projects. Volume 6: Environmental assessment. New 34-meter antenna at Venus site
[NASA-CR-182922] 17 p2332 N88-23919
Evaluation of vertical monopole antennas with elevated radials
[DE88-008339] 19 p2654 N88-25760
Radio astronomy 24 p3364 N88-30031

RADIO ASSISTED DETECTION AND RANGING
U RADAR

RADIO ASTRONOMY
Venusian surface and crust 01 p0010 N88-10054
Imaging at radio wavelengths
01 p0094 N88-10618
Circumstellar radio molecular lines
02 p0252 N88-11595
The Telecommunications and Data Acquisition Report
[NASA-CR-181546] 04 p0432 N88-12679
Intelligent signal analysis and recognition
[NASA-CR-181531] 04 p0501 N88-13084
Nonthermal phenomena in stellar coronae: Evidence from radio observations 04 p0503 N88-13096
A re-examination of the corona-wind dividing line: Diagnostics of non-coronal atmospheres
04 p0504 N88-13101
VLA observations of rapid 6 cm flux variations in alpha Ori 04 p0515 N88-13189
EVN (European VLBI network) and MERLIN observations of 5 superluminal radio sources
[PB87-110730] 04 p0520 N88-13193
Finnish-Soviet Symposium on Radio Astronomy (1st) held at Otaniemi on August 26-27, 1985
[PB87-140661] 07 p0944 N88-15736
Source and event selection for radio-planetary frame-tie measurements using the Phobos Landers
11 p1471 N88-18775
Solar radioimage restoration
[INPE-4312-TDL/279] 11 p1571 N88-19402
The Deep Space Network
[NASA-CR-182700] 13 p1759 N88-20524
Recent observations of the OH radio lines in comets
14 p1999 N88-21917
Thermal-nonthermal relationships in active galactic nuclei
[B8681482] 16 p2289 N88-23707
The polarization of radio galaxies: Its structure at low frequencies
[B8681611] 20 p2884 N88-27123
Laboratory evaluation and application of microwave absorption properties under simulated conditions for planetary atmospheres
[NASA-CR-182443] 23 p3300 N88-29653
Review of Radio Science, 1984-1986
24 p3363 N88-30023
Radio astronomy 24 p3364 N88-30031
The Deep Space Network: An instrument for radio astronomy research
[NASA-CR-183219] 24 p3453 N88-30554

RADIO ATTENUATION
The 6 GHz propagation measurements over a 51 km path in the UK 12 p1617 N88-19673
An EHF telecommunication system engineering model
12 p1618 N88-19674
A propagation campaign in a marine environment utilizing a digital system at 36 GHz 12 p1618 N88-19675

RADIO BEACONS
Antarctic field tests of SARSAT personal locater beacons
[NASA-TM-4008] 01 p0063 N88-10403

RADIO BROADCASTING
U BROADCASTING

RADIO BURSTS
NT SOLAR RADIO BURSTS
NT TYPE 3 BURSTS
Data recorded by the Rome room temperature gravitational wave antenna, during the supernova SN 1987 A in the Large Magellanic Cloud
[NOTA-INTERNA-879] 06 p0806 N88-14922
Solar-geophysical data number 521, January 1988. Part 2: (Comprehensive reports). Data for July 1987 and miscellanea
[PB88-179221] 19 p2743 N88-26285

RADIO COMMUNICATION
NT CODE DIVISION MULTIPLE ACCESS
NT RADIO RELAY SYSTEMS
NT RADIO TELEMETRY
NT TELEPHONY
NT TIME DIVISION MULTIPLE ACCESS
Two-signal cross modulation effects, half-IF effects and interference criteria in land mobile sharing with UHF (Ultra High Frequency) television
[PB87-228037] 05 p0576 N88-13514
MM-wave propagation and application in military communication systems 12 p1617 N88-19669
An investigation of conformable antennas for the astronaut backpack communication system
[NASA-CR-182908] 17 p2333 N88-23929
Development of the network architecture of the Canadian MSAT system 19 p2646 N88-25702

Wave propagation and remote sensing
24 p3364 N88-30029

RADIO CONTROL
Timing control system
[NASA-CASE-NPO-16882-1-CU]
18 p2506 N88-24863
Frequency domain identification of the dynamics of a scaled remotely-piloted helicopter
20 p2786 N88-26524

RADIO ECHOES
JPRS report: Science and technology. China
[JPRS-CST-87-031] 03 p0299 N88-11880
Height profile inversion of ionospheric movement from observed parameters of HF radio echoes
03 p0299 N88-11884
Terrestrial Propagation Characteristics in Modern Systems of Communications, Surveillance, Guidance and Control
[AGARD-CP-407] 12 p1614 N88-19653

RADIO EMISSION
NT CN EMISSION
NT HYDROXYL EMISSION
NT RADIO BURSTS
NT SOLAR RADIO BURSTS
NT SOLAR RADIO EMISSION
NT TYPE 3 BURSTS
Coronal and interplanetary Type 2 radio emission
01 p0114 N88-10731
A VLA survey of dMe flare stars
04 p0513 N88-13154
Radio continuum emission from the ionized stellar winds of the cool supergiants in zeta Aurigae-like systems
04 p0514 N88-13160
Radio emission from RS CVn binaries: A 5 GHz VLA survey of 93 systems 04 p0519 N88-13191
Ray tracing of Jovian low frequency radiation
[NASA-CR-179262] 08 p1101 N88-16620
Self-modulational formation of pulsar microstructures
[NASA-CR-182420] 08 p1104 N88-16622
The radio structure of active nuclei in edge-on spiral and Seyfert galaxies 09 p1264 N88-17576

RADIO EQUIPMENT
NT IONOSONDES
NT MICROWAVE ANTENNAS
NT RADIO ANTENNAS
NT RADIO BEACONS
NT RADIO FILTERS
NT RADIO RECEIVERS
NT RADIO TELESCOPES
NT RADIO TRANSMITTERS
NT RADIOSONDES
NT RADIOTELEPHONES
NT RAWINSONDES
NT RECEPTION DIVERSITY
NT SPACECRAFT ANTENNAS
NT SUPERHETERODYNE RECEIVERS
NT TRANSMITTER RECEIVERS
NT TRANSPONDERS
NT VERY LARGE ARRAY (VLA)
X-band uplink ground systems development: Part 2
04 p0436 N88-12703
MARCE data evaluation 10 p1286 N88-17693
Spread spectrum mobile radio communications
[AD-A187487] 11 p1470 N88-18765
Spread spectrum radio networks
[AD-A188914] 12 p1620 N88-19689
Static and dynamic jamming of networks
[AD-A188921] 12 p1620 N88-19690
Multiple address facility for packet radio: An investigation of performance/complexity trade off
[AD-A191043] 16 p2190 N88-23064
Practical VLF/LF radio test system
[AD-A191768] 18 p2500 N88-24831
A random access algorithm for environments with capture and limited feedback capabilities
[AD-A192233] 20 p2790 N88-26552
Random-access algorithms for environments with capture
[AD-A194303] 23 p3203 N88-29060

RADIO FILTERS
Extending the impulse response in order to reduce errors due to impulse noise and signal fading
19 p2649 N88-25730

RADIO FREQUENCIES
NT EXTREMELY HIGH FREQUENCIES
NT EXTREMELY LOW RADIO FREQUENCIES
NT HIGH FREQUENCIES
NT LOW FREQUENCIES
NT MICROWAVE FREQUENCIES
NT SUPERHIGH FREQUENCIES
NT ULTRAHIGH FREQUENCIES
NT VERY HIGH FREQUENCIES
NT VERY LOW FREQUENCIES
On adaptive signal processing of RF signals
[DE87-014192] 02 p0161 N88-11007
Potential formation in the plasma confinement region of a radio-frequency plugged linear device
[IPPJ-843] 02 p0242 N88-11526
Applications of neutral beam and rf technologies
[DE87-014936] 03 p0379 N88-12382
High-power RF-pulsed modulators for the Los Alamos free-electron laser
[DE88-000514] 04 p0448 N88-12775
Tribological properties of rf-sputtered MoS2 coatings
[DE88-000266] 04 p0452 N88-12802
Fluctuations in frequency of coherent radio signals in solar plasma according to Venera-15 and Venera-16 data 08 p1003 N88-16079
Conceptual design of a radio-frequency driven compact tokamak
[INPE-4364-PRE/1190] 08 p1085 N88-16535
Telemetry applications handbook
[AD-A186825] 09 p1132 N88-16789
F-layer polar cap arcs
[AD-A186592] 09 p1190 N88-17127
Observation of enhanced electric field in an RF-plugged sheet plasma in the RFC-XX-M open-ended machine
[IPPJ-857] 09 p1252 N88-17503
The radio structure of active nuclei in edge-on spiral and Seyfert galaxies 09 p1264 N88-17576
Photoconductor switch and circuit analysis
[AD-A188168] 11 p1478 N88-18821
RF steering in the CEBAF CW superconducting linac
[CEBAF-PR-87-013] 11 p1547 N88-19251
Identification of microwave line-of-sight multipath components 12 p1616 N88-19665
Application of radio frequency superconductivity to recirculating linacs
[CEBAF-PR-88-002] 12 p1690 N88-20107
The preparation, assembly and mounting of RF coaxial cables
[ESA-PSS-01-718-ISSUE-1] 13 p1756 N88-20504
Optical RF distribution links for MMIC phased array antennas
[NASA-TM-100841] 13 p1764 N88-20555
Progress in diagnostic techniques for SC cavities
[CEBAF-PR-88-003] 13 p1772 N88-20600
Theoretical studies of the heating of toroidal plasmas with radiofrequency electromagnetic radiation
[DE88-006913] 15 p2137 N88-22749
RF properties of superconducting Pb electroplated onto Cu
[DE88-005918] 15 p2139 N88-22765
Experimental radio frequency link for Ka-band communications applications
[NASA-TM-100824] 18 p2470 N88-24859
Arcing and rf signal generation during target irradiation by a high-energy, pulsed neutral particle beam
[DE88-007169] 18 p2471 N88-24864
Radio Frequency (RF) strain monitor
[NASA-CASE-LAR-13705-1] 18 p2530 N88-25011
Optical diagnostics for a high power, rf-inductively coupled plasma
[DE88-007822] 18 p2579 N88-25322
Large antenna experiments aboard the space shuttle: Application of nonuniform sampling techniques
19 p2652 N88-25745
Anomalous RF magnetoresistance in copper at 4 K
[DE88-010232] 19 p2722 N88-26162
Coherent RF error statistics
[AD-A193002] 20 p2792 N88-26560
Microwave calibration system 2
[AD-A192976] 20 p2805 N88-26639
Superconducting rf and beam-cavity interactions
[DE88-008598] 20 p2852 N88-26936
Rf cavity primer for cyclic proton accelerators
[DE88-010655] 20 p2853 N88-26938
Bootstrap currents in radio-frequency-driven tokamak equilibria
[DE88-011136] 23 p3285 N88-29561
Study of secondary emission properties of materials used for high power RF components in space
[ESA-CR(P)-2587] 24 p3361 N88-30012
Electromagnetic noise and interference
24 p3363 N88-30028
Radio and infrared properties of young stars
[NASA-CR-183252] 24 p3459 N88-30579

RADIO FREQUENCY HEATING
Fast wave injection into high temperature tokamak plasmas in the lower-hybrid-density regime of JIPP T-IIU
[ISSN-0469-4732] 01 p0099 N88-10649
Microwave superheaters for fusion
[DE88-001656] 05 p0653 N88-14007
A ray-tracing study of electron cyclotron resonance heating in tokamak plasmas with a superthermal electron tail
[INPE-4381-PRE/1201] 08 p1085 N88-16536
Absorption of electron cyclotron radiation in tokamak plasmas with a superthermal tail in the electron velocity distribution
[INPE-4391-PRE/1211] 08 p1086 N88-16541
Modeling considerations for selected rf-plasma edge effects
[DE88-003285] 09 p1252 N88-17500
Ionosonde studies of field-aligned irregularities during high-power HF heating at Arecibo
[AD-A195848] 24 p3401 N88-30256
The study of hydromagnetic waves and RF heating using the TORTUS tokamak, the development of diagnostic techniques based on submillimeter lasers and the gyrotron, and gas discharge 24 p3431 N88-30419

RADIO FREQUENCY INTERFERENCE
NT CHIRP
NT ELECTROMAGNETIC NOISE
NT IONOSPHERIC NOISE
NT SHOT NOISE
NT THERMAL NOISE
NT WHISTLERS
NT WHITE NOISE
Monitoring of harmful interference to the HF (High Frequency) broadcasting service. 3: Results of the June 1986 coordinated monitoring period
[PB87-210274] 01 p0036 N88-10229
A comparative analysis of equatorial and auroral-zone phase scintillation data
[AD-A184509] 03 p0350 N88-12212
An analysis of whistler-mode radiation from the Spacelab-2 electron beam, revision
[AD-A188228] 11 p1552 N88-19287
Analysis, suppression of land clutter characteristics reported 14 p1903 N88-21389
Radio frequency compatibility between IRS and SPOT 3: Preliminary study
[CNES-86/CT/DRT/TIT/TR/011]
14 p1905 N88-21383
Evaluation of the communications impact of a low power arcjet thruster
[NASA-TM-100926] 18 p2475 N88-24682
Propagation management for no-acknowledge HF communications links 18 p2502 N88-24843
Aircraft field degradation and electromagnetic compatibility
[PB88-183975] 19 p2602 N88-25456
Method and apparatus for measuring distance
[NASA-CASE-MSC-20912-1] 20 p2793 N88-26568
Airborne measurement of low frequency atmospheric noise ALFAN 1
[AD-A193056] 21 p2931 N88-27405
A notch filter instrument for measuring ELF (Extremely Low Frequency) MSK (Minimum Shift Keying) signals
[AD-A193324] 21 p2933 N88-27414
New CCIR report on SETI 22 p3067 N88-28204

RADIO FREQUENCY NOISE
U ELECTROMAGNETIC NOISE

RADIO FREQUENCY RADIATION
U RADIO WAVES

RADIO GALAXIES
Long-baseline astrometric interferometers
[AD-A188474] 12 p1713 N88-20250
Infrared astronomy at extremely faint light levels in support of the LAIRTS program
[AD-A191497] 18 p2592 N88-25404
The polarization of radio galaxies: Its structure at low frequencies
[B8681611] 20 p2884 N88-27123

RADIO INTERFERENCE
U RADIO FREQUENCY INTERFERENCE

RADIO INTERFEROMETERS
Long-baseline astrometric interferometers
[AD-A188474] 12 p1713 N88-20250

RADIO JETS (ASTRONOMY)
Long-baseline astrometric interferometers
[AD-A188474] 12 p1713 N88-20250

RADIO METEOROLOGY
Review of recent developments in evaporation ducting assessment 12 p1616 N88-19664

RADIO NAVIGATION
NT LORAN C
The Telecommunications and Data Acquisition Report
[NASA-CR-181546] 04 p0432 N88-12679
Generalized expression for radio navigation parameter error 13 p1787 N88-20691
NAVSTAR global positioning system
[AD-A192609] 20 p2757 N88-26354

RADIO OBSERVATION
Research in geodesy based upon radio interferometric observations of GPS (Global Positioning System) satellites
[AD-A184040] 03 p0346 N88-12187
New approaches to some methodological problems of meteor science 06 p0741 N88-14557

RADIO OCCULTATION
Laboratory evaluation and application of microwave absorption properties under simulated conditions for planetary atmospheres
[NASA-CR-181466] 02 p0254 N88-11606

Laboratory evaluation and application of microwave absorption properties under simulated conditions for planetary atmospheres
[NASA-CR-182443] 23 p3300 N88-29653

RADIO PROPAGATION
U RADIO TRANSMISSION

RADIO RANGE
Correlation between refraction over sea and nature of radar reflections from sea surface
06 p0728 N88-14477

RADIO RANGES
U RADIO BEACONS

RADIO RECEIVERS
NT SUPERHETERODYNE RECEIVERS
NT TRANSMITTER RECEIVERS
X-band uplink ground systems development: Part 2
04 p0436 N88-12703
Construction of a satellite simulator for the frequency range between 11.7 and 12.5 GHz
[IRT-TB-B-84/87] 16 p2166 N88-22917
An outdoor unit for Direct Broadcast Satellite (DBS) digital sound reception
[BMFT-FB-W-86-016] 16 p2189 N88-23050
The Sercel TR5S Global Positioning System (GPS) receiver
[ETN-88-92473] 20 p2757 N88-26357

RADIO REFLECTION
U RADIO ECHOES

RADIO RELAY SYSTEMS
NT CODE DIVISION MULTIPLE ACCESS
NT TIME DIVISION MULTIPLE ACCESS
Improvements to a UHF rebroadcast television link suffering tidal fading: Countisbury UHF relay station
[BBC-RD-1987/14] 05 p0573 N88-13495
Study of a Radio Relay Link (RRL). Cassini mission. Data package for final presentation
[ESA-CR(P)-2472] 07 p0847 N88-15138
A review of the role of surface reflection in multipath propagation over terrestrial microwave links
12 p1615 N88-19655
Space-diversity effects on line-of-sight propagation paths 12 p1617 N88-19670

RADIO SCATTERING
New approaches to some methodological problems of meteor science 06 p0741 N88-14557
Scattering and depolarization by random rough terrain and vegetation covered terrain-unified full wave approach 12 p1615 N88-19657

RADIO SIGNAL ATTENUATION
U RADIO ATTENUATION

RADIO SIGNAL PROPAGATION
U RADIO TRANSMISSION

RADIO SIGNALS
Implications of a simplified signal structure for Navsat
[REPT-63/1439] 01 p0005 N88-10024
Meteor-burst communications: Is this what the Navy needs?
[AD-A184433] 04 p0431 N88-12672
Two-signal cross modulation effects, half-IF effects and interference criteria in land mobile sharing with UHF (Ultra High Frequency) television
[PB87-228037] 05 p0576 N88-13514
Fluctuations in frequency of coherent radio signals in solar plasma according to Venera-15 and Venera-16 data 08 p1003 N88-16079
Indian Ocean validation
[AD-A194458] 23 p3175 N88-28902

RADIO SOURCES (ASTRONOMY)
NT EXTRAGALACTIC RADIO SOURCES
NT PULSARS
NT QUASARS
NT RADIO GALAXIES
NT RADIO JETS (ASTRONOMY)
NT RADIO STARS
USSR report: Space
[JPRS-USP-87-003] 01 p0009 N88-10050
Occultation of compact radio sources by the ion tail of Halley's Comet 01 p0118 N88-10753
Microwave observations of nonthermal phenomena in pre-main sequence stars 04 p0505 N88-13107
EVN (European VLBI network) and MERLIN observations of 5 superluminal radio sources
[PB87-110730] 04 p0520 N88-13193
The Spring 1985 high precision baseline test of the JPL GPS-based geodetic system
[NASA-CR-182586] 14 p1940 N88-21577

RADIO SPECTRA
NT MICROWAVE SPECTRA
Thermal-nonthermal relationships in active galactic nuclei
[B8681482] 16 p2289 N88-23707

RADIO STARS
NT PULSARS
The Parkes radio survey of active chromosphere stars
04 p0511 N88-13141
Infrared astronomy at extremely faint light levels in support of the LAIRTS program
[AD-A191497] 18 p2592 N88-25404
Radio astronomy 24 p3364 N88-30031

RADIO TELEMETRY
Spectral density estimates of coarsely quantized random vibration data 09 p1178 N88-17055
A deep-water OBS (Ocean Bottom Seismometer) array with real-time telemetry
[AD-A187404] 10 p1357 N88-18112

RADIO TELESCOPES
NT VERY LARGE ARRAY (VLA)
Radio astronomy 24 p3364 N88-30031

RADIO TRANSMISSION
NT IONOSPHERIC PROPAGATION
NT MICROWAVE ATTENUATION
NT MICROWAVE TRANSMISSION
NT MULTIPATH TRANSMISSION
NT SHORT WAVE RADIO TRANSMISSION
NT SPREAD SPECTRUM TRANSMISSION
NT TRANSEQUATORIAL PROPAGATION
Meteor-burst communications: Is this what the Navy needs?
[AD-A184433] 04 p0431 N88-12672
A raytrace method for a laterally heterogeneous environment
[AD-A186525] 08 p0978 N88-15912
Experimental Radio Data System (RDS): A survey of reception reliability in the UK
[BBC-RD-1987/17] 09 p1155 N88-16922
MARCE data evaluation 10 p1286 N88-17693
User's guide for the HF (High Frequency) broadcast antenna design and validation summary programs
[PB88-116124] 10 p1317 N88-17875
Source and event selection for radio-planetary frame-tie measurements using the Phobos Landers
11 p1471 N88-18775
Development of a ground-conductivity map for the area of the Federal Republic of Germany from measured field-strength contours 12 p1615 N88-19656
Scattering and depolarization by random rough terrain and vegetation covered terrain-unified full wave approach 12 p1615 N88-19657
VHF/UHF propagation by diffraction: Calculation by numerical integration 12 p1615 N88-19659
A diffraction based theoretical model for prediction of UHF path loss in cities 12 p1616 N88-19661
A program for the calculation of radio-wave transmission loss over the spherical earth and over obstacles
12 p1616 N88-19662
Review of recent developments in evaporation ducting assessment 12 p1616 N88-19664
Refractive index, meteorology and fading in line-of-sight transmission paths 12 p1616 N88-19666
The correlation between methodological and low-level angle-of-arrival measurements 12 p1617 N88-19668
Space-diversity effects on line-of-sight propagation paths 12 p1617 N88-19670
Some measurements of height gain at V.H.F.
12 p1617 N88-19671
An EHF telecommunication system engineering model
12 p1618 N88-19674
A propagation campaign in a marine environment utilizing a digital system at 36 GHz 12 p1618 N88-19675
Construction of a satellite simulator for the frequency range between 11.7 and 12.5 GHz
[IRT-TB-B-84/87] 16 p2166 N88-22917
WAVFLD: A program to compute ionospheric height gain functions and field strengths at VLF
[AD-A191159] 16 p2191 N88-23066
Environmental projects. Volume 6: Environmental assessment. New 34-meter antenna at Venus site
[NASA-CR-182922] 17 p2332 N88-23919
WIPP (Wave Induced Particle Precipitation) experiment logistic support
[AD-A191184] 18 p2499 N88-24824
An evaluation of two millimeter wave propagation models for horizontal atmospheric attenuation at 70-115 GHZ
[AD-A192699] 21 p2931 N88-27403
Rapid-scanning Fourier transform spectrometer for studies of propagation of near-millimeter-wave radiation through clear air and fog
[AD-A193752] 22 p3070 N88-28219
Activities report of the Electromagnetic Environment Division
[FOA-C-30484-3.2/3.3/4.1/4.2]
22 p3071 N88-28233
Electromagnetic interference to radar and radio link systems caused by large scale wind turbines
[FOA-C-30486-3.2] 22 p3071 N88-28234

RADIO TRANSMITTERS
NT IONOSONDES
NT RADIO BEACONS
NT RADIOSONDES
NT RADIOTELEPHONES
NT RAWINSONDES
NT TRANSMITTER RECEIVERS
Analysis of the ICE combiner for multiple antenna arraying 04 p0436 N88-12704
Power density measurements in the near field of the DSS 13 26-meter antenna 04 p0437 N88-12711
KOSPAS-SARSAT satellites used for ocean current study 24 p3450 N88-30534

RADIO WAVE REFRACTION
Terrestrial Propagation Characteristics in Modern Systems of Communications, Surveillance, Guidance and Control
[AGARD-CP-407] 12 p1614 N88-19653
Radio and radar holes and multipath zones: The global and local influences on atmospheric refractive structure and resulting adverse radio and radar performance
12 p1617 N88-19667
MM-wave propagation and application in military communication systems 12 p1617 N88-19669

RADIO WAVES
NT CENTIMETER WAVES
NT CN EMISSION
NT DECAMETRIC WAVES
NT DECIMETER WAVES
NT EXTRATERRESTRIAL RADIO WAVES
NT GALACTIC RADIO WAVES
NT HYDROXYL EMISSION
NT LONG WAVE RADIATION
NT MICROWAVE EMISSION
NT MICROWAVES
NT MILLIMETER WAVES
NT RADIO BURSTS
NT RADIO EMISSION
NT SHORT WAVE RADIATION
NT SOLAR RADIO BURSTS
NT SOLAR RADIO EMISSION
NT SUBMILLIMETER WAVES
NT TYPE 3 BURSTS
NT WHISTLERS
General theory of radio propagation through a stratified atmosphere
[PB87-226197] 04 p0430 N88-12682
Measured characteristics of 800/900 MHz mobile radio channels with high-angle propagation through moderately dense foliage
[CRC-1398] 05 p0573 N88-13493
Correlation between refraction over sea and nature of radar reflections from sea surface
06 p0728 N88-14477
Polar Geophysical Institute's studies of magnetosphere, ionosphere 06 p0728 N88-14480
A Jupiter Data Analysis Program (JDAP) research grant on wave accessibility and attributes
[NASA-CR-182348] 06 p0804 N88-14908
Solar-geophysical data number 515, July 1987. Part 1: (Prompt reports). Data for June 1987, May 1987 and late data
[PB87-233177] 06 p0805 N88-14912
Radar reflectivity and attenuation of radio waves in the melting layer of precipitation
[PB88-121553] 10 p1318 N88-17882
An assessment of the application of in situ ion-density data from DMSP to modeling of transionospheric scintillation
[AD-A188919] 12 p1643 N88-19840
Generalized expression for radio navigation parameter error 13 p1787 N88-20691
Trajectory synthesis of ionograms in presence of artificial ionospheric inhomogeneities 13 p1789 N88-20703
Power source selection for neutral particle beam systems 17 p2407 N88-24314

RADIOACTIVE CONTAMINANTS
The distribution of some chemical elements between dissolved and particulate phases in the ocean
[DE88-010181] 21 p2977 N88-27682

RADIOACTIVE DECAY
NT ALPHA DECAY
NT NEUTRON EMISSION
Summary and conclusions of the 6th Moriond workshop — standard electroweak model
[USIP-87-11] 01 p0092 N88-10602
Few body hypernuclear systems: Weak decays
[DE87-014920] 04 p0488 N88-13010
Nuclear beta decay after Les Houches
[DE87-014921] 04 p0489 N88-13011
Influences of the astrophysical environment on nuclear decay rates
[DE88-001461] 04 p0522 N88-13208
W decays
[NOTA-INTERNA-877] 05 p0648 N88-13966
Double beta decay and nuclear structure
[DE88-001966] 07 p0931 N88-15652
Theory of double beta decay
[DE88-002285] 07 p0931 N88-15653

Properties of nuclei and elementary particles at low and intermediate energies
[DE88-001913] 09 p1244 N88-17456
Calculated late time spectra of supernovae
[DE88-003296] 10 p1428 N88-18530
A look at Supernova 1987A
[DE88-003411] 10 p1429 N88-18531
Spontaneous decay and atomic fluorescence near a metal surface of an absorbing dielectric
[AD-A187508] 13 p1835 N88-20975
Gluino branching ratio effects on the search for supersymmetry
[PREPRINT-572] 14 p1981 N88-21821
A proposed national policy concerning the reentry of space reactors 17 p2415 N88-24359
A method for the analysis of heavy flavor decays
[NOTA-INTERNA-909] 22 p3150 N88-28744
Evidence of the in situ decay of Al-26 in a Semarkona chondrule 24 p3441 N88-30479
Lewis Cliff 86010, a unique Antarctic meteorite: Possible new clues to the early history of the solar system
24 p3442 N88-30482

RADIOACTIVE ELEMENTS
U RADIOACTIVE ISOTOPES

RADIOACTIVE ISOTOPES
NT COBALT 60
NT LAWRENCIUM
NT NEPTUNIUM
NT PLUTONIUM ISOTOPES
NT PLUTONIUM 238
NT TRITIUM
NT URANIUM 238
Content of natural radioactive elements in Venusian rocks determined using data from Vega-1 and Vega-2 stations 13 p1726 N88-20323
The Light-Weight Radioisotope Heater Unit (LWRHU): Development and application 17 p2405 N88-24299
MHW RTG performance during LES 8/9 and Voyager missions 17 p2405 N88-24300
Pioneer 10 and 11 RTG performance update
17 p2405 N88-24301
The radiation sensitivity of select metal chelate polymers: Mechanistic changes at higher energies
[AD-A193467] 23 p3196 N88-29019
The dynamics of transuranics and other radionuclides in natural environments, December 1985
[DE87-014456] 24 p3390 N88-30189

RADIOACTIVE MATERIALS
Airborne lidar experiments at the Savannah River Plant
[NASA-TM-4007] 02 p0194 N88-11209
The dynamic isotope power system: Technology status and demonstration program 17 p2422 N88-24400
RRSAS (Robotic Radiation Survey and Analysis System) Project: A real time sensor driven robotic system
[DE88-006825] 20 p2808 N88-26661

RADIOACTIVE NUCLIDES
U RADIOACTIVE ISOTOPES

RADIOACTIVE WASTES
A comparison of open and closed multimegawatt space power and weapon systems
[DE87-012975] 01 p0089 N88-10579
Highlights of the Chemical Technology Division's research activities
[DE88-000233] 03 p0282 N88-11773
The adaption and use of research codes for performance assessment
[DE88-000552] 06 p0756 N88-14639
JPRS report: Science and technology. Japan
[JPRS-JST-87-030] 16 p2185 N88-23026
Comparison of open and closed multimegawatt space power systems 17 p2414 N88-24353
Space reactor end of life issues
17 p2424 N88-24413
Review of numerical methods for radionuclide transport in three-dimensional porous media, at high Peclet numbers
[CFDU/87/10] 18 p2538 N88-25081
Optimization of mechanical/corrosion properties of TI-CODE 12 plate and sheet. Part 2: Thermomechanical processing effects
[DE88-007493] 19 p2616 N88-25517

RADIOACTIVITY
Radon Research Program, FY-1987
[DE88-002633] 09 p1188 N88-17120
Measurements of astrophysical reaction rates for radioactive samples
[DE88-004309] 10 p1429 N88-18537
Radioactivity as a means of nondestructive testing
[DE88-702778] 23 p3224 N88-29188

RADIOBIOLOGY
Critical phenomena and electromagnetic effects in biological membranes
[AD-A188156] 11 p1518 N88-19064
Biology and Medicine Division
[DE87-009280] 14 p1952 N88-21632

RADIOGENIC MATERIALS
The distribution of some chemical elements between dissolved and particulate phases in the ocean
[DE88-010181] 21 p2977 N88-27682

RADIOGRAPHY
NT AUTORADIOGRAPHY
NT COMPUTER AIDED TOMOGRAPHY
NT NEUTRON RADIOGRAPHY
NT TOMOGRAPHY
Cineradiography
[DE87-013158] 03 p0324 N88-12045
Flaw imaging and ultrasonic techniques for characterizing sintered silicon carbide
[NASA-TM-100177] 03 p0334 N88-12106
Measurement and control of damage in composite materials: Nondestructive controls by thermography, holography, and radiography
[SNIAS-872-430-110] 05 p0559 N88-13403
X-ray imaging: Status and trends
[DE88-000756] 05 p0649 N88-13980
Study on cineradiography
[ISL-R-120/86] 08 p0990 N88-15994
High-resolution Real-Time Radiography (RTR) system design
[AD-A187107] 09 p1166 N88-16992
Performance of a digital real time radiographic imaging system
[MRL-R-1068] 09 p1169 N88-17011
Durability and damage tolerance of aluminum castings
[AD-A186444] 10 p1341 N88-18013
Institute for Materials Science and Engineering, nondestructive evaluation: Technical activities 1987
[PB88-153655] 10 p1342 N88-18020
Characterization of sintered SiC by using NDE
15 p2082 N88-22413
Method of radiographic inspection of wooden members
[NASA-CASE-LAR-13724-1] 17 p2346 N88-23983
Rendering of surfaces from volume data
[AD-A193649] 22 p3143 N88-28689
Analysis of edge detection techniques for radiographic image measurement
[AD-A193650] 23 p3186 N88-28961
Comparison of 2-D Fourier and spatial techniques for removing noise in real-time X-ray radiography
[AD-A193700] 23 p3187 N88-28962
Development of graded reference radiographs for aluminum welds, phase 1
[AD-A195594] 24 p3381 N88-30140

RADIOISOTOPE BATTERIES
NT SNAP 19
Transactions of the Fourth Symposium on Space Nuclear Power Systems
[DE88-006164] 17 p2398 N88-24254
The Light-Weight Radioisotope Heater Unit (LWRHU): Development and application 17 p2405 N88-24299
Foil gas bearing system endurance testing dynamic isotope power system 17 p2405 N88-24302
Two-phase fluid management for a Rankine cycle isotope power system 17 p2405 N88-24303
Innovative methodology and developments in US space radioisotope power safety risk assessments
17 p2415 N88-24362
Status of modular RTG technology
17 p2422 N88-24403
Plasma separation process. Betacell (BCELL) code, user's manual
[DE88-006955] 20 p2859 N88-26981

RADIOLYSIS
Organic molecules on meteoritic solid substrates
[NASA-CR-181570] 05 p0560 N88-13411
Effects of energy, distance and orientation on electron transfer rates studied by pulse radiolysis in organic media
[DE88-002906] 08 p1082 N88-16521
Gas phase pulse radiolysis
[DE88-002981] 10 p1296 N88-17751
Electron transfer to iron(3) oxide colloids
[DE88-002885] 10 p1416 N88-18448

RADIOMETERS
NT ADVANCED VERY HIGH RESOLUTION RADIOMETER
NT DICKE RADIOMETERS
NT INFRARED DETECTORS
NT INFRARED RADIOMETERS
NT INFRARED SCANNERS
NT MICROWAVE RADIOMETERS
NT SPECTRORADIOMETERS
Development of response models for the Earth Radiation Budget Experiment (ERBE) sensors. Part 4: Preliminary nonscanner models and count conversion algorithms
[NASA-CR-178295] 01 p0050 N88-10317
Study on propagation and inverse scattering --- sea studies
[ESA-CR(P)-2394] 01 p0063 N88-10405
The use of fiber optics in the determination of temperature and extent of reaction in detonating explosives
[DE87-012632] 01 p0094 N88-10612
A VAS-numerical model impact study using the Gal-Chen variational approach --- Visible Infrared Spin-Scan Radiometer Atmospheric Sounder (VAS)
02 p0213 N88-11339
NBS (National Bureau of Standards) measurement services: Radiometric standards in the vacuum ultraviolet
[PB87-227625] 03 p0325 N88-12055
Planning for future operational sensors and other priorities
[PB87-220802] 03 p0325 N88-12056
A method for remote sensing of precipitable water vapor and liquid in the atmosphere using a 22-ghz radiometer
[AD-A184204] 03 p0354 N88-12232
Lidar-radiometric method for determining liquid-water content of cirrus clouds 04 p0461 N88-12854
Development of response models for the Earth Radiation Budget Experiment (ERBE) sensors. Part 3: ERBE scanner measurement accuracy analysis due to reduced housekeeping data
[NASA-CR-178294] 05 p0583 N88-13553
Spectral and radiometric calibration of the Airborne Visible/Infrared Imaging Spectrometer
06 p0707 N88-14334
AVHRR/HIRS (Advanced Very High Resolution Radiometer/High Resolution Infra-Red Sounder) operational method for satellite based sea surface temperature determination
[PB88-107594] 06 p0708 N88-14340
An aureolar radiometer for the determination of aerosol size distribution 08 p1018 N88-16174
Design feasibility report on investigation of magnetic bearings for the ocean colour monitor radiometer scanner
[BAE-TP-7849] 09 p1174 N88-17036
A noise-adding radiometer for the Parkes antenna
11 p1473 N88-18788
PbSnTe photovoltaic detectors for operation in the 2-14 micron band
[INPE-4252-PRE/1125] 11 p1508 N88-19008
Remote sensing of atmospheric optical thickness and sea-water attenuation when submerged: Wavelength selection and anticipated errors
[AD-A187609] 11 p1548 N88-19262
Roentgenoradiometric analysis of aerosol in Venusian clouds by Vega-1 and Vega-2 automatic interplanetary stations 13 p1726 N88-20319
Coherence effects in optical physics with special reference to spectroscopy
[AD-A189520] 13 p1840 N88-21007
Activities report of the Toulouse Research Center
[ETN-88-91988] 13 p1850 N88-21077
Investigation into the development of computer aided design software for space based sensors
[NASA-CR-180772] 15 p2107 N88-22552
Description of the MPTR system: Multi Path Transmissometer Radiometer
[FEL-1987-14] 20 p2855 N88-26954
Microwave frequency nondestructive control
[CERT-2/1355-MO] 23 p3189 N88-28976
Improvements in techniques of microwave thermography
[AD-A194613] 23 p3203 N88-29062
NBS (National Bureau of Standards) measurement services: The NBS photodetector spectral response calibration transfer program
[PB88-201595] 24 p3378 N88-30109
Atmospheric corrections for in-flight satellite radiometric calibration
[AD-A196124] 24 p3391 N88-30194
Principles of the optical differential thermal analysis
[AD-A195951] 24 p3429 N88-30408

RADIOMETRIC CORRECTION
Object-dependent atmospheric influence on LANDSAT recordings 01 p0065 N88-10420
First assessment of processing and use of SPOT images by the Institut Geographique Nationale --- French National Geographic Institute 03 p0341 N88-12148
The radiometric processing of SLAR measuring values using the PARES program
[BCRS-86-04] 16 p2227 N88-23301
Some characteristics in synthetic aperture radar (SAR) raw data and SAR images
[FOA-C-30483-3.2] 22 p3071 N88-28232

RADIOMETRIC RECTIFICATION
U RADIOMETRIC CORRECTION

RADIOMETRIC RESOLUTION
The absolute radiometric calibration of space-based sensors 03 p0277 N88-11744
Restoration techniques for redisplay of LANDSAT-5 satellite imagery
[INPE-4189-PRE/1076] 13 p1791 N88-20712

Method for restoration and resampling of TM sensor imagery
[INPE-4491-PRE/1255] 15 p2090 N88-22454

RADIONUCLIDES
U RADIOACTIVE ISOTOPES

RADIOSENSITIVITY
U RADIATION TOLERANCE

RADIOSONDES
NT IONOSONDES
NT RAWINSONDES
VAS products as indices of thunderstorms and severe local storm potential --- Visible and Infrared Spin Scan Radiometer Atmospheric Sounder (VAS) 02 p0201 N88-11253
Forecasting and nowcasting cumulus convection with soundings released from a storm-intercept vehicle 02 p0202 N88-11262
Correlations of TOMS total ozone data (Nimbus-7 satellite) with tropopause height 05 p0617 N88-13788
Middle atmospheric wind measurements using a medium frequency radar
[AD-A185931] 07 p0879 N88-15330
Roys and radiosondes in the region
[INPE-4362-PRE/1188] 13 p1796 N88-20743
Tiros operational vertical sounder (TOVS) and radiosonding in the region 17 p2360 N88-24059

RADIOTELEPHONES
Adaptive digital phase modulation
[PB87-134607] 06 p0693 N88-14253
A diffraction based theoretical model for prediction of UHF path loss in cities 12 p1616 N88-19661
Design mobile satellite system architecture as an integral part of the cellular access digital network 19 p2650 N88-25736

RADIOTHERAPY
U RADIATION THERAPY

RADIUS
U RADII

RADOME MATERIALS
Dielectric behavior of electromagnetic (EM) windows materials irradiated by a CW CO2 high-power laser --- hypersonic/reentry vehicles
[ISL-CO-239/86] 09 p1154 N88-16913

RADON
NT RADON ISOTOPES
Rapid feature extraction via the radon transform
[AD-A190032] 15 p2110 N88-22573

RADON ISOTOPES
Radon-222 in the Antarctic Peninsula
[INPE-4486-PRE/1251] 15 p2092 N88-22468

RAIL TRANSPORTATION
Nowcasting for the national economy needs 02 p0199 N88-11241
Evaluation of the thermal effectiveness of urethane foam and fiberglass as insulation systems for tank cars
[PB88-100797] 06 p0686 N88-14207
TECOM's research efforts in the dynamic environments 08 p0999 N88-16048
Composite materials for rail transit systems
[NASA-CR-178401] 10 p1294 N88-17738
The MBB propulsion concepts for magnetic suspension railways: Retrospective view and prospects
[MBB-Z-141/87] 10 p1316 N88-17865
Identification of lateral operation dynamics of rail vehicles using roll test stand tests 20 p2787 N88-26534

RAILGUN ACCELERATORS
A feasibility study of a hypersonic real-gas facility
[NASA-CR-180423] 01 p0008 N88-10043
Numerical predictions of EML system performance
[DE87-011727] 01 p0011 N88-10061
Switching devices used in the Lethality Test System
[DE87-011734] 01 p0011 N88-10062
Exact solutions to the governing dynamic equations of plasma armature electromagnetic railguns
[DE87-014442] 01 p0011 N88-10063
Effects of barrel joints on hypervelocity projectiles
[DE87-013447] 02 p0157 N88-10983
Current-filamentation instability in railgun arcs
[AD-A184618] 03 p0269 N88-11693
Ultimate velocities for induction launchers
[DE87-012360] 04 p0404 N88-12513
Thermal analysis of electromagnetic launcher rails
[DE88-000166] 04 p0405 N88-12514
Analysis of a series of electromagnetic launcher firings
[AR-005-131] 04 p0405 N88-12516
Efficiency aspects of short, low velocity railguns
[AR-004-847] 04 p0405 N88-12517
Experimental investigation of a three-stage railgun incorporating puff-switching
[MRL-R-1056] 09 p1130 N88-16785
The railgun and its power source
[MRL-R-1058] 09 p1130 N88-16786
Pulsed current transformer for low inductive loads
[AD-A187224] 10 p1324 N88-17913
Structural integrity of metallic armature rail guns
[AD-A188735] 13 p1728 N88-20333
Application of railgun principle to high-velocity hydrogen pellet injection for magnetic fusion reactor refueling
[DE88-005830] 13 p1728 N88-20334
Temperature estimates for a free flowing railgun plasma
[MRL-R-1054] 13 p1843 N88-21032
Analytic solutions to dynamic equations of plasma armature railguns
[DE88-006842] 15 p2023 N88-22057
Structural consequences of railgun augmentation
[DE88-007036] 15 p2023 N88-22058
Railgun rail gouging by hypervelocity sliding contact
[DE88-006865] 16 p2166 N88-22916
Experimental investigation of a three-stage railgun incorporating puff-switching
[AD-A191044] 16 p2166 N88-22918
Fundamental limits to the velocity of solid armatures in railguns 18 p2469 N88-24656
The SRS (Segmented Rail Surface) railgun: A new approach to restrike control
[DE88-007907] 19 p2605 N88-25468
STARFIRE: Hypervelocity railgun development for high-pressure research
[DE88-008348] 19 p2605 N88-25469
Reaming experiments for the lethality test system
[DE88-007902] 20 p2763 N88-26383
Why plasma armature railguns don't work (and what can be done about it)
[DE88-007900] 20 p2763 N88-26384
Application of superconducting technology to earth-to-orbit electromagnetic launch systems
[DE88-010022] 20 p2763 N88-26386
Plasma armature formation in high-pressure, high-velocity hydrogen
[DE88-008347] 20 p2857 N88-26967
An interferometric measurement technique for railgun structures
[AD-A192851] 21 p2901 N88-27217
Slew-induced deformations in a space-based electromagnetic rail gun 21 p2929 N88-27385
Plasma behavior in the boundary layer near a railgun surface
[DE88-008889] 21 p3017 N88-27909
Theoretical modeling of accelerating arc plasmas
[AD-A195606] 24 p3432 N88-30426

RAILROADS
U RAIL TRANSPORTATION

RAILS
Application of Kalker's rolling contact theory to the simulation of rail vehicles
[DFVLR-FB-87-07] 01 p0057 N88-10363
On cleavage in fatigue for rail steels 06 p0716 N88-14388
Composite materials for rail transit systems
[NASA-CR-178401] 10 p1294 N88-17738
Structural integrity of metallic armature rail guns
[AD-A188735] 13 p1728 N88-20333

RAIN
NT ACID RAIN
Estimation from satellite imagery of summertime rainfall over varied space and time scales
[PB87-203246] 01 p0071 N88-10454
The 54-hours continuous post-frontal precipitation north of the Alpine mountain barrier, 22-25 August 1975 02 p0203 N88-11268
Conceptual models of Baiu front and Baiu frontal disturbances in multiscale characteristics --- East Asia 02 p0203 N88-11271
Evaluation of the Rainsat precipitation analysis system in real-time use 02 p0205 N88-11283
Convective scale interaction: Arc cloud lines and the development and evolution of deep convection
[NASA-CR-181469] 02 p0215 N88-11357
Development of a climatic map of rainfall attenuation for Europe
[REPT-372] 02 p0216 N88-11359
Estimates of satellite EHF communication outages due to attenuation by rain
[AD-A183969] 03 p0307 N88-11941
A statistical rain attenuation prediction model with application to the advanced communication technology satellite project. Part 2: Theoretical development of a dynamic model and application to rain fade durations and tolerable control delays for fade countermeasures
[NASA-TM-100242] 03 p0308 N88-11945
On the interannual variability of South American climate and the Southern Oscillation 04 p0470 N88-12905
Effects of rainfall on the seasonal thermocline
[AD-A184432] 04 p0472 N88-12912
Specification of predictors necessary for the determination of over or underestimation of radar derived total rainfall
[AD-A185363] 05 p0628 N88-13838
BARS-1M meteorological complex carried on IL-18 airplane 06 p0725 N88-14458
Estimation of rainfall rates in tropical cyclones by passive microwave radiometry 06 p0744 N88-14577
Improvement of the construction of protective clothing for better wearability and comfort --- rainwear
[IZF-1986-26] 07 p0899 N88-15448
The potential influence of rain on airfoil performance 08 p0952 N88-15774
Radar echo signatures versus relative precipitation
[AD-A186162] 08 p0976 N88-15903
Variations of tropical circulation and associated rainfall anomalies, during 2 years of contrast
[INPE-4359-TDL/300] 08 p1039 N88-16286
Full scale and wind tunnel surface pressure measurements on the T.R.R.L. spray dispersion programme vehicles
[REPT-8623] 09 p1114 N88-16676
Calibration of the ARL (Aeronautical Research Laboratories) rain and icing facility
[AD-A186776] 09 p1121 N88-16710
The structure and dynamics of monsoon depressions 10 p1355 N88-18102
Optimal sampling to provide user-specific climate information 11 p1515 N88-19051
A propagation campaign in a marine environment utilizing a digital system at 36 GHz 12 p1618 N88-19675
Study of cations in the precipation of Estacao Antartica Comandante Ferraz
[INPE-4377-PRE/1197] 12 p1644 N88-19843
Design of the primary pre-TRMM and TRMM ground truth site
[NASA-CR-182609] 12 p1647 N88-19865
A polarimetric rain backscatter model developed for coherent polarization diversity radar applications 13 p1759 N88-20520
Applications of the differential reflectivity radar technique: Focus on estimation of rainfall parameters and microwave attenuation prediction 13 p1759 N88-20521
Numerical simulation of medium scale disturbance on meiyu front 14 p1900 N88-21346
Satellite rainfall retrieval by logistic regression
[NASA-CR-180485] 14 p1946 N88-21607
Some models for rain and cloud attenuation of millimeter waves
[PB88-160809] 14 p1948 N88-21616
The growth potential of corona discharges from aircraft flying in precipitation
[AD-A190507] 15 p2094 N88-22478
Space communication link propagation data for selected cities within the multiple beam and steerable antenna coverage areas of the advanced communications technology satellite
[NASA-TM-100861] 16 p2191 N88-23070
Validate algorithms for the determination of rainfall rates from SSM/I microwave satellite imagery
[AD-A188769] 16 p2233 N88-23337
Fog, rain and aerosol attenuation in the atmosphere
[AD-A190867] 16 p2235 N88-23350
Validate algorithms for the determination of rainfall rates from SSM/I microwave satellite imagery
[AD-A191337] 16 p2236 N88-23353
Rainfall rates and drop-size distributions for environmental testing
[AD-A191342] 16 p2236 N88-23354
Partial likelihood analysis of time series models with application to rainfall-runoff data
[AD-A191157] 16 p2261 N88-23516
Airborne and spaceborne radar images for geologic and environmental mapping in the Amazon rain forest, Brazil 17 p2353 N88-24021
Observation of stratiform rain with 94 GHz and s-b and Doppler radar
[AD-A192013] 18 p2544 N88-25100
Meteorological satellite product support and research for project GALE
[NASA-CR-180989] 19 p2727 N88-26193
Present status of artificial rain making
[DE88-701823] 20 p2826 N88-26769
Rain attenuation at 35 GHz over an 18 km path
[AD-A194504] 22 p3069 N88-28217
Indian monsoon rainfall, 1986-1987 22 p3120 N88-28536
Modes of interannual climate variability and Sahel rainfall anomalies 22 p3121 N88-28547
ENSO, sea-surface temperatures and African rainfall 22 p3122 N88-28550
Sub-Saharan rainfall anomalies and global sea-surface temperature relationships for the recent fifteen year (1970-1984) period 22 p3122 N88-28552
Simulation studies of the influence of sea-surface temperature anomalies on the Sahelian circulation and rainfall 22 p3122 N88-28553

A statistical rain attenuation prediction model with application to the advanced communication technology satellite project. 1: Theoretical development and application to yearly predictions for selected cities in the United States
[NASA-CR-179498] 23 p3205 N88-29077
Effects of precipitation on wind turbine performance
[DE88-001144] 23 p3228 N88-29211
Validate algorithms for the determination of rainfall rates from SSM/I microwave satellite imagery
[AD-A195428] 24 p3404 N88-30270

RAIN FORESTS
Mapping of the mangroves of the Guanabarra Bay through the utilization of remote sensing techniques
[INPE-3942-TDL/229] 12 p1637 N88-19804
Photointerpretation with instrumentation for evaluation of environmental impact: Mata Atlantica in Cubatao 19 p2683 N88-25946
Bibliography on tropical rain forests and the global carbon cycle. Volume 1: An introduction to the literature
[DE88-010761] 22 p3118 N88-28523

RAIN GAGES
Wet deposition and snowpack monitoring operations and quality assurance manual
[PB87-212817] 01 p0064 N88-10413

RAIN IMPACT DAMAGE
In-flight rain damage tests of the shuttle thermal protection system
[NASA-TM-100438] 14 p1881 N88-21241

RAINDROPS
Anthropogenic effects on the droplet formation process, and ion concentrations in droplets — clouds 08 p1018 N88-16175
On the theory of electromagnetic scattering from a raindrop splash
[AD-A188720] 14 p1906 N88-21393
A theoretical model of the washout of trace gases by raindrops in the atmosphere 17 p2375 N88-24125

RAINMAKING
Present status of artificial rain making
[DE88-701823] 20 p2826 N88-26769

RAINSTORMS
NT THUNDERSTORMS
Nowcasting rain/snow transitions and freezing rain 02 p0202 N88-11265
The application of divergence equation in the analysis of heavy rainfall 02 p0207 N88-11299
The mesoscale numerical model for heavy rainfall forecasting in Yangtze River Valley, China 02 p0211 N88-11326
Interactions between the Asian monsoons, the tropical Pacific and the southern hemisphere extratropics 04 p0470 N88-12907
Validate algorithms for the determination of rainfall rates from SSM/I microwave satellite imagery
[AD-A192299] 21 p2974 N88-27664
Passive microwave measurements of water vapor fields and rain for locating fronts in cyclonic storms
[AD-A195632] 24 p3404 N88-30267

RAKES
Calibration of averaging total pressure flight wake rake and natural-laminar-flow airfoil drag certification
[NASA-CR-181630] 19 p2599 N88-25443

RAMAN EFFECT
U RAMAN SPECTRA

RAMAN LASERS
Output power enhancement of AC Raman free-electron laser
[DE88-000503] 04 p0449 N88-12786
Raman microprobe characterization of dielectric films following high-energy pulsed laser irradiation
[DE88-000559] 05 p0588 N88-13587
Studies on nonlinear mechanisms of excimer laser propagation in fused silica fibers
[AD-A186822] 09 p1156 N88-16929
Laser raman studies related to liquid propellants: Structural characteristics inferred from the nitrate anion spectra
[AD-A188462] 12 p1612 N88-19641
Phase preservation cleanup in a double-pass Raman amplifier SBS (Stimulated Brillouin Scattering) conjugator
[AD-A189428] 13 p1761 N88-20536
Theoretical studies of Resonance Enhanced Stimulated Raman Scattering (RESRS) of frequency-doubled Alexandrite laser wavelength in cesium vapor
[NASA-CR-182870] 15 p2036 N88-22133
Unstable behavior of lasers and other optical systems
[AD-A190875] 16 p2213 N88-23204
Laser spectoscopy of plasmas
[AD-A193009] 20 p2861 N88-26991

RAMAN SCATTERING
U RAMAN SPECTRA

RAMAN SPECTRA
The polarization field for pulsed Raman transitions
[DE87-013118] 01 p0035 N88-10227
Large-scale stimulated rotational Raman scattering experiments using the LLNL Nova laser
[DE87-012661] 01 p0051 N88-10328
Spectroscopic studies of shocked and detonating explosives
[DE87-014216] 02 p0155 N88-10972
Theoretical atomic and molecular photophysics
[DE87-014249] 02 p0231 N88-11458
Enhanced noise and Raman scattering in plasma
[DE87-014466] 02 p0238 N88-11501
Enhanced Thomson scattering from laser plasmas
[DE87-014463] 02 p0238 N88-11503
Vibrational spectroscopy of shock-compressed fluid N2 and O2
[DE87-013138] 03 p0313 N88-11979
Raman scattering spectrum along a bevel etched GaAs on Si, TEM (Transmission Electron Microscope) study and GaAs P-I-N photodetector on Si
[DE88-000210] 04 p0498 N88-13066
High energy molecules of high symmetry
[AD-A185385] 05 p0647 N88-13965
Solitons in stimulated Raman scattering: Generation and control of ultrashort optical pulses
[AD-A185141] 05 p0650 N88-13983
Observing effect of laser radiation of low-frequency Raman scattering of light 06 p0772 N88-14742
Raman spectra of adsorbed layers on space shuttle and AOTV thermal protection system surface 06 p0799 N88-14890
Chapter 2: Threshold for Raman conversion of FEL laser pulses in the atmosphere
[DE88-002470] 07 p0859 N88-15215
Cross section of resonant Raman scattering of light by polyenes 07 p0920 N88-15591
Raman spectroscopic investigations of Hg-Cd-Te melts 07 p0926 N88-15625
Stimulated Raman scattering of picosecond light pulses in long dispersive medium 08 p1078 N88-16498
The suppression of stimulated hyper-Raman emission in Na due to parametric four-wave mixing
[DE88-003290] 09 p1172 N88-17030
Concept, construction, and experimental testing of a polychromator for a Raman lidar for the simultaneous telemetering of carbon dioxide and water vapor, relative to oxygen
[GKSS-87/E/20] 09 p1191 N88-17134
Application of state-multipole Heisenberg equations to Raman excitation dynamics
[DE88-003828] 10 p1335 N88-17977
Investigations of stimulated Raman scattering from high density underdense plasmas irradiated by a 0.35 micron laser 10 p1411 N88-18421
Vibrational, mechanical and thermal properties of 3-5 semiconductors
[AD-A187569] 11 p1556 N88-19316
Raman enhancement methods for molecular structure characterization of optical thin films
[DE88-003421] 11 p1558 N88-19324
Laser raman studies related to liquid propellants: Structural characteristics inferred from the nitrate anion spectra
[AD-A188462] 12 p1612 N88-19641
Raman scattering in mixed crystal semiconductors 12 p1686 N88-20149
Phase preservation cleanup in a double-pass Raman amplifier SBS (Stimulated Brillouin Scattering) conjugator
[AD-A189428] 13 p1761 N88-20536
Observation of anomalous low J-value Stokes and anti-Stokes lines in stimulated rotational Raman scattering over long air paths
[DE88-003756] 14 p1911 N88-21418
Three-wave parametric resonance in plasma of relativistic electron flux 14 p1972 N88-21772
Theoretical studies of Resonance Enhanced Stimulated Raman Scattering (RESRS) of frequency-doubled Alexandrite laser wavelength in cesium vapor
[NASA-CR-182870] 15 p2036 N88-22133
The development of high power KrF laser systems for plasma research by the application of stimulated Raman scattering
[ETN-88-92220] 15 p2073 N88-22358
Amplification of signals in fiber optics using the stimulated Raman effect
[AD-A190281] 15 p2133 N88-22727
Surface enhanced Raman scattering applied to surface chemical kinetics
[AD-A191275] 16 p2176 N88-22969
Experimental investigation on stimulated Raman scattering in high-pressure hydrogen by ruby laser 16 p2186 N88-23034
Theoretical studies of Resonance Enhanced Stimulated Raman Scattering (RESRS) of frequency doubled Alexandrite laser wavelength in cesium vapor
[NASA-CR-182871] 17 p2317 N88-23841
Effect of uniaxial stress on the Raman spectra of graphite fibers
[AD-A191730] 18 p2492 N88-24783
Atmospheric propagation of laser beams
[AD-A191447] 18 p2520 N88-24952
Alternative analysis of CO2-laser-produced plasma waves
[DE88-008434] 19 p2730 N88-26215
Raman and absorption spectrophotometric studies of selected lanthanide, californium-doped lanthanide, and actinide trihalides in the solid state
[DE88-008234] 20 p2874 N88-27061
Refractory films from spin-cast carbon
[DE88-011251] 21 p2919 N88-27327
Soliton and polaron dynamics in conducting polymers
[DE88-702539] 23 p3198 N88-29035
Molecular fluorescence measurements with a charge-coupled device detector
[AD-A194437] 23 p3216 N88-29141

RAMAN SPECTROSCOPY
High temperature CO2 study: Anti-Stokes coherent Raman diffusion and infrared spectroscopy
[ESA-TT-1048] 03 p0282 N88-11777
A simplified CARS measurement system for rapid determination of temperature and oxygen concentration
[NASA-TM-100498] 03 p0374 N88-12353
Real-time Raman detection of molecular changes in ceramics undergoing sliding friction
[DE88-000558] 04 p0421 N88-12609
Raman scattering as a diagnostic technique for cathode characterization
[AD-A184434] 04 p0439 N88-12726
Spectroscopic investigations and measurements of certain ARC jet parameters 06 p0796 N88-14877
Raman spectra of adsorbed layers on space shuttle and AOTV thermal protection system surface 06 p0799 N88-14890
Studies of supported metal catalysts
[DE88-002546] 07 p0831 N88-15038
CARS measurements of combustion. 1: Precision of thermometry
[NAL-TR-939] 10 p1299 N88-17769
CARS measurements of combustion. 2: Gas species concentration measurements
[NAL-TR-940] 11 p1453 N88-18863
Some applications of surface Raman and infrared spectroscopies to mechanistic electrochemistry involved adsorbed species
[AD-A188777] 12 p1606 N88-19602
Measurement of detonation temperature of hydrogen-oxygen mixture by CARS (Coherent Anti-Stokes Raman Spectroscopy)
[NASA-TT-20227] 13 p1739 N88-20398
Characterization of redox states of nickel hydroxide film electrodes by in-situ Raman spectroscopy
[AD-A189288] 13 p1741 N88-20411
The use of four-photon Raman spectroscopy for the remote sensing of natural objects
[NASA-TT-20257] 13 p1791 N88-20716
Antistokes coherent Raman diffusion of a nitriding plasma
[ONERA-RF-6/3644-PY] 16 p2175 N88-22962
Requirements for temperature and species concentration measurements in microgravity combustion experiments 17 p2329 N88-23903
Laser Diagnostics for combustion temperature and species measurements 17 p2330 N88-23912
Micro-Raman analysis of dielectric optical thin films
[AD-A191228] 17 p2445 N88-24537
Molecular characterization of structure and bonding in thin film materials
[DE88-006811] 18 p2584 N88-25351
Dual Stokes cars measurements in supersonic combusting flow 19 p2625 N88-25569
Raman, photoluminescence and modulation spectroscopy of semiconductor heterostructures 20 p2861 N88-26997
Mitsubishi Electric Advance (R and D Edition), Volume 41
[PB88-194162] 21 p2929 N88-27388
Polarization selective Raman microspectroscopy 21 p2930 N88-27397
Steady-state approximations in Raman excitation equations
[DE88-011759] 21 p3014 N88-27889
Characterization of crystalline silicon by electrochemical and Raman spectroscopy at the frontier semiconductor/electrolyte
[ETN-88-92354] 21 p3025 N88-27956
Raman spectroscopy on simple molecular systems at very high density
[DE88-010947] 23 p3191 N88-28987

RAMJET ENGINES
NT SUPERSONIC COMBUSTION RAMJET ENGINES

Flame driving of longitudinal instabilities in liquid fueled dump combustors
[AD-A183536] 01 p0006 N88-10033
An experimental investigation of the ignition and flammability limits of various hydrocarbon fuels in a two-dimensional solid fuel ramjet
[AD-A184968] 05 p0549 N88-13342
High-speed inlet research program and supporting analyses 08 p0958 N88-15811
A holographic investigation of particulates in metallized solid fuel ramjet combustion
[AD-A186887] 09 p1140 N88-16831
Military jet fuels, 1944-1987
[AD-A186752] 09 p1150 N88-16890
Application of similarity techniques between reduced and natural scale models of Ramjet engines
[INPE-4269-PRE/1142] 11 p1441 N88-18595
An experimental investigation of rocket ramjet nozzle assembly base pressures
[AD-A189714] 15 p2027 N88-22076
Water flow visualisation of a ramrocket combustion chamber 16 p2202 N88-23138
Aeropropulsive characteristics of isolated combined turbojet/ramjet nozzles at Mach numbers from 0 to 1.20
[NASA-TP-2814] 17 p2299 N88-23757
The 24th JANNAF Combustion Meeting, volume 2
[AD-A190164] 19 p2622 N88-25554
Characteristic time correlations to liquid fuel ramjet combustion efficiency 19 p2624 N88-25566
Low frequency pressure oscillations in a model ramjet combustor 19 p2625 N88-25571
The pressure field generated in a cold-flow side-dump ramjet combustor 19 p2625 N88-25572
Effects of Mach number on acoustic-vortex interactions in a ramjet 19 p2625 N88-25573
Control of combustion instabilities in ramjet motors 19 p2625 N88-25574
Ignition and flammability characteristics of solid fuel ramjets 19 p2626 N88-25575
An efficient computational tool for ramjet combustor research
[DE88-010034] 20 p2760 N88-26369
Combustion of PMMA (polymethylmethacrylate), PE (polyethylene) and PS (polystyrene) in a ramjet
[PB88-186572] 20 p2769 N88-26417
Heterogeneous diffusion flame stabilization
[AD-A193014] 20 p2771 N88-26429
Air intake aerodynamics 24 p3318 N88-29762
Semiempirical methods for airbreathing missiles 24 p3318 N88-29763
Evaluation of the advanced air breathing propulsion concepts, executive summary
[ESA-CR(P)-2540] 24 p3325 N88-29802
Evaluation of advanced air breathing concepts. Volume 1: Executive summary
[ESA-CR(P)-2539] 24 p3326 N88-29806
A new computational capability for ramjet projectiles
[AD-A196061] 24 p3327 N88-29812
Review of research concerning Solid Fuel Ramjet (SOFRAM) at the Research Institute of National Defence (FOA) 2
[FOA-C-20714-2.1] 24 p3327 N88-29813
Ignition and extinguishing of a Solid Fuel Ramjet (SOFRAM)
[FOA-C-20713-2.1] 24 p3337 N88-29865

RAMJET MISSILES
An investigation into the feasibility of using a dual-combustion mode ramjet in a high Mach number tactical missile
[AD-A186906] 09 p1119 N88-16705
Calculation and design of a ramjet missile
[REPT-TR-500] 10 p1311 N88-17832
An experimental investigation of rocket ramjet nozzle assembly base pressures
[AD-A189714] 15 p2027 N88-22076

RANDOM ACCESS
A multi user random access communication system for users with different priorities
[AD-A186041] 07 p0841 N88-15102
On the approximation of the output process of multi-user random access communication networks
[AD-A186197] 07 p0842 N88-15108
An algorithm for random access communication over a noisy channel
[AD-A191315] 16 p2252 N88-23461
An access alternative for mobile satellite networks 19 p2651 N88-25737
Full analysis of a powerful window random access algorithm
[AD-A192437] 21 p2995 N88-27763

RANDOM ACCESS MEMORY
A study of charged particles/radiation damage to VLSI device materials
[NASA-CR-172036] 05 p0577 N88-13518
Comparison of 2D memory SEU transport simulation with experiments
[ATR-86(8139)-2-REV-A] 05 p0656 N88-14025
Fuzzy logic inference processor for real time control: A second generation full custom design
[AD-A188155] 11 p1471 N88-18773
A methodology for hardware verification based on logic simulation
[AD-A188553] 12 p1622 N88-19704
Random access memory testing: Theory and practice. The gains of fault modeling
[EUT-86-E-161] 14 p1955 N88-21649
Self-checking logic arrays
[RR-656-I] 15 p2106 N88-22545
A random access algorithm for environments with capture and limited feedback capabilities
[AD-A192233] 20 p2790 N88-26552
Research on wide area workstations
[AD-A192529] 22 p3136 N88-28643
Random-access algorithms for environments with capture
[AD-A194303] 23 p3203 N88-29060
The effects of total dose on the SEU sensitivity of CMOS static RAMS --- single event upset (SEU), satellite components
[AERE-R-12779] 24 p3428 N88-30401

RANDOM DISTRIBUTIONS
U STATISTICAL DISTRIBUTIONS

RANDOM LOADS
NT GUST LOADS
The effect of fretting corrosion on the fatigue strength of steel and cast iron under sinusoidal and random loading
[LBF-FB-177] 01 p0023 N88-10142
Fatigue under nonnormal random stresses using Monte Carlo method 05 p0607 N88-13723
Random loading fatigue crack growth: Crack closure considerations 06 p0797 N88-14881
Fatigue crack growth due to random loading
[DE88-004641] 10 p1345 N88-18038
Fatigue crack growth due to random loading 18 p2531 N88-25017
Prediction of fatigue life of notched specimens under aircraft loading and importance of the relative method in the case of local strain approach, part 2
[TAE-595-PT-2] 19 p2680 N88-25934

RANDOM NOISE
NT RANDOM SIGNALS
Reception of pseudo noise-modulated signals using digital correlators for satellite navigation tasks
[ETN-87-90426] 01 p0037 N88-10234
Evaluation of a satellite laser ranging technique using pseudonoise code modulated laser diodes
[NASA-CR-182347] 06 p0708 N88-14343
HOC spectral analysis of an almost periodic random sequence in noise
[AD-A185528] 06 p0785 N88-14697
Adaptive detection in non-stationary interference, part 3
[AD-A185622] 07 p0844 N88-15118
Series representations of infinitely divisible random vectors and a generalized shot noise in Banach spaces
[AD-A186429] 07 p0918 N88-15574
Predicting transforms of stable noise and other Gaussian mixtures
[AD-A189280] 12 p1684 N88-20071
Optimal and conventional space-time processing in flow noise
[AD-A189104] 13 p1833 N88-20965
Information and coding capacities of mismatched Gaussian channels
[AD-A190321] 15 p2124 N88-22665
Conditions for information capacity of the discrete-time Gaussian channel to be increased by feedback
[AD-A190317] 15 p2127 N88-22687
Coding capacity of discrete-time Gaussian and nonGaussian channels
[AD-A190318] 15 p2127 N88-22688
Scattering impulse response synthesis using random noise illumination: Initial concept evaluation
[AD-A195086] 24 p3364 N88-30034

RANDOM NUMBERS
RANDOM NUMBER: A syntax-directed package to produce random numbers in user-specified, univariate distributions. User's guide
[DE87-014278] 02 p0228 N88-11436
Components and cycles of a random function
[DE87-014155] 02 p0228 N88-11437
A study of data compactation using numerical methods
[INPE-4317-TDL/284] 13 p1828 N88-20929
A comparison of generators for pseudo-random normal deviates
[DE88-011711] 21 p3010 N88-27859
Random number generation
[USIP-87-15] 22 p3145 N88-28707
A study of the effect of random input motion on low Reynolds number flows
[AD-A195559] 24 p3316 N88-29747

RANDOM PROCESSES
NT RANDOM WALK
Mechanical shock test specification using nonstationary random excitation models
[DE87-013650] 04 p0454 N88-12812
Implementation of a new shock testing procedure using nonstationary random excitation
[DE87-014643] 04 p0456 N88-12827
Propagation of random initial conditions in time 04 p0486 N88-12993
Subcritical branching processes in a two state random environment, and a percolation problem on trees
[PB87-230439] 06 p0762 N88-14677
Von Mises' definition of random sequences reconsidered
[PB87-230512] 06 p0767 N88-14715
Random loading fatigue crack growth: Crack closure considerations 06 p0797 N88-14881
A fast Riemann solver with constant covolume applied to the random choice method
[CAR-87-19] 09 p1231 N88-17375
Nonlinear and diffraction effects in sound beams with random transverse structure 09 p1235 N88-17402
Electronic structure of random alloys and the theory of ordering processes
[DE88-004476] 10 p1407 N88-18394
Random-choice based hybrid methods for one and two dimensional gas dynamics
[CAR-88-01] 14 p1910 N88-21415
Thermal expansion behavior of randomly oriented short carbon fiber reinforced copper composites
[NASA-TT-20175] 15 p2031 N88-22099
Random processes, turbulence and disordering fields
[AD-A190123] 15 p2063 N88-22303
Random Process Simulation for stochastic fatigue analysis
[NASA-TM-100464] 15 p2123 N88-22654
Random processes, turbulence and disordering fields
[AD-A191399] 16 p2209 N88-23181
Periodically correlated processes and their stationary dilations
[NASA-CR-182904] 16 p2263 N88-23530
Computational sciences
[AD-A190826] 18 p2564 N88-25226
Numerical solution of a system of random Volterra integral equations. 1: Successive approximation method 18 p2564 N88-25227
Numerical solutions to stochastic difference equations 18 p2564 N88-25229
Numerical solution to a system of random Volterra integral equations 18 p2565 N88-25230
Approximate solution of random differential equation 18 p2565 N88-25233
A method for the numerical solution of random Cauchy singular integral equation 18 p2565 N88-25234
Numerical solution of random Love's integral equation 18 p2565 N88-25235
On the exceedance random measures for stationary processes
[AD-A192838] 21 p3009 N88-27848
Maximum dynamic responses using matched filter theory and random process theory
[NASA-TM-100653] 22 p3042 N88-28059
Random pseudo-polynomial algorithms and exact problems
[REPT-87-014] 22 p3140 N88-28672

RANDOM SAMPLING
Large antenna experiments aboard the space shuttle: Application of nonuniform sampling techniques 19 p2652 N88-25745

RANDOM SIGNALS
Statistical measures of clipped random signals 08 p1000 N88-16055

RANDOM VARIABLES
On the least squares estimator in moving average models of order one
[AD-A186028] 07 p0909 N88-15508
A new method of estimation in a moving average model of order one
[AD-A186039] 07 p0909 N88-15510
Bounding the expectation of convex functions with limited distribution information
[AD-A186147] 07 p0910 N88-15512
Strong laws of large numbers for arrays of orthogonal random variables
[AD-A186159] 07 p0910 N88-15513
On the asymptotic joint distributions of the eigenvalues of random matrices which arise under components of covariance model
[AD-A186387] 07 p0915 N88-15558
On hypercontractivity of alpha-stable random variables, 0 less than alpha less than 2
[AD-A186425] 07 p0915 N88-15559

An elimination type two-stage procedure for selecting the population with the largest mean from k logistic populations
[AD-A185614] 07 p0916 N88-15566
On selecting the best of k lognormal distributions
[AD-A185628] 07 p0916 N88-15567
Practical applicability of exact and approximate forms of the randomization test for two independent samples
[AD-A186815] 09 p1231 N88-17381
Explicit solutions of moment problems, 1
[AD-A186018] 10 p1397 N88-18325
Some majorization inequalities for functions of exchangeable random variables
[AD-A188207] 11 p1536 N88-19178
Motion in a random gyrotropic environment in D dimensions
[PB87-170650] 12 p1685 N88-20079
Convolution metrics and rates of convergence in the CLT (Central Limit Theorem)
[AD-A189341] 12 p1686 N88-20084
On the expectation of the product of four matrix-valued Gaussian random variables
[EUT-87-E-178] 13 p1828 N88-20927
Effects of state recovery on creep buckling under variable loading 14 p1933 N88-21527
Deterministic approximations of probability inequalities
[REPT-87-43] 14 p1966 N88-21732
Stopping rules and observed significance levels
[AD-A190320] 15 p2124 N88-22664
Effects of randomness of parameters on mean wave propagation in a viscoelastic medium
[REPT-87-60] 16 p2206 N88-23166
Mahler's method in transcendence theory
17 p2393 N88-24227
Additive prophet inequalities for transforms of uniformly bounded pairwise independent random variables
[PB88-173513] 18 p2568 N88-25250
Exact tests for variance component models with unequal cell frequencies in the last stage
[AD-A191645] 18 p2568 N88-25253
Strong law for mixing sequence
[AD-A193615] 23 p3274 N88-29490

RANDOM VIBRATION
The analysis of nonstationary vibration data
05 p0592 N88-13610
Analysis of shock and vibration environments for cargo on C9B transport aircraft 08 p0999 N88-16051
Evaluation of vibration specifications for acoustic environments 08 p0999 N88-16053
Spectral density estimates of coarsely quantized random vibration data 09 p1178 N88-17055
System characterization in nonlinear random vibration
09 p1180 N88-17071
Random vibration (stress screening) of printed wiring assemblies 11 p1499 N88-18953
Nonstationary solution in random vibration theory
[PB88-163746] 14 p1933 N88-21529
The concept of an impact resonance diagram for characterizing the nonlinear response of impact vibration
[DE88-005475] 15 p2086 N88-22432
Random vibration analysis of rattling structures
[DE88-007196] 20 p2813 N88-26691
Diffusion models of crack growth due to random overloads
[DE88-008811] 21 p2962 N88-27595
Analytical and experimental studies of beam waveguide absorbers for structural damping
[AD-A195085] 24 p3382 N88-30144

RANDOM WALK
Dynamic stress at critical locations of a structure as a criterion for mathematical model modification
09 p1180 N88-17066
Mixing properties for random walk in random scenery
[REPT-87-48] 14 p1966 N88-21734
Eigenmodes of a random walk on a 2-D lattice torus with one trap
[DE88-007830] 20 p2844 N88-26874
Range of a constrained random walk
[PB88-126867] 20 p2847 N88-26897

RANGE (EXTREMES)
NT PROPORTIONAL LIMIT
NT RADIO RANGE
Extrema of skewed stable processes
[AD-A185422] 05 p0642 N88-13925
On the characterization of certain point processes
[AD-A186427] 07 p0916 N88-15560
On the extreme order statistics for a stationary sequence
[AD-A186428] 07 p0916 N88-15561
Physics of condensed matter at extreme conditions
[DE88-006232] 13 p1832 N88-20958
Calibration of a hot-wire/hot-film anemometer over a range of temperatures, velocities and pressures
[AD-A189717] 14 p1913 N88-21430
MultiScheme: A parallel processing system based on MIT (Massachusetts Institute of Technology) scheme
[AD-A190383] 15 p2114 N88-22597
Extrema principles of entrophy production and energy dissipation in fluid mechanics
[NASA-TM-100992] 18 p2519 N88-24946

RANGE AND RANGE RATE TRACKING
Range and range rate system
[NASA-CASE-MSC-20867-1] 18 p2521 N88-24958

RANGE CONTROL
U TRAJECTORY CONTROL

RANGE FINDERS
NT LASER RANGE FINDERS
Long range sensor for rendezvous and docking missions 12 p1587 N88-19497
Degradation of downlink distance measurement indexes by the addition of a third tone — tone ranging
[CNES-CT/DRT/TIT/TR-122-T] 15 p2058 N88-22268
Analysis of a range estimator which uses MLS angle measurements
[NASA-CR-182896] 16 p2160 N88-22884

RANGE INDICATORS
U RANGE FINDERS

RANGE MEASUREMENT
U RANGEFINDING

RANGEFINDING
JPRS report: Science and technology. China
[JPRS-CST-87-025] 03 p0300 N88-11888
GPS vertical axis performance enhancement for helicopter precision landing approach
[NASA-CR-177443] 04 p0397 N88-12477
Tau ranging revisited 04 p0437 N88-12710
Range imagery algorithms for the detection of obstacles by autonomous vehicles
[AD-A185421] 05 p0659 N88-14045
The analysis of recent crustal movements in static and kinematic models
[SER-B-279] 09 p1191 N88-17136
The Telecommunications and Data Acquisition Report
[NASA-CR-182545] 11 p1471 N88-18774
Source and event selection for radio-planetary frame-tie measurements using the Phobos Landers
11 p1471 N88-18775
A simplified, general-purpose deep-space ranging correlator design 11 p1473 N88-18786
The effects of atmospheric and thermohaline variability on the validation of the GEOSAT altimeter oceanographic signal between Scotland and Iceland
[AD-A189324] 12 p1650 N88-19882
Range determination of pulsars, taking into account H2 regions
[ETN-88-91492] 14 p1993 N88-21877
Baseline estimation from simultaneous satellite laser tracking
[NASA-CR-182750] 15 p2022 N88-22052
An optical preamplifier for detection of CO2 laser radiation
[AD-A190790] 18 p2520 N88-24949
Range data description based on multiple characteristics 24 p3419 N88-30351

RANGES (FACILITIES)
NT BALLISTIC RANGES
NT TEST RANGES

RANGING
U RANGEFINDING

RANKINE CYCLE
Organic Rankine-cycle power systems working fluids study. Topical report No. 1: Fluorinol 85
[DE87-014604] 02 p0195 N88-11217
Application of Organic Rankine Cycles (ORCs) to decentralized power generation, preliminary study
[DE87-753331] 03 p0347 N88-12197
Design of a condenser-boiler for a binary mercury-organic Rankine cycle solar dynamic space power system
[AD-A184188] 03 p0348 N88-12198
Microwave superheaters for fusion
[DE88-001656] 05 p0653 N88-14007
Supersonic turbines for organic fluid Rankine cycles from 3 to 1300 kW 06 p0713 N88-14375
An experiment to investigate Rankine cycle two-phase microgravity issues
[DE88-004197] 10 p1308 N88-17818
Study on shaft seals for potassium turbine
[EL-891] 15 p2074 N88-22364
Development of an integrated heat pipe-thermal storage system for a solar receiver
[NASA-TM-101099] 15 p2091 N88-22458
Two-phase fluid management for a Rankine cycle isotope power system 17 p2405 N88-24303
An experiment to investigate Rankine cycle two-phase microgravity issues 17 p2409 N88-24322
Design of a high-power-density Ljungstroem turbine using potassium as a working fluid
17 p2409 N88-24323
Nuclear Rankine/flywheel MMW space power concept
17 p2413 N88-24349
Status of the organic Rankine cycle for space applications 17 p2422 N88-24402
Optimization of organic Rankine cycles for space station applications 17 p2423 N88-24407
Dynamic isotope power system critical component verification 17 p2425 N88-24421
SNAP-DYN: Proven technology for wear-term, higher power in space 17 p2425 N88-24422
Energy storage for nuclear burst power systems
17 p2426 N88-24431
Review of alkali metal and refractory alloy compatibility for Rankine cycle applications 17 p2428 N88-24447
Trade study for kWe class space reactors
17 p2430 N88-24454
A high power density radial-in-flow reactor split core design for space power systems
17 p2430 N88-24455
Experimental demonstrations of organic Rankine cycle waste heat rejection systems 17 p2432 N88-24469
Potassium Rankine power system for space power
17 p2433 N88-24476
A combined Rankine/Brayton pulse power cycle
17 p2435 N88-24490
Energy conversion system optimization study for multimegawatt space nuclear power application
17 p2436 N88-24492
C-CAMP: A closed cycle alkali metal power system
[DE88-009715] 19 p2688 N88-25975
Analytical and experimental investigation of ringless piston concept
[AD-A192835] 20 p2810 N88-26673
Reactor applications of the Compact Fusion Advanced Rankine (CFAR) cycle for a D-T tokamak fusion reactor
[DE88-011351] 22 p3153 N88-28762
Study of toluene stability for an Organic Rankine Cycle (ORC) space-based power system
[NASA-CR-180884] 24 p3337 N88-29863
Study of toluene rotary fluid management device and shear flow condenser performance for a space-based organic Rankine power system
[NASA-CR-180885] 24 p3338 N88-29872

RANKING
Contributions to selection and ranking theory with special reference to logistic populations
[AD-A185629] 07 p0917 N88-15568
The r-rank of the groups of exceptional Lie type
[CWI-PM-R8607] 08 p1072 N88-16468
An application of fuzzy set theory to statistical hypothesis testing
[AD-A186705] 09 p1232 N88-17386
Verification of an algorithm for log-time sorting by square comparison
[CWI-CS-R8729] 14 p1956 N88-21656
An assessment of index term ranking
21 p3028 N88-27974

RAOULT LAW
Certain questions of thermodynamic theory of weak solutions 18 p2586 N88-25368

RAPID EYE MOVEMENT STATE
Model based monitoring of human sleep stages
[ISBN-90-9001448-9] 06 p0752 N88-14618

RAPID QUENCHING (METALLURGY)
Investigation of rapidly-solidified dispersion strengthened titanium alloys
[AD-A183882] 01 p0022 N88-10140
Structure of rapidly solidified Ni-Ti
[DE87-012252] 02 p0147 N88-10921
Shock-induced melting and rapid solidification
[DE88-000226] 03 p0288 N88-11810
Effect of rapid solidification on short-range order: A magnetic study
[AD-A185216] 05 p0565 N88-13444
Tensile properties of extrusion consolidated Type 304 SS rapidly solidified powders
[DE87-014875] 05 p0566 N88-13450
Development of iron aluminides
[AD-A185190] 05 p0568 N88-13461
Microstructural modification during laser welding
[DE88-002344] 09 p1144 N88-16860
Remarks on solid state amorphizing transformations
[DE88-006452] 15 p2145 N88-22803
The weldability of consolidated rapidly solidified Type 304 SS powders
[DE88-006738] 16 p2178 N88-22978
Effect of alloying, rapid solidification, and surface kinetics on the high temperature environmental resistance of niobium
[AD-A192093] 18 p2485 N88-24743
Laboratory scale inert gas atomizer for producing rapidly solidified powders
[DE88-006734] 18 p2497 N88-24812
Rapid thermal annealing of silicon layers amorphized by ion implantation
[DE88-702307] 23 p3290 N88-29591

RAPID SOLIDIFICATION
U RAPID QUENCHING (METALLURGY)
U SOLIDIFICATION
RAPID TRANSIT SYSTEMS
Costs and benefits of AC propulsion
[PB88-173380] 16 p2287 N88-23691
Simulation models for the dynamics of tracked vehicle systems: State-of-the-art and open problems
20 p2785 N88-26522
RARE EARTH ALLOYS
Exploratory development in the system Al-Sc-X
[DE88-008242] 19 p2618 N88-25529
RARE EARTH COMPOUNDS
NT CERIUM COMPOUNDS
NT CERIUM OXIDES
NT EUROPIUM COMPOUNDS
NT LANTHANUM TELLURIDES
NT LUTETIUM COMPOUNDS
NT NEODYMIUM COMPOUNDS
Gaining control over rare earth valence fluctuations
[DE87-010116] 01 p0103 N88-10671
Metallurgical processes in multi-component rare earth-transition metal permanent magnet alloys
[AD-A186401] 07 p0832 N88-15045
Superconductivity and phase stability in the heavy rare earth quaternary compounds RBa2Cu3O7 (R = Ho, Er, Tm, Yb, Lu)
[DE88-003478] 10 p1419 N88-18476
Large momentum pairing in one-dimensional systems
[AD-A189228] 13 p1835 N88-20981
Magnetic studies of iron-rare-earth-metalloid alloys
[DE88-006801] 18 p2282 N88-23660
Novel fiber preforms: Rare earth doping
[AD-A191549] 18 p2575 N88-25294
Magnetic phase transitions in 90-K superconductors Ho1Ba2Cu3O(7-delta) and Gd1Ba2Cu3O(7-delta) observed by ZF-muon(+)SR
[DE88-752611] 23 p3290 N88-29588
RARE EARTH ELEMENTS
NT CERIUM
NT DYSPROSIUM
NT ERBIUM
NT EUROPIUM
NT GADOLINIUM
NT HOLMIUM
NT LANTHANUM
NT NEODYMIUM
NT NEODYMIUM ISOTOPES
NT SAMARIUM ISOTOPES
NT YTTERBIUM
NT YTTRIUM
Some electronic factors influencing superconductivity in some rare-Earth-like elements and the beginning of rare-Earth series
[DE87-702582] 01 p0102 N88-10668
Study on substructures of martensite in steels containing rare earth metals
[PB87-143996] 07 p0833 N88-15050
Effect of rare earth elements on the hydrogen-induced cracking in high strength low alloy steel
[PB87-143806] 07 p0833 N88-15052
The synthesis and characterization of some rare earth arsenides
[AD-A186445] 08 p0965 N88-15839
Rare earth elements in heat treatable steels
[PB87-144002] 08 p0966 N88-15858
Energy transfer and non-linear optical properties at near ultraviolet wavelengths: Rare earth 4f yields 5d transitions in crystals and glasses
[DE88-005403] 13 p1840 N88-21012
Thermochemistry and high temperature thermodynamic properties of rare earth-alkaline earth-copper oxide superconductors
[DE88-005976] 15 p2140 N88-22770
Absorption spectra and energy levels of Gd(3+), Nd(3+) and Cr(3+) in the garnet Gd3Sc2Ga3O12
[AD-A193634] 23 p3292 N88-29599
RARE GAS-HALIDE LASERS
NT KRYPTON FLUORIDE LASERS
NT XENON CHLORIDE LASERS
NT XENON FLUORIDE LASERS
Efficiency of ionic noble gas and alkali metal molecules as ultraviolet and far-ultraviolet lasers
09 p1238 N88-17419
RARE GASES
NT ARGON
NT ARGON ISOTOPES
NT HELIUM
NT HELIUM ISOTOPES
NT KRYPTON
NT KRYPTON ISOTOPES
NT LIQUID HELIUM
NT LIQUID HELIUM 2
NT NEON
NT RADON
NT RADON ISOTOPES
NT XENON
Microgravity nucleation and particle coagulation experiments support
[NASA-CR-181541] 04 p0423 N88-12619
Active medium formation in lasers using mixtures of inert gases and optical breakdown pumping
06 p0709 N88-14347
Combustion of a double base fuel in the presence of inert gases
[INPE-4516-RPE/584] 16 p2170 N88-22936
High-order multiphoton ionization of the noble gases
[DE88-007489] 18 p2571 N88-25273
Alternate techniques for noble-gas detection
[DE88-009471] 19 p2613 N88-25507
Method for the isotopically selective detection of inert gases
[DE88-008370] 20 p2769 N88-26421
Rare Gas Halide (RGH) kinetics
[AD-A192352] 20 p2770 N88-26425
The electronic structure of condensed molecular systems
[DE88-007823] 20 p2851 N88-26923
Non-atmospheric noble gases from CO(sub 2) well ga
24 p3441 N88-30476
Noble gases, C,N, and Si isotopes in interstellar SiC form the Murchison carbonaceous chondrite
24 p3442 N88-30483
RAREFACTION
Rarefaction velocities in shocked lead
[DE87-013141] 02 p0146 N88-10917
Low Reynolds number influence on aerodynamic performance of hypersonic lifting vehicles
05 p0531 N88-13230
Experiments on ion-acoustic rarefactive solitons in a multi-component plasma with negative ions
[INPE-4393-PRE/1213] 08 p1086 N88-16542
RAREFACTION WAVES
U ELASTIC WAVES
RAREFIED GAS DYNAMICS
Rarefied gas numerical wind tunnel. 2: Two-dimensional and axially symmetric bodies 05 p0538 N88-13273
Comparisons of Monte-Carlo and PNS (Parabolized Navier-Stokes) calculations for rarefied flow over reentry vehicle configurations
[DE88-004937] 11 p1435 N88-18560
Rarefied gas numerical wind tunnel 3. Universal code for three dimensional bodies 19 p2637 N88-25644
RAREFIED GASES
NT INTERPLANETARY GAS
NT INTERSTELLAR GAS
NT NEUTRAL GASES
Rotational flow of rarefied gas between two coaxial cylinders with slip conditions
[INPE-4277-PRE/1149] 12 p1627 N88-19738
Nozzle lip effects on gas expansion into the plume backflow region
[AD-A192806] 21 p2942 N88-27475
RASERS
U MASERS
RASTER SCANNING
A raster scan algorithm for generating visible parametric surfaces
[DE88-003222] 09 p1220 N88-17321
The US Army Electronic Map Data (EMD) initiative
[AD-A188209] 11 p1565 N88-19372
RATE METERS
U MEASURING INSTRUMENTS
RATES (PER TIME)
NT ACCELERATION (PHYSICS)
NT ACOUSTIC VELOCITY
NT AIRSPEED
NT ANGULAR ACCELERATION
NT ANGULAR VELOCITY
NT ARRHYTHMIA
NT BIT ERROR RATE
NT BURNING RATE
NT COLLISION PARAMETERS
NT COLLISION RATES
NT CRITICAL VELOCITY
NT CURRENT DENSITY
NT DECAY RATES
NT DECELERATION
NT DRIFT RATE
NT ELECTRON ACCELERATION
NT ELECTRON FLUX DENSITY
NT EVAPORATION RATE
NT FLOW VELOCITY
NT FLUX (RATE)
NT FLUX DENSITY
NT GROUP VELOCITY
NT HEART RATE
NT HEAT FLUX
NT HIGH GRAVITY ENVIRONMENTS
NT HIGH SPEED
NT HYPERSONIC SPEED
NT ILLUMINANCE
NT IMPACT ACCELERATION
NT ION PRODUCTION RATES
NT IRRADIANCE
NT LIGHT SPEED
NT LOADING RATE
NT LOW SPEED
NT LUMINANCE
NT LUMINOUS INTENSITY
NT MAGNETIC FLUX
NT MASS FLOW RATE
NT NEUTRON FLUX DENSITY
NT ORBITAL VELOCITY
NT PARTICLE ACCELERATION
NT PARTICLE FLUX DENSITY
NT PHASE VELOCITY
NT PLASMA ACCELERATION
NT PROPAGATION VELOCITY
NT PULSE REPETITION RATE
NT RADIAL VELOCITY
NT RADIANCE
NT RADIANT FLUX DENSITY
NT RECOMBINATION COEFFICIENT
NT RELATIVISTIC VELOCITY
NT RESPIRATORY RATE
NT ROTOR SPEED
NT SOLAR CONSTANT
NT SOLAR FLUX
NT SOLAR FLUX DENSITY
NT SOLAR WIND VELOCITY
NT SOUND INTENSITY
NT SPIN REDUCTION
NT STRAIN ENERGY RELEASE RATE
NT STRAIN RATE
NT SUBSONIC SPEED
NT SUPERSONIC SPEED
NT TACHYCARDIA
NT TERMINAL VELOCITY
NT TIP SPEED
NT TRANSONIC SPEED
NT TRANSVERSE ACCELERATION
NT WIND VELOCITY
Asynchronous rotation in close binary systems with circular orbits 04 p0509 N88-13131
Estimation of rainfall rates in tropical cyclones by passive microwave radiometry 06 p0744 N88-14577
Vapor condensation on a turbulent liquid interface
08 p0982 N88-15939
The effects of data structure on total time on test plots
[AD-A187626] 10 p1389 N88-18296
The convergence rate for the strong law of large numbers: General lattice distributions
[AD-A187560] 10 p1402 N88-18362
Mass loss from evolved stars
11 p1569 N88-19394
Measurement of rate constants of elementary gas reactions of importance to upper atmosphere and combustion systems
[AD-A189432] 13 p1737 N88-20386
Increasing the rate at which ceramic castings undergo preliminary heat-treatment in an ultra-high frequency magnetic field 14 p1886 N88-21275
Two puzzling aspects of protein crystal growth
18 p2580 N88-25329
Kinetics of thermochemical gas-solid reactions important in the Venus sulfur cycle
[NASA-CR-182963] 19 p2742 N88-26280
The rate of volcanism on Venus
[NASA-CR-183039] 19 p2742 N88-26281
A simulation analysis of errors in the measurement of standard electrochemical rate constants from phase-selective impedance data
[AD-A192739] 20 p2770 N88-26426
Effect of double layer structure on the determination of corrosion rates from polarization measurements
[DE88-010097] 20 p2774 N88-26448
Rain attenuation at 35 GHz over an 18 km path
[AD-A194504] 22 p3069 N88-28217
Systolic array fault tolerance performance analysis
[AD-A193521] 23 p3244 N88-29306
Validate algorithms for the determination of rainfall rates from SSM/I microwave satellite imagery
[AD-A195428] 24 p3404 N88-30270
RATINGS
Cetane scale evaluation and possible modification
[AD-A189730] 15 p2048 N88-22200
RATIONS
NT SPACE RATIONS
RATIOS
NT ASPECT RATIO
NT COMPRESSION RATIO
NT DIMENSIONLESS NUMBERS
NT FINENESS RATIO
NT FROUDE NUMBER

NT HIGH ASPECT RATIO
NT HIGH REYNOLDS NUMBER
NT INDEXES (RATIOS)
NT LEAF AREA INDEX
NT LIFT DRAG RATIO
NT LOW ASPECT RATIO
NT LOW REYNOLDS NUMBER
NT MACH NUMBER
NT MASS RATIOS
NT NUSSELT NUMBER
NT PAYLOAD MASS RATIO
NT PECLET NUMBER
NT POISSON RATIO
NT PRANDTL NUMBER
NT PRESSURE RATIO
NT PROPELLANT MASS RATIO
NT RAYLEIGH NUMBER
NT REYNOLDS NUMBER
NT RICHARDSON NUMBER
NT SCALE (RATIO)
NT SIGNAL TO NOISE RATIOS
NT THICKNESS RATIO
NT VOID RATIO

Microgravity nucleation and particle coagulation experiments support
[NASA-CR-181541] 04 p0423 N88-12619

Carbon abundances and C12/C13 ratios in M giants
04 p0515 N88-13167

Hydrogen and deuterium in the local interstellar medium 04 p0521 N88-13204

Determination of the fiber ratio in carbon fiber/resin composites by means of image analysis
[SNIAS-872-422-101] 05 p0558 N88-13398

On the role of the ionization frequency to gyrofrequency ratio in the critical ionization velocity interaction
[TRITA-EPP-86-10] 10 p1410 N88-18414

Isotopic composition of Halley dust
14 p2002 N88-21933

High-fidelity in isotope ratio measurements for resonance ionization mass spectrometry
[DE88-009129] 19 p2613 N88-25506

The ratio of microwaves to X-rays in solar flares: The case for the thick target model
[NASA-CR-183102] 19 p2743 N88-26287

On the estimation of a variance ratio
[AD-A193190] 21 p3009 N88-27854

RATS

The toxicology and metabolism of nickel compounds
[DE87-014801] 04 p0474 N88-12921

Combined effect of microwaves and ionizing radiation
07 p0893 N88-15413

Experiments with rats flown aboard Cosmos-1667 biosatellite (main objectives, conditions and results)
07 p0893 N88-15414

Brain morphogenesis in rats developing in weightlessness 07 p0894 N88-15415

Morphometric analysis of rat aorta endothelium during long-term hypokinesia 07 p0894 N88-15417

Nucleic acid content of skeletal muscles during hypokinesia and in the recovery period
07 p0894 N88-15418

Acid-base equilibrium and some rat blood parameters following exposure to hyperbaric oxygenation
07 p0894 N88-15420

Changes in functional parameters of animals during long-term inhalation of acetic acid
07 p0895 N88-15423

Effect of steroid hormones on biogenic amine levels in lungs during development of pulmonary hypertension in rats submitted to chronic hypobaric hypoxia
07 p0896 N88-15430

Histomorphometric analysis of rat bones after spaceflight aboard Cosmos-1667 biosatellite
10 p1360 N88-18128

Effect of weightlessness on replicative function of rat hepatocyte DNA 10 p1360 N88-18129

RNA-synthesizing activity in rat liver following flight aboard Cosmos-1667 10 p1360 N88-18130

Short- and long-term effects of nonlethal levels of fast high-energy helium ions on retention of developed and formation of new behavioral patterns in rats
10 p1362 N88-18140

Myosin Ca sup (2+), Mg sup (2+)-adenosine triphosphatase activity in ray myocardium following 30-day expose to 1.1 and 2.0 G 10 p1362 N88-18141

Kinetic toxic aspect of potential use of sulfur hexafluoride in closed environments 10 p1362 N88-18142

Comparative evaluation of stress repsonse of rats to different methods of simulating some effects of weightlessness 10 p1363 N88-18144

Experimental measurements of the uptake of ozone in rats and human subjects
[PB88-125422] 10 p1364 N88-18149

Investigation of genetic structures of rat germ cells following flight aboard Cosmos-1514 biosatellite during their prenatal development 10 p1364 N88-18155

Morphological and functional state of the hypothalamo-hypophyseal neurosecretory system of rats flown aboard Cosmos-1667 10 p1365 N88-18156

Investigation of rat skeletal muscles following short-term spaceflight aboard Cosmos-1667 biosatellite
10 p1365 N88-18157

Morphological study of early changes in rat bones in simulated weightlessness 10 p1365 N88-18158

Lipid peroxidation in rat tissues with exposure to antiorthostatic hypokinesia, exercise and immobilization stress 10 p1365 N88-18159

Effect of cardioactive compounds on rat myocardium actomyosin following exposure to accelerations
10 p1365 N88-18161

Effect of external electrostatic field on catecholamine secretion by rat adrenals 10 p1366 N88-18166

New book on metabolic aspects of spaceflight stress
10 p1367 N88-18172

Scaling physiological pharmacokinetic models by physiological time
[DE88-000335] 10 p1368 N88-18173

Response of coronary blood flow to step changes in plasma protein concentration in the isolated rat heart
12 p1651 N88-19892

Life sciences research in space: The requirement for animal models 12 p1654 N88-19909

Does 7-day hindquarters unloading simulate 7 days of weightlessness exposure in rat trabecular bone?
12 p1657 N88-19928

The influence of space flight on water-salt homeostasis in man and animals 12 p1659 N88-19943

Cryopreservation of isolated rat hepathocytes for future use in Spacelab experiments: Preliminary results
12 p1660 N88-19950

Behavior, physiology and energy deposition in rats chronically exposed to 2450 MHz radiation
[PB88-171418] 16 p2237 N88-23363

Behavioral response of rats exposed to high-power microwave radiation
[AD-A192199] 18 p2548 N88-25128

Dexamethasone regulates glutamine synthetase expression in rat skeletal muscles
[NASA-CR-182935] 18 p2549 N88-25129

RAWINSONDES

The use of TOMS-modified VAS data for large-scale NWP 05 p0618 N88-13791

Minimum Energy Routing through Interactive Techniques (MERIT) modeling
[NASA-CR-182535] 10 p1356 N88-18105

RAY ACOUSTICS

U GEOMETRICAL ACOUSTICS

RAY OPTICS

U GEOMETRICAL OPTICS

RAY TRACING

Present status of the high resolution spectrometers
[CEBAF-PR-87-029] 02 p0234 N88-11478

A FORTRAN code for the calculation of probe volume geometry changes in a laser anemometry system caused by window refraction
[NASA-TM-100210] 03 p0364 N88-12288

Coupled acoustic and ocean thermodynamic model
[AD-A184357] 04 p0472 N88-12911

A prototype ray tracer
[AD-A184863] 05 p0634 N88-13874

TRACKER: A 3-D radio ray tracing code
[DE88-003267] 07 p0847 N88-15137

A raytrace method for a laterally heterogeneous environment
[AD-A186525] 08 p0978 N88-15912

A ray-tracing study of electron cyclotron resonance heating in tokamak plasmas with a superthermal electron tail
[INPE-4381-PRE/1201] 08 p1085 N88-16536

Absorption of electron cyclotron waves by superthermal electron velocity distributions in tokamak plasmas
[INPE-4385-PRE/1205] 08 p1086 N88-16539

The effect of asymmetric current-supporting electron velocity distributions on second harmonic electron cyclotron resonance heating: A ray-tracing treatment for the compass tokamak
[INPE-4389-PRE/1209] 08 p1087 N88-16549

Seventy-meter antenna performance predictions: GTD analysis compared with traditional ray-tracing methods
11 p1474 N88-18793

Ray tracing optical analysis of offset solar collector for space station solar dynamic system
[NASA-TM-100853] 15 p2027 N88-22080

Simulation and analysis of wave propagation through random media 21 p2947 N88-27503

A probabilistic model of the apparent radiance of a rough sea
[AD-A193867] 22 p3129 N88-28602

Ionosonde studies of field-aligned irregularities during high-power HF heating at Arecibo
[AD-A195848] 24 p3401 N88-30256

RAYLEIGH DISTRIBUTION

Rayleigh-Taylor instability in compressible fluids
[DE88-002473] 07 p0852 N88-15179

Analytical and numerical analysis of finite amplitude Rayleigh-Taylor instability
[DE88-004056] 11 p1474 N88-18797

Rayleigh-Taylor instability in inertial confinement fusion
[DE88-701411] 15 p2137 N88-22750

Resonant structures for integrated sensors
19 p2673 N88-25893

A multiple-scales partial solution of the pulse-forced Rayleigh-Plesset equation of cavitation bubble dynamics
[AD-A193733] 23 p3212 N88-29118

RAYLEIGH EQUATIONS

The Rayleigh-Taylor instability in ablatively accelerated targets with 1, 1/2 and 1/4 micrometers laser light
[AD-A185945] 07 p0858 N88-15208

Reynold stress closure in jet flows using wave models
[NASA-CR-182662] 12 p1628 N88-19741

RAYLEIGH NUMBER

The numerical and analytical study of bifurcation and multicellular flow instability due to natural convection between narrow horizontal isothermal cylindrical annuli at high Rayleigh numbers
[AD-A186113] 07 p0849 N88-15151

Experimental study of local natural convection heat transfer in inclined and rotating enclosures
09 p1165 N88-16986

Periodic natural convection in a rectangular enclosure of low aspect ratio 10 p1329 N88-17941

High Rayleigh number convection in rectangular enclosures with differentially heated vertical walls and aspect ratios between zero and unity
[NASA-TM-100277] 12 p1628 N88-19739

RAYLEIGH SCATTERING

Optical characterization of silica aerogel glass
[DE87-014617] 02 p0153 N88-10956

Rayleigh scattering measurements of a freejet with homogeneous condensation 03 p0319 N88-12020

All-optical beam control by forced Rayleigh scattering
[AD-A184315] 04 p0490 N88-13018

Chemical reactions in turbulent mixing flows
[AD-A186141] 07 p0849 N88-15153

Mixing in variable density, isothermal turbulent flows and implications for chemically reacting turbulent flows
[PB88-110044] 07 p0852 N88-15176

Rayleigh lidar observations of gravity wave activity in the stratosphere and lower mesosphere
[NASA-CR-182384] 09 p1189 N88-17123

Thermodynamic theory of fluctuations and Rayleigh light scattering in solutions 13 p1785 N88-20681

Laser Diagnostics for combustion temperature and species measurements 17 p2330 N88-23912

Application of Rayleigh scattering to turbulent flow with heat transfer and combustion
[AD-A191565] 18 p2481 N88-24720

Instrumentation for turbulent reacting flows
[AD-A191671] 18 p2515 N88-24923

Developing diagnostic methods for plasma-particle interaction
[DE88-007726] 20 p2858 N88-26973

Investigations on Mie and Rayleigh scattering as basis for the development of Rayleigh temperature lidars with aid of Michelson interferometry
[GKSS-87/E/62] 21 p2976 N88-27675

RAYLEIGH WAVES

A numerical and analytical investigation of Rayleigh-Taylor instability in a solid tungsten plate
[DE87-013593] 01 p0087 N88-10562

Numerical model of Rayleigh instability and spin-off eddies on fronts 13 p1788 N88-20696

Electron-Rayleigh wave interaction in thin film carbons
[AD-A191727] 18 p2492 N88-24781

A comparison of analytical techniques for modeling the Rayleigh-Taylor response of elastic-plastic solids
[DE88-010372] 21 p2962 N88-27596

Finite-difference simulations of Rayleigh-wave scattering by shallow heterogeneity
[AD-A194961] 24 p3402 N88-30259

RAYLEIGH-BENARD CONVECTION

Rayleigh-Benard convection in a Hele-Shaw cell: A numerical study
[KFK-4212] 01 p0044 N88-10280

Special Course on Modern Theoretical and Experimental Approaches to Turbulent Flow Structure and its Modelling
[AGARD-R-755] 03 p0312 N88-11970

Dynamics and routes to chaos from quasiperiodicity
03 p0312 N88-11974

A deterministic approach to turbulence: Chaos in Rayleigh-Benard convection 03 p0313 N88-11975

Determination of fractal dimension, connection of space and temporal chaos and application to experimental results 03 p0313 N88-11977

A dissipation principle and its consequences for structured shock waves in thermoelastic materials
[DE87-013723] 04 p0454 N88-12813
Investigation of surface tension driven convection as a feasibility study for a micro-gravity experiment
[NASA-CR-182504] 11 p1466 N88-18739
RAYLEIGH-RITZ METHOD
Postbuckling of laminated anisotropic panels
[NASA-TM-100509] 08 p0994 N88-16011
RB-57 AIRCRAFT
U B-57 AIRCRAFT
RC CIRCUITS
Realization of active high pass filters for group velocity correction
[MPE-IN-REPT-47] 08 p0979 N88-15918
RC NETWORKS
U RC CIRCUITS
RDX
The effect of RDX particle size on the shock sensitivity of cast PBX formulations. 2: Bimodal compositions
[DE87-009581] 01 p0031 N88-10198
High pressure strand burn rate tests of polyvinylnitrate/nitramine propellants
[AD-A184178] 04 p0422 N88-12615
High explosive moulding powders from RDX and aqueous polyurethane dispersions
[AD-A185026] 05 p0568 N88-13458
Mechanism of and particle size effects on shock sensitivity of heterogeneous pressed explosives: Preliminary assessment of binderless RDX in fuze trains
[MRL-R-1077] 09 p1150 N88-16892
Laser ignition of nitramine composite propellants and crack propagation and branching in burning solid propellants
[AD-A189260] 13 p1753 N88-20483
Laser-RDX aerosol pyrolysis with matrix isolation of unstable intermediates 19 p2632 N88-25614
Theoretical studies of the chemical reactions involved in the ignition of nitramines 19 p2632 N88-25615
Discovery of a low temperature form of TAGN (Triaminoguanidinium Nitrate)
[AD-A196059] 24 p3357 N88-29989
REACTION BONDING
Development of a statistically proven injection molding method for reaction bonded silicon nitride, sintering reaction bonded silicon nitride, and sintered silicon nitride
[ETN-87-90575] 02 p0160 N88-11002
Investigation on diffusion reaction brazing of aluminium
[PB87-143368] 08 p0992 N88-16001
Development, high temperature properties, and microanalysis of nonoxide ceramics
[ETN-88-92103] 14 p1893 N88-21304
Carboxylate formation at the interface between a polyimide coating and cobalt 17 p2320 N88-23859
REACTION JET BACKPACKS
U SELF MANEUVERING UNITS
REACTION JETS
U JET FLOW
U JET THRUST
REACTION KINETICS
Hot-spot reaction in unsustained shocks
[DE87-011781] 01 p0044 N88-10277
Research on one-dimensional two-phase flow. Theory on hydrodynamic balance in two fluid model and its application
[DE87-702615] 01 p0045 N88-10290
Theoretical approaches to chemical dynamics in highly compressed fluids
[DE87-012242] 01 p0046 N88-10296
Kinetics investigations of atmospheric chemical reactions
[PB87-213351] 01 p0069 N88-10439
Aqueous-phase reactions in clouds
[DE86-005249] 01 p0069 N88-10445
Numerical simulation of a supersonic chemically reacting mixing layer 02 p0143 N88-10900
Photolytic processes for measurement of combustion heats of formation and reaction rates
[DE87-014047] 02 p0144 N88-10905
On the modelling of non-reactive and reactive turbulent combustor flows 02 p0169 N88-11061
Some speculations on the mechanisms of abrasive grinding and polishing
[DE87-014242] 02 p0181 N88-11126
Experimental nuclear physics
[DE87-014586] 02 p0231 N88-11459
Solute segregation to phase interfaces and grain boundaries: Studies by analytical electron microscopy and profile deconvolution
[DE87-012129] 02 p0243 N88-11537
Laser spectroscopy and gas-phase chemistry in CVD
[DE87-013715] 03 p0281 N88-11770
Detailed mechanism of benzene oxidation
[NASA-TM-100202] 03 p0282 N88-11775
Detailed kinetic modeling of autoignition chemistry
[DE87-013226] 03 p0283 N88-11782
The calculation of thermal rate constants for gas-phase and heterogeneous reactions in combustion processes
[AD-A184435] 03 p0284 N88-11788
Kinetics of CO adsorption on nickel using time resolved vibration spectroscopy
[ETN-87-90615] 03 p0289 N88-11814
Perturbation and characterization of nonlinear processes
[DE87-014580] 03 p0369 N88-12322
Computer simulations of fragmentation
[DE87-900985] 03 p0375 N88-12358
Development of the non-equilibrium reactive chemical transport code CHMTRNS
[DE88-000682] 04 p0481 N88-12964
Guest-host interactions in thermotropic and lyotropic liquid crystals
[AD-A184402] 04 p0496 N88-13057
Numerical analysis of axisymmetric flow with H2-O2 reactions 05 p0538 N88-13272
Laser probes of propellant combustion chemistry
[AD-A184854] 05 p0561 N88-13415
Detailed mechanism of toluene oxidation and comparison with benzene
[NASA-TM-100261] 05 p0563 N88-13428
Effect of rapid solidification on stainless steel weld metal microstructures and its implications on the Schaeffler diagram
[DE88-001489] 05 p0566 N88-13451
Reactive sticking coefficients of silane on silicon
[DE88-000601] 05 p0570 N88-13473
Theoretical studies of solar lasers and converters
[NASA-CR-181569] 05 p0587 N88-13577
Fracture kinetics of corrosion fatigue 05 p0605 N88-13708
Numerical methods for reaction-diffusion problems with non-differentiable kinetics
[AD-A185405] 05 p0641 N88-13923
Exploitation of the sol-gel route in processing of ceramics and composites
[AD-A185482] 06 p0686 N88-14204
The kinetics and dynamics of iodine monofluoride formation in gas-phase collisions
[AD-A185715] 06 p0709 N88-14352
Quick measurement of individual stress reaction level: Development of the Emotional Stress Reaction Questionnaire (ESRQ)
[FOA-C-50050-5.3] 06 p0752 N88-14617
Theoretical studies of kinetic mechanisms of negative ion formation in plasmas
[AD-A185735] 06 p0784 N88-14812
European reacting flow research: A final assessment
[AD-A185833] 07 p0828 N88-15022
Carbon monoxide and turbulence-chemistry interactions: Blowoff and extinction of turbulent diffusion flames
[AD-A186276] 07 p0828 N88-15025
SRB combustion dynamics analysis computer program (CDA-1)
[NASA-CR-182404] 07 p0830 N88-15032
The carbon dioxide chaperon efficiency for the reaction H + O2 + M yields HO2 + M from ignition delay times behind reflected shock waves
[NASA-TM-100125] 07 p0830 N88-15036
Lyman-alfa/OH-resonance-absorbtion measurements and simulation calculations for the investigation of the induction behavior of methane/ethane/oxygen mixtures in reflected shock waves
[ETN-88-90806] 07 p0831 N88-15042
Chemical reactions in turbulent mixing flows
[AD-A186141] 07 p0849 N88-15153
Feasibility of a complex compound heat pump
[PB88-113022] 07 p0853 N88-15183
Atomic oxygen effects on metals 07 p0924 N88-15617
Non-phonon mechanisms of superconductivity in high T/sub c/ superconducting oxides and other materials and their manifestation
[DE88-002708] 07 p0939 N88-15709
An analytical study of the hydrogen-air reaction mechanism with application to scramjet combustion
[NASA-TP-2791] 08 p0966 N88-15846
Ionic mechanisms of soot formation in flames
[AD-A186195] 08 p0966 N88-15848
Non-steady group combustion of a cloud of char particles
[DE87-010773] 08 p0966 N88-15849
Nb3Al formation in sputter-deposited Nb/Al multi-layer samples
[DE88-003192] 08 p0970 N88-15868
Tin activated reactive ion plating and its application
[PB87-144036] 08 p0970 N88-15871
Nonequilibrium reacting flows 08 p0985 N88-15959
The effects of fuel composition on ignition delay in homogeneous charge and direct injection compression ignition engines
[DE88-003691] 09 p1143 N88-16849
Long-term-aging embrittlement of cast duplex stainless steels: Mechanism and kinetics
[DE88-002929] 09 p1145 N88-16861
Lithium/polymer electrolyte interfacial instability
[AD-A187164] 09 p1147 N88-16874
Morphology control and reinforcing mechanisms using an elastomer in an epoxy network based on diamine menthane
[ISAL-IDI1-87-09] 09 p1148 N88-16881
DSC (Differential Scanning Calorimeter) stability test for liquid propellants: A preliminary report
[AD-A187115] 09 p1150 N88-16888
Computational fluid dynamics and aerothermodynamics
[NASA-CR-182490] 09 p1166 N88-16989
Insights into the mechanisms of chemical reactions: Reaction paths for chemical reactions
[DE88-003041] 10 p1297 N88-17755
Flame propagation in the approximation of straight-line trajectories of burning products
[DE88-700675] 10 p1297 N88-17756
Diffusion description of flame propagation due to the translational motion of burning reaction products
[DE88-700676] 10 p1297 N88-17757
Low temperature reactivity of chars towards oxygen, appendix E2
[DE88-004088] 10 p1298 N88-17760
Kinetic studies following state-selective laser excitation
[DE88-004094] 10 p1335 N88-17981
Chemical activation of molecules by metals: Experimental studies of electron distributions and bonding
[DE88-004465] 10 p1407 N88-18393
Measurements of astrophysical reaction rates for radioactive samples
[DE88-004309] 10 p1429 N88-18537
Combustion of hydrogen and hydrocarbons in fluorine
[AD-A188018] 11 p1453 N88-18662
Voltammetric investigation of porous silicon for integrated circuit applications
[DE88-004024] 11 p1456 N88-18677
Fundamental studies of corrosion of nonoxide structural ceramics
[PB88-141536] 11 p1461 N88-18709
Crystallization and glass formation in electron and laser beam irradiated Cu-Zr alloys
[DE88-003390] 11 p1464 N88-18729
Picosecond laser studies of excited state processes
[AD-A189606] 12 p1607 N88-19607
Instrumentation for collisional energy transfer studies
[AD-A188495] 12 p1689 N88-20105
Kinetic mechanisms for ionization and afterburning suppression
[AD-A189219] 13 p1737 N88-20383
Measurement of rate constants of elementary gas reactions of importance to upper atmosphere and combustion systems
[AD-A189432] 13 p1737 N88-20386
Kinetics of polymer decomposition
[DE88-005500] 13 p1749 N88-20460
Experimental and theoretical constraints on the origin of mid-ocean ridge geothermal fluids 13 p1804 N88-20784
Analytically modeling the carbothermic reduction of alumina in a thermal plasma
[DE88-005535] 13 p1841 N88-21020
Basic research on natural gas combustion phenomena
[PB88-168380] 14 p1887 N88-21278
Infrared absorption spectroscopy and chemical kinetics of free radicals
[DE88-006536] 15 p2033 N88-22112
Molecular dynamics of materials possessing high energy content
[AD-A190034] 15 p2034 N88-22118
The spectroscopy and reaction kinetics of coordinatively unsaturated metal carbonyls
[AD-A190533] 15 p2035 N88-22124
Molecular reaction and energy transfer rate estimation for chemical-laser analysis
[AD-A190664] 15 p2035 N88-22126
Advanced B and Al combustion kinetics over wide temperature ranges
[AD-A190752] 15 p2036 N88-22128
High temperature oxidation and electrochemical studies related to hot corrosion
[AD-A190699] 15 p2040 N88-22156
Effect of vibrational excitation on rate parameters of atmospheric reactions
[AD-A190464] 15 p2094 N88-22477

Lumped model generation and evaluation: Sensitivity and Lie algebraic techniques with applications to combustion
[AD-A190402] 15 p2127 N88-22689
Surface enhanced Raman scattering applied to surface chemical kinetics
[AD-A191275] 16 p2176 N88-22969
Kinetics of electrons and molecules at plasma-beam discharge in molecular gases
[DE88-701196] 16 p2275 N88-23616
Chemical kinetics and photochemical data for use in stratospheric modeling evaluation Number 8
[NASA-CR-182919] 17 p2351 N88-24012
Experiments on reactions of the electronically excited molecule nitron NH (a sup 1 delta) and carbon CH2 (a bar sup 1 A(1)) in gas phase
[MPIS-3/1987] 17 p2397 N88-24249
Calculation of oxidation rates for iron in CO-CO2
[DE88-007313] 18 p2487 N88-24757
The influence of the chemical nature of resins on their reticulation kinetics and the consequences for their nonelastic mechanical properties
[ETN-88-92539] 18 p2493 N88-24788
The burning of HAN-based (hydroxylammonium nitrate) liquid propellants
[DE88-006863] 18 p2494 N88-24800
Chemical kinetics of nitramine propellant combustion
[AD-A191556] 18 p2495 N88-24802
Laboratory experiments on atmospheric OH reactions
18 p2539 N88-25066
Bimolecular reactions and energy-transfer processes of highly vibrationally excited molecules related to energetic materials
[AD-A189013] 18 p2571 N88-25270
A new approach to generating negative ion beams
[AD-A191119] 18 p2572 N88-25276
Spectroscopy and energy transfer kinetics of the interhalogens
[AD-A192103] 18 p2583 N88-25344
An improved external recycle reactor for determining gas-solid reaction kinetics
[NASA-TM-101160] 19 p2611 N88-25492
Next-generation fire extinguishing agent. Phase 1: Suppression concepts
[AD-A192279] 19 p2614 N88-25514
Kinetic measurements of thermal decomposition of energetic materials at high pressures
[AD-A191612] 19 p2622 N88-25552
Chemical kinetics modeling of HMX combustion
19 p2633 N88-25617
Simulation of axisymmetric flow with H2O2 reactions
19 p2638 N88-25651
Kinetics of thermochemical gas-solid reactions important in the Venus sulfur cycle
[NASA-CR-182963] 19 p2742 N88-26280
Rare Gas Halide (RGH) kinetics
[AD-A192352] 20 p2770 N88-26425
The influence of uncompensated solution resistance on the determination and standard electrochemical rate constants using cyclic voltammetry and some comparisons with AC voltammetry
[AD-A192825] 20 p2770 N88-26427
Oxygen reduction in fuel cell electrolytes
[DE88-008240] 20 p2819 N88-26723
Defect characterization of the redox behavior and stability of conducting oxides
[DE88-010799] 20 p2878 N88-27088
Laser probes of natural gas ignition chemistry
[PB88-212568] 21 p2910 N88-27271
Laser probes and numerical modeling as process diagnostics in chemical vapor deposition
[DE88-011622] 21 p2911 N88-27275
Study of crosslinking and nonelastic mechanical properties of epoxy and PSP networks --- epoxy resins; polystyrylpyridine resins (psp)
[ETN-88-92740] 21 p2921 N88-27337
Shock initiation studies on heterogeneous explosives
[DE88-008681] 21 p2923 N88-27351
Methods of quantifying and enhancing reactive oxygen species production 21 p2924 N88-27357
The kinetics of charge-transfer reactions on passive lithium electrodes
[DE88-009256] 21 p2939 N88-27454
Studies of photochemically and electrochemically driven electron transport in zeolites
[DE88-008644] 22 p3155 N88-28769
Reaction dynamics on semiconductor surfaces
[AD-A194305] 22 p3156 N88-28781
Thermodynamic data bases for multivalent elements: An example for ruthenium
[DE88-004395] 23 p3190 N88-28984
Theoretical investigations of nitrocubane decomposition
[AD-A194556] 23 p3200 N88-29047
N2(A3epsilon u+) by reaction of N2F4+H2 in a supersonic flow
[AD-A194493] 23 p3219 N88-29163
Chemical kinetics of hydrogen and P(sub b) centers
[DE88-010528] 23 p3291 N88-29594
Experiments and modeling of multi-component fuel behavior in combustion
[AD-A195011] 24 p3343 N88-29896
Flamelet modeling of turbulent premixed flames
24 p3350 N88-29942
Cosmochemical trends of volatile elements in the solar system 24 p3451 N88-30542

REACTION PRODUCTS
Development of strength in cements
[PB87-232971] 06 p0684 N88-14189
The influence of phosphorus on the solid state reaction between copper and silicon or germanium
[ETN-88-91361] 06 p0789 N88-14838
Investigation of OH reaction products. Excimer laser photolysis/slab laser fluorescence under tropospheric conditions
[REPT-8] 09 p1191 N88-17137
Solar-assisted hydrogen generation by photoelectrocatalysis
[PB88-160932] 12 p1605 N88-19597
Ultraviolet (180 to 300 nm) action spectra for inactivation and DNA photoproduct formation of Bacillus subtilis spores under ultrahigh vacuum 12 p1657 N88-19931
Proton/antiproton yields W(+/-)boson gamma X as a test of the quark charges
[NIKHEF-H/87-11] 13 p1836 N88-20987
New limits on charged Higgs boson mass with CELLO at Petra (Italy) and status of the neutral Higgs boson search
[NOTA-INTERNA-897] 14 p1980 N88-21817
The synthesis of polyphenylene from a CIS-dihydrocatechol biologically produced monomer
18 p2478 N88-24699
Laser-RDX aerosol pyrolysis with matrix isolation of unstable intermediates 19 p2632 N88-25614
Theoretical studies of the chemical reactions involved in the ignition of nitramines 19 p2632 N88-25615
Reaction products of solid propellants after burning at pressures up to 1000 MPa: Comparison between theoretical and experimental results
[ISL-CO-227/87] 22 p3059 N88-28153

REACTION RATE
U REACTION KINETICS

REACTION TIME
Contributions to fast-reacting and high-precision three-phase positioning systems --- machinery
[ETN-87-90427] 01 p0056 N88-10358
Computer response time measurements of mood, fatigue and symptom scale items: Implications for scale response time uses
[AD-A186093] 07 p0888 N88-15384
A deep-water OBS (Ocean Bottom Seismometer) array with real-time telemetry
[AD-A187404] 10 p1357 N88-18112
A comparison of keyboard designs for cockpit applications
[AD-A187775] 12 p1581 N88-19460
Picosecond laser studies of excited state processes
[AD-A189606] 12 p1607 N88-19607
Training in time interval discrimination using verbal feedback 12 p1665 N88-19985
The effects of hypoxia on P300 and reaction time
[DCIEM-87-RR-12] 21 p2979 N88-27697

REACTION WHEELS
Analysis, design, construction and testing of a reaction wheel model for space applications
[INPE-4358-TDL/299] 08 p0963 N88-15834
Reaction wheel experimental model of artificial satellite attitude control: Construction, simulation, and tests
[INPE-4274-PRE/1146] 11 p1490 N88-18896
Spacecraft redesign to reduce microphonic response of a VCO component 11 p1499 N88-18955
Reaction wheel control through digital technique using reference models
[INPE-4220-PRE/1100] 12 p1599 N88-19570
Nutational stability of a satellite equipped with an active magnetic momentum wheel 20 p2784 N88-26513
SIRTF nod maneuvers
[NASA-TM-101007] 22 p3048 N88-28085

REACTIVITY
The effect of additives on the reactivity of palladium surfaces for the chemisorption and hydrogenation of carbon monoxide: A surface science and catalytic study
[DE87-014685] 02 p0145 N88-10909
Reactivity for DT plasma with beam-induced tail in magnetic confinement system
[DE87-753017] 02 p0240 N88-11517
Conductive polymers via reactive aligomer
[AD-A184270] 04 p0419 N88-12597
Reactions of porphyrins in surfactant assemblies, microemulsions and in solutions
[AD-A184797] 05 p0560 N88-13412
Method for preparing hydride configurations and reactive metal surfaces
[DE88-000845] 06 p0679 N88-14161
The use of alloy 117 as a liquid metal current collector
[AD-A185740] 06 p0698 N88-14281
Organic coatings to improve the storageability and safety of pyrotechnic compositions
[AD-A187158] 09 p1150 N88-16889
Low temperature reactivity of chars towards oxygen, appendix E2
[DE88-004088] 10 p1298 N88-17760
Local stoichiometry and atomic interdiffusion during reactive metal/mercury-cadmium-telluride junction formation
[AD-A187554] 10 p1421 N88-18488
Nonmonotonic evolution and thermodynamic trends at metal/(Hg,Cd)Te interfaces: Yb/Hg0.78Cd0.22Te
[AD-A187591] 10 p1422 N88-18490
Metal contacts to cadmium telluride (CdTe)
[AD-A188306] 12 p1698 N88-20159
Properties of reactively sputtered WNx films Zhao, X. -A.
[AD-A188711] 13 p1835 N88-20976
Molecular collision processes in gases and at surfaces
[AD-A189518] 13 p1836 N88-20982
Molecular dynamics of materials possessing high energy content
[AD-A190034] 15 p2034 N88-22118
The Time-Temperature-Transformation (TTT) diagram as a basis for relating the formation and properties of reactive coatings
[AD-A190872] 16 p2182 N88-23006
Agenda for advancing electrochemical science and technology 17 p2321 N88-23861
Effects of space-dependent cross sections on core physics parameters for compact fast spectrum space power reactors 17 p2399 N88-24263
Application of the reactivity constraint approach to the transient control of spacecraft reactors
17 p2406 N88-24305
A review of diffusion barrier technology for application in SP-100 fuel pins 17 p2410 N88-24328
Surface composition-reactivity relationships in heterogeneous catalysis
[DE88-006679] 18 p2480 N88-24714
Structure/property/reactivity relations among nitramine and other energetic materials
[AD-A190878] 18 p2481 N88-24716
The catalytic reactivity of thin film crystal surfaces
[DE88-006387] 19 p2732 N88-26228
In-situ reactive of X-ray optics by glow discharge
[DE88-009840] 20 p2854 N88-26947
Deformation, fracture and explosive properties of reactive materials
[AD-A193080] 21 p2923 N88-27348
Effect of fuel burnup and cross sections on modular HTGR (High-Temperature Gas-cooled Reactor) reactivity coefficients
[DE88-006656] 22 p3151 N88-28748
Active sites and roles of solid acid base catalysts
[NASA-TT-20333] 24 p3345 N88-29909
Reactive plasticizers in negative E-beam resists
[AD-A195161] 24 p3368 N88-30056

REACTOR CORES
Mechanistic model for void distribution in flashing flow
[DE88-002948] 10 p1326 N88-17928
Gas-cooled reactor power systems for space
[DE88-005220] 11 p1545 N88-19240
Transactions of the Fourth Symposium on Space Nuclear Power Systems
[DE88-006164] 17 p2398 N88-24254
Effects of space-dependent cross sections on core physics parameters for compact fast spectrum space power reactors 17 p2399 N88-24263
Considerations pertinent to the Doppler effect for space reactors 17 p2399 N88-24264
Material tradeoffs to minimize flooding reactivity
17 p2399 N88-24265
Thermal-hydraulic considerations for particle bed reactors 17 p2400 N88-24266
Fully passive space reactor conceptual design
17 p2403 N88-24288
Acoustical gas core reactor with MHD power generation for burst power in a bimodal system
17 p2403 N88-24290
Interaction of the control system with core nuclear design for fast spectrum space power reactors
17 p2405 N88-24304
Advanced thermionic converter technology for inductive output coupling 17 p2407 N88-24311
Cermet fuel thermal conductivity
17 p2410 N88-24329

Transient analysis of heat pipe vapor dynamics
17 p2412 N88-24341
Fabrication of a niobium 1 percent zirconium containment for SP-100 primary lithium system materials mass transfer studies 17 p2417 N88-24373
Reactor core coolability with reduced power levels
17 p2425 N88-24425
Benchmark physics experiments for SP-100
17 p2429 N88-24453
A high power density radial-in-flow reactor split core design for space power systems
17 p2430 N88-24455
Effect of fuel burnup and cross sections on modular HTGR (High-Temperature Gas-cooled Reactor) reactivity coefficients
[DE88-006656] 22 p3151 N88-28748

REACTOR DESIGN

Transient modeling of the thermohydraulic behavior of high temperature heat pipes for space reactor applications 02 p0136 N88-10857
Gas-cooled reactor for space power systems
[DE87-011549] 02 p0233 N88-11471
Technical evaluation of major candidate blanket systems for fusion power reactor
[DE87-752989] 02 p0239 N88-11512
Application of a two fluid theoretical plasma transport model on current Tokamak reactor designs
[DE87-013511] 03 p0377 N88-12373
Modular pump limiter systems for large tokamaks
[DE88-001487] 04 p0494 N88-13045
Effect of plasma rotation in tokamak on stabilizing action of electrically conducting wall 06 p0773 N88-14748
Main physics features driving design concept and physics design constraints. Conceptual design study of FY86 FER
[DE88-750309] 07 p0936 N88-15689
Some process control/design considerations in the development of a microgravity mammalian cell bioreactor 09 p1197 N88-17174
A solar receiver-reactor with specularly reflecting walls for high-temperature thermoelectrochemical and thermochemical processes
[AD-A187612] 10 p1351 N88-18077
Plasma physics design and major specifications of candidate reactors for FER design studies. Conceptual design study of FY86 FER
[DE88-751066] 10 p1411 N88-18416
Development of tokamak reactor system analysis code NEW-TORSAC
[DE88-751067] 10 p1411 N88-18417
Conceptual design study of Fusion Experimental Reactor (FY86 FER): Safety
[DE88-751071] 10 p1411 N88-18418
Design issues for a laboratory high gain fusion facility
[DE88-004406] 10 p1413 N88-18434
The 1988 failure rate screening data for fusion reliability and risk analysis
[DE88-006798] 14 p1984 N88-21837
Incorporating reliability into the design of experimental fusion facilities
[DE88-006767] 16 p2275 N88-23618
Transactions of the Fourth Symposium on Space Nuclear Power Systems
[DE88-006164] 17 p2398 N88-24254
Status of CEA design and simulation studies of a 200 KWe turboelectric space power system
17 p2400 N88-24266
Safety constraints and considerations in the development of nuclear powered propulsion
17 p2401 N88-24276
Fully passive space reactor conceptual design
17 p2403 N88-24288
Space based nuclear-pumped laser/reactor concepts
17 p2403 N88-24289
The role of integral experiments and nuclear cross section evaluations in space nuclear reactor design
17 p2404 N88-24293
Sodium heat engine/AMTEC system experiments
17 p2409 N88-24325
Gas-cooled reactor power systems for space
17 p2413 N88-24350
Development and implementation of a space nuclear safety program 17 p2415 N88-24361
Innovative methodology and developments in US space radioisotope power safety risk assessments
17 p2415 N88-24362
Advanced LMMHD space power generation concept
17 p2415 N88-24364
Expert systems approach to modeling systems with the ATHENA thermal-hydraulics code
17 p2416 N88-24365
SOAR: Space orbiting advanced fusion power reactor
17 p2416 N88-24366
Multimegawatt nuclear power system for lunar base applications 17 p2416 N88-24367
Neutronics conceptual design of a UF6-fueled gasesous laser system 17 p2422 N88-24405
The application of high-rate biaxial testing to the design of containment vessels for radioisotope heat sources
17 p2426 N88-24428
Research and development of electrical insulators for thermionic applications 17 p2429 N88-24449
MMW shielding design and analysis
17 p2430 N88-24457
Ceramic electrical insulator development for thermoelectric SACE power system
17 p2430 N88-24459
Comparison of 20-kWe space nuclear power systems: Impact of reactor temperature and technology upon system design and performances 17 p2433 N88-24475
Small particle bed reactors: Sensitivity to Brayton cycle parameters 17 p2435 N88-24487
SP-100 ground engineering systems test facility control systems 17 p2436 N88-24496
TRICE design, evaluation and feasibility tests
17 p2437 N88-24498
Lightweight power bus for a baseload nuclear reactor in space 17 p2438 N88-24505
The safety designs for the TITAN reversed-field pinch reactor study
[DE88-008169] 19 p2729 N88-26205
Fusion programs in applied plasma physics and development and technology at GA Technologies, Inc.
[DE88-008406] 20 p2856 N88-26964

REACTOR FUELS

U NUCLEAR FUELS

REACTOR MATERIALS

Behavior of graphites under intense heat loads
[DE87-012128] 01 p0026 N88-10179
Comparative tests of high temperature creep-rupture behavior of the austenitic CrNi steel DIN W.NR.1.4970 in argon and steam
[KFK-4261] 01 p0063 N88-10402
Development and testing of a system for the partially automated evaluation of holographic interferograms in the experimental stress analysis of reactor components
[ETN-87-90574] 02 p0175 N88-11095
Highlights of the Chemical Technology Division's research activities
[DE88-000233] 03 p0282 N88-11773
Effect of irradiation on the tensile properties of niobium-base alloys
[DE87-002409] 03 p0285 N88-11790
Low activation ferritic alloys for nuclear fusion reactors
[DE87-010711] 03 p0286 N88-11801
Reduced-activation ferritic steels: A comparison with Cr-Mo steels
[DE88-000332] 03 p0290 N88-11826
Data base on the high heat flux behaviour of metals and carbon materials for plasma facing components: Experiments at the 10 MW neutral beam injection test stand of the IPP Nagoya
[IPPJ-AM-53] 04 p0492 N88-13031
Kinetics and mechanism of thermal aging embrittlement of duplex stainless steels
[DE88-002987] 08 p0969 N88-15866
The dishomogeneity of the degree of sensitization in large recirculation pipes in Boiling Water Reactor (BWR) power plants
[CISE-3955] 09 p1247 N88-17473
Mechanisms of intergranular attack and stress corrosion cracking of alloy 600 by high-temperature caustic solutions containing impurities
[DE87-012820] 10 p1300 N88-17773
Weldability of tritium-charged 304L stainless steel
[DP-1740] 12 p1607 N88-19611
IAEA Specialists' Meeting on Graphite Component Structural Design
[DE88-780006] 13 p1746 N88-20439
Fracture criterion of reactor graphite under multiaxial stresses 13 p1746 N88-20442
High temperature Young's modulus of IG-110 graphite
13 p1746 N88-20443
Effects of high temperature neutron irradiation on the physical, chemical and mechanical properties of fine-grained isotropic graphite 13 p1747 N88-20444
Degradations of thermal shock resistance and the fracture toughness of reactor graphite subjected to neutron irradiation 13 p1747 N88-20445
Application of ISRM testing methods to fracture toughness testing of graphite 13 p1747 N88-20446
Notch sensitivity of graphite materials for VHTR
13 p1747 N88-20447
Nondestructive testings of HTGR graphites
13 p1747 N88-20448
Fracture toughness characterization of SA508 and Sa533B RPB steels
[CISE-3908] 14 p1889 N88-21292
The Nordic J-R curve round robin test program --- reactor steel
[VTT-RR-510] 14 p1923 N88-21459
Experiments on the creep behavior of semifinished X10NiCrAlTi 32 20 (Nicrofer 32 20) tubes under multiaxial loading --- nuclear reactors
[JUEL-2127] 14 p1923 N88-21464
The 1988 failure rate screening data for fusion reliability and risk analysis
[DE88-006798] 14 p1984 N88-21837
Development of a computer code CRACK for elastic and elastoplastic fracture mechanics analysis of 2-D structures by finite element technique
[DE88-701231] 15 p2075 N88-22370
Material tradeoffs to minimize flooding reactivity
17 p2399 N88-24265
Thermal-hydraulic considerations for particle bed reactors 17 p2400 N88-24266
Particle bed reactor scaling relationships
17 p2400 N88-24267
Fabrication of reactor shields at the Y-12 plant
17 p2402 N88-24283
Ammonia cleanup of lithium containing components
17 p2403 N88-24287
The role of integral experiments and nuclear cross section evaluations in space nuclear reactor design
17 p2404 N88-24293
Innovative methodology and developments in US space radioisotope power safety risk assessments
17 p2415 N88-24362
Creep behavior of tungsten/niobium and tungsten/niobium-1 percent zirconium composites
17 p2425 N88-24427
Liquid metal testing at ETEC for the SP-100 program
17 p2428 N88-24446
Irradiation effects on tungsten stabilized martensitic steels
[DE88-007074] 18 p2486 N88-24748
The safety designs for the TITAN reversed-field pinch reactor study
[DE88-008169] 19 p2729 N88-26205
Helium induced degradation in the weldability of an austenitic stainless steel
[DE88-009062] 20 p2773 N88-26443
Creep behavior for Hastelloy-XR
[DE88-753428] 21 p2914 N88-27295

REACTOR PHYSICS

Fusion reactor physics and technology studies
[DE87-013691] 01 p0101 N88-10664
Effects of space-dependent cross sections on core physics parameters for compact fast spectrum space power reactors 17 p2399 N88-24263
Fast critical experiment data for space reactors
17 p2403 N88-24286
The role of integral experiments and nuclear cross section evaluations in space nuclear reactor design
17 p2404 N88-24293
ATHENA heat pipe transient model
17 p2412 N88-24344
Neutronics conceptual design of a UF6-fueled gasesous laser system 17 p2422 N88-24405
Benchmark physics experiments for SP-100
17 p2429 N88-24453

REACTOR SAFETY

Research on one-dimensional two-phase flow. Theory on hydrodynamic balance in two fluid model and its application
[DE87-702615] 01 p0045 N88-10290
Development and testing of a system for the partially automated evaluation of holographic interferograms in the experimental stress analysis of reactor components
[ETN-87-90574] 02 p0175 N88-11095
Gas-cooled reactor for space power systems
[DE87-011549] 02 p0233 N88-11471
A long term radiological risk model for plutonium-fueled and fission reactor space nuclear system
[DE87-010466] 06 p0779 N88-14782
Design issues for a laboratory high gain fusion facility
[DE88-004406] 10 p1413 N88-18434
Uncertainties in hydrogen combustion
[DE88-005354] 13 p1739 N88-20395
Potential off-normal events and associated radiological source terms for the compact ignition tokamak: Fusion Safety Program
[DE88-004112] 13 p1842 N88-21024
The 1988 failure rate screening data for fusion reliability and risk analysis
[DE88-006798] 14 p1984 N88-21837
Transactions of the Fourth Symposium on Space Nuclear Power Systems
[DE88-006164] 17 p2398 N88-24254
Operational concerns involving a shadow-shielded nuclear reactor for space station applications
17 p2398 N88-24257
Considerations pertinent to the Doppler effect for space reactors 17 p2399 N88-24264
Material tradeoffs to minimize flooding reactivity
17 p2399 N88-24265

Safety constraints and considerations in the development of nuclear powered propulsion
17 p2401 N88-24276
Fast critical experiment data for space reactors
17 p2403 N88-24286
The role of integral experiments and nuclear cross section evaluations in space nuclear reactor design
17 p2404 N88-24293
Reactor instrumentation and control design and performance simulation for SP-100
17 p2406 N88-24306
Development and implementation of a space nuclear safety program 17 p2415 N88-24361
Innovative methodology and developments in US space radioisotope power safety risk assessments
17 p2415 N88-24362
Inherently safe space reactors
17 p2415 N88-24363
A novel plant protection strategy for transient reactors
17 p2425 N88-24423
Evaluation of UN fuel pin failure modes and motion of fuel during severe accidents for reactors in space
17 p2425 N88-24424
Reactor core coolability with reduced power levels
17 p2425 N88-24425
The application of high-rate biaxial testing to the design of containment vessels for radioisotope heat sources
17 p2426 N88-24428
The NERVA derivative reactor and a systematic approach to multiple space power requirements
17 p2430 N88-24458
Automatic reactor control system for transient operation 17 p2436 N88-24493
An optimal disturbance rejection control system for multimegawatt space nuclear power systems
17 p2436 N88-24495
SP-100 ground engineering systems test facility control systems 17 p2436 N88-24496
Analysis and developments of failure concepts in fracture mechanics based on research results in the field of component safety topics: J-integral concept; crack resistance curves; dynamic criterion
[V-19/86] 18 p2530 N88-25009
Statistical evaluation of light water reactor piping damping data for use in PRA (Probabilistic Risk Assessment) analyses
[DE88-007708] 19 p2661 N88-25828
Health and environmental consequences of the Chernobyl nuclear power plant accident
[DOE/ER-0332] 19 p2689 N88-25985
The safety designs for the TITAN reversed-field pinch reactor study
[DE88-008169] 19 p2729 N88-26205
Overview of the TITAN-2 reversed-field pinch aqueous fusion power core design
[DE88-008170] 20 p2857 N88-26966
An analysis of heat transfer after loss of primary coolant in the SP-100 reactor system
[AD-A194619] 23 p3281 N88-29539

REACTOR TECHNOLOGY
Some new fatigue tests in high temperature water and liquid sodium environment
[DE87-753019] 02 p0192 N88-11197
Gas-cooled reactor for space power systems
[DE87-011549] 02 p0233 N88-11471
Creep test of Hastelloy X for use as the components of OGL-1 in helium environment
[DE88-750289] 07 p0834 N88-15059
Comparative performance of the conjugate gradient and SOR (Successive Over Relaxation) methods for computational thermal hydraulics
[DE88-002553] 08 p0988 N88-15986
Two-phase reduced gravity experiments for a space reactor design
[DE86-015530] 09 p1247 N88-17475
The TITAN Reversed-Field Pinch Reactor: Design-point determination and parametric studies
[DE88-001824] 09 p1251 N88-17498
IAEA Specialists' Meeting on Graphite Component Structural Design
[DE88-780006] 13 p1746 N88-20439
Government research on ceramics coating technology
16 p2184 N88-23019
Transactions of the Fourth Symposium on Space Nuclear Power Systems
[DE88-006164] 17 p2398 N88-24254
Status of CEA design and simulation studies of a 200 KWe turboelectric space power system
17 p2400 N88-24268
Comparison of 20-kWe space nuclear power systems: Impact of reactor temperature and technology upon system design and performances 17 p2433 N88-24475
Potassium Rankine power system for space power
17 p2433 N88-24476
Small particle bed reactors: Sensitivity to Brayton cycle parameters 17 p2435 N88-24487
Systems analysis of INTOR-like designs
[DE88-004422] 18 p2578 N88-25316
The safety designs for the TITAN reversed-field pinch reactor study
[DE88-008169] 19 p2729 N88-26205
Fusion product spectra
[DE88-010912] 23 p3284 N88-29554

READ-ONLY MEMORY DEVICES
Optical laser technology, specifically CD-ROM (Compact Disc - Read Only Memory) and its application to the storage and retrieval of information
[AD-A184111] 03 p0330 N88-12086
Self-checking logic arrays
[RR-656-I] 15 p2106 N88-22545

READING
Data acquisition and processing for surface plate calibration
[AD-A187264] 11 p1564 N88-19366
Working memory capacity: An individual differences approach
[AD-A192359] 20 p2833 N88-26803
The role of working memory in language comprehension
[AD-A192721] 20 p2833 N88-26805

READJUSTMENT
U ADJUSTING

READOUT
Low noise-low power monolithic multiplexing readout electronics for silicon strip detectors
[MPI-PAE/EXP.EL.178] 02 p0168 N88-11057
Performance of a photon counting microchannel plate intensifier with wedge and strip image readout
[DE88-003831] 10 p1334 N88-17970
Comparison of five readout techniques for an integrated magnetometer 19 p2671 N88-25876

REAGENTS
Proposed quality assurance/quality control plan
[AD-A191490] 18 p2525 N88-24978
Method of dispensing reagent chemicals in space
[NASA-CASE-LAR-13607-1-CU]
23 p3200 N88-29048

REAL GASES
PRMIXn: A computer program for thermophysical properties of real gases and gas mixtures
[GKSS-86/E/59] 01 p0020 N88-10125
Hypersonic laminar boundary layer: Parametric study for the representation of real gas effects
05 p0532 N88-13236
On the numerical simulation of three-dimensional hypersonic flow 05 p0532 N88-13237
Hypersonic blunt body computations including real gas effects
[NASA-TM-100074] 10 p1400 N88-18344
Splitting of inviscid fluxes for real gases
[NASA-TM-100856] 14 p1964 N88-21717
High speed inlet calculations with real gas effects
[NASA-CR-182167] 20 p2752 N88-26336
Low density real gas flows about hypersonic vehicles
[AD-A194251] 22 p3075 N88-28253

REAL NUMBERS
NT INTEGERS
Explicit solutions of moment problems, 1
[AD-A186018] 10 p1397 N88-18325
Flexible valued algebras of four-dimensions
[ETN-88-92382] 21 p3008 N88-27844

REAL TIME OPERATION
Real time analysis of detonation products
[DE87-007453] 01 p0031 N88-10195
Aerosol sensor: Real time determination of aerosol mass size distributors using filtering quartz oscillators
[ETN-87-90397] 01 p0049 N88-10311
File management using balanced trees
[ENST-87D001] 01 p0106 N88-10693
Measurements in the functional mock up test of the NAL QSTOL aircraft control system
[NAL-TR-928] 02 p0126 N88-10793
Real-time expert systems: A status report
02 p0129 N88-10817
Rapid toxicity detection in water quality control utilizing automated multispecies biomonitoring for permanent space stations 02 p0135 N88-10848
Use of a 5 cm Doppler radar to detect and forecast severe thunderstorms in a real time forecast operation
02 p0200 N88-11247
A real-time system for automatic single-Doppler wind field analysis 02 p0200 N88-11249
Evaluation of the Rainsat precipitation analysis system in real-time use 02 p0205 N88-11283
Real-time evaluation and prediction of coastal dispersion near the SW tip of Africa — effluents
02 p0210 N88-11318
Short range forecasting of sea breeze generated thunderstorms at the Kennedy Space Center: A real-time experiment using a primitive equation mesoscale numerical model 02 p0211 N88-11324
Methodology of performance evaluation of real time distributed systems
[ENST-87D003] 02 p0228 N88-11440
The Avionics Flight Evaluation System (AFES) of the DFVLR
[ESA-TT-1037] 03 p0266 N88-11677
On the control of a compliant robot arm
03 p0332 N88-12095
Real time analysis of the results from mechanized ultrasonic testing
[DE87-752511] 03 p0334 N88-12107
Concepts and techniques for support of real time distributed operating systems
[AD-A184491] 03 p0367 N88-12307
An inexpensive real-time interactive three-dimensional flight simulation system
[AD-A184340] 04 p0402 N88-12499
Real-time Raman detection of molecular changes in ceramics undergoing sliding friction
[DE88-000558] 04 p0421 N88-12609
Performability modeling based on real data: A casestudy
[NASA-CR-181563] 05 p0633 N88-13870
Presentation of SIGMA (Interactive Assisted Geometry System). A computer assisted shape design program developed at the Aerospatiale Aircraft Division
[SNIAS-872-111-110] 05 p0635 N88-13884
Conceptual issues in measuring the behavior of a distributed real-time process-control computer system
[DE87-009748] 05 p0638 N88-13898
Conceptual issues in measuring the behavior of a distributed real-time process-control computer system
[DE87-014251] 05 p0638 N88-13899
On real-time systems using local area networks
[AD-A185475] 06 p0694 N88-14256
Atmospheric electricity
[NASA-CR-179239] 06 p0744 N88-14575
Objects architecture: A comprehensive design approach for real-time, distributed, fault-tolerant, reactive operating systems
[AD-A185476] 06 p0755 N88-14631
A Multipurpose Adaptive Controller (MAC) for real time digital regulation
[REPT-87-028] 06 p0762 N88-14673
Dynamics formulations for the real-time simulation of constrained motion 06 p0795 N88-14872
A multiple node software development environment
[DE87-010995] 07 p0905 N88-15484
A distributed architecture for intelligent monitoring and anomaly diagnosis of the Hubble Space Telescope
08 p1057 N88-16379
A multiprocessing architecture for real-time monitoring
08 p1059 N88-16390
A framework for real-time distributed expert systems: On-orbit spacecraft fault diagnosis, monitoring and control 08 p1066 N88-16440
TES: A modular systems approach to expert system development for real time space applications
08 p1066 N88-16441
Performance of a digital real time radiographic imaging system
[MRL-R-1068] 09 p1169 N88-17011
Beyond rules: The next generation of expert systems
09 p1210 N88-17256
A conceptual framework for intelligent real-time information processing 09 p1211 N88-17257
TDAS: The Thermal Expert System (TEXSYS) data acquisition system 09 p1211 N88-17258
Real-time artificial intelligence issues in the development of the adaptive tactical navigator
09 p1211 N88-17260
Communication and control in an integrated manufacturing system 09 p1212 N88-17263
Occam/Ada parallel programming system
[ISAL-IDI1-87-11] 09 p1219 N88-17312
Reduction of time delays in Runge-Kutta integration methods — systems simulation
[MBB/LKE-132/S/PUB/241/A]
09 p1229 N88-17363
Investigation of real-time two-dimensional visualization of fuel spray liquid/vapor distribution via exciplex fluorescence
[AD-A188268] 10 p1307 N88-17816
A smart, mapping, charting and geodesy control generator, phase 1
[AD-A188184] 10 p1347 N88-18055
A deep-water OBS (Ocean Bottom Seismometer) array with real-time telemetry
[AD-A187404] 10 p1357 N88-18112
Real time artificial intelligence architecture
10 p1380 N88-18242
Parallelism at the microlevel: Cooperative microcontrollers with real time considerations
10 p1381 N88-18246
Future directions in computer architecture
10 p1383 N88-18257

Shared workspaces for real-time collaboration in distributed networks: Concepts, techniques, problems
[AD-A188150] 10 p1394 N88-18315
Integrated optical synthetic aperture radar processor
[AD-A188019] 11 p1471 N88-18772
Fuzzy logic inference processor for real time control: A second generation full custom design
[AD-A188155] 11 p1471 N88-18773
A microspectroflucrometer system based on real time digital techniques
[REPT-86-014] 11 p1490 N88-18891
Real-time kinematic and dynamic analysis and adaptive model following control of manipulator arms
11 p1495 N88-18927
VAXELN experimentation: Programming a real-time clock and interrupt handling using VAXELN Ada 1.1
[AD-A188100] 11 p1525 N88-19107
Applicability of Ada (trademark) tasking for avionics executives
[AD-A188827] 12 p1578 N88-19445
The use of hardware-in-the-loop-techniques in the development of a modern air-to-surface missile system
12 p1597 N88-19562
Digital method for correction of the phase error in the discrete generation of periodic signals in real time
[INPE-4327-RPE/552] 12 p1618 N88-19676
An intelligent allocation algorithm for parallel processing
[NASA-CR-182648] 12 p1675 N88-20014
Efficient parallel architecture for highly coupled real-time linear system applications
[NASA-CR-182649] 12 p1675 N88-20015
Computer architecture for efficient algorithmic executions in real-time systems: New technology for avionics systems and advanced space vehicles
[NASA-CR-182650] 12 p1675 N88-20016
A prototype for remotely shared textual workspaces
[AD-A188352] 12 p1679 N88-20040
ARCTIC: Programmer's manual and tutorial
[AD-A188619] 12 p1680 N88-20047
Improved flight test productivity using advanced on line data systems 12 p1703 N88-20193
Development of an interactive real-time graphics system for the display of vehicle space positioning
[NASA-TM-100429] 13 p1730 N88-20344
Western aeronautical test range real-time graphics software package MAGIC
[NASA-TM-100425] 13 p1757 N88-20506
The 1987 Airborne Antarctic Ozone Experiment: The Nimbus-7 TOMS data atlas
[NASA-RP-1201] 13 p1791 N88-20714
Configuration management issues and objectives for a real-time research flight test support facility
[NASA-TM-100437] 13 p1813 N88-20832
Dynamic run-time graphics
[DE87-008997] 13 p1820 N88-20879
Development of a real-time aeroperformance analysis technique for the X-29A advanced technology demonstrator
[NASA-TM-100432] 14 p1866 N88-21151
A microprocessor-based real-time simulator of a turbofan engine
[NASA-TM-100889] 14 p1868 N88-21163
Global meteorological data facility for real-time field experiments support and guidance
[NASA-TM-4023] 14 p1947 N88-21608
Real-time flight test data distribution and display
[NASA-TM-100424] 15 p2022 N88-22050
Real-time stressed channel simulator
[AD-A190223] 15 p2025 N88-22067
A review on holography, its principles and applications
[ISL-CO-242/86] 15 p2069 N88-22338
Support for FY87 midlatitude electron-density calibration campaign
[AD-A190174] 15 p2094 N88-22476
Real-time environmental Arctic monitoring (R-TEAM)
[AD-A189946] 15 p2099 N88-22508
Motion sickness: Quantitative, algorithmic malaise indication in real time
[AD-A189674] 15 p2101 N88-22518
Conflict resolution in cooperative systems
[AD-A190351] 15 p2104 N88-22535
Optical switching and control techniques using nonlinear optical wave mixing
[AD-A190467] 15 p2134 N88-22730
A fault tolerant supervision system
[INPE-4419-TDL/307] 15 p2148 N88-22819
Near-real-time TOMS, telecommunications and meteorological support for the 1987 Airborne Antarctic Ozone Experiment
[NASA-CR-4133] 16 p2233 N88-23338
Parallel artificial intelligence search techniques for real time applications
[AD-A190683] 16 p2255 N88-23473
Real time thermal imaging of high temperature semiconductor melts
17 p2330 N88-23914
A timing evaluator for C programs generated by the model system
[AD-A191204] 17 p2385 N88-24174
Genetic algorithms for adaptive real-time control in space systems 17 p2388 N88-24195
TES: A modular systems approach to expert system development for real-time space applications
17 p2388 N88-24197
Evaluating evaporation with satellite thermal data
[AD-A192042] 18 p2531 N88-25019
Beyond Ada: Generating Ada code from equational specifications
[AD-A191866] 18 p2557 N88-25176
Representation and decision mechanisms in artificial intelligence
[AD-A191083] 18 p2560 N88-25197
Real-time optical multiple object recognition and tracking system and method
[NASA-CASE-NPO-17139-1-CU]
18 p2576 N88-25301
Real-time image difference detection using a polarization rotation spacial light modulator
[NASA-CASE-NPO-17144-1-CU]
18 p2576 N88-25305
An intelligent processing environment for real-time simulation
[NASA-CR-183056] 19 p2715 N88-26119
Automation tools for demonstration of goal directed and self-repairing flight control systems
[NASA-CR-179433] 19 p2715 N88-26121
RAGS (Realtime Acquisition and Graphics System): An off-the-shelf hardware and system software small data acquisition computer
[DE88-008399] 19 p2716 N88-26128
An instrument control and data analysis program for NMR imaging and spectroscopy
[DE88-007377] 19 p2717 N88-26132
A high dynamic range acousto-optic image correlator for real-time pattern recognition
[DE88-007933] 19 p2726 N88-26191
A high fidelity real-time simulation of a small turboshaft engine
[NASA-TM-100991] 20 p2761 N88-26378
Environmental monitoring of a titan 34D 5 1/2 segment solid rocket motor static firing
[AD-A192975] 20 p2766 N88-26400
Laser ranging data analysis
[NASA-CR-183115] 20 p2792 N88-26567
RRSAS (Robotic Radiation Survey and Analysis System) Project: A real time sensor driven robotic system
[DE88-006825] 20 p2808 N88-26661
Colored stochastic Petri nets. Application to real time distributed systems
[ENST-87E017] 20 p2839 N88-26843
Definition of an auxiliary processor dedicated to real-time operating system kernels
[NASA-CR-183070] 20 p2841 N88-26860
An investigation of performance improvement in knowledge-based control systems
21 p2928 N88-27382
TDWR (Terminal Doppler Weather Radar) PRF (Pulse Repetition Frequency) selection criteria
[AD-A193089] 21 p2932 N88-27407
FTMP data acquisition environment
[NASA-TM-100636] 21 p2938 N88-27447
Development of a hybrid simulator for robotic manipulators
[AD-A193119] 21 p2956 N88-27557
Army space systems for terrestrial applications
[AD-A192735] 21 p2965 N88-27613
Implementation of an OPS5 derivative on the Novix RISC processor
[DE88-011392] 21 p2994 N88-27758
Simulation of real time problem solving
[AD-A193436] 21 p2997 N88-27778
Notes on operating system requirements for the next millennium
[DE88-010712] 21 p3002 N88-27805
Satellite attitude determination using a CCD (Charge-Coupled-Device) star camera
[AD-A192662] 22 p3046 N88-28080
Using Petri nets for real-time development environments
[REPT-88-005] 22 p3141 N88-28679
Comparison of 2-D Fourier and spatial techniques for removing noise in real-time X-ray radiography
[AD-A193700] 23 p3187 N88-28962
Real-time measurements of the size fractionation of ambient black carbon aerosols at elevated humidities
[DE88-010870] 23 p3215 N88-29138
Machine vision for real time orbital operations
23 p3253 N88-29367
Intelligent test integration system
23 p3254 N88-29371
Distributed cooperating processes in a mobile robot control system 23 p3256 N88-29386
An expert system for a distributed real-time trainer
23 p3261 N88-29411
Real-time space system control with expert systems
23 p3262 N88-29419
Semantic based man-machine interface for real-time communication 23 p3262 N88-29421
Parallel real-time expert systems
[AD-A193673] 23 p3264 N88-29434
Intelligent fault diagnosis and failure management of flight control actuation systems
[NASA-CR-177481] 24 p3323 N88-29790
MIZEX (marginal ice zone experiment) 1987 SAR (Synthetic Aperture Radar) data summary
[AD-A195560] 24 p3364 N88-30035
Geometric modeling for computer aided design
[NASA-CR-183161] 24 p3413 N88-30320
A static scheduler for the computer aided prototyping system: An implementation guide
[AD-A194340] 24 p3414 N88-30322
Achieving real-time performance in FIESTA
24 p3418 N88-30344
Mission telemetry system monitor: A real-time knowledge-based system 24 p3418 N88-30345
Autonomous image data reduction by analysis and interpretation 24 p3418 N88-30347
Automatic mathematical modeling for real time simulation system 24 p3420 N88-30356
A standard architecture for controlling robots
[AD-A195929] 24 p3423 N88-30371
Applications of synchrotron radiation to materials science: Diffraction imaging (topography) and microradiography
[NASA-CR-183265] 24 p3434 N88-30440

REAL VARIABLES

NT ABEL FUNCTION
NT ASYMPTOTES
NT ASYMPTOTIC SERIES
NT BESSEL FUNCTIONS
NT BIHARMONIC EQUATIONS
NT BINARY INTEGRATION
NT BOREL SETS
NT BURGER EQUATION
NT CALCULUS OF VARIATIONS
NT CAUCHY-RIEMANN EQUATIONS
NT COLLINEARITY
NT COPLANARITY
NT COSINE SERIES
NT CUBIC EQUATIONS
NT DELTA FUNCTION
NT DIFFERENTIAL EQUATIONS
NT EINSTEIN EQUATIONS
NT ELLIPTIC DIFFERENTIAL EQUATIONS
NT EULER-CAUCHY EQUATIONS
NT EXISTENCE THEOREMS
NT EXTREMUM VALUES
NT FOKKER-PLANCK EQUATION
NT FOURIER-BESSEL TRANSFORMATIONS
NT GAUSS EQUATION
NT GREEN'S FUNCTIONS
NT HANKEL FUNCTIONS
NT HELMHOLTZ VORTICITY EQUATION
NT HYPERBOLIC DIFFERENTIAL EQUATIONS
NT HYPERBOLIC FUNCTIONS
NT HYPERPLANES
NT INTEGRAL CALCULUS
NT J INTEGRAL
NT JACOBI MATRIX METHOD
NT KERNEL FUNCTIONS
NT LEBESGUE THEOREM
NT LIAPUNOV FUNCTIONS
NT LIMITS (MATHEMATICS)
NT LINEAR EQUATIONS
NT LIPSCHITZ CONDITION
NT MAXIMA
NT MEASURE AND INTEGRATION
NT MINIMA
NT NEUMANN PROBLEM
NT NONLINEAR EQUATIONS
NT NONLINEAR EVOLUTION EQUATIONS
NT NUMERICAL INTEGRATION
NT PADE APPROXIMATION
NT PARABOLIC DIFFERENTIAL EQUATIONS
NT PARTIAL DIFFERENTIAL EQUATIONS
NT PERIODIC FUNCTIONS
NT POISSON EQUATION
NT POWER SERIES
NT QUADRATIC EQUATIONS
NT RICCATI EQUATION
NT RUNGE-KUTTA METHOD
NT SERIES (MATHEMATICS)
NT STURM-LIOUVILLE THEORY
NT TANGENTS
NT TAYLOR SERIES
NT TRIGONOMETRIC FUNCTIONS
NT VECTOR ANALYSIS
NT VLASOV EQUATIONS

NT VORTICITY
NT VORTICITY EQUATIONS
NT WEIERSTRASS FUNCTIONS
NT WEIGHTING FUNCTIONS
Unique normal forms for lambda calculus with surjective pairing
[PB88-173539] 16 p2260 N88-23508

REARWARD FACING STEPS
U BACKWARD FACING STEPS

REATTACHED FLOW
Calculation of the flow through a single-sided sudden expansion with the Computer Program for Parabolic and Elliptic Flows (COPPEF) computer program
[VTH-LR-523] 09 p1163 N88-16973
Surface flow visualization of separated flows on the forebody of an F-18 aircraft and wind-tunnel model
[NASA-TM-100436] 14 p1863 N88-21127
Wave interactions in a three-dimensional attachment line boundary layer
[NASA-CR-181653] 14 p1910 N88-21414
Method and apparatus for detecting laminar flow separation and reattachment
[NASA-CASE-LAR-13952-1-SB] 18 p2513 N88-24910

REB
U RELATIVISTIC ELECTRON BEAMS

REBREATHING
Validation of a modified one-step rebreathing technique for measuring exercise cardiac output
[AD-A192600] 21 p2986 N88-27729
Validation of a modified one-step rebreathing technique for non-invasive measurement of submaximal cardiac output
[AD-A192852] 21 p2987 N88-27735

RECEIVERS
NT RADAR RECEIVERS
NT RADIO RECEIVERS
NT RADIOTELEPHONES
NT SUPERHETERODYNE RECEIVERS
NT TELEVISION RECEIVERS
NT TRANSMITTER RECEIVERS
Reception of pseudo noise-modulated signals using digital correlators for satellite navigation tasks
[ETN-87-90426] 01 p0037 N88-10234
Direct Absorption Receiver (DAR) systems assessment
[DE87-012277] 02 p0196 N88-11222
Tau ranging revisited 04 p0437 N88-12710
Remote sensing of atmospheric crosswinds by utilizing speckle-turbulence interaction and optical heterodyne detection
[AD-A187580] 10 p1347 N88-18052
A solar receiver-reactor with specularly reflecting walls for high-temperature thermoelectrochemical and thermochemical processes
[AD-A187612] 10 p1351 N88-18077
A deep-water OBS (Ocean Bottom Seismometer) array with real-time telemetry
[AD-A187404] 10 p1357 N88-18112
A simplified, general-purpose deep-space ranging correlator design 11 p1473 N88-18786
Quantum limits of superconducting heterodyne receivers
[AD-A188014] 11 p1478 N88-18817
Signal-filter design and system performance for polarimetric radar
[AD-A189257] 13 p1758 N88-20514
System for detecting objects that represent a threat
[NASA-TT-20244] 13 p1760 N88-20528
Bragg-cell receiver study
[NASA-CR-182684] 13 p1761 N88-20535
Performance of single and multiple system AM stereo decoder receivers
[PB88-168307] 15 p2057 N88-22265
A 30 GHz monolithic receive module technology assessment
[NASA-CR-180825] 16 p2194 N88-23084
Requirements for radiation receivers 16 p2272 N88-23593
Mini-station for VHF reception: Argos system simplified description
[INPE-4551-NTE/279] 19 p2655 N88-25764
Design and calibration of a two-channel low-noise heterodyne receiver for use in a CO2 laser Thomson scattering alpha particle diagnostic
[DE88-007866] 19 p2728 N88-26201
Digital communication transmitter and receiver test procedures
[AD-A191218] 20 p2788 N88-26540
SIS (Superconductor-Insulator-Superconductor) mixer research
[AD-A192908] 20 p2879 N88-27092
Airborne measurement of low frequency atmospheric noise ALFAN 1
[AD-A193056] 21 p2931 N88-27405
Multifilter spectrometer (FEB) for microwave atmospheric sounder
[AD-A192312] 21 p2935 N88-27426
Digital carrier demodulation for the DSN Advanced Receiver 22 p3064 N88-28183
Telemetry SNR improvement using the DSN Advanced Receiver with results for Pioneer 10 22 p3064 N88-28184
Advanced Receiver tracking of Voyager 2 near solar conjunction 22 p3065 N88-28185
Performance analysis of a noncoherently combined large aperture optical heterodyne receiver 22 p3065 N88-28189
Direct bit detection receiver performance analyses for 8-DPSK (Differential Phase Shift Keyed) modulated signals operating with improper carrier phase synchronization
[AD-A193839] 22 p3070 N88-28220
Solar energy absorption efficiency of an ellipsoidal receiver-reactor with specularly reflecting walls
[AD-A193726] 22 p3117 N88-28520
On adaptive cell-averaging CFAR (Constant False-Alarm Rate) radar signal detection
[AD-A196286] 24 p3360 N88-30009
Performance of DS/SSMA communications in impulsive channels. Part 1: Correlation receivers
[AD-A195712] 24 p3362 N88-30021

RECEIVING SYSTEMS
U RECEIVERS

RECEPTACLES (CONTAINERS)
U CONTAINERS

RECEPTION DIVERSITY
Space-diversity effects on line-of-sight propagation paths 12 p1617 N88-19670
A polarization diversity meteorological radar system
[AD-A189291] 13 p1758 N88-20515

RECEPTORS (PHYSIOLOGY)
NT CHEMORECEPTORS
NT GRAVIRECEPTORS
NT OTOLITH ORGANS
NT PHOTORECEPTORS
NT PROPRIOCEPTORS

RECHARGING
The MOLICEL(R) rechargeable lithium system: Multicell battery aspects 02 p0163 N88-11024
A new concept in an electrically rechargeable zinc-air alkaline battery
[DE88-003858] 13 p1762 N88-20539

RECIPROCAL THEOREMS
A periodic small-cluster approach to many-body problems
[DE88-002235] 06 p0763 N88-14683

RECIPROCATING ENGINES
U PISTON ENGINES

RECIPROCATION
Reciprocating sliding wear characteristics of copper-carbon fiber composites
[NASA-TT-20176] 15 p2031 N88-22100

RECIPROCITY THEOREM
Time-domain reciprocity theorems for electromagnetic fields in dispersive media
[PB88-126925] 10 p1319 N88-17886
The calibration of photographic and spectroscopic films: Reciprocity failure and thermal responses of IIaO film at liquid nitrogen temperatures
[NASA-CR-181094] 13 p1773 N88-20606

RECIRCULATION
U CIRCULATION

RECIRCULATIVE FLUID FLOW
Improved numerical methods for turbulent viscous recirculating flows 02 p0185 N88-11148
Aerothermal modeling program, phase 2 02 p0185 N88-11149
Efficient numerical techniques for complex fluid flows 02 p0185 N88-11151
Numerical implementation and performance of Reynolds stress closures in finite volume computations of recirculating and strongly swirling flows 08 p0987 N88-15976
Numerical calculation of turbulent recirculating flows
[TUM-LSM-84/29] 09 p1161 N88-16959
Sea duct: A deep-sea computer-controlled recirculating flume for the study of sea floor stability
[AD-A187734] 11 p1516 N88-19056
Improved numerical methods for turbulent viscous recirculating flows
[NASA-CR-180852] 19 p2599 N88-25445

RECLAMATION
NT GAS RECOVERY
NT MATERIALS RECOVERY
NT SOLVOLYSIS
NT WATER RECLAMATION

RECOGNITION
NT CHARACTER RECOGNITION
NT PATTERN RECOGNITION
NT SPEECH RECOGNITION
NT TARGET RECOGNITION
Recognition of isolated non-speech sounds
[AD-A184600] 03 p0306 N88-11933
Windshear training aid. Volume 1: Overview, pilot guide, training program
[PB88-127196] 10 p1276 N88-17637
Applications of mathematical morphology to range imagery
[AD-A189316] 12 p1684 N88-20072
A probabilistic approach to low-level vision
[AD-A189041] 15 p2107 N88-22553
Models of incremental concept formation
[AD-A191597] 18 p2552 N88-25147
Rules, schema and decision making
[AD-A193389] 21 p3027 N88-27967
Visual motion perception and visual attentive processes
[AD-A193640] 23 p3241 N88-29288
Multilevel computational theory of stereoscopic visual image processing
[AD-A195331] 24 p3408 N88-30288
The combinatorics of object recognition in cluttered environments using constrained search
[AD-A196224] 24 p3422 N88-30364
Symbolic construction of a 2D scale-space image
[AD-A195926] 24 p3423 N88-30374

RECOIL IONS
Inelastic ion-surface collisions
[AFGL-TR-87-0206] 19 p2724 N88-26174

RECOMBINATION COEFFICIENT
Nascent vibrational/rotational distribution produced by hydrogen atom recombination
[AD-A193005] 20 p2852 N88-26933

RECOMBINATION REACTIONS
NT ATOMIC RECOMBINATION
NT ELECTRON-ION RECOMBINATION
NT HYDROGEN RECOMBINATIONS
NT ION RECOMBINATION
NT OXYGEN RECOMBINATION
NT RADIATIVE RECOMBINATION
High-efficiency silicon solar cells: Numerical modeling, transient measurements, efficiency goals, and v-shaped grooves
[DE87-012842] 01 p0066 N88-10423
Failure analysis of a 3.5 inch, 50 ampere-hour nickel-hydrogen cell 02 p0164 N88-11030
OH(A-X) fluorescence from photodissociative excitation of HO2 at 157.5 nm
[NASA-CR-181580] 05 p0563 N88-13429
Helium-ion-induced release of hydrogen from graphite
[DE88-002599] 09 p1142 N88-16846
Calculations of rate constants for the three-body recombination of H2 in the presence of H2
[NASA-CR-182548] 11 p1454 N88-18664
Models of recombination lines in radio H2 regions
[INPE-4302-TDL/277] 12 p1710 N88-20232
Study of activationless reactions of point defects with impurities and impurity-defect complexes in alpha-iron
[DE88-701028] 13 p1745 N88-20433
The astrophysics of nebulae and active galactic nuclear emission-line regions: New methods and applications 13 p1858 N88-21111
Studies of molecular biology
[DE88-005906] 15 p2101 N88-22514
A model for nitrogen atom recombination on a silicon dioxide surface
[AD-A189843] 15 p2142 N88-22784
Theoretical studies of dynamics combustion
[DE88-007565] 19 p2611 N88-25495
Auger recombination in GaSb/AlSb-multi quantum well heterostructures 20 p2862 N88-27001
Control of carrier lifetime in PbTe nipi superlattices by external photoinjection 20 p2863 N88-27006
Influence of the temperature-dependence of recombination life-time of free carriers in amorphous semiconductors on thermostimulated photocurrent spectra
[DE88-702726] 23 p3293 N88-29609
Computed potential energy surfaces for chemical reactions
[NASA-CR-183168] 24 p3342 N88-29893
On formulating a simple D-region model
[AD-A195841] 24 p3392 N88-30197

RECOMMENDATIONS
NT SUGGESTION
Observation guidelines for a Total Ozone Mapping Spectrometer (TOMS) in geosynchronous orbit 05 p0619 N88-13801
Space shuttle accident: NASA's actions to address the Presidential Commission report
[PB88-135306] 15 p2024 N88-22059
Engineering research centers and their evaluation
[PB88-180054] 19 p2739 N88-26262
Flight information publication (FLIP) feedback
[AD-A194482] 23 p3174 N88-28897

RECOMPRESSION
U COMPRESSING

RECONNAISSANCE
NT AERIAL RECONNAISSANCE
NT PHOTORECONNAISSANCE
NT SPECTRAL RECONNAISSANCE
Interim review of the possibilities and opportunities for the ONR tropical cyclone motion research initiative
[AD-A185679] 06 p0746 N88-14592
Cooperative analysis expert situation assessment research 09 p1206 N88-17228
Feasibility report: Operation of light air cushion vehicle at McMurdo Sound, Antarctica
[AD-A189057] 13 p1755 N88-20494
Activities report of the Division of Reconnaissance and Seeker Systems
[FOA-C-30479-3.1/3.2/3.3/3.4] 22 p3116 N88-28513

RECONNAISSANCE AIRCRAFT
NT MIRAGE AIRCRAFT
NT U-2 AIRCRAFT
Aquila remotely piloted vehicle: Its potential battlefield contribution still in doubt
[PB88-120241] 13 p1721 N88-20289
The specification and design of a future maritime reconnaissance aircraft 17 p2303 N88-23772

RECONNAISSANCE SPACECRAFT
Specification for an infrared satellite surveillance system for the detection of aircraft
[AD-A189592] 13 p1797 N88-20746

RECONSTRUCTION
NT WAVE FRONT RECONSTRUCTION
Propulsion estimation techniques 07 p0927 N88-15632
Further developments in exact state reconstruction in deterministic digital control systems
[NASA-TP-2812] 11 p1468 N88-18751
More on exact state reconstruction in deterministic digital control systems
[NASA-TP-2847] 22 p3063 N88-28177

RECORDING
NT DATA RECORDING
NT DATA SMOOTHING
NT MAGNETIC RECORDING
Recording multiple signals on a single waveform recorder
[DE87-011632] 01 p0049 N88-10313
Digital imaging techniques for single- and multi-phase reacting flowfields 10 p1327 N88-17933
Development of fiber optic systems for recording and transmitting holographic information
[AD-A189406] 13 p1773 N88-20603
Computer controlled data acquisition system for the NASA 1986 Rocket Triggered Lightning Program
[DE88-008335] 20 p2826 N88-26786
A 1/2-inch high-definition baseband VCR 21 p2930 N88-27393
Maximum-likelihood multichannel deconvolution of P waves at seismic arrays
[AD-A194990] 24 p3391 N88-30191

RECORDING INSTRUMENTS
NT BATHYTHERMOGRAPHS
NT FLIGHT RECORDERS
NT PLOTTERS
NT PRESSURE RECORDERS
NT SEISMOGRAPHS
Recording materials for optical disk memory discussed 06 p0684 N88-14193

RECORDS
Electronic Records Administration at the Savannah River Plant
[DE87-014842] 03 p0364 N88-12415
Quantifying some information processing aspects of the pilot's instrument crosscheck
[AD-A186114] 07 p0898 N88-15443
An introduction to the historical records of China about Mars 23 p3301 N88-29664

RECOVERABILITY
Communications satellite systems operations with the space station. Volume 3: Supplementary technical report
[NASA-CR-180875] 09 p1133 N88-16794
Navigation recovery block design description
[NASA-CR-182473] 10 p1342 N88-18022

RECOVERABLE LAUNCH VEHICLES
A two stage launch vehicle for use as an advanced space transportation system for logistics support of the space station
[NASA-CR-182572] 11 p1443 N88-18606
Space shuttle phase B wind tunnel model and test information. Volume 3: Launch configuration
[NASA-CR-178416-VOL-3-PT-2] 24 p3315 N88-29744
Space shuttle phase B wind tunnel model and test information. Volume 1: Booster configuration
[NASA-CR-178414-VOL-1-PT-1] 24 p3315 N88-29745
Space shuttle phase B wind tunnel model and test information. Volume 1: Booster configuration
[NASA-CR-178414-VOL-1-PT-2] 24 p3320 N88-29770

RECOVERABLE SPACECRAFT
NT AEROSPACE PLANES
NT CHALLENGER (ORBITER)
NT DISCOVERY (ORBITER)
NT HERMES MANNED SPACEPLANE
NT HOTOL LAUNCH VEHICLE
NT REUSABLE SPACECRAFT
NT SPACE SHUTTLE ORBITERS
NT SPACE SHUTTLES
NT X-30 VEHICLE

RECREATION
Spinoff, 1987
[NASA-TM-89652] 02 p0250 N88-11577

RECRYSTALLIZATION
Elimination of subboundaries in 0.5-micron-thick Si-on-insulation films produced by ZMR
[AD-A184590] 03 p0381 N88-12396
Cyclic deformation of an extruded AlMgSi alloy 05 p0598 N88-13654
Dynamic recrystallization during high temperature low cycle fatigue of nickel
[DE88-003224] 10 p1302 N88-17788
Grain refinement during primary breakdown of alloy 718
[DE88-005193] 13 p1743 N88-20423
Fundamental studies on high temperature deformation recrystallization, and grain growth of two-phase materials
[AD-A189725] 15 p2038 N88-22145
Analysis of grain refinement and superplasticity in aluminum-magnesium alloys
[AD-A193029] 21 p2912 N88-27283
Study of feasibility and optimization conditions of laser treatments: Application of the local recrystallization of aluminum
[ISAL-87-0048] 21 p2916 N88-27309
Rapid thermal annealing of silicon layers amorphized by ion implantation
[DE88-702307] 23 p3290 N88-29591

RECTANGLES
An experimental and numerical investigation of swirling flows in a rectangular nozzle 06 p0700 N88-14295
Thermosolutal convection in high-aspect-ratio enclosures
[NASA-TM-100803] 11 p1486 N88-18871
Minimum weight design of rectangular and tapered helicopter rotor blades with frequency constraints
[NASA-TM-100561] 12 p1582 N88-19455
Fingering flow patterns of thermosolutal convection in rectangular enclosures
[NASA-TM-100854] 14 p1911 N88-21417
ALEX results: A comparison of measurements from a round and a rectangular duct with 3-D code predictions
[DE88-005947] 15 p2135 N88-22741
Nonlinear hydroelastic vibrations in rectangular containers
[LRT-WE-9-FB-7(1987)] 22 p3088 N88-28340

RECTANGULAR COORDINATES
U CARTESIAN COORDINATES

RECTANGULAR DRAINAGE
U DRAINAGE PATTERNS

RECTANGULAR PANELS
Advanced radiator concepts utilizing honeycomb panel heat pipes
[NASA-CR-172017] 04 p0443 N88-12747
Geometrically nonlinear analysis of stiffened panels 06 p0722 N88-14440
A summary of experimental results on square plates and stiffened panels subjected to air-blast loading 09 p1178 N88-17057
Predicted and measured strain responses of isotropic panels to base excitation
[NASA-TM-4054] 19 p2679 N88-25928

RECTANGULAR PLANFORMS
NT RECTANGULAR PANELS
NT RECTANGULAR PLATES
The determination of the topological structure of skin friction lines on a rectangular wing-body combination
[NASA-CR-4168] 20 p2753 N88-26343

RECTANGULAR PLATES
Experiments: Test range facilities, part 2 03 p0305 N88-11921
On free decay damping tests 08 p0997 N88-16041
Free vibration of rectangular plates with a small initial curvature
[NASA-CR-179370] 24 p3383 N88-30148

RECTANGULAR WAVEGUIDES
Two-dimensional electron fluid computer calculations of nanosecond pulse, low pressure microwave air breakdown in a rectangular waveguide and their verification by experimental measurement
[DE88-004407] 12 p1618 N88-19678
Calculations of high-frequency parameters of disc-loaded waveguides
[DE88-702178] 21 p2933 N88-27417

RECTANGULAR WIND TUNNELS
Flow visualization on a small scale
[AD-A194728] 23 p3181 N88-28935

RECTIFICATION
NT GEOMETRIC RECTIFICATION (IMAGERY)

RECTIFIERS
NT AVALANCHE DIODES
NT CRYSTAL RECTIFIERS
NT GERMANIUM DIODES
NT THYRATRONS
NT THYRISTORS
Operation of multistage power supplies for electron beam welding installations 03 p0286 N88-11800
Determination of the commutation and angle and load response for a continuous-current, single phase controlled rectifier
[AD-A190602] 15 p2060 N88-22285

RECUPERATORS
U REGENERATORS

RECURSION FORMULAS
U RECURSIVE FUNCTIONS

RECURSIVE FUNCTIONS
Solution methods for bidiagonal and tridiagonal linear systems for parallel and vector computers
[REPT-87-04] 01 p0085 N88-10552
Irreducible *-representations of the Lie superalgebra osp(1,4) with finite-degenerated vacuum
[DE87-703089] 02 p0225 N88-11420
Design of digital filters for electronic instrumentation
[PB87-100418] 04 p0438 N88-12716
Analysis of a parallel solution method for tridiagonal systems
[PB87-230538] 06 p0762 N88-14678
Recursion operator and bihamiltonian structure for integrable multi-dimensional lattices
[PREPRINT-552] 06 p0764 N88-14688
Round-off error propagation in four generally applicable, recursive, least-squares-estimation schemes
[NASA-TM-100055] 06 p0766 N88-14708
Recursive m-estimators of location and scale for dependent sequences
[AD-A186292] 07 p0903 N88-15469
Recursive forward dynamics for multiple robot arms moving a common task object
[NASA-CR-182526] 10 p1340 N88-18008
Dynamic observers as asymptotic limits of recursive filters: Special cases
[AD-A187578] 10 p1397 N88-18324
Recursive inversion of externally defined linear systems
[NASA-TM-100070] 11 p1541 N88-19215
Predicate-transformer semantics of general recursion
[CS-8709] 13 p1820 N88-20876
On the productivity of recursive list definitions
[CS-8707] 14 p1960 N88-21692
The biHamiltonian formulations of integrable evolution equations in multidimensions
[PREPRINT-568] 14 p1968 N88-21745
Recursion operator and Backlund Transformation for the Ruijsenaars-Toda lattice
[PREPRINT-577] 14 p1968 N88-21750
A recursive prediction error parameter estimator for nonlinear models
[RR-326] 17 p2392 N88-24222
Recursive maximum likelihood identification of a nonlinear output-affine model
[RR-322] 18 p2569 N88-25257
Parallel solutions to geometric problems on the scan model of computation
[AD-A192321] 21 p3004 N88-27819
Recursive mass matrix factorization and inversion: An operator approach to open- and closed-chain multibody dynamics
[NASA-CR-182516] 23 p3247 N88-29328
Adaptive identification by systolic arrays
[AD-A193532] 23 p3266 N88-29444

RECYCLING
Biomass recycle as a means to improve the energy efficiency of CELSS algal culture systems 03 p0358 N88-12254
Preliminary experimental results of gas recycling subsystems except carbon dioxide concentration 03 p0359 N88-12261
An overview of Japanese CELSS research activities 03 p0360 N88-12257
Evaluation of bituminous materials used in pavement recycling projects at Tyndall, MacDill, and Hurlburt Air Force Bases
[AD-A188068] 10 p1317 N88-17871
An improved external recycle reactor for determining gas-solid reaction kinetics
[NASA-TM-101160] 19 p2611 N88-25492

Evidence for crustal recycling during the Archean: The parental magmas of the stillwater complex
24 p3396 N88-30226
Continental crustal formation and recycling: Evidence from oceanic basalts 24 p3398 N88-30238
Solid earth as a recycling systems and the lateral growth of Precambrian North America 24 p3400 N88-30249

RED BLOOD CELLS
U ERYTHROCYTES

RED DWARF STARS
The M-type stars
[NASA-SP-492] 02 p0252 N88-11592
Microwave observations of red dwarf flare stars
04 p0513 N88-13153
An astrometric search for a stellar companion to the sun 04 p0520 N88-13195

RED GIANT STARS
NT CARBON STARS
Basic properties and variability
02 p0252 N88-11593
Thermal atmospheric models
02 p0253 N88-11599
Fifth Cambridge Workshop on Cool Stars, Stellar Systems and the Sun 04 p0502 N88-13092
Exploiting the IR: Solar and stellar spectroscopy in the IR 04 p0504 N88-13102
VLA observations of rapid 6 cm flux variations in alpha Ori 04 p0515 N88-13169
Infrared excesses of barium stars
04 p0516 N88-13174
Membership of Cepheids and red giants in 8 open clusters: NGC 129, 6067, 6649, 6664, IC 4725, Ly 6, Ru 79
[PUBL-SER-C-FASC-13] 07 p0944 N88-15739

RED SHIFT
Ultraviolet observations of cataclysmic variables: The IUE archive
[MPE-PREPRINT-91] 02 p0250 N88-11580
Magnitude-redshift relation in a perturbed Friedmann universe
[DE87-753020] 02 p0252 N88-11590
Number count-redshift relation in universe models with nonzero cosmological constant
[DE87-703043] 03 p0388 N88-12435
Flux tube dynamics and solar/stellar redshift measurements 04 p0503 N88-13095
Finnish-Soviet Symposium on Radio Astronomy (1st) held at Otaniemi on August 26-27, 1985
[PB87-140661] 07 p0944 N88-15736
Coherence effects in optical physics with special reference to spectroscopy
[AD-A189520] 13 p1840 N88-21007
Galaxy evolution in dense clusters
13 p1855 N88-21101
Multiple object redshift determinations in clusters of galaxies using OCTOPUS
[INPE-4528-PRE/1278] 15 p2150 N88-22835
New measurements of radial velocities in clusters of galaxies
[INPE-4527-PRE/1277] 15 p2152 N88-22845
Is the 3C273 quasar Mach nearer
[DE88-702235] 21 p3030 N88-27988
Gravitational redshift of self-gravitating systems of dark matter in the universe
[DE88-702688] 23 p3300 N88-29650
A deep redshift survey of field galaxies. Comments on the reality of the Butcher-Oemler effect
[NASA-CR-183255] 24 p3454 N88-30558

REDOX CELLS
Zinc-redox battery: A technology update
[DE87-010737] 01 p0040 N88-10256

REDUCED GRAVITY
Preliminary study of a containerless processing facility for Columbus, executive summary
[ESA-ITT/AO/1-1834/85F] 01 p0032 N88-10203
Preliminary study of a biotechnology research facility for microgravity, executive summary
[MATRA-EPT/AS/VT209/246/NT]
01 p0032 N88-10204
Preliminary study of a gravitational biology facility for Columbus, executive summary
[MATRA-EPT/AS/VT209/255/NT]
01 p0032 N88-10205
Calculation of the eigenvibrations of axisymmetric fluid configurations with a singularity method, taking into account surface tension effects under reduced gravity
[ETN-87-90438] 01 p0048 N88-10304
Aquarack: Aims and Possible Research Projects
[DFVLR-MITT-87-01] 01 p0073 N88-10469
Investigations of the survey of the reproductive biology of Xiphophorus in an Aquarack
01 p0074 N88-10471
Xiphophorus as an experimental system for genetic and biological development studies under microgravity conditions 01 p0074 N88-10472
Research and development at the Marshall Space Flight Center Neutral Buoyancy Simulator
02 p0139 N88-10878
A preliminary study of a fluid science laboratory for space station (Columbus). Part 4: Executive summary
[NLR-TR-87023-L-PT-4] 02 p0170 N88-11072
Consortium for Materials Development in Space. Technical section
[NASA-CR-181508] 03 p0296 N88-11859
Physical vapor transport crystal growth
03 p0296 N88-11860
Highly Non-Linear Optical (NLO) organic crystals
03 p0297 N88-11865
Physical properties of immiscible polymers
03 p0297 N88-11868
High temperature superconductors
03 p0297 N88-11869
Cast iron freezing mechanisms
03 p0298 N88-11870
Access to microgravity: A technical description of the NAE T-33 microgravity facility
[NAE-AN-47] 04 p0405 N88-12518
Microgravity combustion fundamentals
04 p0407 N88-12528
A study of two-phase flow in a reduced gravity environment
[NASA-CR-172035] 04 p0422 N88-12617
Microgravity nucleation and particle coagulation experiments support
[NASA-CR-181540] 04 p0423 N88-12618
Microgravity nucleation and particle coagulation experiments support
[NASA-CR-181541] 04 p0423 N88-12619
Low gravity fluid-thermal experiments
[DE88-000553] 04 p0423 N88-12620
Results from the melting of tungsten composites under microgravity (TEXUS 10 flight)
[FOA-C-20676-2.1] 05 p0571 N88-13482
Feasibility study for gas-grain simulation facility
[NASA-CR-177468] 05 p0646 N88-13954
Electron cytochemical detection of Ca(2)+-ATPase in protonema of moss funaria hygrometrica (H e d w.) under hypogravitation 06 p0749 N88-14602
Prediction of physical workload in reduced gravity environments 06 p0794 N88-14867
Allowable gravity-levels for Spacelab, Columbus and EURECA --- materials science
[BF-R-66.525-2] 07 p0838 N88-15084
Microgravity Particle Research on the Space Station
[NASA-CP-2496] 07 p0883 N88-15354
Astrophysics and the solar nebula
07 p0883 N88-15355
Planetary science 07 p0883 N88-15356
Atmospheric science 07 p0883 N88-15357
Exobiology and life science 07 p0883 N88-15358
Physics and chemistry 07 p0883 N88-15359
Distinctive changes in arterial pressure and blood flow in common carotid artery of monkeys flown aboard Cosmos-1514 biosatellite 07 p0892 N88-15404
Resolution of holograms produced by the fluid experiment system and the holography ground system
07 p0923 N88-15609
Tether Elevator Crawler Systems (TECS)
07 p0927 N88-15631
The effect of microgravity on flame spread over a thin fuel
[NASA-TM-100195] 08 p0967 N88-15853
Cryogenic Fluid Management Technology Workshop. Volume 1: Presentation material and discussion
[NASA-CP-10001] 08 p0980 N88-15924
Low-g propellant gaging 08 p0982 N88-15937
Low gravity liquid motions in spacecraft
08 p0982 N88-15941
Proceedings of the 8th ESA Symposium on European Rocket and Balloon Programs and Related Research
[ESA-SP-270] 08 p1024 N88-16201
The Swedish sounding rocket and balloon program
08 p1025 N88-16205
Preliminary Material Science Experiment Rocket (MASER) 1 results and the evolution of the MASER program 08 p1033 N88-16260
Flight results of the ESA experiment modules in Materials Science Experiment Rocket (MASER) 1
08 p1033 N88-16261
Life sciences experiments on stratospheric balloons and sounding rockets 08 p1033 N88-16262
The D-1 Biorack results: A base for further space biological investigations 08 p1033 N88-16263
Scientific objectives and functional requirements of life sciences in the Space Station 08 p1033 N88-16264
The ESA Anthrorack project: Integrated research in human physiology 08 p1033 N88-16265
Contribution of stratospheric balloon flights in space biology 08 p1033 N88-16266
Skylark sounding rocket development-Skylark 8
08 p1035 N88-16274
Sounding rockets/microgravity products and service
08 p1035 N88-16277
Zero gravity and living organism
08 p1046 N88-16320
Realization of an instrument to measure temperature and concentration gradients in fluids --- microgravity
[CISE-3128] 09 p1168 N88-17003
Space Bioreactor Science Workshop
[NASA-CP-2485] 09 p1196 N88-17168
Suspension cell culture in microgravity and development of a space bioreactor 09 p1196 N88-17169
Space bioreactor: Design/process flow
09 p1197 N88-17170
Computer control of a microgravity mammalian cell bioreactor 09 p1197 N88-17172
Potential use of the bioreactor to determine effects of microgravity and other environmental parameters on growth of hybridoma cells 09 p1198 N88-17178
Cell culture experiments planned for the space bioreactor 09 p1198 N88-17180
Scientific Colloquium in Honor of Prof. Dr. Rer. Nat. Hermann L. Jordan
[DFVLR-MITT-87-11] 09 p1240 N88-17432
Microgravity experiments in space: Compatibility with dynamic perturbing effects 09 p1241 N88-17435
Two-phase reduced gravity experiments for a space reactor design
[DE88-015530] 09 p1247 N88-17475
Microgravity research at the University of Mexico: Experiments in payload G-006 10 p1286 N88-17692
Ten past and ten future GAS/MAUS-payloads
10 p1287 N88-17696
An update to the MITRE/WPI Space Shuttle Program GASCAN G-408 10 p1287 N88-17697
Electrochemical growth of linear conducting crystals in microgravity 10 p1287 N88-17698
Protein-crystal growth experiment (planned)
10 p1287 N88-17700
A payload for investigating the influence of convection on GaAs crystal growth 10 p1288 N88-17702
Application of Hoffman modulation contrast microscopy coupled with three-wavelength two-beam interferometry to the in situ direct observation of the growth process of a crystal in microgravity 10 p1288 N88-17704
The challenge of G-376 10 p1288 N88-17705
A reliable data collection/control system
10 p1289 N88-17706
GAS 450: A space payload for the People Central Coast Student Experimenters 10 p1289 N88-17709
An experiment to investigate Rankine cycle two-phase microgravity issues
[DE88-004197] 10 p1308 N88-17818
NASA Workshop on Biological Adaptation
[NASA-TM-89468] 10 p1368 N88-18174
Non-proprietary research projects of the Center for the Space Processing of Engineering Materials
[AR-2] 10 p1426 N88-18516
Microgravity isolation mount
[ESA-CR(P)-2480] 11 p1443 N88-18604
Mass transport phenomena between bubbles and dissolved gases in liquids under reduced gravity conditions
[NASA-TM-100273] 11 p1455 N88-18672
Investigation of surface tension driven convection as a feasibility study for a micro-gravity experiment
[NASA-CR-182504] 11 p1466 N88-18739
Experimental investigation of low gravity two-phase flow behavior
[DE88-003779] 11 p1466 N88-18741
Microgravity and Materials Processing Facility study (MMPF): Requirements and Analyses of Commercial Operations (RACO) preliminary data release
[NASA-CR-179309] 11 p1466 N88-18742
Study of industry requirements that can be fulfilled by combustion experimentation aboard space station
[NASA-CR-180854] 11 p1566 N88-19377
Computational aspects of robotic experiment manipulation in a microgravity environment
12 p1589 N88-19512
Proceedings of the 3rd European Symposium on Life Sciences Research in Space
[ESA-SP-271] 12 p1652 N88-19893
Life sciences in the framework of the ESA microgravity program and future flight opportunities
12 p1652 N88-19895
ESA's facility for research in human physiology in space: Anthrorack 12 p1652 N88-19896
Second-generation respiratory monitoring system for microgravity studies in man 12 p1653 N88-19906
Plant biology in space 12 p1654 N88-19910
Ecological algal system in microgravity conditions: Preliminary results 12 p1655 N88-19915
Fluid volume changes in astronauts: How they fit our understanding of physiology 12 p1655 N88-19919

Cardiovascular adaptation to zero-g during a long term flight (237 days) on board the Salyut 7 Soviet space station (1984) 12 p1655 N88-19920
Cardiac and peripheral circulation assessment by ultrasound on 3 astronauts during two 7-day space flights (1982 Salyut-7 - 1985 STS 51G) 12 p1656 N88-19921
Physiological reactions upon controlled changes of blood distribution in humans 12 p1656 N88-19924
Effects of cosmic heavy ion radiation and space microgravity on plant systems 12 p1658 N88-19936
Vestibular integrated function and microgravity 12 p1658 N88-19937
Microgravity User Support Center (MUSC) for EURECA, Spacelab and Columbus missions 12 p1660 N88-19947
Biorack experiments in Spacelab D-1 and TML-1: Further developments in gravitational biology 12 p1661 N88-19953
Why life science in space? The next step to go beyond 12 p1661 N88-19954
The suspended Japanese quail as an animal model for experiments related to microgravity 12 p1662 N88-19960
Animal research on the Space Station 12 p1662 N88-19964
Development of an optical diagnostic instrument. Part 2: Instrument development — space laboratories [NLR-TR-87079-L-PT-2] 13 p1841 N88-21016
Mixing fuel particles for space combustion research using acoustics [NASA-TM-100295] 14 p1872 N88-21186
Mechanical design of a ultrahigh gravity UHV facility to launch and recover a low-speed projectile tested on board KC 135 14 p1877 N88-21216
Towards a practical microgravity environment — isolation mount 14 p1878 N88-21223
Vibration characteristics of pumped fluid systems (VCPFS) — microgravity payloads [ESA-CR(P)-2499] 14 p1895 N88-21310
Generation and coalescence of bubbles and stability of foams under microgravity conditions [BMFT-FB-W-86-020] 16 p2184 N88-23017
Microgravity robotics technology program [NASA-TM-100898] 16 p2215 N88-23219
Microgravity mechanisms and robotics program 16 p2219 N88-23237
Base reaction optimization of manipulators with redundant kinematics 16 p2219 N88-23238
Microgravity manipulator demonstration 16 p2219 N88-23242
Noncontact temperature measurements in the microgravity fluids and transport phenomena discipline 17 p2326 N88-23901
Microgravity combustion discipline working group summary of requirements for noncontact temperature measurements 17 p2326 N88-23902
Requirements for temperature and species concentration measurements in microgravity combustion experiments 17 p2329 N88-23903
Separation of biological materials in microgravity [NASA-TM-101142] 17 p2331 N88-23916
An experiment to investigate Rankine cycle two-phase microgravity issues 17 p2409 N88-24322
Theoretical and experimental investigation of swirl flow phase separators for microgravity applications 17 p2411 N88-24335
Microgravity thaw experiment (MITEX) 17 p2427 N88-24439
Reduced-gravity two-phase flow experiments in the NASA KC-135 17 p2431 N88-24465
Analysis and interpretation of low gravity boiling experiments in the KC-135 17 p2432 N88-24466
Microgravity two-phase fluid flow pattern modeling 17 p2432 N88-24467
Experimental investigation of a microgravity separator for two phase mixtures containing small volumes of gas/vapor 17 p2432 N88-24468
Low gravity thermal management using dielectrophoretic forces 17 p2432 N88-24470
Thermodynamic modeling of the r.o-vent fill methodology for transferring cryogens in low gravity [NASA-TM-100932] 18 p2476 N88-24686
Operational facilities of EURECA A1 mission [ETN-88-91939] 18 p2496 N88-24810
Acoustic convective system [NASA-CASE-NPO-17278-1-CU] 18 p2498 N88-24818
Moving belt radiator development status [NASA-TM-100909] 19 p2607 N88-25477
Solid-state combustion synthesis of ceramics and alloys in reduced gravity [NASA-CR-4163] 19 p2608 N88-25479
Industrial processes influenced by gravity [NASA-CR-182140] 20 p2782 N88-26497
Experiments in microgravity environment: Protein crystallization [REPT-881-430-101] 21 p2924 N88-27354
The Marshall Space Flight Center KC-135 microgravity test program for FY84-86 [NASA-TM-4059] 22 p3056 N88-28136
Biorack on Spacelab D1: An overview of the first flight of Biorack, an ESA facility for life sciences research in microgravity [ESA-SP-1091] 22 p3059 N88-28154
A brief overview of the results of the experiments using the ESA Biorack Facility on the German Spacelab D1 mission 22 p3060 N88-28155
The Biorack facility and its performance during the D1 Spacelab mission 22 p3060 N88-28156
The effects of microgravity on genetic recombination in Escherichia coli — Spacelab D1 mission 22 p3060 N88-28157
Growth and differentiation of Bacillus subtilis under microgravity conditions 22 p3060 N88-28158
The Antibio experiment — Spacelab D1 mission 22 p3060 N88-28159
Contraction behavior and protoplasmic streaming in the slime mold Physarum polycephalum (Physarum kinetics) — Spacelab D1 mission 22 p3060 N88-28160
The Paramecium experiment — Spacelab D1 mission 22 p3060 N88-28161
The biological clock of Chlamydomonas reinhardii in space 22 p3061 N88-28162
Effect of microgravity on lymphocyte activation — Spacelab D1 mission 22 p3061 N88-28163
The effect of microgravity on mammalian cell polarization at the ultrastructural level — Spacelab D1 mission 22 p3061 N88-28164
Graviperception of lentil seedling roots grown in space 22 p3061 N88-28165
Effects of short spaceflights on Drosophila melanogaster embryogenesis and life span 22 p3061 N88-28166
Embryogenesis and organogenesis of Carausius morosus under spaceflight conditions 22 p3061 N88-28167
The role of gravity in the establishment of the dorso/ventral axis in the amphibian embryo — Spacelab D1 mission 22 p3062 N88-28168
Microgravity science and applications bibliography, 1987 revision [NASA-TM-4067] 22 p3062 N88-28171
Experimental and analytical study of two-phase flow in zero gravity [AD-A195223] 24 p3358 N88-29993
Containment of a silicone fluid free surface in reduced gravity using barrier coatings [NASA-TM-101314] 24 p3371 N88-30072

REDUCTION
Balanced realizations: Canonical form, parametrization, model reduction [PB87-123360] 06 p0757 N88-14642
Parallel pivoting combined with parallel reduction [NASA-CR-178422] 06 p0760 N88-14662
Reducing adhesion and agglomeration within a cloud of combustible particles [NASA-TM-100902] 20 p2788 N88-26539

REDUCTION (CHEMISTRY)
NT HYDROGENATION
Activated metal oxide surfaces as highly basic and reducing environments [AD-A184958] 05 p0561 N88-13417
Properties of lanthanide oxides as supports for transition metal catalysts [DE88-004520] 11 p1456 N88-18678
Solar-assisted hydrogen generation by photoelectrocatalysis [PB88-160932] 12 p1605 N88-19597
Analytically modeling the carbothermic reduction of alumina in a thermal plasma [DE88-005535] 13 p1841 N88-21020
The evolution of glutathione metabolism in phototrophic microorganisms [NASA-CR-182902] 19 p2695 N88-26015
In situ spectroscopic studies of transition metal macrocycles as catalysts for the electrochemical reduction of oxygen [PB88-203195] 20 p2769 N88-26416
Nickel hydrogen cell positive-electrode studies: Cobalt segregation in reducing environments [AD-A193025] 20 p2796 N88-26587
Super hydrides [AD-A193710] 23 p3192 N88-28995
Breakdown of molecular oxygen by brief pulses of laser radiation [DE88-702687] 23 p3220 N88-29168

REDUCTION (MATHEMATICS)
U OPTIMIZATION

REDUNDANCY
Measurement of fault-tolerant parallel processors [PB87-208328] 01 p0064 N88-10539
Flight test of a resident backup software system 02 p0128 N88-10805
An evaluation plan of bus architectures and protocols using the NASA Ames intelligent redundant actuation system [NASA-CR-177458] 04 p0398 N88-12482
Fault-tolerant computer architecture based on INMOS transputer processor 06 p0797 N88-14880
Inadequacy of conventional dynamic recovery mechanisms in the presence of temporary failures [AD-A186311] 07 p0866 N88-15251
Directions in propulsion control 08 p0956 N88-15799
Construction of control systems with diversified redundancy for electrical machines [BIA-5/86] 11 p1481 N88-18842
On the danger of redundancies in some aerospace mechanisms 14 p1925 N88-21475
Analytical sensor redundancy assessment [NASA-CR-182892] 16 p2163 N88-22901
Dynamic modelling and estimation of the error due to asynchronism in a redundant asynchronous multiprocessor system [NASA-CR-177427] 21 p2898 N88-27205
Investigations on the modification of structural reliability by substitution of aluminum by carbon fiber reinforced plastics in aircraft construction [ILR-MITT-195] 24 p3339 N88-29877

REDUNDANCY ENCODING
Robust control system design 02 p0127 N88-10800

REDUNDANT COMPONENTS
PRAAGE: An interactive IBM-PC code for unreliability/aging analysis [DE87-012124] 04 p0453 N88-12803
On the danger of redundancies in some aerospace mechanisms 14 p1925 N88-21475

REDUNDANT STRUCTURES
U REDUNDANT COMPONENTS

REELS
Tethered diagnostic package for use from the space station [DE88-006264] 16 p2167 N88-22921

REENTRY
NT HYPERSONIC REENTRY
NT SPACECRAFT REENTRY
Thermal stress analysis of space shuttle orbiter subjected to reentry aerodynamic heating [NASA-TM-88286] 01 p0061 N88-10389
Analysis of a nuclear orbital transfer vehicle reentry accident 17 p2425 N88-24426

REENTRY BODIES
U REENTRY VEHICLES

REENTRY EFFECTS
Hypersonic aerodynamics: Applications for HOTOL 05 p0535 N88-13252

REENTRY GLIDERS
U LIFTING REENTRY VEHICLES

REENTRY PHYSICS
Compressible boundary layers — atmospheric reentry [CERT-OA-13/5005-AYD] 20 p2801 N88-26623

REENTRY SHIELDING
Ceramic-ceramic shell tile thermal protection system and method thereof [NASA-CASE-ARC-11641-1] 11 p1448 N88-18628
A model for nitrogen atom recombination on a silicon dioxide surface [AD-A189843] 15 p2142 N88-22784

REENTRY TRAJECTORIES
Maneuverable reentry vehicle trajectory footprints: Calculation and properties [DE88-004726] 10 p1292 N88-17726

REENTRY VEHICLES
NT AEROSPACE PLANES
NT CHALLENGER (ORBITER)
NT DISCOVERY (ORBITER)
NT HERMES MANNED SPACEPLANE
NT HOTOL LAUNCH VEHICLE
NT LIFTING REENTRY VEHICLES
NT MANEUVERABLE REENTRY BODIES
NT REUSABLE SPACECRAFT
NT SPACE SHUTTLE ORBITERS
NT SPACE SHUTTLES
NT X-30 VEHICLE
The aerothermodynamic environment for holes in hypersonic configurations [DE87-014651] 02 p0121 N88-10767
Aerodynamic design and performance of a bent-axis geometry vehicle [DE87-013726] 02 p0124 N88-10786
Scene simulation for passive IR systems 02 p0137 N88-10861
Dual S/X-band RV antenna [DE87-014853] 03 p0305 N88-11923

Proceedings: SDIO/DARPA Workshop on Laser Propulsion. Volume 3: Viewgraphs
[DE88-000964] 04 p0450 N88-12790
High-velocity reverse ballistic rocket sled testing at Sandia National Laboratories 09 p1179 N88-17059
Comparisons of Monte-Carlo and PNS (Parabolized Navier-Stokes) calculations for rarefied flow over reentry vehicle configurations
[DE88-004937] 11 p1435 N88-18560
Three-dimensional flow fields past reentry vehicles 11 p1484 N88-18858
A simplified streamline swallowing procedure for the windward meridian of axisymmetric blunt bodies
[AD-A188413] 12 p1626 N88-19732
Features of Soyuz TM spacecraft 13 p1727 N88-20329
New definition of pressure-center coefficient of reentry craft with asymmetrical configuration 14 p1864 N88-21138
Oil flow patterns on a series of capsule-type re-entry vehicles at hypersonic speeds
[DE88-751805] 16 p2155 N88-22858
Experimental investigation of hypersonic aerodynamics
[NASA-CR-182973] 18 p2458 N88-24591
A simulation of post boost vehicle deployment of multiple reentry vehicles
[DE88-009537] 20 p2764 N88-26391
In-flight motor torque estimates for the second-stage Strypi 9 launch vehicle
[DE88-010833] 21 p2902 N88-27222
Study of hypersonic boundary layers
[CERT-RSF-OA-17/5005-AYD] 23 p3213 N88-29121

REFERENCE ATMOSPHERES
Monthly mean global climatology of temperature, wind, geopotential height, and pressure for 0 - 120 km
[NASA-TM-100697] 15 p2099 N88-22503

REFERENCE STARS
Rigorous compilation of the Northern International Reference Stars (NIRS) 03 p0387 N88-12431
IPS guidestar selection for stellar mode (ASTRO)
[NASA-TM-100336] 21 p2894 N88-27181
Astron observations of supernova 1987A in large magellanic cloud 24 p3445 N88-30504
The guide star catalog
[NASA-CR-183253] 24 p3452 N88-30547

REFERENCES (STANDARDS)
U STANDARDS

REFINING
High-density jet fuels from coal syncrudes, appendix 4
[DE88-003132] 10 p1307 N88-17813
Knowledge base refinement by monitoring abstract control knowledge, revision 1
[AD-A187502] 10 p1397 N88-18323
Aviation turbine fuels from tar sands bitumen and heavy oils. Part 3: Laboratory sample production
[AD-A189278] 13 p1753 N88-20484
Activities of As, Sb, Bi and Pb in copper mattes and their effects on impurity elimination
[TKK-V-A10(1988)] 15 p2041 N88-22165
Turbine fuels from tar sands bitumen and heavy oil. Volume 2, phase 3: Process design specifications for a turbine fuel refinery charging San Ardo heavy crude oil
[AD-A190120] 16 p2183 N88-23011
Feasibility of producing jet fuel from GPGP (Great Plains Gasification Plant) by-products
[DE88-010233] 20 p2781 N88-26492
An adaptive overlapping local grid refinement method for two-dimensional parabolic systems
[AD-A193560] 23 p3271 N88-29464

REFLECTANCE
NT BIDIRECTIONAL REFLECTANCE
NT SPECTRAL REFLECTANCE
Estimating regional evapotranspiration from remotely sensed data by surface energy balance models
[NASA-CR-181400] 01 p0064 N88-10411
Unified Sun and sky illumination for shadows under trees
[DE87-014232] 01 p0083 N88-10535
Estimating scattered and absorbed radiation in plant canopies by remote sensing
[NASA-CR-181390] 02 p0193 N88-11205
Understanding passive cooling systems
[PB87-210464] 02 p0194 N88-11211
Deformation effects on microwave reflectivity
[AD-A185684] 07 p0844 N88-15120
The anisotropy of reflected solar radiation over several types of land surface 08 p1018 N88-16171
High-sensitivity recording of weak reflected or scattered radiation by method of coherent intracavity reception with YAG:Nd(3+) laser 08 p1078 N88-16502
Experimental aspects of high-T/sub c/ superconductors
[DE88-003019] 08 p1090 N88-16564
Statistics of two-dimensional structure elements of mountainous ranges (mosaic model) for calculating three-dimensional reflection functions
[DFVLR-FB-87-33] 09 p1185 N88-17099
Variable band gap materials for thermophotovoltaic generators
[AD-A186858] 09 p1186 N88-17104
Radar reflectivity and attenuation of radio waves in the melting layer of precipitation
[PB88-121553] 10 p1318 N88-17882
Improved canopy reflectance modeling and scene inference through improved understanding of scene pattern
[NASA-CR-182488] 10 p1347 N88-18049
Optical measurements of surface oxide layer formation on metal films
[DE88-003163] 10 p1409 N88-18405
Depolarized infrared reflectance from dry and wetted surfaces
[AD-A188213] 11 p1492 N88-18903
The angular reflectance signature of the canopy hot spot in the optical regime
[DE88-005385] 11 p1505 N88-18991
Target-reflectivity models for various terrain types
[DE88-005510] 11 p1505 N88-18992
An experimental measurement of metal multilayer X-ray reflectivity degradation due to intense X-ray flux
[LA-10989-T] 11 p1547 N88-19255
Running head: What color is it
[NASA-CR-182600] 11 p1551 N88-19280
Measuring and modeling near surface reflected and emitted radiation fluxes at the FIFE site
[NASA-CR-182660] 12 p1640 N88-19818
Applications of the differential reflectivity radar technique: Focus on estimation of rainfall parameters and microwave attenuation prediction 13 p1759 N88-20521
Pseudo-stationary oblique-shock-wave reflections in low gamma gases: Isobutane and sulphur hexafluoride
[UTIAS-TN-267] 13 p1768 N88-20576
Research relative to angular distribution of snow reflectance/snow cover characterization and microwave emission
[NASA-CR-182733] 14 p1941 N88-21582
Experimental research on skin reflection, transmission, absorption of light rays 16 p2187 N88-23039
Spectral measurements for correcting LANDSAT data for atmospheric effects 17 p2353 N88-24020
The use of SLAR and SIRA imagenes for the classification of forest typen in tropical rain forests 17 p2356 N88-24036
Analysis of the parameters responsible for the variations of the illumination conditions in the LANSAT data 17 p2362 N88-24070
An experimental study of the coherent under-ice reflectivity of sound in the Greenland Sea Marginal Ice Zone 18 p2548 N88-25125
Remote sensing of acoustic properties of shallow water sediments: A review
[AD-A192107] 18 p2570 N88-25267
A disposable liquid microcell for near-infrared reflectance analysis
[AD-A192190] 18 p2575 N88-25298
Design and demonstration of a system for the deposition of atomic-oxygen durable coatings for reflective solar dynamic power system concentrators
[NASA-CR-4158] 19 p2606 N88-25474
Canopy reflectance modeling in a tropical wooded grassland
[NASA-CR-182981] 19 p2685 N88-25961
Numerical model for the computation of radiance distributions in natural waters with wind-roughened surfaces
[PB88-192703] 20 p2826 N88-26765
Observation of ferromagnetism in ultrathin f.c.c. films by spin polarised neutron reflection 20 p2865 N88-27015
Picosecond transient reflectivity of unpinned gallium arsenide (100) surfaces
[AD-A193242] 21 p3021 N88-27933
Stratocumulus and cloud-free reflectance from multi-spectral satellite measurements
[AD-A193899] 22 p3128 N88-28599
Seismic reflection experiments imaging the physical nature of crustal structures in southern California 23 p3232 N88-29235
Mars: Spectral signatures seen and unseen 23 p3301 N88-29659
Spectral reflectance of SNC meteorites: Relationships to Martian surface composition 23 p3304 N88-29683
The surface composition of Mars from earthbased observations 23 p3306 N88-29696
Martian surface analogs: Laboratory spectral studies in the mid infrared 23 p3307 N88-29699
The effect of the near earth micrometeoroid environment on a highly reflective mirror surface
[NASA-TM-101307] 24 p3332 N88-29833
Electromagnetic metrology 24 p3363 N88-30024
TM/LANDSAT-5 data to evaluate wheat and bean percent soil cover and leaf area index
[INPE-4609-PRE/1332] 24 p3385 N88-30165
Reflectance pattern and the physical and chemical characteristics of three Brazilian Oxisols
[INPE-4590-PRE/1320] 24 p3387 N88-30172
Study of the spectral response of soybeans
[INPE-4592-PRE/1322] 24 p3387 N88-30174
Deep seismic reflection profiling and continental growth curves 24 p3396 N88-30222
Physical properties of surface materials on Martian volcanoes: Dust-covered lava and ash 24 p3443 N88-30493

REFLECTED RADIATION
U REFLECTED WAVES

REFLECTED RAYS
U REFLECTED WAVES

REFLECTED WAVES
Analytical investigation of reflection of a regular or mach reflection over a secondary wedge
[AD-A185690] 06 p0703 N88-14316
The carbon dioxide chaperon efficiency for the reaction H + O2 + M yields HO2 + M from ignition delay times behind reflected shock waves
[NASA-TM-100125] 07 p0830 N88-15036
Application of correlation method of reception of direct and reflected cosmic radiation to study of plasmaspheres of planet and distribution of radiation brightness 08 p1004 N88-16085
Method of determining atmospheric moisture content by measurement of upward radiation intensity in near IR 08 p1007 N88-16106
Radiation balance components above the tropical evergreen Amazon forests (3rd campaign of data collection)
[INPE-4195-PRE/1079] 11 p1513 N88-19039
Flow/acoustic interaction in duct inflow
[AD-A189264] 13 p1833 N88-20967

REFLECTION
NT INFRARED REFLECTION
NT MACH REFLECTION
NT OPTICAL REFLECTION
NT SIGNAL REFLECTION
NT SPECULAR REFLECTION
NT WAVE REFLECTION
A new approach to modeling and interpreting electromagnetic sounding data
[DE88-000460] 04 p0438 N88-12715
Horn design equations for the NBS (National Bureau of Standards) horn-type noise standards
[PB88-110226] 07 p0844 N88-15122
Accurate boundary conditions for exterior problems in gas dynamics
[NASA-TM-100807] 11 p1537 N88-19182
Electrochromic thin films
[DE88-751099] 11 p1559 N88-19334
Solving reflexive domain equations in a category of complete metric spaces
[CWI-CS-R8709] 13 p1832 N88-20956
Vegetation mapping using high resolution MSS (multispectral scanner) data: Canopy reflectance and shadow problems encountered and possible solutions
[DE88-004273] 14 p1939 N88-21574
Infrared reflection-absorption spectroscopy of hyperfine layers on surfaces of semiconductors and dielectrics 14 p1969 N88-21755
Millimeter and submillimeter waves and frequency selective surfaces
[AD-A191511] 18 p2500 N88-24827
Identification of cascaded microwave circuits with moderate reflections using reflections and transmission measurements
[PB88-171921] 18 p2503 N88-24849
Dielectric compound parabolic concentrating solar collector with frustrated total internal reflection absorber
[DE88-009986] 19 p2688 N88-25976
The use of liquid films for spacecraft survivability to laser radiation
[AD-A192954] 20 p2765 N88-26395
Experimental investigation of the reflection of a planar shock wave over a double wedge
[AD-A193078] 21 p2943 N88-27482
Attachable interferometric strain gages
[AD-A192390] 21 p2950 N88-27522
Effects of low reflection on the collector and source sheaths of a finite ion temperature plasma
[DE88-008929] 21 p3017 N88-27908
Electromagnetic wave incoherent reflection by a half-space of weakly-ionized plasma with an absorbing boundary
[DE88-702413] 21 p3019 N88-27917

Polarization of light reflected by vertically inhomogeneous planetary atmosphere
[DE86-702416] 21 p3031 N88-27992
Arctic ice attenuation model study
[AD-A193382] 22 p3146 N88-28715
Reflection and scattering of acoustic rays computed for parabolic ice keel models
[AD-A193898] 23 p3278 N88-29517

REFLECTION COEFFICIENT
U REFLECTANCE

REFLECTIVITY
U REFLECTANCE

REFLECTOR ANTENNAS
NT PARABOLIC ANTENNAS
NT TWO REFLECTOR ANTENNAS
Physical optics method: Prediction of radar signatures 03 p0304 N88-11914
A simplified approach to axisymmetric dual-reflector antenna design
[NASA-TP-2797] 09 p1111 N88-16662
Compensation of relector antenna surface distortion using an array feed
[NASA-TM-100286] 11 p1476 N88-18805
Multiple-beam ground station reflector antenna system: A preliminary study
[EUT-87-E-171] 14 p1904 N88-21379
An improved method for calculating power density in the Fresnel region of circular parabolic reflector antennas
[AD-A190569] 15 p2060 N88-22284
Analysis and experiments concerning the performance and calibration of compact antenna-test ranges
[PB88-169263] 16 p2188 N88-23047
Analysis and experiments concerning the performance and calibration of compact antenna-test ranges
[ISBN-9-09-001727-5] 16 p2188 N88-23048
Case study of active array feed compensation with sidelobe control for reflector surface distortion
[NASA-TM-100287] 16 p2192 N88-23073
A microstrip array feed for MSAT spacecraft reflector antenna 19 p2652 N88-25747
Active feed array compensation for reflector antenna surface distortions
[NASA-TM-100826] 19 p2654 N88-25762
Analytical approximation of a distorted reflector surface defined by a discrete set of points
[NASA-TM-101323] 21 p2934 N88-27424

REFLECTOR SATELLITES
U PASSIVE SATELLITES

REFLECTORS
NT PARABOLIC REFLECTORS
NT RADAR CORNER REFLECTORS
NT SOLAR COLLECTORS
NT SOLAR REFLECTORS
NT WIGGLER MAGNETS
A new type of lamp and reflector for I.R. simulation 02 p0136 N88-10655
A multibody dynamic analysis of the N-ROSS (Navy Remote Ocean Sensing System) satellite rotating flexible reflector using Kane's method
[AD-A184452] 04 p0462 N88-12860
A simplified approach to axisymmetric dual-reflector antenna design
[NASA-TP-2797] 09 p1111 N88-16662
Study on a double reflector compact range — satellite antennas
[S-201-05] 09 p1153 N88-16908
A new approach for shaping of dual-reflector antennas
[NASA-CR-182561] 11 p1476 N88-18806
Polymer reflectors research during FY86
[DE88-001101] 11 p1508 N88-19009
Workshop on Technology Development Issues for the Large Deployable Reflector (LDR)
[NASA-CP-2407] 12 p1710 N88-20235
Features and applications of the integrated composites analyzer (ICAN) code 15 p2078 N88-22391
LDR structural experiment definition
[NASA-TM-100618] 17 p2312 N88-23826
The radar cross section of some simple reflectors at short wavelengths
[FOA-C-30472-3.3] 18 p2501 N88-24839
Joint services electronics program
[AD-A191749] 18 p2504 N88-24853
Confirmation of slow-waves in a crosstie overlay coplanar waveguide and its application to band-reject gratings and reflectors
[AD-A194981] 24 p3361 N88-30011

REFLEXES
NT VESTIBULAR NYSTAGMUS

REFRACTED RADIATION
U REFRACTED WAVES

REFRACTED RAYS
U REFRACTED WAVES

REFRACTED WAVES
Refraction of shear wave into nonlinearly elastic or elastoplastic half-space 02 p0159 N88-10999
AFAR (Azores Fixed Acoustic Range) measurements of intensity and intensity moments
[AD-A184431] 03 p0355 N88-12237
Mathematical models of sound waves in fluids
[AD-A189270] 13 p1834 N88-20968

REFRACTION
NT ATMOSPHERIC REFRACTION
NT BIREFRINGENCE
NT KERR ELECTROOPTICAL EFFECT
NT RADIO WAVE REFRACTION
Optical characterization of silica aerogel glass
[DE87-014617] 02 p0153 N88-10956
A FORTRAN code for the calculation of probe volume geometry changes in a laser anemometry system caused by window refraction
[NASA-TM-100210] 03 p0364 N88-12288
Low-frequency VLBI in space and interstellar refraction
[PB87-127643] 06 p0696 N88-14267
Correlation between refraction over sea and nature of radar reflections from sea surface 06 p0728 N88-14477
A-scan ultrasound measurement of ocular changes during accommodation
[AD-A186818] 09 p1198 N88-17181
Crystalline sulfur dioxide: Crystal field splittings, absolute band intensities and complex refractive indices derived from infrared spectra
[NASA-CR-182502] 09 p1258 N88-17547
Research on materials and components for opto-electronic signal processing and computing
[AD-A190130] 15 p2143 N88-22788
Refraction in underwater acoustics — navigation systems
[B8735053] 17 p2395 N88-24236
Ray scattering from a collection of ice keels
[AD-A191757] 19 p2722 N88-26163

REFRACTIVE INDEX
U REFRACTIVITY

REFRACTIVITY
A 15 cm aperture LED scintillometer for C(n) squared and crosswind measurements
[KNMI-WR-87-3] 01 p0070 N88-10448
Precise measurement of refractive index and absorption coefficient of near millimeter wave and far infrared materials
[AD-A184536] 03 p0293 N88-11840
Aluminum oxynitride spinel (ALON): A review
[AD-A184753] 03 p0294 N88-11845
Microwave refractive index structure function profiles (Cn2) measured from a small aircraft
[AD-A184343] 04 p0431 N88-12670
Pulse-mode expansions and refractive indices in plane-wave propagation
[DE88-001328] 04 p0437 N88-12714
The application of vector diffraction to the scalar anomalous diffraction approximation of Van de Hulst
[AD-A185930] 07 p0929 N88-15643
A raytrace method for a laterally heterogeneous environment
[AD-A186525] 08 p0978 N88-15912
Christiansen effect in infrared spectra of soil-derived atmospheric dusts
[AD-A187071] 09 p1248 N88-17479
The stability of free-electron lasers against filamentation
[DE88-004712] 10 p1414 N88-18435
An evaluation of the impact of variable temporal and spatial data resolution upon IREPS (Integrated Refractive Effects Prediction System)
[AD-A187764] 11 p1470 N88-18769
Fast switching of far infrared radiation by refractive index change in semiconductors using photoionization
[ETN-88-91490] 11 p1551 N88-19279
Correcting ray field failures caused by focusing in an inhomogeneous duct: A critical look at the Gaussian beam method 12 p1616 N88-19663
Refractive index, meteorology and fading in line-of-sight transmission paths 12 p1616 N88-19666
Optical properties of compressible inhomogeneous shear layers relevant to high power lasers
[AD-A189299] 12 p1633 N88-19774
Analysis of the inter-layer independence of stellar scintillometer profiles of Cn2
[AD-A189372] 12 p1645 N88-19854
Nonlinear optical principles and the photorefractive effect applied to optical phase conjugation
[AD-A188856] 12 p1691 N88-20119
Refractive index gradients in nuclear-reactor-pumped lasers: Gasdynamic effects
[DE88-006099] 13 p1776 N88-20621
Nonlinear refractive index measurements of glasses and crystals
[DE88-005673] 13 p1840 N88-21009
Stellar scintillometer atmospheric optical turbulence profiling experiment: A qualitative comparison of two identical instruments at AMOS (Air Force Maui Optical Station), 1985
[AD-A190589] 15 p2094 N88-22479
Spectral measurements in a disturbed boundary layer over snow
[AD-A190217] 15 p2097 N88-22494
Dispersion measurements of microcrystals in the near ultraviolet and infrared
[DE88-006234] 15 p2145 N88-22800
The optical properties of aerosols
[AD-A191420] 16 p2176 N88-22972
IREPS (Integrated Refractive Effects Prediction System) 3.0, user's manual
[AD-A190398] 16 p2188 N88-23045
Dynamic range compression/expansion of light beams by photorefractive crystals
[NASA-CASE-NPO-17140-1-CU] 17 p2438 N88-24508
Silicon-sapphire waveguides
[AD-A191754] 18 p2504 N88-24854
Construction of approximations to acoustic Green's functions for nonhomogeneous oceans using transmutation
[PB88-185384] 18 p2548 N88-25126
Determination of doping profiles in silicon from resistivity measurements via the four-point probe in combination with layer strippings via anodic oxidation 18 p2583 N88-25347
Numerical investigation of acoustic energy exchange through flow turning 19 p2629 N88-25593
Influence of refractive index and solar concentration on optical power absorption in slabs
[NASA-TM-4056] 19 p2726 N88-26190
Optical characterization of silica aerogel
[DE88-008916] 20 p2854 N88-26946
Predicting optical degradation of a laser beam through a turbulent shear layer 21 p2927 N88-27376
Monte-Carlo estimation of the influence of plant architecture parameters on spectral brightness 24 p3450 N88-30533

REFRACTOMETERS
Fiber optics refractometer for absorption machines
[DE88-002296] 07 p0932 N88-15662
A refractometer for the interferometric determination of the helium abundance in the Jupiter atmosphere
[BONN-IR-86-23] 07 p0946 N88-15749

REFRACTORY COATINGS
Thermal barrier coating life prediction model development 02 p0190 N88-11183
Thermal barrier coating life prediction model development 02 p0190 N88-11184
Thermal barrier coating life prediction model development 02 p0190 N88-11185
Reaction mechanism of sulfur dioxide with single crystal cobalt and chromium and CoCrAlY coatings
[AD-A185989] 09 p1253 N88-17509
Hermetic coating of optical fibers
[AD-A189886] 15 p2044 N88-22177

REFRACTORY MATERIALS
NT CHROMIUM
NT IRIDIUM
NT IRIDIUM ISOTOPES
NT MOLYBDENUM
NT MOLYBDENUM ALLOYS
NT NIOBIUM
NT NIOBIUM ALLOYS
NT NIOBIUM ISOTOPES
NT OSMIUM
NT REFRACTORY METAL ALLOYS
NT REFRACTORY METALS
NT RHENIUM
NT RHENIUM ALLOYS
NT RHENIUM ISOTOPES
NT TANTALUM
NT TANTALUM ALLOYS
NT TUNGSTEN
NT TUNGSTEN ALLOYS
High temperature metal matrix composites for future aerospace systems
[NASA-TM-100212] 02 p0149 N88-10938
Coatings for Advanced Heat Engines Workshop: Book of abstracts
[DE87-012623] 02 p0180 N88-11121
High temperature characterization of ceramic materials
[REPT-NT-3403] 03 p0292 N88-11837
Cu-2 mechanical properties and microstructural stability of advanced steam cycle materials
[DE88-001519] 05 p0566 N88-13452
Material design of high-purpose glass discussed 06 p0675 N88-14133
Projects within the Center for Advanced Materials
[PB88-123054] 06 p0677 N88-14143

Astrophysics and the solar nebula
07 p0883 N88-15355
The synthesis and characterization of some rare earth arsenides
[AD-A186445] 06 p0965 N88-15839
Ethynylated aromatics as high temperature matrix resins
[NASA-TM-89829] 11 p1450 N88-18640
Hot corrosion in gas turbines: A new, unique and informative technique is EASE (Electronic Absorption Spectroscopy Experiments)
[AD-A188508] 12 p1583 N88-19470
Development of metastable processing paths for high temperature alloys
[AD-A188682] 12 p1608 N88-19617
Basic research in ceramic and semiconductor science at selected Japanese laboratories, based on a September 1986 visit: Highlights, summary and overview and detailed notes from selected Japanese laboratories
[DOE/ER-0314] 12 p1696 N88-20150
High-temperature metal matrix composites
[AD-A189516] 13 p1734 N88-20367
Statistical considerations of graphite strength for assessing design allowable stresses
13 p1746 N88-20441
Fracture criterion of reactor graphite under multiaxial stresses 13 p1746 N88-20442
High temperature Young's modulus of IG-110 graphite
13 p1746 N88-20443
Effects of high temperature neutron irradiation on the physical, chemical and mechanical properties of fine-grained isotropic graphite 13 p1747 N88-20444
Degradations of thermal shock resistance and the fracture toughness of reactor graphite subjected to neutron irradiation 13 p1747 N88-20445
JPRS report: Science and technology. China
[JPRS-CST-87-023] 14 p1863 N88-21130
Contemporary ceramics and the new technological revolution 14 p1902 N88-21363
Nonlinear Constitutive Relations for High Temperature Applications, 1986
[NASA-CP-10010] 14 p1928 N88-21498
High temperature materials: What's available
[AERE-R-12632] 15 p2026 N88-22081
Fundamental studies on high temperature deformation recrystallization, and grain growth of two-phase materials
[AD-A189725] 15 p2038 N88-22145
Biaxial experiments supporting the development of constitutive theories for advanced high-temperature materials 15 p2078 N88-22386
Refractory Materials of Zirconate. Part 2: Synthesis and some properties of strontium, zirconate, calcium zirconate and barium zirconate
[NASA-TT-20186] 20 p2779 N88-26483
Radiative heat transfer and selective emission in planar slab coatings on hot emissive substrates
[AD-A193133] 21 p2918 N88-27319
Refractory fibers surface treatment
[REPT-47-803/F] 21 p2922 N88-27339
The High Temperature Materials Laboratory: A new research and user facility at the Oak Ridge National Laboratory
[DE88-010792] 22 p3057 N88-28138
Very high temperature materials for mechanical application
[SNIAS-881-430-106] 23 p3189 N88-28978

REFRACTORY METAL ALLOYS
NT MOLYBDENUM ALLOYS
NT NIOBIUM ALLOYS
NT RHENIUM ALLOYS
NT TANTALUM ALLOYS
NT TUNGSTEN ALLOYS
Properties of refractory metals processed by enhanced sintering treatments
[AD-A184944] 05 p0565 N88-13440
Characterization of precipitates in a niobium-zirconium-carbon alloy
[NASA-TM-100848] 16 p2178 N88-22981
Review of alkali metal and refractory alloy compatibility for Rankine cycle applications 17 p2428 N88-24447
Effect of hydrogen, deuterium and oxygen on the anelastic properties of refractory alloys
[DE88-007349] 18 p2484 N88-24736

REFRACTORY METALS
NT CHROMIUM
NT IRIDIUM
NT IRIDIUM ISOTOPES
NT MOLYBDENUM
NT NIOBIUM
NT NIOBIUM ISOTOPES
NT OSMIUM
NT RHENIUM
NT RHENIUM ISOTOPES
NT TANTALUM
NT TUNGSTEN
Properties of refractory metals processed by enhanced sintering treatments
[AD-A184944] 05 p0565 N88-13440
Development of reliable fuel pins for space reactor applications 17 p2409 N88-24326
Refractory metal alloys and composites for space power systems
[NASA-TM-100946] 21 p2916 N88-27310

REFRASIL (TRADEMARK)
U FIBERS
U SILICON DIOXIDE

REFRIGERANTS
Optimized ground coupled heat pump mechanical package
[DE87-014899] 04 p0441 N88-12738
Development of a low noise 10 K J-T refrigeration system
[AD-A185258] 05 p0571 N88-13484
Investigation of critical heating in narrow flow channels with R12 refrigerant as model fluid
[GKSS-87/E/25] 09 p1163 N88-16972
Investigation on refrigerant R12 critical boiling point in narrow flow pipes considered as model fluid
[ETN-88-92374] 20 p2802 N88-26626
Thermal conductivity of pure fluids in a large region around the critical point
[ETN-88-92135] 20 p2881 N88-27103

REFRIGERATING
Development of a low noise 10 K J-T refrigeration system
[AD-A186004] 07 p0838 N88-15085
Large capacity cryopropellant orbital storage facility
08 p0981 N88-15932

REFRIGERATING MACHINERY
NT REFRIGERATORS
Oxygen chemisorption cryogenic refrigerator
[NASA-CASE-NPO-16734-1-CU]
06 p0689 N88-14223
Air Force cryocooler development for spacecraft
08 p0983 N88-15945
Study of a magnetic refrigerator for space applications for temperatures under 20 K
[NASA-TT-20283] 19 p2641 N88-25668

REFRIGERATORS
A 2.3-GHz cryogenically cooled HEMT amplifier for DSS 13
04 p0434 N88-12689
A cold ejector for closed-cycle helium refrigerators
04 p0434 N88-12690
Traveling-wave maser closed-cycle refrigerator data acquisition and display system 04 p0437 N88-12708
Two-watt, 4-Kelvin closed cycle refrigerator performance 04 p0437 N88-12709
Development of a low noise 10 K J-T refrigeration system
[AD-A185258] 05 p0571 N88-13484
Evaluation of a cryogenic refrigerator for cooling focal plane instrumentation — satellite instruments
[BAE-TP-8095-VOL-1] 05 p0572 N88-13485
Evaluation of a cryogenic refrigerator for cooling focal plane instrumentation. Appendix B: Accommodation study — satellite instruments
[BAE-TP-8095-VOL-2] 05 p0572 N88-13486
Self operating absorption cooling system using solar energy: Small power experimental plant
[DE88-900194] 07 p0874 N88-15299
Cryogenics program overview
08 p0981 N88-15926
Ames Research Center cryogenics program
08 p0981 N88-15927
Cryocooler systems demonstration
[AD-A188025] 11 p1467 N88-18745
Dilution refrigerator with non-valve adsorption system of sup 3/He circulation
[DE88-700974] 15 p2050 N88-22209
Thin superconducting film characterization by surface acoustic waves
[AD-A190417] 15 p2143 N88-22791
Krypton based adsorption type cryogenic refrigerator
[NASA-CASE-NPO-17334-1-CU]
17 p2331 N88-23917
Cryogenic regenerator including saran-carbon heat conduction matrix
[NASA-CASE-NPO-17291-1-CU]
17 p2337 N88-23946
Electrodynamic driver for the space thermoacoustic refrigerator (STAR)
[AD-A192337] 20 p2785 N88-26517
Magnetic heat pumps
[DE88-012058] 21 p2969 N88-27639
CryoSQUID: A SQUID-based magnetic field sensor
[AD-A194237] 23 p3239 N88-29275

REFUELING
NT AIR TO AIR REFUELING
Orbital Spacecraft Consumables Resupply System (OSCRS). Volume 4: Extended study results Part 1: Executive Summary
[NASA-CR-172012] 03 p0268 N88-11686
Orbital Spacecraft Consumables Resupply System (OSCRS): Monopropellant application to space station and OMV automatic refueling impacts of an ELV launch, volume 4
[NASA-CR-172029] 03 p0276 N88-11741
Refueling and density control in the ZT-40M reversed field pinch
[DE88-000504] 04 p0493 N88-13040
Orbital Spacecraft Consumables Resupply System (OSCRS). Volume 1: Executive summary
[NASA-CR-172010] 05 p0553 N88-13368
Safety implications of onboard refueling vapor recovery systems
[PB88-102603] 07 p0839 N88-15088
Investigation of the need for in-use dispensing rate limits and fuel nozzle geometry standardization
[PB88-102611] 07 p0839 N88-15089
Summary and analysis of comments on the recommended practice for the measurement of refueling emissions
[PB88-101530] 07 p0876 N88-15313
SAMSS: An in-progress review of the Spacecraft Assembly, Maintenance, and Servicing Study
08 p0961 N88-15930
Application of railgun principle to high-velocity hydrogen pellet injection for magnetic fusion reactor refueling
[DE88-005830] 13 p1728 N88-20334
Investigation of the misfueling of reciprocating piston aircraft engines
[NASA-TP-2803] 14 p1885 N88-21144
Implementation of a visual servoing system for evaluation of robotic refueling applications
[AD-A189676] 14 p1954 N88-21645
Development and evaluation of an airplane fuel tank ullage composition model. Volume 2: Experimental determination of airplane fuel tank ullage compositions
[AD-A190408] 15 p2017 N88-22025
Fault diagnosis in orbital refueling operations
17 p2381 N88-24154
Thermodynamic modeling of the no-vent fill methodology for transferring cryogens in low gravity
[NASA-TM-100932] 18 p2476 N88-24686
Temperature rise in superfluid helium pumps
[NASA-TM-100997] 21 p2948 N88-27507
Inflight rearming
[AD-A193564] 23 p3176 N88-28909
Technology requirements for an orbiting fuel depot: A necessary element of a space infrastructure
[NASA-TM-101370] 24 p3334 N88-29845
Design and development of a refueling test bed
[FTMS-RP-ER-011] 24 p3357 N88-29986

REGENERATION (ENGINEERING)
Performance of rotary regenerative heat exchanger: A numerical simulation 01 p0046 N88-10292
Heat engine regenerators: Research status and needs
[DE87-013581] 01 p0054 N88-10348
Effects of a regenerating heat treatment on the creep behavior and the lifetime during creep test loading
[ETN-88-91063] 09 p1144 N88-16855
Cryogenic regenerator including saran-carbon heat conduction matrix
[NASA-CASE-NPO-17291-1-CU]
17 p2337 N88-23946
Advanced life support control/monitor instrumentation concepts for flight application
[NASA-CR-177378] 20 p2833 N88-26807
Full analysis of a powerful window random access algorithm
[AD-A192437] 21 p2995 N88-27763
Advancements in oxygen generation and humidity control by water vapor electrolysis
[NASA-CR-172073] 22 p3134 N88-28633

REGENERATION (PHYSIOLOGY)
Limb regeneration in amphibians, a suitable model for investigations of the effects of weightlessness as regards evolution and modifications 07 p0885 N88-15369
Nucleic acid content of skeletal muscles during hypokinesia and in the recovery period
07 p0894 N88-15418
Plant cell cultures in space biology studies
12 p1654 N88-19913
Aspects of bioregenerative life support systems
12 p1655 N88-19917
Organs and tissues regeneration in amphibia under the space flight conditions 12 p1660 N88-19951
Regenerative life support system research
[NASA-CR-182606] 12 p1671 N88-20006
Evaluation of a burned area and the vegetation regeneration affected by the burning in the Parque Nacional de Brazilia through TM/LANDSAT data
17 p2363 N88-24073

REGENERATIVE COOLING
Review of convectively cooled structures for hypersonic flight
[NASA-TM-87740] 17 p2310 N88-23817
REGENERATIVE CYCLES
U REGENERATION (ENGINEERING)
REGENERATIVE FUEL CELLS
Candidate advanced energy storage concepts for multimegawatt burst power systems 17 p2426 N88-24434
Monolithic fuel cell based power source for burst power generation 17 p2429 N88-24450
High power density alkaline fuel cell technology for MMW space burst power 17 p2429 N88-24451
All inorganic ambient temperature rechargeable lithium battery
[DE88-008425] 19 p2662 N88-25834
Regenerative fuel cell energy storage system for a low earth orbit space station
[NASA-CR-174802] 24 p3389 N88-30184
REGENERATORS
NT THERMOSIPHONS
Assessment of energy storage concepts for use in sprint power 17 p2407 N88-24312
Fatigue failure of regenerator screens in a high frequency Stirling engine 17 p2436 N88-24491
Advanced EMU electrochemically regenerable CO2 and moisture absorber module breadboard
[NASA-CR-172054] 21 p2993 N88-27754
REGIMES
On regime selection in global atmospheric flow 17 p2374 N88-24119
REGIONAL PLANNING
NT URBAN PLANNING
Remote sensing with LANDSAT 5 Thematic Mapper (TM) and its application to various planning levels: A case study from the Wuerzburg area, West Germany
[DFVLR-FB-86-62] 01 p0065 N88-10421
The atlas of regional development 16 p2226 N88-23291
Analyses of heliport system plans
[DOT/FAA/PM-87/31] 17 p2306 N88-23810
Topographic data processing for environmental planning 18 p2534 N88-25032
Remote sensing techniques applied to the study of metropolitan regions: The west sector of the Sao Paulo metropolitan area 19 p2681 N88-25941
Territorial management program 19 p2682 N88-25942
Aerial photography as an instrument of municipal and regional planning: Metropolitan area of Sao Paulo (SP) 19 p2684 N88-25957
Remote sensing applied to integrated regional development programs 19 p2685 N88-25958
Utilization of a satellite communication system to protect the national communication network
[FUB-33-1986] 21 p2934 N88-27423
REGIONS
NT AMAZON REGION (SOUTH AMERICA)
NT ANTARCTIC REGIONS
NT ARCTIC REGIONS
NT AURORAL ZONES
NT BRILLOUIN ZONES
NT D REGION
NT E REGION
NT EQUATORIAL REGIONS
NT F REGION
NT F 2 REGION
NT FRESNEL REGION
NT HABITATS
NT NEW ENGLAND (US)
NT NULL ZONES
NT POLAR REGIONS
NT REMOTE REGIONS
NT ROSS ICE SHELF
NT SPORADIC E LAYER
NT SUBARCTIC REGIONS
NT TEMPERATE REGIONS
NT TROPICAL REGIONS
A physical metallurgical basis for heat-affected zone and base-plate properties of a microalloyed HSLA steel
[AD-A180200] 01 p0022 N88-10137
Computation of transonic separated wing flows using an Euler/Navier-Stokes zonal approach
[NASA-TM-88311] 02 p0173 N88-11089
V/STOL aircraft configurations and opportunities in the Pacific Basin
[NASA-TM-100005] 03 p0261 N88-11644
Regional intercomparisons of General Circulation Model predictions and historical climate data: CO2
[DE88-010416] 23 p3235 N88-29248
REGISTERS
Vector performance of register-to-register vector computers
[DE88-004013] 10 p1384 N88-18265
REGISTERS (COMPUTERS)
On proving register atomicity
[CWI-CS-R8707] 13 p1818 N88-20862
Atomic multireader register — computer storage
[CWI-CS-R8722] 14 p1954 N88-21648
Simple multireader registers using time-stamp schemes
[CWI-CS-R8758] 20 p2835 N88-26819
REGOLITH
Energy requirements for HE-3 mining operations on the Moon 17 p2420 N88-24390
Sub-kilometer rampart craters in the equatorial region of Mars: Possible implications for the state and distribution of regolith H2O 23 p3302 N88-29666
Some probable characteristics of the Martian regolith 23 p3303 N88-29678
REGRESSION (STATISTICS)
U REGRESSION ANALYSIS
REGRESSION ANALYSIS
NT REGRESSION COEFFICIENTS
Identification of multivariate outliers and leverage points by means of robust covariance matrices
[REPT-87-15] 01 p0088 N88-10575
PROGRESS: A program for robust regression analysis on the IBM PC
[REPT-85-14] 01 p0088 N88-10576
Tropical cyclone intensity prediction based on empirical orthogonal function representation of wind and shear fields
[AD-A184899] 03 p0353 N88-12229
A computational examination of orthogonal distance regression
[AD-A184374] 03 p0371 N88-12337
Regressed relations for forced convection heat transfer in a direct injection stratified charge rotary engine
[NASA-TM-100124] 05 p0549 N88-13345
An APL workspace for conducting nonparametric statistical inference
[AD-A184971] 05 p0634 N88-13877
Least squares for fuzzy vector data regression
[AD-A185158] 05 p0640 N88-13917
Interactive nonlinear least squares program
[PB88-109855] 06 p0760 N88-14661
Asymptotic normality of poly-t densities with Bayesian applications
[AD-A185718] 06 p0768 N88-14719
Discrete reliability growth models using failure discounting
[AD-A186380] 07 p0866 N88-15252
Objective prediction of monthly mean surface temperature and climatological relationships to mid-tropospheric heights
[DE88-000908] 07 p0880 N88-15340
Estimation and testing in truncated and nontruncated linear median-regression models
[AD-A186317] 07 p0911 N88-15522
Variable selection in logistic regression
[AD-A186032] 07 p0914 N88-15547
Conditionally unbiased bounded influence robust regression with applications to generalized linear models
[AD-A186319] 07 p0915 N88-15556
A continuous oxidizer regression model for the combustion of composite solid propellants
[AD-A186742] 08 p0974 N88-15894
Short data length effects in an asymptotically efficient ARMA (AutoRegressive Moving Average) spectral estimator
[AD-A186561] 08 p1068 N88-16458
Test of linearity in general regression models
[AD-A186036] 08 p1073 N88-16477
Tensorial calibration. Part 1: First order tensorial calibration
[AD-A186708] 09 p1167 N88-16995
Detection of soil erosion with Thematic Mapper (TM) satellite data within Pinyon-Juniper woodlands
[NASA-CR-182476] 09 p1185 N88-17103
A note on computing robust regression estimates via iteratively reweighted least squares
[AD-A186709] 09 p1227 N88-17352
Prediction of polytomous events: Model description, algorithm development and methodological aspects, with an application
[AD-A186549] 09 p1232 N88-17384
Using ridge regression in systematic pointing error corrections 11 p1472 N88-18777
Improving battery reliability by using regression trees
[DE88-004539] 11 p1481 N88-18841
Estimation in linear models with censored data
[AD-A187209] 11 p1540 N88-19203
Department of Defense World Geodetic System 1984: Its definition and relationships with local geodetic systems
[AD-A188815] 12 p1639 N88-19811
Survival analysis using additive risk models
[AD-A189053] 13 p1825 N88-20906
Spatial and temporal distribution of precipitation chemistry across Maryland in 1984, volume 1
[PB88-148929] 14 p1943 N88-21595
Concentration inequalities for Gauss Markov estimators
[CWI-MS-R8706] 14 p1965 N88-21726
Modeling failures of intermittently used machines
[AD-A190298] 15 p2074 N88-22367
Inference for a nonlinear semimartingale regression model
[AD-A190857] 16 p2262 N88-23527
Spectral measurements for correcting LANDSAT data for atmospheric effects 17 p2353 N88-24020
Estimation of an area cultivated with wheat from LANDSAT data through a two-phase sampling method 17 p2357 N88-24041
Evaluation of an estimation system for an irrigated area in a tropical region through TM-LANDSAT imagery 17 p2363 N88-24075
On Hotelling's approach to testing for a nonlinear parameter in regression
[AD-A191189] 17 p2393 N88-24229
Automated analysis of crack growth rate for obtaining da/dN versus delta K relation
[FFA-TN-1987-70] 18 p2527 N88-24996
Asymptotic theory for weighted least squares estimators in Aalen's additive risk model
[AD-A191085] 18 p2562 N88-25210
Symmetrized nearest neighbor regression estimates
[AD-A191998] 18 p2568 N88-25254
A statistical treatment of accelerated life test data for copper-water heat pipes 20 p2783 N88-26509
Asymptotic normality of minimum L1-norm estimates in linear models
[AD-A193399] 21 p3006 N88-27835
On climate prediction for India 22 p3127 N88-28590
Characteristics of regression equations for specifying monthly precipitation amounts over the United States from the field of concurrent mean 700 mb heights 22 p3127 N88-28591
Two biased estimation techniques in linear regression: Application to aircraft
[NASA-TM-100649] 23 p3274 N88-29489
REGRESSION COEFFICIENTS
Estimation of a multivariate continuous variable panel model
[AD-A184472] 04 p0484 N88-12982
Strong consistency of estimation of number of regression variables when the errors are independent and their expectations are not equal to each other
[AD-A186025] 07 p0909 N88-15507
Estimating the solar irradiance of an intermountain region using GOES (Geostationary Operational Environmental Satellite) satellite data: A test of two statistical models
[AD-A188414] 12 p1642 N88-19834
Leave-K-Out diagnostics for time series
[AD-A191343] 16 p2261 N88-23518
Min-max bias robust regression
[AD-A191345] 16 p2263 N88-23529
REGULARITY
Regularity properties of a doubly degenerate equation in hydrology
[REPT-87-07] 01 p0064 N88-10409
Regularity of the Albanese map for nonoriented surfaces
[DE88-006428] 15 p2126 N88-22679
Pairwise complete regularity as a separation axiom
[REPT-87-57] 16 p2264 N88-23539
Regularity of solutions for nonlinear degenerate elliptic boundary value problems
[DE88-702646] 22 p3148 N88-28710
Regularity and numerical solution of eigenvalue problems with piecewise analytic data
[AD-A194993] 24 p3425 N88-30387
REGULATION
U CONTROL
REGULATIONS
Airworthiness of long-life jet transport structures 03 p0265 N88-11674
DOE explosives safety manual
[DE88-000831] 04 p0422 N88-12616
Deterministic uncertainty analysis
[DE88-006139] 13 p1829 N88-20942
The impact of independent research and development regulations on companies not required to negotiate advanced independent research and development agreements
[AD-A190007] 15 p2147 N88-22818
Advisory circular: Noise certification handbook
[FAA-AC-36-4B] 17 p2394 N88-24234
Discussions and agreements in the United Nations on important issues associated with nuclear power in space 17 p2423 N88-24411

International and domestic mobile satellite regulatory proceedings: A comparison of outcomes and discussion of implications 19 p2644 N88-25690
International and domestic regulator issues facing the Canadian MSAT system 19 p2644 N88-25692
Timing regulations to prevent stratospheric-ozone depletion
[R-3495-JMO/RC] 19 p2690 N88-25987
New CCIR report on SETI 22 p3067 N88-28204
The OFP (Operational Flight Program) update cycle needs you
[AD-A194910] 24 p3325 N88-29798

REGULATORS
NT AUTOMATIC FREQUENCY CONTROL
NT FLOW REGULATORS
NT FREQUENCY CONTROL
NT PRESSURE REGULATORS
NT SPEED REGULATORS
NT VOLTAGE REGULATORS
A feasibility study in path planning using optimization techniques
[AD-A193030] 21 p2894 N88-27177

REGULATORY MECHANISMS (BIOLOGY)
Daily dynamics of some physiological indicators of man under desert condition 06 p0750 N88-14605
Physicochemical correlates of human adaptation to extreme environments 06 p0750 N88-14607
Neurophysiological analysis of hypothalamic regulation mechanisms of primary sleep and hypobiosis 06 p0751 N88-14611
Distinctive changes in arterial pressure and blood flow in common carotid artery of monkeys flown aboard Cosmos-1514 biosatellite 07 p0892 N88-15404
Biofeedback control of alveolar carbon dioxide tension to eliminate hypocapnia in man in the presence of hypoxia 07 p0892 N88-15405
NASA Workshop on Biological Adaptation
[NASA-TM-89468] 10 p1368 N88-18174
Regulation of calcium metabolism during prolonged antiorthostatic hypokinesia
[NASA-TT-20219] 11 p1521 N88-19085
Dexamethasone regulates glutamine synthetase expression in rat skeletal muscles
[NASA-CR-182935] 18 p2549 N88-25129

REHEATING
U HEATING

REIGNITION
U IGNITION

REINFORCED PLASTICS
NT CARBON FIBER REINFORCED PLASTICS
NT GLASS FIBER REINFORCED PLASTICS
Short fiber reinforced thermoplastic composites for armor applications: Interfacial bonding
[DE88-004007] 10 p1295 N88-17742
Fiber-reinforced plastic composites. Possibilities and limitations of applications as machine-construction materials
[NASA-TT-20159] 15 p2031 N88-22102
Injection compression for short fiber reinforced plastics
[SNIAS-881-430-118] 21 p2922 N88-27344

REINFORCED PLATES
Optimal ribbing of long plate made of composite material 04 p0426 N88-12641
Interaction of ultrasonic waves with composite plates
[AD-A191879] 18 p2478 N88-24702
Plasma joining of metal matrix composites
[AD-A193939] 22 p3051 N88-28100

REINFORCED SHELLS
Solution of geometrically nonlinear problem for reinforced shell of revolution having arbitrary shape 04 p0426 N88-12637
Rational reinforcement of cylindrical shells with variable stiffness frames subjected to external pressure 04 p0426 N88-12638
Experimental studies on the tripping behavior of narrow T-stiffened flat plates subjected to hydrostatic pressure and underwater shock 05 p0592 N88-13613
Monolithic nature of transversely reinforced composites 14 p1885 N88-21267

REINFORCEMENT (PSYCHOLOGY)
Training in time interval discrimination using verbal feedback 12 p1665 N88-19985

REINFORCEMENT (STRUCTURES)
Reinforced flexural elements for TEMP-STRESS Program
[DE87-012961] 01 p0061 N88-10391
Optimal ribbing of long plate made of composite material 04 p0426 N88-12641
Geometrically nonlinear analysis of stiffened panels 06 p0722 N88-14440
Buckling of braced monosymmetric cantilevers: Timoshenko energy approach
[PB87-133849] 06 p0723 N88-14445
The Shock and Vibration Bulletin. Part 4: Structural Dynamics and Modal Test and Analysis
[AD-A186751] 09 p1179 N88-17062
Analysis of reinforced concrete structures under the effects of localized detonations 09 p1179 N88-17064
Reinforced concrete arches under blast and shock environments 09 p1180 N88-17065
Woven frameworks for three-dimensional reinforcement 14 p1884 N88-21262
Stiffened titanium panels
[NASA-CASE-LAR-13814-1] 18 p2497 N88-24816
A simple unified method for predicting the deflections of reinforced concrete structures 19 p2679 N88-25930
An assessment of modelling techniques for the finite element analysis of reinforced concrete plate and shell structures
[AD-A192263] 20 p2814 N88-26697
Cold worked reinforcing bars in tensile test under high loading rate and low temperatures
[DE88-752993] 21 p2964 N88-27610

REINFORCEMENT RINGS
Redesign of solid rocket booster/external tank attachment ring for the space transportation system
[NASA-TM-100476] 01 p0017 N88-10101
Structural analysis of the space shuttle solid rocket booster/external tank attach ring
[NASA-TM-100510] 11 p1446 N88-18618

REINFORCING FIBERS
NT BORON FIBERS
NT CARBON FIBERS
Pressure effects on the thermal stability of SiC fibers
[NASA-TM-100146] 01 p0019 N88-10120
Interfacial shear strength of pitch and high strain pan fibers in an epoxy matrix
[AD-A185966] 07 p0826 N88-15011
Short fiber reinforced thermoplastic composites for armor applications: Interfacial bonding
[DE88-004007] 10 p1295 N88-17742
Use of reinforced inorganic cement materials for spark wire and drift chamber wire frames
[NASA-CR-180759] 13 p1746 N88-20438
PNL-1 improved ceramic composites through controlled fiber matrix interaction
[DE88-005680] 13 p1750 N88-20462
Creep behavior of tungsten/niobium and tungsten/niobium-1 percent zirconium composites 17 p2425 N88-24427
Properties of two composite materials made of toughened epoxy resin and high-strain graphite fiber
[NASA-TP-2826] 19 p2609 N88-25480
The two isotropic asymptotes of fiber composites
[AD-A192305] 21 p2904 N88-27231
Theoretical and experimental analysis of the toughening behavior of whisker reinforcement in ceramic matrix composites
[DE88-011841] 21 p2906 N88-27241
Wave propagation and vibration of fibre reinforced laminates
[AD-A194144] 22 p3051 N88-28101
Thermoplastic composite with continuous fibers
[FOA-C-20707-2.6] 22 p3051 N88-28103
Elastic wave dispersion in laminated composite plate
[AD-A192289] 23 p3188 N88-28967
A study of the critical factors controlling the synthesis of ceramic matrix composites from preceramic polymers
[AD-A195405] 24 p3340 N88-29881
Some theoretical considerations of the surface tension of liquid metals for metal matrix composites
[AD-A195999] 24 p3340 N88-29882

REINFORCING MATERIALS
Bibliography of textbooks on fibre reinforced plastics (212 books)
[PB87-146080] 07 p0827 N88-15017
Fabrication and materials evaluation of high performance aligned ceramic fibre reinforced glass matrix composite
[AERE-R-12517] 10 p1294 N88-17736
Viscoelastic behavior of a polyetheretherketone (PEEK) composite
[AD-A189545] 13 p1734 N88-20368
Fracture criteria for discontinuously reinforced metal matrix composites
[NASA-CR-182665] 13 p1782 N88-20662
Strength and failure analysis of composite laminate containing a circular hole with reinforcement
[AD-A189629] 14 p1884 N88-21260
Woven frameworks for three-dimensional reinforcement 14 p1884 N88-21262
Monolithic nature of transversely reinforced composites 14 p1885 N88-21267
The two isotropic asymptotes of fiber composites
[AD-A192305] 21 p2904 N88-27231

REISSNER THEORY
Stress strain fields at crack tip and stress intensity factors in Reissner's plate
[PB87-144945] 08 p0994 N88-16014

RELATIVISTIC EFFECTS
Relativistic stochastic mechanics
[PREPRINT-543] 06 p0790 N88-14842
Relativistic corrections for one- and two-photon matrix elements of weakly-bound systems
[NOTA-INTERNA-884] 07 p0929 N88-15645
A note on Fujikawa's method of determining the critical dimension of the relativistic string
[NIKHEF-H/87-5] 08 p1092 N88-16571
Considerations of acceleration effects in relativistic kinematics 09 p1260 N88-17553
Can the causal pathologies of Goedel-type universes be avoided in higher-derivative gravity
[DE88-700185] 11 p1568 N88-19387
Relativistic jet models for the BL Lacertae object Mrk 421 during three epochs of observation
[NASA-TM-89727] 13 p1853 N88-21090
Topics in curved and flat space electromagnetism 13 p1854 N88-21100

RELATIVISTIC ELECTRON BEAMS
A simple self-breaking 2 MV gas switch
[DE87-014346] 02 p0166 N88-11047
Laser induced fluorescent study of relativistic electron beams
[AD-A184456] 04 p0447 N88-12774
Relativistic electron precipitations in a pulsating aurora 04 p0468 N88-12894
Variable collision frequency effects on hose and sausage instabilities in relativistic electron beams
[AD-A184206] 04 p0490 N88-13021
Coherent emission from relativistic beam-plasma interactions 04 p0493 N88-13039
Modulation of an intense beam by an external microwave source: Theory and simulation
[AD-A185683] 07 p0846 N88-15145
Relativistic plasma concentration measuring by Bremsstrahlung
[DE88-700560] 07 p0936 N88-15685
Wave functions for bound states of relativistic electrons in a crystal at electron movement along crystallographic planes
[DE88-700563] 07 p0939 N88-15708
Collective acceleration of electrons and ions in a high relativistic electron beam
[DE88-005261] 13 p1838 N88-20998
Design of electron beam accelerator for microwave application
[DE88-005252] 13 p1838 N88-20999
XeF excimer laser pumped by high-intensity relativistic electron beam 14 p1901 N88-21355
Three-wave parametric resonance in plasma of relativistic electron flux 14 p1972 N88-21772
High pressure operation of beam diodes for generating relativistic electron beams 16 p2279 N88-23643
Deep dielectric charging effects due to high energy electrons in earth's outer magnetosphere
[AD-A192154] 18 p2541 N88-25083
SARLAC: A relativistic electron beam code
[AD-A193134] 21 p2932 N88-27411
Propagation of charged particle beams in the atmosphere
[AD-A193185] 21 p3014 N88-27887
Millimeter wave generation by relativistic electron beams
[AD-A195683] 24 p3362 N88-30016
Research on a two-stage free electron laser oscillator
[AD-A195991] 24 p3377 N88-30115

RELATIVISTIC PARTICLES
NT RELATIVISTIC ELECTRON BEAMS
Analysis of relativistic nucleus-nucleus interactions in emulsion chambers 07 p0926 N88-15624
On a possibility of ion acceleration up to high energies in a high-current electron beam
[DE88-700532] 07 p0931 N88-15657
Relativistic Calogero-Moser systems and solutions
[CWI-PM-R8702] 08 p1092 N88-16570
Single nucleon coincidence cross sections in a relativistic mean field theory
[CEBAF-PR-87-016] 11 p1546 N88-19243
Action-angle maps and scattering theory for some finite-dimensional integrable systems. The pure solution case
[CWI-PM-R8704] 13 p1831 N88-20955
The multistring model VENUS for ultrarelativistic heavy ion collisions
[DE88-007666] 18 p2573 N88-25284
Experiments with high energy nuclear beams at Brookhaven: From AGS to RHIC (Relativistic Heavy Ion Collider)
[DE88-007042] 18 p2574 N88-25287

Experiments on insulation of relativistic electron flows in oblique and tapered magnetic fields
[DE88-007199] 19 p2724 N88-26176
Passage of relativistic magnetic dipole moments through magnetic fields
[DE88-702640] 23 p3295 N88-29624

RELATIVISTIC PLASMAS
A relativistic Monte Carlo binary collision model for use in plasma particle simulation codes
[DE87-013287] 02 p0237 N88-11494
Plasma wave radiative damping of a new type in a relativistic one-dimensional plasma
[DE88-701191] 15 p2135 N88-22739
ECRH current drive in tokamak plasmas
[IPPJ-864] 19 p2729 N88-26209

RELATIVISTIC THEORY
Superluminal velocities within relativity theory
[ETN-87-90958] 02 p0247 N88-11563
Nonlinear, relativistic Langmuir waves in astrophysical magnetospheres
[NASA-CR-182422] 08 p1024 N88-16197
Relativistic electromagnetic waves in an electron-ion plasma
[NASA-CR-182421] 08 p1085 N88-16532
Relativistic Calogero-Moser systems and solutions
[CWI-PM-R8702] 08 p1092 N88-16570
Relativistic theory of gravitation and new concepts about space-time 09 p1240 N88-17431
Hamiltonian approach to relativistic theory of gravity and to general relativity theory
[DE88-700404] 10 p1422 N88-18492
Semileptonic weak interactions in nuclei: A relativistic analysis
[CEBAF-PR-87-024] 11 p1547 N88-19249
Hamiltonian formalism in the model of the relativistic string with rigidity
[DE88-701503] 15 p2147 N88-22815
Bogolyubov transformation in relativistic theory of gravitation
[DE88-701592] 16 p2232 N88-23329
Relativistic theory of gravitation and criticism of General Relativity Theory (GRT)
[DE88-701304] 16 p2284 N88-23673
On the self-trapping of an electromagnetic wave in magnetized plasma
[DE88-701872] 20 p2858 N88-26974
Relativistic theory of the Lamb shift based on self energy
[DE88-702658] 23 p3295 N88-29626

RELATIVISTIC VELOCITY
Superluminal velocities within relativity theory
[ETN-87-90958] 02 p0247 N88-11563
On a possibility of ion acceleration up to high energies in a high-current electron beam
[DE88-700532] 07 p0931 N88-15657
Collective acceleration of electrons and ions in a high relativistic electron beam
[DE88-005261] 13 p1838 N88-20998
The multistring model VENUS for ultrarelativistic heavy ion collisions
[DE88-007666] 18 p2573 N88-25284
A study of mechanisms producing astrophysical jets
[AD-A194100] 23 p3300 N88-29649

RELATIVITY
Volume functions in the general theory of relativity
[ETN-87-90408] 01 p0089 N88-10582
On the theory of the Michelson-Morley experiment in the Earth's gravitational field
[DE87-703077] 02 p0198 N88-11233
Superluminal velocities within relativity theory
[ETN-87-90958] 02 p0247 N88-11563
New notions about space-time and gravitation
[DE87-703259] 03 p0383 N88-12408
Analysis of absolute space-time Lorentz theories
[DE87-703371] 04 p0500 N88-13076
Homogeneous space-time of Goedel type in higher-derivate gravity
[DE87-703690] 04 p0500 N88-13077
Gravity from symmetry breakdown of a gauge affine theory
[DE88-001671] 04 p0500 N88-13079
Cosmological applications of singular hypersurfaces in general relativity 04 p0521 N88-13202
Relativistic stellar pulsations 06 p0801 N88-14902
A simplified model of elementary particles
[NOTA-INTERNA-890] 07 p0930 N88-15647
Criterion of singularity in general theory of relativity 09 p1240 N88-17430
On higher derivative gravity
[DE88-700619] 10 p1354 N88-18090
Hamiltonian approach to relativistic theory of gravity and to general relativity theory
[DE88-700404] 10 p1422 N88-18492
Antimatter: Its history and its properties
[DE88-004308] 10 p1423 N88-18498
Velocity reversal and the arrows of time
[DE88-004237] 10 p1429 N88-18536
Notes on a class of homogeneous space-times
[DE88-700138] 11 p1562 N88-19353
Experimental analysis of absolute space-time Lorentz theories
[DE88-700140] 11 p1563 N88-19355
Seventy years of the general theory of relativity
[DE88-700784] 11 p1563 N88-19356
Relative chaos in stellar systems
[DE88-700148] 12 p1710 N88-20234
Topics in curved and flat space electromagnetism 13 p1854 N88-21100
Galilei relativity principle in classical electrodynamics
[DE87-703203] 14 p1904 N88-21376
Special relativity theory (one-dimensional case) without the postulate on the equality of directions
[DE88-701368] 16 p2284 N88-23674
From general relativity to the theory of superstrings 18 p2587 N88-25369
Dissipative relativistic radiation hydrodynamics
[DE88-702092] 19 p2665 N88-25846
Deviation equation as an equation of motion
[DE88-702134] 19 p2722 N88-26161
General relativity invariance and string field theory
[DE88-702045] 19 p2737 N88-26252
Transcending Newton's legacy
[DE88-010784] 19 p2738 N88-26254
On microphysical principles of thermofluid dynamics
[ETN-88-92095] 20 p2801 N88-26620
Theory of relativity and super-light-speeds-I: Kinematical part
[DE88-701832] 20 p2880 N88-27100
Combining relativity and quantum mechanics: Schroedinger's interpretation of psi
[DE88-701899] 20 p2880 N88-27102
Gravitation electromagnetic theory 22 p3158 N88-28790
On the GKP and BS constructions of C-boundary
[DE88-702643] 22 p3159 N88-28799
Time travel in the homogeneous Som-Raychaudhuri universe
[DE88-702220] 23 p3295 N88-29622
On neutrino fields in Einstein-Cartan theory
[MATH-REPT-208] 23 p3295 N88-29629

RELAXATION (MECHANICS)
NT SPIN-LATTICE RELAXATION
NT STRESS RELAXATION
Pure dephasing of a vibrational adbond
[AD-A185222] 05 p0609 N88-13740
Structure-property relationships in thermoplastic elastomers 4. Dynamic mechanical relaxations in poly(dioxolane), poly(butytrioxocane) and poly(propylene oxide) polyurethanes
[AD-A186278] 07 p0836 N88-15073
Structural relaxation and mechanical properties of amorphous Fe-Zr alloys 07 p0840 N88-15094
Structural relaxation in strained-layer heterostructures
[DE88-002326] 07 p0868 N88-15264
Lattice relaxation of the DX centers in Ga/sub 1-x/Al/sub x/As and of the pressure-induced deep donors in GaAs
[DE88-005452] 13 p1848 N88-21061

RELAXATION METHOD (MATHEMATICS)
Theoretical and practical aspects of multigrid methods in boundary element calculations
[NLR-MP-85021-U] 03 p0370 N88-12328
An application of a gradient relaxation method to noisy infrared images
[AD-A184666] 03 p0377 N88-12371
A note on the use of symmetric line Gauss-Seidel for the steady upwind differenced Euler equations
[AD-A185223] 05 p0580 N88-13540
Matching segments from a map and an aerial image using relaxation techniques
[SNIAS-872-422-103] 05 p0620 N88-13809
Upwind relaxation algorithms for Euler/Navier-Stokes equations 07 p0810 N88-14931
Choice of implicit and explicit operators for the upwind differencing method
[NASA-TM-100857] 14 p1964 N88-21718
Relaxation scheme for compressible flows 19 p2640 N88-25663
Numerical integration of Navier-Stokes equations by application of multigrid concept
[ETN-88-92365] 21 p2949 N88-27513
Relaxed heaps: An alternative to fibonacci heaps
[AD-A194030] 23 p3272 N88-29470

RELAXATION TIME
Ion-matrix coupling in polymer electrolytes from relaxation time studies
[AD-A184632] 03 p0293 N88-11841
Theoretical studies of Resonance Enhanced Stimulated Raman Scattering (RESRS) of frequency-doubled Alexandrite laser wavelength in cesium vapor
[NASA-CR-182870] 15 p2036 N88-22133

RELEASING
Hydrogen retention and release from uranium dioxide
[DE88-002042] 07 p0829 N88-15030
Deployable booms and antennas on AMPTE-IRM 14 p1874 N88-21198
Modification and development of the external tank hydrogen vent umbilical system for the space shuttle vehicle 14 p1928 N88-21496
A plasma wave instrument on the AMPTE/IRM (Active Magnetospheric Particle Tracing Explorers/Ion Release Module) spacecraft
[AD-A191216] 16 p2233 N88-23336
Design, development, fabrication and launch support for a high altitude release of neodymium vapor
[AD-A194196] 22 p3118 N88-28527
Effects of tectonic release on broadband regional distance bodywaves
[AD-A194247] 22 p3119 N88-28529

RELIABILITY
NT AIRCRAFT RELIABILITY
NT CIRCUIT RELIABILITY
NT COMPONENT RELIABILITY
NT SPACECRAFT RELIABILITY
NT STRUCTURAL RELIABILITY
Wire interconnection reliability and moisture levels in hybrid microcircuits with epoxy-attached components
[DE87-012987] 01 p0039 N88-10247
Computing systems dependability and fault tolerance: Basic concepts and terminology 02 p0127 N88-10737
Needs assessment for nondestructive testing and materials characterization for improved reliability in structural ceramics for heat engines
[DE88-000040] 02 p0153 N88-10957
Software reliability models for fault-tolerant avionics computers and related topics
[NASA-CR-181440] 02 p0220 N88-11382
Electronic system reliability and effectiveness
[AD-A184522] 03 p0311 N88-11961
Programmable Logic Arrays (PLA's) design for testability
[PB87-102935] 04 p0438 N88-12718
Reliability of Li/SO2 cells for long-life applications
[DE88-001360] 04 p0440 N88-12735
Software reliability perspectives
[NASA-CR-181523] 04 p0479 N88-12952
Development of an interface for an ultrareliable fault-tolerant control system and an electronic servo-control unit
[NASA-TM-88236] 05 p0553 N88-13367
Electromagnetics and electrothermal approach to evaluate failures in microelectronic devices caused by electrostatic discharges: Stochastical aspects of the device reliability
[AD-A184906] 05 p0577 N88-13522
Composite reliability enhancement via preloading
[AD-A185938] 07 p0826 N88-15010
Reliability and survivability of communication networks
[AD-A186248] 07 p0842 N88-15109
How errors in component reliability affect system reliability
[AD-A186264] 07 p0865 N88-15249
Supportability in aircraft systems through technology and acquisition strategy applications
[AD-A186465] 08 p0949 N88-15759
Reliability issues in distributed operating systems
[PB88-100870] 08 p0993 N88-16009
Experimental Radio Data System (RDS): A survey of reception reliability in the UK
[BBC-RD-1987/17] 09 p1155 N88-16922
Analysis of the reliability of Royal Australian Air force non-destructive inspection
[AD-A186979] 09 p1177 N88-17049
Methods for evaluating the quality and reliability of aerodynamic software programs
[PB87-169793] 09 p1219 N88-17314
Johnson noise thermometer for high radiation and high temperature environments
[DE88-003770] 10 p1323 N88-17911
Analysis and application of the constant tensile load test for polyethylene gas pipe materials
[DE88-002868] 10 p1345 N88-18037
Improving battery reliability by using regression trees
[DE88-004539] 11 p1481 N88-18841
Specialized instrumentation for computational fluid dynamics research
[AD-A188160] 11 p1482 N88-18849
A procedure for estimating the crystal densities of organic explosives
[AD-A189023] 12 p1613 N88-19646
Reliability analyses of a surface mounted package using finite element simulation
[AD-A189488] 12 p1624 N88-19717
Statistical aspects of reliability, maintainability and availability
[AD-A188491] 12 p1634 N88-19783

Estimating system and component reliabilities under partial information on cause of failure
[AD-A189107] 13 p1780 N88-20653
Stochastic comparisons of order statistics, with applications in reliability
[AD-A189408] 13 p1829 N88-20938
Advanced capacitor development
[AD-A189985] 15 p2059 N88-22276
Present, future of automotive hybrid IC applications discussed 16 p2185 N88-23024
Hybrid PV HgCdTe IR detectors technology reliability and failure program: Environmental stress testing plan
[AD-A191165] 16 p2211 N88-23195
Laser comparison study of Nd:BEL and Nd:YAG
[AD-A191084] 16 p2213 N88-23205
Computerized life and reliability modelling for turboprop transmissions
[NASA-TM-100918] 16 p2215 N88-23220
Studies in reliability and inference
[AD-A191389] 16 p2217 N88-23223
Relating design and environmental variables to reliability 17 p2418 N88-24383
Preliminary analysis of helium generation and its effects on the SP-100 system performance 17 p2422 N88-24406
Johnson noise thermometer for high-radiation and high-temperature environments 17 p2434 N88-24480
Descriptions of HF and VHF Loran-C buoys and evaluations as potential datum marker buoys
[AD-A192069] 18 p2462 N88-24618
An extended life and performance test of a low-power arcjet
[NASA-TM-100942] 18 p2476 N88-24687
Sensitivity analysis for the system reliability function
[AD-A191648] 18 p2525 N88-24978
Pyrotechnic system failures: Causes and prevention
[NASA-TM-100633] 20 p2765 N88-26394
An evaluation methodology for dependable multiprocessors
[AD-A192799] 20 p2842 N88-26863
Probabilistic anisotropic failure criteria for composite materials
[AD-A193046] 21 p2904 N88-27232
Test and calibration system for monitoring the Advanced Technologies Testing Aircraft System (ATTAS) data acquisition system 22 p3037 N88-28029
The impact of increased aircraft reliability on maintenance facility design
[AD-A194395] 22 p3042 N88-28057
Another approach for forecasting forecast skill 22 p3126 N88-28580
Estimating reliability with discrete growth models
[AD-A193845] 22 p3143 N88-28692
Use of Markov probability and reliability model generation methods in the analysis of reliability of a fault tolerant hardware and software based system with flexible repair policies
[PNR90467] 22 p3145 N88-28706
Effect of fiber diameter on the reliability of composites - automated laser diffraction implementation
[AD-A193524] 23 p3188 N88-28972
Reliability assessment of Surface Mount Technology (SMT)
[AD-A193759] 23 p3208 N88-29089
Remotely Operated Vehicle (ROV) reliability study, phase 1
[AD-A194367] 23 p3222 N88-29177
Analysis of the effect of faulty spares on the performance of diagnostic algorithms in reliable systems
[AD-A193526] 23 p3223 N88-29186
Reliability and Maintainability (R and M)
[AD-A193857] 23 p3224 N88-29187
Literature review: Validity and potential usefulness of psychomotor ability tests for personnel selection and classification
[AD-A193558] 23 p3241 N88-29267
Reliability and construct validity of reaction time, inspection time and machine-paced tests of cognitive speed
[AD-A193779] 23 p3241 N88-29289
A minitab macro for the Kaplan-Meier product limit estimator and the Tarone-Ware class of tests
[AD-A194298] 23 p3248 N88-29331
An expert system for reliability modeling 23 p3252 N88-29355
Exact lower confidence limits for the reliability of k of n systems for zero failures and nonconservativeness of the maximus method
[AD-A194299] 23 p3274 N88-29485
The cost and performance implications of reliability improvements in the F-16A/B
[AD-A195096] 24 p3324 N88-29796
A reliability-based program for predicting the service life of organic coating systems 24 p3355 N88-29971

RELIABILITY ANALYSIS
Wet deposition and snowpack monitoring operations and quality assurance manual
[PB87-212817] 01 p0064 N88-10413
The reliability of numerical solutions of ordinary differential equations, obtained by implicit calculation schemes
[PTB-W-30] 01 p0085 N88-10549
Application of fracture mechanics theory in the reliability analysis of structural ceramics in multiaxial loading 03 p0335 N88-12113
Investigation of reliability of strength values measured on CFRP test bars by statistical methods. Part 1: Probability distributions for strength analysis
[ESA-TT-1036] 03 p0336 N88-12115
A reliability concept for optimizing aircraft design 04 p0423 N88-12622
Applications of the hybrid automated reliability predictor
[NASA-TP-2760] 04 p0475 N88-12928
On the next generation of reliability analysis tools
[NASA-CR-178380] 04 p0487 N88-13000
Space station software reliability analysis based on failures observed during testing at the multisystem integration facility 06 p0798 N88-14884
An independent evaluation of the CH-46 Safety Reliability and Maintainability Program (SR and M)
[AD-A186310] 07 p0817 N88-14971
Estimating system reliability: Monte Carlo methods, sensitivity and errors in input parameters
[AD-A186182] 07 p0865 N88-15248
Fault tree reliability analysis of the Naval Postgraduate School mini-satellite (ORION)
[AD-A186283] 07 p0866 N88-15250
Discrete reliability growth models using failure discounting
[AD-A186380] 07 p0866 N88-15252
Reliability modelling for fault-tolerant parallel processor
[AD-A185867] 07 p0900 N88-15451
Causes and distribution of failures in semiconductor lasers (a review) 07 p0919 N88-15581
Integrated analysis and applications 08 p0954 N88-15789
Rotor dynamic behavior of centrifugal pumps 08 p0975 N88-15898
SURE reliability analysis: Program and mathematics
[NASA-TP-2764] 09 p1231 N88-17380
An anlysis of the reliability of tree-structured interconnection networks 10 p1378 N88-18228
Derivation of strength factors related to the coordination of the strength of transmission line components --- electric power lines
[S/T-REPT-VOL-5-NO-2] 11 p1500 N88-18959
Reliability based analysis of contact problems
[NASA-CR-182117] 11 p1503 N88-18975
Reliability analyses of a surface mounted package using finite element simulation
[AD-A189488] 12 p1624 N88-19717
An experiment in software reliability: Additional analyses using data from automated replications
[NASA-CR-178395] 12 p1676 N88-20017
A computer code for the solution of large scale network reliability analysis problems
[AD-A188455] 12 p1680 N88-20042
A fault injection experiment using the AIRLAB Diagnostic Emulation Facility
[NASA-CR-178390] 13 p1823 N88-20895
CARE 3 User's Workshop
[NASA-CP-10011] 14 p1954 N88-21646
The 1988 failure rate screening data for fusion reliability and risk analysis
[DE88-006798] 14 p1984 N88-21837
Monte Carlo reliability analysis
[AD-A189972] 15 p2074 N88-22366
Reliability analysis within a Computer Aided Engineering (CAE) infrastructure
[NLR-MP-86059-U] 15 p2074 N88-22369
Whisker-reinforced ceramic composites for heat engine components 15 p2082 N88-22410
Methodology for software reliability prediction, volume 1
[AD-A190018] 15 p2110 N88-22571
Methodology for software reliability prediction, volume 3
[AD-A190019] 15 p2110 N88-22572
Analysis and testing of the SURE program
[NASA-TP-2817] 15 p2123 N88-22653
Digital avionics design and reliability analyzer
[NASA-CR-181641] 16 p2254 N88-23472
The PAWS and STEM reliability analysis programs
[NASA-TM-100572] 16 p2262 N88-23526
Automatically generated acceptance test: A software reliability experiment
[NASA-CR-181667] 17 p2347 N88-23984
Reliability of stochastically forced systems (extended version)
[CWI-AM-R8801] 18 p2526 N88-24985
Semi-Markov adjunction to the Computer-Aided Markov Evaluator (CAME)
[NASA-CR-181645] 19 p2678 N88-25924
Estimating reliability with discrete growth models
[AD-A193845] 22 p3143 N88-28692
Use of Markov probability and reliability model generation methods in the analysis of reliability of a fault tolerant hardware and software based system with flexible repair policies
[PNR90467] 22 p3145 N88-28706
Approximate evaluation of semi-Markov chain reliability models
[AD-A194669] 23 p3223 N88-29185
Investigations on the modification of structural reliability by substitution of aluminum by carbon fiber reinforced plastics in aircraft construction
[ILR-MITT-195] 24 p3339 N88-29877

RELIABILITY CONTROL
U QUALITY CONTROL
U RELIABILITY ENGINEERING

RELIABILITY ENGINEERING
The application of emulation techniques in the analysis of highly reliable, guidance and control computer systems 02 p0127 N88-10798
Some approaches to the design of high integrity software 02 p0127 N88-10799
Reliability modeling of fault-tolerant computer based systems 02 p0127 N88-10801
Software reliability models for fault-tolerant avionics computers and related topics
[NASA-CR-181440] 02 p0220 N88-11382
Reliability-based optimal structural and mechanical design 03 p0335 N88-12109
Reliability of voting in fault-tolerant software systems for small output spaces
[TR-87-16] 05 p0632 N88-13864
Effectiveness of back-to-back testing
[TR-87-08] 05 p0632 N88-13865
A software reliability model with variable fault exposure coefficient
[REPT-87-029] 06 p0757 N88-14648
Evaluate the application of modal test and analysis processes to structural fault detection in MSFC - STS project elements 07 p0927 N88-15630
Innovating systems and techniques for the diagnosis of materials and industrial plants
[CISE-3856] 08 p0976 N88-15901
Hardware/software reliability study --- space programs
[REPT-85.5686] 09 p1218 N88-17307
Probabilistic and reliability design procedures for flexible airfield pavements: Elastic layered method
[AD-A187533] 11 p1442 N88-18600
Modification, implementation, and evaluation of a remote terminal emulator as a software validation and stress testing tool
[AD-A188833] 12 p1678 N88-20034
Comparative analysis of multistage interconnection networks
[AD-A190436] 15 p2115 N88-22598
Information systems for quality. Experience at the Nerviano Aeritalia plant. Avionic systems and equipment group
[ETN-88-92274] 15 p2148 N88-22821
Incorporating reliability into the design of experimental fusion facilities
[DE88-006767] 16 p2275 N88-23618
Integrated avionics reliability 17 p2294 N88-23723
Advanced LMMHD space power generation concept 17 p2415 N88-24364
The VIPER microprocessor
[RSRE-87014] 22 p3135 N88-28640
Reliable onboard computing for critical space systems
[RR-670-I] 22 p3135 N88-28641
Expert systems for MSFC power systems 23 p3255 N88-29375
Blackboard architectures and their relationship to autonomous space systems 23 p3261 N88-29414
A nonlinear filtering process diagnostic system for the Space Station 23 p3262 N88-29417
Intelligent fault diagnosis and failure management of flight control actuation systems
[NASA-CR-177481] 24 p3323 N88-29790

RELIC RADIATION
Dipole component of relict radiation determined from Relikt experiment data 08 p1002 N88-16070
Nonequilibrium ionization of pregalactic plasma and lessening of relic radiation anisotropy 08 p1002 N88-16071
Measurements of the cosmic background radiation
[NASA-CR-182637] 12 p1712 N88-20248
A map of the cosmic background radiaton at 3 millimeters
[INPE-4529-PRE/1279] 15 p2152 N88-22850

RELIEF MAPS
Study of relief of ore regions using space images (on the example of Eastern Yakutia)
08 p1008 N88-16111
Photogrammetric principles for combining remote sounding and three-dimensional mapping
08 p1012 N88-16135
Naval weapons center active fault map series
[AD-A188425] 12 p1643 N88-19835
Topographic data processing for environmental planning 18 p2534 N88-25032

REMAGNETIZATION
U MAGNETIZATION

REMELTING
U MELTING

REMOTE CONSOLES
Modification, implementation, and evaluation of a remote terminal emulator as a software validation and stress testing tool
[AD-A188833] 12 p1678 N88-20034

REMOTE CONTROL
NT RADIO CONTROL
Robotic sensors and actuators for a service manipulator system. Volume 1: Executive summary
[MATRA-EPT/DT/VT187/120]
01 p0053 N88-10341
Robotic sensors and actuators for a service manipulator system. Volume 2: Service Manipulator System (SMS) handbook
[MATRA-EPT/DT/VT187/227]
01 p0053 N88-10342
Robotic sensors and actuators for a service manipulator system. Volume 3, phase A report and program plan
[MATRA-EPT/DT/VT187/228]
01 p0054 N88-10343
Technology survey for a robot which will investigate the condition of underground pipe
[PB87-209979] 01 p0055 N88-10351
Teleoperation and control study — orbital servicing
[BAE-TP-8268] 01 p0076 N88-10489
An autonomous, closed-loop pointing system for use with satellite optics
[DE87-012011] 02 p0235 N88-11483
Low-cost teleoperator-controlled vehicle for damage assessment and dose measurement
[DE88-000713] 04 p0451 N88-12794
Experiences in teleoperation of land vehicles
[DE88-000429] 06 p0711 N88-14355
Experiences in teleoperation of land vehicles
[DE88-001695] 06 p0711 N88-14357
Packet telecommand. System performance assessment study — onboard data handling
[PTC/TNOT/0015/SAAB] 07 p0843 N88-15113
Evaluation of high-voltage, high-power, solid-state remote power controllers for amps
07 p0924 N88-15612
Software simulation of time delay in teleoperation
08 p1056 N88-16371
Promising concepts for ground-to-orbit experiment teleoperation — Columbus 12 p1590 N88-19518
Teleoperation for a Spacelab technology experiment
12 p1590 N88-19521
Utilization of robotics and teleoperation for future in-orbit operations 12 p1591 N88-19527
Human interfaces in remote driving
[DE88-006843] 14 p1953 N88-21643
Test results of high-voltage, high-power, solid-state remote power controllers
[NASA-TM-100322] 16 p2194 N88-23085
Teleoperator human factors study
[NASA-CR-178930] 17 p2382 N88-24162
A control technique for improved robot performance
17 p2391 N88-24212
Computer aided remote control: A general concept for intervention in the nuclear, underwater, and space domains 19 p2699 N88-26046
Airborne remote operated device
[DE88-010324] 21 p2895 N88-27188
Development of remote control welding system of large structures
[PB87-219853] 22 p3083 N88-28309
Remotely Operated Vehicle (ROV) reliability study, phase 1
[AD-A194367] 23 p3222 N88-29177

REMOTE HANDLING
A hydrogen/nickel oxide battery for remote applications
[DE87-009048] 04 p0464 N88-12872
Experiences in teleoperation of land vehicles
[DE88-001695] 06 p0711 N88-14357
Heuristic control of the Utah/MIT dextrous robot hand
06 p0793 N88-14858
Dynamics, control and sensor issues pertinent to robotic hands for the EVA retriever system
06 p0796 N88-14876
Operational experience and design recommendations for teleoperated flight hardware
14 p1927 N88-21489
Space spider crane
[NASA-CASE-LAR-13411-1-SB]
17 p2312 N88-23628
Design study. Manipulator systems for model handling in European transonic wind tunnels
[ETN-88-91944] 18 p2468 N88-24651
Mobile remote manipulator system for a tetrahedral truss
[NASA-CASE-MSC-20985-1] 20 p2765 N88-26398

REMOTE MANIPULATOR SYSTEM
Robotic sensors and actuators for a service manipulator system. Volume 1: Executive summary
[MATRA-EPT/DT/VT187/120]
01 p0053 N88-10341
Robotic sensors and actuators for a service manipulator system. Volume 2: Service Manipulator System (SMS) handbook
[MATRA-EPT/DT/VT187/227]
01 p0053 N88-10342
Teleoperation and control study — orbital servicing
[BAE-TF-8268] 01 p0076 N88-10489
Evaluation of vision systems for teleoperated land vehicles
[DE87-013066] 03 p0333 N88-12100
Telerobotic controller development
06 p1056 N88-16370
Utilization of SMS and EVA for the servicing of European Space Station 12 p1587 N88-19500
Robotic intelligence issues for space manipulator monitoring, control programming
12 p1588 N88-19504
On a knowledge based assisted system for highly autonomous control of experiment-manipulators in the Man-Tended Free Flyer 12 p1588 N88-19505
The Hermes robot arm, its design and verification
12 p1588 N88-19508
Remote manipulation in orbital construction, servicing and repair missions: Is one arm enough? A comparative evaluation of the performance features of robots with one or more arms 12 p1588 N88-19509
Computational aspects of robotic experiment manipulation in a microgravity environment
12 p1589 N88-19512
Covariant control of bilateral servos for in-orbit manipulation 12 p1590 N88-19520
Teleoperation for a Spacelab technology experiment
12 p1590 N88-19521
The Hermes manipulation system (HERA) simulation facility development 12 p1591 N88-19524
A comparative survey of mathematical models for dynamic simulation of in-orbit manipulation operations
12 p1592 N88-19533
Dynamics modeling, simulation, and control of a spacecraft/manipulator system
12 p1592 N88-19534
A teleoperated manipulator system concept for unmanned platforms — Columbus
12 p1593 N88-19537
Multi-axis control of telemanipulators
12 p1593 N88-19539
System and concept design of the SSRMS latching end effector — Space Station 14 p1875 N88-21204
Operational experience and design recommendations for teleoperated flight hardware
14 p1927 N88-21489
Robotic joint experiments under ultravacuum
14 p1927 N88-21490
Design study. Manipulator systems for model handling in European transonic wind tunnels
[ETN-88-91944] 18 p2468 N88-24651
Dynamics of a flexible orbiting platform with MRMS
[ISSN-0285-6808] 18 p2473 N88-24673
Remote servicing of space systems
23 p3260 N88-29409
A teleoperated robotic manipulator system for materials processing experiment servicing
23 p3260 N88-29410
Study of software requirements and artificial intelligence techniques for robotics
[TL-3333] 24 p3422 N88-30365

REMOTE REGIONS
NT ANTARCTIC REGIONS
NT ARCTIC REGIONS
Evaluation of the Shasta Waterless System as a remote site sanitation facility
[AD-A186000] 07 p0898 N88-15442

REMOTE SENSING
Study of Earth from space and strengthening of economy 01 p0010 N88-10055
Study on propagation and inverse scattering — sea studies
[ESA-CR(P)-2394] 01 p0063 N88-10405
Study on the suitability of a European data relay satellite to support a system of remote sensing satellites
[ESA-CR(P)-2400] 01 p0063 N88-10406
Remote Sensing-Arid Lands Workshop, Page, Arizona, June 10-12, 1986
[DE87-012388] 01 p0064 N88-10412
Remote sensing with LANDSAT 5 Thematic Mapper (TM) and its application to various planning levels: A case study from the Wuerzburg area, West Germany
[DFVLR-FB-86-62] 01 p0065 N88-10421
Remote sensing of environmental pollution
[DFVLR-MITT-87-04] 01 p0067 N88-10428
Fiber optic engineering sensor system. Preliminary program management plan, phase 3 revision
[AD-A183663] 01 p0093 N88-10608
Correlation between aircraft MSS and LIDAR remotely sensed data on a forested wetland in South Carolina
[NASA-TM-89643] 02 p0193 N88-11204
Estimating scattered and absorbed radiation in plant canopies by remote sensing
[NASA-CR-181390] 02 p0193 N88-11205
Airborne lidar experiments at the Savannah River Plant
[NASA-TM-4007] 02 p0194 N88-11209
Horizontal shape matching applied to VAS data — Visible and Infrared Spin Scan Radiometer Atmospheric Sounder (VAS) 02 p0201 N88-11254
Statistical remote sensing algorithm development: A complementary process to mesoscale numerical models
02 p0206 N88-11292
Evaluation of one-sided nuclear magnetic resonance for remote detection of explosives
[AD-A184490] 03 p0296 N88-11857
Planning for future operational sensors and other priorities
[PB87-220802] 03 p0325 N88-12056
Commercial Opportunities for Remote Sensing with Polar Platforms
[ESA-SP-269] 03 p0339 N88-12131
Legal protection of the Polar Platform's users
03 p0339 N88-12135
Confidentiality of data — Columbus Polar Platforms
03 p0339 N88-12136
Market potential for commercial remote sensing
03 p0339 N88-12137
An overview of remote sensing users' requirements
03 p0340 N88-12139
MBB-ERNO view of remote sensing commercialization
03 p0340 N88-12140
The CNR/PSN Advanced Microwave Imaging Radiometer (AMIR) — satellite-borne
03 p0340 N88-12141
X-band SAR for a European remote sensing payload
03 p0340 N88-12142
Evolution of remote sensing utilization in geological mapping and ore exploration: Example in Zimbabwe
03 p0343 N88-12165
Vegetation studies in the national Park of Comoe (Ivory Coast) using SPOT 1 satellite data
03 p0343 N88-12166
A comparative thematic mapping analysis of SPOT data: The Vientiane Plain (Laos) 03 p0343 N88-12168
The distinction between different water masses using optical remote sensing applied to data from the Alboran Sea Experiment 1982
[DFVLR-FB-86-48] 03 p0345 N88-12181
The correspondence of surface climate parameters with satellite and terrain data
[NASA-CR-181515] 03 p0346 N88-12185
A method for remote sensing of precipitable water vapor and liquid in the atmosphere using a 22-ghz radiometer
[AD-A184204] 03 p0354 N88-12232
Remote sensing of planets and cartographic results
[HSBW-HEFT-14] 03 p0389 N88-12444
Calibration of a laser-pumped, thermographic phosphor remote thermometry system
[DE88-000452] 04 p0449 N88-12781
The Portable Instant Display and Analysis Spectrometer (PIDAS) 05 p0611 N88-13756
Effective use of principal component analysis with high resolution remote sensing data to delineate hydrothermal alteration and carbonate rocks 05 p0612 N88-13758
Land cover/use classification of Cairns, Queensland, Australia: A remote sensing study involving the conjunctive use of the airborne imaging spectrometer, the large format camera and the thematic mapper simulator
05 p0612 N88-13759
In-orbit calibration adjustment of the Nimbus-7 SMMR
[NASA-TM-100678] 05 p0614 N88-13773
Study on data compression systems for operational remote sensing — meteosat imagery
[NLR-TR-86029-L] 05 p0620 N88-13808
A system overview of the Airborne Visible/Infrared Imaging Spectrometer (AVIRIS)
06 p0705 N88-14326

Airborne Visible/Infrared Imaging Spectrometer (AVIRIS) spectrometer design and performance
06 p0706 N88-14327
AVIRIS foreoptics, fiber optics and on-board calibrator
06 p0706 N88-14328
Evaluation of a satellite laser ranging technique using pseudonoise code modulated laser diodes
[NASA-CR-182347] 06 p0708 N88-14343
Uses of airborne laser Chayka-1 for probing water, land surfaces 06 p0725 N88-14461
Remote acoustic sounding of ferromanganese nodules
06 p0727 N88-14471
Application of remote sensing to agricultural field trials
[ISBN-90-6754-089-7] 06 p0729 N88-14483
Remote sensing in mineral exploration
[PB87-138558] 06 p0729 N88-14484
On-site meteorological program guidance for regulatory modeling applications
[PB87-227542] 06 p0731 N88-14498
Wind shear detection. Forward-looking sensor technology
[NASA-CP-10004] 07 p0817 N88-14970
Review of the potential of satellite remote sensing for marine flood protection
[IOS-237] 07 p0870 N88-15280
Remote sensing of the biosphere
[NASA-CR-182382] 07 p0871 N88-15281
From pattern to process: The strategy of the Earth Observing System: Volume 2: EOS Science Steering Committee report
[NASA-TM-89702] 07 p0871 N88-15283
SAR (Synthetic Aperture Radar). Earth observing system. Volume 2F: Instrument panel report
[NASA-TM-89701] 07 p0871 N88-15284
The influence of yellow substances on remote sensing of sea water constituents from space. Volume 1: Summary
[ESA-CR(P)-2443-VOL-1] 07 p0872 N88-15292
The influence of yellow substances on remote sensing of sea water constituents from space. Volume 2: Appendices
[ESA-CR(P)-2443-VOL-2] 07 p0873 N88-15293
Multistep component analysis of correlations
08 p1009 N88-16115
Commercial applications and scientific research requirements for thermal-infrared observations of terrestrial surfaces
[NASA-TM-89704] 08 p1019 N88-16179
Ocean Colour Workshop --- conference
[ESA-SP-1083] 08 p1042 N88-16292
Overview of ESA's activities in ocean colour remote sensing 08 p1042 N88-16294
Remote sensing of ocean colour for studies of biological productivity and biochemical cycles
08 p1042 N88-16296
Technical aspects of future ocean colour remote sensing 08 p1042 N88-16298
Status and prospects of the Joint Research Commitee (JRC) work on the application of ocean colour monitoring from space 08 p1043 N88-16299
Canadian activities and goals in remote sensing of ocean colour and fluorescence from space
08 p1043 N88-16300
Federal Republic of Germany's interests, activities and goals in remote sensing of ocean colour/fluorescence from space 08 p1043 N88-16302
Italian activities in ocean colour remote sensing
08 p1043 N88-16304
National Remote Sensing Program (NRSP) of the Netherlands 08 p1043 N88-16305
The use of chlorophyll fluorescence measurements from space for separating constituents of sea water
08 p1043 N88-16307
The influence of yellow substances on remote sensing of sea-water constituents from space
08 p1044 N88-16308
Remote measurement of aerosol stream velocity with continuous-wave CO2-laser 08 p1079 N88-16506
Trends in research and development in the Netherlands. The influence of national science policy between 1973 and 1986
[B8701588] 08 p1094 N88-16580
Parallel-processing computer systems and their possible applications in the agency 09 p1128 N88-16774
Tethers: An outline of a new concept for Earth observation 09 p1129 N88-16781
Construction of airborne radars for remote sensing
[PB88-113063] 09 p1154 N88-16916
Fundamental aspects of the physics of remote sensing
[ESA-TT-1045] 09 p1185 N88-17100
Report of the Workshop on Space Systems Possibilities for a Global Energy and Water Cycle Experiment
[WCP-137] 09 p1193 N88-17147
Infrared low-level wind shear work
10 p1275 N88-17628
NROSS (Navy Remote Ocean Sensing System): A force multiplier
[AD-A186853] 10 p1346 N88-18045
Space-based remote sensing of the Earth: A report to the Congress
[NASA-TM-89709] 10 p1346 N88-18046
Earth resources: A continuing bibliography with indexes (supplement 56)
[NASA-SP-7041(56)] 10 p1347 N88-18051
Remote sensing of atmospheric crosswinds by utilizing speckle-turbulence interaction and optical heterodyne detection
[AD-A187580] 10 p1347 N88-18052
Evaluation of a temperature remote sensing technique
[AD-A187885] 10 p1347 N88-18053
Analysis of quasi-geostrophic forcing during the AIMCS (Airborne Investigations of Mesoscale Convective Systems) Project. Volume 2: Results for June 14 through July 16, 1984
[PB88-123807] 10 p1354 N88-18092
Coordination: Southeast continental shelf studies
[DE88-003680] 10 p1357 N88-18110
Multisource context classification methods in remote sensing 11 p1504 N88-18985
General determination of Earth surface type and cloud amount using multispectral AVHRR data
[NOAA-TR-NESDIS-39] 11 p1506 N88-18997
Low cost telemetry and telecommand system for remote measurement of magnitude character
[INPE-4273-PRE/1145] 12 p1598 N88-19564
Principal space programs in the area of microwaves
[INPE-4164-PRE/1064] 12 p1618 N88-19677
Report of the participation in the International Training Course: Remote Sensing in Village Forestry
[INPE-4476-NTE/278] 12 p1637 N88-19802
Mapping of the mangroves of the Guanabarra Bay through the utilization of remote sensing techniques
[INPE-3942-TDL/229] 12 p1637 N88-19804
Research in remote sensing of vegetation
[NASA-CR-182663] 12 p1639 N88-19817
Spectrophotometric remote sensing of the diffuse aurora
[AD-A188599] 12 p1643 N88-19837
National Severe Storms Laboratory, fiscal year 1987
[PB88-140108] 12 p1647 N88-19863
Remote sensing of meteorological parameters with the aid of a clear-air Doppler radar
[PB88-142518] 12 p1647 N88-19864
Relationships between remotely-sensed surface properties and subsurface structure in the ocean
[AD-A189317] 12 p1650 N88-19881
Photographic filters
[INPE-4448-RPE/558] 12 p1692 N88-20124
The radar scattering coefficient as a function of forest stand parameters and viewing angle. An empirical study of the Pinus sylvestris L. in the Kootwijk forest (The Netherlands), extended with observations in the Speulder and Sprielder forest (The Netherlands)
[ETN-88-91348] 13 p1760 N88-20527
Remote fiber fluorimetry techniques for pressure measurements
[DE88-004486] 13 p1773 N88-20604
Remote sensing of earth terrain
[NASA-CR-182677] 13 p1790 N88-20711
Determination of Earth rotation by the combination of data from different space geodetic systems
[NASA-CR-181388] 13 p1791 N88-20713
The use of four-photon Raman spectroscopy for the remote sensing of natural objects
[NASA-TT-20257] 13 p1791 N88-20716
Activities and objectives of the Polar Research Board
[DE88-004543] 13 p1797 N88-20747
Summary of along-track data from the Earth radiation budget satellite for several major desert regions
[NASA-RP-1197] 13 p1802 N88-20772
Activities report in aeronautics and astronautics
[ETN-88-91332] 13 p1859 N88-21115
Lidar active remote sensing. Applications to the atmosphere 14 p1936 N88-21547
The role of remote sensing in the study of polar ice sheets 14 p1939 N88-21570
Vegetation mapping using high resolution MSS (multispectral scanner) data: Canopy reflectance and shadow problems encountered and possible solutions
[DE88-004273] 14 p1939 N88-21574
Investigation of European remote sensing user needs in accessing MOS-1 payload
[ESA-CR(P)-2535] 14 p1940 N88-21580
Research relative to angular distribution of snow reflectance/snow cover characterization and microwave emission
[NASA-CR-182733] 14 p1941 N88-21582
Optical properties of Southern Hemisphere aerosols: Report of the joint CSIRO/NASA study
[NASA-CR-179287] 14 p1945 N88-21605
Satellite rainfall retrieval by logistic regression
[NASA-CR-180485] 14 p1946 N88-21607
Activities report in flight and space travel
[ISSN-0070-3966] 14 p2012 N88-22000
Development of remote sensing techniques capable of delineating soils as an aid to soil survey
[NASA-CR-182610] 15 p2089 N88-22452
Orbital remote sensing: An instrument for monitoring urban growth
[INPE-4456-PRE/1287] 15 p2150 N88-22833
A PC-based receiver-decoder for remote sensor monitoring
[DE88-004733] 16 p2192 N88-23075
Users guide to CAESAR
[BCRS-87-04] 16 p2228 N88-23306
Preparation of the operational phase of the European Remote Sensing Satellite ERS-1
[BCRS-87-06] 16 p2228 N88-23307
Study of the plan for a national data center for the European Remote Sensing Satellite ERS-1
[BCRS-87-11] 16 p2228 N88-23309
International commercialization of remote sensing
[BCRS-87-14] 16 p2228 N88-23310
The multiannual National Remote Sensing Program (NRSP)
[BCRS-87-16] 16 p2229 N88-23311
Earth resources: A continuing bibliography with indexes (issue 57)
[NASA-SP-7041(57)] 16 p2229 N88-23314
Use of energy emission for detecting the necessity of irrigation in wheat in field conditions
[INPE-4461-TDL/318] 16 p2229 N88-23315
Detection, monitoring and analysis of some environmental effects of fires in the Amazon region through utilization of NOAA and LANDSAT satellite imagery and aircraft data
[INPE-4503-TDL/326] 16 p2230 N88-23322
Applications of multitemporal compositions obtained from LANDSAT data in the study of urban growth
[INPE-4480-PRE/1246] 16 p2287 N88-23692
Thermal remote anemometer system
[NASA-CASE-LAR-13508-1] 17 p2342 N88-23962
Prospects of satellite wind sensing systems in the years 1995-2000 17 p2350 N88-24004
The geometric workstation, a new approach for geometric corrections of remotely sensed data
17 p2352 N88-24017
A proposal of adaptation of a knowledge-based scene analysis model to some remote sensing problems
17 p2354 N88-24026
Shape detection in remote sensing through graph isomorphism 17 p2354 N88-24028
Satellite remote sensing of turbidity and sediment concentration in Lagoa dos Patos
17 p2355 N88-24032
Practical image analysis using personal computers: The Canadian experience 17 p2356 N88-24037
International cooperation in remote sensing: The ESA experience 17 p2356 N88-24038
ERS-1 data products and services and their value for tropical countries 17 p2357 N88-24040
Estimation of an area cultivated with wheat from LANDSAT data through a two-phase sampling method
17 p2357 N88-24041
Remote sensing techniques in the estimation of the area cultivated with beans, corn, and castor beans in the Irece County (Bahia State) 17 p2358 N88-24045
A proposal of adaptation of a knowledge-based scene analysis model to some remote sensing problems
17 p2362 N88-24068
Terrain classification using SPOT images and the computer system GOP-300
[FOA-C-20677-2.7] 17 p2368 N88-24102
Soviet remote sensing research and technology
[FASAC-TAR-3130] 17 p2369 N88-24108
An update on remote measurement of soil moisture over vegetation using infrared temperature measurements: A FIFE perspective
[NASA-CR-182926] 17 p2370 N88-24109
Review of power requirements for satellite remote sensing systems 17 p2419 N88-24387
The gamma 1 and gamma 3 bands of (16)O3: Line positions and intensities
[NASA-TM-101162] 17 p2445 N88-24541
Reflectance spectroscopy in planetary science: Review and strategy for the future
[NASA-SP-493] 17 p2451 N88-24564
Evaluating evaporation with satellite thermal data
[AD-A192042] 18 p2531 N88-25019
The application of satellites in connection with the environment
[ETN-88-92474] 18 p2532 N88-25020
Information analysis of integral equations in remote sensing of atmospheric aerosols
18 p2532 N88-25022

DMSP-SSM/1 NASA algorithm validation using primarily LANDSAT and secondarily DMSP and/or AVHRR visible and thermal infrared satellite imagery
[NASA-CR-182979] 18 p2532 N88-25024
Aircraft/lidar turbulence comparison
18 p2546 N88-25111
Remote sensing of acoustic properties of shallow water sediments: A review
[AD-A192107] 18 p2570 N88-25267
Activities report of the Division of Optical Technology
[FOA-C-30477-3] 18 p2576 N88-25299
National Meeting on Remote Sensing Applied to Municipal Planning 19 p2681 N88-25939
Suggested hurricane operational scenario for GOES I-M
[NASA-TM-89729] 19 p2692 N88-26002
Remote determination of chlorophyll concentration in the ocean using an optical pulse radar
[NASA-TT-20301] 19 p2694 N88-26014
Overview of space missions and techniques for ocean monitoring 19 p2700 N88-26053
The contribution of space to maritime activities
19 p2700 N88-26055
Sensors in spaceborne oceanography
19 p2700 N88-26056
Contribution of space to marine activities
19 p2700 N88-26057
The role of space borne imaging radars in environmental monitoring: Some shuttle imaging radar results in Asia
[NASA-TM-101175] 20 p2789 N88-26544
Remote sensing and satellite applications to the needs of the gas and pipeline industry
[PB88-202668] 20 p2817 N88-26714
Surface hydrology, sediment transport dynamics and remote sensing of disturbed watersheds in a humid temperate region
[DE88-008719] 20 p2817 N88-26715
Satellite remote sensing of the wet bulb globe temperature heat stress index, phase 2
[AD-A192798] 20 p2818 N88-26717
Review of methods for remote sensing of atmospheric emissions from stationary sources
[PB88-190483] 20 p2821 N88-26739
Remote sensing of temperature profiles. Performance test of PASS
[DE88-753108] 20 p2826 N88-26768
Methods of determining playa surface conditions using remote sensing
[AD-A192663] 21 p2965 N88-27612
Analysis of remotely sensed imagery using digital morphology
[AD-A192738] 21 p2965 N88-27614
Active and passive remote sensing of ice
[AD-A193307] 21 p2966 N88-27617
Remote sensing of wetlands: Applications overview
[DE88-010695] 21 p2966 N88-27618
The detection and interpretation of long-term changes in ozone from space
[NASA-TM-101135] 21 p2971 N88-27650
Computer simulation procedure for designing airborne aerometric monitoring programs
[DE88-011896] 21 p2975 N88-27674
Fiber optic sensing systems using high frequency resonant sensing heads with intensity sensors
[NASA-TM-101318] 22 p3080 N88-28293
SPOT 1 Image Utilization, Assessment, Results
[ISBN-2-85-426186-8] 22 p3089 N88-28346
The contribution of remote sensing to hydrology and hydrogeology 22 p3090 N88-28347
Mapping of streamflow and soil infiltration of a Sahelian catchment area by SPOT image interpretation: The Oursi pond catchment area in Burkino Faso
22 p3090 N38-28348
The use of SPOT images for water resources surveys in the Kasserine Basin (Tunisia)
22 p3090 N88-28349
SPOT image exploitation for glacial mass balance fluctuation monitoring in the French Alps
22 p3090 N88-28350
SPOT on land and lakes in the Hubei Province (China)
22 p3090 N88-28351
Evaluation of SPOT imagery for monitoring irrigated lands 22 p3090 N88-28352
An evaluation of SPOT imagery for wetland monitoring
22 p3091 N88-28353
Comparative study of crop and soil mapping using multitemporal and multispectral SPOT and LANDSAT data 22 p3091 N88-28354
Water resources and agricultural land use investigations in northeastern Gujarat (India) 22 p3091 N88-28355
Study of the forests on the banks of the Gambia and criteria for detecting mortality 22 p3091 N88-28356
Use of SPOT satellite in agrohydrology: Detection of spring water excess in a grassland region
22 p3091 N88-28357
Review of the studies of geography and environment and studies on spectral characteristics of SPOT HRV data 22 p3091 N88-28358
Evaluation of the grassy biomass in the Sahelian zone in the South Tamesna region (Niger): Prospects and limits of use of SPOT data 22 p3092 N88-28359
Changes in species composition of heathland, monitored by means of remote sensing and field mapping: The results of the HEISPOT project 22 p3092 N88-28360
Topography of an Antartic ice stream
22 p3092 N88-28361
Spatial and spectral registration of Javanese landscape units with SPOT 22 p3092 N88-28362
Comparison between the respective contributions of the TM LANDSAT-4 and HRV SPOT-1 data to the land use mapping of Mediterranean coastal zone
22 p3092 N88-28363
Land use systems and rural landscapes in the center of Veracruz State (Mexico): First results
22 p3092 N88-28364
SPOT for earthquake hazard zoning in southern Italy
22 p3093 N88-28365
Discrimination of sand transport rates and environmental consequences in central Egypt from SPOT data
22 p3093 N88-28366
Delineation of ephemeral fluvial networks on low-relief Piedmont surfaces, Plutonium Valley, Nevada, USA
22 p3093 N88-28367
Following the seasonal evolution of a natural environment in a humid tropical region. Preliminary Evaluation of SPOT (PEPS) number 186: Bangui, Central Africa 22 p3093 N88-28368
Application of SPOT to agricultural information systems in temperate regions 22 p3093 N88-28369
Potential use of SPOT satellite data for the national resources inventory 22 p3093 N88-28370
Methodological developments on crop inventories using SPOT and ground surveys 22 p3094 N88-28371
Evaluation of annual crop surfaces and territorial inventory in the Paris basin by combining classic statistical inquiries and SPOT data (Preliminary Evaluation Program for SPOT 127) 22 p3094 N88-28372
Evaluation of automatic texture analysis for increased crop identification accuracy with SPOT data
22 p3094 N88-28373
Application of SPOT multidate data to wheat yield estimation in Beauce (France) 22 p3094 N88-28374
An evaluation of multidate SPOT data for agriculture and land use mapping in the United Kingdom
22 p3094 N88-28375
The suitability of SPOT imagery for monitoring landscape patterns 22 p3094 N88-28376
Characterization, topology, and cartography of grasslands for the development of fodder resources. (Preliminary Evaluation Program for SPOT number 26)
22 p3095 N88-28377
HRV data for the applications on reneweable resources in Canada — SPOT 22 p3095 N88-28378
SPOT-1 HRV data and vegetation amount
22 p3095 N88-28379
Attempt to inventory vines using oblique SPOT images
22 p3095 N88-28380
Analysis of soils using remote sensing information at the scale of the parcel 22 p3095 N88-28381
Comparative variations of spectral signatures in a cultivated area of the Paris Basin (27 May, 26 June, 1 July 1986) 22 p3095 N88-28382
Monitoring of agricultural production in West Africa. The need to integrate different satellite platforms
22 p3096 N88-28383
Use of SPOT imagery for vegetation/biomass mapping, geotechnical mapping, catchment area determination, and settlement location in the Turkana district, northern Kenya 22 p3096 N88-28384
Digital and visual analysis of SPOT and TM data for crop discrimination in southern Brazil
22 p3096 N88-28385
A comparative thematic mapping analysis of SPOT data: The Vientiane Plain (Lao PDR)
22 p3096 N88-28386
Evaluation of SPOT data for crop inventory and monitoring in Sudanian Africa. Example of Bane area (Burkina Faso) 22 p3096 N88-28388
Identification of farming systems in the cotton area of West Burkina Faso from SPOT-1 data
22 p3097 N88-28389
Monitoring Tunisia's steppes with SPOT
22 p3097 N88-28390
Study of savannah formation in the Sudanian zone. Northwest sector of the La Comoe park, Ivory Coast
22 p3097 N88-28391
Pilot study of rice culture in sub-tropical high population density region (Madagascar) with SPOT 1 multispectral data 22 p3097 N88-28392
Using SPOT HRV data to update the distribution of the paddy field in Taiwan 22 p3097 N88-28393
Agro-ecological mapping from SPOT 1 data in southern Thailand: New questions for an analysis of the farming-systems 22 p3097 N88-28394
SPOT applications on Columbia's coffee zone
22 p3097 N88-28395
Use of SPOT data in preliminary steps of road project studies especially suited for developing countries
22 p3098 N88-28396
SPOT imagery for detecting residential expansion on the rural-urban fringe of Toronto, Canada
22 p3098 N88-28397
Spread of large tropical conurbations
22 p3098 N88-28398
Utilization of remote sensing for the observation of urban populations. Ongoing research in Quito (Ecuador)
22 p3098 N88-28399
Integration of SPOT data into a geocoded information system 22 p3098 N88-28400
Utilizing SPOT data for seismic shot-line mapping and environmental monitoring in oil and gas exploration
22 p3098 N88-28401
Preliminary comparative analysis of LANDSAT and SPOT data for the study of the sanding phenomenon: Zaafrane region (Algeria) 22 p3099 N88-28402
An evaluation of the applicability of SPOT stereoscopic imagery to the Canada Land Use Monitoring Program (CLUMP) 22 p3099 N88-28403
Topographic suppression and advances in classification for land cover mapping using SPOT-1 HRV imagery
22 p3099 N88-28404
Monitoring Moneragala (Sri Lanka) with SPOT imagery
22 p3099 N88-28405
Monitoring urban land cover changes at the urban fringe from SPOT HRV imagery in south-east England
22 p3099 N88-28406
Thematic mapping of central Java (Indonesia)
22 p3100 N88-28412
Utilization of SPOT-1 multispectral data for mapping land cover and phytohygiene monitoring in the central zone of the Mercantour National Park (France)
22 p3100 N88-28413
Applications of SPOT data for urban real estate investment information systems
22 p3101 N88-28414
Mapping and urban multi-experimental assessment of SPOT: Urban results 22 p3101 N88-28415
SPOT-1 over New Zealand: Analysis of SPOT imagery for land use investigations 22 p3101 N88-28416
Comparison of SPOT, LANDSAT TM and combined data for urban studies 22 p3101 N88-28417
Utilization of SPOT multispectral data for urban planning 22 p3101 N88-28418
First results of international investigations of the applications of SPOT-1 data to geologic problems, mineral and energy exploration 22 p3101 N88-28419
Rate of slip on the Altin Dagh Fault (North Tibet, China) 22 p3102 N88-28420
Karst and submarine fresh water discharge in the Antalya area, southern Turkey 22 p3102 N88-28421
Results of the Geosat program to evaluate SPOT data for petroleum and mineral exploration
22 p3102 N88-28422
The application of SPOT data to the structural geology of western Nevada 22 p3102 N88-28423
Application SPOT-1 data to mining activity: Example of the Imiter Silver Mine, Morocco
22 p3102 N88-28424
Evaluation of SPOT imagery contribution to petroleum exploration: The Suez Rift (Egypt)
22 p3102 N88-28425
Evaluation of SPOT imagery for discriminating vegetation communities associated with surficial and bedbrock geology and identifying anomalous and stressed vegetation associated with mineralization
22 p3103 N88-28426
SPOT imagery as an aid to understanding volcanism and tectonics: Examples from the Chilean Andes and the Tibetan Plateau 22 p3103 N88-28427
Role of SPOT in geological application of remote sensing 22 p3103 N88-28428
SPOT imagery preliminary contribution to cartography and geodynamics in the Benue trough (Nigeria)
22 p3103 N88-28429
An evaluation of SPOT imagery for Earth science studies in the Antarctic. Preliminary Evaluation Program (PEPS) 289 for SPOT 22 p3103 N88-28430
Structural analysis of the Jura mountains-Rhine Graben intersection (Switzerland) for petroleum exploration using SPOT stereoscopic data 22 p3103 N88-28431
Methodology for the use of SPOT imagery in petroleum exploration. Example of the Bas-Languedoc area (France) 22 p3104 N88-28432
Analyzing the stratigraphy, tectonism, and mineralization at the Spanish side of the pyrite belt, Huelva province, Spain, using SPOT imagery 22 p3104 N88-28433

Geologic applications of SPOT-1, TM, and NOAA-7 data: Finding and defining unmapped structural features
22 p3104 N88-28434
Comparing different images for ground water survey based on lineament analysis 22 p3104 N88-28435
Spectral and spatial attribute evaluation of SPOT data in geological mapping of precambrian terrains in semiarid environment of Brazil 22 p3104 N88-28436
Geologic results obtained from the use of SPOT imagery along plate boundaries: Examples in the East African rift and of the northern-Caribbean collision
22 p3105 N88-28437
SPOT images and geochemical mapping of lateritic covers in southern Mali 22 p3105 N88-28438
Analysis of the multispectral content and of SPOT subscenes in two regions of Burundi. Lithologic and tectonic interpretations 22 p3105 N88-28439
SPOT imagery for landslide cartography in mountainous areas. Example of the French Maritime Alps
22 p3105 N88-28440
SPOT for slope instability survey in Nepal
22 p3105 N88-28441
Detailed geological mapping of the massif of Sainte Victoire (Provence, France) using SPOT imagery. Comparison with other multisource data. New tectonic interpretation of this region 22 p3105 N88-28442
Satellite remote sensing for forest management. A review illustrated with research results on SPOT 1 data
22 p3106 N88-28443
An evaluation of the utility of SPOT and Thematic Mapper data for providing forest inventory information
22 p3106 N88-28444
Forest mapping by visual interpretation of SPOT images 22 p3106 N88-28446
Forest management applications of SPOT data in Australia 22 p3106 N88-28447
SPOT multispectral data and maritime pine stands in southwest of France 22 p3106 N88-28448
Stand-based forestry inventory from SPOT image
22 p3106 N88-28449
Potential of SPOT imagery as a tool for forest mapping in Quebec 22 p3107 N88-28450
Assessment of large area forest disturbances caused by biotic and abiotic factors on the basis of SPOT images 22 p3107 N88-28451
Study of deforestation in the Vosges (France) by remote sensing 22 p3107 N88-28452
Contribution to the mapping of forests in an intensively divided area, with the help of SPOT image data
22 p3107 N88-28453
SPOT 1: Image utilization, assessment, results. A study of the Elburgon Forest area (Kenya) showing the spectral responses of different forest tree species
22 p3107 N88-28454
SPOT investigations of estuaries and coastal zones: An overview 22 p3107 N88-28455
SPOT: A tool to aid preselection of sites favorable for aquiculture. Evaluation and perspectives of the Preliminary Evaluation Program for SPOT (PEPS) ALIAS Caledonie
22 p3108 N88-28456
The monitoring of sediment transport, water circulation and mixing in estuaries and coastal waters
22 p3108 N88-28457
Evaluation of SPOT data for remote sensing of physical and biological properties of estuaries and coastal zones
22 p3108 N88-28458
Utilization of SPOT in hydrography
22 p3108 N88-28459
Application of SPOT imagery for oil spill contingency planning 22 p3108 N88-28460
The use of SPOT data in mapping coastal areas
22 p3108 N88-28461
SPOT: A satellite for oceanography
22 p3108 N88-28462
Contribution of SPOT satellite to qualitative and quantitative mapping of marine vegetation in the English Channel, North Altantic, western Mediterranean, and South Pacific 22 p3109 N88-28464
Physiography and kinematics of the western coast of the province of Huelva (Andalousia, Spain)
22 p3109 N88-28465
Use of SPOT HRV data in the US Army Corps of Engineers dredging program 22 p3109 N88-28466
Contributions of SPOT imagery to the study of the littoral environments of Saloum (Senegal)
22 p3109 N88-28467
Relevance of a thematic map (SPOT data) with regards to the real flora and structure of the vegetation covering of salt marshes (Mont Saint Michel Bay, France)
22 p3109 N88-28468
Application of SPOT data to renewable resources in the Maldives 22 p3109 N88-28469
The prospects for topographic mapping using SPOT data 22 p3110 N88-28470
The use of SPOT imagery on analytical photogrammetric instruments 22 p3110 N88-28471
Cartographic applications of SPOT imagery
22 p3110 N88-28472
The use of SPOT imagery for topographic mapping
22 p3110 N88-28473
Digital terrain modelling with SPOT data and geological applications 22 p3110 N88-28474
The use of SPOT data for mapping and DEM production — digital elevation model (DEM)
22 p3110 N88-28475
Evaluation of SPOT cartographic capabilities over the Aix Marseille area (France) 22 p3110 N88-28476
Assessment of SPOT imagery for topographic revision and vegetation mapping 22 p3111 N88-28477
A geometrical analysis of SPOT data
22 p3111 N88-28478
Topographic mapping with SPOT 1 data. A practical approach by the Ordnance Survey
22 p3111 N88-28479
Metric applications of SPOT's lateral stereoscopy
22 p3111 N88-28480
Larger scale image mapping with SPOT
22 p3111 N88-28481
Rigorous stereophotogrammetric treatment of SPOT images 22 p3111 N88-28482
Mapping and urban multi-experimental assessment of SPOT: Mapping results 22 p3112 N88-28483
Study of stereoradiometry on SPOT images
22 p3112 N88-28484
Studies on system performance of SPOT (space and ground segments) 22 p3112 N88-28485
Radiometric analysis and potential of SPOT HRV imagery for applications in urban environments and geology 22 p3112 N88-28486
Automatic production of orthophoto using SPOT images 22 p3112 N88-28487
High resolution orthoimage quadrangle maps using SPOT satellite data 22 p3112 N88-28488
Automatic extraction of high resolution elevation data from SPOT stereo images 22 p3113 N88-28489
Automatic creation of digital terrain models from SPOT image pairs 22 p3113 N88-28490
Production of satellite image maps based on SPOT data 22 p3113 N88-28491
Surface reflectance factors derived from SPOT-1 HRV data at two view angles 22 p3113 N88-28492
Digital SPOT stereoplotting: An original approach to the formation of epipolar images and matching
22 p3113 N88-28493
From the extraction of linear networks towards following of them on SPOT images with the help of a knowledge-based interpretation system
22 p3113 N88-28494
Extraction of thin networks by an oriented following of ridges and valleys 22 p3113 N88-28495
SPOT images features extraction
22 p3114 N88-28496
SPOT: A data capture and data updating tool for the French National Geographic Institute's (IGN's) cartographic data base 22 p3114 N88-28497
Use of SPOT imagery in a geographic information system 22 p3114 N88-28498
SEP/VIPS 32 geographic information system. Processing and thematic analysis of images, maps, and associated data 22 p3114 N88-28499
Training of the Group for the Development of Aerospace Remote sensing 22 p3114 N88-28501
Contribution of SPOT to geographic information systems 22 p3114 N88-28502
Summary of analysis and processing techniques used on SPOT imagery 22 p3115 N88-28503
The SPOT program 22 p3115 N88-28504
SPOT data acquisition and distribution
22 p3115 N88-28505
Quality of SPOT images 22 p3115 N88-28506
Survey of SPOT-1 operation 22 p3115 N88-28507
Perspectives for the SPOT program
22 p3115 N88-28508
Closing of the Preliminary Evaluation Program for SPOT (PEPS): Assessment of the acquisition, production, and monitoring of PEPS 22 p3115 N88-28509
The world's water resources: A major neglect. A study in remote sensing in hydrology and water management [ESA-BR-40] 22 p3116 N88-28511
Activities report of the Division of Reconnaissance and Seeker Systems [FOA-C-30479-3.1/3.2/3.3/3.4]
22 p3116 N88-28513
Investigations into the properties, conditions and effects of the ionosphere [AD-A194245] 22 p3118 N88-28528
Genesis of Atlantic lows experiment NASA electra boundary layer flights data report [NASA-TM-100703] 22 p3126 N88-28597
Spectral characteristics and the extent of paleosols of the Palouse formation [NASA-CR-180947] 23 p3228 N88-29210
Activities report in remote sensing [ETN-88-92905] 23 p3309 N88-29714
Wave propagation and remote sensing
24 p3364 N88-30029
Microwave remote sensing in the French industries [ETN-88-93081] 24 p3387 N88-30171
Structure of eastern Turkestan Ridge based on space photographs 24 p3450 N88-30530
Estimation of soil temperature profile from remote microwave and IR measurements
24 p3450 N88-30532

REMOTE SENSORS

NT THEMATIC MAPPERS (LANDSAT)

Efficient placement of structural dynamics sensors on the space station [NASA-CR-172015] 01 p0017 N88-10103
Robotic sensors and actuators for a service manipulator system. Volume 1: Executive summary [MATRA-EPT/DT/VT187/120]
01 p0053 N88-10341
Robotic sensors and actuators for a service manipulator system. Volume 2: Service Manipulator System (SMS) handbook [MATRA-EPT/DT/VT187/227]
01 p0053 N88-10342
Robotic sensors and actuators for a service manipulator system. Volume 3, phase A report and program plan [MATRA-EPT/DT/VT187/228]
01 p0054 N88-10343
Earth resources: A continuing bibliography with indexes (issue 55) [NASA-SP-7041(55)] 01 p0065 N88-10415
The absolute radiometric calibration of space-based sensors 03 p0277 N88-11744
Detector normalization — SPOT remote sensors
03 p0341 N88-12151
Absolute and interband calibration — SPOT
03 p0341 N88-12152
Spectroscopic and retrieval studies in support of SCRIBE (Stratoepheric Cryogenic Interferometer Balloon Experiment) [AD-A184037] 03 p0351 N88-12216
A multibody dynamic analysis of the N-ROSS (Navy Remote Ocean Sensing System) satellite rotating flexible reflector using Kane's method [AD-A184452] 04 p0462 N88-12860
In-situ characterization of the interface of glass reinforced composites [AD-A185136] 05 p0557 N88-13391
Italy's Institute of Research on Electromagnetic Waves--the Istituto di Ricerca sulle Onde Elettromagnetiche [AD-A185020] 05 p0574 N88-13501
Development of response models for the Earth Radiation Budget Experiment (ERBE) sensors. Part 3: ERBE scanner measurement accuracy analysis due to reduced housekeeping data [NASA-CR-178294] 05 p0583 N88-13553
Estimation of marine boundary layer depth and relative humidity with multispectral satellite measurements [AD-A184881] 05 p0620 N88-13804
Software design for an airborne gravity measurement system [AD-A185000] 05 p0634 N88-13878
HIRIS (High-Resolution Imaging Spectrometer: Science opportunities for the 1990s. Earth observing system. Volume 2C: Instrument panel report [NASA-TM-89703] 07 p0871 N88-15282
SAR (Synthetic Aperture Radar). Earth observing system. Volume 2F: Instrument panel report [NASA-TM-89701] 07 p0871 N88-15284
Technical aspects of future ocean colour remote sensing 08 p1042 N88-16298
Developments in ocean colour research in the United Kingdom 08 p1043 N88-16306
Sea surface current estimates off central California as derived from enhanced AVHRR (Advanced Very High Resolution Radiometer) infrared images [AD-A186867] 09 p1194 N88-17155
Remote sensing of atmospheric optical thickness and sea-water attenuation when submerged: Wavelength selection and anticipated errors [AD-A187609] 11 p1548 N88-19262
Long range sensor for rendezvous and docking missions 12 p1587 N88-19497
Airborne electromagnetic sounding of sea ice thickness and sub-ice bathymetry [AD-A188939] 12 p1649 N88-19879
The application of thermal imaging sensors and image processing techniques to a short range surface-to-air missile system [ETN-88-92080] 14 p1982 N88-21829
Instrumentation to provide an active control capability for distributed parameter systems [AD-A190043] 15 p2076 N88-22375

Feasibility study for a 2nd generation system for airborne maritime pollution surveillance
[ETN-88-92108] 15 p2092 N88-22486
Support for FY87 midlatitude electron-density calibration campaign
[AD-A190174] 15 p2094 N88-22476
The multiannual National Remote Sensing Program (NRSP)
[BCRS-87-16] 16 p2229 N88-23311
A new fiber-optic-based ion sensor
[AD-A191322] 16 p2274 N88-23612
Remote sensing of acoustic properties of shallow water sediments: A review
[AD-A192107] 18 p2570 N88-25267
Fiber optic sensors 19 p2670 N88-25870
Satellite remote sensing of the wet bulb globe temperature heat stress index, phase 2
[AD-A192798] 20 p2818 N88-26717
Development of procedures for performing end-to-end tests on the ERS-1 radar altimeter and AMI using a compact antenna test range — Active Microwave Instrument (AMI)
[ESA-CR(P)-2558] 24 p3363 N88-30022

REMOTELY PILOTED VEHICLES
Full-scale transport controlled impact demonstration program
[NASA-TM-89642] 01 p0004 N88-10021
HIMAT flight program: Test results and program assessment overview
[NASA-TM-86725] 01 p0005 N88-10026
Evaluation of vision systems for teleoperated land vehicles
[DE87-013066] 03 p0333 N88-12100
Operator multiple-tasking study for remotely operated platforms
[AD-A184487] 03 p0362 N88-12276
Experiences in teleoperation of land vehicles
[DE88-001695] 06 p0711 N88-14357
An autopilot design for the United States Marine Corps' airborne remotely operated device
[AD-A186379] 07 p0820 N88-14983
A dynamic simulation and feedback control scheme for the U.S. Marine Corps' Airborne Remotely Operated Device (AROD)
[AD-A186597] 06 p0953 N88-15784
Robotic air vehicle. Blending artificial intelligence with conventional software 09 p1210 N88-17252
Search problems in mission planning and navigation of autonomous aircraft
[NASA-CR-182666] 12 p1579 N88-19448
Aquila remotely piloted vehicle: Its potential battlefield contribution still in doubt
[PB88-120241] 13 p1721 N88-20289
A demonstration of retro-traverse using a semi-autonomous land vehicle
[DE88-009851] 21 p2957 N88-27568
Development and design of windtunnel and test facility for RPV (Remote Piloted Vehicle) enhancement devices
[AD-A194842] 24 p3329 N88-29822

REMOVAL
Geometry and reproducibility of a plasma-supported removal of material by laser radiation
[ETN-87-90436] 01 p0052 N88-10335
A new compression method with fast searching on large databases
[DE87-010986] 01 p0106 N88-10691
Cleanliness tests with the Omega Meter: A comparative study for solder flux removal
[DE88-004634] 11 p1460 N88-18704

REMS
U RAPID EYE MOVEMENT STATE

RENAL FUNCTION
Regulation of calcium metabolism during prolonged antiorthostatic hypokinesia
[NASA-TT-20219] 11 p1521 N88-19085
Is ANF implied in the night attenuated renal response to central hypervolemia? 12 p1659 N88-19945
Human adaptation to various hypercapnic conditions in relation to salivary electrolyte dynamics and renal function 12 p1664 N88-19977

RENDEZVOUS
NT ORBITAL RENDEZVOUS
NT SPACE RENDEZVOUS

RENDEZVOUS GUIDANCE
Autonomous control procedures for shuttle rendezvous proximity operations 09 p1208 N88-17244
Space vehicle approach velocity judgments under simulated visual space conditions
[NASA-TM-89437] 11 p1523 N88-19094

RENDEZVOUS TRAJECTORIES
Safe and fuel minimum reference trajectories for closed loop controlled approaches — space stations 12 p1585 N88-19488

REPAIRING
U MAINTENANCE

REPEATERS
The software repeater (an exercise in Z specification)
[RSRE-MEMO-4090] 14 p1958 N88-21677
A 104-km unrepeatered bidirectional fiber optic demonstration link
[AD-A190282] 15 p2134 N88-22728
Spectral modelling of the soft gamma ray repeater
[DE88-007027] 17 p2453 N88-24570

REPETITION
Preliminary evaluation of a micro-based repeated measures testing system
[NASA-CR-172038] 08 p1048 N88-16331

REPLACING
Commonality analysis as a knowledge acquisition problem 08 p1062 N88-16413
A comparative assessment of US and UK explosives qualified as replacements for tetryl
[MRL-R-1094] 13 p1754 N88-20486
Recommended replacements for tetryl in Australian production fuzes and related ordnance
[MRL-R-1089] 13 p1754 N88-20489
Proposal for a new aggressor aircraft
[AD-A194311] 22 p3041 N88-28056

REPLENISHMENT
Study of helium transfer technology for STICCR: Fluid management
[NASA-CR-177463] 10 p1291 N88-17720
Kinetics of thermochemical gas-solid reactions important in the Venus sulfur cycle
[NASA-CR-182963] 19 p2742 N88-26280
The rate of volcanism on Venus
[NASA-CR-183039] 19 p2742 N88-26281

REPORTS
NT CONGRESSIONAL REPORTS
NT PRESIDENTIAL REPORTS
Aircraft accidents
[JB-84] 01 p0004 N88-10020
NASA's new technology reporting system: A review and future prospects
[NASA-CR-180954] 01 p0105 N88-10686
Electronics engineering thrust area report, FY86
[DE87-014616] 03 p0309 N88-11950
National Center for Atmospheric Research
[PB87-228391] 04 p0470 N88-12901
FY 1985 scientific and technical reports, articles, papers and presentations
[NASA-TM-86521] 04 p0501 N88-13083
Workshop on Avionics Corrosion Control
[AGARD-R-733] 05 p0547 N88-13331
Role of technical information in innovation
[PB87-235388] 05 p0658 N88-14039
Role of the technical report in technological innovation
[PB87-232500] 05 p0658 N88-14040
Eddy Current Seminar, 24-26 March 1986
[PB87-124988] 06 p0696 N88-14269
International workshop on two-phase flow fundamentals
[DE88-001478] 06 p0699 N88-14287
Airborne Visible/Infrared Imaging Spectrometer (AVIRIS). A description of the sensor, ground data processing facility, laboratory calibration, and first results
[NASA-CR-182365] 06 p0705 N88-14325
Research reports: 1987 NASA/ASEE Summer Faculty Fellowship Program
[NASA-CR-179219] 07 p0922 N88-15601
Aircraft accident reports: Brief format, US Civil and Foreign Aviation, Issue Number 7 of 1986 accidents
[PB87-916909] 08 p0952 N88-15781
FY87 scientific and technical reports, articles, papers, and presentations
[NASA-TM-100318] 08 p1093 N88-16578
Aircraft accident/incident summary reports, Des Moines, Iowa, November 25, 1985; Chicago, Illinois, August 10, 1986
[PB88-910411] 09 p1115 N88-16685
JPRS report: Science and technology. USSR: Physics and mathematics
[JPRS-UPM-87-009] 09 p1233 N88-17395
Cumulative reports and publications through December 31, 1987
[NASA-CR-181624] 11 p1524 N88-19099
Activities report of Lufthansa
[ISSN-0176-5086] 16 p2155 N88-22855
Aircraft accident/incident summary reports: Modena, Pennsylvania, March 17, 1986; Redwater, Texas, April 4, 1986
[PB88-910403] 16 p2159 N88-22878
Naval research reviews, volume 39, number 3
[AD-A191392] 16 p2264 N88-23543
Acid Precipitation: A current awareness bulletin
[DE88-007987] 20 p2821 N88-26738
RLE progress report, January 1 to December 31, 1987
[RLE-PR-130] 21 p3011 N88-27869
International ultraviolet explorer observatory operations
[NASA-CR-180775] 22 p3145 N88-28708
Activities report in remote sensing
[ETN-88-92905] 23 p3309 N88-29714

REPRESENTATIONS
The total interval of a graph
[AD-A189648] 15 p2119 N88-22625
Approximation and representation of explicit surfaces in the presence of singularities
[ETN-88-92191] 16 p2258 N88-23496
Knowledge representation in geographic information systems
[ETN-88-92470] 20 p2882 N88-27112
An introduction to the nested sequence of tuples data model and algebra
[REPT-87-049] 22 p3145 N88-28702

REPRODUCTION (BIOLOGY)
Investigations of the survey of the reproductive biology of Xiphophorus in an Aquarack 01 p0074 N88-10471
Xiphophorus as an experimental system for genetic and biological development studies under microgravity conditions 01 p0074 N88-10472
Long term investigations of the growth, metabolism, and reproduction of fish under conditions close to weightlessness 01 p0074 N88-10473
Investigations of the reproductive physiology of the rainbow trout (Salmo gairdneri Richardson) 07 p0885 N88-15370
Changes in the morphological and molecular biological processes during early embryo development in amphibians under micro-g conditions 07 p0885 N88-15371
Long duration confinement of aquatic organisms in weightlessness (aquaspace) 07 p0887 N88-15380
Mother-fetus system as object for investigation of mechanisms of physiological effect of weightlessness 07 p0891 N88-15402

REPRODUCTION (COPYING)
NT XEROGRAPHY
The Quick Response Multicolor Printer (QRIMP) system
[AD-A188140] 11 p1504 N88-18982
Data acquisition and processing for surface plate calibration
[AD-A187264] 11 p1564 N88-19366
New duplicating paper with high resolution for aerial photography
[PB87-228706] 19 p2685 N88-25962
The transition from traditional to modern map reproduction
[B8735128] 20 p2818 N88-26718

REPRODUCTIVE SYSTEMS
NT TESTES

REPUBLIC MILITARY AIRCRAFT
U MILITARY AIRCRAFT

REPUBLIC OF CHINA
U TAIWAN

REPULSION
U FORCE

REQUIREMENTS
Space Station Mission Planning System (MPS) development study. Volume 1: Executive summary
[NASA-CR-179202] 01 p0009 N88-10047
Space Station Mission Planning System (MPS) development study. Volume 2
[NASA-CR-179200] 01 p0009 N88-10048
Space Station Mission Planning Study (MPS) development study. Volume 3: Software development plan
[NASA-CR-179203] 01 p0009 N88-10049
Telepresence work station system definition study, part 2
[NASA-CR-172006] 01 p0013 N88-10071
Space Assembly, Maintenance, and Servicing Study (SAMSS) 01 p0015 N88-10089
System Development Working Group report 01 p0016 N88-10092
Structures and Materials Working Group report 01 p0016 N88-10093
Space station contamination considerations 02 p0137 N88-10859
The MOLICEL(R) rechargeable lithium system: Multicell battery aspects 02 p0163 N88-11024
Fault tree safety analysis of a large Li/SOCl(sub)2 spacecraft battery 02 p0163 N88-11025
Rotorcraft Design for Operations
[AGARD-CP-423] 03 p0262 N88-11649
The influence of operational requirements on LHX concept formulation 03 p0262 N88-11650
Apache for the battlefield of today and the 21st century 03 p0265 N88-11670
The EH-101 integrated project: A naval, utility and commercial helicopter system 03 p0265 N88-11672
How space, the fourth operational medium, supports operational maneuver
[AD-A184742] 03 p0373 N88-12346

Advanced Information Processing System (AIPS) proof-of-concept system functional requirements I/O network system services
[NASA-CR-181481] 03 p0384 N88-12412
Fire-related standards and testing 04 p0406 N88-12522
MHD stability and control for mirror machines 04 p0493 N88-13038
Design and assembly sequence analysis of option 3 for CETF reference space station
[NASA-TM-100503] 05 p0553 N88-13369
Roughness and waviness requirements for laminar flow surfaces 07 p0813 N88-14953
Documentation in a software maintenance environment
[AD-A185892] 07 p0901 N88-15459
Derivation of equipment vibration requirements for AV-8B 08 p0997 N88-16037
Requirements and options for communications services in support of the Systems Autonomy Demonstration Project 08 p1057 N88-16374
The role of photodetectors in optical signal processing
[AD-A186804] 09 p1247 N88-17476
Crew interface with windshear systems 10 p1275 N88-17631
Helicopter external vision requirements and visual display characteristics: A report/bibliography, revision A
[AD-A187075] 10 p1276 N88-17641
Specification of an engine and its components starting from a consideration of aircraft missions 10 p1279 N88-17651
An integrated aero/mechanical performance approach to high technology turbine design 10 p1280 N88-17657
A framework for evaluating computer architectures to support systems with security requirements, with applications
[AD-A187082] 10 p1392 N88-18303
Design loads for Swedish military aircraft in a twenty years' perspective 12 p1580 N88-19456
Orbital analysis of a STS (Space Transportation System) external tank in low earth orbit
[AD-A188829] 12 p1593 N88-19542
Low cost mobile robot
[AD-A188507] 12 p1633 N88-19778
Turnaround operations analysis for OTV. Volume 1: Executive summary
[NASA-CR-179316] 13 p1729 N88-20340
Turnaround operations analysis for OTV. Volume 2: Detailed technical report
[NASA-CR-179317] 13 p1729 N88-20341
Intergrated circuit design, phase 2
[AD-A189060] 13 p1760 N88-20530
Space station power system requirements
[NASA-TM-100886] 14 p1881 N88-21245
Large-scale wind turbine structures 15 p2085 N88-22429
Monitoring the usage of a computer system
[DE88-004310] 15 p2106 N88-22542
The modeling, simulation and comparison of interconnection networks for parallel processing
[AD-A190571] 15 p2115 N88-22599
Tactical Rubidium Frequency Standard (TRFS)
[AD-A191049] 16 p2193 N88-23078
Manned Mars mission accommodation: Sprint mission
[NASA-TM-100598] 16 p2290 N88-23711
A structured approach to weapon system design 17 p2303 N88-23773
Advanced EVA system design requirements study 17 p2380 N88-24147
Advisory circular: Noise certification handbook
[FAA-AC-36-4B] 17 p2394 N88-24234
Potassium Rankine power system for space power 17 p2433 N88-24476
Automatic reactor control system for transient operation 17 p2436 N88-24493
Required operational capacity for a 7-1/2 ton capacity, Air Mobile Crane (AMC)
[AD-A192023] 19 p2601 N88-25451
On 3-5 transistors for MM-wave applications
[AD-A191580] 19 p2661 N88-25825
Checkout system software for INPE satellites
[INPE-4554-PRE/1297] 19 p2715 N88-26120
SLAPP: A special multiprocessor array for signal processing and linear algebra
[AD-A191587] 19 p2719 N88-26146
Real time data base management
[AD-A191758] 19 p2739 N88-26265
The free-electron laser: Theoretical innovations and gas-loaded experiment 20 p2806 N88-26646
Electrical load and power source capacity report for the C-130 aircraft Self Contained Navigation System (SCNS): LSI model 6216A, 6216B, 6216C, revision
[AD-A193079] 21 p2895 N88-27186
Sources and nature of cost analysis data base reference manual
[AD-A193099] 21 p3028 N88-27976
A 2.3-GHz low-noise cryo-FET amplifier 22 p3066 N88-28195
Model test of air-exchange efficiency
[DE88-752862] 23 p3201 N88-29049
An overview of technology for spoken interaction with machines
[AD-A194153] 23 p3202 N88-29058
Remotely Operated Vehicle (ROV) reliability study, phase 1
[AD-A194367] 23 p3222 N88-29177
Night lighting and night vision goggle compatibility 23 p3242 N88-29297
Centralized class A flight mishap investigation
[AD-A194397] 24 p3322 N88-29786
Long haul communications in the HF spectrum utilizing high speed modems
[AD-A194683] 24 p3360 N88-30003
Achieving real-time performance in FIESTA 24 p3418 N88-30344

RESCUE OPERATIONS
System for SAR missions 03 p0265 N88-11671
An evaluation of the methods for rescuing EVA (Extravehicular Activities) crewmembers and recovering equipment detached and adrift from the space station
[AD-A189683] 14 p1871 N88-21181
Design and development of an avionics system adapted to helicopter missions 17 p2305 N88-23786
KOSPAS-SARSAT satellites used for ocean current study 24 p3450 N88-30534

RESEARCH
NT DYNAMIC PROGRAMMING
NT LINEAR PROGRAMMING
NT MARKET RESEARCH
NT NONLINEAR PROGRAMMING
NT NUCLEAR RESEARCH
NT QUADRATIC PROGRAMMING
Transactions of the 4th Army Conference on Applied Mathematics and Computing
[AD-A183544] 01 p0085 N88-10547
Research in particles and fields
[NASA-CR-180412] 01 p0119 N88-10763
Crystalline cell research status and direction
[DE87-014214] 03 p0382 N88-12402
The impact of information technology on research in science and engineering
[DE88-000342] 03 p0385 N88-12417
Procedure and program used for data processing in a poll on nuclear energy utilization
[IFSI-87-3] 05 p0649 N88-13977
Budget and programs for 1988 research
[IFSI-88-16] 05 p0660 N88-14048
EISCAT research in Finland in 1986 06 p0691 N88-14234
EISCAT research programs for 1987 06 p0692 N88-14244
Program draft for a special field: Gravitational biology 07 p0887 N88-15381
Index of USA-CERL publications for October 1984 - June 1987
[AD-A186375] 07 p0942 N88-15728
Earth materials research: Report of a Workshop on Physics and Chemistry of Earth Materials
[NASA-CR-182519] 10 p1298 N88-17761
Interdisciplinary research in mathematics, science and technology education
[PB88-131446] 10 p1398 N88-18333
Genetic research in space
[NASA-TT-20216] 11 p1518 N88-19066
Research on algorithms for nonlinear programming
[AD-A188326] 12 p1677 N88-20024
Data base design and implementation
[AD-A190414] 15 p2149 N88-22827
NASA scientific and technical publications: A catalog of Special Publications, Reference Publications, Conference Publications, and Technical Papers, 1987
[NASA-SP-7063(02)] 15 p2149 N88-22830
JPRS report: Science and technology. China
[JPRS-CST-88-009] 16 p2186 N88-23030
Aircraft flight dynamics research in past decade reviewed 16 p2186 N88-23031
JPRS report: Science and technology. China
[JPRS-CST-88-001] 16 p2186 N88-23036
Atmospheric Science and Remote Sensing Laboratory
[NASA-CR-179290] 16 p2236 N88-23355
Fast Algorithm Simulation and Test (FAST) facility
[AD-A191183] 16 p2252 N88-23457
The Engineer Studies Center guide to research and data collection
[AD-A189971] 16 p2285 N88-23680
Soviet combustion research
[PB88-182324] 18 p2483 N88-24730
Activities report of the Communications Department
[ENST-88D003] 21 p2931 N88-27401
Vanderbilt free electron laser project in biomedical and materials research
[AD-A195961] 24 p3378 N88-30121
Center for opto-electronic systems research
[AD-A195159] 24 p3429 N88-30411

RESEARCH AIRCRAFT
NT B-70 AIRCRAFT
NT ROTOR SYSTEMS RESEARCH AIRCRAFT
NT U-2 AIRCRAFT
An integrated study of structures, aerodynamics and controls on the forward swept wing X-29A and the oblique wing research aircraft
[NASA-CR-181548] 04 p0399 N88-12486
First results from the Airborne Visible/Infrared Imaging Spectrometer (AVIRIS) 06 p0707 N88-14335
A perspective on 15 years of proof-of-concept aircraft development and flight research at Ames-Moffett by the Rotorcraft and Powered-Lift Flight Projects Division, 1970-1985
[NASA-RP-1187] 12 p1582 N88-19467
A correlation study of X-29A aircraft and associated analytical development
[NASA-CR-183103] 13 p1722 N88-20296
Development of a real-time aeroperformance analysis technique for the X-29A advanced technology demonstrator
[NASA-TM-100432] 14 p1866 N88-21151
Performance improvements of an F-15 airplane with an integrated engine-flight control system
[NASA-TM-100431] 14 p1867 N88-21159
Development of an integrated set of research facilities for the support of research flight test
[NASA-TM-100427] 14 p1869 N88-21169
The NASA integrated test facility and its impact on flight research
[NASA-TM-100418] 14 p1870 N88-21177
First flight simulator test of the head-up display for NAL QSTOL experimental aircraft (ASUKA)
[DE88-751804] 16 p2162 N88-22896
Development of an airborne facility for advanced avionics research 17 p2307 N88-23801
Taiwan area mesoscale experiment: P-3 aircraft operations summary
[PB88-169073] 18 p2544 N88-25098
The identification of the direct lift control flap system of the research aircraft ATTAS 20 p2786 N88-26527
Investigations into the triggered lightning response of the F106B thunderstorm research aircraft
[NASA-CR-3902] 23 p3236 N88-29258
The NAE atmospheric research aircraft 24 p3313 N88-29730

RESEARCH AND DEVELOPMENT
Blagov commentary on Mir station, first manning 01 p0009 N88-10051
Lithium/iron sulfide batteries: Development and demonstration
[DE87-014222] 01 p0042 N88-10265
Budget reimbursements: The National Aeronautics and Space Administration's reimbursable work
[PB87-207296] 01 p0107 N88-10696
Space technology to meet future needs
[NASA-CR-181473] 02 p0130 N88-10819
Battery development and testing at ESA 02 p0164 N88-11027
Stirling engine research at national and university laboratories in Japan
[DE87-014622] 02 p0180 N88-11123
Planning for US ion cyclotron heating research relevant to the compact ignition tokamak and Alcator C-Mod
[DE88-000022] 02 p0241 N88-11520
JPRS report: Science and technology. China
[JPRS-CST-87-032] 03 p0376 N88-12365
A role for national laboratories in enhancing economic competitiveness. The example of high-temperature superconductors: CNSS papers, No. 1
[DE87-013633] 03 p0379 N88-12386
Materials studies for magnetic fusion energy applications at low temperatures-X
[PB87-232575] 03 p0381 N88-12395
National Science Foundation
[PB87-228375] 03 p0384 N88-12410
National Aeronautics and Space Administration Authorization Act, 1988
[PUB-LAW-100-147] 03 p0385 N88-12422
Solar energy: European research and development
[PB87-107645] 04 p0463 N88-12866
Aerothermodynamics research at NASA Ames 05 p0533 N88-13242
Innovative and alternative technology projects
[PB87-230165] 05 p0623 N88-13818
CELSS Program Meeting 05 p0630 N88-13853
The birth of big science: Nuclear physics as advanced technology source
[NOTA-INTERNA-881] 05 p0648 N88-13967

Role of technical information in innovation
[PB87-235388] 05 p0658 N88-14039
Role of the technical report in technological innovation
[PB87-232500] 05 p0658 N88-14040
AGARD: The NATO Advisory Group for Aerospace Research and Development
[AD-A185062] 05 p0662 N88-14063
Tethers in space handbook
[NASA-CR-181371] 06 p0673 N88-14123
Material design of high-purpose glass discussed 06 p0675 N88-14133
NAL news updated: FY87 business plan, developments 06 p0675 N88-14135
Recent trends in superconductor development discussed 06 p0688 N88-14215
Laser development, evolution of applied technologies described 06 p0689 N88-14221
Strategic management of research and development: A literature search
[NASA-CR-182337] 06 p0790 N88-14847
National Aeronautics and Space Administration (NASA)/American Society for Engineering Education (ASEE) Summer Faculty Fellowship Program, 1987. Volume 1
[NASA-CR-172009-VOL-1] 06 p0792 N88-14855
Federal plan for meteorological services and supporting research, fiscal year 1988
[PB88-118716] 07 p0880 N88-15336
Design and management of research projects
[PB88-106380] 07 p0941 N88-15721
Life prediction technologies for aeronautical propulsion systems 08 p0954 N88-15788
Supersonic STOVL propulsion technology program: An overview 08 p0957 N88-15808
Safety guidelines and procedures for bioscience-based industry and other applied microbiology
[PB87-140521] 08 p1045 N88-16316
Trends in research and development in the Netherlands. The influence of national science policy between 1973 and 1986
[B8701588] 08 p1094 N88-16580
Organizations of intermediation in technology transfer: Its role in technological innovation
[INPE-4354-TDL/297] 08 p1094 N88-16581
Loads and aeroelasticity division research and technology accomplishments for FY 1987 and plans for FY 1988
[NASA-TM-100534] 09 p1114 N88-16680
Impact and promise of NASA aeropropulsion technology 09 p1118 N88-16698
Lewis materials research and technology: An overview 09 p1119 N88-16699
The objectives and methods of the technological research program 09 p1124 N88-16730
Research and technology 1987
[NASA-TM-4021] 09 p1265 N88-17577
Director of R and D institutions (Government of India)
[PB88-127162] 10 p1285 N88-17685
Research and development. Technical-scientific publications (1956-1987): Retrospective view and prospects. Jubilee edition on the occasion of the 75th birthday of Dipl.-Engr. Dr.-Engr. E. H. Ludwig Boelkow
[ISSN-0931-9751] 10 p1309 N88-17819
Research, development, and growth strategy 10 p1309 N88-17820
Research and technology 1987 annual report of the Kennedy Space Center
[NASA-TM-100303] 10 p1431 N88-18548
Lithium/disulfide battery R and D
[DE88-003032] 11 p1481 N88-18839
Research briefing on high-temperature superconductivity
[PB88-133004] 11 p1561 N88-19344
Science and technology in India
[PB88-134747] 11 p1564 N88-19362
Communication satellites: Guidelines for a strategic plan
[NASA-TM-89308] 12 p1599 N88-19569
Technology development of a planar BiPolar transistor
[AD-A188761] 12 p1623 N88-19708
Research and technology, 1987
[NASA-TM-100323] 12 p1713 N88-20253
AGARD Highlights 88/1 14 p2012 N88-22001
The impact of independent research and development regulations on companies not required to negotiate advanced independent research and development agreements
[AD-A190007] 15 p2147 N88-22818
Marshall Space Flight Center 1960-1985: 25th anniversary report
[NASA-TM-100328] 15 p2153 N88-22852
Langley aerospace test highlights, 1987
[NASA-TM-100595] 15 p2153 N88-22853
Space directorate research and technology accomplishments for fiscal year 1987
[NASA-TM-100607] 15 p2153 N88-22854
Government research on ceramics coating technology 16 p2184 N88-23019
Sunshine project for FY 1987 outlined 16 p2184 N88-23021
Activities report of the Department of Systems and Communications
[ENST-87D004] 16 p2189 N88-23053
Computer-assisted cartography research and development report of the Federal Republic of Germany 1984 - 1986 16 p2226 N88-23289
The multiannual National Remote Sensing Program (NRSP)
[BCRS-87-16] 16 p2229 N88-23311
Activities report of the Imagery Department
[ENST-87D008] 16 p2273 N88-23604
DOE (Department of Energy) national laboratories and the semiconductor industry: Continuing the joint planning
[PB88-170295] 16 p2281 N88-23657
Department of Housing and Urban Development independent agencies appropriations for 1989. Part 7: National Aeronautics and Space Administration
[GPO-85-166] 16 p2286 N88-23689
Preparing for the new programs. The ESA technological research and development program 1988-1990
[ESA-SP-1095] 17 p2309 N88-23814
Structural ceramics research 17 p2324 N88-23878
Soviet remote sensing research and technology
[FASAC-TAR-3130] 17 p2369 N88-24108
Research and Technology, 1987, Goddard Space Flight Center
[NAS 1.15:101097] 17 p2453 N88-24572
The application of hydrocarbon bioconversion technology to aerospace materials production 18 p2478 N88-24888
A quality philosophy for research and development
[DE88-006512] 18 p2524 N88-24977
Department of Defense statement on defense agency research and development to the Subcommittee on Defense of the Committee on Appropriations, United States House of Representatives, 100th Congress, second session
[AD-A191840] 18 p2588 N88-25377
The FY 1989 Department of Defense statement on the Science and Technology Program to 100th Congress, second session
[AD-A191843] 18 p2588 N88-25380
Centre for International Co-Operation and Approriate Technology (CICAT)
[PB88-165501] 18 p2590 N88-25389
Electrical and chemical sensors for biological cell research 19 p2669 N88-25866
Procedures for peer review assessments
[DE88-007749] 19 p2739 N88-26263
Exploratory battery technology development and testing report for 1986
[DE88-009870] 20 p2794 N88-26578
Space policy of common sense and moderation
[REPT-49/87] 20 p2883 N88-27118
United States Air Force Graduate Student Summer Support Program, volume 2
[AD-A191122] 21 p2924 N88-27355
Vision research. A national plan: 1983-1987, 1987 evaluation and update
[PB88-192604] 21 p2985 N88-27726
Engineering data compendium. Human perception and performance. User's guide
[LC-87-19560] 21 p2993 N88-27749
Materials research, superconductor and thin layer technology
[REPT-50/87] 21 p3025 N88-27955
High technology space flight orientation program: Overview and recommendations
[ETN-88-92332] 21 p3029 N88-27979
Engineering data compendium. Human perception and performance, volume 1
[LC-87-19560] 22 p3134 N88-28630
Engineering data compendium. Human perception and performance, volume 2
[LC-87-19560] 22 p3134 N88-28631
Engineering data compendium. Human perception and performance, volume 3
[LC-87-19560] 22 p3134 N88-28632
A study of the National Physics Laboratory microdosimetry research programme in collaboration with the University of Leeds (United Kingdom)
[NPL-RS(EXT)-93] 23 p3217 N88-29148
Competition: Issued on establishing and using Federally funded research and development centers
[PB88-178884] 23 p3296 N88-29632
History of aeroelasticity in Germany from the beginning to 1945
[ESA-TT-1082] 24 p3319 N88-29767
With an eye to the future: ESA general studies program 1988
[ESA-SP-1100] 24 p3435 N88-30447

RESEARCH FACILITIES

Aquarack: Aims and Possible Research Projects
[DFVLR-MITT-87-01] 01 p0073 N88-10469
The Aquarack as a potential instrument for basic research work in space biology: Inventory and scientific dispositions 01 p0073 N88-10470
Surveillance systems test and evaluation facilities 02 p0134 N88-10845
Lewis' enhanced laboratory for research into the fatigue and constitutive behavior of high temperature materials 02 p0189 N88-11177
MBB simulation facilities applied for rotorcraft research 03 p0263 N88-11655
Research simulators for helicopters 03 p0263 N88-11656
Experiments: Test range facilities, part 1 03 p0304 N88-11920
FY 1985 scientific and technical reports, articles, papers and presentations
[NASA-TM-86521] 04 p0501 N88-13083
Aerothermodynamics research at NASA Ames 05 p0533 N88-13242
Metrology and calibrating laboratories
[ETN-88-90761] 06 p0670 N88-14104
Polar Geophysical Institute's studies of magnetosphere, ionosphere 06 p0728 N88-14480
Design of the Backscatter Spectroscopy System for the Nova Laser Facility
[DE88-001880] 07 p0859 N88-15214
Research reports: 1987 NASA/ASEE Summer Faculty Fellowship Program
[NASA-CR-179219] 07 p0922 N88-15601
Physics rationale for the engineering specifications for ZTH
[DE88-000938] 07 p0936 N88-15690
Life prediction technologies for aeronautical propulsion systems 08 p0954 N88-15788
CEBAF design overview and project status
[CEBAF-PR-88-001] 09 p1246 N88-17470
Director of R and D institutions (Government of India)
[PB88-127162] 10 p1285 N88-17685
System analysis study of space platform and station accommodations for life sciences research facilities. Volume 1: Executive summary. Phase A: Conceptual design and programmatics
[NASA-CR-179268] 10 p1291 N88-17721
System analysis study of space platform and station accommodations for life sciences research facilities. Volume 2: Study results, attachment 2. Phase A: Conceptual design and programmatics
[NASA-CR-179272] 10 p1291 N88-17722
Relationships between coronary heart disease risk factors and serum ionized calcium in Kennedy Space Center Cohort
[NASA-TM-100979] 10 p1368 N88-18177
Design issues for a laboratory high gain fusion facility
[DE88-004406] 10 p1413 N88-18434
Research and technology 1987 annual report of the Kennedy Space Center
[NASA-TM-100303] 10 p1431 N88-18548
Engineering thrust areas, 1988
[DE88-005103] 11 p1468 N88-18753
Institute for Computational Mechanics in Propulsion (ICOMP)
[NASA-TM-100790] 11 p1540 N88-19202
A perspective on 15 years of proof-of-concept aircraft development and flight research at Ames-Moffett by the Rotorcraft and Powered-Lift Flight Projects Division, 1970-1985
[NASA-RP-1187] 12 p1582 N88-19467
Conceptualization and design of a variable-gravity research facility
[NASA-CR-182574] 12 p1595 N88-19550
Conceptual design and programmatics studies of space station accommodations for Life Sciences Research Facilities (LSRF)
[NASA-CR-179270] 12 p1598 N88-19567
Space station accommodations for life sciences research facilities: Phase A conceptual design and programmatics studies for Missions SAAX0307, SAAX0302 and the transition from SAAX0307 to SAAX0302. Volume 1: Executive summary
[NASA-CR-179267] 12 p1599 N88-19571
Photonic temperature and pressure sensors for biosystems/pulsed microwave. Part 1: Interaction studies
[AD-A188887] 12 p1629 N88-19751
A laboratory facility for research in parallel computation
[AD-A188499] 12 p1680 N88-20044
Basic research in ceramic and semiconductor science at selected Japanese laboratories, based on a September 1986 visit: Highlights, summary and overview and detailed notes from selected Japanese laboratories
[DOE/ER-0314] 12 p1696 N88-20150

A review of technologies applicable to low-speed flight of high-performance aircraft investigated in the Langley 14- x 22-foot subsonic tunnel
[NASA-TP-2796] 13 p1717 N88-20264
Aircraft flight flutter testing at the NASA Ames-Dryden Flight Research Facility
[NASA-TM-100417] 13 p1723 N88-20301
High Reynolds number pump facility for cavitation research
[AD-A189310] 13 p1765 N88-20558
The use of an automated flight test management system in the development of a rapid-prototyping flight research facility
[NASA-TM-100435] 13 p1823 N88-20896
The continuous electron beam accelerator facility
[CEBAF-PR-87-017] 13 p1838 N88-20996
Development of an integrated set of research facilities for the support of research flight test
[NASA-TM-100427] 14 p1869 N88-21169
The NASA integrated test facility and its impact on flight research
[NASA-TM-100418] 14 p1870 N88-21177
Test facilities of the structural dynamics branch of NASA Lewis Research Center
[NASA-TM-100800] 14 p1934 N88-21534
Laboratory Information Management System (LIMS): A case study
[NASA-TM-100835] 14 p1961 N88-21697
Chronology of KSC and KSC related events for 1987
[NASA-CR-182754] 14 p2012 N88-22002
Procedures and requirements for testing in the Langley Research Center unitary plan wind tunnel
[NASA-TM-100529] 15 p2015 N88-22016
Function of Japan Fine Ceramics Center described
15 p2052 N88-22227
Structural dynamics branch research and accomplishments for fiscal year 1987
[NASA-TM-100279] 15 p2088 N88-22446
Marshall Space Flight Center 1960-1985: 25th anniversary report
[NASA-TM-100328] 15 p2153 N88-22852
Development of a mobile research flight test support capability
[NASA-TM-100428] 16 p2159 N88-22883
Development of an airborne facility for advanced avionics research 17 p2307 N88-23801
Structures and Dynamics Division research and technology plans for FY 1988 and accomplishments for FY 1987
[NASA-TM-100585] 17 p2350 N88-24000
Aerospace energy systems laboratory: Requirements and design approach
[NASA-TM-100423] 17 p2390 N88-24206
Analysis procedures and subjective flight results of a simulator validation and cue fidelity experiment
[NASA-TM-88270] 18 p2465 N88-24634
SHaRE: Collaborative materials science research
[DE88-007175] 18 p2467 N88-24646
Preparation for microgravity: The role of the microgravity materials science laboratory
[NASA-TM-100908] 18 p2497 N88-24811
Metals and Ceramics Division
[DE88-006955] 19 p2618 N88-25530
A detailed description of the uncertainty analysis for high area ratio rocket nozzle tests at the NASA Lewis Research Center 19 p2626 N88-25580
Engineering research centers and their evaluation
[PB88-180054] 19 p2739 N88-26262
Solar microwave radiation maps measured at Metsaehovi Radio Research Station in 1980-1981
[PB88-193453] 19 p2741 N88-26276
Building an artificial intelligence capability at Los Alamos
[DE88-009155] 20 p2842 N88-26866
Photovoltaic Measurements and Performance Branch
[DE88-001142] 21 p2968 N88-27633
Publications on acoustics research at the Langley Research Center during 1980-1986
[NASA-TM-100590] 21 p3013 N88-27881
The High Temperature Materials Laboratory: A new research and user facility at the Oak Ridge National Laboratory
[DE88-010792] 22 p3057 N88-28138
Langley Research Center Metrology Program status for fiscal year 1987
[NASA-TM-100651] 22 p3086 N88-28324
Software modifications to total data reporting accessory for metabolic measurement cart
[AD-A193641] 22 p3132 N88-28623
Bibliography of Lewis Research Center technical publications announced in 1987
[NASA-TM-100910] 22 p3162 N88-28832
The NBS/NRL (National Bureau of Standards/Naval Research Laboratory) free electron laser facility
[AD-A194214] 23 p3219 N88-29159
Center for opto-electronic systems research instrumentation grant
[AD-A193711] 23 p3282 N88-29545
Helicopter transmission research at NASA Lewis Research Center
[NASA-TM-100962] 24 p3379 N88-30128
An improvement in the numerical integration procedure used in the NASA Marshall engineering thermosphere model
[NASA-CR-179389] 24 p3392 N88-30200
Science at NASA field centers: Findings and recommendations on the scope, strength and interactions of science and science-related technology programs
[NASA-TM-101188] 24 p3459 N88-30581
Research and technology of the Lyndon B. Johnson Space Center
[NASA-TM-100463] 24 p3460 N88-30583

RESEARCH MANAGEMENT

Documentation as a management strategy for reaching goals in high-risk research-oriented projects
[DE87-012394] 01 p0105 N88-10685
Alternative fuels: Information on DOD's (Department of Defense's) methanol vehicle program
[PB87-213328] 02 p0156 N88-10976
Gallium arsenide and multibandgap solar cell research
[DE87-012260] 02 p0194 N88-11215
Siting and Geotechnical Program Focus and Directions. Report upon the deliberations of a workshop held at the Illinois Institute of Technology, Chicago, Illinois on August 4-5, 1986
[PB87-206272] 02 p0198 N88-11238
Report from the MPP Working Group to the NASA Associate Administrator for Space Science and Applications
[NASA-TM-87819] 02 p0223 N88-11402
Electronics engineering thrust area report, FY86
[DE87-014616] 03 p0309 N88-11950
Materials sciences programs: Fiscal Year 1987
[DE88-000672] 04 p0429 N88-12659
National Center for Atmospheric Research
[PB87-228391] 04 p0470 N88-12901
COLA2: A computer program for the structural synthesis of two components using general modal coordinates
[DE88-001457] 04 p0481 N88-12963
Nuclear techniques in studies of condensed matter
[NASA-RP-1195] 04 p0489 N88-13015
A national model at Howard University demonstrating private sector interrelationships that facilitate research in predominantly Black colleges and universities
[DE88-000160] 04 p0502 N88-13089
The role of basic research in society
[DE88-000459] 04 p0502 N88-13090
The birth of big science: Nuclear physics as advanced technology source
[NOTA-INTERNA-881] 05 p0648 N88-13967
A short introduction to the status and motivation for reversed field pinch and compact toroid research
[DE88-000487] 05 p0652 N88-13999
University research initiative research program summaries
[AD-A184876] 05 p0658 N88-14035
Research for electric energy systems
[DE88-001733] 06 p0695 N88-14265
HOST turbine heat transfer program summary
[NASA-TM-100280] 06 p0704 N88-14320
Research in elementary particle physics
[DE88-002130] 06 p0777 N88-14771
Research and technology objectives and plans. Summary, Fiscal Year 1986
[NASA-TM-87504] 06 p0800 N88-14894
Summaries of FY 1987 engineering research
[DE88-002572] 07 p0840 N88-15096
WOCE Core Project 2 Planning Meeting: The Southern Ocean
[WCP-138] 07 p0882 N88-15348
Research reports: 1987 NASA/ASEE Summer Faculty Fellowship Program
[NASA-CR-179219] 07 p0922 N88-15601
Physics rationale for the engineering specifications for ZTH
[DE88-000938] 07 p0936 N88-15690
Design and management of research projects
[PB88-106380] 07 p0941 N88-15721
German space policy on the threshold of the century. Analysis and proposals for the future
[ETN-88-90573] 07 p0943 N88-15734
Past, present and future role of Black Brant rocket systems to support international space science programs 08 p1034 N88-16272
Research in progress at the Institute for Computer Applications in Science and Engineering
[NASA-CR-181607] 08 p1053 N88-16354
The objectives and methods of the technological research program 09 p1124 N88-16730
The new approach to the definition of the ESA technological research program
09 p1127 N88-16763
Recommendations for a US ice coring program
[PB88-115043] 09 p1185 N88-17102
Performance analysis of parallel branch and bound search with the hypercube architecture
09 p1206 N88-17229
Technical activities 1987, Center for Radiation Research
[PB88-129325] 09 p1245 N88-17464
X-29A forward-swept-wing flight research program status
[NASA-TM-100413] 10 p1277 N88-17644
Study for history of technology developments in European space projects
[REPT-8518-1] 10 p1286 N88-17690
Research, development, and growth strategy
10 p1309 N88-17820
Research studies on extreme ultraviolet and soft X-ray lasers
[AD-A187506] 10 p1338 N88-17996
Features of a TeraFlop supercomputer
[DE88-003540] 10 p1384 N88-18263
Research in experimental nuclear physics
[DE88-004100] 10 p1408 N88-18397
Innovative arrangements for industry/DOE laboratory collaboration in high temperature superconductivity
[DE88-004320] 10 p1420 N88-18482
Journal of Research of the National Bureau of Standards, volume 92, number 5, September-October 1987
[PB88-124409] 10 p1426 N88-18518
Journal of Research of the National Bureau of Standards, volume 92, number 6, November-December 1987
[PB88-138516] 10 p1426 N88-18519
High performance composites research at NASA-Langley
[NASA-TM-100518] 11 p1450 N88-18642
Engineering thrust areas, 1988
[DE88-005103] 11 p1468 N88-18753
AFGL (Air Force Geophysics Laboratory) fiscal year 1988 Air Force technical objectives document
[AD-A187701] 11 p1503 N88-18977
Cumulative reports and publications through December 31, 1987
[NASA-CR-181624] 11 p1524 N88-19099
Institute for Computational Mechanics in Propulsion (ICOMP)
[NASA-TM-100790] 11 p1540 N88-19202
Experimental elementary particle physics at the University of Pittsburgh
[DE88-003542] 11 p1545 N88-19234
Study of industry requirements that can be fulfilled by combustion experimentation aboard space station
[NASA-CR-180854] 11 p1566 N88-19377
Alternative program approaches for the advanced satellite technology program
[AD-A188917] 12 p1600 N88-19576
Research on flow control
[AD-A189014] 12 p1627 N88-19736
Advanced Gas Turbine (AGT) technology development project
[NASA-CR-180891] 12 p1709 N88-20230
Mission directed goals for electric vehicle battery research and development: The Task Force on electric vehicle battery goals
[DE88-005601] 13 p1763 N88-20548
The use of an automated flight test management system in the development of a rapid-prototyping flight research facility
[NASA-TM-100435] 13 p1823 N88-20896
Computation and graphics in mathematical research
[DE88-005796] 13 p1831 N88-20953
Aeronautics and space report of the President: 1986 activities 13 p1852 N88-21087
Development of an integrated set of research facilities for the support of research flight test
[NASA-TM-100427] 14 p1869 N88-21169
Metals. Preliminary study for an Innovation-Oriented research Program (IOP)
[ETN-88-91317] 14 p1889 N88-21290
Innovation-Oriented research Program (IOP) metals. Annexes
[ETN-88-91318] 14 p1889 N88-21291
CTD/O2 data collected in 1985 and 1986 for EPOCS (Equatorial Pacific Ocean Climate Studies)
[PB88-160775] 14 p1951 N88-21629
Activities report in aerospace
[ETN-88-91978] 14 p1991 N88-21866
Engineering support of space shuttle experiment integration
[AD-A190135] 15 p2024 N88-22061
Summary of the 1987 Gordon Research Conference on Corrosion
[AD-A189737] 15 p2041 N88-22161

Structural dynamics branch research and accomplishments for fiscal year 1987
[NASA-TM-100279] 15 p2088 N88-22446
The Department of Defense Superconductivity Research and Development (DSRD) options. A study of possible directions for exploitation of superconductivity in military applications
[AD-A189747] 15 p2142 N88-22780
Space directorate research and technology accomplishments for fiscal year 1987
[NASA-TM-100607] 15 p2153 N88-22854
Advanced electric propulsion research
[NASA-CR-182130] 16 p2170 N88-22937
Ionospheric research in Antarctica
[INPE-4521-PRE/1273] 16 p2232 N88-23331
Naval research reviews, volume 39, number 3
[AD-A191392] 16 p2264 N88-23543
Advice for astronomical research
[ISBN-9-03-460977-4] 16 p2289 N88-23703
Fiber waveguide sensors for intelligent materials
[NASA-CR-183028] 17 p2343 N88-23968
Structures and Dynamics Division research and technology plans for FY 1988 and accomplishments for FY 1987
[NASA-TM-100585] 17 p2350 N88-24000
An overview of advanced battery development at Sandia National Laboratories
[DE88-006823] 18 p2506 N88-24867
Space station architectural elements and issues definition study
[NASA-CR-3941] 18 p2587 N88-25371
The Department of Defense report on the merit review process for competitive selection of university research projects and an analysis of the potential for expanding the geographic distribution of research for the Committees on Appropriations, United States Congress
[AD-A191842] 18 p2586 N88-25379
NASA history data book. Volume 1: NASA resources 1958-1968
[NASA-SP-4012-VOL-1] 18 p2596 N88-25428
NASA historical data book. Volume 2: Programs and projects 1958-1968
[NASA-SP-4012-VOL-2] 18 p2596 N88-25429
NASA historical data book. Volume 3: Programs and projects 1969-1978
[NASA-SP-4012-VOL-3] 18 p2596 N88-25430
Acid rain: Delays and management changes in the Federal research program
[GAO/RCED-87-89] 19 p2690 N88-25988
Computer-aided research
[DE88-007771] 19 p2714 N88-26114
Anatomy of an organizational change effort at the Lewis Research Center
[NASA-CR-4146] 19 p2739 N88-26264
Flight research and testing
[NASA-TM-100439] 20 p2758 N88-26361
Plastic deformation and roughness of free metal surfaces
[PB88-196621] 20 p2772 N88-26439
Novel magnetic materials research using free electron lasers
[DE88-009989] 20 p2807 N88-26652
Building an artificial intelligence capability at Los Alamos
[DE88-009155] 20 p2842 N88-26866
Issues and recommendations associated with distributed computation and data management systems for the space sciences
[NASA-CR-183026] 20 p2881 N88-27108
Aerospace applications studies, 1971-1987
[AGARD-R-759] 21 p2889 N88-27147
Air Force technical objective document, FY89
[AD-A193110] 21 p2896 N88-27194
Soviet dynamic fracture mechanics research
[FASAC-TAR-3140] 21 p2962 N88-27597
Finite element methodology for integrated flow-thermal-structural analysis
[NASA-CR-183144] 21 p2964 N88-27606
Atmospheric turbulence research at DFVLR
[AGARD-R-752] 21 p2975 N88-27669
Federal Council on Science, Engineering and Technology: Committee on Computer Research and Applications, Subcommittee on Science and Engineering Computing: The US Supercomputer Industry
[DE88-011262] 21 p2994 N88-27756
RLE progress report, January 1 to December 31, 1987
[RLE-PR-130] 21 p3011 N88-27869
Publications on acoustics research at the Langley Research Center during 1980-1986
[NASA-TM-100590] 21 p3013 N88-27881
The High Temperature Materials Laboratory: A new research and user facility at the Oak Ridge National Laboratory
[DE88-010792] 22 p3057 N88-28138
Development and verification of NASA Standard Initiator-2 (NSI-2)
[NASA-CR-172069] 23 p3200 N88-29044
Development and verification of NASA Standard Initiator-2 (NSI-2): Appendix
[NASA-CR-172070] 23 p3200 N88-29045
SERI's photovoltaic research project: A foundation for tomorrow's utility-scale electricity
[DE88-001161] 23 p3230 N88-29220
Competition: Issued on establishing and using Federally funded research and development centers
[PB88-178884] 23 p3296 N88-29632
Argonne National Laboratory technology transfer report, FY87
[DE88-010091] 23 p3298 N88-29639
Activities report in remote sensing
[ETN-88-92905] 23 p3309 N88-29714
Space shuttle phase B wind tunnel model and test information. Volume 1: Booster configuration
[NASA-CR-178414-VOL-1-PT-2] 24 p3320 N88-29770
Noncontact photo-thermal sensing
[AD-A195450] 24 p3344 N88-29905
Helicopter transmission research at NASA Lewis Research Center
[NASA-TM-100962] 24 p3379 N88-30128
Science at NASA field centers: Findings and recommendations on the scope, strength and interactions of science and science-related technology programs
[NASA-TM-101188] 24 p3459 N88-30581
Research and technology of the Lyndon B. Johnson Space Center
[NASA-TM-100463] 24 p3460 N88-30583

RESEARCH PROJECTS
University program management information system, fiscal year 1985
[NASA-TM-88381] 06 p0790 N88-14846
Acid rain: Delays and management changes in the Federal research program
[GAO/RCED-87-89] 19 p2690 N88-25988

RESEARCH VEHICLES
NT X-30 VEHICLE
A multiprocessor avionics system for an unmanned research vehicle
[AD-A194806] 24 p3325 N88-29800

RESERVOIRS
Observations of wind waves on a reservoir
[IOS-234] 02 p0193 N88-11206
Understanding passive cooling systems
[PB87-210464] 02 p0194 N88-11211
Study of reservoir water quality utilizing remote sensing techniques: Methodological concepts
17 p2364 N88-24076
Utilization of LANDSAT-TM imagery in the hydroenergetic inventory of the Paraiba de Sul River Basin
17 p2364 N88-24077
Unstable heat pipes
[DE88-010780] 23 p3229 N88-29217

RESIDENTIAL AREAS
Remote sensing techniques applied to the study of metropolitan regions: The west sector of the Sao Paulo metropolitan area
19 p2681 N88-25941
SPOT imagery for detecting residential expansion on the rural-urban fringe of Toronto, Canada
22 p3098 N88-28397
Applications of SPOT data for urban real estate investment information systems
22 p3101 N88-28414
Mapping and urban multi-experimental assessment of SPOT: Urban results
22 p3101 N88-28415

RESIDENTIAL ENERGY
Transient development of stratification in a partially divided enclosure
[DE87-011742] 05 p0572 N88-13490
Heat pump and appliance research
[PB88-102462] 07 p0853 N88-15184
Short Reference Years: Short weather data sets for faster simulations of solar energy systems and energy consumption in buildings
[DE88-900198] 07 p0881 N88-15343
Actual performance and economic feasibility of residential solar water heaters
[INPE-4399-RPE/555] 08 p1023 N88-16191
Effect of storage thermal behavior in seasonal storage solar heating systems
[PB88-114236] 10 p1350 N88-18067

RESIDUAL STRENGTH
Fiber composite structural durability and damage tolerance: Simplified predictive methods
[NASA-TM-100179] 05 p0560 N88-13409
Investigation of low velocity impact damage on filamentary composite materials
07 p0923 N88-15607
Residual stiffness and strength of Kevlar/epoxy laminated impulsively loaded to 7.9 ktaps
[DE88-003724] 09 p1149 N88-16886
Effects of moisture, elevated temperature, and fatigue loading on the behavior of graphite/epoxy buffer strip panels with center cracks
[NASA-TM-100558] 12 p1603 N88-19590

RESIDUAL STRESS
Stress-strain behavior of components subject to residual stresses taking the example of an orifice plate
[FF-10/1986] 01 p0059 N88-10375
Crack initiation life estimations for notched specimens with residual stresses based on local strains
[FF-17/1986] 01 p0060 N88-10385
Stress measurements in sol-gel films
[DE87-014467] 02 p0153 N88-10955
On the stressing of annealed NITINOL: The electrical resistance and calorimetric effects
[AD-A184465] 04 p0414 N88-12569
The evolution of local mechanical properties of Al 2219-T851 during fatigue
05 p0598 N88-13653
The influence of microstructure and residual stresses on the initiation and propagation of short surface cracks on AlMgSi1
05 p0601 N88-13674
Observations on the effect of overloads on fatigue crack growth
05 p0602 N88-13684
The effect of heat treatment on fatigue crack growth in polycarbonate
05 p0606 N88-13714
Analysis of end stresses in glass-metal bimaterial strips
[DE87-007848] 05 p0610 N88-13750
Threshold stress intensity for stable crack growth in high strength steel at ambient temperature and below
06 p0718 N88-14407
Interface characteristics and the mechanical properties of metal matrix composites
[AD-A186441] 08 p0966 N88-15845
Residual stress effect on stability of axially loaded columns
[PB87-143889] 08 p0996 N88-16032
Bias, internal stress and substrate effects on the microstructure and properties of PVD-wear resistant coatings
[AERE-R-12360] 10 p1304 N88-17798
Mechanical response of unidirectional boron/aluminum under combined loading
[NASA-CR-182595] 12 p1604 N88-19591
Evolution of hardening and damage during viscoplastic deformation
[AD-A190714] 15 p2077 N88-22381
Stress corrosion cracking of A723 steel pressure vessels: Two case studies
[AD-A191741] 18 p2527 N88-24990
The stress analysis of ceramic, polymeric, and metallic composite systems by the finite element method
18 p2529 N88-25004
The use of micromachined structures for the management of mechanical properties and adhesion of thin films
19 p2674 N88-25899
Observations on residual stresses in ceramic composites by neutron diffraction techniques
[DE88-009937] 20 p2778 N88-26472
Lattice strain in heteroepitaxial films
20 p2868 N88-27032
Thermo-viscoelastic analysis of composite materials, volume 1
[NASA-CR-183048-VOL-1] 21 p2904 N88-27230
Studies of internal stresses and surface roughness of sputtered Be and BeB films
[DE88-011737] 22 p3086 N88-28327
Theory of acoustoplasticity and ultrasonic measurements of residual stresses
22 p3087 N88-28328
Determination of the residual stresses in welded structures using the elastoplastodynamic method
[ETN-88-92745] 22 p3087 N88-28330
Thin film-residual stress assessment
[AD-A193205] 23 p3196 N88-29018
The mechanical behavior of surface modified ceramics
[DE88-010564] 23 p3196 N88-29022
A dynamic analysis of piezoelectric strained elements
[AD-A196079] 24 p3432 N88-30430

RESIDUES
Implementation of a digital optical matrix-vector multiplier using a holographic look-up table and residue arithmetic
[NASA-CR-180431] 01 p0078 N88-10496
Low extractable wipers for cleaning space flight hardware
02 p0137 N88-10863
Synthesis of high molecular weight peptide polymers and copolymers containing L-dope residues
[AD-A186462] 08 p0973 N88-15887
A programmable global system for the manipulation of residue numbers
[ETN-88-91476] 11 p1530 N88-19139
Carbon residue studies of polyphenyl ethers and ester-based lubricants using a microcarbon residue tester
[AD-A188585] 12 p1611 N88-19632

TDWR (Terminal Doppler Weather Radar) clutter residue map generation and usage
[AD-A191148] 16 p2235 N88-23352
Residual smoothing for accelerating the Alternating Direction Implicit (ADI) iteration method for elliptic difference equations
[CWI-NM-R8721] 16 p2259 N88-23500

RESIN BONDING
Interfacial shear strength of pitch and high strain pan fibers in an epoxy matrix
[AD-A185966] 07 p0826 N88-15011
Adhesion between polystyrene and polymethylmethacrylate
[AD-A192050] 18 p2492 N88-24785

RESIN MATRIX COMPOSITES
NT BORON-EPOXY COMPOSITES
NT GRAPHITE-EPOXY COMPOSITES
Composite structural materials
[NASA-CR-181416] 02 p0190 N88-11186
Time-temperature-stress capabilities of composite materials for advanced supersonic technology application
[NASA-CR-178272] 06 p0677 N88-14144
Fatigue behaviour of hybrid composites
[BR102236] 09 p1138 N88-16819
Mechanics of composite materials: Past, present and future
[NASA-TM-100793] 10 p1295 N88-17744
Ethynylated aromatics as high temperature matrix resins
[NASA-TM-89829] 11 p1450 N88-18640
Interlaminar fracture toughness of thermoplastic composites
[NASA-TM-100532] 15 p2030 N88-22097
Donor acceptor polymerization chemistry as a vehicle to low energy cure matrix resins
[AD-A190119] 15 p2044 N88-22179
Characterization of Mode 1 and Mode 2 delamination growth and thresholds in graphite/peek composites
[NASA-TM-100577] 16 p2172 N88-22947
Influence of fiber reinforcement on the vitreous transition temperature of M 10 matrix composites
[ONERA-RT-44/7086-M] 17 p2316 N88-23835
Proceedings of the American Society for Composites
[AD-A189861] 18 p2477 N88-24693
Current and future molecular structures of aerospace organic matrix resins 18 p2477 N88-24695
Industrial perspective on current and future needs in aerospace matrix resin chemistry
18 p2477 N88-24696
Applications of biotechnology to synthetic chemistry for aerospace matrix resins development
18 p2478 N88-24697
The 700 F properties of autoclave cured PMR-2 composites
[NASA-TM-100923] 18 p2480 N88-24712
The composite aeroengine
[PNR90451] 22 p3045 N88-28070
New acousto-ultrasonic techniques applied to aerospace materials
[NASA-TM-101299] 22 p3086 N88-28323
Novel ladder polymers for use as high temperature stable resins or coatings
[NASA-CASE-LEW-14203-1] 24 p3356 N88-29984

RESINS
NT ACRYLIC RESINS
NT EPOXY RESINS
NT KEVLAR (TRADEMARK)
NT NYLON (TRADEMARK)
NT PEEK
NT PHENOLIC RESINS
NT POLYAMIDE RESINS
NT POLYETHER RESINS
NT POLYIMIDE RESINS
NT POLYMETHYL METHACRYLATE
NT POLYURETHANE RESINS
NT SYNTHETIC RESINS
NT THERMOPLASTIC FILMS
NT THERMOPLASTIC RESINS
NT THERMOSETTING RESINS
NT VINYL COPOLYMERS
Effects of cure pressure on resin flow, voids, and mechanical properties
[AD-A184267] 03 p0295 N88-11853
Influence of carbon fiber surface treatment
[ETN-88-92536] 18 p2492 N88-24787
Electrophoretic coatings. Part 1: Sandia applications
[DE88-008666] 20 p2776 N88-26465

RESISTANCE
Experimental determination of the coefficients of the hydraulic resistance of apertures in the rotary disks
[AD-A190627] 15 p2066 N88-22317

RESISTANCE COEFFICIENTS
U RESISTANCE

RESISTANCE THERMOMETERS
A device for measuring fast temperature fluctuations --- atmospheric temperature
[KNMI-TR-92] 01 p0070 N88-10449
NBS (National Bureau of Standards) measurement services: Platinum resistance thermometer calibrations
[PB88-138367] 10 p1333 N88-17967

RESISTIVITY
U ELECTRICAL RESISTIVITY

RESISTOJET ENGINES
Space station propulsion
[NASA-TM-100216] 03 p0277 N88-11746
Slip casting and extruding shapes of rhenium with metal oxide additives. Part 2: Development of grain stabilized rhenium parts for resistojets
[NASA-CR-180851] 03 p0278 N88-11749
Compatability of dispersion-strengthened platinum with resistojet propellants
[NASA-TP-2765] 04 p0409 N88-12538
Space station resistojet system requirements and interface definition study
[NASA-CR-180832] 04 p0409 N88-12541
Magnetic emissions testing of the space station engineering model resistojet
[NASA-TM-100788] 10 p1292 N88-17728
Component data base for space station resistojet auxiliary propulsion
[NASA-CR-180834] 10 p1293 N88-17731
Electric propulsion options for the SP-100 reference mission 17 p2404 N88-24296
Development of a liquid-fed water resistojet
[NASA-TM-100927] 18 p2523 N88-24968
Experimental evaluation of resistojet thruster plume shields
[NASA-TM-101363] 24 p3338 N88-29868
The dc power control for a liquid-fed resistojet
[NASA-TM-101326] 24 p3338 N88-29869

RESISTOJETS
U RESISTOJET ENGINES

RESISTORS
NT POTENTIOMETERS (RESISTORS)
NT THERMISTORS
Resistor cooling in a vacuum
[DE88-000696] 04 p0440 N88-12733

RESOLUTION
NT ANGULAR RESOLUTION
NT HIGH RESOLUTION
NT IMAGE RESOLUTION
NT RADAR RESOLUTION
NT RADIOMETRIC RESOLUTION
NT SPATIAL RESOLUTION
NT SPECTRAL RESOLUTION
NT TEMPORAL RESOLUTION
Geometric analysis of ensemble of solutions in two-phase flow and complete resolution of problem of choking
[DE88-001687] 04 p0445 N88-12764
Improvement of deep resolution in ultrasonic echographic nondestructive evaluation using signal processing methods
[PB87-147658] 07 p0866 N88-15256
Conflict resolution in cooperative systems
[AD-A190351] 15 p2104 N88-22535
Television monitor field shifter and an opto-electronic method for obtaining a stereo image of optimal depth resolution and reduced depth distrotion on a single screen
[NASA-CASE-NPO-17249-1-CU]
17 p2332 N88-23924
The complexity of AI algorithms
[AD-A193494] 23 p3265 N88-29438
An analysis of results of a high-resolution world ocean circulation model
[AD-A195760] 24 p3405 N88-30272

RESOLVING POWER
U RESOLUTION

RESONANCE
NT CYCLOTRON RESONANCE
NT ELECTRON PARAMAGNETIC RESONANCE
NT MAGNETIC RESONANCE
NT MESON RESONANCE
NT NUCLEAR MAGNETIC RESONANCE
NT OPTICAL RESONANCE
NT ORBITAL RESONANCES (CELESTIAL MECHANICS)
NT PARAMAGNETIC RESONANCE
NT PLASMA RESONANCE
NT RESONANT VIBRATION
NT SPIN RESONANCE
Direct detection of optical radiation through a sampling orifice for inductively coupled plasma atomic emission spectroscopy
[DE87-013609] 01 p0101 N88-10662
Assessment of structural integrity from forced vibration testing
[DE87-014642] 02 p0191 N88-11195
Plasmon resonance absorption in layered structures of silver with periodic corrugation
[DE87-013183] 02 p0231 N88-11453
Singularity expansion method: Target Resonances
03 p0303 N88-11912
The hybrid wavefront resonance method
03 p0303 N88-11913
Surface polariton resonances and reflectance on a bigrating
[AD-A184663] 03 p0377 N88-12370
The itinerant resonating-valence-bond model for superconductivity
[DE87-014794] 03 p0380 N88-12391
The dynamics of solar magnetic flux tubes subjected to resonant foot point shaking 04 p0507 N88-13118
Resonant level lifetime in GaAs/ AlGaAs double-barrier structures
[AD-A185376] 05 p0655 N88-14020
Parametric and resonance interaction of ultrashort light pulses in nonlinear multilevel medium
06 p0773 N88-14746
Modal analyses of the Kernville diagnostic canister
[DE88-003268] 07 p0870 N88-15277
The single particle and collective descriptions of the anomalous Doppler resonance and the role of ion dynamics
[INPE-4390-PRE/1210] 08 p0976 N88-15904
Discovery by Voyager-2 of predicted satellites which determine resonance nature of Uranian rings
08 p1006 N88-16095
Geometric structure, pseudoband gaps, and surface vibrational resonances on metal surfaces
[AD-A187001] 09 p1143 N88-16851
The early years of string theory: The dual resonance model
[DE88-003521] 11 p1563 N88-19359
Resonance energy transfer between carbon monoxide and oxygen molecules using dye laser intracavity absorption spectroscopy
[AD-A188488] 12 p1689 N88-20104
Electromagnetic scattering from and natural resonances of the circular strip 13 p1759 N88-20523
Design, optimization and construction of a dc-SQUID with complete flux transformer circuits
[PB88-160742] 14 p1907 N88-21399
Tunable condensed-media laser with antiresonant ring cavity 14 p1971 N88-21764
Three-wave parametric resonance in plasma of relativistic electron flux 14 p1972 N88-21772
Theoretical studies of Resonance Enhanced Stimulated Raman Scattering (RESRS) of frequency-doubled Alexandrite laser wavelength in cesium vapor
[NASA-CR-182870] 15 p2036 N88-22133
The concept of an impact resonance diagram for characterizing the nonlinear response of impact vibration
[DE88-005475] 15 p2086 N88-22432
Low frequency ocean ambient noise: Measurements and theory
[AD-A191188] 16 p2237 N88-23362
Theoretical studies of Resonance Enhanced Stimulated Raman Scattering (RESRS) of frequency doubled Alexandrite laser wavelength in cesium vapor
[NASA-CR-182871] 17 p2317 N88-23841
Harmonic considerations for electrical distribution feeders
[DE88-007849] 18 p2505 N88-24880
Contributions of autoionizing resonances to the electron collisional excitation rates for Be-like ions
[AD-A190924] 18 p2572 N88-25275
High-fidelity in isotope ratio measurements for resonance ionization mass spectrometry
[DE88-009129] 19 p2613 N88-25506
A proposed Quantum Well Injection Transit Time device (QWITT) 19 p2657 N88-25785
Microwave and millimeter-wave resonant tunneling diodes 19 p2659 N88-25809
Quantum transport calculation of resonant-tunneling response time 19 p2659 N88-25810
Aircraft interior noise reduction by alternate resonance tuning
[NASA-CR-182540] 20 p2849 N88-26909
Resonant tunneling in InGaAs-InP double-barrier structures and superlattices 20 p2871 N88-27047
Excellent negative differential resistance of InGaAs/InAlAs resonant tunneling barrier structures and applications to a new functional device, RHET
20 p2872 N88-27048
Aeromechanical stability analysis of COPTER
21 p2891 N88-27161
Nonlinear stochastic interaction in aeroelastic structures
[AD-A193427] 21 p2961 N88-27589
Orbit determination of 1965-09A for analysis of the eccentricity at 15th-order resonance
[RAE-TR-87059] 22 p3047 N88-28081

Bulk plasmon enhanced photoemission from Nb(100) surface resonances
[AD-A192711] 22 p3154 N88-28767
Resonance excitation of linear and non-linear spiral density waves in a gaseous disk
23 p3299 N88-29643
Storing bits on a DNA polymer chain
[AD-A195701] 24 p3356 N88-29981
Impurity analysis in SIMOX samples by high-efficiency resonance ionization time-of-flight mass spectrometry
[DE88-012061] 24 p3367 N88-30051
Resonance effects accompanying motion with low thrust in earth-moon system 24 p3446 N88-30510

RESONANCE CHARGE EXCHANGE
Charge exchange in low energy (keV) and hyperthermal energy (10-100 eV) ion scattering
[AD-A187643] 11 p1543 N88-19222

RESONANCE FLUORESCENCE
Millimeter-wave studies of moist air
[AD-A184681] 03 p0306 N88-11935
Solitons in stimulated Raman scattering: Generation and control of ultrashort optical pulses
[AD-A185141] 05 p0650 N88-13983
Correlations between photons in resonance fluorescence emitted by an atom near a metal surface
[AD-A188365] 12 p1689 N88-20102

RESONANCE LINES
Formation and passivation of new paramagnetic defects associated with thermal oxides on silicon
[DE88-002720] 07 p0938 N88-15699
Low-power photolytically pumped lasers
[DE88-002448] 08 p0991 N88-15998
Inner-shell X-ray line spectra of highly ionized titanium, chromium, iron and nickel and their appliation to laboratory plasmas
[PB87-225181] 19 p2730 N88-26212

RESONANCE RADIATION
U RESONANCE FLUORESCENCE

RESONANCE SCATTERING
Resonance excitation in gamma gamma collisions at LEP200
[NIKHEF-H/87-3] 08 p1081 N88-16514
Nucleon resonances and nuclei: Experimental aspects
[CEBAF-PR-87-025] 11 p1545 N88-19233

RESONANT CAVITIES
U CAVITY RESONATORS

RESONANT FREQUENCIES
Accurate ab initio calculations which demonstrate a 3 Pi u ground state for Al2
[NASA-TM-89302] 01 p0102 N88-10666
Vibration-absorbing characteristics of metal-polymer shells 02 p0158 N88-10991
Systematic studies of molecular vibrational anharmonicity and vibration-rotation interaction by self-consistent-field higher derivative methods: Applications to asymmetric and symmetric top and linear polyatomic molecules
[DE87-014691] 02 p0232 N88-11465
Two-laser resonance enhanced photoionization spectrum of gas phase benzene
03 p0300 N88-11889
A new method to real-normalize measured complex modes 05 p0593 N88-13618
Initial dynamic load estimates during configuration design 05 p0593 N88-13621
Dynamic behavior of dissymmetric rotor bearings modelled with a periodic coefficient large system
05 p0596 N88-13640
Computation of natural frequencies of planar lattice structure
[AD-A185367] 05 p0641 N88-13920
Finite element method with continuous mass elements
[PB87-143364] 08 p0995 N88-16019
The dynamics of an oscillating four-bar linkage
09 p1181 N88-17074
Centaur G Prime modal test 09 p1181 N88-17075
Using frequency-domain methods to identify XV-15 aeroelastic modes
[NASA-TM-100033] 10 p1277 N88-17846
Time domain wave propagation in multilayered integrated circuits
[AD-A187462] 10 p1324 N88-17916
Electro-mechanical vibratory system
11 p1500 N88-18958
Study of inhomogeneously filled cylindrical resonant cavities by the finite integration technique
[PB88-133707] 12 p1697 N88-20156
Time-domain system for identification of the natural resonant frequencies of aircraft relevant to electromagnetic compatibility testing
[PB88-164520] 13 p1759 N88-20519
The concept of an impact resonance diagram for characterizing the nonlinear response of impact vibration
[DE88-005475] 15 p2086 N88-22432
Single mode levitation and translation
[NASA-CASE-NPO-16675-1-CU] 17 p2395 N88-24241
Open channel flow near the resonance speed
18 p2514 N88-24918
Resonant structures for integrated sensors
19 p2673 N88-25893
FEB structural analysis, revision H
[AD-A192302] 20 p2814 N88-26698
Vibration response of constrained viscoelastically damped plates: Analyses and experiments
[AD-A192329] 20 p2815 N88-26699
Prediction of the aeroelastic behavior of tuned blades. Application to aircraft engines
[ISAL-87-0046] 21 p2897 N88-27199
Natural frequencies and stability of immiscible cylindrical z-independent liquid systems
[LRT-WE-9-FB-1(1987)] 22 p3053 N88-28112
Natural frequencies and stability of immiscible spherical liquid systems
[LRT-WE-9-FB-2(1987)] 22 p3053 N88-28113
Natural frequencies and stability of circular cylindrical immiscible liquid systems
[LRT-WE-9-FB-3(1987)] 22 p3062 N88-28172
Nonlinear oscillations of axially independent liquid column under zero-gravity environment
[LRT-WE-9-FB-12(1987)] 22 p3063 N88-28174
Measure of hydrogen concentration profile in materials by resonant nuclear reactions
[DE88-702599] 23 p3193 N88-28999
Effects on the resonant frequencies caused by loading a spherical cavity with a dielectric sphere
[AD-A193864] 23 p3277 N88-29511
Laser sensing for identification and control of distributed parameter systems
[AD-A195886] 24 p3379 N88-30124

RESONANT VIBRATION
The effect of different packagings on the vibration behavior and the coupling factors of steam turbine blading
[ETN-87-90425] 01 p0056 N88-10357
Equivalent circuit consideration on the rotation of resonant modes of double resonant vibrators
07 p0839 N88-15092
Analyses by equivalent mechanical circuits of bending vibration bars with load-impedance at one end
07 p0840 N88-15093
Sea resonance vibrational source of seismic waves
08 p1010 N88-16126
Theoretical and experimental damping values of piping systems at high ductilities
[DE88-006717] 18 p2526 N88-24986
The role of acoustic resonances in unsteady turbomachinery aerodynamics
[PNR90455] 22 p3147 N88-28720

RESONATORS
NT CAVITY RESONATORS
NT OPTICAL RESONATORS
Measurement and analysis of cryogenic sapphire dielectric resonators and DROs
04 p0433 N88-12686
Equivalent circuit consideration on the rotation of resonant modes of double resonant vibrators
07 p0839 N88-15092
Analyses by equivalent mechanical circuits of bending vibration bars with load-impedance at one end
07 p0840 N88-15093
GERA computer code for calculation of two-dimensional electromagnetic fields in resonators and electron-optical systems by the finite element method
[DE88-700678] 11 p1480 N88-18831
Parametric study of acceleration-induced stresses and frequency changes in doubly-rotated crystal resonators
[AD-A189261] 13 p1781 N88-20532
Quartz oscillator analysis
[DE88-005886] 13 p1784 N88-20550
Semiclassical theory of injected lasers with arbitrary stable and unstable resonators
[AD-A189514] 13 p1775 N88-20615
Resonator coupling of two ring cavity, argon-ion lasers
[AD-A189558] 13 p1775 N88-20616
Method for characterizing end-plate surface resistance of dielectric resonator 14 p1903 N88-21371
Efficient narrow linewidth waveguide dye laser pumped by CuCl laser 16 p2187 N88-23038
Surface wave accelerometer
[ETN-88-92000] 16 p2210 N88-23192
Electrothermal instability in superconducting resonators
[DE88-701684] 16 p2282 N88-23664
Low noise cryogenic dielectric resonator oscillator
[NASA-CASE-NPO-17157-1-CU] 20 p2797 N88-26596
Quartz crystal resonators and oscillators for frequency control and timing applications
[AD-A193310] 21 p2937 N88-27443
X-band resonant ring operation at 450 kW
22 p3064 N88-28181

RESOURCE ALLOCATION
Semi-arid ecosystem development as a function of resource processing and allocation
[DE88-000890] 07 p0875 N88-15308
A software planning and development methodology with resource allocation capability
[AD-A186088] 07 p0902 N88-15462
Physics rationale for the engineering specifications for ZTH
[DE88-000938] 07 p0936 N88-15690
Iterative-deepening heuristic search for optimal and semi-optimal resource allocation
08 p1062 N88-16410
Planning activities in space 08 p1063 N88-16417
An AI approach for scheduling space-station payloads at Kennedy Space Center 08 p1064 N88-16425
Scheduling spacecraft operations
08 p1064 N88-16426
The resource envelope as a basis for space station management system scheduling
08 p1064 N88-16427
Preliminary analysis of an integrated logistics system for OSSA payloads. Volume 2: OSSA integrated logistics support strategy 12 p1584 N88-19479
Dynamic resource allocation in a hierarchical multiprocessor system: A preliminary study
[NASA-CR-183177] 22 p3141 N88-28675

RESOURCES
NT AQUIFERS
NT COAL
NT CRUDE OIL
NT EARTH RESOURCES
NT FORESTS
NT FOSSIL FUELS
NT GEOTHERMAL RESOURCES
NT GLACIERS
NT ICEBERGS
NT LAND ICE
NT MARINE RESOURCES
NT NATURAL GAS
NT OIL FIELDS
NT RAIN FORESTS
NT TAR SANDS
NT UNDERWATER RESOURCES
NT WATER RESOURCES

RESOURCES MANAGEMENT
NT FOREST MANAGEMENT
NT LAND MANAGEMENT
Study of Earth from space and strengthening of economy 01 p0010 N88-10055
Optimum dimensioning of field service centers: Analysis of the problem and solutions thereof
01 p0012 N88-10066
A unified approach to parallel computation: Performance evaluation and architecturally independent parallel programming
[DE87-012519] 01 p0084 N88-10540
Knowledge acquisition issues encountered during the development of an estimating expert system
[DE87-013320] 02 p0248 N88-11568
Spinoff, 1987
[NASA-TM-89652] 02 p0250 N88-11577
Desertification in the Sahelian and Sudanian Zones of West Africa
[PB87-217063] 03 p0345 N88-12183
University research initiative research program summaries
[AD-A184876] 05 p0658 N88-14035
Detection of soil erosion with Thematic Mapper (TM) satellite data within Pinyon-Juniper woodlands
[NASA-CR-182476] 09 p1185 N88-17103
Air Force geographic information and analysis system
[DE88-001420] 10 p1424 N88-18505
Computer-Aided Design Information System (CADIS): User's manual
[DE88-004365] 10 p1424 N88-18509
Wind energy resource survey of New Zealand: National resource assessment
[PB88-139365] 12 p1640 N88-19822
Systems approach to energy quality and efficiency
[PB88-139506] 12 p1640 N88-19823
Orbital remote sensing: An instrument for monitoring urban growth
[INPE-4456-PRE/1287] 15 p2150 N88-22833
Resource management in dialog cell specification (DICE) method
[CWI-CS-R8746] 16 p2248 N88-23433
A proposal for a project entitled assessment of forest resources in Uruguay submitted to the United Nations Industrial Development Organization (UNIDO)
17 p2352 N88-24016
Remote sensing and data integration: Practical solutions for resource managers 17 p2356 N88-24034

Identification of areas cultivated with soybeans in the cerrados regions, through digital processingof satellite images: A methodological approach
17 p2358 N88-24048
Research on enhancing the utilization of digital multispectral data and geographic information systems in global habitability studies
[NASA-CR-182799] 17 p2368 N88-24101
Department of Defense Statement on the Technology Base to the Subcommittee on Defense Industry and Technology of the Committee on Armed Services, United States Senate, 100th Congress, second session
[AD-A191839] 18 p2588 N88-25376
Application of remote sensing in the conservation of natural areas: Ribeira Valley 19 p2683 N88-25949
Remote sensing technique applied to vegetation as an aid to municipal planning 19 p2683 N88-25951
Remote sensing applied to the monitoring of mineral extraction in the proximity of urban areas: Pros and cons
19 p2684 N88-25954
Remote sensing applied to integrated regional development programs 19 p2685 N88-25958
Application of SPOT data to renewable resources in the Maldives 22 p3109 N88-28469
LRS-2: A specialized knowledge system for launch resource scheduling
[AD-A194625] 23 p3182 N88-28941
A scheduling and resource management system for space applications 23 p3256 N88-29383
Intelligent resource management for local area networks: Approach and evolution
23 p3256 N88-29385
Study of the spectral response of soybeans
[INPE-4592-PRE/1322] 24 p3387 N88-30174

RESPIRATION
NT HIGH ALTITUDE BREATHING
Fundamental study on gas monitoring in CELSS
03 p0359 N88-12263
Study of the relationship between photosynthesis, respiration, transpiration, and mineral nutrition in wheat
03 p0360 N88-12268
Human respiratory responses during high performance flight
[AGARD-AG-312] 04 p0474 N88-12923
Short-term in vitro screening studies related to the inhalation toxicology of potentially toxic aerosols
[AD-A184815] 05 p0629 N88-13845
A plethysmograph for measuring pulmonary ventilation in small animals
[AD-A184978] 05 p0629 N88-13846
Maximal cardiorespiratory responses to one- and two-legged cycling during acute and long-term exposure to 4300m
[AD-A185730] 06 p0752 N88-14621
Biorhythmological analysis of dynamics of pulmonary ventilation parameters during orthostatic tests
07 p0891 N88-15400
Role of hemoglobin affinity for oxygen in efficiency of blood respiratory function 07 p0892 N88-15406
Changes in functional parameters of animals during long-term inhalation of acetic acid
07 p0895 N88-15423
Exercise thermoregulation after prolonged wakefulness
[AD-A186224] 08 p1048 N88-16327
Experimental measurements of the uptake of ozone in rats and human subjects
[PB88-125422] 10 p1364 N88-18149
Effect of oxygen inhalation on respiratory function during exercise and exposure to added resistance to respiration
10 p1366 N88-18164
Toxic effects of man-made mineral fibers with particular reference to ceramic fibers
[AD-A187949] 11 p1519 N88-19072
Electromagnetic metrics of mental workload
[AD-A188205] 11 p1523 N88-19093
Respiratory parameters aboard an aircraft performing parabolic flights 12 p1653 N88-19902
Breath-by-breath measurement of alveolar gas exchange 12 p1653 N88-19905
Nitrogen's biological effect on oxygen transport through hematoparenchymal barrier 12 p1662 N88-19967
Human adaptation to various hypercapnic conditions in relation to salivary electrolyte dynamics and renal function 12 p1664 N88-19977
Air quality and human performance, chapter 16
[AD-A188335] 12 p1666 N88-19988
Fibrous glass aerosols: A literature review
[AD-A188420] 12 p1672 N88-20006
Increase in influence of oxygen on the body in the presence of helium 13 p1810 N88-20816
A laser-based photoacoustic spectrometer for direct breath C-13O2/C-12O2 measurement
[DE88-004915] 15 p2101 N88-22516
Vagal tone as an index of mental state
16 p2239 N88-23373
Mathematical modelling of the heat and water vapour transport in the human respiratory tract
17 p2382 N88-24160
Effect of long-term inhalation of acetic acid vapor on some functional parameters of man
19 p2705 N88-26084
Respiration and oxygen tension in the blood of animals exposed to high pressures 20 p2830 N88-26790
Metabolic and cardiorespiratory parameters during three consecutive days of exhaustive running
[AD-A192598] 21 p2985 N88-27728

RESPIRATORY DISEASES
NT ASTHMA

RESPIRATORY PHYSIOLOGY
Load carriage induced alterations of pulmonary function
[AD-A186227] 07 p0889 N88-15386
The respiratory system under weightlessness
12 p1653 N88-19901
Respiratory parameters aboard an aircraft performing parabolic flights 12 p1653 N88-19902
The effect of orthostatic changes in central blood volume on the heart rate response to graded Valsalva maneuvers 12 p1653 N88-19904
Breath-by-breath measurement of alveolar gas exchange 12 p1653 N88-19905
Second-generation respiratory monitoring system for microgravity studies in man 12 p1653 N88-19906
Lung function in simulated microgravity
12 p1654 N88-19907
Closed system physiology: Role of oxygen in the development of wheat 12 p1655 N88-19916

RESPIRATORY RATE
Vital signs rate meter
[AD-A187015] 09 p1198 N88-17183
Desynchronization of heart rate and breathing frequency after transmeridional flight across three time zones
12 p1663 N88-19968

RESPIRATORY SYSTEM
NT ALVEOLI
NT GLOTTIS
NT LARYNX
NT LUNGS
Radon Research Program, FY-1987
[DE88-002633] 09 p1188 N88-17120
JPRS Report: Science and Technology. USSR: Space Biology and Aerospace Medicine, volume 21, no. 6, November - December 1987
[JPRS-USB-88-004] 10 p1364 N88-18150
Effect of hypercapnic-hypoxic test on cariorespiratory parameters of individuals with neurocirculatory dystonia
10 p1367 N88-18169
Modeling of the non-auditory response to blast overpressure
[AD-A187397] 10 p1389 N88-18184
The respiratory system under weightlessness
12 p1653 N88-19901
Mathematical modelling of the heat and water vapour transport in the human respiratory tract
17 p2382 N88-24160
Accidental hypothermia
[AD-A194967] 24 p3406 N88-30278
Models of cerebral-body perfusion and cerebral chemical transport
[AD-A194945] 24 p3407 N88-30283

RESPONDERS
U TRANSPONDERS

RESPONSE BIAS
Response characteristics of dual MOSFET gamma-ray sensors produced by Mitel Corporation
[AD-A189026] 12 p1630 N88-19755
Picosecond optical autocorrelation experiments on fast photodetectors 19 p2659 N88-25802
A nonparametric multidimensional IRT approach with applications to ability estimation and test bias
[AD-A194212] 23 p3273 N88-29483

RESPONSE TIME (COMPUTERS)
Adaptive line of sight algorithms
[DE87-014275] 01 p0081 N88-11523
High performance clause indexing
[DE87-011399] 01 p0106 N88-10688
Indirect solution of static problems using concurrent vector processing computers
[DE87-012105] 05 p0636 N88-13889
An empirical investigation of load indices for load balancing applications
[AD-A185763] 06 p0724 N88-14451
A comparison of the Cray-2 performance before and after the installation of memory pseudo-banking
[NASA-CR-177462] 09 p1215 N88-17287
Graph transformation algorithms for array memory optimization in applicative languages
[DE88-004727] 10 p1387 N88-18283
Modules of nanosecond logic electronics system with computer control
[DE88-700190] 11 p1479 N88-18828
Object recognition on a systolic array
[AD-A187726] 11 p1534 N88-19184
Computer aided fast turnaround laboratory for research in VLSI (Very Large Scale Integration)
[AD-A189451] 12 p1624 N88-19715
Computer program in BASIC language for computation of spectrochemical analytical data
[DE88-701229] 15 p2032 N88-22106
COMESH: A corner mesh finite difference code to solve multigroup diffusion equations in multidimensions
[DE88-701248] 15 p2108 N88-22555
Concepts for robot motion primitives required for space station teleoperations 23 p3257 N88-29387

RESPONSES
NT DYNAMIC RESPONSE
NT HEMODYNAMIC RESPONSES
NT MODAL RESPONSE
NT PHYSIOLOGICAL RESPONSES
NT TRANSIENT RESPONSE
Engine/airframe response evaluation of the HH-60A helicopter equipped with the T700-GE-701 transient droop improvement electronic control unit
[AD-A184443] 04 p0401 N88-12492
Shadow systems and attractors in reaction-diffusion equations
[AD-A185804] 06 p0766 N88-14706
Computer response time measurements of mood, fatigue and symptom scale items: Implications for scale response time uses
[AD-A186093] 07 p0888 N88-15384
Corrosion behavior of sputter-deposited aluminum-based alloys exposed to chloride solutions
[AD-A187262] 10 p1303 N88-17794
Computer aided fast turnaround laboratory for research in VLSI (Very Large Scale Integration)
[AD-A189451] 12 p1624 N88-19715
Distraction and inhibition in continuous CRT performance: A replication and some new findings
[PB88-150941] 13 p1811 N88-20821
The interaction of sensory and perceptual variables: Spatial, temporal and orientation response to figure and ground
[AD-A192897] 20 p2832 N88-26798
Synchronous response modelling and control of an annular momentum control device
[NASA-CR-4166] 24 p3358 N88-29995
Numerical simulation of the function of scientific instrumentation for measuring the speed of electron devices
[AD-A194969] 24 p3376 N88-30103
Dirichlet prior in Bayesian estimation of item response curves
[AD-A195311] 24 p3426 N88-30392

REST
NT BED REST
Influence of altitude and caffeine during rest and exercise on plasma levels of proenkephalin peptide F
[AD-A192659] 22 p3131 N88-28816

RESTORATION
Method for combined image interpolation-restoration through a fir filter design technique
[INPE-4561-PRE/1302] 24 p3413 N88-30315

RESTRAINTS
U CONSTRAINTS

RESTRICTIONS
U CONSTRICTIONS

RESUSCITATION
Accidental hypothermia
[AD-A194967] 24 p3406 N88-30278

RETAINING
Hydrogen retention and release from uranium dioxide
[DE88-002042] 07 p0829 N88-15030

RETARDANTS
NT FLAME RETARDANTS

RETARDING
The generation and suppression of synchrotron sidebands
[DE88-000532] 04 p0449 N88-12787
Fatigue crack retardation in aluminium alloys
05 p0602 N88-13681
Effect of overload ratios on fatigue crack growth behavior in Ti-6Al-4V alloy
[PB87-147082] 07 p0833 N88-15055
The retardation of cold fronts at high mesoscale mountains 09 p1241 N88-17437

RETARDING ION MASS SPECTROMETERS
U MASS SPECTROMETERS

RETENTION (PSYCHOLOGY)
Short- and long-term effects of nonlethal levels of fast high-energy helium ions on retention of developed and formation of new behavioral patterns in rats
10 p1362 N88-18140
Working memory capacity: An individual differences approach
[AD-A192359] 20 p2833 N88-26803

Skilled memory and expertise: Mechanisms of exceptional performance
[AD-A193829] 22 p3133 N88-28628
Low doses of atropine sulfate impair retention of a well-learned spatial task
[AD-A194065] 23 p3237 N88-29266

RETINA
NT FOVEA
Psychophysical, biochemical and histological studies of spectrally selective photic damage to primate retina
[AD-A188115] 11 p1517 N88-19063
Functional assessment of laser irradiation
[AD-A195735] 24 p3408 N88-30287

RETINAL ADAPTATION
NT DARK ADAPTATION
NT LIGHT ADAPTATION

RETIREMENT FOR CAUSE
Engine component retirement for cause. Volume 1: Executive summary
[AD-A192730] 20 p2760 N88-26371

RETORC (TORPEDOES)
U TORPEDOES

RETRACTABLE EQUIPMENT
Development of the Extendable and Retractable Mast (ERM), Design phase 2. Volume 1 — spacecraft payloads
[RP-2010-0000-DS/09] 11 p1467 N88-18750
DARM: A new deployment and retraction mechanism which does not need electric power
14 p1876 N88-21206
The EURECA antenna deployment and retraction mechanisms 14 p1878 N88-21225
The X-beam as a deployable boom for the space station 14 p1925 N88-21473
Motion synchronization of a mechanism to deploy and restow a truss beam 14 p1925 N88-21474

RETRACTABLE LANDING GEAR
U LANDING GEAR
U RETRACTABLE EQUIPMENT

RETRIEVAL
NT DATA RETRIEVAL
NT INFORMATION RETRIEVAL
NT PAYLOAD RETRIEVAL (STS)
Mechanical design of a ultrahigh gravity UHV facility to launch and recover a low-speed projectile tested on board KC 135 14 p1877 N88-21216

RETROFITTING
Computer-aided design analysis of 57-mm, angular-contact, cryogenic turbopump bearings
[NASA-TP-2816] 11 p1496 N88-18933
Servojet retrofit
[AD-A191075] 18 p2522 N88-24964
Aircraft avionics and missile system installation cost study. Volume 1: Technical report and appendices A through E
[AD-A194605] 23 p3178 N88-28923

RETURN TO EARTH SPACE FLIGHT
The comet rendezvous asteroid flyby mission
14 p2005 N88-21956
Retrieving samples from comet nuclei
14 p2006 N88-21959

REUSABLE LAUNCH VEHICLES
NT HOTOL LAUNCH VEHICLE
Ballistic Single Stage Carrier Vehicle (BETA): A single stage reusable ballistic space shuttle concept
[MBB-UR-949/70] 10 p1310 N88-17828
Space shuttle phase B wind tunnel model and test information. Volume 3: Launch configuration
[NASA-CR-178416-VOL-3-PT-2]
24 p3315 N88-29744
Evaluation of the advanced air breathing propulsion concepts, executive summary
[ESA-CR(P)-2540] 24 p3325 N88-29802
Evaluation of advanced air breathing concepts. Volume 1: Executive summary
[ESA-CR(P)-2539] 24 p3326 N88-29806

REUSABLE ROCKET ENGINES
A reusable rocket engine intelligen control
[NASA-TM-100963] 20 p2766 N88-26401

REUSABLE SPACECRAFT
NT AEROSPACE PLANES
NT CHALLENGER (ORBITER)
NT DISCOVERY (ORBITER)
NT HERMES MANNED SPACEPLANE
NT HOTOL LAUNCH VEHICLE
NT SPACE SHUTTLE ORBITERS
NT SPACE SHUTTLES
NT X-30 VEHICLE
Ballistic Single Stage Carrier Vehicle (BETA): A single stage reusable ballistic space shuttle concept
[MBB-UR-949/70] 10 p1310 N88-17828
Trends in the development of space transportation systems
[MBB-UR-911/86] 10 p1315 N88-17857
Three-dimensional Euler solutions for hypersonic Mach numbers
[MBB-UR-944/87] 10 p1315 N88-17859
Space shuttle phase B wind tunnel model and test information. Volume 1: Booster configuration
[NASA-CR-178414-VOL-1-PT-1]
24 p3315 N88-29745
Space shuttle phase B wind tunnel model and test information. Volume 1: Booster configuration
[NASA-CR-178414-VOL-1-PT-2]
24 p3320 N88-29770
Lunar lander conceptual design: Lunar base systems study task 2.2
[NASA-CR-172051] 24 p3335 N88-29854

REUSE
Automated software development workstation
23 p3263 N88-29423

REVERBERATION
The effect of reverberation on active sonar performance
[ARE-TM(UJS)-87104] 03 p0374 N88-12350
Signal, noise, and reverberation in bistatic sonar systems
[FOA-C-20703-2.7] 22 p3147 N88-28721

REVERBERATION CHAMBERS
Measurement of shielding effectiveness of different cable and shielding configurations by mode-stirred techniques
[PB88-155791] 10 p1319 N88-17885
EMR (Electromagnetic Radiation) test facilities evaluation of reverberating chamber located at RADC (Rome Air Development Center), Griffiss AFB (Air Force Base), Rome, New York
[PB88-178827] 15 p2022 N88-22048

REVERSE FIELD PINCH
Steady state theta pinch concept for slow formation of FRC
[ISSN-0469-4732] 01 p0098 N88-10648
A tapered poloidal gap for the reduction of field errors
[DE87-014750] 03 p0377 N88-12375
Interchange stability of noncircular reversed field pinches
[DE88-000177] 03 p0378 N88-12381
Numerical simulation of the Reversed Field Pinch
[AD-A184353] 04 p0491 N88-13023
Transport simulations of the oscillating field current drive experiment in the ZT-40M reversed field pinch
[DE88-000536] 04 p0491 N88-13027
Magnetic fluctuation behaviour of current termination in reversed field pinch
[IPPJ-849] 04 p0492 N88-13034
Refueling and density control in the ZT-40M reversed field pinch
[DE88-000504] 04 p0493 N88-13040
Dynamic processes in field-reversed-configuration compact toroids
[DE87-014756] 05 p0652 N88-13998
A short introduction to the status and motivation for reversed field pinch and compact toroid research
[DE88-000487] 05 p0652 N88-13999
A review of the experimental and theoretical status of the reversed-field pinch
[DE88-000529] 05 p0652 N88-14000
Reversed field pinch plasmas with various boundary conditions
[DE88-000832] 05 p0653 N88-14004
The TITAN oscillating-field current-drive system
[DE88-001823] 06 p0782 N88-14798
Edge plasmas and plasma/wall interactions in an ignition-class reversed field pinch
[DE88-001825] 06 p0782 N88-14799
The TITAN magnet configuration
[DE88-001826] 06 p0782 N88-14800
Reversed field pinch experiments: Summary of progress report
[DE88-002367] 07 p0934 N88-15673
Experimental model of halo plasma observed in small-aspect FRC plasma
[INPE-4159-PRE/1061] 08 p1085 N88-16534
Design, construction and operation of a small RFP for turbulent plasma studies
[INPE-4241-PRE/1116] 08 p1087 N88-16545
Experimental study of the initial plasma formation stage in a linear theta pinch of inverted field
[DE88-700010] 09 p1249 N88-17485
Proceedings of the International Workshop on Engineering Design of Next Step Reversed Field Pinch Devices
[DE88-001915] 09 p1251 N88-17494
The TITAN Reversed-Field Pinch Reactor: Design-point determination and parametric studies
[DE88-001824] 09 p1251 N88-17498
D-3He fuels in a field-reversed configuration
[IPPJ-855] 10 p1411 N88-18419
Stability of an RFP (Reversed-Field Pinch) with resistive and distant boundaries
[DE88-004155] 10 p1413 N88-18431
Zero-dimensional model of a reversed field pinch fusion reactor
[DE88-005213] 10 p1414 N88-18442
Improved zero dimensional model of a reversed field pinch fusion device
[DE88-005212] 12 p1693 N88-20127
Reversed field pinch operation with a thin shell
[DE88-005521] 13 p1843 N88-21027
Electrical circuit modeling of reversed field pinches
[DE88-006942] 15 p2136 N88-22745
QN3D: A 3-dimensional quasi-neutral hybrid particle-in-cell code with applications to the tilt mode instability in field reversed configurations
18 p2580 N88-25325
The safety designs for the TITAN reversed-field pinch reactor study
[DE88-006169] 19 p2729 N88-26205
Overview of the TITAN-2 reversed-field pinch aqueous fusion power core design
[DE88-008170] 20 p2857 N88-26966
RFP (Revised Field Pinch) plasma experiment at INPE
[INPE-4613-PRE/1336] 24 p3431 N88-30420

REVERSE OSMOSIS
Reverse osmosis treatment to remove inorganic contaminants from drinking water
[PB88-147780] 12 p1605 N88-19598

REVERSE TIME
U REACTION TIME

REVERSED FLOW
Dynamics of reverse flows at pump inlet
04 p0425 N88-12636
Comparison of the performance of a reverse flow annular combustion chamber under low and high pressure conditions 24 p3347 N88-29923

REVERSING
A flash spectrum of Cl I, C I, N I, and Ni II absorption in 31 Cygni: A direct observation of the reversing layer
04 p0513 N88-13158
Dislocation free zone model of fracture under reverse loading
[DE88-002676] 07 p0869 N88-15276
Analysis of reversible and irreversible hydrogen trapping in metals
[NPL-DMA(A)-154] 16 p2177 N88-22977
A study on the precipitation and reversion behaviors of Cu-0.3 percent Cr alloy by the step annealing method
[NASA-TT-20169] 18 p2489 N88-24764

REVIEWING
Procedures for peer review assessments
[DE88-007749] 19 p2739 N88-26263

REVISIONS
Revision of the information standards for flight mechanics
[DFVLR-MITT-87-06] 03 p0265 N88-11675
Uniform laws and regulations as adopted by the National Conference on Weights and Measures (72nd), 1987
[PB88-123724] 06 p0689 N88-14225
Model-based building verification in aerial photographs
[AD-A186010] 07 p0870 N88-15278
Influence of base modifications on in-flight base drag in the presence of jet exhaust for Mach numbers from 0.7 to 1.5
[NASA-TP-2802] 11 p1488 N88-18881
Computer-aided design analysis of 57-mm, angular-contact, cryogenic turbopump bearings
[NASA-TP-2816] 11 p1496 N88-18933
HELIOS modelling of point-focusing solar concentrators
[DE88-004933] 12 p1640 N88-19820
Modified theory of gravity
[DE88-700835] 12 p1642 N88-19830
Parametric study of the total cost of aircraft modernization in terms of development and equipment series costs 12 p1700 N88-20177
Systematic behavior of NMC medium range forecasts and the effect of model changes 1985-87
22 p3125 N88-28575

REVOLUTION (MOTION)
U REVOLVING

REVOLVING
Incipient fault detection study for advanced spacecraft systems
[NASA-CR-172014] 02 p0183 N88-11138
The application of the hybrid iterative method to scattering by perfectly conducting bodies of revolution
11 p1475 N88-18802

REYNOLDS EQUATION
Calculations of viscous flows with a multigrid method
13 p1769 N88-20580
High-speed flow calculations past 3-D configurations based on the Reynolds averaged Navier-Stokes equations
[NASA-TM-100082] 14 p1911 N88-21421

REYNOLDS LAW
U REYNOLDS EQUATION
REYNOLDS NUMBER
NT HIGH REYNOLDS NUMBER
NT LOW REYNOLDS NUMBER
Reynolds number effects on the small scale structure of a turbulent channel flow 01 p0001 N88-10004
The structure of separated flow regions occurring near the leading edge of airfoils including transition
[NASA-CR-181434] 01 p0002 N88-10011
Numerical study of the entrance flow and its transition in a circular pipe (2) 03 p0318 N88-12011
The drag of slender axisymmetric cones in rarefied hypersonic flow 05 p0531 N88-13229
Computational study of three-dimensional wake structures
[REPT-2] 05 p0539 N88-13281
Effects of free stream turbulence, Reynolds number and incidence angle on axial turbine cascade performance 05 p0548 N88-13339
Regressed relations for forced convection heat transfer in a direct injection stratified charge rotary engine
[NASA-TM-100124] 05 p0549 N88-13345
Instability and transition in curved channel flow 10 p1328 N88-17938
A low speed wind tunnel investigation of Reynolds number effects on a 60-deg swept wing configuration with leading and trailing edge flaps
[NASA-CR-181684] 19 p2598 N88-25441
Investigation of the validity of Reynolds averaged turbulence models at the frequencies that occur in turbomachinery
[NASA-CR-182162] 22 p3048 N88-28087
Reynolds number effects and the wind tunnel environment 23 p3168 N88-28862
Experimental tools: The tunnel and the model 23 p3168 N88-28864
REYNOLDS STRESS
Turbulence modelling through one point closures-applications-enlightening by large eddy simulation 03 p0312 N88-11972
Reynolds-stress and dissipation rate budgets in a turbulent channel flow
[NASA-TM-89451] 07 p0852 N88-15174
Turbulence models for practical applications 08 p0986 N88-15974
Numerical implementation and performance of Reynolds stress closures in finite volume computations of recirculating and strongly swirling flows 08 p0987 N88-15976
Improvement of the Reynolds-stress model by a new pressure-strain correlation
[NASA-CR-182699] 13 p1783 N88-20667
Development of subminiature multi-sensor hot-wire probes
[NASA-TM-100052] 15 p2069 N88-22336
Studying Turbulence Using Numerical Simulation Databases. Proceedings of the 1987 Summer Program
[NASA-CR-182692] 16 p2194 N88-23086
Study of one-dimensional spectral dynamic equations of the Reynolds stresses in homogeneous anisotropic turbulence: Application to split-spectrum modeling 16 p2196 N88-23095
On local approximations of the pressure-strain term in turbulence models 16 p2197 N88-23102
Local structure of intercomponent energy transfer in homogeneous turbulent shear flow 16 p2197 N88-23103
Test code for the assessment and improvement of Reynolds stress models 16 p2197 N88-23105
Reynolds stress models of homogeneous turbulence 16 p2197 N88-23106
The decay of isotropic turbulence in a rapidly rotating frame 16 p2197 N88-23107
Evaluation of a theory for pressure-strain rate 16 p2198 N88-23108
The simulation of coherent structures in a laminar boundary layer 16 p2198 N88-23111
Active layer model for wall-bounded turbulence 16 p2199 N88-23115
Coherent structures in the axisymmetric turbulent jet mixing layer 21 p2947 N88-27504
Development of a hot-wire measurement technique for moderate intensity three-dimensional flows 22 p3080 N88-28289
Analysis method for the production of Reynolds stresses in compressible turbulent flow (fluid mechanics)
[NASA-TT-20330] 24 p3373 N88-30088
Development of a more general Reynolds stress closure for swirling flow
[AD-A195121] 24 p3374 N88-30092
RF-4 AIRCRAFT
Future air-to-air training for the RF-4
[AD-A194363] 23 p3240 N88-29284
RH-2 HELICOPTER
U UH-1 HELICOPTER
RHENIUM
NT RHENIUM ISOTOPES
Slip casting and extruding shapes of rhenium with metal oxide additives. Part 2: Development of grain stabilized rhenium parts for resistojets
[NASA-CR-180851] 03 p0278 N88-11749
Johnson noise thermometer for high radiation and high temperature environments
[DE88-003770] 10 p1323 N88-17911
Compatibility in space reactor fuel systems
[DE88-005698] 13 p1839 N88-21004
Johnson noise thermometer for high-radiation and high-temperature environments 17 p2434 N88-24480
Iridium-coated rhenium thrusters by CVD
[NASA-TM-101309] 24 p3339 N88-29874
RHENIUM ALLOYS
Equations for determining CVD tungsten-rhenium alloy composition and plating rate
[DE87-008831] 01 p0024 N88-10152
RHENIUM ISOTOPES
A nuclear structure study of the proposed gamma-ray laser candidate nucleus Re-186
[DE88-004299] 10 p1336 N88-17986
Experimental and theoretical investigations of isotope shift and hyperfine structure on 5d elements (especially platinum, iridium and rhenium)
[ETN-88-93121] 24 p3353 N88-29957
RHEOLOGY
Rheological behaviors of an elastomeric membrane
[DE87-013105] 01 p0061 N88-10392
Colloidal structure of bitumens. Relationship between composition-structure behavior
[PC-4] 02 p0146 N88-10912
Rheological and aging characterization of elastomers
[DE87-009598] 02 p0151 N88-10944
Experiments on densely-loaded non-Newtonian slurries in laminar and turbulent pipe flows
[DE88-000719] 04 p0442 N88-12746
TMA-microrheological testing of polymers (thermomechanical analysis)
[PB87-228805] 06 p0683 N88-14187
The effective elastic properties of low-density foams
[DE87-014629] 06 p0684 N88-14194
Physics and chemistry 07 p0883 N88-15359
Thermoplastic elastomers as LOVA binders
[AD-A186563] 10 p1304 N88-17797
Continual capillary viscosimetry using extrusiograph techniques
[PB88-166293] 15 p2046 N88-22195
Experiments on densely-loaded non-Newtonian slurries in laminar and turbulent pipe flows
[DE88-006209] 15 p2067 N88-22323
Electrical dc conductivity of pitch
[AD-A191266] 16 p2182 N88-23008
Characterization of aluminum/RP-1 gel propellant properties
[NASA-TM-100951] 18 p2496 N88-24808
Experiments on densely-loaded non-Newtonian slurries in laminar and turbulent pipe flows
[DE88-010579] 20 p2800 N88-26612
Effects of a temperature-dependent rheology on large scale continental extension
[NASA-CR-183117] 20 p2825 N88-26759
Optimal rheological characteristics in dynamic stability of polymer flow through porous media
[DE88-001225] 21 p2918 N88-27322
A review: Quantitative models for lava flows on Mars 23 p3301 N88-29656
Photogeological inferences of Martian surface composition 23 p3303 N88-29675
Lava flow-field morphology: A case study from Mount Etna, Sicily 23 p3303 N88-29676
Ultrasonic detection of diffusion and adhesion loss 24 p3354 N88-29967
Lava thicknesses: Implications for rheological and crustal development 24 p3443 N88-30490
Small-scale volcanic landforms indicative of distributary tube systems 24 p3444 N88-30496
RHODESIA
U ZIMBABWE
RHODIUM
Laser-induced desorption determinations of surface diffusion on Rh(111)
[DE88-005159] 11 p1454 N88-18667
Model catalyst studies of SMSI (Strong Metal/Support Interactions) and the role of D-electrons in chemisorption and catalysis
[DE88-004518] 13 p1738 N88-20393
The relationship of the chemical bonding topology of high critical temperature copper oxide superconductors to that of the chevrel phases and the ternary lanthanide rhodium borides
[AD-A189255] 13 p1845 N88-21042
Oxide-bound transition metal complexes for methane activation
[PB88-169719] 14 p1887 N88-21277
Mechanism of the nitric oxide-carbon monoxide-oxygen reaction over a single crystal rhodium catalyst
[DE88-006274] 21 p2910 N88-27268
RHODIUM COMPOUNDS
Catalytic activation of carbon dioxide by metal complexes
[AD-A192310] 21 p2909 N88-27262
RHOMBOIDS
Benchmark computation and finite element performance evaluation for a rhombic plate bending problem
[AD-A187402] 10 p1345 N88-18041
RHYTHM (BIOLOGY)
NT CIRCADIAN RHYTHMS
Infradian biorhythms of human vital signs 06 p0750 N88-14606
Biorhythmological analysis of dynamics of pulmonary ventilation parameters during orthostatic tests 07 p0891 N88-15400
New book on space ecology reviewed 07 p0897 N88-15434
Center for the study of rhythmic processes
[AD-A188204] 11 p1520 N88-19078
Interrelationship of heart rhythm indicators and resistance to hypoxia in Antarctic polar workers 12 p1664 N88-19974
Method of assessing changes in biorhythmological structure of human physiological functions 19 p2706 N88-26088
RIBBON PARACHUTES
Parachute characteristics of Titan descent modules --- planetary probe
[BF-3/86-B] 02 p0122 N88-10774
The aerodynamics of supersonic parachutes
[DE87-014846] 04 p0395 N88-12464
RIBBONS
Tape wrapping apparatus and method
[EP-PATENT-0-181-747-A2] 01 p0053 N88-10336
Investigation of boundary layer disturbances caused by periodic heating of a thin ribbon
[AD-A190572] 15 p2065 N88-22314
RIBONUCLEIC ACIDS
RNA-synthesizing activity in rat liver following flight aboard Cosmos-1667 10 p1360 N88-18130
RIBS (SUPPORTS)
Local heat/mass transfer and pressure drop in a two-pass rib-roughened channel for turbine airfoil cooling
[NASA-CR-179635] 03 p0322 N88-12039
Optimal ribbing of long plate made of composite material 04 p0426 N88-12641
The viscous flow on surfaces with streamwise riblets
[DFVLR-FB-87-21] 09 p1162 N88-16961
The viscous flow on surfaces with streamline riblets
[ESA-TT-1091] 24 p3370 N88-30067
RICCATI EQUATION
Oscillation theory for linear second-order differential systems
[DE87-011393] 04 p0484 N88-12983
Strong convergence and convergence rates of approximating solutions for algebraic Riccati equations in Hilbert spaces
[AD-A186190] 08 p1072 N88-16464
A LQG regulator for the angular motion of the rotor at a tuned gyroscope
[INPE-4280-PRE/1152] 12 p1631 N88-19759
Control, stability and filter for a discrete linear stochastic system with correlated noise
[PB88-109525] 21 p3004 N88-27818
Convergence of Galerkin approximations for operator Riccati equations: A nonlinear evolution equation approach
[NASA-CR-181706] 24 p3425 N88-30386
RICE
Pilot study of rice culture in sub-tropical high population density region (Madagascar) with SPOT 1 multispectral data 22 p3097 N88-28392
Using SPOT HRV data to update the distribution of the paddy field in Taiwan 22 p3097 N88-28393
RICHARDSON NUMBER
Some results from the Amazon Forest micrometeorological experiment
[INPE-4631-PRE/1346] 24 p3403 N88-30263
RICHARDSON-DUSHMAN EQUATION
U TEMPERATURE EFFECTS
U THERMIONIC EMISSION
RIDGES
Experimental and theoretical constraints on the origin of mid-ocean ridge geothermal fluids 13 p1804 N88-20784
RIDING QUALITY
Measurement of suspension and ride characteristics of the M1 main battle tank 05 p0596 N88-13637
RIEMANN INTEGRAL
U MEASURE AND INTEGRATION

RIEMANN MANIFOLD
On the cosmological constant in the heterotic string theory
[DE87-703099] 02 p0247 N88-11562
Computer-aided study of a class of Riemannian space-times
[DE87-703367] 05 p0645 N88-13950
A fast Riemann solver with constant covolume applied to the random choice method
[CAR-87-19] 09 p1231 N88-17375
Path integration on the upper half-plane
[DE88-751050] 12 p1682 N88-20057
String theory and algebraic geometry of moduli spaces
[CWI-PM-R8705] 13 p1849 N88-21070
Markov processes applied to control, replacement and signal analysis
[AD-A190563] 15 p2126 N88-22674
Regularity of the Albanese map for nonoriented surfaces
[DE88-006428] 15 p2126 N88-22679
Vortices on the world sheet and string's critical dynamics
[DE88-702116] 21 p3026 N88-27961

RIEMANN PROBLEM
U CAUCHY PROBLEM

RIEMANN SPACE
U RIEMANN MANIFOLD

RIEMANN SPHERE
U RIEMANN MANIFOLD

RIFT VALLEYS
U VALLEYS

RIFTS
U GEOLOGICAL FAULTS

RIGID BODIES
U RIGID STRUCTURES

RIGID ROTOR HELICOPTERS
Time periodic control of a multi-blade helicopter
[AD-A194435] 23 p3180 N88-28931

RIGID ROTORS
An experimental investigation of the flap-lag-torsion aeroelastic stability of a small-scale hingeless helicopter rotor in hover
[NASA-TP-2546] 13 p1715 N88-20257
A comparison of theory and experiment for coupled rotor-body stability of a hingeless rotor model in hover under simulated vacuum conditions
21 p2889 N88-27151
A comparison of theory and experiment for coupled rotor-body stability of a hingeless rotor model in hover
21 p2889 N88-27152
Aeroelastic modeling of rotor blades with spanwise variable elastic axis offset: Classic issues revisited and new formulations 21 p2890 N88-27158
Aeromechanical stability analysis of COPTER
21 p2891 N88-27161

RIGID ROTORS (PLASMA PHYSICS)
NT PLASMA PHYSICS

RIGID STRUCTURES
NT RIGID ROTORS
Flap-lag equations of motion of rigid, articulated rotor blades with three hinge sequences
[NASA-TM-100023] 04 p0401 N88-12495
Numerical simulations of impact tests on a rigid wall --- armor steel
[SNIAS-872-320-102] 05 p0610 N88-13744
Stability analysis of a rigid body with a flexible attachment using the energy-casimir method
[AD-A185646] 06 p0723 N88-14449
Formulation methods of rigid multibody systems for large space structures and some results of computer simulation
[NAL-TR-942] 10 p1293 N88-17730
The dynamics of two coupled rigid bodies
[AD-A187592] 10 p1341 N88-18012
Qualification of frequency response functions using the rigid-body response
[DE88-000745] 10 p1344 N88-18033
The dynamics of coupled planar rigid bodies. Part 1: Reduction, equilibria and stability
[AD-A187487] 10 p1345 N88-18042
Parametric dependence in the equilibrium dynamics of rotating structures
[AD-A187817] 11 p1498 N88-18945
Automatic feedback control of a rigid body for finite displacements 18 p2473 N88-24674
Recursive mass matrix factorization and inversion: An operator approach to open- and closed-chain multibody dynamics
[NASA-CR-182516] 23 p3247 N88-29328
Clevis joint for deployable space structures
[NASA-CASE-LAR-13898-1] 24 p3380 N88-30130

RILLS
U VALLEYS

RING CURRENTS
The duskside plasmapause/ring current interface: Convection and plasma wave observations
[MPE-PREPRINT-93] 02 p0243 N88-11533
Current-driven lower hybrid waves at the inner edge of the ring current --- magnetosphere
[MPE-PREPRINT-94] 02 p0243 N88-11534
Ring current role in dynamics of fluctuating electron and ion fluxes in low-latitude magnetosphere
24 p3447 N88-30514
Plasma of earth's magnetosphere ring currents. Model compared with results of AMPTE/CCE experiment
24 p3447 N88-30515

RING LASERS
Distributed feedback effects in lasers and high gain laser instabilities in optically pumped CH3F
03 p0329 N88-12079
Study on a unidirectional ring laser gyro. Part 1: Proposition of the principle and studies on the components
[NAL-TR-933] 09 p1169 N88-17010
Studies of fluorine combustion
[AD-A187646] 11 p1452 N88-18656
Thirteenth Biennial Guidance Test Symposium, volume 1
[AD-A185782] 12 p1576 N88-19427
Calibration of a ring laser gyro inertial navigation system 12 p1576 N88-19428
The optimum solution to instrument quantization effects 12 p1577 N88-19434
The German Honeywell ring laser gyro: Development and test results 12 p1578 N88-19440
Laser gyro attitude control system feasibility
[AD-A189368] 13 p1720 N88-20285
Resonator coupling of two ring cavity, argon-ion lasers
[AD-A189558] 13 p1775 N88-20616
Solid-state ring laser with acoustooptical phase nonreciprocity of opposing waves
14 p1970 N88-21761
Monolithic integration on a GaAs substrate of a quarter ring laser and an optical guide coupled by an evanescent wave
[ETN-88-92308] 17 p2344 N88-23969
Precision measurement of the Fresnel drag coefficient using a ring laser
[AD-A196025] 24 p3366 N88-30043

RING STRUCTURES
NT REINFORCEMENT RINGS
An experimental and theoretical study of the bending behavior of Kevlar 49/epoxy beams and rings
[DE87-010430] 01 p0061 N88-10394
Investigations of the equilibrium and stability of thin-walled double rings. A contribution to the solution of single-sided contact problems
[ETN-87-90044] 09 p1181 N88-17076
Buckling and breakdown problems in structural mechanics. Failure of prestressed double-walled containers or rings
[MBB-UR-E-956/87] 13 p1783 N88-20671
New wide-band transducer developed
14 p1901 N88-21353
Unrestrained out-of-plane buckling of monosymmetric rings
[PB88-155213] 14 p1923 N88-21458
Tunable condensed-media laser with antiresonant ring cavity 14 p1971 N88-21764
Vibrations of rotating thick or thin rings
18 p2529 N88-25003
Analytical and experimental investigation of ringless piston concept
[AD-A192835] 20 p2810 N88-26673
Transport in GaAs heterojunction ring structures
20 p2864 N88-27011

RINGS
Hot piston ring tests
[NASA-TM-100256] 06 p0729 N88-14486
Hot piston ring/cylinder liner materials: Selection and evaluation
[NASA-TM-100276] 08 p0971 N88-15872
Multi-hundred kilowatt roll ring assembly evaluation results
[NASA-TM-100865] 14 p1904 N88-21375
On the bending response of Kevlar 49/epoxy beams and rings
[DE88-006824] 18 p2530 N88-25012

RINGS (MATHEMATICS)
Class of N-associative rings
[PB87-230421] 06 p0769 N88-14724
The classification problem of finite rings by computable means
[AD-A185869] 07 p0908 N88-15500

RIPPLES
Laser pulse width dependent surface ripples on silicon
[PB88-127311] 10 p1336 N88-17982
Recording a surface acoustic wave on the surface of silicon
[PB88-130372] 11 p1490 N88-18894
Problems in modeling TF ripple loss of fast alphas from a tokamak reactor
[DE88-000612] 11 p1553 N88-19296
Superconductors with structured surfaces: Fields and currents
[AD-A189353] 12 p1699 N88-20164
Helical ripple transport in stellarators at low collision frequency
[DE88-006431] 13 p1843 N88-21031

RISK
Hypersonic aerodynamics: Applications for HOTOL
05 p0535 N88-13252
A long term radiological risk model for plutonium-fueled and fission reactor space nuclear system
[DE87-010486] 06 p0779 N88-14782
Risk analysis methodology survey
07 p0922 N88-15604
Instrumentation utilisation for risk control in safety operations --- balloons and rockets
08 p1030 N88-16240
Group adaptation and individual adjustment in antarctica: A summary of recent research
[AD-A186605] 08 p1051 N88-16347
Sudden in-flight incapacitation in general aviation
[AD-A187044] 09 p1115 N88-16682
Committee on Interagency Radiation Research and Policy Coordination
[DE88-003358] 09 p1188 N88-17121
Medical and psychological problems of assuring flight safety under present conditions
10 p1359 N88-18123
Modeling of the non-auditory response to blast overpressure
[AD-A187397] 10 p1369 N88-18184
Risk reduction cost avoidance for full scale development begins with concept formulation
12 p1700 N88-20174
Post-Challenger evaluation of space shuttle risk assessment and management
[NASA-CR-182461] 12 p1705 N88-20202
The space station assembly phase: Flight telerobotic servicer feasibility, volume 1
[NASA-CR-182669] 13 p1731 N88-20351
Survival analysis using additive risk models
[AD-A189053] 13 p1825 N88-20906
A systems analysis of fire suppression alternatives for the US space station
[AD-A189847] 15 p2025 N88-22064
Asymptotic theory for weighted least squares estimators in Aalen's additive risk model
[AD-A191085] 18 p2562 N88-25210
A perspective of PC-based probabilistic risk assessment
[DE88-006715] 18 p2568 N88-25251
Decision making aids: Methods and risks
22 p3161 N88-28820
Risk analysis in space system safety
22 p3161 N88-28825
Venture theory: A model of decision weights
[AD-A194809] 24 p3426 N88-30391

RITZ AVERAGING METHOD
Predicted and measured strain responses of isotropic panels to base excitation
[NASA-TM-4054] 19 p2679 N88-25928

RIVER BASINS
NT DELAWARE RIVER BASIN (US)
Analysis of squall line based on conventional data
02 p0207 N88-11295
The mesoscale numerical model for heavy rainfall forecasting in Yangtze River Valley, China
02 p0211 N88-11326
Oxidation and reduction rates for organic carbon in the Amazon mainstream tributary and floodplain, inferred from distributions of dissolved gases
[NASA-CR-182943] 18 p2538 N88-25062
Photointerpretation with instrumentation for evaluation of environmental impact: Mata Atlantica in Cubatao
19 p2663 N88-25946
Use of remote sensing in the study of superficial formation certifying the development of integrated economy-case example: Rio Claro (SP) region
19 p2683 N88-25950

RIVERS
NT OHIO RIVER (US)
Evaluation of the magnetic induction conductivity method for detecting frazil ice deposits
[AD-A186940] 09 p1194 N88-17157
Landuse and landform studies of the Mahanadi River Delta with the help of satellite MSS band
17 p2355 N88-24033
Geomorphologic sector maps of Niquizanga-Mayares, province of San Juan, Argentina
17 p2368 N88-24098

Influence of the Yukon River on the Bering Sea
[NASA-CR-182802] 17 p2376 N88-24126
The impact of disorganized occupation of urban sub-basins: Sub-basin of the Cabucu River, metropolitan area of Sao Paulo (SP) 19 p2682 N88-25945
Delineation of ephemeral fluvial networks on low-relief Piedmont surfaces, Plutonium Valley, Nevada, USA 22 p3093 N88-28367

RIVETED JOINTS
Experimental and theoretical investigation of mechanically fastened composites
[AD-A185896] 07 p0826 N88-15008
Damage mechanisms of CFRP riveted joints 11 p1449 N88-18636
On the calculation of stresses in pin-loaded anisotropic plates
[ETN-88-92239] 16 p2222 N88-23261

RIVETING
Automatic riveting machine for spherically-formed airframe structures
[ETN-88-91024] 11 p1495 N88-18924

RIVETS
Crack distribution and growth rates for critical fastener holes in Mirage wing RH79
[AD-A189080] 13 p1722 N88-20293

RNA
U RIBONUCLEIC ACIDS

ROADS
NT HIGHWAYS
Nowcasting for the national economy needs 02 p0199 N88-11241
Feasibility study of a range of products drawn from SPOT satellite imagery and specific to road-laying studies 03 p0342 N88-12157
A texture analysis approach to computer vision for identification of roads in aerial photographs
[AD-A189340] 12 p1639 N88-19815
Computer aided cartographic representation of traffic data: The traffic intensity maps of Baden-Wuerttemberg (Federal Republic of Germany) 16 p2225 N88-23282
Digitizing the traffic network of JOG 250 by scanning --- JOG 250 map 18 p2533 N88-25029
Propagation effects by roadside trees measured at UHF and L-band for mobile satellite systems 19 p2644 N88-25693
Use of SPOT data in preliminary steps of road project studies especially suited for developing countries 22 p3098 N88-28396
Automatic line network extraction from aerial imagery of urban areas through knowledge-based image analysis
[AD-A192399] 23 p3227 N88-29208

ROADWAY POWERED VEHICLES
Simulation models for the dynamics of tracked vehicle systems: State-of-the-art and open problems 20 p2785 N88-26522

ROBOTICS
Telepresence work station system definition study, part 2
[NASA-CR-172006] 01 p0013 N88-10071
Space station platforms 01 p0015 N88-10086
Telerobotics 01 p0015 N88-10090
Robotic sensors and actuators for a service manipulator system. Volume 1: Executive summary
[MATRA-EPT/DT/VT187/120] 01 p0053 N88-10341
Robotic sensors and actuators for a service manipulator system. Volume 2: Service Manipulator System (SMS) handbook
[MATRA-EPT/DT/VT187/227] 01 p0053 N88-10342
Robotic sensors and actuators for a service manipulator system. Volume 3, phase A report and program plan
[MATRA-EPT/DT/VT187/228] 01 p0054 N88-10343
Augmenting the control of a flexible manipulator with passive mechanical damping 01 p0055 N88-10350
Multimedia sensory systems for the solution of the error recovery problem --- robots
[REPT-87-010] 01 p0084 N88-10545
Digital algorithms for the control and dynamic decoupling of industrial robot axes
[ETN-87-90441] 01 p0084 N88-10546
Object-oriented data base management for robot programming
[ETN-87-90367] 01 p0105 N88-10687
Optimization of a controlled two-server maintenance system
[INPE-4202-PRE/1083] 01 p0107 N88-10694
USSR Report: Engineering and Equipment
[JPRS-UEQ-87-007] 02 p0157 N88-10985
Human factors in robotic system design discussed 02 p0158 N88-10988
Robotics and Intelligent Systems Program
[DE87-014561] 02 p0223 N88-11404
Components for measuring robots
[KFK-PFT-126] 03 p0332 N88-12092
On the control of a compliant robot arm 03 p0332 N88-12095
Dynamics and stability of bipedal locomotion robots 03 p0333 N88-12096
A theory for the articulation of robot manipulators 03 p0333 N88-12097
Teleoperator and robotics system analysis
[NASA-CR-179220] 03 p0334 N88-12105
Operator multiple-tasking study for remotely operated platforms
[AD-A184487] 03 p0362 N88-12276
Architecture for dynamic task allocation in a man-robot symbiotic system
[DE87-013872] 03 p0362 N88-12277
Two dimensional path planning with obstacles and shadows
[AD-A184075] 04 p0397 N88-12474
Autonomous Land Vehicle (ALV) planning and navigation system
[AD-A184243] 04 p0397 N88-12475
Correction of inertial navigation system drift errors for an autonomous land vehicle using optical radar terrain data
[AD-A184973] 05 p0544 N88-13311
Towards building a team of intelligent robots
[NASA-CR-181538] 05 p0589 N88-13595
Collision-free motion of two robot arms in a common workspace
[CSE-87-00002] 05 p0589 N88-13596
Behavioral Architecture Robot Control System (BARCS): A new way of building robots
[REPT-87-036] 05 p0638 N88-13902
National Aeronautics and Space Administration (NASA)/American Society for Engineering Education (ASEE) Summer Faculty Fellowship Program, 1987. Volume 1
[NASA-CR-172009-VOL-1] 06 p0792 N88-14855
Heuristic control of the Utah/MIT dextrous robot hand 06 p0793 N88-14858
National Aeronautics and Space Administration (NASA)/American Society for Engineering Education (ASEE) Summer Faculty Fellowship Program, 1987. Volume 2
[NASA-CR-172009-VOL-2] 06 p0796 N88-14874
Dynamics, control and sensor issues pertinent to robotic hands for the EVA retriever system 06 p0796 N88-14876
Time-domain robotic vision application 06 p0798 N88-14886
Proceedings of Image Understanding Workshop, volume 2
[AD-A186104] 07 p0902 N88-15464
Advancing automation and robotics technology for the space station and for the US economy: Submitted to the United States Congress October 1, 1987
[NASA-TM-100777] 08 p0959 N88-15816
Advancing automation and robotics technology for the space station and for the US economy: Submitted to the United States Congress May 15, 1987
[NASA-TM-89811] 08 p0959 N88-15817
Advancing automation and robotics technology for the space station and for the US economy: Submitted to the United States Congress October 1, 1986
[NASA-TM-89190] 08 p0960 N88-15818
Third Conference on Artificial Intelligence for Space Applications, part 1
[NASA-CP-2492-Pt-1] 08 p1055 N88-16360
Issues associated with telerobotic systems in space 08 p1056 N88-16369
Telerobotic controller development 08 p1056 N88-16370
Software simulation of time delay in teleoperation 08 p1056 N88-16371
Task path planning, scheduling and learning for free-ranging robot systems 08 p1058 N88-16386
Goal driven kinematic simulation of flexible arm robot for space station missions 08 p1059 N88-16388
Heuristic search in robot configuration space using variable metric 08 p1059 N88-16389
The power of neural nets 08 p1064 N88-16430
First Annual Workshop on Space Operations Automation and Robotics (SOAR 87)
[NASA-CP-2491] 09 p1203 N88-17206
Robotic planner expert system (RPLANES) 09 p1209 N88-17246
Robotic air vehicle. Blending artificial intelligence with conventional software 09 p1210 N88-17252
Communication and control in an integrated manufacturing system 09 p1212 N88-17263
Development of Moire machine vision 09 p1212 N88-17264
Implementation of a robotic flexible assembly system 09 p1212 N88-17265
System integration of a Telerobotic Demonstration System (TDS) testbed 09 p1212 N88-17266
Vision technology/algorithms for space robotics applications 09 p1212 N88-17267
The use of computer graphic simulation in the development of robotic systems 09 p1214 N88-17275
Intelligent robotic tracker 09 p1214 N88-17276
An efficient representation of spatial information for expert reasoning in robotic vehicles 09 p1214 N88-17278
A generalized method for automatic downhand and wirefeed control of a welding robot and positioner
[NASA-TP-2807] 10 p1316 N88-17869
NASA/NBS (National Aeronautics and Space Administration/National Bureau of Standards) standard reference model for Telerobot Control System Architecture (NASREM)
[PB88-124773] 10 p1338 N88-17999
Design conditions and workspace for the generally-proportioned 3-hinge spherical wrist for robots 10 p1339 N88-18003
Recursive forward dynamics for multiple robot arms moving a common task object
[NASA-CR-182526] 10 p1340 N88-18008
Parameter identification and sensitivity analysis for a robotic manipulator arm
[NASA-CR-181608] 10 p1385 N88-18272
A computer simulation study of an expert system for walking machine motion planning
[AD-A187907] 11 p1438 N88-18577
Robotic assembly and testing of rotary solenoids
[BDX-613-3663] 11 p1480 N88-18834
Voice/natural language interfacing for robotic control
[AD-A187765] 11 p1494 N88-18917
Improvement in robot positioning accuracy by a kinematic identification model 11 p1496 N88-18931
Motion planning and control of robot manipulators via application of a computer graphics animated display 11 p1496 N88-18932
Visual integration and detection of discontinuities: The key role of intensity edges
[AD-A188012] 11 p1520 N88-19076
Research in knowledge representation for natural language communication and planning assistance
[AD-A187355] 11 p1522 N88-19087
Error detection and recovery for robot motion planning with uncertainty
[AD-A187746] 11 p1534 N88-19165
Optically coupled tactile sensor array for robotics 11 p1550 N88-19273
JPRS report. Science and technology: Europe and Latin America
[JPRS-ELS-87-054] 12 p1573 N88-19406
Output aiming control
[AD-A188463] 12 p1583 N88-19473
Robotic intelligence issues for space manipulator monitoring, control programming 12 p1588 N88-19504
On a knowledge based assisted system for highly autonomous control of experiment-manipulators in the Man-Tended Free Flyer 12 p1588 N88-19505
A knowledge-based approach for sensory-controlled assembly operations 12 p1588 N88-19506
Mobile robot activity model for autonomous free flying platforms 12 p1588 N88-19507
Computational aspects of robotic experiment manipulation in a microgravity environment 12 p1589 N88-19512
EPOS: European Proximity Operations Simulation 12 p1589 N88-19515
Ground based supervisory and programming system for automatic experiment execution in orbit 12 p1590 N88-19519
Teleoperation for a Spacelab technology experiment 12 p1590 N88-19521
EUROSIM: A concept of total system support 12 p1590 N88-19523
Utilization of robotics and teleoperation for future in-orbit operations 12 p1591 N88-19527
Robotics servicing experiment --- European space programs 12 p1591 N88-19529
ROTEX: The Robotic Technology Experiment on Spacelab D-2 mission 12 p1592 N88-19530
Definition of the EUROSIM simulation subsystem 12 p1592 N88-19532
A comparative survey of mathematical models for dynamic simulation of in-orbit manipulation operations 12 p1592 N88-19533
Technology requirements for telerobotic satellite servicing in space 12 p1592 N88-19536
Man-tended options for European space robotics 12 p1593 N88-19538
Piezoelectric polymer tactile sensor arrays for robotics
[AD-A188852] 12 p1634 N88-19780

Terrain classification from digital elevation data using slope and curvature information
[AD-A188940] 12 p1639 N88-19812
A representation for serial robotic tasks
12 p1681 N88-20048
Physics for robots
[AD-A189056] 12 p1682 N88-20054
JPRS report. Science and technology: Europe and Latin America
[JPRS-ELS-87-055] 12 p1686 N88-20086
The space station assembly phase: Flight telerobotic servicer feasibility, volume 1
[NASA-CR-182689] 13 p1731 N88-20351
The space station assembly phase: Flight telerobotic servicer feasibility. Volume 2: Methodology and case study
[NASA-CR-182690] 13 p1731 N88-20352
Modelling and simulation of a rate controlled manipulator arm --- Hermes
[NLR-TR-87010-U] 13 p1778 N88-20639
The dynamic control of robotic manipulators in space
[NASA-CR-182710] 13 p1779 N88-20646
Ultrasonic inspection of irregular surfaces
[AERE-R-12465] 13 p1780 N88-20648
Geometry and graphics applied to robotics
[CWI-CS-R8727] 13 p1824 N88-20903
ONR Far East Scientific Bulletin, volume 12, number 3, July-September 1987
[AD-A188554] 13 p1851 N88-21081
Robotic joint experiments under ultravacuum
14 p1927 N88-21490
Improving the man-machine interface to robotic systems
[NPL-DITC-100/87] 14 p1953 N88-21641
Implementation of a visual servoing system for evaluation of robotic refueling applications
[AD-A189676] 14 p1954 N88-21645
Electromagnetic sensor arrays for nondestructive evaluation and robot control
[AD-A190210] 15 p2056 N88-22260
Range image segmentation and surface parameter extraction for a mobile robot
[DE87-013877] 15 p2073 N88-22360
Telerobotic operation of conventional robot manipulators
[DE88-005718] 15 p2073 N88-22363
A probabilistic approach to low-level vision
[AD-A189041] 15 p2107 N88-22553
Microgravity mechanisms and robotics program
16 p2219 N88-23237
Recognizing and locating partially occluded planar objects for assembly routines
[LAAS-87-360] 16 p2247 N88-23422
Contribution to the automatic generation of floor plan placing --- integrated circuit design
[ETN-88-92193] 16 p2247 N88-23426
Contribution to the adaptive dynamic control of a robot manipulator
[LAAS-87-350] 16 p2255 N88-23475
Technology Reports of Kyushu University, volume 61, no. 2
[ISSN-0023-2718] 16 p2256 N88-23485
Realization of natural language style robot task instruction by using the object oriented concept
16 p2257 N88-23487
A design analysis for an automated robotic workpiece manipulator 17 p2344 N88-23975
A software design tool for the analysis of robot dynamics properties
[NLR-MP-86064-U] 17 p2385 N88-24171
A robotic language for cooperative multi-robots
17 p2387 N88-24186
A control technique for improved robot performance
17 p2391 N88-24212
Precise computer controlled positioning of robot end effectors using force sensors
[NASA-CR-182687] 17 p2391 N88-24213
Energy optimal trajectory planning for robot manipulators and autonomous vehicles 17 p2437 N88-24497
A universal computer control system for motors
[NASA-CASE-NPO-17134-1-CU]
18 p2506 N88-24864
The coordination of multiple robotic manipulators
[AD-A190869] 18 p2522 N88-24963
The efficacy of using human myoelectric signals to control the limbs of robots in space
[NASA-CR-182901] 18 p2553 N88-25155
Introduction to compliance in programming of robots
[ETN-88-92189] 18 p2561 N88-25201
Modeling of geometric reasoning for robot programming
[ETN-88-92290] 18 p2561 N88-25202
Analysis of a closed-kinematic chain robot manipulator
[NASA-CR-183031] 18 p2561 N88-25206
Lunar base surface mission operations. Lunar Base Systems Study (LBSS) task 4.1
[NASA-CR-172050] 18 p2594 N88-25415
Design guidelines for robotically serviceable hardware
[NASA-TM-100700] 19 p2606 N88-25472
Flexible tactile sensing arrays for robotics: Architectural robustness and yield considerations
19 p2671 N88-25878
Automatic calibration of space based manipulators and mechanisms
[NASA-CR-182804] 19 p2676 N88-25912
Computer aided remote control: A general concept for intervention in the nuclear, underwater, and space domains 19 p2699 N88-26046
Treatment of systematic errors in the processing of wide angle sonar sensor data for robotic navigation
[DE88-008961] 20 p2756 N88-26352
Design of a controller to reduce residual vibration in the positioning control of flexible robotic manipulators
20 p2808 N88-26658
RRSAS (Robotic Radiation Survey and Analysis System) Project: A real time sensor driven robotic system
[DE88-006825] 20 p2808 N88-26661
An introduction to robot joint control methods
[NLR-TR-86080-U] 20 p2811 N88-26677
Simulation of space manipulator operations (EUROSIM)
[NLR-MP-87017-U] 20 p2811 N88-26678
Experiments in adaptive control of a very flexible one link manipulator 20 p2842 N88-26865
Kinematics of Hooke universal joint robot wrists
[NASA-TM-100567] 20 p2843 N88-26870
Aircraft refueling demonstrator using a microbot alpha 2 robot 21 p2926 N88-27367
Compliant robotic structures, part 3
[AD-A192426] 21 p2955 N88-27556
Development of a hybrid simulator for robotic manipulators
[AD-A193119] 21 p2956 N88-27557
Dexterous hands: Optimizing grasp by design and planning 21 p2958 N88-27572
The VITE model: A neutral command circuit for a generating arm and articulator trajectories
[AD-A192715] 21 p2987 N88-27734
The robust tracking control of nonlinear systems with uncertain dynamics 21 p2999 N88-27788
Intelligent Mobile Autonomous System (IMAS)
[AD-A193181] 21 p3003 N88-27811
Mobile robotics R and D at the Savannah River Laboratory
[DE88-011665] 22 p3083 N88-28310
The analysis and control of robotic manipulators operating at or near kinematically singular configurations
22 p3084 N88-28315
Uncertainty analysis in automatic robot programming
[RR-695-I-IMAG-68-LIFIA] 22 p3142 N88-28685
Motion planning with obstacles and dynamic constraints 23 p3222 N88-29175
Study on design and control of torque-controlled manipulators
[NASA-TT-20197] 23 p3223 N88-29183
Implementation of a flexible link model in a designed robot system, using the finite element method
[ETN-88-92902] 23 p3243 N88-29303
Second Conference on Artificial Intelligence for Space Applications
[NASA-CP-3007] 23 p3251 N88-29351
Space station as a vital focus for advancing the technologies of automation and robotics
[IAF-86-62] 23 p3251 N88-29352
Machine vision for real time orbital operations
23 p3253 N88-29367
A plan for time-phased incorporation of automation and robotics on the US space station
23 p3255 N88-29377
The use of computer graphic simulation in the development of robotic systems
23 p3257 N88-29388
A robotic system for automation of logistics functions on the Space Station 23 p3260 N88-29407
A teleoperated robotic manipulator system for materials processing experiment servicing
23 p3260 N88-29410
Next-generation space manipulator
23 p3263 N88-29428
Study of robotics spacecraft servicing and assembly in space. Volume 1: Executive summary
[ESA-CR(P)-2612-VOL-1] 24 p3333 N88-29839
Low level image processing techniques using the pipeline image processing engine in the flight telerobotic servicer 24 p3418 N88-30346
An automated computerized vision technique for determination of three-dimensional object geometry
24 p3419 N88-30348
Study of software requirements and artificial intelligence techniques for robotics
[TL-3333] 24 p3422 N88-30365
Adaptive control in positioning a rigid-flexible robot arm
[AD-A195194] 24 p3422 N88-30367
Research on problem-solving systems
[AD-A195154] 24 p3423 N88-30370
A standard architecture for controlling robots
[AD-A195929] 24 p3423 N88-30371
Kalman filter-based algorithms for estimating depth from image sequences
[AD-A195818] 24 p3424 N88-30380
Utilizing dynamic stability of orient parts
[AD-A195730] 24 p3427 N88-30397

ROBOTS

Robotic sensors and actuators for a service manipulator system. Volume 1: Executive summary
[MATRA-EPT/DT/VT187/120]
01 p0053 N88-10341
Robotic sensors and actuators for a service manipulator system. Volume 2: Service Manipulator System (SMS) handbook
[MATRA-EPT/DT/VT187/227]
01 p0053 N88-10342
Robotic sensors and actuators for a service manipulator system. Volume 3, phase A report and program plan
[MATRA-EPT/DT/VT187/228]
01 p0054 N88-10343
Traction-drive seven degrees-of-freedom telerobot arm: A concept for manipulation in space
[DE87-010895] 01 p0054 N88-10346
Technology survey for a robot which will investigate the condition of underground pipe
[PB87-209979] 01 p0055 N88-10351
Teleoperation and control study --- orbital servicing
[BAE-TP-8268] 01 p0076 N88-10489
Digital algorithms for the control and dynamic decoupling of industrial robot axes
[ETN-87-90441] 01 p0084 N88-10546
Robotics and Intelligent Systems Program
[DE87-014561] 02 p0223 N88-11404
Components for measuring robots
[KFK-PFT-126] 03 p0332 N88-12092
On the control of a compliant robot arm
03 p0332 N88-12095
A theory for the articulation of robot manipulators
03 p0333 N88-12097
The 3-D world modeling for an autonomous robot
[DE87-013878] 03 p0333 N88-12102
Human motor reactions to dangerous motions in robot operations
[PB87-222196] 03 p0361 N88-12275
Low-cost teleoperator-controlled vehicle for damage assessment and dose measurement
[DE88-000713] 04 p0451 N88-12794
Static standing and dynamic walking of a practical biped robot
[DE88-001367] 04 p0451 N88-12795
Expert robots in nuclear plants
[DE87-014839] 04 p0452 N88-12800
Controlling robots with spoken commands
[DE88-000537] 04 p0452 N88-12801
Ground vehicle convoying
[DE88-000360] 04 p0502 N88-13088
Towards building a team of intelligent robots
[NASA-CR-181538] 05 p0589 N88-13595
Collision-free motion of two robot arms in a common workspace
[CSE-87-00002] 05 p0589 N88-13596
Dealing with unanticipated events in autonomous navigation
[DE88-000590] 05 p0590 N88-13602
Trajectory control of robot manipulators with closed-kinematic chain mechanism
[NASA-TM-89305] 05 p0591 N88-13605
Cartesian path control of a two-degree-of-freedom robot manipulator
[NASA-CR-182331] 05 p0639 N88-13908
Range imagery algorithms for the detection of obstacles by autonomous vehicles
[AD-A185421] 05 p0659 N88-14045
Robot accuracy improvement through kinematic parameter identification 06 p0712 N88-14363
Optical seam tracking in robotic arc welding
[VTT-RR-463] 06 p0713 N88-14376
Self calibration of motion and stereo vision for mobile robot navigation
[AD-A185602] 06 p0781 N88-14794
A demonstration of autonomous navigation and machine vision using the HERMIES-2B robot
[DE88-002298] 07 p0862 N88-15228
Roles of knowledge in motor learning
[AD-A186420] 07 p0897 N88-15438
Software simulation of time delay in teleoperation
08 p1056 N88-16371

Task path planning, scheduling and learning for free-ranging robot systems 08 p1058 N88-16386
Development of a task-level robot programming and simulation system 08 p1058 N88-16387
Goal driven kinematic simulation of flexible arm robot for space station missions 08 p1059 N88-16388
Heuristic search in robot configuration space using variable metric 08 p1059 N88-16389
Real time AI expert system for robotic applications 08 p1061 N88-16408
Solid modelling for the manipulative robot arm (power) and adaptive vision control for space station missions 08 p1061 N88-16409
Planning and scheduling for robotic assembly 08 p1062 N88-16416
Substructure discovery in executed action sequences [AD-A186446] 08 p1069 N88-16462
An optimal resolved rate law for kinematically redundant manipulators 09 p1212 N88-17268
Telerobotic research at NASA Langley Research Center 09 p1213 N88-17269
Manipulator arm design for the Extravehicular Teleoperator Assist Robot (ETAR): Applications on the space station 09 p1213 N88-17270
Development of a facility using robotics for testing automation of inertial instruments 09 p1213 N88-17271
Telerobotic truss assembly 09 p1213 N88-17272
Crew interface with a telerobotic control station 09 p1213 N88-17273
Telerobot for space station 09 p1213 N88-17274
Task-level robot programming: Integral part of evolution from teleoperation to autonomy 09 p1214 N88-17279
Navigation planning using quadtrees [DE88-003706] 09 p1225 N88-17343
A generalized method for automatic downhand and wirefeed control of a welding robot and positioner [NASA-TP-2807] 10 p1316 N88-17869
Design conditions and workspace for the generally-proportioned 3-hinge spherical wrist for robots 10 p1339 N88-18003
Parameter identification and sensitivity analysis for a robotic manipulator arm [NASA-CR-181608] 10 p1385 N88-18272
A computer simulation study of an expert system for walking machine motion planning [AD-A187907] 11 p1438 N88-18577
Fuzzy logic inference processor for real time control: A second generation full custom design [AD-A188155] 11 p1471 N88-18773
Adaptive control of a manipulator with a flexible link [NASA-CR-181637] 11 p1476 N88-18807
Time varying controller design for robot manipulator control [AD-A188094] 11 p1494 N88-18919
Kinematic and dynamic analyses of the Stanford/JPL robot hand [DE88-004637] 11 p1495 N88-18923
Robotics applications in the testing of inertial sensors 12 p1577 N88-19433
In-orbit automatic assembly of reticular structures 12 p1586 N88-19491
Mobile robot activity model for autonomous free flying platforms 12 p1588 N88-19507
The Hermes robot arm, its design and verification 12 p1588 N88-19508
Remote manipulation in orbital construction, servicing and repair missions: Is one arm enough? A comparative evaluation of the performance features of robots with one or more arms 12 p1588 N88-19509
Covariant control of bilateral servos for in-orbit manipulation 12 p1590 N88-19520
The Hermes manipulation system (HERA) simulation facility development 12 p1591 N88-19524
ROTEX: The Robotic Technology Experiment on Spacelab D-2 mission 12 p1592 N88-19530
User's guide: Lower neck transducer for the Hybrid 3 dummy [PB88-133319] 12 p1628 N88-19743
Evaluation tests of lower neck transducer for the Hybrid 3 Dummy [PB88-133327] 12 p1628 N88-19745
Low cost mobile robot [AD-A188507] 12 p1633 N88-19778
Free boundary problems arising in the control of a flexible robot arm [AD-A189124] 12 p1634 N88-19781
Intelligent control of robot manipulators in hazardous environments [DE88-003305] 13 p1778 N88-20638
Force distribution and trajectory control for closed kinematic chains with applications to walking machines 13 p1779 N88-20642
Ultrasonic inspection of irregular surfaces [AERE-R-12465] 13 p1780 N88-20648
Robotic joint prototype for space applications 14 p1878 N88-21222
A joint actuator design for a robotic manipulator 14 p1879 N88-21232
An efficient gradient projection optimization scheme for a seven-degree-of-freedom redundant robot with spherical wrist [DE88-005440] 14 p1919 N88-21453
Implementation of a visual servoing system for evaluation of robotic refueling applications [AD-A189676] 14 p1954 N88-21645
Range image segmentation and surface parameter extraction for a mobile robot [DE87-013877] 15 p2073 N88-22360
Telerobotic operation of conventional robot manipulators [DE88-005718] 15 p2073 N88-22363
The visit problem: Visibility graph-based solution [DE88-000343] 15 p2108 N88-22556
Insertions using geometric analysis and hybrid force-position control: Method and analysis [DE87-013652] 15 p2117 N88-22611
Concurrent algorithms for a mobile robot vision system [DE88-005850] 15 p2117 N88-22614
Path following robot [AD-A190960] 16 p2215 N88-23217
Automatic control of robot motion [AD-A191012] 16 p2215 N88-23218
Microgravity robotics technology program [NASA-TM-100898] 16 p2215 N88-23219
Microgravity mechanisms and robotics program 16 p2219 N88-23237
Accurate positioning of long, flexible ARM's (Articulated Robotic Manipulator) 16 p2219 N88-23243
Point accessibility and primary workspace of simple six-link robots 17 p2345 N88-23976
A control technique for improved robot performance 17 p2391 N88-24212
Induction of models under uncertainty [NASA-TM-101173] 17 p2394 N88-24230
Energy optimal trajectory planning for robot manipulators and autonomous vehicles 17 p2437 N88-24497
Kinematics, dynamics and control of a closed chain mechanism manipulator 18 p2523 N88-24967
Real-time implementation of a kinematic optimization scheme for seven-degree-of-freedom redundant robots with spherical wrists [DE88-006785] 18 p2524 N88-24974
Robot navigation using simple sensor fusion [DE88-006184] 18 p2561 N88-25203
A concurrent on-board vision system for a mobile robot [DE88-007475] 19 p2676 N88-25914
Proceedings of the Colloquium on Space and Sea [ESA-SP-280] 19 p2695 N88-26016
Tasks foreseen for space robots and an example of an associated orbital infrastructure 19 p2699 N88-26044
ELIT: An autonomous underwater observation robot 19 p2699 N88-26048
Underwater robotics in the service of oil field exploitation: The Running and Interconnecting Tool (RIT) in the East Frigg field (North Sea) 19 p2699 N88-26049
Simple 2-D navigation for wheeled vehicles [DE88-007115] 20 p2756 N88-26351
Force servo control of a commercial gantry robot [DE88-006649] 20 p2808 N88-26660
Sensor fusion for robot navigation [DE88-008383] 20 p2809 N88-26663
Mobile robot survival [DE88-009108] 20 p2809 N88-26665
Optimization of performance criteria with bounded joint velocities for robots with one degree of redundancy [DE88-003915] 20 p2810 N88-26670
Local free-space mapping and path guidance for mobile robots [AD-A192970] 20 p2810 N88-26674
Diagnosing faults in autonomous robot plan execution [NASA-CR-182480] 20 p2841 N88-26859
Three-dimensional scene analysis using stero based imaging [AD-A193120] 21 p2894 N88-27178
In-flight load measurements of the Robot-X canards [AD-A193428] 21 p2895 N88-27187
Aircraft refueling demonstrator using a microbot alpha 2 robot 21 p2926 N88-27367
Motor-response learning at a process control panel by an autonomous robot [DE88-005055] 21 p2955 N88-27554
Compliant robotic structures, part 3 [AD-A192426] 21 p2955 N88-27556
Development of a hybrid simulator for robotic manipulators [AD-A193119] 21 p2956 N88-27557
Control of free-flying space robot manipulator systems [NASA-CR-183017] 21 p2956 N88-27562
Control of free-flying space robot manipulator systems [NASA-CR-183104] 21 p2957 N88-27563
Research into the architecture of CAD based robot vision systems [AD-A193330] 21 p2997 N88-27776
Mobile robotics R and D at the Savannah River Laboratory [DE88-011665] 22 p3083 N88-28310
Energy storage considerations for a robotic Mars surface sampler [NASA-TM-100969] 22 p3166 N88-28853
Motion planning for legged locomotion systems on uneven terrain 23 p3221 N88-29170
Implementation of a flexible link model in a designed robot system, using the finite element method [ETN-88-92902] 23 p3243 N88-29303
Motion planning for a free-flying robot 23 p3255 N88-29378
Distributed cooperating processes in a mobile robot control system 23 p3256 N88-29386
Concepts for robot motion primitives required for space station teleoperations 23 p3257 N88-29387
Personnel occupied woven envelope robot 23 p3260 N88-29408
Remote servicing of space systems 23 p3260 N88-29409
Modeling robot flexibility for endpoint force control [AD-A195923] 24 p3380 N88-30132
Haptic exploration in humans and machines: Attribute integration and machine recognition/implementation [AD-A193692] 24 p3410 N88-30299
Simulation of a two link robot manipulator with elastic members [AD-A196014] 24 p3422 N88-30368

ROBUSTNESS (MATHEMATICS)

Identification of multivariate outliers and leverage points by means of robust covariance matrices [REPT-87-15] 01 p0088 N88-10575
Extensions of the small mu test for robust stability [OUEL-1666/87-REV] 02 p0223 N88-11406
New feedback design methodologies for large space structures: A multi-criterion optimization approach 04 p0408 N88-12535
Robust statistical methods for automated outlier detection 04 p0433 N88-12681
Solution of some 3-D viscous and inviscid supersonic flow problems by finite-volume space-marching schemes 05 p0532 N88-13235
Robustness of linear systems [PB87-220042] 05 p0639 N88-13909
Robust prediction operations for stationary processes [AD-A185408] 05 p0641 N88-13924
Maximum entropy/optimal projection design synthesis for decentralized control of large space structures [AD-A186359] 07 p0824 N88-15003
Robust prediction and interpolation for vector stationary processes, 2d enriched version [AD-A185875] 07 p0865 N88-15247
Conditionally unbiased bounded influence robust regression with applications to generalized linear models [AD-A186319] 07 p0915 N88-15556
A methodology for the synthesis of robust feedback systems [NASA-CR-182455] 09 p1225 N88-17342
A note on computing robust regression estimates via iteratively reweighted least squares [AD-A186709] 09 p1227 N88-17352
An integrated pressure sensor for in-vivo use 10 p1333 N88-17965
Stable, robust tracking by sliding mode control [AD-A188278] 10 p1401 N88-18358
Automated radar target recognition based on models of neural nets 11 p1476 N88-18804
Robustness in cost performance models [AD-A187183] 11 p1566 N88-19374
Choice of implicit and explicit operators for the upwind differencing method [NASA-TM-100857] 14 p1964 N88-21718
A robust scale estimator based on the shortest half [REPT-87-36] 14 p1966 N88-21731
Development and application of the p-version of the finite element method [AD-A190036] 15 p2120 N88-22633
Robust adaptive regulation without persistent excitation [NASA-TM-100571] 18 p2561 N88-25204
The robust tracking control of nonlinear systems with uncertain dynamics 21 p2999 N88-27788
Robust prediction for stationary processes: 2D enriched version [AD-A193318] 21 p3006 N88-27833
Robust design of cascade control [REPT-88-006] 22 p3142 N88-28687

Robust control of multivariable and large scale systems
[AD-A194250] 23 p3266 N88-29441

ROCK INTRUSIONS
NT BATHOLITHS
Dike zones on Venus
[NASA-TT-20111] 02 p0254 N88-11607
Drilling investigation of a young magmatic intrusion beneath the Inyo Domes, Long Valley, California: Structural and textural studies
[DE88-006613] 18 p2541 N88-25078
Recycling of lower continental crust through foundering of cumulates from contaminated mafic intrusions 24 p3393 N88-30204
Crustal evolution and the eclogite to granulite phase transition in xenoliths from the West African Craton 24 p3395 N88-30217
Evidence for crustal recycling during the Archean: The parental magmas of the stillwater complex 24 p3396 N88-30226

ROCK MECHANICS
Research needs for hydrocarbon fuels
[DE87-014555] 06 p0687 N88-14209

ROCKET BOOSTERS
U BOOSTER ROCKET ENGINES

ROCKET CHAMBERS
U THRUST CHAMBERS

ROCKET ENGINE CASES
Slip casting and extruding shapes of rhenium with metal oxide additives. Part 2: Development of grain stabilized rhenium parts for resistojets
[NASA-CR-180851] 03 p0278 N88-11749
The structures of large wound propulsion shells --- carbon fiber composites filament winding
[SNIAS-872-430-118] 05 p0559 N88-13406
STA-2A NDT testing
[NASA-CR-179301] 11 p1497 N88-18937
Rocket motor case materials. An evaluation of new fibers for composites
[FOA-C-20696-2.1] 21 p2906 N88-27245

ROCKET ENGINE CONTROL
Selection of efficient correcting motor for an artificial Earth satellite 08 p1007 N88-16102
Intelligent on board control for field emission electric propulsion system 12 p1589 N88-19513

ROCKET ENGINE DESIGN
Hermes propulsion system
[SNIAS-872-422-109] 05 p0556 N88-13383
Skylark sounding rocket development-Skylark 8 08 p1035 N88-16274
Arcjet thruster research and technology
[NASA-CR-180865] 10 p1293 N88-17732
Arcjet thruster research and technology, phase 1
[NASA-CR-182107] 17 p2314 N88-23830
Dual-fuel, dual-mode rocket engine
[NASA-CASE-LAR-13773-1] 18 p2475 N88-24685

ROCKET ENGINES
NT APOGEE BOOST MOTORS
NT ARC JET ENGINES
NT BOOSTER ROCKET ENGINES
NT DUCTED ROCKET ENGINES
NT ELECTRIC ROCKET ENGINES
NT ELECTROSTATIC ENGINES
NT ELECTROTHERMAL ENGINES
NT HYDRAZINE ENGINES
NT HYDROGEN OXYGEN ENGINES
NT ION ENGINES
NT LIQUID AIR CYCLE ENGINES
NT LIQUID PROPELLANT ROCKET ENGINES
NT MERCURY ION ENGINES
NT NOZZLELESS ROCKET ENGINES
NT NUCLEAR ENGINE FOR ROCKET VEHICLES
NT NUCLEAR ROCKET ENGINES
NT RESISTOJET ENGINES
NT REUSABLE ROCKET ENGINES
NT SOLID PROPELLANT ROCKET ENGINES
NT SPACE SHUTTLE BOOSTERS
NT SPACE SHUTTLE MAIN ENGINE
NT UPPER STAGE ROCKET ENGINES
The numerical simulation of an idealised one-dimensional, steady monopropellant rocket
[PDR/CFDU/IC/31] 01 p0018 N88-10107
A life test of a 22-Newton (5-lbf) hydrazine rocket
[NASA-TM-100232] 03 p0278 N88-11750
Plasma thruster development
[AD-A184173] 04 p0408 N88-12536
A two-dimensional finite difference program for thermal analysis of rocket thrust chambers
[NASA-TM-100191] 04 p0409 N88-12539
The VISTA spacecraft: Advantages of ICF (Inertial Confinement Fusion) for interplanetary fusions propulsion applications
[NASA-CR-181549] 04 p0491 N88-13024
Numerical model of the time independent mean flow in a rotating rocket motor 13 p1733 N88-20360
Crack opening and extension in inert solid propellant. An experimental study
[AD-A189808] 15 p2048 N88-22201
Test plan and facilities for qualifying nuclear rocket fuel elements 17 p2434 N88-24482
Thrust chamber thermal barrier coating techniques
[NASA-TM-100933] 18 p2476 N88-24690
The 24th JANNAF Combustion Meeting, volume 2
[AD-A190164] 19 p2622 N88-25554
Numerical grid generation and flow simulation in SSME thrust chamber 19 p2626 N88-25577
A computer program for performance prediction of tripropellant rocket engines with tangential slot injection 19 p2627 N88-25581
Analysis of flow through pump of large rocket engine 19 p2637 N88-25646
Energy conversion measurements in laser-sustained argon plasmas for application to rocket propulsion
[AD-A194931] 24 p3337 N88-29861
Automatic data retrieval from rocket motor holograms
[AD-A195586] 24 p3337 N88-29864
Iridium-coated rhenium thrusters by CVD
[NASA-TM-101309] 24 p3339 N88-29874

ROCKET EXHAUST
The Shock and Vibration Bulletin. Part 4: Structural Dynamics and Modal Test and Analysis
[AD-A186751] 09 p1179 N88-17062
Qualification by analysis of IUS plume deflectors 09 p1179 N88-17063
Kinetic mechanisms for ionization and afterburning suppression
[AD-A189219] 13 p1737 N88-20383
Environmental monitoring of a titan 34D 5 1/2 segment solid rocket motor static firing
[AD-A192975] 20 p2766 N88-26400
Variable Mach number wall jets for control/propulsion on hypervelocity projectiles/interceptors: Tests with an existing model
[AD-A192845] 21 p2892 N88-27167
SRB/SLEEC (Solid Rocket Booster/Shingle Lap Extendible Exit Cone) feasibility study, volume 2. Appendix A: Design study for a SLEEC actuation system
[NASA-CR-178974] 23 p3187 N88-28965
Studies on rocket exhaust plumes and impingement effects related to the Columbus Space Station program: Executive summary
[DFVLR-IB-222-88-A-12] 24 p3337 N88-29862

ROCKET FIRING
Orbital transfer vehicle 3000 LBF thrust chamber assembly hot fire test program
[NASA-CR-182145] 24 p3336 N88-29858

ROCKET FLIGHT
Instrumentation utilisation for risk control in safety operations --- balloons and rockets 08 p1030 N88-16240
Flight results of the ESA experiment modules in Materials Science Experiment Rocket (MASER) 1 08 p1033 N88-16261
Guidance of high-altitude sounding rockets using the S19 and Spinning Rocket Altitude Control (SPINRAC) systems 08 p1034 N88-16273
Zone crystallization experiments in mirror heating facilities
[BMFT-FB-W-86-023] 16 p2184 N88-23016
Wind tunnel investigation of wing and control panel loads at transonic and supersonic speeds on some schematic cruciform missile configurations
[FFA-TN-1986-43] 18 p2457 N88-24585

ROCKET LAUNCHING
NT ORBITAL LAUNCHING
Hydrogen chloride measurements in launch-vehicle exhaust clouds
[DE87-011552] 08 p0964 N88-15837
Esrange (Sweden): New installations, future plans and investments --- rocket range 08 p1029 N88-16235
Facilities and plans for improvements at Andoya (Norway) rocket range 08 p1029 N88-16236
The DFVLR-German Space Operations Center (GSOC) mobile rocket base 08 p1029 N88-16237
High altitude chemical release systems for project BIME (Brazilian Ionospheric Modification Experiments) project IMS (Ionospheric Modification Studies) project PIIE (Polar Ionospheric Irregularities Experiment) project polar arcs
[AD-A188299] 12 p1642 N88-19833

ROCKET MOTOR CASES
U ROCKET ENGINE CASES

ROCKET NOSE CONES
SRB/SLEEC (Solid Rocket Booster/Shingle Lap Extendible Exit Cone) feasibility study, volume 2. Appendix A: Design study for a SLEEC actuation system
[NASA-CR-178974] 23 p3187 N88-28965

ROCKET NOZZLES
Rocket nozzle thermal shock tests in an arc heater facility 02 p0133 N88-10832
Thrust and specific impulse of repetitively-pulsed-laser propulsion rocket 03 p0318 N88-12012
High performance Solid Rocket Motor (SRM) submerged nozzle/combustion cavity flowfield assessment
[NASA-CR-179307] 11 p1446 N88-18622
An experimental investigation of rocket ramjet nozzle assembly base pressures
[AD-A189714] 15 p2027 N88-22076
Aeropropulsive characteristics of isolated combined turbojet/ramjet nozzles at Mach numbers from 0 to 1.20
[NASA-TP-2814] 17 p2299 N88-23757
Arcjet thruster research and technology, phase 1
[NASA-CR-182107] 17 p2314 N88-23830
Nozzle fabrication technique
[NASA-CASE-MSC-21299-1] 18 p2475 N88-24684
A detailed description of the uncertainty analysis for high area ratio rocket nozzle tests at the NASA Lewis Research Center 19 p2626 N88-25580
Boundary layer development as a function of chamber pressure in the NASA Lewis 1030:1 area ratio rocket nozzle
[NASA-TM-100917] 19 p2664 N88-25841
Analysis of edge detection techniques for radiographic image measurement
[AD-A193650] 23 p3186 N88-28961

ROCKET OXIDIZERS
The chemistry of the hypochlorite neutralization of hydrazine fuels
[DE88-002971] 10 p1307 N88-17812

ROCKET PROPELLANT TANKS
U PROPELLANT TANKS

ROCKET PROPELLANTS
NT CRYOGENIC ROCKET PROPELLANTS
NT DOUBLE BASE ROCKET PROPELLANTS
NT GELLED ROCKET PROPELLANTS
NT LIQUID ROCKET PROPELLANTS
NT METAL PROPELLANTS
NT MONOPROPELLANTS
NT NITRAMINE PROPELLANTS
NT RP-1 ROCKET PROPELLANTS
NT SLURRY PROPELLANTS
NT SOLID ROCKET PROPELLANTS
Orbital Spacecraft Consumables Resupply System (OSCRS). Volume 2: Study results
[NASA-CR-172011] 03 p0268 N88-11687
A life test of a 22-Newton (5-lbf) hydrazine rocket
[NASA-TM-100232] 03 p0278 N88-11750
Compatability of dispersion-strengthened platinum with resistojet propellants
[NASA-TP-2765] 04 p0409 N88-12538
Test number 2 of propellant for rocket motor MK52
[PB87-226155] 05 p0571 N88-13480
Space station onboard propulsion system: Technology study
[NASA-CR-179233] 07 p0825 N88-15006
Evidences for distributed combustion 19 p2628 N88-25586
Possibilities of economical improvements for Moon based rocket propulsion using lunar propellants
[ILR-MITT-196] 24 p3338 N88-29871

ROCKET PROPELLED SLEDS
Static force and moment test of the Holloman narrow-gage rocket sled at Mach numbers from 3.5 to 5.5
[AD-A186291] 07 p0822 N88-14995
High-velocity reverse ballistic rocket sled testing at Sandia National Laboratories 09 p1179 N88-17059
Reference position vector 12 p1577 N88-19432

ROCKET SONDES
U SOUNDING ROCKETS

ROCKET SOUNDING
The German scientific balloon and sounding rocket program 08 p1024 N88-16202
The Norwegian scientific balloon and sounding rocket program 1987-1990 08 p1025 N88-16204
The Swedish sounding rocket and balloon program 08 p1025 N88-16205
Swiss scientific balloon and sounding rocket experiments 1985-1987 08 p1025 N88-16206
First results from the Viking associated Aureld-VIP rocket and EISCAT campaign --- auroras; Swedish satellite 08 p1026 N88-16211
Report on ground-based activity at Andoya (Norway) in relation to the Aureld-VIP high rocket and to the Viking satellite --- Swedish satellite 08 p1026 N88-16212
How ground-based observations contribute to rocket, balloon and space shuttle experiments: Experience from the past and outlook for the future 08 p1026 N88-16216
New techniques for rocket and balloon-borne instrumentation for investigations of the structure, dynamics and electrodynamics of the middle atmosphere 08 p1027 N88-16220
ROCOZ-A (improved rocket launched ozone sensor) for middle atmosphere ozone measurements 08 p1029 N88-16233

MAIMIK: A high current electron beam experiment on a sounding rocket from Andoya rocket range (Norway)
08 p1030 N88-16243
CAESAR investigations — Coordinated Auroral Experiment using Scatter And Rockets (CAESAR)
08 p1031 N88-16249
Observations of field-aligned current structures during the Coordinated Auroral Experiment using Scatter And Radar (CAESAR) flight 2 08 p1031 N88-16250
EISCAT measurements of ion velocities during Coordinated Auroral Experiment using Scatter And Rockets (CAESAR) campaign 08 p1031 N88-16251
Remote and in-situ plasma measurements during the Coordinated Auroral Experiment using Scatter And Rockets (CAESAR) flight 08 p1032 N88-16252
Low frequency electrostatic waves observed on board the Coordinated Auroral Experiment using Scatter And Rockets (CAESAR) 2 payload 08 p1032 N88-16253
The rocket and scatter experiment ROSE: Presentation of the scientific payload 08 p1034 N88-16269
Rocket experiments and payloads for Super CAMP — Cold Arctic Mesopause Project (CAMP)
08 p1034 N88-16271
Coordinated Auroral Experiments using Scatter And Rocket investigations (CAESAR investigations)
[MPAE-W-47-87-13] 15 p2096 N88-22487
Rocket measurements within a polar cap arc: Ionospheric modelling
[AD-A192381] 20 p2824 N88-26754

ROCKET TEST FACILITIES
Ground shock profiles for an accidental explosion at the proposed Large Rocket Test Facility at Arnold Engineering Development Center
[DE88-002652] 07 p0853 N88-15180
Test plan and facilities for qualifying nuclear rocket fuel elements 17 p2434 N88-24482

ROCKET THRUST
Thrust and specific impulse of repetitively-pulsed-laser propulsion rocket 03 p0318 N88-12012
A two-dimensional finite difference program for thermal analysis of rocket thrust chambers
[NASA-TM-100191] 04 p0409 N88-12539
Space station propulsion technology
[NASA-CR-179260] 08 p0964 N88-15835

ROCKET VEHICLES
NT ARIANE LAUNCH VEHICLE
NT BLACK BRANT SOUNDING ROCKETS
NT CENTAUR LAUNCH VEHICLE
NT MULTISTAGE ROCKET VEHICLES
NT PAYLOAD ASSIST MODULE
NT SINGLE STAGE ROCKET VEHICLES
NT SKYLARK ROCKET VEHICLE
NT SOUNDING ROCKETS
NT TITAN LAUNCH VEHICLES
Instrumentation package for a shrouded SWERVE/EPW rocket sled test
[DE87-014267] 01 p0008 N88-10045
Effect of rotation on the lateral stability of a free-flying column subjected to an axial thrust with directional control
[AD-A188690] 13 p1728 N88-20338

ROCKET-BORNE INSTRUMENTS
ROCOZ-A (improved rocket launched ozone sensor) for middle atmosphere ozone measurements
08 p1029 N88-16233
A new technique for rocket and space-borne investigations of time-dependant auroral morphology
08 p1030 N88-16241
Ultraviolet rocket-spectra of a sunspot
08 p1032 N88-16257
Preliminary Material Science Experiment Rocket (MASER) 1 results and the evolution of the MASER program 08 p1033 N88-16260
The rocket and scatter experiment ROSE: Presentation of the scientific payload 08 p1034 N88-16269
MRS-3000 meteorological rocket probe for the MMR-06 dart integrated meteorological rocket system
[NASA-TT-20303] 19 p2693 N88-26010

ROCKETS
Vehicle glow observed on the SONDA 3
[INPE-4297-PRE/1168] 12 p1600 N88-19581

ROCKS
NT ANDESITE
NT ANORTHOSITE
NT BASALT
NT BATHOLITHS
NT BEDROCK
NT BRECCIA
NT CARBONACEOUS ROCKS
NT COAL
NT ECLOGITE
NT GNEISS
NT GRANITE
NT IGNEOUS ROCKS
NT LUNAR ROCKS
NT PERIDOTITE
NT REGOLITH
NT SANDSTONES
NT SEDIMENTARY ROCKS
A mineral reconnaissance sampling manual for Costa Rica: Central American energy and resource project
[DE87-014997] 04 p0462 N88-12859
Analysis of airborne imaging spectrometer data for the Ruby Mountains, Montana, by use of absorption-band-depth images 05 p0614 N88-13771
Mapping hydrothermally altered rocks in the Northern Grapevine Mountains, Nevada and California with the airborne imaging spectrometer 05 p0614 N88-13772
X-ray microfluorescence analysis of thin- and thick-sectioned geologic materials
[DE87-009803] 09 p1189 N88-17126
Nature and origin of mineral coatings on volcanic rocks of the Black Mountain, Stonewall Mountain, and Kane Springs Wash volcanic centers, Southern Nevada
[NASA-CR-181437] 09 p1191 N88-17140
Microwave dielectric spectrum of rocks
[NASA-TM-89719] 12 p1642 N88-19831
Elemental composition of Venusian rocks in northeastern part of Terra Aphrodite (determined using data from Vega-2 landing module)
13 p1726 N88-20322
Content of natural radioactive elements in Venusian rocks determined using data from Vega-1 and Vega-2 stations 13 p1726 N88-20323
P/Halley dust coma: Grains or rocks?
14 p2002 N88-21936
Carbon analysis in natural olivine crystals of deep origin
[NASA-TT-20311] 19 p2734 N88-26239
Prospects for hot dry rock in the future
[DE88-010909] 20 p2820 N88-26730
Fine-scale traverses in cumulate rocks, Stillwater Complex: A lunar analogue study
[NASA-CR-183066] 20 p2823 N88-26747
Relationships among earth's gravity field, magnetic field, crustal structure and the magnetic character of crustal rocks
[AD-A195539] 24 p3392 N88-30198
Mid to late proterozoic magmatism within Northeastern North America and its iplications for the growth of the continental crust 24 p3397 N88-30229
Growth of the lower continental crust
24 p3398 N88-30236
Geochronological and lead-isotope evidences for rapid crust formation in middle-proterozoic time: The Labrador example 24 p3398 N88-30239
Trace element differences between Archean, Proterozoic and Phanerozoic crustal components: Implications for crustal growth processes
24 p3399 N88-30243
Exotic minerals in 3,500 million year old rocks: Evidence for large meteorite impacts 24 p3440 N88-30475

RODENTS
NT MICE
NT RATS

RODS
NT CONTROL RODS
Geometrically nonlinear rod mechanism analogy of axisymmetrically loaded spherical shells based on a comprehensive approach to the stability of circular arches
[ETN-87-90419] 01 p0062 N88-10398
A creep measurement of unidirectional epoxy-fiberglass rod
[DE87-014812] 04 p0411 N88-12553
Lightning discharge protection rod
[NASA-CASE-LAR-13470-1] 06 p0666 N88-14083
A direct correlation of strength with impact velocity
[AD-A189251] 13 p1741 N88-20409
Solid hosts for dye laser rods. Part 1: Criteria for choosing a host material
[DE88-006478] 15 p2072 N88-22355
Vibrational power flow analysis of rods and beams
[NASA-CR-183166] 24 p3383 N88-30151

ROENTGEN SATELLITE
U ROSAT MISSION

ROGALLO WINGS
U FOLDING STRUCTURES

ROLL
Investigation of interactions between limb-manipulator dynamics and effective vehicle roll control characteristics
[NASA-CR-3983] 01 p0007 N88-10039
Multi-hundred kilowatt roll ring assembly evaluation results
[NASA-TM-100865] 14 p1904 N88-21375
Aerodynamics in ground effect and predicted landing ground roll of a fighter configuration with a secondary-nozzle thrust reverser
[NASA-TP-2834] 24 p3317 N88-29752
Computer programs for calculation of sting pitch and roll angles required to obtain angles of attack and sideslip on wind tunnel models
[NASA-TM-100659] 24 p3329 N88-29820

ROLL CONTROL
U LATERAL CONTROL

ROLL FORMING
Hardening of metal during production of bent shapes
[BLL-M-37250-(5828.4)] 02 p0148 N88-10928
Interrelation and measurement of formability, strengthening, and thermomechanical processing under metalworking conditions
[DE88-002485] 08 p0967 N88-15850

ROLLER BEARINGS
Improved oil-off survivability of tapered roller bearings
[NASA-CR-180804] 02 p0182 N88-11135
Ceramic bearings for use in gas turbine engines
[NASA-TM-100288] 10 p1340 N88-18007
Corrosion-wear process under rolling-sliding motion
[AD-A189603] 13 p1778 N88-20635
High temperature solid lubrication by catalytically generated carbon
[AD-A190804] 16 p2182 N88-23004

ROLLERS
Requirements for a test stand for plastic rollers for the verification of nonequilibrium force laws
[ILR-MITT-176] 01 p0008 N88-10040
Development, features of roller rocker arm reported
06 p0689 N88-14219
Evaluation of a high-torque backlash-free roller actuator 16 p2219 N88-23239
Roller drive materials performance
16 p2219 N88-23241
Brief evaluation of the alloy 17-4-PH (Z5 CNU 17-04). Semifinished product: 205 mm dia forged roller, test reports
[DF/NH-3616/84] 17 p2322 N88-23866
A study of the floating roller peel test for adhesives
[AD-A194114] 23 p3198 N88-29034

ROLLING
Mode 2 fracture mechanics 15 p2083 N88-22418

ROLLING CONTACT LOADS
Requirements for a test stand for plastic rollers for the verification of nonequilibrium force laws
[ILR-MITT-176] 01 p0008 N88-10040
Application of Kalker's rolling contact theory to the simulation of rail vehicles
[DFVLR-FB-87-07] 01 p0057 N88-10363
Wear of hard steel in rolling lubricated contact
[RP-699] 03 p0332 N88-12094
The numerical solution of the elastohydrodynamically lubricated line and point contact problem, using multigrid techniques
[ISBN-90-9001583-3] 06 p0714 N88-14377
Mechanisms of rolling contact spalling
[NASA-CR-179243] 06 p0714 N88-14380
The quasi-static contact problem with friction for three dimensional elastic bodies
[REPT-87-51] 14 p1918 N88-21447
Calculation of rolling contact of two viscoelastic cylinders with application to the steady state normal contact problem
[ILR-MITT-188] 18 p2530 N88-25008
Energy dissipation in a rolling aircraft tire
[NASA-CR-182978] 19 p2676 N88-25913
Investigation of rolling contact fatigue of ball bearings
[NASA-TT-20196] 19 p2678 N88-25922
Frequency dependent sliding coefficients for general three-dimensional rolling contact in high frequency range
[ILR-MITT-192] 22 p3085 N88-28318

ROLLING MOMENTS
Mechanisms of rolling contact spalling
[NASA-CR-179243] 06 p0714 N88-14380
Parametric estimation of aerodynamic nonlinearities in rolling moment due to sideslip using maximum likelihood method 20 p2786 N88-26528

ROLLUP SOLAR ARRAYS
U SOLAR ARRAYS

ROM DEVICES
U READ-ONLY MEMORY DEVICES

ROOM TEMPERATURE
Behavior of long and short fatigue cracks in a powder metallurgy superalloy at room and at high temperature
05 p0601 N88-13677
Data recorded by the Rome room temperature gravitational wave antenna, during the supernova SN 1987 A in the Large Magellanic Cloud
[NOTA-INTERNA-879] 06 p0806 N88-14922
Lithium fast-ion conductors: Polymer based materials
[AD-A187879] 11 p1461 N88-18712
Photophysics and photochemistry of poly(di-n-hexylsilane) in room temperature solution
[AD-A187890] 11 p1462 N88-18714
High-efficiency Y-Sc-Ga:Cr (sup)3+,Tu (sup)3+,Ho (sup)3+ garnet laser (gl= 2.088 gmm at room temperature 14 p1971 N88-21766

Chemical vapor deposition of TiO2 thin films at room temperature
[DE88-008892] 21 p2953 N88-27542
A new near-infrared tunable-room temperature solid state laser La3Ga5SiO14:Cr(3+)
[DE88-011341] 21 p2953 N88-27543
Relation between strength, creep and relaxation behavior in Cu and Al at room temperature
[ETN-88-92982] 23 p3195 N88-29015
Alternative immersion accelerated testing of coating systems for Naval shoreline facilities
24 p3355 N88-29977

ROOMS
NT CLEAN ROOMS

ROOT-MEAN-SQUARE ERRORS
Detection of signals by weighted integrate-and-dump filter 04 p0435 N88-12696
Spectral- and spatial-domain filtering and sampling approach to the numerical solution of electromagnetic scattering problems
[PB88-106711] 06 p0694 N88-14261
Study of extended least-square iterative techniques in electromagnetic scattering by penetrable objects
[PB88-105879] 06 p0694 N88-14262
Response of wind shear warning systems to turbulence with implication of nuisance alerts
10 p1274 N88-17618
Seismic inversion by a RMS (Root-Mean-Square) Born approximation in the space-time domain
[PB88-165402] 15 p2131 N88-22711
Calculation of root-mean-square loads
[BLL-M-37776-(5828.4)] 18 p2531 N88-25015

ROOTS OF EQUATIONS
Detection of critical points: The first step to automatic line generalization 05 p0619 N88-13803
General solution of certain functional equations
[PREPRINT-554] 06 p0764 N88-14689
Simulation of FELIN logics. Polynomials roots simultaneous computation algorithms
[ETN-88-92182] 16 p2253 N88-23464
A primal-dual algorithm for the computation of the minimum of a convex function on the intersection of convex functions, and its application in data analysis
[RR-638-M] 18 p2563 N88-25217
A full but elementary treatment of systems of homogeneous ordinary linear differential equations with constant coefficients
[REPT-87-82] 20 p2845 N88-26887

ROSAT MISSION
Some highlights on ROSAT mechanisms
14 p1874 N88-21195
Design, construction and performance of the ROSAT high resolution X-ray mirror assembly
[MPE-PREPRINT-101] 15 p2150 N88-22836

ROSS ICE SHELF
Ice-shelf response to ice-stream discharge fluctuation. Part 1: Unconfined ice tongues
[AD-A188147] 10 p1358 N88-18117

ROSSBY REGIMES
Radio emission from RS CVn binaries: A 5 GHz VLA survey of 93 systems 04 p0519 N88-13191
Nonlinear normal mode initialization of a limited area model using nonstationary Rossby modes — numerical weather forecasting
[KNMI-WR-87-10] 14 p1947 N88-21614

ROSSBY WAVES
U PLANETARY WAVES

ROTARY DRIVES
U MECHANICAL DRIVES

ROTARY ENGINES
NT WANKEL ENGINES
Endurance testing of a natural gas-fueled rotary engine
[PB87-215703] 01 p0055 N88-10356
Performance and combustion characteristics of direct-injection stratified-charge rotary engines
[NASA-TM-100134] 04 p0400 N88-12490
Regressed relations for forced convection heat transfer in a direct injection stratified charge rotary engine
[NASA-TM-100124] 05 p0549 N88-13345

ROTARY STABILITY
NT GYROSCOPIC STABILITY
Control and stabilization mechanisms of submunitions
[DFVLR-IB-111-86/9] 03 p0259 N88-11630
Numerical and analytical study of fluid dynamic forces in seals and bearings
[NASA-TM-100268] 11 p1485 N88-18867
Parametric dependence in the equilibrium dynamics of rotating structures
[AD-A187817] 11 p1498 N88-18945

ROTARY WING AIRCRAFT
NT AH-64 HELICOPTER
NT BO-105 HELICOPTER
NT CH-46 HELICOPTER
NT COMPOUND HELICOPTERS
NT HEAVY LIFT HELICOPTERS
NT HELICOPTERS
NT MILITARY HELICOPTERS
NT OH-58 HELICOPTER
NT RIGID ROTOR HELICOPTERS
NT ROTOR SYSTEMS RESEARCH AIRCRAFT
NT TANDEM ROTOR HELICOPTERS
NT TILT ROTOR AIRCRAFT
NT UH-1 HELICOPTER
NT UH-60A HELICOPTER
NT XV-15 AIRCRAFT
Civil applications of high-speed rotorcraft and powered-lift aircraft configurations
[NASA-TM-100035] 03 p0261 N88-11643
Operational load measurements on service helicopters
03 p0263 N88-11658
Test stand performance of a convertible engine for advanced V/STOL and rotorcraft propulsion
[NASA-TM-100211] 03 p0266 N88-11679
NASA/Army Rotorcraft Technology. Volume 3: Systems Integration, Research Aircraft, and Industry
[NASA-CP-2495-VOL-3] 09 p1110 N88-16650
McDonnell Douglas Helicopter Company independent research and development: Preparing for the future
09 p1111 N88-16660
General Rotorcraft Aeromechanical Stability Program (GRASP) version 1.03: User's manual
[NASA-TM-100043] 09 p1219 N88-17313
Helicopter external vision requirements and visual display characteristics: A report/bibliography, revision A
[AD-A187075] 10 p1276 N88-17641
Rotorcraft weight trends in light of structural material characteristics
[AD-A186576] 10 p1276 N88-17642
A perspective on 15 years of proof-of-concept aircraft development and flight research at Ames-Moffett by the Rotorcraft and Powered-Lift Flight Projects Division, 1970-1985
[NASA-RP-1187] 12 p1582 N88-19467
Rotorcraft flight-propulsion control integration: An eclectic design concept
[NASA-TP-2815] 12 p1584 N88-19475
Reasons for increasing development cost of rotary wing aircraft and ideas to reverse the trend
12 p1701 N88-20179
Reducing rotary wing aircraft development time/cost through the use of simulation 12 p1702 N88-20186
Some rotorcraft applications of computational fluid dynamics
[NASA-TM-100066] 18 p2459 N88-24601
Rotorcraft TCAS (traffic alert and collision avoidance system) evaluation: Group 3 results
[AD-A191719] 18 p2461 N88-24614
Zero/zero rotorcraft certification issues. Volume 1: Executive summary
[NASA-CR-177483-VOL-1] 19 p2602 N88-25453
Zero/zero rotorcraft certification issues. Volume 2: Plenary session presentations
[NASA-CR-177483-VOL-2] 19 p2602 N88-25454
Zero/zero rotorcraft certification issues. Volume 3: Working group results
[NASA-CR-177483-VOL-3] 19 p2602 N88-25455
Hover performance tests of baseline metal and Advanced Technology Blade (ATB) rotor systems for the XV-15 tilt rotor aircraft
[NASA-CR-177436] 20 p2759 N88-26367
A general-purpose approach to computer-aided dynamic analysis of a flexible helicopter
[NASA-TM-101002] 20 p2816 N88-26709
Prediction and measurement of human pilot dynamic characteristics in a manned rotorcraft simulation
[NASA-CR-183246] 24 p3410 N88-30297

ROTARY WINGS
NT BEARINGLESS ROTORS
NT CIRCULATION CONTROL ROTORS
NT RIGID ROTORS
NT TILTING ROTORS
NT X WING ROTORS
Analytical modeling of helicopter static and dynamic induced velocity in GRASP
[NASA-TM-100026] 02 p0123 N88-10777
An experimental evaluation of advanced rotorcraft airfoils in the NASA Ames eleven-foot transonic wind tunnel
[NASA-CR-166587] 03 p0261 N88-11640
Analytic investigation of helicopter rotor blade appended aeroelastic devices
[NASA-CR-166525] 03 p0266 N88-11676
Velocity scaled aeroelastic testing of an unducted fan
[GTL-191] 05 p0548 N88-13337
Artificial and natural icing tests of AH-64, phase 2
[AD-A188231] 11 p1439 N88-18585
A code development system for computational fluid dynamics
[AD-A188050] 11 p1482 N88-18848
Verification of the momemtum theory for rotors using measurements on a model helicopter
[R-840-S] 13 p1718 N88-20275
Measurements on a helicopter rotor
[R-764-S] 14 p1861 N88-21119
Investigations on higher harmonic blade pitch control at helicopters
[DFVLR-FB-87-36] 14 p1868 N88-21165
Tip vortices of isolated wings and helicopter rotor blades
[AD-A191336] 16 p2158 N88-22874
Structurally tailorable non-linear snap-through spring system
[NASA-CASE-LAR-13729-1] 18 p2523 N88-24970
Limits of design feasibility of multiwing wind turbines with individual articulated wing structure
[ILR-MITT-180] 18 p2537 N88-25052
Grid generation of a helicopter rotary-wing
19 p2640 N88-25665
Helicopter main-rotor noise: Determination of source contributions using scaled model data
[NASA-TP-2825] 20 p2848 N88-26907
An unsteady helicopter rotor: Fuselage interaction analysis
[NASA-CR-4178] 23 p3171 N88-28880
JUH-1H redesigned pneumatic boot deicing system flight test evaluation
[AD-A194918] 24 p3322 N88-29785

ROTATING
U ROTATION

ROTATING BODIES
NT BEARINGLESS ROTORS
NT CIRCULATION CONTROL ROTORS
NT COMPRESSOR ROTORS
NT FLYWHEELS
NT HELICOPTER TAIL ROTORS
NT IMPELLERS
NT PUMP IMPELLERS
NT RIGID ROTORS
NT ROTARY WINGS
NT ROTATING CYLINDERS
NT ROTATING DISKS
NT ROTATING SPHERES
NT ROTORS
NT TAIL ROTORS
NT TILTING ROTORS
NT TURBINE WHEELS
NT X WING ROTORS
Control and stabilization mechanisms of submunitions
[DFVLR-IB-111-86/9] 03 p0259 N88-11630
Semiempirical method for prediction of aerodynamic forces and moments on a steadily spinning light airplane
[NASA-TM-4009] 04 p0393 N88-12456
Airborne tracking sunphotometer apparatus and system
[NASA-CASE-ARC-11622-1] 06 p0730 N88-14492
Parametric dependence in the equilibrium dynamics of rotating structures
[AD-A187817] 11 p1498 N88-18945
An L-U implicit multigrid algorithm to solve the Euler equations for transonic flow in rotating turbomachinery passages 13 p1718 N88-20270
Topics in curved and flat space electromagnetism
13 p1854 N88-21100
The calculation of transonic flow over the shuttle orbiter using slender body theory 18 p2460 N88-24606
Effects of Coriolis acceleration on the vibrations of spinning structures 18 p2522 N88-24966
Drag measurements on a laminar flow body of revolution in Langley's 13 inch magnetic suspension and balance system
[NASA-CR-182909] 19 p2597 N88-25432

ROTATING CYLINDERS
Experiments on the flow of viscoelastic fluids between eccentric rotating cylinders 12 p1625 N88-19723
Compressible flow in a pie-shaped cylinder rotating about the vertex 18 p2480 N88-24604
Moving belt radiator development status
[NASA-TM-100909] 19 p2607 N88-25477
Numerical simulation of unsteady incompressible flow in a partially-filled rotating cylinder
[AD-A196001] 24 p3371 N88-30073

ROTATING DISKS
Coherent vortex structures in the wake of a stationary disk and of a disk excited to vibration
[ESA-TT-994] 09 p1163 N88-16968
Solution of a rotating Navier-Stokes problem by a nonlinear multigrid algorithm 11 p1538 N88-19194
Life and reliability of rotating disks
15 p2085 N88-22428
Remote temperature-measurement instrumentation for a heated rotating turbine disk
[DE88-006456] 18 p2516 N88-24925
Prediction of the pressure distribution for radial inflow between co-rotating discs
[PNR90464] 22 p3076 N88-28261

Numerical predictions for the flow induced by an enclosed rotating disc
[PNR90463] 22 p3078 N88-28281

ROTATING ENVIRONMENTS
Gastric emptying assessment by echography after a stress (rotating chair) 12 p1661 N88-19955

ROTATING FLUIDS
NT ROTATING LIQUIDS
Linear and nonlinear theories of flow through an actuator disk --- windpowered pumps
[R-803-A] 03 p0316 N88-11995
Turbulent mixing in a rotating, stratified fluid 04 p0445 N88-12759
Compressor large bandwidth noise emission mechanisms
[ETN-88-91177] 05 p0646 N88-13959
Rotational flow of rarefied gas between two coaxial cylinders with slip conditions
[INPE-4277-PRE/1149] 12 p1627 N88-19738
Mushroom-shaped currents (eddy dipoles) under rotation and stratification conditions 13 p1784 N88-20678
Development of a rotary fluid transfer coupling and support mechanism for space station 14 p1928 N88-21493
Experimental demonstrations of organic Rankine cycle waste heat rejection systems 17 p2432 N88-24469
Simulations of a missile with liquid payload under launch conditions
[AD-A191479] 18 p2463 N88-24625
Study of toluene rotary fluid management device and shear flow condenser performance for a space-based organic Rankine power system
[NASA-CR-180885] 24 p3338 N88-29872

ROTATING GENERATORS
NT AC GENERATORS
NT DYNAMOMETERS
NT TURBOGENERATORS
Finnish-Soviet Symposium on Radio Astronomy (1st) held at Otanlemi on August 26-27, 1985
[PB87-140661] 07 p0944 N88-15736

ROTATING LIQUIDS
On rotating sphere-on-a-plate experiments and the questions of whether high angle grain boundaries melt below bulk melting temperatures
[DE88-006627] 15 p2038 N88-22142
Fluid motion in a spinning, coning cylinder via spatial eigenfunction expansion
[AD-A190758] 15 p2066 N88-22319
Computational fluid dynamics methods for low Reynolds number precessing/spinning incompressible flows
[AD-A193891] 23 p3212 N88-29119
Numerical calculations of the response of a spinning spheroidal payload to coning motion
[AD-A195890] 24 p3368 N88-30059
Numerical simulation of unsteady incompressible flow in a partially-filled rotating cylinder
[AD-A196001] 24 p3371 N88-30073

ROTATING MATTER
Can the causal pathologies of Goedel-type universes be avoided in higher-derivative gravity
[DE88-700185] 11 p1568 N88-19387
Plasma rotation in a tokamak
[DE88-700855] 12 p1693 N88-20128

ROTATING PLASMAS
Effect of plasma rotation in tokamak on stabilizing action of electrically conducting wall 06 p0773 N88-14748
Evolution of poloidal variation of impurity density and ambipolar potential in rotating tokamak plasma, part 1
[DE88-006263] 13 p1842 N88-21022
Evolution of poloidal variation of impurity density and ambipolar potential in rotating tokamak plasma, part 2
[DE88-009882] 19 p2731 N88-26218

ROTATING SHAFTS
NT TURBOSHAFTS
Dynamic response of a geared train of rotors subjected to random support excitations 09 p1181 N88-17073
Dynamic stability of elastic rotor-bearing systems via Liapunov's direct method 21 p2958 N88-27571
Development of high temperature, high pressure rotating shaft seals
[DE88-001029] 23 p3221 N88-29172

ROTATING SPHERES
Analytical studies of axially symmetric motion of an incompressible viscous fluid between two concentric rotating spheres 04 p0444 N88-12757
Rotation of magnetized particle in electrically conducting viscous medium 06 p0770 N88-14733
Radiative heat transfer to chemically reacting flow between concentric rotating spheres
[DE88-702538] 22 p3118 N88-28525

ROTATING STALLS
Investigation of the excitation of turbine blade vibration in axial compressors in rotating stall
[ETN-87-90377] 01 p0007 N88-10035
A Navier-Stokes study of cascade flow fields including inlet distortion and rotating stall
[AD-A193109] 21 p2943 N88-27483
A mapping of the viscous flow behavior in a controlled diffusion compressor cascade using laser Doppler velocimetry and preliminary evaluation of codes for the prediction of stall
[AD-A194490] 23 p3211 N88-29112
Modeling of large stall in axial compressors
[VKI-TN-164] 23 p3213 N88-29124

ROTATING VEHICLES
U ROTATING BODIES
U VEHICLES

ROTATION
NT COROTATION
NT COUNTER ROTATION
NT EARTH ROTATION
NT MOLECULAR ROTATION
NT MUON SPIN ROTATION
NT SATELLITE ROTATION
NT SOLAR ROTATION
NT STELLAR ROTATION
The corrosion of iron rotating hemispheres in 1 M sulfuric acid: An electrochemical impedance study
[DE87-014679] 02 p0148 N88-10925
Coolant passage heat transfer with rotation 02 p0186 N88-11160
Filamentation instability of rotating light ion beams in fusion target chambers
[IPPJ-839] 02 p0242 N88-11530
Development, construction and testing of a novel internal combustion engine with conical rotating slide valve
[DE88-900071] 05 p0589 N88-13593
The Jeffcott equations in nonlinear rotordynamics 07 p0928 N88-15636
Application of a simple rotational spherical grating mounting to high resolution soft X-ray spectroscopy
[PB87-164836] 09 p1142 N88-16845
Experimental study of local natural convection heat transfer in inclined and rotating enclosures 09 p1165 N88-16986
Design conditions and workspace for the generally-proportioned 3-hinge spherical wrist for robots 10 p1339 N88-18003
Mathematical modeling of the postbuckling behavior of structural elements 11 p1500 N88-18960
Analysis of a rotating advanced-technology space station for the year 2025
[NASA-CR-178345] 12 p1600 N88-19580
Domain perturbation method in the static equilibrium of masses in rotation
[INPE-4217-PRE/1098] 12 p1686 N88-20085
The effect of combustion gas flow on the rotational dynamics of a spinning solid fuel rocket 13 p1732 N88-20358
Numerical model of the time independent mean flow in a rotating rocket motor 13 p1733 N88-20360
Parametric study of acceleration-induced stresses and frequency changes in doubly-rotated crystal resonators
[AD-A189261] 13 p1761 N88-20532
Eddy current losses induced by rotation of magnetisation
[BLL-M-37634-(5828.4)] 14 p1890 N88-21298
New representation for kinematics of manipulator
[DE88-751446] 14 p1917 N88-21445
Rotation of universe --- metagalaxies 14 p1974 N88-21780
Comparison of active regions on the nucleus of Comet Halley 14 p2004 N88-21948
P/Halley activity in November 1985 14 p2006 N88-21966
Dust tail streamers and Halley's nucleus rotation 14 p2008 N88-21979
The light curve of P/Halley and the rotation of its nucleus 14 p2009 N88-21984
Experimental investigation of a spanwise forced mixing layer
[AD-A190136] 15 p2013 N88-22007
Coupled bending-torsion steady-state response of pretwisted, nonuniform rotating beams using a transfer-matrix method
[NASA-TM-100596] 15 p2086 N88-22435
Density perturbations in a rotating universe
[DE87-703036] 15 p2151 N88-22840
Effects of translational and rotational nonequilibrium on CW (Continuous Wave) chemical laser performance
[AD-A191425] 16 p2214 N88-23210
Kinetic theoretical analysis for propagation of rotating ion beam in ICF 16 p2276 N88-23623
Hybrid particle simulation for focusing of rotating and propagating LIB 16 p2276 N88-23624
Microinstabilities in ion beam propagation 16 p2277 N88-23631
Studies of heat and mass transfer during chemical vapor deposition 17 p2338 N88-23953
The effects of inlet turbulence and rotor/stator interactions on the aerodynamics and heat transfer of a large-scale rotating turbine model. Part 4: Aerodynamic data tabulation
[NASA-CR-179469] 17 p2339 N88-23956
A generic multibody simulation
[NASA-CR-182949] 17 p2388 N88-24198
Spectroscopic measurements of ion temperature, rotation speed and beam deposition profile on DIII-D 17 p2440 N88-24519
Atmospheric autorotating imaging device
[NASA-CASE-NPO-17390-1-CU] 18 p2519 N88-24944
Para-ortho abundance ratio of molecular hydrogen in NGC2023
[ISAS-RN-352] 18 p2573 N88-25286
Some operational aspects of a rotating advanced-technology space station for the year 2025
[NASA-CR-181617] 20 p2765 N88-26397
Rotation symmetric vortex in axiparallel flow
[ETN-88-92364] 21 p2948 N88-27512
Development of high temperature, high pressure rotating shaft seals
[DE88-001029] 23 p3221 N88-29172
The aspect ratio dependence of the attractor dimension in Taylor-Couette flow
[AD-A196297] 24 p3369 N88-30065

ROTATIONAL FLOW
U FLUID FLOW
U VORTICES

ROTOR AERODYNAMICS
A full potential flow analysis with realistic wake influence for helicopter rotor airload prediction
[NASA-CR-4007] 04 p0393 N88-12452
A comparison of experimental and theoretical results for labyrinth gas seals with honeycomb stators
[NASA-CR-182441] 08 p0993 N88-16006
Experimental rotordynamic coefficient results for honeycomb seals
[NASA-CR-182440] 08 p0993 N88-16007
NASA/Army Rotorcraft Technology. Volume 1: Aerodynamics, and Dynamics and Aeroelasticity
[NASA-CP-2495-VOL-1] 09 p1105 N88-16625
Accomplishments at NASA Langley Research Center in rotorcraft aerodynamics technology 09 p1105 N88-16626
The development of CFD methods for rotor applications 09 p1105 N88-16627
A summary of recent NASA/Army contributions to rotorcraft vibrations and structural dynamics technology 09 p1105 N88-16628
A review of research in rotor loads 09 p1106 N88-16629
Comprehensive rotorcraft analysis methods 09 p1106 N88-16630
Rotorcraft aeroelastic stability 09 p1106 N88-16631
NASA/Army Rotorcraft Technology. Volume 2: Materials and Structures, Propulsion and Drive Systems, Flight Dynamics and Control, and Acoustics
[NASA-CP-2495-VOL-2] 09 p1106 N88-16632
Numerical modeling of multidimensional flow in seals and bearings used in rotating machinery
[NASA-TM-100779] 09 p1165 N88-16988
Frequency-response identification of XV-15 tilt-rotor aircraft dynamics 10 p1277 N88-17643
Special flight mechanical features of the bearingless helicopter rotor
[MBB-FM-315/O] 10 p1309 N88-17825
La Recherche Aerospatiale, bimonthly bulletin, number 1987-1, 236/January-February
[ESA-TT-1055] 11 p1433 N88-18549
Verification of the momemtum theory for rotors using measurements on a model helicopter
[R-840-S] 13 p1718 N88-20275
Measurements on a helicopter rotor
[R-764-S] 14 p1861 N88-21119
The 25 m horizontal-axis turbine as a test case for standard Dutch aerodynamic calculation methods for high-speed rotors
[R-762-D] 14 p1942 N88-21589
Advancing-side directivity and retreating-side interactions of model rotor blade-vortex interaction noise
[NASA-TP-2784] 15 p2131 N88-22710
Piezoelectric pushers for active vibration control of rotating machinery 16 p2218 N88-23229
Active control and system identification of rotordynamic structure 16 p2218 N88-23230
Research investigation of helicopter main rotor/tail rotor interaction noise
[NASA-CR-4143] 19 p2722 N88-26165
A review of gear housing dynamics and acoustics literature
[NASA-CR-183110] 20 p2811 N88-26675

Integrated Technology Rotor Methodology Assessment Workshop
[NASA-CP-10007] 21 p2889 N88-27148
Comparison of experimental rotor damping data-reduction techniques 21 p2891 N88-27159
Comparison of experimental coupled helicopter rotor/body stability results with a simple analytical model 21 p2891 N88-27160

ROTOR BLADES
Active control of helicopter vibration using multiloop self-adaptive control 03 p0264 N88-11660
Minimisation of helicopter vibration through active control of structural response 03 p0264 N88-11662
Impacts of rotor hub design criteria on the operational capabilities of rotorcraft systems 03 p0264 N88-11663
Performance measurements of the Kolibrie and FACT rotor blades without tip vanes on the full-scale experimental wind turbine
[IW-R518] 06 p0665 N88-14077
Design and test of a high blade speed, high work capacity transonic turbine 10 p1281 N88-17658
Experimental investigation of a supercritical compressor rotor blade section 10 p1284 N88-17680
A preliminary investigation of finite-element modeling for composite rotor blades
[NASA-TM-100559] 13 p1781 N88-20656
Optimal placement of tuning masses for vibration reduction in helicopter rotor blades
[NASA-TM-100562] 13 p1782 N88-20665
FLAP (Force and Loads Analysis Program) code development and validation
[DE88-001131] 15 p2075 N88-22371
Inflow measurements made with a laser velocimeter on a helicopter model in forward flight. Volume 4: Tapered planform blades at an advance ratio of 0.15
[NASA-TM-100544] 16 p2156 N88-22863
Minimum weight design of rotorcraft blades with multiple frequency and stress constraints
[NASA-TM-100569] 16 p2161 N88-22892
Supersonic axial-flow fan flutter 16 p2221 N88-23255
Hover performance tests of baseline metal and Advanced Technology Blade (ATB) rotor systems for the XV-15 tilt rotor aircraft
[NASA-CR-177436] 20 p2759 N88-26367

ROTOR BLADES (TURBOMACHINERY)
Integration of dynamic, aerodynamic and structural optimization of helicopter rotor blades
[NASA-CR-181441] 01 p0002 N88-10012
ARSPNS: A method to calculate steady and unsteady potential flow about fixed and rotational lifting and nonlifting bodies
[NLR-TR-85114-U] 01 p0044 N88-10282
A method for the efficient calculation of elastic rotor blade dynamic response in forward flight 04 p0394 N88-12460
Measurements and calculations of aerodynamic torques for a vertical-axis wind turbine
[DE88-001783] 04 p0465 N88-12876
Results of the 1986 NASA/FAA/DFVLR main rotor test entry in the German-Dutch wind tunnel (DNW)
[NASA-TM-100507] 04 p0487 N88-13003
Solution procedure for the Navier-Stokes equations applied to rotors 05 p0579 N88-13533
Noise of a model counterrotation propeller with reduced aft rotor diameter at simulated takeoff/approach conditions (F7/A3)
[NASA-TM-100254] 05 p0647 N88-13961
An explicit Runge-Kutta method for unsteady rotor/stator interaction
[NASA-TM-100787] 07 p0816 N88-14967
Blade vibration problems in centrifugal compressors. Fundamental considerations 07 p0851 N88-15165
Blade vibration due to different flow excitation 07 p0851 N88-15166
Blade excitation due to unsteady flow phenomena 07 p0851 N88-15167
Accomplishments at NASA Langley Research Center in rotorcraft aerodynamics technology 09 p1105 N88-16626
A review of research in rotor loads 09 p1106 N88-16629
NASA's rotorcraft icing research program 09 p1108 N88-16641
Three-dimensional incompressible flowfield analysis for establishing rotor designs which optimize power extraction 10 p1329 N88-17943
Design graphs for the first two bending Eigenvibration forms of rotating beams consisting of two beam points
[IW-86006R] 13 p1783 N88-20670
Measurement and analysis of the noise radiated by low Mach numbers centrifugal blowers
[AD-A189226] 13 p1833 N88-20966
Visualisation of the flow at the tip of a high speed axial flow turbine rotor
[AD-A189928] 15 p2063 N88-22300
Visualisation of the flow at the tip of a high speed axial flow turbine rotor: An assessment of flow visualisation techniques and the requirement of the experimental turbine
[AD-A189929] 15 p2063 N88-22301
Improvements to tilt rotor performance through passive blade twist control
[NASA-TM-100583] 15 p2086 N88-22434
Experimental vibration damping characteristics of the third-stage rotor of a three-stage transonic axial-flow compressor
[NASA-TM-100948] 18 p2466 N88-24642
Extensive verification of blade-to-blade flow code based on Denton scheme 19 p2638 N88-25654
The MOD-2 wind turbine: Aeroacoustical noise sources, emissions, and potential impact
[DE88-001132] 19 p2687 N88-25971
Effects of static equilibrium and higher-order nonlinearities on rotor blade stability in hover 21 p2890 N88-27157
A review of non-contacting displacement measurement techniques used to monitor the movement of rotor blades in gas turbine aero engines
[PNR90457] 22 p3045 N88-28071
SR-7A aeroelastic model design report
[NASA-CR-174791] 23 p3179 N88-28928

ROTOR BODY INTERACTIONS
A 0.15-scale study of configuration effects on the aerodynamic interaction between main rotor and fuselage
[NASA-CR-166577] 04 p0395 N88-12462
Integrated Technology Rotor Methodology Assessment Workshop
[NASA-CP-10007] 21 p2889 N88-27148
A comparison of theory and experiment for coupled rotor-body stability of a hingeless rotor model in hover under simulated vacuum conditions 21 p2889 N88-27151
A comparison of theory and experiment for coupled rotor-body stability of a hingeless rotor model in hover 21 p2889 N88-27152
A comparison of theory and experiment for coupled rotor body stability of a bearingless rotor model in hover and forward flight 21 p2890 N88-27154
The importance of steady and dynamic inflow on the stability of rotor-body systems 21 p2890 N88-27156
Comparison of experimental coupled helicopter rotor/body stability results with a simple analytical model 21 p2891 N88-27160
Program user's manual for an unsteady helicopter rotor-fuselage aerodynamic analysis
[NASA-CR-181701] 22 p3039 N88-28047

ROTOR DISKS
U TURBINE WHEELS

ROTOR HUBS
U HUBS
U ROTORS

ROTOR SPEED
Helicopter main-rotor speed effects on far-field acoustic levels
[NASA-TM-100512] 02 p0230 N88-11451
Study on a rotor speed control system for a horizontal axis windmill
[NAL-TR-931] 10 p1349 N88-18062
A LQG regulator for the angular motion of the rotor at a tuned gyroscope
[INPE-4280-PRE/1152] 12 p1631 N88-19759

ROTOR SYSTEMS RESEARCH AIRCRAFT
Flight research at NASA Ames Research Center: A test pilot's perspective
[NASA-TM-100025] 02 p0125 N88-10788

ROTORCRAFT
U ROTARY WING AIRCRAFT

ROTORCRAFT AIRCRAFT
Development of rotorcraft interior noise control concepts. Phase 2: Full scale testing, revision 1
[NASA-CR-172594-REV-1] 06 p0777 N88-14789
Delamination durability of composite materials for rotorcraft 09 p1107 N88-16634
The role of aviation technology in the Caribbean Basin
[NASA-CR-183069] 20 p2745 N88-26289

ROTORS
NT BEARINGLESS ROTORS
NT CIRCULATION CONTROL ROTORS
NT COMPRESSOR ROTORS
NT FLYWHEELS
NT HELICOPTER TAIL ROTORS
NT IMPELLERS
NT PUMP IMPELLERS
NT RIGID ROTORS
NT ROTARY WINGS
NT TAIL ROTORS
NT TILTING ROTORS
NT TURBINE WHEELS
NT X WING ROTORS
Turbines with counterrotating runners for aircraft power plants 02 p0158 N88-10992
A 1987 progress report of manufacturing techniques for Gravity Probe B gyroscope rotors
[NASA-TM-100312] 02 p0176 N88-11101
Measurement of airfoil heat transfer coefficients on a turbine stage 02 p0186 N88-11158
Controlling the dynamic environment during NOE flight 03 p0264 N88-11661
A full potential flow analysis with realistic wake influence for helicopter rotor airload prediction
[NASA-CR-4007] 04 p0393 N88-12452
Flap-lag equations of motion of rigid, articulated rotor blades with three hinge sequences
[NASA-TM-100023] 04 p0401 N88-12495
Calculation of helicopter rotor blade/vortex interaction by Navier-Stokes procedures
[NASA-CR-177441] 05 p0540 N88-13291
Model helicopter rotor rig and associated strain gauge balance for performance studies
[NAL-TM-AE-8704] 05 p0552 N88-13364
Dynamic behavior of dissymmetric rotor bearings modelled with a periodic coefficient large system 05 p0596 N88-13640
Coupled elastic rotor/body vibrations with inplane degrees of freedom 05 p0596 N88-13643
Development of an unsteady wake theory appropriate for aeroelastic analyses of rotors in hover and forward flight
[NASA-CR-182357] 06 p0664 N88-14075
Euler solution of multiblade rotor flow
[NASA-TM-100014] 06 p0704 N88-14322
Creep-fatigue cracking in high temperature turbine rotors 06 p0720 N88-14426
Lift distribution and velocity field measurements for a three-dimensional, steady blade/vortex interaction
[NASA-TM-100013] 07 p0815 N88-14962
Measurement in a wind tunnel of the modification of mean wind and turbulence characteristics due to induction effects near wind turbine rotors
[DE88-000249] 07 p0815 N88-14963
The effects of rotor unbalance on the vertical response of a soft-mounted block 08 p1000 N88-16057
Rotorcraft flight research with emphasis on rotor systems 09 p1111 N88-16656
Dynamic response of a geared train of rotors subjected to random support excitations 09 p1181 N88-17073
The further development of circulation control airfoils 10 p1270 N88-17594
A research program on the aerodynamics of a highly loaded turbine stage 10 p1280 N88-17655
The unsteady gas flow through stator and rotor of a turbomachine 10 p1281 N88-17660
Optimal design and parameter identification of flexible rotor-bearing systems 10 p1339 N88-18002
Electro-mechanical vibratory system 11 p1500 N88-18958
Site effects on wind characteristics at a turbine rotor
[DE88-005135] 11 p1507 N88-19003
Testing of a one-bladed 30-meter-diameter rotor on the DOE/NASA Mod-O wind turbine
[NASA-TM-100274] 11 p1509 N88-19014
Acoustic measurements from a rotor blade-vortex interaction noise experiment in the German-Dutch Wind Tunnel (DNW)
[NASA-TM-4024] 11 p1542 N88-19218
Minimum weight design of rectangular and tapered helicopter rotor blades with frequency constraints
[NASA-TM-100561] 12 p1582 N88-19485
Dynamic modelling of flexible rotor shafts mounted on hydrodynamic bearings 13 p1779 N88-20641
Inflow measurement made with a laser velocimeter on a helicopter model in forward flight. Volume 2: Rectangular planform blades at an advance ratio of 0.23
[NASA-TM-100542] 14 p1864 N88-21139
Inflow measurement made with a laser velocimeter on a helicopter model in forward flight. Volume 3: Rectangular planform blades at an advance ratio of 0.30
[NASA-TM-100543] 15 p2015 N88-22015
Visualisation of the flow at the tip of a high speed axial flow turbine rotor
[AD-A189928] 15 p2063 N88-22300
On the computation of stationary deterministic behavior of nonlinear dynamic systems with applications to rotor-bearing structures
[ETN-88-92241] 16 p2214 N88-23213
Active control and system identification of rotordynamic structure 16 p2218 N88-23230
Development of aeroelastic analysis methods for turborotors and propfans, including mistuning 16 p2219 N88-23244
The 2-D and 3-D time marching transonic potential flow method for propfans 16 p2220 N88-23245

Acoustic characteristics of 1/20-scale model helicopter rotors
[NASA-CR-177355] 16 p2265 N88-23548
Vibration and control of flexible rotor supported by magnetic bearings
[NASA-TM-100888] 17 p2345 N88-23977
Inflow measurements made with a laser velocimeter on a helicopter model in forward flight. Volume 1: Rectangular planform blades at an advance ration of 0.15
[NASA-TM-100541] 18 p2460 N88-24607
Entrance and exit region friction factor models for annular seal analysis
[NASA-CR-183084] 19 p2678 N88-25921
Improved method for stress and compatibility analysis of multicomponent rotating systems
[NASA-TM-100884] 19 p2680 N88-25935
Dynamic stability of elastic rotor-bearing systems via Liapunov's direct method 21 p2958 N88-27571
Euler equation computations for the flow over a hovering helicopter rotor
[NASA-CR-177493] 22 p3038 N88-28037
An analytical investigation of geared system dynamics containing spur and helical gears
22 p3085 N88-28317
Investigation of helicopter rotor blade/wake interactive impulsive noise
[NASA-CR-177435] 23 p3171 N88-28882
The effects of inlet turbulence and rotor/stator interactions on the aerodynamics and heat transfer of a large-scale rotating turbine model. Volume 3: Heat transfer data tabulation 65 percent axial spacing
[NASA-CR-179468] 23 p3180 N88-28930
Three-dimensional Navier-Stokes simulations of turbine rotor-stator interaction
[NASA-TM-100081] 24 p3316 N88-29750
An unconditionally stable Runge-Kutta method for unsteady flows
[NASA-TM-101347] 24 p3321 N88-29780
The effects of inlet turbulence and rotor/stator interactions on the aerodynamics and heat transfer of a large-scale rotating turbine model. Volume 2: Heat transfer data tabulation. 15 percent axial spacing
[NASA-CR-179467] 24 p3326 N88-29804
Spray automated balancing of rotors: Methods and materials
[NASA-CR-182151] 24 p3330 N88-29825

ROUGHNESS
NT SEA ROUGHNESS
NT SURFACE ROUGHNESS
X-ray studies of strain, interface and impurity in semiconductors
[DE87-013856] 01 p0104 N88-10678
Precision metrology comparing ultrasonic and other techniques for the determination of steel thickness
[DE87-011051] 02 p0230 N88-11452
Studies on high-speed electroforming
[DE88-001395] 04 p0429 N88-12656
Computation of turbulent flow of air through smooth and rough pipes using a two-equation turbulence model
06 p0700 N88-14298
Fractal surface finish
[DE88-007972] 22 p3057 N88-28137
Green's function approach to roughening transition of one-dimensional restricted solid on solid model
[DE88-702723] 23 p3278 N88-29512

ROUND TRIP TRAJECTORIES
Mission profiles of the MTFF co-orbiting with the US Space Station 12 p1585 N88-19487

ROUTES
Two dimensional path planning with obstacles and shadows
[AD-A184075] 04 p0397 N88-12474
Single-layer wire routing
[AD-A186990] 09 p1157 N88-16932
Automatic routing module 09 p1210 N88-17251
Minimum Energy Routing through Interactive Techniques (MERIT) modeling
[NASA-CR-182535] 10 p1356 N88-18105
Deadlock-free message routing in processor networks
[CS-8706] 14 p1960 N88-21691
Implementation of a distributed adaptive routing algorithm on the Intel iPSC (Intel Personal Super-Computer)
[AD-A189849] 15 p2109 N88-22567
Contribution of space to marine activities
19 p2700 N88-26057
Indian Ocean validation
[AD-A194458] 23 p3175 N88-28902

ROVER PROJECT
History of some direct nuclear propulsion developments since 1946 17 p2400 N88-24270
A critique of NERVA based nuclear reactor design and performance for MMW space propulsion applications
17 p2404 N88-24297
Nuclear propulsion: Past, present and future
17 p2427 N88-24441
The NERVA derivative reactor and a systematic approach to multiple space power requirements
17 p2430 N88-24458

ROVING VEHICLES
Aerosols in Martian Atmosphere and Natural Dust Observation (AMANDO). Proposal for the Mars orbiter balloon and rover to study the Martian atmosphere, its thermal content, and its interaction with the soil
[IFSI-87-9] 08 p1100 N88-16619
Mars Lander/Rover vehicle development: An advanced space design project for USRA and NASA/OAST
[NASA-CR-182562] 12 p1709 N88-20226
Electromagnetic powered vehicles (EMPV) for Mars exploration 17 p2419 N88-24388
Energy storage considerations for a robotic Mars surface sampler
[NASA-TM-100969] 22 p3166 N88-28853

RP-1 ROCKET PROPELLANTS
Characterization of aluminum/RP-1 gel propellant properties
[NASA-TM-100951] 18 p2496 N88-24808

RPV
U REMOTELY PILOTED VEHICLES

RUANDA-URUNDI
U BURUNDI

RUBBER
NT BUNA (TRADEMARK)
NT ELASTOMERS
NT LATEX
NT SYNTHETIC RUBBERS
NT VULCANIZED ELASTOMERS
Basic research on macromolecular dynamics
[PB88-141643] 10 p1305 N88-17805
Numerical-experimental investigation of singularity at a crack in nonlinear rubber elasticity
11 p1500 N88-18961
Rubber-modified epoxies: Interfacial tension and morphology
[AD-A192464] 21 p2917 N88-27313
Elastic behavior of a rubber layer bonded between two rigid spheres
[AD-A193698] 23 p3198 N88-29030
Determination of the hydroperoxide potential of jet fuels
[AD-A195975] 24 p3357 N88-29991

RUBIDIUM
NT RUBIDIUM ISOTOPES
On-orbit frequency stability analysis of the GPS NAVSTAR 8 rubidium clock and NAVSTARs 9 and 10 cesium clocks
[AD-A184984] 05 p0544 N88-13312
A rubidium-stabilised laser diode for interferometry
[NPL-MOM-85] 14 p1914 N88-21433
Ultrahigh coherent semiconductor lasers and their applications to Rb atomic clock
14 p1976 N88-21789
Tactical Rubidium Frequency Standard (TRFS)
[AD-A191049] 16 p2193 N88-23078
Tactical Rubidium Frequency Standard (TRFS), volume 2
[AD-A191190] 18 p2503 N88-24850
Tactical Rubidium Frequency Standard (TRFS), volume 1
[AD-A192981] 20 p2805 N88-26640

RUBIDIUM ISOTOPES
Development and applications of new technical advances to problems of fluid/electrolyte/mineral imbalance in military personnel
[AD-A186437] 07 p0889 N88-15388

RUBY LASERS
A mode-locked ruby laser with chlorophyll d as saturable absorber 03 p0327 N88-12064
Noncontact temperature measurements of hot steel bodies using an electromagnetic acoustic transducer (EMAT)
[DE88-000560] 04 p0446 N88-12765
Formation of high-coherence radiation in free-running mode ruby laser for pulse holography
08 p1077 N88-16497
Multipoint Thomson scattering diagnostic for DIII-D
[DE88-008737] 20 p2857 N88-26969

RUDDERS
The use of aeroelastic wind tunnel models to prove structural design 05 p0551 N88-13355

RULES
NT FLIGHT RULES
NT INSTRUMENT FLIGHT RULES
NT SELECTION RULES (NUCLEAR PHYSICS)
NT VISUAL FLIGHT RULES
A rule-based system for arrival sequencing and scheduling in air traffic control 02 p0129 N88-10815
Genie inference engine rule writer's guide
[AD-A185709] 06 p0762 N88-14675
FORTRAN 77 programming guidelines
[DFVLR-MITT-87-10] 07 p0905 N88-15487
Using output to evaluate and refine rules in rule-based expert systems 08 p1055 N88-16362
Approaches to the verification of rule-based expert systems 09 p1206 N88-17232
A rule-based Lisp dialect translator using paramodulation 10 p1380 N88-18238
Directions for programming in FORTRAN 77
[NASA-TT-20317] 20 p2839 N88-26842
Towards knowledge bases-semantics, rules and object-oriented programming
[PB88-108154] 20 p2882 N88-27110
Rules, schema and decision making
[AD-A193389] 21 p3027 N88-27967
Generating semi-Gaussian two dimensional quadrature rules
[REPT-205] 23 p3272 N88-29476

RUN TIME (COMPUTERS)
File usage analysis and resource usage prediction: A measurement-based study
[NASA-CR-181553] 05 p0633 N88-13867
Predictability of process resource usage: A measurement-based study of UNIX
[NASA-CR-181562] 05 p0633 N88-13869
Nonpreemptive run-time scheduling issues on a multitasked, multiprogrammed multiprocessor with dependencies, bidimensional tasks, folding and dynamic graphs
[DE88-003598] 09 p1223 N88-17335
A digital logic simulator with concurrent programming considerations
[AD-A188823] 12 p1678 N88-20032
Modeling and optimum time performance for concurrent processing
[NASA-CR-4167] 20 p2797 N88-26595
Matrix substructuring, domain decomposition and particle methods: Current trends for solving PDEs in parallel
[DE88-009826] 21 p3007 N88-27836

RUNGE-KUTTA METHOD
Navier-Stokes cascade analysis with a stiff Kappa-Epsilon turbulence solver
[NASA-TM-100218] 02 p0123 N88-10778
Implementation and evaluation of several continuously imbedded methods of Sarafyan
[DE88-000025] 02 p0221 N88-11393
Implementation of the Runge-Kutta-Fehlberg method for solution of ordinary differential equations on a parallel processor
[AD-A184660] 03 p0370 N88-12331
Application of Runge Kutta time marching scheme for the computation of transonic flows in turbomachines
[NASA-TM-86997] 04 p0394 N88-12461
An explicit Runge-Kutta method for unsteady rotor/stator interaction
[NASA-TM-100787] 07 p0816 N88-14967
Diagonally implicit Runge-Kutta-Nystrom methods for oscillatory problems
[CWI-NM-R8704] 09 p1228 N88-17356
A note on a diagonally implicit Runge-Kutta-Nystrom method
[CWI-NM-R8706] 09 p1228 N88-17358
Reduction of time delays in Runge-Kutta integration methods --- systems simulation
[MBB/LKE-132/S/PUB/241/A]
09 p1229 N88-17363
Applications of a multigrid finite volume method with Runge-Kutta time integrations for solving the Euler and Navier-Stokes equations 11 p1539 N88-19201
Numerical methods in the resolution of control electrovalve model
[INPE-4154-RPE/540] 13 p1764 N88-20554
An adaptive grid technique for solution of the Euler equations 13 p1768 N88-20579
Convergence of Runge-Kutta methods on classes of stiff initial value problems
[CWI-NM-R8717] 13 p1827 N88-20924
Effects of numerical dissipation on finite-volume solutions of compressible flow problems
[AD-A193173] 21 p2944 N88-27485
KRYSI, an ODE solver combining a semi-implicit Runge-Kutta method and a preconditioned Krylov method
[DE88-012245] 21 p3008 N88-27841
Runge-Kutta finite-volume simulation of laminar transonic flow over the ONERA M6 wing using the Navier-Stokes equations
[FFA-TN-1987-06] 22 p3039 N88-28045
An unconditionally stable Runge-Kutta method for unsteady flows
[NASA-TM-101347] 24 p3321 N88-29780

RUNNING
Metabolic and cardiorespiratory parameters during three consecutive days of exhaustive running
[AD-A192598] 21 p2985 N88-27728

Gastric emptying during walking and running: Effects of varied exercise intensity
[AD-A194025] 23 p3240 N88-29281

RUNOFFS
U DRAINAGE

RUNWAY CONDITIONS
A new look at the use of linear methods to predict aircraft dynamic response to taxi over bomb damaged and repaired airfields 09 p1180 N88-17069
Aircraft and ground vehicle friction correlation test results obtained under winter runway conditions during joint FAA/NASA Runway Friction Program
[NASA-TM-100506] 11 p1438 N88-18582
An investigation of the spray produced by a yawed wheel, including measurement of impact forces --- aircraft wheels
[BU-363] 14 p1866 N88-21150
Airplane runway performance monitoring system
[NASA-CASE-LAR-13854-1-CU] 18 p2462 N88-24621

RUNWAYS
The ability of modified pavement quality concrete to resist ground erosion caused by VTOL aircraft
[BAE-ARG-238] 03 p0267 N88-11683
Optimum take-off run of aircraft on ground airfields 04 p0423 N88-12623
A laboratory study of asphalt concrete mix designs for high-contact pressure aircraft traffic
[AD-A185753] 06 p0670 N88-14106
Chicago's O'Hare Runway Configuration Management System (RCMS). Volume 1: Description of the operational software
[AD-A185886] 07 p0821 N88-14990
Comparative study of nondestructive pavement testing, MacDill Air Force Base, Florida
[AD-A186082] 07 p0822 N88-14993
Chicago's O'Hare Runway Configuration Management System (RCMS). Volume 2: Users guide
[AD-A186222] 08 p0953 N88-15783
A new look at the use of linear methods to predict aircraft dynamic response to taxi over bomb damaged and repaired airfields 09 p1180 N88-17069
Evaluation of bituminous materials used in pavement recycling projects at Tyndall, MacDill, and Hurlburt Air Force Bases
[AD-A188068] 10 p1317 N88-17871
Micro PAVER concept and development airport pavement management system
[AD-A187360] 11 p1441 N88-18598
Probabilistic and reliability design procedures for flexible airfield pavements: Elastic layered method
[AD-A187533] 11 p1442 N88-18600
Profilometer for bomb-damage-repaired airfield pavements and measurement of pavement upheaval. Report 1: Technology evaluation
[AD-A187985] 11 p1442 N88-18601
Soft-ground aircraft arresting systems
[AD-A190838] 16 p2165 N88-22912
Microwave landing system mathematical modeling study for Midway Airport Runway 22L, Chicago, Illinois
[AD-A191721] 18 p2462 N88-24616
Airplane runway performance monitoring system
[NASA-CASE-LAR-13854-1-CU] 18 p2462 N88-24621
Takeoff predictions for powered-lift aircraft
[NASA-CR-177491] 19 p2597 N88-25431
Alternate/modified binders for airfield pavements
[AD-A192781] 21 p2899 N88-27206
Improvement of head-up display standards. Volume 5: Head up display ILS (Instrument Landing System) accuracy flight tests
[AD-A194602] 23 p3178 N88-28922
Airport surface traffic automation study
[AD-A194553] 23 p3181 N88-28934
An analysis of time and space requirements for aircraft turnrounds
[TT-8705] 24 p3322 N88-29783

RUPTURING
Stress rupture behavior of silicon carbide coated, low modulus carbon/carbon composites
[NASA-CR-180863] 06 p0678 N88-14150
Ductile failure
[AD-A189429] 13 p1781 N88-20654
Internal fluid dynamics within a nonspinning partially liquid-filled shell due to burster rupture
[AD-A191055] 18 p2507 N88-24874
Critical conditions for failure in materials subjected to high rates of loading
[AD-A194697] 23 p3226 N88-29201

RURAL AREAS
Land-use classification in a region north-west of Wuerzburg (Federal Republic of Germany) using digital, multispectral LANDSAT 5 Thematic Mapper data
[DFVLR-FB-87-37] 14 p1940 N88-21579

RURAL LAND USE
The contribution of satellite data in drawing up maps used in rural development 03 p0343 N88-12167
A comparative thematic mapping analysis of SPOT data: The Vientiane Plain (Laos) 03 p0343 N88-12168
Water resources and agricultural land use investigations in northeastern Gujarat (India) 22 p3091 N88-28355
Spatial and spectral registration of Javanese landscape units with SPOT 22 p3092 N88-28362
Land use systems and rural landscapes in the center of Veracruz State (Mexico): First results 22 p3092 N88-28364
An evaluation of multidate SPOT data for agriculture and land use mapping in the United Kingdom 22 p3094 N88-28375
Discrimination methods of traditional fields in a humid tropical region (Shaba, Zaire) using digital classification on SPOT data 22 p3096 N88-28387
Monitoring Tunisia's steppes with SPOT 22 p3097 N88-28390
Agro-ecological mapping from SPOT 1 data in southern Thailand: New questions for an analysis of the farming-systems 22 p3097 N88-28394
SPOT-1 over New Zealand: Analysis of SPOT imagery for land use investigations 22 p3101 N88-28416

RUSTING
Reduced time frame for predicting coating performance 24 p3356 N88-29979

RUTHENIUM
Ruthenium catalysts and their use in ammonia production
[GB-PATENT-2-136-704-A] 01 p0020 N88-10123
Determination, by X-ray fluorescence, of platinum, palladium, ruthenium, iron and chromium in special steels
[PB87-132114] 06 p0683 N88-14183
Contrast between the chemical, structural and electronic properties of thin films of Cu and Ni on the Ru(0001) surface
[DE88-002360] 07 p0938 N88-15698
Superconductivity and crystal structure of high-pressure phases in V-Ru-H system 09 p1239 N88-17426
Growth and electronic properties of strained metal overlayers
[DE87-010956] 10 p1417 N88-18463
Thermodynamic data bases for multivalent elements: An example for ruthenium
[DE88-004395] 23 p3190 N88-28984

RUTHENIUM COMPOUNDS
Intramolecular energy transfer reactions as a method for metal complex assisted production of hydrogen
[DE88-001621] 05 p0562 N88-13425

RUTILE
Electrochemical and optical investigations on ion-implanted TiO2 samples
[ETN-88-91485] 11 p1455 N88-18670

RYDBERG SERIES
Two-laser resonance enhanced photoionization spectrum of gas phase benzene 03 p0300 N88-11889
Study of energy levels and decay mechanisms for singlet Rydberg states of molecular nitrogen
[AD-A192505] 21 p3014 N88-27886
The 2D Rydberg series in Al I
[NASA-TM-101189] 22 p3150 N88-28740

S

S BAND
U SUPERHIGH FREQUENCIES
U ULTRAHIGH FREQUENCIES

S CURVES
Electromagnetic fields backscattered from an s-shaped inlet cavity with an absorber coating on its inner walls
[NASA-CR-182401] 07 p0845 N88-15130
Electromagnetic propagation in PEC and absorbing curved S-ducts
[NASA-TM-100833] 12 p1621 N88-19698

S GLASS
S-glass analysis by X-ray spectroscopy
[DE88-004636] 11 p1454 N88-18666

S MATRIX THEORY
Integrable quantum systems and classical Lie algebras
[DE88-700872] 12 p1683 N88-20063
Action-angle maps and scattering theory for some finite-dimensional integrable systems. The pure solution case
[CWI-PM-R8704] 13 p1831 N88-20955
Analysis of networks with parameters S: Generalization of junction matrix
[INPE-4535-PRE/1282] 20 p2793 N88-26570
Polarization of light reflected by vertically inhomogeneous planetary atmosphere
[DE88-702416] 21 p3031 N88-27992
Theory of quark mixing matrix and invariant functions of mass matrices
[USIP-87-14] 22 p3159 N88-28800

S STARS
Emission features in IRAS LRS spectra of MS, S and CS stars 04 p0514 N88-13163
Radial velocities monitoring of a sample of barium and S stars using CORAVEL: Towards an evolutionary link between barium and S stars?
[SER-C-PREPUBL-FASC-19] 18 p2593 N88-25410

S WAVES
Refraction of shear wave into nonlinearly elastic or elastoplastic half-space 02 p0159 N88-10999
Lg wave excitation and propagation in the presence of one-, two-, and three-dimensional heterogeneities
[AD-A187364] 11 p1510 N88-19022
Investigation of the use of horizontally polarised shear waves for TOFD studies on austenitic steel
[AERE-R-12145] 13 p1780 N88-20649
Earthquakes from peninsular India: Data from the Gauribidanur seismic array
[DE88-701232] 15 p2093 N88-22471
Input-output characterization of fiber composites by SH waves
[NASA-CR-4153] 17 p2347 N88-23986

S-A-W DEVICES
U SURFACE ACOUSTIC WAVE DEVICES

S-N DIAGRAMS
Cyclic fatigue damage characteristics observed for simple loadings extended to multiaxial life prediction
[NASA-CR-182126] 18 p2531 N88-25016

SABOT PROJECTILES
A feasibility study of a hypersonic real-gas facility
[NASA-CR-180423] 01 p0008 N88-10043
Combined calculation of deformation and stress for the body and sabot of an APFSDS 03 p0302 N88-11899
Launchability of base-driven electromagnetic projectiles
[AD-A189635] 15 p2023 N88-22055

SACCADIC EYE MOVEMENTS
Influence of moving visual environment on saccadic eye movements and fixation 21 p2926 N88-27368

SACCHARIDES
U CARBOHYDRATES

SADDLE POINTS
Transient periodic behavior related to a saddle-node bifurcation
[ETN-88-91321] 05 p0642 N88-13928

SAFETY
NT AEROSPACE SAFETY
NT AIRCRAFT SAFETY
NT FLIGHT SAFETY
NT INDUSTRIAL SAFETY
NT REACTOR SAFETY
Human motor reactions to dangerous motions in robot operations
[PB87-222196] 03 p0361 N88-12275
General-Purpose Heat Source Safety Verification Test Program: Edge-on flyer plate tests
[DE87-006309] 03 p0376 N88-12362
DOE explosives safety manual
[DE88-000831] 04 p0422 N88-12616
Comparison of fire resistance of metallic and nonmetallic structures
[SNIAS-872-551-101] 05 p0572 N88-13489
Establishment of complete minimum test sets for digital circuits with safety engineering significance
[ETN-88-90599] 05 p0578 N88-13526
An independent evaluation of the CH-46 Safety Reliability and Maintainability Program (SR and M)
[AD-A186310] 07 p0817 N88-14971
Fault tree reliability analysis of the Naval Postgraduate School mini-satellite (ORION)
[AD-A186283] 07 p0866 N88-15250
Summary of the report of the Senior Committee on Environmental, Safety and Economic Aspects of Magnetic Fusion Energy
[DE88-003270] 07 p0937 N88-15692
Solid mechanics research for quantitative non-destructive evaluation
[AD-A186599] 08 p0993 N88-16010
ESSAA: Embedded system safety analysis assistant 08 p1060 N88-16396
Helicopter human factors research 09 p1109 N88-16644
Organic coatings to improve the storageability and safety of pyrotechnic compositions
[AD-A187158] 09 p1150 N88-16889
The TITAN Reversed-Field Pinch Reactor: Design-point determination and parametric studies
[DE88-001824] 09 p1251 N88-17498
Minimizing development flight test time and cost in the US Air Force 12 p1703 N88-20192
Characteristics of the positive lighting flash
[DE88-005854] 13 p1800 N88-20760

Burning characteristics and flammability of PVC cables in groups
[NASA-TT-20226] 14 p1893 N88-21303
Orbital transfer vehicle: Concept definition and system analysis study
[NASA-CR-179315] 15 p2024 N88-22060
United Nations deliberations of the use of nuclear power sources in space: 1978-1987 17 p2423 N88-24410
Discussions and agreements in the United Nations on important issues associated with nuclear power in space 17 p2423 N88-24411
Critical nuclear launch issues: A perspective from the State of Florida 17 p2423 N88-24412
Space reactor end of life issues 17 p2424 N88-24413
Designing to safe power limits in hybrid circuits
[DE88-005533] 18 p2506 N88-24865
Quality and productivity drive innovation and improvement at United Technologies Aerospace Operations, Inc.
[NASA-CR-182944] 18 p2525 N88-24983
Radiation safety in commercial air traffic
[NASA-TM-101156] 19 p2600 N88-25447
Pressure/temperature sensitive inorganic phosphors 19 p2627 N88-25583
Risk analysis in space system safety 22 p3161 N88-28825
Avionics system design for high energy fields: A guide for the designer and airworthiness specialist
[NASA-CR-181590] 23 p3178 N88-28919
Numerical field model simulation of full scale fire tests in a closed spherical/cylindrical vessel
[AD-A195067] 24 p3359 N88-29998
Improvement of head-up display standards. Volume 3: An evaluation of head-up display safety
[AD-A195787] 24 p3410 N88-30300

SAFETY DEVICES
NT ARRESTING GEAR
NT ESCAPE CAPSULES
The use of Kevlar on aero-engine fan containment casings
[PNR90410] 02 p0182 N88-11134
Spinoff, 1987
[NASA-TM-89652] 02 p0250 N88-11577
Experimental and mathematical investigation of response characteristics and aging phenomena in safety fuse elements
[ETN-88-91478] 11 p1480 N88-18832
Variable response load limiting device
[NASA-CASE-LAR-12801-1] 17 p2346 N88-23982
Timing control system
[NASA-CASE-NPO-16882-1-CU] 18 p2506 N88-24863

SAFETY FACTORS
Computer simulation of thermal modeling of primary lithium cells 02 p0163 N88-11022
Chemical analysis of charged Li/SO(sub)2 cells 02 p0163 N88-11026
Small space reactor power systems for unmanned solar system exploration missions
[NASA-TM-100228] 05 p0660 N88-14054
Safety implications of onboard refueling vapor recovery systems
[PB88-102603] 07 p0839 N88-15088
Safety philosophy, policy, and requirements for manned spaceflight. Volume 1: Executive summary
[HEG-0886/1036-VOL-1] 08 p0962 N88-15826
Post-Challenger evaluation of space shuttle risk assessment and management
[NASA-CR-182461] 12 p1705 N88-20202
Technical challenges in the development of a European space suit system and comparison with underwater suits 19 p2696 N88-26024
Safety aspects in design and operation practice of GKSS underwater simulation plant GUSI 19 p2698 N88-26037
Safety of extravehicular space activities 19 p2698 N88-26038
Reducing risks inherent in operating underwater craft: The contribution of classification, the example of the SAGA highly autonomous support submarine 19 p2699 N88-26042
Control of flight through microburst wind shear using deterministic trajectory optimization 20 p2761 N88-26375
The VIPER microprocessor
[RSRE-87014] 22 p3135 N88-28640
Study on long-term evolution towards European manned spaceflight. Volume 1: Executive summary
[ERNO-OX1-002/88-VOL-1] 24 p3330 N88-29827

SAFETY MANAGEMENT
Aircraft accident/incident summary reports: Unalaska, Alaska, September 25, 1985; Jenkinsburg, Georgia, September 29, 1985; Boston, Massachusetts, December 15, 1985; Dekalb, Texas, December 31, 1985; and Erie, Pennsylvania, February 21, 1986
[PB87-910408] 02 p0123 N88-10780
UV radiation: Human exposure to ultraviolet radiation
[PB87-137410] 06 p0752 N88-14619
Risk analysis methodology survey 07 p0922 N88-15604
Evaluate the application of modal test and analysis processes to structural fault detection in MSFC - STS project elements 07 p0927 N88-15630
Safety guidelines and procedures for bioscience-based industry and other applied microbiology
[PB87-140521] 08 p1045 N88-16316
Environmental projects. Volume 4: Asbestos survey
[NASA-CR-182527] 10 p1353 N88-18083
Conceptual design study of Fusion Experimental Reactor (FY86 FER): Safety
[DE88-751071] 10 p1411 N88-18418
Research field of fire technology in Finland
[DE88-751094] 11 p1467 N88-18747
Procedures for quantitative sensitivity and performance validation studies of a deterministic fire safety model
[NBS/GCR-88/544] 11 p1469 N88-18762
Spacecraft fire-safety experiments for space station: Technology development mission
[NASA-CR-182114] 13 p1731 N88-20353
Flame retardants
[NASA-TT-20250] 13 p1739 N88-20400
Safety research of insulating materials of cable for nuclear power generating station
[NASA-TT-20202] 13 p1752 N88-20477
EDF's studies and first choices regarding the design of electrical equipment
[NASA-TT-20222] 13 p1764 N88-20553
Environmental projects. Volume 5, part 1: Study of subsurface contamination. Part 2: Guide to implement environmental compliance programs
[NASA-CR-182691] 13 p1796 N88-20741
Nuclear safety as applied to space power reactor systems 17 p2415 N88-24360

SAGE SATELLITE
European validation of SAGE-2 aerosol profiles
[AERONOMICA-ACTA-A-327-1988] 23 p3234 N88-29243

SAHARA DESERT (AFRICA)
Discrimination of sand transport rates and environmental consequences in central Egypt from SPOT data 22 p3093 N88-28366

SAILPLANES
U GLIDERS

SALICYLATES
Method for sampling of methyl salicylate vapor in air using passivated stainless steel syringes and analysis by gas chromatography
[AD-A187838] 11 p1447 N88-18624

SALINITY
Porosity influence on the strength and elasticity of first-year sea ice
[AD-A184493] 03 p0354 N88-12233
Effects of rainfall on the seasonal thermocline
[AD-A184432] 04 p0472 N88-12912
Progress in the measurement of salinity and oxygen at the Woods Hole Oceanographic Institution
[PB88-108089] 06 p0748 N88-14598
Seasonal cycling of sulfur and iron in porewaters of a Delaware salt marsh
[NASA-CR-182385] 07 p0876 N88-15311
Multipurpose corrosion inhibitors for aerospace materials in Naval environments
[AD-A186728] 09 p1143 N88-16853
Physical properties of summer sea ice in the Fram Strait, June-July 1984
[AD-A186937] 09 p1194 N88-17156
Editing master oceanographic observation data set 4
[AD-A188405] 12 p1649 N88-19876
Determination of mean thermohaline characteristics of the ocean 13 p1784 N88-20675
Estimates of ocean-atmosphere thermal interaction in Gulf Stream energy-active test range in winter of 1984 13 p1785 N88-20679
Propagation of subsurface salinity maximum in tropical Atlantic 13 p1786 N88-20686
Space-time analysis of oceanographic fields by modified empirical orthogonal functions method 13 p1786 N88-20687
Intrathermocline lens of Mediterranean water in tropical North Atlantic 13 p1786 N88-20688
Model of hydrodynamic adjustment of temperature, salinity and current fields 13 p1789 N88-20700
Microwave and structural properties of saline ice
[AD-A189307] 13 p1803 N88-20779
YABLED cruises part 2: Data from YABLED-17 through YABLED-26, January-October 1985
[PB88-163597] 14 p1950 N88-21627
Physical, chemical and CTD (Conductivity/Temperature/Depth) data from the Marathon 2 expedition
[AD-A189930] 15 p2099 N88-22507
Hydrographic observations in the northwestern Weddell Sea Marginal Ice Zone during March 1986
[PB88-173240] 16 p2237 N88-23359
Influence of the Yukon River on the Bering Sea
[NASA-CR-182802] 17 p2376 N88-24126
Expendable conductivity, temperature and depth system (XCTD) development program
[AD-A192182] 18 p2547 N88-25121

SALIVA
Human adaptation to various hypercapnic conditions in relation to salivary electrolyte dynamics and renal function 12 p1664 N88-19977

SALT SPRAY TESTS
Corrosion behavior of sputter-deposited aluminum-based alloys exposed to chloride solutions
[AD-A187262] 10 p1303 N88-17794
Stress corrosion of C ring specimen in salt spray tests
[I-186/87] 21 p2916 N88-27307

SALTS
Turbine airfoil deposition models and their hot corrosion implications 02 p0189 N88-11178

SALYUT SPACE STATION
Basic results of medical studies during prolonged manned flights on-board the Salyut-7/Soyuz-T orbital complex
[NASA-TT-20217] 10 p1369 N88-18182
The USSR space systems for remote sensing of earth resources and the environment (sensor systems, processing techniques, applications) 17 p2356 N88-24035
The Soviet MIR space station
[AD-A194040] 23 p3184 N88-28951

SAMARIUM
NT SAMARIUM ISOTOPES

SAMARIUM ISOTOPES
Nd isotopes and crustal growth rate 24 p3392 N88-30203
Changing styles of crustal growth in Southern Africa: Constraints from geochemical and Sr-Nd isotope studies in Archaean to Pan African terrains 24 p3396 N88-30227

SAMPLED DATA
U DATA SAMPLING

SAMPLED DATA SYSTEMS
U DATA SAMPLING

SAMPLERS
Wet deposition and snowpack monitoring operations and quality assurance manual
[PB87-212817] 01 p0064 N88-10413

SAMPLES
Rosetta: A mission to sample the nucleus of a comet 14 p2005 N88-21958

SAMPLING
NT AIR SAMPLING
NT CORE SAMPLING
NT DATA SAMPLING
NT PARTICULATE SAMPLING
NT RANDOM SAMPLING
Fast dynamic studies with PC384-7B; system improvements and development of an automated blood sampling system --- tomography
[USIP-87-05] 01 p0075 N88-10481
Measurements in the functional mock up test of the NAL QSTOL aircraft control system
[NAL-TR-928] 02 p0126 N88-10793
The correspondence of surface climate parameters with satellite and terrain data
[NASA-CR-181515] 03 p0346 N88-12185
Superoxide dismutase assays
[AD-A183972] 03 p0356 N88-12242
Microcomputer control of a hydraulically actuated piston
[AD-A184130] 03 p0368 N88-12317
A mineral reconnaissance sampling manual for Costa Rica: Central American energy and resource project
[DE87-014997] 04 p0462 N88-12859
RRS DISCOVERY cruise 160, 30 June-25 July, 1986. Geochemical sampling over the Madeira and Porcupine Abyssal Plains
[PB87-222030] 04 p0471 N88-12910
An urn model for the multi-sample capture/recapture sequential tagging process
[AD-A184470] 04 p0496 N88-12998
Sample reuse in statistical remodeling
[AD-A184916] 05 p0643 N88-13938
Aviation turbine fuels from tar sands bitumen and heavy oils. Part 2: Laboratory sample production
[AD-A185744] 06 p0687 N88-14211

On determining the weight for obtaining a large number of items
[AD-A186181] 07 p0915 N88-15553
Regulation of nonlinear and generalized linear systems
[AD-A186706] 09 p1224 N88-17338
Practical applicability of exact and approximate forms of the randomization test for two independent samples
[AD-A186815] 09 p1231 N88-17381
The accommodative status in the dark of US Navy fighter pilots
[AD-A188188] 10 p1370 N88-18186
Using SIR (Scientific Information Retrival) system for data management during a field program
[DE88-001555] 10 p1424 N88-18508
Frequency-sampling design of two-dimensional FIR digital filters with nonuniform samples
[AD-A187773] 11 p1477 N88-18815
Ideal shrinking and expansion of discrete sequences
[NASA-TM-88202] 11 p1524 N88-19100
Sampling intervals
[AD-A189445] 12 p1573 N88-19408
Isotopic and chemical studies of early crustal metasedimentary rocks
[NASA-CR-182711] 14 p1944 N88-21601
Analysis of meteorological conditions and haze distribution for the Second Arctic Gas and Aerosol Sampling Program (AGASP 2), March-April 1986
[PB88-164140] 14 p1948 N88-21618
High speed, bandpass sampling of digital communications waveforms
[AD-A189842] 15 p2056 N88-22254
Empirical and hierarchical Bayes competitors of preliminary test estimators in two sample problems
[AD-A190327] 15 p2125 N88-22670
Instrumentation for ultrafast electronics
[AD-A191379] 16 p2193 N88-23080
Evaluation of an estimation system for an irrigated area in a tropical region through TM-LANDSAT imagery
17 p2363 N88-24075
A disposable liquid microcell for near-infrared reflectance analysis
[AD-A192190] 18 p2575 N88-25298
A non-contact picosecond prober for integrated circuit testing 19 p2655 N88-25766
Picosecond sampling of integrated circuits
19 p2655 N88-25767
Electro-optic sampling of high-speed, InP-based integrated circuits 19 p2655 N88-25769
An optically strobed sample and hold circuit
19 p2656 N88-25772
Comparison of sampling oscilloscopes with less than 35 ps transition durations 19 p2658 N88-25793
Asynchronous optical sampling for laser-based combustion diagnostics in high pressure flames
[AD-A192920] 20 p2770 N88-26428
Analysis of debris from accelerated life test of the Hughes five-year Vuilleumier cryocooler
[AD-A193101] 21 p2931 N88-27400
Sampling strategies for Monte-Carlo forecasting methods 22 p3126 N88-28583
Importance sampling for stochastic simulations
[AD-A193585] 22 p3138 N88-28654
Elemental composition of the Martian surface
23 p3302 N88-29665
Viking Landers and remote sensing
23 p3304 N88-29685
Recent observations of carbon monoxide in the Amazon Rain Forest
[INPE-4478-PRE/1245] 24 p3390 N88-30186
The dynamics of transuranics and other radionuclides in natural environments, December 1985
[DE87-014456] 24 p3390 N88-30189
New type of primitive meteorite found in Antarcitca
24 p3441 N88-30478

SAMPLING DEVICES
U SAMPLERS

SAN ANDREAS FAULT
Correlation of data on strain accumulation adjacent to the San Andreas Fault with available models
[NASA-CR-180757] 13 p1796 N88-20742
Geodetic measurement of deformation east of the San Andreas fault in Central California
[NASA-CR-182709] 13 p1798 N88-20754

SAND DUNES
U DUNES

SANDS
NT TAR SANDS
Environmental processes and spectral reflectance characteristics associated with soil erosion in desert fringe regions
[NASA-CR-182332] 05 p0620 N88-13811

SANDSTONES
Geological characterization and statistical comparison of outcrop and subsurface facies: Shannon Shelf sand ridges
[DE87-001243] 03 p0348 N88-12202
Abundance and distribution of ultramafic microbreccia in Moses Rock Dike: Quantitative application of AIS data
05 p0613 N88-13766

SANDWICH CONSTRUCTION
U SANDWICH STRUCTURES

SANDWICH STRUCTURES
Mechanical properties characterization of composite sandwich materials intended for space antenna applications
[NASA-TM-88893] 01 p0020 N88-10121
Process for producing sandwich mouldings
[EP-PATENT-0-191-623-A2] 04 p0426 N88-12642
Analysis of the voltage-current characteristics of metal-isolator-tin-telluride sandwich structures
[ETN-88-91089] 09 p1256 N88-17528

SANITATION
Evaluation of the Shasta Waterless System as a remote site sanitation facility
[AD-A186000] 07 p0898 N88-15442

SAPPHIRE
Measurement and analysis of cryogenic sapphire dielectric resonators and DROs
04 p0433 N88-12686
Laser enhanced adhesion of copper films to sapphire substrates
[DE88-006802] 15 p2038 N88-22144

SARCOMA
U CANCER

SARSAT
Antarctic field tests of SARSAT personal locater beacons
[NASA-TM-4008] 01 p0063 N88-10403
Search and rescue satellite system (SERES), phase A0
[ETN-88-92335] 18 p2472 N88-24669
COSPAS/SARSAT 406-MHz emergency beacon digital controller
[NASA-TM-100859] 20 p2792 N88-26566
KOSPAS-SARSAT satellites used for ocean current study 24 p3450 N88-30534

SAS
Annotated computer output for illustrative examples of clustering using the mixture method and two comparable methods from SAS
[AD-A184887] 03 p0364 N88-12292

SAS-D
U IUE

SATAN (SENSOR)
U TERRAIN ANALYSIS

SATELLITE ALTIMETRY
Precise orbit computation, gravity model adjustment and altimeter data processing for the ERS-1 altimetry mission
[ESA-CR(P)-2436] 02 p0130 N88-10820
An exploratory study of inland water and land altimetry using Seasat data
[ESA-CR(P)-2433] 02 p0193 N88-11208
GEOSAT altimeter geophysical data record user handbook
[PB87-213336] 03 p0276 N88-11743
Radial orbit error reduction and sea surface topography determination using satellite altimetry
04 p0462 N88-12861
Error assessments of widely-used orbit error approximations in satellite altimetry
[NASA-CR-182390] 07 p0823 N88-14998
An efficient algorithm for computing the crossovers in satellite altimetry
[NASA-CR-182389] 07 p0871 N88-15286
On estimating the basin-scale ocean circulation from satellite altimetry. Part 1: Straightforward spherical harmonic expansion
[NASA-CR-182387] 07 p0882 N88-15352
The effects of atmospheric and thermohaline variability on the validation of the GEOSAT altimeter oceanographic signal between Scotland and Iceland
[AD-A189324] 12 p1650 N88-19882
Seasat orbit determination experiments in preparation for the ERS-1 altimetry mission
[ETN-88-91842] 14 p1871 N88-21182
Study of the dynamic topography of oceans by means of satellite altimetry 14 p1938 N88-21567
From satellite altimetry to ocean topography, a survey of data processing techniques
[ETN-88-91841] 14 p1939 N88-21575
Determination of the ocean circulation by spaceborne radar altimeter 19 p2701 N88-26060
FORTRAN programs for computation of time dependent sea levels and trajectory errors from satellite altimeter data
[BONN-MITT-73] 21 p2901 N88-27216

Microwave instrument for planetary mission (Titan/CASSINI mission orbiter spacecraft)
[BAE-CS/TP-8359] 24 p3375 N88-30102
A study of the feasibility of using sea and wind information from the ERS-1 satellite. Part 1: Wind scatterometer data
[NASA-CR-182833] 24 p3386 N88-30167
A study of the feasibility of using sea and wind information from the ERS-1 satellite. Part 2: Use of scatterometer and altimeter data in wave modeling and assimilation
[ESA-CR(P)-2604-PT-2] 24 p3387 N88-30176

SATELLITE ANTENNAS
Study of advanced satellite concept using a multifeed reconfigurable antenna
[ESA-CR(P)-2406-VOL-1] 01 p0013 N88-10073
Study of advanced satellite concept using a multifeed reconfigurable antenna. Detailed report on mission definition, coverage analysis and performance requirements, antenna geometry
[ITS-TR-014.C/85] 01 p0013 N88-10074
Study of advanced satellite concept using a multifeed reconfigurable antenna. Detailed report on Polarization Sensitive Reflector (PSR) and offset parabolic antennas, Appendix 1
[ESA-CR(P)-2406-VOL-3] 01 p0013 N88-10075
Study of advanced satellite concept using a multifeed reconfigurable antenna. Appendix 3 : Feeding network, final performance analysis, study of reconfiguration possibilities
[ITS-TR-032/85] 01 p0014 N88-10076
Data Relay Satellite antenna subsystem study
[ESA-CR(P)-2435-VOL-2] 02 p0162 N88-11014
Study of antenna configuration for Data Relay Satellite (DRS) user spacecraft
[A5/516/86] 02 p0162 N88-11018
DRS (Data Relay Satellite) antenna subsystem study
[ESA-CR(P)-2435-VOL-1] 02 p0162 N88-11019
Studies of the structural dynamic behavior of satellite antenna system
[AD-A185526] 06 p0673 N88-14121
Space environmental effects on polymeric materials
[NASA-CR-182418] 07 p0838 N88-15082
ESA Bulletin No. 8
[ETN-87-90513] 09 p1122 N88-16718
European developments in antenna technology
09 p1123 N88-16725
Study of dual beam antenna systems for the data relay satellite, volume 1
[S-272-02-VOL-1] 09 p1152 N88-16905
Study of dual beam antenna systems for the data relay satellite. Volume 2: Executive summary
[S-272-03-VOL-2] 09 p1153 N88-16906
Study on a double reflector compact range — satellite antennas
[S-201-05] 09 p1153 N88-16908
Hemispherical pointing mechanism drive unit — satellite payloads antennas 14 p1874 N88-21193
A pointing mechanism for intersatellite link system
14 p1874 N88-21194
Some highlights on ROSAT mechanisms
14 p1874 N88-21195
Deployable booms and antennas on AMPTE-IRM
14 p1874 N88-21198
Aerospatiale unfurlable reflector and associated mechanisms 14 p1875 N88-21203
Design of a linear actuator and breadboard test result — far IR telescope 14 p1877 N88-21217
Photoelastic model tests of the Dornier linear actuator — far IR telescope 14 p1877 N88-21218
Fine adjustment mechanism for FIRST
14 p1878 N88-21219
The EURECA antenna deployment and retraction mechanisms 14 p1878 N88-21225
Development and qualification of the OLYMPUS antenna pointing mechanism 14 p1879 N88-21227
Antenna system for MSAT mission
19 p2651 N88-25742
Antenna technology for advanced mobile communication systems 19 p2651 N88-25743
Large antenna experiments aboard the space shuttle: Application of nonuniform sampling techniques
19 p2652 N88-25745
The 15-meter antenna performance optimization using an interdisciplinary approach 19 p2652 N88-25746
A microstrip array feed for MSAT spacecraft reflector antenna 19 p2652 N88-25747
Technologies for antenna shape and vibration control
19 p2652 N88-25748
Dynamics of satellites with radial wire antennas
20 p2784 N88-26514
Development of procedures for performing end-to-end tests on the ERS-1 radar altimeter and AMI using a compact antenna test range — Active Microwave Instrument (AMI)
[ESA-CR(P)-2558] 24 p3363 N88-30022

A 30/20 GHz multibeam array antenna suitable for future high rate TDMA European satellite networks
[ETN-88-93079] 24 p3365 N88-30037

SATELLITE ATMOSPHERES
Microwave instrument for planetary mission (Titan/CASSINI mission orbiter spacecraft)
[BAE-CS/TP-8359] 24 p3375 N88-30102

SATELLITE ATTITUDE CONTROL
Aerospace research at the National Aerospace Laboratory (NLR)
[ETN-87-90821] 01 p0107 N88-10697
The mechanical properties of solid state diffusion bonds between Ti-6Al-4V and 304L stainless steel
[BAJ-TR-113-1967] 03 p0332 N88-12093
Advanced gyros in spacecraft control. Digital capture loops for dry tuned gyros
[LITEF-120046] 08 p0962 N88-15827
Exploring hypotheses in attitude control fault diagnosis 08 p1058 N88-16384
Control and stabilization of ESA satellites 09 p1124 N88-16734
Fine attitude measurement system study. Volume 1: Executive summary
[BAE-TP-7831-VOL-1] 09 p1133 N88-16795
Fine attitude measurement system study, volume 2
[BAE-TP-7831-VOL-2] 09 p1133 N88-16796
Fine attitude measurement system study. Volume 3: Appendices
[BAE-TP-7831-VOL-3] 09 p1133 N88-16797
Preliminary design of the ORION attitude control system
[AD-A187179] 10 p1292 N88-17729
Investigation of the spin stability of the NPS (Naval Postgraduate School) mini-satellite (Orion)
[AD-A187781] 11 p1445 N88-18613
Construction aspects of testbeds for attitude control systems simulation of artificial satellites
[INPE-4283-PRE/1155] 11 p1445 N88-18616
Table with aerostatic bearings for simulation in one degree of freedom of Attitude Control Systems of artificial satellites
[INPE-4320-TDL/287] 11 p1445 N88-18617
Reaction wheel experimental model of artificial satellite attitude control: Construction, simulation, and tests
[INPE-4274-PRE/1146] 11 p1490 N88-18896
Design of a spherical air bearing simulator for tests of the attitude control system of artificial satellites
[INPE-4284-PRE/1155] 12 p1595 N88-19551
Table with aerostatic bearings for simulation in one degree of freedom attitude control systems of artificial satellites
[INPE-4272-PRE/1144] 12 p1595 N88-19552
Reaction wheel control through digital technique using reference models
[INPE-4220-PRE/1100] 12 p1599 N88-19570
Simulation and tests of a satellite attitude and orbit control system. General considerations concerning an example case (INPE) and design of a servo rate table
[INPE-4282-PRE/1154] 12 p1599 N88-19572
Attitude control of an artificial satellite through the extension of the linear quadratic regulator theory
[INPE-4407-TDL/304] 12 p1600 N88-19577
Cold gas jet system for satellite attitude control-modeling and simulation
[INPE-4279-PRE/1150] 12 p1601 N88-19583
Modeling of a nutation damper for satellite stabilization through rotation
[INPE-4275-PRE/1147] 12 p1601 N88-19584
Development of integrated detectors for attitude sensors
[INPE-4409-PRE/1222] 12 p1602 N88-19586
Gas consumption estimation of an attitude control system of an artificial satellite (utilizing DRF) in limit cycle phase
[INPE-4338-RPE/553] 13 p1731 N88-20350
An advanced low-cost 2-axis active magnetic bearing flywheel — satellite attitude control 14 p1877 N88-21213
High lifetime mechanisms implemented in infrared horizon scanning sensors — SPOT 14 p1877 N88-21214
Evolution of large momentum and reaction wheels 14 p1879 N88-21230
Nutational stability of a satellite equipped with an active magnetic momentum wheel 20 p2784 N88-26513
Dynamics of satellites with radial wire antennas 20 p2784 N88-26514
Study of a safe attitude for the Infrared Space Observatory (ISO) during perigee pass
[SNIAS-881-440-113] 23 p3185 N88-28954
SCARES: A Spacecraft Control Anomaly Resolution Expert System 23 p3256 N88-29381

SATELLITE ATTITUDE DISTURBANCE
U SPACECRAFT STABILITY

SATELLITE CAPTURE
U SPACECRAFT RECOVERY

SATELLITE COMMUNICATION
The criterion of equal integrated quality: An improved method of planning DBS systems
[BBC-RD-1987/10] 02 p0161 N88-11012
Estimates of satellite EHF communication outages due to attenuation by rain
[AD-A183969] 03 p0307 N88-11941
An allotment planning concept and related computer software for planning the fixed satellite service at the 1988 space WARC
[NASA-TM-100244] 03 p0308 N88-11944
A statistical rain attenuation prediction model with application to the advanced communication technology satellite project. Part 2: Theoretical development of a dynamic model and application to rain fade durations and tolerable control delays for fade countermeasures
[NASA-TM-100242] 03 p0308 N88-11945
Design description report for a photovoltaic power system for a remote satellite earth terminal
[NASA-CR-179586] 04 p0465 N88-12875
Error control techniques for satellite and space communications
[NASA-CR-181581] 05 p0576 N88-13516
Round table on the future of satellite communications and broadcasting in Europe
[ESA-STR-221] 07 p0843 N88-15112
Transient electromagnetic scattering from heterogeneous lossy spheres
[AD-A186869] 09 p1152 N88-16903
Comparison of direct and heterodyne detection optical intersatellite communication links 09 p1169 N88-17013
Complementary satellite sound broadcasting systems: A NASA assessment for the Voice of America
[NASA-TM-100300] 10 p1321 N88-17899
Digital bit error rate estimator for telemetry links
[INPE-4351-TDL/295] 12 p1598 N88-19563
Alternative force structuring strategies for military satellite communication systems
[AD-A189492] 13 p1758 N88-20516
Effect of atmospheric turbulence on the bit error probability of a space to ground near infrared laser communications link using binary pulse position modulation and an avalanche photodiode detector
[NASA-TM-100699] 14 p1873 N88-21189
Real-time environmental Arctic monitoring (R-TEAM)
[AD-A189948] 15 p2099 N88-22508
Error control techniques for satellite and space communications
[NASA-CR-182886] 17 p2332 N88-23922
Experiments applications guide: Advanced Communications Technology Satellite (ACTS)
[NASA-TM-100265] 22 p3048 N88-28082
A statistical rain attenuation prediction model with application to the advanced communication technology satellite project. 1: Theoretical development and application to yearly predictions for selected cities in the United States
[NASA-CR-179496] 23 p3205 N88-29077
Comparative analysis of passive communications satellites employing the SHF and HF spectrum for use in a strategic role
[AD-A194682] 24 p3362 N88-30019
Signals and systems 24 p3363 N88-30026

SATELLITE CONFIGURATIONS
Evaluation of a cryogenic refrigerator for cooling focal plane instrumentation. Appendix B: Accommodation study — satellite instruments
[BAE-TP-8095-VOL-2] 05 p0572 N88-13486
Study of reconfigurable payloads for direct broadcast satellites, summary
[DBS87-0004] 09 p1135 N88-16808
System configuration management — space systems 22 p3160 N88-28813
PSDE/SAT 2: Preliminary spacecraft configuration study, executive summary
[ESA-CR(P)-2618] 24 p3333 N88-29840

SATELLITE CONTROL
NT SATELLITE ATTITUDE CONTROL
ESA Bulletin No. 10
[ETN-87-90514] 09 p1123 N88-16728
Range and mission scheduling automation using combined AI and operations research techniques 09 p1209 N88-17249
Attitude and orbit control for the AMPTE-UKS (Active Magnetospheric Particle Tracer Explores-UK Subsatellite): Evaluation of the in-flight performance
[PB87-225199] 19 p2604 N88-25467

SATELLITE DEFENSE
U SPACECRAFT DEFENSE

SATELLITE DESIGN
The new generation of SPOT satellites 03 p0345 N88-12178
Mechanical design of the ac bracket package for the RETE experiment
[IFSI-87-4] 05 p0555 N88-13379
A geostationary imaging spectrometer TOMS instrument 05 p0619 N88-13802
Fault tree reliability analysis of the Naval Postgraduate School mini-satellite (ORION)
[AD-A186283] 07 p0866 N88-15250
Specialist support for projects: Activities, methods and infrastructure 09 p1124 N88-16729
Lightsats and their attraction to budget oriented Federal agencies 10 p1289 N88-17711
Into the thermosphere: The atmosphere explorers
[NASA-SP-490] 10 p1353 N88-18084
Investigation of the spin stability of the NPS (Naval Postgraduate School) mini-satellite (Orion)
[AD-A187781] 11 p1445 N88-18613
A logical structuration for an administration of space projects
[INPE-4435-TDL/310] 12 p1585 N88-19482
Study of the optimization of satellite system design for transfer orbit
[MBB-URV-135] 13 p1727 N88-20332
CRRES chemical release mechanisms 14 p1874 N88-21192
Definition and implementation study for the Varan-S radar
[CNES-CT/DRT/TIT/RL-143-T] 15 p2058 N88-22267
Structural acoustics design manual
[ESA-PSS-03-1201-ISSUE-1] 17 p2311 N88-23821
MSAT-X: A technical introduction and status report
[NASA-CR-182921] 17 p2334 N88-23933
The high-throughput X-ray spectroscopy mission E6889478 MN513835 — ESA program
[ESA-SP-1092] 17 p2450 N88-24554
Starting point of a project: Decision mechanisms — space projects 22 p3159 N88-28806
PSDE/SAT 2: Preliminary spacecraft configuration study, executive summary
[ESA-CR(P)-2618] 24 p3333 N88-29840
Low cost satellite
[ESA-CR(P)-2560] 24 p3334 N88-29844

SATELLITE DOPPLER POSITIONING
The sequential evaluation of Doppler satellite observations
[REPT-141] 01 p0010 N88-10057
Solid Earth mission end-to-end data system study
[C04825.08/FR] 17 p2309 N88-23811
Specifications and performance of ultrastable oscillators in the DORIS orbitography and positioning system
[ETN-88-92761] 24 p3331 N88-29831

SATELLITE DRAG
Gradiometer accommodation on board a drag-free satellite 12 p1645 N88-19650
Using nonstationary models of the atmosphere to describe satellite drag 24 p3445 N88-30502

SATELLITE GROUND SUPPORT
Training in satellite ground system operations 09 p1129 N88-16775

SATELLITE GROUND TRACKS
An intelligent tutor for the space domain 09 p1204 N88-17217

SATELLITE IMAGERY
Object-dependent atmospheric influence on LANDSAT recordings 01 p0065 N88-10420
GOES observations for the FIRE/SRB Wisconsin experiment region from October 11 through November 2, 1986
[NASA-TM-100485] 01 p0071 N88-10453
Estimation from satellite imagery of summertime rainfall over varied space and time scales
[PB87-203246] 01 p0071 N88-10454
Tropical cyclone center locations from enhanced infrared satellite imagery
[PB87-213450] 01 p0071 N88-10455
Study, design, and evaluation of data reduction by encoding or information extraction. Part 1: Data generation analysis — multispectral satellite imagery
[NLR-TR-85094-L-PT-1] 01 p0078 N88-10501
Study, design and evaluation of data reduction by encoding or information extraction. Part 2: Operational considerations — multispectral satellite imagery
[NLR-TR-85094-L-PT-2] 01 p0079 N88-10502
Study, design and evaluation of data reduction by encoding or information extraction. Part 3: Algorithm design — multispectral satellite imagery
[NLR-TR-85094-L-PT-3] 01 p0079 N88-10503
Study, design and evaluation of data reduction by encoding or information extraction. Part 4: Performance demonstration — multispectral satellite imagery
[NLR-TR-85094-L-PT-4] 01 p0079 N88-10504
Study, design and evaluation of data reduction by encoding or information extraction. Part 5: Algorithm implementation aspects — multispectral satellite imagery
[NLR-TR-85094-L-PT-5] 01 p0079 N88-10505
An introduction to the GOES I-M imager and sounder instruments and the GVAR retransmission format
[NOAA-TR-NESDIS-39] 02 p0140 N88-10884

Operational cloud-clearing techniques of VAS radiance data --- Visible and Infrared Spin Scan Radiometer Atmospheric Sounder (VAS) 02 p0201 N88-11256
Observation of the development of mesoscale systems by operational meteorological satellites 02 p0201 N88-11259
The use of satellite IR data in the enhancement of surface thermal fields 02 p0202 N88-11260
The importance of mesoscale waves in the upper troposphere for formation of cloud and precipitation areas 02 p0203 N88-11273
On the interaction between radar and satellite image nowcasting systems and mesoscale numerical models 02 p0204 N88-11277
Satellite imagery and conceptual models in mesoscale forecasting 02 p0205 N88-11282
Evaluation of the Rainsat precipitation analysis system in real-time use 02 p0205 N88-11283
The Pacific Weather Center Satellite Facility: An overview 02 p0205 N88-11286
Simulation of mesoscale satellite sounder data from a mesoscale numerical model 02 p0214 N88-11345
Mesoscale forecasting with satellite data: Challenges and opportunities for today and tomorrow 02 p0215 N88-11353
SPOT 1: First In-Flight Results --- conferences [ISBN-2-85428-177-2] 03 p0340 N88-12143
Development of the SPOT commercial service: Preliminary conclusions after six months of operations 03 p0340 N88-12144
Satimage and the Nordic SPOT market 03 p0340 N88-12145
SPOT Image Corporation: Early results 03 p0340 N88-12146
The Canadian SPOT program 03 p0340 N88-12147
First assessment of processing and use of SPOT images by the Institut Geographique Nationale --- French National Geographic Institute 03 p0341 N88-12148
Results of the satellite and the Toulouse (France) receiving station operator --- SPOT 03 p0341 N88-12149
Signal to noise ratios --- SPOT images 03 p0341 N88-12150
Modulation transfer function --- SPOT 03 p0341 N88-12153
Intrinsic and extrinsic geometric quality --- SPOT images 03 p0341 N88-12154
Registration of SPOT images 03 p0341 N88-12155
Evaluation of SPOT stereoscopic possibilities for cartography 03 p0342 N88-12156
Feasibility study of a range of products drawn from SPOT satellite imagery and specific to road-laying studies 03 p0342 N88-12157
Adaptation of numerical SPOT data to an urban environment 03 p0342 N88-12158
Cartography and topography with SPOT 03 p0342 N88-12159
Application of SPOT-1 data to mineral exploration in Nevada 03 p0343 N88-12163
Geological interpretation of a SPOT image over Kenya: The Gregory rift network of faults 03 p0343 N88-12164
Vegetation studies in the national Park of Comoe (Ivory Coast) using SPOT 1 satellite data 03 p0343 N88-12166
The contribution of satellite data in drawing up maps used in rural development 03 p0343 N88-12167
SPOT data for crop discrimination in southern Brazil 03 p0343 N88-12169
SPOT: A tool for agricultural statistics 03 p0344 N88-12170
Stand based forest inventory from SPOT IMAGE. First experiments 03 p0344 N88-12173
Use of SPOT images for coastal development and inventory of aquacultural sites in New Caledonia (ALIAS project). First results 03 p0344 N88-12175
Contribution of SPOT data to the physiographic study of coastal environment: La Pointe d'Arcay and l'Anse de l'Aiguillon (France) 03 p0344 N88-12176
The use of SPOT images for water resources surveys. The examples of the Kasserine area (Tunisia) and the Jebel Amour (Algeria) 03 p0345 N88-12179
Eastern - western Arctic Sea ice analysis 1986 [AD-A184016] 03 p0355 N88-12235
Cloud cover determination in polar regions from satellite imagery [NASA-CR-181544] 04 p0471 N88-12908
Tropical easterly jet located using TOMS data 05 p0616 N88-13783
Application of TOMS data to weather analysis models 05 p0617 N88-13787
National Point Of Contact (NPOC)-SPOT inquiry 1986 [NLR-MP-86055-U] 05 p0620 N88-13807
Study on data compression systems for operational remote sensing --- meteosat imagery [NLR-TR-86029-L] 05 p0620 N88-13808
High resolution satellite imagery simulation --- treaty verification [FOA-C-30462-3.3,9.3] 05 p0620 N88-13810
Mesoscale applications of high resolution imagery [AD-A185039] 05 p0627 N88-13833
AVHRR/HIRS (Advanced Very High Resolution Radiometer/High Resolution Infra-Red Sounder) operational method for satellite based sea surface temperature determination [PB88-107594] 06 p0708 N88-14340
Remote sensing in mineral exploration [PB87-138558] 06 p0729 N88-14484
Automated satellite cloud analysis: A multispectral approach to the problem of snow/cloud discrimination [AD-A185672] 06 p0746 N88-14591
Solar-geophysical activity reports for STIP (Study of Travelling Interplanetary Phenomena) Interval 15, 12-21 February 1984 ground level event and STIP Interval 16, 20 April-4 May 1984 Forbush decrease [PB87-232658] 06 p0805 N88-14915
Review of the potential of satellite remote sensing for marine flood protection [IOS-237] 07 p0870 N88-15280
An investigation of offshore circulation using satellite data and feature tracking techniques [AD-A186271] 07 p0881 N88-15347
Space photographs of the Onega-Ladoga isthmus and prediction of useful minerals 08 p1008 N88-16108
French activities in ocean colour observations 08 p1043 N88-16303
Earthnet's experience with Seasat SAR image processing 09 p1127 N88-16760
Technical assessment of the joint CSIRO/Bureau of Meteorology proposal for a geostationary imager/sounder over the Australian region [RTP-15] 09 p1135 N88-16811
Detection of soil erosion with Thematic Mapper (TM) satellite data within Pinyon-Juniper woodlands [NASA-CR-182476] 09 p1185 N88-17103
A multiple-satellite observation of the high-latitude auroral activity on 11 January 1983 [AD-A175170] 09 p1189 N88-17122
Nature and origin of mineral coatings on volcanic rocks of the Black Mountain, Stonewall Mountain, and Kane Springs Wash volcanic centers, Southern Nevada [NASA-CR-181437] 09 p1191 N88-17140
Meteorological Information Extraction Center (MIEC) processing --- Meteosat imagery [ESA-STR-224] 09 p1192 N88-17143
Introduction to the Meteosat system [ESA-SP-1041] 09 p1193 N88-17146
Application of satellite data in variational analysis for global cyclonic systems [NASA-CR-182468] 09 p1193 N88-17152
Handbook of the GEMS image processing system [RAE-TR-86062] 09 p1219 N88-17310
Inexpensive solution for the mass distribution of satellite images [PB88-114038] 10 p1317 N88-17873
Analysis of quasi-geostrophic forcing during the AIMCS (Airborne Investigations of Mesoscale Convective Systems) Project. Volume 2: Results for June 14 through July 16, 1984 [PB88-123807] 10 p1354 N88-18092
Character of five selected LANDSAT lineaments in southwestern Pennsylvania: Report of investigations, 1987 [PB88-133517] 11 p1505 N88-18988
An application of digital cartography updating middle and small scale thematic maps using orbital data [INPE-4460-TDL/317] 12 p1637 N88-19805
Influence of solar illumination conditions on TM/Landsat data [INPE-4463-TDL/320] 12 p1638 N88-19806
Comparison of simulation modeling and satellite techniques for monitoring ecological processes [NASA-CR-182592] 12 p1641 N88-19825
Mesoscale monitoring of the soil freeze/thaw boundary from orbital microwave radiometry [NASA-CR-182659] 12 p1645 N88-19855
Dynamical and photometric studies of Saturn's rings 12 p1711 N88-20241
An investigation of Doppler satellite positioning multi-station adjustment software 13 p1730 N88-20345
Restoration techniques for redisplay of LANDSAT-5 satellite imagery [INPE-4189-PRE/1076] 13 p1791 N88-20712
Analysis for architecture for image processing [INPE-4294-PRE/1165] 13 p1791 N88-20715
Aspects and applications of primary processing of visual information [INPE-4290-PRE/1161] 13 p1841 N88-21015
IUE program SUGSD: Varability time scale of H Ly-alpha from Uranus [NASA-CR-182706] 13 p1856 N88-21107
Optical properties of Southern Hemisphere aerosols: Report of the joint CSIRO/NASA study [NASA-CR-179287] 14 p1945 N88-21605
Image processing on VEGA pictures 14 p2009 N88-21983
Geometric restoration of satellite image data [AD-A190462] 15 p2089 N88-22450
Satellite UV image processing [AD-A190466] 15 p2089 N88-22451
Project CODEAMA/FUNCATE (test-area of Barreirinha-AM): Field report [INPE-4500-RPE/563] 15 p2090 N88-22455
Comparative utilization of analog and digital processes in the treatment of MSS-LANDSAT data for studying the national parks of Brazil [INPE-4011-TDL/240] 15 p2090 N88-22456
Calibration and processing of AVHRR data for temperature estimation [INPE-4493-PRE/1257] 15 p2095 N88-22485
Detection, monitoring and analysis of some environmental effects of fires in the Amazon region through utilization of NOAA and LANDSAT satellite imagery and aircraft data [INPE-4503-TDL/326] 16 p2230 N88-23322
Validate algorithms for the determination of rainfall rates from SSM/I microwave satellite imagery [AD-A188769] 16 p2233 N88-23337
NOAA-ERL-ARL (National Oceanic and Atmospheric Administration-Environmental Research Laboratories-Air Resources Laboratory) solar UV radiation and climate research project: Program description [PB88-169396] 16 p2233 N88-23339
Validate algorithms for the determination of rainfall rates from SSM/I microwave satellite imagery [AD-A191337] 16 p2236 N88-23353
Updating land-use of the Sao Jose dos Campos municipality through remote sensing data [INPE-4479-RPE/562] 16 p2287 N88-23693
A low cost automatic Earth observation satellite tracking ground receiving station 17 p2309 N88-23815
Meteorological Satellite Center Technical Note No. 16 [ISSN-0388-9653] 17 p2350 N88-24003
Latitudinal and seasonal variation of the cloud characteristic parameters and their effects on the cloud classification 17 p2351 N88-24005
Some problems with regard to the TOVS processing detected by using NOAA-HRPT data check program 17 p2351 N88-24009
Enhanced infra-red picture of LR-FAX for spring and autumn seasons 17 p2351 N88-24011
Latin American Symposium on Remote Sensing, 4th Brazilian Remote Sensing Symposium and 6th SELPER Plenary Meeting, volume 1 17 p2352 N88-24013
A comparison of supervised maximum likelihood and decision tree classification for crop cover estimation from multitemporal LANDSAT MSS data 17 p2352 N88-24014
Mapping from LANDSAT and SPOT satellite imagery 17 p2352 N88-24018
Spectral measurements for correcting LANDSAT data for atmospheric effects 17 p2353 N88-24020
Mapping soil and rock variation from satellite images in the Sahel 17 p2354 N88-24023
An integrated study of the Alto Paranaiba Kimberlite Province, Minas Gerais, Brazil: A possible tool for diamond exploration 17 p2355 N88-24031
Satellite remote sensing of turbidity and sediment concentration in Lagoa dos Patos 17 p2355 N88-24032
Practical image analysis using personal computers: The Canadian experience 17 p2356 N88-24037
Presentation of the METEOSAT system and the roles of EUMETSAT within the meteorological community 17 p2357 N88-24039
ERS-1 data products and services and their value for tropical countries 17 p2357 N88-24040
Estimation of an area cultivated with wheat from LANDSAT data through a two-phase sampling method 17 p2357 N88-24041
Utilization of TM/LANDSAT images in the implanted forests mapping in the Mogi-Guacu Region (SP-Brazil) 17 p2357 N88-24042
Anomalies in the vegetation in the Alto Xingu - MT 17 p2357 N88-24043
Remote sensing techniques in the estimation of the area cultivated with beans, corn, and castor beans in the Irece County (Bahia State) 17 p2358 N88-24045
CANASATE: Sugar cane mapping by satellite 17 p2358 N88-24046
Spectral behavior of crops through analysis of LANDSAT-TM data 17 p2358 N88-24047

Identification of areas cultivated with soybeans in the cerrados regions, through digital processingof satellite images: A methodological approach
17 p2358 N88-24048
Structure and dynamics of vegetation in the middle semi-arid tropics. Quixaba's Caatinga (PE): Terrain analysis of MSS/LANDSAT data 17 p2358 N88-24049
Study of fracturing for groundwater research in the Sergipe state with remote sensing products
17 p2359 N88-24052
A system for determination of wind fields using geostationary meterological satellites
17 p2360 N88-24056
Digital processing of infrared and visible images from the GOES satellite and its integration with meteorological radar data 17 p2360 N88-24057
Thematic mapping utilizing data from the Thematic Mapper sensor of the LANDSAT satellite
17 p2361 N88-24060
Geometric image correction: An approach for the registration of LANDSAT-TM digital images supported by topographical maps of medium and great scales
17 p2361 N88-24061
Generation of thematic maps for updating aeronautical pilot charts utilizing LANDSAT-TM images
17 p2361 N88-24062
Evolution of a family of image processing systems at INPE 17 p2361 N88-24065
Spectral measurements for correcting LANDSAT data for atmospheric effects 17 p2362 N88-24066
Analysis of the parameters responsible for the variations of the illumination conditions in the LANSAT data
17 p2362 N88-24070
Tornado tracks in Southwestern Brazil, Eastern Paraguay, and Northwestern Argentina
17 p2362 N88-24071
Interpretation of MSS/LANDSAT data for evaluation of physical distribution of mangroves in Cananeia-Iguape (SP) 17 p2363 N88-24072
Evaluation of an estimation system for an irrigated area in a tropical region through TM-LANDSAT imagery
17 p2363 N88-24075
Study of reservoir water quality utilizing remote sensing techniques: Methodological concepts
17 p2364 N88-24076
Utilization of LANDSAT-TM imagery in the hydroenergetic inventory of the Paraiba de Sul River Basin 17 p2364 N88-24077
Evaluation of the floodable area of the canal of Sao Goncalo through TM-LANDSAT 5 imagery
17 p2364 N88-24078
Automatic registration of satellite imagery
17 p2364 N88-24080
Visualization of digital terrain models
17 p2364 N88-24081
Application of its transformation in color enhancement of LANDSAT imagery 17 p2365 N88-24082
Evaluation of a flood period (June, 1984) in the southern region of Laguna dos Patos, through remote sensing data, meteorological and oceanographic
17 p2365 N88-24083
Detection of biomass burning and smoke plumes in the Amazon region through NOAA satellite imagery
17 p2365 N88-24085
Evaluation of the mangrove area at the Piaui River (SE) through remote sensing 17 p2365 N88-24086
Dune fields in central Western Argentina
17 p2366 N88-24088
The breaked anticlines, cuesta and crest homoclines, ortoclinal valleys, and other forms of relief outcrops delineated with the help of remote sensing imagery
17 p2366 N88-24089
Mapping of plant associations and the variation of surface water in the Pantanal Mato-Grossense National Park, through remote sensing techniques
17 p2366 N88-24092
Temporal analysis of the changes in Parque Estadual de Jacupiranga vegetation through digital treatment of LANDSAT imagery 17 p2367 N88-24094
Evaluation of TM false color composites for crop discrimination 17 p2367 N88-24096
Some geological aspects of the Pirapemas Lineament Belt 17 p2368 N88-24099
Lithostructural interpretation of Chapda do Cachimbo (Pa-Am-Mt), based on radar and LANDSAT imagery
17 p2368 N88-24100
Research on enhancing the utilization of digital multispectral data and geographic information systems in global habitability studies
[NASA-CR-182799] 17 p2368 N88-24101
Terrain classification using SPOT images and the computer system GOP-300
[FOA-C-20677-2.7] 17 p2368 N88-24102
Coupling of satellite remote sensing to digitized topographic map to detect changes in land use
[B8735129] 17 p2369 N88-24104
Influence of the Yukon River on the Bering Sea
[NASA-CR-182802] 17 p2376 N88-24126
Ice conditions along the Ohio River as observed on LANDSAT images, 1972-1985
[AD-A191172] 18 p2531 N88-25018
DMSP-SSM/1 NASA algorithm validation using primarily LANDSAT and secondarily DMSP and/or AVHRR visible and thermal infrared satellite imagery
[NASA-CR-182979] 18 p2532 N88-25024
Monitoring biological impacts of space shuttle launches from Vandenberg Air Force Base: Establishment of baseline conditions
[NASA-TM-100982] 18 p2549 N88-25133
Application of dynamic programming to image registration
[ENST-87E022] 18 p2557 N88-25180
The Io sulfur torus in 1981
[NASA-TM-101139] 18 p2595 N88-25419
National Meeting on Remote Sensing Applied to Municipal Planning 19 p2681 N88-25939
Mapping of land use in Sao Jose dos Campos municipality by remote sensing, an aid for the elaboration of its PDDI 19 p2681 N88-25940
Technique to obtain the agricultural ownership limits by satellite imagery, to approve control, and to accompany agricultural activity 19 p2682 N88-25943
The use of satellite imagery for municipal conditions in rural recording in Pereira Barreto (SP)
19 p2682 N88-25944
The impact of hemp production on the development of the municipalities of Araras, Leme, Santa Cruz da Conceicao and Pirassununga 19 p2683 N88-25948
Application of remote sensing in the conservation of natural areas: Ribeira Valley 19 p2683 N88-25949
Use of remote sensing in the study of superficial formation certifying the development of integrated economy-case example: Rio Claro (SP) region
19 p2683 N88-25950
Canopy reflectance modeling in a tropical wooded grassland
[NASA-CR-182981] 19 p2685 N88-25961
Separability of cultivation through digital analysis of SPOT and TM data
[INPE-4541-PRE/1287] 19 p2685 N88-25963
Suggested hurricane operational scenario for GOES I-M
[NASA-TM-89729] 19 p2692 N88-26002
Bathymetry estimation by analyzing swell on SPOT images 19 p2701 N88-26062
Image processing applied to quantitative numerical cartography of ocean circulation
19 p2702 N88-26065
Methods for processing satellite images and their application to underwater operations
19 p2702 N88-26066
Checkout system software for INPE satellites
[INPE-4554-PRE/1297] 19 p2715 N88-26120
Meteorological satellite product support and research for project GALE
[NASA-CR-180989] 19 p2727 N88-26193
Voyager imaging photometry and radiative transfer modeling of the spoke-like features in Saturn's outer B-ring 19 p2742 N88-26278
Interpreting forest biome productivity and cover utilizing nested scales of image resolution and biogeographical analysis
[NASA-CR-183036] 20 p2817 N88-26711
Hydrologic models for land-atmosphere retrospective studies of the use of LANDSAT and AVHRR data
[NASA-CR-182861] 20 p2817 N88-26712
Hydrologic models for land-atmosphere retrospective studies of the use of LANDSAT and AVHRR data
[NASA-CR-182862] 20 p2818 N88-26716
Validate algorithms for the determination of rainfall rates from SSM/I microwave satellite imagery
[AD-A192299] 21 p2974 N88-27664
SPOT 1 Image Utilization, Assessment, Results
[ISBN-2-85-428188-8] 22 p3089 N88-28346
The contribution of remote sensing to hydrology and hydrogeology 22 p3090 N88-28347
Mapping of streamflow and soil infiltration of a Sahelian catchment area by SPOT image interpretation: The Oursi pond catchment area in Burkino Faso
22 p3090 N88-28348
The use of SPOT images for water resources surveys in the Kasserine Basin (Tunisia)
22 p3090 N88-28349
SPOT image exploitation for glacial mass balance fluctuation monitoring in the French Alps
22 p3090 N88-28350
SPOT on land and lakes in the Hubei Province (China)
22 p3090 N88-28351
Evaluation of SPOT imagery for monitoring irrigated lands 22 p3090 N88-28352
An evaluation of SPOT imagery for wetland monitoring
22 p3091 N88-28353
Comparative study of crop and soil mapping using multitemporal and multispectral SPOT and LANDSAT data 22 p3091 N88-28354
Water resources and agricultural land use investigations in northeastern Gujarat (India) 22 p3091 N88-28355
Study of the forests on the banks of the Gambia and criteria for detecting mortality 22 p3091 N88-28356
Use of SPOT satellite in agrohydrology: Detection of spring water excess in a grassland region
22 p3091 N88-28357
Review of the studies of geography and environment and studies on spectral characteristics of SPOT HRV data 22 p3091 N88-28358
Evaluation of the grassy biomass in the Sahelian zone in the South Tamesna region (Niger): Prospects and limits of use of SPOT data 22 p3092 N88-28359
Changes in species composition of heathland, monitored by means of remote sensing and field mapping: The results of the HEISPOT project 22 p3092 N88-28360
Topography of an Antartic ice stream
22 p3092 N88-28361
Spatial and spectral registration of Javanese landscape units with SPOT 22 p3092 N88-28362
Comparison between the respective contributions of the TM LANDSAT-4 and HRV SPOT-1 data to the land use mapping of Mediterranean coastal zone
22 p3092 N88-28363
Land use systems and rural landscapes in the center of Veracruz State (Mexico): First results
22 p3092 N88-28364
SPOT for earthquake hazard zoning in southern Italy
22 p3093 N88-28365
Discrimination of sand transport rates and environmental consequences in central Egypt from SPOT data
22 p3093 N88-28366
Delineation of ephemeral fluvial networks on low-relief Piedmont surfaces, Plutonium Valley, Nevada, USA
22 p3093 N88-28367
Following the seasonal evolution of a natural environment in a humid tropical region. Preliminary Evaluation of SPOT (PEPS) number 186: Bangui, Central Africa 22 p3093 N88-28368
Application of SPOT to agricultural information systems in temperate regions 22 p3093 N88-28369
Potential use of SPOT satellite data for the national resources inventory 22 p3093 N88-28370
Methodological developments on crop inventories using SPOT and ground surveys 22 p3094 N88-28371
Evaluation of annual crop surfaces and territorial inventory in the Paris basin by combining classic statistical inquiries and SPOT data (Preliminary Evaluation Program for SPOT 127) 22 p3094 N88-28372
Evaluation of automatic texture analysis for increased crop identification accuracy with SPOT data
22 p3094 N88-28373
Application of SPOT multidate data to wheat yield estimation in Beauce (France) 22 p3094 N88-28374
An evaluation of multidate SPOT data for agriculture and land use mapping in the United Kingdom
22 p3094 N88-28375
The suitability of SPOT imagery for monitoring landscape patterns 22 p3094 N88-28376
Characterization, topology, and cartography of grasslands for the development of fodder resources. (Preliminary Evaluation Program for SPOT number 26)
22 p3095 N88-28377
HRV data for the applications on reneweable resources in Canada --- SPOT 22 p3095 N88-28378
SPOT-1 HRV data and vegetation amount
22 p3095 N88-28379
Attempt to inventory vines using oblique SPOT images
22 p3095 N88-28380
Analysis of soils using remote sensing information at the scale of the parcel 22 p3095 N88-28381
Comparative variations of spectral signatures in a cultivated area of the Paris Basin (27 May, 26 June, 1 July 1986) 22 p3095 N88-28382
Monitoring of agricultural production in West Africa. The need to integrate different satellite platforms
22 p3096 N88-28383
Use of SPOT imagery for vegetation/biomass mapping, geotechnical mapping, catchment area determination, and settlement location in the Turkana district, northern Kenya 22 p3096 N88-28384
Digital and visual analysis of SPOT and TM data for crop discrimination in southern Brazil
22 p3096 N88-28385
A comparative thematic mapping analysis of SPOT data: The Vientiane Plain (Lao PDR)
22 p3096 N88-28386
Discrimination methods of traditional fields in a humid tropical region (Shaba, Zaire) using digital classification on SPOT data 22 p3096 N88-28387
Evaluation of SPOT data for crop inventory and monitoring in Sudanian Africa. Example of Bane area (Burkina Faso) 22 p3096 N88-28388

Identification of farming systems in the cotton area of West Burkina Faso from SPOT-1 data
22 p3097 N88-28389

Monitoring Tunisia's steppes with SPOT
22 p3097 N88-28390

Study of savannah formation in the Sudanian zone. Northwest sector of the La Comoe park, Ivory Coast
22 p3097 N88-28391

Pilot study of rice culture in sub-tropical high population density region (Madagascar) with SPOT 1 multispectral data
22 p3097 N88-28392

Using SPOT HRV data to update the distribution of the paddy field in Taiwan
22 p3097 N88-28393

Agro-ecological mapping from SPOT 1 data in southern Thailand: New questions for an analysis of the farming-systems
22 p3097 N88-28394

SPOT applications on Columbia's coffee zone
22 p3097 N88-28395

Use of SPOT data in preliminary steps of road project studies especially suited for developing countries
22 p3098 N88-28396

SPOT imagery for detecting residential expansion on the rural-urban fringe of Toronto, Canada
22 p3098 N88-28397

Spread of large tropical conurbations
22 p3098 N88-28398

Utilization of remote sensing for the observation of urban populations. Ongoing research in Quito (Ecuador)
22 p3098 N88-28399

Integration of SPOT data into a geocoded information system
22 p3098 N88-28400

Utilizing SPOT data for seismic shot-line mapping and environmental monitoring in oil and gas exploration
22 p3098 N88-28401

Preliminary comparative analysis of LANDSAT and SPOT data for the study of the sanding phenomenon: Zaafrane region (Algeria)
22 p3099 N88-28402

An evaluation of the applicability of SPOT stereoscopic imagery to the Canada Land Use Monitoring Program (CLUMP)
22 p3099 N88-28403

Topographic suppression and advances in classification for land cover mapping using SPOT-1 HRV imagery
22 p3099 N88-28404

Monitoring Moneragala (Sri Lanka) with SPOT imagery
22 p3099 N88-28405

Monitoring urban land cover changes at the urban fringe from SPOT HRV imagery in south-east England
22 p3099 N88-28406

Preliminary analyses of SPOT HRV multispectral products for arid and temperate environments
22 p3099 N88-28407

Assessment of SPOT satellite based system in humid tropical vegetation identification, classification and monitoring
22 p3100 N88-28408

A comparison between SPOT and LANDSAT TM for mapping of vegetation and bedrock outcrops
22 p3100 N88-28409

Accuracy of land use classification for SPOT image data
22 p3100 N88-28410

Analysis of SPOT multispectral data concerning a border zone between two geographical regions in southern Belgium
22 p3100 N88-28411

Thematic mapping of central Java (Indonesia)
22 p3100 N88-28412

Utilization of SPOT-1 multispectral data for mapping land cover and phytohygiene monitoring in the central zone of the Mercantour National Park (France)
22 p3100 N88-28413

Applications of SPOT data for urban real estate investment information systems
22 p3101 N88-28414

Mapping and urban multi-experimental assessment of SPOT: Urban results
22 p3101 N88-28415

SPOT-1 over New Zealand: Analysis of SPOT imagery for land use investigations
22 p3101 N88-28416

Comparison of SPOT, LANDSAT TM and combined data for urban studies
22 p3101 N88-28417

Utilization of SPOT multispectral data for urban planning
22 p3101 N88-28418

First results of international investigations of the applications of SPOT-1 data to geologic problems, mineral and energy exploration
22 p3101 N88-28419

Rate of slip on the Altin Dagh Fault (North Tibet, China)
22 p3102 N88-28420

Karst and submarine fresh water discharge in the Antalya area, southern Turkey
22 p3102 N88-28421

Results of the Geosat program to evaluate SPOT data for petroleum and mineral exploration
22 p3102 N88-28422

The application of SPOT data to the structural geology of western Nevada
22 p3102 N88-28423

Application SPOT-1 data to mining activity: Example of the Imiter Silver Mine, Morocco
22 p3102 N88-28424

Evaluation of SPOT imagery contribution to petroleum exploration: The Suez Rift (Egypt)
22 p3102 N88-28425

Evaluation of SPOT imagery for discriminating vegetation communities associated with surficial and bedbrock geology and identifying anomalous and stressed vegetation associated with mineralization
22 p3103 N88-28426

SPOT imagery as an aid to understanding volcanism and tectonics: Examples from the Chilean Andes and the Tibetan Plateau
22 p3103 N88-28427

Role of SPOT in geological application of remote sensing
22 p3103 N88-28428

SPOT imagery preliminary contribution to cartography and geodynamics in the Benue trough (Nigeria)
22 p3103 N88-28429

An evaluation of SPOT imagery for Earth science studies in the Antarctic. Preliminary Evaluation Program (PEPS) 289 for SPOT
22 p3103 N88-28430

Structural analysis of the Jura mountains-Rhine Graben intersection (Switzerland) for petroleum exploration using SPOT stereoscopic data
22 p3103 N88-28431

Methodology for the use of SPOT imagery in petroleum exploration. Example of the Bas-Languedoc area (France)
22 p3104 N88-28432

Analyzing the stratigraphy, tectonism, and mineralization at the Spanish side of the pyrite belt, Huelva province, Spain, using SPOT imagery
22 p3104 N88-28433

Geologic applications of SPOT-1, TM, and NOAA-7 data: Finding and defining unmapped structural features
22 p3104 N88-28434

Comparing different images for ground water survey based on lineament analysis
22 p3104 N88-28435

Spectral and spatial attribute evaluation of SPOT data in geological mapping of precambrian terrains in semiarid environment of Brazil
22 p3104 N88-28436

Geologic results obtained from the use of SPOT imagery along plate boundaries: Examples in the East African rift and of the northern-Caribbean collision
22 p3105 N88-28437

SPOT images and geochemical mapping of lateritic covers in southern Mali
22 p3105 N88-28438

Analysis of the multispectral content and of SPOT subscenes in two regions of Burundi. Lithologic and tectonic interpretations
22 p3105 N88-28439

SPOT imagery for landslide cartography in mountainous areas. Example of the French Maritime Alps
22 p3105 N88-28440

SPOT for slope instability survey in Nepal
22 p3105 N88-28441

Detailed geological mapping of the massif of Sainte Victoire (Provence, France) using SPOT imagery. Comparison with other multisource data. New tectonic interpretation of this region
22 p3105 N88-28442

Satellite remote sensing for forest management. A review illustrated with research results on SPOT 1 data
22 p3106 N88-28443

An evaluation of the utility of SPOT and Thematic Mapper data for providing forest inventory information
22 p3106 N88-28444

SPOT-1 satellite imagery for forest inventory in Sweden
22 p3106 N88-28445

Forest mapping by visual interpretation of SPOT images
22 p3106 N88-28446

Forest management applications of SPOT data in Australia
22 p3106 N88-28447

SPOT multispectral data and maritime pine stands in southwest of France
22 p3106 N88-28448

Stand-based forestry inventory from SPOT image
22 p3106 N88-28449

Potential of SPOT imagery as a tool for forest mapping in Quebec
22 p3107 N88-28450

Assessment of large area forest disturbances caused by biotic and abiotic factors on the basis of SPOT images
22 p3107 N88-28451

Study of deforestation in the Vosges (France) by remote sensing
22 p3107 N88-28452

Contribution to the mapping of forests in an intensively divided area, with the help of SPOT image data
22 p3107 N88-28453

SPOT 1: Image utilization, assessment, results. A study of the Elburgon Forest area (Kenya) showing the spectral responses of different forest tree species
22 p3107 N88-28454

SPOT investigations of estuaries and coastal zones: An overview
22 p3107 N88-28455

SPOT: A tool to aid preselection of sites favorable for aquiculture. Evaluation and perspectives of the Preliminary Evaluation Program for SPOT (PEPS) ALIAS Caledonie
22 p3108 N88-28456

The monitoring of sediment transport, water circulation and mixing in estuaries and coastal waters
22 p3108 N88-28457

Evaluation of SPOT data for remote sensing of physical and biological properties of estuaries and coastal zones
22 p3108 N88-28458

Utilization of SPOT in hydrography
22 p3108 N88-28459

Application of SPOT imagery for oil spill contingency planning
22 p3108 N88-28460

The use of SPOT data in mapping coastal areas
22 p3108 N88-28461

SPOT: A satellite for oceanography
22 p3108 N88-28462

Contribution of SPOT satellite to qualitative and quantitative mapping of marine vegetation in the English Channel, North Atlantic, western Mediterranean, and South Pacific
22 p3109 N88-28464

Physiography and kinematics of the western coast of the province of Huelva (Andalousia, Spain)
22 p3109 N88-28465

Use of SPOT HRV data in the US Army Corps of Engineers dredging program
22 p3109 N88-28466

Contributions of SPOT imagery to the study of the littoral environments of Saloum (Senegal)
22 p3109 N88-28467

Relevance of a thematic map (SPOT data) with regards to the real flora and structure of the vegetation covering of salt marshes (Mont Saint Michel Bay, France)
22 p3109 N88-28468

Application of SPOT data to renewable resources in the Maldives
22 p3109 N88-28469

The prospects for topographic mapping using SPOT data
22 p3110 N88-28470

The use of SPOT imagery on analytical photogrammetric instruments
22 p3110 N88-28471

Cartographic applications of SPOT imagery
22 p3110 N88-28472

The use of SPOT imagery for topographic mapping
22 p3110 N88-28473

Digital terrain modelling with SPOT data and geological applications
22 p3110 N88-28474

The use of SPOT data for mapping and DEM production — digital elevation model (DEM)
22 p3110 N88-28475

Evaluation of SPOT cartographic capabilities over the Aix Marseille area (France)
22 p3110 N88-28476

Assessment of SPOT imagery for topographic revision and vegetation mapping
22 p3111 N88-28477

Topographic mapping with SPOT 1 data. A practical approach by the Ordnance Survey
22 p3111 N88-28479

Metric applications of SPOT's lateral stereoscopy
22 p3111 N88-28480

Larger scale image mapping with SPOT
22 p3111 N88-28481

Rigorous stereophotogrammetric treatment of SPOT images
22 p3111 N88-28482

Mapping and urban multi-experimental assessment of SPOT: Mapping results
22 p3112 N88-28483

Study of stereoradiometry on SPOT images
22 p3112 N88-28484

Studies on system performance of SPOT (space and ground segments)
22 p3112 N88-28485

Radiometric analysis and potential of SPOT HRV imagery for applications in urban environments and geology
22 p3112 N88-28486

Automatic production of orthophoto using SPOT images
22 p3112 N88-28487

High resolution orthoimage quadrangle maps using SPOT satellite data
22 p3112 N88-28488

Automatic extraction of high resolution elevation data from SPOT stereo images
22 p3113 N88-28489

Automatic creation of digital terrain models from SPOT image pairs
22 p3113 N88-28490

Production of satellite image maps based on SPOT data
22 p3113 N88-28491

Surface reflectance factors derived from SPOT-1 HRV data at two view angles
22 p3113 N88-28492

Digital SPOT stereoplotting: An original approach to the formation of epipolar images and matching
22 p3113 N88-28493

From the extraction of linear networks towards following of them on SPOT images with the help of a knowledge-based interpretation system
22 p3113 N88-28494

Extraction of thin networks by an oriented following of ridges and valleys
22 p3113 N88-28495

SPOT images features extraction
22 p3114 N88-28496

SPOT: A data capture and data updating tool for the French National Geographic Institute's (IGN's) cartographic data base
22 p3114 N88-28497

Use of SPOT imagery in a geographic information system
22 p3114 N88-28498

SEP/VIPS 32 geographic information system. Processing and thematic analysis of images, maps, and associated data
22 p3114 N88-28499

Space imagery as a teaching aid in secondary education
22 p3114 N88-28500

Training of the Group for the Development of Aerospace Remote sensing
22 p3114 N88-28501

Contribution of SPOT to geographic information systems 22 p3114 N88-28502
Summary of analysis and processing techniques used on SPOT imagery 22 p3115 N88-28503
The SPOT program 22 p3115 N88-28504
SPOT data acquisition and distribution 22 p3115 N88-28505
Quality of SPOT images 22 p3115 N88-28506
Survey of SPOT-1 operation 22 p3115 N88-28507
Perspectives for the SPOT program 22 p3115 N88-28508
Closing of the Preliminary Evaluation Program for SPOT (PEPS): Assessment of the acquisition, production, and monitoring of PEPS 22 p3115 N88-28509
Use of LANDSAT images of vegetation cover to estimate effective hydraulic properties of soils
[NASA-CR-183185] 22 p3116 N88-28514
The patterns of tropical convection during the 1986-87 ENSO 22 p3120 N88-28537
An objective technique for Arctic cloud analysis using multispectral AVHRR (Advanced Very High Resolution Radiometer) satellite imagery
[AD-A194732] 23 p3235 N88-29250
Surface composition of Mars: A Viking multispectral view 23 p3300 N88-29655
The history of Martian volcanism determined from a revised relative chronology 23 p3301 N88-29657
High resolution Viking Orbiter images: A useful data source for testing the viability of geomorphic processes attributed to Martian landforms 23 p3307 N88-29703
Microwave instrument for planetary mission (Titan/CASSINI mission orbiter spacecraft)
[BAE-CS/TP-8359] 24 p3375 N88-30102
TM/LANDSAT-5 data to evaluate wheat and bean percent soil cover and leaf area index
[INPE-4609-PRE/1332] 24 p3385 N88-30165
Evaluation of LANDSAT-TM data for geomorphological mapping
[INPE-4593-PRE/1324] 24 p3386 N88-30168
Imaging instrument of the vegetation payload (SPOT 4)
[SNIAS-881-440-107] 24 p3386 N88-30169
The use of orbital remote sensing data for low cost ground-water survey
[INPE-4587-PRE/1318] 24 p3386 N88-30170
Reflectance pattern and the physical and chemical characteristics of three Brazilian Oxisols
[INPE-4590-PRE/1320] 24 p3387 N88-30172
Use of digital images as a mineral prospecting tool in the tin province of Goias, Brazil
[INPE-4537-PRE/1284] 24 p3387 N88-30173
Relief effect correction on LANDSAT imagery for forest applications using digital terrain models
[INPE-4611-PRE/1334] 24 p3388 N88-30179
LANDSAT TM and agrometeorological data for wheat yield estimation at the farm level
[INPE-4591-PRE/1321] 24 p3388 N88-30180
Volcanic contribution to crustal growth in the Central Andes: A new estimate and a discussion of uncertainties 24 p3401 N88-30255
Validate algorithms for the determination of rainfall rates from SSM/I microwave satellite imagery
[AD-A195428] 24 p3404 N88-30270
Compression and decompression of imaging sensor signals (CADISS): A multiprocessor system for image compression/decompression on board scientific satellites
[NLR-TR-87076-L] 24 p3414 N88-30323
Analytical method for approximate geodetic referencing of scanner images of meteorological artificial earth satellites using control points 24 p3449 N88-30527
Determining the spatial structure of fields of precipitation from space radar images in two orthogonal polarizations 24 p3450 N88-30531

SATELLITE INSTRUMENTS

Evaluation of a satellite laser ranging technique using pseudonoise code modulated laser diodes
[NASA-CR-182347] 06 p0708 N88-14343
Into the thermosphere: The atmosphere explorers
[NASA-SP-490] 10 p1353 N88-18084
Investigation of the diffuse ultraviolet background with DE data
[NASA-CR-182863] 19 p2741 N88-26271
Research and development objectives: Installation, startup, and test operation of a remote and program controlled measuring table for the calibration of EGRET experiment
[ETN-88-92105] 22 p3152 N88-28752

SATELLITE LAUNCHING

U SPACECRAFT LAUNCHING

SATELLITE LIFETIME

Forward-biased current annealing of radiation damaged gallium arsenide and silicon solar cells
[AD-A186904] 09 p1186 N88-17105

SATELLITE MANEUVERS

U SPACECRAFT MANEUVERS

SATELLITE NAVIGATION SYSTEMS

Reception of pseudo noise-modulated signals using digital correlators for satellite navigation tasks
[ETN-87-90426] 01 p0037 N88-10234
GPS vertical axis performance enhancement for helicopter precision landing approach
[NASA-CR-177443] 04 p0397 N88-12477
A demonstration of high precision GPS orbit determination for geodetic applications 04 p0432 N88-12680
Precise near-earth navigation with GPS: A survey of techniques 04 p0433 N88-12682
A positioning system based on NAVSAT
[NLR-MP-87018-U] 20 p2757 N88-26358
Study on NAVSAT system evaluation, phase 2. Part 1: Study results
[NLR-TR-87061-L-PT-1] 22 p3041 N88-28054
Study on NAVSAT system evaluation, phase 2. Part 2: Detailed simulation results
[NLR-TR-87061-L-PT-2] 22 p3041 N88-28055
Accuracy of satellite data navigation
[AD-A195877] 24 p3322 N88-29787
Low cost satellite
[ESA-CR(P)-2560] 24 p3334 N88-29844

SATELLITE NETWORKS

NT ARGOS SYSTEM
Accurate position measuring spacecraft package
[ESA-CR(P)-2398-VOL-1] 01 p0004 N88-10022
Accurate position measuring spacecraft package, executive summary
[ESA-CR(P)-2398-VOL-2] 01 p0004 N88-10023
Study of mobile communications payload for Columbus Polar Platforms
[ITS-TR-056A/86] 01 p0034 N88-10220
Study on the suitability of a European data relay satellite to support a system of remote sensing satellites
[ESA-CR(P)-2400] 01 p0063 N88-10406
Study into a data relay satellite mission analysis tool
[ESA-CR(P)-2422] 02 p0220 N88-11384
The Black College satellite telecommunications network planning in support of energy-related collaborative research
[DE88-000182] 03 p0307 N88-11940
Interoperability and integration of data relay satellite systems 03 p0339 N88-12134
Study of the feasiblity of a satellite communication system for road transportation home office to vehicle communication. Volume 1: Conceptual analysis
[SC/87-E/6-VOL-1] 05 p0575 N88-13505
Study of the feasibility of a satellite communication system for road transportation home office to vehicle communication. Volume 2: Market study
[SC/87-E/6-VOL-2] 05 p0575 N88-13506
Low frequency VLBI in space using GAS-Can satellites: Report on the May 1987 JPL Workshop
[NASA-CR-182362] 06 p0801 N88-14904
Round table on the future of satellite communications and broadcasting in Europe
[ESA-STR-221] 07 p0843 N88-15112
Method for joint adjustment of satellite and surface geodetic networks 08 p1007 N88-16105
Study of reconfigurable payloads for direct broadcast satellites, summary
[DBS87-0004] 09 p1135 N88-16808
An introduction to military satellite communications
[RSRE-MEMO-3976] 09 p1153 N88-16911
Introduction to the Meteosat system
[ESA-SP-1041] 09 p1193 N88-17148
The orientation of global satellite networks 11 p1506 N88-18996
On-board processing for mobile satellite communications
[ESA-CR(P)-2519] 14 p1905 N88-21382
Activities report in flight and space travel
[ISSN-0070-3966] 14 p2012 N88-22000
Degradation of downlink distance measurement indexes by the addition of a third tone — tone ranging
[CNES-CT/DRT/TIT/TR-122-T] 15 p2058 N88-22268
MSAT-X: A technical introduction and status report
[NASA-CR-182921] 17 p2334 N88-23933
Satellites at sea — INMARSAT 19 p2700 N88-26054
Document transfer by a digital satellite link
[NLR-MP-86071-U] 20 p2792 N88-26564
The Frequency Division Multiple Access/Time Domain Multiplex (FDMA/TDM) system reviewed 22 p3069 N88-28214
Business telecommunications using satellite microterminals: Gaining the competitive edge
[ESA-BR-49] 22 p3070 N88-28225
Determination of satcom access power levels within the ground segment
[RSRE-MEMO-4097] 22 p3070 N88-28226
Performance of a rapid carrier acquisition circuit for satellite ground terminal modems
[RSRE-TEST-REPORT-87/CC3/2] 22 p3071 N88-28227
NOA: A Network Operator Assistant for scheduling Tracking and Data Relay Satellite System (TDRSS) 23 p3259 N88-29403
Optical multiple access intersatellite links
[BAE-TP-8502] 24 p3361 N88-30013

SATELLITE OBSERVATION

USSR report: Space
[JPRS-USP-87-003] 01 p0009 N88-10050
The sequential evaluation of Doppler satellite observations
[REPT-141] 01 p0010 N88-10057
Study on the suitability of a European data relay satellite to support a system of remote sensing satellites
[ESA-CR(P)-2400] 01 p0063 N88-10406
How we get pictures from space, revised edition
[NF-151/7-87-REV] 02 p0193 N88-11203
Observation of the development of mesoscale systems by operational meteorological satellites 02 p0201 N88-11259
Use of simulated satellite radiances from a mesoscale numerical model to understand kinematic and dynamic processes 02 p0202 N88-11261
Research in geodesy based upon radio interferometric observations of GPS (Global Positioning System) satellites
[AD-A184040] 03 p0346 N88-12187
IRAS and near IR observations of active binaries 04 p0518 N88-13186
Budget and programs for 1986 research
[IFSI-86-16] 05 p0660 N88-14048
Satellite observations of extreme ultraviolet radiation
[AD-A185043] 05 p0661 N88-14059
Report of the International Satellite Cloud Climatology Project (ISCCP) workshop on cloud algorithms in the polar regions
[WCP-131] 06 p0745 N88-14581
Review of the potential of satellite remote sensing for marine flood protection
[IOS-237] 07 p0870 N88-15280
The influence of yellow substances on remote sensing of sea water constituents from space. Volume 1: Summary
[ESA-CR(P)-2443-VOL-1] 07 p0872 N88-15292
The influence of yellow substances on remote sensing of sea water constituents from space. Volume 2: Appendices
[ESA-CR(P)-2443-VOL-2] 07 p0873 N88-15293
The use of chlorophyll fluorescence measurements from space for separating constituents of sea water. Volume 1: Summary
[ESA-CR(P)-2444-VOL-1] 07 p0873 N88-15294
The use of chlorophyll fluorescence measurements from space for separating constituents of sea water. Volume 2: Appendices
[ESA-CR(P)-2444-VOL-2] 07 p0873 N88-15295
Feasibility studies of optical processing of image bandwidth compression schemes
[AD-A186073] 07 p0932 N88-15660
Longitudinal variations of equatorial ionosphere determined from Intercosmos-19 artificial Earth satellite data 08 p1003 N88-16074
Satellite monitoring of earthquake precursor effects in magnetosphere 08 p1007 N88-16103
Research work at the Meteorological Institute of the University of Munich (Federal Republic of Germany)
[MITT-56] 08 p1013 N88-16141
Inversion of simulated satellite signals 08 p1017 N88-16168
Commercial applications and scientific research requirements for thermal-infrared observations of terrestrial surfaces
[NASA-TM-89704] 08 p1019 N88-16179
Global views of the aurora from the Viking satellite — Swedish satellite 08 p1025 N88-16208
Instantaneous pictures of the high-latitude electrodynamics using Viking and DMSP/F7 observations — Swedish satellite 08 p1025 N88-16209
The Meteosat operational program 09 p1127 N88-16759
Fine attitude measurement system study. Volume 1: Executive summary
[BAE-TP-7831-VOL-1] 09 p1133 N88-16795
Fine attitude measurement system study, volume 2
[BAE-TP-7831-VOL-2] 09 p1133 N88-16796
Fine attitude measurement system study. Volume 3: Appendices
[BAE-TP-7831-VOL-3] 09 p1133 N88-16797
A multiple-satellite observation of the high-latitude auroral activity on 11 January 1983
[AD-A175170] 09 p1189 N88-17122

NROSS (Navy Remote Ocean Sensing System): A force multiplier
[AD-A186853] 10 p1346 N88-18045
Earth resources: A continuing bibliography with indexes (supplement 56)
[NASA-SP-7041(56)] 10 p1347 N88-18051
Application of satellite data in observational and theoretical studies of the evolving structure of baroclinic waves
[NASA-CR-179277] 10 p1354 N88-18091
Proceedings of an ESA-NASA Workshop on a Joint Solid Earth Program
[NASA-CR-182642] 12 p1644 N88-19844
Spaceborne magnetometry 12 p1644 N88-19846
Terrestrial gravity data and comparisons with satellite data 12 p1644 N88-19848
Calibration of the solar radiation estimation method by satellites
[INPE-4349-PRE/1185] 12 p1646 N88-19861
An investigation of Doppler satellite positioning multi-station adjustment software 13 p1730 N88-20345
Analysis of spectral reflectance characteristics of targets under satellites and automatic cloud recognition 13 p1755 N88-20498
Radiative processes affecting ocean mixed-layer heat content and their monitoring from satellite 13 p1806 N88-20800
Climatology and space observations
[ISBN-2-85-428179-9] 14 p1935 N88-21536
The Earth radiation budget and its spatial and temporal variations 14 p1936 N88-21548
Net radiative flux at the Earth surface: Estimation from satellite observations 14 p1936 N88-21550
Satellite estimations of the solar radiation flux at the surface 14 p1936 N88-21551
Satellite retrieval of cloud cover parameters and the International Satellite Cloud Climatology Program (ISCCP) 14 p1937 N88-21552
Measurement from satellites of land surface parameters and fluxes in the thermal infrared bands: Problems and methods 14 p1937 N88-21557
The role of remote sensing in the study of polar ice sheets 14 p1939 N88-21570
Elements of sea ice dynamics and thermodynamics 14 p1939 N88-21571
Extension of the vegetation mission to thermal infrared spectral bands
[CNES-T-86/224-CT/DRT/TIT/IO] 16 p2227 N88-23299
Turbidity patterns in the delta waters of southwest Netherlands on Thematic Mapper (TM) and multispectral scanner (MSS) satellite images
[BCRS-86-06] 16 p2227 N88-23303
Near-real-time TOMS, telecommunications and meteorological support for the 1987 Airborne Antarctic Ozone Experiment
[NASA-CR-4133] 16 p2233 N88-23338
Prospects of satellite wind sensing systems in the years 1995-2000 17 p2350 N88-24004
Latitudinal and seasonal variation of the cloud characteristic parameters and their effects on the cloud classification 17 p2351 N88-24005
Estimation of total Outgoing Longwave Radiation (OLR) flux from geostationary meteorological satellite infrared window radiance 17 p2351 N88-24006
The application of satellites in connection with the environment
[ETN-88-92474] 18 p2532 N88-25020
Satellite observed Mesoscale Convective System (MCS) propagation characteristics and a 3-12 hour heavy precipitation forecast index
[PB88-180161] 19 p2692 N88-26004
Sensors in spaceborne oceanography 19 p2700 N88-26056
Remote sensing and satellite applications to the needs of the gas and pipeline industry
[PB88-202668] 20 p2817 N88-26714
Diffusion of slight solar induced disturbances in the middle atmosphere
[MITT-53] 20 p2825 N88-26758
Cyrogenic test facilities for an optical cryomechanism qualification
[REPT-881-440-116] 21 p2901 N88-27219
Optimized observation periods required to achieve geodetic accuracies using the global positioning system
[AD-A193844] 22 p3041 N88-28052
The world's water resources: A major neglect. A study in remote sensing in hydrology and water management
[ESA-BR-40] 22 p3116 N88-28511
Stratocumulus and cloud-free reflectance from multi-spectral satellite measurements
[AD-A193899] 22 p3128 N88-28599
Oblique metallogenic zones recognized by interpreting space photographs of southern Tien Shan 24 p3450 N88-30529

SATELLITE ORBIT CALCULATION
U ORBIT CALCULATION

SATELLITE ORBITS
NT GEOSYNCHRONOUS ORBITS
NT POLAR ORBITS
NT STATIONARY ORBITS
The contraction of satellite orbits under the influence of air drag. Part 8: Orbital lifetime in an oblate atmosphere, when perigee distance is perturbed by odd zonal harmonics in the geopotential
[RAE-TR-86069-PT-8] 01 p0010 N88-10058
Satellite orbits: Plot routines
[UIO-SR-87-02] 01 p0011 N88-10060
Precise orbit computation, gravity model adjustment and altimeter data processing for the ERS-1 altimetry mission
[ESA-CR(P)-2436] 02 p0130 N88-10820
On air-drag perturbation of transit satellite and selection of parameters in orbit improvement 03 p0269 N88-11691
Advanced simulation and analysis of a geopotential research mission
[NASA-CR-182355] 06 p0670 N88-14108
Simulation and analysis of a geopotential research mission
[NASA-CR-182354] 06 p0670 N88-14109
An orbit simulation study of a geopotential research mission including satellite-to-satellite tracking and disturbance compensation systems
[NASA-CR-182353] 07 p0823 N88-14997
Investigation of the feasibility of an analytical method of accounting for the effects of atmospheric drag on satellite motion 07 p0923 N88-15608
An evaluation of semianalytical satellite theory against long arcs of real data for highly eccentric orbits
[AD-A185825] 08 p0960 N88-15819
An intelligent tutor for the space domain 09 p1204 N88-17217
Relative motion of two satellites in close-elliptical orbits
[AD-A188851] 12 p1594 N88-19543
Analysis of orbital geometry and orbit maintenance of an Earth observation satellite
[INPE-4276-PRE/1148] 12 p1594 N88-19549
NAVARES: A prototype expert system for NAVSTAR anomaly resolution
[AD-A189491] 12 p1600 N88-19579
The evaluation and selection of a 5th ground antenna site for the global positioning system
[AD-A189495] 13 p1720 N88-20286
Orbit accuracy requirement of GPS for precise positioning and orbit determination within local area 13 p1756 N88-20499
Analysis of the orbit of Cosmos 1335 (1982-07A) at 3:12 resonance
[RAE-TR-87041] 14 p1872 N88-21185
Baseline estimation from simultaneous satellite laser tracking
[NASA-CR-182750] 15 p2022 N88-22052
The prediction of satellite lifetimes
[RAE-TR-87030] 17 p2310 N88-23818
Orbit determination of 1965-09A for analysis of the eccentricity at 15th-order resonance
[RAE-TR-87059] 22 p3047 N88-28081
A standard library for modeling satellite orbits on a microcomputer
[AD-A195759] 24 p3331 N88-29830
Experimental and analytical study of two-phase flow in zero gravity
[AD-A195223] 24 p3358 N88-29993
Plane periodic satellite motions relative to center of mass in neighborhood of collinear libration point 24 p3445 N88-30507
Resonance effects accompanying motion with low thrust in earth-moon system 24 p3446 N88-30510

SATELLITE ORIENTATION
Analysis of free molecular effects on the attitude of satellites in geostationary transfer orbit. Part 1: Theoretical analysis
[DFVLR-IB-222-86-A/08] 01 p0014 N88-10077
Analysis of free molecular effects on the attitude of satellites in geostationary transfer orbit. Part 2: Force and torque measurement in free molecular wind tunnel tests
[DFVLR-IB-222-86-A/07] 01 p0014 N88-10078
An autonomous, closed-loop pointing system for use with satellite optics
[DE87-012011] 02 p0235 N88-11483
Fine attitude measurement system study. Volume 1: Executive summary
[BAE-TP-7831-VOL-1] 09 p1133 N88-16795
Fine attitude measurement system study, volume 2
[BAE-TP-7831-VOL-2] 09 p1133 N88-16796
Fine attitude measurement system study. Volume 3: Appendices
[BAE-TP-7831-VOL-3] 09 p1133 N88-16797

SATELLITE PERTURBATION
The contraction of satellite orbits under the influence of air drag. Part 8: Orbital lifetime in an oblate atmosphere, when perigee distance is perturbed by odd zonal harmonics in the geopotential
[RAE-TR-86069-PT-8] 01 p0010 N88-10058
A study of a satellite-to-satellite tracking configuration by application of linear perturbation theory
[REPT-86.3] 01 p0011 N88-10059
Analysis of free molecular effects on the attitude of satellites in geostationary transfer orbit. Part 1: Theoretical analysis
[DFVLR-IB-222-86-A/08] 01 p0014 N88-10077
Analysis of free molecular effects on the attitude of satellites in geostationary transfer orbit. Part 2: Force and torque measurement in free molecular wind tunnel tests
[DFVLR-IB-222-86-A/07] 01 p0014 N88-10078
Estimability of potential coefficients from orbit perturbations --- satellite geodesy
[REPT-86.1] 01 p0064 N88-10408
Prevention of radiation induced degradations and of electrostatic perturbations on the Arabsat spacecraft in flight results 03 p0275 N88-11734
Simulation and analysis of a geopotential research mission
[NASA-CR-182354] 06 p0670 N88-14109
Orbit correction requirements for a natural resources satellite
[INPE-4286-PRE/1158] 12 p1594 N88-19548
Analysis of orbital geometry and orbit maintenance of an Earth observation satellite
[INPE-4276-PRE/1148] 12 p1594 N88-19549

SATELLITE POWER TRANSMISSION (TO EARTH)
ESA Bulletin No. 25
[ISSN-0376-4265] 09 p1128 N88-16767
Satellite power systems under consideration by the United Nations 09 p1128 N88-16773

SATELLITE RENDEZVOUS
U ORBITAL RENDEZVOUS

SATELLITE REPAIR
U ORBITAL SERVICING

SATELLITE ROTATION
A multibody dynamic analysis of the N-ROSS (Navy Remote Ocean Sensing System) satellite rotating flexible reflector using Kane's method
[AD-A184452] 04 p0462 N88-12860
Preliminary design of the ORION attitude control system
[AD-A187179] 10 p1292 N88-17729
A spin and deployment mechanism 14 p1926 N88-21479
Rotational evolution of dynamically symmetric gyrostat with internal friction 24 p3446 N88-30509

SATELLITE SOUNDING
An introduction to the GOES I-M imager and sounder instruments and the GVAR retransmission format
[NOAA-TR-NESDIS-33] 02 p0140 N88-10884
Improved geostationary satellite soundings for the mesoscale weather analysis/forecast operation 02 p0200 N88-11252
Horizontal shape matching applied to VAS data --- Visible and Infrared Spin Scan Radiometer Atmospheric Sounder (VAS) 02 p0201 N88-11254
Automated detection of severe thunderstorms using geosynchronous infrared data 02 p0201 N88-11257
Mesoscale analysis and nowcasting via a numerical model coupled with satellite sounder data 02 p0211 N88-11328
Methods of incorporating satellite data into mesoscale numerical forecast models 02 p0212 N88-11336
Simulation of mesoscale satellite sounder data from a mesoscale numerical model 02 p0214 N88-11345
The effect of enhanced conventional and VAS moisture analysis on RAFS short-range precipitation forecasts --- Regional Analysis and Forecasting System (RAFS) 02 p0215 N88-11352
Scientific and Operational Requirements for TOMS Data
[NASA-CP-2497] 05 p0615 N88-13774
Dobson-stations performance assessment using TOMS data 05 p0618 N88-13792
Volcanic eruption detection with TOMS 05 p0618 N88-13793
Analysis of SO2 signals in SBUV/TOMS data 05 p0618 N88-13794
Comparison of ground based and TOMS measurements of SO2 from volcanic emissions 05 p0618 N88-13795
Use of satellite data in volcano monitoring 05 p0618 N88-13797
Selection of optimum wavelengths for ozone mapping from satellites 05 p0619 N88-13798
Determination of total ozone from HIRS2/MSU sounding data 05 p0619 N88-13799
Complementary information between UV and IR for remote sensing of total ozone 05 p0619 N88-13800

Observation guidelines for a Total Ozone Mapping Spectrometer (TOMS) in geosynchronous orbit
05 p0619 N88-13801
Electric field measurements on Viking: First results
[TRITA-EPP-87-04] 05 p0625 N88-13826
High Resolution Picture Transmission (HRPT) data processing from NOAA series satellites
[INPE-4372-PRE/1195] 08 p0963 N88-15831
Limiting accuracy of scatterometer determination of wind speed over ocean from satellite
08 p1007 N88-16107
The German scientific balloon and sounding rocket program 08 p1024 N88-16202
Viking: The first Swedish satellite
08 p1025 N88-16207
Report on ground-based activity at Andoya (Norway) in relation to the Aureld-VIP high rocket and to the Viking satellite --- Swedish satellite 08 p1026 N88-16212
Vertical atmospheric sounding
[INPE-4370-PRE/1195] 08 p1036 N88-16283
Microphysics of the auroral acceleration region of other regions of the magnetosphere 08 p1096 N88-16592
Preliminary results from the dc electric field experiment on Viking --- Swedish satellite
[TRITA-EPP-87-03] 09 p1190 N88-17130
Roys and radiosondes in the region
[INPE-4362-PRE/1188] 13 p1796 N88-20743
Satellite gradiometry
[B8735057] 16 p2229 N88-23313
Simultaneous observation of upward moving field aligned energetic electrons and ions on auroral zone field lines
[IRF-PREPRINT-102] 16 p2231 N88-23326
Some problems with regard to the TOVS processing detected by using NOAA-HRPT data check program
17 p2351 N88-24009
Processing of HRPT data from the NOAA series satellites 17 p2359 N88-24053
Tiros operational vertical sounder (TOVS) and radiosonding in the region 17 p2360 N88-24059
Suggested hurricane operational scenario for GOES I-M
[NASA-TM-89729] 19 p2692 N88-26002
Field-aligned structure of the storm time Pc 5 wave of November 14-15, 1979
[AD-A193022] 21 p2972 N88-27653
Snapshots of high-latitude electrodynamics using Viking and DMSP/F7 observations
[TRITA-EPP-88-01] 23 p3234 N88-29244
Possibilities of determining vertical profiles of microphysical characteristics of stratospheric aerosol using space measurements of transparency and solar halo 24 p3449 N88-30526

SATELLITE SURFACES
NT LUNAR SURFACE

SATELLITE TELEVISION
The role of the L-Sat program in the evolution of European communications satellites
09 p1127 N88-16758
Image processing on VEGA pictures
14 p2009 N88-21983

SATELLITE TEMPERATURE
COS-B in-orbit study
[ESA-CR(P)-2420] 01 p0017 N88-10102
Thermal analysis in steady state conditions for satellites
[INPE-4429-TDL/309] 12 p1599 N88-19574
A study of satellite emission computed tomography
[AD-A189567] 13 p1797 N88-20745
Far infrared spectroscopy telescope (FIRST) inflatable thermal shield, phase 1
[SR/FIS/108(87)CZ] 24 p3453 N88-30552

SATELLITE TRACKING
NT SATELLITE-TO-SATELLITE TRACKING
Precise orbit computation, gravity model adjustment and altimeter data processing for the ERS-1 altimetry mission
[ESA-CR(P)-2436] 02 p0130 N88-10820
Research in geodesy based upon radio interferometric observations of GPS (Global Positioning System) satellites
[AD-A184040] 03 p0346 N88-12187
Optimized tracking of RF carriers with phase noise, including Pioneer 10 results 04 p0434 N88-12694
An intelligent tutor for the space domain
09 p1204 N88-17217
Estimation of geopotential from satellite-to-satellite range rate data: Numerical results
[NASA-CR-180771] 14 p1941 N88-21583
Baseline estimation from simultaneous satellite laser tracking
[NASA-CR-182750] 15 p2022 N88-22052
A low cost automatic Earth observation satellite tracking ground receiving station 17 p2309 N88-23815
The Telecommunications and Data Acquisition Report
[NASA-CR-183131] 22 p3063 N88-28178
The limits of direct satellite tracking with the Global Positioning System (GPS) 22 p3064 N88-28179
Approximation of atmospheric density by Chebyshev polynomials in predicting motion of low artificial earth satellites 24 p3445 N88-30503

SATELLITE TRANSMISSION
Implications of a simplified signal structure for Navsat
[REPT-63/1439] 01 p0005 N88-10024
The Black College satellite telecommunications network planning in support of energy-related collaborative research
[DE88-000182] 03 p0307 N88-11940
Propagation effects on satellite systems at frequencies below 10 GHz: A handbook for satellite systems design
[NASA-RP-1108/2] 06 p0690 N88-14226
The role of the L-Sat program in the evolution of European communications satellites
09 p1127 N88-16758
MARCE data evaluation 10 p1286 N88-17693
Construction of a satellite simulator for the frequency range between 11.7 and 12.5 GHz
[IRT-TB-B-84/87] 16 p2166 N88-22917
Atmospheric corrections for in-flight satellite radiometric calibration
[AD-A196124] 24 p3391 N88-30194

SATELLITE-BORNE INSTRUMENTS
NT ADVANCED VERY HIGH RESOLUTION RADIOMETER
NT TOTAL OZONE MAPPING SPECTROMETER
A VAS-numerical model impact study using the Gal-Chen variational approach --- Visible Infrared Spin-Scan Radiometer Atmospheric Sounder (VAS)
02 p0213 N88-11339
Planning for future operational sensors and other priorities
[PB87-220802] 03 p0325 N88-12056
The CNR/PSN Advanced Microwave Imaging Radiometer (AMIR) --- satellite-borne
03 p0340 N88-12141
Absolute and interband calibration --- SPOT
03 p0341 N88-12152
The new generation of SPOT satellites
03 p0345 N88-12178
Evaluation of a cryogenic refrigerator for cooling focal plane instrumentation --- satellite instruments
[BAE-TP-8095-VOL-1] 05 p0572 N88-13485
Evaluation of a cryogenic refrigerator for cooling focal plane instrumentation. Appendix B: Accommodation study --- satellite instruments
[BAE-TP-8095-VOL-2] 05 p0572 N88-13486
Development of response models for the Earth Radiation Budget Experiment (ERBE) sensors. Part 3: ERBE scanner measurement accuracy analysis due to reduced housekeeping data
[NASA-CR-178294] 05 p0583 N88-13553
HIRIS (High-Resolution Imaging Spectrometer: Science opportunities for the 1990s. Earth observing system. Volume 2C: Instrument panel report
[NASA-TM-89703] 07 p0871 N88-15282
LANDSAT thematic mapper radiometric calibration study
[NASA-CR-182410] 07 p0872 N88-15287
Alouette-ISIS program summary
[NASA-CR-180747] 08 p1023 N88-16195
Contribution of stratospheric balloon flights in space biology 08 p1033 N88-16266
Design feasibility report on investigation of magnetic bearings for the ocean colour monitor radiometer scanner
[BAE-TP-7849] 09 p1174 N88-17036
Statistical studies of low frequency oscillations in satellite-observed stratospheric temperatures
10 p1353 N88-18086
High efficiency, long life traveling wave tubes for future communications satellites
[NASA-TM-100837] 12 p1598 N88-19565
Spaceborne gravity gradiometry characterizing the data type 12 p1644 N88-19847
GRADIO three-axis electrostatic accelerometers
12 p1645 N88-19849
Gradiometer accommodation on board a drag-free satellite 12 p1645 N88-19850
Concept of an Opto-electronic Accelerometer System (OAS) 12 p1645 N88-19852
Polar mesospheric cloud experiment
[AD-A188936] 12 p1648 N88-19872
The bit-error rate performance of a satellite microwave matrix switch
[NASA-TM-100285] 16 p2167 N88-22920
Prospects of satellite wind sensing systems in the years 1995-2000 17 p2350 N88-24004
The high-throughput X-ray spectroscopy mission E6889478 MN513835 --- ESA program
[ESA-SP-1092] 17 p2450 N88-24554
The French spaceborne oceanography program
19 p2701 N88-26058
The Oak Ridge National Laboratory strategic defense initiative shield optimization program: Executive summary
[DE88-008016] 20 p2847 N88-26899
Basic research for the geodynamics program
[NASA-CR-183149] 21 p2973 N88-27662

SATELLITE-BORNE PHOTOGRAPHY
Evaluation of digital, multitemporal LANDSAT 5 thematic mapper data for the determination of the aerial snowcover extent and spectral separation of various surface types in the inner Oetztal (West Germany) with special regard to the significance of aerial snowcover information for water resources management
[DFVLR-FB-86-46] 03 p0345 N88-12180
Varifront 3 expedition data report (USNS DE STEIGUER CRUISE 1202-82). Bioluminescence, hydrographic, nutrient, and satellite data from the Gulf of California (November-December 1981)
[AD-A185011] 05 p0620 N88-13805
Modeling cloudy and clear interval length probabilities using space shuttle imagery
[AD-A185290] 05 p0627 N88-13837
Investigations on the application of space photographs (Spacelab metric camera) for routine inventories of extensively managed forest areas
[DFVLR-FB-87-22] 09 p1185 N88-17098
Oceanographic features of the east and southeast Indian Ocean for June 1983
[AD-A186948] 09 p1195 N88-17158
An objective technique for Arctic cloud analysis using multispectral AVHRR (Advanced Very High Resolution Radiometer) satellite imagery
[AD-A194732] 23 p3235 N88-29250
Structure of eastern Turkestan Ridge based on space photographs 24 p3450 N88-30530

SATELLITE-BORNE RADAR
Review of inversion techniques for spaceborne lidar systems
[AD-A184164] 04 p0447 N88-12772
The role of space borne imaging radars in environmental monitoring: Some shuttle imaging radar results in Asia
[NASA-TM-101175] 20 p2789 N88-26544

SATELLITE-TO-SATELLITE TRACKING
A study of a satellite-to-satellite tracking configuration by application of linear perturbation theory
[REPT-86.3] 01 p0011 N88-10059
Study of a satellite-to-satellite tracking gravity mission
[ESA-CR(P)-2419] 02 p0198 N88-11237
An orbit simulation study of a geopotential research mission including satellite-to-satellite tracking and disturbance compensation systems
[NASA-CR-182353] 07 p0823 N88-14997
Continued design of a Pointing, Acquisition, and Tracking (PAT) subsystem for InterSatellite Laser links (ISL2)
[TELDIX-15-093-178] 14 p1905 N88-21384

SATELLITES
Toward a comprehensive theory for the sweeping of trapped radiation by inert orbiting matter
[NASA-CR-182584] 11 p1569 N88-19395

SATURABLE REACTORS
Low power consumption current transducer
[NASA-CASE-NPO-16888-1-CU]
17 p2335 N88-23937

SATURATED HYDROCARBONS
U ALKANES

SATURATION
Design for performance enhancement in feedback control systems with multiple saturating nonlinearities
[NASA-CR-182614] 11 p1535 N88-19168
Design of feedback control systems for stable plants with saturating actuators
[NASA-CR-182613] 12 p1681 N88-20050
Measurements of optical nonlinearities in MOCVD-grown GaAs/GaAlAs multiple quantum wells
14 p1975 N88-21787
Saturation and the limit of jet mixing enhancement by single frequency plane wave excitation: Experiment and theory
[NASA-TM-100882] 17 p2295 N88-23732

SATURATION (CHEMISTRY)
Optimizing the application of high temperature corrosion resistant aluminium-silicon-base coatings
[BLL-M-37222-(5828.4)] 01 p0018 N88-10112

SATURN
Astron observations of supernova 1987A in large magellanic cloud 24 p3445 N88-30504

SATURN ATMOSPHERE
An analysis of longitude variations in the equatorial spectrum of Saturn 10 p1430 N88-18539
Extended atmospheres of outer planet satellites and comets
[NASA-CR-181449] 10 p1430 N88-18540
Extended atmospheres of outer planet satellites and comets
[NASA-CR-183157] 24 p3457 N88-30572

SATURN RINGS
Study of a Radio Relay Link (RRL). Cassini mission. Data package for final presentation
[ESA-CR(P)-2472] 07 p0847 N88-15138
Simulation of the plasma interaction with thin dust clouds 11 p1552 N88-19291
Dynamical and photometric studies of Saturn's rings 12 p1711 N88-20241
Voyager imaging photometry and radiative transfer modeling of the spoke-like features in Saturn's outer B-ring 19 p2742 N88-26278
SATURN SATELLITES
NT TITAN
Extended atmospheres of outer planet satellites and comets
[NASA-CR-181449] 10 p1430 N88-18540
SAVANNAHS
U GRASSLANDS
SCALARS
Scalar densities and baryon mass differences in lattice QCD with Wilson fermions
[PREPRINT-544] 06 p0778 N88-14773
The application of vector diffraction to the scalar anomalous diffraction approximation of Van de Hulst
[AD-A185930] 07 p0929 N88-15643
On the expectation of the product of four matrix-valued Gaussian random variables
[EUT-87-E-178] 13 p1828 N88-20927
Direct numerical simulation of buoyantly driven turbulence 16 p2196 N88-23097
Existence of periodic solutions in n-dimensional retarded functional differential equations
[RR-325] 17 p2392 N88-24221
Direct numerical simulations of the PDF's (Probability Density Functions) of a passive scalar in a forced mixing layer
[AD-A192134] 18 p2568 N88-25256
The covariance of scalar fields scattered by pressure-release randomly rough surfaces
[AD-A192489] 22 p3146 N88-28714
SCALE (CORROSION)
Carbon dioxide treatment for scale removal and control in potable water systems
[AD-A184346] 04 p0412 N88-12556
Beneficial and detrimental effects of silica in the high temperature oxidation of 20Cr/25Ni/Nb stainless steel
[AERE-R-12667] 10 p1301 N88-17779
Point defect structure of Cr2O3
[AD-A187620] 11 p1556 N88-19317
SCALE (RATIO)
Detection of critical points: The first step to automatic line generalization 05 p0619 N88-13803
SCALE EFFECT
Cavitation inception scale effects. 1. Nuclei distributions in natural waters. 2. Cavitation inception in a turbulent shear flow
[AD-A186553] 08 p0988 N88-15987
Dynamic interaction of convective cumulus with large-scale environment
[MITT-55] 20 p2827 N88-26773
Size effects in linear elastic fracture mechanics 21 p2964 N88-27609
SCALE HEIGHT
An analysis of apparent-motion vectors in, and the structure of, A mid-latitude sporadic E layer using a 2.66 MHz radar
[AD-A186126] 07 p0877 N88-15321
SCALE MODELS
Evaluation of a scale-model experiment to investigate long-range acoustic propagation
[NASA-TP-2748] 02 p0230 N88-11450
Underwater acoustic backscatter from a model of arctic ice open leads and pressure ridges
[AD-A184693] 03 p0354 N88-12234
A 0.15-scale study of configuration effects on the aerodynamic interaction between main rotor and fuselage
[NASA-CR-166577] 04 p0395 N88-12462
Analytical investigation of the dynamics of tethered constellations in Earth orbit (phase 2)
[NASA-CR-179218] 04 p0408 N88-12533
Measurement of model deformation in wind tunnels 05 p0551 N88-13358
A system identification technique based on the random decrement signatures. Part 2: Experimental results 05 p0594 N88-13626
On the subgrid-scale modeling of compressible turbulence
[NASA-CR-178420] 06 p0702 N88-14309
ASSESS-2: An aircraft simulation of Spacelab 09 p1123 N88-16723
Aerodynamic performance of a scale-model, counter-rotating unducted fan 10 p1282 N88-17666
The assessment of the sound insulation requirements for a large broadcasting studio, using a scale model: Practical details
[BBC-RD-1987/21] 10 p1318 N88-17878
Application of similarity techniques between reduced and natural scale models of Ramjet engines
[INPE-4269-PRE/1142] 11 p1441 N88-18595
Sub-scaling of projectile/target system damaged by hypervelocity
[AD-A186683] 12 p1634 N88-19779
An investigation of classical dynamic scaling techniques applied to an oleo-pneumatic landing gear strut
[AD-A187664] 13 p1721 N88-20292
Scale model development for aeroelasticity studies
[ETN-88-91887] 14 p1868 N88-21164
Space station full-scale docking/berthing mechanisms development 14 p1927 N88-21491
Visualization of the air flowing through a dynamic model of the vocal folds
[ISVR-TR-154] 14 p1952 N88-21634
Model-scale sound propagation experiment
[NASA-TM-100602] 15 p2130 N88-22709
MPD (magnetoplasmadynamic) thruster advanced pumping system concepts
[AD-A190513] 15 p2138 N88-22756
Limits of design feasibility of multiwing wind turbines with individual articulated wing structure
[ILR-MITT-180] 18 p2537 N88-25052
Frequency domain identification of the dynamics of a scaled remotely-piloted helicopter 20 p2786 N88-26524
Flow visualization on a small scale
[AD-A194728] 23 p3181 N88-28935
Model test of air-exchange efficiency
[DE88-752862] 23 p3201 N88-29049
Test of an 0.8-scale model of the AH-64 Apache in the NASA Langley full-scale wind tunnel
[AD-A196129] 24 p3319 N88-29768
SCALERS
Multichannel scaling analyzer
[DE88-700541] 07 p0905 N88-15481
SCALING
A multiple-time-scale turbulence model based on variable partitioning of turbulent kinetic energy spectrum
[NASA-CR-179222] 04 p0444 N88-12754
Transport scaling in the collisionless-detrapping regime in stellarators
[DE88-001511] 05 p0653 N88-14006
Collider constraints in the choices for wavelength and gradient scaling
[PB87-123691] 06 p0779 N88-14783
On the smallest scale for the incompressible Navier-Stokes equations
[NASA-CR-181628] 11 p1434 N88-18558
The scaling of the threshold conditions for solid propellant erosive burning 19 p2630 N88-25601
SCALING LAWS
Reynolds number effects on the small scale structure of a turbulent channel flow 01 p0001 N88-10004
An analysis of an available set of linear programming test problems
[DE87-014578] 02 p0221 N88-11392
Relative merits of size, field, and current on ignited Tokamak performance: A comparison of CITs and Super-JETs
[DE88-000038] 02 p0241 N88-11521
Finite size scaling and lattice gauge theory
[DE87-014139] 02 p0245 N88-11549
An experimental investigation of unsteadiness in swept shock wave/turbulent boundary layer interactions 04 p0445 N88-12760
Improvement of modal scaling factors using mass additive technique 05 p0593 N88-13620
Nonlinear evolution equations, rescalings, model partial differential equations (PDES) and their integrability, 2
[PREPRINT-560] 06 p0764 N88-14691
The effect of response scaling on the detection of singularities in multiresponse estimation
[AD-A185964] 07 p0908 N88-15503
Anomalous scaling laws in multifractal objects
[NOTA-INTERNA-883] 07 p0916 N88-15565
A crude scaling law for lasertrons
[DE88-003880] 09 p1173 N88-17032
Plasma physics design and major specifications of candidate reactors for FER design studies. Conceptual design study of FY86 FER
[DE88-751066] 10 p1411 N88-18416
Atomic-scale simulation in materials science
[DE88-005204] 11 p1544 N88-19230
Cavitation inception
[AD-A189220] 13 p1765 N88-20557
Similarity theories and microturbulence in the atmospheric mixed layer 13 p1806 N88-20802
Scale model development for aeroelasticity studies
[ETN-88-91887] 14 p1868 N88-21164
Transport processes during directional solidification and crystal growth: Scaling and experimental study 14 p1988 N88-21857
Pusherless implosion, pulse tailoring and ignition scaling law for laser fusion 16 p2277 N88-23629
Scaling laws for homogeneous turbulent shear flows in a rotating frame
[NASA-CR-181672] 19 p2665 N88-25847
Scaling laws for geomagnetic tail current sheet acceleration
[AD-A193379] 19 p2691 N88-25998
The scaled-sized model: A revision of Amdahl's law
[DE88-008114] 20 p2844 N88-26875
Optimization and scale-up performance of polymer electrolyte batteries
[AD-A193987] 22 p3073 N88-28243
Faster scaling algorithms for network problems
[AD-A194032] 23 p3251 N88-29348
SCANNERS
NT COASTAL ZONE COLOR SCANNER
NT HORIZON SCANNERS
NT INFRARED SCANNERS
NT MULTISPECTRAL BAND SCANNERS
NT OCEAN COLOR SCANNER
NT OPTICAL SCANNERS
NT THEMATIC MAPPERS (LANDSAT)
NT ULTRASONIC SCANNERS
Fast dynamic studies with PC384-7B; system improvements and development of an automated blood sampling system --- tomography
[USIP-87-05] 01 p0075 N88-10481
Scene simulation for passive IR systems 02 p0137 N88-10861
Development of response models for the Earth Radiation Budget Experiment (ERBE) sensors. Part 3: ERBE scanner measurement accuracy analysis due to reduced housekeeping data
[NASA-CR-178294] 05 p0583 N88-13553
ISTP SBIR phase 1 Full-Sky Scanner: A feasibility study
[NASA-CR-180749] 10 p1333 N88-17964
Multidimensional system analysis of electro-optic sensors with sampled deterministic output
[AD-A187083] 10 p1408 N88-18399
Report on desktop publishing
[AD-A187698] 11 p1528 N88-19128
OCR vision system, an alternative to bar code
[DE88-003761] 15 p2149 N88-22828
Orbital navigation, docking and obstacle avoidance as a form of three dimensional model-based image understanding 17 p2388 N88-24194
Atmospheric autorotating imaging device
[NASA-CASE-NPO-17390-1-CU] 18 p2519 N88-24944
Use of modern scanner techniques in cartography 18 p2535 N88-25040
Fracture physics of delamination of composite materials
[AD-A192021] 19 p2609 N88-25482
Equipment for an advanced electron beam lithography system
[AD-A192956] 21 p2936 N88-27435
Parallel solutions to geometric problems on the scan model of computation
[AD-A192321] 21 p3004 N88-27819
Rapid-scanning Fourier transform spectrometer for studies of propagation of near-millimeter-wave radiation through clear air and fog
[AD-A193752] 22 p3070 N88-28219
SCANNING
NT CONICAL SCANNING
NT PANORAMIC SCANNING
NT RADAR SCANNING
NT RASTER SCANNING
Estimation filters with adaptive scanning time for flying target tracking
[ETN-87-90401] 01 p0036 N88-10232
Digital receiver structures and methods for the determination of the scanning frequency in modems for fast data transmission via telephone channels
[ETN-87-90429] 01 p0037 N88-10235
In-orbit calibration adjustment of the Nimbus-7 SMMR
[NASA-TM-100678] 05 p0614 N88-13773
AVIRIS scan drive design and performance 06 p0706 N88-14330
Quantifying some information processing aspects of the pilot's instrument crosscheck
[AD-A186114] 07 p0898 N88-15443
Scanning finite element calculation method
[PB87-143442] 08 p0995 N88-16017
High-speed assembly language (80386/80387) programming for laser spectra scan control and data acquisition providing improved resolution water vapor spectroscopy
[NASA-CR-4117] 08 p1053 N88-16355

Orbital navigation, docking and obstacle avoidance as a form of three dimensional model-based image understanding 08 p1061 N88-16406
Future television systems: Comparison of sequent ial and interlaced scanning
[BBC-RD-1987/18] 09 p1155 N88-16923
Soft maps for US Army electronic map background applications
[AD-A188427] 12 p1638 N88-19809
Systems for ultrasonic scanning, analysis and imagery 15 p2082 N88-22414
Flaw characterization in structural ceramics using scanning laser acoustic microscopy 15 p2082 N88-22415
Nondestructive evaluation of sintered ceramics 15 p2083 N88-22416
Three-dimensional flow visualization using laser-sheet scanning 16 p2203 N88-23143
Digitizing the traffic network of JOG 250 by scanning — JOG 250 map 18 p2533 N88-25029
SEGMERGE: A scanline visible surface algorithm with adaptive span selection and inexpensive antialiasing
[DE88-009186] 20 p2836 N88-26826
Scanning tunneling microscopy as a surface chemical probe
[AD-A192710] 21 p2909 N88-27263
Investigations on multiport antennas for polarimetric and modal field scanning
[REPT-5-87] 23 p3205 N88-29073
Scanning electron microscopy study of adhesion in sea urchin blastulae
[NASA-CR-183136] 24 p3406 N88-30275

SCANNING DEVICES
U SCANNERS

SCANNING LASER ACOUSTIC MICROSCOPE (SLAM)
U ACOUSTIC MICROSCOPES

SCAR PROGRAM
U SUPERSONIC CRUISE AIRCRAFT RESEARCH

SCARS (GEOLOGY)
U EROSION

SCATHA SATELLITE
Survey of the Air Force P78-2 (SCATHA) satellite plasma wave data during electron gun operations
[AD-A191014] 16 p2168 N88-22926
A severe spacecraft-charging event on SCATHA in September 1982
[AD-A193007] 20 p2765 N88-26396
Ion gun generated electromagnetic interference on the SCATHA satellite
[AD-A195179] 24 p3335 N88-29853

SCATTER PROPAGATION
Active and passive remote sensing of ice
[AD-A186685] 09 p1195 N88-17162
Multiple scattering of waves in discrete random media
[AD-A191068] 18 p2499 N88-24823

SCATTERERS
U SCATTERING

SCATTERING
NT ACOUSTIC SCATTERING
NT ATMOSPHERIC SCATTERING
NT BACKSCATTERING
NT COHERENT SCATTERING
NT COMPTON EFFECT
NT ELASTIC SCATTERING
NT ELECTROMAGNETIC SCATTERING
NT ELECTRON SCATTERING
NT FORWARD SCATTERING
NT HALOS
NT INCOHERENT SCATTERING
NT INELASTIC SCATTERING
NT INVERSE SCATTERING
NT ION SCATTERING
NT LIGHT SCATTERING
NT MICROWAVE SCATTERING
NT MIE SCATTERING
NT NEUTRON SCATTERING
NT NUCLEAR SCATTERING
NT PROTON SCATTERING
NT RADAR SCATTERING
NT RAMAN SPECTRA
NT RAYLEIGH SCATTERING
NT RESONANCE SCATTERING
NT REVERBERATION
NT THOMSON SCATTERING
NT TROPOSPHERIC SCATTERING
NT WAVE SCATTERING
NT X RAY SCATTERING
Surface scattering characteristics and the measurement of particulate contamination 02 p0137 N88-10862
Theoretical atomic and molecular photophysics
[DE87-014249] 02 p0231 N88-11458
JPRS report: Science and technology. China
[JPRS-CST-87-034] 03 p0301 N88-11897
New physical explanation of phase-conjugate waves produced in backward stimulated scattering 03 p0302 N88-11900
Uniform geometrical theory of diffraction 03 p0303 N88-11911
Singularity expansion method: Target Resonances 03 p0303 N88-11912
Numerical modeling: Integral equation method 03 p0304 N88-11919
Experiments: Test range facilities, part 2 03 p0305 N88-11921
Anti-Stokes generation of 226 nm light
[DE88-001612] 05 p0589 N88-13590
Atomic beam studies of the interaction of hydrogen with transition metal surfaces
[DE88-000208] 05 p0648 N88-13970
Energy dependence of ion-induced sputtering yields of monatomic solids in the low energy region
[IPPJ-AM-52] 05 p0651 N88-13988
Helium atom surface scattering apparatus for studies of crystalline surface dynamics
[DE88-002104] 06 p0787 N88-14826
Raman spectroscopic investigations of Hg-Cd-Te melts 07 p0926 N88-15625
Scattering of optical radiation by bursting water particles in fog 09 p1236 N88-17410
High-temperature charge-density studies of CeO/sub 2-x/ using X-ray and neutron diffraction techniques
[DE88-002988] 09 p1257 N88-17536
Investigation of a ray-mode representation of the Green's function in a rectangular cavity
[PB88-131677] 11 p1469 N88-18763
Electromagnetic scattering by an exponentially distributed rough surface with the introduction of a rough surface generation technique
[AD-A189678] 14 p1905 N88-21392
Observation of anomalous low J-value Stokes and anti-Stokes lines in stimulated rotational Raman scattering over long air paths
[DE88-003756] 14 p1911 N88-21418
Exciton relaxation phenomena in a disordered system 14 p1978 N88-21802
The elastic properties of monoclinic ZrO2
[DE88-005920] 14 p1986 N88-21847
Experimental studies of elastic properties of crystals by Brillouin scattering
[DE88-005923] 14 p1986 N88-21848
Brillouin scattering and transmission electron microscopy studies of radiation-induced elastic softening, disordering and amorphization of intermetallic compounds
[DE88-005927] 14 p1987 N88-21850
Theory of the dissociation dynamics of small molecules on metal surfaces: Finite temperature studies
[DE88-006495] 15 p2132 N88-22716
The optical properties of aerosols
[AD-A191420] 16 p2176 N88-22972
K-pulse estimation from incomplete multiple-frequency scattering data and target identification
[AD-A190827] 16 p2190 N88-23061
Enhanced backscattering from rough surfaces
[AD-A190995] 16 p2190 N88-23063
An experimental study of the coherent under-ice reflectivity of sound in the Greenland Sea Marginal Ice Zone 18 p2548 N88-25125
Changes in seismic velocity and apparent attenuation due to isotropic and anisotropic scattering: Results from physical modeling 19 p2691 N88-25997
Solution of Faddeev-Yakubovsky differential equations by the finite-dimensional approximation method for four spinless particles in the 1+3 scattering problem
[DE87-702983] 19 p2719 N88-26145
Ray scattering from a collection of ice keels
[AD-A191757] 19 p2722 N88-26163
Microwave image understanding and its application to radar cross section management 20 p2788 N88-26542
The theory of electron-polar phonon scattering rates in semiconductor micro-structures 20 p2871 N88-27043
Radar information from the partial derivatives of the echo signal phase from a point scatterer
[AD-A193402] 21 p2923 N88-27415
The effect of particle properties on radiative heat transfer 24 p3350 N88-29941
Scattering impulse response synthesis using random noise illumination: Initial concept evaluation
[AD-A195088] 24 p3364 N88-30034
Finite-difference simulations of Rayleigh-wave scattering by shallow heterogeneity
[AD-A194961] 24 p3402 N88-30259

SCATTERING AMPLITUDE
On the spin structure of the elastic ppbar scattering amplitude
[NOTA-INTERNA-892] 06 p0778 N88-14772
Absorption, scattering, and thermal radiation by conductive fibers
[AD-A186105] 07 p0842 N88-15106
Eikonal solutions to optical model coupled-channel equations
[NASA-TP-2830] 24 p3428 N88-30402

SCATTERING COEFFICIENTS
High-sensitivity recording of weak reflected or scattered radiation by method of coherent intracavity reception with YAG:Nd(3+) laser 08 p1078 N88-16502
Active and passive remote sensing of ice
[AD-A186685] 09 p1195 N88-17162
Acoustic backscattering from bottom sediment at normal incidence in the laboratory
[AD-A186905] 09 p1242 N88-17443
Effect of translucence of engineering ceramics on heat transfer in diesel engines
[DE88-003732] 10 p1305 N88-17804
Atmospheric backscatter at 10.6 microns; a compendium of measurements made outside the United Kingdom by the airborne LATAS coherent laser radar velocimeter
[RSRE-87002] 12 p1631 N88-19763
The radar scattering coefficient as a function of forest stand parameters and viewing angle. An empirical study of the Pinus sylvestris L. in the Kootwijk forest (The Netherlands), extended with observations in the Speulder and Sprielder forest (The Netherlands)
[ETN-88-91348] 13 p1760 N88-20527
Ray scattering from a collection of ice keels
[AD-A191757] 19 p2722 N88-26163

SCATTERING CROSS SECTIONS
Ab initio methods for electron-molecule collisions
[DE87-011728] 01 p0092 N88-10598
Heavy-particle collisions in the plasma edge
[DE87-012928] 02 p0237 N88-11493
Applied nuclear science research and development
[LA-10915-PR] 03 p0374 N88-12355
Magnetic diffuse scattering
[DE87-013539] 04 p0489 N88-13014
Electromagnetic wave probing of Earth's environment
[NASA-CR-182358] 06 p0690 N88-14232
On the spin structure of the elastic ppbar scattering amplitude
[NOTA-INTERNA-892] 06 p0778 N88-14772
Cross section of resonant Raman scattering of light by polyenes 07 p0920 N88-15591
The application of vector diffraction to the scalar anomalous diffraction approximation of Van de Hulst
[AD-A185930] 07 p0929 N88-15643
Hyperspherical coordinate theory of two-electron processes: Future plans
[DE87-010653] 08 p1081 N88-16516
Status of cross section data for photon scattering by atoms
[DE87-011281] 08 p1081 N88-16517
Introductory review: Physics of electron slowing-down processes
[DE88-002918] 09 p1246 N88-17466
The application of the hybrid iterative method to scattering by perfectly conducting bodies of revolution 11 p1475 N88-18802
Single nucleon coincidence cross sections in a relativistic mean field theory
[CEBAF-PR-87-016] 11 p1546 N88-19243
An efficient numerical algorithm for solving scattering and inverse scattering problems of electromagnetic waves
[AD-A188479] 12 p1619 N88-19684
Experimental set-up for measurements of Compton scattering cross section on light nuclei
[DE88-700161] 12 p1688 N88-20097
Vibration spectra of oxygen and vanadium atoms in vanadium-oxygen disordered interstitial alloys
[DE87-703166] 13 p1740 N88-20404
Measurement of the sup 4He(gamma, p)sup 3H total cross section and charge symmetry
[NOTA-INTERNA-902] 14 p1981 N88-21820
Inelastic two composite particle systems scattering at high energy
[DE88-701841] 20 p2851 N88-26928
Effect of a laser field in the electron inelastic scattering into plasma fields
[DE88-702295] 23 p3218 N88-29157
Neutrino detection primer
[AD-A193805] 23 p3280 N88-29529

SCATTERING FUNCTIONS
Developments related to scattering eigen elements in Schroedinger operators for particles with spin
[ETN-88-91077] 09 p1229 N88-17361
Synchronous measurements of effective photon path length in visible and near-IR spectral regions in real cloud systems 13 p1790 N88-20706

SCATTERING MATRIX
U S MATRIX THEORY

SCATTEROMETERS
Study of a payload for Columbus Polar Platform Earth observation demonstration mission, executive summary
[ESA-CR(P)-2412] 01 p0014 N88-10079

Deployment, hold down and release mechanisms for Wind Scatterometer Antenna (WSA) --- ERS-1 wind scatterometer antenna (WSA) 14 p1876 N88-21207
Preparation and execution of calibration measurements for handling of airborne SAR data (AGRISAR) [ETN-88-92338] 17 p2333 N88-23926
A study of the feasibility of using sea and wind information from the ERS-1 satellite. Part 1: Wind scatterometer data [NASA-CR-182833] 24 p3386 N88-30167
A study of the feasibility of using sea and wind information from the ERS-1 satellite. Part 2: Use of scatterometer and altimeter data in wave modeling and assimilation [ESA-CR(P)-2604-PT-2] 24 p3387 N88-30176

SCAVENGING
Auxiliary propulsion technology for advanced Earth-to-orbit vehicles [NASA-TM-100237] 06 p0674 N88-14127
Atmospheric science 07 p0883 N88-15357
STS propellant scavenging systems study. Part 2, volume 1: Executive summary and study results [NASA-CR-179275] 10 p1290 N88-17716
STS propellant scavenging systems study. Part 2, volume 2: Cost and WBS/dictionary [NASA-CR-179276] 10 p1290 N88-17717
Weight savings in aerospace vehicles through propellant scavenging [NASA-TM-100900] 19 p2605 N88-25470

SCENE ANALYSIS
The 3-D world modeling for an autonomous robot [DE87-013878] 03 p0333 N88-12102
Methods for design and evaluation of integrated hardware/software systems for concurrent computation [NASA-CR-181522] 04 p0479 N88-12953
Television motion measurement for DATV and other applications [BBC-RD-1987/11] 05 p0573 N88-13496
Some vision algorithms 06 p0795 N88-14871
Proceedings of Image Understanding Workshop, volume 1 [AD-A186103] 07 p0902 N88-15463
Recognition of polyhedral objects under structured illumination [PB88-106703] 07 p0932 N88-15661
Estimation of broadband planetary albedo from operational narrowband satellite measurements [PB88-107644] 07 p0945 N88-15748
Thematic mapper research in the earth sciences: Small scale patches of suspended matter and phytoplankton in the Elbe River Estuary, German Bight and Tidal Flats [NASA-CR-182378] 08 p1019 N88-16180
Image chunking: Defining spatial building blocks for scene analysis [AD-A187072] 09 p1200 N88-17191
Development of Moire machine vision 09 p1212 N88-17264
General determination of Earth surface type and cloud amount using multispectral AVHRR data [NOAA-TR-NESDIS-39] 11 p1506 N88-18997
Three-dimensional scene analysis using stero based imaging [AD-A193120] 21 p2894 N88-27178

SCF
U SELF CONSISTENT FIELDS

SCHEDULES
The development of laboratory vibration test schedules: Philosophies and techniques 08 p0999 N88-16049
Laboratory vibration test schedules development beyond MIL-STD-810D 08 p0999 N88-16050
Operational aspects of a spacecraft planning/scheduling expert system 08 p1052 N88-16415
Timetable control in a management system (space program) 22 p3160 N88-28815
Inflight rearming [AD-A193564] 23 p3176 N88-28909

SCHEDULING
NT PREDICTION ANALYSIS TECHNIQUES
A rule-based system for arrival sequencing and scheduling in air traffic control 02 p0129 N88-10815
Optimal pre-scheduling of problem remappings [NASA-CR-178378] 06 p0756 N88-14633
On stochastic optimality of policies in first passage problems [AD-A186293] 07 p0915 N88-15554
Third Conference on Artificial Intelligence for Space Applications, part 1 [NASA-CP-2492-PT-1] 08 p1055 N88-16360
Intelligent process development of foam molding for the Thermal Protection System (TPS) of the space shuttle external tank 08 p1060 N88-16397
Knowledge-based simulation 08 p1061 N88-16404
Planning and scheduling for robotic assembly 08 p1062 N88-16416
An AI approach for scheduling space-station payloads at Kennedy Space Center 08 p1064 N88-16425
Scheduling spacecraft operations 08 p1064 N88-16426
The resource envelope as a basis for space station management system scheduling 08 p1064 N88-16427
Prototype resupply scheduler 08 p1064 N88-16428
Performance analysis of parallel branch and bound search with the hypercube architecture 09 p1206 N88-17229
Expert mission planning and replanning scheduling system for NASA KSC payload operations 09 p1209 N88-17247
Range and mission scheduling automation using combined AI and operations research techniques 09 p1209 N88-17249
Nonpreemptive run-time scheduling issues on a multitasked, multiprogrammed multiprocessor with dependencies, bidimensional tasks, folding and dynamic graphs [DE88-003598] 09 p1223 N88-17335
A note on the effect of preemptive policies on the stability of a priority queue [AD-A186871] 09 p1227 N88-17345
An evaluation of project scheduling techniques in a dynamic environment [AD-A187057] 09 p1260 N88-17554
Dynamic processor self-scheduling for general parallel nested loops [DE88-003572] 10 p1393 N88-18311
Deadlock prevention in processor self-scheduling for parallel nested loops [DE88-003573] 10 p1393 N88-18313
A traveling-salesman-based approach to aircraft scheduling in the terminal area [NASA-TM-100062] 12 p1576 N88-19424
Schedule and cost control of development 12 p1704 N88-20196
Approximation algorithms for scheduling unrelated parallel machines [CWI-OS-R8714] 13 p1817 N88-20861
Satellite acquisition: Global positioning system acquisition changes after Challenger's accident [PB88-155536] 14 p1880 N88-21236
Discrete generalized networks: Application to integer constrained flow problems [AD-A190823] 16 p2190 N88-23060
Elementary and middle school science improvement project [NASA-CR-179328] 16 p2285 N88-23679
Performance effectiveness and the work/rest cycle [AD-A191448] 18 p2551 N88-25145
A mixed-integer linear programming problem which is efficiently solvable [AD-A191028] 18 p2556 N88-25168
LRS-2: A specialized knowledge system for launch resource scheduling [AD-A194625] 23 p3182 N88-28941
A knowledge-based decision support system for payload scheduling 23 p3252 N88-29358
A scheduling and resource management system for space applications 23 p3256 N88-29383
A space station onboard scheduling assistant 23 p3259 N88-29402
NOA: A Network Operator Assistant for scheduling Tracking and Data Relay Satellite System (TDRSS) 23 p3259 N88-29403
Experiment scheduling for Spacelab missions 23 p3259 N88-29404
A static scheduler for the computer aided prototyping system: An implementation guide [AD-A194340] 24 p3414 N88-30322
Contingency rescheduling of spacecraft operations 24 p3416 N88-30337
Knowledge based tools for Hubble Space Telescope planning and scheduling: Constraints and strategies 24 p3417 N88-30338
The proposal entry processor: Telescience applications for Hubble Space Telescope science operations 24 p3417 N88-30339
Candidate functions for advanced technology implementation in the Columbus mission planning environment 24 p3417 N88-30340
Integrated resource scheduling in a distributed scheduling environment 24 p3417 N88-30342
Lisp Object State Saver (LOSS): A facility used to save partial schedules of the Hubble Space Telescope 24 p3421 N88-30360
The P-3 Scheduling Support System (P-3 S3) [AD-A194824] 24 p3436 N88-30450

SCHEMATICS
U CIRCUIT DIAGRAMS

SCHIFF BASES
U IMINES

SCHIZOPHRENIA
Information processing deficits in psychiatric populations: Implications for normal workload assessment 16 p2241 N88-23390

SCHLIEREN PHOTOGRAPHY
Development of flow visualization techniques for use in the Hot Gas Laboratory [BAE-ARG-233] 03 p0325 N88-12052
Development of an optical diagnostic instrument. Part 2: Instrument development --- space laboratories [NLR-TR-87079-L-PT-2] 13 p1841 N88-21016

SCHOOLS
A summary of the Naval Postgraduate School research program [AD-A186362] 07 p0942 N88-15727
Elementary and middle school science improvement project [NASA-CR-179328] 16 p2285 N88-23679

SCHOTTKY BARRIER DIODES
U SCHOTTKY DIODES

SCHOTTKY DIODES
Study and realization of Schottky diodes for forthcoming integrated hyperfrequency devices [LAAS-87-062] 02 p0167 N88-11054
Comparative investigation of heterodyne mixers at 1000 GHz [FTL-068827] 09 p1158 N88-16940
Development of a high speed InGaAs/InP Schottky barrier photodetector for millimeter-wave fiber optical links [AD-A188594] 12 p1629 N88-19750
Characterization of enhanced Schottky-barrier InGaAs/Al(1-x)As strained channel modulation-doped field-effect transistors [AD-A188820] 12 p1698 N88-20162
The influence of current stressing on the structure of Ag contacts to GaAs [DE88-005988] 15 p2140 N88-22771
Research investigation directed toward extending the useful range of the electromagnetic spectrum [AD-A190198] 17 p2332 N88-23920
Research investigation directed toward extending the useful range of the electromagnetic spectrum, appendix [AD-A190199] 17 p2332 N88-23921
Novel silicon Schottky barrier infrared imaging arrays 17 p2439 N88-24510
Schottky-barrier formation on a covalent semiconductor without Fermi-level pinning: The Metal-MoS2(0001) interface [AD-A193044] 21 p3021 N88-27931
Blue-green laser diode research program [AD-A191980] 23 p3218 N88-29153

SCHOTTKY EFFECT
U WORK FUNCTIONS

SCHROEDINGER EQUATION
Numerical studies of the dual HEMT/algorithm development and numerical studies of Schrodinger's equation [AD-A184471] 04 p0478 N88-12946
Darboux and Baecklund transformations for the Schroedinger equation [PREPRINT-545] 06 p0763 N88-14685
Equations of nonlinear Schroedinger type in 1 + 1 and 2 + 1 dimensions, obtained from integrable Partial Differential Equations (PDEs) [PREPRINT-548] 06 p0764 N88-14687
Nonisospectral deformations and Darboux transformations for the 3rd order spectral problem [PREPRINT-558] 06 p0764 N88-14690
The inverse back scattering problem for the Schroedinger equation in two space dimensions [AD-A185603] 06 p0765 N88-14701
Modified quantum mechanics of small composite systems [NIKHEF-H/87-1] 06 p0790 N88-14845
Developments related to scattering eigen elements in Schroedinger operators for particles with spin [ETN-88-91077] 09 p1229 N88-17361
On exact solutions of multidimensional Schroedinger equation with polynomial potentials [DE88-700460] 09 p1230 N88-17373
Further study of relation of von Karman equation for elastic large deflection problem and Schrodinger equation for quantum eigenvalues problem 14 p1899 N88-21341
Geometric methods and the gauge structure of Berry's phase [DE88-006538] 15 p2127 N88-22682
Free Laplacian with attractive boundary conditions [DE87-702971] 16 p2256 N88-23482
Combining relativity and quantum mechanics: Schroedinger's interpretation of pai [DE88-701899] 20 p2880 N88-27102
Cauchy problem for the nonlinear Schroedinger equation [DE88-702454] 21 p3011 N88-27867

SCHUMANN-RUNGE BANDS
Aeronomic problems of the molecular oxygen photodissociation. Part 3: Solar spectral irradiances in the region of the O2 Herzberg continuum, Schumann-Runge bands and continuum
[AERONOMICA-ACTA-A-332-1988] 24 p3343 N88-29897
Aeronomic problems of molecular oxygen photodissociation. Part 2: Theoretical absorption cross sections of the Schumann-Runge bands at 79 K
[AERONOMICA-ACTA-A-331-1988] 24 p3344 N88-29907

SCHWARTZ INEQUALITY
Baecklund transformation and the Schwarzian derivative
[AD-A190277] 15 p2127 N88-22684

SCHWARZSCHILD METRIC
Criterion of singularity in general theory of relativity 09 p1240 N88-17430

SCIENCE
Interdisciplinary research in mathematics, science and technology education
[PB88-131446] 10 p1398 N88-18333

SCIENTIFIC SATELLITES
NT AMPTE (SATELLITES)
NT ASTRONOMICAL SATELLITES
NT AZUR SATELLITE
NT COSMIC BACKGROUND EXPLORER SATELLITE
NT DYNAMICS EXPLORER 1 SATELLITE
NT EXOSAT SATELLITE
NT EXPLORER SATELLITES
NT EXPLORER 47 SATELLITE
NT EXPLORER 51 SATELLITE
NT EXPLORER 54 SATELLITE
NT EXPLORER 55 SATELLITE
NT GAMMA RAY OBSERVATORY
NT GEOPOTENTIAL RESEARCH MISSION
NT HUBBLE SPACE TELESCOPE
NT INTERNATIONAL SUN EARTH EXPLORER 3
NT INTERNATIONAL SUN EARTH EXPLORERS
NT MAGSAT SATELLITES
NT SOLAR MESOSPHERE EXPLORER
NT SPACE INFRARED TELESCOPE FACILITY
NT UK SATELLITES
NT X RAY ASTROPHYSICS FACILITY
Report on the scientific satellites of the European Space Agency
[ESA-SP-1090] 01 p0014 N88-10081
Viking quick look plots: A short description --- Swedish satellite 06 p0692 N88-14243
Analysis and interpretation of satellite fragmentation data 06 p0798 N88-14885
Viking: The first Swedish satellite 08 p1025 N88-16207
MAXIE 1
[AD-A189688] 14 p1882 N88-21247
Evaluating evaporation with satellite thermal data
[AD-A192042] 18 p2531 N88-25019
MAXIE-1 (Magnetospheric Atmospheric X-ray Imaging Experiment)
[AD-A192846] 21 p2902 N88-27221

SCIENTISTS
Report from the MPP Working Group to the NASA Associate Administrator for Space Science and Applications
[NASA-TM-87819] 02 p0223 N88-11402
On the occasion of the 50th anniversary of the death of Professor Hugo Junkers
[MBB/LW-3016/S/PUB/201] 02 p0257 N88-11627
National Center for Atmospheric Research
[PB87-228391] 04 p0470 N88-12901
A study of the minority college programs at the NASA Johnson Space Center 06 p0798 N88-14887
Research reports: 1987 NASA/ASEE Summer Faculty Fellowship Program
[NASA-CR-179219] 07 p0922 N88-15601
Networking requirements and future alternatives
[NASA-TM-89711] 10 p1426 N88-18517

SCINTILLATION
A comparative analysis of equatorial and auroral-zone phase scintillation data
[AD-A184509] 03 p0350 N88-12212
Study on cineradiography
[ISL-R-120/86] 08 p0990 N88-15994
F-layer polar cap arcs
[AD-A186592] 09 p1190 N88-17127
An assessment of the application of in situ ion-density data from DMSP to modeling of transionospheric scintillation
[AD-A188919] 12 p1643 N88-19840
Analysis of the inter-layer independence of stellar scintillometer profiles of Cn2
[AD-A189372] 12 p1645 N88-19854
Measurements of the scintillation time constants of inorganic crystals for the development of a triple-Phoswich detector for high-energy X-ray quanta
[ETN-88-91501] 14 p1993 N88-21875
Stellar scintillometer atmospheric optical turbulence profiling experiment: A qualitative comparison of two identical instruments at AMOS (Air Force Maui Optical Station), 1985
[AD-A190589] 15 p2094 N88-22479
Design, fabricate, calibrate, test and deliver two satellite electron flux detectors
[AD-A190799] 16 p2169 N88-22930
Radio-wave scintillations and ionospheric irregularities at high latitudes
[AD-A192140] 18 p2501 N88-24837
Spectral estimation of received phase in the presence of amplitude scintillation 22 p3064 N88-28180

SCINTILLATION COUNTERS
A layered scintillation detector for solar neutron observations
[DE87-011354] 01 p0049 N88-10314
A 15 cm aperture LED scintillometer for C(n) squared and crosswind measurements
[KNMI-WR-87-3] 01 p0070 N88-10448
A program to study antiprotons in the cosmic rays: Arizona collaboration
[NASA-CR-180702] 01 p0120 N88-10764
Multichannel electron counter with high space resolution
[DE88-700564] 07 p0857 N88-15204
The response of a small liquid scintillation counter for low energy (gamma, p) experiments
[NOTA-INTERNA-901] 14 p1980 N88-21819
Measurements of the scintillation time constants of inorganic crystals for the development of a triple-Phoswich detector for high-energy X-ray quanta
[ETN-88-91501] 14 p1993 N88-21875
Stellar scintillometer atmospheric optical turbulence profiling experiment: A qualitative comparison of two identical instruments at AMOS (Air Force Maui Optical Station), 1985
[AD-A190589] 15 p2094 N88-22479
Study of light transmission methods from scintillators to optical fiber with wave length shifter
[DE88-701587] 18 p2574 N88-25292

SCINTILLATORS
U SCINTILLATION COUNTERS

SCINTILLOMETERS
U SCINTILLATION COUNTERS

SCISSION
U CLEAVAGE

SCORPIO CONSTELLATION
U SCORPIUS CONSTELLATION

SCORPIUS CONSTELLATION
The angular diameter of alpha Scorpii in the near-infrared Ca II triplet 04 p0514 N88-13162

SCOTLAND
SeaSoar profiles in the Iceland-Scotland area, May 1987
[IOS-253] 18 p2548 N88-25124

SCPC TRANSMISSION
U SINGLE CHANNEL PER CARRIER TRANSMISSION

SCRAMJET ENGINES
U SUPERSONIC COMBUSTION RAMJET ENGINES

SCRAMJETS
U SUPERSONIC COMBUSTION RAMJET ENGINES

SCREEN EFFECT
Sensitivity of F-106B leading-edge-vortex images to flight and vapor-screen parameters
[NASA-TP-2818] 17 p2300 N88-23760

SCREW DISLOCATIONS
The effects of thin anodic films on the cyclic microstrain/macrostrain behavior of tungsten 05 p0597 N88-13650

SCREW PINCH
FOM contributions to the 14th European Conference on Controlled Fusion and Plasma Physics
[REPT-87-174] 12 p1693 N88-20129
Formation of high-Beta plasmas in various modes of operation in TPE-2 12 p1693 N88-20132
The stability of a screw-pinch plasma to global MHD modes 12 p1694 N88-20133
Improved confinement of screw pinch plasmas in SPICA 2 12 p1694 N88-20137

SCREWS
An advanced extruder-feeder biomass liquefaction reactor system 18 p2535 N88-25042
Empirical fatigue crack growth data for a tension loaded threaded fastener
[AD-A194112] 22 p3088 N88-28334

SCRUBBERS
Compact regenerable sulfur scrubber for phosphoric acid fuel cells
[AD-A191356] 16 p2230 N88-23318

SCRUBBING
U WASHING

SEA BREEZE
Short range forecasting of sea breeze generated thunderstorms at the Kennedy Space Center: A real-time experiment using a primitive equation mesoscale numerical model 02 p0211 N88-11324
Validation of a three dimensional numerical model of the sea breeze in complex terrain 02 p0211 N88-11325
Mesoscale analysis and forecasting for the 1987 America's Cup, Fremantle, Western Australia 02 p0214 N88-11350
Atmospheric diffusion at coastal site in presence of sea-breeze
[DE88-700038] 07 p0876 N88-15314

SEA GRASSES
Five New South Wales barrier lagoons: Their macrobenthic fauna and seagrass communities 11 p1517 N88-19059

SEA ICE
NT ICE FLOES
NT ICEBERGS
NT PRESSURE ICE
Porosity influence on the strength and elasticity of first-year sea ice
[AD-A184493] 03 p0354 N88-12233
Eastern - western Arctic Sea ice analysis 1986
[AD-A184016] 03 p0355 N88-12235
The ice conditions in the Greenland waters, 1981
[ISBN-87-7478-276-2] 05 p0629 N88-13844
Electromagnetic wave probing of Earth's environment
[NASA-CR-182358] 06 p0690 N88-14232
Report of the second session of the working group on sea ice and climate
[WCP-128] 06 p0745 N88-14580
Navarin Basin Ice Drift Program
[PB88-104021] 06 p0748 N88-14599
Predictability of ice concentration in the high-latitude North Atlantic from statistical analysis of SST (Sea Surface Temperature) and ice concentration data
[AD-A186621] 08 p1045 N88-16315
Physical properties of summer sea ice in the Fram Strait, June-July 1984
[AD-A186937] 09 p1194 N88-17156
Active and passive remote sensing of ice
[AD-A186685] 09 p1195 N88-17162
NASA Oceanic Processes Program
[NASA-TM-4025] 10 p1357 N88-18109
Physical and structural characteristics of Weddell Sea pack ice
[AD-A188189] 10 p1358 N88-18119
Airborne electromagnetic sounding of sea ice thickness and sub-ice bathymetry
[AD-A188939] 12 p1649 N88-19879
Predictions and studies with a one-dimensional ice/ocean model
[AD-A189158] 13 p1803 N88-20776
Microwave and structural properties of saline ice
[AD-A189307] 13 p1803 N88-20779
Mechanical properties of sea ice and sea ice deformation in the near-shore zone
[PB88-147889] 13 p1804 N88-20782
Elements of sea ice dynamics and thermodynamics 14 p1939 N88-21571
Sea ice observations and models 14 p1939 N88-21572
The Greenland Sea Project: The Arctemiz project 14 p1939 N88-21573
The effects of time-dependent winds and ocean eddies on ice motion in a marginal ice zone
[AD-A190105] 15 p2100 N88-22511
Hydrographic observations in the northwestern Weddell Sea Marginal Ice Zone during March 1986
[PB88-173240] 16 p2237 N88-23359
An investigation of Soviet capabilities in extended range arctic ice forecasting
[AD-A191082] 17 p2376 N88-24127
Sea ice kinematics: Space and time scales
[AD-A191162] 17 p2376 N88-24128
Examples of ice pack rigidity and mobility characteristics determined from ice motion
[AD-A191163] 17 p2377 N88-24129
DMSP-SSM/1 NASA algorithm validation using primarily LANDSAT and secondarily DMSP and/or AVHRR visible and thermal infrared satellite imagery
[NASA-CR-182979] 18 p2532 N88-25024
Higher frequency ambient noise in the arctic ocean
[AD-A192203] 18 p2547 N88-25122
Ray scattering from a collection of ice keels
[AD-A191757] 19 p2722 N88-26163
Active and passive remote sensing of ice
[AD-A193307] 21 p2966 N88-27617
The relationship between polar sea ice and the position of the near equatorial convergence zone 22 p3123 N88-28563
Arctic ice attenuation model study
[AD-A193382] 22 p3146 N88-28715

An objective technique for Arctic cloud analysis using multispectral AVHRR (Advanced Very High Resolution Radiometer) satellite imagery
[AD-A194732] 23 p3235 N88-29250
Meteorological features during the marginal ice zone experiment from 20 March to 10 April 1987
[AD-A193960] 23 p3235 N88-29251
Sea ice processes
[AD-A193980] 23 p3237 N88-29262
Reflection and scattering of acoustic rays computed for parabolic ice keel models
[AD-A193898] 23 p3278 N88-29517
MIZEX (marginal ice zone experiment) 1987 SAR (Synthetic Aperture Radar) data summary
[AD-A195560] 24 p3364 N88-30035

SEA KNIGHT HELICOPTER
U CH-46 HELICOPTER

SEA LAUNCHING
The effect of a turbulent airstream on a vertically-launched missile at high angles of attack
[AD-A192408] 20 p2758 N88-26363

SEA LEVEL
Regime dependent analysis experiments --- sea level pressure field 02 p0209 N88-11314
Mesoscale surface field analysis from routine observations --- pressure, wind fields 02 p0209 N88-11315
Sea level changes
[DE87-014357] 04 p0472 N88-12913
Expectations for water level deviations at the delta works: Zierikzee (Netherlands), November 1981-February 1986
[KNMI-TR-93] 05 p0628 N88-13840
FORTRAN programs for computation of time dependent sea levels and trajectory errors from satellite altimeter data
[BONN-MITT-73] 21 p2901 N88-27216
Reduce uncertainty in projection of future sea-level changes due to ice wastage
[DE88-009863] 22 p3129 N88-28601

SEA ROUGHNESS
Studies of thin surface films aim at seeing deep ocean processes 04 p0460 N88-12847
Impact force as a part of the total breaking wave force on a vertical cylinder
[RR-CE78] 24 p3384 N88-30154

SEA STATES
Cavitation inception scale effects. 1. Nuclei distributions in natural waters. 2. Cavitation incaption in a turbulent shear flow
[AD-A186553] 08 p0988 N88-15987
A propagation campaign in a marine environment utilizing a digital system at 36 GHz 12 p1618 N88-19675
Low frequency ocean ambient noise: Measurements and theory
[AD-A191188] 16 p2237 N88-23362
A probabilistic model of the apparent radiance of a rough sea
[AD-A193867] 22 p3129 N88-28602

SEA SURFACE TEMPERATURE
The distinction between different water masses using optical remote sensing applied to data from the Alboran Sea Experiment 1982
[DFVLR-FB-86-48] 03 p0345 N88-12181
A multibody dynamic analysis of the N-ROSS (Navy Remote Ocean Sensing System) satellite rotating flexible reflector using Kane's method
[AD-A184452] 04 p0462 N88-12860
On the interannual variability of South American climate and the Southern Oscillation 04 p0470 N88-12905
AVHRR/HIRS (Advanced Very High Resolution Radiometer/High Resolution Infra-Red Sounder) operational method for satellite based sea surface temperature determination
[PB88-107594] 06 p0708 N88-14340
The effect of latitude on the development of tropical cyclones
[AD-A185670] 06 p0746 N88-14590
Predictability of ice concentration in the high-latitude North Atlantic from statistical analysis of SST (Sea Surface Temperature) and ice concentration data
[AD-A186621] 08 p1045 N88-16315
NASA Oceanic Processes Program
[NASA-TM-4025] 10 p1357 N88-18109
Spatial-temporal variability of North Pacific sea surface temperature anomaly patterns 11 p1516 N88-19058
Tropic heat MR (Meteorological Recorder) meteorological data (April 1984 - June 1985)
[PB88-161286] 14 p1948 N88-21620
Influence of the Yukon River on the Bering Sea
[NASA-CR-182802] 17 p2376 N88-24126
Determination of mesoscale variability of sea surface temperature and attenuation in the North Atlantic from satellite measurement
[REPT-162] 18 p2548 N88-25127
The active layer of the upper Atlantic Ocean 22 p3124 N88-28566

SEA URCHINS
Scanning electron microscopy study of adhesion in sea urchin blastulae
[NASA-CR-183136] 24 p3406 N88-30275
Immunofluorescence localization of dissociation supernatant and extracellular matrix components in Lytechinus pictus sectioned embryos
[NASA-CR-183137] 24 p3406 N88-30276

SEA WALLS
U BREAKWATERS

SEA WATER
Power flow in terms of Poynting vector for Extremely Low Frequency (ELF) dipole sources in seawater
[ARE-TM(UTM)-87102] 01 p0035 N88-10221
Hydrochemical structure of Gulf Stream frontal zone waters 06 p0727 N88-14476
Foam generation and air entrainment near a free surface
[AD-A185986] 07 p0848 N88-15149
The influence of yellow substances on remote sensing of sea water constituents from space. Volume 1: Summary
[ESA-CR(P)-2443-VOL-1] 07 p0872 N88-15292
The influence of yellow substances on remote sensing of sea water constituents from space. Volume 2: Appendices
[ESA-CR(P)-2443-VOL-2] 07 p0873 N88-15293
The use of chlorophyll fluorescence measurements from space for separating constituents of sea water. Volume 1: Summary
[ESA-CR(P)-2444-VOL-1] 07 p0873 N88-15294
The use of chlorophyll fluorescence measurements from space for separating constituents of sea water. Volume 2: Appendices
[ESA-CR(P)-2444-VOL-2] 07 p0873 N88-15295
Cavitation inception scale effects. 1. Nuclei distributions in natural waters. 2. Cavitation inception in a turbulent shear flow
[AD-A186553] 08 p0988 N88-15987
The use of chlorophyll fluorescence measurements from space for separating constituents of sea water 08 p1043 N88-16307
The influence of yellow substances on remote sensing of sea-water constituents from space 08 p1044 N88-16308
Sea surface current estimates off central California as derived from enhanced AVHRR (Advanced Very High Resolution Radiometer) infrared images
[AD-A186867] 09 p1194 N88-17155
The analytical exponential decay coefficient of the submarine light field
[AD-A187215] 11 p1548 N88-19261
Remote sensing of atmospheric optical thickness and sea-water attenuation when submerged: Wavelength selection and anticipated errors
[AD-A187609] 11 p1548 N88-19262
Editing master oceanographic observation data set 4
[AD-A188405] 12 p1649 N88-19876
Cavitation inception
[AD-A189220] 13 p1765 N88-20557
Determination of mean thermohaline characteristics of the ocean 13 p1784 N88-20675
Research on influence of individual sea water components on spectral brightness coefficient of outgoing radiation 13 p1785 N88-20682
Predictions and studies with a one-dimensional ice/ocean model
[AD-A189158] 13 p1803 N88-20776
Experimental and theoretical constraints on the origin of mid-ocean ridge geothermal fluids 13 p1804 N88-20784
Relationship between optical transfer function and natural light field in sea or atmosphere 15 p2054 N88-22247
Physical, chemical and CTD (Conductivity/Temperature/Depth) data from the Marathon 2 expedition
[AD-A189930] 15 p2099 N88-22507
MIZPAC (marginal ice zone Pacific) 84-86 CTD (Conductivity, Temperature, Depth) data report
[AD-A192478] 21 p2976 N88-27679
Evaluation of organic coating deterioration and substrate corrosion in seawater using electrochemical impedance measurements 24 p3355 N88-29976

SEALANTS
U SEALERS

SEALERS
Process for the production of a thermoplastic elastomer composition
[EP-PATENT-0-202-782-A2] 05 p0569 N88-13465
Examination of polysulfide sealants by scanning electron microscopy
[MRL-R-1096] 13 p1752 N88-20478
Determination of the modulus of elasticity of structural silicone sealants
[PB88-157458] 14 p1893 N88-21307
Inadequacies of EMI-seal material: A corrosion study 17 p2319 N88-23852
Primerless RTV silicones
[BDX-613-3807] 24 p3356 N88-29980

SEALING
The axisymmetric sealing gap with variable viscosity. A variable hydraulic resistance
[ETN-87-90604] 03 p0314 N88-11987
Metal modification for improved glass-ceramic to metal seals: 1. Auger results on ion implantation and vapor deposition films
[DE88-005244] 10 p1339 N88-18006
Processing of glass to aluminum (low melting metals) seals via an injection molding technique
[DE88-004689] 13 p1751 N88-20468
Composite repair of cracked aluminum alloy aircraft structure
[AD-A190514] 18 p2455 N88-24573
Sample decomposition in sealed teflon vessels
[NASA-TT-20189] 18 p2494 N88-24798
Optical pressure sealing couping (light joint)
[NASA-CASE-MFS-29348-1] 18 p2576 N88-25303

SEALS (STOPPERS)
NT HERMETIC SEALS
NT LABYRINTH SEALS
NT O RING SEALS
NT PACKINGS (SEALS)
NT PLUGS
NT PUMP SEALS
Coatings for high-temperature bearings and seals
[NASA-TM-100249] 05 p0567 N88-13453
Three-dimensional dynamic labyrinth seal analysis
[AD-A185353] 05 p0590 N88-13599
Seal technology for liquid oxygen (LOX) turbopumps
[NASA-CR-174866] 05 p0591 N88-13603
Processing and interfacial analysis of glass-ceramic to metal seals
[DE88-002999] 08 p0971 N88-15873
Numerical modeling of multidimensional flow in seals and bearings used in rotating machinery
[NASA-TM-100779] 09 p1185 N88-16988
Tribological properties of alumina-boria-silicate fabric from 25 to 850 C
[NASA-TM-100806] 11 p1464 N88-18726
Numerical and analytical study of fluid dynamic forces in seals and bearings
[NASA-TM-100268] 11 p1485 N88-18867
Properties to seals made with Li2O-Al2O3-SiO2-glass ceramics and aluminum-containing austenitic stainless steels
[DE88-004688] 12 p1633 N88-19776
Thermal stress minimized, two component, turbine shroud seal
[NASA-CASE-LEW-14212-1] 17 p2345 N88-23978
Botany Facility: Magnetic fluid seal considerations for the centrifuge
[SIRA-A/7373/WP110/MAC004] 17 p2378 N88-24138
Entrance and exit region friction factor models for annular seal analysis
[NASA-CR-183084] 19 p2678 N88-25921
Development of high temperature, high pressure rotating shaft seals
[DE88-001029] 23 p3221 N88-29172

SEAMOUNTS
Bathymetric hazard survey test
[AD-A189150] 13 p1803 N88-20775
Identification and acoustic characterization of seamounts
[AD-A192204] 18 p2548 N88-25123

SEAMS (JOINTS)
Automatic seam welding with infrared sensor feedback
[DE87-013556] 01 p0055 N88-10352

SEARCH AND RESCUE SATELLITE
U SARSAT

SEARCH FOR EXTRATERRESTRIAL INTELLIGENCE
U PROJECT SETI

SEARCH PROFILES
Parallel artificial intelligence search techniques for real time applications
[AD-A190683] 16 p2255 N88-23473
A flexible search strategy for production systems 23 p3262 N88-29420

SEARCH RADAR
NT OVER-THE-HORIZON RADAR
A preliminary assessment of thunderstorm outflow wind measurement with airport surveillance radars
[AD-A189064] 13 p1799 N88-20757
Automated test device for FASR (Fixed Array Surveillance Radar) beam steering componentry
[AD-A191650] 18 p2500 N88-24829

Analysis of ATCRBS (Air Traffic Control Radar Beacon System), mode select (Mode S) in combat operations
[AD-A193140] 22 p3040 N88-28050

SEARCHING
NT SEARCH PROFILES
A new compression method with fast searching on large databases
[DE87-010986] 01 p0106 N88-10691
System for SAR missions 03 p0265 N88-11671
An astrometric search for a stellar companion to the sun 04 p0520 N88-13195
An automated supernova search and the design strategy
[DE88-001827] 05 p0660 N88-14051
Investigation and implementation of an algorithm for computing optimal search paths
[AD-A185927] 07 p0902 N88-15461
Investigation of candidate data structures and search algorithms to support a knowledge based fault diagnosis system 07 p0923 N88-15606
Research on visual information processing with special reference to oculomotor behavior in the areas of exploration, recognition and search
[AD-A186598] 08 p1051 N88-16346
Effects of uniform target density on random search
[AD-A186468] 08 p1073 N88-16473
Visual attention effects on discrimination of line orientation and line arrangement
[AD-A187013] 09 p1200 N88-17190
Hierachical object recognition using libraries of parameterized model sub-parts
[AD-A187476] 10 p1396 N88-18322
Search problems in mission planning and navigation of autonomous aircraft
[NASA-CR-182666] 12 p1579 N88-19448

SEAS
NT ADRIATIC SEA
NT BEAUFORT SEA (NORTH AMERICA)
NT BERING SEA
NT BLACK SEA
NT CARIBBEAN SEA
NT MEDITERRANEAN SEA
NT NORTH SEA
Hydrographic observations in the northwestern Weddell Sea Marginal Ice Zone during March 1986
[PB88-173240] 16 p2237 N88-23359
Eigenmatrix representations of radiance distributions in layered natural waters with wind-roughened surfaces
[PB88-188701] 20 p2828 N88-26780

SEASAT SATELLITES
An exploratory study of inland water and land altimetry using Seasat data
[ESA-CR(P)-2433] 02 p0193 N88-11208
Earthnet's experience with Seasat SAR image processing 09 p1127 N88-16760
Tidal estimation in the Pacific with application to SEASAT altimetry
[NASA-TM-100694] 13 p1803 N88-20780
Seasat orbit determination experiments in preparation for the ERS-1 altimetry mission
[ETN-88-91842] 14 p1871 N88-21182

SEASONAL VARIATIONS
U ANNUAL VARIATIONS

SEASONS
NT SPRING (SEASON)
NT SUMMER
NT WINTER
Modes of surface circulation and climate over the tropical Atlantic, Eastern Pacific, and Indian Oceans 06 p0742 N88-14564
Effect of storage thermal behavior in seasonal storage solar heating systems
[PB88-114236] 10 p1350 N88-18067
Northern Hemisphere 700 mb teleconnections based on half-monthly mean anomaly data stratified by season and by sign 22 p3123 N88-28561
On the modes of growing-season precipitation over central North America 22 p3124 N88-28567
Differences in radiation budget parameters over Asia in relation to contrasting Indian monsoons 22 p3125 N88-28574
Typical weather months in the past (1973-1983) in Central Europe
[AD-A194701] 23 p3235 N88-29249

SEATS
NT BARANY CHAIR
Variable response load limiting device
[NASA-CASE-LAR-12801-1] 17 p2346 N88-23982

SEAWEEDS
Contribution of SPOT satellite to qualitative and quantitative mapping of marine vegetation in the English Channel, North Atlantic, western Mediterranean, and South Pacific 22 p3109 N88-28464

SECONDARY BATTERIES
U STORAGE BATTERIES

SECONDARY EMISSION
External surface charging mechanisms — spacecraft 03 p0273 N88-11719
Analysis of relativistic nucleus-nucleus interactions in emulsion chambers 07 p0926 N88-15624
The magnitude of secondary electron contributions in photon stimulated desorption
[AD-A189094] 13 p1835 N88-20980
Secondary electron emission characteristics improved by ion implantation 14 p1903 N88-21370
Question on the measurement of the metal work function in an electron spectrometer by the secondary-electron emission threshold method
[NASA-TT-20190] 16 p2178 N88-22979
Effects of secondary electron emission on the collector and source sheaths of a finite ion temperature plasma
[DE88-008930] 20 p2858 N88-26971
Plasma theory and simulation
[AD-A194674] 23 p3286 N88-29565
Study of secondary emission properties of materials used for high power RF components in space
[ESA-CR(P)-2587] 24 p3361 N88-30012

SECONDARY FLOW
Flow field measurements in a 90 degree turning duct 02 p0186 N88-11157
Secondary subharmonic instability of boundary layers with pressure gradient and suction
[NASA-CR-4112] 07 p0848 N88-15148
Mean velocities and Reynolds stresses in the juncture flow and in the shear layer downstream of an appendage
[AD-A185819] 08 p0980 N88-15923
Experimental study of secondary flow in the presence of two jet arrays on the wall of a turbine blade
[ECL-87-11] 08 p0987 N88-15981
Investigation of dihedral effects in compressor cascades 10 p1282 N88-17672
Secondary flow measurements with L2F-technique in centrifugal compressors 10 p1283 N88-17676
Design and testing of a front stage for an advanced high pressure compressor 10 p1283 N88-17679
Computation of secondary flows in an axial multistage compressor 10 p1284 N88-17681
Flow patterns induced by vortices
[NAL-TR-932] 10 p1332 N88-17963
Disk pumping test
[AD-A187199] 11 p1440 N88-18591
A review of approaches to the study of turbulence modification by means of non-Newtonian additives
[AD-A188799] 12 p1627 N88-19734
Secondary instability of compressible boundary layer to subharmonic three-dimensional disturbances
[NASA-CR-4144] 16 p2200 N88-23122
The aspect ratio dependence of the attractor dimension in Taylor-Couette flow
[AD-A196297] 24 p3369 N88-30065

SECONDARY RADAR
Validate algorithms for the determination of rainfall rates from SSM/I microwave satellite imagery
[AD-A191337] 16 p2236 N88-23353
Fine resolution errors in secondary surveillance radar altitude reporting
[RSRE-87019] 23 p3175 N88-28906

SECONDARY WAVES
U S WAVES

SECRETIONS
NT ALDOSTERONE
NT CORTICOSTEROIDS
NT HORMONES
NT PITUITARY HORMONES
Effect of external electrostatic field on catecholamine secretion by rat adrenals 10 p1366 N88-18166
Gastric emptying during walking and running: Effects of varied exercise intensity
[AD-A194025] 23 p3240 N88-29281

SECULAR PERTURBATION
U LONG TERM EFFECTS

SECULAR VARIATIONS
Statistics of the geomagnetic secular variation for the past 5Ma
[NASA-CR-181558] 04 p0467 N88-12890

SECURITY
NT AIRPORT SECURITY
NT COMPUTER INFORMATION SECURITY
Assessment of the impacts of transferring certain nuclear reactor technologies to the Soviet Union and Eastern Europe
[DE87-014388] 02 p0249 N88-11576
Bar code document accountability system performance update
[DE88-002256] 06 p0791 N88-14849
Application of a database system for inventory management of classified material
[AD-A186986] 09 p1261 N88-17558
Use of fiber optic equipment for security
[DE88-007898] 20 p2853 N88-26943
Technology security, volume 1
[DE88-008612] 21 p3029 N88-27978
Report to Congress on the effectiveness of the Civil Aviation Security Program
[AD-A195282] 24 p3322 N88-29784
Antisatellite weapons and satellite deployment strategies
[AD-A195014] 24 p3427 N88-30396

SEDATIVES
Pharmacological resetting of the Circadian sleep-wake cycle
[AD-A186194] 07 p0889 N88-15385
Selected aspects of triazolam in relation to aviator performance in naval flight operations
[AD-A189322] 12 p1667 N88-19996
Role of opioid peptides in pathogenesis of vestibulovegetative disorders 19 p2704 N88-26079

SEDIMENT TRANSPORT
Sea duct: A deep-sea computer-controlled recirculating flume for the study of sea floor stability
[AD-A187734] 11 p1516 N88-19056
Surface hydrology, sediment transport dynamics and remote sensing of disturbed watersheds in a humid temperate region
[DE88-008719] 20 p2817 N88-26715
Prediction of continental shelf sediment transport using a theoretical model of the wave-current boundary layer
[AD-A192272] 20 p2829 N88-26783

SEDIMENTARY ROCKS
NT CARBONACEOUS ROCKS
NT COAL
NT SANDSTONES
Preliminary results from an investigation of AIS-1 data over an area of epithermal alteration: Plateau, Northern Queensland, Australia 05 p0613 N88-13768
Isotopic and chemical studies of early crustal metasedimentary rocks
[NASA-CR-182711] 14 p1944 N88-21601

SEDIMENTS
NT SANDS
NT TAR SANDS
Geoacoustic models of the Hudson Canyon area
[AD-A183535] 01 p0073 N88-10465
A mineral reconnaissance sampling manual for Costa Rica: Central American energy and resource project
[DE87-014997] 04 p0462 N88-12859
Two-layer stratified flow analysis of gravity currents and turbidity currents in lakes, reservoirs and the ocean 04 p0463 N88-12864
RRS DISCOVERY cruise 160, 30 June-25 July, 1986. Geochemical sampling over the Madeira and Porcupine Abyssal Plains
[PB87-222030] 04 p0471 N88-12910
Colloidal stability of oxidized silicon particles in ethanolic and aqueous media
[DE87-014783] 05 p0562 N88-13421
Concentration coefficients of elements in ferromanganese nodules relative to ocean sediments 06 p0726 N88-14464
Tectonics of sedimentary cover and basement of Labrador Sea 06 p0726 N88-14468
Modern concept concerning transport of bottom sediments in abyssal regions of world ocean 06 p0728 N88-14478
Formation of sediments in fuels containing added sulphonic acids — marine diesel fuels
[RAE-TM-NAV-ENG-1163] 09 p1150 N88-16891
Acoustic backscattering from bottom sediment at normal incidence in the laboratory
[AD-A186905] 09 p1242 N88-17443
Geological evolution and analysis of confirmed or suspected gas hydrate localities. Volume 10: Basin analysis, formation and stability of gas hydrates of the Aleutian Trench and the Bering Sea
[DE88-001008] 10 p1346 N88-18048
Data-base of Antarctic pre-Pleistocene sediment cores
[PB88-124151] 10 p1354 N88-18094
Rapid underway sediment classification by electrical methods
[AD-A187477] 10 p1357 N88-18114
Resolution of the magnetotelluric method for determining local inhomogeneities in the sedimentary cover 13 p1789 N88-20701
Satellite remote sensing of turbidity and sediment concentration in Lagoa dos Patos 17 p2355 N88-24032
Geological evolution and analysis of confirmed or suspected gas hydrate localities. Volume 2: Basin analysis, formation and stability of gas hydrates in the Black Sea
[DE88-001052] 18 p2532 N88-25023
Evaluation of the biot coefficients
[AD-A191643] 18 p2570 N88-25265
Remote sensing of acoustic properties of shallow water sediments: A review
[AD-A192107] 18 p2570 N88-25267

The Martian sedimentary record
23 p3302 N88-29669
Surface units on Mars: The assemblage in the Valles Marineris
23 p3304 N88-29680
Early cratering rates and the nature of the Martian cratered uplands
23 p3306 N88-29694
Constraints on continental accretion from sedimentation
24 p3392 N88-30202
The growth of continents and some consequences since 1.5 Ga
24 p3395 N88-30220
Solid earth as a recycling systems and the lateral growth of Precambrian North America
24 p3400 N88-30249
Spectral analysis of the Elatina varve series
[NASA-CR-183085]
24 p3402 N88-30260

SEEBECK COEFFICIENT
U SEEBECK EFFECT

SEEBECK EFFECT
Optimisation of the thermoelectric figure of merit of modified silicon germanium alloys
[AD-A191347]
16 p2283 N88-23670

SEEDS
Simulation of effect on biological systems of impact wave from heavy charged particle track
07 p0896 N88-15429
Research on cotton plants grown in space
08 p1006 N88-16098
Effect of spaceflight factors on biological material flown aboard Cosmos-1514 biosatellite
10 p1364 N88-18154

SEEKERS
U HOMING DEVICES

SEEPAGE
Nonseismic, surface geophysical and geochemical prospecting technology
[PB88-196613]
23 p3227 N88-29207

SEGMENTS
Segmented hollow cathode discharges for copper ion lasers
[ETN-87-90403]
01 p0052 N88-10333
Numerical arc segmentation algorithm for a radio conference-NASARC (version 2.0) technical manual
[NASA-TM-100160]
08 p0977 N88-15910
Image segmentation via fractal dimension
[AD-A186825]
12 p1678 N88-20033
Results of the testing of the segmentation program on RESEDA
[BCRS-87-01]
16 p2228 N88-23304
Adaptive segmentation evaluation
[AD-A190965]
16 p2274 N88-23609
Automatic registration of satellite imagery
17 p2364 N88-24080
The SRS (Segmented Rail Surface) railgun: A new approach to restrike control
[DE88-007907]
19 p2605 N88-25468

SEGREGATION
U SEPARATION

SEISMIC WAVES
NT RAYLEIGH WAVES
Institute of Geophysics and Planetary Physics at Lawrence Livermore National Laboratory
[DE87-014618]
02 p0251 N88-11583
A new approach to modeling and interpreting electromagnetic sounding data
[DE88-000460]
04 p0438 N38-12715
Multichannel deconvolution of P waves at seismic arrays and three component stations
[AD-A184450]
04 p0467 N88-12688
NORSAR detection processing system
[AD-A185968]
07 p0877 N88-15318
Sea resonance vibrational source of seismic waves
08 p1010 N88-16126
Correlation between seismic activity and variations of microseismic oscillations
08 p1011 N88-16131
Determining trajectory of ground movement accompanying seismic phenomena
08 p1011 N88-16132
Materials of the World Data Center B. Deep Seismic Sounding (DSS): Pacific data
09 p1196 N88-17167
Regional wave attenuation and seismic moment from the inversion of NORESS spectra
[AD-A187399]
11 p1510 N88-19023
State-of-the-art for assessing earthquake hazards in the US. Parameters for specifying intensity-related earthquake ground motions
[AD-A188230]
11 p1512 N88-19032
Ultrasonic physical modeling of seismic wave propagation from graben-like structures
[AD-A189066]
13 p1796 N88-20744
Geodetic measurement of deformation east of the San Andreas fault in Central California
[NASA-CR-182709]
13 p1798 N88-20754
Earthquakes from peninsular India: Data from the Gauribidanur seismic array
[DE88-701232]
15 p2093 N88-22471
Characteristics of seismic sources of some Asian earthquakes and Soviet underground explosions from Gauribidanur array records
[DE88-701233]
15 p2093 N88-22472
Seismic inversion by a RMS (Root-Mean-Square) Born approximation in the space-time domain
[PB88-165402]
15 p2131 N88-22711
The determination of gravity and topography from seismic velocities, accounting for dynamic behavior of the Earth's mantle
[ETN-88-92420]
17 p2374 N88-24117
Remote sensing of acoustic properties of shallow water sediments: A review
[AD-A192107]
18 p2570 N88-25267
Statistical evaluation of light water reactor piping damping data for use in PRA (Probabilistic Risk Assessment) analyses
[DE88-007708]
19 p2661 N88-25828
Influence of scattering on seismic waves: Physical mechanisms contributing to attenuation in the crust
[AD-A191699]
19 p2690 N88-25992
Seismic body waves and the earth's inner core
[DE88-007395]
19 p2691 N88-25994
Changes in seismic velocity and apparent attenuation due to isotropic and anisotropic scattering: Results from physical modeling
19 p2691 N88-25997
Proceedings of the Array Signal Processing Symposium: Treaty Verification Program
[DE88-008346]
20 p2790 N88-26548
Stochastic geologic effects on near-field ground motions in alluvium
[AD-A192315]
21 p2972 N88-27652
Effects of tectonic release on broadband regional distance bodywaves
[AD-A194247]
22 p3119 N88-28529
Interactions between air and ground sound at the Earth surface
22 p3149 N88-28733
Acoustic-seismic helicopter detection
22 p3149 N88-28734
Seismic reflection experiments imaging the physical nature of crustal structures in southern California
23 p3232 N88-29235
Maximum-likelihood multichannel deconvolution of P waves at seismic arrays
[AD-A194990]
24 p3391 N88-30191
Deep seismic reflection profiling and continental growth curves
24 p3396 N88-30222
Discrimination studies using short-period P waves at upper mantle distances
[AD-A195468]
24 p3401 N88-30257

SEISMOGRAPHS
Research and development activities of the Seismology Section
[DE88-701235]
16 p2231 N88-23323

SEISMOLOGY
NT HELIOSEISMOLOGY
The interpretation of crustal dynamics data in terms of plate motions and regional deformation near plate boundaries
[NASA-CR-181475]
03 p0349 N88-12205
Earthquake source mechanisms and transform fault tectonics in the Gulf of California
03 p0349 N88-12206
Interseismic deformation for normal fault earthquakes
03 p0349 N88-12207
Transform fault earthquakes in the North Atlantic: Source mechanisms and depth of faulting
03 p0350 N88-12208
RRS DISCOVERY Cruise 161, 15 August (227)-19 September (262) 1986. Portuguese Ocean-continent boundary, plate boundaries west of Iberia and seismic structure of sediments off Madeira
[PB87-222006]
06 p0747 N88-14596
NORSAR detection processing system
[AD-A185968]
07 p0877 N88-15318
State-of-the-art for assessing earthquake hazards in the United States. Report 26: Parameters for specifying magnitude-related earthquake ground motions
[AD-A185997]
07 p0877 N88-15319
Use of space photographs for paleoseismogeological studies (on the example of Mongolian Altay)
08 p1008 N88-16110
New data on structure of earth's crust and seismicity of basins in Atlantic and Indian Oceans
08 p1010 N88-16123
Sea resonance vibrational source of seismic waves
08 p1010 N88-16126
Geomechanical model of seismofocal zone of active continental margin
08 p1011 N88-16128
Comprehensive method for defining seismogenic zones
08 p1011 N88-16129
A deep-water OBS (Ocean Bottom Seismometer) array with real-time telemetry
[AD-A187404]
10 p1357 N88-18112
Regional wave attenuation and seismic moment from the inversion of NORESS spectra
[AD-A187399]
11 p1510 N88-19023
Applications and limitations of the spectral-analysis-of-surface-waves method
[PB88-136619]
11 p1513 N88-19038
Numerical modeling of wave migration of seismic data
13 p1786 N88-20684
Interactive automated system for testing analog units of digital seismic stations
13 p1789 N88-20702
Correlation of data on strain accumulation adjacent to the San Andreas Fault with available models
[NASA-CR-180757]
13 p1796 N88-20742
Research and development activities of the Seismology Section
[DE88-701235]
16 p2231 N88-23323
The determination of gravity and topography from seismic velocities, accounting for dynamic behavior of the Earth's mantle
[ETN-88-92420]
17 p2374 N88-24117
Stochastic geologic effects on near-field ground motions in alluvium
[AD-A192315]
21 p2972 N88-27652
SPOT for earthquake hazard zoning in southern Italy
22 p3093 N88-28365
Utilizing SPOT data for seismic shot-line mapping and environmental monitoring in oil and gas exploration
22 p3098 N88-28401
Maximum-likelihood multichannel deconvolution of P waves at seismic arrays
[AD-A194990]
24 p3391 N88-30191

SEISMOMETERS
U SEISMOGRAPHS

SELECTION
NT PERSONNEL SELECTION
NT PILOT SELECTION
NT SITE SELECTION
On detection of change points using mean vectors
[AD-A185581]
06 p0767 N88-14717
Maximum likelihood principle and model selection when the true model is unspecified
[AD-A186027]
07 p0914 N88-15544
Variable selection in logistic regression
[AD-A186032]
07 p0914 N88-15547
Control variate selection for multiresponse simulation
[AD-A186637]
08 p1069 N88-16463
Advanced human factors engineering tool technologies
[AD-A189390]
13 p1812 N88-20825
Structure and surface characterizations of high strength carbon fibers
[AD-A189642]
15 p2029 N88-22087
On two-stage allocation procedures for selection problems
[AD-A190766]
15 p2126 N88-22675
Sensor and actuator selection for large space structure control
[AD-A194912]
24 p3333 N88-29842

SELECTION RULES (NUCLEAR PHYSICS)
On selection rules and inelastic electron scattering at intermediate energies
[DE88-701833]
23 p3280 N88-29526

SELECTIVE SURFACES
Millimeter and submillimeter waves and frequency selective surfaces
[AD-A191511]
18 p2500 N88-24827

SELECTIVITY
Selective growth velocity in needle crystals
14 p1988 N88-21858
Synthesis and analysis of novel polymers with potential for providing both high permselectivity and permeability in gas separation applications
[DE88-006533]
15 p2043 N88-22174

SELECTORS
Selection and effects of channels in distributed communication and decision making tasks: A theoretical review and a proposed research paradigm
[AD-A191807]
18 p2587 N88-25375

SELENIDES
NT CADMIUM SELENIDES
NT COPPER SELENIDES
NT ZINC SELENIDES
Tunable optical sources/growth and characterization of nonlinear optical materials
[AD-A190874]
16 p2274 N88-23608

SELENIUM
Phase equilibrium and crystal growth studies on AgGaSe2 and related nonlinear optical materials
[AD-A184768]
03 p0382 N88-12400
Thermal expansion of some Ge-Se-Te glasses
[PD-MT-8722]
04 p0420 N88-12606
Studies on some Ge-Se-Te glasses
[PD-MT-8721]
04 p0420 N88-12607
J = O Task Force
[DE88-001326]
04 p0450 N88-12788

SELENIUM COMPOUNDS
NT CADMIUM SELENIDES
NT COPPER SELENIDES
NT SELENIDES
NT ZINC SELENIDES
Review of selenium thermodynamic data
[DE88-006194] 13 p1849 N88-21068
SELF ADAPTIVE CONTROL SYSTEMS
Active control of helicopter vibration using multiloop self-adaptive control 03 p0264 N88-11660
Wavefront error sensing
[NASA-CR-181504] 03 p0321 N88-12030
Simplified self-tuning control algorithms
[OUEL-1657/86] 07 p0907 N88-15494
Self-adaptive data bases
[AD-A186414] 07 p0942 N88-15729
SELF ALIGNMENT
Self-alignment of ions drifting in plasma 06 p0774 N88-14752
Design, manufacture and spin test of high contact ratio helicopter transmission utilizing Self-Aligning Bearingless Planetary (SABP)
[NASA-CR-4155] 18 p2524 N88-24975
SELF CONSISTENT FIELDS
Self-consistent modification of a fast tail distribution by resonant fields in nonuniform plasmas
[AD-A183790] 01 p0099 N88-10650
The H5(+) potential energy hypersurface: Characterization of ten distinct energetically low-lying stationary points 16 p2267 N88-23561
Quantum Monte Carlo study of the MIES associated with H2(X 1 sigma g +) and H2(B 1 sigma u +) 16 p2268 N88-23564
Raychaudhuri equation in the self-consistent Einstein-Cartan theory with spin-density
[NASA-TM-101145] 17 p2447 N88-24546
SELF DEPLOYING SPACE STATIONS
U SELF ERECTING DEVICES
U SPACE STATIONS
SELF DIFFUSION (SOLID STATE)
Investigations of crystallization velocity and boron diffusion in glassy iron-boron alloys and of activity coefficients of boron in crystalline iron-boron alloys
[ETN-87-90613] 03 p0381 N88-12393
The influence of phosphorus on the solid state reaction between copper and silicon or germanium
[ETN-88-91361] 06 p0789 N88-14838
Heterogeneous isotope exchange between solid cesium iodide and gaseous methyl iodide
[ETN-88-91085] 09 p1141 N88-16840
Transport and relaxation processes in supercritical fluids
[DE88-004804] 10 p1419 N88-18474
A multigrid approach for the solution of a nonlinear diffusion equation in a time-dependent area using Cartesian coordinates
[GMD-STUDIEN-122] 16 p2257 N88-23491
SELF ERECTING DEVICES
The 15-meter antenna performance optimization using an interdisciplinary approach 19 p2652 N88-25746
SELF EXCITATION
Dynamics of reverse flows at pump inlet 04 p0425 N88-12636
Longitudinal mode combustion instabilities in air breathing engines 06 p0680 N88-14166
The design and performance of a real-time self excited vocoder 19 p2653 N88-25753
SELF FOCUSING
Numerical simulation of laser filamentation experiments
[ETN-87-90959] 02 p0179 N88-11118
Theory of transient thermal self-focusing of sound beams 09 p1234 N88-17401
On the self-focusing of electric helicons
[DE88-701870] 20 p2848 N88-26905
SELF INDUCED VIBRATION
NT SUPERSONIC FLUTTER
NT TRANSONIC FLUTTER
Investigations on higher harmonic blade pitch control at helicopters
[DFVLR-FB-87-36] 14 p1868 N88-21165
SELF LUBRICATION
Coatings for high-temperature bearings and seals
[NASA-TM-100249] 05 p0567 N88-13453
Self-lubricating coatings for high-temperature applications 09 p1119 N88-16703
SELF MANEUVERING UNITS
Personnel occupied woven envelope robot 23 p3260 N88-29408
SELF ORGANIZING SYSTEMS
Experiments in isolated digit recognition using the multilayer perceptron
[RSRE-MEMO-4073] 17 p2333 N88-23927
Hierarchical organization for large, dynamic radio networks
[AD-A193942] 23 p3204 N88-29067
Radial basis functions, multi-variable functional interpolation and adaptive networks
[RSRE-MEMO-4148] 23 p3265 N88-29436
SELF REGULATING
U AUTOMATIC CONTROL
SELF REPAIRING DEVICES
Automation tools for demonstration of goal directed and self-repairing flight control systems
[NASA-CR-179433] 19 p2715 N88-26121
SELF TESTS
Programmable Logic Arrays (PLA's) design for testability
[PB87-102935] 04 p0438 N88-12718
SELSYNS (TRADEMARK)
U SERVOMOTORS
SEMANTICS
Semantic network processing systems --- artificial intelligence
[OUEL-1677/87] 02 p0223 N88-11401
Integrating syntax, semantics, and discourse DARPA (Defense Advanced Research Projects Agency) Natural Language Understanding Program
[AD-A184505] 03 p0364 N88-12289
Near-horn prolog
[AD-A185172] 05 p0634 N88-13880
Annotated algebraic specification of the static semantics of pool
[PB88-106695] 07 p0912 N88-15533
Ada (trade name) compiler validation summary report. Systems designers' PLC SD Ada-plus VAX/VMS x MC68020. Version 2B.00. Host: VAX 8600. Target: Motorola MC68020. Completion of on-site testing
[AD-A186571] 08 p1053 N88-16356
The use and generation of illustrative examples in computer-based instructional systems 08 p1060 N88-16400
Conceptual information processing: A robust approach to KBS-DBMS integration 08 p1063 N88-16422
Semantics of EqL
[AD-A188151] 10 p1389 N88-18297
Research in knowledge representation for natural language communication and planning assistance
[AD-A187355] 11 p1522 N88-19087
KR: An efficient knowledge representation system
[AD-A187705] 11 p1529 N88-19129
EqL: The language and its implementation
[AD-A188161] 11 p1530 N88-19137
An evaluation of historical algebras
[AD-A188350] 12 p1684 N88-20067
Using design axioms and topology to model database semantics
[CWI-CS-R8711] 13 p1818 N88-20863
Algebra of Communicating Processes (ACP)tau: A universal axiom system for process specification
[CWI-CS-R8725] 13 p1819 N88-20869
Designing equivalent semantic models for process creation
[CWI-CS-R8732] 13 p1819 N88-20872
Predicate-transformer semantics of general recursion
[CS-8709] 13 p1820 N88-20876
A fully abstract semantics for data flow nets
[CWI-CS-R8724] 13 p1822 N88-20893
A convergence theorem in process algebra
[CWI-CS-R8733] 13 p1827 N88-20920
A fully abstract semantics for event-based simulation
[AD-A190560] 15 p2060 N88-22283
Inference engine for expert systems
[INPE-4465-TDL/321] 15 p2113 N88-22590
Semantics for Prolog via term rewrite systems
[CWI-CS-R8739] 16 p2247 N88-23428
Semantics for logic programs without occur check
[CWI-CS-R8740] 16 p2248 N88-23429
Towards fully abstract semantics for local variables: Preliminary report
[AD-A191065] 16 p2251 N88-23456
Readiness and failures in the algebra of communicating processes
[CWI-CS-R8748] 16 p2258 N88-23499
Contractions in comparing concurrency semantics
[CWI-CS-R8755] 20 p2840 N88-26850
A semantic approach to fairness
[CWI-CS-R8759] 20 p2840 N88-26853
Towards knowledge bases-semantics, rules and object-oriented programming
[PB88-108154] 20 p2882 N88-27110
Hiding in stream semantics of uniform concurrency
[PB88-121579] 20 p2882 N88-27114
A cockpit natural language study: Vocabulary and grammar analyses
[AD-A193289] 21 p2993 N88-27753
Linguistic semantics for parallel computation
[PB88-105960] 21 p2995 N88-27761
Unification and set-valued functions for functional and logic programming
[AD-A193643] 23 p3250 N88-29341
Validation of expert systems 23 p3262 N88-29416
Semantic based man-machine interface for real-time communication 23 p3262 N88-29421
An expert system for natural language processing 23 p3263 N88-29426
Exploiting lexical regularities in designing natural language systems
[AD-A195922] 24 p3423 N88-30375
SEMICIRCULAR CANALS
Membrane model of cupula or vestibular semicircular canals 10 p1361 N88-18132
SEMICONDUCTING FILMS
Excimer laser-assisted deposition of GaAs, AlAs and (Al,Ga)As from Lewis acid-base adducts
[AD-A184588] 03 p0329 N88-12081
Some investigations of molecular beam epitaxial growth of 3-5 semiconductor films via Monte-Carlo computer simulations, carrier tunnelling and spectroscopic ellipsometry
[AD-A185520] 06 p0789 N88-14839
Neutron and X-ray scattering studies of layered solids 09 p1246 N88-17469
Gas source MBE (Molecular Beam Epitaxy)
[AD-A189763] 15 p2142 N88-22782
Beam assisted fabrication of 3-5/Si monolithic devices
[AD-A189979] 15 p2142 N88-22785
Fundamental properties and devices applications of Ge(x)Si(1-x)/Si superlattices
[AD-A190129] 15 p2143 N88-22787
Thin superconducting film characterization by surface acoustic waves
[AD-A190417] 15 p2143 N88-22791
Silicon-on-insulator pin diodes
[AD-A193359] 21 p2937 N88-27445
Molecular beam epitaxy of GaP films on Si substrates
[PB88-131974] 21 p3020 N88-27923
Laser induced chemical vapor epitaxial growth of gallium arsenide films
[AD-A194254] 23 p3291 N88-29595
SEMICONDUCTOR DEVICES
NT AVALANCHE DIODES
NT BIPOLAR TRANSISTORS
NT CHARGE COUPLED DEVICES
NT CHARGE TRANSFER DEVICES
NT CMOS
NT FIELD EFFECT TRANSISTORS
NT GALLIUM ARSENIDE LASERS
NT GERMANIUM DIODES
NT HETEROJUNCTION DEVICES
NT HIGH ELECTRON MOBILITY TRANSISTORS
NT JFET
NT JUNCTION DIODES
NT JUNCTION TRANSISTORS
NT LIGHT EMITTING DIODES
NT METAL OXIDE SEMICONDUCTORS
NT MIM (SEMICONDUCTORS)
NT MIM DIODES
NT MIS (SEMICONDUCTORS)
NT MODFETS
NT MSM (SEMICONDUCTORS)
NT PHOTODIODES
NT PHOTOVOLTAIC CELLS
NT SCHOTTKY DIODES
NT SEMICONDUCTOR LASERS
NT SILICON TRANSISTORS
NT SOI (SEMICONDUCTORS)
NT SOLAR CELLS
NT SOS (SEMICONDUCTORS)
NT THERMISTORS
NT THYRISTORS
NT TRANSFERRED ELECTRON DEVICES
NT TRANSISTOR AMPLIFIERS
NT TRANSISTORS
NT VARISTORS
NT VERTICAL JUNCTION SOLAR CELLS
Calorimetric Absorption Spectroscopy (CAS): A new method for the characterization of the optical properties of semiconductor systems
[ETN-87-90407] 01 p0098 N88-10645
Electrical behavior of layers implanted with low energy pions in Si
[INPE-4199-PRE/1051] 01 p0102 N88-10670
Variations in semiconductor device response in a medium-energy x-ray dose-enhancing environment
[DE87-012400] 02 p0243 N88-11538
Ohmic contacting schemes to gallium arsenide devices
[DE87-014627] 02 p0244 N88-11544
RADC/NBS (Rome Air Development Center/National Bureau of Standards) Workshop. Moisture Measurement and Control for Microelectronics (4)
[PB87-224614] 03 p0309 N88-11947
Vectorial electron transfer on designed surfaces
[PB87-232229] 03 p0381 N88-12394
Epitaxial reactor development for growth of silicon-on-insulator devices
[AD-A184758] 03 p0382 N88-12399

Molecular beam epitaxial growth and characterization of 3-5 compound semiconductor single and multiple interface structures
[AD-A185400] 05 p0656 N88-14021
Area detectors for X-ray spectroscopy
[DE88-001429] 06 p0679 N88-14163
High frequency periodic time domain waveform measurement system
[PB87-225256] 06 p0695 N88-14264
Structure of layered crystals studied by high energy ion beams
[DE88-001675] 06 p0786 N88-14822
Analytical investigations of bulk wave resonators in the piezoelectric thin film on gallium-arsenide configuration
[AD-A185716] 06 p0789 N88-14840
High-temperature electronics
08 p0956 N88-15797
Crystal diffraction lenses for imaging gamma-ray telescope
[DE88-003084] 08 p1083 N88-16529
Relaxation of metastable semiconductor strained-layer structures by plastic flow
[DE88-002729] 08 p1090 N88-16560
Nanoelectronics
[AD-A186969] 09 p1156 N88-16930
Acceleration techniques for decoupling algorithms in semiconductor simulation
[DE88-003593] 09 p1221 N88-17323
Study of quantum mechanical effects in deep submicron, grating-gate field effect transistors
[AD-A188283] 10 p1325 N88-17923
Microwave semiconductor research-materials, devices and circuits
[AD-A187121] 10 p1415 N88-18444
Corner compensation structures for (110) oriented silicon
[DE88-003300] 10 p1417 N88-18455
An electro-optic explosive igniter
[DE88-004728] 11 p1466 N88-18738
Microelectronic applications of the conductor-thin insulator-semiconductor (CIS) structure
11 p1560 N88-19341
Electronic properties of semiconductor inversion layers in sub-micron structures
[AD-A188635] 12 p1698 N88-20161
Electrical properties of medium field, chem-prep varistors
[DE88-006147] 13 p1762 N88-20540
Improvements in end point detection --- semiconductor fabrication
[RSRE-MEMO-4035/A] 14 p1899 N88-21336
JPRS report: Science and technology. China
[JPRS-CST-87-038] 14 p1901 N88-21350
Applications of lasers to semiconductor studies
14 p1901 N88-21356
Laser pulse detection with infrared range semiconductor detectors
[DE88-700857] 14 p1914 N88-21432
The Shubnikov de Haas effect in narrow-gap semimagnetic semiconductors
[ETN-88-92249] 14 p1988 N88-21861
Application of copper-carbon fiber composites to power semiconductor devices
[NASA-TT-20171] 15 p2031 N88-22101
Temperature-dependent conductivity of oxygen-depleted YBCO ceramics
[AD-A190340] 15 p2044 N88-22182
Growth of Pb/sub 1-x/Eu/sub x/Te epitaxial layers by the liquid phase epitaxy technique
[DE88-701022] 15 p2139 N88-22763
Development program for 1.93-micron lasers
[NASA-CR-4148] 16 p2212 N88-23198
Radiation effects in silicon
[DE88-006642] 16 p2282 N88-23659
Limited reaction processing for semiconductor device fabrication
[AD-A190913] 16 p2283 N88-23666
Development of 20 GHz monolithic transmit modules
[NASA-CR-182134] 17 p2445 N88-24539
Simple high speed camera with CCD-sensor
[MPIS-8/1987] 18 p2518 N88-24940
Advanced development of double-injection, deep-impurity semiconductor switches
[NASA-CR-182118] 18 p2583 N88-25346
Ceramic substrates for semiconductor applications reported: AlN substrates 19 p2633 N88-25621
Organization of a Topical Meeting on Picosecond Electronics and Optoelectronics
[AD-A187136] 19 p2655 N88-25765
Molecular Beam Epitaxy (MBE) for high speed devices
19 p2656 N88-25770
Multigigahertz logic based on InP-MISFET's exhibiting extremely high transconductance
19 p2656 N88-25771
Millimeter-wave integrated circuits
19 p2656 N88-25774
Fast GaAs photoconductive detectors with high sensitivity integrated in coplanar systems onto GaAs substrates 19 p2658 N88-25790
Non-stationary transport in MODFET's and heterojunction devices 19 p2659 N88-25804
Carrier transport in semiconductor magnetic sensors under nonuniform fields 19 p2672 N88-25888
Tin oxide microsensors on thin silicon membranes
19 p2673 N88-25897
Workshop report and presentations from the Semiconductor Research Corporation-DOE Semiconductor Task Force Workshop
[DE88-007690] 19 p2733 N88-26232
Ion implantation processing of 3-5 strained-layer semiconductors
[DE88-005270] 19 p2734 N88-26240
Plasma separation process. Betacell (BCELL) code, user's manual
[DE88-006955] 20 p2859 N88-26981
Raman, photoluminescence and modulation spectroscopy of semiconductor heterostructures
20 p2861 N88-26997
Energy levels and magneto-electric effects in some quasi uni-dimensional semiconductor heterostructures
20 p2864 N88-27009
Quantum transport in an electron waveguide
20 p2864 N88-27010
Random quantum interference in microdevices
20 p2866 N88-27021
Recent applications of Monte Carlo methods for semiconductor microdevice simulation
20 p2871 N88-27046
Excellent negative differential resistance of InGaAs/InAlAs resonant tunneling barrier structures and applications to a new functional device, RHET
20 p2872 N88-27048
Fermi level dependent native defect formation: Consequences for metal-semiconductor and semiconductor-semiconductor interfaces
[DE88-009247] 20 p2875 N88-27066
Studying the physics and operation of multi-terminal near-micron and sub-micron length, hot electron semiconductor devices
[AD-A193380] 21 p2938 N88-27446
Solid state research
[AD-A192837] 21 p3020 N88-27929
Investigation of electronic band structure of semiconductors by photoemission
[ETN-88-92370] 21 p3025 N88-27957
Further improvements relating to the temperature compensation of semiconductor strain gauge pressure transducers
[RAE-TR-87061] 22 p3081 N88-28298
Semiconductor bridge (SCB) igniter studies. 1: Comparison of SCB and hot-wire pyrotechnic actuators
[DE88-008802] 23 p3200 N88-29046
Studies on strained (In,Ga)As/GaAs semiconductors and optical devices 23 p3287 N88-29575
Electronic and optical devices and applications
24 p3363 N88-30027
Automatic prober for the dc characterisation of gallium arsenide devices. Part 2: The data sorting and display facility
[AD-A195408] 24 p3377 N88-30111
Tolerances for phase locking of semiconductor laser arrays
[AD-A195974] 24 p3378 N88-30120
Application of nondestructive testing techniques to materials testing
[AD-A195718] 24 p3381 N88-30138
Light-millimeter wave interactions in semiconductor devices
[AD-A195898] 24 p3432 N88-30428
Waveform relaxation applied to transient device simulation
[AD-A194992] 24 p3432 N88-30429

SEMICONDUCTOR DIODES
NT AVALANCHE DIODES
NT GERMANIUM DIODES
NT GUNN DIODES
NT JUNCTION DIODES
NT LIGHT EMITTING DIODES
NT PHOTODIODES
NT SCHOTTKY DIODES
NT TUNNEL DIODES
Blue-green laser diode research program
[AD-A183517] 01 p0051 N88-10323
AlGaAs heterojunction lasers
[NASA-CR-4119] 09 p1171 N88-17020
Ultra-high speed integrated optical waveguide devices for optical computing
[AD-A188470] 12 p1691 N88-20118
Growth of Pb/sub 1-x/Eu/sub x/Te epitaxial layers by the liquid phase epitaxy technique
[DE88-701022] 15 p2139 N88-22763
Design and evaluation of single-lobed far-field pattern laser arrays: AlGaAs/GaAs and InGaAsP/InP systems --- optical communication
[LAAS-88-023] 16 p2214 N88-23211
Diode laser ignition of high explosives and pyrotechnics
[DE88-008771] 21 p2923 N88-27352
A GaAs solid state device model for high power applications
[DE88-011320] 21 p2939 N88-27457
Photodiodes for optical communication in the near infrared
[ETN-88-92379] 21 p3016 N88-27900
Blue-green laser diode research program
[AD-A191980] 23 p3218 N88-29153

SEMICONDUCTOR INSULATOR SEMICONDUCTORS
U SIS (SEMICONDUCTORS)

SEMICONDUCTOR JUNCTIONS
NT HETEROJUNCTIONS
NT N-P-N JUNCTIONS
NT P-I-N JUNCTIONS
NT P-N JUNCTIONS
NT P-N-P JUNCTIONS
NT P-N-P-N JUNCTIONS
NT SILICON JUNCTIONS
Optimization of SIS mixer elements
[NASA-CR-180710] 01 p0104 N88-10680
Investigation of silicon surface passivation by silicon nitride film deposition
[NASA-CR-182350] 06 p0729 N88-14487
Photoluminescence study of InP surfaces and InP-insulator interfaces
[ECL-87-13] 08 p1089 N88-16555
Electron tunneling in junctions doped with semiconductors and metals 19 p2734 N88-26236
A comparison of the radiation tolerance characteristics of multijunction solar cells with series and voltage-matched configurations
[NASA-TM-101177] 21 p2967 N88-27624

SEMICONDUCTOR LASERS
NT GALLIUM ARSENIDE LASERS
Blue-green laser diode research program
[AD-A183517] 01 p0051 N88-10323
Status, development of laser devices in China
03 p0303 N88-11907
High power phased array and tailored gain semiconductor lasers 03 p0329 N88-12078
Phase-locked semiconductor quantum well laser arrays
[AD-A185155] 05 p0588 N88-13583
Nonconventional optical techniques for optical wavefront processing
[AD-A185099] 05 p0650 N88-13982
Causes and distribution of failures in semiconductor lasers (a review) 07 p0919 N88-15581
Generation of light pulses in semiconductor laser upon excitation by several electron beams
07 p0920 N88-15589
Electro-optical studies of semiconductor compounds for electroluminescent and laser devices
[PH-155] 07 p0937 N88-15693
Semiconductor laser with electron-beam pumping and fiber-optic output waveguide 09 p1235 N88-17405
Dye lasers pumped by radiation from high-power semiconductor lasers 09 p1237 N88-17417
Periodic-pulse semiconductor laser with electron-beam pumping 09 p1238 N88-17422
Ultra-high speed integrated optical waveguide devices for optical computing
[AD-A188470] 12 p1691 N88-20118
Fiber-coupled external-cavity semiconductor high power laser
[AD-A188454] 13 p1774 N88-20611
High power, high efficiency, 2D laser diode arrays for pumping solid state lasers
[DE88-004042] 13 p1777 N88-20632
Dynamic and spectral properties of semiconductor lasers with quantum well, quantum wire, and quantum box structures 14 p1975 N88-21788
Ultrahigh coherent semiconductor lasers and their applications to Rb atomic clock
14 p1976 N88-21789
Generation of number-phase minimum uncertainty states 14 p1978 N88-21803
Fabrication and characterization of semiconductor lasers of Pb(1-x)Sn(x)Te
[INPE-4253-PRE/1126] 15 p2072 N88-22357
Generation of tunable coherent radiation in 3 micrometers-5 micrometers region using semiconductor lasers in external cavities
[AD-A190860] 16 p2212 N88-23202
Design and evaluation of single-lobed far-field pattern laser arrays: AlGaAs/GaAs and InGaAsP/InP systems --- optical communication
[LAAS-88-023] 16 p2214 N88-23211

Distributed feedback lasers
[NASA-CR-4154] 18 p2520 N88-24948
Characteristics, packaging and physics of ultra high speed diode lasers and detectors
19 p2658 N88-25797
Frequency chirping in pulse modulated gain and real index guided single quantum well lasers
19 p2658 N88-25798
Picosecond measurements of gain-switching in a semiconductor laser driven by ultrashort electrical pulses
19 p2658 N88-25800
New semiconductor laser structure for an optical communication system
[ETN-88-92353] 20 p2807 N88-26854
Blue-green laser diode research program
[AD-A191980] 23 p3218 N88-29153
Mode locking of semiconductor laser with external cavity
[AD-A196018] 24 p3378 N88-30117

SEMICONDUCTOR PLASMAS
Fundamental studies and device development in beta silicon carbide
[AD-A189540] 12 p1699 N88-20165
Modeling and transport in semiconductor devices
[AD-A188760] 13 p1844 N88-21037

SEMICONDUCTORS (MATERIALS)
NT ACCEPTOR MATERIALS
NT AMORPHOUS SEMICONDUCTORS
NT AMORPHOUS SILICON
NT CMOS
NT DONOR MATERIALS
NT METAL OXIDE SEMICONDUCTORS
NT MIM (SEMICONDUCTORS)
NT MIS (SEMICONDUCTORS)
NT N-TYPE SEMICONDUCTORS
NT ORGANIC SEMICONDUCTORS
NT P-TYPE SEMICONDUCTORS
NT PHOTOCONDUCTORS
NT SOS (SEMICONDUCTORS)
NT SUPERLATTICES
Construction and characterization of amorphous-silicon test structures
[DE87-013595] 01 p0029 N88-10182
Toward pulsed power uses for photoconductive semiconductor switches: Closing switches
[DE87-012020] 01 p0041 N88-10262
Recent developments in opening photoconductive semiconductor switches
[DE87-012130] 01 p0041 N88-10263
Metal-sensing layer-semiconductor and metal-sensing layer-metal heterostructure gas sensors
[DE87-011293] 01 p0103 N88-10674
X-ray studies of strain, interface and impurity in semiconductors
[DE87-013856] 01 p0104 N88-10678
Reduction of CO2 to methanol and methane by photo and dark reactions on semiconductor and metal electrodes
[PB87-226825] 02 p0156 N88-10975
Semiconductor detector performance for low-energy X-rays
[DE87-014132] 02 p0244 N88-11542
Coupling and absorption phenomena in semiconductor-clad dielectric optical waveguides
[DE87-013446] 03 p0307 N88-11939
Measurement of the electron density and the attachment rate coefficient in silane/helium discharges
[AD-A184268] 04 p0496 N88-13051
Valence bond cluster studies of alkali metal/semiconductor bonding
[AD-A184276] 04 p0496 N88-13054
Novel dynamical investigations of excitons and their structure in semiconductors
[DE87-014868] 04 p0499 N88-13070
Far infrared Fourier transform spectroscopy of semiconductors
[DE88-000188] 04 p0499 N88-13072
Supersonic beam observations of semiconductor clusters
[AD-A184991] 05 p0655 N88-14018
The pseudopotential density functional method applied to semiconducting crystals
[ETN-88-91362] 05 p0656 N88-14024
JPRS report: Science and technology. USSR: Physics and mathematics
[JPRS-UPM-87-008] 06 p0769 N88-14727
Population inversion in gapless semiconductors as result of interband pumping 06 p0770 N88-14732
Heteroepitaxial growth of 3-5 semiconductor compounds by metal-organic chemical vapor deposition for device applications
[NASA-CR-182346] 06 p0788 N88-14832
Some investigations of molecular beam epitaxial growth of 3-5 semiconductor films via Monte-Carlo computer simulations, carrier tunnelling and spectroscopic ellipsometry
[AD-A185520] 06 p0789 N88-14839
Improving the method of calculating electronic properties of narrow bandgap semiconductors
07 p0926 N88-15627
Electro-optical studies of semiconductor compounds for electroluminescent and laser devices
[PH-155] 07 p0937 N88-15693
Effect of the band-gap characteristics on laser-induced dry etching of semiconductors
[DE88-001853] 07 p0937 N88-15695
A flux analysis of the solar cells
[INPE-4247-PRE/1120] 08 p1022 N88-16186
JPRS report: Science and technology. USSR: Physics and mathematics
[JPRS-UPM-87-010] 08 p1075 N88-16485
Instability of strong-absorption domain in semiconductor 08 p1077 N88-16495
Photoluminescence study of InP surfaces and InP-insulator interfaces
[ECL-87-13] 08 p1089 N88-16555
Interpretation of the temperature dependence of conductivity in superconducting oxides
[DE88-003028] 08 p1091 N88-16565
Plasma and ion etching for failure analysis. Part 2. The etching of plastic encapsulant and other semiconductor device materials, using the Technics Giga Etch 100-E plasma etch system
[AERE-R-12212] 09 p1177 N88-17050
JPRS report: Science and technology. USSR: Physics and mathematics
[JPRS-UPM-87-009] 09 p1233 N88-17395
Linear theory of generation of longitudinal sound waves in semiconductors upon interband absorption of optical radiation 09 p1234 N88-17397
Visible InGaAsP/GaAsP lasers produced by epitaxial growth from liquid phase 09 p1237 N88-17416
A report on the effects of neutron irradiation of GaAs semiconductors
[AD-A186816] 09 p1253 N88-17510
Control of solid-excitation-based photochemical dry etching of semiconductors by ion-bombardment-induced damage
[DE88-003214] 09 p1257 N88-17537
Stability and metastability in semiconductor strained-layer structures
[DE88-003308] 09 p1258 N88-17544
An advanced microcomputer design for processing of semiconductor materials 10 p1288 N88-17703
Application of nondestructive testing techniques to materials testing
[AD-A187645] 10 p1342 N88-18021
Photochemical solar energy conversion utilizing semiconductors localized in membrane mimetic systems
[DE88-002887] 10 p1349 N88-18065
Microwave semiconductor research-materials, devices and circuits
[AD-A187121] 10 p1415 N88-18444
Tight binding theory of semiconductors
10 p1415 N88-18447
Microscopic control of metallization stability
[AD-A187553] 10 p1421 N88-18487
Local stoichiometry and atomic interdiffusion during reactive metal/mercury-cadmium-telluride junction formation
[AD-A187554] 10 p1421 N88-18488
Nonmonotonic evolution and thermodynamic trends at metal/(Hg,Cd)Te interfaces: Yb/Hg0.78Cd0.22Te
[AD-A187591] 10 p1422 N88-18490
CdTe(110)-Mn interface reaction and the formation of non-equilibrium ternary semimagnetic semiconductor alloys
[AD-A187593] 10 p1422 N88-18491
PbSnTe photovoltaic detectors for operation in the 2-14 micron band
[INPE-4252-PRE/1125] 11 p1508 N88-19008
Digital control of the Czochralski growth of Gallium arsenide-controller software reference manual
[AD-A187210] 11 p1528 N88-19127
Atomic-scale simulation in materials science
[DE88-005204] 11 p1544 N88-19230
Fast switching of far infrared radiation by refractive index change in semiconductors using photoionization
[ETN-88-91490] 11 p1551 N88-19279
Theoretical studies of the interface electronic properties of tetrahedrally coordinated semiconductors
[AD-A187216] 11 p1555 N88-19306
High pressure electronic transport in semiconductors
[AD-A187428] 11 p1555 N88-19308
Laser measurements of state-resolved Ga and in atom sticking and desorption on metal and semiconductor surfaces
[AD-A187644] 11 p1555 N88-19310
Vibrational, mechanical and thermal properties of 3-5 semiconductors
[AD-A187569] 11 p1556 N88-19316
Electron paramagnetic resonance studies of Mn(2+) in 2-6 semiconductor alloys 11 p1560 N88-19340
Feasibility studies of the growth of 3-5 compounds of boron by MOCVD
[NASA-CR-181622] 11 p1561 N88-19343
Raman scattering in mixed crystal semiconductors
12 p1696 N88-20149
Basic research in ceramic and semiconductor science at selected Japanese laboratories, based on a September 1986 visit: Highlights, summary and overview and detailed notes from selected Japanese laboratories
[DOE/ER-0314] 12 p1696 N88-20150
Metal contacts to cadmium telluride (CdTe)
[AD-A188306] 12 p1698 N88-20159
Thin-film diffusion barriers for metal-semiconductor contacts
[AD-A188712] 13 p1844 N88-21035
New method of examining microninhomogeneity of local centers in high-resistivity semiconductor materials under scanning electron microscope 14 p1969 N88-21754
Infrared reflection-absorption spectroscopy of hyperfine layers on surfaces of semiconductors and dielectrics
14 p1969 N88-21755
United States - Japan Seminar on Quantum Mechanical Aspects of Quantum Electronics
[AD-A186938] 14 p1974 N88-21781
Enhanced excitonic optical nonlinearity and exciton dynamics in semiconductor microstructures
14 p1977 N88-21795
Free carrier nonlinear optics 14 p1977 N88-21796
High density femtosecond excitation of nonthermal carrier distributions in intrinsic and modulation doped GaAs quantum wells 14 p1977 N88-21798
Dynamical aspects of carrier tunneling in semiconductor superlattices 14 p1977 N88-21799
Experimental and theoretical studies of coherent and nonthermal processes in semiconductors probed by femtosecond laser techniques 14 p1977 N88-21800
Femtosecond studies in hot carrier relaxation in GaAs and AlGaAs 14 p1977 N88-21801
Amorphous semiconductors made in space
15 p2051 N88-22221
Pb(1-x)Sn(x)Te crystal growth in space
15 p2051 N88-22223
Absolute pressure derivatives of deep level defects in 3-5 semiconductors
[DE88-006318] 15 p2140 N88-22772
Examination of temperature effects on gate-to-drain avalanche breakdown in GaAs MESFETs (Metal-Semiconductor Field Effect Transistors) by measuring light emission under RF drive
[AD-A189634] 15 p2141 N88-22778
Repetitive opening switches using optically activated semiconductors
[AD-A190196] 15 p2143 N88-22790
Interface formation and precursory dynamics
[AD-A190741] 15 p2144 N88-22794
Fermi level stabilization in semiconductors: Implications for implant activation efficiency
[DE88-006332] 15 p2145 N88-22801
UV-Laser reactions of molecular adsorbates
[AD-A190796] 16 p2212 N88-23201
Investigation of non-linear optical behavior of semiconductors for optical switching, volume 1
[AD-A191297] 16 p2274 N88-23611
DOE (Department of Energy) national laboratories and the semiconductor industry: Continuing the joint planning
[PB88-170295] 16 p2281 N88-23657
Radiation effects in silicon
[DE88-006642] 16 p2282 N88-23659
Limited reaction processing for semiconductor device fabrication
[AD-A190913] 16 p2283 N88-23666
Microscopic control of semiconductor interface reactivity
[AD-A191193] 16 p2283 N88-23668
Optimisation of the thermoelectric figure of merit of modified silicon germanium alloys
[AD-A191347] 16 p2283 N88-23670
Non-contact temperature measurement requirements for electronic materials processing
17 p2328 N88-23898
Real time thermal imaging of high temperature semiconductor melts 17 p2330 N88-23914
Preparation of improved PbSnTe thermoelectric alloys and evaluation of their figure of merit
[AD-A191346] 17 p2445 N88-24538
Liquid encapsulated float zone process and apparatus
[NASA-CASE-MFS-28144-1] 17 p2446 N88-24545
Time resolved spectroscopy facility for the study of nonlinear optical properties of semiconducting polymers
[AD-A191221] 18 p2490 N88-24768

Stress measurements in graphite fibers by laser raman spectroscopy
[AD-A191710] 18 p2491 N88-24779
Joint services electronics program
[AD-A190239] 18 p2503 N88-24848
Mathematical models for VLSI device simulation
[AD-A191125] 18 p2562 N88-25212
Electronic structure, elementary excitations, optical and transport properties of semiconductor superlattices
[AD-A190795] 18 p2581 N88-25333
An investigation of 2-6 superlattice deposition by laser photochemical techniques
[AD-A191547] 18 p2581 N88-25336
Recent data on Si:As impurity band conduction multiplexed arrays
[AD-A191752] 18 p2582 N88-25340
Studies of metal-silicon, silicon-metal and silicide based interfaces: Synchrotron radiation photo emission and inverse photoemission investigations of interface formation and compound nucleation
[AD-A191808] 19 p2619 N88-25536
Nonequilibrium phonons and disorder in Al sub x Ga sub 1-x As 19 p2657 N88-25788
Direct subpicosecond measurement of carrier mobility of photoexcited electrons in GaAs
19 p2659 N88-25803
Longitudinally localized optical carrier injection for femtosecond transport studies 19 p2659 N88-25806
Optical sensing of magnetic fields
19 p2670 N88-25871
Digital control of the czochralski growth of gallium arsenide. System reference manual. Valid for Czochralski growth controller software version 2.4
[AD-A191997] 19 p2732 N88-26227
Workshop report and presentations from the Semiconductor Research Corporation-DOE Semiconductor Task Force Workshop
[DE88-007690] 19 p2733 N88-26232
Ion implantation processing of 3-5 strained-layer semiconductors
[DE88-005270] 19 p2734 N88-26240
Auger recombination in GaSb/AlSb-multi quantum well heterostructures 20 p2862 N88-27001
Piezoelectric effects in strained layer superlattices
20 p2863 N88-27002
Semiconductor microcrystallites in porous glass and their applications in optics 20 p2863 N88-27005
Ferromagnetic/semiconductor hybrid structures
20 p2865 N88-27013
Properties of synthetic magnetic superlattices
20 p2865 N88-27014
EXAFS studies of the microstructure of semiconductor alloys, defects and semiconductor-metal interfaces
20 p2868 N88-27031
Phonons in semiconductor superlattices
20 p2869 N88-27035
Electron-phonon interactions in In(0.53)Ga(0.47)As and in In(0.53)Ga(0.47)As/InP quantum wells
20 p2869 N88-27037
Electronic structure of quantum-well states revealed under high pressures 20 p2870 N88-27038
The theory of electron-polar phonon scattering rates in semiconductor micro-structures
20 p2871 N88-27043
Vertical electronic transport in novel semiconductor heterojunction structures 20 p2871 N88-27045
Influence of interfaces on electronic and magnetic properties of MnSe/ZnSe superlattices near monolayer limit 20 p2872 N88-27050
Atomistic simulation of stability, metastability and growth of strained layer structures 20 p2873 N88-27053
Electrical study of metal/group 3-5 semiconductor interfaces: Comparison with the atomic-level studies
20 p2874 N88-27059
Growth and characterization of thin films of ZnSnP(sub)2
[DE88-001164] 20 p2874 N88-27060
Defects in high-mobility semiconductor systems
[AD-A192298] 20 p2879 N88-27090
Epitaxy and properties of two dimensional GaInAs semiconductor structures
[ETN-88-92357] 20 p2879 N88-27094
Numerical calculations of dopent diffusion involving flashlamp heating of silicon 21 p2929 N88-27384
Polarization selective Raman microspectroscopy
21 p2930 N88-27397
NDP (Neutron Depth Profiling) evaluations of boron-implanted compound semiconductors
[AD-A192306] 21 p2934 N88-27425
Studying the physics and operation of multi-terminal near-micron and sub-micron length, hot electron semiconductor devices
[AD-A193380] 21 p2938 N88-27446
Solid state research
[AD-A192837] 21 p3020 N88-27929
Schottky-barrier formation on a covalent semiconductor without Fermi-level pinning: The Metal-MoS2(0001) interface
[AD-A193044] 21 p3021 N88-27931
Ultrafast physics in semiconductor microstructures
[AD-A193300] 21 p3022 N88-27936
Prediction of deep levels and equilibrium concentrations of defects in semiconductors 21 p3023 N88-27945
Deep level defects in semiconductors: Stress and pressure studies
[DE88-010855] 21 p3024 N88-27948
X-ray studies of strain, interface and impurities in semiconductors
[DE88-012460] 21 p3025 N88-27954
Techniques and instrumentation for transient characterization of metal-insulator-semiconductor diodes. Applications to metal-insulator InP system
[ECL-87-17] 21 p3025 N88-27959
The p-well or n-well CMOS technology for advanced SEU-hard SRAMs
[DE88-006845] 22 p3156 N88-28777
Reaction dynamics on semiconductor surfaces
[AD-A194305] 22 p3156 N88-28781
The VPE-hydride technique with alloy source: Equilibrium analysis
[AD-A194036] 22 p3157 N88-28784
Multiphoton transitions in semiconductors in the non-perturbative approach
[DE88-702664] 22 p3157 N88-28786
Infrared devices using semiconductor quantum wells
[RSRE-MEMO-4018] 22 p3157 N88-28788
DARPA-URI consortium meetings on submicron heterostructures of diluted magnetic semiconductors
[AD-A193499] 23 p3206 N88-29081
The diamond as a new electronic material
[NASA-TT-20354] 23 p3209 N88-29098
Local environment approach for deep-level defects in semiconductors: Application to the vacancy in silicon
[DE88-702017] 23 p3287 N88-29573
Intrinsic and extrinsic energy states of semiconductors and heterostructures using novel techniques
[DE88-008560] 23 p3289 N88-29582
Electronic states in tunneling semiconductor superlattices
[DE88-011571] 23 p3290 N88-29587
Study of superconducting properties in some many valley semiconductors
[DE88-702325] 23 p3291 N88-29593
Lattice-matched HgZnTe epitaxy development
[AD-A193677] 23 p3292 N88-29600
Hot electron emission in semiconductors
[AD-A194101] 23 p3292 N88-29601
System suitable for observing surface plasmon in a semi-infinite semiconductor superlattice
[DE88-702686] 23 p3293 N88-29606
Vibration spectra induced by impurities in 3-5-compounds semiconductors
[DE88-702730] 23 p3293 N88-29610
Power MISFETs on OnP
[AD-A195242] 24 p3433 N88-30436
Joint services electronics program
[AD-A195731] 24 p3434 N88-30439

SEMISOLIDS
Electrochromic cells with lutetium diphthalocyanine and semisolid polymer electrolytes
[AD-A188031] 10 p1352 N88-18076

SEMISPAN MODELS
Tip aerodynamics from wind tunnel test of semi-span wing
[NASA-TM-88253] 05 p0540 N88-13290

SENDERS
U TRANSMITTERS

SENSE ORGANS
NT CHEMORECEPTORS
NT COCHLEA
NT CORNEA
NT EAR
NT EYE (ANATOMY)
NT FOVEA
NT GRAVIRECEPTORS
NT MIDDLE EAR
NT OCULOMOTOR NERVES
NT OTOLITH ORGANS
NT PHOTORECEPTORS
NT PROPRIOCEPTORS
NT PUPILS
NT RETINA
NT SEMICIRCULAR CANALS
NT VESTIBULES
Functional development of gravity receptors in insects and amphibians 07 p0886 N88-15376
Regulatory biochemical and metabolic responses in photoreceptors
[AD-A192898] 20 p2831 N88-26794

SENSES
U SENSORY PERCEPTION

SENSIBILITY
U SENSITIVITY

SENSING
U DETECTION

SENSITIVITY
NT IMPACT RESISTANCE
NT LIGHT ADAPTATION
NT NOTCH SENSITIVITY
NT PHOTOSENSITIVITY
NT PHOTOTROPISM
NT PROPELLANT SENSITIVITY
NT RADIATION TOLERANCE
NT SPECTRAL SENSITIVITY
The effect of RDX particle size on the shock sensitivity of cast PBX formulations. 2: Bimodal compositions
[DE87-009581] 01 p0031 N88-10198
Microstructural effects in shock initiation of granular explosives
[DE87-011282] 01 p0031 N88-10200
Scotopic sensitivity with 10 percent oxygen
[AD-A183973] 03 p0356 N88-12243
Aerodynamic sensitivities from subsonic, sonic and supersonic unsteady, nonplanar lifting-surface theory
[NASA-TM-100502] 04 p0394 N88-12459
Investigation, development and application of optimal output feedback theory. Vol. 4: Measures of eigenvalue/eigenvector sensitivity to system parameters and unmodeled dynamics
[NASA-CR-4108] 04 p0482 N88-12969
Sensitivity of the H alpha line to expansion, geometrical extent and temperature gradient in the G and K supergiant chromospheres 04 p0514 N88-13159
Langlie Test Method Program for use with the HP-41CV/X calculator
[DE88-001935] 06 p0687 N88-14210
Tailorable infrared sensing device with strain layer superlattice structure
[NASA-CASE-NPO-16607-1-CU]
06 p0788 N88-14836
Estimating system reliability: Monte Carlo methods, sensitivity and errors in input parameters
[AD-A186182] 07 p0865 N88-15248
Comparison of sensitivity and precision of holographic and speckle-interferometry methods with Fourier-plane recording 08 p1078 N88-16500
Mechanism of and particle size effects on shock sensitivity of heterogeneous pressed explosives: Preliminary assessment of binderless RDX in fuze trains
[MRL-R-1077] 09 p1150 N88-16892
Design of a charge sensitive preamplifier on high resistivity silicon
[DE88-003491] 10 p1323 N88-17907
A semianalytical technique for sensitivity analysis of unsteady aerodynamic computations
[NASA-TM-100810] 11 p1503 N88-18976
Visual contrast sensitivity functions obtained from untrained observers using tracking and staircase procedures
[AD-A187715] 11 p1522 N88-19089
Analysis of the sensitivity of the attitude control system of an artificial satellite
[INPE-4285-PRE/1157] 12 p1599 N88-19573
Sensitivity reduction over a frequency band
[AD-A189123] 12 p1621 N88-19694
Computer aided fast turnaround laboratory for research in VLSI (Very Large Scale Integration)
[AD-A189451] 12 p1624 N88-19715
Metal contacts to cadmium telluride (CdTe)
[AD-A188306] 12 p1698 N88-20159
Anomalous shock sensitivity/density relationship for RDX-polyethylene wax and related formulations from MRL Small Scale Gap Test (SSGT) measurements
[MRL-R-1099] 13 p1739 N88-20399
Some properties of Australian produced explosive composition H-6
[MRL-TN-525] 13 p1754 N88-20490
Computational aspects of sensitivity calculations in transient structural analysis
[NASA-TM-100589] 14 p1924 N88-21467
Sensitivity of control-augmented structure obtained by a system decomposition method
[NASA-TM-100535] 14 p1954 N88-21647
Shape sensitivity analysis of wing static aeroelastic characteristics
[NASA-TP-2808] 15 p2018 N88-22031
Infrared-sensitive spatial light modulator
[AD-A190391] 15 p2134 N88-22729
French evaluation of Japanese biosensors
16 p2184 N88-23020
Sensitivity analysis and multidisciplinary optimization for aircraft design: Recent advances and results
[NASA-TM-100630] 17 p2302 N88-23766
On quench sensitivity of Cu-Cr alloys
[NASA-TT-20174] 18 p2489 N88-24785

A multi-frame ion pinhole camera for intense ion beam transport and focusing experiments
[DE88-007283] 18 p2516 N88-24926
Reducing sensitivity to errors in free electron laser amplifiers
[DE88-007017] 18 p2522 N88-24960
Sensitivity analysis for the system reliability function
[AD-A191648] 18 p2525 N88-24979
Simulation of diaphragm-type IC pressure sensors
19 p2672 N88-25887
A mixed-modem solution for sensitive data segregation on a broadband network
[DE88-001765] 19 p2718 N88-26139
The T-T-T curve in Cu-Cr alloy
[NASA-TT-20167] 20 p2774 N88-26453
Performance sensitivities for point-focus dish systems with secondary concentrators
[DE88-001152] 21 p2968 N88-27629
The radiation sensitivity of select metal chelate polymers: Mechanistic changes at higher energies
[AD-A193467] 23 p3196 N88-29019
Acoustic-optical detector of gravitational waves based on high-quality crystals
[DE88-702459] 23 p3232 N88-29232
Phase sensitive amplification with SIS (Superconductor-Insulator-Superconductor) quasiparticle mixers
[AD-A194594] 23 p3291 N88-29596

ENSITIZING
Study of stainless steel time-temperature sensitization diagrams, part 1
[ETN-87-90762] 03 p0289 N88-11815
The dishomogeneity of the degree of sensitization in large recirculation pipes in Boiling Water Reactor (BWR) power plants
[CISE-3955] 09 p1247 N88-17473

ENSORIMOTOR PERFORMANCE
NT PSYCHOMOTOR PERFORMANCE
Measurement and modification of sensorimotor system function during visual-motor performance
[AD-A186351] 07 p0889 N88-15387
Risk of hypertension and functional cerebral laterality in oil expedition works in far north
12 p1665 N88-19980
Neurophysiological precursors of accurate visuomotor performance 21 p2981 N88-27706
Alterations in upper extremity motor function in soldiers during acute high altitude exposure
[AD-A192676] 23 p3238 N88-29272

SENSORS
Metal-sensing layer-semiconductor and metal-sensing layer-metal heterostructure gas sensors
[DE87-011293] 01 p0103 N88-10674
Optimal detection of sensor failures in flight control systems using deterministic observers
02 p0128 N88-10803
Combustion control with smart sensors
[DE87-013688] 03 p0281 N88-11768
On the root locus method applied to flexural vibration control systems 03 p0320 N88-12022
Limits to the precision of electro-optic and magneto-optic sensors
[PB87-212536] 03 p0323 N88-12040
Turbine flow meter with optical fiber pick-up
[NAL-TR-923] 09 p1169 N88-17009
A quantitative method for evaluating sensor layouts
09 p1178 N88-17056
Multichannel anisotropic single-mode fiber optics for transducers 09 p1240 N88-17429
ISTP SBIR phase 1 Full-Sky Scanner: A feasibility study
[NASA-CR-180749] 10 p1333 N88-17964
Signal and data processing for IR sensors
10 p1374 N88-18199
Prototype thin-film thermocouple/heat-flux sensor for a ceramic-insulated diesel engine
[NASA-TM-100798] 11 p1490 N88-18892
Optically coupled tactile sensor array for robotics
11 p1550 N88-19273
Spectral contents readout of birefringent sensors
[NASA-CR-179430] 13 p1784 N88-20673
Electromagnetic sensor arrays for nondestructive evaluation and robot control
[AD-A190210] 15 p2056 N88-22260
Analytical sensor redundancy assessment
[NASA-CR-182892] 16 p2163 N88-22901
A comparison of integrated and separate systems for flight control and navigation 17 p2303 N88-23779
Fiber waveguide sensors for intelligent materials
[NASA-CR-183028] 17 p2343 N88-23968
Design considerations for the development of an implantable sensor for the continuous measurement of glucose in the diabetic patient 17 p2382 N88-24159
User's guide to the Fault Inferring Nonlinear Detection System (FINDS) computer program
[NASA-CR-178410] 18 p2462 N88-24619
Automatic calibration of space based manipulators and mechanisms
[NASA-CR-182804] 19 p2676 N88-25912
Fiber optic sensors with internal referencing
[NASA-TM-100893] 20 p2806 N88-26644
RRSAS (Robotic Radiation Survey and Analysis System) Project: A real time sensor driven robotic system
[DE88-006825] 20 p2808 N88-26661
Nuclear and ionic charge distribution experiment on ISEE-1 and ISEE-3
[NASA-CR-180776] 23 p3183 N88-28947
Sensor and actuator selection for large space structure control
[AD-A194912] 24 p3333 N88-29842

SENSORY DISCRIMINATION
NT BRIGHTNESS DISCRIMINATION
NT TACTILE DISCRIMINATION
NT VISUAL DISCRIMINATION

SENSORY FEEDBACK
Center for the study of rhythmic processes
[AD-A188204] 11 p1520 N88-19078
Steady-state evoked potentials possibilities for mental-state estimation 16 p2240 N88-23380

SENSORY PERCEPTION
NT AUDITORY PERCEPTION
NT CONSCIOUSNESS
NT PROPRIOCEPTION
NT SPACE PERCEPTION
NT TACTILE DISCRIMINATION
NT TOUCH
NT VISUAL DISCRIMINATION
NT VISUAL PERCEPTION
Brain potentials and personality: A new look at stress susceptibility
[AD-A186931] 09 p1199 N88-17189
Engineering data compendium. Human perception and performance. User's guide
[LC-87-19560] 21 p2993 N88-27749
Engineering data compendium. Human perception and performance, volume 1
[LC-87-19560] 22 p3134 N88-28630
Engineering data compendium. Human perception and performance, volume 2
[LC-87-19560] 22 p3134 N88-28631
Engineering data compendium. Human perception and performance, volume 3
[LC-87-19560] 22 p3134 N88-28632

SENSORY STIMULATION
Sleep induced in cat by electric stimulation of acoustic and motor areas in brain cortex
06 p0751 N88-14612
Vestibular response to caloric stimulation during orbital flight 12 p1658 N88-19939
Significance of sensory signal phase mismatch in mechanisms of motion sickness development
20 p2830 N88-26787

SENTENCES
NT SYLLABLES
NT WORDS (LANGUAGE)

SEO (INDIAN SPACECRAFT)
U INDIAN SPACECRAFT

SEPAC (PAYLOAD)
Space experiments with particle accelerators (SEPAC): Description of instrumentation
[NASA-TM-89728] 14 p1945 N88-21606

SEPARATED FLOW
NT BOUNDARY LAYER SEPARATION
The structure of separated flow regions occurring near the leading edge of airfoils including transition
[NASA-CR-181434] 01 p0002 N88-10011
Investigations of separated flow states on wings of medium aspect ratio taking into account the wind tunnel interference problem
[ETN-87-90437] 01 p0003 N88-10016
An inviscid model of planar, separated flows of finite extent
[RAE-TR-86070] 01 p0044 N88-10279
Intergration effects of D-shaped, underwing, aft-mounted, separate-flow, flow-through nacelles on a high-wing transport
[NASA-TM-4018] 02 p0122 N88-10773
Computation of transonic separated wing flows using an Euler/Navier-Stokes zonal approach
[NASA-TM-88311] 02 p0173 N88-11089
Three-dimensional unsteady flow elicited by finite wings and complex configurations 04 p0395 N88-12468
Investigation of low-speed turbulent separated flow around airfoils
[NASA-CR-177450] 04 p0396 N88-12471
Numerical simulation of unsteady separated flows
[AD-A184132] 04 p0442 N88-12741
Driving mechanism of unsteady separation shock motion in hypersonic interactive flow 05 p0530 N88-13226
Application of discrete vortex method to analysis of separated flow around aerofoils
05 p0537 N88-13268
Characteristics of a separating confluent boundary layer and the downstream wake
[NASA-TM-100046] 06 p0704 N88-14323
A theory for the core flow of leading-edge vortices
07 p0810 N88-14935
Vortex dynamics 07 p0812 N88-14945
A flow visualization study of the leading edge separation bubble on a NACA 0012 airfoil with simulated glaze ice
[NASA-CR-180846] 07 p0816 N88-14966
Analysis of three-dimensional viscous internal flows
[AD-A186254] 07 p0849 N88-15155
Unsteady three-dimensional flow separation
[NASA-CR-182412] 08 p0949 N88-15761
Calculation of symmetric and asymmetric vortex seperation on cones and tangent ogives based on discrete vortex models
[NASA-CR-4122] 08 p0950 N88-15768
Three-dimensional unsteady flow elicited by finite wings and complex configurations
[AD-A186464] 08 p0951 N88-15770
Wind tunnel investigations of periodic vortex separation on rough-surface circular cylinders using acoustic measuring methods
[DFVLR-FB-87-24] 09 p1112 N88-16665
Solution of the three-dimensional Navier-Stokes equations for transonic flow using a multigrid method
10 p1267 N88-17579
Control of vortical separation on conical bodies
10 p1267 N88-17580
Fluctuations and massive separation in three-dimensional shock-wave/boundary-layer interactions
[NASA-TM-89224] 11 p1434 N88-18559
Some aspects of aircraft dynamic loads due to flow separation
[AGARD-R-750] 11 p1439 N88-18588
Numerical model of the time independent mean flow in a rotating rocket motor 13 p1733 N88-20360
Surface flow visualization of separated flows on the forebody of an F-18 aircraft and wind-tunnel model
[NASA-TM-100436] 14 p1863 N88-21127
A flight test investigation into flow separation and structural response for a transport aircraft at buffet onset
[RAE-TR-87006] 14 p1867 N88-21156
On the prediction of highly vortical flows using an Euler equation model, part 2
[AD-A190245] 15 p2064 N88-22305
Dense-spray structure and phenomena. Part 1. Turbulence/dispersed-phase interactions
[AD-A190606] 15 p2065 N88-22315
A new laminar water tunnel to study the transition process in a blasius layer and in a separation bubble and a new tool for industrial aerodynamics and hydrodynamic research 16 p2204 N88-23150
Propfan model wind tunnel aeroelastic research results 16 p2220 N88-23246
Stall flutter analysis of propfans
16 p2221 N88-23256
Unsteady flow about cambered plates
[AD-A191226] 17 p2337 N88-23945
Accounting for the effects of unsteady, separated boundary layers in transonic two dimensional calculations
[ONERA-RT-30/3064-RY-063-R]
17 p2338 N88-23952
Theoretical and experimental investigation of swirl flow phase separators for microgravity applications
17 p2411 N88-24335
Experimental investigation of a microgravity separator for two phase mixtures containing small volumes of gas/vapor 17 p2432 N88-24488
Unsteady flow in a supercritical supersonic inlet
18 p2460 N88-24605
Instability of laminar separation bubbles: Causes and effects
[AD-A191168] 18 p2508 N88-24876
Computation of the turbulent boundary layer downstream of vortex generators
[AD-A191544] 18 p2508 N88-24881
Improving the performance of a finite element method using vector analysis on CRAY 1
[ETN-88-92153] 18 p2513 N88-24907
Method and apparatus for detecting laminar flow separation and reattachment
[NASA-CASE-LAR-13952-1-SB]
18 p2513 N88-24910
Turbulent heat transfer and fluid flow measurements downstream of abrupt expansions and in a cavity of a circular tube at a uniform wall temperature
18 p2515 N88-24920
Method of forming a multiple layer dielectric and a hot film sensor therewith
[NASA-CASE-LAR-13678-1] 18 p2584 N88-25355

Development of a method of calculating unstable flows of cascades separated at the leading edge
[PB87-228714] 19 p2598 N88-25437
Vortex methods for separated flows
[NASA-TM-100068] 20 p2753 N88-26342
A study of flow separation in transonic flow using inviscid and viscous computational fluid dynamics (CFD) schemes
[NASA-CR-183119] 20 p2801 N88-26618
Treatment of the separated flow around profiles (nonviscous, incompressible, two dimensional flow) by the singularities method
[ISL-R-106/87] 20 p2803 N88-26633
Experimental study of unsteady separating turbulent boundary layers
[AD-A192997] 21 p2943 N88-27477
Physical mechanisms in shock-induced turbulent separated flow
[AD-A193165] 21 p2944 N88-27484
A documentation of two- and three-dimensional shock-separated turbulent boundary layers
[NASA-TM-101008] 21 p2949 N88-27519
Study of three-dimensional transonic flow separations
[AD-A193018] 22 p3037 N88-28032
The dynamic behavior of a turbulent boundary layer subjected to a shock-induced separation
[AD-A194164] 22 p3075 N88-28252
Development and analysis of turbulent non-equilibrium boundary layers 23 p3169 N88-28872
Shock boundary layer interaction 23 p3170 N88-28873
Classical separation, trailing-edge flows and buffeting 23 p3170 N88-28874
Vortex flows 23 p3170 N88-28875
Direct-solution techniques for viscous flows and their control
[AD-A194775] 23 p3211 N88-29114
Numerical methods: Euler time dependent solver 24 p3318 N88-29760
The effects of incoming boundary layer thickness on unsteady shock-induced turbulent separations induced by cylinders
[AD-A196190] 24 p3368 N88-30060
Numerical simulation of nozzle flows
[AD-A195144] 24 p3369 N88-30064

SEPARATION
Segregation effects in welded stainless steels
[DE88-701224] 15 p2037 N88-22139

SEPARATORS
NT AIR FILTERS
NT DUST COLLECTORS
NT EVAPORATORS
NT FLUID FILTERS
NT SIEVES
Grace DAKASEP alkaline battery separator 02 p0164 N88-11031
Qualification testing of General Electric 50 Ah nickel-cadmium cells with Pellon 2536 separator and passivated positive plates 02 p0165 N88-11036
Physical properties of immiscible polymers 03 p0297 N88-11868
Plasma centrifuge development at INPE
[INPE-4243-PRE/1117] 08 p1067 N88-16546
Research on fluid dynamic energy separation
[DE88-002776] 10 p1339 N88-18001
A graph separator theorem and its application to Gaussian elimination to optimize Boolean expressions for parallel evaluation
[AD-A188527] 14 p1962 N88-21706
Theoretical and experimental investigation of swirl flow phase separators for microgravity applications 17 p2411 N88-24335
Experimental investigation of a microgravity separator for two phase mixtures containing small volumes of gas/vapor 17 p2432 N88-24468
Flotation processes
[PB88-180302] 18 p2540 N88-25075
Fundamental studies of separation processes
[DE88-007487] 19 p2611 N88-25494

SEQUENCING
Cross-correlation of uniform cyclic difference set sequences
[AD-A184879] 05 p0640 N88-13913
HOC spectral analysis of an almost periodic random sequence in noise
[AD-A185528] 06 p0765 N88-14697
Von Mises' definition of random sequences reconsidered
[PB87-230512] 06 p0767 N88-14715
Recursive m-estimators of location and scale for dependent sequences
[AD-A186292] 07 p0903 N88-15469
On the characterization of certain point processes
[AD-A186427] 07 p0916 N88-15560
On the extreme order statistics for a stationary sequence
[AD-A186428] 07 p0916 N88-15561
Future television systems: Comparison of sequent ial and interlaced scanning
[BBC-RD-1987/18] 09 p1155 N88-16923
Strongly sequential term rewriting systems
[PB88-126693] 10 p1398 N88-18334
Linear prediction of stationary vector sequences
[NASA-TM-100069] 10 p1403 N88-18366
Ideal shrinking and expansion of discrete sequences
[NASA-TM-88202] 11 p1524 N88-19100
The roll back chip: Hardware support for distributed simulation using time warp
[AD-A187823] 11 p1529 N88-19132
Computer aided fast turnaround laboratory for research in VLSI (Very Large Scale Integration)
[AD-A189451] 12 p1624 N88-19715
An automatic system for extraction of information from a Computer Aided Design (CAD), selection, sequencing, and execution of turning processes
[INPE-4350-TDL/294] 12 p1676 N88-20020
A graph separator theorem and its application to Gaussian elimination to optimize Boolean expressions for parallel evaluation
[AD-A188527] 14 p1962 N88-21706
SSME technology test bed fast shutdown assessment
[NASA-CR-179354] 17 p2314 N88-23831
Spatial organization of homopolymer chains inside spherical polybutadiene domains of SB diblock copolymers
[AD-A193390] 21 p2918 N88-27321
Robust prediction for stationary processes: 2D enriched version
[AD-A193318] 21 p3006 N88-27833
Strong law for mixing sequence
[AD-A193615] 23 p3274 N88-29490
Performance of DS/SSMA communications in impulsive channels. Part 1: Correlation receivers
[AD-A195712] 24 p3362 N88-30021

SEQUENTIAL ANALYSIS
The sequential evaluation of Doppler satellite observations
[REPT-141] 01 p0010 N88-10057
Explicit formulate for the distributions of stopping variables under Wald's truncated SPRT (Sequential Probability Radio Tests) for a poisson process
[AD-A185053] 05 p0640 N88-13914
Statistical selection procedures
[AD-A185868] 07 p0913 N88-15538
Strongly sequential term rewriting systems
[PB88-126693] 10 p1398 N88-18334
DASM: A tool for Decomposition and Analysis of Sequential Machines
[EUT-87-E-170] 14 p1956 N88-21660
Efficient monotone sequential design
[CWI-MS-R8705] 14 p1962 N88-21707
Sequential tests for the drift of a Wiener process with a smooth prior and the heat equation
[AD-A190322] 15 p2121 N88-22638

SEQUENTIAL COMPUTERS
A model for architectural comparison
[AD-A195993] 24 p3411 N88-30302

SEQUENTIAL CONTROL
Substructure discovery in executed action sequences
[AD-A186446] 08 p1069 N88-16462

SERIES (MATHEMATICS)
NT ASYMPTOTIC SERIES
NT COSINE SERIES
NT PADE APPROXIMATION
NT POWER SERIES
NT TAYLOR SERIES
Recursive m-estimators of location and scale for dependent sequences
[AD-A186292] 07 p0903 N88-15469
Series representations of infinitely divisible random vectors and a generalized shot noise in banach spaces
[AD-A186502] 08 p1073 N88-16474
A representation for serial robotic tasks 12 p1681 N88-20048
Detecting serial correlation in the error structure of a cross-lagged panel model
[AD-A189070] 12 p1685 N88-20077
Distributions of quadratic forms
[AD-A190224] 15 p2124 N88-22663

SERIES EXPANSION
Spherical harmonic expansion of the Levitus Sea surface topography
[NASA-CR-181448] 02 p0216 N88-11362
Asymptotic form of stationary solutions of the Navier-Stokes equations for large Reynolds numbers 04 p0459 N88-12838
The shifted Adams method for ordinary differential equations
[DE88-000810] 04 p0486 N88-12994
The simulation of the viscous flow around a cylinder by the random vortex method 05 p0579 N88-13534
Contributions to selection and ranking theory with special reference to logistic populations
[AD-A185629] 07 p0917 N88-15568
On the Edgeworth expansion and the bootstrap approximation for a Studentized U-statistic
[CWI-MS-R8708] 14 p1965 N88-21728
On a biorthogonal system associated with uniform asymptotic expansions
[CWI-AM-R8709] 18 p2566 N88-25240
Accurate solution of parabolic equations by expansion in ultraspherical polynomials
[DE88-701829] 20 p2845 N88-26880
Asymptotic orders of reachability in perturbed linear systems
[AD-A192718] 22 p3143 N88-28688
Why are certain nonlinear Partial Differential Equations (PDE) both widely applicable and integrable
[PREPRINT-582] 22 p3144 N88-28698
Solution of large order Fourier-Bessel equations
[ARE-TM(UHA)-88504] 23 p3272 N88-29475
On the meaning of perturbation expansions in quantum field theory
[DE88-702138] 23 p3294 N88-29620
An improved spherical earth diffraction algorithm for SEKE
[AD-A195847] 24 p3360 N88-30005

SEROTONIN
Effect of low-frequency whole-body vertical vibration on the serotonergic system of the brain and spinal cord 19 p2704 N88-26081

SERPENTINE
Impact-induced devolatilization and hydrogen isotopic fractionation of serpentine: Implications for planetary accretion
[NASA-CR-182877] 16 p2175 N88-22966

SERVICE LIFE
Ensuring the service life of designs (experience in aircraft construction) 02 p0157 N88-10986
Improving repairability of gears 02 p0158 N88-10989
Space station propulsion
[NASA-TM-100216] 03 p0277 N88-11746
Ultra-fine grained alloy material
[AD-A184500] 03 p0290 N88-11820
Durability (lifetime) predictions adhesively bonded structures
[AD-A184069] 03 p0335 N88-12110
Investigation of instability, dynamic forces, and effect of dynamic loading on strength of cages for the bearings in the high pressure oxygen turbopumps for the space shuttle main engine
[NASA-CR-178970] 06 p0714 N88-14378
Turbine engine monitoring systems: Can they benefit component improvement program management?
[AD-A186992] 09 p1120 N88-16706
Evaluation of bituminous materials used in pavement recycling projects at Tyndall, MacDill, and Hurlburt Air Force Bases
[AD-A188068] 10 p1317 N88-17871
Computer-aided design analysis of 57-mm, angular-contact, cryogenic turbopump bearings
[NASA-TP-2816] 11 p1496 N88-18933
Sodium-sulfur technology evaluation at Argonne National Laboratory
[DE88-002852] 13 p1762 N88-20544
Failure mechanism of He-Ne lasers 14 p1902 N88-21362
Experience with duplex bearings in narrow angle oscillating applications 14 p1926 N88-21484
Titanium carbide coatings for aerospace ball bearings 14 p1927 N88-21486
Two gimbal bearing case studies: Some lessons learned 14 p1927 N88-21487
Robotic joint experiments under ultravacuum 14 p1927 N88-21490
Evaluation of structural analysis methods for life prediction 14 p1930 N88-21511
MPD (magnetoplasmadynamic) thruster advanced pumping system concepts
[AD-A190513] 15 p2138 N88-22756
Development of a flexible and economic helicopter engine monitoring system
[PB88-165147] 16 p2160 N88-22887
The effect of titanium reinforcement on the life of positive grids in lead-acid batteries 17 p2320 N88-23857
Pioneer 10 and 11 RTG performance update 17 p2405 N88-24301
Foil gas bearing system endurance testing dynamic isotope power system 17 p2405 N88-24302
AMTEC electrode development 17 p2409 N88-24324
Gas-cooled reactor power systems for space 17 p2413 N88-24350

Analysis of closed cycle megawatt class space power systems with nuclear reactor heat sources
17 p2413 N88-24351
Performance and long duration test of a 30 kw thermal arcjet engine
[AD-A190962] 18 p2474 N88-24677
An extended life and performance test of a low-power arcjet
[NASA-TM-100942] 18 p2476 N88-24687
Harmfulness of defects: Behaviour in service of a delamination in a composite containing many differently oriented layers
[PB88-124714] 18 p2479 N88-24705
Nickel hydrogen low earth orbit life testing
[AD-A191946] 18 p2504 N88-24855
Effect of LEO cycling at shallow depths of discharge on MANTECH IPV nickel-hydrogen cells
[NASA-TM-101300] 19 p2688 N88-25978
Engine component retirement for cause. Volume 1: Executive summary
[AD-A192730] 20 p2760 N88-26371
A statistical treatment of accelerated life test data for copper-water heat pipes 20 p2783 N88-26509
Results from life test in progress on eagle-picher nickel cadmium cells
[AD-A192816] 21 p2936 N88-27434
Sodium/sulfur cell evaluation results
[DE88-011488] 21 p2938 N88-27451
Background to the UK military requirements for engine usage, condition and maintenance management systems
22 p3033 N88-28004
Corrosion and stress corrosion of metals in decontamination solutions 22 p3054 N88-28118
Modeling discrete bathtub and upside down bathtub mean residual life functions
[AD-A192000] 22 p3085 N88-28320
Burn-in with mixed populations
[AD-A194651] 22 p3085 N88-28321
Life-span knowledge engineering for space operations
23 p3259 N88-29401
Fuel effects on flame radiation and hot-section durability 24 p3347 N88-29925
A reliability-based program for predicting the service life of organic coating systems 24 p3355 N88-29971
In-house capacitor technology program
[AD-A194804] 24 p3367 N88-30049

SERVICES
NT MEDICAL SERVICES
NT METEOROLOGICAL SERVICES
Freedom of Information Act: Fee waiver practices at the FBI (Federal Bureau of Investigation)
[PB87-216727] 02 p0249 N88-11573
Reuse: A Reliable Unified Service Environment for distributed systems 10 p1379 N88-18231

SERVOCONTROL
A new state space model for the NASA/JPL 70-meter antenna servo controls 04 p0436 N88-12702
A modern control theory based algorithm for control of the NASA/JPL 70-meter antenna axis servos
04 p0436 N88-12706
Development of an interface for an ultrareliable fault-tolerant control system and an electronic servo-control unit
[NASA-TM-88236] 05 p0553 N88-13367
Description and analysis of a cascade control of fluid flow
[PB87-112686] 06 p0698 N88-14282
Covariant control of bilateral servos for in-orbit manipulation 12 p1590 N88-19520
Servo-actuator control for sampled-data feedback disturbance rejection --- helicopters
[ESA-TT-1002] 16 p2163 N88-22903
Study on design and control of torque-controlled manipulators
[NASA-TT-20197] 23 p3223 N88-29183

SERVOMECHANISMS
NT SERVOMOTORS
Application of prediction of equilibrium to servo-controlled calorimetry measurements
[DE87-013745] 03 p0324 N88-12046
Design of a velocity and position control laboratory servo system
[AD-A186596] 08 p0990 N88-15997
Control system simulation for a single-link flexible arm
[AD-A187037] 09 p1174 N88-17035
Adaptive proximate time-optimal servomechanisms
09 p1175 N88-17043
Covariant control of bilateral servos for in-orbit manipulation 12 p1590 N88-19520
Implementation of a visual servoing system for evaluation of robotic refueling applications
[AD-A189676] 14 p1954 N88-21645
Photo-optical converter of angular displacements in digital servomechanisms
[DE87-703208] 14 p1961 N88-21698
Servo-actuator control for sampled-data feedback disturbance rejection --- helicopters
[ESA-TT-1002] 16 p2163 N88-22903
Path following robot
[AD-A190960] 16 p2215 N88-23217
Roller drive materials performance
16 p2219 N88-23241
Force servo control of a commercial gantry robot
[DE88-006649] 20 p2808 N88-26660
Study on design and control of torque-controlled manipulators
[NASA-TT-20197] 23 p3223 N88-29183
A standard architecture for controlling robots
[AD-A195929] 24 p3423 N88-30371

SERVOMOTORS
Modelling of a hydraulic motor and servo-valve to produce a desired system response using analogue and digital compensation techniques
[ETN-88-92079] 14 p1899 N88-21337

SERVOS
U SERVOMOTORS

SERVOSTABILITY CONTROL
U SERVOCONTROL

SET THEORY
NT BOREL SETS
NT EQUIVALENCE
Maintaining state constraints in relational databases: A proof theoretic basis
[DE87-014329] 02 p0248 N88-11569
A characterization of separating pairs and triplets in a graph
[AD-A184278] 04 p0477 N88-12941
On the number of minimum size separating vertex sets in a graph
[AD-A184279] 04 p0478 N88-12942
Foundations of O-theory 2: Measurements and relation to fuzzy set theory
[DE88-000013] 04 p0485 N88-12986
Diagonalisation methods in polynomial setting
[PB87-136616] 06 p0769 N88-14726
Theoretical investigations of chaotic dynamics
[AD-A186404] 07 p0867 N88-15261
An O(n3L) interior point algorithm for convex quadratic programming
[AD-A186001] 07 p0909 N88-15504
An elementary approach to the Danieli-Kolmogorov theorem and some related results
[AD-A186011] 07 p0909 N88-15505
On the extreme points of the set of all 2xn bivariate positive quadrant dependent distributions with fixed marginals and some applications
[AD-A186316] 07 p0911 N88-15521
Stationary regenerative sets and subordinators
[AD-A186298] 07 p0918 N88-15573
A fast bottom-up algorithm for computing the cut sets of noncoherent fault trees
[DE88-003741] 09 p1220 N88-17320
Norm inequalities for derivatives and differences
[DE88-002920] 09 p1230 N88-17371
An application of fuzzy set theory to statistical hypothesis testing
[AD-A186705] 09 p1232 N88-17386
A unified approach for digital image processing problems: Mathematical morphology
[INPE-4311-TDL/278] 11 p1537 N88-19183
Measures of similarity between fuzzy concepts: A comparative analysis
[AD-A189430] 13 p1825 N88-20910
Compact representation of the separating k-sets of a graph
[AD-A189650] 14 p1965 N88-21723
Data management and language enhancement for generalized set theory computer language for operation of large relational databases
[NASA-CR-182868] 16 p2250 N88-23446
Algorithms and data structures for an expanded family of matroid intersection problems
[AD-A191482] 18 p2562 N88-25213
A primal-dual algorithm for the computation of the minimum of a convex function on the intersection of convex functions, and its application in data analysis
[RR-638-M] 18 p2563 N88-25217
Multicriteria integer programming for problems involving linear and nonlinear utility functions
[AD-A194530] 23 p3249 N88-29336
Unification and set-valued functions for functional and logic programming
[AD-A193643] 23 p3250 N88-29341
A methodology for multiple rule system integration and resolution within a singular knowledge base
23 p3261 N88-29413
Mathematical algorithms for approximate reasoning
23 p3262 N88-29418
Practical higher-order functional and logic programming based on lambda-calculus and set-abstraction
[AD-A193645] 23 p3271 N88-29486

SETI
U PROJECT SETI

SEX FACTOR
Gender and cognitive style differences at the human-computer interface
[NPL-DITC-90/87] 01 p0077 N88-10493
Meta-analysis of leadership differences between males and females and the effect on performance
[AD-A187769] 11 p1564 N88-19361

SEX GLANDS
NT TESTES

SEYFERT GALAXIES
Comparison of global and nuclear properties of starburst and Seyfert 1 galaxies 03 p0388 N88-12438
The radio structure of active nuclei in edge-on spiral and Seyfert galaxies 09 p1264 N88-17576
IUE evidence on the nature of the innermost broad-line region in Seyfert 1 galaxies 17 p2450 N88-24552
AGN (OIII) emission line profiles: Dependencies on galaxy inclination and Balmer decrement
[INPE-4596-PRE/1324] 24 p3459 N88-30577

SFAR
U SOUND FIXING AND RANGING

SHADOWGRAPH PHOTOGRAPHY
NT SCHLIEREN PHOTOGRAPHY
Development of flow visualization techniques for use in the Hot Gas Laboratory
[BAE-ARG-233] 03 p0325 N88-12052

SHADOWGRAPHS
U SHADOWGRAPH PHOTOGRAPHY

SHADOWS
NT PENUMBRAS
Unified Sun and sky illumination for shadows under trees
[DE87-014232] 01 p0083 N88-10535
Shadow systems and attractors in reaction-diffusion equations
[AD-A185804] 06 p0766 N88-14706
Color shadow methods of analyzing reconstructed wave front 09 p1236 N88-17407
Manual for obscuration code with space station applications
[NASA-CR-178099] 17 p2334 N88-23931
Shape from shading, occlusion and texture
[AD-A184840] 18 p2571 N88-25269
Curvature of blended rolled edge reflectors at the shadow boundary contour
[NASA-CR-182974] 18 p2576 N88-25300

SHAFTS (MACHINE ELEMENTS)
NT ROTATING SHAFTS
NT TURBOSHAFTS
Digital algorithms for the control and dynamic decoupling of industrial robot axes
[ETN-87-90441] 01 p0084 N88-10546
Analysis of 7- X 10-foot high speed wind tunnel shaft loads in support of fan blade failure investigation
[NASA-TM-100504] 04 p0402 N88-12496
Exact finite element method analysis of viscoelastic tapered structures to transient loads
05 p0595 N88-13632
The Jeffcott equations in nonlinear rotordynamics
07 p0928 N88-15636
Dynamic modelling of flexible rotor shafts mounted on hydrodynamic bearings 13 p1779 N88-20641
Study on shaft seals for potassium turbine
[EL-891] 15 p2074 N88-22364
Angular position measurements at high temperatures and high radiation environments
17 p2434 N88-24479
SRB/SLEEC (Solid Rocket Booster/Shingle Lap Extendible Exit Cone) feasibility study, volume 2. Appendix A: Design study for a SLEEC actuation system
[NASA-CR-178974] 23 p3187 N88-28965

SHALLOW SHELL EQUATIONS
Effective treatment of membrane and shear locking phenomena in curved shear-deformable axisymmetric shell element 04 p0428 N88-12652
Forced motion of initially stressed shells and plates
18 p2529 N88-25005

SHALLOW SHELLS
Blade vibration problems in centrifugal compressors. Fundamental considerations 07 p0851 N88-15165
Nonlinear dynamic analysis and optimal control of shallow shells 23 p3224 N88-29191

SHALLOW WATER
Nearshore wave transformation study of sites near Port Canaveral Inlet, Florida
[AD-A186965] 09 p1195 N88-17159
Remote sensing of acoustic properties of shallow water sediments: A review
[AD-A192107] 18 p2570 N88-25267
Fully implicit splitting method for accurate tidal computations
[PB88-183637] 20 p2828 N88-26781

SHANKS
U JOINTS (JUNCTIONS)

SHANNON INFORMATION THEORY
U INFORMATION THEORY

SHAPE CONTROL
Multisurface control mechanism for a deployable antenna: Far Infrared and Submillimeter Space Telescope (FIRST) technology study
[RP-FA-D003] 09 p1135 N88-16807
Development of metastable processing paths for high temperature alloys
[AD-A188682] 12 p1608 N88-19617
The 15-meter diameter hoop/column antenna surface control actuator system 14 p1924 N88-21469
Technologies for antenna shape and vibration control 19 p2652 N88-25748
Robust design of distributed controllers for large flexible space structures
[NASA-CR-183202] 24 p3380 N88-30134

SHAPE MEMORY ALLOYS
NT NITINOL ALLOYS
A comparison of high damping shape memory alloys with Cu-Mn-based and Fe-Cr-based alloys
[AD-A184110] 04 p0414 N88-12566
Martensitic transformation and microstructures in sintered NiAl alloys
[NASA-TT-20192] 19 p2616 N88-25519
Shape memory alloys: New materials for future engineering
[NASA-TT-20193] 20 p2775 N88-26455

SHAPED CHARGES
Jet formation and characterization of a conical shaped charge
[DE87-012102] 02 p0155 N88-10969
Destruction test of small scaled solid propellant motors
[ISAS-R-620] 03 p0278 N88-11752
Jet initiation of PBX 9502
[DE88-000493] 05 p0571 N88-13481
Developments in instrumental techniques for observations of magnetospheric and ionospheric shaped charge releases 08 p1031 N88-16248
Penetration theory for inclined and moving shaped charges
[MBB-UA-940/86] 10 p1315 N88-17861

SHAPES
NT CONVEXITY
NT ELLIPTICITY
NT LINE SHAPE
NT T SHAPE
Shape optimization of linear antennas
[ETN-87-90413] 01 p0036 N88-10233
Theory and methods for design of pulse shapes for broadcast teletext
[CRC-1405] 02 p0162 N88-11013
A shape preserving interpolant which has tension controls
[DE87-014615] 02 p0229 N88-11443
Observations on the hydrodynamic flow visualization at ONERA
[PD-FM-8718] 04 p0444 N88-12753
An approach to object recognition: Aligning pictorial descriptions
[AD-A184462] 04 p0482 N88-12972
Shape optimization of damping layers 05 p0595 N88-13635
The statistics of the shape of small fatigue cracks 05 p0599 N88-13666
Electromagnetic fields backscattered from an s-shaped inlet cavity with an absorber coating on its inner walls
[NASA-CR-182401] 07 p0845 N88-15130
An experimental mapping of the flow field behind a glaze ice shape on a NACA 0012 airfoil
[NASA-CR-180847] 08 p0950 N88-15766
Shape isomers as candidates for the gamma ray laser storage state
[DE88-005228] 11 p1492 N88-18909
Design modeling for shape optimization 11 p1527 N88-19122
Shape optimization of three-dimensional stamped and solid automotive components
[GMR-5168] 11 p1528 N88-19123
An investigation of cruciform parachutes and towed targets
[BU-360] 14 p1862 N88-21122
Electrohydrodynamic migration of charged droplets in an insulating fluid
[NASA-TM-100849] 14 p1912 N88-21424
Study of mean free path effects on growth of ultrafine metallic aerosols
[AD-A190206] 15 p2039 N88-22149
Mixed finite element formulation applied to shape optimization 16 p2221 N88-23252
Implications of the trapping-desorption and direct inelastic scattering channels on Dicke-narrowed lineshapes
[AD-A191410] 16 p2270 N88-23581
Shape detection in remote sensing through graph isomorphism 17 p2354 N88-24026
An analytic model for aerodynamic shapes
[AD-A191573] 18 p2456 N88-24583
Shape stability in composites 18 p2479 N88-24706
Stiffened titanium panels
[NASA-CASE-LAR-13814-1] 18 p2497 N88-24816
Shape from shading, occlusion and texture
[AD-A184840] 18 p2571 N88-25269
Flexible tactile sensing arrays for robotics: Architectural robustness and yield considerations 19 p2671 N88-25878
Theoretical predictions of precipitate shapes in cubic alloys
[DE88-010856] 21 p2914 N88-27291
Texture perception and shape from texture
[AD-A192923] 21 p2996 N88-27771
Distortion functions
[DE88-752634] 21 p3015 N88-27896
Three-dimensional zonal grids about arbitrary shapes by Poisson's equation
[NASA-TM-101018] 22 p3039 N88-28042
Using primal sketch primitives as the basis for the Hough transform
[INPE-4564-PRE/1305] 24 p3412 N88-30310
Symbolic construction of a 2D scale-space image
[AD-A195926] 24 p3423 N88-30374

SHARP LEADING EDGES
Tests on the AFWAL 65 deg delta wing at NLR: A study of vortex flow development between Mach = 0.4 and 4
[NLR-MP-86058-U] 13 p1717 N88-20266
Development of a method of calculating unstable flows of cascades separated at the leading edge
[PB87-228714] 19 p2598 N88-25437

SHATTERING
U FRAGMENTATION

SHEAR
An analytical study of the effects of transverse shear deformation and anisotropy on buckling loads of laminated cylinders
[NASA-TM-100508] 05 p0557 N88-13387
Temperature-dependent tensile and shear response of graphite/aluminum
[NASA-CR-182914] 19 p2609 N88-25484

SHEAR CREEP
Viscoelastic properties of EA951 adhesive: A source of creep deformations of a strongback
[DE88-001581] 06 p0685 N88-14197

SHEAR DISTURBANCES
U S WAVES

SHEAR FATIGUE
U SHEAR STRESS

SHEAR FLOW
Two-dimensional shear flow turbulence: A statistical theory of vortex filaments
[DE87-012234] 01 p0046 N88-10295
Shearing flow over Stokes wave. Part one: General theory
[ETN-87-90957] 02 p0171 N88-11074
Analysis of the motions and effects of hairpin vortices 03 p0316 N88-11997
Nonequilibrium fluctuations and transport in sheared fluids 03 p0316 N88-11999
Heat and moisture transport in the atmospheric boundary layer
[AD-A184222] 04 p0470 N88-12904
Three-dimensional structure of boundary layers in transition to turbulence
[AD-A185466] 06 p0702 N88-14311
Turbulence in hypersonic flow
[AD-A185624] 07 p0815 N88-14961
Nonlinear and nonparallel stability problems
[AD-A186406] 07 p0850 N88-15159
Interpretation of equatorial current meter data as internal waves
[PB88-108113] 08 p1044 N88-16309
Investigation of the influence of wind shear on the aerodynamic characteristics of aircraft using a vortex-lattice method 10 p1274 N88-17619
Analysis of shear-layer probe data for holes in hypersonic configurations
[DE88-003992] 11 p1435 N88-18564
Structure of shear flow turbulence and its control
[AD-A187909] 11 p1482 N88-18846
Transport and stability properties of free shear flows 13 p1768 N88-20577
Research on turbulence in bottom boundary layer in ocean 13 p1788 N88-20697
Mixed-layer shear related to wind stress in the central equatorial Pacific 13 p1805 N88-20793
Mixed-layer fronts in the California current 13 p1805 N88-20794
Enhancement of data acquisition and numerical computation capabilities for unsteady fluid dynamics
[AD-A190115] 15 p2063 N88-22302
A new method of measuring multigrade oil shear elasticity and viscosity at high shear rates
[AD-A190145] 15 p2064 N88-22304
Instruments for use in experimental studies of complex turbulent shear flow: Three component LDVs
[AD-A190526] 15 p2065 N88-22312
Direct numerical simulation of buoyantly driven turbulence 16 p2196 N88-23097
Modeling of turbulent transport as a volume process 16 p2196 N88-23099
A statistical investigation of the single-point pdf of velocity and vorticity based on direct numerical simulations 16 p2196 N88-23101
Local structure of intercomponent energy transfer in homogeneous turbulent shear flow 16 p2197 N88-23103
A general form for the dissipation length scale in turbulent shear flows 16 p2197 N88-23104
Relations between two-point correlations and pressure strain terms 16 p2198 N88-23109
Conditionally-averaged structures in wall-bounded turbulent flows 16 p2198 N88-23112
Structure of turbulent shear flows 16 p2198 N88-23113
Inflectional instabilities in the wall region of bounded turbulent shear flows 16 p2199 N88-23114
An investigation of ducted propellers in axisymmetric shear flow 16 p2202 N88-23136
Experimental study of vortex sheets in plane flow 16 p2203 N88-23142
Dynamics and control of turbulent shear flows
[AD-A191527] 18 p2508 N88-24879
LLNL granular solids flow project
[DE88-007492] 18 p2513 N88-24906
A single streamwise vortical structure and its instability in shear flows 18 p2515 N88-24921
Atomization in a turbulent shear layer: Preliminary measurements 19 p2624 N88-25565
Scaling laws for homogeneous turbulent shear flows in a rotating frame
[NASA-CR-181672] 19 p2665 N88-25847
Influence of wind shear on the aerodynamic characteristics of airplanes
[NASA-TP-2827] 20 p2755 N88-26344
A numerical simulation of two-dimensional transient shear flow
[ISAS-RN-627] 20 p2797 N88-26600
Stability of a coastal upwelling front over topography
[AD-A192354] 20 p2829 N88-26784
Evolution of hairpin vortices in a shear flow
[NASA-TM-100858] 20 p2845 N88-26885
Cavitation inception in a turbulent shear flow
[DE88-011486] 21 p2946 N88-27497
Granular flow: Particle-dynamics simulations of steady flow
[DE88-011342] 21 p2948 N88-27506
Direct simulation of stable stratified homogeneous turbulent shear flows
[DFVLR-FB-88-04] 21 p2949 N88-27516
The Kelvin-Helmholtz instability in a stratified shear flow
[CFD/88/2] 22 p3076 N88-28265
Stability of parallel inviscid shear flow with mean spanwise variation
[FFA-TN-1987-57] 22 p3079 N88-28285
Nonlinear surface and internal waves on shear flow
[PREPRINT-584] 22 p3129 N88-28604
Study of toluene rotary fluid management device and shear flow condenser performance for a space-based organic Rankine power system
[NASA-CR-180885] 24 p3338 N88-29872

SHEAR LAYERS
A note on the instability of a vortex sheet leaving a semi-infinite plate
[DFVLR-FB-87-16] 01 p0004 N88-10019
On the instability of thin circular shear layers 04 p0395 N88-12467
Blowup for a nonlinear evolution equation and self-reproducing strained shear layers 04 p0444 N88-12755
Combustion related shear-flow dynamics in elliptic supersonic jets 05 p0531 N88-13232
Experimental investigation of heterogeneous compressible shear layers 06 p0700 N88-14294
Nonlinear and nonparallel stability problems
[AD-A186406] 07 p0850 N88-15159
Mean velocities and Reynolds stresses in the juncture flow and in the shear layer downstream of an appendage
[AD-A185819] 08 p0980 N88-15923
Cavitation inception scale effects. 1. Nuclei distributions in natural waters. 2. Cavitation inception in a turbulent shear flow
[AD-A186553] 08 p0988 N88-15987
Active feedback interaction with a shear layer
[AD-A188525] 12 p1573 N88-19410

Time-accurate simulations of a shear layer forced at a single frequency
[NASA-TM-100836] 12 p1628 N88-19740
Optical properties of compressible inhomogeneous shear layers relevant to high power lasers
[AD-A189299] 12 p1633 N88-19774
Three-dimensional shear layer experiments and their use as test cases for calculation methods
[NLR-MP-86036-U] 13 p1767 N88-20570
Numerical model of Rayleigh instability and spin-off eddies on fronts 13 p1788 N88-20696
Instruments for use in experimental studies of complex turbulent shear flow: Three component LDVs
[AD-A190526] 15 p2065 N88-22312
Shear-layer structures in near-wall turbulence 16 p2198 N88-23110
Dynamics and control of turbulent shear flows
[AD-A191527] 18 p2508 N88-24879
Characteristics of merging shear layers and turbulent wakes of a multi-element airfoil
[NASA-TM-100053] 18 p2511 N88-24900
Stability of a coastal upwelling front over topography
[AD-A192354] 20 p2829 N88-26784
Predicting optical degradation of a laser beam through a turbulent shear layer 21 p2927 N88-27376
An analysis of horizontal temperature gradients and heat content in the mixed layer and the surface forcing during PATCHEX
[AD-A192330] 21 p2976 N88-27678
Aerodynamics of seeing on large transport aircraft
[NASA-CR-183122] 23 p3174 N88-28896

SHEAR PROPERTIES
NT SHEAR STRENGTH
Two-dimensional shear flow turbulence: A statistical theory of vortex filaments
[DE87-012234] 01 p0046 N88-10295
Refraction of shear wave into nonlinearly elastic or elastoplastic half-space 02 p0159 N88-10999
Stability of low-shear Tokamaks
[DE88-000305] 03 p0379 N88-12383
Determination of through-plane shear moduli for glass-reinforced plastics
[PB87-106274] 04 p0418 N88-12592
Steady shearing in a viscoplastic solid
[AD-A184341] 04 p0454 N88-12810
The evolution of plastic strain in steady, plastic shock waves
[DE87-013812] 04 p0456 N88-12826
Studies of unsteadiness in boundary layers
[AD-A185662] 06 p0703 N88-14315
The effect of shear lips on fatigue crack growth in Al-2024 sheet material 06 p0718 N88-14408
Shear failure in round bar tensile tests of Al-Zn-Mg-Cu alloys
[PB87-143632] 07 p0869 N88-15271
Successful mixed formulation for axisymmetric shell analysis employing discontinuous stress fields of the same order as the displacement field
[DE88-700021] 09 p1178 N88-17052
Boundary stabilization of thin elastic plates
[AD-A187123] 10 p1343 N88-18025
On stress collapse in adiabatic shear bands
[AD-A187185] 11 p1498 N88-18942
High shear rate rheometry of low-viscosity liquids
[AD-A188447] 12 p1627 N88-19733
Parametric study of acceleration-induced stresses and frequency changes in doubly-rotated crystal resonators
[AD-A189261] 13 p1761 N88-20532
The buckling and vibration of composite plates using the Levy method considering shear deformation and rotary inertia
[AD-A189743] 15 p2076 N88-22374
The influence of cathodic protection on erosion-corrosion of metals and model alloys
[AD-A191613] 18 p2485 N88-24742
Pulsed spray structure and atomisation techniques
[AD-A192280] 20 p2800 N88-26614
An experimental and analytical evaluation of a biaxial test for determining shear properties of composite materials
[NASA-CR-182928] 21 p2962 N88-27593
Small scale mixing in the initial region of a jet
[AD-A193500] 23 p3192 N88-28994
Critical conditions for failure in materials subjected to high rates of loading
[AD-A194697] 23 p3226 N88-29201
Kinetic theory for electrostatic waves due to transverse velocity shears
[AD-A193404] 23 p3284 N88-29557
Large displacement and rotational formulation for laminated cylindrical shells including parabolic transverse shear
[AD-A194871] 24 p3384 N88-30158

SHEAR STRAIN
Plastic strain localization between voids in shear deformation fields 04 p0427 N88-12648
Effective treatment of membrane and shear locking phenomena in curved shear-deformable axisymmetric shell element 04 p0428 N88-12652
Vibration and buckling of geometrically imperfect laminated cylindrical shells 04 p0456 N88-12822
Plasticity of aluminum and iron at high shear strain rate and high pressure 05 p0563 N88-13430
The analysis of deformations and strains in composites by moire interferometry
[AD-A187482] 10 p1345 N88-18043
Geodetic measurement of deformation east of the San Andreas fault in Central California
[NASA-CR-182709] 13 p1798 N88-20754
An efficient Mindlin finite strip plate element based on assumed strain distribution 15 p2081 N88-22407
Dynamic shear band development in plane strain
[AD-A190915] 18 p2526 N88-24988
Improved finite strip Mindlin plate bending element using assumed shear strain distributions
[NASA-TM-100928] 23 p3225 N88-29195

SHEAR STRENGTH
Shear strength of the ASDEX upgrade Toroidal Field (TF) coil insulation: Rupture, fatigue and creep behavior --- tokamak
[IPP-1/230] 01 p0059 N88-10376
Spatial strength variation and statistical size effect of laminated orthotropic composite materials 04 p0427 N88-12646
Flexibilized copolyimide adhesives
[NASA-TM-89303] 05 p0570 N88-13474
Effect of interface on mechanical properties of graphite/201 aluminum composites 05 p0606 N88-13717
Interfacial shear strength of pitch and high strain pan fibers in an epoxy matrix
[AD-A185966] 07 p0826 N88-15011
Improving the interlaminar shear strength of carbon fiber-epoxy composites through carbon fiber bromination
[NASA-TM-100248] 07 p0827 N88-15018
A nonlinear computational model for the strength and failure of composite plates and shells 11 p1501 N88-18964
An investigation of the mechanical properties of improved carbon fibre composite materials
[RAE-TR-86021] 14 p1884 N88-21259
Evaluation of a thermoplastic polyimide (422) for bonding GR/PI composite
[NASA-TM-100584] 16 p2182 N88-23003

SHEAR STRESS
NT TORSIONAL STRESS
Free-edge delamination: Laminate width and loading conditions effects
[NASA-TM-100238] 04 p0411 N88-12551
A refined nonlinear analysis of laminated composite plates and shells
[AD-A184436] 04 p0454 N88-12811
Analysis of end stresses in glass-metal bimaterial strips
[DE87-007848] 05 p0610 N88-13750
A method for the approximate calculation of the skin friction coefficient of horizontal wavy plates
[VKI-TN-160] 07 p0851 N88-15172
The NASA aircraft icing research program 08 p0957 N88-15803
Shear and mixing effects on cells in agitated microcarrier tissue culture reactors 09 p1197 N88-17173
Strength and structure of Ga sub 1-xIn sub xAs alloys
[AD-A188092] 10 p1303 N88-17795
Ethynylated aromatics as high temperature matrix resins
[NASA-TM-89829] 11 p1450 N88-18640
On stress collapse in adiabatic shear bands
[AD-A187185] 11 p1498 N88-18942
Variation of the wind stress related to frontal passages during FASINEX (Frontal Air-Sea Interaction Experiment) 1986
[AD-A187180] 11 p1514 N88-19042
Sea duct: A deep-sea computer-controlled recirculating flume for the study of sea floor stability
[AD-A187734] 11 p1516 N88-19056
Mechanical response of unidirectional boron/aluminum under combined loading
[NASA-CR-182595] 12 p1604 N88-19591
Three-dimensional scattering of impulsive acoustic waves by a semi-infinite crack in the plane interface of a half space and a layer
[PB88-146998] 12 p1687 N88-20089
Bodies in unsteady flow
[AD-A190416] 15 p2064 N88-22308
Stochastic estimation of conditional eddies in turbulent channel flow 16 p2194 N88-23087
Coherent structure 16 p2199 N88-23117
Computation and characteristics of pulsatile multi-bifurcation flow 18 p2483 N88-24729
Method and apparatus for detecting laminar flow separation and reattachment
[NASA-CASE-LAR-13952-1-SB] 18 p2513 N88-24910
Resolved shear stress intensity coefficient and fatigue crack growth in large crystals
[NASA-CR-182137] 18 p2528 N88-24997
Characterization of accelerating pipe flow
[AD-A189065] 21 p2943 N88-27481
Liquid crystals for unsteady surface shear stress visualization
[DE88-010570] 21 p2951 N88-27527
Shear stress at a film-substrate interface due to mismatch strain
[AD-A193461] 23 p3288 N88-29577
Experimental determination of drag modifications due to elastic compliant surfaces using quantitative visual techniques
[AD-A194785] 24 p3372 N88-30082
Development of a more general Reynolds stress closure for swirling flow
[AD-A195121] 24 p3374 N88-30092

SHEAR WAVES
U S WAVES

SHEARING
Coronal magnetic fields produced by photospheric shear
[NASA-CR-181514] 03 p0390 N88-12447
Steady shearing in a viscoplastic solid
[AD-A184341] 04 p0454 N88-12810
An analytical study of the effects of transverse shear deformation and anisotropy on natural vibration frequencies of laminated cylinders
[NASA-TM-100554] 10 p1295 N88-17739
Applications of the lateral shearing interferometer in measurement of synchrotron radiation optical elements
[DE88-005184] 13 p1840 N88-21011

SHEARING STRESS
U SHEAR STRESS

SHEATHS
NT ION SHEATHS
NT PLASMA SHEATHS
Research and development of electrical insulators for thermionic applications 17 p2429 N88-24449
Effects of low reflection on the collector and source sheaths of a finite ion temperature plasma
[DE88-008929] 21 p3017 N88-27908
Collector and source sheaths of a finite ion temperature plasma
[DE88-003934] 23 p3286 N88-29564

SHEET METAL
U METAL SHEETS

SHELL STABILITY
Geometrically nonlinear rod mechanism analogy of axisymmetrically loaded spherical shells based on a comprehensive approach to the stability of circular arches
[ETN-87-90419] 01 p0062 N88-10398
Determination of the ultimate loads for corrugated-steel, barrel-type shell structures
[AD-A187716] 11 p1498 N88-18944
Tripping of stiffened plates using a refined beam theory
[AD-A193989] 22 p3087 N88-28333
Thickness effects on the stability of shell like structures 23 p3224 N88-29192
Computational aerodynamic analysis for a range-limited 25mm training round
[AD-A185270] 24 p3320 N88-29772

SHELL THEORY
Nonsteady-state vibrations in acoustic medium of elastic elliptical shell subjected to instantaneously applied uniform pressure 02 p0160 N88-11000
An integral equation analysis of inelastic shells 03 p0336 N88-12118
Solution of geometrically nonlinear problem for reinforced shell of revolution having arbitrary shape 04 p0426 N88-12637
Rational reinforcement of cylindrical shells with variable stiffness frames subjected to external pressure 04 p0426 N88-12638
Finite deformations of shell with rigid inclusion 04 p0426 N88-12639
Effective treatment of membrane and shear locking phenomena in curved shear-deformable axisymmetric shell element 04 p0428 N88-12652
Calculation of displacement, constraints and eigenmodes of rotating blades
[ETN-88-92296] 16 p2224 N88-23277
An electron-scattering study of N-15
[ETN-88-92479] 16 p2266 N88-23552

SHELLFISH
Irradiation preservation of seafood: Literature review
[DE88-001691] 05 p0631 N88-13858

SHELLS (STRUCTURAL FORMS)
NT ANISOTROPIC SHELLS
NT CONICAL SHELLS
NT CYLINDRICAL SHELLS
NT DOMES (STRUCTURAL FORMS)
NT ELASTIC SHELLS
NT FLUID FILLED SHELLS
NT LIQUID FILLED SHELLS
NT METAL SHELLS
NT ORTHOTROPIC SHELLS
NT REINFORCED SHELLS
NT SHALLOW SHELLS
NT SPHERICAL SHELLS
NT THIN WALLED SHELLS
NT TOROIDAL SHELLS
Analysis of shell-type structures subjected to time-dependent mechanical and thermal loading
[NASA-CR-181409] 01 p0060 N88-10388
USSR report: Engineering and equipment
[JPRS-UEQ-87-008] 04 p0423 N88-12621
Finite deformations of shell with rigid inclusion
04 p0426 N88-12639
The structures of large wound propulsion shells --- carbon fiber composites filament winding
[SNIAS-872-430-118] 05 p0559 N88-13406
Optical deformation measurement on shells following the raster principle
[ETN-88-90608] 05 p0609 N88-13741
An element of a multilayer shell for the computation of composite structures
[ONERA-RT-14/3542-RY-051-R]
05 p0610 N88-13742
Development of a shell system for DS moulds at RR precision casting facility --- directional solidification (DS)
[PNR90400] 09 p1151 N88-16893
Consistent linearization of the element-independent corotational formulation for the structural analysis of general shells
[NASA-CR-178418] 09 p1181 N88-17078
A nonlinear computational model for the strength and failure of composite plates and shells
11 p1501 N88-18964
Optimal filament shells loaded with internal pressure in a centrifugal force field 14 p1885 N88-21266
Preliminary 2-D shell analysis of the space shuttle solid rocket boosters
[NASA-TM-100515] 17 p2348 N88-23989
Three-dimensional curved shell and solid-shell transition finite elements with temperature and temperature gradients as primary variables for steady state heat conduction
17 p2349 N88-23997
Adaptive finite element methods for shells
[AD-A193221] 21 p2960 N88-27565
Parameter identification of material constants in a composite shell structure
[DE88-008115] 22 p3086 N88-28326
Experimental investigation of the effects of underwater exposure on the damping characteristics of bolted structural connections for plates and shells
[AD-A194486] 23 p3226 N88-29200
SHIELDING
NT ELECTROMAGNETIC SHIELDING
NT HEAT SHIELDING
NT MAGNETIC SHIELDING
NT RADIATION SHIELDING
NT REENTRY SHIELDING
NT SOLAR RADIATION SHIELDING
NT SPACECRAFT SHIELDING
Review of diffusion barrier technology for application in SP-100 fuel pins
[DE88-000021] 02 p0234 N88-11480
On the role of crack tip shielding in influencing the behavior of long and small fatigue cracks in aluminum-lithium alloy 2090 05 p0600 N88-13671
Effect of plasma rotation in tokamak on stabilizing action of electrically conducting wall 06 p0773 N88-14748
Laminar flow control leading edge glove flight test article development
[NASA-CR-172137] 07 p0815 N88-14960
An estimate of the noise shielding on the fuselage resulting from installing a short duct around an advanced propeller
[NASA-TM-100262] 10 p1405 N88-18379
Laser countermeasure impacts and penalties
[DE88-006871] 18 p2520 N88-24947
Trailer shield assembly for a welding torch
[NASA-CASE-MFS-29260-1] 18 p2524 N88-24972
Systems analysis of INTOR-like designs
[DE88-004422] 18 p2578 N88-25316
Self shielding of surfaces irradiated by intense energy fluxes
[DE88-007094] 18 p2579 N88-25318
Experimental evaluation of resistojet thruster plume shields
[NASA-TM-101383] 24 p3338 N88-29868
SHIELDS (GEOLOGY)
U BEDROCK
SHIFT REGISTERS
A labeling procedure for linear finite-state codes
11 p1472 N88-18781
Novel silicon Schottky barrier infrared imaging arrays
17 p2439 N88-24510
SHIP HULLS
Experimental studies on the tripping behavior of narrow T-stiffened flat plates subjected to hydrostatic pressure and underwater shock 05 p0592 N88-13613
Validation of the Underwater Shock Analysis (USA) program. Part 1: Theoretical considerations --- ship design
[REPT-5073713-86-01] 06 p0702 N88-14308
Steady ship waves at low Froude numbers, part 2
[AD-A176805] 09 p1160 N88-16953
Mechanisms in thermal mechanical forming of plates
[AD-A187797] 11 p1466 N88-18744
An investigation of ducted propellers in axisymmetric shear flow 16 p2202 N88-23136
Revised Impact Dynamic Design-Analysis Method (RIDDAM)
[AD-A190479] 16 p2217 N88-23225
Tripping of stiffened plates using a refined beam theory
[AD-A193989] 22 p3087 N88-28333
Numerical field model simulation of full scale fire tests in a closed spherical/cylindrical vessel
[AD-A195067] 24 p3359 N88-29998
Response of SMA (Shielded Metal Arc) and narrow gap HY80 weldments to explosive shock loading
[AD-A195994] 24 p3385 N88-30162
SHIPS
NT AIRCRAFT CARRIERS
NT SUBMARINES
The EH-101 integrated project: A naval, utility and commercial helicopter system 03 p0265 N88-11672
Visualization of the flow field around a generic destroyer model in a simulated turbulent atmospheric boundary layer
[AD-A184658] 03 p0320 N88-12023
Integrated control and display research for transition and vertical flight on the NASA V/STOL Research Aircraft (VSRA)
[NASA-TM-100029] 05 p0551 N88-13359
A summary of experimental results on square plates and stiffened panels subjected to air-blast loading
09 p1178 N88-17057
The evolution of naval warfare technology and the impact of space systems
[AD-A186900] 09 p1233 N88-17392
Application of a database system for inventory management of classified material
[AD-A186986] 09 p1261 N88-17558
A pyrotechnic delay ignition system for a submarine launched marine signal
[MRL-R-1079] 13 p1754 N88-20487
CTD/O2 data collected in 1985 and 1986 for EPOCS (Equatorial Pacific Ocean Climate Studies)
[PB88-160775] 14 p1951 N88-21629
Measurements of the time dependent velocity field surrounding a model propeller in uniform water flow
16 p2205 N88-23155
Low frequency ocean ambient noise: Measurements and theory
[AD-A191188] 16 p2237 N88-23362
Satellites at sea --- INMARSAT
19 p2700 N88-26054
Contribution of space to marine activities
19 p2700 N88-26057
Vertical ship motions and sea loads considering nonlinear effects
[TAE-592] 20 p2784 N88-26515
SHIVERING
Influence of skeletal muscle glycogen on passive rewarming after hypothermia
[AD-A186451] 08 p1049 N88-16334
Manipulation of muscle glycogen concentrations using high and low carbohydrate diets and exercise
[AD-A187732] 11 p1519 N88-19069
SHOCK
The Shock and Vibration Digest, Volume 19, No. 11
03 p0265 N88-11673
The Shock and Vibration Digest, Volume 19, No. 10
03 p0335 N88-12112
Impact-induced devolatilization and hydrogen isotopic fractionation of serpentine: Implications for planetary accretion
[NASA-CR-182877] 16 p2175 N88-22966
SHOCK ABSORBERS
Steering mechanism --- vehicles
[EP-PATENT-0-181-700-A1] 01 p0053 N88-10338
Non-linear shipboard shock analysis of the Tomahawk missile shock isolation system 05 p0592 N88-13614
Liquid spring design methodology for shock isolation system applications 08 p0998 N88-16043
Design and test of a spacecraft instrument shock isolator 08 p0998 N88-16044
Suspension design for a satellite transport container
[INPE-4352-TDL/296] 12 p1600 N88-19578
Variable response load limiting device
[NASA-CASE-LAR-12801-1] 17 p2346 N88-23982
SHOCK DIFFUSERS
U DIFFUSERS
U SHOCK WAVE ATTENUATION
SHOCK FRONTS
Monitoring of Pc3 pulsations in solar wind and at Earth by interplanetary magnetic field
08 p1002 N88-16069
Vehicle glow observed on the SONDA 3
[INPE-4297-PRE/1168] 12 p1600 N88-19581
SHOCK HEATING
Theoretical studies of mass loss and shock phenomena in cool star envelopes
[NASA-CR-182433] 08 p1099 N88-16616
SHOCK LAYERS
Absorption characteristics of Si3N4 ablation layer plasma 20 p2783 N88-26504
Research in applied mathematics
[AD-A192385] 21 p3004 N88-27820
SHOCK LOADS
NT BLAST LOADS
Shock-chemistry in natural materials and evolution of planetary surfaces
[DE87-012737] 02 p0254 N88-11604
Shock-induced chemical synthesis of phases similar to the high temperature superconductor oxides
[DE87-013725] 03 p0380 N88-12387
Shock compression of solids as a physical-chemical-mechanical process
[DE88-001674] 05 p0563 N88-13427
Experimental studies on the tripping behavior of narrow T-stiffened flat plates subjected to hydrostatic pressure and underwater shock 05 p0592 N88-13613
On the simulation of ballistic shock loads
05 p0593 N88-13615
Response of a sequential damper to shock inputs
08 p0998 N88-16042
Liquid spring design methodology for shock isolation system applications 08 p0998 N88-16043
A modal control based limiting performance formulation for shock excited systems 08 p0998 N88-16046
Analysis of shock and vibration environments for cargo on C9B transport aircraft 08 p0999 N88-16051
The Shock and Vibration Bulletin. Part 2: Instrumentation, shock analysis, and shock testing
[AD-A186749] 09 p1178 N88-17053
Retarded potential technique applied for shock wave loading of doubly symmetric submerged structures
09 p1179 N88-17058
Measurement, data analysis and prediction of pyrotechnic shock from pin-pullers and separation joints
09 p1179 N88-17061
Suspension design for a satellite transport container
[INPE-4352-TDL/296] 12 p1600 N88-19578
Investigations into shock-induced enhancement of mixing and combustion in supersonic burners
[AD-A189609] 12 p1607 N88-19608
The effects of incoming boundary layer thickness on unsteady shock-induced turbulent separations induced by cylinders
[AD-A196190] 24 p3365 N88-30060
Response of SMA (Shielded Metal Arc) and narrow gap HY80 weldments to explosive shock loading
[AD-A195994] 24 p3385 N88-30162
SHOCK RESISTANCE
NT IMPACT RESISTANCE
SHOCK SIMULATORS
Scaling the electromagnetically driven explosive shock simulator 05 p0592 N88-13612
SHOCK SPECTRA
Conservatism implications of shock test tailoring for multiple design environments 05 p0592 N88-13611
Designing electronics for pyrotechnic shock
08 p0997 N88-16038
Dynamic substructuring for shock spectrum analysis using component mode synthesis
11 p1499 N88-18950
La Recherche Aerospatiale, bimonthly bulletin, no. 1986-5, 234/September-October
[ESA-TT-1032] 19 p2641 N88-25671
SHOCK TESTS
Conservatism implications of shock test tailoring for multiple design environments
[DE87-013927] 03 p0338 N88-12127
Mechanical shock test specification using nonstationary random excitation models
[DE87-013650] 04 p0454 N88-12812

Implementation of a new shock testing procedure using nonstationary random excitation
[DE87-014643] 04 p0456 N88-12827
The 58th Shock and Vibration Symposium, volume 1
[NASA-CP-2488-VOL-1] 05 p0592 N88-13609
Conservatism implications of shock test tailoring for multiple design environments 05 p0592 N88-13611
Scaling the electromagnetically driven explosive shock simulator 05 p0592 N88-13612
Non-linear shipboard shock analysis of the Tomahawk missile shock isolation system 05 p0592 N88-13614
Ground shock profiles for an accidental explosion at the proposed Large Rocket Test Facility at Arnold Engineering Development Center
[DE88-002652] 07 p0853 N88-15180
The Shock and Vibration Bulletin. Part 1: Welcome, Keynote Address, Invited Papers, Nondevelopment Items Workshop and Pyrotechnic Shock Workshop
[AD-A186748] 08 p0997 N88-16034
Guidelines for qualifying non-development equipment to shock and vibration 08 p0997 N88-16036
Designing electronics for pyrotechnic shock 08 p0997 N88-16038
The Shock and Vibration Bulletin. Part 3: Isolation and damping, vibration test criteria, and vibration analysis and test
[AD-A186750] 08 p0997 N88-16040
The Shock and Vibration Bulletin. Part 2: Instrumentation, shock analysis, and shock testing
[AD-A186749] 09 p1178 N88-17053
A quantitative method for evaluating sensor layouts 09 p1178 N88-17056
Measurement, data analysis and prediction of pyrotechnic shock from pin-pullers and separation joints 09 p1179 N88-17061
Design and dynamic testing of an instrumented spacecraft component 11 p1499 N88-18952
Experimental comparison of lightning simulation techniques to CV-580 airborne lightning strike measurements
[AD-A190576] 15 p2098 N88-22496

SHOCK TUBES
NT SHOCK TUNNELS
Fast shock tube assemblies
[DE87-011732] 01 p0008 N88-10042
Production of flows for aeroballistic investigation in the shock tubes of the Franco-German Research Institute (ISL), Saint-Louis (France)
[ISL-R-113/86] 05 p0541 N88-13295
Velocity interferometry in shock tubes and shock tunnels
[ISL-CO-203/87] 09 p1122 N88-16713
A review of some flow visualization experiments carried out at the Institut Franco-Allemand de Recherches (ISL) shock tubes
[ISL-CO-243/86] 09 p1163 N88-16974
Blast waves generated by planar detonations
[DE88-002219] 09 p1164 N88-16979
Production by pyrolysis of diffusion particles for velocimetry in shock tubes
[ISL-R-119/86] 11 p1455 N88-18671
Computational studies of wave-shaping in a blast simulator by perforated plates in the driver
[AD-A188200] 11 p1483 N88-18850
Investigation of heat transfer to a flat plate in a shock tube
[AD-A189538] 13 p1766 N88-20561
Plate response analysis using shock tube
[AD-A190828] 18 p2523 N88-24987
Test of a prototype gate with fast opening equipping the shock tube 0 2.40 m at CEG
[PB87-227864] 19 p2604 N88-25465
Numerical simulation of the shock tube flows by TVD scheme 19 p2638 N88-25648
Surface temperature thermal fluxmeters for shock tubes
[NASA-TT-20319] 20 p2762 N88-26381
A shock-tube experiment on gases mixing processes associated with CO2/N2 mixing gasdynamic laser
[ISAS-RN-350] 20 p2797 N88-26598
Navier-Stokes simulation of shock-tube flows over a wedge-type step by finite volume method
[ISAS-RN-628] 20 p2797 N88-26599

SHOCK TUNNELS
Shock tunnels for real gas hypersonics 05 p0530 N88-13223
Velocity interferometry in shock tubes and shock tunnels
[ISL-CO-203/87] 09 p1122 N88-16713
A numerical study of the test time in a hypersonic shock tunnel
[AD-A194057] 23 p3172 N88-28888

SHOCK WAVE ATTENUATION
Static magnetization and microwave loss in shock-modified ferrites
[DE87-012362] 02 p0146 N88-10916

SHOCK WAVE GENERATORS
NT SHOCK TUBES
NT SHOCK TUNNELS

SHOCK WAVE INTERACTION
Interaction of interplanetary shocks with nonuniform ambient solar wind 01 p0116 N88-10740
Large-scale interaction of the solar wind with comets Halley and Giacobini-Zinner 01 p0117 N88-10745
The global interaction of comets with the solar wind 01 p0117 N88-10746
Effect of dissipation on propagation of spherical detonation shock wave 02 p0159 N88-10998
Spectroscopy and nonthermal processes 02 p0252 N88-11594
The effects of sweep and bluntness on a glancing shock wave turbulent boundary layer interaction 05 p0531 N88-13227
Interferometric data for a shock-wave/boundary-layer interaction
[NASA-TM-88227] 05 p0543 N88-13306
The effect of collision angle on mach reflection
[AD-A185798] 06 p0704 N88-14319
Separated flow 07 p0812 N88-14944
Examination of the development of a compressible turbulent boundary layer on a rough and porous wall
[PB87-148266] 07 p0815 N88-14964
Experimental research on swept shock wave/boundary layer interactions
[AD-A187250] 10 p1331 N88-17957
Velocity measurements in a 3D (three dimensional) shock wave laminar boundary layer interaction
[AD-A187334] 10 p1332 N88-17959
The structure and control of three-dimensional shock wave turbulent boundary layer interactions
[AD-A187642] 10 p1332 N88-17961
Shock wave/turbulent boundary layer interaction in high-Reynolds-number hypersonic flows
[AD-A188029] 11 p1434 N88-18555
Fluctuations and massive separation in three-dimensional shock-wave/boundary-layer interactions
[NASA-TM-89224] 11 p1434 N88-18559
Resonant Alfven wave instabilities driven by streaming fast particles 13 p1855 N88-21104
An experimental-computational investigation of transonic shock wave-turbulent boundary layer interaction in a curved test section
[CWI-NM-R8716] 14 p1909 N88-21408
Numerical and experimental investigation of multiple shock wave/turbulent boundary layer interactions in a rectangular duct
[AD-A190772] 15 p2066 N88-22320
Numerical study of unsteady viscous hypersonic blunt body flows with an impinging shock
[NASA-TM-100096] 15 p2122 N88-22650
High-resolution shock-capturing schemes for inviscid and viscous hypersonic flows
[NASA-TM-100097] 15 p2122 N88-22651
La Recherche Aerospatiale, bimonthly bulletin, number 1987-3, 238/May-June
[ESA-TT-1075] 16 p2206 N88-23161
Technology Reports of Kyushu University, volume 61, no. 2
[ISSN-0023-2718] 16 p2256 N88-23485
Theoretical investigation of 3-D shock wave-turbulent boundary layer interactions, part 6
[AD-A191546] 18 p2509 N88-24882
Gone with the solar wind: A study of protons accelerated by interplanetary shocks 19 p2743 N88-26283
Compressible boundary layers --- atmospheric reentry
[CERT-OA-13/5005-AYD] 20 p2801 N88-26623
A documentation of two- and three-dimensional shock-separated turbulent boundary layers
[NASA-TM-101008] 21 p2949 N88-27519
The dynamic behavior of a turbulent boundary layer subjected to a shock-induced separation
[AD-A194164] 22 p3075 N88-28252
Shock boundary layer interaction 23 p3170 N88-28873
Noise generation and boundary layer effects in vortex-airfoil interaction and methods of digital hologram analysis for these flow fields
[AD-A194191] 23 p3171 N88-28883
Shock waves in unsteady flows
[NASA-TT-20329] 23 p3214 N88-29134
Numerical simulation of nozzle flows
[AD-A195144] 24 p3369 N88-30064
Experimental and numerical investigation of the effect of distributed suction on oblique shock wave/turbulent boundary layer interaction
[NASA-TM-101334] 24 p3372 N88-30084

SHOCK WAVE PROFILES
Effect of dissipation on propagation of spherical detonation shock wave 02 p0159 N88-10998
Theoretical and experimental investigations on the structure of stationary shock waves in gas particle dispersions
[ETN-88-92983] 23 p3213 N88-29122
Influence of peak pressure on the substructure evolution and shock wave profiles of Ti-6Al-4V
[DE88-006458] 23 p3225 N88-29197

SHOCK WAVE PROPAGATION
Change in interplanetary shock acceleration preceding STIP Interval 17 01 p0112 N88-10719
Rarefaction velocities in shocked lead
[DE87-013141] 02 p0146 N88-10917
Explicit and implicit soil modelling for dynamic soil-structure interaction problems 04 p0428 N88-12650
Theoretical and numerical analysis of shock wave propagation through different dusty-gas mixture layers 06 p0699 N88-14292
Validation of the Underwater Shock Analysis (USA) program. Part 1: Theoretical considerations --- ship design
[REPT-5073713-86-01] 06 p0702 N88-14308
Steady waves in a nonlinear theory of viscoelasticity
[AD-A185548] 06 p0723 N88-14448
Misty picture weather-watch and microbarograph project: Experiments 9412-14-18
[DE88-003949] 11 p1514 N88-19047
On the possibility of high velocity deflagration front propagation by radiative energy transfer
[AD-A189022] 12 p1613 N88-19645
Research in applied mathematics
[AD-A192385] 21 p3004 N88-27820

SHOCK WAVES
NT DETONATION WAVES
NT OBLIQUE SHOCK WAVES
NT SONIC BOOMS
Shock-wave studies using plastic flyers driven by an electric gun for hypervelocity impact on selected materials
[DE87-012631] 01 p0008 N88-10046
Real time analysis of detonation products
[DE87-007453] 01 p0031 N88-10195
The effect of RDX particle size on the shock sensitivity of cast PBX formulations. 2: Bimodal compositions
[DE87-009581] 01 p0031 N88-10198
Hot-spot reaction in unsustained shocks
[DE87-011781] 01 p0044 N88-10277
Time-resolved measurements of shock-induced vapor-pressure profiles
[DE87-012972] 01 p0045 N88-10289
Rayleigh-Taylor instability in compressible fluids
[DE87-013494] 01 p0047 N88-10297
Relation between shock strength and strain-rate plasticity at maximum deviatoric stress
[DE87-011736] 01 p0061 N88-10390
Propagating shocks in the corona 01 p0112 N88-10718
Interactions of oblique interplanetary discontinuities and their manifestations during STIP intervals 15-19 01 p0119 N88-10758
Hot spots: Subnanometer femtosecond energy localization
[DE87-010276] 02 p0155 N88-10968
Visible emission from granular explosives during shock initiation
[DE87-012361] 02 p0155 N88-10970
Spectroscopic studies of shocked and detonating explosives
[DE87-014216] 02 p0155 N88-10972
Computations of hypervelocity impact using the CTH shock wave physics code
[DE87-013067] 02 p0169 N88-11062
Modeling shockwave deformation via molecular dynamics
[DE87-013157] 02 p0169 N88-11063
Shock-induced cooling in dense fluids
[DE87-014343] 02 p0170 N88-11067
Vibrational spectroscopy of shock-compressed fluid N2 and O2
[DE87-013138] 03 p0313 N88-11979
Numerical calculation of two dimensional fluid flow with strong shocks
[KFK-4191] 03 p0314 N88-11986
Steady tonation and flagration waves in reactive continua
[RARDE-2/73] 03 p0315 N88-11989
Application of an upwind algorithm to the parabolized Navier-Stokes equations 03 p0316 N88-12000
An experimental investigation of quasi-conical shock wave/turbulent boundary layer interactions 03 p0317 N88-12004
On the scheme dependency of the three-dimensional Euler solutions 03 p0318 N88-12010
Thrust and specific impulse of repetitively-pulsed-laser propulsion rocket 03 p0318 N88-12012

Nonequilibrium characteristics of nitrogen plasmas appropriate to an AOTV flight 03 p0319 N88-12019
A study of chaos and mixing in Rayleigh-Taylor and Richtmyer-Meshkov unstable interfaces
[AD-A184751] 03 p0320 N88-12026
Particle velocity and stress gage measurements in spherical diverging flow
[DE87-007333] 03 p0321 N88-12033
Models for penetration of thin plates
[DE87-013727] 03 p0332 N88-12090
Numerical experiments with a symmetric high-resolution shock-capturing scheme
[NASA-TM-88325] 03 p0370 N88-12332
Shock-induced chemical synthesis of phases similar to the high temperature superconductor oxides
[DE87-013725] 03 p0380 N88-12387
Adiabatic supernova expansion into the circumstellar medium
[DE87-014241] 03 p0387 N88-12433
Neutrinos in supernovae
[DE87-014295] 03 p0387 N88-12434
Particle injection and cosmic ray acceleration at collisionless parallel shocks
[DE88-000507] 04 p0430 N88-12665
Three-dimensional, free-Lagrange hydrodynamics
[DE88-000494] 04 p0443 N88-12749
An experimental investigation of unsteadiness in swept shock wave/turbulent boundary layer interactions
04 p0445 N88-12760
Numerical modeling of slow shocks
[DE87-014768] 04 p0454 N88-12808
A dissipation principle and its consequences for structured shock waves in thermoelastic materials
[DE87-013723] 04 p0454 N88-12813
The evolution of plastic strain in steady, plastic shock waves
[DE87-013812] 04 p0456 N88-12826
Slow-mode shocks in the earth's magnetosphere
[DE88-000483] 04 p0468 N88-12895
Prompt simultaneous acceleration of protons and electrons to relativistic energies by shock waves in solar flares
[IPPJ-851] 04 p0493 N88-13037
Core bounce supernovae
[DE87-014910] 04 p0520 N88-13197
Driving mechanism of unsteady separation shock motion in hypersonic interactive flow 05 p0530 N88-13226
On the numerical simulation of three-dimensional hypersonic flow 05 p0532 N88-13237
Numerical experiments with hypersonic flows beneath a cone-delta-wing combination 05 p0532 N88-13238
The off-design performance of hypersonic waveriders
05 p0533 N88-13244
Influence of shock wave and gas pressure on the behavior of a pyrotechnical device
[SNIAS-872-430-111] 05 p0570 N88-13477
On the simulation of ballistic shock loads
05 p0593 N88-13615
The Shock and Vibration Digest, Volume 19, No. 12
05 p0610 N88-13746
Analytical investigation of reflection of a regular or mach reflection over a secondary wedge
[AD-A185690] 06 p0703 N88-14316
Dynamic high pressure process for fabricating superconducting and permanent magnetic materials
[DE88-000848] 06 p0785 N88-14817
Breakdown of the conservative potential equation
07 p0809 N88-14929
Upwind relaxation algorithms for Euler/Navier-Stokes equations 07 p0810 N88-14931
The carbon dioxide chaperon efficiency for the reaction H + O2 + M yields HO2 + M from ignition delay times behind reflected shock waves
[NASA-TM-100125] 07 p0830 N88-15036
Lyman-alfa/OH-resonance-absorbtion measurements and simulation calculations for the investigation of the induction behavior of methane/ethane/oxygen mixtures in reflected shock waves
[ETN-88-90806] 07 p0831 N88-15042
The Shock and Vibration Bulletin. Part 3: Isolation and damping, vibration test criteria, and vibration analysis and test
[AD-A186750] 08 p0997 N88-16040
Analytical study of the effect of early warning on optimal shock isolation 08 p0998 N88-16047
Criteria of interplanetary parameters causing intense magnetic storms (Dst less than -100nT)
[NASA-CR-182423] 08 p1024 N88-16200
Shock structure and noise of supersonic jets in simulated flight to Mach 0.4
[NASA-TP-2785] 08 p1080 N88-16510
Bidirectional electron heat flux events in space
[DE88-001791] 08 p1084 N88-16531
AMPTE-UKS ion observations at a quasi-parallel bow shock 08 p1095 N88-16589
Experimental investigation of shock-induced disturbances on transonic airfoils
[DFVLR-FB-87-28] 09 p1112 N88-16666
Mechanism of and particle size effects on shock sensitivity of heterogeneous pressed explosives: Preliminary assessment of binderless RDX in fuze trains
[MRL-R-1077] 09 p1150 N88-16892
A guide to the transient three phase porous flow model implemented in the two-dimensional CRAY-TENSOR code: Physics, numerics, and code description
[DE88-003709] 09 p1165 N88-16983
Multi-component stress history measurements and analysis
[DE88-000977] 09 p1168 N88-17004
Reinforced cocnrete arches under blast and shock environments 09 p1180 N88-17065
Transverse flow deflections associated with fast coronal mass ejecta in interplanetary space
[DE88-003180] 09 p1263 N88-17566
NF85: A three-dimensional, air-dynamics computer code for analyzing explosions in structures
[DE88-005085] 10 p1331 N88-17953
The use of optical fibers for shock pressure and timing measurements at high pressures
[DE88-004012] 10 p1334 N88-17971
Supernova mechanisms: Before and after SN1987a
[DE88-003489] 10 p1429 N88-18533
Operating loading of piping systems
[ETN-88-91057] 11 p1484 N88-18856
A lecture on detonation-shock dynamics
[DE88-004313] 11 p1487 N88-18879
Preparation of thin film polyvinylidene fluoride shock wave pressure transducers
[PB88-156070] 11 p1490 N88-18893
Approximate method for predicting the permanent set in a beam in vacuo and in water subject to a shock wave 11 p1500 N88-18957
Reynold stress closure in jet flows using wave models
[NASA-CR-182662] 12 p1628 N88-19741
Wave curves for simple isotropic elastic solids
[AD-A188865] 12 p1636 N88-19798
To what extent is mass loading responsible for the Venus bowshock precursor?
[NASA-TM-89307] 12 p1711 N88-20239
Anomalous shock sensitivity/density relationship for RDX-polyethylene wax and related formulations from MRL Small Scale Gap Test (SSGT) measurements
[MRL-R-1099] 13 p1739 N88-20399
Use of the LLNL 40 kV electric gun to study the shock response of 21-6-9 stainless steel
[DE87-014550] 13 p1742 N88-20418
Investigation of heat transfer to a flat plate in a shock tube
[AD-A189538] 13 p1766 N88-20561
An interferometric investigation of the diffraction of planar shock waves over a half-diamond cylinder in air
[UTIAS-322] 13 p1768 N88-20575
Pseudo-stationary oblique-shock-wave reflections in low gamma gases: Isobutane and sulphur hexafluoride
[UTIAS-TN-267] 13 p1768 N88-20576
Theoretical investigation of the wave shaping process in a section of ladder fracture tape
[MRL-R-1081] 13 p1771 N88-20595
Impact shock generator from explosively driven plates
[DE88-003596] 14 p1918 N88-21452
Buckling of blast loaded cylinder
[AD-A190124] 15 p2076 N88-22376
The structure of sonic underexpanded turbulent air jets in still air
[AD-A190856] 16 p2157 N88-22870
Efficient implementation of essentially non-oscillatory shock capturing schemes, 2
[NASA-CR-181656] 17 p2392 N88-24217
Passive shock wave-boundary layer control for the Bell FX69-H-098 airfoil 18 p2457 N88-24588
On symmetric TVD schemes
19 p2639 N88-25659
Non-oscillatory spectral Fourier methods for shock wave calculations
[NASA-CR-181675] 19 p2720 N88-26148
Numerical modeling of the effect of particle size of explosives on shock initiation properties
[DE88-010479] 20 p2780 N88-26491
Australian structures response evaluation: Ground shock and air blast measurements for site investigation survey
[MRL-TN-526] 20 p2813 N88-26685
Shock wave compression and metallization of simple molecules
[DE88-008031] 20 p2851 N88-26925
On linear relationship between shock velocity and particle velocity
[DE88-701827] 20 p2880 N88-27099
Experimental investigation of the reflection of a planar shock wave over a double wedge
[AD-A193078] 21 p2943 N88-27482
A documentation of two- and three-dimensional shock-separated turbulent boundary layers
[NASA-TM-101008] 21 p2949 N88-27519
Solution to the compressible Navier-Stokes equations of motion by Chebyshev polynomials with implicit time stepping
[AD-A194119] 22 p3075 N88-28257
Influence of peak pressure on the substructure evolution and shock wave profiles of Ti-6Al-4V
[DE88-006458] 23 p3225 N88-29197

SHOOTING STAR AIRCRAFT
U T-33 AIRCRAFT

SHORELINES
Atmospheric diffusion at coastal site in presence of sea-breeze
[DE88-700038] 07 p0876 N88-15314
Trace element geochemistry of the South Atlantic Bight
[DE88-003515] 10 p1356 N88-18108
Meteorological features during the marginal ice zone experiment from 20 March to 10 April 1987
[AD-A193960] 23 p3235 N88-29251

SHORT CIRCUITS
The Pierce diode with an external circuit. 2: Non-uniform equilibria
[AD-A188027] 11 p1478 N88-18818
Shorts in self-checking circuits
[RR-657-I] 14 p1908 N88-21402
Pierce diode with external circuit. Part 3: Chaotic behavior
[AD-A194837] 24 p3365 N88-30041

SHORT CRACKS
Fracture mechanics analysis for short cracks
[AD-A192002] 18 p2527 N88-24992

SHORT HAUL AIRCRAFT
NT A-300 AIRCRAFT
NT A-320 AIRCRAFT
NT EUROPEAN AIRBUS
Flight researh at NASA Ames Research Center: A test pilot's perspective
[NASA-TM-100025] 02 p0125 N88-10788
Current fire safety design aspects of commuter aircraft
[DOT/FAA/CT-87/32] 19 p2600 N88-25448

SHORT TAKEOFF AIRCRAFT
Civil applications of high-speed rotorcraft and powered-lift aircraft configurations
[NASA-TM-100035] 03 p0261 N88-11643
V/STOL aircraft configurations and opportunities in the Pacific Basin
[NASA-TM-100005] 03 p0261 N88-11644
Flaps-up takoff performance of the OV-1D aircraft with YT53-L-704 engine installed
[AD-A185960] 07 p0819 N88-14979
Study on a unidirectional ring laser gyro. Part 1: Proposition of the principle and studies on the components
[NAL-TR-933] 09 p1169 N88-17010
Recommendations for ground effects research for V/STOL and STOL aircraft and associated equipment for large scale testing
[NASA-CR-177429] 10 p1268 N88-17585
An aerodynamic comparison of blown and mechanical high lift airfoils 10 p1272 N88-17606
Development of circulation control technology for powered-lift STOL aircraft 10 p1272 N88-17608
Circulation control STOL aircraft design aspects
10 p1272 N88-17610
A review of technologies applicable to low-speed flight of high-performance aircraft investigated in the Langley 14- x 22-foot subsonic tunnel
[NASA-TP-2796] 13 p1717 N88-20264
Parametric study of supersonic STOVL flight characteristics
[NASA-CR-177330] 16 p2161 N88-22893
A numerical study of the hot gas environment around a STOVL aircraft in ground proximity
[NASA-TM-100895] 17 p2295 N88-23729
Method for prediction and determination of takeoff performance for vectored thrust vehicles
[AD-A191809] 18 p2463 N88-24626
Takeoff predictions for powered-lift aircraft
[NASA-CR-177491] 19 p2597 N88-25431
Low-speed wind-tunnel test of a STOL supersonic-cruise fighter concept
[NASA-TM-4050] 20 p2761 N88-26374
Aerodynamics in ground effect and predicted landing ground roll of a fighter configuration with a secondary-nozzle thrust reverser
[NASA-TP-2834] 24 p3317 N88-29752

SHORT WAVE RADIATION
NT CENTIMETER WAVES
NT DECIMETER WAVES
NT MICROWAVE EMISSION
NT MICROWAVES
NT MILLIMETER WAVES
NT SUBMILLIMETER WAVES

Studies on nonlinear mechanisms of excimer laser propagation in fused silica fibers
[AD-A186822] 09 p1156 N88-16929
A MININEC model of the miniloop antenna
[AD-A191759] 18 p2500 N88-24830
Angular radiation models for Earth-atmosphere system. Volume 1: Shortwave radiation
[NASA-RP-1184] 21 p2976 N88-27677

SHORT WAVE RADIO TRANSMISSION
Meteor-burst communications: Is this what the Navy needs?
[AD-A184433] 04 p0431 N88-12672
Digital correlator for the portable channel prober measurement instrument
[AD-A189065] 14 p1904 N88-21377

SHORTENING
U REDUCTION

SHOT NOISE
Series representations of infinitely divisible random vectors and a generalized shot noise in Banach spaces
[AD-A186429] 07 p0918 N88-15574
Series representations of infinitely divisible random vectors and a generalized shot noise in banach spaces
[AD-A186502] 08 p1073 N88-16474

SHRINKAGE
Process for producing sandwich mouldings
[EP-PATENT-0-191-623-A2] 04 p0426 N88-12642

SHROUDED BODIES
U SHROUDS

SHROUDED PROPELLERS
Ducted propeller design and analysis
[DE88-001925] 06 p0664 N88-14069
An estimate of the noise shielding on the fuselage resulting from installing a short duct around an advanced propeller
[NASA-TM-100262] 10 p1405 N88-18379
An investigation of ducted propellers in axisymmetric shear flow 16 p2202 N88-23136

SHROUDED TURBINES
Thermal stress minimized, two component, turbine shroud seal
[NASA-CASE-LEW-14212-1] 17 p2345 N88-23978

SHROUDS
Instrumentation package for a shrouded SWERVE/EPW rocket sled test
[DE87-014267] 01 p0008 N88-10045
Degradation of beam brightness by field emission from a cathode shroud
[DE88-008345] 20 p2794 N88-26576

SHUNTS
U CIRCUITS

SHUTDOWNS
Failure control techniques for the SSME
[NASA-CR-179224] 04 p0409 N88-12537
SSME technology test bed fast shutdown assessment
[NASA-CR-179354] 17 p2314 N88-23831
Evaluation and improvement of liquid propellant rocket chugging analysis techniques. Part 1: A one-dimensional analysis of low frequency combustion instability in the fuel preburner of the space shuttle main engine
[NASA-CR-183106] 21 p2903 N88-27224
Evaluation and improvement of liquid propellant rocket chugging analysis techniques. Part 2: A study of low frequency combustion instability in rocket engine preburners using a heterogeneous stirred tank reactor model
[NASA-CR-182724] 21 p2903 N88-27225

SHUTTERS
Mode locking in Nd-laser by means of Gd-Sc-Ga-garnet shutter 09 p1237 N88-17412
Nonlinear stage of ultrashort-pulse formation in solid-state laser 14 p1971 N88-21765
Pulse duration control of XeCl*-laser by means of plasma shutter 14 p1973 N88-21774

SHUTTLE BOOSTERS
U SPACE SHUTTLE BOOSTERS

SHUTTLE GLOW
U SPACECRAFT GLOW

SHUTTLE IMAGING RADAR
The Shuttle Imaging Radar B (SIR-B) experiment report
[NASA-CR-182923] 17 p2334 N88-23932
Subsurface morphology and geoarchaeology revealed by spaceborne and airborne radar
17 p2353 N88-24022
The role of space borne imaging radars in environmental monitoring: Some shuttle imaging radar results in Asia
[NASA-TM-101178] 18 p2502 N88-24844
The role of space borne imaging radars in environmental monitoring: Some shuttle imaging radar results in Asia
[NASA-TM-101175] 20 p2789 N88-26544

SHUTTLE ORBITERS
U SPACE SHUTTLE ORBITERS

SHUTTLE PALLET SATELLITES
Testing of heat pipes on SPAS-01
[BMFT-FB-W-86-014] 06 p0672 N88-14119
The Cryogenic Infrared Spectrometer and Telescope for the Atmosphere (CRISTA) experiment on Astro-SPAS
08 p1034 N88-16270

SI
U INTERNATIONAL SYSTEM OF UNITS

SIALON
High temperature characterization of ceramic materials
[REPT-NT-3403] 03 p0292 N88-11837

SIC (COEFFICIENT)
U STRUCTURAL INFLUENCE COEFFICIENTS

SICKNESSES
NT ALTITUDE SICKNESS
NT DECOMPRESSION SICKNESS
Attitudes towards the cold: Effects on psychological mood and subjective reports of illness during cold weather training
[AD-A194777] 23 p3239 N88-29274

SID (IONOSPHERIC DISTURBANCES)
U SUDDEN IONOSPHERIC DISTURBANCES

SIDE INLETS
Hot-wire measurements of compressor blade wakes in a cascade wind tunnel
[AD-A194737] 23 p3181 N88-28936

SIDE-LOOKING RADAR
Construction of airborne radars for remote sensing
[PB88-113063] 09 p1154 N88-16916
Marginal Ice Zone Experiment (MIZEX) 1984 VARAN-S data set
[ETN-88-92032] 14 p1950 N88-21625
Definition and implementation study for the Varan-S radar
[CNES-CT/DRT/TIT/RL-143-T]
15 p2058 N88-22267
The radiometric processing of SLAR measuring values using the PARES program
[BCRS-86-04] 16 p2227 N88-23301
Investigation of the usefulness of speckle analysis in imaging radar systems
[BCRS-86-05] 16 p2227 N88-23302

SIDEBANDS
Sideband suppression by an intracavity optical filter in the Los Alamos free-electron laser oscillator
[DE87-011740] 02 p0177 N88-11103
Spectral evolution equation for the sideband instability in a free-electron laser oscillator
[DE88-000510] 04 p0447 N88-12771
The free electron laser sideband instability reconsidered
[AD-A184269] 04 p0447 N88-12773
Analysis of sideband spectra from untapered undulator using analytical technique
[DE87-014763] 04 p0448 N88-12778
The generation and suppression of synchrotron sidebands
[DE88-000532] 04 p0449 N88-12787
Comparison of sideband spectra obtained from analytical formula and from numerical simulation in free-electron laser
[DE88-000521] 04 p0450 N88-12789
HF sidebands in the ionosphere
05 p0574 N88-13497
The structure of the sideband spectrum in free electron lasers
[AD-A186952] 09 p1170 N88-17015

SIDELOBE REDUCTION
Adaptive interference techniques for mobile antennas
19 p2647 N88-25714

SIDELOBES
Adaptive detection in non-stationary interference, part 3
[AD-A185622] 07 p0844 N88-15118
Compensation of relector antenna surface distortion using an array feed
[NASA-TM-100286] 11 p1476 N88-18805
Conformal microstrip slot antenna and antenna array
[AD-A189623] 15 p2055 N88-22252
An improved method for calculating power density in the Fresnel region of circular parabolic reflector antennas
[AD-A190569] 15 p2060 N88-22284
Case study of active array feed compensation with sidelobe control for reflector surface distortion
[NASA-TM-100287] 16 p2192 N88-23073
TDWR (Terminal Doppler Weather Radar) clutter residue map generation and usage
[AD-A191148] 16 p2235 N88-23352
Sidelobe level of an adaptive array using the SMI (Sampled Matrix Inversion) algorithm
[AD-A193131] 21 p2932 N88-27409

SIDERITE METEORITES
U IRON METEORITES

SIDESLIP
Effects of winglets on a first-generation jet transport wing. 7: Sideslip effects on winglet loads and selected wing loads at subsonic speeds for a full-span model
[NASA-TP-2619] 11 p1436 N88-18567
Parametric estimation of aerodynamic nonlinearities in rolling moment due to sideslip using maximum likelihood method 20 p2786 N88-26528
Angle of attack and sideslip estimation using an inertial reference platform
[AD-A194876] 24 p3319 N88-29769
Computer programs for calculation of sting pitch and roll angles required to obtain angles of attack and sideslip on wind tunnel models
[NASA-TM-100659] 24 p3329 N88-29820

SIERRA LEONE
Global solar radiation in Sierra Leone (West Africa)
[DE88-702725] 23 p3235 N88-29252

SIERRA NEVADA MOUNTAINS (CA)
Structure and modification of winter mountain clouds in the Sierra Nevada: Nowcasting/forecasting the onset of supercooled liquid water 02 p0202 N88-11263

SIEVES
The flow downstream of screens and the formation of longitudinal vortices in the stagnation point flow
[DFVLR-FB-87-27] 09 p1162 N88-16963
Size-reduction and sorting behavior in sieve hammer mills
[ETN-88-91480] 11 p1467 N88-18749

SIGHT
U VISUAL PERCEPTION

SIGNAL ANALYSIS
NT CEPSTRAL ANALYSIS
Intelligent signal analysis and recognition
[NASA-CR-181531] 04 p0501 N88-13084
The Newcastle meteor radar
06 p0741 N88-14556
Flow diagnostics and visualization in wind tunnels and flight 07 p0811 N88-14940
Backscattering signal analysis concerning a three-dimensional object configuration on the basis of object motion
[ESA-TT-1044] 09 p1154 N88-16915
Markov processes applied to control, replacement and signal analysis
[AD-A190563] 15 p2126 N88-22674
Software development for the reconstruction of source parameters using research and development arrays
[REPT-840445-TW] 16 p2246 N88-23417
Acoustic emission frequency discrimination
[NASA-CASE-MSC-20467-1] 17 p2342 N88-23966
Evaluation of the communications impact of a low power arcjet thruster
[NASA-TM-100926] 18 p2475 N88-24682
Artificial intelligence applied to process signal analysis
23 p3252 N88-29359

SIGNAL ANALYZERS
Analysis of counting errors in the phase/Doppler particle analyzer
[NASA-TM-100231] 03 p0323 N88-12043
Lower bounds on bearing accuracy for closely spaced sources
[AD-A184258] 04 p0486 N88-12997
An interface for the connection of the SCP2160A pulse analyser to a Hewlett-Packard desk-top computer
[RSRE-MEMO-4030] 22 p3073 N88-28245

SIGNAL DETECTION
NT CORRELATION DETECTION
Nonlinear techniques for detection and filtering of discrete-time signals 02 p0160 N88-11004
Radar ECCM's new area: Anti-STEALTH and anti-ARM 03 p0299 N88-11881
Detection of signals by the digital integrate-and-dump filter with offset sampling 04 p0435 N88-12695
Detection of signals by weighted integrate-and-dump filter 04 p0435 N88-12696
Development of an acoustic echosounder for detection of lower level atmospheric turbulence
[AD-A184877] 05 p0626 N88-13831
Adaptive detection in non-stationary interference, part 3
[AD-A185622] 07 p0844 N88-15118
Transient classifier systems and man-machine interface research
[AD-A186213] 07 p0899 N88-15446
High frequency acoustic underwater communication with low probability of being traced
[REPT-4-87] 09 p1242 N88-17447
Detection of signals in non-Gaussian correlated noise derived from Cauchy processes
[AD-A187488] 10 p1320 N88-17894
A deep-water OBS (Ocean Bottom Seismometer) array with real-time telemetry
[AD-A187404] 10 p1357 N88-18112
The Telecommunications and Data Acquisition Report
[NASA-CR-182545] 11 p1471 N88-18774

Simulated performance of an order statistic threshold strategy for detection of narrowband signals
11 p1474 N88-18796

On the design of suboptimal matched filters for three-dimensional moving target detection
[AD-A188384] 12 p1619 N88-19682

Detection and angle estimation of coherent plane waves 13 p1759 N88-20522

Method for set-up for researching signal curve development
[NASA-TT-20235] 13 p1760 N88-20526

Masking of motion cues by random motion: Comparison of human performance with a signal detection model
[UTIAS-313] 14 p1953 N88-21639

Earthquakes from peninsular India: Data from the Gauribidanur seismic array
[DE88-701232] 15 p2093 N88-22471

Characteristics of seismic sources of some Asian earthquakes and Soviet underground explosions from Gauribidanur array records
[DE88-701233] 15 p2093 N88-22472

Study of microcomputer-based real-time programmable optical signal processor and application
[AD-A190076] 15 p2133 N88-22726

Research and development activities of the Seismology Section
[DE88-701235] 16 p2231 N88-23323

Utilization of dense packed planar acoustic echosounders to identify turbulence structure in the lowest levels of the atmosphere
[AD-A191006] 16 p2233 N88-23335

Information and stochastic systems
[AD-A192167] 16 p2501 N88-24838

Identification and acoustic characterization of seamounts
[AD-A192204] 18 p2548 N88-25123

An optically strobed sample and hold circuit
19 p2656 N88-25772

Comparison of sampling oscilloscopes with less than 35 ps transition durations 19 p2658 N88-25793

Noise in piezoresistive and capacitive sensors
19 p2670 N88-25874

Comparison of five readout techniques for an integrated magnetometer 19 p2671 N88-25876

Proceedings of the Array Signal Processing Symposium: Treaty Verification Program
[DE88-008346] 20 p2790 N88-26548

Surface disturbances produced by low-level, subsonic B-1 aircraft
[AD-A192257] 20 p2824 N88-26752

Direct bit detection receiver performance analyses for 8-DPSK (Differential Phase Shift Keyed) modulated signals operating with improper carrier phase synchronization
[AD-A193839] 22 p3070 N88-28220

Effects of tectonic release on broadband regional distance bodywaves
[AD-A194247] 22 p3119 N88-28529

Computer-controlled measurements of nonlinear standing waves
[AD-A193840] 22 p3147 N88-28717

SQUID (superconducting quantum interference device) arrays for simultaneous magnetic measurements: Calibration and source localization performance
[AD-A193815] 23 p3216 N88-29143

Evaluation of atmospheric effects for operational tactical decision aid
[AD-A194205] 23 p3232 N88-29236

Improvements in techniques of microwave thermography
[AD-A193620] 23 p3239 N88-29276

On the design and optimization of distributed signal detection and parameter estimation systems
[AD-A193934] 23 p3266 N88-29446

On adaptive cell-averaging CFAR (Constant False-Alarm Rate) radar signal detection
[AD-A196286] 24 p3360 N88-30009

A detection theory analysis of visual display performance
[AD-A196291] 24 p3409 N88-30292

SIGNAL DETECTORS

Icing detector with early warning capability
[AOA-4.1.0055] 03 p0325 N88-12050

Surface acoustic wave deposition sensor
[DE87-006527] 09 p1243 N88-17452

A deep-water OBS (Ocean Bottom Seismometer) array with real-time telemetry
[AD-A187404] 10 p1357 N88-18112

Computation of LMS (Least-Mean-Square) and matched digital filters for optical clutter suppression
[AD-A188885] 12 p1687 N88-20093

Preliminary comparison of some coincidence methods for gravitational wave detectors
[NOTA-INTERNA-903] 14 p1945 N88-21604

Applications research studies of microtubules
[AD-A190855] 16 p2182 N88-23005

Method and apparatus for detecting laminar flow separation and reattachment
[NASA-CASE-LAR-13952-1-SB]
18 p2513 N88-24910

Design and testing of a luminance and chrominance stabilization system for a computer-controlled color display
[AD-A191922] 18 p2554 N88-25159

Novel nonlinear signal processing principles
[AD-A191644] 19 p2707 N88-26097

Local free-space mapping and path guidance for mobile robots
[AD-A192970] 20 p2810 N88-26674

Laboratory feasibility study of a composite embedded fiber optic sensor for measurement of structural vibrations
[AD-A194270] 22 p3152 N88-28754

Analytical methods in stochastic control and nonlinear filtering
[AD-A194272] 24 p3426 N88-30388

SIGNAL DISCRIMINATORS

U SIGNAL DETECTORS

SIGNAL DISTORTION

A generalization of order statistic filters: The alpha-trimmed linear filter
[AD-A186125] 07 p0842 N88-15107

Solution of the Lloyd-Max quantizer parameters by the method of successive substitution
[AD-A187829] 11 p1540 N88-19207

The effects of solar cycle and latitude dependence on the formation of ionospheric C layer
[INPE-4342-TDL/293] 16 p2232 N88-23332

SIGNAL ENCODING

NT AMPLITUDE MODULATION
NT DELTA MODULATION
NT DIFFERENTIAL PULSE CODE MODULATION
NT FREQUENCY MODULATION
NT FREQUENCY SHIFT KEYING
NT PHASE MODULATION
NT PHASE SHIFT KEYING
NT PULSE AMPLITUDE MODULATION
NT PULSE CODE MODULATION
NT PULSE DURATION MODULATION
NT PULSE MODULATION
NT PULSE POSITION MODULATION

Study of a coding and modulation system for the V32 call of the CCITT
[ENST-87E007] 02 p0162 N88-11015

Bandwidth efficient block codes for M-ary PSK modulation
[NASA-CR-181543] 04 p0437 N88-12712

Study of synthetic aperture radar data compression and encoding. Part 3: Performance evaluation of speckle suppression and data compression algorithms
[NLR-TR-85085-L-PT-3] 06 p0692 N88-14248

Study of synthetic aperture radar data compression and encoding. Part 4: Algorithm implementation aspects
[NLR-TR-85085-L-PT-4] 06 p0692 N88-14249

Study of synthetic aperture radar data compression and encoding. Part 1: SAR image data analysis
[NLR-TR-85085-L-PT-1] 07 p0843 N88-15115

Study of synthetic aperture radar data compression and encoding. Part 2: SAR image speckle suppression and data compression algorithms
[NLR-TR-85085-L-PT-2] 07 p0843 N88-15116

Multichannel 2-D power spectral estimation and applications
[AD-A191273] 18 p2191 N88-23068

Coding for write-unidirectional memories and conflict resolution
[ENST-87C005] 16 p2245 N88-23408

A new code for Galileo 22 p3065 N88-28186

Direct bit detection receiver performance analyses for 8-DPSK (Differential Phase Shift Keyed) modulated signals operating with improper carrier phase synchronization
[AD-A193839] 22 p3070 N88-28220

SIGNAL FADEOUT

U SIGNAL FADING

SIGNAL FADING

Measured characteristics of 800/900 MHz mobile radio channels with high-angle propagation through moderately dense foliage
[CRC-1398] 05 p0573 N88-13493

Improvements to a UHF rebroadcast television link suffering tidal fading: Countisbury UHF relay station
[BBC-RD-1987/14] 05 p0573 N88-13495

An additional study and implementation of tone calibrated technique of modulation
[NASA-CR-182377] 07 p0844 N88-15117

The design of trellis codes for fading channels
[NASA-CR-182523] 10 p1320 N88-17891

Propagation effects by roadside trees measured at UHF and L-band for mobile satellite systems
19 p2644 N88-25693

Propagation modeling for land mobile satellite systems
19 p2645 N88-25694

Attenuated direct and scattered wave propagation on simulated land mobile satellite service paths in the presence of trees 19 p2645 N88-25695

Trellis-coded MPSK modulation techniques for MSAT-X(sup)1 19 p2648 N88-25721

Performance of the ICAO standard core service modulation and coding techniques
19 p2648 N88-25723

Extending the impulse response in order to reduce errors due to impulse noise and signal fading
19 p2649 N88-25730

SIGNAL GENERATORS

NT FREQUENCY SYNTHESIZERS
NT FUNCTION GENERATORS

Results of the use of an automated electrical measuring instrument calibration system
[SNIAS-881-430-107] 23 p3217 N88-29146

SIGNAL MEASUREMENT

NBS (National Bureau of Standards) wideband sampling wattmeter
[PB87-210324] 03 p0323 N88-12041

Wave propagation experiments on 22-bay lattice
[AD-A186140] 07 p0824 N88-15002

The optimum solution to instrument quantization effects 12 p1577 N88-19434

The effects of atmospheric and thermohaline variability on the validation of the GEOSAT altimeter oceanographic signal between Scotland and Iceland
[AD-A189324] 12 p1650 N88-19682

Alaska Loran C probe test results
[AD-A189131] 13 p1720 N88-20284

Bragg-cell receiver study
[NASA-CR-182684] 13 p1761 N88-20535

An analysis of the efficiency and directivity of the sound generated by a moving laser source
[AD-A192220] 20 p2849 N88-26914

A notch filter instrument for measuring ELF (Extremely Low Frequency) MSK (Minimum Shift Keying) signals
[AD-A193324] 21 p2933 N88-27414

SIGNAL MIXING

Four-wave mixing used in optical amplitude encoding
03 p0376 N88-12366

Self-pumped phase conjugation in a supersonically flowing medium
[AD-A188281] 10 p1338 N88-17998

Optical signal processing using nonlinear optics
[AD-A188461] 12 p1691 N88-20117

Studies of coherent beam processing concepts, phase 1
[AD-A194749] 22 p3083 N88-28306

SIGNAL PROCESSING

Monitoring of harmful interference to the HF (High Frequency) broadcasting service. 3: Results of the June 1986 coordinated monitoring period
[PB87-210274] 01 p0036 N88-10229

Independence in sonar observations
[ARE-TR-87102] 01 p0088 N88-10572

White noise calculus for two-parameter filtering
[ENST-87C003] 01 p0088 N88-10578

Measurements in the functional mock up test of the NAL QSTOL aircraft control system
[NAL-TR-928] 02 p0126 N88-10793

Nonlinear techniques for detection and filtering of discrete-time signals 02 p0160 N88-11004

On adaptive signal processing of RF signals
[DE87-014192] 02 p0161 N88-11007

A digital audio link to the Channel Islands in the UHF television band: Protection of television signals from digitally modulated interference
[BBC-RD-1987/7] 02 p0161 N88-11010

Experiments: Test range facilities, part 1
03 p0304 N88-11920

An antenna array processing system for multiple source bearing estimation 03 p0305 N88-11927

Research in monolithic signal-processing circuits
[AD-A184680] 03 p0311 N88-11962

SBNR (Signed Binary Number Representations) digital signal processor architecture
[AD-A184603] 03 p0364 N88-12290

End of year report for parallel vision algorithm design and implementation
[AD-A184327] 03 p0366 N88-12301

The effect of reverberation on active sonar performance
[ARE-TM(UJS)-87104] 03 p0374 N88-12350

Optical alignment of Centaur's inertial guidance system
[NASA-TM-88844] 04 p0405 N88-12515

On a circular correlation technique for filtering randomly noisy data
[AD-A184317] 04 p0431 N88-12669

Application of lattice filtering techniques to CW measured time domain data
[AD-A184351] 04 p0431 N88-12671

Accommodating the residue of processed or computed digital video signals within the 8 bit CCIR recommendation 601
[BBC-RD-1987/12] 04 p0432 N88-12676
Robust statistical methods for automated outlier detection 04 p0433 N88-12681
Frequency doubling conversion efficiencies for deep space optical communications 04 p0434 N88-12691
Design of digital filters for electronic instrumentation
[PB87-100418] 04 p0438 N88-12716
Interferometry theory for the block 2 processor
[NASA-CR-181551] 04 p0440 N88-12730
Measured characteristics of 800/900 MHz mobile radio channels with high-angle propagation through moderately dense foliage
[CRC-1398] 05 p0573 N88-13493
Italy's Institute of Research on Electromagnetic Waves--the Istituto di Ricerca sulle Onde Elettromagnetiche
[AD-A185020] 05 p0574 N88-13501
Analysis of SO2 signals in SBUV/TOMS data 05 p0618 N88-13794
Estimation of marine boundary layer depth and relative humidity with multispectral satellite measurements
[AD-A184881] 05 p0620 N88-13804
Cross-correlation of uniform cyclic difference set sequences
[AD-A184879] 05 p0640 N88-13913
Two digital X-ray imaging systems for applications in X-ray diffraction
[PB87-123683] 06 p0669 N88-14103
Theory of displaced phase center antenna for space based radar applications
[PB87-229837] 06 p0690 N88-14227
Discussion on the modelling and processing of signals from an acousto-optic spectrum analyzer
[AD-A185639] 06 p0694 N88-14257
Statistical techniques for signal processing
[AD-A185774] 06 p0694 N88-14259
Signal chain for the Airborne Visible/Infrared Imaging Spectrometer (AVIRIS) 06 p0706 N88-14331
Fast algorithms for structural optimization and least squares
[AD-A185766] 06 p0724 N88-14452
Fiber optic single mode sensors
[FOA-C-30453-3.1] 06 p0780 N88-14790
Digital signal processing algorithms for automatic voice recognition 06 p0793 N88-14862
Time-domain robotic vision application 06 p0798 N88-14886
A generalization of order statistic filters: The alpha-trimmed linear filter
[AD-A186125] 07 p0842 N88-15107
An additional study and implementation of tone calibrated technique of modulation
[NASA-CR-182377] 07 p0844 N88-15117
Improvement of deep resolution in ultrasonic echographic nondestructive evaluation using signal processing methods
[PB87-147658] 07 p0866 N88-15256
Strong consistency of maximum likelihood parameter estimation of superimposed exponential signals in noise
[AD-A186384] 07 p0911 N88-15526
On simultaneous estimation of the number of signals and frequencies under a model with multiple sinusoids
[AD-A186026] 07 p0913 N88-15543
On the direction of arrival estimation
[AD-A186031] 07 p0914 N88-15546
On rate of convergence of equivariation linear prediction estimates of the number of signals and frequencies of multiple sinusoids
[AD-A186034] 07 p0914 N88-15549
High Resolution Picture Transmission (HRPT) data processing from NOAA series satellites
[INPE-4372-PRE/1195] 08 p0963 N88-15831
A simultaneous M-ary channel hypothesis test with least-mean-square signal amplitude estimation
[AD-A186526] 08 p0978 N88-15913
Optical communication with semiconductor laser diodes
[NASA-CR-182464] 09 p1154 N88-16918
Limiting of YUV digital video signals
[BBC-RD-1987/22] 09 p1155 N88-16924
High performance VLSI algorithms and architectures for digital signal processing 09 p1155 N88-16926
Spectral density estimates of coarsely quantized random vibration data 09 p1178 N88-17055
Fractal images: Procedure and theory
[AD-A187014] 09 p1217 N88-17293
Space-time processing of field produced by moving source 09 p1234 N88-17399
The role of photodetectors in optical signal processing
[AD-A186804] 09 p1247 N88-17476
A report on the effects of neutron irradiation of GaAs semiconductors
[AD-A186816] 09 p1253 N88-17510
Response of wind shear warning systems to turbulence with implication of nuisance alerts 10 p1274 N88-17618
Signal processing for an optical wide band data transmission system
[DE88-003854] 10 p1319 N88-17888
Detection of signals in non-Gaussian correlated noise derived from Cauchy processes
[AD-A187488] 10 p1320 N88-17894
Signal processing studies program optical signal amplification, volume 2
[AD-A188054] 10 p1320 N88-17896
Signal processing studies program optical signal amplification, volume 1
[AD-A188055] 10 p1321 N88-17897
Signal processing studies program VLSI designs for unary functions
[AD-A188053] 10 p1325 N88-17922
An integrated pressure sensor for in-vivo use 10 p1333 N88-17965
Optically controlled devices and ultrafast laser sources for signal processing
[AD-A187417] 10 p1338 N88-17995
Signal and data processing for IR sensors 10 p1374 N88-18199
Wafer scale implementation of a GaAs systolic signal processor cell 10 p1381 N88-18247
Ground clutter processing for wind measurements with airport surveillance radars
[AD-A187708] 11 p1514 N88-19044
A signal processing approach to the numerical solution of parabolic differential equations 11 p1539 N88-19197
Digital method for correction of the phase error in the discrete generation of periodic signals in real time
[INPE-4327-RPE/552] 12 p1618 N88-19676
Optimum filters and smoothers design for carrier phase and frequency tracking
[NASA-CR-182654] 12 p1618 N88-19679
Mathematical foundations of signal processing. 2: The role of group theory
[AD-A188482] 12 p1620 N88-19685
VLSI implementations for digital signal processing
[AD-A189612] 12 p1624 N88-19719
Structural-acoustic interior noise modeling and analysis from experimental data
[PB88-141775] 12 p1687 N88-20088
Optical signal processing using nonlinear optics
[AD-A188461] 12 p1691 N88-20117
Architecture specification for PAVE PILLAR avionics
[AD-A188722] 13 p1723 N88-20303
The acoustic-modeling problem in automatic speech recognition
[AD-A188529] 13 p1757 N88-20510
Statistical signal processing using a class of iterative estimation algorithms
[AD-A189050] 13 p1757 N88-20511
System for detecting objects that represent a threat
[NASA-TT-20244] 13 p1760 N88-20528
Bragg-cell receiver study
[NASA-CR-182684] 13 p1761 N88-20535
Analysis for architecture for image processing
[INPE-4294-PRE/1165] 13 p1791 N88-20715
Study of photochromic materials for use in optical signal processing
[AD-A189068] 13 p1839 N88-21006
Digital correlator for the portable channel prober measurement instrument
[AD-A189065] 14 p1904 N88-21377
On-board processing for mobile satellite communications
[ESA-CR(P)-2519] 14 p1905 N88-21382
Squeezed state in degenerate parametric amplification discussed by H. Takahasi in 1963 14 p1976 N88-21790
Generating squeezed microwave radiation with a Josephson parametric amplifier 14 p1978 N88-21805
Merit of Hadamard transform active absorption spectrometer described 15 p2053 N88-22232
Optimum signal processing in distributed sensor systems
[AD-A189443] 15 p2055 N88-22250
Direct bit detection receiver noise performance analysis for 32-PSK and 64-PSK modulated signals
[AD-A190009] 15 p2056 N88-22256
A hardware/software system for implementing geophysical diffraction tomography
[DE88-006411] 15 p2094 N88-22480
Auditory perception of complex sounds
[AD-A190528] 15 p2103 N88-22529
Selective mechanisms in auditory and bimodal signal processing
[AD-A190529] 15 p2103 N88-22530
Auditory pattern memory: Mechanisms of tonal sequence discrimination by human observers
[AD-A190337] 15 p2104 N88-22534
Investigation into the development of computer aided design software for space based sensors
[NASA-CR-180772] 15 p2107 N88-22552
Memory efficient evaluations of nonlinear stochastic equations and C3 applications
[AD-A189872] 15 p2110 N88-22569
Design and implementation of VLSI prime factor algorithm processor
[AD-A190483] 15 p2112 N88-22580
Cholesky downdating on a hypercube
[DE88-006780] 15 p2113 N88-22586
The adjoint process in stochastic optimal control
[AD-A189720] 15 p2116 N88-22605
Nonlinear signal processing using neural networks: Prediction and system modelling
[DE88-006479] 15 p2118 N88-22621
Near optimal blind deconvolution
[REPT-87-016] 15 p2123 N88-22655
Filtering of jump processes
[AD-A189701] 15 p2123 N88-22656
The partially observed stochastic minimum principle
[AD-A189787] 15 p2124 N88-22658
Multivariate analysis and its application
[AD-A189983] 15 p2124 N88-22661
Spatial matched processing for multipath propagation
[AD-A189790] 15 p2129 N88-22701
Space time processing, environmental-acoustic effects
[AD-A190764] 15 p2130 N88-22708
Space-variant optical systems
[AD-A189967] 15 p2133 N88-22724
Infrared-sensitive spatial light modulator
[AD-A190391] 15 p2134 N88-22729
Autonomous control system for Czochralski growth of LEC GaAs
[AD-A189726] 15 p2141 N88-22779
Research on materials and components for opto-electronic signal processing and computing
[AD-A190130] 15 p2143 N88-22788
Analysis of a range estimator which uses MLS angle measurements
[NASA-CR-182896] 16 p2160 N88-22884
A compact high resolution piezoresistive digital tactile sensor
[DE88-000430] 16 p2210 N88-23188
The TMS32010 evaluation module controller --- signal processor
[EUT-86-E-162] 16 p2245 N88-23407
HIFI: A design method for implementing signal processing algorithms on VLSI processor arrays
[ETN-88-92238] 16 p2247 N88-23421
The PROMISE simulation system: Software for the simulation of parallel processes
[NLR-MP-86077-U] 16 p2247 N88-23427
Error control techniques for satellite and space communications
[NASA-CR-182886] 17 p2332 N88-23922
Doppler radar with multiphase modulation of transmitted and reflected signal
[NASA-CASE-MSC-18808-1] 17 p2332 N88-23923
Processing of HRPT data from the NOAA series satellites 17 p2359 N88-24053
Near surface current determined from INPE's satellite-tracked buoy, during 6-26 November, 1985 17 p2360 N88-24058
Angular position measurements at high temperatures and high radiation environments 17 p2434 N88-24479
Time-frequency representations for speech signals
[AD-A188661] 18 p2498 N88-24819
Signal processing with degenerate four-wave mixing
[AD-A191496] 18 p2499 N88-24825
A method for discrimination of radar targets using complex natural resonances
[AD-A191848] 18 p2500 N88-24832
Propagation management for no-acknowledge HF communications links 18 p2502 N88-24843
Optics: Perspectives for Measurement Techniques and Signal Processing for Flight Guidance --- conference
[DFVLR-MITT-87-21] 18 p2516 N88-24928
Investigations in electro-optical multistability for signal processing 18 p2518 N88-24938
Low frequency electrostatic turbulence in the polar cap E-region
[DRI-3-88] 18 p2540 N88-25077
An experimental study of the coherent under-ice reflectivity of sound in the Greenland Sea Marginal Ice Zone 18 p2548 N88-25125
Optical computing based on neuronal models
[AD-A191481] 18 p2575 N88-25293
Optical nonlinearities in GaAs/GaAlAs multiple quantum wells fabricated by metalorganic chemical vapor deposition for use in optical signal processing
[AD-A191558] 18 p2582 N88-25337

Signal processing computational needs
[AD-A191756] 19 p2642 N88-25674
Multipath measurements for land mobile satellite service using global positioning system signals
19 p2645 N88-25700
Adaptive interference techniques for mobile antennas
19 p2647 N88-25714
Interleaver design for trellis-coded differential 8-PSK modulation with non-coherent detection
19 p2648 N88-25719
Mini-station for VHF reception: Argos system simplified description
[INPE-4551-NTE/279] 19 p2655 N88-25764
Organization of a Topical Meeting on Picosecond Electronics and Optoelectronics
[AD-A187136] 19 p2655 N88-25765
A simple technique to generate or gate microwave pulses with picosecond speeds 19 p2657 N88-25784
Characteristics and application of wideband guided-wave devices 19 p2660 N88-25817
Active control of 2-D instability waves on an axisymmetric body
[AD-A191578] 19 p2663 N88-25835
Novel nonlinear signal processing principles
[AD-A191644] 19 p2707 N88-26097
SLAPP: A special multiprocessor array for signal processing and linear algebra
[AD-A191587] 19 p2719 N88-26146
Proceedings of the Array Signal Processing Symposium: Treaty Verification Program
[DE88-008346] 20 p2790 N88-26548
Signal processing in digital speech transmission systems
[ETN-88-92122] 20 p2792 N88-26561
A microcomputer based frequency-domain processor for laser Doppler anemometry
[NASA-TM-100998] 20 p2803 N88-26634
Display and processing of multidimensional signals with the aid of fractal image sequences
[ETN-88-92131] 20 p2806 N88-26642
MAXIE-1 (Magnetospheric Atmospheric X-ray Imaging Experiment)
[AD-A192846] 21 p2902 N88-27221
A numerically efficient digital matched filter for periodic and windowed periodic radar waveforms
[AD-A193132] 21 p2932 N88-27410
Fourth generation neurocognitive pattern analysis system 21 p2977 N88-27686
The application of non-stationary data analysis techniques in the identification of changes in the electroencephalogram associated with the onset of drowsiness 21 p2978 N88-27688
A statistical procedure for the evaluation of presence/non-presence of stimulus-related EEG activity
21 p2978 N88-27689
Demodulation processes in auditory perception
[AD-A193421] 21 p2988 N88-27740
Robust methods for array signal processing
[AD-A192854] 21 p3012 N88-27871
Solid state research
[AD-A192837] 21 p3020 N88-27929
Experiments applications guide: Advanced Communications Technology Satellite (ACTS)
[NASA-TM-100265] 22 p3048 N88-28082
The Telecommunications and Data Acquisition Report
[NASA-CR-183131] 22 p3063 N88-28178
Spectral estimation of received phase in the presence of amplitude scintillation 22 p3064 N88-28180
Telemetry SNR improvement using the DSN Advanced Receiver with results for Pioneer 10
22 p3064 N88-28184
Advanced Receiver tracking of Voyager 2 near solar conjunction 22 p3065 N88-28185
Strawman Optical Reception Development Antenna (SORDA) 22 p3065 N88-28187
Performance analysis of a noncoherently combined large aperture optical heterodyne receiver
22 p3065 N88-28189
Effect of detector dead time on the performance of optical direct-detection communication links
22 p3065 N88-28190
A wideband, high-resolution spectrum analyzer
22 p3066 N88-28194
A digitally implemented phase-locked loop detection scheme for analysis of the phase and power stability of a calibration tone 22 p3066 N88-28196
The behavior of a C stas loop in the presence of space telemetry signals 22 p3067 N88-28198
DSN very long baseline interferometry system Mark IV-88 22 p3067 N88-28199
Baseband assembly analog-to-digital converter board
22 p3067 N88-28201
An evaluation of Interactive Laboratory System software, ILS-PC/DOS: A digital signal processing software package
[AD-A193838] 22 p3138 N88-28657
Application of the Hilbert transform to Doppler radar signals from a hypervelocity gun
[AD-A193690] 22 p3146 N88-28716
Method and apparatus for non-destructive testing of temper embrittlement in steels
[NASA-CASE-LAR-13817-1] 23 p3195 N88-29012
Signal processing software for ground penetrating radar, user's manual
[AD-A194286] 23 p3203 N88-29059
Automatic classification of digitally modulated signals
[AD-A194623] 23 p3203 N88-29064
Basic research in electronics (JSEP) Joint Services Electronics Program
[AD-A193072] 23 p3206 N88-29079
Anti-aliasing filters for dynamics and control experiments
[AD-A193758] 23 p3226 N88-29203
A computer program package for introductory one-dimensional digital signal processing applications
[AD-A194656] 23 p3249 N88-29338
Object discrimination via bulk temperature/velocity filtering, phase 1
[AD-A194533] 23 p3274 N88-29487
Acoustooptic processing of two-dimensional signals using temporal and spatial integration
[AD-A194803] 24 p3359 N88-29999
Doppler-corrected differential detection system
[NASA-CASE-NPO-16987-1-CU]
24 p3359 N88-30001
Review of Radio Science, 1984-1986
24 p3363 N88-30023
Signals and systems 24 p3363 N88-30026
Quantitative surface temperature measurement using two-color thermographic phosphors and video equipment
[NASA-CASE-LAR-13740-1] 24 p3376 N88-30105
Reconstruction of multidimensional signals from multiple level threshold crossings
[AD-A195561] 24 p3425 N88-30383
Spectroscopic studies with multiple quantum well materials with applications to optical signal processing at room temperature
[AD-A194171] 24 p3429 N88-30409

SIGNAL RECEPTION
NT SYLLABLES
NT SYMBOLS
NT TELEVISION RECEPTION
Optimized tracking of RF carriers with phase noise, including Pioneer 10 results 04 p0434 N88-12694
An analysis of simplified feed architectures for MMIC (Monolithic Microwave Integrated Circuit) T/R (Transmit/Receive) module arrays
[AD-A185474] 06 p0697 N88-14275
Automatic antenna switching design for Extra Vehicular Activity (EVA) communication system
06 p0797 N88-14883
Adaptive detection in non-stationary interference, part 3
[AD-A185622] 07 p0844 N88-15118
High-sensitivity recording of weak reflected or scattered radiation by method of coherent intracavity reception with YAG:Nd(3+) laser 08 p1078 N88-16502
Fabrication and packaging of discontinuous MIM (Metal-Insulator-Metal) film arrays for efficient MM wave and IR detection and mixing
[AD-A186809] 09 p1146 N88-16869
Spread spectrum mobile radio communications
[AD-A187487] 11 p1470 N88-18765
Phase calibration generator 11 p1473 N88-18785
Target localization in an inhomogeneous medium
[AD-A190008] 15 p2130 N88-22703
Digital communication transmitter and receiver test procedures
[AD-A191218] 20 p2788 N88-26540
The focal plane reception pattern calculation for a paraboloidal antenna with a nearby fence
[NASA-TM-100691] 24 p3365 N88-30039

SIGNAL REFLECTION
Delay-Doppler radar imaging
[AD-A184165] 03 p0308 N88-11943
Correlation between refraction over sea and nature of radar reflections from sea surface
06 p0728 N88-14477
Adaptive detection in non-stationary interference, part 3
[AD-A185622] 07 p0844 N88-15118
The characteristics of two broadband (2 MHz to 10 MHz) switched vee antennas
[AD-A187874] 11 p1471 N88-18770
Remote determination of chlorophyll concentration in the ocean using an optical pulse radar
[NASA-TT-20301] 19 p2694 N88-26014

SIGNAL STABILIZATION
Optimized tracking of RF carriers with phase noise, including Pioneer 10 results 04 p0434 N88-12694
X-band uplink ground systems development: Part 2
04 p0436 N88-12703
Some properties of the Hilbert transform
[DE88-002465] 09 p1227 N88-17350
Comparison of five readout techniques for an integrated magnetometer 19 p2671 N88-25876

SIGNAL TO NOISE RATIOS
Masking effects of fine and coarse grain pictorial noise
[IZF-1985-21] 01 p0076 N88-10485
Maximum likelihood estimates of parameters in linear systems with process and measurement noise
[DFVLR-FB-87-20] 01 p0083 N88-10532
ISIS: Image reconstruction methods and signal-to-noise ratio investigations --- spaceborne interferometry
01 p0094 N88-10619
Signal to noise ratios --- SPOT images
03 p0341 N88-12150
Detector normalization --- SPOT remote sensors
03 p0341 N88-12151
Optimized tracking of RF carriers with phase noise, including Pioneer 10 results 04 p0434 N88-12694
Detection of signals by the digital integrate-and-dump filter with offset sampling 04 p0435 N88-12695
Detection of signals by weighted integrate-and-dump filter 04 p0435 N88-12696
Lower bounds on bearing accuracy for closely spaced sources
[AD-A184258] 04 p0486 N88-12997
Measured noise performance of a direct-sequence spread-spectrum system and a comparison of single vice dual-channel delay-lock loops
[AD-A186288] 07 p0843 N88-15110
Adaptive detection in non-stationary interference, part 3
[AD-A185622] 07 p0844 N88-15118
A simultaneous M-ary channel hypothesis test with least-mean-square signal amplitude estimation
[AD-A186526] 08 p0978 N88-15913
High-sensitivity recording of weak reflected or scattered radiation by method of coherent intracavity reception with YAG:Nd(3+) laser 08 p1078 N88-16502
On the signal strength dependency on pressure in laser sub-Doppler saturation spectroscopy with special attention to gaseous diatonic molecules
[USIP-87-13] 09 p1171 N88-17023
The relationship between vision carrier-to-noise ratio and picture signal-to-noise ratio in a System I television receiver
[BBC-RD-1987/23] 10 p1318 N88-17877
New monostatic balanced Doppler velocimeter using a polarization preserving fiber
[PB88-130869] 11 p1490 N88-18895
Envelope and phase statistics for non-Gaussian noise and resulting error probabilities for digital communications systems 12 p1617 N88-19672
Signal-filter design and system performance for polarimetric radar
[AD-A189257] 13 p1758 N88-20514
Detection and angle estimation of coherent plane waves 13 p1759 N88-20522
A preliminary assessment of thunderstorm outflow wind measurement with airport surveillance radars
[AD-A189064] 13 p1799 N88-20757
Preliminary comparison of some coincidence methods for gravitational wave detectors
[NOTA-INTERNA-903] 14 p1945 N88-21604
Masking of motion cues by random motion: Comparison of human performance with a signal detection model
[UTIAS-313] 14 p1953 N88-21639
Direct bit detection receiver noise performance analysis for 32-PSK and 64-PSK modulated signals
[AD-A190009] 15 p2056 N88-22256
The 2 FSK/QPSK (Frequency Shift Keying/Quadrature Phase Shift Keying) transmitter and receiver: Design and performance
[AD-A190028] 15 p2056 N88-22258
Multiplex methods in infrared spectrometry
16 p2271 N88-23588
Loran-C monitor correlation over a 92-mile baseline in Ohio 17 p2293 N88-23720
Analysis of binarized Hartley phase-only filter performance with respect to stochastic noise
[DE88-007604] 18 p2519 N88-24945
Codes for QPSK modulation with invariance under 90 degrees rotation 19 p2648 N88-25720
Signal processing in digital speech transmission systems
[ETN-88-92122] 20 p2792 N88-26561
Detection of acceleration (+Gz) induced blackout by matched-filtering of visual evoked potentials
21 p2982 N88-27710
The behavior of a Costas loop in the presence of space telemetry signals 22 p3067 N88-28198

Direct bit detection receiver performance analyses for 8-DPSK (Differential Phase Shift Keyed) modulated signals operating with improper carrier phase synchronization
[AD-A193839] 22 p3070 N88-28220
Effect of phase errors in stepped-frequency radar systems
[AD-A194476] 23 p3203 N88-29061
Multi-sensory tracking mount control
[AD-A194675] 23 p3249 N88-29339
Analytical methods in stochastic control and nonlinear filtering
[AD-A194272] 24 p3426 N88-30388

SIGNAL TRANSMISSION
NT ALOHA SYSTEM
NT AUTOMATIC PICTURE TRANSMISSION
NT BIOTELEMETRY
NT CODE DIVISION MULTIPLE ACCESS
NT DATA TRANSMISSION
NT FREQUENCY DIVISION MULTIPLE ACCESS
NT IONOSPHERIC PROPAGATION
NT MICROWAVE ATTENUATION
NT MICROWAVE TRANSMISSION
NT MULTIPATH TRANSMISSION
NT MULTIPLE ACCESS
NT PACKET TRANSMISSION
NT PCM TELEMETRY
NT RADAR TRANSMISSION
NT RADIO TELEMETRY
NT RADIO TRANSMISSION
NT SATELLITE TRANSMISSION
NT SHORT WAVE RADIO TRANSMISSION
NT SINGLE CHANNEL PER CARRIER TRANSMISSION
NT TELEMETRY
NT TELEVISION TRANSMISSION
NT TRANSEQUATORIAL PROPAGATION
The absolute radiometric calibration of space-based sensors 03 p0277 N88-11744
Experiments: Test range facilities, part 2
03 p0305 N88-11921
Design of digital filters for electronic instrumentation
[PB87-100418] 04 p0438 N88-12716
Measured characteristics of 800/900 MHz mobile radio channels with high-angle propagation through moderately dense foliage
[CRC-1398] 05 p0573 N88-13493
Time domain electromagnetic waves in multilayered media
[AD-A185055] 05 p0574 N88-13502
Fiber optic video link
[FOA-C-30444-3.1] 06 p0780 N88-14789
An additional study and implementation of tone calibrated technique of modulation
[NASA-CR-182377] 07 p0844 N88-15117
Waveform for short-dwell-time meteorological Doppler radars
[PB88-102199] 07 p0845 N88-15126
High Resolution Picture Transmission (HRPT) data processing from NOAA series satellites
[INPE-4372-PRE/1195] 08 p0963 N88-15831
Method for set-up for researching signal curve development
[NASA-TT-20235] 13 p1760 N88-20526
Upward propagating electric fields from thunderstorms and VLF transmitters 13 p1801 N88-20767
Results of one way transit time measuring in navigation experiment NAVEX
[DFVLR-MITT-87-17] 14 p1865 N88-21145
Target localization in an inhomogeneous medium
[AD-A190008] 15 p2130 N88-22703
Trellis-coded CPM for satellite-based mobile communications 19 p2648 N88-25718
An error floor in tone calibrated transmission
19 p2649 N88-25729
Extending the impulse response in order to reduce errors due to impulse noise and signal fading
19 p2649 N88-25730
Non-stationary transport in MODFET's and heterojunction devices 19 p2659 N88-25804
Radar and EW applications of multi-gigahertz optical components and systems 19 p2660 N88-25816
A 1/2-inch high-definition baseband VCR
21 p2930 N88-27393
Dependence effects in unique signal transmission
[DE88-010331] 21 p2933 N88-27419

SIGNALS
Controlling XeCl-laser by means of external signal with less than 2 W/cm (sup)2 intensity
14 p1972 N88-21768

SIGNATURE ANALYSIS
Fundamental aspects of the physics of remote sensing
[ESA-TT-1045] 09 p1185 N88-17100
Open questions in closed-loop photodetection
14 p1979 N88-21812
Autoregressive moving average modeling of radar target signatures
[AD-A194612] 22 p3069 N88-28218
Variability in spectral signatures of terrestrial volcanic rocks and implications for volcanology on Mars
23 p3303 N88-29672

SIGNATURES
NT INFRARED SIGNATURES
NT MAGNETIC SIGNATURES
NT RADAR SIGNATURES
NT SPECTRAL SIGNATURES
A system identification technique based on the random decrement signatures. Part 1: Theory and simulation
05 p0594 N88-13625
A system identification technique based on the random decrement signatures. Part 2: Experimental results
05 p0594 N88-13626
Interaction of a vortex pair with a free surface
[AD-A186619] 08 p0988 N88-15988
The angular reflectance signature of the canopy hot spot in the optical regime
[DE88-005385] 11 p1505 N88-18991
Toward a comprehensive theory for the sweeping of trapped radiation by inert orbiting matter
[NASA-CR-182584] 11 p1569 N88-19395
Polarimetric ISAR imaging using either measured or calculated transient signatures
[AD-A190077] 15 p2056 N88-22259
Anomalies in the heat-capacity signatures of submonolayer adsorbates with attractive lateral interactions
[AD-A190736] 15 p2147 N88-22817

SIGNIFICANCE
Determining differences in rates corresponding to a given significance level
[AD-A185004] 05 p0644 N88-13940

SIGNS (SYMBOLS)
U SYMBOLS

SIGNS AND SYMPTOMS
Computer response time measurements of mood, fatigue and symptom scale items: Implications for scale response time uses
[AD-A186093] 07 p0888 N88-15384
Motion sickness: Quantitative, algorithmic malaise indication in real time
[AD-A189674] 15 p2101 N88-22518
Simulator sickness in the AH-64 Apache combat mission simulator
[AD-A193419] 21 p2988 N88-27739
Alterations in upper extremity motor function in soldiers during acute high altitude exposure
[AD-A192676] 23 p3238 N88-29272

SIKORSKY AIRCRAFT
NT UH-60A HELICOPTER
Recent Sikorsky R and D progress
09 p1111 N88-16659

SILANES
Laser spectroscopy and gas-phase chemistry in CVD
[DE87-013715] 03 p0281 N88-11770
Measurement of the electron density and the attachment rate coefficient in silane/helium discharges
[AD-A184268] 04 p0496 N88-13051
Reactive sticking coefficients of silane on silicon
[DE88-000601] 05 p0570 N88-13473
Soluble polysilane derivatives: Chemistry and spectroscopy
[AD-A187889] 11 p1461 N88-18713
Photophysics and photochemistry of poly(di-n-hexylsilane) in room temperature solution
[AD-A187890] 11 p1462 N88-18714
High-performance polymeric materials
[AD-A190708] 15 p2046 N88-22190
Polymer precursors for ceramic composites
17 p2326 N88-23890
Boron-containing organosilane polymers and ceramic materials thereof
[NASA-CASE-ARC-11649-1-SB]
23 p3199 N88-29040
Ion kinetics in silane plasmas
[AD-A196202] 24 p3431 N88-30423

SILENCERS
Silencium resonators (Silators) for the attenuation and elimination of sound
[MBB-Z-546/83] 10 p1312 N88-17841

SILICA
U SILICON DIOXIDE

SILICA GEL
Separation of anionic from nonionic alkoxy compounds using silica gel
[GB-PATENT-2-140-415-A] 01 p0020 N88-10122
Structure of sol-gel-derived inorganic polymers. 2: Silicates and borates
[DE87-013068] 01 p0027 N88-10172
Optical characterization of silica aerogel glass
[DE87-014617] 02 p0153 N88-10956
Mass transfer mechanisms for water adsorbed on silica gel
[DE88-005993] 15 p2032 N88-22107
Structure of sol-gel silica
[DE88-006870] 15 p2033 N88-22114
A model for insulated wires in the method of moments code NEC (Numerical Electromagnetics Code)
[DE88-008920] 20 p2794 N88-26577
Optical characterization of silica aerogel
[DE88-008916] 20 p2854 N88-26946
Precursor chemistry and the structure of silica aerogels
[DE88-011253] 21 p2920 N88-27328

SILICA GLASS
Optical characterization of silica aerogel glass
[DE87-014617] 02 p0153 N88-10956
Environmental fracture toughness and static fatigue crack propagation of silica glass
05 p0606 N88-13716
Novel fiber preforms: Rare earth doping
[AD-A191549] 18 p2575 N88-25294
Adhesion of hydrated silicate films
[DE88-011250] 21 p2920 N88-27333
Development of high efficiency q-switched glass laser via sol-gel processing
[AD-A192301] 23 p3218 N88-29154

SILICATES
NT ALUMINUM SILICATES
NT ANDESITE
NT CALCIUM SILICATES
NT GARNETS
NT YTTRIUM-ALUMINUM GARNET
NT ZEOLITES
Structure of sol-gel-derived inorganic polymers. 2: Silicates and borates
[DE87-013068] 01 p0027 N88-10172
Some speculations on the mechanisms of abrasive grinding and polishing
[DE87-014242] 02 p0181 N88-11126
The effect of temperature on fatigue crack initiation from aluminosilicate inclusions 06 p0720 N88-14427
Electron microscopy study of morphology and composition of a ferrisilicate catalyst
[DE88-005754] 11 p1562 N88-19352
High-performance polymeric materials
[AD-A190708] 15 p2046 N88-22190
Point defects in irradiated silicates
17 p2408 N88-24319
The evolution of cometary activity
18 p2594 N88-25416
Adhesion of hydrated silicate films
[DE88-011250] 21 p2920 N88-27333
Recycling of lower continental crust through foundering of cumulates from contaminated mafic intrusions
24 p3393 N88-30204

SILICIDES
NT DISILICIDES
Cohesive energies of transition metal silicides and phosphides — Knudsen effusion
[AD-A186691] 09 p1254 N88-17519
Initial development of high-temperature titanium silicide alloys
[DE88-007860] 20 p2772 N88-26437
Rocket-propellant burn tests of silicide-coated niobium and tantalum
[DE88-010729] 20 p2781 N88-26496

SILICON
NT AMORPHOUS SILICON
Si - SiO2 interfaces: A High Resolution Transmission Electron Microscopy (HRTEM) study
[DE87-012255] 01 p0028 N88-10181
Construction and characterization of amorphous-silicon test structures
[DE87-013595] 01 p0029 N88-10182
Effect of high-temperature annealing on the microstructure and thermoelectric properties of GaP doped SiGe
[NASA-TM-100164] 01 p0029 N88-10188
Monocrystalline silicon gradiometer for gravity experiments in space
[NASA-CR-181452] 01 p0050 N88-10321
Electrical behavior of layers implanted with low energy pions in Si
[INPE-4199-PRE/1051] 01 p0102 N88-10670
Chemical vapor deposition of B6P and B6As films
[DE87-009288] 02 p0151 N88-10942
Hydrogen annealing of P(sub) b and E prime defect centers in oxidized silicon wafers
[DE87-014293] 02 p0152 N88-10951
Preparation of oxide glasses from metal alkoxides by sol-gel method
[NASA-TT-20124] 02 p0154 N88-10965
Voltammetric investigation of porous silicon for integrated circuit applications
[DE87-009287] 02 p0166 N88-11042

Wide bandgap passivation layers on silicon
[DE87-014307] 02 p0244 N88-11543
Bond character at a silicon/copper surface
[AD-A184167] 03 p0295 N88-11851
Integrated fiber-optic coupler
[AD-A184494] 03 p0377 N88-12369
Elimination of subboundaries in 0.5-micron-thick Si-on-insulation films produced by ZMR
[AD-A184590] 03 p0381 N88-12396
Dramatically improved radiation hardness for CMOS silicon gate integrated circuits even down to cryogenic temperatures
[AD-A184672] 03 p0381 N88-12398
Epitaxial reactor development for growth of silicon-on-insulator devices
[AD-A184758] 03 p0382 N88-12399
Performance of GaAs and silicon concentrator cells under 37 MeV proton irradiation
[NASA-TM-100144] 04 p0465 N88-12877
Colloidal stability of oxidized silicon particles in ethanolic and aqueous media
[DE87-014783] 05 p0562 N88-13421
Reactive sticking coefficients of silane on silicon
[DE88-000601] 05 p0570 N88-13473
Technology upgrade of a silicon compiler
[AD-A184873] 05 p0655 N88-14016
Preparation of amorphous silicon semiconductors
[GB-PATENT-2-176-054-A] 05 p0656 N88-14022
Effects of hydrolysis on metallo-organic solution deposition of PZT films
[ATR-86(8443)-1] 06 p0679 N88-14160
Theoretical aspects of channeling, damage, and range distributions for low (keV) and high (MeV) energy implantation
[DE88-000949] 06 p0786 N88-14818
Silicon microscale mechanisms from (110) oriented wafers
[DE88-002096] 06 p0787 N88-14825
The influence of phosphorus on the solid state reaction between copper and silicon or germanium
[ETN-88-91361] 06 p0789 N88-14838
Diamond turning of silicon for optics applications
[DE88-002501] 07 p0840 N88-15095
Formation and passivation of new paramagnetic defects associated with thermal oxides on silicon
[DE88-002720] 07 p0938 N88-15699
Radiant power degradation of silicon-doped gallium arsenide and gallium aluminum arsenide infrared light-emitting diodes
[AD-A186726] 09 p1157 N88-16935
IRAC test report. Gallium doped silicon band 2: Read noise and dark current
[NASA-TM-87813] 09 p1159 N88-16945
Forward-biased current annealing of radiation damaged gallium arsenide and silicon solar cells
[AD-A186904] 09 p1186 N88-17105
The mechanism of anisotropic silicon etching and its relevance for micromachinings
[MBB-UA-1013/86] 10 p1311 N88-17838
Laser pulse width dependent surface ripples on silicon
[PB88-127311] 10 p1336 N88-17982
Optical measurements of surface oxide layer formation on metal films
[DE88-003163] 10 p1409 N88-18405
Corner compensation structures for (110) oriented silicon
[DE88-003300] 10 p1417 N88-18455
Recording a surface acoustic wave on the surface of silicon
[PB88-130372] 11 p1490 N88-18894
Measurement of the gamma-ray response of some commercial silicon detectors
[AD-A187431] 11 p1543 N88-19221
Atomistic simulation of low-energy beam deposition
[DE88-004344] 11 p1544 N88-19228
Development of VLSI optical data link
[AD-A187883] 11 p1549 N88-19265
Silicon and indium doping of GaAs: Measurements of the effect of doping on mechanical behavior and relation with dislocation formation
[DE88-003862] 11 p1554 N88-19303
Formation of buried nitride layers in (110) silicon
[DE88-003255] 11 p1557 N88-19323
Silicon containing photoresists
[AD-A188666] 12 p1605 N88-19601
Preparation and characterization of thin films of alumina by metalorganic chemical vapor deposition
[AD-A188366] 12 p1608 N88-19614
Polymeric materials for electro-optic testing
[AD-A188382] 12 p1610 N88-19627
Hydrodynamic simulation of forced convection in the Czochralski process
[INPE-4471-TDL/323] 12 p1697 N88-20158
Thermal oxide growth on silicon: Intrinsic stress and silicon cleaning effects
[AD-A188790] 13 p1736 N88-20377
Focused ion beam fabrication of graded channel FET's in GaAs and Si
[AD-A189166] 13 p1845 N88-21040
Pressure-dependent DLTS (Deep Level Transient Spectroscopy) experiments on Si-doped AlGaAs
[DE88-003842] 13 p1846 N88-21047
X-ray diffraction study of a thin GaAs film on Si(100)
[DE88-005290] 13 p1847 N88-21055
Initial stages of silicon growth on the (100) surface of silicon by localized laser CVD
[DE88-005420] 13 p1848 N88-21059
Modeling growth of interdendritic silicon ribbons
14 p1897 N88-21322
Breathing mode lattice relaxation associated with carrier emission and capture by deep electronic levels in silicon
[DE88-003844] 14 p1985 N88-21842
Fabrication and electrical characterization of multilevel aluminum interconnects used to achieve silicon-hybrid wafer-scale integration
[AD-A190519] 15 p2060 N88-22282
High-efficiency thin-film silicon-on-GaP solar cell for improved radiation resistance
[AD-A190268] 15 p2091 N88-22460
Fundamental properties and devices applications of Ge(x)Si(1-x)/Si superlattices
[AD-A190129] 15 p2143 N88-22787
The structure of the boron-hydrogen complex in silicon
[DE88-005433] 15 p2144 N88-22795
Neutron radiation tolerance of Au-activated silicon
17 p2408 N88-24316
Improved GaP doped SiGe thermoelectric material
17 p2437 N88-24503
Observation of injected silicon in heliotron E
17 p2441 N88-24524
Metastability in SiGe/Si strained-layer structures
[DE88-007603] 18 p2585 N88-25361
On the use of convergent beam electron diffraction for identification of antiphase boundaries in GaAs grown on Si
[DE88-008220] 18 p2585 N88-25362
Silicon pulse sharpening diodes-switching kilovolts in 10's of picoseconds 19 p2661 N88-25824
Microminiature fluidic amplifier
19 p2669 N88-25865
Anomalous emissivity from periodic micro-machined silicon surfaces 19 p2670 N88-25872
Stress modeling of microdiaphragm pressure sensors
19 p2670 N88-25873
Application-specific packaging for custom micromechanical structures 19 p2671 N88-25879
High dose uranium ion implantation into silicon
[LBL-23509] 19 p2725 N88-26182
Defects in high-mobility semiconductor systems
[AD-A191618] 19 p2732 N88-26224
X-ray response of GaAlAs/GaAs radiation hardened double: Heterostructure photodiode compared to Si:PIN photodiodes
[DE88-007425] 19 p2733 N88-26231
Ductile-brittle transition of cutting behavior in diamond turning of single crystal Si
[DE88-008890] 20 p2809 N88-26664
Kinetic of oxidation to air of a Fe-Al-Mn alloy system at 600-800(sup 0)C temperature range
[DE88-702309] 21 p2920 N88-27330
Studying the physics and operation of multi-terminal near-micron and sub-micron length, hot electron semiconductor devices
[AD-A193380] 21 p2938 N88-27446
Molecular beam epitaxy of GaP films on Si substrates
[PB88-131974] 21 p3020 N88-27923
Development of 30 micrometers extrinsic silicon multiplexed infrared deterctor array
[NASA-CR-177446] 22 p3082 N88-28301
Atomistic simulation of silicon grain boundaries
[DE88-009925] 22 p3155 N88-28771
Sol-gel processing of metal-oxide-semiconductor structures
[DE88-009853] 22 p3156 N88-28778
Sol-gel kinetics: Si(sup)29 NMR and a statistical reaction model
[DE88-011545] 23 p3191 N88-28988
Stress corrosion of ceramic materials
[AD-A191979] 23 p3195 N88-29016
Local environment approach for deep-level defects in semiconductors: Application to the vacancy in silicon
[DE88-702017] 23 p3287 N88-29573
Ultrafast processes and spectroscopy with free electron lasers
[AD-A195248] 24 p3379 N88-30126

SILICON ALLOYS
Factors determining the morphology of precipitation in aluminum-germanium and aluminum-silicon alloys
[DE87-014682] 03 p0287 N88-11806
Cyclic deformation of an extruded AlMgSi alloy
05 p0598 N88-13654
Stability diagrams for epitaxial strained layers
[DE88-003935] 10 p1418 N88-18470
Brittle to ductile transition to cleavage fracture
[DE88-004074] 10 p1420 N88-18481
Optimisation of the thermoelectric figure of merit of modified silicon germanium alloys
[AD-A191347] 16 p2283 N88-23670
Preparation of improved PbSnTe thermoelectric alloys and evaluation of their figure of merit
[AD-A191346] 17 p2445 N88-24538
Improved properties of SiGe/GaP alloys
[NASA-CASE-NPO-17259-1-CU] 18 p2585 N88-25358
Hydrogenated amorphous silicon-germanium alloys
[DE88-001147] 19 p2620 N88-25546
Low-band-gap, amorphous-silicon-based alloys by photochemical vapor deposition
[DE88-001165] 21 p3023 N88-27944
Calculation of the specific and volumetric enthalpies of Ge-Si alloys
[DE88-008949] 21 p3026 N88-27965

SILICON CARBIDES
Pressure effects on the thermal stability of SiC fibers
[NASA-TM-100146] 01 p0019 N88-10120
Physics and chemistry of packing fine ceramic powders
[DE87-013709] 01 p0029 N88-10183
Laser chemically vapor deposited silicon-carbide: Growth features, topography, microstructure, and composition
[DE87-013767] 01 p0029 N88-10184
Fiber-reinforced composite hot-gas filters
[DE87-012257] 01 p0033 N88-10208
An investigation of the high strain rate deformation of SiCw/2124 Al composite
[OUEL-1675/87] 02 p0142 N88-10895
Processing and properties of SiC/Nicalon composites
[DE87-013885] 03 p0279 N88-11757
The infiltration kinetics of aluminum in silicon carbide compacts
[AD-A184682] 03 p0290 N88-11823
Characterization and thermal conductivity of hot-pressed silicon carbide
[DKG-25] 03 p0292 N88-11834
Flaw imaging and ultrasonic techniques for characterizing sintered silicon carbide
[NASA-TM-100177] 03 p0334 N88-12106
Carbon-fiber reinforced aluminum
04 p0403 N88-12507
Composite materials with glass matrix
[SGR/PR-4305/86-SV/JC] 05 p0558 N88-13394
Fabrication of composites by chemical vapor deposition
[DE87-014565] 05 p0559 N88-13408
Structural characterization of ion implanted beta-SiC thin films
[DE87-014567] 05 p0656 N88-14027
Stress rupture behavior of silicon carbide coated, low modulus carbon/carbon composites
[NASA-CR-180863] 06 p0678 N88-14150
Sintering and densification of particulate composites: Inclusion size and clustering
[DE88-002230] 06 p0685 N88-14199
Cyclic fatigue of ceramics at high temperatures
[PB87-127700] 06 p0685 N88-14200
Micromechanisms of fatigue crack growth and fracture toughness in metal matrix composites
[AD-A186941] 09 p1137 N88-16816
Investigation of microstructural factors that cause low fracture toughness in silicon carbide whisker/Al alloy composites
[AD-A186443] 09 p1137 N88-16817
Microstructures and properties of SiC whisker-reinforced mullite composites
[DE88-002611] 09 p1139 N88-16826
Wire-cut electrical discharge machinability of ceramics
[AD-A186989] 09 p1146 N88-16870
Fabrication and materials evaluation of high performance aligned ceramic fibre reinforced glass matrix composite
[AERE-R-12517] 10 p1294 N88-17736
Micro-mechanisms of deformation in SiC/Al composites
[AD-A188282] 10 p1296 N88-17749
Friction and wear of monolithic and fiber reinforced silicon-ceramics sliding against IN-718 alloy at 25 to 800 C in atmospheric air at ambient pressure
[NASA-TM-100294] 10 p1304 N88-17796
NMR (Nuclear Magnetic Resonance) imaging for detecting binder/plasticizers in green-state structural ceramics
[DE88-003111] 10 p1304 N88-17800
Fabrication, phase transformation studies and characterization of SiC-AlN-Al2OC ceramics
[DE88-004053] 10 p1306 N88-17807

Plasma deposition of silicon carbide thin films
[AD-A188093] 11 p1556 N88-19314
Effect of rigid inclusions on sintering
[DE88-005745] 12 p1609 N88-19623
Fundamental studies and device development in beta silicon carbide
[AD-A189540] 12 p1699 N88-20165
Composites strengthening
[AD-A189258] 13 p1734 N88-20364
The influence of the fiber-matrix bond on the mechanical behavior of NICALON/SiC composites
[DE88-006155] 13 p1734 N88-20369
Nondestructive evaluation of carbon-carbon coatings
[AD-A189524] 13 p1748 N88-20453
Ultrasonic characterization of non-uniform porosity distributions in SiC ceramic
[DE88-004814] 13 p1749 N88-20459
Development, high temperature properties, and microanalysis of nonoxide ceramics
[ETN-88-92103] 14 p1893 N88-21304
Processing, texture and mechanical properties of sintered silicon carbide
[NASA-TT-20253] 14 p1893 N88-21305
Microwave sintering of alumina-SiC composites at 2.45 and 60 GHz
[DE88-006455] 15 p2030 N88-22095
Processing, microstructure, and mechanical properties of silicon carbide particulate reinforced aluminum alloys
[AD-A188981] 15 p2037 N88-22136
Characterization of sintered SiC by using NDE
15 p2082 N88-22413
Strength and cracking resistance of ceramics. Report 3: SiC ceramics 16 p2180 N88-22994
Structure and mechanical properties of metal matrix composites made using semi-solid processes: The case of the system Al-Si/SiC
[ETN-88-92299] 17 p2316 N88-23836
Nondestructive evaluation of structural ceramics
17 p2324 N88-23876
Improved silicon carbide for advanced heat engines
17 p2324 N88-23879
Strength optimization of alpha-SiC by improved processing 17 p2324 N88-23880
Colloidal characterization of silicon nitride and silicon carbide 17 p2325 N88-23883
Molten salt corrosion of SiC and Si3N4
17 p2325 N88-23885
Thermal cyclic durability testing of ceramic materials for turbine engines 17 p2325 N88-23886
Ceramic matrix composites 17 p2325 N88-23888
Polymer precursors for SiC ceramic materials
17 p2326 N88-23889
SiC fiber analysis 17 p2326 N88-23891
SiC fiber reinforced reaction-bonded Si3N4 composites 17 p2326 N88-23892
High frequency ultrasonic characterization of sintered SiC
[NASA-TM-100825] 17 p2347 N88-23985
Defects in cubic silicon carbide on silicon
17 p2408 N88-24317
An investigation of ceramic coatings for protection of SiC from high-temperature corrosion
[DE88-007873] 18 p2493 N88-24790
Auger analysis of a fiber/matrix interface in a ceramic matrix composite
[NASA-TM-100892] 19 p2610 N88-25487
Interface modification in Nicalon (trademark)/SiC composites
[DE88-009708] 20 p2767 N88-26409
Observations on residual stresses in ceramic composites by neutron diffraction techniques
[DE88-009937] 20 p2778 N88-26472
Factors influencing the toughening behavior of whisker reinforced ceramics
[DE88-011396] 20 p2779 N88-26479
As-received microstructure of a SiC/Ti-15-3 composite
[NASA-TM-100938] 22 p3050 N88-28095
Investigation of a SiC/Ti-24Al-11Nb composite
[NASA-TM-100956] 23 p3190 N88-28980
Determination of impurities in silicon carbide by ICP AES (inductively coupled plasma atomic emission spectrometry) after coprecipitation with lanthanum hydroxide
[NASA-TT-20332] 23 p3193 N88-29003
Sinterable ceramic powders from laser-heated gases
[AD-A194162] 23 p3197 N88-29024
Boron-containing organosilane polymers and ceramic materials thereof
[NASA-CASE-ARC-11649-1-SB]
23 p3199 N88-29040
Processing technology research in composites
[AD-A195693] 24 p3341 N88-29890
Electrical properties of materials for elevated temperature resistance strain gage application
[NASA-CR-182214] 24 p3376 N88-30106

SILICON COMPOUNDS
NT ALUMINUM SILICATES
NT ANDESITE
NT CALCIUM SILICATES
NT DISILICIDES
NT GARNETS
NT ORGANIC SILICON COMPOUNDS
NT QUARTZ
NT SILANES
NT SILICATES
NT SILICIDES
NT SILICON CARBIDES
NT SILICON DIOXIDE
NT SILICON NITRIDES
NT SILICON OXIDES
NT YTTRIUM-ALUMINUM GARNET
NT ZEOLITES
Flash threshold of shocked aluminum silicofluoride
[DE88-003978] 10 p1339 N88-18005
Silicon-germanium heterostructures
13 p1844 N88-21034
Recent data on SiAs impurity band conduction multiplexed arrays
[AD-A191752] 18 p2582 N88-25340
Photorefractive damage mechanism in electro-optic materials
[AD-A194560] 23 p3282 N88-29543

SILICON DIOXIDE
NT QUARTZ
Mechanism of mechanical fatigue of fused silica
[DE87-014199] 02 p0152 N88-10950
Formation and passivation of new paramagnetic defects associated with thermal oxides on silicon
[DE88-002720] 07 p0938 N88-15699
Studies on nonlinear mechanisms of excimer laser propagation in fused silica fibers
[AD-A186822] 09 p1156 N88-16929
Dispersive hole transport in SiO2
[AD-A187077] 09 p1254 N88-17513
Beneficial and detrimental effects of silica in the high temperature oxidation of 20Cr/25Ni/Nb stainless steel
[AERE-R-12667] 10 p1301 N88-17779
A viscoelastic BEM (Boundary Element Method) for modeling oxidation
[AD-A187490] 11 p1452 N88-18653
High temperature oxidation studies on alloys containing dispersed phase particles and clarification of the mechanism of growth of SiO2
[AD-A188158] 11 p1457 N88-18688
SiO2 film stress distribution during thermal oxidation of Si
[AD-A189552] 12 p1612 N88-19637
Oxide-bound transition metal complexes for methane activation
[PB88-169719] 14 p1887 N88-21277
Chemical vapor deposited silica coatings for solar mirror protection
[NASA-TM-100834] 14 p1893 N88-21306
Abrasion resistant porous silica antireflective coatings
[DE88-006230] 14 p1894 N88-21308
Infrared reflection-absorption spectroscopy of hyperfine layers on surfaces of semiconductors and dielectrics
14 p1969 N88-21755
A model for nitrogen atom recombination on a silicon dioxide surface
[AD-A189843] 15 p2142 N88-22784
Studies of boron implantation through photochemically deposited SiO2 films on Hg(sub 1-x)Cd(sub x)Te
[SD-TR-87-26] 19 p2621 N88-25548
Improved adhesion for SiO2 particles in silica substrates using helium-ion irradiation
[DE88-008915] 21 p2920 N88-27332
Silicon oxidation studies: A review of recent studies on thin film silicon dioxide formation in the physics and chemistry of SiO2 and the Si-SiO2 interface
[AD-A193176] 21 p3021 N88-27932

SILICON FILMS
Laser chemically vapor deposited silicon-carbide: Growth features, topography, microstructure, and composition
[DE87-013767] 01 p0029 N88-10184
Understanding the transport properties of silicon grain boundaries and how they relate to I.C. applications of polysilicon
[DE87-013809] 01 p0104 N88-10677
The soft/hard wet anodization of aluminum oxide and its use in a thin film multilayered capacitor
[AD-A187575] 10 p1325 N88-17919
Apparatus for the study of silicon film deposition and silicon etching
[AD-A187616] 10 p1334 N88-17972
Grazing incidence X-ray scattering study of defect structures in MBE GaAs/Si using synchrotron radiation
[DE88-004556] 10 p1420 N88-18483
Synthesis and characterization of thin films
[AD-A187335] 10 p1421 N88-18485
Development of VLSI optical data link
[AD-A187884] 11 p1549 N88-19266
Studies of boron implantation through photochemically deposited SiO2 films on Hg(sub 1-x)Cd(sub x)Te
[SD-TR-87-26] 19 p2621 N88-25548
Chemical multisensors with selective encapsulation of ion-selective membranes 19 p2670 N88-25889
Air loading effects on a capacitively sensed membrane supported silicon accelerometer
19 p2672 N88-25886
Tin oxide microsensors on thin silicon membranes
19 p2673 N88-25897
Deposition techniques and properties of strain compensated LPCVD silicon nitride films
19 p2673 N88-25898
The use of micromachined structures for the management of mechanical properties and adhesion of thin films 19 p2674 N88-25899
Stability of uncapsulated weight cells with thin film elongation measurement bands under influence of humidity, temperature and operation voltage
[ETN-88-92383] 21 p2951 N88-27531
Silicon oxidation studies: A review of recent studies on thin film silicon dioxide formation in the physics and chemistry of SiO2 and the Si-SiO2 interface
[AD-A193176] 21 p3021 N88-27932
Laser crystallized silicon films on alumina ceramic substrates and application to thin film c-Si solar cells
[PB88-131966] 22 p3116 N88-28515

SILICON JUNCTIONS
An investigation of the equivalent circuit and carrier lifetimes of Si/SiGe heterostructure p-n diodes for frequencies between 0.5 and 18.5 MHz
[FOA-C-30469-3.2] 09 p1256 N88-17529
Characterization of crystalline silicon by electrochemical and Raman spectroscopy at the frontier semiconductor/electrolyte
[ETN-88-92354] 21 p3025 N88-27956

SILICON NITRIDES
Development of a statistically proven injection molding method for reaction bonded silicon nitride, sintering reaction bonded silicon nitride, and sintered silicon nitride
[ETN-87-90575] 02 p0160 N88-11002
Electron microscopy studies of tensile cyclic fatigue-tested silicon nitride ceramics
[DE88-001438] 06 p0685 N88-14196
Investigation of silicon surface passivation by silicon nitride film deposition
[NASA-CR-182350] 06 p0729 N88-14487
Improved silicon nitride for advanced heat engines
[NASA-CR-175006] 08 p0973 N88-15886
Wire-cut electrical discharge machinability of ceramics
[AD-A186989] 09 p1146 N88-16870
Focused ultrasonic backscatter technique for near-surface flaw detection in structural ceramics
[DE88-003112] 09 p1183 N88-17091
NMR (Nuclear Magnetic Resonance) imaging for detecting binder/plasticizers in green-state structural ceramics
[DE88-003111] 10 p1304 N88-17800
A viscoelastic BEM (Boundary Element Method) for modeling oxidation
[AD-A187490] 11 p1452 N88-18653
Investigations of surface coatings based on silicon and nitrogen: From amorphous Si to silicon nitride
[DE88-004995] 12 p1609 N88-19622
A new process for synthesis of silicon nitride powders for advanced ceramics
[AD-A189354] 13 p1748 N88-20451
Dynamic tensile cyclic fatigue of Si3N4
[DE88-003919] 13 p1781 N88-20658
Optical study of germanium, germanium plus arsenic, and germanium plus gallium implants in gallium arsenide
[AD-A189600] 13 p1845 N88-21045
Photon-controlled growth of multilayered structures
[DE88-005061] 13 p1847 N88-21054
Development, high temperature properties, and microanalysis of nonoxide ceramics
[ETN-88-92103] 14 p1893 N88-21304
Effect of oxidation on strength and thermal stability of material based on Si3N4 14 p1896 N88-21319
Fracture toughness of silicon nitride-silicon nitride joints bonded with oxynitride glass
[DE88-005548] 15 p2043 N88-22172
Flaw characterization in structural ceramics using scanning laser acoustic microscopy
15 p2082 N88-22415
Nondestructive evaluation of structural ceramics
17 p2324 N88-23876
Improved silicon nitride for advanced heat engines
17 p2324 N88-23881
Improved processing of Si3N4
17 p2325 N88-23882
Colloidal characterization of silicon nitride and silicon carbide 17 p2325 N88-23883

Molten salt corrosion of SiC and Si3N4
17 p2325 N88-23885
Thermal cyclic durability testing of ceramic materials for turbine engines 17 p2325 N88-23886
SiC fiber reinforced reaction-bonded Si3N4 composites 17 p2326 N88-23892
Environmental effects on slow crack growth in silicon nitride
[DE88-007206] 18 p2494 N88-24795
Auger analysis of a fiber/matrix interface in a ceramic matrix composite
[NASA-TM-100892] 19 p2610 N88-25487
Deposition techniques and properties of strain compensated LPCVD silicon nitride films
19 p2673 N88-25898
Application of electron microscopy for the analysis of the mechanical behavior of advanced ceramics
[DE88-005049] 20 p2777 N88-26469
Application of magnification xeroradiography to advanced ceramics
[DE88-009965] 20 p2778 N88-26473
Absorption characteristics of Si3N4 ablation layer plasma 20 p2783 N88-26504
The high temperature creep deformation of Si3N4-6Y2O3-2Al2O3
[NASA-CR-183204] 23 p3190 N88-28981
Sinterable ceramic powders from laser-heated gases
[AD-A194162] 23 p3197 N88-29024

SILICON OXIDES
NT QUARTZ
NT SILICON DIOXIDE
Holographically correcting synthetic aperture aberrations
[AD-A189510] 12 p1692 N88-20123
Thermal oxide growth on silicon: Intrinsic stress and silicon cleaning effects
[AD-A188790] 13 p1736 N88-20377
Polarization properties of SiO masers
13 p1858 N88-21113
Hot electrons in silicon dioxide: Ballistic to steady-state transport 20 p2871 N88-27042

SILICON POLYMERS
NT SILICONES
NT SILOXANES
High yield synthesis of B4C/BN ceramic materials by pyrolysis of polymeric Lewis base adducts of decaborane(14)
[AD-A188154] 11 p1462 N88-18717
The 1986 IEEE Solid-State Sensor Workshop
[AD-A190922] 19 p2668 N88-25860
Characteristics of polysilicon layers and their application in sensors 19 p2669 N88-25861
Design and construction techniques for planar polysilicon pressure transducers with piezoresistive read-out 19 p2669 N88-25862
Integrated polysilicon tactile sensor
19 p2669 N88-25863
Thermal management of integrated microsensors
19 p2670 N88-25875
Deposition techniques and properties of strain compensated LPCVD silicon nitride films
19 p2673 N88-25898
Photovoltaic cells with n-silicon and conductive polymers
[ETN-88-92133] 20 p2821 N88-26734
Silicon-on-insulator pin diodes
[AD-A193359] 21 p2937 N88-27445
Boron-containing organosilane polymers and ceramic materials thereof
[NASA-CASE-ARC-11649-1-SB]
23 p3199 N88-29040

SILICON RADIATION DETECTORS
Low noise-low power monolithic multiplexing readout electronics for silicon strip detectors
[MPI-PAE/EXP.EL.178] 02 p0168 N88-11057
Design of a charge sensitive preamplifier on high resistivity silicon
[DE88-003491] 10 p1323 N88-17907
The silicon microstrip detector --- particle position measurement
[ETN-88-92235] 16 p2210 N88-23189

SILICON RECTIFIERS
U CRYSTAL RECTIFIERS

SILICON SOLAR CELLS
U SOLAR CELLS

SILICON TRANSISTORS
NT SOS (SEMICONDUCTORS)
Development of Si/SiGe heterostructures
[AD-A189527] 13 p1845 N88-21044
Thermal vacuum sensors based on integrated silicon thermopiles
[ETN-88-92237] 16 p2210 N88-23190
Integrated magnetic field sensor using high magnetotransistors
[ETN-88-92356] 21 p2941 N88-27465

SILICON-ON-INSULATOR SEMICONDUCTORS
U SOI (SEMICONDUCTORS)

SILICON-ON-SAPPHIRE JUNCTIONS
U SOS (SEMICONDUCTORS)

SILICON-ON-SAPPHIRE SEMICONDUCTORS
U SOS (SEMICONDUCTORS)

SILICON-ON-SAPPHIRE TRANSISTORS
U SOS (SEMICONDUCTORS)

SILICONES
NT SILOXANES
Investigation of structure-permeability relationships of silicone polymer membranes
[PB87-230181] 03 p0293 N88-11839
Determination of the modulus of elasticity of structural silicone sealants
[PB88-157458] 14 p1893 N88-21307
Primerless RTV silicones
[BDX-613-3807] 24 p3356 N88-29980
Containment of a silicone fluid free surface in reduced gravity using barrier coatings
[NASA-TM-101314] 24 p3371 N88-30072

SILOXANES
Synthesis, NMR characterization and electrical properties of siloxane-based polymer electrolytes
[AD-A184184] 04 p0418 N88-12596
Synthesis and structure property studies of toughened epoxy resins via functionalized polysiloxanes
[AD-A187984] 11 p1462 N88-18715
Ionic conductive polymers based on crosslinked elastic siloxane-ethylene oxide copolymers
[DE88-011243] 21 p2917 N88-27311
Functional study of the Si/SiO2 structures. Application to the implementation of an integrated ion sensor
[ECL-87-16] 22 p3073 N88-28246
Quasi-liquid crystalline materials with special electro-optic properties
[AD-A194579] 23 p3282 N88-29544

SILTS
U SEDIMENTS

SILVER
Plasmon resonance absorption in layered structures of silver with periodic corrugation
[DE87-013183] 02 p0231 N88-11453
Study of IR laser photoacoustic spectra of organic molecules adsorbed on metal surface
03 p0301 N88-11891
Simulation of the layer-growth dynamics in silver films: Dynamics of adatom clusters and vacancy clusters on Ag(100)
[DE87-014764] 03 p0380 N88-12390
Phase equilibrium and crystal growth studies on AgGaSe2 and related nonlinear optical materials
[AD-A184768] 03 p0382 N88-12400
Coverage dependence of adsorbate-substrate bond lengths: Chlorine and caesium adsorbed on silver single crystals
[PB87-125142] 06 p0788 N88-14833
Sputtered silver films to improve chromium carbide based solid lubricant coatings for use to 900 C
[NASA-TM-100783] 08 p0973 N88-15885
Adhesion of vapour phase deposited ultra-thin polyimide films on polycrystalline silver
[AD-A187930] 10 p1306 N88-17810
Photoacoustic studies of surface plasmons in metallic microstructures
[DE88-004423] 11 p1460 N88-18703
Optical waveguide formation by ion implantation of Ti or Ag
[DE88-004595] 11 p1551 N88-19278
Tunable optical sources/growth and characterization of nonlinear optical materials
[AD-A190874] 16 p2274 N88-23608
Interface characterization of Cu-Cu and Cu-Ag-Cu low temperature solid state bonds
[AD-A191015] 16 p2283 N88-23667
Electronic and geometric structure of silver and palladium on aluminum (111) in monoatomic surface layers
[ETN-88-92120] 20 p2879 N88-27093
Functional study of the Si/SiO2 structures. Application to the implementation of an integrated ion sensor
[ECL-87-16] 22 p3073 N88-28246

SILVER ALLOYS
In-situ vibrational spectroscopy of specifically adsorbed azide on silver electrodes
[AD-A188511] 12 p1605 N88-19600

SILVER CHLORIDES
Silver multi-layers for planar Ag/AgCl reference electrodes 19 p2672 N88-25883

SILVER COMPOUNDS
NT SILVER CHLORIDES
NT SILVER IODIDES
Investigation of effect of silver compounds on microflora in water reclaimed from atmospheric moisture condensate in a closed environment 07 p0892 N88-15407

SILVER HALIDES
NT SILVER CHLORIDES
NT SILVER IODIDES

SILVER IODIDES
Altered and enhanced iodargyrite with bismuth triiodide for use in precipitation enhancement operations
[AD-A185229] 05 p0561 N88-13419

SIMD (COMPUTERS)
A parallel computer based on cube connected cycles
10 p1378 N88-18227
Introduction to a system for implementing neural net connections on SIMD architectures
[NASA-CR-181612] 10 p1386 N88-18279
BLITZ: Blitzen's micron-code assembly language design document, version 1.0
[TR88-14] 12 p1676 N88-20019
An emulation tool for simulating matrix operations on an SIMD (Single Instruction Multiple Data stream) multiprocessor
[AD-A188654] 12 p1678 N88-20030
The physical structure of concurrent problems and concurrent computers
[DE88-005812] 13 p1814 N88-20835
An analysis of multiple grain CHiP architectures
[AD-A189942] 15 p2110 N88-22570
What have we learnt from using real parallel machines to solve real problems
[DE88-011227] 22 p3135 N88-28636

SIMICOR (IMAGE CORRELATOR)
U IMAGE CORRELATORS

SIMILARITIES
U ANALOGIES

SIMILARITY THEOREM
NT LAGRANGE SIMILARITY HYPOTHESIS
Clustering by means of medoids
[REPT-87-03] 01 p0085 N88-10551
Similar solutions for viscous hypersonic flow over a slender three-fourths-power body of revolution
[NASA-TM-100205] 04 p0443 N88-12752
Determining Langmuir circulation parameters on basis of similarity theory 13 p1785 N88-20680
On a class of similarity solutions of the equation u sub t = (absolute value of u sup m-1 u sub x) sub x with m greater than -1
[REPT-87-54] 14 p1963 N88-21713

SIMILITUDE LAW
Scale model development for aeroelasticity studies
[ETN-88-91887] 14 p1868 N88-21164

SIMPLEX METHOD
A new pivoting rule for the dual network simplex method
[REPT-87-17] 01 p0080 N88-10511
An exponential example for Terlaky's pivoting rule for the criss-cross simplex method
[REPT-87-18] 01 p0080 N88-10512
On the volume of a n-dimensional simplex
[REPT-87-16] 01 p0086 N88-10557
An analysis of an available set of linear programming test problems
[DE87-014578] 02 p0221 N88-11392
Progress in mathematical programming
[AD-A185729] 06 p0759 N88-14658
Eliminating columns in the simplex method for linear programming
[DE88-004191] 10 p1386 N88-18277
Continuous deformation algorithm on the product space of unit simplices, revised version
[PB88-114210] 10 p1387 N88-18281
Primal-dual parallel solution of very large sparse linear programs
[AD-A188500] 12 p1680 N88-20045
An extension of the MS pivoting rule to capacitated network flow problems
[REPT-87-33] 14 p1963 N88-21711
Making progress during a stall in the simplex algorithm
[DE88-007120] 18 p2558 N88-25182
Linear programming for Air Force decision aiding
21 p2928 N88-27378

SIMULATED ALTITUDE
U ALTITUDE SIMULATION

SIMULATION
NT ALTITUDE SIMULATION
NT ANALOG SIMULATION
NT COMPUTER SYSTEMS SIMULATION
NT COMPUTERIZED SIMULATION
NT CONTROL SIMULATION
NT DIGITAL SIMULATION
NT ENVIRONMENT SIMULATION
NT EXHAUST FLOW SIMULATION
NT FLIGHT SIMULATION
NT LANDING SIMULATION
NT MOTION SIMULATION
NT NEUTRAL BUOYANCY SIMULATION
NT SOLAR SIMULATION

NT SPACE ENVIRONMENT SIMULATION
NT SYSTEMS SIMULATION
NT WEIGHTLESSNESS SIMULATION
Simulations using the pseudo-current algorithm
[DE87-012403] 01 p0040 N88-10255
Multidimensional modeling of convective heat transfer with application to IC engines
[DE87-011046] 01 p0055 N88-10353
Description of the Mountain Cloud Chemistry Program version of the PLUVIUS MOD 5.0 reactive storm simulation model
[DE87-012846] 01 p0070 N88-10450
A simulation study of interfaces in Ni, Al and Ni3Al with and without boron
[DE87-013156] 01 p0102 N88-10667
Comparison of MHD simulation for the February 1986 events with interplanetary observations by the spacecraft Sakigake 01 p0113 N88-10722
A simulation of the IPS variations from a magnetohydrodynamical simulation 01 p0118 N88-10755
Fourteenth Space Simulation Conference: Testing for a Permanent Presence in Space
[NASA-CP-2446] 02 p0132 N88-10829
Rocket nozzle thermal shock tests in an arc heater facility 02 p0133 N88-10832
Surveillance systems test and evaluation facilities 02 p0134 N88-10845
Thermal testing by internal IR heating of the FEP module 02 p0136 N88-10854
A new type of lamp and reflector for I.R. simulation 02 p0136 N88-10855
Scene simulation for passive IR systems 02 p0137 N88-10861
Numerical simulation of transient two-phase flow
[CFDU/87/4] 02 p0171 N88-11077
Impact of turbulence modeling on numerical accuracy and efficiency of compressible flow simulations
[NASA-TM-88333] 02 p0173 N88-11088
The numerical simulation of the mesoscale characteristics associated with Baiu front. Part 1: Structure, low-level jet and radiation characteristics 02 p0203 N88-11272
RANDOM NUMBER: A syntax-directed package to produce random numbers in user-specified, univariate distributions. User's guide
[DE87-014278] 02 p0228 N88-11436
Saturn: A large area X-ray simulation accelerator
[DE87-012021] 02 p0233 N88-11472
High explosive simulations of supernovae and the supernova shell fragmentation model of solar system formation
[DE87-014708] 02 p0251 N88-11584
Wake shield 03 p0298 N88-11871
Fundamentals of turbulence for turbulence modeling and simulation 03 p0312 N88-11971
Turbulence modelling through one point closures-applications-enlightening by large eddy simulation 03 p0312 N88-11972
Lattice gas hydrodynamics 03 p0313 N88-11978
A modular BLSS simulation model 03 p0359 N88-12260
Monte Carlo simulation of primitive atom-transfer reactions in solution
[AD-A183977] 03 p0375 N88-12360
Gravitational accretion of hot dark matter 03 p0388 N88-12439
Some experiences with the viscous-inviscid interaction approach
[NASA-TM-100015] 04 p0395 N88-12466
Analysis of sideband spectra from untapered undulator using analytical technique
[DE87-014763] 04 p0448 N88-12778
A network definition and solution of simulation problems
[DE88-000675] 04 p0481 N88-12962
Transport simulations of the oscillating field current drive experiment in the ZT-40M reversed field pinch
[DE88-000538] 04 p0491 N88-13027
A comparison of the basket method and the stratified random sampling for contract change order negotiations
[AD-A184170] 04 p0500 N88-13080
European hypersonic wind tunnels 05 p0530 N88-13221
The simulation of the viscous flow around a cylinder by the random vortex method 05 p0579 N88-13534
The statistics of the shape of small fatigue cracks 05 p0599 N88-13666
Numerical simulations of impact tests on a rigid wall — armor steel
[SNIAS-872-320-102] 05 p0610 N88-13744
Feasibility study for gas-grain simulation facility
[NASA-CR-177468] 05 p0646 N88-13954
Comparison of 2D memory SEU transport simulation with experiments
[ATR-86(8139)-2-REV-A] 05 p0656 N88-14025
On the influence of false plots on tracking relaibility: Simulations and preliminary analyses
[FOA-C-30443-3.2] 06 p0692 N88-14245
Satellite ground-terminal user simulation
[NASA-TM-100234] 06 p0694 N88-14260
Numerical simulation of boundary layers. Part 3: Turbulence and relaminarization in sink flows
[NASA-TM-88220] 06 p0698 N88-14283
A process study of the biothermal conversion of water hyacinths to methane
[DE88-000554] 06 p0730 N88-14488
Wind tunnel wall interference 07 p0811 N88-14938
Incompressible viscous flow simulations of the NFAC wind tunnel
[NASA-CR-177431] 07 p0816 N88-14969
European reacting flow research: A final assessment
[AD-A185833] 07 p0828 N88-15022
Developing an accelerated endurance test for greases: A status report
[AD-A185963] 07 p0836 N88-15072
An approach to validation and verification of the communications load model with supporting user's guide
[AD-A185926] 07 p0840 N88-15098
The determination of equivalent bearing loading for the BSMT that simulate SSME high pressure oxidizer turbopump conditions using the SHABERTH/SINDA computer programs 07 p0925 N88-15623
Plasma theory and simulation
[DE88-000412] 07 p0934 N88-15670
An experimental mapping of the flow field behind a glaze ice shape on a NACA 0012 airfoil
[NASA-CR-180847] 08 p0950 N88-15766
A multistage mesh generator for solving the average-passage equation system
[NASA-CR-179539] 08 p0951 N88-15769
Development of an emulation-simulation thermal control model for space station application
[NASA-CR-182409] 08 p0962 N88-15823
Vapor condensation on a turbulent liquid interface 08 p0982 N88-15939
Numerical simulation of turbulent spots in channel and boundary layer flows 08 p0983 N88-15948
Temporal and contextual knowledge in model-based expert systems 08 p1055 N88-16363
Rapid prototyping and AI programming environments applied to payload modeling 08 p1061 N88-16405
Numerical simulation of heat transfer turbulence, volume 4
[AD-A185132] 09 p1159 N88-16947
Proceedings of the Energy Independence Conference: Fusion Energy and Plasma Physics
[DE88-700657] 09 p1253 N88-17507
Numerical simulation of axisymmetric turbulent flow in combustors and diffusors
[NASA-CR-4115] 10 p1268 N88-17582
NASA wind shear model: Summary of model analyses 10 p1273 N88-17617
Satellite interference analysis and simulation using personal computers
[NASA-CR-182522] 10 p1319 N88-17890
Evaluation of regional-scale air quality models: Chairmen reports from four workshops
[DE88-001397] 10 p1352 N88-18080
Comparative evaluation of stress repsonse of rats to different methods of simulating some effects of weightlessness 10 p1363 N88-18144
Morphological study of early changes in rat bones in simulated weightlessness 10 p1365 N88-18158
Vector performance of register-to-register vector computers
[DE88-004013] 10 p1384 N88-18265
Parallel discrete event simulation: A shared memory approach
[NASA-CR-182521] 10 p1393 N88-18312
Performance and optimization of direct implicit time integration schemes for use in electrostatic particle simulation codes
[DE88-003254] 10 p1406 N88-18381
Supernova mechanisms: Before and after SN1987a
[DE88-003489] 10 p1429 N88-18533
Gamma-ray and neutron spectroscopy of planetary surfaces and atmospheres
[DE88-004287] 10 p1430 N88-18541
Simulated performance of an order statistic threshold strategy for detection of narrowband signals 11 p1474 N88-18796
Extrema of Gaussian process by simulation 11 p1541 N88-19211
Atomic-scale simulation in materials science
[DE88-005204] 11 p1544 N88-19230
Two dimensional simulations of multipass beam breakup
[CEBAF-PR-87-008] 11 p1547 N88-19254
Manned simulation: Helpful means to determine and improve structural load criteria 12 p1581 N88-19459
Table with aerostatic bearings for simulation in one degree of freedom attitude control systems of artificial satellites
[INPE-4272-PRE/1144] 12 p1595 N88-19552
Simulation and tests of a satellite attitude and orbit control system. General considerations concerning an example case (INPE) and design of a servo rate table
[INPE-4282-PRE/1154] 12 p1599 N88-19572
A methodology for hardware verification based on logic simulation
[AD-A188553] 12 p1622 N88-19704
Reliability analyses of a surface mounted package using finite element simulation
[AD-A189488] 12 p1624 N88-19717
Wavenumber - frequency structure of turbulent flow in a channel from a direct simulation
[AD-A189079] 12 p1627 N88-19737
Gradiometer mission spectral analysis and simulation studies: Past and future 12 p1645 N88-19851
Full scale architectural simulation techniques for space stations 12 p1651 N88-19887
OMV man/system simulation integration: A preliminary analysis and recommendation
[NASA-CR-182602] 12 p1671 N88-20005
Experimental analysis of algorithms
[AD-A188528] 12 p1677 N88-20028
Analysis of simulated annealing type algorithms
[AD-A189382] 12 p1679 N88-20037
Reducing rotary wing aircraft development time/cost through the use of simulation 12 p1702 N88-20186
The use of simulation in the development of the Airbus 12 p1702 N88-20188
Interaction between two-dimensional sonic jets and supersonic flow to model heat addition in a supersonic combustor
[AD-A189572] 13 p1716 N88-20261
Numerical simulation of subsonic and transonic propeller flow
[NASA-TM-100163] 13 p1716 N88-20262
The effect of combustion gas flow on the rotational dynamics of a spinning solid fuel rocket 13 p1732 N88-20358
Simulated impact damage in a thick graphite/epoxy laminate using spherical indenters
[NASA-TM-100539] 13 p1733 N88-20363
Model catalyst studies of SMSI (Strong Metal/Support Interactions) and the role of D-electrons in chemisorption and catalysis
[DE88-004518] 13 p1738 N88-20393
Applications of the differential reflectivity radar technique: Focus on estimation of rainfall parameters and microwave attenuation prediction 13 p1759 N88-20521
Center for Turbulence Research 1987 activities
[NASA-CR-182693] 13 p1769 N88-20583
Corrosion-wear process under rolling-sliding motion
[AD-A189603] 13 p1778 N88-20635
Structural clearances and internal friction: Simulation by Eigen distortions
[ISSN-0208-5658] 13 p1779 N88-20640
Two dimensional uncorrelated bias in fix algorithms
[NASA-CR-182683] 13 p1815 N88-20647
Predictive monitoring research: Summary of the PREMON system
[NASA-CR-182687] 13 p1824 N88-20905
Very high energy gamma ray astrophysics
[DE88-005821] 13 p1854 N88-21095
Potential applications of computational fluid dynamics to biofluid analysis
[NASA-TM-100089] 14 p1911 N88-21422
A general 2D electrical model for diagonally connected MHD generators
[DE88-004283] 14 p1984 N88-21835
Numerical simulation of turbulent flames using vortex methods
[AD-A189813] 15 p2034 N88-22116
A fully abstract semantics for event-based simulation
[AD-A190560] 15 p2060 N88-22283
Finite element simulation of perforation of aluminum plates
[DE88-002092] 15 p2073 N88-22362
Monte Carlo reliability analysis
[AD-A189972] 15 p2074 N88-22366
Experimental comparison of lightning simulation techniques to CV-580 airborne lightning strike measurements
[AD-A190576] 15 p2098 N88-22496
Exhaustive and pseudo-exhaustive testing
[AD-A190140] 15 p2111 N88-22574
A direct-execution parallel architecture for the Advanced Continuous Simulation Language (ACSL)
[NASA-CR-182809] 15 p2115 N88-22602
An approximation technique for solving a system of Fredholm integral equations for asymmetric detector response functions
[AD-A190577] 15 p2121 N88-22645

Random Process Simulation for stochastic fatigue analysis
[NASA-TM-100464] 15 p2123 N88-22654
The application of linear maximum likelihood estimation of aerodynamic derivatives for the Bell-205 and Bell-206
[AD-A191279] 16 p2161 N88-22894
Pulsed power simulation problems in magic
[AD-A191110] 16 p2191 N88-23065
Modeling scalar flux and the energy and dissipation equations 16 p2196 N88-23096
Direct numerical simulation of buoyantly driven turbulence 16 p2196 N88-23097
Premixed turbulent flame calculation
16 p2196 N88-23098
Coherent structure 16 p2199 N88-23117
Fast algorithms for Euler and Navier-Stokes simulations
[AD-A190897] 16 p2208 N88-23175
Calculation of displacement, constraints and eigenmodes of rotating blades
[ETN-88-92296] 16 p2224 N88-23277
Numerical simulation of coastal upwelling phenomena in Cabo Frio (RJ) through a two layer finite element model
[INPE-4502-RPE/561] 16 p2237 N88-23361
Fast Algorithm Simulation and Test (FAST) facility
[AD-A191183] 16 p2252 N88-23457
Hybrid particle simulation for focusing of rotating and propagating LIB 16 p2276 N88-23624
Single phase liquid immersion cooling of discrete heat sources in a vertical channel
[AD-A191224] 17 p2337 N88-23944
Finite element simulation of the atmosphere's electromagnetic response to charge perturbations associated with lightning 17 p2375 N88-24124
Simulating futures in extended common LISP
[NASA-TM-101000] 18 p2559 N88-25192
NAS: The first year
[NASA-TM-101006] 18 p2560 N88-25196
A constraint algorithm for maintaining rigid bonds in molecular dynamics simulations of large molecules
[AD-A191663] 18 p2572 N88-25277
Effects of Mach number on acoustic-vortex interactions in a ramjet 19 p2625 N88-25573
Numerical simulations of astrophysical jets
19 p2636 N88-25635
Numerical simulation of supersonic free-jets
19 p2636 N88-25639
Numerical calculation of three dimensional flow by TVD scheme 19 p2638 N88-25649
Simulation of axisymmetric flow with H2O2 reactions
19 p2638 N88-25651
Numerical simulation of turbulent flow using the exponential expression of k-Epsilon equation
19 p2640 N88-25662
Attenuated direct and scattered wave propagation on simulated land mobile satellite service paths in the presence of trees 19 p2645 N88-25695
Modulation efficiency limited high frequency performance of the MODFET 19 p2657 N88-25786
Accurate, productive aerodynamic simulation on patched mesh systems
[AD-A192040] 19 p2714 N88-26110
Simulated measurement of power flow in structures near to simple sources and simple boundaries
[NASA-TM-89124] 19 p2722 N88-26166
A simulation analysis of errors in the measurement of standard electrochemical rate constants from phase-selective impedance data
[AD-A192739] 20 p2770 N88-26426
Research in electromagnetic shielding theory. Part 2: EMP (electromagnetic pulse) simulation using small loops
[AD-A192882] 20 p2791 N88-26558
Navier-Stokes simulation of shock-tube flows over a wedge-type step by finite volume method
[ISAS-RN-626] 20 p2797 N88-26599
A numerical simulation of two-dimensional transient shear flow
[ISAS-RN-627] 20 p2797 N88-26600
Monte Carlo simulations of femtosecond relaxation of photoexcited electrons in AlGaAs/GaAs quantum wells
20 p2869 N88-27036
Atomistic simulation of stability, metastability and growth of strained layer structures 20 p2873 N88-27053
Documentation of the Benson Diesel Engine Simulation Program
[NASA-TM-100940] 21 p2898 N88-27201
Implicit finite-difference simulation of an internal flow in a nozzle: An example of a physical application on a hypercube
[AD-A192475] 21 p2942 N88-27472
Numerical experiments on turbulent mixing
[AD-A192572] 21 p2942 N88-27473
Granular flow: Particle-dynamics simulations of steady flow
[DE88-011342] 21 p2948 N88-27506
Direct simulation of stable stratified homogeneous turbulent shear flows
[DFVLR-FB-88-04] 21 p2949 N88-27516
Cloud simulation warm cloud experiments: Droplet growth and aerosol scavenging
[AD-A192944] 21 p2974 N88-27666
Electroencephalographic correlates of pilot performance: Simulation and in-flight studies
21 p2982 N88-27711
Analysis of lower hybrid current drive and rampup experiments on the JT-60 tokamak
[DE88-753136] 21 p3018 N88-27915
Method to predict external store carriage characteristics at transonic speeds
[NASA-CR-4170] 22 p3037 N88-28034
HPM (High Power Microwave) simulation fidelity studies
[DE88-012229] 22 p3068 N88-28209
Some screening experiments in objective prediction of monthly mean temperature over the United States during the winter season 22 p3127 N88-28589
Importance sampling for stochastic simulations
[AD-A193585] 22 p3138 N88-28654
Atomistic simulation of silicon grain boundaries
[DE88-009925] 22 p3155 N88-28771
Boundary layer simulation and control in wind tunnels
[AGARD-AR-224] 23 p3167 N88-28857
Missiles, fuselage and similar bodies
23 p3167 N88-28858
Empirical tools for simulation methodologies
23 p3168 N88-28866
Transport-type configurations
23 p3169 N88-28867
Introduction and critical flow phenomena
23 p3169 N88-28870
Shock boundary layer interaction
23 p3170 N88-28873
Classical separation, trailing-edge flows and buffeting
23 p3170 N88-28874
Vortex flows 23 p3170 N88-28875
Boundary layer manipulation 23 p3170 N88-28877
Natural convection immersion cooling of an array of simulated chips in an enclosure filled with dielectric liquid
[AD-A193594] 23 p3207 N88-29088
Typical weather months in the past (1973-1983) in Central Europe
[AD-A194701] 23 p3235 N88-29249
The gradient method for interface tracking
[AD-A194477] 23 p3248 N88-29334
Fusion product spectra
[DE88-010912] 23 p3284 N88-29554
Systematic properties of clusters of galaxies in different cosmological scenarios 23 p3299 N88-29646
Laboratory evaluation and application of microwave absorption properties under simulated conditions for planetary atmospheres
[NASA-CR-182443] 23 p3300 N88-29653
Variation in the thickness of ejecta cover on Mars with increasing crater density 23 p3307 N88-29701
Simulation of Vulcain engine operation at low inlet pressure
[ETN-88-93083] 24 p3339 N88-29875
Finite-difference simulations of Rayleigh-wave scattering by shallow heterogeneity
[AD-A194961] 24 p3402 N88-30259
Simulation of a two link robot manipulator with elastic members
[AD-A196014] 24 p3422 N88-30368
Waveform relaxation applied to transient device simulation
[AD-A194992] 24 p3432 N88-30429
Simulations of lava flows on Mars
24 p3443 N88-30495

SIMULATOR TRAINING

U TRAINING SIMULATORS

SIMULATORS

NT COCKPIT SIMULATORS
NT CONTROL SIMULATION
NT FLIGHT SIMULATORS
NT MOTION SIMULATORS
NT SHOCK SIMULATORS
NT SOLAR SIMULATORS
NT SPACE SIMULATORS
NT TRAINING SIMULATORS
NT VERTICAL MOTION SIMULATORS
NT VIBRATION SIMULATORS
Infra-red lamp panel study and assessment application to thermal vacuum testing of sigma telescope
02 p0132 N88-10830
The Hermes-3 program
[DE87-012132] 02 p0234 N88-11473
New main reflector, subreflector and dual chamber concepts for compact range applications
[NASA-CR-181506] 04 p0402 N88-12498
SCRAM JET (Supersonic Combustion Ramjet) combustion experiments 04 p0404 N88-12512
On the simulation of ballistic shock loads
05 p0593 N88-13615
Tutoring electronic troubleshooting in a simulated maintenance work environment
09 p1204 N88-17215
Design of a neural network simulator on a transputer array 09 p1205 N88-17221
Table with aerostatic bearings for simulation in one degree of freedom of Attitude Control Systems of artificial satellites
[INPE-4320-TDL/287] 11 p1445 N88-18617
A dynamic analysis of the parallel-plate EMP (electromagnetic pulse) simulator using a wire mesh approximation and the numerical electromagnetics code
[AD-A187535] 11 p1470 N88-18767
RELIC: A reliability simulator for integrated circuits
[AD-A187493] 11 p1477 N88-18811
Computational studies of wave-shaping in a blast simulator by perforated plates in the driver
[AD-A188200] 11 p1483 N88-18850
Reaction wheel experimental model of artificial satellite attitude control: Construction, simulation, and tests
[INPE-4274-PRE/1146] 11 p1490 N88-18896
The Hermes manipulation system (HERA) simulation facility development 12 p1591 N88-19524
A methodology for hardware verification based on logic simulation
[AD-A188553] 12 p1622 N88-19704
A digital circuit design environment
[AD-A188831] 12 p1623 N88-19709
Engine flow simulation for wind tunnel testing at NLR
[NLR-MP-87011-U] 13 p1723 N88-20305
A microprocessor-based real-time simulator of a turbofan engine
[NASA-TM-100889] 14 p1868 N88-21163
A packet-switched wide-area communication network simulator
[FUB-3-1986] 14 p1905 N88-21381
The effects of torque response and time delay on rotorcraft vertical axis handling qualities
[AD-A189873] 15 p2017 N88-22023
Development and evaluation of an airplane fuel tank ullage composition model. Volume 2: Experimental determination of airplane fuel tank ullage compositions
[AD-A190408] 15 p2017 N88-22025
Real-time stressed channel simulator
[AD-A190223] 15 p2025 N88-22067
A UNIX-based interactive VHDL (hardware description language) simulator
[AD-A189749] 15 p2109 N88-22565
Construction of a satellite simulator for the frequency range between 11.7 and 12.5 GHz
[IRT-TB-B-84/87] 16 p2166 N88-22917
Preliminary measurements of heat flux in a subsonic gun simulator
[AD-A191090] 16 p2208 N88-23178
Development of an airborne facility for advanced avionics research 17 p2307 N88-23801
Safety aspects in design and operation practice of GKSS underwater simulation plant GUSI
19 p2698 N88-26037
Research in electromagnetic shielding theory. Part 2: EMP (electromagnetic pulse) simulation using small loops
[AD-A192882] 20 p2791 N88-26558
The UMAC simulator 20 p2834 N88-26811
Can CNV amplitude predict ability to accomplish a demanding task? 21 p2980 N88-27700
Block Oriented Simulation System (BOSS)
[NASA-CR-182947] 21 p2995 N88-27760
Goldstone solar system radar performance analysis
22 p3068 N88-28206
The p-well or n-well CMOS technology for advanced SEU-hard SRAMs
[DE88-006845] 22 p3156 N88-28777

SIMULTANEOUS IMAGE CORRELATOR

U IMAGE CORRELATORS

SINE WAVES

On simultaneous estimation of the number of signals and frequencies under a model with multiple sinusoids
[AD-A186026] 07 p0913 N88-15543
On rate of convergence of equivariation linear prediction estimates of the number of signals and frequencies of multiple sinusoids
[AD-A186034] 07 p0914 N88-15549
Fatigue effects of a swept sine test
08 p0999 N88-16054
Overview of multi-input frequency domain modal testing methods with an emphasis on sine testing
11 p1499 N88-18949
Sinusoidal transform coding 19 p2653 N88-25752

SINGLE CHANNEL PER CARRIER TRANSMISSION
Ionospheric total electron content estimation for single-frequency global positioning system receivers
02 p0161 N88-11005
Measured noise performance of a direct-sequence spread-spectrum system and a comparison of single vice dual-channel delay-lock loops
[AD-A186288] 07 p0843 N88-15110
SINGLE CRYSTALS
Energy-selected electron diffraction experiments using the rocking-crystal method in the raster microscope for the investigation of localization effects in single crystals
[ETN-87-90409] 01 p0104 N88-10682
Constitutive modeling for single crystal superalloys
02 p0187 N88-11168
Constitutive modeling of superalloy single crystals with verification testing 02 p0188 N88-11169
Creep-fatigue behavior of NiCoCrAlY coated PWA 1480 02 p0189 N88-11176
Production of metallic monocrystals described
03 p0286 N88-11796
Consortium for Materials Development in Space. Technical section
[NASA-CR-181508] 03 p0296 N88-11859
Materials preparation and longevity in hyperthermal atomic oxygen 03 p0297 N88-11862
Investigation of two laser beam coupling and amplification in Ce-doped SBN single crystals
03 p0327 N88-12069
Determination of the origin of self-pumped phase conjugation in barium titanate
[AD-A184697] 03 p0377 N88-12372
Monocrystal sputtering by the computer simulation code ACOCT
[IPPJ-848] 04 p0493 N88-13035
Evaluation of the Mellen EDG furnace for growth of large diameter GaAs single crystals in a horizontal configuration
[DE88-000463] 04 p0498 N88-13068
The structure of adsorbed sulfur and carbon on molybdenum and rhenium single crystal surfaces, and their influence on carbon monoxide and hydrocarbon chemisorption
[DE88-001393] 04 p0499 N88-13073
Environmentally assisted cracking: Overview of evidence for an adsorption-induced localised-slip process
[AD-A185175] 05 p0565 N88-13443
Surface deformation and fatigue crack initiation of alpha-iron 05 p0598 N88-13651
Low cycle fatigue behaviour of notched specimens of nickel based superalloy single crystal
05 p0605 N88-13712
An overview of fatigue 05 p0608 N88-13729
Preparation and characterization of members of the system (Zn,Se)1-xGaPx
[AD-A185073] 05 p0655 N88-14019
New application of transition metal carbides detailed
06 p0675 N88-14132
Growth of solid solution single crystals
[NASA-TP-2787] 06 p0688 N88-14212
High temperature low cycle fatigue of oxide dispersion strengthened and single crystal nickel base superalloys
06 p0720 N88-14422
Orientation effects in copper single crystals fatigued at elevated temperatures 06 p0720 N88-14423
Coverage dependence of adsorbate-substrate bond lengths: Chlorine and caesium adsorbed on silver single crystals
[PB87-125142] 06 p0788 N88-14833
Grain boundary and surface diffusion in oxides
[DE88-002348] 07 p0938 N88-15697
Low field characterization of YBa2Cu3O sub 7-delta single crystals
[DE88-002895] 07 p0938 N88-15700
A laboratory study of tin whisker growth
[ESA-STR-223] 08 p1089 N88-16553
Epitaxial growth and new phase of single crystal Dy by molecular beam epitaxy
[DE88-002850] 09 p1256 N88-17531
CdTe(110)-Mn interface reaction and the formation of non-equilibrium ternary semimagnetic semiconductor alloys
[AD-A187593] 10 p1422 N88-18491
Single-crystal structural study of La2Cu/sub 0.95/Li/sub 0.05/O4
[DE88-003482] 11 p1554 N88-19302
Silicon and indium doping of GaAs: Measurements of the effect of doping on mechanical behavior and relation with dislocation formation
[DE88-003862] 11 p1554 N88-19303
Autonomous Liquid Encapsulated Czochralski (LEC) growth of single crystal GaAs by intelligent digital control
[AD-A187211] 11 p1555 N88-19305
Preparation and characterization of Cu2Zn1-xMnxGeS4
[AD-A188113] 11 p1556 N88-19315
An in situ annealing study of lead implanted single crystal calcium titanate
[DE88-005435] 11 p1562 N88-19351
The cyclic stress-strain behavior of a single crystal nickel-base superalloy
[NASA-TM-100269] 12 p1607 N88-19610
Contact and current noise in beta alumina and Nasicon ceramics
[AD-A189168] 12 p1611 N88-19635
The effects of temperature and strain rate on the yielding behavior of the single crystal superalloy PWA 1480
14 p1931 N88-21517
The elastic properties of monoclinic ZrO2
[DE88-005920] 14 p1986 N88-21847
Bithermal fatigue of a nickel-base superalloy single crystal
[NASA-TM-100885] 15 p2042 N88-22168
Single crystal growth by laser CVD
15 p2050 N88-22213
Unified constitutive model for single crystal deformation behavior with applications 15 p2078 N88-22388
The kinetics of contact noise in NaBeta alumina
[AD-A190651] 15 p2130 N88-22707
An investigation of the crystalchemistry and thermochemistry of selected mineral systems
[AD-A189758] 15 p2142 N88-22781
Dispersion measurements of microcrystals in the near ultraviolet and infrared
[DE88-006234] 15 p2145 N88-22800
Fatigue crack growth behavior of a single crystal alloy as observed through an in situ fatigue loading stage
[NASA-TM-100863] 16 p2179 N88-22986
UV-Laser reactions of molecular adsorbates
[AD-A190796] 16 p2212 N88-23201
SSME single-crystal turbine blade dynamics
16 p2221 N88-23257
Defects in cubic silicon carbide on silicon
17 p2408 N88-24317
Interaction of slow neutrons with Ge74 single crystals
[DE87-703010] 17 p2445 N88-24536
Isothermal and bithermal thermomechanical fatigue behavior of a NiCoCrAlY-coated single crystal superalloy
[NASA-TM-100907] 18 p2489 N88-24766
Resolved shear stress intensity coefficient and fatigue crack growth in large crystals
[NASA-CR-182137] 18 p2528 N88-24997
Electronic controller for reciprocating rotary crystallizer
[NASA-TM-101140] 18 p2584 N88-25354
Stress modeling of microdiaphragm pressure sensors
19 p2670 N88-25873
Accelerated fatigue crack growth behavior of PWA 1480 single crystal alloy and its dependence on the deformation mode
[NASA-TM-100943] 20 p2772 N88-26436
Development of a model procedure for the determination of volume diffusion lengths by transient measurements on monocrystal silicon solar cells
[ETN-88-92119] 20 p2821 N88-26733
Anisotropic characteristic lengths in single crystal YBa2Cu3O(sub 7-Delta)
[DE88-009959] 20 p2877 N88-27080
Pure metallic bridge and point-contact tunneling into single- and polycrystal YBa2Cu3O(sub 7-y)
[DE88-010030] 20 p2878 N88-27084
Electron irradiation effects in YBa2Cu3O7-Delta single crystals
[DE88-010050] 20 p2878 N88-27085
Mechanism of the nitric oxide-carbon monoxide-oxygen reaction over a single crystal rhodium catalyst
[DE88-006274] 21 p2910 N88-27268
Energy migration, motion and order in synthetic polymers
[AD-A193334] 21 p2918 N88-27320
Silicon-on-insulator pin diodes
[AD-A193359] 21 p2937 N88-27445
Experimental fabrication of thin film single crystalline solar cells
[PB88-131958] 21 p2967 N88-27627
Growth and characterization of CuGaS2, CuAlS2 and CuGa0.9Al0.1S2 single crystals
[AD-A192963] 21 p3021 N88-27930
Experimental fabrication of thin film single crystalline solar cells
[PB88-131958] 22 p3116 N88-28516
Effect of neutron irradiation on critical magnetization current in single crystal YBa2Cu3O(sub 7-delta)
[DE88-009970] 22 p3156 N88-28775
Preparation and testing of Nb-Zr and Nb-ZrO2 single crystals for deformation studies
[DE88-702798] 23 p3293 N88-29613
Anisotropic constitutive modeling for nickel-base single crystal superalloys
[NASA-CR-182157] 24 p3353 N88-29961
Streaking images that appear only in the plane of diffraction in undoped GaAs single crystals: Diffraction imaging (topography) by monochromatic synchrotron radiation
[NASA-CR-183267] 24 p3433 N88-30437
SINGLE ENGINE AIRCRAFT
NT F-16 AIRCRAFT
NT F-106 AIRCRAFT
NT MIG AIRCRAFT
NT MIRAGE AIRCRAFT
NT T-33 AIRCRAFT
SINGLE EVENT UPSETS
MARECS-A case 03 p0274 N88-11729
Comparison of 2D memory SEU transport simulation with experiments
[ATR-86(8139)-2-REV-A] 05 p0656 N88-14025
Effects of cosmic rays on single event upsets
[NASA-CR-183053] 20 p2793 N88-26569
The effects of total dose on the SEU sensitivity of CMOS static RAMS — single event upset (SEU), satellite components
[AERE-R-12779] 24 p3428 N88-30401
The Single Event Upset (SEU) test facility on the Hardwell tandem generator for cosmic ray simulation
[AERE-R-12896] 24 p3459 N88-30580
SINGLE INSTRUCTION MULTIPLE DATA STREAM
U SIMD (COMPUTERS)
SINGLE STAGE ROCKET VEHICLES
NT BLACK BRANT SOUNDING ROCKETS
Ballistic Single Stage Carrier Vehicle (BETA): A single stage reusable ballistic space shuttle concept
[MBB-UR-949/70] 10 p1310 N88-17828
SINGLE STAGE TO ORBIT VEHICLES
NT HOTOL LAUNCH VEHICLE
SINGLE-PHASE FLOW
Theoretical prediction of single phase turbulent flow distribution in particulate bed reactors
17 p2419 N88-24386
SINGULAR INTEGRAL EQUATIONS
A quadrature formula for a double-pole singular integral
[PD-FM-8725] 04 p0485 N88-12990
Potential flow around two-dimensional airfoils using a singular integral method
[NASA-CR-182345] 06 p0664 N88-14070
A spline collocation method for integral equations of the first kind with logarithmic singularity — boundary value problems
[REPT-87-39] 14 p1963 N88-21712
SINGULARITY (MATHEMATICS)
Breakdown of steady and unsteady interacting boundary layers
[NLR-MP-86047-U] 01 p0045 N88-10284
Study of closed loop control singularity in dynamic systems with a constraint on the final state
[LAAS-87-180] 02 p0223 N88-11405
Singularity expansion method: Target Resonances
03 p0303 N88-11912
The hybrid wavefront resonance method
03 p0303 N88-11913
Singularities in X-ray spectra of metals
[DE88-001440] 06 p0681 N88-14174
The effect of response scaling on the detection of singularities in multiresponse estimation
[AD-A185964] 07 p0908 N88-15503
Anomalous scaling laws in multifractal objects
[NOTA-INTERNA-883] 07 p0916 N88-15565
Boundary elements combined with singular fields for three-dimensional cracked solids
[RAE-TR-87038] 09 p1183 N88-17088
Criterion of singularity in general theory of relativity
09 p1240 N88-17430
Numerical-experimental investigation of singularity at a crack in nonlinear rubber elasticity
11 p1500 N88-18961
Singular Lagrangians. Classical dynamics and quantization. Lectures for young scientists
[DE88-701158] 15 p2146 N88-22806
Formal solution of differential linear systems in the proximity of a singularity
[ETN-88-92190] 16 p2258 N88-23495
Approximation and representation of explicit surfaces in the presence of singularities
[ETN-88-92191] 16 p2258 N88-23496
Analysis and modeling of complex non-stationary flows
[PB88-127188] 19 p2664 N88-25842
Linearization along invariant manifolds and a generalization of the Hartman-Grobman theorems for degenerate singularities of vector fields in R cubed
[REPT-87-80] 20 p2845 N88-26886
The analysis and control of robotic manipulators operating at or near kinematically singular configurations
22 p3084 N88-28315

A singular perturbation analysis of the weakly nonlinear evolution of long and short water waves and waves in boundary layers 23 p3209 N88-29102
A minimax method for a class of Hamiltonian systems with singular potentials
[AD-A193478] 23 p3270 N88-29453

SINKS
NT HEAT SINKS

SINKS (GEOLOGY)
U STRUCTURAL BASINS

SINTERED ALUMINUM POWDER
Microdesigning of lightweight/high strength ceramic materials
[AD-A188526] 12 p1610 N88-19631
Characterization of 7090 and 7091 profiles made with Cegedur powder — powder metallurgy, aircraft construction materials
[REPT-48-441/F] 18 p2487 N88-24752

SINTERING
Toughening of alpha-alumina: Preliminary results
[DE87-702776] 01 p0028 N88-10178
Analytical electron microscopy characterization of boron in sintered alpha-SiC
[DE87-012532] 02 p0142 N88-10889
Needs assessment for NDT and characterization of ceramics: Assessment of inspection technology for green state and sintered ceramics
[DE87-013550] 02 p0151 N88-10947
Structure and grain coarsening during the processing of engineering ceramics
[NASA-TM-100235] 03 p0293 N88-11838
Cast iron freezing mechanisms 03 p0298 N88-11870
Research and development on high strength ceramic heaters discussed 04 p0404 N88-12508
Sintered steels of high resistance alloyed to Nb, Mo, Mn and Si
[DE87-703546] 04 p0415 N88-12573
Studies of alumina additions in zirconia - magnesia
[DE87-703500] 04 p0419 N88-12602
Fatigue failure of thin porous strips 04 p0426 N88-12640
Corrosion resistance of sintered alloy steels
[BLL-M-37363-(5828.4)] 05 p0564 N88-13438
Properties of refractory metals processed by enhanced sintering treatments
[AD-A184944] 05 p0565 N88-13440
Results from the melting of tungsten composites under microgravity (TEXUS 10 flight)
[FOA-C-20676-2.1] 05 p0571 N88-13482
Crack propagation properties of sintered steel 05 p0604 N88-13698
Metallurgical processes in multi-component rare earth-transition metal permanent magnet alloys
[AD-A186401] 07 p0832 N88-15045
Techniques for ceramic sintering using microwave energy
[DE88-001416] 07 p0837 N88-15080
The use of NMR imaging to measure porosity and binder distributions in green-state and partially sintered ceramics
[DE88-003099] 08 p0972 N88-15881
Improved silicon nitride for advanced heat engines
[NASA-CR-175006] 08 p0973 N88-15886
The migration of grain boundaries in ceramic materials with particular reference to the sintering process
[DE88-004085] 10 p1306 N88-17808
High temperature processing of superconducting Y1Ba2Cu3O6.9
[DE88-003002] 10 p1416 N88-18449
Improved magnetization for YBa2Cu3O/sub 7-delta annealed in oxygen above 1000 C
[DE88-003934] 10 p1418 N88-18469
Freestanding films of YBa2Cu3O/sub 6.9/
[DE88-003995] 10 p1419 N88-18471
Deactivation of alumina based catalysts 11 p1455 N88-18673
Composite ceramic superconducting filaments for superconducting cable
[AD-A187833] 11 p1556 N88-19312
Effect of rigid inclusions on sintering
[DE88-005745] 12 p1609 N88-19623
Mass transport and chemical demixing of Y-Ba-Cu-O compounds during sintering in temperature gradients
[DE88-004887] 12 p1696 N88-20151
Processing of nanophase ceramics
[DE88-005985] 13 p1752 N88-20475
The unique characteristics of the structure of composite materials made on a base of sphalerite-analogous boron nitride 14 p1886 N88-21273
Development, high temperature properties, and microanalysis of nonoxide ceramics
[ETN-88-92103] 14 p1893 N88-21304
Processing, texture and mechanical properties of sintered silicon carbide
[NASA-TT-20253] 14 p1893 N88-21305
Microwave sintering of alumina-SiC composites at 2.45 and 60 GHz
[DE88-006455] 15 p2030 N88-22095
Titanium powder frit made during the transformation alpha-beta
[ETN-88-91999] 16 p2177 N88-22976
Improved silicon carbide for advanced heat engines 17 p2324 N88-23879
Strength optimization of alpha-SiC by improved processing 17 p2324 N88-23880
Improved silicon nitride for advanced heat engines 17 p2324 N88-23881
Improved processing of Si3N4 17 p2325 N88-23882
High frequency ultrasonic characterization of sintered SiC
[NASA-TM-100825] 17 p2347 N88-23985
Martensitic transformation and microstructures in sintered NiAl alloys
[NASA-TT-20178] 18 p2488 N88-24761
Martensitic transformation and microstructures in sintered NiAl alloys
[NASA-TT-20192] 19 p2616 N88-25519
Assessment of opportunities for gas-fired sintering in the advanced ceramics and powdered metals industries
[PB88-197157] 19 p2620 N88-25545
Sintering of the heterogeneous MgO compacts
[DE88-010357] 20 p2767 N88-26408
Manufacturing of a ceramic-ceramic composite matrix using the sol-gel procedure
[ETN-88-92157] 20 p2768 N88-26414
Preparation of oxide superconductors
[DE88-009136] 20 p2875 N88-27063

SINUSOIDS
U SINE WAVES

SIR-A
U SHUTTLE IMAGING RADAR

SIR-B
U SHUTTLE IMAGING RADAR

SIRTF
U SPACE INFRARED TELESCOPE FACILITY

SIS (SEMICONDUCTORS)
Optimization of SIS mixer elements
[NASA-CR-180710] 01 p0104 N88-10680
Quantum limits of superconducting heterodyne receivers
[AD-A188014] 11 p1478 N88-18817

SITE SELECTION
Siting and Geotechnical Program Focus and Directions. Report upon the deliberations of a workshop held at the Illinois Institute of Technology, Chicago, Illinois on August 4-5, 1986
[PB87-206272] 02 p0198 N88-11238
On the exact solution of large-scale simple plant location problems
[FI-032-TB-22E] 02 p0229 N88-11441
Use of SPOT images for coastal development and inventory of aquacultural sites in New Caledonia (ALIAS project). First results 03 p0344 N88-12175
Variability of wind power near Oklahoma City and implications for siting of wind turbines
[DE88-000444] 04 p0470 N88-12902
Cape Blanco wind farm feasibility study
[DE88-003748] 10 p1348 N88-18059
The evaluation and selection of a 5th ground antenna site for the global positioning system
[AD-A189495] 13 p1720 N88-20286
Environmental assessment for the compact ignition Tokamak
[DE88-005633] 15 p2135 N88-22740
Utilization of LANDSAT-TM, for aiding in the localization of archeological sites in the state of Sao Paulo 17 p2362 N88-24069
Review of numerical methods for radionuclide transport in three-dimensional porous media, at high Peclet numbers
[CFDU/87/10] 18 p2538 N88-25061
Extremely Low Frequency (ELF) communications system ecological monitoring program: Summary of 1986 progress
[AD-A192014] 19 p2642 N88-25676
Australian structures response evaluation: Ground shock and air blast measurements for site investigation survey
[MRL-TN-526] 20 p2813 N88-26685
Review of geographic processing techniques applicable to regional analysis
[DE88-010759] 21 p2970 N88-27643
SPOT: A tool to aid preselection of sites favorable for aquiculture. Evaluation and perspectives of the Preliminary Evaluation Program for SPOT (PEPS) ALIAS Caledonie 22 p3108 N88-28456
Geology of six possible Martian landing sites 23 p3304 N88-29682

SITES
NT LANDING SITES
NT LAUNCHING PADS
NT LAUNCHING SITES
Atmospheric diffusion at coastal site in presence of sea-breeze
[DE88-700038] 07 p0876 N88-15314
An analytic model for ionization distributions produced in nanometer sites by protons
[DE88-003943] 10 p1406 N88-18385
Lunar fiberglass: Properties and process design
[NASA-CR-182580] 11 p1466 N88-18740
Site effects on wind characteristics at a turbine rotor
[DE88-005135] 11 p1507 N88-19003
Crustal Dynamics Project: Catalogue of site information
[NASA-RP-1198] 11 p1513 N88-19037
Maps for tourists. A systematic approach to tourist cartography 16 p2227 N88-23296

SITTING POSITION
Sitting posture of helicopter pilots of the Royal Netherlands Air Force; preliminary recommendations
[IZF-1986-16] 05 p0631 N88-13857
Sitting posture of pilots in the Boelkow 105c helicopter
[IZF-1986-22] 09 p1202 N88-17202

SIZE (DIMENSIONS)
NT GRAIN SIZE
The effect of size and surface on the lifetime prediction of StE 460 notched bars
[FD-6/1986] 01 p0058 N88-10374
Estimating payload internal temperatures and radiator size for multimegawatt space platforms
[DE88-000244] 03 p0275 N88-11738
Rayleigh scattering measurements of a freejet with homogeneous condensation 03 p0319 N88-12020
Scaling of size/time/temperature associated with dilatation and distortion in uniaxial specimens 03 p0336 N88-12117
Titanium oxide absorption and spot sizes in II Peg, HR 1099 and UX Ari 04 p0508 N88-13126
The filtering problem for infinite dimensional stochastic processes
[AD-A186431] 07 p0916 N88-15562
Size effects in linear elastic fracture mechanics 21 p2964 N88-27609

SIZE DETERMINATION
Results from a questionnaire on particulate metrology in the UK
[NPL-MOM-81] 09 p1141 N88-16841
Electrohydrodynamic migration of charged droplets in an insulating fluid
[NASA-TM-100849] 14 p1912 N88-21424
Combined aerodynamic size, charge-to-mass, and velocity measurements of aerosol particles
[ST-REPT-VOL-5-NO-4] 14 p1944 N88-21599
Consequences of the size determination of P/Halley by space probes on the scale of sizes of cometary nuclei 14 p2009 N88-21986
Gas turbine smoke measurement: A smoke generator for the assessment of current and future techniques 24 p3348 N88-29930
Particle size measurements in sooting combustion systems 24 p3348 N88-29931
The effect of particle properties on radiative heat transfer 24 p3350 N88-29941

SIZE DISTRIBUTION
NT PARTICLE SIZE DISTRIBUTION
Cavitation inception scale effects. 1. Nuclei distributions in natural waters. 2. Cavitation inception in a turbulent shear flow
[AD-A186553] 08 p0988 N88-15987
Approximating the size of a dynamically growing asynchronous distributed network
[AD-A187011] 09 p1152 N88-16899
Cometary magnitude distribution: The tabulated data 14 p1995 N88-21888
Information analysis of integral equations in remote sensing of atmospheric aerosols 18 p2532 N88-25022
Small-droplet spray measurements with a scattered-light scanner
[NASA-TM-100973] 20 p2806 N88-26645
Holographic determination of droplet size distributions
[DFVLR-MITT-88-05] 22 p3074 N88-28250

SIZE SEPARATION
Size-reduction and sorting behavior in sieve hammer mills
[ETN-88-91480] 11 p1467 N88-18749

SIZING (SEPARATION)
U SIZE SEPARATION

SIZING (SHAPING)
Mission requirements and aircraft sizing 05 p0545 N88-13317

SKELETON
U MUSCULOSKELETAL SYSTEM

SKEWNESS
Extrema of skewed stable processes
[AD-A185422] 05 p0642 N88-13925
Dual cylindrical wave Laser-Doppler method for measurement of skin friction in fluid flow
06 p0700 N88-14297
SKILLS
U ABILITIES
SKIN (ANATOMY)
Local human skin potential: Spatial distribution, magnitude and origin
[DE87-012882] 01 p0075 N88-10480
DNA damage and repair in human skin in situ
[DE87-014288] 03 p0356 N88-12241
Effect of antiorthostatic position and different illumination on sensitivity of skin in upper half of the body to ultraviolet radiation 10 p1363 N88-18145
Experimental research on skin reflection, transmission, absorption of light rays 16 p2187 N88-23039
SKIN (STRUCTURAL MEMBER)
Damage tolerance of stiffened-skin structures: Prediction and experimental verification
[NLR-MP-86041-U] 06 p0667 N88-14091
Absorption of cyclotron radiation in skin layer in Araks experiment 08 p1003 N88-16076
Low frequency eddy current detection and evaluation of corrosion in aircraft skins
[ETN-88-91664] 09 p1144 N88-16859
SKIN FRICTION
NT AERODYNAMIC DRAG
NT FRICTION DRAG
NT SUPERSONIC DRAG
NT VISCOUS DRAG
Effect of viscosity on a vertical cylinder due to surface waves
[ETN-87-90960] 02 p0171 N88-11075
Dual cylindrical wave Laser-Doppler method for measurement of skin friction in fluid flow
06 p0700 N88-14297
Overview of the Langley viscous drag reduction program 07 p0812 N88-14946
Riblets for aircraft skin-friction reduction
07 p0814 N88-14955
Airfoil large eddy breakup devices for turbulent drag reduction 07 p0814 N88-14956
A method for the approximate calculation of the skin friction coefficient of horizontal wavy plates
[VKI-TN-160] 07 p0851 N88-15172
A review of approaches to the study of turbulence modification by means of non-Newtonian additives
[AD-A188799] 12 p1627 N88-19734
Enhanced viscous flow drag reduction using acoustic excitation
[NASA-CR-182734] 15 p2062 N88-22295
Boundary layer measurements using hot-film sensors
17 p2297 N88-23743
Manipulation of the structure of a turbulent boundary layer 18 p2512 N88-24901
The determination of the topological structure of skin friction lines on a rectangular wing-body combination
[NASA-CR-4168] 20 p2753 N88-26343
A new method of calculating the boundary layer characteristics downstream of manipulators. Part 2: Skin friction and net drag reduction
[PNR90456] 22 p3078 N88-28280
Skin friction balance
[NASA-CASE-LAR-13710-1] 23 p3216 N88-29145
Development and design of windtunnel and test facility for RPV (Remote Piloted Vehicle) enhancement devices
[AD-A194842] 24 p3329 N88-29822
SKIN RESISTANCE
Interaction of acoustic and electromagnetic waves involved in anomalous skin effect
08 p1079 N88-16503
Estimation of body fluid shift by electrical impedance in various postures 12 p1661 N88-19956
SKIN TEMPERATURE (BIOLOGY)
Temperature regulation at rest and exercise during the human menstrual cycle
[AD-A186461] 08 p1050 N88-16341
Analysis of annular microstrip antennas for hyperthermic applicators
[PB88-181508] 19 p2643 N88-25679
Physiological responses to acute exercise-heat stress
[AD-A192606] 21 p2986 N88-27732
Depressed sweating during exercise at altitude
[AD-A192603] 22 p3130 N88-28609
SKIN TEMPERATURE (NON-BIOLOGICAL)
Correlations of velocity and temperature fluctuations in the stagnation-point flow of circular cylinder in turbulent flow
[NASA-TM-100930] 19 p2597 N88-25435
SKIS
Airworthiness and flight characteristics test of a ski assembly for the UH-60A Black Hawk helicopter
[AD-A191414] 16 p2162 N88-22895
SKULL
Realistic conductivity geometry model of the human head for interpretation of neuromagnetic data
[PB88-112230] 10 p1369 N88-18179
SKY
NT NIGHT SKY
Unified Sun and sky illumination for shadows under trees
[DE87-014232] 01 p0083 N88-10535
ISTP SBIR phase 1 Full-Sky Scanner: A feasibility study
[NASA-CR-180749] 10 p1333 N88-17964
Analysis of deep sky sources found by the infrared astronomy satellite
[AD-A189605] 13 p1853 N88-21089
Effects of atmospheric model layering on LOWTRAN 6 calculations of 8-12 micrometers near-horizon sky radiances
[AD-A192969] 20 p2791 N88-26559
SKY BRIGHTNESS
IR (infrared) sky radiance distributions in the marine boundary layer
[AD-A193683] 22 p3119 N88-28531
SKY RADIATION
NT AIRGLOW
NT DAYGLOW
NT GEOCORONAL EMISSIONS
NT NIGHTGLOW
Sky radiance distributions for thermal imaging backgrounds
[AD-A191135] 17 p2373 N88-24115
SKY SURVEYS (ASTRONOMY)
A search for X-ray luminous late type stars in NIPSS data 04 p0511 N88-13143
A search for very low mass (brown dwarf) stars as wide binaries using a seven element infrared camera-photometer 04 p0512 N88-13150
A VLA survey of dMe flare stars
04 p0513 N88-13154
An automated supernova search and the design strategy
[DE88-001827] 05 p0660 N88-14051
A sky temperature survey at 19.2 GHz using a balloon borne Dicke radiometer for anisotropy tests of the cosmic microwave background 11 p1571 N88-19403
The imaging of extra-galactic low-energy gamma-ray sources prospects, techniques, and instrumentation
[NASA-CR-182536] 12 p1713 N88-20251
Survival analysis, or what to do with upper limits in astronomical surveys
[NASA-CR-182936] 17 p2449 N88-24551
Ultraviolet spectra of subluminous objects found in the Kiso Schmidt survey and systematic reanalysis of the archived ultraviolet spectra of white dwarfs observed with the IUE satellite under the Astrophysics Data Program (ADP)
[NASA-CR-182976] 18 p2592 N88-25406
Investigation of the diffuse ultraviolet background with DE data
[NASA-CR-182863] 19 p2741 N88-26271
A survey of the Ap stars for rapid variability
20 p2884 N88-27127
SKY WAVES
NT WHISTLERS
SKYLAB PROGRAM
Earth resources: A continuing bibliography with indexes (issue 55)
[NASA-SP-7041(55)] 01 p0065 N88-10415
SKYLARK
U SKYLARK ROCKET VEHICLE
SKYLARK ROCKET VEHICLE
Skylark sounding rocket development-Skylark 8
08 p1035 N88-16274
SLABS
Fracture mechanisms and strengthening of slab lasers
[DE88-004002] 11 p1493 N88-18914
SLANT
U SLOPES
SLANT PERCEPTION
U SPACE PERCEPTION
SLEDS
NT ROCKET PROPELLED SLEDS
SLEEP
NT HYPNOSIS
Sleep and wakefulness: Handbook for flight medical officers, second edition
[AGARD-AG-270(E)] 02 p0217 N88-11366
Neurophysiological analysis of hypothalamic regulation mechanisms of primary sleep and hypobiosis
06 p0751 N88-14611
Sleep induced in cat by electric stimulation of acoustic and motor areas in brain cortex
06 p0751 N88-14612
Model based monitoring of human sleep stages
[ISBN-90-9001448-9] 06 p0752 N88-14618
Pharmacological resetting of the Circadian sleep-wake cycle
[AD-A186194] 07 p0889 N88-15385
Discrete adaptation to sensory conflict
10 p1363 N88-18146
Neurohumoral aspects of sleep
[AD-A188653] 12 p1667 N88-19992
The application of non-stationary data analysis techniques in the identification of changes in the electroencephalogram associated with the onset of drowsiness 21 p2978 N88-27688
Psychophysiological measures of drowsiness as estimators of mental fatigue and performance degradation during sleep deprivation 21 p2980 N88-27702
SLEEP DEPRIVATION
Sleep and wakefulness: Handbook for flight medical officers, second edition
[AGARD-AG-270(E)] 02 p0217 N88-11366
Assessment of physical activity intensity by heart rate during sleep limited military operations
[AD-A185913] 07 p0888 N88-15382
Pharmacological resetting of the Circadian sleep-wake cycle
[AD-A186194] 07 p0889 N88-15385
Role of adenosine analogs and growth hormone in waking and sleep
[AD-A187897] 11 p1519 N88-19070
Napping and human functioning during prolonged work
[AD-A190228] 15 p2102 N88-22525
Psychophysiological measures of drowsiness as estimators of mental fatigue and performance degradation during sleep deprivation 21 p2980 N88-27702
SLENDER BODIES
NT SLENDER CONES
Computational study of three-dimensional wake structures
[REPT-2] 05 p0539 N88-13281
Calculations of the turbulent wake behind a slender self-propelled double-body and comparisons with experiment
[AD-A185661] 06 p0703 N88-14314
Centerplane source distribution for slender bodies
10 p1328 N88-17940
Experimental research on center of pressure of slender body with two pointed ends 14 p1864 N88-21137
The calculation of transonic flow over the shuttle orbiter using slender body theory 18 p2460 N88-24606
Finite element solution of 3-D turbulent Navier-Stokes equations for propeller-driven slender bodies
18 p2515 N88-24919
Forces and moments on a slender, cavitating body
[DE88-007208] 21 p2945 N88-27491
A calculation of the turbulent boundary layer on a slender ellipsoid at low incidence
[FFA-TN-1988-02] 23 p3213 N88-29126
Semi-empirical methods for conventional and unconventional missiles 24 p3318 N88-29758
SLENDER CONES
The drag of slender axisymmetric cones in rarefied hypersonic flow 05 p0531 N88-13229
SLENDER WINGS
A theory for the core flow of leading-edge vortices
07 p0810 N88-14935
Calculated unsteady aerodynamics of wings
[AD-A189608] 12 p1574 N88-19415
Optimal control of the wing rock phenomenon
21 p2927 N88-27373
High-aspect-ratio wings 23 p3167 N88-28859
Delta wing configurations 23 p3167 N88-28860
SLEWING
Dynamics of spacecraft control laboratory experiment (SCOLE) slew maneuvers
[NASA-CR-4098] 01 p0014 N88-10082
Recent advances in structural dynamics of large space structures
[NASA-TM-100513] 02 p0138 N88-10867
Combined problem of slew maneuver control and vibration suppression
[NASA-CR-181537] 04 p0455 N88-12817
The dynamics and control of large-flexible space structures, part 10
[NASA-CR-182426] 08 p0963 N88-15830
Large-angle slewing maneuvers for flexible spacecraft
[NASA-CR-4123] 08 p1000 N88-16060
Slew-induced deformations in a space-based electromagnetic rail gun 21 p2929 N88-27385
SLIDING
The wear process during the RUNNING-IN of steel in lubricated sliding
[NAL-TR-922T] 02 p0181 N88-11130
Dynamic analysis of a structure with sliding base
08 p0998 N88-16045
Sliding charge density waves and related problems
[AD-A186720] 09 p1157 N88-16934

Friction and wear of monolithic and fiber reinforced silicon-ceramics sliding against IN-718 alloy at 25 to 800 C in atmospheric air at ambient pressure
[NASA-TM-100294] 10 p1304 N88-17796
Stable, robust tracking by sliding mode control
[AD-A188278] 10 p1401 N88-18358
The flying characteristics of the membrane slider bearing 18 p2522 N88-24965

SLIDING CONTACT
Traction model development
[AD-A188450] 15 p2073 N88-22359

SLIDING FRICTION
The development of a friction model predicting the sliding behavior of materials pairs, especially at low temperatures: Progress report and renewal proposal
[DE87-013941] 01 p0055 N88-10354
Application of Kalker's rolling contact theory to the simulation of rail vehicles
[DFVLR-FB-87-07] 01 p0057 N88-10363
The friction and wear of TPS fibers
[NASA-CR-181496] 03 p0291 N88-11830
Real-time Raman detection of molecular changes in ceramics undergoing sliding friction
[DE88-000558] 04 p0421 N88-12609
Literature review of solid lubrication mechanisms
[AD-A185010] 05 p0567 N88-13456
Surface gouging by hypervelocity sliding contact between metallic materials
[DE88-001937] 06 p0682 N88-14178
The use of alloy 117 as a liquid metal current collector
[AD-A185740] 06 p0698 N88-14281
Mechanisms of wear in single- and two-phase materials
[DE88-003846] 10 p1305 N88-17806
Reciprocating sliding wear characteristics of copper-carbon fiber composites
[NASA-TT-20176] 15 p2031 N88-22100
Railgun rail gouging by hypervelocity sliding contact
[DE88-006866] 16 p2166 N88-22916
Study of temperature and stress fields of two sliding cylinders
[ETN-88-92134] 20 p2815 N88-26704
Studies of dynamic contact of ceramics and alloys for advanced heat engines
[DE88-008996] 21 p2919 N88-27324
Frequency dependent sliding coefficients for general three-dimensional rolling contact in high frequency range
[ILR-MITT-192] 22 p3085 N88-28318
Static and dynamic metal-metal friction at plastic stress levels
[DE88-011281] 23 p3222 N88-29176
Stability of stick-slip phenomenon by using constitutive friction laws of Dietrich and Ruina
[ILR-MITT-197] 24 p3379 N88-30127

SLIP BANDS
U EDGE DISLOCATIONS

SLIP CASTING
Slip casting and extruding shapes of rhenium with metal oxide additives. Part 2: Development of grain stabilized rhenium parts for resistojets
[NASA-CR-180851] 03 p0276 N88-11749
Slip casting of advanced ceramics and composites
[DE88-003424] 11 p1467 N88-18746

SLIP FLOW
Rotational flow of rarefied gas between two coaxial cylinders with slip conditions
[INPE-4277-PRE/1149] 12 p1627 N88-19738
Slip velocity method for three-dimensional compressible turbulent boundary layers
[NASA-TM-100586] 13 p1771 N88-20592

SLIPSTREAMS
NT PROPELLER SLIPSTREAMS
An investigation of the effects of the propeller slipstream on a wing boundary layer 06 p0700 N88-14293

SLITS
Experimental investigation of simplest inhomogeneities in cylindrical slit line
[DE88-702368] 21 p2933 N88-27418

SLOPES
Computational study of three-dimensional wake structures
[REPT-2] 05 p0539 N88-13281
Wind and temperature structure on the slopes of a mountain valley
[DE88-000080] 07 p0880 N88-15338
Detecting and interval estimation about a slope change point
[AD-A186030] 07 p0909 N88-15509
Numerical modeling results for mode propagation in a wedge
[AD-A193998] 22 p3147 N88-28718
A preliminary investigation of drag reduction and mechanism for a blunt body of revolution with slanted base
[NASA-TT-20349] 24 p3317 N88-29753

SLOSHING
U LIQUID SLOSHING

SLOT ANTENNAS
Performance evaluation of a half-wave resonant slot antenna over perfect ground using NEC (Numerical Electromagnetic Code)
[AD-A184004] 03 p0308 N88-11942
Mutual admittance between slots in cylinders of arbitrary shape
[AD-A184254] 04 p0439 N88-12723
Conformal microstrip slot antenna and antenna array
[AD-A189623] 15 p2055 N88-22252
Current-drive on the Versator-2 tokamak with a slotted-waveguide fast-wave coupler
[DE88-006261] 15 p2136 N88-22743
Picosecond photoconductive transceivers 19 p2656 N88-25777

SLOTS
Fin gaps and body slots of guided projectiles: Effects, data correlation and modeling
[AD-A184440] 03 p0270 N88-11698
Mutual admittance between slots in cylinders of arbitrary shape
[AD-A184254] 04 p0439 N88-12723
Optical communication with semiconductor laser diodes
[NASA-CR-182464] 09 p1154 N88-16918
Experimental verification of a finite-difference time-domain thin slot algorithm
[DE88-005572] 13 p1817 N88-20859
Cavitation inception in rectangular two-dimensional slots
[AD-A190677] 15 p2066 N88-22318
Solid rocket motor aft field joint flow field analysis
[NASA-CR-179288] 18 p2474 N88-24675
Electromagnetic penetration into a conducting circular cylinder through a narrow slot, TE case
[AD-A191602] 18 p2500 N88-24828
Characteristics of merging shear layers and turbulent wakes of a multi-element airfoil
[NASA-TM-100053] 18 p2511 N88-24900

SLOTTED ANTENNAS
U SLOT ANTENNAS

SLOTTED WIND TUNNELS
Theoretical and experimental studies of the transonic flow field and associated boundary conditions near a longitudinally-slotted wind-tunnel wall
[NASA-CR-181169] 08 p0959 N88-15815
Wall interference assessment/correction of data from tests of a CAST 10-2/DOA 2 airfoil in the Langley 0.3-m transonic cryogenic tunnel 20 p2751 N88-26331

SLOW NEUTRONS
U THERMAL NEUTRONS

SLURRIES
Two-phase non-Newtonian hydrodynamic modeling of slurries
[DE87-011519] 01 p0047 N88-10298
Experiments on densely-loaded non-Newtonian slurries in laminar and turbulent pipe flows
[DE88-000719] 04 p0442 N88-12745
Heat transfer investigations in a slurry bubble column
[DE88-001445] 06 p0699 N88-14286
Laser velocimeter measurements of solids in multiphase flow
[DE88-000196] 11 p1487 N88-18876
Fluidization mechanisms in slurry flows
[DE88-005191] 13 p1766 N88-20563
Experiments on densely-loaded non-Newtonian slurries in laminar and turbulent pipe flows
[DE88-006209] 15 p2067 N88-22323
An advanced extruder-feeder biomass liquefaction reactor system 18 p2535 N88-25042
Experiments on densely-loaded non-Newtonian slurries in laminar and turbulent pipe flows
[DE88-010579] 20 p2800 N88-26612

SLURRY PROPELLANTS
Fuels combustion research
[AD-A187688] 11 p1453 N88-18657
Liquid phase decomposition in slurry fuels 19 p2624 N88-25564

SMALL ASTRONOMY SATELLITES
U SAS

SMALL PERTURBATION FLOW
A transonic-small-disturbance wing design methodology
[NASA-TP-2806] 10 p1273 N88-17614
Steady and unsteady transonic small disturbance analysis of realistic aircraft configurations
[NASA-TM-100557] 13 p1717 N88-20269
Transonic flow field analysis for real fuselage configurations 14 p1864 N88-21133

SMEAR
Extending the impulse response in order to reduce errors due to impulse noise and signal fading 19 p2649 N88-25730

SMELTING
LFCM (Liquid-Fed Ceramic Melter) vitrification technology
[DE88-003441] 09 p1149 N88-16887
Activities of As, Sb, Bi and Pb in copper mattes and their effects on impurity elimination
[TKK-V-A10(1988)] 15 p2041 N88-22165
Plasma technology: Preliminary studies 2
[DE88-752815] 22 p3154 N88-28763

SMOG
Ozone in the atmosphere 18 p2539 N88-25064

SMOKE
Summary report of the history and events pertinent to the Civil Aeromedical Institute's evaluation of providing smoke/fume protective breathing equipment for airline passenger use
[AD-A184499] 03 p0261 N88-11645
Structural characteristics of dean vortices in a curved channel
[AD-A184724] 03 p0320 N88-12024
The development of low level coastal flow fields when solar radiation is blocked by smoke
[DE87-014348] 03 p0354 N88-12230
Flammability, smoke and toxicity test on fire barrier fabric from the Porcher company --- Airbus aircraft
[ETN-88-91168] 06 p0666 N88-14085
A holographic investigation of particulates in metallized solid fuel ramjet combustion
[AD-A186887] 09 p1140 N88-16831
Effects of additives on fire properties of polyethylene
[AD-A187064] 09 p1145 N88-16871
The visioceilometer and its tactical applications
[AD-A188216] 12 p1647 N88-19866
Detection of biomass burning and smoke plumes in the Amazon region through NOAA satellite imagery 17 p2365 N88-24085
Enhanced emergency smoke venting
[DOT/FAA/CT-88/22] 20 p2758 N88-26350
A study relating to the fog oil replacement program
[AD-A192536] 21 p2923 N88-27347
Application of laser diffraction techniques to particle sizing in solid propellant rocket motors
[AD-A193841] 22 p3049 N88-28089
Project wind, phase 4 (smoke test), Meadow Brook Valley, Red Bluff, California
[AD-A194742] 22 p3128 N88-28596
Smoke hoods: Net safety benefit analysis --- aircraft accidents
[CAA-PAPER-87017] 23 p3174 N88-28898
Flow visualization on a small scale
[AD-A194728] 23 p3181 N88-28935
Flow visualization by laser sheet
[AD-A194481] 23 p3211 N88-29111
Gas turbine smoke measurement: A smoke generator for the assessment of current and future techniques 24 p3348 N88-29930
Numerical field model simulation of full scale fire tests in a closed spherical/cylindrical vessel
[AD-A195067] 24 p3359 N88-29998

SMOKE ABATEMENT
Military jet fuels, 1944-1987
[AD-A186752] 09 p1150 N88-16890

SMOKE TRAILS
Development of flow visualization techniques for use in the Hot Gas Laboratory
[BAE-ARG-233] 03 p0325 N88-12052

SMOOTHING
NT DATA SMOOTHING
Computation of turbulent flow of air through smooth and rough pipes using a two-equation turbulence model 06 p0700 N88-14298
Analysis of smoothing matrices for the preconditioning of elliptic difference equations
[CWI-NM-R8705] 09 p1228 N88-17357
Improving the stability of predictor-corrector methods by residue smoothing
[CWI-NM-R8707] 09 p1228 N88-17359
Optimal application of Morrison's iterative noise removal for deconvolution. Appendices
[NASA-CR-182477] 09 p1231 N88-17376
Optimum filters and smoothers design for carrier phase and frequency tracking
[NASA-CR-182654] 12 p1618 N88-19679
The existence of smooth densities for the prediction filtering and smoothing problems
[AD-A189865] 15 p2119 N88-22629
The effects of optical smoothing techniques on filamentation in laser plasmas
[AD-A188719] 16 p2275 N88-23614
A comparative study of Chebyshev acceleration and residue smoothing in the solution of nonlinear elliptic difference equations
[CWI-NM-R8723] 18 p2569 N88-25259

Distributive iteration for indefinite systems as smoothing method in multigrid process on example of Stokes and Navier-Stokes equations with emphasis on incomplete decompositions
[ETN-88-92127] 21 p2948 N88-27509
Outliner resistant filtering and smoothing: 2D version
[AD-A193319] 21 p3012 N88-27874

SMU (MANEUVERING UNITS)
U SELF MANEUVERING UNITS

SNAILS
The influence of weightlessness on the metabolism of the Biomphalaria glabrata 01 p0074 N88-10475

SNAP
NT FISSION ELECTRIC CELLS
NT SNAP 19
SNAP-DYN: Proven technology for wear-term, higher power in space 17 p2425 N88-24422
SNAP fuel performance 17 p2435 N88-24484
SNAP-DYN: Concepts for multikilowatt space power applications 17 p2435 N88-24486

SNAP 19
Pioneer 10 and 11 RTG performance update 17 p2405 N88-24301

SNATCHING
U SPACECRAFT RECOVERY

SNOW
On the role of snow in the redistribution of precipitation by small scale topography 02 p0203 N88-11267
Thunderstorms with snow: A comprehensive, empirical study of their occurrence, development and structure
[AD-A185929] 07 p0879 N88-15329
Active and passive remote sensing of ice
[AD-A186685] 09 p1195 N88-17162
Aircraft and ground vehicle friction correlation test results obtained under winter runway conditions during joint FAA/NASA Runway Friction Program
[NASA-TM-100506] 11 p1438 N88-18582
Determination of the ultimate loads for corrugated-steel, barrel-type shell structures
[AD-A187716] 11 p1498 N88-18944
Characteristics of coherent and incoherent waves in snow at microwave and millimeter wave frequencies
[AD-A188990] 12 p1620 N88-19692
Study of cations in the precipation of Estacao Antartica Comandante Ferraz
[INPE-4377-PRE/1197] 12 p1644 N88-19843
Reduce uncertainty in projection of future sea-level changes due to ice wastage
[DE88-009883] 22 p3129 N88-28601

SNOW COVER
Evaluation of digital, multitemporal LANDSAT 5 thematic mapper data for the determination of the aerial snowcover extent and spectral separation of various surface types in the inner Oetztal (West Germany) with special regard to the significance of aerial snowcover information for water resources management
[DFVLR-FB-86-46] 03 p0345 N88-12180
Remote sensing of earth terrain
[NASA-CR-182677] 13 p1790 N88-20711
Research relative to angular distribution of snow reflectance/snow cover characterization and microwave emission
[NASA-CR-182733] 14 p1941 N88-21582
Spectral measurements in a disturbed boundary layer over snow
[AD-A190217] 15 p2097 N88-22494
Ice conditions along the Ohio River as observed on LANDSAT images, 1972-1985
[AD-A191172] 18 p2531 N88-25018
Higher frequency ambient noise in the arctic ocean
[AD-A192203] 18 p2547 N88-25122
Active and passive remote sensing of ice
[AD-A193307] 21 p2966 N88-27617

SNOWPLOW EFFECT
U PLASMA DYNAMICS

SNOWSTORMS
Nowcasting rain/snow transitions and freezing rain 02 p0202 N88-11265

SOAPS
The elliptic Sinh-Gordon equation and the construction of toroidal soap bubbles
[DE88-006426] 15 p2113 N88-22585

SOCIAL FACTORS
Problems in integrating geographic data
[DE87-012880] 01 p0106 N88-10689
The role of basic research in society
[DE88-000459] 04 p0502 N88-13090
Activities report of the Technical University of Twente
[ETN-88-90620] 06 p0799 N88-14892
Some aspects of sociopsychological screening of flying school applicants 07 p0890 N88-15392
Antarctica as a model for the human exploration of Mars
[AD-A185835] 08 p1051 N88-16342
Social factors in space station interiors 12 p1651 N88-19888
Do we need a new cartography? 16 p2225 N88-23283
Stress in relation to the physical and social environment 19 p2695 N88-26020
Selection and training of subjects to live and work in hostile and unusual environments 19 p2696 N88-26026

SOCIAL ISOLATION
Stress in relation to the physical and social environment 19 p2695 N88-26020

SOCIOLOGY
NT SOCIAL FACTORS

SODIUM
NT LIQUID SODIUM
NT SODIUM VAPOR
Blue-green laser diode research program
[AD-A183517] 01 p0051 N88-10323
Theoretical and lidar studies of the seasonal and nocturnal variations of the mesospheric sodium layer at Urbana, Illinois 01 p0068 N88-10435
Lidar investigations of M-zone 06 p0741 N88-14558
The sodium layer at 69 N latitude in wintertime 08 p1027 N88-16218
Lidar metal density measurements in the upper atmosphere 08 p1027 N88-16219
The suppression of stimulated hyper-Raman emission in Na due to parametric four-wave mixing
[DE88-003290] 09 p1172 N88-17030
A modeling analysis program for the JPL table mountain Io sodium cloud data
[NASA-CR-182555] 11 p1570 N88-19400
Quantitative determination of a hydrogen impurity in a sodium coolant by hydride thermal dissociation
[NASA-TT-20239] 13 p1740 N88-20402
Use of long-distance pair potentials in calculations of defect characteristics in metals
[DE88-701039] 15 p2037 N88-22138
The kinetics of contact noise in NaBeta alumina
[AD-A190651] 15 p2130 N88-22707
Associative two-body condensation in laser-cooled sodium and hydrogen 16 p2267 N88-23559
Theoretical studies of solar-pumped lasers
[NASA-CR-182929] 17 p2344 N88-23971
Cardiac rhythm of animals consuming reclaimed water differing in concentration of sodium and potassium ions 19 p2705 N88-26085
Production of powdered sodium hydride with large specific surface by the catalyzed reaction of molten sodium with hydrogen-1
[NASA-TT-20185] 20 p2776 N88-26462
Spectral line shapes from highly ionized sodium plasmas
[AD-A193401] 21 p3017 N88-27907

SODIUM CHLORIDES
Electronic conduction in molten sodium chloride
[DE87-010063] 02 p0144 N88-10901
Experimental verification of vapor deposition rate theory in high velocity burner rigs 02 p0189 N88-11179
The role of inclusions in corrosion fatigue crack initiation in Q1N 05 p0604 N88-13699
Geochemistry of freezing brines, low-temperature properties of sodium chloride
[AD-A185751] 06 p0680 N88-14168
The factors which govern the acceleration of corrosion fatigue crack growth rate of a ferritic stainless steel 06 p0717 N88-14402
Fatigue thresholds of C.Mn steels in saline environments 06 p0717 N88-14403
A rapid polishing method for KBr and NaCl infrared windows
[DE88-002480] 07 p0862 N88-15229
The influence of strain on hydrogen entry, transport, and embrittlement of a high strength steel in aqueous sodium chloride solution
[AD-A189302] 12 p1608 N88-19619
The effect of H2S concentration and pH on hydrogen permeation in AISI 410 stainless steel in 5 percent NaCl
[NPL-DMA(A)-148] 14 p1890 N88-21293
Corrosion of tungsten alloys in marine environments 17 p2320 N88-23854
Nuclear magnetic resonance spectrometer
[AD-A192928] 21 p2950 N88-27523
Alternative immersion accelerated testing of coating systems for Naval shoreline facilities 24 p3355 N88-29977

SODIUM COMPOUNDS
NT SODIUM CHLORIDES
NT SODIUM FLUORIDES
NT SODIUM HYDRIDES
NT SODIUM HYDROXIDES
NT SODIUM NITRATES
Corrosion-wear process under rolling-sliding motion
[AD-A189603] 13 p1778 N88-20635

SODIUM FLUORIDES
Prevention of disuse osteoporosis: Effect of sodium fluoride during five weeks of bed rest
[NASA-CR-172018] 01 p0075 N88-10483
Interatomic Auger rates for the sodium fluoride crystal
[DE87-013012] 03 p0382 N88-12401
Intracavity spectrum analyzer with NaF:F2(+):F3(-) crystal laser for long-wave IR wave band 07 p0919 N88-15584
High temperature solar electrothermal processing-3. Zinc from zinc oxide at 1200-1675K using a non-consumable anode
[AD-A186600] 09 p1141 N88-16836

SODIUM HYDRIDES
Production of powdered sodium hydride with large specific surface by the catalyzed reaction of molten sodium with hydrogen-1
[NASA-TT-20185] 20 p2776 N88-26462

SODIUM HYDROXIDES
Improvements to Raney copper zinc methanol synthesis catalysts 17 p2318 N88-23844
Titrimetric analysis of HAN-based liquid propellants
[AD-A196225] 24 p3357 N88-29990

SODIUM NITRATES
Performance characteristics of magnesium-sodium nitrate flares in oxygen-nitrogen atmospheres
[AD-A185274] 05 p0570 N88-13476

SODIUM SULFUR BATTERIES
Extended abstracts: Eighth Battery and Electrochemical Contractors' Conference
[DE88-000960] 06 p0730 N88-14489
Improve the lifetime of the hollow fiber sodium sulfur cell
[DE88-004881] 13 p1751 N88-20469
Sodium-sulfur technology evaluation at Argonne National Laboratory
[DE88-002852] 13 p1762 N88-20544
A novel class of positive electrodes for rechargeable batteries
[DE88-004559] 13 p1783 N88-20545
Failure analysis of Chloride Silent Power, Ltd. PB cells
[DE88-010567] 21 p2938 N88-27448
Component stress during freeze/thaw cycling
[DE88-011204] 21 p2938 N88-27449
Sodium/sulfur cell evaluation results
[DE88-011488] 21 p2938 N88-27451
Effect of thermal cycling on CSPL (Chloride Silent Power Ltd.) sodium/sulfur cells
[DE88-011205] 21 p2939 N88-27455
Post-test observations on CSPL (Chloride Silent Power Limited) cells
[DE88-011975] 21 p2940 N88-27461
Considerations and measurements of latent-heat-storage salts for secondary thermal battery applications
[DE88-011091] 23 p3228 N88-29213

SODIUM VAPOR
Solar pumped, alkali vapor laser
[AD-A187156] 09 p1170 N88-17016
Alkali metal diffuse band lasers
[AD-A190244] 15 p2071 N88-22350

SOFAR
U SOUND FIXING AND RANGING

SOFT LANDING SPACECRAFT
NT AEROSPACE PLANES
NT HOTOL LAUNCH VEHICLE
NT LANDING MODULES
NT LUNAR LANDING MODULES
NT X-30 VEHICLE

SOFTENING
Large-strain softening of aluminum at elevated temperature
[DE87-011559] 01 p0024 N88-10153
Study of the characteristic curve of hardening and softening during low-cycle fatigue process 06 p0719 N88-14414
Brillouin scattering and transmission electron microscopy studies of radiation-induced elastic softening, disordering and amorphization of intermetallic compounds
[DE88-005927] 14 p1987 N88-21850

SOFTWARE (COMPUTERS)
U COMPUTER PROGRAMS
U COMPUTER SYSTEMS PROGRAMS

SOFTWARE ENGINEERING
NT COMPUTER PROGRAMMING
NT LANGUAGE PROGRAMMING
NT LOGIC PROGRAMMING
NT MICROPROGRAMMING
NT PARALLEL PROGRAMMING
NT SYMBOLIC PROGRAMMING
Color display programming for aviation
[DFVLR-MITT-87-03] 01 p0006 N88-10031
Space Station Mission Planning System (MPS) development study. Volume 1: Executive summary
[NASA-CR-179202] 01 p0009 N88-10047

Space Station Mission Planning System (MPS) development study. Volume 2
[NASA-CR-179200] 01 p0009 N88-10048
Space Station Mission Planning Study (MPS) development study. Volume 3: Software development plan
[NASA-CR-179203] 01 p0009 N88-10049
Attitude Control Working Group report
01 p0016 N88-10099
Collection and analysis of specific ELINT Signal Parameters
[NASA-CR-181419] 01 p0033 N88-10213
A brief discussion of formally based approaches to rapid prototyping
[BAE-WAA-RP-RES-SWE-440]
01 p0079 N88-10508
Analysis and synthesis of abstract data types through generalization from examples
[NASA-CR-178369] 01 p0081 N88-10519
Some approaches to the design of high integrity software 02 p0127 N88-10799
Assessment of software quality for the AIRBUS A310 automatic pilot 02 p0128 N88-10804
Software reliability models for fault-tolerant avionics computers and related topics
[NASA-CR-181440] 02 p0220 N88-11382
A design methodology for the utilization of metrics within various phases of software lifecycle models
[DE87-010519] 02 p0220 N88-11385
Prototype Rendezvous Onboard Software (PROBS)
[MATRA-EPT-DT-PRB-2A-00068]
02 p0222 N88-11396
Dynamic image interpretation for autonomous vehicle navigation
[AD-A184043] 03 p0262 N88-11647
JPRS report: Science and technology. China
[JPRS-CST-87-026] 03 p0269 N88-11688
An allotment planning concept and related computer software for planning the fixed satellite service at the 1988 space WARC
[NASA-TM-100244] 03 p0308 N88-11944
Technology applications branch graphics projects
[AD-A184621] 03 p0364 N88-12291
Issues in image processing software development for a multi-user, multi-programming environment
[DE88-000358] 03 p0365 N88-12298
National Science Foundation
[PB87-228375] 03 p0384 N88-12410
Programmable real-time digital video image processing
[PB87-104162] 04 p0430 N88-12661
Software reliability perspectives
[NASA-CR-181523] 04 p0479 N88-12952
Software maintenance in scientific and engineering environments: An introduction and guide
[NASA-CR-177409] 04 p0479 N88-12954
Managing distributed derived data: A preliminary proposal
[DE88-000714] 04 p0481 N88-12966
Intelligent signal analysis and recognition
[NASA-CR-181531] 04 p0501 N88-13084
Towards building a team of intelligent robots
[NASA-CR-181538] 05 p0589 N88-13595
A rudimentary database for three-dimensional objects using structural representation
[CSE-87-00004] 05 p0590 N88-13597
Experiments in fault tolerant software reliability
[NASA-CR-181554] 05 p0632 N88-13863
Reliability of voting in fault-tolerant software systems for small output spaces
[TR-87-16] 05 p0632 N88-13864
Effectiveness of back-to-back testing
[TR-87-08] 05 p0632 N88-13865
RSDIMU acceptance testing system: Overview of acceptance software and procedures
05 p0632 N88-13866
Software design for an airborne gravity measurement system
[AD-A185000] 05 p0634 N88-13878
An Ada graphical tool to support software development
[DE87-014854] 05 p0636 N88-13891
Sandia software guidelines: Software quality planning
[DE88-001931] 05 p0636 N88-13894
A requirements specification for a software design support system
[NASA-CR-182333] 05 p0637 N88-13896
Role of technical information in innovation
[PB87-235388] 05 p0658 N88-14039
Approaches and possible improvements in the area of multibody dynamics modeling
[NASA-CR-179227] 06 p0663 N88-14067
Atmospheric electricity
[NASA-CR-179239] 06 p0744 N88-14575
Window system: A toolbox for interactive computer graphics
[PB87-234262] 06 p0756 N88-14637
A software reliability model with variable fault exposure coefficient
[REPT-87-029] 06 p0757 N88-14646
How to estimate the total number of errors in a software system
[PB87-132130] 06 p0758 N88-14647
Virtual image processor: A prototype implementation
[AD-A185560] 06 p0758 N88-14652
National Aeronautics and Space Administration (NASA)/American Society for Engineering Education (ASEE) Summer Faculty Fellowship Program, 1987. Volume 2
[NASA-CR-172009-VOL-2] 06 p0796 N88-14874
Space station software reliability analysis based on failures observed during testing at the multisystem integration facility 06 p0798 N88-14884
A plan for collecting ada software development cost, schedule and environment data
[AD-A185905] 07 p0902 N88-15460
A software planning and development methodology with resource allocation capability
[AD-A186088] 07 p0902 N88-15462
Software enhancements and modifications to Program FDTD executable on the Cray X-MP computer
[DE88-001877] 07 p0904 N88-15476
Modelling of clustering effects in point processes: An application to failures in SPC-systems (stored program control-systems)
[PB87-149241] 07 p0904 N88-15480
A multiple node software development environment
[DE87-010995] 07 p0905 N88-15484
Enhancement of computer system for applications software branch 07 p0923 N88-15610
An easy-to-use diagnostic system development shell
08 p1055 N88-16366
Interactive knowledge acquisition tools
08 p1060 N88-16401
A learning apprentice for software parts composition
08 p1065 N88-16436
Automatic program generation from specifications using Prolog 08 p1065 N88-16437
On acquisition of programming knowledge
08 p1065 N88-16438
Information handling architecture and software for CIM (Computer Integrated Manufacturing)
[PB88-105820] 08 p1067 N88-16453
Standardization of software development
[INPE-4330-NTE/272] 08 p1068 N88-16455
Proposal of a methodology for the conceptual design of the Distributed Data Base
[INPE-4315-TDL/282] 08 p1093 N88-16576
Development of a comprehensive software engineering environment 09 p1203 N88-17211
Simplifying the construction of domain-specific automatic programming systems: The NASA automated software development workstation project
09 p1204 N88-17212
The knowledge-based software assistant
09 p1204 N88-17213
Algorithm design for scientific computation for highly parallel multiprocessor systems
[AD-A186713] 09 p1217 N88-17299
Design and implementation of elementary functions in Ada
[CWI-NM-R8710] 09 p1218 N88-17304
Hardware/software reliability study — space programs
[REPT-65.5686] 09 p1218 N88-17307
Description of a limited VAX-Ada program support environment developed within UDP division version 1.0
[ARE-TM(UDP)-87103] 09 p1219 N88-17308
Software program validity: A survey
[PB87-170593] 09 p1219 N88-17315
A proposal for a feasibility study on the design of software interfaces in large systems
[NPL-DITC-89/87] 09 p1222 N88-17330
An approach to the hierarchical specification, design and verification of software
[RSRE-MEMO-4063] 09 p1223 N88-17332
Advances in reliable numerical computation: A summary — conference
[NPL-DITC-102/87] 09 p1229 N88-17367
An expert system to support the verification/validation of flight-critical software
[MBB-UT-102/87] 10 p1314 N88-17852
Design sensitivity analysis of nonlinear structural systems and numerical implementation with established finite element codes 10 p1344 N88-18032
Why reusable software isn't 10 p1376 N88-18212
Towards reusable software designs and implementations 10 p1376 N88-18213
Archetyping: A knowledge-based reuse paradigm
10 p1376 N88-18214
Developing a standard taxonomy or software engineering standards 10 p1379 N88-18234
Future directions in computer architecture and software workshop 10 p1383 N88-18258
A method for assessing the software engineering capability of contractors: Preliminary version
[AD-A187230] 10 p1388 N88-18290
The design and implementation of pedagogical software for the multi-backend/multi-lingual database system
[AD-A188106] 11 p1530 N88-19135
Compact high order schemes for the Euler equations
[NASA-CR-181625] 11 p1530 N88-19138
KA-Prolog: Language definition
[GMD-249] 11 p1532 N88-19155
The SAS (Statistical Analysis System) by forms: Putting statistical power into the hands of an end-user
[DE88-002217] 11 p1541 N88-19212
Accessing hierarchical databases via SQL transactions in a multi-model database system
[AD-A187878] 11 p1565 N88-19369
Prototype on-board software for rendezvous and docking 12 p1586 N88-19496
Robotic intelligence issues for space manipulator monitoring, control programming
12 p1588 N88-19504
EUROSIM: A design concept for an in-orbit operations simulator 12 p1589 N88-19517
EUROSIM: A concept of total system support
12 p1590 N88-19523
Definition of the EUROSIM simulation subsystem
12 p1592 N88-19532
A production-quality UNIX Very High Speed Integrated Circuit (VHSIC) Hardware Description Language (VHDL) subset analyzer
[AD-A188832] 12 p1623 N88-19710
Computer architecture for efficient algorithmic executions in real-time systems: New technology for avionics systems and advanced space vehicles
[NASA-CR-182650] 12 p1675 N88-20016
An experiment in software reliability: Additional analyses using data from automated replications
[NASA-CR-178395] 12 p1676 N88-20017
Building software systems economically with mechanized logic: Initial design proposal
[AD-A188791] 12 p1678 N88-20031
Investigation of low energy space plasma
[NASA-CR-182611] 12 p1694 N88-20138
Martian Clouds Data Workshop
[NASA-CR-182431] 12 p1711 N88-20238
Theoretical investigation of EM wave generation and radiation in the ULF, ELF and VLF bands by the electrodynamic orbiting tether
[NASA-CR-182720] 13 p1760 N88-20529
Algebra of Communicating Processes (ACP)tau: A universal axiom system for process specification
[CWI-CS-R8725] 13 p1819 N88-20869
Two normal form theorems for Communicating Sequential Processes (CSP) program
[CWI-CS-R8735] 13 p1819 N88-20874
Type-checking Mini-ML: An algebraic specification with user-defined syntax
[CWI-CS-R8737] 13 p1827 N88-20921
On the design of some systolic algorithms
[CS-8705] 14 p1957 N88-21666
Software quality assurance workstation
[P-1124/RT-14791] 14 p1957 N88-21670
Design method for Ada programs
[ESA-CR(P)-2528] 14 p1958 N88-21671
Public tool interfaces for software development environments
[RSRE-87004] 14 p1958 N88-21674
Procedures for updating dynamic mathematical models
[EMSB-23/86] 14 p1964 N88-21716
Common database interface for heterogeneous software engineering tools
[AD-A189628] 14 p1991 N88-21870
Sigma system: Overview, prospects
15 p2052 N88-22230
Investigation into the development of computer aided design software for space based sensors
[NASA-CR-180772] 15 p2107 N88-22552
Using Colored Stochastic Petri Net (CS-PN) software for protocol specification, validation, and evaluation
[ENST-87C004] 15 p2113 N88-22588
Nonlinear normal mode initialization of the NCAR (National Center for Atmospheric Research) CCM (Community Climate Model)
[PB88-171814] 16 p2235 N88-23347
Portability of software. The use of software in the hardware mixture
[MBB/LWD-11/S/PUB/253] 16 p2246 N88-23416
Software development for the reconstruction of source parameters using research and development arrays
[REPT-840445-TW] 16 p2246 N88-23417
The official handbook of MASCOT, version 3.1, issue 1 — software tool
[BR103975] 16 p2246 N88-23419
The synthesizer generator, a useful tool?
[REPT-87-77] 16 p2250 N88-23443

The Design, Development and Testing of Complex Avionics Systems
[AGARD-CP-417] 17 p2302 N88-23767
The avionics software architecture impact on system architecture 17 p2303 N88-23778
Testing complex avionics software: A practical experience 17 p2306 N88-23794
Interfacing and integrating hardware and software design systems 17 p2306 N88-23796
Software engineering for the British Aerospace Experimental Aircraft Programme (EAP) 17 p2306 N88-23798
A software life cycle support environment 17 p2306 N88-23800
Implantation of a geo-cartographical information system through microcomputers 17 p2361 N88-24064
COMTAL vision one/20 programming processor system from the VAX 11/780 17 p2364 N88-24079
Protection and security mechanisms in the SMITE capability computer
[RSRE-MEMO-4117] 17 p2384 N88-24167
Development environment for secure software
[RSRE-87015] 17 p2386 N88-24179
Separability and security models --- software
[RSRE-87020] 17 p2386 N88-24180
The Environment for Application Software Integration and Execution (EASIE) version 1.0. Volume 4: System installation and maintenance guide
[NASA-TM-100576] 17 p2386 N88-24185
Knowledge based system verification and validation as related to automation of space station subsystems: Rationale for a knowledge based system lifecycle 17 p2387 N88-24192
TALOS: A distributed architecture for intelligent monitoring and anomaly diagnosis of the Hubble Space Telescope 17 p2388 N88-24193
Models and metrics for software management and engineering
[NASA-CR-182953] 17 p2389 N88-24200
An OOD (Object-Oriented Design) paradigm for flight simulators
[AD-A191097] 18 p2467 N88-24647
The Environment for Application Software Integration and Execution (EASIE), version 1.0. Volume 3: Program execution guide
[NASA-TM-100575] 18 p2558 N88-25184
Algorithms and software for solving finite element equations on serial and parallel architectures
[NASA-CR-183027] 18 p2559 N88-25191
Theory of numerical information environment and its applications 19 p2640 N88-25666
Checkout system software for INPE satellites
[INPE-4554-PRE/1297] 19 p2715 N88-26120
Position and velocity determination using a Global Positioning System: An outline
[B8735052] 20 p2757 N88-26355
Research in computer science 1985/6
[PB88-113840] 20 p2835 N88-26815
Script editor: An editor for the specification phase in the development of computer based learning
[REPT-87-68] 20 p2839 N88-26846
Fixpoint representations of characteristic sets of linear-time temporal formulas
[CWI-CS-R8754] 20 p2840 N88-26849
NEXT: An expert system development tool to support engineering design
[NLR-MP-86070-U] 20 p2843 N88-26871
Design and development of courseware for goniometry
[REPT-87-73] 20 p2881 N88-27106
Control of free-flying space robot manipulator systems
[NASA-CR-183104] 21 p2957 N88-27563
Space shuttle natural environment analysis
[NASA-CR-179337] 21 p2976 N88-27676
Block Oriented Simulation System (BOSS)
[NASA-CR-182947] 21 p2995 N88-27760
The programmer's apprentice project: A research overview
[AD-A192784] 21 p2996 N88-27769
Software engineering guidelines for RASP and ANDECS: Requirements and architectural design
[DFVLR-MITT-88-07] 21 p3000 N88-27793
FORTRAN 77 implementation of abstract datatype models
[DFVLR-MITT-88-08] 21 p3000 N88-27794
A PRELUDE (analysis and design of control systems-preliminary utilities depository). A data-based interactive system of control software, user's guid e
[DFVLR-MITT-88-12] 21 p3000 N88-27795
The management of software in airborne recording systems 22 p3035 N88-28019
Software engineering for the EBR-2 data acquisition system conversion
[DE88-009950] 22 p3136 N88-28647
Appraisal of prototype PASCAL program validation suite
[NPL-DITC-112/88] 22 p3139 N88-28665
ALGRES: A system for the specification and prototyping of complex databases
[REPT-87-018] 22 p3140 N88-28668
On eclecticism in specifications: A case study centered around Petri nets --- software engineering
[REPT-87-008] 22 p3140 N88-28671
Using Petri nets for real-time development environments
[REPT-88-005] 22 p3141 N88-28679
Verification and tests --- space projects 22 p3160 N88-28814
The SMITE object oriented backing store
[RSRE-MEMO-4147] 23 p3244 N88-29308
Investigation of the use of High Order Languages (HOLs) for on-board software
[CRI/FR/HOL-C/1/87] 23 p3251 N88-29349
A software engineering approach to expert system design and verification 23 p3252 N88-29356
Automated software development workstation 23 p3263 N88-29423
An expert system for natural language processing 23 p3263 N88-29426
Advanced information processing system: Input/output network management software
[NASA-CR-181678] 23 p3264 N88-29431
Central user and browse service --- ERS-1 ground segment
[CU-PG-MDA-SY-0005] 23 p3297 N88-29637
Improvements of DCAP 1, phase 2-3/A
[D2-RP-AI-106] 24 p3414 N88-30325
The need for a comprehensive expert system development methodology 24 p3421 N88-30362
Study of software requirements and artificial intelligence techniques for robotics
[TL-3333] 24 p3422 N88-30365
The P-3 Scheduling Support System (P-3 S3)
[AD-A194824] 24 p3436 N88-30450

SOFTWARE TOOLS

An evaluation of WPS-Plus word processing software for the IBM PC and compatibles
[DE87-011972] 01 p0081 N88-10518
Benchmarking the Connection Machine
[DE87-013500] 02 p0218 N88-11374
The VAXONLINE software system at Fermilab
[DE87-013565] 02 p0220 N88-11387
A general approach to error propagation
[DE87-014287] 02 p0224 N88-11412
Electronic authoring tools
[DE87-011797] 02 p0248 N88-11567
Microcomputer control of spectroscopic instruments
[ATR-86(8431)-4] 03 p0326 N88-12058
A scientific workstation operator-interface for accelerator control
[DE87-014689] 03 p0362 N88-12278
The structure-mapping engine: Algorithm and examples
[AD-A184042] 03 p0368 N88-12315
Image processing for optical engineering applications
[PB87-210035] 03 p0376 N88-12364
IDMS application documentation made easy
[DE88-000199] 03 p0384 N88-12416
Guidelines for preparing software user documentation
[NASA-CR-181550] 04 p0480 N88-12959
A network definition and solution of simulation problems
[DE88-000675] 04 p0481 N88-12962
On the next generation of reliability analysis tools
[NASA-CR-178380] 04 p0487 N88-13000
A requirements specification for a software design support system
[NASA-CR-182333] 05 p0637 N88-13896
Software-implemented fault insertion: An FTMP example
[NASA-CR-178423] 06 p0761 N88-14668
Documentation in a software maintenance environment
[AD-A185892] 07 p0901 N88-15459
After ten years of metafiles: Where does the Computer Graphics Metafile fit
[DE88-001840] 07 p0904 N88-15474
A multiple node software development environment
[DE87-010995] 07 p0905 N88-15484
Integration of symbolic and algorithmic hardware and software for the automation of space station subsystems
[NASA-TM-89705] 07 p0907 N88-15497
Research in progress at the Institute for Computer Applications in Science and Engineering
[NASA-CR-181607] 08 p1053 N88-16354
CLIPS: An expert system tool for delivery and training 08 p1056 N88-16368
Interactive knowledge acquisition tools 08 p1060 N88-16401
Standardization of software development
[INPE-4330-NTE/272] 08 p1068 N88-16455
Development of a comprehensive software engineering environment 09 p1203 N88-17211
Building validation tools for knowledge-based systems 09 p1207 N88-17235
Hardware/software reliability study --- space programs
[REPT-65.5686] 09 p1218 N88-17307
An approach to the hierarchical specification, design and verification of software
[RSRE-MEMO-4063] 09 p1223 N88-17332
Concept of a programmable maintenance processor applicable to multiprocessing systems
[NASA-TM-100406] 09 p1223 N88-17333
Nonpreemptive run-time scheduling issues on a multitasked, multiprogrammed multiprocessor with dependencies, bidimensional tasks, folding and dynamic graphs
[DE88-003598] 09 p1223 N88-17335
Navigation recovery block design description
[NASA-CR-182473] 10 p1342 N88-18022
On parallelism in software/hardware design tools 10 p1374 N88-18200
An applicative programmer's approach to matrix algebra, lessons for hardware and software 10 p1382 N88-18251
Factors causing unexpected variations in Ada benchmarks
[AD-A187231] 10 p1388 N88-18291
Chips: A tool for developing software interfaces interactively
[AD-A187499] 10 p1389 N88-18295
The performance of software-managed multiprocessor caches on parallel numerical programs
[DE88-003590] 10 p1393 N88-18308
EUROSIM: A concept of total system support 12 p1590 N88-19523
Quality control of upper air conventional data (TEMP and PILOT)
[INPE-4223-RPE/546] 12 p1647 N88-19862
A knowledge acquisition tool for the intelligent processing of materials
[AD-A188982] 12 p1679 N88-20036
Investigation of low energy space plasma
[NASA-CR-182611] 12 p1694 N88-20138
Development of a dependency theory toolbox for database design
[AD-A188872] 12 p1707 N88-20216
Western aeronautical test range real-time graphics software package MAGIC
[NASA-TM-100425] 13 p1757 N88-20506
Advanced human factors engineering tool technologies
[AD-A189390] 13 p1812 N88-20825
MacCAD (Macintosh Computer Aided Design), computer aided design tool for system analysis
[AD-A189241] 13 p1815 N88-20843
Steps into a geometer's workbench
[CWI-CS-R8726] 13 p1819 N88-20870
A packet-switched wide-area communication network simulator
[FUB-3-1986] 14 p1905 N88-21381
Public tool interfaces for software development environments
[RSRE-87004] 14 p1958 N88-21674
Ada tasking in Ten15
[RSRE-MEMO-4074] 14 p1958 N88-21676
The software repeater (an exercise in Z specification)
[RSRE-MEMO-4090] 14 p1958 N88-21677
Reliability analysis within a Computer Aided Engineering (CAE) infrastructure
[NLR-MP-86059-U] 15 p2074 N88-22369
Supercomputer environment
[AD-A190633] 15 p2107 N88-22551
A graphics editor for structured analysis with a data dictionary
[AD-A190618] 15 p2112 N88-22584
Using Colored Stochastic Petri Net (CS-PN) software for protocol specification, validation, and evaluation
[ENST-87C004] 15 p2113 N88-22588
The Colored Stochastic Petri Net (CS-PN) software: Application to the validation and the performance evaluation of distributed systems
[ENST-87D005] 15 p2113 N88-22589
Two-dimensional graphics tools for a transputer based display board
[NASA-TM-100820] 15 p2113 N88-22591
A fault tolerant supervision system
[INPE-4419-TDL/307] 15 p2148 N88-22819
An integrated and modular digital modeling approach for the space station electrical power system development
[NASA-TM-100904] 16 p2170 N88-22935
Integrated multidisciplinary analysis tool IMAT users' guide
[NASA-TM-100605] 16 p2223 N88-23273

The official handbook of MASCOT, version 3.1, issue 1 — software tool
[BR103975] 16 p2246 N88-23419
HIFI: A design method for implementing signal processing algorithms on VLSI processor arrays
[ETN-88-92238] 16 p2247 N88-23421
The PROMISE simulation system: Software for the simulation of parallel processes
[NLR-MP-86077-U] 16 p2247 N88-23427
The synthesizer generator, a useful tool?
[REPT-87-77] 16 p2250 N88-23443
A description of an automated database comparison program
[NASA-TM-100609] 16 p2253 N88-23463
The Design, Development and Testing of Complex Avionics Systems
[AGARD-CP-417] 17 p2302 N88-23767
Managing advanced avionic system design
17 p2304 N88-23783
Advanced development of a cockpit automation design support system 17 p2304 N88-23785
Design and development of an avionics system adapted to helicopter missions 17 p2305 N88-23786
Testing complex avionics software: A practical experience 17 p2306 N88-23794
Developing systems using state-of-the-art CAD/CAM technology 17 p2306 N88-23795
Software engineering for the British Aerospace Experimental Aircraft Programme (EAP)
17 p2306 N88-23798
Avionics systems: Development method and computer tools 17 p2306 N88-23799
A software life cycle support environment
17 p2306 N88-23800
Workshops for the design of avionics systems and the development of onboard software
17 p2307 N88-23802
Coherent functional development: Key to successful future system integration 17 p2307 N88-23803
Automatically generated acceptance test: A software reliability experiment
[NASA-CR-181667] 17 p2347 N88-23984
A software design tool for the analysis of robot dynamics properties
[NLR-MP-86064-U] 17 p2385 N88-24171
The Environment for Application Software Integration and Execution (EASIE) version 1.0. Volume 4: System installation and maintenance guide
[NASA-TM-100576] 17 p2386 N88-24185
Parallel processors and nonlinear structural dynamics algorithms and software
[NASA-CR-182925] 17 p2387 N88-24187
Third Conference on Artificial Intelligence for Space Applications, part 2
[NASA-CP-2492-PT-2] 17 p2387 N88-24188
Integration of symbolic and algorithmic hardware and software for the automation of space station subsystems
17 p2387 N88-24190
Automatic program generation from specifications using PROLOG 17 p2388 N88-24196
Graphics software tool for VT terminals (VTGRAPH)
[NASA-TM-100331] 17 p2389 N88-24201
Description of graphics translation software between Intergraph and Tektronix systems
[NASA-TM-100335] 17 p2389 N88-24202
New York TRACON demonstration of program recoding requirements analysis document
[DOT/FAA/CT-87/34] 18 p2462 N88-24622
The Environment for Application Software Integration and Execution (EASIE), version 1.0. Volume 3: Program execution guide
[NASA-TM-100575] 18 p2558 N88-25184
The -mdoc macro package: A software tool to support computer documentation standards
[DE88-000500] 18 p2559 N88-25188
NFEARS: A nonlinear adaptive finite element solver, part 1
[AD-A191823] 18 p2563 N88-25215
PHOTODIGITIZE: A software/hardware system
[DE88-009575] 19 p2716 N88-26125
GRAPHICS MANAGER (GFXMGR): An interactive graphics software program for the Advanced Electronics Design (AED) graphics controller, Model 767
[DE88-010370] 19 p2717 N88-26131
The UMAC simulator 20 p2834 N88-26811
A multiprocess operating system for 16 bit microcomputers or porting Unix (trademark) to a NS32016 with enhancements 20 p2836 N88-26822
Numerical optimization, system theoretic and software tools for the integrated design of flexible structures and their control systems
[AD-A192927] 21 p2895 N88-27183
User's manual for the two-dimensional transputer graphics toolkit
[NASA-TM-100974] 21 p3001 N88-27799
Improving the performance of AI algorithms
[AD-A192848] 21 p3003 N88-27809
Software modifications to total data reporting accessory for metabolic measurement cart
[AD-A193641] 22 p3132 N88-28623
Software quality measurement demonstration project (1)
[AD-A193429] 22 p3136 N88-28646
Software engineering for the EBR-2 data acquisition system conversion
[DE88-009950] 22 p3136 N88-28647
Appraisal of prototype PASCAL program validation suite
[NPL-DITC-112/88] 22 p3139 N88-28665
Validation code for the Whetstone Benchmark
[NPL-DITC-107/88] 22 p3140 N88-28667
ALGRES: A system for the specification and prototyping of complex databases
[REPT-87-018] 22 p3140 N88-28668
Artificial intelligence software acquisition program, volume 2
[AD-A194239] 22 p3141 N88-28680
Signal processing software for ground penetrating radar, user's manual
[AD-A194286] 23 p3203 N88-29059
Software development without languages
23 p3257 N88-29392
Knowledge based programming environments: A perspective 23 p3258 N88-29393
Requirements for a tool to aid in the development of expert systems for space station applications
23 p3258 N88-29398
Benchmarking expert system tools
23 p3259 N88-29399
Two implementations of the Expert System for the Flight Analysis System (ESFAS) project
23 p3259 N88-29400
A flexible search strategy for production systems
23 p3262 N88-29420
AI tools in computer based problem solving
23 p3263 N88-29424
Networking and AI systems: Requirements and benefits 23 p3263 N88-29425
Expert system technology as a data processing tool
23 p3263 N88-29427
Artificial intelligence software acquisition program, volume 1
[AD-A194104] 23 p3267 N88-29447
Central user and browse service — ERS-1 ground segment
[CU-PG-MDA-SY-0005] 23 p3297 N88-29637
Quality measures and assurance for AI (Artificial Intelligence) software
[NASA-CR-4187] 24 p3411 N88-30304
An operations manual for the digital data system
[NASA-CR-181688] 24 p3415 N88-30329
The proposal entry processor: Telescience applications for Hubble Space Telescope science operations
24 p3417 N88-30339

SOI (SEMICONDUCTORS)
Epitaxial reactor development for growth of silicon-on-insulator devices
[AD-A184758] 03 p0382 N88-12399
Silicon-on-insulator electronics for a space nuclear power system 17 p2431 N88-24461
JFET/SOS (Junction Field-Effect Transistor/Silicon-on-Sapphire) devices: Gamma-radiation-induced effects
[AD-A193001] 20 p2795 N88-26586
Silicon-on-insulator pin diodes
[AD-A193359] 21 p2937 N88-27445
Evaluation of silicon-on-insulator MOS (Metal-Oxide-Semiconductor) transistor response to 10-keV X-ray and cobalt-60 irradiation
[DE88-006102] 23 p3206 N88-29082

SOIL EROSION
Remote Sensing-Arid Lands Workshop, Page, Arizona, June 10-12, 1986
[DE87-012368] 01 p0064 N88-10412
Environmental processes and spectral reflectance characteristics associated with soil erosion in desert fringe regions
[NASA-CR-182332] 05 p0620 N88-13811
Soil erosion and causative factors at Vandenberg Air Force Base, California
[NASA-TM-100981] 17 p2381 N88-24156

SOIL MAPPING
The Earthnet Heat Capacity Mapping Mission (HCMM) data-processing system at Lannion (France)
09 p1127 N88-16761
Development of remote sensing techniques capable of delineating soils as an aid to soil survey
[NASA-CR-182610] 15 p2089 N88-22452
Comparative study of crop and soil mapping using multitemporal and multispectral SPOT and LANDSAT data 22 p3091 N88-28354
SPOT images and geochemical mapping of lateritic covers in southern Mali 22 p3105 N88-28438

SOIL MECHANICS
Enhancement of surface-atmosphere fluxes by desert-fringe vegetation through reduction of surface albedo and of soil heat flux
[NASA-CR-181442] 02 p0197 N88-11231
Explicit and implicit soil modelling for dynamic soil-structure interaction problems
04 p0428 N88-12650
Error analysis for geotechnical engineering
[AD-A186795] 09 p1189 N88-17124
Computer Applications in Geotechnical Engineering (CAGE) and Geotechnical aspects of the Computer-Aided Structural Engineering (G-CASE) projects. User's guide. UTEXAS2 slope-stability package. Volume 1: User's manual
[AD-A187674] 11 p1511 N88-19025
A parametric study of embedded cantilever retaining walls: The results of a finite element study
[RR-CE83] 24 p3383 N88-30152
Computer-Aided Structural Engineering (CASE) project. Development of design formulas for ribbed mat foundations on expansive soils
[AD-A194807] 24 p3412 N88-30307

SOIL MOISTURE
Moisture determinations in and under vegetation canopies. Part 2: Results after parameterization of the CLOUD model
[FEL-1986-63] 01 p0064 N88-10410
Characterization of 6 soils in the X-band, through measurements of complex permittivity
[INPE-4376-TDL/302] 12 p1639 N88-19814
An introduction to the parameterization of land-surface processes 14 p1937 N88-21554
Measurement of the water content of soil from space and application to the regional water balance
14 p1938 N88-21561
Theory of neutron moisture probes and interpretation of measurements in complex soil and water systems
17 p2342 N88-23965
An update on remote measurement of soil moisture over vegetation using infrared temperature measurements: A FIFE perspective
[NASA-CR-182926] 17 p2370 N88-24109
Microwave remote sensing at INPE (Institute for Space Research) Brazil: Concepts and future prospects of soil moisture studies
[INPE-4569-PRE/1310] 24 p3388 N88-30178

SOIL SCIENCE
Significance of foundation-soil separation in dynamic soil-structure interaction 05 p0596 N88-13641
The unsteady ground heat flow at the contact surface between a glacier run and the subsoil
08 p1014 N88-16147
A semianalytical solution of the heat conduction equation for several boundary conditions
08 p1014 N88-16148
Aerosols in Martian Atmosphere and Natural Dust Observation (AMANDO). Proposal for the Mars orbiter balloon and rover to study the Martian atmosphere, its thermal content, and its interaction with the soil
[IFSI-87-9] 08 p1100 N88-16619
Critical comparison of moving average and cumulative summation control charts for trace analysis data
[AD-A188312] 12 p1705 N88-20203

SOILS
NT ALLUVIUM
NT LATERITES
NT LUNAR SOIL
NT SANDS
NT TAR SANDS
Significance of foundation-soil separation in dynamic soil-structure interaction 05 p0596 N88-13641
Analysis of airborne imaging spectrometer data for the Ruby Mountains, Montana, by use of absorption-band-depth images 05 p0614 N88-13771
An analytical soil thermodynamic model for the diurnal variation of ground surface temperature
[AD-A185388] 05 p0625 N88-13823
Computer-aided analysis for the Mechanics of Granular Materials (MGM) experiment, part 2
07 p0926 N88-15626
Global digital data sets of soil type, soil texture, surface slope and other properties: Documentation of archived data tape
[NASA-TM-100685] 09 p1185 N88-17097
Detection of soil erosion with Thematic Mapper (TM) satellite data within Pinyon-Juniper woodlands
[NASA-CR-182476] 09 p1185 N88-17103
Thermal properties of soil: A case study
[INPE-4332-TDL/289] 12 p1637 N88-19803
Characterization of 6 soils in the X-band, through measurements of complex permittivity
[INPE-4376-TDL/302] 12 p1639 N88-19814

Modeling surface exchanges: The soil-vegetation-atmosphere continuum
14 p1937 N88-21553
Sensitivity of general circulation models to surface processes
14 p1937 N88-21556
Development of remote sensing techniques capable of delineating soils as an aid to soil survey
[NASA-CR-182610] 15 p2089 N88-22452
Mapping soil and rock variation from satellite images in the Sahel
17 p2354 N88-24023
Indentification of shallow groundwater regions in semi-arid Brazil by remote sensing methods
17 p2355 N88-24030
Characteristics of drainage determinations in aerial photographs and relief determination on different scales planialtimetric charts for three soils in the state of Sao Paulo
17 p2367 N88-24095
Botany Facility: Problems of water supply, plant nutrients and soil in the Botany Facility
[SIRA-A/7373/WP220/RJS/003]
17 p2379 N88-24141
Monitoring biological impacts of space shuttle launches from Vandenberg Air Force Base: Establishment of baseline conditions
[NASA-TM-100982] 18 p2549 N88-25133
The impact of hemp production on the development of the municipalities of Araras, Leme, Santa Cruz da Conceicao and Pirassununga
19 p2683 N88-25948
Vegetation studies on Vandenberg Air Force Base, California
[NASA-TM-100985] 20 p2831 N88-26795
Direct determination of part-per-billion levels of volatile organics in water and soil samples using glow discharge mass spectrometry
[DE88-011389] 21 p2910 N88-27272
Analysis of soils using remote sensing information at the scale of the parcel
22 p3095 N88-28381
Use of LANDSAT images of vegetation cover to estimate effective hydraulic properties of soils
[NASA-CR-183185] 22 p3116 N88-28514
Nonseismic, surface geophysical and geochemical prospecting technology
[PB88-196613] 23 p3227 N88-29207
Spectral characteristics and the extent of paleosols of the Palouse formation
[NASA-CR-180947] 23 p3228 N88-29210
Regional environmental studies using national data bases and GIS (Geographic Information System)
[DE88-008368] 23 p3230 N88-29225
Viking Landers and remote sensing
23 p3304 N88-29685
The surface composition of Mars from earthbased observations
23 p3306 N88-29696
Reflectance pattern and the physical and chemical characteristics of three Brazilian Oxisols
[INPE-4590-PRE/1320] 24 p3387 N88-30172
The dynamics of transuranics and other radionuclides in natural environments, December 1985
[DE87-014456] 24 p3390 N88-30189
Estimation of soil temperature profile from remote microwave and IR measurements
24 p3450 N88-30532

SOL-GEL PROCESSES

Stress measurements in sol-gel films
[DE87-014467] 02 p0153 N88-10955
Preparation of oxide glasses from metal alkoxides by sol-gel method
[NASA-TT-20124] 02 p0154 N88-10965
Study of ceramic-fiber/ceramic sol-gel based matrix composites
[SNIAS-872-430-120] 05 p0569 N88-13469
Exploitation of the sol-gel route in processing of ceramics and composites
[AD-A185482] 06 p0686 N88-14204
On 1064 nm and 350 nm laser damage thresholds of high index oxide films deposited from organic solutions and sols
[DE88-001636] 07 p0859 N88-15217
The influence of processing variables on physical properties of sol-gel derived TiO2 films
[DE88-005155] 11 p1559 N88-19331
Structure of sol-gel silica
[DE88-006870] 15 p2033 N88-22114
Sol/gel processing techniques for glass matrix composites
[AD-A191748] 18 p2478 N88-24701
Manufacturing of a ceramic-ceramic composite matrix using the sol-gel procedure
[ETN-88-92157] 20 p2766 N88-26414
Characterization of the surface area and porosity of sol-gel films using saw devices
[DE88-008794] 20 p2875 N88-27069
Preparation and properties of new inorganic glasses and gel-derived solids
[AD-A192922] 21 p2917 N88-27315
Ellipsometric imaging of drying sol-gel films
[DE88-011785] 21 p2921 N88-27335
Application of sol-gel procedures to ceramic composites
[ETN-88-92741] 21 p2921 N88-27338
Comparison of sol-gel procedures for zircon and alumina
[REPT-881-430-108] 21 p2922 N88-27342
Sol-gel processing of metal-oxide-semiconductor structures
[DE88-009853] 22 p3156 N88-28778
Electrical properties of metal-oxide-silicon structures with sol-gel oxides
[DE88-011791] 22 p3156 N88-28779
Sol-gel kinetics: Si(sup)29 NMR and a statistical reaction model
[DE88-011545] 23 p3191 N88-28988
The sol-gel synthesis of ceramics
[SNIAS-881-430-114] 23 p3199 N88-29037
Al2O3-TiO2 and Al2TiO5 ceramic materials
[SNIAS-881-430-122] 23 p3199 N88-29038
Development of high efficiency q-switched glass laser via sol-gel processing
[AD-A192301] 23 p3218 N88-29154

SOLAR ACTIVITY

NT FACULAE
NT SOLAR FLARES
NT SOLAR PROMINENCES
NT SPICULES
NT SUNSPOTS

Low altitude flux and dose measurements during two solar flare events
01 p0111 N88-10713
Probable detection of solar neutrons by ground-level neutron monitors during STIP interval 16
01 p0111 N88-10715
Solar energetic particles events observed by Prognoz-10 Intercosmos (May-October 1985)
01 p0111 N88-10716
The large Type 4 radio burst event of 24 April 1985 interpreted by dynamic spectral recordings and associated recordings
01 p0112 N88-10717
Propagating shocks in the corona
01 p0112 N88-10718
Solar origins of coronal mass ejections
01 p0113 N88-10726
Radio studies of large scale structures of the Sun's corona and transient activity
01 p0114 N88-10728
Solar events and their influence on the interplanetary medium
01 p0115 N88-10734
Solar activity, magnetic clouds, and geomagnetic storms
01 p0115 N88-10735
Quantification of the background signal to solar neutrino detection from cosmogenic activation of the atmosphere
[DE87-013830] 01 p0119 N88-10762
Magnetic fields in the overshoot zone: The great escape
02 p0256 N88-11616
A numerical study of the thermal stability of solar loops
02 p0256 N88-11619
The Sun and the solar activity
03 p0271 N88-11704
Irradiations. Accumulated doses. Heavy ions — space environment
03 p0272 N88-11708
Solar magnetic and velocity fields
[AD-A184360] 03 p0390 N88-12449
Asymmetry and variations of solar limb darkening along the diameter defined by diurnal motion in April 1981
04 p0506 N88-13111
Calibration of the Ca II K line-core density and the magnetic flux density in stars using solar data
04 p0507 N88-13116
Three-halves law in sunspot cycle shape
[NASA-CR-181520] 04 p0525 N88-13210
The appearance and disappearance of magnetic flux on the quiet sun
[AD-A185432] 05 p0661 N88-14055
Solar-geophysical data number 515, July 1987. Part 1: (Prompt reports). Data for June 1987, May 1987 and late data
[PB87-233177] 06 p0805 N88-14912
Solar-geophysical data number 515, July 1987. Part 2: (Comprehensive reports). Data for January 1987 and miscellanea
[PB87-233185] 06 p0805 N88-14913
Solar-geophysical activity reports for STIP (Study of Travelling Interplanetary Phenomena) interval 15, 12-21 February 1964 ground level event and STIP interval 16, 20 April-4 May 1984 Forbush decrease
[PB87-232658] 06 p0805 N88-14915
Quasiperiodic variations in manifestations of solar activity
08 p1004 N88-16083
Prediction of the next solar activity cycle
08 p1035 N88-16276
Bern solar observations. Solar data for January-December 1986
[REPT-53] 09 p1263 N88-17569
Neutrino magnetic moment and time variation of solar neutrino flux
[DE88-700687] 10 p1430 N88-18542
Development of high stability fiber optic spectrophotometric systems for study of solar/stellar magnetic activity
[AD-A189327] 13 p1852 N88-21088
Sunspot frequency and solar activity
[PUBL-17/87] 14 p2011 N88-21996
Table of solar activity associated with coronal mass ejections observed by the SMM coronagraph/polarimeter in 1980
[PB88-170881] 14 p2011 N88-21998
Solar-geophysical data number 520, December 1987. Part 2: (Comprehensive reports). Data for June 1987 and miscellanea
[PB88-164207] 15 p2152 N88-22849
Development of a digital sun sensor for a spin-stabilized satellite
[INPE-4508-TDL/327] 16 p2169 N88-22929
The gamma-ray spectrometer experiment on the solar maximum mission satellite
[NASA-CR-182977] 17 p2452 N88-24569
The SAMEX vector magnetograph: A design study for a space-based solar vector magnetograph
[NASA-TM-4048] 18 p2596 N88-25424
Automated spectrometric unit for the study of radiation characteristics of cosmic radiation aboard Prognoz-9 space stations
19 p2706 N88-26090
Solar microwave radiation maps measured at Metsaehovi Radio Research Station in 1980-1981
[PB88-193453] 19 p2741 N88-26276
Solar-geophysical data number 521, January 1988. Part 1: (Prompt reports). Data for December 1987, November 1987 and late data
[PB88-179213] 19 p2743 N88-26284
Diffusion of slight solar induced disturbances in the middle atmosphere
[MITT-53] 20 p2825 N88-26758
Solar-geophysical data number 522, February 1988. Part 2: (Comprehensive reports). Data for August 1987 and miscellanea
[PB88-194741] 20 p2886 N88-27138
Solar-geophysical data number 522, February 1988. Part 1: (Prompt reports). Data for January 1988, December 1987 and late data
[PB88-194733] 20 p2886 N88-27139
Modeling, designing and simulating a pointing control system for balloon-borne solar experiments
[NASA-TM-100337] 22 p3082 N88-28300

SOLAR ACTIVITY EFFECTS

The Sun and the solar activity
03 p0271 N88-11704
Contributions of lidar measurements to the study of long term variations of the middle atmosphere
[ETN-88-91237] 05 p0625 N88-13824
Characteristics of atmospheric disturbances with a quasi-two day period
06 p0734 N88-14515
On the dependence of the lower thermospheric wind regime on the solar cycle
06 p0736 N88-14524
Radar observations of high-latitude lower-thermospheric and upper-mesospheric winds and their response to geomagnetic activity
06 p0742 N88-14563
Solar-geophysical data number 515, July 1987. Supplement (explanation of data reports)
[PB87-233169] 06 p0805 N88-14914
New book on space ecology reviewed
07 p0897 N88-15434
Dynamics and turbulence of solar wind in area of its formation based on radio transmission data measured with Venera-15 and Venera-16 spacecraft
08 p1003 N88-16080
Peculiarities of daytime ionosphere of Venus during years of low and high solar activity
08 p1005 N88-16091
Distribution of electron concentration in nightime atmosphere of Venus based on radio transmission data
08 p1005 N88-16092
Interplanetary and geophysical effects of a coronal transient
08 p1095 N88-16587
Solar-geophysical data number 516, August 1987. Part 1: (Prompt reports). Data for July 1987, June 1987 and late data
[PB88-114368] 09 p1263 N88-17570
Solar-geophysical data number 516, August 1987. Part 2: (Comprehensive reports). Data for February 1987
[PB88-114376] 09 p1264 N88-17571
Upper-thermospheric observations and neutral-gas dynamics at high latitudes during solar maximum
[AD-A188058] 11 p1512 N88-19031
The effects of solar cycle and latitude dependence on the formation of ionospheric C layer
[INPE-4342-TDL/293] 16 p2232 N88-23332
Diffusion of slight solar induced disturbances in the middle atmosphere
[MITT-53] 20 p2825 N88-26758

Advanced Receiver tracking of Voyager 2 near solar conjunction 22 p3065 N88-28185
X-band noise temperature near the Sun at a 34-meter high efficiency antenna 22 p3067 N88-28200
Variations in the atmosphere associated with the 11-year solar cycle 22 p3122 N88-28557

SOLAR ARRAYS
Phase 3 study of selected tether applications in space. Volume 2: Study results
[NASA-CR-179186] 02 p0132 N88-10828
Imaging interferometry with non-redundant arrays 02 p0257 N88-11624
Environmental interactions of solar generators in space 03 p0274 N88-11730
Electricity from photovoltaic solar cells. Flat-Plate Solar Array Project of the US Department of Energy's National Photovoltaics Program: 10 years of progress
[NASA-TM-89653] 03 p0346 N88-12188
Characteristics of current solar central receiver projects
[DE88-001314] 04 p0466 N88-12880
The high performance solar array GSR3
[SNIAS-872-422-108] 05 p0622 N88-13814
Study of large solar arrays (SOLA), phase 2A
[BAE-SS/1109] 09 p1186 N88-17106
Study of Large Solar Arrays (SOLA). Phase 2A: Amplifying information to final report (SS/1109)
[BAE-SS/1110] 09 p1248 N88-17480
Oxidation and protection of fiberglass-epoxy composite masts for photovoltaic arrays in the low Earth orbital environment
[NASA-TM-100839] 11 p1485 N88-18734
Mast material test program (MAMATEP)
[NASA-TM-100821] 12 p1604 N88-19592
Vega-1 and Vega-2 automatic stations: Functioning of flyby vehicles during encounter with Halley's comet 13 p1725 N88-20314
Direct absorption receiver control studies
[DE87-013653] 13 p1795 N88-20737
The development status of the strongback array --- spacecraft structure 14 p1875 N88-21201
The SPOT solar array. Box opening mechanisms physical vapor deposition (PVD)-MoS2: Lubricated slides. Functional evaluation 14 p1876 N88-21211
Qualification testing of the EUROSTAR Solar Array Drive Mechanism (SADM) 14 p1879 N88-21229
Solar cell experiment on the first satellite of the Brazilian complete space mission
[INPE-4248-PRE/1121] 14 p1880 N88-21238
Contamination of optical surfaces --- Space Station 18 p2592 N88-25400
Assessment of the effects of space debris and meteoroids environment on the space station solar array assembly
[NASA-TM-101315] 23 p3185 N88-28959
Advanced planar array development for space station
[NASA-CR-179373] 24 p3389 N88-30181
Alternative module configurations for advanced solar arrays on low orbit and extended lifetime missions (AMOC 2)
[ESA-CR(P)-2581] 24 p3389 N88-30182

SOLAR ATMOSPHERE
What's needed in the UV and EUV 02 p0255 N88-11612
First results on quiet and magnetic granulation from SOUP 02 p0255 N88-11613
Solar ultraviolet spectrum obtained from a balloon gondola 08 p1032 N88-16258
Small scale MHD wave processes in the solar atmosphere and solar wind 08 p1096 N88-16608
MHD waves in the solar atmosphere 08 p1096 N88-16609
Negative viscosity in global circulations 13 p1786 N88-20685
On the magnetic structure and energy balance of EUV-emitting plasma in the quiet Sun 17 p2452 N88-24567
The SAMEX vector magnetograph: A design study for a space-based solar vector magnetograph
[NASA-TM-4048] 18 p2596 N88-25424

SOLAR AZIMUTH
U AZIMUTH
U SOLAR POSITION

SOLAR BACKSCATTER UV SPECTROMETER
Nimbus 7 Solar Backscatter Ultraviolet (SBUV) spectral scan solar irradiance and Earth radiance product user's guide
[NASA-RP-1199] 09 p1184 N88-17096

SOLAR CELLS
NT VERTICAL JUNCTION SOLAR CELLS
Effects of electron and proton irradiations on n/p and p/n GaAs cells grown by MOCVD
[NASA-TM-100199] 01 p0042 N88-10266
High-efficiency silicon solar cells: Numerical modeling, transient measurements, efficiency goals, and v-shaped grooves
[DE87-012842] 01 p0066 N88-10423
The fundamentals of photovoltaic system electrical design
[DE87-009061] 02 p0194 N88-11214
Gallium arsenide and multibandgap solar cell research
[DE87-012260] 02 p0194 N88-11215
CuInSe2 solar cell research by sputter deposition
[DE87-001184] 02 p0195 N88-11219
Wide bandgap passivation layers on silicon
[DE87-014307] 02 p0244 N88-11543
Recent progress in space photovoltaic systems
[NASA-TM-100208] 03 p0311 N88-11966
Mechanically stacked multijunction solar cells: An update on Sandia programs
[DE87-014641] 03 p0347 N88-12190
Crystalline cell research status and direction
[DE87-014214] 03 p0382 N88-12402
Performance of GaAs and silicon concentrator cells under 37 MeV proton irradiation
[NASA-TM-100144] 04 p0465 N88-12877
Radiation performance of AlGaAs concentrator cells and expected performance of cascade structures
[NASA-TM-100145] 04 p0465 N88-12878
Characteristics of current solar central receiver projects
[DE88-001314] 04 p0466 N88-12880
The high performance solar array GSR3
[SNIAS-872-422-108] 05 p0622 N88-13814
Development of mechanically stacked tandem concentrator cells
[DE88-001926] 06 p0730 N88-14490
Surface modification using ion beams: Recent developments at ORNL
[DE88-000951] 06 p0786 N88-14619
The results of the 1984/1985 Round-Robin Calibration of Reference Solar Cells for the Summit Working Group on Technology, Growth and Employment
[DE88-900215] 07 p0874 N88-15303
Further study of inversion layer MOS solar cells 07 p0925 N88-15621
A flux analysis of the solar cells
[INPE-4247-PRE/1120] 08 p1022 N88-16186
Variable band gap materials for thermophotovoltaic generators
[AD-A186858] 09 p1186 N88-17104
Forward-biased current annealing of radiation damaged gallium arsenide and silicon solar cells
[AD-A186904] 09 p1186 N88-17105
Physico-chemical studies on copper sulfide behavior in the CdS-Cu2S solar cell
[ETN-88-91068] 09 p1187 N88-17109
A comparison of different module configurations for multibandgap solar cells
[DE88-002718] 09 p1187 N88-17113
Investigation of the subsequent treatment and the stability of CuxS-CdS thin-film solar cells
[ETN-88-91488] 11 p1507 N88-19006
Proceedings of the 1987 High-Efficiency Photovoltaic Subcontractors' Review Meeting
[DE88-003354] 11 p1508 N88-19011
Positron annihilation spectroscopy of AlGaAs/GaAs interfaces in MOCVD-grown GaAs heterojunction solar cells
[DE88-003903] 11 p1508 N88-19012
Results of the 1987 NASA/JPL balloon flight solar cell calibration program
[NASA-CR-182617] 12 p1574 N88-19413
Acoustic phonons, surface plasmons and surface acoustic plasmons in a superlattice and their nonreciprocal device applications
[AD-A188918] 12 p1698 N88-20163
Research on multibandgap solar cells
[DE87-012261] 13 p1792 N88-20721
Research on high-efficiency, stacked, multijunction, amorphous silicon alloy thin-film solar cells
[DE88-001108] 13 p1793 N88-20723
CdZnTe as a wide-band-gap absorber for a tandem, thin-film solar cell
[DE88-001114] 13 p1793 N88-20724
Research on single-crystal CdTe solar cells
[DE88-001115] 13 p1793 N88-20725
Stable, high-efficiency, CuInSe2-based, polycrystalline, thin-film tandem solar cells
[DE88-001116] 13 p1793 N88-20726
Cadmium sulfide/copper ternary heterojunction cell research
[DE88-001122] 13 p1793 N88-20727
SERI's Photovoltaic R and D Project: Recent progress and future directions
[DE88-001129] 13 p1794 N88-20728
Progress of amorphous silicon based solar cells and modules
[DE88-004666] 13 p1794 N88-20733
Thin-film cadmium telluride solar cells
[DE88-001107] 13 p1846 N88-21050
Investigations of the origins of metastable, light-induced changes in hydrogenated amorphous silicon
[DE88-001117] 13 p1846 N88-21051
Solar cell experiment on the first satellite of the Brazilian complete space mission
[INPE-4248-PRE/1121] 14 p1880 N88-21238
Polysilicon-contacted p+ emitters for silicon solar cell applications
[DE88-005106] 14 p1942 N88-21586
Considerations in GaAs standard cell design
[DE88-003310] 14 p1985 N88-21840
Thermal analysis of heat storage canisters for a solar dynamic, space power system
[DE88-004199] 15 p2027 N88-22075
Solar cell cover glasses for satellites 15 p2052 N88-22225
High-efficiency thin-film silicon-on-GaP solar cell for improved radiation resistance
[AD-A190268] 15 p2091 N88-22460
Optimization of organic Rankine cycles for space station applications 17 p2423 N88-24407
Progress in InP solar cell research
[NASA-TM-100914] 18 p2507 N88-24870
Aging behavior of Au-based ohmic contacts to GaAs
[NASA-CR-182146] 19 p2662 N88-25831
Fast parametrization procedure for solar cells
[PB88-186416] 19 p2686 N88-25966
Photovoltaic energy systems
[DE88-007504] 19 p2687 N88-25968
Study of Staebler-Wronsky degradation effect in a Si:H based P-I-N solar cells
[NASA-CR-182564] 19 p2687 N88-25970
Electrophoretic coatings. Part 1: Sandia applications
[DE88-008666] 20 p2776 N88-26465
Photovoltaic concentrator technology: Recent results
[DE88-009588] 20 p2819 N88-26726
Development of a model procedure for the determination of volume diffusion lengths by transient measurements on monocrystal silicon solar cells
[ETN-88-92119] 20 p2821 N88-26733
Photovoltaic cells with n-silicon and conductive polymers
[ETN-88-92133] 20 p2821 N88-26734
Analytical determination of critical crack size in solar cells
[NASA-CR-183128] 20 p2821 N88-26736
Solar cell modeling and simulation
[AD-A193249] 21 p2966 N88-27620
Solar energy conversion through the interaction of plasmons with tunnel junctions. Part A: Solar cell analysis. Part B: Photoconductor analysis
[NASA-CR-183044] 21 p2967 N88-27621
Device physics related to the granular nature of CuInSe2 solar cells
[DE88-001159] 21 p2967 N88-27622
Laser-heated CVD process for depositing thin films for low-cost solar-cell applications
[DE88-001162] 21 p2967 N88-27623
A comparison of the radiation tolerance characteristics of multijunction solar cells with series and voltage-matched configurations
[NASA-TM-101177] 21 p2967 N88-27624
Experimental fabrication of thin film single crystalline solar cells
[PB88-131958] 21 p2967 N88-27627
Amorphous silicon solar cells using a metal substrate
[PB88-131941] 21 p2968 N88-27628
Space photovoltaic generators. State of the art, trends
[REPT-881-440-106] 21 p2970 N88-27640
Low-band-gap, amorphous-silicon-based alloys by photochemical vapor deposition
[DE88-001165] 21 p3023 N88-27944
Laser crystallized silicon films on alumina ceramic substrates and application to thin film c-Si solar cells
[PB88-131966] 22 p3116 N88-28515
Experimental fabrication of thin film single crystalline solar cells
[PB88-131958] 22 p3116 N88-28516
Theoretical investigation on heterojunction solar cell
[DE88-701837] 23 p3229 N88-29219
Construction of gallium arsenide solar concentrator for space use
[AD-A194658] 23 p3230 N88-29222
Long-term behavior of energy production systems with the example of HELIOS and SYMPHONIE
[ETN-88-92988] 23 p3230 N88-29223
Alternative module configurations for advanced solar arrays on low orbit and extended lifetime missions (AMOC 2)
[ESA-CR(P)-2581] 24 p3389 N88-30182

SOLAR COLLECTORS
Focusing solar energy collector 02 p0159 N88-10996

Development of an innovative, low-cost solar collector
[PB87-206819] 02 p0194 N88-11210
DTA/DSC studies of phase equilibria in binary mixtures of barium carbonate with alkali carbonates
[DE87-001195] 02 p0194 N88-11213
Proceedings of the Solar Thermal Technology Conference
[DE87-014441] 02 p0195 N88-11220
Direct Absorption Receiver flow experiments
[DE87-014655] 02 p0196 N88-11221
Direct Absorption Receiver (DAR) systems assessment
[DE87-012277] 02 p0196 N88-11222
An evaluation of the LEC-460 solar collector
[DE88-000052] 02 p0196 N88-11224
Polymers in solar technologies
[DE88-001102] 03 p0294 N88-11849
Numerical and experimental investigation of the unsteady temperature distribution in solar central receivers
[ESA-TT-1050] 03 p0347 N88-12193
Crystalline cell research status and direction
[DE87-014214] 03 p0382 N88-12402
Light funnel concentrator panel for solar power
[NASA-CR-179223] 04 p0464 N88-12870
Performance of GaAs and silicon concentrator cells under 37 MeV proton irradiation
[NASA-TM-100144] 04 p0465 N88-12877
International Energy Agency (IEA) Small Solar Power Systems (SSPS) sodium cavity and external receiver performance comparison
[DE88-001310] 04 p0465 N88-12879
Characteristics of current solar central receiver projects
[DE88-001314] 04 p0466 N88-12880
Design, fabrication and delivery of a miniature Cassegrainian concentrator solar array system
[NASA-CR-179237] 06 p0730 N88-14493
Mean and peak wind load reduction on heliostats
[DE87-012281] 07 p0873 N88-15296
Satellite techniques of solar resource assessment for focusing and non-focusing solar collector systems
[DE88-001657] 07 p0874 N88-15298
Performance of highly concentrating mirror collectors and collector systems
[DFVLR-FB-87-29] 09 p1186 N88-17107
Side-by-side comparisons of evacuated compound parabolic concentrator and flat plate solar collector systems at temperatures of 90 to 100°C
[DE88-004717] 10 p1351 N88-18073
A solar receiver-reactor with specularly reflecting walls for high-temperature thermoelectrochemical and thermochemical processes
[AD-A187612] 10 p1351 N88-18077
Los Alamos optical materials reliability, maintainability, and exposure testing program
[DE88-001953] 10 p1409 N88-18404
HELIOS modelling of point-focusing solar concentrators
[DE88-004933] 12 p1640 N88-19820
Control strategies and hardware used in solar thermal applications
[DE88-004631] 13 p1794 N88-20731
Direct absorption receiver control studies
[DE87-013653] 13 p1795 N88-20737
A five year weathering experiment with solar collectors
[DE88-900369] 13 p1796 N88-20740
Advanced sensible heat solar receiver for space power
[NASA-TM-100847] 14 p1882 N88-21249
Space station solar concentrator materials research
[NASA-TM-100862] 14 p1882 N88-21250
Direct conversion of solar energy to thermal energy
[BMFT-FB-T-86-220] 14 p1943 N88-21592
Thermal modeling of solar central receiver cavities
[DE88-004940] 14 p1943 N88-21594
Ray tracing optical analysis of offset solar collector for space station solar dynamic system
[NASA-TM-100853] 15 p2027 N88-22080
Development of an integrated heat pipe-thermal storage system for a solar receiver
[NASA-TM-101099] 15 p2091 N88-22458
Progress in InP solar cell research
[NASA-TM-100914] 18 p2507 N88-24870
Evaluation of the chromium oxide arc spraying treatment on solar energy collectors
[ETN-88-92564] 18 p2537 N88-25053
Design and demonstration of a system for the deposition of atomic-oxygen durable coatings for reflective solar dynamic power system concentrators
[NASA-CR-4158] 19 p2606 N88-25474
Thermal distortion analysis of the space station solar dynamic concentrator
[NASA-TM-100868] 19 p2606 N88-25475
Dielectric compound parabolic concentrating solar collector with frustrated total internal reflection absorber
[DE88-009986] 19 p2688 N88-25976
Advanced heat receiver conceptual design study
[NASA-CR-180901] 19 p2688 N88-25977
Influence of refractive index and solar concentration on optical power absorption in slabs
[NASA-TM-4056] 19 p2726 N88-26190
Performance sensitivities for point-focus dish systems with secondary concentrators
[DE88-001152] 21 p2968 N88-27629
Calculation of the specific and volumetric enthalpies of Ge-Si alloys
[DE88-008949] 21 p3026 N88-27965
Lewis Research Center space station electric power system test facilities
[NASA-TM-100924] 23 p3182 N88-28942
Construction of gallium arsenide solar concentrator for space use
[AD-A194658] 23 p3230 N88-29222
The effect of the near earth micrometeoroid environment on a highly reflective mirror surface
[NASA-TM-101307] 24 p3332 N88-29833

SOLAR COMPANION STAR
U NEMESIS (STAR)

SOLAR CONSTANT
Aerosol optical depth and ratios of diffuse-sky to total solar irradiance measured from aircraft following the eruption of El Chichon
[PB88-100789] 07 p0878 N88-15326

SOLAR CONVERTERS
U SOLAR GENERATORS

SOLAR CORONA
NT CORONAL HOLES
NT CORONAL LOOPS
Propagating shocks in the corona
01 p0112 N88-10718
Magnetic field twist driven by remote convective motions: Characteristics and twist rates 01 p0113 N88-10724
Solar origins of coronal mass ejections
01 p0113 N88-10726
On the association of erupting magnetic fields with eruptive prominences and coronal mass ejections
01 p0113 N88-10727
Radio studies of large scale structures of the Sun's corona and transient activity 01 p0114 N88-10728
Observations of the brightness temperature distribution of the quiet solar corona at decametric wavelengths
01 p0114 N88-10729
Meterwave observations of a coronal hole
01 p0114 N88-10730
Coronal and interplanetary Type 2 radio emission
01 p0114 N88-10731
Coronal mass ejections: The long-term variation of their occurrence rate and the solar wind mass flux
01 p0114 N88-10732
Was the eclipse comet of 1893 a disconnected coronal transient? 01 p0115 N88-10733
High-resolution continuum observations of the Sun
02 p0255 N88-11614
Statistical properties of small high-velocity events in the solar transition region 04 p0506 N88-13112
Magnetic field draping about coronal mass ejecta
[DE88-001805] 05 p0661 N88-14057
Astrophysics and the solar nebula
07 p0883 N88-15355
Exobiology and life science 07 p0883 N88-15358
Total light flux and colour of solar corona
[PB87-143335] 07 p0946 N88-15754
Proceedings of the 21st ESLAB Symposium on Small Scale Processes in the Chromosphere/Corona, Interplanetary Medium and Planetary Magnetospheres
[ESA-SP-275] 08 p1094 N88-16582
Solar corona and solar wind 08 p1094 N88-16584
Observations and modeling of the prominence/corona transition region 08 p1094 N88-16585
Gasflows in the transition region above sunspot
08 p1095 N88-16586
Interplanetary and geophysical effects of a coronal transient 08 p1095 N88-16587
Flux tubes and loops in the solar chromosphere and corona 08 p1095 N88-16591
Emerging flux, magnetic reconnection, plasma turbulence and waves in the transition zone of the solar atmosphere 08 p1096 N88-16597
The effects of viscosity on resistive ballooning modes in line-tied coronal magnetic fields
08 p1097 N88-16599
Coronal heating by means of helical magnetohydrodynamic turbulence
[AD-A187084] 10 p1410 N88-18413
Table of solar activity associated with coronal mass ejections observed by the SMM coronagraph/polarimeter in 1980
[PB88-170881] 14 p2011 N88-21998
The properties of solar coronal active regions deduced from X-ray line spectra
[AD-A193026] 20 p2886 N88-27141
More than a solar cycle of synoptic solar and coronal data: A video presentation
[NASA-CR-181459] 23 p3308 N88-29708
Corona-solar wind coupling review
[AFGL-TR-87-0203] 24 p3458 N88-30575

SOLAR CORPUSCULAR RADIATION
NT SOLAR ELECTRONS
NT SOLAR NEUTRINOS
NT SOLAR NEUTRONS
NT SOLAR PROTONS

SOLAR COSMIC RAYS
Solar cosmic ray propagation in high-velocity solar wind stream 08 p1002 N88-16073
Automated spectrometric unit for the study of radiation characteristics of cosmic radiation aboard Prognoz-9 space stations 19 p2706 N88-26090
Solar flares and magnetospheric particles: Investigations based upon the ONR-602 and ONR-604 experiments
[AD-A193396] 21 p3031 N88-27994

SOLAR CYCLES
NT SUNSPOT CYCLE
STIP Symposium on Physical Interpretation of Solar/Interplanetary and Cometary Intervals
[NASA-CR-181201] 01 p0110 N88-10709
Overview of STIP intervals 15-19
01 p0110 N88-10710
Quantification of the background signal to solar neutrino detection from cosmogenic activation of the atmosphere
[DE87-013830] 01 p0119 N88-10762
The impact of varves on solar physics
[NASA-CR-181519] 03 p0390 N88-12448
Drought, solar activity link established by Leningrad geophysicists 04 p0458 N88-12835
Spectral analysis of APT RS CVn binary light curves
04 p0508 N88-13122
Starspots on the short-period RS CVn system SV Cam: 45 years of activity 04 p0508 N88-13123
Stellar cycle variability of solar-like stars: A sneak preview 04 p0510 N88-13136
A comprehensive exploration of late-type stars in the far-ultraviolet 04 p0520 N88-13194
Long-period variations of wind parameters in the mesopause region and the solar cycle dependence
06 p0733 N88-14509
On the dependence of the lower thermospheric wind regime on the solar cycle 06 p0736 N88-14524
Max '91: Flare research at the next solar maximum
[NASA-TM-89700] 06 p0806 N88-14919
Prediction of the next solar activity cycle
08 p1035 N88-16276
Solar-geophysical data number 516, August 1987. Part 1: (Prompt reports). Data for July 1987, June 1987 and late data
[PB88-114368] 09 p1263 N88-17570
Variations in the atmosphere associated with the 11-year solar cycle 22 p3122 N88-28557
Basic causes of amplitude modulation in climatic/weather parameters
[DE88-702743] 23 p3236 N88-29254
Neutrino electrodynamics and possible effects for solar neutrinos
[DE88-701647] 23 p3308 N88-29705
More than a solar cycle of synoptic solar and coronal data: A video presentation
[NASA-CR-181459] 23 p3308 N88-29708
Spectral analysis of the Elatina varve series
[NASA-CR-183085] 24 p3402 N88-30260

SOLAR DISK
U SUN

SOLAR DYNAMIC POWER SYSTEMS
Electrical Power Working Group report
01 p0016 N88-10095
Photovoltaic power modules for NASA's manned space station
[NASA-TM-100229] 03 p0277 N88-11745
Design of a condenser-boiler for a binary mercury-organic Rankine cycle solar dynamic space power system
[AD-A184188] 03 p0348 N88-12198
Status of 20 kHz space station power distribution technology
[NASA-TM-100781] 08 p0964 N88-15838
Solar concentrator advanced development program, task 1
[NASA-CR-179489] 10 p1350 N88-18068
Computer-aided modeling and prediction of performance of the modified Lundell class of alternators in space station solar dynamic power systems
[NASA-CR-182538] 11 p1507 N88-19000
Solar dynamic power system definition study
[NASA-CR-180877] 13 p1733 N88-20361
Space station power system requirements
[NASA-TM-100886] 14 p1881 N88-21245

Advanced sensible heat solar receiver for space power
[NASA-TM-100847] 14 p1882 N88-21249
Space station solar concentrator materials research
[NASA-TM-100862] 14 p1882 N88-21250
Power systems for production, construction, life support and operations in space
[NASA-TM-100838] 14 p1883 N88-21254
Ray tracing optical analysis of offset solar collector for space station solar dynamic system
[NASA-TM-100853] 15 p2027 N88-22080
Structural assessment of a space station solar dynamic heat receiver thermal energy storage canister
15 p2081 N88-22406
Solar dynamic heat rejection technology. Task 2: Heat pipe radiator development
[NASA-CR-182141] 16 p2209 N88-23182
The multi-disciplinary design study: A life cycle cost algorithm
[NASA-CR-4156] 17 p2385 N88-24172
Speculations on future opportunities to evolve Brayton powerplants aboard the space station
17 p2398 N88-24258
Design and demonstration of a system for the deposition of atomic-oxygen durable coatings for reflective solar dynamic power system concentrators
[NASA-CR-4158] 19 p2606 N88-25474
Thermal distortion analysis of the space station solar dynamic concentrator
[NASA-TM-100868] 19 p2606 N88-25475
Liquid metal thermal electric converter theoretical and experimental studies
[DE88-006806] 19 p2688 N88-25974
Advanced heat receiver conceptual design study
[NASA-CR-180901] 19 p2688 N88-25977
Solar dynamic power systems
[ETN-88-92969] 23 p3230 N88-29224
Study of toluene stability for an Organic Rankine Cycle (ORC) space-based power system
[NASA-CR-180884] 24 p3337 N88-29863
Study of toluene rotary fluid management device and shear flow condenser performance for a space-based organic Rankine power system
[NASA-CR-180885] 24 p3338 N88-29872

SOLAR DYNAMICS
U HELIOSEISMOLOGY

SOLAR ECLIPSES
Observations of the solar chromosphere in Kunming
[PB87-143319] 07 p0944 N88-15737

SOLAR ELECTRONS
Structural dynamics of high-latitude magnetosphere determined from solar electron data
24 p3444 N88-30500

SOLAR ENERGY
Focusing solar energy collector
02 p0159 N88-10996
Proceedings of the Solar Thermal Technology Conference
[DE87-014441] 02 p0195 N88-11220
Application of solar technology to fuel production chemical processing, and thermochemical energy transport: Status and future
[DE87-014172] 03 p0346 N88-12189
Solar energy: European research and development
[PB87-107645] 04 p0463 N88-12866
Technical evaluation of a solar-powered absorption cooling system (LiBr-H2O)
[PB87-108254] 04 p0463 N88-12867
International Energy Agency (IEA) Small Solar Power Systems (SSPS) sodium cavity and external receiver performance comparison
[DE88-001310] 04 p0465 N88-12879
A study of the optimal transition temperatue of PCM (Phase Change Material) wallboard for solar energy storage
[DE88-001522] 04 p0466 N88-12882
Proceedings of the Eleventh DOE Solar Photochemistry Research Conference
[DE88-000678] 04 p0466 N88-12883
The developmental status of solar thermochemical hydrogen production
[DE88-001778] 04 p0466 N88-12884
Self operating absorption cooling system using solar energy: Small power experimental plant
[DE88-900194] 07 p0874 N88-15299
Definition and economic evaluation of Space Solar Power Systems (SSPS), part 1
[ILR-MITT-184-1(1987)] 08 p1022 N88-16189
Definition and economic evaluation of Space Solar Power Systems (SSPS), part 2
[ILR-MITT-184-2(1987)] 08 p1022 N88-16190
Solar assisted absorption or motor driven heat pump with earth seasonal storage, part 1
[DE88-900191] 09 p1187 N88-17114
Proceedings of the 12th Symposium of Japan Solar Energy Society
[DE88-770029] 11 p1507 N88-19005
Solar generation and storage of O2 (a 1 delta g)
[NASA-CR-4127] 14 p1913 N88-21431
Solar assisted absorption or motor driven heat pump with earth seasonal storage. Part 2: Tables and figures
[DE88-900226] 19 p2686 N88-25964
Integrated solar reforming for thermochemical energy transport
[DE88-005010] 19 p2686 N88-25967
Dielectric compound parabolic concentrating solar collector with frustrated total internal reflection absorber
[DE88-009986] 19 p2688 N88-25976
Photovoltaic Measurements and Performance Branch
[DE88-001142] 21 p2968 N88-27633

SOLAR ENERGY ABSORBERS
Development of an innovative, low-cost solar collector
[PB87-206819] 02 p0194 N88-11210
Characterization of transparent insulation materials --- solar energy absorbers
[ETN-88-91052] 09 p1163 N88-16970
Development of a manufacturing unit for selective coating of solar absorbers made out of aluminum
[BMFT-FB-T-86-204] 14 p1942 N88-21590
Technical applications of solar energy. Project: Selective coatings
[BMFT-FB-T-86-213] 14 p1943 N88-21591
Direct conversion of solar energy to thermal energy
[BMFT-FB-T-86-220] 14 p1943 N88-21592
Solar energy absorption efficiency of an ellipsoidal receiver-reactor with specularly reflecting walls
[AD-A193726] 22 p3117 N88-28520

SOLAR ENERGY CONVERSION
NT PHOTOTHERMAL CONVERSION
NT PHOTOVOLTAIC CONVERSION
Engineering principles and concepts for active solar systems
[DE87-001181] 01 p0066 N88-10425
The fundamentals of photovoltaic system electrical design
[DE87-009061] 02 p0194 N88-11214
Solar thermal technology
[DE87-001171] 02 p0195 N88-11218
Proceedings of the Solar Thermal Technology Conference
[DE87-014441] 02 p0195 N88-11220
An evaluation of the LEC-460 solar collector
[DE88-000052] 02 p0196 N88-11224
Polymers in solar technologies
[DE88-001102] 03 p0294 N88-11849
Energy transfer and photochemistry in biomimetic solar conversion
[PB88-130026] 10 p1348 N88-18057
Photochemical solar energy conversion utilizing semiconductors localized in membrane mimetic systems
[DE88-002887] 10 p1349 N88-18065
Design of the Sandia-Israel 20-kW reflux heat-pipe solar receiver/reactor
[DE88-001312] 13 p1794 N88-20729
Control strategies and hardware used in solar thermal applications
[DE88-004631] 13 p1794 N88-20731
Oxidation/sulfidation of materials in an SO3/SO2/O2 thermochemical-transport, distributed-receiver, solar-energy system
[DE88-005875] 13 p1795 N88-20739
Direct conversion of solar energy to thermal energy
[BMFT-FB-T-86-220] 14 p1943 N88-21592
Comparison of electrically driven lasers for space power transmission
[NASA-TM-4045] 16 p2212 N88-23197
Performance sensitivities for point-focus dish systems with secondary concentrators
[DE88-001152] 21 p2968 N88-27629
Reflux heat-pipe solar receivers for dish-electric systems
[DE88-008671] 21 p2968 N88-27631
SERI's photovoltaic research project: A foundation for tomorrow's utility-scale electricity
[DE88-001161] 23 p3230 N88-29220

SOLAR FACULAE
U FACULAE

SOLAR FLARES
A layered scintillation detector for solar neutron observations
[DE87-011354] 01 p0049 N88-10314
STIP Symposium on Physical Interpretation of Solar/Interplanetary and Cometary Intervals
[NASA-CR-181201] 01 p0110 N88-10709
Solar-terrestrial observations during STIP interval 15 (12-21 February 1984) 01 p0111 N88-10711
Overview of the MONSEE UAG report on STIP intervals No. 15 and 16: The 24-25 April 1984 Forbush decrease period 01 p0111 N88-10712
Low altitude flux and dose measurements during two solar flare events 01 p0111 N88-10713
The largest white light flare ever observed: 25 April 1984, 0001 UT 01 p0111 N88-10714
Probable detection of solar neutrons by ground-level neutron monitors during STIP interval 16
01 p0111 N88-10715
Solar energetic particles events observed by Prognoz-10 Intercosmos (May-October 1985)
01 p0111 N88-10716
Two dimensional imaging observations of meter-decameter bursts associated with the February 1986 flare activity 01 p0113 N88-10723
Solar origins of coronal mass ejections
01 p0113 N88-10726
Radio studies of large scale structures of the Sun's corona and transient activity 01 p0114 N88-10728
An account of a flare related shock event recorded by the energetic particle detector EPONA of the Giotto spacecraft during September 1985 (STIP interval 18)
01 p0118 N88-10757
Solar-geophysical data number 513, May 1987. Part 1: (Prompt reports). Data for April, March 1987 and late data
[PB87-204939] 01 p0119 N88-10760
Solar-geophysical data number 513, May 1987. Part 2: (Comprehensive reports). Data for November 1986 and miscellanea
[PB87-204974] 01 p0119 N88-10761
Loop interaction in the visible emission corona: Morphological details 02 p0256 N88-11622
Sunspot observations from the SOUP instrument on Spacelab 2 02 p0257 N88-11623
Solar-geophysical data number 514, June 1987. Part 2: (Comprehensive reports). Data for December 1986
[PB87-217279] 03 p0390 N88-12450
Prompt simultaneous acceleration of protons and electrons to relativistic energies by shock waves in solar flares
[IPPJ-851] 04 p0493 N88-13037
A large X-ray flare on Sigma 2 coronae borealis observed with exosat 04 p0508 N88-13121
The appearance and disappearance of magnetic flux on the quiet sun
[AD-A185432] 05 p0661 N88-14055
Flares: Solar and stellar
[PB87-124962] 06 p0806 N88-14917
Max '91: Flare research at the next solar maximum
[NASA-TM-89700] 06 p0806 N88-14919
Energetics and dynamics of simple impulsive solar flares
[NASA-TM-87816] 07 p0947 N88-15755
Flare doublet: Interplanetary and geomagnetic effects
08 p1001 N88-16066
Unusually strong density decrease in near-Earth interplanetary plasma and magnetically quiet day as effects of isolated solar flare 08 p1002 N88-16072
Solar event of 27 April 1981 08 p1004 N88-16084
Magnetic reconnection and solar flare loops
08 p1094 N88-16583
Interplanetary and geophysical effects of a coronal transient 08 p1095 N88-16587
Small-scale structure in solar flare radio emission
08 p1097 N88-16598
Dynamic evolution of the source volumes of gradual and impulsive solar flare emissions
[NASA-TM-87815] 08 p1102 N88-16621
Solar-geophysical data number 517, September 1987. Part 1: (Prompt reports). Data for August, July 1987 and late data
[PB88-128426] 10 p1430 N88-18544
Solar-geophysical data number 517, September 1987. Part 2: (Comprehensive reports). Data for March 1987 and miscellanea
[PB88-128434] 10 p1431 N88-18545
Solar flares and magnetic topology
[AD-A188692] 12 p1712 N88-20244
Solar-geophysical data number 519, November 1987. Part 2: (Comprehensive reports). Data for May 1987 and miscellanea
[PB88-158910] 14 p2011 N88-21997
Solar-geophysical data number 520, December 1987. Part 1: (Prompt reports). Data for November 1987, October 1987 and late data
[PB88-164199] 16 p2290 N88-23712
The gamma-ray spectrometer experiment on the solar maximum mission satellite
[NASA-CR-182977] 17 p2452 N88-24569
The 2-D magnetohydrostatic configurations leading to flares or quiescent filament eruptions
[NASA-TM-101147] 18 p2595 N88-25423
Preliminary estimates of radiation exposures for manned interplanetary missions from anomalously large solar flare events
[NASA-TM-100620] 18 p2596 N88-25427

Solar-geophysical data number 521, January 1988. Part 2: (Comprehensive reports). Data for July 1987 and miscellanea
[PB88-179221] 19 p2743 N88-26285
The solar flare of 18 August 1979: Incoherent scatter radar data and photochemical model comparisons
[DE88-007616] 19 p2743 N88-26286
The ratio of microwaves to X-rays in solar flares: The case for the thick target model
[NASA-CR-183102] 19 p2743 N88-26287
The properties of solar coronal active regions deduced from X-ray line spectra
[AD-A193026] 20 p2886 N88-27141
The hard X-ray burst spectrometer event listing 1980-1987
[NASA-TM-4036] 20 p2887 N88-27144
Measurement of macroscopic electric fields in solar plasma structures
[AD-A193291] 21 p3031 N88-27993
Solar flares and magnetospheric particles: Investigations based upon the ONR-602 and ONR-604 experiments
[AD-A193396] 21 p3031 N88-27994
Solar-geophysical data number 523, March 1988. Part 1: (Prompt reports). Data for February 1988, January 1988 and late data
[PB88-212766] 24 p3458 N88-30574
Solar-geophysical data number 523, March 1988. Part 2: (Comprehensive reports). Data for September 1987 and miscellanea
[PB88-212774] 24 p3458 N88-30576

SOLAR FLUX
High-resolution continuum observations of the Sun
02 p0255 N88-11614
Total light flux and colour of solar corona
[PB87-143335] 07 p0946 N88-15754
Solar event of 27 April 1981 08 p1004 N88-16084
Neutrino magnetic moment and time variation of solar neutrino flux
[DE88-700687] 10 p1430 N88-18542
Reflux heat-pipe solar receivers for dish-electric systems
[DE88-008671] 21 p2968 N88-27631

SOLAR FLUX DENSITY
NT SOLAR CONSTANT
Short term variability between 120 and 300 mm from Solar Mesosphere Explorer (SME) observations
[AERONOMICA-ACTA-A-328-1988]
23 p3308 N88-29709

SOLAR FURNACES
A solar receiver-reactor with specularly reflecting walls for high-temperature thermoelectrochemical and thermochemical processes
[AD-A187612] 10 p1351 N88-18077
Polymer reflectors research during FY86
[DE88-001101] 11 p1508 N88-19009
Photolytic formation of free radicals and their effect on hydrocarbon pyrolysis chemistry in a concentrated solar environment
[DE88-004129] 13 p1794 N88-20730
Solar energy absorption efficiency of an ellipsoidal receiver-reactor with specularly reflecting walls
[AD-A193726] 22 p3117 N88-28520

SOLAR GENERATORS
NT SOLAR CELLS
NT SOLAR DYNAMIC POWER SYSTEMS
NT VERTICAL JUNCTION SOLAR CELLS
Environmental interactions of solar generators in space 03 p0274 N88-11730
Recent progress in space photovoltaic systems
[NASA-TM-100208] 03 p0311 N88-11966
Solar converging method 04 p0403 N88-12504
Design description report for a photovoltaic power system for a remote satellite earth terminal
[NASA-CR-179586] 04 p0465 N88-12875
International Energy Agency (IEA) Small Solar Power Systems (SSPS) sodium cavity and external receiver performance comparison
[DE88-001310] 04 p0465 N88-12879
A 1,000-watt solar power unit for Far North
06 p0728 N88-14481
Short Reference Years: Short weather data sets for faster simulations of solar energy systems and energy consumption in buildings
[DE88-900198] 07 p0881 N88-15343
Definition and economic evaluation of Space Solar Power Systems (SSPS), part 1
[ILR-MITT-184-1(1987)] 08 p1022 N88-16189
Definition and economic evaluation of Space Solar Power Systems (SSPS), part 2
[ILR-MITT-184-2(1987)] 08 p1022 N88-16190
Oxidation/sulfidation of materials in an SO3/SO2/O2 thermochemical-transport, distributed-receiver, solar-energy system
[DE88-005875] 13 p1795 N88-20739
Thermal analysis of heat storage canisters for a solar dynamic, space power system
[DE88-004199] 15 p2027 N88-22075
Reflux heat-pipe solar receivers for dish-electric systems
[DE88-008671] 21 p2968 N88-27631
Photovoltaic Energy. Electricity from Sunlight: A current awareness bulletin
[DE88-008289] 21 p2969 N88-27634
Space photovoltaic generators. State of the art, trends
[REPT-881-440-106] 21 p2970 N88-27640
SERI's photovoltaic research project: A foundation for tomorrow's utility-scale electricity
[DE88-001161] 23 p3230 N88-29220

SOLAR GRANULATION
First results on quiet and magnetic granulation from SOUP 02 p0255 N88-11613
High-resolution continuum observations of the Sun
02 p0255 N88-11614
Large-scale horizontal flows from SOUP observations of solar granulation 02 p0256 N88-11621
Loop interaction in the visible emission corona: Morphological details 02 p0256 N88-11622
Sunspot observations from the SOUP instrument on Spacelab 2 02 p0257 N88-11623

SOLAR HEATING
Statistical distribution of solar radiation (hourly sums): Cumulative frequency curves preparation of a European data set and direction for use
[PB87-107454] 04 p0467 N88-12886
Transient development of stratification in a partially divided enclosure
[DE87-011742] 05 p0572 N88-13490
Evaluation of thermal storage for solar heating systems: Executive summary
[DE88-900219] 07 p0874 N88-15304
Short Reference Years: Short weather data sets for faster simulations of solar energy systems and energy consumption in buildings
[DE88-900198] 07 p0881 N88-15343
Actual performance and economic feasibility of residential solar water heaters
[INPE-4399-RPE/555] 08 p1023 N88-16191
Solar tides in the upper equatorial thermosphere: A comparison between AE-E data and the NCAR thermospheric general circulation model
[AD-A186160] 08 p1023 N88-16196
Solar assisted absorption or motor driven heat pump with earth seasonal storage, part 1
[DE88-900191] 09 p1187 N88-17114
Effect of storage thermal behavior in seasonal storage solar heating systems
[PB88-114236] 10 p1350 N88-18067
Application of the estimation method to parameter performance date of solar water heating systems
[INPE-4268-PRE/1141] 11 p1508 N88-19007
Advanced utilization of solar energy: Utilization for biotechnology
[DE88-770031] 12 p1640 N88-19819

SOLAR HOUSES
Advanced utilization of solar energy: Utilization for biotechnology
[DE88-770031] 12 p1640 N88-19819

SOLAR INSTRUMENTS
NT SPECTROHELIOGRAPHS

SOLAR INTERIOR
Oscillations of solar models with internal element diffusion
[DE88-003156] 09 p1264 N88-17573

SOLAR LASERS
U SOLAR-PUMPED LASERS

SOLAR LIMB
Small-scale energy storage and release as the cause of the stellar X-ray corona 02 p0255 N88-11615

SOLAR MAGNETIC FIELD
On the association of erupting magnetic fields with eruptive prominences and coronal mass ejections
01 p0113 N88-10727
Theoretical Problems in High Resolution Solar Physics, 2
[NASA-CP-2483] 02 p0254 N88-11609
First results on quiet and magnetic granulation from SOUP 02 p0255 N88-11613
Small-scale energy storage and release as the cause of the stellar X-ray corona 02 p0255 N88-11615
Magnetic fields in the overshoot zone: The great escape 02 p0256 N88-11616
Theoretical modelling of the fine structures in sunspots 02 p0256 N88-11617
Pressure structure of solar coronal loops
02 p0256 N88-11618
The Sun and the solar activity
03 p0271 N88-11704
The solar wind 03 p0271 N88-11705
Solar magnetic and velocity fields
[AD-A184360] 03 p0390 N88-12449
Development of optical modulators for measurements of solar magnetic fields
[NASA-TM-100315] 04 p0490 N88-13016
Large scale solar and stellar magnetic fields
04 p0507 N88-13117
The appearance and disappearance of magnetic flux on the quiet sun
[AD-A185432] 05 p0661 N88-14055
Magnetic reconnection and solar flare loops
08 p1094 N88-16583
Flux tubes and loops in the solar chromosphere and corona 08 p1095 N88-16591
Emerging flux, magnetic reconnection, plasma turbulence and waves in the transition zone of the solar atmosphere 08 p1096 N88-16597
The effects of viscosity on resistive ballooning modes in line-tied coronal magnetic fields
08 p1097 N88-16599
Solar-geophysical data number 517, September 1987. Part 1: (Prompt reports). Data for August, July 1987 and late data
[PB88-128426] 10 p1430 N88-18544
Development of high stability fiber optic spectrophotometric systems for study of solar/stellar magnetic activity
[AD-A189327] 13 p1852 N88-21088
Magnetic field hourly averages from the Rome-GSFC experiment aboard Helios 1 and Helio 2
[NASA-TM-89782] 14 p2011 N88-21995
The SAMEX vector magnetograph: A design study for a space-based solar vector magnetograph
[NASA-TM-4048] 18 p2596 N88-25424

SOLAR MAXIMUM MISSION
In-orbit and laboratory exchange of ORUs designed/not designed for servicing 12 p1587 N88-19499
Remote repair demonstration of Solar Maximum main electronics box 12 p1588 N88-19510

SOLAR MESOSPHERE EXPLORER
Short term variability between 120 and 300 mm from Solar Mesosphere Explorer (SME) observations
[AERONOMICA-ACTA-A-328-1988]
23 p3308 N88-29709

SOLAR NEBULA
U SOLAR CORONA

SOLAR NEIGHBORHOOD
A spectral survey of 26 G9-M6 flare stars in the solar neighborhood 04 p0512 N88-13149
A VLA survey of dMe flare stars
04 p0513 N88-13154
An astrometric search for a stellar companion to the sun 04 p0520 N88-13195
Hydrogen and deuterium in the local interstellar medium 04 p0521 N88-13204

SOLAR NEUTRINOS
Superfluid He4 as a solar neutrino detector
[DE87-014477] 02 p0257 N88-11625
A possible accelerator experiment to solve the solar neutrino puzzle
[PREPRINT-556] 06 p0778 N88-14778
Solar oscillations, gravitational multipole field of the Sun and the solar neutrino paradox
[DE88-002100] 07 p0946 N88-15752
Stable, heavy, neutral particles in the sun and in toponium decay 17 p2452 N88-24568
Cosmions and stars
[DE88-010886] 20 p2887 N88-27145
Neutrino electrodynamics and possible effects for solar neutrinos
[DE88-701647] 23 p3308 N88-29705
Resonant spin-flavor precession of solar and supernova neutrinos
[DE88-752604] 23 p3308 N88-29707

SOLAR NEUTRONS
A layered scintillation detector for solar neutron observations
[DE87-011354] 01 p0049 N88-10314
Probable detection of solar neutrons by ground-level neutron monitors during STIP interval 16
01 p0111 N88-10715

SOLAR NOISE
U SOLAR RADIO EMISSION

SOLAR OBSERVATORIES
NT PINHOLE OCCULTER FACILITY
Theoretical Problems in High Resolution Solar Physics, 2
[NASA-CP-2483] 02 p0254 N88-11609
Bern solar observations. Solar data for January-December 1986
[REPT-53] 09 p1263 N88-17569
NASA Marshall Space Flight Center solar observatory
[NASA-TM-100339] 24 p3332 N88-29832
Coordinated study of Solar-Terrestrial Observatory (STO) payloads on space station
[NASA-CR-183142] 24 p3334 N88-29848

SOLAR ORBITS
Single-burn transfer to nominally periodic orbit in the vicinity of point L2 of Earth-Sun system and related problems 08 p1006 N88-16100
Numerical evidence that the motion of Pluto is chaotic [AD-A195920] 24 p3455 N88-30568

SOLAR OSCILLATIONS
First results on quiet and magnetic granulation from SOUP 02 p0255 N88-11613
Large-scale horizontal flows from SOUP observations of solar granulation 02 p0256 N88-11621
Sunspot observations from the SOUP instrument on Spacelab 2 02 p0257 N88-11623
Perturbations of the Sun's gravitational field due to solar oscillations [DE88-002099] 07 p0946 N88-15751
Solar oscillations, gravitational multipole field of the Sun and the solar neutrino paradox [DE88-002100] 07 p0946 N88-15752
Global solar oscillations observed in the visible to near infrared continuum 13 p1858 N88-21110

SOLAR PHYSICS
About the interest of solar interferometric observations 01 p0094 N88-10615
Solar-geophysical data number 513, May 1987. Part 1: (Prompt reports). Data for April, March 1987 and late data [PB87-204939] 01 p0119 N88-10760
Solar-geophysical data number 513, May 1987. Part 2: (Comprehensive reports). Data for November 1986 and miscellanea [PB87-204974] 01 p0119 N88-10761
Theoretical Problems in High Resolution Solar Physics, 2 [NASA-CP-2483] 02 p0254 N88-11609
High-resolution continuum observations of the Sun 02 p0255 N88-11614
Solar-geophysical data number 514, June 1987. Part 1: (Prompt reports). Data for May 1987, April 1987 and late data [PB87-217261] 02 p0257 N88-11626
The impact of varves on solar physics [NASA-CR-181519] 03 p0390 N88-12448
Solar-geophysical data number 514, June 1987. Part 2: (Comprehensive reports). Data for December 1986 [PB87-217279] 03 p0390 N88-12450
Exploiting the IR: Solar and stellar spectroscopy in the IR 04 p0504 N88-13102
Three-halves law in sunspot cycle shape [NASA-CR-181520] 04 p0525 N88-13210
Solar-geophysical data number 515, July 1987. Part 1: (Prompt reports). Data for June 1987, May 1987 and late data [PB87-233177] 06 p0805 N88-14912
Solar-geophysical data number 515, July 1987. Part 2: (Comprehensive reports). Data for January 1987 and miscellanea [PB87-233185] 06 p0805 N88-14913
Solar-geophysical activity reports for STIP (Study of Travelling Interplanetary Phenomena) Interval 15, 12-21 February 1984 ground level event and STIP Interval 16, 20 April-4 May 1984 Forbush decrease [PB87-232658] 06 p0805 N88-14915
On the potential role of concentrated field-aligned currents in solar physics 06 p1099 N88-16614
Solar-geophysical data number 516, August 1987. Part 2: (Comprehensive reports). Data for February 1987 [PB88-114376] 09 p1264 N88-17571
Solar-geophysical data number 518, October 1987. Part 2: (Comprehensive reports). Data for April 1987 [PB88-138060] 12 p1711 N88-20242
Solar-geophysical data number 518, October 1987. Part 1: (Prompt reports). Data for September 1987, August 1987 and late data [PB88-138078] 12 p1712 N88-20243
Research and technology, 1987 [NASA-TM-100323] 12 p1713 N88-20253
Solar-geophysical data number 519, November 1987. Part 2: (Comprehensive reports). Data for May 1987 and miscellanea [PB88-158910] 14 p2011 N88-21997
Solar-geophysical data number 520, December 1987. Part 1: (Prompt reports). Data for November 1987, October 1987 and late data [PB88-164199] 16 p2290 N88-23712
Stable, heavy, neutral particles in the sun and in toponium decay 17 p2452 N88-24568
An image processing system for research in solar physics [AD-A191673] 18 p2595 N88-25421
Solar-geophysical data number 521, January 1988. Part 1: (Prompt reports). Data for December 1987, November 1987 and late data [PB88-179213] 19 p2743 N88-26284
Solar-geophysical data number 521, January 1988. Part 2: (Comprehensive reports). Data for July 1987 and miscellanea [PB88-179221] 19 p2743 N88-26285
Solar-geophysical data number 523, March 1988. Part 1: (Prompt reports). Data for February 1988, January 1988 and late data [PB88-212766] 24 p3458 N88-30574
Solar-geophysical data number 523, March 1988. Part 2: (Comprehensive reports). Data for September 1987 and miscellanea [PB88-212774] 24 p3458 N88-30576

SOLAR PLANETARY INTERACTIONS
NT SOLAR TERRESTRIAL INTERACTIONS
Peculiarities of daytime ionosphere of Venus during years of low and high solar activity 08 p1005 N88-16091
Solar-geophysical data number 516, August 1987. Part 2: (Comprehensive reports). Data for February 1987 [PB88-114376] 09 p1264 N88-17571

SOLAR PLASMA (RADIATION)
U SOLAR WIND

SOLAR POSITION
Influence of solar illumination conditions on TM/Landsat data [INPE-4463-TDL/320] 12 p1638 N88-19806

SOLAR POWER GENERATION
U SOLAR GENERATORS

SOLAR POWER SATELLITES
Technology for large space systems: A bibliography with indexes (supplement 18) [NASA-SP-7046(18)] 21 p2901 N88-27214

SOLAR POWER SOURCES
U SOLAR GENERATORS

SOLAR PROBES
NT HELIOS 1
NT HELIOS 2

SOLAR PROMINENCES
STIP Symposium on Physical Interpretation of Solar/Interplanetary and Cometary Intervals [NASA-CR-181201] 01 p0110 N88-10709
Solar-geophysical data number 513, May 1987. Part 2: (Comprehensive reports). Data for November 1986 and miscellanea [PB87-204974] 01 p0119 N88-10761
Solar-geophysical data number 514, June 1987. Part 2: (Comprehensive reports). Data for December 1986 [PB87-217279] 03 p0390 N88-12450
Observations and modeling of the prominence/corona transition region 08 p1094 N88-16585
Emerging flux, magnetic reconnection, plasma turbulence and waves in the transition zone of the solar atmosphere 08 p1096 N88-16597
Solar-geophysical data number 517, September 1987. Part 2: (Comprehensive reports). Data for March 1987 and miscellanea [PB88-128434] 10 p1431 N88-18545
Magnetohydrodynamic (MHD) simulation of solar prominence formation 13 p1858 N88-21109
Solar-geophysical data number 519, November 1987. Part 2: (Comprehensive reports). Data for May 1987 and miscellanea [PB88-158910] 14 p2011 N88-21997
Measurement of macroscopic electric fields in solar plasma structures [AD-A193291] 21 p3031 N88-27993

SOLAR PROPULSION
NT SOLAR THERMAL PROPULSION

SOLAR PROTONS
Automated spectrometric unit for the study of radiation characteristics of cosmic radiation aboard Prognoz-9 space stations 19 p2706 N88-26090

SOLAR RADIATION
NT SOLAR COSMIC RAYS
NT SOLAR ELECTRONS
NT SOLAR NEUTRINOS
NT SOLAR NEUTRONS
NT SOLAR PROTONS
NT SOLAR RADIO BURSTS
NT SOLAR RADIO EMISSION
NT SOLAR WIND
NT SOLAR X-RAYS
NT SUNLIGHT
NT TYPE 3 BURSTS
Balloon-based infrared solar occultation measurements of stratospheric O3, H2O, HNO3 and CFC-12 [NOAA-TR-NESDIS-34] 01 p0068 N88-10438
Solar Energy Meteorological Research and Training Site, Alaska [DE87-013706] 01 p0069 N88-10440
Status of the solar and infrared radiation submodels in the LLNL 1-D and 2-D chemical-transport models [DE87-014320] 01 p0069 N88-10441
Solar modulation of the cosmic radiation in the heliosphere 01 p0112 N88-10720
Mathematical modelling of solar ultraviolet radiation induced optical degradation in anodized aluminum 02 p0135 N88-10846
A quasi-physical model for converting hourly global horizontal to direct normal insolation [DE87-012273] 03 p0349 N88-12204
Calendar year 1985 solar and weather data for Austin, Texas [PB87-220174] 03 p0352 N88-12219
The development of low level coastal flow fields when solar radiation is blocked by smoke [DE87-014348] 03 p0354 N88-12230
Statistical distribution of solar radiation (hourly sums): Cumulative frequency curves preparation of a European data set and direction for use [PB87-107454] 04 p0467 N88-12886
A comprehensive exploration of late-type stars in the far-ultraviolet 04 p0520 N88-13194
Finnish contributions to EISCAT science in 1986 06 p0691 N88-14235
Latitude coverage of observations of the middle atmosphere by solar absorption spectrometry from a heliosynchronous orbit [AERONOMICA-ACTA-A-316-1987] 06 p0742 N88-14566
Rome Neutron Monitor (NM) - 64 data for 5 solar particle ground-level events [IFSI-86-7] 06 p0806 N88-14918
Satellite techniques of solar resource assessment for focusing and non-focusing solar collector systems [DE88-001857] 07 p0874 N88-15298
The solar radiation incident at the top of the atmosphere of Uranus and Neptune [AERONOMICA-ACTA-A-317-1987] 07 p0878 N88-15323
Short Reference Years: Short weather data sets for faster simulations of solar energy systems and energy consumption in buildings [DE88-900198] 07 p0881 N88-15343
Finnish-Soviet Symposium on Radio Astronomy (1st) held at Otaniemi on August 26-27, 1985 [PB87-140661] 07 p0944 N88-15736
The use of the direct measurement of solar radiation for the determination of Pasquill Stability Parameter [AD-A186084] 07 p0946 N88-15750
The anisotropy of reflected solar radiation over several types of land surface 08 p1018 N88-16171
An aureolar radiometer for the determination of aerosol size distribution 08 p1018 N88-16174
Aerosol size distribution from measurements of the radiance in the solar aureole 08 p1019 N88-16176
The iterative radiance model of the Meteorological Institute of the University of Munich (West Germany) 08 p1019 N88-16178
Solar ultraviolet spectrum obtained from a balloon gondola 08 p1032 N88-16258
Dynamic evolution of the source volumes of gradual and impulsive solar flare emissions [NASA-TM-87815] 08 p1102 N88-16621
Nimbus 7 Solar Backscatter Ultraviolet (SBUV) spectral scan solar irradiance and Earth radiance product user's guide [NASA-RP-1199] 09 p1184 N88-17096
Solar-geophysical data number 516, August 1987. Part 1: (Prompt reports). Data for July 1987, June 1987 and late data [PB88-114368] 09 p1263 N88-17570
Solar-geophysical data number 516, August 1987. Part 2: (Comprehensive reports). Data for February 1987 [PB88-114376] 09 p1264 N88-17571
Parameterization of radiative transfer in the Earth's atmosphere with specific applications to clouds 10 p1353 N88-18087
Evaluation of surface energy and radiation balance systems on the Konza Prairie [NASA-CR-182534] 10 p1355 N88-18097
Radiation balance components above the tropical evergreen Amazon forests (3rd campaign of data collection) [INPE-4195-PRE/1079] 11 p1513 N88-19039
Influence of radiation and thermal conduction on temperature distribution in the thin wall of a hollow cylinder [INPE-4428-TDL/308] 12 p1626 N88-19730
Calibration of the solar radiation estimation method by satellites [INPE-4349-PRE/1185] 12 p1646 N88-19861
Vertical turbulent transfer of matter in thin ocean surface layer during daytime heating 13 p1787 N88-20693
Direct absorption receiver control studies [DE87-013653] 13 p1795 N88-20737
Radiative processes affecting ocean mixed-layer heat content and their monitoring from satellite 13 p1806 N88-20800
Satellite estimations of the solar radiation flux at the surface 14 p1936 N88-21551

Solar-geophysical data number 520, December 1987. Part 2: (Comprehensive reports). Data for June 1987 and miscellanea
[PB88-164207] 15 p2152 N88-22849
NOAA-ERL-ARL (National Oceanic and Atmospheric Administration-Environmental Research Laboratories-Air Resources Laboratory) solar UV radiation and climate research project: Program description
[PB88-169396] 16 p2233 N88-23339
Comparison of the solar radiation estimation method by satellites 17 p2360 N88-24055
Photovoltaic Advanced Research and Development Project, solar radiation research
[DE88-001143] 18 p2537 N88-25056
Results of radiation measurements in West Germany and from special measurement series in the Meteorological Observatory of Hamburg
[REPT-11] 18 p2542 N88-25088
Observations of cosmic rays in the outer heliosphere
[NASA-CR-182942] 18 p2596 N88-25425
Preliminary estimates of radiation exposures for manned interplanetary missions from anomalously large solar flare events
[NASA-TM-100620] 18 p2596 N88-25427
The ratio of microwaves to X-rays in solar flares: The case for the thick target model
[NASA-CR-183102] 19 p2743 N88-26287
Determination and application of bidirectional solar-optical properties of fenestration systems
[DE88-010364] 20 p2820 N88-26727
On the global radiation incident variously orientated surfaces on the South Coast of Finland
[FMI-5] 20 p2823 N88-26746
Solar-geophysical data number 522, February 1988. Part 1: (Prompt reports). Data for January 1988, December 1987 and late data
[PB88-194733] 20 p2886 N88-27139
Overview and future direction for blackbody solar-pumped lasers
[NASA-TM-100621] 21 p2955 N88-27553
Development of radiation and cloud parameterization programs for AFGL (Air Force Geophysics Laboratory) global models
[AD-A193369] 21 p2973 N88-27658
SERI standard broadband format: A solar and meteorological data archival format
[DE88-001145] 21 p3028 N88-27975
IR (infrared) sky radiance distributions in the marine boundary layer
[AD-A193683] 22 p3119 N88-28531
Differences in radiation budget parameters over Asia in relation to contrasting Indian monsoons 22 p3125 N88-28574
A comparison of typical meteorological year solar radiation information with the SOLMET data base
[DE88-009242] 23 p3234 N88-29247
Global solar radiation in Sierra Leone (West Africa)
[DE88-702725] 23 p3235 N88-29252
Mathematical correlation between variations in solar radiation parameters. Part 1: Daily sums of global radiation and midday global radiation
[DE88-702742] 23 p3236 N88-29253
Basic causes of amplitude modulation in climatic/weather parameters
[DE88-702743] 23 p3236 N88-29254
Short term variability between 120 and 300 mm from Solar Mesosphere Explorer (SME) observations
[AERONOMICA-ACTA-A-328-1988] 23 p3308 N88-29709
Energy budget and ground temperatures in hot regions
[AD-A196298] 24 p3404 N88-30268

SOLAR RADIATION SHIELDING
A near-earth optical communications terminal with a corevolving planetary sun shield 04 p0434 N88-12693
Air temperature shield tests
[AD-A187459] 11 p1514 N88-19043
OLYMPUS shuttle specific radiator shield 14 p1879 N88-21234

SOLAR RADIO BURSTS
NT TYPE 3 BURSTS
The large Type 4 radio burst event of 24 April 1985 interpreted by dynamic spectral recordings and associated recordings 01 p0112 N88-10717
Two dimensional imaging observations of meter-decameter bursts associated with the February 1986 flare activity 01 p0113 N88-10723
Coronal and interplanetary Type 2 radio emission 01 p0114 N88-10731
Solar-geophysical data number 513, May 1987. Part 1: (Prompt reports). Data for April, March 1987 and late data
[PB87-204939] 01 p0119 N88-10760
Solar-geophysical data number 513, May 1987. Part 2: (Comprehensive reports). Data for November 1986 and miscellanea
[PB87-204974] 01 p0119 N88-10761
Solar-geophysical data number 514, June 1987. Part 2: (Comprehensive reports). Data for December 1986
[PB87-217279] 03 p0390 N88-12450
Solar-geophysical data number 517, September 1987. Part 2: (Comprehensive reports). Data for March 1987 and miscellanea
[PB88-128434] 10 p1431 N88-18545
Solar-geophysical data number 519, November 1987. Part 2: (Comprehensive reports). Data for May 1987 and miscellanea
[PB88-158910] 14 p2011 N88-21997
Solar-geophysical data number 523, March 1988. Part 2: (Comprehensive reports). Data for September 1987 and miscellanea
[PB88-212774] 24 p3458 N88-30576

SOLAR RADIO EMISSION
NT SOLAR RADIO BURSTS
NT TYPE 3 BURSTS
Variations of the semi-diurnal tidal wind in the meteor region with periods of about 27 and 13.5 days 06 p0734 N88-14516
Solar-geophysical activity reports for STIP (Study of Travelling Interplanetary Phenomena) interval 15, 12-21 February 1984 ground level event and STIP interval 16, 20 April-4 May 1984 Forbush decrease
[PB88-101274] 06 p0802 N88-14906
Observation and interpretation of solar S-component radiation at millimetre waves
[PB87-225207] 06 p0805 N88-14916
Finnish-Soviet Symposium on Radio Astronomy (1st) held at Otaniemi on August 26-27, 1985
[PB87-140661] 07 p0944 N88-15736
Solar-geophysical data number 517, September 1987. Part 1: (Prompt reports). Data for August, July 1987 and late data
[PB88-128426] 10 p1430 N88-18544
Solar-geophysical data number 520, December 1987. Part 1: (Prompt reports). Data for November 1987, October 1987 and late data
[PB88-164199] 16 p2290 N88-23712
Solar-geophysical data number 523, March 1988. Part 1: (Prompt reports). Data for February 1988, January 1988 and late data
[PB88-212766] 24 p3458 N88-30574

SOLAR RADIO WAVES
U SOLAR RADIO EMISSION

SOLAR RECEIVERS
U SOLAR COLLECTORS

SOLAR REFLECTORS
NT SOLAR COLLECTORS
Design concepts to improve high performance solar simulator 02 p0136 N88-10852
Solar thermal technology
[DE87-001171] 02 p0195 N88-11218
Solar converging method 04 p0403 N88-12504
Point-focus concentrator reflector assembly, phase 1
[DE88-003616] 13 p1792 N88-20720
Chemical vapor deposited silica coatings for solar mirror protection
[NASA-TM-100834] 14 p1893 N88-21306
Contamination of optical surfaces --- Space Station 18 p2592 N88-25400
Specular steel surfaces for solar mirror substrates
[DE88-001153] 21 p2968 N88-27630
Planarization of metal substrates for solar mirrors
[DE88-011492] 23 p3229 N88-29214

SOLAR ROTATION
Variations of the semi-diurnal tidal wind in the meteor region with periods of about 27 and 13.5 days 06 p0734 N88-14516

SOLAR SEISMOLOGY
U HELIOSEISMOLOGY

SOLAR SELECTIVE COATINGS
U SELECTIVE SURFACES

SOLAR SENSORS
Airborne tracking sunphotometer apparatus and system
[NASA-CASE-ARC-11622-1] 06 p0730 N88-14492
Development of integrated detectors for attitude sensors
[INPE-4409-PRE/1222] 12 p1602 N88-19586
Characterization of integrated photovoltaic detectors for MECB solar sensors
[INPE-4408-PRE/1221] 12 p1630 N88-19754

SOLAR SIMULATION
ESA Bulletin No. 25
[ISSN-0376-4265] 09 p1128 N88-16767
Development of infrared techniques for testing spacecraft 09 p1128 N88-16772

SOLAR SIMULATORS
Design concepts to improve high performance solar simulator 02 p0136 N88-10852
Development of infrared techniques for testing spacecraft 09 p1128 N88-16772

SOLAR SPECTRA
Loop interaction in the visible emission corona: Morphological details 02 p0256 N88-11622
Solar magnetic and velocity fields
[AD-A184360] 03 p0390 N88-12449
Calibrating AIS images using the surface as a reference 05 p0612 N88-13760
Short-term temporal variations of Nimbus-7 measurements of the solar UV spectral irradiance
[PB88-102132] 07 p0946 N88-15753
Measurement of macroscopic electric fields in solar plasma structures
[AD-A193291] 21 p3031 N88-27993
Aeronomic problems of the molecular oxygen photodissociation. Part 3: Solar spectral irradiances in the region of the O2 Herzberg continuum, Schumann-Runge bands and continuum
[AERONOMICA-ACTA-A-332-1988] 24 p3343 N88-29897
Atmospheric corrections for in-flight satellite radiometric calibration
[AD-A196124] 24 p3391 N88-30194
Spectral analysis of the Elatina varve series
[NASA-CR-183085] 24 p3402 N88-30260

SOLAR SPECTROMETERS
Small-scale structure in solar flare radio emission 08 p1097 N88-16598
The hard X-ray burst spectrometer event listing 1980-1987
[NASA-TM-4036] 20 p2887 N88-27144

SOLAR SYSTEM
High explosive simulations of supernovae and the supernova shell fragmentation model of solar system formation
[DE87-014708] 02 p0251 N88-11584
Royal Observatory, Edinburgh: Research and Facilities
[ISSN-0267-6281] 14 p1993 N88-21881
Space infrared telescope facility project
[NASA-CR-183058] 20 p2883 N88-27121
Activities report of the Institute for Extraterrestrial Physics
[MPE-206] 21 p3029 N88-27981
Lewis Cliff 86010, a unique Antarctic meteorite: Possible new clues to the early history of the solar system 24 p3442 N88-30482
Noble gases, C,N, and Si isotopes in interstellar SiC form the Murchison carbonaceous chondrite 24 p3442 N88-30483
Workshop on the Origins of Solar Systems
[NASA-CR-183025] 24 p3451 N88-30536
Star formation and molecular clouds 24 p3451 N88-30537
Observations of star formation 24 p3451 N88-30538
Cosmochemical trends of volatile elements in the solar system 24 p3451 N88-30542
Terrestrial versus giant planet formation 24 p3451 N88-30543

SOLAR TEMPERATURE
Observations and modeling of the prominence/corona transition region 08 p1094 N88-16585

SOLAR TERRESTRIAL INTERACTIONS
STIP Symposium on Physical Interpretation of Solar/Interplanetary and Cometary Intervals
[NASA-CR-181201] 01 p0110 N88-10709
Overview of STIP intervals 15-19 01 p0110 N88-10710
Solar-terrestrial observations during STIP interval 15 (12-21 February 1984) 01 p0111 N88-10711
Overview of the MONSEE UAG report on STIP intervals No. 15 and 16: The 24-25 April 1984 Forbush decrease period 01 p0111 N88-10712
The large Type 4 radio burst event of 24 April 1985 interpreted by dynamic spectral recordings and associated recordings 01 p0112 N88-10717
Solar-terrestrial research in the space station era 01 p0117 N88-10747
Space Environment Technology --- conference
[ISBN-2-85428-170-5] 03 p0271 N88-11702
The solar wind 03 p0271 N88-11705
Hot plasmas in the Earth's magnetosphere 03 p0272 N88-11710
Magnetospheric storms 03 p0272 N88-11711
Configurations of the quiet polar cap and its response to a sudden increase of the energy input rate epsilon
[DMI-GEOPHYS-PAPERS-R-74] 03 p0350 N88-12210
Drought, solar activity link established by Leningrad geophysicists 04 p0458 N88-12835
Solar-geophysical activity reports for STIP (Study of Travelling Interplanetary Phenomena) interval 15, 12-21 February 1984 ground level event and STIP interval 16, 20 April-4 May 1984 Forbush decrease
[PB88-101274] 06 p0802 N88-14906

Solar-geophysical activity reports for STIP (Study of Travelling Interplanetary Phenomena) Interval 15, 12-21 February 1984 ground level event and STIP Interval 16, 20 April-4 May 1984 Forbush decrease
[PB87-232658] 06 p0805 N88-14915
New book on space ecology reviewed
07 p0697 N88-15434
Flare doublet: Interplanetary and geomagnetic effects
08 p1001 N88-16066
Monitoring of Pc3 pulsations in solar wind and at Earth by interplanetary magnetic field
08 p1002 N88-16069
Unusually strong density decrease in near-Earth interplanetary plasma and magnetically quiet day as effects of isolated solar flare 08 p1002 N88-16072
Interplanetary and geophysical effects of a coronal transient 08 p1095 N88-16587
The formation of boundary layers by the entry of low-energy electrons and energetic ions into the Earth's magnetosphere 08 p1095 N88-16590
International geosphere-biosphere program: A study of global change
[PB88-142393] 11 p1510 N88-19021
Interpretation of the northward B sub z (NBZ) Birkeland current system and polar cap convection patterns in terms of the impulsive penetration model
[AERONOMICA-ACTA-A-321-1987]
18 p2595 N88-25422
Diffusion of slight solar induced disturbances in the middle atmosphere
[MITT-53] 20 p2825 N88-26758
Coordinated study of Solar-Terrestrial Observatory (STO) payloads on space station
[NASA-CR-183142] 24 p3334 N88-29848
Corona-solar wind coupling review
[AFGL-TR-87-0203] 24 p3458 N88-30575

SOLAR THERMAL ELECTRIC POWER PLANTS
Performance analysis of solar thermal power systems
[DE88-000563] 04 p0465 N88-12874
Definition and economic evaluation of Space Solar Power Systems (SSPS), part 1
[ILR-MITT-184-1(1987)] 08 p1022 N88-16189
Definition and economic evaluation of Space Solar Power Systems (SSPS), part 2
[ILR-MITT-184-2(1987)] 08 p1022 N88-16190
Power from the sun: Principles of high temperature solar thermal technology
[DE87-001104] 13 p1795 N88-20736

SOLAR THERMAL PROPULSION
Solar thermal propulsion for orbit transfer vehicles
17 p2426 N88-24445

SOLAR WIND
Change in interplanetary shock acceleration preceding STIP Interval 17 01 p0112 N88-10719
Evolution of the solar wind structure in the outer heliosphere 01 p0112 N88-10721
Study of pickup of cometary ions in turbulent solar winds 01 p0113 N88-10725
Coronal mass ejections: The long-term variation of their occurrence rate and the solar wind mass flux
01 p0114 N88-10732
Dynamics of magnetic clouds in interplanetary space
01 p0115 N88-10736
A numerical study of transient, thermally-conductive solar wind 01 p0115 N88-10738
A two-fluid model for solar wind fluid with higher order moments 01 p0116 N88-10739
Interaction of interplanetary shocks with nonuniform ambient solar wind 01 p0116 N88-10740
An overview of STIP interval 18: September 1985, the G-Z encounter 01 p0116 N88-10741
Comparative plasma tails of Venus and comets
01 p0116 N88-10742
Large-scale interaction of the solar wind with comets Halley and Giacobini-Zinner 01 p0117 N88-10745
The global interaction of comets with the solar wind
01 p0117 N88-10746
Solar wind-cometary interaction at the ionopause and associated phenomena 01 p0117 N88-10748
Solar wind effects on the outer ion coma of Comet Halley 01 p0117 N88-10750
The solar wind interaction with comets: A post encounter view 01 p0118 N88-10751
Plasma-tail activity and the interplanetary medium at Halley's Comet during Armada Week: 6-14 March 1986
01 p0118 N88-10752
Study of the mechanism for solar wind formation
01 p0118 N88-10756
A numerical study of the thermal stability of solar loops 02 p0256 N88-11619
Solar transition region and coronal response to heating rate perturbations 02 p0256 N88-11620
The solar wind 03 p0271 N88-11705
Hot plasmas in the Earth's magnetosphere
03 p0272 N88-11710
Magnetospheric storms 03 p0272 N88-11711
High latitude F-region drift studies
[AD-A184466] 04 p0467 N88-12889
Model of solar-wind magnetosphere coupling
04 p0525 N88-13211
Observations of turbulence and fluctuations in the solar wind 04 p0525 N88-13212
A fluid simulation of the AMPTE lithium gas releases in the solar wind
[TRITA-EPP-87-06] 05 p0661 N88-14056
Magnetic field draping about coronal mass ejecta
[DE88-001805] 05 p0661 N88-14057
Interplanetary magnetic field effects on the interaction of the solar wind with Venus 06 p0805 N88-14910
Monitoring of Pc3 pulsations in solar wind and at Earth by interplanetary magnetic field
08 p1002 N88-16069
Solar cosmic ray propagation in high-velocity solar wind stream 08 p1002 N88-16073
Fluctuations in frequency of coherent radio signals in solar plasma according to Venera-15 and Venera-16 data 08 p1003 N88-16079
Dynamics and turbulence of solar wind in area of its formation based on radio transmission data measured with Venera-15 and Venera-16 spacecraft
08 p1003 N88-16080
Bidirectional electron heat flux events in space
[DE88-001791] 08 p1084 N88-16531
Solar corona and solar wind 08 p1094 N88-16584
The formation of boundary layers by the entry of low-energy electrons and energetic ions into the Earth's magnetosphere 08 p1095 N88-16590
Numerical simulation of solar wind and magnetospheric phenomena 08 p1097 N88-16600
Small scale MHD wave processes in the solar atmosphere and solar wind 08 p1098 N88-16608
Observations of small scale structures using data from the wave experiment on the AMPTE-UKS spacecraft
08 p1099 N88-16612
Transverse flow deflections associated with fast coronal mass ejecta in interplanetary space
[DE88-003180] 09 p1263 N88-17566
Data reduction and analysis of HELIOS plasma wave data
[NASA-CR-182466] 09 p1264 N88-17572
Universal power spectra for wave turbulence: Applications to wind waves, flicker noise, solar wind spectrum and classical second sound
10 p1318 N88-17879
Personal overview of solar wind 6
[DE88-003147] 10 p1430 N88-18543
The relation of solar wind structure to hydromagnetic discontinuities
[DE88-004304] 10 p1431 N88-18546
Electric fields in Earth orbital space. Magnetospheric structural dynamic response to external variables
[AD-A188592] 12 p1643 N88-19836
To what extent is mass loading responsible for the Venus bowshock precursor?
[NASA-TM-89307] 12 p1711 N88-20239
Solar wind observation at the time of closest encounter with Comet Halley 14 p1995 N88-21890
Calculation of the shape of the contact surface at Comet Halley 14 p1995 N88-21892
A comparison between wave observations performed in the environments of Comets Halley and Giacobini-Zinner 14 p1996 N88-21896
Magnetic cavity formation at Comet Halley and at the AMPTE Li release 14 p1996 N88-21898
Plasmapause formation
[AERONOMICA-ACTA-A-319-1987]
15 p2138 N88-22759
Observation of nonlinear wave decay processes in the solar wind by the AMPTE IRM plasma wave experiment
[AD-A191409] 16 p2290 N88-23713
Interpretation of the northward B sub z (NBZ) Birkeland current system and polar cap convection patterns in terms of the impulsive penetration model
[AERONOMICA-ACTA-A-321-1987]
18 p2595 N88-25422
Spacecraft requirements for predictions of geomagnetic activity (a tutorial)
[AD-A191943] 19 p2685 N88-25959
Gone with the solar wind: A study of protons accelerated by interplanetary shocks 19 p2743 N88-26283
Generation of Adlam-Allen waves by plasma release experiments in the solar wind
[PB88-106000] 20 p2886 N88-27140
Magnetohydrodynamic wave propagation in the solar wind
[DE88-702411] 21 p3032 N88-27995
Stability of Venusian ionopause
24 p3448 N88-30523
Corona-solar wind coupling review
[AFGL-TR-87-0203] 24 p3458 N88-30575

SOLAR WIND VELOCITY
Nature and the nonlinear evolution of electrostatic waves associated with the AMPTE (Active Magnetosphere Particle Tracer Explorers) solar wind releases
[AD-A185471] 06 p0806 N88-14920
Dynamics and turbulence of solar wind in area of its formation based on radio transmission data measured with Venera-15 and Venera-16 spacecraft
08 p1003 N88-16080

SOLAR X-RAYS
Small-scale energy storage and release as the cause of the stellar X-ray corona 02 p0255 N88-11615
A large X-ray flare on Sigma 2 coronae borealis observed with exosat 04 p0508 N88-13121
Magnetic reconnection and solar flare loops
08 p1094 N88-16583
Dynamic evolution of the source volumes of gradual and impulsive solar flare emissions
[NASA-TM-87815] 08 p1102 N88-16621
Solar-geophysical data number 517, September 1987. Part 2: (Comprehensive reports). Data for March 1987 and miscellanea
[PB88-128434] 10 p1431 N88-18545
The properties of solar coronal active regions deduced from X-ray line spectra
[AD-A193026] 20 p2886 N88-27141
Solar-geophysical data number 523, March 1988. Part 2: (Comprehensive reports). Data for September 1987 and miscellanea
[PB88-212774] 24 p3458 N88-30576

SOLAR-PUMPED LASERS
Design studies for a solar pumped laser device
[DFVLR-FB-87-39] 13 p1777 N88-20629
Direct solar-pumped iodine laser amplifier
[NASA-CR-182674] 13 p1777 N88-20630
Theoretical studies of solar-pumped lasers
[NASA-CR-182929] 17 p2344 N88-23971
Theoretical studies of solar lasers and converters
[NASA-CR-182927] 17 p2344 N88-23972

SOLDERED JOINTS
Fatigue and thermal fatigue of Pb-Sn solder joints
[DE87-012881] 01 p0024 N88-10150
Microstructural observations of the Sn-Pb solder/Cu system and thermal fatigue of the solder joint
[DE88-001392] 07 p0832 N88-15048
The inspection of metallurgical bounds in electronic systems
[AD-A192064] 18 p2582 N88-25343
Thermal cycling tests on surface-mount assemblies
[DE88-007695] 21 p2939 N88-27453

SOLDERING
The effect of organic inhibitors on the atmospheric corrosion and solderability of copper
[DE88-000261] 04 p0414 N88-12565
Cleanliness tests with the Omega Meter: A comparative study for solder flux removal
[DE88-004834] 11 p1460 N88-18704
Comparison of isopropyl alcohol and trichloroethylene in removing solder flux
[DE88-005556] 14 p1889 N88-21288
The inspection of electronic metallurgical bonds
[AD-A192197] 18 p2486 N88-24745
Conductivity mechanism and operating behavior of electrically conductive adhesives on the example of a power transistor
[ETN-88-92355] 21 p2940 N88-27464

SOLDERS
Fatigue and thermal fatigue of Pb-Sn solder joints
[DE87-012881] 01 p0024 N88-10150
Effect of hold time on fatigue of lead rich PbSn solder
06 p0715 N88-14387
Thermomechanical fatigue of lead-base low tin solder
06 p0721 N88-14432
Evaluation of solder flux solvents in a vapor-degreasing application for hybrid microcircuits
[BDX-613-3638] 11 p1488 N88-18752

SOLENOIDS
High repetition rate electron beam RF-acceleration and sub-millimeter wave generation via a free electron laser
[AD-A186066] 07 p0858 N88-15209
Harmonic expansion for the magnetic field of the helical solenoid
[DE88-700100] 07 p0928 N88-15638
Robotic assembly and testing of rotary solenoids
[BDX-613-3663] 11 p1480 N88-18834
Use of magnetic materials in excimer laser circuits
[DE88-006449] 19 p2674 N88-25903

SOLID ELECTRODES
Fundamental studies of surfaces processes and trace analysis using solid electrodes
[AD-A186156] 07 p0828 N88-15024
The overcharge behavior of polymer electrolyte cells
[AD-A193984] 22 p3117 N88-28522

SOLID ELECTROLYTES
Nuclear magnetic resonance studies of ion motion in solid electrolytes
[DE87-014547] 02 p0232 N88-11464
Studies of alumina additions in zirconia - magnesia
[DE87-703500] 04 p0419 N88-12602
Effect of sidechain length and crosslinking on ionic conductivity in polyphosphazene solid electrolytes
[AD-A184419] 04 p0497 N88-13058
JPRS report: Science and technology. Japan
[JPRS-JST-87-028] 06 p0675 N88-14130
Gas separation using solid electrolytes described
06 p0675 N88-14131
Ionically conducting polymers: Principles and properties of solid electrolytes
[DE88-001552] 06 p0684 N88-14190
Lithium/polymer electrolyte interfacial instability
[AD-A187164] 09 p1147 N88-16874
Interfacial effects in thin Li/PEO cells at room temperature
[AD-A186974] 09 p1157 N88-16931
Thermogravimetric analysis of polymeric materials for an intermediate temperature solid electrolyte
[DE88-004854] 10 p1306 N88-17809
Electrochromic cells with lutetium diphthalocyanine and semisolid polymer electrolytes
[AD-A188031] 10 p1352 N88-18078
Electronic and ionic transport in polymers
[AD-A187253] 11 p1452 N88-18651
Lithium fast-ion conductors: Polymer based materials
[AD-A187879] 11 p1461 N88-18712
Fast protonic conducting solid electrolytes
[AD-A188524] 12 p1698 N88-20160
Contrasting conductance/viscosity relations in liquid states of vitreous and polymer solid electrolytes
[AD-A189378] 13 p1748 N88-20452
Recent advances in solid polymer electrolyte fuel cell technology
[DE88-005380] 15 p2092 N88-22464
The kinetics of contact noise in NaBeta alumina
[AD-A190651] 15 p2130 N88-22707
Preparation technology for thin film solid electrolyte fuel cells
[PB88-131925] 20 p2821 N88-26735
Failure analysis of Chloride Silent Power, Ltd. PB cells
[DE88-010567] 21 p2938 N88-27448
The overcharge behavior of polymer electrolyte cells
[AD-A193984] 22 p3117 N88-28522
Polymeric electrolytes
[AD-A193766] 23 p3198 N88-29031

SOLID LUBRICANTS
Composite bearing materials containing solid lubricant in filamentary form, stages 3 and 4
[IRD-87/2] 01 p0054 N88-10344
The wear process during the RUNNING-IN of steel in lubricated sliding
[NAL-TR-922T] 02 p0181 N88-11130
Calculation of the tribological properties of surfaces by semi-empirical methods
[AD-A184283] 04 p0450 N88-12791
Coatings for high-temperature bearings and seals
[NASA-TM-100249] 05 p0567 N88-13453
Literature review of solid lubrication mechanisms
[AD-A185010] 05 p0567 N88-13456
The tribological properties of MoS2 coatings in vacuum, low relative humidity and high relative humidity environments
[DE88-001611] 06 p0711 N88-14356
Sputtered silver films to improve chromium carbide based solid lubricant coatings for use to 900 C
[NASA-TM-100783] 08 p0973 N88-15885
Tribological properties of alumina-boria-silicate fabric from 25 to 850 C
[NASA-TM-100806] 11 p1464 N88-18726
The performance of thin solid films for satellite gears
14 p1876 N88-21209
A test facility for the in-vacuo assessment of dry lubricants and small mechanisms at cryogenic temperatures
14 p1878 N88-21224
High temperature solid lubrication by catalytically generated carbon
[AD-A190804] 16 p2182 N88-23004
Investigation of rolling contact fatigue of ball bearings
[NASA-TT-20196] 19 p2678 N88-25922
Status and directions of modified tribological surfaces by ion processes
[NASA-TM-101304] 22 p3063 N88-28176
Evaluation of transfer films of Salox M on 440C for HPOTP bearing cage applications, task 119
[NASA-CR-179020] 23 p3223 N88-29184

SOLID MECHANICS
Solid mechanics research for quantitative non-destructive evaluation
[AD-A186599] 08 p0993 N88-16010
A collaborative program of research in engineering sciences
[DE88-003383] 10 p1423 N88-18504
Symmetry and global bifurcation in nonlinear solid mechanics
[AD-A190521] 15 p2121 N88-22642
Probabilistic finite element methods
18 p2564 N88-25223
Analytical determination of critical crack size in solar cells
[NASA-CR-183128] 20 p2821 N88-26736
Finite element method for plate structures with inclined angles
[ILR-MITT-182] 21 p3008 N88-27842
Some stability criteria in fluid and solid mechanics
21 p3027 N88-27966

SOLID PHASES
Grain boundary phase equilibria in metallic systems
[DE87-014123] 01 p0104 N88-10679
Microgravity thaw experiment (MITEX)
17 p2427 N88-24439

SOLID PROPELLANT COMBUSTION
NT SOLID PROPELLANT IGNITION
Measurement of solid propellant combustion velocity by means of microwaves
[CERT-1/1316-MO] 03 p0283 N88-11778
Influence of shock wave and gas pressure on the behavior of a pyrotechnical device
[SNIAS-872-430-111] 05 p0570 N88-13477
Advantages of internal thermal protection in a pyrotechnical plunger
[SNIAS-872-430-114] 05 p0571 N88-13478
Numerical simulation applied to the development of a pyrotechnical system
[SNIAS-872-430-115] 05 p0571 N88-13479
A continuous oxidizer regression model for the combustion of composite solid propellants
[AD-A186742] 08 p0974 N88-15894
Holographic investigation of metallized solid propellant combustion in two-dimensional and three-dimensional rocket motors
[AD-A187000] 09 p1140 N88-16832
The correlation of HMX (cyclotetramethylenetetranitramine) particle characterization techniques to propellant burn rate
[AD-A187119] 09 p1140 N88-16833
Design of a solid fuel combustion chamber
[VTH-LR-447] 09 p1141 N88-16837
Investigation of the flow and combustion behavior in a solid fuel combustion chamber, including the measuring program
[VTH-LR-460] 09 p1141 N88-16838
Design of a gas mass flow control system for the gas inlet installation of a solid fuel combustion chamber
[VTH-LR-471] 09 p1141 N88-16839
Solid fuel combustion chamber
[VTH-LR-515] 09 p1141 N88-16842
Combustion mechanisms
[AD-A187979] 11 p1453 N88-18660
Speed control of a missile with throttleable ducted rocket propulsion 12 p1597 N88-19561
Combustion theory and related questions
[AD-A189160] 13 p1737 N88-20382
Laser ignition of nitramine composite propellants and crack propagation and branching in burning solid propellants
[AD-A189260] 13 p1753 N88-20483
Combustion behavior of the vitiator. Experimental results of a second test series
[VTH-LR-509] 18 p2484 N88-24734
Development of a computerized analysis for solid propellant combustion instability with turbulence
[NASA-CR-182351] 19 p2611 N88-25497
Combustion of PMMA (polymethylmethacrylate), PE (polyethylene) and PS (polystyrene) in a ramjet
[PB88-186572] 20 p2769 N88-26417
Reaction products of solid propellants after burning at pressures up to 1000 MPa: Comparison between theoretical and experimental results
[ISL-CO-227/87] 22 p3059 N88-28153

SOLID PROPELLANT IGNITION
Ignition studies in a two-stage closed vessel using various igniter materials
[ISL-CO-231/86] 09 p1142 N88-16843
Laser ignition of nitramine composite propellants and crack propagation and branching in burning solid propellants
[AD-A189260] 13 p1753 N88-20483
Some properties of ignition gases. Review of measuring results in the years 1981-1986)
[PB88-106968] 21 p2908 N88-27259

SOLID PROPELLANT ROCKET ENGINES
NT APOGEE BOOST MOTORS
NT SPACE SHUTTLE BOOSTERS
Results of the development motor 8 test firing
[GPO-78-692] 03 p0278 N88-11751
Destruction test of small scaled solid propellant motors
[ISAS-R-620] 03 p0278 N88-11752
Structural analysis of a bolted joint concept for the space shuttle's solid rocket motor casing
[NASA-TM-89092] 04 p0407 N88-12531
Modal survey of the space shuttle solid rocket motor using multiple input methods 05 p0593 N88-13617
Measurement of particle size distribution in a solid propellant rocket motor using light scattering
[AD-A184875] 06 p0673 N88-14124
Verification of FANTASTIC integrated code
07 p0924 N88-15613
A European apogee boost motor for GEOS
09 p1123 N88-16719
Holographic investigation of metallized solid propellant combustion in two-dimensional and three-dimensional rocket motors
[AD-A187000] 09 p1140 N88-16832
Measurements of particulates in solid propellant rocket motors
[AD-A187777] 11 p1446 N88-18621
NASA (National Aeronautics and Space Administration) procurement: The 1973 space shuttle solid rocket motor contractor selection
[PB88-135264] 11 p1447 N88-18623
Speed control of a missile with throttleable ducted rocket propulsion 12 p1597 N88-19561
Transient Pressure Test Article (TPTA) 1.1 and 1.1A, volume 1
[NASA-CR-179322-VOL-1] 12 p1603 N88-19588
A study of combustion and flow behaviour in solid-propellant rocket motors
[UTIAS-280] 13 p1732 N88-20357
The effect of combustion gas flow on the rotational dynamics of a spinning solid fuel rocket
13 p1732 N88-20358
Space shuttle solid rocket motor Profile Measuring Device (PMD) 14 p1928 N88-21495
Combustion of a double base fuel in the presence of inert gases
[INPE-4516-RPE/564] 16 p2170 N88-22936
Preliminary 2-D shell analysis of the space shuttle solid rocket boosters
[NASA-TM-100515] 17 p2348 N88-23989
Solid rocket motor aft field joint flow field analysis
[NASA-CR-179288] 18 p2474 N88-24675
SRM propellant and polymer materials structural test program
[NASA-TP-2821] 18 p2530 N88-25013
Driving of axial acoustic fields by side-wall stabilized premixed flames 19 p2629 N88-25592
Motor test data comparisons with laboratory data and stability predictions 19 p2629 N88-25594
One person's view of velocity-coupled instability
19 p2629 N88-25595
Measurement of particulate size in solid propellant rocket motors 19 p2630 N88-25599
An interactive computer code for preliminary design of solid propellant rocket motors
[AD-A192869] 20 p2766 N88-26399
Environmental monitoring of a titan 34D 5 1/2 segment solid rocket motor static firing
[AD-A192975] 20 p2766 N88-26400
Application of laser diffraction techniques to particle sizing in solid propellant rocket motors
[AD-A193841] 22 p3049 N88-28089
SRM (Solid Rocket Motor) propellant and polymer materials structural modeling
[NASA-TP-2824] 22 p3089 N88-28343
SRB/SLEEC (Solid Rocket Booster/Shingle Lap Extendible Exit Cone) feasibility study, volume 1
[NASA-CR-178973] 23 p3187 N88-28964

SOLID PROPELLANTS
NT COMPOSITE PROPELLANTS
NT DOUBLE BASE ROCKET PROPELLANTS
NT HMX
NT HTPB PROPELLANTS
NT METAL PROPELLANTS
NT NITRAMINE PROPELLANTS
NT PLASTIC PROPELLANTS
NT SOLID ROCKET PROPELLANTS
High pressure strand burn rate tests of polyvinylnitrate/nitramine propellants
[AD-A184178] 04 p0422 N88-12615
SRB combustion dynamics analysis computer program (CDA-1)
[NASA-CR-182404] 07 p0830 N88-15032
An investigation into the feasibility of using a dual-combustion mode ramjet in a high Mach number tactical missile
[AD-A186906] 09 p1119 N88-16705
Advanced B and Al combustion kinetics over wide temperature ranges
[AD-A190752] 15 p2036 N88-22128

Technical instructions for a control operating system of the gas flow installation for the solid fuel combustion chamber
[LR-507] 20 p2788 N88-26537
SOLID ROCKET BINDERS
Thermoplastic elastomers as LOVA binders
[AD-A185864] 07 p0835 N88-15067
SOLID ROCKET BOOSTERS (SPACE SHUTTLE)
U SPACE SHUTTLE BOOSTERS
SOLID ROCKET PROPELLANTS
NT DOUBLE BASE ROCKET PROPELLANTS
NT HMX
NT HTPB PROPELLANTS
NT METAL PROPELLANTS
Modal survey of the space shuttle solid rocket motor using multiple input methods 05 p0593 N88-13617
Measurements of particulates in solid propellant rocket motors
[AD-A187777] 11 p1446 N88-18621
LGM-30B stage 2 disected motor test report
[AD-A190771] 15 p2027 N88-22079
Advanced B and Al combustion kinetics over wide temperature ranges
[AD-A190752] 15 p2036 N88-22128
Crack opening and extension in inert solid propellant. An experimental study
[AD-A189808] 15 p2048 N88-22201
The 24th JANNAF Combustion Meeting, volume 1
[AD-A190163] 19 p2627 N88-25585
Characterization of a modified Rijke burner for measurement of distributed combustion 19 p2628 N88-25587
Propellant combustion response to oscillatory radiant heat flux 19 p2628 N88-25589
New instability phenomena in solid propellant combustion 19 p2628 N88-25591
A review of particle sizing methods in rocket propulsion 19 p2630 N88-25597
The scaling of the threshold conditions for solid propellant erosive burning 19 p2630 N88-25601
Dimensional analysis and experimental observation of the coupling phenomena between combustion and fracture of damaged propellant samples 19 p2630 N88-25603
Analysis of microwave burner measurement system using a microwave network analysis computer program 19 p2631 N88-25604
Pressure differential scanning calorimetry (DSC) evaluation of solid rocket propellant burn rate mod 19 p2631 N88-25606
Solid rocket motor performance: A workshop report 19 p2631 N88-25607
Structure of laminar, premixed flames of CH2O/NO2/O2 mixtures 19 p2632 N88-25613
Reaction products of solid propellants after burning at pressures up to 1000 MPa: Comparison between theoretical and experimental results
[ISL-CO-227/87] 22 p3059 N88-28153
Automatic data retrieval from rocket motor holograms
[AD-A195586] 24 p3337 N88-29864
Ignition and extinguishing of a Solid Fuel Ramjet (SOFRAM)
[FOA-C-20713-2.1] 24 p3337 N88-29865
Combustion diagnostics of propellant with new grain geometries
[AD-A194944] 24 p3342 N88-29895
Descriptive characterization of propellant particles
[AD-A195176] 24 p3356 N88-29985
Preliminary investigation of flow modeling during solid propellant processing
[AD-A196168] 24 p3357 N88-29987
SOLID ROTATION
U ROTATING BODIES
SOLID SOLUTIONS
Non-lattice matched metallic superlattices
[DE87-011512] 04 p0497 N88-13062
Growth of solid solution single crystals
[NASA-TP-2787] 06 p0688 N88-14212
The physics of metallic superlattices: An experimental point of view
[DE88-003080] 10 p1416 N88-18452
Positron-annihilation 2D-ACAR studies of disordered and defected alloys
[DE88-003118] 10 p1416 N88-18454
Irreversible dissolution of solid solutions: A kinetic and stoichometric model
[DE88-009194] 19 p2614 N88-25513
SOLID STATE
Formation of amorphous alloys by solid state reactions
[DE87-013175] 02 p0146 N88-10918
Survey state of the art: Electrical load management techniques and equipment
[AD-A184083] 05 p0577 N88-13517
Study of solid state photomultiplier
[NASA-CR-177465] 05 p0583 N88-13556
New branch of solid-state physics 08 p1079 N88-16508
Solid state research
[AD-A185987] 09 p1253 N88-17508
Studies of nonlinear and chaotic phenomena in solid state systems
[DE88-002330] 09 p1254 N88-17515
Solid-state voltage standard performance and design guidelines
[PB88-123757] 10 p1322 N88-17905
Studies in solid state ionics
[DE88-700830] 11 p1559 N88-19333
Test results of high-voltage, high-power, solid-state remote power controllers
[NASA-TM-100322] 16 p2194 N88-23085
Interface characterization of Cu-Cu and Cu-Ag-Cu low temperature solid state bonds
[AD-A191015] 16 p2283 N88-23667
Reactor instrumentation and control design and performance simulation for SP-100 17 p2406 N88-24306
Solid-state combustion synthesis of ceramics and alloys in reduced gravity
[NASA-CR-4163] 19 p2608 N88-25479
Raman and absorption spectrophotometric studies of selected lanthanide, californium-doped lanthanide, and actinide trihalides in the solid state
[DE88-008234] 20 p2874 N88-27061
SOLID STATE DEVICES
NT AVALANCHE DIODES
NT BIPOLAR TRANSISTORS
NT CHARGE COUPLED DEVICES
NT CHARGE TRANSFER DEVICES
NT CMOS
NT CRYSTAL RECTIFIERS
NT FIELD EFFECT TRANSISTORS
NT GALLIUM ARSENIDE LASERS
NT GERMANIUM DIODES
NT HETEROJUNCTION DEVICES
NT HIGH ELECTRON MOBILITY TRANSISTORS
NT JFET
NT JUNCTION DIODES
NT JUNCTION TRANSISTORS
NT LIGHT EMITTING DIODES
NT METAL OXIDE SEMICONDUCTORS
NT MIM (SEMICONDUCTORS)
NT MIM DIODES
NT MIS (SEMICONDUCTORS)
NT MODFETS
NT MSM (SEMICONDUCTORS)
NT PHOTODIODES
NT PHOTOVOLTAIC CELLS
NT RUBY LASERS
NT SCHOTTKY DIODES
NT SEMICONDUCTOR DEVICES
NT SEMICONDUCTOR LASERS
NT SILICON TRANSISTORS
NT SIS (SEMICONDUCTORS)
NT SOI (SEMICONDUCTORS)
NT SOLAR CELLS
NT SOLID STATE LASERS
NT SOS (SEMICONDUCTORS)
NT THERMISTORS
NT THYRISTORS
NT TRANSFERRED ELECTRON DEVICES
NT TRANSISTOR AMPLIFIERS
NT TRANSISTORS
NT VARISTORS
NT VERTICAL JUNCTION SOLAR CELLS
NT YAG LASERS
Chemically modified microelectrode arrays. New kinds of electronic devices
[AD-A184389] 04 p0439 N88-12724
Fabricate, calibrate and test a dosimeter for integration into the CRRES (Combined Release and Radiation Effects Satellite) satellite
[AD-A185439] 05 p0585 N88-13564
Evaluation of high-voltage, high-power, solid-state remote power controllers for amps 07 p0924 N88-15612
Joint services electronics program
[AD-A187587] 10 p1325 N88-17920
Electrochromic cells with lutetium diphthalocyanine and semisolid polymer electrolytes
[AD-A188031] 10 p1352 N88-18078
The physics of very small structures
[AD-A187672] 11 p1556 N88-19311
Solid state research
[AD-A188388] 12 p1699 N88-20166
Solid-state electrochemical processes in dye films
[AD-A188756] 13 p1844 N88-21036
Instrumentation for the characterization and development of millimeter wave components compatible with monolithic integration
[AD-A189724] 15 p2059 N88-22275
Hermetically sealable package for hybrid solid-state electronic devices and the like
[NASA-CASE-MSC-20181-1] 17 p2335 N88-23941
Characterization of a 30-GHz IMPATT solid state amplifier
[NASA-TM-100876] 18 p2503 N88-24847
Joint services electronics program
[AD-A192076] 18 p2504 N88-24856
Organization of a Topical Meeting on Picosecond Electronics and Optoelectronics
[AD-A187136] 19 p2655 N88-25765
On 3-5 transistors for MM-wave applications
[AD-A191580] 19 p2661 N88-25825
The 1986 IEEE Solid-State Sensor Workshop
[AD-A190922] 19 p2668 N88-25860
Development of a GaAs solid state device model for high power applications
[DE88-009048] 19 p2734 N88-26242
A GaAs solid state device model for high power applications
[DE88-011320] 21 p2939 N88-27457
Solid state research
[AD-A192837] 21 p3020 N88-27929
Space-charge-wave solid state microwave amplifier
[AD-A193792] 23 p3208 N88-29091
Phase sensitive amplification with SIS (Superconductor-Insulator-Superconductor) quasiparticle mixers
[AD-A194594] 23 p3291 N88-29596
High power storage system based on thin film solid ionics
[AD-A193623] 23 p3291 N88-29598
SOLID STATE LASERS
NT GALLIUM ARSENIDE LASERS
NT RUBY LASERS
NT YAG LASERS
Diode pumped solid-state laser oscillators for spectroscopic applications
[NASA-CR-180576] 01 p0052 N88-10331
High energy efficient solid state laser sources
[NASA-CR-181362] 01 p0052 N88-10332
High average power solid state laser power conditioning system
[DE87-013558] 03 p0328 N88-12071
Laser development, evolution of applied technologies described 06 p0689 N88-14221
Super-short yttrium aluminate pulse generator with controlled resonator Q-factor 06 p0772 N88-14740
Laser Program
[DE87-011009] 07 p0858 N88-15212
The YAlO(sub 3):Er laser
[PB88-130877] 11 p1493 N88-18911
Growth of Cr,Nd:Gd3Sc2Al3O12 (Cr,Nd:GSAG) crystals by the Heat Exchanger Method (HEM)(trademark)
[DE88-004041] 11 p1558 N88-19326
High power, high efficiency 770 nm laser diode array
[DE88-004043] 12 p1631 N88-19762
Direct solar-pumped iodine laser amplifier
[NASA-CR-182674] 13 p1777 N88-20630
High power, high efficiency, 2D laser diode arrays for pumping solid state lasers
[DE88-004042] 13 p1777 N88-20632
Energy transfer and non-linear optical properties at near ultraviolet wavelengths: Rare earth 4f yields 5d transitions in crystals and glasses
[DE88-005403] 13 p1840 N88-21012
Time characteristics of ultrashort light pulses from dye lasers with distributed feedback 14 p1970 N88-21759
Solid-state ring laser with acoustooptical phase nonreciprocity of opposing waves 14 p1970 N88-21761
Nonlinear stage of ultrashort-pulse formation in solid-state laser 14 p1971 N88-21765
Tunable optical sources/growth and characterization of nonlinear optical materials
[AD-A190874] 16 p2274 N88-23608
Fracture of solid state lasers
[DE88-007023] 18 p2522 N88-24961
Laser spectroscopy investigations of materials for solid state laser systems
[AD-A192514] 21 p2952 N88-27535
A new near-infrared tunable-room temperature solid state laser La3Ga5SiO14:Cr(3+)
[DE88-011341] 21 p2953 N88-27543
Solid-state laser research report: Energy transfer in non-uniform codoped crystals
[AD-A194358] 23 p3219 N88-29161
Spectral properties of semiconductor lasers with external resonators
[ETN-88-93119] 24 p3379 N88-30125
SOLID SURFACES
NT CRYSTAL SURFACES
An investigation of the behavior of outgassed molecules in thermal vacuums 02 p0133 N88-10836

Application of spin-sensitive electron spectroscopies to investigations of electronic and magnetic properties of solid surfaces and epitaxial systems
[DE87-014235] 02 p0245 N88-11550
Pure dephasing of a vibrational adbond
[AD-A185222] 05 p0609 N88-13740
Unified study of plasma-surface interactions for space power and propulsion
[AD-A186211] 07 p0825 N88-15007
A model for nitrogen atom recombination on a silicon dioxide surface
[AD-A189843] 15 p2142 N88-22784

SOLID SUSPENSIONS
Stochastic model of the motion of suspended particles in turbulent flow
[HSBW-MITT-21/1987] 03 p0315 N88-11990
The influence of yellow substances on remote sensing of sea-water constituents from space
08 p1044 N88-16308
A small concentration expansion for the effective heat conductivity of a random disperse two-component material; an assessment of Batchelor's renormalization method
[REPT-87-71] 16 p2207 N88-23168

SOLID-SOLID INTERFACES
Behavior of metal ceramic interfaces
[PB87-147500] 07 p0837 N88-15076
Formation and passivation of new paramagnetic defects associated with thermal oxides on silicon
[DE88-002720] 07 p0938 N88-15699
Interfacial effects in thin Li/PEO cells at room temperature
[AD-A186974] 09 p1157 N88-16931
Thermodynamics of wetting by liquid metals
[DE88-003634] 11 p1563 N88-19360
Friction and wear of ceramics
17 p2323 N88-23874
Studies of metal-silicon, silicon-metal and silicide based interfaces: Synchrotron radiation photo emission and inverse photoemission investigations of interface formation and compound nucleation
[AD-A191808] 19 p2619 N88-25536
Thermo-mechanical cracking in coated media with a cavity by a moving asperity friction
[AD-A193311] 21 p2961 N88-27586
Green's function approach to roughening transition of one-dimensional restricted solid on solid model
[DE88-702723] 23 p3278 N88-29512

SOLIDIFICATION
NT MELT SPINNING
Formation of amorphous alloys by solid state reactions
[DE87-013175] 02 p0146 N88-10918
Structure of rapidly solidified Ni-Ti
[DE87-012252] 02 p0147 N88-10921
On the role of convective motion during dendrite growth: Experiments under variable gravity, revised
[NASA-CR-179213] 02 p0156 N88-10979
Shock-induced melting and rapid solidification
[DE88-000226] 03 p0288 N88-11810
Influence of boron on porosity in nickel-base superalloy castings 03 p0299 N88-11877
Analytical treatment of the melting and solidification of latent heat store materials in finned tube geometries
[IKE-5-223] 03 p0314 N88-11985
Microstructure of amorphous and crystalline zirconium alloys rapidly solidified
[DE87-703700] 05 p0564 N88-13432
Effect of rapid solidification on short-range order: A magnetic study
[AD-A185216] 05 p0565 N88-13444
Tensile properties of extrusion consolidated Type 304 SS rapidly solidified powders
[DE87-014875] 05 p0566 N88-13450
Effect of rapid solidification on stainless steel weld metal microstructures and its implications on the Schaeffler diagram
[DE88-001489] 05 p0566 N88-13451
Development of iron aluminides
[AD-A185190] 05 p0568 N88-13461
Thermo-mechanical behavior of high temperature fiber composites 06 p0678 N88-14149
Behavior and structure of metal vapor arc plasma between molten electrodes
[DE88-001854] 06 p0782 N88-14801
Cellular solidification in a monotectic system
[NASA-TM-100317] 07 p0829 N88-15027
A numerical thermal model of the rapid solidification parameters in the capacitor discharge welding process
[DE88-002206] 07 p0864 N88-15244
Investigations in field of surface forces in metallurgy
[BLL-M-47406-(5828.4)] 08 p0969 N88-15860
Transparent metal model study of the use of a cellular growth front to form aligned monotectic composite materials
[NASA-CR-182414] 08 p0969 N88-15861
Spray deposition: A fundamental study of droplet impingement, spreading and consolidation
[AD-A186627] 08 p0970 N88-15869
Microstructural modification during laser welding
[DE88-002344] 09 p1144 N88-16860
Microgravity research at the University of Mexico: Experiments in payload G-006 10 p1286 N88-17692
Application of Onsager's reciprocity relations to interface motion
[DE88-003286] 10 p1397 N88-18327
Void formation in solidification
[DE88-003895] 11 p1452 N88-18650
Effect of density change on rapid liquid-solid interface kinetics and heat flow
[DE88-004286] 11 p1487 N88-18878
Development of metastable processing paths for high temperature alloys
[AD-A188682] 12 p1608 N88-19617
A fundamental understanding of the effect of alloying elements on the corrosion resistance of rapidly solidified Mg alloys
[AD-A189385] 13 p1741 N88-20413
Experimental and theoretical methods for investigating helium effects in rapidly solidified metals
[DE88-005542] 13 p1743 N88-20425
Growth and deformation mechanisms of refractory alloy hybrid materials
[AD-A190492] 15 p2039 N88-22152
Characterization of an explosively consolidated rapidly solidified Fe-16Ni-9Cr-5Mo-2Cu alloy powder
[DE88-006733] 15 p2041 N88-22162
Remarks on solid state amorphizing transformations
[DE88-006452] 15 p2145 N88-22803
The weldability of consolidated rapidly solidified Type 304 SS powders
[DE88-006738] 16 p2178 N88-22978
Deformation of rapidly solidified dispersion strengthened titanium alloys
[AD-A190793] 16 p2179 N88-22984
Effect of alloying, rapid solidification, and surface kinetics on the high temperature environmental resistance of niobium
[AD-A192093] 18 p2485 N88-24743
Laboratory scale inert gas atomizer for producing rapidly solidified powders
[DE88-006734] 18 p2497 N88-24812
Survey of the literature on fractals with possible applications to phase change processes
[DE88-012240] 21 p2911 N88-27277
A computer model for the flow of a molten polymer in a narrow cavity
[NPL-DMA(A)-157] 22 p3058 N88-28146
Solidification with natural circulation
[DE88-011197] 22 p3074 N88-28248
A fundamental study of P/M processed elevated temperature aluminum alloys
[AD-A192958] 23 p3194 N88-29005
An investigation into the metallurgical aspects of joining rapidly-solidified aluminum alloys
[AD-A194677] 23 p3194 N88-29009

SOLIDS
TIPS-1 user's manual: Cray-1 version
[DE87-013297] 01 p0081 N88-10522
Theory of defects in non-metallic solids
[DE87-014068] 02 p0152 N88-10949
Electron capture from solids by positrons
[DE87-014355] 02 p0232 N88-11463
Optical instrumentation and study of gas-solid suspension flows
[DE88-000147] 04 p0442 N88-12744
Monocrystal sputtering by the computer simulation code ACOCT
[IPPJ-848] 04 p0493 N88-13035
Shock compression of solids as a physical-chemical-mechanical process
[DE88-001674] 05 p0563 N88-13427
Vibrational properties of disordered solids. Far infrared studies: Performance report
[DE88-001474] 06 p0786 N88-14821
Impact of solids on composite materials
[NASA-CR-182395] 07 p0827 N88-15015
Pressure and mass velocity measurements in solids subjected to dynamic loadings 07 p0921 N88-15595
Equation of state of condensed materials physical principles and applications
[NASA-TT-20007] 08 p0968 N88-15855
A guide to the transient three phase porous flow model implemented in the two-dimensional CRAY-TENSOR code: Physics, numerics, and code description
[DE88-003709] 09 p1165 N88-16983
A modified version of the phase sensitive technique for measurements of absolute sound velocity in solids
[DE88-002303] 10 p1405 N88-18378
Pulsed laser photothermal spectroscopy of liquids and solids
[DE88-003839] 11 p1455 N88-18675
Wave curves for simple isotropic elastic solids
[AD-A188865] 12 p1636 N88-19798
Stress analysis in elastic solids with many cracks
[AD-A189015] 12 p1636 N88-19799
Material instabilities in solids
[AD-A189525] 13 p1738 N88-20388
Properties of molecular solids and fluids at high pressure and temperature
[DE88-004195] 13 p1738 N88-20391
Innovative, counterflow gas/fine solids, direct contact heat exchanger
[DE88-004744] 13 p1770 N88-20585
Particle-dynamics calculations of gravity flow of inelastic, frictional spheres
[DE88-005224] 13 p1770 N88-20586
Kinetics of combustion of finely divided solid fuel in granules
[BLL-M-37626-(5828.4)] 14 p1888 N88-21283
Theory of Muon method for study of solid and liquid hydrogen 14 p1972 N88-21770
Density measurements on solids and liquids
[PB88-164934] 15 p2036 N88-22129
A 3-D solid rendering of NDT data
[DE88-006199] 15 p2076 N88-22373
Dynamical optimization techniques for the calculation of electronic structure in solids
[DE88-006010] 15 p2140 N88-22768
Thermal and power availability transient responses for the Argonne monolithic solid oxide fuel cell
17 p2419 N88-24384
Self-consistent model for the brittle response of solids
18 p2528 N88-24999
An evaluation of some thermodynamic and transport properties of solid and liquid lithium over the temperature range 200 to 1700 K
[DE88-008947] 19 p2614 N88-25512
A general qualitative study of point and extended defects and their interactions in non-metallic systems
[AD-A191687] 19 p2618 N88-25532
Equation of state of solid neon from X-ray diffraction measurements to 110 GPa
[DE88-008723] 19 p2734 N88-26241
Research on the kinetics of phase changes in solids
[AD-A192222] 20 p2814 N88-26696
Lattice theory of fracture of solids with layered structure
[DE88-701867] 20 p2876 N88-27073
A comparison of analytical techniques for modeling the Rayleigh-Taylor response of elastic-plastic solids
[DE88-010372] 21 p2962 N88-27596
Monolithic fuel cells
[DE88-012004] 21 p2969 N88-27638

SOLIDS FLOW
Laser velocimeter measurements of solids in multiphase flow
[DE88-000196] 11 p1487 N88-18876
LLNL granular solids flow project
[DE88-007492] 18 p2513 N88-24906
LLNL Granular Solids Flow Project
[DE88-008023] 19 p2664 N88-25844

SOLITARY WAVES
Intensive synoptic eddies and quasigeostrophic approximation 04 p0460 N88-12844
Dynamics of isolated intrathermocline eddy
04 p0460 N88-12845
Soliton twin boundaries of the cubic-tetragonal martensitic transformations in ferroelastic materials
[DE87-014741] 04 p0495 N88-13047
Solitons in stimulated Raman scattering: Generation and control of ultrashort optical pulses
[AD-A185141] 05 p0650 N88-13983
The Eckhaus Partial Differential Equation (PDE) I psi t + psi xx + 2(psi/sq)x psi +2(/psi/) to the 4th power psi = 0
[PREPRINT-546] 06 p0763 N88-14686
Soliton mode of propagation of light pulses through single-mode optical fibers and problems of its experimental realization 07 p0920 N88-15592
Experiments on ion-acoustic rarefactive solitons in a multi-component plasma with negative ions
[INPE-4393-PRE/1213] 08 p1086 N88-16542
Relativistic Calogero-Moser systems and solutions
[CWI-PM-R8702] 08 p1092 N88-16570
Low frequency waves and small scale solitary structures observed by Viking --- Swedish satellite; auroras
08 p1099 N88-16611
Advanced studies of integrable systems
[AD-A186792] 09 p1151 N88-16895
The 80 fsec soliton-like pulses from an optical-nonlinear fiber resonator
[PB88-127303] 10 p1409 N88-18403
Super Virasoro algebra and solvable supersymmetric quantum field theories
[DE88-752299] 15 p2127 N88-22681
Interaction of solitons in single mode optical fibres
17 p2439 N88-24511

Nonlinear surface polaritons
[AD-A191046] 18 p2499 N88-24822
Nonlinear surface and internal waves on shear flow
[PREPRINT-584] 22 p3129 N88-28604
The construction of implicit and explicit solitary wave solutions of nonlinear partial differential equations
[AD-A193475] 23 p3269 N88-29452
On nonlinear equations admitting soliton solutions with a deBroglie phase
[DE88-702694] 23 p3277 N88-29508
Characteristics of solitary waves and weak double layers in the magnetospheric plasma
[IRF-PREPRINT-105] 24 p3431 N88-30418

SOLITONS
U SOLITARY WAVES

SOLUBILITY
Aqueous-phase reactions in clouds
[DE86-005249] 01 p0069 N88-10445
Thermodynamics of interaction between nitrogen and molten nickel alloys
[BLL-M-37309-(5828.4)] 02 p0149 N88-10934
Near-infrared dichroism of a mesogenic transition metal complex and its solubility in nematic hosts
[DE87-014471] 03 p0287 N88-11805
Investigation of structure-permeability relationships of silicone polymer membranes
[PB87-230181] 03 p0293 N88-11839
Physical properties of immiscible polymers
03 p0297 N88-11868
High temperature superconductors
03 p0297 N88-11869
Conducting hybrid polymeric systems
[DE88-000527] 04 p0421 N88-12611
Electrochemical characteristics of acid electrolytes for fuel cells
[PB88-104641] 06 p0731 N88-14497
Soluble polysilane derivatives: Chemistry and spectroscopy
[AD-A187889] 11 p1461 N88-18713
Physics of immiscible flow in porous media
[PB88-131008] 11 p1487 N88-18873
Evaluation and prediction of Henry's law constants and aqueous solubilities for solvents and hydrocarbon fuel components. Volume 1: Technical discussion
[AD-A188571] 12 p1613 N88-19843
Prediction of thermodynamic properties, including solubility equilibria and vapor pressures, for mixed aqueous electrolytes to high temperatures
[DE88-006317] 14 p1990 N88-21863
Improved structural polymer alloys and composites
[AD-A192092] 19 p2619 N88-25538
Synthesis of model polymers and related structures in support of vinyl monomer grafting studies
[DE88-010245] 20 p2778 N88-26476
Critical point wetting drop tower experiment
[NASA-CR-183062] 20 p2798 N88-26603
A method for determining the solubility of hydrogen in molten aluminum-lithium alloys
[DE88-009807] 21 p2910 N88-27270
Interfacial tension of immiscible polymer blends: Temperature and molecular weight dependence
[AD-A192463] 21 p2917 N88-27312
Soluble metal chelate polymers of coordination numbers six, seven and eight
[AD-A192485] 21 p2917 N88-27314
Natural frequencies and stability of immiscible cylindrical z-independent liquid systems
[LRT-WE-9-FB-1(1987)] 22 p3053 N88-28112

SOLUTES
Van der Waals clusters of aromatic molecules studied using supersonic molecular jet spectroscopy
[AD-A186087] 07 p0929 N88-15644
Thermosolutal convection in high-aspect-ratio enclosures
[NASA-TM-100803] 11 p1486 N88-18871
The coordination cluster theory for metallic solutions
[DE88-005934] 13 p1738 N88-20389
High resolution detection of solute segregation to the cores of dislocations in grain boundaries
[DE88-009168] 20 p2877 N88-27078

SOLUTION
Numerical solution of weak forms of conservation laws on optimal unstructured triangular grids
20 p2797 N88-26597
Solution of the Orr-Sommerfeld equation for the Blausius boundary-layer documentation of program ORRBL and a test case
[NASA-CR-4169] 20 p2841 N88-26858
A systolic array for efficient execution of the Faddeev algorithm
[DE88-011330] 22 p3135 N88-28635

SOLUTIONS
NT AIR
NT ALVEOLAR AIR
NT AQUEOUS SOLUTIONS
NT DETONABLE GAS MIXTURES
NT GAS MIXTURES
NT HIGH TEMPERATURE AIR
NT SOLID SOLUTIONS
Accurate, stable, explicit solution of the parabolized Navier-Stokes equations 01 p0043 N88-10276
Theory of interstitial solutions
[BLL-M-37314-(5828.4)] 02 p0233 N88-11469
A 13C and 15N solid state NMR characterization of aramid-containing nylon-6 polymers synthesized by in situ polymerization of caprolactam with benzoyl caprolactam derivatives
[AD-A187067] 09 p1147 N88-16872
On the barotropic model of the ocean circulation
[AD-A188148] 10 p1358 N88-18118
The coordination cluster theory for metallic solutions
[DE88-005934] 13 p1738 N88-20389
Prediction of high-temperature thermodynamic properties of mixed electrolyte solutions including solubility equilibria, vapor pressure depression and boiling point elevation
[DE88-006344] 13 p1849 N88-21069
Fingering flow patterns of thermosolutal convection in rectangular enclosures
[NASA-TM-100854] 14 p1911 N88-21417
Almost-periodic solutions of nonlinear parabolic equations
[DE88-006423] 15 p2118 N88-22618
Bayesian solutions to a 2 x 2 decision matrix using interval scaled payoffs with an application to foreign policy decisions
[AD-A190863] 16 p2260 N88-23511
Certain questions of thermodynamic theory of weak solutions 18 p2586 N88-25368
The influence of uncompensated solution resistance on the determination and standard electrochemical rate constants using cyclic voltammetry and some comparisons with AC voltammetry
[AD-A192825] 20 p2770 N88-26427
A matroid algorithm and its application to the efficient solution of two optimization problems on graphs, revision
[AD-A192709] 20 p2838 N88-26838
Ill-posed problems and integral equations
[AD-A193709] 22 p3143 N88-28691
The construction of implicit and explicit solitary wave solutions of nonlinear partial differential equations
[AD-A193475] 23 p3269 N88-29452
Weak solution of the Langevin equation on a generalized functional space
[AD-A194290] 23 p3270 N88-29456
Structure and dynamics of solutions of lithium salts relevant to battery construction
[AD-A195399] 24 p3366 N88-30044

SOLVENTS
Effects of solvent exposures on poly(etheretherketone) (PEEK) and PEEK-fiberglass composites
[MLM-3405] 03 p0281 N88-11766
Saturable absorbers for colliding pulse-locked Nd:YAG lasers 03 p0302 N88-11902
Re-usable thin-layer spectroelectrochemical cell for non-aqueous solvent systems
[AD-A186951] 09 p1248 N88-17478
Cleanliness tests with the Omega Meter: A comparative study for solder flux removal
[DE88-004634] 11 p1460 N88-18704
Comparison of isopropyl alcohol and trichloroethylene in removing solder flux
[DE88-005556] 14 p1889 N88-21288
A study of solvent effects on the synthesis of pure component and composite ceramic powders by metal alkoxide hydrolysis
[DE88-008381] 20 p2777 N88-26470
Hydrogen storage by molecular polyhydrides
[AD-A194207] 23 p3191 N88-28989

SOLVOLYSIS
Descriptive characterization of propellant particles
[AD-A195176] 24 p3356 N88-29985

SONAR
Independence in sonar observations
[ARE-TR-87102] 01 p0088 N88-10572
The effect of reverberation on active sonar performance
[ARE-TM(UJS)-87104] 03 p0374 N88-12350
Correction of inertial navigation system drift errors for an autonomous land vehicle using optical radar terrain data
[AD-A184973] 05 p0544 N88-13311
User manual for ATILA, a finite-element code for modeling piezoelectric transducers
[AD-A185948] 07 p0847 N88-15141
Transient classifier systems and man-machine interface research
[AD-A186213] 07 p0899 N88-15446
Observations of the upper ocean using a multi-beam Doppler sonar
[AD-A188896] 12 p1649 N88-19878
Human efficiency for visual detection of targets on CRT displays using a two-level multiple channel time history format
[AD-A188419] 12 p1670 N88-20001
Observations of waves and Langmuir circulation with Doppler sonars 13 p1805 N88-20790
Robot navigation using simple sensor fusion
[DE88-006184] 18 p2561 N88-25203
Treatment of systematic errors in the processing of wide angle sonar sensor data for robotic navigation
[DE88-008961] 20 p2756 N88-26352
Sensor fusion for robot navigation
[DE88-008383] 20 p2809 N88-26663
Signal, noise, and reverberation in bistatic sonar systems
[FOA-C-20703-2.7] 22 p3147 N88-28721
Basic research in electronics (JSEP) Joint Services Electronics Program
[AD-A193072] 23 p3206 N88-29079

SONDES
NT IONOSONDES
NT RADIOSONDES
NT RAWINSONDES
Ozonesonde observations at Lauder, New Zealand during the Spring and early Summer of 1986
[PB88-173273] 16 p2232 N88-23328

SONIC BOOMS
MOAOPS and BOOM-MAP computer programs for sonic boom research, volume 1
[AD-A189548] 12 p1574 N88-19414

SONIC FATIGUE
U ACOUSTIC FATIGUE

SONIC FLOW
U TRANSONIC FLOW

SONIC SPEED
U ACOUSTIC VELOCITY

SOOT
An instrument for the quasi-continuous determination of atmospheric soot content
[DFVLR-FB-87-04] 01 p0068 N88-10433
Investigation of fuel additive effects on sooting flames
[AD-A186403] 07 p0829 N88-15026
Ionic mechanisms of soot formation in flames
[AD-A186195] 08 p0966 N88-15848
Measurements of gas turbine combustor and engine augmentor tube sooting characteristics
[AD-A187831] 11 p1440 N88-18592
Fuels combustion research
[AD-A187688] 11 p1453 N88-18657
Experimental and theoretical analysis of the radiative transfer within a sooty pool fire
[DE88-007099] 20 p2769 N88-26419
Real-time measurements of the size fractionation of ambient black carbon aerosols at elevated humidities
[DE88-010870] 23 p3215 N88-29138
Combustion and fuels in gas turbine engines
[AGARD-CP-422] 24 p3345 N88-29910
The performance of a surrogate blend in simulating JP-4 in a spray-fueled combustor 24 p3347 N88-29926
Radiation from soot-containing flames
24 p3347 N88-29927
Flamelet chemistry modelling of soot formation for radiation 24 p3348 N88-29928
Large ionic species in sooting acetylene and benzene flames 24 p3348 N88-29932
Rates of formation of soot from hydrocarbon flames and its destruction 24 p3349 N88-29933
The influence of pressure on soot formation
24 p3349 N88-29934
Particle sizing in combustion systems, using scattered laser light
[AD-A196231] 24 p3352 N88-29953
Optical measurements of soot and temperature profiles in premixed propane-oxygen flames
[NASA-TM-101343] 24 p3358 N88-29997
Optical measurements of soot in premixed flames
[NASA-TM-101305] 24 p3373 N88-30090

SORBENTS
NT ADSORBENTS

SORPTION
NT ADSORPTION
NT CHEMISORPTION
Working fluids for sorption heat pumps
[DE88-900203] 07 p0874 N88-15301
Synthesis and analysis of novel polymers with potential for providing both high permselectivity and permeability in gas separation applications
[DE88-006533] 15 p2043 N88-22174

SORTING
U CLASSIFYING

SOS (SEMICONDUCTORS)
Silicon-sapphire waveguides
[AD-A191754] 18 p2504 N88-24854
Investigation of photoconductive picosecond microstripline switches on self-implanted Silicon On Sapphire (SOS) 19 p2657 N88-25789

Carrier lifetime versus ion-implantation dose in Silicon On Sapphire 19 p2658 N88-25791
Picosecond optoelectronic switches using composite electronic materials 19 p2658 N88-25792
JFET/SOS (Junction Field-Effect Transistor/Silicon-on-Sapphire) devices: Gamma-radiation-induced effects
[AD-A193001] 20 p2795 N88-26586

SOUND
U ACOUSTICS

SOUND ABSORPTION
U SOUND TRANSMISSION

SOUND AMPLIFICATION
A continued study of optical sound generation and amplification
[AD-A188362] 12 p1691 N88-20116

SOUND BARRIER
U ACOUSTIC VELOCITY

SOUND DETECTING AND RANGING
A method of improving remote reproduction of a sound field by one-third-octave analysis and digital filtering
[RAE-TM-FS(F)-679] 22 p3147 N88-28722

SOUND DETECTORS
U SOUND TRANSDUCERS

SOUND FIELDS
Excitation of natural oscillations of a boundary layer by an external acoustic field 04 p0425 N88-12634
RADSPHERE: A computer program for calculating the steady-state, axially symmetric, forced response and radiation field of a submerged spherical shell
[AD-A185025] 05 p0609 N88-13738
Development of a new method of measuring the characteristic impedance and complex wave number of a porous acoustic material
[AD-A185038] 05 p0646 N88-13957
Mode pattern of field generated by parametric radiator in acoustic waveguide 08 p1076 N88-16488
Acoustic field in waveguide with sloping bed 08 p1076 N88-16490
Sound propagation through a turbulent atmosphere: Experimental techniques and data analysis
[AD-A188891] 12 p1688 N88-20094
Invariant characteristics of acoustic field in stratified ocean 13 p1788 N88-20698
Measurement and analysis of the noise radiated by low Mach numbers centrifugal blowers
[AD-A189226] 13 p1833 N88-20966
Flow/acoustic interaction in duct inflow
[AD-A189264] 13 p1833 N88-20967
Acoustic radiation from line- and point-loaded plates: Uniformly asymptotic solutions
[AD-A189367] 13 p1834 N88-20969
A computerized investigation using the method of images to predict the sound field in a fluid wedge overlying a slow fluid half-space
[AD-A190013] 15 p2130 N88-22704
Driving of axial acoustic fields by side-wall stabilized premixed flames 19 p2629 N88-25592
Numerical investigation of acoustic energy exchange through flow turning 19 p2629 N88-25593
Velocity coupling 19 p2629 N88-25596
Vertical directionality of ambient noise at 32 deg N as a function of longitude: Tape number 86180
[AD-A193228] 21 p3012 N88-27872
The covariance of scalar fields scattered by pressure-release randomly rough surfaces
[AD-A192489] 22 p3146 N88-28714
A method of improving remote reproduction of a sound field by one-third-octave analysis and digital filtering
[RAE-TM-FS(F)-679] 22 p3147 N88-28722
Acoustic pressure distribution on the bottom of a wedge-shaped ocean
[AD-A193961] 23 p3278 N88-29518

SOUND FIXING AND RANGING
Outdoor sound propagation, its implications for unattended ground sensors
[FEL-1986-64] 20 p2850 N88-26917

SOUND FREQUENCIES
U ACOUSTIC FREQUENCIES

SOUND GENERATORS
Flow induced pulsations in pipe systems
[ETN-88-91367] 06 p0702 N88-14307
Linear theory of generation of longitudinal sound waves in semiconductors upon interband absorption of optical radiation 09 p1234 N88-17397
A continued study of optical sound generation and amplification
[AD-A188362] 12 p1691 N88-20116
Design of a sound neck in connection with the model-support system of a transonic wind tunnel test section
[ILR-MITT-186(1987)] 14 p1869 N88-21171
Software development for the reconstruction of source parameters using research and development arrays
[REPT-840445-TW] 16 p2246 N88-23417

SOUND INTENSITY
Sound power measurements in situ using a reference sound source
[PB88-182571] 20 p2849 N88-26910

SOUND LOCALIZATION
Method for determining the coordinates of sound sources by means of a sound measurement system
[NASA-TT-20242] 13 p1834 N88-20972
Software development for the reconstruction of source parameters using research and development arrays
[REPT-840445-TW] 16 p2246 N88-23417
Proceedings of the French-German Colloquium on Helicopter Detection
[ISL-R-104/87] 22 p3147 N88-28723
Acoustic helicopter positioning 22 p3148 N88-28726
Acoustic detection of helicopters: Experiments 22 p3148 N88-28727
Acoustic direction finding of flying helicopters 22 p3148 N88-28728
Examples of the application of acoustics for the detection and classification of targets 22 p3148 N88-28729
Detection of helicopters using ground-controlled microphones 22 p3148 N88-28730

SOUND MEASUREMENT
U ACOUSTIC MEASUREMENT

SOUND PERCEPTION
U AUDITORY PERCEPTION

SOUND PRESSURE
Sound pressure distribution in front of a serrated boundary: Standing wave suppression and diffusion 07 p0928 N88-15639
Diffraction of sound at junction of two waveguides 08 p1076 N88-16491
Sound propagation through a turbulent atmosphere: Experimental techniques and data analysis
[AD-A188891] 12 p1688 N88-20094
Development of a computerized analysis for solid propellant combustion instability with turbulence
[NASA-CR-182351] 19 p2611 N88-25497
An analysis of the efficiency and directivity of the sound generated by a moving laser source
[AD-A192220] 20 p2849 N88-26914
Acoustic pressure distribution on the bottom of a wedge-shaped ocean
[AD-A193961] 23 p3278 N88-29518

SOUND PROPAGATION
NT VOICE
Sound propagation over uneven ground and irregular topography
[NASA-CR-182352] 06 p0776 N88-14763
The properties of sound propagation in liquid constrained viscoelastic and polymeric structures
[AD-A185944] 07 p0929 N88-15640
Use of boundary-layer method for problem of sound propagation through channel with variable cross-section containing stream of fluid 09 p1233 N88-17396
Comparison of the rough surface reflection coefficient with specularly scattered acoustic data
[AD-A187086] 09 p1242 N88-17444
Optically stimulated sound from gas bubbles in water 12 p1686 N88-20087
Sound propagation through a turbulent atmosphere: Experimental techniques and data analysis
[AD-A188891] 12 p1688 N88-20094
Construction of approximations to acoustic Green's functions for nonhomogeneous oceans using transmutation
[PB88-185384] 18 p2548 N88-25126
Linear and nonlinear acoustic wave propagation in the atmosphere
[NASA-CR-4157] 18 p2571 N88-25268
Outdoor sound propagation, its implications for unattended ground sensors
[FEL-1986-64] 20 p2850 N88-26917
Sound propagation at low altitude 22 p3148 N88-28725

SOUND TRANSDUCERS
NT ELECTROACOUSTIC TRANSDUCERS
NT HYDROPHONES
NT MICROPHONES
Noncontact temperature measurements of hot steel bodies using an electromagnetic acoustic transducer (EMAT)
[DE88-000560] 04 p0446 N88-12765
Mode pattern of field generated by parametric radiator in acoustic waveguide 08 p1076 N88-16488
Acoustic helicopter positioning 22 p3148 N88-28726
Sensors adapted for acoustic detection 22 p3148 N88-28731
Correlation method and sensors adapted to the environment 22 p3149 N88-28732

SOUND TRANSMISSION
Active minimisation of acoustic fields. A review of research into the active control of sound undertaken at ISVR from 1983 to 1986
[ISVR-TR-146] 01 p0091 N88-10593
The effect of ocean fluctuations on sound transmission in the ocean
[AD-A184382] 03 p0355 N88-12236
Nonlinear acoustics
[AD-A184271] 04 p0488 N88-13004
Aircraft interior noise reduction by alternate resonance tuning
[NASA-CR-181530] 04 p0488 N88-13005
An analysis of sound absorbing linings for the interior of the NASA Ames 80 x 120-foot wind tunnel
[NASA-CR-177396] 04 p0488 N88-13006
Theoretical and practical aspects of the functional absorber method of arranging sound absorbing panels
[BBC-RD-1987/15] 05 p0646 N88-13955
Multipath time-delay estimation via the EM algorithm
[PB88-106851] 07 p0845 N88-15124
The properties of sound propagation in liquid constrained viscoelastic and polymeric structures
[AD-A185944] 07 p0929 N88-15640
Identification and proposed control of helicopter transmission noise at the source 09 p1109 N88-16647
Comparison of the rough surface reflection coefficient with specularly scattered acoustic data
[AD-A187086] 09 p1242 N88-17444
Silencium resonators (Silators) for the attenuation and elimination of sound
[MBB-Z-546/83] 10 p1312 N88-17841
Sound transmission through the walls of light aircraft: An investigation of structure-borne noise in a Handley Page 137 Jetstream 3 aircraft
[NASA-CR-182509] 10 p1405 N88-18376
A study of methods to predict and measure the transmission of sound through the walls of light aircraft
[NASA-CR-182656] 12 p1687 N88-20090
Sound propagation through a turbulent atmosphere: Experimental techniques and data analysis
[AD-A188891] 12 p1688 N88-20094
A continued study of optical sound generation and amplification
[AD-A188362] 12 p1691 N88-20116
Spatial matched processing for multipath propagation
[AD-A189790] 15 p2129 N88-22701
Target localization in an inhomogeneous medium
[AD-A190008] 15 p2130 N88-22703
A computerized investigation using the method of images to predict the sound field in a fluid wedge overlying a slow fluid half-space
[AD-A190013] 15 p2130 N88-22704
An outdoor unit for Direct Broadcast Satellite (DBS) digital sound reception
[BMFT-FB-W-86-016] 16 p2189 N88-23050
Sources and levels of background noise in the NASA Ames 40- by 80-foot wind tunnel
[NASA-TM-100077] 17 p2395 N88-24239
Signal processing in digital speech transmission systems
[ETN-88-92122] 20 p2792 N88-26561
Aircraft interior noise reduction by alternate resonance tuning
[NASA-CR-182540] 20 p2849 N88-26909
Acoustic diffraction by an absorbing finite strip in a moving fluid
[PB88-191382] 20 p2849 N88-26912
Reflection and scattering of acoustic rays computed for parabolic ice keel models
[AD-A193898] 23 p3278 N88-29517
Acoustic pressure distribution on the bottom of a wedge-shaped ocean
[AD-A193961] 23 p3278 N88-29518
Analysis of the transmission of sound into the passenger compartment of a propeller aircraft using the finite element method
[FFA-TN-1988-15] 23 p3279 N88-29520

SOUND VELOCITY
U ACOUSTIC VELOCITY

SOUND WAVES
NT AERODYNAMIC NOISE
NT AIRCRAFT NOISE
NT BLADE SLAP NOISE
NT ENGINE NOISE
NT ION ACOUSTIC WAVES
NT JET AIRCRAFT NOISE
NT LAMB WAVES
NT NOISE (SOUND)
NT SONIC BOOMS
NT THERMAL NOISE
Geoacoustic models of the Hudson Canyon area
[AD-A183535] 01 p0073 N88-10465

Finite difference solution of a generic differential equation
[PB87-205878] 01 p0087 N88-10568
A new method for determining acoustic properties of the seabed from the ambient noise field in the ocean
[RAE-TR-86035] 01 p0090 N88-10590
The phenomenology of Karman vortex streets via sound in oscillatory flow
[MPIS-MITT-84-1987] 02 p0122 N88-10775
Boundary effects on the drag of an oscillating sphere: Applications to the magnetic sphere rheometer. Attenuation and dispersion of acoustic waves in nematic liquid crystals 04 p0488 N88-13007
Theoretical and practical aspects of the functional absorber method of arranging sound absorbing panels
[BBC-RD-1987/15] 05 p0646 N88-13955
Full field visualization of surface and bulk acoustic waves using heterodyne holographic interferometry
[AD-A185071] 05 p0646 N88-13958
Nonlinear reflection of sound wave in gas mixture 06 p0769 N88-14728
Dependence of acoustical characteristics of laser-induced breakdown in dielectric materials on shape of inelastic region 06 p0774 N88-14753
Waves and vibrations in elastic superlattice composites 06 p0776 N88-14765
The properties of sound propagation in liquid constrained viscoelastic and polymeric structures
[AD-A185944] 07 p0929 N88-15640
Characterizing particle combustion in a Rijke burner
[AD-A186157] 08 p0966 N88-15847
Approximation of noncorrelated reflections in problem of sound propagation through waveguide with rough boundary 08 p1076 N88-16487
Diffraction of sound at junction of two waveguides 08 p1076 N88-16491
Equation of acoustic and gravitational waves in stratified moving medium 08 p1077 N88-16493
Stimulated Mandelstam-Brillouin scattering during forward scattering of light 08 p1078 N88-16499
Interaction of acoustic and electromagnetic waves involved in anomalous skin effect 08 p1079 N88-16503
The assessment of the sound insulation requirements for a large broadcasting studio, using a scale model: Theoretical considerations
[BBC-RD-1987/20] 09 p1155 N88-16921
Linear theory of generation of longitudinal sound waves in semiconductors upon interband absorption of optical radiation 09 p1234 N88-17397
Theory of transient thermal self-focusing of sound beams 09 p1234 N88-17401
Nonlinear and diffraction effects in sound beams with random transverse structure 09 p1235 N88-17402
Transient sound radiation from infinite thin plate
[ARE-TM(UHA)-87508] 09 p1243 N88-17449
Surface acoustic wave deposition sensor
[DE87-006527] 09 p1243 N88-17452
Cryogenic acoustic microscopy
[AD-A187274] 10 p1299 N88-17767
The assessment of the sound insulation requirements for a large broadcasting studio, using a scale model: Practical details
[BBC-RD-1987/21] 10 p1318 N88-17878
Johnson noise thermometer for high radiation and high temperature environments
[DE88-003770] 10 p1323 N88-17911
Microscopic modeling of sound waves in granular material
[DE88-000348] 10 p1405 N88-18375
Scattering of impulsive acoustic waves by a semi-infinite crack in the plane interface of a half-space and a layer
[PB88-126396] 10 p1405 N88-18377
A modified version of the phase sensitive technique for measurements of absolute sound velocity in solids
[DE88-002303] 10 p1405 N88-18378
Evolution of acoustic gravity wave packet in spatially and temporally varying wind 11 p1469 N88-18760
Acoustic wave electroless deposition monitor
[DE88-004023] 11 p1489 N88-18887
Recording a surface acoustic wave on the surface of silicon
[PB88-130372] 11 p1490 N88-18894
The temporal and spatial acoustical response of a point-driven fluid-loaded plate
[AD-A188504] 12 p1636 N88-19794
Method for determination of the wind velocity and direction
[NASA-TT-20233] 13 p1802 N88-20769
Flow/acoustic interaction in duct inflow
[AD-A189264] 13 p1833 N88-20967
Mathematical models of sound waves in fluids
[AD-A189270] 13 p1834 N88-20968
Acoustic radiation from line- and point-loaded plates: Uniformly asymptotic solutions
[AD-A189367] 13 p1834 N88-20969
Modeling of laser ultrasound generation in a weld pool
[DE88-005546] 13 p1834 N88-20971
Method for determining artillery position
[NASA-TT-20238] 13 p1834 N88-20973
Perception of complex auditory patterns
[AD-A190218] 15 p2102 N88-22524
Mechanisms mediating the perception of complex acoustic patterns
[AD-A190112] 15 p2130 N88-22705
Generation and propagation of sound waves in a collapsing or anti-collapsing star with uniform density
[DE87-703034] 15 p2151 N88-22839
Propagation of acoustic gravity wave spectrum through vertical wind shear region 16 p2186 N88-23035
Study of the boundary layer of a flow pulsed by acoustic waves
[ETN-88-91998] 16 p2206 N88-23163
Refraction in underwater acoustics --- navigation systems
[B8735053] 17 p2395 N88-24236
Johnson noise thermometer for high-radiation and high-temperature environments 17 p2434 N88-24480
Evaluation of the biot coefficients
[AD-A191643] 18 p2570 N88-25265
Acoustic wave dispersion in a viscous, compressible, liquid-filled cylindrical elastic tube 19 p2722 N88-26164
Dynamics and stability of combustion driven self oscillations in presence of various frequencies. Extensive stability criteria
[ETN-88-92123] 20 p2771 N88-26432
Studying materials using acoustic waves
[AD-A192234] 20 p2850 N88-26915
On the possibility of the soliton description of acoustic emission during plastic deformation of crystals
[DE88-701878] 20 p2876 N88-27075
Reflection of sound in open ended ducts
[PB88-103478] 21 p3012 N88-27870
Propagation of acoustic disturbances in transonic flow fields of lifting wings
[DFVLR-FB-88-13] 21 p3013 N88-27880
Computer-controlled measurements of nonlinear standing waves
[AD-A193840] 22 p3147 N88-28717
The role of acoustic resonances in unsteady turbomachinery aerodynamics
[PNR90455] 22 p3147 N88-28720
Interactions between air and ground sound at the Earth surface 22 p3149 N88-28733
Acoustic-seismic helicopter detection 22 p3149 N88-28734
In situ fault detection by the hybrid ray mode method
[AD-A195226] 24 p3381 N88-30137

SOUNDERS
U SOUNDING

SOUNDING
NT ACOUSTIC SOUNDING
NT ATMOSPHERIC SOUNDING
NT BALLOON SOUNDING
NT ECHO SOUNDING
NT IONOSPHERIC SOUNDING
NT MICROWAVE SOUNDING
NT ROCKET SOUNDING
NT SATELLITE SOUNDING
A new approach to modeling and interpreting electromagnetic sounding data
[DE88-000460] 04 p0438 N88-12715
Materials of the World Data Center B. Deep Seismic Sounding (DSS): Pacific data 09 p1196 N88-17167
Airborne electromagnetic sounding of sea ice thickness and sub-ice bathymetry
[AD-A188939] 12 p1649 N88-19879
HF (High Frequency) Maximum Usable Frequency (MUF) model uncertainty assessment
[AD-A189132] 13 p1757 N88-20513

SOUNDING ROCKETS
NT BLACK BRANT SOUNDING ROCKETS
NT SKYLARK ROCKET VEHICLE
Proceedings of the 8th ESA Symposium on European Rocket and Balloon Programs and Related Research
[ESA-SP-270] 08 p1024 N88-16201
Esrange (Sweden): New installations, future plans and investments --- rocket range 08 p1029 N88-16235
Facilities and plans for improvements at Andoya (Norway) rocket range 08 p1029 N88-16236
Preliminary Material Science Experiment Rocket (MASER) 1 results and the evolution of the MASER program 08 p1033 N88-16260
Future plans for the NASA suborbital program 08 p1034 N88-16267
Guidance of high-altitude sounding rockets using the S19 and Spinning Rocket Altitude Control (SPINRAC) systems 08 p1034 N88-16273
Sounding rockets/microgravity products and service 08 p1035 N88-16277
In-situ plasma bubble observations associated with equatorial spread-F over Natal
[INPE-4488-PRE/1252] 15 p2095 N88-22482
Electric field measurement by S-520-9 sounding rocket using the time of flight technique of lithium ion beam
[ISAS-RN-367] 18 p2543 N88-25095
Rocket-borne low energy ion measurements in space 18 p2593 N88-25412
MRS-3000 meteorological rocket probe for the MMR-06 dart integrated meteorological rocket system
[NASA-TT-20303] 19 p2693 N88-26010
Design, development, fabrication and launch support for a high altitude release of neodymium vapor
[AD-A194196] 22 p3118 N88-28527
Aerospace payload support systems
[AFGL-TR-87-0241] 24 p3334 N88-29843

SOUNDS (TOPOGRAPHIC FEATURES)
The physical oceanography of the northern Baffin Bay-Nares Strait region
[AD-A190015] 15 p2100 N88-22509

SOUTH AMERICA
On the interannual variability of South American climate and the Southern Oscillation 04 p0470 N88-12905
A study on electric fields and conductivity associated with electrified clouds in the region of South America
[INPE-4487-TDL/325] 15 p2096 N88-22486

SOUTH WEST AFRICA
U NAMIBIA

SOUTHERN HEMISPHERE
NT ANTARCTIC REGIONS
NT ROSS ICE SHELF
October lower stratospheric Antarctic temperature and total ozone from 1979-1985 05 p0615 N88-13776
Atmosphere of Venus in south polar area based on radio transmission data 08 p1005 N88-16089
Meteorological atlas of the Southern Hemisphere lower stratosphere for August and September 1987
[NASA-TM-4049] 20 p2825 N88-26763
Recent secular changes in the wintertime circulation of the Southern Hemisphere 22 p3122 N88-28555

SOUTHERN OSCILLATION
On the interannual variability of South American climate and the Southern Oscillation 04 p0470 N88-12905
Variations of tropical circulation and associated rainfall anomalies, during 2 years of contrast
[INPE-4359-TDL/300] 08 p1039 N88-16286
Survey of acoustic techniques for monitoring El Nino
[PB88-157615] 13 p1804 N88-20783

SOVIET SATELLITES
NT COSMOS SATELLITES
NT INTERCOSMOS SATELLITES
NT PROGNOZ SATELLITES

SOVIET SPACECRAFT
NT MIR SPACE STATION
NT SALYUT SPACE STATION
NT SOYUZ SPACECRAFT
Soviet spacecraft engineering research
[FASAC-TAR-3090] 17 p2311 N88-23823
Soviet space program handbook
[AD-A194332] 22 p3046 N88-28077

SOVIET UNION
U U.S.S.R.

SOYBEANS
Estimating scattered and absorbed radiation in plant canopies by remote sensing
[NASA-CR-181390] 02 p0193 N88-11205
Spectral behavior of crops through analysis of LANDSAT-TM data 17 p2358 N88-24047
Identification of areas cultivated with soybeans in the cerrados regions, through digital processingof satellite images: A methodological approach 17 p2358 N88-24048
Evaluation of TM false color composites for crop discrimination 17 p2367 N88-24096
Study of the spectral response of soybeans
[INPE-4592-PRE/1322] 24 p3387 N88-30174

SOYUZ SPACECRAFT
USSR report: Space
[JPRS-USP-87-003] 01 p0009 N88-10050
Basic results of medical studies during prolonged manned flights on-board the Salyut-7/Soyuz-T orbital complex
[NASA-TT-20217] 10 p1369 N88-18182
Soviet space transport systems 13 p1727 N88-20328
Features of Soyuz TM spacecraft 13 p1727 N88-20329
The USSR space systems for remote sensing of earth resources and the environment (sensor systems, processing techniques, applications) 17 p2356 N88-24035

SPACE
State-of-the-art in true space-time finite element method 17 p2391 N88-24215

Space station as a vital focus for advancing the technologies of automation and robotics
[IAF-86-62] 23 p3251 N88-29352

SPACE ADAPTATION SYNDROME
Cosmonauts' hormonal responses after brief spaceflights 07 p0890 N88-15394
Experiments with rats flown aboard Cosmos-1667 biosatellite (main objectives, conditions and results) 07 p0893 N88-15414
JPRS Report: Science and Technology. USSR: Space Biology and Aerospace Medicine, volume 21, no. 5, September - October 1987
[JPRS-USB-88-003] 10 p1359 N88-18122
Inflight simian circadian rhythms and temperature homeostasis aboard Cosmos-1514 biosatellite 10 p1359 N88-18125
Discrete adaptation to sensory conflict 10 p1363 N88-18146
Genetic research in space
[NASA-TT-20216] 11 p1518 N88-19066
Cardiovascular adaptation to zero-g during a long term flight (237 days) on board the Salyut 7 Soviet space station (1984) 12 p1655 N88-19920
Cardiac and peripheral circulation assessment by ultrasound on 3 astronauts during two 7-day space flights (1982 Salyut-7 - 1985 STS 51G) 12 p1656 N88-19921
Load and control of the cardiocirculatory system in weightlessness 12 p1656 N88-19922
Neuro-reflex mechanisms of circulation regulation in simulated microgravity 12 p1656 N88-19923
The rate of adaptation to altered g in the human centrifuge: Implications for simulations of mass-discrimination in space flight 12 p1659 N88-19941
Gastric emptying assessment by echography after a stress (rotating chair) 12 p1661 N88-19955
The relationship between preflight underwater training and space motion sickness 19 p2696 N88-26025
Results of medical research conducted in 1985 during long-term spaceflights 19 p2702 N88-26070

SPACE BASED RADAR
Theory of displaced phase center antenna for space based radar applications
[PB87-229837] 06 p0690 N88-14227
Parametric analysis of power requirements for space-based radar 17 p2399 N88-24260
Space based radar application to air traffic control 17 p2399 N88-24262
The role of space borne imaging radars in environmental monitoring: Some shuttle imaging radar results in Asia
[NASA-TM-101178] 18 p2502 N88-24844

SPACE BASES
NT LUNAR BASES
NT SPACE COLONIES
Small reactor power systems for manned planetary surface bases
[NASA-TM-100223] 04 p0524 N88-13209

SPACE BIOLOGY
U EXOBIOLOGY

SPACE CAPSULES
NT ESCAPE CAPSULES

SPACE CHARGE
Filamentation instability of rotating light ion beams in fusion target chambers
[IPPJ-839] 02 p0242 N88-11530
Intense electron beams
[DE88-002456] 09 p1247 N88-17474
A ring model of the lasertron
[DE88-004656] 10 p1323 N88-17908
Generalized equations for emittance and field energy of high-current beams in periodic focusing
[DE88-004448] 10 p1404 N88-18372
Experimental results of a high-gain microwave FEL operating at 140 GHz
[DE88-004358] 11 p1492 N88-18907
Wiggler taper optimization for free-electron-laser amplifiers with moderate space-charge effects
[DE88-003758] 13 p1775 N88-20618
Theoretical model of the cathode spot on a unipolar arc
[AD-A190109] 15 p2059 N88-22277
Deep dielectric charging effects due to high energy electrons in earth's outer magnetosphere
[AD-A192154] 18 p2541 N88-25083
Accelerator research studies
[DE88-007124] 18 p2574 N88-25290
Spacecraft requirements for predictions of geomagnetic activity (a tutorial)
[AD-A191943] 19 p2685 N88-25959
Results from the SLAC lasertron
[DE88-007816] 20 p2806 N88-26647
Space-charge-wave solid state microwave amplifier
[AD-A193792] 23 p3208 N88-29091
Beam optics test stand
[AD-A193901] 23 p3216 N88-29144

SPACE COLONIES
Steps toward lunar settlement
[DE88-009141] 21 p2900 N88-27213

SPACE COMMERCIALIZATION
Space station: Leadership for the future
[NASA-PAM-509/8-87] 01 p0013 N88-10072
Moving the factory into orbit 02 p0134 N88-10844
Commercial Opportunities for Remote Sensing with Polar Platforms
[ESA-SP-269] 03 p0339 N88-12131
Possible commercial use of the polar platforms --- Columbus 03 p0339 N88-12132
Market potential for commercial remote sensing 03 p0339 N88-12137
Commercial perspective of an imaging spectrometer development program 03 p0340 N88-12138
MBB-ERNO view of remote sensing commercialization 03 p0340 N88-12140
SPOT 1: First In-Flight Results --- conferences
[ISBN-2-85428-177-2] 03 p0340 N88-12143
Development of the SPOT commercial service: Preliminary conclusions after six months of operations 03 p0340 N88-12144
Satimage and the Nordic SPOT market 03 p0340 N88-12145
SPOT Image Corporation: Early results 03 p0340 N88-12146
Definition and economic evaluation of Space Solar Power Systems (SSPS), part 2
[ILR-MITT-184-2(1987)] 08 p1022 N88-16190
The ILV: A new commercial expendable launch vehicle --- Industrial Launch Vehicle (ILV) 08 p1035 N88-16275
The prospects of space utilization
[MBB-UR-931/86] 10 p1314 N88-17856
Space-based remote sensing of the Earth: A report to the Congress
[NASA-TM-89709] 10 p1346 N88-18046
Preparation for microgravity: The role of the microgravity materials science laboratory
[NASA-TM-100906] 18 p2497 N88-24811
Business telecommunications using satellite microterminals: Gaining the competitive edge
[ESA-BR-49] 22 p3070 N88-28225
Applications of SPOT data for urban real estate investment information systems 22 p3101 N88-28414
SPOT data acquisition and distribution 22 p3115 N88-28505
Commercialization and export --- aerospace industry 22 p3161 N88-28824

SPACE COMMUNICATION
NT SATELLITE COMMUNICATION
NT SPACECRAFT COMMUNICATION
The Telecommunications and Data Acquisition Report
[NASA-CR-181546] 04 p0432 N88-12679
An evolutionary communications scenario for Mars exploration
[NASA-TM-100263] 05 p0576 N88-13515
High data rate modem simulation for the space station multiple-access communications system 06 p0795 N88-14870
Optically controlled phased-array antenna technology for space communication systems
[NASA-TM-100852] 11 p1476 N88-18809
Monolithic microwave integrated circuit technology for advanced space communication
[NASA-TM-100829] 14 p1906 N88-21389
Error control techniques for satellite and space communications
[NASA-CR-182886] 17 p2332 N88-23922
Service offerings and interfaces for the ACTS network of Earth stations
[NASA-TM-100809] 18 p2471 N88-24663
Telescience testbed pilot program
[NASA-CR-183207] 24 p3412 N88-30309
The Deep Space Network: An instrument for radio astronomy research
[NASA-CR-183219] 24 p3453 N88-30554

SPACE COOLING (BUILDINGS)
Engineering principles and concepts for active solar systems
[DE87-001181] 01 p0066 N88-10425
Understanding passive cooling systems
[PB87-210464] 02 p0194 N88-11211
Life-cycle cost analysis of residential heat pumps and alternative HVAC (Heating, Ventilating and Air-Conditioning) systems
[DE88-003701] 07 p0839 N88-15090
Heat pump and appliance research
[PB88-102462] 07 p0853 N88-15184
Water source heat pump: How to get home heating and cooling from your own back yard
[DE88-900180] 07 p0875 N88-15306
Short Reference Years: Short weather data sets for faster simulations of solar energy systems and energy consumption in buildings
[DE88-900198] 07 p0881 N88-15343
Field experience with aquifer thermal energy storage
[DE88-007075] 18 p2538 N88-25058

SPACE DEBRIS
Space environmental considerations for a long-term cryogenic storage vessel 08 p0981 N88-15933
Space station integrated wall damage and penetration damage control. Task 5: Space debris measurement, mapping and characterization system
[NASA-CR-179281] 10 p1285 N88-17688
Nuclear-powered space debris sweeper 17 p2418 N88-24380
Effects of meteoroids and space debris on the particulate environment for space station 18 p2591 N88-25399
Assessment of the effects of space debris and meteoroids environment on the space station solar array assembly
[NASA-TM-101315] 23 p3185 N88-28959

SPACE DENSITY
Galactic interstellar abundance surveys with IUE and IRAS 04 p0522 N88-13206

SPACE DIVERSITY
U RECEPTION DIVERSITY

SPACE ENVIRONMENT
U AEROSPACE ENVIRONMENTS

SPACE ENVIRONMENT SIMULATION
NT NEUTRAL BUOYANCY SIMULATION
NT WEIGHTLESSNESS SIMULATION
Irradiation testing 03 p0274 N88-11727
Laboratory simulation of the electrodynamic interactions of a tethered satellite with an ionospheric plasma
[IFSI-86-3] 08 p0961 N88-15822
Experimental evidence of micro-nonequilibrium on the magnetopause and further predictions 08 p1098 N88-16606
ASSESS-2: An aircraft simulation of Spacelab 09 p1123 N88-16723
Major spacecraft hardware testing in Europe 09 p1125 N88-16740
Development of infrared techniques for testing spacecraft 09 p1128 N88-16772
Seven year thermal vacuum real life test of a medium speed (despin) mechanism manufactured by Dornier System
[ESA-ESTL-64] 09 p1175 N88-17038
EUROSIM: A design concept for an in-orbit operations simulator 12 p1589 N88-19517
Ultraviolet (180 to 300 nm) action spectra for inactivation and DNA photoproduct formation of Bacillus subtilis spores under ultrahigh vacuum 12 p1657 N88-19931
Survival and mutation induction of dehydrated yeast cells after UV exposure 12 p1657 N88-19932
Cellular effects of heavy ions: Experimental results and theoretical approaches --- space radiation 12 p1658 N88-19933
Activities report of the Toulouse Research Center
[ETN-88-91988] 13 p1850 N88-21077
Simulation of cometary nuclei 14 p2005 N88-21954
Development of a slip-ring system for energy transfer in space conditions. Space flight qualification and extended life tests
[BMFT-FB-W-86-019] 16 p2169 N88-22932
Different techniques for intervening under the sea: Possible links with space applications 19 p2697 N88-26030
Contribution to the study of materials behavior in space environment
[SNIAS-881-430-104] 23 p3189 N88-28977
The effects of total dose on the SEU sensitivity of CMOS static RAMS — single event upset (SEU), satellite components
[AERE-R-12779] 24 p3428 N88-30401
The Single Event Upset (SEU) test facility on the Hardwell tandem generator for cosmic ray simulation
[AERE-R-12896] 24 p3459 N88-30580

SPACE ENVIRONMENTAL LUBRICATION
U SPACECRAFT LUBRICATION

SPACE ERECTABLE STRUCTURES
Access flight hardware design and development 02 p0139 N88-10873
Planning and scheduling for robotic assembly 08 p1062 N88-16416
Satellite assembly in geostationary orbit: A plug-and-socket concept 09 p1128 N88-16769
Space station structures development
[NASA-CR-179261] 09 p1133 N88-16792
The integration of a mesh reflector to a 15-foot box truss structure. Task 3: Box truss analysis and technology development
[NASA-CR-178228] 11 p1497 N88-18941

A 60-meter erectable assembly concept for a control of flexible structures flight experiment
[NASA-TM-100497] 14 p1873 N88-21190
Bi-stem gripping apparatus
[NASA-CASE-MFS-28185-1] 17 p2345 N88-23979
Development of a space deployable radiator using heat pipes
[SNIAS-881-440-104] 23 p3214 N88-29128
Clevis joint for deployable space structures
[NASA-CASE-LAR-13898-1] 24 p3380 N88-30130
Far infrared spectroscopy telescope (FIRST) inflatable thermal shield, phase 1
[SR/FIS/108(87)CZ] 24 p3453 N88-30552

SPACE EXPER WITH PARTICLE ACCELERATORS
U SEPAC (PAYLOAD)

SPACE EXPLORATION
USSR report: Space
[JPRS-USP-87-003] 01 p0009 N88-10050
A matter-antimatter propulsion system for manned interstellar flight
[DE87-013311] 02 p0141 N88-10885
How we get pictures from space, revised edition
[NF-151/7-87-REV] 02 p0193 N88-11203
Small reactor power systems for manned planetary surface bases
[NASA-TM-100223] 04 p0524 N88-13209
An evolutionary communications scenario for Mars exploration
[NASA-TM-100263] 05 p0576 N88-13515
Small space reactor power systems for unmanned solar system exploration missions
[NASA-TM-100228] 05 p0660 N88-14054
Unispace 82 09 p1128 N88-16756
America plans for space
[AD-A187465] 10 p1289 N88-17713
Deep space target location with Hubble Space Telescope (HST) and Hipparcos data
[NASA-CR-182520] 10 p1427 N88-18524
Interplanetary mission design handbook. Volume 1, Part 5: Mars-to-Earth ballistic mission opportunities, 1992-2007
[NASA-CR-182525] 10 p1430 N88-18538
Soviet space transport systems 13 p1727 N88-20328
The Deep Space Network
[NASA-CR-182700] 13 p1759 N88-20524
Electromagnetic powered vehicles (EMPV) for Mars exploration 17 p2419 N88-24388
Reflectance spectroscopy in planetary science: Review and strategy for the future
[NASA-SP-493] 17 p2451 N88-24564
Planetary Geology: Goals, Future Directions, and Recommendations
[NASA-CP-3005] 19 p2742 N88-26279
Reports of planetary astronomy, 1988
[NASA-TM-4063] 22 p3163 N88-28835
The NASA Electric Propulsion Program
[NASA-TM-101324] 24 p3336 N88-29859
Volatiles on Mars
[NASA-CR-183113] 24 p3456 N88-30571

SPACE FLIGHT
NT INTERPLANETARY FLIGHT
NT INTERSTELLAR TRAVEL
NT LONG DURATION SPACE FLIGHT
NT MANNED SPACE FLIGHT
NT RETURN TO EARTH SPACE FLIGHT
NT SPACE SHUTTLE MISSION 31-A
NT SPACE SHUTTLE MISSION 31-B
NT SPACE SHUTTLE MISSION 41-C
NT SPACE SHUTTLE MISSION 51-L
NT SPACE SHUTTLE MISSION 61-B
NT SPACE SHUTTLE MISSIONS
Radiation effects in space
[DE87-012529] 01 p0075 N88-10479
The Proceedings of the Symposium on Mechanics for Space Flight
[ISAS-SP-5] 03 p0317 N88-12006
USSR Space Life Sciences Digest index to issues 10-14
[NASA-CR-3922(17)] 07 p0883 N88-15361
Development of methods for the study of space motion sickness 07 p0892 N88-15408
Research on cotton plants grown in space 08 p1006 N88-16098
Advantages of manned lunar base 08 p1009 N88-16118
Possible use of plasmids for study of effect of space flight factors on biological objects 08 p1046 N88-16319
Electrochemical carbon dioxide concentrator subsystem development
[NASA-CR-177411] 08 p1053 N88-16353
Organs and tissues regeneration in amphibia under the space flight conditions 12 p1660 N88-19951
Advanced space propulsion study - antiproton and beamed power propulsion
[AD-A189218] 13 p1732 N88-20355
Langley aerospace test highlights, 1987
[NASA-TM-100595] 15 p2153 N88-22853
Possibilities and limits for use of laser propulsion systems in interorbital space flight
[ILR-MITT-185] 18 p2475 N88-24683
Soviet space program handbook
[AD-A194332] 22 p3046 N88-28077

SPACE FLIGHT FEEDING
National Aeronautics and Space Administration (NASA)/American Society for Engineering Education (ASEE) Summer Faculty Fellowship Program, 1987. Volume 1
[NASA-CR-172009-VOL-1] 06 p0792 N88-14855
The determination of nutritional requirements for Safe Haven Food Supply System (emergency/survival foods) 06 p0792 N88-14856
Design concepts for bioreactors in space 09 p1198 N88-17179

SPACE FLIGHT STRESS
JPRS report: Science and technology. USSR: Space Biology and Aerospace Medicine, volume 21, no. 3, May - June 1987
[JPRS-USB-88-001] 07 p0889 N88-15389
Cosmonauts' hormonal responses after brief spaceflights 07 p0890 N88-15394
Third Soviet-French Symposium on Space Cytology 07 p0893 N88-15411
Effect of spaceflight factors on primate's blood circulation 10 p1359 N88-18124
Effect of weightlessness on replicative function of rat hepatocyte DNA 10 p1360 N88-18129
RNA-synthesizing activity in rat liver following flight aboard Cosmos-1667 10 p1360 N88-18130
Comparative evaluation of stress repsonse of rats to different methods of simulating some effects of weightlessness 10 p1363 N88-18144
JPRS Report: Science and Technology. USSR: Space Biology and Aerospace Medicine, volume 21, no. 6, November - December 1987
[JPRS-USB-88-004] 10 p1364 N88-18150
New book on metabolic aspects of spaceflight stress 10 p1367 N88-18172
Cytomorphology and ultrastructure of corn root meristem in weightlessness 12 p1651 N88-19891
Hypnosis: Possible applications for cosmonauts 12 p1665 N88-19984
JPRS report: Science and technology. USSR: Space Biology and Aerospace Medicine, volume 22, no. 1, January - February 1988
[JPRS-USB-88-005] 19 p2702 N88-26069
Growth and differentiation of cells in organotypical rat embryo cerebellar culture developing in weightlessness 19 p2703 N88-26076
Macaca rhesus tolerance to +Gz accelerations 19 p2704 N88-26080
Method for measuring absolute linear parameters of chromosomes 19 p2707 N88-26095
Effect of weightlessness on brain development (results of flight of pregnant rats on Kosmos-1514 biosatellite and study of subsequent development of their progeny on earth 20 p2829 N88-26786

SPACE FLIGHT TRAINING
Summary of Payload Integration Plan (PIP) for Starlab-1 flight experiment, enclosure 3
[NASA-TM-89713] 11 p1522 N88-19086
An expert system for a distributed real-time trainer 23 p3261 N88-29411
An intelligent training system for space shuttle flight controllers 24 p3415 N88-30331

SPACE GLIDERS
U LIFTING REENTRY VEHICLES

SPACE HABITATS
Design concepts for bioreactors in space 09 p1198 N88-17179

SPACE HEATING (BUILDINGS)
Engineering principles and concepts for active solar systems
[DE87-001181] 01 p0066 N88-10425
Life-cycle cost analysis of residential heat pumps and alternative HVAC (Heating, Ventilating and Air-Conditioning) systems
[DE88-003701] 07 p0839 N88-15090
Heat pump and appliance research
[PB88-102462] 07 p0853 N88-15184
Water source heat pump: How to get home heating and cooling from your own back yard
[DE88-900180] 07 p0875 N88-15306
Use of a general control simulation program to evaluate HVAC control stability
[DE88-000476] 08 p0975 N88-15896
Advanced utilization of solar energy: Utilization for biotechnology
[DE88-770031] 12 p1640 N88-19819
Field experience with aquifer thermal energy storage
[DE88-007075] 18 p2538 N88-25058

SPACE INDUSTRIALIZATION
NT SPACE MANUFACTURING
NT SPACE PROCESSING
Microgravity and Materials Processing Facility study (MMPF): Requirements and Analyses of Commercial Operations (RACO) preliminary data release
[NASA-CR-179309] 11 p1466 N88-18742
Economic impact of space flight activities in West Germany. Influence of allocations of Bundesministerium fuer Forschung und Technologie
[ETN-88-92106] 21 p2901 N88-27215

SPACE INFRARED TELESCOPE FACILITY
Space Infrared Telescope Facility (SIRTF) design and thermal analysis 08 p0982 N88-15934
Study of helium transfer technology for STICCR: Fluid management
[NASA-CR-177463] 10 p1291 N88-17720
Space infrared telescope facility project
[NASA-CR-183058] 20 p2883 N88-27121
SIRTF nod maneuvers
[NASA-TM-101007] 22 p3048 N88-28085
Survey of material for an infrared-opaque coating
[NASA-TM-88204] 22 p3153 N88-28757

SPACE LABORATORIES
NT MANNED ORBITAL LABORATORIES
NT SPACELAB
Preliminary study of a biotechnology research facility for microgravity, executive summary
[MATRA-EPT/AS/VT209/246/NT] 01 p0032 N88-10204
Preliminary study of a gravitational biology facility for Columbus, executive summary
[MATRA-EPT/AS/VT209/255/NT] 01 p0032 N88-10205
System analysis study of space platform and station accommodations for life sciences research facilities. Volume 2: Study results. Appendix E: Work breakdown structure and dictionary
[NASA-CR-179274] 10 p1292 N88-17723
System analysis study of space platform and station accommodations for life sciences research facilities. Volume 2: Study results. Appendix D: Life sciences research facility requirements
[NASA-CR-179273] 10 p1292 N88-17724
Development of an optical diagnostic instrument. Part 2: Instrument development — space laboratories
[NLR-TR-87079-L-PT-2] 13 p1841 N88-21016
Microgravity mechanisms and robotics program 16 p2219 N88-23237
Botany Facility pre-phase C/D. Core payload for EURECA, volume 1
[BF-RP-ER-015-VOL-1] 17 p2379 N88-24144
Simulation of space manipulator operations (EUROSIM)
[NLR-MP-87017-U] 20 p2811 N88-26678

SPACE LAW
Legal protection of the Polar Platform's users 03 p0339 N88-12135
JPRS report: Science and technology. USSR: Space
[JPRS-USP-88-001] 24 p3444 N88-30498

SPACE LOGISTICS
Orbital Spacecraft Consumables Resupply System (OSCRS): Monopropellant application to space station and OMV automatic refueling impacts of an ELV launch, volume 4
[NASA-CR-172029] 03 p0276 N88-11741
Inventory behavior at remote sites 06 p0796 N88-14873
A robotic system for automation of logistics functions on the Space Station 23 p3260 N88-29407

SPACE MAINTENANCE
Expert system study for spacecraft management
[TL-2699-ISS-1] 07 p0824 N88-15004
Orbital Replaceable Unit (ORU)/cold plate thermal interface study. Volume 1: Executive Summary
[BAE-TP-8430] 07 p0855 N88-15195
SAMSS: An in-progress review of the Spacecraft Assembly, Maintenance, and Servicing Study 08 p0981 N88-15930
Man-Tended Free Flyer operational design features 12 p1585 N88-19485
Operational experience and design recommendations for teleoperated flight hardware 14 p1927 N88-21489
Remote servicing of space systems 23 p3260 N88-29409

SPACE MANUFACTURING
Moving the factory into orbit 02 p0134 N88-10844
Physical vapor transport crystal growth 03 p0296 N88-11860
Microgravity nucleation and particle coagulation experiments support
[NASA-CR-181540] 04 p0423 N88-12618

Potential for on-orbit manufacture of large space structures using the pultrusion process
[NASA-TM-4016] 05 p0557 N88-13388
LISP based simulation generators for modeling complex space processes 08 p1061 N88-16403
Lunar fiberglass: Properties and process design
[NASA-CR-182580] 11 p1466 N88-18740
Some operational aspects of a rotating advanced-technology space station for the year 2025
[NASA-CR-181617] 20 p2765 N88-26397
Steps toward lunar settlement
[DE88-009141] 21 p2900 N88-27213
Homogeneity of glasses: Experiment WL-IHF-05 in D1 mission --- Spacelab
[ETN-88-92339] 21 p2924 N88-27353
Experiments in microgravity environment: Protein crystallization
[REPT-881-430-101] 21 p2924 N88-27354

SPACE MECHANICS
NT ASTRODYNAMICS
NT CELESTIAL MECHANICS
NT KEPLER LAWS
NT ORBITAL MECHANICS

SPACE MISSIONS
NT ASTEROID MISSIONS
NT CASSINI MISSION
NT FLYBY MISSIONS
NT GIOTTO MISSION
NT MANNED MARS MISSIONS
NT SOLAR MAXIMUM MISSION
NT ULYSSES MISSION
Recent progress in space photovoltaic systems
[NASA-TM-100208] 03 p0311 N88-11966
Relating service doctrine to space system requirements
[AD-A186620] 08 p1074 N88-16483
Critical issues for establishment of a permanently-occupied lunar base
[AD-A187128] 09 p1263 N88-17567
America plans for space
[AD-A187465] 10 p1289 N88-17713
Rendezvous and docking verification and demonstration in orbit, executive summary
[MBB-303-16/86] 10 p1291 N88-17719
A technique for capture analysis of low thrust missions in a planetary system
[AD-A188934] 12 p1594 N88-19544
The German Spacelab mission D1: Payload integration
[ETN-88-91507] 14 p1871 N88-21179
A comparison of propulsion systems for potential space mission applications
[DE88-005637] 14 p1882 N88-21248
Retrieving samples from comet nuclei
14 p2006 N88-21959
Electric propulsion options for the SP-100 reference mission 17 p2404 N88-24296
Safety of extravehicular space activities
19 p2698 N88-26038
Launch operations to support future space forces
[AD-A192679] 20 p2881 N88-27107
LRS-2: A specialized knowledge system for launch resource scheduling
[AD-A194625] 23 p3182 N88-28941
The principles of mass and maneuver applied to space operations
[AD-A194037] 23 p3276 N88-29500

SPACE NAVIGATION
Calibration of attitude control sensors
02 p0159 N88-10995
The navigation experiment NAVEX: Experimental results of clock synchronization
[DFVLR-MITT-87-05] 03 p0271 N88-11701
Satellite autonomous navigation with SHAD (Stellar Horizon Atmospheric Dispersion)
[AD-A184988] 05 p0544 N88-13313
Orbital navigation, docking and obstacle avoidance as a form of three dimensional model-based image understanding 08 p1061 N88-16406
The navigation experment NAVEX: Experimental results of clock synchronization
[ESA-TT-1084] 09 p1132 N88-16791
Space shuttle onboard navigation console expert/trainer system 09 p1203 N88-17208
Verifying shuttle onboard software using expert systems 09 p1207 N88-17237
Orbital navigation, docking and obstacle avoidance as a form of three dimensional model-based image understanding 17 p2388 N88-24194

SPACE OBSERVATIONS (FROM EARTH)
A comparison of interferometry from space and ground 01 p0094 N88-10614
Fiber-linked telescope arrays on the ground and in space 01 p0095 N88-10626
Ground-based optical interferometry
01 p0096 N88-10631
Ground-based interferometry with the European Very Large Telescope (VLT) 01 p0096 N88-10632
CERGA high angular resolution optical network --- astronomical interferometry 01 p0096 N88-10633
Practical limits to ground based interferometry and its impact on space interferometry
01 p0096 N88-10634
Milliarcsecond ground-based imaging with single telescopes 01 p0097 N88-10637
Activities report in astronomy
[ISSN-0531-4496] 01 p0108 N88-10701
How we get pictures from space, revised edition
[NF-151/7-87-REV] 02 p0193 N88-11203
An automated supernova search and the design strategy
[DE88-001827] 05 p0660 N88-14051
Max '91: Flare research at the next solar maximum
[NASA-TM-89700] 06 p0806 N88-14919
The French balloon and sounding rocket space program 08 p1025 N88-16203
The Swedish sounding rocket and balloon program
08 p1025 N88-16205
Swiss scientific balloon and sounding rocket experiments 1985-1987 08 p1025 N88-16206
How ground-based observations contribute to rocket, balloon and space shuttle experiments: Experience from the past and outlook for the future
08 p1026 N88-16216
Some ground-based optical observations of Comet Halley during its post-perihelion passage
08 p1033 N88-16259
Bern solar observations. Solar data for January-December 1986
[REPT-53] 09 p1263 N88-17569
Dust coma morphology of Comet Halley during the Giotto encounter 14 p2000 N88-21921
Investigation of the Sun-aligned F-region walls and related phenomena in the auroral latitude range
[AFGL-TR-87-0248] 19 p2692 N88-26000
Amateur astronomy in the space age
[RAE-TM-SS-4] 22 p3163 N88-28836
The surface composition of Mars from earthbased observations 23 p3306 N88-29696
Mars earth-based radar: 1986 results and 1988-1990 opportunities 23 p3306 N88-29697
Activities report in astronomy
[ISSN-0531-4496] 24 p3451 N88-30535

SPACE PERCEPTION
A parallel model of the kinetic depth effect using local computations
[AD-A181945] 01 p0083 N88-10536
Computer-controlled testing of visual-spatial ability
[AD-A183971] 03 p0357 N88-12249
Latency differences and effects of selective attention to gratings in the central and right visual fields: 2
[DE87-014730] 04 p0473 N88-12918
Interaction of different modules in depth perception: Stereo and shading
[AD-A185607] 06 p0759 N88-14855
Perception and control of simulated self motion
[AD-A187444] 10 p1372 N88-18188
Visual evoked potentials
[AD-A187942] 11 p1519 N88-19071
Position, scale, and rotation invariant target recognition using range imagery
[AD-A188828] 12 p1633 N88-19772
Spatial cognition 17 p2380 N88-24152
The interaction of sensory and perceptual variables: Spatial, temporal and orientation response to figure and ground
[AD-A192897] 20 p2832 N88-26798
A model for visual attention
[AD-A193061] 21 p2991 N88-27744
Visual motion perception and visual attentive processes
[AD-A193640] 23 p3241 N88-29288
Central serous chorioretinopathy in USAF aviators: A review
[AD-A195697] 24 p3407 N88-30280

SPACE PHOTOGRAPHY
U SPACEBORNE PHOTOGRAPHY

SPACE PLASMAS
NT SOLAR WIND
NT STELLAR WINDS
Local spectra and wave distribution functions --- space plasma
[KGI-PREPRINT-099] 01 p0100 N88-10659
Comparative plasma tails of Venus and comets
01 p0116 N88-10742
Overview of plasma observations during the Halley flybys 01 p0116 N88-10743
The geosynchronous plasma environment
03 p0273 N88-11716
Three-dimensional charging effects --- spacecraft
03 p0273 N88-11720
Flux tube dynamics and solar/stellar redshift measurements 04 p0503 N88-13095
Nonthermal phenomena in stellar coronae: Evidence from radio observations 04 p0503 N88-13096
Observational constraints and evidence for saturation
04 p0503 N88-13097
Observations of turbulence and fluctuations in the solar wind 04 p0525 N88-13212
Activities report of the Ionospheric Observatory
[UIO-SR-87-01] 05 p0625 N88-13827
Evolution of spectral densities in weakly inhomogeneous plasmas
[PB87-137402] 06 p0784 N88-14811
Neutron stars observations as astrophysical probes
06 p0800 N88-14896
Unusually strong density decrease in near-Earth interplanetary plasma and magnetically quiet day as effects of isolated solar flare 08 p1002 N88-16072
Viking: The first Swedish satellite
08 p1025 N88-16207
Bidirectional electron heat flux events in space
[DE88-001791] 08 p1084 N88-16531
Proceedings of the 21st ESLAB Symposium on Small Scale Processes in the Chromosphere/Corona, Interplanetary Medium and Planetary Magnetospheres
[ESA-SP-275] 08 p1094 N88-16582
Coupling of microscopic and macroscopic processes in the Earth's magnetotail 08 p1095 N88-16588
AMPTE-UKS ion observations at a quasi-parallel bow shock 08 p1095 N88-16589
Microphysics of the auroral acceleration region of other regions of the magnetosphere 08 p1096 N88-16592
Acceleration/heating processes on auroral field lines as observed by the Viking spacecraft
08 p1096 N88-16596
Small scale plasma density structures observed by the Viking double probe instrument --- Swedish satellite
08 p1098 N88-16604
Self-modulational formation of pulsar microstructures
[NASA-CR-182420] 08 p1104 N88-16622
Laser simulation of light and plasma action on comets and planets 09 p1237 N88-17413
Electric field measurement by S-520-9 sounding rocket using the time of flight technique of lithium ion beam
[ISAS-RN-367] 18 p2543 N88-25095
Contaminant ions and waves in the space station environment 18 p2590 N88-25393
Kinetic modulational instability of electron cyclotron waves in plasmas
[DE88-701893] 20 p2859 N88-26978
Generation of Adlam-Allen waves by plasma release experiments in the solar wind
[PB88-106000] 20 p2886 N88-27140

SPACE PLATFORMS
NT COLUMBUS SPACE STATION
NT EURECA (ESA)
NT SPACE STATION POLAR PLATFORMS
NT SYNCHRONOUS PLATFORMS
A test-bed for space interferometry: Space Platform Interferometer (SPI) 01 p0097 N88-10640
Moving the factory into orbit 02 p0134 N88-10844
Mission Peculiar Equipment Support Structure: A platform for space construction
02 p0139 N88-10874
Estimating payload internal temperatures and radiator size for multimegawatt space platforms
[DE88-000244] 03 p0275 N88-11738
Considerations concerning a thermal joint for a deployable or steerable battery radiator for the Columbus Polar Platform
[NLR-TR-86055-U] 03 p0276 N88-11739
Commercial Opportunities for Remote Sensing with Polar Platforms
[ESA-SP-269] 03 p0339 N88-12131
Possible commercial use of the polar platforms --- Columbus 03 p0339 N88-12132
Payload configurations and serviceability --- Columbus Polar Platforms 03 p0339 N88-12133
Legal protection of the Polar Platform's users
03 p0339 N88-12135
Confidentiality of data --- Columbus Polar Platforms
03 p0339 N88-12136
X-band SAR for a European remote sensing payload
03 p0340 N88-12142
The effect of maximum-allowable payload temperature on the mass of a multimegawatt space-based platform
[DE88-001921] 05 p0555 N88-13381
Communications payload concepts for geostationary facilities
[NASA-TM-100154] 05 p0576 N88-13513
Carbon Dioxide observational platform system (CO-OPS) Feasibility Study
[NASA-CR-179225] 06 p0671 N88-14113
Feasibility study of a carbon dioxide observational platform system. Volume 2: Programmatics
[NASA-CR-180404] 06 p0672 N88-14114

Polar platform element of Space Station: Mission objectives, European priorities, candidate instrumentation and selection procedure 09 p1129 N88-16779
Model of space platform electromagnetic (EMC) configuration
[ESA-CR(P)-2500] 09 p1135 N88-16809
System analysis study of space platform and station accommodations for life sciences research facilities. Volume 1: Executive summary. Phase A: Conceptual design and programmatics
[NASA-CR-179268] 10 p1291 N88-17721
System analysis study of space platform and station accommodations for life sciences research facilities. Volume 2: Study results, attachment 2. Phase A: Conceptual design and programmatics
[NASA-CR-179272] 10 p1291 N88-17722
Mobile robot activity model for autonomous free flying platforms 12 p1588 N88-19507
Explorer Platform on-orbit servicing operations 12 p1591 N88-19526
A thermal equilibrium model for multi-megawatt space platforms 17 p2410 N88-24332
Individual satellite power requirements calculated from specified constellation performance 17 p2420 N88-24392
The effect of maximum allowable payload temperature on the mass of a multimegawatt space based platform 17 p2424 N88-24416
Space Power Reference Source (SPRS): A user's guide to SDI Space Power Technology Programs 17 p2427 N88-24440
A nuclear powered space based multimegawatt MHD disc power system 17 p2432 N88-24471
Tasks foreseen for space robots and an example of an associated orbital infrastructure 19 p2699 N88-26044
Defensive platform size and survivability
[DE88-011634] 23 p3184 N88-28948
Analytical investigation of the dynamics of tethered constellations in earth orbit
[NASA-CR-179371] 23 p3184 N88-28950
Expandable pallet for space station interface attachments
[NASA-CASE-MSC-21117-1] 23 p3185 N88-28958
Technology requirements for an orbiting fuel depot: A necessary element of a space infrastructure
[NASA-TM-101370] 24 p3334 N88-29845
Interim Flight Opportunity (IFO). Volume 1: Executive summary — space platform
[SE/LS/AP-36-818/CN-VOL-1] 24 p3334 N88-29849

SPACE POWER REACTORS

NT FISSION ELECTRIC CELLS
Fast critical experiment data for space reactors
[DE87-007005] 01 p0093 N88-10605
Gas-cooled reactor for space power systems
[DE87-011549] 02 p0233 N88-11471
Review of diffusion barrier technology for application in SP-100 fuel pins
[DE88-000021] 02 p0234 N88-11480
Low gravity fluid-thermal experiments
[DE88-000553] 04 p0423 N88-12620
Small space reactor power systems for unmanned solar system exploration missions
[NASA-TM-100228] 05 p0660 N88-14054
A long term radiological risk model for plutonium-fueled and fission reactor space nuclear system
[DE87-010466] 06 p0779 N88-14782
Value-assessment of energy storage concepts in burst power systems
[DE87-013756] 09 p1187 N88-17115
Two-phase reduced gravity experiments for a space reactor design
[DE86-015530] 09 p1247 N88-17475
Molybdenum-base cermet fuel development
[DE88-005529] 13 p1839 N88-21003
Power transmission studies for tethered SP-100
[NASA-TM-100864] 14 p1883 N88-21251
Requirements and cost considerations for a Combined Space Nuclear Reactor Test Facility
[DE88-006763] 15 p2132 N88-22719
Transactions of the Fourth Symposium on Space Nuclear Power Systems
[DE88-006164] 17 p2398 N88-24254
Overview of NASA Lewis Research Center free-piston Stirling engine technology activities applicable to space power systems 17 p2398 N88-24255
Speculations on future opportunities to evolve Brayton powerplants aboard the space station 17 p2398 N88-24258
The results of application studies for space nuclear power 17 p2398 N88-24259
Effects of space-dependent cross sections on core physics parameters for compact fast spectrum space power reactors 17 p2399 N88-24263
Considerations pertinent to the Doppler effect for space reactors 17 p2399 N88-24264
Status of CEA design and simulation studies of a 200 KWe turboelectric space power system 17 p2400 N88-24268
Magnet shielding analysis for SOAR: A space fusion reactor 17 p2400 N88-24269
A fusion based plasma propulsion system 17 p2401 N88-24274
Preliminary study of niobium alloy contamination by transport through helium 17 p2402 N88-24279
Fabrication of lithium hydride shields for space nuclear power systems 17 p2402 N88-24282
Conceptual design of the SP-100 GES test site 17 p2402 N88-24284
Fast critical experiment data for space reactors 17 p2403 N88-24286
Fully passive space reactor conceptual design 17 p2403 N88-24288
Space based nuclear-pumped laser/reactor concepts 17 p2403 N88-24289
Acoustical gas core reactor with MHD power generation for burst power in a bimodal system 17 p2403 N88-24290
Fluid dynamics of spherical cavity reactors 17 p2403 N88-24291
BIFOLD: A dual-mode nuclear space power system 17 p2404 N88-24292
Electric propulsion options for the SP-100 reference mission 17 p2404 N88-24296
Interaction of the control system with core nuclear design for fast spectrum space power reactors 17 p2405 N88-24304
Application of the reactivity constraint approach to the transient control of spacecraft reactors 17 p2406 N88-24305
An adaptive load-following control system for a space nuclear power system 17 p2406 N88-24307
The effect of elevated temperature on irradiated MOS devices 17 p2406 N88-24308
The response of a power MOSFET (N-channel) and a dielectric isolated operational amplifier to the combined environmental effects of high temperature and total dose gamma radiation 17 p2406 N88-24309
Advanced thermionic converter technology for inductive output coupling 17 p2407 N88-24311
Monolithic fuel cell based power source for sprint power generation 17 p2407 N88-24313
Power source selection for neutral particle beam systems 17 p2407 N88-24314
Radiation hardening design of nuclear powered spacecraft 17 p2407 N88-24315
Space nuclear reactor shielding optimization studies 17 p2408 N88-24320
Design of a high-power-density Ljungstroem turbine using potassium as a working fluid 17 p2409 N88-24323
Development of reliable fuel pins for space reactor applications 17 p2409 N88-24326
Helium-3 fusion fuel resources for space power 17 p2410 N88-24330
Thermal management for multi-modal nuclear power plants 17 p2410 N88-24331
A thermal equilibrium model for multi-megawatt space platforms 17 p2410 N88-24332
A review of impact design criteria for space power heat rejection systems 17 p2410 N88-24333
Fundamental analysis of space nuclear-MHD generator for gigawatt-level power 17 p2411 N88-24337
Liquid-metal MHD power conversion for space electric systems 17 p2411 N88-24338
Studies for the definition of a Faraday converter for space nuclear systems 17 p2411 N88-24339
Design of a superconducting alternator for space-based power generation 17 p2412 N88-24340
Progress in the computer modeling of the liquid phase behavior of a liquid metal heat pipe 17 p2412 N88-24342
A liquid metal MHD concept for multimegawatt space power application 17 p2413 N88-24348
Nuclear Rankine/flywheel MMW space power concept 17 p2413 N88-24349
Gas-cooled reactor power systems for space 17 p2413 N88-24350
Analysis of closed cycle megawatt class space power systems with nuclear reactor heat sources 17 p2413 N88-24351
A dynamic model for the aft accumulator in the TE SP-100 system 17 p2414 N88-24354
RSMASS: A simple model for estimating reactor/shield masses 17 p2414 N88-24355
SP-100 control system modeling 17 p2414 N88-24356
ATHENA simulation of the 300 kW SP-100 17 p2414 N88-24357
Parametric analyses of the TE SP-100 system performance 17 p2415 N88-24358
A proposed national policy concerning the reentry of space reactors 17 p2415 N88-24359
Nuclear safety as applied to space power reactor systems 17 p2415 N88-24360
Development and implementation of a space nuclear safety program 17 p2415 N88-24361
Innovative methodology and developments in US space radioisotope power safety risk assessments 17 p2415 N88-24362
Inherently safe space reactors 17 p2415 N88-24363
Advanced LMMHD space power generation concept 17 p2415 N88-24364
SOAR: Space orbiting advanced fusion power reactor 17 p2416 N88-24366
Multimegawatt nuclear power system for lunar base applications 17 p2416 N88-24367
Radiation effects testing capabilities of the Texas A and M Nuclear Science Center 17 p2416 N88-24368
A generalized method for optimizing the mass of space power systems 17 p2416 N88-24369
Fabrication of SP-100 fuel barrier structures by chemical vapor deposition 17 p2416 N88-24371
SP-100 system modeling: SNPSAM update 17 p2417 N88-24372
Fabrication of a niobium 1 percent zirconium containment for SP-100 primary lithium system materials mass transfer studies 17 p2417 N88-24373
Transactions of the Fifth Symposium on Space Nuclear Power Systems
[DE88-006165] 17 p2417 N88-24374
SP-100 GES test site 17 p2417 N88-24375
Civil missions applications study 17 p2417 N88-24376
Applications of nuclear power to lunar and Mars missions 17 p2417 N88-24377
Air Force space power requirements and nuclear power assessment methodology 17 p2418 N88-24378
Nuclear-powered space debris sweeper 17 p2418 N88-24380
EETAP (End-to-End Transient Analysis Program) for space nuclear power system simulation 17 p2418 N88-24381
Optimization of SP-100 thermoelectric electromagnetic pump 17 p2418 N88-24382
Relating design and environmental variables to reliability 17 p2418 N88-24383
Power requirements for mining and microwave processing of extraterrestrial resources 17 p2420 N88-24389
Power and energy requirements for electromagnetic launchers 17 p2420 N88-24391
Possible creep studies of lithium with a compact device 17 p2422 N88-24404
Neutronics conceptual design of a UF6-fueled gaseous laser system 17 p2422 N88-24405
Preliminary analysis of helium generation and its effects on the SP-100 system performance 17 p2422 N88-24406
Optimization of organic Rankine cycles for space station applications 17 p2423 N88-24407
Assessment of nuclear reactor concepts for low power space applications 17 p2423 N88-24409
United Nations deliberations of the use of nuclear power sources in space: 1978-1987 17 p2423 N88-24410
Discussions and agreements in the United Nations on important issues associated with nuclear power in space 17 p2423 N88-24411
Critical nuclear launch issues: A perspective from the State of Florida 17 p2423 N88-24412
Space reactor end of life issues 17 p2424 N88-24413
SP-100 flight qualification testing assessment 17 p2424 N88-24414
Liquid droplet radiator development 17 p2424 N88-24415
The effect of maximum allowable payload temperature on the mass of a multimegawatt space based platform 17 p2424 N88-24416
Space vehicle/nuclear reactor thermal radiation integration issues 17 p2424 N88-24417
MACRAD: A mass analysis code for radiators 17 p2424 N88-24418
The Curie point radiator 17 p2424 N88-24420
Dynamic isotope power system critical component verification 17 p2425 N88-24421
Evaluation of UN fuel pin failure modes and motion of fuel during severe accidents for reactors in space 17 p2425 N88-24424
Reactor core coolability with reduced power levels 17 p2425 N88-24425
Analysis of a nuclear orbital transfer vehicle reentry accident 17 p2425 N88-24426

Creep behavior of tungsten/niobium and tungsten/niobium-1 percent zirconium composites
17 p2425 N88-24427
The application of high-rate biaxial testing to the design of containment vessels for radioisotope heat sources
17 p2426 N88-24428
Value assessment of energy storage concepts in burst power systems 17 p2426 N88-24432
A multimegawatt space power source radiator design
17 p2427 N88-24436
An irradiation performance data base for nitride fuels
17 p2427 N88-24438
Liquid metal testing at ETEC for the SP-100 program
17 p2428 N88-24446
Review of alkali metal and refractory alloy compatibility for Rankine cycle applications 17 p2428 N88-24447
Development of materials for fabric radiators
17 p2429 N88-24448
Polymer fuel cell as an energy storage component for space power applications 17 p2429 N88-24452
Benchmark physics experiments for SP-100
17 p2429 N88-24453
Trade study for kWe class space reactors
17 p2430 N88-24454
A high power density radial-in-flow reactor split core design for space power systems
17 p2430 N88-24455
Transient analyses of multimegawatt space reactors
17 p2430 N88-24456
MMW shielding design and analysis
17 p2430 N88-24457
The NERVA derivative reactor and a systematic approach to multiple space power requirements
17 p2430 N88-24458
Ceramic electrical insulator development for thermoelectric SACE power system
17 p2430 N88-24459
Apparatus for the measurement of resistivity of glasses and ceramics 17 p2431 N88-24460
Silicon-on-insulator electronics for a space nuclear power system 17 p2431 N88-24461
Experimental demonstrations of organic Rankine cycle waste heat rejection systems 17 p2432 N88-24469
A nuclear powered space based multimegawatt MHD disc power system 17 p2432 N88-24471
Burst power gas core reactor with MHD power generation 17 p2433 N88-24472
Molybdenum-base cermet fuel development
17 p2434 N88-24481
Test plan and facilities for qualifying nuclear rocket fuel elements 17 p2434 N88-24482
A comparison of uranium nitride and mixed carbide fuels swelling 17 p2435 N88-24485
Energy conversion system optimization study for multimegawatt space nuclear power application
17 p2436 N88-24492
Automatic reactor control system for transient operation 17 p2436 N88-24493
Experimental evaluation of the MIT-SNL period-generated minimum time control laws for the rapid adjustment of reactor power 17 p2436 N88-24494
An optimal disturbance rejection control system for multimegawatt space nuclear power systems
17 p2436 N88-24495
SP-100 ground engineering systems test facility control systems 17 p2436 N88-24496
TRICE design, evaluation and feasibility tests
17 p2437 N88-24498
Multimegawatt power conditioning requirements study
17 p2438 N88-24504
Lightweight power bus for a baseload nuclear reactor in space 17 p2438 N88-24505
SP-100 Ground Engineering Systems: Test facility control systems
[DE88-009195] 21 p3015 N88-27895
Comparative analysis of the space power architecture studies
[NASA-TM-100977] 22 p3049 N88-28090
Customizing Space Nuclear Power System Analysis Model (SNPSAM): Introducing a secondary coolant loop
[AD-A194620] 22 p3151 N88-28750
Lewis Research Center space station electric power system test facilities
[NASA-TM-100924] 23 p3182 N88-28942
Transient thermal analysis of three fast-charging latent heat storage configurations for a space-based power system
[DE88-009714] 23 p3186 N88-28960
An analysis of heat transfer after loss of primary coolant in the SP-100 reactor system
[AD-A194619] 23 p3281 N88-29539

SPACE PROBES
NT GALILEO PROBE
NT GALILEO SPACECRAFT
NT GIOTTO MISSION
NT HELIOS 1
NT HELIOS 2
NT MARS OBSERVER
NT MARS PROBES
Parachute characteristics of Titan descent modules --- planetary probe
[BF-3/86-B] 02 p0122 N88-10774
Study of fault tolerant techniques for satellite data handling
[FTT/REP/0001/SAAB] 05 p0632 N88-13860
Study of descent of probes with high lift-drag ratio into the atmosphere of Jupiter 08 p1006 N88-16101
Applications of expert systems for satellite autonomy
08 p1066 N88-16443
Rocket and airjet propulsion for ballistic and aerodynamic space probes
[REPT-TR-527] 10 p1310 N88-17826

SPACE PROCESSING
Preliminary study of a containerless processing facility for Columbus, executive summary
[ESA-ITT/AO/1-1834/85F] 01 p0032 N88-10203
Prephase A study of a crystallization laboratory for Columbus, executive summary
[ESA-ITT/AO/1-1866/85F] 01 p0032 N88-10206
Consortium for Materials Development in Space. Technical section
[NASA-CR-181508] 03 p0296 N88-11859
Materials preparation and longevity in hyperthermal atomic oxygen 03 p0297 N88-11862
Physical properties of immiscible polymers
03 p0297 N88-11868
High temperature superconductors
03 p0297 N88-11869
Cast iron freezing mechanisms
03 p0298 N88-11870
Materials processing in space program support
[NASA-CR-179217] 03 p0298 N88-11872
Design study for asteroidal exploitation
03 p0389 N88-12445
Center for the Space Processing of Engineering Materials 07 p0838 N88-15083
Preliminary Material Science Experiment Rocket (MASER) 1 results and the evolution of the MASER program 08 p1033 N88-16260
Space Bioreactor Science Workshop
[NASA-CP-2485] 09 p1196 N88-17168
Suspension cell culture in microgravity and development of a space bioreactor 09 p1196 N88-17169
Space bioreactor: Design/process flow
09 p1197 N88-17170
Plant cell technologies in space: Background, strategies and prospects 09 p1198 N88-17177
Cell culture experiments planned for the space bioreactor 09 p1198 N88-17180
Materials processing in space: An introduction to the G-480 payload 10 p1287 N88-17695
Ten past and ten future GAS/MAUS-payloads
10 p1287 N88-17696
An update to the MITRE/WPI Space Shuttle Program GASCAN G-408 10 p1287 N88-17697
The challenge of G-376 10 p1288 N88-17705
Non-proprietary research projects of the Center for the Space Processing of Engineering Materials
[AR-2] 10 p1426 N88-18516
Microgravity and Materials Processing Facility study (MMPF): Requirements and Analyses of Commercial Operations (RACO) preliminary data release
[NASA-CR-179309] 11 p1466 N88-18742
Cell cultures in space: From basic research to biotechnology 2 12 p1660 N88-19948
Preliminary market analysis for large zeolite crystals
[NASA-CR-182882] 15 p2049 N88-22207
JPRS report: Science and technology. Japan
[JPRS-JST-88-001] 15 p2051 N88-22218
Space utilization plans 15 p2051 N88-22219
Space experiment plan FMPT
15 p2051 N88-22220
Amorphous semiconductors made in space
15 p2051 N88-22221
Pb(1-x)Sn(x)Te crystal growth in space
15 p2051 N88-22223
On-orbit technology experiment facility definition
[NASA-TM-100614] 17 p2311 N88-23824
Non-contact temperature measurement requirements for electronic materials processing
17 p2328 N88-23898
Noncontact temperature measurement: Requirements and applications for metals and alloys research
17 p2328 N88-23899
Multi-color pyrometer for materials processing in space 17 p2329 N88-23905
Separation of biological materials in microgravity
[NASA-TM-101142] 17 p2331 N88-23916
Power requirements for mining and microwave processing of extraterrestrial resources
17 p2420 N88-24389
Microgravity thaw experiment (MITEX)
17 p2427 N88-24439
Preparation for microgravity: The role of the microgravity materials science laboratory
[NASA-TM-100906] 18 p2497 N88-24811
Analysis of the performance of the space ultravacuum research facility in attached and free-flyer mode
[NASA-TM-100325] 20 p2763 N88-26387
Industrial processes influenced by gravity
[NASA-CR-182140] 20 p2782 N88-26497
Method of dispensing reagent chemicals in space
[NASA-CASE-LAR-13607-1-CU]
23 p3200 N88-29048
Optimization of low gravity materials processing experiments using expert systems
23 p3252 N88-29361
A generic expert system for materials processing in space 23 p3255 N88-29376
A teleoperated robotic manipulator system for materials processing experiment servicing
23 p3260 N88-29410

SPACE PROGRAMS
NT BRAZILIAN SPACE PROGRAM
NT CANADIAN SPACE PROGRAM
NT CHINESE SPACE PROGRAM
NT EARTH RESOURCES PROGRAM
NT EUROPEAN SPACE PROGRAMS
NT FRENCH SPACE PROGRAMS
NT GALILEO PROJECT
NT JAPANESE SPACE PROGRAM
NT NASA SPACE PROGRAMS
NT PROJECT SETI
NT ROVER PROJECT
NT SKYLAB PROGRAM
NT SWEDISH SPACE PROGRAM
NT U.S.S.R. SPACE PROGRAM
NT UK SPACE PROGRAM
National Aeronautics and Space Administration space station proposal, fiscal year 1988
[S-HRG-100-328] 05 p0659 N88-14043
Advantages of manned lunar base
08 p1009 N88-16118
Hardware/software reliability study --- space programs
[REPT-65.5686] 09 p1218 N88-17307
An update to the MITRE/WPI Space Shuttle Program GASCAN G-408 10 p1287 N88-17697
A logical structuration for an administration of space projects
[INPE-4435-TDL/310] 12 p1585 N88-19482
Principal space programs in the area of microwaves
[INPE-4164-PRE/1064] 12 p1618 N88-19677
Proceedings of the 3rd European Symposium on Life Sciences Research in Space
[ESA-SP-271] 12 p1652 N88-19893
Aeronautics and space report of the President: 1986 activities 13 p1852 N88-21087
Space projects for the 90's relevant to climatology
14 p1935 N88-21539
Space policy of common sense and moderation
[REPT-49/87] 20 p2883 N88-27118
High technology space flight orientation program: Overview and recommendations
[ETN-88-92332] 21 p3029 N88-27979
History of manned spaceflight
[CNES-NT-121] 21 p3032 N88-28000
Management of large space projects --- conference
[ISBN-2-85-428192-6] 22 p3159 N88-28803
Management 22 p3159 N88-28804
Large space projects --- management
22 p3159 N88-28805
The development phases of a project --- space projects 22 p3159 N88-28807
Human organization --- space projects
22 p3160 N88-28808
Carrying out space projects 22 p3160 N88-28811
Timetable control in a management system (space program) 22 p3160 N88-28815
Costs --- space projects 22 p3160 N88-28816
Value engineering --- space projects
22 p3160 N88-28817
Price estimates and analysis
22 p3161 N88-28818
Management of large space projects. Financial means. Part 1: Financing of constructors
22 p3161 N88-28822
Means of financing --- space projects
22 p3161 N88-28823
The role and the place of insurance of large space projects 22 p3161 N88-28826

SPACE PSYCHOLOGY
Selecting the right crew for future space stations: An analysis of selection research on offshore divers, aviation pilots and other high risk groups in Scandinavia
19 p2698 N88-26021

SPACE RADIATION
U EXTRATERRESTRIAL RADIATION

SPACE RADIATORS
U SPACECRAFT RADIATORS
SPACE RATIONS
Space and sea: Is there a place for ionization?
19 p2699 N88-26043
SPACE RENDEZVOUS
NT ORBITAL RENDEZVOUS
Prototype Rendezvous Onboard Software (PROBS) [MATRA-EPT-DT-PRB-2A-00068]
02 p0222 N88-11396
Rendezvous and Docking Verification (RVDV) and in-orbit demonstration, executive summary [RVD-RVDV-FR-AS-01] 06 p0673 N88-14120
Rendezvous and docking verification and demonstration in orbit, executive summary [MBB-303-16/86] 10 p1291 N88-17719
The RVD mission: The on-board data processing requirements 12 p1586 N88-19495
Prototype on-board software for rendezvous and docking 12 p1586 N88-19496
Long range sensor for rendezvous and docking missions 12 p1587 N88-19497
Motion simulation for in-orbit operations
12 p1589 N88-19514
A software engineering approach to expert system design and verification 23 p3252 N88-29356
SPACE SCIENCES
U AEROSPACE SCIENCES
SPACE SELF MANEUVERING UNITS
U SELF MANEUVERING UNITS
SPACE SHUTTLE BOOSTERS
Redesign of solid rocket booster/external tank attachment ring for the space transportation system [NASA-TM-100476] 01 p0017 N88-10101
Stability of mechanical joints in launching vehicles: Local and global stationary values of energy density
03 p0270 N88-11696
Results of the development motor 8 test firing [GPO-78-692] 03 p0278 N88-11751
Shuttle rocket booster computational fluid dynamics [NASA-CR-182518] 10 p1293 N88-17733
Structural analysis of the space shuttle solid rocket booster/external tank attach ring [NASA-TM-100510] 11 p1446 N88-18618
High performance Solid Rocket Motor (SRM) submerged nozzle/combustion cavity flowfield assessment [NASA-CR-179307] 11 p1446 N88-18622
NASA (National Aeronautics and Space Administration) procurement: The 1973 space shuttle solid rocket motor contractor selection [PB88-135264] 11 p1447 N88-18623
STA-2A NDT testing [NASA-CR-179301] 11 p1497 N88-18937
Calculation of flow about posts and powerhead model [NASA-CR-179305] 12 p1625 N88-19722
Preliminary 2-D shell analysis of the space shuttle solid rocket boosters [NASA-TM-100515] 17 p2348 N88-23989
Effects of natural environment on first generation solid rocket booster thermal protection system materials [NASA-TM-100329] 17 p2373 N88-24113
Quality and productivity drive innovation and improvement at United Technologies Aerospace Operations, Inc. [NASA-CR-182944] 18 p2525 N88-24983
SRM propellant and polymer materials structural test program [NASA-TP-2821] 18 p2530 N88-25013
Assembly Test Article (ATA) [NASA-CR-179361] 21 p2903 N88-27226
SPACE SHUTTLE MAIN ENGINE
Configuration evaluation and criteria plan. Volume 2: Evaluation criteria plan (update). Space Transportation Main Engine (STME) configuration study [NASA-CR-181429] 03 p0270 N88-11699
Failure control techniques for the SSME [NASA-CR-179224] 04 p0409 N88-12537
The 58th Shock and Vibration Symposium, volume 1 [NASA-CP-2488-VOL-1] 05 p0592 N88-13609
Fluid mass and thermal loading effects on the modal characteristics of space shuttle main engine liquid oxygen inlet splitter vanes 05 p0594 N88-13628
Incipient failure detection of space shuttle main engine turbopump bearings using vibration envelope detection
05 p0595 N88-13629
High frequency data acquisition system for space shuttle main engine testing 05 p0595 N88-13630
Space shuttle main engine vibration data base
05 p0595 N88-13631
Thermal finite-element analysis of space shuttle main engine turbine blade [NASA-TM-100117] 05 p0610 N88-13745
Analysis of internal flows relative to the space shuttle main engine [NASA-CR-179240] 06 p0674 N88-14125
Evaluation of load tracks and wear of two sets of bearings from space shuttle main engine high pressure oxygen turbopumps [NASA-CR-178969] 07 p0861 N88-15223
Pattern recognition techniques for failure trend detection in SSME ground tests 07 p0924 N88-15614
Equilibrium retention in the nozzle of oxygen hydrogen propulsion systems 07 p0924 N88-15616
The determination of equivalent bearing loading for the BSMT that simulate SSME high pressure oxidizer turbopump conditions using the SHABERTH/SINDA computer programs 07 p0925 N88-15623
SSME environment database development [NASA-CR-179245] 08 p0964 N88-15836
Embedded expert system for space shuttle main engine maintenance 08 p1058 N88-16382
Space shuttle main engine anomaly data and inductive knowledge based systems: Automated corporate expertise 08 p1060 N88-16398
An expert system to analyze high frequency dependent data for the space shuttle main engine turbopumps
08 p1060 N88-16399
Automatic mathematical modeling for space application 08 p1060 N88-16402
RB-ARD: A proof of concept rule-based abort
08 p1065 N88-16435
Computer-aided design analysis of 57-mm, angular-contact, cryogenic turbopump bearings [NASA-TP-2816] 11 p1496 N88-18933
Rocketdyne automated dynamics data analysis and management system 11 p1499 N88-18954
Calculation of flow about posts and powerhead model [NASA-CR-179305] 12 p1625 N88-19722
Duct flow nonuniformities: Effect of struts in SSME HGM II(+) [NASA-CR-179285] 15 p2062 N88-22296
Advanced probabilistic methods for quantifying the effects of various uncertainties in structural response
15 p2080 N88-22401
Thermal-structural analyses of Space Shuttle Main Engine (SSME) hot section components
15 p2081 N88-22404
SSME single-crystal turbine blade dynamics
16 p2221 N88-23257
SSME technology test bed fast shutdown assessment [NASA-CR-179354] 17 p2314 N88-23831
Research study: Space shuttle main engine plume flowfield model [NASA-CR-179336] 18 p2474 N88-24676
Duct flow nonuniformities for Space Shuttle Main Engine (SSME) [NASA-CR-179338] 18 p2511 N88-24899
Numerical grid generation and flow simulation in SSME thrust chamber 19 p2626 N88-25577
Evaluation and improvement of liquid propellant rocket chugging analysis techniques. Part 1: A one-dimensional analysis of low frequency combustion instability in the fuel preburner of the space shuttle main engine [NASA-CR-183106] 21 p2903 N88-27224
Evaluation and improvement of liquid propellant rocket chugging analysis techniques. Part 2: A study of low frequency combustion instability in rocket engine preburners using a heterogeneous stirred tank reactor model [NASA-CR-182724] 21 p2903 N88-27225
Evaluation of transfer films of Salox M on 440C for HPOTP bearing cage applications, task 119 [NASA-CR-179020] 23 p3223 N88-29184
Automatic mathematical modeling for real time simulation system 24 p3420 N88-30356
SPACE SHUTTLE MISSION 31-A
Comparison of flight-measured and calculated temperatures on the space shuttle orbiter [NASA-TM-88278] 03 p0321 N88-12029
Studies of the vestibulo-ocular reflex on STS 4, 5 and 6 [NASA-TM-100461] 12 p1666 N88-19987
SPACE SHUTTLE MISSION 31-B
Studies of the vestibulo-ocular reflex on STS 4, 5 and 6 [NASA-TM-100461] 12 p1666 N88-19987
SPACE SHUTTLE MISSION 41-C
In-orbit and laboratory exchange of ORUs designed/not designed for servicing 12 p1587 N88-19499
SPACE SHUTTLE MISSION 51-L
Space shuttle accident: NASA's actions to address the Presidential Commission report [PB88-135306] 15 p2024 N88-22059
SPACE SHUTTLE MISSION 61-B
A synopsis of the EVA training conducted on EASE/ACCESS for STS-61-B 02 p0140 N88-10879
Overview of crew member energy expenditure during Shuttle Flight 61-8 EASE/ACCESS task performance
02 p0140 N88-10882
SPACE SHUTTLE MISSIONS
NT SPACE SHUTTLE MISSION 31-A
NT SPACE SHUTTLE MISSION 31-B
NT SPACE SHUTTLE MISSION 41-C
NT SPACE SHUTTLE MISSION 51-L
NT SPACE SHUTTLE MISSION 61-B
Meteorological systems support to critical shuttle requirements on the Eastern Test Range — STS
02 p0205 N88-11281
The 1987 Get Away Special Experimenter's Symposium [NASA-CP-2500] 10 p1286 N88-17691
Spacelab: An international success story [NASA-SP-487] 11 p1566 N88-19375
SPACE SHUTTLE ORBITAL FLIGHT TEST 4
U SPACE TRANSPORTATION SYSTEM 4 FLIGHT
SPACE SHUTTLE ORBITER 099
U CHALLENGER (ORBITER)
SPACE SHUTTLE ORBITER 103
U DISCOVERY (ORBITER)
SPACE SHUTTLE ORBITERS
NT CHALLENGER (ORBITER)
NT DISCOVERY (ORBITER)
The composition of the gas in the loading inlet of the Space Shuttle Orbiter [ETN-87-90430] 01 p0012 N88-10069
Effects of forced and free convections on structural temperatures of space shuttle orbiter during reentry flight [NASA-TM-86800] 01 p0043 N88-10275
Thermal stress analysis of space shuttle orbiter subjected to reentry aerodynamic heating [NASA-TM-88286] 01 p0061 N88-10389
Contamination control of the space shuttle Orbiter crew compartment 02 p0133 N88-10834
Pinhole occulter experiment [NASA-CR-179206] 02 p0235 N88-11481
Comparison of flight-measured and calculated temperatures on the space shuttle orbiter [NASA-TM-88278] 03 p0321 N88-12029
Numerical simulation of the hypersonic flow around lifting vehicles 05 p0532 N88-13234
The effects of RCS jet firing on the isolated Orbiter and mated coast phases of the glide return to launch site maneuver at Mach number 6 (IA302B) [NASA-CR-180223] 20 p2766 N88-26403
SPACE SHUTTLE PAYLOADS
NT ASTRO MISSIONS (STS)
NT EARTH RADIATION BUDGET EXPERIMENT
NT GET AWAY SPECIALS (STS)
NT PHYSICS AND CHEMISTRY EXPERIMENT IN SPACE
NT SPACELAB
NT X RAY ASTROPHYSICS FACILITY
Phase 3 study of selected tether applications in space. Volume 2: Study results [NASA-CR-179186] 02 p0132 N88-10828
An investigation of the behavior of outgassed molecules in thermal vacuums 02 p0133 N88-10836
Space Construction [NASA-CP-2490] 02 p0138 N88-10870
The flight demonstration program and selection process 02 p0138 N88-10871
Mission Peculiar Equipment Support Structure: A platform for space construction
02 p0139 N88-10874
Marshall Space Flight Center's role in EASE/ACCESS mission management 02 p0139 N88-10875
A monograph of the National Space Transportation System Office (NSTSO) integration activities conducted at the NASA Lyndon B. Johnson Space Center for the EASE/ACCESS payload flown on STS 61-B
02 p0139 N88-10876
EASE/ACCESS ground processing at Kennedy Space Center 02 p0139 N88-10877
Overview of crew member energy expenditure during Shuttle Flight 61-8 EASE/ACCESS task performance
02 p0140 N88-10882
High power ion thruster performance [NASA-TM-100127] 04 p0409 N88-12542
Potential for on-orbit manufacture of large space structures using the pultrusion process [NASA-TM-4016] 05 p0557 N88-13388
Mechanistic studies of polymeric samples exposed aboard STS 8 [NASA-CR-182364] 06 p0686 N88-14202
NASA (National Aeronautics and Space Administration) ADP (Automated Data Processing) system: Information on the automated mission and the payload tracking system [PB88-104989] 07 p0942 N88-15730
The dynamics and control of large-flexible space structures, part 10 [NASA-CR-182426] 08 p0963 N88-15830
Experiment control and data system for an infrared detector array with maximum sensitivity [ETN-88-91497] 09 p1136 N88-16813

POCC capabilities document. Payload support capabilities description: MCC, JSC POCC, remote POCC interface
[NASA-TM-89708] 09 p1260 N88-17555
Payload bay atmospheric vent airflow testing at the Vibration and Acoustic Test Facility
[NASA-TM-100460] 11 p1437 N88-18572
Modification of integrated partial payload lifting assembly
[NASA-CR-182573] 11 p1443 N88-18607
Project SKYLITE: A design exploration
[AD-A187906] 11 p1511 N88-19030
Explorer Platform on-orbit servicing operations 12 p1591 N88-19526
Research and technology, 1987
[NASA-TM-100323] 12 p1713 N88-20253
Deployable/retrievable boom: One application to tethered satellite 14 p1874 N88-21197
Payload deployment system --- STS 14 p1875 N88-21199
OLYMPUS shuttle specific radiator shield 14 p1879 N88-21234
Space experiment plan FMPT 15 p2051 N88-22220
The Shuttle Imaging Radar B (SIR-B) experiment report
[NASA-CR-182923] 17 p2334 N88-23932
High power ion thruster performance 17 p2404 N88-24295
Payload deployment method and system
[NASA-CASE-MSC-21330-1] 18 p2470 N88-24660
The detection and interpretation of long-term changes in ozone from space
[NASA-TM-101135] 21 p2971 N88-27650
Design considerations for the ORION satellite: Structure, propulsion and attitude control subsystems for a small, general purpose spacecraft
[AD-A193837] 22 p3048 N88-28086
Aerospace payload support systems
[AFGL-TR-87-0241] 24 p3334 N88-29843
Containment of a silicone fluid free surface in reduced gravity using barrier coatings
[NASA-TM-101314] 24 p3371 N88-30072
Spacelab data processing facility (SLDPF) Quality Assurance (QA)/Data Accounting (DA) expert systems: Transition from prototypes to operational systems 24 p3420 N88-30353

SPACE SHUTTLE SOLID ROCKET MOTORS
U SPACE SHUTTLE BOOSTERS

SPACE SHUTTLES
NT HERMES MANNED SPACEPLANE
Fourteenth Space Simulation Conference: Testing for a Permanent Presence in Space
[NASA-CP-2446] 02 p0132 N88-10829
Redistribution of particulates in shuttle bay during launch 02 p0133 N88-10837
Moving the factory into orbit 02 p0134 N88-10844
Spacecraft material flammability testing and configurations 04 p0407 N88-12529
Structural analysis of a bolted joint concept for the space shuttle's solid rocket motor casing
[NASA-TM-89092] 04 p0407 N88-12531
Proceedings: SDIO/DARPA Workshop on Laser Propulsion. Volume 3: Viewgraphs
[DE88-000964] 04 p0450 N88-12790
The analysis of nonstationary vibration data 05 p0592 N88-13610
Modal survey of the space shuttle solid rocket motor using multiple input methods 05 p0593 N88-13617
Modeling cloudy and clear interval length probabilities using space shuttle imagery
[AD-A185290] 05 p0627 N88-13837
An analytical method for ditching analysis of an airborne vehicle
[NASA-CR-4120] 07 p0816 N88-14968
Propulsion estimation techniques 07 p0927 N88-15632
The Jeffcott equations in nonlinear rotordynamics 07 p0928 N88-15636
SSME environment database development
[NASA-CR-179245] 08 p0964 N88-15836
Zero-G thermodynamic vent system for shuttle/Centaur 08 p0983 N88-15943
Third Conference on Artificial Intelligence for Space Applications, part 1
[NASA-CP-2492-Pt-1] 08 p1055 N88-16360
Telerobotic controller development 08 p1056 N88-16370
Space shuttle main engine anomaly data and inductive knowledge based systems: Automated corporate expertise 08 p1060 N88-16398
Prototype resupply scheduler 08 p1064 N88-16428
RB-ARD: A proof of concept rule-based abort 08 p1065 N88-16435
Lateral stability and control derivatives extracted from space shuttle Challenger flight data
[NASA-TM-100520] 09 p1132 N88-16788
Centaur G Prime modal test 09 p1181 N88-17075
Space shuttle onboard navigation console expert/trainer system 09 p1203 N88-17208
Expert system verification concerns in an operations environment 09 p1207 N88-17234
Verifying shuttle onboard software using expert systems 09 p1207 N88-17237
Analysis of shear-layer probe data for holes in hypersonic configurations
[DE88-003992] 11 p1435 N88-18564
Cornering characteristics of the main-gear tire of the space shuttle orbiter
[NASA-TP-2790] 11 p1438 N88-18583
Space shuttle phase B wind tunnel test database
[NASA-CR-4121] 11 p1444 N88-18611
Structural analysis of the space shuttle solid rocket booster/external tank attach ring
[NASA-TM-100510] 11 p1446 N88-18618
Effect of element size on the solution accuracies of finite-element heat transfer and thermal stress analyses of space shuttle orbiter
[NASA-TM-88292] 11 p1502 N88-18971
Orbital analysis of a STS (Space Transportation System) external tank in low earth orbit
[AD-A188829] 12 p1593 N88-19542
Transient Pressure Test Article (TPTA) 1.1 and 1.1A, volume 1
[NASA-CR-179322-VOL-1] 12 p1603 N88-19588
Lateral and longitudinal stability and control parameters for the space shuttle discovery as determined from flight test data
[NASA-TM-100555] 13 p1724 N88-20309
Soviet space transport systems 13 p1727 N88-20328
A 60-meter erectable assembly concept for a control of flexible structures flight experiment
[NASA-TM-100497] 14 p1873 N88-21190
In-flight rain damage tests of the shuttle thermal protection system
[NASA-TM-100438] 14 p1881 N88-21241
Analysis of contamination data recorded by the IECM camera/photometer
[NASA-TM-100324] 14 p1882 N88-21246
Chronology of KSC and KSC related events for 1987
[NASA-CR-182754] 14 p2012 N88-22002
Engineering support of space shuttle experiment integration
[AD-A190135] 15 p2024 N88-22061
A method of atmospheric density measurements during space shuttle entry using ultraviolet-laser Rayleigh scattering
[NASA-TM-100056] 15 p2069 N88-22337
Survey of the Air Force P78-2 (SCATHA) satellite plasma wave data during electron gun operations
[AD-A191014] 16 p2168 N88-22926
A decade of computer simulations for space shuttle aerodynamics
[NASA-TM-100990] 18 p2459 N88-24603
Structural margins assessment approach
[NASA-TM-100332] 18 p2473 N88-24672
Numerical simulations of flow around shuttle orbiter 19 p2635 N88-25633
Book analysis. Challenger: A major malfunction
[AD-A182458] 20 p2764 N88-26388
Space shuttle phase B wind tunnel model and test information. Volume 2: Orbiter configuration
[NASA-CR-178415-VOL-2-PT-2] 21 p2893 N88-27172
Space shuttle natural environment analysis
[NASA-CR-179337] 21 p2976 N88-27676
Space shuttle phase B wind tunnel model and test information. Volume 2: Orbiter configuration
[NASA-CR-178415-VOL-2-PT-1] 23 p3171 N88-28881
Progress on a Monte Carlo shuttle contamination model
[AD-A193694] 23 p3183 N88-28945
Preloaded brake disc
[NASA-CASE-MSC-21132-1] 23 p3223 N88-29181
Space shuttle phase B wind tunnel model and test information. Volume 3: Launch configuration
[NASA-CR-178416-VOL-3-PT-2] 24 p3315 N88-29744
Space shuttle phase B wind tunnel model and test information. Volume 1: Booster configuration
[NASA-CR-178414-VOL-1-PT-1] 24 p3315 N88-29745
Space shuttle phase B wind tunnel model and test information. Volume 1: Booster configuration
[NASA-CR-178414-VOL-1-PT-2] 24 p3320 N88-29770
Ascent guidance for a winged boost vehicle
[NASA-CR-172083] 24 p3334 N88-29846

SPACE SIMULATORS
A modern space simulation facility to accommodate high production acceptance testing 02 p0134 N88-10841
Characteristics and performance of the ESTEC large space simulator cryogenic system 02 p0135 N88-10849
Structural Assembly Demonstration Experiment (SADE)
[NASA-CR-179205] 02 p0138 N88-10868
Research and development at the Marshall Space Flight Center Neutral Buoyancy Simulator 02 p0139 N88-10878
Environment test laboratory
[ETN-88-91885] 14 p1869 N88-21166
Simulation of cometary nuclei 14 p2005 N88-21954

SPACE STATION PAYLOADS
Phase 3 study of selected tether applications in space. Volume 2: Study results
[NASA-CR-179186] 02 p0132 N88-10828
Communications payload concepts for geostationary facilities
[NASA-TM-100154] 05 p0576 N88-13513
Microgravity Particle Research on the Space Station
[NASA-CP-2496] 07 p0883 N88-15354
Astrophysics and the solar nebula 07 p0883 N88-15355
Planetary science 07 p0883 N88-15356
Atmospheric science 07 p0883 N88-15357
Exobiology and life science 07 p0883 N88-15358
Physics and chemistry 07 p0883 N88-15359
System analysis study of space platform and station accommodations for life sciences research facilities. Volume 2: Study results. Appendix E: Work breakdown structure and dictionary
[NASA-CR-179274] 10 p1292 N88-17723
System analysis study of space platform and station accommodations for life sciences research facilities. Volume 2: Study results. Appendix D: Life sciences research facility requirements
[NASA-CR-179273] 10 p1292 N88-17724
Progress toward a cosmic dust collection facility on space station
[NASA-CR-182427] 12 p1598 N88-19566
Conceptual design and programmatics studies of space station accommodations for Life Sciences Research Facilities (LSRF)
[NASA-CR-179270] 12 p1598 N88-19567
Space station accommodations for life sciences research facilities: Phase A conceptual design and programmatics studies for Missions SAAX0307, SAAX0302 and the transition from SAAX0307 to SAAX0302. Volume 1: Executive summary
[NASA-CR-179267] 12 p1599 N88-19571
Analysis of low gravity tolerance of model experiments for space station: Preliminary results for directional solidification
[NASA-CR-182657] 12 p1614 N88-19648
Research and technology, 1987
[NASA-TM-100323] 12 p1713 N88-20253
Requirements for temperature and species concentration measurements in microgravity combustion experiments 17 p2329 N88-23903
Mars rover/sample return mission requirements affecting space station
[NASA-CR-172048] 18 p2594 N88-25414
A knowledge-based decision support system for payload scheduling 23 p3252 N88-29358
Coordinated study of Solar-Terrestrial Observatory (STO) payloads on space station
[NASA-CR-183142] 24 p3334 N88-29848

SPACE STATION POLAR PLATFORMS
A teleoperated manipulator system concept for unmanned platforms --- Columbus 12 p1593 N88-19537
P-Plus: Polar Platform utilization study, executive summary
[BAE-TP-8391] 18 p2469 N88-24653

SPACE STATION POWER SUPPLIES
Space station assembly/servicing capabilities 01 p0016 N88-10100
Solar converging method 04 p0403 N88-12504
Space station systems: A bibliography with indexes
[NASA-SP-7056(05)] 05 p0556 N88-13382
Power components for the space station 20-kHz power distribution system
[NASA-TM-100866] 14 p1904 N88-21374
Structural assessment of a space station solar dynamic heat receiver thermal energy storage canister 15 p2081 N88-22406
Benefits of 20 kHz PMAD in a nuclear space station 17 p2398 N88-24256
Operational concerns involving a shadow-shielded nuclear reactor for space station applications 17 p2398 N88-24257

Speculations on future opportunities to evolve Brayton powerplants aboard the space station
17 p2398 N88-24258
Hydrogen turbines for space power systems: A simplified axial flow gas turbine model 17 p2419 N88-24385
AC power system breadboard
[NASA-CR-179369] 22 p3049 N88-28091
Lewis Research Center space station electric power system test facilities
[NASA-TM-100924] 23 p3182 N88-28942
Expert systems for MSFC power systems
23 p3255 N88-29375
Utilization of artificial intelligence techniques for the Space Station power system 23 p3261 N88-29412
Regenerative fuel cell energy storage system for a low earth orbit space station
[NASA-CR-174802] 24 p3389 N88-30184

SPACE STATION PROPULSION

Space station propulsion technology: Space station propulsion system test bed test plan
[NASA-CR-179201] 01 p0017 N88-10104
Space station integrated propulsion and fluid system study: Fluid systems configuration databook
[NASA-CR-179215] 03 p0278 N88-11753
Space station systems: A bibliography with indexes
[NASA-SP-7056(05)] 05 p0556 N88-13382

SPACE STATION STRUCTURES

Space station resistojet system requirements and interface definition study
[NASA-CR-180832] 04 p0409 N88-12541
Advanced radiator concepts utilizing honeycomb panel heat pipes
[NASA-CR-172017] 04 p0443 N88-12747
Space station systems: A bibliography with indexes
[NASA-SP-7056(05)] 05 p0556 N88-13382
Personnel occupied woven envelope robot power
[NASA-CR-182367] 07 p0856 N88-15196
Solar concentrator advanced development program, task 1
[NASA-CR-179489] 10 p1350 N88-18068
LDR structural experiment definition
[NASA-TM-100618] 17 p2312 N88-23826
Mobile remote manipulator system for a tetrahedral truss
[NASA-CASE-MSC-20985-1] 20 p2765 N88-26398

SPACE STATIONS

NT COLUMBUS SPACE STATION
NT MIR SPACE STATION
NT SALYUT SPACE STATION
NT SPACE STATION POLAR PLATFORMS
Space Station Mission Planning System (MPS) development study. Volume 1: Executive summary
[NASA-CR-179202] 01 p0009 N88-10047
Space Station Mission Planning System (MPS) development study. Volume 2
[NASA-CR-179200] 01 p0009 N88-10048
Space Station Mission Planning Study (MPS) development study. Volume 3: Software development plan
[NASA-CR-179203] 01 p0009 N88-10049
Space station integrated wall design and penetration damage control
[NASA-CR-179169] 01 p0013 N88-10070
Space station: Leadership for the future
[NASA-PAM-509/8-87] 01 p0013 N88-10072
Study of a payload for Columbus Polar Platform Earth observation demonstration mission, executive summary
[ESA-CR(P)-2412] 01 p0014 N88-10079
Columbus preparatory program. Payload element study on a technology demonstration mission, executive summary
[CS-RP-AI-016] 01 p0014 N88-10080
Spacecraft 2000
[NASA-CP-2473] 01 p0015 N88-10084
Space station platforms 01 p0015 N88-10086
Space station assembly/servicing capabilities
01 p0016 N88-10100
Efficient placement of structural dynamics sensors on the space station
[NASA-CR-172015] 01 p0017 N88-10103
Preliminary study of a containerless processing facility for Columbus, executive summary
[ESA-ITT/AO/1-1834/85F] 01 p0032 N88-10203
Prephase A study of a crystallization laboratory for Columbus, executive summary
[ESA-ITT/AO/1-1866/85F] 01 p0032 N88-10206
Study of mobile communications payload for Columbus Polar Platforms
[ITS-TR-056A/86] 01 p0034 N88-10220
Catalytic processes for space station waste conversion
[NASA-CR-177423] 01 p0077 N88-10491
Space station based interferometry
01 p0096 N88-10628
Solar-terrestrial research in the space station era
01 p0117 N88-10747
Fourteenth Space Simulation Conference: Testing for a Permanent Presence in Space
[NASA-CP-2446] 02 p0132 N88-10829
Columbus pressurized module verification
02 p0134 N88-10842
Moving the factory into orbit 02 p0134 N88-10844
Rapid toxicity detection in water quality control utilizing automated multispecies biomonitoring for permanent space stations 02 p0135 N88-10848
Space station contamination considerations
02 p0137 N88-10859
Contamination control concepts for space station customer servicing 02 p0137 N88-10860
Predictive momentum management for a space station measurement and computation requirements
[NASA-CR-172026] 02 p0138 N88-10868
Space Construction
[NASA-CP-2490] 02 p0138 N88-10870
Space station: National Aeronautics and Space Administration's 1987 cost estimate
[PB87-220760] 02 p0140 N88-10883
Pinhole occulter experiment
[NASA-CR-179206] 02 p0235 N88-11481
Orbital Spacecraft Consumables Resupply System (OSCRS). Volume 4: Extended study results Part 1: Executive Summary
[NASA-CR-172012] 03 p0268 N88-11686
Orbital Spacecraft Consumables Resupply System (OSCRS): Monopropellant application to space station and OMV automatic refueling impacts of an ELV launch, volume 4
[NASA-CR-172029] 03 p0276 N88-11741
Photovoltaic power modules for NASA's manned space station
[NASA-TM-100229] 03 p0277 N88-11745
Space station propulsion
[NASA-TM-100216] 03 p0277 N88-11746
Space station integrated propulsion and fluid system study: Fluid systems configuration databook
[NASA-CR-179215] 03 p0278 N88-11753
An allotment planning concept and related computer software for planning the fixed satellite service at the 1988 space WARC
[NASA-TM-100244] 03 p0308 N88-11944
Potential applications of expert systems and operations research to space station logistics functions
[NASA-CR-180473] 03 p0372 N88-12342
Department of Housing and Urban Development-Independent Agencies Appropriations for fiscal year 1988, Thursday, 9 April 1987: National Aeronautics and Space Administration
03 p0386 N88-12424
Department of Housing and Urban Development-Independent Agencies Appropriations for fiscal year 1988, Friday, 10 April 1987: National Aeronautics and Space Administration
03 p0386 N88-12425
Spacecraft Fire Safety
[NASA-CP-2476] 04 p0406 N88-12520
Space station internal environmental and safety concerns 04 p0407 N88-12527
Optimization techniques applied to passive measures for in-orbit spacecraft survivability
[NASA-CR-179216] 04 p0408 N88-12532
An assessment of clinical chemical sensing technology for potential use in space station health maintenance facility
[NASA-CR-172013] 04 p0475 N88-12926
Space suit extravehicular hazards protection development
[NASA-TM-100458] 04 p0475 N88-12927
Orbital Spacecraft Consumables Resupply System (OSCRS). Volume 1: Executive summary
[NASA-CR-172010] 05 p0553 N88-13368
Design and assembly sequence analysis of option 3 for CETF reference space station
[NASA-TM-100503] 05 p0553 N88-13369
Space station systems: A bibliography with indexes
[NASA-SP-7056(05)] 05 p0556 N88-13382
Feasibility study for gas-grain simulation facility
[NASA-CR-177468] 05 p0646 N88-13954
National Aeronautics and Space Administration space station proposal, fiscal year 1988
[S-HRG-100-328] 05 p0659 N88-14043
The 1988 NASA (National Aeronautics and Space Administration) authorization
[GPO-80-245] 05 p0659 N88-14044
Approaches and possible improvements in the area of multibody dynamics modeling
[NASA-CR-179227] 06 p0663 N88-14067
Controlled Ecological Life Support Systems (CELSS) conceptual design option study
[NASA-CR-177421] 06 p0754 N88-14625
Controlled Ecological Life Support Systems (CELSS) physiochemical waste management systems evaluation
[NASA-CR-177422] 06 p0754 N88-14626
National Aeronautics and Space Administration (NASA)/American Society for Engineering Education (ASEE) Summer Faculty Fellowship Program, 1987. Volume 2
[NASA-CR-172009-VOL-2] 06 p0796 N88-14874
Performance considerations for the astrometric telescope facility on the phase 1 space station
[NASA-TM-100040] 06 p0800 N88-14898
Space station accommodations for lunar base elements: A study
[NASA-TM-100501] 06 p0804 N88-14907
A space transportation system operations model
[NASA-TM-100481] 07 p0823 N88-14999
Space station onboard propulsion system: Technology study
[NASA-CR-179233] 07 p0825 N88-15006
Chromic acid anodizing of aluminum foil
[NASA-CR-178417] 07 p0837 N88-15077
Space environmental effects on polymeric materials
[NASA-CR-182418] 07 p0838 N88-15082
Integration of symbolic and algorithmic hardware and software for the automation of space station subsystems
[NASA-TM-89705] 07 p0907 N88-15497
Some considerations on measuring the Newtonian gravitational constant G in an orbiting laboratory
07 p0922 N88-15603
The feasibility of using TAE as the UIL for the space station and for other internal NASA tasks and projects
07 p0925 N88-15618
Can space station software be specified through Ada?
07 p0925 N88-15622
Advancing automation and robotics technology for the space station and for the US economy: Submitted to the United States Congress October 1, 1987
[NASA-TM-100777] 08 p0959 N88-15816
Advancing automation and robotics technology for the space station and for the US economy: Submitted to the United States Congress May 15, 1987
[NASA-TM-89811] 08 p0959 N88-15817
Advancing automation and robotics technology for the space station and for the US economy: Submitted to the United States Congress October 1, 1986
[NASA-TM-89190] 08 p0960 N88-15818
Development of an emulation-simulation thermal control model for space station application
[NASA-CR-182409] 08 p0962 N88-15823
Space station accommodations for life sciences research facilities. Phase 1: Conceptual design and programmatics studies for Missions SAAX0307, SAAX0302 and the transition from SAAX0307 to SAAX0302. Volume 2: Study results
[NASA-CR-179244] 08 p0962 N88-15829
Space station propulsion technology
[NASA-CR-179260] 08 p0964 N88-15835
Status of 20 kHz space station power distribution technology
[NASA-TM-100781] 08 p0964 N88-15838
Third Conference on Artificial Intelligence for Space Applications, part 1
[NASA-CP-2492-Pt-1] 08 p1055 N88-16360
Telerobotic controller development
08 p1056 N88-16370
MTK: An AI tool for model-based reasoning
08 p1056 N88-16372
Integration of symbolic and algorithmic hardware and software for the automation of space station subsystems
08 p1056 N88-16373
KBS V and V as related to automation of space station subsystems: Rationale for a KBS lifecycle
08 p1057 N88-16375
Monitoring of space station life support systems with miniature mass spectrometry and artificial intelligence
08 p1057 N88-16376
Artificial intelligence and space power systems automation 08 p1058 N88-16381
Goal driven kinematic simulation of flexible arm robot for space station missions 08 p1059 N88-16388
FMEAssist: A knowledge-based approach to Failure Modes and Effects Analysis 08 p1060 N88-16395
Solid modelling for the manipulative robot arm (power) and adaptive vision control for space station missions
08 p1061 N88-16409
Planning and scheduling for robotic assembly
08 p1062 N88-16416
Planning activities in space 08 p1063 N88-16417
Intelligent man/machine interfaces on the space station 08 p1063 N88-16418
An AI approach for scheduling space-station payloads at Kennedy Space Center 08 p1064 N88-16425
The resource envelope as a basis for space station management system scheduling
08 p1064 N88-16427
Prototype resupply scheduler
08 p1064 N88-16428
Prototype space station automation system delivered and demonstrated at NASA 08 p1066 N88-16442

Applications of expert systems for satellite autonomy
08 p1066 N88-16443
Space station structures development
[NASA-CR-179261] 09 p1133 N88-16792
Communications satellite systems operations with the space station. Volume 3: Supplementary technical report
[NASA-CR-180875] 09 p1133 N88-16794
Development of a coupled expert system for the spacecraft attitude control problem
09 p1205 N88-17223
User interface devices for mission control
09 p1205 N88-17224
Design knowledge capture for the space station
09 p1208 N88-17239
Vision technology/algorithms for space robotics applications 09 p1212 N88-17267
Manipulator arm design for the Extravehicular Teleoperator Assist Robot (ETAR): Applications on the space station 09 p1213 N88-17270
Telerobot for space station 09 p1213 N88-17274
Space station integrated wall damage and penetration damage control. Task 5: Space debris measurement, mapping and characterization system
[NASA-CR-179281] 10 p1285 N88-17688
The 1987 Get Away Special Experimenter's Symposium
[NASA-CP-2500] 10 p1286 N88-17691
Simulation test beds for the space station electrical power system
[NASA-TM-100786] 10 p1290 N88-17715
System analysis study of space platform and station accommodations for life sciences research facilities. Volume 1: Executive summary. Phase A: Conceptual design and programmatics
[NASA-CR-179268] 10 p1291 N88-17721
System analysis study of space platform and station accommodations for life sciences research facilities. Volume 2: Study results, attachment 2. Phase A: Conceptual design and programmatics
[NASA-CR-179272] 10 p1291 N88-17722
Report of the Committee on the Space Station of the National Research Council
[NASA-CR-181602] 10 p1292 N88-17727
Magnetic emissions testing of the space station engineering model resistojet
[NASA-TM-100788] 10 p1292 N88-17728
Component data base for space station resistojet auxiliary propulsion
[NASA-CR-180834] 10 p1293 N88-17731
NASA/NBS (National Aeronautics and Space Administration/National Bureau of Standards) standard reference model for Telerobot Control System Architecture (NASREM)
[PB88-124773] 10 p1338 N88-17999
Assessment of mixed fleet potential for space station launch and assembly
[NASA-TM-100550] 11 p1443 N88-18608
Orbiter transfer vehicle concept definition and system analysis study. Volume 4: Space station accommodations. Revision 1
[NASA-CR-179293] 11 p1444 N88-18609
Orbital transfer vehicle concept definition and system analysis study. Volume 4, Appendix A: Space station accommodations. Revision 1
[NASA-CR-179294] 11 p1444 N88-18610
Space station operating system study
[NASA-CR-179308] 11 p1446 N88-18619
Microgravity and Materials Processing Facility study (MMPF): Requirements and Analyses of Commercial Operations (RACO) preliminary data release
[NASA-CR-179309] 11 p1466 N88-18742
Phase calibration generator 11 p1473 N88-18785
Computer-aided modeling and prediction of performance of the modified Lundell class of alternators in space station solar dynamic power systems
[NASA-CR-182538] 11 p1507 N88-19000
Space vehicle approach velocity judgments under simulated visual space conditions
[NASA-TM-89437] 11 p1523 N88-19094
Study of industry requirements that can be fulfilled by combustion experimentation aboard space station
[NASA-CR-180854] 11 p1566 N88-19377
A lunar transportation system
[NASA-CR-182561] 11 p1567 N88-19379
Preliminary analysis of an integrated logistics system for OSSA payloads
[NASA-CR-4114] 12 p1584 N88-19477
Preliminary analysis of an integrated logistics system for OSSA payloads. Volume 1: Executive summary
12 p1584 N88-19478
Preliminary analysis of an integrated logistics system for OSSA payloads. Volume 2: OSSA integrated logistics support strategy 12 p1584 N88-19479
Preliminary analysis of an integrated logistics system for OSSA payloads. Volume 3: OSSA integrated logistics support planning document 12 p1584 N88-19480
Preliminary analysis of an integrated logistics system for OSSA payloads. Volume 4: Supportability analysis of the 1.8m centrifuge 12 p1584 N88-19481
State-of-the-art technologies for construction in space: A review
[AD-A188412] 12 p1585 N88-19483
Proceedings of the 1st European In-Orbit Operations Technology Symposium
[ESA-SP-272] 12 p1585 N88-19484
Safe rendezvous approach to a space station by impulsive transfers and continuous thrust arcs
12 p1585 N88-19486
Assembly and servicing of a European Space Station
12 p1586 N88-19492
Utilization of SMS and EVA for the servicing of European Space Station 12 p1587 N88-19500
Robotic intelligence issues for space manipulator monitoring, control programming
12 p1588 N88-19504
EUROSIM: A concept of total system support
12 p1590 N88-19523
Technology requirements for telerobotic satellite servicing in space 12 p1592 N88-19536
Analysis of a rotating advanced-technology space station for the year 2025
[NASA-CR-178345] 12 p1600 N88-19580
Space Station Human Factors Research Review. Volume 3: Space Station Habitability and Function: Architectural Research
[NASA-CP-2426-VOL-3] 12 p1650 N88-19883
Space station architectural elements model study. Space station human factors research review
12 p1650 N88-19884
Space station architectural elements model study
[REPT-31799] 12 p1650 N88-19885
Space station group activities habitability module study: A synopsis 12 p1651 N88-19886
Full scale architectural simulation techniques for space stations 12 p1651 N88-19887
Social factors in space station interiors
12 p1651 N88-19888
Vega-1 and Vega-2 automatic stations: Functioning of flyby vehicles during encounter with Halley's comet
13 p1725 N88-20314
Study on long term evolution Towards European Autonomous Manned Spaceflight (STEAMS)
[SNIAS-SE/LS/AP-35-073] 13 p1727 N88-20330
Turnaround operations analysis for OTV. Volume 1: Executive summary
[NASA-CR-179316] 13 p1729 N88-20340
Turnaround operations analysis for OTV. Volume 2: Detailed technical report
[NASA-CR-179317] 13 p1729 N88-20341
The space station assembly phase: Flight telerobotic servicer feasibility, volume 1
[NASA-CR-182689] 13 p1731 N88-20351
The space station assembly phase: Flight telerobotic servicer feasibility. Volume 2: Methodology and case study
[NASA-CR-182690] 13 p1731 N88-20352
Spacecraft fire-safety experiments for space station: Technology development mission
[NASA-CR-182114] 13 p1731 N88-20353
Solar dynamic power system definition study
[NASA-CR-180877] 13 p1733 N88-20361
The dynamic control of robotic manipulators in space
[NASA-CR-182710] 13 p1779 N88-20646
An evaluation of the methods for rescuing EVA (Extravehicular Activities) crewmembers and recovering equipment detached and adrift from the space station
[AD-A189683] 14 p1871 N88-21181
Space station heavy lift launch vehicle utilization
[NASA-TM-100604] 14 p1873 N88-21188
Incorporation of privacy elements in space station design
[NASA-CR-182748] 14 p1881 N88-21242
Space station power system requirements
[NASA-TM-100886] 14 p1881 N88-21245
Multi-hundred kilowatt roll ring assembly evaluation results
[NASA-TM-100865] 14 p1904 N88-21375
Space station mobile transporter
14 p1927 N88-21488
Superconducting magnet technique for ASTROMAG on the space station
[DE88-004560] 15 p2025 N88-22063
A systems analysis of fire suppression alternatives for the US space station
[AD-A189847] 15 p2025 N88-22064
Ray tracing optical analysis of offset solar collector for space station solar dynamic system
[NASA-TM-100853] 15 p2027 N88-22080
Japanese space station module
15 p2052 N88-22224
Solar cell cover glasses for satellites
15 p2052 N88-22225
Vibrations of structures with parametric uncertainties
[AD-A190400] 15 p2076 N88-22378
Research and technology
[NASA-TM-100172] 15 p2153 N88-22851
Tethered diagnostic package for use from the space station
[DE88-006264] 16 p2167 N88-22921
An integrated and modular digital modeling approach for the space station electrical power system development
[NASA-TM-100904] 16 p2170 N88-22935
JPRS report: Science and technology. Japan
[JPRS-JST-87-030] 16 p2185 N88-23026
Microgravity mechanisms and robotics program
16 p2219 N88-23237
Base reaction optimization of manipulators with redundant kinematics 16 p2219 N88-23238
Department of Housing and Urban Development independent agencies appropriations for 1989. Part 7: National Aeronautics and Space Administration
[GPO-85-166] 16 p2286 N88-23689
Manned Mars mission accommodation: Sprint mission
[NASA-TM-100598] 16 p2290 N88-23711
On-orbit technology experiment facility definition
[NASA-TM-100614] 17 p2311 N88-23824
LDR structural experiment definition
[NASA-TM-100618] 17 p2312 N88-23826
Locking hinge
[NASA-CASE-MSC-21056-1] 17 p2312 N88-23827
Manual for obscuration code with space station applications
[NASA-CR-178099] 17 p2334 N88-23931
Space Station Human Factors Research Review. Volume 1: EVA Research and Development
[NASA-CP-2426-VOL-1] 17 p2379 N88-24145
Advanced EVA system design requirements study
17 p2380 N88-24147
Space Station Human Factors Research Review. Volume 4: Inhouse Advanced Development and Research
[NASA-CP-2426-VOL-4] 17 p2380 N88-24148
Space station proximity operations and window design
17 p2380 N88-24149
Spatial cognition 17 p2380 N88-24152
Fault diagnosis in orbital refueling operations
17 p2381 N88-24154
Third Conference on Artificial Intelligence for Space Applications, part 2
[NASA-CP-2492-PT-2] 17 p2387 N88-24188
MTK: An AI tool for model-based reasoning
17 p2387 N88-24189
Integration of symbolic and algorithmic hardware and software for the automation of space station subsystems
17 p2387 N88-24190
Connecting remote systems for demonstration of automation technologies 17 p2387 N88-24191
Knowledge based system verification and validation as related to automation of space station subsystems: Rationale for a knowledge based system lifecycle
17 p2387 N88-24192
Status of the organic Rankine cycle for space applications 17 p2422 N88-24402
Optimization of organic Rankine cycles for space station applications 17 p2423 N88-24407
Research and Technology, 1987, Goddard Space Flight Center
[NAS 1.15:101097] 17 p2453 N88-24572
Space station architectural elements model study
[NASA-CR-4027] 18 p2464 N88-24632
Possibilities and limits for use of laser propulsion systems in interorbital space flight
[ILR-MITT-185] 18 p2475 N88-24683
Human performance issues arising from manned space station missions
[NASA-CR-3942] 18 p2553 N88-25156
Space station architectural elements and issues definition study
[NASA-CR-3941] 18 p2587 N88-25371
Space station habitability recommendations based on a systematic comparative analysis of analogous conditions
[NASA-CR-3943] 18 p2587 N88-25372
A Study of Space Station Contamination Effects --- conference
[NASA-CP-3002] 18 p2590 N88-25390
Neutral environment for space station
18 p2590 N88-25391
Space station neutral external environment
18 p2590 N88-25392
Contaminant ions and waves in the space station environment 18 p2590 N88-25393
Space station induced electromagnetic effects
18 p2591 N88-25394
Space station contamination study: Assessment of contaminant spectral brightness
18 p2591 N88-25395

Calculation of space station infrared irradiance from atmosphere-induced emissions
18 p2591 N88-25396
Space station particulate contamination environment
18 p2591 N88-25397
The particulate environment surrounding the space station: Estimates from the PACS data
18 p2591 N88-25398
Effects of meteoroids and space debris on the particulate environment for space station 18 p2591 N88-25399
Contamination of optical surfaces — Space Station
18 p2592 N88-25400
Surface interactions relevant to space station contamination problems 18 p2592 N88-25401
Laboratory experiments of relevance to the space station environment 18 p2592 N88-25402
Contamination of the space station environment by vented chemicals 18 p2592 N88-25403
Centaur operations at the space station
[NASA-CR-179593] 19 p2606 N88-25473
Evaluation of the ion trap mass spectrometer for potential application in the space station
[DE88-008940] 19 p2674 N88-25902
Selecting the right crew for future space stations: An analysis of selection research on offshore divers, aviation pilots and other high risk groups in Scandinavia
19 p2696 N88-26021
The US space programme spacewalk/extravehicular activity experience: Past, present and future
19 p2697 N88-26031
Habitability of the Space Station: From vehicle to living space 19 p2697 N88-26033
Recent research on crew wardroom habitability for the Space Station 19 p2698 N88-26039
Tasks foreseen for space robots and an example of an associated orbital infrastructure
19 p2699 N88-26044
Some operational aspects of a rotating advanced-technology space station for the year 2025
[NASA-CR-181617] 20 p2765 N88-26397
Vapor Compression Distillation Subsystem (VCDS) component enhancement, testing and expert fault diagnostics development, volume 2
[NASA-CR-172076] 21 p2994 N88-27755
Block Oriented Simulation System (BOSS)
[NASA-CR-182947] 21 p2995 N88-27760
Vapor Compression Distillation Subsystem (VCDS) component enhancement, testing and expert fault diagnostics development, volume 1
[NASA-CR-172072] 22 p3134 N88-28634
Ariane 5, HERMES and European vehicles for space station servicing
[SNIAS-881-422-102] 23 p3183 N88-28943
Space transportation nodes assumptions and requirements: Lunar base systems study task 2.1
[NASA-CR-172052] 23 p3183 N88-28944
Expandable pallet for space station interface attachments
[NASA-CASE-MSC-21117-1] 23 p3185 N88-28958
Assessment of the effects of space debris and meteoroids environment on the space station solar array assembly
[NASA-TM-101315] 23 p3185 N88-28959
Collet lock joint for space station truss
[NASA-CASE-MSC-21207-1] 23 p3222 N88-29180
Second Conference on Artificial Intelligence for Space Applications
[NASA-CP-3007] 23 p3251 N88-29351
A plan for time-phased incorporation of automation and robotics on the US space station
23 p3255 N88-29377
A space station onboard scheduling assistant
23 p3259 N88-29402
A robotic system for automation of logistics functions on the Space Station 23 p3260 N88-29407
Definition of common support equipment and space station interface requirements for IOC model technology experiments
[NASA-TM-100656] 24 p3336 N88-29856
Study of toluene rotary fluid management device and shear flow condenser performance for a space-based organic Rankine power system
[NASA-CR-180885] 24 p3338 N88-29872
Advanced planar array development for space station
[NASA-CR-179373] 24 p3389 N88-30181
Space station proximity operations windows: Human factors design guidelines
[NASA-TM-88233] 24 p3410 N88-30301
A shared-world conceptual model for integrating space station life sciences telescience operations
24 p3416 N88-30333
Integrated resource scheduling in a distributed scheduling environment 24 p3417 N88-30342
The space station assembly phase: System design trade-offs for the flight telerobotic servicer
24 p3420 N88-30357

SPACE SUITS
NT EXTRAVEHICULAR MOBILITY UNITS
Space suit extravehicular hazards protection development
[NASA-TM-100458] 04 p0475 N88-12927
EVA, the technological challenge
12 p1592 N88-19535
Space cabin atmosphere and extracurricular sortie — embolisms 19 p2696 N88-26023
Technical challenges in the development of a European space suit system and comparison with underwater suits
19 p2696 N88-26024

SPACE SURVEILLANCE (GROUND BASED)
Photographic observations of the large scale features of Comet Halley 16 p2288 N88-23698
SSTS (Space Surveillance and Tracking System): The importance of early test and evaluation organizational participation
[AD-A193745] 23 p3276 N88-29499

SPACE SURVEILLANCE (SPACEBORNE)
Surveillance systems test and evaluation facilities
02 p0134 N88-10845
Strategic Defense Initiative Program: Status of space surveillance and tracking system
[PB88-150438] 14 p1967 N88-21739

SPACE SYSTEMS ENGINEERING
U AEROSPACE ENGINEERING

SPACE TELESCOPE
U HUBBLE SPACE TELESCOPE

SPACE TOOLS
An introduction to robot joint control methods
[NLR-TR-86080-U] 20 p2811 N88-26677
Study of software requirements and artificial intelligence techniques for robotics
[TL-3333] 24 p3422 N88-30365

SPACE TRANSPORTATION
NT SPACE TRANSPORTATION SYSTEM
Soviet space transport systems
13 p1727 N88-20328

SPACE TRANSPORTATION SYSTEM
Space Construction
[NASA-CP-2490] 02 p0138 N88-10870
The flight demonstration program and selection process 02 p0138 N88-10871
A monograph of the National Space Transportation System Office (NSTSO) integration activities conducted at the NASA Lyndon B. Johnson Space Center for the EASE/ACCESS payload flown on STS 61-B
02 p0139 N88-10876
Pinhole occulter experiment
[NASA-CR-179206] 02 p0235 N88-11481
Results of the development motor 8 test firing
[GPO-78-692] 03 p0278 N88-11751
Department of Housing and Urban Development-Independent Agencies Appropriations for fiscal year 1988, Friday, 10 April 1987: National Aeronautics and Space Administration
03 p0386 N88-12425
The determination of exhaust cloud dimensions from films of space shuttle launches
[NASA-CR-4103] 06 p0732 N88-14500
A space transportation system operations model
[NASA-TM-100481] 07 p0823 N88-14999
Evaluate the application of modal test and analysis processes to structural fault detection in MSFC - STS project elements 07 p0927 N88-15830
NASA (National Aeronautics and Space Administration) ADP (Automated Data Processing) system: Information on the automated mission and the payload tracking system
[PB88-104989] 07 p0942 N88-15730
A study to evaluate STS heads-up ascent trajectory performance employing a minimum-Hamiltonian optimization strategy
[NASA-TP-2793] 08 p0960 N88-15820
Lateral stability and control derivatives extracted from space shuttle Challenger flight data
[NASA-TM-100520] 09 p1132 N88-16788
STS propellant scavenging systems study. Part 2, volume 1: Executive summary and study results
[NASA-CR-179275] 10 p1290 N88-17716
STS propellant scavenging systems study. Part 2, volume 2: Cost and WBS/dictionary
[NASA-CR-179276] 10 p1290 N88-17717
Ballistic Single Stage Carrier Vehicle (BETA): A single stage reusable ballistic space shuttle concept
[MBB-UR-949/70] 10 p1310 N88-17828
Trends in the development of space transportation systems
[MBB-UR-911/86] 10 p1315 N88-17857
Research and technology 1987 annual report of the Kennedy Space Center
[NASA-TM-100303] 10 p1431 N88-18548
A two stage launch vehicle for use as an advanced space transportation system for logistics support of the space station
[NASA-CR-182572] 11 p1443 N88-18606
Assessment of mixed fleet potential for space station launch and assembly
[NASA-TM-100550] 11 p1443 N88-18608
Orbital analysis of a STS (Space Transportation System) external tank in low earth orbit
[AD-A188829] 12 p1593 N88-19542
Post-Challenger evaluation of space shuttle risk assessment and management
[NASA-CR-182461] 12 p1705 N88-20202
Research and technology, 1987
[NASA-TM-100323] 12 p1713 N88-20253
Department of Housing and Urban Development independent agencies appropriations for 1989. Part 7: National Aeronautics and Space Administration
[GPO-85-166] 16 p2286 N88-23689
Technology development program for twenty-first century aerospace vehicles 17 p2302 N88-23768
Large antenna experiments aboard the space shuttle: Application of nonuniform sampling techniques
19 p2652 N88-25745
Mark IV-85 mission support planning and future mission set 22 p3067 N88-28202
Space transportation nodes assumptions and requirements: Lunar base systems study task 2.1
[NASA-CR-172052] 23 p3183 N88-28944
SRB/SLEEC (Solid Rocket Booster/Shingle Lap Extendible Exit Cone) feasibility study, volume 1
[NASA-CR-178973] 23 p3187 N88-28964

SPACE TRANSPORTATION SYSTEM FLIGHTS
NT SPACE TRANSPORTATION SYSTEM 4 FLIGHT

SPACE TRANSPORTATION SYSTEM 4 FLIGHT
Studies of the vestibulo-ocular reflex on STS 4, 5 and 6
[NASA-TM-100461] 12 p1666 N88-19987

SPACE VEHICLE CHECKOUT PROGRAM
RETE experiment Assembly, Integration, and Verification (AIV) activities
[IFSI-87-6] 05 p0555 N88-13380
The KATE shell: An implementation of model-based control, monitor and diagnosis 09 p1210 N88-17255
Study of the assembly, integration and verification programs of telecommunication satellites applicable to other satellite programs
[MATRA-100/CC/MLG/031/87] 24 p3334 N88-29847

SPACE VEHICLE CONTROL
U SPACECRAFT CONTROL

SPACE WEAPONS
A comparison of open and closed multimegawatt space power and weapon systems
[DE87-012975] 01 p0089 N88-10579
The impact of deployment rates on the effectiveness of strategic defenses
[AD-A186907] 09 p1233 N88-17393
A strategy for space warfare
[AD-A186658] 09 p1233 N88-17394
AFAL (Air Force Astronautics Laboratory) technical objective document FY89
[AD-A187861] 11 p1567 N88-19378
Vapor-mist for lightweight high voltage space insulation systems
[DE87-011704] 13 p1762 N88-20538
Constellation sizing for modest directed energy platforms
[DE88-007033] 15 p2070 N88-22343
Parametric analysis of power requirements for space-based radar 17 p2399 N88-24260
Monolithic fuel cell based power source for sprint power generation 17 p2407 N88-24313
Analysis of closed cycle megawatt class space power systems with nuclear reactor heat sources
17 p2413 N88-24351
The effect of operating temperature on open, multimegawatt space power systems
17 p2414 N88-24352
Comparison of open and closed multimegawatt space power systems 17 p2414 N88-24353
RSMASS: A simple model for estimating reactor/shield masses 17 p2414 N88-24355
Hydrogen turbines for space power systems: A simplified axial flow gas turbine model 17 p2419 N88-24385
Power and energy requirements for electromagnetic launchers 17 p2420 N88-24391
Individual satellite power requirements calculated from specified constellation performance
17 p2420 N88-24392
Candidate advanced energy storage concepts for multimegawatt burst power systems
17 p2426 N88-24434
Monitoring space weaponry: Detection and verification issues
[DE88-008726] 20 p2847 N88-26900
SDI and/or arms control
[RAND-P-7357] 20 p2848 N88-26903
Launch operations to support future space forces
[AD-A192679] 20 p2881 N88-27107

Slew-induced deformations in a space-based electromagnetic rail gun 21 p2929 N88-27385
Future SDI (Strategic Defense Initiative) decision making
[AD-A192794] 21 p3010 N88-27860
Overview of the SDI (Strategic Defense Initiative) Program in short wavelength chemical lasers
[DE88-007912] 21 p3010 N88-27861
Electronic combat roadmap for space
[AD-A194262] 22 p3146 N88-28709
SDI (Strategic Defense Initiative) battle management/C3 (Command, Control and Communications) algorithms technology program plan
[AD-A194357] 23 p3275 N88-29495
A submillimeter wavelength space-based imaging radar
[AD-A195846] 24 p3364 N88-30033
Looking beyond the strategic defense initiative
[AD-A195079] 24 p3427 N88-30394
Antisatellite weapons and satellite deployment strategies
[AD-A195014] 24 p3427 N88-30396

SPACE-TIME CONTINUUM
U RELATIVITY

SPACE-TIME FUNCTIONS
Volume functions in the general theory of relativity
[ETN-87-90408] 01 p0089 N88-10582
Inequivalent quantizations and fundamentally perfect spaces
[DE87-014225] 02 p0229 N88-11446
Superconformal invariance and superstring in background fields
[DE87-703097] 02 p0247 N88-11561
Our universe as an attractor in a superstring model
[DE87-703066] 02 p0251 N88-11585
New notions about space-time and gravitation
[DE87-703259] 03 p0383 N88-12408
Analysis of absolute space-time Lorentz theories
[DE87-703371] 04 p0500 N88-13076
Homogeneous space-time of Goedel type in higher-derivate gravity
[DE87-703690] 04 p0500 N88-13077
Computer-aided study of a class of Riemannian space-times
[DE87-703367] 05 p0645 N88-13950
Superstrings on quantum spacetime
[DE88-700106] 07 p0940 N88-15715
Space-time processing of field produced by moving source 09 p1234 N88-17399
Criterion of singularity in general theory of relativity 09 p1240 N88-17430
Relativistic theory of gravitation and new concepts about space-time 09 p1240 N88-17431
Machine models and simulations
[PB88-118690] 10 p1386 N88-18280
Spatial-temporal variability of North Pacific sea surface temperature anomaly patterns 11 p1516 N88-19058
Notes on a class of homogeneous space-times
[DE88-700138] 11 p1562 N88-19353
Experimental analysis of absolute space-time Lorentz theories
[DE88-700140] 11 p1563 N88-19355
Space-time analysis of oceanographic fields by modified empirical orthogonal functions method 13 p1786 N88-20687
Space-time structure of ultrashort light pulses formed during stimulated backscattering of laser beam 14 p1972 N88-21767
Strings in four dimensions
[DE88-006435] 14 p1990 N88-21864
Seismic inversion by a RMS (Root-Mean-Square) Born approximation in the space-time domain
[PB88-165402] 15 p2131 N88-22711
Einstein metrics and Brans-Dicke superfields
[DE88-006992] 15 p2146 N88-22809
Quantization of axial electrodynamics
[DE88-701498] 15 p2147 N88-22813
Cosmology for high energy physicists
[DE88-005705] 15 p2151 N88-22842
Big whorls carry little whorls 16 p2195 N88-23094
Local time displacement as a symmetry of nature in flat space-time
[NASA-TM-100610] 16 p2264 N88-23542
Raychaudhuri equation in the self-consistent Einstein-Cartan theory with spin-density
[NASA-TM-101145] 17 p2447 N88-24546
Photon limited image processing in the space-time domain
[AD-A193142] 21 p2972 N88-27655
Electromagnetic theory of the gravitation 22 p3158 N88-28793
Global gauge anomaly of classical groups in even dimension
[DE88-008572] 22 p3158 N88-28797
On the GKP and BS constructions of C-boundary
[DE88-702643] 22 p3159 N88-28799
Open bosonic string in background electromagnetic field
[DE88-702140] 23 p3201 N88-29053
Time travel in the homogeneous Som-Raychaudhuri universe
[DE88-702220] 23 p3295 N88-29622
Image focusing in space and time
[AD-A195839] 24 p3429 N88-30410

SPACE-TIME METRIC
U SPACE-TIME FUNCTIONS

SPACEBORNE ASTRONOMY
ESA Workshop on Optical Interferometry in Space
[ESA-SP-273] 01 p0094 N88-10613
A comparison of interferometry from space and ground 01 p0094 N88-10614
Imaging strategies for a spaceborne interferometer 01 p0094 N88-10617
ISIS: Image reconstruction methods and signal-to-noise ratio investigations --- spaceborne interferometry 01 p0094 N88-10619
ISIS: Image reconstruction experiments and comparison of various array configurations --- spaceborne interferometry 01 p0095 N88-10620
OASIS: A mission concept --- Optical Aperture Synthesis Space Interferometry (OASIS) 01 p0095 N88-10622
Binary Star Explorer 01 p0095 N88-10624
ISIS: Imaging Speckle Interfereometer in Space 01 p0095 N88-10625
Proposed studies of a 30 meter imaging interferometer concept --- spaceborne astronomy 01 p0096 N88-10627
Space station based interferometry 01 p0096 N88-10628
NASA/JPL study on optical imaging interferometry in space 01 p0096 N88-10630
Aperture synthesis in space: Technical problems 01 p0097 N88-10638
Solar interferometry with a 4-aperture nonredundant and stabilized network 01 p0097 N88-10639
A test-bed for space interferometry: Space Platform Interferometer (SPI) 01 p0097 N88-10640
Dike zones on Venus
[NASA-TT-20111] 02 p0254 N88-11607
The Swedish sounding rocket and balloon program 08 p1025 N88-16205
Swiss scientific balloon and sounding rocket experiments 1985-1987 08 p1025 N88-16206
Infrared astronomy: Why and how? 09 p1123 N88-16722
Use of Space Station for space science 09 p1129 N88-16782
Microgravity payloads and missions for Space Station: Some issues affecting compatibility with other payloads 09 p1129 N88-16783
Experiment control and data system for an infrared detector array with maximum sensitivity
[ETN-88-91497] 09 p1136 N88-16813
Preparation of photometric measurements on a million stars in the framework of the satellite project HIPPARCOS/TYCHO
[ETN-88-91502] 13 p1853 N88-21093
The X-ray properties of AM Her stars
[MPE-PREPRINT-106] 16 p2289 N88-23704
SW UMa and V426 Oph: EXOSAT surprises 19 p2740 N88-26269
International ultraviolet explorer observatory operations
[NASA-CR-180775] 22 p3145 N88-28708
EXOSAT observations of Hercules X-1
[MPE-PREPRINT-119] 22 p3164 N88-28841
Beyond the visible: A decade of observations with the International Ultraviolet Explorer (IUE)
[ESA-F09] 24 p3331 N88-29828
ESA report to the 27th COSPAR meeting
[ESA-SP-1098] 24 p3453 N88-30556
The high-throughput X-ray spectroscopy mission: The mission-science report
[ESA-SP-1097] 24 p3453 N88-30557

SPACEBORNE EXPERIMENTS
NT PHYSICS AND CHEMISTRY EXPERIMENT IN SPACE
Blagov commentary on Mir station, first manning 01 p0009 N88-10051
Final phase of Project Vega 01 p0009 N88-10053
The Aquarack as a potential instrument for basic research work in space biology: Inventory and scientific dispositions 01 p0073 N88-10470
Xiphophorus as an experimental system for genetic and biological development studies under microgravity conditions 01 p0074 N88-10472
Life support systems for biological experiments under weightlessness in the German and European space programs 01 p0074 N88-10477
Trickle water and feeding system in plant culture and light-dark cycle effects on plant growth 03 p0361 N88-12273
Microgravity nucleation and particle coagulation experiments support
[NASA-CR-181540] 04 p0423 N88-12618
Microgravity nucleation and particle coagulation experiments support
[NASA-CR-181541] 04 p0423 N88-12619
Study of certain biological characteristics of bacteria during the French-Soviet CYTOS-2 space experiment 04 p0473 N88-12917
Research on Electrodynamic Tether Effects (RETE) experiment Electrical Ground Support Equipment (EGSE) --- tethered satellite
[IFSI-87-2] 05 p0555 N88-13378
RETE experiment Assembly, Integration, and Verification (AIV) activities
[IFSI-87-6] 05 p0555 N88-13380
Partial analysis of experiment LDEF A-0114
[NASA-CR-179236] 06 p0780 N88-14787
Allowable gravity-levels for Spacelab, Columbus and EURECA --- materials science
[BF-R-66.525-2] 07 p0838 N88-15084
Microgravity Particle Research on the Space Station
[NASA-CP-2496] 07 p0883 N88-15354
Astrophysics and the solar nebula 07 p0883 N88-15355
Planetary science 07 p0883 N88-15356
Atmospheric science 07 p0883 N88-15357
Exobiology and life science 07 p0883 N88-15358
Physics and chemistry 07 p0883 N88-15359
Proceedings and program draft in Gravitational Biology in the Federal Republic of Germany --- Effects of Weightlessness on the Human Organism
[ESA-TT-988] 07 p0884 N88-15363
The role of the DFVLR project management life sciences in the space program of the Federal Republic of Germany 07 p0884 N88-15364
A theoretical concept for state changes and shape changes in weightlessness 07 p0884 N88-15365
Experiments with rats flown aboard Cosmos-1667 biosatellite (main objectives, conditions and results) 07 p0893 N88-15414
Multiply charged particles in primary cosmic rays with energy less than or equal to 2 TeV 07 p0921 N88-15596
Space station accommodations for life sciences research facilities. Phase 1: Conceptual design and programmatics studies for Missions SAAX0307, SAAX0302 and the transition from SAAX0307 to SAAX0302. Volume 2: Study results
[NASA-CR-179244] 08 p0962 N88-15829
LeRC cryogenic fluid management program overview 08 p0981 N88-15928
Cryogenic fluid management program flight concept definition 08 p0981 N88-15929
How ground-based observations contribute to rocket, balloon and space shuttle experiments: Experience from the past and outlook for the future 08 p1026 N88-16216
Scheduling spacecraft operations 08 p1064 N88-16426
Microgravity experiments in space: Compatibility with dynamic perturbing effects 09 p1241 N88-17435
Microgravity research at the University of Mexico: Experiments in payload G-006 10 p1286 N88-17692
An update to the MITRE/WPI Space Shuttle Program GASCAN G-408 10 p1287 N88-17697
The photons payload, G-494: A learning experience 10 p1288 N88-17701
The challenge of G-376 10 p1288 N88-17705
Project Explorer takes its second step: GAS-608 in engineering development 10 p1288 N88-17707
The NORSTAR Program: Space shuttle to space station 10 p1289 N88-17710
Into the thermosphere: The atmosphere explorers
[NASA-SP-490] 10 p1353 N88-18084
Preliminary analysis of an integrated logistics system for OSSA payloads
[NASA-CR-4114] 12 p1584 N88-19477
Preliminary analysis of an integrated logistics system for OSSA payloads. Volume 4: Supportability analysis of the 1.8m centrifuge 12 p1584 N88-19481
Promising concepts for ground-to-orbit experiment teleoperation --- Columbus 12 p1590 N88-19518
Ground based supervisory and programming system for automatic experiment execution in orbit 12 p1590 N88-19519
Robotics servicing experiment --- European space programs 12 p1591 N88-19529
Cytomorphology and ultrastructure of corn root meristem in weightlessness 12 p1651 N88-19891
The European Space Agency's role in life sciences and research in space 12 p1652 N88-19894
Exobiology and botany facilities for EURECA 12 p1652 N88-19898
Life sciences research in space: The requirement for animal models 12 p1654 N88-19909

Fish as a tool for testing fitness in space
12 p1662 N88-19963
Animal research on the Space Station
12 p1662 N88-19964
Thermal structure of Venusian Atmosphere determined from results of measurements from Vega-2 landing module
13 p1725 N88-20315
Vibration characteristics of pumped fluid systems (VCPFS) --- microgravity payloads
[ESA-CR(P)-2499] 14 p1895 N88-21310
Engineering support of space shuttle experiment integration
[AD-A190135] 15 p2024 N88-22061
Space utilization plans 15 p2051 N88-22219
Amorphous semiconductors made in space
15 p2051 N88-22221
Containerless glass melting 15 p2051 N88-22222
Pb(1-x)Sn(x)Te crystal growth in space
15 p2051 N88-22223
Solar cell cover glasses for satellites
15 p2052 N88-22225
Noncontact temperature measurements in the microgravity fluids and transport phenomena discipline
17 p2328 N88-23901
Microgravity combustion discipline working group summary of requirements for noncontact temperature measurements 17 p2328 N88-23902
Requirements for temperature and species concentration measurements in microgravity combustion experiments 17 p2329 N88-23903
Non-contact temperature measurements for biotechnology discipline working group
17 p2329 N88-23904
Airborne and spaceborne radar images for geologic and environmental mapping in the Amazon rain forest, Brazil
17 p2353 N88-24021
Botany Facility pre-phase C/D. Core payload for EURECA, volume 2
[BF-RP-ER-015-VOL-2] 17 p2377 N88-24130
Botany Facility: The problems of plant fixation
[SIRA-A/7373/WP220/RJS/001]
17 p2379 N88-24140
Theoretical plasma physics research of active space experiments
[AD-A192075] 18 p2577 N88-25309
Contamination of the space station environment by vented chemicals 18 p2592 N88-25403
Application of AI to space systems
19 p2634 N88-25626
Microgravity science and applications bibliography, 1987 revision
[NASA-TM-4067] 22 p3062 N88-28171
Experimental proof of quasilongitudinal propagation of low-frequency waves in middle latitudes in upper ionosphere 24 p3447 N88-30516
Influence of plasma parameters on VLF radiation in near-rocket region 24 p3448 N88-30518
Charge composition of primary cosmic ray nuclei with z greater than or equal to 2 in energy region greater than or equal to 2 TeV 24 p3448 N88-30519

SPACEBORNE LASERS
Atmospheric Lidar Experiment In Space (ALEXIS)
[DFVLR-MITT-88-10] 22 p3118 N88-28526
Spaceborne lidar: Development of a laboratory test system
[BF-R-66.090-1] 24 p3378 N88-30118

SPACEBORNE PHOTOGRAPHY
NT SATELLITE-BORNE PHOTOGRAPHY
Remote sensing of planets and cartographic results
[HSBW-HEFT-14] 03 p0389 N88-12444
Space applications in geography
08 p1007 N88-16104
Use of space photographs for geomorphological studies in southwestern Tajikistan 08 p1008 N88-16109
Academic course Space Methods for Studying Modern Landscapes of Continents 08 p1012 N88-16133
Photogrammetric principles for combining remote sounding and three-dimensional mapping
08 p1012 N88-16135
Using space photography of the Earth in the classroom: Drought in Africa
[NASA-CR-182948] 19 p2685 N88-25960

SPACEBORNE TELESCOPES
NT GERMAN INFRARED LABORATORY
NT HUBBLE SPACE TELESCOPE
NT INFRARED SPACE OBSERVATORY (ISO)
NT SPACE INFRARED TELESCOPE FACILITY
NT X RAY ASTROPHYSICS FACILITY
OASIS: A mission concept --- Optical Aperture Synthesis Space Interferometry (OASIS) 01 p0095 N88-10622
COSMIC --- Coherent Optical System of Modular Image Collectors (COSMIC); spaceborne telescope
01 p0095 N88-10623
Fiber-linked telescope arrays on the ground and in space 01 p0095 N88-10626
Wavefront error sensing
[NASA-CR-181504] 03 p0321 N88-12030
Study of solid state photomultiplier
[NASA-CR-177485] 05 p0583 N88-13556
Multisurface control mechanism for a deployable antenna: Far Infrared and Submillimeter Space Telescope (FIRST) technology study
[RP-FA-D003] 09 p1135 N88-16807
Design of a linear actuator and breadboard test result --- far IR telescope 14 p1877 N88-21217
Fine adjustment mechanism for FIRST
14 p1878 N88-21219
Design, construction and performance of the ROSAT high resolution X-ray mirror assembly
[MPE-PREPRINT-101] 15 p2150 N88-22836

SPACECRAFT ANTENNAS
Mechanical properties characterization of composite sandwich materials intended for space antenna applications
[NASA-TM-88893] 01 p0020 N88-10121
Thermal testing by internal IR heating of the FEP module 02 p0136 N88-10854
Dual S/X-band RV antenna
[DE87-014853] 03 p0305 N88-11923
MBA payload testing by Compact Antenna Test Range (CATR)
[ESA-CR(P)-2473] 08 p0977 N88-15906
The ESTEC Mini Compact Antenna Test Range
[ESA-CR(P)-2475] 08 p0977 N88-15907
Latching mechanisms for IOC --- EURECA
14 p1875 N88-21205
Features and applications of the integrated composites analyzer (ICAN) code 15 p2078 N88-22391
Development of a general software package for the analysis and synthesis of planar antenna arrays for space applications
[S-247-02] 24 p3359 N88-30000

SPACECRAFT CABIN ATMOSPHERES
Progress in European CELSS activities
03 p0356 N88-12252
Space cabin atmosphere and extracurricular sortie --- embolisms 19 p2696 N88-26023

SPACECRAFT CABINS
Contamination control of the space shuttle Orbiter crew compartment 02 p0133 N88-10834
Space station group activities habitability module study: A synopsis 12 p1651 N88-19886

SPACECRAFT CHARGING
Space Environment Technology --- conference
[ISBN-2-85428-170-5] 03 p0271 N88-11702
The geosynchronous plasma environment
03 p0273 N88-11716
Introduction to the problem of environmentally induced discharges 03 p0273 N88-11717
External surface charging mechanisms --- spacecraft
03 p0273 N88-11719
Three-dimensional charging effects --- spacecraft
03 p0273 N88-11720
Modeling of environmentally-induced effects within satellites. Part 1: NASCAP modeling of satellites
03 p0273 N88-11721
Modeling of environmentally-induced transients within satellites. Part 2: Discharge coupling transients
03 p0273 N88-11722
Discharge phenomena --- spacecraft
03 p0274 N88-11723
In-flight diagnosis: Analysis of spurious events --- spacecraft 03 p0274 N88-11724
Electromagnetic interaction between an electric discharge and cabling inside a satellite
03 p0274 N88-11725
Electromagnetic effects of a discharge on circuitry --- spacecraft 03 p0274 N88-11726
Charging calculations for the HIPPARCOS satellite
03 p0274 N88-11728
MARECS-A case 03 p0274 N88-11729
Electromagnetic compatibility (EMC) phenomena and prevention of the effects --- spacecraft
03 p0274 N88-11731
Electrostatic discharges in geostationary orbit: The case of Telecom 1 03 p0275 N88-11733
Flight model discharge system
[AD-A185657] 06 p0673 N88-14122
MAIMIK: A high current electron beam experiment on a sounding rocket from Andoya rocket range (Norway)
08 p1030 N88-16243
Spacecraft dielectric surface charging property determination
[NASA-CR-180879] 14 p1881 N88-21243
Simulations of the electrostatic charging of ESA communications satellites
[ESA-STM-239] 18 p2472 N88-24670
Deep dielectric charging effects due to high energy electrons in earth's outer magnetosphere
[AD-A192154] 18 p2541 N88-25083
Spacecraft requirements for predictions of geomagnetic activity (a tutorial)
[AD-A191943] 19 p2685 N88-25959
Ion gun generated electromagnetic interference on the SCATHA satellite
[AD-A195179] 24 p3335 N88-29853

SPACECRAFT COMMUNICATION
NT SATELLITE COMMUNICATION
Coherent infrared detection, volume B --- CO2 laser intersatellite data link
[ESA-CR(P)-2392-VOL-1] 01 p0034 N88-10218
Coherent infrared detection, volume D --- CO2 laser intersatellite data link
[ESA-CR(P)-2392-VOL-2] 01 p0034 N88-10219
A conformal aircraft phased array antenna for airplane-satellite communication in the L band
[ESA-TT-1057] 03 p0305 N88-11926
Error control techniques for satellite and space communications
[NASA-CR-181581] 05 p0576 N88-13516
Results on the low elevation angle propagation experiment, part 1
[TUD-R-328] 06 p0693 N88-14250
Satellite ground-terminal user simulation
[NASA-TM-100234] 06 p0694 N88-14260
Study of a Radio Relay Link (RRL). Cassini mission. Data package for final presentation
[ESA-CR(P)-2472] 07 p0847 N88-15138
The Telecommunications and Data Acquisition Report
[NASA-CR-182545] 11 p1471 N88-18774
Spacecraft telecommunications system mass estimates 11 p1473 N88-18784
The evaluation and selection of a 5th ground antenna site for the global positioning system
[AD-A189495] 13 p1720 N88-20286
A pointing mechanism for intersatellite link system
14 p1874 N88-21194
Continued design of a Pointing, Acquisition, and Tracking (PAT) subsystem for InterSatellite Laser links (ISL2)
[TELDIX-15-093-178] 14 p1905 N88-21384
Construction of a 60 GHz Traveling Wave Tube (TWT) for intersatellite link on geostationary orbit (ISL/TWT)
[BMFT-FB-W-86-015] 16 p2192 N88-23076
Environmental projects. Volume 6: Environmental assessment. New 34-meter antenna at Venus site
[NASA-CR-182922] 17 p2332 N88-23919
Connecting remote systems for demonstration of automation technologies 17 p2387 N88-24191
Assessment of optical communications systems for the Data Relay Satellite
[ESA-CR(P)-2488-VOL-2] 18 p2502 N88-24842
Document transfer by a digital satellite link
[NLR-MP-86071-U] 20 p2792 N88-26564
Optical multiple access intersatellite links
[BAE-TP-8502] 24 p3361 N88-30013
The LTPP communication processor --- Columbus and Hermes
[CL/CP/SES/FR/004] 24 p3415 N88-30328
A rule-based systems approach to spacecraft communications configuration optimization
24 p3417 N88-30341

SPACECRAFT COMPONENTS
NT COMMAND MODULES
NT LANDING MODULES
NT LUNAR LANDING MODULES
NT SPACECRAFT CABINS
NT SPACECRAFT MODULES
Telemetry conditioning units for the European launcher Ariane 01 p0012 N88-10068
Mobile test fixture system for use in a thermal vacuum facility 02 p0134 N88-10843
Mathematical modelling of solar ultraviolet radiation induced optical degradation in anodized aluminum
02 p0135 N88-10846
A nondissipative Pyrotechnic Arming and Firing Unit (PAFU)
[CRA/REPO/8019] 02 p0155 N88-10974
Incipient fault detection study for advanced spacecraft systems
[NASA-CR-172014] 02 p0183 N88-11138
Electromagnetic effects of a discharge on circuitry --- spacecraft 03 p0274 N88-11726
Fire-related standards and testing
04 p0406 N88-12522
Fire extinguishment and inhibition in spacecraft environments 04 p0406 N88-12523
High energy density rechargeable batteries for aerospace power requirements
[AD-A184883] 05 p0577 N88-13519
Natural frequencies and structural integrity assessment of large space structures
[AD-A186139] 07 p0824 N88-15001
Heat pipes for space use 09 p1124 N88-16736
Major spacecraft hardware testing in Europe
09 p1125 N88-16740

Promotion of European components for ESA projects
09 p1128 N88-16764
Space station structures development
[NASA-CR-179261] 09 p1133 N88-16792
Activities report in tribology
[ESA-ESTL-79] 09 p1174 N88-17037
The 58th Shock and Vibration Symposium, volume 2
[NASA-CP-2488-VOL-2] 11 p1499 N88-18948
Design and dynamic testing of an instrumented spacecraft component 11 p1499 N88-18952
SOAR: Space orbiting advanced fusion power reactor
[AD-A189234] 13 p1732 N88-20356
Proceedings of the 3rd European Space Mechanisms and Tribology Symposium
[ESA-SP-279] 14 p1874 N88-21191
Models for steady and nonsteady Coulomb torque in ball bearings 14 p1876 N88-21208
Towards a practical microgravity environment — isolation mount 14 p1878 N88-21223
Cryogenic test facilities for an optical cryomechanism qualification 14 p1879 N88-21228
Structural latches for modular assembly of spacecraft and space mechanisms 14 p1925 N88-21471
A pyrotechnical opening valve
[SNIAS-MU/TYS-NT-2-06(0)] 16 p2167 N88-22922
TES: A modular systems approach to expert system development for real-time space applications
17 p2388 N88-24197
The use of liquid films for spacecraft survivability to laser radiation
[AD-A192954] 20 p2765 N88-26395
Study of secondary emission properties of materials used for high power RF components in space
[ESA-CR(P)-2587] 24 p3361 N88-30012
Heavy ion and proton tests for subsystem upset
[AD-A195267] 24 p3434 N88-30442

SPACECRAFT CONFIGURATIONS
NT SATELLITE CONFIGURATIONS
Adaptive control of Large Space Structure (LSS)
[ISAS-R-621] 03 p0276 N88-11740
Payload configurations and serviceability — Columbus Polar Platforms 03 p0339 N88-12133
The 1988 NASA (National Aeronautics and Space Administration) authorization
[GPO-80-245] 05 p0659 N88-14044
Zero-G thermodynamic vent system for shuttle/Centaur 08 p0983 N88-15943
Space station overview 09 p1129 N88-16780
Space station structures development
[NASA-CR-179261] 09 p1133 N88-16792
Coorbiting Platform Utilization Study (CPLUS), executive summary — Columbus
[SN-WP-4000-DOC-8609/85/F]
09 p1133 N88-16798
Analysis of a rotating advanced-technology space station for the year 2025
[NASA-CR-178345] 12 p1600 N88-19580
Ludwig Prandtl collected treatises on applied mechanics, hydro- and aerodynamics, part 1
[NASA-TT-20316] 20 p2752 N88-26337
EXSAT: Expert system to configure telecommunication satellites
[SNIAS-881-440-101] 21 p2902 N88-27223
Space shuttle phase B wind tunnel model and test information. Volume 2: Orbiter configuration
[NASA-CR-178415-VOL-2-PT-1]
23 p3171 N88-28881

SPACECRAFT CONSTRUCTION MATERIALS
Outgassing data for selecting spacecraft materials
[NASA-RP-1124] 01 p0019 N88-10117
High intensity 5 eV O-atom exposure facility for material degradation studies 02 p0135 N88-10847
Spacecraft surface exposure to atomic oxygen in low Earth orbit 03 p0273 N88-11715
Discharge phenomena — spacecraft
03 p0274 N88-11723
Discharge prevention of geosynchronous orbit conductive thermal control materials and grounding systems 03 p0274 N88-11732
Fire-related standards and testing
04 p0406 N88-12522
Spacecraft material flammability testing and configurations 04 p0407 N88-12529
Carbon fiber reinforced glass matrix composites for space based applications
[AD-A184355] 04 p0410 N88-12546
Influence of bonding shop moisture on metal-honeycomb junctions bonded with ultra-thin adhesive films
[SNIAS-872-422-112] 05 p0558 N88-13399
First International Week of Adhesive Bonding and Assembling
[SNIAS-872-430-106] 05 p0569 N88-13468
Time-temperature-stress capabilities of composite materials for advanced supersonic technology application
[NASA-CR-178272] 06 p0677 N88-14144
Spectroscopic investigations and measurements of certain ARC jet parameters 06 p0796 N88-14877
Multipurpose corrosion inhibitors for aerospace materials in Naval environments
[AD-A186728] 09 p1143 N88-16853
Space environmental effects on polymeric materials
[NASA-CR-182454] 09 p1148 N88-16879
Soviet spacecraft engineering research
[FASAC-TAR-3090] 17 p2311 N88-23823
Aluminum alloy
[NASA-CASE-LAR-13924-1-CU]
18 p2487 N88-24753
Reinforced plastics: Winding and weaving technologies for space products
[SNIAS-881-430-103] 21 p2922 N88-27341
The technical reporting and approval procedure for materials and processes
[ESA-PSS-01-700-ISSUE-1] 22 p3162 N88-28833
Contribution to the study of materials behavior in space environment
[SNIAS-881-430-104] 23 p3189 N88-28977
Very high temperature materials for mechanical application
[SNIAS-881-430-106] 23 p3189 N88-28978
Material and process selection and quality control for ESA space systems and associated equipment
[ESA-PSS-01-70-ISSUE-3] 23 p3224 N88-29190
Study of secondary emission properties of materials used for high power RF components in space
[ESA-CR(P)-2587] 24 p3361 N88-30012

SPACECRAFT CONTAMINATION
Fourteenth Space Simulation Conference: Testing for a Permanent Presence in Space
[NASA-CP-2446] 02 p0132 N88-10829
Contamination control concepts for space station customer servicing 02 p0137 N88-10860
Surface scattering characteristics and the measurement of particulate contamination 02 p0137 N88-10862
Low extractable wipers for cleaning space flight hardware 02 p0137 N88-10863
Spacecraft surface exposure to atomic oxygen in low Earth orbit 03 p0273 N88-11715
Analysis of geophysical data bases and models for spacecraft interactions
[AD-A184809] 05 p0555 N88-13375
Analysis of contamination data recorded by the IECM camera/photometer
[NASA-TM-100324] 14 p1882 N88-21246
A Study of Space Station Contamination Effects — conference
[NASA-CP-3002] 18 p2590 N88-25390
Neutral environment for space station
18 p2590 N88-25391
Space station neutral external environment
18 p2590 N88-25392
Contaminant ions and waves in the space station environment 18 p2590 N88-25393
Space station induced electromagnetic effects
18 p2591 N88-25394
Space station contamination study: Assessment of contaminant spectral brightness
18 p2591 N88-25395
Space station particulate contamination environment
18 p2591 N88-25397
The particulate environment surrounding the space station: Estimates from the PACS data
18 p2591 N88-25398
Effects of meteoroids and space debris on the particulate environment for space station 18 p2591 N88-25399
Contamination of optical surfaces — Space Station
18 p2592 N88-25400
Surface interactions relevant to space station contamination problems 18 p2592 N88-25401
Laboratory experiments of relevance to the space station environment 18 p2592 N88-25402
Contamination of the space station environment by vented chemicals 18 p2592 N88-25403
Progress on a Monte Carlo shuttle contamination model
[AD-A193694] 23 p3183 N88-28945
Studies on rocket exhaust plumes and impingement effects related to the Columbus Space Station program: Executive summary
[DFVLR-IB-222-88-A-12] 24 p3337 N88-29862

SPACECRAFT CONTROL
NT SATELLITE ATTITUDE CONTROL
NT SATELLITE CONTROL
Dynamics of spacecraft control laboratory experiment (SCOLE) slew maneuvers
[NASA-CR-4098] 01 p0014 N88-10082
Telemetry, Tracking, and Control Working Group report
01 p0016 N88-10096
Attitude Control Working Group report
01 p0016 N88-10099
Predictive momentum management for a space station measurement and computation requirements
[NASA-CR-172026] 02 p0138 N88-10866
Equal-modulus vector programmed frequency control of minimally redundant structure of powered, single-degree-of-freedom gyroscopes for spacecraft attitude control system 02 p0159 N88-10994
A linear quadratic Gaussian with loop transfer recovery proximity operations autopilot for spacecraft
[NASA-CR-172028] 02 p0227 N88-11433
Adaptive control of Large Space Structure (LSS)
[ISAS-R-621] 03 p0276 N88-11740
New feedback design methodologies for large space structures: A multi-criterion optimization approach
04 p0408 N88-12535
Combined problem of slew maneuver control and vibration suppression
[NASA-CR-181537] 04 p0455 N88-12817
Modeling and control of large flexible vehicles in the atmosphere and space
[AD-A185368] 05 p0555 N88-13377
Optimal control of large space structures via generalized inverse matrix
[NASA-CR-182336] 05 p0639 N88-13907
Guidance and control strategies for aerospace vehicles
[NASA-CR-181579] 05 p0643 N88-13935
Expert system study for spacecraft management
[TL-2699-ISS-1] 07 p0824 N88-15004
The dynamics and control of large-flexible space structures, part 10
[NASA-CR-182426] 08 p0963 N88-15830
Large-angle slewing maneuvers for flexible spacecraft
[NASA-CR-4123] 08 p1000 N88-16060
Gyrostabilizer system of Kvant module
08 p1006 N88-16099
Study of descent of probes with high lift-drag ratio into the atmosphere of Jupiter 08 p1006 N88-16101
Third Conference on Artificial Intelligence for Space Applications, part 1
[NASA-CP-2492-Pt-1] 08 p1055 N88-16360
KBS V and V as related to automation of space station subsystems: Rationale for a KBS lifecycle
08 p1057 N88-16375
A distributed architecture for intelligent monitoring and anomaly diagnosis of the Hubble Space Telescope
08 p1057 N88-16379
Expert systems relations in space applications
08 p1059 N88-16391
Application of parallel distributed processing to space based systems 08 p1059 N88-16393
ESSAA: Embedded system safety analysis assistant
08 p1060 N88-16396
Similarity networks as a knowledge representation for space applications 08 p1062 N88-16411
A framework for real-time distributed expert systems: On-orbit spacecraft fault diagnosis, monitoring and control 08 p1066 N88-16440
TES: A modular systems approach to expert system development for real time space applications
08 p1066 N88-16441
Applications of expert systems for satellite autonomy
08 p1066 N88-16443
MPAD MCC workstation system: ADDAM and EEVE
09 p1203 N88-17209
Development of a coupled expert system for the spacecraft attitude control problem
09 p1205 N88-17223
Verifying shuttle onboard software using expert systems 09 p1207 N88-17237
Expert system applications in spacecraft subsystem controllers 09 p1210 N88-17254
Formulation methods of rigid multibody systems for large space structures and some results of computer simulation
[NAL-TR-942] 10 p1293 N88-17730
Intelligent on board control for field emission electric propulsion system 12 p1589 N88-19513
Activities report in aeronautics and astronautics
[ETN-88-91332] 13 p1859 N88-21115
A feedback double path compensating control structure for the attitude control of a flexible spacecraft
[INPE-4464-PRE/1239] 14 p1880 N88-21240
Technology development program for twenty-first century aerospace vehicles 17 p2302 N88-23768
Three axis attitude control system
[NASA-CASE-GSC-12970-1] 17 p2308 N88-23808
Travelling wave concepts for the modeling and control of space structures
[AD-A191235] 17 p2310 N88-23819
TALOS: A distributed architecture for intelligent monitoring and anomaly diagnosis of the Hubble Space Telescope 17 p2388 N88-24193

Genetic algorithms for adaptive real-time control in space systems 17 p2388 N88-24195
Guidance and control strategies for aerospace vehicles
[NASA-CR-183032] 18 p2467 N88-24644
Low authority control of large space structures using a constrained threshold control formulation 18 p2472 N88-24667
A feedback linearization approach to spacecraft control using momentum exchange devices
[NASA-CR-172057] 18 p2472 N88-24668
Spacecraft applications of advanced global positioning system technology
[NASA-CR-172063] 20 p2757 N88-26359
Simulation of attitude and maneuvers for the Brazilian spin-stabilized satellite
[INPE-4271-PRE/1143] 22 p3046 N88-28079
Study of standard generic approach for spacecraft (S/C) autonomy and automation (phase 3). Book A: Autonomy concept description
[ESA-CR(P)-2555-VOL-1] 23 p3185 N88-28955
Study of standard generic approach for spacecraft (S/C) autonomy and automation (phase 3). Book B: Autonomy concept application example
[ESA-CR(P)-2555-VOL-2] 23 p3185 N88-28956
Study of standard generic approach for spacecraft (S/C) autonomy and automation (phase 3). Book C: Autonomy concept summary
[ESA-CR(P)-2555-VOL-3] 23 p3185 N88-28957
Intelligent interfaces for expert systems 23 p3258 N88-29397
Theory of filtering and control with application to control of large space structures
[AD-A195500] 24 p3335 N88-29851
Synchronous response modelling and control of an annular momentum control device
[NASA-CR-4186] 24 p3358 N88-29995
Robust design of distributed controllers for large flexible space structures
[NASA-CR-183202] 24 p3380 N88-30134
Automated space vehicle control for rendezvous proximity operations 24 p3416 N88-30335
An approach to CMG steering using feedback linearization
[NASA-CR-183172] 24 p3422 N88-30369
Increasing accuracy in evaluating vector of state under conditions of incomplete observability of expanded system 24 p3446 N88-30511

SPACECRAFT DEFENSE
An examination of the Advanced Communications Technology Satellite (ACTS) and its application to the Defense Data Network (DDN)
[AD-A184003] 03 p0276 N88-11742
ADAM (Acquisition Deployment and Maneuvering): The space game
[AD-A189512] 12 p1685 N88-20078
Alternative force structuring strategies for military satellite communication systems
[AD-A189492] 13 p1758 N88-20516
Antisatellite weapons and satellite deployment strategies
[AD-A195014] 24 p3427 N88-30396

SPACECRAFT DESIGN
NT SATELLITE DESIGN
Spacecraft 2000 program overview 01 p0015 N88-10085
Space station platforms 01 p0015 N88-10086
Space Assembly, Maintenance, and Servicing Study (SAMSS) 01 p0015 N88-10089
Spacecraft Systems Working Group report 01 p0015 N88-10091
System Development Working Group report 01 p0016 N88-10092
Structures and Materials Working Group report 01 p0016 N88-10093
Thermal Control Working Group report 01 p0016 N88-10094
COSMIC — Coherent Optical System of Modular Image Collectors (COSMIC); spaceborne telescope 01 p0095 N88-10623
Proposed studies of a 30 meter imaging interferometer concept — spaceborne astronomy 01 p0096 N88-10627
NASA/JPL study on optical imaging interferometry in space 01 p0096 N88-10630
Aerospace research at the National Aerospace Laboratory (NLR)
[ETN-87-90821] 01 p0107 N88-10697
Determination of life cycle costs in astronautics
[MBB-UR-E-910/86-PUB] 02 p0249 N88-11572
Electromagnetic compatibility (EMC) phenomena and prevention of the effects — spacecraft 03 p0274 N88-11731
Aeroassisted manned transfer vehicle (TAXI) for advanced Mars Transportation: NASA/USRA 1987 Senior Design Project
[NASA-CR-181478] 03 p0275 N88-11736
Adaptive control of Large Space Structure (LSS)
[ISAS-R-621] 03 p0276 N88-11740
Space station integrated propulsion and fluid system study: Fluid systems configuration databook
[NASA-CR-179215] 03 p0278 N88-11753
Design study for asteroidal exploitation 03 p0389 N88-12445
New feedback design methodologies for large space structures: A multi-criterion optimization approach 04 p0408 N88-12535
General aerodynamic-aerothermodynamic concepts for Hermes 05 p0535 N88-13251
Hermes propulsion system
[SNIAS-872-422-109] 05 p0556 N88-13383
Introduction to local area network design on Ariane 5 and future launchers
[SNIAS-872-422-102] 05 p0635 N88-13886
Auxiliary propulsion technology for advanced Earth-to-orbit vehicles
[NASA-TM-100237] 06 p0674 N88-14127
NAL news updated: FY87 business plan, developments 06 p0675 N88-14135
Airborne particulate matter in spacecraft
[NASA-CP-2499] 06 p0753 N88-14623
Safety philosophy, policy, and requirements for manned spaceflight. Volume 1: Executive summary
[HEG-0886/1036-VOL-1] 08 p0962 N88-15826
Space station accommodations for life sciences research facilities. Phase 1: Conceptual design and programmatics studies for Missions SAAX0307, SAAX0302 and the transition from SAAX0307 to SAAX0302. Volume 2: Study results
[NASA-CR-179244] 08 p0962 N88-15829
The TV-SAT/TDF/TELE-X pyrotechnical system
[CNES-87/CT/DRT/TVE/IL/358] 08 p0974 N88-15891
Space Infrared Telescope Facility (SIRTF) design and thermal analysis 08 p0982 N88-15934
FMEAssist: A knowledge-based approach to Failure Modes and Effects Analysis 08 p1060 N88-16395
Space station overview 09 p1129 N88-16780
The Columbus program, an overview 09 p1130 N88-16784
Columbus feasibility studies. Volume 1: Requirements and system concept
[ETN-88-91073] 09 p1134 N88-16799
Columbus feasibility studies. Volume 2: Element constituents, mechanical
[ETN-88-91074] 09 p1134 N88-16800
Columbus feasibility studies. Volume 3: Avionics, systems
[ETN-88-91075] 09 p1134 N88-16801
Model of space platform electromagnetic (EMC) configuration
[ESA-CR(P)-2500] 09 p1135 N88-16809
Kinetic isolation tether experiment
[NASA-CR-182458] 09 p1135 N88-16810
Design knowledge capture for the space station 09 p1208 N88-17239
Apollo Lightcraft project
[NASA-CR-182575] 11 p1445 N88-18615
Spacecraft telecommunications system mass estimates 11 p1473 N88-18784
The 58th Shock and Vibration Symposium, volume 2
[NASA-CP-2488-VOL-2] 11 p1499 N88-18948
Spacecraft redesign to reduce microphonic response of a VCO component 11 p1499 N88-18955
Man-Tended Free Flyer operational design features 12 p1585 N88-19485
Multimission Modular Spacecraft (MMS). A serviceable design spacecraft 12 p1587 N88-19501
Columbus Simulation Facility (CSF) 12 p1590 N88-19522
Alternative program approaches for the advanced satellite technology program
[AD-A188917] 12 p1600 N88-19576
Space Station Human Factors Research Review. Volume 3: Space Station Habitability and Function: Architectural Research
[NASA-CP-2426-VOL-3] 12 p1650 N88-19883
Space station architectural elements model study. Space station human factors research review 12 p1650 N88-19884
Radiation problems in manned space flight with a view to the Space Station 12 p1658 N88-19934
Flight Vehicle Development Time and Cost Reduction
[AGARD-CP-424] 12 p1700 N88-20173
Mars Lander/Rover vehicle development: An advanced space design project for USRA and NASA/OAST
[NASA-CR-182562] 12 p1709 N88-20226
Mars Lander/Rover vehicle development: An advanced space design project for USRA and NASA/OAST
[NASA-CR-182571] 12 p1709 N88-20227
Study on long term evolution Towards European Autonomous Manned Spaceflight (STEAMS)
[SNIAS-SE/LS/AP-35-073] 13 p1727 N88-20330
On the sensitivity of complex, internally coupled systems
[NASA-TM-100537] 13 p1813 N88-20829
Docking/berthing subsystem: Design and breadboard test 14 p1879 N88-21233
Nonlinear analysis and optimal design of dynamic mechanical systems for spacecraft application
[AD-A190644] 15 p2026 N88-22070
Study of surface discharges
[ONERA-12/7236-PY] 15 p2026 N88-22073
Japanese space station module 15 p2052 N88-22224
External tank gamma ray imaging telescope study. Final review, phase 2
[NASA-CR-179320] 15 p2150 N88-22634
A pyrotechnical opening valve
[SNIAS-MU/TYS-NT-2-06(0)] 16 p2167 N88-22922
Manned Mars mission accommodation: Sprint mission
[NASA-TM-100598] 16 p2290 N88-23711
Technology development program for twenty-first century aerospace vehicles 17 p2302 N88-23768
Colombus feasibility studies, executive summary
[ETN-88-92334] 17 p2311 N88-23820
Advanced EVA system design requirements study 17 p2380 N88-24147
Space Station Human Factors Research Review. Volume 4: Inhouse Advanced Development and Research
[NASA-CP-2426-VOL-4] 17 p2380 N88-24148
Space station proximity operations and window design 17 p2380 N88-24149
Radiation hardening design of nuclear powered spacecraft 17 p2407 N88-24315
A review of impact design criteria for space power heat rejection systems 17 p2410 N88-24333
Relating design and environmental variables to reliability 17 p2418 N88-24383
Progress and future directions in computational fluid dynamics
[NASA-TM-100091] 18 p2456 N88-24579
High speed and high angle of attack aerodynamic characteristics of winged space vehicle
[ISSN-0285-6808] 18 p2459 N88-24599
Attitude control laws for gas-jet spacecraft 18 p2467 N88-24643
Structural margins assessment approach
[NASA-TM-100332] 18 p2473 N88-24672
Mars rover/sample return mission requirements affecting space station
[NASA-CR-172048] 18 p2594 N88-25414
Weight savings in aerospace vehicles through propellant scavenging
[NASA-TM-100900] 19 p2605 N88-25470
Boundary layer simulator (BLIMPJ) improvement 19 p2627 N88-25582
Numerical simulations of aerodynamic contribution of flows about a space-plane-type configuration 19 p2635 N88-25632
Considerations for spacecraft design for MSAT 19 p2651 N88-25741
Recent research on crew wardroom habitability for the Space Station 19 p2698 N88-26039
Marine techniques: R and D axes, identification of areas of common interest with space techniques 19 p2699 N88-26047
Design and testing of a high power spacecraft thermal management system
[NASA-TM-4051] 20 p2764 N88-26389
EXSAT: Expert system to configure telecommunication satellites
[SNIAS-881-440-101] 21 p2902 N88-27223
Design of booster wound structures — spacecraft structures
[SNIAS-881-430-102] 21 p2903 N88-27228
Literal dynamic modeling
[REPT-881-440-114] 22 p3048 N88-28083
Performance and technical tolerance — space projects 22 p3160 N88-28812
Study of standard generic approach for spacecraft (S/C) autonomy and automation (phase 3). Book A: Autonomy concept description
[ESA-CR(P)-2555-VOL-1] 23 p3185 N88-28955
Study of standard generic approach for spacecraft (S/C) autonomy and automation (phase 3). Book B: Autonomy concept application example
[ESA-CR(P)-2555-VOL-2] 23 p3185 N88-28956
Study of standard generic approach for spacecraft (S/C) autonomy and automation (phase 3). Book C: Autonomy concept summary
[ESA-CR(P)-2555-VOL-3] 23 p3185 N88-28957

Space station as a vital focus for advancing the technologies of automation and robotics
[IAF-86-62] 23 p3251 N88-29352
Study on long-term evolution towards European manned spaceflight. Volume 1: Executive summary
[ERNO-OX1-002/88-VOL-1] 24 p3330 N88-29827
Spacecraft mass estimation, relationships and engine data: Task 1.1 of the lunar base systems study
[NASA-CR-172061] 24 p3332 N88-29836
Maintenance and supply options
[NASA-CR-172062] 24 p3332 N88-29837
Study on conceptual design of spacecraft using Computer Aided Engineering (CAE)
[SNIAS-920-CA/TS] 24 p3333 N88-29841
Interim Flight Opportunity (IFO). Volume 1: Executive summary — space platform
[SE/LS/AP-36-818/CN-VOL-1] 24 p3334 N88-29849
MANIP — spacecraft modeling program
[MANIP-217A] 24 p3335 N88-29855

SPACECRAFT DOCKING

Blagov commentary on Mir station, first manning 01 p0009 N88-10051
Rendezvous and Docking Verification (RVDV) and in-orbit demonstration, executive summary
[RVD-RVDV-FR-AS-01] 06 p0673 N88-14120
Docking/Berthing Subsystem (DBS). Development part 1: Latching analysis — Columbus
[ESA-CR(P)-2479] 08 p0962 N88-15825
Orbital navigation, docking and obstacle avoidance as a form of three dimensional model-based image understanding 08 p1061 N88-16406
Rendezvous and docking verification and demonstration in orbit, executive summary
[MBB-303-16/86] 10 p1291 N88-17719
Space vehicle approach velocity judgments under simulated visual space conditions
[NASA-TM-89437] 11 p1523 N88-19094
Analysis of RVD operations in manned space missions 12 p1586 N88-19494
The RVD mission: The on-board data processing requirements 12 p1586 N88-19495
Prototype on-board software for rendezvous and docking 12 p1586 N88-19496
Long range sensor for rendezvous and docking missions 12 p1587 N88-19497
Motion simulation for in-orbit operations 12 p1589 N88-19514
EPOS: European Proximity Operations Simulation 12 p1589 N88-19515
Dynamic testing of a docking system — ground-based simulator 12 p1589 N88-19516
Rendezvous and docking (RVD) verification and demonstration in-orbit 12 p1592 N88-19531
Development of an intermodule connector for serviceable spacecraft 14 p1877 N88-21212
Docking/berthing subsystem: Design and breadboard test 14 p1879 N88-21233
Space station full-scale docking/berthing mechanisms development 14 p1927 N88-21491
Orbital navigation, docking and obstacle avoidance as a form of three dimensional model-based image understanding 17 p2388 N88-24194
Range and range rate system
[NASA-CASE-MSC-20867-1] 18 p2521 N88-24958
OMV docking simulator 23 p3255 N88-29379

SPACECRAFT ELECTRONIC EQUIPMENT

Spacecraft 2000
[NASA-CP-2473] 01 p0015 N88-10084
The ESA centralized management system for satellite electronic test and checkout instrumentation 09 p1124 N88-16731
Multicarrier demodulator design, volume 1 — communication satellites
[ESA-CR(P)-2468-VOL-1] 09 p1158 N88-16941
Multicarrier demodulator design. Volume 2: Executive summary — communication satellites
[ESA-CR(P)-2468-VOL-2] 09 p1158 N88-16942
Development of a multiplexer module for use in a spaceborne cryogenic environment based on GaAs MESFET technology
[RPT/CRY/62463/BOP] 11 p1559 N88-19335
Specifications and performance of ultrastable oscillators in the DORIS orbitography and positioning system
[ETN-88-92761] 24 p3331 N88-29831
The effects of total dose on the SEU sensitivity of CMOS static RAMS — single event upset (SEU), satellite components
[AERE-R-12779] 24 p3428 N88-30401

SPACECRAFT ENVIRONMENTS

Fourteenth Space Simulation Conference: Testing for a Permanent Presence in Space
[NASA-CP-2446] 02 p0132 N88-10829
Contamination control of the space shuttle Orbiter crew compartment 02 p0133 N88-10834
Space station contamination considerations 02 p0137 N88-10859
Contamination control concepts for space station customer servicing 02 p0137 N88-10860
Environmental life support system technology study — space flight
[ESA-CR(P)-2432] 02 p0218 N88-11371
Spacecraft Fire Safety
[NASA-CP-2476] 04 p0406 N88-12520
Fire extinguishment and inhibition in spacecraft environments 04 p0406 N88-12523
Inerting and atmospheres 04 p0406 N88-12524
Fire-related medical science 04 p0406 N88-12525
Aircraft fire safety research 04 p0406 N88-12526
Space station internal environmental and safety concerns 04 p0407 N88-12527
Microgravity combustion fundamentals 04 p0407 N88-12528
Spacecraft material flammability testing and configurations 04 p0407 N88-12529
Analysis of geophysical data bases and models for spacecraft interactions
[AD-A184809] 05 p0555 N88-13375
Flight model discharge system
[AD-A185657] 06 p0673 N88-14122
Controlled Ecological Life Support Systems (CELSS) conceptual design option study
[NASA-CR-177421] 06 p0754 N88-14625
Controlled Ecological Life Support Systems (CELSS) physiochemical waste management systems evaluation
[NASA-CR-177422] 06 p0754 N88-14626
Physiological and immunological aspects of human adaptation to temperature elevation in a closed environment 07 p0895 N88-15424
Some considerations on measuring the Newtonian gravitational constant G in an orbiting laboratory 07 p0922 N88-15603
Goal driven kinematic simulation of flexible arm robot for space station missions 08 p1059 N88-16388
GAS eleven node thermal model (GEM) 10 p1289 N88-17712
Spacecraft fire detection and extinguishment: A bibliography
[NASA-CR-180880] 11 p1444 N88-18612
NASDA's new test facilities for satellites and rockets 11 p1499 N88-18951
Survey of the Air Force P78-2 (SCATHA) satellite plasma wave data during electron gun operations
[AD-A191014] 16 p2168 N88-22926
Advancements in oxygen generation and humidity control by water vapor electrolysis
[NASA-CR-172073] 22 p3134 N88-28633

SPACECRAFT EQUIPMENT

NT SPACECRAFT ELECTRONIC EQUIPMENT
A modern space simulation facility to accommodate high production acceptance testing 02 p0134 N88-10841
Transient modeling of the thermohydraulic behavior of high temperature heat pipes for space reactor applications 02 p0136 N88-10857
Microgravity nucleation and particle coagulation experiments support
[NASA-CR-181540] 04 p0423 N88-12618
Microgravity nucleation and particle coagulation experiments support
[NASA-CR-181541] 04 p0423 N88-12619
Space station accommodations for life sciences research facilities. Phase 1: Conceptual design and programmatics studies for Missions SAAX0307, SAAX0302 and the transition from SAAX0307 to SAAX0302. Volume 2: Study results
[NASA-CR-179244] 08 p0962 N88-15829
Air Force cryocooler development for spacecraft 08 p0983 N88-15945
Issues associated with telerobotic systems in space 08 p1056 N88-16369
Task path planning, scheduling and learning for free-ranging robot systems 08 p1058 N88-16386
Heuristic search in robot configuration space using variable metric 08 p1059 N88-16389
Development of a facility using robotics for testing automation of inertial instruments 09 p1213 N88-17271
Microgravity isolation mount
[ESA-CR(P)-2480] 11 p1443 N88-18604
Development of the Extendable and Retractable Mast (ERM), Design phase 2. Volume 1 — spacecraft payloads
[RP-2010-0000-DS/09] 11 p1467 N88-18750
Covariant control of bilateral servos for in-orbit manipulation 12 p1590 N88-19520
A comparative survey of mathematical models for dynamic simulation of in-orbit manipulation operations 12 p1592 N88-19533
High efficiency, long life traveling wave tubes for future communications satellites
[NASA-TM-100837] 12 p1598 N88-19565
The preparation, assembly and mounting of RF coaxial cables
[ESA-PSS-01-718-ISSUE-1] 13 p1756 N88-20504
Proceedings of the 3rd European Space Mechanisms and Tribology Symposium
[ESA-SP-279] 14 p1874 N88-21191
The CTM program of masts and the CTM engineering model — spacecraft mechanism 14 p1874 N88-21196
The development status of the strongback array — spacecraft structure 14 p1875 N88-21201
DARM: A new deployment and retraction mechanism which does not need electric power 14 p1876 N88-21206
Robotic joint prototype for space applications 14 p1878 N88-21222
A joint actuator design for a robotic manipulator 14 p1879 N88-21232
Development of an engineering model dynamic cooler — spacecraft payloads
[F+W-TF-B-1885] 14 p1895 N88-21311
Accurate positioning of long, flexible ARM's (Articulated Robotic Manipulator) 16 p2219 N88-23243
Acoustic convective system
[NASA-CASE-NPO-17278-1-CU] 18 p2498 N88-24818
Range and range rate system
[NASA-CASE-MSC-20867-1] 18 p2521 N88-24958
Study of a magnetic refrigerator for space applications for temperatures under 20 K
[NASA-TT-20283] 19 p2641 N88-25668
Automatic calibration of space based manipulators and mechanisms
[NASA-CR-182804] 19 p2676 N88-25912
Different techniques for intervening under the sea: Possible links with space applications 19 p2697 N88-26030
Computer aided remote control: A general concept for intervention in the nuclear, underwater, and space domains 19 p2699 N88-26046
Heat pump augmented radiator for low-temperature space applications
[DE88-008369] 20 p2765 N88-26393
Transient thermal analysis of three latent heat storage configurations for rapid thermal charging
[DE88-008943] 20 p2881 N88-27104
Surface Tension Confined Liquid Cryogen Cooler (STCLCC)
[NASA-CASE-GSC-13112-1] 23 p3201 N88-29050
Material and process selection and quality control for ESA space systems and associated equipment
[ESA-PSS-01-70-ISSUE-3] 23 p3224 N88-29190
Qualification test levels for units to be derived from mechanical test data analysis — ESA
[REPT-87-158-EI/ET/AG] 24 p3381 N88-30139

SPACECRAFT GLOW

Mechanistic studies of polymeric samples exposed aboard STS 8
[NASA-CR-182364] 06 p0686 N88-14202
Vehicle glow observed on the SONDA 3
[INPE-4297-PRE/1168] 12 p1600 N88-19581
Space station contamination study: Assessment of contaminant spectral brightness 18 p2591 N88-25395
Calculation of space station infrared irradiance from atmosphere-induced emissions 18 p2591 N88-25396

SPACECRAFT GUIDANCE

Guidance and control strategies for aerospace vehicles
[NASA-CR-181579] 05 p0643 N88-13935
An analysis of the effect of aeroassist maneuvers on orbital transfer vehicle performance
[NASA-TM-89117] 06 p0672 N88-14116
Verifying shuttle onboard software using expert systems 09 p1207 N88-17237
Aeroassisted orbit transfer vehicle trajectory analysis
[NASA-TM-89138] 12 p1599 N88-19575
Computer architecture for efficient algorithmic executions in real-time systems: New technology for avionics systems and advanced space vehicles
[NASA-CR-182650] 12 p1675 N88-20016
Aeroassist flight experiment guidance Quiet Time
[NASA-TM-100556] 14 p1881 N88-21244
Identification of a star field from a spinning satellite
[CNES-NT-120] 15 p2026 N88-22074
Guidance and control strategies for aerospace vehicles
[NASA-CR-183032] 18 p2457 N88-24644
A design study of onboard navigation and guidance during aerocapture at Mars
[NASA-CR-172053] 18 p2469 N88-24654
Time minimal computation of feedback control schemes for optimal guidance problems used in space flight
[ETN-88-92989] 23 p3184 N88-28953

Ascent guidance for a winged boost vehicle
[NASA-CR-172083] 24 p3334 N88-29848

SPACECRAFT INSTRUMENTS
NT SATELLITE INSTRUMENTS
Calibration of attitude control sensors
02 p0159 N88-10995
Roentgenoradiometric analysis of aerosol in Venusian clouds by Vega-1 and Vega-2 automatic interplanetary stations 13 p1726 N88-20319
A method of atmospheric density measurements during space shuttle entry using ultraviolet-laser Rayleigh scattering
[NASA-TM-100056] 15 p2069 N88-22337
NIMBUS-7 CZCS. Coastal Zone Color Scanner imagery for selected coastal regions. North America - Europe. South America - Africa - Antarctica. Level 2 photographic product
[NASA-CR-180755] 15 p2089 N88-22447
A plasma wave instrument on the AMPTE/IRM (Active Magnetospheric Particle Tracing Explorers/Ion Release Module) spacecraft
[AD-A191216] 16 p2233 N88-23336
Measurement of galactic radio emission at frequency 37 GHz from aboard spacecraft
24 p3448 N88-30520

SPACECRAFT LANDING
NT MARS LANDING
NT PLANETARY LANDING
Applications of expert systems for satellite autonomy
08 p1066 N88-16443
Lunar base launch and landing facility conceptual design, 2nd edition
[NASA-CR-172049] 20 p2885 N88-27135

SPACECRAFT LAUNCHING
Analysis of the bivariate parameter wind differences between Jimsphere and Windsonde
[NASA-TM-4014] 01 p0072 N88-10461
Meteorological systems support to critical shuttle requirements on the Eastern Test Range --- STS
02 p0205 N88-11281
Department of Housing and Urban Development-Independent Agencies Appropriations for fiscal year 1988, Thursday, 9 April 1987: National Aeronautics and Space Administration
03 p0386 N88-12424
The determination of exhaust cloud dimensions from films of space shuttle launches
[NASA-CR-4103] 06 p0732 N88-14500
Ariane localization technique by Data Relay Satellite (DRS)
[SES/ENG/TN-548/86] 08 p0961 N88-15821
Ariane launch performance 09 p1125 N88-16743
SYLDA: A dual-launch system for Ariane
09 p1125 N88-16745
Preliminary orbit determination algorithms: Application to the Brazilian satellite
[INPE-4411-NTE/276] 12 p1594 N88-19546
Satellite acquisition: Global positioning system acquisition changes after Challenger's accident
[PB88-155536] 14 p1880 N88-21236
Radio frequency compatibility between IRS and SPOT 3: Preliminary study
[CNES-86/CT/DRT/TIT/TR/011]
14 p1905 N88-21383
JPRS report: Science and technology. China
[JPRS-CST-87-043] 15 p2053 N88-22233
Chronology of China's successful satellite launchings
15 p2053 N88-22234
Direct nuclear propulsion for Earth-to-orbit vehicles
17 p2400 N88-24271
Monitoring biological impacts of space shuttle launches from Vandenberg Air Force Base: Establishment of baseline conditions
[NASA-TM-100982] 18 p2549 N88-25133
Launch operations to support future space forces
[AD-A192679] 20 p2881 N88-27107
Design considerations for the ORION satellite: Structure, propulsion and attitude control subsystems for a small, general purpose spacecraft
[AD-A193837] 22 p3048 N88-28086
Reduced flexibility in processing Titan 4 space launch vehicles at Cape Canaveral Air Force Station
[AD-A194908] 24 p3332 N88-29834

SPACECRAFT LUBRICATION
The performance of thin solid films for satellite gears
14 p1876 N88-21209
The SPOT solar array. Box opening mechanisms physical vapor deposition (PVD)-MoS2: Lubricated slides. Functional evaluation 14 p1876 N88-21211
A test facility for the in-vacuo assessment of dry lubricants and small mechanisms at cryogenic temperatures 14 p1878 N88-21224

SPACECRAFT MAINTENANCE
A data structure and algorithm for fault diagnosis
08 p1065 N88-16432
Remote manipulation in orbital construction, servicing and repair missions: Is one arm enough? A comparative evaluation of the performance features of robots with one or more arms 12 p1588 N88-19509
Remote repair demonstration of Solar Maximum main electronics box 12 p1588 N88-19510
Treatment of unforeseen situations by online knowledge-based diagnostic systems --- spacecraft maintenance 12 p1589 N88-19511
Review of commercial spacecraft: Recovery and repair experiences. Implications for future spacecraft designs and operations 12 p1591 N88-19528

SPACECRAFT MANEUVERS
NT ORBITAL MANEUVERS
An analysis of the effect of aeroassist maneuvers on orbital transfer vehicle performance
[NASA-TM-89117] 06 p0672 N88-14116
Dynamics formulations for the real-time simulation of constrained motion 06 p0795 N88-14872
The dynamics and control of large-flexible space structures, part 10
[NASA-CR-182426] 08 p0963 N88-15830
Large-angle slewing maneuvers for flexible spacecraft
[NASA-CR-4123] 08 p1000 N88-16060
EPOS: European Proximity Operations Simulation
12 p1589 N88-19515
Aeroassist flight experiment guidance Quiet Time
[NASA-TM-100556] 14 p1881 N88-21244
Orbital navigation, docking and obstacle avoidance as a form of three dimensional model-based image understanding 17 p2388 N88-24194
SIRTF nod maneuvers
[NASA-TM-101007] 22 p3048 N88-28085

SPACECRAFT MODELS
Efficient placement of structural dynamics sensors on the space station
[NASA-CR-172015] 01 p0017 N88-10103
Evaluation of the infrared test method for the olympus thermal balance tests 02 p0136 N88-10956
Modeling of environmentally-induced effects within satellites. Part 1: NASCAP modeling of satellites
03 p0273 N88-11721
Modeling of environmentally-induced transients within satellites. Part 2: Discharge coupling transients
03 p0273 N88-11722
Flight model discharge system
[AD-A185657] 06 p0673 N88-14122
Thermal structural control modelling techniques --- spacecraft
[FOK-TR-R-86-030] 08 p0962 N88-15828
Dynamic tests of the Ariane launch vehicle
09 p1126 N88-16749
GAS eleven node thermal model (GEM)
10 p1289 N88-17712
Columbus Simulation Facility (CSF)
12 p1590 N88-19522
Dynamics modeling, simulation, and control of a spacecraft/manipulator system
12 p1592 N88-19534
Literal dynamic modeling
[REPT-881-440-114] 22 p3048 N88-28083
Procedures for updating dynamic mathematical models, test phase --- spacecraft hardware
[MEBS-38/87] 24 p3335 N88-29852
MANIP --- spacecraft modeling program
[MANIP-217A] 24 p3335 N88-29855

SPACECRAFT MODULES
NT COMMAND MODULES
NT LANDING MODULES
NT LUNAR LANDING MODULES
Space station internal environmental and safety concerns 04 p0407 N88-12527
Controlled Ecological Life Support Systems (CELSS) conceptual design option study
[NASA-CR-177421] 06 p0754 N88-14625
Columbus pressurized module utilization study, executive summary
[CS-RP-AI-027] 07 p0825 N88-15005
Flight results of the ESA experiment modules in Materials Science Experiment Rocket (MASER) 1
08 p1033 N88-16261
Satellite assembly in geostationary orbit: A plug-and-socket concept 09 p1128 N88-16769
Space station overview 09 p1129 N88-16780
Columbus feasibility studies. Volume 2: Element constituents, mechanical
[ETN-88-91074] 09 p1134 N88-16800
In-orbit and laboratory exchange of ORUs designed/not designed for servicing 12 p1587 N88-19499
Multimission Modular Spacecraft (MMS). A serviceable design spacecraft 12 p1587 N88-19501
CRRES chemical release mechanisms
14 p1874 N88-21192
Development of an intermodule connector for serviceable spacecraft 14 p1877 N88-21212
Docking/berthing subsystem: Design and breadboard test 14 p1879 N88-21233
Space station architectural elements model study
[NASA-CR-4027] 18 p2464 N88-24632
Habitability of the Space Station: From vehicle to living space 19 p2697 N88-26033
Recent research on crew wardroom habitability for the Space Station 19 p2698 N88-26039
Maintenance and supply options
[NASA-CR-172062] 24 p3332 N88-29837
Alternative module configurations for advanced solar arrays on low orbit and extended lifetime missions (AMOC 2)
[ESA-CR(P)-2581] 24 p3389 N88-30182

SPACECRAFT MOTION
Relative motion near the triangular libration points in the Earth-Moon system 01 p0097 N88-10636
Concept definition study for recovery of tumbling satellites. Volume 2: Supporting research and technology report
[NASA-CR-179229] 06 p0672 N88-14117
Concept definition study for recovery of tumbling satellites. Volume 1: Executive summary, study results
[NASA-CR-179228] 06 p0672 N88-14118
Low gravity liquid motions in spacecraft
08 p0982 N88-15941
Single-burn transfer to nominally periodic orbit in the vicinity of point L2 of Earth-Sun system and related problems 08 p1006 N88-16100
The nonlinear dynamics of a spacecraft coupled to the vibration of a contained fluid
[DE88-007035] 16 p2168 N88-22925
Contribution to the numerical solution of airplane spin motion
[ETN-88-92368] 21 p2896 N88-27190
Approximation of atmospheric density by Chebyshev polynomials in predicting motion of low artificial earth satellites 24 p3445 N88-30503

SPACECRAFT ORBITAL ASSEMBLY
U ORBITAL ASSEMBLY

SPACECRAFT ORBITS
NT GEOSYNCHRONOUS ORBITS
NT POLAR ORBITS
NT SATELLITE ORBITS
NT STATIONARY ORBITS
NT TRANSFER ORBITS
Thermal testing by internal IR heating of the FEP module 02 p0136 N88-10854
Limitation of spacecraft orbit near colinear libration center of limited elliptical three body problem
08 p1003 N88-16075
Orbital navigation, docking and obstacle avoidance as a form of three dimensional model-based image understanding 08 p1061 N88-16406
Optimal thrust vector control of coplanar orbital evasive maneuvers
[AD-A189544] 13 p1730 N88-20346
Canonical variables and canonical integrals for motion in near-circular orbits 24 p3446 N88-30512

SPACECRAFT PERFORMANCE
COS-B in-orbit study
[ESA-CR(P)-2420] 01 p0017 N88-10102
MARECS-A case 03 p0274 N88-11729
RETE experiment Assembly, Integration, and Verification (AIV) activities
[IFSI-87-6] 05 p0555 N88-13380
Why mechanisms are critical to spacecraft performance 09 p1125 N88-16737
Predictive monitoring research: Summary of the PREMON system
[NASA-CR-182687] 13 p1824 N88-20905
Design and testing of a high power spacecraft thermal management system
[NASA-TM-4051] 20 p2764 N88-26389
Survey of SPOT-1 operation 22 p3115 N88-28507
Verification and tests --- space projects
22 p3160 N88-28814
A scheduling and resource management system for space applications 23 p3256 N88-29383
Study of the assembly, integration and verification programs of telecommunication satellites applicable to other satellite programs
[MATRA-100/CC/MLG/031/87]
24 p3334 N88-29847

SPACECRAFT POWER SUPPLIES
Electrical Power Working Group report
01 p0016 N88-10095
A matter-antimatter propulsion system for manned interstellar flight
[DE87-013311] 02 p0141 N88-10885
BRASILSAT A2: Ground and in-orbit anomalies
02 p0164 N88-11032
International Ultraviolet Explorer (IUE) spacecraft battery performance update 02 p0164 N88-11033
Earth Radiation Budget Satellite (ERBS) orbiting profiles and Ni-Cd use 02 p0165 N88-11034

Flight experience of solar mesosphere explorer's power system over high temperatures ranges
02 p0165 N88-11037
Real time charge efficiency monitoring for nickel electrodes in NICD and NIH2 cells
02 p0165 N88-11038
Gas-cooled reactor for space power systems
[DE87-011549] 02 p0233 N88-11471
Environmental interactions of solar generators in space 03 p0274 N88-11730
Photovoltaic power modules for NASA's manned space station
[NASA-TM-100229] 03 p0277 N88-11745
SPRE 1 free-piston Stirling engine testing at NASA Lewis Research Center
[NASA-TM-100241] 03 p0277 N88-11747
The ac power system testbed
[NASA-CR-175068] 03 p0309 N88-11948
Recent progress in space photovoltaic systems
[NASA-TM-100208] 03 p0311 N88-11966
Overview of free-piston Stirling engine technology for space power application
[NASA-TM-88886] 03 p0386 N88-12427
Low Earth orbit environmental effects on the space station photovoltaic power generation systems
[NASA-TM-100230] 03 p0387 N88-12429
Study of Plasma Motor Generator (PMG) tether system for orbit reboost
[NASA-CR-172016] 04 p0403 N88-12501
Space station resistojet system requirements and interface definition study
[NASA-CR-180832] 04 p0409 N88-12541
Low gravity fluid-thermal experiments
[DE88-000553] 04 p0423 N88-12620
The effect of maximum-allowable payload temperature on the mass of a multimegawatt space-based platform
[DE88-001921] 05 p0555 N88-13381
Making space nickel/hydrogen batteries lighter and less expensive
[DE88-000168] 05 p0578 N88-13530
The high performance solar array GSR3
[SNIAS-872-422-108] 05 p0622 N88-13814
Progress toward the evolution of a Stirling space engine
[NASA-TM-100221] 05 p0659 N88-14046
Status of 20 kHz space station power distribution technology
[NASA-TM-100781] 08 p0964 N88-15838
A knowledge-based system for monitoring the electrical power system of the Hubble Space Telescope
08 p1058 N88-16380
Artificial intelligence and space power systems automation 08 p1058 N88-16381
The European space battery test center
09 p1125 N88-16738
Solar pumped, alkali vapor laser
[AD-A187156] 09 p1170 N88-17016
Study of large solar arrays (SOLA), phase 2A
[BAE-SS/1109] 09 p1186 N88-17106
Study of Large Solar Arrays (SOLA). Phase 2A: Amplifying information to final report (SS/1109)
[BAE-SS/1110] 09 p1248 N88-17480
Simulation test beds for the space station electrical power system
[NASA-TM-100786] 10 p1290 N88-17715
ESL batteries and multi-segment applications — ESA Simulation Language (ESL)
[CS-1029/00-QFIN4] 10 p1322 N88-17901
Creep behavior of tungsten/niobium and tungsten/niobium-1 percent zirconium composites
[NASA-TM-100804] 11 p1460 N88-18707
Computer-aided modeling and prediction of performance of the modified Lundell class of alternators in space station solar dynamic power systems
[NASA-CR-182538] 11 p1507 N88-19000
Development of encapsulated lithium hydride thermal energy storage for space power systems
[DE88-004762] 11 p1507 N88-19001
Solar dynamic power system definition study
[NASA-CR-180877] 13 p1733 N88-20361
Advanced sensible heat solar receiver for space power
[NASA-TM-100847] 14 p1882 N88-21249
Power systems for production, construction, life support and operations in space
[NASA-TM-100838] 14 p1883 N88-21254
Test facilities of the structural dynamics branch of NASA Lewis Research Center
[NASA-TM-100800] 14 p1934 N88-21534
Thermophotovoltaic space power system, phase 3
[NASA-CR-179327] 14 p1942 N88-21585
Thermal analysis of heat storage canisters for a splar dynamic, space power system
[DE88-004199] 15 p2027 N88-22075
Development of an integrated heat pipe-thermal storage system for a solar receiver
[NASA-TM-101099] 15 p2091 N88-22458
Development of a slip-ring system for energy transfer in space conditions. Space flight qualification and extended life tests
[BMFT-FB-W-86-019] 16 p2169 N88-22932
The 1988 overview of free-piston Stirling technology for space power at the NASA Lewis Research Center
[NASA-TM-100795] 16 p2170 N88-22934
An integrated and modular digital modeling approach for the space station electrical power system development
[NASA-TM-100904] 16 p2170 N88-22935
Value of energy storage in pulsed space power systems
[AD-A191311] 16 p2170 N88-22938
The application of high temperature superconductors to space electrical power distribution components
[NASA-TM-100901] 16 p2171 N88-22939
Comparison of electrically driven lasers for space power transmission
[NASA-TM-4045] 16 p2212 N88-23197
Aerospace energy systems laboratory: Requirements and design approach
[NASA-TM-100423] 17 p2390 N88-24206
Parametric analysis of power requirements for space-based radar 17 p2399 N88-24260
Megawatt level electric propulsion perspectives
17 p2404 N88-24294
The Light-Weight Radioisotope Heater Unit (LWRHU): Development and application 17 p2405 N88-24299
MHW RTG performance during LES 8/9 and Voyager missions 17 p2405 N88-24300
Foil gas bearing system endurance testing dynamic isotope power system 17 p2405 N88-24302
Two-phase fluid management for a Rankine cycle isotope power system 17 p2405 N88-24303
Reactor instrumentation and control design and performance simulation for SP-100
17 p2406 N88-24306
A review of thermionic power conversion systems for SDI applications 17 p2407 N88-24310
Radiation hardening design of nuclear powered spacecraft 17 p2407 N88-24315
The effect of operating temperature on open, multimegawatt space power systems
17 p2414 N88-24352
Transactions of the Fifth Symposium on Space Nuclear Power Systems
[DE88-006165] 17 p2417 N88-24374
Air Force space power requirements and nuclear power assessment methodology 17 p2418 N88-24378
Thermal and power availability transient responses for the Argonne monolithic solid oxide fuel cell
17 p2419 N88-24384
Review of power requirements for satellite remote sensing systems 17 p2419 N88-24387
Individual satellite power requirements calculated from specified constellation performance
17 p2420 N88-24392
A transient model for liquid metal heat pipes
17 p2421 N88-24398
The dynamic isotope power system: Technology status and demonstration program 17 p2422 N88-24400
Characteristics of the closed Brayton cycle for dynamic isotope power systems 17 p2422 N88-24401
Status of the organic Rankine cycle for space applications 17 p2422 N88-24402
Status of modular RTG technology
17 p2422 N88-24403
Optimization of organic Rankine cycles for space station applications 17 p2423 N88-24407
Energy storage evaluation for burst power applications
17 p2426 N88-24430
Energy storage for nuclear burst power systems
17 p2426 N88-24431
Candidate advanced energy storage concepts for multimegawatt burst power systems
17 p2426 N88-24434
A multimegawatt space power source radiator design
17 p2427 N88-24436
The liquid droplet radiator in space: A parametric approach 17 p2427 N88-24437
Space Power Reference Source (SPRS): A user's guide to SDI Space Power Technology Programs
17 p2427 N88-24440
Gigawatt, closed cycle, vapor core-MHD space power system conceptual design study
17 p2433 N88-24473
Critical issues for SOAR: The space orbiting advanced fusion power reactor 17 p2433 N88-24474
Comparison of 20-kWe space nuclear power systems: Impact of reactor temperature and technology upon system design and performances 17 p2433 N88-24475
Potassium Rankine power system for space power
17 p2433 N88-24476
Low cross-section Mo-Nb thermocouples for nuclear application: The state-of-the-art
17 p2433 N88-24477
Material property and irradiation performance correlations for nitride fuels 17 p2434 N88-24483
SNAP fuel performance 17 p2435 N88-24484
SNAP-DYN: Concepts for multikilowatt space power applications 17 p2435 N88-24486
The closed Brayton cycle: An energy conversion system for near-term military space missions
17 p2435 N88-24488
The effect of operating temperature and turbine blade cooling on Brayton cycle space power systems
17 p2435 N88-24489
A combined Rankine/Brayton pulse power cycle
17 p2435 N88-24490
Energy conversion system optimization study for multimegawatt space nuclear power application
17 p2436 N88-24492
Automatic reactor control system for transient operation 17 p2436 N88-24493
Alkali metal thermoelectric converter design for space power systems applications 17 p2437 N88-24499
A capillary pumped SHE/AMTEC system
17 p2437 N88-24500
High power density electrodes for AMTEC
17 p2437 N88-24501
Multimegawatt power conditioning requirements study
17 p2438 N88-24504
Lightweight power bus for a baseload nuclear reactor in space 17 p2438 N88-24505
Component improvement of free-piston Stirling engine key technology for space power
[NASA-TM-100950] 19 p2607 N88-25476
Hydrogen turbines for space power systems: A simplified axial flow gas turbine model
[DE88-009585] 19 p2677 N88-25920
Effect of LEO cycling at shallow depths of discharge on MANTECH IPV nickel-hydrogen cells
[NASA-TM-101300] 19 p2688 N88-25978
The design and fabrication of a Stirling engine heat exchanger module with an integral heat pipe
[NASA-TM-101296] 20 p2820 N88-26732
Refractory metal alloys and composites for space power systems
[NASA-TM-100946] 21 p2916 N88-27310
Space photovoltaic generators. State of the art, trends
[REPT-881-440-106] 21 p2970 N88-27640
Arcjet power supply and start circuit
[NASA-CASE-LEW-14374-1] 23 p3181 N88-28939
Thin film coatings for space electrical power system applications
[NASA-TM-101325] 23 p3187 N88-28966
Solar dynamic power systems
[ETN-88-92969] 23 p3230 N88-29224
Possibilities of economical improvements for Moon based rocket propulsion using lunar propellants
[ILR-MITT-196] 24 p3338 N88-29871
Alternative module configurations for advanced solar arrays on low orbit and extended lifetime missions (AMOC 2)
[ESA-CR(P)-2581] 24 p3389 N88-30182
Fuel cells for space use
[FCP-TR-DOS-SY-026] 24 p3389 N88-30183

SPACECRAFT PRELAUNCH TESTS
U SPACE VEHICLE CHECKOUT PROGRAM

SPACECRAFT PROPULSION
NT ELECTROMAGNETIC PROPULSION
NT ELECTROSTATIC PROPULSION
NT ION PROPULSION
NT MASS DRIVERS (PAYLOAD DELIVERY)
NT PLASMA PROPULSION
NT SOLAR THERMAL PROPULSION
Spacecraft 2000
[NASA-CP-2473] 01 p0015 N88-10084
A matter-antimatter propulsion system for manned interstellar flight
[DE87-013311] 02 p0141 N88-10885
Auxiliary propulsion system flight package
[NASA-CR-180828] 02 p0141 N88-10886
High temperature metal matrix composites for future aerospace systems
[NASA-TM-100212] 02 p0149 N88-10938
Space station propulsion
[NASA-TM-100216] 03 p0277 N88-11746
A low-power arcjet cyclic lifetest
[NASA-TM-100233] 03 p0278 N88-11748
Thrust and specific impulse of repetitively-pulsed-laser propulsion rocket 03 p0318 N88-12012
Design study for asteroidal exploitation
03 p0389 N88-12445
Interplanetary propulsion using inertial fusion
[NASA-TM-89661] 04 p0409 N88-12540

The VISTA spacecraft: Advantages of ICF (Inertial Confinement Fusion) for interplanetary fusions propulsion applications
[NASA-CR-181549] 04 p0491 N88-13024
Space station onboard propulsion system: Technology study
[NASA-CR-179233] 07 p0825 N86-15006
Advanced fusion power: A preliminary assessment
[AD-A185903] 07 p0933 N88-15664
Space station propulsion technology
[NASA-CR-179260] 08 p0964 N88-15835
Selection of efficient correcting motor for an artificial Earth satellite 08 p1007 N88-16102
Electric propulsion: A controversial must for long-lived applications satellites 09 p1124 N88-16735
Rocket and airjet propulsion for ballistic and aerodynamic space probes
[REPT-TR-527] 10 p1310 N88-17826
Soviet space transport systems
13 p1727 N88-20328
Advanced space propulsion study - antiproton and beamed power propulsion
[AD-A189218] 13 p1732 N88-20355
Cermet-fueled reactors for advanced space applications
[DE88-005528] 13 p1839 N88-21002
Test facilities of the structural dynamics branch of NASA Lewis Research Center
[NASA-TM-100800] 14 p1934 N88-21534
Prospects for antiproton production and propulsion
16 p2267 N88-23556
Heat transfer in aerospace propulsion
[NASA-TM-100874] 17 p2339 N88-23957
The results of application studies for space nuclear power 17 p2398 N88-24259
History of some direct nuclear propulsion developments since 1946 17 p2400 N88-24270
Interplanetary propulsion using inertial fusion
17 p2401 N88-24273
A fusion based plasma propulsion system
17 p2401 N88-24274
Ultra high temperature direct propulsion
17 p2401 N88-24275
Safety constraints and considerations in the development of nuclear powered propulsion
17 p2401 N88-24276
A critique of NERVA based nuclear reactor design and performance for MMW space propulsion applications
17 p2404 N88-24297
Gas core reactors for direct nuclear propulsion
17 p2428 N88-24442
Status of high power electric propulsion technology
17 p2428 N88-24443
Performance and long duration test of a 30 kw thermal arcjet engine
[AD-A190962] 18 p2474 N88-24677
Development of a liquid-fed water resistojet
[NASA-TM-100927] 18 p2523 N88-24968
Propulsion analysis and application potential of air breathing combined propulsion for ballistic space transporter
[ETN-88-92369] 21 p2903 N88-27227
Performance of 10-kW class xenon ion thrusters
[NASA-TM-101292] 22 p3049 N88-28088
Gravitational propulsion 22 p3158 N88-28796
Orbital Propulsion Module (OPM). Study on coni-spherical surface tension tanks (COSTA)
[MBB-URV-170/87] 23 p3187 N88-28963
Spacecraft mass estimation, relationships and engine data: Task 1.1 of the lunar base systems study
[NASA-CR-172061] 24 p3332 N88-29836
Possibilities of economical improvements for Moon based rocket propulsion using lunar propellants
[ILR-MITT-196] 24 p3338 N88-29871

SPACECRAFT RADIATORS

Membrane heat pipe development for space radiator applications
[DE86-008015] 01 p0045 N88-10285
Considerations concerning a thermal joint for a deployable or steerable battery radiator for the Columbus Polar Platform
[NLR-TR-86055-U] 03 p0276 N88-11739
The effect of maximum-allowable payload temperature on the mass of a multimegawatt space-based platform
[DE88-001921] 05 p0555 N88-13381
Moveable thermal joints for deployable or steerable spacecraft radiator systems
[NLR-MP-87016-U] 13 p1730 N88-20347
OLYMPUS shuttle specific radiator shield
14 p1879 N88-21234
Fabric space radiators
[DE88-005569] 14 p1880 N88-21237
Development of a lightweight structure with load bearing capability and high thermal conductance
17 p2420 N88-24393
A reflux tube fabric radiator 17 p2421 N88-24394
Liquid droplet radiator development
17 p2424 N88-24415
Fabric radiators 17 p2427 N88-24435
A multimegawatt space power source radiator design
17 p2427 N88-24436
The liquid droplet radiator in space: A parametric approach 17 p2427 N88-24437
Space power radiation cooled dc transmission line analysis 17 p2438 N88-24506
Arc-textured metal surfaces for high thermal emittance space radiators
[NASA-TM-100894] 18 p2487 N88-24754
Moving belt radiator development status
[NASA-TM-100909] 19 p2607 N88-25477
Heat pump augmented radiators for spacecraft thermal management
[DE88-007890] 20 p2764 N88-26392
Development of a space deployable radiator using heat pipes
[SNIAS-881-440-104] 23 p3214 N88-29128

SPACECRAFT RECOVERY

Concept definition study for recovery of tumbling satellites. Volume 2: Supporting research and technology report
[NASA-CR-179229] 06 p0672 N88-14117
Concept definition study for recovery of tumbling satellites. Volume 1: Executive summary, study results
[NASA-CR-179228] 06 p0672 N88-14118
Rendezvous and Docking Verification (RVDV) and in-orbit demonstration, executive summary
[RVD-RVDV-FR-AS-01] 06 p0673 N88-14120
Review of commercial spacecraft: Recovery and repair experiences. Implications for future spacecraft designs and operations 12 p1591 N88-19528

SPACECRAFT REENTRY

Effects of forced and free convections on structural temperatures of space shuttle orbiter during reentry flight
[NASA-TM-86800] 01 p0043 N88-10275
Ceramic-ceramic shell tile thermal protection system and method thereof
[NASA-CASE-ARC-11641-1] 11 p1448 N88-18628
A method of atmospheric density measurements during space shuttle entry using ultraviolet-laser Rayleigh scattering
[NASA-TM-100056] 15 p2069 N88-22337
New concepts for atmospheric braking deceleration in planetary atmosphere entry
[SNIAS-CAS-DECE-P003-DPAA]
16 p2168 N88-22923
A proposed national policy concerning the reentry of space reactors 17 p2415 N88-24359

SPACECRAFT RELIABILITY

Configuration evaluation and criteria plan. Volume 2: Evaluation criteria plan (update). Space Transportation Main Engine (STME) configuration study
[NASA-CR-181429] 03 p0270 N88-11699
Natural frequencies and structural integrity assessment of large space structures
[AD-A186139] 07 p0824 N88-15001
Risk analysis in space system safety
22 p3161 N88-28825
Case study: The Hermes program product assurance
22 p3162 N88-28831
A scheduling and resource management system for space applications 23 p3256 N88-29383
Hermes: Study of propulsion system for reusable man-rated spacecraft
[PSRM-TN-0000-00-04A] 24 p3337 N88-29866

SPACECRAFT RENDEZVOUS

U SPACE RENDEZVOUS

SPACECRAFT SENSORS

U SPACECRAFT INSTRUMENTS

SPACECRAFT SHIELDING

Consortium for Materials Development in Space. Technical section
[NASA-CR-181506] 03 p0296 N88-11859
Wake shield 03 p0296 N88-11871
Optimization techniques applied to passive measures for in-orbit spacecraft survivability
[NASA-CR-179216] 04 p0408 N88-12532

SPACECRAFT STABILITY

Pinhole occulter experiment
[NASA-CR-179206] 02 p0235 N88-11481
Concept definition study for recovery of tumbling satellites. Volume 2: Supporting research and technology report
[NASA-CR-179229] 06 p0672 N88-14117
Concept definition study for recovery of tumbling satellites. Volume 1: Executive summary, study results
[NASA-CR-179228] 06 p0672 N88-14118
Modeling of a nutation damper for satellite stabilization through rotation
[INPE-4275-PRE/1147] 12 p1601 N88-19584
Vibrations of structures with parametric uncertainties
[AD-A190400] 15 p2076 N88-22378
The Proceedings of the Symposium on Mechanics for Space Flight 1987
[ISAS-SP-6] 20 p2782 N88-26499
Nutational stability of a satellite equipped with an active magnetic momentum wheel 20 p2784 N88-26513

SPACECRAFT STRUCTURES

Spacecraft surface exposure to atomic oxygen in low Earth orbit 03 p0273 N88-11715
Computational methods for problems in aerodynamics and large space structure using parallel and vector architectures
[AD-A185401] 05 p0541 N88-13294
Viscous damped space structure for reduced jitter
05 p0594 N88-13623
Evaluate the application of modal test and analysis processes to structural fault detection in MSFC - STS project elements 07 p0927 N88-15630
The development of test methodology for testing glassy materials 07 p0927 N88-15633
Thermal structural control modelling techniques — spacecraft
[FOK-TR-R-86-030] 08 p0962 N88-15828
Mechanical in-flight environment of Ariane payloads
09 p1126 N88-16748
Analytical interactive approach for phenomena involving structures, thermal and control aspects. Volume 1: Theory — spacecraft structures
[ESA-CR(P)-2503-VOL-1] 09 p1134 N88-16803
Analytical interactive approach for phenomena involving structures, thermal, and control aspects. Volume 2: Toward the solution — spacecraft structures
[ESA-CR(P)-2503-VOL-2] 09 p1134 N88-16804
Analytical interactive approach for phenomena involving structures, thermal, and control aspects. Volume 3: Executive summary — spacecraft structures
[ESA-CR(P)-2503-VOL-3] 09 p1134 N88-16805
Optimized approach to damage tolerance — spacecraft
[FOK-FSS-R-87-024] 09 p1134 N88-16806
Integrity control of carbon fiber reinforced plastics (CFRP) structural elements. Conclusion with respect to the control methodology of CFRP primary structures in manned space flight and the implications to the design, analysis and testing of CFRP structural elements, executive summary
[MBB-TR-RB517-014/85] 09 p1139 N88-16824
Measurement, data analysis and prediction of pyrotechnic shock from pin-pullers and separation joints
09 p1179 N88-17061
In-orbit automatic assembly of reticular structures
12 p1586 .N88-19491
Suspension design for a satellite transport container
[INPE-4352-TDL/296] 12 p1600 N88-19578
Development of isostatic mounts and associated guidelines — spacecraft payloads
[CASA-IM-WP-301] 13 p1731 N88-20354
Numerical solution of multibody systems in space applications 14 p1875 N88-21200
The development status of the strongback array — spacecraft structure 14 p1875 N88-21201
A sequentially deployable structure for space applications 14 p1875 N88-21202
Optimal control and identification of space structures
[AD-A190033] 15 p2025 N88-22065
Wave propagation and dynamics of lattice structures
[AD-A190037] 15 p2025 N88-22066
Vibration control of large structures
[AD-A191358] 16 p2168 N88-22928
Lewis Structures Technology, 1988. Volume 1: Structural Dynamics
[NASA-CP-3003-VOL-1] 16 p2217 N88-23226
Base reaction optimization of manipulators with redundant kinematics 16 p2219 N88-23238
Travelling wave concepts for the modeling and control of space structures
[AD-A191235] 17 p2310 N88-23819
Structural acoustics design manual
[ESA-PSS-03-1201-ISSUE-1] 17 p2311 N88-23821
Insert design handbook
[ESA-PSS-03-1202-ISSUE-1] 17 p2311 N88-23822
Progress and future directions in computational fluid dynamics
[NASA-TM-100091] 18 p2456 N88-24579
Study of the influence of metallurgical factors on fatigue and fracture of aerospace structural materials
[AD-A192909] 20 p2774 N88-26452
Design of booster wound structures — spacecraft structures
[SNIAS-881-430-102] 21 p2903 N88-27228
Reinforced plastics: Winding and weaving technologies for space products
[SNIAS-881-430-103] 21 p2922 N88-27341
Vibration control of large structures
[AD-A193317] 21 p2961 N88-27587

Optical method to measure the deformations of structures loaded by hydraulic pressure
[SNIAS-881-430-111] 22 p3088 N88-28338
Nondestructive investigations for space use
[SNIAS-881-430-105] 23 p3224 N88-29189
Dynamics of articulated aerospace structures
[AD-A195685] 24 p3324 N88-29794
Sensor and actuator selection for large space structure control
[AD-A194912] 24 p3333 N88-29842
Laser sensing for identification and control of distributed parameter systems
[AD-A195886] 24 p3379 N88-30124

SPACECRAFT SURVIVABILITY
Spacecraft fire detection and extinguishment: A bibliography
[NASA-CR-180880] 11 p1444 N88-18612
The use of liquid films for spacecraft survivability to laser radiation
[AD-A192954] 20 p2765 N88-26395
SCARES: A Spacecraft Control Anomaly Resolution Expert System 23 p3256 N88-29381

SPACECRAFT TELEVISION
NT SATELLITE TELEVISION

SPACECRAFT TEMPERATURE
Effects of forced and free convections on structural temperatures of space shuttle orbiter during reentry flight
[NASA-TM-86800] 01 p0043 N88-10275
The effect of maximum-allowable payload temperature on the mass of a multimegawatt space-based platform
[DE88-001921] 05 p0555 N88-13381
EUREX D: An expert system for failure diagnosis and recovery in the TCS of the European retrievable carrier EURECA 08 p1058 N88-16385
Moveable thermal joints for deployable or steerable spacecraft radiator systems
[NLR-MP-87016-U] 13 p1730 N88-20347
Feasibility demonstration of a sensor for high-quality two-phase flow --- Space Station
[NLR-TR-87009-U] 13 p1767 N88-20569
MTK: An AI tool for model-based reasoning 17 p2387 N88-24189
Heat pump-augmented systems for spacecraft thermal management 17 p2424 N88-24419
The Curie point radiator 17 p2424 N88-24420
Design and testing of a high power spacecraft thermal management system
[NASA-TM-4051] 20 p2764 N88-26389
Biorack thermal performance during the D1 mission --- Spacelab 22 p3062 N88-28170
The heat pipe network of TDF-1/TV-SAT. Review of the development at completion
[SNIAS-881-440-103] 23 p3213 N88-29127
Reasoning about fault diagnosis for the space station common module thermal control system 23 p3258 N88-29395
MANIP --- spacecraft modeling program
[MANIP-217A] 24 p3335 N88-29855

SPACECRAFT TRACKING
NT SATELLITE TRACKING
NT SATELLITE-TO-SATELLITE TRACKING
Spacecraft 2000
[NASA-CP-2473] 01 p0015 N88-10084
Telemetry, Tracking, and Control Working Group report 01 p0016 N88-10096
Media calibrations of the Doppler signal for a gravitational wave experiment --- interplanetary medium
[IFSI-86-13] 05 p0625 N88-13825
Investigation of design considerations for Telemetry, Tracking and Command (TT and C) antenna system on Naval Postgraduate School Orion mini-satellite
[AD-A187130] 10 p1291 N88-17718
Using ridge regression in systematic pointing error corrections 11 p1472 N88-18777
Spacecraft applications of advanced global positioning system technology
[NASA-CR-172055] 21 p2894 N88-27180
Advanced Receiver tracking of Voyager 2 near solar conjunction 22 p3065 N88-28185
Determination of the Venus flyby orbits of the Soviet Vega probes using VLBI techniques 22 p3067 N88-28203

SPACECRAFT TRAJECTORIES
NT INTERPLANETARY TRAJECTORIES
Safe and fuel minimum reference trajectories for closed loop controlled approaches --- space stations 12 p1585 N88-19488
A technique for capture analysis of low thrust missions in a planetary system
[AD-A188934] 12 p1594 N88-19544
Optimal thrust vector control of coplanar orbital evasive maneuvers
[AD-A189544] 13 p1730 N88-20346
IMP 7 (Explorer 47) trajectory, September 26, 1972 to September 25, 1978
[NASA-CR-182697] 14 p1871 N88-21183
Spacecraft trajectories
[ISBN-2-85-428166-7] 15 p2023 N88-22054

SPACECREWS
An assessment of clinical chemical sensing technology for potential use in space station health maintenance facility
[NASA-CR-172013] 04 p0475 N88-12926
Antarctica as a model for the human exploration of Mars
[AD-A185835] 08 p1051 N88-16342
Hemolysis in runners as evidenced by low serum haptoglobin: Implications for preflight monitoring of astronauts
[NASA-TM-100304] 11 p1518 N88-19067
Studies of the vestibulo-ocular reflex on STS 4, 5 and 6
[NASA-TM-100461] 12 p1666 N88-19987
An evaluation of the methods for rescuing EVA (Extravehicular Activities) crewmembers and recovering equipment detached and adrift from the space station
[AD-A189683] 14 p1871 N88-21181
Space station habitability recommendations based on a systematic comparative analysis of analogous conditions
[NASA-CR-3943] 18 p2587 N88-25372
Selecting the right crew for future space stations: An analysis of selection research on offshore divers, aviation pilots and other high risk groups in Scandinavia 19 p2696 N88-26021
Selection of isolated space crews 19 p2697 N88-26028
The US space programme spacewalk/extravehicular activity experience: Past, present and future 19 p2697 N88-26031
The human element in space: Lessons from Antarctica
[AD-A193440] 21 p2988 N88-27741
History of manned spaceflight
[CNES-NT-121] 21 p3032 N88-28000
An expert system for a distributed real-time trainer 23 p3261 N88-29411

SPACELAB
Space Station Mission Planning System (MPS) development study. Volume 1: Executive summary
[NASA-CR-179202] 01 p0009 N88-10047
Space lab system analysis
[NASA-CR-179207] 02 p0138 N88-10869
Allowable gravity-levels for Spacelab, Columbus and EURECA --- materials science
[BF-R-66.525-2] 07 p0838 N88-15084
Spacelab Data Processing Facility (SLDPF) quality assurance expert systems development 08 p1059 N88-16394
Rapid prototyping and AI programming environments applied to payload modeling 08 p1061 N88-16405
Project management in astronautics: From Spacelab to Columbus
[MBB-URE-943/87] 10 p1315 N88-17858
Spacelab: An international success story
[NASA-SP-487] 11 p1566 N88-19375
Second-generation respiratory monitoring system for microgravity studies in man 12 p1653 N88-19906
Implications of shiftwork in space for human physiology experiments 12 p1659 N88-19942
Microgravity User Support Center (MUSC) for EURECA, Spacelab and Columbus missions 12 p1660 N88-19947
The German Spacelab mission D1: Payload integration
[ETN-88-91507] 14 p1871 N88-21179
Space experiments with particle accelerators (SEPAC): Description of instrumentation
[NASA-TM-89728] 14 p1945 N88-21606
Space experiment plan FMPT 15 p2051 N88-22220
Amorphous semiconductors made in space 15 p2051 N88-22221
Containerless glass melting 15 p2051 N88-22222
Pb(1-x)Sn(x)Te crystal growth in space 15 p2051 N88-22223
Experiment scheduling for Spacelab missions 23 p3259 N88-29404
Spacelab data processing facility (SLDPF) Quality Assurance (QA)/Data Accounting (DA) expert systems: Transition from prototypes to operational systems 24 p3420 N88-30353

SPACELAB PAYLOADS
Space Station Mission Planning System (MPS) development study. Volume 2
[NASA-CR-179200] 01 p0009 N88-10048
Planning and execution of the NAVEX experiment in the Spacelab Mission D1
[DFVLR-FB-87-03] 01 p0010 N88-10056
The navigation experiment NAVEX: Experimental results of clock synchronization
[DFVLR-MITT-87-05] 03 p0271 N88-11701
First flight of the ATMOS instrument during the Spacelab 3 Mission, April 29 through May 6, 1985
[NASA-CR-182360] 06 p0728 N88-14482
Resolution of holograms produced by the fluid experiment system and the holography ground system 07 p0923 N88-15609
A backscatter lidar proposed for the second German Spacelab mission 08 p1018 N88-16173
The D-1 Biorack results: A base for further space biological investigations 08 p1033 N88-16263
The ESA Anthrorack project: Integrated research in human physiology 08 p1033 N88-16265
ESA Bulletin No. 8
[ETN-87-90513] 09 p1122 N88-16718
ASSESS-2: An aircraft simulation of Spacelab 09 p1123 N88-16723
White blood cells in space: An experiment for the first Spacelab mission 09 p1127 N88-16757
The navigation experment NAVEX: Experimental results of clock synchronization
[ESA-TT-1084] 09 p1132 N88-16791
Investigations on the application of space photographs (Spacelab metric camera) for routine inventories of extensively managed forest areas
[DFVLR-FB-87-22] 09 p1185 N88-17098
Teleoperation for a Spacelab technology experiment 12 p1590 N88-19521
ROTEX: The Robotic Technology Experiment on Spacelab D-2 mission 12 p1592 N88-19530
ESA's facility for research in human physiology in space: Anthrorack 12 p1652 N88-19896
The ESA facility Biorack 12 p1652 N88-19897
BIOTEX, a project for biotechnological basic experiments under microgravity --- Spacelab 12 p1652 N88-19899
The respiratory system under weightlessness 12 p1653 N88-19901
Gravisensing in lentil seedling roots grown in space (Spacelab D-1 mission) 12 p1654 N88-19911
The use of plant protoplasts in biotechnological space research 12 p1655 N88-19914
Vestibular response to caloric stimulation during orbital flight 12 p1658 N88-19939
Synopsis of the Spacelab D-1 frog statolith experiment STATEX 12 p1659 N88-19940
Cyropreservation of isolated rat hepathocytes for future use in Spacelab experiments: Preliminary results 12 p1660 N88-19950
Biorack experiments in Spacelab D-1 and TML-1: Further developments in gravitational biology 12 p1661 N88-19953
Application of ARIADNE: A data bank-based information system for human physiology research --- Spacelab Anthrorack 12 p1662 N88-19962
Results of one way transit time measuring in navigation experiment NAVEX
[DFVLR-MITT-87-17] 14 p1865 N88-21145
The German Spacelab mission D1: Payload integration
[ETN-88-91507] 14 p1871 N88-21179
Securing the timescale of the NAVEX-reference clock and rate determinations by time comparisons with the help of the Global Positioning System (GPS) --- Spacelab D1 mission
[DFVLR-MITT-87-20] 16 p2159 N88-22879
Navigation experiment NAVEX. The reading differences between all ground station measuring clocks during each Spacelab pass of the D1 mission
[DFVLR-MITT-87-23] 16 p2159 N88-22880
The NAVEX experiment in the Spacelab D1 mission: Planning and execution
[ESA-TT-1078] 16 p2166 N88-22913
Zone crystallization experiments in mirror heating facilities
[BMFT-FB-W-86-023] 16 p2184 N88-23016
Liquid motions in partially filled containers: Preliminary results of the D-1 mission --- Spacelab
[NLR-MP-86042-U] 20 p2802 N88-26629
Homogeneity of glasses: Experiment WL-IHF-05 in D1 mission --- Spacelab
[ETN-88-92339] 21 p2924 N88-27353
Biorack on Spacelab D1: An overview of the first flight of Biorack, an ESA facility for life sciences research in microgravity
[ESA-SP-1091] 22 p3059 N88-28154
A brief overview of the results of the experiments using the ESA Biorack Facility on the German Spacelab D1 mission 22 p3060 N88-28155
The Biorack facility and its performance during the D1 Spacelab mission 22 p3060 N88-28156
The effects of microgravity on genetic recombination in Escherichia coli --- Spacelab D1 mission 22 p3060 N88-28157

Growth and differentiation of Bacillus subtilis under microgravity conditions 22 p3060 N88-28158
The Antibio experiment — Spacelab D1 mission 22 p3060 N88-28159
Contraction behavior and protoplasmic streaming in the slime mold Physarum polycephalum (Physarum kinetics) — Spacelab D1 mission 22 p3060 N88-28160
The Paramecium experiment — Spacelab D1 mission 22 p3060 N88-28161
The biological clock of Chlamydomonas reinhardii in space 22 p3061 N88-28162
Effect of microgravity on lymphocyte activation — Spacelab D1 mission 22 p3061 N88-28163
The effect of microgravity on mammalian cell polarization at the ultrastructural level — Spacelab D1 mission 22 p3061 N88-28164
Graviperception of lentil seedling roots grown in space 22 p3061 N88-28165
Effects of short spaceflights on Drosophila melanogaster embryogenesis and life span 22 p3061 N88-28166
Embryogenesis and organogenesis of Carausius morosus under spaceflight conditions 22 p3061 N88-28167
The role of gravity in the establishment of the dorso/ventral axis in the amphibian embryo — Spacelab D1 mission 22 p3062 N88-28168
Dosimetric mapping inside Biorack — Spacelab D1 mission 22 p3062 N88-28169
Biorack thermal performance during the D1 mission — Spacelab 22 p3062 N88-28170
Biosample: Preservation, handling and observation system synthesis and breadboarding — Spacelab [ESA-CR(P)-2609] 24 p3336 N88-29857
Fluid physics double rack — Spacelab [SD-TN-AI-012] 24 p3358 N88-29992
Accommodation concept for fluid physics facilities, volume 2 — Spacelab [SG-TN-AI-027-VOL-2] 24 p3358 N88-29994

SPAIN
Physiography and kinematics of the western coast of the province of Huelva (Andalousia, Spain) 22 p3109 N88-28465

SPALLATION
Experimental measurements and numerical simulations of metal spallation by detonating solid explosives [DE87-013227] 01 p0054 N88-10347
Study of adherent oxide scales [AD-A187368] 11 p1456 N88-18680
Impact shock generator from explosively driven plates [DE88-003596] 14 p1918 N88-21452
Spallation and dynamic fracture as an effect of laser induced shock-waves [AD-A193513] 23 p3188 N88-28971

SPALLING
Mechanisms of rolling contact spalling [NASA-CR-179243] 06 p0714 N88-14380

SPANWISE BLOWING
Numerical study of delta wing leading edge blowing [NASA-CR-183101] 20 p2752 N88-26335

SPARE PARTS
A problem of machine repair with a variable number of heterogeneous servers [INPE-4245-PRE/1118] 08 p1074 N88-16482
Systems integrated human engineering on the Navy's rapid acquisition of manufactured parts/test and integration facility 09 p1206 N88-17226
Computation of ECM (Electronic Counter-Measures) war reserve materiel spare requirements [AD-A193301] 21 p2897 N88-27195
Computers in weapons systems: A look at the F-15 [AD-A194498] 23 p3178 N88-28920

SPARK CHAMBERS
Use of reinforced inorganic cement materials for spark wire and drift chamber wire frames [NASA-CR-180759] 13 p1746 N88-20438

SPARK DISCHARGES
U ELECTRIC SPARKS

SPARK GAPS
Development of a repetitive 1-MV, 22-kJ Marx generator [DE87-011286] 01 p0038 N88-10242
Characterization of surface discharge switches and high performance applications [DE87-011763] 01 p0041 N88-10261
Development of a high-energy crowbar for the Los Alamos free-electron laser [DE87-014748] 02 p0179 N88-11113
A tapered poloidal gap for the reduction of field errors [DE87-014750] 03 p0377 N88-12375

SPARK IGNITION
Japanese industrial research on lean combustion: A case study: International Research Monitoring Program [DE87-013839] 02 p0144 N88-10904
The role of low temperature chemistry in the autoignition of n-butane [DE88-002385] 07 p0829 N88-15031
Fuel nitrogen conversion in a supercharged spark ignition engine [DE88-003739] 08 p0974 N88-15893
The effects of fuel composition on ignition delay in homogeneous charge and direct injection compression ignition engines [DE88-003691] 09 p1143 N88-16849
Status of alcohol fuels utilization technology for highway transportation: A 1986 perspective. Volume 2: Compression ignition engines [DE88-006059] 13 p1753 N88-20485
Combustion and performance characteristics of methanol plus higher alcohols in a spark ignition engine [PB88-147962] 14 p1918 N88-21451
Minimum ignition energy measurements using laser induced spark initiation 19 p2632 N88-25610
Summary of discussions at the Tenth Meeting of the Sandia Cooperative Group on the Aerothermochemistry of Turbulent Combustion [DE88-008467] 21 p2910 N88-27269
Experimental validation of a zero-dimensional computer model for spark-ignition engines [DE88-009034] 21 p2957 N88-27565

SPARK MACHINING
Wire-cut electrical discharge machinability of ceramics [AD-A186989] 09 p1146 N88-16870

SPARK SHADOWGRAPH PHOTOGRAPHY
U SHADOWGRAPH PHOTOGRAPHY

SPARKS
NT ELECTRIC SPARKS
Coupling of a spark source mass spectrograph and a ND-YAG laser [DE88-012116] 21 p2951 N88-27530

SPAS (ESA PLATFORMS)
U SHUTTLE PALLET SATELLITES

SPATIAL DEPENDENCIES
Spatial strength variation and statistical size effect of laminated orthotropic composite materials 04 p0427 N88-12646

SPATIAL DISTRIBUTION
NT STAR DISTRIBUTION
Method for single-shot measurement of picosecond laser pulse-lengths without electronic time dispersion [DE87-013171] 02 p0178 N88-11107
Forecasting stratus over the British Isles 02 p0209 N88-11310
Structural frequency functions for an impulsive, distributed forcing function [DE87-013811] 03 p0333 N88-12101
Illustrations of a density-equalizing map projection technique [DE87-013892] 03 p0339 N88-12130
Cloud cover determination in polar regions from satellite imagery [NASA-CR-181544] 04 p0471 N88-12908
The giant spot on ll Peg in 1986 04 p0508 N88-13120
Structural frequency functions for an impulsive, distributed forcing function 05 p0594 N88-13627
Meteor velocity distribution and an optimum monitoring mathematical model 06 p0739 N88-14546
On the spatial structure of the Perseids meteor stream 06 p0740 N88-14550
The use of chlorophyll fluorescence measurements from space for separating constituents of sea water. Volume 1: Summary [ESA-CR(P)-2444-VOL-1] 07 p0673 N88-15294
The use of chlorophyll fluorescence measurements from space for separating constituents of sea water. Volume 2: Appendices [ESA-CR(P)-2444-VOL-2] 07 p0673 N88-15295
Acoustic scattering from composite wind-wave surfaces 3: Forward scatter intensities and spatial coherence at low and high frequencies and small grazing angles for Bubble-free regimes [AD-A185908] 07 p0681 N88-15345
A directed method for locating the focus of expansion [AD-A185840] 07 p0906 N88-15491
Study on the mechanical stresses in the elements of the model of a toroidal magnet of a tokamak with strong field [DE88-700343] 07 p0935 N88-15679
Longitudinal variations of equatorial ionosphere determined from Intercosmos-19 artificial Earth satellite data 08 p1003 N88-16074
Predictability of ice concentration in the high-latitude North Atlantic from statistical analysis of SST (Sea Surface Temperature) and ice concentration data [AD-A186621] 08 p1045 N88-16315
Convective wind fields as investigated with doppler lidar [PB88-115472] 09 p1193 N88-17151
Image chunking: Defining spatial building blocks for scene analysis [AD-A187072] 09 p1200 N88-17191
Study of quantum mechanical effects in deep submicron, grating-gate field effect transistors [AD-A188283] 10 p1325 N88-17923
Evolution of acoustic gravity wave packet in spatially and temporally varying wind 11 p1489 N88-18760
Visual contrast sensitivity functions obtained from untrained observers using tracking and staircase procedures [AD-A187715] 11 p1522 N88-19089
Spatial distribution of carbon and native defects in large-diameter bulk grown GaAs [DE88-003870] 11 p1562 N88-19348
To the problem of determining true volume steam content by measured values of mean density of a mixture in thermally unsteady two-phase flows [DE88-700840] 12 p1626 N88-19726
A segmented calorimeter for low-energy particle beams in space [DE88-001806] 13 p1838 N88-20997
Arcs in cesium seeded noble gases resulting from a magnetically induced electric field [EUT-87-E-177] 13 p1843 N88-21028
Spatial distribution of traffic in a cellular mobile data network [EUT-87-E-168] 14 p1904 N88-21378
Experimental and numerical study of liquid distribution in dispersive-annular flow [DE88-700844] 14 p1909 N88-21406
Spatial and temporal distribution of precipitation chemistry across Maryland in 1984, volume 1 [PB88-148929] 14 p1943 N88-21595
Spatial and temporal distribution of precipitation chemistry across Maryland in 1984, volume 2 [PB88-148937] 14 p1944 N88-21596
Spatial distribution of O(supra 1D) from Comet Halley 14 p1999 N88-21913
The representational code of the internal model of dynamic systems: An individual differences and dual task approach [AD-A190876] 16 p2244 N88-23403
Thomson scattering for determining electron concentrations and temperatures in an inductively coupled plasma. 1: Assessment of the technique for a low-flow, low-power plasma [AD-A191323] 16 p2280 N88-23651
Anomalies in the vegetation in the Alto Xingu - MT 17 p2357 N88-24043
An investigation of Soviet capabilities in extended range arctic ice forecasting [AD-A191082] 17 p2376 N88-24127
Sea ice kinematics: Space and time scales [AD-A191162] 17 p2376 N88-24128
Instantaneous two-dimensional multiple particle sizing diagnostic 19 p2630 N88-25600
Spatial organization of homopolymer chains inside spherical polybutadiene domains of SB diblock copolymers [AD-A193390] 21 p2918 N88-27321
Radar information from the partial derivatives of the echo signal phase from a point scatterer [AD-A193402] 21 p2933 N88-27415
A three-dimensional model of the gas-cell atomic frequency standard [AD-A193218] 21 p3011 N88-27868
Flow dynamics stimulated by hairpin-like vortices in initially laminar boundary layers [AD-A194253] 22 p3075 N88-28254
Distribution of hydroxyl clouds in the galaxy [DE88-702415] 22 p3164 N88-28844
The spatial and temporal variability of the arctic atmospheric boundary layer and its effect on electromagnetic (EM) propagation [AD-A193958] 23 p3204 N88-29068
HPM (High-Power Microwave) coupling into realistic targets [DE88-011788] 23 p3207 N88-29084
Low doses of atropine sulfate impair retention of a well-learned spatial task [AD-A194065] 23 p3237 N88-29266
Eye movements and spatial pattern vision [AD-A195496] 24 p3408 N88-30290
A detection theory analysis of visual display performance [AD-A196291] 24 p3409 N88-30292
Determining the spatial structure of fields of precipitation from space radar images in two orthogonal polarizations 24 p3450 N88-30531

SPATIAL FILTERING
Analysis of airborne imaging spectrometer data for the Ruby Mountains, Montana, by use of absorption-band-depth images 05 p0614 N88-13771
Spectral- and spatial-domain filtering and sampling approach to the numerical solution of electromagnetic scattering problems [PB88-106711] 06 p0694 N88-14261

Large-aperture sparse array antenna systems of moderate bandwidth for multiple emitter location
[AD-A188409] 12 p1619 N88-19683
Infrared-sensitive spatial light modulator
[AD-A190391] 15 p2134 N88-22729
Generation of thematic maps for updating aeronautical pilot charts utilizing LANDSAT-TM images
17 p2361 N88-24062
Real-time optical multiple object recognition and tracking system and method
[NASA-CASE-NPO-17139-1-CU]
18 p2576 N88-25301
Optical correlation using the magneio-optic device
[AD-A192342] 20 p2854 N88-26950
The predictability of low frequency patterns in the NMC MRF 22 p3127 N88-28587
Comparison of 2-D Fourier and spatial techniques for removing noise in real-time X-ray radiography
[AD-A193700] 23 p3187 N88-28962

SPATIAL ISOTROPY
U ISOTROPY
U SPATIAL DISTRIBUTION

SPATIAL MARCHING
A spatial marching technique for the inviscid blunt body problem 05 p0533 N88-13239
Leeside crossflow modeling in Euler space-marching computations
[NASA-TM-89710] 10 p1325 N88-17924
Split-coefficient matrix solution and experimental study of axisymmetric underexpanded exhaust plumes
15 p2054 N88-22242

SPATIAL ORIENTATION
U ATTITUDE (INCLINATION)

SPATIAL RESOLUTION
Estimation from satellite imagery of summertime rainfall over varied space and time scales
[PB87-203246] 01 p0071 N88-10454
What's needed in the UV and EUV
02 p0255 N88-11612
Visual evoked responses to sinusoidal gratings presented in central and right visual fields: 1
[DE87-014731] 04 p0473 N88-12919
Resolution limitations and optimization of the LLNL streak camera focus
[DE88-001633] 05 p0586 N88-13572
High-spatial-resolution TOVS observations for the FIRE/SRB Wisconsin experiment region from October 14 through November 2, 1986
[NASA-TM-100522] 06 p0747 N88-14593
High spatial resolution observations of dust and gas in NGC 7027 and the M8 Hourglass
06 p0801 N88-14903
Multichannel electron counter with high space resolution
[DE88-700564] 07 p0857 N88-15204
HIRIS (High-Resolution Imaging Spectrometer: Science opportunities for the 1990s. Earth observing system. Volume 2C: Instrument panel report
[NASA-TM-89703] 07 p0871 N88-15282
Method for restoration and resampling of TM sensor imagery
[INPE-4491-PRE/1255] 15 p2090 N88-22454
Sources of digital spatial data for geographic information systems
[AD-A189788] 15 p2148 N88-22824
A compact high resolution piezoresistive digital tactile sensor
[DE88-000430] 16 p2210 N88-23188
Spatial filtering on digital images
17 p2354 N88-24025
Effects of spatial resolution in CARS measurements
[PB88-121900] 18 p2482 N88-24727
Spatial stability of a compressible mixing layer
[NASA-CR-181671] 18 p2514 N88-24916
Investigation of the potential impact of new photonic materials on optical processing systems
21 p2924 N88-27359
Perception of motion in statistically-defined displays
[AD-A193076] 21 p2991 N88-27745
Research for reducing the labor intensive nature of high-resolution terrain analysis feature extraction
[AD-A192661] 22 p3089 N88-28345
Spectral and spatial attribute evaluation of SPOT data in geological mapping of precambrian terrains in semiarid environment of Brazil 22 p3104 N88-28436
Comparison of 2-D Fourier and spatial techniques for removing noise in real-time X-ray radiography
[AD-A193700] 23 p3187 N88-28962

SPECIES DIFFUSION
Species biology and potential for controlling four exotic plants (Ammophila arenaria, Carpobrotus edulis, Cortaderia jubata and Gasoul crystallinum) on Vandenberg Air Force Base, California
[NASA-TM-100980] 10 p1363 N88-18148

SPECIFIC GRAVITY
U DENSITY (MASS/VOLUME)

SPECIFIC HEAT
Specific heat of the high T/sub c superconductors (La,M)2CuO4 and YBa2Cu3O7 in magnetic fields
[DE87-014680] 03 p0380 N88-12388
Magnetic field dependence of the specific heat of some high-T/sub c/ superconductors
[DE87-014078] 04 p0497 N88-13063
Heavy Fermions and coherence in Kondo lattices: Specific heat of low energy excitation in Cer systems
[ETN-88-91080] 09 p1255 N88-17525
Specific heat of novel thin-film material systems
10 p1415 N88-18446
Research on high-specific-heat dielectrics
[AD-A187248] 11 p1461 N88-18710
Thermal conductivity, electrical conductivity and specific heat of copper-carbon fiber composite
[NASA-TT-20172] 16 p2172 N88-22948
Long-time tunneling in amorphous metals at helium temperatures
[DE88-701150] 16 p2281 N88-23654
Transient analysis of Li and LiH thermal storage spheres 17 p2411 N88-24334
The thermodynamic properties of quinoline and isoquinoline
[DE88-001218] 18 p2484 N88-24735
The precipitation processes of Cu-Zr-Cr alloys
[NASA-TT-20168] 18 p2488 N88-24758
Interactions between superconductivity and Kondo-grid properties in CeCu2Si2. Measurement results of specific heat under high pressure
[ETN-88-92377] 21 p3025 N88-27958
Discovery of a low temperature form of TAGN (Triaminoguanidinium Nitrate)
[AD-A196059] 24 p3357 N88-29989

SPECIFIC IMPULSE
Advanced energy conversion concept for beamed-energy propulsion
[AD-A187336] 10 p1324 N88-17914
Megawatt level electric propulsion perspectives
17 p2404 N88-24294
High power ion thruster performance
17 p2404 N88-24295
Nuclear electric propulsion system: Nuclear plant and thermomechanical conversion system
17 p2405 N88-24298
Solar thermal propulsion for orbit transfer vehicles
17 p2428 N88-24445
Performance of a hydrogen pulsed electrothermal thruster. Strategic defense initiative organization innovative science and technology. SBIR, phase 1
[AD-A191999] 18 p2475 N88-24679
Unified study of plasma/surface interactions for space power and propulsion
[AD-A195971] 24 p3338 N88-29870

SPECIFICATIONS
NT AIRCRAFT SPECIFICATIONS
NT EQUIPMENT SPECIFICATIONS
NT FUNCTIONAL DESIGN SPECIFICATIONS
Operating experiences and test results of six cold helium compressors
[DE87-012115] 02 p0157 N88-10982
Dual S/X-band RV antenna
[DE87-014853] 03 p0305 N88-11923
The aerodynamics of supersonic parachutes
[DE87-014846] 04 p0395 N88-12464
Mechanical shock test specification using nonstationary random excitation models
[DE87-013650] 04 p0454 N88-12812
Conservatism implications of shock test tailoring for multiple design environments 05 p0592 N88-13611
LISP: A language for stratified design
[AD-A185606] 06 p0759 N88-14654
FAA air traffic control operations concepts. Volume 5: ATCT/TCCC (Airport Traffic Control Tower/Tower Control Computer Complex) tower controllers
[AD-A185983] 07 p0818 N88-14977
DOE data exchange format specification, mechanical products/drafting: Version 1.2.2: CADCAM-045
[DE88-001923] 07 p0904 N88-15477
Annotated algebraic specification of the static semantics of pool
[PB88-106695] 07 p0912 N88-15533
Study on the model of a toroidal magnet for a tokamak with a strong field
[DE88-700346] 07 p0935 N88-15681
Main physics features driving design concept and physics design constraints. Conceptual design study of FY86 FER
[DE88-750309] 07 p0936 N88-15689
Evaluation of CWMS (Continuous-Wave Measurement System) single-wire dipole antenna
[DE88-003979] 09 p1155 N88-16920
Specification of an engine and its components starting from a consideration of aircraft missions
10 p1279 N88-17651
Plasma physics design and major specifications of candidate reactors for FER design studies. Conceptual design study of FY86 FER
[DE88-751066] 10 p1411 N88-18416
Conceptual design study of Fusion Experimental Reactor (FY86 FER): Safety
[DE88-751071] 10 p1411 N88-18418
Workshop on Design Loads for Advanced Fighters
[AGARD-R-746] 12 p1579 N88-19449
Changes in USAF structural loads requirements
12 p1580 N88-19452
A methodology for hardware verification based on logic simulation
[AD-A188553] 12 p1622 N88-19704
The formal specification of computer systems
[AD-A188947] 12 p1675 N88-20013
Engine testing for synfuel operation
[DE88-006044] 13 p1779 N88-20645
Algebraic specifications for parameterized data types: The case of minimal computable algebras and parameters with equality
[CWI-CS-R8714] 13 p1826 N88-20916
Type-checking Mini-ML: An algebraic specification with user-defined syntax
[CWI-CS-R8737] 13 p1827 N88-20921
Performance of elastomeric bearings
[PB88-159470] 14 p1918 N88-21450
The effects of torque response and time delay on rotorcraft vertical axis handling qualities
[AD-A189873] 15 p2017 N88-22023
Program profiling in Cedar
[AD-A190683] 16 p2250 N88-23449
The specification and design of a future maritime reconnaissance aircraft 17 p2303 N88-23772
Systems engineering technique
17 p2303 N88-23776
Modeling of functional specifications for onboard software: Experience with the Rafale avionics system
17 p2303 N88-23777
Interfacing and integrating hardware and software design systems 17 p2306 N88-23796
Development of complex avionics systems: Experience from French military programs 17 p2307 N88-23804
Specification for IBM/IBM compatible 3480 tape cartridge
[NASA-TM-100702] 17 p2384 N88-24168
Nonlinear flying quality parameters based on dynamic inversion
[AD-A192146] 18 p2464 N88-24627
Use of a two-stage light-gas gun as an injector for electromagnetic railguns
[DE88-007200] 18 p2469 N88-24657
The -mdoc macro package: A software tool to support computer documentation standards
[DE88-000500] 18 p2559 N88-25188
Miltipath measurements for land mobile satellite service using global positioning system signals
19 p2645 N88-25700
Analytical determination of critical crack size in solar cells
[NASA-CR-183128] 20 p2821 N88-26736
Script editor: An editor for the specification phase in the development of computer based learning
[REPT-87-68] 20 p2839 N88-26846
The evaluation of a deformable diffraction grating for a stigmatic EUV spectroheliometer
[NASA-CR-183064] 20 p2853 N88-26941
Assembly Test Article (ATA)
[NASA-CR-179361] 21 p2903 N88-27226
The MELMUX MX-7100 series high-speed digital multiplexers 21 p2930 N88-27396
The Ariane 5 program management specifications
22 p3162 N88-28829
The technical reporting and approval procedure for materials and processes
[ESA-PSS-01-700-ISSUE-1] 22 p3162 N88-28833
High hot-hardness gear lubricant evaluations, phase 2
[AD-A192309] 23 p3196 N88-29017
Material and process selection and quality control for ESA space systems and associated equipment
[ESA-PSS-01-70-ISSUE-3] 23 p3224 N88-29190
Level 1 Ada/SQL (Structured Query Language) database language interface user's guide
[AD-A194480] 23 p3249 N88-29335

SPECIMEN GEOMETRY
A mixed finite element method for the computation of stress in a composite with loaded holes
[ONERA-RT-34/4242-RY-054-R]
01 p0062 N88-10395
Nondestructive control: Modeling of electromagnetic phenomena, defect characterization, and sensor optimization
[ECL-86-14] 08 p0993 N88-16008

The relationship of tensile specimen size and geometry effects to unique constitutive parameters for ductile materials
[AD-A186020] 08 p0994 N88-16012
Application of ISRM testing methods to fracture toughness testing of graphite 13 p1747 N88-20446
Damage in a perforated graphite-epoxy plate under monotonic, cyclic biaxial loading
[ONERA-NT-1987-5] 20 p2816 N88-26708
Stress corrosion of C ring specimen in salt spray tests
[I-186/87] 21 p2916 N88-27307
An experimental and analytical evaluation of a biaxial test for determining shear properties of composite materials
[NASA-CR-182928] 21 p2962 N88-27593
Mixed finite element methods to compute stress in a load composite specimen with holes: Numerical results
[ONERA-RT-37/4242-RY-062-R] 22 p3088 N88-28336

SPECIMENS
The influence of small defects on tensile specimen ductility and symmetry of deformation
[AD-A187983] 10 p1346 N88-18044
Cyropreservation of isolated rat hepathocytes for future use in Spacelab experiments: Preliminary results 12 p1660 N88-19950
Specimen preparation techniques for the examination of ceramic and metal-matrix composites
[DE88-005157] 15 p2030 N88-22094
Method of radiographic inspection of wooden members
[NASA-CASE-LAR-13724-1] 17 p2346 N88-23983
Sample decomposition in sealed teflon vessels
[NASA-TT-20189] 18 p2494 N88-24798
Low temperature storage container for transporting perishables to space station
[NASA-CASE-MFS-28248-1] 18 p2498 N88-24817

SPECKLE HOLOGRAPHY
Comparison of sensitivity and precision of holographic and speckle-interferometry methods with Fourier-plane recording 08 p1078 N88-16500

SPECKLE INTERFEROMETRY
New results from high angular resolution observations of alpha Ori 04 p0514 N88-13161
Comparison of sensitivity and precision of holographic and speckle-interferometry methods with Fourier-plane recording 08 p1078 N88-16500
Investigations of high resolution imaging through the Earth's atmosphere using speckle interferometry
[AD-A189295] 12 p1692 N88-20121
Speckle interferometry of asteroids
[NASA-CR-180438] 15 p2151 N88-22843
Speckle imaging of active galactic nuclei: NGC 1068 and NGC 4151 18 p2592 N88-25407
An upper limit on the primordial He4 abundance from speckle interferometric observations of muon Cassiopeiae 23 p3298 N88-29641
Binary star measurements using digital speckle interferometer of 6-m telescope 24 p3448 N88-30521

SPECKLE PATTERNS
ISIS: Imaging Speckle Interferometer in Space 01 p0095 N88-10625
Study of synthetic aperture radar data compression and encoding. Part 3: Performance evaluation of speckle suppression and data compression algorithms
[NLR-TR-85085-L-PT-3] 06 p0692 N88-14248
Study of synthetic aperture radar data compression and encoding. Part 2: SAR image speckle suppression and data compression algorithms
[NLR-TR-85085-L-PT-2] 07 p0843 N88-15116
Calculation of noise in spatial speckle-field holograms under conditions of saturated photoresponse 09 p1235 N88-17403
Investigation of the usefulness of speckle analysis in imaging radar systems
[BCRS-86-05] 16 p2227 N88-23302
Speckle imaging of active galactic nuclei: NGC 1068 and NGC 4151 18 p2592 N88-25407
Digital image processing from speckle interferograms by correlation methods: Application in atmospheric optics, astronomy, and biology
[ETN-88-92125] 20 p2855 N88-26953
Methods for inoarect imaging through the atmosphere
[ONERA-NT-1987-4] 20 p2884 N88-27124

SPECTRA
NT ABSORPTION SPECTRA
NT ATOMIC SPECTRA
NT BALMER SERIES
NT ELECTROMAGNETIC SPECTRA
NT ELECTRONIC SPECTRA
NT EMISSION SPECTRA
NT ENERGY SPECTRA
NT FRAUNHOFER LINES
NT GAMMA RAY SPECTRA
NT H ALPHA LINE
NT H BETA LINE
NT H LINES
NT HERZBERG BANDS
NT INFRARED SPECTRA
NT K LINES
NT LINE SPECTRA
NT LYMAN SPECTRA
NT MASS SPECTRA
NT MICROWAVE SPECTRA
NT MOLECULAR SPECTRA
NT NEUTRON SPECTRA
NT NOISE SPECTRA
NT OXYGEN SPECTRA
NT PLASMA SPECTRA
NT POWER SPECTRA
NT RADIATION SPECTRA
NT RADIO SPECTRA
NT RAMAN SPECTRA
NT RYDBERG SERIES
NT SCHUMANN-RUNGE BANDS
NT SHOCK SPECTRA
NT SOLAR SPECTRA
NT SPECTRAL BANDS
NT STELLAR SPECTRA
NT ULTRAVIOLET SPECTRA
NT VIBRATIONAL SPECTRA
NT VISIBLE SPECTRUM
NT X RAY SPECTRA
EVA reference manual
[DE87-014073] 01 p0082 N88-10526
Comparison of sideband spectra obtained from analytical formula and from numerical simulation in free-electron laser
[DE88-000521] 04 p0450 N88-12789
SUSIE reference manual
[DE88-001462] 05 p0636 N88-13893
The structure of the sideband spectrum in free electron lasers
[AD-A186952] 09 p1170 N88-17015
Scattering of optical radiation by bursting water particles in fog 09 p1236 N88-17410
Systematic errors of the FSU global spectral model 10 p1356 N88-18103
Well-posedness and spectral estimation for infinite dimensional systems
[AD-A187621] 10 p1401 N88-18354
Lg wave excitation and propagation in the presence of one-, two-, and three-dimensional heterogeneities
[AD-A187364] 11 p1510 N88-19022
Estimation of sea surface wave spectra using acoustic tomography
[AD-A187837] 11 p1516 N88-19057
Emission of gamma rays from various materials pulsed with 14-MeV neutrons
[DE88-003837] 11 p1544 N88-19227
Inversion algorithms for geophysical problems
[AD-A189252] 13 p1815 N88-20845
New method of examining micrononhomogeneity of local centers in high-resistivity semiconductor materials under scanning electron microscope 14 p1969 N88-21754
Multichannel 2-D power spectral estimation and applications
[AD-A191273] 16 p2191 N88-23068
Time-frequency representations for speech signals
[AD-A188661] 18 p2498 N88-24819
Molecular-beam, mass-spectrometric studies of wood vapor and model compounds over HZSM-5 catalyst 18 p2535 N88-25044
Wavenumber spectra from THIR 6.7 micron water vapor data 20 p2824 N88-26756
Qualitative characteristics of open waveguide resonator spectra
[DE88-702387] 23 p3202 N88-29056

SPECTRAL ABSORPTION
U ABSORPTION SPECTRA

SPECTRAL ANALYSIS
U SPECTRUM ANALYSIS

SPECTRAL BANDS
NT ABSORPTION SPECTRA
NT FRAUNHOFER LINES
NT HERZBERG BANDS
NT SCHUMANN-RUNGE BANDS
Analysis of SO2 signals in SBUV/TOMS data 05 p0618 N88-13794
Analysis of hydrocarbon band 3.35 in spectrum of Halley's Comet using data from infrared spectrometer on Vega-1 spacecraft 13 p1727 N88-20327
The gamma 1 and gamma 3 bands of (16)O3: Line positions and intensities
[NASA-TM-101162] 17 p2445 N88-24541
Line positions and intensities for the gamma 1 + gamma 2 and gamma 2 + gamma 3 bands of (16)O3
[NASA-TM-101161] 17 p2446 N88-24542
Spectral characteristics and the extent of paleosols of the Palouse formation
[NASA-CR-180947] 23 p3228 N88-29210
Atmospheric corrections for in-flight satellite radiometric calibration
[AD-A196124] 24 p3391 N88-30194

SPECTRAL CORRELATION
Multistep component analysis of correlations 08 p1009 N88-16115
Correlation and spectral density measurements by LDA — flow measurement
[ISL-CO-244/86] 14 p1910 N88-21412
Spectrometry and spectral radiometry 16 p2271 N88-23586
Selective radiation absorption in aluminized composite propellant combustion 19 p2630 N88-25598

SPECTRAL EMISSION
PG 0308 + 096: A short-period white dwarf + dM binary with strongly modulated H-alpha emission 04 p0509 N88-13132
Evidence for expanding magnetic loops in coronae of cool stars 04 p0510 N88-13134
X-rays, color, and the Vaughan-Preston gap 04 p0510 N88-13135
Determination of cloud base height and emissivity from downwelling angular radiances
[AD-A185985] 07 p0879 N88-15331
NBS (National Bureau of Standards) measurement services: Spectral irradiance calibrations
[PB88-123781] 10 p1408 N88-18401
Research on influence of individual sea water components on spectral brightness coefficient of outgoing radiation 13 p1785 N88-20682
A spectroscopic study of absorption and emission features of interstellar dust components
[B8681462] 16 p2289 N88-23706
Space station contamination study: Assessment of contaminant spectral brightness 18 p2591 N88-25395
Calculation of space station infrared irradiance from atmosphere-induced emissions 18 p2591 N88-25396
Speckle imaging of active galactic nuclei: NGC 1068 and NGC 4151 18 p2592 N88-25407
Design, development, fabrication and launch support for a high altitude release of neodymium vapor
[AD-A194196] 22 p3118 N88-28527

SPECTRAL ENERGY DISTRIBUTION
Local spectra and wave distribution functions — space plasma
[KGI-PREPRINT-099] 01 p0100 N88-10659
A spectral survey of 26 G9-M6 flare stars in the solar neighborhood 04 p0512 N88-13149
Evolution of spectral densities in weakly inhomogeneous plasmas
[PB87-137402] 06 p0784 N88-14811
Power spectral density analysis of wind-shear turbulence for related flight simulations
[NASA-CR-182721] 13 p1802 N88-20773
Inversion algorithms for geophysical problems
[AD-A189252] 13 p1815 N88-20845
Three dimensional spectral energy measurement on turbulence subjected to a high degree of plane deformation
[ETN-88-92537] 18 p2511 N88-24896
Study of the structure of turbulence in accelerating transitional boundary layers
[AD-A191698] 19 p2663 N88-25837
Statistical description of stochastic dynamics
[AD-A192924] 21 p3009 N88-27852

SPECTRAL LINE WIDTH
Statistical fine structure in inhomogeneously broadened absorption lines in solids
[AD-A190341] 16 p2174 N88-22957
Studies of spectral line ratio fluctuations using Inductively Coupled Plasma (ICP) light
[IRF-PREPRINT-100] 18 p2578 N88-25311
Spectral line shapes from highly ionized sodium plasmas
[AD-A193401] 21 p3017 N88-27907

SPECTRAL LINES
U LINE SPECTRA

SPECTRAL METHODS
An adaptive pseudo-spectral method for reaction diffusion problems
[NASA-CR-178394] 02 p0224 N88-11414
Airborne Visible/Infrared Imaging Spectrometer (AVIRIS) spectrometer design and performance 06 p0706 N88-14327
Spectral methods: Analysis and applications to flow problems
[AD-A186265] 07 p0850 N88-15156
Spectral representation of infinitely divisible processes
[AD-A186210] 07 p0910 N88-15515
Spectral dilation of L(B,H)-valued measures and its application to stationary dilation for Banach space valued processes
[NASA-CR-182388] 07 p0913 N88-15536

Prognosis using spectral embedding — weather forecasting 08 p1016 N88-16157
High-speed assembly language (80386/80387) programming for laser spectra scan control and data acquisition providing improved resolution water vapor spectroscopy
[NASA-CR-4117] 08 p1053 N88-16355
Short data length effects in an asymptotically efficient ARMA (AutoRegressive Moving Average) spectral estimator
[AD-A186561] 08 p1068 N88-16458
Analysis of the spectral vanishing viscosity method for periodic conservation laws
[NASA-CR-181613] 09 p1231 N88-17378
Coupling finite element and spectral methods: First results
[NASA-CR-181606] 09 p1231 N88-17379
Kinetics and spectrum of light pulse used in picosecond holography 09 p1236 N88-17409
Conjugate gradient spectral iterative technique
[PB88-126917] 10 p1398 N88-18337
Spectral iterative technique with Gram-Schmidt orthoganalization
[PB88-127451] 10 p1399 N88-18338
Domain decomposition preconditioners for the spectral collocation method
[NASA-CR-181620] 10 p1400 N88-18345
On the smallest scale for the incompressible Navier-Stokes equations
[NASA-CR-181628] 11 p1434 N88-18558
Recursive inversion of externally defined linear systems
[NASA-TM-100070] 11 p1541 N88-19215
How to generate equal probability design load conditions — aircraft design
[NLR-TR-86060-U] 13 p1722 N88-20295
Low-order spectral models of atmospheric circulation: A survey
[CWI-AM-R8705] 13 p1797 N88-20748
Spectral element methods: Algorithms and architectures
[NASA-CR-182701] 13 p1820 N88-20878
Spectrum fatigue testing for materials characterization
[VTT-RR-502] 15 p2088 N88-22443
Development of remote sensing techniques capable of delineating soils as an aid to soil survey
[NASA-CR-182610] 15 p2089 N88-22452
Propagation of acoustic gravity wave spectrum through vertical wind shear region 16 p2186 N88-23035
An efficient parallel algorithm for the simulation of three-dimensional compressible transition on a 20 processor Flex/32 multicomputer
[NASA-CR-178340] 17 p2337 N88-23943
Effects of spatial resolution in CARS measurements
[PB88-121900] 18 p2482 N88-24727
Analysis of a six-component barotropic spectral model: Chaotic motion, predictability and vacillation — atmospheric circulation
[CWI-AM-R8710] 18 p2542 N88-25090
La Recherche Aerospatiale, bimonthly bulletin, no. 1986-5, 234/September-October
[ESA-TT-1032] 19 p2641 N88-25671
Non-oscillatory spectral Fourier methods for shock wave calculations
[NASA-CR-181675] 19 p2720 N88-26148
Semi-discrete approximations to nonlinear systems of conservation laws; consistency and L(infinity)-stability imply convergence
[NASA-CR-181683] 19 p2721 N88-26157
Study and implementation of ultrahigh frequency coupling devices using the fin line technology — millimeter waves
[ETN-88-92307] 20 p2796 N88-26588
Spectral resolution of the Navier-Stokes equations in multi-domain curved complex geometries
[ONERA-NT-1987-2] 20 p2802 N88-26631
Solution of the Orr-Sommerfeld equation for the Blausius boundary-layer documentation of program ORRBL and a test case
[NASA-CR-4169] 20 p2841 N88-26858

SPECTRAL NOISE
U WHITE NOISE

SPECTRAL RECONNAISSANCE
The role of anisotropy in the long range reconnaissance of the albedo of land surfaces 08 p1017 N88-16169
Radiation absorption in the infrared spectral range: A comparison between laboratory measurements and theoretical calculation illustrated by a H2O 2.7 micrometer 08 p1018 N88-16170
Long range reconnaissance of trace gases: A special aspect of emission spectroscopy 08 p1018 N88-16172
Earth resources: A continuing bibliography with indexes (supplement 56)
[NASA-SP-7041(56)] 10 p1347 N88-18051

SPECTRAL REFLECTANCE
Development of response models for the Earth Radiation Budget Experiment (ERBE) sensors. Part 2: Analysis of the ERBE integrating sphere ground calibration
[NASA-CR-178293] 01 p0049 N88-10316
Surface polariton resonances and reflectance on a bigrating
[AD-A184663] 03 p0377 N88-12370
AIS-2 radiometry and a comparison of methods for the recovery of ground reflectance 05 p0611 N88-13757
Calibrating AIS images using the surface as a reference 05 p0612 N88-13760
AIS-2 spectra of California wetland vegetation 05 p0613 N88-13763
Toward detecting California shrubland canopy chemistry with AIS data 05 p0613 N88-13764
Measuring near infrared spectral reflectance changes from water stressed conifer stands with AIS-2 05 p0613 N88-13765
Preliminary results from an investigation of AIS-1 data over an area of epithermal alteration: Plateau, Northern Queensland, Australia 05 p0613 N88-13768
Causes of spurious features in spectral reflectance data 05 p0614 N88-13769
Automatic continuum analysis of reflectance spectra 05 p0614 N88-13770
Mapping hydrothermally altered rocks in the Northern Grapevine Mountains, Nevada and California with the airborne imaging spectrometer 05 p0614 N88-13772
Environmental processes and spectral reflectance characteristics associated with soil erosion in desert fringe regions
[NASA-CR-182332] 05 p0620 N88-13811
NBS (National Bureau of Standards) measurement services: Spectral reflectance
[PB88-109905] 06 p0779 N88-14785
Monte Carlo method calculation of spectral brightness coefficient of vegetation cover as function of illumination conditions 08 p1008 N88-16113
Transport properties of conductive polymers
[AD-A188411] 12 p1610 N88-19628
Influence of solar illumination conditions on TM/Landsat data
[INPE-4463-TDL/320] 12 p1638 N88-19806
Research in remote sensing of vegetation
[NASA-CR-182663] 12 p1639 N88-19817
Analysis of spectral reflectance characteristics of targets under satellites and automatic cloud recognition 13 p1755 N88-20498
Spectral reflective characteristics of sea surface 13 p1784 N88-20676
Space station solar concentrator materials research
[NASA-TM-100862] 14 p1882 N88-21250
Reflectance spectroscopy in planetary science: Review and strategy for the future
[NASA-SP-493] 17 p2451 N88-24564
Optical constants of minerals and other materials from the millimeter to the ultraviolet
[AD-A192210] 18 p2482 N88-24724
Methods of determining playa surface conditions using remote sensing
[AD-A192663] 21 p2965 N88-27612
SPOT 1: Image utilization, assessment, results. A study of the Elburgon Forest area (Kenya) showing the spectral responses of different forest tree species 22 p3107 N88-28454
Study of stereoradiometry on SPOT images 22 p3112 N88-28484
Surface reflectance factors derived from SPOT-1 HRV data at two view angles 22 p3113 N88-28492
Variations in spectral reflectance signature in healthy stands of pine and spruce
[FOA-C-30468-3.1] 22 p3116 N88-28512
Monte-Carlo estimation of the influence of plant architecture parameters on spectral brightness 24 p3450 N88-30533

SPECTRAL RESOLUTION
What's needed in the UV and EUV 02 p0255 N88-11612
Preliminary results from an investigation of AIS-1 data over an area of epithermal alteration: Plateau, Northern Queensland, Australia 05 p0613 N88-13768
HIRIS (High-Resolution Imaging Spectrometer: Science opportunities for the 1990s. Earth observing system. Volume 2C: Instrument panel report
[NASA-TM-89703] 07 p0871 N88-15282
Velocity resolved far-infrared spectroscopy of galactic sources 13 p1854 N88-21099
Merit of Hadamard transform active absorption spectrometer described 15 p2053 N88-22232
Dispersive spectral apparatus 16 p2271 N88-23587
Spectral resolution of the Navier-Stokes equations in multi-domain curved complex geometries
[ONERA-NT-1987-2] 20 p2802 N88-26631
Time-resolved doubly bent crystal X-ray spectrometer
[DE88-007899] 20 p2805 N88-26637
The collection of statistics on the frequency of cloud cover over North America
[AD-A193093] 21 p2974 N88-27667
Spectral and spatial attribute evaluation of SPOT data in geological mapping of precambrian terrains in semiarid environment of Brazil 22 p3104 N88-28436
On the multiple grating spectrometer resolving power
[PREPRINT-585] 22 p3153 N88-28761

SPECTRAL SENSITIVITY
Hard- and software problems of spaced meteor observations by optical electronics 06 p0741 N88-14560
Improvements in profiler wind estimates using smoothed data in the spectrum finder algorithm
[PB88-102181] 07 p0881 N88-15342
High-temperature photoelectron spectroscopy. An increased sensitivity spectrometer for studying vapor-phase species produced at furnace temperatures greater than 2000K
[AD-A186542] 09 p1140 N88-16835
Psychophysical, biochemical and histological studies of spectrally selective photic damage to primate retina
[AD-A188115] 11 p1517 N88-19063
Spectral properties of semiconductor lasers with external resonators
[ETN-88-93119] 24 p3379 N88-30125

SPECTRAL SIGNATURES
Solar-geophysical data number 514, June 1987. Part 1: (Prompt reports). Data for May 1987, April 1987 and late data
[PB87-217261] 02 p0257 N88-11626
Analysis of the parameters responsible for the variations of the illumination conditions in the LANSAT data 17 p2362 N88-24070
Comparative variations of spectral signatures in a cultivated area of the Paris Basin (27 May, 26 June, 1 July 1986) 22 p3095 N88-28382
Mars: Spectral signatures seen and unseen 23 p3301 N88-29659
Variability in spectral signatures of terrestrial volcanic rocks and implications for volcanology on Mars 23 p3303 N88-29672
Spectral reflectance of SNC meteorites: Relationships to Martian surface composition 23 p3304 N88-29683
Integrating multispectral imagery and ground level hyperspectral signature data
[AD-A195976] 24 p3386 N88-30166

SPECTROGRAMS
Spectrograms of the visible region in the JT-60 tokamak (wavelength range from 2210 A to 5250 A)
[DE87-753002] 02 p0240 N88-11513
Variations of the vertical and horizontal velocities of the small-scale structures and the physical problems related to overshoot layers 04 p0507 N88-13115

SPECTROGRAPHS
AURIO: A proposal for flying auroral imaging observatory on the Polar Platform in the Space Station/Columbus program 08 p1034 N88-16268
Mechanisms mediating perception of complex acoustic patterns
[AD-A189765] 15 p2102 N88-22520
Rutherford magnetic spectrograph for intense ion beam measurements on PBFA 2
[DE88-007281] 19 p2725 N88-26181
Coupling of a spark source mass spectrograph and a ND-YAG laser
[DE88-012116] 21 p2951 N88-27530

SPECTROHELIOGRAPHS
The evaluation of a deformable diffraction grating for a stigmatic EUV spectroheliometer
[NASA-CR-182371] 06 p0707 N88-14337
The evaluation of a deformable diffraction grating for a stigmatic EUV spectroheliometer
[NASA-CR-183064] 20 p2853 N88-26941

SPECTROHELIOSCOPES
U SPECTROHELIOGRAPHS

SPECTROMETERS
NT EBERT SPECTROMETERS
NT FABRY-PEROT SPECTROMETERS
NT GAMMA RAY SPECTROMETERS
NT IMAGING SPECTROMETERS
NT INFRARED SPECTROMETERS
NT LASER SPECTROMETERS
NT MASS SPECTROMETERS
NT MICROWAVE SPECTROMETERS
NT NEUTRON SPECTROMETERS
NT SOLAR BACKSCATTER UV SPECTROMETER
NT SOLAR SPECTROMETERS
NT SPECTROHELIOGRAPHS
NT TIME OF FLIGHT SPECTROMETERS
NT TOTAL OZONE MAPPING SPECTROMETER
NT ULTRAVIOLET SPECTROMETERS

The wavenumber: An alternative to the directional coupler for multimode analysis in oversized waveguides
[IPF-87-2] 01 p0037 N88-10237
Diode pumped solid-state laser oscillators for spectroscopic applications
[NASA-CR-180576] 01 p0052 N88-10331
Spectrometric test of a linear array sensor
[NASA-TM-100676] 01 p0064 N88-10414
Instrumental and operational aspects of an EXELFS system connected to JEOL 100C STEM
[USIP-87-09] 01 p0092 N88-10601
Present status of the high resolution spectrometers
[CEBAF-PR-87-029] 02 p0234 N88-11478
Conceptual design of a high-resolution pion (0) spectrometer
[DE87-014757] 03 p0324 N88-12047
Commercial perspective of an imaging spectrometer development program 03 p0340 N88-12138
Evidence for expanding magnetic loops in coronae of cool stars 04 p0510 N88-13134
Airborne Visible/Infrared Imaging Spectrometer (AVIRIS). A description of the sensor, ground data processing facility, laboratory calibration, and first results
[NASA-CR-182365] 06 p0705 N88-14325
A system overview of the Airborne Visible/Infrared Imaging Spectrometer (AVIRIS) 06 p0705 N88-14326
Astromag: A particle spectrometer for the Space Station
[PREPRINT-557] 06 p0707 N88-14336
Characteristics of an Ebert monochromator for an infrared spectrometer in the wavelength range 1 micrometer to 15 micrometers
[AD-A186945] 09 p1166 N88-16991
A comparison of measurements from the A/E35U-3 and PWMA (Portable Wear Metal Analyzer) spectrometers
[AD-A186855] 09 p1177 N88-17047
Error modeling and confidence interval estimation for inductively coupled plasma calibration curves
[AD-A186711] 09 p1250 N88-17488
A combined cosmic ray muon spectrometer and high energy air shower array
[DE88-003057] 09 p1264 N88-17574
Characterization of the arc/spark excitation sources used in the spectrometric oil analysis program
[AD-A187131] 10 p1297 N88-17758
Evaluation of a temperature remote sensing technique
[AD-A187885] 10 p1347 N88-18053
Atomic and molecular gas phase spectrometry
[AD-A187562] 11 p1452 N88-18655
A microspectrofluorometer system based on real time digital techniques
[REPT-86-014] 11 p1490 N88-18891
Interfacing of a microcomputer with a simultaneous atomic-emission spectrometer
[PB88-139571] 11 p1526 N88-19109
Development of a cryogenic stepping drive for ISO/LWS 14 p1878 N88-21220
Quantitative AES: The establishment of a standard reference spectrum for the accurate determination of spectrometer transmission functions
[NPL-DMA(A)-151] 14 p1887 N88-21279
Digital filter unit for selection of spectrometric information
[DE87-702990] 16 p2246 N88-23415
Spectral radiometry: Methods, measuring techniques, and applications --- conference
[PTB-OPT-24] 16 p2271 N88-23585
Spectrometry and spectral radiometry 16 p2271 N88-23586
Dispersive spectral apparatus 16 p2271 N88-23587
Heterodyne spectrometer for the very high frequency range between 300 and 3000 GHz (1 mm to 0.1 mm) using a mixer in open structure 16 p2271 N88-23589
Spectral radiation measurement using a photodiode array as receiver 16 p2271 N88-23591
A new fiber-optic-based phase-resolved phosphorescence spectrometer
[AD-A191325] 16 p2275 N88-23613
X-ray spectroscopic diagnostics on JIPPT-IIU and HELIOTRON-E 17 p2440 N88-24515
Automated spectrometric unit for the study of radiation characteristics of cosmic radiation aboard Prognoz-9 space stations 19 p2706 N88-26090
The XRD (X-Ray Diode) array, the grazing incidence spectrometer and the X-ray imaging camera on PBFA 2
[DE88-007282] 19 p2728 N88-26200
Scanning tunneling microscopy as a surface chemical probe
[AD-A192710] 21 p2909 N88-27263
Multifilter spectrometer (FEB) for microwave atmospheric sounder
[AD-A192312] 21 p2935 N88-27426
Nuclear magnetic resonance spectrometer
[AD-A192928] 21 p2950 N88-27523
Calibration of the portable wear metal analyzer
[AD-A192971] 21 p2950 N88-27524
Rapid-scanning Fourier transform spectrometer for studies of propagation of near-millimeter-wave radiation through clear air and fog
[AD-A193752] 22 p3070 N88-28219
Molecular fluorescence measurements with a charge-coupled device detector
[AD-A194437] 23 p3216 N88-29141

SPECTROMETRY
U SPECTROMETERS

SPECTROPHOTOGRAPHY
The calibration of photographic and spectroscopic films: Reciprocity failure and thermal responses of IIaO film at liquid nitrogen temperatures
[NASA-CR-181094] 13 p1773 N88-20606

SPECTROPHOTOMETERS
NT INFRARED SPECTROPHOTOMETERS
NT ULTRAVIOLET SPECTROPHOTOMETERS
Comparison of ground based and TOMS measurements of SO2 from volcanic emissions 05 p0618 N88-13795
NBS (National Bureau of Standards) measurement services: Spectral reflectance
[PB88-109905] 06 p0779 N88-14785
A new class of multiple dispersion grating spectrometers
[PREPRINT-569] 14 p1983 N88-21830
Ground-based facility for spectrophotometric studies of the airflow and aurora
[AP-29] 22 p3119 N88-28532
NBS (National Bureau of Standards) measurement services: The NBS photodetector spectral response calibration transfer program
[PB88-201595] 24 p3376 N88-30109

SPECTROPHOTOMETRY
NT STELLAR SPECTROPHOTOMETRY
High resolution electron and ion microscopy
[AERE-R-12502] 10 p1297 N88-17754
Electrochemical and optical investigations on ion-implanted TiO2 samples
[ETN-88-91485] 11 p1455 N88-18670
Spectrophotometric remote sensing of the diffuse aurora
[AD-A188599] 12 p1643 N88-19837
The type Ia supernova 1986G in NGC5128: Optical photometry and spectra
[INPE-4426-PRE/1230] 12 p1710 N88-20231
Development of high stability fiber optic spectrophotometric systems for study of solar/stellar magnetic activity
[AD-A189327] 13 p1852 N88-21088
Color fluctuations in the inner coma of Comet Halley as measured from VEGA-2 14 p2000 N88-21925
The evolution of CN emission in Halley's comet with heliocentric distance 14 p2006 N88-21961
Outburst of Halley's comet 14 p2007 N88-21967
Spectrophotometric observations of Comet Halley 14 p2007 N88-21972
Single-laboratory evaluation of SW-846 methods 7090/7091 determination of beryllium by flame and furnace atomic absorption spectrophotometry
[PB88-171434] 16 p2175 N88-22963
The dynamics of SBO galaxies. Part 1: The data
[SER-C-PREPUBL-FASC-22] 24 p3455 N88-30567

SPECTROPOLARIMETERS
U POLARIMETERS

SPECTRORADIOMETERS
Spectrometric test of a linear array sensor
[NASA-TM-100676] 01 p0064 N88-10414
AIS-2 radiometry and a comparison of methods for the recovery of ground reflectance 05 p0611 N88-13757
Characteristics of an Ebert monochromator for an infrared spectrometer in the wavelength range 1 micrometer to 15 micrometers
[AD-A186945] 09 p1166 N88-16991
Spectral radiometry: Methods, measuring techniques, and applications --- conference
[PTB-OPT-24] 16 p2271 N88-23585
Spectrometry and spectral radiometry 16 p2271 N88-23586
Differential spectral radiometry 16 p2272 N88-23594
Reflection standards for spectroradiometry: Realization and calibration 16 p2272 N88-23595
Ultraviolet radiometry: Radiation sources and measuring methods 16 p2272 N88-23596
Spectroradiometry in the industrial test laboratory 16 p2272 N88-23598
Spectroradiometry in meteorology 16 p2272 N88-23599
Spectroradiometry in industrial safety 16 p2272 N88-23600
Spectroradiometry in materials testing 16 p2273 N88-23601
Study of stereoradiometry on SPOT images 22 p3112 N88-28484

SPECTROSCOPES
U SPECTROMETERS

SPECTROSCOPIC ANALYSIS
Auger electron spectroscopy of oxidized titanium overlayers: Speciation of homogeneous and heterogeneous samples
[KFK-4221] 02 p0146 N88-10913
Chemical analysis for excimer laser systems
[DE88-001941] 05 p0589 N88-13591
Determination, by X-ray fluorescence, of platinum, palladium, ruthenium, iron and chromium in special steels
[PB87-132114] 06 p0683 N88-14183
Re-usable thin-layer spectroelectrochemical cell for non-aqueous solvent systems
[AD-A186951] 09 p1248 N88-17478
Method for sampling of methyl salicylate vapor in air using passivated stainless steel syringes and analysis by gas chromatography
[AD-A187838] 11 p1447 N88-18624
An experimental method for species concentration measurements in a welding arc using laser-induced fluorescence
[DE88-005638] 13 p1778 N88-20636
Computer program in BASIC language for computation of spectrochemical analytical data
[DE88-701229] 15 p2032 N88-22106
In situ spectroscopic studies of transition metal macrocycles as catalysts for the electrochemical reduction of oxygen
[PB88-203195] 20 p2769 N88-26416
Array detectors for plasma spectrochemistry
[AD-A194220] 22 p3052 N88-28105
Applications of charge transfer devices in spectroscopy
[AD-A194408] 23 p3192 N88-28992

SPECTROSCOPIC TELESCOPES
NT STRATOSCOPE TELESCOPES
Crystal diffraction lenses for imaging gamma-ray telescope
[DE88-003084] 08 p1083 N88-16529

SPECTROSCOPY
NT ABSORPTION SPECTROSCOPY
NT ASTRONOMICAL SPECTROSCOPY
NT AUGER SPECTROSCOPY
NT AURORAL SPECTROSCOPY
NT ELECTRON SPECTROSCOPY
NT FLAME SPECTROSCOPY
NT GAS SPECTROSCOPY
NT INFRARED SPECTROSCOPY
NT LASER SPECTROSCOPY
NT MAGNETIC SPECTROSCOPY
NT MASS SPECTROSCOPY
NT MOLECULAR SPECTROSCOPY
NT NUCLEAR RADIATION SPECTROSCOPY
NT OPTICAL EMISSION SPECTROSCOPY
NT PHOTOACOUSTIC SPECTROSCOPY
NT PHOTOELECTRON SPECTROSCOPY
NT RAMAN SPECTROSCOPY
NT SPECTROPHOTOGRAPHY
NT SPECTROPHOTOMETRY
NT SPECTROSCOPIC ANALYSIS
NT STELLAR SPECTROPHOTOMETRY
NT ULTRAVIOLET SPECTROSCOPY
NT X RAY SPECTROSCOPY
A CAMAC system controlled by an IBM AT computer for time-resolved spectroscopy
[DE87-010111] 01 p0060 N88-10514
Spectroscopic studies of shocked and detonating explosives
[DE87-014216] 02 p0155 N88-10972
Third-harmonic generation and multiphoton ionization spectroscopy
[DE87-013545] 03 p0281 N88-11769
Supercritical fluid chromatography/supersonic jet spectroscopy
[DE88-000297] 03 p0282 N88-11774
Spectroscopic and retrieval studies in support of SCRIBE (Stratospheric Cryogenic Interferometer Balloon Experiment)
[AD-A184037] 03 p0351 N88-12216
Interatomic Auger rates for the sodium fluoride crystal
[DE87-013012] 03 p0382 N88-12401
Doppler snapshots 04 p0508 N88-13125
Spectroscopic monitoring of RS CVn stars at Kitt Peak using the Penn State fiber optic echelle 04 p0509 N88-13127
H alpha and Ca II emission line variability of FK comae 04 p0509 N88-13128
Evidence for an additional source of opacity during the impulsive phase of stellar flares 04 p0510 N88-13133

Contemporaneous B,V,R,I photometry and H alpha spectroscopy of YY Gem 04 p0513 N88-13155
Applications of nonlinear hole burning spectroscopy [AD-A184943] 05 p0587 N88-13580
Design of the Backscatter Spectroscopy System for the Nova Laser Facility [DE88-001880] 07 p0859 N88-15214
USSR report: Physics and mathematics [JPRS-UPM-87-002] 07 p0918 N88-15575
Raman spectroscopic investigations of Hg-Cd-Te melts 07 p0926 N88-15625
High-speed assembly language (80386/80387) programming for laser spectra scan control and data acquisition providing improved resolution water vapor spectroscopy [NASA-CR-4117] 08 p1053 N88-16355
JPRS report: Science and technology. USSR: Physics and mathematics [JPRS-UPM-87-009] 09 p1233 N88-17395
Product kinetic and internal energy distributions via velocity-aligned Doppler spectroscopy [DE88-003510] 10 p1298 N88-17764
Overview of applications of Laser-Induced Breakdown Spectroscopy (LIBS) [DE88-004314] 10 p1336 N88-17987
Spectroscopic studies of energy transfer in photosynthetic reaction centers of higher plants [DE88-003850] 10 p1359 N88-18121
Rovibrational spectroscopy of ArCO van der Waals complex [DE88-004291] 10 p1406 N88-18387
Soluble polysilane derivatives: Chemistry and spectroscopy [AD-A187889] 11 p1461 N88-18713
Positron annihilation spectroscopy of AlGaAs/GaAs interfaces in MOCVD-grown GaAs heterojunction solar cells [DE88-003903] 11 p1508 N88-19012
Multicomponent analysis using synchronous-excitation phase-resolved fluorescence spectroscopy [AD-A188883] 12 p1606 N88-19604
Millimeter and submillimeter wave research: Spectroscopy, energy transfer, and techniques [AD-A188952] 12 p1620 N88-19691
Advanced electron optics for vibrational spectroscopy [AD-A188469] 12 p1629 N88-19747
An electrochemical and spectroscopic study of electrode systems [AD-A189274] 13 p1737 N88-20384
Supercritical fluid chromatography/supersonic jet spectroscopy [DE88-004438] 13 p1738 N88-20392
Coherence effects in optical physics with special reference to spectroscopy [AD-A189520] 13 p1840 N88-21007
Development and evaluation of instrumentation and methods for multi-element analysis [AD-A189345] 13 p1841 N88-21018
Measurement of species concentrations in flames by laser-induced fluorescence [DE88-007096] 14 p1889 N88-21286
Optical cooling and trapping 14 p1974 N88-21782
Spectrographic detection of nitrogen impurity in helium [DE88-752301] 15 p2033 N88-22111
Summary report on the Japan-US Workshop on the Assessment of Spectroscopic Data for Temperature and Density Measurements --- plasma diagnostics [IPPJ-861] 17 p2439 N88-24512
Helium-like titanium spectra from tokamak plasmas 17 p2440 N88-24516
Spectroscopic study of heliotron E plasmas: Stark profile, CXR, poloidal rotation and carbon coating 17 p2441 N88-24523
Spectral diagnostics for temperature and density measurements on ATF 17 p2442 N88-24525
Spectroscopic data relevant to alpha particle diagnostics 17 p2442 N88-24527
Polarization spectroscopy: Prospect and data needs 17 p2443 N88-24531
Availability and quality of spectroscopic data and standards for tokamak studies 17 p2443 N88-24534
Reflectance spectroscopy in planetary science: Review and strategy for the future [NASA-SP-493] 17 p2451 N88-24564
Optical diagnostics for a high power, rf-inductively coupled plasma [DE88-007822] 18 p2579 N88-25322
Spectroscopy and energy transfer kinetics of the interhalogens [AD-A192103] 18 p2583 N88-25344
XUV source for ultra-high resolution photoionization spectroscopy [DE88-007531] 19 p2614 N88-25510
Supercritical fluid chromatography/supersonic jet spectroscopy [DE88-007935] 19 p2614 N88-25511
Simultaneously time- and space-resolved spectroscopic characterization of laser-produced plasmas [DE88-008038] 19 p2728 N88-26202
Velocity measurements and flow visualization in turbulent three-dimensional supersonic flows using oxygen flow tagging [AD-A192551] 21 p2892 N88-27165
Optical diagnostics for metallurgical processes [DE88-009255] 21 p2913 N88-27289
Calibration of the portable wear metal analyzer [AD-A192971] 21 p2950 N88-27524
Use of Moessbauer spectroscopy to study implanted surfaces [DE88-010452] 21 p3023 N88-27942
Recent advances in optical spectroscopy using high performance array detectors [AD-A194219] 22 p3152 N88-28753
International ultraviolet explorer spectral atlas of planetary nebulae, central stars, and related objects [NASA-RP-1203] 22 p3164 N88-28843
Determination of impurities in silicon carbide by ICP AES (inductively coupled plasma atomic emission spectrometry) after coprecipitation with lanthanum hydroxide [NASA-TT-20332] 23 p3193 N88-29003
Electrochemical evaluation of the long term corrosion resistance of polymer coated steel 24 p3355 N88-29974
An electrochemical impedance spectroscopy study of reactions at the metal/coating interface 24 p3355 N88-29975
Ultrafast processes and spectroscopy with free electron lasers [AD-A195248] 24 p3379 N88-30126
Observations of faint field galaxies [NASA-CR-183251] 24 p3453 N88-30555
A deep redshift survey of field galaxies. Comments on the reality of the Butcher-Oemler effect [NASA-CR-183255] 24 p3454 N88-30558

SPECTRUM ANALYSIS
NT CEPSTRAL ANALYSIS
NT FLAME SPECTROSCOPY
NT MAXIMUM ENTROPY METHOD
A work station for EXELFS data acquisition and analysis [USIP-87-10] 01 p0078 N88-10498
Mathematics applied to nuclear geophysics [INPE-4234-PRE/1109] 01 p0086 N88-10561
An application of L1 to astronomy --- stellar velocity [REPT-87-10] 01 p0108 N88-10702
Design and development of a database for spectral data and analysis results [DE87-011323] 02 p0247 N88-11564
Analysis of sideband spectra from untapered undulator using analytical technique [DE87-014763] 04 p0448 N88-12778
Evidence for expanding magnetic loops in coronae of cool stars 04 p0510 N88-13134
Magnetic fields on K and M stars 04 p0510 N88-13137
A spectral survey of 26 G9-M6 flare stars in the solar neighborhood 04 p0512 N88-13149
Proceedings of the Third Airborne Imaging Spectrometer Data Analysis Workshop [NASA-CR-181552] 05 p0611 N88-13755
Evaluation of AIS-2 (1986) data over hydrothermally altered granitoid rocks of the Singatse Range (Yerington) Nevada and comparison with 1985 AIS-1 data 05 p0613 N88-13767
Application of Vandermonde decomposition to directional and modal analysis of broadband transients [AD-A185007] 05 p0646 N88-13956
Incoherent radar spectra 06 p0691 N88-14239
Discussion on the modelling and processing of signals from an acousto-optic spectrum analyzer [AD-A185639] 06 p0694 N88-14257
Spectral and radiometric calibration of the Airborne Visible/Infrared Imaging Spectrometer 06 p0707 N88-14334
HOC spectral analysis of an almost periodic random sequence in noise [AD-A185528] 06 p0765 N88-14697
Intracavity spectrum analyzer with NaF:F2(+):F3(-) crystal laser for long-wave IR wave band 07 p0919 N88-15584
Effect of multiplication of spectral components of multi-frequency lasing of pulsed tunable laser 07 p0920 N88-15586
HEAO-1 observations of gamma-ray bursts 07 p0947 N88-15756
Comparative analysis of ultraviolet observations of Halley's comet on ASTRON astrophysical station before and after perihelion 08 p1004 N88-16086
Spectral analysis of an orographically structured area in the forefield of mesoscale flow simulations 08 p1016 N88-16160
Orographically influenced cold fronts in a spectral approach 08 p1016 N88-16161
Mesospheric dynamics and chemistry from SME data [NASA-CR-182465] 09 p1191 N88-17139
Nature and origin of mineral coatings on volcanic rocks of the Black Mountain, Stonewall Mountain, and Kane Springs Wash volcanic centers, Southern Nevada [NASA-CR-181437] 09 p1191 N88-17140
Growth and characteristics of materials for tunable lasers in the near infrared spectral region [NASA-CR-182501] 11 p1491 N88-18901
The 58th Shock and Vibration Symposium, volume 2 [NASA-CP-2488-VOL-2] 11 p1499 N88-18948
Dynamic substructuring for shock spectrum analysis using component mode synthesis 11 p1499 N88-18950
Regional wave attenuation and seismic moment from the inversion of NORESS spectra [AD-A187399] 11 p1510 N88-19023
Applications and limitations of the spectral-analysis-of-surface-waves method [PB88-136619] 11 p1513 N88-19038
Running head: What color is it [NASA-CR-182600] 11 p1551 N88-19280
Spectral images and multi-component models of the chromospheres of AR Lacertae 11 p1568 N88-19384
High resolution infrared absorption spectra of various trace gases present in the upper atmosphere of the Earth [NASA-CR-182590] 12 p1642 N88-19829
Microwave dielectric spectrum of rocks [NASA-TM-89719] 12 p1642 N88-19831
Gradiometer mission spectral analysis and simulation studies: Past and future 12 p1645 N88-19851
Elemental composition of Venusian rocks in northeastern part of Terra Aphrodite (determined using data from Vega-2 landing module) 13 p1726 N88-20322
Analysis of hydrocarbon band 3.35 in spectrum of Halley's Comet using data from infrared spectrometer on Vega-1 spacecraft 13 p1727 N88-20327
Spectral contents readout of birefringent sensors [NASA-CR-179430] 13 p1784 N88-20673
Stratospheric trace gas distributions from fair infrared thermal emission spectroscopy 13 p1797 N88-20749
Planetary scale barotropic spectral model 13 p1801 N88-20766
Computer programs for calculating group cross-section covariances from uncertainty parameters in the ENDF/B-V format. UNC 32/33 --- neutron physics [ECN-202] 13 p1837 N88-20995
Development and evaluation of instrumentation and methods for multi-element analysis [AD-A189345] 13 p1841 N88-21018
On the interpretation of the 3 micron emission feature in the spectrum of Comet Halley: Abundances in Comet Halley and in interstellar matter 14 p2002 N88-21935
Optical and hydrodynamic implications of Comet Halley dust size distribution 14 p2003 N88-21939
Development of remote sensing techniques capable of delineating soils as an aid to soil survey [NASA-CR-182610] 15 p2089 N88-22452
Spectral measurements in a disturbed boundary layer over snow [AD-A190217] 15 p2097 N88-22494
Multiple object redshift determinations in clusters of galaxies using OCTOPUS [INPE-4528-PRE/1278] 15 p2150 N88-22835
Multichannel 2-D power spectral estimation and applications [AD-A191273] 16 p2191 N88-23068
Spectral analysis in the linear geodetic boundary value problem [B8735056] 16 p2259 N88-23502
Spectral measurements for correcting LANDSAT data for atmospheric effects 17 p2353 N88-24020
Utilization of LANDSAT-TM , for aiding in the localization of archeological sites in the state of Sao Paulo 17 p2362 N88-24069
Study of reservoir water quality utilizing remote sensing techniques: Methodological concepts 17 p2364 N88-24076
Differential spectral synthesis of the stellar populations in the bulges of spiral galaxies 17 p2451 N88-24558
Studies of spectral line ratio fluctuations using Inductively Coupled Plasma (ICP) light [IRF-PREPRINT-100] 18 p2578 N88-25311
Measurement of HO2 and other trace gases in the stratosphere using a high resolution far-infrared spectrometer at 28 KM [NASA-CR-180400] 20 p2821 N88-26737

Multifilter spectrometer (FEB) for microwave atmospheric sounder
[AD-A192312] 21 p2935 N88-27426
Statistical analysis of dyadic stationary processes
[AD-A193057] 21 p3009 N88-27853
Array detectors for plasma spectrochemistry
[AD-A194220] 22 p3052 N88-28105
A wideband, high-resolution spectrum analyzer 22 p3066 N88-28194
ENSO, sea-surface temperatures and African rainfall 22 p3122 N88-28550
Backlund transformations associated with a Riemann-Hilbert spectral problem
[PREPRINT-596] 22 p3146 N88-28712
Qualitative characteristics of open waveguide resonator spectra
[DE88-702387] 23 p3202 N88-29056
Large aperture multi-dimensional laser radar testbed
[AD-A193447] 23 p3218 N88-29155
Surface composition of Mars: A Viking multispectral view 23 p3300 N88-29655
The optical spectroscopy of copper-blue luminescence in zinc sulfide crystals. Zero-phonon line spectra under the influence of magnetic field, temperature and excitation intensity
[ETN-88-93122] 24 p3344 N88-29903
Acoustooptic processing of two-dimensional signals using temporal and spatial integration
[AD-A194803] 24 p3359 N88-29999
Spectral analysis of the Elatina varve series
[NASA-CR-183085] 24 p3402 N88-30260

SPECULAR REFLECTION
Radiative heat transfer solutions in plane-parallel participating media: Application to multilayer insulations for space vehicles
[NPE-4221-PRE/1101] 08 p0962 N88-15824
Polymer reflectors research during FY86
[DE88-001101] 11 p1508 N88-19009
Deformation, fracture and explosive properties of reactive materials
[AD-A193080] 21 p2923 N88-27348
Solar energy absorption efficiency of an ellipsoidal receiver-reactor with specularly reflecting walls
[AD-A193726] 22 p3117 N88-28520

SPEECH
NT PHONETICS
NT SYLLABLES
NT WORDS (LANGUAGE)
Recognition of isolated non-speech sounds
[AD-A184600] 03 p0306 N88-11933
Studies of the processing of single words using positron tomographic measures of cerebral blood flow change
[AD-A184058] 03 p0356 N88-12244
Neural network based speech synthesizer: A preliminary report 08 p1064 N88-16429
Voice stress analysis 16 p2242 N88-23395
Time-frequency representations for speech signals
[AD-A188661] 18 p2498 N88-24819
Sinusoidal transform coding 19 p2653 N88-25752
Analysis and improvement of the vector quantization in SELP (Stochastically Excited Linear Prediction) 19 p2653 N88-25756
A cockpit natural language study: Vocabulary and grammar analyses
[AD-A193289] 21 p2993 N88-27753

SPEECH BASEBAND COMPRESSION
Speech coding at 4800 bps for mobile satellite communications 19 p2652 N88-25749

SPEECH DEFECTS
A study of the performance of automatic speech recognisers with speech impaired children
[RSRE-MEMO-4040] 01 p0076 N88-10486

SPEECH DISCRIMINATION
U SPEECH RECOGNITION

SPEECH RECOGNITION
A study of the performance of automatic speech recognisers with speech impaired children
[RSRE-MEMO-4040] 01 p0076 N88-10486
Language modelling for automatic speech recognition: A review
[RSRE-MEMO-4038] 01 p0084 N88-10544
Integrated voice and visual systems research topics
[NASA-CR-177417] 03 p0356 N88-12246
Controlling robots with spoken commands
[DE88-000537] 04 p0452 N88-12801
National Aeronautics and Space Administration (NASA)/American Society for Engineering Education (ASEE) Summer Faculty Fellowship Program, 1987. Volume 1
[NASA-CR-172009-VOL-1] 06 p0792 N88-14855
Digital signal processing algorithms for automatic voice recognition 06 p0793 N88-14862
Speech recognition: Acoustic-phonetic knowledge acquisition and representation
[AD-A185897] 07 p0840 N88-15097
Comparison of alphanumeric data entry methods for advanced helicopter cockpits
[AD-A186934] 09 p1201 N88-17201
Mathematical structures for speech recognition
[AD-A187063] 09 p1217 N88-17295
Voice technology using personal computers
[AD-A186743] 09 p1218 N88-17300
Speech recognition: Acoustic-phonetic knowledge acquisition and representation
[AD-A187293] 10 p1320 N88-17893
A two-stage isolated-word recognition system using discriminant analysis
[AD-A187425] 10 p1402 N88-18360
Voice/natural language interfacing for robotic control
[AD-A187765] 11 p1494 N88-18917
Evaluating the performance of the LPC (Linear Predictive Coding) 2.4 kbps (kilobits per second) processor with bit errors using a sentence verification task
[AD-A188573] 12 p1620 N88-19686
Spire based speaker-independent continuous speech recognition using mixed feature sets
[AD-A188834] 12 p1620 N88-19688
Northeast Artificial Intelligence Consortium (NAIC) administrative matters and ancillary functions, volume 1
[AD-A189466] 12 p1682 N88-20055
The acoustic-modeling problem in automatic speech recognition
[AD-A188529] 13 p1757 N88-20510
Perception of complex auditory patterns
[AD-A190218] 15 p2102 N88-22524
Auditory perception of complex sounds
[AD-A190526] 15 p2103 N88-22529
Algorithms and architectures for acoustic phonetical detection of continuous speech
[ENST-87E016] 16 p2189 N88-23054
Investigation of air transportation technology at Massachusetts Institute of Technology, 1986 17 p2293 N88-23716
Experiments in isolated digit recognition using the multilayer perceptron
[RSRE-MEMO-4073] 17 p2333 N88-23927
Experimental evaluation of algorithms for connected speech recognition using hidden Markov models
[RSRE-MEMO-4099] 17 p2333 N88-23928
ACSB: A minimum performance assessment 19 p2649 N88-25731
Novel nonlinear signal processing principles
[AD-A191644] 19 p2707 N88-26097
Signal processing in digital speech transmission systems
[ETN-88-92122] 20 p2792 N88-26561
A review of workload measurement in relation to verbal comprehension 21 p2925 N88-27360
Demodulation processes in auditory perception
[AD-A193421] 21 p2988 N88-27740
Survey of neural net paradigms for specification of discrete networks
[AD-A192682] 22 p3141 N88-28674
An overview of technology for spoken interaction with machines
[AD-A194153] 23 p3202 N88-29058
Effect of hypoxia on speech recognition in noise
[AD-A193943] 23 p3240 N88-29280
Hidden Markov models for automatic speech recognition: Theory and application
[RSRE-MEMO-4135] 23 p3251 N88-29350

SPEECHES
U LECTURES

SPEED
U VELOCITY

SPEED CONTROL
A simulation study of a speed control system for autonomous on-road operation of automotive vehicles
[AD-A184030] 03 p0362 N88-12279
The theory and implementation of a high quality pulse width modulated waveform synthesiser applicable to voltage FED inverters
[ETN-87-90712] 09 p1157 N88-16937
Speed control of a missile with throttleable ducted rocket propulsion 12 p1597 N88-19561
Contribution to speed regulation of small motors with phase-locked loops
[ETN-88-92373] 20 p2796 N88-26590
Reduction in mill air compressor power requirements through installation of a variable frequency speed control
[DE88-008493] 23 p3221 N88-29171

SPEED INDICATORS
NT TACHOMETERS

SPEED REGULATION
U SPEED CONTROL

SPEED REGULATORS
The design of a turboshaft speed governor using modern control techniques
[NASA-CR-175046] 01 p0053 N88-10339
Engine/airframe response evaluation of the HH-60A helicopter equipped with the T700-GE-701 transient droop improvement electronic control unit
[AD-A184443] 04 p0401 N88-12492
Contribution to speed regulation of small motors with phase-locked loops
[ETN-88-92373] 20 p2796 N88-26590

SPENT FUELS
Atlas of atomic spectral lines of neptunium emitted by an inductively coupled plasma
[DE88-000640] 06 p0782 N88-14796
Numerical computations of natural convection heat transfer in irregular geometries
[DE88-002358] 07 p0852 N88-15178

SPERMATOGENESIS
Investigations of the reproductive physiology of the rainbow trout (Salmo gairdneri Richardson) 07 p0885 N88-15370

SPHERES
NT CONCENTRIC SPHERES
NT FALLING SPHERES
NT ROTATING SPHERES
Development of response models for the Earth Radiation Budget Experiment (ERBE) sensors. Part 2: Analysis of the ERBE integrating sphere ground calibration
[NASA-CR-178293] 01 p0049 N88-10316
Division algebras and sphere fibrations
[ETN-87-90677] 01 p0087 N88-10566
Particle velocity and stress gage measurements in spherical diverging flow
[DE87-007333] 03 p0321 N88-12033
Dynamical analysis of molecular decay at spherical surfaces
[AD-A184908] 05 p0647 N88-13964
Nonuniformity of electromagnetic field at Lambda = 10.6 micron wavelength inside atmospheric aerosol particles 06 p0772 N88-14743
Assessment of anomalous gravitational field of elastic Earth 07 p0921 N88-15594
Application of a simple rotational spherical grating mounting to high resolution soft X-ray spectroscopy
[PB87-164836] 09 p1142 N88-16845
Light absorption by an atom moving inside a spherical box
[AD-A187241] 10 p1407 N88-18395
The application of the hybrid iterative method to scattering by perfectly conducting bodies of revolution 11 p1475 N88-18802
A program for the calculation of radio-wave transmission loss over the spherical earth and over obstacles 12 p1616 N88-19662
Simulated impact damage in a thick graphite/epoxy laminate using spherical indenters
[NASA-TM-100539] 13 p1733 N88-20363
Distribution of chain ends inside the polybutadiene microspheres of SB diblock copolymers
[AD-A191257] 16 p2182 N88-23007
The structure and stability of spherically expanding flames 17 p2318 N88-23842
Theoretical predictions of precipitate shapes in cubic alloys
[DE88-010856] 21 p2914 N88-27291
Light scattering by charged spheres
[AD-A193753] 22 p3153 N88-28759
Elastic behavior of a rubber layer bonded between two rigid spheres
[AD-A193698] 23 p3198 N88-29030
Effects on the resonant frequencies caused by loading a spherical cavity with a dielectric sphere
[AD-A193864] 23 p3277 N88-29511

SPHERICAL COORDINATES
Density variations of meteor flux along the Earth's orbit 06 p0739 N88-14545
Hyperspherical coordinate theory of two-electron processes: Future plans
[DE87-010653] 08 p1081 N88-16516
Generation of surface grids through elliptic partial differential equations for aircraft and missile configurations
[AD-A186631] 11 p1535 N88-19169
Adiabatic representation of three-body problem in hyperspherical coordinates. Statement of the problem
[DE88-701162] 15 p2126 N88-22678
A formulation for the boundary-layer equations in general coordinates
[NASA-TM-100079] 18 p2459 N88-24600
An improved spherical earth diffraction algorithm for SEKE
[AD-A195847] 24 p3360 N88-30005

SPHERICAL HARMONICS
Atlas of wide-field-of-view outgoing longwave radiation derived from Nimbus 7 Earth radiation budget data set - November 1978 to October 1985
[NASA-RP-1186] 01 p0070 N88-10451
Ab initio methods for electron-molecule collisions
[DE87-011728] 01 p0092 N88-10598

Spherical harmonic expansion of the Levitus Sea surface topography
[NASA-CR-181448] 02 p0216 N88-11362
Statistics of the geomagnetic secular variation for the past 5Ma
[NASA-CR-181558] 04 p0467 N88-12890
Rotation of magnetized particle in electrically conducting viscous medium 06 p0770 N88-14733
Modeling and estimation of a low degree geopotential model from terrestrial gravity data
[NASA-CR-182808] 16 p2232 N88-23330

SPHERICAL PLASMAS
Stability of spheroidal spheromak plasma by use of force-free approximation
[IPPJ-846] 02 p0241 N88-11523

SPHERICAL SHELLS
Geometrically nonlinear rod mechanism analogy of axisymmetrically loaded spherical shells based on a comprehensive approach to the stability of circular arches
[ETN-87-90419] 01 p0062 N88-10398
Microgravity nucleation and particle coagulation experiments support
[NASA-CR-181541] 04 p0423 N88-12619
RADSPHERE: A computer program for calculating the steady-state, axially symmetric, forced response and radiation field of a submerged spherical shell
[AD-A185025] 05 p0609 N88-13738
A vectorized Poisson solver over a spherical shell and its application to the quasi-geostrophic omega-equation
[NASA-CR-4116] 08 p1039 N88-16285
Retarded potential technique applied for shock wave loading of doubly symmetric submerged structures
09 p1179 N88-17058
Cubic spline solution of symmetric buckling problems of clamped shallow spherical shells
15 p2053 N88-22239
Method and apparatus for growing crystals
[NASA-CASE-MFS-28137-1] 17 p2446 N88-24544

SPHERICAL TANKS
Mass transport in annular spherical system
[LRT-WE-9-FB-11(1987)] 22 p3077 N88-28271
Orbital Propulsion Module (OPM). Study on coni-spherical surface tension tanks (COSTA)
[MBB-URV-170/87] 23 p3187 N88-28963

SPHEROIDS
NT OBLATE SPHEROIDS
NT PROLATE SPHEROIDS

SPHEROMAKS
Acceleration to hypervelocities using minimum energy concepts
[DE87-011796] 01 p0089 N88-10583
Stability of spheroidal spheromak plasma by use of force-free approximation
[IPPJ-846] 02 p0241 N88-11523
Magnetohydrodynamic stability of spheromak plasma in toroidal flux conserver with rectangular cross section 3. Stability for symmetric modes
[IPPJ-845] 02 p0241 N88-11524
Reversed field pinch experiments: Summary of progress report
[DE88-002367] 07 p0934 N88-15673
Stability of spheromak against current driven modes: Effects of flux hole on stability
[IPPJ-868] 19 p2730 N88-26211

SPICULES
Active region flows 02 p0255 N88-11611

SPIKE ANTENNAS
U MONOPOLE ANTENNAS

SPIKING
Distributed feedback effects in lasers and high gain laser instabilities in optically pumped CH3F
03 p0329 N88-12079

SPILLING
Products of the neutralization of hydrazine fuels with hypochlorite, 2
[DE87-011454] 01 p0030 N88-10193
Hydrocarbon fuel spill dispersion on water: Literature review
[AD-A192486] 21 p2922 N88-27346

SPIN
NT ELECTRON CAPTURE
NT ISOTOPIC SPIN
NT NUCLEAR SPIN
NT PARTICLE SPIN
NT SPIN-SPIN COUPLING
Gravitational interaction of massless fields with higher spins (s greater than 2) 06 p0775 N88-14760
ISTP SBIR phase 1 Full-Sky Scanner: A feasibility study
[NASA-CR-180749] 10 p1333 N88-17964
Spin precession in stationary gravitational fields
[DE88-701107] 15 p2093 N88-22470
Effective electron interactions due to virtual charge and spin excitations in an extended Hubbard model for Cu-O superconductors
[DE88-005971] 15 p2139 N88-22766
Refractory films from spin-cast carbon
[DE88-011251] 21 p2919 N88-27327

SPIN DYNAMICS
Laminar flow over a spinning projectile at an angle of attack 02 p0121 N88-10766
Plasmon resonance absorption in layered structures of silver with periodic corrugation
[DE87-013183] 02 p0231 N88-11453
Torsion as a source of expansion in a Bianchi type I universe in the self-consistent Einstein-Cartan theory of a perfect fluid with spin density
[AD-A184200] 03 p0322 N88-12037
Fundamental properties of spin-polarized quantum systems
[DE88-004425] 10 p1423 N88-18499
Investigation of the spin stability of the NPS (Naval Postgraduate School) mini-satellite (Orion)
[AD-A187781] 11 p1445 N88-18613
Laser measurements of state-resolved Ga and in atom sticking and desorption on metal and semiconductor surfaces
[AD-A187644] 11 p1555 N88-19310
Can the causal pathologies of Goedel-type universes be avoided in higher-derivative gravity
[DE88-700185] 11 p1568 N88-19387
The effect of combustion gas flow on the rotational dynamics of a spinning solid fuel rocket
13 p1732 N88-20358
Fluid motion in a spinning, coning cylinder via spatial eigenfunction expansion
[AD-A190758] 15 p2066 N88-22319
Energy transfer processes in free radicals: A collaborative experimental and theoretical investigation
[AD-A191264] 16 p2269 N88-23578
Raychaudhuri equation in the self-consistent Einstein-Cartan theory with spin-density
[NASA-TM-101145] 17 p2447 N88-24546
Inflation in Einstein-Cartan theory with energy-momentum tensor with spin
[NASA-TM-101164] 17 p2447 N88-24547
A scientific basis for an alternate cathode architecture
[AD-A191498] 18 p2481 N88-24717
Theoretical investigation of the development of the normal fluid and superfluid velocity distributions during spin-up for a He2-filled cylinder
[MPIS-6/1987] 18 p2510 N88-24892
Dynamics of satellites with radial wire antennas
20 p2784 N88-26514
Properties of synthetic magnetic superlattices
20 p2865 N88-27014
A method for reducing the coning of a spinning vehicle
[DE88-010971] 21 p2896 N88-27189
Contribution to the numerical solution of airplane spin motion
[ETN-88-92368] 21 p2896 N88-27190
Dissolution rates of polymers and copolymers based on methyl, ethyl and butyl methacrylate
[AD-A194713] 23 p3197 N88-29027
Passage of relativistic magnetic dipole moments through magnetic fields
[DE88-702640] 23 p3295 N88-29624
Resonant spin-flavor precession of solar and supernova neutrinos
[DE88-752604] 23 p3308 N88-29707

SPIN GLASS
Nonlinear relaxation and ergodicity breakdown in random anisotropy spin glasses
[PREPRINT-565] 06 p0764 N88-14693
Superconductive analogue of spin glasses
[DE88-702059] 19 p2733 N88-26233

SPIN REDUCTION
Seven year thermal vacuum real life test of a medium speed (despin) mechanism manufactured by Dornier System
[ESA-ESTL-64] 09 p1175 N88-17038

SPIN RESONANCE
Nuclear structure studies at intermediate energies
[DE88-006683] 18 p2571 N88-25271
Paramagnetic spins in oxygen-loaded ceramic La2CuO4/sub 4+delta/
[DE88-007114] 19 p2619 N88-25539

SPIN STABILIZATION
Effect of void gas lying between fluid slugs in nutation dampers 03 p0319 N88-12015
Country plans three-axis weather satellite
06 p0688 N88-14218
Attitude dynamics for satellites stabilized through spin
[INPE-4403-NTE/275] 08 p0963 N88-15833
Control and stabilization of ESA satellites
09 p1124 N88-16734
Investigation of the spin stability of the NPS (Naval Postgraduate School) mini-satellite (Orion)
[AD-A187781] 11 p1445 N88-18613
Separation dynamics for the last stage of a launch vehicle and satellite
[INPE-4281-PRE/1153] 12 p1601 N88-19582
Modeling of a nutation damper for satellite stabilization through rotation
[INPE-4275-PRE/1147] 12 p1601 N88-19584
Identification of a star field from a spinning satellite
[CNES-NT-120] 15 p2026 N88-22074
Development of a digital sun sensor for a spin-stabilized satellite
[INPE-4508-TDL/327] 16 p2169 N88-22929
Dynamics of satellites with radial wire antennas
20 p2784 N88-26514
A method for reducing the coning of a spinning vehicle
[DE88-010971] 21 p2896 N88-27189
Simulation of attitude and maneuvers for the Brazilian spin-stabilized satellite
[INPE-4271-PRE/1143] 22 p3046 N88-28079
Computational aerodynamic analysis for a range-limited 25mm training round
[AD-A185270] 24 p3320 N88-29772

SPIN TEMPERATURE
Spin disorder resistivity and bare Curie temperature in the ferromagnetic superconductor ErRh4B4
[DE88-003016] 10 p1415 N88-18445

SPIN WAVES
U MAGNONS

SPIN-LATTICE RELAXATION
Nuclear magnetic resonance studies of ion motion in solid electrolytes
[DE87-014547] 02 p0232 N88-11464
Nonlinear relaxation and ergodicity breakdown in random anisotropy spin glasses
[PREPRINT-565] 06 p0764 N88-14693
Transport and relaxation processes in supercritical fluids
[DE88-004804] 10 p1419 N88-18474
Nuclear magnetic ordering and paramagnetic relaxation of diatomic molecules in Ca (OH)2
[B8681469] 23 p3281 N88-29532
Static and dynamic behavior of a quasi one-dimensional Heisenberg antiferromagnet in the long-range ordered state. A nuclear magnetic resonance study performed with a He3-He4 dilution refrigerator
[B8705564] 23 p3281 N88-29533
Fluctuation and relaxation phenomena studied by means of nuclear orientation
[B8679671] 23 p3281 N88-29534

SPIN-ORBIT INTERACTIONS
NT ELECTRON CAPTURE

SPIN-SPIN COUPLING
Example of correlation between space and spin coordinates
[DE87-703366] 05 p0657 N88-14030

SPINAL CORD
Neuropeptides in experimental head injury
[AD-A188067] 11 p1520 N88-19077
Effect of low-frequency whole-body vertical vibration on the serotoninergic system of the brain and spinal cord
19 p2704 N88-26081

SPINEL
Aluminum oxynitride spinel (ALON): A review
[AD-A184753] 03 p0294 N88-11845
Precipitation in alumina-rich spinel: A transformation-toughened ceramic single crystal
[DE87-012380] 06 p0785 N88-14815
The migration of grain boundaries in ceramic materials with particular reference to the sintering process
[DE88-004085] 10 p1306 N88-17808
Research on high-specific-heat dielectrics
[AD-A187248] 11 p1481 N88-18710

SPIRAL GALAXIES
NT ANDROMEDA GALAXY
NT BARRED GALAXIES
NT MILKY WAY GALAXY
Comments on H. Arp The persistent problem of spiral galaxies
[TRITA-EPP-87-05] 05 p0660 N88-14052
Infrared emission and tidal interactions of spiral galaxies 07 p0923 N88-15611
The radio structure of active nuclei in edge-on spiral and Seyfert galaxies 09 p1264 N88-17576
Global properties of star formation in spiral galaxies
14 p1994 N88-21883
Molecular gas in Virgo cluster spiral galaxies
17 p2450 N88-24557
Surface photometric investigations for spiral galaxies of large dimension structures in edge-on gemetry
[ETN-88-92126] 21 p3030 N88-27985
The dynamics of SBO galaxies. Part 1: The data
[SER-C-PREPUBL-FASC-22] 24 p3455 N88-30567

SPLASHING
Numerical simulation of splash of droplet at unit gravity 05 p0538 N88-13275
SPLEEN
Spleen lymphocyte nucleic acids in pregnant rats flown in space and their offspring 07 p0892 N88-15403
SPLINE FUNCTIONS
The use of splines in the modelling of a photodiode response
[NPL-DITC-88/87] 01 p0085 N88-10550
An adaptive subdivision method with crack prevention for rendering beta-spline objects
[AD-A184249] 04 p0477 N88-12940
Stability properties of spline approximations for retarded systems
[PB87-220919] 05 p0639 N88-13910
The Wilson-Fowler spline in a global IGES (Initial Graphics Exchange Specification) coordinate frame
[DE88-001942] 06 p0757 N88-14840
Solution in vibration problems of rectangular plates with spline function
[PB87-143459] 08 p0996 N88-16029
Strategies for knot placement in least squares data fitting by splines
[NPL-DITC-101/87] 09 p1229 N88-17366
The NPL data approximation subroutine library: Current and planned facilities
[NPL-DITC-104/87] 14 p1959 N88-21681
A spline collocation method for integral equations of the first kind with logarithmic singularity --- boundary value problems
[REPT-87-39] 14 p1963 N88-21712
Cubic spline solution of symmetric buckling problems of clamped shallow spherical shells
15 p2053 N88-22239
Application of spline functions to digital image processing
[ETN-88-92194] 17 p2392 N88-24218
Open or closed curves by regularized B-splines
[RR-652-M] 18 p2563 N88-25218
SPLINES
Knot selection for least squares thin plate splines
[AD-A185681] 06 p0759 N88-14857
Core spline method for solution of quantum-mechanical systems of differential equations for bound states
[DE88-700492] 09 p1259 N88-17551
Procedure for converting a Wilson-Fowler spline to a cubic B-spline with double knots
[DE88-008971] 20 p2844 N88-26878
SPLITS (GEOLOGY)
U GEOLOGICAL FAULTS
SPLITTING
A survey of upwind principles for the multidimensional Euler equations 08 p0984 N88-15953
Schwarz splitting and template operators
[AD-A187956] 10 p1404 N88-18370
The splitting of Comet Halley 1986
14 p2010 N88-21989
Fully implicit splitting method for accurate tidal computations
[PB88-183637] 20 p2828 N88-26781
SPOILERS
A numerical procedure for conformal mapping of the exterior of a circle onto the exterior of a wing profile with a spoiler
[ISL-R-110/86] 11 p1536 N88-19180
Air-jet spoiler
[BU-364] 13 p1722 N88-20299
Theoretical and experimental investigations of a vortex drag behind a wing profile with spoiler
[ISL-PU-309/87] 21 p2892 N88-27169
Investigations of aircraft control with jet spoilers
[ISL-R-112/87] 21 p2898 N88-27202
SPONGES (MATERIALS)
The origin of the spicule skeleton of fresh water sponges (Spongillides). 07 p0885 N88-15368
SPONTANEOUS COMBUSTION
Fire tests on loose-fill insulation materials
[DE88-751182] 11 p1467 N88-18748
SPONTANEOUS EMISSION
Effect of off-axis radiation in amplified spontaneous emission
[DE88-007001] 14 p1915 N88-21440
Investigation of ultrashort traveling-wave amplified spontaneous emission 16 p2187 N88-23040
SPORADIC E LAYER
An analysis of apparent-motion vectors in, and the structure of, A mid-latitude sporadic E layer using a 2.66 MHz radar
[AD-A186126] 07 p0877 N88-15321
SPORADIC METEOROIDS
Models of sporadic meteor body distributions
06 p0739 N88-14543
Lidar investigations of M-zone
06 p0741 N88-14558
Optical electronics for meteor observations
06 p0741 N88-14559
SPORES
NT MICROSPORES
SPOT (FRENCH SATELLITE)
SPOT 1: First In-Flight Results --- conferences
[ISBN-2-85428-177-2] 03 p0340 N88-12143
Development of the SPOT commercial service: Preliminary conclusions after six months of operations
03 p0340 N88-12144
Satimage and the Nordic SPOT market
03 p0340 N88-12145
SPOT Image Corporation: Early results
03 p0340 N88-12146
The Canadian SPOT program
03 p0340 N88-12147
First assessment of processing and use of SPOT images by the Institut Geographique Nationale --- French National Geographic Institute 03 p0341 N88-12148
Results of the satellite and the Toulouse (France) receiving station operator --- SPOT
03 p0341 N88-12149
Signal to noise ratios --- SPOT images
03 p0341 N88-12150
Detector normalization --- SPOT remote sensors
03 p0341 N88-12151
Absolute and interband calibration --- SPOT
03 p0341 N88-12152
Modulation transfer function --- SPOT
03 p0341 N88-12153
Intrinsic and extrinsic geometric quality --- SPOT images 03 p0341 N88-12154
Registration of SPOT images
03 p0341 N88-12155
Evaluation of SPOT stereoscopic possibilities for cartography 03 p0342 N88-12156
Feasibility study of a range of products drawn from SPOT satellite imagery and specific to road-laying studies
03 p0342 N88-12157
Adaptation of numerical SPOT data to an urban environment 03 p0342 N88-12158
Cartography and topography with SPOT
03 p0342 N88-12159
Vegetation classification, land systems and mapping using SPOT multispectral data: Preliminary results
03 p0342 N88-12160
SPOT for earthquake hazard zoning in southern Italy, a provisional report 03 p0342 N88-12161
Flood monitoring using SPOT
03 p0342 N88-12162
Application of SPOT-1 data to mineral exploration in Nevada 03 p0343 N88-12163
Geological interpretation of a SPOT image over Kenya: The Gregory rift network of faults
03 p0343 N88-12164
Evolution of remote sensing utilization in geological mapping and ore exploration: Example in Zimbabwe
03 p0343 N88-12165
Vegetation studies in the national Park of Comoe (Ivory Coast) using SPOT 1 satellite data
03 p0343 N88-12166
SPOT data for crop discrimination in southern Brazil
03 p0343 N88-12169
SPOT: A tool for agricultural statistics
03 p0344 N88-12170
Application of multitemporal SPOT data for crop monitoring: Effects of frost and drought
03 p0344 N88-12171
Use of SPOT panchromatic imagery to update forest maps of northern Quebec, Canada
03 p0344 N88-12172
Stand based forest inventory from SPOT IMAGE. First experiments 03 p0344 N88-12173
Applicability of SPOT for forest inventory, mapping and change monitoring 03 p0344 N88-12174
Use of SPOT images for coastal development and inventory of aquacultural sites in New Caledonia (ALIAS project). First results 03 p0344 N88-12175
Contribution of SPOT data to the physiographic study of coastal environment: La Pointe d'Arcay and l'Anse de l'Aiguillon (France) 03 p0344 N88-12176
Coastal dynamics of the mouth of the Saloum (Senegal) --- SPOT imagery 03 p0345 N88-12177
The new generation of SPOT satellites
03 p0345 N88-12178
The use of SPOT images for water resources surveys. The examples of the Kasserine area (Tunisia) and the Jebel Amour (Algeria) 03 p0345 N88-12179
National Point Of Contact (NPOC)-SPOT inquiry 1986
[NLR-MP-86055-U] 05 p0620 N88-13807
The SPOT solar array. Box opening mechanisms physical vapor deposition (PVD)-MoS2: Lubricated slides. Functional evaluation 14 p1876 N88-21211
High lifetime mechanisms implemented in infrared horizon scanning sensors --- SPOT
14 p1877 N88-21214
Radio frequency compatibility between IRS and SPOT 3: Preliminary study
[CNES-86/CT/DRT/TIT/TR/011]
14 p1905 N88-21383
Terrain classification using SPOT images and the computer system GOP-300
[FOA-C-20677-2.7] 17 p2368 N88-24102
Bathymetry estimation by analyzing swell on SPOT images 19 p2701 N88-26062
Contribution of spaceborne high resolution radiometers to mapping of precoastal depths
19 p2701 N88-26063
SPOT 1 Image Utilization, Assessment, Results
[ISBN-2-85-428188-8] 22 p3089 N88-28346
The contribution of remote sensing to hydrology and hydrogeology 22 p3090 N88-28347
Mapping of streamflow and soil infiltration of a Sahelian catchment area by SPOT image interpretation: The Oursi pond catchment area in Burkino Faso
22 p3090 N88-28348
The use of SPOT images for water resources surveys in the Kasserine Basin (Tunisia)
22 p3090 N88-28349
SPOT image exploitation for glacial mass balance fluctuation monitoring in the French Alps
22 p3090 N88-28350
SPOT on land and lakes in the Hubei Province (China)
22 p3090 N88-28351
Evaluation of SPOT imagery for monitoring irrigated lands 22 p3090 N88-28352
An evaluation of SPOT imagery for wetland monitoring
22 p3091 N88-28353
Comparative study of crop and soil mapping using multitemporal and multispectral SPOT and LANDSAT data 22 p3091 N88-28354
Water resources and agricultural land use investigations in northeastern Gujarat (India) 22 p3091 N88-28355
Study of the forests on the banks of the Gambia and criteria for detecting mortality 22 p3091 N88-28356
Use of SPOT satellite in agrohydrology: Detection of spring water excess in a grassland region
22 p3091 N88-28357
Review of the studies of geography and environment and studies on spectral characteristics of SPOT HRV data 22 p3091 N88-28358
Evaluation of the grassy biomass in the Sahelian zone in the South Tamesna region (Niger): Prospects and limits of use of SPOT data 22 p3092 N88-28359
Changes in species composition of heathland, monitored by means of remote sensing and field mapping: The results of the HEISPOT project 22 p3092 N88-28360
Topography of an Antartic ice stream
22 p3092 N88-28361
Spatial and spectral registration of Javanese landscape units with SPOT 22 p3092 N88-28362
Comparison between the respective contributions of the TM LANDSAT-4 and HRV SPOT-1 data to the land use mapping of Mediterranean coastal zone
22 p3092 N88-28363
Land use systems and rural landscapes in the center of Veracruz State (Mexico): First results
22 p3092 N88-28364
SPOT for earthquake hazard zoning in southern Italy
22 p3093 N88-28365
Discrimination of sand transport rates and environmental consequences in central Egypt from SPOT data
22 p3093 N88-28366
Delineation of ephemeral fluvial networks on low-relief Piedmont surfaces, Plutonium Valley, Nevada, USA
22 p3093 N88-28367
Following the seasonal evolution of a natural environment in a humid tropical region. Preliminary Evaluation of SPOT (PEPS) number 186: Bangui, Central Africa 22 p3093 N88-28368
Application of SPOT to agricultural information systems in temperate regions 22 p3093 N88-28369
Potential use of SPOT satellite data for the national resources inventory 22 p3093 N88-28370
Methodological developments on crop inventories using SPOT and ground surveys 22 p3094 N88-28371
Evaluation of annual crop surfaces and territorial inventory in the Paris basin by combining classic statistical inquiries and SPOT data (Preliminary Evaluation Program for SPOT 127) 22 p3094 N88-28372
Evaluation of automatic texture analysis for increased crop identification accuracy with SPOT data
22 p3094 N88-28373
Application of SPOT multidate data to wheat yield estimation in Beauce (France) 22 p3094 N88-28374
An evaluation of multidate SPOT data for agriculture and land use mapping in the United Kingdom
22 p3094 N88-28375
The suitability of SPOT imagery for monitoring landscape patterns 22 p3094 N88-28376

Characterization, topology, and cartography of grasslands for the development of fodder resources. (Preliminary Evaluation Program for SPOT number 26)
22 p3095 N88-28377
HRV data for the applications on reneweable resources in Canada — SPOT 22 p3095 N88-28378
SPOT-1 HRV data and vegetation amount
22 p3095 N88-28379
Attempt to inventory vines using oblique SPOT images
22 p3095 N88-28380
Analysis of soils using remote sensing information at the scale of the parcel 22 p3095 N88-28381
Comparative variations of spectral signatures in a cultivated area of the Paris Basin (27 May, 26 June, 1 July 1986) 22 p3095 N88-28382
Monitoring of agricultural production in West Africa. The need to integrate different satellite platforms
22 p3096 N88-28383
Use of SPOT imagery for vegetation/biomass mapping, geotechnical mapping, catchment area determination, and settlement location in the Turkana district, northern Kenya 22 p3096 N88-28384
Digital and visual analysis of SPOT and TM data for crop discrimination in southern Brazil
22 p3096 N88-28385
A comparative thematic mapping analysis of SPOT data: The Vientiane Plain (Lao PDR)
22 p3096 N88-28386
Discrimination methods of traditional fields in a humid tropical region (Shaba, Zaire) using digital classification on SPOT data 22 p3096 N88-28387
Evaluation of SPOT data for crop inventory and monitoring in Sudanian Africa. Example of Bane area (Burkina Faso) 22 p3096 N88-28388
Identification of farming systems in the cotton area of West Burkina Faso from SPOT-1 data
22 p3097 N88-28389
Monitoring Tunisia's steppes with SPOT
22 p3097 N88-28390
Study of savannah formation in the Sudanian zone. Northwest sector of the La Comoe park, Ivory Coast
22 p3097 N88-28391
Pilot study of rice culture in sub-tropical high population density region (Madagascar) with SPOT 1 multispectral data 22 p3097 N88-28392
Using SPOT HRV data to update the distribution of the paddy field in Taiwan 22 p3097 N88-28393
Agro-ecological mapping from SPOT 1 data in southern Thailand: New questions for an analysis of the farming-systems 22 p3097 N88-28394
SPOT applications on Columbia's coffee zone
22 p3097 N88-28395
Use of SPOT data in preliminary steps of road project studies especially suited for developing countries
22 p3098 N88-28396
SPOT imagery for detecting residential expansion on the rural-urban fringe of Toronto, Canada
22 p3098 N88-28397
Spread of large tropical conurbations
22 p3098 N88-28398
Utilization of remote sensing for the observation of urban populations. Ongoing research in Quito (Ecuador)
22 p3098 N88-28399
Integration of SPOT data into a geocoded information system 22 p3098 N88-28400
Utilizing SPOT data for seismic shot-line mapping and environmental monitoring in oil and gas exploration
22 p3098 N88-28401
Preliminary comparative analysis of LANDSAT and SPOT data for the study of the sanding phenomenon: Zaafrane region (Algeria) 22 p3099 N88-28402
An evaluation of the applicability of SPOT stereoscopic imagery to the Canada Land Use Monitoring Program (CLUMP) 22 p3099 N88-28403
Topographic suppression and advances in classification for land cover mapping using SPOT-1 HRV imagery
22 p3099 N88-28404
Monitoring Moneragala (Sri Lanka) with SPOT imagery
22 p3099 N88-28405
Monitoring urban land cover changes at the urban fringe from SPOT HRV imagery in south-east England
22 p3099 N88-28406
Preliminary analyses of SPOT HRV multispectral products for arid and temperate environments
22 p3099 N88-28407
Assessment of SPOT satellite based system in humid tropical vegetation identification, classification and monitoring 22 p3100 N88-28408
A comparison between SPOT and LANDSAT TM for mapping of vegetation and bedrock outcrops
22 p3100 N88-28409
Accuracy of land use classification for SPOT image data 22 p3100 N88-28410
Analysis of SPOT multispectral data concerning a border zone between two geographical regions in southern Belgium 22 p3100 N88-28411
Thematic mapping of central Java (Indonesia)
22 p3100 N88-28412
Utilization of SPOT-1 multispectral data for mapping land cover and phytohygiene monitoring in the central zone of the Mercantour National Park (France)
22 p3100 N88-28413
Applications of SPOT data for urban real estate investment information systems
22 p3101 N88-28414
Mapping and urban multi-experimental assessment of SPOT: Urban results 22 p3101 N88-28415
SPOT-1 over New Zealand: Analysis of SPOT imagery for land use investigations 22 p3101 N88-28416
Comparison of SPOT, LANDSAT TM and combined data for urban studies 22 p3101 N88-28417
Utilization of SPOT multispectral data for urban planning 22 p3101 N88-28418
First results of international investigations of the applications of SPOT-1 data to geologic problems, mineral and energy exploration 22 p3101 N88-28419
Rate of slip on the Altin Dagh Fault (North Tibet, China) 22 p3102 N88-28420
Karst and submarine fresh water discharge in the Antalya area, southern Turkey 22 p3102 N88-28421
Results of the Geosat program to evaluate SPOT data for petroleum and mineral exploration
22 p3102 N88-28422
The application of SPOT data to the structural geology of western Nevada 22 p3102 N88-28423
Application SPOT-1 data to mining activity: Example of the Imiter Silver Mine, Morocco
22 p3102 N88-28424
Evaluation of SPOT imagery contribution to petroleum exploration: The Suez Rift (Egypt)
22 p3102 N88-28425
Evaluation of SPOT imagery for discriminating vegetation communities associated with surficial and bedbrock geology and identifying anomalous and stressed vegetation associated with mineralization
22 p3103 N88-28426
SPOT imagery as an aid to understanding volcanism and tectonics: Examples from the Chilean Andes and the Tibetan Plateau 22 p3103 N88-28427
Role of SPOT in geological application of remote sensing 22 p3103 N88-28428
SPOT imagery preliminary contribution to cartography and geodynamics in the Benue trough (Nigeria)
22 p3103 N88-28429
An evaluation of SPOT imagery for Earth science studies in the Antarctic. Preliminary Evaluation Program (PEPS) 289 for SPOT 22 p3103 N88-28430
Structural analysis of the Jura mountains-Rhine Graben intersection (Switzerland) for petroleum exploration using SPOT stereoscopic data 22 p3103 N88-28431
Methodology for the use of SPOT imagery in petroleum exploration. Example of the Bas-Languedoc area (France) 22 p3104 N88-28432
Analyzing the stratigraphy, tectonism, and mineralization at the Spanish side of the pyrite belt, Huelva province, Spain, using SPOT imagery 22 p3104 N88-28433
Geologic applications of SPOT-1, TM, and NOAA-7 data: Finding and defining unmapped structural features
22 p3104 N88-28434
Comparing different images for ground water survey based on lineament analysis 22 p3104 N88-28435
Spectral and spatial attribute evaluation of SPOT data in geological mapping of precambrian terrains in semiarid environment of Brazil 22 p3104 N88-28436
Geologic results obtained from the use of SPOT imagery along plate boundaries: Examples in the East African rift and of the northern-Caribbean collision
22 p3105 N88-28437
SPOT images and geochemical mapping of lateritic covers in southern Mali 22 p3105 N88-28438
Analysis of the multispectral content and of SPOT subscenes in two regions of Burundi. Lithologic and tectonic interpretations 22 p3105 N88-28439
SPOT imagery for landslide cartography in mountainous areas. Example of the French Maritime Alps
22 p3105 N88-28440
SPOT for slope instability survey in Nepal
22 p3105 N88-28441
Detailed geological mapping of the massif of Sainte Victoire (Provence, France) using SPOT imagery. Comparison with other multisource data. New tectonic interpretation of this region 22 p3105 N88-28442
Satellite remote sensing for forest management. A review illustrated with research results on SPOT 1 data
22 p3106 N88-28443
An evaluation of the utility of SPOT and Thematic Mapper data for providing forest inventory information
22 p3106 N88-28444
SPOT-1 satellite imagery for forest inventory in Sweden 22 p3106 N88-28445
Forest mapping by visual interpretation of SPOT images 22 p3106 N88-28446
Forest management applications of SPOT data in Australia 22 p3106 N88-28447
SPOT multispectral data and maritime pine stands in southwest of France 22 p3106 N88-28448
Stand-based forestry inventory from SPOT image
22 p3106 N88-28449
Potential of SPOT imagery as a tool for forest mapping in Quebec 22 p3107 N88-28450
Assessment of large area forest disturbances caused by biotic and abiotic factors on the basis of SPOT images 22 p3107 N88-28451
Study of deforestation in the Vosges (France) by remote sensing 22 p3107 N88-28452
Contribution to the mapping of forests in an intensively divided area, with the help of SPOT image data
22 p3107 N88-28453
SPOT 1: Image utilization, assessment, results. A study of the Elburgon Forest area (Kenya) showing the spectral responses of different forest tree species
22 p3107 N88-28454
SPOT investigations of estuaries and coastal zones: An overview 22 p3107 N88-28455
SPOT: A tool to aid preselection of sites favorable for aquiculture. Evaluation and perspectives of the Preliminary Evaluation Program for SPOT (PEPS) ALIAS Caledonie
22 p3108 N88-28456
The monitoring of sediment transport, water circulation and mixing in estuaries and coastal waters
22 p3108 N88-28457
Evaluation of SPOT data for remote sensing of physical and biological properties of estuaries and coastal zones
22 p3108 N88-28458
Utilization of SPOT in hydrography
22 p3108 N88-28459
Application of SPOT imagery for oil spill contingency planning 22 p3108 N88-28460
The use of SPOT data in mapping coastal areas
22 p3108 N88-28461
SPOT: A satellite for oceanography
22 p3108 N88-28462
Contribution of SPOT satellite to qualitative and quantitative mapping of marine vegetation in the English Channel, North Altantic, western Mediterranean, and South Pacific 22 p3109 N88-28464
Physiography and kinematics of the western coast of the province of Huelva (Andalousia, Spain)
22 p3109 N88-28465
Use of SPOT HRV data in the US Army Corps of Engineers dredging program 22 p3109 N88-28466
Contributions of SPOT imagery to the study of the littoral environments of Saloum (Senegal)
22 p3109 N88-28467
Relevance of a thematic map (SPOT data) with regards to the real flora and structure of the vegetation covering of salt marshes (Mont Saint Michel Bay, France)
22 p3109 N88-28468
Application of SPOT data to renewable resources in the Maldives 22 p3109 N88-28469
The prospects for topographic mapping using SPOT data 22 p3110 N88-28470
The use of SPOT imagery on analytical photogrammetric instruments 22 p3110 N88-28471
Cartographic applications of SPOT imagery
22 p3110 N88-28472
The use of SPOT imagery for topographic mapping
22 p3110 N88-28473
Digital terrain modelling with SPOT data and geological applications 22 p3110 N88-28474
The use of SPOT data for mapping and DEM production — digital elevation model (DEM)
22 p3110 N88-28475
Evaluation of SPOT cartographic capabilities over the Aix Marseille area (France) 22 p3110 N88-28476
Assessment of SPOT imagery for topographic revision and vegetation mapping 22 p3111 N88-28477
A geometrical analysis of SPOT data
22 p3111 N88-28478
Topographic mapping with SPOT 1 data. A practical approach by the Ordnance Survey
22 p3111 N88-28479
Metric applications of SPOT's lateral stereoscopy
22 p3111 N88-28480
Larger scale image mapping with SPOT
22 p3111 N88-28481
Rigorous stereophotogrammetric treatment of SPOT images 22 p3111 N88-28482
Mapping and urban multi-experimental assessment of SPOT: Mapping results 22 p3112 N88-28483
Study of stereoradiometry on SPOT images
22 p3112 N88-28484
Studies on system performance of SPOT (space and ground segments) 22 p3112 N88-28485
Radiometric analysis and potential of SPOT HRV imagery for applications in urban environments and geology 22 p3112 N88-28486

Automatic production of orthophoto using SPOT images 22 p3112 N88-28487
High resolution orthoimage quadrangle maps using SPOT satellite data 22 p3112 N88-28488
Automatic extraction of high resolution elevation data from SPOT stereo images 22 p3113 N88-28489
Automatic creation of digital terrain models from SPOT image pairs 22 p3113 N88-28490
Production of satellite image maps based on SPOT data 22 p3113 N88-28491
Surface reflectance factors derived from SPOT-1 HRV data at two view angles 22 p3113 N88-28492
Digital SPOT stereoplotting: An original approach to the formation of epipolar images and matching 22 p3113 N88-28493
From the extraction of linear networks towards following of them on SPOT images with the help of a knowledge-based interpretation system 22 p3113 N88-28494
Extraction of thin networks by an oriented following of ridges and valleys 22 p3113 N88-28495
SPOT images features extraction 22 p3114 N88-28496
SPOT: A data capture and data updating tool for the French National Geographic Institute's (IGN's) cartographic data base 22 p3114 N88-28497
Use of SPOT imagery in a geographic information system 22 p3114 N88-28498
SEP/VIPS 32 geographic information system. Processing and thematic analysis of images, maps, and associated data 22 p3114 N88-28499
Space imagery as a teaching aid in secondary education 22 p3114 N88-28500
Training of the Group for the Development of Aerospace Remote sensing 22 p3114 N88-28501
Contribution of SPOT to geographic information systems 22 p3114 N88-28502
Summary of analysis and processing techniques used on SPOT imagery 22 p3115 N88-28503
The SPOT program 22 p3115 N88-28504
SPOT data acquisition and distribution 22 p3115 N88-28505
Quality of SPOT images 22 p3115 N88-28506
Survey of SPOT-1 operation 22 p3115 N88-28507
Perspectives for the SPOT program 22 p3115 N88-28508
Closing of the Preliminary Evaluation Program for SPOT (PEPS): Assessment of the acquisition, production, and monitoring of PEPS 22 p3115 N88-28509
Imaging instrument of the vegetation payload (SPOT 4) [SNIAS-881-440-107] 24 p3386 N88-30169

SPOT WELDS
Development of research on fatigue of spot-weld in automobile structures in Japan 05 p0608 N88-13728
The use of photoelastic methods to study the stressed states of spot-welded joints 14 p1898 N88-21335

SPRAY CHARACTERISTICS
Fuel-injector/air-swirl characterization [NASA-CR-180864] 07 p0820 N88-14985
Liquid sprays and flow studies in the direct-injection diesel engine under motored conditions [NASA-TM-100135] 11 p1440 N88-18594
An investigation of the spray produced by a yawed wheel, including measurement of impact forces --- aircraft wheels [BU-363] 14 p1866 N88-21150
Experimental research of combustion systems 21 p2927 N88-27371
Holographic determination of droplet size distributions [DFVLR-MITT-88-05] 22 p3074 N88-28250
Turbulence effects on the droplet distribution behind airblast atomizers 24 p3346 N88-29915
Nozzle airflow influences on fuel patternation 24 p3346 N88-29916
Spray performance of a vaporizing fuel injector 24 p3346 N88-29919

SPRAYED COATINGS
Development and production of new and modified powders for sprayed coatings and components for saving important raw materials [BMFT-FB-T-86-129] 01 p0025 N88-10159
Cost 501 Project UK10 part 3: Thermal fatigue damage of Fecralloy steel-sprayed and co-extruded tubing [AERE-R-12230] 10 p1343 N88-18026
Stability of uncapsulated weight cells with thin film elongation measurement bands under influence of humidity, temperature and operation voltage [ETN-88-92383] 21 p2951 N88-27531
Spray automated balancing of rotors: Methods and materials [NASA-CR-182151] 24 p3330 N88-29825

SPRAYED PROTECTIVE COATINGS
U PROTECTIVE COATINGS
U SPRAYED COATINGS

SPRAYERS
Shear stress cleaning for surface deparriculation 02 p0134 N88-10838
The TAB method for numerical calculation of spray droplet breakup [DE87-011756] 04 p0442 N88-12743
The KIVA-2 computer program for transient multidimensional chemically reactive flows with sprays [DE88-000502] 07 p0854 N88-15191
Spray deposition: A fundamental study of droplet impingement, spreading and consolidation [AD-A186627] 08 p0970 N88-15869
Dense-spray structure and phenomena. Part 2: Pressure-atomized sprays [AD-A190312] 15 p2064 N88-22307
Laser measurement of particle velocities in vacuum plasma spray deposition [DE88-007111] 19 p2728 N88-26198
Pulsed spray structure and atomisation techniques [AD-A192280] 20 p2800 N88-26614

SPRAYING
NT ARC SPRAYING
NT FLAME SPRAYING
NT PLASMA SPRAYING
Ceramics thin film 04 p0403 N88-12505
Fire extinguishment and inhibition in spacecraft environments 04 p0406 N88-12523
Comparison of UNL laser imaging and sizing system and a phase/Doppler system for analyzing sprays from a NASA nozzle [NASA-CR-182437] 09 p1161 N88-16956
Dense-spray structure and phenomena. Part 1. Turbulence/dispersed-phase interactions [AD-A190606] 15 p2065 N88-22315
Mixing and thermodynamic critical phenomena of combusting monopropellant sprays 19 p2623 N88-25558
Atomization in a turbulent shear layer: Preliminary measurements 19 p2624 N88-25565
Anatomy of group burning mode transitions in spray group combustion 19 p2626 N88-25578
Small-droplet spray measurements with a scattered-light scanner [NASA-TM-100973] 20 p2806 N88-26645

SPRAYING APPARATUS
U SPRAYERS

SPRAYS
U SPRAYERS

SPREAD F
Large scale plasma irregularities observed in the nighttime ionosphere over Natal using a rocket-borne Langmuir probe [INPE-4422-PRE/1226] 12 p1694 N88-20139
In-situ plasma bubble observations associated with equatorial spread-F over Natal [INPE-4488-PRE/1252] 15 p2095 N88-22482

SPREAD SPECTRUM TRANSMISSION
The role of spread spectrum in packet radio networks [AD-A184511] 03 p0306 N88-11929
SBNR (Signed Binary Number Representations) digital signal processor architecture [AD-A184603] 03 p0364 N88-12290
Performance analysis of coded frequency-hopped spread-spectrum systems with unknown interference [AD-A186069] 07 p0841 N88-15103
Packet error probabilities in frequency-hopped spread spectrum packet radio networks. Markov frequency hopping patterns considered [AD-A186071] 07 p0841 N88-15104
Measured noise performance of a direct-sequence spread-spectrum system and a comparison of single vice dual-channel delay-lock loops [AD-A186288] 07 p0843 N88-15110
Coding for spread-spectrum communications networks [AD-A185667] 07 p0844 N88-15119
Adaptive spread spectrum networks [AD-A187154] 09 p1152 N88-16900
Wideband HF (High Frequency) modeling and simulation [PB88-116116] 10 p1317 N88-17874
Spread spectrum mobile radio communications [AD-A187487] 11 p1470 N88-18765
Spread spectrum radio networks [AD-A188914] 12 p1620 N88-19689
Propagation effects on spread-spectrum mobile satellite systems 19 p2645 N88-25699
Coding for meteor-burst communications channel and side information for channels with block-interference 23 p3202 N88-29054
Statistical analysis of the LMS (Last Mean Squares) and modified stochastic gradient [AD-A195497] 24 p3424 N88-30376

SPREADING
Dependence of the expectancy of hitting on the number of spread shots. Determination of the expectancy of hitting using a spread salvo [REPT-FM6] 10 p1310 N88-17829
Investigation of several spread shot conditions [REPT-TR-164] 10 p1310 N88-17830
Tectonics and three-dimensional structure of spreading centers: Microearthquake studies and tomographic inversions [PB88-163290] 14 p1945 N88-21602
The spreading and mixing of dense gas clouds in still air [KNMI-WR-87-12] 16 p2230 N88-23320
A study of flame spreading and combustion phenomena of stick propellants [AD-A193598] 22 p3052 N88-28106

SPRING (SEASON)
Insights into the general circulation of the lower stratosphere from TOMS 05 p0616 N88-13780
Use of SPOT satellite in agrohydrology: Detection of spring water excess in a grassland region 22 p3091 N88-28357

SPRINGS (ELASTIC)
Non-linear shipboard shock analysis of the Tomahawk missile shock isolation system 05 p0592 N88-13614
Pin joints, gears, springs, cranks and other novel micromechanical structures [DE88-002504] 07 p0864 N88-15245
The paradoxical asymptotic status of massless springs [AD-A185625] 07 p0928 N88-15637
Nonlinear line-spring model for surface crack analysis with particular reference to work hardening materials [PB87-144838] 08 p0994 N88-16016
Liquid spring design methodology for shock isolation system applications 08 p0998 N88-16043
Payload deployment system --- STS 14 p1875 N88-21199
Locking hinge [NASA-CASE-MSC-21056-1] 17 p2312 N88-23827
Structurally tailorable non-linear snap-through spring system [NASA-CASE-LAR-13729-1] 18 p2523 N88-24970
Stability of dynamical systems supported by rubber springs 19 p2680 N88-25932
Leaf spring [GB-PATENT-2-192-689-A] 23 p3222 N88-29179

SPRINKLING
Test results and predictions for the response of near-ceiling sprinkler links in a full-scale compartment fire [NBSIR-87/3633] 01 p0033 N88-10209

SPUTTERING
NT MAGNETRON SPUTTERING
Metallic superlattices with monolayer modulation [DE87-012724] 01 p0023 N88-10145
Synergism of electroplating and vacuum processes [DE87-013496] 01 p0033 N88-10211
Electron sputtering in the analytical electron microscope: Calculations and experimental data [DE87-011457] 01 p0049 N88-10312
CuInSe2 solar cell research by sputter deposition [DE87-001184] 02 p0195 N88-11219
Corrosion-resistant amorphous metallic coatings: Engineering development [NASA-CR-181487] 03 p0287 N88-11802
Tribological properties of rf-sputtered MoS2 coatings [DE88-000266] 04 p0452 N88-12802
Monocrystal sputtering by the computer simulation code ACOCT [IPPJ-848] 04 p0493 N88-13035
Non-lattice matched metallic superlattices [DE87-011512] 04 p0497 N88-13062
An investigation of unipolar arcing at atmospheric pressure in aluminum 2024 and aluminum coated glass slides [AD-A184903] 05 p0577 N88-13521
Energy dependence of ion-induced sputtering yields of monatomic solids in the low energy region [IPPJ-AM-52] 05 p0651 N88-13988
The tribological properties of MoS2 coatings in vacuum, low relative humidity and high relative humidity environments [DE88-001611] 06 p0711 N88-14356
Nb3Al formation in sputter-deposited Nb/Al mutli-layer samples [DE88-003192] 08 p0970 N88-15868
Sputtered silver films to improve chromium carbide based solid lubricant coatings for use to 900 C [NASA-TM-100783] 08 p0973 N88-15885
Depth of origin of sputtered atoms: Experimental and theoretical study of Cu/Ru(0001) [DE88-002848] 08 p1082 N88-16520

Calculated sputtering and atomic displacement cross-sections for applications to medium voltage analytical electron microscopy
[DE88-002904] 09 p1166 N88-17006
Modeling considerations for selected rf-plasma edge effects
[DE88-003285] 09 p1252 N88-17500
The effect of varying sputtering parameters on the microstructure and mechanical properties of 10 percent Ni + TiB2 thin films
[DE88-002600] 09 p1254 N88-17517
Corrosion behavior of sputter-deposited aluminum-based alloys exposed to chloride solutions
[AD-A187262] 10 p1303 N88-17794
Apparatus for the study of silicon film deposition and silicon etching
[AD-A187616] 10 p1334 N88-17972
Fabrication and evaluation of transmissive multilayer optics for 8 keV X-rays
[DE88-003999] 10 p1409 N88-18402
Synthesis and characterization of thin films
[AD-A187335] 10 p1421 N88-18485
Electrochromic thin films
[DE88-751099] 11 p1559 N88-19334
Properties of reactively sputtered WNx films Zhao, X. -A.
[AD-A188711] 13 p1835 N88-20976
Superconducting superlattice structures
[DE88-005346] 13 p1847 N88-21058
A novel method for sputter-deposition of high T(sub c) superconductor films via a computer-controlled mass analyzed ion beam
[DE88-006001] 13 p1848 N88-21064
Recent advances in solid polymer electrolyte fuel cell technology
[DE88-005380] 15 p2092 N88-22464
Preparation of large area NbN/AlN/NbN Josephson junctions
[DE88-006074] 15 p2145 N88-22799
Auger electron spectroscopy of contrast-forming layers on metals
[NASA-TT-20182] 16 p2178 N88-22980
The effects of thin compressive films on indentation fracture toughness measurements
[AD-A192243] 20 p2779 N88-26480
Laser desorption/ablation studies by resonance ionization mass spectrometry
[DE88-009124] 20 p2807 N88-26650
Formation of metastable structures and amorphous phases in Cu-W alloys using the triod sputtering technique
[DE88-009051] 21 p2915 N88-27298
Erosion/redeposition modeling and calculations for carbon
[DE88-010382] 22 p3057 N88-28139
Status and directions of modified tribological surfaces by ion processes
[NASA-TM-101304] 22 p3063 N88-28176
Preparation of superconducting YBa2Cu3O(sub 7-x) films by magnetron sputtering
[DE88-009977] 23 p3289 N88-29583

SQUALLS
The combined use of diagnosed mesoscale frontogenesis and satellite imagery in forecasting squall line formation 02 p0201 N88-11258
Analysis of squall line based on conventional data 02 p0207 N88-11295
Observations of a midlatitude squall line boundary layer wake
[AD-A185609] 06 p0746 N88-14589
Density flows at the mountain edge 08 p1016 N88-16156

SQUARE WAVES
Study on the square wave alternating plasma arc welding for aluminum alloys
[PB87-143772] 07 p0863 N88-15239
Use of a coherent square wave reference to demodulate BPSK (Binary Phase Shift Keying) carriers and a visual indicator of the quality of received QPSK (Quadrature Phase Shift Keying) carriers
[AD-A193528] 23 p3204 N88-29065

SQUEEZE FILMS
Magnetohydrodynamic squeeze film
[DE88-701876] 20 p2810 N88-26669

SQUEEZED STATES (QUANTUM THEORY)
United States - Japan Seminar on Quantum Mechanical Aspects of Quantum Electronics
[AD-A186938] 14 p1974 N88-21781
Squeezed state in degenerate parametric amplification discussed by H. Takahasi in 1963 14 p1976 N88-21790
Squeezed states of light 14 p1976 N88-21791
Pulsed squeezed light 14 p1976 N88-21792
Generation of number-phase minimum uncertainty states 14 p1978 N88-21803
Squeezing via travelling-wave forward four-wave mixing in atomic vapors: Comparison with nondegenerate theory 14 p1978 N88-21804
Generating squeezed microwave radiation with a Josephson parametric amplifier 14 p1978 N88-21805
Detecting squeezed states by cross-correlation 14 p1978 N88-21806
Nonclassical lights 14 p1979 N88-21810
Quantum statistics of parametric oscillators above threshold 14 p1979 N88-21811

SQUEEZING
U COMPRESSING

SQUID (DETECTORS)
Capacitive resonant transducer for the Frascati gravitational antenna
[IFSI-86-9] 05 p0578 N88-13528
Hitachi develops ceramic superconducting device 06 p0688 N88-14214
Design, optimization and construction of a dc-SQUID with complete flux transformer circuits
[PB88-160742] 14 p1907 N88-21399
Inductive spurious coupling of a dc-SQUID to resonant input circuit
[NOTA-INTERNA-894] 14 p1908 N88-21401
Squid instrumentation for neuromagnetic study of complex brain activity 21 p2978 N88-27691
CryoSQUID: A SQUID-based magnetic field sensor
[AD-A194237] 23 p3239 N88-29275
Planar thin film SQUID with integral flux concentrator
[NASA-CASE-MFS-26282-1] 23 p3292 N88-29602

SR (REACTORS)
U SATURABLE REACTORS

SRB (SOLID ROCKET BOOSTERS)
U SPACE SHUTTLE BOOSTERS

SRI LANKA
Monitoring Moneragala (Sri Lanka) with SPOT imagery 22 p3099 N88-28405

STABILITY
NT ACOUSTIC INSTABILITY
NT AERODYNAMIC STABILITY
NT AIRCRAFT STABILITY
NT BAROCLINIC INSTABILITY
NT BOUNDARY LAYER STABILITY
NT COMBUSTION STABILITY
NT CONTROL STABILITY
NT DIMENSIONAL STABILITY
NT DIRECTIONAL STABILITY
NT DYNAMIC STABILITY
NT FLAME STABILITY
NT FLOW STABILITY
NT FREQUENCY STABILITY
NT GOERTLER INSTABILITY
NT GYROSCOPIC STABILITY
NT LATERAL STABILITY
NT LONGITUDINAL STABILITY
NT LOW SPEED STABILITY
NT MAGNETOHYDRODYNAMIC STABILITY
NT MOTION STABILITY
NT ROTARY STABILITY
NT SHELL STABILITY
NT SPACECRAFT STABILITY
NT STATIC STABILITY
NT STORAGE STABILITY
NT STRUCTURAL STABILITY
NT SURFACE STABILITY
NT SYSTEMS STABILITY
NT THERMAL STABILITY
Rayleigh-Taylor instability in compressible fluids
[DE87-013494] 01 p0047 N88-10297
Models of high spatial frequency thermal blooming instabilities
[DE87-014280] 01 p0052 N88-10330
The atomic weight and isotopic composition of nitrogen and their variation in nature
[DE87-012867] 02 p0144 N88-10902
Organic Rankine-cycle power systems working fluids study. Topical report No. 1: Fluorinol 85
[DE87-014604] 02 p0195 N88-11217
Stability of semidiscrete approximations for hyperbolic initial-boundary-value problems: An eigenvalue analysis
[NASA-TM-88328] 02 p0227 N88-11434
Filamentation instability of rotating light ion beams in fusion target chambers
[IPPJ-839] 02 p0242 N88-11530
Dynamics and stability of bipedal locomotion robots 03 p0333 N88-12096
Interchange stability of noncircular reversed field pinches
[DE88-000177] 03 p0378 N88-12381
Atomic frequency standards for ultra-high-frequency stability 04 p0433 N88-12685
The shifted Adams method for ordinary differential equations
[DE88-000810] 04 p0486 N88-12994
Variable collision frequency effects on hose and sausage instabilities in relativistic electron beams
[AD-A184206] 04 p0490 N88-13021
Computational methods for problems in aerodynamics and large space structure using parallel and vector architectures
[AD-A185401] 05 p0541 N88-13294
Colloidal stability of oxidized silicon particles in ethanolic and aqueous media
[DE87-014783] 05 p0562 N88-13421
Stability properties of spline approximations for retarded systems
[PB87-220919] 05 p0639 N88-13910
Extrema of skewed stable processes
[AD-A185422] 05 p0642 N88-13925
Tutorial on elementary bifurcation theory
[DE87-014849] 05 p0642 N88-13932
Asymptotically stable all-pass transfer functions: Canonical form, parametrization and realization
[PB87-123972] 06 p0763 N88-14684
Existence and stability of transition layers
[AD-A185806] 06 p0766 N88-14707
High temperature stability of superconducting YBa2Cu3O subx as characterized by X-ray diffraction
[DE88-001856] 06 p0787 N88-14824
Nonlinear and nonparallel stability problems
[AD-A186406] 07 p0850 N88-15159
Structural relaxation in strained-layer heterostructures
[DE88-002326] 07 p0868 N88-15264
Analysis of stable crack growth with isotropic and kinematic hardening
[PB87-144911] 07 p0868 N88-15266
Weak convergence of sums of moving averages in the alpha-stable domain of attraction
[AD-A186430] 07 p0912 N88-15529
Local properties of index-alpha stable fields
[AD-A186432] 07 p0912 N88-15530
Some new approaches to multivariate probability distributions
[AD-A186038] 07 p0914 N88-15551
Admissible and singular translates of stable processes
[AD-A186426] 07 p0917 N88-15571
The use of the direct measurement of solar radiation for the determination of Pasquill Stability Parameter
[AD-A186084] 07 p0946 N88-15750
Elastic-plastic fracture investigation on stable crack growth for plane stress
[PB87-144820] 08 p0995 N88-16022
Matrix functions in the stability of higher-order numerical schemes
[INPE-4246-PRE/1119] 08 p1073 N88-16472
DSC (Differential Scanning Calorimeter) stability test for liquid propellants: A preliminary report
[AD-A187115] 09 p1150 N88-16888
A control system for maintaining high stability in gas pressure
[DE88-003712] 09 p1175 N88-17042
A note on the effect of preemptive policies on the stability of a priority queue
[AD-A186871] 09 p1227 N88-17345
Cohesive energies of transition metal silicides and phosphides --- Knudsen effusion
[AD-A186691] 09 p1254 N88-17519
Stability and metastability in semiconductor strained-layer structures
[DE88-003308] 09 p1258 N88-17544
Molecular dynamics study of high-temperature grain-boundary stability in a (100) sigma = 29 bicrystal model
[DE88-002955] 09 p1258 N88-17546
Diffusion studies in amorphous NiZr alloys
[DE88-003009] 10 p1301 N88-17781
One-dimensional leakage-flow vibration instabilities
[DE88-002875] 10 p1330 N88-17947
Instabilities and chaos in a multimode, standing-wave, CW dye laser
[DE88-005028] 10 p1337 N88-17993
Comparative evaluation of orthostatic stability following immersion in horizontal and vertical positions 10 p1363 N88-18143
Stable, robust tracking by sliding mode control
[AD-A188278] 10 p1401 N88-18358
Electronic structure of random alloys and the theory of ordering processes
[DE88-004476] 10 p1407 N88-18394
Electronic structure and phase stability of alloys
[DE88-004574] 11 p1562 N88-19350
Preliminary investigation of stability of a fin-stiffened slender strut
[NASA-TM-4034] 12 p1599 N88-19568
Design of feedback control systems for stable plants with saturating actuators
[NASA-CR-132613] 12 p1681 N88-20050
The lattice nonlinearities and the long term stability of the SSC
[CEBAF-PR-87-009] 12 p1690 N88-20108

Stability and uniqueness in nonlinear continuum mechanics
[AD-A189616] 12 p1699 N88-20172
An experimental investigation of the flap-lag-torsion aeroelastic stability of a small-scale hingeless helicopter rotor in hover
[NASA-TP-2546] 13 p1715 N88-20257
Some properties of Australian produced explosive composition H-6
[MRL-TN-525] 13 p1754 N88-20490
Numerical experiments on the stability of controlled boundary layers
[NASA-CR-181649] 13 p1771 N88-20591
Three-wave parametric resonance in plasma of relativistic electron flux 14 p1972 N88-21772
Comprehensive model for laser instability in a CO2 laser with gaseous saturable absorber 14 p1979 N88-21808
Recent progress in optical bistability and tristability 14 p1979 N88-21809
Stability limits in the monoclinic-tetragonal transformations of zirconia
[DE88-005924] 14 p1986 N88-21849
Convection effects on stability at the solidification front 14 p1988 N88-21860
Equilibrium stability of strained epitaxial layers on a rigid substrate
[INPE-4254-PRE/1127] 15 p2145 N88-22804
Stability and control methodology for conceptual aircraft design. Volume 1: Methodology manual
[AD-A191314] 16 p2164 N88-22906
Secondary instability of compressible boundary layer to subharmonic three-dimensional disturbances
[NASA-CR-4144] 16 p2200 N88-23122
Experimental study of vortex sheets in plane flow 16 p2203 N88-23142
Method and models for R-curve instability calculations
[NASA-TM-100935] 16 p2224 N88-23278
Microinstabilities in ion beam propagation 16 p2277 N88-23631
Stability requirement FOT ignition and high gain implosion = 2-D simulation for high neutron yield experiment = 16 p2278 N88-23633
Electrothermal instability in superconducting resonators
[DE88-701684] 16 p2282 N88-23664
Mechanics of instability-related delimination growth
[NASA-TM-100622] 17 p2349 N88-23998
Observations of frontal instabilities on an upwelling filament
[AD-A191051] 17 p2375 N88-24122
Shape stability in composites 18 p2479 N88-24706
Spatial stability of a compressible mixing layer
[NASA-CR-181671] 18 p2514 N88-24916
Investigations in electro-optical multistability for signal processing 18 p2518 N88-24938
Theoretical investigations of drift waves in a magnetic quadrupole 18 p2578 N88-25312
Stability of dynamical systems supported by rubber springs 19 p2680 N88-25932
Instability-related delamination growth of embedded and edge delaminations 20 p2767 N88-26406
The protonic Beta double prime aluminas: Preparation, stability, conductivity and structure
[DE88-008442] 20 p2768 N88-26415
Modelling of premixed combustion using a thin flame sheet and the effect of the hydrodynamic instability
[DE88-009467] 20 p2770 N88-26423
Phase stability and alloy design of ordered intermetallics
[DE88-007479] 20 p2772 N88-26435
The effects of gradients on boundary stability
[DE88-009592] 20 p2773 N88-26445
A numerical study of Rayleigh-Taylor instability in aluminum and steel plates
[DE88-010475] 20 p2774 N88-26449
Resistance of polyamide-6 against long time effects of various media at various temperatures
[NASA-TT-20297] 20 p2779 N88-26484
An experimental study of the effect of pitch rate on delta wing aerodynamics and stability
[NASA-CR-183159] 21 p2893 N88-27173
Research opportunities below 300 nm at the NBS Free-Electron Laser Facility
[AD-A193100] 21 p2953 N88-27538
Transverse resistive wall instability in a high-power, short-wavelength free-electron laser
[DE88-011730] 21 p2954 N88-27549
On plasma stability under anisotropic random electric field influence
[DE88-702422] 21 p3019 N88-27918
Migration and stability of HgCdTe lattice defects
[AD-A193293] 21 p3021 N88-27935
Some stability criteria in fluid and solid mechanics 21 p3027 N88-27966
Modification of YBa2Cu3O(7-x) ceramics by adsorbed water and other gases
[DE88-011518] 22 p3057 N88-28140
A digitally implemented phase-locked loop detection scheme for analysis of the phase and power stability of a calibration tone 22 p3066 N88-28196
Unstable heat pipes
[DE88-010780] 23 p3229 N88-29217
Stability of semidiscrete approximations for hyperbolic initial-boundary-value problems: Stationary modes
[NASA-TM-100994] 23 p3270 N88-29455
Stability experimental results of cable-in-conduit superconductor for fusion
[DE88-753424] 23 p3290 N88-29589
Study of toluene stability for an Organic Rankine Cycle (ORC) space-based power system
[NASA-CR-180884] 24 p3337 N88-29863
Circuit design criteria for stable lateral inhibition neural networks
[AD-A195066] 24 p3366 N88-30046
Recent insights into instability and transition to turbulence in open-flow systems
[NASA-CR-181693] 24 p3372 N88-30079
Stability of Venusian ionopause 24 p3448 N88-30523
The stability of disk galaxies and constraints on their mass-luminosity ratio
[SER-C-PREPUBL-FASC-27] 24 p3455 N88-30565

STABILITY AUGMENTATION
A wind tunnel model with dynamic control
[BU-352] 13 p1724 N88-20310
Conceptual final paper on the preliminary design of an oblique flying wing SST
[NASA-CR-182879] 16 p2161 N88-22891

STABILITY DERIVATIVES
NT PITCHING MOMENTS
NT ROLLING MOMENTS
NT YAWING MOMENTS
Controlling the dynamic environment during NOE flight 03 p0264 N88-11661
Low speed wind tunnel investigation of propeller slipstream aerodynamic effects on different nacelle/wing combinations. Part 1: Total forces and moments and pressure distributions on nacelle/wing at different angles of attack and yaw and at different thrust coefficients
[FFA-TN-1987-22] 05 p0542 N88-13302

STABILITY TESTS
NT FLIGHT STABILITY TESTS
NT WIND TUNNEL STABILITY TESTS
Stability analysis of a rigid body with a flexible attachment using the energy-casimir method
[AD-A185646] 06 p0723 N88-14449
DSC (Differential Scanning Calorimeter) stability test for liquid propellants: A preliminary report
[AD-A187115] 09 p1150 N88-16888

STABILIZATION
NT SIGNAL STABILIZATION
NT SPIN STABILIZATION
NT THREE AXIS STABILIZATION
Performances of an Actively Stabilized Stellar Interferometer (ASSI): Faint magnitudes, low fringe contrast measurements and operationality 01 p0097 N88-10641
Control and stabilization mechanisms of submunitions
[DFVLR-IB-111-86/9] 03 p0259 N88-11630
Slip casting and extruding shapes of rhenium with metal oxide additives. Part 2: Development of grain stabilized rhenium parts for resistojets
[NASA-CR-180851] 03 p0278 N88-11749
Processing, fabrication, applications and limitations of inherently conducting polymers
[DE88-003210] 08 p0973 N88-15883
The structure of the sideband spectrum in free electron lasers
[AD-A186952] 09 p1170 N88-17015
Feedback stabilization of distributed systems
[AD-A187111] 09 p1222 N88-17328
Boundary stabilization of thin elastic plates
[AD-A187123] 10 p1343 N88-18025
Time delays and boundary feedback stabilization in one-dimensional viscoelasticity, appendices A through H
[AD-A187534] 10 p1401 N88-18353
Fermi level stabilization in semiconductors: Implications for implant activation efficiency
[DE88-006332] 15 p2145 N88-22801
Concepts for a laser gyroscope of the highest precision 18 p2517 N88-24929
Heterogeneous diffusion flame stabilization
[AD-A193014] 20 p2771 N88-26429
Feedback stabilization of du/dt=Au + bl in Hilbert space when the normalization function is less than or equal to r
[AD-A193510] 23 p3277 N88-29506

STABILIZED PLATFORMS
Vega-1 and Vega-2 automatic stations: Functioning of flyby vehicles during encounter with Halley's comet 13 p1725 N88-20314

STABILIZERS (FLUID DYNAMICS)
Pointwise stabilization for coupled quasilinear and linear wave equations
[AD-A190031] 15 p2120 N88-22632

STABLE OSCILLATIONS
Mode priming in an overmoded gyrotron oscillator
[AD-A189151] 13 p1772 N88-20602
Oscillating airfoils: Achievements and conjectures
[AD-A190490] 15 p2014 N88-22008

STACKING FAULTS
U CRYSTAL DEFECTS

STACKS
Mechanically stacked multijunction solar cells: An update on Sandia programs
[DE87-014641] 03 p0347 N88-12190
Development of mechanically stacked tandem concentrator cells
[DE88-001926] 06 p0730 N88-14490
Changing the layers of mind
[AD-A186648] 08 p1052 N88-16350
Portable (and disposable) interpreters 10 p1380 N88-18237
Phosphoric acid electric utility fuel cell technology development
[DE88-010187] 20 p2795 N88-26582

STAGE SEPARATION
The TV-SAT/TDF/TELE-X pyrotechnical system
[CNES-87/CT/DRT/TVE/IL/358] 08 p0974 N88-15891
Stage separation testing of Ariane 09 p1126 N88-16752
The Ariane fairing and its separation systems 09 p1126 N88-16754
Separation dynamics for the last stage of a launch vehicle and satellite
[INPE-4281-PRE/1153] 12 p1601 N88-19582
Investigation of Super°Zip separation joint
[NASA-TM-4031] 15 p2026 N88-22072

STAGING (ROCKETS)
U STAGE SEPARATION

STAGNATION FLOW
Efficient shell implosion and target design 16 p2277 N88-23630
Correlations of velocity and temperature fluctuations in the stagnation-point flow of circular cylinder in turbulent flow
[NASA-TM-100930] 19 p2597 N88-25435
A simple, analytic 3-dimensional downburst model based on boundary layer stagnation flow
[NASA-TM-100632] 22 p3042 N88-28058

STAGNATION POINT
The flow downstream of screens and the formation of longitudinal vortices in the stagnation point flow
[DFVLR-FB-87-27] 09 p1162 N88-16963
Computational fluid dynamics and aerothermodynamics
[NASA-CR-182490] 09 p1166 N88-16989
Stagnating turbulent reacting flows
[AD-A191449] 18 p2508 N88-24877
Correlations of velocity and temperature fluctuations in the stagnation-point flow of circular cylinder in turbulent flow
[NASA-TM-100930] 19 p2597 N88-25435

STAGNATION PRESSURE
Time-resolved measurements of shock-induced vapor-pressure profiles
[DE87-012972] 01 p0045 N88-10289
Low thrust viscous nozzle flow fields prediction
[NASA-CR-182334] 05 p0582 N88-13551
Pusherless implosion, pulse tailoring and ignition scaling law for laser fusion 16 p2277 N88-23629

STAGNATION REGION
U STAGNATION POINT

STAINING
Use of lasers with F sub A(II)-color center KCl:Li crystals in the intraresonator laser spectroscopy method 06 p0769 N88-14729

STAINLESS STEELS
NT AUSTENITIC STAINLESS STEELS
NT FERRITIC STAINLESS STEELS
NT MARTENSITIC STAINLESS STEELS
Studies on temporal field emission from stainless steel surfaces
[DE87-014237] 02 p0147 N88-10919
Experimental determination of flow potential surfaces supporting a multiaxial formulation of viscoplasticity 02 p0187 N88-11167
Damping characteristics of a composite-reinforced stainless-steel tube
[DE87-012455] 02 p0191 N88-11192

Investigation on ductile fracture behavior of 3-inch diameter Type 304 stainless steel pipe with a circumferential through-wall crack
[DE87-753016] 02 p0191 N88-11196
Precision metrology comparing ultrasonic and other techniques for the determination of steel thickness
[DE87-011051] 02 p0230 N88-11452
Investigations of creep cavitation in Type 304 stainless steel
[DE87-014198] 03 p0287 N88-11803
Crevice corrosion of stainless steels and related alloys. Part 2: Summary of experimental test data for input to mathematical model
[BR99871-PT-2] 03 p0289 N88-11816
Effect of helium on irradiation creep in an austenitic stainless steel
[DE87-013754] 03 p0290 N88-11824
The mechanical properties of solid state diffusion bonds between Ti-6Al-4V and 304L stainless steel
[BAJ-TR-113-1987] 03 p0332 N88-12093
Mechanical properties of a microalloyed steel with high niobium content
[DE87-703545] 04 p0415 N88-12572
Partial substitution of vanadium by niobium in AISI H13 steel
[DE87-703548] 04 p0415 N88-12575
The aging behavior of types 308 and 308CRE stainless steels and its effect on mechanical properties
[DE87-012541] 04 p0417 N88-12590
Creep life prediction based on stochastic model of microstructurally short crack growth
[NASA-TM-100245] 04 p0456 N88-12825
Damping characteristics of a composite-reinforced stainless-steel plate
[DE88-000303] 04 p0457 N88-12828
Pulsed eddy-current inspection of thin-walled stainless steel tubing
[DE88-001492] 04 p0457 N88-12830
Data base on the high heat flux behaviour of metals and carbon materials for plasma facing components: Experiments at the 10 MW neutral beam injection test stand of the IPP Nagoya
[IPPJ-AM-53] 04 p0492 N88-13031
Study of the influence of mechanical - thermal treatments on the creep behavior of a niobium stainless steel
[DE87-703506] 05 p0563 N88-13431
Tensile properties of extrusion consolidated Type 304 SS rapidly solidified powders
[DE87-014875] 05 p0566 N88-13450
Effect of rapid solidification on stainless steel weld metal microstructures and its implications on the Schaeffler diagram
[DE88-001489] 05 p0566 N88-13451
Cu-2 mechanical properties and microstructural stability of advanced steam cycle materials
[DE88-001519] 05 p0566 N88-13452
Coupling effects between the ferrite and austenite phases during corrosion fatigue of a ferrite/austenite duplex stainless steel 05 p0605 N88-13706
Fractographic and microstructural aspects of fracture toughness testing in irradiated 304 stainless steel
[DE88-000795] 06 p0681 N88-14172
Determination, by X-ray fluorescence, of platinum, palladium, ruthenium, iron and chromium in special steels
[PB87-132114] 06 p0683 N88-14183
The factors which govern the acceleration of corrosion fatigue crack growth rate of a ferritic stainless steel 06 p0717 N88-14402
Near-threshold fatigue crack growth behavior at cryogenic temperature 06 p0718 N88-14409
Mixed mode fatigue crack growth using the Brasilian disc 06 p0719 N88-14416
Axial creep-fatigue damage assessment in type 316 SS material 06 p0721 N88-14430
Study on the cryogenic toughness of stainless steel weld metals
[PB87-143830] 07 p0834 N88-15057
The effect of deformation rate on JBK-75 stainless steel forgings
[DE88-001696] 07 p0834 N88-15061
A pulsed eddy current method for examining thin-walled stainless steel tubing
[DE88-002294] 07 p0866 N88-15255
Kinetics and mechanism of thermal aging embrittlement of duplex stainless steels
[DE88-002987] 08 p0969 N88-15866
Study on the fracture behavior of 9 percent Ni steel welded joint
[PB87-143863] 08 p0995 N88-16023
Long-term-aging embrittlement of cast duplex stainless steels: Mechanism and kinetics
[DE88-002929] 09 p1145 N88-16861
Long-term aging of cast stainless steels: Mechanisms and resulting properties
[DE88-002888] 09 p1145 N88-16864
Characterization of duplex stainless steel by TEM (Transmission Electron Microscopy), SANS (Small-Angle Neutron Scattering) and APFIM (Atom-Probe Field Ion Microscopy) techniques
[DE88-002916] 09 p1145 N88-16865
Aging degradation of cast stainless steels: Effects on mechanical properties
[DE88-003053] 09 p1145 N88-16866
Application of ac-impedance method on determination of corrosion rate of metals
[DE88-750307] 10 p1300 N88-17771
Effect of low-temperature aging on the mechanical properties of cast stainless steels
[DE88-002872] 10 p1300 N88-17774
Studies of the initiation of pitting corrosion on stainless steels
[AERE-M-3615] 10 p1301 N88-17778
Beneficial and detrimental effects of silica in the high temperature oxidation of 20Cr/25Ni/Nb stainless steel
[AERE-R-12667] 10 p1301 N88-17779
Cost 501 Project UK10 part 3: Thermal fatigue damage of Fecralloy steel-sprayed and co-extruded tubing
[AERE-R-12230] 10 p1343 N88-18026
In situ ultrahigh vacuum friction measurement and wear track analysis of ion implanted 304 stainless steel
[DE88-004537] 11 p1494 N88-18922
Weldability of tritium-charged 304L stainless steel
[DP-1740] 12 p1607 N88-19611
Hydrogen induced cracks in armor steel weldments fabricated with austenitic filler alloys
[AD-A188733] 13 p1740 N88-20406
Use of the LLNL 40 kV electric gun to study the shock response of 21-6-9 stainless steel
[DE87-014550] 13 p1742 N88-20418
Creep behavior of consolidated rapidly solidified Type 304 stainless steel powder containing helium
[DE88-005536] 13 p1743 N88-20424
Study of defects in metals by positron annihilation
[DE88-701042] 13 p1745 N88-20432
The effect of H2S concentration and pH on hydrogen permeation in AISI 410 stainless steel in 5 percent NaCl
[NPL-DMA(A)-148] 14 p1890 N88-21293
The effect of H2S concentration and pH on the cracking resistance of AISI 410 stainless steel in 5 percent brine
[NPL-DMA(A)-149] 14 p1890 N88-21294
Statistical analysis of feasibility of non-destructive inspection of mechanical properties of hot worked pipes of alloy steels
[BLL-M-37598-(5828.4)] 14 p1922 N88-21455
Cyclic uniaxial and biaxial hardening of type 304 stainless steel modeled by the viscoplasticity theory based on overstress 14 p1931 N88-21514
Some implications for cyclic plastic and viscoplastic equations based on nonproportional loading experiments 14 p1931 N88-21515
Segregation effects in welded stainless steels
[DE88-701224] 15 p2037 N88-22139
Grain growth behavior of extrusion consolidated centrifugally atomized Type 304 stainless steel powder
[DE88-006788] 15 p2038 N88-22143
The weldability of consolidated rapidly solidified Type 304 SS powders
[DE88-006738] 16 p2178 N88-22978
Enhanced emittance of oxidized 304 stainless steel 17 p2423 N88-24408
The effects of Hertzian stress and test ambient on the friction coefficient of MoS2 coatings
[DE88-008118] 20 p2777 N88-26467
GTAW characterization for weld penetration on 304L stainless steel
[DE88-010611] 20 p2810 N88-26672
Investigation of hydrogen isotope penetration through stainless steels Kh18N10T and Kh3M2BFR
[DE88-702189] 21 p2915 N88-27297
Thermal conductivity and thermal expansion of stainless steels D9 and HT9
[DE88-011973] 21 p2916 N88-27306
Distribution of weld quality in thin section stainless steel tube attachment welds
[PB88-109632] 21 p2955 N88-27555
Method of forming dynamic membrane on stainless steel support
[NASA-CASE-MSC-18172-3] 23 p3201 N88-29052
State variable approach to deformation phenomena in Face Centered Cubic (FCC) metals
[VTT-44] 24 p3354 N88-29964
An experimental study of biaxial yield in modified 9Cr-1Mo steel at room temperature
[NASA-CR-175012] 24 p3385 N88-30164

STALLING
Post stall behavior in axial-flow compressors
[AD-A185712] 06 p0685 N88-14081
Possibilities for on-line surge suppression by fast guide vane adjustment in axial compressors 10 p1283 N88-17674

STAMPING
Contribution to the study of wrinkling in metal stamping
[ISAL-IDI1-87-08] 08 p0976 N88-15900
Shape optimization of three-dimensional stamped and solid automotive components
[GMR-5168] 11 p1528 N88-19123

STANDARD ATMOSPHERES
U REFERENCE ATMOSPHERES

STANDARD DEVIATION
Coherent RF error statistics
[AD-A193002] 20 p2792 N88-26560

STANDARDIZATION
NT COMMONALITY
Fabrication of standardized piezoelectric polymer shock gauges by the Bauer method
[DE87-012738] 01 p0049 N88-10315
Study of aeropropulsion laboratory pressure drop rig and recommended test procedure
[AD-A184333] 03 p0322 N88-12038
Formalizing reusable software components in the programmer's apprentice
[AD-A185843] 07 p0901 N88-15457
The use of heart rate in the prescription and evaluation of exercise programs
[AD-A186454] 08 p1049 N88-16336
Standardization of software development
[INPE-4330-NTE/272] 08 p1068 N88-16455
Effects of additives on fire properties of polyethylene
[AD-A187064] 09 p1146 N88-16871
Interfacing slave designs to Fastbus: Practical experience
[DE88-002807] 09 p1215 N88-17286
An evaluation of perceptions of form, fit, function (F3) standardization on the Standard Inertial Navigation Unit (STD INU) program
[AD-A188955] 12 p1579 N88-19446
Some reflections on the standardization of bed-rest procedures for weightlessness simulation (cardiovascular and endocrine apsects) 12 p1662 N88-19961
European approaches in standard spectrum development --- aircraft load spectra
[NLR-MP-87007-U] 13 p1782 N88-20661
Public tool interfaces for software development environments
[RSRE-87004] 14 p1958 N88-21674
Inventory of topographic mapping and standardization of geographic names as the basis of a Geographic Information System (GIS) 16 p2225 N88-23281
Interfacing and integrating hardware and software design systems 17 p2306 N88-23796
Characterization of lubricants in terms of transition diagram data
[AD-A194264] 23 p3197 N88-29025
Improvement of head-up display standards. Volume 3: An evaluation of head-up display safety
[AD-A195787] 24 p3410 N88-30300
Strategic, organizational and standardization aspects of integrated information systems, volume 6
[AD-A195855] 24 p3437 N88-30457

STANDARDS
NT FREQUENCY STANDARDS
NT REFERENCE ATMOSPHERES
Viscosity measurements at high temperatures on a standard reference material supplied by BCR --- Bureau Communite de Reference (BCR)
[NPL-DMA(A)-146] 01 p0020 N88-10126
Center for Electronics and Electrical Engineering Technical Progress Bulletin covering center programs, October to December 1986 with 1987 CEEE events calendar
[PB87-226890] 02 p0168 N88-11058
Center for Electronics and Electrical Engineering technical publication announcements covering center programs, July to September 1986 with 1987 CEEE events calendar
[PB87-223442] 02 p0168 N88-11059
AGARD standard aeroelastic configurations for dynamic response. Candidate configuration I.-wing 445.6
[NASA-TM-100492] 02 p0192 N88-11202
Evaluating computers and their performance: Perspectives, pitfalls, and paths
[DE87-014264] 02 p0218 N88-11375
Definitions as database records
[DE87-014057] 02 p0248 N88-11570
Revision of the information standards for flight mechanics
[DFVLR-MITT-87-06] 03 p0265 N88-11675
Center for Electronics and Electrical Engineering Technical Progress Bulletin covering center programs, January to March 1987 with 1987 CEEE events calendar
[PB87-224648] 03 p0309 N88-11948
Requirements for the calibration of mechanical shock transducers
[PB87-227591] 03 p0325 N88-12054

NBS (National Bureau of Standards) measurement services: Radiometric standards in the vacuum ultraviolet
[PB87-227625] 03 p0325 N88-12055
Calibration standard for metallographic microscopes
[RFP-3956-REV] 03 p0326 N88-12057
Balloon track data analysis
[AD-A184750] 03 p0350 N88-12213
FORTRAN compiler performance benchmarks for the IBM personal computer
[LA-10883-MS] 03 p0363 N88-12284
Los Alamos National Laboratory computer benchmarking 1986
[LA-10898-MS] 03 p0363 N88-12285
Fire-related standards and testing
04 p0406 N88-12522
The atomic weight and isotopic composition of oxygen and their variation in nature
[DE87-014397] 04 p0413 N88-12558
Atomic frequency standards for ultra-high-frequency stability 04 p0433 N88-12685
Optimization of dilatometer test procedures
[DE87-014998] 04 p0447 N88-12769
Standard fatigue test specimens for fastener evaluation
[AGARD-AG-304] 04 p0455 N88-12818
Metrology and calibrating laboratories
[ETN-88-90761] 06 p0670 N88-14104
Uniform laws and regulations as adopted by the National Conference on Weights and Measures (72nd), 1987
[PB86-123724] 06 p0689 N88-14225
Nonconformity testing for the Graphical Kernel System (GKS)
[GMD/VAL-86-104] 06 p0757 N88-14844
NBS (National Bureau of Standards) measurement services: Spectral reflectance
[PB88-109905] 06 p0779 N88-14785
Horn design equations for the NBS (National Bureau of Standards) horn-type noise standards
[PB88-110226] 07 p0844 N88-15122
Development of Soviet state ergonomic standards (GOST)
[AD-A185536] 07 p0899 N88-15449
Soviet state ergonomic standards (GOST)
[AD-A185537] 07 p0900 N88-15450
After ten years of metafiles: Where does the Computer Graphics Metafile fit
[DE88-001840] 07 p0904 N88-15474
Thermodynamic values from computer summation of group additivity data
[AD-A186131] 07 p0940 N88-15711
Summary record of presentations to the Federal Telecommunication Standards Committee/Fiber optics task group
[PB88-110853] 08 p0978 N88-15911
PCM telemetry standard
[ESA-PSS-48(TTC.A.02)ISSUE-1]
09 p1132 N88-16790
Results from a questionnaire on particulate metrology in the UK
[NPL-MOM-81] 09 p1141 N88-16841
The ISO narrow spectrum series of filtered X-radiations at NPL
[NPL-RS(EXT)-92] 09 p1245 N88-17462
Influence of non-metallic elements in the mechanical properties of 20 Mn Mo Ni 55 steel
[DE88-700412] 10 p1300 N88-17775
Solid-state voltage standard performance and design guidelines
[PB88-123757] 10 p1322 N88-17905
NBS (National Bureau of Standards) measurement services: Platinum resistance thermometer calibrations
[PB88-138367] 10 p1333 N88-17967
NASA/NBS (National Aeronautics and Space Administration/National Bureau of Standards) standard reference model for Telerobot Control System Architecture (NASREM)
[PB88-124773] 10 p1338 N88-17999
Developing a standard taxonomy or software engineering standards 10 p1379 N88-18234
NBS (National Bureau of Standards) measurement services: Spectral irradiance calibrations
[PB88-123781] 10 p1408 N88-18401
Journal of Research of the National Bureau of Standards, volume 92, number 5, September-October 1987
[PB88-124409] 10 p1426 N88-18518
Journal of Research of the National Bureau of Standards, volume 92, number 6, November-December 1987
[PB88-138516] 10 p1426 N88-18519
Running head: What color is it
[NASA-CR-182600] 11 p1551 N88-19280
Ultrasonic measurements research: Progress in 1987
[AD-A188506] 12 p1687 N88-20092
Standardized environmental fatigue sequence for the evaluation of composite components in combat aircraft (ENSTAFF = ENvironmental faISTAFF)
[LBF-FB-179] 13 p1722 N88-20300
Orbital transfer vehicle concept definition and system analysis study. Volume 2: OTV concept definition and evaluation. Book 1: Mission and system requirements
[NASA-CR-179321] 13 p1729 N88-20339
The preparation, assembly and mounting of RF coaxial cables
[ESA-PSS-01-718-ISSUE-1] 13 p1756 N88-20504
Quantitative AES: The establishment of a standard reference spectrum for the accurate determination of spectrometer transmission functions
[NPL-DMA(A)-151] 14 p1887 N88-21279
An overview of the army GIS (Geographic Information Systems) Research Program
[AD-A189711] 14 p1992 N88-21871
Computer grading of extensometers (BS 3846)
[NPL-DMA(A)-152] 15 p2108 N88-22560
NASA and the challenge of ISDN: The role of satellites in an ISDN world
[NASA-CR-182749] 15 p2126 N88-22676
COBOL Analysis System (CAS) users manual
[PB88-171442] 16 p2250 N88-23445
Radiation standards 16 p2272 N88-23592
Requirements for radiation receivers
16 p2272 N88-23593
Reflection standards for spectroradiometry. Realization and calibration 16 p2272 N88-23595
Unified interchange format for computer data (standard file format)
[ESA-STR-225] 17 p2386 N88-24183
Discussions and agreements in the United Nations on important issues associated with nuclear power in space
17 p2423 N88-24411
Mobile satellite services: International co-ordination, co-operation and competition 19 p2644 N88-25691
Reducing risks inherent in operating underwater craft: The contribution of classification, the example of the SAGA highly autonomous support submarine
19 p2699 N88-26042
Center for Electronics and Electrical Engineering technical publication announcements covering Center programs, July to September 1987
[PB88-196530] 20 p2793 N88-26572
Fiber optic sensors with internal referencing
[NASA-TM-100893] 20 p2806 N88-26644
Improvement of head-up display standards. Volume 1: Head-up display design guide, appendix
[AD-A192973] 20 p2834 N88-26809
Unified methods of accelerated laboratory tests of the preparations for temporary protection of cars
[NASA-TT-20298] 21 p2921 N88-27336
A 1/2-inch high-definition baseband VCR
21 p2930 N88-27393
Ada (trade name) compiler validation summary report: Verdix Corporation VAda-010-03315, version 5.5 MicroVAX 2 host ISBC 386/20P Intel target
[AD-A193226] 21 p2997 N88-27774
Ada (trade name) compiler validation summary report: Verdix corporation VAda-010-13125, version 5.41 Sun Microsystems Sun-3/160 host microbar GPC68020 target
[AD-A193415] 21 p2997 N88-27777
The exploitation of Aircraft Integrated Monitoring System (AIMS) data in height-keeping studies for aircraft operating above FL 290 22 p3036 N88-28026
A new code for Galileo 22 p3065 N88-28186
Langley Research Center Metrology Program status for fiscal year 1987
[NASA-TM-100651] 22 p3086 N88-28324
Validation code for the Whetstone Benchmark
[NPL-DITC-107/88] 22 p3140 N88-28667
High hot-hardness gear lubricant evaluations, phase 2
[AD-A192309] 23 p3196 N88-29017
Vision and visual protection in fast jet aircraft
23 p3241 N88-29292
Ada (trade name) compiler validation summary report: Verdix Corporation VAda-010-03205, version 5.42 MicroVAX 2 host and national DB32000 (NS32032 target
[AD-A193485] 23 p3247 N88-29326
Integration of LANTIRN (Low Altitude Navigation and Targeting Infrared for Night) into operational fighter training
[AD-A194906] 24 p3325 N88-29799
Using standards to break down information transfer barriers 24 p3439 N88-30467

STANDING WAVES
Sound pressure distribution in front of a serrated boundary: Standing wave suppression and diffusion
07 p0928 N88-15639
Instabilities and chaos in a multimode, standing-wave, CW dye laser
[DE88-005028] 10 p1337 N88-17993
Solid-state ring laser with acoustooptical phase nonreciprocity of opposing waves
14 p1970 N88-21761
Computer-controlled measurements of nonlinear standing waves
[AD-A193840] 22 p3147 N88-28717

STANDS
U SUPPORTS

STANNIDES
NT NIOBIUM STANNIDES

STAPHYLOCOCCUS
Study of certain biological characteristics of bacteria during the French-Soviet CYTOS-2 space experiment
04 p0473 N88-12917

STAR CLUSTERS
NT GLOBULAR CLUSTERS
Membership of Cepheids and red giants in 8 open clusters: NGC 129, 6067, 6649, 6664, IC 4725, Ly 6, Ru 79
[PUBL-SER-C-FASC-13] 07 p0944 N88-15739
Color-magnitude diagrams of star clusters in the Magellanic clouds from wide-field electronography. Part 3: NGC 1841
[PUBL-SER-C-FASC-14] 07 p0944 N88-15740
Clustering of galaxies and clusters of galaxies in a decaying-particle cosmological model with a massive decay product
[DE88-753434] 23 p3298 N88-29642

STAR DISTRIBUTION
Basic properties and variability
02 p0252 N88-11593

STAR FIELDS
U STAR DISTRIBUTION

STAR FORMATION
The Einstein survey of the young stars in the Orion Nebula 04 p0518 N88-13182
VLBI research on OH-maser IN W33
08 p1001 N88-16064
Global properties of star formation in spiral galaxies
14 p1994 N88-21883
Submillimeter and far infrared line observations of M17 SW: A clumpy molecular cloud penetrated by UV radiation
[NASA-CR-182866] 16 p2288 N88-23701
Infrared astronomy at extremely faint light levels in support of the LAIRTS program
[AD-A191497] 18 p2592 N88-25404
Star formation and molecular clouds
24 p3451 N88-30537
Observations of star formation
24 p3451 N88-30538
Starbursts and their dynamics
[NASA-CR-180227] 24 p3452 N88-30549

STAR TRACKERS
Satellite autonomous navigation with SHAD (Stellar Horizon Atmospheric Dispersion)
[AD-A184988] 05 p0544 N88-13313
Fine attitude measurement system study. Volume 1: Executive summary
[BAE-TP-7831-VOL-1] 09 p1133 N88-16795
Fine attitude measurement system study, volume 2
[BAE-TP-7831-VOL-2] 09 p1133 N88-16796
Fine attitude measurement system study. Volume 3: Appendices
[BAE-TP-7831-VOL-3] 09 p1133 N88-16797
Integrated focal plane star sensor
[OG-RT/86-0156] 09 p1262 N88-17562
Identification of a star field from a spinning satellite
[CNES-NT-120] 15 p2026 N88-22074
Satellite attitude determination using a CCD (Charge-Coupled-Device) star camera
[AD-A192662] 22 p3046 N88-28080

STAR TRACKING
U STAR TRACKERS

STARBURST GALAXIES
Comparison of global and nuclear properties of starburst and Seyfert 1 galaxies 03 p0388 N88-12438
Galaxy evolution in dense clusters
13 p1855 N88-21101
Starbursts and their dynamics
[NASA-CR-180227] 24 p3452 N88-30549

STARCHES
Identification of hydroxypropyl starch hydrolysate components 17 p2315 N88-23832

STARK EFFECT
Relaxation effect of stark split levels for two-level system interacting with symmetrical strong resonant bichromatic field 03 p0299 N88-11882
Experimental and theoretical studies of coherent and nonthermal processes in semiconductors probed by femtosecond laser techniques 14 p1977 N88-21800
Stark effect in intense field. Perturbation theory and 1/n-expansion
[DE87-702947] 16 p2266 N88-23550

Time-resolved spectroscopic measurement of anode plasma in magnetically-insulated diode
16 p2279 N88-23641
Spectroscopic study of heliotron E plasmas: Stark profile, CXR, poloidal rotation and carbon coating
17 p2441 N88-24523
High-order multiphoton ionization of the noble gases
[DE88-007489] 18 p2571 N88-25273
Quantum-confined stark effect in InGaAs/InP quantum wells grown by metal-organic chemical vapor deposition
19 p2660 N88-25814
Dynamics of below-gap photoexcitation in GaAs quantum wells 19 p2660 N88-25815
Novel quantum well optical devices
20 p2868 N88-27028

STARS
NT A STARS
NT ASYMPTOTIC GIANT BRANCH STARS
NT B STARS
NT BINARY STARS
NT BLACK HOLES (ASTRONOMY)
NT CARBON STARS
NT CATACLYSMIC VARIABLES
NT CEPHEID VARIABLES
NT COOL STARS
NT DOUBLE STARS
NT DWARF NOVAE
NT DWARF STARS
NT EARLY STARS
NT ECLIPSING BINARY STARS
NT F STARS
NT FLARE STARS
NT G STARS
NT GIANT STARS
NT HERCULES NOVA
NT HOT STARS
NT INFRARED STARS
NT K STARS
NT LATE STARS
NT M STARS
NT MAGNETIC STARS
NT MAIN SEQUENCE STARS
NT MIRA VARIABLES
NT NEMESIS (STAR)
NT NEUTRON STARS
NT NOVAE
NT O STARS
NT PRE-MAIN SEQUENCE STARS
NT PROTOSTARS
NT PULSARS
NT RADIO STARS
NT RED DWARF STARS
NT RED GIANT STARS
NT REFERENCE STARS
NT S STARS
NT SUBGIANT STARS
NT SUN
NT SUPERGIANT STARS
NT SUPERMASSIVE STARS
NT SUPERNOVA 1987A
NT SUPERNOVAE
NT T TAURI STARS
NT VARIABLE STARS
NT WHITE DWARF STARS
NT WOLF-RAYET STARS
NT X RAY BINARIES
NT X RAY STARS
Calibration of the Ca II K line-core density and the magnetic flux density in stars using solar data
04 p0507 N88-13116
Active phases on II Peg 04 p0507 N88-13119
The giant spot on II Peg in 1986
04 p0508 N88-13120
Spectral analysis of APT RS CVn binary light curves
04 p0508 N88-13122
Starspots on the short-period RS CVn system SV Cam: 45 years of activity 04 p0508 N88-13123
The short-period RS CVn stars: Starspots and fundamental properties 04 p0508 N88-13124
Doppler snapshots 04 p0508 N88-13125
Titanium oxide absorption and spot sizes in II Peg, HR 1099 and UX Ari 04 p0508 N88-13126
Spectroscopic monitoring of RS CVn stars at Kitt Peak using the Penn State fiber optic echelle
04 p0509 N88-13127
The X-ray orbital lightcurves of AR Lac and TY Pyx
04 p0509 N88-13129
X-rays, color, and the Vaughan-Preston gap
04 p0510 N88-13135
Stellar activity and the rotation of Hyades stars
04 p0510 N88-13139
Relativistic stellar pulsations 06 p0801 N88-14902
Galaxy evolution in dense clusters
13 p1855 N88-21101
Stars, gas and dust in the Andromeda galaxy
[B8679680] 16 p2289 N88-23708
Research and Technology, 1987, Goddard Space Flight Center
[NAS 1.15:101097] 17 p2453 N88-24572
Cosmions and stars
[DE88-010886] 20 p2887 N88-27145
Apparent brightness of stars and lasers
22 p3065 N88-28188
Study of modern instrumentation and methods for astronomic positioning in the field
[AD-A196173] 24 p3452 N88-30548

STARSPOTS
NT SUNSPOTS
The giant spot on II Peg in 1986
04 p0508 N88-13120
Spectral analysis of APT RS CVn binary light curves
04 p0508 N88-13122
Starspots on the short-period RS CVn system SV Cam: 45 years of activity 04 p0508 N88-13123
The short-period RS CVn stars: Starspots and fundamental properties 04 p0508 N88-13124
Titanium oxide absorption and spot sizes in II Peg, HR 1099 and UX Ari 04 p0508 N88-13126
Flares: Solar and stellar
[PB87-124962] 06 p0806 N88-14917
Mapping stellar surface features
09 p1262 N88-17564

STARTING
NT AIR START
Performance of supersonic impingement radial turbines 06 p0712 N88-14367
Experimental study of two-dimensional vortex patterns for impulsively started bodies in comparison with other configurations 11 p1435 N88-18562
On the start up of supersonic underexpanded jets --- Mach disks 11 p1435 N88-18563
Possible creep studies of lithium with a compact device 17 p2422 N88-24404
Arcjet power supply and start circuit
[NASA-CASE-LEW-14374-1] 23 p3181 N88-28939

STATE EQUATIONS
U EQUATIONS OF STATE

STATE ESTIMATION
Maximum likelihood estimates of parameters in linear systems with process and measurement noise
[DFVLR-FB-87-20] 01 p0083 N88-10532
Propulsion estimation techniques
07 p0927 N88-15632
Reduction of time delays in Runge-Kutta integration methods --- systems simulation
[MBB/LKE-132/S/PUB/241/A]
09 p1229 N88-17363
Further developments in exact state reconstruction in deterministic digital control systems
[NASA-TP-2812] 11 p1468 N88-18751
Control test and validation for a large diameter high stability centrifuge 12 p1577 N88-19437
A state-space approach to super-optimal H sup infinity control problems
[OUEL-1690/87] 14 p1962 N88-21702
Estimation of time- and state-dependent delays and other parameters in functional differential equations
[NASA-CR-181663] 17 p2383 N88-24164
Computer aided design for linear control State Variable System (SVS)
[AD-A193282] 21 p2997 N88-27775
More on exact state reconstruction in deterministic digital control systems
[NASA-TP-2847] 22 p3063 N88-28177
Increasing accuracy in evaluating vector of state under conditions of incomplete observability of expanded system 24 p3446 N88-30511

STATE VECTORS
Inequivalent quantizations and fundamentally perfect spaces
[DE87-014225] 02 p0229 N88-11446
Teleoperator and robotics system analysis
[NASA-CR-179220] 03 p0334 N88-12105
SDVS (State Delta Verification System): Program verification system development fiscal year 1986
[AD-A184338] 03 p0366 N88-12302
Optimal observers for ARMA models
[OUEL-1659/86] 07 p0907 N88-15495
Linear state space modeling of a turbofan engine
[AD-A190110] 15 p2019 N88-22035
A state-space approach to discrete-time super-optimal H sup inf control problems
[OUEL-1712/87] 17 p2391 N88-24211
A design study of onboard navigation and guidance during aerocapture at Mars
[NASA-CR-172053] 18 p2469 N88-24654
Increasing accuracy in evaluating vector of state under conditions of incomplete observability of expanded system 24 p3446 N88-30511

STATIC AERODYNAMIC CHARACTERISTICS
The physics and mathematical description of the Achilles heel of stationary wind turbine aerodynamics: The tip flow
[R-812-D] 03 p0260 N88-11635

STATIC CHARACTERISTICS
NT STATIC AERODYNAMIC CHARACTERISTICS
The Lewis Strain Gauge Laboratory: Status and plans
02 p0184 N88-11146
Attitude determination of artificial satellites through joint application of static and dynamic optimal estimation techniques
[INPE-4415-TDL/306] 08 p0963 N88-15832
Static and dynamic jamming of networks
[AD-A188921] 12 p1620 N88-19690
Domain perturbation method in the static equilibrium of masses in rotation
[INPE-4217-PRE/1098] 12 p1686 N88-20085
Experimental research on center of pressure of slender body with two pointed ends 14 p1864 N88-21137

STATIC DEFORMATION
Influence of the static deformation on a wing in the unsteady aerodynamic 05 p0551 N88-13357
Optical method to measure the deformations of structures loaded by hydraulic pressure
[SNIAS-881-430-111] 22 p3088 N88-28338

STATIC DISCHARGERS
Antistatic coating compositions
[GB-PATENT-2-177-413-A] 05 p0568 N88-13463

STATIC ELECTRICITY
Development of test methods for the electrostatic properties of nonhomogeneous fabrics, phase 2
[AD-A190853] 18 p2489 N88-24767
Light scattering by charged spheres
[AD-A193753] 22 p3153 N88-28759

STATIC FIRING
Altitude simulation testing of Ariane's second-stage engine 09 p1126 N88-16747
Integration testing of the propulsion system of Ariane's first stage 09 p1126 N88-16751
Transient Pressure Test Article (TPTA) 1.1 and 1.1A, volume 1
[NASA-CR-179322-VOL-1] 12 p1603 N88-19588
Environmental monitoring of a titan 34D 5 1/2 segment solid rocket motor static firing
[AD-A192975] 20 p2766 N88-26400

STATIC FRICTION
Further refinement and applications of the mixed computational algorithm for plane elastic contact problems
[AD-A188308] 12 p1683 N88-20065
Static and dynamic metal-metal friction at plastic stress levels
[DE88-011281] 23 p3222 N88-29176

STATIC LOADS
Reinforced flexural elements for TEMP-STRESS Program
[DE87-012961] 01 p0061 N88-10391
Investigation on ductile fracture behavior of 3-inch diameter Type 304 stainless steel pipe with a circumferential through-wall crack
[DE87-753016] 02 p0191 N88-11196
Static standing and dynamic walking of a practical biped robot
[DE88-001367] 04 p0451 N88-12795
Experimental studies on the tripping behavior of narrow T-stiffened flat plates subjected to hydrostatic pressure and underwater shock 05 p0592 N88-13613
Static force and moment test of the Holloman narrow-gage rocket sled at Mach numbers from 3.5 to 5.5
[AD-A186291] 07 p0822 N88-14995
A comparison of the predicted and measured gravitational stresses in VAWT (Vertical Axis Wind Turbine) blades
[DE88-002113] 09 p1187 N88-17111
Durability of compound cylinder under static internal-pressure repeat load of long duration
16 p2180 N88-22991
Diffusion models of crack growth due to random overloads
[DE88-008811] 21 p2962 N88-27595
Static and dynamic metal-metal friction at plastic stress levels
[DE88-011281] 23 p3222 N88-29176

STATIC MODELS
The analysis of recent crustal movements in static and kinematic models
[SER-B-279] 09 p1191 N88-17136

STATIC PRESSURE
NT HYDROSTATIC PRESSURE
Effect of empennage arrangement on single-engine nozzle/afterbody static pressures at transonic speeds
[NASA-TP-2753] 02 p0122 N88-10771

The structure of sonic underexpanded turbulent air jets in still air
[AD-A190856] 16 p2157 N88-22870

STATIC STABILITY
NT DIMENSIONAL STABILITY
NT SHELL STABILITY
NT STRUCTURAL STABILITY
Handling qualities of a wide-body transport airplane utilizing Pitch Active Control Systems (PACS) for relaxed static stability application
[NASA-TP-2482] 07 p0821 N88-14987
Material instabilities in solids
[AD-A189525] 13 p1738 N88-20386
An experimental study to determine the flow and the subsonic static and dynamic stability characteristics of aircraft operating at high angles-of-attack
16 p2201 N88-23129
Stability of stick-slip phenomenon by using constitutive friction laws of Dietrich and Ruina
[ILR-MITT-197] 24 p3379 N88-30127

STATIC TESTS
NT STATIC FIRING
Static force and moment test of the Holloman narrow-gage rocket sled at Mach numbers from 3.5 to 5.5
[AD-A186291] 07 p0822 N88-14995
Static performance of an axisymmetric nozzle with post-exit vanes for multiaxis thrust vectoring
[NASA-TP-2800] 13 p1719 N88-20280
Static performance of nonaxisymmetric nozzles with yaw thrust-vectoring vanes
[NASA-TP-2813] 14 p1861 N88-21118
Static mechanical properties of 30 x 11.5 - 14.5, type 8 aircraft tires of bias-ply and radial-belted design
[NASA-TP-2810] 14 p1867 N88-21157

STATIC THRUST
Static performance of nonaxisymmetric nozzles with yaw thrust-vectoring vanes
[NASA-TP-2813] 14 p1861 N88-21118

STATICS
NT AEROSTATICS
NT ELECTROSTATICS
NT HYDROSTATICS
Development of methods for the analysis of the frequency and voltage statics of electricity users and electrical networks
[ETN-87-90412] 01 p0043 N88-10271
Static aeroelastic considerations in the definition of design loads for fighter airplanes
05 p0550 N88-13351
Research in applied mathematics related to identification of noisy systems
[AD-A189355] 13 p1825 N88-20908
Static dielectric breakdown strength of condensed heterogeneous high explosives
[AD-A191035] 16 p2183 N88-23014
A static scheduler for the computer aided prototyping system: An implementation guide
[AD-A194340] 24 p3414 N88-30322

STATIONARY ORBITS
Numerical arc segmentation algorithm for a radio conference: A software tool for communication satellite systems planning
[NASA-TM-100789] 16 p2167 N88-22919

STATIONKEEPING
Phase 3 study of selected tether applications in space. Volume 2: Study results
[NASA-CR-179186] 02 p0132 N88-10828
A linear quadratic Gaussian with loop transfer recovery proximity operations autopilot for spacecraft
[NASA-CR-172028] 02 p0227 N88-11433
Development and qualification of an Augmented Electro-Thermal Hydrazine-Thruster (AEHT) with 0.1 to 0.2 N vacuum thrust
[BMFT-FB-W-86-012] 16 p2169 N88-22931
On the collision hazard of colocated geostationary satellites
[DFVLR-FB-88-02] 23 p3184 N88-28952

STATIONS
NT AUTOMATIC WEATHER STATIONS
NT COLUMBUS SPACE STATION
NT CREW WORKSTATIONS
NT GROUND STATIONS
NT HYDROELECTRIC POWER STATIONS
NT INTEGRATED MISSION CONTROL CENTER
NT MIR SPACE STATION
NT POLYSTATION DOPPLER TRACKING SYSTEM
NT SALYUT SPACE STATION
NT SPACE STATION POLAR PLATFORMS
NT SPACE STATIONS
NT TRACKING STATIONS
NT WEATHER STATIONS
NT WORKSTATIONS
The significance of orientation unknowns in station and net adjustments 11 p1506 N88-18994

STATISTICAL ANALYSIS
NT AMPLITUDE DISTRIBUTION ANALYSIS
NT ANALYSIS OF VARIANCE
NT BIVARIATE ANALYSIS
NT CORRELATION COEFFICIENTS
NT COVARIANCE
NT DISCRIMINANT ANALYSIS (STATISTICS)
NT FACTOR ANALYSIS
NT GOODNESS OF FIT
NT LIKELIHOOD RATIO
NT MAXWELL-BOLTZMANN DENSITY FUNCTION
NT MULTIVARIATE STATISTICAL ANALYSIS
NT NONPARAMETRIC STATISTICS
NT NORMAL DENSITY FUNCTIONS
NT ORTHOGONALITY
NT POISSON DENSITY FUNCTIONS
NT PROBABILITY DENSITY FUNCTIONS
NT PROBABILITY DISTRIBUTION FUNCTIONS
NT QUANTILES
NT RAYLEIGH DISTRIBUTION
NT REGRESSION ANALYSIS
NT REGRESSION COEFFICIENTS
NT SEQUENTIAL ANALYSIS
NT STANDARD DEVIATION
NT STATISTICAL CORRELATION
NT STATISTICAL DECISION THEORY
NT STATISTICAL TESTS
NT VARIANCE (STATISTICS)
NT WEIBULL DENSITY FUNCTIONS
Analyses and assessments of span wise gust gradient data from NASA B-57B aircraft
[NASA-CR-178288] 01 p0002 N88-10007
Low cycle fatigue on isotropic fine-grained graphite
[DE87-702627] 01 p0028 N88-10177
Two-dimensional shear flow turbulence: A statistical theory of vortex filaments
[DE87-012234] 01 p0046 N88-10295
Analysis of the bivariate parameter wind differences between Jimsphere and Windsonde
[NASA-TM-4014] 01 p0072 N88-10461
Statistically determined nickel cadmium performance relationships 02 p0165 N88-11039
Software reliability models for fault-tolerant avionics computers and related topics
[NASA-CR-181440] 02 p0220 N88-11382
An antenna array processing system for multiple source bearing estimation 03 p0305 N88-11927
Geological characterization and statistical comparison of outcrop and subsurface facies: Shannon Shelf sand ridges
[DE87-001243] 03 p0348 N88-12202
Spatial strength variation and statistical size effect of laminated orthotropic composite materials
04 p0427 N88-12646
Robust statistical methods for automated outlier detection 04 p0433 N88-12681
Statistics of the geomagnetic secular variation for the past 5Ma
[NASA-CR-181558] 04 p0467 N88-12890
Statistical inference: Computer oriented algorithmic approach
[DE87-013874] 04 p0478 N88-12948
An urn model for the multi-sample capture/recapture sequential tagging process
[AD-A184470] 04 p0486 N88-12998
Statistical properties of small high-velocity events in the solar transition region 04 p0506 N88-13112
Statistical process control applied to the liquid-fed ceramic melter process
[DE88-000271] 05 p0569 N88-13471
A system identification technique based on the random decrement signatures. Part 1: Theory and simulation
05 p0594 N88-13625
A system identification technique based on the random decrement signatures. Part 2: Experimental results
05 p0594 N88-13626
Fatigue crack growth: Statistical considerations
05 p0606 N88-13718
Global atmospheric circulation statistics: Four year averages
[NASA-TM-100690] 05 p0628 N88-13842
An APL workspace for conducting nonparametric statistical inference
[AD-A184971] 05 p0634 N88-13877
Sample reuse in statistical remodeling
[AD-A184916] 05 p0643 N88-13938
Quantile based unified distribution of extreme values and order statistics
[AD-A185171] 05 p0644 N88-13942
Quantile statistical data analysis
[AD-A185181] 05 p0644 N88-13943
Presentation of a computer program permitting the exploitation of tests designed to determine the sensitivity of one shot devices to a parameter. Application to a degenerate one shot sequence
[SNIAS-872-430-117] 05 p0644 N88-13945
Boeing 727 MLS (Microwave Landing System) terminal instrument procedures (TERPS) approach data collection and processing, data report
[AD-A185523] 06 p0667 N88-14090
Statistical techniques for signal processing
[AD-A185774] 06 p0694 N88-14259
Statistical structure of temperature field over South Pacific Ocean 06 p0726 N88-14485
Geophysical-geomorphological statistical regionalization of North Atlantic
06 p0726 N88-14486
A statistical study of variations of internal gravity wave energy characteristics in meteor zone
06 p0735 N88-14523
A unified mathematical approach to image analysis
[AD-A185719] 06 p0765 N88-14703
Adaptive detection in non-stationary interference, part 3
[AD-A185622] 07 p0844 N88-15118
Statistical analyses of measured directional wave and current data
[PB87-144523] 07 p0853 N88-15185
Robust prediction and interpolation for vector stationary processes, 2d enriched version
[AD-A185875] 07 p0865 N88-15247
How errors in component reliability affect system reliability
[AD-A186264] 07 p0865 N88-15249
On two methods of identifying influential sets of observations
[AD-A186270] 07 p0910 N88-15518
Statistical selection procedures
[AD-A185868] 07 p0913 N88-15538
Mathematical techniques for system realization and identification
[AD-A186352] 07 p0915 N88-15557
On the extreme order statistics for a stationary sequence
[AD-A186428] 07 p0916 N88-15561
Increasing time resolution of picosecond absorption spectrometer by selection of length of laser light pulses
07 p0919 N88-15579
Turbulence models for practical applications
08 p0986 N88-15974
Statistical measures of clipped random signals
08 p1000 N88-16055
Statistical model of interaction of electromagnetic waves with natural objects being sensed
08 p1008 N88-16112
Predictability of ice concentration in the high-latitude North Atlantic from statistical analysis of SST (Sea Surface Temperature) and ice concentration data
[AD-A186621] 08 p1045 N88-16315
Conditional sampling in plasma turbulence
08 p1097 N88-16603
Fracture-mechanical, statistics and fractographic investigations on the steel 20 MnMoNi 55 in the ductile-brittle transition domain
[ETN-88-91064] 09 p1144 N88-16856
Strength and toughness of a brittle material
[VTT-RR-479] 09 p1183 N88-17089
Statistics of two-dimensional structure elements of mountainous ranges (mosaic model) for calculating three-dimensional reflection functions
[DFVLR-FB-87-33] 09 p1185 N88-17099
Error analysis for geotechnical engineering
[AD-A186795] 09 p1189 N88-17124
An application of fuzzy set theory to statistical hypothesis testing
[AD-A186705] 09 p1232 N88-17386
Outlier resistant predictive source encoding for a Gaussian stationary nominal source
[AD-A186725] 09 p1232 N88-17387
Calculating measurement imprecision and uncertainty
[DE88-003981] 09 p1233 N88-17391
Statistics of breakdown centers appearing during propagation of laser radiation through turbulent atmosphere 09 p1236 N88-17411
Helicopter activities in Germany
[MBB-UD-487/86] 10 p1314 N88-17853
Radar reflectivity and attenuation of radio waves in the melting layer of precipitation
[PB88-121553] 10 p1318 N88-17882
Statistical studies of low frequency oscillations in satellite-observed stratospheric temperatures
10 p1353 N88-18086
On precision and accuracy (bias) statements for measurement procedures
[DE88-004434] 10 p1402 N88-18359
A generalized quantile estimator under censoring
[AD-A188280] 10 p1402 N88-18364
Los Alamos optical materials reliability, maintainability, and exposure testing program
[DE88-001953] 10 p1409 N88-18404
Advances in calculating macroionic solution structure
[DE88-003799] 10 p1409 N88-18406

A semianalytical technique for sensitivity analysis of unsteady aerodynamic computations
[NASA-TM-100810] 11 p1503 N88-18976
Causes and prevention of occupational Repetition Strain Injuries (RSI) 11 p1521 N88-19083
Joint moments of the maximum in a critical branching process
[AD-A188157] 11 p1541 N88-19209
The SAS (Statistical Analysis System) by forms: Putting statistical power into the hands of an end-user
[DE88-002217] 11 p1541 N88-19212
Optimal arrangement of components via pairwise rearrangements
[AD-A187633] 11 p1541 N88-19213
Robustness in cost performance models
[AD-A187183] 11 p1566 N88-19374
Sampling intervals
[AD-A189445] 12 p1573 N88-19408
Systems approach to energy quality and efficiency
[PB88-139506] 12 p1640 N88-19823
Comparison of simulation modeling and satellite techniques for monitoring ecological processes
[NASA-CR-182592] 12 p1641 N88-19825
Estimating the solar irradiance of an intermountain region using GOES (Geostationary Operational Environmental Satellite) satellite data: A test of two statistical models
[AD-A188414] 12 p1642 N88-19834
Pre-convective environmental conditions indicative of non-tornadic severe thunderstorm winds over Southeast Florida
[AD-A188679] 12 p1648 N88-19870
Worldwide distributions of shipboard surface meteorological observations for EM propagation analysis
[AD-A188771] 12 p1648 N88-19871
Experimental analysis of algorithms
[AD-A188528] 12 p1677 N88-20028
Predicting transforms of stable noise and other Gaussian mixtures
[AD-A189280] 12 p1684 N88-20071
Detecting serial correlation in the error structure of a cross-lagged panel model
[AD-A189070] 12 p1685 N88-20077
Pion absorption in nuclei: The pion(+ or -),proton reactions
[LA-10997-T] 12 p1688 N88-20098
Management information systems design implications: The effect of cognitive style and information presentation on problem solving
[AD-A188850] 12 p1705 N88-20205
Design methodology for allocating data in a distributed database
[AD-A188826] 12 p1706 N88-20215
Statistical considerations of graphite strength for assessing design allowable stresses
13 p1746 N88-20441
Statistical signal processing using a class of iterative estimation algorithms
[AD-A189050] 13 p1757 N88-20511
HF (High Frequency) Maximum Usable Frequency (MUF) model uncertainty assessment
[AD-A189132] 13 p1757 N88-20513
Tests for uniformity arising from a series of events
[AD-A189069] 13 p1828 N88-20935
Stochastic comparisons of order statistics, with applications in reliability
[AD-A189408] 13 p1829 N88-20938
Application of expert systems in project management decision aiding
[NASA-CR-180762] 13 p1850 N88-21074
Electromagnetic scattering by an exponentially distributed rough surface with the introduction of a rough surface generation technique
[AD-A189678] 14 p1908 N88-21392
Statistical analysis of feasibility of non-destructive inspection of mechanical properties of hot worked pipes of alloy steels
[BLL-M-37596-(5828.4)] 14 p1922 N88-21455
Assimilation of meteorological observations
14 p1936 N88-21544
Spatial and temporal distribution of precipitation chemistry across Maryland in 1984, volume 2
[PB88-148937] 14 p1944 N88-21596
Analysis of winter season precipitation bands over the Southern Plains 14 p1947 N88-21609
Quasi-loglinear models for test and item analysis -- psychometrics
[B8716249] 14 p1952 N88-21636
The NPL data approximation subroutine library: Cu rrent and planned facilities
[NPL-DITC-104/87] 14 p1959 N88-21681
Using a parallel computer system for statistical resampling methods
[REPT-87-47] 14 p1960 N88-21690
General aviation activity and avionics survey: 1986 data
[AD-A189986] 15 p2013 N88-22003
Results of the International Comparison of Absolute Gravimeters (2nd) held in Sevres, France in June-July 1985
[AD-A189869] 15 p2093 N88-22474
The collection of statistics on the frequency of cloud cover over North America
[AD-A190456] 15 p2097 N88-22495
Properties of some Bayesian scoring procedures for computerized adaptive tests
[AD-A189925] 15 p2124 N88-22660
Empirical and hierarchical Bayes competitors of preliminary test estimators in two sample problems
[AD-A190327] 15 p2125 N88-22670
Statistical fine structure in inhomogeneously broadened absorption lines in solids
[AD-A190341] 16 p2174 N88-22957
Statistical fine structure in the inhomogeneously broadened electronic origin of pentacene in p-terphenyl
[AD-A191211] 16 p2176 N88-22968
Modeling of turbulent transport as a volume process
16 p2196 N88-23099
A statistical investigation of the single-point pdf of velocity and vorticity based on direct numerical simulations 16 p2196 N88-23101
Seasonal variation for structural strength value
[PB88-169248] 16 p2222 N88-23260
Analysis of means in some nonstandard situations
[ETN-88-92247] 16 p2262 N88-23522
Remote sensing techniques in the estimation of the area cultivated with beans, corn, and castor beans in the Irece County (Bahia State) 17 p2358 N88-24045
Characteristics of drainage determinations in aerial photographs and relief determination on different scales planialtimetric charts for three soils in the state of Sao Paulo 17 p2367 N88-24095
An investigation of Soviet capabilities in extended range arctic ice forecasting
[AD-A191082] 17 p2376 N88-24127
Survival analysis, or what to do with upper limits in astronomical surveys
[NASA-CR-182936] 17 p2449 N88-24551
Performance estimates for operations conducted while wearing individual protective equipment: User manual
[AD-A191871] 18 p2553 N88-25154
Annotated computer output for split plot design: SAS GLM
[AD-A190800] 18 p2555 N88-25167
A method for the numerical solution of random Cauchy singular integral equation 18 p2565 N88-25234
Exact tests for variance component models with unequal cell frequencies in the last stage
[AD-A191645] 18 p2568 N88-25253
On path properties of certain infinitely divisible processes
[AD-A192016] 18 p2568 N88-25255
Statistical evaluation of light water reactor piping damping data for use in PRA (Probabilistic Risk Assessment) analyses
[DE88-007708] 19 p2661 N88-25828
Determining system maintainability as a probability
[DE88-007722] 19 p2679 N88-25927
Circulation statistics from seasonal and perpetual January and July simulations with the NCAR (National Center for Atmospheric Research) Community Climate Model (CCM1):R15
[PB88-192620] 20 p2823 N88-26748
Kinetic theory for plane flows of rough, inelastic, circular disks 21 p2946 N88-27499
The low-latitude auroral boundary: Steady-state and time-dependent representations
[AD-A193200] 21 p2972 N88-27656
The collection of statistics on the frequency of cloud cover over North America
[AD-A193093] 21 p2974 N88-27667
A statistical procedure for the evaluation of presence/non-presence of stimulus-related EEG activity 21 p2978 N88-27689
Computation of filters by sampling and quantization
[AD-A192839] 21 p3005 N88-27826
On the exceedance random measures for stationary processes
[AD-A192838] 21 p3009 N88-27848
Statistical analysis of dyadic stationary processes
[AD-A193057] 21 p3009 N88-27853
The SAS System by forms: Putting statistical power into the hands of an end-user
[DE88-010512] 21 p3010 N88-27857
Comparison of results based on a deterministic versus a statistical uncertainty analysis
[DE88-010751] 21 p3010 N88-27858
Analysis of lower hybrid current drive and rampup experiments on the JT-60 tokamak
[DE88-753136] 21 p3018 N88-27915
Modeling discrete bathtub and upside down bathtub mean residual life functions
[AD-A192000] 22 p3085 N88-28320
Evaluation of annual crop surfaces and territorial inventory in the Paris basin by combining classic statistical inquiries and SPOT data (Preliminary Evaluation Program for SPOT 127) 22 p3094 N88-28372
Complex EOF analysis of intraseasonal tropical wind fluctuations 22 p3121 N88-28544
Sub-Saharan rainfall anomalies and global sea-surface temperature relationships for the recent fifteen year (1970-1984) period 22 p3122 N88-28552
Northern Hemisphere 700 mb teleconnections based on half-monthly mean anomaly data stratified by season and by sign 22 p3123 N88-28561
On the modes of growing-season precipitation over central North America 22 p3124 N88-28567
Correction of systematic errors in NMC medium range forecasts 22 p3126 N88-28584
Theoretical and practical limits of predictability of the NMC medium-range model 22 p3127 N88-28586
A comparison of typical meteorological year solar radiation information with the SOLMET data base
[DE88-009242] 23 p3234 N88-29247
A minitab macro for the Kaplan-Meier product limit estimator and the Tarone-Ware class of tests
[AD-A194298] 23 p3248 N88-29331
Multi-sensory tracking mount control
[AD-A194675] 23 p3249 N88-29339
Commentary on Harold Hotelling's articles on the teaching of statistics
[AD-A194215] 23 p3273 N88-29484
Limiting distributions of non-linear vector functions of stationary Gaussian processes
[AD-A194569] 23 p3274 N88-29488
Asymptotic modal analysis and statistical energy analysis
[NASA-CR-183077] 23 p3278 N88-29514
Measurement and analysis of low altitude atmospheric turbulence obtained using a specially instrumented Gnat aircraft 24 p3313 N88-29728
Re-assessment of gust statistics using CAADRP data
24 p3313 N88-29732
Fatigue crack propagation: Probabilistic modeling and statistical analysis
[AD-A195885] 24 p3384 N88-30155
Statistical analysis of the LMS (Last Mean Squares) and modified stochastic gradient
[AD-A195497] 24 p3424 N88-30376
Instrumentation for computational statistical research
[AD-A195887] 24 p3426 N88-30390

STATISTICAL COMMUNICATION THEORY
U COMMUNICATION THEORY

STATISTICAL CORRELATION
Independence in sonar observations
[ARE-TR-87102] 01 p0088 N88-10572
An application of L1 to astronomy — stellar velocity
[REPT-87-10] 01 p0108 N88-10702
The velocity structure and turbulence at the center of the Orion Nebula 04 p0521 N88-13201
Control charts when the observations are correlated
[AD-A186388] 07 p0866 N88-15253

STATISTICAL DECISION THEORY
Bayesian solutions to a 2 x 2 decision matrix using interval scaled payoffs with an application to foreign policy decisions
[AD-A190863] 16 p2260 N88-23511

STATISTICAL DISTRIBUTIONS
NT BRIGHTNESS DISTRIBUTION
NT PROBABILITY DISTRIBUTION FUNCTIONS
NT RAYLEIGH DISTRIBUTION
RANDOM NUMBER: A syntax-directed package to produce random numbers in user-specified, univariate distributions. User's guide
[DE87-014278] 02 p0228 N88-11436
Light scattering by oriented and randomly dispersed chiral particles
[DE87-014758] 03 p0376 N88-12368
On the geometrical description of fatigue crack surfaces 05 p0607 N88-13727
The application of doubly-truncated hydrometeor distributions to numerical cloud models
[AD-A185273] 05 p0627 N88-13836
Quantile based unified distribution of extreme values and order statistics
[AD-A185171] 05 p0644 N88-13942
Tracking procedure for non-normally distributed measurement errors
[AD-A186287] 07 p0903 N88-15468
Recursive m-estimators of location and scale for dependent sequences
[AD-A186292] 07 p0903 N88-15469
Detecting and interval estimation about a slope change point
[AD-A186030] 07 p0909 N88-15509
Additional investigations in landing process of aircraft: Test distributions
[DFVLR-MITT-87-13] 09 p1115 N88-16686

Analysis of gases in the earth's crust
[PB88-141619] 10 p1354 N88-18093
Five New South Wales barrier lagoons: Their macrobenthic fauna and seagrass communities
11 p1517 N88-19059
Position finding and tolerances
[AD-A187685] 11 p1540 N88-19205
Analysis of impact crater arrangement on the Venutian surface (from photographic materials of the Venera-15 and -16 spacecraft)
[NASA-TT-20211] 11 p1571 N88-19401
Design of the primary pre-TRMM and TRMM ground truth site
[NASA-CR-182609] 12 p1647 N88-19865
On the theory of electromagnetic scattering from a raindrop splash
[AD-A188720] 14 p1906 N88-21393
Grain boundary oxidation and low-cycle fatigue at elevated temperatures 15 p2083 N88-22420
Statistical inference for stochastic processes
[AD-A190491] 15 p2126 N88-22673
Evaluation of an estimation system for an irrigated area in a tropical region through TM-LANDSAT imagery
17 p2363 N88-24075
Evaluation of the floodable area of the canal of Sao Goncalo through TM-LANDSAT 5 imagery
17 p2364 N88-24078
Restrictions in activity monitoring through remote sensing 17 p2365 N88-24084
The 35 mm vertical aerial photographs for mapping stands of bracatinga in different age classes
17 p2366 N88-24087
Preliminary study on the application of digital processing of TM-LANDSAT data in the mapping of apple orchards in Fraiburgo (SC) 17 p2367 N88-24093
Some geological aspects of the Pirapemas Lineament Belt 17 p2368 N88-24099
The theory of random alloys
[DE88-006408] 18 p2487 N88-24756
Interpreting forest biome productivity and cover utilizing nested scales of image resolution and biogeographical analysis
[NASA-CR-183036] 20 p2817 N88-26711
Range of a constrained random walk
[PB88-126867] 20 p2847 N88-26897
Aperiodic superlattices: Structured randomness
20 p2873 N88-27055
The computation of stationary distributions on Markov chains through perturbations
[AD-A193191] 21 p3009 N88-27855
A probabilistic model of the apparent radiance of a rough sea
[AD-A193867] 22 p3129 N88-28602
Additional investigations into the aircraft landing process: Test distributions
[ESA-TT-1090] 23 p3177 N88-28913
Selecting the best binomial population: Parametric empirical Bayes approach
[AD-A193341] 23 p3269 N88-29450
Sequential approach to Colombeau's theory of generalized functions
[DE88-701869] 23 p3276 N88-29503
AGN (OIII) emission line profiles: Dependencies on galaxy inclination and Balmer decrement
[INPE-4596-PRE/1324] 24 p3459 N88-30577

STATISTICAL MECHANICS
Statistical mechanical theory of condensed explosives
[DE87-009137] 01 p0031 N88-10197
Chaos: Chto Delat? (What is to be done?)
[DE88-000513] 05 p0643 N88-13933
Relativistic stochastic mechanics
[PREPRINT-543] 06 p0790 N88-14842
A study of the free energy of the Lenz-Ising model using the cluster variation method of Morita
[AD-A186023] 08 p1073 N88-16476
Electronic structure and phase stability of alloys
[DE88-004574] 11 p1562 N88-19350
Integral equation theory of polymer blends
[DE88-005305] 13 p1751 N88-20471
Memory efficient evaluations of nonlinear stochastic equations and C3 applications
[AD-A189872] 15 p2110 N88-22569
A small concentration expansion for the effective heat conductivity of a random disperse two-component material; an assessment of Batchelor's renormalization method
[REPT-87-71] 16 p2207 N88-23168
The two-dimensional one component plasma in a doubly periodic background: Exact results
[AD-A191260] 16 p2280 N88-23650
Introduction to lattice gauge theory
[DE88-006073] 18 p2584 N88-25349
Thermo field dynamics and para statistical mechanics
[DE88-702057] 19 p2737 N88-26253
On microphysical principles of thermofluid dynamics
[ETN-88-92095] 20 p2801 N88-26620
Extension of Boltzmann's theory to a liquid
[DE88-009153] 20 p2880 N88-27097
Statistical description of stochastic dynamics
[AD-A192924] 21 p3009 N88-27852
A virtual statistical mechanical neural computer
[AD-A193962] 22 p3139 N88-28660

STATISTICAL MOMENTS
U DISTRIBUTION MOMENTS

STATISTICAL PROBABILITY
U PROBABILITY THEORY

STATISTICAL TESTS
Determining differences in rates corresponding to a given significance level
[AD-A185004] 05 p0644 N88-13940
Contributions to selection and ranking theory with special reference to logistic populations
[AD-A185629] 07 p0917 N88-15568
Asymptotic error bounds for power approximations to multinomial tests of fit
[MEMO-640] 08 p1072 N88-16470
An application of fuzzy set theory to statistical hypothesis testing
[AD-A186705] 09 p1232 N88-17386
Statistical aspects of reliability, maintainability and availability
[AD-A188491] 12 p1634 N88-19783
On the Edgeworth expansion and the bootstrap approximation for a Studentized U-statistic
[CWI-MS-R8708] 14 p1965 N88-21728
Distributions of quadratic forms
[AD-A190224] 15 p2124 N88-22663
Stopping rules and observed significance levels
[AD-A190320] 15 p2124 N88-22664
Admissible Bayes tests for structural relationship
[AD-A190326] 15 p2125 N88-22669
On Hotelling's approach to testing for a nonlinear parameter in regression
[AD-A191189] 17 p2393 N88-24229
A minitab macro for the Kaplan-Meier product limit estimator and the Tarone-Ware class of tests
[AD-A194298] 23 p3248 N88-29331
A nonparametric multidimensional IRT approach with applications to ability estimation and test bias
[AD-A194212] 23 p3273 N88-29483
Exact lower confidence limits for the reliability of k of n systems for zero failures and nonconservativeness of the maximus method
[AD-A194299] 23 p3274 N88-29485
Instrumentation for computational statistical research
[AD-A195887] 24 p3426 N88-30390

STATISTICAL WEATHER FORECASTING
Forecasting the kind of precipitation in winter
02 p0202 N88-11266
Statistical very short-range forecasting via analogues
02 p0206 N88-11290
Statistical remote sensing algorithm development: A complementary process to mesoscale numerical models
02 p0206 N88-11292
A severe weather forecast software package
02 p0206 N88-11294
Statistical relationships between the mesoscale organization of convection and the large-scale wind profiles during GATE --- GARP Atlantic Tropical Experiment (GATE) 02 p0208 N88-11302
Mesoscale MOS forecast support for 1988 winter Olympics ski events --- model output statistics (MOS)
02 p0209 N88-11312
Extrapolation of extremum values of the wind velocity
08 p1015 N88-16150
The bimodality of large scale averaged flow parameters --- statistical weather forecasting
08 p1016 N88-16159
A drought watch system
[WCP-134] 16 p2234 N88-23345
Comparative verification between GEM model and official aviation terminal forecasts
18 p2546 N88-25115

STATOR BLADES
Computational study on thermal efficiency of ceramic gas turbine
[DE88-753114] 20 p2809 N88-26667
Numerical solutions of unsteady inviscid transonic turbine cascade flows
[AD-A196111] 24 p3316 N88-29748

STATORS
Measurement of airfoil heat transfer coefficients on a turbine stage 02 p0186 N88-11158
Flow in a model turbine stator
02 p0187 N88-11163
Turbine airfoil deposition models and their hot corrosion implications 02 p0189 N88-11178
An explicit Runge-Kutta method for unsteady rotor/stator interaction
[NASA-TM-100787] 07 p0816 N88-14967
A comparison of experimental and theoretical results for labyrinth gas seals with honeycomb stators
[NASA-CR-182441] 08 p0993 N88-16006
Experimental rotordynamic coefficient results for honeycomb seals
[NASA-CR-182440] 08 p0993 N88-16007
The unsteady gas flow through stator and rotor of a turbomachine 10 p1281 N88-17660
Parametric study of choke flutter with a linear theory
10 p1283 N88-17673
Computer-aided modeling and prediction of performance of the modified Lundell class of alternators in space station solar dynamic power systems
[NASA-CR-182538] 11 p1507 N88-19000
Piezoelectric pushers for active vibration control of rotating machinery 16 p2218 N88-23229
Study on the heat resisting and cooling property of the ceramics-metal hybrid stator vanes
[DE88-753117] 20 p2810 N88-26668
The effects of inlet turbulence and rotor/stator interactions on the aerodynamics and heat transfer of a large-scale rotating turbine model. Volume 3: Heat transfer data tabulation 65 percent axial spacing
[NASA-CR-179468] 23 p3180 N88-28930
Three-dimensional Navier-Stokes simulations of turbine rotor-stator interaction
[NASA-TM-100081] 24 p3316 N88-29750
An unconditionally stable Runge-Kutta method for unsteady flows
[NASA-TM-101347] 24 p3321 N88-29780
The effects of inlet turbulence and rotor/stator interactions on the aerodynamics and heat transfer of a large-scale rotating turbine model. Volume 2: Heat transfer data tabulation. 15 percent axial spacing
[NASA-CR-179467] 24 p3326 N88-29804

STAYS
U GUY WIRES

STEADY FLOW
NT COUETTE FLOW
Calculation of stationary and low frequency unsteady flows in a steam turbine end stage
[MITT-23] 01 p0057 N88-10364
Instability of steady flow with constant vorticity in vessels with elliptical cross-section 02 p0159 N88-10997
SHARP simulation of discontinuities in highly convective steady flow
[NASA-TM-100240] 05 p0642 N88-13931
Measurements of the time dependent velocity field surrounding a model propeller in uniform water flow
16 p2205 N88-23155
A variational finite element method for three-dimensional, steady, compressible, viscous flows
18 p2512 N88-24904
An h-p adaptive finite element method for steady compressible flow 21 p2941 N88-27467
An efficient patched grid Navier-Stokes solution for multiple bodies, phase 1
[AD-A194166] 23 p3211 N88-29110
Contamination and distortion of steady flow field induced by discrete frequency disturbances in aircraft gas engines
[AD-A195440] 24 p3370 N88-30069

STEADY STATE
A baroclinic wavy basic state model: Description and preliminary experiments
[KNMI-WR-87-1] 01 p0068 N88-10436
A two-fluid model for solar wind fluid with higher order moments 01 p0116 N88-10739
Blade loss transient dynamics analysis, volume 1. Task 2: TETRA 2 theoretical development
[NASA-CR-179632] 02 p0125 N88-10791
Blade loss transient dynamics analysis, volume 2. Task 2: TETRA 2 user's manual
[NASA-CR-179633] 02 p0126 N88-10792
Proceedings of the Japan-US Workshop P-92 on Plasma Material Interaction/High Heat Flux Data Needs for the Next Step Ignition and Steady State Devices
[DE87-013568] 04 p0494 N88-13042
PISCES: Plasma-surface interactions and materials research
[DE88-001323] 04 p0494 N88-13044
An experimental investigation of the aerodynamics of a NACA 64A010 airfoil-flap combination with and without flap oscillations. Part 1: Steady-state characteristics
[NASA-TM-88217] 05 p0542 N88-13305
RADSPHERE: A computer program for calculating the steady-state, axially symmetric, forced response and radiation field of a submerged spherical shell
[AD-A185025] 05 p0609 N88-13738
Numerical methods for reaction-diffusion problems with non-differentiable kinetics
[AD-A185405] 05 p0641 N88-13923
Gas diffusion studies in steady and nonsteady cavities
[AD-A185795] 06 p0704 N88-14318

A loading system for creep testing under constant compressive stress
[NASA-TT-20119] 06 p0722 N88-14441
Steady-state deformation of some lithium ceramics
[DE88-003116] 08 p0972 N88-15882
Influence of viscosity on the structure of a magnetic neutral layer 08 p1098 N88-16605
Dynamic evolution of the source volumes of gradual and impulsive solar flare emissions
[NASA-TM-87815] 08 p1102 N88-16621
Optimization of volume produced H(-) ions in a low-pressure hydrogen plasma
[IPPJ-853] 09 p1252 N88-17505
On the barotropic model of the ocean circulation
[AD-A188148] 10 p1358 N88-18118
Thermal analysis in steady state conditions for satellites
[INPE-4429-TDL/309] 12 p1599 N88-19574
Accelerating the computation of steady state solutions for non-equilibrium, chemically reacting flow fields
12 p1625 N88-19724
Optimum duration of steady-state stage in friction welding of metals without artificial braking
14 p1898 N88-21330
Coupled bending-torsion steady-state response of pretwisted, nonuniform rotating beams using a transfer-matrix method
[NASA-TM-100596] 15 p2086 N88-22435
Magnetic fusion energy plasma interactive and high heat flux components. Volume 5: Technical assessment of critical issues in the steady state operation of fusion confinement devices
[DE88-006920] 15 p2136 N88-22744
Analysis of closed cycle megawatt class space power systems with nuclear reactor heat sources
17 p2413 N88-24351
EETAP (End-to-End Transient Analysis Program) for space nuclear power system simulation
17 p2418 N88-24381
HTPIPE: A steady state heat pipe analysis program
17 p2421 N88-24396
Periodic solutions in aircraft cruise-dash optimization
18 p2464 N88-24631
Steady state and transient behavior of the Pd-SnO(sub x) MIS oxygen sensors 19 p2672 N88-25890
Evolution of poloidal variation of impurity density and ambipolar potential in rotating tokamak plasma, part 2
[DE88-009882] 19 p2731 N88-26218
Periodic oscillations in nonlinear mechanical systems
21 p2963 N88-27599
The low-latitude auroral boundary: Steady-state and time-dependent representations
[AD-A193200] 21 p2972 N88-27656
Steady-state approximations in Raman excitation equations
[DE88-011759] 21 p3014 N88-27889
Steady and unsteady transonic pressure measurements on a clipped delta wing for pitching and control-surface oscillations
[NASA-TP-2594] 23 p3173 N88-28895
An exponential decay estimate for the stationary perturbation of Poiseuille flow
[AD-A193480] 23 p3210 N88-29105
Finite element analysis of steady and transiently moving/rolling nonlinear viscoelastic structure. Part 1: Theory
[NASA-CR-179886] 23 p3273 N88-29480

STEADY STATE FLOW
U EQUILIBRIUM FLOW

STEAM
Development of creep resistant austenitic stainless steels for advanced steam cycle superheater application
[DE87-012929] 01 p0023 N88-10147
Comparative tests of high temperature creep-rupture behavior of the austenitic CrNi steel DIN W.NR.1.4970 in argon and steam
[KFK-4261] 01 p0063 N88-10402
National Aerospace Laboratory experiment
04 p0404 N88-12509
Cu-2 mechanical properties and microstructural stability of advanced steam cycle materials
[DE88-001519] 05 p0586 N88-13452
To the problem of determining true volume steam content by measured values of mean density of a mixture in thermally unsteady two-phase flows
[DE88-700840] 12 p1626 N88-19726

STEAM FLOW
National Aerospace Laboratory experiment
04 p0404 N88-12509
Study of a water-steam two phase flow in a T-branch
[ETN-88-92306] 20 p2801 N88-26624

STEAM GENERATORS
U BOILERS

STEAM TURBINES
The effect of different packagings on the vibration behavior and the coupling factors of steam turbine blading
[ETN-87-90425] 01 p0056 N88-10357
Calculation of stationary and low frequency unsteady flows in a steam turbine end stage
[MITT-23] 01 p0057 N88-10364
Development of a supersonic steam turbine with a single stage pressure ratio of 200 for generator and mechanical drive 06 p0713 N88-14374
On line instrument systems for monitoring steam turbogenerators
[CISE-3860] 08 p0990 N88-15995
Open-cycle centrifugal vapor-compression heat pump
[PB88-157391] 11 p1488 N88-18885
Design of a high-power-density Ljungstroem turbine using potassium as a working fluid
17 p2409 N88-24323

STEEL STRUCTURES
The effect of fretting corrosion on the fatigue strength of steel and cast iron under sinusoidal and random loading
[LBF-FB-177] 01 p0023 N88-10142
Deformation induced cracking in steel girder bridges and retrofit guidelines
[PB88-102710] 07 p0868 N88-15265
A summary of experimental results on square plates and stiffened panels subjected to air-blast loading
09 p1178 N88-17057
Removal of out-of-plane distortion in mild steel panels using flame heating, volume 1
[AD-A187802] 11 p1457 N88-18684
Removal of out-of-plane distortion in mild steel panels using flame heating, volume 2
[AD-A187803] 11 p1457 N88-18685
Characteristics of welds joining parts of high-strength pipe steels and produced by beam of continuous-wave CO2-laser 14 p1897 N88-21325

STEELS
NT AUSTENITIC STAINLESS STEELS
NT BAINITIC STEEL
NT CARBON STEELS
NT CHROMIUM STEELS
NT FERRITIC STAINLESS STEELS
NT HIGH STRENGTH STEELS
NT LOW CARBON STEELS
NT MARAGING STEELS
NT MARTENSITIC STAINLESS STEELS
NT NICKEL STEELS
NT STAINLESS STEELS
Optimizing the application of high temperature corrosion resistant aluminium-silicon-base coatings
[BLL-M-37222-(5828.4)] 01 p0018 N88-10112
A physical metallurgical basis for heat-affected zone and base-plate properties of a microalloyed HSLA steel
[AD-A180200] 01 p0022 N88-10137
Development of ultrafine grains and related properties in Hadfield manganese steels
[DE87-011884] 01 p0024 N88-10154
Crack propagation behavior of the materials StE 460 and AlMg 4.5Mn
[FD-1/1986] 01 p0058 N88-10373
The effect of size and surface on the lifetime prediction of StE 460 notched bars
[FD-6/1986] 01 p0058 N88-10374
Fatigue crack propagation of low-alloy steel in a vacuum environment
[DE87-013770] 01 p0061 N88-10393
The water permeability of multi-layer coatings
[BLL-M-37252-(5828.4)] 02 p0148 N88-10927
Anelastic behaviour of materials under multiaxial strains. Part 3: Order-disorder transition, Shoek effect and Poisson's ratio in AISI-1080 steel
[DE87-703087] 02 p0191 N88-11193
Microstructural characterization of irradiated PWR steels using the atom probe field-ion microscope
[DE88-000341] 03 p0291 N88-11828
Sintered steels of high resistance alloyed to Nb, Mo, Mn and Si
[DE87-703546] 04 p0415 N88-12573
Progress in the development of niobium alloyed high speed steel
[DE87-703549] 04 p0415 N88-12576
Hadfield steels with Nb and Ti carbides
[DE87-703706] 04 p0416 N88-12579
Corrosion of ferritic steels by molten lithium: Influence of competing thermal gradient mass transfer and surface product reactions
[DE88-000334] 04 p0417 N88-12585
Effects of stress-relieving on the mechanical properties and the structure of specimens of high-temperature fine-grained structural steels heat-treated to simulate welding
[BLL-CE-TRANS-8258-(9022.09)]
04 p0417 N88-12586
Influence of creep on the precipitate structure under conditions of long-term creep. 4: Experiments on 10 CrMo 9 10 steel
[BLL-CE-TRANS-8256-(9022.09)]
04 p0417 N88-12589
Corrosion resistance of sintered alloy steels
[BLL-M-37363-(5828.4)] 05 p0564 N88-13438
Master plots for predicting the case-depth in laser surface treatments
[PB87-221875] 05 p0586 N88-13574
The mechanics of fatigue-crack nucleation in a low-alloy steel under fretting conditions 05 p0597 N88-13649
The influence of the topography of fracture surfaces on crack closure 05 p0598 N88-13657
Striations and the fatigue growth mechanism in a micro-alloyed steel 05 p0599 N88-13661
Fatigue of 30CrMnSiNi2A notched specimens under spectrum loading 05 p0602 N88-13689
Interaction of microstructure and fatigue in tool steels
05 p0603 N88-13693
Tensile mean stress effects on uniaxial fatigue behavior of 1045 HR steel 05 p0603 N88-13694
The initiation and growth of fatigue cracks in carburised 9Cr1Mo steel 05 p0603 N88-13696
Crack propagation properties of sintered steel
05 p0604 N88-13698
The role of inclusions in corrosion fatigue crack initiation in Q1N 05 p0604 N88-13699
The influence of crack conditions on hydrogen uptake by steels 05 p0604 N88-13702
Modeling the effect of sulfur on the threshold environmental cracking rate of steels in high temperature water 05 p0604 N88-13703
Fracture analysis of drawn composite dual-phase steel wire
[DE88-001396] 06 p0681 N88-14173
Ion-beam nitriding of steels
[NASA-CASE-LEW-14104-2] 06 p0682 N88-14179
An investigation of fatigue crack growth in a ductile material at high growth rates 06 p0715 N88-14383
Life prediction of steel cords
06 p0715 N88-14386
On cleavage in fatigue for rail steels
06 p0716 N88-14388
Fatigue crack growth behavior in hydrogen gas environment 06 p0716 N88-14391
The relationship between microstructural size and fatigue threshold in iron and steel
06 p0716 N88-14396
Threshold behaviour of semi-elliptic hydrogen-induced and fatigue-induced cracks 06 p0717 N88-14397
A model for ultra-low fatigue crack growth
06 p0717 N88-14404
The effects of loading history on fatigue crack growth threshold 06 p0718 N88-14406
Study of the characteristic curve of hardening and softening during low-cycle fatigue process
06 p0719 N88-14414
Fatigue oxidation interaction in low cycle fatigue
06 p0719 N88-14420
Thermal mechanical low cycle fatigue of 25CDV4-10 steel 06 p0721 N88-14429
Transients in elevated temperature crack growth
[DE87-013189] 06 p0724 N88-14454
Characterization of current steels. The 35 NCD 16 alloy in 30 mm diam laminated bars made by Aubert and Duval
[CEAT-41/N/76] 07 p0832 N88-15048
Study on substructures of martensite in steels containing rare earth metals
[PB87-143996] 07 p0833 N88-15050
Tribological studies on high speed steel cutting tools
[DE88-002550] 07 p0864 N88-15246
Study on characteristics of SCC propagation da/dt for welded joint
[PB87-143640] 07 p0869 N88-15270
Analysis of load-bearing capacity of nitrided layer
[PB87-144176] 08 p0968 N88-15857
Rare earth elements in heat treatable steels
[PB87-144002] 08 p0968 N88-15858
Investigations in field of surface forces in metallurgy
[BLL-M-47406-(5828.4)] 08 p0969 N88-15860
TiN coatings on M2 steel produced by plasma assisted chemical vapor deposition
[DE88-003189] 08 p0970 N88-15867
Mechanical properties of steel-to-steel adhesive bonds
[PB88-111299] 08 p0971 N88-15877
The relationship of tensile specimen size and geometry effects to unique constitutive parameters for ductile materials
[AD-A186020] 08 p0994 N88-16012
Fracture-resistant characteristics of medium-strength plates with regard to the initiation, stable and unstable propagation of surface cracks
[PB87-144804] 08 p0996 N88-16025

Study of the temperature dependence of the mechanical characteristics of the steels GX 5 CrNi 13 4 and GGG 40 in tensile and bending tests
[DE88-001469] 09 p1143 N88-16850
Influence of non-metallic elements in the mechanical properties of 20 Mn Mo Ni 55 steel
[DE88-700412] 10 p1300 N88-17775
A detailed microstructural examination of the cause of HAZ cracking in type 316 steel
[AERE-R-12428] 10 p1301 N88-17777
Effects of commercial cladding on the fracture behavior of pressure vessel steel plates
[DE88-004333] 10 p1303 N88-17790
Acoustic emission-microstructural relations in ferritic steels. Part 3: The effect of inclusion content
[AERE-R-12041] 10 p1341 N88-18015
Acoustic emission measurements of PWR weld materials with inserted defects
[AERE-R-12386] 10 p1341 N88-18016
The measurement of stress in steels of varying microstructure by Barkhausen and magneto-acoustic emission
[AERE-R-12387] 10 p1343 N88-18027
Effects of sulfur content on the plain strain fracture toughness of inertia welds in 4340 steel
[AD-A188192] 11 p1458 N88-18689
Influence of grain boundary phosphorus segregation on hydrogen embrittlement in steel
[DE88-700176] 11 p1459 N88-18696
Protecting old oil tanks made of steel against internal corrosion using organic coatings
[DE88-751089] 11 p1459 N88-18698
Hydrogen embrittlement of gun steel
[AD-A188972] 13 p1740 N88-20407
Non-destructive evaluation techniques applied to the study of fatigue microcrack growth in steel alloys
[DE88-004090] 13 p1742 N88-20420
Transformation, metallurgical response and behavior of the weld fusion zone and heat affected zone in Cr-Mo steels for fossil energy application
[DE88-006037] 13 p1744 N88-20430
Corrosion-wear process under rolling-sliding motion
[AD-A189603] 13 p1778 N88-20635
Influence of hydrogen on crack formation tendency in heat-affected zone with stress concentrator 14 p1887 N88-21276
Rust converters
[AD-A188767] 14 p1891 N88-21299
Some structural aspects of crack propagation in heat-resistant steels under cyclic thermal and mechanical load 14 p1896 N88-21317
Efficiency of fusion during periodic-pulse laser-beam welding 14 p1897 N88-21324
Simulation of thermo-mechanical forming processes: A mixed Eulerian-Langrangian finite element method
[PB88-155247] 14 p1933 N88-21530
Influence of temperature on the tensile strength and toughness characteristics. Material 35NCD16 ESR. Test report M5-521800
[M5-521800] 15 p2041 N88-22163
Characterization of HYTUF steel. Semifinished product: 160 mm dia forging block. Processor: CSI. Test Report M3-434600
[M3-434600] 15 p2041 N88-22164
Analysis of reversible and irreversible hydrogen trapping in metals
[NPL-DMA(A)-154] 16 p2177 N88-22977
Dynamic fracture toughness evaluation by measurement of CTOD
[WNS/ASD-88-02] 16 p2178 N88-22982
Corrosion of electroless nickel-coated steel
[AD-A191045] 16 p2179 N88-22985
Environment effects on crack propagation with tensile stress
[GKSS-87/E/46] 16 p2223 N88-23267
Technology Reports of Kyushu University, volume 61, no. 2
[ISSN-0023-2718] 16 p2256 N88-23485
Irradiation effects on tungsten stabilized martensitic steels
[DE88-007074] 18 p2486 N88-24748
Stress corrosion cracking of A723 steel pressure vessels: Two case studies
[AD-A191741] 18 p2527 N88-24990
Prediction of fatigue life of notched specimens under aircraft loading and importance of the relative method in the case of local strain approach, part 2
[TAE-595-PT-2] 19 p2680 N88-25934
A numerical study of Rayleigh-Taylor instability in aluminum and steel plates
[DE88-010475] 20 p2774 N88-26449
Ultrasonic studies of stresses and plastic deformation in steel during tension and compression
[AD-A192308] 21 p2912 N88-27280
Cold worked reinforcing bars in tensile test under high loading rate and low temperatures
[DE88-752993] 21 p2964 N88-27610
Specular steel surfaces for solar mirror substrates
[DE88-001153] 21 p2968 N88-27630
Influence of dispersed additives reinforcement on the wear reinforcement mechanisms of the alumina-steel couple. Macroscopic and structural aspects
[ECL-88-01] 22 p3059 N88-28148
Method and apparatus for non-destructive testing of temper embrittlement in steels
[NASA-CASE-LAR-13817-1] 23 p3195 N88-29012
High hot-hardness gear lubricant evaluations, phase 2
[AD-A192309] 23 p3196 N88-29017
Critical conditions for failure in materials subjected to high rates of loading
[AD-A194697] 23 p3226 N88-29201
Damage initiation in the short beam shear test of composite materials using stiffness reduction
[AD-A194880] 24 p3340 N88-29863
Crystal structures of ordered carbon metal alloys
[AD-A195597] 24 p3353 N88-29959
Performance Prediction for Coatings. Proceedings of a Workshop
[AD-A188973] 24 p3354 N88-29966
Degradation of protective coatings on steel in corrosive environments 24 p3354 N88-29969
Electrical detection of coating deterioration 24 p3355 N88-29973
Electrochemical evaluation of the long term corrosion resistance of polymer coated steel 24 p3355 N88-29974
An electrochemical impedance spectroscopy study of reactions at the metal/coating interface 24 p3355 N88-29975
Evaluation of organic coating deterioration and substrate corrosion in seawater using electrochemical impedance measurements 24 p3355 N88-29976
Alternative immersion accelerated testing of coating systems for Naval shoreline facilities 24 p3355 N88-29977
The effect of notch root radius on the determination of toughness in ultrahigh strength steel friction welds
[AD-A195952] 24 p3384 N88-30156
Response of SMA (Shielded Metal Arc) and narrow gap HY80 weldments to explosive shock loading
[AD-A195994] 24 p3385 N88-30162

STEEP GRADIENT AIRCRAFT
U V/STOL AIRCRAFT

STEEPEST ASCENT METHOD
U STEEPEST DESCENT METHOD

STEEPEST DESCENT METHOD
Dynamical optimization techniques for the calculation of electronic structure in solids
[DE88-006010] 15 p2140 N88-22768

STEEPNESS
U SLOPES

STEERABLE ANTENNAS
MSAT mobile electronically steered phased array antenna development 19 p2647 N88-25711
MSAT-X electronically steered phased array antenna system 19 p2647 N88-25712
The JPL mechanically steered antenna 19 p2647 N88-25715

STEERING
Steering mechanism — vehicles
[EP-PATENT-0-181-700-A1] 01 p0053 N88-10338
GPS vertical axis performance enhancement for helicopter precision landing approach
[NASA-CR-177443] 04 p0397 N88-12477
RF steering in the CEBAF CW superconducting linac
[CEBAF-PR-87-013] 11 p1547 N88-19251
Aberrations: Their effect on off-axis beam steering
[AD-A189601] 13 p1840 N88-21008
Null steering applications of polynomials with unimodular coefficients
[AD-A191087] 18 p2562 N88-25211
Local free-space mapping and path guidance for mobile robots
[AD-A192970] 20 p2810 N88-26674
Time-Optimal Adaptive Shaped Torque (TOAST) technical note
[AD-A192719] 20 p2843 N88-26869
Guided radiation beams in free electron lasers
[AD-A194525] 22 p3082 N88-28305

STELLAR ACTIVITY
NT FACULAE
NT SOLAR ACTIVITY
NT SOLAR FLARES
NT SOLAR PROMINENCES
NT SPICULES
NT STARSPOTS
NT STELLAR FLARES
NT SUNSPOTS
Fifth Cambridge Workshop on Cool Stars, Stellar Systems and the Sun 04 p0502 N88-13092
The photospheric magnetic fields of cool stars: Recent results of survey and time-variability programs 04 p0503 N88-13094
Observational constraints and evidence for saturation 04 p0503 N88-13097
Heating of stellar chromospheres and coronae: Evidence for non-magnetic basal heating 04 p0503 N88-13098
Active phases on II Peg 04 p0507 N88-13119
Stellar activity and the rotation of Hyades stars 04 p0510 N88-13139
Activity in warm stars 04 p0511 N88-13142
Measurements of stellar magnetic fields: Empirical constraints on dynamo and rotational evolution theories 04 p0518 N88-13185
The EUV line flux variations and activity in Alpha Orionis 08 p1032 N88-16256
EXOSAT observations of Hercules X-1
[MPE-PREPRINT-119] 22 p3164 N88-28841
On the origin of gamma ray bursts
[MPE-PREPRINT-120] 22 p3166 N88-28855
Activity-rotation relations for lower main sequence stars 23 p3298 N88-29640
Starbursts and their dynamics
[NASA-CR-180227] 24 p3452 N88-30549

STELLAR ATMOSPHERES
NT CHROMOSPHERE
NT SOLAR ATMOSPHERE
Analysis of the carbon star G77-61
[ETN-87-90422] 01 p0109 N88-10707
The M-type stars
[NASA-SP-492] 02 p0252 N88-11592
Spectroscopy and nonthermal processes 02 p0252 N88-11594
Thermal atmospheric models 02 p0253 N88-11599
Quasi-thermal models 02 p0253 N88-11600
The atmospheres of M dwarfs: Observations 02 p0253 N88-11601
M dwarfs: Theoretical work 02 p0253 N88-11602
X-ray pulsars: Accretion flow deceleration 03 p0390 N88-12451
Atmospheres of stars in the limits of thin and thick convection zones: The M dwarfs 04 p0505 N88-13104
Atmospheres of stars in the limits of thick and thin convection zones: M giants 04 p0505 N88-13105
Spectroscopic monitoring of RS CVn stars at Kitt Peak using the Penn State fiber optic echelle 04 p0509 N88-13127
Magnetic fields on K and M stars 04 p0510 N88-13137
Activity in warm stars 04 p0511 N88-13142
Empirical relations between photospheric magnetic fields and atmospheric radiative losses for cool dwarf stars 04 p0511 N88-13145
A flash spectrum of Cl I, C I, N I, and Ni II absorption in 31 Cygni: A direct observation of the reversing layer 04 p0513 N88-13158
Application of dynamic atmosphere models to the analysis of angular diameter observations of Mira variables 04 p0515 N88-13168
IUE observations of the hybrid K3 II star Iota Aurigae and constraints on the outer atmospheric structure 04 p0516 N88-13171
Time series infrared spectroscopy of long period variables 04 p0516 N88-13172
Water masers associated with 2 carbon stars: EU Andromedae and V778 Cygni 04 p0517 N88-13176
Gamma ray lines from novae 04 p0526 N88-13214
Onset of type 2 supernova in circumstellar envelope created by the stellar wind from presupernova
[DE88-700448] 10 p1428 N88-18526
A spherical, non-LTE, blanketed model stellar atmosphere for Phi Cas (FOIa) 10 p1428 N88-18528
Consistent transport coefficients in astrophysics
[NASA-TM-101154] 17 p2451 N88-24560
Evolutionary helium and CNO anomalies in the atmospheres and winds of massive hot stars
[NASA-CR-183254] 24 p3452 N88-30550

STELLAR COLOR
Stellar activity and the rotation of Hyades stars 04 p0510 N88-13139
JHK photometry of CN-rich field giants 04 p0516 N88-13175
Radio emission from RS CVn binaries: A 5 GHz VLA survey of 93 systems 04 p0519 N88-13191
The type Ia supernova 1986G in NGC5128: Optical photometry and spectra
[INPE-4426-PRE/1230] 12 p1710 N88-20231
Differential spectral synthesis of the stellar populations in the bulges of spiral galaxies 17 p2451 N88-24558

Spectral classification of Low Mass X-ray Binaries (LMXB) energy spectra with color-color diagrams
[MPE-PREPRINT-111] 22 p3163 N88-28837

STELLAR COMPOSITION
The M-type stars
[NASA-SP-492] 02 p0252 N88-11592
Radial velocity measurements of a sample of northern metal-deficient stars
[SER-C-PREPUBL-FASC-25] 24 p3455 N88-30564

STELLAR CORES
Speckle imaging of active galactic nuclei: NGC 1068 and NGC 4151 18 p2592 N88-25407
Microwave spectroscopy and gravitational collapse 18 p2594 N88-25413

STELLAR CORONAS
NT CORONAL HOLES
NT CORONAL LOOPS
NT SOLAR CORONA
Small-scale energy storage and release as the cause of the stellar X-ray corona 02 p0255 N88-11615
A re-examination of the corona-wind dividing line: Diagnostics of non-coronal atmospheres 04 p0504 N88-13101
X-rays, color, and the Vaughan-Preston gap 04 p0510 N88-13135
Relations between chromospheric and coronal structure, flux-flux correlations and convective zone properties 04 p0510 N88-13138

STELLAR DOPPLER SHIFT
U DOPPLER EFFECT
U EXTRATERRESTRIAL RADIATION

STELLAR ENVELOPES
The M-type stars
[NASA-SP-492] 02 p0252 N88-11592
Spectroscopy and nonthermal processes 02 p0252 N88-11594
Circumstellar radio molecular lines 02 p0252 N88-11595
Circumstellar shells, the formation of grains, and radiation transfer 02 p0252 N88-11596
Mass loss 02 p0253 N88-11597
Circumstellar chemistry 02 p0253 N88-11598
Adiabatic supernova expansion into the circumstellar medium
[DE87-014241] 03 p0387 N88-12433
Emission features in IRAS LRS spectra of MS, S and CS stars 04 p0514 N88-13163
Winds and shells around low-mass supergiants 04 p0514 N88-13164
Far infrared circumstellar debris shells of red supergiant stars 04 p0515 N88-13165
Consistent spherical Nonlocal Thermal Equilibrium (NLTE) models for objects with B-star-like luminosities
[ETN-88-90601] 06 p0800 N88-14897
Low mass stars with mass loss and low-luminosity carbon star formation 06 p0801 N88-14900
Onset of type 2 supernova in circumstellar envelope created by the stellar wind from presupernova
[DE88-700448] 10 p1428 N88-18526
Mass loss from evolved stars 11 p1569 N88-19394
Polarization properties of SiO masers 13 p1858 N88-21113

STELLAR EVOLUTION
NT STAR FORMATION
NT STELLAR MASS ACCRETION
Soft X-ray observations of pre-main sequence stars in the chamaeleon dark cloud
[NASA-CR-181457] 02 p0250 N88-11579
Basic properties and variability 02 p0252 N88-11593
Grids of evolutionary models of massive stars with mass loss and overshooting. Properties of Wolf-Rayet stars sensitive to overshooting
[PUBL-SER-C-FASC-12] 03 p0388 N88-12437
Angular momentum evolution of young stars 04 p0504 N88-13099
Post-zero-age main sequence rotation 04 p0504 N88-13100
Atmospheres of stars in the limits of thick and thin convection zones: M giants 04 p0505 N88-13105
Disk accretion during the early stages of stellar evolution 04 p0505 N88-13106
The onset of chromospheric activity among the A- and F- type stars 04 p0511 N88-13144
Neutron capture nucleosynthesis in low mass AGB stars 04 p0517 N88-13178
Spin-up and spin-down on the way to the main sequence 04 p0518 N88-13181
The Einstein survey of the young stars in the Orion Nebula 04 p0518 N88-13182
Measurements of stellar magnetic fields: Empirical constraints on dynamo and rotational evolution theories 04 p0518 N88-13185
Stromgren photometry of RSCVn and HD108102 04 p0519 N88-13187
Influences of the astrophysical environment on nuclear decay rates
[DE88-001461] 04 p0522 N88-13208
The role of fragmentation in interaction of meteoroids with the Earth's atmosphere 06 p0737 N88-14532
Low mass stars with mass loss and low-luminosity carbon star formation 06 p0801 N88-14900
Physics and chemistry 07 p0883 N88-15359
AGB (Asymptotic Giant Branch): Star evolution
[DE88-001829] 07 p0945 N88-15742
HEAO-1 observations of gamma-ray bursts 07 p0947 N88-15756
An introduction to nuclear astrophysics
[DE88-002761] 08 p1100 N88-16618
The distances and absolute magnitudes of RR Lyrae variable stars 11 p1568 N88-19386
Intermixing processes in massive stars and their influence on stellar evolution and nucleosynthesis
[ETN-88-91484] 11 p1568 N88-19388
A global model for planetary nebulae, taking into account central stellar evolution and influence on halo ionization
[ETN-88-91491] 11 p1568 N88-19389
Pre-supernova evolution of SN 1987A
[SER-C-PREPUBL-FASC-15] 18 p2593 N88-25409
Radial velocities monitoring of a sample of barium and S stars using CORAVEL: Towards an evolutionary link between barium and S stars?
[SER-C-PREPUBL-FASC-19] 18 p2593 N88-25410
Review of the theoretical changes of surface chemistry during massive star evolution
[SER-C-PREPUBL-FASC-17] 18 p2593 N88-25411
Asymptotic giant branch stars in the Infrared Astronomical Satellite (IRAS) catalogs: Selection and analysis of the population characteristics
[MPE-PREPRINT-116] 22 p3163 N88-28840
The evolution of low-mass X-ray binaries
[MPE-PREPRINT-118] 22 p3165 N88-28851
Evolutionary helium and CNO anomalies in the atmospheres and winds of massive hot stars
[NASA-CR-183254] 24 p3452 N88-30550
Radio and infrared properties of young stars
[NASA-CR-183252] 24 p3459 N88-30579

STELLAR FIELDS
U STAR DISTRIBUTION

STELLAR FLARES
NT SOLAR FLARES
Atmospheres of stars in the limits of thin and thick convection zones: The M dwarfs 04 p0505 N88-13104
Evidence for an additional source of opacity during the impulsive phase of stellar flares 04 p0510 N88-13133
The Parkes radio survey of active chromosphere stars 04 p0511 N88-13141
Excess emission in the wings of the Hydrogen Balmer lines during a flare on the late-type dMe star YZ CMi 04 p0511 N88-13146
Exosat results on the dMe flare Star Wolf 630AB and on VB 8 04 p0512 N88-13151
IUE/Optical/VLA flares on AD Leo 04 p0512 N88-13152
A helium flare on the active G5 dwarf Kappa Ceti 04 p0519 N88-13189
Flares: Solar and stellar
[PB87-124962] 06 p0806 N88-14917

STELLAR GRAVITATION
Relativistic stellar pulsations 06 p0801 N88-14902
Spectroscopic determinations of surface gravities of giant stars, and ultraviolet observations of RR Lyrae and X Arietis 11 p1569 N88-19391

STELLAR INTERIORS
NT SOLAR INTERIOR
NT STELLAR CORES
Magnetic fields in the overshoot zone: The great escape 02 p0256 N88-11616

STELLAR LUMINOSITY
The atmospheres of M dwarfs: Observations 02 p0253 N88-11601
The closest solar analogs in the bright star catalogue 04 p0506 N88-13110
The Wilson-Bappu relationship: A barometric effect 04 p0516 N88-13170
Pre-main sequence activity: How far is magnetism involved 04 p0517 N88-13179
The contribution of accretion luminosity to the infrared spectra of T Tauri stars: A possible test 04 p0518 N88-13183
M dwarfs from the Einstein medium sensitivity survey 04 p0519 N88-13188
Radio emission from RS CVn binaries: A 5 GHz VLA survey of 93 systems 04 p0519 N88-13191
Consistent spherical Nonlocal Thermal Equilibrium (NLTE) models for objects with B-star-like luminosities
[ETN-88-90601] 06 p0800 N88-14897
Low mass stars with mass loss and low-luminosity carbon star formation 06 p0801 N88-14900
A survey study of energy distribution in component stars of Algol-type binary systems 06 p0801 N88-14901
Differential spectral synthesis of the stellar populations in the bulges of spiral galaxies 17 p2451 N88-24558
Ultraviolet spectra of subluminous objects found in the Kiso Schmidt survey and systematic reanalysis of the archived ultraviolet spectra of white dwarfs observed with the IUE satellite under the Astrophysics Data Program (ADP)
[NASA-CR-182976] 18 p2592 N88-25406

STELLAR MAGNETIC FIELDS
NT SOLAR MAGNETIC FIELD
Coronal magnetic fields produced by photospheric shear
[NASA-CR-181514] 03 p0390 N88-12447
Fifth Cambridge Workshop on Cool Stars, Stellar Systems and the Sun 04 p0502 N88-13092
Measurements of stellar magnetic fields 04 p0503 N88-13093
The photospheric magnetic fields of cool stars: Recent results of survey and time-variability programs 04 p0503 N88-13094
Nonthermal phenomena in stellar coronae: Evidence from radio observations 04 p0503 N88-13096
Calibration on the Sun for stellar magnetic fields 04 p0506 N88-13113
Large scale solar and stellar magnetic fields 04 p0507 N88-13117
The short-period RS CVn stars: Starspots and fundamental properties 04 p0508 N88-13124
Evidence for expanding magnetic loops in coronae of cool stars 04 p0510 N88-13134
Magnetic fields on K and M stars 04 p0510 N88-13137
Activity in warm stars 04 p0511 N88-13142
Empirical relations between photospheric magnetic fields and atmospheric radiative losses for cool dwarf stars 04 p0511 N88-13145
Pre-main sequence activity: How far is magnetism involved 04 p0517 N88-13179
Measurements of stellar magnetic fields: Empirical constraints on dynamo and rotational evolution theories 04 p0518 N88-13185
Observations and analysis of the photospheric magnetic fields on dwarf G, K and M stars 04 p0520 N88-13196
Polarization properties of SiO masers 13 p1858 N88-21113
EXO033319-2554.2: A 55-MG eclipsing AM Herculis binary
[MPE-PREPRINT-114] 22 p3163 N88-28838

STELLAR MAGNITUDE
The closest solar analogs in the bright star catalogue 04 p0506 N88-13110
The distances and absolute magnitudes of RR Lyrae variable stars 11 p1568 N88-19385

STELLAR MASS
Mass loss 02 p0253 N88-11597
Circumstellar chemistry 02 p0253 N88-11598
The atmospheres of M dwarfs: Observations 02 p0253 N88-11601
Flux tube dynamics and solar/stellar redshift measurements 04 p0503 N88-13095
Atmospheres of stars in the limits of thick and thin convection zones: M giants 04 p0505 N88-13105
Disk accretion during the early stages of stellar evolution 04 p0505 N88-13106
Microwave observations of nonthermal phenomena in pre-main sequence stars 04 p0505 N88-13107
The closest solar analogs in the bright star catalogue 04 p0506 N88-13110
Application of dynamic atmosphere models to the analysis of angular diameter observations of Mira variables 04 p0515 N88-13168
Neutron capture nucleosynthesis in low mass AGB stars 04 p0517 N88-13178
A survey study of energy distribution in component stars of Algol-type binary systems 06 p0801 N88-14901
EXOSAT guest observer program. Binary parameters of the X-ray Pulsar 4U1626-67
[NASA-CR-182374] 06 p0802 N88-14905
BE Ursae Majoris: A detached binary with a unique reprocessing spectrum
[NASA-CR-182419] 08 p1083 N88-16526
A spherical, non-LTE, blanketed model stellar atmosphere for Phi Cas (FOIa) 10 p1428 N88-18528
Spectroscopic determinations of surface gravities of giant stars, and ultraviolet observations of RR Lyrae and X Arietis 11 p1569 N88-19391
Hydrodynamical models of supernova SN 1987 A in the LMC
[DE88-701123] 15 p2151 N88-22837
A review of the Initial Mass Function (IMF) — stellar mass
[MPE-PREPRINT-112] 22 p3165 N88-28848

Mass transfer instabilities due to angular momentum flows in close binaries — stars
[MPE-PREPRINT-113] 22 p3165 N88-28849

The evolution of low-mass X-ray binaries
[MPE-PREPRINT-118] 22 p3165 N88-28851

STELLAR MASS ACCRETION

The contribution of accretion luminosity to the infrared spectra of T Tauri stars: A possible test
04 p0518 N88-13183

STELLAR MASS EJECTION

Solar origins of coronal mass ejections
01 p0113 N88-10726

On the association of erupting magnetic fields with eruptive prominences and coronal mass ejections
01 p0113 N88-10727

Coronal mass ejections: The long-term variation of their occurrence rate and the solar wind mass flux
01 p0114 N88-10732

The M-type stars
[NASA-SP-492] 02 p0252 N88-11592

IRAS and cool stellar mass loss
04 p0515 N88-13166

Magnetic field draping about coronal mass ejecta
[DE88-001805] 05 p0661 N88-14057

AGB (Asymptotic Giant Branch): Star evolution
[DE88-001829] 07 p0945 N88-15742

Numerical modelling of the classical nova outburst
[NASA-TM-89707] 07 p0945 N88-15746

Theoretical studies of mass loss and shock phenomena in cool star envelopes
[NASA-CR-182433] 08 p1099 N88-16616

Transverse flow deflections associated with fast coronal mass ejecta in interplanetary space
[DE88-003180] 09 p1263 N88-17566

Stellar energy loss and anomalous contributions to the (photon photon) (neutrino antineutrino) interaction
[DE86-700618] 10 p1428 N88-18529

Mass loss from evolved stars
11 p1569 N88-19394

Magnetohydrodynamic (MHD) simulation of solar prominence formation 13 p1858 N88-21109

Solar-geophysical data number 519, November 1987. Part 2: (Comprehensive reports). Data for May 1987 and miscellanea
[PB88-158910] 14 p2011 N88-21997

Table of solar activity associated with coronal mass ejections observed by the SMM coronagraph/polarimeter in 1980
[PB88-170681] 14 p2011 N88-21998

STELLAR MODELS

Dynamic effects of stellar winds and associated HII regions on the interstellar medium
[ETN-87-90421] 01 p0109 N88-10706

Analysis of the carbon star G77-61
[ETN-87-90422] 01 p0109 N88-10707

High explosive simulations of supernovae and the supernova shell fragmentation model of solar system formation
[DE87-014708] 02 p0251 N88-11584

The M-type stars
[NASA-SP-492] 02 p0252 N88-11592

Grids of evolutionary models of massive stars with mass loss and overshooting. Properties of Wolf-Rayet stars sensitive to overshooting
[PUBL-SER-C-FASC-12] 03 p0388 N88-12437

Relations between chromospheric and coronal structure, flux-flux correlations and convective zone properties
04 p0510 N88-13138

Theoretical studies of mass loss and shock phenomena in cool star envelopes
[NASA-CR-182433] 08 p1099 N88-16616

A spherical, non-LTE, blanketed model stellar atmosphere for Phi Cas (FOIa)
10 p1428 N88-18528

Intermixing processes in massive stars and their influence on stellar evolution and nucleosynthesis
[ETN-88-91484] 11 p1568 N88-19388

A global model for planetary nebulae, taking into account central stellar evolution and influence on halo ionization
[ETN-88-91491] 11 p1568 N88-19389

The effects of rotation on the winds from hot stars
11 p1569 N88-19393

Galaxy evolution in dense clusters
13 p1855 N88-21101

Hydrodynamical models of supernova SN 1987 A in the LMC
[DE88-701123] 15 p2151 N88-22837

Pre-supernova evolution of SN 1987A
[SER-C-PREPUBL-FASC-15] 18 p2593 N88-25409

On the origin of gamma ray bursts
[MPE-PREPRINT-120] 22 p3166 N88-28855

STELLAR MOTIONS

NT SOLAR OSCILLATIONS
NT SOLAR ROTATION
NT STELLAR ORBITS
NT STELLAR OSCILLATIONS
NT STELLAR ROTATION

On the (lack of) proper motion of the Vela pulsar
01 p0097 N88-10635

Basic properties and variability
02 p0252 N88-11593

The kinematics of late-type supergiants
[SER-C-PREPUBL-FASC-28] 24 p3454 N88-30560

STELLAR ORBITS

Asynchronous rotation in close binary systems with circular orbits 04 p0509 N88-13131

Regular orbital variations in the ultraviolet resonance lines of YZ Cnc
[MPE-PREPRINT-117] 22 p3165 N88-28850

Duplicity in the solar neighborhood: Part 4: Spectroscopic orbits for four dwarf M stars
[SER-C-PREPUBL-FASC-21] 24 p3454 N88-30561

Orbital stability in rotating triaxial stellar systems
[SER-C-PREPUBL-FASC-24] 24 p3455 N88-30569

STELLAR OSCILLATIONS

NT SOLAR OSCILLATIONS

The ultrashort period dwarf nova SW Ursae Majoris
24 p3453 N88-30553

STELLAR PHYSICS

NT SOLAR PHYSICS

The M-type stars
[NASA-SP-492] 02 p0252 N88-11592

The atmospheres of M dwarfs: Observations
02 p0253 N88-11601

Active phases on II Peg 04 p0507 N88-13119

The short-period RS CVn stars: Starspots and fundamental properties 04 p0508 N88-13124

Relativistic stellar pulsations 06 p0801 N88-14902

Activities in astrophysics
[INPE-4582-PRE/1316] 24 p3456 N88-30570

STELLAR RADIATION

NT STELLAR WINDS

Ultraviolet observations of AM Her — cataclysmic variable
[MPE-PREPRINT-92] 02 p0250 N88-11581

The M-type stars
[NASA-SP-492] 02 p0252 N88-11592

Basic properties and variability
02 p0252 N88-11593

Spectroscopy and nonthermal processes
02 p0252 N88-11594

Circumstellar shells, the formation of grains, and radiation transfer 02 p0252 N88-11596

The pulsation modes of CO Aur
[PUBL-SER-C-FASC-10] 03 p0387 N88-12430

VLA observations of rapid 6 cm flux variations in alpha Ori 04 p0515 N88-13169

A comprehensive exploration of late-type stars in the far-ultraviolet 04 p0520 N88-13194

The history and development of nonlinear stellar pulsation codes
[DE88-001828] 06 p0801 N88-14899

Relativistic stellar pulsations 06 p0801 N88-14902

Observations of gamma bursts from GBS 0526-66
08 p1001 N88-16065

The EUV line flux variations and activity in Alpha Orionis 08 p1032 N88-16256

On the time delay of the ultrahigh-energy radiation signal from the source Cygnus X-3
[DE88-700649] 10 p1431 N88-18547

Thermal radiation from neutron stars
[MPE-203] 11 p1571 N88-19404

Analysis of the inter-layer independence of stellar scintillometer profiles of Cn2
[AD-A189372] 12 p1645 N88-19854

To the opportunities of cluster analysis of light curves of supernovae
[DE88-701642] 21 p3030 N88-27982

EXO033319-2554.2: A 55-MG eclipsing AM Herculis binary
[MPE-PREPRINT-114] 22 p3163 N88-28838

Radio and infrared properties of young stars
[NASA-CR-183252] 24 p3459 N88-30579

STELLAR ROTATION

NT SOLAR ROTATION

Angular momentum evolution of young stars
04 p0504 N88-13099

Post-zero-age main sequence rotation
04 p0504 N88-13100

Large scale solar and stellar magnetic fields
04 p0507 N88-13117

Asynchronous rotation in close binary systems with circular orbits 04 p0509 N88-13131

Relations between chromospheric and coronal structure, flux-flux correlations and convective zone properties
04 p0510 N88-13138

Stellar activity and the rotation of Hyades stars
04 p0510 N88-13139

Broadband linear polarization and chromospheric CaII H and K line emission in late-type main sequence stars
04 p0511 N88-13140

Spin-up and spin-down on the way to the main sequence 04 p0518 N88-13181

Observations and analysis of the photospheric magnetic fields on dwarf G, K and M stars
04 p0520 N88-13196

The effects of rotation on the winds from hot stars
11 p1569 N88-19393

Activity-rotation relations for lower main sequence stars 23 p3298 N88-29640

Orbital stability in rotating triaxial stellar systems
[SER-C-PREPUBL-FASC-24] 24 p3455 N88-30569

STELLAR SPECTRA

NT SOLAR SPECTRA

An application of L1 to astronomy — stellar velocity
[REPT-87-10] 01 p0108 N88-10702

Ultraviolet observations of cataclysmic variables: The IUE archive
[MPE-PREPRINT-91] 02 p0250 N88-11580

The M-type stars
[NASA-SP-492] 02 p0252 N88-11592

Spectroscopy and nonthermal processes
02 p0252 N88-11594

Comparison of global and nuclear properties of starburst and Seyfert 1 galaxies 03 p0388 N88-12438

A large X-ray flare on Sigma 2 coronae borealis observed with exosat 04 p0508 N88-13121

Spectroscopic monitoring of RS CVn stars at Kitt Peak using the Penn State fiber optic echelle
04 p0509 N88-13127

H alpha and Ca II emission line variability of FK comae 04 p0509 N88-13128

PG 0308 + 096: A short-period white dwarf + dM binary with strongly modulated H-alpha emission
04 p0509 N88-13132

Evidence for an additional source of opacity during the impulsive phase of stellar flares
04 p0510 N88-13133

Magnetic fields on K and M stars
04 p0510 N88-13137

The Wilson-Bappu relationship: A barometric effect
04 p0516 N88-13170

IUE observations of the hybrid K3 II star Iota Aurigae and constraints on the outer atmospheric structure
04 p0516 N88-13171

Time series infrared spectroscopy of long period variables 04 p0516 N88-13172

Synthetic spectra for the N-type carbon star TX Psc
04 p0516 N88-13173

Water masers associated with 2 carbon-stars: EU Andromedae and V778 Cygni 04 p0517 N88-13176

The delta upsilon = 1 fundamental bands of carbon monoxide in late-type stars 04 p0517 N88-13177

Pre-main sequence activity: How far is magnetism involved 04 p0517 N88-13179

Chromospheric variability mechanisms affecting pre-main sequence stars 04 p0517 N88-13180

Measurements of stellar magnetic fields: Empirical constraints on dynamo and rotational evolution theories
04 p0518 N88-13185

IRAS and near IR observations of active binaries
04 p0518 N88-13186

M dwarfs from the Einstein medium sensitivity survey
04 p0519 N88-13188

A helium flare on the active G5 dwarf Kappa Ceti
04 p0519 N88-13189

A comprehensive exploration of late-type stars in the far-ultraviolet 04 p0520 N88-13194

Observations of gamma bursts from GBS 0526-66
08 p1001 N88-16065

BE Ursae Majoris: A detached binary with a unique reprocessing spectrum
[NASA-CR-182419] 08 p1083 N88-16526

Theoretical studies of mass loss and shock phenomena in cool star envelopes
[NASA-CR-182433] 08 p1099 N88-16616

Gamma-ray imaging observations of the Crab and Cygnus regions 10 p1427 N88-18522

Calculated late time spectra of supernovae
[DE88-003296] 10 p1428 N88-18530

The type Ia supernova 1986G in NGC5128: Optical photometry and spectra
[INPE-4426-PRE/1230] 12 p1710 N88-20231

A 23 hour EXOSAT observation of the X-ray pulsar 1E2259+586 and the associated supernova remnant G109.1-1.0
[MPE-PREPRINT-99] 14 p1994 N88-21882

The X-ray properties of AM Her stars
[MPE-PREPRINT-106] 16 p2289 N88-23704

IUE evidence on the nature of the innermost broad-line region in Seyfert 1 galaxies 17 p2450 N88-24552

Duplicity in the solar neighborhood. Part 3: New spectroscopic elements for nine solar-type binary stars
[SER-C-PREPUBL-FASC-18-PT-3] 18 p2592 N88-25405
Analysis of emission features in IRAS LRS spectra 21 p2928 N88-27380
Spectral classification of Low Mass X-ray Binaries (LMXB) energy spectra with color-color diagrams
[MPE-PREPRINT-111] 22 p3163 N88-28837
International ultraviolet explorer spectral atlas of planetary nebulae, central stars, and related objects
[NASA-RP-1203] 22 p3164 N88-28843
The ultrashort period dwarf nova SW Ursae Majoris 24 p3453 N88-30553
Duplicity in the solar neighborhood: Part 5: Spectroscopic orbit for the nearby double-lined solar-type star HR 8581
[SER-C-PREPUBL-FASC-23] 24 p3455 N88-30562

STELLAR SPECTROPHOTOMETRY
The M-type stars
[NASA-SP-492] 02 p0252 N88-11592
Basic properties and variability 02 p0252 N88-11593
Infrared excesses of barium stars 04 p0516 N88-13174
JHK photometry of CN-rich field giants 04 p0516 N88-13175
Stromgren photometry of RSCVn and HD108102 04 p0519 N88-13187
Mapping stellar surface features 09 p1262 N88-17564
Preparation of photometric measurements on a million stars in the framework of the satellite project HIPPARCOS/TYCHO
[ETN-88-91502] 13 p1853 N88-21093
A new determination of the Geneva photometric passbands and their absolute calibration
[SER-C-PREPUBL-FASC-26] 24 p3452 N88-30546

STELLAR STRUCTURE
Pressure structure of solar coronal loops 02 p0256 N88-11618
The onset of chromospheric activity among the A- and F- type stars 04 p0511 N88-13144
Surface photometric investigations for spiral galaxies of large dimension structures in edge-on gemetry
[ETN-88-92126] 21 p3030 N88-27985

STELLAR SYSTEMS
Fifth Cambridge Workshop on Cool Stars, Stellar Systems and the Sun 04 p0502 N88-13092
Relative chaos in stellar systems
[DE88-700148] 12 p1710 N88-20234
Asymptotic giant branch populations in composite stellar systems 13 p1854 N88-21098
Orbital stability in rotating triaxial stellar systems
[SER-C-PREPUBL-FASC-24] 24 p3455 N88-30569

STELLAR TEMPERATURE
Application of dynamic atmosphere models to the analysis of angular diameter observations of Mira variables 04 p0515 N88-13168
Pre-main sequence activity: How far is magnetism involved 04 p0517 N88-13179
BE Ursae Majoris: A detached binary with a unique reprocessing spectrum
[NASA-CR-182419] 08 p1083 N88-16526
A spherical, non-LTE, blanketed model stellar atmosphere for Phi Cas (FOIa) 10 p1428 N88-18528
The astrophysics of nebulae and active galactic nuclear emission-line regions: New methods and applications 13 p1858 N88-21111

STELLAR WINDS
Dynamic effects of stellar winds and associated HII regions on the interstellar medium
[ETN-87-90421] 01 p0109 N88-10706
A re-examination of the corona-wind dividing line: Diagnostics of non-coronal atmospheres 04 p0504 N88-13101
The acceleration of winds by MHD waves in open magnetic structures 04 p0506 N88-13109
Radio continuum emission from the ionized stellar winds of the cool supergiants in zeta Aurigae-like systems 04 p0514 N88-13160
Winds and shells around low-mass supergiants 04 p0514 N88-13164
Theoretical studies of mass loss and shock phenomena in cool star envelopes
[NASA-CR-182433] 08 p1099 N88-16616
Onset of type 2 supernova in circumstellar envelope created by the stellar wind from presupernova
[DE88-700448] 10 p1428 N88-18526
The effects of rotation on the winds from hot stars 11 p1569 N88-19393
Colliding stellar winds in the eclipsing Wolf-Rayet binary V444 Cygni
[NASA-CR-182937] 17 p2451 N88-24563
Propagation of linear gravity waves in a relativistic atmosphere
[DE88-702062] 19 p2691 N88-25995
Time-dependent mass loss from hot stars with and without radiative driving
[DE88-008899] 20 p2884 N88-27128
Regular orbital variations in the ultraviolet resonance lines of YZ Cnc
[MPE-PREPRINT-117] 22 p3165 N88-28850
Evolutionary helium and CNO anomalies in the atmospheres and winds of massive hot stars
[NASA-CR-183254] 24 p3452 N88-30550

STELLARATORS
Mode purity measurements on gyrotrons for plasma heating at the stellarator W 7-AS
[IPF-87-3] 01 p0101 N88-10660
Computational study of three-dimensional magnetohydrodynamic equilibria in toroidal helical systems
[DE87-753007] 02 p0240 N88-11514
Progress in stellarator/heliotron research, 1981-1986: Executive summary
[DE88-000017] 02 p0241 N88-11519
The role of stellarators in the advanced toroidal program
[DE87-014815] 04 p0491 N88-13025
Transport scaling in the collisionless-detrapping regime in stellarators
[DE88-001511] 05 p0653 N88-14006
High midplane accessibility stellarator windings for high current toroidal accelerators
[AD-A186235] 07 p0933 N88-15665
Activities report of the Institute of Plasma Physics
[ETN-88-91020] 07 p0933 N88-15668
Benchmarks of neutral beam injection codes for stellarators
[DE88-003786] 10 p1412 N88-18428
Diagnostics for ATF
[DE88-004175] 10 p1414 N88-18438
ATF experimental plans
[DE88-004177] 10 p1414 N88-18439
Low aspect ratio torsatrons
[DE88-004173] 11 p1552 N88-19284
Summaries of FY86 research in the Applied Plasma Physics Fusion Theory Program
[DE88-004242] 11 p1554 N88-19298
Proceedings of US-Japan Heliotron-Stellarator Workshop, volume 3
[DE88-004788] 11 p1554 N88-19299
Proceedings of US-Japan Heliotron-Stellarator Workshop, volume 2
[DE88-004789] 11 p1554 N88-19300
Proceedings of US-Japan Heliotron-Stellarator Workshop, volume 4
[DE88-004787] 12 p1693 N88-20126
Comparison of analytic and full guiding center behavior at a trapped-passing interface in stellarators
[DE88-004174] 13 p1842 N88-21025
Helical ripple transport in stellarators at low collision frequency
[DE88-006431] 13 p1843 N88-21031
Spectral diagnostics for temperature and density measurements on ATF 17 p2442 N88-24525
Neoclassical diffusion due to trapping/detrapping orbits in stellarators
[DE88-008566] 20 p2857 N88-26968

STEP FAULTS
U GEOLOGICAL FAULTS

STEP FUNCTIONS
Effect of phase errors in stepped-frequency radar systems
[AD-A194476] 23 p3203 N88-29061

STEPPES
Monitoring Tunisia's steppes with SPOT 22 p3097 N88-28390

STEPPING MOTORS
Theoretical and experimental investigations on a linear, permanently excited stepping motor
[ETN-88-91061] 09 p1158 N88-16939
Development of a cryogenic stepping drive for ISO/LWS 14 p1878 N88-21220

STEREOCHEMISTRY
The mechanism of stereo regulation during anionic polymerization of polar monomers
[AD-A186530] 08 p0973 N88-15888
New phosphorus based polymer systems
[AD-A190457] 15 p2045 N88-22186
Topological stereochemistry
[AD-A191867] 18 p2477 N88-24691

STEREOGRAPHY
U STEREOPHOTOGRAPHY

STEREOPHONICS
Performance of single and multiple system AM stereo decoder receivers
[PB88-168307] 15 p2057 N88-22265

STEREOPHOTOGRAPHY
Evaluation of SPOT stereoscopic possibilities for cartography 03 p0342 N88-12158
Pulsed laser stereophotography of plasmas and dynamically moving surfaces
[DE88-003170] 09 p1173 N88-17031
Automated stereophotogrammetry
[AD-A189617] 12 p1630 N88-19757
Relative orientation
[AD-A190385] 15 p2089 N88-22449
Stereoscopic photographs, ground and aerial, of trees used in the arborization of Curitiba (PR) 17 p2366 N88-24091
Finding wheels of vehicles in stereo images
[AD-A194372] 22 p3080 N88-28292
Metric applications of SPOT's lateral stereoscopy 22 p3111 N88-28480
Rigorous stereophotogrammetric treatment of SPOT images 22 p3111 N88-28482
Study of stereoradiometry on SPOT images 22 p3112 N88-28484
Automatic extraction of high resolution elevation data from SPOT stereo images 22 p3113 N88-28489
Automatic creation of digital terrain models from SPOT image pairs 22 p3113 N88-28490
Digital SPOT stereoplotting: An original approach to the formation of epipolar images and matching 22 p3113 N88-28493
Determining vehicle motion from stereo image sequences
[AD-A194371] 23 p3216 N88-29140

STEREOSCOPIC PHOTOGRAPHY
U STEREOPHOTOGRAPHY

STEREOSCOPIC VISION
Self calibration of motion and stereo vision for mobile robot navigation
[AD-A185602] 06 p0781 N88-14794
Computing 3-D structure of rigid objects using stereo and motion 08 p1061 N88-16407
Visual evoked potentials
[AD-A187942] 11 p1519 N88-19071
Three-dimensional information from stereovision process 12 p1593 N88-19540
Television monitor field shifter and an opto-electronic method for obtaining a stereo image of optimal depth resolution and reduced depth distrotion on a single screen
[NASA-CASE-NPO-17249-1-CU] 17 p2332 N88-23924
Multilevel computational theory of stereoscopic visual image processing
[AD-A195331] 24 p3408 N88-30288

STEREOSCOPY
NT STEREOPHOTOGRAPHY
Stereo and eye movement
[AD-A193588] 22 p3142 N88-28681

STERILIZATION
Controlled ecological life support systems: Development of a plant growth module 05 p0630 N88-13854

STERNS
U AFTERBODIES

STEROIDS
NT ALDOSTERONE
NT CORTICOSTEROIDS

STIFF STRUCTURES
U RIGID STRUCTURES

STIFFENING
Interactive buckling effects in stiffened FRP panels
[ARE-TM(UMS)-87204] 01 p0059 N88-10378
Vibration and buckling of geometrically imperfect laminated cylindrical shells 04 p0456 N88-12822
Experimental studies on the tripping behavior of narrow T-stiffened flat plates subjected to hydrostatic pressure and underwater shock 05 p0592 N88-13613
Geometrically nonlinear analysis of stiffened panels 06 p0722 N88-14440
Optimum design of geodesically stiffened composite plates
[NASA-CR-182499] 10 p1344 N88-18035
Preliminary investigation of stability of a fin-stiffened slender strut
[NASA-TM-4034] 12 p1599 N88-19568
Postbuckling delamination of a stiffened composite panel using finite element methods
[NASA-CR-182803] 15 p2030 N88-22098
Local buckling and crippling of composite stiffener sections
[NASA-TM-101133] 17 p2317 N88-23840
Stiffened titanium panels
[NASA-CASE-LAR-13814-1] 18 p2497 N88-24816
Nonlinear vibrations of periodically stiffened plates 21 p2963 N88-27598

STIFFNESS
Control of a flexible one-link manipulator
[AD-A185035] 05 p0590 N88-13598

A comparison of experimental and theoretical results for labyrinth gas seals with honeycomb stators
[NASA-CR-182441] 08 p0993 N88-16006
Development of a new generation of high-temperature composite materials 09 p1119 N88-16702
Reliability of structures with stiffness and strength degradation 09 p1180 N88-17068
A superelement component dynamic synthesis method 11 p1500 N88-18956
Wave propagation in laminated composite plates
[AD-A188999] 12 p1604 N88-19594
Investigation of the inter-relationship between base pavement stiffness and asphalt overlay compaction
[DOT/FAA/ES-88/1] 14 p1869 N88-21170
Investigation and synthesis of high temperature and increased stiffness RSP aluminum alloys
[AD-A190407] 15 p2039 N88-22151
Dynamic characteristics of a vibrating beam with periodic variation in bending stiffness
[NASA-TP-2697] 17 p2348 N88-23988
Stiffness degradation of composite laminates 20 p2767 N88-26405
A micromechanics model of the stiffness and strength of laminates with fiber waviness
[NASA-CR-181670] 20 p2768 N88-26413
Nonlinear interaction between overall and local buckling of stiffened panels with symmetric cross-sections
[PB88-104054] 21 p2960 N88-27580
Analysis of stiffness reduction, failure and stress concentration in fiber composite laminates
[AD-A193519] 22 p3050 N88-28096
Two-dimensional sequential and concurrent finite element analysis of unstiffened and stiffened aluminum and composite panels with hole
[NASA-CR-183083] 22 p3086 N88-28325
Damage initiation in the short beam shear test of composite materials using stiffness reduction
[AD-A194880] 24 p3340 N88-29883
Nonlinear stress-strain and inelastic rebound with exponential stiffness
[AD-A195667] 24 p3384 N88-30159

STIFFNESS MATRIX
Frequency domain identification of structural dynamic systems with general damping matrices 03 p0337 N88-12120
Identification of linear structural models 03 p0337 N88-12121
Hybrid FEM (Finite Element Method) approach to stress distribution in the vicinity of a notch in non-homogeneous materials
[PB87-143392] 07 p0868 N88-15268
An efficient Mindlin finite strip plate element based on assumed strain distribution 15 p2081 N88-22407
Improved finite strip Mindlin plate bending element using assumed shear strain distributions
[NASA-TM-100928] 23 p3225 N88-29195
Geometric and material nonlinear analysis of structures comprising rectangular hollow sections
[CE-79] 24 p3382 N88-30141

STIGMATISM
The evaluation of a deformable diffraction grating for a stigmatic EUV spectroheliometer
[NASA-CR-182371] 06 p0707 N88-14337

STIMULANTS
NT ATROPINE
NT CAFFEINE
NT NOREPINEPHRINE
Propranolol and the compensatory circulatory responses to orthostasis at high altitude
[AD-A192675] 22 p3131 N88-28618

STIMULATED EMISSION
A simplified approach to axisymmetric dual-reflector antenna design
[NASA-TP-2797] 09 p1111 N88-16662
Optically stimulated sound from gas bubbles in water 12 p1686 N88-20087
Stimulated Emission of Energetic Particles (SEEP)
[AD-A188724] 13 p1853 N88-21094
Survey of the Air Force P78-2 (SCATHA) satellite plasma wave data during electron gun operations
[AD-A191014] 16 p2168 N88-22926
Theoretical studies of solar-pumped lasers
[NASA-CR-182929] 17 p2344 N88-23971
Monolithic fuel cell based power source for sprint power generation 17 p2407 N88-24313

STIMULATED EMISSION DEVICES
NT AIRBORNE LASERS
NT ARGON LASERS
NT ATMOSPHERIC LASERS
NT CARBON DIOXIDE LASERS
NT CARBON MONOXIDE LASERS
NT CHEMICAL LASERS
NT CONTINUOUS WAVE LASERS
NT DISTRIBUTED FEEDBACK LASERS
NT DYE LASERS
NT EXCIMER LASERS
NT FREE ELECTRON LASERS
NT GALLIUM ARSENIDE LASERS
NT GAMMA RAY LASERS
NT GAS LASERS
NT GASDYNAMIC LASERS
NT GLASS LASERS
NT HCN LASERS
NT HELIUM-NEON LASERS
NT HF LASERS
NT HIGH POWER LASERS
NT HYDROGEN MASERS
NT INFRARED LASERS
NT INTERSTELLAR MASERS
NT IODINE LASERS
NT KRYPTON FLUORIDE LASERS
NT LASERS
NT LIQUID LASERS
NT MASERS
NT METAL VAPOR LASERS
NT NEODYMIUM LASERS
NT NITROGEN LASERS
NT NOVA LASER SYSTEM
NT NUCLEAR PUMPED LASERS
NT PULSED LASERS
NT Q SWITCHED LASERS
NT RAMAN LASERS
NT RARE GAS-HALIDE LASERS
NT RING LASERS
NT RUBY LASERS
NT SEMICONDUCTOR LASERS
NT SOLAR-PUMPED LASERS
NT SOLID STATE LASERS
NT SPACEBORNE LASERS
NT TEA LASERS
NT TRAVELING WAVE MASERS
NT TUNABLE LASERS
NT TWO-WAVELENGTH LASERS
NT ULTRASHORT PULSED LASERS
NT ULTRAVIOLET LASERS
NT WATER MASERS
NT WAVEGUIDE LASERS
NT X RAY LASERS
NT XENON CHLORIDE LASERS
NT XENON FLUORIDE LASERS
NT YAG LASERS
Laser countermeasure impacts and penalties
[DE88-006871] 18 p2520 N88-24947

STIMULATION
NT AUDITORY STIMULI
NT SENSORY STIMULATION
Advancing automation and robotics technology for the space station and for the US economy: Submitted to the United States Congress October 1, 1986
[NASA-TM-89190] 08 p0960 N88-15818
Role of optokinetic stimulation in vesibulospinal reflexes 10 p1360 N88-18131
Disuse condition stimulates bone resorption in organ culture 12 p1656 N88-19925
Neck receptor stimulation in 0 and 1 g 12 p1658 N88-19938
Phase preservation cleanup in a double-pass Raman amplifier SBS (Stimulated Brillouin Scattering) conjugator
[AD-A189428] 13 p1761 N88-20536
Amplification of signals in fiber optics using the stimulated Raman effect
[AD-A190281] 15 p2133 N88-22727
Unstable behavior of lasers and other optical systems
[AD-A190875] 16 p2213 N88-23204

STIMULI
Cognitive task demands as reflected in physiological measures 21 p2980 N88-27699

STIRLING CYCLE
Heat engine regenerators: Research status and needs
[DE87-013581] 01 p0054 N88-10348
RE-1000 free-piston Stirling engine hydraulic output system description
[NASA-TM-100185] 01 p0108 N88-10700
Overview of free-piston Stirling engine technology for space power application
[NASA-TM-88886] 03 p0386 N88-12427
Design concepts for the ASTROMAG cryogenic system
[NASA-CR-181505] 04 p0497 N88-13060
The Goddard Space Flight Center mechanical cooler program 08 p0983 N88-15944
Cryocooler systems demonstration
[AD-A188025] 11 p1467 N88-18745
Test results of a 40-kW Stirling engine and comparison with the NASA Lewis computer code predictions
[NASA-TM-87050] 11 p1508 N88-19013
Magnetic heat pump design
[DE88-007730] 20 p2798 N88-26605

STIRLING ENGINES
Study of free-piston Stirling engine driven linear alternators
[NASA-CR-181425] 01 p0055 N88-10355
RE-1000 free-piston Stirling engine hydraulic output system description
[NASA-TM-100185] 01 p0108 N88-10700
Stirling engine research at national and university laboratories in Japan
[DE87-014622] 02 p0180 N88-11123
Stirling engines and irrigation pumping
[DE88-000020] 02 p0181 N88-11125
Automotive Stirling engine: Mod 2 design report
[NASA-CR-175106] 02 p0250 N88-11578
SPRE 1 free-piston Stirling engine testing at NASA Lewis Research Center
[NASA-TM-100241] 03 p0277 N88-11747
Overview of free-piston Stirling engine technology for space power application
[NASA-TM-88886] 03 p0386 N88-12427
Progress toward the evolution of a Stirling space engine
[NASA-TM-100221] 05 p0659 N88-14046
Hot piston ring tests
[NASA-TM-100256] 06 p0729 N88-14486
Report to Congress on the Automotive Technology Development Program
[DE88-003742] 07 p0864 N88-15242
Hot piston ring/cylinder liner materials: Selection and evaluation
[NASA-TM-100276] 08 p0971 N88-15872
Overview of heat transfer and fluid flow problem areas encountered in Stirling engine modeling
[NASA-TM-100131] 09 p1262 N88-17561
Free-piston Stirling engine diaphragm-coupled heat-actuated heat pump component technology program, phase 1C
[DE88-003654] 10 p1330 N88-17949
Free-piston Stirling engine diaphragm-coupled heat-actuated heat pump component technology program, phase 1B
[DE88-003653] 11 p1483 N88-18854
Test results of a 40-kW Stirling engine and comparison with the NASA Lewis computer code predictions
[NASA-TM-87050] 11 p1508 N88-19013
Cast iron-base alloy for cylinder/regenerator housing
[NASA-CR-182116] 12 p1608 N88-19613
A survey of oscillating flow in Stirling engine heat exchangers
[NASA-CR-182108] 15 p2067 N88-22322
Description of an oscillating flow pressure drop test rig
[NASA-TM-100905] 16 p2170 N88-22933
The 1988 overview of free-piston Stirling technology for space power at the NASA Lewis Research Center
[NASA-TM-100795] 16 p2170 N88-22934
Overview of NASA Lewis Research Center free-piston Stirling engine technology activities applicable to space power systems 17 p2398 N88-24255
Fatigue failure of regenerator screens in a high frequency Stirling engine 17 p2436 N88-24491
Component improvement of free-piston Stirling engine key technology for space power
[NASA-TM-100950] 19 p2607 N88-25476
The design and fabrication of a Stirling engine heat exchanger module with an integral heat pipe
[NASA-TM-101296] 20 p2820 N88-26732
Phase 1 results from the Stirling-powered vehicle project
[NASA-TM-100978] 21 p3029 N88-27980
Testing of a variable-stroke Stirling engine
[NASA-TM-100899] 24 p3440 N88-30472

STIRRING
Coagulation in stirred tanks
[B8711373] 05 p0562 N88-13420

STOCHASTIC PROCESSES
NT MARKOV CHAINS
NT MARKOV PROCESSES
NT RANDOM PROCESSES
NT RANDOM WALK
Processing of fractal functions by linear and nonlinear operators
[RAE-TR-85079] 01 p0088 N88-10571
A problem in quantum probability --- statistical invariants problem
[REPT-87-06] 01 p0088 N88-10573
Stochastic integration for operator valued processes on Hilbert spaces and on nuclear spaces
[ENST-87D002] 01 p0089 N88-10580
A stochastic delamination growth model for fatigue loaded laminated composite materials 02 p0141 N88-10888
Stochastic model of the motion of suspended particles in turbulent flow
[HSBW-MITT-21/1987] 03 p0315 N88-11990
Operator multiple-tasking study for remotely operated platforms
[AD-A184487] 03 p0362 N88-12276

Stochastic model of the NASA/MSFC ground facility for large space structures with uncertain parameters: The maximum entropy approach
[NASA-CR-181489] 03 p0372 N88-12343
Some stochastic aspects of intergranular creep cavitation
[DE88-000065] 04 p0416 N88-12581
The TAB method for numerical calculation of spray droplet breakup
[DE87-011756] 04 p0442 N88-12743
Electromagnetics and electrothermal approach to evaluate failures in microelectronic devices caused by electrostatic discharges: Stochastical aspects of the device reliability
[AD-A184906] 05 p0577 N88-13522
Conditional second order closure for turbulent shear flows
[AD-A185369] 05 p0581 N88-13542
Fatigue crack growth under random overloads 05 p0602 N88-13682
Computer aided modeling and fatigue failure forecast under stochastic loading 05 p0607 N88-13720
On the geometrical description of fatigue crack surfaces 05 p0607 N88-13727
Comparing hard and soft prior bounds in geophysical inverse problems
[NASA-CR-181557] 05 p0624 N88-13820
Explicit formulate for the distributions of stopping variables under Wald's truncated SPRT (Sequential Probability Radio Tests) for a poisson process
[AD-A185053] 05 p0640 N88-13914
Point processes
[AD-A185398] 05 p0641 N88-13921
Robust prediction operations for stationary processes
[AD-A185408] 05 p0641 N88-13924
Isotropic probability measures in infinite dimensional spaces: Inverse problems/prior information/stochastic inversion
[NASA-CR-181555] 05 p0643 N88-13936
Freidlin-Wentzell type estimates and the law of the iterated logarithm for a class of stochastic processes related to symmetric statistics
[AD-A185366] 05 p0644 N88-13944
On the correlation free forms for nonlinear stochastic systems
[DE87-011169] 05 p0645 N88-13947
Computing block-angular Karmarker projections with applications to stochastic programming, revision
[AD-A185647] 06 p0759 N88-14656
On the relations between increasing functions associated with two-parameter continuous martingales
[AD-A185572] 06 p0765 N88-14699
Stochastic approximation and large deviations: General results for w.p.l. Convergence
[AD-A185818] 06 p0768 N88-14721
Relativistic stochastic mechanics
[PREPRINT-543] 06 p0790 N88-14842
A multicut algorithm for two-stage stochastic linear programs
[AD-A186148] 07 p0903 N88-15466
Stochastic filtering solutions for ill-posed linear problems and their extension to measurable transformations
[AD-A186016] 07 p0909 N88-15506
Strong laws of large numbers for arrays of orthogonal random variables
[AD-A186159] 07 p0910 N88-15513
Spectral representation of infinitely divisible processes
[AD-A186210] 07 p0910 N88-15515
Upper bounds on the expected value of a convex function using gradient and conjugate function information
[AD-A186246] 07 p0910 N88-15517
Remark on the multiple Wiener integral
[AD-A186015] 07 p0913 N88-15541
Point processes in the plane
[AD-A186017] 07 p0913 N88-15542
On stochastic optimality of policies in first passage problems
[AD-A186293] 07 p0915 N88-15554
On hypercontractivity of alpha-stable random variables, 0 less than alpha less than 2
[AD-A186425] 07 p0915 N88-15559
The filtering problem for infinite dimensional stochastic processes
[AD-A186431] 07 p0916 N88-15562
Sublinear upper bounds for stochastic programs with recourse, revision
[AD-A186436] 07 p0916 N88-15564
Validation of a stochastic model to determine failure rates for communication-electronic systems
[AD-A186536] 08 p0980 N88-15920
Optimal correction problem of a multidimensional stochastic system
[AD-A186727] 09 p1228 N88-17353
A Prohorov bound for a Poisson process and a Bernoulli process
[CWI-MS-R8701] 09 p1232 N88-17388
Persistence characteristics of 500 mb blocking and zonal flows in the mid-latitudes of the Northern and Southern Hemispheres 10 p1353 N88-18088
Explicit solutions of moment problems, 1
[AD-A186018] 10 p1397 N88-18325
Prediction of the response and optimal control of stochastic parametrically and externally excited nonlinear systems 11 p1496 N88-18930
Deterministic equivalent for a continuous linear-convex stochastic control problem
[AD-A187818] 11 p1540 N88-19206
Stochastic heuristics in network design: Parameter tuning and performance evaluation
[REPT-87-017] 11 p1541 N88-19210
Extrema of Gaussian process by simulation 11 p1541 N88-19211
Recursive inversion of externally defined linear systems
[NASA-TM-100070] 11 p1541 N88-19215
On relaxation algorithms based on Markov random fields
[AD-A189043] 13 p1814 N88-20840
Stochasticity in nonlinear Hamiltonian systems
[DE88-005499] 13 p1826 N88-20915
Stochastic comparisons of order statistics, with applications in reliability
[AD-A189408] 13 p1829 N88-20938
Stochastic and chaotic oscillations
[CWI-AM-R8704] 13 p1829 N88-20940
Nonstationary solution in random vibration theory
[PB88-163746] 14 p1933 N88-21529
Identification of nonlinear rational systems using a prediction-error estimation algorithm
[RR-317] 14 p1959 N88-21680
An orthogonal parameter estimation algorithm for nonlinear stochastic systems
[RR-307] 14 p1966 N88-21736
Open questions in closed-loop photodetection 14 p1979 N88-21812
Stochastic acceleration of cometary ions: The effects of composition and source strength distributions 14 p1997 N88-21902
Random processes, turbulence and disordering fields
[AD-A190123] 15 p2063 N88-22303
Vibrations of structures with parametric uncertainties
[AD-A190400] 15 p2076 N88-22378
Probabilistic structural analysis computer code (NESSUS) 15 p2079 N88-22397
Memory efficient evaluations of nonlinear stochastic equations and C3 applications
[AD-A189872] 15 p2110 N88-22569
Using Colored Stochastic Petri Net (CS-PN) software for protocol specification, validation, and evaluation
[ENST-87C004] 15 p2113 N88-22588
The Colored Stochastic Petri Net (CS-PN) software: Application to the validation and the performance evaluation of distributed systems
[ENST-87D005] 15 p2113 N88-22589
The adjoint process in stochastic optimal control
[AD-A189720] 15 p2116 N88-22605
Martingale representation and the Malliavin calculus
[AD-A189721] 15 p2119 N88-22626
The existence of smooth densities for the prediction filtering and smoothing problems
[AD-A189865] 15 p2119 N88-22629
Normed Bellman equation with degenerate diffusion coefficients and its application to differential equations
[AD-A190319] 15 p2120 N88-22637
Random Process Simulation for stochastic fatigue analysis
[NASA-TM-100464] 15 p2123 N88-22654
The partially observed stochastic minimum principle
[AD-A189787] 15 p2124 N88-22658
Approximations in extreme value theory
[AD-A189817] 15 p2124 N88-22659
Stopping rules and observed significance levels
[AD-A190320] 15 p2124 N88-22664
Estimation of convolution tails
[AD-A190323] 15 p2125 N88-22666
Continuity of symmetric stable processes
[AD-A190324] 15 p2125 N88-22667
Extreme value for dependent sequences via the Stein-Chen method of poisson approximation
[AD-A190325] 15 p2125 N88-22668
Detection of the number, locations and magnitudes of jumps
[AD-A190328] 15 p2125 N88-22671
Statistical inference for stochastic processes
[AD-A190491] 15 p2126 N88-22673
Stochastic evolution equations driven by nuclear space valued martingales
[AD-A189342] 15 p2126 N88-22677
Conditions for information capacity of the discrete-time Gaussian channel to be increased by feedback
[AD-A190317] 15 p2127 N88-22687
Studying Turbulence Using Numerical Simulation Databases. Proceedings of the 1987 Summer Program
[NASA-CR-182692] 16 p2194 N88-23086
Stochastic estimation of conditional eddies in turbulent channel flow 16 p2194 N88-23087
Optimal control, estimation compensation of linear discrete-time systems with stochastic parameters
[REPT-87-56] 16 p2255 N88-23478
An algebraic construction of a class of one-dependent processes
[REPT-87-65] 16 p2259 N88-23507
A note on phase-type, almost phase-type, generalized hyperexponential and Coxian distribution, revision
[AD-A191236] 16 p2261 N88-23517
Stochastic approach of image segmentation. A model of cooperation between region primitives and boundaries
[ETN-88-92192] 16 p2262 N88-23523
Modeling, filtering and control of stochastic processes --- communication networks
[ENST-87E021] 17 p2333 N88-23925
Parallel discrete-event simulation of FCFS stochastic queueing networks
[NASA-CR-181669] 17 p2389 N88-24203
Stochasticity in elliptical galaxies
[SER-C-PREPUBL-FASC-20] 17 p2450 N88-24556
Information and stochastic systems
[AD-A192167] 18 p2501 N88-24838
Analysis of binarized Hartley phase-only filter performance with respect to stochastic noise
[DE88-007604] 18 p2519 N88-24945
Reliability of stochastically forced systems (extended version)
[CWI-AM-R8801] 18 p2526 N88-24985
Computational sciences
[AD-A190826] 18 p2564 N88-25226
Numerical solutions to stochastic difference equations 18 p2564 N88-25229
On path properties of certain infinitely divisible processes
[AD-A192016] 18 p2568 N88-25255
Stochasticity in a Q-machine plasma 18 p2578 N88-25315
Study of probabilistic fatigue crack growth and associated scatter under constant-and-variable amplitude loading spectrum
[AD-A192027] 19 p2679 N88-25929
Stochastic modeling of EM scattering from foliage
[AD-A192258] 20 p2790 N88-26553
Two classes of self-similar stable processes with stationary increments
[AD-A192842] 20 p2846 N88-26894
Simulation and analysis of wave propagation through random media 21 p2947 N88-27503
Nonlinear stochastic interaction in aeroelastic structures
[AD-A193427] 21 p2961 N88-27589
Stochastic geologic effects on near-field ground motions in alluvium
[AD-A192315] 21 p2972 N88-27652
Simulation methodology
[AD-A192548] 21 p2995 N88-27764
Control, stability and filter for a discrete linear stochastic system with correlated noise
[PB88-109525] 21 p3004 N88-27818
A Wong-Zakai type theorem for certain discontinuous semimartingales
[AD-A192713] 21 p3005 N88-27822
Approximations of stochastic equations driven by predictable processes
[AD-A192714] 21 p3005 N88-27823
Computation of filters by sampling and quantization
[AD-A192839] 21 p3005 N88-27826
On the exceedance random measures for stationary processes
[AD-A192838] 21 p3009 N88-27848
A note on vector bimeasures
[AD-A192841] 21 p3009 N88-27849
A study on Lebesgue decomposition of measures induced by stable processes
[AD-A192893] 21 p3009 N88-27850
Multiple integration with respect to Poisson and Levy processes
[AD-A192895] 21 p3009 N88-27851
Statistical description of stochastic dynamics
[AD-A192924] 21 p3009 N88-27852
A virtual statistical mechanical neural computer
[AD-A193962] 22 p3139 N88-28660
Theory of Laplacian fractals: Diffusion limited aggregation and dielectric breakdown model
[PREPRINT-590] 22 p3144 N88-28701
Extremal two-correlations of two-valued stationary one-dependent processes
[REPT-88-01] 22 p3145 N88-28704

Dynamic analysis of computer and communications sytems: Semi-Markov approach
23 p3244 N88-29305
Weak solution of the Langevin equation on a generalized functional space
[AD-A194290] 23 p3270 N88-29456
An asymptotic evaluation of the tail of a multiple symmetric alpha-stable integral
[AD-A194570] 23 p3270 N88-29460
On Wiener-Masani's algorithm for finding the generating function of multivariate stochastic processes
[NASA-CR-182905] 23 p3273 N88-29481
Stochastic game approach to guidance design
[AD-A194574] 23 p3276 N88-29498
Theory of filtering and control with application to control of large space structures
[AD-A195500] 24 p3335 N88-29851
Statistical analysis of the LMS (Last Mean Squares) and modified stochastic gradient
[AD-A195497] 24 p3424 N88-30376
Stability, stochastic stationarity and generalized Lyapunov equations for two-point boundary-value descriptor systems
[AD-A195645] 24 p3425 N88-30385
Analytical methods in stochastic control and nonlinear filtering
[AD-A194272] 24 p3426 N88-30388

STOICHIOMETRY
Structural properties of high-T/sub c/ oxide super conductors
[DE88-002974] 08 p1090 N88-16563
Copper oxidation states, vacancy ordering and their effect on high temperature superconductivity
[DE88-003079] 09 p1258 N88-17542
Local stoichiometry and atomic interdiffusion during reactive metal/mercury-cadmium-telluride junction formation
[AD-A187554] 10 p1421 N88-18488
Processing relationships in YBa2Cu3O(7-x) superconductors
[DE88-005137] 11 p1559 N88-19330
Investigations of surface coatings based on silicon and nitrogen: From amorphous Si to silicon nitride
[DE88-004995] 12 p1609 N88-19622
Electron diffraction evidence for the ordering of excess nickel atoms by relation to stoichiometry in nickel-rich beta'-NiAl formation of a nickel-aluminum (Ni2Al) superlattices
[NASA-TT-20177] 14 p1890 N88-21297
Irreversible dissolution of solid solutions: A kinetic and stoichiometric model
[DE88-009194] 19 p2614 N88-25513
A study of the interaction of diffusion flames with a vortex pair flowfield 21 p2908 N88-27258
Premixed turbulent flame propagation
[AD-A192955] 21 p2909 N88-27265

STOKES FLOW
Shearing flow over Stokes wave. Part one: General theory
[ETN-87-90957] 02 p0171 N88-11074
Rotation of magnetized particle in electrically conducting viscous medium 06 p0770 N88-14733
Chaos, mappings and spatial complexity in fluids
11 p1484 N88-18860
New mixed finite element methods
18 p2567 N88-25248
High performance solutions of the Stokes problem using mini-elements, self-adaptive grids, and multigrid methods: Applications
[ECL-87-15] 22 p3077 N88-28266

STOKES LAW
Two domain decomposition techniques for Stokes problems
[DE88-008724] 19 p2720 N88-26149

STOKES LAW (FLUID MECHANICS)
La Recherche Aerospatiale, bimonthly bulletin, number 1987-1, 236/January-February
[ESA-TT-1055] 11 p1433 N88-18549
Boundary effects on the drag of a cylinder in axial motion at low Reynolds number 13 p1768 N88-20578
A simple explanation of the Stokes phenomenon
[AD-A193253] 21 p3006 N88-27832

STOL AIRCRAFT
U SHORT TAKEOFF AIRCRAFT

STOMACH
Gastric emptying during exercise: Effects of acute heat stress, acclimation and hypohydration
[AD-A188008] 11 p1519 N88-19073
Gastric emptying during walking and running: Effects of varied exercise intensity
[AD-A194025] 23 p3240 N88-29281

STONES (ROCKS)
U ROCKS

STONY METEORITES
NT ACHONDRITES
NT CARBONACEOUS CHONDRITES
NT CARBONACEOUS METEORITES
NT CHONDRITES

STOPPING
Algorithms with conic termination for nonlinear optimization
[DE88-005893] 13 p1816 N88-20851
Merge and termination in process algebra
[CWI-CS-R8716] 13 p1826 N88-20918
Stopping rules and observed significance levels
[AD-A190320] 15 p2124 N88-22664
Soft-ground aircraft arresting systems
[AD-A190838] 16 p2165 N88-22912

STOPPING POWER
Studies of HZE particle interactions and transport for space radiation protection purposes
[NASA-TM-101159] 20 p2886 N88-27142

STORAGE
Solar generation and storage of O2 (a 1 delta g)
[NASA-CR-4127] 14 p1913 N88-21431

STORAGE BATTERIES
NT LEAD ACID BATTERIES
NT NICKEL CADMIUM BATTERIES
NT NICKEL HYDROGEN BATTERIES
NT NICKEL ZINC BATTERIES
NT ZINC-BROMIDE BATTERIES
High energy density rechargeable batteries for aerospace power requirements
[AD-A184883] 05 p0577 N88-13519
Interfacial effects in thin Li/PEO cells at room temperature
[AD-A186974] 09 p1157 N88-16931
A novel class of positive electrodes for rechargeable batteries
[DE88-004559] 13 p1763 N88-20545
Candidate advanced energy storage concepts for multimegawatt burst power systems
17 p2426 N88-24434
Small scale bipolar nickel-hydrogen testing
[NASA-TM-100936] 18 p2538 N88-25059
All inorganic ambient temperature rechargeable lithium battery
[DE88-008425] 19 p2662 N88-25834
Ambient temperature secondary lithium batteries using LiAl lithium insertion anodes
[DE88-006394] 20 p2793 N88-26574
Exploratory battery technology development and testing report for 1986
[DE88-009870] 20 p2794 N88-26578
Considerations and measurements of latent-heat-storage salts for secondary thermal battery applications
[DE88-011091] 23 p3228 N88-29213
Structure and dynamics of solutions of lithium salts relevant to battery construction
[AD-A195399] 24 p3386 N88-30044

STORAGE RINGS (PARTICLE ACCELERATORS)
Brightness and coherence of radiation from undulators and high-gain free electron lasers
[DE87-011093] 02 p0177 N88-11102
Interactive Design of Accelerators (IDA)
[DE87-013298] 02 p0234 N88-11476
Compact electron storage rings
[DE87-013301] 02 p0234 N88-11477
High energy polarized electron beams
[CEBAF-R-87-002] 11 p1548 N88-19244
ZAP user's manual
[LBL-21270] 11 p1546 N88-19248
On bunch lengthening using the fourth harmonic cavity in the NSLS VUV ring
[DE88-007392] 18 p2574 N88-25288
Activities report of the Werner-Heisenberg Institute of Physics
[ETN-88-92946] 21 p3015 N88-27893
Distortion functions
[DE88-752634] 21 p3015 N88-27896

STORAGE STABILITY
Pyrotechnic component development at Sandia National Laboratory
[DE87-006899] 02 p0154 N88-10967
Effects of long term storage on aerospace nickel cadmium cell performance 02 p0165 N88-11035
Shelf life degradation of selected anaerobic threadlocking adhesives at various storage temperatures
[AD-A187712] 11 p1461 N88-18711
Cyropreservation of isolated rat hepathocytes for future use in Spacelab experiments: Preliminary results
12 p1660 N88-19950
Material degradation in a barium hydroxide latent heat storage pilot unit
[DFVLR-FB-87-49] 16 p2175 N88-22961
Aging of CFRP due to longterm storage in heated air
[DFVLR-FB-88-05] 21 p2922 N88-27345

STORAGE TANKS
Electrical heating method --- pipelines, metal tanks
[GB-PATENT-2-137-059-A] 01 p0043 N88-10274
Orbital Spacecraft Consumables Resupply System (OSCRS). Volume 2: Study results
[NASA-CR-172011] 03 p0268 N88-11687
Contribution of acoustic analysis to assess damage in fluid storage tanks under high pressure --- composite materials, filament winding
[SNIAS-872-430-119] 05 p0559 N88-13407
Space environmental considerations for a long-term cryogenic storage vessel 08 p0981 N88-15933
Space Infrared Telescope Facility (SIRTF) design and thermal analysis 08 p0982 N88-15934
Thermal analysis for the Cryogenic Fluid Management Flight Experiment (CFMFE) 08 p0982 N88-15935
Protecting old oil tanks made of steel against internal corrosion using organic coatings
[DE88-751069] 11 p1459 N88-18698
Examination of methods for pollen storage and dispersal
[TN-RB524-097/86] 17 p2378 N88-24134
Prediction of velocity and temperature profiles in thermally driven gravity currents applied to stratified thermal storage tanks
[DE88-004452] 21 p2946 N88-27496

STORE RELEASE
U EXTERNAL STORE SEPARATION

STORM DAMAGE
Forecast of Atlantic seasonal hurricane activity for 1988 15 p2098 N88-22500

STORM ENHANCEMENT
The effect of latitude on the development of tropical cyclones
[AD-A185670] 06 p0746 N88-14590
Tropical cyclones, 1987: Central North Pacific
[PB88-188081] 18 p2547 N88-25119

STORM SUPPRESSION
The studies of physical models on hailstorms and their applications in nowcasting 02 p0207 N88-11300

STORM SURGES
An hourly analysis, updating and short-range forecasting system --- numerical weather forecasting
02 p0206 N88-11288
Hurricane Elena storm surge data
[AD-A184573] 03 p0353 N88-12228
Hurricane Danny storm surge data, report 4
[AD-A186373] 07 p0879 N88-15334
Hurricane Kate storm surge data, report 5
[AD-A186374] 07 p0880 N88-15335
Hurricane climatology for the Atlantic and Gulf coasts of the United States
[PB88-114657] 08 p1039 N88-16288

STORMS
NT CYCLONES
NT HAILSTORMS
NT HURRICANES
NT MAGNETIC STORMS
NT MICROBURSTS (METEOROLOGY)
NT RAINSTORMS
NT SNOWSTORMS
NT STORMS (METEOROLOGY)
NT SUDDEN IONOSPHERIC DISTURBANCES
NT THUNDERSTORMS
NT TORNADOES
NT TROPICAL STORMS
NT TYPHOONS
NWS (National Weather Service) watch/warning verification flash flood, winter storm and high wind, January 1980 - June 1986
[PB87-223053] 04 p0469 N88-12898
Ozone, jet streaks and severe weather
05 p0616 N88-13781
Model investigations of atmospheric ammonia scavenging
[DE88-002337] 09 p1194 N88-17153
Using SIR (Scientific Information Retrival) system for data management during a field program
[DE88-001555] 10 p1424 N88-18508
Effects of stress on judgement and decision making in dynamic tasks
[AD-A188203] 11 p1523 N88-19092
National Severe Storms Laboratory, fiscal year 1987
[PB88-140108] 12 p1647 N88-19863
Research and development to acquire and reduce melting layer cloud physics and evaluate a prototype M-meter
[AD-A188390] 12 p1648 N88-19873
TDWR (Terminal Doppler Weather Radar) PRF (Pulse Repetition Frequency) selection criteria
[AD-A193089] 21 p2932 N88-27407
Passive microwave measurements of water vapor fields and rain for locating fronts in cyclonic storms
[AD-A195632] 24 p3404 N88-30267

STORMS (METEOROLOGY)
NT CYCLONES
NT HAILSTORMS
NT HURRICANES
NT MICROBURSTS (METEOROLOGY)
NT RAINSTORMS
NT SNOWSTORMS
NT THUNDERSTORMS
NT TORNADOES
NT TROPICAL STORMS
NT TYPHOONS
Description of the Mountain Cloud Chemistry Program version of the PLUVIUS MOD 5.0 reactive storm simulation model
[DE87-012846] 01 p0070 N88-10450
The use of McIDAS as a Mesoscale forecasting tool during the Canadian Atlantic storms programs — Man-computer Interactive Data Access System (McIDAS) 02 p0205 N88-11284
A short-range forecasting experiment conducted during the Canadian Atlantic storms program 02 p0205 N88-11285
A severe weather forecast software package 02 p0206 N88-11294
A review of the analysis forecasting and research about severe local storms in Guangdong province (China) 02 p0207 N88-11298
Severe weather potential (SPOT) plotfile generator [PB87-217717] 02 p0216 N88-11360
Theory of heat and moisture exchange between finely disperse storm-generated spray and turbulent air flow 04 p0481 N88-12851
Prediction of polytomous events: Model description, algorithm development and methodological aspects, with an application
[AD-A186549] 09 p1232 N88-17384
Pre-convective environmental conditions indicative of non-tornadic severe thunderstorm winds over Southeast Florida
[AD-A188679] 12 p1648 N88-19870
STOSS-AND-LEE TOPOGRAPHY
U GLACIAL DRIFT
STOWAGE (ONBOARD EQUIPMENT)
Locking hinge
[NASA-CASE-MSC-21056-1] 17 p2312 N88-23827
Expandable pallet for space station interface attachments
[NASA-CASE-MSC-21117-1] 23 p3185 N88-28958
STRAIN AGING
U PRECIPITATION HARDENING
STRAIN DISTRIBUTION
Experimental and theoretical investigation of mechanically fastened composites
[AD-A185896] 07 p0826 N88-15008
Structural relaxation in strained-layer heterostructures
[DE88-002326] 07 p0868 N88-15264
A summary of experimental results on square plates and stiffened panels subjected to air-blast loading 09 p1178 N88-17057
Computed stress and strain distributions under interference fit and after coldworking
[AD-A186950] 10 p1342 N88-18024
Development of reliable fuel pins for space reactor applications 17 p2409 N88-24326
Design and construction techniques for planar polysilicon pressure transducers with piezoresistive read-out 19 p2669 N88-25862
Compression creep of filamentary composites
[NASA-CR-182550] 20 p2798 N88-26601
STRAIN ENERGY METHODS
Fatigue life evaluation according to local strain concept
[FF-14/1985] 01 p0059 N88-10381
Estimation multiaxial elastic-plastic notch stresses and strains in combined loading
[FB-2/1986] 01 p0060 N88-10382
A comparison of plastic work energy and external input for fatigue crack propagation 05 p0607 N88-13722
Design and dynamic testing of an instrumented spacecraft component 11 p1499 N88-18952
Vibration response of constrained viscoelastically damped plates: Analyses and experiments
[AD-A192329] 20 p2815 N88-26699
STRAIN ENERGY RELEASE RATE
Strain-energy-release rate analysis of the end-notched flexure specimen using the finite-element method
[NASA-TM-100494] 05 p0608 N88-13735
Subliminate damage mechanisms in composite structures
[AD-A186807] 09 p1137 N88-16815
Three-dimensional analysis of a postbuckled embedded delamination
[NASA-TP-2823] 20 p2812 N88-26684
STRAIN FATIGUE
U FATIGUE (MATERIALS)
STRAIN GAGE ACCELEROMETERS
Zeroshift of piezoelectric accelerometers in pyroshock measurements 08 p0997 N88-16039
STRAIN GAGES
Balancing strain gauge bridges
[GB-PATENT-2-129-567-A] 01 p0048 N88-10307
Strain gages in engineering geodesy
[SER-C-320] 01 p0048 N88-10309
Fabrication of standardized piezoelectric polymer shock gauges by the Bauer method
[DE87-012738] 01 p0049 N88-10315
Notes on transducer design based on resistance strain gages with applied temperature compensation
[FFA-MEMO-129] 01 p0050 N88-10319
The development of a high temperature static strain gage system 02 p0184 N88-11142
Elevated temperature strain gages 02 p0184 N88-11144
The Lewis Strain Gauge Laboratory: Status and plans 02 p0184 N88-11146
Model helicopter rotor rig and associated strain gauge balance for performance studies
[NAL-TM-AE-8704] 05 p0552 N88-13364
Earth penetrator strain gage applications
[DE88-002260] 09 p1166 N88-16993
Strain gage balance for half models 302-6. Calibration report — wind tunnels
[F+W-FO-1803] 09 p1168 N88-17001
Strain gage sting balance 204-6. Calibration report — wind tunnels
[F+W-FO-1838] 09 p1168 N88-17002
Multi-component stress history measurements and analysis
[DE88-000977] 09 p1168 N88-17004
Manoeuvres by default, by demand and by design 12 p1580 N88-19455
Determination of the toughness of a brittle material using strain gages
[ETN-88-92540] 18 p2527 N88-24993
Design and construction techniques for planar polysilicon pressure transducers with piezoresistive read-out 19 p2669 N88-25862
Deposition techniques and properties of strain compensated LPCVD silicon nitride films 19 p2673 N88-25898
In-flight load measurements of the Robot-X canards
[AD-A193428] 21 p2895 N88-27187
Attachable interferometric strain gages
[AD-A192390] 21 p2950 N88-27522
Further improvements relating to the temperature compensation of semiconductor strain gauge pressure transducers
[RAE-TR-87061] 22 p3081 N88-28298
Electrical properties of materials for elevated temperature resistance strain gage application
[NASA-CR-182214] 24 p3376 N88-30106
Method of attaching strain gauges to various materials
[NASA-CASE-LAR-13797-1] 24 p3376 N88-30108
STRAIN HARDENING
Dugdale solutions for strain hardening materials
[FD-6/1985] 01 p0059 N88-10380
Tensile behavior of superplastic Al-Cu-Li-Zr alloy 2090 at cryogenic temperatures
[DE87-014084] 02 p0147 N88-10923
Hadfield steels with Nb and Ti carbides
[DE87-703706] 04 p0416 N88-12579
Fatigue, fracture and strain hardening of high carbon hardened alloy steel
[AD-A186101] 07 p0831 N88-15043
Processing, structure and properties of heavily deformed in situ composites
[AD-A189611] 13 p1742 N88-20416
Response of aluminum alloys to erosive particle impacts
[DE88-005910] 15 p2041 N88-22159
Strain hardening at large strains in aluminum alloys
[DE88-007415] 18 p2484 N88-24737
STRAIN MEASUREMENT
The development of a high temperature static strain gage system 02 p0184 N88-11142
The Lewis Strain Gauge Laboratory: Status and plans 02 p0184 N88-11146
High temperature stress-strain analysis 02 p0188 N88-11170
Measurement of model deformation in wind tunnels 05 p0551 N88-13358
Application of finite element methods with cyclic elasto-plastic strain analysis to low cycle fatigue analysis of engine components
[AR-004-512] 05 p0596 N88-13642
Axial creep-fatigue damage assessment in type 316 SS material 06 p0721 N88-14430
Thermomechanical fatigue of lead-base low tin solder 06 p0721 N88-14432
A quantitative method for evaluating sensor layouts 09 p1178 N88-17056
Optical analysis of stress and strain in photoelastic particle assemblies
[ETN-88-91591] 09 p1182 N88-17082
The influence of strain on hydrogen entry, transport, and embrittlement of a high strength steel in aqueous sodium chloride solution
[AD-A189302] 12 p1608 N88-19619
Correlation of data on strain accumulation adjacent to the San Andreas Fault with available models
[NASA-CR-180757] 13 p1796 N88-20742
The mechanical properties of card measured by photographic Moire
[NPL-DMOM-87] 14 p1923 N88-21463
Research sensors 15 p2085 N88-22430
Strain intensity factor approach for predicting the strength of continuously reinforced metal matrix composites
[NASA-TM-100617] 17 p2317 N88-23838
Radio Frequency (RF) strain monitor
[NASA-CASE-LAR-13705-1] 18 p2530 N88-25011
Uniaxial tensile strain measurement for ceramic testing at elevated temperature: Requirements, problems and solutions
[DE88-008090] 19 p2621 N88-25550
Predicted and measured strain responses of isotropic panels to base excitation
[NASA-TM-4054] 19 p2679 N88-25928
Ion implantation processing of 3-5 strained-layer semiconductors
[DE88-005270] 19 p2734 N88-26240
Component stress during freeze/thaw cycling
[DE88-011204] 21 p2938 N88-27449
Optical method to measure the deformations of structures loaded by hydraulic pressure
[SNIAS-881-430-111] 22 p3088 N88-28338
Piezoelectric and electrostrictive materials for transducer applications, volume 2
[AD-A194956] 24 p3376 N88-30104
STRAIN RATE
An investigation of the high strain rate deformation of SiCw/2124 Al composite
[OUEL-1675/87] 02 p0142 N88-10895
Strain rate effects in fast-gas-cooled uranium-titanium and uranium-niobium alloys
[OUEL-1683/87] 02 p0149 N88-10937
Experimental determination of flow potential surfaces supporting a multiaxial formulation of viscoplasticity 02 p0187 N88-11167
Material behaviour at high rates of strain
[OUEL-1684/87] 02 p0192 N88-11200
Work-in-progress presented at the Army Symposium on Solid Mechanics, 1986: Lightening of the Force
[AD-A184791] 04 p0427 N88-12644
A direct method to obtain constitutive model constants from cylinder impact test results 04 p0427 N88-12647
Influence of strain rate and notch depth on tensile properties of HITCO 6250
[DE88-001324] 04 p0455 N88-12816
The evolution of plastic strain in steady, plastic shock waves
[DE87-013812] 04 p0456 N88-12826
Plasticity of aluminum and iron at high shear strain rate and high pressure 05 p0563 N88-13430
A critical review of the development of several viscoplastic constitutive theories
[AD-A185652] 07 p0867 N88-15262
Theory of deformation. Part 1: Kinematics
[DE88-003007] 08 p1001 N88-16062
The effect of strain rate on the strength and ductility of SiCw/2124 Al composite
[OUEL-1692/87] 14 p1924 N88-21486
An internal variable constitutive model for the large deformation of metals at high temperatures 14 p1929 N88-21503
Constitutive modeling and thermoviscoplasticity 14 p1930 N88-21506
Creep rupture analysis of a beam resting on high temperature foundation 14 p1930 N88-21509
Controlled-strain rate tests at very low strain rates of 2618 aluminum at 200 C 14 p1931 N88-21513
The effects of temperature and strain rate on the yielding behavior of the single crystal superalloy PWA 1480 14 p1931 N88-21517
Nonlinear structural analysis of a turbine airfoil using the Walker viscoplastic material model for B1900 + Hf 14 p1932 N88-21522
Unified constitutive models for high-temperature structural applications 14 p1932 N88-21523
Effect of strain rate on high-temperature low-cycle fatigue behavior of Hastelloy X and Hastelloy XR
[DE88-752302] 15 p2037 N88-22140
The CRREL (Cold Regions Research and Engineering Laboratory) Hopkinson bar apparatus
[AD-A190599] 15 p2077 N88-22380

Unified constitutive model development for metal matrix composites at high temperature
15 p2078 N88-22387
Unified constitutive model for single crystal deformation behavior with applications
15 p2078 N88-22388
Phenomenological modelling of rate-dependent plasticity for high strain rate problems
[DE88-006647] 15 p2087 N88-22440
Evaluation of a theory for pressure-strain rate
16 p2198 N88-23108
Relations between two-point correlations and pressure strain terms
16 p2198 N88-23109
Superplasticity: A fundamental investigation on deformation mechanism and cavitation phenomena
[AD-A191548] 18 p2485 N88-24741
The variation of torsional ductility of high-purity aluminum with temperature and strain rate
[DE88-005618] 18 p2487 N88-24755
Metastability in SiGe/Si strained-layer structures
[DE88-007603] 18 p2585 N88-25361
Influence of strain rate on the substructure evolution and yield behavior of Ti-6Al-4V
[DE88-006457] 19 p2616 N88-25520
Apparatus for pressure welding of titanium structures with a controlled rate of deformation
[RAE-TRANS-2161] 19 p2677 N88-25915
Temperature, moisture and strain rate effects on the compressive mechanical behavior of Nylon 6/6
[DE88-010734] 21 p2961 N88-27591
Environmental cracking of a superferritic stainless steel under slow strain rate conditions
22 p3053 N88-28117
Development of sensors for ceramic components in advanced propulsion systems: Survey and evaluation of measurement techniques for temperature, strain and heat flux for ceramic components in advanced propulsion systems
[NASA-CR-182111] 22 p3081 N88-28299
A transversely isotropic thermoelastic theory
[NASA-TM-101302] 22 p3087 N88-28332
Plastic flow and failure modeling under high strain rate loading
[AD-A194223] 23 p3226 N88-29199

STRAIN SOFTENING
U PLASTIC DEFORMATION

STRAKES
Transonic Navier-Stokes computations of strake-generated vortex interactions for a fighter-like configuration
[NASA-TM-100009] 15 p2014 N88-22010
Wind-tunnel investigation of actuated forebody strakes for yaw control at high angles of attack
17 p2299 N88-23754
Helicopter anti-torque system using fuselage strakes
[NASA-CASE-LAR-13630-1] 17 p2308 N88-23809
Actuated forebody strakes
[NASA-CASE-LAR-13983-1] 18 p2464 N88-24628

STRANGE ATTRACTORS
Dimension densities for turbulent systems with spatially decaying correlation functions
[DE87-010119] 02 p0169 N88-11066
Anomalous scaling laws in multifractal objects
[NOTA-INTERNA-883] 07 p0916 N88-15565

STRAPDOWN INERTIAL GUIDANCE
Test equipment with fiber optic data bus and laser gyro strapdown system LTN-90 for the helicopter BO-105
[ESA-TT-1038] 01 p0005 N88-10025
NAVSIM 2: A computer program for simulating aided-inertial navigation for aircraft
[NASA-CR-177438] 04 p0398 N88-12478
Advances in Air-Launched Weapon Guidance and Control
[AGARD-CP-431] 12 p1596 N88-19553
A prototype fibre optic gyroscope for missile guidance applications
12 p1596 N88-19554
A fiber optic gyro strapdown reference system for guided weapons
12 p1597 N88-19560
An analysis of DREO's (Defence Research Establishment Ottawa) analog rebalance loops for the CSG-2 (Canadian Strapdown Gyroscope) tuned-rotor gyroscope
[AD-A188577] 12 p1629 N88-19749
Utilization of strapdown inertial and non-inertial sensors in determination of satellite attitude by Kalman filters
[INPE-4313-TDL/280] 13 p1731 N88-20349
Design, simulation and laboratory testing of an inertial system for measuring the attitude and narrow-spaced motions
[DFVLR-FB-87-42] 14 p1912 N88-21426
The NAE atmospheric research aircraft
24 p3313 N88-29730

STRATA
NT SUBSTRATES

STRATEGIC MATERIALS
International role of US geoscience
[NASA-CR-182407] 08 p1035 N88-16281

STRATEGY
Technology transfer to China
[PB87-223418] 04 p0502 N88-13087
Strategic management of research and development: A literature search
[NASA-CR-182337] 06 p0790 N88-14847
Investigation of design concepts for large space structures to support military applications
[AD-A186098] 07 p0824 N88-15000
Performance analysis of coded frequency-hopped spread-spectrum systems with unknown interference
[AD-A186069] 07 p0841 N88-15103
Strategies of data analysis
[AD-A186033] 07 p0914 N88-15548
Cirrus: An automated protocol analysis tool
[AD-A186646] 08 p1052 N88-16348
Research, development, and growth strategy
10 p1309 N88-17820
State-of-the-art technologies for construction in space: A review
[AD-A188412] 12 p1585 N88-19483
Static and dynamic jamming of networks
[AD-A188921] 12 p1620 N88-19690
Alternative force structuring strategies for military satellite communication systems
[AD-A189492] 13 p1758 N88-20516
Parallel image compression
[NASA-CR-180758] 13 p1814 N88-20837
Johnson Space Center's strategic game plan: Charting a course to the year 2000 and beyond
[NASA-TM-89733] 13 p1850 N88-21078
Anatomy of an organizational change effort at the Lewis Research Center
[NASA-CR-4146] 19 p2739 N88-26264
SDI: Myth or reality
[DE88-009121] 20 p2847 N88-26901
The strategic defense initiative: Strategic implications
[AD-A192341] 20 p2847 N88-26902
Rules, schema and decision making
[AD-A193389] 21 p3027 N88-27967
Technology transfer for DOE's Office of Transportation Systems: Assessment and strategies
[DE88-010760] 21 p3029 N88-27977
Electronic combat roadmap for space
[AD-A194282] 22 p3146 N88-28709
Defensive platform size and survivability
[DE88-011634] 23 p3184 N88-28948
The advice taker/inquirer: A system for high-level acquisition of expert knowledge
24 p3421 N88-30359
Antisatellite weapons and satellite deployment strategies
[AD-A195014] 24 p3427 N88-30396

STRATIFICATION
NT ATMOSPHERIC STRATIFICATION
NT INTERCALATION
The correspondence of surface climate parameters with satellite and terrain data
[NASA-CR-181515] 03 p0346 N88-12185
Influence of stratification in near-surface water layer on intensity of gas exchange between atmosphere and water
04 p0459 N88-12841
Transient development of stratification in a partially divided enclosure
[DE87-011742] 05 p0572 N88-13490
Two-layer model of circulation in world ocean with detailed description of seasonal evolution of upper quasihomogeneous layer
06 p0727 N88-14470
North Pacific Ocean. Gulf of Alaska, R/V Thomas G. Thompson: 1 February - 8 March 1987. STD data report
[AD-A186569] 06 p1045 N88-16314
Dynamics of the Oceanic Surface Mixed Layer
[AD-A188348] 13 p1804 N88-20785
Structures and fluxes in a deep convecting mixed layer
13 p1804 N88-20786
Equatorial turbulence: Mixed layer and thermocline
13 p1804 N88-20787
On the zonal momentum balance at the equator
13 p1805 N88-20788
The mixed layer of the western equatorial Pacific Ocean
[HIG-1861] 13 p1805 N88-20789
Unsteady shallowing mixed layer
13 p1805 N88-20791
Horizontal scales of wind forced inertial motions
13 p1806 N88-20795
Subduction
13 p1806 N88-20796
Hamiltonian description of the interaction of surface waves with mixed-layer currents
13 p1806 N88-20799
Monitoring ocean surface layer processes
13 p1806 N88-20801
The main ocean thermocline
14 p1938 N88-21563
Role of ordinary to extraordinary mode wave coupling in ionospheric heating experiments
[AD-A195335] 24 p3362 N88-30017
Mathematical problems of nonlinear wave propagation and of waves in heterogeneous media
[AD-A195970] 24 p3368 N88-30057

STRATIFIED FLOW
Regressed relations for forced convection heat transfer in a direct injection stratified charge rotary engine
[NASA-TM-100124] 05 p0549 N88-13345
Far field of steady waves produced by local perturbation sources in stream of stratified fluid
06 p0771 N88-14736
Mushroom-shaped currents (eddy dipoles) under rotation and stratification conditions
13 p1784 N88-20678
Direct simulation of stable stratified homogeneous turbulent shear flows
[DFVLR-FB-88-04] 21 p2949 N88-27516

STRATIGRAPHY
Geoacoustic models of the Hudson Canyon area
[AD-A183535] 01 p0073 N88-10465
Research needs for hydrocarbon fuels
[DE87-014555] 06 p0687 N88-14209
Neogene paleoclimate in Pacific Ocean subarctic region determined from study of diatoms
08 p1010 N88-16125
Geological evolution and analysis of confirmed or suspected gas hydrate localities. Volume 10: Basin analysis, formation and stability of gas hydrates of the Aleutian Trench and the Bering Sea
[DE88-001008] 10 p1346 N88-18048
Geological evolution and analysis of confirmed or suspected gas hydrate localities. Volume 2: Basin analysis, formation and stability of gas hydrates in the Black Sea
[DE88-001052] 18 p2532 N88-25023
Analyzing the stratigraphy, tectonism, and mineralization at the Spanish side of the pyrite belt, Huelva province, Spain, using SPOT imagery
22 p3104 N88-28433
Stratigraphy of the Kasei Valles region, Mars
23 p3305 N88-29690
Documenting volcano-tectonic episodes in Mars' stratigraphic record
23 p3306 N88-29695
Ridged and gullied terrains in the Martian uplands
23 p3307 N88-29700
Variation in the thickness of ejecta cover on Mars with increasing crater density
23 p3307 N88-29701
Deep seismic reflection profiling and continental growth curves
24 p3396 N88-30222

STRATOCUMULUS CLOUDS
Mesoscale applications of high resolution imagery
[AD-A185039] 05 p0627 N88-13833

STRATOPAUSE
Ion composition measurements in the upper stratosphere --- parachute-borne mass spectrometer
[ETN-87-90423] 01 p0069 N88-10442

STRATOSCOPE TELESCOPES
Vibration isolation system for the Stratospheric Observatory For Infrared Astronomy (SOFIA)
14 p1926 N88-21483

STRATOSCOPE 1 TELESCOPE
U STRATOSCOPE TELESCOPES

STRATOSCOPE 2 TELESCOPE
U STRATOSCOPE TELESCOPES

STRATOSPHERE
NT OZONOSPHERE
NT STRATOPAUSE
Balloon-based infrared solar occultation measurements of stratospheric O3, H2O, HNO3 and CFC-12
[NOAA-TR-NESDIS-34] 01 p0068 N88-10438
Kinetics investigations of atmospheric chemical reactions
[PB87-213351] 01 p0069 N88-10439
Airborne lidar studies of Arctic polar stratospheric clouds
01 p0069 N88-10443
ECC (Electrochemical Concentration Cell) ozonesonde observations at South Pole, Antarctica during 1986
[PB87-207502] 02 p0197 N88-11228
Production of NO by galactic cosmic rays and lightning
[DE87-014613] 02 p0197 N88-11230
Stratospheric particles: Synchrotron X-ray fluorescence determination of trace element contents
[DE87-012482] 02 p0198 N88-11234
Spectroscopic and retrieval studies in support of SCRIBE (Stratospheric Cryogenic Interferometer Balloon Experiment)
[AD-A184037] 03 p0351 N88-12216
October lower stratospheric Antarctic temperature and total ozone from 1979-1985
05 p0615 N88-13776
Insights into the general circulation of the lower stratosphere from TOMS
05 p0616 N88-13780
Lower-stratospheric/upper-tropospheric exchange processes associated with tropical cyclones as observed by TOMS
05 p0616 N88-13782

Comparison of ground based and TOMS measurements of SO2 from volcanic emissions
05 p0618 N88-13795
Observations of inertial period waves and vertical velocities in the tropical middle atmosphere using the MST radar technique
06 p0742 N88-14562
Description of data on the Nimbus 7 LIMS map archive tape: Water vapor and nitrogen dioxide
[NASA-TP-2761] 06 p0744 N88-14572
Middle atmospheric wind measurements using a medium frequency radar
[AD-A185931] 07 p0879 N88-15330
Large-scale dynamics of the mean flow breakdown in the stratosphere and mesosphere during the winter 1983/84
08 p1028 N88-16228
In-situ stratospheric water vapor measurements on board long duration balloons
08 p1029 N88-16232
Rayleigh lidar observations of gravity wave activity in the stratosphere and lower mesosphere
[NASA-CR-182384] 09 p1189 N88-17123
Measurement of vertical distributions of halogenated hydrocarbons in the stratosphere
[ETN-88-91065] 09 p1191 N88-17135
Statistical studies of low frequency oscillations in satellite-observed stratospheric temperatures
10 p1353 N88-18086
An analysis of longitude variations in the equatorial spectrum of Saturn
10 p1430 N88-18539
Initial results with the LLNL 2-D chemical-radiative-transport model of the troposphere and stratosphere
[DE88-004355] 11 p1512 N88-19033
High altitude chemical release systems for project BIME (Brazilian Ionospheric Modification Experiments) project IMS (Ionospheric Modification Studies) project PIIE (Polar Ionospheric Irregularities Experiment) project polar arcs
[AD-A188299] 12 p1642 N88-19833
Stratospheric trace gas distributions from fair infrared thermal emission spectroscopy
13 p1797 N88-20749
Ultraviolet absorption cross sections of methylbromide at stratospheric temperatures
[AERONOMICA-ACTA-A-320-1987]
15 p2036 N88-22132
Stratospheric electric field and conductivity measurements over electrified convective clouds in the South American region, revised
[INPE-4046-PRE/1012-REV-3]
15 p2095 N88-22483
A study on electric fields and conductivity associated with electrified clouds in the region of South America
[INPE-4487-TDL/325] 15 p2096 N88-22486
Chemical kinetics and photochemical data for use in stratospheric modeling evaluation Number 8
[NASA-CR-182919] 17 p2351 N88-24012
Stratospheric positive ion composition measurements and acetonitrile detection: A consistent picture
[AERONOMICA-ACTA-A-326-1987]
18 p2542 N88-25084
Three-dimensional temperature fields in the atmosphere up to 50 km altitude
[ETN-88-92150] 18 p2542 N88-25089
SAM 2 data user's guide
[NASA-RP-1200] 18 p2543 N88-25094
Radiation safety in commercial air traffic
[NASA-TM-101156] 19 p2600 N88-25447
Theory on conductivity measurement technique for Langmuir probes in the stratosphere
[INPE-4514-PRE/1268] 19 p2692 N88-25999
Meteorological atlas of the Southern Hemisphere lower stratosphere for August and September 1987
[NASA-TM-4049] 20 p2825 N88-26763
Design, development, fabrication and launch support for a high altitude release of neodymium vapor
[AD-A194196] 22 p3118 N88-28527
Ultraviolet absorption cross sections of chloro- and chlorofluoromethanes at stratospheric temperatures
[AERONOMICA-ACTA-A-324-1988]
23 p3231 N88-29228
Present state of knowledge of the upper atmosphere 1988: An assessment report
[NASA-RP-1208] 23 p3232 N88-29233
Forty-eight-inch lidar aerosol measurements taken at the Langley Research Center, May 1974 to December 1987
[NASA-RP-1209] 23 p3232 N88-29234
Changes in stratospheric ozone: Observations and theories
[AERONOMICA-ACTA-A-334-1988]
24 p3390 N88-30188
Possibilities of determining vertical profiles of microphysical characteristics of stratospheric aerosol using space measurements of transparency and solar halo
24 p3449 N88-30526

STRATOSPHERE RADIATION
Long range reconnaissance of trace gases: A special aspect of emission spectroscopy
08 p1018 N88-16172

STRATOSPHERIC AEROSOL & GAS EXPERIMENT
U SAGE SATELLITE

STRATOTANKER AIRCRAFT
U C-135 AIRCRAFT

STRATUS CLOUDS
Forecasting stratus over the British Isles
02 p0209 N88-11310
Stratocumulus and cloud-free reflectance from multi-spectral satellite measurements
[AD-A193899] 22 p3128 N88-28599

STREAK CAMERAS
Progress toward a crystal streak camera using tungsten bronze crystals for the electrooptic material
[DE87-013110] 03 p0323 N88-12044
Evaluation system for crystal streak cameras
[DE88-000238] 03 p0324 N88-12048
Streak camera dynamic range optimization
[DE88-001632] 05 p0586 N88-13571
Resolution limitations and optimization of the LLNL streak camera focus
[DE88-001633] 05 p0586 N88-13572
Flat-field response and geometric distortion measurements of optical streak cameras
[DE88-002394] 09 p1168 N88-17005
Resolution limitations and optimization of the ITT F4157 streak tube focus for fast (10 ps) operation
[DE88-003727] 09 p1169 N88-17007
The 5-GHz operation of the ITT and RCA streak tubes with a 7.5-ns time window
[DE88-003342] 09 p1169 N88-17008
Zoom versus full-field sensitivity at the ETS (Experimental Test System)
[AD-A188162] 12 p1628 N88-19742
Laser-heterodyne interferometry with streak camera detection
[DE88-003292] 14 p1914 N88-21437
Summary and conclusions on electrooptical streak camera project
[DE88-006616] 15 p2069 N88-22334

STREAK PHOTOGRAPHY
Programmable 10 MHz optical fiducial system for hydrodiagnostic cameras
[DE87-013223] 02 p0175 N88-11091
Evaluation system for crystal streak cameras
[DE88-000238] 03 p0324 N88-12048

STREAM FUNCTIONS (FLUIDS)
Optimization of explicit time-stepping algorithms and Stream-Function-Coordinate (SFC) concept for fluid dynamics problems
04 p0445 N88-12762
Extensions of the control volume based finite element method for fluid flow problems
06 p0700 N88-14296
Inviscid flows, part 1: Formulation of inviscid rotational flow problems by velocity potential and stream function methods. Applications to turbomachines
08 p0985 N88-15984
Viscous flows. Part 3: Formulation of the Navier-Stokes equations by stream function vorticity methods
08 p0986 N88-15969
Resonant Alfven wave instabilities driven by streaming fast particles
13 p1855 N88-21104

STREAMLINE FLOW
U LAMINAR FLOW

STREAMLINED BODIES
NT FAIRINGS

STREAMLINING
Observations on the hydrodynamic flow visualization at ONERA
[PD-FM-8718] 04 p0444 N88-12753
Predictive wall adjustment strategy for two-dimensional flexible walled adaptive wind tunnel: A detailed description of the first one-step method
[NASA-CR-181635] 12 p1573 N88-19409
An evaluation in a modern wind tunnel of the transonic adaptive wall adjustment strategy developed by NPL in the 1940's
[NASA-CR-181623] 12 p1575 N88-19417
A simplified streamline swallowing procedure for the windward meridian of axisymmetric blunt bodies
[AD-A188413] 12 p1626 N88-19732
The effects of two Carlucci initiatives concurrency and streamlining, on the test and evaluation phase of system acquisitions
12 p1704 N88-20198
Streamlining invitation for bids
[AD-A188941] 12 p1705 N88-20206
Empty test section streamlining of the transonic self-streamlining wind tunnel fitted with new walls
[NASA-CR-181680] 19 p2598 N88-25442
The determination of the topological structure of skin friction lines on a rectangular wing-body combination
[NASA-CR-4168] 20 p2753 N88-26343

STREAMS
NT GAS STREAMS
Ice-shelf response to ice-stream discharge fluctuation. Part 1: Unconfined ice tongues
[AD-A188147] 10 p1358 N88-18117
A queueing system with independent Markov input streams
[AD-A187601] 10 p1402 N88-18363
Hiding in stream semantics of uniform concurrency
[PB88-121579] 20 p2882 N88-27114
Stream function-vorticity finite elements and the resolution of the Navier-Stokes equations
[DE88-702318] 21 p2945 N88-27494

STRENGTH OF MATERIALS
U MECHANICAL PROPERTIES

STRESS (PHYSIOLOGY)
NT ACCELERATION STRESSES (PHYSIOLOGY)
Assessment of the reliability of a correction procedure for WGT (Wet Globe Thermometer) (Botsball) measurements of heat stress
[AD-A185193] 05 p0584 N88-13559
Microwave challenges to the thermoregulatory system
[AD-A185391] 05 p0629 N88-13847
Physiological determinants of load bearing capacity
[AD-A184977] 05 p0629 N88-13848
A device and methodology for measuring repetitive lifting VO2max (oxygen consumption rate)
[AD-A185195] 05 p0630 N88-13850
Daily dynamics of some physiological indicators of man under desert condition
06 p0750 N88-14605
Quick measurement of individual stress reaction level: Development of the Emotional Stress Reaction Questionnaire (ESRQ)
[FOA-C-50050-5.3] 06 p0752 N88-14617
Exercise in the heat: Effects of dinitrophenol administration
[AD-A185731] 06 p0752 N88-14622
Polycythemia and hydration status: Effects on blood volume and thermoregulation during exercise-heat stress
[AD-A185945] 07 p0888 N88-15383
Load carriage induced alterations of pulmonary function
[AD-A186227] 07 p0889 N88-15386
General biological character of adaptive capacity of mammalian metabolism in response to diverse and extreme environmental factors
08 p1047 N88-16324
Prediction of human thermoregulatory responses and endurance time in water at 20 and 24C
[AD-A186223] 08 p1048 N88-16326
Portable, ambient air microclimate cooling in simulated desert and tropic conditions
[AD-A186457] 08 p1050 N88-16338
Brain potentials and personality: A new look at stress susceptibility
[AD-A186931] 09 p1199 N88-17189
Comparative evaluation of stress repsonse of rats to different methods of simulating some effects of weightlessness
10 p1363 N88-18144
Second All-Union Conference on Physiology of Extreme States and Individual Protection of Man
10 p1363 N88-18147
Manipulation of muscle glycogen concentrations using high and low carbohydrate diets and exercise
[AD-A187732] 11 p1519 N88-19069
Gastric emptying during exercise: Effects of acute heat stress, acclimation and hypohydration
[AD-A188008] 11 p1519 N88-19073
Development of a coping strategies questionnaire to assess endurance performance
[AD-A188010] 11 p1520 N88-19074
Operation Everest 2: Alterations in the immune system at high altitude
[AD-A188011] 11 p1520 N88-19075
Causes and prevention of occupational Repetition Strain Injuries (RSI)
11 p1521 N88-19083
Conceptualization and design of a variable-gravity research facility
[NASA-CR-182574] 12 p1595 N88-19550
Endocrine responses to resistance exercise
[AD-A188681] 12 p1667 N88-19993
Motion sickness: A study of its effects on human physiology
[AD-A188821] 12 p1667 N88-19995
Plasma cortisol, renin and aldosterone during an intense heat acclimation program
[AD-A189387] 13 p1809 N88-20810
Challenges of physiological monitoring in a Navy operational setting
16 p2239 N88-23374
Stress in relation to the physical and social environment
19 p2695 N88-26020
Ergonomy and interior furnishing of the cabins of deep diving manned submarines: The Nautile example --- couch
19 p2697 N88-26032
Significance of nutrition to change in human carbohydrate and lipid metabolism under emotional stress
19 p2703 N88-26073

Analysis of clinical symptoms of human decompression sickness during altitude chamber studies
19 p2703 N88-26074
Satellite remote sensing of the wet bulb globe temperature heat stress index, phase 2
[AD-A192798] 20 p2818 N88-26717
Effect of weightlessness on brain development (results of flight of pregnant rats on Kosmos-1514 biosatellite and study of subsequent development of their progeny on earth 20 p2829 N88-26786
Can CNV amplitude predict ability to accomplish a demanding task? 21 p2980 N88-27700
Hyperthermia: New thoughts on an old problem
[AD-A192602] 21 p2986 N88-27731
Variability in intake and dehydration in young men during a simulated desert walk
[AD-A192654] 22 p3131 N88-28613
Hormonal regulation of fluid and electrolytes: Effects of heat exposure and exercise in the heat
[AD-A192655] 22 p3131 N88-28614
The impact of hyperthermia and hypohydration on circulation, strength, endurance and health
[AD-A192657] 22 p3131 N88-28615
Stress/fatigue and the ARNG (Army National Guard) aviator
[AD-A194184] 22 p3132 N88-28621
Hierarchical structure in polymeric solids and its influence on properties
[AD-A194720] 23 p3197 N88-29029
Currents induced in a human being for electromagnetic fields to 10 kHz-50 MHz
[AD-A191977] 23 p3238 N88-29268
Visual related accidents/incidents
23 p3242 N88-29293
Nutrient requirements for high stress environments
[AD-A194595] 23 p3243 N88-29301
Accidental hypothermia
[AD-A194967] 24 p3406 N88-30278

STRESS (PSYCHOLOGY)

Antarctica as a model for the human exploration of Mars
[AD-A185835] 08 p1051 N88-16342
Overlearning and positive thinking alleviate negative effects of stress on performance
[FOA-C-50051-5.3] 08 p1051 N88-16344
Brain potentials and personality: A new look at stress susceptibility
[AD-A186931] 09 p1199 N88-17189
Second All-Union Conference on Physiology of Extreme States and Individual Protection of Man
10 p1363 N88-18147
Hemodynamic effects of beta-adrenergic blocking with obsidan in clinostatic and orthostatic positions
10 p1367 N88-18171
Development of a coping strategies questionnaire to assess endurance performance
[AD-A188010] 11 p1520 N88-19074
Conceptualization and design of a variable-gravity research facility
[NASA-CR-182574] 12 p1595 N88-19550
Protection from stress 12 p1664 N88-19978
Individual functional typology of sympathoadrenal system as indicator of physiological status in adverse environments 12 p1665 N88-19979
Mental-State Estimation, 1987
[NASA-CP-2504] 16 p2239 N88-23370
Chronic stress as a factor in aircraft mishaps
16 p2239 N88-23376
Acute stress 16 p2239 N88-23377
Voice-stress measure of mental workload
16 p2240 N88-23381
A correlational approach to predicting operator status
16 p2242 N88-23393
Voice stress analysis 16 p2242 N88-23395
Stress in relation to the physical and social environment 19 p2695 N88-26020
Significance of nutrition to change in human carbohydrate and lipid metabolism under emotional stress 19 p2703 N88-26073
Thermal stress and its effects on fine motor skill and decoding tasks 21 p2926 N88-27369
Stress and the military pilot
[AD-A194313] 22 p3133 N88-28626
Attitudes towards the cold: Effects on psychological mood and subjective reports of illness during cold weather training
[AD-A194777] 23 p3239 N88-29274
Nutrient requirements for high stress environments
[AD-A194595] 23 p3243 N88-29301
Central adrenergic receptors as mediators of central response to stress: Study with Positron Emission Tomography (PET)
[AD-A194947] 24 p3407 N88-30284

STRESS ANALYSIS

NT BOUNDARY ELEMENT METHOD

Compendium of post-failure analysis techniques for composite materials
[AD-A183783] 01 p0018 N88-10113
Polymer chain segment orientation during stress relaxation
[DE87-013392] 01 p0027 N88-10174
Ion-implantation-induced stress in glasses: Variation of damage mode efficiency with changes in glass structure
[DE87-013523] 01 p0028 N88-10175
Low cycle fatigue on isotropic fine-grained graphite
[DE87-702627] 01 p0028 N88-10177
A generalized least-squares determination of triaxial stress states by X-ray diffraction and the associated errors
[AD-A183851] 01 p0058 N88-10371
The use of Hencky's equations for the estimation of multiaxial elastic-plastic notch stresses and strains
[FB-3/1986] 01 p0060 N88-10383
Stress-strain analysis and life predictions of a notched shaft under multiaxial loading
[FB-5/1986] 01 p0060 N88-10384
Criteria for determination of significant load cycles in variable amplitude load sequences
[NLR-MP-86013-U] 01 p0060 N88-10386
Relation between shock strength and strain-rate plasticity at maximum deviatoric stress
[DE87-011736] 01 p0061 N88-10390
A user's guide for BIE3D: A boundary integral equation computer program for three-dimensional elastostatic analysis
[RAE-TM-MAT-STR-1078] 01 p0079 N88-10509
Shearing flow over Stokes wave. Part one: General theory
[ETN-87-90957] 02 p0171 N88-11074
Development and testing of a system for the partially automated evaluation of holographic interferograms in the experimental stress analysis of reactor components
[ETN-87-90574] 02 p0175 N88-11095
3D inelastic analysis methods for hot section components 02 p0187 N88-11164
Component specific modeling
02 p0187 N88-11166
Constitutive modeling of superalloy single crystals with verification testing 02 p0188 N88-11169
Constitutive modeling for isotropic materials
02 p0188 N88-11171
Applications of dislocation theory to crack growth problems 02 p0190 N88-11188
Energy changes in transforming solids
[DE87-011257] 02 p0191 N88-11194
Diffraction moire: The dynamic regime
[DE87-014883] 03 p0335 N88-12111
Nonlinear thermoviscoelastic analysis of metallic plane curved beams 03 p0336 N88-12119
Kinetics of crack growth: Thermal/mechanical interaction 03 p0337 N88-12124
Failure analysis of composite structure materials
[AD-A184468] 04 p0410 N88-12548
On the stressing of annealed NITINOL: The electrical resistance and calorimetric effects
[AD-A184465] 04 p0414 N88-12569
Effects of stress-relieving on the mechanical properties and the structure of specimens of high-temperature fine-grained structural steels heat-treated to simulate welding
[BLL-CE-TRANS-8258-(9022.09)]
04 p0417 N88-12586
Influence of creep on the precipitate structure under conditions of long-term creep. 4: Experiments on 10 CrMo 9 10 steel
[BLL-CE-TRANS-8256-(9022.09)]
04 p0417 N88-12589
Influence of strain rate and notch depth on tensile properties of HITCO 6250
[DE88-001324] 04 p0455 N88-12816
Higher order theory analysis of a modified free-edge delamination specimen 04 p0455 N88-12820
The evolution of plastic strain in steady, plastic shock waves
[DE87-013812] 04 p0456 N88-12826
A comparison of structural frequency response functions measured with forces from 500 to 250,000 lb
[DE88-000668] 04 p0457 N88-12829
Large change-of-curvature effects in quadratic finite elements for CAD of membrane structures
04 p0480 N88-12958
Development of an integrated BEM approach for hot fluid structure interaction
[NASA-CR-181577] 05 p0556 N88-13384
Micromechanics of the degradation of composite materials
[SNIAS-872-430-113] 05 p0559 N88-13405
Finite element model for the stress and flexibility analysis of curved pipes
[DE87-703632] 05 p0592 N88-13608
Fatigue under nonnormal random stresses using Monte Carlo method 05 p0607 N88-13723
Analysis of end stresses in glass-metal bimaterial strips
[DE87-007848] 05 p0610 N88-13750
Stresses and displacements in two, three and four layered structures submitted to flexible or rigid loads
[AD-A185707] 06 p0723 N88-14450
Transient welding strain measurement by Moire technique: A comparison between experimental measurement and numerical analysis for strain-stress cycles during GTA spot-welding
[PB87-143871] 07 p0868 N88-15269
Thermal stress analysis of a cooled monochromator crystal
[DE88-002116] 07 p0937 N88-15696
Composite/metal jointing technology for vehicle weight reduction
[DE88-900228] 08 p0992 N88-16005
Generalized displacement method in the finite element analysis of incompressible material
[PB87-143434] 08 p0995 N88-16018
Study of the technique of stress determination by measuring magnetism
[PB87-143905] 08 p0996 N88-16028
Fatigue effects of a swept sine test
08 p0999 N88-16054
Review of fatigue and fracture research at NASA Langley Research Center 09 p1106 N88-16633
Optical analysis of stress and strain in photoelastic particle assemblies
[ETN-88-91591] 09 p1182 N88-17082
A comparison of the predicted and measured gravitational stresses in VAWT (Vertical Axis Wind Turbine) blades
[DE88-002113] 09 p1187 N88-17111
Finite element substructuring methods for composite mechanics
[NASA-TM-100297] 10 p1296 N88-17745
Analytical and experimental characterization of damage processes in composite laminates
[AD-A187221] 10 p1296 N88-17746
Basic research on macromolecular dynamics
[PB88-141643] 10 p1305 N88-17805
Flaw identification from forced vibration testing
[DE88-002641] 10 p1342 N88-18018
Computed stress and strain distributions under interference fit and after coldworking
[AD-A186950] 10 p1342 N88-18024
Frequency response function estimation at level
[DE88-002644] 10 p1344 N88-18034
On delamination of (+ or - theta sub m/90 sub n/2) sub s laminates subject to tensile loading
[AD-A188095] 11 p1447 N88-18626
Fracture mechanisms and strengthening of slab lasers
[DE88-004002] 11 p1493 N88-18914
Development of encapsulated lithium hydride thermal energy storage for space power systems
[DE88-004762] 11 p1507 N88-19001
SiO2 film stress distribution during thermal oxidation of Si
[AD-A189552] 12 p1612 N88-19637
A hybrid-stress finite element approach for stress and vibration analysis in linear anisotropic elasticity
[NASA-CR-179311] 12 p1634 N88-19784
Stress analysis in elastic solids with many cracks
[AD-A189015] 12 p1636 N88-19799
Modification, implementation, and evaluation of a remote terminal emulator as a software validation and stress testing tool
[AD-A188833] 12 p1678 N88-20034
Delamination stresses in semicircular laminated composite bars
[NASA-TM-4026] 13 p1735 N88-20375
The use of photoelastic methods to study the stressed states of spot-welded joints 14 p1898 N88-21335
JPRS report: Science and technology. China
[JPRS-CST-87-042] 14 p1899 N88-21338
Mathematical stress analysis of composite materials
14 p1900 N88-21349
Nonlinear Constitutive Relations for High Temperature Applications, 1986
[NASA-CP-10010] 14 p1928 N88-21498
A constitutive model with damage for high temperature superalloys 14 p1930 N88-21510
Cyclic uniaxial and biaxial hardening of type 304 stainless steel modeled by the viscoplasticity theory based on overstress 14 p1931 N88-21514
On 3-D inelastic analysis methods for hot section components. Volume 1: Special finite element models
[NASA-CR-180893] 14 p1934 N88-21535
Efficient method for structural optimization
15 p2054 N88-22240

Development of a computer code CRACK for elastic and elastoplastic fracture mechanics analysis of 2-D structures by finite element technique
[DE88-701231] 15 p2075 N88-22370
Lewis Structures Technology, 1988. Volume 2: Structural Mechanics
[NASA-CP-3003-VOL-2] 15 p2077 N88-22382
Finite element (MARC) solution technologies for viscoplastic analyses 15 p2078 N88-22389
Three-dimensional inelastic approximate analysis code (MOMM) 15 p2079 N88-22392
Specialty three-dimensional finite element analysis codes 15 p2079 N88-22393
Probabilistic structural analysis computer code (NESSUS) 15 p2079 N88-22397
Structural tailoring of advanced turboprops 15 p2080 N88-22400
Thermal-structural analyses of Space Shuttle Main Engine (SSME) hot section components 15 p2081 N88-22404
Structural assessment of a space station solar dynamic heat receiver thermal energy storage canister 15 p2081 N88-22406
Whisker-reinforced ceramic composites for heat engine components 15 p2082 N88-22410
Minimum weight design of rotorcraft blades with multiple frequency and stress constraints
[NASA-TM-100589] 16 p2161 N88-22892
Hybrid PV HgCdTe IR detectors technology reliability and failure program: Environmental stress testing plan
[AD-A191165] 16 p2211 N88-23195
On the calculation of stresses in pin-loaded anisotropic plates
[ETN-88-92239] 16 p2222 N88-23261
On the calculation of stresses in pin-loaded anisotropic plates
[LR-529] 16 p2223 N88-23268
A generalized variational method for solving stress intensity factors at cracks on the edge of holes in orthotropic plates
[IC-AERO-87-02] 17 p2348 N88-23992
Possible creep studies of lithium with a compact device 17 p2422 N88-24404
Analysis of notched metal matrix composites under tension loading
[NASA-TM-100629] 18 p2480 N88-24713
On the reversion phenomena of Cu-3 percent Ti alloys
[NASA-TT-20170] 18 p2488 N88-24762
Stress measurements in graphite fibers by laser raman spectroscopy
[AD-A191710] 18 p2491 N88-24779
Effect of uniaxial stress on the Raman spectra of graphite fibers
[AD-A191730] 18 p2492 N88-24783
Computational fluid dynamics applied to the prediction of the heat-transfer, mechanical and thermal-stress behavior of heat exchangers
[CFDU/87/7] 18 p2510 N88-24893
Plate response analysis using shock tube
[AD-A190828] 18 p2526 N88-24987
Advanced development of the boundary element method for elastic and inelastic thermal stress analysis 18 p2529 N88-25002
Forced motion of initially stressed shells and plates 18 p2529 N88-25005
Fatigue crack growth due to random loading 18 p2531 N88-25017
Influence of strain rate on the substructure evolution and yield behavior of Ti-6Al-4V
[DE88-006457] 19 p2616 N88-25520
Simulation of diaphragm-type IC pressure sensors 19 p2672 N88-25887
Static analysis of thin plates using the finite strip-element method 19 p2679 N88-25931
Improved method for stress and compatibility analysis of multicomponent rotating systems
[NASA-TM-100884] 19 p2680 N88-25935
A constitutive model with damage for high-temperature superalloys 20 p2771 N88-26434
Observations on residual stresses in ceramic composites by neutron diffraction techniques
[DE88-009937] 20 p2778 N88-26472
Vertical ship motions and sea loads considering nonlinear effects
[TAE-592] 20 p2784 N88-26515
Stress concentration around circular hole in a composite material specimen representative of the X-29A forward-swept wing aircraft
[NASA-CR-179435] 20 p2814 N88-26694
Dynamical stress concentration problems, from every side, bordered and perforated plates
[ETN-88-92128] 20 p2815 N88-26703
Study of temperature and stress fields of two sliding cylinders
[ETN-88-92134] 20 p2815 N88-26704
Stress analysis using infrared thermography
[ETN-88-92169] 20 p2816 N88-26705
Stress-related phenomena in transient radiation-induced absorption in optical fibers
[DE88-010956] 20 p2854 N88-26949
Lattice strain in heteroepitaxial films 20 p2868 N88-27032
Boundary layer solutions for the free-edge problem in composite laminates 21 p2904 N88-27229
Thermal stress and its effects on fine motor skill and decoding tasks 21 p2926 N88-27369
An experimental and analytical evaluation of a biaxial test for determining shear properties of composite materials
[NASA-CR-182928] 21 p2962 N88-27593
Verification of the ADINA finite element code for creep analysis: Problems from the open literature
[DE88-011826] 21 p2962 N88-27594
Analyses and correlations of environment assisted fatigue crack propagation for attachment lugs 22 p3053 N88-28116
Environmental cracking of a superferritic stainless steel under slow strain rate conditions 22 p3053 N88-28117
Studies of internal stresses and surface roughness of sputtered Be and BeB films
[DE88-011737] 22 p3086 N88-28327
Mixed finite element methods to compute stress in a load composite specimen with holes: Numerical results
[ONERA-RT-37/4242-RY-062-R] 22 p3088 N88-28336
Structural dynamics of maneuvering aircraft
[AD-A192376] 23 p3176 N88-28908
Thin film-residual stress assessment
[AD-A193205] 23 p3196 N88-29018
Aeroelastic response of metallic and composite propfan models in yawed flow
[NASA-TM-100964] 24 p3326 N88-29807
Thermal stress analysis in PMR-15 carbon fibre laminates
[ETN-88-93123] 24 p3341 N88-29886
Stresses in cylindrical shells with tangential nozzles submitted to external loads and internal pressure
[CRIF-MT-172] 24 p3382 N88-30146
Determination of multiaxial flow surfaces at elevated temperatures using the concept of dissipation potential
[ORNL/TM-10787] 24 p3383 N88-30149

STRESS CALCULATIONS
U STRESS ANALYSIS

STRESS CONCENTRATION
On the relations between cyclic contraction ratio, flow stress, and deformation mechanisms in bainitic CrMoV steels
[VTT-36] 01 p0025 N88-10158
Theoretical investigation of stress concentrations in damaged carbon fibre reinforced plastic plate structures. Volume 1: Main text
[BR99872-VOL-1] 03 p0280 N88-11761
Theoretical investigation of stress concentrations in damaged carbon fibre reinforced plastic plate structures. Volume 2: Tables, figures and plates
[BR99873-VOL-2] 03 p0280 N88-11762
Stress state of welded joints of dissimilar materials obtained by diffusion welding 03 p0286 N88-11799
Evaluation method of the brittle fracture strength in structurally stress-concentrated regions
[PB87-129490] 06 p0721 N88-14435
Effect of rare earth elements on the hydrogen-induced cracking in high strength low alloy steel
[PB87-143806] 07 p0833 N88-15052
Hybrid FEM (Finite Element Method) approach to stress distribution in the vicinity of a notch in non-homogeneous materials
[PB87-143392] 07 p0868 N88-15268
SiO2 film stress distribution during thermal oxidation of Si
[AD-A189552] 12 p1612 N88-19637
Influence of hydrogen on crack formation tendency in heat-affected zone with stress concentrator 14 p1887 N88-21276
Evolution of hardening and damage during viscoplastic deformation
[AD-A190714] 15 p2077 N88-22381
Stress concentration around circular hole in a composite material specimen representative of the X-29A forward-swept wing aircraft
[NASA-CR-179435] 20 p2814 N88-26694
Dynamical stress concentration problems, from every side, bordered and perforated plates
[ETN-88-92128] 20 p2815 N88-26703
Failure analysis of quasi-isotropic composite laminates with free edges under off-axis loading 22 p3049 N88-28092
Analysis of stiffness reduction, failure and stress concentration in fiber composite laminates
[AD-A193519] 22 p3050 N88-28096
Mixed finite element methods to compute stress in a load composite specimen with holes: Numerical results
[ONERA-RT-37/4242-RY-062-R] 22 p3088 N88-28336
A comprehensive study on damage tolerance properties of notched composite laminates
[AD-A192952] 23 p3188 N88-28968
Development and experimental verification of a two-dimensional numerical model of piezoelectrically induced threshold voltage shifts in GaAs MESFETs
[AD-A193462] 23 p3206 N88-29080
Shear stress at a film-substrate interface due to mismatch strain
[AD-A193461] 23 p3288 N88-29577

STRESS CORROSION
NT STRESS CORROSION CRACKING
The application of group radiators for the determination of tension crack corrosion
[BAM-06264] 01 p0022 N88-10141
Influence of some parameters on the stress corrosion of a ABNT 304 stainless steel in MgCl/sub 2/
[DE87-703707] 04 p0416 N88-12580
A study of corrosion fatigue crack initiation, growth and the threshold condition under variable amplitude loading 05 p0604 N88-13701
The influence of crack conditions on hydrogen uptake by steels 05 p0604 N88-13702
Occurance and growth of fatigue cracks in corrosion environment 05 p0604 N88-13704
The role of composition and microstructure gradients on weld metal properties and behavior
[DE88-004956] 10 p1303 N88-17791
Aircraft corrosion problems and research in the Netherlands
[NLR-MP-86066-U] 13 p1744 N88-20427
Stress corrosion of C ring specimen in salt spray tests
[I-186/87] 21 p2916 N88-27307
Phenomena of the ionic transport in the stress corrosion of metals
[DE88-702502] 23 p3195 N88-29013
Stress corrosion of ceramic materials
[AD-A191979] 23 p3195 N88-29016

STRESS CORROSION CRACKING
Stress corrosion cracking of high-strength steels in aqueous environments 03 p0289 N88-11818
Effects of stress-relieving on the mechanical properties and the structure of specimens of high-temperature fine-grained structural steels heat-treated to simulate welding
[BLL-CE-TRANS-8258-(9022.09)] 04 p0417 N88-12586
Environmentally assisted cracking: Overview of evidence for an adsorption-induced localised-slip process
[AD-A185175] 05 p0565 N88-13443
Fatigue crack propagation in Al-Zn-Mg bicrystals and its dependence on the environment 05 p0605 N88-13707
Fracture kinetics of corrosion fatigue 05 p0605 N88-13708
The influence of grain boundary chemistry and structure on the intergranular attack and intergranular stress corrosion cracking of austenitic alloys
[DE88-002436] 07 p0835 N88-15063
Study on characteristics of SCC propagation da/dt for welded joint
[PB87-143640] 07 p0869 N88-15270
Multipurpose corrosion inhibitors for aerospace materials in Naval environments
[AD-A186728] 09 p1143 N88-16853
Mechanisms of intergranular attack and stress corrosion cracking of alloy 600 by high-temperature caustic solutions containing impurities
[DE87-012820] 10 p1300 N88-17773
Computer aided testing procedure for stress corrosion cracking investigations
[GKSS-86/E/63] 11 p1460 N88-18706
Reduction of residual stresses and distortion in girth welded pipes
[AD-A187728] 11 p1494 N88-18920
Comparative investigations of indirect crack length measurement under fatigue loading in a corrosive environment
[GKSS-86/E/64] 11 p1502 N88-18972
Stress corrosion cracking and metal-induced embrittlement: Comparative studies of local chemistries
[DE88-003235] 13 p1742 N88-20419
Controlling stress corrosion cracking in mechanism components of ground support equipment 14 p1926 N88-21480
Effect of loading conditions on environment-sensitive fracture
[BR102697] 14 p1934 N88-21533
Stress corrosion of ceramic materials
[AD-A190501] 15 p2045 N88-22187

Environmentally assisted crack growth in structural alloys: Perspectives and new directions
[AD-A190137] 15 p2076 N88-22377
Environment effects on crack propagation with tensile stress
[GKSS-87/E/46] 16 p2223 N88-23267
Stress corrosion cracking properties of Al-Li alloys 17 p2320 N88-23853
Stress corrosion cracking of A723 steel pressure vessels: Two case studies
[AD-A191741] 18 p2527 N88-24990
Stress corrosion evaluation of powder metallurgy aluminum alloy 7091 with the breaking load test method 22 p3053 N88-28115
Corrosion and stress corrosion of metals in decontamination solutions 22 p3054 N88-28118
Design guidelines for prevention of corrosion in combat and tactical vehicles
[AD-A194172] 22 p3055 N88-28126

STRESS CYCLES
Fracture morphologies of carbon-black-loaded SBR (Styrene-Butadiene Rubber) subjected to low-cycle, high-stress fatigue
[DE88-006808] 16 p2181 N88-23002
Theory of viscoplasticity based on overstress with applications 18 p2529 N88-25007

STRESS DISTRIBUTION
NT STRESS CONCENTRATION
The use of Hencky's equations for the estimation of multiaxial elastic-plastic notch stresses and strains
[FB-3/1986] 01 p0060 N88-10383
Stress-strain analysis and life predictions of a notched shaft under multiaxial loading
[FB-5/1986] 01 p0060 N88-10384
Crack initiation life estimations for notched specimens with residual stresses based on local strains
[FF-17/1986] 01 p0060 N88-10385
Three-dimensional finite element based, interative approach for analysis of laminated composites 03 p0280 N88-11763
Free-edge delamination: Laminate width and loading conditions effects
[NASA-TM-100238] 04 p0411 N88-12551
Plastic strain localization between voids in shear deformation fields 04 p0427 N88-12648
Constraint effects in fatigue crack growth 05 p0606 N88-13719
Telemetric laser extensometry technique for monitoring deflections in small cracks 05 p0607 N88-13724
On the geometrical description of fatigue crack surfaces 05 p0607 N88-13727
Profiles of self stress and of load stress at notches 06 p0719 N88-14419
Wave propagation experiments on 22-bay lattice
[AD-A186140] 07 p0824 N88-15002
Experimental and theoretical investigation of mechanically fastened composites
[AD-A185696] 07 p0826 N88-15008
A method for the approximate calculation of the skin friction coefficient of horizontal wavy plates
[VKI-TN-160] 07 p0851 N88-15172
Deformation induced cracking in steel girder bridges and retrofit guidelines
[PB88-102710] 07 p0868 N88-15265
Stress strain fields at crack tip and stress intensity factors in Reissner's plate
[PB87-144945] 08 p0994 N88-16014
Successful mixed formulation for axisymmetric shell analysis employing discontinuous stress fields of the same order as the displacement field
[DE88-700021] 09 p1178 N88-17052
To determine the stress distribution in the vicinity of GRP end pads where the specimen is held and loaded (CFC coupon specimens) --- glass reinforced plastic (GRP) carbon fiber composite (CFC)
[BAE-WST-R-RES-CFC-12023] 09 p1182 N88-17080
Further tests to determine the stress distribution in the vicinity of GRP end pads where the specimen is held and loaded (CFC coupon specimens) --- glass reinforced plastic (GRP) carbon fiber composite (CFC)
[BAE-WST-R-RES-CFC-12023-ADD-1] 09 p1182 N88-17081
Computed stress and strain distributions under interference fit and after coldworking
[AD-A186950] 10 p1342 N88-18024
A study of the mechanical behavior of a 2-D carbon-carbon composite 11 p1449 N88-18638
Matrix-fiber stress transfer in composite materials: Elasto-plastic model with an interphase layer
[PB88-136635] 11 p1450 N88-18643
Reduction of residual stresses and distortion in girth welded pipes
[AD-A187728] 11 p1494 N88-18920
The stress field surrounding the tip of a crack propagating in a finite body 11 p1500 N88-19362
Thermal-mechanical fatigue testing of a titanium-aluminide alloy
[AD-A189555] 12 p1609 N88-19620
SiO2 film stress distribution during thermal oxidation of Si
[AD-A189552] 12 p1612 N88-19637
A technique for local refinement of the stress field by finite element method
[INPE-4219-PRE/1099] 12 p1683 N88-20061
Cyclic crack growth emanating at a round notch considering viscoplasticity
[AD-A189577] 13 p1781 N88-20655
Local refinement of stress field by finite element method
[INPE-4321-TDL/288] 13 p1828 N88-20930
The use of photoelastic methods to study the stressed states of spot-welded joints 14 p1898 N88-21335
Mathematical stress analysis of composite materials 14 p1900 N88-21349
Data requirements to model creep in 9Cr-1Mo-V steel 14 p1931 N88-21512
A test for interfacial effects and stress transfer in ceramic matrix composites
[NASA-CR-182758] 15 p2046 N88-22194
Phenomenological modelling of rate-dependent plasticity for high strain rate problems
[DE88-006647] 15 p2087 N88-22440
Durability of compound cylinder under static internal-pressure repeat load of long duration 16 p2180 N88-22991
Stress modeling of microdiaphragm pressure sensors 19 p2670 N88-25873
Study of temperature and stress fields of two sliding cylinders
[ETN-88-92134] 20 p2815 N88-26704
Boundary layer solutions for the free-edge problem in composite laminates 21 p2904 N88-27229
The three-dimensional stress field around a cylindrical inclusion in a plate of arbitrary thickness 21 p2963 N88-27602
Mechanics of thrust fault formation 23 p3231 N88-29229
Shear stress at a film-substrate interface due to mismatch strain
[AD-A193461] 23 p3288 N88-29577
A test for interfacial effects and stress transfer in ceramic matrix composites
[NASA-CR-182873] 24 p3340 N88-29880
Particle size measurements in sooting combustion systems 24 p3348 N88-29931

STRESS FIELDS
U STRESS DISTRIBUTION

STRESS FUNCTIONS
Non- and semi-parametric maximum likelihood estimators and the von Misis Method, part 1
[CWI-MS-R8709] 13 p1829 N88-20941
A central limit theorem for M-estimators by the von Mises method
[CWI-MS-R8713] 16 p2262 N88-23525
Dynamic shear band development in plane strain
[AD-A190915] 18 p2526 N88-24988
Dynamical stress concentration problems, from every side, bordered and perforated plates
[ETN-88-92128] 20 p2815 N88-26703

STRESS INTENSITY FACTORS
Crack propagation behavior of the materials StE 460 and AlMg 4.5Mn
[FD-1/1986] 01 p0058 N88-10373
Crack behavior in ceramic materials under static, slowly increasing, and cyclic loading conditions
[KFK-4209] 02 p0154 N88-10964
Development and testing of a system for the partially automated evaluation of holographic interferograms in the experimental stress analysis of reactor components
[ETN-87-90574] 02 p0175 N88-11095
Large change-of-curvature effects in quadratic finite elements for CAD of membrane structures 04 p0480 N88-12958
Stress intensity factors for cracking metal structures under rapid thermal loading, phase 1
[AD-A184112] 05 p0591 N88-13606
Finite element model for the stress and flexibility analysis of curved pipes
[DE87-703632] 05 p0592 N88-13608
Closure behavior under constant effective stress intensity loading conditions 05 p0598 N88-13656
Fatigue crack propagation of short and long cracks: Phys. basis, prediction methods and engineering significance 05 p0599 N88-13664
Behavior of short cracks in a 2024 aluminum alloy sheet tested at several stress ratios 05 p0600 N88-13669
the influence of temper embrittlement on fatigue crack growth in hydrogen 05 p0605 N88-13709
Constraint effects in fatigue crack growth 05 p0606 N88-13719
Development of research on fatigue of spot-weld in automobile structures in Japan 05 p0608 N88-13728
Fatigue crack growth 05 p0608 N88-13734
Influence of crack closure on fatigue crack propagation and threshold 06 p0718 N88-14394
A re-evaluation of fatigue threshold test methods 06 p0717 N88-14401
Influence of stress ratio R on fatigue threshold delta K(th) for 40Cr steel 06 p0718 N88-14405
The effects of loading history on fatigue crack growth threshold 06 p0718 N88-14406
Threshold stress intensity for stable crack growth in high strength steel at ambient temperature and below 06 p0718 N88-14407
The effect of shear lips on fatigue crack growth in Al-2024 sheet material 06 p0718 N88-14408
Threshold and crack-growth tests on pre-cracked specimens produced in cyclic compression 06 p0718 N88-14412
Fracture study of windshield glass panes 06 p0799 N88-14891
Stress strain fields at crack tip and stress intensity factors in Reissner's plate
[PB87-144945] 08 p0994 N88-16014
Stress intensity and crack displacement for small edge cracks
[NASA-TP-2801] 09 p1184 N88-17095
Threshold fatigue crack growth in Ti-6Al-2Sn-4Zr-6Mo
[AD-A189560] 13 p1741 N88-20415
Growth of fatigue cracks in nickel alloys at high temperatures 14 p1896 N88-21318
Stress-intensity factors for small surface and corner cracks in plates
[NASA-TM-100599] 15 p2088 N88-22445
Strain intensity factor approach for predicting the strength of continuously reinforced metal matrix composites
[NASA-TM-100617] 17 p2317 N88-23838
Hydrogen embrittlement susceptibility of high strength ESR 4340 steel alloys for ballistically resistant/tolerant components 17 p2319 N88-23848
Fracture mechanics 17 p2324 N88-23877
A generalized variational method for solving stress intensity factors at cracks on the edge of holes in orthotropic plates
[IC-AERO-87-02] 17 p2348 N88-23992
Determination of the toughness of a brittle material using strain gages
[ETN-88-92540] 18 p2527 N88-24993
Some stress intensity factor equations
[FFA-TN-1987-07] 18 p2527 N88-24995
Automated analysis of crack growth rate for obtaining da/dN versus delta K relation
[FFA-TN-1987-70] 18 p2527 N88-24996
Resolved shear stress intensity coefficient and fatigue crack growth in large crystals
[NASA-CR-182137] 18 p2528 N88-24997
The surface crack problem in an orthotropic plate under bending and tension
[NASA-CR-178281] 18 p2531 N88-25014
A method for the numerical solution of random Cauchy singular integral equation 18 p2565 N88-25234
Dimensional analysis and experimental observation of the coupling phenomena between combustion and fracture of damaged propellant samples 19 p2630 N88-25603
Lattice theory of fracture of solids with layered structure
[DE88-701867] 20 p2876 N88-27073
Stress intensity factors for cracked metallic structures under rapid thermal loading
[AD-A191219] 23 p3193 N88-29004
The use of a surface acoustic wave technique to study the growth behavior of small cracks in a high strength steel alloy 23 p3225 N88-29193
Elastic-plastic analysis of part-through crack propagation in piping and pressure vessels
[DE88-701619] 23 p3225 N88-29198
Stress intensity factors for cracked metallic structures under rapid thermal loading
[AES-8609709F-1] 24 p3353 N88-29962
Wide range stress intensity factor expression for an edge-cracked round bar bend specimen
[AD-A196285] 24 p3382 N88-30147
Obtaining stress intensity factors on cracks, by means of fitting techniques on numerical results calculated with the finite element method 24 p3384 N88-30153

STRESS MEASUREMENT
Stress measurements in sol-gel films
[DE87-014467] 02 p0153 N88-10955
Particle velocity and stress gage measurements in spherical diverging flow
[DE87-007333] 03 p0321 N88-12033

Multi-component stress history measurements and analysis
[DE88-000977] 09 p1168 N88-17004
Optical analysis of stress and strain in photoelastic particle assemblies
[ETN-88-91591] 09 p1182 N88-17082
The measurement of stress in steels of varying microstructure by Barkhausen and magneto-acoustic emission
[AERE-R-12387] 10 p1343 N88-18027
SiO2 film stress distribution during thermal oxidation of Si
[AD-A189552] 12 p1612 N88-19637
Stress measurements in graphite fibers by laser raman spectroscopy
[AD-A191710] 18 p2491 N88-24779
In-flight load measurements of the Robot-X canards
[AD-A193428] 21 p2895 N88-27187
Polarization selective Raman microspectroscopy
21 p2930 N88-27397
Effects of applied stress and temperature on the nonlinear elastic properties of graphite fibers
[AD-A194469] 22 p3050 N88-28093
Report on an overseas visit to USA relating to the thermoelastic measurement of stresses, 16-21 August 1987
[AD-A195313] 24 p3385 N88-30161

STRESS PROPAGATION
Instability-related delamination growth of embedded and edge delaminations 20 p2767 N88-26406
User's manual for C-HEMP: A two-dimensional wave propagation code. Volume 1: Description and derivations of the code
[AD-A193197] 21 p2944 N88-27486

STRESS RELAXATION
Polymer chain segment orientation during stress relaxation
[DE87-013392] 01 p0027 N88-10174
Tensile mean stress effects on uniaxial fatigue behavior of 1045 HR steel 05 p0603 N88-13694
Relaxation of metastable semiconductor strained-layer structures by plastic flow
[DE88-002729] 08 p1090 N88-16560
Stability and metastability in semiconductor strained-layer structures
[DE88-003308] 09 p1258 N88-17544
SiO2 film stress distribution during thermal oxidation of Si
[AD-A189552] 12 p1612 N88-19637
Effects of state recovery on creep buckling under variable loading 14 p1933 N88-21527
Corrosion Research Center, University of Minnesota
[DE88-006681] 15 p2041 N88-22160
Effect of uniaxial compression on physical and mechanical properties of ferroelectric ceramic material
16 p2180 N88-22993
Stress relaxation of a titanium (Ti-6Al-4V) threaded joint
[DE88-010102] 21 p2961 N88-27590
The mechanical behavior of surface modified ceramics
[DE88-010564] 23 p3196 N88-29022

STRESS RUPTURE STRENGTH
U CREEP RUPTURE STRENGTH

STRESS TENSORS
Characteristics of thermooptical sound excitation in metals 08 p1076 N88-16486
Optical analysis of stress and strain in photoelastic particle assemblies
[ETN-88-91591] 09 p1182 N88-17082
A simplified orthotropic formulation of the viscoplasticity theory based on overstress 14 p1929 N88-21505
Investigation of the components of the energy-momentum tensor in the neighborhood of crack tips under special materials and loading conditions
[W-4/87] 14 p1934 N88-21531
Phenomenological modelling of rate-dependent plasticity for high strain rate problems
[DE88-006647] 15 p2087 N88-22440

STRESS WAVES
Shearing flow over Stokes wave. Part one: General theory
[ETN-87-90957] 02 p0171 N88-11074
Numerical and experimental research on propagation of elastic stress waves in conical shell under axial impulsive loading 15 p2053 N88-22238
Acousto-ultrasonic input-output characterization of unidirectional fiber composite plate by SV waves
[NASA-CR-4152] 16 p2217 N88-23224

STRESS-STRAIN DIAGRAMS
The relationship of tensile specimen size and geometry effects to unique constitutive parameters for ductile materials
[AD-A186020] 08 p0994 N88-16012
Development of a unified constitutive model for an isotropic nickel base superalloy Rene 80
14 p1929 N88-21501
A simplified key-curve approach for J-R-curve testing of CT specimens
[VTT-RR-503] 15 p2088 N88-22444

STRESS-STRAIN RELATIONSHIPS
On the relations between cyclic contraction ratio, flow stress, and deformation mechanisms in bainitic CrMoV steels
[VTT-36] 01 p0025 N88-10158
Stress-strain behavior of components subject to residual stresses taking the example of an orifice plate
[FF-10/1986] 01 p0059 N88-10375
Constitutive modeling of superalloy single crystals with verification testing 02 p0188 N88-11169
High temperature stress-strain analysis
02 p0188 N88-11170
Constitutive modeling for isotropic materials
02 p0188 N88-11172
Material behaviour at high rates of strain
[OUEL-1684/87] 02 p0192 N88-11200
Generalized hybrid variational principle, corresponding finite element model 03 p0301 N88-11895
Particle velocity and stress gage measurements in spherical diverging flow
[DE87-007333] 03 p0321 N88-12033
A direct method to obtain constitutive model constants from cylinder impact test results
04 p0427 N88-12647
The effect of temperature on the tensile properties of HSLA-100 steel
[AD-A184951] 05 p0565 N88-13441
Cyclic deformation and crack initiation
05 p0597 N88-13646
Fatigue of 30CrMnSiNi2A notched specimens under spectrum loading 05 p0602 N88-13689
Thermo-mechanical behavior of high temperature fiber composites 06 p0678 N88-14149
Near-threshold fatigue 06 p0716 N88-14392
Dependence of strainrange partitioned fatigue life at elevated temperature on monotonic stress-strain properties 06 p0721 N88-14428
Stresses and displacements in two, three and four layered structures submitted to flexible or rigid loads
[AD-A185707] 06 p0723 N88-14450
Composite reliability enhancement via preloading
[AD-A185938] 07 p0826 N88-15010
Study on the mechanical stresses in the elements of the model of a toroidal magnet of a tokamak with strong field
[DE88-700343] 07 p0935 N88-15679
On the relations between cyclic contraction ratio flowstress and deformation mechanisms in bainitic CrMoV steels
[DE87-753043] 08 p0968 N88-15856
Stress strain fields at crack tip and stress intensity factors in Reissner's plate
[PB87-144945] 08 p0994 N88-16014
Theory of deformation. Part 1: Kinematics
[DE88-003007] 08 p1001 N88-16062
Dynamic stress at critical locations of a structure as a criterion for mathematical model modification
09 p1180 N88-17066
Stability and metastability in semiconductor strained-layer structures
[DE88-003308] 09 p1258 N88-17544
Relationship between fatigue life in the creep-fatigue region and stress-strain response
[NASA-TM-100796] 10 p1345 N88-18040
On delamination of (+ or - theta sub m/90 sub n/2) sub s laminates subject to tensile loading
[AD-A188095] 11 p1447 N88-18626
The cyclic stress-strain behavior of a single crystal nickel-base superalloy
[NASA-TM-100269] 12 p1607 N88-19610
Development of a constitutive equation for HSLA (High-Strength Low-Alloy)-100 at cryogenic temperatures
[AD-A189243] 13 p1740 N88-20408
Parametric study of acceleration-induced stresses and frequency changes in doubly-rotated crystal resonators
[AD-A189261] 13 p1761 N88-20532
Body tensor formalism in finite deformation elasticity and application to the torsion of a circular cylinder
13 p1780 N88-20651
Improvement of the Reynolds-stress model by a new pressure-strain correlation
[NASA-CR-182699] 13 p1783 N88-20667
Stress-strain behaviour of a bolt hole in carbon fibre composite plates
[BU-354] 14 p1923 N88-21460
The effect of strain rate on the strength and ductility of SiCw/2124 Al composite
[OUEL-1692/87] 14 p1924 N88-21466
A simplified orthotropic formulation of the viscoplasticity theory based on overstress 14 p1929 N88-21505
Constitutive response of Rene 80 under thermal mechanical loads 14 p1932 N88-21524
The CRREL (Cold Regions Research and Engineering Laboratory) Hopkinson bar apparatus
[AD-A190599] 15 p2077 N88-22380
Biaxial experiments supporting the development of constitutive theories for advanced high-temperature materials 15 p2078 N88-22386
Fatigue damage mapping 15 p2084 N88-22423
Bithermal fatigue: A simplified alternative to thermomechanical fatigue 15 p2084 N88-22424
Behaviour of fibre-reinforced composites under dynamic loading
[AD-A191310] 16 p2174 N88-22955
Analysis of crack-tip fields in a viscoplastic material
17 p2349 N88-23996
Analysis of notched metal matrix composites under tension loading
[NASA-TM-100629] 18 p2480 N88-24713
Role of cracks in the creep of structural polycrystalline ceramics
[AD-A191485] 18 p2490 N88-24770
A transversely isotropic thermoelastic theory
[NASA-TM-101302] 22 p3087 N88-28332
Relation between strength, creep and relaxation behavior in Cu and Al at room temperature
[ETN-88-92982] 23 p3195 N88-29015
Plastic flow and failure modeling under high strain rate loading
[AD-A194223] 23 p3226 N88-29199
Intraplate deformation, stress in the lithosphere and the driving mechanism for plate motions
[NASA-CR-183121] 23 p3231 N88-29231
Shear stress at a film-substrate interface due to mismatch strain
[AD-A193461] 23 p3288 N88-29577
Anisotropic constitutive modeling for nickel-base single crystal superalloys
[NASA-CR-182157] 24 p3353 N88-29961
Nonlinear stress-strain and inelastic rebound with exponential stiffness
[AD-A195667] 24 p3384 N88-30159

STRESS-STRAIN-TIME RELATIONS
Analysis of crack-tip fields in a viscoplastic material
17 p2349 N88-23996

STRESSES
NT AXIAL STRESS
NT COMBINED STRESS
NT CRITICAL LOADING
NT PLANE STRESS
NT RESIDUAL STRESS
NT REYNOLDS STRESS
NT SHEAR STRESS
NT TENSILE STRESS
NT THERMAL STRESSES
NT TORSIONAL STRESS
NT TRIAXIAL STRESSES
Component specific modeling
02 p0187 N88-11166
Anelastic behaviour of materials under multiaxial strains. Part 3: Order-disorder transition, Shoek effect and Poisson's ratio in AISI-1080 steel
[DE87-703087] 02 p0191 N88-11193
Investigations of creep cavitation in Type 304 stainless steel
[DE87-014198] 03 p0287 N88-11803
Superoxide dismutase assays
[AD-A183972] 03 p0356 N88-12242
Initial dynamic load estimates during configuration design 05 p0593 N88-13621
A study of fatigue crack growth life under random stresses 05 p0602 N88-13685
Tensile mean stress effects on uniaxial fatigue behavior of 1045 HR steel 05 p0603 N88-13694
Stress effects and the optimum format of a scrolling seven-line VDT text window
[AD-A185559] 06 p0758 N88-14651
Assessment of anomalous gravitational field of elastic Earth 07 p0921 N88-15594
Study on the mechanical stresses in the elements of the model of a toroidal magnet of a tokamak with strong field
[DE88-700343] 07 p0935 N88-15679
Study on the model of a toroidal magnet for a tokamak with a strong field
[DE88-700346] 07 p0935 N88-15681
Failure modes of laminate structures
[DE88-002579] 08 p0996 N88-16033
Creep and fatigue research efforts on advanced materials 09 p1119 N88-16701
A large strain thermomechanical forming model for elastic-viscoplastic behavior in metals
10 p1301 N88-17780
Effects of the neutron spectrum on mechanical property changes in low dose irradiations
[DE88-003429] 10 p1302 N88-17786
A component synthesis method using Lanczos vectors
[DE88-002263] 10 p1403 N88-18368

Kinetic and turbulence models for granular and two-phase flows
11 p1484 N88-18862
Random vibration (stress screening) of printed wiring assemblies
11 p1499 N88-18953
Ion beam modification of film stress and the effectiveness of thin film encapsulants on GaAs
[DE88-004458] 11 p1558 N88-19328
Thermal oxide growth on silicon: Intrinsic stress and silicon cleaning effects
[AD-A188790] 13 p1736 N88-20377
Real-time stressed channel simulator
[AD-A190223] 15 p2025 N88-22067
Elasto-plastic analysis using a stress-based finite element method and an endochronic theory of plasticity
[DE88-003001] 15 p2075 N88-22372
Does the pipe diffusion of self-interstitials in crystals under stresses exist
[DE88-701027] 15 p2139 N88-22762
A dynamic analysis of piezoelectric strained elements
[AD-A191478] 18 p2503 N88-24851
Theory of viscoplasticity based on overstress with applications
18 p2529 N88-25007
A new boundary integral equation formulation for elastodynamic and elastostatic crack analysis
[AD-A192967] 20 p2815 N88-26702
Ultrasonic studies of stresses and plastic deformation in steel during tension and compression
[AD-A192308] 21 p2912 N88-27280
Granular flow: Particle-dynamics simulations of steady flow
[DE88-011342] 21 p2948 N88-27506
Fiber-optics used to record high-speed photographs inside a pressurized tank during lethality testing
[DE88-011283] 21 p2951 N88-27529
Deep level defects in semiconductors: Stress and pressure studies
[DE88-010855] 21 p3024 N88-27948
Stress related failures causing open metallization
[AD-A195061] 24 p3383 N88-30150

STRETCHING

Spectral dilation of L(B,H)-valued measures and its application to stationary dilation for Banach space valued processes
[NASA-CR-182388] 07 p0913 N88-15536
Optical evaluation of prototype stretched-membrane mirror modules for solar central receivers
[DE88-011884] 21 p2969 N88-27637

STRIATION

Surface gouging by hypervelocity sliding contact between metallic materials
[DE88-001937] 06 p0682 N88-14178
Interaction of a vortex pair with a free surface
[AD-A186619] 08 p0988 N88-15988
The striae in the dust tails of great comets: A formal comparison of the goodness of fit by various theories, and a new proposal
14 p2002 N88-21937

STRING THEORY

Research program in elementary particle theory
[DE88-000159] 02 p0233 N88-11468
Superconformal invariance and superstring in background fields
[DE87-703097] 02 p0247 N88-11561
On the cosmological constant in the heterotic string theory
[DE87-703099] 02 p0247 N88-11562
Our universe as an attractor in a superstring model
[DE87-703066] 02 p0251 N88-11585
Cosmological applications of singular hypersurfaces in general relativity
04 p0521 N88-13202
Introduction to string field theory
[DE87-014583] 05 p0657 N88-14032
Superstrings on quantum spacetime
[DE88-700106] 07 p0940 N88-15715
A note on Fujikawa's method of determining the critical dimension of the relativistic string
[NIKHEF-H/87-5] 08 p1092 N88-16571
Ambiguity in determining the effective action for string-corrected Einstein gravity
[PB87-166153] 09 p1259 N88-17550
Research in theoretical physics: Results from last year 1986/87
[DE88-004922] 10 p1423 N88-18502
Cosmic strings: A problem or a solution
[DE88-003410] 10 p1429 N88-18535
The early years of string theory: The dual resonance model
[DE88-003521] 11 p1563 N88-19359
Simulation of nuclear collisions at high energies in the frames of quark-gluon string model
[DE88-700914] 12 p1690 N88-20113
String theory and algebraic geometry of moduli spaces
[CWI-PM-R8705] 13 p1849 N88-21070
Introduction to classical mechanics of systems with constraints, part 3
[DE88-701057] 13 p1850 N88-21073
Early reheating and cosmic strings
13 p1855 N88-21103
Analysis of hadron production in deep inelastic muon-proton collisions through the fire-string model
[PREPRINT-578] 14 p1981 N88-21822
Strings in four dimensions
[DE88-006435] 14 p1990 N88-21864
Recent developments in the path integral approach to anomalies
[DE87-703032] 15 p2118 N88-22616
Path integral, BRS symmetry, and string and membrane theories
[DE88-752300] 15 p2146 N88-22810
Involution-dependent constants and the cancellation of divergences in the 1-loop open string amplitude
[DE88-006537] 15 p2146 N88-22811
Finite width corrections to the Nambu action for the Nielsen-Olesen string
[DE88-006996] 15 p2147 N88-22812
Cosmology for high energy physicists
[DE88-005705] 15 p2151 N88-22842
Hyperelliptic statsums in superstring theory
[DE88-701646] 16 p2284 N88-23676
Integrability of fermionic string in superfluid Hamiltonian approach
[DE88-701662] 16 p2284 N88-23678
Introduction to covariant formulation of superstring (field) theory
[DE87-703038] 18 p2586 N88-25363
The geometry of the Virasoro group for physicists
[DE88-007374] 18 p2586 N88-25366
Comment on non-renormalization theorem in the four dimensional superstrings
[DE88-752551] 18 p2586 N88-25367
From general relativity to the theory of superstrings
18 p2587 N88-25369
Superstrings
[DE87-702982] 19 p2737 N88-26249
General relativity invariance and string field theory
[DE88-702045] 19 p2737 N88-26252
Topics in gauge theories and the unification of elementary particle interactions
[DE88-008112] 19 p2738 N88-26256
Algebraic and arithmetic geometry in string theory
[CWI-PM-R8708] 20 p2848 N88-26904
Research in theoretical particle physics
[DE88-008230] 20 p2851 N88-26927
Geometry of superconformal manifolds, part 1
[DE88-702405] 21 p3011 N88-27863
Closed string fields as parameters of extra gauge symmetry of open string field theory
[DE88-702046] 21 p3026 N88-27960
Vortices on the world sheet and string's critical dynamics
[DE88-702116] 21 p3026 N88-27961
Dynamical evolution of cosmic strings
[DE88-011724] 21 p3030 N88-27989
The ground state of the bosonic string
[USIP-88-01] 22 p3151 N88-28746
The Hilbert space of the closed bosonic string
[USIP-88-04] 22 p3151 N88-28747
Calculations in perturbative string field theory
[DE88-011616] 22 p3158 N88-28798
Open bosonic string in background electromagnetic field
[DE88-702140] 23 p3201 N88-29053
Holomorphic geometry of interacting string
[DE88-702714] 23 p3295 N88-29627
The Hilbert space of the open bosonic string
[USIP-88-02] 23 p3295 N88-29628
Introduction to string theory
[DE88-702706] 24 p3435 N88-30445

STRINGS

Verification of a systolic algorithm for string comparison
[CWI-CS-R8734] 13 p1819 N88-20873
Hamiltonian formalism in the model of the relativistic string with rigidity
[DE88-701503] 15 p2147 N88-22815
String driven inflation
[DE88-006994] 15 p2151 N88-22841

STRIP TRANSMISSION LINES

NT MICROSTRIP TRANSMISSION LINES
Time domain electromagnetic waves in multilayered media
[AD-A185055] 05 p0574 N88-13502
Time domain wave propagation in multilayered integrated circuits
[AD-A187462] 10 p1324 N88-17916
Conformal microstrip slot antenna and antenna array
[AD-A189623] 15 p2055 N88-22252
Investigation of radiating and guiding structures in microstrip patch antennas
[AD-A191445] 16 p2193 N88-23082
Time domain wave propagation in multilayered integrated circuits
[AD-A193821] 22 p3073 N88-28241

STRONG INTERACTIONS (FIELD THEORY)

An introduction to charm and heavy quark physics
[DE87-013589] 02 p0231 N88-11455

STRONGLY COUPLED PLASMAS

Error modeling and confidence interval estimation for inductively coupled plasma calibration curves
[AD-A186711] 09 p1250 N88-17486
Development and evaluation of instrumentation and methods for multi-element analysis
[AD-A189345] 13 p1841 N88-21018
The two-dimensional one component plasma in a doubly periodic background: Exact results
[AD-A191260] 16 p2280 N88-23650
Thomson scattering for determining electron concentrations and temperatures in an inductively coupled plasma. 1: Assessment of the technique for a low-flow, low-power plasma
[AD-A191323] 16 p2280 N88-23651
Thomson scattering for determining electron concentrations and temperatures in an inductively coupled plasma. 2: Description and evaluation of a multichannel instrument
[AD-A191324] 16 p2280 N88-23652
MACH2: A two-dimensional magnetohydrodynamic simulation code for complex experimental configurations
[AD-A192285] 20 p2860 N88-26988
Role of ordinary to extraordinary mode wave coupling in ionospheric heating experiments
[AD-A195335] 24 p3362 N88-30017

STRONTIUM

Superconducting properties and structural characterization of high T/sub c/ oxides
[DE88-003479] 10 p1420 N88-18477
High temperature superconductivity
[AD-A190259] 16 p2281 N88-23655
Lewis Cliff 86010, a unique Antarctic meteorite: Possible new clues to the early history of the solar system
24 p3442 N88-30482

STRONTIUM COMPOUNDS

Superconductivity in La/sub 1.85-x/Nd/sub x/Sr/sub .15/CuO
[DE88-003014] 09 p1258 N88-17540

STRUCTURAL ANALYSIS

NT BERNSTEIN ENERGY PRINCIPLE
NT DYNAMIC STRUCTURAL ANALYSIS
NT ENERGY METHODS
NT EQUILIBRIUM METHODS
NT FLUTTER ANALYSIS
NT MATRIX METHODS
NT STRAIN ENERGY METHODS
Redesign of solid rocket booster/external tank attachment ring for the space transportation system
[NASA-TM-100476] 01 p0017 N88-10101
Structural reliability and damage tolerance of ceramic composites for high-temperature applications
[PB87-208310] 01 p0019 N88-10119
Mean flow structure of a turbulent junction vortex
[PB87-206231] 01 p0047 N88-10301
Assessment of the COFSI/MAST I project
[NASA-CR-181366] 01 p0053 N88-10340
Analysis of shell-type structures subjected to time-dependent mechanical and thermal loading
[NASA-CR-181409] 01 p0060 N88-10388
Reinforced flexural elements for TEMP-STRESS Program
[DE87-012961] 01 p0061 N88-10391
Dynamical simulation of structural multiplicity in grain boundaries
[DE87-012746] 01 p0103 N88-10676
Reliability of finite element methods in North America
[AGARD-R-748] 02 p0184 N88-11139
Turbine Engine Hot Section Technology, 1985
[NASA-CP-2405] 02 p0184 N88-11140
3D inelastic analysis methods for hot section components
02 p0187 N88-11164
3-D inelastic analysis methods for hot section components
02 p0187 N88-11165
High temperature stress-strain analysis
02 p0188 N88-11170
Constitutive modeling for isotropic materials
02 p0188 N88-11171
Combined calculation of deformation and stress for the body and sabot of an APFSDS
03 p0302 N88-11899
Reliability-based optimal structural and mechanical design
03 p0335 N88-12109
The Shock and Vibration Digest, Volume 19, No. 10
03 p0335 N88-12112
Reduced complexity structural modeling for automated airframe synthesis
[NASA-CR-177440] 04 p0393 N88-12453

An integrated study of structures, aerodynamics and controls on the forward swept wing X-29A and the oblique wing research aircraft
[NASA-CR-181548] 04 p0399 N88-12486
USSR report: Engineering and equipment
[JPRS-UEQ-87-008] 04 p0423 N88-12621
Work-in-progress presented at the Army Symposium on Solid Mechanics, 1986: Lightening of the Force
[AD-A184791] 04 p0427 N88-12644
Explicit and implicit soil modelling for dynamic soil-structure interaction problems
04 p0428 N88-12650
Corrosion control by composite material substitution with application to the M-939 5-ton truck
04 p0428 N88-12654
Detection of defects on structures
[EP-PATENT-0-210-794-A2] 04 p0453 N88-12807
A refined nonlinear analysis of laminated composite plates and shells
[AD-A184436] 04 p0454 N88-12811
Extremum methods of structural analysis for system reliability assessment 04 p0456 N88-12824
Light funnel concentrator panel for solar power
[NASA-CR-179223] 04 p0464 N88-12870
Methods for design and evaluation of integrated hardware/software systems for concurrent computation
[NASA-CR-181522] 04 p0479 N88-12953
Large change-of-curvature effects in quadratic finite elements for CAD of membrane structures
04 p0480 N88-12958
COLA2: A computer program for the structural synthesis of two components using general modal coordinates
[DE88-001457] 04 p0481 N88-12963
Nuclear techniques in studies of condensed matter
[NASA-RP-1195] 04 p0489 N88-13015
Novel dynamical investigations of excitons and their structure in semiconductors
[DE87-014868] 04 p0499 N88-13070
Static Aeroelastic Effects on High Performance Aircraft
[AGARD-CP-403] 05 p0550 N88-13348
Space station systems: A bibliography with indexes
[NASA-SP-7056(05)] 05 p0556 N88-13382
Micromechanics of the degradation of composite materials
[SNIAS-872-430-113] 05 p0559 N88-13405
Fiber composite structural durability and damage tolerance: Simplified predictive methods
[NASA-TM-100179] 05 p0560 N88-13409
Mechanical property evaluation of a series of commercial tungsten alloys
[AD-A185440] 05 p0565 N88-13446
The matrix exponential in transient structural analysis
05 p0593 N88-13619
Simultaneous structural and control optimization via linear quadratic regulator eigenstructure assignment
05 p0594 N88-13622
Structural frequency functions for an impulsive, distributed forcing function 05 p0594 N88-13627
Exact finite element method analysis of viscoelastic tapered structures to transient loads
05 p0595 N88-13632
Optimal shock isolation with minimum settling time
05 p0595 N88-13633
Significance of foundation-soil separation in dynamic soil-structure interaction 05 p0596 N88-13641
An element of a multilayer shell for the computation of composite structures
[ONERA-RT-14/3542-RY-051-R]
05 p0610 N88-13742
Experimental studies on acoustic emission monitoring of crack propagation in offshore structures: A literature survey 05 p0610 N88-13748
Structural tests and development of a laminar flow control wing surface composite chordwise joint
[NASA-CR-172462] 06 p0663 N88-14066
Design verification and fabrication of active control systems for the DAST ARW-2 high aspect ratio wing, part 1
[NASA-CR-177959-PT-1] 06 p0669 N88-14101
Continuum modeling of large lattice structures: Status and projections
[NASA-TP-2767] 06 p0672 N88-14115
Geometric nonlinear analysis of asymmetric thin-walled members
[PB87-133856] 06 p0723 N88-14446
Fundamental aspects of the structure of supersonic turbulent boundary
[AD-A186366] 07 p0815 N88-14959
Natural frequencies and structural integrity assessment of large space structures
[AD-A186139] 07 p0824 N88-15001
New mechanism of the high temperature (reversible) temper brittleness of alloy steels
[PB87-143954] 07 p0833 N88-15056
Experimental investigation of damping characteristics of bolted structural connections for plates and shells
[AD-A186075] 07 p0867 N88-15259
Structural relaxation in strained-layer heterostructures
[DE88-002326] 07 p0868 N88-15264
Typhoon structural evolution
[AD-A186090] 07 p0879 N88-15333
Contrast between the chemical, structural and electronic properties of thin films of Cu and Ni on the Ru(0001) surface
[DE88-002360] 07 p0938 N88-15698
Aeropropulsion '87. Session 2: Aeropropulsion Structures Research
[NASA-CP-10003-SESS-2] 08 p0954 N88-15785
Integrated analysis and applications
08 p0954 N88-15789
Overview of NASA PTA propfan flight test program
08 p0957 N88-15805
Mixed method of finite strip and finite element
[PB87-143467] 08 p0996 N88-16027
The Shock and Vibration Bulletin. Part 3: Isolation and damping, vibration test criteria, and vibration analysis and test
[AD-A186750] 08 p0997 N88-16040
Evaluation of vibration specifications for acoustic environments 08 p0999 N88-16053
North Pacific Ocean. Subtropical front north of Hawaii, R/V Thomas G. Thompson: 7 January - 10 February 1974. CTD data report
[AD-A186565] 08 p1044 N88-16310
Analytical interactive approach for phenomena involving structures, thermal and control aspects. Volume 1: Theory --- spacecraft structures
[ESA-CR(P)-2503-VOL-1] 09 p1134 N88-16803
Analytical interactive approach for phenomena involving structures, thermal, and control aspects. Volume 2: Toward the solution --- spacecraft structures
[ESA-CR(P)-2503-VOL-2] 09 p1134 N88-16804
Analytical interactive approach for phenomena involving structures, thermal, and control aspects. Volume 3: Executive summary --- spacecraft structures
[ESA-CR(P)-2503-VOL-3] 09 p1134 N88-16805
Gas erosion of impeller housing in the operation of a high-temperature, high-pressure helium circulator
[DE88-002607] 09 p1175 N88-17041
The Shock and Vibration Bulletin. Part 4: Structural Dynamics and Modal Test and Analysis
[AD-A186751] 09 p1179 N88-17062
Analysis of reinforced concrete structures under the effects of localized detonations
09 p1179 N88-17064
Reinforced cocnrete arches under blast and shock environments 09 p1180 N88-17065
Optimized structure design using reanalysis techniques 09 p1180 N88-17067
Consistent linearization of the element-independent corotational formulation for the structural analysis of general shells
[NASA-CR-178418] 09 p1181 N88-17078
FABSTRAN: A computer program for frame and beam static and transient response analysis (nonlinear)
[ARE-TR-86205] 09 p1182 N88-17079
Self-adaptive analysis of three-dimensional structures using a p-version of finite element method
[FFA-TN-1987-31] 09 p1182 N88-17084
Rotorcraft weight trends in light of structural material characteristics
[AD-A186576] 10 p1276 N88-17642
Structural analysis of the space shuttle solid rocket booster/external tank attach ring
[NASA-TM-100510] 11 p1446 N88-18618
Study of the mechanical behavior of a 2-D carbon-carbon composite
[NASA-CR-182594] 11 p1451 N88-18649
Structural analysis using X-ray scattering and neutron scattering on binary amorphous (Co,Cu)Ti alloys
[ETN-88-91487] 11 p1459 N88-18699
Study of the production of some superconducting and magnetic materials by solidification in the drop tube and drop tower
[NASA-CR-182494] 11 p1461 N88-18708
Experimental set-up and mathematical modeling of H-shaped beam type structure
[AD-A187196] 11 p1466 N88-18743
Structure of shear flow turbulence and its control
[AD-A187909] 11 p1482 N88-18846
Dynamic substructuring for shock spectrum analysis using component mode synthesis
11 p1499 N88-18950
Approximate method for predicting the permanent set in a beam in vacuo and in water subject to a shock wave 11 p1500 N88-18957
Mathematical modeling of the postbuckling behavior of structural elements 11 p1500 N88-18960
Structural analysis methods development for turbine hot section components
[NASA-TM-100298] 11 p1501 N88-18967
Deformations in VLBI antennas
[NASA-TM-100696] 11 p1502 N88-18970
Dynamic analysis of plane frames by microcomputer
11 p1531 N88-19143
An interdisciplinary approach to predictive modeling of structural adhesive bonding: Factors affecting the durability of titanium/epoxy bonds
[AD-A189503] 12 p1611 N88-19636
Structural shape optimization in multidisciplinary system synthesis
[NASA-TM-100538] 12 p1614 N88-19650
Advanced durability analysis. Volume 1: Analytical methods
[AD-A188341] 12 p1635 N88-19789
On analysis of viscoelastic structures
[AD-A188445] 12 p1636 N88-19793
Structural-acoustic interior noise modeling and analysis from experimental data
[PB88-141775] 12 p1687 N88-20088
Dynamical and photometric studies of Saturn's rings
12 p1711 N88-20241
A correlation study of X-29A aircraft and associated analytical development
[NASA-CR-183103] 13 p1722 N88-20296
Viscoelastic behavior of a polyetheretherketone (PEEK) composite
[AD-A189545] 13 p1734 N88-20368
Materials Research Laboratory at Brown University
[AD-A188006] 13 p1739 N88-20396
A fundamental understanding of the effect of alloying elements on the corrosion resistance of rapidly solidified Mg alloys
[AD-A189385] 13 p1741 N88-20413
Recent developments in nondestructive evaluation for structural ceramics
[DE88-005889] 13 p1751 N88-20473
Time-domain system for identification of the natural resonant frequencies of aircraft relevant to electromagnetic compatibility testing
[PB88-164520] 13 p1759 N88-20519
Control of structure in turbulent flows: Bifurcating and blooming jets
[AD-A189607] 13 p1766 N88-20562
Structural clearances and internal friction: Simulation by Eigen distortions
[ISSN-0208-5658] 13 p1779 N88-20640
Sixteenth NASTRAN (trademark) Users' Colloquium
[NASA-CP-2505] 13 p1780 N88-20652
A preliminary investigation of finite-element modeling for composite rotor blades
[NASA-TM-100559] 13 p1781 N88-20656
Component mode synthesis using experimental modes enhanced by mass loading
[DE88-006097] 13 p1781 N88-20657
Finite element methodology for nonlinear free and harmonic forced vibrations of beam and plate structures
13 p1782 N88-20663
Fluid-thermal-structural study of aerodynamically heated leading edges
[NASA-TM-100579] 13 p1783 N88-20666
Analysis of shell-type structures subjected to time-dependent mechanical and thermal loading
[NASA-CR-182705] 13 p1783 N88-20668
Activities report of the Structures Department
[ETN-88-91986] 13 p1783 N88-20672
Microwave and structural properties of saline ice
[AD-A189307] 13 p1803 N88-20779
Biophysical applications of solid state and tritium NMR
[DE88-005328] 13 p1808 N88-20806
Robustifying the Kalman filter
[AD-A189240] 13 p1825 N88-20907
The synthesis, characterization and structural studies of In(C5H4Me) by X-ray diffraction and electron diffraction techniques and a reinvestigation of the crystalline state of In(C5H5) by X-ray diffraction studies
[AD-A189110] 13 p1844 N88-21038
Exploring the relation between interface structure and mechanical properties in multilayer structures
[DE88-005428] 13 p1848 N88-21060
Spacecraft dielectric surface charging property determination
[NASA-CR-180879] 14 p1881 N88-21243
Unrestrained out-of-plane buckling of monosymmetric rings
[PB88-155213] 14 p1923 N88-21458
Structural and material testing of a composite microlite wing model
[BU-355] 14 p1923 N88-21461
Experiments on the creep behavior of semifinished X10NiCrAlTi 32 20 (Nicrofer 32 20) tubes under multiaxial loading --- nuclear reactors
[JUEL-2127] 14 p1923 N88-21464

Probabilistic analysis of crack containing structures with the PARIS code
[KFK-4286] 14 p1924 N88-21465
Nonlinear Constitutive Relations for High Temperature Applications, 1986
[NASA-CP-10010] 14 p1928 N88-21498
Evaluation of structural analysis methods for life prediction 14 p1930 N88-21511
On the global/local time incrementing for viscoplastic analysis 14 p1932 N88-21519
Nonlinear structural analysis of a turbine airfoil using the Walker viscoplastic material model for B1900 + Hf 14 p1932 N88-21522
Sensitivity of control-augmented structure obtained by a system decomposition method
[NASA-TM-100535] 14 p1954 N88-21647
Aero/structural tailoring of engine blades (AERO/STAEBL)
[NASA-CR-180805] 14 p1959 N88-21662
Implementing embedded artificial intelligence rules within algorithmic programming languages
[NASA-CR-178393] 14 p1959 N88-21686
Properties of the nucleus of P/Halley 14 p2004 N88-21952
Galvanic corrosion initiatives
[AD-A190658] 15 p2040 N88-22155
Transformation toughening of ceramics
[AD-A190399] 15 p2045 N88-22183
Developments in ceramic superconducting materials 15 p2052 N88-22229
JPRS report: Science and technology. China
[JPRS-CST-87-043] 15 p2053 N88-22233
Efficient method for structural optimization 15 p2054 N88-22240
UARS spacecraft recorder
[NASA-CR-180768] 15 p2068 N88-22331
Buckling of blast loaded cylinder
[AD-A190124] 15 p2076 N88-22376
Environmentally assisted crack growth in structural alloys: Perspectives and new directions
[AD-A190137] 15 p2076 N88-22377
Vibrations of structures with parametric uncertainties
[AD-A190400] 15 p2076 N88-22378
The composite blade structural analyzer (COBSTRAN) 15 p2078 N88-22390
Three-dimensional inelastic approximate analysis code (MOMM) 15 p2079 N88-22392
METCAN: The metal matrix composite analyzer 15 p2079 N88-22395
Probabilistic structural analysis computer code (NESSUS) 15 p2079 N88-22397
Structural tailoring of high-speed turbine blades (SSME/STAEBL) 15 p2080 N88-22398
Computational structural mechanics for engine structures 15 p2080 N88-22399
Structural tailoring of advanced turboprops 15 p2080 N88-22400
Advanced probabilistic methods for quantifying the effects of various uncertainties in structural response 15 p2080 N88-22401
Thermostructural analysis of simulated cowl lips 15 p2080 N88-22403
Thermal-structural analyses of Space Shuttle Main Engine (SSME) hot section components 15 p2081 N88-22404
Structural analyses of engine wall cooling concepts and materials 15 p2081 N88-22405
Structural assessment of a space station solar dynamic heat receiver thermal energy storage canister 15 p2081 N88-22406
Whisker-reinforced ceramic composites for heat engine components 15 p2082 N88-22410
Continuous fiber ceramic matrix composites for heat engine components 15 p2082 N88-22411
Flaw characterization in structural ceramics using scanning laser acoustic microscopy 15 p2082 N88-22415
Improvements to tilt rotor performance through passive blade twist control
[NASA-TM-100583] 15 p2086 N88-22434
Experimental design and structural optimization
[PB88-169255] 15 p2087 N88-22436
Bilateral symmetry elements of the Zhamanshin impact crater
[NASA-TT-20288] 15 p2096 N88-22490
Structural decomposition of multiple time scale Markov processes
[AD-A189739] 15 p2123 N88-22657
An investigation of the crystalchemistry and thermochemistry of selected mineral systems
[AD-A189758] 15 p2142 N88-22781
Path integral, BRS symmetry, and string and membrane theories
[DE88-752300] 15 p2146 N88-22810
Research and technology
[NASA-TM-100172] 15 p2153 N88-22851
Coherent structure 16 p2199 N88-23117
Coherent structures: Comments on mechanisms 16 p2199 N88-23118
Coherent structures and dynamical systems 16 p2199 N88-23119
Coherent structures and modeling: Some background comments 16 p2199 N88-23120
Multigrid for structures analysis 16 p2218 N88-23232
Vibration and flutter analysis of the SR-7L large-scale propfan 16 p2221 N88-23254
A nonlinear computation for composite structures
[ONERA-RT-15/3542-RY-062-R] 16 p2222 N88-23265
STRUTEX: A prototype knowledge-based system for initially configuring a structure to support point loads in two dimensions
[NASA-TM-100613] 16 p2250 N88-23448
Applicability and limitations of probability models in connection with the reliability of large-scale technical installations
[W-3/87] 16 p2261 N88-23520
Travelling wave concepts for the modeling and control of space structures
[AD-A191235] 17 p2310 N88-23819
Structural acoustics design manual
[ESA-PSS-03-1201-ISSUE-1] 17 p2311 N88-23821
Nondestructive Evaluation (NDE) of structural ceramics by photoacoustic microscopy 17 p2325 N88-23884
Remote sensing and structural rupture: Application examples in the study of tectonics 17 p2359 N88-24050
Analysis and interpretation of image lithostructure: An application of the multiconcept in the metamorphic belt of Sul de Santana da Boa Vista (RS) 17 p2359 N88-24051
Study of fracturing for groundwater research in the Sergipe state with remote sensing products 17 p2359 N88-24052
Lithostructural interpretation of Chapda do Cachimbo (Pa-Am-Mt), based on radar and LANDSAT imagery 17 p2366 N88-24100
The structural analysis of some crystalline and semi-crystalline substances using X-ray and neutron diffraction 17 p2445 N88-24540
Analysis of dust grain properties in two star forming regions through comparison of theoretical models to observations 17 p2451 N88-24559
Research on aero-thermodynamic distortion induced structural dynamic response of multi-stage compressor blading
[AD-A192169] 18 p2456 N88-24584
Electromagnetic damping and vibration isolation of space structures
[AD-A191492] 18 p2471 N88-24665
Fundamental studies of beta phase decomposition modes in titanium alloys
[AD-A191495] 18 p2485 N88-24740
Calculation of rolling contact of two viscoelastic cylinders with application to the steady state normal contact problem
[ILR-MITT-188] 18 p2530 N88-25008
Probabilistic finite element methods 18 p2564 N88-25223
Simulated measurement of power flow in structures near to simple sources and simple boundaries
[NASA-TM-89124] 19 p2722 N88-26166
Sensitivity to crack initiation in thick assemblies. Test report 48-444
[REPT-48-444] 20 p2758 N88-26365
Surface phases and their influence on metal-oxide interfaces
[DE88-007938] 20 p2769 N88-26420
Australian structures response evaluation: Ground shock and air blast measurements for site investigation survey
[MRL-TN-526] 20 p2813 N88-26685
FEB structural analysis, revision H
[AD-A192302] 20 p2814 N88-26698
Vibrational impacts of hush house operation
[DE88-006983] 21 p2899 N88-27207
Microchemical analysis of polycrystalline Ni3Al and other ordered alloys using the field-ion microscope atom probe
[DE88-011519] 21 p2914 N88-27294
Finite element method for plate structures with inclined angles
[ILR-MITT-182] 21 p3008 N88-27842
Structural Tailoring of Advanced Turboprops (STAT)
[NASA-CR-180861] 22 p3045 N88-28074
The effect of microgravity on mammalian cell polarization at the ultrastructural level --- Spacelab D1 mission 22 p3061 N88-28164
Application of differential quadrature to the analysis of structural components 22 p3087 N88-28331
Parametric identification of mechanical structures
[ETN-88-92881] 22 p3088 N88-28339
Modal synthesis by use of substructures with fixed or free coupling points
[ILR-MITT-191] 22 p3089 N88-28341
SRM (Solid Rocket Motor) propellant and polymer materials structural modeling
[NASA-TP-2824] 22 p3089 N88-28343
Structural analysis of the Jura mountains-Rhine Graben intersection (Switzerland) for petroleum exploration using SPOT stereoscopic data 22 p3103 N88-28431
Laboratory feasibility study of a composite embedded fiber optic sensor for measurement of structural vibrations
[AD-A194270] 22 p3152 N88-28754
A fundamental study of P/M processed elevated temperature aluminum alloys
[AD-A192958] 23 p3194 N88-29005
Structural relationship between icosahedral and Frank-Kasper phases of Al-Li-Cu
[AD-A193768] 23 p3195 N88-29011
Nondestructive investigations for space use
[SNIAS-881-430-105] 23 p3224 N88-29189
Experimental investigation of the effects of underwater exposure on the damping characteristics of bolted structural connections for plates and shells
[AD-A194486] 23 p3226 N88-29200
Interactive plotting of NASTRAN aerodynamic models using NPLOT and DISSPLA
[AD-A194115] 23 p3226 N88-29204
Computer programs for generation of NASTRAN and VIBRA-6 aircraft models
[AD-A195467] 24 p3323 N88-29792
Constitutive modeling for isotropic materials
[NASA-CR-182132] 24 p3327 N88-29811
Attenuated total reflectance FT-IR spectroscopy to measure interfacial reaction kinetics at silica surfaces
[AD-A196330] 24 p3344 N88-29908
Stress intensity factors for cracked metallic structures under rapid thermal loading
[AES-8809709F-1] 24 p3353 N88-29962
Analytical and experimental studies of beam waveguide absorbers for structural damping
[AD-A195085] 24 p3382 N88-30144
Computer-Aided Structural Engineering (CASE) project. Development of design formulas for ribbed mat foundations on expansive soils
[AD-A194807] 24 p3412 N88-30307
Computer-Aided Structural Engineering (CASE) project. Computer program for analysis of planar grid structures (CGRID), user's guide
[AD-A195977] 24 p3413 N88-30317
Structuring processes in expanding laser-produced plasmas
[AD-A195249] 24 p3431 N88-30424
Structural dynamics of high-latitude magnetosphere determined from solar electron data 24 p3444 N88-30500

STRUCTURAL BASINS
NT DELAWARE RIVER BASIN (US)
NT GREAT BASIN (US)
NT RIVER BASINS
NT WATERSHEDS
Typhoon structural evolution
[AD-A186090] 07 p0879 N88-15333
On estimating the basin-scale ocean circulation from satellite altimetry. Part 1: Straightforward spherical harmonic expansion
[NASA-CR-182387] 07 p0882 N88-15352
New data on structure of earth's crust and seismicity of basins in Atlantic and Indian Oceans 08 p1010 N88-16123
Bathymetric hazard survey test
[AD-A189150] 13 p1803 N88-20775
The impact of disorganized occupation of urban sub-basins: Sub-basin of the Cabucu River, metropolitan area of Sao Paulo (SP) 19 p2682 N88-25945

STRUCTURAL BEAMS
U BEAMS (SUPPORTS)

STRUCTURAL DESIGN
NT PRESSURE VESSEL DESIGN
Integration of dynamic, aerodynamic and structural optimization of helicopter rotor blades
[NASA-CR-181441] 01 p0002 N88-10012
A feasibility study of a hypersonic real-gas facility
[NASA-CR-180423] 01 p0008 N88-10043
Blagov commentary on Mir station, first manning 01 p0009 N88-10051
Space station integrated wall design and penetration damage control
[NASA-CR-179169] 01 p0013 N88-10070
Telepresence work station system definition study, part 2
[NASA-CR-172006] 01 p0013 N88-10071
Propulsion Working Group report 01 p0016 N88-10098

Space station propulsion technology: Space station propulsion system test bed test plan
[NASA-CR-179201] 01 p0017 N88-10104
Linear emittance damper with megagauss fields
[DE87-013562] 01 p0093 N88-10606
Phase 3 study of selected tether applications in space. Volume 2: Study results
[NASA-CR-179186] 02 p0132 N88-10828
Models of degradation of stratified composite structures
[ONERA-RT-13/3542-RY-061-R] 02 p0142 N88-10892
Advances in nickel hydrogen technology at Yardney Battery Division 02 p0164 N88-11029
International Ultraviolet Explorer (IUE) spacecraft battery performance update 02 p0164 N88-11033
Qualification testing of General Electric 50 Ah nickel-cadmium cells with Pellon 2536 separator and passivated positive plates 02 p0165 N88-11036
Test summary for advanced H2 cycle NI-CD cell 02 p0165 N88-11040
Prediction of fatigue cracking and rupture of large structures
[ONERA-RT-31/7169-RY-055-R] 02 p0192 N88-11199
The Shock and Vibration Digest, Volume 19, No. 11 03 p0265 N88-11673
Airworthiness of long-life jet transport structures 03 p0265 N88-11674
Pump assisted heat pipe 03 p0319 N88-12018
Structural characteristics of dean vortices in a curved channel
[AD-A184724] 03 p0320 N88-12024
Reliability-based optimal structural and mechanical design 03 p0335 N88-12109
The Shock and Vibration Digest, Volume 19, No. 10 03 p0335 N88-12112
Parachute materials
[DE87-014845] 04 p0411 N88-12550
Design of digital filters for electronic instrumentation
[PB87-100418] 04 p0438 N88-12716
Design of efficient FIR filters with minimal delay
[PB87-100434] 04 p0438 N88-12717
Lifting bodies: An attractive aerodynamic configuration choice for hypervelocity vehicles 05 p0534 N88-13248
Static aeroelastic considerations in the definition of design loads for fighter airplanes 05 p0550 N88-13351
The use of aeroelastic wind tunnel models to prove structural design 05 p0551 N88-13355
Design and assembly sequence analysis of option 3 for CETF reference space station
[NASA-TM-100503] 05 p0553 N88-13369
Space station systems: A bibliography with indexes
[NASA-SP-7056(05)] 05 p0556 N88-13382
Surface treatment problems found in new aircraft designed using structural composites
[SNIAS-872-111-113] 05 p0558 N88-13397
A complete linearized theory for the analysis and design of two-dimensional hydrofoils near a free surface
[UTIAS-TN-264] 05 p0579 N88-13531
Initial dynamic load estimates during configuration design 05 p0593 N88-13621
The high performance solar array GSR3
[SNIAS-872-422-108] 05 p0622 N88-13814
Structural optimization in the design process — aircraft
[SNIAS-872-111-115] 05 p0635 N88-13885
Small space reactor power systems for unmanned solar system exploration missions
[NASA-TM-100228] 05 p0660 N88-14054
Design, fabrication and delivery of a miniature Cassegrainian concentrator solar array system
[NASA-CR-179237] 06 p0730 N88-14493
Aircraft engine hot section technology: An overview of the HOST Project 08 p0957 N88-15804
Design and test of a spacecraft instrument shock isolator 08 p0998 N88-16044
Comprehensive rotorcraft analysis methods 09 p1106 N88-16630
Advanced composite airframe program: Today's technology 09 p1107 N88-16636
Integrity control of carbon fiber reinforced plastics (CFRP) structural elements. Conclusion with respect to the control methodology of CFRP primary structures in manned space flight and the implications to the design, analysis and testing of CFRP structural elements, executive summary
[MBB-TR-RB517-014/85] 09 p1139 N88-16824
Three-dimensional incompressible flowfield analysis for establishing rotor designs which optimize power extraction 10 p1329 N88-17943
Optimal design and parameter identification of flexible rotor-bearing systems 10 p1339 N88-18002
Design conditions and workspace for the generally-proportioned 3-hinge spherical wrist for robots 10 p1339 N88-18003
Design sensitivity analysis of nonlinear structural systems and numerical implementation with established finite element codes 10 p1344 N88-18032
Physical and structural characteristics of Weddell Sea pack ice
[AD-A188189] 10 p1358 N88-18119
Apollo Lightcraft project
[NASA-CR-182575] 11 p1445 N88-18615
An optimal structure for a 34-meter millimeter-wave center-fed BWG antenna: The Cross-Box concept 11 p1472 N88-18778
Derivation of strength factors related to the coordination of the strength of transmission line components --- electric power lines
[S/T-REPT-VOL-5-NO-2] 11 p1500 N88-18959
Problems in modeling TF ripple loss of fast alphas from a tokamak reactor
[DE88-000612] 11 p1553 N88-19296
Interaction between structural considerations and system design in advanced flight controls 12 p1580 N88-19458
Manned simulation: Helpful means to determine and improve structural load criteria 12 p1581 N88-19459
Presentation of structural component designs for the family of commuter airplanes
[NASA-CR-182568] 12 p1581 N88-19463
A class 2 weight assessment for the implementation of commonality and preliminary structural designs for the family of commuter airplanes
[NASA-CR-182565] 12 p1581 N88-19464
Presentation of flight control design and handling quality commonality by separate surface stability augmentation for the family of commuter airplanes
[NASA-CR-182567] 12 p1583 N88-19471
Automatic in-orbit payload deployment mechanisms, logistic operations and transport vehicle design compatibilities 12 p1586 N88-19493
Conceptualization and design of a variable-gravity research facility
[NASA-CR-182574] 12 p1595 N88-19550
Progress toward a cosmic dust collection facility on space station
[NASA-CR-182427] 12 p1598 N88-19566
Conceptual design and programmatics studies of space station accommodations for Life Sciences Research Facilities (LSRF)
[NASA-CR-179270] 12 p1598 N88-19567
Space station accommodations for life sciences research facilities: Phase A conceptual design and programmatics studies for Missions SAAX0307, SAAX0302 and the transition from SAAX0307 to SAAX0302. Volume 1: Executive summary
[NASA-CR-179267] 12 p1599 N88-19571
Concentrating photovoltaic collectors: Fabrication design
[PB88-148051] 12 p1640 N88-19821
Optics of the CEBAF CW superconducting accelerator
[CEBAF-PR-87-012] 12 p1690 N88-20110
Orbital transfer vehicle concept definition and system analysis study. Volume 2: OTV concept definition and evaluation. Book 1: Mission and system requirements
[NASA-CR-179321] 13 p1729 N88-20339
Development of isostatic mounts and associated guidelines --- spacecraft payloads
[CASA-IM-WP-301] 13 p1731 N88-20354
X-ray computed tomography for structural ceramic applications: Beam hardening corrections
[DE88-005891] 13 p1752 N88-20474
Aluminum-air battery development
[DE88-006617] 13 p1762 N88-20542
Structural clearances and internal friction: Simulation by Eigen distortions
[ISSN-0208-5658] 13 p1779 N88-20640
Potential off-normal events and associated radiological source terms for the compact ignition tokamak: Fusion Safety Program
[DE88-004112] 13 p1842 N88-21024
Space infrared telescope facility wide field and diffraction limited array camera (IRAC)
[NASA-CR-182704] 13 p1853 N88-21092
A sequentially deployable structure for space applications 14 p1875 N88-21202
Thermophotovoltaic space power system, phase 3
[NASA-CR-179327] 14 p1942 N88-21585
Large-scale wind turbine structures 15 p2085 N88-22429
Design studies of primary aircraft structures in ARALL laminates
[LR-520] 16 p2160 N88-22888
Experimental design and structural optimization
[ETN-88-92232] 16 p2257 N88-23492
Insert design handbook
[ESA-PSS-03-1202-ISSUE-1] 17 p2311 N88-23822
LDR structural experiment definition
[NASA-TM-100618] 17 p2312 N88-23826
Ceramics for turbine engines 17 p2323 N88-23873
Gigawatt, closed cycle, vapor core-MHD space power system conceptual design study 17 p2433 N88-24473
Small particle bed reactors: Sensitivity to Brayton cycle parameters 17 p2435 N88-24487
A combined Rankine/Brayton pulse power cycle 17 p2435 N88-24490
Alkali metal thermoelectric converter design for space power systems applications 17 p2437 N88-24499
A capillary pumped SHE/AMTEC system 17 p2437 N88-24500
Performance of vapor-fed sodium heat engine/AMTEC systems 17 p2437 N88-24502
Multimegawatt power conditioning requirements study 17 p2438 N88-24504
Experimental vibration damping characteristics of the third-stage rotor of a three-stage transonic axial-flow compressor
[NASA-TM-100948] 18 p2466 N88-24642
Design of overlays for rigid airport pavements
[DOT/FAA/PM-87/19] 18 p2468 N88-24652
Fundamental limits to the velocity of solid armatures in railguns 18 p2469 N88-24656
Use of a two-stage light-gas gun as an injector for electromagnetic railguns
[DE88-007200] 18 p2469 N88-24657
Structural margins assessment approach
[NASA-TM-100332] 18 p2473 N88-24672
Dynamics of a flexible orbiting platform with MRMS
[ISSN-0285-6808] 18 p2473 N88-24673
Internal erosion rates of a 10-kW xenon ion thruster
[NASA-TM-100954] 18 p2476 N88-24688
Calculation of assemblies bonded with quasi-elastic adhesives
[REPT-47-632/F] 18 p2493 N88-24793
Space station architectural elements and issues definition study
[NASA-CR-3941] 18 p2587 N88-25371
Modulation efficiency limited high frequency performance of the MODFET 19 p2657 N88-25786
Advanced energy system program
[PB88-183025] 19 p2686 N88-25965
Accelerator research studies
[DE88-008236] 19 p2726 N88-26187
Computer-Aided Engineering (CAE) for engineering design 21 p2929 N88-27390
Optimal design of viscoelastic structures 21 p2959 N88-27579
A hidden-surface removal algorithm for structures defined by triangular and rectangular surface patches
[DFVLR-MITT-88-03] 21 p3000 N88-27792
Probabilistic structural analysis to quantify uncertainties associated with turbopump blades
[NASA-TM-100278] 22 p3050 N88-28094
Missiles, fuselages and similar bodies 23 p3169 N88-28869
Comparison of the influence of different gust models on structural design 24 p3312 N88-29722
Lunar lander conceptual design: Lunar base systems study task 2.2
[NASA-CR-172051] 24 p3335 N88-29854
Gas turbine combustion modeling 24 p3349 N88-29936
A small annular combustor of high power density, wide operating range and low manufacturing cost 24 p3351 N88-29951
Alternative module configurations for advanced solar arrays on low orbit and extended lifetime missions (AMOC 2)
[ESA-CR(P)-2581] 24 p3389 N88-30182
The space station assembly phase: System design trade-offs for the flight telerobotic servicer 24 p3420 N88-30357

STRUCTURAL DESIGN CRITERIA

Rational reinforcement of cylindrical shells with variable stiffness frames subjected to external pressure 04 p0426 N88-12638
Simultaneous structural and control optimization via linear quadratic regulator eigenstructure assignment 05 p0594 N88-13622
Evaluation of vibration specifications for acoustic environments 08 p0999 N88-16053
Rotorcraft handling-qualities design criteria development 09 p1109 N88-16645
Workshop on Design Loads for Advanced Fighters
[AGARD-R-746] 12 p1579 N88-19449
Structural design requirements for aircraft incorporating active control technology 12 p1580 N88-19453
Manoeuvres by default, by demand and by design 12 p1580 N88-19455

How to generate equal probability design load conditions — aircraft design
[NLR-TR-86060-U] 13 p1722 N88-20295
Some design considerations for ceramic components in heat engine applications 17 p2323 N88-23875
Frequency dependent sliding coefficients for general three-dimensional rolling contact in high frequency range
[ILR-MITT-192] 22 p3065 N88-28318
SR-7A aeroelastic model design report
[NASA-CR-174791] 23 p3179 N88-29928

STRUCTURAL DYNAMICS
U DYNAMIC STRUCTURAL ANALYSIS

STRUCTURAL ENGINEERING
Efficient placement of structural dynamics sensors on the space station
[NASA-CR-172015] 01 p0017 N88-10103
Strain gages in engineering geodesy
[SER-C-320] 01 p0048 N88-10309
Activities report in metal manufacturing
[ISSN-0524-7705] 07 p0839 N88-15086
Index of USA-CERL publications for October 1984 - June 1987
[AD-A186375] 07 p0942 N88-15728
Aeropropulsion structures 08 p0954 N88-15786
Computer Applications in Geotechnical Engineering (CAGE) and Geotechnical aspects of the Computer-Aided Structural Engineering (G-CASE) projects. User's guide. UTEXAS2 slope-stability package. Volume 1: User's manual
[AD-A187674] 11 p1511 N88-19025
Stabilization and control problems in structural dynamics
[AD-A190197] 15 p2073 N88-22361
Travelling wave concepts for the modeling and control of space structures
[AD-A191235] 17 p2310 N88-23819
Probabilistic anisotropic failure criteria for composite materials
[AD-A193046] 21 p2904 N88-27232
An investigation of techniques for determination of optimum/self-optimizing systems
21 p2963 N88-27600
Development of remote control welding system of large structures
[PB87-219853] 22 p3083 N88-28309
Computer-Aided Structural Engineering (CASE) project. Development of design formulas for ribbed mat foundations on expansive soils
[AD-A194807] 24 p3412 N88-30307
Computer-Aided Structural Engineering (CASE) project. Computer program for analysis of planar grid structures (CGRID), user's guide
[AD-A195977] 24 p3413 N88-30317

STRUCTURAL FAILURE
Assessment of structural integrity from forced vibration testing
[DE87-014642] 02 p0191 N88-11195
Natural frequencies and structural integrity assessment of large space structures
[AD-A186139] 07 p0824 N88-15001
Postbuckling of laminated anisotropic panels
[NASA-TM-100509] 08 p0994 N88-16011
Damage mechanics of fiber reinforced plastics: A general view 11 p1448 N88-18631
Buckling and breakdown problems in structural mechanics. Failure of prestressed double-walled containers or rings
[MBB-UR-E-956/87] 13 p1783 N88-20671
Analysis and developments of failure concepts in fracture mechanics based on research results in the field of component safety topics: J-integral concept; crack resistance curves; dynamic criterion
[V-19/86] 18 p2530 N88-25009
Loading rate sensitivity of open hole composites in compression
[NASA-TM-100634] 19 p2610 N88-25490
Critical issues and directions for fracture mechanics and structural integrity
[AD-A193050] 21 p2960 N88-27584
Durability of continuous fiber reinforced metal matrix composites
[AD-A193868] 22 p3050 N88-28097
The development of acoustic emission for structural integrity monitoring of aircraft
[AD-A196264] 24 p3427 N88-30398

STRUCTURAL FATIGUE
U FATIGUE (MATERIALS)

STRUCTURAL FOUNDATIONS
U FOUNDATIONS

STRUCTURAL INFLUENCE COEFFICIENTS
The nonlinear dynamic response of an elastic-plastic thin plate under impulse loading
[AD-A182147] 08 p0994 N88-16013

STRUCTURAL MATERIALS
U CONSTRUCTION MATERIALS

STRUCTURAL MEMBERS
NT ANISOTROPIC PLATES
NT ANNULAR PLATES
NT BEAMS (SUPPORTS)
NT BOX BEAMS
NT CANTILEVER BEAMS
NT CIRCULAR PLATES
NT COLUMNS (SUPPORTS)
NT CORRUGATED PLATES
NT CURVED BEAMS
NT ELASTIC PLATES
NT END PLATES
NT FLAT PLATES
NT GIRDERS
NT I BEAMS
NT LONGERONS
NT MEMBRANE STRUCTURES
NT METAL PLATES
NT ORTHOTROPIC PLATES
NT PERFORATED PLATES
NT PLASTIC PLATES
NT PLATES (STRUCTURAL MEMBERS)
NT POROUS PLATES
NT RECTANGULAR PLATES
NT REINFORCED PLATES
NT SKIN (STRUCTURAL MEMBER)
NT STRAKES
NT STRUTS
NT TIMOSHENKO BEAMS
NT TRUSSES
NT WING PANELS
Possibilities for the modeling of dynamically loaded cylindrical structural parts in the wind tunnel
[KU-SFB-210/T/24] 01 p0001 N88-10005
NDE (Nondestructive Evaluation) of advanced structural ceramics
[DE87-014417] 03 p0292 N88-11832
Performance evaluation of a half-wave resonant slot antenna over perfect ground using NEC (Numerical Electromagnetic Code)
[AD-A184004] 03 p0308 N88-11942
Potential for on-orbit manufacture of large space structures using the pultrusion process
[NASA-TM-4016] 05 p0557 N88-13388
Distortional buckling formulae for thin-walled channel columns
[PB87-124012] 06 p0722 N88-14437
Geometric nonlinear analysis of asymmetric thin-walled members
[PB87-133856] 06 p0723 N88-14446
Chromic acid anodizing of aluminum foil
[NASA-CR-178417] 07 p0837 N88-15077
Fastening high resistance bolts in real assemblies
[CRIF-MT-171] 07 p0861 N88-15221
High-resolution Real-Time Radiography (RTR) system design
[AD-A187107] 09 p1166 N88-16992
Laboratory studies related to in-flight acoustic emission monitoring
[AD-A186714] 09 p1242 N88-17445
Environment assisted degradation mechanisms in aluminum-lithium alloys
[NASA-CR-182482] 10 p1301 N88-17782
Modern materials for light constructions — aircraft
[MBB-Z-136/86] 10 p1312 N88-17839
Dynamic response of some structural elements fabricated from a non-linear elastic material
10 p1344 N88-18031
Optimum design of geodesically stiffened composite plates
[NASA-CR-182499] 10 p1344 N88-18035
Characterization of damped structural connections for multi-component systems
[NASA-TM-100801] 11 p1502 N88-18974
The place for thermoplastic composites in structural components
[AD-A189149] 12 p1604 N88-19596
A study of damage tolerance in curved composite panels
[AD-A190617] 15 p2029 N88-22092
Characterization of structural connections for multicomponent systems 16 p2220 N88-23251
Experimental and theoretical investigation of passive damping concepts for member forced and free vibration
[NASA-CR-183082] 20 p2814 N88-26693
Critical issues and directions for fracture mechanics and structural integrity
[AD-A193050] 21 p2960 N88-27584
Application of differential quadrature to the analysis of structural components 22 p3087 N88-28331
Dynamics of articulated aerospace structures
[AD-A195685] 24 p3324 N88-29794

STRUCTURAL PROPERTIES (GEOLOGY)
Interseismic deformation for normal fault earthquakes
03 p0349 N88-12207
Studies in Aeolian geology
[NASA-CR-182328] 05 p0625 N88-13828
Petrogenesis of basalts from the Archean Matachewan Dike Swarm Superior Province of Canada
06 p0796 N88-14878
New data on structure of earth's crust and seismicity of basins in Atlantic and Indian Oceans
08 p1010 N88-16123
Statistics of two-dimensional structure elements of mountainous ranges (mosaic model) for calculating three-dimensional reflection functions
[DFVLR-FB-87-33] 09 p1185 N88-17099
Character of five selected LANDSAT lineaments in southwestern Pennsylvania: Report of investigations, 1987
[PB88-133517] 11 p1505 N88-18988
New data on the formation conditions and age of the Kamensk and Gusev astroblemes
[NASA-TT-20212] 11 p1513 N88-19040
Synthesis of finite displacements and displacements in continental margins
[NASA-CR-182616] 12 p1642 N88-19832
Geophysical study of the structure and processes of the continental convergence zones: Alpine-Himalayan Belt
[NASA-CR-182647] 12 p1644 N88-19842
Martian geomorphology and its relation to subsurface volatiles
[NASA-CR-182428] 12 p1711 N88-20237
Relationship between oceanic geological formations and tectonic structures 13 p1785 N88-20683
Bilateral symmetry elements of the Zhamanshin impact crater
[NASA-TT-20288] 15 p2096 N88-22490
A three-dimensional gravity model of the geologic structure of Long Valley caldera
[DE88-006331] 16 p2231 N88-23324
Subsurface morphology and geoarchaeology revealed by spaceborne and airborne radar
17 p2353 N88-24022
An integrated study of the Alto Paranaiba Kimberlite Province, Minas Gerais, Brazil: A possible tool for diamond exploration 17 p2355 N88-24031
Landuse and landform studies of the Mahanadi River Delta with the help of satellite MSS band
17 p2355 N88-24033
Remote sensing and structural rupture: Application examples in the study of tectonics
17 p2359 N88-24050
Analysis and interpretation of image lithostructure: An application of the multiconcept in the metamorphic belt of Sul de Santana da Boa Vista (RS)
17 p2359 N88-24051
Dune fields in central Western Argentina
17 p2366 N88-24088
The breaked anticlines, cuesta and crest homoclines, ortoclinal valleys, and other forms of relief outcrops delineated with the help of remote sensing imagery
17 p2366 N88-24089
Some geological aspects of the Pirapemas Lineament Belt 17 p2368 N88-24099
Lithostructural interpretation of Chapda do Cachimbo (Pa-Am-Mt), based on radar and LANDSAT imagery
17 p2368 N88-24100
A sedimentological and mineralogical study of the Koogah Formation, New South Wales
18 p2542 N88-25087
Use of remote sensing in the study of superficial formation certifying the development of integrated economy-case example: Rio Claro (SP) region
19 p2683 N88-25950
Stochastic geologic effects on near-field ground motions in alluvium
[AD-A192315] 21 p2972 N88-27652
Structural analysis of the Jura mountains-Rhine Graben intersection (Switzerland) for petroleum exploration using SPOT stereoscopic data 22 p3103 N88-28431
Analyzing the stratigraphy, tectonism, and mineralization at the Spanish side of the pyrite belt, Huelva province, Spain, using SPOT imagery 22 p3104 N88-28433
Geologic applications of SPOT-1, TM, and NOAA-7 data: Finding and defining unmapped structural features
22 p3104 N88-28434
Comparing different images for ground water survey based on lineament analysis 22 p3104 N88-28435
The Martian sedimentary record
23 p3302 N88-29669
Photogeological inferences of Martian surface composition 23 p3303 N88-29675
Some probable characteristics of the Martian regolith
23 p3303 N88-29678
Surface units on Mars: The assemblage in the Valles Marineris 23 p3304 N88-29680
Stratigraphy of the Kasei Valles region, Mars
23 p3305 N88-29690

Diapirs of the Mediterranean ridge: The tectonic regime of an incipient accreted terrane
24 p3396 N88-30224
The tectonic setting of the Seychelles, Mascarene and Amirante Plateaus in the Western Equatorial Indian Ocean 24 p3396 N88-30225
Ridge-trench collision in Archean and Post-Archean crustal growth: Evidence from southern Chile
24 p3397 N88-30233
Reappraisal of the geology of Kangimut Sammisoq, Ameralik Fjord, Southern West Greenland: Crustal structure and interpretation of isotopic data
24 p3398 N88-30234
Archean crustal evolution of the northern North China Craton 24 p3398 N88-30235
Evolution of the Dharwar Craton: A terrain of early Archean crustal stability, long term orogenic cycles and large scale palaeobiological activity
24 p3399 N88-30241
Spectral analysis of the Elatina varve series
[NASA-CR-183085] 24 p3402 N88-30260
Debris flows of the Simud-Tiu outflow system of Mars
24 p3442 N88-30485
High-resolution (30 m) lunar radar images
24 p3442 N88-30486
Mars: Volcanism in the Valles Marineris overlooked
24 p3443 N88-30491
The Martian highland paterae: Evidence for explosive volcanism on Mars 24 p3443 N88-30492
Physical properties of surface materials on Martian volcanoes: Dust-covered lava and ash
24 p3443 N88-30493
Rifts of deeply eroded Hawaiian basaltic shields: A structural analog for large Martian volcanoes
24 p3443 N88-30494
Small-scale volcanic landforms indicative of distributary tube systems 24 p3444 N88-30496

STRUCTURAL RELIABILITY
Ensuring the service life of designs (experience in aircraft construction) 02 p0157 N88-10986
A reliability concept for optimizing aircraft design
04 p0423 N88-12622
The strength of hybrid composites
[BR101991] 09 p1138 N88-16821
Integrity control of carbon fiber reinforced plastics (CFRP) structural elements. Conclusion with respect to the control methodology of CFRP primary structures in manned space flight and the implications to the design, analysis and testing of CFRP structural elements, executive summary
[MBB-TR-RB517-014/85] 09 p1139 N88-16824
The Shock and Vibration Bulletin. Part 4: Structural Dynamics and Modal Test and Analysis
[AD-A186751] 09 p1179 N88-17062
Reliability of structures with stiffness and strength degradation 09 p1180 N88-17068
Micro PAVER concept and development airport pavement management system
[AD-A187360] 11 p1441 N88-18598
Structural integrity of metallic armature rail guns
[AD-A188735] 13 p1728 N88-20333
Crack opening and extension in inert solid propellant. An experimental study
[AD-A189808] 15 p2048 N88-22201
Applicability and limitations of probability models in connection with the reliability of large-scale technical installations
[W-3/87] 16 p2261 N88-23520
Critical issues and directions for fracture mechanics and structural integrity
[AD-A193050] 21 p2960 N88-27584
Computation of failure probability of fatigue loaded cracked structures
[ETN-88-92360] 21 p2964 N88-27607
Durability of continuous fiber reinforced metal matrix composites
[AD-A193868] 22 p3050 N88-28097
Automated early fatigue damage sensing system
[AD-A195717] 24 p3382 N88-30143

STRUCTURAL RIGIDITY
U STRUCTURAL STABILITY

STRUCTURAL STABILITY
NT SHELL STABILITY
Models of degradation of stratified composite structures
[ONERA-RT-13/3542-RY-061-R]
02 p0142 N88-10892
Stability of mechanical joints in launching vehicles: Local and global stationary values of energy density
03 p0270 N88-11696
Vibration and buckling of geometrically imperfect laminated cylindrical shells 04 p0456 N88-12822
Three-dimensional structure of boundary layers in transition to turbulence
[AD-A185466] 06 p0702 N88-14311
Flow in labyrinth seals and its influence on rotor stability of turbocompressors 07 p0851 N88-15168
Analysis of reinforced concrete structures under the effects of localized detonations
09 p1179 N88-17064
Reinforced concrete arches under blast and shock environments 09 p1180 N88-17065
Investigations of the stability of the cell opening of soft polyurethane foams
[ETN-88-91481] 11 p1463 N88-18724
Vibrations of structures with parametric uncertainties
[AD-A190400] 15 p2076 N88-22378
Rigidity and smoothness of motion
[AD-A190555] 15 p2128 N88-22694
A thermally modified polymer matrix composite material with structural integrity to 371 C
[NASA-TM-100922] 19 p2609 N88-25483
Structure and refinement of ordered aromatic heterocyclic polymers by diffraction methods: Application of results to electro-optic phenomena
[AD-A191859] 19 p2619 N88-25537
Stability control of leakage flow channels
[DE88-009995] 23 p3210 N88-29107

STRUCTURAL STRAIN
Stresses and displacements in two, three and four layered structures submitted to flexible or rigid loads
[AD-A185707] 06 p0723 N88-14450
Predicted and measured strain responses of isotropic panels to base excitation
[NASA-TM-4054] 19 p2679 N88-25928

STRUCTURAL VIBRATION
NT BENDING VIBRATION
NT FLUTTER
NT LINEAR VIBRATION
NT SELF INDUCED VIBRATION
NT SUPERSONIC FLUTTER
NT TRANSONIC FLUTTER
Test of the Hipparcos payload in the Liege vacuum facility focal 02 p0135 N88-10850
Active control of helicopter vibration using multiloop self-adaptive control 03 p0264 N88-11660
Controlling the dynamic environment during NOE flight
03 p0264 N88-11661
Minimisation of helicopter vibration through active control of structural response 03 p0264 N88-11662
Identification of perturbations in turbomachines by the analysis of pressure signals, vibrations and wavelike motions
[ETN-88-90602] 05 p0590 N88-13600
The 58th Shock and Vibration Symposium, volume 1
[NASA-CP-2488-VOL-1] 05 p0592 N88-13609
The analysis of nonstationary vibration data
05 p0592 N88-13610
Simultaneous structural and control optimization via linear quadratic regulator eigenstructure assignment
05 p0594 N88-13622
Viscous damped space structure for reduced jitter
05 p0594 N88-13623
On the glitches in the force transmitted by an electrodynamic exciter to a structure
05 p0594 N88-13624
Fluid mass and thermal loading effects on the modal characteristics of space shuttle main engine liquid oxygen inlet splitter vanes 05 p0594 N88-13628
Incipient failure detection of space shuttle main engine turbopump bearings using vibration envelope detection
05 p0595 N88-13629
Space shuttle main engine vibration data base
05 p0595 N88-13631
Optimal shock isolation with minimum settling time
05 p0595 N88-13633
A passive vibration-cancelling isolation mount
05 p0595 N88-13636
Advanced joining concepts for passive vibration control 05 p0596 N88-13638
Dynamic response of laminated composite plates using a three-dimensional hybrid-stress finite-element formulation 05 p0596 N88-13639
Studies on fluid-structural vibration using boundary element method
[PB87-129508] 06 p0699 N88-14291
Flow in Centrifugal Compressors --- conference
[VKI-LS-1987-01] 07 p0850 N88-15160
Blade vibration due to different flow excitation
07 p0851 N88-15166
Blade excitation due to unsteady flow phenomena
07 p0851 N88-15167
Data acquisition, reduction and analysis of shock and vibration testing using a super microcomputer
[AD-A186123] 07 p0867 N88-15260
Parametric and experimental analysis using a power flow approach
[NASA-CR-182460] 09 p1116 N88-16693
Mechanical in-flight environment of Ariane payloads
09 p1126 N88-16748
A review of two-phase flow-induced vibration
[DE88-001955] 09 p1160 N88-16955
The Shock and Vibration Bulletin. Part 4: Structural Dynamics and Modal Test and Analysis
[AD-A186751] 09 p1179 N88-17062
Optimized structure design using reanalysis techniques 09 p1180 N88-17067
Reliability of structures with stiffness and strength degradation 09 p1180 N88-17068
A new look at the use of linear methods to predict aircraft dynamic response to taxi over bomb damaged and repaired airfields 09 p1180 N88-17069
Frequency response functions of a nonlinear system
09 p1180 N88-17070
System characterization in nonlinear random vibration
09 p1180 N88-17071
A review of flow-induced vibration in two-phase flow
[DE88-002873] 10 p1329 N88-17946
Strategic placement of accelerometers to measure forces by the sum of weighted accelerations
[DE88-002262] 10 p1333 N88-17968
Dynamic response of some structural elements fabricated from a non-linear elastic material
10 p1344 N88-18031
The 58th Shock and Vibration Symposium, volume 2
[NASA-CP-2488-VOL-2] 11 p1499 N88-18948
Overview of multi-input frequency domain modal testing methods with an emphasis on sine testing
11 p1499 N88-18949
Spacecraft redesign to reduce microphonic response of a VCO component 11 p1499 N88-18955
Electro-mechanical vibratory system
11 p1500 N88-18958
The Shock and Vibration Digest, volume 20, no. 3
12 p1635 N88-19786
Wave propagation and dynamics of lattice structures
[AD-A190037] 15 p2025 N88-22066
Wave propagation and dynamics of lattice structures
[AD-A190611] 15 p2025 N88-22069
Stabilization and control problems in structural dynamics
[AD-A190197] 15 p2073 N88-22361
Instrumentation to provide an active control capability for distributed parameter systems
[AD-A190043] 15 p2076 N88-22375
Vibrations of structures with parametric uncertainties
[AD-A190400] 15 p2076 N88-22378
Vibration control of large structures
[AD-A191358] 16 p2168 N88-22928
Lewis Structures Technology, 1988. Volume 1: Structural Dynamics
[NASA-CP-3003-VOL-1] 16 p2217 N88-23226
Piezoelectric pushers for active vibration control of rotating machinery 16 p2218 N88-23229
Structural acoustics design manual
[ESA-PSS-03-1201-ISSUE-1] 17 p2311 N88-23821
Vibration testing of ACT fuselage
19 p2634 N88-25627
Predicted and measured strain responses of isotropic panels to base excitation
[NASA-TM-4054] 19 p2679 N88-25928
Modeling and parameter identification of motor vehicles 20 p2785 N88-26521
Vibration control of large structures
[AD-A193317] 21 p2961 N88-27587
Coupled thermal vibrations of beams with temperature-dependent properties
21 p2963 N88-27601
Laboratory feasibility study of a composite embedded fiber optic sensor for measurement of structural vibrations
[AD-A194270] 22 p3152 N88-28754
Nonlinear vibrations of imperfect thin walled cylindrical shells
[ETN-88-92904] 23 p3227 N88-29205
ASKA-acoustics: Theory and applications --- vibro acoustics
[FFA-TN-1988-13] 23 p3279 N88-29519

STRUCTURAL WEIGHT
Assessment of energy storage concepts for use in sprint power 17 p2407 N88-24312
RSMASS: A simple model for estimating reactor/shield masses 17 p2414 N88-24355
A generalized method for optimizing the mass of space power systems 17 p2416 N88-24389

STRUCTURES
Comparison of measured temperatures, thermal stresses and creep residues with predictions on a built-up titanium structure
[NASA-TM-86814] 03 p0337 N88-12125
NF85: A three-dimensional, air-dynamics computer code for analyzing explosions in structures
[DE88-005085] 10 p1331 N88-17953
Engine structures: A bibliography of Lewis Research Center's research for 1980-1987
[NASA-TM-100842] 17 p2350 N88-24002

STRUTS
Effect of a model support strut on measurement of aerodynamic longitudinal and lateral coefficients
[PB87-170288] 09 p1113 N88-16670
Preliminary investigation of stability of a fin-stiffened slender strut
[NASA-TM-4034] 12 p1599 N88-19568
An investigation of classical dynamic scaling techniques applied to an oleo-pneumatic landing gear strut
[AD-A187664] 13 p1721 N88-20292
The X-beam as a deployable boom for the space station 14 p1925 N88-21473
Duct flow nonuniformities: Effect of struts in SSME HGM II(+)
[NASA-CR-179285] 15 p2062 N88-22296
Test of an 0.8-scale model of the AH-64 Apache in the NASA Langley full-scale wind tunnel
[AD-A196129] 24 p3319 N88-29768

STS
U SPACE TRANSPORTATION SYSTEM

STS-4
U SPACE TRANSPORTATION SYSTEM 4 FLIGHT

STS-5
U SPACE SHUTTLE MISSION 31-A

STS-6
U SPACE SHUTTLE MISSION 31-B

STS-13
U SPACE SHUTTLE MISSION 41-C

STS-31
U SPACE SHUTTLE MISSION 61-B

STS-33
U SPACE SHUTTLE MISSION 51-L

STUDENTS
Field evaluation of interactive simulation for maintenance training: SH-3 helicopter electro-mechanical bladefold system
[AD-A185923] 07 p0821 N88-14991
The sine and cosine function for class 4-VWO. Exploration of possible bottlenecks
[REPT-87-72] 20 p2881 N88-27105
Computer-aided decision making
[AD-A194210] 22 p3137 N88-28651

STUDIES
U INVESTIGATION

STURM-LIOUVILLE OPERATOR
U STURM-LIOUVILLE THEORY

STURM-LIOUVILLE THEORY
Discontinuous inverse Sturm-Liouville problems with symmetric potentials
[DE88-009803] 19 p2720 N88-26152

STYRENES
NT POLYSTYRENE

SUBARCTIC REGIONS
North Pacific Ocean. Subarctic front central Pacific, R/V Thomas G. Thompson: 8 September - 9 October 1975. CTD data report
[AD-A186567] 08 p1044 N88-16312
North Pacific Ocean. Northwest Pacific Transition Zone, R/V Thomas G. Thompson: 19 March - 1 May 1971. STD data report
[AD-A186568] 08 p1044 N88-16313
North Pacific Ocean. Gulf of Alaska, R/V Thomas G. Thompson: 1 February - 8 March 1967. STD data report
[AD-A186569] 08 p1045 N88-16314
North Pacific Ocean. Central Pacific Transition Zone, R/V Thomas G. Thompson: 25 March - 3 May 1968. STD data report
[AD-A186570] 09 p1195 N88-17160

SUBASSEMBLIES
Components for measuring robots
[KFK-PFT-126] 03 p0332 N88-12092

SUBCARRIER WAVES
U CARRIER WAVES

SUBCIRCUITS
U CIRCUITS
U SUBASSEMBLIES

SUBDIVISIONS
Taper sectioning to magnify the interface thickness of a dissimilar metal joint
[RFP-3890-REV] 03 p0333 N88-12099
An adaptive subdivision method with crack prevention for rendering beta-spline objects
[AD-A184249] 04 p0477 N88-12940

SUBDUCTION (GEOLOGY)
Relationship between oceanic geological formations and tectonic structures 13 p1785 N88-20683
Recycling of lower continental crust through foundering of cumulates from contaminated mafic intrusions 24 p3393 N88-30204
Pluton emplacement and magmatic arc construction: A model from the Patagonian batholith 24 p3393 N88-30206
An illustration of the complexity of continent formation 24 p3393 N88-30207
Does subduction zone magmatism produce average continental crust 24 p3394 N88-30214
Decoupled Rb-Sr and Sm-Nd isotopic evolution of the continental crust 24 p3395 N88-30216
Continental crustal formation and recycling: Evidence from oceanic basalts 24 p3398 N88-30238
Continental growth through time by underplating of subducted oceanic crust: Evidence from kimberlites in South Africa and SW Pacific 24 p3399 N88-30244

SUBGIANT STARS
Infrared excesses of barium stars 04 p0516 N88-13174

SUBGRAVITY
U REDUCED GRAVITY

SUBHARMONIC GENERATORS
Secondary subharmonic instability of boundary layers with pressure gradient and suction
[NASA-CR-4112] 07 p0848 N88-15148

SUBLATTICES
U LATTICES (MATHEMATICS)

SUBLAYERS
U SUBSTRATES

SUBLIMATION
Sublimation characteristics of H2O comet nucleus with CO2 impurities 14 p2010 N88-21988
The evolution of cometary activity 18 p2594 N88-25416

SUBLIMINAL STIMULI
Two attentional models of classical conditioning: Variations in CS effectiveness revisited
[AD-A187697] 11 p1522 N88-19088

SUBMARINES
Experimental studies on the tripping behavior of narrow T-stiffened flat plates subjected to hydrostatic pressure and underwater shock 05 p0592 N88-13613
Interaction of a vortex pair with a free surface
[AD-A186619] 08 p0988 N88-15988
A pyrotechnic delay ignition system for a submarine launched marine signal
[MRL-R-1079] 13 p1754 N88-20487
Experiments to investigate the vortices shed from a submarine-like body of revolution 16 p2205 N88-23156
Revised Impact Dynamic Design-Analysis Method (RIDDAM)
[AD-A190479] 16 p2217 N88-23225
Ergonomy and interior furnishing of the cabins of deep diving manned submarines: The Nautile example --- couch 19 p2697 N88-26032
The SAGA highly autonomous assistance submarine 19 p2698 N88-26034
Reducing risks inherent in operating underwater craft: The contribution of classification, the example of the SAGA highly autonomous support submarine 19 p2699 N88-26042
ELIT: An autonomous underwater observation robot 19 p2699 N88-26048
Tripping of stiffened plates using a refined beam theory
[AD-A193989] 22 p3087 N88-28333
Numerical field model simulation of full scale fire tests in a closed spherical/cylindrical vessel
[AD-A195067] 24 p3359 N88-29998
Response of SMA (Shielded Metal Arc) and narrow gap HY80 weldments to explosive shock loading
[AD-A195994] 24 p3385 N88-30162

SUBMERGED BODIES
NT DIVING (UNDERWATER)
Breaking wave forces on vertical cylinders
[RR-CE71] 03 p0338 N88-12126
Validation of the Underwater Shock Analysis (USA) program. Part 1: Theoretical considerations --- ship design
[REPT-5073713-86-01] 06 p0702 N88-14308
Retarded potential technique applied for shock wave loading of doubly symmetric submerged structures 09 p1179 N88-17058
The use of a water towing tank for aerodynamic testing and methods for quantitative evaluation of photographs 16 p2202 N88-23140
Computer aided remote control: A general concept for intervention in the nuclear, underwater, and space domains 19 p2699 N88-26046
Marine techniques: R and D axes, identification of areas of common interest with space techniques 19 p2699 N88-26047
Underwater robotics in the service of oil field exploitation: The Running and Interconnecting Tool (RIT) in the East Frigg field (North Sea) 19 p2699 N88-26049

SUBMERGING
Natural convection immersion cooling of an array of simulated chips in an enclosure filled with dielectric liquid
[AD-A193594] 23 p3207 N88-29088
Alternative immersion accelerated testing of coating systems for Naval shoreline facilities 24 p3355 N88-29977

SUBMILLIMETER WAVES
High repetition rate electron beam RF-acceleration and sub-millimeter wave generation via a free electron laser
[AD-A186066] 07 p0858 N88-15209
Holes in OI 130 nm emission fields of upper atmosphere during day 08 p1004 N88-16082
PRONAOS: A submillimeter facility --- astronomical balloon 08 p1032 N88-16255
Quantum limits of superconducting heterodyne receivers
[AD-A188014] 11 p1478 N88-18817
Millimeter and submillimeter wave research: Spectroscopy, energy transfer, and techniques
[AD-A188952] 12 p1620 N88-19691
An attempt to measure the diffuse brightness of the sky at submillimeter wavelengths 12 p1710 N88-20233
Development and applications of optical interferometric micrometrology in the angstrom and subangstrom range
[NASA-TM-100299] 16 p2211 N88-23196
Heterodyne spectrometer for the very high frequency range between 300 and 3000 GHz (1 mm to 0.1 mm) using a mixer in open structure 16 p2271 N88-23589
Telescope illumination and beam measurements for submillimeter astronomy
[MPE-PREPRINT-88] 16 p2288 N88-23699
The galactic nucleus at mm-, sub-mm and far-infrared wavelengths
[MPE-PREPRINT-102] 16 p2288 N88-23700
Balloon-borne three-meter telescope for far-infrared and submillimeter astronomy
[NASA-CR-182924] 17 p2449 N88-24550
Millimeter and submillimeter waves and frequency selective surfaces
[AD-A191511] 18 p2500 N88-24827
Apparatus for submillimeter laser diagnostics of high-temperature plasma
[DE88-702464] 23 p3285 N88-29563
A submillimeter wavelength space-based imaging radar
[AD-A195846] 24 p3364 N88-30033
The study of hydromagnetic waves and RF heating using the TORTUS tokamak, the development of diagnostic techniques based on submillimeter lasers and the gyrotron, and gas discharge 24 p3431 N88-30419

SUBMINIATURIZATION
Development of subminiature multi-sensor hot-wire probes
[NASA-TM-100052] 15 p2069 N88-22336

SUBROUTINE LIBRARIES (COMPUTERS)
The SUPRENUM communications subroutine library for grid-oriented problems
[DE88-000137] 04 p0479 N88-12950
A new library of CAMAC routines for the control of the system CRATE by a microVAX in the VAXELN environment
[NOTA-INTERNA-893] 06 p0761 N88-14667
Implementation of elementary functions in Ada
[CWI-NM-R8709] 09 p1218 N88-17303
Contributions to a numerical library in Ada
[NPL-DITC-98/87] 09 p1219 N88-17309
FORTRAN 77 error handling of the RASP library
[DFVLR-MITT-87-14] 14 p1957 N88-21669
The NPL data approximation subroutine library: Cu rrent and planned facilities
[NPL-DITC-104/87] 14 p1959 N88-21681
Ada user library
[FOA-C-20657-2.7] 16 p2246 N88-23418
Proposal for standard mathematical packages in Ada
[CWI-NM-R8718] 16 p2249 N88-23439
PLOT300: A Tektronics PLOT10 emulator for HP 9000 series 200/300 computers
[NASA-TM-100606] 16 p2250 N88-23447
TRANSL: A PATRAN translator subroutine library
[DE88-010976] 21 p2998 N88-27784

SUBROUTINES
Using MINOS (Modular In-core Nonlinear Optimization System) as a subroutine for decomposition
[DE87-013086] 02 p0221 N88-11390
The circular serial autocorrelation computer program
[AD-A184795] 03 p0365 N88-12295
MODTRAN: A moderate resolution model for LOWTRAN
[AD-A185384] 05 p0574 N88-13503
Mixing Microsoft C and Microsoft FORTRAN program modules on the IBM Personal Computer
[DE88-001947] 05 p0637 N88-13895
Rationale for the design of the Ada (tradename) programming language
[AD-A187106] 09 p1217 N88-17297
Wave group analysis based on Kimura's method
[AD-A187610] 11 p1516 N88-19055
Subroutines for solving the equation of diffusion in media with anisotropic properties
[DE88-700743] 11 p1536 N88-19179

Design of an aeroelastic composite wing wind tunnel model
[AD-A188855] 12 p1582 N88-19466
BLITZ: Blitzen's micron-code assembly language design document, version 1.0
[TR88-14] 12 p1676 N88-20019
Computer programs for calculating group cross-section covariances from uncertainty parameters in the ENDF/B-V format. UNC 32/33 --- neutron physics
[ECN-202] 13 p1837 N88-20995
Finite area combustor theoretical rocket performance
[NASA-TM-100785] 14 p1883 N88-21252
Expressing mathematical subroutines constructively
[AD-A190559] 15 p2121 N88-22644
CIMAG2: The computer program to generate color images
[AD-A191847] 18 p2557 N88-25175
Photocurrent modeling of modern microcircuit PN junctions
[DE88-007037] 19 p2662 N88-25832
Effective communication between a microVAX and a specialized high-speed subprocessor
[DE88-007967] 19 p2714 N88-26115
Using IMSL mathematical and statistical computer subroutines in physiological and biomechanical research
[AD-A192594] 21 p2995 N88-27765

SUBSETS (MATHEMATICS)
U SET THEORY

SUBSONIC FLOW
Three-dimensional calculation in high subsonic axial compressor rotor and its comparison with L2F velocity measurement 03 p0300 N88-11886
Solution of the two-dimensional Euler equations on unstructured triangular meshes 04 p0396 N88-12469
Wakes of two dimensional bluff bodies in subsonic flow. Influence of a separating plate and of a pulsed injection of momentum
[IMFL-4200-86/75] 05 p0541 N88-13297
A numerical model of unsteady, subsonic aeroelastic behavior
[NASA-TM-100487] 06 p0663 N88-14064
A direct calculation method for perturbation fields of moving bodies in compressible media at subsonic Mach numbers
[ETN-88-90808] 06 p0701 N88-14305
Boundary layer transition 07 p0811 N88-14942
Experimental investigation of the subsonic high-altitude operation of the NASA Lewis 10- by 10-foot supersonic wind tunnel
[NASA-TM-100214] 08 p0959 N88-15814
Navier-Stokes computations for circulation control airfoils 10 p1269 N88-17592
A numerical study of unsteady two-dimensional subsonic compressible base flow 10 p1327 N88-17931
Conditions at infinity for theories of oscillating wings and propellers in subsonic flow
[NAL-TR-937] 11 p1434 N88-18556
A discretization of the integral equation for the time dependent linearized subsonic potential flow over a wing
[AD-A188534] 12 p1574 N88-19411
Numerical simulation of subsonic and transonic propeller flow
[NASA-TM-100163] 13 p1716 N88-20262
ARSPNSC: A method to calculate subsonic steady and unsteady potential flow about complex configurations
[NLR-TR-86122-U] 13 p1717 N88-20265
Finite element calculations for aerodynamic coefficients of a 3-dimensional body in subsonic flow using Green's function method
[NASA-TT-20208] 13 p1718 N88-20272
Effect of flow convergence on turbulence level in stream 14 p1973 N88-21773
Study of the boundary layer of a flow pulsed by acoustic waves
[ETN-88-91998] 16 p2206 N88-23163
Numerical simulations of the flat-plate laminar boundary layer in subsonic and supersonic flow
[PDR/CFDU/IC/36] 18 p2511 N88-24895
Influence of rear body geometry on the velocity characteristics of the near wake
[ISL-R-113/87] 20 p2753 N88-26339
Three-dimensional viscous flow computations of a circular jet in subsonic and supersonic cross flow
[NASA-CR-182153] 20 p2800 N88-26616
Navier-Stokes calculations of transonic flows past cavities
[NASA-CR-180484] 23 p3212 N88-29116

SUBSONIC SPEED
Aerodynamic sensitivities from subsonic, sonic and supersonic unsteady, nonplanar lifting-surface theory
[NASA-TM-100502] 04 p0394 N88-12459
Effects of winglets on a first-generation jet transport wing. 7: Sideslip effects on winglet loads and selected wing loads at subsonic speeds for a full-span model
[NASA-TP-2619] 11 p1436 N88-18567
Preliminary measurements of heat flux in a subsonic gun simulator
[AD-A191090] 16 p2208 N88-23178
Integrated Application of Active Controls (IAAC) technology to an advanced subsonic transport project: Program review
[NASA-CR-3880] 17 p2301 N88-23763
Theoretical-numerical study of feasibility of use of winglets on low aspect ration wings at subsonic and transonic Mach numbers at reduce drag
[NASA-CR-4174] 21 p2892 N88-27168
Pressure distributions from subsonic tests of an advanced laminar-flow-control wing with leading- and trailing-edge flaps
[NASA-TM-4040-PT-2] 24 p3321 N88-29776

SUBSONIC WIND TUNNELS
The vertical test section (VMK) of DFVLR in Cologne-Porz, Federal Republic of Germany (status 1986)
[ESA-TT-1053] 03 p0267 N88-11682
Effect of flow convergence on turbulence level in stream 14 p1973 N88-21773
A comparative study of vortex flows in wind and water tunnels 16 p2204 N88-23151

SUBSTITUTES
Concept and analysis of a direct-injection alcohol layer charge motor
[ETN-88-91482] 11 p1495 N88-18925
Solution of the Lloyd-Max quantizer parameters by the method of successive substitution
[AD-A187829] 11 p1540 N88-19207

SUBSTITUTION
U SUBSTITUTES

SUBSTRATES
Laser chemically vapor deposited silicon-carbide: Growth features, topography, microstructure, and composition
[DE87-013767] 01 p0029 N88-10184
The water permeability of multi-layer coatings
[BLL-M-37252-(5828.4)] 02 p0148 N88-10927
Epitaxial reactor development for growth of silicon-on-insulator devices
[AD-A184758] 03 p0382 N88-12399
Effectiveness of electrodeposited coatings in reducing atmospheric corrosion of copper substrates
[DE87-013651] 05 p0566 N88-13448
Water disbondment characterization of organic Coating/metal substrate systems
[AD-A184847] 05 p0567 N88-13454
Reactive sticking coefficients of silane on silicon
[DE88-000601] 05 p0570 N88-13473
Raman microprobe characterization of dielectric films following high-energy pulsed laser irradiation
[DE88-000559] 05 p0588 N88-13587
Tribology of thin film systems
[ETN-88-91365] 05 p0590 N88-13601
Effects of hydrolysis on metallo-organic solution deposition of PZT films
[ATR-86(8443)-1] 06 p0679 N88-14160
Investigation of silicon surface passivation by silicon nitride film deposition
[NASA-CR-182350] 06 p0729 N88-14487
Coverage dependence of adsorbate-substrate bond lengths: Chlorine and caesium adsorbed on silver single crystals
[PB87-125142] 06 p0788 N88-14833
Monolayer films prepared by the spontaneous self-assembly of symmetrical and unsymmetrical dialkyl sulfides from solution onto gold substrates: Structure, properties, and reactivity of constituent functional groups
[AD-A186717] 09 p1137 N88-16814
Adhesion of vapour phase deposited ultra-thin polyimide films on polycrystalline silver
[AD-A187930] 10 p1306 N88-17810
The soft/hard wet anodization of aluminum oxide and its use in a thin film multilayered capacitor
[AD-A187575] 10 p1325 N88-17919
Interactions of cultured human endothelial cells with polymeric surfaces
[PB88-112255] 10 p1369 N88-18178
The deposition rate dependence of plasma polymerization on the radius of curvature of the substrate
[DE88-003811] 10 p1412 N88-18429
Optical characterization of GaAs/sub 1-x/Sb/sub x/ and GaAs/sub 1-x/Sb/sub x/GaAs strained layer superlattices
[DE88-003393] 10 p1418 N88-18464
Adhesion of PVD titanium coatings to beryllium substrates
[DE88-005147] 11 p1483 N88-18721
Surface mediated photocatalysis
[AD-A188882] 12 p1603 N88-19589
Preparation and characterization of thin films of alumina by metalorganic chemical vapor deposition
[AD-A188366] 12 p1608 N88-19614
Research on mercury cadmium telluride
[AD-A189155] 13 p1845 N88-21039
X-ray diffraction study of a thin GaAs film on Si(100)
[DE88-005290] 13 p1847 N88-21055
Vapor phase deposition and growth of polyimide films on copper
[AD-A189969] 15 p2044 N88-22178
Laser evaporation studies
[AD-A189815] 15 p2071 N88-22346
Processing defects and strength of alumina substrates
[W-10/87] 15 p2087 N88-22441
High-efficiency thin-film silicon-on-GaP solar cell for improved radiation resistance
[AD-A190268] 15 p2091 N88-22460
RF properties of superconducting Pb electroplated onto Cu
[DE88-005918] 15 p2139 N88-22765
A model for nitrogen atom recombination on a silicon dioxide surface
[AD-A189843] 15 p2142 N88-22784
Equilibrium stability of strained epitaxial layers on a rigid substrate
[INPE-4254-PRE/1127] 15 p2145 N88-22804
Synthesis and characterization of high-T(sub c) screen-printed Y-Ba-Cu-O films on alumina
[NASA-TM-100860] 15 p2146 N88-22805
Surface enhanced Raman scattering applied to surface chemical kinetics
[AD-A191275] 16 p2176 N88-22969
Monolithic integration on a GaAs substrate of a quarter ring laser and an optical guide coupled by an evanescent wave
[ETN-88-92308] 17 p2344 N88-23969
On the use of convergent beam electron diffraction for identification of antiphase boundaries in GaAs grown on Si
[DE88-008220] 18 p2585 N88-25362
JPRS report: Science and technology. Japan
[JPRS-JST-88-005] 19 p2633 N88-25619
Ceramic substrates for semiconductor applications reported: AIN substrates 19 p2633 N88-25621
AIN substrate applications 19 p2634 N88-25622
Plasma deposition: Investigations on a new approach
[ETN-88-92619] 20 p2861 N88-26992
MBE growth of HgTe/CdTe superlattices on Si(100) substrates 20 p2869 N88-27033
Preparation of high-T(sub)c Y1Ba2Cu3O(sub 7-Delta) superconducting thin films by MBE (Molecular-Beam-Epitaxy) techniques
[DE88-009999] 20 p2877 N88-27082
Improved adhesion for SiO2 particles in silica substrates using helium-ion irradiation
[DE88-008915] 21 p2920 N88-27332
Amorphous silicon solar cells using a metal substrate
[PB88-131941] 21 p2968 N88-27628
Specular steel surfaces for solar mirror substrates
[DE88-001153] 21 p2968 N88-27630
Chemistry of adhesion at the polyimide-metal interface
[AD-A194647] 22 p3058 N88-28143
Low temperature film growth of the oxides of zinc, aluminum and vanadium (and related systems, oxides of gold and germanium, nitrides of aluminum and tungsten) by reactive sputter deposition
[AD-A193497] 23 p3191 N88-28986
Planarization of metal substrates for solar mirrors
[DE88-011492] 23 p3229 N88-29214
Evaluation of organic coating deterioration and substrate corrosion in seawater using electrochemical impedance measurements 24 p3355 N88-29976
Ion exchange processes for fabrication of integrated optical waveguide structures into glass substrates
[VTT-46] 24 p3429 N88-30405

SUBSTRUCTURES
Mechanical strength and niobium and niobium-base alloys substructures
[DE87-703692] 04 p0415 N88-12577
Substructure discovery in executed action sequences
[AD-A186446] 08 p1069 N88-16462
Finite element substructuring methods for composite mechanics
[NASA-TM-100297] 10 p1296 N88-17745
Influence of strain rate on the substructure evolution and yield behavior of Ti-6Al-4V
[DE88-006457] 19 p2616 N88-25520

SUBTROPICAL REGIONS
U TEMPERATE REGIONS
U TROPICAL REGIONS

SUCTION
Investigation of viscous/inviscid interaction in transonic flow over airfoils with suction 06 p0664 N88-14074
Laminar flow control leading edge glove flight test article development
[NASA-CR-172137] 07 p0815 N88-14960
Control of laminar flow around of the wing in free-air conditions
[AD-A187479] 15 p2013 N88-22004

Flow quality of NAL two-dimensional transonic wind tunnel. Part 1: Mach number distributions, flow angularities and preliminary study of side wall boundary layer suction
[NASA-TT-20209] 16 p2165 N88-22911

Operational considerations for laminar flow aircraft
17 p2298 N88-23748

Investigation of viscous/inviscid interaction in transonic flow over airfoils with suction
[NASA-CR-183112] 21 p2945 N88-27490

Method for maintaining precise suction strip porosities
[NASA-CASE-LAR-13638-1] 23 p3201 N88-29051

Experimental and numerical investigation of the effect of distributed suction on oblique shock wave/turbulent boundary layer interaction
[NASA-TM-101334] 24 p3372 N88-30084

SUD AVIATION AIRCRAFT
NT CONCORDE AIRCRAFT

SUDDEN IONOSPHERIC DISTURBANCES

Solar-geophysical data number 513, May 1987. Part 1: (Prompt reports). Data for April, March 1987 and late data
[PB87-204939] 01 p0119 N88-10760

Solar-geophysical data number 515, July 1987. Part 1: (Prompt reports). Data for June 1987, May 1987 and late data
[PB87-233177] 06 p0805 N88-14912

Solar-geophysical data number 517, September 1987. Part 1: (Prompt reports). Data for August, July 1987 and late data
[PB88-126426] 10 p1430 N88-18544

Solar-geophysical data number 520, December 1987. Part 1: (Prompt reports). Data for November 1987, October 1987 and late data
[PB88-164199] 16 p2290 N88-23712

Solar-geophysical data number 521, January 1988. Part 1: (Prompt reports). Data for December 1987, November 1987 and late data
[PB88-179213] 19 p2743 N88-26284

SUDDEN STORM COMMENCEMENTS

A compilation of Sudden Storm Commencements (SSCs), associated interplanetary disturbances, and cosmic ray variations
[IFSI-86-11] 06 p0807 N88-14923

A possible role for ionospheric ions in triggering a geomagnetic substorm onset 08 p1096 N88-16594

National Severe Storms Laboratory, fiscal year 1987
[PB88-140108] 12 p1647 N88-19863

SUGAR CANE

Report on phase 1 of the project estimate development of a model for yield estimation of sugar cane based on LANDSAT and agromet data
[INPE-4466-RPE/560] 12 p1638 N88-19807

CANASATE: Sugar cane mapping by satellite
17 p2358 N88-24046

Spectral behavior of crops through analysis of LANDSAT-TM data 17 p2358 N88-24047

Evaluation of TM false color composites for crop discrimination 17 p2367 N88-24096

Application of interactive graphic system (CAD/CAM) in the determination of process evolution in land use in the Ribeirao Preto municipality 19 p2684 N88-25956

SUGARS
NT GLUCOSE

SUGGESTION

Hypnosis: Possible applications for cosmonauts
12 p1665 N88-19984

SUITS
NT EXTRAVEHICULAR MOBILITY UNITS
NT PRESSURE SUITS
NT SPACE SUITS

SULFATES

Copper electroforming from acid sulfate baths: Preliminary studies
[INPE-4375-RPE/554] 08 p0969 N88-15864

Meteorological aspects of wet deposition in Southern Finland
[FMI-3] 19 p2693 N88-26007

Kinetics of thermochemical gas-solid reactions important in the Venus sulfur cycle
[NASA-CR-182963] 19 p2742 N88-26280

SULFIDATION

Oxidation/sulfidation of materials in an SO3/SO2/O2 thermochemical-transport, distributed-receiver, solar-energy system
[DE88-005875] 13 p1795 N88-20739

SULFIDES
NT BISMUTH SULFIDES
NT CADMIUM SULFIDES
NT COPPER SULFIDES
NT DISULFIDES
NT HYDROGEN SULFIDE
NT LEAD SULFIDES
NT MOLYBDENUM DISULFIDES
NT MOLYBDENUM SULFIDES
NT POLYSULFIDES
NT PYRITES
NT ZINC SULFIDES

Lithium/iron sulfide batteries: Development and demonstration
[DE87-014222] 01 p0042 N88-10265

The effect of non-metallic inclusions on fatigue and fatigue thresholds of 25Mn-5Cr-1Ni steel
06 p0718 N88-14410

Monolayer films prepared by the spontaneous self-assembly of symmetrical and unsymmetrical dialkyl sulfides from solution onto gold substrates: Structure, properties, and reactivity of constituent functional groups
[AD-A186717] 09 p1137 N88-16814

The crystallization of tough thermoplastic resins in the presence of carbon fibers
[NASA-CR-182984] 20 p2776 N88-26464

Weathering of sulfides on Mars
23 p3301 N88-29662

SULFONATES

Thermogravimetric analysis of polymeric materials for an intermediate temperature solid electrolyte
[DE88-004854] 10 p1306 N88-17809

SULFONES

Reinforcing of thermoplastic polycarbonate and polysulfone with carbon fibers: Production and characteristics of UD-compound objects
[NASA-TT-20158] 13 p1735 N88-20374

SULFONIC ACID

Formation of sediments in fuels containing added sulphonic acids --- marine diesel fuels
[RAE-TM-NAV-ENG-1163] 09 p1150 N88-16891

Molecular composites processing and properties, 1
[AD-A194113] 23 p3189 N88-28974

SULFUR

The effect of sulfur and zirconium Co-doping on the oxidation of NiCrAl
[NASA-TM-100209] 02 p0150 N88-10940

Modeling the effect of sulfur on the threshold environmental cracking rate of steels in high temperature water 05 p0604 N88-13703

Sulfur-induced ductility-dip cracking in weld metal of low-carbon steel
[PB87-143814] 07 p0833 N88-15051

Seasonal cycling of sulfur and iron in porewaters of a Delaware salt marsh
[NASA-CR-182385] 07 p0876 N88-15311

Acoustic emission-microstructural relations in ferritic steels. Part 3: The effect of inclusion content
[AERE-R-12041] 10 p1341 N88-18015

Study of adherent oxide scales
[AD-A187368] 11 p1456 N88-18680

Preparation and characterization of Cu2Zn1-xMnxGeS4
[AD-A188113] 11 p1556 N88-19315

The Io sulfur torus in 1981
[NASA-TM-101139] 18 p2595 N88-25419

Hydrogen embrittlement of iron-nickel alloys
[AD-A195909] 24 p3353 N88-29958

SULFUR COMPOUNDS
NT BISMUTH SULFIDES
NT CADMIUM SULFIDES
NT COPPER SULFIDES
NT DISULFIDES
NT HYDROGEN SULFIDE
NT LEAD SULFIDES
NT MOLYBDENUM DISULFIDES
NT MOLYBDENUM SULFIDES
NT POLYSULFIDES
NT PYRITES
NT SULFATES
NT SULFIDES
NT SULFONATES
NT SULFONES
NT SULFUR DIOXIDES
NT SULFUR FLUORIDES
NT SULFURIC ACID
NT THIOLS
NT ZINC SULFIDES

Investigations of the influence of chemical reactions of the vertical flow of gaseous and particulate compounds
08 p1017 N88-16165

Electronic and ionic transport in polymers
[AD-A191642] 18 p2490 N88-24772

Uses of lunar sulfur
[DE88-009119] 21 p3031 N88-27990

SULFUR DIOXIDES

Volcanic eruption detection with TOMS
05 p0618 N88-13793

Analysis of SO2 signals in SBUV/TOMS data
05 p0618 N88-13794

TOMS and the NOAA/FAA volcano support plan
05 p0618 N88-13796

Use of satellite data in volcano monitoring
05 p0618 N88-13797

Crystalline sulfur dioxide: Crystal field splittings, absolute band intensities and complex refractive indices derived from infrared spectra
[NASA-CR-182502] 09 p1258 N88-17547

The role of repowering in America's power generation future
[DOE/FE-0096] 10 p1351 N88-18076

The role of analytical chemistry in assessing atmospheric effects of combustion
[DE88-003909] 10 p1352 N88-18082

Assessment of crop loss from air pollutants: Meteorology-atmospheric chemistry and long range transport
[PB88-146857] 15 p2089 N88-22448

A theoretical model of the washout of trace gases by raindrops in the atmosphere 17 p2375 N88-24125

Kinetics of thermochemical gas-solid reactions important in the Venus sulfur cycle
[NASA-CR-182963] 19 p2742 N88-26280

Episodic vs. epochal release of SO2 on Mars
23 p3305 N88-29688

SULFUR FLUORIDES

Optical determination of the virial coefficients of the gases C2H4, C2H6 and SF6
[ETN-87-90610] 03 p0282 N88-11778

Interaction of intense electromagnetic fields with SF/sub 6/ molecules and clusters in supersonic expansion
[DE88-700310] 07 p0846 N88-15132

Kinetic toxic aspect of potential use of sulfur hexafluoride in closed environments 10 p1362 N88-18142

Pseudo-stationary oblique-shock-wave reflections in low gamma gases: Isobutane and sulphur hexafluoride
[UTIAS-TN-267] 13 p1768 N88-20576

SULFUR OXIDES
NT SULFUR DIOXIDES

SULFURIC ACID

The corrosion of iron rotating hemispheres in 1 M sulfuric acid: An electrochemical impedance study
[DE87-014679] 02 p0148 N88-10925

A modified sulphuric acid anodising process used as a pretreatment for the adhesive bonding of aluminum alloys
[ARE-TM(UMM)-87410] 16 p2177 N88-22974

The rate of volcanism on Venus
[NASA-CR-183039] 19 p2742 N88-26281

Kinetic of martensitic transformations induced by hydrogen in the austenite
[DE88-701623] 23 p3194 N88-29007

SUMMARIES
NT ABSTRACTS

Summaries of physical research in the geosciences
[DE88-000833] 04 p0468 N88-12696

University research initiative research program summaries
[AD-A184876] 05 p0658 N88-14035

Summary of comparison between experimental and analytical (including empirical) results for initiation of crack growth for surface cracks
[DE88-001604] 06 p0721 N88-14433

Summaries of FY 1987 engineering research
[DE88-002572] 07 p0840 N88-15096

Summary of the report of the Senior Committee on Environmental, Safety and Economic Aspects of Magnetic Fusion Energy
[DE88-003270] 07 p0937 N88-15692

A summary of the Naval Postgraduate School research program
[AD-A186362] 07 p0942 N88-15727

Annual data summary and climatological evaluation CERC (Coastal Engineering Research Center) field research facility, 1985. Volume 1. Main text and appendixes A and B
[AD-A186442] 08 p1039 N88-16289

Aircraft accident/incident summary reports, Des Moines, Iowa, November 25, 1985; Chicago, Illinois, August 10, 1986
[PB88-910411] 09 p1115 N88-16685

Summaries of FY86 research in the Applied Plasma Physics Fusion Theory Program
[DE88-004242] 11 p1554 N88-19298

Whither many-body theory. A summary of the Oulu Conference
[DE88-003095] 11 p1563 N88-19358

Revised Uniform Summary of Surface Weather Observations, Loring AFB, Maine, Parts A - F
[AD-A188201] 14 p1947 N88-21610

Summary and conclusions on electrooptical streak camera project
[DE88-006616] 15 p2089 N88-22334

Narrative domain implementation
[AD-A192265] 20 p2843 N88-26868

SUMMER

The role of low-level cooling in a conceptual model of the Australian summertime cool change: Implications for very-short-range forecasting 02 p0204 N88-11275

Physical properties of summer sea ice in the Fram Strait, June-July 1984
[AD-A186937] 09 p1194 N88-17156
Report on project WIND: Preliminary experiments w ith the UK Meteorological Office mesoscale model, September 1987
[AD-A191621] 18 p2544 N88-25099
MIZPAC (marginal ice zone Pacific) 84-86 CTD (Conductivity, Temperature, Depth) data report
[AD-A192478] 21 p2976 N88-27679
Factors influencing summer temperatures and precipitation in the southwest 22 p3124 N88-28565

SUMS
Weak convergence of sums of moving averages in the alpha-stable domain of attraction
[AD-A186430] 07 p0912 N88-15529
Fast serial input-serial output pipelined inner product units
[REPT-87-031] 11 p1530 N88-19142

SUN
Unified Sun and sky illumination for shadows under trees
[DE87-014232] 01 p0083 N88-10535
About the interest of solar interferometric observations 01 p0094 N88-10615
Solar interferometry with a 4-aperture nonredundant and stabilized network 01 p0097 N88-10639
The Sun and the solar activity 03 p0271 N88-11704
Fifth Cambridge Workshop on Cool Stars, Stellar Systems and the Sun 04 p0502 N88-13092
Calibration on the Sun for stellar magnetic fields 04 p0506 N88-13113
Variations of the vertical and horizontal velocities of the small-scale structures and the physical problems related to overshoot layers 04 p0507 N88-13115
The dynamics of solar magnetic flux tubes subjected to resonant foot point shaking 04 p0507 N88-13118
The appearance and disappearance of magnetic flux on the quiet sun
[AD-A185432] 05 p0661 N88-14055
Perturbations of the Sun's gravitational field due to solar oscillations
[DE88-002099] 07 p0946 N88-15751
Oscillations of solar models with internal element diffusion
[DE88-003156] 09 p1264 N88-17573
Solar microwave radiation maps measured at Metsaehovi Radio Research Station in 1978-1979
[PB88-127543] 13 p1857 N88-21108
Stable, heavy, neutral particles in the sun and in toponium decay 17 p2452 N88-24568
MHD bending waves in a current sheet
[NASA-TM-101149] 18 p2579 N88-25323

SUN SENSORS
U SOLAR SENSORS

SUNLIGHT
Sunlight supply and gas exchange systems in microalgal bioreactor 03 p0359 N88-12258
Influence of solar illumination conditions on TM/Landsat data
[INPE-4463-TDL/320] 12 p1638 N88-19806

SUNRISE
The lengthening and shortening of the day
[KNMI-TR-91] 05 p0628 N88-13839
Computing basic solar and lunar data from the Air Almanac
[AD-A190777] 16 p2290 N88-23710

SUNSET
The lengthening and shortening of the day
[KNMI-TR-91] 05 p0628 N88-13839
Computing basic solar and lunar data from the Air Almanac
[AD-A190777] 16 p2290 N88-23710

SUNSPOT CYCLE
Three-halves law in sunspot cycle shape
[NASA-CR-181520] 04 p0525 N88-13210
Development of high stability fiber optic spectrophotometric systems for study of solar/stellar magnetic activity
[AD-A189327] 13 p1852 N88-21088
Sunspot frequency and solar activity
[PUBL-17/87] 14 p2011 N88-21996

SUNSPOTS
The large Type 4 radio burst event of 24 April 1985 interpreted by dynamic spectral recordings and associated recordings 01 p0112 N88-10717
Quantification of the background signal to solar neutrino detection from cosmogenic activation of the atmosphere
[DE87-013830] 01 p0119 N88-10762
Magnetic field morphology in the upper layers 02 p0255 N88-11610
Theoretical modelling of the fine structures in sunspots 02 p0256 N88-11617
Large-scale horizontal flows from SOUP observations of solar granulation 02 p0256 N88-11621
Sunspot observations from the SOUP instrument on Spacelab 2 02 p0257 N88-11623
Variations of the semi-diurnal tidal wind in the meteor region with periods of about 27 and 13.5 days 06 p0734 N88-14516
Solar Dynamics and G-modes
[NASA-CR-180737] 06 p0805 N88-14911
Flares: Solar and stellar
[PB87-124962] 06 p0806 N88-14917
Ultraviolet rocket-spectra of a sunspot 08 p1032 N88-16257
Gasflows in the transition region above sunspot 08 p1095 N88-16586
Solar-geophysical data number 516, August 1987. Part 1: (Prompt reports). Data for July 1987, June 1987 and late data
[PB88-114368] 09 p1263 N88-17570
Spectral analysis of the Elatina varve series
[NASA-CR-183085] 24 p3402 N88-30260

SUPERALLOYS
U HEAT RESISTANT ALLOYS

SUPERCHARGERS
Fuel nitrogen conversion in a supercharged spark ignition engine
[DE88-003739] 08 p0974 N88-15893
Technology developments for a compound cycle engine 09 p1107 N88-16637
Servojet retrofit
[AD-A191075] 18 p2522 N88-24964
New super alloys used in turbochargers 19 p2634 N88-25628

SUPERCHARGING
U SUPERCHARGERS

SUPERCOMPUTERS
NT CRAY COMPUTERS
NBS (National Bureau of Standards) research reports (April 1987)
[PB87-210258] 01 p0018 N88-10111
NOSTRADAMUS programmable translator user's manual and programmer's manual
[DE87-013414] 01 p0083 N88-10533
Approximate polynomial preconditioning applied to biharmonic equations on vector supercomputers
[NASA-TM-100217] 01 p0087 N88-10563
An embedded multiprocessor computer for proof-of-principle testing of exploratory systems concepts
[DE87-012735] 02 p0218 N88-11372
Implementation of preconditioned s-step conjugate gradient methods on a multiprocessor system with memory hierarchy
[DE87-014401] 02 p0222 N88-11400
Report from the MPP Working Group to the NASA Associate Administrator for Space Science and Applications
[NASA-TM-87819] 02 p0223 N88-11402
Energy transformation in molecular electronic systems
[DE87-013916] 03 p0282 N88-11771
Numerical simulation system 04 p0404 N88-12511
Center for Supercomputing Research and Development (CEDAR)
[DE88-000807] 04 p0475 N88-12930
The SUPRENUM communications subroutine library for grid-oriented problems
[DE88-000137] 04 p0479 N88-12950
Programming techniques for high-speed processing of large scale numerical simulation on supercomputers 05 p0537 N88-13269
Vectorizing the FFTs on supercomputer SX system 05 p0537 N88-13270
Tridiagonal approximate factorization method: A preconditioning technique for solving nonsymmetric linear systems suitable to supercomputers 05 p0537 N88-13271
Supercomputing at Florida State University (FSU)
[DE87-013900] 05 p0654 N88-14009
Some performance comparisons for a fluid dynamics code
[PB88-113709] 07 p0852 N88-15175
Internal fluid mechanics research on supercomputers for aerospace propulsion systems
[NASA-TM-100289] 07 p0854 N88-15188
Monte Carlo photon transport on vector and parallel supercomputers
[DE88-002503] 07 p0905 N88-15486
Applicative parallelism: Potential and challenge
[DE87-011885] 08 p1068 N88-16459
Supercomputers for solving PDE (Partial Differential Equations) problems
[AD-A186583] 09 p1215 N88-17283
A performance comparison of the Cray-2 and the Cray X-MP
[NASA-CR-177461] 09 p1216 N88-17288
Interdisciplinary research in applied mathematics
[AD-A186793] 09 p1226 N88-17344
Emerging supercomputer architectures
[DE88-003539] 10 p1384 N88-18262
Features of a TeraFlop supercomputer
[DE88-003540] 10 p1384 N88-18263
Supercomputer performance: The theory, practice, and results
[DE88-004697] 10 p1384 N88-18266
Using program structure to achieve prefetching for cache memories
[DE88-003599] 10 p1387 N88-18282
Dynamic processor self-scheduling for general parallel nested loops
[DE88-003572] 10 p1393 N88-18311
Performance and evaluation at the Center for Supercomputing Research and Development
[DE88-003563] 10 p1417 N88-18456
Center for Supercomputing Research and Development
[DE88-003564] 10 p1418 N88-18466
The Livermore FORTRAN Kernels: A computer test of the numerical performance range — benchmark tests
[UCRL-53745] 11 p1531 N88-19144
Data flow graph optimization in IF1
[DE88-004396] 11 p1532 N88-19151
A report on the study of algorithms to enhance vector computer performance for the discretized one-dimensional time-dependent heat conduction equation: EPIC research, phase 1
[DE88-005642] 13 p1820 N88-20880
Activities report of the Toulouse Research Center
[ETN-88-91988] 13 p1850 N88-21077
Supercomputer-aided generalized mixer analysis and optimization
[FUB-15-1986] 14 p1957 N88-21668
Supercomputer environment
[AD-A190633] 15 p2107 N88-22551
Implementation of a distributed adaptive routing algorithm on the Intel iPSC (Intel Personal Super-Computer)
[AD-A189849] 15 p2109 N88-22567
The good, the bad and the ugly: Comparing high-speed computer systems
[DE88-007498] 16 p2245 N88-23412
Supercomputer programming environments
[AD-A190887] 16 p2251 N88-23452
Effective use of shared memory multiprocessors
[DE88-007019] 18 p2560 N88-25195
Computer science research, 1987: Computation Directorate
[DE88-008637] 20 p2834 N88-26812
The performance of the NEC SX-2 and Cray X-MP supercomputers
[DE88-009177] 20 p2835 N88-26813
Federal Council on Science, Engineering and Technology: Committee on Computer Research and Applications, Subcommittee on Science and Engineering Computing: The US Supercomputer Industry
[DE88-011262] 21 p2994 N88-27756
Supercomputer for parallel data analysis
[DE88-702148] 21 p2995 N88-27759
Hypervelocity impact analysis with supercomputers
[DE88-008907] 21 p3001 N88-27797
Notes on operating system requirements for the next millennium
[DE88-010712] 21 p3002 N88-27805
Microsupercomputers: Design and implementation
[AD-A194712] 22 p3*35 N88-28638
Supermap for Cray FORTRAN: A user's guide
[NASA-CR-177410] 24 p3412 N88-30308

SUPERCONDUCTING MAGNETS
Modeling of proximity coupling between superconducting filaments in superconducting dipole magnets
[DE87-014684] 03 p0382 N88-12403
Design concepts for the ASTROMAG cryogenic system
[NASA-CR-181505] 04 p0497 N88-13060
Completely magnetically contained electrothermal thrusters
[AD-A185674] 06 p0674 N88-14129
Astromag: A particle spectrometer for the Space Station
[PREPRINT-557] 06 p0707 N88-14336
The TITAN magnet configuration
[DE88-001826] 06 p0782 N88-14800
Study on the model of a toroidal magnet for a tokamak with a strong field
[DE88-700346] 07 p0935 N88-15681
The superconducting gravimeter: Application, calibration, and further development
[SER-C-329] 09 p1167 N88-16998
Development activities for a 21-T superconducting magnet and cryostat
[DE88-004370] 11 p1558 N88-19327

Advances in applied superconductivity: A preliminary evaluation of goals and impacts
[DE88-006441] 14 p1986 N88-21844
Superconducting magnet technique for ASTROMAG on the space station
[DE88-004560] 15 p2025 N88-22083
Fluids, gels and glasses under extreme conditions of pressure and temperature
[AD-A190655] 15 p2035 N88-22125
Magnet strength fluctuations in the SSC (Superconducting Super Collider) lattice. Part 2: Frequency modulation
[DE88-006491] 15 p2141 N88-22774
The Department of Defense Superconductivity Research and Development (DSRD) options. A study of possible directions for exploitation of superconductivity in military applications
[AD-A189747] 15 p2142 N88-22780
SSC (Superconducting Super Collider) magnet technology
[DE88-007386] 19 p2733 N88-26230
Magnetic heat pumps
[DE88-012058] 21 p2969 N88-27639
High-T(sub c) superconductor and its use in superconducting magnets
[DE88-008403] 23 p3289 N88-29581

SUPERCONDUCTING POWER TRANSMISSION
The status of R and D for superconducting power transmission systems
[DE88-003499] 11 p1561 N88-19346
Conductor loss in superconducting power transmission cables
[DE88-011414] 23 p3290 N88-29586

SUPERCONDUCTING QUANTUM INTERFEROMETERS
U SQUID (DETECTORS)

SUPERCONDUCTING SUPER COLLIDER
Characteristics of multimuon events from fourth generation quarks at the SSC (Superconducting Super Collider)
[DE88-002954] 09 p1257 N88-17535
Advanced nonlinear theory: Long-term stability at the SSC
[CEBAF-PR-87-027] 11 p1546 N88-19246
A practical guide to modern high energy particle accelerators
[DE88-004035] 11 p1548 N88-19260
The lattice nonlinearities and the long term stability of the SSC
[CEBAF-PR-87-009] 12 p1690 N88-20108
Optics of the CEBAF CW superconducting accelerator
[CEBAF-PR-87-012] 12 p1690 N88-20110
Physics at large transverse momenta
[DE88-005758] 13 p1836 N88-20986
Magnet strength fluctuations in the SSC (Superconducting Super Collider) lattice. Part 2: Frequency modulation
[DE88-006491] 15 p2141 N88-22774
SSC (Superconducting Super Collider) magnet technology
[DE88-007386] 19 p2733 N88-26230

SUPERCONDUCTIVITY
NT KONDO EFFECT
Superconducting properties of metallic superlattices
[DE87-012725] 01 p0023 N88-10146
Design and testing of electrical insulation for superconducting coils
[DE87-012256] 01 p0039 N88-10246
Some electronic factors influencing superconductivity in some rare-Earth-like elements and the beginning of rare-Earth series
[DE87-702582] 01 p0102 N88-10668
Simple instrumentation for testing of ceramic superconductors
[DE87-013849] 01 p0103 N88-10672
Grain boundary effects in processing high T/sub c/ superconductors
[DE87-009297] 01 p0103 N88-10673
Optimization of SIS mixer elements
[NASA-CR-180710] 01 p0104 N88-10680
Progress toward a superconducting opening switch
[DE87-014170] 02 p0167 N88-11051
Theory of the one- and two-dimensional electron gas
[DE87-012864] 02 p0244 N88-11540
High gradient superconducting quadrupoles
[DE87-013590] 02 p0244 N88-11541
Electrical properties of high T/sub c/ superconductors under high pressures
[DE87-012818] 02 p0245 N88-11546
Superconductivity of pseudobinary compounds Al5 (V-Cr)3Si, (V-MO)3Si, Mo3(Si-Re), bombarded with fast neutrons 03 p0285 N88-11792
High temperature superconductors
03 p0297 N88-11869
A role for national laboratories in enhancing economic competitiveness. The example of high-temperature superconductors: CNSS papers, No. 1
[DE87-013633] 03 p0379 N88-12386
Superconductivity as a synchronous spatial alternation of valence bonds
[AD-A184208] 03 p0382 N88-12405
Experimental perspectives on heavy electron metals
[DE87-014766] 04 p0416 N88-12583
Valence bond theory and superconductivity
[AD-A184274] 04 p0496 N88-13052
The chemical bond and superconductivity
[AD-A184275] 04 p0496 N88-13053
Non-lattice matched metallic superlattices
[DE87-011512] 04 p0497 N88-13062
Pressure induced phase transitions, superconductivity of phosphorus described 06 p0675 N88-14134
Superconducting material development
06 p0688 N88-14217
The use of alloy 117 as a liquid metal current collector
[AD-A185740] 06 p0698 N88-14281
Studies of tunneling in metals under high pressure
06 p0775 N88-14757
High temperature stability of superconducting YBa2Cu3O subx as characterized by X-ray diffraction
[DE88-001856] 06 p0787 N88-14824
Effect of high pressure oxygen loading on the superconductivity of La2CuO4
[DE88-002108] 06 p0787 N88-14827
Atomic-level studies of superconducting YBa2Cu3O sub 7-x
[DE88-002522] 06 p0788 N88-14831
L2,3 XANES of the high T sub c superconductor YBa2Cu3O7 with variable oxygen content
[NOTA-INTERNA-888] 06 p0788 N88-14837
Accelerators and Superconductivity: A Marriage of Convenience. Second John Adams Memorial Lecture
[DE88-700005] 07 p0931 N88-15656
Low field characterization of YBa2Cu3O sub 7-delta single crystals
[DE88-002895] 07 p0938 N88-15700
On the coexistence of phonon and non-phonon (plasmon) mechanisms in new high T/sub c/ superconductors
[DE88-003188] 07 p0938 N88-15703
Metal-oxide superconductor BaPbsub1-xBisubxO3: Unusual properties and new applications
08 p1077 N88-16494
Magnetic investigations of superconductive, polycrystalline (RE)1Ba2Cu3O(7-x) compounds (RE = Y, Gd, Ho, Dy)
[DE88-002537] 08 p1090 N88-16558
Experimental aspects of high-T/sub c/ superconductors
[DE88-003019] 08 p1090 N88-16564
Microstructure modifications of micron thick NbN films to improve J/sub c/ and H/sub c2/
[DE88-003078] 08 p1091 N88-16567
JPRS report: Science and technology. USSR: Physics and mathematics
[JPRS-UPM-87-009] 09 p1233 N88-17395
Phenomenological model of superconductivity of heavy fermions in U(sub 1-x)ThsubxBesub13
09 p1238 N88-17423
Properties of superconducting tunnel structures in microwave radiation field 09 p1239 N88-17424
Superconductivity and crystal structure of high-pressure phases in V-Ru-H system 09 p1239 N88-17426
Bulk superconductivity in La2CuO4
[DE88-002509] 09 p1254 N88-17516
Nonequilibrium superconductivity for particle detectors
[DE88-002876] 09 p1257 N88-17539
Superconductivity in La/sub 1.85-x/Nd/sub x/Sr/sub .15/CuO
[DE88-003014] 09 p1258 N88-17540
High temperature superconductivity research at Argonne National Laboratory
[DE88-003055] 09 p1258 N88-17541
Copper oxidation states, vacancy ordering and their effect on high temperature superconductivity
[DE88-003079] 09 p1258 N88-17542
Electrochemical growth of linear conducting crystals in microgravity 10 p1287 N88-17698
Spin disorder resistivity and bare Curie temperature in the ferromagnetic superconductor ErRh4B4
[DE88-003016] 10 p1415 N88-18445
Normal and superconducting state properties of La2-xSr/sub x/CuO4
[DE88-003013] 10 p1416 N88-18450
Superconducting and magnetic properties of Fe-doped oxide superconductors
[DE88-003024] 10 p1416 N88-18451
The physics of metallic superlattices: An experimental point of view
[DE88-003080] 10 p1416 N88-18452
Electronic structure, charge transfer excitations and high temperature superconductivity
[DE88-003096] 10 p1416 N88-18453
Positron-annihilation 2D-ACAR studies of disordered and defected alloys
[DE88-003118] 10 p1416 N88-18454
Performance and evaluation at the Center for Supercomputing Research and Development
[DE88-003563] 10 p1417 N88-18456
Comparative evaluation of resistive and inductive techniques for measuring temperature of superconducting transition
[DE88-700603] 10 p1417 N88-18457
The structure and properties of twin boundaries in superconducting YBa2Cu3O7
[DE88-003864] 10 p1418 N88-18468
Freestanding films of YBa2Cu3O/sub 6.9/
[DE88-003995] 10 p1419 N88-18471
Grain boundaries, planar defects and superconducting properties of YBa2Cu3O7
[DE88-003477] 10 p1419 N88-18475
Superconductivity and phase stability in the heavy rare earth quaternary compounds RBa2Cu3O7 (R = Ho, Er, Tm, Yb, Lu)
[DE88-003478] 10 p1419 N88-18476
Superconducting properties and structural characterization of high T/sub c/ oxides
[DE88-003479] 10 p1420 N88-18477
Penetration depth measurements of YBa2Cu3O/sub 7-delta/ at 4 MHz
[DE88-003493] 10 p1420 N88-18478
The electronic structure of YBa2Cu3O/sub 7-delta/ above and below T/sub c/
[DE88-003495] 10 p1420 N88-18479
Simulation and processing of high resolution images of defects and interfaces in superconducting YBa2Cu3O7
[DE88-003856] 10 p1420 N88-18480
Innovative arrangements for industry/DOE laboratory collaboration in high temperature superconductivity
[DE88-004320] 10 p1420 N88-18482
Superconductivity of thin film intermetallic compounds
[AD-A187563] 10 p1421 N88-18489
The injector for the CEBAF CW superconducting linac
[CEBAF-PR-87-011] 11 p1546 N88-19241
RF steering in the CEBAF CW superconducting linac
[CEBAF-PR-87-013] 11 p1547 N88-19251
Single-crystal structural study of La2Cu/sub 0.95/Li/sub 0.05/O4
[DE88-003482] 11 p1554 N88-19302
Composite ceramic superconducting filaments for superconducting cable
[AD-A187833] 11 p1556 N88-19312
An electron spectroscopic investigation of high-temperature superconducting oxides
[DE88-003807] 11 p1558 N88-19325
Processing relationships in YBa2Cu3O(7-x) superconductors
[DE88-005137] 11 p1559 N88-19330
Research briefing on high-temperature superconductivity
[PB88-133004] 11 p1561 N88-19344
Mass transport and chemical demixing of Y-Ba-Cu-O compounds during sintering in temperature gradients
[DE88-004887] 12 p1696 N88-20151
An overview of recent developments in high-temperature superconductivity
[DE88-005477] 12 p1697 N88-20155
Progress in diagnostic techniques for SC cavities
[CEBAF-PR-88-003] 13 p1772 N88-20600
Large momentum pairing in one-dimensional systems
[AD-A189228] 13 p1835 N88-20981
Theoretical studies on the electronic structure and properties of complex ceramic crystals and glasses
[DE88-005837] 13 p1845 N88-21049
Competing interactions in metallic superlattices
[DE88-005344] 13 p1847 N88-21057
Superconducting superlattice structures
[DE88-005346] 13 p1847 N88-21058
Design, optimization and construction of a dc-SQUID with complete flux transformer circuits
[PB88-160742] 14 p1907 N88-21399
Superconducting transition temperature of Cu-Nb microcomposites 14 p1973 N88-21775
Thermal model describing development of normal region in superconductor film carrying electric current
14 p1973 N88-21776
Giant Josephson signal in wide superconducting films
14 p1973 N88-21777
Properties of superconductors with strong electron-phonon interaction 14 p1974 N88-21779
Advances in applied superconductivity: A preliminary evaluation of goals and impacts
[DE88-006441] 14 p1986 N88-21844
Magnetic impurities in superconductors
[DE88-006917] 14 p1986 N88-21846

Temperature-dependent conductivity of oxygen-depleted YBCO ceramics
[AD-A190340] 15 p2044 N88-22182
Developments in ceramic superconducting materials
15 p2052 N88-22229
RF properties of superconducting Pb electroplated onto Cu
[DE88-005918] 15 p2139 N88-22765
Superconductivity and the tailoring of lattice parameters of the compound YBa2Cu3O(sub x)
[DE88-005904] 15 p2140 N88-22769
Superconductivity in power engineering
[DE88-701414] 15 p2141 N88-22776
The Department of Defense Superconductivity Research and Development (DSRD) options. A study of possible directions for exploitation of superconductivity in military applications
[AD-A189747] 15 p2142 N88-22780
Thin superconducting film characterization by surface acoustic waves
[AD-A190417] 15 p2143 N88-22791
Magnetic anomalies in the rare earth oxide superconductors GdBa2Cu3O(7-x) and YbBa2Cu3O(7-x)
[AD-A190713] 15 p2144 N88-22793
Status of RF superconductivity at Argonne National Laboratory
[DE88-005913] 15 p2144 N88-22796
High-T(sub c) superconducting wire fabrication and testing
[DE88-005989] 15 p2144 N88-22798
High temperature superconductors in the La(sub 1+x)Ba(sub 2-x)Cu O(sub y system
[DE88-006367] 15 p2145 N88-22802
Synthesis and characterization of high-T(sub c) screen-printed Y-Ba-Cu-O films on alumina
[NASA-TM-100860] 15 p2146 N88-22805
The superconducting phase shifter in the development of a terahertz imaging radar system
[AD-A190666] 16 p2188 N88-23046
High temperature superconductivity
[AD-A190259] 16 p2281 N88-23655
Electrothermal instability in superconducting resonators
[DE88-701684] 16 p2282 N88-23664
Effects of 67.5 MeV electron irradiation on Y-Ba-Cu-O and Gd-Ba-Cu-O high-temperature superconductors
[AD-A191271] 16 p2283 N88-23669
Materials science with muon spin rotation
[NASA-CR-182891] 17 p2396 N88-24242
Systematic variation of magnetic-field penetration depth in high-T(c) superconductors studied by muon spin relaxation
17 p2396 N88-24243
Coexisting static magnetic ordering and superconductivity in CeCu2.1Si2 found by muon spin relaxation
17 p2396 N88-24245
Superconducting thin film vertex detector for SSC (Superconducting Super Collider) applications
[DE88-005951] 17 p2445 N88-24535
Method of producing high T(subc) superconducting NBN films
[NASA-CASE-NPO-16681-1-CU]
17 p2446 N88-24543
Crystalline metal-semiconductor superlattices
[DE88-007063] 18 p2581 N88-25332
A role for high frequency superconducting devices in free space power transmission systems
[NASA-TM-100971] 19 p2662 N88-25830
Superconductive analogue of spin glasses
[DE88-702059] 19 p2733 N88-26233
Effect of a weak magnetic field on high temperature superconductivity in Y-Ba-Cu-O ceramics
[DE88-702192] 19 p2733 N88-26235
Magnetization studies of multifilamentary Nb3Sn wires
[DE88-009103] 19 p2735 N88-26243
All-electron local density theory of electronic structure and superconductivity in YBa2Cu3O7 and YBa2Cu3O6
[DE88-009944] 19 p2735 N88-26246
Structural and magnetic properties of Fe impurities in YBa2Cu3O(sub 7-delta)
[DE88-009961] 19 p2735 N88-26247
Application of superconducting technology to earth-to-orbit electromagnetic launch systems
[NASA-TM-101134] 20 p2763 N88-26385
Application of superconducting technology to earth-to-orbit electromagnetic launch systems
[DE88-010022] 20 p2763 N88-26386
Superconducting rf and beam-cavity interactions
[DE88-008598] 20 p2852 N88-26936
Superconductivity of Cr/V superlattices
20 p2874 N88-27057
To the twinning plane superconductivity theory
[DE88-702195] 20 p2874 N88-27058
Effects of grain boundary composition on properties of YBa2Cu3O/sub 7-x/
[DE88-007679] 20 p2875 N88-27064
Superconductivity of heavy-electron uranium compounds
[DE88-007901] 20 p2875 N88-27065
The superconducting transition in oxygen deficient YBa2Cu3O(sub 7-Delta)
[DE88-009957] 20 p2877 N88-27079
Anisotropy of the lower critical field in YBa2Cu3O(sub 7-Delta)
[DE88-009971] 20 p2877 N88-27081
Preparation of high-T(sub)c Y1Ba2Cu3O(sub 7-Delta) superconducting thin films by MBE (Molecular-Beam-Epitaxy) techniques
[DE88-009999] 20 p2877 N88-27082
Oxygen vacancy ordering and superconductivity in YBa2Cu3O(sub 7-x)
[DE88-010005] 20 p2877 N88-27083
Superconducting electronic film structures
[AD-A192907] 20 p2879 N88-27091
On the chemistry of superconductivity
[DE88-010714] 20 p2880 N88-27096
Compilation of NRL publications on high temperature superconductivity
[AD-A189137] 21 p3019 N88-27921
Effect of high-amplitude high-frequency current on non-isothermal equilibrium of NS-boundary in inhomogeneous superconductor
[DE88-701682] 21 p3019 N88-27922
Anharmonic model for high-Tc superconductors
[DE88-702196] 21 p3020 N88-27924
High-temperature superconductivity: An overview
[DE88-702051] 21 p3020 N88-27925
Coupled even-parity superconducting states: Square lattice
[AD-A193432] 21 p3022 N88-27938
Properties of new low dimensional materials and mechanisms of high T(sub c) superconductivity
[DE88-012026] 21 p3024 N88-27951
Superconducting properties of LaBa2Cu3O(sub x) and YBa2Cu3O(sub y)
[DE88-012038] 21 p3024 N88-27952
X-ray studies of strain, interface and impurities in semiconductors
[DE88-012460] 21 p3025 N88-27954
High Tc superconducting HoBa2Cu(sub 1-x)Fe(sub x)3O(sub 7-y)
[DE88-008909] 22 p3155 N88-28768
Effect of neutron irradiation on critical magnetization current in single crystal YBa2Cu3O(sub 7-delta)
[DE88-009970] 22 p3156 N88-28775
Gravitation electromagnetic theory
22 p3158 N88-28790
SQUID (superconducting quantum interference device) arrays for simultaneous magnetic measurements: Calibration and source localization performance
[AD-A193815] 23 p3216 N88-29143
CryoSQUID: A SQUID-based magnetic field sensor
[AD-A194237] 23 p3239 N88-29275
Effects of metal substitutions (Fe and Ga) in YBa2Cu3O7 on its superconducting properties and microstructures
[DE88-007393] 23 p3287 N88-29572
Properties of strong coupled superconductors
[DE88-702050] 23 p3287 N88-29574
Possible mechanism for high-temperature superconductivity in the BaSr-La(Y)-CuO systems
[DE88-702060] 23 p3288 N88-29576
Electron microscopy of ceramic superconductors
[DE88-006446] 23 p3288 N88-29580
High-T(sub c) superconductor and its use in superconducting magnets
[DE88-008403] 23 p3289 N88-29581
An HVEM study of displacement cascade damage in Nb3Sn at 13 K
[DE88-009997] 23 p3289 N88-29584
Band electronic structures and crystal packing forces
[DE88-010247] 23 p3289 N88-29585
Stability experimental results of cable-in-conduit superconductor for fusion
[DE88-753424] 23 p3290 N88-29589
Development of Nb-Ti multifilamentar superconducting wires
[DE88-702324] 23 p3290 N88-29592
Study of superconducting properties in some many valley semiconductors
[DE88-702325] 23 p3291 N88-29593
Planar thin film SQUID with integral flux concentrator
[NASA-CASE-MFS-28282-1] 23 p3292 N88-29602
Dependence of high critical temperature of ceramic superconductors on the nominal Cu(sup 3+)Cu(sup 2+) ratio
[DE88-702734] 23 p3293 N88-29611
The thermal conductivity of dirty type 2 superconductors
[B6681488] 23 p3294 N88-29615
Theory of superconductivity in oxides
[AD-A195647] 24 p3433 N88-30432
Behaviour and hysteresis losses of irreversible type-2 superconducting cylindrical shell
[DE88-702708] 24 p3433 N88-30434

SUPERCONDUCTORS

NT HIGH TEMPERATURE SUPERCONDUCTORS
Simple instrumentation for testing of ceramic superconductors
[DE87-013849] 01 p0103 N88-10672
Abrikosov vortex motion and elementary pinning force in a SNS Josephson junction
[DE87-013807] 01 p0105 N88-10683
Multidimensional elemental analysis with the Sandia nuclear microprobe
[DE87-014158] 02 p0183 N88-11136
Properties of Nb3Sn superconductor wires with composite cores
[KFK-4263] 02 p0246 N88-11557
Consortium for Materials Development in Space. Technical section
[NASA-CR-181508] 03 p0296 N88-11859
Powder-metallurgical preparation of A15 superconductors
[ETN-87-90584] 03 p0380 N88-12392
Topological aspects of infinite metal clusters and superconductors
[AD-A184104] 04 p0495 N88-13049
Magnetic field dependence of the specific heat of some high-T/sub c/ superconductors
[DE87-014078] 04 p0497 N88-13063
Anomalous phonon behavior of superconductor Y-Ba-Cu-O
[DE87-703401] 05 p0654 N88-14010
JPRS report: Science and technology. Japan
[JPRS-JST-87-023] 06 p0684 N88-14191
JPRS report: Science and technology. Japan
[JPRS-JST-87-027] 06 p0688 N88-14213
Hitachi develops ceramic superconducting device
06 p0688 N88-14214
Recent trends in superconductor development discussed
06 p0688 N88-14215
Superconducting material development
06 p0688 N88-14217
Study of some superconducting and magnetic materials on high T sub c oxide superconductors
[NASA-CR-182330] 06 p0785 N88-14813
The consequences of intergrain Josephson coupling in ceramic high-temperature superconductors
[DE87-013713] 06 p0785 N88-14816
Dynamic high pressure process for fabricating superconducting and permanent magnetic materials
[DE88-000848] 06 p0785 N88-14817
Superconducting switch program
[AD-A185682] 07 p0848 N88-15144
Fabrication of YBa2Cu3O7 superconducting ceramics
[DE88-003012] 07 p0938 N88-15701
Non-phonon mechanisms of superconductivity in high T/sub c/ superconducting oxides and other materials and their manifestation
[DE88-002708] 07 p0939 N88-15709
Localization of Cu 3d levels in the high Tc superconductor YBa2Cu3O approximately 7 by Cu2p X-ray photoelectron spectroscopy
[NOTA-INTERNA-887] 07 p0939 N88-15710
Metal-oxide superconductor BaPbsub1-xBisubxO3: Unusual properties and new applications
08 p1077 N88-16494
Soft X-ray absorption and emission spectra and the electronic structure of the Ba2YCu3O/sub 7-x/ superconductor
[DE88-002609] 08 p1090 N88-16559
Coulomb interactions and effective strong coupling Hamiltonians in Cu-O superconductors
[DE88-002942] 08 p1090 N88-16561
Oxygen diffusion in high T/sub c/-superconductors
[DE88-002965] 08 p1090 N88-16562
Structural properties of high-T/sub c/ oxide super conductors
[DE88-002974] 08 p1090 N88-16563
Experimental aspects of high-T/sub c/ superconductors
[DE88-003019] 08 p1090 N88-16564
Interpretation of the temperature dependence of conductivity in superconducting oxides
[DE88-003028] 08 p1091 N88-16565
High T/sub c/ superconductor as a strongly correlated state
[DE88-003194] 08 p1091 N88-16569
Powder metallurgical preparation of A15 superconductors
[ETN-88-91072] 09 p1144 N88-16858
Mechanism of change of vortex structure orientation in type-2 superconductors 09 p1239 N88-17425
Magnetic properties of heavy fermion superconductors
[ETN-88-91078] 09 p1255 N88-17524
Forces on neutral atoms due to electromagnetic fields
[AD-A187461] 10 p1408 N88-18396

Spin disorder resistivity and bare Curie temperature in the ferromagnetic superconductor ErRh4B4
[DE88-003016] 10 p1415 N88-18445

High temperature processing of superconducting Y1Ba2Cu3O6.9
[DE88-003002] 10 p1416 N88-18449

Normal and superconducting state properties of La2-xSr/sub x/CuO4
[DE88-003013] 10 p1416 N88-18450

Superconducting and magnetic properties of Fe-doped oxide superconductors
[DE88-003024] 10 p1416 N88-18451

Positron-annihilation 2D-ACAR studies of disordered and defected alloys
[DE88-003118] 10 p1416 N88-18454

Improved magnetization for YBa2Cu3O/sub 7-delta annealed in oxygen above 1000 C
[DE88-003934] 10 p1418 N88-18469

The effect of magnetic impurities and barriers on the magnetization and critical current of fine filament NbTi composites
[DE88-004443] 10 p1419 N88-18472

Simulation and processing of high resolution images of defects and interfaces in superconducting YBa2Cu3O7
[DE88-003656] 10 p1420 N88-18480

Superconductivity of thin film intermetallic compounds
[AD-A187563] 10 p1421 N88-18489

Study of the production of some superconducting and magnetic materials by solidification in the drop tube and drop tower
[NASA-CR-182494] 11 p1461 N88-18708

Cryocooler systems demonstration
[AD-A188025] 11 p1467 N88-18745

Perturbation effects in the CEBAF beam transport system
[CEBAF-PR-87-010] 11 p1546 N88-19242

Atom probe microanalysis of superconducting YBa2Cu3O(sub 7-x)
[DE88-003203] 11 p1557 N88-19322

An electron spectroscopic investigation of high-temperature superconducting oxides
[DE88-003807] 11 p1558 N88-19325

Processing relationships in YBa2Cu3O(7-x) superconductors
[DE88-005137] 11 p1559 N88-19330

Proceedings of the First International Symposium on Physical and Technical Problems of Superconductivity Application in Power Generation
[DE88-700618] 11 p1559 N88-19332

Multipass beam breakup in recirculating linacs
[CEBAF-PR-87-007] 12 p1690 N88-20111

Artificially structured superconductors
[DE88-005345] 12 p1697 N88-20153

An overview of recent developments in high-temperature superconductivity
[DE88-005477] 12 p1697 N88-20155

Phase transitions in two-dimensional superconducting arrays in a transverse magnetic field
[INPE-4457-RPE/559] 12 p1697 N88-20157

Superconductors with structured surfaces: Fields and currents
[AD-A189353] 12 p1699 N88-20164

Large momentum pairing in one-dimensional systems
[AD-A189228] 13 p1835 N88-20981

The relationship of the chemical bonding topology of high critical temperature copper oxide superconductors to that of the chevrel phases and the ternary lanthanide rhodium borides
[AD-A189255] 13 p1845 N88-21042

Discussion of radiation effects and high-temperature oxide superconductors
[DE88-001427] 13 p1846 N88-21046

A hydroxycarbonate route to superconductor precursor powders
[DE88-003638] 13 p1846 N88-21052

Superconducting superlattice structures
[DE88-005346] 13 p1847 N88-21058

A novel method for sputter-deposition of high T(sub c) superconductor films via a computer-controlled mass analyzed ion beam
[DE88-006001] 13 p1848 N88-21064

Superconducting transition temperature of Cu-Nb microcomposites 14 p1973 N88-21775

Thermal model describing development of normal region in superconductor film carrying electric current 14 p1973 N88-21776

Organic metal (ET)4Hg3Br8A quasi-two-dimensional superconductor 14 p1974 N88-21778

Properties of superconductors with strong electron-phonon interaction 14 p1974 N88-21779

Advances in applied superconductivity: A preliminary evaluation of goals and impacts
[DE88-006441] 14 p1986 N88-21844

Magnetic impurities in superconductors
[DE88-006917] 14 p1986 N88-21846

Temperature-dependent conductivity of oxygen-depleted YBCO ceramics
[AD-A190340] 15 p2044 N88-22182

Melt processing ceramic YBa2Cu3O(sub 6.9)
[DE88-007039] 15 p2047 N88-22199

Function of Japan Fine Ceramics Center described 15 p2052 N88-22227

Synthesis of metastable superconductors by high dynamic pressure
[DE88-005620] 15 p2139 N88-22764

Effective electron interactions due to virtual charge and spin excitations in an extended Hubbard model for Cu-O superconductors
[DE88-005971] 15 p2139 N88-22766

Superconductivity in power engineering
[DE88-701414] 15 p2141 N88-22776

Magnetic anomalies in the rare earth oxide superconductors GdBa2Cu3O(7-x) and YbBa2Cu3O(7-x)
[AD-A190713] 15 p2144 N88-22793

A sup 57 Fe Mossbauer study of the superconductor YBa sub 2 (Fe sub x Cu sub 1-x) sub 3 O sub y
[DE88-701543] 16 p2282 N88-23661

Effects of 67.5 MeV electron irradiation on Y-Ba-Cu-O and Gd-Ba-Cu-O high-temperature superconductors
[AD-A191271] 16 p2283 N88-23669

Materials science with muon spin rotation
[NASA-CR-182891] 17 p2396 N88-24242

Coexisting static magnetic ordering and superconductivity in CeCu2.1Si2 found by muon spin relaxation 17 p2396 N88-24245

Static magnetic ordering of CeCu2.1Si2 found by muon spin relaxation 17 p2396 N88-24246

Design of a superconducting alternator for space-based power generation 17 p2412 N88-24340

Lightweight power bus for a baseload nuclear reactor in space 17 p2438 N88-24505

Research work completed at the Naval Surface Warfare Center Solid State Group of the Radiation Division
[AD-A191627] 18 p2582 N88-25339

Vacancy ordering in the basal plane of YBa2Cu3O(sub)z
[DE88-004572] 18 p2583 N88-25348

Quench detection by fluid dynamic means in cable-in-conduit superconductors
[DE88-007269] 18 p2585 N88-25359

Workshop report and presentations from the Semiconductor Research Corporation-DOE Semiconductor Task Force Workshop
[DE88-007690] 19 p2733 N88-26232

Superconductive analogue of spin glasses
[DE88-702059] 19 p2733 N88-26233

RCL model for the development of hysteresis in superconductors
[DE88-702061] 19 p2733 N88-26234

Dimensional crossover in layered superconductors 19 p2734 N88-26237

Superfluidity of a two dimensional Boson Coulomb gas
[DE88-009827] 19 p2735 N88-26244

Theory of oxygen content, atomic ordering and oxygen diffusion in 1,2,3 superconducting oxides as a function of temperature and oxygen pressure
[DE88-007961] 19 p2735 N88-26248

Preparation of oxide superconductors
[DE88-009136] 20 p2875 N88-27063

Recent advances in atom-probe field ion microscopy
[DE88-008799] 20 p2876 N88-27070

HeFlow: A program for calculating pressure and temperature of helium in forced-flow superconductors. Part 1: Numerical solutions. Part 2: HeFlow user's manual
[DE88-008941] 20 p2876 N88-27071

Phenomenological approach to high T/sub c/ oxide superconductors
[DE88-701868] 20 p2876 N88-27074

Anisotropic characteristic lengths in single crystal YBa2Cu3O(sub 7-Delta)
[DE88-009959] 20 p2877 N88-27080

Ceramic processing of high-T(sub)c superconductors
[DE88-010090] 20 p2878 N88-27087

SIS (Superconductor-Insulator-Superconductor) mixer research
[AD-A192908] 20 p2879 N88-27092

Mitsubishi Electric Advance (R and D Edition), Volume 41
[PB88-194162] 21 p2929 N88-27388

Superconducting oxides with high critical temperatures 21 p2930 N88-27392

Effect of high-amplitude high-frequency current on non-isothermal equilibrium of NS-boundary in inhomogeneous superconductor
[DE88-701682] 21 p3019 N88-27922

Probing the electronic and defect structure of perovskite superconductors
[DE88-008349] 21 p3022 N88-27939

Thermodynamics of oxygen-vacancy ordering in YBa2Cu3O(sub z)
[DE88-009816] 21 p3022 N88-27940

Superconductor consolidation
[DE88-010938] 21 p3024 N88-27949

Study of the friction and wear-related properties of ceramic superconductors
[DE88-011844] 21 p3024 N88-27950

Ceramic fabrication technology for high-T(sub)c materials
[DE88-012060] 21 p3024 N88-27953

Materials research, superconductor and thin layer technology
[REPT-50/87] 21 p3025 N88-27955

Interactions between superconductivity and Kondo-grid properties in CeCu2Si2. Measurement results of specific heat under high pressure
[ETN-88-92377] 21 p3025 N88-27958

Modification of YBa2Cu3O(7-x) ceramics by adsorbed water and other gases
[DE88-011518] 22 p3057 N88-28140

Investigation of magnetic anisotropy and spin wave modes in transition metal multilayers
[DE88-009007] 22 p3154 N88-28765

Fabrication of bulk superconducting ceramics
[DE88-009956] 22 p3155 N88-28773

Possible occurrence of band interplay in high Tc superconductor
[PREPRINT-593] 22 p3157 N88-28789

Gravitation control 22 p3158 N88-28795

Gravitational propulsion 22 p3158 N88-28796

Properties of strong coupled superconductors
[DE88-702050] 23 p3287 N88-29574

Electron microscopy of ceramic superconductors
[DE88-006446] 23 p3288 N88-29580

High-T(sub c) superconductor and its use in superconducting magnets
[DE88-008403] 23 p3289 N88-29581

Preparation of superconducting YBa2Cu3O(sub 7-x) films by magnetron sputtering
[DE88-009977] 23 p3289 N88-29583

Magnetic phase transitions in 90-K superconductors Ho1Ba2Cu3O(7-delta) and Gd1Ba2Cu3O(7-delta) observed by ZF-muon(+)SR
[DE88-752611] 23 p3290 N88-29588

Phase sensitive amplification with SIS (Superconductor-Insulator-Superconductor) quasiparticle mixers
[AD-A194594] 23 p3291 N88-29596

Fluctuations of order parameters in the high T(sub c) superconductors
[DE88-702549] 23 p3292 N88-29603

Anomalous dependence of the thermoelectric power on the temperature in YBaCuO high-T(sub c) superconducting samples
[DE88-702682] 23 p3292 N88-29605

SUPERCOOLING
NT CRYOGENIC COOLING

Structure and modification of winter mountain clouds in the Sierra Nevada: Nowcasting/forecasting the onset of supercooled liquid water 02 p0202 N88-11263

SUPERCRITICAL AIRFOILS
NT SUPERCRITICAL WINGS

A transonic model representation for two-dimensional wall interference assessment
[NLR-TR-86026-U] 01 p0001 N88-10006

Influence of the static deformation on a wing in the unsteady aerodynamic 05 p0551 N88-13357

Design and experimental evaluation of a swept supercritical Laminar Flow Control (LFC) airfoil 07 p0813 N88-14951

An aerodynamic comparison of blown and mechanical high lift airfoils 10 p1272 N88-17606

The NASA Langley Laminar-Flow-Control (LFC) experiment on a swept, supercritical airfoil: Design overview
[NASA-TP-2809] 14 p1861 N88-21117

Investigation of side-wall effects in wind tunnel with supercritical airfoil testing 15 p2054 N88-22241

Aerodynamic performance and pressure distributions for a NASA SC(2)-0714 airfoil tested in the Langley 0.3-meter transonic cryogenic tunnel
[NASA-TM-4044] 18 p2456 N88-24580

Calculation of 2-D unsteady transonic full potential flow about oscillating airfoils by two complementary approaches
[PB88-127519] 20 p2753 N88-26341

SUPERCRITICAL FLOW

Unsteady flow in a supercritical supersonic inlet 18 p2460 N88-24605

Electrochemistry in near-critical and supercritical fluids. 6: The electrochemistry of ferrocene and phenazine in acetonitrile between 25C and 300C
[AD-A192171] 18 p2482 N88-24723

SUPERCRITICAL FLUIDS

Supercritical fluid chromatography/supersonic jet spectroscopy
[DE88-000297] 03 p0282 N88-11774

Retention processes in supercritical fluid chromatography
[DE88-000079] 04 p0413 N88-12559
Thermodynamic properties of supercritical mixtures
[DE88-000809] 04 p0413 N88-12562
Supercritical fluid extraction-gas chromatography of Volatile Organic Compounds (VOC) from tenax devices
[PB88-124300] 10 p1298 N88-17759
Transport and relaxation processes in supercritical fluids
[DE88-004804] 10 p1419 N88-18474
Supercritical fluid chromatography/supersonic jet spectroscopy
[DE88-004438] 13 p1738 N88-20392
Development and evaluation of supercritical fluid chromatography-mass spectrometry
[DE88-005122] 13 p1738 N88-20394
Instrumental aspects of capillary supercritical fluid chromatography
[ETN-88-92242] 16 p2174 N88-22960
Electrochemistry in near-critical and supercritical fluids. 5: The dimerization of quinoline and acridine radical anions and dianions in ammonia from -70 C to 150 C
[AD-A190058] 16 p2175 N88-22967
Electrochemistry in near-critical and supercritical fluids. 6: The electrochemistry of ferrocene and phenazine in acetonitrile between 25C and 300C
[AD-A192171] 18 p2482 N88-24723
Supercritical fluid chromatography/supersonic jet spectroscopy
[DE88-007935] 19 p2614 N88-25511

SUPERCRITICAL WINGS
Investigations on a transonic airfoil with a 30 mm wide perforation/cavity arrangement
[ESA-TT-1072] 03 p0260 N88-11634
Static aeroelastic effects on the flutter of a supercritical wing 05 p0550 N88-13353
Testing of a schematic transport plane model in several European windtunnels
[PB87-170270] 09 p1113 N88-16671
Unsteady pressure and structural response measurements of an elastic supercritical wing
[NASA-TM-100591] 17 p2299 N88-23756
Analysis of experimental data for cast 10-2/DOA2 supercritical airfoil at high Reynolds numbers
[AD-A192827] 21 p2892 N88-27166

SUPERFLUID FLOW
U SUPERFLUIDITY

SUPERFLUIDITY
Superfluid He4 as a solar neutrino detector
[DE87-014477] 02 p0257 N88-11625
Design concepts for the ASTROMAG cryogenic system
[NASA-CR-181505] 04 p0497 N88-13060
Method of two-time Green functions in molecular hydrodynamics of superfluid liquid 06 p0771 N88-14735
Cryogenic acoustic microscopy
[AD-A187274] 10 p1299 N88-17767
Superfluid turbulence in He II at elevated pressures 10 p1422 N88-18493
Development of a motorized cryovalve for the control of superfluid liquid helium 14 p1925 N88-21477
Peculiarities of non-stationary heat transfer to superfluid helium
[DE88-701174] 16 p2200 N88-23124
Integrability of fermionic string in superfluid Hamiltonian approach
[DE88-701662] 16 p2284 N88-23678
Theoretical investigation of the development of the normal fluid and superfluid velocity distributions during spin-up for a He2-filled cylinder
[MPIS-6/1987] 18 p2510 N88-24892
Superfluid turbulence in counterflowing helium II 19 p2665 N88-25849
Superfluidity of a two dimensional Boson Coulomb gas
[DE88-009827] 19 p2735 N88-26244
Temperature rise in superfluid helium pumps
[NASA-TM-100997] 21 p2948 N88-27507
Superfluid Helium On-Orbit Transfer (SHOOT) operatons
[NASA-TM-101009] 22 p3048 N88-28084
Stability experimental results of cable-in-conduit superconductor for fusion
[DE88-753424] 23 p3290 N88-29589

SUPERGIANT STARS
Basic properties and variability 02 p0252 N88-11593
Spectroscopy and nonthermal processes 02 p0252 N88-11594
Circumstellar shells, the formation of grains, and radiation transfer 02 p0252 N88-11596
Fifth Cambridge Workshop on Cool Stars, Stellar Systems and the Sun 04 p0502 N88-13092
The acceleration of winds by MHD waves in open magnetic structures 04 p0506 N88-13109
An analysis of the photospheric line profiles in F, G, and K supergiants 04 p0513 N88-13157
A flash spectrum of Cl I, C I, N I, and Ni II absorption in 31 Cygni: A direct observation of the reversing layer 04 p0513 N88-13158
Sensitivity of the H alpha line to expansion, geometrical extent and temperature gradient in the G and K supergiant chromospheres 04 p0514 N88-13159
Radio continuum emission from the ionized stellar winds of the cool supergiants in zeta Aurigae-like systems 04 p0514 N88-13160
Winds and shells around low-mass supergiants 04 p0514 N88-13164
Far infrared circumstellar debris shells of red supergiant stars 04 p0515 N88-13165
VLA observations of rapid 6 cm flux variations in alpha Ori 04 p0515 N88-13169
A comprehensive exploration of late-type stars in the far-ultraviolet 04 p0520 N88-13194
The EUV line flux variations and activity in Alpha Orionis 08 p1032 N88-16256
Evolutionary helium and CNO anomalies in the atmospheres and winds of massive hot stars
[NASA-CR-183254] 24 p3452 N88-30550
The kinematics of late-type supergiants
[SER-C-PREPUBL-FASC-28] 24 p3454 N88-30560

SUPERGRAVITY
Spontaneous symmetry breaking in N=2 supergravity
[DE87-702749] 01 p0109 N88-10704
Spontaneous symmetry breaking in N=3 supergravity
[DE87-702753] 01 p0109 N88-10705
New class of spherically symmetric interior solution with cosmological constant
[DE87-703095] 02 p0226 N88-11422
Our universe as an attractor in a superstring model
[DE87-703066] 02 p0251 N88-11585
Geometrization of Planck length in composite gravity and supergravity
[DE87-703085] 02 p0251 N88-11588
Chiral U(1) anomaly in D = 4 super Yang-Mills theory coupled to supergravity
[DE87-753022] 02 p0252 N88-11591
Research in theoretical physics: Results from last year 1986/87
[DE88-004922] 10 p1423 N88-18502
Freund-Rubin type solutions for different compactifications of the eleven-dimensional space
[DE88-700869] 12 p1686 N88-20082
Ten dimensional N = 1 supergravity coupled to supersymmetric Yang-Mills fields in superspace
[DE87-703033] 15 p2146 N88-22808
N=2 supergravity in superspace: Solution to the constraints
[DE88-702135] 19 p2741 N88-26272
N=2 supergravity in superspace: The invariant action
[DE88-702136] 19 p2741 N88-26273
N=2 supergravity in superspace: different versions and matter couplings
[DE88-702137] 19 p2741 N88-26274
Lagrangian of the self-duality equation and d = 10, N = 2b supergravity
[DE88-701554] 24 p3455 N88-30563

SUPERHARMONICS
N=2 supergravity in superspace: Solution to the constraints
[DE88-702135] 19 p2741 N88-26272
N=2 supergravity in superspace: different versions and matter couplings
[DE88-702137] 19 p2741 N88-26274

SUPERHEATING
Development of creep resistant austenitic stainless steels for advanced steam cycle superheater application
[DE87-012929] 01 p0023 N88-10147
Microwave superheaters for fusion
[DE88-001656] 05 p0653 N88-14007
Review of nucleation and incipient boiling under pool and forced convection conditions 08 p0982 N88-15938
The effect of asymmetric current-supporting electron velocity distributions on second harmonic electron cyclotron resonance heating: A ray-tracing treatment for the compass tokamak
[INPE-4389-PRE/1209] 08 p1087 N88-16549
Kinetics of homogeneous nucleation in superheated F-11 and F-21 liquid freons
[NASA-TT-20286] 19 p2613 N88-25503
Solidification with natural circulation
[DE88-011197] 22 p3074 N88-28248
Initiation of explosive molten aluminum-water interactions at wet or underwater surfaces
[DE88-004686] 23 p3194 N88-29006

SUPERHETERODYNE RECEIVERS
Comparative investigation of heterodyne mixers at 1000 GHz
[FTL-068627] 09 p1158 N88-16940

SUPERHIGH FREQUENCIES
Phase 2 development of a 12 GHz MMIC FET amplifier
[IM-I86-1010] 01 p0038 N88-10240
Performance of high power S-band klystrons focused with permanent magnet
[DE87-753024] 02 p0167 N88-11053
X-band SAR for a European remote sensing payload 03 p0340 N88-12142
X-band uplink ground systems development: Part 2 04 p0436 N88-12703
Optically tuned MM-wave IMPATT source
[AD-A185250] 05 p0577 N88-13523
Results on the low elevation angle propagation experiment, part 1
[TUD-R-32B] 06 p0693 N88-14250
GaAs MMIC yield evaluation --- monolithic microwave integrated circuits (MMIC)
[ESA-CR(P)-2470] 08 p0979 N88-15916
Investigation of the quantitative determination of two dimensional sea surface wave spectra from shipborne radar measurements
[GKSS-87/E/10] 09 p1195 N88-17163
X-band system performance of the very large array 11 p1473 N88-18789
DSS 14 64-meter antenna S- and X-band efficiency and system noise temperature calibrations, September 1987 11 p1473 N88-18790
Characterization of 6 soils in the X-band, through measurements of complex permittivity
[INPE-4376-TDL/302] 12 p1639 N88-19814
Preparation and execution of calibration measurements for handling of airborne SAR data (AGRISAR)
[ETN-88-92338] 17 p2333 N88-23926
Monolithic GaAs Ku-band one watt constant phase variable power amplifier
[DE88-006272] 18 p2506 N88-24866
An overview of the OmniTRACS: The first operational mobile Ku-band satellite communications 19 p2644 N88-25689
X-band resonant ring operation at 450 kW 22 p3064 N88-28181
X-band noise temperature near the Sun at a 34-meter high efficiency antenna 22 p3067 N88-28200
DSS 14 antenna calibrations for GSSR/VLA Saturn radar experiments 22 p3068 N88-28207

SUPERHYBRID MATERIALS
NT GRAPHITE-EPOXY COMPOSITES

SUPERIMPOSITION (MATHEMATICS)
U SUPERPOSITION (MATHEMATICS)

SUPERLATTICES
Metallic superlattices with monolayer modulation
[DE87-012724] 01 p0023 N88-10145
Superconducting properties of metallic superlattices
[DE87-012725] 01 p0023 N88-10146
Photoluminescence studies of GaAs/AlAs superlattices
[DE87-013817] 02 p0245 N88-11548
Interaction between defects and the formation of dissipative structures in irradiated impure crystals
[DE87-703125] 02 p0246 N88-11552
Non-lattice matched metallic superlattices
[DE87-011512] 04 p0497 N88-13062
MBE growth of InAsSb strained-layer superlattices
[DE88-000365] 05 p0654 N88-14011
Waves and vibrations in elastic superlattice composites 06 p0776 N88-14765
Structure of layered crystals studied by high energy ion beams
[DE88-001675] 06 p0786 N88-14822
Tailorable infrared sensing device with strain layer superlattice structure
[NASA-CASE-NPO-16607-1-CU] 06 p0788 N88-14836
The role of thermodynamic phase diagrams and lattice matching in superlattice growth
[DE88-003113] 08 p1091 N88-16568
Hydrogen in niobium-tantalum superlattices 09 p1146 N88-16867
Neutron and X-ray scattering studies of layered solids 09 p1246 N88-17469
Superlattice photodetectors
[AD-A186956] 09 p1253 N88-17511
Optical characterization of GaAs/sub 1-x/Sb/sub x/ and GaAs/sub 1-x/Sb/sub x/GaAs strained layer superlattices
[DE88-003393] 10 p1418 N88-18464
Magnetic rare earth superlattices
[DE88-003483] 10 p1418 N88-18465
MBE growth, characterization and electronic device processing of HgCdTe, HgZnTe related heterojunctions and HgCdTe-CdTe superlattices
[AD-A187456] 10 p1421 N88-18486
Theoretical studies of the interface electronic properties of tetrahedrally coordinated semiconductors
[AD-A187216] 11 p1555 N88-19306

MBE (Molecular Beam Epitaxial) growth characterization and electronic device processing of HgCdTe, HgZnTe related heterojunctions and HgCdTe-CdTe superlattices
[AD-A187416] 11 p1555 N88-19307
Atomic monolayer metallic superlattices
[DE88-005348] 12 p1607 N88-19612
Brillouin scattering from collective spin waves in magnetic superlattices
[DE88-005347] 12 p1697 N88-20154
Silicon-germanium heterostructures 13 p1844 N88-21034
Photon-controlled growth of multilayered structures
[DE88-005061] 13 p1847 N88-21054
Competing interactions in metallic superlattices
[DE88-005344] 13 p1847 N88-21057
Superconducting superlattice structures
[DE88-005346] 13 p1847 N88-21058
Dynamical aspects of carrier tunneling in semiconductor superlattices 14 p1977 N88-21799
The Shubnikov de Haas effect in narrow-gap semimagnetic semiconductors
[ETN-88-92249] 14 p1988 N88-21861
Experimental studies on electronic properties of HgTe/CdTe and Hg sub 1-z Cd sub x Te/CdTe heterostructures and superlattices
[AD-A189826] 15 p2142 N88-22783
Fundamental properties and devices applications of Ge(x)Si(1-x)/Si superlattices
[AD-A190129] 15 p2143 N88-22787
Neutron diffraction refinement of CsHSO4 superionic phase structure
[DE88-701496] 18 p2580 N88-25326
Crystalline metal-semiconductor superlattices
[DE88-007063] 18 p2581 N88-25332
Electronic structure, elementary excitations, optical and transport properties of semiconductor superlattices
[AD-A190795] 18 p2581 N88-25333
Magnetic superlattices
[AD-A191450] 18 p2581 N88-25334
Optical properties of heterostructures and superlattices
[AD-A191542] 18 p2581 N88-25335
An investigation of 2-6 superlattice deposition by laser photochemical techniques
[AD-A191547] 18 p2581 N88-25336
Molecular Beam Epitaxy (MBE) for high speed devices 19 p2656 N88-25770
Defects in high-mobility semiconductor systems
[AD-A191618] 19 p2732 N88-26224
Third International Conference on Superlattices, Microstructures and Microdevices
[AD-A191416] 20 p2861 N88-26995
Piezoelectric effects in strained layer superlattices 20 p2863 N88-27002
Control of carrier lifetime in PbTe nipi superlattices by external photoinjection 20 p2863 N88-27006
Metallic superlattices 20 p2864 N88-27012
Properties of synthetic magnetic superlattices 20 p2865 N88-27014
Superlattice doping interfaces 20 p2866 N88-27019
A 10 microns photoexcited avalanche gain due to electron impact ionization from GaAs quantum well superlattices 20 p2867 N88-27026
Transport study on Si/Si(1-x)Ge(x) superlattices selectively doped by secondary implantation of Sb 20 p2867 N88-27027
Electrical properties of p-type and n-type ZnSe-ZnTe strained-layer superlattices 20 p2868 N88-27029
MBE growth of HgTe/CdTe superlattices on Si(100) substrates 20 p2869 N88-27033
Growth of high quality CoSi2/Si superstructures on Si(111) 20 p2869 N88-27034
Phonons in semiconductor superlattices 20 p2869 N88-27035
Electronic structure of quantum-well states revealed under high pressures 20 p2870 N88-27038
On a-SiH/a-SiN(x):H superlattices: Confinement or contamination 20 p2870 N88-27040
Extended and local plasmons in a lateral superlattice 20 p2870 N88-27041
Resonant tunneling in InGaAs-InP double-barrier structures and superlattices 20 p2871 N88-27047
Non-effective-mass matching in superlattices 20 p2872 N88-27049
Influence of interfaces on electronic and magnetic properties of MnSe/Zn Se superlattices near monolayer limit 20 p2872 N88-27050
Structural studies of (Ga,In)(As,P) alloys and (InAs) sub m (GaAs) sub n strained-layer superlattices by fluorescence-detected EXAFS 20 p2872 N88-27051
Type 3 - type 1 transition and strain effect in Hg(1-x)Cd(x)Te-CdTe and Hg(1-x)Zn(x)Te-CdTe superlattices 20 p2872 N88-27052
Ordering transitions of ternary alloys A(1-x)B(x)C 20 p2873 N88-27054
Aperiodic superlattices: Structured randomness 20 p2873 N88-27055
Characterization of structural and magnetic order of Er/Y superlattices 20 p2873 N88-27056
Superconductivity of Cr/V superlattices 20 p2874 N88-27057
Thermal conductivity of isotopically pure semiconductors, superlattices, semiconductor alloys and semiconductors as a function of temperature; control of the segregation coefficient in LEC crystal growth; and photo-Hall measurements of GaAs 21 p2927 N88-27375
Solar energy conversion through the interaction of plasmons with tunnel junctions. Part A: Solar cell analysis. Part B: Photoconductor analysis
[NASA-CR-183044] 21 p2967 N88-27621
Laser spectroscopy of quantum well and superlattice structures
[AD-A193336] 21 p3022 N88-27937
Investigations on the MBE (Molecular Beam Epitaxy) growth and properties of Al(sub y)Ga(sub y)In(sub 1-x-y)AsInP and InGaAs-InAlAs superlattices
[DE88-009105] 21 p3022 N88-27941
Meaning of energy diagrams used to describe hetero-structures
[DE88-702219] 21 p3023 N88-27943
Studies on strained (In,Ga)As/GaAs semiconductors and optical devices 23 p3287 N88-29575
Intrinsic and extrinsic energy states of semiconductors and heterostructures using novel techniques
[DE88-008560] 23 p3289 N88-29582
Electronic states in tunneling semiconductor superlattices
[DE88-011571] 23 p3290 N88-29587

SUPERMASSIVE STARS
Intermixing processes in massive stars and their influence on stellar evolution and nucleosynthesis
[ETN-88-91484] 11 p1568 N88-19388
IUE evidence on the nature of the innermost broad-line region in Seyfert 1 galaxies 17 p2450 N88-24552

SUPERNOVA REMNANTS
On the (lack of) proper motion of the Vela pulsar 01 p0097 N88-10635
Recent X-ray observations of supernova remnants and their interpretation
[MPE-PREPRINT-96] 09 p1262 N88-17563
A 23 hour EXOSAT observation of the X-ray pulsar 1E2259+586 and the associated supernova remnant G109.1-1.0
[MPE-PREPRINT-99] 14 p1994 N88-21882

SUPERNOVA 1987A
Data recorded by the Rome room temperature gravitational wave antenna, during the supernova SN 1987 A in the Large Magellanic Cloud
[NOTA-INTERNA-879] 06 p0806 N88-14922
A look at Supernova 1987A
[DE88-003411] 10 p1429 N88-18531
Particle physics and cosmology
[DE88-004944] 13 p1854 N88-21096
Astron observations of supernova 1987A in large magellanic cloud 24 p3445 N88-30504

SUPERNOVAE
NT SUPERNOVA 1987A
High explosive simulations of supernovae and the supernova shell fragmentation model of solar system formation
[DE87-014708] 02 p0251 N88-11584
Adiabatic supernova expansion into the circumstellar medium
[DE87-014241] 03 p0387 N88-12433
Neutrinos in supernovae
[DE87-014295] 03 p0387 N88-12434
Core bounce supernovae
[DE87-014910] 04 p0520 N88-13197
An automated supernova search and the design strategy
[DE88-001827] 05 p0660 N88-14051
Numerical modelling of the classical nova outburst
[NASA-TM-89707] 07 p0945 N88-15746
An introduction to nuclear astrophysics
[DE88-002761] 08 p1100 N88-16618
Onset of type 2 supernova in circumstellar envelope created by the stellar wind from presupernova
[DE88-700448] 10 p1428 N88-18526
Calculated late time spectra of supernovae
[DE88-003296] 10 p1428 N88-18530
Supernova mechanisms: Before and after SN1987a
[DE88-003489] 10 p1429 N88-18533
The type Ia supernova 1986G in NGC5128: Optical photometry and spectra
[INPE-4426-PRE/1230] 12 p1710 N88-20231
Hydrodynamical models of supernova SN 1987 A in the LMC
[DE88-701123] 15 p2151 N88-22837
Research and Technology, 1987, Goddard Space Flight Center
[NAS 1.15:101097] 17 p2453 N88-24572
Nuclear and astrophysical evidence on the equation of state
[DE88-007397] 18 p2572 N88-25279
Pre-supernova evolution of SN 1987A
[SER-C-PREPUBL-FASC-15] 18 p2593 N88-25409
To the opportunities of cluster analysis of light curves of supernovae
[DE88-701642] 21 p3030 N88-27982
Strange, quark and metastable neutron stars
[DE88-702404] 21 p3030 N88-27984
Resonant spin-flavor precession of solar and supernova neutrinos
[DE88-752604] 23 p3308 N88-29707
Gamma radiation expected from supernova 1987A in large magellanic cloud 24 p3445 N88-30505
Activities report in astronomy
[ISSN-0531-4496] 24 p3451 N88-30535

SUPERPLASTICITY
Superplastic deformation and post forming tensile properties of Ti-6Al-4V sheet
[RAE-TR-86015] 01 p0023 N88-10144
Tensile behavior of superplastic Al-Cu-Li-Zr alloy 2090 at cryogenic temperatures
[DE87-014084] 02 p0147 N88-10923
Investigation by differential scanning calorimetry of microstructure in a superplastic Al-Mg-Zr alloy
[AD-A184902] 05 p0564 N88-13439
Micromechanical and microstructural studies of ceramic superplasticity
[DE88-005793] 13 p1751 N88-20472
Superplastic flow of mullite-zirconia composites
[DE88-005905] 15 p2028 N88-22085
Superplasticity: A fundamental investigation on deformation mechanism and cavitation phenomena
[AD-A191548] 18 p2485 N88-24741
Optimizing superplastic response in lithium containing aluminum-magnesium alloys
[AD-A192217] 20 p2774 N88-26451
Thermomechanical processing of Al alloy 2090 for grain refinement and superplasticity
[AD-A192333] 21 p2912 N88-27281
Analysis of grain refinement and superplasticity in aluminum-magnesium alloys
[AD-A193029] 21 p2912 N88-27283
Equipment for the pressure welding of metals and alloys utilising the effects of superplasticity
[RAE-TRANS-2162] 22 p3055 N88-28129

SUPERPOSITION (MATHEMATICS)
A new method of calculating the boundary layer characteristics downstream of manipulators. Part 1: Boundary layer integral parameters
[PNR90455] 22 p3078 N88-28279

SUPERSATURATION
Microgravity nucleation and particle coagulation experiments support
[NASA-CR-181540] 04 p0423 N88-12618
Microgravity nucleation and particle coagulation experiments support
[NASA-CR-181541] 04 p0423 N88-12619
Precipitation in alumina-rich spinel: A transformation-toughened ceramic single crystal
[DE87-012380] 06 p0785 N88-14815
Nucleation in super-saturated products
[NASA-TT-20275] 15 p2037 N88-22134

SUPERSONIC AIRCRAFT
NT B-70 AIRCRAFT
NT CONCORDE AIRCRAFT
NT F-4 AIRCRAFT
NT F-14 AIRCRAFT
NT F-15 AIRCRAFT
NT F-16 AIRCRAFT
NT F-106 AIRCRAFT
NT F-111 AIRCRAFT
NT MIG AIRCRAFT
NT MIRAGE AIRCRAFT
NT RF-4 AIRCRAFT
NT SUPERSONIC TRANSPORTS
Experiences using the Mark IV supersonic hypersonic arbitrary body program 05 p0534 N88-13249
Time-temperature-stress capabilities of composite materials for advanced supersonic technology application
[NASA-CR-178272] 06 p0677 N88-14144
Aeropropulsion '87. Session 6: High-Speed Propulsion Technology
[NASA-CP-10003-SESS-6] 08 p0957 N88-15807
Shock structure and noise of supersonic jets in simulated flight to Mach 0.4
[NASA-TP-2785] 08 p1080 N88-16510
The design and use of a temperature-compensated hot-film anemometer system for boundary-layer flow transition detection on supersonic aircraft
[NASA-TM-100421] 13 p1723 N88-20304

Propulsion and airframe aerodynamic interactions of supersonic V/STOL configurations. Volume 1: Wind tunnel test pressure data report
[NASA-CR-177343-VOL-1] 16 p2157 N88-22866
Propulsion and airframe aerodynamic interactions of supersonic V/STOL configurations. Volume 2: Wind tunnel test force and moment data report
[NASA-CR-177343-VOL-2] 16 p2157 N88-22867
Propulsion and airframe aerodynamic interactions of supersonic V/STOL configurations. Volume 4: Summary
[NASA-CR-177343-VOL-4] 16 p2157 N88-22868
Parametric study of supersonic STOVL flight characteristics
[NASA-CR-177330] 16 p2161 N88-22893
PAN AIR analysis of the NASA/MCAIR 279-3: An advanced supersonic V/STOL fighter/attack aircraft
[NASA-TM-86838] 17 p2298 N88-23750
The challenges and opportunities of supersonic transport propulsion technology
[NASA-TM-100921] 17 p2307 N88-23806
Navier-Stokes analysis of transonic transport aircraft empennage 19 p2636 N88-25637
Low-speed wind-tunnel test of a STOL supersonic-cruise fighter concept
[NASA-TM-4050] 20 p2761 N88-26374
Supersonic transport/hypersonic transport (SST/HST) development
[REPT-881-111-101] 21 p2896 N88-27192
An analysis of lateral-directional handling qualities and Eigenstructure of high performance aircraft
[AD-A194874] 24 p3328 N88-29814

SUPERSONIC AIRFOILS
Supersonic aerodynamics of delta wings
[NASA-TP-2771] 10 p1273 N88-17615

SUPERSONIC BOUNDARY LAYERS
Supersonic boundary layer on a heated wall
[ETN-88-91617] 08 p0950 N88-15763
Fundamental aspects of the structure of supersonic turbulent boundary layers
[AD-A191494] 18 p2456 N88-24581

SUPERSONIC COMBUSTION
Interaction between two-dimensional sonic jets and supersonic flow to model heat addition in a supersonic combustor
[AD-A189572] 13 p1716 N88-20261
Turbulent reacting flows and supersonic combustion
[AD-A189690] 15 p2034 N88-22115
JPRS report: Science and technology. Japan
[JPRS-JST-88-005] 19 p2633 N88-25619
Basic research in supersonic combustion 19 p2634 N88-25623

SUPERSONIC COMBUSTION RAMJET ENGINES
SCRAM JET (Supersonic Combustion Ramjet) combustion experiments 04 p0404 N88-12512
Aerodynamics of Hypersonic Lifting Vehicles
[AGARD-CP-428] 05 p0529 N88-13219
Hypersonic airbreathing propulsion: Evolution and opportunities 05 p0531 N88-13231
Numerical analysis of flow through scramjet engine inlets 05 p0532 N88-13233
Ignition and flameholding in supersonic flow by injection of dissociated hydrogen 05 p0560 N88-13410
Advanced fabrication techniques for hydrogen-cooled engine structures
[NASA-CR-3949] 06 p0723 N88-14447
Analysis and performance prediction of scramjet inlets utilizing a three-dimensional Navier-Stokes code 07 p0811 N88-14936
Aeropropulsion '87. Session 6: High-Speed Propulsion Technology
[NASA-CP-10003-SESS-6] 08 p0957 N88-15807
Hypersonic propulsion research 08 p0958 N88-15812
An analytical study of the hydrogen-air reaction mechanism with application to scramjet combustion
[NASA-TP-2791] 08 p0966 N88-15846
An investigation into the feasibility of using a dual-combustion mode ramjet in a high Mach number tactical missile
[AD-A186906] 09 p1119 N88-16705
Investigations into shock-induced enhancement of mixing and combustion in supersonic burners
[AD-A189609] 12 p1607 N88-19608
Active cooling design for scramjet engines using optimization methods
[NASA-TM-100581] 13 p1783 N88-20669
Numerical and experimental investigation of multiple shock wave/turbulent boundary layer interactions in a rectangular duct
[AD-A190772] 15 p2066 N88-22320
Measurement data processing system based on personal computer: For scramjet combustion test
[DE88-751807] 16 p2174 N88-22959
Numerical simulation of scramjet inlet flow fields
[NASA-TP-2517] 17 p2296 N88-23735
Two-dimensional viscous flow computations of hypersonic scramjet nozzle flowfields at design and off-design conditions
[NASA-CR-182150] 19 p2603 N88-25459
Mach 2 combustion characteristics of hydrogen/hydrocarbon fuel mixtures 19 p2625 N88-25568

SUPERSONIC COMPRESSORS
Application of highly loaded single-stage mixed-flow compressors in small jet-engines 10 p1280 N88-17652
Design and testing of a front stage for an advanced high pressure compressor 10 p1283 N88-17679

SUPERSONIC CRUISE AIRCRAFT RESEARCH
Concept development of a Mach 3.0 high-speed civil transport
[NASA-TM-4058] 21 p2895 N88-27182

SUPERSONIC DRAG
Submunitions simulations, volume 2
[TR-CR-RD-SS-87-7-VOL-2] 19 p2641 N88-25669

SUPERSONIC FLIGHT
Time-temperature-stress capabilities of composite materials for advanced supersonic technology application
[NASA-CR-178272] 06 p0677 N88-14144
Wind tunnel investigation of wing and control panel loads at transonic and supersonic speeds on some schematic cruciform missile configurations
[FFA-TN-1986-43] 18 p2457 N88-24585

SUPERSONIC FLOW
Intergration effects of D-shaped, underwing, aft-mounted, separate-flow, flow-through nacelles on a high-wing transport
[NASA-TM-4018] 02 p0122 N88-10773
Numerical simulation of a supersonic chemically reacting mixing layer 02 p0143 N88-10900
Optical fiber interferometric sensor to measure temperature in gas flow
[ENST-87E006] 02 p0170 N88-11071
A supersonic potential gradient method for the calculation of unsteady aerodynamic pressures on harmonically oscillating wings
[ESA-TT-930] 03 p0259 N88-11631
Efficient numerical approaches for predicting supersonic flows with viscous/inviscid interaction 03 p0260 N88-11637
Supercritical fluid chromatography/supersonic jet spectroscopy
[DE88-000297] 03 p0282 N88-11774
A hybrid numerical technique for predicting the aerodynamic and acoustic fields of advanced turboprops
[NASA-CR-174926] 03 p0374 N88-12352
Experimental and theoretical study of condensation in multicomponent mixtures
[DE88-000897] 04 p0413 N88-12563
Conical wing with maximum lift-to-drag ratio in supersonic gas flow 04 p0425 N88-12633
Numerical study of supersonic flow around blunt bodies with extended needle nose 04 p0425 N88-12635
Combustion related shear-flow dynamics in elliptic supersonic jets 05 p0531 N88-13232
Solution of some 3-D viscous and inviscid supersonic flow problems by finite-volume space-marching schemes 05 p0532 N88-13235
The role of computation fluid dynamics in aeronautical engineering (4). The development and applications of implicit TVD finite volume code 05 p0536 N88-13259
Numerical analysis of supersonic flows using panel method 05 p0537 N88-13266
Interferometric data for a shock-wave/boundary-layer interaction
[NASA-TM-88227] 05 p0543 N88-13306
Ignition and flameholding in supersonic flow by injection of dissociated hydrogen 05 p0560 N88-13410
A Cartesian finite-volume method for the Euler equations 05 p0579 N88-13532
Investigation of the effect of laterally ejected gas jets on flows
[ISL-R-107/86] 05 p0581 N88-13545
Hot wire and laser velocimeter studies of turbulent flow at supersonic velocities
[ETN-88-91172] 05 p0585 N88-13566
Studies of supersonic turbulence and hot-wire response using Laser-Induced Fluorescence (LIF) 06 p0664 N88-14072
NASA supersonic STOVL propulsion technology program
[NASA-TM-100227] 06 p0668 N88-14093
Numerical study of chemically reacting flows using an LU scheme
[NASA-CR-180862] 06 p0668 N88-14094
Performance of supersonic impingement radial turbines 06 p0712 N88-14367
Aerodynamic design and test performance of supersonic turbines for the Vulcain rocket engine 06 p0713 N88-14373
Supersonic turbines for organic fluid Rankine cycles from 3 to 1300 kW 06 p0713 N88-14375
Raman spectra of adsorbed layers on space shuttle and AOTV thermal protection system surface 06 p0799 N88-14890
Application of a full potential method for analysis of complex aircraft geometries 07 p0809 N88-14930
Fundamental aspects of the structure of supersonic turbulent boundary
[AD-A186366] 07 p0815 N88-14959
Supersonic boundary layer on a heated wall
[ETN-88-91617] 08 p0950 N88-15763
The simulation of three-dimensional viscous supersonic flow past blunt bodies with a hybrid implicit/explicit finite difference method
[DFVLR-FB-87-32] 08 p0950 N88-15765
Supersonic throughflow fans for high-speed aircraft 08 p0958 N88-15810
New techniques in computational aerodynamics
[AD-A186719] 09 p1112 N88-16664
Application of highly loaded single-stage mixed-flow compressors in small jet-engines 10 p1280 N88-17652
Development and application of oxygen flow tagging for velocity measurements and flow visualization in turbulent three-dimensional supersonic flows
[AD-A187982] 10 p1289 N88-17714
On the interaction of Tollmein-Schlichting waves in axisymmetric supersonic flows
[NASA-CR-181619] 10 p1331 N88-17955
Experimental research on swept shock wave/boundary layer interactions
[AD-A187250] 10 p1331 N88-17957
The structure and control of three-dimensional shock wave turbulent boundary layer interactions
[AD-A187642] 10 p1332 N88-17961
Self-pumped phase conjugation in a supersonically flowing medium
[AD-A188281] 10 p1338 N88-17998
On the stability of the supersonic boundary layer 11 p1435 N88-18561
Nonaxisymmetric body supersonic, aerodynamic prediction
[AD-A189338] 13 p1716 N88-20259
Interaction between two-dimensional sonic jets and supersonic flow to model heat addition in a supersonic combustor
[AD-A189572] 13 p1716 N88-20261
Tests on the AFWAL 65 deg delta wing at NLR: A study of vortex flow development between Mach = 0.4 and 4
[NLR-MP-86058-U] 13 p1717 N88-20266
The international vortex flow experiment: A test case for compressible Euler codes
[NLR-MP-86076-U] 13 p1717 N88-20267
Supercritical fluid chromatography/supersonic jet spectroscopy
[DE88-004438] 13 p1738 N88-20392
Investigation of supersonic chemically reacting and radiating channel flow
[NASA-CR-182726] 14 p1862 N88-21125
Basic instability mechanisms in chemically reacting subsonic and supersonic flows
[AD-A190101] 15 p2034 N88-22120
JPRS report: Science and technology. China
[JPRS-CST-87-043] 15 p2053 N88-22233
Zero-lift drag predictions in supersonic flow for complex configurations 15 p2054 N88-22246
Numerical and experimental investigation of multiple shock wave/turbulent boundary layer interactions in a rectangular duct
[AD-A190772] 15 p2066 N88-22320
Analysis for high compressible supersonic flow in converging nozzle
[IPPJ-860] 16 p2157 N88-22869
An integral equation for the linearized supersonic flow over a wing
[AD-A191408] 16 p2158 N88-22875
User's manual for EULER3DS
[AD-A191048] 16 p2208 N88-23177
Multi-body aircraft with an all-movable center fuselage actively controlling fuselage pressure drag
[NASA-CASE-LAR-13511-1] 17 p2301 N88-23765
An efficient parallel algorithm for the simulation of three-dimensional compressible transition on a 20 processor Flex/32 multicomputer
[NASA-CR-178340] 17 p2337 N88-23943
Fundamental aspects of the structure of supersonic turbulent boundary layers
[AD-A191494] 18 p2456 N88-24581
Numerical simulations of the flat-plate laminar boundary layer in subsonic and supersonic flow
[PDR/CFDU/IC/36] 18 p2511 N88-24895

Numerical solutions of the complete Navier-Stokes equations
[NASA-CR-183023] 18 p2514 N88-24914
A characteristic method for calculating the generalized flat flutter aerodynamic forces
[NASA-TT-20300] 19 p2598 N88-25438
Aerodynamic focusing of particles and heavy molecules
[DE88-007145] 19 p2598 N88-25440
Cascades with harmonically oscillating blades in supersonic flow
[NASA-TT-20323] 19 p2599 N88-25446
Supercritical fluid chromatography/supersonic jet spectroscopy
[DE88-007935] 19 p2614 N88-25511
Dual Stokes cars measurements in supersonic combusting flow 19 p2625 N88-25569
Numerical simulation of supersonic free-jets 19 p2636 N88-25639
Relaxation scheme for compressible flows 19 p2640 N88-25663
Non equilibrium expansion of a radiating gas in a channel of varying section
[DE88-702063] 19 p2665 N88-25845
Navier-Stokes code NS3D for blunt bodies. Part 1: Analysis, results and verification
[DE88-010105] 19 p2666 N88-25855
Three-dimensional viscous flow computations of a circular jet in subsonic and supersonic cross flow
[NASA-CR-182153] 20 p2800 N88-26616
Nonaxisymmetric viscous lower branch modes in axisymmetric supersonic flows
[NASA-CR-181687] 21 p2891 N88-27164
Velocity measurements and flow visualization in turbulent three-dimensional supersonic flows using oxygen flow tagging
[AD-A192551] 21 p2892 N88-27165
Cryogenic free jets
[DFVLR-FB-88-16] 21 p2900 N88-27210
An improved version of NCOREL: A computer program for 3-D nonlinear supersonic potential flow computations
[NASA-CR-4165] 22 p3038 N88-28039
Chemically-produced N2(A) to NO(X) energy transfer in a supersonic flow
[AD-A192501] 22 p3082 N88-28302
NF (a 1 delta) production in a supersonic flow using N2F4+H2 in a BCL-16 nozzle
[AD-A194478] 22 p3082 N88-28304
An integral equation for the linearized unsteady supersonic flow over a wing
[AD-A193773] 23 p3172 N88-28887
Preliminary studies of NF3+H2 production of N2(A3 sigma(+)u) in a supersonic flow
[AD-A194479] 23 p3219 N88-29162
N2(A3epsilon u+) by reaction of N2F4+H2 in a supersonic flow
[AD-A194493] 23 p3219 N88-29163
Accuracy criteria for evaluating supersonic aerodynamic coefficient predictions 24 p3317 N88-29756
Compression pylon
[NASA-CASE-LAR-13777-1] 24 p3323 N88-29789

SUPERSONIC FLOW INLETS
U SUPERSONIC INLETS

SUPERSONIC FLUTTER
Detailed on-blade measurements on a transonic fan in unstalled supersonic flutter
[PNR90424] 22 p3039 N88-28043

SUPERSONIC INLETS
Unsteady flow in a supercritical supersonic inlet 18 p2460 N88-24605

SUPERSONIC JET FLOW
Numerical analysis of flow characteristics of supersonic free-jets 05 p0538 N88-13274
On the start up of supersonic underexpanded jets --- Mach disks 11 p1435 N88-18563
The thermal evolution of the jets in SS433 --- galactic object
[MPE-PREPRINT-107] 16 p2269 N88-23705
Velocity measurements and flow visualization in turbulent three-dimensional supersonic flows using oxygen flow tagging
[AD-A192551] 21 p2892 N88-27165

SUPERSONIC NOZZLES
Design of supersonic Coanda jet nozzles 10 p1270 N88-17599

SUPERSONIC SPEED
Aerodynamic sensitivities from subsonic, sonic and supersonic unsteady, nonplanar lifting-surface theory
[NASA-TM-100502] 04 p0394 N88-12459
The aerodynamics of supersonic parachutes
[DE87-014846] 04 p0395 N88-12464
Vortex formation over delta, double-delta and wave rider configurations at supersonic speeds 05 p0533 N88-13243
Design of wings and wing/body configurations for transonic and supersonic speeds 05 p0545 N88-13318
Supersonic beam observations of semiconductor clusters
[AD-A184991] 05 p0655 N88-14018
Supersonic aerodynamics of delta wings
[NASA-TP-2771] 10 p1273 N88-17615
Aerodynamic characteristics of wings designed with a combined-theory method to cruise at a Mach number of 4.5
[NASA-TP-2799] 12 p1575 N88-19420
Nonaxisymmetric body supersonic, aerodynamic prediction
[AD-A189338] 13 p1716 N88-20259
The structure of sonic underexpanded turbulent air jets in still air
[AD-A190856] 16 p2157 N88-22870
Submunitions simulations, volume 2
[TR-CR-RD-SS-87-7-VOL-2] 19 p2641 N88-25669
High speed and high angle of attack wind tunnel test results of the winged space vehicle C-2
[ISAS-RN-623] 20 p2751 N88-26329
Wind tunnel tests of elliptical missile body configurations at Mach numbers 0.4 to 5.0
[AD-A193525] 22 p3038 N88-28040
Wind tunnel investigation of wing and control panel loads at transonic and supersonic speeds on some schematic cruciform missile configurations
[FFA-TN-1986-43-SUPPL-1] 22 p3039 N88-28044

SUPERSONIC TRANSPORTS
NT CONCORDE AIRCRAFT
Propulsion challenges and opportunities for high-speed transport aircraft 08 p0958 N88-15809
Conceptual final paper on the preliminary design of an oblique flying wing SST
[NASA-CR-182879] 16 p2161 N88-22891
The challenges and opportunities of supersonic transport propulsion technology
[NASA-TM-100921] 17 p2307 N88-23806
Concept development of a Mach 3.0 high-speed civil transport
[NASA-TM-4058] 21 p2895 N88-27182

SUPERSONIC TURBINES
Design and test of a high blade speed, high work capacity transonic turbine 10 p1281 N88-17658
Numerical solutions of unsteady inviscid transonic turbine cascade flows
[AD-A196111] 24 p3316 N88-29748

SUPERSONIC WIND TUNNELS
The 0.6m x 0.6m trisonic test section (TMK) of DFVLR in Cologne-Porz, Federal Republic of Germany (status 1986)
[ESA-TT-1052] 03 p0267 N88-11681
Experimental investigation of the subsonic high-altitude operation of the NASA Lewis 10- by 10-foot supersonic wind tunnel
[NASA-TM-100214] 08 p0959 N88-15814
Design of a supersonic wind tunnel
[ETN-88-92078] 14 p1870 N88-21176
Numerical and experimental investigation of multiple shock wave/turbulent boundary layer interactions in a rectangular duct
[AD-A190772] 15 p2066 N88-22320
A comparative study of vortex flows in wind and water tunnels 16 p2204 N88-23151
Supersonic wall adaptation in the rubber tube test section of the DFVLR Goettingen
[IB-222-87-A-08] 24 p3330 N88-29824

SUPERSONICS
Planform effects on the supersonic aerodynamics of multibody configurations
[NASA-TP-2762] 04 p0393 N88-12454

SUPERSTRING THEORY
U STRING THEORY

SUPERSYMMETRY
Spontaneous symmetry breaking in N=2 supergravity
[DE87-702749] 01 p0109 N88-10704
New class of spherically symmetric interior solution with cosmological constant
[DE87-703095] 02 p0226 N88-11422
Anomalies in gauge theories
[DE87-014087] 02 p0229 N88-11444
Superconformal invariance and superstring in background fields
[DE87-703097] 02 p0247 N88-11561
Geometrization of Planck length in composite gravity and supergravity
[DE87-703085] 02 p0251 N88-11588
Chiral U(1) anomaly in D = 4 super Yang-Mills theory coupled to supergravity
[DE87-753022] 02 p0252 N88-11591
A supersymmetric Lagrangian for Poincare gauge theories of gravity
[DE88-001670] 04 p0500 N88-13078
Breaking of supersymmetry degeneracy and phenomenological conditions
[PREPRINT-559] 06 p0790 N88-14843
Instanton in supersymmetric theory with static disorder
[DE88-700357] 07 p0940 N88-15716
On the dynamical supersymmetry of atomic hydrogen
[DE88-700713] 10 p1422 N88-18495
Research in theoretical physics: Results from last year 1986/87
[DE88-004922] 10 p1423 N88-18502
SUSY anomaly in quantum-mechanical systems
[DE88-700890] 12 p1699 N88-20170
Summary of supersymmetric particle search with the CELLO detector at Petra (Italy)
[NOTA-INTERNA-898] 14 p1980 N88-21818
Gluino branching ratio effects on the search for supersymmetry
[PREPRINT-572] 14 p1981 N88-21821
Strings in four dimensions
[DE88-006435] 14 p1990 N88-21864
On the Hilbert space of supersymmetric quantum systems
[DE88-701648] 16 p2284 N88-23677
Introduction to covariant formulation of superstring (field) theory
[DE87-703038] 18 p2586 N88-25363
Comment on non-renormalization theorem in the four dimensional superstrings
[DE88-752551] 18 p2586 N88-25367
General relativity invariance and string field theory
[DE88-702045] 19 p2737 N88-26252
Superalgebras with Grassmann algebra-valued structure constants from superfields
[DE88-702239] 21 p3011 N88-27862
Research in the theory of condensed matter and elementary particles
[DE88-010180] 22 p3151 N88-28749
Lagrangian of the self-duality equation and d = 10, N = 2b supergravity
[DE88-701554] 24 p3455 N88-30563

SUPPLEMENTS
NASA thesaurus supplement: A four part cumulative supplement to the 1985 edition of the NASA Thesaurus
[NASA-SP-7053(SUPP-4)] 08 p1093 N88-16575

SUPPLYING
Prototype resupply scheduler 08 p1064 N88-16428
Steps toward lunar settlement
[DE88-009141] 21 p2900 N88-27213
Maintenance and supply options
[NASA-CR-172062] 24 p3332 N88-29837

SUPPORT SYSTEMS
NT CLOSED ECOLOGICAL SYSTEMS
NT GROUND SUPPORT SYSTEMS
NT LIFE SUPPORT SYSTEMS
Repulsive force support system feasibility study
[NASA-CR-178400] 04 p0402 N88-12497
The effect of mass, wind angle and erection technique on the aeroelastic behaviour of a cable-stayed bridge model
[NAE-AN-46] 04 p0455 N88-12819
Space station accommodations for lunar base elements: A study
[NASA-TM-100501] 06 p0804 N88-14907
A space transportation system operations model
[NASA-TM-100481] 07 p0823 N88-14999
Global meteorological data facility for real-time field experiments support and guidance
[NASA-TM-4023] 14 p1947 N88-21608
Engine component retirement for cause. Volume 1: Executive summary
[AD-A192730] 20 p2760 N88-26371
Inflight rearming
[AD-A193564] 23 p3176 N88-28909
Definition of common support equipment and space station interface requirements for IOC model technology experiments
[NASA-TM-100656] 24 p3336 N88-29856

SUPPORTS
NT PYLONS
A passive vibration-cancelling isolation mount 05 p0595 N88-13636
Strain gage sting balance 204-6. Calibration report --- wind tunnels
[F+W-FO-1838] 09 p1168 N88-17002
Dynamic response of a geared train of rotors subjected to random support excitations 09 p1181 N88-17073
Centaur G Prime modal test 09 p1181 N88-17075
Microgravity isolation mount
[ESA-CR(P)-2480] 11 p1443 N88-18604
Development of isostatic mounts and associated guidelines --- spacecraft payloads
[CASA-IM-WP-301] 13 p1731 N88-20354

Design of a sound neck in connection with the model-support system of a transonic wind tunnel test section
[ILR-MITT-186(1987)] 14 p1869 N88-21171
Kinematic support using elastic elements
14 p1926 N88-21481
Almond test body — for microwave anechoic chambers
[NASA-CASE-LAR-13747-1] 18 p2502 N88-24845
Thermal compensating mount
[NASA-CASE-LAR-13794-1] 18 p2519 N88-24942
FEB (Multifilter Electronics Box) lifting device analysis, revision A
[AD-A192313] 21 p2935 N88-27427
Method of forming dynamic membrane on stainless steel support
[NASA-CASE-MSC-18172-3] 23 p3201 N88-29052

SUPPRESSION
U RETARDING

SUPPRESSORS
Investigation of fuel additive effects on sooting flames
[AD-A186403] 07 p0829 N88-15026
Computation of LMS (Least-Mean-Square) and matched digital filters for optical clutter suppression
[AD-A188885] 12 p1687 N88-20093
Kinetic mechanisms for ionization and afterburning suppression
[AD-A189219] 13 p1737 N88-20383

SURFACE ACOUSTIC WAVE DEVICES
The design and implementation of surface acoustic wave devices for linear FM and a new non-linear FM pulse compression technique for radar applications
[AD-A186741] 08 p0980 N88-15922
The acoustic-electric field analysis of multilayered surface acoustic wave devices
[ETN-88-91592] 09 p1242 N88-17446
Surface acoustic wave deposition sensor
[DE87-006527] 09 p1243 N88-17452
Measuring thin film properties using SAW (Surface Acoustic Wave) devices: Diffusivity and surface area
[DE88-002216] 13 p1834 N88-20970
Isothermal measurement and thermal desorption using SAW devices 19 p2671 N88-25881
Thermodynamic study of hygroscopic polymers using surface acoustic waves 19 p2672 N88-25882
Surface acoustic wave gas sensor based on film conductivity changes 19 p2673 N88-25894
The covariance of scalar fields scattered by pressure-release randomly rough surfaces
[AD-A192489] 22 p3146 N88-28714
Large aperture multi-dimensional laser radar testbed
[AD-A193447] 23 p3218 N88-29155
The use of a surface acoustic wave technique to study the growth behavior of small cracks in a high strength steel alloy 23 p3225 N88-29193
A theoretical and experimental investigation into the use of SAW weighting techniques in optical diffraction gratings
[RSRE-MEMO-4128] 23 p3283 N88-29549

SURFACE COOLING
Transient cooling of a hot surface by droplets evaporation, March 1986 - March 1987
[PB88-153341] 10 p1330 N88-17950
Investigation of annular flow at high evaporation rates in view of liquid film cooling
[DFVLR-FB-88-08] 21 p2949 N88-27517
Studies of gas turbine heat transfer airfoil surface and end-wall cooling effects
[AD-A195165] 24 p3326 N88-29805

SURFACE CRACKS
Thermomechanical cracking in coated media due to high speed asperity excitation
[AD-A184176] 04 p0454 N88-12809
The effect of microstructure on the surface crack length: Crack depth relationship for short cracks
05 p0600 N88-13670
Summary of comparison between experimental and analytical (including empirical) results for initiation of crack growth for surface cracks
[DE88-001604] 06 p0721 N88-14433
Study on the correlation of polystyrene (PS) film craze to its fracture behaviour by TEM (Transmission Electron Microscopy)
[PB87-143343] 08 p0970 N88-15870
Nonlinear line-spring model for surface crack analysis with particular reference to work hardening materials
[PB87-144838] 08 p0994 N88-16016
Fracture-resistant characteristics of medium-strength plates with regard to the initiation, stable and unstable propagation of surface cracks
[PB87-144804] 08 p0996 N88-16025
Finite element analysis for the calculation of calibration curves of fracture mechanics specimen for semicircular surface cracks with several starting depths, for the crack depth measurement following the dc potential method
[GKSS-87/E/19] 09 p1183 N88-17086
Stress-intensity factors for small surface and corner cracks in plates
[NASA-TM-100599] 15 p2088 N88-22445
Surface crack analysis applied to impact damage in a thick graphite-epoxy composite
[NASA-TM-100600] 16 p2173 N88-22950
Fracture morphologies of carbon-black-loaded SBR (Styrene-Butadiene Rubber) subjected to low-cycle, high-stress fatigue
[DE88-006808] 16 p2181 N88-23002
On governing equations for crack layer propagation
[NASA-CR-182120] 16 p2223 N88-23272
The surface crack problem in an orthotropic plate under bending and tension
[NASA-CR-178281] 18 p2531 N88-25014
Boundary element method for contact heat transfer
[DE88-011013] 20 p2800 N88-26613
A critical review of IR drops and electrode potentials within pits, crevices and cracks
[AD-A192481] 21 p2935 N88-27431
Thermo-mechanical cracking in coated media with a cavity by a moving asperity friction
[AD-A193311] 21 p2961 N88-27586
Empirical fatigue crack growth data for a tension loaded threaded fastener
[AD-A194112] 22 p3088 N88-28334

SURFACE DEFECTS
Ultrasonic testing of near-surface zones using scattered signals
[ETN-88-90813] 07 p0929 N88-15642
Ultrasonic inspection of irregular surfaces
[AERE-R-12465] 13 p1780 N88-20648
Measurement of the elastic-plastic surface flaw back surface topology and its relation to constraint
[DE88-006765] 15 p2087 N88-22437

SURFACE DIFFUSION
De-alloying
[DE87-012488] 01 p0022 N88-10139
Studies of supported metal catalysts
[DE88-002546] 07 p0831 N88-15038
Numerical computations of natural convection heat transfer in irregular geometries
[DE88-002358] 07 p0852 N88-15178
Grain boundary and surface diffusion in oxides
[DE88-002348] 07 p0938 N88-15697
Laser-induced desorption determinations of surface diffusion on Rh(111)
[DE88-005159] 11 p1454 N88-18667
Depolarized infrared reflectance from dry and wetted surfaces
[AD-A188213] 11 p1492 N88-18903
On the global radiation incident variously orientated surfaces on the South Coast of Finland
[FMI-5] 20 p2823 N88-26748

SURFACE DISTORTION
Removal of out-of-plane distortion in mild steel panels using flame heating, volume 1
[AD-A187802] 11 p1457 N88-18684
Removal of out-of-plane distortion in mild steel panels using flame heating, volume 2
[AD-A187803] 11 p1457 N88-18685
Compensation of relector antenna surface distortion using an array feed
[NASA-TM-100286] 11 p1476 N88-18805
Case study of active array feed compensation with sidelobe control for reflector surface distortion
[NASA-TM-100287] 16 p2192 N88-23073
Thermal distortion analysis of the space station solar dynamic concentrator
[NASA-TM-100868] 19 p2606 N88-25475
Active feed array compensation for reflector antenna surface distortions
[NASA-TM-100826] 19 p2654 N88-25782

SURFACE ENERGY
Estimating regional evapotranspiration from remotely sensed data by surface energy balance models
[NASA-CR-181400] 01 p0064 N88-10411
Evaluation of surface energy and radiation balance systems on the Konza Prairie
[NASA-CR-182534] 10 p1355 N88-18097
Surface free energy of laser-produced bond percolators
[PB88-130885] 11 p1493 N88-18913

SURFACE FINISHING
Surface treatment problems found in new aircraft designed using structural composites
[SNIAS-872-111-113] 05 p0558 N88-13397
The analysis of metal finishing solutions by ion chromatography
[AD-A184812] 05 p0561 N88-13414
Fatigue characteristics of ion treated surfaces
05 p0606 N88-13713
New application of transition metal carbides detailed
06 p0675 N88-14132
Ion-beam nitriding of steels
[NASA-CASE-LEW-14104-2] 06 p0682 N88-14179
Study of surface treatment before bonding of light alloys
[DCQ/L-48-287/F] 06 p0682 N88-14181
Surface modification using ion beams: Recent developments at ORNL
[DE88-000951] 06 p0786 N88-14819
Chemical cleaning of metal surfaces in vacuum systems by exposure to reactive gases
[AD-A188588] 12 p1608 N88-19616
Comparison of isopropyl alcohol and trichloroethylene in removing solder flux
[DE88-005556] 14 p1889 N88-21288
Specimen preparation techniques for the examination of ceramic and metal-matrix composites
[DE88-005157] 15 p2030 N88-22094
Auger electron spectroscopy of contrast-forming layers on metals
[NASA-TT-20182] 16 p2178 N88-22980
Surface conditioning products as tools for corrosion removal and corrosion prevention
17 p2320 N88-23856
Influence of carbon fiber surface treatment
[ETN-88-92536] 18 p2492 N88-24787
Evaluation of the chromium oxide arc spraying treatment on solar energy collectors
[ETN-88-92564] 18 p2537 N88-25053
The knowledge based automatic extraction of the machinable surfaces for automatic CAD-CAM system
[INPE-4542-PRE/1288] 20 p2836 N88-26824
Fabrication technology
[DE88-010598] 20 p2855 N88-26955
Study of surface treatments before adhesive bonding of light alloys — aircraft industry
[ETN-88-92743] 21 p2916 N88-27308
Optimization of fatigue and friction properties of titanium by means of surface treatments
[ECL-87-22] 22 p3056 N88-28133
Fractal surface finish
[DE88-007972] 22 p3057 N88-28137

SURFACE GEOMETRY
Approximation and representation of explicit surfaces in the presence of singularities
[ETN-88-92191] 16 p2258 N88-23496
Cylindrical surface profile and diameter measuring tool and method
[NASA-CASE-MFS-28287-1] 17 p2341 N88-23959

SURFACE INTERACTIONS
U SURFACE REACTIONS

SURFACE IONIZATION
Laser post-ionization secondary neutral mass spectroscopy
[DE88-002979] 09 p1172 N88-17027

SURFACE LAYERS
NT MONOMOLECULAR FILMS
Auger electron spectroscopy of oxidized titanium overlayers: Speciation of homogeneous and heterogeneous samples
[KFK-4221] 02 p0146 N88-10913
Bond character at a silicon/copper surface
[AD-A184167] 03 p0295 N88-11851
Far-infrared spectra of lithium deposited on a gold electrode: Interpretation using a cluster model
[AD-A184231] 04 p0495 N88-13050
Atomic and electronic structure of surfaces and chemisorbed layers
[DE87-014987] 04 p0498 N88-13065
Cosmological applications of singular hypersurfaces in general relativity 04 p0521 N88-13202
The effect of ion beam mixed Ni-Al surface layers on PSB extrusion morphology in fatigued nickel
05 p0598 N88-13652
Model Cu/ZnO catalysts for methanol synthesis: The role of surface structure
[DE88-002354] 07 p0830 N88-15037
Foam generation and air entrainment near a free surface
[AD-A185986] 07 p0848 N88-15149
Analysis of load-bearing capacity of nitrided layer
[PB87-144176] 08 p0968 N88-15857
Monolayer films prepared by the spontaneous self-assembly of symmetrical and unsymmetrical dialkyl sulfides from solution onto gold substrates: Structure, properties, and reactivity of constituent functional groups
[AD-A186717] 09 p1137 N88-16814
Geometric structure, pseudoband gaps, and surface vibrational resonances on metal surfaces
[AD-A187001] 09 p1143 N88-16851
Tactile sensing and inverse problems
[AD-A187464] 10 p1340 N88-18011
Cost 501 Project U.K.10. Part 4: The oxidation of fecralloy steel co-extruded onto strong steel substrates
[AERE-R-12432-PT-4] 11 p1456 N88-18679
Characterization of enhanced Schottky-barrier InGaAs/Al(1-x)As strained channel modulation-doped field-effect transistors
[AD-A188820] 12 p1698 N88-20162

Characterization of redox states of nickel hydroxide film electrodes by in-situ Raman spectroscopy
[AD-A189288] 13 p1741 N88-20411
Vertical turbulent transfer of matter in thin ocean surface layer during daytime heating 13 p1787 N88-20693
High-efficiency thin-film silicon-on-GaP solar cell for improved radiation resistance
[AD-A190268] 15 p2091 N88-22480
Studies of surfaces using optical sum-frequency generation
[DE88-006334] 15 p2131 N88-22715
Calculating depletion region carrier concentrations with capacitance-voltage measurements and etching
[AD-A189630] 15 p2141 N88-22777
On governing equations for crack layer propagation
[NASA-CR-182120] 16 p2223 N88-23272
Evaluating evaporation with satellite thermal data
[AD-A192042] 18 p2531 N88-25019
Surface phases and their influence on metal-oxide interfaces
[DE88-007938] 20 p2769 N88-26420
Fundamental optical studies of competitive adsorption and thin film phenomena
[DE88-008780] 20 p2875 N88-27068
Electronic and geometric structure of silver and palladium on aluminum (111) in monoatomic surface layers
[ETN-88-92120] 20 p2879 N88-27093
Thermo-mechanical cracking in coated media with a cavity by a moving asperity friction
[AD-A193311] 21 p2961 N88-27586
Elastic behavior of a rubber layer bonded between two rigid spheres
[AD-A193698] 23 p3198 N88-29030

SURFACE NAVIGATION

Dynamic image interpretation for autonomous vehicle navigation
[AD-A184043] 03 p0262 N88-11647
Autonomous Land Vehicle (ALV) planning and navigation system
[AD-A184243] 04 p0397 N88-12475
A computer simulation study of an expert system for walking machine motion planning
[AD-A187907] 11 p1438 N88-18577
A comparison of terrain association and resection as methods of position location
[AD-A189480] 13 p1790 N88-20710
Assessment of the differential technique for land navigation within 1000 km of Omega Australia
[AD-A191036] 16 p2160 N88-22685
The integration of digital maps in vehicle navigation systems 16 p2225 N88-23286
Joint University Program for Air Transportation Research, 1986
[NASA-CP-2502] 17 p2293 N88-23715
Navigation system for land vehicles
[NASA-CASE-LAR-13322-1] 18 p2462 N88-24620
Navigation using the Teldix fiber-optic gyroscope 18 p2517 N88-24933
Contribution of space to marine activities 19 p2700 N88-26057
Automatic omega station and LOP (Line Of Position) selection
[AD-A193302] 21 p2894 N88-27179
Measurement and interpretation of North Atlantic Ocean marine radar sea scatter
[AD-A196239] 24 p3364 N88-30036

SURFACE PRESSURE

U PRESSURE

SURFACE PROPERTIES

NT ADHESION
NT ADSORPTIVITY
NT COEFFICIENT OF FRICTION
NT INTERFACIAL TENSION
NT SKIN TEMPERATURE (NON-BIOLOGICAL)
NT SPECTRAL REFLECTANCE
NT SURFACE CRACKS
NT SURFACE DEFECTS
NT SURFACE ENERGY
NT SURFACE ROUGHNESS
NT SURFACE STABILITY
NT SURFACE TEMPERATURE
NT WALL TEMPERATURE

Recovery of vacuum gaps after arcing
[DE87-013852] 01 p0039 N88-10250
High-efficiency silicon solar cells: Numerical modeling, transient measurements, efficiency goals, and v-shaped grooves
[DE87-012842] 01 p0066 N88-10423
A surface science investigation of potential intermediates, catalysts, and promoters in the synthesis of higher alcohols by metals
[DE87-014188] 02 p0144 N88-10906
Field ion microscope studies of surface reconstructions
[DE87-014644] 02 p0147 N88-10924
Investigation of the structure of coatings of self fluxing alloys fused by laser energy
[BLL-M-37301-(5828.4)] 02 p0148 N88-10930
Surface topography and electrical response of metal-electrolyte interface
[DE87-013553] 02 p0166 N88-11046
Surface effects and low frequency noises in GaAs field effect transistors
[LAAS-87-179] 02 p0168 N88-11055
Analytical caustic surfaces
[NASA-TM-87805] 02 p0168 N88-11060
A preliminary taxonomy of visible surface algorithms
[DE87-013559] 02 p0220 N88-11386
Plasmon resonance absorption in layered structures of silver with periodic corrugation
[DE87-013183] 02 p0231 N88-11453
The structure and reactivity of heterogeneous surfaces and study of the geometry of surface complexes
[DE88-000158] 03 p0279 N88-11754
Materials preparation and longevity in hyperthermal atomic oxygen 03 p0297 N88-11862
The formation of optical membrane reflector surfaces using uniform pressure loading
[DE87-012275] 03 p0376 N88-12367
Characterization of catalysts with metal-support effects and of the species adsorbed on their surfaces
[DE87-014636] 04 p0414 N88-12564
Characterization of thin layers for optics
[PB87-217949] 04 p0490 N88-13017
Calibration on the Sun for stellar magnetic fields 04 p0506 N88-13113
The dynamics of solar magnetic flux tubes subjected to resonant foot point shaking 04 p0507 N88-13118
A complete linearized theory for the analysis and design of two-dimensional hydrofoils near a free surface
[UTIAS-TN-264] 05 p0579 N88-13531
Dynamical analysis of molecular decay at spherical surfaces
[AD-A184908] 05 p0647 N88-13964
Effect of metal surface properties on the fatigue crack growth behavior 06 p0716 N88-14390
Investigation of silicon surface passivation by silicon nitride film deposition
[NASA-CR-182350] 06 p0729 N88-14487
Automated satellite cloud analysis: A multispectral approach to the problem of snow/cloud discrimination
[AD-A185672] 06 p0746 N88-14591
A surface plasmon waveguide sensor: A new type of chemical transducer based on optical phenomena
[ETN-88-91322] 06 p0780 N88-14792
Extending the range of Low Energy Electron Diffraction (LEED) surface structure determination: Co-adsorbed molecules, incommensurate overlayers and alloy surface order studied by new video and electron counting LEED techniques
[DE88-001401] 06 p0786 N88-14820
Helium atom surface scattering apparatus for studies of crystalline surface dynamics
[DE88-002104] 06 p0787 N88-14826
Photon stimulated desorption from oxidized Al(110)
[DE88-002209] 06 p0787 N88-14828
A jet in a crossflow
[NASA-CR-182469] 09 p1113 N88-16674
Surface composition-reactivity relationships in heterogeneous catalysis
[DE87-003450] 09 p1140 N88-16834
Surface and interface electronic structure
[DE88-003363] 09 p1258 N88-17545
Monitoring interfacial dynamics by pulsed laser techniques
[DE88-003362] 10 p1335 N88-17976
Interactions of cultured human endothelial cells with polymeric surfaces
[PB88-112255] 10 p1369 N88-18178
Solving complex and disordered surface structures with electron diffraction
[DE88-003863] 10 p1418 N88-18467
Preliminary experiments on surface flow visualization in the cryogenic wind tunnel by use of condensing or freezing gases
[NASA-CR-181634] 11 p1442 N88-18602
In situ ultrahigh vacuum friction measurement and wear track analysis of ion implanted 304 stainless steel
[DE88-004537] 11 p1494 N88-18922
Scanning tunneling microscopy of silver, gold, and aluminium monomers and small clusters on graphite
[DE88-003871] 11 p1562 N88-19349
Some applications of surface Raman and infrared spectroscopies to mechanistic electrochemistry involved adsorbed species
[AD-A188777] 12 p1606 N88-19602
Measuring and modeling near surface reflected and emitted radiation fluxes at the FIFE site
[NASA-CR-182660] 12 p1640 N88-19818
Airborne electromagnetic sounding of sea ice thickness and sub-ice bathymetry
[AD-A188939] 12 p1649 N88-19879
Relationships between remotely-sensed surface properties and subsurface structure in the ocean
[AD-A189317] 12 p1650 N88-19881
Superconductors with structured surfaces: Fields and currents
[AD-A189353] 12 p1699 N88-20164
A study of the interaction of light with sub-micron metallic surfaces
[DE88-003138] 13 p1776 N88-20624
Computer aided surface representation
[DE88-005408] 13 p1817 N88-20854
Optics for large telescope 13 p1840 N88-21014
Hydrogen pumping and release by graphite under high flux plasma bombardment
[DE88-005880] 13 p1842 N88-21021
Advances in contact algorithms and their application to tires
[NASA-TP-2781] 14 p1922 N88-21456
Measurement from satellites of land surface parameters and fluxes in the thermal infrared bands: Problems and methods 14 p1937 N88-21557
Technical applications of solar energy. Project: Selective coatings
[BMFT-FB-T-86-213] 14 p1943 N88-21591
The nucleus of Comet Halley 14 p2004 N88-21947
Properties of the nucleus of P/Halley 14 p2004 N88-21952
Physical-mechanical properties of matrices on the comet nuclei surface models 14 p2010 N88-21987
Study of surface discharges
[ONERA-12/7236-PY] 15 p2026 N88-22073
Structure of sol-gel silica
[DE88-006870] 15 p2033 N88-22114
Measurement of emissivity of industrial surfaces using a simple method
[NASA-TT-20165] 15 p2036 N88-22130
The thermal radiative properties of metals at high temperature
[DE88-006825] 15 p2038 N88-22141
JPRS report: Science and technology. Japan
[JPRS-JST-88-002] 15 p2050 N88-22210
Material surface improvement by laser 15 p2051 N88-22217
First-principles calculations of quasiparticle energies at surfaces and interfaces: Semiconductor surface-state spectra and band offsets
[DE88-006340] 15 p2141 N88-22773
Experimental investigation of the hypersonic flow over a six finned configuration
[AD-A190870] 16 p2157 N88-22871
Surface and interfacial properties of carbon fibers
[NASA-CR-182890] 16 p2173 N88-22951
Method of digital surface photometry of galaxies and its application to the edge-on galaxy NGC 5907 16 p2287 N88-23695
Thematic mapping utilizing data from the Thematic Mapper sensor of the LANDSAT satellite 17 p2361 N88-24060
Analysis of the parameters responsible for the variations of the illumination conditions in the LANSAT data 17 p2362 N88-24070
Arc-textured metal surfaces for high thermal emittance space radiators
[NASA-TM-100894] 18 p2487 N88-24754
The electrokinetic behavior of calcium oxalate monohydrate in macromolecular solutions
[NASA-TM-101144] 18 p2493 N88-24791
Evidences for distributed combustion 19 p2628 N88-25586
How much do edges affect the ignition of a homogeneous reactive solid: Summary to date 19 p2631 N88-25608
Surface fatigue life of CBN and vitreous ground carburized and hardened AISI 9310 spur gears
[NASA-TM-100960] 19 p2677 N88-25916
X-ray and optical analysis of surface properties of metal optics
[DE88-004033] 19 p2727 N88-26195
Epitaxial iron films
[AD-A191815] 19 p2732 N88-26225
The catalytic reactivity of thin film crystal surfaces
[DE88-006387] 19 p2732 N88-26228
Production of powdered sodium hydride with large specific surface by the catalyzed reaction of molten sodium with hydrogen-1
[NASA-TT-20185] 20 p2776 N88-26462
Scattering patterns of dihedral corner reflectors with impedance surface impedances
[NASA-CR-183078] 20 p2789 N88-26545
Evaluation of surface energy and radiation balance systems for FIFE
[NASA-CR-183118] 20 p2828 N88-26778

Eigenmatrix representations of radiance distributions in layered natural waters with wind-roughened surfaces
[PB88-188701] 20 p2828 N88-26780
SEGMERGE: A scanline visible surface algorithm with adaptive span selection and inexpensive antialiasing
[DE88-009186] 20 p2836 N88-26826
Sound propagation over uneven ground and irregular topography
[NASA-CR-182956] 20 p2849 N88-26911
Fermi level dependent native defect formation: Consequences for metal-semiconductor and semiconductor-semiconductor interfaces
[DE88-008247] 20 p2875 N88-27066
Computer modeling for surface properties of carbon fibers 21 p2928 N88-27383
Analytical approximation of a distorted reflector surface defined by a discrete set of points
[NASA-TM-101323] 21 p2934 N88-27424
Methods of determining playa surface conditions using remote sensing
[AD-A192663] 21 p2965 N88-27612
Self-energies and the interactions of particles with surfaces
[DE88-010451] 21 p3014 N88-27885
Characterization of crystalline silicon by electrochemical and Raman spectroscopy at the frontier semiconductor/electrolyte
[ETN-88-92354] 21 p3025 N88-27956
Surface photometric investigations for spiral galaxies of large dimension structures in edge-on gemetry
[ETN-88-92126] 21 p3030 N88-27985
Fractal surface finish
[DE88-007972] 22 p3057 N88-28137
Modification of YBa2Cu3O(7-x) ceramics by adsorbed water and other gases
[DE88-011518] 22 p3057 N88-28140
Comparison of the bidirectional reflectance distribution function of various surfaces
[NASA-TM-101317] 22 p3153 N88-28760
Bulk plasmon enhanced photoemission from Nb(100) surface resonances
[AD-A192711] 22 p3154 N88-28767
Techniques for boundary layer tripping and control 23 p3168 N88-28863
Measure of hydrogen concentration profile in materials by resonant nuclear reactions
[DE88-702599] 23 p3193 N88-28999
Influence of local volume forces on surface relaxation of pure metals and alloys: Applications to Ni, Al, Ni3Al
[DE88-702718] 23 p3195 N88-29014
The mechanical behavior of surface modified ceramics
[DE88-010564] 23 p3196 N88-29022
Liquid thickness gauge
[NASA-CASE-LAR-13826-1] 23 p3217 N88-29150
Surface properties in electric discharge machining
[NASA-TT-20243] 23 p3223 N88-29182
Green's function approach to roughening transition of one-dimensional restricted solid on solid model
[DE88-702723] 23 p3278 N88-29512
Optical emission from surface waves supported in thin metal films 23 p3282 N88-29540
Potential induced structural transformations of the Au(100) and Au(111) surfaces
[DE88-005446] 23 p3287 N88-29571
Theoretical investigation of image states of the hydrogen covered Cu (100)
[DE88-702662] 23 p3292 N88-29604
System suitable for observing surface plasmon in a semi-infinite semiconductor superlattice
[DE88-702686] 23 p3293 N88-29606
Morphologic contrasts between Nirgal and Auqakuh Valles, Mars: Evidence of different crustal properties 23 p3304 N88-29681
Preliminary analysis of recent 2.2-4.2 micrometers telescopic observations of Elysium, Mars: Implications for crystallinity and hydration state of surface materials 23 p3306 N88-29692
Experimental determination of drag modifications due to elastic compliant surfaces using quantitative visual techniques
[AD-A194785] 24 p3372 N88-30082

SURFACE REACTIONS

Surface modification by metal deposition and laser irradiation 01 p0023 N88-10148
Gases released by surface flashover of insulators
[DE87-013851] 01 p0039 N88-10249
Silicon oxidation photoassisted with a continuous wave CO2 laser beam and contribution to the study of silica layers obtained
[LAAS-87-158] 02 p0179 N88-11115
Enhancement of surface-atmosphere fluxes by desert-fringe vegetation through reduction of surface albedo and of soil heat flux
[NASA-CR-181442] 02 p0197 N88-11231
Spacecraft surface exposure to atomic oxygen in low Earth orbit 03 p0273 N88-11715
Surface chemistry of transition metal carbides: A theoretical analysis
[AD-A184237] 03 p0291 N88-11829
Study of IR laser photoacoustic spectra of organic molecules adsorbed on metal surface 03 p0301 N88-11891
Deformation mechanisms of thermostructural materials
[AD-A184070] 03 p0338 N88-12128
Vectorial electron transfer on designed surfaces
[PB87-232229] 03 p0381 N88-12394
Surface catalytic degradation study of two linear perfluoropolyalkylethers at 345 C
[NASA-TP-2774] 04 p0410 N88-12543
Simulation studies for surfaces and materials strength
[NASA-CR-181535] 04 p0412 N88-12557
Influence of stratification in near-surface water layer on intensity of gas exchange between atmosphere and water 04 p0459 N88-12841
Reactions of porphyrins in surfactant assemblies, microemulsions and in solutions
[AD-A184797] 05 p0560 N88-13412
A study of the interaction of laser light with liquid propellant drops
[AD-A185117] 05 p0587 N88-13582
Pure dephasing of a vibrational adbond
[AD-A185222] 05 p0609 N88-13740
Energy dependence of ion-induced sputtering yields of monatomic solids in the low energy region
[IPPJ-AM-52] 05 p0651 N88-13988
Method for preparing hydride configurations and reactive metal surfaces
[DE88-000845] 06 p0679 N88-14161
Partial analysis of experiment LDEF A-0114
[NASA-CR-179236] 06 p0780 N88-14787
Unified study of plasma-surface interactions for space power and propulsion
[AD-A186211] 07 p0825 N88-15007
Studies of metal/carbon surface chemistry
[DE87-009545] 07 p0829 N88-15029
Surface chemistry of chemically sensitive field effect transistors
[AD-A185917] 07 p0847 N88-15139
Phonon dispersion for several surfaces with ordered overlayers: A lattice dynamical study 07 p0876 N88-15315
Investigations in field of surface forces in metallurgy
[BLL-M-47406-(5828.4)] 08 p0969 N88-15860
Beneficial and detrimental effects of silica in the high temperature oxidation of 20Cr/25Ni/Nb stainless steel
[AERE-R-12667] 10 p1301 N88-17779
Apparatus for the study of silicon film deposition and silicon etching
[AD-A187616] 10 p1334 N88-17972
Nonmonotonic evolution and thermodynamic trends at metal/(Hg,Cd)Te interfaces: Yb/Hg0.78Cd0.22Te
[AD-A187591] 10 p1422 N88-18490
An application of active surface heating for augmenting lift and reducing drag of an airfoil
[NASA-TM-100563] 11 p1436 N88-18570
Theoretical studies of the potential surface for the F - H2 greater than HF + H reaction
[NASA-CR-182551] 11 p1557 N88-19319
FTIR (Fourier Transform Infrared) and FTNMR (Fourier Transform Nuclear Magnetic Resonance) study of organophosphorus surface reactions
[AD-A188337] 12 p1609 N88-19625
An interdisciplinary approach to predictive modeling of structural adhesive bonding: Factors affecting the durability of titanium/epoxy bonds
[AD-A189503] 12 p1611 N88-19636
Advanced electron optics for vibrational spectroscopy
[AD-A188469] 12 p1629 N88-19747
Photochemistry at structured surfaces: A classical electromagnetic approach
[AD-A189519] 13 p1737 N88-20387
Model catalyst studies of SMSI (Strong Metal/Support Interactions) and the role of D-electrons in chemisorption and catalysis
[DE88-004518] 13 p1738 N88-20393
Laser surface melting
[BMFT-FB-T-86-072] 14 p1914 N88-21435
Methods of measurement for the evaluation of monolayer properties. Development and applications — lung surfactants
[ETN-88-92229] 15 p2104 N88-22532
Surface enhanced Raman scattering applied to surface chemical kinetics
[AD-A191275] 16 p2176 N88-22969
A study of surface tension driven segregation in monotectic alloy systems
[NASA-CR-182894] 16 p2178 N88-22983
The application of Rutherford backscattering for analyzing multilayered structure change induced by pulsed ion beam bombardment 16 p2278 N88-23638
Microscopic control of semiconductor interface reactivity
[AD-A191193] 16 p2283 N88-23668
Surface interactions relevant to space station contamination problems 18 p2592 N88-25401
New instability phenomena in solid propellant combustion 19 p2628 N88-25591
Interactions of molecules with surfaces
[DE88-007950] 19 p2723 N88-26169
Laser induced surface emission of neutral species and its relationship to optical surface damage processes
[DE88-008035] 19 p2726 N88-26192
Numerical model for the computation of radiance distributions in natural waters with wind-roughened surfaces
[PB88-192703] 20 p2826 N88-26765
An IETS (Inelastic Electron Tunneling Spectroscopy) study of surface reactions applicable to adhesion
[AD-A192274] 21 p2909 N88-27261
Scanning tunneling microscopy as a surface chemical probe
[AD-A192710] 21 p2909 N88-27263
Self-energies and the interactions of particles with surfaces
[DE88-010451] 21 p3014 N88-27885
Initiation of explosive molten aluminum-water interactions at wet or underwater surfaces
[DE88-004686] 23 p3194 N88-29006
Quantitative surface temperature measurement using two-color thermographic phosphors and video equipment
[NASA-CASE-LAR-13740-1] 24 p3376 N88-30105
Cosmochemical trends of volatile elements in the solar system 24 p3451 N88-30542

SURFACE ROUGHNESS

Experience about the application and valuation of roughness strips for boundary layer transition control in wind tunnel tests in the high-speed range
[ESA-TT-1028] 01 p0044 N88-10278
The effect of size and surface on the lifetime prediction of StE 460 notched bars
[FD-6/1986] 01 p0058 N88-10374
Structure and grain coarsening during the processing of engineering ceramics
[NASA-TM-100235] 03 p0293 N88-11838
Roughness and waviness requirements for laminar flow surfaces 07 p0813 N88-14953
Wind tunnel model surface gauge for measuring roughness
[NASA-CR-182392] 07 p0822 N88-14996
Backscatter from a periodic rough surface at near grazing incidence
[NASA-CR-182397] 07 p0845 N88-15128
A new look at the use of linear methods to predict aircraft dynamic response to taxi over bomb damaged and repaired airfields 09 p1180 N88-17069
Propagation of creep waves around rough cylindrical surface 09 p1234 N88-17400
Comparison of the rough surface reflection coefficient with specularly scattered acoustic data
[AD-A187086] 09 p1242 N88-17444
Interferometric study of natural convection heat transfer from a vertical flat plate with transverse roughness elements 10 p1327 N88-17935
Comparison of methods for the calculation of thermal contact resistance of the first Brazilian satellite
[NASA-TT-20180] 14 p1880 N88-21239
Electromagnetic shadowing by an exponentially distributed rough surface
[AD-A189677] 14 p1906 N88-21391
Electromagnetic scattering by an exponentially distributed rough surface with the introduction of a rough surface generation technique
[AD-A189678] 14 p1906 N88-21392
Effect of freestream turbulence on a two dimensional cascade, with different surface roughness, at high Reynolds number
[AD-A190615] 15 p2065 N88-22316
Enhanced backscattering from rough surfaces
[AD-A190995] 16 p2190 N88-23063
Enhanced backscattering from rough surfaces
[AD-A191089] 16 p2274 N88-23610
Manufacturing requirements 17 p2297 N88-23745
An experimental study of the coherent under-ice reflectivity of sound in the Greenland Sea Marginal Ice Zone 18 p2548 N88-25125
Plastic deformation and roughness of free metal surfaces
[PB88-196621] 20 p2772 N88-26439
Numerical model for the computation of radiance distributions in natural waters with wind-roughened surfaces
[PB88-192703] 20 p2826 N88-26765
Eigenmatrix representations of radiance distributions in layered natural waters with wind-roughened surfaces
[PB88-188701] 20 p2828 N88-26780

Investigations of rough surface effects on friction factors in turbulent pipe flow
[AD-A193774] 22 p3075 N88-28255
Studies of internal stresses and surface roughness of sputtered Be and BeB films
[DE88-011737] 22 p3086 N88-28327
Analysis of soils using remote sensing information at the scale of the parcel 22 p3095 N88-28381
The covariance of scalar fields scattered by pressure-release randomly rough surfaces
[AD-A192489] 22 p3146 N88-28714

SURFACE ROUGHNESS EFFECTS
A preliminary demonstration of the use of boundary-layer models of flow in complex terrain for high resolution surface wind forecasting 02 p0212 N88-11330
Effects of enviromentally imposed roughness on airfoil performance 08 p0952 N88-15778
Adhesive bond strengths on aluminium alloys as a function of surface topographies and their wetting properties
[ARE-TM(UMM)-87403] 09 p1148 N88-16880

SURFACE STABILITY
Colloidal stability of oxidized silicon particles in ethanolic and aqueous media
[DE87-014783] 05 p0562 N88-13421
Microscopic control of metallization stability
[AD-A187553] 10 p1421 N88-18487
Computer Applications in Geotechnical Engineering (CAGE) and Geotechnical aspects of the Computer-Aided Structural Engineering (G-CASE) projects. User's guide. UTEXAS2 slope-stability package. Volume 1: User's manual
[AD-A187674] 11 p1511 N88-19025
The sensitivity of boundary layer instability growth rates to compliant wall properties
[AD-A190433] 15 p2064 N88-22309
Empirical flutter prediction method
[AD-A195699] 24 p3327 N88-29810
Mathematical problems of nonlinear wave propagation and of waves in heterogeneous media
[AD-A195970] 24 p3368 N88-30057

SURFACE TEMPERATURE
NT SKIN TEMPERATURE (NON-BIOLOGICAL)
NT WALL TEMPERATURE
Cooling effect of a single evaporating droplet on a hot semi-infinite metal body
[PB87-201802] 01 p0046 N88-10294
Estimating regional evapotranspiration from remotely sensed data by surface energy balance models
[NASA-CR-181400] 01 p0064 N88-10411
The use of satellite IR data in the enhancement of surface thermal fields 02 p0202 N88-11260
Use of time changes of surface data parameters in short range forecasting 02 p0206 N88-11291
Comparison of flight-measured and calculated temperatures on the space shuttle orbiter
[NASA-TM-88278] 03 p0321 N88-12029
Properties of the atmospheric boundary layer above a subtropical oceanic front
[AD-A184006] 03 p0351 N88-12215
An analytical soil thermodynamic model for the diurnal variation of ground surface temperature
[AD-A185388] 05 p0625 N88-13823
Role of anomalous currents in formation of ocean surface temperature field 06 p0727 N88-14474
Sea surface current estimates off central California as derived from enhanced AVHRR (Advanced Very High Resolution Radiometer) infrared images
[AD-A186867] 09 p1194 N88-17155
Relationships between remotely-sensed surface properties and subsurface structure in the ocean
[AD-A189317] 12 p1650 N88-19881
Radiative processes affecting ocean mixed-layer heat content and their monitoring from satellite 13 p1806 N88-20800
Monitoring ocean surface layer processes 13 p1806 N88-20801
Research sensors 15 p2085 N88-22430
Infrared radiometric technique in temperature measurement 17 p2330 N88-23913
Indentification of shallow groundwater regions in semi-arid Brazil by remote sensing methods 17 p2355 N88-24030
The potential impact on atmospheric ozone and temperature of increasing trace gas concentrations
[NASA-CR-182965] 17 p2373 N88-24112
Evaluating evaporation with satellite thermal data
[AD-A192042] 18 p2531 N88-25019
Surface temperature thermal fluxmeters for shock tubes
[NASA-TT-20319] 20 p2762 N88-26381
An empirical surface temperature model
[AD-A192737] 21 p2974 N88-27665
Surface energy balance of three general circulation models: Current climate and response to increasing atmospheric CO2
[DE88-010967] 21 p2975 N88-27673
Interannual variability in the Atlantic and Indian Oceans and its relationship to the southern oscillation 22 p3121 N88-28548
DERF forecasts of thickness 22 p3126 N88-28579
Measurement and interpretation of North Atlantic Ocean marine radar sea scatter
[AD-A196239] 24 p3384 N88-30036
Measurement of local high-level, transient surface heat flux
[NASA-TP-2840] 24 p3375 N88-30099
Energy budget and ground temperatures in hot regions
[AD-A196298] 24 p3404 N88-30268

SURFACE TENSION
U INTERFACIAL TENSION

SURFACE TO AIR MISSILES
A study of infrared missile seekers and the countermeasure techniques employed to defeat them
[ETN-87-90927] 02 p0131 N88-10822
Development of a computer model for missile simulation, or simulation of a kinetic coverage area for a target detection missile
[FOA-C-20666-2.5] 08 p1067 N88-16449
Development of a computer model for missile simulation, or simulation of a kinetic coverage area for a collimation guided missile
[FOA-C-20667-2.5] 08 p1067 N88-16450
The application of thermal imaging sensors and image processing techniques to a short range surface-to-air missile system
[ETN-88-92080] 14 p1982 N88-21829
The effect of a turbulent airstream on a vertically-launched missile at high angles of attack
[AD-A192408] 20 p2758 N88-26363
Future air-to-air training for the RF-4
[AD-A194363] 23 p3240 N88-29284

SURFACE TO SURFACE MISSILES
NT ANTITANK MISSILES
NT CRUISE MISSILES
NT MX MISSILE
NT TOMAHAWK MISSILES
The effects of data structure on total time on test plots
[AD-A187628] 10 p1389 N88-18296
LGM-30B stage 2 disected motor test report
[AD-A190771] 15 p2027 N88-22079

SURFACE TREATMENT
U SURFACE FINISHING

SURFACE VEHICLES
NT AIRCRAFT CARRIERS
NT AUTOMOBILES
NT ELECTRIC AUTOMOBILES
NT ELECTRIC MOTOR VEHICLES
NT MAGNETIC LEVITATION VEHICLES
NT MOTOR VEHICLES
NT ROADWAY POWERED VEHICLES
NT ROCKET PROPELLED SLEDS
NT ROVING VEHICLES
NT TANKS (COMBAT VEHICLES)
NT TRACKED VEHICLES
NT TRANSPORTER
NT TRUCKS
NT WALKING MACHINES
Correction of inertial navigation system drift errors for an autonomous land vehicle using optical radar terrain data
[AD-A184973] 05 p0544 N88-13311
Range imagery algorithms for the detection of obstacles by autonomous vehicles
[AD-A185421] 05 p0659 N88-14045
An overview of vision-based navigation for autonomous land vehicles 1986
[AD-A188186] 10 p1276 N88-17640
On the maneuvering of vehicles
[AD-A187632] 10 p1427 N88-18521
Low cost mobile robot
[AD-A188507] 12 p1633 N88-19778
Terrain classification from digital elevation data using slope and curvature information
[AD-A188940] 12 p1639 N88-19812
Feasibility report: Operation of light air cushion vehicle at McMurdo Sound, Antarctica
[AD-A189057] 13 p1755 N88-20494
Articulated suspension system
[NASA-CASE-NPO-17354-1-CU] 18 p2524 N88-24973
Local free-space mapping and path guidance for mobile robots
[AD-A192970] 20 p2810 N88-26674
Assessments of maneuverability with the TeleOperated Vehicle (TOV)
[AD-A191584] 21 p2993 N88-27751

SURFACE WATER
Influence of the Yukon River on the Bering Sea
[NASA-CR-182802] 17 p2376 N88-24126

SURFACE WAVES
NT BAROCLINIC WAVES
NT CAPILLARY WAVES
NT ELECTROMAGNETIC SURFACE WAVES
NT GRAVITY WAVES
NT RIPPLES
Effect of viscosity on a vertical cylinder due to surface waves
[ETN-87-90960] 02 p0171 N88-11075
Determination of fractal dimension, connection of space and temporal chaos and application to experimental results 03 p0313 N88-11977
Effect of plasma resonance on properties of surface waves 06 p0773 N88-14749
Materials for acceleration by surface electromagnetic waves
[DE88-700312] 07 p0846 N88-15133
Acoustic scattering from composite wind-wave surfaces 3: Forward scatter intensities and spatial coherence at low and high frequencies and small grazing angles for Bubble-free regimes
[AD-A185908] 07 p0881 N88-15345
Investigation of the quantitative determination of two dimensional sea surface wave spectra from shipborne radar measurements
[GKSS-87/E/10] 09 p1195 N88-17163
Surface acoustic wave deposition sensor
[DE87-006527] 09 p1243 N88-17452
Numerical studies of propagation of Lg waves across ocean continent boundaries using the Representation Theorem (RT) 10 p1353 N88-18085
Research and development of surface skimming bulk wave devices for sensor applications
[AD-A187504] 11 p1470 N88-18766
Lg wave excitation and propagation in the presence of one-, two-, and three-dimensional heterogeneities
[AD-A187364] 11 p1510 N88-19022
Applications and limitations of the spectral-analysis-of-surface-waves method
[PB88-136619] 11 p1513 N88-19038
Estimation of sea surface wave spectra using acoustic tomography
[AD-A187837] 11 p1516 N88-19057
Investigation of surface wave blindness in microstrip phased array antennas
[AD-A189326] 12 p1621 N88-19696
Energy and momentum fluxes through the sea surface 13 p1806 N88-20798
Hamiltonian description of the interaction of surface waves with mixed-layer currents 13 p1806 N88-20799
Thin superconducting film characterization by surface acoustic waves
[AD-A190417] 15 p2143 N88-22791
Surface wave accelerometer
[ETN-88-92000] 16 p2210 N88-23192
Investigation of the imaging of ocean surface waves using a synthetic aperture radar
[SER-A-WISS-ABHANDL-84] 16 p2236 N88-23357
Surface-wave model uncertainty assessment
[AD-A193094] 21 p2932 N88-27408
Nonlinear surface and internal waves on shear flow
[PREPRINT-584] 22 p3129 N88-28604
Optical emission from surface waves supported in thin metal films 23 p3282 N88-29540

SURFACE-ACTIVE AGENTS
U SURFACTANTS

SURFACES
Shear stress cleaning for surface departiculation 02 p0134 N88-10838
Aerodynamic sensitivities from subsonic, sonic and supersonic unsteady, nonplanar lifting-surface theory
[NASA-TM-100502] 04 p0394 N88-12459
Calculation of the distributed loads on the blades of individual multiblade propellers in axial flow using linear and nonlinear lifting surface theories
[NASA-TT-20173] 13 p1719 N88-20278

SURFACTANTS
Separation of anionic from nonionic alkoxy compounds using silica gel
[GB-PATENT-2-140-415-A] 01 p0020 N88-10122
Influence of surfactants on damping of gravity-capillary waves. 1: Frequency dependence 04 p0459 N88-12843
Reactions of porphyrins in surfactant assemblies, microemulsions and in solutions
[AD-A184797] 05 p0560 N88-13412
Precipitation of surfactants and surfactant mixtures in aqueous solutions
[DE88-003333] 10 p1298 N88-17763

A review of approaches to the study of turbulence modification by means of non-Newtonian additives
[AD-A188799] 12 p1627 N88-19734
Methods of measurement for the evaluation of monolayer properties. Development and applications --- lung surfactants
[ETN-88-92229] 15 p2104 N88-22532
Attenuated total reflectance FT-IR spectroscopy to measure interfacial reaction kinetics at silica surfaces
[AD-A196330] 24 p3344 N88-29908

SURGERY
Does the knife open perspectives for the myopic pilot?
[ETN-87-90166] 09 p1199 N88-17187

SURGES
Radio studies of large scale structures of the Sun's corona and transient activity 01 p0114 N88-10728
Was the eclipse comet of 1893 a disconnected coronal transient? 01 p0115 N88-10733
A numerical study of transient, thermally-conductive solar wind 01 p0115 N88-10738
Radiation-induced transient attenuation of optical fibers at 800 and 1300 nm
[DE87-013165] 02 p0235 N88-11485
Departmental report on program EMTP-machine windings surge transients: Travelling wave method
[PB87-123733] 04 p0438 N88-12719
Transient processes in the interaction between pulsed laser radiation and matter
[ISL-R-115/86] 05 p0588 N88-13586
Application of Vandermonde decomposition to directional and modal analysis of broadband transients
[AD-A185007] 05 p0646 N88-13956
A unified model for the WTS and the generation on Pi 2 pulsations --- Westward Traveling Surge (WTS)
08 p1096 N88-16593
Possibilities for on-line surge suppression by fast guide vane adjustment in axial compressors
10 p1283 N88-17674
Equipment test methods for externally produced electromagnetic transients
[RAE-TM-FS(F)-457] 14 p1865 N88-21140
Techniques for studying fast reactions in liquids
[DE88-005917] 14 p1888 N88-21285
Bloch oscillations in small Josephson junctions: Their manifestation in switching effects
14 p1969 N88-21756
Effects of emission energy transient in periodic-pulse XeCl excimer laser of approximately 400 W average power 14 p1971 N88-21763
Molecular dynamics of materials possessing high energy content
[AD-A190034] 15 p2034 N88-22118
Polarimetric ISAR imaging using either measured or calculated transient signatures
[AD-A190077] 15 p2056 N88-22259
Application of the reactivity constraint approach to the transient control of spacecraft reactors
17 p2406 N88-24305
EETAP (End-to-End Transient Analysis Program) for space nuclear power system simulation
17 p2418 N88-24381
Characterization of accelerating pipe flow
[AD-A193065] 21 p2943 N88-27481
Investigation of the quasi-steady approach used in transient two-phase flow analysis
[DE88-004303] 21 p2944 N88-27489

SURVEILLANCE
NT SPACE SURVEILLANCE (GROUND BASED)
NT SPACE SURVEILLANCE (SPACEBORNE)
Pyroelectric line scanner for remote IR imaging of vehicles
[DE87-012127] 02 p0235 N88-11484
Cooperative analysis expert situation assessment research 09 p1206 N88-17228
Terrestrial Propagation Characteristics in Modern Systems of Communications, Surveillance, Guidance and Control
[AGARD-CP-407] 12 p1614 N88-19653
Automatic knowledge acquisition for aerial image interpretation
[AD-A188616] 12 p1638 N88-19810
Specification for an infrared satellite surveillance system for the detection of aircraft
[AD-A189592] 13 p1797 N88-20746
A preliminary assessment of thunderstorm outflow wind measurement with airport surveillance radars
[AD-A189064] 13 p1799 N88-20757
The Effect of the Ionosphere on Communication, Navigation and Surveillance Systems Based on Ionospheric Effects Symposium held on 5-7 May 1987 in Springfield, Virginia
[AD-A191855] 18 p2541 N88-25081
Aerodynamics of seeing on large transport aircraft
[NASA-CR-183122] 23 p3174 N88-28896

SURVEILLANCE RADAR
NT AIRBORNE SURVEILLANCE RADAR
NT MULTISTATIC RADAR
Development of an airborne facility for advanced avionics research 17 p2307 N88-23801
Automated test device for FASR (Fixed Array Surveillance Radar) beam steering componentry
[AD-A191650] 18 p2500 N88-24829
Multi-target tracking algorithms for cluttered environments 20 p2789 N88-26543
Fine resolution errors in secondary surveillance radar altitude reporting
[RSRE-87019] 23 p3175 N88-28906
Evaluation of LISBON TAR SSR radar
[EEC/NOTE-5/87] 24 p3362 N88-30015

SURVEYING
U SURVEYS

SURVEYS
NT GEODETIC SURVEYS
NT GEOLOGICAL SURVEYS
NT SKY SURVEYS (ASTRONOMY)
Subjective probability, combination of expert opinion and probabilistic approaches to information retrieval
04 p0501 N88-13085
The Parkes radio survey of active chromosphere stars
04 p0511 N88-13141
A survey of existing hypersonic ground test facilities: North America 05 p0529 N88-13220
Survey state of the art: Electrical load management techniques and equipment
[AD-A184083] 05 p0577 N88-13517
Varifront 3 expedition data report (USNS DE STEIGUER CRUISE 1202-82). Bioluminescence, hydrographic, nutrient, and satellite data from the Gulf of California (November-December 1981)
[AD-A185011] 05 p0620 N88-13805
Survey of electronic measurement needs below 10 MHz
[PB88-110366] 07 p0844 N88-15121
NASA JSC neural network survey results
09 p1205 N88-17220
Environmental projects. Volume 4: Asbestos survey
[NASA-CR-182527] 10 p1353 N88-18083
Surveying with GPS in Australia
11 p1504 N88-18986
A study of technology transfer arrangements for national laboratories
[DE88-005423] 11 p1567 N88-19382
An evaluation of perceptions of form, fit, function (F3) standardization on the Standard Inertial Navigation Unit (STD INU) program
[AD-A188955] 12 p1579 N88-19446
A study on local level inertial surveying systems. Error model for the stationary system
[B8736714] 16 p2229 N88-23312
Study of reservoir water quality utilizing remote sensing techniques: Methodological concepts
17 p2364 N88-24076
Human performance issues arising from manned space station missions
[NASA-CR-3942] 18 p2553 N88-25156
Territorial management program
19 p2682 N88-25942
RRSAS (Robotic Radiation Survey and Analysis System) Project: A real time sensor driven robotic system
[DE88-006825] 20 p2808 N88-26661
Australian structures response evaluation: Ground shock and air blast measurements for site investigation survey
[MRL-TN-526] 20 p2813 N88-26685
Development of sensors for ceramic components in advanced propulsion systems: Survey and evaluation of measurement techniques for temperature, strain and heat flux for ceramic components in advanced propulsion systems
[NASA-CR-182111] 22 p3081 N88-28299
Signal processing software for ground penetrating radar, user's manual
[AD-A194286] 23 p3203 N88-29059
Seismic reflection experiments imaging the physical nature of crustal structures in southern California
23 p3232 N88-29235
The use of orbital remote sensing data for low cost ground-water survey
[INPE-4587-PRE/1318] 24 p3386 N88-30170
A dynamic analysis of piezoelectric strained elements
[AD-A196079] 24 p3432 N88-30430
A deep redshift survey of field galaxies. Comments on the reality of the Butcher-Oemler effect
[NASA-CR-183255] 24 p3454 N88-30558
Antarctic Meteorite Newsletter, Volume 11, Number 2, August 1988
[NASA-TM-89801] 24 p3457 N88-30573

SURVIVAL
Improved oil-off survivability of tapered roller bearings
[NASA-CR-180804] 02 p0182 N88-11135
The determination of nutritional requirements for Safe Haven Food Supply System (emergency/survival foods)
06 p0792 N88-14856
Survival analysis using additive risk models
[AD-A189053] 13 p1825 N88-20906
Validation of mathematical model predictions of immersion survival times
[IAM-652] 14 p1952 N88-21635
Radiation effects testing capabilities of the Texas A and M Nuclear Science Center 17 p2416 N88-24368
Survival analysis, or what to do with upper limits in astronomical surveys
[NASA-CR-182936] 17 p2449 N88-24551
Mobile robot survival
[DE88-009108] 20 p2809 N88-26665
Accidental hypothermia
[AD-A194967] 24 p3406 N88-30278

SUSCEPTIBILITY (MAGNETISM)
U MAGNETIC PERMEABILITY

SUSPENDING (HANGING)
NT MAGNETIC SUSPENSION
Comparative evaluation of stress repsonse of rats to different methods of simulating some effects of weightlessness 10 p1363 N88-18144
Morphological study of early changes in rat bones in simulated weightlessness 10 p1365 N88-18158
General equilibrium characteristics of a dual-lift helicopter system
[NASA-TP-2615] 12 p1573 N88-19407
Does 7-day hindquarters unloading simulate 7 days of weightlessness exposure in rat trabecular bone?
12 p1657 N88-19928
The suspended Japanese quail as an animal model for experiments related to microgravity
12 p1662 N88-19960
Oscillation damped movement of suspended objects
[DE88-005715] 15 p2086 N88-22433
Human response to prolonged motionless suspension in four types of full body harnesses
21 p2929 N88-27387

SUSPENDING (MIXING)
Optical instrumentation and study of gas-solid suspension flows
[DE88-000147] 04 p0442 N88-12744
Thematic mapper research in the earth sciences: Small scale patches of suspended matter and phytoplankton in the Elbe River Estuary, German Bight and Tidal Flats
[NASA-CR-182378] 08 p1019 N88-16180
Suspension cell culture in microgravity and development of a space bioreactor 09 p1196 N88-17169
Christiansen effect in infrared spectra of soil-derived atmospheric dusts
[AD-A187071] 09 p1248 N88-17479
Suspension of small metallic plates: A versatile sensor
[PB88-130901] 11 p1487 N88-18874
Velocity and concentration measurements in flowing suspensions by nuclear magnetic resonance
[DE88-006225] 13 p1770 N88-20589
LLNL Granular Solids Flow Project
[DE88-008023] 19 p2664 N88-25844

SUSPENSION SYSTEMS (VEHICLES)
Measurement of suspension and ride characteristics of the M1 main battle tank 05 p0596 N88-13637
The MBB propulsion concepts for magnetic suspension railways: Retrospective view and prospects
[MBB-Z-141/87] 10 p1316 N88-17865
Articulated suspension system
[NASA-CASE-NPO-17354-1-CU] 18 p2524 N88-24973
A review of gear housing dynamics and acoustics literature
[NASA-CR-183110] 20 p2811 N88-26675
Leaf spring
[GB-PATENT-2-192-689-A] 23 p3222 N88-29179

SWALLOWING
A simplified streamline swallowing procedure for the windward meridian of axisymmetric blunt bodies
[AD-A188413] 12 p1626 N88-19732

SWAMPS
U MARSHLANDS

SWASH
U SPLASHING

SWEAT COOLING
Polycythemia and hydration status: Effects on blood volume and thermoregulation during exercise-heat stress
[AD-A185946] 07 p0888 N88-15383
Temperature regulation at rest and exercise during the human menstrual cycle
[AD-A186461] 08 p1050 N88-16341
The effects of different combinations of inlet air conditions used for cooling as measured on a heated manikin
[AD-A191116] 18 p2552 N88-25151

SWEATING
U PERSPIRATION

SWEDEN
Esrange (Sweden): New installations, future plans and investments — rocket range 08 p1029 N88-16235
Surface ozone measurements at a Swedish mountain site
[CM-72] 09 p1191 N88-17138
SWEDISH SPACE PROGRAM
Satimage and the Nordic SPOT market 03 p0340 N88-12145
Electric field measurements on Viking: First results
[TRITA-EPP-87-04] 05 p0625 N88-13826
Viking quick look plots: A short description — Swedish satellite 06 p0692 N88-14243
The Swedish sounding rocket and balloon program 08 p1025 N88-16205
Viking: The first Swedish satellite 08 p1025 N88-16207
Global views of the aurora from the Viking satellite — Swedish satellite 08 p1025 N88-16208
Instantaneous pictures of the high-latitude electrodynamics using Viking and DMSP/F7 observations — Swedish satellite 08 p1025 N88-16209
First results from the Viking associated Aureld-VIP rocket and EISCAT campaign — auroras; Swedish satellite 08 p1026 N88-16211
Small scale plasma density structures observed by the Viking double probe instrument — Swedish satellite 08 p1098 N88-16604
Low frequency waves and small scale solitary structures observed by Viking — Swedish satellite; auroras 08 p1099 N88-16611
Preliminary results from the dc electric field experiment on Viking — Swedish satellite
[TRITA-EPP-87-03] 09 p1190 N88-17130
SWEEP ANGLE
NT LEADING EDGE SWEEP
NT SWEEPBACK
The effects of sweep and bluntness on a glancing shock wave turbulent boundary layer interaction 05 p0531 N88-13227
SWEEP EFFECT
Three-dimensional unsteady flow elicited by finite wings and complex configurations 04 p0395 N88-12468
SWEEP FREQUENCY
Material parameter measurements at high temperatures
[NASA-CR-182707] 13 p1739 N88-20397
SWEEPBACK
NT LEADING EDGE SWEEP
Structural Tailoring of Advanced Turboprops (STAT)
[NASA-CR-180861] 22 p3045 N88-28074
SWEEPBACK ANGLES
U SWEEPBACK
SWELLING
Swelling behavior of ferritic/martensitic steels
[DE88-001757] 06 p0662 N88-14177
Uranium nitride fuel swelling and thermal conductivity correlations 17 p2409 N88-24327
A comparison of uranium nitride and mixed carbide fuels swelling 17 p2435 N88-24485
SWEPT FORWARD WINGS
Wing divergence of trimmed aircraft 05 p0550 N88-13354
X-29A forward-swept-wing flight research program status
[NASA-TM-100413] 10 p1277 N88-17644
The aerodynamic design optimisation of a forward swept wing fighter aircraft
[CAR-87-18] 11 p1433 N88-18553
A correlation study of X-29A aircraft and associated analytical development
[NASA-CR-183103] 13 p1722 N88-20296
Development of a real-time aeroperformance analysis technique for the X-29A advanced technology demonstrator
[NASA-TM-100432] 14 p1866 N88-21151
Experiment investigation on longitudinal characteristics of the forward swept wing
[AD-A191553] 18 p2456 N88-24582
Current flight test experience related to structural divergence of forward-swept wings
[NASA-TM-100445] 18 p2464 N88-24633
High performance forward swept wing aircraft
[NASA-CASE-ARC-11636-1] 23 p3177 N88-28914
SWEPT WINGS
NT ARROW WINGS
NT DELTA WINGS
NT SWEPT FORWARD WINGS
NT SWEPTBACK WINGS
Investigations of separated flow states on wings of medium aspect ratio taking into account the wind tunnel interference problem
[ETN-87-90437] 01 p0003 N88-10016
Measurement techniques in low-speed turbulent flows: A report on EUROMECH 202
[NLR-MP-86038-U] 01 p0045 N88-10283
Three-dimensional unsteady flow elicited by finite wings and complex configurations 04 p0395 N88-12468
Calculation of three-dimensional stationary turbulent boundary layer on root section of wing ignoring compressibility 04 p0424 N88-12630
A swept wing panel in a low speed flexible walled test section
[NASA-CR-4106] 05 p0540 N88-13292
Static aeroelastic effects on the flutter of a supercritical wing 05 p0550 N88-13353
Flight research on natural laminar flow 07 p0813 N88-14950
Pressure distributions and oil-flow patterns for a swept circulation-control wing 10 p1270 N88-17596
Boundary-layer and wake measurements on a swept, circulation-control wing 10 p1270 N88-17597
Development of disturbances in swept wing flows
[NASA-CR-182675] 13 p1768 N88-20574
Preliminary in-flight boundary layer transition measurements on a 45 deg swept wing at Mach Numbers between 0.9 and 1.8
[NASA-TM-100412] 13 p1772 N88-20598
The NASA Langley Laminar-Flow-Control (LFC) experiment on a swept, supercritical airfoil: Design overview
[NASA-TP-2809] 14 p1861 N88-21117
Wave interactions in a three-dimensional attachment line boundary layer
[NASA-CR-181653] 14 p1910 N88-21414
Boundary-layer and wake measurements on a swept, circulation-control wing
[NASA-TM-89426] 15 p2014 N88-22013
Theoretical investigation of secondary instability of three-dimensional boundary-layer flows with application to the DFVLR-F5 model wing
[DFVLR-FB-87-44] 15 p2068 N88-22330
Nonlinear wave interactions in swept wing flows
[NASA-CR-4142] 16 p2206 N88-23160
A low speed wind tunnel investigation of Reynolds number effects on a 60-deg swept wing configuration with leading and trailing edge flaps
[NASA-CR-181684] 19 p2598 N88-25441
AGARD standard aeroelastic configurations for dynamic response. 1: Wing 445.6
[AGARD-R-765] 21 p2896 N88-27193
Method to predict external store carriage characteristics at transonic speeds
[NASA-CR-4170] 22 p3037 N88-28034
Techniques used in the F-14 variable-sweep transition flight experiment
[NASA-TM-100444] 24 p3374 N88-30093
SWEPTBACK WINGS
NT ARROW WINGS
NT DELTA WINGS
Variable sweep wings 10 p1309 N88-17823
SWIRLING
Numerical simulation of turbulent premixed combustion and decay of turbulent swirling flow
[DE87-014253] 03 p0284 N88-11787
An experimental and numerical investigation of swirling flows in a rectangular nozzle 06 p0700 N88-14295
Fuel-injector/air-swirl characterization
[NASA-CR-180864] 07 p0820 N88-14985
Numerical implementation and performance of Reynolds stress closures in finite volume computations of recirculating and strongly swirling flows 08 p0987 N88-15976
Calculation on film preparation and film motion of a swirl atomizer
[DFVLR-FB-87-25] 09 p1162 N88-16962
Numerical simulation of turbulent premixed combustion and decay of turbulent swirling flow
[DE88-006588] 14 p1888 N88-21284
Theoretical and experimental investigation of swirl flow phase separators for microgravity applications 17 p2411 N88-24335
Effect of initial tangential velocity distribution on the mean evolution of a swirling turbulent free jet
[NASA-TM-100934] 18 p2458 N88-24592
Development of a liquid-fed water resistojet
[NASA-TM-100927] 18 p2523 N88-24968
Turbulence structure of mixing swirling flows
[AD-A193063] 21 p2943 N88-27478
Euler analysis of a swirl recovery vane design for use with an advanced single-rotation propfan
[NASA-TM-101357] 24 p3320 N88-29771
Analysis of the flow through double swirl airblast atomizers 24 p3351 N88-29949
Development of a more general Reynolds stress closure for swirling flow
[AD-A195121] 24 p3374 N88-30092
SWIRLING WAKES
U TURBULENT WAKES
SWITCHES
NT ELECTRIC SWITCHES
NT SWITCHING CIRCUITS
NT VACUUM ARC SWITCHES
Switching devices used in the Lethality Test System
[DE87-011734] 01 p0011 N88-10062
New concepts for high current self-sustained diffuse discharge closing switches
[DE87-011678] 01 p0040 N88-10252
A high-voltage multistage laser-triggered gas switch
[DE87-011725] 01 p0040 N88-10253
Investigations into the design of multi-terawatt magnetic switches
[DE87-012014] 01 p0040 N88-10254
Characterization of surface discharge switches and high performance applications
[DE87-011763] 01 p0041 N88-10261
Toward pulsed power uses for photoconductive semiconductor switches: Closing switches
[DE87-012020] 01 p0041 N88-10262
A simple self-breaking 2 MV gas switch
[DE87-014346] 02 p0166 N88-11047
The design and construction of a thermally controlled single mode fiber switch
[ETN-87-90929] 02 p0236 N88-11491
Loss measurement of 3-port ferrite switches in the 90 GHz range
[ESA-TT-1054] 03 p0310 N88-11958
Low jitter laser-triggered high-voltage vacuum switch using low laser energies
[DE88-001922] 05 p0587 N88-13576
Program to development an optical transistor and switch
[AD-A185666] 06 p0697 N88-14278
Superconducting switch program
[AD-A185682] 07 p0848 N88-15144
Photoconductor switch and circuit analysis
[AD-A188168] 11 p1478 N88-18821
Analysis of anomalous resistivity during the conduction phase of the plasma erosion opening switch
[DE88-006382] 15 p2061 N88-22286
Repetitive opening switches using optically activated semiconductors
[AD-A190196] 15 p2143 N88-22790
Investigation of non-linear optical behavior of semiconductors for optical switching, volume 1
[AD-A191297] 16 p2274 N88-23611
A monolithic reduced-size Ku-Band SPOT (Single-Pole Double Throw) FET switch
[DE88-006273] 18 p2505 N88-24858
The SRS (Segmented Rail Surface) railgun: A new approach to restrike control
[DE88-007907] 19 p2605 N88-25468
Picosecond electrical pulses for VLSI electronics characterization 19 p2655 N88-25768
Graphite as a picosecond laser activated opening switch 19 p2657 N88-25783
Investigation of photoconductive picosecond microstripline switches on self-implanted Silicon On Sapphire (SOS) 19 p2657 N88-25789
Fast GaAs photoconductive detectors with high sensitivity integrated in coplanar systems onto GaAs substrates 19 p2658 N88-25790
Picosecond optoelectronic switches using composite electronic materials 19 p2658 N88-25792
A new optoelectronic CW microwave source 19 p2660 N88-25818
Optical modulation above 20 GHz using a waveguide electrooptic switch 19 p2660 N88-25819
Electron-impact-ionization and electron-attachment cross sections of radicals important in transient gaseous discharges
[AD-A192248] 20 p2770 N88-26424
Development of liquid metal field-emission sources for use in fast repetitive opening switches
[AD-A192230] 20 p2795 N88-26583
Pseudospark switches
[DE88-702227] 23 p3207 N88-29085
Consideration of plasma opening switches from a wave propagation perspective
[AD-A195681] 24 p3431 N88-30421
SWITCHING
NT BEAM SWITCHING
NT MAGNETIC SWITCHING
NT MICROWAVE SWITCHING
NT OPTICAL SWITCHING
NT PACKET SWITCHING
Measuring technical and mathematical investigation of multiple reignitions at the switching of a motor using vacuum circuit breakers
[ETN-87-90406] 01 p0042 N88-10270
Contribution to the study of circuit switched networks: Modeling and numerical solutions
[LAAS-87-174] 02 p0162 N88-11017

Automatic antenna switching design for Extra Vehicular Activity (EVA) communication system
06 p0797 N88-14883
Experimental investigation of a three-stage railgun incorporating puff-switching
[MRL-R-1056] 09 p1130 N88-16785
Transient electromagnetic scattering from heterogeneous lossy spheres
[AD-A186669] 09 p1152 N88-16903
The characteristics of two broadband (2 MHz to 10 MHz) switched vee antennas
[AD-A187874] 11 p1471 N88-18770
New mode switching algorithm for the JPL 70-meter antenna servo controller 11 p1474 N88-18791
Fast switching of far infrared radiation by refractive index change in semiconductors using photoionization
[ETN-88-91490] 11 p1551 N88-19279
Two queues with alternating service and switching times
[CWI-OS-R8712] 13 p1831 N88-20949
Bloch oscillations in small Josephson junctions: Their manifestation in switching effects
14 p1969 N88-21756
Optical switching and control techniques using nonlinear optical wave mixing
[AD-A190467] 15 p2134 N88-22730
Experimental investigation of a three-stage railgun incorporating puff-switching
[AD-A191044] 16 p2166 N88-22918
Investigation of non-linear optical behavior of semiconductors for optical switching, volume 1
[AD-A191297] 16 p2274 N88-23611
Photoconductive generation of sub-picosecond electrical pulses and their measurement applications
19 p2656 N88-25778
Picosecond switching in Josephson tunnel junctions
19 p2657 N88-25780
High speed, high repetition rate, high voltage photoconductive switching 19 p2657 N88-25781
Generation and forming of ultrashort high voltage pulses 19 p2657 N88-25782
Energy variations in optical pulses from gain-switched AlGaAs diode lasers 19 p2658 N88-25796
Picosecond measurements of gain-switching in a semiconductor laser driven by ultrashort electrical pulses
19 p2658 N88-25800
Experiments applications guide: Advanced Communications Technology Satellite (ACTS)
[NASA-TM-100265] 22 p3048 N88-28082
Charge storage and switching phenomena in metal complexes
[AD-A193778] 23 p3192 N88-28996
Optics and symbolic computing
[AD-A195119] 24 p3360 N88-30004
Piezoelectric and electrostrictive materials for transducer applications, volume 2
[AD-A194956] 24 p3376 N88-30104
Use of depletion edge translation for high-speed modulation and switching of lightwaves
[AD-A195611] 24 p3430 N88-30417

SWITCHING CIRCUITS
Recent developments in opening photoconductive semiconductor switches
[DE87-012130] 01 p0041 N88-10263
Recording multiple signals on a single waveform recorder
[DE87-011632] 01 p0049 N88-10313
Progress toward a superconducting opening switch
[DE87-014170] 02 p0167 N88-11051
Evaluation of device figure of merit in microwave switching circuit design
[AD-A184896] 05 p0577 N88-13520
Digital control of a direct current converter for a hybrid vehicle
[LAAS-87-266] 05 p0578 N88-13527
Trip electrical circuit of the gyrotron
[INPE-4336-NTE/273] 12 p1622 N88-19701
RF-switches: Application and design — satellite communication 14 p1877 N88-21215
The modeling, simulation and comparison of interconnection networks for parallel processing
[AD-A190571] 15 p2115 N88-22599
The bit-error rate performance of a satellite microwave matrix switch
[NASA-TM-100285] 16 p2167 N88-22920
Neutron effects on the electrical and switching characteristics of NPN bipolar power transistors
17 p2431 N88-24463
High speed opto-isolator for radar applications
19 p2658 N88-25795
Silicon pulse sharpening diodes-switching kilovolts in 10's of picoseconds 19 p2661 N88-25824
Extinction behavior of low voltage switching arc under consideration of cathodic coatings and dynamic arc column
[ETN-88-92384] 20 p2796 N88-26591

SWITCHING ELEMENTS
U SWITCHING CIRCUITS

SWITCHING THEORY
An exact analysis and performance of framed ALOHA with capture
[AD-A185006] 05 p0574 N88-13500

SWITZERLAND
Swiss scientific balloon and sounding rocket experiments 1985-1987 08 p1025 N88-16206
Research in Switzerland on ocean and inland-water colour monitoring 08 p1043 N88-16301

SYLLABLES
Motor theory of auditory perception
[AD-A192095] 18 p2550 N88-25136

SYMBIOSIS
The development of ODE methods: A symbiosis between hardware and numerical analysis
[DE87-014925] 03 p0370 N88-12325

SYMBOLIC PROGRAMMING
Petri nets as a support to symbolic execution of concurrent Ada programs
[REPT-87-007] 01 p0082 N88-10529
Integration of symbolic and algorithmic hardware and software for the automation of space station subsystems
[NASA-TM-89705] 07 p0907 N88-15497
Optical symbolic processor for expert system execution
[AD-A187494] 10 p1385 N88-18268
Deriving abstractions from a software object network
[AD-A187472] 10 p1389 N88-18294
Center for Supercomputing Research and Development
[DE88-003564] 10 p1418 N88-18466
Optical symbolic processor for expert system execution
[AD-A187882] 11 p1525 N88-19103
Integration of symbolic and algorithmic hardware and software for the automation of space station subsystems
17 p2387 N88-24190
Computer systems for the representation and manipulation of mathematical knowledge
[AD-A193547] 23 p3249 N88-29340
AI tools in computer based problem solving
23 p3263 N88-29424
MACSYMA program for the painleve test of nonlinear ordinary and partial differential equations
[AD-A194293] 23 p3270 N88-29458
Optics and symbolic computing
[AD-A195119] 24 p3360 N88-30004
Optical symbolic computing
[AD-A195690] 24 p3429 N88-30406

SYMBOLS
Symbolic, algebraic, and numeric solutions to heat conduction problems using Green's functions
09 p1165 N88-16987
Computer-assisted symbolization by raster data processing — mapping 16 p2225 N88-23284
Extraction of texts and symbols from unstructured vector data — mapping 16 p2225 N88-23287
Optical symbolic processor for expert system execution
[AD-A192005] 18 p2575 N88-25296

SYMMETRICAL BODIES
NT AXISYMMETRIC BODIES
NT BODIES OF REVOLUTION
NT CONCENTRIC SPHERES
NT CONICAL BODIES
NT CYLINDRICAL BODIES
NT ELLIPSOIDS
NT FAIRINGS
NT FALLING SPHERES
NT PARABOLIC BODIES
NT ROTATING CYLINDERS
NT ROTATING SPHERES
NT SLENDER CONES
NT SPHERES
NT TORUSES

SYMMETRY
NT BROKEN SYMMETRY
NT SUPERSYMMETRY
Observations of localized grain boundary dislocations in series of (001) and (110) symmetrical tilt boundaries in aluminum
[DE87-014011] 01 p0025 N88-10156
Summary and conclusions of the 6th Moriond workshop — standard electroweak model
[USIP-87-11] 01 p0092 N88-10602
Systematic studies of molecular vibrational anharmonicity and vibration-rotation interaction by self-consistent-field higher derivative methods: Applications to asymmetric and symmetric top and linear polyatomic molecules
[DE87-014691] 02 p0232 N88-11465
Numerical experiments with a symmetric high-resolution shock-capturing scheme
[NASA-TM-88325] 03 p0370 N88-12332
Dynamics of atoms in low-symmetry systems
[AD-A184318] 03 p0375 N88-12361
Light scattering by oriented and randomly dispersed chiral particles
[DE87-014758] 03 p0376 N88-12368
The finite element method for electronic structure
[DE88-001708] 04 p0485 N88-12989
Conditional second order closure for turbulent shear flows
[AD-A185369] 05 p0581 N88-13542
RADSPHERE: A computer program for calculating the steady-state, axially symmetric, forced response and radiation field of a submerged spherical shell
[AD-A185025] 05 p0609 N88-13738
High energy molecules of high symmetry
[AD-A185385] 05 p0647 N88-13965
Buckling of braced monosymmetric cantilevers: Timoshenko energy approach
[PB87-133849] 06 p0723 N88-14445
On the work needed to factor a symmetric positive definite matrix
[AD-A185781] 06 p0759 N88-14660
Improved understanding of the loss-of-symmetry phenomenon in the conventional Kalman filter
[NASA-TM-100041] 06 p0766 N88-14709
Model of earlier stage of universe's evolution
06 p0775 N88-14758
Global bifurcation of periodic solutions with symmetry
[AD-A185881] 07 p0908 N88-15501
Nonsymmetric metrics in nonlinear field theory
[DE88-700509] 07 p0913 N88-15537
Calculation of symmetric and asymmetric vortex seperation on cones and tangent ogives based on discrete vortex models
[NASA-CR-4122] 08 p0950 N88-15768
Dynamical characteristics of weak turbulence
[AD-A186724] 09 p1161 N88-16957
An application of eigenspace methods to symmetric flutter suppression
[NASA-CR-181618] 10 p1284 N88-17684
The influence of small defects on tensile specimen ductility and symmetry of deformation
[AD-A187983] 10 p1346 N88-18044
Symmetries in nonlinear control systems and their applications 11 p1496 N88-18929
Symmetry and equivalence restrictions in electronic structure calculations
[NASA-TM-89252] 11 p1557 N88-19320
Symmetry problems in particle physics
[DE88-004927] 12 p1688 N88-20099
Chiral symmetry in the path-integral approach
[DE88-700833] 12 p1699 N88-20168
A symmetric set of Euler angles and oblique orientation space sections
[DE88-005317] 13 p1847 N88-21056
Symmetry and global bifurcation in nonlinear solid mechanics
[AD-A190521] 15 p2121 N88-22642
Ten dimensional N = 1 supergravity coupled to supersymmetric Yang-Mills fields in superspace
[DE87-703033] 15 p2146 N88-22808
Path integral, BRS symmetry, and string and membrane theories
[DE88-752300] 15 p2146 N88-22810
Local time displacement as a symmetry of nature in flat space-time
[NASA-TM-100610] 16 p2264 N88-23542
Rigid symmetries and BRST-invariance in gauge theories
[PB88-180948] 18 p2572 N88-25280
Symmetrized magnetic field configuration of low aspect ratio helical system
[IPPJ-869] 20 p2855 N88-26956
Nonlinear interaction between overall and local buckling of stiffened panels with symmetric cross-sections
[PB88-104054] 21 p2960 N88-27580
Closed string fields as parameters of extra gauge symmetry of open string field theory
[DE88-702046] 21 p3026 N88-27960
Symmetry problem of energy-momentum tensor and the creation of gravitational field
[DE88-702442] 21 p3026 N88-27964
Small scale mixing in the initial region of a jet
[AD-A193500] 23 p3192 N88-28994

SYMMETRY BREAKING
U BROKEN SYMMETRY

SYMPATHETIC NERVOUS SYSTEM
Individual functional typology of sympathoadrenal system as indicator of physiological status in adverse environments 12 p1665 N88-19979
Direct interaction between autonomic nerves and the immune system
[AD-A188576] 12 p1667 N88-19991

SYMPATHOMIMETICS
U ADRENERGICS

SYMPTOMS
U SIGNS AND SYMPTOMS
SYNAPSES
Large-scale neuronal circuits for selective storage and recognition of complex stimuli, a pilot study
[AD-A184134] 04 p0474 N88-12920
Biophysical and biochemical mechanisms in synaptic transmitter release
[AD-A187059] 09 p1199 N88-17184
Long term synaptic plasticity and learning in neuronal networks
[AD-A186834] 09 p1199 N88-17188
Synapses that compute motion
[AD-A190389] 15 p2116 N88-22607
SYNCHRONISM
NT BIT SYNCHRONIZATION
The navigation experiment NAVEX: Experimental results of clock synchronization
[DFVLR-MITT-87-05] 03 p0271 N88-11701
Comparing barrier algorithms
[NASA-CR-178377] 04 p0476 N88-12934
Asynchronous rotation in close binary systems with circular orbits 04 p0509 N88-13131
On detection of change points using mean vectors
[AD-A185581] 06 p0767 N88-14717
Super-short yttrium aluminate pulse generator with controlled resonator Q-factor 06 p0772 N88-14740
High repetition rate electron beam RF-acceleration and sub-millimeter wave generation via a free electron laser
[AD-A186066] 07 p0858 N88-15209
The navigation experment NAVEX: Experimental results of clock synchronization
[ESA-TT-1084] 09 p1132 N88-16791
Parallel access to synchronization variables
[DE88-003570] 10 p1392 N88-18306
Frame synchronization performance and analysis 11 p1473 N88-18787
Electro-mechanical vibratory system 11 p1500 N88-18958
A neuronal model of classical conditioning
[AD-A188378] 12 p1670 N88-19999
On proving register atomicity
[CWI-CS-R8707] 13 p1818 N88-20862
A survey of provably correct fault-tolerant clock synchronization techniques
[NASA-TM-100553] 13 p1823 N88-20894
Approximate agreement
[AD-A191030] 16 p2251 N88-23455
Asynchronous optical sampling for laser-based combustion diagnostics in high pressure flames
[AD-A192920] 20 p2770 N88-26428
A modular proof of correctness for a network synchronizer
[AD-A192726] 21 p3002 N88-27802
Heating efficiency of beat wave excitation in a density gradient
[AD-A193066] 21 p3017 N88-27905
Synchronous response modelling and control of an annular momentum control device
[NASA-CR-4166] 24 p3358 N88-29995
SYNCHRONIZATION
U SYNCHRONISM
SYNCHRONIZED OSCILLATORS
Mode priming in an overmoded gyrotron oscillator
[AD-A189151] 13 p1772 N88-20602
SYNCHRONIZERS
A review of the semiconductor storage of television signals. Part 2: Applications 1975-1986
[BBC-RD-1987/6] 02 p0161 N88-11009
Interleaver design for trellis-coded differential 8-PSK modulation with non-coherent detection 19 p2648 N88-25719
SYNCHRONOUS DETECTORS
U CORRELATORS
SYNCHRONOUS MOTORS
The method of rigid armature flux orientation for the field-oriented control of highly dynamic drives with synchronous machines
[ETN-87-90405] 01 p0042 N88-10269
Contributions to fast-reacting and high-precision three-phase positioning systems --- machinery
[ETN-87-90427] 01 p0056 N88-10358
Computerized system for studies on creep of irradiated materials in the BR-10 reactor. Control system for electric motor
[DE87-702888] 03 p0310 N88-11952
The operational behavior of microprocessor-controlled and pulsed inverter-fed synchronous machines with permanent magnet excitation
[ETN-88-91479] 11 p1480 N88-18833
A high performance inverter-fed drive system of an interior permanent magnet synchronous machine
[DE88-006753] 15 p2061 N88-22288
Permanent magnet excitation of axial flow synchronous machines with high rotation moment
[ETN-88-92385] 20 p2796 N88-26592
Voltage directive drive with claw pole motor and control without rotor position indicator
[ETN-88-93120] 24 p3366 N88-30047
SYNCHRONOUS PLATFORMS
Communications payload concepts for geostationary facilities
[NASA-TM-100154] 05 p0576 N88-13513
Latitude coverage of observations of the middle atmosphere by solar absorption spectrometry from a heliosynchronous orbit
[AERONOMICA-ACTA-A-316-1987] 06 p0742 N88-14566
Coorbiting Platform Utilization Study (CPLUS), executive summary --- Columbus
[SN-WP-4000-DOC-6609/85/F] 09 p1133 N88-16798
SYNCHRONOUS SATELLITES
NT GOES SATELLITES
Low-g propellant gaging 08 p0982 N88-15937
Satellite assembly in geostationary orbit: A plug-and-socket concept 09 p1128 N88-16769
Investigations of high resolution imaging through the Earth's atmosphere using speckle interferometry
[AD-A189295] 12 p1692 N88-20121
Survey of the Air Force P78-2 (SCATHA) satellite plasma wave data during electron gun operations
[AD-A191014] 16 p2168 N88-22926
Construction of a 60 GHz Traveling Wave Tube (TWT) for intersatellite link on geostationary orbit (ISL/TWT)
[BMFT-FB-W-86-015] 16 p2192 N88-23076
On the collision hazard of colocated geostationary satellites
[DFVLR-FB-88-02] 23 p3184 N88-28952
SYNCHROTRON RADIATION
Brightness and coherence of radiation from undulators and high-gain free electron lasers
[DE87-011093] 02 p0177 N88-11102
Stratospheric particles: Synchrotron X-ray fluorescence determination of trace element contents
[DE87-012482] 02 p0198 N88-11234
Compact electron storage rings
[DE87-013301] 02 p0234 N88-11477
Resistor cooling in a vacuum
[DE88-000696] 04 p0440 N88-12733
Center for X-Ray Optics, 1986
[DE88-000715] 04 p0449 N88-12783
The generation and suppression of synchrotron sidebands
[DE88-000532] 04 p0449 N88-12787
The production of ultrasmall and superfine holographic diffraction gratings using synchrotron radiation and lithographic techniques
[AD-A185395] 05 p0585 N88-13562
Microwave superheaters for fusion
[DE88-001656] 05 p0653 N88-14007
JPRS report: Science and technology. Japan
[JPRS-JST-87-027] 06 p0688 N88-14213
HEAO-1 observations of gamma-ray bursts 07 p0947 N88-15756
The structure of the sideband spectrum in free electron lasers
[AD-A186952] 09 p1170 N88-17015
Grazing incidence X-ray scattering study of defect structures in MBE GaAs/Si using synchrotron radiation
[DE88-004556] 10 p1420 N88-18483
Initial operation of the Tevatron collider
[FNAL-TM-1449] 11 p1547 N88-19252
Multilayer-coated mirrors as power filters in synchrotron radiation beamlines
[DE88-003872] 11 p1550 N88-19276
Applications of the lateral shearing interferometer in measurement of synchrotron radiation optical elements
[DE88-005184] 13 p1840 N88-21011
Advances in geochemistry and cosmochemistry: Trace element microdistributions with the synchrotron X-ray fluorescence microprobe
[DE88-006355] 15 p2032 N88-22108
Transport simulations of ohmic ignition experiment: IGNITEX
[DE88-006055] 15 p2138 N88-22757
On bunch lengthening using the fourth harmonic cavity in the NSLS VUV ring
[DE88-007392] 18 p2574 N88-25288
An undulator radiation source for spin-polarized photoemission studies of novel magnetic materials
[AD-A193756] 22 p3083 N88-28307
Fourier transform of gravitational synchrotron radiation
[PREPRINT-588] 22 p3144 N88-28700
X-ray diffraction imaging (topography) of electrooptic crystals by synchrotron radiation
[NASA-CR-183266] 24 p3432 N88-30427
Diffraction imaging (topography) with monochromatic synchrotron radiation
[NASA-CR-183264] 24 p3433 N88-30431
Streaking images that appear only in the plane of diffraction in undoped GaAs single crystals: Diffraction imaging (topography) by monochromatic synchrotron radiation
[NASA-CR-183267] 24 p3433 N88-30437
Applications of synchrotron radiation to materials science: Diffraction imaging (topography) and microradiography
[NASA-CR-183265] 24 p3434 N88-30440
SYNCHROTRONS
NT STORAGE RINGS (PARTICLE ACCELERATORS)
National Synchrotron Light Source users manual: Guide to the VUV and X-ray beam lines
[DE88-001464] 04 p0490 N88-13020
Accelerators and Superconductivity: A Marriage of Convenience. Second John Adams Memorial Lecture
[DE88-700005] 07 p0931 N88-15656
A two-wavelength infrared interferometer/polarimeter system for CIT (Compact Ignition Tokamak)
[DE88-007681] 18 p2579 N88-25321
Optical guiding in the separable beam limit
[AD-A192452] 21 p2952 N88-27534
SYNCOPE
NT BLACKOUT (PHYSIOLOGY)
SYNDROMES
U SIGNS AND SYMPTOMS
SYNOPTIC MEASUREMENT
Analysis of winter season precipitation bands over the Southern Plains 14 p1947 N88-21609
The role of space borne imaging radars in environmental monitoring: Some shuttle imaging radar results in Asia
[NASA-TM-101175] 20 p2789 N88-26544
Meteorological features during the marginal ice zone experiment from 20 March to 10 April 1987
[AD-A193960] 23 p3235 N88-29251
SYNOPTIC METEOROLOGY
An illustrative example of the nowcasting challenge 02 p0199 N88-11243
Conceptual models of Baiu front and Baiu frontal disturbances in multiscale characteristics --- East Asia 02 p0203 N88-11271
A review of the analysis forecasting and research about severe local storms in Guangdong province (China) 02 p0207 N88-11298
Properties of the atmospheric boundary layer above a subtropical oceanic front
[AD-A184006] 03 p0351 N88-12215
Isentropic analysis and interpretation: Operational applications to synoptic and mesoscale forecast problems
[AD-A184814] 05 p0626 N88-13830
Global atmospheric circulation statistics: Four year averages
[NASA-TM-100690] 05 p0628 N88-13842
Synoptic perturbations and climate 08 p1016 N88-16158
Northern winter circulations for the period 1974-1983
[AD-A187779] 11 p1511 N88-19028
Dynamics of synoptic ocean eddies 13 p1786 N88-20689
Analysis of a six-component barotropic spectral model: Chaotic motion, predictability and vacillation --- atmospheric circulation
[CWI-AM-R8710] 18 p2542 N88-25090
Verification of regional climates of GISS GCM. Part 1: Winter
[NASA-TM-100695] 19 p2694 N88-26012
Synoptic patterns related to tropical cyclone recurvature
[AD-A192338] 20 p2827 N88-26771
Solar-geophysical data number 522, February 1988. Part 2: (Comprehensive reports). Data for August 1987 and miscellanea
[PB88-194741] 20 p2886 N88-27138
Some evidence for a Northern Hemispheric extratropic trigger mechanism of ENSO events 22 p3123 N88-28558
SYNTAX
NT SYLLABLES
NT WORDS (LANGUAGE)
Integrating syntax, semantics, and discourse DARPA (Defense Advanced Research Projects Agency) Natural Language Understanding Program
[AD-A184505] 03 p0364 N88-12289
Ada (trade name) compiler validation summary report. Systems designers' PLC SD Ada-plus VAX/VMS x MC68020. Version 2B.00. Host: VAX 8600. Target: Motorola MC68020. Completion of on-site testing
[AD-A186571] 08 p1053 N88-16356
Substructure discovery in executed action sequences
[AD-A186446] 08 p1069 N88-16462
Experience with Omega: Implementation of a prototype programming environment, part 6
[AD-A187080] 10 p1385 N88-18270
KA-Prolog: Language definition
[GMD-249] 11 p1532 N88-19155

A parser generator for finitely ambiguous context-free grammars
[CWI-CS-R8712] 13 p1818 N88-20864
WORDNET: An electronic lexical reference system based on theories of lexical memory
[AD-A193086] 21 p3027 N88-27970
Unification and set-valued functions for functional and logic programming
[AD-A193643] 23 p3250 N88-29341
Experiments in automatic phrase indexing for document retrieval: A comparison of syntactic and non-syntactic methods 23 p3296 N88-29634
Exploiting lexical regularities in designing natural language systems
[AD-A195922] 24 p3423 N88-30375

SYNTHESIS
Reduced complexity structural modeling for automated airframe synthesis
[NASA-CR-177440] 04 p0393 N88-12453
A method for designing robust multivariable feedback systems
[NASA-CR-182459] 09 p1225 N88-17341
A methodology for the synthesis of robust feedback systems
[NASA-CR-182455] 09 p1225 N88-17342
Structural shape optimization in multidisciplinary system synthesis
[NASA-TM-100538] 12 p1614 N88-19650

SYNTHESIS (CHEMISTRY)
NT COPOLYMERIZATION
NT DIMERIZATION
NT POLYMERIZATION
Process for the preparation of acyl halides
[GB-PATENT-2-133-792-A] 01 p0020 N88-10124
Novel polymers and copolymers and production of poly(acetylene)
[EP-PATENT-0-173-473-A2] 01 p0026 N88-10161
A process for producing phenolic foams
[EP-PATENT-0-170-357-A1] 01 p0026 N88-10162
Novel conductive polymers
[EP-PATENT-0-182-548-A2] 01 p0026 N88-10163
Crosslinkable elastomeric materials
[EP-PATENT-0-181-735-A1] 01 p0026 N88-10165
Boronium complexes as polymer catalysts
[GB-PATENT-2-161-475-A] 01 p0026 N88-10166
Synthesis and characterization of processable polyimides with enhanced thermal stability
[NASA-CR-181447] 01 p0030 N88-10191
Synthesis of novel acid electrolytes for phosphoric acid fuel cells
[PB87-221305] 01 p0066 N88-10426
Preparation of polymer polyols
[EP-PATENT-0-162-589-A1] 01 p0102 N88-10665
Formation of amorphous alloys by solid state reactions
[DE87-013175] 02 p0146 N88-10918
Urea-polyurethane and polydimethylsiloxane mixtures. Morphology control using a block copolymer
[ISAL-IDI1-87-05] 02 p0153 N88-10959
Wittig synthesis of conductive segmented block polymer compositions
[AD-A184018] 03 p0295 N88-11850
Synthesis and characterization of block copolymers
[AD-A184405] 03 p0295 N88-11855
Synthesis and characterization of block copolymers
[AD-A184406] 03 p0296 N88-11856
Highly Non-Linear Optical (NLO) organic crystals 03 p0297 N88-11865
Shock-induced chemical synthesis of phases similar to the high temperature superconductor oxides
[DE87-013725] 03 p0380 N88-12387
Ceramics thin film 04 p0403 N88-12505
Synthesis, NMR characterization and electrical properties of siloxane-based polymer electrolytes
[AD-A184184] 04 p0418 N88-12596
Conductive polymers via reactive aligomer
[AD-A184270] 04 p0419 N88-12597
Thermoplastic elastomers as LOVA (Low Vulnerability Ammunition) binders
[AD-A184350] 04 p0419 N88-12599
Proton abstraction as a route to conductive polymers
[AD-A184019] 04 p0421 N88-12612
Studies on syntheses of amine-carboxyboranes (boron analogues of amino acids) and derivatives
[AD-A184838] 05 p0557 N88-13386
Molecular-level synthesis and characterization of metal-polymer interfaces
[AD-A184956] 05 p0567 N88-13455
Preparation and characterization of members of the system (Zn,Se)1-xGaPx
[AD-A185073] 05 p0655 N88-14019
Method for preparing hydride configurations and reactive metal surfaces
[DE88-000845] 06 p0679 N88-14161
Model Cu/ZnO catalysts for methanol synthesis: The role of surface structure
[DE88-002354] 07 p0830 N88-15037
Biopolymers: Protein and nucleic acids
[AD-A185837] 07 p0835 N88-15066
The synthesis and characterization of some rare earth arsenides
[AD-A186445] 08 p0965 N88-15839
A 13C and 15N solid state NMR characterization of aramid-containing nylon-6 polymers synthesized by in situ polymerization of caprolactam with benzoyl caprolactam derivatives
[AD-A187067] 09 p1147 N88-16872
Thermoplastic elastomers as LOVA binders
[AD-A186563] 10 p1304 N88-17797
Electrically conducting polymer-copper sulphide composite films, preparation by treatment of polymer-copper (2) acetate composites with hydrogen sulfide
[NASA-TT-20204] 10 p1305 N88-17803
Effect of weightlessness on replicative function of rat hepatocyte DNA 10 p1360 N88-18129
RNA-synthesizing activity in rat liver following flight aboard Cosmos-1667 10 p1360 N88-18130
Electronic and ionic transport in polymers
[AD-A187253] 11 p1452 N88-18651
Synthesis and structure property studies of toughened epoxy resins via functionalized polysiloxanes. Friction and wear studies
[AD-A188258] 11 p1462 N88-18718
Preparation of thin film polyvinylidene fluoride shock wave pressure transducers
[PB88-156070] 11 p1490 N88-18893
Nonlinear optical waveguides containing a transition metal-based dye molecule
[DE88-003257] 11 p1550 N88-19275
The preparation of titanium nitride and titanium carbonitride by the preceramic polymer route
[AD-A188357] 12 p1610 N88-19626
Ordered polymers for space applications
[AD-A188460] 12 p1610 N88-19630
Synthesis and characterization of 1,2-cyclobutenedicarboxamides: Thermally generated polymers and Diels-Alder adducts
[AD-A188591] 12 p1611 N88-19633
A procedure for estimating the crystal densities of organic explosives
[AD-A189023] 12 p1613 N88-19646
Synthesis of energetic materials
[AD-A189115] 13 p1753 N88-20482
A hydroxycarbonate route to superconductor precursor powders
[DE88-003638] 13 p1846 N88-21052
The combustion synthesis of boride composites
[DE88-005474] 15 p2028 N88-22084
Research on stable processible conducting polymers for electronic applications
[AD-A190246] 15 p2044 N88-22180
New phosphorus based polymer systems
[AD-A190457] 15 p2045 N88-22186
A new approach to highly fluorinated lubricants
[AD-A190523] 15 p2045 N88-22188
Evaluation of direct methane conversion to higher hydrocarbons and oxygenates
[DE88-003812] 15 p2049 N88-22204
Synthesis of metastable superconductors by high dynamic pressure
[DE88-005620] 15 p2139 N88-22764
Remarks on solid state amorphizing transformations
[DE88-006452] 15 p2145 N88-22803
Synthesis and characterization of high-T(sub c) screen-printed Y-Ba-Cu-O films on alumina
[NASA-TM-100860] 15 p2146 N88-22805
Synthesis and properties of novel cluster phases
[DE88-006816] 16 p2175 N88-22964
Evaluation of a thermoplastic polyimide (422) for bonding GR/PI composite
[NASA-TM-100584] 16 p2182 N88-23003
Key problems and hydrogen atom formation 16 p2269 N88-23573
Improvements to Raney copper zinc methanol synthesis catalysts 17 p2318 N88-23844
Polymer precursors for SiC ceramic materials 17 p2326 N88-23889
Topological stereochemistry
[AD-A191867] 18 p2477 N88-24691
Aromatic cyclotriphosphazenes
[NASA-CASE-ARC-11428-3] 18 p2477 N88-24692
Proceedings of the American Society for Composites
[AD-A189861] 18 p2477 N88-24693
Current and future molecular structures of aerospace organic matrix resins 18 p2477 N88-24695
Industrial perspective on current and future needs in aerospace matrix resin chemistry 18 p2477 N88-24696
Applications of biotechnology to synthetic chemistry for aerospace matrix resins development 18 p2478 N88-24697
The application of hydrocarbon bioconversion technology to aerospace materials production 18 p2478 N88-24698
The synthesis of polyphenylene from a CIS-dihydrocatechol biologically produced monomer 18 p2478 N88-24699
Update of low temperature catalyst development
[DE88-007032] 18 p2480 N88-24715
Synthesis and characterization of new phosphazene polymers
[AD-A191508] 18 p2490 N88-24771
High strength/sigh modulus aromatic heterocyclic ABA block copolymers
[AD-A191666] 18 p2491 N88-24774
A cardiostimulant protein from the Australian Red Waratah Sea anemone, Actinia tenebrosa 18 p2550 N88-25138
Solid-state combustion synthesis of ceramics and alloys in reduced gravity
[NASA-CR-4163] 19 p2608 N88-25479
Improved structural polymer alloys and composites
[AD-A192092] 19 p2619 N88-25538
Substituted 1,1,1-Triaryl-2,2,2-Trifluoroethanes and processes for their synthesis
[NASA-CASE-LEW-14345-1] 20 p2767 N88-26404
Glass forming ranges of amorphous alloys
[DE88-007897] 20 p2772 N88-26438
Dual mechanism bifunctional polymers: Design, synthesis and application of a new category of metal ion complexing agents
[DE88-008233] 20 p2777 N88-26468
A study of solvent effects on the synthesis of pure component and composite ceramic powders by metal alkoxide hydrolysis
[DE88-006381] 20 p2777 N88-26470
Fundamental studies of elastomers
[DE88-009679] 20 p2778 N88-26471
Refractory Materials of Zirconate. Part 2: Synthesis and some properties of strontium, zirconate, calcium zirconate and barium zirconate
[NASA-TT-20186] 20 p2779 N88-26483
Cosmological helium production simplified
[DE88-009578] 20 p2885 N88-27130
Ionic conductive polymers based on crosslinked elastic siloxane-ethylene oxide copolymers
[DE88-011243] 21 p2917 N88-27311
Soluble metal chelate polymers of coordination numbers six, seven and eight
[AD-A192485] 21 p2917 N88-27314
Preparation and properties of high Q microwave dielectrics in the (CA, SR, BA) zirconate system
[AD-A193127] 21 p2918 N88-27317
Energy migration, motion and order in synthetic polymers
[AD-A193334] 21 p2918 N88-27320
New synthetic approaches to boron hydride transformations
[AD-A193872] 22 p3052 N88-28108
Super hydrides
[AD-A193710] 23 p3192 N88-28995
Polymerization of azaethylenes (imines) and aza-1,3-dienes: Potential reactive monomers
[AD-A194717] 23 p3197 N88-29026
Boron-containing organosilane polymers and ceramic materials thereof
[NASA-CASE-ARC-11649-1-SB] 23 p3199 N88-29040
Diamond film by hot filament CVD method
[NASA-TT-20335] 23 p3294 N88-29618
Novel ladder polymers for use as high temperature stable resins or coatings
[NASA-CASE-LEW-14203-1] 24 p3356 N88-29984

SYNTHESIZERS
Neural network based speech synthesizer: A preliminary report 08 p1064 N88-16429

SYNTHETIC APERTURE RADAR
NT SIDE-LOOKING RADAR
Study of a payload for Columbus Polar Platform Earth observation demonstration mission, executive summary
[ESA-CR(P)-2412] 01 p0014 N88-10079
X-band SAR for a European remote sensing payload 03 p0340 N88-12142
Inverse scattering analysis of diffraction limited SAR
[FOA-C-30459-3.2] 05 p0576 N88-13512
Arrays for discrete Fourier transform
[REPT-87-019] 05 p0632 N88-13861
Study of synthetic aperture radar data compression and encoding. Part 3: Performance evaluation of speckle suppression and data compression algorithms
[NLR-TR-85085-L-PT-3] 06 p0692 N88-14248
Study of synthetic aperture radar data compression and encoding. Part 4: Algorithm implementation aspects
[NLR-TR-85085-L-PT-4] 06 p0692 N88-14249

Texture study of Synthetic Aperture Radar (SAR) images of ocean surfaces
[AD-A186021] 07 p0841 N88-15101
Study of synthetic aperture radar data compression and encoding. Part 1: SAR image data analysis
[NLR-TR-85085-L-PT-1] 07 p0843 N88-15115
Study of synthetic aperture radar data compression and encoding. Part 2: SAR image speckle suppression and data compression algorithms
[NLR-TR-85085-L-PT-2] 07 p0843 N88-15116
SAR (Synthetic Aperture Radar). Earth observing system. Volume 2F: Instrument panel report
[NASA-TM-89701] 07 p0871 N88-15284
Earthnet's experience with Seasat SAR image processing 09 p1127 N88-16760
Radar backscatter from airports and surrounding areas 10 p1274 N88-17823
Rotor SAR (ROSAR): A new high-resolution all-weather vision method for helicopters
[MBB-UA-1046/87] 10 p1314 N88-17855
SAR (Synthetic Aperture Radar) imaging of ship wakes in the Gulf of Alaska
[AD-A186554] 10 p1317 N88-17872
Integrated optical synthetic aperture radar processor
[AD-A188019] 11 p1471 N88-18772
The complex point spread function of the RSRE SAR (Synthetic Aperture Radar)
[AD-A189011] 12 p1621 N88-19693
Synthetic-aperture radars viewed as interferometers with matched filter processing of the collected data
[AD-A190608] 15 p2057 N88-22262
Preliminary study of a coherent radar
[BCRS-86-03] 16 p2189 N88-23051
Investigation of the imaging of ocean surface waves using a synthetic aperture radar
[SER-A-WISS-ABHANDL-84] 16 p2236 N88-23357
Preparation and execution of calibration measurements for handling of airborne SAR data (AGRISAR)
[ETN-88-92338] 17 p2333 N88-23926
The role of space borne imaging radars in environmental monitoring: Some shuttle imaging radar results in Asia
[NASA-TM-101178] 18 p2502 N88-24844
Data volume reduction for imaging radar polarimetry
[NASA-CASE-NPO-17184-1-CU] 20 p2788 N88-26541
The role of space borne imaging radars in environmental monitoring: Some shuttle imaging radar results in Asia
[NASA-TM-101175] 20 p2789 N88-26544
Some characteristics in synthetic aperture radar (SAR) raw data and SAR images
[FOA-C-30483-3.2] 22 p3071 N88-28232
Effect of phase errors in stepped-frequency radar systems
[AD-A194476] 23 p3203 N88-29061
Acoustooptic processing of two-dimensional signals using temporal and spatial integration
[AD-A194803] 24 p3359 N88-29999
A submillimeter wavelength space-based imaging radar
[AD-A195846] 24 p3364 N88-30033
MIZEX (marginal ice zone experiment) 1987 SAR (Synthetic Aperture Radar) data summary
[AD-A195560] 24 p3364 N88-30035

SYNTHETIC APERTURES
High precision ultrasonic scanning system and SAFT-UT development
[DE87-010038] 01 p0008 N88-10044
Imaging of planar defects with synthetic aperture focusing technique (LSAFT) --- ultrasonic inspection
[VTT-468] 01 p0058 N88-10370
On the concept of resolution ellipse in aperture synthesis matched deconvolution with error analysis --- astronomical interferometry 01 p0095 N88-10621
OASIS: A mission concept --- Optical Aperture Synthesis Space Interferometry (OASIS) 01 p0095 N88-10622
Aperture synthesis in space: Technical problems 01 p0097 N88-10638
Holographically correcting synthetic aperture aberrations
[AD-A189510] 12 p1692 N88-20123

SYNTHETIC ARRAYS
ISIS: Image reconstruction experiments and comparison of various array configurations --- spaceborne interferometry 01 p0095 N88-10620
Fiber-linked telescope arrays on the ground and in space 01 p0095 N88-10626

SYNTHETIC FIBERS
NT CERAMIC FIBERS
NT GLASS FIBERS
NT NYLON (TRADEMARK)
Molecular composites: Processing, post-treatment and mechanics
[AD-A184458] 04 p0410 N88-12547
Structure of thermotropic polyesters with large substituents
[AD-A184086] 04 p0418 N88-12595
Solid state C-13 NMR characterization of textiles: Qualitative and quantitative analysis
[AD-A184349] 04 p0419 N88-12598
Development of test methods for the electrostatic properties of nonhomogeneous fabrics, phase 2
[AD-A190853] 18 p2489 N88-24767

SYNTHETIC FUELS
NT GASOHOL (FUEL)
Fifty years in synthetic fuels information: Have we lost a strategic national resource
[DE87-010902] 02 p0155 N88-10973
Emerging environmental constraints on the use of gasoline and diesel fuel and tradeoffs associated with the use of alternative fuels
[DE87-011504] 04 p0422 N88-12614
Combustion characteristics of gas turbine alternative fuels
[NASA-TM-100247] 05 p0548 N88-13338
Fuel nitrogen conversion in a supercharged spark ignition engine
[DE88-003739] 08 p0974 N88-15893
Engine testing for synfuel operation
[DE88-006044] 13 p1779 N88-20645
Production costs of hydrocarbon fuels from biomass
[DE88-006667] 18 p2495 N88-24804
Development of an equation of state for computation of supercompressibility factors, critical flow factors and other properties for wet, sour natural gases, synthetic gases and admixtures
[PB88-202676] 20 p2798 N88-26602
An outdoor test facility for the large-scale production of microalgae
[DE88-001146] 21 p2984 N88-27723
The behaviour of synthetic fuels in a small transparent combustor 24 p3351 N88-29950

SYNTHETIC RESINS
NT ACRYLIC RESINS
NT EPOXY RESINS
NT KEVLAR (TRADEMARK)
NT NYLON (TRADEMARK)
NT PEEK
NT PHENOLIC RESINS
NT POLYAMIDE RESINS
NT POLYETHER RESINS
NT POLYMETHYL METHACRYLATE
NT THERMOPLASTIC FILMS
NT THERMOPLASTIC RESINS
NT THERMOSETTING RESINS
NT VINYL COPOLYMERS
Flame retardation treatment of synthetic rubbers and synthetic resins
[NASA-TT-20285] 19 p2620 N88-25544

SYNTHETIC RUBBERS
NT BUNA (TRADEMARK)
NT ELASTOMERS
NT VULCANIZED ELASTOMERS
Flame retardation treatment of synthetic rubbers and synthetic resins
[NASA-TT-20285] 19 p2620 N88-25544
Development of a nitrile rubber for dynamic damping
[AD-A194060] 22 p3058 N88-28145

SYRIA
International manned flight, USSR-SAR
[NASA-TT-20260] 16 p2166 N88-22914

SYSTEM EFFECTIVENESS
Measurement of fault-tolerant parallel processors
[PB87-208328] 01 p0084 N88-10539
Experiments in fault tolerant software reliability
[NASA-CR-181554] 05 p0632 N88-13863
Field evaluation of interactive simulation for maintenance training: SH-3 helicopter electro-mechanical bladefold system
[AD-A185923] 07 p0821 N88-14991
Measurement and effects of transport delays in a state-of-the-art F-16C flight simulator
[AD-A187367] 11 p1441 N88-18599
The integration of artificial intelligence techniques to improve the effectiveness of electronic countermeasure strategies in a tactical environment
[AD-A189483] 12 p1682 N88-20056
A low cost automatic Earth observation satellite tracking ground receiving station 17 p2309 N88-23815
An enumeration of research to determine the optimal design and use of Army flight training simulators
[AD-A191242] 18 p2468 N88-24649
Vapor Compression Distillation Subsystem (VCDS) component enhancement, testing and expert fault diagnostics development, volume 1
[NASA-CR-172072] 22 p3134 N88-28634
The OFP (Operational Flight Program) update cycle needs you
[AD-A194910] 24 p3325 N88-29798
Controlled degradation of resolution of high-quality flight simulator images for training effectiveness evaluation
[AD-A196189] 24 p3330 N88-29823

SYSTEM FAILURES
Inadequacy of conventional dynamic recovery mechanisms in the presence of temporary failures
[AD-A186311] 07 p0866 N88-15251
Modelling of clustering effects in point processes: An application to failures in SPC-systems (stored program control-systems)
[PB87-149241] 07 p0904 N88-15480
Validation of a stochastic model to determine failure rates for communication-electronic systems
[AD-A186536] 08 p0980 N88-15920
Pattern-recognition software detecting the onset of failures in complex systems
[DE88-002861] 09 p1220 N88-17318
Airworthiness considerations 10 p1276 N88-17636
Failure mechanism of He-Ne lasers 14 p1902 N88-21362
On the danger of redundancies in some aerospace mechanisms 14 p1925 N88-21475
Orbiter processing facility service platform failure and redesign 14 p1928 N88-21494
Modeling failures of intermittently used machines
[AD-A190298] 15 p2074 N88-22367
Aircraft accident/incident summary reports: Modena, Pennsylvania, March 17, 1986; Redwater, Texas, April 4, 1986
[PB88-910403] 16 p2159 N88-22878
Expanded envelope concepts for aircraft control-element failure detection and identification
[NASA-CR-181664] 16 p2160 N88-22886
Design of the Detector 2: A CMOS gate array for the study of concurrent error detection techniques
[AD-A191247] 16 p2193 N88-23079
Compilation of preprints
[AD-A191245] 16 p2252 N88-23460
Modeling of functional specifications for onboard software: Experience with the Rafale avionics system 17 p2303 N88-23777
MTK: An AI tool for model-based reasoning 17 p2387 N88-24189
Applications of fault tree analysis to the design process
[DE88-007048] 18 p2525 N88-24982
Failure rate prediction of electronic components
[PB87-228953] 19 p2678 N88-25925
Electronic failure analysis-corrosion of avionics 22 p3054 N88-28122

SYSTEM IDENTIFICATION
Digital algorithms for the control and dynamic decoupling of industrial robot axes
[ETN-87-90441] 01 p0084 N88-10546
Effect of installation and calibration errors of sensors on system identification results of an aircraft
[ESA-TT-1059] 03 p0266 N88-11678
A system identification technique based on the random decrement signatures. Part 1: Theory and simulation 05 p0594 N88-13625
A system identification technique based on the random decrement signatures. Part 2: Experimental results 05 p0594 N88-13626
Lie algebraic method in filtering and identification
[CWI-PM-R8606] 08 p1072 N88-16467
A state space approach to the problem of adaptive pole assignment
[CWI-OS-R8704] 09 p1224 N88-17339
Identification of nonlinear output-affine systems using an orthogonal least squares algorithm
[RR-313] 14 p1958 N88-21678
Identification of nonlinear rational systems using a prediction-error estimation algorithm
[RR-317] 14 p1959 N88-21680
Application of the NARMAX method to nonlinear frequency response estimation
[RR-319] 14 p1964 N88-21721
Active control and system identification of rotordynamic structure 16 p2218 N88-23230
Identification of control structures --- expert systems
[REPT-87-66] 18 p2255 N88-23479
TVC (Thrust Vector Control) jet vane thermal modeling using parametric system identification
[AD-A191518] 18 p2474 N88-24678
System identification in vehicle dynamics
[DFVLR-MITT-87-22] 20 p2785 N88-26518
Flight vehicle system identification: Status and prospects 20 p2785 N88-26520
Vehicle dynamics: Identification in the frequency domain 20 p2785 N88-26523
Frequency domain identification of the dynamics of a scaled remotely-piloted helicopter 20 p2786 N88-26524
Multivariable identification of a flexible transport aircraft 20 p2786 N88-26525
A two-point aerodynamic model for identification 20 p2786 N88-26526

The identification of the direct lift control flap system of the research aircraft ATTAS
20 p2786 N88-26527
Identification methods for transport dynamical investigations
20 p2787 N88-26531
Utilization of identification methods in the time and frequency domain for the determination of the XV-15 (tilt-rotor) dynamics for lateral motion in hover flight
20 p2787 N88-26532
Identification of lateral operation dynamics of rail vehicles using roll test stand tests
20 p2787 N88-26534
Nonlinear identification of an aircraft for the direct calculation of an anticipatory control
20 p2787 N88-26535
Estimation of aircraft parameters using filter error methods and extended Kalman filter
[DFVLR-FB-88-15] 23 p3176 N88-28911

SYSTEMS ANALYSIS
NT SYSTEM IDENTIFICATION
Digital system bus integrity
[NASA-CR-181446] 01 p0006 N88-10030
A feasibility study of a hypersonic real-gas facility
[NASA-CR-180423] 01 p0008 N88-10043
Numerical predictions of EML system performance
[DE87-011727] 01 p0011 N88-10061
Spacecraft 2000
[NASA-CP-2473] 01 p0015 N88-10084
Space Assembly, Maintenance, and Servicing Study (SAMSS)
01 p0015 N88-10089
Spacecraft Systems Working Group report
01 p0015 N88-10091
System Development Working Group report
01 p0016 N88-10092
The periodic Lyapunov equations
[REPT-86-007] 01 p0087 N88-10567
Recent advances in structural dynamics of large space structures
[NASA-TM-100513] 02 p0138 N88-10867
Space lab system analysis
[NASA-CR-179207] 02 p0138 N88-10869
Direct Absorption Receiver (DAR) systems assessment
[DE87-012277] 02 p0196 N88-11222
Software reliability models for fault-tolerant avionics computers and related topics
[NASA-CR-181440] 02 p0220 N88-11382
Balloon track data analysis
[AD-A184750] 03 p0350 N88-12213
UNIX benchmark system
[AD-A184492] 03 p0367 N88-12308
Institute for Computational Mechanics in Propulsion (ICOMP) first year summary
[NASA-TM-100225] 03 p0370 N88-12330
Mathematical models for the S.D.I.
[AD-A184667] 03 p0373 N88-12345
Development and evaluation of a Monte Carlo code system for analysis of ionization chamber responses
[AD-A183970] 03 p0375 N88-12359
The impact of information technology on research in science and engineering
[DE88-000342] 03 p0385 N88-12417
CNET (Chief of Naval Education and Training) Program Automated Tracking System (CPATS): A comprehensive study
[AD-A184694] 03 p0385 N88-12418
An evaluation plan of bus architectures and protocols using the NASA Ames intelligent redundant actuation system
[NASA-CR-177458] 04 p0398 N88-12482
On dynamic loads in parallel shaft transmissions. 1: Modelling and analysis
[NASA-TM-100180] 04 p0451 N88-12797
PRAAGE: An interactive IBM-PC code for unreliability/aging analysis
[DE87-012124] 04 p0453 N88-12803
Extremum methods of structural analysis for system reliability assessment
04 p0456 N88-12824
Performance analysis of solar thermal power systems
[DE88-000563] 04 p0465 N88-12874
Applications of the hybrid automated reliability predictor
[NASA-TP-2760] 04 p0475 N88-12928
Software maintenance in scientific and engineering environments: An introduction and guide
[NASA-CR-177409] 04 p0479 N88-12954
Investigation, development and application of optimal output feedback theory. Vol. 4: Measures of eigenvalue/eigenvector sensitivity to system parameters and unmodeled dynamics
[NASA-CR-4108] 04 p0482 N88-12969
Propagation of random initial conditions in time
04 p0486 N88-12993
RSDIMU acceptance testing system: Overview of acceptance software and procedures
05 p0632 N88-13866
Post stall behavior in axial-flow compressors
[AD-A185712] 06 p0665 N88-14081
Controlled Ecological Life Support Systems (CELSS) physiochemical waste management systems evaluation
[NASA-CR-177422] 06 p0754 N88-14626
Characteristic trajectories of generalized Lanchester equations
[AD-A185762] 06 p0766 N88-14705
Summaries of FY 1987 engineering research
[DE88-002572] 07 p0840 N88-15096
How errors in component reliability affect system reliability
[AD-A186264] 07 p0865 N88-15249
Mathematical techniques for system realization and identification
[AD-A186352] 07 p0915 N88-15557
Risk analysis methodology survey
07 p0922 N88-15604
Orbital transfer vehicle studies overview
08 p0981 N88-15931
Adaptive exponential stabilization of a first order continuous-time system
[CWI-OS-R8705] 08 p1069 N88-16461
System analysis in rotorcraft design: The past decade
09 p1110 N88-16652
Dynamic analysis of multimesh-gear helicopter transmissions
[NASA-TP-2789] 09 p1176 N88-17045
Cooperative analysis expert situation assessment research
09 p1206 N88-17228
Approaches to the verification of rule-based expert systems
09 p1206 N88-17232
Building validation tools for knowledge-based systems
09 p1207 N88-17235
A performance comparison of the Cray-2 and the Cray X-MP
[NASA-CR-177461] 09 p1216 N88-17288
Concept of a programmable maintenance processor applicable to multiprocessing systems
[NASA-TM-100406] 09 p1223 N88-17333
A methodology for the synthesis of robust feedback systems
[NASA-CR-182455] 09 p1225 N88-17342
Latent failures and coverage in fault-tolerant systems. A VLSI CMOS circuit design technique to aid test generation
[AD-A187615] 10 p1325 N88-17921
Comprehensive analysis of helicopters with bearingless rotors
[NASA-CR-182537] 10 p1390 N88-18300
A two-stage isolated-word recognition system using discriminant analysis
[AD-A187425] 10 p1402 N88-18360
Linear prediction of stationary vector sequences
[NASA-TM-100069] 10 p1403 N88-18366
Multidimensional system analysis of electro-optic sensors with sampled deterministic output
[AD-A187083] 10 p1408 N88-18399
Development of tokamak reactor system analysis code NEW-TORSAC
[DE88-751067] 10 p1411 N88-18417
Orbiter transfer vehicle concept definition and system analysis study. Volume 4: Space station accommodations. Revision 1
[NASA-CR-179293] 11 p1444 N88-18609
Orbital transfer vehicle concept definition and system analysis study. Volume 4, Appendix A: Space station accommodations. Revision 1
[NASA-CR-179294] 11 p1444 N88-18610
Space station operating system study
[NASA-CR-179308] 11 p1446 N88-18619
Simulated performance of an order statistic threshold strategy for detection of narrowband signals
11 p1474 N88-18796
Design for performance enhancement in feedback control systems with multiple saturating nonlinearities
[NASA-CR-182614] 11 p1535 N88-19168
Generating the states of a probabilistic system
[AD-A187896] 11 p1540 N88-19208
Optimal arrangement of components via pairwise rearrangements
[AD-A187633] 11 p1541 N88-19213
ICF special studies
[DE88-004057] 11 p1551 N88-19281
Preliminary analysis of an integrated logistics system for OSSA payloads. Volume 2: OSSA integrated logistics support strategy
12 p1584 N88-19479
Motion simulation for in-orbit operations
12 p1589 N88-19514
Structural shape optimization in multidisciplinary system synthesis
[NASA-TM-100538] 12 p1614 N88-19650
Systems approach to energy quality and efficiency
[PB88-139506] 12 p1640 N88-19823
Analysis, estimation, and control for perturbed and singular systems and for systems subject to discrete events
[AD-A188496] 12 p1677 N88-20026
Knowledge-based system analysis and control
[AD-A188163] 12 p1681 N88-20049
Systems analysis and simulation techniques: Essential tools for balanced complex weapon system designs in terms of performance and cost
12 p1702 N88-20187
The TempIS Project: Performance analysis of temporal queries
[AD-A188354] 12 p1706 N88-20213
Study of the optimization of satellite system design for transfer orbit
[MBB-URV-135] 13 p1727 N88-20332
Solar dynamic power system definition study
[NASA-CR-180877] 13 p1733 N88-20361
Activities report of the Systems Department
[ETN-88-91987] 13 p1756 N88-20505
Coherent laser radar system theory
[AD-A188759] 13 p1774 N88-20612
On the sensitivity of complex, internally coupled systems
[NASA-TM-100537] 13 p1813 N88-20829
MacCAD (Macintosh Computer Aided Design), computer aided design tool for system analysis
[AD-A189241] 13 p1815 N88-20843
Further results on the McMillan degree and the Kronecker indices of ARMA models --- input-output relations of linear systems
[EUT-87-E-175] 13 p1827 N88-20925
MANPRINT handbook for RFP (Request For Proposal) development
[AD-A188321] 13 p1850 N88-21075
Advanced avionics system analysis. Modular avionics cost benefit study formulation
[AD-A189019] 14 p1867 N88-21158
Sensitivity of control-augmented structure obtained by a system decomposition method
[NASA-TM-100535] 14 p1954 N88-21647
Parametric methods of analysing linear and nonlinear systems
[RR-318] 14 p1967 N88-21741
A systems analysis of fire suppression alternatives for the US space station
[AD-A189847] 15 p2025 N88-22064
Comparative analysis
[AD-A190556] 15 p2065 N88-22313
Monitoring the usage of a computer system
[DE88-004310] 15 p2106 N88-22542
Fault tree analysis and synthesis
[ETN-88-92235] 16 p2261 N88-23521
Liquid droplet radiator development
17 p2424 N88-24415
MACRAD: A mass analysis code for radiators
17 p2424 N88-24418
Dynamic isotope power system critical component verification
17 p2425 N88-24421
Possibilities and limits for use of laser propulsion systems in interorbital space flight
[ILR-MITT-185] 18 p2475 N88-24683
Reliability of stochastically forced systems (extended version)
[CWI-AM-R8801] 18 p2526 N88-24985
Systems analysis of INTOR-like designs
[DE88-004422] 18 p2578 N88-25316
Diagnosing faults in autonomous robot plan execution
[NASA-CR-182480] 20 p2841 N88-26859
Finite-dimensional approximation for optimal fixed-order compensation of distributed parameter systems
[NASA-CR-181674] 20 p2843 N88-26873
The influence of weld metal properties, weld geometry and applied load on weld system performance
[AD-A193403] 21 p2961 N88-27588
Performability analysis: Measures, an algorithm and a case study
[AD-A192477] 21 p3001 N88-27800
Sources and nature of cost analysis data base reference manual
[AD-A193099] 21 p3028 N88-27976
Test and calibration system for monitoring the Advanced Technologies Testing Aircraft System (ATTAS) data acquisition system
22 p3037 N88-28029
Air Force Systems Command software independent verification and validation implementation analysis and guidance
[AD-A194309] 22 p3137 N88-28653
Combined and-or parallel execution of logic programs
[AD-A193648] 22 p3138 N88-28656
Modularity in the PASCAL model compiler
[NPL-DITC-111/88] 22 p3139 N88-28664
On the pseudo-linearization problem for nonlinear systems
[AD-A194021] 22 p3142 N88-28683

Use of Markov probability and reliability model generation methods in the analysis of reliability of a fault tolerant hardware and software based system with flexible repair policies
[PNR90467] 22 p3145 N88-28706
Analysis of the effect of faulty spares on the performance of diagnostic algorithms in reliable systems
[AD-A193526] 23 p3223 N88-29186
An analysis of heat transfer after loss of primary coolant in the SP-100 reactor system
[AD-A194619] 23 p3281 N88-29539
Center for opto-electronic systems research instrumentation grant
[AD-A193711] 23 p3282 N88-29545
Knowledge based simulation: An artificial intelligence approach to system modeling and automating the simulation life cycle
[AD-A195838] 24 p3423 N88-30372
Center for opto-electronic systems research
[AD-A195159] 24 p3429 N88-30411

SYSTEMS COMPATIBILITY
Interoperability and integration of data relay satellite systems 03 p0339 N88-12134

SYSTEMS DESIGN
U SYSTEMS ENGINEERING

SYSTEMS ENGINEERING
NT COMPUTER SYSTEMS DESIGN
NT CONTROL SYSTEMS DESIGN
The ISA test system: A catalog of automatic support facilities 01 p0012 N88-10067
Preliminary study of a biotechnology research facility for microgravity, executive summary
[MATRA-EPT/AS/VT209/246/NT] 01 p0032 N88-10204
Prephase A study of a crystallization laboratory for Columbus, executive summary
[ESA-ITT/AO/1-1866/85F] 01 p0032 N88-10206
Robotic sensors and actuators for a service manipulator system. Volume 2: Service Manipulator System (SMS) handbook
[MATRA-EPT/DT/VT187/227] 01 p0053 N88-10342
A brief discussion of formally based approaches to rapid prototyping
[BAE-WAA-RP-RES-SWE-440] 01 p0079 N88-10508
Fiber optic engineering sensor system. Preliminary program management plan, phase 3 revision
[AD-A183663] 01 p0093 N88-10608
Aperture synthesis in space: Technical problems 01 p0097 N88-10638
AI expert system technology issues for guidance and control applications 02 p0128 N88-10808
Vacuum pumps and systems: A review of current practice 02 p0134 N88-10839
A modern space simulation facility to accommodate high production acceptance testing 02 p0134 N88-10841
Transient modeling of the thermohydraulic behavior of high temperature heat pipes for space reactor applications 02 p0136 N88-10857
A nondissipative Pyrotechnic Arming and Firing Unit (PAFU)
[CRA/REPO/8019] 02 p0155 N88-10974
A preliminary study of a fluid science laboratory for space station (Columbus). Part 4: Executive summary
[NLR-TR-87023-L-PT-4] 02 p0170 N88-11072
Study of closed loop control singularity in dynamic systems with a constraint on the final state
[LAAS-87-180] 02 p0223 N88-11405
Pinhole occulter experiment
[NASA-CR-179206] 02 p0235 N88-11481
Research simulators for helicopters 03 p0263 N88-11656
A129 advanced solutions for meeting today's combat helicopter requirement 03 p0265 N88-11669
The Avionics Flight Evaluation System (AFES) of the DFVLR
[ESA-TT-1037] 03 p0266 N88-11677
Mass spectroscopic facility 03 p0296 N88-11861
A design-philosophy for grounding and inter-unit wiring
[EMCR-20/85] 03 p0310 N88-11954
Discussions in support of the design-philosophy for grounding and inter-unit wiring
[EMCR-21/85] 03 p0310 N88-11955
The CNR/PSN Advanced Microwave Imaging Radiometer (AMIR) --- satellite-borne 03 p0340 N88-12141
Design and implementation of a debugger for an abstract machine
[AD-A184691] 03 p0363 N88-12283
The warp computer: Architecture, implementation, and performance
[AD-A184329] 03 p0363 N88-12286
Concepts and techniques for support of real time distributed operating systems
[AD-A184491] 03 p0367 N88-12307
National Science Foundation
[PB87-228375] 03 p0384 N88-12410
Multicast gateway design considerations
[PB87-219960] 04 p0430 N88-12663
Plant Growth Module (PGM) conceptual design 05 p0631 N88-13855
Carbon Dioxide observational platform system (CO-OPS) Feasibility Study
[NASA-CR-179225] 06 p0671 N88-14113
Objects architecture: A comprehensive design approach for real-time, distributed, fault-tolerant, reactive operating systems
[AD-A185476] 06 p0755 N88-14631
Design, production, and characterization of broadband optical waveguides
[DFVLR-FB-85-52] 06 p0780 N88-14791
Study of a Radio Relay Link (RRL). Cassini mission. Data package for final presentation
[ESA-CR(P)-2472] 07 p0847 N88-15138
SAR (Synthetic Aperture Radar). Earth observing system. Volume 2F: Instrument panel report
[NASA-TM-89701] 07 p0871 N88-15284
A software planning and development methodology with resource allocation capability
[AD-A186088] 07 p0902 N88-15462
Docking/Berthing Subsystem (DBS). Development part 1: Latching analysis --- Columbus
[ESA-CR(P)-2479] 08 p0962 N88-15825
Cryogenics program overview 08 p0981 N88-15926
Space Infrared Telescope Facility (SIRTF) design and thermal analysis 08 p0982 N88-15934
JPRS report: Science and technology. USSR: Space
[JPRS-USP-87-006] 08 p1001 N88-16063
Telescope design for Michelson Interferometer for Passive Atmospheric Sounding (MIPAS) B 08 p1017 N88-16167
A backscatter lidar proposed for the second German Spacelab mission 08 p1018 N88-16173
CLIPS: An expert system tool for delivery and training 08 p1056 N88-16368
Requirements and options for communications services in support of the Systems Autonomy Demonstration Project 08 p1057 N88-16374
Expert systems relations in space applications 08 p1059 N88-16391
FMEAssist: A knowledge-based approach to Failure Modes and Effects Analysis 08 p1060 N88-16395
LISP based simulation generators for modeling complex space processes 08 p1061 N88-16403
Knowledge-based simulation 08 p1061 N88-16404
Commonality analysis as a knowledge acquisition problem 08 p1062 N88-16413
Qualitative models for planning: A gentle introduction 08 p1062 N88-16414
Telemetry applications handbook
[AD-A186825] 09 p1132 N88-16789
Columbus feasibility studies. Volume 2: Element constituents, mechanical
[ETN-88-91074] 09 p1134 N88-16800
Columbus feasibility studies. Volume 3: Avionics, systems
[ETN-88-91075] 09 p1134 N88-16801
Design of a solid fuel combustion chamber
[VTH-LR-447] 09 p1141 N88-16837
A substructure method for dynamic simulation of flexible mechanical systems with geometric nonlinearities 09 p1176 N88-17044
Bioreactor design concepts 09 p1197 N88-17171
User engineering: A new look at system engineering 09 p1206 N88-17231
Design knowledge capture for the space station 09 p1208 N88-17239
CONFIG: Qualitative simulation tool for analyzing behavior of engineering devices 09 p1208 N88-17240
Evaluating software testing methods to reduce testing duplication in US Army communications equipment acquisition
[AD-A186961] 09 p1216 N88-17292
Application of a database system for inventory management of classified material
[AD-A186986] 09 p1261 N88-17558
Knowledge base refinement by monitoring abstract control knowledge, revision 1
[AD-A187502] 10 p1397 N88-18323
Multidimensional system analysis of electro-optic sensors with sampled deterministic output
[AD-A187083] 10 p1408 N88-18399
Plasma physics design and major specifications of candidate reactors for FER design studies. Conceptual design study of FY86 FER
[DE88-751066] 10 p1411 N88-18416
Development of the Extendable and Retractable Mast (ERM), Design phase 2. Volume 1 — spacecraft payloads
[RP-2010-0000-DS/09] 11 p1467 N88-18750
A worked example of an application of the SAINT simulation program
[AD-A188198] 11 p1524 N88-19097
Evaluating expert system tools: A framework and methodology-workshops
[AD-A187190] 11 p1533 N88-19159
The design of the POSTGRES storage system
[AD-A187244] 11 p1564 N88-19365
UNIVERS product, phase 1
[AD-A187405] 11 p1564 N88-19367
Accessing hierarchical databases via SQL transactions in a multi-model database system
[AD-A187878] 11 p1565 N88-19369
The Hermes robot arm, its design and verification 12 p1588 N88-19508
Guidance and control of air-launched armaments: An aeroengineer's perspective 12 p1597 N88-19557
Alternative program approaches for the advanced satellite technology program
[AD-A188917] 12 p1600 N88-19576
An EHF telecommunication system engineering model 12 p1618 N88-19674
Emerging technologies program 3-5: Microelectronics Panel report
[AD-A189463] 12 p1624 N88-19716
Aspects of bioregenerative life support systems 12 p1655 N88-19917
Visual display representation of multidimensional systems: The effect of information correlation and display integrality
[AD-A188655] 12 p1672 N88-20010
Management information systems design implications: The effect of cognitive style and information presentation on problem solving
[AD-A188850] 12 p1705 N88-20205
A comparison of information system development methodologies
[AD-A188957] 12 p1707 N88-20219
Activities report of the Systems Department
[ETN-88-91987] 13 p1756 N88-20505
The acoustic-modeling problem in automatic speech recognition
[AD-A188529] 13 p1757 N88-20510
Design of a supersonic wind tunnel
[ETN-88-92078] 14 p1870 N88-21176
The development status of the strongback array --- spacecraft structure 14 p1875 N88-21201
System and concept design of the SSRMS latching end effector --- Space Station 14 p1875 N88-21204
Latching mechanisms for IOC --- EURECA 14 p1875 N88-21205
The EURECA antenna deployment and retraction mechanisms 14 p1878 N88-21225
Evolution of large momentum and reaction wheels 14 p1879 N88-21230
Development of an engineering model dynamic cooler --- spacecraft payloads
[F+W-TF-B-1885] 14 p1895 N88-21311
Continued design of a Pointing, Acquisition, and Tracking (PAT) subsystem for InterSatellite Laser links (ISL2)
[TELDIX-15-093-178] 14 p1905 N88-21384
DataViews: A personalizable, interactive, data display system for the decisionmaker
[AD-A188509] 14 p1991 N88-21868
Aluminum-air battery development
[DE88-006620] 15 p2061 N88-22287
Designs of profiles for cascades
[NASA-TT-20161] 15 p2067 N88-22326
Reliability analysis within a Computer Aided Engineering (CAE) infrastructure
[NLR-MP-86059-U] 15 p2074 N88-22369
Basic design studies for the realization of liquid crystal display systems in aircraft
[VA-87-001] 16 p2163 N88-22900
Toward a mathematical formalism of performance, task difficulty, and activation 16 p2239 N88-23372
The Design, Development and Testing of Complex Avionics Systems
[AGARD-CP-417] 17 p2302 N88-23767
Systems for the 21st century 17 p2302 N88-23769
Architecture and role of the Sensor Subsystem in future aircraft weapon systems 17 p2302 N88-23770
Rapid prototyping of complex avionic system architectures 17 p2302 N88-23771
The specification and design of a future maritime reconnaissance aircraft 17 p2303 N88-23772
A structured approach to weapon system design 17 p2303 N88-23773
Development of a generic architecture 17 p2303 N88-23774

Test philosophy of the EH101 integrated avionic
17 p2303 N88-23775
Systems engineering technique
17 p2303 N88-23776
A comparison of integrated and separate systems for flight control and navigation 17 p2303 N88-23779
Development and testing of a predictive methodology for optimization of man-machine interface in future avionics systems 17 p2304 N88-23780
A change in system design emphasis: From machine to man 17 p2304 N88-23782
Managing advanced avionic system design
17 p2304 N88-23783
Psychosensory cockpit ergonomics, advantages of intelligent information systems 17 p2304 N88-23784
Design for interoperability (interchangeability)
17 p2305 N88-23789
The integration, characterisation and trialling of a modern complex airborne radar 17 p2305 N88-23791
Experience in the integration of human engineering effort with avionics systems development
17 p2305 N88-23793
Developing systems using state-of-the-art CAD/CAM technology 17 p2306 N88-23795
Workshops for the design of avionics systems and the development of onboard software
17 p2307 N88-23802
Coherent functional development: Key to successful future system integration 17 p2307 N88-23803
Development of complex avionics systems: Experience from French military programs 17 p2307 N88-23804
Ariane 4 pyrotechnics system: Definition of the chains and pyrotechnic devices
[CNES-88/CT/DRT/TVE/IL/25]
17 p2310 N88-23816
Life Support Subsystem (LSS). Concept for the Botany Facility --- EURECA
[TN-RB524-107/86] 17 p2377 N88-24131
Botany Facility: Considerations and analyses of the balancing system philosophy proposed for the BF centrifuge
[SIRA-A/7373/WP110/PWF001]
17 p2378 N88-24139
Selection of a handling and maintenance option for the SP-100 ground engineering system test
17 p2402 N88-24285
The Curie point radiator 17 p2424 N88-24420
The high-throughput X-ray spectroscopy mission E6889478 MN513835 --- ESA program
[ESA-SP-1092] 17 p2450 N88-24554
Concepts for a laser gyroscope of the highest precision 18 p2517 N88-24929
A systems engineering based methodology for analyzing human electrocortical responses
[AD-A190809] 18 p2550 N88-25135
The ATF (Advanced Toroidal Facility) Data M Management System
[DE88-007265] 18 p2589 N88-25385
System capacity and economic modeling computer tool for satellite mobile communications systems
19 p2644 N88-25686
Development of the network architecture of the Canadian MSAT system 19 p2646 N88-25702
System architecture for the Canadian interim mobile satellite system 19 p2646 N88-25703
Design, development and trials of an airline passenger telephone system 19 p2646 N88-25704
Space cabin atmosphere and extracurricular sortie --- embolisms 19 p2696 N88-26023
Technical challenges in the development of a European space suit system and comparison with underwater suits
19 p2696 N88-26024
The SAGA highly autonomous assistance submarine
19 p2698 N88-26034
Safety aspects in design and operation practice of GKSS underwater simulation plant GUSI
19 p2698 N88-26037
Improvement of head-up display standards. Volume 1: Head-up display design guide, appendix
[AD-A192973] 20 p2834 N88-26809
An overview of the development of a linear broadband analog fiber-optic link
[DE88-008668] 20 p2854 N88-26945
Database design and management in engineering optimization
[AD-A193325] 21 p3003 N88-27813
New generation of integrated monitoring systems for modern aircraft 22 p3035 N88-28015
Artificial intelligence software acquisition program, volume 2
[AD-A194239] 22 p3141 N88-28680
Study of standard generic approach for spacecraft (S/C) autonomy and automation (phase 3). Book A: Autonomy concept description
[ESA-CR(P)-2555-VOL-1] 23 p3185 N88-28955
Study of standard generic approach for spacecraft (S/C) autonomy and automation (phase 3). Book B: Autonomy concept application example
[ESA-CR(P)-2555-VOL-2] 23 p3185 N88-28956
Study of standard generic approach for spacecraft (S/C) autonomy and automation (phase 3). Book C: Autonomy concept summary
[ESA-CR(P)-2555-VOL-3] 23 p3185 N88-28957
Computer aided filter design
[AD-A193959] 23 p3208 N88-29093
A proof of the Kahn principle for input/output automata
[AD-A194454] 23 p3248 N88-29333
Level 1 Ada/SQL (Structured Query Language) database language interface user's guide
[AD-A194480] 23 p3249 N88-29335
Computer systems for the representation and manipulation of mathematical knowledge
[AD-A193547] 23 p3249 N88-29340
Space station as a vital focus for advancing the technologies of automation and robotics
[IAF-86-62] 23 p3251 N88-29352
Artificial intelligence applied to process signal analysis
23 p3252 N88-29359
On recognizing ignorance 23 p3254 N88-29372
Strategic defense initiative architecture dataflow modeling technique version 1.5
[AD-A194356] 23 p3275 N88-29494
Dynamically reconfigurable distributed database systems
[AD-A194716] 23 p3297 N88-29636
Study of robotics spacecraft servicing and assembly in space. Volume 1: Executive summary
[ESA-CR(P)-2612-VOL-1] 24 p3333 N88-29839
Accommodation concept for fluid physics facilities, volume 2 --- Spacelab
[SG-TN-AI-027-VOL-2] 24 p3358 N88-29994
A detection theory analysis of visual display performance
[AD-A196291] 24 p3409 N88-30292
Study of human factors engineering criteria for extravehicular activity (EVA) systems, volume 1
[STF23-F87025-VOL-1] 24 p3410 N88-30298
Knowledge-based integrated information systems engineering: Highlights and bibliography. Knowledge-Based Integrated Information Systems Engineering (KBIISE) Project, volume 1
[AD-A195850] 24 p3435 N88-30449
Technical opinions regarding knowledge-based integrated information systems engineering, volume 8
[AD-A195857] 24 p3436 N88-30454
Knowledge-Based Integrated Information Systems Development Methodologies Plan. Knowledge-Based Integrated Information Systems Engineering (KBIISE) report, volume 2
[AD-A195851] 24 p3436 N88-30455

SYSTEMS FOR NUCLEAR AUXILIARY POWER

U SNAP

SYSTEMS INTEGRATION

Design principles and practices for implementation of MIL-STD-1760 in aircraft and stores
[AD-A183724] 01 p0005 N88-10027
Mid infrared LHS system packaging using flexible waveguides
[NASA-CR-181192] 01 p0093 N88-10607
Space station integrated propulsion and fluid system study: Fluid systems configuration databook
[NASA-CR-179215] 03 p0278 N88-11753
A modular BLSS simulation model
03 p0359 N88-12260
Methods for design and evaluation of integrated hardware/software systems for concurrent computation
[NASA-CR-181522] 04 p0479 N88-12953
GOLD: Integration of model-based control systems with artificial intelligence and workstations
[DE88-000706] 04 p0483 N88-12977
Small space reactor power systems for unmanned solar system exploration missions
[NASA-TM-100228] 05 p0660 N88-14054
Carbon Dioxide observational platform system (CO-OPS) Feasibility Study
[NASA-CR-179225] 06 p0671 N88-14113
Development of a graphical display on the DMS test bed 06 p0794 N88-14864
Space station software reliability analysis based on failures observed during testing at the multisystem integration facility 06 p0798 N88-14884
Fiber optics for controls 08 p0956 N88-15798
Servicer system demonstration plan and capability development
[NASA-CR-179246] 08 p0975 N88-15895
Rotorcraft flight-propulsion control integration
09 p1108 N88-16643
NASA/Army Rotorcraft Technology. Volume 3: Systems Integration, Research Aircraft, and Industry
[NASA-CP-2495-VOL-3] 09 p1110 N88-16650
Avionics systems integration technology
09 p1110 N88-16654
Integrated diagnostics 09 p1111 N88-16655
Systems integrated human engineering on the Navy's rapid acquisition of manufactured parts/test and integration facility 09 p1206 N88-17226
The IDEAL (Integrated Design and Engineering Analysis Languages) modeling methodology: Capabilities and Applications 09 p1206 N88-17227
Implementing clips on a parallel computer
09 p1211 N88-17259
Software for integrated manufacturing systems, part 1
09 p1211 N88-17261
Software for integrated manufacturing systems, part 2
09 p1211 N88-17262
Communication and control in an integrated manufacturing system 09 p1212 N88-17263
System integration of a Telerobotic Demonstration System (TDS) testbed 09 p1212 N88-17266
Columbus feasibility studies. Volume 4: Integration, test, and operations
[ETN-88-90576] 11 p1445 N88-18614
Interfacing of a microcomputer with a simultaneous atomic-emission spectrometer
[PB88-139571] 11 p1526 N88-19109
Workshop on the Integration of Finite Element Modeling with Geometric Modeling
[NASA-CR-182515] 11 p1526 N88-19111
Integration of finite element modeling with solid modeling through a dynamic interface 11 p1526 N88-19112
Integration of geometric modeling and advanced finite element preprocessing 11 p1526 N88-19114
Solid/FEM integration at SNLA
[SAND-87-0882A] 11 p1526 N88-19116
Workshop on Design Loads for Advanced Fighters
[AGARD-R-746] 12 p1579 N88-19449
Interaction between structural considerations and system design in advanced flight controls
12 p1580 N88-19458
Advanced propfan analysis for the family of commuter airplanes
[NASA-CR-182566] 12 p1582 N88-19468
A digital logic simulator with concurrent programming considerations
[AD-A188823] 12 p1678 N88-20032
Development cost reduction using integrated CAE-CAD-CAM techniques 12 p1701 N88-20182
Digital correlator for the portable channel prober measurement instrument
[AD-A189065] 14 p1904 N88-21377
Common database interface for heterogeneous software engineering tools
[AD-A189628] 14 p1991 N88-21870
AGARD Highlights 88/1 14 p2012 N88-22001
Supercomputer environment
[AD-A190633] 15 p2107 N88-22551
Integrated avionics reliability 17 p2294 N88-23723
Rule-based fault-tolerant flight control
17 p2294 N88-23725
The Design, Development and Testing of Complex Avionics Systems
[AGARD-CP-417] 17 p2302 N88-23767
A comparison of integrated and separate systems for flight control and navigation 17 p2303 N88-23779
Development and testing of a predictive methodology for optimization of man-machine interface in future avionics systems 17 p2304 N88-23780
Crewstation Information and Development System (CIDS) 17 p2304 N88-23781
Design for interoperability (interchangeability)
17 p2305 N88-23789
The electromagnetic threat to future avionic systems
17 p2305 N88-23790
The integration, characterisation and trialling of a modern complex airborne radar 17 p2305 N88-23791
Experience in the integration of human engineering effort with avionics systems development
17 p2305 N88-23793
A look toward the future of complex avionics systems development using the USAF Test Pilot School's avionics systems test training aircraft 17 p2306 N88-23797
Coherent functional development: Key to successful future system integration 17 p2307 N88-23803
Space vehicle/nuclear reactor thermal radiation integration issues 17 p2424 N88-24417
Dynamic resource allocation in a hierarchical multiprocessor system: A preliminary study
[NASA-CR-183177] 22 p3141 N88-28675
A relational data-knowledge base system and its potential in developing a distributed data-knowledge system 23 p3251 N88-29353
Coupling expert systems and simulation
23 p3252 N88-29360
Intelligent test integration system
23 p3254 N88-29371

Requirements for a tool to aid in the development of expert systems for space station applications
23 p3258 N88-29398

A methodology for multiple rule system integration and resolution within a singular knowledge base
23 p3261 N88-29413

Knowledge-based integrated information systems engineering: Highlights and bibliography. Knowledge-Based Integrated Information Systems Engineering (KBIISE) Project, volume 1
[AD-A195850] 24 p3435 N88-30449

Knowledge-Based Integrated Information Systems Development Methodologies Plan. Knowledge-Based Integrated Information Systems Engineering (KBIISE) report, volume 2
[AD-A195851] 24 p3436 N88-30455

Integrating information systems in a major decentralized international organization, volume 7
[AD-A195856] 24 p3439 N88-30458

SYSTEMS MANAGEMENT

Critical issues for establishment of a permanently-occupied lunar base
[AD-A187128] 09 p1263 N88-17567

The design and implementation of the Technical Facilities Controller (TFC) for the Goldstone deep space communications complex 11 p1474 N88-18794

UNIVERS product, phase 1
[AD-A187405] 11 p1564 N88-19367

National Informatics Centre: Profile of services
[PB88-134135] 12 p1706 N88-20211

Data management strategies in the industrial environment
[NLR-MP-87002-U] 16 p2286 N88-23684

Life-span knowledge engineering for space operations
23 p3259 N88-29401

A nonlinear filtering process diagnostic system for the Space Station 23 p3262 N88-29417

Real-time space system control with expert systems
23 p3262 N88-29419

SYSTEMS SIMULATION

Rivista Tecnica Selenia, volume 10, number 2
[ETN-87-90763] 01 p0011 N88-10064

The importance sampling and its application to radar simulation 01 p0012 N88-10065

System adaptivity and the modelling of stereotypes — human-computer interaction
[NPL-DITC-91/87] 01 p0077 N88-10494

Study into a data relay satellite mission analysis tool
[ESA-CR(P)-2422] 02 p0220 N88-11384

Simulation of the perpendicular magnetic recording process
[B8713537] 05 p0586 N88-13570

An interactive-graphics method for dynamic system modelling, applying consistency rules
09 p1181 N88-17072

Reduction of time delays in Runge-Kutta integration methods — systems simulation
[MBB/LKE-132/S/PUB/241/A]
09 p1229 N88-17363

Columbus Simulation Facility (CSF)
12 p1590 N88-19522

A comparative survey of mathematical models for dynamic simulation of in-orbit manipulation operations
12 p1592 N88-19533

AVSCOM'S modifications to Teledyne Systems Company's air-to-air fire control system simulation model
[AD-A189136] 13 p1722 N88-20294

SIMSAT: Simulation package for flexible systems. Beams in space
[TW-278] 13 p1730 N88-20348

Activities report of the Systems Department
[ETN-88-91987] 13 p1756 N88-20505

Model structure selection for multivariable systems by cross-validation methods
[EUT-87-E-176] 13 p1827 N88-20926

Numerical solution of multibody systems in space applications 14 p1875 N88-21200

An intelligent simulation model generator
[REPT-87-053] 15 p2109 N88-22562

Infrared simulation model Sensor Atmosphere Target (SENSAT)-2A
[DFVLR-FB-88-01] 16 p2165 N88-22910

On the computation of stationary deterministic behavior of nonlinear dynamic systems with applications to rotor-bearing structures
[ETN-88-92241] 16 p2214 N88-23213

The PROMISE simulation system: Software for the simulation of parallel processes
[NLR-MP-86077-U] 16 p2247 N88-23427

Tape versus queue and stacks: The lower bounds
[CWI-CS-R8752] 16 p2249 N88-23437

Monte Carlo analysis of lateral collection diode arrays
[RSRE-MEMO-4080] 17 p2335 N88-23938

Virtual interface environment
17 p2381 N88-24153

Recursive maximum likelihood identification of a nonlinear output-affine model
[RR-322] 18 p2569 N88-25257

Simulation of space manipulator operations (EUROSIM)
[NLR-MP-87017-U] 20 p2811 N88-26678

Study on NAVSAT system evaluation, phase 2. Part 1: Study results
[NLR-TR-87061-L-PT-1] 22 p3041 N88-28054

Study on NAVSAT system evaluation, phase 2. Part 2: Detailed simulation results
[NLR-TR-87061-L-PT-2] 22 p3041 N88-28055

Design and development of a refueling test bed
[FTMS-RP-ER-011] 24 p3357 N88-29986

Improvements of DCAP 1, phase 2-3/A
[D2-RP-AI-106] 24 p3414 N88-30325

SYSTEMS STABILITY

Closed-loop system analysis using Lyapunov stability theory 04 p0483 N88-12978

Robustness of linear systems
[PB87-220042] 05 p0639 N88-13909

Investigations of the equilibrium and stability of thin-walled double rings. A contribution to the solution of single-sided contact problems
[ETN-87-90044] 09 p1181 N88-17076

Modelling and control of an annular momentum control device
[NASA-CR-4138] 13 p1754 N88-20491

Boundary stabilization of the reaction-diffusion equation with unilateral conditions
[RR-315] 14 p1964 N88-21720

Natural frequencies and stability of immiscible cylindrical z-independent liquid systems
[LRT-WE-9-FB-1(1987)] 22 p3053 N88-28112

Natural frequencies and stability of immiscible spherical liquid systems
[LRT-WE-9-FB-2(1987)] 22 p3053 N88-28113

SYSTOLIC ARRAYS

Implementation and performance of a complex vision system on a systolic array machine
[AD-A184331] 04 p0482 N88-12971

Correctness proofs for systolic algorithms: Palindromes and sorting
[PB88-106075] 07 p0912 N88-15534

SAGE: The Clemson University Systolic Array Generating Engine 10 p1379 N88-18235

Wafer scale implementation of a GaAs systolic signal processor cell 10 p1381 N88-18247

On systolic architectures for interpolation and integration 10 p1382 N88-18250

Systolic array adaptive beamforming
[AD-A187496] 10 p1385 N88-18269

Object recognition on a systolic array
[AD-A187726] 11 p1534 N88-19164

On the design of some systolic algorithms
[CS-8705] 14 p1957 N88-21666

Proposal for a parallel system with image processing applications
[INPE-4293-PRE/1164] 14 p1961 N88-21696

Systolic determination of absolute stability in feedback control systems
[OUEL-1704/87] 14 p1962 N88-21705

HIFI: A design method for implementing signal processing algorithms on VLSI processor arrays
[ETN-88-92238] 16 p2247 N88-23421

Synthesis and simulation of systolic algorithms
[ETN-88-92183] 16 p2247 N88-23423

Efficient bit-level, word-level and block-level systolic arrays for matrix-matrix multiplication
[DE88-011331] 20 p2841 N88-26856

A programmable systolic array for factorial analysis. Part 2: The symmetric eigenvalue problem
[AD-A192396] 21 p2995 N88-27762

A systolic array for efficient execution of the Faddeev algorithm
[DE88-011330] 22 p3135 N88-28635

Systolic array fault tolerance performance analysis
[AD-A193521] 23 p3244 N88-29306

Adaptive identification by systolic arrays
[AD-A193532] 23 p3266 N88-29444

T

T SHAPE

Two-phase flow forms and pressure drop in horizontal T tube joints with vertical branch
[GKSS-87/E/12] 09 p1183 N88-16969

Study of a water-steam two phase flow in a T-branch
[ETN-88-92306] 20 p2801 N88-26624

T TAURI STARS

Angular momentum evolution of young stars
04 p0504 N88-13099

Disk accretion during the early stages of stellar evolution 04 p0505 N88-13106

Pre-main sequence activity: How far is magnetism involved 04 p0517 N88-13179

The contribution of accretion luminosity to the infrared spectra of T Tauri stars: A possible test
04 p0518 N88-13183

Theoretical studies of mass loss and shock phenomena in cool star envelopes
08 p1099 N88-16616

T-33 AIRCRAFT

Access to microgravity: A technical description of the NAE T-33 microgravity facility
[NAE-AN-47] 04 p0405 N88-12518

TABLES (DATA)

Implementation of a digital optical matrix-vector multiplier using a holographic look-up table and residue arithmetic
[NASA-CR-180431] 01 p0078 N88-10496

TeXting the FORMULARY: A collection of examples of the use of TeX to produce ruled tables and displayed equations
[AD-A185920] 07 p0921 N88-15598

Bern solar observations. Solar data for January-December 1986
[REPT-53] 09 p1263 N88-17569

Evaluation and compilation of thermodynamic properties of high temperature chemical species
[AD-A187509] 11 p1452 N88-18654

Tabulation of Mie scattering calculation results for microwave radiative transfer modeling
[NASA-CR-4130] 14 p1947 N88-21612

Table of solar activity associated with coronal mass ejections observed by the SMM coronagraph/polarimeter in 1980
[PB88-170881] 14 p2011 N88-21998

The effects of inlet turbulence and rotor/stator interactions on the aerodynamics and heat transfer of a large-scale rotating turbine model. Part 4: Aerodynamic data tabulation
[NASA-CR-179469] 17 p2339 N88-23956

TABS (CONTROL SURFACES)

Analytic investigation of helicopter rotor blade appended aeroelastic devices
[NASA-CR-166525] 03 p0266 N88-11676

TACHISTOSCOPES

Mechanisms of early light and dark adaptations
12 p1663 N88-19972

TACHOMETERS

Design of a velocity and position control laboratory servo system
[AD-A186596] 08 p0990 N88-15997

TACHYCARDIA

Propranolol and the compensatory circulatory responses to orthostasis at high altitude
[AD-A192675] 22 p3131 N88-28618

TACTICS

An interactive computer graphics network monitor for a tactical communications network
[AD-A184131] 04 p0477 N88-12938

Impact of flying qualities on mission effectiveness for helicopter air combat, volume 1
[NASA-CR-166568] 06 p0669 N88-14100

Computer aided tactics for air combat
12 p1597 N88-19559

Aircrew training devices: Utility and utilization of advanced instructional features, phase 4
[AD-A188418] 12 p1670 N88-20000

Flight simulator: Field of view utilized in performing tactical maneuvers
[AD-A192412] 20 p2762 N88-26379

Biomedical aspects of military operations at high altitude
[AD-A192677] 22 p3132 N88-28619

Tactical air force night/adverse weather training
[AD-A194243] 22 p3133 N88-28625

TACTILE DISCRIMINATION

Optically coupled tactile sensor array for robotics
11 p1550 N88-19273

The rate of adaptation to altered g in the human centrifuge: Implications for simulations of mass-discrimination in space flight
12 p1659 N88-19941

Integrated polysilicon tactile sensor
19 p2669 N88-25863

Flexible tactile sensing arrays for robotics: Architectural robustness and yield considerations
19 p2671 N88-25878

TACTILE SENSATION

U TOUCH

TAGGING

U MARKING

TAIL ASSEMBLIES

Effect of empennage arrangement on single-engine nozzle/afterbody static pressures at transonic speeds
[NASA-TP-2753] 02 p0122 N88-10771

Base pressure measurements on a missile body with cruciform tail
[ESA-TT-1062] 03 p0270 N88-11695
Effect of permissible variations of center-of-gravity locations of cargo airplane on its mass
04 p0424 N88-12625
Navier-Stokes analysis of transonic transport aircraft empennage 19 p2636 N88-25637

TAIL MOUNTINGS
U TAIL ASSEMBLIES

TAIL ROTORS
NT HELICOPTER TAIL ROTORS
New aerodynamic design of the fenestron for improved performance 03 p0264 N88-11664
Aeroelastic characteristics of the AH-64 bearingless tail rotor 21 p2891 N88-27162

TAIL SURFACES
Effect of permissible variations of center-of-gravity locations of cargo airplane on its mass
04 p0424 N88-12625

TAILLESS AIRCRAFT
NT F-106 AIRCRAFT
Conceptual final paper on the preliminary design of an oblique flying wing SST
[NASA-CR-182879] 16 p2161 N88-22891

TAILS (ASSEMBLIES)
U TAIL ASSEMBLIES

TAIWAN
Observational analysis of the interaction between fronts and the orography in Taiwan during the late winter monsoon season 02 p0203 N88-11270
Taiwan area mesoscale experiment: P-3 aircraft operations summary
[PB88-169073] 18 p2544 N88-25098

TAKEOFF
NT VERTICAL TAKEOFF
Noise of a model high speed counterrotation propeller at simulated takeoff/approach conditions (F7/A7)
[NASA-TM-100206] 01 p0091 N88-10592
Optimum take-off run of aircraft on ground airfields
04 p0423 N88-12623
High speed propeller performance and noise predictions at takeoff/landing conditions
[NASA-TM-100267] 05 p0646 N88-13960
Flaps-up takoff performance of the OV-1D aircraft with YT53-L-704 engine installed
[AD-A185960] 07 p0819 N88-14979
Verification of obstacle accountability areas using a simple mathematical model. Part 1: Description of general model and application for a specific case --- engine failure at takeoff
[NLR-TR-85069-U] 09 p1115 N88-16683
Aerodynamic and acoustic characteristics of an advanced propeller under take-off and landing conditions
[NAL-TR-935] 09 p1243 N88-17453
Radar returns from ground clutter in vicinity of airports
10 p1274 N88-17624
Simulator investigation of wind shear recovery techniques 10 p1275 N88-17630
Changes in USAF structural loads requirements
12 p1580 N88-19452
Flight simulator experiments concerning take-off visibility minima
[NLR-TR-86050-U] 13 p1719 N88-20281
Advanced turboprop aircraft flyover noise: Annoyance to counter-rotating-propeller configurations with an equal number of blades on each rotor, preliminary results
[NASA-TM-100612] 16 p2265 N88-23547
Aircraft accident report: Air New Orleans, DBA continental express flight 962 British Aerospace 3101 (Jetstream 31), N331CY, New Orleans International Airport, Kenner, Louisiana, May 26, 1987
[PB88-910408] 19 p2601 N88-25450

TALKING
NT SYLLABLES
NT WORDS (LANGUAGE)

TANDEM MIRRORS
Massachusetts Institute of Technology Plasma Fusion Center: 1986-1987 Report to the President
[DE87-013518] 01 p0101 N88-10661
Fusion reactor physics and technology studies
[DE87-013691] 01 p0101 N88-10664
New methods of confinement and heating of plasma in magnetic fields
[DE88-701021] 15 p2135 N88-22738
Hot electron diagnostics using X-ray imaging on GAMMA10 17 p2443 N88-24530

TANDEM ROTOR HELICOPTERS
NT CH-46 HELICOPTER
Computer program for conceptual tandem rotor helicopter design
[AD-A187832] 11 p1439 N88-18584

TANGENTS
Calculation of symmetric and asymmetric vortex seperation on cones and tangent ogives based on discrete vortex models
[NASA-CR-4122] 08 p0950 N88-15768

TANKS (COMBAT VEHICLES)
Weldability of 2219-T851 and 2519-T87 aluminum armor alloys for use in Army vehicle systems
[AD-A184296] 04 p0451 N88-12792
Measurement of suspension and ride characteristics of the M1 main battle tank 05 p0596 N88-13637
Failure of filament lamps subjected to vibration with special reference to the 26 volt 5 Watt tank lamp
[EL-135] 09 p1158 N88-16938
An investigation of steep descent guidance for terminally-guided sub-munitions
12 p1596 N88-19555
Armoured vehicle track elastomers: Research and development at MRL
[MRL-GD-0012] 19 p2620 N88-25541
Design guidelines for prevention of corrosion in combat and tactical vehicles
[AD-A194172] 22 p3055 N88-28126
Advanced development waste processing unit for combat vehicles, phase 2
[AD-A193793] 23 p3243 N88-29302

TANKS (CONTAINERS)
NT EXTERNAL TANKS
NT FUEL TANKS
NT PROPELLANT TANKS
NT SPHERICAL TANKS
NT STORAGE TANKS
NT WING TANKS
Evaluation of the thermal effectiveness of urethane foam and fiberglass as insulation systems for tank cars
[PB88-100797] 06 p0686 N88-14207
Use of water towing tanks for aerodynamics and hydrodynamics 16 p2204 N88-23149
Technical feasibility study of applying auto-control methods to plating process solutions
[DE88-008014] 19 p2641 N88-25670
Nonlinear oscillations in paraboloidal containers
[LRT-WE-9-FB-3(1988)] 22 p3078 N88-28275
Liquid oscillations in a prolate spheroidal container
[LRT-WE-9-FB-4(1988)] 22 p3078 N88-28276
Nonlinear hydroelastic vibrations in rectangular containers
[LRT-WE-9-FB-7(1987)] 22 p3088 N88-28340

TANTALUM
Metallic superlattices with monolayer modulation
[DE87-012724] 01 p0023 N88-10145
Superconducting properties of metallic superlattices
[DE87-012725] 01 p0023 N88-10146
Computer simulations of knock-on processes in bcc Ta crystal
[DE87-752980] 02 p0246 N88-11554
Use of nonporous metals membranes for the separation of hydrogen from gas mixtures
[BMFT-FB-T-86-206] 14 p1888 N88-21280
Rocket-propellant burn tests of silicide-coated niobium and tantalum
[DE88-010729] 20 p2781 N88-26496

TANTALUM ALLOYS
Reduced-activation ferritic steels: A comparison with Cr-Mo steels
[DE88-000332] 03 p0290 N88-11826

TANTALUM COMPOUNDS
NT TANTALUM OXIDES
Hydrogen in niobium-tantalum superlattices
09 p1146 N88-16867

TANTALUM OXIDES
On 1064 nm and 350 nm laser damage thresholds of high index oxide films deposited from organic solutions and sols
[DE88-001636] 07 p0859 N88-15217

TAPE RECORDERS
UARS spacecraft recorder
[NASA-CR-180768] 15 p2068 N88-22331
Mechanisms mediating perception of complex acoustic patterns
[AD-A189765] 15 p2102 N88-22520

TAPER
U TAPERING

TAPERED WINGS
U SWEPT WINGS

TAPERING
Improved oil-off survivability of tapered roller bearings
[NASA-CR-180804] 02 p0182 N88-11135
Taper sectioning to magnify the interface thickness of a dissimilar metal joint
[RFP-3890-REV] 03 p0333 N88-12099
Exact finite element method analysis of viscoelastic tapered structures to transient loads
05 p0595 N88-13632
Minimum weight design of rectangular and tapered helicopter rotor blades with frequency constraints
[NASA-TM-100561] 12 p1582 N88-19465
Inflow measurements made with a laser velocimeter on a helicopter model in forward flight. Volume 4: Tapered planform blades at an advance ratio of 0.15
[NASA-TM-100544] 16 p2156 N88-22863
Telescope illumination and beam measurements for submillimeter astronomy
[MPE-PREPRINT-88] 16 p2288 N88-23699
AGARD standard aeroelastic configurations for dynamic response. 1: Wing 445.6
[AGARD-R-765] 21 p2896 N88-27193

TAR SANDS
Aviation turbine fuels from tar sands bitumen and heavy oils. Part 2: Laboratory sample production
[AD-A185744] 06 p0687 N88-14211
Aviation turbine fuels from tar sands bitumen and heavy oils. Part 3: Laboratory sample production
[AD-A189278] 13 p1753 N88-20484
Turbine fuels from tar sands bitumen and heavy oil. Volume 2, phase 3: Process design specifications for a turbine fuel refinery charging San Ardo heavy crude oil
[AD-A190120] 16 p2183 N88-23011

TARE (DATA REDUCTION)
U DATA REDUCTION

TARGET ACQUISITION
Problems and possible solutions involved in hard target calibration of coherent Doppler lidar
07 p0922 N88-15602
Development of a computer model for missile simulation, or simulation of a kinetic coverage area for a target detection missile
[FOA-C-20666-2.5] 08 p1067 N88-16449
A piloted simulation investigating handling qualities and performance requirements of a single-pilot helicopter in air combat employing a helmet-driven turreted gun
[AD-A186878] 09 p1116 N88-16689
On the design of suboptimal matched filters for three-dimensional moving target detection
[AD-A188384] 12 p1619 N88-19682
Continued design of a Pointing, Acquisition, and Tracking (PAT) subsystem for InterSatellite Laser links (ISL2)
[TELDIX-15-093-178] 14 p1905 N88-21384
A study of Radar Cross Section (RCS) characteristics and their application in future weapon systems
[ETN-88-92081] 14 p1906 N88-21390
Strategic Defense Initiative Program: Status of space surveillance and tracking system
[PB88-150438] 14 p1967 N88-21739
Design and implementation of VLSI prime factor algorithm processor
[AD-A190483] 15 p2112 N88-22580
The superconducting phase shifter in the development of a terahertz imaging radar system
[AD-A190666] 16 p2188 N88-23046
Air-to-air radar flight testing
[AGARD-AG-300-VOL-7] 21 p2932 N88-27406
Interactive, networked moving platform simulators
[AD-A192374] 23 p3182 N88-28940
Evaluation of atmospheric effects for operational tactical decision aid
[AD-A194205] 23 p3232 N88-29236

TARGET PENETRATION
U TERMINAL BALLISTICS

TARGET RECOGNITION
Feature selection applied to radar target identification
[AD-A183880] 01 p0034 N88-10215
Detection of targets in the presence of clutter using target echo modulations caused by rotating structures
[REPT-12-86] 01 p0036 N88-10231
Independence in sonar observations
[ARE-TR-87102] 01 p0088 N88-10572
Scene simulation for passive IR systems
02 p0137 N88-10861
Theoretical Aspects of Target Classification
[AGARD-LS-152] 03 p0303 N88-11909
Input signal shaping: K-pulse
03 p0304 N88-11917
On the influence of false plots on tracking relaibility: Simulations and preliminary analyses
[FOA-C-30443-3.2] 06 p0692 N88-14245
Investigation and implementation of an algorithm for computing optimal search paths
[AD-A185927] 07 p0902 N88-15461
Interaction of a vortex pair with a free surface
[AD-A186619] 08 p0988 N88-15988
Object detection in images from outdoor scenes using evidential reasoning
[FOA-C-30481-3.3] 08 p1020 N88-16183
Research on visual information processing with special reference to oculomotor behavior in the areas of exploration, recognition and search
[AD-A186598] 08 p1051 N88-16346

Visual attention effects on discrimination of line orientation and line arrangement
[AD-A187013] 09 p1200 N88-17190
Management Information and Downloader Interface System (MIDIS)
[AD-A186978] 09 p1261 N88-17557
Automated radar target recognition based on models of neural nets 11 p1476 N88-18804
On the design of suboptimal matched filters for three-dimensional moving target detection
[AD-A188384] 12 p1619 N88-19682
Position, scale, and rotation invariant target recognition using range imagery
[AD-A188828] 12 p1833 N88-19772
Human efficiency for visual detection of targets on CRT displays using a two-level multiple channel time history format
[AD-A188419] 12 p1670 N88-20001
An optimal branch-and-bound procedure for the constrained path, moving target search problem
[AD-A188962] 12 p1685 N88-20075
Analysis of spectral reflectance characteristics of targets under satellites and automatic cloud recognition 13 p1755 N88-20498
Passive autonomous infrared sensor technology
[AD-A186698] 13 p1839 N88-21005
Effect of friction and control parameters on the tracking accuracy of a target seeker
[AD-A190010] 15 p2056 N88-22257
Polarimetric ISAR imaging using either measured or calculated transient signatures
[AD-A190077] 15 p2056 N88-22259
Multi-disciplinary techniques for understanding time-varying space-based imagery
[AD-A190711] 15 p2117 N88-22610
Rigidity and smoothness of motion
[AD-A190555] 15 p2128 N88-22694
Method and device for the detection and identification of a helicopter
[NASA-TT-20251] 15 p2129 N88-22698
K-pulse estimation from incomplete multiple-frequency scattering data and target identification
[AD-A190827] 16 p2190 N88-23061
Parametric analysis of power requirements for space-based radar 17 p2399 N88-24260
Joint services electronics program
[AD-A191749] 18 p2504 N88-24853
Real-time optical multiple object recognition and tracking system and method
[NASA-CASE-NPO-17139-1-CU] 18 p2576 N88-25301
Multi-target tracking algorithms for cluttered environments 20 p2789 N88-26543
Optical data processing
[AD-A193024] 20 p2839 N88-26841
Outdoor sound propagation, its implications for unattended ground sensors
[FEL-1986-64] 20 p2850 N88-26917
An empirical surface temperature model
[AD-A192737] 21 p2974 N88-27665
Distributed algorithms for probabilistic solution of computational vision problems
[AD-A193150] 21 p2997 N88-27773
Autoregressive moving average modeling of radar target signatures
[AD-A194612] 22 p3069 N88-28218
Activities report of the Division of Reconnaissance and Seeker Systems
[FOA-C-30479-3.1/3.2/3.3/3.4] 22 p3116 N88-28513
Helicopter recognition using laser radars 22 p3149 N88-28736
Object discrimination via bulk temperature/velocity filtering, phase 1
[AD-A194533] 23 p3274 N88-29487
Modeling and performance of HF/OTH (High-Frequency/Over-the-Horizon) radar target identification systems
[AD-A196287] 24 p3365 N88-30038

TARGET THICKNESS
The Rayleigh-Taylor instability in ablatively accelerated targets with 1, 1/2 and 1/4 micrometers laser light
[AD-A185945] 07 p0858 N88-15208

TARGETS
NT LASER TARGETS
NT PARTICLE ACCELERATOR TARGETS
NT RADAR TARGETS
Shock-wave studies using plastic flyers driven by an electric gun for hypervelocity impact on selected materials
[DE87-012631] 01 p0008 N88-10046
Electron interactions with nuclei
[DE87-014587] 02 p0232 N88-11460
Helicopter fire control: Advantages of an automatic target tracker 03 p0264 N88-11667
Analysis of compressible flow on high-velocity jet penetration 03 p0302 N88-11898
Singularity expansion method: Target Resonances 03 p0303 N88-11912
Analytic model of an imploding Z-pinch plasma colliding inelastically with a thin-shelled cylindrical target
[DE88-000051] 03 p0378 N88-12379
Design and implementation of the ESL compact range underhung bridge crane
[NASA-CR-182396] 07 p0862 N88-15231
Effects of uniform target density on random search
[AD-A186468] 08 p1073 N88-16473
Target-reflectivity models for various terrain types
[DE88-005510] 11 p1505 N88-18992
Lower bounds on acceleration estimation accuracy
[AD-A188383] 12 p1619 N88-19681
Cramer-Rao bounds on the accuracy of location and velocity estimations using CCD optical sensors
[AD-A188481] 12 p1629 N88-19748
Sub-scaling of projectile/target system damaged by hypervelocity
[AD-A188663] 12 p1634 N88-19779
Properties of reactively sputtered WNx films Zhao, X. -A.
[AD-A188711] 13 p1835 N88-20976
An investigation of cruciform parachutes and towed targets
[BU-360] 14 p1862 N88-21122
Advanced guidance algorithms for homing missiles with bearings-only measurements
[AD-A190435] 15 p2017 N88-22026
A multiple model adaptive tracking algorithm against airborne targets
[AD-A190619] 15 p2057 N88-22263
TDWR (Terminal Doppler Weather Radar) clutter residue map generation and usage
[AD-A191148] 16 p2235 N88-23352
Numerical analysis of target implosion in LIB ICF 16 p2277 N88-23628
The application of Rutherford backscattering for analyzing multilayered structure change induced by pulsed ion beam bombardment 16 p2278 N88-23638
Self shielding of surfaces irradiated by intense energy fluxes
[DE88-007094] 18 p2579 N88-25318
High dose uranium ion implantation into silicon
[LBL-23509] 19 p2725 N88-26182
Analysis of the perforation of monolithic and simple laminate aluminium targets as a test of analytical deformation models
[MRL-R-1111] 20 p2813 N88-26686
Fiber-optics used to record high-speed photographs inside a pressurized tank during lethality testing
[DE88-011283] 21 p2951 N88-27529
HPM (High-Power Microwave) coupling into realistic targets
[DE88-011788] 23 p3207 N88-29084
Multi-sensory tracking mount control
[AD-A194675] 23 p3249 N88-29339
Comparative aspects of multiple processes of attention
[AD-A195805] 24 p3408 N88-30291

TASK COMPLEXITY
Examining the relative efficiency of Part- versus whole-task practice for multiple-task situations
[AD-A185056] 05 p0631 N88-13856
Artificial Intelligence (AI), Operations Research (OR), and Decision Support Systems (DSS): A conceptual framework 09 p1209 N88-17245
Cardiovascular and subjective measures of task demand in a low workload monitoring task
[REPT-8804] 10 p1368 N88-18176
Distraction and inhibition in continuous CRT performance: A replication and some new findings
[PB88-150941] 13 p1811 N88-20821
Toward a mathematical formalism of performance, task difficulty, and activation 16 p2239 N88-23372
Simultaneous multiple control force exertion capabilities of males and females versus helicopter control force design limits
[AD-A191653] 18 p2553 N88-25153
The relationship between system response time, working memory, and task complexity: An empirical investigation
[DE88-000976] 19 p2711 N88-26105

TASKS
Architecture for dynamic task allocation in a man-robot symbiotic system
[DE87-013872] 03 p0362 N88-12277
Some data processing requirements for precision Nap-Of-the-Earth (NOE) guidance and control of rotorcraft
[NASA-CR-177453] 04 p0401 N88-12493
The characterization of diagnostic tasks for engineering systems
[DE88-000093] 04 p0483 N88-12973
Taskomat, a task battery for information processing
[IZF-1987-2] 05 p0630 N88-13851
Examining the relative efficiency of Part- versus whole-task practice for multiple-task situations
[AD-A185056] 05 p0631 N88-13856
A study of the minority college programs at the NASA Johnson Space Center 06 p0798 N88-14887
Evoked brain activity and personnel performance
[AD-A185922] 07 p0897 N88-15436
Development of a task-level robot programming and simulation system 08 p1058 N88-16387
Crew procedures for microwave landing system operations
[NASA-CR-178359] 09 p1116 N88-16688
Dynamic function allocation in fighter cockpits
[AD-A185397] 09 p1201 N88-17199
Performance analysis of parallel branch and bound search with the hypercube architecture 09 p1206 N88-17229
Task-level robot programming: Integral part of evolution from teleoperation to autonomy 09 p1214 N88-17279
A note on the effect of preemptive policies on the stability of a priority queue
[AD-A186871] 09 p1227 N88-17345
Trends in the distribution of tasks between commercial pilots and flight control systems
[MBB-UT-008/87] 10 p1314 N88-17851
Investigation of effects of short-term exposure to high concentrations of carbon monoxide on operator's psychophysiological functions 10 p1361 N88-18133
On the number of task assignments in distributed computing systems 10 p1378 N88-18230
Deadlock prevention in processor self-scheduling for parallel nested loops
[DE88-003573] 10 p1393 N88-18313
Motor control in man and monkey 11 p1518 N88-19065
Brain activity during tactical decision-making. Part 2: Probe-evoked potentials and workload
[AD-A188688] 12 p1667 N88-19994
A representation for serial robotic tasks 12 p1681 N88-20048
Task allocation for efficient performance of a decentralized organization
[AD-A188699] 12 p1705 N88-20204
The space station assembly phase: Flight telerobotic servicer feasibility. Volume 2: Methodology and case study
[NASA-CR-182690] 13 p1731 N88-20352
Lifting and carrying capacities relative to physical fitness measures
[AD-A189305] 13 p1809 N88-20808
Proceedings of the Workshop on the Assessment of Crew Workload Measurements Methods, Techniques and Procedures. Volume 1: Preliminary Selection of Measures
[AD-A189004] 13 p1812 N88-20827
Method to evaluate image-recovery algorithms based on task performance
[DE88-005382] 13 p1816 N88-20853
POPEYE: A production rule-based model of multitask supervisory control (POPCORN) 16 p2240 N88-23384
Realization of natural language style robot task instruction by using the object oriented concept 16 p2257 N88-23487
NASA-Ames workload research program 17 p2380 N88-24151
Fault diagnosis in orbital refueling operations 17 p2381 N88-24154
Performance estimates for operations conducted while wearing individual protective equipment: User manual
[AD-A191871] 18 p2553 N88-25154
Lunar base surface mission operations. Lunar Base Systems Study (LBSS) task 4.1
[NASA-CR-172050] 18 p2594 N88-25415
Diagnosing faults in autonomous robot plan execution
[NASA-CR-182480] 20 p2841 N88-26859

TAURID METEOROIDS
On orbits and association of meteor streams with Comets P/Halley and P/Encke 14 p2003 N88-21945

TAXIING
A new look at the use of linear methods to predict aircraft dynamic response to taxi over bomb damaged and repaired airfields 09 p1180 N88-17069
Takeoff predictions for powered-lift aircraft
[NASA-CR-177491] 19 p2597 N88-25431

TAXONOMY
A preliminary taxonomy of visible surface algorithms
[DE87-013559] 02 p0220 N88-11386
A taxonomy of analytical computer performance models for computer design
[AD-A185561] 06 p0755 N88-14632

Developing a standard taxonomy or software engineering standards 10 p1379 N88-18234
A taxonomy for conjugate gradient methods [DE88-008574] 21 p3004 N88-27817

TAYLOR INSTABILITY
A numerical and analytical investigation of Rayleigh-Taylor instability in a solid tungsten plate [DE87-013593] 01 p0087 N88-10562
Numerical simulation of transient two-phase flow [CFDU/87/4] 02 p0171 N88-11077
Computer modeling of two-phase flow [CFDU/87/5] 02 p0171 N88-11078
Magnetic fields in the overshoot zone: The great escape 02 p0256 N88-11616
The dynamics of bubble growth for Rayleigh-Taylor unstable interfaces [AD-A184752] 03 p0321 N88-12027
Rayleigh-Taylor instability in compressible fluids [DE88-002473] 07 p0852 N88-15179
The Rayleigh-Taylor instability in ablatively accelerated targets with 1, 1/2 and 1/4 micrometers laser light [AD-A185945] 07 p0858 N88-15208
Analytical and numerical analysis of finite amplitude Rayleigh-Taylor instability [DE88-004056] 11 p1474 N88-18797
Rayleigh-Taylor instability in inertial confinement fusion [DE88-701411] 15 p2137 N88-22750
Efficient shell implosion and target design 16 p2277 N88-23630
A comparison of analytical techniques for modeling the Rayleigh-Taylor response of elastic-plastic solids [DE88-010372] 21 p2962 N88-27596

TAYLOR SERIES
Efficient method for structural optimization 15 p2054 N88-22240
Expressing mathematical subroutines constructively [AD-A190559] 15 p2121 N88-22644

TAYLOR THEOREM
U TAYLOR SERIES

TAYLOR-GOERTLER INSTABILITY
U GOERTLER INSTABILITY

TDMA
U TIME DIVISION MULTIPLE ACCESS

TDR SATELLITES
Study on the suitability of a European data relay satellite to support a system of remote sensing satellites [ESA-CR(P)-2400] 01 p0063 N88-10406
Data Relay Satellite antenna subsystem study [ESA-CR(P)-2435-VOL-2] 02 p0162 N88-11014
Study of antenna configuration for Data Relay Satellite (DRS) user spacecraft [A5/516/86] 02 p0162 N88-11018
DRS (Data Relay Satellite) antenna subsystem study [ESA-CR(P)-2435-VOL-1] 02 p0162 N88-11019
Study into a data relay satellite mission analysis tool [ESA-CR(P)-2422] 02 p0220 N88-11384
Interoperability and integration of data relay satellite systems 03 p0339 N88-12134
Ariane localization technique by Data Relay Satellite (DRS) [SES/ENG/TN-548/86] 08 p0961 N88-15821
Operational aspects of a spacecraft planning/scheduling expert system 08 p1062 N88-16415
Study of dual beam antenna systems for the data relay satellite, volume 1 [S-272-02-VOL-1] 09 p1152 N88-16905
Study of dual beam antenna systems for the data relay satellite. Volume 2: Executive summary [S-272-03-VOL-2] 09 p1153 N88-16906
Assessment of optical communications systems for Data Relay Satellite. Volume 1: Executive summary [ESA-CR(P)-2488-VOL-1] 18 p2502 N88-24841
Assessment of optical communications systems for the Data Relay Satellite [ESA-CR(P)-2488-VOL-2] 18 p2502 N88-24842
NOA: A Network Operator Assistant for scheduling Tracking and Data Relay Satellite System (TDRSS) 23 p3259 N88-29403
Optical multiple access intersatellite links [BAE-TP-8502] 24 p3361 N88-30013

TEA LASERS
TEA-TE: Powerful nitrogen-based laser system 07 p0919 N88-15583
Laser CO2/TEA frequency-stabilized by phase conjugation 22 p3082 N88-28303

TEACHING
U EDUCATION

TEACHING MACHINES
The associative memory ME7 [ESA-TT-1033] 01 p0079 N88-10506

TEAMS
Operational groups at the Aerospatiale Aircraft Division [SNIAS-872-111-107] 05 p0658 N88-14036

TEARING
An investigation of fatigue crack growth in a ductile material at high growth rates 06 p0715 N88-14383

TEARING MODES (PLASMAS)
An unusual magnetopause encounter by AMPTE-UKS 08 p1097 N88-16602
A quadratic-form analysis of the collisionless tearing mode [AD-A188886] 12 p1695 N88-20144

TECHNICAL WRITING
Role of the technical report in technological innovation [PB87-232500] 05 p0658 N88-14040
Genie inference engine rule writer's guide [AD-A185709] 06 p0762 N88-14675
Preliminary analysis of an integrated logistics system for OSSA payloads. Volume 3: OSSA integrated logistics support planning document 12 p1584 N88-19480
Directory of Japanese technical resources, 1987 [PB87-205258] 12 p1706 N88-20212
Text organization and comprehensibility in technical writing [AD-A188913] 12 p1707 N88-20217
Computer-aided writing [AD-A192516] 20 p2838 N88-26837
Technical communication in the computer industry: An information-development process to track, measure and ensure quality 23 p3297 N88-29635

TECHNIQUES
U METHODOLOGY

TECHNOLOGICAL FORECASTING
NT DELPHI METHOD (FORECASTING)
Spacecraft 2000 program overview 01 p0015 N88-10085
Military needs and forecast, 2 01 p0015 N88-10087
Propulsion Working Group report 01 p0016 N88-10098
Attitude Control Working Group report 01 p0016 N88-10099
New nowcasting opportunities using modern meteorological radar 02 p0199 N88-11245
Future directions in computer architecture and software workshop 10 p1383 N88-18258
Emerging supercomputer architectures [DE88-003539] 10 p1384 N88-18262
TABLET: The personal computer of the year 2000 [NASA-CR-182528] 10 p1384 N88-18267
New generation imager system [NASA-CR-180464] 10 p1408 N88-18398
AFGL (Air Force Geophysics Laboratory) fiscal year 1988 Air Force technical objectives document [AD-A187701] 11 p1503 N88-18977
AFAL (Air Force Astronautics Laboratory) technical objective document FY89 [AD-A187861] 11 p1567 N88-19378
Study on long term evolution Towards European Autonomous Manned Spaceflight (STEAMS) [SNIAS-SE/LS/AP-35-073] 13 p1727 N88-20330
European Progress on Space (EPOS): Participation in the creation of long term European space programs [ILR-MITT-189] 14 p1871 N88-21180
Notes on artificial intelligence. Part 1: Technical forecast [FOA-C-30448-3.3-PT-1] 17 p2390 N88-24208
Speculations on future opportunities to evolve Brayton powerplants aboard the space station 17 p2398 N88-24258
Possibilities and limits for use of laser propulsion systems in interorbital space flight [ILR-MITT-185] 18 p2475 N88-24683
Air Force technical objective document, FY89 [AD-A193110] 21 p2896 N88-27194
Future trends in aviation propulsion [PNR90443] 22 p3044 N88-28068

TECHNOLOGIES
NT BIOTECHNOLOGY
NT BUBBLE TECHNIQUE
NT ENERGY TECHNOLOGY
NT GEOTHERMAL TECHNOLOGY
NT MARINE TECHNOLOGY
NT MILITARY TECHNOLOGY
NT REACTOR TECHNOLOGY
JPRS report: Science and technology. China [JPRS-CST-87-031] 03 p0299 N88-11880
JPRS report: Science and Technology. Europe and Latin America [JPRS-ELS-88-002] 10 p1316 N88-17870
JPRS report: Science and technology. Europe and Latin America [JPRS-ELS-88-003] 11 p1468 N88-18754
JPRS report: Science and technology. China [JPRS-CST-87-029] 11 p1468 N88-18755
Conditions and mechanisms of the process of technological innovation in Brazil: The role of research institutes [INPE-4175-TDL/274] 11 p1567 N88-19383
Science, technology and the Constitution: Background paper [PB88-142534] 12 p1708 N88-20222
JPRS report: Science and technology. China [JPRS-CST-88-003] 13 p1755 N88-20495
JPRS report: Science and technology. China [JPRS-CST-87-030] 13 p1756 N88-20501
JPRS report: Science and technology. China [JPRS-CST-88-009] 16 p2186 N88-23030
JPRS report: Science and technology. China [JPRS-CST-88-001] 16 p2186 N88-23036
On-orbit technology experiment facility definition [NASA-TM-100614] 17 p2311 N88-23824
Center for Electronics and Electrical Engineering technical publication announcements covering Center programs, July to September 1987 [PB88-196530] 20 p2793 N88-26572
Resources: NASA for entrepreneurs [NASA-CR-182152] 20 p2883 N88-27119

TECHNOLOGY ASSESSMENT
Investigation of the suitability of the 8ft x 6ft transonic wind-tunnel for aeroacoustic research on propellers [RAE-TM-AERO-2093] 01 p0008 N88-10041
Spacecraft 2000 program overview 01 p0015 N88-10085
Communication satellite technology trends 01 p0015 N88-10088
Spacecraft Systems Working Group report 01 p0015 N88-10091
System Development Working Group report 01 p0016 N88-10092
Electrical Power Working Group report 01 p0016 N88-10095
Propulsion Working Group report 01 p0016 N88-10098
Attitude Control Working Group report 01 p0016 N88-10099
Study on the suitability of a European data relay satellite to support a system of remote sensing satellites [ESA-CR(P)-2400] 01 p0063 N88-10406
Practical limits to ground based interferometry and its impact on space interferometry 01 p0096 N88-10634
NASA's new technology reporting system: A review and future prospects [NASA-CR-180954] 01 p0105 N88-10686
The British Technology Group [ONRL-7-022-R] 01 p0107 N88-10698
A survey of aircraft integrated control technology [AR-004-561] 02 p0126 N88-10794
Space technology to meet future needs [NASA-CR-181473] 02 p0130 N88-10819
Center for Electronics and Electrical Engineering Technical Progress Bulletin covering center programs, October to December 1986 with 1987 CEEE events calendar [PB87-226890] 02 p0168 N88-11058
Center for Electronics and Electrical Engineering technical publication announcements covering center programs, July to September 1986 with 1987 CEEE events calendar [PB87-223442] 02 p0168 N88-11059
Transmission efficiency in advanced aerospace powerplant [PNR90391] 02 p0182 N88-11133
Identifying areas of leading edge Japanese science and technology: Activity analysis using SIC (Standard Industrial Classes) categories and scientific subfields [PB87-204087] 02 p0249 N88-11574
A critical assessment of wind tunnel results for the NACA 0012 airfoil [NASA-TM-100019] 03 p0260 N88-11636
Comparative testing of wind measuring equipment. Part 1: Inventory and selection [R-814-D-PT-1] 03 p0325 N88-12053
Laser sources today and tomorrow [DE87-014247] 03 p0330 N88-12083
Potential applications of expert systems and operations research to space station logistics functions [NASA-CR-180473] 03 p0372 N88-12342
Progress in improving weather forecasting viewed 04 p0458 N88-12833
The role of basic research in society [DE88-000459] 04 p0502 N88-13090
Hypersonic airbreathing propulsion: Evolution and opportunities 05 p0531 N88-13231
The RAE experimental data-base for missiles at high Mach number and its use in assessing CFD methods 05 p0534 N88-13250
Hypersonic aerodynamics: Applications for HOTOL 05 p0535 N88-13252
A perspective of computational fluid dynamics 05 p0538 N88-13279
Fundamentals of fighter aircraft design 05 p0544 N88-13316

Progress toward the evolution of a Stirling space engine
[NASA-TM-100221] 05 p0659 N88-14046
Astronautics and aeronautics, 1978: A chronology
[NASA-SP-4023] 05 p0662 N88-14062
Radiation curing: Comparison of heat, UV, and radiation curing
[OEFZS-4393] 06 p0689 N88-14224
Selected aspects of microelectronics technology and applications: Numerically controlled machine tools. Technology trends series no. 2
[PB87-132973] 06 p0696 N88-14268
Interim review of the possibilities and opportunities for the ONR tropical cyclone motion research initiative
[AD-A185679] 06 p0746 N88-14592
Research and technology objectives and plans. Summary, Fiscal Year 1986
[NASA-TM-87504] 06 p0800 N88-14894
Wind tunnel wall interference 07 p0811 N88-14938
Survey of electronic measurement needs below 10 MHz
[PB88-110366] 07 p0844 N88-15121
The technology of centrifugal compressors: A design approach and new goals for research 07 p0850 N88-15163
Remote sensing of the biosphere
[NASA-CR-182382] 07 p0871 N88-15281
The results of the 1984/1985 Round-Robin Calibration of Reference Solar Cells for the Summit Working Group on Technology, Growth and Employment
[DE88-900215] 07 p0874 N88-15303
Risk analysis methodology survey 07 p0922 N88-15604
Expert system technology 07 p0926 N88-15628
Supersonic throughflow fans for high-speed aircraft 08 p0958 N88-15810
Advancing automation and robotics technology for the space station and for the US economy: Submitted to the United States Congress May 15, 1987
[NASA-TM-89811] 08 p0959 N88-15817
Advancing automation and robotics technology for the space station and for the US economy: Submitted to the United States Congress October 1, 1986
[NASA-TM-89190] 08 p0960 N88-15818
Advanced gyros in spacecraft control. Digital capture loops for dry tuned gyros
[LITEF-120046] 08 p0962 N88-15827
Summary record of presentations to the Federal Telecommunication Standards Committee/Fiber optics task group
[PB88-110853] 08 p0978 N88-15911
An overview of key technology thrusts at Bell Helicopter Textron 09 p1111 N88-16657
The wind tunnel as a yardstick for aircraft design
[NLR-MP-85032-U] 09 p1121 N88-16712
Electric propulsion: A controversial must for long-lived applications satellites 09 p1124 N88-16735
Satellite power systems under consideration by the United Nations 09 p1128 N88-16773
Microwave tubes: Literature study no. 8 comprising the year 1986
[FOA-C-30457-3] 09 p1159 N88-16944
Thermal energy storage by means of an absorption cycle
[ETN-88-91614] 09 p1186 N88-17108
Value-assessment of energy storage concepts in burst power systems
[DE87-013756] 09 p1187 N88-17115
An examination of the impact of potential advances in component technology for future military engines 10 p1279 N88-17650
Helicopter activities in Germany
[MBB-UD-487/86] 10 p1314 N88-17853
Future directions in computer architecture and software: The year 2000 10 p1377 N88-18218
Networking requirements and future alternatives
[NASA-TM-89711] 10 p1426 N88-18517
Technical-economical evaluation of a novel propfan concept in comparison with the turbofan for the nineties
[ETN-88-91022] 11 p1441 N88-18596
High performance composites research at NASA-Langley
[NASA-TM-100518] 11 p1450 N88-18642
Free-piston Stirling engine diaphragm-coupled heat-actuated heat pump component technology program, phase 1B
[DE88-003653] 11 p1483 N88-18854
Review of the state of the art and projected technology of low heat rejection engines
[PB88-131255] 11 p1496 N88-18934
Status of emerging technologies: An economic/technological assessment to the year 2000
[PB88-155775] 11 p1567 N88-19381
Assessment, development and application of combustor aerothermal models
[NASA-TM-100290] 12 p1582 N88-19469
Remote manipulation in orbital construction, servicing and repair missions: Is one arm enough? A comparative evaluation of the performance features of robots with one or more arms 12 p1588 N88-19509
Robotics servicing experiment --- European space programs 12 p1591 N88-19529
ROTEX: The Robotic Technology Experiment on Spacelab D-2 mission 12 p1592 N88-19530
Technology requirements for telerobotic satellite servicing in space 12 p1592 N88-19536
Space station accommodations for life sciences research facilities: Phase A conceptual design and programmatics studies for Missions SAAX0307, SAAX0302 and the transition from SAAX0307 to SAAX0302. Volume 1: Executive summary
[NASA-CR-179267] 12 p1599 N88-19571
Computer aided fast turnaround laboratory for research in VLSI (Very Large Scale Integration)
[AD-A189451] 12 p1624 N88-19715
Parametric study of the total cost of aircraft modernization in terms of development and equipment series costs 12 p1700 N88-20177
The increased time and cost of development: Causes and (some) remedies 12 p1701 N88-20178
Advanced Gas Turbine (AGT) technology development project
[NASA-CR-180891] 12 p1709 N88-20230
Workshop on Technology Development Issues for the Large Deployable Reflector (LDR)
[NASA-CP-2407] 12 p1710 N88-20235
A review of technologies applicable to low-speed flight of high-performance aircraft investigated in the Langley 14- x 22-foot subsonic tunnel
[NASA-TP-2796] 13 p1717 N88-20264
Spacecraft fire-safety experiments for space station: Technology development mission
[NASA-CR-182114] 13 p1731 N88-20353
A comparative assessment of US and UK explosives qualified as replacements for tetryl
[MRL-R-1094] 13 p1754 N88-20486
Cryogenic Fluid Management Technology Workshop. Volume 2: Roundtable Discussion of Technology Requirements
[NASA-CP-10009] 13 p1772 N88-20599
The evaluation of automatic barometers, illustrated by the Nakaasa barometer
[KNMI-TR-95] 13 p1774 N88-20610
Power from the sun: Principles of high temperature solar thermal technology
[DE87-001104] 13 p1795 N88-20736
Biophysical applications of solid state and tritium NMR
[DE88-005328] 13 p1808 N88-20806
The concept of intelligent integrated interactive CAD systems
[CWI-CS-R8717] 13 p1818 N88-20865
Energy loss of particles in dense matter-calorimetry
[NIKHEF-H/87-12] 13 p1836 N88-20988
Johnson Space Center's strategic game plan: Charting a course to the year 2000 and beyond
[NASA-TM-89733] 13 p1850 N88-21076
Development of a real-time aeroperformance analysis technique for the X-29A advanced technology demonstrator
[NASA-TM-100432] 14 p1866 N88-21151
Power systems for production, construction, life support and operations in space
[NASA-TM-100838] 14 p1883 N88-21254
Monolithic microwave integrated circuit technology for advanced space communication
[NASA-TM-100829] 14 p1906 N88-21389
X-ray lasers: State of art and prospect
[ETN-88-92003] 14 p1914 N88-21434
Laser technology: CO2 lasers and laser optics
[ETN-88-91469] 14 p1915 N88-21441
What has been done and what will be done by subnatural linewidth spectroscopy 14 p1978 N88-21807
Extension of free-electron lasers into the extreme ultraviolet
[DE88-005373] 15 p2070 N88-22341
Energy from the wind
[DE88-006897] 15 p2091 N88-22459
A method for estimating and controlling the cost of extending technology
[AD-A190717] 15 p2150 N88-22631
Development and qualification of an Augmented Electro-Thermal Hydrazine-Thruster (AEHT) with 0.1 to 0.2 N vacuum thrust
[BMFT-FB-W-86-012] 16 p2169 N88-22931
Status of CAD/CAM in medium-sized industries described 16 p2184 N88-23022
A 30 GHz monolithic receive module technology assessment
[NASA-CR-180825] 16 p2194 N88-23084
Microgravity robotics technology program
[NASA-TM-100898] 16 p2215 N88-23219
Soviet magnetic confinement fusion research
[PB88-182316] 16 p2279 N88-23644
Microelectronics the next fifteen years 17 p2305 N88-23792
Soviet spacecraft engineering research
[FASAC-TAR-3090] 17 p2311 N88-23823
Current stage of remote sensing system for cartographic application 17 p2366 N88-24090
Soviet remote sensing research and technology
[FASAC-TAR-3130] 17 p2369 N88-24108
Teleoperator human factors study
[NASA-CR-178930] 17 p2382 N88-24162
Applications of nuclear power to lunar and Mars missions 17 p2417 N88-24377
The dynamic isotope power system: Technology status and demonstration program 17 p2422 N88-24400
Assessment of nuclear reactor concepts for low power space applications 17 p2423 N88-24409
Value assessment of energy storage concepts in burst power systems 17 p2426 N88-24432
Low cross-section Mo-Nb thermocouples for nuclear application: The state-of-the-art 17 p2433 N88-24477
SNAP-DYN: Concepts for multikilowatt space power applications 17 p2435 N88-24486
Air Force ultrafast optical electronics center
[AD-A191491] 17 p2438 N88-24507
Proceedings of the American Society for Composites
[AD-A189861] 18 p2477 N88-24693
Industrial perspective on current and future needs in aerospace matrix resin chemistry 18 p2477 N88-24696
Differential technology in plastics industries differentiation in combination technology nonflammability technology
[NASA-TT-20256] 18 p2494 N88-24797
Assessment of optical communications systems for Data Relay Satellite. Volume 1: Executive summary
[ESA-CR(P)-2488-VOL-1] 18 p2502 N88-24841
Assessment of optical communications systems for the Data Relay Satellite
[ESA-CR(P)-2488-VOL-2] 18 p2502 N88-24842
Technical and economic evaluation of emerging biomass pyrolysis processes for gasoline production 18 p2536 N88-25048
Recent advances in low-thrust propulsion technology
[NASA-TM-100959] 18 p2569 N88-25260
Liquid Engine Jet Atomization Workshop report 19 p2627 N88-25584
Millimeter-wave integrated circuits 19 p2656 N88-25774
High performance quarter-micron-gate MODFETs 19 p2656 N88-25776
Remote sensing technique applied to vegetation as an aid to municipal planning 19 p2683 N88-25951
Man versus machine: The role of astronauts in extravehicular activity 19 p2699 N88-26045
Flight Mechanics Panel Symposium on Rotorcraft Design for Operations: Technical evaluation report
[AGARD-AR-243] 20 p2758 N88-26362
Pyrotechnic system failures: Causes and prevention
[NASA-TM-100633] 20 p2765 N88-26394
The outlook for ceramics in heat engines, 1990-2010: Results of a worldwide Delphi survey
[DE88-010075] 20 p2778 N88-26475
Photovoltaic concentrator technology: Recent results
[DE88-009588] 20 p2819 N88-26726
Design of booster wound structures --- spacecraft structures
[SNIAS-881-430-102] 21 p2903 N88-27228
Recent developments in nickel hydrogen technology
[DE88-011248] 21 p2939 N88-27456
Ceramic fabrication technology for high-T(sub)c materials
[DE88-012060] 21 p3024 N88-27953
Technology transfer for DOE's Office of Transportation Systems: Assessment and strategies
[DE88-010760] 21 p3029 N88-27977
Phase 1 results from the Stirling-powered vehicle project
[NASA-TM-100978] 21 p3029 N88-27980
The anatomy of the gyroscope
[AGARD-AG-313] 22 p3079 N88-28287
Recent advances in high-power microwave amplifiers
[DE88-007820] 23 p3206 N88-29083
Reliability assessment of Surface Mount Technology (SMT)
[AD-A193759] 23 p3208 N88-29089
Remotely Operated Vehicle (ROV) reliability study, phase 1
[AD-A194367] 23 p3222 N88-29177
Constitutive modeling for isotropic materials
[NASA-CR-182132] 24 p3327 N88-29811

Study on conceptual design of spacecraft using Computer Aided Engineering (CAE)
[SNIAS-920-CA/TS] 24 p3333 N88-29841
Study of the assembly, integration and verification programs of telecommunication satellites applicable to other satellite programs
[MATRA-100/CC/MLG/031/87] 24 p3334 N88-29847
Space structure (dynamics and control) theme development
[NASA-TM-100597] 24 p3335 N88-29850
Definition of common support equipment and space station interface requirements for IOC model technology experiments
[NASA-TM-100656] 24 p3336 N88-29856

TECHNOLOGY TRANSFER
NT AEROSPACE TECHNOLOGY TRANSFER
NASA's new technology reporting system: A review and future prospects
[NASA-CR-180954] 01 p0105 N88-10686
New technologies and intellectual property: An economic analysis
[N-2601-NSF] 01 p0107 N88-10695
The British Technology Group
[ONRL-7-022-R] 01 p0107 N88-10698
Using bibliographic databases in technology transfer
[NASA-CR-181403] 02 p0222 N88-11399
Assessment of the impacts of transferring certain nuclear reactor technologies to the Soviet Union and Eastern Europe
[DE87-014388] 02 p0249 N88-11576
Materials studies for magnetic fusion energy applications at low temperatures-X
[PB87-232575] 03 p0381 N88-12395
Spinoff
[NASA-TM-89651] 03 p0386 N88-12426
The attitudes of science policy, environmental, and utility leaders on US energy issues and fusion
[DE88-000784] 04 p0494 N88-13041
Technology transfer to China
[PB87-223418] 04 p0502 N88-13087
University research initiative research program summaries
[AD-A184876] 05 p0658 N88-14035
Tools and technologies for expert systems: A human factors perspective 06 p0797 N88-14882
Impressions, observations and comments on science and technology in Japan
[PB87-235743] 06 p0799 N88-14893
Research and technology objectives and plans. Summary, Fiscal Year 1986
[NASA-TM-87504] 06 p0800 N88-14894
Faraday cup characterization of electron beam welding parameters
[DE88-001896] 07 p0864 N88-15241
Biotechnology in western Europe
[PB88-105887] 07 p0883 N88-15360
Organizations of intermediation in technology transfer: Its role in technological innovation
[INPE-4354-TDL/297] 08 p1094 N88-16581
A study of federal technology transfer to the commercial sector
[AD-A187017] 09 p1262 N88-17560
Research and technology 1987
[NASA-TM-4021] 09 p1265 N88-17577
Mathematical modeling of two-state classification technology transfer summary and user's guide
[DE88-003849] 11 p1526 N88-19110
The status of R and D for superconducting power transmission systems
[DE88-003499] 11 p1561 N88-19346
AITI Test Report 87-002: Pratt and Whitney technical order transfer tests
[DE88-004045] 11 p1564 N88-19363
AITI Report 87-003: Honeywell technical order transfer tests
[DE88-004046] 11 p1564 N88-19364
A study of technology transfer arrangements for national laboratories
[DE88-005423] 11 p1567 N88-19382
JPRS report. Science and technology: Europe and Latin America
[JPRS-ELS-87-054] 12 p1573 N88-19406
JPRS report. Science and technology: Europe and Latin America
[JPRS-ELS-87-055] 12 p1686 N88-20086
Directory of Japanese technical resources, 1987
[PB87-205258] 12 p1706 N88-20212
NASA/UK TAP
[NASA-CR-180350] 12 p1708 N88-20223
A project to transfer technology from NASA centers in support of industrial innovation in the midwest
[NASA-CR-180360] 12 p1708 N88-20224
Development of a nationwide network for technology transfer
[NASA-CR-181058] 12 p1709 N88-20225
Technology transfer from US Federal laboratories: Report of a roundtable
[PB88-144803] 12 p1709 N88-20228
Technology '87: Research and Development Laboratory Technology Transfer Program
[DE88-003142] 13 p1852 N88-21084
Spin off businesses as mechanisms for transferring technologies
[DE88-005640] 13 p1852 N88-21085
Applicability of aerospace thermal insulation technologies to the civilian sector
[DE88-003717] 13 p1852 N88-21086
Technology transfer to China. Volume 2: Working papers, part 1
[PB88-158704] 14 p1992 N88-21872
Technology transfer to China. Volume 2: Working papers, part 2
[PB88-158712] 14 p1992 N88-21873
Recent advances in photovoltaic concentrator technology
[DE88-003948] 15 p2091 N88-22462
Small and medium power reactors 1987
[DE88-701435] 15 p2132 N88-22720
Developing systems using state-of-the-art CAD/CAM technology 17 p2306 N88-23795
The contribution of space to maritime activities 19 p2700 N88-26055
Workshop report and presentations from the Semiconductor Research Corporation-DOE Semiconductor Task Force Workshop
[DE88-007690] 19 p2733 N88-26232
Technology transfer, Sandia National Laboratories
[DE88-009790] 19 p2740 N88-26268
Wind Energy Technology: Generating power from the wind, a current awareness bulletin
[DE88-008292] 20 p2820 N88-26729
Thermal energy storage
[DE88-010753] 21 p2967 N88-27625
Technology transfer for DOE's Office of Transportation Systems: Assessment and strategies
[DE88-010760] 21 p3029 N88-27977
Argonne National Laboratory technology transfer report, FY87
[DE88-010091] 23 p3298 N88-29639
China's acquisition and use of foreign aviation technology
[AD-A194827] 24 p3440 N88-30471
Research and technology of the Lyndon B. Johnson Space Center
[NASA-TM-100463] 24 p3460 N88-30583

TECHNOLOGY UTILIZATION
Space station: Leadership for the future
[NASA-PAM-509/8-87] 01 p0013 N88-10072
Spacecraft 2000 program overview 01 p0015 N88-10085
Space station platforms 01 p0015 N88-10086
Military needs and forecast, 2 01 p0015 N88-10087
System Development Working Group report 01 p0016 N88-10092
Electrical Power Working Group report 01 p0016 N88-10095
Space station based interferometry 01 p0096 N88-10628
NASA's new technology reporting system: A review and future prospects
[NASA-CR-180954] 01 p0105 N88-10686
New technologies and intellectual property: An economic analysis
[N-2601-NSF] 01 p0107 N88-10695
The use of McIDAS as a Mesoscale forecasting tool during the Canadian Atlantic storms programs — Man-computer Interactive Data Access System (McIDAS) 02 p0205 N88-11284
Spinoff, 1987
[NASA-TM-89652] 02 p0250 N88-11577
An examination of the Advanced Communications Technology Satellite (ACTS) and its application to the Defense Data Network (DDN)
[AD-A184003] 03 p0276 N88-11742
Optical laser technology, specifically CD-ROM (Compact Disc - Read Only Memory) and its application to the storage and retrieval of information
[AD-A184111] 03 p0330 N88-12086
Market potential for commercial remote sensing 03 p0339 N88-12137
Feasibility study of a range of products drawn from SPOT satellite imagery and specific to road-laying studies 03 p0342 N88-12157
Spinoff
[NASA-TM-89651] 03 p0386 N88-12426
Lasers measure atmosphere 04 p0461 N88-12849
Carbon-carbon composites and Aerospatiale. State of the art and prospects
[SNIAS-872-430-108] 05 p0559 N88-13401
A 40-kW fuel cell field test summary utilities activities report
[PB88-112800] 06 p0731 N88-14496
Artificial intelligence systems 06 p0761 N88-14670
Columbus pressurized module utilization study, executive summary
[CS-RP-AI-027] 07 p0825 N88-15005
Biotechnology in western Europe
[PB88-105887] 07 p0883 N88-15360
Advantages of manned lunar base 08 p1009 N88-16118
Technology developments to meet tomorrow's need for higher satellite frequencies 09 p1124 N88-16732
Introducing new technology into onboard handling systems 09 p1124 N88-16733
Heat pipes for space use 09 p1124 N88-16736
Parallel-processing computer systems and their possible applications in the agency 09 p1128 N88-16774
Microwave tubes: Literature study no. 8 comprising the year 1986
[FOA-C-30467-3] 09 p1159 N88-16944
The use of computer graphic simulation in the development of robotic systems 09 p1214 N88-17275
Study for history of technology developments in European space projects
[REPT-8518-1] 10 p1286 N88-17690
The NORSTAR Program: Space shuttle to space station 10 p1289 N88-17710
The prospects of space utilization
[MBB-UR-931/86] 10 p1314 N88-17856
Minutes of the meeting of the Indo-US Subcommission on Science and Technology (8th) held at Washington, D.C. on September 22-24, 1986
[PB88-130158] 10 p1423 N88-18503
Networking requirements and future alternatives
[NASA-TM-89711] 10 p1426 N88-18517
Science and technology in India
[PB88-134747] 11 p1564 N88-19362
Utilization of robotics and teleoperation for future in-orbit operations 12 p1591 N88-19527
NASA/UK TAP
[NASA-CR-180350] 12 p1708 N88-20223
A project to transfer technology from NASA centers in support of industrial innovation in the midwest
[NASA-CR-180360] 12 p1708 N88-20224
Development of a nationwide network for technology transfer
[NASA-CR-181058] 12 p1709 N88-20225
Johnson Space Center's strategic game plan: Charting a course to the year 2000 and beyond
[NASA-TM-89733] 13 p1850 N88-21076
Contemporary ceramics and the new technological revolution 14 p1902 N88-21363
Microprocessors in space instrumentation
[RR-321] 14 p1955 N88-21655
External tank gamma ray imaging telescope study. Final review, phase 2
[NASA-CR-179320] 15 p2150 N88-22834
Spectroradiometry in materials testing 16 p2273 N88-23601
Data management strategies in the industrial environment
[NLR-MP-87002-U] 16 p2286 N88-23684
Clinical applications of computerized thermography 17 p2330 N88-23915
The results of application studies for space nuclear power 17 p2398 N88-24259
P-Plus: Polar Platform utilization study, executive summary
[BAE-TP-8391] 18 p2469 N88-24653
Personal computer as a workstation in a cartographic automation system? 18 p2535 N88-25039
Different techniques for intervening under the sea: Possible links with space applications 19 p2697 N88-26030
Tasks foreseen for space robots and an example of an associated orbital infrastructure 19 p2699 N88-26044
The contribution of space to maritime activities 19 p2700 N88-26055
The role of aviation technology in the Caribbean Basin
[NASA-CR-183069] 20 p2745 N88-26289
Resources: NASA for entrepreneurs
[NASA-CR-182152] 20 p2883 N88-27119
High technology space flight orientation program: Overview and recommendations
[ETN-88-92332] 21 p3029 N88-27979
The use of AIMS data for operational and research purposes in atmospheric sciences 22 p3036 N88-28025
A 400 kV ion implanter: Operating principles and applications 22 p3069 N88-28213

Utilization of remote sensing for the observation of urban populations. Ongoing research in Quito (Ecuador)
22 p3098 N88-28399
China's acquisition and use of foreign aviation technology
[AD-A194827] 24 p3440 N88-30471

TECTONIC MOVEMENT
U TECTONICS

TECTONICS
Accuracy of GPS surveying technique and its possible application to the Wegener project — Mediterranean tectonics
[REPT-85.3] 01 p0063 N88-10407
Tectonics of the Caroline Oceanic Step (southwestern Pacific Ocean) 06 p0725 N88-14462
Tectonics and magmatism of Walvis Ridge and Discovery Rise (Atlantic Ocean)
06 p0726 N88-14463
Tectonics of sedimentary cover and basement of Labrador Sea 06 p0726 N88-14468
Mid-tertiary volcano-tectonic development of the Southwestern Cordillera of North America
06 p0797 N88-14879
Geomechanical model of seismofocal zone of active continental margin 08 p1011 N88-16128
Comprehensive method for defining seismogenic zones 08 p1011 N88-16129
Thematic mapper study of Alaskan ophiolites
[NASA-CR-182554] 11 p1504 N88-18984
Experimental and theoretical constraints on the origin of mid-ocean ridge geothermal fluids
13 p1804 N88-20784
Tectonics and three-dimensional structure of spreading centers: Microearthquake studies and tomographic inversions
[PB88-163290] 14 p1945 N88-21602
Remote sensing and structural rupture: Application examples in the study of tectonics
17 p2359 N88-24050
Some geological aspects of the Pirapemas Lineament Belt 17 p2358 N88-24099
Specific features of emanation, temperature and hydrodynamic fields in the epicentral zone of tectonic earthquake
[DE88-701140] 17 p2373 N88-24114
Effects of a temperature-dependent rheology on large scale continental extension
[NASA-CR-183117] 20 p2825 N88-26759
SPOT imagery as an aid to understanding volcanism and tectonics: Examples from the Chilean Andes and the Tibetan Plateau 22 p3103 N88-28427
Analyzing the stratigraphy, tectonism, and mineralization at the Spanish side of the pyrite belt, Huelva province, Spain, using SPOT imagery 22 p3104 N88-28433
Analysis of the multispectral content and of SPOT subscenes in two regions of Burundi. Lithologic and tectonic interpretations 22 p3105 N88-28439
Effects of tectonic release on broadband regional distance bodywaves
[AD-A194247] 22 p3119 N88-28529
Documenting volcano-tectonic episodes in Mars' stratigraphic record 23 p3306 N88-29695
Workshop on the Growth of Continental Crust
[NASA-CR-183073] 24 p3392 N88-30201
Structure of Southwestern Michipicoten Greenstone Belt, Ontario: Evidence for Archean accretion
24 p3397 N88-30228
The tectonic setting of Archean anorthosites
24 p3397 N88-30231
Crustal growth in the Archean: The geochemical evidence 24 p3400 N88-30246
NASA MEVTV Program Working Group Meeting: Volcanism on Mars
[NASA-CR-183074] 24 p3442 N88-30487

TED
U TRANSFERRED ELECTRON DEVICES

TEDLAR (TRADEMARK)
U POLYVINYL FLUORIDE

TEE
U T SHAPE

TEFLON (TRADEMARK)
Sample decomposition in sealed teflon vessels
[NASA-TT-20189] 18 p2494 N88-24798

TELECHIRICS
U REMOTE HANDLING

TELECOMMUNICATION
NT AIRCRAFT COMMUNICATION
NT ALOHA SYSTEM
NT AUTOMATIC PICTURE TRANSMISSION
NT BIOTELEMETRY
NT BROADCASTING
NT CODE DIVISION MULTIPLE ACCESS
NT COMMUNICATION
NT DATA LINKS
NT DEMAND ASSIGNMENT MULTIPLE ACCESS
NT ELECTRONIC MAIL
NT FACSIMILE COMMUNICATION
NT FLEET SATELLITE COMMUNICATION SYSTEM
NT FREQUENCY DIVISION MULTIPLE ACCESS
NT LINE OF SIGHT COMMUNICATION
NT MULTICHANNEL COMMUNICATION
NT MULTIPLE ACCESS
NT OPTICAL COMMUNICATION
NT PACKET TRANSMISSION
NT PCM TELEMETRY
NT PULSE COMMUNICATION
NT RADIO COMMUNICATION
NT RADIO RELAY SYSTEMS
NT RADIO TELEMETRY
NT RADIOTELEPHONES
NT SATELLITE COMMUNICATION
NT SATELLITE TELEVISION
NT SINGLE CHANNEL PER CARRIER TRANSMISSION
NT SPACE COMMUNICATION
NT SPACECRAFT ANTENNAS
NT SPACECRAFT COMMUNICATION
NT TELEMETRY
NT TELEPHONY
NT TIME DIVISION MULTIPLE ACCESS
NT UNDERWATER COMMUNICATION
NT VIDEO COMMUNICATION
NT VOICE COMMUNICATION
NT WIDEBAND COMMUNICATION
ELF/VLF/LF propagation and system design
[AD-A183261] 01 p0033 N88-10212
Monitoring of harmful interference to the HF (High Frequency) broadcasting service. 3: Results of the June 1986 coordinated monitoring period
[PB87-210274] 01 p0036 N88-10229
HF (High Frequency) broadcasting planning model: A comparison of two versions
[PB87-210282] 01 p0036 N88-10230
An examination of the Advanced Communications Technology Satellite (ACTS) and its application to the Defense Data Network (DDN)
[AD-A184003] 03 p0276 N88-11742
Compilation of 1986 annual reports of the Navy ELF (Extremely Low Frequency) communications system ecological monitoring program, volume 3
[AD-A184563] 03 p0306 N88-11932
The design and testing of an analog optical communication link capable of the simultaneous transmission of four frequency division multiplexed audio signals
[AD-A184695] 03 p0307 N88-11936
The Black College satellite telecommunications network planning in support of energy-related collaborative research
[DE88-000182] 03 p0307 N88-11940
Heterogeneous multi-trunking queueing systems
[AD-A184255] 04 p0431 N88-12668
The Telecommunications and Data Acquisition Report
[NASA-CR-181546] 04 p0432 N88-12679
JPRS report: Science and technology. Japan
[JPRS-JST-87-023] 06 p0684 N88-14191
JPRS report: Science and technology. Japan
[JPRS-JST-87-027] 06 p0688 N88-14213
Status, outlook of optical technology in information equipment field 06 p0689 N88-14222
Channel access protocols for multihop packet radio networks
[AD-A186074] 07 p0842 N88-15105
Correctness proofs for systolic algorithms: Palindromes and sorting
[PB88-106075] 07 p0912 N88-15534
Summary record of presentations to the Federal Telecommunication Standards Committee/Fiber optics task group
[PB88-110853] 08 p0978 N88-15911
Team problem solving: Effects of communication and function overlap
[AD-A187010] 09 p1152 N88-16898
Crosstalk analysis of a broadband data communications system
[DE88-003652] 09 p1156 N88-16927
Communications patterns in a symbolic multiprocessor
[AD-A186896] 09 p1215 N88-17282
ELF (Extremely Low Frequency) communications system ecological monitoring program: Electromagnetic field measurements and engineering support, 1986
[AD-A188057] 11 p1509 N88-19017
Communication satellites: Guidelines for a strategic plan
[NASA-TM-89306] 12 p1599 N88-19569
JPRS report: Science and technology. Europe and Latin America
[JPRS-ELS-88-001] 12 p1614 N88-19649
Terrestrial Propagation Characteristics in Modern Systems of Communications, Surveillance, Guidance and Control
[AGARD-CP-407] 12 p1614 N88-19653
Envelope and phase statistics for non-Gaussian noise and resulting error probabilities for digital communications systems 12 p1617 N88-19672
A prototype for remotely shared textual workspaces
[AD-A188352] 12 p1679 N88-20040
Defending secrets, sharing data: New locks and keys for electronic information
[PB88-143185] 12 p1706 N88-20210
A simulation study of a parallel processor with unbalanced loads
[AD-A189573] 13 p1822 N88-20887
Near-real-time TOMS, telecommunications and meteorological support for the 1987 Airborne Antarctic Ozone Experiment
[NASA-CR-4133] 16 p2233 N88-23338
IPC for modular software requires a third party connect
[AD-A189199] 16 p2246 N88-23414
An algorithm for random access communication over a noisy channel
[AD-A191315] 16 p2252 N88-23461
Development of a generic architecture
17 p2303 N88-23774
An FSK (Frequency Shift Keying) telemetry module for vector measuring current meters
[AD-A192142] 18 p2470 N88-24661
Practical VLF/LF radio test system
[AD-A191768] 18 p2500 N88-24831
Information and stochastic systems
[AD-A192167] 18 p2501 N88-24838
The Effect of the Ionosphere on Communication, Navigation and Surveillance Systems Based on Ionospheric Effects Symposium held on 5-7 May 1987 in Springfield, Virginia
[AD-A191855] 18 p2541 N88-25081
Design, implementation and evaluation of an operating system for a network of transputers
[AD-A186593] 18 p2559 N88-25193
Selection and effects of channels in distributed communication and decision making tasks: A theoretical review and a proposed research paradigm
[AD-A191807] 18 p2587 N88-25375
Narrative compression coding for a channel with errors
[AD-A191577] 19 p2642 N88-25673
Extremely Low Frequency (ELF) communications system ecological monitoring program: Summary of 1986 progress
[AD-A192014] 19 p2642 N88-25676
Extremely Low Frequency (ELF) communications program: Non-ionizing electromagnetic radiation literature evaluation and assessment, 1986-1987 literature review
[AD-A192024] 19 p2642 N88-25677
Activities report of the Communications Department
[ENST-88D003] 21 p2931 N88-27401
An evaluation of two millimeter wave propagation models for horizontal atmospheric attenuation at 70-115 GHZ
[AD-A192699] 21 p2931 N88-27403
Experiments applications guide: Advanced Communications Technology Satellite (ACTS)
[NASA-TM-100265] 22 p3048 N88-28082
Basic research in electronics (JSEP) Joint Services Electronics Program
[AD-A193072] 23 p3206 N88-29079
Long haul communications in the HF spectrum utilizing high speed modems
[AD-A194683] 24 p3360 N88-30003
Design of a self-timed VLSI multicomputer communication controller
[AD-A194567] 24 p3361 N88-30014
A static scheduler for the computer aided prototyping system: An implementation guide
[AD-A194340] 24 p3414 N88-30322
Statistical analysis of the LMS (Last Mean Squares) and modified stochastic gradient
[AD-A195497] 24 p3424 N88-30376
Integrating images, applications, and communications networks, volume 5
[AD-A195854] 24 p3436 N88-30452
Information technology to facilitate group interaction
24 p3438 N88-30463
Using standards to break down information transfer barriers 24 p3439 N88-30467

TELECONNECTIONS (METEOROLOGY)
The atmosphere as a component of the climate system: Structure and variability 14 p1935 N88-21540

TELEGRAPH SYSTEMS
Fluxons and order in long Josephson junctions
[AD-A190879] 16 p2282 N88-23665

TELEGRAPHY
U TELEGRAPH SYSTEMS

TELEMETERS
U TELEMETRY

TELEMETRY
NT BIOTELEMETRY
NT PCM TELEMETRY
NT RADIO TELEMETRY
TIROS-N/NOAA A-J space environment monitor subsystem
[PB87-203998] 01 p0015 N88-10083
Spacecraft 2000
[NASA-CP-2473] 01 p0015 N88-10084
Telemetry, Tracking, and Control Working Group report 01 p0016 N88-10096
Fiber optic engineering sensor system. Preliminary program management plan, phase 3 revision
[AD-A183663] 01 p0093 N88-10608
How we get pictures from space, revised edition
[NF-151/7-87-REV] 02 p0193 N88-11203
Detection of signals by weighted integrate-and-dump filter 04 p0435 N88-12696
Analysis of the ICE combiner for multiple antenna arraying 04 p0436 N88-12704
New approach to telemetry development will significantly increase productivity of Joint Test Assembly (JTA) teams
[DE88-001676] 05 p0554 N88-13373
A distributed architecture for intelligent monitoring and anomaly diagnosis of the Hubble Space Telescope 08 p1057 N88-16379
A knowledge-based system for monitoring the electrical power system of the Hubble Space Telescope 08 p1058 N88-16380
Exploring hypotheses in attitude control fault diagnosis 08 p1058 N88-16384
A multiprocessing architecture for real-time monitoring 08 p1059 N88-16390
Spacelab Data Processing Facility (SLDPF) quality assurance expert systems development 08 p1059 N88-16394
Telemetry applications handbook
[AD-A186825] 09 p1132 N88-16789
Concept, construction, and experimental testing of a polychromator for a Raman lidar for the simultaneous telemetering of carbon dioxide and water vapor, relative to oxygen
[GKSS-87/E/20] 09 p1191 N88-17134
POCC capabilities document. Payload support capabilities description: MCC, JSC POCC, remote POCC interface
[NASA-TM-89708] 09 p1260 N88-17555
Investigation of design considerations for Telemetry, Tracking and Command (TT and C) antenna system on Naval Postgraduate School Orion mini-satellite
[AD-A187130] 10 p1291 N88-17718
Digital bit error rate estimator for telemetry links
[INPE-4351-TDL/295] 12 p1598 N88-19563
Low cost telemetry and telecommand system for remote measurement of magnitude character
[INPE-4273-PRE/1145] 12 p1598 N88-19564
Estimating the solar irradiance of an intermountain region using GOES (Geostationary Operational Environmental Satellite) satellite data: A test of two statistical models
[AD-A188414] 12 p1642 N88-19834
The imaging of extra-galactic low-energy gamma-ray sources prospects, techniques, and instrumentation
[NASA-CR-182536] 12 p1713 N88-20251
Geometric restoration of satellite image data
[AD-A190462] 15 p2089 N88-22450
Survey of the Air Force P78-2 (SCATHA) satellite plasma wave data during electron gun operations
[AD-A191014] 16 p2168 N88-22926
Soviet remote sensing research and technology
[FASAC-TAR-3130] 17 p2369 N88-24108
TALOS: A distributed architecture for intelligent monitoring and anomaly diagnosis of the Hubble Space Telescope 17 p2388 N88-24193
An FSK (Frequency Shift Keying) telemetry module for vector measuring current meters
[AD-A192142] 18 p2470 N88-24661
Adaptive data acquisition multiplexing system and method
[NASA-CASE-MSC-21170-1] 18 p2471 N88-24662
A VLSI single-chip (225,223) Reed-Solomon encoder with interleaver
[NASA-CASE-NPO-17280-1-CU] 21 p2902 N88-27220
The Telecommunications and Data Acquisition Report
[NASA-CR-183131] 22 p3063 N88-28178
Telemetry SNR improvement using the DSN Advanced Receiver with results for Pioneer 10 22 p3064 N88-28184
Advanced Receiver tracking of Voyager 2 near solar conjunction 22 p3065 N88-28185
A new code for Galileo 22 p3065 N88-28186
The behavior of a Costas loop in the presence of space telemetry signals 22 p3067 N88-28198
Baseband assembly analog-to-digital converter board 22 p3067 N88-28201
Research and development objectives: installation, startup, and test operation of a remote and program controlled measuring table for the calibration of EGRET experiment
[ETN-88-92105] 22 p3152 N88-28752
Multi-sensory tracking mount control
[AD-A194675] 23 p3249 N88-29339
An expert systems application to space base data processing 23 p3256 N88-29384
Long haul underwater fiber optic link
[AD-A194487] 23 p3282 N88-29542
Accuracy of satellite data navigation
[AD-A195877] 24 p3322 N88-29787
Mission telemetry system monitor: A real-time knowledge-based system 24 p3418 N88-30345
Automated cataloging and characterization of space-derived data 24 p3420 N88-30354

TELEOPERATOR MANEUVERING SYSTEM
U TELEOPERATORS

TELEOPERATORS
Telepresence work station system definition study, part 2
[NASA-CR-172006] 01 p0013 N88-10071
Telerobotics 01 p0015 N88-10090
Robotic sensors and actuators for a service manipulator system. Volume 3, phase A report and program plan
[MATRA-EPT/DT/VT187/228] 01 p0054 N88-10343
Traction-drive seven degrees-of-freedom telerobot arm: A concept for manipulation in space
[DE87-010895] 01 p0054 N88-10346
Teleoperation and control study — orbital servicing
[BAE-TP-8268] 01 p0076 N88-10489
A methodology for dynamic task allocation in a man-machine system
[DE87-007373] 01 p0077 N88-10492
Evaluation of vision systems for teleoperated land vehicles
[DE87-013066] 03 p0333 N88-12100
Teleoperator and robotics system analysis
[NASA-CR-179220] 03 p0334 N88-12105
Operator multiple-tasking study for remotely operated platforms
[AD-A184487] 03 p0362 N88-12276
Experiences in teleoperation of land vehicles
[DE88-000429] 06 p0711 N88-14355
Experiences in teleoperation of land vehicles
[DE88-001695] 06 p0711 N88-14357
Issues associated with telerobotic systems in space 08 p1056 N88-16369
Telerobotic controller development 08 p1056 N88-16370
Software simulation of time delay in teleoperation 08 p1056 N88-16371
System integration of a Telerobotic Demonstration System (TDS) testbed 09 p1212 N88-17266
Manipulator arm design for the Extravehicular Teleoperator Assist Robot (ETAR): Applications on the space station 09 p1213 N88-17270
Crew interface with a telerobotic control station 09 p1213 N88-17273
NASA/NBS (National Aeronautics and Space Administration/National Bureau of Standards) standard reference model for Telerobot Control System Architecture (NASREM)
[PB88-124773] 10 p1338 N88-17999
Technology requirements for telerobotic satellite servicing in space 12 p1592 N88-19536
A teleoperated manipulator system concept for unmanned platforms — Columbus 12 p1593 N88-19537
Multi-axis control of telemanipulators 12 p1593 N88-19539
The space station assembly phase: Flight telerobotic servicer feasibility, volume 1
[NASA-CR-182689] 13 p1731 N88-20351
The space station assembly phase: Flight telerobotic servicer feasibility. Volume 2: Methodology and case study
[NASA-CR-182690] 13 p1731 N88-20352
The 22nd Aerospace Mechanisms Symposium
[NASA-CP-2506] 14 p1924 N88-21468
Operational experience and design recommendations for teleoperated flight hardware 14 p1927 N88-21489
Design, development and evaluation of Stanford/Ames EVA prehensors
[NASA-CR-182688] 15 p2105 N88-22540
Teleoperator human factors study
[NASA-CR-178930] 17 p2382 N88-24162
A universal computer control system for motors
[NASA-CASE-NPO-17134-1-CU] 18 p2506 N88-24864
Underwater simulation for space teleoperation 19 p2698 N88-26040
Simulation of space manipulator operations (EUROSIM)
[NLR-MP-87017-U] 20 p2811 N88-26878
A demonstration of retro-traverse using a semi-autonomous land vehicle
[DE88-009851] 21 p2957 N88-27568
Assessments of maneuverability with the TeleOperated Vehicle (TOV)
[AD-A191584] 21 p2993 N88-27751
Mobile robotics R and D at the Savannah River Laboratory
[DE88-011665] 22 p3083 N88-28310
Concepts for robot motion primitives required for space station teleoperations 23 p3257 N88-29387
A teleoperated robotic manipulator system for materials processing experiment servicing 23 p3260 N88-29410
Low level image processing techniques using the pipeline image processing engine in the flight telerobotic servicer 24 p3418 N88-30346
The space station assembly phase: System design trade-offs for the flight telerobotic servicer 24 p3420 N88-30357

TELEPHONES
NT RADIOTELEPHONES
Land mobile satellite transmission measurements at 869 MHz. A comparison of error probabilities for various message block durations and fade margins as a function of vegetation shadowing
[NASA-CR-179929] 06 p0693 N88-14255
Inexpensive solution for the mass distribution of satellite images
[PB88-114038] 10 p1317 N88-17873
Design, development and trials of an airline passenger telephone system 19 p2648 N88-25704
MSAT mobile electronically steered phased array antenna development 19 p2647 N88-25711

TELEPHONY
Digital receiver structures and methods for the determination of the scanning frequency in modems for fast data transmission via telephone channels
[ETN-87-90429] 01 p0037 N88-10235
Digital to analog and analog to digital conversion using pulse duration modulation
[ETN-87-90415] 01 p0078 N88-10499
Study of a coding and modulation system for the V32 call of the CCITT
[ENST-87E007] 02 p0162 N88-11015
AUSSAT mobile satellite services 19 p2643 N88-25684
Development of the network architecture of the Canadian MSAT system 19 p2646 N88-25702

TELESCOPES
NT GAMMA RAY TELESCOPES
NT GERMAN INFRARED LABORATORY
NT HUBBLE SPACE TELESCOPE
NT INFRARED SPACE OBSERVATORY (ISO)
NT INFRARED TELESCOPES
NT PARTICLE TELESCOPES
NT RADIO TELESCOPES
NT SPACE INFRARED TELESCOPE FACILITY
NT SPACEBORNE TELESCOPES
NT SPECTROSCOPIC TELESCOPES
NT STRATOSCOPE TELESCOPES
NT ULTRAVIOLET TELESCOPES
NT VERY LARGE ARRAY (VLA)
NT X RAY ASTROPHYSICS FACILITY
NT X RAY TELESCOPES
An optoelectronic alignment telescope for straightness measurements
[ETN-87-90383] 01 p0093 N88-10609
Ground-based interferometry with the European Very Large Telescope (VLT) 01 p0096 N88-10632
Activities report in astronomy
[ISSN-0531-4496] 01 p0108 N88-10701
Automatic photometric monitoring of cool stars 04 p0504 N88-13103
Statistical properties of small high-velocity events in the solar transition region 04 p0506 N88-13112
Spectral analysis of APT RS CVn binary light curves 04 p0508 N88-13122
H alpha and Ca II emission line variability of FK cornae 04 p0509 N88-13128
Automatic telescope operations 04 p0519 N88-13190
Optical photometer for the Tirgo telescope
[IFSI-87-5] 05 p0650 N88-13985
An automated supernova search and the design strategy
[DE88-001827] 05 p0660 N88-14051
Telescope design for Michelson Interferometer for Passive Atmospheric Sounding (MIPAS) B 08 p1017 N88-16167
Balloon-borne three-meter telescope for far-infrared and submillimeter astronomy
[NASA-CR-182310] 09 p1262 N88-17565

Optics for large telescope 13 p1840 N88-21014
Very high energy gamma ray astrophysics
[DE88-005821] 13 p1854 N88-21095
External tank gamma ray imaging telescope study. Final review, phase 2
[NASA-CR-179320] 15 p2150 N88-22834
Performance of the Los Alamos expanding telescope
[DE88-010924] 22 p3151 N88-28751
Martian surface analogs: Laboratory spectral studies in the mid infrared 23 p3307 N88-29699
Very high energy cosmic gamma rays from radio and X-ray pulsars 23 p3309 N88-29711
NASA Marshall Space Flight Center solar observatory
[NASA-TM-100339] 24 p3332 N88-29832
Binary star measurements using digital speckle interferometer of 6-m telescope 24 p3448 N88-30521
Activities report in astronomy
[ISSN-0531-4496] 24 p3451 N88-30535

TELESCOPING STRUCTURES
U FOLDING STRUCTURES

TELEVISION CAMERAS
Sensor fusion for robot navigation
[DE88-006383] 20 p2809 N88-26863

TELEVISION EQUIPMENT
NT IMAGE DISSECTOR TUBES
NT TELEVISION CAMERAS
NT TELEVISION RECEIVERS
A 1/2-inch high-definition baseband VCR 21 p2930 N88-27393

TELEVISION RECEIVERS
Receiver susceptibility measurements relating to interference between UHF (Ultra High Frequency) television and land mobile radio services
[PB87-226029] 06 p0690 N88-14228
Considerations concerning the basic bandwidth reduction of high definition television systems (HDTV) component signals, based on psychophysiological properties of the eye
[IRT-B-83/87] 09 p1153 N88-16909
An outdoor unit for Direct Broadcast Satellite (DBS) digital sound reception
[BMFT-FB-W-86-016] 16 p2189 N88-23050

TELEVISION RECEPTION
A review of the semiconductor storage of television signals. Part 2: Applications 1975-1986
[BBC-RD-1987/6] 02 p0161 N88-11009

TELEVISION SYSTEMS
NT SATELLITE TELEVISION
Lewis Information Network (LINK): Background and overview
[NASA-TM-100162] 03 p0305 N88-11925
Cineradiography
[DE87-013158] 03 p0324 N88-12045
Through-transmission/pulse-echo ultrasonic equipment evaluation
[AD-A186340] 07 p0929 N88-15641
Considerations concerning the basic bandwidth reduction of high definition television systems (HDTV) component signals, based on psychophysiological properties of the eye
[IRT-B-83/87] 09 p1153 N88-16909
Future television systems: Comparison of sequent ial and interlaced scanning
[BBC-RD-1987/18] 09 p1155 N88-16923
Optical data processing
[AD-A193024] 20 p2839 N88-26841
High definition television: Evaluation for remote task performance
[DE88-011573] 23 p3202 N88-29057

TELEVISION TRANSMISSION
A review of the semiconductor storage of television signals. Part 2: Applications 1975-1986
[BBC-RD-1987/6] 02 p0161 N88-11009
A digital audio link to the Channel Islands in the UHF television band: Protection of television signals from digitally modulated interference
[BBC-RD-1987/7] 02 p0161 N88-11010
A digital audio link to the Channel Islands in the UHF television band: Preliminary experimental results
[BBC-RD-1987/9] 02 p0161 N88-11011
Improvements to a UHF rebroadcast television link suffering tidal fading: Countisbury UHF relay station
[BBC-RD-1987/14] 05 p0573 N88-13495
Television motion measurement for DATV and other applications
[BBC-RD-1987/11] 05 p0573 N88-13496
Two-signal cross modulation effects, half-IF effects and interference criteria in land mobile sharing with UHF (Ultra High Frequency) television
[PB87-228037] 05 p0576 N88-13514
Future television systems: Comparison of sequent ial and interlaced scanning
[BBC-RD-1987/18] 09 p1155 N88-16923
The relationship between vision carrier-to-noise ratio and picture signal-to-noise ratio in a System I television receiver
[BBC-RD-1987/23] 10 p1318 N88-17877
Digital television routing systems: A survey of optical and electrical techniques
[BBC-RD-1988/3] 19 p2654 N88-25763
Organization of the TDF1/TDF2 program 22 p3161 N88-28827

TELLEGEN THEORY
U NETWORK ANALYSIS
U NETWORK SYNTHESIS

TELLURIDES
NT CADMIUM TELLURIDES
NT LANTHANUM TELLURIDES
NT LEAD TELLURIDES
NT MERCURY TELLURIDES
NT TIN TELLURIDES
NT ZINC TELLURIDES

TELLURIUM
Thermal expansion of some Ge-Se-Te glasses
[PD-MT-8722] 04 p0420 N88-12606
Studies on some Ge-Se-Te glasses
[PD-MT-8721] 04 p0420 N88-12607
Lattice-matched HgZnTe epitaxy development
[AD-A193677] 23 p3292 N88-29600

TELLURIUM ALLOYS
PbSnTe photovoltaic detectors for operation in the 2-14 micron band
[INPE-4252-PRE/1125] 11 p1508 N88-19008

TELLURIUM COMPOUNDS
NT CADMIUM TELLURIDES
NT LANTHANUM TELLURIDES
NT LEAD TELLURIDES
NT MERCURY TELLURIDES
NT TIN TELLURIDES
NT ZINC TELLURIDES

TEMPEL 2 COMET
Anisotropic emission from comets: Fans versus jets. 2: Periodic Comet Tempel 2 14 p2001 N88-21928
The comet rendezvous asteroid flyby mission 14 p2005 N88-21956

TEMPER (METALLURGY)
the influence of temper embrittlement on fatigue crack growth in hydrogen 05 p0605 N88-13709

TEMPERATE REGIONS
An analysis of apparent-motion vectors in, and the structure of, A mid-latitude sporadic E layer using a 2.66 MHz radar
[AD-A186126] 07 p0877 N88-15321
Preliminary analyses of SPOT HRV multispectral products for arid and temperate environments 22 p3099 N88-28407

TEMPERATURE
NT ABSOLUTE ZERO
NT AMBIENT TEMPERATURE
NT ATMOSPHERIC TEMPERATURE
NT AURORAL TEMPERATURE
NT BODY TEMPERATURE
NT BRIGHTNESS TEMPERATURE
NT COMBUSTION TEMPERATURE
NT CRITICAL TEMPERATURE
NT CRYOGENIC TEMPERATURE
NT CURIE TEMPERATURE
NT FLAME TEMPERATURE
NT FLASH POINT
NT GAS TEMPERATURE
NT GLASS TRANSITION TEMPERATURE
NT HIGH TEMPERATURE
NT IGNITION TEMPERATURE
NT INLET TEMPERATURE
NT ION TEMPERATURE
NT IONOSPHERIC TEMPERATURE
NT LOW TEMPERATURE
NT NOISE TEMPERATURE
NT OCEAN TEMPERATURE
NT OPERATING TEMPERATURE
NT PLASMA TEMPERATURE
NT ROOM TEMPERATURE
NT SATELLITE TEMPERATURE
NT SEA SURFACE TEMPERATURE
NT SKIN TEMPERATURE (BIOLOGY)
NT SKIN TEMPERATURE (NON-BIOLOGICAL)
NT SOLAR TEMPERATURE
NT SPIN TEMPERATURE
NT STELLAR TEMPERATURE
NT SURFACE TEMPERATURE
NT TRANSITION TEMPERATURE
NT WALL TEMPERATURE
NT WATER TEMPERATURE
Estimation from satellite imagery of summertime rainfall over varied space and time scales
[PB87-203246] 01 p0071 N88-10454
Estimating payload internal temperatures and radiator size for multimegawatt space platforms
[DE88-000244] 03 p0275 N88-11738
Temperature hysteresis and magnetic transitions in amorphous Fe-Ni-Zr alloys
[DE88-000228] 03 p0294 N88-11848
Scaling of size/time/temperature associated with dilatation and distortion in uniaxial specimens 03 p0336 N88-12117
Improper ferroelectricity: A theoretical and experimental study
[AD-A184614] 03 p0381 N88-12397
Studies of pressure-velocity coupling schemes for analysis of incompressible and compressible flows
[NASA-CR-181526] 04 p0443 N88-12748
Controlled ecological life support systems: Development of a plant growth module 05 p0630 N88-13854
Strength and structure of Ga sub 1-xIn sub xAs alloys
[AD-A188092] 10 p1303 N88-17795
Thermal analysis of transistor packages, part 2
[DE88-005091] 10 p1323 N88-17909
Calibration of a hot-wire/hot-film anemometer over a range of temperatures, velocities and pressures
[AD-A189717] 14 p1913 N88-21430
Calibration and processing of AVHRR data for temperature estimation
[INPE-4493-PRE/1257] 15 p2095 N88-22485
Monthly mean global climatology of temperature, wind, geopotential height, and pressure for 0 - 120 km
[NASA-TM-100697] 15 p2099 N88-22503
Physical, chemical and CTD (Conductivity/Temperature/Depth) data from the Marathon 2 expedition
[AD-A189930] 15 p2099 N88-22507
Global atmospheric circulation statistics, 1000-1 mb
[PB88-168240] 16 p2234 N88-23340
Analysis of crack-tip fields in a viscoplastic material 17 p2349 N88-23996
Theory of oxygen content, atomic ordering and oxygen diffusion in 1,2,3 superconducting oxides as a function of temperature and oxygen pressure
[DE88-007961] 19 p2735 N88-26248
Interfacial tension of immiscible polymer blends: Temperature and molecular weight dependence
[AD-A192463] 21 p2917 N88-27312
Object discrimination via bulk temperature/velocity filtering, phase 1
[AD-A194533] 23 p3274 N88-29487

TEMPERATURE COMPENSATION
Notes on transducer design based on resistance strain gages with applied temperature compensation
[FFA-MEMO-129] 01 p0050 N88-10319
Development of an electronically-scanned pressure module for operation at cryogenic temperatures
[NASA-CR-181610] 12 p1629 N88-19746
The design and use of a temperature-compensated hot-film anemometer system for boundary-layer flow transition detection on supersonic aircraft
[NASA-TM-100421] 13 p1723 N88-20304
Thermal compensating mount
[NASA-CASE-LAR-13794-1] 18 p2519 N88-24942
Further improvements relating to the temperature compensation of semiconductor strain gauge pressure transducers
[RAE-TR-87061] 22 p3081 N88-28298

TEMPERATURE CONTROL
Thermal Control Working Group report 01 p0016 N88-10094
Considerations concerning a thermal joint for a deployable or steerable battery radiator for the Columbus Polar Platform
[NLR-TR-86055-U] 03 p0276 N88-11739
Traveling-wave maser closed-cycle refrigerator data acquisition and display system 04 p0437 N88-12708
Two-watt, 4-Kelvin closed cycle refrigerator performance 04 p0437 N88-12709
Testing of heat pipes on SPAS-01
[BMFT-FB-W-86-014] 06 p0672 N88-14119
Orbital Replaceable Unit (ORU)/cold plate thermal interface study. Volume 1: Executive Summary
[BAE-TP-8430] 07 p0855 N88-15195
Development of an emulation-simulation thermal control model for space station application
[NASA-CR-182409] 08 p0962 N88-15823
Thermal structural control modelling techniques --- spacecraft
[FOK-TR-R-86-030] 08 p0962 N88-15828
MTK: An AI tool for model-based reasoning 08 p1056 N88-16372
Integration of symbolic and algorithmic hardware and software for the automation of space station subsystems 08 p1058 N88-16373
EUREX D: An expert system for failure diagnosis and recovery in the TCS of the European retrievable carrier EURECA 08 p1058 N88-16385
Heat pipes for space use 09 p1124 N88-16736

Analytical interactive approach for phenomena involving structures, thermal and control aspects. Volume 1: Theory --- spacecraft structures
[ESA-CR(P)-2503-VOL-1] 09 p1134 N88-16803
Analytical interactive approach for phenomena involving structures, thermal, and control aspects. Volume 2: Toward the solution --- spacecraft structures
[ESA-CR(P)-2503-VOL-2] 09 p1134 N88-16804
Analytical interactive approach for phenomena involving structures, thermal, and control aspects. Volume 3: Executive summary --- spacecraft structures
[ESA-CR(P)-2503-VOL-3] 09 p1134 N88-16805
TDAS: The Thermal Expert System (TEXSYS) data acquisition system 09 p1211 N88-17258
Moveable thermal joints for deployable or steerable spacecraft radiator systems
[NLR-MP-87016-U] 13 p1730 N88-20347
Feasibility demonstration of a sensor for high-quality two-phase flow --- Space Station
[NLR-TR-87009-U] 13 p1767 N88-20569
Development, manufacturing and testing of a gas-loaded variable conductance methanol heat pipe
[NLR-MP-87010-U] 13 p1767 N88-20571
High output paraffin actuators: Utilization in aerospace mechanisms 14 p1924 N88-21470
Advanced capacitor development
[AD-A189985] 15 p2059 N88-22276
Multi-color pyrometer for materials processing in space 17 p2329 N88-23905
The role of fiberoptics in remote temperature measurement 17 p2329 N88-23909
Real time thermal imaging of high temperature semiconductor melts 17 p2330 N88-23914
MTK: An AI tool for model-based reasoning 17 p2387 N88-24189
The effect of elevated temperature on irradiated MOS devices 17 p2406 N88-24308
Turbomachinery in space 17 p2408 N88-24321
Thermal management for multi-modal nuclear power plants 17 p2410 N88-24331
Silicon-on-insulator electronics for a space nuclear power system 17 p2431 N88-24461
Low gravity thermal management using dielectrophoretic forces 17 p2432 N88-24470
Method and apparatus for growing crystals
[NASA-CASE-MFS-28137-1] 17 p2446 N88-24544
Field experience with aquifer thermal energy storage
[DE88-007075] 18 p2538 N88-25058
Design and testing of a high power spacecraft thermal management system
[NASA-TM-4051] 20 p2764 N88-26389
Heat pump augmented radiators for spacecraft thermal management
[DE88-007890] 20 p2764 N88-26392
Modeling and thermal management of advanced batteries
[DE88-010023] 20 p2794 N88-26580
Thermal-sensation control: A new method of controlling cooled/heated environments 21 p2930 N88-27394
Biorack thermal performance during the D1 mission --- Spacelab 22 p3062 N88-28170
The heat pipe network of TDF-1/TV-SAT. Review of the development at completion
[SNIAS-881-440-103] 23 p3213 N88-29127
Testing degradation of a sample under thermal cycling
[GB-PATENT-2-188-163-A] 23 p3227 N88-29206
Reasoning about fault diagnosis for the space station common module thermal control system 23 p3258 N88-29395
Experimental and analytical study of two-phase flow in zero gravity
[AD-A195223] 24 p3358 N88-29993

TEMPERATURE DEPENDENCE

Hot-spot reaction in unsustained shocks
[DE87-011781] 01 p0044 N88-10277
Anelastic behaviour of materials under multiaxial strains. Part 3: Order-disorder transition, Shoek effect and Poisson's ratio in AISI-1080 steel
[DE87-703087] 02 p0191 N88-11193
Ignition and combustion of metals in oxygen 04 p0407 N88-12530
Retention processes in supercritical fluid chromatography
[DE88-000079] 04 p0413 N88-12559
Experimental perspectives on heavy electron metals
[DE87-014766] 04 p0416 N88-12583
Magnetic field dependence of the specific heat of some high-T/sub c/ superconductors
[DE87-014078] 04 p0497 N88-13063
Temperature dependent mechanical properties of an alumina fiber reinforced aluminum composite 06 p0677 N88-14147
Fatigue oxidation interaction in low cycle fatigue 06 p0719 N88-14420
Study of some superconducting and magnetic materials on high T sub c oxide superconductors
[NASA-CR-182330] 06 p0785 N88-14813
Effect of point defects on graphite lattice parameters
[DE88-700340] 07 p0827 N88-15019
Use of a local heat source for determining temperature of inlet heat section in ring channels
[DE88-700332] 07 p0854 N88-15187
Change of europium crystallographic symmetry at helicoidal magnetic ordering
[DE88-700559] 07 p0939 N88-15707
Study of the temperature dependence of the mechanical characteristics of the steels GX 5 CrNi 13 4 and GGG 40 in tensile and bending tests
[DE88-001469] 09 p1143 N88-16850
Hydrogen in niobium-tantalum superlattices 09 p1146 N88-16867
Structural relationships in high temperature superconductors
[DE88-002924] 09 p1257 N88-17534
Renormalization group analysis of the temperature dependent coupling constant in massless theory
[DE88-751059] 09 p1259 N88-17552
Flame propagation in the approximation of straight-line trajectories of burning products
[DE88-700675] 10 p1297 N88-17756
EXPLO: Explosives thermal analysis computer code
[DE88-001938] 10 p1307 N88-17814
Capacitor analysis for RF antennas
[DE88-004178] 10 p1318 N88-17883
Optical absorption in doped CdxHg1-xTe
[AD-A187434] 11 p1560 N88-19338
Increasing the rate at which ceramic castings undergo preliminary heat-treatment in an ultra-high frequency magnetic field 14 p1886 N88-21275
Data requirements to model creep in 9Cr-1Mo-V steel 14 p1931 N88-21512
Temperature-dependent conductivity of oxygen-depleted YBCO ceramics
[AD-A190340] 15 p2044 N88-22182
Strength and cracking resistance of ceramics. Report 3: SiC ceramics 16 p2180 N88-22994
Ultra high temperature direct propulsion 17 p2401 N88-24275
High-temperature thermal conductivity of a carbon-bonded carbon-fiber insulation 17 p2402 N88-24281
Temperature dependence of ultraviolet absorption cross sections of chlorofluoroethanes
[AERONOMICA-ACTA-A-325-1987] 18 p2482 N88-24726
Temperature-dependent tensile and shear response of graphite/aluminum
[NASA-CR-182914] 19 p2609 N88-25484
Anomalous temperature-dependent negative magnetoresistance in pregraphitic carbons
[AD-A191725] 19 p2619 N88-25535
Dimensional crossover in layered superconductors 19 p2734 N88-26237
Effects of a temperature-dependent rheology on large scale continental extension
[NASA-CR-183117] 20 p2825 N88-26759
Photoluminescence studies of InGaAlAs quaternary alloys
[DE88-007197] 20 p2874 N88-27062
Properties of strong coupled superconductors
[DE88-702050] 23 p3287 N88-29574
Intrinsic and extrinsic energy states of semiconductors and heterostructures using novel techniques
[DE88-008560] 23 p3289 N88-29582
Anomalous dependence of the thermoelectric power on the temperature in YBaCuO high-T(sub c) superconducting samples
[DE88-702682] 23 p3292 N88-29605
Influence of the temperature-dependence of recombination life-time of free carriers in amorphous semiconductors on thermostimulated photocurrent spectra
[DE88-702728] 23 p3293 N88-29609
Thermostimulated conductivity in amorphous semiconductors with non-exponential density of localized states
[DE88-702737] 23 p3293 N88-29612

TEMPERATURE DIFFERENCES

U TEMPERATURE GRADIENTS

TEMPERATURE DISTRIBUTION

Automatic seam welding with infrared sensor feedback
[DE87-013556] 01 p0055 N88-10352
Satellite and synoptic studies of chemical fronts in the California current and coastal upwelling zone
[AD-A183909] 01 p0073 N88-10466
An approximate solution to the problem of heating massive bodies by both radiation and convection
[BLL-M-37315-(5828.4)] 02 p0170 N88-11068
On the mixing of a row of jets with a confined crossflow 02 p0185 N88-11154
The use of satellite IR data in the enhancement of surface thermal fields 02 p0202 N88-11260
Finite element analysis of three-dimensional steady and unsteady temperature fields (computation of temperature distribution of turbine blade with composite cooling) 03 p0300 N88-11887
Numerical and experimental investigation of the unsteady temperature distribution in solar central receivers
[ESA-TT-1050] 03 p0347 N88-12193
Thermal analysis of electromagnetic launcher rails
[DE88-000166] 04 p0405 N88-12514
Microgravity nucleation and particle coagulation experiments support
[NASA-CR-181540] 04 p0423 N88-12618
Microgravity nucleation and particle coagulation experiments support
[NASA-CR-181541] 04 p0423 N88-12619
Resistivity of EuBa2(Cu/sub 1-y/Zn/sub y/)3O/sub x/ as a ffunction of temperature, magnetic field, pressure and Zn concentration
[DE87-014740] 04 p0499 N88-13069
Flux tube dynamics and solar/stellar redshift measurements 04 p0503 N88-13095
Occurance and growth of fatigue cracks in corrosion environment 05 p0604 N88-13704
Statistical structure of temperature field over South Pacific Ocean 06 p0726 N88-14465
Role of anomalous currents in formation of ocean surface temperature field 06 p0727 N88-14474
Structure-property relationships in thermoplastic elastomers 4. Dynamic mechanical relaxations in poly(dioxolane), poly(butyltrioxocane) and poly(propylene oxide) polyurethanes
[AD-A186278] 07 p0836 N88-15073
Supersonic boundary layer on a heated wall
[ETN-88-91617] 08 p0950 N88-15763
Determination of the heat conduction coefficient of the soil from the advance of the diurnal temperature wave 08 p1015 N88-16151
Observations and modeling of the prominence/corona transition region 08 p1094 N88-16585
Symbolic, algebraic, and numeric solutions to heat conduction problems using Green's functions 09 p1165 N88-16987
Approximate solutions of heat conduction in a medium with variable properties
[AD-A186933] 10 p1326 N88-17925
Influence of radiation and thermal conduction on temperature distribution in the thin wall of a hollow cylinder
[INPE-4428-TDL/308] 12 p1626 N88-19730
Retrieval of three-dimensional wind and temperature fields from single-Doppler radar data 12 p1646 N88-19858
Roys and radiosondes in the region
[INPE-4362-PRE/1188] 13 p1796 N88-20743
Arcs in cesium seeded noble gases resulting from a magnetically induced electric field
[EUT-87-E-177] 13 p1843 N88-21028
Comparison of methods for the calculation of thermal contact resistance of the first Brazilian satellite
[NASA-TT-20180] 14 p1880 N88-21239
Modeling growth of interdendritic silicon ribbons 14 p1897 N88-21322
Finite element explicit algorithm for solving temporal temperature fields 14 p1899 N88-21339
Thermal instability and heat transfer characteristics in water/ice systems
[AD-A189627] 15 p2062 N88-22297
Hydrographic observations in the northwestern Weddell Sea Marginal Ice Zone during March 1986
[PB88-173240] 16 p2237 N88-23359
Studies of heat and mass transfer during chemical vapor deposition 17 p2338 N88-23953
Tiros operational vertical sounder (TOVS) and radiosonding in the region 17 p2360 N88-24059
Specific features of emanation, temperature and hydrodynamic fields in the epicentral zone of tectonic earthquake
[DE88-701140] 17 p2373 N88-24114
Observations of frontal instabilities on an upwelling filament
[AD-A191051] 17 p2375 N88-24122
Botany Facility: Test report on breadboard tests for the determination of the heat transfer at the glass disk and of the temperature distribution in the fluorescent tube
[BF-TN-ER-053] 17 p2378 N88-24136
A thermal equilibrium model for multi-megawatt space platforms 17 p2410 N88-24332
An irradiation performance data base for nitride fuels 17 p2427 N88-24438
Noncontact temperature pattern measuring device
[NASA-CASE-NPO-17024-1-CU] 18 p2519 N88-24943

Optical investigations of the thermal boundary layer in arc plasmas 18 p2578 N88-25313
Thermal distortion analysis of the space station solar dynamic concentrator
[NASA-TM-100868] 19 p2606 N88-25475
Coal particle behaviour in a counter-current combustor
[TAE-606] 19 p2612 N88-25498
Fuel droplet vaporization and temperature distributions of axisymmetric unsteady sprays 19 p2626 N88-25579
Energy dissipation in a rolling aircraft tire
[NASA-CR-182978] 19 p2676 N88-25913
A statistical treatment of accelerated life test data for copper-water heat pipes 20 p2783 N88-26509
Characteristics of long size thermosyphons made of corrugated tube 20 p2784 N88-26511
Study of temperature and stress fields of two sliding cylinders
[ETN-88-92134] 20 p2815 N88-26704
Cryogenic free jets
[DFVLR-FB-88-16] 21 p2900 N88-27210
A lubrication study of engine bearings 21 p2958 N88-27574
Analysis of lower hybrid current drive and rampup experiments on the JT-60 tokamak
[DE88-753136] 21 p3018 N88-27915
Effect of high-amplitude high-frequency current on non-isothermal equilibrium of NS-boundary in inhomogeneous superconductor
[DE88-701682] 21 p3019 N88-27922
Steady conduction of heat in prolate spheroidal systems
[LRT-WE-9-FB-16(1987)] 22 p3077 N88-28272
Heat transport in a parabolic tube of circular cross-section
[LRT-WE-9-FB-2(1988)] 22 p3078 N88-28274
Currents induced in a human being for electromagnetic fields to 10 kHz-50 MHz
[AD-A191977] 23 p3238 N88-29268
Reasoning about fault diagnosis for the space station common module thermal control system 23 p3256 N88-29395
The thermal behavior of film cooled turbulent boundary layers as affected by longitudinal vortices
[AD-A195155] 24 p3374 N88-30095
Theoretical modeling of accelerating arc plasmas
[AD-A195606] 24 p3432 N88-30426

TEMPERATURE EFFECTS

Stability relationship for water droplet crystallization with the NASA Lewis icing spray
[NASA-TM-100220] 02 p0125 N88-10790
Study of improved methods for predicting chemical equilibria
[DE87-014647] 02 p0145 N88-10908
The effect of temperature on fatigue crack initiation from aluminosilicate inclusions
[PNR90377] 02 p0154 N88-10962
Preparative electrophoresis for space
[NASA-TP-2777] 02 p0156 N88-10977
Qualification testing of General Electric 50 Ah nickel-cadmium cells with Pellon 2536 separator and passivated positive plates 02 p0165 N88-11036
Flight experience of solar mesosphere explorer's power system over high temperatures ranges 02 p0165 N88-11037
Reduction of temperature rise in high-speed photography
[NASA-TM-100222] 02 p0176 N88-11100
Creep-fatigue behavior of NiCoCrAlY coated PWA 1480 02 p0189 N88-11176
A one-dimensional model of thermally-driven coastal front evolution 02 p0204 N88-11274
Fracture mechanism of fine grain graphite under high heat fluxes
[IPPJ-842] 02 p0242 N88-11527
Processing and properties of SiC/Nicalon composites
[DE87-013885] 03 p0279 N88-11757
Stress corrosion cracking of high-strength steels in aqueous environments 03 p0289 N88-11818
A fundamental study of the mechanical and microstructural response of elevated temperature PM aluminum-titanium alloys 03 p0289 N88-11819
Investigation of structure-permeability relationships of silicone polymer membranes
[PB87-230181] 03 p0293 N88-11839
Estimations of gravitational effects on thermal denaturation process in a biopolymer 03 p0318 N88-12013
Kinetics of crack growth: Thermal/mechanical interaction 03 p0337 N88-12124
Structure of thermotropic polyesters with large substituents
[AD-A184086] 04 p0418 N88-12595
Effect of time and temperature on transformation toughened zirconias
[AD-A184356] 04 p0419 N88-12600
Pipe and bend erosion by pneumatic transport of solids at high temperature
[DE88-001345] 04 p0429 N88-12658
Combustion characteristics of gas turbine alternative fuels
[NASA-TM-100247] 05 p0548 N88-13338
The effect of temperature on the tensile properties of HSLA-100 steel
[AD-A184951] 05 p0565 N88-13441
Development of response models for the Earth Radiation Budget Experiment (ERBE) sensors. Part 1: Dynamic models and computer simulations for the ERBE nonscanner, scanner and solar monitor sensors
[NASA-CR-178292] 05 p0584 N88-13557
The initiation and growth of small fatigue cracks in copper at room and cryogenic temperatures 05 p0600 N88-13668
Effect of test temperature and frequency on fatigue crack propagation in PVC 05 p0606 N88-13715
Material design of high-purpose glass discussed 06 p0675 N88-14133
Pressure induced phase transitions, superconductivity of phosphorus described 06 p0675 N88-14134
Polymer material for heat sensors 06 p0676 N88-14142
Fractographic and microstructural aspects of fracture toughness testing in irradiated 304 stainless steel
[DE88-000795] 06 p0681 N88-14172
Mechanisms of rolling contact spalling
[NASA-CR-179243] 06 p0714 N88-14380
Cyclic deformation behaviour of cast irons with various graphite shapes in the temperature range 20 C less than or = T less than or = 500 C 06 p0715 N88-14384
Near-threshold fatigue 06 p0716 N88-14392
Near-threshold fatigue crack growth behavior at cryogenic temperature 06 p0718 N88-14409
Effect of temperature exposure on fatigue crack propagation 06 p0720 N88-14421
High temperature low cycle fatigue behavior and creep-fatigue interation of MA 6000 ODS alloy 06 p0720 N88-14425
The effect of temperature on fatigue crack initiation from aluminosilicate inclusions 06 p0720 N88-14427
An analysis of temperature effect on LCF crack growth rates in superalloy GH36 06 p0721 N88-14431
Thermomechanical fatigue of lead-base low tin solder 06 p0721 N88-14432
Daily dynamics of some physiological indicators of man under desert condition 06 p0750 N88-14605
Exercise in the heat: Effects of dinitrophenol administration
[AD-A185731] 06 p0752 N88-14622
Precipitation in alumina-rich spinel: A transformation-toughened ceramic single crystal
[DE87-012380] 06 p0785 N88-14815
The role of low temperature chemistry in the autoignition of n-butane
[DE88-002385] 07 p0829 N88-15031
Supersonic boundary layer on a heated wall
[ETN-88-91617] 08 p0950 N88-15763
Structural study of the impregnating resins of the type TGMDA/DDS — expoxy resins
[ETN-88-91616] 08 p0965 N88-15842
Kinetics and mechanism of thermal aging embrittlement of duplex stainless steels
[DE88-002987] 08 p0969 N88-15866
Description of tests run in the T2 cryogenic wind tunnel
[PB87-170296] 09 p1113 N88-16672
Mechanical properties of carbon fiber reinforced thermoplastic matrix composites
[NAL-TR-934] 09 p1139 N88-16827
Surface composition-reactivity relationships in heterogeneous catalysis
[DE87-003450] 09 p1140 N88-16834
Influence of post-anneal cooling treatments on suppression of cryogenic intergranular fracture in experimental Ni-free high-Mn austenitic steels
[DE88-002766] 09 p1145 N88-16863
Theory of transient thermal self-focusing of sound beams 09 p1234 N88-17401
Molecular dynamics study of high-temperature grain-boundary stability in a (100) sigma = 29 bicrystal model
[DE88-002955] 09 p1258 N88-17546
The influence of the heating procedure on the oxidation behaviour of NiAl studied by XPS
[AERE-R-12498] 10 p1300 N88-17776
A detailed microstructural examination of the cause of HAZ cracking in type 316 steel
[AERE-R-12428] 10 p1301 N88-17777
A review of pitting corrosion in high temperature aqueous solutions
[DE88-003547] 10 p1302 N88-17787
The measurement of stress in steels of varying microstructure by Barkhausen and magneto-acoustic emission
[AERE-R-12387] 10 p1343 N88-18027
Radiation and temperature effects on the time-dependent response of T300/934 graphite/epoxy
[NASA-CR-182603] 11 p1451 N88-18646
Gastric emptying during exercise: Effects of acute heat stress, acclimation and hypohydration
[AD-A188008] 11 p1519 N88-19073
MBE (Molecular Beam Epitaxial) growth characterization and electronic device processing of HgCdTe, HgZnTe related heterojunctions and HgCdTe-CdTe superlattices
[AD-A187416] 11 p1555 N88-19307
Convective heat transfer and its effect on inertial measurement units 12 p1578 N88-19442
Effects of moisture, elevated temperature, and fatigue loading on the behavior of graphite/epoxy buffer strip panels with center cracks
[NASA-TM-100558] 12 p1603 N88-19590
Thermal cracking and variable properties effects on free boundary layer diffusion flames
[NBS/GCR-88/542] 12 p1614 N88-19652
The fatigue behavior of ferritic and austenitic steels at elevated temperatures
[DE88-006304] 13 p1744 N88-20431
The calibration of photographic and spectroscopic films: Reciprocity failure and thermal responses of IIaO film at liquid nitrogen temperatures
[NASA-CR-181094] 13 p1773 N88-20606
A study of the dynamics of high temperature brittle intergranular fracture by acoustic emission
[AERE-R-12479] 13 p1780 N88-20650
Environmental effects on the post-impact compressive strength of CFC
[RAE-TM-MAT-STR-1088] 14 p1884 N88-21258
Influence of hydrogen on crack formation tendency in heat-affected zone with stress concentrator 14 p1887 N88-21276
Friction welding: Advanced method of producing end cutting tool 14 p1897 N88-21327
The effect of surface tension in the weld pool on seam formation when welding thin sheet with light rays 14 p1898 N88-21334
An internal variable constitutive model for the large deformation of metals at high temperatures 14 p1929 N88-21503
The effects of temperature and strain rate on the yielding behavior of the single crystal superalloy PWA 1480 14 p1931 N88-21517
An automated procedure for material parameter evaluation for viscoplastic constitutive models 14 p1932 N88-21520
Diversity of comets, synergic temperature effects and the stability of organic compounds in icy nuclei 14 p2005 N88-21955
Corrosion Research Center, University of Minnesota
[DE88-006681] 15 p2041 N88-22160
Influence of temperature on the tensile strength and toughness characteristics. Material 35NCD16 ESR. Test report M5-521800
[M5-521800] 15 p2041 N88-22163
Grain boundary oxidation and low-cycle fatigue at elevated temperatures 15 p2083 N88-22420
Examination of temperature effects on gate-to-drain avalanche breakdown in GaAs MESFETs (Metal-Semiconductor Field Effect Transistors) by measuring light emission under RF drive
[AD-A189634] 15 p214' N88-22778
Contribution to the study of modern materials for cutting tools
[ISAL-IDI1-87-17] 16 p2185 N88-23029
Analysis for fuel implosion in ICF target and pellet gain 16 p2276 N88-23620
Influence of fiber reinforcement on the vitreous transition temperature of M 10 matrix composites
[ONERA-RT-44/7086-M] 17 p2316 N88-23835
Polymer precursors for ceramic composites 17 p2326 N88-23890
SiC fiber analysis 17 p2326 N88-23891
The effect of elevated temperature on irradiated MOS devices 17 p2406 N88-24308
Analysis of thermal and radiation effects in materials using the GEMAT process 17 p2408 N88-24318
The effect of operating temperature on open, multimegawatt space power systems 17 p2414 N88-24352
The response of selected semiconductor technologies to the combined environmental effects of high temperature and total dose gamma radiation 17 p2431 N88-24462
Effect of alloying, rapid solidification, and surface kinetics on the high temperature environmental resistance of niobium
[AD-A192093] 18 p2485 N88-24743

High temperature embrittleness of Cu-Cr alloy
[NASA-TT-20184] 18 p2488 N88-24759
Critical cooling rates on solution treatment of Cu-Cr and Cu-Be alloys
[NASA-TT-20163] 18 p2488 N88-24760
On the reversion phenomena of Cu-3 percent Ti alloys
[NASA-TT-20170] 18 p2488 N88-24762
Effect of size of precipitates on recrystallization temperatures in Cu-Cr, Cu-Zr, and Cu-Zr-Cr alloys
[NASA-TT-20166] 18 p2489 N88-24763
Rapidly solidified lightweight durable disk material
[AD-A191697] 18 p2491 N88-24775
Thermal distortion analysis of the space station solar dynamic concentrator
[NASA-TM-100868] 19 p2606 N88-25475
Pressure/temperature sensitive inorganic phosphors 19 p2627 N88-25583
Last spring frosts and first autumn frosts in Finland
[FMI-6] 19 p2693 N88-26008
RCL model for the development of hysteresis in superconductors
[DE88-702061] 19 p2733 N88-26234
Electron tunneling in junctions doped with semiconductors and metals 19 p2734 N88-26236
Critical point wetting drop tower experiment
[NASA-CR-183062] 20 p2798 N88-26603
Our climate in danger
[DE88-701824] 20 p2822 N88-26743
Photosynthetic water splitting
[DE88-007809] 20 p2830 N88-26791
Thermal inhibition by megagauss field due to variation of electron temperature in laser plasma
[DE88-701887] 20 p2859 N88-26977
Phase transformations and thermodynamic behavior of the YBa2Cu3O(sub)x system via EMF measurements
[DE88-010054] 20 p2878 N88-27086
Compilation of temperature factors of cubic elements
[PB88-108170] 21 p2908 N88-27260
Determination of lumped-mass thermal properties associated with autoclave curing of graphite/epoxy composites 21 p2925 N88-27364
Thermal stress and its effects on fine motor skill and decoding tasks 21 p2926 N88-27369
Temperature, moisture and strain rate effects on the compressive mechanical behavior of Nylon 6/6
[DE88-010734] 21 p2961 N88-27591
Photodiodes for optical communication in the near infrared
[ETN-88-92379] 21 p3016 N88-27900
Development and application of a finite element method to compute strongly heated turbulent flows
[ECL-88-02] 22 p3077 N88-28267
Marangoni convection in finite cylindrical liquid bridges
[LRT-WE-9-FB-5(1988)] 22 p3078 N88-28277
Effect of fuel burnup and cross sections on modular HTGR (High-Temperature Gas-cooled Reactor) reactivity coefficients
[DE88-006656] 22 p3151 N88-28748
Ultraviolet absorption cross sections of chloro- and chlorofluoromethanes at stratospheric temperatures
[AERONOMICA-ACTA-A-324-1988] 23 p3231 N88-29228
Intraplate deformation, stress in the lithosphere and the driving mechanism for plate motions
[NASA-CR-183121] 23 p3231 N88-29231
Thermodynamical, optical and X-rays studies of some thermotropic liquid crystals
[DE88-702301] 23 p3290 N88-29590
Temperature dependence of conductivity and of Hall coefficients for noble metal films
[ETN-88-92981] 23 p3294 N88-29616
Thermal stress analysis in PMR-15 carbon fibre laminates
[ETN-88-93123] 24 p3341 N88-29886
Effect of interfacial phenomena on contact line heat Transfer-3
[AD-A194941] 24 p3343 N88-29901
The thermal behavior of film cooled turbulent boundary layers as affected by longitudinal vortices
[AD-A195155] 24 p3374 N88-30095
Study of human factors engineering criteria for Extra Vehicular Activity (EVA) systems, volume 2
[STF23-F87025-VOL-2] 24 p3409 N88-30293

TEMPERATURE FIELDS
U TEMPERATURE DISTRIBUTION

TEMPERATURE GRADIENTS
NT THERMOCLINES
Icing detector with early warning capability
[AOA-4.1.0055] 03 p0325 N88-12050
Crack initiation and propagation due to cyclic thermal gradients — aircraft turbine blades
[ESA-TT-1023] 03 p0336 N88-12114
Nonlinear thermoviscoelastic analysis of metallic plane curved beams 03 p0336 N88-12119
Corrosion of ferritic steels by molten lithium: Influence of competing thermal gradient mass transfer and surface product reactions
[DE88-000334] 04 p0417 N88-12585
Influence of stratification in near-surface water layer on intensity of gas exchange between atmosphere and water 04 p0459 N88-12841
Thermophoresis of spherical aerosol particle at arbitrary Knudsen numbers 04 p0461 N88-12850
Evaluation of the Mellen EDG furnace for growth of large diameter GaAs single crystals in a horizontal configuration
[DE88-000463] 04 p0498 N88-13068
Sensitivity of the H alpha line to expansion, geometrical extent and temperature gradient in the G and K supergiant chromospheres 04 p0514 N88-13159
An analytical soil thermodynamic model for the diurnal variation of ground surface temperature
[AD-A185388] 05 p0625 N88-13823
Thin film and gradient-driven instability mechanisms
[PB88-101522] 07 p0853 N88-15182
A calorimeter for measuring the neutral beam power reaching the plasma
[DE88-001412] 07 p0937 N88-15691
Investigation of thermoacoustic heat transport using a thermoacoustic couple
[AD-A186889] 09 p1242 N88-17442
Side-by-side comparisons of evacuated compound parabolic concentrator and flat plate solar collector systems at temperatures of 90 to 100°C
[DE88-004717] 10 p1351 N88-18073
A neutral-beam diagnostic for fast confined alpha particles in a burning plasma: Applicatoin on CIT (Compact Ignition Tokamak)
[DE88-004890] 11 p1554 N88-19301
Remote sensing of meteorological parameters with the aid of a clear-air Doppler radar
[PB88-142518] 12 p1647 N88-19864
Vertical turbulent transfer of matter in thin ocean surface layer during daytime heating 13 p1787 N88-20693
The mixed layer of the western equatorial Pacific Ocean
[HIG-1861] 13 p1805 N88-20789
High output paraffin actuators: Utilization in aerospace mechanisms 14 p1924 N88-21470
Kinematic support using elastic elements 14 p1926 N88-21481
Two gimbal bearing case studies: Some lessons learned 14 p1927 N88-21487
Proceedings of the Seminar on Hydrodynamics and Crystal Growth
[ETN-88-92025] 14 p1987 N88-21853
Hydrodynamical regimes in molten metals under a horizontal temperature gradient 14 p1988 N88-21859
Experiments investigating advanced materials under thermomechanical loading 15 p2077 N88-22385
Ocean, Wave, and Tidal Energy Systems: Current abstracts
[DE88-008299] 19 p2687 N88-25973
The effects of gradients on boundary stability
[DE88-009592] 20 p2773 N88-26445
An experimental investigation of transient characteristics in a gravity-assisted heat pipe 20 p2783 N88-26506
HeFlow: A program for calculating pressure and temperature of helium in forced-flow superconductors. Part 1: Numerical solutions. Part 2: HeFlow user's manual
[DE88-008941] 20 p2876 N88-27071
Prediction of velocity and temperature profiles in thermally driven gravity currents applied to stratified thermal storage tanks
[DE88-004452] 21 p2946 N88-27496
An analysis of horizontal temperature gradients and heat content in the mixed layer and the surface forcing during PATCHEX
[AD-A192330] 21 p2976 N88-27678

TEMPERATURE INDICATORS
U INDICATING INSTRUMENTS
U TEMPERATURE MEASURING INSTRUMENTS

TEMPERATURE INSTRUMENTS
U TEMPERATURE MEASURING INSTRUMENTS

TEMPERATURE INVERSIONS
North Pacific Ocean. Gulf of Alaska, R/V Thomas G. Thompson: 1 February - 8 March 1967. STD data report
[AD-A186569] 08 p1045 N88-16314

TEMPERATURE MEASUREMENT
Estimating regional evapotranspiration from remotely sensed data by surface energy balance models
[NASA-CR-181400] 01 p0064 N88-10411
A device for measuring fast temperature fluctuations — atmospheric temperature
[KNMI-TR-92] 01 p0070 N88-10449
Psychophysical considerations in measuring MRTD with staring arrays — minimum resolvable temperature difference (MRTD)
[RSRE-MEMO-4031] 01 p0076 N88-10487
The use of fiber optics in the determination of temperature and extent of reaction in detonating explosives
[DE87-012632] 01 p0094 N88-10612
Evaluation of the infrared test method for the olympus thermal balance tests 02 p0136 N88-10656
Optical fiber interferometric sensor to measure temperature in gas flow
[ENST-87E006] 02 p0170 N88-11071
Evaluating and testing thermographic phosphors for turbine-engine temperature measurements
[DE87-011772] 02 p0174 N88-11090
Further development of the dynamic gas temperature measurement system 02 p0184 N88-11141
Correlation of velocity and velocity-density turbulence in the exhaust of an atmospheric burner 02 p0185 N88-11147
Forecasting the kind of precipitation in winter 02 p0202 N88-11266
Time-resolved temperature and density measurements in ionizing, uniformly irradiated UV-laser-produced plasmas
[DE87-014649] 02 p0238 N88-11504
Comparison of flight-measured and calculated temperatures on the space shuttle orbiter
[NASA-TM-88278] 03 p0321 N88-12029
Comparison of measured temperatures, thermal stresses and creep residues with predictions on a built-up titanium structure
[NASA-TM-86814] 03 p0337 N88-12125
A simplified CARS measurement system for rapid determination of temperature and oxygen concentration
[NASA-TM-100498] 03 p0374 N88-12353
Resistor cooling in a vacuum
[DE88-000696] 04 p0440 N88-12733
Noncontact temperature measurements of hot steel bodies using an electromagnetic acoustic transducer (EMAT)
[DE88-000560] 04 p0446 N88-12765
Calibration of a laser-pumped, thermographic phosphor remote thermometry system
[DE88-000452] 04 p0449 N88-12781
A mathematical model of high alloy nickel base high temperature alloys
[BLL-M-37381-(5828.4)] 05 p0564 N88-13436
October lower stratospheric Antarctic temperature and total ozone from 1979-1985 05 p0615 N88-13776
Development of a Doppler wind lidar system for atmospheric wind measurements 08 p1027 N88-16217
Aerosols in Martian Atmosphere and Natural Dust Observation (AMANDO). Proposal for the Mars orbiter balloon and rover to study the Martian atmosphere, its thermal content, and its interaction with the soil
[IFSI-87-9] 08 p1100 N88-16619
MARCE data evaluation 10 p1286 N88-17693
A reliable data collection/control system 10 p1289 N88-17708
CARS measurements of combustion. 1: Precision of thermometry
[NAL-TR-939] 10 p1299 N88-17769
NBS (National Bureau of Standards) measurement services: Platinum resistance thermometer calibrations
[PB88-138367] 10 p1333 N88-17967
Comparative evaluation of resistive and inductive techniques for measuring temperature of superconducting transition
[DE88-700603] 10 p1417 N88-18457
A noise-adding radiometer for the Parkes antenna 11 p1473 N88-18788
Measurement of velocity and temperature profiles in low-speed, turbulent non-isothermal flows
[PB88-155833] 11 p1486 N88-18872
Error evaluation of some practical thermocouple probes for gas turbine combustor tests
[NAL-TR-936] 11 p1489 N88-18886
A sky temperature survey at 19.2 GHz using a balloon borne Dicke radiometer for anisotropy tests of the cosmic microwave background 11 p1571 N88-19403
Vestibular response to caloric stimulation during orbital flight 12 p1658 N88-19939
Electron temperature measurements in an argon/cesium plasma diode
[AD-A188835] 12 p1695 N88-20141
Exhaust-gas pressure and temperature survey of F404-GE-400 turbofan engine
[NASA-TM-88273] 13 p1724 N88-20307
Measurement of detonation temperature of hydrogen-oxygen mixture by CARS (Coherent Anti-Stokes Raman Spectroscopy)
[NASA-TT-20227] 13 p1739 N88-20398
Remote fiber fluorimetry techniques for pressure measurements
[DE88-004486] 13 p1773 N88-20604

Noncontact thermometry via laser pumped, thermographic phosphors: Characterization of systematic errors and industrial applications
[DE88-005599] 13 p1777 N88-20628
Phenomenological description of eddy registered in Gulf Stream 13 p1787 N88-20694
Monitoring ocean surface layer processes 13 p1806 N88-20801
On the structure of pulsed plasma jets 13 p1843 N88-21030
The astrophysics of nebulae and active galactic nuclear emission-line regions: New methods and applications 13 p1858 N88-21111
Tropic heat MR (Meteorological Recorder) meteorological data (April 1984 - June 1985)
[PB88-161286] 14 p1948 N88-21620
Temperature of the nucleus of Comet Halley 14 p2009 N88-21985
Measurement of emissivity of industrial surfaces using a simple method
[NASA-TT-20165] 15 p2036 N88-22130
Rocket measurements of ionospheric electron temperature over Natal
[INPE-4485-PRE/1250] 15 p2096 N88-22489
Validate algorithms for the determination of rainfall rates from SSM/I microwave satellite imagery
[AD-A188769] 16 p2233 N88-23337
Noncontact Temperature Measurement
[NASA-CP-2503] 17 p2327 N88-23895
Radiation thermometry: The measurement problem 17 p2328 N88-23896
The NBS scale of radiance temperature 17 p2328 N88-23897
Non-contact temperature measurement requirements for electronic materials processing 17 p2328 N88-23898
Noncontact temperature measurement: Requirements and applications for metals and alloys research 17 p2328 N88-23899
Noncontact temperature measurement in glass and other transparent materials 17 p2328 N88-23900
Noncontact temperature measurements in the microgravity fluids and transport phenomena discipline 17 p2328 N88-23901
Microgravity combustion discipline working group summary of requirements for noncontact temperature measurements 17 p2328 N88-23902
Requirements for temperature and species concentration measurements in microgravity combustion experiments 17 p2329 N88-23903
Non-contact temperature measurements for biotechnology discipline working group 17 p2329 N88-23904
Multi-color pyrometer for materials processing in space 17 p2329 N88-23905
Direct emissivity measurements on liquids and corrections to multi-color pyrometers 17 p2329 N88-23906
Common but unappreciated sources of error in one, two, and multiple-color pyrometry 17 p2329 N88-23907
Fast optical pyrometry 17 p2329 N88-23908
The role of fiberoptics in remote temperature measurement 17 p2329 N88-23909
Laser pyrometry 17 p2330 N88-23910
Noncontact true temperature measurement, 2 17 p2330 N88-23911
Laser Diagnostics for combustion temperature and species measurements 17 p2330 N88-23912
Infrared radiometric technique in temperature measurement 17 p2330 N88-23913
Real time thermal imaging of high temperature semiconductor melts 17 p2330 N88-23914
Clinical applications of computerized thermography 17 p2330 N88-23915
Summary report on the Japan-US Workshop on the Assessment of Spectroscopic Data for Temperature and Density Measurements --- plasma diagnostics
[IPPJ-861] 17 p2439 N88-24512
Effects of spatial resolution in CARS measurements
[PB88-121900] 18 p2482 N88-24727
Remote temperature-measurement instrumentation for a heated rotating turbine disk
[DE88-006456] 18 p2516 N88-24925
Special observations 18 p2545 N88-25108
Analysis of annular microstrip antennas for hyperthermic applicators
[PB88-181508] 19 p2643 N88-25679
Studies of error in temperature measurement with thermistors in the range between continual and free-molecule flows
[NASA-TT-20302] 19 p2674 N88-25900
Examination of the termalization of confined ions
[PB87-227815] 19 p2723 N88-26171
Evaluation of thermophosphor temperature technique
[DE88-007654] 20 p2805 N88-26638
Remote sensing of temperature profiles. Performance test of PASS
[DE88-753108] 20 p2826 N88-26768
Global-scale temperature changes to August 1987 and a comparison of satellite and conventional data 22 p3125 N88-28572
Energy conversion measurements in laser-sustained argon plasmas for application to rocket propulsion
[AD-A194931] 24 p3337 N88-29861
Measurement of local high-level, transient surface heat flux
[NASA-TP-2840] 24 p3375 N88-30099
Quantitative surface temperature measurement using two-color thermographic phosphors and video equipment
[NASA-CASE-LAR-13740-1] 24 p3376 N88-30105
Estimation of soil temperature profile from remote microwave and IR measurements 24 p3450 N88-30532

TEMPERATURE MEASURING INSTRUMENTS
NT BATHYTHERMOGRAPHS
NT OPTICAL PYROMETERS
NT PNEUMATIC PROBES
NT PYROMETERS
NT RADIATION PYROMETERS
NT RESISTANCE THERMOMETERS
NT THERMOMETERS
Realization of an instrument to measure temperature and concentration gradients in fluids --- microgravity
[CISE-3128] 09 p1168 N88-17003
Forward looking wind shear detection 10 p1275 N88-17629
Evaluation of a temperature remote sensing technique
[AD-A187885] 10 p1347 N88-18053
Boundary layer measurements using hot-film sensors 17 p2297 N88-23743
Noncontact Temperature Measurement
[NASA-CP-2503] 17 p2327 N88-23895
Measurement of local high-level, transient surface heat flux
[NASA-TP-2840] 24 p3375 N88-30099

TEMPERATURE PROBES
NT PNEUMATIC PROBES

TEMPERATURE PROFILES
Effect of NASA advanced designs on thermal behavior of Ni-H2 cells
[NASA-TM-100197] 01 p0021 N88-10132
Diagnosing short term changes in temperature and moisture profiles from single Doppler radar 02 p0200 N88-11251
Method for determining atmospheric temperature profiles from observations of astronomical refraction of stars 08 p1013 N88-16139
A study of finite difference and finite element vertical discretization schemes for baroclinic prediction equations
[AD-A186617] 08 p1040 N88-16291
GAS eleven node thermal model (GEM) 10 p1289 N88-17712
Suggested severe local storm operational scenario for GOES I-M
[NASA-TM-100688] 11 p1515 N88-19052
Editing master oceanographic observation data set 4
[AD-A188405] 12 p1649 N88-19876
Basic networks of TOGA: Determination of thermal profiles by XBT and of sea level by tide gage 14 p1939 N88-21568
Large ice masses: Characteristics, behaviour and relation to climate 14 p1939 N88-21569
Aerodynamic aspects of the Amazon Forest
[INPE-4445-TDL/313] 15 p2098 N88-22501
Antistokes coherent Raman diffusion of a nitriding plasma
[ONERA-RF-6/3644-PY] 16 p2175 N88-22962
Utilization of dense packed planar acoustic echosounders to identify turbulence structure in the lowest levels of the atmosphere
[AD-A191006] 16 p2233 N88-23335
Ion temperature profile measurement using charge exchange recombination spectroscopy on JIPP T-IIU 17 p2440 N88-24518
Spectroscopic measurements of ion temperature, rotation speed and beam deposition profile on DIII-D 17 p2440 N88-24519
Three-dimensional temperature fields in the atmosphere up to 50 km altitude
[ETN-88-92150] 18 p2542 N88-25089
Superthermal electron processes in the upper atmosphere of Uranus: Aurora and electroglow
[NASA-TM-101150] 18 p2594 N88-25417
Diurnal variations in optical depth at Mars: Observations and interpretations
[NASA-TM-100057] 18 p2595 N88-25420
Temperature and species profiles in propellant ignition and combustion 19 p2633 N88-25616
An arranging method on L/D of two-phase closed thermosyphons 20 p2783 N88-26508
Remote sensing of temperature profiles. Performance test of PASS
[DE88-753108] 20 p2826 N88-26768
Prediction of velocity and temperature profiles in thermally driven gravity currents applied to stratified thermal storage tanks
[DE88-004452] 21 p2946 N88-27496
Retrieval of temperature and concentration profiles from a limited number of absorption measurements 21 p2947 N88-27501
Temperature profile construction methods: An evaluation
[AD-A195919] 24 p3403 N88-30262

TEMPERATURE SCALES
The NBS scale of radiance temperature 17 p2328 N88-23897

TEMPERATURE SENSORS
NT THERMISTORS
Development of heat flux sensors for turbine airfoils 02 p0184 N88-11143
Icing detector with early warning capability
[AOA-4.1.0055] 03 p0325 N88-12050
Instrument for radiation testing/screening electronic devices over an extended temperature range
[AD-A184245] 03 p0326 N88-12060
Polymer material for heat sensors 06 p0676 N88-14142
Evaluation of a temperature remote sensing technique
[AD-A187885] 10 p1347 N88-18053
La Recherche Aerospatiale, bimonthly bulletin, number 1987-1, 236/January-February
[ESA-TT-1055] 11 p1433 N88-18549
Photonic temperature and pressure sensors for biosystems/pulsed microwave. Part 1: Interaction studies
[AD-A188887] 12 p1629 N88-19751
Characteristics of polysilicon layers and their application in sensors 19 p2669 N88-25861
Flexible tactile sensing arrays for robotics: Architectural robustness and yield considerations 19 p2671 N88-25878
Thermodynamic study of hygroscopic polymers using surface acoustic waves 19 p2672 N88-25882
Modulated-splitting-ratio fiber-optic temperature sensor
[NASA-TM-101332] 22 p3042 N88-28062
Development of sensors for ceramic components in advanced propulsion systems: Survey and evaluation of measurement techniques for temperature, strain and heat flux for ceramic components in advanced propulsion systems
[NASA-CR-182111] 22 p3081 N88-28299

TEMPERING
Partial substitution of vanadium by niobium in AISI H13 steel
[DE87-703548] 04 p0415 N88-12575
Study on substructures of martensite in steels containing rare earth metals
[PB87-143996] 07 p0833 N88-15050
Investigation of the auto-tempering of low-carbon martensite
[PB87-143970] 07 p0833 N88-15053
New mechanism of the high temperature (reversible) temper brittleness of alloy steels
[PB87-143954] 07 p0833 N88-15056
The measurement of stress in steels of varying microstructure by Barkhausen and magneto-acoustic emission
[AERE-R-12387] 10 p1343 N88-18027

TEMPLATES
Schwarz splitting and template operators
[AD-A187956] 10 p1404 N88-18370
Defect detection and classification in VLSI pattern inspection 18 p2507 N88-24871

TEMPORAL DISTRIBUTION
Optimization of explicit time-stepping algorithms and Stream-Function-Coordinate (SFC) concept for fluid dynamics problems 04 p0445 N88-12762
Convective wind fields as investigated with doppler lidar
[PB88-115472] 09 p1193 N88-17151
Evolution of acoustic gravity wave packet in spatially and temporally varying wind 11 p1469 N88-18760
Temporal evolution of ionospheric electric field driven by field-aligned current 11 p1469 N88-18761
Spatial and temporal distribution of precipitation chemistry across Maryland in 1984, volume 1
[PB88-148929] 14 p1943 N88-21595
Spatial and temporal distribution of precipitation chemistry across Maryland in 1984, volume 2
[PB88-148937] 14 p1944 N88-21596
The spatial and temporal variability of the arctic atmospheric boundary layer and its effect on electromagnetic (EM) propagation
[AD-A193958] 23 p3204 N88-29068

Mineralization through geologic time: Evolution of continental crust 24 p3400 N88-30250

TEMPORAL RESOLUTION

Estimation from satellite imagery of summertime rainfall over varied space and time scales
[PB87-203246] 01 p0071 N88-10454

A CAMAC system controlled by an IBM AT computer for time-resolved spectroscopy
[DE87-010111] 01 p0080 N88-10514

Evaluation of digital, multitemporal LANDSAT 5 thematic mapper data for the determination of the aerial snowcover extent and spectral separation of various surface types in the inner Oetztal (West Germany) with special regard to the significance of aerial snowcover information for water resources management
[DFVLR-FB-86-46] 03 p0345 N88-12180

Visual evoked responses to sinusoidal gratings presented in central and right visual fields: 1
[DE87-014731] 04 p0473 N88-12919

Resolution limitations and optimization of the LLNL streak camera focus
[DE88-001633] 05 p0586 N88-13572

Investigation of the evolution of the fusion processes in the plasma focus using time-resolved neutron spectroscopy
[IPF-87-4] 09 p1251 N88-17493

Time-resolved spectroscopic measurement of anode plasma in magnetically-insulated diode 16 p2279 N88-23641

Applications of multitemporal compositions obtained from LANDSAT data in the study of urban growth
[INPE-4480-PRE/1246] 16 p2287 N88-23692

Fast optical pyrometry 17 p2329 N88-23908

Electron device probing in the femtosecond time scale 19 p2660 N88-25821

TENDENCIES

Reference filters for electrostatic charging tendency measurements of fuels
[AD-A191717] 18 p2495 N88-24803

TENSILE DEFORMATION

Polymer chain segment orientation during stress relaxation
[DE87-013392] 01 p0027 N88-10174

An investigation of the high strain rate deformation of SiCw/2124 Al composite
[OUEL-1675/87] 02 p0142 N88-10895

The effect of deformation rate on JBK-75 stainless steel forgings
[DE88-001696] 07 p0834 N88-15061

Fatigue and uniaxial deformation behavior of Hastelloy XR at elevated temperatures
[DE88-751058] 09 p1145 N88-16862

The influence of small defects on tensile specimen ductility and symmetry of deformation
[AD-A187983] 10 p1346 N88-18044

An investigation of the influence of dislocation substructures on the deformation behavior of AK, DQ steel sheets
[DE88-006337] 14 p1889 N88-21289

TENSILE PROPERTIES

Superplastic deformation and post forming tensile properties of Ti-6Al-4V sheet
[RAE-TR-86015] 01 p0023 N88-10144

Tensile behavior of superplastic Al-Cu-Li-Zr alloy 2090 at cryogenic temperatures
[DE87-014084] 02 p0147 N88-10923

A shape preserving interpolant which has tension controls
[DE87-014615] 02 p0229 N88-11443

Effect of irradiation on the tensile properties of niobium-base alloys
[DE87-002409] 03 p0285 N88-11790

The effect of strain rate on the yield behavior of iron-base LRO alloys at elevated temperatures
[DE87-014893] 03 p0288 N88-11808

Carbon fiber reinforced glass matrix composites for space based applications
[AD-A184355] 04 p0410 N88-12546

Molecular composites: Processing, post-treatment and mechanics
[AD-A184458] 04 p0410 N88-12547

Mechanical behavior of a controlled rolled high-strength low alloy steeel plate, microalloyed with Nb and V
[DE87-703507] 04 p0415 N88-12571

Welding and weldability of ductile intermetallic alloys
[DE87-014061] 04 p0416 N88-12582

The accommodation of precipitate plates modelled as a tensile test
[DE88-000207] 04 p0454 N88-12814

Small-diameter wire tensile testing
[DE88-000835] 04 p0455 N88-12815

Influence of strain rate and notch depth on tensile properties of HITCO 6250
[DE88-001324] 04 p0455 N88-12816

The effect of temperature on the tensile properties of HSLA-100 steel
[AD-A184951] 05 p0565 N88-13441

Tensile properties of extrusion consolidated Type 304 SS rapidly solidified powders
[DE87-014875] 05 p0566 N88-13450

Basic energy sciences research in the Metals and Ceramics Division of Oak Ridge National Laboratory
[DE87-013538] 06 p0681 N88-14171

The effect of neutron irradiation on the tensile properties and microstructure of several vanadium alloys
[DE88-001755] 06 p0682 N88-14176

Electron microscopy studies of tensile cyclic fatigue-tested silicon nitride ceramics
[DE88-001438] 06 p0685 N88-14196

Effect of hold time on fatigue of lead rich PbSn solder 06 p0715 N88-14387

High temperature low cycle fatigue behavior and creep-fatigue interation of MA 6000 ODS alloy 06 p0720 N88-14425

The relationship of tensile specimen size and geometry effects to unique constitutive parameters for ductile materials
[AD-A186020] 08 p0994 N88-16012

Influence of post-anneal cooling treatments on suppression of cryogenic intergranular fracture in experimental Ni-free high-Mn austenitic steels
[DE88-002766] 09 p1145 N88-16863

Effects of the neutron spectrum on mechanical property changes in low dose irradiations
[DE88-003429] 10 p1302 N88-17786

Durability and damage tolerance of aluminum castings
[AD-A186444] 10 p1341 N88-18013

Analysis and application of the constant tensile load test for polyethylene gas pipe materials
[DE88-002868] 10 p1345 N88-18037

The effects of low doses of 14 MeV neutrons on the tensile properties of three binary copper alloys
[DE88-003400] 11 p1458 N88-18691

Development of a constitutive equation for HSLA (High-Strength Low-Alloy)-100 at cryogenic temperatures
[AD-A189243] 13 p1740 N88-20408

The effect of microstructure on the fatigue crack growth resistance of nickel base superalloys
[AD-A189526] 13 p1741 N88-20414

Behaviour of fibre-reinforced composites under dynamic loading
[AD-A191310] 16 p2174 N88-22955

Effects of natural environment on first generation solid rocket booster thermal protection system materials
[NASA-TM-100329] 17 p2373 N88-24113

Creep behavior of tungsten/niobium and tungsten/niobium-1 percent zirconium composites 17 p2425 N88-24427

Dynamic consolidation of metal powders
[AD-A192126] 18 p2485 N88-24744

Temperature-dependent tensile and shear response of graphite/aluminum
[NASA-CR-182914] 19 p2609 N88-25484

The postirradiation tensile properties and microstructure of several vanadium alloys
[DE88-007140] 19 p2615 N88-25515

Exploratory development in the system Al-Sc-X
[DE88-008242] 19 p2618 N88-25529

Uniaxial tensile strain measurement for ceramic testing at elevated temperature: Requirements, problems and solutions
[DE88-008090] 19 p2621 N88-25550

Initial development of high-temperature titanium silicide alloys
[DE88-007860] 20 p2772 N88-26437

Helium induced degradation in the weldability of an austenitic stainless steel
[DE88-009062] 20 p2773 N88-26443

Nickel aluminides: A new family of nickel + aluminum alloys featuring simple composition, low density, excellent oxidation resistance and high yield strength that increases with temperature
[DE88-010692] 20 p2776 N88-26461

Thermomechanical processing of Al alloy 2090 for grain refinement and superplasticity
[AD-A192333] 21 p2912 N88-27281

Some effects of nitrates on the tensile properties of Al 7075-T7351
[AD-A195118] 24 p3354 N88-29965

TENSILE STRENGTH

Gas tungsten arc welding of Al-10Fe-5Ce
[AD-A184202] 03 p0334 N88-12104

Weldability of 2219-T851 and 2519-T87 aluminum armor alloys for use in Army vehicle systems
[AD-A184296] 04 p0451 N88-12792

Fatigue strength of alloy A286 at cryogenic temperature 05 p0603 N88-13695

Effect of interface on mechanical properties of graphite/201 aluminum composites 05 p0606 N88-13717

Deformation, fatigue and fracture behavior of two cast anisotropic superalloys 05 p0608 N88-13732

Temperature dependent mechanical properties of an alumina fiber reinforced aluminum composite 06 p0677 N88-14147

Threshold stress intensity for stable crack growth in high strength steel at ambient temperature and below 06 p0718 N88-14407

Structural relaxation and mechanical properties of amorphous Fe-Zr alloys 07 p0840 N88-15094

Cavitation inception scale effects. 1. Nuclei distributions in natural waters. 2. Cavitation inception in a turbulent shear flow
[AD-A186553] 08 p0988 N88-15987

Computation of the tensile and bending restraint intensities of welded specimens by finite element method
[PB87-143798] 08 p0995 N88-16024

Investigation of microstructural factors that cause low fracture toughness in silicon carbide whisker/Al alloy composites
[AD-A186443] 09 p1137 N88-16817

Long-term aging of cast stainless steels: Mechanisms and resulting properties
[DE88-002888] 09 p1145 N88-16864

Aging degradation of cast stainless steels: Effects on mechanical properties
[DE88-003053] 09 p1145 N88-16866

Materials Research Laboratory at Brown University
[AD-A188006] 13 p1739 N88-20396

A direct correlation of strength with impact velocity
[AD-A189251] 13 p1741 N88-20409

Use of reinforced inorganic cement materials for spark wire and drift chamber wire frames
[NASA-CR-180759] 13 p1746 N88-20438

The statistical characterization of tensile strengths for a nuclear-type graphite 13 p1746 N88-20440

Statistical considerations of graphite strength for assessing design allowable stresses 13 p1746 N88-20441

High temperature Young's modulus of IG-110 graphite 13 p1746 N88-20443

Dynamic tensile cyclic fatigue of Si3N4
[DE88-003919] 13 p1781 N88-20658

The age hardening response of thermomechanically processed Al-Mg-Li alloys
[AD-A189870] 15 p2039 N88-22147

Cracking tendencies of restrained welds in high strength low alloy steels under hyperbaric conditions
[AD-A190255] 15 p2039 N88-22150

Influence of temperature on the tensile strength and toughness characteristics. Material 35NCD16 ESR. Test report M5-521800
[M5-521800] 15 p2041 N88-22163

Characterization of HYTUF steel. Semifinished product: 160 mm dia forging block. Processor: C3f. Test Report M3-434600
[M3-434600] 15 p2041 N88-22164

Strength and cracking resistance of ceramics. Report 3: SiC ceramics 16 p2180 N88-22994

Fracture morphologies of carbon-black-loaded SBR (Styrene-Butadiene Rubber) subjected to low-cycle, high-stress fatigue
[DE88-006808] 16 p2181 N88-23002

High strength/sigh modulus aromatic heterocyclic ABA block copolymers
[AD-A191666] 18 p2491 N88-24774

High temperature testing of C/C (Carbon/Carbon) composites
[AD-A193012] 20 p2768 N88-26411

Development of a biaxial test system for thin-walled metal tubes using tensile-compressive axial load and internal-external pressure
[DE88-011279] 21 p2962 N88-27592

A technique for measuring area under a curve
[AD-A193559] 23 p3271 N88-29483

TENSILE STRESS

Constitutive modeling of superalloy single crystals with verification testing 02 p0188 N88-11169

Tensile mean stress effects on uniaxial fatigue behavior of 1045 HR steel 05 p0603 N88-13694

Mixed mode fatigue crack growth using the Brasilian disc 06 p0719 N88-14416

Effect of overload ratios on fatigue crack growth behavior in Ti-6Al-4V alloy
[PB87-147062] 07 p0833 N88-15055

Deformation effects on microwave reflectivity
[AD-A185684] 07 p0844 N88-15120

Shear failure in round bar tensile tests of Al-Zn-Mg-Cu alloys
[PB87-143632] 07 p0869 N88-15271

Pressure and tension dependence of phase shift of polarization modes in birefringent single-mode fiber-optic waveguide 08 p1078 N88-16501

Elastoplastic response of unidirectional graphite/aluminum under combined tension-compression cyclic loading
[CCMS-88-01] 11 p1451 N88-18647
Fracture criterion of reactor graphite under multiaxial stresses 13 p1746 N88-20442
Environment effects on crack propagation with tensile stress
[GKSS-87/E/46] 16 p2223 N88-23267
Peak Acceleration Device (PAD)
[AD-A191639] 18 p2461 N88-24611
Stress corrosion cracking of A723 steel pressure vessels: Two case studies
[AD-A191741] 18 p2527 N88-24990
The surface crack problem in an orthotropic plate under bending and tension
[NASA-CR-178281] 18 p2531 N88-25014
Nonlinear stress-strain and inelastic rebound with exponential stiffness
[AD-A195667] 24 p3384 N88-30159

TENSILE TESTS
Cumulative fatigue and life prediction of fibre composites. Part 2: Experimental techniques and results
[BR101014] 02 p0142 N88-10894
An investigation of the high strain rate deformation of SiCw/2124 Al composite
[OUEL-1675/87] 02 p0142 N88-10895
Creep fatigue life prediction for engine hot section materials (isotropic): Third year progress review 02 p0188 N88-11173
Elevated temperature crack growth 02 p0188 N88-11174
The accommodation of precipitate plates modelled as a tensile test
[DE88-000207] 04 p0454 N88-12814
Test number 2 of propellant for rocket motor MK52
[PB87-226155] 05 p0571 N88-13480
Crack growth in contrasting titanium alloys under the conjoint action of high and low cycle fatigue 05 p0602 N88-13686
Device for measuring hole elongation in a bolted joint
[NASA-CASE-LAR-13453-1] 06 p0712 N88-14361
Shear failure in round bar tensile tests of Al-Zn-Mg-Cu alloys
[PB87-143632] 07 p0869 N88-15271
High temperature tensile testing of ceramic composites
[NASA-CR-180888] 08 p0990 N88-15996
Study of the temperature dependence of the mechanical characteristics of the steels GX 5 CrNi 13 4 and GGG 40 in tensile and bending tests
[DE88-001469] 09 p1143 N88-16850
High-temperature properties of ceramic fibers and insulations for thermal protection of atmospheric entry and hypersonic cruise vehicles
[NASA-TM-100059] 10 p1295 N88-17743
A study of the mechanical behavior of a 2-D carbon-carbon composite 11 p1449 N88-18638
Ethynylated aromatics as high temperature matrix resins
[NASA-TM-89829] 11 p1450 N88-18640
An experimental and numerical study of notch sensitivity of ARALL laminates
[CCMS-88-04] 11 p1450 N88-18644
Microstructural characterization of the heat affected zone of HSLA (High Strength Low Alloy)-100 steel GMA (Gas Metal Arc)-weldment
[AD-A187825] 11 p1457 N88-18686
Effects of moisture, elevated temperature, and fatigue loading on the behavior of graphite/epoxy buffer strip panels with center cracks
[NASA-TM-100558] 12 p1603 N88-19590
Development of a constitutive equation for HSLA (High-Strength Low-Alloy)-100 at cryogenic temperatures
[AD-A189243] 13 p1740 N88-20408
High temperature Young's modulus of IG-110 graphite 13 p1746 N88-20443
Notch sensitivity of graphite materials for VHTR 13 p1747 N88-20447
An investigation of the mechanical properties of improved carbon fibre composite materials
[RAE-TR-88021] 14 p1884 N88-21259
Materials testing at cryogenic temperatures
[BU-359] 14 p1923 N88-21462
The effective fracture toughness of aluminum at rapid heating rates
[AD-A189745] 15 p2038 N88-22146
A test for interfacial effects and stress transfer in ceramic matrix composites
[NASA-CR-182758] 15 p2046 N88-22194
A study of failure characteristics in thermoplastic composite material
[AD-A190613] 16 p2171 N88-22940
Test procedures and standards for mechanical property measurements on metal matrix composites
[NPL-DMA(A)-153] 16 p2172 N88-22944
Behaviour of fibre-reinforced composites under dynamic loading
[AD-A191310] 16 p2174 N88-22955
Mechanical and structural characterization of aluminum ceramic fibers
[ETN-88-92168] 17 p2323 N88-23870
Bearing-bypass material system test
[NASA-CASE-LAR-13458-1] 17 p2342 N88-23967
Fracture physics of delamination of composite materials
[AD-A192021] 19 p2609 N88-25482
High temperature testing of C/C (Carbon/Carbon) composites
[AD-A193012] 20 p2768 N88-26411
Investigation of structure and surface state effect on hydrogen embrittlement of steels, under consideration of acoustic emission analysis
[ETN-88-92350] 20 p2775 N88-26457
Cold worked reinforcing bars in tensile test under high loading rate and low temperatures
[DE88-752993] 21 p2964 N88-27610

TENSOR ANALYSIS
Nonlinear parametric least-squares adjustment
[AD-A184039] 03 p0371 N88-12336
Tensorial calibration. Part 1: First order tensorial calibration
[AD-A186708] 09 p1167 N88-16995
Relative chaos in stellar systems
[DE88-700148] 12 p1710 N88-20234

TENSOR FIELDS
U TENSORS

TENSORS
NT STRESS TENSORS
Direction dependent connections of complex manifolds and their submanifolds
[DE87-703073] 02 p0225 N88-11419
Fundamentals of turbulence for turbulence modeling and simulation 03 p0312 N88-11971
Lagrangian procedures for higher order field equations
[DE87-703365] 05 p0640 N88-13911
Eigenvalues and eigenvectors of field tensors and associated energy tensors
[DE88-001951] 06 p0763 N88-14682
Tensorial calibration. 2. Second order tensorial calibration
[AD-A186614] 09 p1167 N88-16994
Tensorial calibration. Part 1: First order tensorial calibration
[AD-A186708] 09 p1167 N88-16995
Estimates of green tensors for certain boundary value problems
[NASA-TT-20203] 11 p1535 N88-19172
Irreducible tensor operators and multiple-quantum NMR 11 p1542 N88-19217
Connection between general observers and Lanczos potential
[DE88-700139] 11 p1563 N88-19354
Body tensor formalism in finite deformation elasticity and application to the torsion of a circular cylinder 13 p1780 N88-20651
A piecewise quadratic strength tensor theory for composites
[AD-A190929] 16 p2173 N88-22952
Inflation in Einstein-Cartan theory with energy-momentum tensor with spin
[NASA-TM-101164] 17 p2447 N88-24547
Inevitable inflation in Einstein-Cartan theory with improved energy-momentum tensor with spin
[NASA-TM-101146] 18 p2586 N88-25365
Dissipative relativistic radiation hydrodynamics
[DE88-702092] 19 p2665 N88-25846
Symmetry problem of energy-momentum tensor and the creation of gravitational field
[DE88-702442] 21 p3026 N88-27964
On nonlinear equations admitting soliton solutions with a deBroglie phase
[DE88-702694] 23 p3277 N88-29508
Waves and instabilities in an electron-positron plasma in an ultra-strong magnetic field 23 p3283 N88-29551
New methods for nonlinear optimization
[AD-A195982] 24 p3412 N88-30313
The triangle: A multiprocessor architecture for fast curve and surface generation
[AD-A195862] 24 p3414 N88-30324

TERMINAL BALLISTICS
Mechanical property evaluation of a series of commercial tungsten alloys
[AD-A185440] 05 p0565 N88-13446
On the simulation of ballistic shock loads 05 p0593 N88-13615
Structural frequency functions for an impulsive, distributed forcing function 05 p0594 N88-13627
High-velocity reverse ballistic rocket sled testing at Sandia National Laboratories 09 p1179 N88-17059
Penetration theory for inclined and moving shaped charges
[MBB-UA-940/86] 10 p1315 N88-17861
A laboratory railgun for terminal ballistics and arc armature research studies
[AD-A187225] 11 p1442 N88-18603
Crack arrest fracture toughness of armor steels
[AD-A187711] 11 p1456 N88-18681
Splinter generator
[MBB-UA-1048/87] 11 p1491 N88-18897
Ballistic evaluation of applique armours: Presentation and interpretation of ballistic data
[MRL-TN-527] 19 p2635 N88-25629
Review of research concerning Solid Fuel Ramjet (SOFRAM) at the Research Institute of National Defence (FOA) 2
[FOA-C-20714-2.1] 24 p3327 N88-29813

TERMINAL FACILITIES
Issues in air transport and airport management
[PB87-204509] 02 p0124 N88-10782
FAA air traffic control operations concepts. Volume 2: ACF/ACCC (Area Control Facility/Area Control Computer Complex) terminal and en route controll ers
[AD-A185980] 07 p0818 N88-14974
FAA air traffic control operations concepts. Volume 3: ISSS (Initial Sector Suite System) en route controllers
[AD-A185981] 07 p0818 N88-14975
FAA air traffic control operations concepts. Volume 4: TAAS (Terminal Advanced Automation System) terminal controllers
[AD-A185982] 07 p0818 N88-14976
FAA air traffic control operations concepts. Volume 5: ATCT/TCCC (Airport Traffic Control Tower/Tower Control Computer Complex) tower controllers
[AD-A185983] 07 p0818 N88-14977
A traveling-salesman-based approach to aircraft scheduling in the terminal area
[NASA-TM-100062] 12 p1576 N88-19424
Estimates of potential increases in airport capacity through ATC (Air Traffic Control) system improvements in the airport and terminal areas
[AD-A188533] 12 p1578 N88-19444

TERMINAL GUIDANCE
NT LASER GUIDANCE
An investigation of steep descent guidance for terminally-guided sub-munitions 12 p1596 N88-19555

TERMINAL VELOCITY
Efficiency aspects of short, low velocity railguns
[AR-004-847] 04 p0405 N88-12517
Phenomenological piercing characteristics of composite materials 14 p1895 N88-21315

TERMINATING
U STOPPING

TERMINOLOGY
Digital Name Data Base Antarctic as a component of a landscape data base of the Antarctic 01 p0065 N88-10419
Abregrams or deleweds: A forty-year view of acronyms
[DE87-010808] 01 p0106 N88-10690
Definitions as database records
[DE87-014057] 02 p0248 N88-11570
Energy Data Base: Subject Thesaurus
[DE87-008007] 03 p0384 N88-12414
NASA thesaurus supplement: A four part cumulative supplement to the 1985 edition of the NASA Thesaurus
[NASA-SP-7053(SUPP-4)] 08 p1093 N88-16575
NASA thesaurus: Astronomy vocabulary
[NASA-SP-7069] 17 p2450 N88-24553
NASA combined file postings statistics based on NASA thesaurus, Jan. 1968 - July 1988
[NASA-CR-182985] 18 p2589 N88-25384

TERMS
Radar descriptors for the classification of terrain features
[AD-A188145] 11 p1504 N88-18983
An assessment of index term ranking 21 p3028 N88-27974

TERNARY ALLOYS
NT ASTROLOY (TRADEMARK)
A geometrical model for determining the physicochemical properties of ternary metallic systems
[BLL-M-37303-(5828.4)] 02 p0149 N88-10931
CdTe(110)-Mn interface reaction and the formation of non-equilibrium ternary semimagnetic semiconductor alloys
[AD-A187593] 10 p1422 N88-18491
Ordering transitions of ternary alloys A(1-x)B(x)C 20 p2873 N88-27054

TERNARY SYSTEMS
Thermodynamic properties of supercritical mixtures
[DE88-000809] 04 p0413 N88-12562
Electronic structure calculations and binding analyses for selected binary and ternary metal hydrides
[ETN-88-91087] 09 p1256 N88-17527

TERNARY SYSTEMS (DIGITAL)
U DIGITAL SYSTEMS
TERPENES
NT AZULENE
TERRACES (LANDFORMS)
NT PIEDMONTS
NT PLATEAUS
TERRAIN
Evaluation of a scale-model experiment to investigate long-range acoustic propagation
[NASA-TP-2748] 02 p0230 N88-11450
The correspondence of surface climate parameters with satellite and terrain data
[NASA-CR-181515] 03 p0346 N88-12185
Disturbance and recovery of Arctic Alaskan tundra terrain. A review of recent investigations
[AD-A184442] 04 p0467 N88-12887
Large bandwidth ground scattering model --- radar scattering
[FOA-C-30458-3.2] 05 p0576 N88-13511
Electromagnetic wave probing of Earth's environment
[NASA-CR-182358] 06 p0690 N88-14232
Fast, colour displays of digital terrain elevation data
[AD-A185596] 06 p0729 N88-14485
Sound propagation over uneven ground and irregular topography
[NASA-CR-182352] 06 p0776 N88-14763
Academic course Space Methods for Studying Modern Landscapes of Continents 08 p1012 N88-16133
Radar returns from ground clutter in vicinity of airports 10 p1274 N88-17624
The digital landmass simulation production overview
[AD-A187978] 11 p1503 N88-18978
Three-dimensional image generation from an aerial photograph
[AD-A188039] 11 p1503 N88-18979
Contour-to-grid interpolation with nonlinear finite elements: A feasibility study
[AD-A188108] 11 p1503 N88-18980
Terrain Analyst Work Station (TAWS) demonstrations
[AD-A188139] 11 p1504 N88-18981
Radar descriptors for the classification of terrain features
[AD-A188145] 11 p1504 N88-18983
A digital terrain system for microcomputers
[INPE-4170-PRE/1067] 11 p1505 N88-18987
An investigation of terrain related variables for predicting the multipath fade depth distribution on terrestrial microwave lines 12 p1615 N88-19654
Development of a ground-conductivity map for the area of the Federal Republic of Germany from measured field-strength contours 12 p1615 N88-19656
Scattering and depolarization by random rough terrain and vegetation covered terrain-unified full wave approach 12 p1615 N88-19657
VHF/UHF propagation by diffraction: Calculation by numerical integration 12 p1615 N88-19659
Mono- and bistatic radar coverage diagrams including diffractive wave propagation 12 p1616 N88-19660
Development of a digital terrain modeling system for microcomputers
[INPE-4406-TDL/303] 12 p1639 N88-19816
Modification of the BLUEMAX 2 terrain following model to incorporate radar detection
[AD-A190594] 15 p2017 N88-22028
The visit problem: Visibility graph-based solution
[DE88-000343] 15 p2108 N88-22556
The use of LANDSAT-TM pictures for the detection of space-limiting elements for the benefit of landscape photomapping
[BCRS-87-02] 16 p2228 N88-23305
Visualization of digital terrain models 17 p2364 N88-24081
Terrain classification using SPOT images and the computer system GOP-300
[FOA-C-20677-2.7] 17 p2368 N88-24102
Digital monoplotting, part 1
[B8735122-PT-1] 17 p2369 N88-24106
Digital monoplotting, part 2
[B8735122-PT-2] 17 p2369 N88-24107
Land mobile satellite propagation results 19 p2645 N88-25698
Development of an atmospheric diffusion evaluation method incorporating topographical effects. Part 1: Literature review of atmospheric diffusion models incorporating terrain effects
[DE88-753104] 20 p2822 N88-26742
Sound propagation over uneven ground and irregular topography
[NASA-CR-182956] 20 p2849 N88-26911
Surface-wave model uncertainty assessment
[AD-A193094] 21 p2932 N88-27408
Army space systems for terrestrial applications
[AD-A192735] 21 p2965 N88-27613
Analysis of remotely sensed imagery using digital morphology
[AD-A192738] 21 p2965 N88-27614
Active and passive remote sensing of ice
[AD-A193307] 21 p2966 N88-27617
Land use systems and rural landscapes in the center of Veracruz State (Mexico): First results 22 p3092 N88-28364
The suitability of SPOT imagery for monitoring landscape patterns 22 p3094 N88-28376
Digital terrain modelling with SPOT data and geological applications 22 p3110 N88-28474
Automatic production of orthophoto using SPOT images 22 p3112 N88-28487
Automatic creation of digital terrain models from SPOT image pairs 22 p3113 N88-28490
Constraints on the origin of fractured terrane, Northern Martian plains 23 p3304 N88-29684
Ridged and gullied terrains in the Martian uplands 23 p3307 N88-29700
Evolution of the Dharwar Craton: A terrain of early Archean crustal stability, long term orogenic cycles and large scale palaeobiological activity 24 p3399 N88-30241
Crustal growth in the Archean: The geochemical evidence 24 p3400 N88-30246
TERRAIN ANALYSIS
A Workshop on Desert Processes, September 24-28, 1984: Report on the conference
[AD-A184599] 03 p0345 N88-12184
A review of computer-assisted photo interpretation research at USAETL (US Army Engineer Topographic Laboratories)
[AD-A184034] 03 p0346 N88-12186
Correction of inertial navigation system drift errors for an autonomous land vehicle using optical radar terrain data
[AD-A184973] 05 p0544 N88-13311
An inexpensive real-time interactive three dimensional flight simulation system
[AD-A184868] 07 p0821 N88-14989
Determination of network attributes from a high resolution terrain data base
[AD-A186078] 07 p0870 N88-15279
Statistics of two-dimensional structure elements of mountainous ranges (mosaic model) for calculating three-dimensional reflection functions
[DFVLR-FB-87-33] 09 p1185 N88-17099
Target-reflectivity models for various terrain types
[DE88-005510] 11 p1505 N88-18992
Digital data dubbing capability
[AD-A188252] 11 p1525 N88-19105
Digital Topographic Support System (DTSS)
[AD-A188304] 12 p1638 N88-19808
Terrain classification from digital elevation data using slope and curvature information
[AD-A188940] 12 p1639 N88-19812
A comparison of terrain association and resection as methods of position location
[AD-A189480] 13 p1790 N88-20710
Remote sensing of earth terrain
[NASA-CR-182677] 13 p1790 N88-20711
Interpolation algorithms for digital terrain models
[INPE-4373-PRE/1196] 13 p1820 N88-20877
Modification of the BLUEMAX 2 terrain following model to incorporate radar detection
[AD-A190594] 15 p2017 N88-22028
Study of fracturing for groundwater research in the Sergipe state with remote sensing products 17 p2359 N88-24052
Updating of municipal official register of real estate through the geographical information system 19 p2684 N88-25952
Aerial photography as an instrument of atmospheric analysis: Maps of the middle atmosphere and its dynamics, Baixada Santista (SP) 19 p2684 N88-25955
Linear feature extraction from radar imagery. Phase 2: Base contract report
[AD-A192828] 21 p2931 N88-27404
Methods of determining playa surface conditions using remote sensing
[AD-A192663] 21 p2965 N88-27612
Research for reducing the labor intensive nature of high-resolution terrain analysis feature extraction
[AD-A192661] 22 p3089 N88-28345
Motion planning for legged locomotion systems on uneven terrain 23 p3221 N88-29170
Relief effect correction on LANDSAT imagery for forest applications using digital terrain models
[INPE-4611-PRE/1334] 24 p3388 N88-30179
A digital terrain model system for a microcomputer
[INPE-4610-PRE/1333] 24 p3413 N88-30316
TERRESTRIAL DUST BELT
The dust ring of the Earth
[RAE-TRANS-2163] 22 p3119 N88-28530
TERRESTRIAL MAGNETISM
U GEOMAGNETISM
TERRESTRIAL PLANETS
NT EARTH (PLANET)
NT MARS (PLANET)
NT VENUS (PLANET)
A bibliography of dunes: Earth, Mars, and Venus
[NASA-CR-4149] 20 p2885 N88-27134
TERRESTRIAL RADIATION
Radiation belts 03 p0272 N88-11707
Nimbus 7 Solar Backscatter Ultraviolet (SBUV) spectral scan solar irradiance and Earth radiance product user's guide
[NASA-RP-1199] 09 p1184 N88-17096
Net radiative flux at the Earth surface: Estimation from satellite observations 14 p1936 N88-21550
Results of radiation measurements in West Germany and from special measurement series in the Meteorological Observatory of Hamburg
[REPT-11] 18 p2542 N88-25088
Angular radiation models for Earth-atmosphere system. Volume 1: Shortwave radiation
[NASA-RP-1184] 21 p2976 N88-27677
Energy budget and ground temperatures in hot regions
[AD-A196298] 24 p3404 N88-30268
TEST BEDS
U TEST EQUIPMENT
TEST CHAMBERS
NT ANECHOIC CHAMBERS
NT HYPERBARIC CHAMBERS
NT PRESSURE CHAMBERS
NT REVERBERATION CHAMBERS
NT VACUUM CHAMBERS
Design, construction, activation, and operation of a high intensity acoustic test chamber 02 p0137 N88-10864
Man rating the b-1B molecular sieve oxygen generation system
[AD-A186275] 07 p0899 N88-15447
MBA payload testing by Compact Antenna Test Range (CATR)
[ESA-CR(P)-2473] 08 p0977 N88-15906
The ESTEC Mini Compact Antenna Test Range
[ESA-CR(P)-2475] 08 p0977 N88-15907
Environment test laboratory
[ETN-88-91885] 14 p1869 N88-21166
Study of mean free path effects on growth of ultrafine metallic aerosols
[AD-A190206] 15 p2039 N88-22149
Development of computer-controlled thermogravimetric instrumentation for measurement of environmental and high temperature volatilization and desorption of contaminants from polymeric materials
[AD-A195934] 24 p3343 N88-29900
TEST EQUIPMENT
Shielding effectiveness against electromagnetic interference
[DE88-003864] 07 p0846 N88-15131
Space station propulsion technology
[NASA-CR-179260] 08 p0964 N88-15835
Simulation test beds for the space station electrical power system
[NASA-TM-100786] 10 p1290 N88-17715
Construction aspects of testbeds for attitude control systems simulation of artificial satellites
[INPE-4283-PRE/1155] 11 p1445 N88-18616
Almond test body --- for microwave anechoic chambers
[NASA-CASE-LAR-13747-1] 18 p2502 N88-24845
Techniques utilized in the simulated altitude testing of a 2D-CD vectoring and reversing nozzle
[NASA-TM-100872] 19 p2604 N88-25464
AC power system breadboard
[NASA-CR-179369] 22 p3049 N88-28091
TEST FACILITIES
NT ANECHOIC CHAMBERS
NT BALLISTIC RANGES
NT BLOWDOWN WIND TUNNELS
NT CASCADE WIND TUNNELS
NT COMBUSTION WIND TUNNELS
NT CRYOGENIC WIND TUNNELS
NT ENVIRONMENTAL LABORATORIES
NT HOTSHOT WIND TUNNELS
NT HYDRAULIC TEST TUNNELS
NT HYPERSONIC WIND TUNNELS
NT HYPERVELOCITY WIND TUNNELS
NT LOW SPEED WIND TUNNELS
NT RECTANGULAR WIND TUNNELS
NT REVERBERATION CHAMBERS
NT ROCKET TEST FACILITIES
NT SHOCK TUNNELS
NT SLOTTED WIND TUNNELS
NT SUBSONIC WIND TUNNELS
NT SUPERSONIC WIND TUNNELS
NT TEST RANGES

NT TEST STANDS
NT TRANSIENT REACTOR TEST FACILITY
NT TRANSONIC WIND TUNNELS
NT TRISONIC WIND TUNNELS
NT WIND TUNNELS

High precision ultrasonic scanning system and SAFT-UT development
[DE87-010038] 01 p0008 N88-10044

Switching devices used in the Lethality Test System
[DE87-011734] 01 p0011 N88-10062

Anechoic Chamber test of the Electromagnetic Measurement System ground test unit
[DE87-012998] 01 p0035 N88-10226

Fourteenth Space Simulation Conference: Testing for a Permanent Presence in Space
[NASA-CP-2446] 02 p0132 N88-10829

Surveillance systems test and evaluation facilities
02 p0134 N88-10845

High intensity 5 eV O-atom exposure facility for material degradation studies 02 p0135 N88-10847

A digital control system for high level acoustic noise generation 02 p0138 N88-10865

Experiments: Test range facilities, part 2
03 p0305 N88-11921

The ac power system testbed
[NASA-CR-175068] 03 p0309 N88-11948

The LPX (Long Pulse Experiment) facility
[DE87-010493] 03 p0311 N88-11964

The LLNL 150-mm equation-of-state gun system
[DE88-000423] 04 p0405 N88-12519

Measured performance of the heat exchanger in the NASA icing research tunnel under severe icing and dry-air conditions
[NASA-TM-100116] 04 p0451 N88-12796

A survey of existing hypersonic ground test facilities: North America 05 p0529 N88-13220

High frequency data acquisition system for space shuttle main engine testing 05 p0595 N88-13630

An overview of the DOE/SANDIA/USDA vertical axis wind turbine Test Bed Project
[DE88-000604] 05 p0622 N88-13812

Feasibility study for gas-grain simulation facility
[NASA-CR-177468] 05 p0646 N88-13954

Atomic beam studies of the interaction of hydrogen with transition metal surfaces
[DE88-000208] 05 p0648 N88-13970

Aerodynamic testing of small turbines
06 p0713 N88-14371

Ground shock profiles for an accidental explosion at the proposed Large Rocket Test Facility at Arnold Engineering Development Center
[DE88-002652] 07 p0853 N88-15180

Long duration confinement of aquatic organisms in weightlessness (aquaspace) 07 p0887 N88-15380

Enhancement of computer system for applications software branch 07 p0923 N88-15610

Cavitation inception scale effects. 1. Nuclei distributions in natural waters. 2. Cavitation inception in a turbulent shear flow
[AD-A186553] 08 p0986 N88-15987

Calibration of the ARL (Aeronautical Research Laboratories) rain and icing facility
[AD-A186776] 09 p1121 N88-16710

ESA Bulletin No. 8
[ETN-87-90513] 09 p1122 N88-16718

Coordinated use of European test facilities
09 p1123 N88-16726

ESA Bulletin No. 10
[ETN-87-90514] 09 p1123 N88-16728

The European space battery test center
09 p1125 N88-16738

Major spacecraft hardware testing in Europe
09 p1125 N88-16740

Study on a double reflector compact range — satellite antennas
[S-201-05] 09 p1153 N88-16908

The assessment of the sound insulation requirements for a large broadcasting studio, using a scale model: Theoretical considerations
[BBC-RD-1987/20] 09 p1155 N88-16921

NASDA's new test facilities for satellites and rockets
11 p1499 N88-18951

Robotics applications in the testing of inertial sensors
12 p1577 N88-19433

Cost effective development of a national test bed
[NASA-TM-100321] 12 p1601 N88-19585

Transient Pressure Test Article (TPTA) 1.1 and 1.1A, volume 1
[NASA-CR-179322-VOL-1] 12 p1603 N88-19588

Aircraft flight flutter testing at the NASA Ames-Dryden Flight Research Facility
[NASA-TM-100417] 13 p1723 N88-20301

Western aeronautical test range real-time graphics software package MAGIC
[NASA-TM-100425] 13 p1757 N88-20506

Overview of recent activities in the Heat Cycle Research Program
[DE88-005544] 13 p1795 N88-20738

Configuration management issues and objectives for a real-time research flight test support facility
[NASA-TM-100437] 13 p1813 N88-20832

Activities report of the Physics Department
[ETN-88-91985] 13 p1833 N88-20964

JPRS report: Science and technology. China
[JPRS-CST-87-038] 14 p1901 N88-21350

China constructing high-altitude test cell
14 p1901 N88-21351

Materials testing at cryogenic temperatures
[BU-359] 14 p1923 N88-21462

Test facilities of the structural dynamics branch of NASA Lewis Research Center
[NASA-TM-100800] 14 p1934 N88-21534

Procedures and requirements for testing in the Langley Research Center unitary plan wind tunnel
[NASA-TM-100529] 15 p2015 N88-22016

Small engine components test facility turbine testing cell
[NASA-TM-100887] 15 p2019 N88-22037

Investigation of aeroacoustic mechanisms by remote thermal imaging
[DE88-002612] 15 p2021 N88-22046

EMR (Electromagnetic Radiation) test facilities evaluation of reverberating chamber located at RADC (Rome Air Development Center), Griffiss AFB (Air Force Base), Rome, New York
[PB88-178827] 15 p2022 N88-22048

Investigations of test methodology for the stress loading facility
[PB88-186095] 15 p2022 N88-22049

Description of ground motion data processing codes, volume 2
[DE88-007137] 15 p2095 N88-22481

Requirements and cost considerations for a Combined Space Nuclear Reactor Test Facility
[DE88-006763] 15 p2132 N88-22719

Space directorate research and technology accomplishments for fiscal year 1987
[NASA-TM-100607] 15 p2153 N88-22854

Airworthiness and flight characteristics test of a ski assembly for the UH-60A Black Hawk helicopter
[AD-A191414] 16 p2162 N88-22895

Analysis and experiments concerning the performance and calibration of compact antenna-test ranges
[ISBN-9-09-001727-5] 16 p2188 N88-23048

Aerodynamic and Related Hydrodynamic Studies Using Water Facilities
[AGARD-CP-413] 16 p2200 N88-23125

Fast Algorithm Simulation and Test (FAST) facility
[AD-A191183] 16 p2252 N88-23457

Benefits of 20 kHz PMAD in a nuclear space station
17 p2398 N88-24256

Requirements and cost considerations for a combined space nuclear reactor test facility
17 p2401 N88-24277

Conceptual design of the SP-100 GES test site
17 p2402 N88-24284

Selection of a handling and maintenance option for the SP-100 ground engineering system test
17 p2402 N88-24285

SP-100 GES test site 17 p2417 N88-24375

Liquid metal testing at ETEC for the SP-100 program
17 p2428 N88-24446

SHaRE: Collaborative materials science research
[DE88-007175] 18 p2467 N88-24646

Safety aspects in design and operation practice of GKSS underwater simulation plant GUSI
19 p2698 N88-26037

Development of a model procedure for the determination of volume diffusion lengths by transient measurements on monocrystal silicon solar cells
[ETN-88-92119] 20 p2821 N88-26733

Vibrational impacts of hush house operation
[DE88-006983] 21 p2899 N88-27207

Development of a free-electron laser user facility for the extreme ultraviolet
[DE88-007892] 21 p2953 N88-27541

Atmospheric turbulence research at DFVLR
[AGARD-R-752] 21 p2975 N88-27669

An outdoor test facility for the large-scale production of microalgae
[DE88-001146] 21 p2984 N88-27723

SP-100 Ground Engineering Systems: Test facility control systems
[DE88-009195] 21 p3015 N88-27895

Unsteady water channel
[AD-A194231] 23 p3171 N88-28884

Lewis Research Center space station electric power system test facilities
[NASA-TM-100924] 23 p3182 N88-28942

Testing degradation of a sample under thermal cycling
[GB-PATENT-2-188-163-A] 23 p3227 N88-29206

Development and design of windtunnel and test facility for RPV (Remote Piloted Vehicle) enhancement devices
[AD-A194842] 24 p3329 N88-29822

Design and development of a refueling test bed
[FTMS-RP-ER-011] 24 p3357 N88-29986

Numerical field model simulation of full scale fire tests in a closed spherical/cylindrical vessel
[AD-A195067] 24 p3359 N88-29998

Development and installation of an instrumentation package for GE F404 investigative testing
[AD-A196265] 24 p3376 N88-30107

The dynamics of transuranics and other radionuclides in natural environments, December 1985
[DE87-014456] 24 p3390 N88-30189

Maximum-likelihood multichannel deconvolution of P waves at seismic arrays
[AD-A194990] 24 p3391 N88-30191

TEST FIRING
NT STATIC FIRING

Results of the development motor 8 test firing
[GPO-78-692] 03 p0278 N88-11751

Failure control techniques for the SSME
[NASA-CR-179224] 04 p0409 N88-12537

Mechanical property evaluation of a series of commercial tungsten alloys
[AD-A185440] 05 p0565 N88-13446

Experimental investigation of a three-stage railgun incorporating puff-switching
[AD-A191044] 16 p2166 N88-22918

Orbital transfer vehicle 3000 LBF thrust chamber assembly hot fire test program
[NASA-CR-182145] 24 p3336 N88-29858

TEST PATTERN GENERATORS

Programmable Logic Arrays (PLA's) design for testability
[PB87-102935] 04 p0438 N88-12718

Short pseudorandom test sequences
[AD-A185863] 08 p1054 N88-16357

A new approach on test generation for array structures using the behavior of the system — VLSI chips
[INF-87-27] 14 p1907 N88-21397

TEST RANGES
NT BALLISTIC RANGES

AFAR (Azores Fixed Acoustic Range) measurements of intensity and intensity moments
[AD-A184431] 03 p0355 N88-12237

The PC/AT compatible computer as a mission control center display processor at Ames-Dryden Flight Research Facility
[NASA-TM-100426] 14 p1955 N88-21654

Analysis and experiments concerning the performance and calibration of compact antenna-test ranges
[PB88-169263] 16 p2188 N88-23047

Radar cross section studies/compact range research
[NASA-CR-183124] 20 p2792 N88-26565

Development of procedures for performing end-to-end tests on the ERS-1 radar altimeter and AMI using a compact antenna test range — Active Microwave Instrument (AMI)
[ESA-CR(P)-2558] 24 p3363 N88-30022

TEST STANDS

Requirements for a test stand for plastic rollers for the verification of nonequilibrium force laws
[ILR-MITT-176] 01 p0008 N88-10040

Description of an oscillating flow pressure drop test rig
[NASA-TM-100905] 16 p2170 N88-22933

Identification of lateral operation dynamics of rail vehicles using roll test stand tests
20 p2787 N88-26534

Beam optics test stand
[AD-A193901] 23 p3216 N88-29144

TEST VEHICLES

Vehicle dynamics: Identification in the frequency domain 20 p2785 N88-26523

TESTERS
U TEST EQUIPMENT

TESTES

Investigation of genetic structures of rat germ cells following flight aboard Cosmos-1514 biosatellite during their prenatal development 10 p1364 N88-18155

TESTING
U TESTS

TESTING MACHINES
U TEST EQUIPMENT

TESTS

Fire-related standards and testing
04 p0406 N88-12522

Announced United States nuclear tests: July 1945 through December 1986
[NVO-209-REV-7] 11 p1546 N88-19247

The design and fabrication of a Stirling engine heat exchanger module with an integral heat pipe
[NASA-TM-101296] 20 p2820 N88-26732

TETHERED SATELLITES
Research on Electrodynamic Tether Effects (RETE) experiment Electrical Ground Support Equipment (EGSE) --- tethered satellite
[IFSI-87-2] 05 p0555 N88-13378
RETE experiment Assembly, Integration, and Verification (AIV) activities
[IFSI-87-6] 05 p0555 N88-13380
Tethers in space handbook
[NASA-CR-181371] 06 p0673 N88-14123
Laboratory simulation of the electrodynamic interactions of a tethered satellite with an ionospheric plasma
[IFSI-86-3] 08 p0961 N88-15822
Tethers: An outline of a new concept for Earth observation 09 p1129 N88-16781
Kinetic isolation tether experiment
[NASA-CR-182458] 09 p1135 N88-16810
Deployable/retrievable boom: One application to tethered satellite 14 p1874 N88-21197
Analytical investigation of the dynamics of tethered constellations in earth orbit
[NASA-CR-179371] 23 p3184 N88-28950

TETHERING
Phase 3 study of selected tether applications in space. Volume 2: Study results
[NASA-CR-179186] 02 p0132 N88-10828
Electrodynamic tether system study
[NASA-CR-172024] 03 p0275 N88-11737
Hollow cathode plasma coupling study, 1986
[NASA-CR-171985] 03 p0309 N88-11949
Analytical investigation of the dynamics of tethered constellations in Earth orbit (phase 2)
[NASA-CR-179218] 04 p0408 N88-12533
Tethers in space handbook
[NASA-CR-181371] 06 p0673 N88-14123
Tether Elevator Crawler Systems (TECS) 07 p0927 N88-15631
Plasma contactors for use with electodynamic tethers for power generation
[NASA-CR-182424] 08 p1087 N88-16547
Kinetic isolation tether experiment
[NASA-CR-182458] 09 p1135 N88-16810
General equilibrium characteristics of a dual-lift helicopter system
[NASA-TP-2615] 12 p1573 N88-19407
Space plasma contactor research, 1987
[NASA-CR-182148] 16 p2280 N88-23649
Study of Plasma Motor Generator (PMG) tether system for orbit reboost
[NASA-CR-172074] 23 p3184 N88-28949
Analytical investigation of the dynamics of tethered constellations in earth orbit
[NASA-CR-179371] 23 p3184 N88-28950

TETHERLINES
Study of Plasma Motor Generator (PMG) tether system for orbit reboost
[NASA-CR-172016] 04 p0403 N88-12501
Tethers in space handbook
[NASA-CR-181371] 06 p0673 N88-14123
Power and charge dissipation from an electrodynamic tether 06 p0795 N88-14869
Theoretical investigation of EM wave generation and radiation in the ULF, ELF and VLF bands by the electrodynamic orbiting tether
[NASA-CR-182720] 13 p1760 N88-20529
Power transmission studies for tethered SP-100
[NASA-TM-100864] 14 p1883 N88-21251
Tethered diagnostic package for use from the space station
[DE88-006264] 16 p2167 N88-22921
Technologies applicable to space tethers
[NASA-CR-183055] 19 p2606 N88-25471

TETRAGONS
NT RECTANGLES
NT RHOMBOIDS

TETRANITROTETRAZACYCLOOCTANE
U HMX

TETRYL
A comparative assessment of US and UK explosives qualified as replacements for tetryl
[MRL-R-1094] 13 p1754 N88-20486
Recommended replacements for tetryl in Australian production fuzes and related ordnance
[MRL-R-1089] 13 p1754 N88-20489

TEXAS
Calendar year 1985 solar and weather data for Austin, Texas
[PB87-220174] 03 p0352 N88-12219
An overview of the DOE/SANDIA/USDA vertical axis wind turbine Test Bed Project
[DE88-000604] 05 p0622 N88-13812

TEXTBOOKS
Bibliography of textbooks on fibre reinforced plastics (212 books)
[PB87-146080] 07 p0827 N88-15017

TEXTILES
Solid state C-13 NMR characterization of textiles: Qualitative and quantitative analysis
[AD-A184349] 04 p0419 N88-12598
The role of textile material in clothing on thermoregulatory responses to intermittent exercise
[AD-A192599] 22 p3130 N88-28608

TEXTS
Stress effects and the optimum format of a scrolling seven-line VDT text window
[AD-A185559] 06 p0758 N88-14651
Extraction of texts and symbols from unstructured vector data --- mapping 16 p2225 N88-23287

TEXTURES
Cloud cover determination in polar regions from satellite imagery
[NASA-CR-181544] 04 p0471 N88-12908
The effect of texture on the crack growth resistance of alumina
[NASA-TM-100250] 06 p0686 N88-14206
The microstructure and texture of torsion-reverse torsion experiments
[DE88-001801] 06 p0721 N88-14434
Texture study of Synthetic Aperture Radar (SAR) images of ocean surfaces
[AD-A186021] 07 p0841 N88-15101
Textural features for image classification in remote sensing
[INPE-4169-PRE/1066] 08 p1020 N88-16181
A texture analysis approach to computer vision for identification of roads in aerial photographs
[AD-A189340] 12 p1639 N88-19815
Texture profile in thermomechanically processed 2-inch-thick 5 Ni-steel armor plate
[AD-A189275] 13 p1741 N88-20410
Micromechanical and microstructural studies of ceramic superplasticity
[DE88-005793] 13 p1751 N88-20472
A symmetric set of Euler angles and oblique orientation space sections
[DE88-005317] 13 p1847 N88-21056
Materials dependence of deformation texture development in various deformation modes
[DE88-004312] 14 p1922 N88-21457
Finding texture boundaries in images
[AD-A190554] 15 p2117 N88-22609
Investigation into the use of texturing for real-time computer animation
[AD-A191008] 16 p2251 N88-23454
Textural features for image classification in remote sensing 17 p2354 N88-24027
Remote sensing and structural rupture: Application examples in the study of tectonics 17 p2359 N88-24050
Shape from shading, occlusion and texture
[AD-A184840] 18 p2571 N88-25269
Texture perception and shape from texture
[AD-A192923] 21 p2996 N88-27771
Evaluation of automatic texture analysis for increased crop identification accuracy with SPOT data 22 p3094 N88-28373

TF-30 ENGINE
Fuel property effects on the US Navy's TF30 engine 24 p3345 N88-29911

TF-34 ENGINE
Knowledge based jet engine diagnostics 09 p1203 N88-17210
Noise assessment of unsuppressed TF-34-GE-100A engine at Warfield ANG, Baltimore, Maryland
[AD-A189966] 15 p2129 N88-22702

TFX AIRCRAFT
U F-111 AIRCRAFT

THAILAND
Thailand in maps. Application of the mapping system THEMAK2 for specific purpose atlas preparation 16 p2226 N88-23295

THALAMUS
The interaction of thalamo-cortical systems in the 40 Hz following response 21 p2979 N88-27694

THALLIUM ALLOYS
Studies of transverse phonon modes in premartensitic indium-thallium alloys
[DE88-003481] 13 p1744 N88-20428

THALLIUM COMPOUNDS
Non-linear materials (TAS)
[AD-A189197] 12 p1633 N88-19775

THAWING
U MELTING

THEMATIC MAPPERS (LANDSAT)
LANDSAT thematic mapper radiometric calibration study
[NASA-CR-182410] 07 p0872 N88-15287
Thematic mapper research in the earth sciences: Small scale patches of suspended matter and phytoplankton in the Elbe River Estuary, German Bight and Tidal Flats
[NASA-CR-182378] 08 p1019 N88-16180
Evaluation of the flooding areas of the Sao Goncalo Canal through LANDSAT 5 thematic mapper images
[INPE-4118-PRE/1039] 08 p1020 N88-16185
Detection of soil erosion with Thematic Mapper (TM) satellite data within Pinyon-Juniper woodlands
[NASA-CR-182476] 09 p1185 N88-17103
Land-use classification in a region north-west of Wuerzburg (Federal Republic of Germany) using digital, multispectral LANDSAT 5 Thematic Mapper data
[DFVLR-FB-87-37] 14 p1940 N88-21579
Method for restoration and resampling of TM sensor imagery
[INPE-4491-PRE/1255] 15 p2090 N88-22454
Turbidity patterns in the delta waters of southwest Netherlands on Thematic Mapper (TM) and multispectral scanner (MSS) satellite images
[BCRS-86-06] 16 p2227 N88-23303
The use of LANDSAT-TM pictures for the detection of space-limiting elements for the benefit of landscape photomapping
[BCRS-87-02] 16 p2228 N88-23305
Evaluation of an estimation system for an irrigated area in a tropical region through TM-LANDSAT imagery 17 p2363 N88-24075
Study of the Arachon (France) underwater delta using Thematic Mapper data 19 p2702 N88-26064
Digital and visual analysis of SPOT and TM data for crop discrimination in southern Brazil 22 p3096 N88-28385
A comparison between SPOT and LANDSAT TM for mapping of vegetation and bedrock outcrops 22 p3100 N88-28409
Accuracy of land use classification for SPOT image data 22 p3100 N88-28410
An evaluation of the utility of SPOT and Thematic Mapper data for providing forest inventory information 22 p3106 N88-28444
Evaluation of SPOT data for remote sensing of physical and biological properties of estuaries and coastal zones 22 p3108 N88-28458
TM/LANDSAT-5 data to evaluate wheat and bean percent soil cover and leaf area index
[INPE-4609-PRE/1332] 24 p3385 N88-30165
LANDSAT-TM data to map flooded areas
[INPE-4594-PRE/1324] 24 p3387 N88-30177

THEMATIC MAPPING
Remote sensing with LANDSAT 5 Thematic Mapper (TM) and its application to various planning levels: A case study from the Wuerzburg area, West Germany
[DFVLR-FB-86-62] 01 p0065 N88-10421
Development of a climatic map of rainfall attenuation for Europe
[REPT-372] 02 p0216 N88-11359
First assessment of processing and use of SPOT images by the Institut Geographique Nationale --- French National Geographic Institute 03 p0341 N88-12148
Evaluation of SPOT stereoscopic possibilities for cartography 03 p0342 N88-12156
Cartography and topography with SPOT 03 p0342 N88-12159
Vegetation classification, land systems and mapping using SPOT multispectral data: Preliminary results 03 p0342 N88-12160
The contribution of satellite data in drawing up maps used in rural development 03 p0343 N88-12167
A comparative thematic mapping analysis of SPOT data: The Vientiane Plain (Laos) 03 p0343 N88-12168
Applicability of SPOT for forest inventory, mapping and change monitoring 03 p0344 N88-12174
Evaluation of digital, multitemporal LANDSAT 5 thematic mapper data for the determination of the aerial snowcover extent and spectral separation of various surface types in the inner Oetztal (West Germany) with special regard to the significance of aerial snowcover information for water resources management
[DFVLR-FB-86-46] 03 p0345 N88-12180
New precipitation map of world ocean 04 p0458 N88-12834
Land cover/use classification of Cairns, Queensland, Australia: A remote sensing study involving the conjunctive use of the airborne imaging spectrometer, the large format camera and the thematic mapper simulator 05 p0612 N88-13759
Overview of Austrian Airborne Imaging Spectrometer (AIS) programme and first results 05 p0612 N88-13762
Mapping hydrothermally altered rocks in the Northern Grapevine Mountains, Nevada and California with the airborne imaging spectrometer 05 p0614 N88-13772
Use of space photographs for geomorphological studies in southwestern Tajikistan 08 p1008 N88-16109
Thematic mapper research in the earth sciences: Small scale patches of suspended matter and phytoplankton in the Elbe River Estuary, German Bight and Tidal Flats
[NASA-CR-182378] 08 p1019 N88-16180

Design and implementation of a data base system for Digital Land Mass System (DLMS) data
[FEL-IR-1987-19] 09 p1185 N88-17101
Mapping stellar surface features
09 p1262 N88-17564
Thematic mapper study of Alaskan ophiolites
[NASA-CR-182554] 11 p1504 N88-18984
An application of digital cartography updating middle and small scale thematic maps using orbital data
[INPE-4460-TDL/317] 12 p1637 N88-19805
Naval weapons center active fault map series
[AD-A188425] 12 p1643 N88-19835
Terrestrial gravity data and comparisons with satellite data 12 p1644 N88-19848
Inventory of topographic mapping and standardization of geographic names as the basis of a Geographic Information System (GIS) 16 p2225 N88-23281
Developments in the design of topographic maps in the Federal Republic of Germany: Activities and suggestions
16 p2226 N88-23290
The atlas of regional development
16 p2226 N88-23291
The use of LANDSAT-TM pictures for the detection of space-limiting elements for the benefit of landscape photomapping
[BCRS-87-02] 16 p2228 N88-23305
Latin American Symposium on Remote Sensing, 4th Brazilian Remote Sensing Symposium and 6th SELPER Plenary Meeting, volume 1 17 p2352 N88-24013
Utilization of TM/LANDSAT images in the implanted forests mapping in the Mogi-Guacu Region (SP-Brazil)
17 p2357 N88-24042
Thematic mapping utilizing data from the Thematic Mapper sensor of the LANDSAT satellite
17 p2361 N88-24060
Geometric image correction: An approach for the registration of LANDSAT-TM digital images supported by topographical maps of medium and great scales
17 p2361 N88-24061
Generation of thematic maps for updating aeronautical pilot charts utilizing LANDSAT-TM images
17 p2361 N88-24062
Utilization of LANDSAT-TM , for aiding in the localization of archeological sites in the state of Sao Paulo
17 p2362 N88-24069
Interpretation of MSS/LANDSAT data for evaluation of physical distribution of mangroves in Cananeia-Iguape (SP) 17 p2363 N88-24072
Utilization of LANDSAT-TM imagery in the hydroenergetic inventory of the Paraiba do Sul River Basin 17 p2364 N88-24077
Evaluation of a flood period (June, 1984) in the southern region of Laguna dos Patos, through remote sensing data, meteorological and oceanographic
17 p2365 N88-24083
Evaluation of the mangrove area at the Piaui River (SE) through remote sensing 17 p2365 N88-24086
Evaluation of TM false color composites for crop discrimination 17 p2367 N88-24096
Presentation of map information on a color display
[FOA-C-20667-2.7] 17 p2368 N88-24103
Mapping of land use in Sao Jose dos Campos municipality by remote sensing, an aid for the elaboration of its PDDI 19 p2681 N88-25940
Technique to obtain the agricultural ownership limits by satellite imagery, to approve control, and to accompany agricultural activity 19 p2682 N88-25943
The use of satellite imagery for municipal conditions in rural recording in Pereira Barreto (SP)
19 p2682 N88-25944
Use of remote sensing in the study of superficial formation certifying the development of integrated economy-case example: Rio Claro (SP) region
19 p2683 N88-25950
Canopy reflectance modeling in a tropical wooded grassland
[NASA-CR-182981] 19 p2685 N88-25961
Study of the Arachon (France) underwater delta using Thematic Mapper data 19 p2702 N88-26064
Development of automatic names placement software
[AD-A192786] 21 p2996 N88-27770
Mapping of streamflow and soil infiltration of a Sahelian catchment area by SPOT image interpretation: The Oursi pond catchment area in Burkino Faso
22 p3090 N88-28348
Comparison between the respective contributions of the TM LANDSAT-4 and HRV SPOT-1 data to the land use mapping of Mediterranean coastal zone
22 p3092 N88-28363
Delineation of ephemeral fluvial networks on low-relief Piedmont surfaces, Plutonium Valley, Nevada, USA
22 p3093 N88-28367
Use of SPOT imagery for vegetation/biomass mapping, geotechnical mapping, catchment area determination, and settlement location in the Turkana district, northern Kenya 22 p3096 N88-28384
A comparative thematic mapping analysis of SPOT data: The Vientiane Plain (Lao PDR)
22 p3096 N88-28386
Monitoring Tunisia's steppes with SPOT
22 p3097 N88-28390
Study of savannah formation in the Sudanian zone, Northwest sector of the La Comoe park, Ivory Coast
22 p3097 N88-28391
Agro-ecological mapping from SPOT 1 data in southern Thailand: New questions for an analysis of the farming-systems 22 p3097 N88-28394
A comparison between SPOT and LANDSAT TM for mapping of vegetation and bedrock outcrops
22 p3100 N88-28409
Thematic mapping of central Java (Indonesia)
22 p3100 N88-28412
Utilization of SPOT-1 multispectral data for mapping land cover and phytohygiene monitoring in the central zone of the Mercantour National Park (France)
22 p3100 N88-28413
Applications of SPOT data for urban real estate investment information systems
22 p3101 N88-28414
Mapping and urban multi-experimental assessment of SPOT: Urban results 22 p3101 N88-28415
SPOT imagery preliminary contribution to cartography and geodynamics in the Benue trough (Nigeria)
22 p3103 N88-28429
Forest mapping by visual interpretation of SPOT images 22 p3106 N88-28446
Contribution to the mapping of forests in an intensively divided area, with the help of SPOT image data
22 p3107 N88-28453
Contribution of SPOT satellite to qualitative and quantitative mapping of marine vegetation in the English Channel, North Atlantic, western Mediterranean, and South Pacific 22 p3109 N88-28464
Relevance of a thematic map (SPOT data) with regards to the real flora and structure of the vegetation covering of salt marshes (Mont Saint Michel Bay, France)
22 p3109 N88-28468
The prospects for topographic mapping using SPOT data 22 p3110 N88-28470
The use of SPOT data for mapping and DEM production -- digital elevation model (DEM)
22 p3110 N88-28475
Evaluation of SPOT cartographic capabilities over the Aix Marseille area (France) 22 p3110 N88-28476
Assessment of SPOT imagery for topographic revision and vegetation mapping 22 p3111 N88-28477
SEP/VIPS 32 geographic information system. Processing and thematic analysis of images, maps, and associated data 22 p3114 N88-28499
Spectral characteristics and the extent of paleosols of the Palouse formation
[NASA-CR-180947] 23 p3228 N88-29210

THEODOLITES
Optical alignment of Centaur's inertial guidance system
[NASA-TM-88844] 04 p0405 N88-12515

THEOREM PROVING
A note on compactifications of products of semigroups
[CWI-PM-R8701] 08 p1072 N88-16469
A proof rule process creation
[CWI-CS-R8710] 13 p1822 N88-20891
About disequations simplification
[RR-645-I-IMAG-55-LIFIA] 15 p2119 N88-22624
Correctness proofs for systolic algorithms: A palindrome recognizer
[CWI-CS-R8747] 16 p2248 N88-23434
On a classification of problems on sets of bilinear forms by formal polynomials
[RR-642-I-IMAG-53-LIFIA] 17 p2392 N88-24219
Challenge problems focusing on equality and combinatory logic: Evaluating automated theorem-proving programs
[DE88-010057] 20 p2844 N88-26879

THEOREMS
NT BAYES THEOREM
NT BERNOULLI THEOREM
NT DUALITY THEOREM
NT EXISTENCE THEOREMS
NT GAUSS-MARKOV THEOREM
NT LAGRANGE SIMILARITY HYPOTHESIS
NT LEBESGUE THEOREM
NT LIOUVILLE THEOREM
NT POYNTING THEOREM
NT RECIPROCAL THEOREMS
NT RECIPROCITY THEOREM
NT SIMILARITY THEOREM
NT UNIQUENESS THEOREM
Homogeneous space-time of Goedel type in higher-derivate gravity
[DE87-703690] 04 p0500 N88-13077
Comment on the Adler-Bardeen theorem and related problems
[DE88-751051] 10 p1403 N88-18367
Nonlinear dynamic maximum power theorem
[AD-A187491] 11 p1477 N88-18810
A graph separator theorem and its application to Gaussian elimination to optimize Boolean expressions for parallel evaluation
[AD-A188527] 14 p1962 N88-21706
Decomposition of graphs on surfaces and a homotopic circulation theorem
[CWI-OS-R8719] 16 p2264 N88-23538
Comparison theorems and their use in the analysis of some nonlinear diffusion problems
[DE88-010032] 20 p2845 N88-26884
Challenge equality problems in lattice theory
[DE88-010094] 20 p2876 N88-27072
A Wong-Zakai type theorem for certain discontinuous semimartingales
[AD-A192713] 21 p3005 N88-27822
Ill-posed problems and integral equations
[AD-A193709] 22 p3143 N88-28691

THEORETICAL PHYSICS
NT BOHR THEORY
NT NEWTON THEORY
NT QUANTUM THEORY
Theoretical plasma physics
[DE88-001475] 04 p0492 N88-13029
Theoretical atomic and molecular physics
[DE88-001625] 05 p0649 N88-13974
JPRS report: Science and technology. USSR: Physics and mathematics
[JPRS-UPM-87-008] 06 p0769 N88-14727
Computers in theoretical physics
[DE88-700516] 07 p0941 N88-15720
Theoretical nuclear physics
[DE87-004504] 09 p1244 N88-17455
Activities report in nuclear physics
[ETN-88-91609] 09 p1245 N88-17458
Research in theoretical physics
[DE88-003201] 09 p1259 N88-17548
Research in theoretical physics: Results from last year 1986/87
[DE88-004922] 10 p1423 N88-18502
Theoretical studies in few-body intermediate energy physics
[DE88-004101] 12 p1689 N88-20106
Lie groups in prolongation theory
[B8721781] 14 p1967 N88-21743
On the Fefferman class of metrics associated with a 3-dimensional Cauchy-Riemann (CR)-space
[PREPRINT-579] 14 p1991 N88-21865
Theoretical plasma physics research of active space experiments
[AD-A192075] 18 p2577 N88-25309
Theoretical atomic and molecular physics
[DE88-007122] 19 p2724 N88-26175
Theoretical studies in elementary particle physics
[DE88-006929] 20 p2851 N88-26926
Research in theoretical particle physics
[DE88-008230] 20 p2851 N88-26927
Evidence for laser emission from the TICT exciplex of coumarin dyes
[DE88-702544] 23 p3220 N88-29167
Weak interaction physics: From its birth to the electroweak model
[DE88-702494] 23 p3280 N88-29531
Theoretical studies in high energy physics
[DE88-011606] 23 p3281 N88-29538
Theoretical particle physics
[DE88-011499] 23 p3295 N88-29621
Time travel in the homogeneous Som-Raychaudhuri universe
[DE88-702220] 23 p3295 N88-29622
Holomorphic geometry of interacting string
[DE88-702714] 23 p3295 N88-29627
Introduction to string theory
[DE88-702706] 24 p3435 N88-30445

THERAPY
NT CHEMOTHERAPY
NT RADIATION THERAPY
The effects of normal and therapeutic baths on the central vascular organs of persons with healthy hearts, as measured by X-ray
[NASA-TT-20252] 13 p1811 N88-20818

THERMAL ABSORPTION
Instability of strong-absorption domain in semiconductor 08 p1077 N88-16495
Isothermal measurement and thermal desorption using SAW devices 19 p2671 N88-25881

THERMAL AGITATION
U THERMAL ENERGY

THERMAL ANALYSIS
Effects of forced and free convections on structural temperatures of space shuttle orbiter during reentry flight
[NASA-TM-86800] 01 p0043 N88-10275
Evaluation of the infrared test method for the olympus thermal balance tests 02 p0136 N88-10856
Analysis of phase equilibria in NiTi-C system in high nickel regions
[BLL-M-37304-(5828.4)] 02 p0149 N88-10932
Flammability limits in cocurrent smoldering combustion
[DE87-014102] 03 p0284 N88-11785
Comparison of flight-measured and calculated temperatures on the space shuttle orbiter
[NASA-TM-88278] 03 p0321 N88-12029
Thermal analysis of electromagnetic launcher rails
[DE88-000166] 04 p0405 N88-12514
A two-dimensional finite difference program for thermal analysis of rocket thrust chambers
[NASA-TM-100191] 04 p0409 N88-12539
Synthesis of the monoclinic yttria by thermal plasma processing
[DE88-000496] 04 p0421 N88-12608
Light funnel concentrator panel for solar power
[NASA-CR-179223] 04 p0464 N88-12870
Space station systems: A bibliography with indexes
[NASA-SP-7056(05)] 05 p0556 N88-13382
Development of an integrated BEM approach for hot fluid structure interaction
[NASA-CR-181577] 05 p0556 N88-13384
Investigation by differential scanning calorimetry of microstructure in a superplastic Al-Mg-Zr alloy
[AD-A184902] 05 p0564 N88-13439
Thermal finite-element analysis of space shuttle main engine turbine blade
[NASA-TM-100117] 05 p0610 N88-13745
Modeling of thermal effects on TIBER 2 (Thermal Ignition/Burn Experimental Reactor) divertor during plasma disruptions
[DE88-001893] 06 p0783 N88-14805
A numerical thermal model of the rapid solidification parameters in the capacitor discharge welding process
[DE88-002206] 07 p0864 N88-15244
Development of an emulation-simulation thermal control model for space station application
[NASA-CR-182409] 08 p0962 N88-15823
Space Infrared Telescope Facility (SIRTF) design and thermal analysis 08 p0982 N88-15934
Thermal analysis for the Cryogenic Fluid Management Flight Experiment (CFMFE) 08 p0982 N88-15935
Analytical interactive approach for phenomena involving structures, thermal and control aspects. Volume 1: Theory --- spacecraft structures
[ESA-CR(P)-2503-VOL-1] 09 p1134 N88-16803
Analytical interactive approach for phenomena involving structures, thermal, and control aspects. Volume 2: Toward the solution --- spacecraft structures
[ESA-CR(P)-2503-VOL-2] 09 p1134 N88-16804
Analytical interactive approach for phenomena involving structures, thermal, and control aspects. Volume 3: Executive summary --- spacecraft structures
[ESA-CR(P)-2503-VOL-3] 09 p1134 N88-16805
Review of thermal properties of graphite composite materials
[NASA-TM-100049] 09 p1139 N88-16825
Thermal wave imaging
[AD-A186810] 09 p1177 N88-17046
EXPLO: Explosives thermal analysis computer code
[DE88-001938] 10 p1307 N88-17814
Thermal analysis of transistor packages, part 2
[DE88-005091] 10 p1323 N88-17909
Microcomputer analysis of regenerative heat exchangers for oscillating flow
[DE88-001773] 10 p1329 N88-17945
Simple renormalization group method for calculating thermal equations of states
[DE88-700143] 11 p1454 N88-18668
Effect of element size on the solution accuracies of finite-element heat transfer and thermal stress analyses of space shuttle orbiter
[NASA-TM-88292] 11 p1502 N88-18971
Thermal analysis in steady state conditions for satellites
[INPE-4429-TDL/309] 12 p1599 N88-19574
Thermal properties of soil: A case study
[INPE-4332-TDL/289] 12 p1637 N88-19803
Fluid-thermal-structural study of aerodynamically heated leading edges
[NASA-TM-100579] 13 p1783 N88-20666
Analysis of shell-type structures subjected to time-dependent mechanical and thermal loading
[NASA-CR-182705] 13 p1783 N88-20668
Investigation of Super*Zip separation joint
[NASA-TM-4031] 15 p2026 N88-22072
Thermal analysis of heat storage canisters for a solar dynamic, space power system
[DE88-004199] 15 p2027 N88-22075
Boundary shape identification problems in two-dimensional domains related to thermal testing of materials
[NASA-CR-181654] 15 p2105 N88-22541
Thermal remote anemometer system
[NASA-CASE-LAR-13508-1] 17 p2342 N88-23962
Application of integrated fluid-thermal-structural analysis methods
[NASA-TM-100625] 17 p2350 N88-24001
Cermet fuel thermal conductivity
17 p2410 N88-24329
HTPIPE: A steady state heat pipe analysis program
17 p2421 N88-24396
A scientific basis for an alternate cathode architecture
[AD-A191498] 18 p2481 N88-24717
Evaluating evaporation with satellite thermal data
[AD-A192042] 18 p2531 N88-25019
Nondestructive evaluation methods for determination of thermal history and mechanical properties of aluminum-lithium alloys
[DE88-007352] 19 p2615 N88-25516
MHD (magnetohydrodynamic) thermal hydraulic analysis of three-dimensional liquid metal flows in fusion blanket ducts
[DE88-009929] 19 p2731 N88-26219
Thermal and mechanical analysis of the Faraday shield for the compact ignition tokamak
[DE88-007855] 20 p2856 N88-26962
Transient thermal analysis of three latent heat storage configurations for rapid thermal charging
[DE88-008943] 20 p2881 N88-27104
Transient thermal analysis of three fast-charging latent heat storage configurations for a space-based power system
[DE88-009714] 23 p3186 N88-28960
Adaptive computational methods for aerothermal heating analysis
[NASA-CR-181636] 23 p3212 N88-29115
Free electron lasers with small period wigglers
[DE88-011627] 23 p3218 N88-29156
Construction of gallium arsenide solar concentrator for space use
[AD-A194658] 23 p3230 N88-29222
An analysis of heat transfer after loss of primary coolant in the SP-100 reactor system
[AD-A194619] 23 p3281 N88-29539
Principles of the optical differential thermal analysis
[AD-A195951] 24 p3429 N88-30408
Evolution of thermal structure of Benguela upswelling system according to satellite and shipboard data
24 p3449 N88-30525

THERMAL BARRIERS (PLASMA CONTROL)
First and second harmonic ECRH experience at gyrotron frequencies at LLNL
[DE88-003998] 10 p1413 N88-18430
Hot electron diagnostics using X-ray imaging on GAMMA10 17 p2443 N88-24530
Thrust chamber thermal barrier coating techniques
[NASA-TM-100933] 18 p2476 N88-24690

THERMAL BATTERIES
A case study of the development of a military specification - zirconium powder for thermal batteries
[AD-A188751] 13 p1792 N88-20717
Considerations and measurements of latent-heat-storage salts for secondary thermal battery applications
[DE88-011091] 23 p3228 N88-29213

THERMAL BLOOMING
Models of high spatial frequency thermal blooming instabilities
[DE87-014280] 01 p0052 N88-10330
High spatial frequency thermal blooming instability: A linear stability analysis
[DE88-010711] 20 p2807 N88-26655

THERMAL BOUNDARY LAYER
Optical investigations of the thermal boundary layer in arc plasmas 18 p2578 N88-25313
Thermal models pertaining to continental growth
24 p3397 N88-30230

THERMAL BUCKLING
A comparison of experimental and calculated thin-shell leading-edge buckling due to thermal stresses
[NASA-TM-100416] 17 p2349 N88-23999

THERMAL CONDUCTIVITY
A numerical study of transient, thermally-conductive solar wind 01 p0115 N88-10738
Thermal resistance of contacting metal surfaces at helium temperatures
[BLL-RISLEY-TR-5500-(9091.9F)] 02 p0148 N88-10929
Development of highly porous calcium silicate hydrate materials with extremely low thermal conductivity
[BMFT-FB-T-86-164] 02 p0150 N88-10941
LLE review
[DE87-014468] 02 p0178 N88-11110
A heat transfer model for a heated helium airship
[AD-A183786] 03 p0259 N88-11629
Characterization and thermal conductivity of hot-pressed silicon carbide
[DKG-25] 03 p0292 N88-11834
Pump assisted heat pipe 03 p0319 N88-12018
Development of response models for the Earth Radiation Budget Experiment (ERBE) sensors. Part 1: Dynamic models and computer simulations for the ERBE nonscanner, scanner and solar monitor sensors
[NASA-CR-178292] 05 p0584 N88-13557
Methods and first results of plasma non-isothermal parameters measurements in meteor trails
06 p0737 N88-14531
A calorimeter for measuring the neutral beam power reaching the plasma
[DE88-001412] 07 p0937 N88-15691
Characteristics of thermooptical sound excitation in metals 08 p1076 N88-16486
Bistable cellular flames
[DE88-003074] 09 p1142 N88-16848
Characterization of transparent insulation materials --- solar energy absorbers
[ETN-88-91052] 09 p1163 N88-16970
EXPLO: Explosives thermal analysis computer code
[DE88-001938] 10 p1307 N88-17814
Influence of radiation and thermal conduction on temperature distribution in the thin wall of a hollow cylinder
[INPE-4428-TDL/308] 12 p1626 N88-19730
Effects of high temperature neutron irradiation on the physical, chemical and mechanical properties of fine-grained isotropic graphite 13 p1747 N88-20444
A segmented calorimeter for low-energy particle beams in space
[DE88-001806] 13 p1838 N88-20997
Guidelines for estimation and characterization of the thermo-mechanical properties of new optical materials
[DE88-004359] 13 p1840 N88-21010
Thermal model describing development of normal region in superconductor film carrying electric current
14 p1973 N88-21776
Thermal conductivity of oxide ceramics
[DE88-005842] 15 p2042 N88-22169
Material surface improvement by laser
15 p2051 N88-22217
Thermal conductivity, electrical conductivity and specific heat of copper-carbon fiber composite
[NASA-TT-20172] 16 p2172 N88-22948
Some aspects of the unified model of non-ideal high-parameter plasmas: Electron EOS and conduction coefficients 16 p2277 N88-23632
Optimisation of the thermoelectric figure of merit of modified silicon germanium alloys
[AD-A191347] 16 p2283 N88-23670
High-temperature thermal conductivity of a carbon-bonded carbon-fiber insulation
17 p2402 N88-24281
Uranium nitride fuel swelling and thermal conductivity correlations 17 p2409 N88-24327
Cermet fuel thermal conductivity
17 p2410 N88-24329
Development of a lightweight structure with load bearing capability and high thermal conductance
17 p2420 N88-24393
Consistent transport coefficients in astrophysics
[NASA-TM-101154] 17 p2451 N88-24580
On the magnetic structure and energy balance of EUV-emitting plasma in the quiet Sun
17 p2452 N88-24567
Analytic and numerical modeling of heat and material transport in electrical hypervelocity guns
[AD-A192178] 18 p2469 N88-24655
Thermal conductivity of hard anodized coatings on aluminum
[AD-A191755] 18 p2492 N88-24784
Thermophysical properties of argon
[DE88-010376] 19 p2613 N88-25509
Ceramic substrates for semiconductor applications reported: AlN substrates 19 p2633 N88-25621
AlN substrate applications 19 p2634 N88-25622
Thermal management of integrated microsensors
19 p2670 N88-25875
Ion thermal conductivity and ion distribution function in the banana regime
[IPPJ-865] 19 p2729 N88-26208
Thermal conductivity of selected foams and systems from 100 to 300 K
[PB88-201553] 20 p2777 N88-26466
An experimental investigation of transient characteristics in a gravity-assisted heat pipe 20 p2783 N88-26506
Boundary element method for contact heat transfer
[DE88-011013] 20 p2800 N88-26613

Physical-chemical reactions at welding arc/molten pool interfaces
[DE88-007717] 20 p2808 N88-26662
Thermal conductivity of pure fluids in a large region around the critical point
[ETN-88-92135] 20 p2881 N88-27103
Thermal conductivity and thermal expansion of stainless steels D9 and HT9
[DE88-011973] 21 p2916 N88-27306
Ceramic technology for advanced heat engines project
[DE88-008945] 21 p2919 N88-27323
Studies of dynamic contact of ceramics and alloys for advanced heat engines
[DE88-008996] 21 p2919 N88-27324
Data compilation for radiation damage on ceramic insulators. Revised with updated data and reviews
[DE88-753426] 21 p2920 N88-27329
Determination of radiative properties of fiberglass and foam insulations
[DE88-007845] 21 p2920 N88-27331
Deformation, fracture and explosive properties of reactive materials
[AD-A193080] 21 p2923 N88-27348
Thermal conductivity of isotopically pure semiconductors, superlattices, semiconductor alloys and semiconductors as a function of temperature; control of the segregation coefficient in LEC crystal growth; and photo-Hall measurements of GaAs
21 p2927 N88-27375
Coupled thermal vibrations of beams with temperature-dependent properties
21 p2963 N88-27601
Measurement of the thermal conductivity of dielectric thin solid films with a thermal comparator
[DE88-008468] 21 p3016 N88-27898
The thermal conductivity of dirty type 2 superconductors
[B8681488] 23 p3294 N88-29615
Viking Landers and remote sensing
23 p3304 N88-29685

THERMAL CONTROL COATINGS
Thermal expansion mismatch and oxidation in thermal barrier coatings 02 p0189 N88-11182
The study of excited oxygen molecule gas species production and quenching on thermal protection system materials
[NASA-CR-172027] 02 p0233 N88-11470
Discharge prevention of geosynchronous orbit conductive thermal control materials and grounding systems 03 p0274 N88-11732
Low Earth orbit environmental effects on the space station photovoltaic power generation systems
[NASA-TM-100230] 03 p0387 N88-12429
Space environmental considerations for a long-term cryogenic storage vessel 08 p0981 N88-15933
Strength and failure rate of composite materials with carbon in ceramic matrix 16 p2180 N88-22995
Evaluation of ceramic thermal barrier coatings for gas turbine engine components
[ETN-88-91947] 16 p2181 N88-22998
Space vehicle/nuclear reactor thermal radiation integration issues 17 p2424 N88-24417

THERMAL CONVECTION
U FREE CONVECTION

THERMAL CURRENTS
U CONVECTIVE FLOW

THERMAL CYCLING TESTS
Contributions to the investigation of mechanical behavior of gamma/gamma NbC Cotac composites at medium and at high temperature
[ESA-TT-1031] 03 p0280 N88-11760
Effect of long-term thermal aging on coated Celion/LARC-160 composites
[NASA-TM-100498] 04 p0410 N88-12544
Stress intensity factors for cracking metal structures under rapid thermal loading, phase 1
[AD-A184112] 05 p0591 N88-13606
The effect of thermal shock on carbon fiber epoxy composites
[FOA-C-20675-2.6] 08 p0965 N88-15841
Cost 501 Project UK10 part 3: Thermal fatigue damage of Fecralloy steel-sprayed and co-extruded tubing
[AERE-R-12230] 10 p1343 N88-18026
Dynamic tensile cyclic fatigue of Si3N4
[DE88-003919] 13 p1781 N88-20658
Overview of recent activities in the Heat Cycle Research Program
[DE88-005544] 13 p1795 N88-20738
Effect of nonuniform state of thermal stress on resistance of EI826 alloy to thermal fatigue
14 p1895 N88-21313
Some structural aspects of crack propagation in heat-resistant steels under cyclic thermal and mechanical load 14 p1896 N88-21317
A fundamental understanding of the interfacial compatibility in hybrid material systems
[AD-A192921] 21 p2909 N88-27264
Thermal cycling tests on surface-mount assemblies
[DE88-007695] 21 p2939 N88-27453
Testing degradation of a sample under thermal cycling
[GB-PATENT-2-188-163-A] 23 p3227 N88-29206

THERMAL DECOMPOSITION
NT PYROLYSIS
Surface modification by metal deposition and laser irradiation 01 p0023 N88-10148
Low temperature reactivity of chars towards oxygen, appendix E2
[DE88-004088] 10 p1298 N88-17760
Kinetics of polymer decomposition
[DE88-005500] 13 p1749 N88-20460
Analytically modeling the carbothermic reduction of alumina in a thermal plasma
[DE88-005535] 13 p1841 N88-21020
Analysis of thermal and radiation effects in materials using the GEMAT process 17 p2408 N88-24318
Thermal decomposition studies of explosives for component applications
[DE88-007201] 18 p2495 N88-24805
Kinetic measurements of thermal decomposition of energetic materials at high pressures
[AD-A191612] 19 p2622 N88-25552
Pressure differential scanning calorimetry (DSC) evaluation of solid rocket propellant burn rate mod
19 p2631 N88-25608
Simultaneous thermogravimetric modulated beam mass spectrometry and time-of-flight velocity spectra measurements: Thermal decomposition mechanisms of RDX and HMX 19 p2632 N88-25612
Laser-RDX aerosol pyrolysis with matrix isolation of unstable intermediates 19 p2632 N88-25614
Theoretical studies of the chemical reactions involved in the ignition of nitramines 19 p2632 N88-25615

THERMAL DEFOCUSING
U THERMAL BLOOMING

THERMAL DEGRADATION
Behavior of graphites under intense heat loads
[DE87-012128] 01 p0028 N88-10179
Thermo-optical modeling of flashlamp-pumped zig-zag slabs
[DE87-011878] 01 p0051 N88-10326
Glassy GeO2 obtained by the gel process
[NASA-TT-20125] 06 p0685 N88-14201
Kinetics and mechanism of thermal aging embrittlement of duplex stainless steels
[DE88-002987] 08 p0969 N88-15866
Shelf life degradation of selected anaerobic threadlocking adhesives at various storage temperatures
[AD-A187712] 11 p1481 N88-18711
Degradations of thermal shock resistance and the fracture toughness of reactor graphite subjected to neutron irradiation 13 p1747 N88-20445
Interfacial chemistry-structure and fracture of ceramic composites
[DE88-005516] 13 p1750 N88-20461
On the use of thermal degradation data to predict cable ignition performance
[DE88-002276] 19 p2621 N88-25549
Antimisting kerosene: Low temperature degradation and blending
[NASA-CR-182725] 20 p2781 N88-26495
T55-L-714 engine development and qualification. Engine M11 low cycle fatigue test report. (0213-005-87)
[AD-A192765] 21 p2897 N88-27197
Aging of CFRP due to longterm storage in heated air
[DFVLR-FB-88-05] 21 p2922 N88-27345
Perfluoropolyalkylether lubricants under boundary conditions: Iron catalysis of lubricant degradation
[AD-A193241] 21 p2956 N88-27560
Testing degradation of a sample under thermal cycling
[GB-PATENT-2-188-163-A] 23 p3227 N88-29206

THERMAL DIFFUSION
Transient development of stratification in a partially divided enclosure
[DE87-011742] 05 p0572 N88-13490
Influence of fast alpha diffusion and thermal alpha buildup on Tokamak reactor performance
[DE88-003661] 09 p1251 N88-17496
Plasma confinement calculations for TIBER-2
[DE88-004044] 10 p1412 N88-18425
Interaction of a strong vortex with decaying turbulence
[DE88-007102] 14 p1911 N88-21420
Heating at a propagating crack tip in a viscoplastic material
[AD-A190952] 16 p2224 N88-23274
The structure and stability of spherically expanding flames 17 p2318 N88-23842
High spatial frequency thermal blooming instability: A linear stability analysis
[DE88-010711] 20 p2807 N88-26655
Numerical calculations of dopent diffusion involving flashlamp heating of silicon 21 p2929 N88-27384
Heat and mass transfer in a transport channel
[DE88-701968] 21 p2945 N88-27493
Time-dependent thermal convection of Earth mantle and double diffusive convection in magma chambers
[MITT-52] 21 p2974 N88-27663

THERMAL DIFFUSIVITY
Analysis of energy confinement of slideaway discharges
[DE87-753008] 02 p0240 N88-11515
Thermal wave imaging
[AD-A186810] 09 p1177 N88-17046
Effect of experimental variables on flash thermal diffusivity data analysis
[DE88-003631] 11 p1487 N88-18877
Thermophysical properties of argon
[DE88-010376] 19 p2613 N88-25509

THERMAL DISSOCIATION
Quantitative determination of a hydrogen impurity in a sodium coolant by hydride thermal dissociation
[NASA-TT-20239] 13 p1740 N88-20402

THERMAL EFFECTS
U TEMPERATURE EFFECTS

THERMAL EFFICIENCY
U THERMODYNAMIC EFFICIENCY

THERMAL EMISSION
NT THERMIONIC EMISSION
Thermal atmospheric models
02 p0253 N88-11599
Microwave observations of nonthermal phenomena in pre-main sequence stars 04 p0505 N88-13107
Unsteady heat transfer in turbine blade ducts: Focus on combustor sources
[NASA-TM-100815] 11 p1486 N88-18870
Stratospheric trace gas distributions from fair infrared thermal emission spectroscopy
13 p1797 N88-20749
Arc-textured metal surfaces for high thermal emittance space radiators
[NASA-TM-100894] 18 p2487 N88-24754
Gamma rays from Cygnus X-1: Modeling and nonthermal pair production
[DE88-006830] 18 p2596 N88-25426
Anomalous emissivity from periodic micro-machined silicon surfaces 19 p2670 N88-25872
An objective technique for Arctic cloud analysis using multispectral AVHRR (Advanced Very High Resolution Radiometer) satellite imagery
[AD-A194732] 23 p3235 N88-29250

THERMAL ENERGY
Physical design of parameters of Nd:YAG disk laser
03 p0302 N88-11904
Heats of mixing for thermal energy storage systems. Phase 1: Selection of suitable liquid-liquid mixtures
[DE87-014971] 03 p0347 N88-12196
The numerical and analytical study of bifurcation and multicellular flow instability due to natural convection between narrow horizontal isothermal cylindrical annuli at high Rayleigh numbers 10 p1328 N88-17937
Determination of atmospheric moisture structure from high resolution MAMS radiance data
11 p1515 N88-19049
An assessment methodology for thermal energy storage evaluation
[DE88-004642] 13 p1794 N88-20732
Direct conversion of solar energy to thermal energy
[BMFT-FB-T-86-220] 14 p1943 N88-21592
Storage of thermal energy by means of an absorption cycle
[PB88-190814] 21 p2966 N88-27619
Thermal energy storage
[DE88-010753] 21 p2967 N88-27625

THERMAL ENERGY STORAGE
U HEAT STORAGE

THERMAL ENVIRONMENTS
Fourteenth Space Simulation Conference: Testing for a Permanent Presence in Space
[NASA-CP-2446] 02 p0132 N88-10829
Integration of symbolic and algorithmic hardware and software for the automation of space station subsystems
[NASA-TM-89705] 07 p0907 N88-15497
MARCE data evaluation 10 p1286 N88-17693
Characteristics of the thermal environment
[AD-A188359] 12 p1641 N88-19827
The role of water in the thermal balance of the coma
14 p1999 N88-21916
Integration of symbolic and algorithmic hardware and software for the automation of space station subsystems
17 p2387 N88-24190
Variability in intake and dehydration in young men during a simulated desert walk
[AD-A192654] 22 p3131 N88-28613
Experimental and analytical study of two-phase flow in zero gravity
[AD-A195223] 24 p3358 N88-29993

THERMAL EXPANSION
The effect of bromination of carbon fibers on the coefficient of thermal expansion of graphite fiber-epoxy composites
[NASA-TM-100236] 02 p0143 N88-10899
Carbon-fiber reinforced plastics
04 p0403 N88-12506
Study of zero CTE (Coefficients of Thermal Expansion) of graphite/epoxy composites
[DE87-013557] 04 p0412 N88-12554
Thermal expansion of some Ge-Se-Te glasses
[PD-MT-8722] 04 p0420 N88-12606
Advanced materials for solid oxide fuel cells
[DE88-002338] 10 p1350 N88-18071
The effects of various conductor components on Nb3Sn filament prestrain in cable-in-conduit conductors
[DE88-003956] 11 p1479 N88-18824
Determination of the equilibrium concentration of characteristic defects by the measurement of thermal expansion using neutron scattering and laser interferometry
[ETN-88-91489] 11 p1490 N88-18890
Properties fo seals made with Li2O-Al2O3-SiO2-glass ceramics and aluminum-containing austenitic stainless steels
[DE88-004688] 12 p1633 N88-19776
Effects of high temperature neutron irradiation on the physical, chemical and mechanical properties of fine-grained isotropic graphite 13 p1747 N88-20444
Guidelines for estimation and characterization of the thermo-mechanical properties of new optical materials
[DE88-004359] 13 p1840 N88-21010
Thermal deformation and strength of composite materials at high temperatures 14 p1885 N88-21263
Materials testing at cryogenic temperatures
[BU-359] 14 p1923 N88-21462
Thermally stable deployable structure
14 p1925 N88-21472
Thermal expansion behavior of randomly oriented short carbon fiber reinforced copper composites
[NASA-TT-20175] 15 p2031 N88-22099
Features and applications of the integrated composites analyzer (ICAN) code 15 p2078 N88-22391
Thermal stress in high temperature cylindrical fasteners
[NASA-TM-100611] 15 p2087 N88-22438
Thermal compensating mount
[NASA-CASE-LAR-13794-1] 18 p2519 N88-24942
Thermal conductivity and thermal expansion of stainless steels D9 and HT9
[DE88-011973] 21 p2916 N88-27306
Thin film-residual stress assessment
[AD-A193205] 23 p3196 N88-29018
High effectiveness contour matching contact heat exchanger
[NASA-CASE-MSC-20840-1] 23 p3214 N88-29132
Transverse expansion of individual carbon and graphite filaments
[AD-A195073] 24 p3342 N88-29891

THERMAL FATIGUE
Fatigue and thermal fatigue of Pb-Sn solder joints
[DE87-012881] 01 p0024 N88-10150
Determination of the fatigue strength of mechanically, thermally and corrosively loaded multilayer materials
[ETN-87-90375] 01 p0058 N88-10372
Fracture mechanical analysis of the initiation and propagation of matrix and surface cracks in thermally loaded fiber composite models
[ETN-87-90439] 01 p0062 N88-10400
The effect of temperature on fatigue crack initiation from aluminosilicate inclusions
[PNR90377] 02 p0154 N88-10962
Some new fatigue tests in high temperature water and liquid sodium environment
[DE87-753019] 02 p0192 N88-11197
Deformation mechanisms of thermostructural materials
[AD-A184070] 03 p0338 N88-12128
Thermal mechanical low cycle fatigue of 25CDV4-10 steel 06 p0721 N88-14429
Microstructural observations of the Sn-Pb solder/Cu system and thermal fatigue of the solder joint
[DE88-001392] 07 p0832 N88-15048
Creep and fatigue research efforts on advanced materials 09 p1119 N88-16701
Fatigue and uniaxial deformation behavior of Hastelloy XR at elevated temperatures
[DE88-751058] 09 p1145 N88-16862
Dynamic recrystallization during high temperature low cycle fatigue of nickel
[DE88-003224] 10 p1302 N88-17788
Cost 501 Project UK10 part 3: Thermal fatigue damage of Fecralloy steel-sprayed and co-extruded tubing
[AERE-R-12230] 10 p1343 N88-18026
Thermal fatigue of stainless steel
[DE88-004146] 11 p1458 N88-18694
Thermal-mechanical fatigue testing of a titanium-aluminide alloy
[AD-A189555] 12 p1609 N88-19620
Effect of nonuniform state of thermal stress on resistance of EI826 alloy to thermal fatigue
14 p1895 N88-21313
Effect of protective coatings on high-temperature fatigue of heat-resistant alloys 14 p1895 N88-21314
Effect of strain rate on high-temperature low-cycle fatigue behavior of Hastelloy X and Hastelloy XR
[DE88-752302] 15 p2037 N88-22140
Bithermal fatigue of a nickel-base superalloy single crystal
[NASA-TM-100885] 15 p2042 N88-22168
Unified constitutive model for single crystal deformation behavior with applications 15 p2078 N88-22388
Elevated temperature crack growth
15 p2084 N88-22421
Bithermal fatigue: A simplified alternative to thermomechanical fatigue 15 p2084 N88-22424
Analyses and experiments on the integrity and lifetime predictions of plasma-facing components in fusion reactors
[DE87-702957] 15 p2135 N88-22735

THERMAL GRAVIMETRY
U THERMOGRAVIMETRY

THERMAL INSTABILITY
Thermal instability and heat transfer characteristics in water/ice systems
[AD-A189627] 15 p2062 N88-22297

THERMAL INSULATION
Shear strength of the ASDEX upgrade Toroidal Field (TF) coil insulation: Rupture, fatigue and creep behavior --- tokamak
[IPP-1/230] 01 p0059 N88-10376
Thermal resistance of contacting metal surfaces at helium temperatures
[BLL-RISLEY-TR-5500-(9091.9F)]
02 p0148 N88-10929
Evaluation of the thermal effectiveness of urethane foam and fiberglass as insulation systems for tank cars
[PB88-100797] 06 p0686 N88-14207
Radiative heat transfer solutions in plane-parallel participating media: Application to multilayer insulations for space vehicles
[INPE-4221-PRE/1101] 08 p0962 N88-15824
Space environmental considerations for a long-term cryogenic storage vessel 08 p0981 N88-15933
Characterization of transparent insulation materials --- solar energy absorbers
[ETN-88-91052] 09 p1163 N88-16970
High-temperature properties of ceramic fibers and insulations for thermal protection of atmospheric entry and hypersonic cruise vehicles
[NASA-TM-100059] 10 p1295 N88-17743
Thermal analysis of transistor packages, part 2
[DE88-005091] 10 p1323 N88-17909
Ceramic-ceramic shell tile thermal protection system and method thereof
[NASA-CASE-ARC-11641-1] 11 p1448 N88-18628
Fire tests on loose-fill insulation materials
[DE88-751182] 11 p1467 N88-18748
Multilayer thermal insulation tests
[INPE-4475-PRE/1243] 12 p1626 N88-19729
Applicability of aerospace thermal insulation technologies to the civilian sector
[DE88-003717] 13 p1852 N88-21086
Fabric space radiators
[DE88-005569] 14 p1880 N88-21237
High-temperature thermal conductivity of a carbon-bonded carbon-fiber insulation
17 p2402 N88-24281
Development of refractory thermocouples for space nuclear power tests 17 p2434 N88-24478
Thermal conductivity of hard anodized coatings on aluminum
[AD-A191755] 18 p2492 N88-24784
Calculational model development for fibrous thermal insulation transient test procedures
[DE88-007843] 18 p2493 N88-24789
A monolithic gas flow sensor with polyimide as thermal insulator 19 p2669 N88-25864
Contribution to the development of coated fiber ceramic insolation material
[ETN-88-92361] 21 p2906 N88-27243
Determination of radiative properties of fiberglass and foam insulations
[DE88-007845] 21 p2920 N88-27331
The mechanical behavior of surface modified ceramics
[DE88-010564] 23 p3196 N88-29022

THERMAL MAPPING
Evaluation and certification of heater assemblies developed for thermal vacuum acceptance testing
02 p0136 N88-10853
Investigation of aeroacoustic mechanisms by remote thermal imaging
[DE88-002612] 15 p2021 N88-22046
Real time thermal imaging of high temperature semiconductor melts 17 p2330 N88-23914
Clinical applications of computerized thermography
17 p2330 N88-23915
Sky radiance distributions for thermal imaging backgrounds
[AD-A191135] 17 p2373 N88-24115
Noncontact temperature pattern measuring device
[NASA-CASE-NPO-17024-1-CU]
18 p2519 N88-24943
Image processing applied to quantitative numerical cartography of ocean circulation
19 p2702 N88-26065

THERMAL NEUTRONS
Defects in cubic silicon carbide on silicon
17 p2408 N88-24317
Interaction of slow neutrons with Ge74 single crystals
[DE87-703010] 17 p2445 N88-24536

THERMAL NOISE
Generating squeezed microwave radiation with a Josephson parametric amplifier
14 p1978 N88-21805

THERMAL PLASMAS
Synthesis of the monoclinic yttria by thermal plasma processing
[DE88-000496] 04 p0421 N88-12608
Analytically modeling the carbothermic reduction of alumina in a thermal plasma
[DE88-005535] 13 p1841 N88-21020
The effects of optical smoothing techniques on filamentation in laser plasmas
[AD-A188719] 16 p2275 N88-23614
Modelling of thermal plasma systems
18 p2578 N88-25314
Reconstruction of wave distribution functions in warm plasmas
[IRF-PREPRINT-104] 24 p3431 N88-30422

THERMAL POWER
U TURBOGENERATORS

THERMAL PROPERTIES
U THERMODYNAMIC PROPERTIES

THERMAL PROTECTION
Thermal barrier coating life prediction model development 02 p0190 N88-11183
Thermal barrier coating life prediction model development 02 p0190 N88-11184
Thermal barrier coating life prediction model development 02 p0190 N88-11185
The friction and wear of TPS fibers
[NASA-CR-181496] 03 p0291 N88-11830
Performance analysis of advanced spacecraft TPS
[NASA-CR-181532] 04 p0399 N88-12484
Space suit extravehicular hazards protection development
[NASA-TM-100458] 04 p0475 N88-12927
Advantages of internal thermal protection in a pyrotechnical plunger
[SNIAS-872-430-114] 05 p0571 N88-13478
National Aeronautics and Space Administration (NASA)/American Society for Engineering Education (ASEE) Summer Faculty Fellowship Program, 1987. Volume 2
[NASA-CR-172009-VOL-2] 06 p0796 N88-14874
Spectroscopic investigations and measurements of certain ARC jet parameters 06 p0798 N88-14877
Raman spectra of adsorbed layers on space shuttle and AOTV thermal protection system surface
06 p0799 N88-14890
Life modeling of thermal barrier coatings for aircraft gas turbine engines
[NASA-TM-100283] 07 p0834 N88-15060
In-flight rain damage tests of the shuttle thermal protection system
[NASA-TM-100438] 14 p1881 N88-21241
Aerothermal tests of quilted dome models on a flat plate at a Mach number of 6.5
[NASA-TP-2804] 15 p2067 N88-22325
Thermal stress minimized, two component, turbine shroud seal
[NASA-CASE-LEW-14212-1] 17 p2345 N88-23978
Effects of natural environment on first generation solid rocket booster thermal protection system materials
[NASA-TM-100329] 17 p2373 N88-24113

THERMAL RADIATION
NT BLACK BODY RADIATION
NT PHONON BEAMS
The effects of minor trace gases on the transfer of thermal infrared radiation through the Earth's atmosphere 04 p0468 N88-12893
Radiation curing: Comparison of heat, UV, and radiation curing
[OEFZS-4393] 06 p0689 N88-14224

Nonuniformity of electromagnetic field at Lambda = 10.6 micron wavelength inside atmospheric aerosol particles
06 p0772 N88-14743

Absorption, scattering, and thermal radiation by conductive fibers
[AD-A186105] 07 p0842 N88-15106

Commercial applications and scientific research requirements for thermal-infrared observations of terrestrial surfaces
[NASA-TM-89704] 08 p1019 N88-16179

Group 2A metastable collision complexes: Spectroscopy and behavior in intense radiation fields
[AD-A186737] 08 p1082 N88-16524

Thermal radiation from neutron stars
[MPE-203] 11 p1571 N88-19404

Fabric space radiators
[DE88-005569] 14 p1880 N88-21237

Combustion and fuels in gas turbine engines
[AGARD-CP-422] 24 p3345 N88-29910

Radiation from soot-containing flames
24 p3347 N88-29927

Flamelet chemistry modelling of soot formation for radiation
24 p3348 N88-29928

Radiation transfer in gas turbine combustors
24 p3348 N88-29929

Degradation of protective coatings on steel in corrosive environments
24 p3354 N88-29969

THERMAL REACTORS

Influence of fast alpha diffusion and thermal alpha buildup on Tokamak reactor performance
[DE88-003661] 09 p1251 N88-17496

THERMAL RESISTANCE

Polymers in solar technologies
[DE88-001102] 03 p0294 N88-11849

Technology development of a planar BiPolar transistor
[AD-A186761] 12 p1623 N88-19706

Degradations of thermal shock resistance and the fracture toughness of reactor graphite subjected to neutron irradiation
13 p1747 N88-20445

Comparison of methods for the calculation of thermal contact resistance of the first Brazilian satellite
[NASA-TT-20180] 14 p1880 N88-21239

High temperature testing of C/C (Carbon/Carbon) composites
[AD-A193012] 20 p2768 N88-26411

Heat transfer of mesh-wick heat-pipes (bottom heat mode)
20 p2783 N88-26507

THERMAL RESOURCES

NT GEOTHERMAL RESOURCES

THERMAL SHIELDING

U HEAT SHIELDING

THERMAL SHOCK

Rocket nozzle thermal shock tests in an arc heater facility
02 p0133 N88-10832

Comparison of high purity fine grain graphites from different suppliers with regard to physical, mechanical, and thermal properties — Joint European Torus wall protection
[JUEL-SPEZ-401] 02 p0154 N88-10963

Performance of low upper-shelf material under pressurized-thermal-shock loading (PTSE-2)
[DE88-002297] 07 p0832 N88-15049

The effect of thermal shock on carbon fiber epoxy composites
[FOA-C-20675-2.6] 08 p0965 N88-15841

Photohydrodynamical processes near compact objects
11 p1569 N88-19390

Degradations of thermal shock resistance and the fracture toughness of reactor graphite subjected to neutron irradiation
13 p1747 N88-20445

Notch sensitivity of graphite materials for VHTR
13 p1747 N88-20447

Response of aluminum alloys to erosive particle impacts
[DE88-005910] 15 p2041 N88-22159

Fracture mechanics 17 p2324 N88-23877

Strength optimization of alpha-SiC by improved processing 17 p2324 N88-23880

Ceramic matrix composites 17 p2325 N88-23888

An analysis of the efficiency and directivity of the sound generated by a moving laser source
[AD-A192220] 20 p2849 N88-26914

Studies of dynamic contact of ceramics and alloys for advanced heat engines
[DE88-008996] 21 p2919 N88-27324

Evaluation of fracture models through pressurized-thermal-shock testing
[DE88-011834] 21 p2963 N88-27603

THERMAL SINKS

U HEAT SINKS

THERMAL STABILITY

Pressure effects on the thermal stability of SiC fibers
[NASA-TM-100146] 01 p0019 N88-10120

Viscosity measurements at high temperatures on a standard reference material supplied by BCR — Bureau Communite de Reference (BCR)
[NPL-DMA(A)-146] 01 p0020 N88-10126

Synthesis and characterization of processable polyimides with enhanced thermal stability
[NASA-CR-181447] 01 p0030 N88-10191

A numerical study of the thermal stability of solar loops 02 p0256 N88-11619

Thermally stable aromatic structures from acyclic precursors. 1. Para polyphenylene model compounds from 3-Dimethyl amino hex-5-EN-1-YNES
[AD-A185300] 05 p0568 N88-13462

High temperature stability of superconducting YBa2Cu3O subx as characterized by X-ray diffraction
[DE88-001856] 06 p0787 N88-14824

Development and applications of new technical advances to problems of fluid/electrolyte/mineral imbalance in military personnel
[AD-A186437] 07 p0889 N88-15388

Improved perfluoroalkylether fluid development
[NASA-CR-180872] 08 p0967 N88-15851

Self-lubricating coatings for high-temperature applications 09 p1119 N88-16703

Correlations of norbornenyl crosslinked polyimide resin structures with resin thermo-oxidative stability, resin glass transition temperature and composite initial mechanical properties
[NASA-TM-100791] 09 p1147 N88-16877

Polymerization of fluorinated diacetylenes
[AD-A188051] 11 p1462 N88-18716

A novel class of positive electrodes for rechargeable batteries
[DE88-004559] 13 p1763 N88-20545

Thermal deformation and strength of composite materials at high temperatures 14 p1885 N88-21263

Effect of nonuniform state of thermal stress on resistance of EI826 alloy to thermal fatigue
14 p1895 N88-21313

Effect of oxidation on strength and thermal stability of material based on Si3N4 14 p1896 N88-21319

Dependence of formation of radiative color centers in optical glass fibers on technological factors
14 p1896 N88-21321

Thermally stable deployable structure
14 p1925 N88-21472

High-performance polymeric materials
[AD-A190708] 15 p2046 N88-22190

Stability of the high-temperature G-16 primer composition
[DE88-006201] 15 p2049 N88-22206

Electronic structure and stability of small cation and anion hydrogen clusters 16 p2267 N88-23562

SiC fiber analysis 17 p2326 N88-23891

Current and future molecular structures of aerospace organic matrix resins 18 p2477 N88-24695

A thermally modified polymer matrix composite material with structural integrity to 371 C
[NASA-TM-100922] 19 p2609 N88-25483

Defect characterization of the redox behavior and stability of conducting oxides
[DE88-010799] 20 p2878 N88-27088

Reaction-theoretical aspects of the thermal behavior of lubricating oils and working fluids
[NASA-TT-20304] 23 p3199 N88-29041

THERMAL STRESSES

Thermal stress analysis of space shuttle orbiter subjected to reentry aerodynamic heating
[NASA-TM-88286] 01 p0061 N88-10389

Reinforced flexural elements for TEMP-STRESS Program
[DE87-012961] 01 p0061 N88-10391

Thermal testing by internal IR heating of the FEP module 02 p0136 N88-10854

Stress state of welded joints of dissimilar materials obtained by diffusion welding 03 p0286 N88-11799

Comparison of measured temperatures, thermal stresses and creep residues with predictions on a built-up titanium structure
[NASA-TM-86814] 03 p0337 N88-12125

Welding and weldability of ductile intermetallic alloys
[DE87-014061] 04 p0416 N88-12582

Thermal stress in the edge cladding of Nova glass laser disks
[DE88-000425] 04 p0448 N88-12780

Thermomechanical cracking in coated media due to high speed asperity excitation
[AD-A184176] 04 p0454 N88-12809

United States - Japan Workshop on Dielectric and Piezoelectric Ceramics (3rd) held in Toyama, Japan on November 9-12, 1986
[AD-A185113] 05 p0568 N88-13460

Fluid mass and thermal loading effects on the modal characteristics of space shuttle main engine liquid oxygen inlet splitter vanes 05 p0594 N88-13628

Fracture kinetics of corrosion fatigue
05 p0605 N88-13708

The effect of heat treatment on fatigue crack growth in polycarbonate 05 p0606 N88-13714

Thermo-mechanical behavior of high temperature fiber composites 06 p0678 N88-14149

Geometrically nonlinear analysis of stiffened panels
06 p0722 N88-14440

Thermoplastic elastomers as LOVA binders
[AD-A185864] 07 p0835 N88-15067

Thermal stress analysis of a cooled monochromator crystal
[DE88-002116] 07 p0937 N88-15696

Study of the mechanical behavior of a 2-D carbon-carbon composite
[NASA-CR-182594] 11 p1451 N88-18649

Oxidation and protection of fiberglass-epoxy composite masts for photovoltaic arrays in the low Earth orbital environment
[NASA-TM-100839] 11 p1485 N88-18734

The effects of various conductor components on Nb3Sn filament prestrain in cable-in-conduit conductors
[DE88-003956] 11 p1479 N88-18824

Effect of element size on the solution accuracies of finite-element heat transfer and thermal stress analyses of space shuttle orbiter
[NASA-TM-88292] 11 p1502 N88-18971

Monolithic nature of transversely reinforced composites 14 p1885 N88-21267

JPRS report: Science and technology. USSR: Materials science
[JPRS-UMS-87-007] 14 p1895 N88-21312

Thermally stable deployable structure
14 p1925 N88-21472

The viscoplasticity theory based on overstress applied to the modeling of a nickel base superalloy at 815 C
14 p1928 N88-21499

A unified creep-plasticity model suitable for thermo-mechanical loading 14 p1932 N88-21518

Constitutive response of Rene 80 under thermal mechanical loads 14 p1932 N88-21524

Thermal analysis of heat storage canisters for a solar dynamic, space power system
[DE88-004199] 15 p2027 N88-22075

Fundamental studies on high temperature deformation recrystallization, and grain growth of two-phase materials
[AD-A189725] 15 p2038 N88-22145

A test for interfacial effects and stress transfer in ceramic matrix composites
[NASA-CR-182758] 15 p2046 N88-22194

High-temperature combustor liner tests in structural component response test facility
15 p2077 N88-22383

Specialty three-dimensional finite element analysis codes 15 p2079 N88-22393

MHOST: An efficient finite element program for inelastic analysis of solids and structures
15 p2079 N88-22394

METCAN: The metal matrix composite analyzer
15 p2079 N88-22395

Structural tailoring of high-speed turbine blades (SSME/STAEBL) 15 p2080 N88-22398

Thermostructural analysis of simulated cowl lips
15 p2080 N88-22403

Thermal-structural analyses of Space Shuttle Main Engine (SSME) hot section components
15 p2081 N88-22404

Structural analyses of engine wall cooling concepts and materials 15 p2081 N88-22405

Elevated temperature crack growth
15 p2084 N88-22421

Thermal stress in high temperature cylindrical fasteners
[NASA-TM-100611] 15 p2087 N88-22438

JPRS report: Science and technology. USSR: Materials science
[JPRS-UMS-88-006] 16 p2179 N88-22988

Model study of thermal stresses in gas-turbine blades with protective coating 16 p2179 N88-22989

Thermal stress minimized, two component, turbine shroud seal
[NASA-CASE-LEW-14212-1] 17 p2345 N88-23978

A comparison of experimental and calculated thin-shell leading-edge buckling due to thermal stresses
[NASA-TM-100416] 17 p2349 N88-23999

Computational fluid dynamics applied to the prediction of the heat-transfer, mechanical and thermal-stress behavior of heat exchangers
[CFDU/87/7] 18 p2510 N88-24893

Advanced development of the boundary element method for elastic and inelastic thermal stress analysis
18 p2529 N88-25002

Study on the heat resisting and cooling property of the ceramics-metal hybrid stator vanes
[DE88-753117] 20 p2810 N88-26668

Thermal cycling tests on surface-mount assemblies
[DE88-007695] 21 p2939 N88-27453
Coupled thermal vibrations of beams with temperature-dependent properties
21 p2963 N88-27601
Stress intensity factors for cracked metallic structures under rapid thermal loading
[AD-A191219] 23 p3193 N88-29004
Thin film-residual stress assessment
[AD-A193205] 23 p3196 N88-29018
Analytical study of graphite-epoxy tube response to thermal loads
[NASA-CR-183215] 24 p3341 N88-29884
Thermal stress analysis in PMR-15 carbon fibre laminates
[ETN-88-93123] 24 p3341 N88-29886
Transverse expansion of individual carbon and graphite filaments
[AD-A195073] 24 p3342 N88-29891
Stress intensity factors for cracked metallic structures under rapid thermal loading
[AES-8609709F-1] 24 p3353 N88-29962

THERMAL VACUUM TESTS
Meeting today's requirements for large thermal vacuum test facilities 02 p0134 N88-10840
Mobile test fixture system for use in a thermal vacuum facility 02 p0134 N88-10843
Irradiation testing 03 p0274 N88-11727
Seven year thermal vacuum real life test of a medium speed (despin) mechanism manufactured by Dornier System
[ESA-ESTL-64] 09 p1175 N88-17038
Development of a slip-ring system for energy transfer in space conditions. Space flight qualification and extended life tests
[BMFT-FB-W-86-019] 16 p2169 N88-22932
Thermal vacuum sensors based on integrated silicon thermopiles
[ETN-88-92237] 16 p2210 N88-23190

THERMALIZATION (ENERGY ABSORPTION)
The role of hydrogen thermalization in shaping the Lyman-alpha coma --- comets 14 p2007 N88-21971

THERMIONIC CATHODES
A synthetic plasma source
[TRITA-EPP-86-15] 05 p0652 N88-13995

THERMIONIC CONVERSION SYSTEMS
U THERMIONIC POWER GENERATION

THERMIONIC CONVERTERS
Irradiation test results on thermionic fuel element sheath insulators 17 p2402 N88-24280
MHW RTG performance during LES 8/9 and Voyager missions 17 p2405 N88-24300
A review of thermionic power conversion systems for SDI applications 17 p2407 N88-24310
Advanced thermionic converter technology for inductive output coupling 17 p2407 N88-24311
AMTEC electrode development
17 p2409 N88-24324
Sodium heat engine/AMTEC system experiments
17 p2409 N88-24325
Research and development of electrical insulators for thermionic applications 17 p2429 N88-24449
High power density alkaline fuel cell technology for MMW space burst power 17 p2429 N88-24451
Liquid metal thermal-electric converter electrode development
[DE88-009252] 23 p3230 N88-29221

THERMIONIC DIODES
Limiting efficiency of a thermionic diode
[DE88-700598] 11 p1479 N88-18830

THERMIONIC EMISSION
A scientific basis for an alternate cathode architecture
[AD-A191498] 18 p2481 N88-24717
Thermionic integrated circuit program
[DE88-010119] 19 p2662 N88-25833

THERMIONIC EMITTERS
A review of thermionic power conversion systems for SDI applications 17 p2407 N88-24310
Advanced thermionic converter technology for inductive output coupling 17 p2407 N88-24311

THERMIONIC POWER GENERATION
Energy storage for nuclear burst power systems
17 p2426 N88-24431
Candidate advanced energy storage concepts for multimegawatt burst power systems
17 p2426 N88-24434

THERMIONIC REACTORS
U ION ENGINES
U NUCLEAR ROCKET ENGINES

THERMIONICS
Physics and device design of vacuum integrated circuits 01 p0039 N88-10251
Thermionic Technology Program. A: Insulator test and evaluation
[DE88-004707] 13 p1795 N88-20735

THERMISTORS
Air temperature shield tests
[AD-A187459] 11 p1514 N88-19043
Studies of error in temperature measurement with thermistors in the range between continual and free-molecule flows
[NASA-TT-20302] 19 p2674 N88-25900
Effect of interfacial phenomena on contact line heat Transfer-3
[AD-A194941] 24 p3343 N88-29901

THERMOCHEMICAL PROPERTIES
NT HEAT OF COMBUSTION
NT HEAT OF FORMATION
NT HEAT OF FUSION
NT LATENT HEAT
The formation and thermochemical properties of multiligand complexes
[AD-A184935] 05 p0561 N88-13416
Phase diagrams in materials science and the use of the computer in their calculation
[PB88-155262] 18 p2586 N88-25364

THERMOCHEMISTRY
NT AEROTHERMOCHEMISTRY
NT COMBUSTION CHEMISTRY
Ultra-fine grained alloy material
[AD-A184500] 03 p0290 N88-11820
Application of solar technology to fuel production chemical processing, and thermochemical energy transport: Status and future
[DE87-014172] 03 p0346 N88-12189
The developmental status of solar thermochemical hydrogen production
[DE88-001778] 04 p0466 N88-12884
Phase diagram and thermochemical properties of the Al-Cu system
[ETN-88-91015] 05 p0566 N88-13447
A process study of the biothermal conversion of water hyacinths to methane
[DE88-000554] 06 p0730 N88-14488
Study of the vapor-liquid equilibria used in the fabrication process of hydrogen by thermochemistry
[DE88-900239] 07 p0830 N88-15035
A solar receiver-reactor with specularly reflecting walls for high-temperature thermoelectrochemical and thermochemical processes
[AD-A187612] 10 p1351 N88-18077
Evaluation and compilation of thermodynamic properties of high temperature chemical species
[AD-A187509] 11 p1452 N88-18654
Analysis of model fuels and their compatibility with selected elastomers, part 1
[AD-A188361] 12 p1612 N88-19639
Thermochemistry and high temperature thermodynamic properties of rare earth-alkaline earth-copper oxide superconductors
[DE88-005976] 15 p2140 N88-22770
An investigation of the crystalchemistry and thermochemistry of selected mineral systems
[AD-A189758] 15 p2142 N88-22781
Thermochemical analysis of mass transfer in a NB-1ZR-potassium heat pipe 17 p2412 N88-24346
Structure/property/reactivity relations among nitramine and other energetic materials
[AD-A190878] 18 p2481 N88-24716
Proceedings of the 1987 Biomass Thermochemical Conversion Contractors' Review Meeting
[DE88-006730] 18 p2535 N88-25041
Low-temperature thermochemical converaion of high moisture biomass feedstocks 18 p2536 N88-25047
Solid rocket motor performance: A workshop report
19 p2631 N88-25607
Chemical kinetics modeling of HMX combustion
19 p2633 N88-25617
Integrated solar reforming for thermochemical energy transport
[DE88-005010] 19 p2686 N88-25967
Kinetics of thermochemical gas-solid reactions important in the Venus sulfur cycle
[NASA-CR-182963] 19 p2742 N88-26280
Silicon oxidation studies: A review of recent studies on thin film silicon dioxide formation in the physics and chemistry of SiO2 and the Si-SiO2 interface
[AD-A193176] 21 p3021 N88-27932
Theoretical investigations of nitrocubane decomposition
[AD-A194556] 23 p3200 N88-29047
Chemical interactions between the present-day Martian atmosphere and surface minerals
23 p3305 N88-29689
Gas phase combustion chemistry of nitramine propellants
[AD-A195082] 24 p3344 N88-29902
Three-dimensional combustor predictors: A comparison of equilibrium and laminar flamelet chemistry models
24 p3350 N88-29940

THERMOCHROMATIC MATERIALS
Quasi-liquid crystalline materials with special electro-optic properties
[AD-A194579] 23 p3282 N88-29544

THERMOCLINES
Dynamics of isolated intrathermocline eddy
04 p0460 N88-12845
Effects of rainfall on the seasonal thermocline
[AD-A184432] 04 p0472 N88-12912
Intrathermocline lens of Mediterranean water in tropical North Atlantic 13 p1786 N88-20688
Dynamics of the Oceanic Surface Mixed Layer
[AD-A188348] 13 p1804 N88-20785
Structures and fluxes in a deep convecting mixed layer 13 p1804 N88-20786
Equatorial turbulence: Mixed layer and thermocline
13 p1804 N88-20787
Subduction 13 p1806 N88-20796
Wind forcing and observed oceanic wavenumber spectra 13 p1806 N88-20797
Monitoring ocean surface layer processes
13 p1806 N88-20801
The main ocean thermocline
14 p1938 N88-21563
An analysis of horizontal temperature gradients and heat content in the mixed layer and the surface forcing during PATCHEX
[AD-A192330] 21 p2976 N88-27678

THERMOCOUPLES
NT THERMOPILES
Temperature Metrology '86
[DE88-700236] 08 p0989 N88-15990
Investigation of thermoacoustic heat transport using a thermoacoustic couple
[AD-A186889] 09 p1242 N88-17442
Error evaluation of some practical thermocouple probes for gas turbine combustor tests
[NAL-TR-938] 11 p1489 N88-18886
Prototype thin-film thermocouple/heat-flux sensor for a ceramic-insulated diesel engine
[NASA-TM-100798] 11 p1490 N88-18892
Botany Facility. Thermal Control (TC) subsystem test report on experiment container of laboratory model and breadboard centrifuge
[BF-TN-ER-061/86] 17 p2378 N88-24135
Low cross-section Mo-Nb thermocouples for nuclear application: The state-of-the-art
17 p2433 N88-24477
Development of refractory thermocouples for space nuclear power tests 17 p2434 N88-24478
Thermocouple for heating and cooling of memory metal actuators
[NASA-CASE-NPO-17068-1-CU]
23 p3217 N88-29151

THERMODYNAMIC COUPLING
Specific heat of novel thin-film material systems
10 p1415 N88-18446
Predictions and studies with a one-dimensional ice/ocean model
[AD-A189158] 13 p1803 N88-20776
Advanced thermionic converter technology for inductive output coupling 17 p2407 N88-24311
Coupled even-parity superconducting states: Square lattice
[AD-A193432] 21 p3022 N88-27938

THERMODYNAMIC CYCLES
NT BRAYTON CYCLE
NT RANKINE CYCLE
NT STIRLING CYCLE
Analysis of shell-type structures subjected to time-dependent mechanical and thermal loading
[NASA-CR-181409] 01 p0060 N88-10388
Two-watt, 4-Kelvin closed cycle refrigerator performance 04 p0437 N88-12709
The application of liquid-metal MHD (magnetohydrodynamics) to renewable energy sources
[DE88-003083] 09 p1251 N88-17495
Nuclear electric propulsion system: Nuclear plant and thermomechanical conversion system
17 p2405 N88-24298
Studies for the definition of a Faraday converter for space nuclear systems 17 p2411 N88-24339
The liquid droplet radiator in space: A parametric approach 17 p2427 N88-24437

THERMODYNAMIC EFFICIENCY
Advanced natural gas fueled engine development. Part 1: Design and analyses
[PB87-224804] 03 p0331 N88-12087
Performance of highly concentrating mirror collectors and collector systems
[DFVLR-FB-87-29] 09 p1186 N88-17107
Nuclear electric propulsion system: Nuclear plant and thermomechanical conversion system
17 p2405 N88-24298

Preparation of improved PbSnTe thermoelectric alloys and evaluation of their figure of merit
[AD-A191346] 17 p2445 N88-24538
Computational study on thermal efficiency of ceramic gas turbine
[DE88-753114] 20 p2809 N88-26667
An analysis of the efficiency and directivity of the sound generated by a moving laser source
[AD-A192220] 20 p2849 N88-26914

THERMODYNAMIC EQUILIBRIUM
Evaluation of the infrared test method for the olympus thermal balance tests 02 p0136 N88-10656
Quasi-thermal models 02 p0253 N88-11600
Undercooling and nucleation in iron nickel alloys
[AD-A185500] 06 p0683 N88-14184
Review of nucleation and incipient boiling under pool and forced convection conditions 06 p0982 N88-15938
Spatial and temporal monitoring of the Jovian atmosphere 12 p1711 N88-20240
A thermal equilibrium model for multi-megawatt space platforms 17 p2410 N88-24332

THERMODYNAMIC PROPERTIES
NT CRITICAL POINT
NT CRITICAL TEMPERATURE
NT EMISSIVITY
NT ENTHALPY
NT ENTROPY
NT FREE ENERGY
NT GIBBS FREE ENERGY
NT HEAT OF COMBUSTION
NT HEAT OF FORMATION
NT HEAT OF FUSION
NT LATENT HEAT
NT MELTING POINTS
NT PYROELECTRICITY
NT SPECIFIC HEAT
NT SURFACE ENERGY
NT THERMAL CONDUCTIVITY
NT THERMAL DIFFUSION
NT THERMAL DIFFUSIVITY
NT THERMAL EXPANSION
NT THERMAL INSTABILITY
NT THERMAL STABILITY
NT THERMOCHEMICAL PROPERTIES
NT THERMOPHYSICAL PROPERTIES
NT VAPOR PRESSURE
NT VOLATILITY
The dissociation of dense liquid nitrogen and shock cooling
[DE87-013490] 01 p0022 N88-10136
Description of NCAR (National Center for Atmospheric Research) Community Climate Model (CCM1)
[PB87-203782] 01 p0072 N88-10462
Application of new conformal solution of theories
[PB87-214557] 01 p0105 N88-10684
Study of improved methods for predicting chemical equilibria
[DE87-014647] 02 p0145 N88-10908
The M-type stars
[NASA-SP-492] 02 p0252 N88-11592
Magnetic field morphology in the upper layers 02 p0255 N88-11610
Modelling and theories of alloy phase behavior
[DE87-014399] 03 p0287 N88-11804
The correlation between microstructure and thermomechanical properties of two-phase materials and porous sintered materials
[KFK-4205] 03 p0292 N88-11835
China report: Science and technology
[JPRS-CST-87-015] 03 p0298 N88-11873
Integrated 3-parameter diagram for determining thermodynamic properties of fluids 03 p0298 N88-11874
Study of IR laser photoacoustic spectra of organic molecules adsorbed on metal surface 03 p0301 N88-11891
Conjugated heat transfer from a radiating fluid in a rectangular channel 03 p0317 N88-12003
Effects of state recovery on creep buckling induced by thermomechanical loading 03 p0336 N88-12116
Phase transition of multifractals
[DE87-014344] 03 p0383 N88-12409
Research and development on high strength ceramic heaters discussed 04 p0404 N88-12508
Thermodynamic properties of supercritical mixtures
[DE88-000809] 04 p0413 N88-12562
Experimental study of thermocapillary flows in a thin liquid layer with heat fluxes imposed on the free surface
[NASA-TM-100252] 04 p0445 N88-12763
Thermodynamic properties for natural gas binaries
[PB87-226833] 04 p0500 N88-13074
Atmospheres of stars in the limits of thick and thin convection zones: M giants 04 p0505 N88-13105
An analytical soil thermodynamic model for the diurnal variation of ground surface temperature
[AD-A185388] 05 p0625 N88-13823
Molecular dynamics studies of aromatic hydrocarbon liquids
[DE88-001473] 05 p0648 N88-13973
Geochemistry of freezing brines, low-temperature properties of sodium chloride
[AD-A185751] 06 p0680 N88-14168
TMA-microrheological testing of polymers (thermomechanical analysis)
[PB87-228805] 06 p0683 N88-14187
Material design of high performance glasses discussed 06 p0688 N88-14216
Excess thermodynamic properties of aqueous electrolytes to high temperatures and pressures
[DE88-001768] 07 p0940 N88-15712
Determination of thermodynamic function of minerals at high temperatures
[DE88-001911] 07 p0940 N88-15713
Determination of thermodynamic function of minerals at high temperatures
[DE88-002311] 07 p0940 N88-15714
North Pacific Ocean. Subtropical front north of Hawaii, R/V Thomas G. Thompson: 7 January - 10 February 1974. CTD data report
[AD-A186565] 08 p1044 N88-16310
Thermodynamic and conductivity studies of nonstoichiometric cerium dioxide by Coulometric titration: A simultaneous measurement
[DE88-003054] 08 p1091 N88-16566
Analysis of the decomposition of transparent polymer materials (blocks) under the action of laser beams in free generation mode
[AD-A187090] 09 p1147 N88-16873
Numerical solutions of two moving boundary problems by both finite difference and finite element methods with applications
[DE88-002867] 09 p1230 N88-17374
Calculation and design of a ramjet missile
[REPT-TR-500] 10 p1311 N88-17832
Chemical activation of molecules by metals: Experimental studies of electron distributions and bonding
[DE88-004465] 10 p1407 N88-18393
Utilization of the JANAF (Joint Army Navy Air Force) database for chemical thermodynamic calculations
[DE88-004571] 10 p1423 N88-18501
Evaluation and compilation of thermodynamic properties of high temperature chemical species
[AD-A187509] 11 p1452 N88-18654
Documentation for computer code NACL
[LBL-21859] 11 p1531 N88-19145
Vibrational, mechanical and thermal properties of 3-5 semiconductors
[AD-A187569] 11 p1556 N88-19316
Hot corrosion in gas turbines: A new, unique and informative technique is EASE (Electronic Absorption Spectroscopy Experiments)
[AD-A188508] 12 p1583 N88-19470
Thermal properties of soil: A case study
[INPE-4332-TDL/289] 12 p1637 N88-19803
MOPAC manual: A general molecular orbital package, fourth edition
[AD-A188623] 13 p1733 N88-20362
High-temperature metal matrix composites
[AD-A189516] 13 p1734 N88-20367
Properties of molecular solids and fluids at high pressure and temperature
[DE88-004195] 13 p1738 N88-20391
Liquid alloys: New perspectives and challenges
[DE88-005935] 13 p1750 N88-20463
Thermodynamic theory of fluctuations and Rayleigh light scattering in solutions 13 p1785 N88-20681
The thermodynamic properties of organic oxygen compounds
[DE88-001208] 13 p1849 N88-21065
Rapid e-beam heating for measuring thermodynamics of metastable materials
[DE88-003565] 13 p1849 N88-21066
Review of selenium thermodynamic data
[DE88-006194] 13 p1849 N88-21068
Prediction of high-temperature thermodynamic properties of mixed electrolyte solutions including solubility equilibria, vapor pressure depression and boiling point elevation
[DE88-006344] 13 p1849 N88-21069
On the theory of the conversion of metallic mixed phases. 5: Fluctuations and nucleation in sub-cooled phases
[NASA-TT-20249] 14 p1890 N88-21296
Prediction of thermodynamic properties, including solubility equilibria and vapor pressures, for mixed aqueous electrolytes to high temperatures
[DE88-006317] 14 p1990 N88-21863
The thermal radiative properties of metals at high temperature
[DE88-006625] 15 p2038 N88-22141
Thermochemistry and high temperature thermodynamic properties of rare earth-alkaline earth-copper oxide superconductors
[DE88-005976] 15 p2140 N88-22770
Value of energy storage in pulsed space power systems
[AD-A191311] 16 p2170 N88-22938
TVC (Thrust Vector Control) jet vane thermal modeling using parametric system identification
[AD-A191518] 18 p2474 N88-24678
The thermodynamic properties of quinoline and isoquinoline
[DE88-001218] 18 p2484 N88-24735
Dynamic consolidation of metal powders
[AD-A192126] 18 p2485 N88-24744
An evaluation of some thermodynamic and transport properties of solid and liquid lithium over the temperature range 200 to 1700 K
[DE88-008947] 19 p2614 N88-25512
Mixing and thermodynamic critical phenomena of combusting monopropellant sprays 19 p2623 N88-25558
The development of a user friendly thermodynamic code for the personal computer 19 p2623 N88-25559
Dimensional analysis and experimental observation of the coupling phenomena between combustion and fracture of damaged propellant samples 19 p2630 N88-25603
On 3-5 transistors for MM-wave applications
[AD-A191580] 19 p2661 N88-25825
Radiative heat transfer and selective emission in planar slab coatings on hot emissive substrates
[AD-A193133] 21 p2918 N88-27319
An analysis of horizontal temperature gradients and heat content in the mixed layer and the surface forcing during PATCHEX
[AD-A192330] 21 p2976 N88-27678
Some theoretical considerations of the surface tension of liquid metals for metal matrix composites
[AD-A195999] 24 p3340 N88-29882
Thermomechanical computations for GAP, a high energy binder for composite propellants
[FOA-C-20718-2.1] 24 p3357 N88-29988
Particle trajectories and potentials in a plane sheath moving in a magnetoplasma
[AD-A196228] 24 p3390 N88-30190
The origin of the moon: Further studies of the giant impact 24 p3440 N88-30474

THERMODYNAMICS
NT AEROTHERMODYNAMICS
NT COMBUSTION PHYSICS
NT NONEQUILIBRIUM THERMODYNAMICS
Hot-spot reaction in unsustained shocks
[DE87-011781] 01 p0044 N88-10277
Thermodynamics of interaction between nitrogen and molten nickel alloys
[BLL-M-37309-(5828.4)] 02 p0149 N88-10934
Energy changes in transforming solids
[DE87-011257] 02 p0191 N88-11194
Application of new conformal solution theories
[PB87-211934] 02 p0247 N88-11558
A heat transfer model for a heated helium airship
[AD-A183786] 03 p0259 N88-11629
The Proceedings of the Symposium on Mechanics for Space Flight
[ISAS-SP-5] 03 p0317 N88-12006
Retention processes in supercritical fluid chromatography
[DE88-000079] 04 p0413 N88-12559
Model for ultrasonic attenuation and elastic constant in chromium and its alloys
[DE87-703478] 04 p0415 N88-12570
Use of a thermodynamic analog for pneumatic transport in horizontal pipes
[AD-A184076] 04 p0441 N88-12740
Coupled acoustic and ocean thermodynamic model
[AD-A184357] 04 p0472 N88-12911
Non-lattice matched metallic superlattices
[DE87-011512] 04 p0497 N88-13062
Ionic transport and electrical relaxation in glass
[DE88-000887] 05 p0657 N88-14028
Calendar of selected aeronautical and space meetings
[AGARD-CAL-87/1] 05 p0657 N88-14033
Thermo-mechanical behavior of high temperature fiber composites 06 p0678 N88-14149
Reactions and bonding between glasses and titanium
[DE88-000603] 06 p0685 N88-14195
On the interconnection of dynamic processes in the lower thermosphere with meteorological phenomena in the tropostratosphere 06 p0734 N88-14512
The nonlinear thermodynamics of meteors, noctilucent clouds, enhanced airglow and global atmospheric circulation 06 p0738 N88-14538

Thermodynamic values from computer summation of group additivity data
[AD-A186131] 07 p0940 N88-15711
Investigations in field of surface forces in metallurgy
[BLL-M-47406-(5828.4)] 08 p0969 N88-15860
Zero-G thermodynamic vent system for shuttle/Centaur 08 p0983 N88-15943
Use of the thermodynamic evaporation formula of Hoffmann in energy balance models for flowing water 08 p1013 N88-16143
A study of the free energy of the Lenz-Ising model using the cluster variation method of Morita
[AD-A186023] 08 p1073 N88-16476
Thermodynamic and conductivity studies of nonstoichiometric cerium dioxide by Coulometric titration: A simultaneous measurement
[DE88-003054] 08 p1091 N88-16566
The role of thermodynamic phase diagrams and lattice matching in superlattice growth
[DE88-003113] 08 p1091 N88-16568
An analysis of the closure conditions for two-fluid models of two-phase flow
[DE88-003355] 09 p1164 N88-16982
Investigation of thermoacoustic heat transport using a thermoacoustic couple
[AD-A186889] 09 p1242 N88-17442
Metal hydrides
[DE88-005083] 10 p1299 N88-17766
A large strain thermomechanical forming model for elastic-viscoplastic behavior in metals 10 p1301 N88-17780
Collaborative studies of polar cap ionospheric dynamics
[AD-A187888] 10 p1355 N88-18098
Nonmonotonic evolution and thermodynamic trends at metal/(Hg,Cd)Te interfaces: Yb/Hg0.78Cd0.22Te
[AD-A187591] 10 p1422 N88-18490
Studies in finite time thermodynamics
[DE88-004531] 10 p1423 N88-18500
Utilization of the JANAF (Joint Army Navy Air Force) database for chemical thermodynamic calculations
[DE88-004571] 10 p1423 N88-18501
Velocity reversal and the arrows of time
[DE88-004237] 10 p1429 N88-18536
Analysis of shear-layer probe data for holes in hypersonic configurations
[DE88-003992] 11 p1435 N88-18564
Fundamental studies of corrosion of nonoxide structural ceramics
[PB88-141536] 11 p1461 N88-18709
Mechanisms in thermal mechanical forming of plates
[AD-A187797] 11 p1466 N88-18744
Thermodynamics of wetting by liquid metals
[DE88-003634] 11 p1563 N88-19360
A continuum damage model for viscoelastic materials
[AD-A189426] 12 p1637 N88-19800
Oxidation/sulfidation of materials in an SO3/SO2/O2 thermochemical-transport, distributed-receiver, solar-energy system
[DE88-005875] 13 p1795 N88-20739
Dynamical modeling of marine boundary layer convection 13 p1797 N88-20750
Predicting oscillatory finite difference solutions to the heat equation: A comparative study of the coefficient and matrix methods
[AD-A189591] 13 p1825 N88-20911
Two studies of nonlinear processes in irreversible thermodynamics
[DE88-005794] 13 p1849 N88-21067
Electrohydrodynamic migration of charged droplets in an insulating fluid
[NASA-TM-100849] 14 p1912 N88-21424
A viscoplastic theory applied to copper
[NASA-TM-100831] 14 p1928 N88-21497
Elements of sea ice dynamics and thermodynamics 14 p1939 N88-21571
Nucleation in super-saturated products
[NASA-TT-20275] 15 p2037 N88-22134
The age hardening response of thermomechanically processed Al-Mg-Li alloys
[AD-A189870] 15 p2039 N88-22147
Comparison of entropy generation and conventional design methods for heat exchangers
[AD-A190256] 15 p2064 N88-22306
Nondestructive evaluation of sintered ceramics 15 p2083 N88-22416
Sequential tests for the drift of a Wiener process with a smooth prior and the heat equation
[AD-A190322] 15 p2121 N88-22638
Advanced chemical heat pumps using liquid-vapor reactions
[DE88-006760] 16 p2205 N88-23159
Models in nonlinear thermomechanics. Finite element models and constitutive models for large deformation elastoplasticity
[ETN-88-92240] 16 p2222 N88-23262
Thermodynamic modeling of the no-vent fill methodology for transferring cryogens in low gravity
[NASA-TM-100932] 18 p2476 N88-24686
Isothermal and bithermal thermomechanical fatigue behavior of a NiCoCrAlY-coated single crystal superalloy
[NASA-TM-100907] 18 p2489 N88-24766
Advanced development of double-injection, deep-impurity semiconductor switches
[NASA-CR-182118] 18 p2583 N88-25346
Vacancy ordering in the basal plane of YBa2Cu3O(sub)z
[DE88-004572] 18 p2583 N88-25348
The morphological stability of continuous intergranular phases: Thermodynamic considerations
[DE88-006328] 18 p2584 N88-25350
Phase diagrams in materials science and the use of the computer in their calculation
[PB88-155262] 18 p2586 N88-25364
Study of data distributions and functions for the development of thermodynamic equations of state
[PB88-196365] 18 p2587 N88-25370
Mass spectrometric high temperature measurements of the barium oxide-zirconium dioxide system and the determination of thermodynamic data for barium zirconate. Clarification of the counter-stopping capacity of coated particles for solid fission products by zirconium dioxide addition
[NASA-TT-20187] 19 p2611 N88-25496
Next-generation fire extinguishing agent. Phase 1: Suppression concepts
[AD-A192279] 19 p2614 N88-25514
Initial value problems for nonlinear heat equations
[DE88-702021] 19 p2737 N88-26251
Thermo field dynamics and para statistical mechanics
[DE88-702057] 19 p2737 N88-26253
Thermostatistical estimations of vapor-state molecules affected by gravity in a heat pipe 20 p2783 N88-26505
Electrodynamic driver for the space thermoacoustic refrigerator (STAR)
[AD-A192337] 20 p2785 N88-26517
On microphysical principles of thermofluid dynamics
[ETN-88-92095] 20 p2801 N88-26620
Thermodynamic analysis of chemical heat storage system for heat pump
[DE88-753121] 20 p2820 N88-26728
Non-equilibrium phases and phase diagrams
[DE88-008896] 20 p2880 N88-27098
Thermomechanical processing of Al alloy 2090 for grain refinement and superplasticity
[AD-A192333] 21 p2912 N88-27281
Finite element methodology for integrated flow-thermal-structural analysis
[NASA-CR-183144] 21 p2964 N88-27606
Air-sea interaction in the vicinity of a land-sea boundary in the presence of upwelling 21 p2973 N88-27661
A study of tunneling phenomena in gallium arsenide-aluminum gallium arsenide heterostructures 21 p3023 N88-27946
The dynamics and thermodynamics of a 30-60 day oscillation 22 p3121 N88-28543
Thermodynamic data bases for multivalent elements: An example for ruthenium
[DE88-004395] 23 p3190 N88-28984
The construction of the thermoelasticity equations on the basis of contemporary notions of nonlinear continua mechanics
[NASA-TT-20307] 23 p3296 N88-29631
Experimental and analytical study of two-phase flow in zero gravity
[AD-A195223] 24 p3358 N88-29993

THERMOELASTICITY
A comparison of high damping shape memory alloys with Cu-Mn-based and Fe-Cr-based alloys
[AD-A184110] 04 p0414 N88-12566
A dissipation principle and its consequences for structured shock waves in thermoelastic materials
[DE87-013723] 04 p0454 N88-12813
On stress collapse in adiabatic shear bands
[AD-A187185] 11 p1498 N88-18942
Coupled thermal vibrations of beams with temperature-dependent properties 21 p2963 N88-27601
A transversely isotropic thermoelastic theory
[NASA-TM-101302] 22 p3087 N88-28332
The construction of the thermoelasticity equations on the basis of contemporary notions of nonlinear continua mechanics
[NASA-TT-20307] 23 p3296 N88-29631
Report on an overseas visit to USA relating to the thermoelastic measurement of stresses, 16-21 August 1987
[AD-A195313] 24 p3385 N88-30161

THERMOELECTRIC CONVERSION SYSTEMS
U THERMOELECTRIC POWER GENERATION

THERMOELECTRIC COOLING
Comparison of a thermoelectric cooling system and a groundwater heat pump
[DE88-001753] 08 p0984 N88-15950

THERMOELECTRIC GENERATORS
NT SNAP 19
General-Purpose Heat Source Safety Verification Test Program: Edge-on flyer plate tests
[DE87-006309] 03 p0376 N88-12362
Speculations on future opportunities to evolve Brayton powerplants aboard the space station 17 p2398 N88-24258
The Light-Weight Radioisotope Heater Unit (LWRHU): Development and application 17 p2405 N88-24299
Pioneer 10 and 11 RTG performance update 17 p2405 N88-24301
A review of thermionic power conversion systems for SDI applications 17 p2407 N88-24310
Optimization of SP-100 thermoelectric electromagnetic pump 17 p2418 N88-24382
Status of modular RTG technology 17 p2422 N88-24403
Weldability of general purpose heat source iridium capsules 17 p2426 N88-24429
Ceramic electrical insulator development for thermoelectric SACE power system 17 p2430 N88-24459
Study on iron disilicide thermoelectric generator
[AD-A193082] 22 p3116 N88-28517

THERMOELECTRIC MATERIALS
Improved GaP doped SiGe thermoelectric material 17 p2437 N88-24503

THERMOELECTRIC POWER GENERATION
Point defect structure of Cr2O3
[AD-A187620] 11 p1556 N88-19317
The results of application studies for space nuclear power 17 p2398 N88-24259
MHW RTG performance during LES 8/9 and Voyager missions 17 p2405 N88-24300
AMTEC electrode development 17 p2409 N88-24324
Sodium heat engine/AMTEC system experiments 17 p2409 N88-24325
A dynamic model for the aft accumulator in the TE SP-100 system 17 p2414 N88-24354
Parametric analyses of the TE SP-100 system performance 17 p2415 N88-24358
SP-100 system modeling: SNPSAM update 17 p2417 N88-24372
A nuclear powered space based multimegawatt MHD disc power system 17 p2432 N88-24471
Alkali metal thermoelectric converter design for space power systems applications 17 p2437 N88-24499
A capillary pumped SHE/AMTEC system 17 p2437 N88-24500
High power density electrodes for AMTEC 17 p2437 N88-24501
Performance of vapor-fed sodium heat engine/AMTEC systems 17 p2437 N88-24502
Preparation of improved PbSnTe thermoelectric alloys and evaluation of their figure of merit
[AD-A191346] 17 p2445 N88-24538
Liquid metal thermal electric converter theoretical and experimental studies
[DE88-008806] 19 p2688 N88-25974
Study on iron disilicide thermoelectric generator
[AD-A193082] 22 p3116 N88-28517

THERMOELECTRICITY
Effect of high-temperature annealing on the microstructure and thermoelectric properties of GaP doped SiGe
[NASA-TM-100164] 01 p0029 N88-10188
Thermoelectric power in disordered electronic systems near the Anderson transition
[PREPRINT-547] 06 p0731 N88-14494
Electrothermal instability in superconducting resonators
[DE88-701684] 16 p2282 N88-23664
Optimisation of the thermoelectric figure of merit of modified silicon germanium alloys
[AD-A191347] 16 p2283 N88-23670
Preparation of improved PbSnTe thermoelectric alloys and evaluation of their figure of merit
[AD-A191346] 17 p2445 N88-24538
Improved properties of SiGe/GaP alloys
[NASA-CASE-NPO-17259-1-CU] 18 p2585 N88-25358
Anomalous dependence of the thermoelectric power on the temperature in YBaCuO high-T(sub c) superconducting samples
[DE88-702682] 23 p3292 N88-29605

THERMOGRAMS
U RECORDING INSTRUMENTS
U TEMPERATURE MEASURING INSTRUMENTS

THERMOGRAPHY
Evaluating and testing thermographic phosphors for turbine-engine temperature measurements
[DE87-011772] 02 p0174 N88-11090
Calibration of a laser-pumped, thermographic phosphor remote thermometry system
[DE88-000452] 04 p0449 N88-12781
Measurement and control of damage in composite materials: Nondestructive controls by thermography, holography, and radiography
[SNIAS-872-430-110] 05 p0559 N88-13403
Geological evolution and analysis of confirmed or suspected gas hydrate localities. Volume 10: Basin analysis, formation and stability of gas hydrates of the Aleutian Trench and the Bering Sea
[DE88-001008] 10 p1346 N88-18048
Noncontact thermometry via laser pumped, thermographic phosphors: Characterization of systematic errors and industrial applications
[DE88-005599] 13 p1777 N88-20628
Clinical applications of computerized thermography
17 p2330 N88-23915
Thermographic detection of buried debonds
[AD-A192115] 18 p2475 N88-24680
Nondestructive testing using ultrahigh frequencies
[CERT-5/1333-MO] 18 p2526 N88-24984
Image processing applied to quantitative numerical cartography of ocean circulation
19 p2702 N88-26085
Stress analysis using infrared thermography
[ETN-88-92169] 20 p2816 N88-26705
Improvements in techniques of microwave thermography
[AD-A194613] 23 p3203 N88-29062
Improvements in techniques of microwave thermography
[AD-A193620] 23 p3239 N88-29276

THERMOGRAVIMETRY
Simultaneous TG/DSC (thermogravimetry/Differential Scanning Calorimetry) and TG/MS (thermogravimetry/Mass Spectrometry) analyses of polymeric and energetic materials
[DE88-000727] 04 p0413 N88-12561
Thermogravimetric analysis of polymeric materials for an intermediate temperature solid electrolyte
[DE88-004854] 10 p1306 N88-17809
Analysis of thermal and radiation effects in materials using the GEMAT process 17 p2408 N88-24318
Simultaneous thermogravimetric modulated beam mass spectrometry and time-of-flight velocity spectra measurements: Thermal decomposition mechanisms of RDX and HMX 19 p2632 N88-25612
Development of computer-controlled thermogravimetric instrumentation for measurement of environmental and high temperature volatilization and desorption of contaminants from polymeric materials
[AD-A195934] 24 p3343 N88-29900

THERMOHYDRAULICS
Low gravity fluid-thermal experiments
[DE88-000553] 04 p0423 N88-12620
A model for stationary and dynamic impression of undercooled boiling in coupled thermohydraulic and neutron physics calculations of nuclear reactors
[IKE-6-171] 09 p1247 N88-17472
Thermal-hydraulic considerations for particle bed reactors 17 p2400 N88-24266
ATHENA heat pipe transient model
17 p2412 N88-24344
Transient thermohydraulic heat pipe modeling
17 p2413 N88-24347
SP-100 control system modeling
17 p2414 N88-24356
ATHENA simulation of the 300 kW SP-100
17 p2414 N88-24357
Expert systems approach to modeling systems with the ATHENA thermal-hydraulics code
17 p2416 N88-24365
The THROHPUT code: Thermohydraulic heat pipe modeling 17 p2421 N88-24399
Study of a water-steam two phase flow in a T-branch
[ETN-88-92306] 20 p2801 N88-26624

THERMOMECHANICAL TREATMENT
NT HOT ISOSTATIC PRESSING
NT HOT PRESSING
Development of iron aluminides
[AD-A185190] 05 p0568 N88-13461
Interrelation and measurement of formability, strengthening, and thermomechanical processing under metalworking conditions
[DE88-002485] 08 p0967 N88-15850
Grain refinement during primary breakdown of alloy 718
[DE88-005193] 13 p1743 N88-20423
Simulation of thermo-mechanical forming processes: A mixed Eulerian-Langrangian finite element method
[PB88-155247] 14 p1933 N88-21530
Experiments investigating advanced materials under thermomechanical loading 15 p2077 N88-22385
METCAN: The metal matrix composite analyzer
15 p2079 N88-22395

THERMOMECHANICS
U THERMODYNAMICS

THERMOMETERS
NT RESISTANCE THERMOMETERS
Assessment of the reliability of a correction procedure for WGT (Wet Globe Thermometer) (Botsball) measurements of heat stress
[AD-A185193] 05 p0584 N88-13559
Temperature Metrology '86
[DE88-700236] 08 p0989 N88-15990
Johnson noise thermometer for high radiation and high temperature environments
[DE88-003770] 10 p1323 N88-17911
Air temperature shield tests
[AD-A187459] 11 p1514 N88-19043
Radiation thermometry: The measurement problem
17 p2328 N88-23896
Johnson noise thermometer for high-radiation and high-temperature environments
17 p2434 N88-24480
Evaluation of thermophosphor temperature technique
[DE88-007654] 20 p2805 N88-26638

THERMOMETRY
U TEMPERATURE MEASUREMENT

THERMONUCLEAR ENERGY
U THERMONUCLEAR POWER GENERATION

THERMONUCLEAR POWER GENERATION
Applications of neutral beam and rf technologies
[DE87-014936] 03 p0379 N88-12382
Study of Plasma Motor Generator (PMG) tether system for orbit reboost
[NASA-CR-172016] 04 p0403 N88-12501

THERMONUCLEAR PROPULSION
U NUCLEAR PROPULSION

THERMONUCLEAR REACTIONS
NT CONTROLLED FUSION
NT NUCLEAR FUSION
Fusion reactivity enhancement due to ion tail formation by beam and ion cyclotron heating
[DE87-753018] 02 p0240 N88-11518
A model for stationary and dynamic impression of undercooled boiling in coupled thermohydraulic and neutron physics calculations of nuclear reactors
[IKE-6-171] 09 p1247 N88-17472
Flame propagation in the approximation of straight-line trajectories of burning products
[DE88-700675] 10 p1297 N88-17756
Diffusion description of flame propagation due to the translational motion of burning reaction products
[DE88-700676] 10 p1297 N88-17757
Preliminary analysis on plasma equilibrium control. Conceptual design study of FY86 FER
[DE88-751441] 14 p1984 N88-21834
Rayleigh-Taylor instability in inertial confinement fusion
[DE88-701411] 15 p2137 N88-22750
BIFOLD: A dual-mode nuclear space power system
17 p2404 N88-24292
TIBER (Tokamak Ignition/Burn Experimental Reactor) 2 as a precursor to an international thermonuclear experimental reactor
[DE88-008906] 20 p2858 N88-26970
The classical nova outburst
[DE88-009138] 21 p3030 N88-27987

THERMOPHILIC PLANTS
NT BLUE GREEN ALGAE

THERMOPHORESIS
Thermophoresis of spherical aerosol particle at arbitrary Knudsen numbers 04 p0461 N88-12850
Atmospheric science 07 p0883 N88-15357

THERMOPHYSICAL PROPERTIES
NT CRITICAL POINT
NT CRITICAL TEMPERATURE
NT EMISSIVITY
NT HEAT OF FUSION
NT LATENT HEAT
NT MELTING POINTS
NT PYROELECTRICITY
NT SPECIFIC HEAT
NT THERMAL CONDUCTIVITY
NT THERMAL DIFFUSION
NT THERMAL DIFFUSIVITY
NT THERMAL STABILITY
NT VAPOR PRESSURE
NT VOLATILITY
PRMIXn: A computer program for thermophysical properties of real gases and gas mixtures
[GKSS-86/E/59] 01 p0020 N88-10125
Thermophysical Properties Measurement Facility (TPMF) — Columbus space station
[ESA-CR(P)-2417] 02 p0157 N88-10981
Growth of solid solution single crystals
[NASA-TP-2787] 06 p0688 N88-14212
A theoretical and experimental study of the thermophysical properties of lithium hydride
[NASA-TT-20179] 16 p2175 N88-22965
Phase equilibria and density calculations in the critical region: A phenomenological correction for a classical equation of state
[PB88-185335] 19 p2723 N88-26167

THERMOPHYSICS
U THERMODYNAMICS

THERMOPILES
Thermal vacuum sensors based on integrated silicon thermopiles
[ETN-88-92237] 16 p2210 N88-23190

THERMOPLASTIC FILMS
Molecular composites: Processing, post-treatment and mechanics
[AD-A184458] 04 p0410 N88-12547

THERMOPLASTIC RESINS
NT PEEK
NT THERMOPLASTIC FILMS
Interfacial strength development in thermoplastic resins and fiber-reinforced thermoplastic composites
[NASA-CR-181525] 04 p0411 N88-12549
Thermoplastic elastomer compositions — cable jackets
[EP-PATENT-0-204-453-A1] 04 p0418 N88-12593
Thermoplastic elastomers as LOVA (Low Vulnerability Ammunition) binders
[AD-A184350] 04 p0419 N88-12599
Process for the production of a thermoplastic elastomer composition
[EP-PATENT-0-202-782-A2] 05 p0569 N88-13465
Flexibilized copolyimide adhesives
[NASA-TM-89303] 05 p0570 N88-13474
Development of an impact- and solvent-resistant thermoplastic composite matrix, phase 4
[NASA-CR-178413] 06 p0677 N88-14145
An investigation of physical properties of thermoplastic polyimides
[NASA-TM-100530] 06 p0678 N88-14151
Thermoplastic elastomers as LOVA binders
[AD-A185865] 07 p0835 N88-15068
Structure-property relationships in thermoplastic elastomers 4. Dynamic mechanical relaxations in poly(dioxolane), poly(butyltrioxocane) and poly(propylene oxide) polyurethanes
[AD-A186278] 07 p0836 N88-15073
Thermoplastic elastomers as LOVA binders
[AD-A186563] 10 p1304 N88-17797
The place for thermoplastic composites in structural components
[AD-A189149] 12 p1604 N88-19596
A continuum damage model for viscoelastic materials
[AD-A189426] 12 p1637 N88-19800
Reinforcing of thermoplastic polycarbonate and polysulfone with carbon fibers: Production and characteristics of UD-compound objects
[NASA-TT-20158] 13 p1735 N88-20374
Interlaminar fracture toughness of thermoplastic composites
[NASA-TM-100532] 15 p2030 N88-22097
Mechanical behaviour of particle filled thermoplastics
[PB88-169297] 15 p2047 N88-22196
A study of failure characteristics in thermoplastic composite material
[AD-A190613] 16 p2171 N88-22940
The adhesive bonding of thermoplastic composites
[AD-A190994] 16 p2173 N88-22953
The mechanical behavior of particle filled thermoplastics
[ETN-88-92234] 16 p2181 N88-22999
Evaluation of a thermoplastic polyimide (422) for bonding GR/PI composite
[NASA-TM-100584] 16 p2182 N88-23003
Loading rate sensitivity of open hole composites in compression
[NASA-TM-100634] 19 p2610 N88-25490
Thermoplastic coating of carbon fibers
[NASA-CR-183067] 20 p2767 N88-26407
Irreversible deformations during fracture in polymers
[W-7/86] 20 p2780 N88-26485
Characterization of elastic-plastic properties of AS4/APC-2 thermoplastic composite
[NASA-CR-183145] 21 p2906 N88-27242
Thermoplastic composite with continuous fibers
[FOA-C-20707-2.6] 22 p3051 N88-28103
An investigation of some basic properties of hybrid composite materials
[AD-A194136] 23 p3189 N88-28975

THERMOPLASTICITY
Constitutive modeling and thermoviscoplasticity
14 p1930 N88-21506
A unified creep-plasticity model suitable for thermo-mechanical loading 14 p1932 N88-21518
The adhesive bonding of thermoplastic composites
[AD-A190994] 16 p2173 N88-22953

The mechanical behavior of particle filled thermoplastics
[ETN-88-92234] 16 p2181 N88-22999
The crystallization of tough thermoplastic resins in the presence of carbon fibers
[NASA-CR-182984] 20 p2776 N88-26464

THERMOREGULATION
Microwave challenges to the thermoregulatory system
[AD-A185391] 05 p0629 N88-13847
Human thermoregulatory model for whole body immersion in water at 20 and 28 C
[AD-A185052] 05 p0629 N88-13849
Exercise in the heat: Effects of dinitrophenol administration
[AD-A185731] 06 p0752 N88-14622
Polycythemia and hydration status: Effects on blood volume and thermoregulation during exercise-heat stress
[AD-A185946] 07 p0888 N88-15383
Prediction of human thermoregulatory responses and endurance time in water at 20 and 24C
[AD-A186223] 08 p1048 N88-16326
Exercise thermoregulation after prolonged wakefulness
[AD-A186224] 08 p1048 N88-16327
Rational considerations for modelling human thermoregulation during cold water immersion
[AD-A186226] 08 p1048 N88-16329
Temperature regulation at rest and exercise during the human menstrual cycle
[AD-A186461] 08 p1050 N88-16341
Manipulation of muscle glycogen concentrations using high and low carbohydrate diets and exercise
[AD-A187732] 11 p1519 N88-19069
Validation of mathematical model predictions of immersion survival times
[IAM-652] 14 p1952 N88-21635
Further development of a mathematical model for the specification of immersion clothing insulation
[IAM-653] 14 p1954 N88-21644
Physiological responses to acute exercise-heat stress
[AD-A192606] 21 p2986 N88-27732
Plasma volume expansion in rats: Effects on thermoregulation and exercise
[AD-A192656] 22 p3130 N88-28606
The role of textile material in clothing on thermoregulatory responses to intermittent exercise
[AD-A192599] 22 p3130 N88-28608
Depressed sweating during exercise at altitude
[AD-A192603] 22 p3130 N88-28609
Accidental hypothermia
[AD-A194967] 24 p3406 N88-30278

THERMOSETTING RESINS
NT EPOXY RESINS
NT KEVLAR (TRADEMARK)
NT NYLON (TRADEMARK)
NT PHENOLIC RESINS
NT POLYAMIDE RESINS
Addition polyimide composition
[EP-PATENT-0-167-304-A1] 01 p0053 N88-10337
Study of the morphology of thermosetting matrices
[ONERA-RT-5/3346-M] 02 p0153 N88-10961
Composite structural materials
[NASA-CR-181416] 02 p0190 N88-11186
Cure and properties of thermosetting polymers
[AD-A184669] 03 p0293 N88-11843
High-temperature thermosets derived from the Diels-Alder polymerization of bisbenzocyclobutenes and bimaleimides
[AD-A188800] 13 p1747 N88-20449
Optimization of binary pigment coatings
[AD-A189103] 13 p1748 N88-20450
Correlation between dielectric and structural properties during epoxy cure
[AD-A190696] 16 p2181 N88-22997
Cellular thermosetting fluoropolymers and process for making them
[NASA-CASE-GSC-13008-1] 17 p2326 N88-23894
Injection compression for short fiber reinforced plastics
[SNIAS-881-430-118] 21 p2922 N88-27344

THERMOSIPHONS
Heat transfer of mesh-wick heat-pipes (bottom heat mode) 20 p2783 N88-26507
An arranging method on L/D of two-phase closed thermosyphons 20 p2783 N88-26508
Characteristics of long size thermosyphons made of corrugated tube 20 p2784 N88-26511

THERMOSPHERE
The climatic wind regime in the lower thermosphere from meteor radar observations 06 p0733 N88-14506
The lower thermosphere wind regime from simultaneous observations over Euroasia (Collm, Dushanbe, Frunze) 06 p0733 N88-14510
Wind regime peculiarities in the lower thermosphere in the winter of 1983/84 06 p0733 N88-14511
On the interconnection of dynamic processes in the lower thermosphere with meteorological phenomena in the tropostratosphere 06 p0734 N88-14512
Circulation in the mesosphere and lower thermosphere during the MAP (Middle Atmosphere Program)/WINE (Winter in the Northern Europe) period 06 p0734 N88-14514
Main results of atmospheric fine structure parameter observation in the lower thermosphere 06 p0735 N88-14518
On connection between evolution of troposphere fronts and changes of circulation regime in meteor zone 06 p0735 N88-14519
On the dependence of the lower thermospheric wind regime on the solar cycle 06 p0736 N88-14524
Longitudinal peculiarities of meridional circulation in lower thermosphere and mesosphere 06 p0736 N88-14525
Lower thermosphere wind regime according to radiometeor measurements in Kazan 06 p0736 N88-14526
Mesoscale density variability in the mesosphere and thermosphere: Effects of vertical flow accelerations 06 p0736 N88-14529
Some aspects of metallic ion chemistry and dynamics in the mesosphere and thermosphere 06 p0737 N88-14534
Monte Carlo modeling and meteor showers 06 p0740 N88-14549
Radar observations of high-latitude lower-thermospheric and upper-mesospheric winds and their response to geomagnetic activity 06 p0742 N88-14563
An analysis of apparent-motion vectors in, and the structure of, A mid-latitude sporadic E layer using a 2.66 MHz radar
[AD-A186126] 07 p0877 N88-15321
Solar tides in the upper equatorial thermosphere: A comparison between AE-E data and the NCAR thermospheric general circulation model
[AD-A186160] 08 p1023 N88-16196
TOTAL: A new instrument to study turbulent parameters in the mesosphere and lower thermosphere 08 p1029 N88-16234
The effects of a geomagnetic storm on thermospheric circulation
[AD-A186638] 09 p1190 N88-17128
The photons payload, G-494: A learning experience 10 p1288 N88-17701
Into the thermosphere: The atmosphere explorers
[NASA-SP-490] 10 p1353 N88-18084
USU (Utah State University) Center of Excellence in Theory and Analysis of the Geo-Plasma Environment
[AD-A187687] 11 p1511 N88-19026
Upper-thermospheric observations and neutral-gas dynamics at high latitudes during solar maximum
[AD-A188058] 11 p1512 N88-19031
Effect of nitrogen dioxide release on thermosphere 13 p1789 N88-20704
The NASA Marshall engineering thermosphere model
[NASA-CR-179359] 20 p2825 N88-26760
Wave structures in thermospheric density from satellite electrostatic triaxial accelerometer measurements
[AD-A194134] 23 p3233 N88-29240
An improvement in the numerical integration procedure used in the NASA Marshall engineering thermosphere model
[NASA-CR-179389] 24 p3392 N88-30200

THERMOSTABILITY
U THERMAL STABILITY

THERMOTROPISM
U ANISOTROPY
U TEMPERATURE EFFECTS

THERMOVISCOELASTICITY
Nonlinear thermoviscoelastic analysis of metallic plane curved beams 03 p0336 N88-12119

THESAURI
Energy Data Base: Subject Thesaurus
[DE87-008007] 03 p0384 N88-12414
NASA thesaurus supplement: A four part cumulative supplement to the 1985 edition of the NASA Thesaurus
[NASA-SP-7053(SUPP-4)] 08 p1093 N88-16575
NASA thesaurus: Astronomy vocabulary
[NASA-SP-7069] 17 p2450 N88-24553
NASA combined file postings statistics based on NASA thesaurus, Jan. 1968 - July 1988
[NASA-CR-182985] 18 p2589 N88-25384
WORDNET: An electronic lexical reference system based on theories of lexical memory
[AD-A193086] 21 p3027 N88-27970
Capitalizing on experience with intelligence gateway software
[AD-A193362] 21 p3028 N88-27971
Exploiting lexical regularities in designing natural language systems
[AD-A195922] 24 p3423 N88-30375

THESES
Down-to-Earth approach for final projects in Karlsruhe (Federal Republic of Germany) 16 p2226 N88-23292

THETA PINCH
Steady state theta pinch concept for slow formation of FRC
[ISSN-0469-4732] 01 p0098 N88-10648
Experimental study of the initial plasma formation stage in a linear theta pinch of inverted field
[DE88-700010] 09 p1249 N88-17485

THICK FILMS
Elimination of subboundaries in 0.5-micron-thick Si-on-insulation films produced by ZMR
[AD-A184590] 03 p0381 N88-12396
Microstructure modifications of micron thick NbN films to improve J/sub c/ and H/sub c2/
[DE88-003078] 08 p1091 N88-16567
Synthesis and characterization of high-T(sub c) screen-printed Y-Ba-Cu-O films on alumina
[NASA-TM-100860] 15 p2146 N88-22805
The effects of thin compressive films on indentation fracture toughness measurements
[AD-A192243] 20 p2779 N88-26480
Superconducting electronic film structures
[AD-A192907] 20 p2879 N88-27091

THICK PLATES
Solution in vibration problems of rectangular plates with spline function
[PB87-143459] 08 p0996 N88-16029
Detection sensitivity in thick assemblies — eddy currents, light alloys, aircraft construction materials
[REPT-48-912/F] 16 p2216 N88-23221

THICKNESS
Analysis of thickness fields retrieved from NOAA-7 observations through the 3I (Improved Initialization Inversion) method. Interest for weather forecasting 02 p0201 N88-11255
Taper sectioning to magnify the interface thickness of a dissimilar metal joint
[RFP-3890-REV] 03 p0333 N88-12099
Microstructure modifications of micron thick NbN films to improve J/sub c/ and H/sub c2/
[DE88-003078] 08 p1091 N88-16567
Analysis of a turbulent premixed V-flame (influence of flame-thickening)
[NAL-TR-941] 10 p1299 N88-17770
Composition and thickness of multilayer foils using MeV ion-beam techniques
[DE88-004360] 11 p1448 N88-18629
Airborne electromagnetic sounding of sea ice thickness and sub-ice bathymetry
[AD-A188939] 12 p1649 N88-19879
Simulated impact damage in a thick graphite/epoxy laminate using spherical indenters
[NASA-TM-100539] 13 p1733 N88-20363
A new method of measuring multigrade oil shear elasticity and viscosity at high shear rates
[AD-A190145] 15 p2064 N88-22304
Surface crack analysis applied to impact damage in a thick graphite-epoxy composite
[NASA-TM-100600] 16 p2173 N88-22950
Gravity currents with heat transfer effects
[PB88-180047] 16 p2205 N88-23158
Thermal conductivity of hard anodized coatings on aluminum
[AD-A191755] 18 p2492 N88-24784
Heating and evaporation of turbulent liquid films: Measurement of film thickness and the onset of nucleate boiling
[DE88-006388] 18 p2512 N88-24905
Vibrations of rotating thick or thin rings 18 p2529 N88-25003
Forced motion of initially stressed shells and plates 18 p2529 N88-25005
Effect of thickness on downward flame spread over paper
[NASA-TT-20282] 19 p2612 N88-25501
Dimensional crossover in layered superconductors 19 p2734 N88-26237
GTAW characterization for weld penetration on 304L stainless steel
[DE88-010611] 20 p2810 N88-26672
Ice detector
[NASA-CASE-LAR-13776-1] 23 p3217 N88-29149
Liquid thickness gauge
[NASA-CASE-LAR-13826-1] 23 p3217 N88-29150
Thickness effects on the stability of shell like structures 23 p3224 N88-29192
Progress in determining the thickness and distribution of volcanic materials on Mars 23 p3302 N88-29670
Variation in the thickness of ejecta cover on Mars with increasing crater density 23 p3307 N88-29701
The use of hot-film technique for boundary layer studies on a 21 percent thick airfoil
[NAE-AN-45] 24 p3321 N88-29781

Predicting the durability of adhesives and coatings by remote detection of hidden defects and coating-thickness irregularities: A theoretical and numerical study
24 p3355 N88-29972

THICKNESS RATIO
Stress state of welded joints of disimilar materials obtained by diffusion welding
03 p0286 N88-11799

THIN AIRFOILS
NT THIN WINGS
The effects of rotational flow, viscosity, thickness, and shape on transonic flutter dip phenomena
[NASA-TM-100811] 11 p1502 N88-18969
Technology for pressure-instrumented thin airfoil models
[NASA-CR-4173] 23 p3180 N88-28933

THIN FILMS
NT ENERGY ABSORPTION FILMS
NT MONOMOLECULAR FILMS
Use of sol-gels in the application of ceramic oxide thin films
[DE87-013610] 01 p0028 N88-10178
Direct formation of thin films and epitaxial overlayers at low temperatures using a low-energy (10-500 eV) ion beam deposition system
[DE87-012291] 01 p0103 N88-10675
Chemical vapor deposition of B6P and B6As films
[DE87-009288] 02 p0151 N88-10942
Stress measurements in sol-gel films
[DE87-014467] 02 p0153 N88-10955
The development of a new and novel Hadamard transform infrared spectrometer for analytical chemistry
[DE87-014804] 02 p0175 N88-11094
Multilayered foils as radiation entrance windows and spectral filters for image converters in the ultrasoft X-ray wavelength region
[MPE-PREPRINT-90] 02 p0176 N88-11099
The preparation of thin films for photovoltaic conversion by novel MOCVD techniques
[DE87-001185] 02 p0194 N88-11212
Preparation and properties of evaporated CdTe films
[DE87-012270] 02 p0195 N88-11216
CuInSe2 solar cell research by sputter deposition
[DE87-001184] 02 p0195 N88-11219
Wide bandgap passivation layers on silicon
[DE87-014307] 02 p0244 N88-11543
Ohmic contacting schemes to gallium arsenide devices
[DE87-014627] 02 p0244 N88-11544
Thin film microstructures: Simulation and theory
[DE87-014732] 02 p0246 N88-11553
Highly Non-Linear Optical (NLO) organic crystals
03 p0297 N88-11865
Highly Non-Linear Optical (NLO) organic crystals and films. Electrooptical organic materials
03 p0297 N88-11866
Ion plating: Fundamental processing studies and synthesis of high performance coatings
[AD-A184766] 03 p0303 N88-11908
Thin films for geothermal sensing
[DE88-000154] 03 p0326 N88-12061
Taper sectioning to magnify the interface thickness of a dissimilar metal joint
[RFP-3890-REV] 03 p0333 N88-12099
Investigation of hexagonal ferrite film growth techniques for millimeter-wave systems applications
[AD-A184335] 03 p0383 N88-12406
Experimental study of thermocapillary flows in a thin liquid layer with heat fluxes imposed on the free surface
[NASA-TM-100252] 04 p0445 N88-12763
Studies of thin surface films aim at seeing deep ocean processes
04 p0460 N88-12847
Theory and simulations of Zone 2 microstructures in thin films
[DE87-014752] 04 p0499 N88-13071
Influence of bonding shop moisture on metal-honeycomb junctions bonded with ultra-thin adhesive films
[SNIAS-872-422-112] 05 p0558 N88-13399
Raman microprobe characterization of dielectric films following high-energy pulsed laser irradiation
[DE88-000559] 05 p0588 N88-13587
Tribology of thin film systems
[ETN-88-91365] 05 p0590 N88-13601
The effects of thin anodic films on the cyclic microstrain/macrostrain behavior of tungsten
05 p0597 N88-13650
Develop techniques for ion implantation of (lead-lanthanum-zirconate-titanate) for adaptive optics
[DE88-000642] 05 p0650 N88-13986
Structural characterization of ion implanted beta-SiC thin films
[DE87-014567] 05 p0656 N88-14027
Effects of hydrolysis on metallo-organic solution deposition of PZT films
[ATR-86(8443)-1] 06 p0679 N88-14160
Determination, by X-ray fluorescence, of platinum, palladium, ruthenium, iron and chromium in special steels
[PB87-132114] 06 p0683 N88-14183
An analysis of the effect of system variables on the quality of thin films and powders produced by laser-breakdown chemical vapor deposition
[DE88-001793] 06 p0708 N88-14342
Partial analysis of experiment LDEF A-0114
[NASA-CR-179236] 06 p0780 N88-14787
Structure of layered crystals studied by high energy ion beams
[DE88-001675] 06 p0786 N88-14822
Analytical investigations of bulk wave resonators in the piezoelectric thin film on gallium-arsenide configuration
[AD-A185716] 06 p0789 N88-14840
Very thin VLSI-layouts (Very Large Scale Integration-Layouts) of complete binary trees
[PB88-100847] 06 p0789 N88-14841
Microstructure and magnetic properties of cobalt-chromium alloys
[DE88-002762] 07 p0835 N88-15064
Superconducting switch program
[AD-A185682] 07 p0848 N88-15144
Radiation hardness evaluation of thin film ferroelectric capacitors
[DE88-001357] 07 p0848 N88-15147
Thin film and gradient-driven instability mechanisms
[PB88-101522] 07 p0853 N88-15182
Thin film electret boundary layer transition detector: A feasibility study
[AD-A185675] 07 p0856 N88-15199
Contrast between the chemical, structural and electronic properties of thin films of Cu and Ni on the Ru(0001) surface
[DE88-002360] 07 p0938 N88-15698
Research sensors
08 p0955 N88-15795
TiN coatings on M2 steel produced by plasma assisted chemical vapor deposition
[DE88-003189] 08 p0970 N88-15867
Sputtered silver films to improve chromium carbide based solid lubricant coatings for use to 900 C
[NASA-TM-100783] 08 p0973 N88-15885
Depth of origin of sputtered atoms: Experimental and theoretical study of Cu/Ru(0001)
[DE88-002848] 08 p1082 N88-16520
Experimental aspects of high-T/sub c/ superconductors
[DE88-003019] 08 p1090 N88-16564
The role of thermodynamic phase diagrams and lattice matching in superlattice growth
[DE88-003113] 08 p1091 N88-16568
Monolayer films prepared by the spontaneous self-assembly of symmetrical and unsymmetrical dialkyl sulfides from solution onto gold substrates: Structure, properties, and reactivity of constituent functional groups
[AD-A186717] 09 p1137 N88-16814
The effect of varying sputtering parameters on the microstructure and mechanical properties of 10 percent Ni + TiB2 thin films
[DE88-002600] 09 p1254 N88-17517
Crystalline sulfur dioxide: Crystal field splittings, absolute band intensities and complex refractive indices derived from infrared spectra
[NASA-CR-182502] 09 p1258 N88-17547
Diffusion studies in amorphous NiZr alloys
[DE88-003009] 10 p1301 N88-17781
The migration of grain boundaries in ceramic materials with particular reference to the sintering process
[DE88-004085] 10 p1306 N88-17808
Adhesion of vapour phase deposited ultra-thin polyimide films on polycrystalline silver
[AD-A187930] 10 p1306 N88-17810
The soft/hard wet anodization of aluminum oxide and its use in a thin film multilayered capacitor
[AD-A187575] 10 p1325 N88-17919
Apparatus for the study of silicon film deposition and silicon etching
[AD-A187616] 10 p1334 N88-17972
Monitoring interfacial dynamics by pulsed laser techniques
[DE88-003362] 10 p1335 N88-17976
Optical measurements of surface oxide layer formation on metal films
[DE88-003163] 10 p1409 N88-18405
Specific heat of novel thin-film material systems
10 p1415 N88-18446
The physics of metallic superlattices: An experimental point of view
[DE88-003080] 10 p1416 N88-18452
Synthesis and characterization of thin films
[AD-A187335] 10 p1421 N88-18485
Superconductivity of thin film intermetallic compounds
[AD-A187563] 10 p1421 N88-18489
Evaluation of centrifugal barrel tumbling process for impregnation of molybdenum disulfide powder lubricant
[BDX-613-3698] 11 p1464 N88-18727
Ceramic decomposition under irradiation
[DE88-004327] 11 p1464 N88-18732
Cryocooler systems demonstration
[AD-A188025] 11 p1467 N88-18745
Prototype thin-film thermocouple/heat-flux sensor for a ceramic-insulated diesel engine
[NASA-TM-100798] 11 p1490 N88-18892
Preparation of thin film polyvinylidene fluoride shock wave pressure transducers
[PB88-156070] 11 p1490 N88-18893
Plasma deposition of silicon carbide thin films
[AD-A188093] 11 p1556 N88-19314
Proceedings of the Polycrystalline Thin Film Program Meeting
[DE87-001169] 11 p1557 N88-19321
Raman enhancement methods for molecular structure characterization of optical thin films
[DE88-003421] 11 p1558 N88-19324
Ion beam modification of film stress and the effectiveness of thin film encapsulants on GaAs
[DE88-004458] 11 p1558 N88-19328
Electrochromic thin films
[DE88-751099] 11 p1559 N88-19334
Preparation and characterization of thin films of alumina by metalorganic chemical vapor deposition
[AD-A188366] 12 p1608 N88-19614
Electrophoretically deposited styrene-acrylate coatings for suppression of internal electromagnetic pulse effects
[DE88-003820] 12 p1609 N88-19621
Polymeric materials for electro-optic testing
[AD-A188382] 12 p1610 N88-19627
The effects of thin polymeric surface films in reducing fretting corrosion and wear
[AD-A188633] 12 p1611 N88-19634
SiO2 film stress distribution during thermal oxidation of Si
[AD-A189552] 12 p1612 N88-19637
Artificially structured superconductors
[DE88-005345] 12 p1697 N88-20153
Characterization of redox states of nickel hydroxide film electrodes by in-situ Raman spectroscopy
[AD-A189288] 13 p1741 N88-20411
Improved methods for high resolution electron microscopy
[DE88-005731] 13 p1774 N88-20609
Research on high-efficiency, stacked, multijunction, amorphous silicon alloy thin-film solar cells
[DE88-001108] 13 p1793 N88-20723
CdZnTe as a wide-band-gap absorber for a tandem, thin-film solar cell
[DE88-001114] 13 p1793 N88-20724
Stable, high-efficiency, CuInSe2-based, polycrystalline, thin-film tandem solar cells
[DE88-001116] 13 p1793 N88-20726
Cadmium sulfide/copper ternary heterojunction cell research
[DE88-001122] 13 p1793 N88-20727
Direct absorption receiver control studies
[DE87-013653] 13 p1795 N88-20737
Measurement of the properties of lossy materials inside a finite conducting cylinder
[NASA-CR-182664] 13 p1832 N88-20962
Measuring thin film properties using SAW (Surface Acoustic Wave) devices: Diffusivity and surface area
[DE88-002216] 13 p1834 N88-20970
Thin-film diffusion barriers for metal-semiconductor contacts
[AD-A188712] 13 p1844 N88-21035
Modulatable thin film field emission space gun
[AD-A189279] 13 p1845 N88-21043
Thin-film cadmium telluride solar cells
[DE88-001107] 13 p1846 N88-21050
X-ray diffraction study of a thin GaAs film on Si(100)
[DE88-005290] 13 p1847 N88-21055
Superconducting superlattice structures
[DE88-005346] 13 p1847 N88-21058
Initial stages of silicon growth on the (100) surface of silicon by localized laser CVD
[DE88-005420] 13 p1848 N88-21059
A novel method for sputter-deposition of high T(sub c) superconductor films via a computer-controlled mass analyzed ion beam
[DE88-006001] 13 p1848 N88-21064
The performance of thin solid films for satellite gears
14 p1876 N88-21209
Space station solar concentrator materials research
[NASA-TM-100862] 14 p1882 N88-21250
On the torque and wear behavior of selected thin film MOS2 lubricated gimbal bearings
14 p1926 N88-21485
Infrared reflection-absorption spectroscopy of hyperfine layers on surfaces of semiconductors and dielectrics
14 p1969 N88-21755

Giant Josephson signal in wide superconducting films
14 p1973 N88-21777
Femtosecond studies in hot carrier relaxation in GaAs and AlGaAs
14 p1977 N88-21801
Structure and properties of titanium nitride and zirconium nitride thin films prepared by reactive ion plating --- cutting tools
[ETN-88-92218] 15 p2042 N88-22167
Vapor phase deposition and growth of polyimide films on copper
[AD-A189969] 15 p2044 N88-22178
Development of a laboratory test for multiport injector deposits: Approaches 1 and 2
[AD-A190697] 15 p2048 N88-22203
Laser evaporation studies
[AD-A189815] 15 p2071 N88-22346
High-efficiency thin-film silicon-on-GaP solar cell for improved radiation resistance
[AD-A190268] 15 p2091 N88-22460
Fundamental studies of the mechanical behavior of microelectronic thin film materials
[AD-A190038] 15 p2143 N88-22786
Thin superconducting film characterization by surface acoustic waves
[AD-A190417] 15 p2143 N88-22791
Thin film research diagnostics instrumentation
[AD-A191240] 16 p2213 N88-23207
Magnetic studies of iron-rare-earth-metalloid alloys
[DE88-006801] 16 p2282 N88-23660
Boundary layer measurements using hot-film sensors
17 p2297 N88-23743
Superconducting thin film vertex detector for SSC (Superconducting Super Collider) applications
[DE88-005951] 17 p2445 N88-24535
Micro-Raman analysis of dielectric optical thin films
[AD-A191228] 17 p2445 N88-24537
Method of producing high T(subc) superconducting NBN films
[NASA-CASE-NPO-16681-1-CU]
17 p2446 N88-24543
Electrical conduction in thin film carbons
[AD-A191726] 18 p2491 N88-24780
Electron-Rayleigh wave interaction in thin film carbons
[AD-A191727] 18 p2492 N88-24781
Joint services electronics program research in electronics
[AD-A192206] 18 p2504 N88-24857
Magnetic superlattices
[AD-A191450] 18 p2581 N88-25334
Molecular characterization of structure and bonding in thin film materials
[DE88-006811] 18 p2584 N88-25351
Electrode films of porous agarose: The effects of physical structure on electron transport processes
[DE88-007366] 19 p2611 N88-25493
Hydrogenated amorphous silicon-germanium alloys
[DE88-001147] 19 p2620 N88-25546
Picosecond optoelectronic study of a thin film transmission line structure
19 p2661 N88-25823
The 1986 IEEE Solid-State Sensor Workshop
[AD-A190922] 19 p2668 N88-25860
The structure and properties of RF reactive sputtered IrO2 films
19 p2672 N88-25884
Effect of process conditions on aluminum oxide thin film used in pH ISFET
19 p2673 N88-25892
Surface acoustic wave gas sensor based on film conductivity changes
19 p2673 N88-25894
Zinc-oxide thin films for integrated-sensor applications
19 p2673 N88-25896
Tin oxide microsensors on thin silicon membranes
19 p2673 N88-25897
The use of micromachined structures for the management of mechanical properties and adhesion of thin films
19 p2674 N88-25899
Systematics of excimer laser ablation: Thin film preparation of high T(sub c) material
[DE88-010569] 19 p2675 N88-25909
Study of Staebler-Wronsky degradation effect in a Si:H based P-I-N solar cells
[NASA-CR-182564] 19 p2687 N88-25970
Center for thin film studies
[AD-A191996] 19 p2732 N88-26226
The catalytic reactivity of thin film crystal surfaces
[DE88-006387] 19 p2732 N88-26228
The use of liquid films for spacecraft survivability to laser radiation
[AD-A192954] 20 p2765 N88-26395
The effects of thin compressive films on indentation fracture toughness measurements
[AD-A192243] 20 p2779 N88-26480
Preparation technology for thin film solid electrolyte fuel cells
[PB88-131925] 20 p2821 N88-26735
Properties of multilayers for soft X-ray optics
20 p2867 N88-27025
Growth and characterization of thin films of ZnSnP(sub)2
[DE88-001164] 20 p2874 N88-27060
Fundamental optical studies of competitive adsorption and thin film phenomena
[DE88-008780] 20 p2875 N88-27068
Characterization of the surface area and porosity of sol-gel films using saw devices
[DE88-008794] 20 p2875 N88-27069
Preparation of high-T(sub)c Y1Ba2Cu3O(sub 7-Delta) superconducting thin films by MBE (Molecular-Beam-Epitaxy) techniques
[DE88-009999] 20 p2877 N88-27082
Thin film and near-surface characterization using a mechanical properties microprobe
[DE88-011399] 21 p2915 N88-27302
Equipment for building and testing superconductive flux flow electronic devices
[AD-A192959] 21 p2936 N88-27436
Superconducting thin films, composites and junctions
[AD-A193123] 21 p2937 N88-27440
Effects of surface tension and contact angle on sensible heating and boiling incipience in dielectric falling films
[DE88-007057] 21 p2945 N88-27492
Chemical vapor deposition of TiO2 thin films at room temperature
[DE88-008892] 21 p2953 N88-27542
Laser-heated CVD process for depositing thin films for low-cost solar-cell applications
[DE88-001162] 21 p2967 N88-27623
Experimental fabrication of thin film single crystalline solar cells
[PB88-131958] 21 p2967 N88-27627
Amorphous silicon solar cells using a metal substrate
[PB88-131941] 21 p2968 N88-27628
Measurement of the thermal conductivity of dielectric thin solid films with a thermal comparator
[DE88-008468] 21 p3016 N88-27896
Materials research, superconductor and thin layer technology
[REPT-50/87] 21 p3025 N88-27955
Studies of internal stresses and surface roughness of sputtered Be and BeB films
[DE88-011737] 22 p3086 N88-28327
Experimental fabrication of thin film single crystalline solar cells
[PB88-131958] 22 p3116 N88-28516
Computer simulation of electromigration in thin films
[AD-A194526] 22 p3157 N88-28782
Thin film coatings for space electrical power system applications
[NASA-TM-101325] 23 p3187 N88-28966
Thin film-residual stress assessment
[AD-A193205] 23 p3196 N88-29018
Dissolution rates of polymers and copolymers based on methyl, ethyl and butyl methacrylate
[AD-A194713] 23 p3197 N88-29027
Theoretical investigation on heterojunction solar cell
[DE88-701837] 23 p3229 N88-29219
Shear stress at a film-substrate interface due to mismatch strain
[AD-A193461] 23 p3288 N88-29577
Preparation of superconducting YBa2Cu3O(sub 7-x) films by magnetron sputtering
[DE88-009977] 23 p3289 N88-29583
Research on crystal and film ferroelectric materials for optoelectronic applications
[AD-A193512] 23 p3291 N88-29597
High power storage system based on thin film solid ionics
[AD-A193623] 23 p3291 N88-29598
New method for preparation of (Cd, Hg)Te thin films
[DE88-702727] 23 p3293 N88-29608
Temperature dependence of conductivity and of Hall coefficients for noble metal films
[ETN-88-92981] 23 p3294 N88-29616
Diamond film by hot filament CVD method
[NASA-TT-20335] 23 p3294 N88-29618
Stress related failures causing open metallization
[AD-A195061] 24 p3383 N88-30150
A review of melt and vapor growth techniques for polydiacetylene thin films for nonlinear optical applications
[NASA-TM-100340] 24 p3430 N88-30412
Cluster beam studies
[AD-A195182] 24 p3434 N88-30443

THIN PLATES

Generalized hybrid variational principle, corresponding finite element model
03 p0301 N88-11895
Models for penetration of thin plates
[DE87-013727] 03 p0332 N88-12090
On the instability of thin circular shear layers
04 p0395 N88-12467
Fatigue failure of thin porous strips
04 p0426 N88-12640
The accommodation of precipitate plates modelled as a tensile test
[DE88-000207] 04 p0454 N88-12814
Knot selection for least squares thin plate splines
[AD-A185681] 06 p0759 N88-14657
Transient welding strain measurement by Moire technique: A comparison between experimental measurement and numerical analysis for strain-stress cycles during GTA spot-welding
[PB87-143871] 07 p0868 N88-15269
Bending analysis of thin plates with openings
[PB87-143400] 07 p0869 N88-15274
The nonlinear dynamic response of an elastic-plastic thin plate under impulse loading
[AD-A182147] 08 p0994 N88-16013
Solution in vibration problems of rectangular plates with spline function
[PB87-143459] 08 p0996 N88-16029
Integral equation method for the analysis of plates and shells
[PB87-144788] 08 p0996 N88-16030
A note on the aerodynamic design of thin parallel-sided aerofoil sections
[ARL-AERO-TM-388] 09 p1114 N88-16677
Investigation of thermoacoustic heat transport using a thermoacoustic couple
[AD-A186889] 09 p1242 N88-17442
Transient sound radiation from infinite thin plate
[ARE-TM(UHA)-87508] 09 p1243 N88-17449
Boundary stabilization of thin elastic plates
[AD-A187123] 10 p1343 N88-18025
Numerical simulation of the perforation of thin plates
[ISL-R-122/86] 11 p1495 N88-18926
Investigation into the operation of the new special drills for drilling holes in thin components made of composite materials --- aircraft components
[LR-519] 16 p2215 N88-23215
Dynamic response of plates to moving loads: Structural impedance and finite element methods
18 p2528 N88-25000
Static analysis of thin plates using the finite strip-element method
19 p2679 N88-25931
An investigation of soft launch and instability breakup with a two-stage light gas gun
[DE88-010371] 21 p2901 N88-27218

THIN WALLED SHELLS

Analysis of shell-type structures subjected to time-dependent mechanical and thermal loading
[NASA-CR-181409] 01 p0060 N88-10388
Analytic model of an imploding Z-pinch plasma colliding inelastically with a thin-shelled cylindrical target
[DE88-000051] 03 p0378 N88-12379
Integral equation method for the analysis of plates and shells
[PB87-144788] 08 p0996 N88-16030
Successful mixed formulation for axisymmetric shell analysis employing discontinuous stress fields of the same order as the displacement field
[DE88-700021] 09 p1178 N88-17052
Investigations of the equilibrium and stability of thin-walled double rings. A contribution to the solution of single-sided contact problems
[ETN-87-90044] 09 p1181 N88-17076
Analysis of shell-type structures subjected to time-dependent mechanical and thermal loading
[NASA-CR-182705] 13 p1783 N88-20668
Reversed field pinch operation with a thin shell
[DE88-005521] 13 p1843 N88-21027
Topics in curved and flat space electromagnetism
13 p1854 N88-21100
A comparison of experimental and calculated thin-shell leading-edge buckling due to thermal stresses
[NASA-TM-100416] 17 p2349 N88-23999
Nonlinear vibrations of imperfect thin walled cylindrical shells
[ETN-88-92904] 23 p3227 N88-29205
Geometric and material nonlinear analysis of structures comprising rectangular hollow sections
[CE-79] 24 p3382 N88-30141

THIN WALLS

Pulsed eddy-current inspection of thin-walled stainless steel tubing
[DE88-001492] 04 p0457 N88-12830
Development on thin wall tubes of dispersion type
[DE87-703384] 05 p0571 N88-13483
Distortional buckling formulae for thin-walled channel columns
[PB87-124012] 06 p0722 N88-14437
Geometric nonlinear analysis of asymmetric thin-walled members
[PB87-133856] 06 p0723 N88-14446
Influence of radiation and thermal conduction on temperature distribution in the thin wall of a hollow cylinder
[INPE-4428-TDL/308] 12 p1626 N88-19730

The elastic analysis of a thin toroidal shell
[AD-A187801] 12 p1635 N88-19785

THIN WINGS
Calculation of aerodynamic heat transfer for blunt-nosed thin wings at different angles of attack at supersonic speeds
[NASA-TT-20127] 02 p0123 N88-10776
A supersonic potential gradient method for the calculation of unsteady aerodynamic pressures on harmonically oscillating wings
[ESA-TT-930] 03 p0259 N88-11631

THINNERS
U SOLVENTS

THIOLS
Reactions of some thiol collectors at noble-metal and pyrite electrodes
[PB88-138318] 11 p1455 N88-18674
Determination of low molecular weight thiols using monobromobimane fluorescent labeling and high-performance liquid chromatography
[NASA-CR-182932] 19 p2608 N88-25478
The evolution of glutathione metabolism in phototrophic microorganisms
[NASA-CR-182902] 19 p2695 N88-26015
Correlations between wettability and structure in monolayers of alkanethiols adsorbed on gold
[AD-A194348] 23 p3191 N88-28991

THIXOTROPIC PROPELLANTS
U GELLED ROCKET PROPELLANTS

THIXOTROPY
Thixotropic surface composition for phenolaldehyde resin laminates
[GB-PATENT-2-180-251-A] 04 p0410 N88-12545

THOMAS-FERMI MODEL
Semiclassical theory of the nuclear response function. Quasielastic electron scattering
[ETN-88-91082] 09 p1245 N88-17459

THOMAS-FERMI THEORY
U THOMAS-FERMI MODEL

THOMSON EFFECT
U THERMOELECTRICITY

THOMSON SCATTERING
Enhanced Thomson scattering from laser plasmas
[DE87-014463] 02 p0238 N88-11503
Feasibility of alpha particle measurement in a magnetically confined plasma by CO2 laser Thomson scattering
[DE88-000039] 02 p0241 N88-11522
Tangential Thomson scattering --- plasma diagnostics
[REPT-87-173] 08 p1087 N88-16548
Thomson scattering for determining electron concentrations and temperatures in an inductively coupled plasma. 1: Assessment of the technique for a low-flow, low-power plasma
[AD-A191323] 16 p2280 N88-23651
Measurement of time evolution of plasma electron component parameters on the Ogra-4 device by the Thomson scattering method
[DE88-701575] 16 p2282 N88-23662
Design and calibration of a two-channel low-noise heterodyne receiver for use in a CO2 laser Thomson scattering alpha particle diagnostic
[DE88-007866] 19 p2728 N88-26201
A CO2 laser Thomson scattering diagnostic for fusion product alpha particle measurement
[DE88-007683] 20 p2857 N88-26965
Multipoint Thomson scattering diagnostic for DIII-D
[DE88-008737] 20 p2857 N88-26969
Multi-mode optical fibers for simultaneous 13-position measurements Thomson scattering apparatus in the JFT-2M tokamak
[DE88-753133] 21 p3015 N88-27897

THORIUM
Phenomenological model of superconductivity of heavy fermions in U(sub 1-x)ThsubxBesub13
09 p1238 N88-17423
Effects of galactic chemical evolution on thorium/neodymium cosmochronology
[DE88-003829] 11 p1570 N88-19397

THORON
U RADON ISOTOPES

THREADS
Empirical fatigue crack growth data for a tension loaded threaded fastener
[AD-A194112] 22 p3088 N88-28334

THREAT EVALUATION
Military needs and forecast, 2
01 p0015 N88-10087
System for detecting objects that represent a threat
[NASA-TT-20244] 13 p1760 N88-20528
Investigations of test methodology for the stress loading facility
[PB88-166095] 15 p2022 N88-22049
Threat expert system technology advisor
[NASA-CR-177479] 24 p3328 N88-29816

THREE AXIS STABILIZATION
Country plans three-axis weather satellite
06 p0688 N88-14218
Control and stabilization of ESA satellites
09 p1124 N88-16734
Three axis attitude control system
[NASA-CASE-GSC-12970-1] 17 p2308 N88-23808
Wave structures in thermospheric density from satellite electrostatic triaxial accelerometer measurements
[AD-A194134] 23 p3233 N88-29240

THREE BODY PROBLEM
Asymptotics of the effective potentials and wave functions of a three-body problem in suitable coordinates
[DE87-703323] 03 p0370 N88-12326
Physics of few-body lambda hypernuclei
[DE87-014746] 03 p0375 N88-12357
Study on orbits near the triangular libration points in the perturbed restricted three body problem
[ESA-CR(P)-2440] 07 p0944 N88-15741
Limitation of spacecraft orbit near colinear libration center of limited elliptical three body problem
08 p1003 N88-16075
Periodic orbits of limited elliptical three body problem
08 p1004 N88-16081
Hyperspherical coordinate theory of two-electron processes: Future plans
[DE87-010653] 08 p1081 N88-16516
Adiabatic representation of three-body problem in hyperspherical coordinates. Statement of the problem
[DE88-701162] 15 p2126 N88-22678
A generic multibody simulation
[NASA-CR-182949] 17 p2388 N88-24198
Families of periodic solutions in problem of solid body rotation at triangular libration point in restricted three-body problem 24 p3446 N88-30508

THREE DIMENSIONAL BODIES
Problem and solution formulations for the generation of 3D block-structured grids --- aircraft design
[NLR-MP-86020-U] 01 p0005 N88-10028
A user's guide for BIE3D: A boundary integral equation computer program for three-dimensional elastostatic analysis
[RAE-TM-MAT-STR-1078] 01 p0079 N88-10509
Three dimensional reconstruction of optical microscope pictures using the three dimensional microscopic inverse point spread function
[ETN-87-90420] 01 p0098 N88-10646
The Green's function method for fully unsteady aerodynamics around three-dimensional bodies and its application to flutter analysis
[UTIAS-298] 03 p0260 N88-11639
The 3-D world modeling for an autonomous robot
[DE87-013878] 03 p0333 N88-12102
On the recognition of curved objects
[AD-A184441] 04 p0478 N88-12945
Finite-element method for three-dimensional electric and electromagnetic field problems
[PB87-138731] 06 p0696 N88-14274
Shuttle computational grid generation
06 p0794 N88-14863
A knowledge-based object recognition system for applications in the space station
[NASA-CR-182411] 08 p0989 N88-15991
Numerical analysis of motion of solid bodies in atmosphere 08 p1079 N88-16505
Self-adaptive analysis of three-dimensional structures using a p-version of finite element method
[FFA-TN-1987-31] 09 p1182 N88-17084
Boundary elements combined with singular fields for three-dimensional cracked solids
[RAE-TR-87038] 09 p1183 N88-17088
Solid modelling with faceted primitives
[ETN-88-91593] 09 p1218 N88-17305
Shape optimization of three-dimensional stamped and solid automotive components
[GMR-5168] 11 p1528 N88-19123
Measuring accuracy of 3-dimensional bodies by the GOMER-1 device
[DE87-703230] 12 p1628 N88-19744
Retrieval of three-dimensional wind and temperature fields from single-Doppler radar data
12 p1646 N88-19858
An interactive user-friendly approach to surface-fitting three-dimensional geometries
[NASA-CR-4126] 12 p1682 N88-20058
High-speed flow calculations past 3-D configurations based on the Reynolds averaged Navier-Stokes equations
[NASA-TM-100082] 14 p1911 N88-21421
Tectonics and three-dimensional structure of spreading centers: Microearthquake studies and tomographic inversions
[PB88-163290] 14 p1945 N88-21602
Definition and display of profiled sweep-objects --- computer graphics
[REPT-87-45] 14 p1957 N88-21665
A three-dimensional model for the elastic properties of a foam
[DE88-006197] 15 p2046 N88-22192
A 3-D solid rendering of NDT data
[DE88-006199] 15 p2076 N88-22373
On the geometric interpretation of image contours
[RR-647-I-IMAG-57-LIFIA] 15 p2109 N88-22563
Maximum likelihood parameter identification of flexible spacecraft
[LR-508] 16 p2168 N88-22924
Three-dimensional curved shell and solid-shell transition finite elements with temperature and temperature gradients as primary variables for steady state heat conduction
17 p2349 N88-23997
A survey of freeform solid modeling methods
[REPT-87-81] 20 p2839 N88-26847
The construction of composite grids for general three-dimensional regions 20 p2843 N88-26872
An aspect graph-based control strategy for 3-D object recognition 21 p2927 N88-27377
Creating aspect graphs for use in object recognition
21 p2928 N88-27379
Enhancement of modeling and image generation techniques for high-resolution 3-dimensional imagery
[DE88-008923] 21 p2998 N88-27782
Three-dimensional zonal grids about arbitrary shapes by Poisson's equation
[NASA-TM-101018] 22 p3039 N88-28042

THREE DIMENSIONAL BOUNDARY LAYER
Three-dimensional structure of boundary layers in transition to turbulence
[AD-A185466] 06 p0702 N88-14311
Unsteady behavior of three-dimensional vortices relevant to turbulent boundary layers
[AD-A186767] 09 p1161 N88-16958
Velocity measurements in a 3D (three dimensional) shock wave laminar boundary layer interaction
[AD-A187334] 10 p1332 N88-17959
The structure and control of three-dimensional shock wave turbulent boundary layer interactions
[AD-A187642] 10 p1332 N88-17961
General fuselage coordinates for the calculation of three-dimensional boundary layers
[MBB/LKE-122/S/PUB/244] 13 p1771 N88-20596
Wave interactions in a three-dimensional attachment line boundary layer
[NASA-CR-181653] 14 p1910 N88-21414
Theoretical investigation of secondary instability of three-dimensional boundary-layer flows with application to the DFVLR-F5 model wing
[DFVLR-FB-87-44] 15 p2068 N88-22330
Boundary layer transition
[CERT-OA-37/5018-AYD] 18 p2458 N88-24595
A documentation of two- and three-dimensional shock-separated turbulent boundary layers
[NASA-TM-101008] 21 p2949 N88-27519
Study of hypersonic boundary layers
[CERT-RSF-OA-17/5005-AYD]
23 p3213 N88-29121
User's manual for three dimensional boundary layer (BL3-D) code
[NASA-CR-174899] 24 p3369 N88-30063
Assessment of a 3-D boundary layer analysis to predict heat transfer and flow field in a turbine passage
[NASA-CR-174894] 24 p3370 N88-30066

THREE DIMENSIONAL COMPOSITES
Woven frameworks for three-dimensional reinforcement 14 p1884 N88-21262
Fracture behavior in multidimensional fiber-reinforced composites 22 p3051 N88-28099
An investigation of some basic properties of hybrid composite materials
[AD-A194136] 23 p3189 N88-28975

THREE DIMENSIONAL FLOW
NT SECONDARY FLOW
NASA-VOF3D: A three-dimensional computer program for incompressible flows with free surfaces
[DE87-011849] 01 p0045 N88-10288
Characteristics and boundary elements for three dimensional nonstationary Navier Stokes flows
[PREPRINT-1051] 02 p0172 N88-11086
Flow in a model turbine stator
02 p0187 N88-11163
IMPSOR: A fully vectorized FORTRAN code for three dimensional moving boundary problems with Dirichlet or Neumann boundary conditions
[DE87-014964] 02 p0226 N88-11427
On the onset of three-dimensionality and time-dependence in the Goertler vortex problem
[NASA-CR-178404] 03 p0260 N88-11638
Three-dimensional calculation in high subsonic axial compressor rotor and its comparison with L2F velocity measurement 03 p0300 N88-11886

Calculation of the three dimensional flow in the impeller of hydraulic turbomachines using a finite element method
[ETN-87-90612] 03 p0315 N88-11988
Theoretical analysis of primary instabilities in three dimensional boundary layer flows
[ESA-TT-1063] 03 p0315 N88-11992
On the scheme dependency of the three-dimensional Euler solutions 03 p0318 N88-12010
Development and application of computational aerothermodynamics flowfield computer codes
[NASA-CR-181534] 04 p0395 N88-12465
An analysis of the compressible-viscous flow field around a 3D-oscillating wing 05 p0535 N88-13254
Three-dimensional flow past a two-dimensional body 05 p0539 N88-13280
Computational study of three-dimensional wake structures
[REPT-2] 05 p0539 N88-13281
Time-marching finite-difference methods for the three-dimensional Euler equations of contravariant velocity components 05 p0539 N88-13285
Numerical simulation of transonic aircraft in comparison to wind tunnel test 05 p0540 N88-13289
A numerical study of the effects of curvature and convergence on dilution jet mixing
[NASA-TM-89878] 05 p0549 N88-13347
Displaying three-dimensional data
[AD-A185347] 05 p0580 N88-13541
The development and evaluation of three-dimensional models of cold flow in internal combustion engines
[DE88-900077] 05 p0589 N88-13594
Three-dimensional dynamic labyrinth seal analysis
[AD-A185353] 05 p0590 N88-13599
A system of three-dimensional complex variables
[NASA-TM-88318] 05 p0645 N88-13951
Numerical simulation of flight body circumference flow 06 p0676 N88-14137
Analysis of three-dimensional viscous internal flows
[AD-A186254] 07 p0849 N88-15155
Numerical calculation of appendage, flat plate junction flow
[AD-A186371] 07 p0850 N88-15158
Multitasked embedded multigrid for three-dimensional flow simulation
[NASA-CR-182398] 07 p0852 N88-15173
Acta Aerodynamica Sinica (selected articles)
[AD-A185723] 08 p0949 N88-15757
Unsteady three-dimensional flow separation
[NASA-CR-182412] 08 p0949 N88-15761
Consistent boundary conditions for Reduced Navier-Stokes (RNS) scheme applied to 3-dimensional internal viscous flows
[NASA-CR-180874] 08 p0950 N88-15762
The simulation of three-dimensional viscous supersonic flow past blunt bodies with a hybrid implicit/explicit finite difference method
[DFVLR-FB-87-32] 08 p0950 N88-15765
Turbomachinery 08 p0955 N88-15792
Finite Element Calculation Methods and Their Application to Turbomachinery, volume 2
[VKI-LS-1987-05-VOL-2] 08 p0985 N88-15965
Mesh generation 08 p0986 N88-15971
Active control of jet flowfields
[AD-A186736] 08 p0989 N88-15989
Numerical resolution of the equations of three-dimensional stable compressible transonic flows
[PB87-168415] 09 p1113 N88-16673
Techniques of flow visualization
[AGARD-AG-302] 09 p1164 N88-16977
Numerical modeling of multidimensional flow in seals and bearings used in rotating machinery
[NASA-TM-100779] 09 p1165 N88-16988
Numerical solutions of three-dimensional Navier-Stokes equations for closed-bluff bodies
[NASA-CR-182359] 09 p1166 N88-16990
Three dimensional Monte Carlo simulation of molecular movement and heat radiation in vacuum devices: Computer code MOVAK3D --- fusion reactors
[KFK-4292] 09 p1246 N88-17471
Development and application of oxygen flow tagging for velocity measurements and flow visualization in turbulent three-dimensional supersonic flows
[AD-A187982] 10 p1289 N88-17714
Three-dimensional Euler solutions for hypersonic Mach numbers
[MBB-UR-944/87] 10 p1315 N88-17859
An experimental investigation of pressure driven three-dimensional turbulent boundary layers 10 p1327 N88-17934
A three-dimensional dual potential procedure for rotational flows 10 p1329 N88-17942
Three-dimensional incompressible flowfield analysis for establishing rotor designs which optimize power extraction 10 p1329 N88-17943
Boundary-integral-equation method for computing the three-dimensional flow of groundwater
[PB88-126891] 10 p1330 N88-17951
Fluctuations and massive separation in three-dimensional shock-wave/boundary-layer interactions
[NASA-TM-89224] 11 p1434 N88-18559
Three-dimensional flow fields past reentry vehicles 11 p1484 N88-18858
Two and three dimensional elliptic flows 11 p1485 N88-18866
Topology and grid adaption for high-speed flow computations
[NASA-CR-182586] 11 p1487 N88-18875
Implementation of multigrid in SOLA algorithm --- fluid flow 11 p1538 N88-19191
Three-dimensional incompressible Navier-Stokes computations of internal flows
[NASA-TM-100076] 12 p1576 N88-19425
Numerical simulation of subsonic and transonic propeller flow
[NASA-TM-100163] 13 p1716 N88-20262
The construction of a three-dimensional finite volume grid generator for a wing in a wind tunnel with application to Navier-Stokes flow solvers
[FFA-TN-1987-58] 13 p1719 N88-20277
Three-dimensional shear layer experiments and their use as test cases for calculation methods
[NLR-MP-86036-U] 13 p1767 N88-20570
Development of disturbances in swept wing flows
[NASA-CR-182675] 13 p1768 N88-20574
Slip velocity method for three-dimensional compressible turbulent boundary layers
[NASA-TM-100586] 13 p1771 N88-20592
Numerical analysis of three-dimensional viscous internal flows
[NASA-TM-100878] 14 p1861 N88-21116
Problems appearing at interface balances --- flames 14 p1987 N88-21855
Experimental investigation of a spanwise forced mixing layer
[AD-A190136] 15 p2013 N88-22007
Trends in Computational Fluid Dynamics (CFD) for aeronautical 3D steady applications: The Dutch situation
[NLR-MP-86074-U] 15 p2015 N88-22017
Secondary instability of compressible boundary layer to subharmonic three-dimensional disturbances
[NASA-CR-4144] 16 p2200 N88-23122
Three-dimensional flow visualization using laser-sheet scanning 16 p2203 N88-23143
Application of high speed holography to aerodynamic and hydrodynamic three-dimensional velocimetry 16 p2203 N88-23144
Nonlinear wave interactions in swept wing flows
[NASA-CR-4142] 16 p2206 N88-23160
Accuracy versus convergence rates for a three dimensional multistage Euler code
[NASA-CR-181665] 16 p2261 N88-23519
Numerical simulation of scramjet inlet flow fields
[NASA-TP-2517] 17 p2296 N88-23735
An efficient parallel algorithm for the simulation of three-dimensional compressible transition on a 20 processor Flex/32 multicomputer
[NASA-CR-178340] 17 p2337 N88-23943
Development and improvement of a code to calculate small, three dimensional, unsteady transonic perturbations
[ONERA-RTS-31/3064-RY-062-R] 17 p2338 N88-23951
A variational finite element method for three-dimensional, steady, compressible, viscous flows 18 p2512 N88-24904
SOLA-DM: A numerical solution algorithm for transient three-dimensional flows
[DE88-007159] 18 p2514 N88-24913
Finite element solution of 3-D turbulent Navier-Stokes equations for propeller-driven slender bodies 18 p2515 N88-24919
Review of numerical methods for radionuclide transport in three-dimensional porous media, at high Peclet numbers
[CFDU/87/10] 18 p2538 N88-25061
Analysis of flow through pump of large rocket engine 19 p2637 N88-25646
Numerical analysis of three dimensional cascade flow by solving Navier-Stokes equations 19 p2638 N88-25650
Numerical analysis of duct flow using three-dimensional parabolized Navier-Stokes equation 19 p2638 N88-25652
On the stationary solutions of three-dimensional Euler equations by the TVD difference schemes 19 p2639 N88-25660
MHD (magnetohydrodynamic) thermal hydraulic analysis of three-dimensional liquid metal flows in fusion blanket ducts
[DE88-009929] 19 p2731 N88-26219
Use of direct solvers for multidimensional fluid flow computations
[DE88-010063] 20 p2799 N88-26611
Three-dimensional viscous flow computations of a circular jet in subsonic and supersonic cross flow
[NASA-CR-182153] 20 p2800 N88-26616
Improved 3-D turbomachinery CFD algorithm
[NASA-CR-179364] 20 p2801 N88-26619
Velocity measurements and flow visualization in turbulent three-dimensional supersonic flows using oxygen flow tagging
[AD-A192551] 21 p2892 N88-27165
Numerical methods for incompressible viscous flows with engineering applications
[NASA-CR-183143] 21 p2948 N88-27508
Study of three-dimensional transonic flow separations
[AD-A193018] 22 p3037 N88-28032
An improved version of NCOREL: A computer program for 3-D nonlinear supersonic potential flow computations
[NASA-CR-4165] 22 p3038 N88-28039
The application of the two-fluid model of turbulence to the 3-D simulation of turbulent combustion in reciprocating engines
[PDR/CFDU/IC/37] 22 p3052 N88-28110
Mass transport in flow of sources
[LRT-WE-9-FB-4(1987)] 22 p3077 N88-28268
Holographic flow visualization
[PNR90466] 22 p3079 N88-28283
Development of a hot-wire measurement technique for moderate intensity three-dimensional flows 22 p3080 N88-28289
Shock boundary layer interaction 23 p3170 N88-28873
Small scale mixing in the initial region of a jet
[AD-A193500] 23 p3192 N88-28994
Direct-solution techniques for viscous flows and their control
[AD-A194775] 23 p3211 N88-29114
Navier-Stokes calculations of transonic flows past cavities
[NASA-CR-180484] 23 p3212 N88-29116
Study of hypersonic boundary layers
[CERT-RSF-OA-17/5005-AYD] 23 p3213 N88-29121
Experience with three dimensional composite grids 23 p3247 N88-29324
Three-dimensional Navier-Stokes simulations of turbine rotor-stator interaction
[NASA-TM-100081] 24 p3316 N88-29750
Three-dimensional combustor predictors: A comparison of equilibrium and laminar flamelet chemistry models 24 p3350 N88-29940
An analysis of finite-difference and finite-volume formulations of conservation laws
[NASA-CR-177416] 24 p3370 N88-30071

THREE DIMENSIONAL MODELS

Three-dimensional adaptive grid generation for body-fitted coordinate system
[NASA-CR-182192] 21 p2950 N88-27520
The three-dimensional stress field around a cylindrical inclusion in a plate of arbitrary thickness 21 p2963 N88-27602
Prediction of regional pollutant dispersion using a nested-grid, three-dimensional numerical model 21 p2971 N88-27649
A three-dimensional model of the gas-cell atomic frequency standard
[AD-A193218] 21 p3011 N88-27868
A simple, analytic 3-dimensional downburst model based on boundary layer stagnation flow
[NASA-TM-100632] 22 p3042 N88-28058
Three-dimensional elliptic grid generation technique with application to turbomachinery cascades
[NASA-TM-101330] 24 p3372 N88-30078
Geometric modeling for computer aided design
[NASA-CR-183161] 24 p3413 N88-30320

THREE DIMENSIONAL MOTION

NT SECONDARY FLOW
NT THREE DIMENSIONAL FLOW
Three-dimensional transient electromagnetic modeling for exploration geophysics 10 p1346 N88-18047
On the design of suboptimal matched filters for three-dimensional moving target detection
[AD-A188384] 12 p1619 N88-19682
Simulation of measuring points for three dimensional measurements
[WPB-0115] 13 p1821 N88-20883
A three dimensional non-singular modelling of rigid manipulators
[AD-A189707] 15 p2116 N88-22604
Rigidity and smoothness of motion
[AD-A190555] 15 p2126 N88-22694

Minimal parameter solution of the orthogonal matrix differential equation
[NASA-TM-4043] 17 p2383 N88-24165
A generic multibody simulation
[NASA-CR-182949] 17 p2388 N88-24198
The avoidance of collisions for Newtonian bodies with hidden variables
[RSRE-87013] 22 p3041 N88-28053
Determining vehicle motion from stereo image sequences
[AD-A194371] 23 p3216 N88-29140

THRESHOLD CURRENTS
Total photoionization cross sections of atomic oxygen from threshold to 44.3A
[NASA-CR-182992] 17 p2397 N88-24252

THRESHOLD DETECTORS (DOSIMETERS)
Miniature radiation dosimeter for in vivo radiation measurements 19 p2672 N88-25889

THRESHOLD VOLTAGE
Development and experimental verification of a two-dimensional numerical model of piezoelectrically induced threshold voltage shifts in GaAs MESFETs
[AD-A193462] 23 p3206 N88-29080

THRESHOLDS (PERCEPTION)
Psychophysical considerations in measuring MRTD with staring arrays — minimum resolvable temperature difference (MRTD)
[RSRE-MEMO-4031] 01 p0076 N88-10487

THROTTLING
Integrated autopilot/autothrottle based on a total energy control concept: Design and evaluation of additional autopilot modes
[NASA-CR-4131] 13 p1724 N88-20308

THRUST
NT HIGH THRUST
NT JET THRUST
NT LOW THRUST
NT ROCKET THRUST
NT STATIC THRUST
High power ion thruster performance
[NASA-TM-100127] 04 p0409 N88-12542
An experimental investigation of an arcjet thruster exhaust using Langmuir probes
[NASA-TM-100258] 14 p1883 N88-21253
Development of a liquid-fed water resistojet
[NASA-TM-100927] 18 p2523 N88-24968
Low-speed wind-tunnel test of a STOL supersonic-cruise fighter concept
[NASA-TM-4050] 20 p2761 N88-26374
Iridium-coated rhenium thrusters by CVD
[NASA-TM-101309] 24 p3339 N88-29874

THRUST AUGMENTATION
Reduction of tilt rotor download using circulation control 10 p1271 N88-17605
Circulation control STOL aircraft design aspects 10 p1272 N88-17610
A computational study of thrust augmenting ejectors based on a viscous-inviscid approach 10 p1326 N88-17929
Augmentor performance of an F100 engine model derivative engine in an F-15 airplane
[NASA-TM-86745] 17 p2307 N88-23805

THRUST CHAMBER PRESSURE
Boundary layer development as a function of chamber pressure in the NASA Lewis 1030:1 area ratio rocket nozzle
[NASA-TM-100917] 19 p2664 N88-25841

THRUST CHAMBERS
A two-dimensional finite difference program for thermal analysis of rocket thrust chambers
[NASA-TM-100191] 04 p0409 N88-12539
MPD (magnetoplasmadynamic) thrust chamber flow dynamics
[AD-A189940] 15 p2137 N88-22751
Orbital transfer vehicle 3000 LBF thrust chamber assembly hot fire test program
[NASA-CR-182145] 24 p3336 N88-29858

THRUST CONTROL
NT THRUST VECTOR CONTROL

THRUST DISTRIBUTION
Low speed wind tunnel investigation of propeller slipstream aerodynamic effects on different nacelle/wing combinations. Part 1: Total forces and moments and pressure distributions on nacelle/wing at different angles of attack and yaw and at different thrust coefficients
[FFA-TN-1987-22] 05 p0542 N88-13302
Fixed wing CCW aerodynamics with and without supplementary thrust deflection 10 p1272 N88-17607
Development of circulation control technology for powered-lift STOL aircraft 10 p1272 N88-17608

THRUST FAULTS
U GEOLOGICAL FAULTS

THRUST MEASUREMENT
Space station propulsion technology
[NASA-CR-179260] 08 p0964 N88-15835

THRUST POWER
U THRUST

THRUST PROGRAMMING
The eivaN: A forward-looking interactive orbital trajectory plotting tool for use with proximity operations (PROX OPS) and other maneuvers: Description and user's manual
[NASA-CR-177490] 24 p3414 N88-30327

THRUST REVERSAL
Aerodynamics in ground effect and predicted landing ground roll of a fighter configuration with a secondary-nozzle thrust reverser
[NASA-TP-2834] 24 p3317 N88-29752

THRUST VECTOR CONTROL
Effects of the installation and operation of jet-exhaust yaw vanes on the longitudinal and lateral-directional characteristics of the F-14 airplane
[NASA-TP-2769] 04 p0393 N88-12455
An experimental and numerical investigation of swirling flows in a rectangular nozzle 06 p0700 N88-14295
Design of supersonic Coanda jet nozzles 10 p1270 N88-17599
Manoeuvres by default, by demand and by design 12 p1580 N88-19455
Static performance of an axisymmetric nozzle with post-exit vanes for multiaxis thrust vectoring
[NASA-TP-2800] 13 p1719 N88-20280
Optimal thrust vector control of coplanar orbital evasive maneuvers
[AD-A189544] 13 p1730 N88-20348
Static performance of nonaxisymmetric nozzles with yaw thrust-vectoring vanes
[NASA-TP-2813] 14 p1861 N88-21118
Pressure measurements of impinging jet with asymmetric nozzle
[NASA-CR-182759] 15 p2014 N88-22011
Heat transfer modeling of jet vane Thrust Vector Control (TVC) systems
[AD-A190106] 15 p2019 N88-22034
Experimental investigation of two-dimensional confined jet thrust vector control
[AD-A189845] 15 p2027 N88-22077
Method for prediction and determination of takeoff performance for vectored thrust vehicles
[AD-A191809] 18 p2463 N88-24626
Attitude control laws for gas-jet spacecraft 18 p2467 N88-24643
TVC (Thrust Vector Control) jet vane thermal modeling using parametric system identification
[AD-A191518] 18 p2474 N88-24678
The effects of RCS jet firing on the isolated Orbiter and mated coast phases of the glide return to launch site maneuver at Mach number 6 (IA302B)
[NASA-CR-180223] 20 p2766 N88-26403

THUNDERSTORMS
The physics of charge separation preceding lightning strokes in thunderclouds
[NASA-CR-178371] 01 p0071 N88-10452
Use of a 5 cm Doppler radar to detect and forecast severe thunderstorms in a real time forecast operation 02 p0200 N88-11247
Thunderstorm nowcasting using Doppler radar and soundings 02 p0200 N88-11248
The use of advanced data sets in the short-range forecasting of the development of a tornadic thunderstorm along a mesoscale convergence zone 02 p0200 N88-11250
VAS products as indices of thunderstorms and severe local storm potential — Visible and Infrared Spin Scan Radiometer Atmospheric Sounder (VAS) 02 p0201 N88-11253
Automated detection of severe thunderstorms using geosynchronous infrared data 02 p0201 N88-11257
Forecasting and nowcasting cumulus convection with soundings released from a storm-intercept vehicle 02 p0202 N88-11262
Mesoscale thunderstorm forecasting using RAOB data, surface mesonet observations, and an expert system 02 p0206 N88-11293
Cumulus and thunderstorm initiation by mountains 02 p0207 N88-11301
The importance of the lower level windshear profile in tornado/non-tornado discrimination 02 p0208 N88-11304
Short range forecasting of sea breeze generated thunderstorms at the Kennedy Space Center: A real-time experiment using a primitive equation mesoscale numerical model 02 p0211 N88-11324
Severe weather potential (SPOT) plotfile generator
[PB87-217717] 02 p0216 N88-11360
Definition and use of sensors for measuring electrical conductivity in thunderclouds
[ESA-TT-1047] 03 p0352 N88-12222
Experimental and analytic studies of the triggered lightning environment of the F106B
[NASA-CR-4104] 04 p0469 N88-12897
Atmospheric electricity
[NASA-CR-179239] 06 p0744 N88-14575
Radar observations of changes in precipitation size spectra associated with lightning 06 p0744 N88-14576
Thunderstorms with snow: A comprehensive, empirical study of their occurrence, development and structure
[AD-A185929] 07 p0879 N88-15329
Applicability of extremely low frequency global resonances for study of Venusian storm activity 08 p1005 N88-16093
Suggested severe local storm operational scenario for GOES I-M
[NASA-TM-100688] 11 p1515 N88-19052
Radio and radar holes and multipath zones: The global and local influences on atmospheric refractive structure and resulting adverse radio and radar performance 12 p1617 N88-19667
Pre-convective environmental conditions indicative of non-tornadic severe thunderstorm winds over Southeast Florida
[AD-A188679] 12 p1648 N88-19870
A preliminary assessment of thunderstorm outflow wind measurement with airport surveillance radars
[AD-A189064] 13 p1799 N88-20757
Wind shear as a predictor of severe weather for the eastern United States
[PB88-157144] 13 p1800 N88-20762
Upward propagating electric fields from thunderstorms and VLF transmitters 13 p1801 N88-20767
Stratospheric electric field and conductivity measurements over electrified convective clouds in the South American region, revised
[INPE-4046-PRE/1012-REV-3] 15 p2095 N88-22483
Atmospheric Science and Remote Sensing Laboratory
[NASA-CR-179290] 16 p2236 N88-23355
Analysis of lightning field changes during active thunderstorms in Florida 18 p2545 N88-25103
Satellite observed Mesoscale Convective System (MCS) propagation characteristics and a 3-12 hour heavy precipitation forecast index
[PB88-180161] 19 p2692 N88-26004
A radar study of the interaction between lightning and precipitation
[DE88-009120] 20 p2827 N88-26770
Investigations into the triggered lightning response of the F106B thunderstorm research aircraft
[NASA-CR-3902] 23 p3236 N88-29258

THYMINE
Survival and mutation induction of dehydrated yeast cells after UV exposure 12 p1657 N88-19932

THYRATRONS
Linear thyratron
[AD-A194111] 23 p3208 N88-29094

THYRISTORS
Study on the dynamics of executive electromechanism with thyristor commutator for cryogenic systems
[DE87-703209] 12 p1622 N88-19702

TIBET
SPOT imagery as an aid to understanding volcanism and tectonics: Examples from the Chilean Andes and the Tibetan Plateau 22 p3103 N88-28427

TIBIA
Changes in the status of the human tibia during antiorthostatic hypokinesia
[NASA-TT-20221] 13 p1810 N88-20813

TID
U TRAVELING IONOSPHERIC DISTURBANCES

TIDAL OSCILLATION
U TIDES

TIDE POWERED GENERATORS
Ocean, Wave, and Tidal Energy Systems: Current abstracts
[DE88-008299] 19 p2687 N88-25973

TIDEPOWER
Ocean, Wave, and Tidal Energy Systems: Current abstracts
[DE88-008299] 19 p2687 N88-25973
Survey on utility technology of a tidal and ocean current energy
[DE88-770148] 20 p2819 N88-26722

TIDES
NT ATMOSPHERIC TIDES
NT EARTH TIDES
Seasonal cycling of sulfur and iron in porewaters of a Delaware salt marsh
[NASA-CR-182385] 07 p0876 N88-15311
Tide- and wind-forced currents in Buzzards Bay, Massachusetts
[PB88-110580] 07 p0882 N88-15350
Infrared emission and tidal interactions of spiral galaxies 07 p0923 N88-15611
Tidal estimation in the Pacific with application to SEASAT altimetry
[NASA-TM-100694] 13 p1803 N88-20780

Fully implicit splitting method for accurate tidal computations
[PB88-183637] 20 p2828 N88-26781
TIG WELDING
U GAS TUNGSTEN ARC WELDING
TILES
Ceramic-ceramic shell tile thermal protection system and method thereof
[NASA-CASE-ARC-11641-1] 11 p1448 N88-18628
In-flight rain damage tests of the shuttle thermal protection system
[NASA-TM-100438] 14 p1881 N88-21241
Implementation of nonsquare tilings on an image processing system
[FOA-C-30487-3.3] 22 p3140 N88-28669
TILT
U ATTITUDE (INCLINATION)
TILT ROTOR AIRCRAFT
NT XV-15 AIRCRAFT
Rotorcraft designs for the year 2000
03 p0264 N88-11665
Rotorcraft aeroelastic stability
09 p1106 N88-16631
Reduction of tilt rotor download using circulation control 10 p1271 N88-17605
Frequency-response identification of XV-15 tilt-rotor aircraft dynamics 10 p1277 N88-17643
Improvements to tilt rotor performance through passive blade twist control
[NASA-TM-100583] 15 p2086 N88-22434
The role of aviation technology in the Caribbean Basin
[NASA-CR-183069] 20 p2745 N88-26289
TILT ROTOR RESEARCH AIRCRAFT PROGRAM
Flight researh at NASA Ames Research Center: A test pilot's perspective
[NASA-TM-100025] 02 p0125 N88-10788
Hover performance tests of baseline metal and Advanced Technology Blade (ATB) rotor systems for the XV-15 tilt rotor aircraft
[NASA-CR-177436] 20 p2759 N88-26367
TILTING
U ATTITUDE (INCLINATION)
TILTING ROTORS
Using frequency-domain methods to identify XV-15 aeroelastic modes
[NASA-TM-100033] 10 p1277 N88-17646
TILTMETERS
Evaluation of a miniature horizontal pendulum tilt transducer 12 p1577 N88-19435
TIMBER INVENTORY
Stand based forest inventory from SPOT IMAGE. First experiments 03 p0344 N88-12173
Applicability of SPOT for forest inventory, mapping and change monitoring 03 p0344 N88-12174
TIME
NT EPHEMERIS TIME
NT FLIGHT TIME
NT MTBF
NT REACTION TIME
NT RELAXATION TIME
NT RESPONSE TIME (COMPUTERS)
NT TRANSIT TIME
Nonlinear techniques for detection and filtering of discrete-time signals 02 p0160 N88-11004
Modeling XV-15 tilt-rotor aircraft dynamics by frequency and time-domain identification techniques
03 p0263 N88-11657
Scaling of size/time/temperature associated with dilatation and distortion in uniaxial specimens
03 p0336 N88-12117
A multiple-time-scale turbulence model based on variable partitioning of turbulent kinetic energy spectrum
[NASA-CR-179222] 04 p0444 N88-12754
Propagation of random initial conditions in time
04 p0486 N88-12993
On-orbit frequency stability analysis of the GPS NAVSTAR 8 rubidium clock and NAVSTARs 9 and 10 cesium clocks
[AD-A184984] 05 p0544 N88-13312
Time domain electromagnetic waves in multilayered media
[AD-A185055] 05 p0574 N88-13502
Timing variation in dual loop benchmarks
[AD-A185697] 06 p0707 N88-14338
Time characteristics of travelling wave lasing with two-photon picosecond optical pumping
07 p0918 N88-15578
Optical communication with semiconductor laser diodes
[NASA-CR-182464] 09 p1154 N88-16918
Time domain wave propagation in multilayered integrated circuits
[AD-A187462] 10 p1324 N88-17916
Time varying controller design for robot manipulator control
[AD-A188094] 11 p1494 N88-18919
Dynamics of production and oxidation of boranes
[AD-A188988] 12 p1606 N88-19605
Hypnosis: Possible applications for cosmonauts
12 p1665 N88-19984
An evaluation of historical algebras
[AD-A188350] 12 p1684 N88-20067
Flight Vehicle Development Time and Cost Reduction
[AGARD-CP-424] 12 p1700 N88-20173
The increased time and cost of development: Causes and (some) remedies 12 p1701 N88-20178
Reducing time required for the development of avionic systems 12 p1702 N88-20185
Minimizing development flight test time and cost in the US Air Force 12 p1703 N88-20192
The TEMPIS project: Current status
[AD-A188963] 12 p1707 N88-20220
Time characteristics of ultrashort light pulses from dye lasers with distributed feedback
14 p1970 N88-21759
CK-LOG system conversion (user's manual and user interface)
[AD-A190273] 15 p2111 N88-22577
State-of-the-art in true space-time finite element method 17 p2391 N88-24215
Optimal discrete-time LQR problems for parabolic systems with unbounded input: Approximation and convergence
[NASA-CR-181673] 18 p2567 N88-25247
Test of a prototype gate with fast opening equipping the shock tube 0 2.40 m at CEG
[PB87-227864] 19 p2604 N88-25465
A numerical study of the test time in a hypersonic shock tunnel
[AD-A194057] 23 p3172 N88-28888
A linear-time algorithm for finding a minimum spanning pseudoforest
[AD-A194029] 23 p3250 N88-29346
Improved time bounds for the maximum flow problem
[AD-A194034] 23 p3272 N88-29471
Time travel in the homogeneous Som-Raychaudhuri universe
[DE88-702220] 23 p3295 N88-29622
TIME CONSTANT
Measurements of the scintillation time constants of inorganic crystals for the development of a triple-Phoswich detector for high-energy X-ray quanta
[ETN-88-91501] 14 p1993 N88-21875
TIME DELAY
U TIME LAG
TIME DEPENDENCE
The analysis of moisture absorption in multi-layered media
[NPL-DMA(A)-147] 01 p0019 N88-10115
Analysis of shell-type structures subjected to time-dependent mechanical and thermal loading
[NASA-CR-181409] 01 p0060 N88-10388
3D inelastic analysis methods for hot section components 02 p0187 N88-11164
The impact on short-term precipitation forecast skill of time-dependent lateral and lower boundary conditions within a meso-beta numerical cloud prediction model
02 p0211 N88-11327
On the onset of three-dimensionality and time-dependence in the Goertler vortex problem
[NASA-CR-178404] 03 p0260 N88-11638
Effect of time and temperature on transformation toughened zirconias
[AD-A184356] 04 p0419 N88-12600
Alternating current circuit theory and pulsed NMR (Nuclear Magnetic Resonance)
[DE88-000641] 04 p0440 N88-12732
Canonical transformations and exact invariants for dissipative systems
[DE87-703663] 04 p0485 N88-12985
On the numerical simulation of three-dimensional hypersonic flow 05 p0532 N88-13237
Noise modelling in the time domain with the aid of Spice
[PB87-221941] 05 p0573 N88-13492
Numerical and analytical methods in nonlinear partial differential equations
[AD-A185210] 05 p0641 N88-13918
Time-dependent hypersonic viscous interactions
[AD-A185764] 06 p0665 N88-14082
Implicit time dependent methods for inviscid and viscous compressible flows 06 p0701 N88-14304
Photoionization of atoms and ions: Application of time-dependent response method within the density functional theory
[AD-A185686] 07 p0930 N88-15649
A new technique for rocket and space-borne investigations of time-dependant auroral morphology
08 p1030 N88-16241
Nonlinear diffusion in the presence of a time-dependent external electric field
[INPE-4378-PRE/1198] 08 p1085 N88-16533
Additional investigations in landing process of aircraft: Test distributions
[DFVLR-MITT-87-13] 09 p1115 N88-16686
A method for designing robust multivariable feedback systems
[NASA-CR-182459] 09 p1225 N88-17341
Explicit-implicit methods for time-dependent partial differential equations
[CWI-NM-R8703] 09 p1228 N88-17355
Time dependent degradation of energetic electrons in gaseous and condensed media
[DE88-002912] 09 p1246 N88-17465
Physics modeling support contract
[DE88-004039] 10 p1335 N88-17980
Scaling physiological pharmacokinetic models by physiological time
[DE88-000335] 10 p1368 N88-18173
Performance and optimization of direct implicit time integration schemes for use in electrostatic particle simulation codes
[DE88-003254] 10 p1406 N88-18381
Velocity reversal and the arrows of time
[DE88-004237] 10 p1429 N88-18536
Radiation and temperature effects on the time-dependent response of T300/934 graphite/epoxy
[NASA-CR-182603] 11 p1451 N88-18646
A new computational technique for generating algorithms, with application to the solution of the time-dependent incompressible Navier-Stokes equations
11 p1485 N88-18864
An adaptive grid finite difference method for time-dependent Magnetohydrodynamic (MHD) flows and its astrogeophysical applications
11 p1553 N88-19294
A discretization of the integral equation for the time dependent linearized subsonic potential flow over a wing
[AD-A188534] 12 p1574 N88-19411
Time-dependent Slow-Time-Scale theory of free-running and phase-locked gyrotron oscillators
[AD-A188910] 12 p1629 N88-19752
A representation for serial robotic tasks
12 p1681 N88-20048
Structural materials: The changing scene
12 p1703 N88-20190
Numerical model of the time independent mean flow in a rotating rocket motor 13 p1733 N88-20360
The calibration of photographic and spectroscopic films: Reciprocity failure and thermal responses of IIaO film at liquid nitrogen temperatures
[NASA-CR-181094] 13 p1773 N88-20606
Analysis of shell-type structures subjected to time-dependent mechanical and thermal loading
[NASA-CR-182705] 13 p1783 N88-20668
Applications of elastic-viscoplastic constitutive models in dynamic analyses of crack run-arrest events
14 p1930 N88-21507
Data requirements to model creep in 9Cr-1Mo-V steel
14 p1931 N88-21512
On the global/local time incrementing for viscoplastic analysis 14 p1932 N88-21519
Time dependent MHD models for the cometary magnetosphere 14 p1997 N88-21900
Short duration flow establishment on a profile in a Water-Ludwieg-Tunnel 16 p2201 N88-23134
Measurements of the time dependent velocity field surrounding a model propeller in uniform water flow
16 p2205 N88-23155
Nanosecond laser photolysis of opaque heterogeneous photosensitizers
[AD-A191424] 16 p2213 N88-23209
Study of mechanisms of time-dependent crack growth at elevated temperature
[DE88-006918] 16 p2223 N88-23271
Vectorization of the odd-even hopscotch scheme and the alternating direction implicit scheme for the two-dimensional Burgers' equations
[CWI-NM-R8720] 16 p2249 N88-23440
A multigrid approach for the solution of a nonlinear diffusion equation in a time-dependent area using Cartesian coordinates
[GMD-STUDIEN-122] 16 p2257 N88-23491
Measurement of time evolution of plasma electron component parameters on the Ogra-4 device by the Thomson scattering method
[DE88-701575] 16 p2282 N88-23662
Analysis of crack-tip fields in a viscoplastic material
17 p2349 N88-23996
Solving time-dependent two-dimensional eddy current problems
[NASA-TM-100875] 18 p2566 N88-25239
US participation in the TOGA (Tropical Ocean and the Global Atmosphere) Program: A research strategy
[DE88-010986] 19 p2681 N88-25938
Computer modeling of time dependent SBS (Stimulated Brillouin Scattering) in two and three dimensions
[DE88-008922] 19 p2720 N88-26150

Resistance of polyamide-6 against long time effects of various media at various temperatures
[NASA-TT-20297] 20 p2779 N88-26484
A new trajectory following polynomial-time algorithm for the linear programming problem
[REPT-87-87] 20 p2840 N88-26848
A nodal method for time-dependent transport equation
[DE88-004285] 20 p2844 N88-26876
The low-latitude auroral boundary: Steady-state and time-dependent representations
[AD-A193200] 21 p2972 N88-27656
Time-dependent thermal convection of Earth mantle and double diffusive convection in magma chambers
[MITT-52] 21 p2974 N88-27663
Staggered-grid finite element solution technique for the Maxwell's equations in the time domain
[DE88-011731] 21 p3007 N88-27838
The calculation of time dependent eddy currents in tokamaks
[REPT-206] 23 p3286 N88-29568
Chaotic behaviour in quantum dynamics
[AD-A193936] 23 p3295 N88-29623
Numerical methods: Euler time dependent solver
24 p3318 N88-29760

TIME DISCRIMINATION
Visual attention effects on discrimination of line orientation and line arrangement
[AD-A187013] 09 p1200 N88-17190
Comparative aspects of multiple processes of attention
[AD-A195805] 24 p3408 N88-30291

TIME DIVISION MULTIPLE ACCESS
Satellite ground-terminal user simulation
[NASA-TM-100234] 06 p0694 N88-14260
A 30/20 GHz multibeam array antenna suitable for future high rate TDMA European satellite networks
[ETN-88-93079] 24 p3365 N88-30037

TIME DIVISION MULTIPLEXING
Digital television routing systems: A survey of optical and electrical techniques
[BBC-RD-1988/3] 19 p2654 N88-25763
Rivista Tecnica Selenia, volume 10, no. 3, 1987
[ETN-88-92717] 22 p3068 N88-28210
The Frequency Division Multiple Access/Time Domain Multiplex (FDMA/TDM) system reviewed
22 p3069 N88-28214

TIME FUNCTIONS
Time accurate techniques using characteristic flux averaging with application to unsteady aerodynamics
08 p0985 N88-15957
Calculated late time spectra of supernovae
[DE88-003296] 10 p1428 N88-18530
Supporting valid time: An historical algebra
[AD-A187740] 11 p1565 N88-19368
Simple multireader registers using time-stamp schemes
[CWI-CS-R8758] 20 p2835 N88-26819
Study and temporal simulation of the electromagnetic susceptibility of interconnected systems
[ECL-87-19] 22 p3071 N88-28228

TIME LAG
Teleoperation and control study --- orbital servicing
[BAE-TP-8268] 01 p0076 N88-10489
Flap-lag equations of motion of rigid, articulated rotor blades with three hinge sequences
[NASA-TM-100023] 04 p0401 N88-12495
CGI delay compensation
[NASA-TM-86703] 04 p0476 N88-12932
The carbon dioxide chaperon efficiency for the reaction H + O2 + M yields HO2 + M from ignition delay times behind reflected shock waves
[NASA-TM-100125] 07 p0830 N88-15035
Multipath time-delay estimation via the EM algorithm
[PB88-106851] 07 p0845 N88-15124
Software simulation of time delay in teleoperation
08 p1056 N88-16371
Sojourn times in the M/G/1 queue with deterministic feedback
[CWI-OS-R8708] 08 p1074 N88-16479
Time delays and boundary feedback stabilization in one-dimensional viscoelasticity, appendices A through H
[AD-A187534] 10 p1401 N88-18353
Measurement and effects of transport delays in a state-of-the-art F-16C flight simulator
[AD-A187367] 11 p1441 N88-18599
Realtime pilot model parameter identification
[AD-A188873] 12 p1584 N88-19476
Sojourn times in feedback queues
[CWI-OS-R8710] 13 p1830 N88-20947
Radial track of moving objects determined by HF backscatter technique 14 p1901 N88-21354
Practical considerations for structural control: System uncertainty, system time delay and truncation of small control forces
[PB88-163738] 14 p1933 N88-21528
The effects of torque response and time delay on rotorcraft vertical axis handling qualities
[AD-A189873] 15 p2017 N88-22023
Loran-C monitor correlation over a 92-mile baseline in Ohio 17 p2293 N88-23720
Electro-optic sampling of high-speed, InP-based integrated circuits 19 p2655 N88-25769
Multigigahertz logic based on InP-MISFET's exhibiting extremely high transconductance
19 p2656 N88-25771
Concepts for robot motion primitives required for space station teleoperations 23 p3257 N88-29387

TIME MARCHING
Theoretical investigations of three turbine cascades using a two dimensional time marching procedure
[DFVLR-FB-87-02] 01 p0057 N88-10362
Application of Runge Kutta time marching scheme for the computation of transonic flows in turbomachines
[NASA-TM-86997] 04 p0394 N88-12461
Computation of flow past conical hypersonic wings using a second order Godunov method
05 p0533 N88-13241
Time-marching finite-difference methods for the three-dimensional Euler equations of contravariant velocity components 05 p0539 N88-13285
Electromagnetic scattering problem in the wave-vector-time domain
[PB88-106083] 06 p0694 N88-14263
Theoretical investigations of three turbine cascades using a 2-D time marching procedure
[ESA-TT-1077] 16 p2207 N88-23170
The 2-D and 3-D time marching transonic potential flow method for propfans 16 p2220 N88-23245
Reduced order models for nonlinear aerodynamics
16 p2220 N88-23248

TIME MEASUREMENT
Planning and execution of the NAVEX experiment in the Spacelab Mission D1
[DFVLR-FB-87-03] 01 p0010 N88-10056
Timing variation in dual loop benchmarks
[AD-A185697] 06 p0707 N88-14338
Electronics for the External Muon Detector (EMD) of ICARUS
[NOTA-INTERNA-880] 07 p0847 N88-15143
Chemical reactions in turbulent mixing flows
[AD-A186141] 07 p0849 N88-15153
Increasing time resolution of picosecond absorption spectrometer by selection of length of laser light pulses
07 p0919 N88-15579
The use of optical fibers for shock pressure and timing measurements at high pressures
[DE88-004012] 10 p1334 N88-17971
Electromechanical timing measurement technique
[DE88-005098] 11 p1489 N88-18889
Application of the Global Positioning System (GPS) time receivers to the fundamental station Wettzell
11 p1506 N88-18995
Results of one way transit time measuring in navigation experiment NAVEX
[DFVLR-MITT-87-17] 14 p1865 N88-21145
Securing the timescale of the NAVEX-reference clock and rate determinations by time comparisons with the help of the Global Positioning System (GPS) --- Spacelab D1 mission
[DFVLR-MITT-87-20] 16 p2159 N88-22879
Navigation experiment NAVEX. The reading differences between all ground station measuring clocks during each Spacelab pass of the D1 mission
[DFVLR-MITT-87-23] 16 p2159 N88-22880
The NAVEX experiment in the Spacelab D1 mission: Planning and execution
[ESA-TT-1078] 16 p2166 N88-22913
Timing for subnanosecond pulses
[DE88-701390] 16 p2192 N88-23074
A simulation analysis of errors in the measurement of standard electrochemical rate constants from phase-selective impedance data
[AD-A192739] 20 p2770 N88-26426
Quartz crystal resonators and oscillators for frequency control and timing applications
[AD-A193310] 21 p2937 N88-27443

TIME MEASURING INSTRUMENTS
NT ATOMIC CLOCKS
NT CLOCKS
NT TIMING DEVICES

TIME OF FLIGHT SPECTROMETERS
A program to study antiprotons in the cosmic rays: Arizona collaboration
[NASA-CR-180702] 01 p0120 N88-10764
Laser post-ionization secondary neutral mass spectroscopy
[DE88-002979] 09 p1172 N88-17027
High-voltage inverse-square function generator
[DE88-701109] 15 p2058 N88-22270
Ultrasonic Time-Of-Flight Diffraction (TOFD) measurements of crack depths in an acceleration reservoir of a high velocity research gun
[DE88-006644] 16 p2164 N88-22907
Timing for subnanosecond pulses
[DE88-701390] 16 p2192 N88-23074
Synopsis of a computer program designed to interface a personal computer with the fast data acquisition system of a time-of-flight mass spectrometer
[NASA-CR-177474] 21 p3001 N88-27798
Impurity analysis in SIMOX samples by high-efficiency resonance ionization time-of-flight mass spectrometry
[DE88-012061] 24 p3367 N88-30051

TIME OPTIMAL CONTROL
Optimal control, estimation compensation of linear discrete-time systems with stochastic parameters
[REPT-87-56] 16 p2255 N88-23478
Time-Optimal Adaptive Shaped Torque (TOAST) technical note
[AD-A192719] 20 p2843 N88-26869
Approximations and optimal control for the pathwise average cost per unit time and discounted problems for wideband noise driven systems
[AD-A192712] 21 p3008 N88-27847

TIME SERIES ANALYSIS
Time series infrared spectroscopy of long period variables 04 p0516 N88-13172
Quantile based unified distribution of extreme values and order statistics
[AD-A185171] 05 p0644 N88-13942
New approaches to some methodological problems of meteor science 06 p0741 N88-14557
On the least squares estimator in moving average models of order one
[AD-A186028] 07 p0909 N88-15508
Quasiperiodic variations in manifestations of solar activity 08 p1004 N88-16083
The linear dependency structure of covariance nonstationary time series
[AD-A186548] 09 p1232 N88-17383
Neutrino magnetic moment and time variation of solar neutrino flux
[DE88-700687] 10 p1430 N88-18542
Spectral measurements in a disturbed boundary layer over snow
[AD-A190217] 15 p2097 N88-22494
Simulation analysis of moored fluorometer time series from the Mid-Atlantic Bight
[DE88-006066] 15 p2099 N88-22505
Partial likelihood analysis of time series models with application to rainfall-runoff data
[AD-A191157] 16 p2261 N88-23516
Leave-K-Out diagnostics for time series
[AD-A191343] 16 p2261 N88-23518
Comparison of surface current determined from satellite-tracked buoy with shipboard wind data during the 4th Brazilian antarctic expedition, 10-14 March, 1986
17 p2354 N88-24024
Sea ice kinematics: Space and time scales
[AD-A191162] 17 p2376 N88-24128
Adaptive time series analysis using predictive inference and entropy
[AD-A191858] 18 p2560 N88-25199
Comparison of experimental rotor damping data-reduction techniques 21 p2891 N88-27159
Definition of long ocean wave slope for radar applications
[AD-A193198] 21 p2933 N88-27412
Solution to the compressible Navier-Stokes equations of motion by Chebyshev polynomials with implicit time stepping
[AD-A194119] 22 p3075 N88-28257
Tropospheric biennial variability and its relationship to the southern oscillation 22 p3121 N88-28549
A method to adjust climatological time series for discontinuous inhomogeneities
22 p3124 N88-28570
Atmospheric angular momentum and length of day
[AD-A194505] 23 p3233 N88-29238

TIME SHARING
IPC for modular software requires a third party connect
[AD-A189199] 16 p2248 N88-23414
Piecewise linear approach for timing simulation of VLSI (Very-Large-Scale-Integrated) circuits on serial and parallel computers
[AD-A191328] 16 p2252 N88-23462
Timesharing performance as an indicator of pilot mental workload
[NASA-CR-182807] 18 p2552 N88-25150
The emergence of multi-user expert systems
23 p3260 N88-29406
Networking and AI systems: Requirements and benefits 23 p3263 N88-29425

TIME TEMPERATURE PARAMETER
Effect of time and temperature on transformation toughened zirconias
[AD-A184356] 04 p0419 N88-12600
Time-temperature-stress capabilities of composite materials for advanced supersonic technology application
[NASA-CR-178272] 06 p0677 N88-14144
Finite element explicit algorithm for solving temporal temperature fields 14 p1899 N88-21339
The Time-Temperature-Transformation (TTT) diagram as a basis for relating the formation and properties of reactive coatings
[AD-A190872] 16 p2182 N88-23006
TIMERS
U TIMING DEVICES
TIMING
U TIME MEASUREMENT
TIMING DEVICES
Response of helical structures to high speed pulses or when can a helix be called an inductor
[DE87-014347] 01 p0090 N88-10587
Parallel binary and parallel coded decimal time code formats
[AD-A190126] 17 p2384 N88-24170
Timing control system
[NASA-CASE-NPO-16882-1-CU] 18 p2506 N88-24863
TIMOSHENKO BEAMS
Buckling of braced monosymmetric cantilevers: Timoshenko energy approach
[PB87-133849] 06 p0723 N88-14445
Boundary stabilization of thin elastic plates
[AD-A187123] 10 p1343 N88-18025
Behavior of a two-layered beam under impact loading
[OUEL-1716/87] 17 p2349 N88-23993
Refining finite element models. Numerical application to a lattice structure. Study of a macroelement of Timoshenko beam type
[ONERA-RT-8/3313-RY-070-R] 22 p3144 N88-28696
Analytical and experimental studies of beam waveguide absorbers for structural damping
[AD-A195085] 24 p3382 N88-30144
TIN
Effect of hold time on fatigue of lead rich PbSn solder 06 p0715 N88-14387
A laboratory study of tin whisker growth
[ESA-STR-223] 08 p1089 N88-16553
The effects of various conductor components on Nb3Sn filament prestrain in cable-in-conduit conductors
[DE88-003956] 11 p1479 N88-18824
Properties of reactively sputtered WNx films Zhao, X. -A.
[AD-A188711] 13 p1835 N88-20976
Photoionization dynamics and abundance patterns in laser vaporized tin and lead clusters
[AD-A191604] 18 p2482 N88-24722
Use of digital images as a mineral prospecting tool in the tin province of Goias, Brazil
[INPE-4537-PRE/1284] 24 p3387 N88-30173
TIN ALLOYS
Thermomechanical fatigue of lead-base low tin solder 06 p0721 N88-14432
PbSnTe photovoltaic detectors for operation in the 2-14 micron band
[INPE-4252-PRE/1125] 11 p1508 N88-19008
Fraction eutectic measurements in slowly cooled Pb - 15 wt percent Sn alloys
[NASA-CR-180830] 19 p2618 N88-25531
Magnetization studies of multifilamentary Nb3Sn wires
[DE88-009103] 19 p2735 N88-26243
An HVEM study of displacement cascade damage in Nb3Sn at 13 K
[DE88-009997] 23 p3289 N88-29584
TIN COMPOUNDS
NT NIOBIUM STANNIDES
NT TIN OXIDES
NT TIN TELLURIDES
The Moessbauer effect of SnI4 at high pressure
[DE87-014771] 04 p0495 N88-13048
TIN OXIDES
Steady state and transient behavior of the Pd-SnO(sub x) MIS oxygen sensors 19 p2672 N88-25890
Tin oxide microsensors on thin silicon membranes 19 p2673 N88-25897
TIN TELLURIDES
Analysis of the voltage-current characteristics of metal-isolator-tin-telluride sandwich structures
[ETN-88-91089] 09 p1256 N88-17528
TIP SPEED
Visualisation of the flow at the tip of a high speed axial flow turbine rotor
[AD-A189928] 15 p2063 N88-22300
Visualisation of the flow at the tip of a high speed axial flow turbine rotor: An assessment of flow visualisation techniques and the requirement of the experimental turbine
[AD-A189929] 15 p2063 N88-22301
TIPS
NT BLADE TIPS
NT CRACK TIPS
NT WING TIPS
TIRES
NT AIRCRAFT TIRES
Cornering characteristics of the main-gear tire of the space shuttle orbiter
[NASA-TP-2790] 11 p1438 N88-18583
Advances in contact algorithms and their application to tires
[NASA-TP-2781] 14 p1922 N88-21456
TIROS N SERIES SATELLITES
Assimilation of high resolution TOVS data into a mesoscale NWP model --- numerical weather prediction (NWP) 02 p0213 N88-11338
TIROS OPERATIONAL SATELLITE SYSTEM
Some problems with regard to the TOVS processing detected by using NOAA-HRPT data check program 17 p2351 N88-24009
TIROS SATELLITES
NT TIROS N SERIES SATELLITES
High-spatial-resolution TOVS observations for the FIRE/SRB Wisconsin experiment region from October 14 through November 2, 1986
[NASA-TM-100522] 06 p0747 N88-14593
TISSUES (BIOLOGY)
NT ADIPOSE TISSUES
NT ENDOTHELIUM
Space Bioreactor Science Workshop
[NASA-CP-2485] 09 p1196 N88-17168
Shear and mixing effects on cells in agitated microcarrier tissue culture reactors 09 p1197 N88-17173
Plant cell technologies in space: Background, strategies and prospects 09 p1198 N88-17177
Muscle preservation in the study of bioenergetic effects of hypokinesia 10 p1362 N88-18139
Lipid peroxidation in rat tissues with exposure to antiorthostatic hypokinesia, exercise and immobilization stress 10 p1365 N88-18159
Interactions of cultured human endothelial cells with polymeric surfaces
[PB88-112255] 10 p1369 N88-18178
Critical phenomena and electromagnetic effects in biological membranes
[AD-A188156] 11 p1518 N88-19064
Biophysical applications of solid state and tritium NMR
[DE88-005328] 13 p1808 N88-20806
Studies of model ion channels in defect-free multibilayers of phospholipids
[AD-A188740] 16 p2238 N88-23365
Leg volume change under Lower Body Negative Pressure (LBNP) in dependence on stratification
[DFVLR-FB-87-47] 16 p2238 N88-23367
Photochrome from green plants: Assay, purification and characterization
[DE88-007511] 19 p2702 N88-26067
Improvements in techniques of microwave thermography
[AD-A194613] 23 p3203 N88-29062
Improvements in techniques of microwave thermography
[AD-A193620] 23 p3239 N88-29276
TITAN
Parachute characteristics of Titan descent modules --- planetary probe
[BF-3/86-B] 02 p0122 N88-10774
Study of a Radio Relay Link (RRL). Cassini mission. Data package for final presentation
[ESA-CR(P)-2472] 07 p0847 N88-15138
New concepts for atmospheric braking deceleration in planetary atmosphere entry
[SNIAS-CAS-DECE-P003-DPAA] 16 p2168 N88-22923
Microwave instrument for planetary mission (Titan/CASSINI mission orbiter spacecraft)
[BAE-CS/TP-8359] 24 p3375 N88-30102
TITAN LAUNCH VEHICLES
Reduced flexibility in processing Titan 4 space launch vehicles at Cape Canaveral Air Force Station
[AD-A194908] 24 p3332 N88-29834
TITANATES
NT BARIUM TITANATES
NT LEAD TITANATES
NT LEAD ZIRCONATE TITANATES
NT PEROVSKITES
NT PIEZOELECTRIC CERAMICS
Modeling of irradiation-induced amorphization in a titanate ceramic
[DE87-014751] 03 p0292 N88-11833
Develop techniques for ion implantation of (lead-lanthanum-zirconate-titanate) for adaptive optics
[DE88-000642] 05 p0650 N88-13986
TITANIA
Hafnia-rich mixed oxide ceramics of the system HfO2-ZrO2-TiO2 for heaters and heat exchangers in electrothermal thrusters: The effects of titania on selected electrical and mechanical properties of Hafnia-rich mixed oxides in the system Hafnia-Zirconia-Titania, volume 1
[NASA-CR-182800-VOL-1] 15 p2047 N88-22197
TITANIUM
Comparison of measured temperatures, thermal stresses and creep residues with predictions on a built-up titanium structure
[NASA-TM-86814] 03 p0337 N88-12125
TiN coatings on M2 steel produced by plasma assisted chemical vapor deposition
[DE88-003189] 08 p0970 N88-15867
Tunable Al2O3:Ti3+ laser with optical pumping 09 p1237 N88-17415
Effects of ion implantation on cavitation erosion of a cobalt based metal/carbide alloy
[AD-A187239] 10 p1303 N88-17793
Adhesion of PVD titanium coatings to beryllium substrates
[DE88-005147] 11 p1483 N88-18721
Optical waveguide formation by ion implantation of Ti or Ag
[DE88-004595] 11 p1551 N88-19278
Microprobe examination of composite materials produced by burning of Ti, Cr, C powders with powder of any one Fe-group metal 14 p1886 N88-21269
The effect of titanium reinforcement on the life of positive grids in lead-acid batteries 17 p2320 N88-23857
Stiffened titanium panels
[NASA-CASE-LAR-13814-1] 18 p2497 N88-24816
PLZT (Lead-Lathanium-Zirconium-Titanium) electro-optic photographic system
[AD-A193473] 23 p3215 N88-29137
Electrical properties of materials for elevated temperature resistance strain gage application
[NASA-CR-182214] 24 p3376 N88-30106
TITANIUM ALLOYS
NT NITINOL ALLOYS
Investigation of rapidly-solidified dispersion strengthened titanium alloys
[AD-A183882] 01 p0022 N88-10140
Contribution to the study of the Ti-Al phase diagram by conventional and high resolution electron microscopy
[ESA-TT-1021] 01 p0023 N88-10143
Superplastic deformation and post forming tensile properties of Ti-6Al-4V sheet
[RAE-TR-86015] 01 p0023 N88-10144
Structure of rapidly solidified Ni-Ti
[DE87-012252] 02 p0147 N88-10921
Strain rate effects in fast-gas-cooled uranium-titanium and uranium-niobium alloys
[OUEL-1683/87] 02 p0149 N88-10937
Corrosion-electrochemical and mechanical properties of composite graphite-carbide metal materials based on titanium and its alloys 03 p0285 N88-11794
A fundamental study of the mechanical and microstructural response of elevated temperature PM aluminum-titanium alloys 03 p0289 N88-11819
China report: Science and technology
[JPRS-CST-87-015] 03 p0298 N88-11873
Status of titanium alloys R and D described 03 p0298 N88-11876
The mechanical properties of solid state diffusion bonds between Ti-6Al-4V and 304L stainless steel
[BAJ-TR-113-1987] 03 p0332 N88-12093
The effect of microstructure on the surface crack length: Crack depth relationship for short cracks 05 p0600 N88-13670
Crack growth in contrasting titanium alloys under the conjoint action of high and low cycle fatigue 05 p0602 N88-13686
Characterization of the microstructures of various materials
[AD-A184961] 05 p0655 N88-14017
Reactions and bonding between glasses and titanium
[DE88-000603] 06 p0685 N88-14195
Effect of overload ratios on fatigue crack growth behavior in Ti-6Al-4V alloy
[PB87-147062] 07 p0833 N88-15055
The effect of varying sputtering parameters on the microstructure and mechanical properties of 10 percent Ni + TiB2 thin films
[DE88-002600] 09 p1254 N88-17517
Transmission electron microscopy studies of titanium-containing braze/alumina seals
[DE88-005243] 10 p1303 N88-17792
Structural analysis using X-ray scattering and neutron scattering on binary amorphous (Co,Cu)Ti alloys
[ETN-88-91487] 11 p1459 N88-18699

Elevated temperature crack growth studies of advanced titanium aluminides
[AD-A189025] 12 p1608 N88-19618
Thermal-mechanical fatigue testing of a titanium-aluminide alloy
[AD-A189555] 12 p1609 N88-19620
An interdisciplinary approach to predictive modeling of structural adhesive bonding: Factors affecting the durability of titanium/epoxy bonds
[AD-A189503] 12 p1611 N88-19636
Threshold fatigue crack growth in Ti-6Al-2Sn-4Zr-6Mo
[AD-A189560] 13 p1741 N88-20415
Phenomenological piercing characteristics of composite materials 14 p1895 N88-21315
Optimization of oxygen cutting process for titanium alloys 14 p1897 N88-21323
Characteristics of joint formation during friction welding of Ti alloys to Nb alloys 14 p1898 N88-21329
Growth and deformation mechanisms of refractory alloy hybrid materials
[AD-A190492] 15 p2039 N88-22152
Investigation of laser diagnostics of PACVD processes for depositing hard face coatings
[DE88-007083] 15 p2043 N88-22176
Titanium powder frit made during the transformation alpha-beta
[ETN-88-91999] 16 p2177 N88-22976
Deformation of rapidly solidified dispersion strengthened titanium alloys
[AD-A190793] 16 p2179 N88-22984
Fundamental studies of beta phase decomposition modes in titanium alloys
[AD-A191495] 18 p2485 N88-24740
On the reversion phenomena of Cu-3 percent Ti alloys
[NASA-TT-20170] 18 p2488 N88-24762
Optimization of mechanical/corrosion properties of TI-CODE 12 plate and sheet. Part 2: Thermomechanical processing effects
[DE88-007493] 19 p2616 N88-25517
Apparatus for pressure welding of titanium structures with a controlled rate of deformation
[RAE-TRANS-2161] 19 p2677 N88-25915
Study of probabilistic fatigue crack growth and associated scatter under constant-and-variable amplitude loading spectrum
[AD-A192027] 19 p2679 N88-25929
Prediction of fatigue life of notched specimens under aircraft loading and importance of the relative method in the case of local strain approach, part 2
[TAE-595-PT-2] 19 p2680 N88-25934
Initial development of high-temperature titanium silicide alloys
[DE88-007860] 20 p2772 N88-26437
Glass forming ranges of amorphous alloys
[DE88-007897] 20 p2772 N88-26438
A fundamental understanding of the interfacial compatibility in hybrid material systems
[AD-A192921] 21 p2909 N88-27264
Constant amplitude fatigue life data for notched and unnotched annealed Ti-6Al-4V sheet
[AD-A193420] 21 p2913 N88-27287
Influence of microstructure and microdamage processes on fracture at high loading rates
[AD-A192957] 21 p2960 N88-27583
Stress relaxation of a titanium (Ti-6Al-4V) threaded joint
[DE88-010102] 21 p2961 N88-27590
JTDE 1 XTE34 materials research and development report
[AD-A194268] 22 p3044 N88-28063
As-received microstructure of a SiC/Ti-15-3 composite
[NASA-TM-100938] 22 p3050 N88-28095
Optimization of fatigue and friction properties of titanium by means of surface treatments
[ECL-87-22] 22 p3056 N88-28133
Investigation of a SiC/Ti-24Al-11Nb composite
[NASA-TM-100956] 23 p3190 N88-28980
Influence of peak pressure on the substructure evolution and shock wave profiles of Ti-6Al-4V
[DE88-006458] 23 p3225 N88-29197
Development of Nb-Ti multifilamentar superconducting wires
[DE88-702324] 23 p3290 N88-29592

TITANIUM BORIDES
Carbon-fiber reinforced aluminum
04 p0403 N88-12507
Wire-cut electrical discharge machinability of ceramics
[AD-A186989] 09 p1146 N88-16870
The effect of varying sputtering parameters on the microstructure and mechanical properties of 10 percent Ni + TiB2 thin films
[DE88-002600] 09 p1254 N88-17517

TITANIUM CARBIDES
Analysis of phase equilibria in NiTi-C system in high nickel regions
[BLL-M-37304-(5828.4)] 02 p0149 N88-10932
Hadfield steels with Nb and Ti carbides
[DE87-703706] 04 p0416 N88-12579
New application of transition metal carbides detailed
06 p0675 N88-14132
Ball bearings with chemical vapor deposition (CVD)-TiC coated components 14 p1876 N88-21210
Titanium carbide coatings for aerospace ball bearings
14 p1927 N88-21486

TITANIUM COMPOUNDS
NT BARIUM TITANATES
NT LEAD TITANATES
NT LEAD ZIRCONATE TITANATES
NT PEROVSKITES
NT PIEZOELECTRIC CERAMICS
NT RUTILE
NT TITANATES
NT TITANIUM BORIDES
NT TITANIUM CARBIDES
NT TITANIUM NITRIDES
NT TITANIUM OXIDES
Optical frequency doubling in Ti:LiMbO3 waveguide resonators
[ETN-88-91486] 11 p1550 N88-19271
Muon motion in titanium hydride
17 p2396 N88-24247

TITANIUM DIOXIDE
U TITANIUM OXIDES

TITANIUM NITRIDES
Tin activated reactive ion plating and its application
[PB87-144036] 08 p0970 N88-15871
Bias, internal stress and substrate effects on the microstructure and properties of PVD-wear resistant coatings
[AERE-R-12360] 10 p1304 N88-17798
The preparation of titanium nitride and titanium carbonitride by the preceramic polymer route
[AD-A188357] 12 p1610 N88-19626
Structure and properties of titanium nitride and zirconium nitride thin films prepared by reactive ion plating --- cutting tools
[ETN-88-92218] 15 p2042 N88-22167

TITANIUM OXIDES
NT RUTILE
Auger electron spectroscopy of oxidized titanium overlayers: Speciation of homogeneous and heterogeneous samples
[KFK-4221] 02 p0146 N88-10913
Characterization of catalysts with metal-support effects and of the species adsorbed on their surfaces
[DE87-014636] 04 p0414 N88-12564
Titanium oxide absorption and spot sizes in II Peg, HR 1099 and UX Ari 04 p0508 N88-13126
On 1064 nm and 350 nm laser damage thresholds of high index oxide films deposited from organic solutions and sols
[DE88-001636] 07 p0859 N88-15217
Point defect structure of Cr2O3
[AD-A187620] 11 p1556 N88-19317
The influence of processing variables on physical properties of sol-gel derived TiO2 films
[DE88-005155] 11 p1559 N88-19331
Model catalyst studies of SMSI (Strong Metal/Support Interactions) and the role of D-electrons in chemisorption and catalysis
[DE88-004518] 13 p1738 N88-20393
Oxide-bound transition metal complexes for methane activation
[PB88-169719] 14 p1887 N88-21277
Chemical vapor deposition of TiO2 thin films at room temperature
[DE88-008892] 21 p2953 N88-27542
Al2O3-TiO2 and Al2TiO5 ceramic materials
[SNIAS-881-430-122] 23 p3199 N88-29038

TITRATION
Titrimetric analysis of HAN-based liquid propellants
[AD-A196225] 24 p3357 N88-29990

TNT (TRINITROTOLUENE)
U TRINITROTOLUENE

TOILETS
Evaluation of the Shasta Waterless System as a remote site sanitation facility
[AD-A186000] 07 p0898 N88-15442

TOKAMAK DEVICES
NT JOINT EUROPEAN TORUS
Behavior of graphites under intense heat loads
[DE87-012128] 01 p0028 N88-10179
Shear strength of the ASDEX upgrade Toroidal Field (TF) coil insulation: Rupture, fatigue and creep behavior --- tokamak
[IPP-1/230] 01 p0059 N88-10376
Millimeter wave tokamak heating and current drive with a high power free electron laser
[DE87-011324] 01 p0099 N88-10651
Massachusetts Institute of Technology Plasma Fusion Center: 1986-1987 Report to the President
[DE87-013518] 01 p0101 N88-10661
Thermally driven convective cells and tokamak edge turbulence
[DE87-014424] 02 p0238 N88-11499
On tokamak equilibrium
[DE87-014811] 02 p0239 N88-11507
System studies of compact ignition tokamaks
[DE87-014976] 02 p0239 N88-11508
Improvement of energy confinement of neutral beam heated plasma by lower hybrid current drive in JT-60
[DE87-752983] 02 p0239 N88-11509
Two dimensional neutral transport analysis in tokamak plasma
[DE87-752984] 02 p0239 N88-11510
Transport analysis of OH and NBI heated discharges in JT-60
[DE87-752985] 02 p0239 N88-11511
Spectrograms of the visible region in the JT-60 tokamak (wavelength range from 2210 A to 5250 A)
[DE87-753002] 02 p0240 N88-11513
Analysis of energy confinement of slideaway discharges
[DE87-753008] 02 p0240 N88-11515
Vectorization of MHD equilibrium and stability codes
[DE87-753013] 02 p0240 N88-11516
Planning for US ion cyclotron heating research relevant to the compact ignition tokamak and Alcator C-Mod
[DE88-000022] 02 p0241 N88-11520
Relative merits of size, field, and current on ignited Tokamak performance: A comparison of CITs and Super-JETs
[DE88-000038] 02 p0241 N88-11521
Fracture mechanism of fine grain graphite under high heat fluxes
[IPPJ-842] 02 p0242 N88-11527
Simulation of tokamak runaway-electron events. Study of the response of materials by use of an electron linear accelerator
[IPPJ-841] 02 p0242 N88-11528
Wavepacket propagation and current startup near the lower hybrid frequency in the torus
[IPPJ-840] 02 p0242 N88-11529
Limit of possible operation of crescent and bean shaped Tokamaks
[IPPJ-837] 02 p0242 N88-11532
Laser blow-off experiments on ASDEX --- tokamak
[IPP-III/119] 02 p0243 N88-11535
A microwave FEL (Free Electron Laser) code using waveguide modes
[DE88-000225] 03 p0330 N88-12084
Application of a two fluid theoretical plasma transport model on current Tokamak reactor designs
[DE87-013511] 03 p0377 N88-12373
Mathematical models of plasma discharge control in a tokamak
[DE87-702891] 03 p0378 N88-12377
Stability of low-shear Tokamaks
[DE88-000305] 03 p0379 N88-12383
Negative ion beams for heating and current-drive in NET
[AD-A184390] 04 p0489 N88-13012
Data base on the high heat flux behaviour of metals and carbon materials for plasma facing components: Experiments at the 10 MW neutral beam injection test stand of the IPP Nagoya
[IPPJ-AM-53] 04 p0492 N88-13031
Refueling and density control in the ZT-40M reversed field pinch
[DE88-000504] 04 p0493 N88-13040
Modular pump limiter systems for large tokamaks
[DE88-001487] 04 p0494 N88-13045
ICRF launcher studies
[DE88-001710] 04 p0495 N88-13046
ALT-1 pump limiter experiments
[DE88-000822] 05 p0651 N88-13989
Subcommittee for MHD theory
[DE88-000596] 05 p0653 N88-14003
Effect of plasma rotation in tokamak on stabilizing action of electrically conducting wall 06 p0773 N88-14748
Confinement of energy in tokamak-10 plasma during electron-cyclotron-resonance heating
06 p0773 N88-14750
TIBER 2 (Tokamak Ignition/Burn Experimental Reactor) parameters with neutral beams at high energies
[DE88-001891] 06 p0783 N88-14803
Overview of the TIBER 2 (Thermal Ignition/Burn Experimental Reactor) design
[DE88-001892] 06 p0783 N88-14804
Modeling of thermal effects on TIBER 2 (Thermal Ignition/Burn Experimental Reactor) divertor during plasma disruptions
[DE88-001893] 06 p0783 N88-14805
Slowing down tail enhanced, neoclassical and classical alpha particle fluxes in tokamak reactors
[DE88-001930] 06 p0783 N88-14806
Poloidal magnetics of compact ignition tokamaks
[DE88-001774] 07 p0934 N88-15672

Reversed field pinch experiments: Summary of progress report
[DE88-002367] 07 p0934 N88-15673
Method of plasma diagnostics by a heavy ion beam for the T-15 tokamak
[DE88-700342] 07 p0935 N88-15678
Study on the mechanical stresses in the elements of the model of a toroidal magnet of a tokamak with strong field
[DE88-700343] 07 p0935 N88-15679
Study on the model of a toroidal magnet for a tokamak with a strong field
[DE88-700346] 07 p0935 N88-15681
Gas feed system for the T-15 tokamak discharge chamber
[DE88-700351] 07 p0935 N88-15682
Simulation an experiment on plasma instability investigation in a tokamak with a divertor
[DE88-700352] 07 p0935 N88-15683
Model for plasma equilibrium configuration evolution in a tokamak with adiabatic compression
[DE88-700354] 07 p0936 N88-15684
Simple model for hot ion plasmas
[DE88-750045] 07 p0936 N88-15688
Conceptual design of a radio-frequency driven compact tokamak
[INPE-4364-PRE/1190] 08 p1085 N88-16535
A ray-tracing study of electron cyclotron resonance heating in tokamak plasmas with a superthermal electron tail
[INPE-4381-PRE/1201] 08 p1085 N88-16536
Shape of the plasma boundary in TBR
[INPE-4388-PRE/1208] 08 p1086 N88-16540
Absorption of electron cyclotron radiation in tokamak plasmas with a superthermal tail in the electron velocity distribution
[INPE-4391-PRE/1211] 08 p1086 N88-16541
Tangential Thomson scattering --- plasma diagnostics
[REPT-87-173] 08 p1087 N88-16548
Nonlinear evolution of the internal kink mode in toroidal geometry for shaped tokamak plasmas
[DE88-003655] 08 p1087 N88-16550
Microwave system for the microwave Tokamak experiment (MTX)
[DE88-002391] 09 p1250 N88-17487
Influence of fast alpha diffusion and thermal alpha buildup on Tokamak reactor performance
[DE88-003661] 09 p1251 N88-17496
Two-dimensional analysis for a scrapeoff and divertor regions with an MHD model. Conceptual design study of FY86 FER
[DE88-751069] 09 p1251 N88-17497
Pump limiter experiments and analysis in the TEXTOR tokamak 09 p1252 N88-17506
Proceedings of the Energy Independence Conference: Fusion Energy and Plasma Physics
[DE88-700657] 09 p1253 N88-17507
Application of high temperature ceramic superconductors (CSC) to commercial tokamak reactors
[DE88-003973] 09 p1257 N88-17538
Tokamak with highly elongated cross-section of a plasma
[DE88-700356] 10 p1410 N88-18412
Plasma physics design and major specifications of candidate reactors for FER design studies. Conceptual design study of FY86 FER
[DE88-751066] 10 p1411 N88-18416
Development of tokamak reactor system analysis code NEW-TORSAC
[DE88-751067] 10 p1411 N88-18417
Toroidal confinement research concepts evaluation and tradeoff studies
[DE88-004277] 11 p1551 N88-19282
Magnetic and inertial fusion status and development plans
[DE88-004405] 11 p1552 N88-19288
Problems in modeling TF ripple loss of fast alphas from a tokamak reactor
[DE88-000612] 11 p1553 N88-19296
A neutral-beam diagnostic for fast confined alpha particles in a burning plasma: Applicatoin on CIT (Compact Ignition Tokamak)
[DE88-004890] 11 p1554 N88-19301
CIT (Compact Ignition Tokamak) fueling
[DE88-002709] 12 p1692 N88-20125
Plasma rotation in a tokamak
[DE88-700855] 12 p1693 N88-20128
FOM contributions to the 14th European Conference on Controlled Fusion and Plasma Physics
[REPT-87-174] 12 p1693 N88-20129
Microturbulent fluctuations in the TORTUR tokamak 12 p1693 N88-20131
Flux coordinate studies of elongated plasmas at high Beta 12 p1694 N88-20134
A high field launch for electron cyclotron heating using an external window
[DE88-005350] 13 p1838 N88-21000
Observations on energy transport in tokamaks: A new formula for turbulent transport
[DE88-005309] 13 p1841 N88-21019
Evolution of poloidal variation of impurity density and ambipolar potential in rotating tokamak plasma, part 1
[DE88-006263] 13 p1842 N88-21022
Potential off-normal events and associated radiological source terms for the compact ignition tokamak: Fusion Safety Program
[DE88-004112] 13 p1842 N88-21024
Consistency between current ramp-up/recharging scenario by non-inductive current drive and dense and cold divertor plasma. Conceptual design study of FY86 FER
[DE88-751438] 14 p1984 N88-21833
Preliminary analysis on plasma equilibrium control. Conceptual design study of FY86 FER
[DE88-751441] 14 p1984 N88-21834
Preparing the Alcator C bolometer system for use on MTX (Microwave Tokamak Experiment)
[DE88-006724] 15 p2134 N88-22733
Analyses and experiments on the integrity and lifetime predictions of plasma-facing components in fusion reactors
[DE87-702957] 15 p2135 N88-22735
Environmental assessment for the compact ignition Tokamak
[DE88-005633] 15 p2135 N88-22740
Long-time impurity confinement as a precursor to disruptions in ohmically heated tokamaks
[DE88-006183] 15 p2136 N88-22742
Current-drive on the Versator-2 tokamak with a slotted-waveguide fast-wave coupler
[DE88-006261] 15 p2136 N88-22743
Improvement of plasma confinement due to electron Landau damping in tokamaks
[DE88-752339] 15 p2136 N88-22747
Transport simulations of ohmic ignition experiment: IGNITEX
[DE88-006055] 15 p2138 N88-22757
Incorporating reliability into the design of experimental fusion facilities
[DE88-006767] 16 p2275 N88-23618
Soviet magnetic confinement fusion research
[PB88-182316] 16 p2279 N88-23644
Remote maintenance design activities and research and development accomplishments for the compact ignition tokamak
[DE88-006980] 16 p2279 N88-23645
Corpuscular plasma diagnostics complex on a tokamak with a strong field
[DE88-701576] 16 p2279 N88-23646
Ion temperature measurement with spectroscopy in JT-60 17 p2439 N88-24513
X-ray emission from tokamaks 17 p2439 N88-24514
X-ray spectroscopic diagnostics on JIPPT-IIU and HELIOTRON-E 17 p2440 N88-24515
Helium-like titanium spectra from tokamak plasmas 17 p2440 N88-24516
Spectroscopic results from JET: Some examples of data comparison and data needs 17 p2440 N88-24517
Tokamak studies of density sensitive line ratios 17 p2441 N88-24521
Flux density measurements of neutral iron in TEXTOR with laser induced fluorescence 17 p2442 N88-24528
Measurements of Z(sub eff) profile with a visible bremsstrahlung continuum detector array 17 p2443 N88-24529
Availability and quality of spectroscopic data and standards for tokamak studies 17 p2443 N88-24534
Systems analysis of INTOR-like designs
[DE88-004422] 18 p2578 N88-25316
A study of runaway electron confinement in the ASDEX tokamak
[DE88-007327] 18 p2579 N88-25319
A two-wavelength infrared interferometer/polarimeter system for CIT (Compact Ignition Tokamak)
[DE88-007681] 18 p2579 N88-25321
ECRH current drive in tokamak plasmas
[IPPJ-864] 19 p2729 N88-26209
Parallel gradient effects on ICRH (Ion Cyclotron Resonance Heating) in tokamaks
[DE88-009038] 19 p2730 N88-26216
Evolution of poloidal variation of impurity density and ambipolar potential in rotating tokamak plasma, part 2
[DE88-009882] 19 p2731 N88-26218
Thermal and mechanical analysis of the Faraday shield for the compact ignition tokamak
[DE88-007855] 20 p2856 N88-26962
Fusion programs in applied plasma physics and development and technology at GA Technologies, Inc.
[DE88-008406] 20 p2856 N88-26964
Multipoint Thomson scattering diagnostic for DIII-D
[DE88-008737] 20 p2857 N88-26969
TIBER (Tokamak Ignition/Burn Experimental Reactor) 2 as a precursor to an international thermonuclear experimental reactor
[DE88-008906] 20 p2858 N88-26970
Requirements for neutral beam current drive in tokamaks
[DE88-006180] 20 p2859 N88-26980
Impurity transport calculations for a drift-dependent tokamak scrape-off plasma
[DE88-010053] 20 p2859 N88-26984
Full-wave calculations in flux coordinates for toroidal geometry
[DE88-010131] 20 p2860 N88-26985
Toroidal and poloidal soft X-ray imaging system on the D3-D tokamak
[DE88-010585] 20 p2860 N88-26986
Vertical viewing ECE diagnostic for the D3-D tokamak
[DE88-010586] 20 p2860 N88-26987
MTX (Microwave Tokamak Experiment) plasma diagnostic system
[DE88-011326] 20 p2861 N88-26993
Multi-mode optical fibers for simultaneous 13-position measurements Thomson scattering apparatus in the JFT-2M tokamak
[DE88-753133] 21 p3015 N88-27897
Moment approach to neoclassical flows, currents and transport in auxiliary heated tokamaks
[DE88-008024] 21 p3016 N88-27901
Tokamak magnetic turbulence over the safety factor range 0.6 less than q less than 3
[DE88-008421] 21 p3017 N88-27904
ITER plasma equilibrium and poloidal field system design
[DE88-011005] 21 p3018 N88-27912
Global and local magnetohydrodynamic relaxations
[DE88-752602] 21 p3018 N88-27913
Design of divertor plate and measurements of double-null open divertor plasma in the JFT-2M tokamak
[DE88-753130] 21 p3018 N88-27914
Analysis of lower hybrid current drive and rampup experiments on the JT-60 tokamak
[DE88-753136] 21 p3018 N88-27915
Reactor applications of the Compact Fusion Advanced Rankine (CFAR) cycle for a D-T tokamak fusion reactor
[DE88-011351] 22 p3153 N88-28762
A survey of the current experimental database for lower hybrid current-drive and heating
[DE88-009830] 23 p3283 N88-29552
Numerical simulations of resistive magnetohydrodynamic instabilities in a poloidal divertor tokamak
[DE88-010768] 23 p3285 N88-29559
Bootstrap currents in radio-frequency-driven tokamak equilibria
[DE88-011136] 23 p3285 N88-29561
Tokamak plasma interaction with limiters
[UTIAS-325] 23 p3286 N88-29566
The calculation of time dependent eddy currents in tokamaks
[REPT-206] 23 p3286 N88-29568
Stability experimental results of cable-in-conduit superconductor for fusion
[DE88-753424] 23 p3290 N88-29589
The study of hydromagnetic waves and RF heating using the TORTUS tokamak, the development of diagnostic techniques based on submillimeter lasers and the gyrotron, and gas discharge 24 p3431 N88-30419

TOLERANCES (MECHANICS)
NT IMPACT TOLERANCES
Effects of barrel joints on hypervelocity projectiles
[DE87-013447] 02 p0157 N88-10983
Pinhole occulter experiment
[NASA-CR-179206] 02 p0235 N88-11481
Damage considerations in sizing aircraft cells. Life predictions
[SNIAS-872-111-116] 05 p0548 N88-13330
A study of damage tolerance in curved composite panels
[AD-A190617] 15 p2029 N88-22092
Manufacturing requirements 17 p2297 N88-23745
Fuel containment and damage tolerance in large composite primary aircraft structures. Phase 2: Testing
[NASA-CR-172519] 19 p2601 N88-25452
A comprehensive study on damage tolerance properties of notched composite laminates
[AD-A192952] 23 p3188 N88-28968

TOLERANCES (PHYSIOLOGY)
NT ACCELERATION TOLERANCE
NT ALTITUDE TOLERANCE
NT COLD TOLERANCE

NT HEAT TOLERANCE
NT HUMAN TOLERANCES
NT RADIATION TOLERANCE
Superoxide dismutase assays
[AD-A183972] 03 p0356 N88-12242
Microwave challenges to the thermoregulatory system
[AD-A185391] 05 p0629 N88-13847
Possible use of plasmids for study of effect of space flight factors on biological objects
08 p1046 N88-16319
Exercise thermoregulation after prolonged wakefulness
[AD-A186224] 08 p1048 N88-16327
Rational considerations for modelling human thermoregulation during cold water immersion
[AD-A186226] 08 p1048 N88-16329
Portable, ambient air microclimate cooling in simulated desert and tropic conditions
[AD-A186457] 08 p1050 N88-16338
Respiratory and cardiovascular responses to cold stress following repeated cold water immersion
[AD-A186460] 08 p1050 N88-16340
The role of hydration on peripheral response to cold
[AD-A186448] 09 p1199 N88-17186
Brain potentials and personality: A new look at stress susceptibility
[AD-A186931] 09 p1199 N88-17189
Annoyance caused by advanced turboprop aircraft flyover noise: Single-rotating propeller configuration
[NASA-TP-2782] 09 p1242 N88-17441
The precision of limits on bodily fluids when using beta-expectation inner tolerance limits
[AD-A187966] 10 p1369 N88-18185
Psychophysical, biochemical and histological studies of spectrally selective photic damage to primate retina
[AD-A188115] 11 p1517 N88-19063
Toxic effects of man-made mineral fibers with particular reference to ceramic fibers
[AD-A187949] 11 p1519 N88-19072
Interrelationship of heart rhythm indicators and resistance to hypoxia in Antarctic polar workers
12 p1664 N88-19974
Air quality and human performance, chapter 16
[AD-A188335] 12 p1666 N88-19988
Medical problems related to altitude in: Human performance physiology and environmental medicine at terrestrial extremes, chapter 14
[AD-A188340] 12 p1666 N88-19989
Direct interaction between autonomic nerves and the immune system
[AD-A188576] 12 p1667 N88-19991
Behavioral response of rats exposed to high-power microwave radiation
[AD-A192199] 18 p2548 N88-25128
Extremely Low Frequency (ELF) communications system ecological monitoring program: Summary of 1986 progress
[AD-A192014] 19 p2642 N88-25676
Assessment of cochlear damage after microwave irradiation
[AD-A193237] 21 p2987 N88-27737
Evaluation of the potential health hazards associated with the machining of carbon fiber composites
[AD-A194835] 24 p3408 N88-30286

TOLLMEIN-SCHLICHTING WAVES
Numerical simulation of Tollmien-Schlichting waves by use of a modified vortex particle-in-cell method
[IC-AERO-85-02] 02 p0171 N88-11079
Time-dependent hypersonic viscous interactions
[AD-A185764] 06 p0665 N88-14082
Computational design of natural laminar flow wings for transonic transport application 07 p0813 N88-14948
On the interaction of Tollmein-Schlichting waves in axisymmetric supersonic flows
[NASA-CR-181619] 10 p1331 N88-17955
Development of disturbances in swept wing flows
[NASA-CR-182675] 13 p1768 N88-20574
Ejection mechanisms in the sublayer of a turbulent channel 16 p2195 N88-23090
Wave-growth associated with turbulent spot in plane Poiseuille flow 16 p2199 N88-23116
Active control of 2-D instability waves on an axisymmetric body
[AD-A191578] 19 p2663 N88-25835
Variable Sweep Transition Flight Experiment (VSTFE)-parametric pressure distribution boundary layer stability study and wing glove design task
[NASA-CR-3992] 23 p3173 N88-28894
Nonlinear Tollmien-Schlichting/vortex interaction in boundary layers
[NASA-CR-181698] 24 p3311 N88-29715
The strong nonlinear interaction of Tollmien-Schlichting waves and Taylor-Goertler vortices in curved channel flow
[NASA-CR-181697] 24 p3311 N88-29716
On the generation of mean flows by the interaction of Goertler vortices and Tollmien-Schlichting waves in curved channel flows
[NASA-CR-181690] 24 p3315 N88-29743

TOLUENE
Detailed mechanism of toluene oxidation and comparison with benzene
[NASA-TM-100261] 05 p0563 N88-13428
Characterization of the dimensions of colloidal calcium carbonate dispersions in toluene with neutron small-angle scattering
[ECN-197] 06 p0680 N88-14167
Study of toluene stability for an Organic Rankine Cycle (ORC) space-based power system
[NASA-CR-180884] 24 p3337 N88-29863
Study of toluene rotary fluid management device and shear flow condenser performance for a space-based organic Rankine power system
[NASA-CR-180885] 24 p3338 N88-29872

TOMAHAWK MISSILES
Non-linear shipboard shock analysis of the Tomahawk missile shock isolation system 05 p0592 N88-13614

TOMOGRAPHY
NT COMPUTER AIDED TOMOGRAPHY
Model-based ultrasonic tomography
[DE87-013786] 01 p0058 N88-10369
A comparison of film-based tomography and computed tomography for advanced ceramic materials
[DE88-003114] 07 p0837 N88-15079
A new technique for rocket and space-borne investigations of time-dependant auroral morphology
08 p1030 N88-16241
The Quick Response Multicolor Printer (QRMP) system
[AD-A188140] 11 p1504 N88-18982
Geophysical diffraction tomography for imaging isolated subsurface inclusions
[DE88-003918] 11 p1505 N88-18990
Estimation of sea surface wave spectra using acoustic tomography
[AD-A187837] 11 p1516 N88-19057
Three-dimensional image reconstruction in object space
[DE88-900279] 12 p1712 N88-20246
A study of satellite emission computed tomography
[AD-A189567] 13 p1797 N88-20745
Studies toward observing and modelling large energetic ocean regions
[AD-A189267] 13 p1803 N88-20778
Survey of acoustic techniques for monitoring El Nino
[PB88-157615] 13 p1804 N88-20783
Tectonics and three-dimensional structure of spreading centers: Microearthquake studies and tomographic inversions
[PB88-163290] 14 p1945 N88-21602
XDATAP
[DE88-007161] 20 p2837 N88-26827
The design of a digital Eprom oscillator for electrical impedance tomography
[DE88-012243] 21 p2940 N88-27462
Interferometric tomography of continuous fields with incomplete projections
[NASA-CR-183181] 22 p3081 N88-28295
Variation of carotid flow under load, studied by the Doppler echo method --- acceleration tolerance
[REPT-1149] 23 p3240 N88-29282
Positron emission tomography: A new technique for observing fluid behavior in engineering systems
[PNR90471] 24 p3374 N88-30091
Central adrenergic receptors as mediators of central response to stress: Study with Positron Emission Tomography (PET)
[AD-A194947] 24 p3407 N88-30284

TOMS
U TOTAL OZONE MAPPING SPECTROMETER

TONE
U PITCH

TONOMETRY
U PRESSURE MEASUREMENT

TONUS
U MUSCULAR TONUS

TOOLS
NT GRINDING MACHINES
NT LATHES
NT MACHINE TOOLS
NT MILLING MACHINES
NT SPACE TOOLS
Human engineering laboratory grounding analysis (HELGA)-2
[AD-A185367] 05 p0578 N88-13524
Interaction of microstructure and fatigue in tool steels
05 p0603 N88-13693
Tool and process for miniature explosive joining of tubes
[NASA-CASE-LAR-13662-1] 06 p0711 N88-14359
Proceedings of the DOD Workload Assessment Workshop on Workload Assessment Techniques and Tools held in Dayton, Ohio on 27-28 September 1986
[AD-A185650] 08 p1052 N88-16352
Friction welding: Advanced method of producing end cutting tool 14 p1897 N88-21327

TOPEX
Specifications and performance of ultrastable oscillators in the DORIS orbitography and positioning system
[ETN-88-92761] 24 p3331 N88-29831

TOPOGRAPHY
NT TERRAIN
Venusian surface and crust 01 p0010 N88-10054
The program DSMME: Digital Situation Model, Measurement --- mapping 01 p0065 N88-10418
Geoacoustic models of the Hudson Canyon area
[AD-A183535] 01 p0073 N88-10465
Surface topography and electrical response of metal-electrolyte interface
[DE87-013553] 02 p0166 N88-11046
On the role of snow in the redistribution of precipitation by small scale topography 02 p0203 N88-11267
Validation of a three dimensional numerical model of the sea breeze in complex terrain
02 p0211 N88-11325
Spherical harmonic expansion of the Levitus Sea surface topography
[NASA-CR-181448] 02 p0216 N88-11362
Cartography and topography with SPOT
03 p0342 N88-12159
Considering refraction in leveling with laser plane
04 p0462 N88-12857
Radial orbit error reduction and sea surface topography determination using satellite altimetry
04 p0462 N88-12861
The influence of the topography of fracture surfaces on crack closure 05 p0598 N88-13657
Sound propagation over uneven ground and irregular topography
[NASA-CR-182352] 06 p0776 N88-14763
Wind and temperature structure on the slopes of a mountain valley
[DE88-000080] 07 p0880 N88-15338
Laser system for automating topographic terrain survey 08 p1012 N88-16136
Estimation of gravity vector components from Bell gravity gradiometer and auxiliary data under consideration of topography and associated analytical upward continuation aspects
[AD-A188146] 10 p1355 N88-18099
NASA Oceanic Processes Program
[NASA-TM-4025] 10 p1357 N88-18109
Terrain Analyst Work Station (TAWS) demonstrations
[AD-A188139] 11 p1504 N88-18981
Digital data dubbing capability
[AD-A188252] 11 p1525 N88-19105
Silicon containing photoresists
[AD-A188666] 12 p1605 N88-19601
Influence of solar illumination conditions on TM/Landsat data
[INPE-4483-TDL/320] 12 p1638 N88-19806
Automatic knowledge acquisition for aerial image interpretation
[AD-A188616] 12 p1638 N88-19810
Research on the physical oceanography of the Gulf Stream
[AD-A188512] 12 p1649 N88-19877
Airborne electromagnetic sounding of sea ice thickness and sub-ice bathymetry
[AD-A188939] 12 p1649 N88-19879
A comparison of terrain association and resection as methods of position location
[AD-A189480] 13 p1790 N88-20710
Comparisons of global topographic/isostatic models to the Earth's observed gravity field
[NASA-CR-182696] 13 p1798 N88-20752
Planetary scale barotropic spectral model
13 p1801 N88-20766
Bathymetric hazard survey test
[AD-A189150] 13 p1803 N88-20775
Study of the dynamic topography of oceans by means of satellite altimetry 14 p1938 N88-21567
From satellite altimetry to ocean topography, a survey of data processing techniques
[ETN-88-91841] 14 p1939 N88-21575
Inventory of topographic mapping and standardization of geographic names as the basis of a Geographic Information System (GIS) 16 p2225 N88-23281
Mass digitization of topographic-cartographic information 16 p2226 N88-23288
Developments in the design of topographic maps in the Federal Republic of Germany: Activities and suggestions
16 p2226 N88-23290

The use of LANDSAT-TM pictures for the detection of space-limiting elements for the benefit of landscape photomapping
[BCRS-87-02] 16 p2228 N88-23305
Geometric image correction: An approach for the registration of LANDSAT-TM digital images supported by topographical maps of medium and great scales
17 p2361 N88-24061
Criteria for planimetric and altimetric correction of maps restituted from aerial photographs in 1:100,000 scale
17 p2367 N88-24097
The determination of gravity and topography from seismic velocities, accounting for dynamic behavior of the Earth's mantle
[ETN-88-92420] 17 p2374 N88-24117
Reports on cartography and geodesy. Series 1, no. 99
[ETN-88-92387] 18 p2533 N88-25025
West German Geodetic Working Group: Official topographic-cartographic information system (ATKIS), content description 18 p2533 N88-25026
West German Geodetic Working Group: Official topographic-cartographic information system (ATKIS), technical conception 18 p2533 N88-25027
Creation of digital topographic models with the ALK-GIAP. The DLM 25 as an example
18 p2534 N88-25031
Topographic data processing for environmental planning 18 p2534 N88-25032
State of development of ALK (October 1986)
18 p2534 N88-25035
Vectorization of raster algorithms for elevation data processing 18 p2534 N88-25036
Recent developments in software and hardware by Scitex Co. --- computer aided mapping
18 p2535 N88-25038
Use of remote sensing in the study of superficial formation certifying the development of integrated economy-case example: Rio Claro (SP) region
19 p2683 N88-25950
Updating of municipal official register of real estate through the geographical information system
19 p2684 N88-25952
Aerial photography as an instrument of atmospheric analysis: Maps of the middle atmosphere and its dynamics, Baixada Santista (SP) 19 p2684 N88-25955
Development of an atmospheric diffusion evaluation method incorporating topographical effects. Part 1: Literature review of atmospheric diffusion models incorporating terrain effects
[DE88-753104] 20 p2822 N88-26742
Influence of microstructure and microdamage processes on fracture at high loading rates
[AD-A192957] 21 p2960 N88-27583
X-ray studies of strain, interface and impurities in semiconductors
[DE88-012460] 21 p3025 N88-27954
Topography of an Antartic ice stream
22 p3092 N88-28361
Land use systems and rural landscapes in the center of Veracruz State (Mexico): First results
22 p3092 N88-28364
The suitability of SPOT imagery for monitoring landscape patterns 22 p3094 N88-28376
Topographic suppression and advances in classification for land cover mapping using SPOT-1 HRV imagery
22 p3099 N88-28404
The prospects for topographic mapping using SPOT data 22 p3110 N88-28470
Cartographic applications of SPOT imagery
22 p3110 N88-28472
The use of SPOT imagery for topographic mapping
22 p3110 N88-28473
The use of SPOT data for mapping and DEM production --- digital elevation model (DEM)
22 p3110 N88-28475
Assessment of SPOT imagery for topographic revision and vegetation mapping 22 p3111 N88-28477
Topographic mapping with SPOT 1 data. A practical approach by the Ordnance Survey
22 p3111 N88-28479
Extratropical response to tropical heating as a function of period of model integrations
22 p3125 N88-28577
Intraplate deformation, stress in the lithosphere and the driving mechanism for plate motions
[NASA-CR-183121] 23 p3231 N88-29231
Mars: Near-infrared comparative spectroscopy during the 1986 opposition 23 p3301 N88-29658
Topography of large craters on Mars: Implications for the highlands resurfacing history
23 p3306 N88-29691
Finite-difference simulations of Rayleigh-wave scattering by shallow heterogeneity
[AD-A194961] 24 p3402 N88-30259
X-ray diffraction imaging (topography) : of electroopticcrystals by synchrotron radiation
[NASA-CR-183266] 24 p3432 N88-30427
Streaking images that appear only in the plane of diffraction in undoped GaAs single crystals: Diffraction imaging (topography) by monochromatic synchrotron radiation
[NASA-CR-183267] 24 p3433 N88-30437
Physical properties of surface materials on Martian volcanoes: Dust-covered lava and ash
24 p3443 N88-30493
Obligue metallogenic zones recognized by interpreting space photographs of southern Tien Shan
24 p3450 N88-30529
Structure of eastern Turkestan Ridge based on space photographs 24 p3450 N88-30530

TOPOLOGY
NT FIXED POINTS (MATHEMATICS)
NT HOMOTOPY THEORY
NT INVARIANT IMBEDDINGS
NT METRIC SPACE
Control of the German main triangulation network by macrometer measurement 1983-1985 (KONMAC)
[SER-B-282] 01 p0063 N88-10404
TIPS-1 user's manual: Cray-1 version
[DE87-013297] 01 p0081 N88-10522
Smooth dynamics on the interval (with an emphasis on unimodal maps)
[REPT-87-09] 01 p0086 N88-10555
Covariant Lorentz anomalies in higher dimensional space
[DE87-753021] 02 p0230 N88-11448
Topological aspects of infinite metal clusters and superconductors
[AD-A184104] 04 p0495 N88-13049
Topological equivalence of certain function spaces 2
[PB88-100904] 06 p0767 N88-14712
Embedding topological median algebras in products of dendrons
[PB88-100888] 06 p0767 N88-14713
Monte Carlo simulation of triangulated random surfaces in grand canonical ensemble
[DE88-700378] 07 p0941 N88-15718
The design of impedance- matching networks for broadband antennas
[AD-A187600] 10 p1320 N88-17695
Topology and grid adaption for high-speed flow computations
[NASA-CR-182586] 11 p1487 N88-18875
Geometrical and topological issues in octree based automatic meshing 11 p1527 N88-19118
Finite octree meshing through topologically driven geometric operators 11 p1527 N88-19121
On exterior variational calculus
[DE88-700861] 12 p1683 N88-20062
Using design axioms and topology to model database semantics
[CWI-CS-R8711] 13 p1818 N88-20863
Measurement of the elastic-plastic surface flaw back surface topology and its relation to constraint
[DE88-006765] 15 p2087 N88-22437
Efficient, high resolution computations of projectile and missile flow fields
[AD-A191086] 16 p2158 N88-22873
Topological stereochemistry
[AD-A191867] 18 p2477 N88-24691
The determination of the topological structure of skin friction lines on a rectangular wing-body combination
[NASA-CR-4168] 20 p2753 N88-26343
Some remarks on geodesics in gauge groups and harmonic maps
[DE88-702665] 22 p3115 N88-28510
On the GKP and BS constructions of C-boundary
[DE88-702643] 22 p3159 N88-28799
Optimization-driven machine-oriented motion measurement 23 p3245 N88-29312
Monotone recurrence relations, their Birkhoff orbits and topological entropy
[AD-A193481] 23 p3276 N88-29504

TORCHES
Optimization of oxygen cutting process for titanium alloys 14 p1897 N88-21323
Studies of heat and mass transfer during chemical vapor deposition 17 p2338 N88-23953
Welding torch gas cup extension
[NASA-CASE-MFS-29252-1] 17 p2345 N88-23980

TORNADO AIRCRAFT
U MRCA AIRCRAFT

TORNADOES
The importance of the lower level windshear profile in tornado/non-tornado discrimination
02 p0208 N88-11304
The Windsor Locks, Connecticut tornado of 3 October 1979: An analysis of an intermittant severe weather event 02 p0208 N88-11305
Severe weather potential (SPOT) plotfile generator
[PB87-217717] 02 p0216 N88-11360
Tornado tracks in Southwestern Brazil, Eastern Paraguay, and Northwestern Argentina
17 p2362 N88-24071

TOROIDAL PLASMAS
Fast wave injection into high temperature tokamak plasmas in the lower-hybrid-density regime of JIPP T-IIU
[ISSN-0469-4732] 01 p0099 N88-10649
Nonlinear fluid equations for a low collisionality toroidal plasma
[DE87-013006] 01 p0100 N88-10655
Computational study of three-dimensional magnetohydrodynamic equilibria in toroidal helical systems
[DE87-753007] 02 p0240 N88-11514
Magnetohydrodynamic stability of spheromak plasma in toroidal flux conserver with rectangular cross section 3. Stability for symmetric modes
[IPPJ-845] 02 p0241 N88-11524
Limit of possible operation of crescent and bean shaped Tokamaks
[IPPJ-837] 02 p0242 N88-11532
A tapered poloidal gap for the reduction of field errors
[DE87-014750] 03 p0377 N88-12375
Interchange stability of noncircular reversed field pinches
[DE88-000177] 03 p0378 N88-12381
Ballooning modes or Fourier modes in a toroidal plasma?
[AD-A184299] 04 p0491 N88-13022
The role of stellarators in the advanced toroidal program
[DE87-014815] 04 p0491 N88-13025
A three-barrel repeating pneumatic pellet injector for plasma fueling of the Joint European Torus
[DE88-000330] 04 p0491 N88-13026
Transport simulations of the oscillating field current drive experiment in the ZT-40M reversed field pinch
[DE88-000538] 04 p0491 N88-13027
Dynamic processes in field-reversed-configuration compact toroids
[DE87-014756] 05 p0652 N88-13998
High midplane accessibility stellarator windings for high current toroidal accelerators
[AD-A186235] 07 p0933 N88-15665
A calorimeter for measuring the neutral beam power reaching the plasma
[DE88-001412] 07 p0937 N88-15691
Nonlinear evolution of the internal kink mode in toroidal geometry for shaped tokamak plasmas
[DE88-003655] 08 p1087 N88-16550
Evaluation of magnetic coordinates in finite-beta, asymmetric plasmas
[DE88-003665] 10 p1412 N88-18424
ATF experimental plans
[DE88-004177] 10 p1414 N88-18439
Toroidal confinement research concepts evaluation and tradeoff studies
[DE88-004841] 11 p1552 N88-19285
Improved confinement of screw pinch plasmas in SPICA 2 12 p1694 N88-20137
Effects of toroidal forces in current loops embedded in a background plasma
[AD-A188878] 12 p1695 N88-20143
Fully implicit three-dimensional MHD (magnetohydrodynamics) stability and evolution in toroidal geometry
[DE88-000624] 13 p1842 N88-21023
Theoretical studies of the heating of toroidal plasmas with radiofrequency electromagnetic radiation
[DE88-006913] 15 p2137 N88-22749
Ion thermal conductivity and ion distribution function in the banana regime
[IPPJ-865] 19 p2729 N88-26208
Full-wave calculations in flux coordinates for toroidal geometry
[DE88-010131] 20 p2860 N88-26985
Toroidal and poloidal soft X-ray imaging system on the D3-D tokamak
[DE88-010585] 20 p2860 N88-26986
Density fluctuations in currentless high beta plasmas in Heliotron E
[DE88-752310] 23 p3283 N88-29550
RFP (Revised Field Pinch) plasma experiment at INPE
[INPE-4613-PRE/1336] 24 p3431 N88-30420

TOROIDAL SHELLS
The elastic analysis of a thin toroidal shell
[AD-A187801] 12 p1635 N88-19785

TOROIDS
Shear strength of the ASDEX upgrade Toroidal Field (TF) coil insulation: Rupture, fatigue and creep behavior --- tokamak
[IPP-1/230] 01 p0059 N88-10376

A short introduction to the status and motivation for reversed field pinch and compact toroid research
[DE88-000487] 05 p0652 N88-13999
An introduction to poloidal and toroidal fields
[MITT-54] 17 p2394 N88-24232
TORPEDOES
Revised Impact Dynamic Design-Analysis Method (RIDDAM)
[AD-A190479] 16 p2217 N88-23225
TORQUE
Predictive momentum management for a space station measurement and computation requirements
[NASA-CR-172026] 02 p0138 N88-10866
Measurements and calculations of aerodynamic torques for a vertical-axis wind turbine
[DE88-001783] 04 p0465 N88-12876
Solar Dynamics and G-modes
[NASA-CR-180737] 06 p0805 N88-14911
Preliminary design of the ORION attitude control system
[AD-A187179] 10 p1292 N88-17729
Reaction wheel control through digital technique using reference models
[INPE-4220-PRE/1100] 12 p1599 N88-19570
Efficiency characteristics of speed modulated drives at predicted torque conditions for air-to-air heat pumps
[DE88-005846] 13 p1770 N88-20588
Models for steady and nonsteady Coulomb torque in ball bearings 14 p1876 N88-21208
On the torque and wear behavior of selected thin film MOS2 lubricated gimbal bearings
14 p1926 N88-21485
Two gimbal bearing case studies: Some lessons learned 14 p1927 N88-21487
The effects of torque response and time delay on rotorcraft vertical axis handling qualities
[AD-A189873] 15 p2017 N88-22023
Evaluation of a high-torque backlash-free roller actuator 16 p2219 N88-23239
Helicopter anti-torque system using fuselage strakes
[NASA-CASE-LAR-13630-1] 17 p2306 N88-23809
Time-Optimal Adaptive Shaped Torque (TOAST) technical note
[AD-A192719] 20 p2843 N88-26869
In-flight motor torque estimates for the second-stage Strypi 9 launch vehicle
[DE88-010633] 21 p2902 N88-27222
TORQUE MEASURING APPARATUS
U TORQUEMETERS
TORQUE MOTORS
A high performance inverter-fed drive system of an interior permanent magnet synchronous machine
[DE88-006753] 15 p2061 N88-22288
Study on design and control of torque-controlled manipulators
[NASA-TT-20197] 23 p3223 N88-29183
TORQUEMETERS
Analysis of free molecular effects on the attitude of satellites in geostationary transfer orbit. Part 2: Force and torque measurement in free molecular wind tunnel tests
[DFVLR-IB-222-86-A/07] 01 p0014 N88-10078
TORSION
Torsion as a source of expansion in a Bianchi type I universe in the self-consistent Einstein-Cartan theory of a perfect fluid with spin density
[AD-A184200] 03 p0322 N88-12037
Vibration and buckling of geometrically imperfect laminated cylindrical shells 04 p0456 N88-12822
Micromechanics of fatigue crack initiation under axial and torsional loadings 06 p0719 N88-14413
Multiaxial fatigue failure criterion: A new approach
06 p0719 N88-14418
The microstructure and texture of torsion-reverse torsion experiments
[DE88-001801] 06 p0721 N88-14434
Piezoelectric laminates for torsional and bending model control: Theory and experiment
10 p1343 N88-18029
An experimental investigation of the flap-lag-torsion aeroelastic stability of a small-scale hingeless helicopter rotor in hover
[NASA-TP-2546] 13 p1715 N88-20257
Development of a torsion balance for adhesion measurements
[NASA-TM-100799] 13 p1748 N88-20454
Coupled bending-torsion steady-state response of pretwisted, nonuniform rotating beams using a transfer-matrix method
[NASA-TM-100596] 15 p2086 N88-22435
Strain hardening at large strains in aluminum alloys
[DE88-007415] 18 p2484 N88-24737
The variation of torsional ductility of high-purity aluminum with temperature and strain rate
[DE88-005618] 18 p2487 N88-24755
TORSIONAL STRESS
Theory of deformation. Part 1: Kinematics
[DE88-003007] 08 p1001 N88-16062
TORSO
Analysis of head response to torso acceleration. Volume 1: Development of performance requirements
[PB88-156757] 14 p1953 N88-21640
TORUSES
Compact torus studies
[DE87-014254] 02 p0237 N88-11496
On meteor stream spatial structure theory
06 p0739 N88-14544
Unfoldings of quasi-periodic tori
[ZW-8706] 13 p1828 N88-20928
A high field launch for electron cyclotron heating using an external window
[DE88-005350] 13 p1838 N88-21000
Eigenmodes of a random walk on a 2-D lattice torus with one trap
[DE88-007830] 20 p2844 N88-26874
Unfoldings of quasi-periodic tori
[B8811118] 23 p3278 N88-29513
TOTAL ENERGY SYSTEMS
An analysis of gas-steam total power recovery energy system 20 p2784 N88-26512
TOTAL OZONE MAPPING SPECTROMETER
Scientific and Operational Requirements for TOMS Data
[NASA-CP-2497] 05 p0615 N88-13774
TOMS: The Antarctic ozone hole and ozone trends
05 p0615 N88-13775
Analysis of the breakdown of the Antarctic circumpolar vortex using TOMS ozone data
05 p0615 N88-13779
Insights into the general circulation of the lower stratosphere from TOMS 05 p0616 N88-13780
Lower-stratospheric/upper-tropospheric exchange processes associated with tropical cyclones as observed by TOMS 05 p0616 N88-13782
Tropical easterly jet located using TOMS data
05 p0616 N88-13783
The use of TOMS data for tropospheric ozone studies
05 p0616 N88-13784
TOMS as a monitor of the ultraviolet radiation environment: Applications to photobiology
05 p0617 N88-13785
Application of TOMS data to weather analysis models
05 p0617 N88-13787
Correlations of TOMS total ozone data (Nimbus-7 satellite) with tropopause height
05 p0617 N88-13788
TOMS ozone data compared at mesoscale resolution to tropopause heights from the AVE radiosonde network and to VAS radiances over the south-central United States 05 p0617 N88-13790
The use of TOMS-modified VAS data for large-scale NWP 05 p0618 N88-13791
Dobson-stations performance assessment using TOMS data 05 p0618 N88-13792
Volcanic eruption detection with TOMS
05 p0618 N88-13793
Analysis of SO2 signals in SBUV/TOMS data
05 p0618 N88-13794
Comparison of ground based and TOMS measurements of SO2 from volcanic emissions
05 p0618 N88-13795
TOMS and the NOAA/FAA volcano support plan
05 p0618 N88-13796
Observation guidelines for a Total Ozone Mapping Spectrometer (TOMS) in geosynchronous orbit
05 p0619 N88-13801
A geostationary imaging spectrometer TOMS instrument 05 p0619 N88-13802
The 1987 Airborne Antarctic Ozone Experiment: The Nimbus-7 TOMS data atlas
[NASA-RP-1201] 13 p1791 N88-20714
Near-real-time TOMS, telecommunications and meteorological support for the 1987 Airborne Antarctic Ozone Experiment
[NASA-CR-4133] 16 p2233 N88-23338
TOUCH
NT TACTILE DISCRIMINATION
Tactile sensing and inverse problems
[AD-A187464] 10 p1340 N88-18011
Integrated polysilicon tactile sensor
19 p2669 N88-25863
The interaction of thalamo-cortical systems in the 40 Hz following response 21 p2979 N88-27694
TOUGHNESS
NT NOTCH SENSITIVITY
Carbon fiber reinforced glass matrix composites for space based applications
[AD-A184355] 04 p0410 N88-12546
Interfacial strength development in thermoplastic resins and fiber-reinforced thermoplastic composites
[NASA-CR-181525] 04 p0411 N88-12549
The effect of temperature on the tensile properties of HSLA-100 steel
[AD-A184951] 05 p0565 N88-13441
Micromechanisms of fatigue crack growth and fracture toughness in metal matrix composites
[AD-A186941] 09 p1137 N88-16816
Strength and toughness of a brittle material
[VTT-RR-479] 09 p1183 N88-17089
Finite element substructuring methods for composite mechanics
[NASA-TM-100297] 10 p1296 N88-17745
The influence of small defects on tensile specimen ductility and symmetry of deformation
[AD-A187983] 10 p1346 N88-18044
Interaction of particulate and transformation toughening
[AD-A189321] 13 p1741 N88-20412
Degradations of thermal shock resistance and the fracture toughness of reactor graphite subjected to neutron irradiation 13 p1747 N88-20445
Fracture toughness testing of a ceramic matrix composite
[AD-A189846] 15 p2029 N88-22089
Influence of temperature on the tensile strength and toughness characteristics. Material 35NCD16 ESR. Test report M5-521800
[M5-521800] 15 p2041 N88-22163
Characterization of HYTUF steel. Semifinished product: 160 mm dia forging block. Processor: C3f. Test Report M3-434600
[M3-434600] 15 p2041 N88-22164
Transformation toughening of ceramics
[AD-A190399] 15 p2045 N88-22183
Determination of the toughness of a brittle material using strain gages
[ETN-88-92540] 18 p2527 N88-24993
Theoretical and experimental analysis of the toughening behavior of whisker reinforcement in ceramic matrix composites
[DE88-011841] 21 p2906 N88-27241
Development of high strength and toughness microcomposite HSLA Fe/Cr/Mn/C steel with and without Nb
[DE88-009813] 21 p2913 N88-27290
Effects of near interfacial microstructure on toughness and subcritical crack growth in ceramic/metal systems
[DE88-009842] 21 p2919 N88-27325
The influence of weld metal properties, weld geometry and applied load on weld system performance
[AD-A193403] 21 p2961 N88-27588
A technique for measuring area under a curve
[AD-A193559] 23 p3271 N88-29463
TOWED BODIES
Australian aerodynamic design codes for aerial tow bodies
[AD-A189048] 13 p1715 N88-20258
An investigation of cruciform parachutes and towed targets
[BU-360] 14 p1862 N88-21122
Bodies in unsteady flow
[AD-A190416] 15 p2064 N88-22308
TOWED TARGETS
U TARGETS
U TOWED BODIES
TOWERS
NT AIRPORT TOWERS
Build, install and demonstrate a variable stroke pump control and windmill system
[DE87-014656] 03 p0347 N88-12191
Facilities for research and weather observations on the 213 m tower at Cabauw (Netherlands) and at remote locations
[KNMI-WR-87-5] 06 p0746 N88-14587
TOWING
The use of a water towing tank for aerodynamic testing and methods for quantitative evaluation of photographs
16 p2202 N88-23140
Use of water towing tanks for aerodynamics and hydrodynamics 16 p2204 N88-23149
TOWNSEND DISCHARGE
NT GAS DISCHARGES
TOXIC HAZARDS
Hydride generation from the Exide load-leveling cells
[DE87-011361] 01 p0041 N88-10259
Opportunities for nowcasting air pollution episodes and accidental toxic and radioactive releases
02 p0210 N88-11317
Space station internal environmental and safety concerns 04 p0407 N88-12527
Investigation of the exposure to harmful compounds in the workshop of nondestructive materials testing at Gilze-Rijen (Netherlands)
[PML-1985-42] 05 p0623 N88-13816
Monitoring of space station life support systems with miniature mass spectrometry and artificial intelligence
08 p1057 N88-16376

Critical comparison of moving average and cumulative summation control charts for trace analysis data
[AD-A188312] 12 p1705 N88-20203

TOXICITY

Rapid toxicity detection in water quality control utilizing automated multispecies biomonitoring for permanent space stations 02 p0135 N88-10848
Aircraft fire safety research 04 p0406 N88-12526
Evaluation of the sensidyne toxic gas sensor for HF (Hydrogen Fluoride) vapor
[DE88-000647] 04 p0446 N88-12767
The toxicology and metabolism of nickel compounds
[DE87-014801] 04 p0474 N88-12921
Short-term in vitro screening studies related to the inhalation toxicology of potentially toxic aerosols
[AD-A184815] 05 p0629 N88-13845
Flammability, smoke and toxicity test on fire barrier fabric from the Porcher company --- Airbus aircraft
[ETN-88-91168] 06 p0666 N88-14085
Physiological and biochemical aspects of toxic effects of oxidants in man's environment (air, water) 07 p0890 N88-15391
Specific organic compounds in excreta 07 p0895 N88-15422
Kinetic toxic aspect of potential use of sulfur hexafluoride in closed environments 10 p1362 N88-18142
Toxic effects of man-made mineral fibers with particular reference to ceramic fibers
[AD-A187949] 11 p1519 N88-19072
Fibrous glass aerosols: A literature review
[AD-A188420] 12 p1672 N88-20008
Evaluation of the acute toxicity of a synthetic polyalphaolefin-based hydraulic fluid
[AD-A190412] 15 p2045 N88-22184
Reclamation of water contaminated with fuel system icing inhibitor. Phase 1: Literature review and information compilation
[DE88-006575] 16 p2183 N88-23013
Evaluation of the toxicity of products from the thermal degradation of materials
[ETN-88-91995] 18 p2549 N88-25130
Experimental study of protective effect of antioxidant enzymes-superoxide dismutase and catalase-when using intermittent toxic modes of hyperbaric oxygenation 19 p2707 N88-26094
National air toxics information clearinghouse: NATICH data base users guide for data viewing, February 1988
[PB88-197470] 21 p2970 N88-27645

TOXICITY AND SAFETY HAZARD

Investigation of the exposure to harmful compounds in the workshop of nondestructive materials testing at Gilze-Rijen (Netherlands)
[PML-1985-42] 05 p0623 N88-13816
Investigation of the nature and concentration of vapor and mist during the cleaning of aircraft
[PML-1985-29] 05 p0623 N88-13817
Waste destruction by plasma
[SNIAS-881-430-113] 21 p2971 N88-27651

TOXICOLOGY

JPRS report: Science and technology. USSR: Life sciences
[JPRS-ULS-87-012] 03 p0355 N88-12238
JPRS report: Science and technology. USSR: Life sciences
[JPRS-ULS-87-013] 06 p0750 N88-14608
Changes in functional parameters of animals during long-term inhalation of acetic acid 07 p0895 N88-15423
USSR report: Life sciences. Biomedical and behavioral sciences
[JPRS-UBB-87-010] 12 p1651 N88-19889
JPRS report: Science and technology. USSR: Life sciences
[JPRS-ULS-88-002] 12 p1665 N88-19982
JPRS report: Science and technology. USSR: Life sciences
[JPRS-ULS-88-009] 20 p2829 N88-26785

TOXINS AND ANTITOXINS

EURECA Botany Facility. Technical note: Removal of phytotoxins
[SIRA-A/7373/WP220/RJS/005] 17 p2379 N88-24143

TRACE CONTAMINANTS

First flight of the ATMOS instrument during the Spacelab 3 Mission, April 29 through May 6, 1985
[NASA-CR-182360] 06 p0728 N88-14482
Layered-capacitor method for dielectric bridge measurements. Algorithms for inversion and parameter fitting: Documentation, verification, data analysis
[PB88-131479] 11 p1505 N88-18989
High resolution infrared absorption spectra of various trace gases present in the upper atmosphere of the Earth
[NASA-CR-182590] 12 p1642 N88-19829
Critical comparison of moving average and cumulative summation control charts for trace analysis data
[AD-A188312] 12 p1705 N88-20203
A data acquisition system for atmospheric tracer studies
[DE88-006211] 14 p1991 N88-21869
Analytical Chemistry Division
[DE88-701236] 16 p2174 N88-22956
The potential impact on atmospheric ozone and temperature of increasing trace gas concentrations
[NASA-CR-182965] 17 p2373 N88-24112
Preliminary study of niobium alloy contamination by transport through helium 17 p2402 N88-24279

TRACE ELEMENTS

The effects of minor trace gases on the transfer of thermal infrared radiation through the Earth's atmosphere 04 p0468 N88-12893
Development of FTMS methods for the detection of trace chemical species and development of FTMS methods for the analysis of various chemical species
[AD-A185857] 07 p0828 N88-15023
Trace-element metabolism in man and animals in the presence of hypoxic states of diverse etiology 07 p0889 N88-15390
Long range reconnaissance of trace gases: A special aspect of emission spectroscopy 08 p1018 N88-16172
Trace element geochemistry of the South Atlantic Bight
[DE88-003515] 10 p1356 N88-18108
Stratospheric trace gas distributions from fair infrared thermal emission spectroscopy 13 p1797 N88-20749
Advances in geochemistry and cosmochemistry: Trace element microdistributions with the synchrotron X-ray fluorescence microprobe
[DE88-006355] 15 p2032 N88-22108
A theoretical model of the washout of trace gases by raindrops in the atmosphere 17 p2375 N88-24125
Trace gas measurements in the troposphere using tunable diode lasers 18 p2540 N88-25072
Review of methods for remote sensing of atmospheric emissions from stationary sources
[PB88-190483] 20 p2821 N88-26739
Tracer water transport and subgrid precipitation variation within atmospheric general circulation models
[NASA-CR-182897] 20 p2823 N88-26745
Physical oceanography and tracer chemistry of the southern ocean
[DE88-006852] 20 p2826 N88-26779
Application of Auger electron spectroscopy to the study of trace element effects on weldability
[DE88-010457] 21 p2915 N88-27301
The 1985-86 measurements with the tunable diode laser absorption spectrometer
[PB88-214002] 23 p3231 N88-29226
Role of zircon in tracing crustal growth and recycling 24 p3394 N88-30211
Trace element differences between Archean, Proterozoic and Phanerozoic crustal components: Implications for crustal growth processes 24 p3399 N88-30243

TRACKED VEHICLES

Armoured vehicle track elastomers: Research and development at MRL
[MRL-GD-0012] 19 p2620 N88-25541

TRACKING (POSITION)

NT COMPENSATORY TRACKING
NT INFRARED TRACKING
NT MISSILE TRACKING
NT OPTICAL TRACKING
NT POLYSTATION DOPPLER TRACKING SYSTEM
NT PURSUIT TRACKING
NT RADAR TRACKING
NT RANGE AND RANGE RATE TRACKING
NT SATELLITE TRACKING
NT SATELLITE-TO-SATELLITE TRACKING
NT SPACECRAFT TRACKING
NT STAR TRACKERS

Tropical cyclone center locations from enhanced infrared satellite imagery
[PB87-213450] 01 p0071 N88-10455
Advanced dead reckoning navigation for mobile robots 03 p0262 N88-11646
Helicopter fire control: Advantages of an automatic target tracker 03 p0264 N88-11667
CNET (Chief of Naval Education and Training) Program Automated Tracking System (CPATS): A comprehensive study
[AD-A184694] 03 p0385 N88-12418
Effect of motion cues during complex curved approach and landing tasks: A piloted simulation study
[NASA-TP-2773] 04 p0398 N88-12480
A modern control theory based algorithm for control of the NASA/JPL 70-meter antenna axis servos 04 p0436 N88-12706
Supertracks: The building blocks of chaos
[DE88-001513] 04 p0522 N88-13207
Opportunities for tropical cyclone motion research in the Northwest Pacific region
[AD-A185068] 05 p0627 N88-13834
Boeing 727 MLS (Microwave Landing System) terminal instrument procedures (TERPS) approach data collection and processing, data report
[AD-A185523] 06 p0667 N88-14090
Optical seam tracking in robotic arc welding
[VTT-RR-463] 06 p0713 N88-14376
Experimental design of a piloted helicopter off-axis-tracking simulation using a helmet mounted display
[AD-A186228] 07 p0820 N88-14982
Tracking procedure for non-normally distributed measurement errors
[AD-A186287] 07 p0903 N88-15468
A piloted simulation investigating handling qualities and performance requirements of a single-pilot helicopter in air combat employing a helmet-driven turreted gun
[AD-A186878] 09 p1116 N88-16689
Role of optokinetic stimulation in vesibulospinal reflexes 10 p1360 N88-18131
Stable, robust tracking by sliding mode control
[AD-A188278] 10 p1401 N88-18358
An investigation of Doppler satellite positioning multi-station adjustment software 13 p1730 N88-20345
Robustifying the Kalman filter
[AD-A189240] 13 p1825 N88-20907
Multiple model parameter adaptive control for in-flight simulation
[AD-A190568] 15 p2021 N88-22044
Moving-bank multiple model adaptive estimation applied to flexible spacestructure control
[AD-A190761] 15 p2026 N88-22071
Effect of friction and control parameters on the tracking accuracy of a target seeker
[AD-A190010] 15 p2056 N88-22257
A multiple model adaptive tracking algorithm against airborne targets
[AD-A190619] 15 p2057 N88-22263
Comparison of surface current determined from satellite-tracked buoy with shipboard wind data during the 4th Brazilian antarctic expedition, 10-14 March, 1986 17 p2354 N88-24024
A system for determination of wind fields using geostationary meterological satellites 17 p2360 N88-24056
Near surface current determined from INPE's satellite-tracked buoy, during 6-26 November, 1985 17 p2360 N88-24058
Descriptions of HF and VHF Loran-C buoys and evaluations as potential datum marker buoys
[AD-A192069] 18 p2462 N88-24618
F-14 modeling study
[NASA-CR-4164] 19 p2603 N88-25462
MSAT mobile electronically steered phased array antenna development 19 p2647 N88-25711
Multi-target tracking algorithms for cluttered environments 20 p2789 N88-26543
A human factors evaluation of the Advanced Visual Technology System (AVTS) eye tracking oculometer 21 p2925 N88-27361
Passive multipath target tracking in an inhomogeneous acoustic medium
[AD-A193284] 21 p3012 N88-27873
Apparent brightness of stars and lasers 22 p3065 N88-28188
DSS 13 microprocessor antenna controller 22 p3066 N88-28192
A system for determination of wind fields from cloud tracks: INPE experiment
[INPE-4492-PRE/1256] 22 p3128 N88-28594
Interactive, networked moving platform simulators
[AD-A192374] 23 p3182 N88-28940
The gradient method for interface tracking
[AD-A194477] 23 p3248 N88-29334
Multi-sensory tracking mount control
[AD-A194675] 23 p3249 N88-29339
SSTS (Space Surveillance and Tracking System): The importance of early test and evaluation organizational participation
[AD-A193745] 23 p3276 N88-29499
Observed track-keeping performance of DC10 aircraft equipped with the Collins AINS-70 area navigation system: Karlsruhe and Masstricht UACs (Upper Area Control centres)
[EEC-202] 24 p3323 N88-29788
Analysis of environmental parameters from the Panama City tower radar experiment
[AD-A194994] 24 p3404 N88-30264
Dynamical systems and motion vision
[AD-A195932] 24 p3422 N88-30366

TRACKING AND DATA RELAY SATELLITES
U TDR SATELLITES
TRACKING ANTENNAS
U DIRECTIONAL ANTENNAS
TRACKING FILTERS
A multiple model adaptive tracking algorithm against airborne targets
[AD-A190619] 15 p2057 N88-22263
Object discrimination via bulk temperature/velocity filtering, phase 1
[AD-A194533] 23 p3274 N88-29487
TRACKING NETWORKS
NT DEEP SPACE NETWORK
NT POLYSTATION DOPPLER TRACKING SYSTEM
NT RADAR NETWORKS
Determination of TRANET (tracking station coordinates for tracking network) and SMTP (Special Mission Tracking Program) tracking station coordinates for use in the WGS (World Geodetic System) 84
[AD-A185863] 07 p0817 N88-14972
NASA (National Aeronautics and Space Administration) ADP (Automated Data Processing) system: Information on the automated mission and the payload tracking system
[PB88-104989] 07 p0942 N88-15730
Horizontal estimation and information fusion in multitarget and multisensor environments
[AD-A186935] 09 p1224 N88-17336
Surface disturbances produced by low-level, subsonic B-1 aircraft
[AD-A192257] 20 p2824 N88-26752
An investigation of the uses of time domain capable vector network analyzers as a diagnostic for helix traveling-wave circuits
[AD-A192460] 21 p2935 N88-27430
TRACKING PROBLEM
Synthesizing controllers for uncertain systems by a quantitative pole-placement
[PB87-195590] 02 p0223 N88-11403
The robust tracking control of nonlinear systems with uncertain dynamics 21 p2999 N88-27788
TRACKING STATIONS
NT POLYSTATION DOPPLER TRACKING SYSTEM
Determination of TRANET (tracking station coordinates for tracking network) and SMTP (Special Mission Tracking Program) tracking station coordinates for use in the WGS (World Geodetic System) 84
[AD-A185863] 07 p0817 N88-14972
TRACKING STUDIES
U TRACKING (POSITION)
TRACTION
Traction model development
[AD-A188450] 15 p2073 N88-22359
Roller drive materials performance 16 p2219 N88-23241
A critical speed study for aircraft bias ply tires
[AD-A193616] 22 p3084 N88-28313
TRACTORS
NT TRACKED VEHICLES
TRACTS
U SITES
TRADEOFFS
Toroidal confinement research concepts evaluation and tradeoff studies
[DE88-004277] 11 p1551 N88-19282
On 3-5 transistors for MM-wave applications
[AD-A191580] 19 p2661 N88-25825
Array trade-off study using multilayer parasitic subarrays
[NASA-TM-101321] 22 p3070 N88-28222
TRADESCANTIA
Zero gravity and living organism 08 p1046 N88-16320
TRAFFIC
NT AIR TRAFFIC
Pyroelectric line scanner for remote IR imaging of vehicles
[DE87-012127] 02 p0235 N88-11484
Computer aided cartographic representation of traffic data: The traffic intensity maps of Baden-Wuerttemberg (Federal Republic of Germany) 16 p2225 N88-23262
Digital maps for an electronic traffic guide 18 p2534 N88-25033
TRAFFIC CONTROL
NT AIR TRAFFIC CONTROL
Simulation of an enhanced TCAS 2 system in operation
[NASA-CR-181545] 04 p0398 N88-12479
The estimation of basic matrices using travel intensity theorems
[REPT-87-13] 05 p0642 N88-13926
A traveling-salesman-based approach to aircraft scheduling in the terminal area
[NASA-TM-100062] 12 p1576 N88-19424
A three dimensional assignment method in the time space
[REPT-87-49] 16 p2287 N88-23690
Airport surface traffic automation study
[AD-A194553] 23 p3181 N88-28934
TRAILING EDGE FLAPS
Static aeroelastic considerations in the definition of design loads for fighter airplanes 05 p0550 N88-13351
Flight and wind-tunnel measurements showing base drag reduction provided by a trailing disk for high Reynolds number turbulent flow for subsonic and transonic Mach numbers
[NASA-TP-2638] 06 p0701 N88-14299
High-flaps for natural laminar flow airfoils 17 p2296 N88-23739
Pressure distributions from subsonic tests of an advanced laminar-flow-control wing with leading- and trailing-edge flaps
[NASA-TM-4040-PT-1] 17 p2300 N88-23758
A low speed wind tunnel investigation of Reynolds number effects on a 60-deg swept wing configuration with leading and trailing edge flaps
[NASA-CR-181684] 19 p2598 N88-25441
Pressure distributions from subsonic tests of an advanced laminar-flow-control wing with leading- and trailing-edge flaps
[NASA-TM-4040-PT-2] 24 p3321 N88-29776
TRAILING EDGES
A study of rotor broadband noise mechanisms and helicopter tail rotor noise 06 p0777 N88-14766
Navier-Stokes calculations and turbulence modeling in the trailing edge region of a circulation control airfoil 10 p1268 N88-17587
Investigations of a circulation control airfoil flowfield using an advanced laser velocimeter 10 p1269 N88-17589
Experimental investigation of the transonic flow at the leeward side of a delta wing at high incidence
[LR-518] 16 p2156 N88-22861
Structure of unsteady flows at leading- and trailing-edges: Flow visualization and its interpretation 16 p2205 N88-23154
Axisymmetric viscid-inviscid interaction by a frozen vorticity approximation
[AD-A191743] 18 p2509 N88-24885
Characteristics of merging shear layers and turbulent wakes of a multi-element airfoil
[NASA-TM-100053] 18 p2511 N88-24900
The influence of surface rounding on trailing edge noise
[AD-A193387] 21 p3012 N88-27876
Classical separation, trailing-edge flows and buffeting 23 p3170 N88-28874
Experiments on the dissipation of sound by separated flow at an edge
[ISVR-TR-151] 23 p3279 N88-29522
TRAINEES
U STUDENTS
TRAINERS
U TRAINING DEVICES
TRAINING
U EDUCATION
TRAINING AIRCRAFT
NT T-33 AIRCRAFT
A look toward the future of complex avionics systems development using the USAF Test Pilot School's avionics systems test training aircraft 17 p2306 N88-23797
TRAINING ANALYSIS
The construction of a pedagogy to promote meaningful learning of strategies and tactics for solving problems of elementary combinatorics
[AD-A187928] 11 p1542 N88-19216
Report of the participation in the International Training Course: Remote Sensing in Village Forestry
[INPE-4476-NTE/278] 12 p1637 N88-19802
Hypnosis: Possible applications for cosmonauts 12 p1665 N88-19984
TRAINING DEVICES
NT TEACHING MACHINES
Examining the relative efficiency of Part- versus whole-task practice for multiple-task situations
[AD-A185056] 05 p0631 N88-13856
Learning to program methodically. 3: The newly designed course of the elementary programming
[PB87-119871] 06 p0757 N88-14643
Application of the analysis phase of the instructional system development to the MK-105 magnetic minesweeping mission of the MH-53E helicopter
[AD-A186282] 07 p0822 N88-14994
Human performance data needed for training device design decisions
[AD-A185988] 07 p0898 N88-15441
Air Force Human Resources Laboratory technical reports and technical papers
[AD-A186830] 09 p1201 N88-17200
Space shuttle onboard navigation console expert/trainer system 09 p1203 N88-17208
Aircrew training devices: Utility and utilization of advanced instructional features, phase 4
[AD-A188418] 12 p1670 N88-20000
Parachute for in-flight training on parachute ejection
[REPT-87-11] 18 p2458 N88-24593
TRAINING EVALUATION
Investigation of pilot behavior in a training program for assessing handling qualities using a ground simulator
[ESA-TT-999] 03 p0357 N88-12247
Field evaluation of interactive simulation for maintenance training: SH-3 helicopter electro-mechanical bladefold system
[AD-A185923] 07 p0821 N88-14991
A validity study of a selection procedure for student airline pilots
[DFVLR-FB-87-34] 09 p1201 N88-17196
Measurement and effects of transport delays in a state-of-the-art F-16C flight simulator
[AD-A187367] 11 p1441 N88-18599
Visual recognition training: Effectiveness of computer graphics
[AD-A188302] 12 p1689 N88-19997
Utility NDE personnel qualification/certification: Enhanced personnel qualification requirements for ASME (American Society for Mechanical Engineers) Code Section 11 examinations
[DE88-006748] 16 p2216 N88-23222
Personality, attitudes, and pilot training performance: Preliminary analysis
[AD-A193102] 21 p2991 N88-27746
An expert system for a distributed real-time trainer 23 p3261 N88-29411
Controlled degradation of resolution of high-quality flight simulator images for training effectiveness evaluation
[AD-A196189] 24 p3330 N88-29823
Improvement of head-up display standards. Volume 3: An evaluation of head-up display safety
[AD-A195787] 24 p3410 N88-30300
TRAINING SIMULATORS
NT COCKPIT SIMULATORS
NT FLIGHT SIMULATORS
An enumeration of research to determine the optimal design and use of Army flight training simulators
[AD-A191242] 18 p2468 N88-24649
Development of training implying man-machine interface: From the aircraft to the spacecraft 19 p2700 N88-26052
Controlled degradation of resolution of high-quality flight simulator images for training effectiveness evaluation
[AD-A196189] 24 p3330 N88-29823
LANTIRN simulator training in the F-16C
[AD-A195201] 24 p3330 N88-29826
TRAJECTORIES
NT ABORT TRAJECTORIES
NT ASCENT TRAJECTORIES
NT BALLISTIC TRAJECTORIES
NT DESCENT TRAJECTORIES
NT ELECTRON TRAJECTORIES
NT HYPERBOLIC TRAJECTORIES
NT INTERPLANETARY TRAJECTORIES
NT MISSILE TRAJECTORIES
NT MOLECULAR TRAJECTORIES
NT PARTICLE TRAJECTORIES
NT REENTRY TRAJECTORIES
NT RENDEZVOUS TRAJECTORIES
NT ROUND TRIP TRAJECTORIES
NT SPACECRAFT TRAJECTORIES
NT UNDERWATER TRAJECTORIES
On the degree of generality of inflationary solutions in cosmological models with a scalar field
[DE87-703079] 02 p0251 N88-11586
A dissipation principle and its consequences for structured shock waves in thermoelastic materials
[DE87-013723] 04 p0454 N88-12813
Supertracks: The building blocks of chaos
[DE88-001513] 04 p0522 N88-13207
Trajectory control of robot manipulators with closed-kinematic chain mechanism
[NASA-TM-89305] 05 p0591 N88-13605
Cartesian path control of a two-degree-of-freedom robot manipulator
[NASA-CR-182331] 05 p0639 N88-13908
An evaluation of semianalytical satellite theory against long arcs of real data for highly eccentric orbits
[AD-A185825] 08 p0960 N88-15819
Heuristic search in robot configuration space using variable metric 08 p1059 N88-16389
POCC capabilities document. Payload support capabilities description: MCC, JSC POCC, remote POCC interface
[NASA-TM-89708] 09 p1260 N88-17555
Simulator investigation of wind shear recovery techniques 10 p1275 N88-17630

Orbital analysis of a STS (Space Transportation System) external tank in low earth orbit
[AD-A188829] 12 p1593 N88-19542
Base reaction optimization of manipulators with redundant kinematics 16 p2219 N88-23238
Microgravity manipulator demonstration 16 p2219 N88-23242
Comparison of surface current determined from satellite-tracked buoy with shipboard wind data during the 4th Brazilian antarctic expedition, 10-14 March, 1986 17 p2354 N88-24024
Tornado tracks in Southwestern Brazil, Eastern Paraguay, and Northwestern Argentina 17 p2362 N88-24071
A centered projective algorithm for linear programming
[AD-A192100] 18 p2557 N88-25178
Accelerator research studies
[DE88-007124] 18 p2574 N88-25290
A simulation of post boost vehicle deployment of multiple reentry vehicles
[DE88-009537] 20 p2764 N88-26391
Multi-target tracking algorithms for cluttered environments 20 p2789 N88-26543

TRAJECTORY ANALYSIS
Instrumentation package for a shrouded SWERVE/EPW rocket sled test
[DE87-014267] 01 p0008 N88-10045
Development and testing of an air-mass transformation trajectory model 02 p0209 N88-11309
Approach trajectory planning system for maximum concealment
[NASA-TM-88258] 02 p0227 N88-11435
Analysis of the motions and effects of hairpin vortices 03 p0316 N88-11997
Optoelectronic measurement methods for ballistic experiments
[PB87-110706] 05 p0583 N88-13554
Pattern recognition techniques for failure trend detection in SSME ground tests 07 p0924 N88-15614
An evaluation of semianalytical satellite theory against long arcs of real data for highly eccentric orbits
[AD-A185825] 08 p0960 N88-15819
Aircraft flight test trajectory control
[NASA-CR-179428] 09 p1120 N88-16707
Maneuverable reentry vehicle trajectory footprints: Calculation and properties
[DE88-004726] 10 p1292 N88-17726
Interplanetary mission design handbook. Volume 1, Part 5: Mars-to-Earth ballistic mission opportunities, 1992-2007
[NASA-CR-182525] 10 p1430 N88-18538
Three-dimensional trajectory analyses of two drop sizing instruments: PMS OAP and PMS FSSP
[NASA-CR-4113] 11 p1437 N88-18574
Store separation and missile firing from aircraft: Experimental methods for trajectory projection
[NASA-TT-20214] 11 p1439 N88-18589
Effect of transition aerodynamics on aeroassist flight experiment trajectories
[NASA-TM-100546] 11 p1446 N88-18620
The stress field surrounding the tip of a crack propagating in a finite body 11 p1500 N88-18962
Trajectory characteristics and heating of hypervelocity projectiles having large ballistic coefficients
[NASA-TP-2614] 12 p1574 N88-19412
Aeroassisted orbit transfer vehicle trajectory analysis
[NASA-TM-89138] 12 p1599 N88-19575
A method and measures to evaluate trackers for air traffic control
[NLR-TR-86072-U] 13 p1720 N88-20287
Trajectory code studies, 1987
[DE88-006218] 13 p1728 N88-20335
Linear programming along the trajectory of the problem
[REPT-87-41] 14 p1956 N88-21662
Distribution of neutral gas molecules at large distances from Halley's comet 14 p1999 N88-21914
Spacecraft trajectories
[ISBN-2-85-428166-7] 15 p2023 N88-22054
On the trajectory of a linear programming problem
[REPT-87-53] 16 p2250 N88-23442
Underwater optical trajectography and video image mosaics 19 p2700 N88-26051
A new trajectory following polynomial-time algorithm for the linear programming problem
[REPT-87-87] 20 p2840 N88-26848
A numerical simulation of side force effects by aerodynamic flight trajectory correction
[ISL-CO-211/87] 21 p2896 N88-27191
FORTRAN programs for computation of time dependent sea levels and trajectory errors from satellite altimeter data
[BONN-MITT-73] 21 p2901 N88-27216
A theoretical determination of the density at a traveling source that emitts particles
[ISAS-RN-351] 21 p3013 N88-27883
Asymptotic orders of reachability in perturbed linear systems
[AD-A192718] 22 p3143 N88-28688
Computational aerodynamic analysis for a range-limited 25mm training round
[AD-A185270] 24 p3320 N88-29772
Ascent guidance for a winged boost vehicle
[NASA-CR-172083] 24 p3334 N88-29846

TRAJECTORY CONTROL
NT TRAJECTORY OPTIMIZATION
Trajectory control using laterally ejected jets. Literature review
[ISL-R-117/85] 05 p0581 N88-13544
Cartesian path control of a two-degree-of-freedom robot manipulator
[NASA-CR-182331] 05 p0639 N88-13908
Optimal guidance of homing missiles 06 p0671 N88-14111
Real-time kinematic and dynamic analysis and adaptive model following control of manipulator arms 11 p1495 N88-18927
Aerodynamic possibilities for the realization of trajectory corrections
[ISL-CO-251/86] 14 p1862 N88-21120
A numerical simulation of side force effects by aerodynamic flight trajectory correction
[ISL-CO-211/87] 21 p2896 N88-27191
The VITE model: A neutral command circuit for a generating arm and articulator trajectories
[AD-A192715] 21 p2987 N88-27734
Time minimal computation of feedback control schemes for optimal guidance problems used in space flight
[ETN-88-92989] 23 p3184 N88-28953
The eivaN: A forward-looking interactive orbital trajectory plotting tool for use with proximity operations (PROX OPS) and other maneuvers: Description and user's manual
[NASA-CR-177490] 24 p3414 N88-30327

TRAJECTORY MEASUREMENT
Flightpath reconstruction and systematic radar error estimation from multiradar range-azimuth measurements
[NLR-MP-85064-U] 06 p0693 N88-14251
Determining trajectory of ground movement accompanying seismic phenomena 08 p1011 N88-16132
Spacecraft trajectories
[ISBN-2-85-428166-7] 15 p2023 N88-22054
A multiple model adaptive tracking algorithm against airborne targets
[AD-A190619] 15 p2057 N88-22263
Trajectory measurement of the Fokker 100 aircraft during autoland testing
[NLR-MP-86010-U] 20 p2758 N88-26366

TRAJECTORY OPTIMIZATION
Performance and optimization of direct implicit time integration schemes for use in electrostatic particle simulation codes
[DE88-003254] 10 p1406 N88-18381
Safe rendezvous approach to a space station by impulsive transfers and continuous thrust arcs 12 p1585 N88-19486
Safe and fuel minimum reference trajectories for closed loop controlled approaches --- space stations 12 p1585 N88-19488
Optimal thrust vector control of coplanar orbital evasive maneuvers
[AD-A189544] 13 p1730 N88-20346
Performance optimization of a cruise missile using dynamic-stall induced lift augmentation
[AD-A190497] 15 p2017 N88-22027
Periodic solutions in aircraft cruise-dash optimization 18 p2464 N88-24631
Optimum-Path-to-Go guidance of command adjusted trajectory projectiles
[AD-A193377] 22 p3040 N88-28051
The analysis and control of robotic manipulators operating at or near kinematically singular configurations 22 p3084 N88-28315
The eivaN: A forward-looking interactive orbital trajectory plotting tool for use with proximity operations (PROX OPS) and other maneuvers: Description and user's manual
[NASA-CR-177490] 24 p3414 N88-30327

TRANQUILIZERS
Carbamates, atropine, and diazepam: Effects on performance in the running rat
[AD-A188009] 11 p1517 N88-19062

TRANSATMOSPHERIC VEHICLES
Apollo Lightcraft project
[NASA-CR-182575] 11 p1445 N88-18615

TRANSCEIVERS
U TRANSMITTER RECEIVERS

TRANSCENDENTAL FUNCTIONS
NT COSINE SERIES
NT EXPONENTIAL FUNCTIONS
NT LOGARITHMS
NT PERIODIC FUNCTIONS
NT TANGENTS
NT TRIGONOMETRIC FUNCTIONS
High speed transcendental elementary function architecture in support of the Vector Wave Equation (VWE)
[AD-A189746] 15 p2119 N88-22627
Mahler's method in transcendence theory 17 p2393 N88-24227
General analytic solution of certain functional equations of addition type
[PREPRINT-583] 22 p3144 N88-28699

TRANSCONDUCTANCE
Characterization of enhanced Schottky-barrier InGaAs/Al(1-x)As strained channel modulation-doped field-effect transistors
[AD-A188820] 12 p1698 N88-20162

TRANSDUCERS
NT DIGITAL TRANSDUCERS
NT ELECTROACOUSTIC TRANSDUCERS
NT ELECTRONIC TRANSDUCERS
NT HYDROPHONES
NT IMAGE TRANSDUCERS
NT INTERDIGITAL TRANSDUCERS
NT MAGNETIC TRANSDUCERS
NT MICROPHONES
NT MODE TRANSFORMERS
NT PIEZOELECTRIC GAGES
NT PIEZOELECTRIC TRANSDUCERS
NT PIEZORESISTIVE TRANSDUCERS
NT PRESSURE SENSORS
NT QUARTZ TRANSDUCERS
NT SOUND TRANSDUCERS
NT THERMOPILES
NT ULTRASONIC WAVE TRANSDUCERS
Notes on transducer design based on resistance strain gages with applied temperature compensation
[FFA-MEMO-129] 01 p0050 N88-10319
Capacitive resonant transducer for the Frascati gravitational antenna
[IFSI-86-9] 05 p0578 N88-13528
A surface plasmon waveguide sensor: A new type of chemical transducer based on optical phenomena
[ETN-88-91322] 06 p0780 N88-14792
Statistical measures of clipped random signals 08 p1000 N88-16055
Investigation of thermoacoustic heat transport using a thermoacoustic couple
[AD-A186889] 09 p1242 N88-17442
Evaluation of a miniature horizontal pendulum tilt transducer 12 p1577 N88-19435
User's guide: Lower neck transducer for the Hybrid 3 dummy
[PB88-133319] 12 p1628 N88-19743
Evaluation tests of lower neck transducer for the Hybrid 3 Dummy
[PB88-133327] 12 p1628 N88-19745
Development of an electronically-scanned pressure module for operation at cryogenic temperatures
[NASA-CR-181610] 12 p1629 N88-19748
Computer grading of extensometers (BS 3846)
[NPL-DMA(A)-152] 15 p2108 N88-22560
Low power consumption current transducer
[NASA-CASE-NPO-16888-1-CU] 17 p2335 N88-23937
Characterization of noncontact piezoelectric transducer with conically shaped piezoelement
[NASA-CR-4151] 17 p2347 N88-23987
Single mode levitation and translation
[NASA-CASE-NPO-16675-1-CU] 17 p2395 N88-24241
Navigation system for land vehicles
[NASA-CASE-LAR-13322-1] 18 p2462 N88-24620
Thermodynamic study of hygroscopic polymers using surface acoustic waves 19 p2672 N88-25882
Air loading effects on a capacitively sensed membrane supported silicon accelerometer 19 p2672 N88-25886
Deposition techniques and properties of strain compensated LPCVD silicon nitride films 19 p2673 N88-25898
Acoustic emission calibration instrumentation
[DE88-010817] 21 p2951 N88-27528
Direct measurement of solids: High temperature sensing. Experimental development and testing of high temperature pulsed EMATs
[DE88-009859] 21 p2954 N88-27546
Piezoelectric and electrostrictive materials for transducer applications, volume 1
[AD-A194957] 24 p3374 N88-30096
Piezoelectric and electrostrictive materials for transducer applications, volume 2
[AD-A194956] 24 p3376 N88-30104
Piezoelectric and electrostrictive materials for transducer applications, volume 3
[AD-A194949] 24 p3377 N88-30112

TRANSEQUATORIAL PROPAGATION
Solar tides in the upper equatorial thermosphere: A comparison between AE-E data and the NCAR thermospheric general circulation model
[AD-A186160] 08 p1023 N88-16196

TRANSFER
U TRANSFERRING

TRANSFER FUNCTIONS
NT MODULATION TRANSFER FUNCTION
NT OPTICAL TRANSFER FUNCTION
Electromagnetic tests
[SNIAS-872-430-103] 05 p0575 N88-13508
Equivalence of input-output stability and exponential stability for infinite dimensional systems
[TW-276] 05 p0638 N88-13903
Asymptotically stable all-pass transfer functions: Canonical form, parametrization and realization
[PB87-123972] 06 p0763 N88-14684
Statistical analyses of measured directional wave and current data
[PB87-144523] 07 p0853 N88-15185
Characterization of all controlled invariant sub-spaces for spectral systems
[PB88-106638] 07 p0912 N88-15532
Frequency-response identification of XV-15 tilt-rotor aircraft dynamics 10 p1277 N88-17643
Dynamic modelling of an electromechanical valve using frequency response data
[AD-A187908] 11 p1494 N88-18918
Identification of microwave line-of-sight multipath components 12 p1616 N88-19665
Sensitivity reduction over a frequency band
[AD-A189123] 12 p1621 N88-19694
Multipass beam breakup in recirculating linacs
[CEBAF-PR-87-007] 12 p1690 N88-20111
Elimination of quantifiers of linear variables and corresponding transfer principles
[DE88-005692] 13 p1826 N88-20912
On a bound of the modeling errors of black-box transfer function estimates
[EUT-87-E-173] 14 p1963 N88-21708
Coupled bending-torsion steady-state response of pretwisted, nonuniform rotating beams using a transfer-matrix method
[NASA-TM-100596] 15 p2086 N88-22435
Method for restoration and resampling of TM sensor imagery
[INPE-4491-PRE/1255] 15 p2090 N88-22454
Experimental comparison of lightning simulation techniques to CV-580 airborne lightning strike measurements
[AD-A190576] 15 p2098 N88-22496
Development of a digital sun sensor for a spin-stabilized satellite
[INPE-4508-TDL/327] 16 p2169 N88-22929

TRANSFER OF TRAINING
National Aeronautics and Space Administration (NASA)/American Society for Engineering Education (ASEE) Summer Faculty Fellowship Program, 1987. Volume 1
[NASA-CR-172009-VOL-1] 06 p0792 N88-14855
Teaching artificial neural systems to drive: Manual training techniques for autonomous systems
09 p1207 N88-17238

TRANSFER ORBITS
Analysis of free molecular effects on the attitude of satellites in geostationary transfer orbit. Part 1: Theoretical analysis
[DFVLR-IB-222-86-A/08] 01 p0014 N88-10077
Analysis of free molecular effects on the attitude of satellites in geostationary transfer orbit. Part 2: Force and torque measurement in free molecular wind tunnel tests
[DFVLR-IB-222-86-A/07] 01 p0014 N88-10078
Single-burn transfer to nominally periodic orbit in the vicinity of point L2 of Earth-Sun system and related problems 08 p1006 N88-16100
Application of artificial intelligence to impulsive orbital transfers 08 p1066 N88-16439
Safe rendezvous approach to a space station by impulsive transfers and continuous thrust arcs
12 p1585 N88-19486
Cost-effective orbit transfer modes for satellite retrieval and servicing --- Space Station
12 p1586 N88-19489
Study of the optimization of satellite system design for transfer orbit
[MBB-URV-135] 13 p1727 N88-20332
Solar thermal propulsion for orbit transfer vehicles
17 p2428 N88-24445
Impact of ETO propellants on the aerothermodynamic analyses of propulsion components
[NASA-TM-101303] 24 p3374 N88-30094

TRANSFER TUNNELS
Modification of integrated partial payload lifting assembly
[NASA-CR-182573] 11 p1443 N88-18607

TRANSFERRED ELECTRON DEVICES
A planar IC-compatible transferred electron device for millimeter-wave operation
[AD-A192692] 21 p2936 N88-27433

TRANSFERRING
Personal computers and All-In-1: Document transfer and translation
[DE88-003760] 10 p1384 N88-18264
USAF hyperbaric animal transfer chamber system
[AD-A193633] 23 p3237 N88-29265

TRANSFORM INTEGRALS
U INTEGRAL TRANSFORMATIONS

TRANSFORMATION TENSORS
U TENSORS

TRANSFORMATIONS (MATHEMATICS)
NT COORDINATE TRANSFORMATIONS
NT FAST FOURIER TRANSFORMATIONS
NT FOURIER TRANSFORMATION
NT FOURIER-BESSEL TRANSFORMATIONS
NT HILBERT TRANSFORMATION
NT INTEGRAL TRANSFORMATIONS
NT LAPLACE TRANSFORMATION
NT LINEAR TRANSFORMATIONS
Theoretical aspects of target classification: Physical optics and radon transform methods
03 p0304 N88-11915
A theory for the articulation of robot manipulators
03 p0333 N88-12097
Frequency domain identification of structural dynamic systems with general damping matrices
03 p0337 N88-12120
Group analysis of equations arising in ocean acoustics
04 p0472 N88-12914
Canonical transformations and exact invariants for dissipative systems
[DE87-703663] 04 p0485 N88-12985
Darboux and Baecklund transformations for the Schroedinger equation
[PREPRINT-545] 06 p0763 N88-14685
Nonisospectral deformations and Darboux transformations for the 3rd order spectral problem
[PREPRINT-558] 06 p0764 N88-14690
Darboux transformation and special solutions for the two-dimensional Toda-lattice
[PREPRINT-562] 06 p0764 N88-14692
Loop coalescing: A compiler transformation for parallel machines
[DE88-003571] 10 p1392 N88-18307
The significance of orientation unknowns in station and net adjustments 11 p1506 N88-18994
Predicting transforms of stable noise and other Gaussian mixtures
[AD-A189280] 12 p1684 N88-20071
Introduction to classical mechanics of systems with constraints, part 1
[DE88-701055] 13 p1832 N88-20957
Introduction to classical mechanics of systems with constraints, part 2
[DE88-701056] 13 p1849 N88-21072
Introduction to classical mechanics of systems with constraints, part 3
[DE88-701057] 13 p1850 N88-21073
Iteration of transformation passes over attributed program trees --- compilers
[INF-87-28] 14 p1956 N88-21661
Recursion operator and Backlund Transformation for the Ruijsenaars-Toda lattice
[PREPRINT-577] 14 p1968 N88-21750
Utilization of space color transformation, linear contrast and filtration for enhancement of colored digital images
[INPE-4310-PRE/1176] 14 p1983 N88-21831
Remarks on the time transformation of path-integral measures
[DE87-703040] 15 p2118 N88-22617
Baecklund transformation and the Schwarzian derivative
[AD-A190277] 15 p2127 N88-22684
Space time processing, environmental-acoustic effects
[AD-A190764] 15 p2130 N88-22708
Reduced order models for nonlinear aerodynamics
16 p2220 N88-23248
Bogolyubov transformation in relativistic theory of gravitation
[DE88-701592] 16 p2232 N88-23329
New stable, vectorisable Kalman filter algorithms based on orthogonal transformations
[DFVLR-FB-87-52] 16 p2258 N88-23494
Mathematical morphology: An algebraic approach
[CWI-AM-R8707] 16 p2258 N88-23497
The 1 and 2D symmetric Helmert transformation: An exact nonlinear least squares solution
[REPT-87-1] 16 p2259 N88-23503
Application of its transformation in color enhancement of LANDSAT imagery 17 p2365 N88-24082
An analytic model for aerodynamic shapes
[AD-A191573] 18 p2456 N88-24583
Additive prophet inequalities for transforms of uniformly bounded pairwise independent random variables
[PB88-173513] 18 p2568 N88-25250
Numerical simulation of viscous flows over transonic aircraft configurations 19 p2637 N88-25642
Thermal inhibition by megagauss field due to variation of electron temperature in laser plasma
[DE88-701887] 20 p2859 N88-26977
Backlund transformations associated with a Riemann-Hilbert spectral problem
[PREPRINT-596] 22 p3146 N88-28712
DATATRAN: Datum transformation software
[AD-A195723] 24 p3387 N88-30175
Using primal sketch primitives as the basis for the Hough transform
[INPE-4564-PRE/1305] 24 p3412 N88-30310
Reconstruction of multidimensional signals from multiple level threshold crossings
[AD-A195561] 24 p3425 N88-30383

TRANSFORMERS
NT INSTRUMENT TRANSFORMERS
NT MODE TRANSFORMERS
NT VOLTAGE CONVERTERS (AC TO AC)
Analysis of the electromagnetic performance characteristics of stripline transformers
[DE87-012515] 01 p0042 N88-10264
The railgun and its power source
[MRL-R-1058] 09 p1130 N88-16786
Pulsed current transformer for low inductive loads
[AD-A187224] 10 p1324 N88-17913
Optimum transformer design for a pulsed power system
[DE88-006054] 13 p1760 N88-20525
The application of high temperature superconductors to space electrical power distribution components
[NASA-TM-100901] 16 p2171 N88-22939

TRANSFORMS
U TRANSFORMATIONS (MATHEMATICS)

TRANSIENT HEATING
NT PULSE HEATING
NT SHOCK HEATING
A numerical study of transient heat and mass transfer in crystal growth 07 p0925 N88-15619
Transient radiative energy transfer in incompressible laminar flows
[NASA-CR-182605] 11 p1488 N88-18883
Calculational model development for fibrous thermal insulation transient test procedures
[DE88-007843] 18 p2493 N88-24789
Transient thermal analysis of three latent heat storage configurations for rapid thermal charging
[DE88-008943] 20 p2881 N88-27104
Measurement of local high-level, transient surface heat flux
[NASA-TP-2840] 24 p3375 N88-30099

TRANSIENT LOADS
NT BLAST LOADS
NT GUST LOADS
NT IMPACT LOADS
NT LANDING LOADS
NT SHOCK LOADS
Exact finite element method analysis of viscoelastic tapered structures to transient loads
05 p0595 N88-13632
Boundary element analysis for dynamic loading of a circular plate on an elastic medium
[CI-86] 06 p0722 N88-14443
Transient dynamics of fibre reinforced composite plates
[IIT-B/CE/RR/87-1] 13 p1734 N88-20370
Transient analysis of a plate on an elastic foundation under a moving load 19 p2680 N88-25933

TRANSIENT OSCILLATIONS
An asymptotic theory for a class of initial-boundary value problems for weakly nonlinear wave equations with an application to a model of the galloping oscillations of overhead transmission lines
[REPT-87-12] 01 p0086 N88-10556
Asymptotics for a system of nonlinearly coupled wave equations with an application to the galloping oscillations of overhead transmission lines
[REPT-87-78] 17 p2348 N88-23991

TRANSIENT REACTOR TEST FACILITY
A novel plant protection strategy for transient reactors
17 p2425 N88-24423

TRANSIENT RESPONSE
A transient model for thermal detonation
[IKE-2-75] 03 p0314 N88-11984
Time domain electromagnetic waves in multilayered media
[AD-A185055] 05 p0574 N88-13502
Structuring data for concurrent vectorized processing in a transient dynamics finite element program
[DE87-013082] 05 p0636 N88-13890

The KIVA-2 computer program for transient multidimensional chemically reactive flows with sprays
[DE88-000502] 07 p0854 N88-15191
FABSTRAN: A computer program for frame and beam static and transient response analysis (nonlinear)
[ARE-TR-86205] 09 p1182 N88-17079
Experimental and mathematical investigation of response characteristics and aging phenomena in safety fuse elements
[ETN-88-91478] 11 p1480 N88-18832
Computational aspects of sensitivity calculations in transient structural analysis
[NASA-TM-100589] 14 p1924 N88-21467
Transient compressible flow in porous materials
[DE88-006685] 15 p2067 N88-22324
Progress in the computer modeling of the liquid phase behavior of a liquid metal heat pipe
17 p2412 N88-24342
Transient thermohydraulic heat pipe modeling
17 p2413 N88-24347
Thermal and power availability transient responses for the Argonne monolithic solid oxide fuel cell
17 p2419 N88-24384
The THROHPUT code: Thermohydraulic heat pipe modeling 17 p2421 N88-24399
Transient analyses of multimegawatt space reactors
17 p2430 N88-24456
SOLA-DM: A numerical solution algorithm for transient three-dimensional flows
[DE88-007159] 18 p2514 N88-24913
Steady state and transient behavior of the Pd-SnO(sub x) MIS oxygen sensors 19 p2672 N88-25890
An experimental investigation of transient characteristics in a gravity-assisted heat pipe 20 p2783 N88-26506
Techniques and instrumentation for transient characterization of metal-insulator-semiconductor diodes. Applications to metal-insulator InP system
[ECL-87-17] 21 p3025 N88-27959
Finite element analysis of steady and transiently moving/rolling nonlinear viscoelastic structure. Part 1: Theory
[NASA-CR-179886] 23 p3273 N88-29480

TRANSIENTS (SURGES)
U SURGES

TRANSISTOR AMPLIFIERS
Phase 2 development of a 12 GHz MMIC FET amplifier
[IM-I86-1010] 01 p0038 N88-10240
A 2.3-GHz cryogenically cooled HEMT amplifier for DSS 13 04 p0434 N88-12689

TRANSISTOR CIRCUITS
Formal multilevel hierarchical verification of synchronous MOS VLSI circuits
[AD-A187532] 10 p1324 N88-17918
Improved description of base dynamics in the modeling of bipolar transistors
[PB88-181516] 19 p2732 N88-26229

TRANSISTOR LOGIC
Development of a planar heterojunction bipolar transistor for very high speed logic
[AD-A188137] 11 p1478 N88-18820
Generating layouts for random logic: Cell generation schemes
[EUT-86-E-164] 14 p1956 N88-21658

TRANSISTORS
NT BIPOLAR TRANSISTORS
NT FIELD EFFECT TRANSISTORS
NT HIGH ELECTRON MOBILITY TRANSISTORS
NT JFET
NT JUNCTION TRANSISTORS
NT MODFETS
NT SILICON TRANSISTORS
NT SOS (SEMICONDUCTORS)
Chemically modified microelectrode arrays. New kinds of electronic devices
[AD-A184389] 04 p0439 N88-12724
Reevaluating the worst-case radiation response of MOS transistors
[DE87-014157] 04 p0497 N88-13059
Thermal analysis of transistor packages, part 2
[DE88-005091] 10 p1323 N88-17909
Numerical methods in the resolution of control electrovalve model
[INPE-4154-RPE/540] 13 p1764 N88-20554
Hot electron transistors grown by MOCVD
20 p2861 N88-26996
Excellent negative differential resistance of InGaAs/InAlAs resonant tunneling barrier structures and applications to a new functional device, RHET
20 p2872 N88-27048
Evaluation of silicon-on-insulator MOS (Metal-Oxide-Semiconductor) transistor response to 10-keV X-ray and cobalt-60 irradiation
[DE88-006102] 23 p3206 N88-29082
Metal grid base heterojunction transistor operating at 60 and 94 GHz
[AD-A194763] 23 p3207 N88-29087

TRANSIT TIME
A proposed Quantum Well Injection Transit Time device (QWITT) 19 p2657 N88-25785

TRANSITION
Temperature hysteresis and magnetic transitions in amorphous Fe-Ni-Zr alloys
[DE88-000228] 03 p0294 N88-11848

TRANSITION FLOW
Numerical study of the entrance flow and its transition in a circular pipe (2) 03 p0318 N88-12011
A numerical study of the effects of curvature and convergence on dilution jet mixing
[NASA-TM-89878] 05 p0549 N88-13347
Effect of transition aerodynamics on aeroassist flight experiment trajectories
[NASA-TM-100546] 11 p1446 N88-18620
The design and use of a temperature-compensated hot-film anemometer system for boundary-layer flow transition detection on supersonic aircraft
[NASA-TM-100421] 13 p1723 N88-20304
A new laminar water tunnel to study the transition process in a blasius layer and in a separation bubble and a new tool for industrial aerodynamics and hydrodynamic research 16 p2204 N88-23150
Simulation of laminar-turbulent transition in the vicinity of a wall
[AD-A191380] 16 p2208 N88-23180
An efficient parallel algorithm for the simulation of three-dimensional compressible transition on a 20 processor Flex/32 multicomputer
[NASA-CR-178340] 17 p2337 N88-23943
Modeling of cavitation phenomena in homogeneous flow in transitory regimes in pipes
[ISAL-IDI1-87-15] 17 p2337 N88-23948
Prediction of laminar and turbulent flows past single and twin airfoils 18 p2457 N88-24589
Turbulence transition in a circular pipe
20 p2782 N88-26503
Transition at hypersonic speeds
[NASA-CR-178315] 24 p3368 N88-30058
Transition mixing study empirical model report
[NASA-CR-182139] 24 p3371 N88-30076
Recent insights into instability and transition to turbulence in open-flow systems
[NASA-CR-181693] 24 p3372 N88-30079

TRANSITION LAYERS
Existence and stability of transition layers
[AD-A185806] 06 p0766 N88-14707

TRANSITION METALS
NT CADMIUM
NT CHROMIUM
NT COBALT
NT COBALT 60
NT GOLD
NT HAFNIUM
NT IRIDIUM
NT IRIDIUM ISOTOPES
NT IRON
NT IRON ISOTOPES
NT IRON 57
NT MANGANESE
NT MOLYBDENUM
NT NICKEL
NT NIOBIUM
NT NIOBIUM ISOTOPES
NT OSMIUM
NT PALLADIUM
NT PLATINUM
NT PLATINUM ISOTOPES
NT RHENIUM
NT RHENIUM ISOTOPES
NT RHODIUM
NT RUTHENIUM
NT SILVER
NT TANTALUM
NT TITANIUM
NT TUNGSTEN
NT VANADIUM
NT YTTRIUM
NT ZINC
NT ZIRCONIUM
Near-infrared dichroism of a mesogenic transition metal complex and its solubility in nematic hosts
[DE87-014471] 03 p0287 N88-11805
A theoretical analysis of the deactivation of metal surfaces upon carburization
[AD-A184556] 03 p0290 N88-11821
Surface chemistry of transition metal carbides: A theoretical analysis
[AD-A184237] 03 p0291 N88-11829
K-CO on transition metals: A local ionic interaction
[AD-A184342] 04 p0496 N88-13056
Atomic beam studies of the interaction of hydrogen with transition metal surfaces
[DE88-000208] 05 p0648 N88-13970
Cohesive energies of transition metal silicides and phosphides --- Knudsen effusion
[AD-A186691] 09 p1254 N88-17519
Nonlinear optical waveguides containing a transition metal-based dye molecule
[DE88-003257] 11 p1550 N88-19275
Gas phase reactions of electrons, negative ions and free-radicals with transition metal complexes
11 p1560 N88-19339
Transition metal cluster chemistry
[AD-A188731] 13 p1740 N88-20405
Clusters of transition metal atoms
[AD-A191265] 16 p2270 N88-23579
In situ spectroscopic studies of transition metal macrocycles as catalysts for the electrochemical reduction of oxygen
[PB88-203195] 20 p2769 N88-26416
Magnetic excitations in transition metal systems
[DE88-011022] 21 p2912 N88-27279
Investigation of magnetic anisotropy and spin wave modes in transition metal multilayers
[DE88-009007] 22 p3154 N88-28765

TRANSITION POINTS
On the search for experimentally observed grain boundary phase transitions
[DE87-012747] 02 p0244 N88-11539
Visible boundary layer transition points through flight tests 06 p0675 N88-14136
Nature of Western Pacific transition zone
08 p1010 N88-16122
Characterization of lubricants in terms of transition diagram data
[AD-A194264] 23 p3197 N88-29025

TRANSITION PROBABILITIES
Passage from two-parameters to infinite dimension
[ENST-87C002] 01 p0088 N88-10577

TRANSITION TEMPERATURE
Superconductivity of pseudobinary compounds Al5 (V-Cr)3Si, (V-MO)3Si, Mo3(Si-Re), bombarded with fast neutrons 03 p0285 N88-11792
Impact behavior of 9-Cr and 12-Cr ferritic steels after low-temperature irradiation
[DE88-000333] 03 p0291 N88-11827
Analytical treatment of the melting and solidification of latent heat store materials in finned tube geometries
[IKE-5-223] 03 p0314 N88-11985
Soliton twin boundaries of the cubic-tetragonal martensitic transformations in ferroelastic materials
[DE87-014741] 04 p0495 N88-13047
Metal-oxide superconductor BaPbsub1-xBisubxO3: Unusual properties and new applications
08 p1077 N88-16494
Study of the micromechanical properties of fluor glasses based on ZrF4
[ISAL-ITC1-87-03] 09 p1148 N88-16882
Study of molecular mobility of noncrystaline polymer alloys of different compatibility using mechanical spectrometry
[ISAL-87-0032] 09 p1149 N88-16883
High temperature superconductivity research at Argonne National Laboratory
[DE88-003055] 09 p1258 N88-17541
Superconductivity and phase stability in the heavy rare earth quaternary compounds RBa2Cu3O7 (R = Ho, Er, Tm, Yb, Lu)
[DE88-003478] 10 p1419 N88-18476
Rapid e-beam heating for measuring thermodynamics of metastable materials
[DE88-003565] 13 p1849 N88-21066
Superconducting transition temperature of Cu-Nb microcomposites 14 p1973 N88-21775
Properties of superconductors with strong electron-phonon interaction 14 p1974 N88-21779
Influence of fiber reinforcement on the vitreous transition temperature of M 10 matrix composites
[ONERA-RT-44/7086-M] 17 p2316 N88-23835
Method of producing high T(subc) superconducting NBN films
[NASA-CASE-NPO-16881-1-CU] 17 p2446 N88-24543
Crystalline metal-semiconductor superlattices
[DE88-007063] 18 p2581 N88-25332
The superconducting transition in oxygen deficient YBa2Cu3O(sub 7-Delta)
[DE88-009957] 20 p2877 N88-27079
High-temperature superconductivity: An overview
[DE88-702051] 21 p3020 N88-27925
Thermodynamics of oxygen-vacancy ordering in YBa2Cu3O(sub z)
[DE88-009816] 21 p3022 N88-27940
Properties of new low dimensional materials and mechanisms of high T(sub c) superconductivity
[DE88-012026] 21 p3024 N88-27951

Preparation and characterization of isotopic oxygen-enriched yttrium barium copper oxide
[DE88-010939] 22 p3154 N88-28766
High Tc superconducting HoBa2Cu(sub 1-x)Fe(sub x)3O(sub 7-y)
[DE88-008909] 22 p3155 N88-28768
Effect of neutron irradiation on critical magnetization current in single crystal YBa2Cu3O(sub 7-delta)
[DE88-009970] 22 p3156 N88-28775
High-T(sub c) superconductor and its use in superconducting magnets
[DE88-008403] 23 p3289 N88-29581
Thermodynamical, optical and X-rays studies of some thermotropic liquid crystals
[DE88-702301] 23 p3290 N88-29590
Fluctuations of order parameters in the high T(sub c) superconductors
[DE88-702549] 23 p3292 N88-29603
Dependence of high critical temperature of ceramic superconductors on the nominal Cu(sup 3+)Cu(sup 2+) ratio
[DE88-702734] 23 p3293 N88-29611
Theory of superconductivity in oxides
[AD-A195647] 24 p3433 N88-30432
Theoretical model of high temperature superconductors
[DE88-702707] 24 p3434 N88-30441

TRANSITS
NT THEODOLITES

TRANSLATING
NT MACHINE TRANSLATION
Errors associated with Russian name transliteration
[DE87-011717] 02 p0248 N88-11566
A data translation method for heterogeneous database systems 04 p0501 N88-13081
Programming language translation for multicomputers 10 p1381 N88-18244
Translations of scientific and technical literature: A guide to their location 16 p2286 N88-23686
Description of graphics translation software between Intergraph and Tektronix systems
[NASA-TM-100335] 17 p2389 N88-24202
The UMAC simulator 20 p2834 N88-26811
TRANSL: A PATRAN translator subroutine library
[DE88-010976] 21 p2998 N88-27784
Conversion of productions in OPS5 to their equivalent English
[ORNL/TM-10246] 24 p3411 N88-30306

TRANSLATIONAL MOTION
NT SECONDARY FLOW
NT THREE DIMENSIONAL FLOW
NT THREE DIMENSIONAL MOTION
Diffusion description of flame propagation due to the translational motion of burning reaction products
[DE88-700676] 10 p1297 N88-17757
Effects of translational and rotational nonequilibrium on CW (Continuous Wave) chemical laser performance
[AD-A191425] 16 p2214 N88-23210
A generic multibody simulation
[NASA-CR-182949] 17 p2388 N88-24198
Large planar maneuvers for articulated flexible manipulators
[NASA-CR-183079] 19 p2711 N88-26104

TRANSLUCENCE
Effect of translucence of engineering ceramics on heat transfer in diesel engines
[DE88-003732] 10 p1305 N88-17804

TRANSLUNAR SPACE
U INTERPLANETARY SPACE

TRANSMISSION
NT ACOUSTIC PROPAGATION
NT AERODYNAMIC HEAT TRANSFER
NT ALOHA SYSTEM
NT AUTOMATIC PICTURE TRANSMISSION
NT BIOTELEMETRY
NT CODE DIVISION MULTIPLE ACCESS
NT CONDUCTIVE HEAT TRANSFER
NT CONVECTIVE HEAT TRANSFER
NT DATA TRANSMISSION
NT DEMAND ASSIGNMENT MULTIPLE ACCESS
NT DIFFRACTION PROPAGATION
NT ELECTRIC POWER TRANSMISSION
NT ELECTROMAGNETIC WAVE TRANSMISSION
NT FREQUENCY DIVISION MULTIPLE ACCESS
NT FREQUENCY DIVISION MULTIPLEXING
NT GROUND WAVE PROPAGATION
NT HALOS
NT HEAT TRANSFER
NT HEAT TRANSMISSION
NT IONOSPHERIC PROPAGATION
NT LAMINAR HEAT TRANSFER
NT LIGHT SCATTERING
NT LIGHT TRANSMISSION
NT MICROWAVE ATTENUATION
NT MICROWAVE TRANSMISSION
NT MULTIPATH TRANSMISSION
NT MULTIPLE ACCESS
NT MULTIPLEXING
NT PACKET TRANSMISSION
NT PCM TELEMETRY
NT RADAR TRANSMISSION
NT RADIATIVE HEAT TRANSFER
NT RADIO TELEMETRY
NT RADIO TRANSMISSION
NT SATELLITE TRANSMISSION
NT SCATTER PROPAGATION
NT SHOCK WAVE PROPAGATION
NT SHORT WAVE RADIO TRANSMISSION
NT SIGNAL TRANSMISSION
NT SINGLE CHANNEL PER CARRIER TRANSMISSION
NT SOUND TRANSMISSION
NT SPREAD SPECTRUM TRANSMISSION
NT STRESS PROPAGATION
NT TELEMETRY
NT TELEPHONY
NT TELEVISION TRANSMISSION
NT TIME DIVISION MULTIPLE ACCESS
NT TIME DIVISION MULTIPLEXING
NT TRANSEQUATORIAL PROPAGATION
NT TURBULENT HEAT TRANSFER
NT WAVE PROPAGATION
NT WAVELENGTH DIVISION MULTIPLEXING
An analysis of simplified feed architectures for MMIC (Monolithic Microwave Integrated Circuit) T/R (Transmit/Receive) module arrays
[AD-A185474] 06 p0697 N88-14275
Parametric and experimental analysis using a power flow approach
[NASA-CR-182460] 09 p1116 N88-16693
Development of fiber optic systems for recording and transmitting holographic information
[AD-A189406] 13 p1773 N88-20603
Millimeter-wave integrated circuits 19 p2656 N88-25774

TRANSMISSION EFFICIENCY
Transmission efficiency in advanced aerospace powerplant
[PNR90391] 02 p0182 N88-11133
Developments in optical sensor technologies described 06 p0689 N88-14220
Land mobile satellite transmission measurements at 869 MHz. A comparison of error probabilities for various message block durations and fade margins as a function of vegetation shadowing
[NASA-CR-179929] 06 p0693 N88-14255
Designing variable-length codes with good error-recovery properties
[BBC-RD-1987/19] 10 p1317 N88-17876
Phase calibration generator 11 p1473 N88-18785
A concatenated coded modulation scheme for error control
[NASA-CR-182639] 12 p1621 N88-19697
Results of one way transit time measuring in navigation experiment NAVEX
[DFVLR-MITT-87-17] 14 p1865 N88-21145
Spatial distribution of traffic in a cellular mobile data network
[EUT-87-E-168] 14 p1904 N88-21378

TRANSMISSION LINES
NT BEAM WAVEGUIDES
NT CIRCULAR WAVEGUIDES
NT COAXIAL CABLES
NT COMMUNICATION CABLES
NT FLUID TRANSMISSION LINES
NT MICROSTRIP TRANSMISSION LINES
NT OPTICAL FIBERS
NT OPTICAL WAVEGUIDES
NT PLASMAGUIDES
NT POWER LINES
NT RECTANGULAR WAVEGUIDES
NT STRIP TRANSMISSION LINES
NT UNDERGROUND TRANSMISSION LINES
NT WAVEGUIDES
Crosstalk in braided shield coaxial cables 01 p0035 N88-10224
The development of diagnostic fuses
[SAND-86-0395] 03 p0311 N88-11963
Low-noise cryogenic transmission line 04 p0434 N88-12688
Departmental report on program EMTP-machine windings surge transients: Travelling wave method
[PB87-123733] 04 p0438 N88-12719
The use of coaxial transmission line elements in log-periodic dipole arrays
[AD-A184864] 05 p0574 N88-13499
Safety research of insulating materials of cable for nuclear power generating station
[NASA-TT-20202] 13 p1752 N88-20477
Harmonic and rectangular pulse reproduction through current transformers
[EUT-86-E-159] 14 p1907 N88-21395
The application of high temperature superconductors to space electrical power distribution components
[NASA-TM-100901] 16 p2171 N88-22939
A computer model investigation of a half square log-periodic array
[AD-A190955] 16 p2190 N88-23062
High frequency power distribution system
[NASA-CR-175071] 17 p2335 N88-23939
Space power radiation cooled dc transmission line analysis 17 p2438 N88-24506
Carrier lifetime versus ion-implantation dose in Silicon On Sapphire 19 p2658 N88-25791
Experimental investigation of simplest inhomogeneities in cylindrical slit line
[DE88-702388] 21 p2933 N88-27418
Multichannel data transmission through a fiber optic cable
[AD-A193842] 22 p3070 N88-28221
A fiber optic beamforming processor for wideband direction finding
[AD-A194862] 24 p3428 N88-30404
Ultra-wideband direction finding using a fiber optic beamforming processor
[AD-A194861] 24 p3430 N88-30413

TRANSMISSION LOSS
Loss measurement of 3-port ferrite switches in the 90 GHz range
[ESA-TT-1054] 03 p0310 N88-11958
Analysis of counting errors in the phase/Doppler particle analyzer
[NASA-TM-100231] 03 p0323 N88-12043
Photoinduced low-temperature changes in optical losses in fiber optics based on chalcogenide glasses 06 p0770 N88-14731
A diffraction based theoretical model for prediction of UHF path loss in cities 12 p1616 N88-19661
A program for the calculation of radio-wave transmission loss over the spherical earth and over obstacles 12 p1616 N88-19662
Low-loss, high-isolation, fiber-optic isolator
[NASA-CASE-NPO-17207-1-CU] 18 p2576 N88-25304
Surface-wave model uncertainty assessment
[AD-A193094] 21 p2932 N88-27408

TRANSMISSIONS (MACHINE ELEMENTS)
Transmission efficiency in advanced aerospace powerplant
[PNR90391] 02 p0182 N88-11133
Improved oil-off survivability of tapered roller bearings
[NASA-CR-180804] 02 p0182 N88-11135
The flight evaluation of an advanced engine display and monitoring system 03 p0264 N88-11659
A129 advanced solutions for meeting today's combat helicopter requirement 03 p0265 N88-11669
Multipath gear-friction planetary transmissions 04 p0424 N88-12629
On dynamic loads in parallel shaft transmissions. 1: Modelling and analysis
[NASA-TM-100180] 04 p0451 N88-12797
On dynamic loads in parallel shaft transmissions. 2: Parameter study
[NASA-TM-100181] 04 p0452 N88-12798
Efficiency testing of a helicopter transmission planetary reduction stage
[NASA-TP-2795] 07 p0861 N88-15224
Experimental investigation on the bending fatigue performance of gas carbonitrided and carburized gears
[PB87-147997] 08 p0992 N88-16003
Results of NASA/Army transmission research 09 p1108 N88-16640
Dynamic analysis of multimesh-gear helicopter transmissions
[NASA-TP-2789] 09 p1176 N88-17045
Advanced transmission studies
[NASA-TM-100857] 14 p1919 N88-21454
Computerized life and reliability modelling for turboprop transmissions
[NASA-TM-100918] 16 p2215 N88-23220
Magnetic drive coupling
[NASA-CASE-MSC-21171-1] 17 p2344 N88-23973
Design, manufacture and spin test of high contact ratio helicopter transmission utilizing Self-Aligning Bearingless Planetary (SABP)
[NASA-CR-4155] 18 p2524 N88-24975
Optimization of planetary gears
[ETN-88-92375] 21 p2958 N88-27573
Helicopter transmission research at NASA Lewis Research Center
[NASA-TM-100962] 24 p3379 N88-30128

TRANSMISSIVITY
National Aerospace Laboratory experiment 04 p0404 N88-12509
Determination of cloud base height and emissivity from downwelling angular radiances
[AD-A185985] 07 p0879 N88-15331

Experimental research on skin reflection, transmission, absorption of light rays 16 p2187 N88-23039

TRANSMISSOMETERS

Description of the MPTR system: Multi Path Transmissometer Radiometer
[FEL-1987-14] 20 p2855 N88-26954

TRANSMITTANCE

Distortion of wideband carbon dioxide laser radar waveforms due to atmospheric dispersion and absorption
[AD-A188687] 12 p1632 N88-19771

Enhancements to the atmospheric transmittance/radiance program FASCODE
[AD-A188863] 12 p1643 N88-19839

Spectral measurements for correcting LANDSAT data for atmospheric effects 17 p2362 N88-24066

Optical constants of minerals and other materials from the millimeter to the ultraviolet
[AD-A192210] 18 p2482 N88-24724

Development and validation of transmission measurements techniques of image contrast, utilizing existing IR imagers
[AD-A191471] 18 p2541 N88-25079

Filling of the atmospheric transmission window due to emission from very high rotational levels of NO and O3
[AD-A194670] 23 p3233 N88-29239

TRANSMITTER RECEIVERS

A laser communication experiment utilizing the ACT satellite and an airborne laser transceiver
[NASA-TM-100792] 11 p1492 N88-18910

The 2 FSK/QPSK (Frequency Shift Keying/Quadrature Phase Shift Keying) transmitter and receiver: Design and performance
[AD-A190028] 15 p2056 N88-22258

Picosecond photoconductive transceivers 19 p2656 N88-25777

Digital communication transmitter and receiver test procedures
[AD-A191218] 20 p2788 N88-26540

TRANSMITTERS

NT EMERGENCY LOCATOR TRANSMITTERS
NT IONOSONDES
NT RADAR TRANSMITTERS
NT RADIO BEACONS
NT RADIO TRANSMITTERS
NT RADIOSONDES
NT RADIOTELEPHONES
NT RAWINSONDES
NT REPEATERS
NT TRANSMITTER RECEIVERS

Ultrafast photoconductor detector-laser-diode transmitter
[DE87-013803] 03 p0329 N88-12082

Inductance effects in the high-power transmitter crowbar system 04 p0433 N88-12687

Receiver susceptibility measurements relating to interference between UHF (Ultra High Frequency) television and land mobile radio services
[PB87-228029] 06 p0690 N88-14228

A 104-km unrepeatered bidirectional fiber optic demonstration link
[AD-A190282] 15 p2134 N88-22728

Development of 20 GHz monolithic transmit modules
[NASA-CR-182134] 17 p2445 N88-24539

WIPP (Wave Induced Particle Precipitation) experiment logistic support
[AD-A191184] 18 p2499 N88-24824

Outer zone electron precipitation produced by a VLF transmitter
[AD-A191944] 19 p2691 N88-25993

TRANSMUTATION

Construction of approximations to acoustic Green's functions for nonhomogeneous oceans using transmutation
[PB88-185384] 18 p2548 N88-25126

TRANSOCEANIC FLIGHT

Desynchronization of heart rate and breathing frequency after transmeridional flight across three time zones 12 p1663 N88-19968

TRANSONIC AIRCRAFT

U SUPERSONIC AIRCRAFT

TRANSONIC COMPRESSORS

Radial compressor design using an Euler solver 10 p1283 N88-17675

Studies of unsteady axial-compressor functioning 24 p3380 N88-30129

TRANSONIC FLIGHT

Sensitivity of F-106B leading-edge-vortex images to flight and vapor-screen parameters
[NASA-TP-2818] 17 p2300 N88-23760

Wind tunnel investigation of wing and control panel loads at transonic and supersonic speeds on some schematic cruciform missile configurations
[FFA-TN-1986-43] 18 p2457 N88-24585

TRANSONIC FLOW

Transonic analysis and design of axisymmetric bodies in nonuniform flow
[NASA-CR-4101] 01 p0003 N88-10013

A method for the calculation of transonic flows for the control of adaptive wind tunnels
[ETN-87-90411] 01 p0003 N88-10015

A flow function method for the axisymmetric calculation of the transonic turbomachine flow taking into account the flow differences in circumferential direction
[ETN-87-90428] 01 p0056 N88-10359

Computation of transonic separated wing flows using an Euler/Navier-Stokes zonal approach
[NASA-TM-88311] 02 p0173 N88-11089

Investigations on a transonic airfoil with a 30 mm wide perforation/cavity arrangement
[ESA-TT-1072] 03 p0260 N88-11634

Fin gaps and body slots of guided projectiles: Effects, data correlation and modeling
[AD-A184440] 03 p0270 N88-11698

Application of the finite difference method to the solution of mixed partial differential equations for the case of transonic flow
[ETN-87-90760] 03 p0370 N88-12327

Application of Runge Kutta time marching scheme for the computation of transonic flows in turbomachines
[NASA-TM-86997] 04 p0394 N88-12461

Concepts for radically increasing the numerical convergence rate of the Euler equations
[NASA-CR-177456] 04 p0395 N88-12463

Solution of the two-dimensional Euler equations on unstructured triangular meshes 04 p0396 N88-12469

Some asymptotic modes of transonic vortex flow 04 p0425 N88-12632

The role of computation fluid dynamics in aeronautical engineering (4). The development and applications of implicit TVD finite volume code 05 p0536 N88-13259

Navier-Stokes simulation of transonic transportation aircraft configurations. 1: Flow-field simulation over wing-fuselage combinations 05 p0540 N88-13288

Numerical simulation of transonic aircraft in comparison to wind tunnel test 05 p0540 N88-13289

Study of the effect of mass transfer on a transonic boundary layer. Application to flow relaminarization
[ETN-88-91169] 05 p0541 N88-13296

Computation of transonic flows with nacelle simulation
[SNIAS-872-111-117] 05 p0542 N88-13300

Investigation of viscous/inviscid interaction in transonic flow over airfoils with suction 06 p0664 N88-14074

A zonal approach for the solution of coupled Euler and potential solutions of flows with complex geometries
[AD-A185465] 06 p0702 N88-14310

Finite-volume scheme for transonic potential flow about airfoils and bodies in an arbitrarily shaped channel 07 p0809 N88-14928

Breakdown of the conservative potential equation 07 p0809 N88-14929

Development of direct-inverse 3-D methods for applied aerodynamic design and analysis
[NASA-CR-182436] 08 p0950 N88-15767

Theoretical and experimental studies of the transonic flow field and associated boundary conditions near a longitudinally-slotted wind-tunnel wall
[NASA-CR-181169] 08 p0959 N88-15815

An initial investigation into methods of computing transonic aerodynamics sensitivity coefficients
[NASA-CR-182444] 09 p1112 N88-16663

Experimental investigation of shock-induced disturbances on transonic airfoils
[DFVLR-FB-87-28] 09 p1112 N88-16666

Numerical resolution of the equations of three-dimensional stable compressible transonic flows
[PB87-168415] 09 p1113 N88-16673

Mach number effects on transonic aeroelastic forces and flutter characteristics
[NASA-TM-100547] 09 p1113 N88-16675

Solution of the three-dimensional Navier-Stokes equations for transonic flow using a multigrid method 10 p1267 N88-17579

Navier-Stokes simulation of wind-tunnel flow using LU-ADI factorization algorithm
[NASA-TM-100042] 10 p1268 N88-17584

Navier-Stokes computations for circulation control airfoils 10 p1269 N88-17592

Wall jet analysis for circulation control aerodynamics. Part 2: Zonal modeling concepts for wall jet/potential flow coupling 10 p1269 N88-17593

A transonic-small-disturbance wing design methodology
[NASA-TP-2806] 10 p1273 N88-17614

The unsteady gas flow through stator and rotor of a turbomachine 10 p1281 N88-17660

The effects of rotational flow, viscosity, thickness, and shape on transonic flutter dip phenomena
[NASA-TM-100811] 11 p1502 N88-18969

A multigrid solver for two-dimensional transonic full potential flow calculations 11 p1538 N88-19189

A multigrid full potential transonic code for arbitrary configurations --- aircraft 11 p1539 N88-19195

Wing flutter calculations with the CAP-TSD unsteady transonic small disturbance program
[NASA-TM-100580] 12 p1575 N88-19419

Application of a flux vector splitting methodology towards the solution of unsteady transonic flows, with future emphasis on the blade flutter problem
[AD-A189500] 13 p1716 N88-20260

Numerical simulation of subsonic and transonic propeller flow
[NASA-TM-100163] 13 p1716 N88-20262

Tests on the AFWAL 65 deg delta wing at NLR: A study of vortex flow development between Mach = 0.4 and 4
[NLR-MP-86058-U] 13 p1717 N88-20266

The international vortex flow experiment: A test case for compressible Euler codes
[NLR-MP-86076-U] 13 p1717 N88-20267

Steady and unsteady transonic small disturbance analysis of realistic aircraft configurations
[NASA-TM-100557] 13 p1717 N88-20269

An L-U implicit multigrid algorithm to solve the Euler equations for transonic flow in rotating turbomachinery passages 13 p1718 N88-20270

An adaptive grid technique for solution of the Euler equations 13 p1768 N88-20579

Multigrid solution of the Euler equations 13 p1769 N88-20582

Wall interference assessment and corrections for transonic adaptive wall airfoil data 14 p1863 N88-21129

Transonic flow field analysis for real fuselage configurations 14 p1864 N88-21133

An experimental-computational investigation of transonic shock wave-turbulent boundary layer interaction in a curved test section
[CWI-NM-R8716] 14 p1909 N88-21408

Computational fluid dynamics drag prediction: Results from the Viscous Transonic Airfoil Workshop
[NASA-TM-100095] 15 p2014 N88-22009

Mixed direct-inverse problem of transonic cascade 15 p2054 N88-22244

A zonal approach for the solution of coupled Euler and potential solutions of flows with complex geometries
[AD-A189752] 15 p2114 N88-22595

A physically consistent model for artificial dissipation in transonic potential flow computations
[NASA-TM-100846] 15 p2122 N88-22652

Experimental investigation of the transonic flow at the leeward side of a delta wing at high incidence
[LR-518] 16 p2156 N88-22861

The 2-D and 3-D time marching transonic potential flow method for propfans 16 p2220 N88-23245

Development and improvement of a code to calculate small, three dimensional, unsteady transonic perturbations
[ONERA-RTS-31/3064-RY-062-R] 17 p2338 N88-23951

Accounting for the effects of unsteady, separated boundary layers in transonic two dimensional calculations
[ONERA-RT-30/3064-RY-063-R] 17 p2338 N88-23952

A transonic small disturbance wing design methodology 18 p2457 N88-24590

The calculation of transonic flow over the shuttle orbiter using slender body theory 18 p2460 N88-24606

Computational Fluid Mechanics
[NASA-CR-183022] 18 p2514 N88-24915

Navier-Stokes analysis of transonic transport aircraft empennage 19 p2636 N88-25637

Navier-Stokes code NS3D for blunt bodies. Part 1: Analysis, results and verification
[DE88-010105] 19 p2666 N88-25855

An initial investigation into methods of computing transonic aerodynamic sensitivity coefficients
[NASA-CR-183061] 20 p2752 N88-26332

Finite element approximation to a model problem of transonic flow
[DE88-701835] 20 p2752 N88-26333

Calculation of 2-D unsteady transonic full potential flow about oscillating airfoils by two complementary approaches
[PB88-127519] 20 p2753 N88-26341

A study of flow separation in transonic flow using inviscid and viscous computational fluid dynamics (CFD) schemes
[NASA-CR-183119] 20 p2801 N88-26818

Theoretical-numerical study of feasibility of use of winglets on low aspect ration wings at subsonic and transonic Mach numbers at reduce drag
[NASA-CR-4174] 21 p2892 N88-27168
Experimental determination of aerodynamic damping in a three-stage transonic axial-flow compressor
[NASA-TM-100953] 21 p2897 N88-27200
Investigation of viscous/inviscid interaction in transonic flow over airfoils with suction
[NASA-CR-183112] 21 p2945 N88-27490
Study of three-dimensional transonic flow separations
[AD-A193018] 22 p3037 N88-28032
Method to predict external store carriage characteristics at transonic speeds
[NASA-CR-4170] 22 p3037 N88-28034
Transonic blade-vortex interactions
22 p3037 N88-28035
Runge-Kutta finite-volume simulation of laminar transonic flow over the ONERA M6 wing using the Navier-Stokes equations
[FFA-TN-1987-06] 22 p3039 N88-28045
Boundary layer development and transition
23 p3169 N88-28871
The influence of numerical boundary conditions on transonic flow
[DFVLR-FB-88-06] 23 p3172 N88-28890
Navier-Stokes calculations of transonic flows past cavities
[NASA-CR-180484] 23 p3212 N88-29116
Three-dimensional elliptic grid generation for an F-16
23 p3246 N88-29315
A streamwise upwind algorithm for the Euler and Navier-Stokes equations applied to transonic flows
[NASA-TM-101019] 24 p3316 N88-29751
Application of unsteady aerodynamic methods for transonic aeroelastic analysis
[NASA-TM-100665] 24 p3317 N88-29754
Computational methods for the problems of the tip vortex
[NASA-CR-181436] 24 p3320 N88-29775
Theoretical aerodynamics, transonic flow
[AD-A196247] 24 p3321 N88-29777

TRANSONIC FLUTTER
Unsteady transonic algorithm improvements for realistic aircraft applications
[NASA-TM-100516] 08 p0949 N88-15760
Unsteady transonic small-disturbance theory including entropy and vorticity effects
[NASA-TM-100568] 12 p1575 N88-19418
Wing flutter calculations with the CAP-TSD unsteady transonic small disturbance program
[NASA-TM-100580] 12 p1575 N88-19419
Propagation of acoustic disturbances in transonic flow fields of lifting wings
[DFVLR-FB-88-13] 21 p3013 N88-27880

TRANSONIC INLETS
U SUPERSONIC INLETS

TRANSONIC NOZZLES
A research program on the aerodynamics of a highly loaded turbine stage 10 p1280 N88-17655

TRANSONIC SPEED
Comparison of wind tunnel and flight test afterbody and nozzle pressures for a twin-jet fighter aircraft at transonic speeds
[NASA-TP-2588] 02 p0121 N88-10765
Effect of empennage arrangement on single-engine nozzle/afterbody static pressures at transonic speeds
[NASA-TP-2753] 02 p0122 N88-10771
An experimental evaluation of advanced rotorcraft airfoils in the NASA Ames eleven-foot transonic wind tunnel
[NASA-CR-166587] 03 p0261 N88-11640
Design of wings and wing/body configurations for transonic and supersonic speeds
05 p0545 N88-13318
Development of transonic speed cascade design method using Euler code and inverse solution
06 p0676 N88-14139
Unsteady transonic algorithm improvements for realistic aircraft applications
[NASA-TM-100516] 08 p0949 N88-15760
Comparison of two transonic noise prediction formulations using the aircraft noise prediction program
[NASA-CR-181609] 12 p1688 N88-20095
Parametric flutter studies of an arrow-wing configuration: Some early results
[NASA-TM-100608] 19 p2599 N88-25444
Wind tunnel investigation of wing and control panel loads at transonic and supersonic speeds on some schematic cruciform missile configurations
[FFA-TN-1988-43-SUPPL-1] 22 p3039 N88-28044
Test results at transonic speeds on a contoured over-the-wing propfan model
[NASA-TM-88206] 23 p3177 N88-28918
Recent advances in transonic computational aeroelasticity
[NASA-TM-100663] 24 p3321 N88-29778

TRANSONIC TURBINES
U SUPERSONIC TURBINES

TRANSONIC WIND TUNNELS
A method for the calculation of transonic flows for the control of adaptive wind tunnels
[ETN-87-90411] 01 p0003 N88-10015
Investigation of the suitability of the 8ft x 6ft transonic wind-tunnel for aeroacoustic research on propellers
[RAE-TM-AERO-2093] 01 p0008 N88-10041
Wall interference tests of a CAST 10-2/DOA 2 airfoil in an adaptive-wall test section
[NASA-TM-4015] 02 p0122 N88-10772
Intergration effects of D-shaped, underwing, aft-mounted, separate-flow, flow-through nacelles on a high-wing transport
[NASA-TM-4018] 02 p0122 N88-10773
The 0.6m x 0.6m trisonic test section (TMK) of DFVLR in Cologne-Porz, Federal Republic of Germany (status 1986)
[ESA-TT-1052] 03 p0267 N88-11681
Status of magnetic suspension technology
07 p0811 N88-14939
Preliminary calibration and test results from the National Transonic Facility 07 p0811 N88-14941
Effect of an optimized fiber orientation on transonic flutter characteristics of a high-aspect-ratio composite wing
[NAL-TR-930] 09 p1120 N88-16709
Transonic wind tunnel calibration 1986: Force measurements on three ONERA-C5 models and three half sphere cylinder calibration bodies in the F+W transonic test section
[F+W-FO-1854] 09 p1122 N88-16714
Influence of the wall boundary layer on force measurements on half models in the transonic wind tunnel
[F+W-TF-1876] 09 p1122 N88-16715
Pressure distributions from high Reynolds number transonic tests of an NACA 0012 airfoil in the Langley 0.3-meter transonic cryogenic tunnel
[NASA-TM-100526] 11 p1435 N88-18565
High Reynolds number transonic tests on a NACA 0012 airfoil in the Langley 0.3-meter transonic cryogenic tunnel
[NASA-TM-100527] 11 p1436 N88-18571
An evaluation in a modern wind tunnel of the transonic adaptive wall adjustment strategy developed by NPL in the 1940's
[NASA-CR-181623] 12 p1575 N88-19417
Design of a sound neck in connection with the model-support system of a transonic wind tunnel test section
[ILR-MITT-186(1987)] 14 p1869 N88-21171
Modifications to the Langley 8-foot transonic pressure tunnel for the laminar flow control experiment
[NASA-TM-4032] 15 p2021 N88-22047
Aerofoil testing in a self-streamlining flexible walled wind tunnel
[NASA-CR-4128] 16 p2156 N88-22865
The transonic wind tunnel (TWB) at DFVLR, Brunswick (Federal Republic of Germany)
[DFVLR-MITT-88-01] 16 p2164 N88-22909
Flow quality of NAL two-dimensional transonic wind tunnel. Part 1: Mach number distributions, flow angularities and preliminary study of side wall boundary layer suction
[NASA-TT-20209] 16 p2165 N88-22911
Design study. Manipulator systems for model handling in European transonic wind tunnels
[ETN-88-91944] 18 p2468 N88-24651
Empty test section streamlining of the transonic self-streamlining wind tunnel fitted with new walls
[NASA-CR-181680] 19 p2598 N88-25442
Wall interference assessment/correction of data from tests of a CAST 10-2/DOA 2 airfoil in the Langley 0.3-m transonic cryogenic tunnel 20 p2751 N88-26331
European transonic wind tunnel project: Assistance to the design group
[ONERA-RSF-11/0694-GY-010-G]
21 p2900 N88-27208
Studies concerning the European transonic wind tunnel
[ONERA-RSF-10/0694-GY-010-G]
21 p2900 N88-27209
Hybrid procedure for dynamic measurements in transonic wind tunnels: Demonstrated by pitch oscillation
[DFVLR-FB-88-19] 21 p2900 N88-27211
Boundary layer simulation and control in wind tunnels
[AGARD-AR-224] 23 p3167 N88-28857

TRANSONICS
U TRANSONIC FLOW

TRANSPARENCE
Spatial characterization of acid rain stress in Canadian Shield Lakes
[NASA-CR-181136] 01 p0067 N88-10430
Spatial characterization of acid rain stress in Canadian Shield Lakes
[NASA-CR-180577] 01 p0067 N88-10431
Aluminum oxynitride spinel (ALON): A review
[AD-A184753] 03 p0294 N88-11845
Resistance of canopy materials against chemicals
[PML-1985-22] 05 p0569 N88-13466
Photoinduced low-temperature changes in optical losses in fiber optics based on chalcogenide glasses
06 p0770 N88-14731
Method for investigating the formation of crystals in a transparent material
[NASA-CASE-MFS-26008-1-CU]
06 p0788 N88-14835
Analysis of the decomposition of transparent polymer materials (blocks) under the action of laser beams in free generation mode
[AD-A187090] 09 p1147 N88-16873
Characterization of transparent insulation materials --- solar energy absorbers
[ETN-88-91052] 09 p1163 N88-16970
The interaction of small particles with laser beams
[AD-A190716] 15 p2072 N88-22354
Noncontact temperature measurement in glass and other transparent materials 17 p2328 N88-23900
Direct visualization of surfaces from computed tomography data
[AD-A193646] 22 p3153 N88-28758
Vision through aircraft transparencies
23 p3242 N88-29294
Maintenance of vision-related components
23 p3242 N88-29296
Precision measurement of the Fresnel drag coefficient using a ring laser
[AD-A196025] 24 p3366 N88-30043

TRANSPARENT MATERIALS
U TRANSPARENCE

TRANSPIRATION
A calculation method for the propulsive jet and its aerodynamic interaction with an afterbody
[ESA-TT-1039] 03 p0259 N88-11632
Study of the relationship between photosynthesis, respiration, transpiration, and mineral nutrition in wheat
03 p0360 N88-12268

TRANSPIRATION COOLING
U SWEAT COOLING

TRANSPONDERS
RF-switches: Application and design --- satellite communication 14 p1877 N88-21215
Refraction in underwater acoustics --- navigation systems
[B8735053] 17 p2395 N88-24236

TRANSPORT AIRCRAFT
NT A-300 AIRCRAFT
NT A-320 AIRCRAFT
NT BOEING 737 AIRCRAFT
NT BOEING 747 AIRCRAFT
NT C-130 AIRCRAFT
NT C-135 AIRCRAFT
NT CARGO AIRCRAFT
NT CH-46 HELICOPTER
NT CONCORDE AIRCRAFT
NT DC 9 AIRCRAFT
NT EUROPEAN AIRBUS
NT F-27 AIRCRAFT
NT SHORT HAUL AIRCRAFT
NT UH-60A HELICOPTER
NT VC-10 AIRCRAFT
Full-scale transport controlled impact demonstration program
[NASA-TM-89642] 01 p0004 N88-10021
Intergration effects of D-shaped, underwing, aft-mounted, separate-flow, flow-through nacelles on a high-wing transport
[NASA-TM-4018] 02 p0122 N88-10773
An aerodynamic performance evaluation of the NASA/Ames Research Center advanced concepts flight simulator
[NASA-TM-89659] 03 p0268 N88-11685
Investigation of pilot behavior in a training program for assessing handling qualities using a ground simulator
[ESA-TT-999] 03 p0357 N88-12247
Effect of permissible variations of center-of-gravity locations of cargo airplane on its mass
04 p0424 N88-12625
Computation of nacelle interference using boundary element method 05 p0537 N88-13267
Navier-Stokes simulation of transonic transportation aircraft configurations. 1: Flow-field simulation over wing-fuselage combinations 05 p0540 N88-13288
Aeroelastic analysis of modern transport aircraft
05 p0550 N88-13352

A study of the utilization of advanced composites in fuselage structures of commercial aircraft
[NASA-CR-172405] 06 p0679 N88-14157
Natural laminar flow nacelle for transport aircraft 07 p0813 N88-14949
Laminar flow integration: Flight tests status and plans 07 p0813 N88-14952
Handling qualities of a wide-body transport airplane utilizing Pitch Active Control Systems (PACS) for relaxed static stability application
[NASA-TP-2482] 07 p0821 N88-14987
Study on utilization of advanced composites in fuselage structures of large transports
[NASA-CR-172406] 07 p0827 N88-15014
Aeropropulsion '87. Session 6: High-Speed Propulsion Technology
[NASA-CP-10003-SESS-6] 08 p0957 N88-15807
Analysis of shock and vibration environments for cargo on C9B transport aircraft 08 p0999 N88-16051
Experimental study on the effect of fiber orientation on flutter characteristics of high-aspect-ratio transport wing
[NAL-TR-936] 09 p1120 N88-16708
Are windshear training aid recommendations appropriate for other than large jet transports? Pilot procedures: Shear models 10 p1275 N88-17635
Gear systems for advanced turboprops 10 p1282 N88-17667
Research and development. Technical-scientific publications (1956-1987): Retrospective view and prospects. Jubilee edition on the occasion of the 75th birthday of Dipl.-Engr. Dr.-Engr. E. H. Ludwig Boelkow
[ISSN-0931-9751] 10 p1309 N88-17819
High performance composites research at NASA-Langley
[NASA-TM-100518] 11 p1450 N88-18642
Application of hybrid laminar flow control to global range military transport aircraft
[NASA-CR-181638] 14 p1862 N88-21124
Trends in Computational Fluid Dynamics (CFD) for aeronautical 3D steady applications: The Dutch situation
[NLR-MP-86074-U] 15 p2015 N88-22017
KRASH parametric sensitivity study: Transport category airplanes
[AD-A189962] 15 p2017 N88-22024
Computational wing design studies relating to natural laminar flow 17 p2297 N88-23740
Integrated Application of Active Controls (IAAC) technology to an advanced subsonic transport project: Program review
[NASA-CR-3880] 17 p2301 N88-23763
Fuel containment concepts: Transport category airplanes
[AD-A189818] 18 p2494 N88-24799
Multivariable identification of a flexible transport aircraft 20 p2786 N88-26525
Application of complementary parameter identification techniques to flight test data of a transport aircraft 20 p2787 N88-26533
Concept development of a Mach 3.0 high-speed civil transport
[NASA-TM-4058] 21 p2895 N88-27182
Critical joints in large composite primary aircraft structures. Volume 1: Technical summary
[NASA-CR-3914] 23 p3190 N88-28983
Low-speed longitudinal flying qualities of modern transport aircraft 24 p3314 N88-29738

TRANSPORT COEFFICIENTS
U TRANSPORT PROPERTIES

TRANSPORT PROPERTIES
NT ATMOSPHERIC CONDUCTIVITY
NT CARRIER MOBILITY
NT DIFFUSION COEFFICIENT
NT EDDY VISCOSITY
NT ELECTRICAL RESISTIVITY
NT ELECTRON MOBILITY
NT GAS VISCOSITY
NT GASEOUS DIFFUSION
NT HOLE MOBILITY
NT IONIC MOBILITY
NT KONDO EFFECT
NT MAGNETORESISTIVITY
NT PHOTOCONDUCTIVITY
NT PLASMA CONDUCTIVITY
NT SUPERCONDUCTIVITY
NT THERMAL CONDUCTIVITY
NT THERMAL DIFFUSIVITY
NT VISCOSITY
Studies of transport processes in porous and ion exchange membranes
[ISBN-951-99847-0-4] 01 p0021 N86-10133
Aqueous-phase reactions in clouds
[DE86-005249] 01 p0069 N88-10445
Understanding the transport properties of silicon grain boundaries and how they relate to I.C. applications of polysilicon
[DE87-013809] 01 p0104 N88-10677
Conservation and transport properties of turbulence with large density variations
[LA-10911-MS] 03 p0321 N88-12032
Development and evaluation of a Monte Carlo code system for analysis of ionization chamber responses
[AD-A183970] 03 p0375 N88-12359
Novel macrocyclic carriers for proton-coupled liquid membrane transport
[DE88-000636] 04 p0413 N88-12560
Heat and moisture transport in the atmospheric boundary layer
[AD-A184222] 04 p0470 N88-12904
Numerical analysis of axisymmetric flow with H2-O2 reactions 05 p0538 N88-13272
Conditional second order closure for turbulent shear flows
[AD-A185369] 05 p0581 N88-13542
Monte Carlo photon transport on vector and parallel supercomputers
[DE88-002503] 07 p0905 N88-15486
Weak interactions and local order in strong turbulence 09 p1159 N88-16948
Transport delay compensation for computer-generated imagery systems
[NASA-TM-100084] 10 p1277 N88-17645
Models for ionic transport in glass
[DE88-002860] 10 p1304 N88-17799
Electronic and ionic transport in polymers
[AD-A187253] 11 p1452 N88-18651
High pressure electronic transport in semiconductors
[AD-A187428] 11 p1555 N88-19308
The physics of very small structures
[AD-A187672] 11 p1556 N88-19311
The influence of strain on hydrogen entry, transport, and embrittlement of a high strength steel in aqueous sodium chloride solution
[AD-A189302] 12 p1608 N88-19619
Transport properties of conductive polymers
[AD-A188411] 12 p1610 N88-19628
Competing interactions in metallic superlattices
[DE88-005344] 13 p1847 N88-21057
Electronic and ionic transport in polymers
[AD-A190434] 15 p2045 N88-22185
Noncontact temperature measurements in the microgravity fluids and transport phenomena discipline 17 p2328 N88-23901
Centrifugal acceleration of ions in the polar magnetosphere
[NASA-TM-101148] 17 p2374 N88-24120
An evaluation of energy-independent heavy ion transport coefficient approximations
[NASA-TM-101158] 17 p2397 N88-24251
Simplified curve fits for the transport properties of equilibrium air
[NASA-CR-178411] 18 p2513 N88-24911
Stochasticity in a Q-machine plasma 18 p2578 N88-25315
NASA research Program: The roles of fluid motion and other transport phenomena in the morphology of materials
[NASA-CR-182801] 18 p2580 N88-25327
Electronic structure, elementary excitations, optical and transport properties of semiconductor superlattices
[AD-A190795] 18 p2581 N88-25333
An evaluation of some thermodynamic and transport properties of solid and liquid lithium over the temperature range 200 to 1700 K
[DE88-008947] 19 p2614 N88-25512
Simulation of axisymmetric flow with H2O2 reactions 19 p2638 N88-25651
Longitudinally localized optical carrier injection for femtosecond transport studies 19 p2659 N88-25806
Ballistic transport and hot electron spectroscopy in Tunneling Hot Electron Transfer Amplifier (THETA) 19 p2659 N88-25808
Heavy ion fusion system assessment: Final focus and transport model
[LBL-23040] 19 p2725 N88-26183
Drift wave vortices and anomalous transport
[DE88-009562] 20 p2859 N88-26982
Impurity transport calculations for a drift-dependent tokamak scrape-off plasma
[DE88-010053] 20 p2859 N88-26984
Third International Conference on Superlattices, Microstructures and Microdevices
[AD-A191416] 20 p2861 N88-26995
Transport in GaAs heterojunction ring structures 20 p2864 N88-27011
Theoretical aspects of electron transport in modulated structures 20 p2865 N88-27016
Transport study on Si/Si(1-x)Ge(x) superlattices selectively doped by secondary implantation of Sb 20 p2867 N88-27027
Resonant tunneling in InGaAs-InP double-barrier structures and superlattices 20 p2871 N88-27047
Type 3 - type 1 transition and strain effect in Hg(1-x)Cd(x)Te-CdTe and Hg(1-x)Zn(x)Te-CdTe superlattices 20 p2872 N88-27052
Studies of HZE particle interactions and transport for space radiation protection purposes
[NASA-TM-101159] 20 p2886 N88-27142
Application of acoustic-Doppler current profiler and expendable bathythermograph measurements to the study of the velocity structure and transport of the Gulf Stream
[NASA-CR-183188] 22 p3129 N88-28605
A study of electronic transport and breakdown in SiO2
[AD-A194258] 22 p3156 N88-28780
Phenomena of the ionic transport in the stress corrosion of metals
[DE88-702502] 23 p3195 N88-29013
Transport of organic vapors in multiphase polymer system
[AD-A194097] 23 p3198 N88-29033
Development of computer-controlled thermogravimetric instrumentation for measurement of environmental and high temperature volatilization and desorption of contaminants from polymeric materials
[AD-A195934] 24 p3343 N88-29900
Experimental and analytical study of two-phase flow in zero gravity
[AD-A195223] 24 p3358 N88-29993
Models of cerebral-body perfusion and cerebral chemical transport
[AD-A194945] 24 p3407 N88-30283

TRANSPORT THEORY
NT MIXING LENGTH FLOW THEORY
Interactive Design of Accelerators (IDA)
[DE87-013298] 02 p0234 N88-11476
Computer models for kinetic equations of magnetically confined plasmas
[DE87-011571] 02 p0236 N88-11492
Two dimensional neutral transport analysis in tokamak plasma
[DE87-752984] 02 p0239 N88-11510
Transport analysis of OH and NBI heated discharges in JT-60
[DE87-752985] 02 p0239 N88-11511
Progress in stellarator/heliotron research, 1981-1986: Executive summary
[DE88-000017] 02 p0241 N88-11519
Nonequilibrium fluctuations and transport in sheared fluids 03 p0316 N88-11999
Momentum transport and particle dynamics in turbulent shear flows 03 p0317 N88-12002
Two-layer stratified flow analysis of gravity currents and turbidity currents in lakes, reservoirs and the ocean 04 p0463 N88-12864
Development of the non-equilibrium reactive chemical transport code CHMTRNS
[DE88-000682] 04 p0481 N88-12964
Transport simulations of the oscillating field current drive experiment in the ZT-40M reversed field pinch
[DE88-000538] 04 p0491 N88-13027
Transport scaling in the collisionless-detrapping regime in stellarators
[DE88-001511] 05 p0653 N88-14006
Comparison of 2D memory SEU transport simulation with experiments
[ATR-86(8139)-2-REV-A] 05 p0656 N88-14025
Theoretical studies of multicomponent mixtures: Phase equilibrium and transport
[DE88-002717] 07 p0831 N88-15040
Use of back air trajectories in interpreting atmospheric chemistry data: A review and bibliography
[PB88-102108] 07 p0876 N88-15312
Particle transport in microdetonations — inertial confinement fusion pellets
[OEFZS-4402] 09 p1164 N88-16976
Time dependent degradation of energetic electrons in gaseous and condensed media
[DE88-002912] 09 p1246 N88-17465
Two-dimensional analysis for a scrapeoff and divertor regions with an MHD model. Conceptual design study of FY86 FER
[DE88-751069] 09 p1251 N88-17497
Applied mathematics of transport theory
[DE88-004098] 10 p1404 N88-18369
Studies in finite time thermodynamics
[DE88-004531] 10 p1423 N88-18500
Boltzmann-Fokker-Planck calculations using standard discrete-ordinates codes
[DE88-005393] 11 p1537 N88-19185
Propagator solutions of partial differential equations applied to plasma transport
[DE88-006432] 13 p1816 N88-20852
Conservative finite volume solutions of a linear hyperbolic transport equation in two and three dimensions using multiple grids
[NASA-CR-182715] 13 p1828 N88-20934
FLOSIN: A fluid loop analyzer for SINDA 15 p2066 N88-22321

Transport simulations of ohmic ignition experiment: IGNITEX
[DE88-006055] 15 p2138 N88-22757
Analysis of reversible and irreversible hydrogen trapping in metals
[NPL-DMA(A)-154] 16 p2177 N88-22977
Modeling of turbulent transport as a volume process 16 p2196 N88-23099
A statistical investigation of the single-point pdf of velocity and vorticity based on direct numerical simulations 16 p2196 N88-23101
BRYNTRN: A baryon transport computer code, computation procedures and data base
[NASA-TM-4037] 16 p2290 N88-23714
Effects of space-dependent cross sections on core physics parameters for compact fast spectrum space power reactors 17 p2399 N88-24263
Consistent transport coefficients in astrophysics
[NASA-TM-101154] 17 p2451 N88-24560
A benchmark for galactic cosmic ray transport codes
[NASA-TM-101157] 17 p2453 N88-24571
Physical properties of f electron systems
[DE88-006886] 18 p2581 N88-25331
Electrode films of porous agarose: The effects of physical structure on electron transport processes
[DE88-007366] 19 p2611 N88-25493
Quantum transport calculation of resonant-tunneling response time 19 p2659 N88-25810
Multidimensional nodal transport methods for multiple-instruction multiple-data distributed memory machines
[DE88-004732] 19 p2713 N88-26108
Tracer water transport and subgrid precipitation variation within atmospheric general circulation models
[NASA-CR-182897] 20 p2823 N88-26745
Eigenmodes of a random walk on a 2-D lattice torus with one trap
[DE88-007830] 20 p2844 N88-26874
A nodal method for time-dependent transport equation
[DE88-004285] 20 p2844 N88-26876
Quantum transport theory of resonant-tunneling heterostructure devices 20 p2865 N88-27017
Quantum interference and transport in microstructures 20 p2866 N88-27022
Kinetic theory for plane flows of rough, inelastic, circular disks 21 p2946 N88-27499
Introduction to laser plasma diagnostics
[DE88-011056] 23 p3265 N88-29560
Bootstrap currents in radio-frequency-driven tokamak equilibria
[DE88-011136] 23 p3285 N88-29561

TRANSPORTATION
NT AIR TRANSPORTATION
NT RAIL TRANSPORTATION
NT RAPID TRANSIT SYSTEMS
NT SPACE TRANSPORTATION
NT SPACE TRANSPORTATION SYSTEM
NT URBAN TRANSPORTATION
Aircraft accident/incident summary reports: Unalaska, Alaska, September 25, 1985; Jenkinsburg, Georgia, September 29, 1985; Boston, Massachusetts, December 15, 1985; Dekalb, Texas, December 31, 1985; and Erie, Pennsylvania, February 21, 1986
[PB87-910408] 02 p0123 N88-10780
Spinoff, 1987
[NASA-TM-89652] 02 p0250 N88-11577
The development of laboratory vibration test schedules: Philosophies and techniques 08 p0999 N88-16049
The DFVLR-German Space Operations Center (GSOC) mobile rocket base 08 p1029 N88-16237
A lunar transportation system
[NASA-CR-182561] 11 p1567 N88-19379
A model of intrazonal trip distribution considering centrality index 16 p2257 N88-23486
A three dimensional assignment method in the time space
[REPT-87-49] 16 p2287 N88-23690
Technology transfer for DOE's Office of Transportation Systems: Assessment and strategies
[DE88-010760] 21 p3029 N88-27977

TRANSPORTATION NETWORKS
Study of the feasibility of a satellite communication system for road transportation home office to vehicle communication. Volume 1: Conceptual analysis
[SC/87-E/6-VOL-1] 05 p0575 N88-13505
Study of the feasibility of a satellite communication system for road transportation home office to vehicle communication. Volume 2: Market study
[SC/87-E/6-VOL-2] 05 p0575 N88-13506
Determination of network attributes from a high resolution terrain data base
[AD-A186078] 07 p0870 N88-15279
Computer aided cartographic representation of traffic data: The traffic intensity maps of Baden-Wuerttemberg (Federal Republic of Germany) 16 p2225 N88-23282
From the extraction of linear networks towards following of them on SPOT images with the help of a knowledge-based interpretation system 22 p3113 N88-28494
Extraction of thin networks by an oriented following of ridges and valleys 22 p3113 N88-28495

TRANSPORTER
Space station mobile transporter 14 p1927 N88-21488

TRANSURANIUM ELEMENTS
NT LAWRENCIUM
NT NEPTUNIUM
NT PLUTONIUM ISOTOPES
NT PLUTONIUM 238

TRANSVERSE ACCELERATION
Determination of the drag of missiles with variable lateral acceleration possibility
[REPT-FM15] 10 p1310 N88-17831

TRANSVERSE OSCILLATION
NT H WAVES

TRANSVERSE WAVES
NT H WAVES
TE/TM (Transverse Electric/Transverse Magnetic) height profile measurements of transpolar VLF (Very Low Frequency) signals
[AD-A194503] 22 p3069 N88-28216

TRANSVERSELY EXCITED ATMOSPHERIC LASERS
U TEA LASERS

TRAPATT DIODES
U AVALANCHE DIODES

TRAPPED MAGNETIC FIELDS
Magnetic trapping of neutral atoms
[AD-A188473] 12 p1889 N88-20103
Comparison of analytic and full guiding center behavior at a trapped-passing interface in stellarators
[DE88-004174] 13 p1842 N88-21025
New methods of confinement and heating of plasma in magnetic fields
[DE88-701021] 15 p2135 N88-22738

TRAPPED PARTICLES
NT INNER RADIATION BELT
NT MAGNETICALLY TRAPPED PARTICLES
NT RADIATION BELTS
The free electron laser sideband instability reconsidered
[AD-A184269] 04 p0447 N88-12773
Forces on neutral atoms due to electromagnetic fields
[AD-A187461] 10 p1408 N88-18396
The JPL trapped mercury ion frequency standard 11 p1471 N88-18776
Toward a comprehensive theory for the sweeping of trapped radiation by inert orbiting matter
[NASA-CR-182584] 11 p1569 N88-19395
Theory of laser cooling and spectroscopy of harmonically trapped single atoms
[AD-A189576] 13 p1775 N88-20617
Comparison of analytic and full guiding center behavior at a trapped-passing interface in stellarators
[DE88-004174] 13 p1842 N88-21025
United States - Japan Seminar on Quantum Mechanical Aspects of Quantum Electronics
[AD-A186938] 14 p1974 N88-21781
Optical trapping of neutral atoms and dielectric particles by radiation pressure 14 p1974 N88-21783
Modeling the effects of heavy charged particles on MOSFETs (Metal-Oxide-Semiconductor Field Effect Transistors)
[AD-A190575] 15 p2143 N88-22792
Numerical simulation for particle acceleration and trapping by an electromagnetic wave 16 p2277 N88-23626
JFET/SOS (Junction Field-Effect Transistor/Silicon-on-Sapphire) devices: Gamma-radiation-induced effects
[AD-A193001] 20 p2795 N88-26586
Investigation of the potential impact of new photonic materials on optical processing systems 21 p2924 N88-27359
The dust ring of the Earth
[RAE-TRANS-2163] 22 p3119 N88-28530
Large area nuclear particle detectors using ET materials
[NASA-CR-180777] 23 p3215 N88-29136
Spontaneous force optical traps
[AD-A196103] 24 p3377 N88-30114
Research on a two-stage free electron laser oscillator
[AD-A195991] 24 p3377 N88-30115

TRAPPING
Conditions for geomagnetically trapping sub-micron lunar ejecta between L = 1.2 and L = 3.1 04 p0521 N88-13203
Propagation in longitudinally varying ducts, with emphasis on guiding to antiguiding transitions 12 p1615 N88-19658
MOSFET performance degradation due to hot carriers 13 p1848 N88-21083
Analysis of reversible and irreversible hydrogen trapping in metals
[NPL-DMA(A)-154] 16 p2177 N88-22977
Autoionization for lower level detrapping in X-ray lasers
[AD-A195845] 24 p3379 N88-30123

TRAPS
NT COLD TRAPS
NT ION TRAPS (INSTRUMENTATION)
Implications of the trapping-desorption and direct inelastic scattering channels on Dicke-narrowed lineshapes
[AD-A191410] 16 p2270 N88-23581

TRAVELING IONOSPHERIC DISTURBANCES
Interplanetary Magnetic Field (IMF) influence on the magnetic configuration and particle fluxes at geostationary orbit and on the substorm onset 08 p1031 N88-16247
A unified model for the WTS and the generation on Pi 2 pulsations — Westward Traveling Surge (WTS) 08 p1096 N88-16593
Moving ionospheric perturbations induced by wave trains propagating through ocean 09 p1239 N88-17427
On the dynamics of the auroral ionosphere during the breakup of a substorm
[AD-A193368] 21 p2972 N88-27657

TRAVELING SALESMAN PROBLEM
Progress in mathematical programming
[AD-A185729] 06 p0759 N88-14658
A traveling-salesman-based approach to aircraft scheduling in the terminal area
[NASA-TM-100062] 12 p1576 N88-19424
Local search for constrained routing problems — traveling salesman
[CWI-OS-R8711] 13 p1830 N88-20948
A concurrent neural network algorithm for the traveling salesman problem
[DE88-006981] 18 p2562 N88-25208
An extension of the Hopfield-Tank model for solution of the multiple traveling salesmen problem
[DE88-008377] 19 p2715 N88-26122

TRAVELING WAVE AMPLIFIERS
Solid-state travelling wave amplifiers based on multi-stream instability
[AD-A189566] 12 p1624 N88-19718
Construction of a 60 GHz Traveling Wave Tube (TWT) for intersatellite link on geostationary orbit (ISL/TWT)
[BMFT-FB-W-86-015] 16 p2192 N88-23076
Wide band gyrotron traveling wave amplifier analysis
[AD-A194269] 23 p3216 N88-29139

TRAVELING WAVE MASERS
A 2.3-GHz maser at Usuda, Japan, for TDRSS-orbiting VLBI experiment 11 p1472 N88-18779
A 2.3-GHz low-noise cryo-FET amplifier 22 p3066 N88-28195
An 8.4-GHz dual maser front end for Parkes reimplementation 22 p3066 N88-28197

TRAVELING WAVE MODULATION
A high frequency GaAlAs travelling wave electro-optic modulator at 0.82 micrometers
[NASA-TM-100970] 22 p3073 N88-28240

TRAVELING WAVE TUBES
Performance of a small, graphite electrode, multistage depressed collector with a 500-W, continuous wave, 4.8- to 9.6-GHz traveling wave tube
[NASA-TP-2788] 07 p0848 N88-15146
High efficiency, long life traveling wave tubes for future communications satellites
[NASA-TM-100837] 12 p1598 N88-19565
Construction of a 60 GHz Traveling Wave Tube (TWT) for intersatellite link on geostationary orbit (ISL/TWT)
[BMFT-FB-W-86-015] 16 p2192 N88-23076
Miniature traveling wave tube and method of making
[NASA-CASE-LEW-14520-1] 17 p2335 N88-23936
An investigation of the uses of time domain capable vector network analyzers as a diagnostic for helix traveling-wave circuits
[AD-A192460] 21 p2935 N88-27430
A millimeter-wave tunneLadder TWT
[NASA-CR-182184] 22 p3072 N88-28239

TRAVELING WAVES
NT SOLITARY WAVES
Intracavity absorption spectroscopy with ring traveling-wave dye laser 03 p0300 N88-11890
Determination of fractal dimension, connection of space and temporal chaos and application to experimental results 03 p0313 N88-11977
The 8.4-GHz low-noise maser pump source assembly 04 p0436 N88-12705
Traveling-wave maser closed-cycle refrigerator data acquisition and display system 04 p0437 N88-12708
Departmental report on program EMTP-machine windings surge transients: Travelling wave method
[PB87-123733] 04 p0438 N88-12719

Modeling and control of large flexible vehicles in the atmosphere and space
[AD-A185368] 05 p0555 N88-13377
Time characteristics of travelling wave lasing with two-photon picosecond optical pumping
07 p0918 N88-15578
Travelling waves and chaos in double-diffusive convection 11 p1484 N88-18857
Harmonic and rectangular pulse reproduction through current transformers
[EUT-86-E-159] 14 p1907 N88-21395
Squeezing via travelling-wave forward four-wave mixing in atomic vapors: Comparison with nondegenerate theory 14 p1978 N88-21804
Travelling wave concepts for the modeling and control of space structures
[AD-A191235] 17 p2310 N88-23819
Asymptotics for a system of nonlinearly coupled wave equations with an application to the galloping oscillations of overhead transmission lines
[REPT-87-78] 17 p2348 N88-23991
Electrical pulse compression by traveling-wave photoconductivity 19 p2661 N88-25822

TREADS
Armoured vehicle track elastomers: Research and development at MRL
[MRL-GD-0012] 19 p2620 N88-25541
A critical speed study for aircraft bias ply tires
[AD-A193616] 22 p3084 N88-28313

TREAT (TEST FACILITY)
U TRANSIENT REACTOR TEST FACILITY

TREES (MATHEMATICS)
NT FAULT TREES
File management using balanced trees
[ENST-87D001] 01 p0106 N88-10693
Subcritical branching processes in a two state random environment, and a percolation problem on trees
[PB87-230439] 06 p0762 N88-14677
Very thin VLSI-layouts (Very Large Scale Integration-Layouts) of complete binary trees
[PB88-100847] 06 p0789 N88-14841
A note on the partitioning shortest path algorithm
[CWI-OS-R8703] 08 p1067 N88-16451
An anlysis of the reliability of tree-structured interconnection networks 10 p1378 N88-18228
Improving battery reliability by using regression trees
[DE88-004539] 11 p1481 N88-18841
Finite octree meshing through topologically driven geometric operators 11 p1527 N88-19121
Iteration of transformation passes over attributed program trees — compilers
[INF-87-28] 14 p1956 N88-21661
A comparison of supervised maximum likelihood and decision tree classification for crop cover estimation from multitemporal LANDSAT MSS data
17 p2352 N88-24014
Automatic routing in symbolic IC design environment
19 p2714 N88-26112

TREES (PLANTS)
NT CONIFERS
Effects of fire on composition, biomass, and nutrients in oak scrub vegetation on John F. Kennedy Space Center, Florida
[NASA-TM-100305] 08 p1020 N88-16182
Vegetation mapping using high resolution MSS (multispectral scanner) data: Canopy reflectance and shadow problems encountered and possible solutions
[DE88-004273] 14 p1939 N88-21574
Utilization of TM/LANDSAT images in the implanted forests mapping in the Mogi-Guacu Region (SP-Brazil)
17 p2357 N88-24042
Interpretation of MSS/LANDSAT data for evaluation of physical distribution of mangroves in Cananeia-Iguape (SP) 17 p2363 N88-24072
Evaluation of the mangrove area at the Piaui River (SE) through remote sensing 17 p2365 N88-24086
Stereoscopic photographs, ground and aerial, of trees used in the arborization of Curitiba (PR)
17 p2366 N88-24091
Propagation effects by roadside trees measured at UHF and L-band for mobile satellite systems
19 p2644 N88-25693
Attenuated direct and scattered wave propagation on simulated land mobile satellite service paths in the presence of trees 19 p2645 N88-25695
Propagation measurements for an Australian land mobile satellite system 19 p2645 N88-25697
Canopy reflectance modeling in a tropical wooded grassland
[NASA-CR-182981] 19 p2685 N88-25961
SPOT 1: Image utilization, assessment, results. A study of the Elburgon Forest area (Kenya) showing the spectral responses of different forest tree species
22 p3107 N88-28454

TRENDS
Communication satellite technology trends
01 p0015 N88-10088
Earth Radiation Budget Satellite (ERBS) orbiting profiles and Ni-Cd use 02 p0165 N88-11034
Technology transfer to China
[PB87-223418] 04 p0502 N88-13087
The technology of centrifugal compressors: A design approach and new goals for research
07 p0850 N88-15163
Long-term variation of total ozone
[INPE-4307-PRE/1173] 08 p1023 N88-16192
Trends in research and development in the Netherlands. The influence of national science policy between 1973 and 1986
[B8701588] 08 p1094 N88-16580
Lewis materials research and technology: An overview
09 p1119 N88-16699
Avionics acquisition, trends and future approaches
12 p1702 N88-20184
Function of Japan Fine Ceramics Center described
15 p2052 N88-22227
Marshall Space Flight Center 1960-1985: 25th anniversary report
[NASA-TM-100328] 15 p2153 N88-22852
Development of a multipurpose smart recorder for general aviation aircraft
[NASA-CR-168353] 18 p2465 N88-24637
The application of hydrocarbon bioconversion technology to aerospace materials production
18 p2478 N88-24698
Millimeter-wave integrated circuits
19 p2656 N88-25774
Trends in civil aircraft propulsion
[PNR90441] 22 p3044 N88-28067
Future trends in aviation propulsion
[PNR90443] 22 p3044 N88-28068

TRIANGLES
Solution of the two-dimensional Euler equations on unstructured triangular meshes
04 p0396 N88-12469
Non-rigid motion and Regge calculus
[AD-A190387] 15 p2121 N88-22640
The triangle: A multiprocessor architecture for fast curve and surface generation
[AD-A195882] 24 p3414 N88-30324

TRIANGULAR WINGS
U DELTA WINGS

TRIANGULATION
Control of the German main triangulation network by macrometer measurement 1983-1985 (KONMAC)
[SER-B-282] 01 p0063 N88-10404
Optimization of photogrammetric image adjustment
[SER-C-323] 07 p0872 N88-15289
Discovery and problem solving: Triangulation as a weak heuristic 08 p1062 N88-16412
Contour-to-grid interpolation with nonlinear finite elements: A feasibility study
[AD-A188108] 11 p1503 N88-18980
Adjustment in photogrammetry: Methods, programs and applications
[B8735130] 17 p2369 N88-24105
Adaptive mesh generation for viscous flows using Delaunay triangulation
[NASA-CR-181699] 24 p3316 N88-29749

TRIAXIAL STRESSES
A generalized least-squares determination of triaxial stress states by X-ray diffraction and the associated errors
[AD-A183851] 01 p0058 N88-10371
Periodic orbits around a satellite modelled as a triaxial ellipsoid
[AD-A190592] 15 p2022 N88-22051
Creep of carbon yarn and carbon-carbon composites at high temperatures and high stresses
[AD-A195224] 24 p3340 N88-29878

TRIAXIALITY
U TRIAXIAL STRESSES

TRIBOLOGY
Coatings for Advanced Heat Engines Workshop: Book of abstracts
[DE87-012623] 02 p0180 N88-11121
Boundary lubrication. Experiments with boundary lubrication and plain bearings at +60...-60 deg C temperatures
[DE87-752869] 02 p0180 N88-11124
Piston ring friction and vehicle fuel economy
[DE87-014536] 02 p0181 N88-11127
Double-effect absorption heat pump, phase 3
[PB87-232195] 03 p0317 N88-12005
Adiabatic diesel engine component development: Reference engine for on-highway applications
[NASA-CR-179531] 03 p0386 N88-12428
Calculation of the tribological properties of surfaces by semi-empirical methods
[AD-A184283] 04 p0450 N88-12791
Tribological properties of rf-sputtered MoS2 coatings
[DE88-000266] 04 p0452 N88-12802
Tribology of thin film systems
[ETN-88-91365] 05 p0590 N88-13601
Projects within the Center for Advanced Materials
[PB88-123054] 06 p0677 N88-14143
The tribological properties of MoS2 coatings in vacuum, low relative humidity and high relative humidity environments
[DE88-001611] 06 p0711 N88-14358
Tribological studies on high speed steel cutting tools
[DE88-002550] 07 p0864 N88-15246
The WAFTER: A versatile wear and friction tester
[MRL-TN-519] 09 p1169 N88-17012
Activities report in tribology
[ESA-ESTL-79] 09 p1174 N88-17037
Seven year thermal vacuum real life test of a medium speed (despin) mechanism manufactured by Dornier System
[ESA-ESTL-64] 09 p1175 N88-17038
Adhesion, friction and micromechanical properties of ceramics
[NASA-TM-100782] 10 p1305 N88-17801
Tribology of ceramics: Report of the Committee on Tribology of Ceramics
[NASA-CR-182506] 10 p1305 N88-17802
Tribological properties of alumina-boria-silicate fabric from 25 to 850 C
[NASA-TM-100806] 11 p1464 N88-18726
Overview of the DOE-ECUT Tribology Program
[DE88-002878] 13 p1778 N88-20637
Proceedings of the 3rd European Space Mechanisms and Tribology Symposium
[ESA-SP-279] 14 p1874 N88-21191
Models for steady and nonsteady Coulomb torque in ball bearings 14 p1876 N88-21208
Ball bearings with chemical vapor deposition (CVD)-TiC coated components 14 p1876 N88-21210
Separable electrical connectors for space: A tribological and electrical assessment 14 p1879 N88-21231
Towards a tribology information system: The results of a Planning Workshop held at the National Bureau of Standards, July-August 1985
[PB88-168604] 14 p1918 N88-21448
Structural Ceramics
[NASA-CP-2427] 17 p2323 N88-23872
Ceramics for turbine engines
17 p2323 N88-23873
Development of test methods for the electrostatic properties of nonhomogeneous fabrics, phase 2
[AD-A190853] 18 p2489 N88-24767
The lubricating properties of magnetron sputtered MoS2
[ESA-ESTL-76] 24 p3381 N88-30136

TRICHLORIDES
U CHLORIDES

TRIGGER CIRCUITS
Pseudospark switches
[DE88-702227] 23 p3207 N88-29085

TRIGGERS
U ACTUATORS

TRIGONOMETRIC FUNCTIONS
NT COSINE SERIES
NT TANGENTS
High speed transcendental elementary function architecture in support of the Vector Wave Equation (VWE)
[AD-A189746] 15 p2119 N88-22627

TRIM (BALANCE)
U AERODYNAMIC BALANCE

TRINITROTOLUENE
The viscosity of molten TNT
[MRL-R-1100] 19 p2622 N88-25553

TRINITROTRIAZOCYCLOHEXANE
U RDX

TRIPLE AXIS SPECTROMETERS
U NEUTRON SPECTROMETERS

TRIPLET EXCITATION
U ATOMIC ENERGY LEVELS

TRIPLET STATE
U ATOMIC ENERGY LEVELS

TRIPROPELLANTS
U LIQUID ROCKET PROPELLANTS

TRISONIC WIND TUNNELS
The 0.6m x 0.6m trisonic test section (TMK) of DFVLR in Cologne-Porz, Federal Republic of Germany (status 1986)
[ESA-TT-1052] 03 p0267 N88-11681

TRITIUM
Magneto-Inertia Confinement Approach (MICA) to fusion in dynamic Z-pinch formed from a frozen deuterium-tritium tube
[IPPJ-856] 09 p1252 N88-17504
Weldability of tritium-charged 304L stainless steel
[DP-1740] 12 p1607 N88-19611

Biophysical applications of solid state and tritium NMR
[DE88-005328] 13 p1808 N88-20806
Outlook for the fusion hybrid and tritium-breeding fusion reactors
[PB88-149281] 13 p1843 N88-21029
Infrared spectroscopy of H3(+)
16 p2268 N88-23565
Analysis of containerless condensation of polyatomic hydrogen ions, with emphasis on H3(+,-) association channels and a future workshop to study related topics
16 p2269 N88-23576
Helium-3 fusion fuel resources for space power
17 p2410 N88-24330
The hole of a blanket tritium system on the fusion fuel cycle
[DE88-010007] 20 p2859 N88-26983

TRITONS
Physics of few-body lambda hypernuclei
[DE87-014746] 03 p0375 N88-12357

TROCHOIDS
U PIVOTS

TROPICAL METEOROLOGY
Annual tropical cyclone report, 1986
[AD-A184082] 04 p0470 N88-12903
Interactions between the Asian monsoons, the tropical Pacific and the southern hemisphere extratropics
04 p0470 N88-12907
A method to obtain a wind model for the boundary layer in a representative tropical region
[R-818-D] 06 p0743 N88-14569
The effect of latitude on the development of tropical cyclones
[AD-A185670] 06 p0746 N88-14590
US participation in the TOGA (Tropical Ocean and the Global Atmosphere) Program: A research strategy
[DE88-010986] 19 p2681 N88-25938
Dynamic interaction of convective cumulus with large-scale environment
[MITT-55] 20 p2827 N88-26773
Westward moving atmospheric wave disturbances over the African tropics: Dynamic and energetic aspects
[MITT-57] 20 p2827 N88-26774
The patterns of tropical convection during the 1986-87 ENSO 22 p3120 N88-28537
Climatology of various synoptic systems over the tropical North Pacific 22 p3121 N88-28542
Complex EOF analysis of intraseasonal tropical wind fluctuations 22 p3121 N88-28544
On the impact of low-latitude anomalous forcing on local and remote circulation: Winters(DJF) 1978/79 to 1986/87 22 p3123 N88-28560
An observational study of interaction between large scale tropical cumulus convection and the equatorial circulation anomalies 22 p3124 N88-28564
The impact of the El Nino event on the ECMWF model performance 22 p3125 N88-28576
Extratropical response to tropical heating as a function of period of model integrations
22 p3125 N88-28577
Observed normal mode structure of low frequency oscillations 22 p3126 N88-28595

TROPICAL REGIONS
NT AMAZON REGION (SOUTH AMERICA)
The challenge of very short range forecasting in the tropics 02 p0205 N88-11287
Statistical relationships between the mesoscale organization of convection and the large-scale wind profiles during GATE --- GARP Atlantic Tropical Experiment (GATE) 02 p0208 N88-11302
The contribution of satellite data in drawing up maps used in rural development 03 p0343 N88-12167
On the interannual variability of South American climate and the Southern Oscillation 04 p0470 N88-12905
The use of TOMS data for tropospheric ozone studies
05 p0616 N88-13784
Modes of surface circulation and climate over the tropical Atlantic, Eastern Pacific, and Indian Oceans
06 p0742 N88-14564
A method to obtain a wind model for the boundary layer in a representative tropical region
[R-818-D] 06 p0743 N88-14569
Tropical hydrology
[WMO-655] 06 p0745 N88-14584
Geosat crossover analysis in the tropical Pacific. Part 1: Constrained sinusoidal crossover adjustment
[NASA-CR-182391] 07 p0871 N88-15285
Variations of tropical circulation and associated rainfall anomalies, during 2 years of contrast
[INPE-4359-TDL/300] 08 p1039 N88-16286
Corrosion and deterioration testing in humid tropic environments
[AD-A186917] 10 p1302 N88-17783
Mapping of the mangroves of the Guanabarra Bay through the utilization of remote sensing techniques
[INPE-3942-TDL/229] 12 p1637 N88-19804
JEDA (Joint Environmental Data Analysis) Center report on tropical Pacific subsurface thermal data management, 1986
[PB88-140090] 12 p1649 N88-19875
Perspectives in microclimate cooling involving protective clothing in hot environments
[AD-A188370] 12 p1671 N88-20007
Basic networks of TOGA: Determination of thermal profiles by XBT and of sea level by tide gage
14 p1939 N88-21588
Ground-based column abundance measurements of atmospheric hydroxyl
[NASA-CR-182676] 14 p1944 N88-21598
Tropical and monsoonal studies
[AD-A188387] 14 p1947 N88-21611
Tropic heat MR (Meteorological Recorder) meteorological data (April 1984 - June 1985)
[PB88-161286] 14 p1948 N88-21620
Current velocity and hydrographic observations in the Straits of Florida, the Caribbean Sea and offshore of the Antillean Archipelago: Subtropical Atlantic Climate Studies (STACS) 1986
[PB88-160767] 14 p1951 N88-21628
Tropical circulations and the associated rainfall anomalies during two contrasting years
[INPE-4506-PRE/1261-REV] 15 p2098 N88-22502
A study of the dynamics of the Intertropical Convergence Zone (ITCZ) in a symmetric atmosphere-ocean model
[NASA-TM-86220] 19 p2693 N88-26005
Following the seasonal evolution of a natural environment in a humid tropical region. Preliminary Evaluation of SPOT (PEPS) number 186: Bangui, Central Africa 22 p3093 N88-28368
Discrimination methods of traditional fields in a humid tropical region (Shaba, Zaire) using digital classification on SPOT data 22 p3096 N88-28387
Assessment of SPOT satellite based system in humid tropical vegetation identification, classification and monitoring 22 p3100 N88-28408
Bibliography on tropical rain forests and the global carbon cycle. Volume 1: An introduction to the literature
[DE88-010761] 22 p3118 N88-28523
The patterns of tropical convection during the 1986-87 ENSO 22 p3120 N88-28537
Some diagnostic results concerning the tropical 40-50 day oscillation 22 p3121 N88-28546
Evolution of thermal structure of Benguela upswelling system according to satellite and shipboard data
24 p3449 N88-30525

TROPICAL STORMS
NT HURRICANES
NT TYPHOONS
Tropical cyclone center locations from enhanced infrared satellite imagery
[PB87-213450] 01 p0071 N88-10455
Summary of 1987 Atlantic tropical cyclone activity and verification of author's seasonal forecast
02 p0215 N88-11356
Opportunities for tropical cyclone motion research in the Northwest Pacific region
[AD-A185068] 05 p0627 N88-13834
Environmental and convective influence on tropical cyclone development versus non-development
[AD-A185231] 05 p0627 N88-13835
Estimation of rainfall rates in tropical cyclones by passive microwave radiometry 06 p0744 N88-14577
The effect of latitude on the development of tropical cyclones
[AD-A185670] 06 p0746 N88-14590
Interim review of the possibilities and opportunities for the ONR tropical cyclone motion research initiative
[AD-A185879] 06 p0746 N88-14592
Recent Colorado State University tropical cyclone research of interest to forecasters
[AD-A185996] 07 p0879 N88-15332
Annual data summary and climatological evaluation CERC (Coastal Engineering Research Center) field research facility, 1985. Volume 1. Main text and appendixes A and B
[AD-A186442] 08 p1039 N88-16289
Northern winter circulations for the period 1974-1983
[AD-A187779] 11 p1511 N88-19028
The role of vortex structure in tropical cyclone motion
[AD-A190961] 16 p2235 N88-23351
Tropical cyclones, 1987: Central North Pacific
[PB88-188081] 18 p2547 N88-25119
Tropical cyclone report
[AD-A191883] 19 p2693 N88-26009

TROPICS
U TROPICAL REGIONS

TROPISM
NT GRAVITROPISM

TROPOPAUSE
Photochemical ozone overburden correction
05 p0615 N88-13778
Northwest Airlines flight experiments
05 p0617 N88-13786
Application of TOMS data to weather analysis models
05 p0617 N88-13787
Correlations of TOMS total ozone data (Nimbus-7 satellite) with tropopause height
05 p0617 N88-13788
An analysis of tropopause pressure and total ozone correlations 05 p0617 N88-13789
TOMS ozone data compared at mesoscale resolution to tropopause heights from the AVE radiosonde network and to VAS radiances over the south-central United States 05 p0617 N88-13790
The use of TOMS-modified VAS data for large-scale NWP 05 p0618 N88-13791

TROPOSPHERE
NT TROPOPAUSE
The importance of mesoscale waves in the upper troposphere for formation of cloud and precipitation areas 02 p0203 N88-11273
Scientific and Operational Requirements for TOMS Data
[NASA-CP-2497] 05 p0615 N88-13774
Lower-stratospheric/upper-tropospheric exchange processes associated with tropical cyclones as observed by TOMS 05 p0616 N88-13782
Tropical easterly jet located using TOMS data
05 p0616 N88-13783
The use of TOMS data for tropospheric ozone studies
05 p0616 N88-13784
Numerical modeling of troposphere-induced gravity wave propagation 06 p0735 N88-14522
Observations of inertial period waves and vertical velocities in the tropical middle atmosphere using the MST radar technique 06 p0742 N88-14562
Investigation of OH reaction products. Excimer laser photolysis/slab laser fluorescence under tropospheric conditions
[REPT-8] 09 p1191 N88-17137
Optical characterization of tropospheric aerosols
[AD-A187839] 11 p1511 N88-19029
Initial results with the LLNL 2-D chemical-radiative-transport model of the troposphere and stratosphere
[DE88-004355] 11 p1512 N88-19033
Photoacoustic measurements of atmospheric aerosol absorption coefficients at ultraviolet, visible and infrared wavelengths 11 p1512 N88-19036
A paper on horizontal deformation in the frontogenesis in south Brazil
[INPE-4469-TDL/322] 12 p1647 N88-19867
Pre-convective environmental conditions indicative of non-tornadic severe thunderstorm winds over Southeast Florida
[AD-A188679] 12 p1648 N88-19870
Computer simulation of tropospheric chemistry
[JUEL-2144] 13 p1798 N88-20756
IREPS (Integrated Refractive Effects Prediction System) 3.0, user's manual
[AD-A190398] 16 p2188 N88-23045
SAGE 1 and SAM 2 measurements of 1 micron aerosol extinction in the free troposphere
[NASA-CR-182945] 17 p2374 N88-24121
A theoretical model of the washout of trace gases by raindrops in the atmosphere 17 p2375 N88-24125
Workshop on Atmospheric OH
[BPT-7/87] 18 p2538 N88-25063
Effect of carbohydrate oxidation on the tropospheric HOx-system 18 p2539 N88-25067
Trace gas measurements in the troposphere using tunable diode lasers 18 p2540 N88-25072
Development of continuous wave laser frequency modulation of OH in tropospheric concentrations range
18 p2540 N88-25073
Tropospheric biennial variability and its relationship to the southern oscillation 22 p3121 N88-28549
Atmospheric deposition of nitrate to the ocean surface
23 p3231 N88-29227
Forty-eight-inch lidar aerosol measurements taken at the Langley Research Center, May 1974 to December 1987
[NASA-RP-1209] 23 p3232 N88-29234
Global vertical mass transport by clouds: A two-dimensional model study
[CM-74] 24 p3391 N88-30192

TROPOSPHERIC RADIATION
Tropospheric ultraviolet radiation: Assessment of existing data and effect on ozone formation
[PB88-130133] 10 p1354 N88-18095

TROPOSPHERIC SCATTERING
Results on the low elevation angle propagation experiment, part 1
[TUD-R-328] 06 p0693 N88-14250
Optical characterization of tropospheric aerosols
[AD-A187839] 11 p1511 N88-19029

Corrections for differential scattering by aerosols in the measurement of ozone by DIAL --- differential absorption lidar (DIAL)
[NPL-QU-78] 14 p1945 N88-21603

TROPOSPHERIC WAVES
NT PLANETARY WAVES
The importance of mesoscale waves in the upper troposphere for formation of cloud and precipitation areas 02 p0203 N88-11273

TROUBLESHOOTING
U MAINTENANCE

TRUCKS
Adiabatic diesel engine component development: Reference engine for on-highway applications
[NASA-CR-179531] 03 p0386 N88-12428
Full scale and wind tunnel surface pressure measurements on the T.R.R.L. spray dispersion programme vehicles
[REPT-8623] 09 p1114 N88-16676
Ethanol as a fuel of a lorry. Use experience from a diesel engine modified to an otto engine
[DE88-752870] 21 p2958 N88-27569

TRUNCATION (MATHEMATICS)
U APPROXIMATION

TRUNCATION ERRORS
Spectral analysis in the linear geodetic boundary value problem
[B8735056] 16 p2259 N88-23502

TRUNKS (LINES)
U TRANSMISSION LINES

TRUNNIONS
U SHAFTS (MACHINE ELEMENTS)

TRUSSES
Simultaneous structural and control optimization via linear quadratic regulator eigenstructure assignment 05 p0594 N88-13622
Continuum modeling of large lattice structures: Status and projections
[NASA-TP-2767] 06 p0672 N88-14115
Buckling of braced monosymmetric cantilevers: Timoshenko energy approach
[PB87-133849] 06 p0723 N88-14445
Chromic acid anodizing of aluminum foil
[NASA-CR-178417] 07 p0837 N88-15077
Space station structures development
[NASA-CR-179261] 09 p1133 N88-16792
Optimized structure design using reanalysis techniques 09 p1180 N88-17067
Solar concentrator advanced development program, task 1
[NASA-CR-179489] 10 p1350 N88-18068
The integration of a mesh reflector to a 15-foot box truss structure. Task 3: Box truss analysis and technology development
[NASA-CR-178228] 11 p1497 N88-18941
Control augmented structural synthesis
[NASA-CR-4132] 13 p1721 N88-20290
A 60-meter erectable assembly concept for a control of flexible structures flight experiment
[NASA-TM-100497] 14 p1873 N88-21190
A sequentially deployable structure for space applications 14 p1875 N88-21202
Aerospatiale unfurlable reflector and associated mechanisms 14 p1875 N88-21203
Motion synchronization of a mechanism to deploy and restow a truss beam 14 p1925 N88-21474
Continuum modeling and dynamic analysis of large truss structures 17 p2349 N88-23995
Mobile remote manipulator system for a tetrahedral truss
[NASA-CASE-MSC-20985-1] 20 p2765 N88-26398
Collet lock joint for space station truss
[NASA-CASE-MSC-21207-1] 23 p3222 N88-29180
Clevis joint for deployable space structures
[NASA-CASE-LAR-13898-1] 24 p3380 N88-30130

TRYPTAMINES
NT SEROTONIN

TSUNAMI WAVES
Moving ionospheric perturbations induced by wave trains propagating through ocean 09 p1239 N88-17427

TUBE CATHODES
NT PHOTOCATHODES
NT THERMIONIC CATHODES
Improved cathode life testing
[REPT-3189-T] 02 p0168 N88-11056
High-current density, high-brightness electron beams from large-area lanthanum hexaboride cathodes
[AD-A187700] 11 p1477 N88-18813
Program to research laser-driven thermionic electron sources for free electron lasers
[AD-A190473] 15 p2072 N88-22353

TUBE HEAT EXCHANGERS
Qualification of expansion and joint welding procedures of tube-to-tubesheet joints for heat exchangers in nuclear power plants
[DE87-703526] 05 p0589 N88-13592
Test methodology for infrared tubular heaters
[PB88-160916] 12 p1626 N88-19728
Development of protective coatings for ceramic tubular components
[PB88-197165] 20 p2776 N88-26463
Qualification of expansion and welding procedures of tube-to-tubesheet joints for heat exchangers in nuclear power plants
[DE88-701621] 23 p3221 N88-29174

TUBES
Studies of heat and mass transfer during chemical vapor deposition 17 p2338 N88-23953

TUBING
U PIPES (TUBES)

TUMORS
NT CANCER
NT NEOPLASMS

TUNABLE LASERS
Status, development of laser devices in China 03 p0303 N88-11907
NO2 heterodyne frequency measurements with a tunable diode laser, a CO laser transfer oscillator and CO2 laser standards
[NASA-CR-182393] 06 p0710 N88-14353
Dynamic restructuring of pulsed CO2 laser frequency and multiple-peak generation in a cell with IR-absorbing gas in the resonator 07 p0919 N88-15580
Effect of multiplication of spectral components of multi-frequency lasing of pulsed tunable laser 07 p0920 N88-15586
Characteristics of LKI-501 tunable dye laser with dyes in solid matrix 07 p0920 N88-15587
Dye laser for holographic interferometry 07 p0920 N88-15588
Tunable Al2O3:Ti3+-laser with optical pumping 09 p1237 N88-17415
Continuously frequency-tunable high-pressure CO2-laser with plasmatic cathode 09 p1238 N88-17418
Growth and characteristics of materials for tunable lasers in the near infrared spectral region
[NASA-CR-182501] 11 p1491 N88-18901
Resonantly-enhanced, four-photon ionization of krypton at laser intensities exceeding 10(12) W/sq cm
[DE88-005038] 11 p1544 N88-19229
Projected performance of RF-linac-driven free-electron lasers in the VUV and soft X-ray regions
[DE88-004294] 13 p1776 N88-20625
A picosecond tunable ultrashort cavity dye laser 14 p1902 N88-21361
Nonlinearly tunable wideband emission of infrared radiation by Al2O3:Ti laser 14 p1970 N88-21758
Tunable condensed-media laser with antiresonant ring cavity 14 p1971 N88-21764
Diode laser spectroscopy of chemical moieties at surfaces
[AD-A190710] 15 p2036 N88-22127
Efficient narrow linewidth waveguide dye laser pumped by CuCl laser 16 p2187 N88-23038
Observation of synchronously transient pumped mode-locking dye laser under negative cavity detuning 16 p2187 N88-23041
Generation of tunable coherent radiation in 3 micrometers-5 micrometers region using semiconductor lasers in external cavities
[AD-A190860] 16 p2212 N88-23202
Isotope separation using tuned laser and electron beam
[NASA-CASE-NPO-16907-1-CU] 18 p2483 N88-24732
A new near-infrared tunable-room temperature solid state laser La3Ga5SiO14:Cr(3+)
[DE88-011341] 21 p2953 N88-27543
Initial testing of the tunable diode laser absorption spectrometer for measuring HNO3 in diesel engine exhaust, stage 2
[PB88-193073] 21 p2970 N88-27641
The 1985-86 measurements with the tunable diode laser absorption spectrometer
[PB88-214002] 23 p3231 N88-29226
Growth and characterization of materials for tunable lasers in the near infrared spectral region
[NASA-CR-183132] 24 p3377 N88-30113
Spectroscopic studies with multiple quantum well materials with applications to optical signal processing at room temperature
[AD-A194171] 24 p3429 N88-30409

TUNDRA
Disturbance and recovery of Arctic Alaskan tundra terrain. A review of recent investigations
[AD-A184442] 04 p0467 N88-12887

TUNGSTEN
Progress toward a crystal streak camera using tungsten bronze crystals for the electrooptic material
[DE87-013110] 03 p0323 N88-12044
The effects of thin anodic films on the cyclic microstrain/macrostrain behavior of tungsten 05 p0597 N88-13650
Anomalies in electromagnetic absorption of circularly polarized ultrasonic waves by tungsten within Doppler-shifted cyclotron resonance range 06 p0775 N88-14756
Shielding analysis of a small compact space nuclear reactor
[AD-A185566] 06 p0779 N88-14784
Growth and electronic properties of strained metal overlayers
[DE87-010956] 10 p1417 N88-18463
Creep behavior of tungsten/niobium and tungsten/niobium-1 percent zirconium composites
[NASA-TM-100804] 11 p1460 N88-18707
The effects of various conductor components on Nb3Sn filament prestrain in cable-in-conduit conductors
[DE88-003956] 11 p1479 N88-18824
Tungsten-carbon multilayer system studied with X-ray scattering
[DE88-005749] 13 p1735 N88-20373
Properties of reactively sputtered WNx films Zhao, X. -A.
[AD-A188711] 13 p1835 N88-20976
Compatibility in space reactor fuel systems
[DE88-005698] 13 p1839 N88-21004
Dynamic fracture toughness evaluation by measurement of CTOD
[WNS/ASD-88-02] 16 p2178 N88-22982
Creep behavior of tungsten/niobium and tungsten/niobium-1 percent zirconium composites 17 p2425 N88-24427
Irradiation effects on tungsten stabilized martensitic steels
[DE88-007074] 18 p2486 N88-24748
Low temperature film growth of the oxides of zinc, aluminum and vanadium (and related systems, oxides of gold and germanium, nitrides of aluminum and tungsten) by reactive sputter deposition
[AD-A193497] 23 p3191 N88-28986

TUNGSTEN ALLOYS
Equations for determining CVD tungsten-rhenium alloy composition and plating rate
[DE87-008831] 01 p0024 N88-10152
Reduced-activation ferritic steels: A comparison with Cr-Mo steels
[DE88-000332] 03 p0290 N88-11826
Mechanical property evaluation of a series of commercial tungsten alloys
[AD-A185440] 05 p0585 N88-13446
The effect of ion implantation on the corrosion behavior of a high-density sintered tungsten alloy
[AD-A185713] 06 p0683 N88-14185
Corrosion behavior of high density tungsten alloys
[AD-A187108] 09 p1143 N88-16852
Corrosion of tungsten alloys in marine environments 17 p2320 N88-23854
Irradiation effects on tungsten stabilized martensitic steels
[DE88-007074] 18 p2486 N88-24748
Low-chromium reduced-activation ferritic steels
[DE88-009060] 19 p2617 N88-25524
Formation of metastable structures and amorphous phases in Cu-W alloys using the triod sputtering technique
[DE88-009051] 21 p2915 N88-27298
Hot isostatic pressing of tungsten-nickel-iron composites
[FOA-C-20698-2.1] 22 p3056 N88-28135

TUNGSTEN CARBIDES
Surface chemistry of transition metal carbides: A theoretical analysis
[AD-A184237] 03 p0291 N88-11829

TUNGSTEN COMPOUNDS
NT TUNGSTEN CARBIDES
Improved cathode life testing
[REPT-3189-T] 02 p0168 N88-11056
Results from the melting of tungsten composites under microgravity (TEXUS 10 flight)
[FOA-C-20676-2.1] 05 p0571 N88-13482

TUNGSTEN INERT GAS WELDING
U GAS TUNGSTEN ARC WELDING

TUNING
Fast autotuning of a hydrogen maser by cavity Q modulation 04 p0436 N88-12707
Optically tuned MM-wave IMPATT source
[AD-A185250] 05 p0577 N88-13523
Tailorable infrared sensing device with strain layer superlattice structure
[NASA-CASE-NPO-16607-1-CU] 06 p0788 N88-14836
Simplified self-tuning control algorithms
[OUEL-1657/86] 07 p0907 N88-15494
Operation of electron-beam controlled CO2 laser at 6 atmospheres 11 p1468 N88-18758

Polarization effects in laser-pumped Nd:YAG lasers
[DE88-004019] 11 p1492 N88-18904
Optimal placement of tuning masses for vibration reduction in helicopter rotor blades
[NASA-TM-100562] 13 p1782 N88-20665
Development of aeroelastic analysis methods for turborotors and propfans, including mistuning
16 p2219 N88-23244
State of tuning
[NASA-TT-20195] 18 p2561 N88-25205
Tuning a major part of a clustering algorithm
[AD-A191446] 20 p2836 N88-26821
Aircraft interior noise reduction by alternate resonance tuning
[NASA-CR-182540] 20 p2849 N88-26909
Visible tunable source
[DE88-006442] 20 p2854 N88-26944
Prediction of the aeroelastic behavior of tuned blades. Application to aircraft engines
[ISAL-87-0046] 21 p2897 N88-27199
An electronically tuned, stable 8415-MHz dielectric resonator FET oscillator for space applications
22 p3068 N88-28205
Experimental investigation of propfan aeroelastic response in off-axis flow with mistuning
[NASA-TM-101320] 22 p3089 N88-28344

TUNING FORK GYROSCOPES
An analysis of DREO's (Defence Research Establishment Ottawa) analog rebalance loops for the CSG-2 (Canadian Strapdown Gyroscope) tuned-rotor gyroscope
[AD-A188577] 12 p1629 N88-19749
A LQG regulator for the angular motion of the rotor at a tuned gyroscope
[INPE-4280-PRE/1152] 12 p1631 N88-19759

TUNISIA
Monitoring Tunisia's steppes with SPOT
22 p3097 N88-28390

TUNNEL DIODES
Nanoelectronics
[AD-A186969] 09 p1156 N88-16930
SIS (Superconductor-Insulator-Superconductor) mixer research
[AD-A192908] 20 p2879 N88-27092

TUNNEL RESISTORS
U ELECTRON TUNNELING
U RESISTORS

TURBIDITY
Two-layer stratified flow analysis of gravity currents and turbidity currents in lakes, reservoirs and the ocean
04 p0463 N88-12864
Turbidity patterns in the delta waters of southwest Netherlands on Thematic Mapper (TM) and multispectral scanner (MSS) satellite images
[BCRS-86-06] 16 p2227 N88-23303
Satellite remote sensing of turbidity and sediment concentration in Lagoa dos Patos
17 p2355 N88-24032

TURBINE BLADES
Modeling and measurement of heat transfer on turbine blade tips 01 p0006 N88-10032
Investigation of the excitation of turbine blade vibration in axial compressors in rotating stall
[ETN-87-90377] 01 p0007 N88-10035
Experimental determination of the oscillatory forces on two turbine blade profiles
[ETN-87-90417] 01 p0007 N88-10037
The effect of different packagings on the vibration behavior and the coupling factors of steam turbine blading
[ETN-87-90425] 01 p0056 N88-10357
The influence of high free stream turbulence, intensive cooling and wake on the external heat transfer of convectively cooled gas turbine blades
[ETN-87-90432] 01 p0056 N88-10360
Blade loss transient dynamics analysis, volume 1. Task 2: TETRA 2 theoretical development
[NASA-CR-179632] 02 p0125 N88-10791
Blade loss transient dynamics analysis, volume 2. Task 2: TETRA 2 user's manual
[NASA-CR-179633] 02 p0126 N88-10792
Comparison between numerical solutions and measurements for a high speed turbine blade
[PNR90402] 02 p0172 N88-11082
Blade excitation criteria developed for aero derived engines in Arctic Alaska
[PNR90368] 02 p0182 N88-11131
Turbine Engine Hot Section Technology, 1985
[NASA-CP-2405] 02 p0184 N88-11140
Development of heat flux sensors for turbine airfoils
02 p0184 N88-11143
Prediction of turbine blade heat transfer
02 p0187 N88-11162
3D inelastic analysis methods for hot section components 02 p0187 N88-11164
3-D inelastic analysis methods for hot section components 02 p0187 N88-11165
Component specific modeling
02 p0187 N88-11166
Constitutive modeling of superalloy single crystals with verification testing 02 p0188 N88-11169
Constitutive modeling for isotropic materials
02 p0188 N88-11171
Constitutive modeling for isotropic materials
02 p0188 N88-11172
Turbine airfoil deposition models and their hot corrosion implications 02 p0189 N88-11178
Experimental verification of vapor deposition rate theory in high velocity burner rigs 02 p0189 N88-11179
Thermal expansion mismatch and oxidation in thermal barrier coatings 02 p0189 N88-11182
Finite element analysis of three-dimensional steady and unsteady temperature fields (computation of temperature distribution of turbine blade with composite cooling)
03 p0300 N88-11887
Local heat/mass transfer and pressure drop in a two-pass rib-roughened channel for turbine airfoil cooling
[NASA-CR-179635] 03 p0322 N88-12039
Crack initiation and propagation due to cyclic thermal gradients — aircraft turbine blades
[ESA-TT-1023] 03 p0336 N88-12114
National Aerospace Laboratory experiment
04 p0404 N88-12509
Simulated service test behavior of various internal and external coatings applied on CF6-50 first stage turbine blades
[NLR-MP-86018-U] 05 p0549 N88-13343
Thermal finite-element analysis of space shuttle main engine turbine blade
[NASA-TM-100117] 05 p0610 N88-13745
STAEBL/general composites with hygrothermal effects (STAEBL/GENCOM)
[NASA-TM-100266] 05 p0611 N88-13754
Accurate rotor loads prediction using the FLAP (Force and Loads Analysis Program) dynamics code
[DE88-001109] 05 p0623 N88-13815
Research on internal fluid mechanism between turbine blades 06 p0676 N88-14138
Development of transonic speed cascade design method using Euler code and inverse solution
06 p0676 N88-14139
Experimental study of secondary flow in the presence of two jet arrays on the wall of a turbine blade
[ECL-87-11] 08 p0967 N88-15981
Creep and fatigue research efforts on advanced materials 09 p1119 N88-16701
VAWT (Vertical-Axis Wind Turbine) stochastic loads produced by atmospheric turbulence
[DE88-001355] 09 p1187 N88-17110
A comparison of the predicted and measured gravitational stresses in VAWT (Vertical Axis Wind Turbine) blades
[DE88-002113] 09 p1187 N88-17111
Advanced Technology for Aero Gas Turbine Components
[AGARD-CP-421] 10 p1279 N88-17647
A research program on the aerodynamics of a highly loaded turbine stage 10 p1280 N88-17655
Advanced techniques employed in blade cooling research 10 p1281 N88-17659
Transonic blade design on rotational stream surfaces
10 p1282 N88-17671
Wake interaction effects on the transition process on turbine blades
[AD-A188020] 10 p1332 N88-17962
Unsteady heat transfer in turbine blade ducts: Focus on combustor sources
[NASA-TM-100815] 11 p1486 N88-18870
Testing of a one-bladed 30-meter-diameter rotor on the DOE/NASA Mod-O wind turbine
[NASA-TM-100274] 11 p1509 N88-19014
Fatigue load measurements and evaluation of the 25m Horizontal Axis Wind Turbine (HAWT) at Petten, The Netherlands
[NLR-MP-86054-U] 13 p1782 N88-20660
Nonlinear structural analysis of a turbine airfoil using the Walker viscoplastic material model for B1900 + Hf
14 p1932 N88-21522
New airfoil sections for straight bladed turbine
[DE88-701075] 14 p1942 N88-21588
Aero/structural tailoring of engine blades (AERO/STAEBL)
[NASA-CR-180805] 14 p1959 N88-21682
Structural tailoring of high-speed turbine blades (SSME/STAEBL) 15 p2080 N88-22398
Advanced probabilistic methods for quantifying the effects of various uncertainties in structural response
15 p2080 N88-22401
Model study of thermal stresses in gas-turbine blades with protective coating 16 p2179 N88-22989
Dependence of structure of stabilized ZrO2 coatings on condensation rate 16 p2180 N88-22990
Two-equation low-Reynolds-number turbulence modeling of transitional boundary layer flows characteristic of gas turbine blades
[NASA-CR-4145] 16 p2209 N88-23185
Lewis Structures Technology, 1988. Volume 1: Structural Dynamics
[NASA-CP-3003-VOL-1] 16 p2217 N88-23226
Low-cost optical data acquisition system for blade vibration measurement 16 p2219 N88-23240
SSME single-crystal turbine blade dynamics
16 p2221 N88-23257
Vanadic hot corrosion of gas turbine blade coating materials 17 p2321 N88-23864
The effect of operating temperature and turbine blade cooling on Brayton cycle space power systems
17 p2435 N88-24489
A 3 MW wood fired gas turbine at Red Boiling Springs, Tennessee 18 p2536 N88-25051
Recent advances in capacitance type of blade tip clearance measurements
[NASA-TM-101291] 19 p2603 N88-25460
New super alloys used in turbochargers
19 p2634 N88-25628
Computational study on thermal efficiency of ceramic gas turbine
[DE88-753114] 20 p2809 N88-26667
T55-L-714 engine development and qualification. Engine M11 low cycle fatigue test report. (0213-005-87)
[AD-A192765] 21 p2897 N88-27197
Prediction of the aeroelastic behavior of tuned blades. Application to aircraft engines
[ISAL-87-0046] 21 p2897 N88-27199
Advanced computational methods for turbomachinery blade design
[PNR90438] 22 p3044 N88-28065
Structural Tailoring of Advanced Turboprops (STAT)
[NASA-CR-180861] 22 p3045 N88-28074
Probabilistic structural analysis to quantify uncertainties associated with turbopump blades
[NASA-TM-100278] 22 p3050 N88-28094
Thermal barrier coating life-prediction model development
[NASA-CR-179507] 22 p3058 N88-28142
Optimization of nondestructive control of ceramic pieces for aeronautical turbines
[ETN-88-92884] 22 p3059 N88-28149
Interaction of creep and fatigue damage in gas turbine blade material
[PNR90440] 22 p3088 N88-28335
The mechanical behavior of surface modified ceramics
[DE88-010564] 23 p3196 N88-29022
Dynamic response of a 330-kW horizontal axis wind turbine generator
[DE88-001136] 23 p3228 N88-29212
Numerical solutions of unsteady inviscid transonic turbine cascade flows
[AD-A196111] 24 p3316 N88-29748
User's manual for three dimensional boundary layer (BL3-D) code
[NASA-CR-174899] 24 p3369 N88-30063
Impact of ETO propellants on the aerothermodynamic analyses of propulsion components
[NASA-TM-101303] 24 p3374 N88-30094

TURBINE ENGINES
NT CONVERTIBLE FAN-SHAFT ENGINES
NT GAS TURBINE ENGINES
NT J-57 ENGINE
NT JET ENGINES
NT RAMJET ENGINES
NT SUPERSONIC COMBUSTION RAMJET ENGINES
NT TF-30 ENGINE
NT TURBOFAN ENGINES
NT TURBOJET ENGINES
NT TURBOPROP ENGINES
Blade loss transient dynamics analysis, volume 1. Task 2: TETRA 2 theoretical development
[NASA-CR-179632] 02 p0125 N88-10791
Blade loss transient dynamics analysis, volume 2. Task 2: TETRA 2 user's manual
[NASA-CR-179633] 02 p0126 N88-10792
Evaluating and testing thermographic phosphors for turbine-engine temperature measurements
[DE87-011772] 02 p0174 N88-11090
Development of heat flux sensors for turbine airfoils
02 p0184 N88-11143
Film cooling heat transfer on a turbine airfoil
02 p0186 N88-11156
Thermal barrier coating life prediction model development 02 p0190 N88-11185
USSR report: Engineering and equipment
[JPRS-UEQ-87-008] 04 p0423 N88-12621
Thermal finite-element analysis of space shuttle main engine turbine blade
[NASA-TM-100117] 05 p0610 N88-13745

Recent advances in high temperature instrumentation for hot section applications
[NASA-TM-100282] 06 p0707 N88-14339
Creep-fatigue cracking in high temperature turbine rotors 06 p0720 N88-14426
Directions in propulsion control 08 p0956 N88-15799
Improved silicon nitride for advanced heat engines
[NASA-CR-175006] 08 p0973 N88-15886
Turbine engine monitoring systems: Can they benefit component improvement program management?
[AD-A186992] 09 p1120 N88-16706
Turbine flow meter with optical fiber pick-up
[NAL-TR-923] 09 p1169 N88-17009
Measurements of gas turbine combustor and engine augmentor tube sooting characteristics
[AD-A187831] 11 p1440 N88-18592
Utilization of parallel processing in solving the inviscid form of the average-passage equation system for multistage turbomachinery
[NASA-TM-89845] 14 p1868 N88-21160
NNEPEQ: Chemical equilibrium version of the Navy/NASA Engine Program
[NASA-TM-100851] 14 p1868 N88-21161
Aeropropulsive characteristics of isolated combined turbojet/ramjet nozzles at Mach numbers from 0 to 1.20
[NASA-TP-2814] 17 p2299 N88-23757
Ceramics for turbine engines 17 p2323 N88-23873
Thermal cyclic durability testing of ceramic materials for turbine engines 17 p2325 N88-23886
A high fidelity real-time simulation of a small turboshaft engine
[NASA-TM-100991] 20 p2761 N88-26378
JTDE 1 XTE34 materials research and development report
[AD-A194268] 22 p3044 N88-28063

TURBINE PUMPS
Seal technology for liquid oxygen (LOX) turbopumps
[NASA-CR-174866] 05 p0591 N88-13603
Incipient failure detection of space shuttle main engine turbopump bearings using vibration envelope detection 05 p0595 N88-13629
Thermal finite-element analysis of space shuttle main engine turbine blade
[NASA-TM-100117] 05 p0610 N88-13745
STAEBL/general composites with hygrothermal effects (STAEBL/GENCOM)
[NASA-TM-100266] 05 p0611 N88-13754
Evaluation of load tracks and wear of two sets of bearings from space shuttle main engine high pressure oxygen turbopumps
[NASA-CR-178969] 07 p0861 N88-15223
The determination of equivalent bearing loading for the BSMT that simulate SSME high pressure oxidizer turbopump conditions using the SHABERTH/SINDA computer programs 07 p0925 N88-15623
An expert system to analyze high frequency dependent data for the space shuttle main engine turbopumps 08 p1060 N88-16399
Disk pumping test
[AD-A187199] 11 p1440 N88-18591
Computer-aided design analysis of 57-mm, angular-contact, cryogenic turbopump bearings
[NASA-TP-2816] 11 p1496 N88-18933
Electromagnetic dampers for cryogenic applications 16 p2218 N88-23231
SSME single-crystal turbine blade dynamics 16 p2221 N88-23257
Rotor self-lubricating axial stop
[NASA-CASE-MFS-28273-1] 17 p2344 N88-23974
Analysis of flow through pump of large rocket engine 19 p2637 N88-25646
Probabilistic structural analysis to quantify uncertainties associated with turbopump blades
[NASA-TM-100278] 22 p3050 N88-28094
Evaluation of transfer films of Salox M on 440C for HPOTP bearing cage applications, task 119
[NASA-CR-179020] 23 p3223 N88-29184

TURBINE WHEELS
Determination of the critical crack length a (sub IC) in turbine discs
[PB87-144812] 07 p0820 N88-14986

TURBINES
NT AXIAL FLOW TURBINES
NT GAS TURBINES
NT SHROUDED TURBINES
NT STEAM TURBINES
NT SUPERSONIC TURBINES
NT WIND TURBINES
Performance of supersonic impingement radial turbines 06 p0712 N88-14367
Design and testing of a small radial turbine for auxiliary power units 10 p1281 N88-17661
Research on fluid dynamic energy separation
[DE88-002776] 10 p1339 N88-18001
A combined Rankine/Brayton pulse power cycle 17 p2435 N88-24490
Remote temperature-measurement instrumentation for a heated rotating turbine disk
[DE88-006456] 18 p2516 N88-24925
Extensive verification of blade-to-blade flow code based on Denton scheme 19 p2638 N88-25654
C-CAMP: A closed cycle alkali metal power system
[DE88-009715] 19 p2688 N88-25975
Numerical computation of three-dimensional turbulent flow in tightly curved ducts and spiral turbine casings
[ETN-88-92362] 21 p2948 N88-27511
Calibration of the portable wear metal analyzer
[AD-A192971] 21 p2950 N88-27524
The effects of inlet turbulence and rotor/stator interactions on the aerodynamics and heat transfer of a large-scale rotating turbine model. Volume 3: Heat transfer data tabulation 65 percent axial spacing
[NASA-CR-179468] 23 p3180 N88-28930
The effects of inlet turbulence and rotor/stator interactions on the aerodynamics and heat transfer of a large-scale rotating turbine model. Volume 2: Heat transfer data tabulation. 15 percent axial spacing
[NASA-CR-179467] 24 p3326 N88-29804
Studies of gas turbine heat transfer airfoil surface and end-wall cooling effects
[AD-A195165] 24 p3326 N88-29805
An investigation of constitutive models for predicting viscoplastic response during cyclic loading
[AD-A194875] 24 p3385 N88-30163

TURBOCHARGERS
U SUPERCHARGERS
U TURBOCOMPRESSORS

TURBOCOMPRESSORS
Modeling and measurement of heat transfer on turbine blade tips 01 p0006 N88-10032
Investigation of the excitation of turbine blade vibration in axial compressors in rotating stall
[ETN-87-90377] 01 p0007 N88-10035
Design verification tests for an axial gap permanent magnet compressor motor
[DE87-014360] 02 p0167 N88-11049
Three-dimensional calculation in high subsonic axial compressor rotor and its comparison with L2F velocity measurement 03 p0300 N88-11886
Automated design of controlled diffusion blades
[NASA-TM-100251] 05 p0542 N88-13304
Effects of free stream turbulence, Reynolds number and incidence angle on axial turbine cascade performance 05 p0548 N88-13339
Post stall behavior in axial-flow compressors
[AD-A185712] 06 p0665 N88-14081
Flow in labyrinth seals and its influence on rotor stability of turbocompressors 07 p0851 N88-15168
Technology developments for a compound cycle engine 09 p1107 N88-16637
Advanced Technology for Aero Gas Turbine Components
[AGARD-CP-421] 10 p1279 N88-17647
Optimisation of military compressors for weight and volume 10 p1279 N88-17649
Operation of gas turbine engines in dust-laden environments 10 p1280 N88-17654
Investigation of dihedral effects in compressor cascades 10 p1282 N88-17672
Possibilities for on-line surge suppression by fast guide vane adjustment in axial compressors 10 p1283 N88-17674
Design and development of an advanced F100 compressor 10 p1283 N88-17678
Experimental investigation of a supercritical compressor rotor blade section 10 p1284 N88-17680
Radial mixing in turbomachines
[AD-A188028] 11 p1482 N88-18847
Small engine components test facility turbine testing cell
[NASA-TM-100887] 15 p2019 N88-22037
Supersonic axial-flow fan flutter 16 p2221 N88-23255
Research on aero-thermodynamic distortion induced structural dynamic response of multi-stage compressor blading
[AD-A192169] 18 p2456 N88-24584
Servojet retrofit
[AD-A191075] 18 p2522 N88-24964
New super alloys used in turbochargers 19 p2634 N88-25628
Experimental determination of aerodynamic damping in a three-stage transonic axial-flow compressor
[NASA-TM-100953] 21 p2897 N88-27200
Modeling of large stall in axial compressors
[VKI-TN-164] 23 p3213 N88-29124

TURBOCONVERTERS
U TURBOGENERATORS

TURBOELECTRIC CONVERSION
U TURBOGENERATORS

TURBOFAN AIRCRAFT
NT BOEING 737 AIRCRAFT
NT CONCORDE AIRCRAFT
NT F-111 AIRCRAFT
Multiple-Purpose Subsonic Naval Aircraft (MPSNA): Multiple Application Propfan Study (MAPS)
[NASA-CR-175104] 23 p3177 N88-28917

TURBOFAN ENGINES
NT CONVERTIBLE FAN-SHAFT ENGINES
NT TF-30 ENGINE
NT TF-34 ENGINE
First article test noise survey of the A/F32T-9 large turbo fan engine enclosed noise suppressor system, Sky Harbor IAP (International Airport), Phoenix, Arizona
[AD-A183799] 01 p0090 N88-10588
The wide chord fan blade: A Rolls Royce first
[PNR90416] 02 p0125 N88-10789
Impact and promise of NASA aeropropulsion technology 09 p1118 N88-16698
Turbine engine monitoring systems: Can they benefit component improvement program management?
[AD-A186992] 09 p1120 N88-16706
Engine flow simulation for wind tunnel testing at NLR
[NLR-MP-87011-U] 13 p1723 N88-20305
Exhaust-gas pressure and temperature survey of F404-GE-400 turbofan engine
[NASA-TM-88273] 13 p1724 N88-20307
A microprocessor-based real-time simulator of a turbofan engine
[NASA-TM-100889] 14 p1868 N88-21163
Linear state space modeling of a turbofan engine
[AD-A190110] 15 p2019 N88-22035
Noise assessment of unsuppressed TF-34-GE-100A engine at Warfield ANG, Baltimore, Maryland
[AD-A189966] 15 p2129 N88-22702
Augmentor performance of an F100 engine model derivative engine in an F-15 airplane
[NASA-TM-86745] 17 p2307 N88-23805
Euler analysis of a swirl recovery vane design for use with an advanced single-rotation propfan
[NASA-TM-101357] 24 p3320 N88-29771
Developing the Rolls-Royce Tay
[PNR90447] 24 p3327 N88-29809
High performance turbofan afterburner systems 24 p3347 N88-29922
Contamination and distortion of steady flow field induced by discrete frequency disturbances in aircraft gas engines
[AD-A195440] 24 p3370 N88-30069
Development and installation of an instrumentation package for GE F404 investigative testing
[AD-A196265] 24 p3376 N88-30107

TURBOFANS
Technical-economical evaluation of a novel propfan concept in comparison with the turbofan for the nineties
[ETN-88-91022] 11 p1441 N88-18596
Measurement and analysis of the noise radiated by low Mach numbers centrifugal blowers
[AD-A189226] 13 p1833 N88-20966
Holographic interferometry for flow visualization studies in high speed fans
[PNR90459] 22 p3045 N88-28072

TURBOGENERATORS
Innovating systems and techniques for the diagnosis of materials and industrial plants
[CISE-3856] 08 p0976 N88-15901
Status of CEA design and simulation studies of a 200 KWe turboelectric space power system 17 p2400 N88-24268
Power source selection for neutral particle beam systems 17 p2407 N88-24314
Turbomachinery in space 17 p2408 N88-24321
Rotating-hoop, pulsed-energy converter 17 p2426 N88-24433

TURBOJET AIRCRAFT
U JET AIRCRAFT

TURBOJET ENGINE CONTROL
Testing of the engine compartment fire extinguishing system in the F/EF-111 aircraft
[AD-A188801] 12 p1576 N88-19423

TURBOJET ENGINES
NT J-57 ENGINE
NT TF-30 ENGINE
NT TURBOFAN ENGINES
NT TURBOPROP ENGINES
High-speed inlet research program and supporting analyses 08 p0958 N88-15811
The coming revolution in turbine engine technology 10 p1279 N88-17648
Numerical simulation of diffuser/combustor dome interaction 10 p1281 N88-17663
Development of vertical takeoff aircraft with turbojet engines in Germany 10 p1309 N88-17822
Aircraft emissions characterization: TF41-A2, TF30-P103 and TF30-P109 engines
[AD-A192053] 18 p2466 N88-24638

Vibrational impacts of hush house operation
[DE88-006963] 21 p2899 N88-27207
Air intake aerodynamics 24 p3318 N88-29762
Semiempirical methods for airbreathing missiles 24 p3318 N88-29763
Evaluation of the advanced air breathing propulsion concepts, executive summary
[ESA-CR(P)-2540] 24 p3325 N88-29802
Evaluation of advanced air breathing concepts. Volume 1: Executive summary
[ESA-CR(P)-2539] 24 p3326 N88-29806

TURBOMACHINE BLADES
NT COMPRESSOR BLADES
NT ROTOR BLADES (TURBOMACHINERY)
NT STATOR BLADES
NT TURBINE BLADES
A flow function method for the axisymmetric calculation of the transonic turbomachine flow taking into account the flow differences in circumferential direction
[ETN-87-90428] 01 p0056 N88-10359
The use of holographic interferometry for turbomachinery fan evaluation during rotating tests
[PNR90390] 02 p0176 N88-11098
The unsteady gas flow through stator and rotor of a turbomachine 10 p1281 N88-17660
High Reynolds number pump facility for cavitation research
[AD-A189310] 13 p1765 N88-20558
Calculation of displacement, constraints and eigenmodes of rotating blades
[ETN-88-92296] 16 p2224 N88-23277
Structural optimization of fiber composite turbomachine blades
[ETN-88-92351] 20 p2760 N88-26372
Coupled inviscid - boundary layer methods for turbomachinery blading design
[PNR90437] 22 p3078 N88-28260

TURBOMACHINERY
NT AXIAL FLOW TURBINES
NT CENTRIFUGAL COMPRESSORS
NT CENTRIFUGAL PUMPS
NT GAS TURBINES
NT SHROUDED TURBINES
NT STEAM TURBINES
NT SUPERSONIC TURBINES
NT TURBINE PUMPS
NT TURBINES
NT TURBOCOMPRESSORS
NT TURBOFANS
NT TURBOGENERATORS
NT WIND TURBINES
Navier-Stokes cascade analysis with a stiff Kappa-Epsilon turbulence solver
[NASA-TM-100218] 02 p0123 N88-10778
Optical flow diagnostic measurements in turbomachinery
[PNR90396] 02 p0172 N88-11081
Calculation of the three dimensional flow in the impeller of hydraulic turbomachines using a finite element method
[ETN-87-90612] 03 p0315 N88-11988
Application of Runge Kutta time marching scheme for the computation of transonic flows in turbomachines
[NASA-TM-86997] 04 p0394 N88-12461
Identification of perturbations in turbomachines by the analysis of pressure signals, vibrations and wavelike motions
[ETN-88-90602] 05 p0590 N88-13600
Numerical simulation of flows in axial and radial turbomachines using Euler solvers 06 p0713 N88-14372
Supersonic turbines for organic fluid Rankine cycles from 3 to 1300 kW 06 p0713 N88-14375
Blade vibration due to different flow excitation 07 p0851 N88-15166
Blade excitation due to unsteady flow phenomena 07 p0851 N88-15167
A multistage mesh generator for solving the average-passage equation system
[NASA-CR-179539] 08 p0951 N88-15789
Aeropropulsion '87. Session 3: Internal Fluid Mechanics Research
[NASA-CP-10003-SESS-3] 08 p0954 N88-15790
Turbomachinery 08 p0955 N88-15792
The Goddard Space Flight Center mechanical cooler program 08 p0983 N88-15944
Finite Element Calculation Methods and Their Application to Turbomachinery Flows, volume 1
[VKI-LS-1987-05-VOL-1] 08 p0985 N88-15960
Inviscid flows, part 1: Formulation of inviscid rotational flow problems by velocity potential and stream function methods. Applications to turbomachines 08 p0985 N88-15964
Inviscid flows, part 2 08 p0985 N88-15966
Viscous flows, part 1 08 p0986 N88-15967
Viscous flows, part 2 08 p0986 N88-15968
Modeling the unsteady flow found in axial turbomachinery
[ECL-87-07] 08 p0987 N88-15980
Numerical modeling of multidimensional flow in seals and bearings used in rotating machinery
[NASA-TM-100779] 09 p1165 N88-16988
The unsteady gas flow through stator and rotor of a turbomachine 10 p1281 N88-17660
Transonic blade design on rotational stream surfaces 10 p1282 N88-17671
An L-U implicit multigrid algorithm to solve the Euler equations for transonic flow in rotating turbomachinery passages 13 p1718 N88-20270
Numerical analysis of three-dimensional viscous internal flows
[NASA-TM-100878] 14 p1861 N88-21116
Utilization of parallel processing in solving the inviscid form of the average-passage equation system for multistage turbomachinery
[NASA-TM-89845] 14 p1868 N88-21160
Visualization of flows in turbomachinery
[AD-A189927] 15 p2063 N88-22299
Aeroelastic forced response analysis of turbomachinery 16 p2220 N88-23247
Forced response unsteady aerodynamics in a multistage compressor 18 p2512 N88-24903
Fluid dynamics of high performance turbomachines
[AD-A192073] 19 p2664 N88-25840
Improved method for stress and compatibility analysis of multicomponent rotating systems
[NASA-TM-100884] 19 p2680 N88-25935
A diagonally inverted LU implicit multigrid scheme
[NASA-TM-100911] 20 p2753 N88-26340
Improved 3-D turbomachinery CFD algorithm
[NASA-CR-179364] 20 p2801 N88-26619
Advanced computational methods for turbomachinery blade design
[PNR90438] 22 p3044 N88-28065
Investigation of the validity of Reynolds averaged turbulence models at the frequencies that occur in turbomachinery
[NASA-CR-182162] 22 p3048 N88-28087
Two-dimensional flow through a turbine cascade
[PDR/CFDU/IC/34] 22 p3076 N88-28264
Non-reflecting boundary conditions for computations of unsteady flows in turbomachines
[PNR90469] 22 p3079 N88-28284
The role of acoustic resonances in unsteady turbomachinery aerodynamics
[PNR90455] 22 p3147 N88-28720
Three-dimensional Navier-Stokes simulations of turbine rotor-stator interaction
[NASA-TM-100081] 24 p3316 N88-29750
An unconditionally stable Runge-Kutta method for unsteady flows
[NASA-TM-101347] 24 p3321 N88-29780
Three-dimensional elliptic grid generation technique with application to turbomachinery cascades
[NASA-TM-101330] 24 p3372 N88-30078

TURBOPROP AIRCRAFT
NT C-130 AIRCRAFT
NT F-27 AIRCRAFT
NT OV-1 AIRCRAFT
Noise of a model high speed counterrotation propeller at simulated takeoff/approach conditions (F7/A7)
[NASA-TM-100206] 01 p0091 N88-10592
A hybrid numerical technique for predicting the aerodynamic and acoustic fields of advanced turboprops
[NASA-CR-174926] 03 p0374 N88-12352
Noise of a model counterrotation propeller with reduced aft rotor diameter at simulated takeoff/approach conditions (F7/A3)
[NASA-TM-100254] 05 p0647 N88-13961
Are windshear training aid recommendations appropriate for other than large jet transports? Pilot procedures: Shear models 10 p1275 N88-17635
Sound transmission through the walls of light aircraft: An investigation of structure-borne noise in a Handley Page 137 Jetstream 3 aircraft
[NASA-CR-182509] 10 p1405 N88-18376
Analysis of in-flight acoustic data for a twin-engined turboprop airplane
[NASA-CR-178389] 11 p1543 N88-19220
NASA advanced turboprop research and concept validation program
[NASA-TM-100891] 16 p2163 N88-22902
NASA/industry advanced turboprop technology program
[NASA-TM-100929] 16 p2466 N88-24641
Multiple-Purpose Subsonic Naval Aircraft (MPSNA): Multiple Application Propfan Study (MAPS)
[NASA-CR-175104] 23 p3177 N88-28917

TURBOPROP ENGINES
Advanced turboprop wing installation effects measured by unsteady blade pressure and noise
[NASA-TM-100200] 01 p0002 N88-10008
Analysis and test evaluation of the dynamic stability of three advanced turboprop models at zero forward speed
[NASA-CR-175025] 06 p0668 N88-14095
Analysis and test evaluation of the dynamic response and stability of three advanced turboprop models at low forward speed
[NASA-CR-175026] 06 p0668 N88-14096
Flaps-up takoff performance of the OV-1D aircraft with YT53-L-704 engine installed
[AD-A185960] 07 p0819 N88-14979
Impact and promise of NASA aeropropulsion technology 09 p1118 N88-16698
Design and aerodynamic performance of a small mixed-flow gas generator turbine 10 p1281 N88-17662
Gear systems for advanced turboprops 10 p1282 N88-17667
Computerized life and reliability modelling for turboprop transmissions
[NASA-TM-100918] 16 p2215 N88-23220
Development of aeroelastic analysis methods for turborotors and propfans, including mistuning 16 p2219 N88-23244
Vibration and flutter analysis of the SR-7L large-scale propfan 16 p2221 N88-23254
Experimental and analytical evaluation of the effects of simulated engine inlets on the blade vibratory stresses of the SR-3 model prop-fan
[NASA-CR-174959] 23 p3179 N88-28927

TURBOPUMPS
U TURBINE PUMPS

TURBOROTORS
U TURBINE WHEELS

TURBOSHAFTS
The design of a turboshaft speed governor using modern control techniques
[NASA-CR-175046] 01 p0053 N88-10339
Test stand performance of a convertible engine for advanced V/STOL and rotorcraft propulsion
[NASA-TM-100211] 03 p0266 N88-11679
The convertible engine: A dual-mode propulsion system 09 p1108 N88-16639
A high fidelity real-time simulation of a small turboshaft engine
[NASA-TM-100991] 20 p2761 N88-26378

TURBULENCE
NT ATMOSPHERIC TURBULENCE
NT CLEAR AIR TURBULENCE
NT GUSTS
NT HOMOGENEOUS TURBULENCE
NT ISOTROPIC TURBULENCE
NT LOW LEVEL TURBULENCE
NT MAGNETOHYDRODYNAMIC TURBULENCE
NT PLASMA TURBULENCE
Study of pickup of cometary ions in turbulent solar winds 01 p0113 N88-10725
Impact of turbulence modeling on numerical accuracy and efficiency of compressible flow simulations
[NASA-TM-88333] 02 p0173 N88-11088
Prediction of turbine blade heat transfer 02 p0187 N88-11162
Flow in a model turbine stator 02 p0187 N88-11163
Thermally driven convective cells and tokamak edge turbulence
[DE87-014424] 02 p0238 N88-11499
Fundamentals of turbulence for turbulence modeling and simulation 03 p0312 N88-11971
A deterministic approach to turbulence: Chaos in Rayleigh-Benard convection 03 p0313 N88-11975
On helicity fluctuations and the energy cascade in turbulence
[NASA-CR-178403] 03 p0321 N88-12028
Conservation and transport properties of turbulence with large density variations
[LA-10911-MS] 03 p0321 N88-12032
Investigation of low-speed turbulent separated flow around airfoils
[NASA-CR-177450] 04 p0396 N88-12471
Fully developed turbulence via Feigenbaum's period-doubling bifurcations
[DE88-000242] 04 p0441 N88-12739
Optical instrumentation and study of gas-solid suspension flows
[DE88-000147] 04 p0442 N88-12744
A multiple-time-scale turbulence model based on variable partitioning of turbulent kinetic energy spectrum
[NASA-CR-179222] 04 p0444 N88-12754
Tracking through turbulence at the Tonopah Test Range
[DE88-001448] 04 p0446 N88-12766
Input turbulence features at a megawatt-size wind turbine, Medicine Bow, Wyoming
[DE88-000098] 04 p0464 N88-12873

Using a new characterization of turbulent wind for accurate correlation of wind turbine response with wind speed
[DE88-001453] 04 p0466 N88-12881
The velocity structure and turbulence at the center of the Orion Nebula 04 p0521 N88-13201
A perspective of computational fluid dynamics 05 p0538 N88-13279
Effects of free stream turbulence, Reynolds number and incidence angle on axial turbine cascade performance 05 p0548 N88-13339
Vortical Flows Research Program of the Fluid Dynamics Research Branch
[NASA-TM-88332] 05 p0582 N88-13549
Measurement of local convective heat transfer coefficients from a smooth and roughened NACA-0012 airfoil: Flight test data
[NASA-TM-100284] 05 p0582 N88-13552
Isentropic analysis and interpretation: Operational applications to synoptic and mesoscale forecast problems
[AD-A184814] 05 p0626 N88-13830
Chaos: Chto Delat? (What is to be done?)
[DE88-000513] 05 p0643 N88-13933
Studies of supersonic turbulence and hot-wire response using Laser-Induced Fluorescence (LIF) 06 p0664 N88-14072
Turbulence, turbulence control, and drag reduction
[AD-A185643] 06 p0665 N88-14080
The production of turbulence in boundary layers: The role of microscale coherent motions
[AD-A185568] 06 p0703 N88-14313
European reacting flow research: A final assessment
[AD-A185833] 07 p0828 N88-15022
Reynolds-stress and dissipation rate budgets in a turbulent channel flow
[NASA-TM-89451] 07 p0852 N88-15174
Numerical solution of turbulent flow past a backward facing step using a nonlinear K-epsilon model
[NASA-CR-178421] 07 p0854 N88-15189
Feasibility studies of optical processing of image bandwidth compression schemes
[AD-A186073] 07 p0932 N88-15660
Velocity and density measurements in a turbulent nonpremixed flame with comparison to numerical model predictions
[DE87-014695] 08 p0967 N88-15854
On the correlation of plume centerline velocity decay of turbulent acoustically excited jets
[NASA-TM-100193] 09 p1114 N88-16681
Numerical simulation of heat transfer turbulence, volume 4
[AD-A185132] 09 p1159 N88-16947
Analysis of a turbulent premixed V-flame (influence of flame-thickening)
[NAL-TR-941] 10 p1299 N88-17770
Universal power spectra for wave turbulence: Applications to wind waves, flicker noise, solar wind spectrum and classical second sound 10 p1318 N88-17879
One-dimensional leakage-flow vibration instabilities
[DE88-002875] 10 p1330 N88-17947
Remote sensing of atmospheric crosswinds by utilizing speckle-turbulence interaction and optical heterodyne detection
[AD-A187580] 10 p1347 N88-18052
Wake effects in a Fayette 95-IIS wind turbine array
[DE88-001103] 10 p1349 N88-18063
Turbulence loads on the Howden 26-m-diameter wind turbine
[DE88-001118] 10 p1351 N88-18075
Study of resistive pressure-gradient-driven turbulence
[DE88-005062] 10 p1414 N88-18441
Superfluid turbulence in He II at elevated pressures 10 p1422 N88-18493
An experimental investigation of straight and curved annular wall jets
[NASA-CR-182546] 11 p1434 N88-18557
Turbulence modeling in non-inertial frames of reference
[NASA-CR-181646] 11 p1488 N88-18880
Sound propagation through a turbulent atmosphere: Experimental techniques and data analysis
[AD-A188891] 12 p1688 N88-20094
Systems near the onset and in the well-developed regimes of turbulence
[DE88-005365] 13 p1766 N88-20565
Calculations of viscous flows with a multigrid method 13 p1769 N88-20580
Power spectral density analysis of wind-shear turbulence for related flight simulations
[NASA-CR-182721] 13 p1802 N88-20773
On the zonal momentum balance at the equator 13 p1805 N88-20788
Observations on energy transport in tokamaks: A new formula for turbulent transport
[DE88-005309] 13 p1841 N88-21019
The 30 x 30 inch wind tunnel
[IC-AERO-87-01] 14 p1869 N88-21168
Problems in fluid dynamics
[NASA-CR-182678] 14 p1909 N88-21410
The turbulent heat flux in low Mach number flows with large density variations
[DE88-006445] 14 p1911 N88-21419
Interaction of a strong vortex with decaying turbulence
[DE88-007102] 14 p1911 N88-21420
Effect of flow convergence on turbulence level in stream 14 p1973 N88-21773
Numerical simulation of turbulent flames using vortex methods
[AD-A189813] 15 p2034 N88-22116
Basic instability mechanisms in chemically reacting subsonic and supersonic flows
[AD-A190101] 15 p2034 N88-22120
Random processes, turbulence and disordering fields
[AD-A190123] 15 p2063 N88-22303
Film cooling effectiveness on a flat plate in high free-stream turbulence using a single row of 30 deg slant-hole injectors
[AD-A190500] 15 p2147 N88-22816
On the validation of a code and a turbulence model appropriate to circulation control airfoils
[NASA-TM-100090] 16 p2156 N88-22864
On local approximations of the pressure-strain term in turbulence models 16 p2197 N88-23102
Shear-layer structures in near-wall turbulence 16 p2198 N88-23110
Wave-growth associated with turbulent spot in plane Poiseuille flow 16 p2199 N88-23116
On the prediction of equilibrium states in homogeneous turbulence
[NASA-CR-181659] 16 p2207 N88-23174
Simulation of laminar-turbulent transition in the vicinity of a wall
[AD-A191380] 16 p2208 N88-23180
Random processes, turbulence and disordering fields
[AD-A191399] 16 p2209 N88-23181
Two-equation low-Reynolds-number turbulence modeling of transitional boundary layer flows characteristic of gas turbine blades
[NASA-CR-4145] 16 p2209 N88-23185
Experimental study of bypass transition in a boundary layer
[NASA-TM-100913] 16 p2209 N88-23186
A proposal for the establishment of a center of excellence in theoretical geoplasma research
[AD-A189742] 16 p2231 N88-23327
Measurements of edge turbulence with Langmuir probes in currentless Heliotron E plasmas
[DE88-752313] 16 p2275 N88-23617
Surface curvature and pressure gradient effects on turbulent flow: An assessment based on numerical solution of the Reynolds equations 17 p2338 N88-23954
The effects of inlet turbulence and rotor/stator interactions on the aerodynamics and heat transfer of a large-scale rotating turbine model. Part 4: Aerodynamic data tabulation
[NASA-CR-179469] 17 p2339 N88-23956
Generation of flux tube waves in stellar convection zones. 1: Longitudinal tube waves
[NASA-TM-101152] 17 p2451 N88-24561
Prediction of laminar and turbulent flows past single and twin airfoils 18 p2457 N88-24589
Cross stream differencing for integral boundary layer equations
[AD-A191744] 18 p2509 N88-24886
Fast algorithm development for large-eddy simulation of circular-jet turbulence
[AD-A192044] 18 p2509 N88-24887
Three dimensional spectral energy measurement on turbulence subjected to a high degree of plane deformation
[ETN-88-92537] 18 p2511 N88-24896
Computational Fluid Mechanics
[NASA-CR-183022] 18 p2514 N88-24915
Modelling of thermal plasma systems 18 p2578 N88-25314
Correlations of velocity and temperature fluctuations in the stagnation-point flow of circular cylinder in turbulent flow
[NASA-TM-100930] 19 p2597 N88-25435
Turbulence and flame propagation
[PB87-228912] 19 p2612 N88-25499
Noise generation by air bubbles in water: An experimental study of creation and splitting
[AD-A192063] 19 p2664 N88-25839
Scaling laws for homogeneous turbulent shear flows in a rotating frame
[NASA-CR-181672] 19 p2665 N88-25847
Wind flow study: July 1987 and November-December 1987
[DE88-008969] 20 p2828 N88-26776
Summary of discussions at the Tenth Meeting of the Sandia Cooperative Group on the Aerothermochemistry of Turbulent Combustion
[DE88-008467] 21 p2910 N88-27269
Coupled experimental and theoretical investigations of instability, chaos and turbulence in an axisymmetric jet flow
[AD-A192943] 21 p2942 N88-27476
Characterization of accelerating pipe flow
[AD-A193065] 21 p2943 N88-27481
Tokamak magnetic turbulence over the safety factor range 0.6 less than q less than 3
[DE88-008421] 21 p3017 N88-27904
Project wind, phase 4 (smoke test), Meadow Brook Valley, Red Bluff, California
[AD-A194742] 22 p3128 N88-28596
Aerodynamics of seeing on large transport aircraft
[NASA-CR-183122] 23 p3174 N88-28896
The effects of inlet turbulence and rotor/stator interactions on the aerodynamics and heat transfer of a large-scale rotating turbine model. Volume 3: Heat transfer data tabulation 65 percent axial spacing
[NASA-CR-179468] 23 p3180 N88-28930
The effects of inlet turbulence and rotor/stator interactions on the aerodynamics and heat transfer of a large-scale rotating turbine model. Volume 2: Heat transfer data tabulation. 15 percent axial spacing
[NASA-CR-179467] 24 p3326 N88-29804
Recent insights into instability and transition to turbulence in open-flow systems
[NASA-CR-181693] 24 p3372 N88-30079
Comparisons of solar nebula models 24 p3451 N88-30539

TURBULENCE EFFECTS

Vortex/boundary-layer interactions: Data report, volume 1
[NASA-CR-181462] 02 p0121 N88-10768
Turbulence generation in combustion
[AD-A184810] 05 p0561 N88-13413
Measurement in a wind tunnel of the modification of mean wind and turbulence characteristics due to induction effects near wind turbine rotors
[DE88-000249] 07 p0815 N88-14963
Effects of turbulence on stationary and non-stationary processes in C-systems
[AD-A186215] 07 p0849 N88-15154
Numerical simulation of heat transfer turbulence, volume 2
[AD-A185130] 08 p0983 N88-15947
Numerical simulation of turbulent spots in channel and boundary layer flows 08 p0983 N88-15948
Heat transfer from impinging flame jets
[ETN-88-91610] 09 p1162 N88-16964
Effect of freestream turbulence on a two dimensional cascade, with different surface roughness, at high Reynolds number
[AD-A190615] 15 p2065 N88-22316
High power, high frequency radiation from beam-plasma interactions
[AD-A190207] 15 p2137 N88-22752
Investigation of intensity and phase fluctuations of an acoustic wave after crossing thermal turbulence
[ETN-88-92542] 17 p2395 N88-24238
Design of a mechanism to control wind tunnel turbulence 21 p2926 N88-27370
Turbulence effects on the droplet distribution behind airblast atomizers 24 p3346 N88-29915
Radiation transfer in gas turbine combustors 24 p3348 N88-29929

TURBULENCE METERS

Flight test equipment for the on-board measurement of wind turbulence 24 p3311 N88-29719
A summary of atmospheric turbulence measurements with specially-equipped aircraft in the US 24 p3312 N88-29727
Measurement and analysis of low altitude atmospheric turbulence obtained using a specially instrumented Gnat aircraft 24 p3313 N88-29728

TURBULENCE MODELS

NT K-EPSILON TURBULENCE MODEL

Investigation of the validity of Reynolds averaged turbulence models at the frequencies that occur in turbomachinery
[NASA-CR-182162] 22 p3048 N88-28087
Turbulence modelling of flows with non-uniform density 22 p3075 N88-28258

TURBULENT BOUNDARY LAYER

Experimental study of three-dimensional turbulent jet-solid boundary interaction 01 p0046 N88-10293
Heat transfer with very high free stream turbulence 02 p0186 N88-11161

Computation of turbulent flows using an extended k-epsilon turbulence closure model
[NASA-CR-179204] 03 p0312 N88-11969
An experimental investigation of quasi-conical shock wave/turbulent boundary layer interactions
03 p0317 N88-12004
Visualization of the flow field around a generic destroyer model in a simulated turbulent atmospheric boundary layer
[AD-A184658] 03 p0320 N88-12023
Calculation of three-dimensional stationary turbulent boundary layer on root section of wing ignoring compressibility 04 p0424 N88-12630
An experimental investigation of unsteadiness in swept shock wave/turbulent boundary layer interactions
04 p0445 N88-12760
Heat and moisture transport in the atmospheric boundary layer
[AD-A184222] 04 p0470 N88-12904
The effects of sweep and bluntness on a glancing shock wave turbulent boundary layer interaction
05 p0531 N88-13227
Development of the computer program for turbulent boundary layers 05 p0536 N88-13264
Interferometric data for a shock-wave/boundary-layer interaction
[NASA-TM-88227] 05 p0543 N88-13306
Experimental study of the fluid mechanics of unsteady turbulent boundary layers
[AD-A184856] 05 p0580 N88-13536
Asymptotic analysis of a turbulent boundary layer in a strong adverse pressure gradient
[AD-A185406] 05 p0581 N88-13543
Fluctuating pressure loads under high speed boundary layers
[NASA-TM-100517] 05 p0647 N88-13962
The production of turbulence in boundary layers: The role of microscale coherent motions
[AD-A185568] 06 p0703 N88-14313
Studies of unsteadiness in boundary layers
[AD-A185662] 06 p0703 N88-14315
Measurements of the free stream fluctuations above a turbulent boundary layer
[NASA-TM-100036] 06 p0704 N88-14321
Wall turbulence control 07 p0812 N88-14943
Airfoil large eddy breakup devices for turbulent drag reduction 07 p0814 N88-14956
Fundamental aspects of the structure of supersonic turbulent boundary
[AD-A186366] 07 p0815 N88-14959
Examination of the development of a compressible turbulent boundary layer on a rough and porous wall
[PB87-148266] 07 p0815 N88-14964
Mean velocities and Reynolds stresses in the juncture flow and in the shear layer downstream of an appendage
[AD-A185819] 08 p0980 N88-15923
Approximation of noncorrelated reflections in problem of sound propagation through waveguide with rough boundary 08 p1076 N88-16487
Unsteady behavior of three-dimensional vortices relevant to turbulent boundary layers
[AD-A186767] 09 p1161 N88-16958
Numerical simulation of the interaction of pressure waves with laminar and turbulent boundary layers
[DFVLR-FB-87-18] 09 p1161 N88-16960
A dynamical system/coherent structure approach to the fully developed turbulent wall layer
10 p1267 N88-17578
Burst vortex/boundary layer interaction
[NASA-CR-182510] 10 p1268 N88-17583
Boundary layer calculation using digital computers
[REPT-MM-4] 10 p1309 N88-17821
An experimental investigation of pressure driven three-dimensional turbulent boundary layers
10 p1327 N88-17934
An analysis of the motion and effects of hairpin vortices
[AD-A187261] 10 p1331 N88-17958
The structure and control of three-dimensional shock wave turbulent boundary layer interactions
[AD-A187642] 10 p1332 N88-17961
Shock wave/turbulent boundary layer interaction in high-Reynolds-number hypersonic flows
[AD-A186029] 11 p1434 N88-18555
Fluctuations and massive separation in three-dimensional shock-wave/boundary-layer interactions
[NASA-TM-89224] 11 p1434 N88-18559
Structure of shear flow turbulence and its control
[AD-A187909] 11 p1482 N88-18846
Changes in the turbulent boundary layer structure associated with net drag reduction by outer layer manipulators
[NASA-CR-178152] 11 p1483 N88-18853
A simplified streamline swallowing procedure for the windward meridian of axisymmetric blunt bodies
[AD-A188413] 12 p1626 N88-19732
Research on flow control
[AD-A189014] 12 p1627 N88-19736
Interaction between two-dimensional sonic jets and supersonic flow to model heat addition in a supersonic combustor
[AD-A189572] 13 p1716 N88-20261
Coherent structure-reflective turbulent viscous flow modeling
[AD-A188339] 13 p1765 N88-20556
Slip velocity method for three-dimensional compressible turbulent boundary layers
[NASA-TM-100586] 13 p1771 N88-20592
Research on turbulence in bottom boundary layer in ocean 13 p1788 N88-20697
Unsteady shallowing mixed layer
13 p1805 N88-20791
Flow/acoustic interaction in duct inflow
[AD-A189264] 13 p1833 N88-20967
JPRS report: Science and technology. China
[JPRS-CST-87-023] 14 p1863 N88-21130
Propagation of artificial disturbances immersed in thick turbulent boundary layer 14 p1864 N88-21136
An experimental-computational investigation of transonic shock wave-turbulent boundary layer interaction in a curved test section
[CWI-NM-R8716] 14 p1909 N88-21408
Enhanced viscous flow drag reduction using acoustic excitation
[NASA-CR-182734] 15 p2062 N88-22295
Bodies in unsteady flow
[AD-A190416] 15 p2064 N88-22308
Effect of freestream turbulence on a two dimensional cascade, with different surface roughness, at high Reynolds number
[AD-A190615] 15 p2065 N88-22316
Numerical and experimental investigation of multiple shock wave/turbulent boundary layer interactions in a rectangular duct
[AD-A190772] 15 p2066 N88-22320
Aerothermal tests of quilted dome models on a flat plate at a Mach number of 6.5
[NASA-TP-2804] 15 p2067 N88-22325
Studying Turbulence Using Numerical Simulation Databases. Proceedings of the 1987 Summer Program
[NASA-CR-182692] 16 p2194 N88-23086
Self similarity of two point correlations in wall bounded turbulent flows 16 p2195 N88-23089
Ejection mechanisms in the sublayer of a turbulent channel 16 p2195 N88-23090
Structure of turbulent shear flows
16 p2198 N88-23113
Coherent structures: Comments on mechanisms
16 p2199 N88-23118
Some visualization studies on turbulent boundary layers using multiwire hydrogen bubble generation
16 p2204 N88-23153
Laser Doppler anemometry
[NASA-TM-100072] 16 p2210 N88-23187
Technology Reports of Kyushu University, volume 61, no. 2
[ISSN-0023-2718] 16 p2256 N88-23485
Natural laminar flow and airplane stability and control
17 p2298 N88-23747
Unsteady flow about cambered plates
[AD-A191226] 17 p2337 N88-23945
Fundamental aspects of the structure of supersonic turbulent boundary layers
[AD-A191494] 18 p2456 N88-24581
Computation of the turbulent boundary layer downstream of vortex generators
[AD-A191544] 18 p2508 N88-24881
Theoretical investigation of 3-D shock wave-turbulent boundary layer interactions, part 6
[AD-A191546] 18 p2509 N88-24882
The behavior of drop-containing turbulent eddies
[AD-A191669] 18 p2509 N88-24883
Manipulation of the structure of a turbulent boundary layer 18 p2512 N88-24901
Hypersonic turbulent wall boundary layer computations
[NASA-CR-182147] 18 p2514 N88-24917
Correlations of velocity and temperature fluctuations in the stagnation-point flow of circular cylinder in turbulent flow
[NASA-TM-100930] 19 p2597 N88-25435
Study of the structure of turbulence in accelerating transitional boundary layers
[AD-A191698] 19 p2663 N88-25837
Comparison of the wall pressure fluctuations in artificially generated turbulent spots, natural transition and turbulent boundary layers
[AD-A191777] 19 p2663 N88-25838
Boundary layer development as a function of chamber pressure in the NASA Lewis 1030:1 area ratio rocket nozzle
[NASA-TM-100917] 19 p2664 N88-25841
Drag reduction of turbulent boundary layers by means of grooved surfaces
[ETN-88-92618] 20 p2802 N88-26630
Wind tunnel study of atmospheric diffusion in unstable stratified boundary layer. Part 2: Characteristic scale and diffusion
[DE88-753109] 20 p2823 N88-26749
The diffusion of vorticity from a plane boundary
[AD-A192706] 21 p2942 N88-27474
Experimental study of unsteady separating turbulent boundary layers
[AD-A192997] 21 p2943 N88-27477
The heat transfer and fluid dynamics of concave surface curvature
[AD-A193064] 21 p2943 N88-27479
A documentation of two- and three-dimensional shock-separated turbulent boundary layers
[NASA-TM-101008] 21 p2949 N88-27519
Plasma behavior in the boundary layer near a railgun surface
[DE88-008889] 21 p3017 N88-27909
The dynamic behavior of a turbulent boundary layer subjected to a shock-induced separation
[AD-A194164] 22 p3075 N88-28252
Coupled inviscid - boundary layer methods for turbomachinery blading design
[PNR90437] 22 p3076 N88-28260
A new method of calculating the boundary layer characteristics downstream of manipulators. Part 1: Boundary layer integral parameters
[PNR90455] 22 p3078 N88-28279
Development and analysis of turbulent non-equilibrium boundary layers 23 p3169 N88-28872
Environmental effects on transition and boundary layer characteristics 23 p3170 N88-28876
Stability and drag reduction in a boundary layer with microbubbles
[AD-A191975] 23 p3209 N88-29099
A mapping of the viscous flow behavior in a controlled diffusion compressor cascade using laser Doppler velocimetry and preliminary evaluation of codes for the prediction of stall
[AD-A194490] 23 p3211 N88-29112
A calculation of the turbulent boundary layer on a slender ellipsoid at low incidence
[FFA-TN-1988-02] 23 p3213 N88-29126
Studies of gas turbine heat transfer airfoil surface and end-wall cooling effects
[AD-A195165] 24 p3326 N88-29805
The effects of incoming boundary layer thickness on unsteady shock-induced turbulent separations induced by cylinders
[AD-A196190] 24 p3368 N88-30060
Numerical simulation of the interaction of pressure waves with laminar and turbulent boundary layers
[ESA-TT-1089] 24 p3371 N88-30075
Experimental and numerical investigation of the effect of distributed suction on oblique shock wave/turbulent boundary layer interaction
[NASA-TM-101334] 24 p3372 N88-30084
The thermal behavior of film cooled turbulent boundary layers as affected by longitudinal vortices
[AD-A195155] 24 p3374 N88-30095
Vortex formation and particle transport in a cross-field plasma sheath
[AD-A194838] 24 p3432 N88-30425

TURBULENT DIFFUSION

Experimental study of turbulent diffusion parameters in ocean 04 p0459 N88-12840
Active and passive plume distribution models in the convective boundary layer using a large eddy simulation model
[KNMI-TR-90] 05 p0581 N88-13546
Extinguishing diffusion flames with dry powder and halon at low Froude numbers
[PB87-111365] 06 p0679 N88-14159
Carbon monoxide and turbulence-chemistry interactions: Blowoff and extinction of turbulent diffusion flames
[AD-A186276] 07 p0828 N88-15025
Continuum theories for fluid-particle flows: Some aspects of lift forces and turbulence
[DE88-007038] 18 p2511 N88-24898
Turbulence and flame propagation
[PB87-228912] 19 p2612 N88-25499
Development of an atmospheric diffusion evaluation method incorporating topographical effects. Part 1: Literature review of atmospheric diffusion models incorporating terrain effects
[DE88-753104] 20 p2822 N88-26742

Wind tunnel study of atmospheric diffusion in unstable stratified boundary layer. Part 2: Characteristic scale and diffusion
[DE88-753109] 20 p2823 N88-26749

TURBULENT FLOW
NT CAVITATION FLOW
Reynolds number effects on the small scale structure of a turbulent channel flow 01 p0001 N88-10004
Measurement techniques in low-speed turbulent flows: A report on EUROMECH 202
[NLR-MP-86038-U] 01 p0045 N88-10283
Influence of a magnetic field on the diffusion of small particles in a turbulent flow
[DE87-702877] 01 p0046 N88-10291
Two-dimensional shear flow turbulence: A statistical theory of vortex filaments
[DE87-012234] 01 p0046 N88-10295
Mean flow structure of a turbulent junction vortex
[PB87-208231] 01 p0047 N88-10301
Numerical calculation of the turbulent flow about a cubic body
[ETN-87-90418] 01 p0047 N88-10302
Determination of the dynamic parameters of annular clearances with turbulent flow and incompressible media
[ETN-87-90434] 01 p0047 N88-10303
The influence of high free stream turbulence, intensive cooling and wake on the external heat transfer of convectively cooled gas turbine blades
[ETN-87-90432] 01 p0056 N88-10360
Navier-Stokes cascade analysis with a stiff Kappa-Epsilon turbulence solver
[NASA-TM-100218] 02 p0123 N88-10778
Radiative and free-convective heat transfer from a finite horizontal plate inside an enclosure
02 p0133 N88-10833
On the modelling of non-reactive and reactive turbulent combustor flows 02 p0169 N88-11061
Dimension densities for turbulent systems with spatially decaying correlation functions
[DE87-010119] 02 p0169 N88-11066
Large scale structures in turbulent pipe flow
[MPIS-MITT-83-1987] 02 p0172 N88-11085
The four spot time-of-flight laser anemometer
02 p0184 N88-11145
Correlation of velocity and velocity-density turbulence in the exhaust of an atmospheric burner
02 p0185 N88-11147
Improved numerical methods for turbulent viscous recirculating flows 02 p0185 N88-11148
Aerothermal modeling program, phase 2
02 p0185 N88-11149
Fuel-injector/air-swirl characterization
02 p0185 N88-11150
Measurement of airfoil heat transfer coefficients on a turbine stage 02 p0186 N88-11158
A calculation method for the propulsive jet and its aerodynamic interaction with an afterbody
[ESA-TT-1039] 03 p0259 N88-11632
Numerical simulation of turbulent premixed combustion and decay of turbulent swirling flow
[DE87-014253] 03 p0284 N88-11787
Computation of turbulent flows using an extended k-epsilon turbulence closure model
[NASA-CR-179204] 03 p0312 N88-11969
Special Course on Modern Theoretical and Experimental Approaches to Turbulent Flow Structure and its Modelling
[AGARD-R-755] 03 p0312 N88-11970
Turbulence modelling through one point closures-applications-enlightening by large eddy simulation 03 p0312 N88-11972
Homogeneous turbulence two-point closures and applications to one-point closures
03 p0312 N88-11973
Transition to turbulence via spatio-temporal intermittency 03 p0313 N88-11976
Determination of fractal dimension, connection of space and temporal chaos and application to experimental results 03 p0313 N88-11977
Stochastic model of the motion of suspended particles in turbulent flow
[HSBW-MITT-21/1987] 03 p0315 N88-11990
Analysis of the motions and effects of hairpin vortices
03 p0316 N88-11997
Numerical study of the entrance flow and its transition in a circular pipe (2) 03 p0318 N88-12011
Multidimensional modeling of convective heat transfer with application to I.C. engines
[DE87-014983] 03 p0322 N88-12036
Numerical simulation of internal combustion engine flows: Development and users guide for MAGIC radial-azimuthal version
[DE87-014453] 03 p0332 N88-12091
Optical instrumentation and study of gas-solid suspension flows
[DE88-000147] 04 p0442 N88-12744
Experiments on densely-loaded non-Newtonian slurries in laminar and turbulent pipe flows
[DE88-000719] 04 p0442 N88-12746
Theory of heat and moisture exchange between finely disperse storm-generated spray and turbulent air flow
04 p0461 N88-12851
Numerical analysis of flow through scramjet engine inlets 05 p0532 N88-13233
Numerical prediction of turbulent flows in dump diffusers 05 p0537 N88-13265
Delta wing in incompressible flow. Experimental study in F2
[ONERA-RT-36/1147-AN-249-G]
05 p0541 N88-13298
Interferometric data for a shock-wave/boundary-layer interaction
[NASA-TM-88227] 05 p0543 N88-13306
A numerical study of the effects of curvature and convergence on dilution jet mixing
[NASA-TM-89878] 05 p0549 N88-13347
Statistical theory of turbulent incompressible multimaterial flow
[DE88-000435] 05 p0579 N88-13535
Physical analysis and numerical simulation of coherent turbulent structures in mixed layers, jets, and wakes
[ETN-88-91183] 05 p0581 N88-13548
Hot wire and laser velocimeter studies of turbulent flow at supersonic velocities
[ETN-88-91172] 05 p0585 N88-13566
Analysis of internal flows relative to the space shuttle main engine
[NASA-CR-179240] 06 p0674 N88-14125
Visible boundary layer transition points through flight tests 06 p0675 N88-14136
Summary of discussions at the Ninth Meeting of the Sandia Cooperative Group on the Aerothermochemistry of Turbulent Combustion
[DE88-002281] 06 p0680 N88-14165
Experimental investigation of heterogeneous compressible shear layers 06 p0700 N88-14294
An experimental and numerical investigation of swirling flows in a rectangular nozzle 06 p0700 N88-14295
Extensions of the control volume based finite element method for fluid flow problems 06 p0700 N88-14296
Computation of turbulent flow of air through smooth and rough pipes using a two-equation turbulence model
06 p0700 N88-14298
Flight and wind-tunnel measurements showing base drag reduction provided by a trailing disk for high Reynolds number turbulent flow for subsonic and transonic Mach numbers
[NASA-TP-2638] 06 p0701 N88-14299
Approximate solutions for the momentum transport in turbulent flows in narrow rod array bundles using the finite element method
[ETN-88-90810] 06 p0701 N88-14306
On the subgrid-scale modeling of compressible turbulence
[NASA-CR-178420] 06 p0702 N88-14309
Three-dimensional structure of boundary layers in transition to turbulence
[AD-A185466] 06 p0702 N88-14311
The acoustic source created by turbulent flow over orifices and louvers
[REPT-97674] 06 p0776 N88-14764
A multistage time-stepping scheme for the thin-layer Navier-Stokes equations 07 p0810 N88-14932
Flow diagnostics and visualization in wind tunnels and flight 07 p0811 N88-14940
Overview of the Langley viscous drag reduction program 07 p0812 N88-14946
Natural laminar flow nacelle for transport aircraft
07 p0813 N88-14949
Fundamental aspects of the structure of supersonic turbulent boundary
[AD-A186366] 07 p0815 N88-14959
Turbulence in hypersonic flow
[AD-A185624] 07 p0815 N88-14961
High resolution simulation of turbulent flow in a channel
[AD-A186022] 07 p0848 N88-15150
Effects of turbulence on stationary and non-stationary processes in C-systems
[AD-A186215] 07 p0849 N88-15154
Identification and avoidance of instabilities in high performance turbomachinery 07 p0850 N88-15164
Reynolds-stress and dissipation rate budgets in a turbulent channel flow
[NASA-TM-89451] 07 p0852 N88-15174
Mixing in variable density, isothermal turbulent flows and implications for chemically reacting turbulent flows
[PB88-110044] 07 p0852 N88-15176
Numerical solution of turbulent flow past a backward facing step using a nonlinear K-epsilon model
[NASA-CR-178421] 07 p0854 N88-15189
Chemical reacting flows 08 p0955 N88-15793
Optical measurement systems
08 p0955 N88-15796
Viscous flows, part 1 08 p0986 N88-15967
Introduction to the Modeling of Turbulence
[VKI-LS-81-06] 08 p0986 N88-15972
Examples of turbulence-model applications
08 p0987 N88-15975
Direct and large eddy simulation of turbulence. Summary of the state of art 1987 08 p0987 N88-15977
Turbulence modeling for compressible flows
08 p0987 N88-15978
The effect of eddy distribution on momentum and heat transfer near the wall in turbulent pipe flow
[NASA-TM-100257] 08 p0988 N88-15984
Cavitation inception scale effects. 1. Nuclei distributions in natural waters. 2. Cavitation inception in a turbulent shear flow
[AD-A186553] 08 p0988 N88-15987
Fully turbulent internal flow excitation of pipe systems
08 p1000 N88-16056
Numerical calculation of turbulent recirculating flows
[TUM-LSM-84/29] 09 p1161 N88-16959
Numerical and physical aspects of large eddy simulation of turbulent flows
[ETN-88-91611] 09 p1162 N88-16965
The dynamics of heat transfer at a turbulent pipe flow
[OEFZS-4400] 09 p1164 N88-16975
Solution of the three-dimensional Navier-Stokes equations for transonic flow using a multigrid method
10 p1267 N88-17579
Numerical simulation of axisymmetric turbulent flow in combustors and diffusors
[NASA-CR-4115] 10 p1268 N88-17582
Navier-Stokes calculations and turbulence modeling in the trailing edge region of a circulation control airfoil
10 p1268 N88-17587
Wall jet analysis for circulation control aerodynamics. Part 1: Fundamental CFD and turbulence modeling concepts 10 p1269 N88-17588
Investigations of a circulation control airfoil flowfield using an advanced laser velocimeter
10 p1269 N88-17589
A theory for turbulent curved wall jets
10 p1269 N88-17590
Evaluation of a research circulation control airfoil using Navier-Stokes methods 10 p1269 N88-17591
Development and application of oxygen flow tagging for velocity measurements and flow visualization in turbulent three-dimensional supersonic flows
[AD-A187982] 10 p1289 N88-17714
Fully Lagrangian Renormalized Approximation theory of fluid turbulence
[DE88-004960] 10 p1330 N88-17952
An analysis of the motion and effects of hairpin vortices
[AD-A187261] 10 p1331 N88-17958
La Recherche Aerospatiale, bimonthly bulletin, number 1987-1, 236/January-February
[ESA-TT-1055] 11 p1433 N88-18549
Diagnostics for research in atomization and turbulent two-phase flows
[AD-A187338] 11 p1482 N88-18843
Structure of shear flow turbulence and its control
[AD-A187909] 11 p1482 N88-18846
Kinetic and turbulence models for granular and two-phase flows 11 p1484 N88-18862
A review of approaches to the study of turbulence modification by means of non-Newtonian additives
[AD-A188799] 12 p1627 N88-19734
Wavenumber - frequency structure of turbulent flow in a channel from a direct simulation
[AD-A189079] 12 p1627 N88-19737
Time-accurate simulations of a shear layer forced at a single frequency
[NASA-TM-100836] 12 p1628 N88-19740
Reynold stress closure in jet flows using wave models
[NASA-CR-182662] 12 p1628 N88-19741
Coherent structure-reflective turbulent viscous flow modeling
[AD-A188339] 13 p1765 N88-20556
Control of structure in turbulent flows: Bifurcating and blooming jets
[AD-A189607] 13 p1766 N88-20562
The influence of Mach number and heat transfer on the turbulent flow wall law
[NASA-TT-20230] 13 p1771 N88-20594
Research on flow around bluff bodies, flow induced vibrations 14 p1864 N88-21135
Numerical simulation of turbulent premixed combustion and decay of turbulent swirling flow
[DE88-006588] 14 p1888 N88-21284
Study on the burnout with variations of flow twisting over tube length
[DE87-703170] 14 p1909 N88-21405

Mean flow structure in the near wake of a turbulent junction vortex
[PB88-150115] 14 p1910 N88-21416
Accuracy requirements and benchmark experiments for CFD validation
[NASA-TM-100087] 14 p1911 N88-21423
Two-fluid turbulence models and reciprocating engines
[CFD/87/6] 14 p1918 N88-21449
Turbulent reacting flows and supersonic combustion
[AD-A189690] 15 p2034 N88-22115
An investigation of flow structure, mixing and chemical reaction in combusting turbulent flows
[AD-A189980] 15 p2034 N88-22117
Duct flow nonuniformities: Effect of struts in SSME HGM II(+)
[NASA-CR-179285] 15 p2062 N88-22296
Chemically reacting turbulent flow
[AD-A190522] 15 p2065 N88-22311
Experiments on densely-loaded non-Newtonian slurries in laminar and turbulent pipe flows
[DE88-006209] 15 p2067 N88-22323
Development of subminiature multi-sensor hot-wire probes
[NASA-TM-100052] 15 p2069 N88-22336
Describing the source created by turbulent flow over orifices and louvers
[AD-A190254] 15 p2130 N88-22706
Studying Turbulence Using Numerical Simulation Databases. Procedings of the 1987 Summer Program
[NASA-CR-182692] 16 p2194 N88-23086
Stochastic estimation of conditional eddies in turbulent channel flow 16 p2194 N88-23087
A low dimensional dynamical system for the wall layer
16 p2194 N88-23088
Self similarity of two point correlations in wall bounded turbulent flows 16 p2195 N88-23089
Validation of EDQNM for subgrid and supergrid models 16 p2195 N88-23092
Angular distribution of turbulence in wave space
16 p2195 N88-23093
Big whorls carry little whorls 16 p2195 N88-23094
Study of one-dimensional spectral dynamic equations of the Reynolds stresses in homogeneous anisotropic turbulence: Application to split-spectrum modeling
16 p2196 N88-23095
Modeling scalar flux and the energy and dissipation equations 16 p2196 N88-23096
Direct numerical simulation of buoyantly driven turbulence 16 p2196 N88-23097
Premixed turbulent flame calculation
16 p2196 N88-23098
Modeling of turbulent transport as a volume process
16 p2196 N88-23099
Analysis of non-premixed turbulent reacting flows
16 p2196 N88-23100
A statistical investigation of the single-point pdf of velocity and vorticity based on direct numerical simulations 16 p2196 N88-23101
Local structure of intercomponent energy transfer in homogeneous turbulent shear flow
16 p2197 N88-23103
A general form for the dissipation length scale in turbulent shear flows 16 p2197 N88-23104
Test code for the assessment and improvement of Reynolds stress models 16 p2197 N88-23105
The decay of isotropic turbulence in a rapidly rotating frame 16 p2197 N88-23107
Evaluation of a theory for pressure-strain rate
16 p2198 N88-23108
Conditionally-averaged structures in wall-bounded turbulent flows 16 p2198 N88-23112
Structure of turbulent shear flows
16 p2198 N88-23113
Inflectional instabilities in the wall region of bounded turbulent shear flows 16 p2199 N88-23114
Active layer model for wall-bounded turbulence
16 p2199 N88-23115
Coherent structures: Comments on mechanisms
16 p2199 N88-23118
Coherent structures and dynamical systems
16 p2199 N88-23119
Coherent structures and modeling: Some background comments 16 p2199 N88-23120
Coherent structures --- in turbulent flows
16 p2199 N88-23121
Experimental studies of vortex flows
[NASA-CR-182874] 16 p2207 N88-23171
Random processes, turbulence and disordering fields
[AD-A191399] 16 p2209 N88-23181
Investigation of subgrid models in homogeneous incompressible turbulence
[ONERA-RSF-13/3419-AY-106-A]
16 p2209 N88-23183
Numerical simulation of scramjet inlet flow fields
[NASA-TP-2517] 17 p2296 N88-23735

Theoretical prediction of single phase turbulent flow distribution in particulate bed reactors
17 p2419 N88-24386
Fundamental aspects of the structure of supersonic turbulent boundary layers
[AD-A191494] 18 p2456 N88-24581
Wave growth associated with turbulent spots in plane Poiseuille flow
[FFA-TN-1988-08] 18 p2457 N88-24587
Application of Rayleigh scattering to turbulent flow with heat transfer and combustion
[AD-A191585] 18 p2481 N88-24720
Analysis of molecular mixing and chemical reaction in mixing layer
[AD-A191600] 18 p2482 N88-24721
Stagnating turbulent reacting flows
[AD-A191449] 18 p2508 N88-24877
Study of mixing and reaction in the field of a vortex
[AD-A191489] 18 p2508 N88-24878
Dynamics and control of turbulent shear flows
[AD-A191527] 18 p2508 N88-24879
Injection of drag reducing additives into turbulent water flows
[AD-A192072] 18 p2509 N88-24888
CFD benefits, goals, stepping-stones and techniques. Proposals for the scientific programme of the European Reserch Centre on flow, turbulence and combustion --- computational fluid dynamics
[CFDU/88/1] 18 p2510 N88-24894
Duct flow nonuniformities for Space Shuttle Main Engine (SSME)
[NASA-CR-179338] 18 p2511 N88-24899
Numerical solutions of the complete Navier-Stokes equations
[NASA-CR-183023] 18 p2514 N88-24914
Finite element solution of 3-D turbulent Navier-Stokes equations for propeller-driven slender bodies
18 p2515 N88-24919
Instrumentation for turbulent reacting flows
[AD-A191671] 18 p2515 N88-24923
Low frequency electrostatic turbulence in the polar cap E-region
[DRI-3-88] 18 p2540 N88-25077
Improved numerical methods for turbulent viscous recirculating flows
[NASA-CR-180852] 19 p2599 N88-25445
Coal particle behaviour in a counter-current combustor
[TAE-606] 19 p2612 N88-25498
Atomization in a turbulent shear layer: Preliminary measurements 19 p2624 N88-25565
Anatomy of group burning mode transitions in spray group combustion 19 p2626 N88-25578
Numerical simulation of transition to turbulence in plane Poiseuille flow by a spectral method
19 p2640 N88-25661
Numerical simulation of turbulent flow using the exponential expression of k-Epsilon equation
19 p2640 N88-25662
Superfluid turbulence in counterflowing helium II
19 p2665 N88-25849
Numerical simulation studies of laminar-turbulent transition in the plan channel 19 p2665 N88-25850
Pressure drop and heat transfer in turbulent non-Newtonian pipe flow of advanced energy transmission fluids
[DE88-010021] 19 p2666 N88-25853
Navier-Stokes code NS3D for blunt bodies. Part 1: Analysis, results and verification
[DE88-010105] 19 p2666 N88-25855
Direct simulations of chemically reacting turbulent mixing layers, part 2
[NASA-CR-180853] 19 p2667 N88-25857
Influence of rear body geometry on the velocity characteristics of the near wake
[ISL-R-113/87] 20 p2753 N88-26339
The effect of a turbulent airstream on a vertically-launched missile at high angles of attack
[AD-A192408] 20 p2758 N88-26363
An efficient computational tool for ramjet combustor research
[DE88-010034] 20 p2760 N88-26369
Heterogeneous diffusion flame stabilization
[AD-A193014] 20 p2771 N88-26429
Turbulence transition in a circular pipe
20 p2782 N88-26503
Nonlinear equation of state effects and the momentum-dilution trade-off in a turbulent buoyant jet
[DE88-701839] 20 p2799 N88-26610
Experiments on densely-loaded non-Newtonian slurries in laminar and turbulent pipe flows
[DE88-010579] 20 p2800 N88-26612
Experimental investigation of turbulent flow in smooth and longitudinal grooved tubes
[NASA-TM-77480] 20 p2800 N88-26615

Treatment of the separated flow around profiles (nonviscous, incompressible, two dimensional flow) by the singularities method
[ISL-R-106/87] 20 p2803 N88-26633
Evolution of hairpin vortices in a shear flow
[NASA-TM-100858] 20 p2845 N88-26885
Velocity measurements and flow visualization in turbulent three-dimensional supersonic flows using oxygen flow tagging
[AD-A192551] 21 p2892 N88-27165
The structure and stability of nonpremixed gas jet flames 21 p2908 N88-27257
Premixed turbulent flame propagation
[AD-A192955] 21 p2909 N88-27265
Summary of discussions at the Tenth Meeting of the Sandia Cooperative Group on the Aerothermochemistry of Turbulent Combustion
[DE88-008467] 21 p2910 N88-27269
Design of a mechanism to control wind tunnel turbulence 21 p2926 N88-27370
Predicting optical degradation of a laser beam through a turbulent shear layer 21 p2927 N88-27376
Numerical experiments on turbulent mixing
[AD-A192572] 21 p2942 N88-27473
Turbulence structure of mixing swirling flows
[AD-A193063] 21 p2943 N88-27478
Physical mechanisms in shock-induced turbulent separated flow
[AD-A193165] 21 p2944 N88-27484
Cavitation inception in a turbulent shear flow
[DE88-011486] 21 p2946 N88-27497
Laser-Doppler measurements of turbulence structures in free streams behind flat and rotation symmetrical profiles
[ETN-88-92336] 21 p2948 N88-27510
Numerical computation of three-dimensional turbulent flow in tightly curved ducts and spiral turbine casings
[ETN-88-92362] 21 p2948 N88-27511
Investigations on drag reduction in turbulent pipe flows by addition of ionic and nonionic high polymers
[ETN-88-92380] 21 p2949 N88-27515
Turbulent flow field visualization with integral interferometric imaging and computed tomography
21 p2950 N88-27521
Photon limited image processing in the space-time domain
[AD-A193142] 21 p2972 N88-27655
The influence of surface rounding on trailing edge noise
[AD-A193387] 21 p3012 N88-27876
The application of the two-fluid model of turbulence to the 3-D simulation of turbulent combustion in reciprocating engines
[PDR/CFDU/IC/37] 22 p3052 N88-28110
Interactions between coherent structures and premixed flame fronts
[ETN-88-92885] 22 p3053 N88-28111
Flow dynamics stimulated by hairpin-like vortices in initially laminar boundary layers
[AD-A194253] 22 p3075 N88-28254
Investigations of rough surface effects on friction factors in turbulent pipe flow
[AD-A193774] 22 p3075 N88-28255
Development and application of a finite element method to compute strongly heated turbulent flows
[ECL-88-02] 22 p3077 N88-28267
Calibration of a triple wire probe for turbulence measurements
[AD-A193956] 22 p3081 N88-28296
Small scale mixing in the initial region of a jet
[AD-A193500] 23 p3192 N88-28994
Three-dimensional laser Doppler velocimeter studies of flow in a 90 deg curved duct having a square cross-section 23 p3209 N88-29101
A numerical study of turbulent plane jets in still and flowing environments employing two-equation k-epsilon model 23 p3211 N88-29109
Modeling of momentum transport of axially parallel turbulent flows in rod cascades
[ETN-88-92978] 23 p3214 N88-29131
Aerodynamic heating of missiles
24 p3319 N88-29764
Flamelet modeling of turbulent premixed flames
24 p3350 N88-29942
Modeling the stability of a turbulent premixed flame, downstream from a step by a Lagrangian method
24 p3350 N88-29943
Modeling and experimental study of a reactive flow confined with well injection 24 p3351 N88-29946
Approximation of viscoelastic stresses from Newtonian turbulent kinematics
[AD-A194317] 24 p3371 N88-30077
Boltzmann equation approach to two-phase flow turbulence
[AD-A196153] 24 p3373 N88-30086

Analysis method for the production of Reynolds stresses in compressible turbulent flow (fluid mechanics)
[NASA-TT-20330] 24 p3373 N88-30088
Development of a more general Reynolds stress closure for swirling flow
[AD-A195121] 24 p3374 N88-30092

TURBULENT HEAT TRANSFER
The influence of high free stream turbulence, intensive cooling and wake on the external heat transfer of convectively cooled gas turbine blades
[ETN-87-90432] 01 p0056 N88-10360
Heat and moisture transport in the atmospheric boundary layer
[AD-A184222] 04 p0470 N88-12904
The development and evaluation of three-dimensional models of cold flow in internal combustion engines
[DE88-900077] 05 p0589 N88-13594
Effects of turbulence on stationary and non-stationary processes in C-systems
[AD-A186215] 07 p0849 N88-15154
Weak interactions and local order in strong turbulence 09 p1159 N88-16948
Heat transfer from impinging flame jets
[ETN-88-91610] 09 p1162 N88-16964
Wake interaction effects on the transition process on turbine blades
[AD-A188020] 10 p1332 N88-17962
Mixed turbulent convective heat transfer in vertical ducts 11 p1485 N88-18865
Turbulent transfer of momentum and heat in boundary layer of fluid beyond an obstacle. 1: Hydrodynamic characteristics 13 p1787 N88-20690
Vertical turbulent transfer of matter in thin ocean surface layer during daytime heating 13 p1787 N88-20693
Equatorial turbulence: Mixed layer and thermocline 13 p1804 N88-20787
Application of Rayleigh scattering to turbulent flow with heat transfer and combustion
[AD-A191565] 18 p2481 N88-24720
Stagnating turbulent reacting flows
[AD-A191449] 18 p2508 N88-24877
Turbulent heat transfer and fluid flow measurements downstream of abrupt expansions and in a cavity of a circular tube at a uniform wall temperature 18 p2515 N88-24920
Study of the structure of turbulence in accelerating transitional boundary layers
[AD-A191698] 19 p2663 N88-25837
Multidimensional modeling of convective heat transfer with application to I.C. engines
[DE88-007446] 19 p2738 N88-26257
The heat transfer and fluid dynamics of concave surface curvature
[AD-A193064] 21 p2943 N88-27479
Studies of gas turbine heat transfer airfoil surface and end-wall cooling effects
[AD-A195165] 24 p3326 N88-29805

TURBULENT JETS
Experimental study of three-dimensional turbulent jet-solid boundary interaction 01 p0046 N88-10293
Combustion in turbulent jets and buoyant flames
[PB87-232674] 03 p0283 N88-11779
Laser Doppler measurements in a turbulent free jet
[ESA-TT-1067] 03 p0315 N88-11994
Comparative studies in the near-field of turbulent transports of heated and unheated jets normal to a cross stream 04 p0444 N88-12756
Conditional second order closure for turbulent shear flows
[AD-A185369] 05 p0581 N88-13542
A computational study of thrust augmenting ejectors based on a viscous-inviscid approach 10 p1326 N88-17929
Turbulence interactions in single- and multi-phase turbulent mixing and combustion processes
[AD-A187505] 10 p1332 N88-17960
Active feedback interaction with a shear layer
[AD-A188525] 12 p1573 N88-19410
Control of structure in turbulent flows: Bifurcating and blooming jets
[AD-A189607] 13 p1766 N88-20562
The structure of sonic underexpanded turbulent air jets in still air
[AD-A190856] 16 p2157 N88-22870
Noncondensing round turbulent gas jets in liquids
[AD-A191191] 16 p2208 N88-23179
Effect of initial tangential velocity distribution on the mean evolution of a swirling turbulent free jet
[NASA-TM-100934] 18 p2458 N88-24592
Particle-laden weakly swirling free jets: Measurements and predictions
[NASA-TM-100920] 18 p2466 N88-24639
Hydroacoustic pulsating jet generator
[MPIS-7/1987] 18 p2510 N88-24891
Coherent structures in the axisymmetric turbulent jet mixing layer 21 p2947 N88-27504

TURBULENT MIXING
Momentum transport and particle dynamics in turbulent shear flows 03 p0317 N88-12002
Blowup for a nonlinear evolution equation and self-reproducing strained shear layers 04 p0444 N88-12755
Turbulent mixing in a rotating, stratified fluid 04 p0445 N88-12759
Chemical reactions in turbulent mixing flows
[AD-A186141] 07 p0849 N88-15153
On the pairing process in an excited, plane, turbulent mixing layer
[AD-A186355] 07 p0850 N88-15157
Mixing in variable density, isothermal turbulent flows and implications for chemically reacting turbulent flows
[PB88-110044] 07 p0852 N88-15176
Turbulence interactions in single- and multi-phase turbulent mixing and combustion processes
[AD-A187505] 10 p1332 N88-17960
Unsteady shallowing mixed layer 13 p1805 N88-20791
Radiative processes affecting ocean mixed-layer heat content and their monitoring from satellite 13 p1806 N88-20800
Coherent structure 16 p2199 N88-23117
Experimental studies of vortex flows
[NASA-CR-182874] 16 p2207 N88-23171
The spreading and mixing of dense gas clouds in still air
[KNMI-WR-87-12] 16 p2230 N88-23320
Study of mixing and reaction in the field of a vortex
[AD-A191489] 18 p2508 N88-24878
Measurement of burning rates of NOSOL-363 propellants under cross-flow and strand burner conditions using real-time X-ray radiography 19 p2623 N88-25560
Direct simulations of chemically reacting turbulent mixing layers, part 2
[NASA-CR-180853] 19 p2667 N88-25857
Numerical experiments on turbulent mixing
[AD-A192572] 21 p2942 N88-27473
Coherent structures in the axisymmetric turbulent jet mixing layer 21 p2947 N88-27504

TURBULENT WAKES
NT PROPELLER SLIPSTREAMS
NT SLIPSTREAMS
The influence of high free stream turbulence, intensive cooling and wake on the external heat transfer of convectively cooled gas turbine blades
[ETN-87-90432] 01 p0056 N88-10360
A natural low frequency oscillation in the wake of an airfoil near stalling conditions
[NASA-TM-100213] 02 p0123 N88-10779
Calculations of the turbulent wake behind a slender self-propelled double-body and comparisons with experiment
[AD-A185661] 06 p0703 N88-14314
Investigation of large-scale structures in the near wake of a parallel flat plate
[DFVLR-FB-87-31] 09 p1162 N88-16967
Coherent vortex structures in the wake of a stationary disk and of a disk excited to vibration
[ESA-TT-994] 09 p1163 N88-16968
SAR (Synthetic Aperture Radar) imaging of ship wakes in the Gulf of Alaska
[AD-A186554] 10 p1317 N88-17872
Wake interaction effects on the transition process on turbine blades
[AD-A188020] 10 p1332 N88-17962
Structure of shear flow turbulence and its control
[AD-A187909] 11 p1482 N88-18846
Active feedback interaction with a shear layer
[AD-A188525] 12 p1573 N88-19410
Effect of freestream turbulence on a two dimensional cascade, with different surface roughness, at high Reynolds number
[AD-A190615] 15 p2065 N88-22316
Characteristics of merging shear layers and turbulent wakes of a multi-element airfoil
[NASA-TM-100053] 18 p2511 N88-24900
Numerical simulation and stability analysis of the absolutely and convectively unstable wake
[DFVLR-FB-88-09] 21 p2949 N88-27518
Hot-wire measurements of compressor blade wakes in a cascade wind tunnel
[AD-A194737] 23 p3181 N88-28936
Investigation of large-scale structures in the near wake of a parallel flat plate
[ESA-TT-1100] 24 p3372 N88-30080

TURING MACHINES
Machine models and simulations
[PB88-118690] 10 p1386 N88-18280
A labeling procedure for linear finite-state codes 11 p1472 N88-18781
Further results on finite-state codes 11 p1472 N88-18782
ESKISS: A program for optimal state assignment
[EUT-87-E-167] 14 p1956 N88-21659
Tape versus queue and stacks: The lower bounds
[CWI-CS-R8752] 16 p2249 N88-23437
Simple multireader registers using time-stamp schemes
[CWI-CS-R8758] 20 p2835 N88-26819

TURKEY
Karst and submarine fresh water discharge in the Antalya area, southern Turkey 22 p3102 N88-28421

TVC (CONTROL)
U THRUST VECTOR CONTROL

TWENTY-SEVEN DAY VARIATION
Short term variability between 120 and 300 mm from Solar Mesosphere Explorer (SME) observations
[AERONOMICA-ACTA-A-328-1988] 23 p3308 N88-29709

TWINNING
The structure and properties of twin boundaries in superconducting YBa2Cu3O7
[DE88-003864] 10 p1418 N88-18468
Single-crystal structural study of La2Cu/sub 0.95/Li/sub 0.05/O4
[DE88-003482] 11 p1554 N88-19302
Materials dependence of deformation texture development in various deformation modes
[DE88-004312] 14 p1922 N88-21457
To the twinning plane superconductivity theory
[DE88-702195] 20 p2874 N88-27058

TWISTING
Magnetic field twist driven by remote convective motions: Characteristics and twist rates 01 p0113 N88-10724
Twisted cube
[PB87-162814] 09 p1220 N88-17316
Magnetization studies of multifilamentary Nb3Sn wires
[DE88-009103] 19 p2735 N88-26243

TWO BODY ORBITS
U TWO BODY PROBLEM

TWO BODY PROBLEM
Propagation of random initial conditions in time 04 p0486 N88-12993
The avoidance of collisions for Newtonian bodies with hidden variables
[RSRE-87013] 22 p3041 N88-28053

TWO DIMENSIONAL BODIES
A critical assessment of wind tunnel results for the NACA 0012 airfoil
[NASA-TM-100019] 03 p0260 N88-11636
Development of the computer program for turbulent boundary layers 05 p0536 N88-13264
Rarefied gas numerical wind tunnel. 2: Two-dimensional and axially symmetric bodies 05 p0538 N88-13273
Three-dimensional flow past a two-dimensional body 05 p0539 N88-13280
Computation of flow around 2-D circular cylinder 05 p0539 N88-13284
Navier-Stokes analysis of laminar flow control of a two-dimensional airfoil 05 p0540 N88-13286
SUSIE reference manual
[DE88-001462] 05 p0636 N88-13893
Potential flow around two-dimensional airfoils using a singular integral method
[NASA-CR-182345] 06 p0664 N88-14070
Electromagnetic propagation in PEC and absorbing curved S-ducts
[NASA-TM-100833] 12 p1621 N88-19698
Nonlinear resonance of two-dimensional ion layers
[AD-A188890] 12 p1695 N88-20145
Organic metal (ET)4Hg3Br8A quasi-two-dimensional superconductor 14 p1974 N88-21778
Boundary shape identification problems in two-dimensional domains related to thermal testing of materials
[NASA-CR-181654] 15 p2105 N88-22541
Two-dimensional graphics tools for a transputer based display board
[NASA-TM-100820] 15 p2113 N88-22591
A finite-element alternating method for two-dimensional Mode-1 crack configurations
[NASA-TM-100616] 16 p2224 N88-23276
Preliminary 2-D shell analysis of the space shuttle solid rocket boosters
[NASA-TM-100515] 17 p2348 N88-23989

TWO DIMENSIONAL BOUNDARY LAYER
Prediction of turbine blade heat transfer 02 p0187 N88-11162
Numerical simulation of unsteady separated flows
[AD-A184132] 04 p0442 N88-12741
An experimental investigation of the ignition and flammability limits of various hydrocarbon fuels in a two-dimensional solid fuel ramjet
[AD-A184968] 05 p0549 N88-13342
Boundary layer calculation using digital computers
[REPT-MM-4] 10 p1309 N88-17821

Experimental investigation of two-dimensional confined jet thrust vector control
[AD-A189845] 15 p2027 N88-22077

TWO DIMENSIONAL FLOW
NT COUETTE FLOW
A transonic model representation for two-dimensional wall interference assessment
[NLR-TR-86026-U] 01 p0001 N88-10006
An inviscid model of planar, separated flows of finite extent
[RAE-TR-86070] 01 p0044 N88-10279
Rayleigh-Benard convection in a Hele-Shaw cell: A numerical study
[KFK-4212] 01 p0044 N88-10280
Generation of body-fitted grids for two dimensional interior domains by the solution of a system of Poisson equations using multigrid techniques
[GMD-246] 01 p0044 N88-10281
Two-dimensional shear flow turbulence: A statistical theory of vortex filaments
[DE87-012234] 01 p0046 N88-10295
Locating parallel numerical tasks in the solution of viscous fluid flows
[DE87-013510] 02 p0169 N88-11064
Point vortex dynamics: Recent results and open problems
[DE87-014759] 03 p0314 N88-11982
Numerical calculation of two dimensional fluid flow with strong shocks
[KFK-4191] 03 p0314 N88-11986
Conjugated heat transfer from a radiating fluid in a rectangular channel 03 p0317 N88-12003
Solution of the two-dimensional Euler equations on unstructured triangular meshes
04 p0396 N88-12469
A free-Lagrange method for 2-D compressible flows
[DE88-000216] 04 p0442 N88-12745
Continuation finite element analysis of viscoelastic fluids 04 p0445 N88-12761
Computation of dynamic stall of NACA0012 airfoil by block pentadiagonal matrix scheme
05 p0535 N88-13255
Practical application of two-dimensional viscous flow computation 05 p0535 N88-13257
The role of computation fluid dynamics in aeronautical engineering (4). The development and applications of implicit TVD finite volume code
05 p0536 N88-13259
Numerical analysis of cascade flow isolving Navier-Stokes equations 05 p0536 N88-13262
Inverse design method for two-dimensional transonic cascades 05 p0536 N88-13263
Numerical prediction of turbulent flows in dump diffusers 05 p0537 N88-13265
Three-dimensional structure of boundary layers in transition to turbulence
[AD-A185466] 06 p0702 N88-14311
Upwind relaxation algorithms for Euler/Navier-Stokes equations 07 p0810 N88-14931
An explicit method for the solution of the Euler equations, applied to unsteady two dimensional flows
[ETN-88-90807] 07 p0855 N88-15194
Parametric study of choke flutter with a linear theory
10 p1283 N88-17673
A numerical study of unsteady two-dimensional subsonic compressible base flow 10 p1327 N88-17931
Well-posedness and spectral estimation for infinite dimensional systems
[AD-A187621] 10 p1401 N88-18354
An experimental investigation of straight and curved annular wall jets
[NASA-CR-182546] 11 p1434 N88-18557
Experimental study of two-dimensional vortex patterns for impulsively started bodies in comparison with other configurations 11 p1435 N88-18562
Two and three dimensional elliptic flows
11 p1485 N88-18866
A generalisation of Hall's scheme for solving the Euler equations for two-dimensional flows
11 p1537 N88-19188
A multigrid solver for two-dimensional transonic full potential flow calculations 11 p1538 N88-19189
Application of a flux vector splitting methodology towards the solution of unsteady transonic flows, with future emphasis on the blade flutter problem
[AD-A189500] 13 p1716 N88-20260
Solution of two-dimensional Euler equations: Experience with a finite volume code
[DFVLR-FB-87-41] 13 p1767 N88-20572
An explicit method for the solution of the Euler equations applied to unsteady two-dimensional flows
[MBB/LKE-121/S/PUB/257] 14 p1910 N88-21411
Random-choice based hybrid methods for one and two dimensional gas dynamics
[CAR-88-01] 14 p1910 N88-21415
Flexiwall 3 SO: A second order predictive strategy for rapid wall adjustment in two-dimensional compressible flow
[NASA-CR-181662] 15 p2015 N88-22018
Effect of freestream turbulence on a two dimensional cascade, with different surface roughness, at high Reynolds number
[AD-A190615] 15 p2065 N88-22316
Application of a multigrid method for solving the Navier-Stokes equation in two-dimensional flow problems
[KU-SFB-210/T/32] 16 p2206 N88-23164
Accounting for the effects of unsteady, separated boundary layers in transonic two dimensional calculations
[ONERA-RT-30/3064-RY-063-R]
17 p2338 N88-23952
Surface curvature and pressure gradient effects on turbulent flow: An assessment based on numerical solution of the Reynolds equations 17 p2338 N88-23954
Prediction of laminar and turbulent flows past single and twin airfoils 18 p2457 N88-24589
Gas diffusion studies in steady and nonsteady cavities
18 p2512 N88-24902
A characteristic method for calculating the generalized flat flutter aerodynamic forces
[NASA-TT-20300] 19 p2598 N88-25438
Two-dimensional viscous flow computations of hypersonic scramjet nozzle flowfields at design and off-design conditions
[NASA-CR-182150] 19 p2603 N88-25459
One person's view of velocity-coupled instability
19 p2629 N88-25595
An initial investigation into methods of computing transonic aerodynamic sensitivity coefficients
[NASA-CR-183061] 20 p2752 N88-26332
Calculation of 2-D unsteady transonic full potential flow about oscillating airfoils by two complementary approaches
[PB88-127519] 20 p2753 N88-26341
Heterogeneous diffusion flame stabilization
[AD-A193014] 20 p2771 N88-26429
A numerical simulation of two-dimensional transient shear flow
[ISAS-RN-627] 20 p2797 N88-26600
Treatment of the separated flow around profiles (nonviscous, incompressible, two dimensional flow) by the singularities method
[ISL-R-106/87] 20 p2803 N88-26633
Implicit finite-difference simulation of an internal flow on a hypercube
[AD-A192474] 21 p2942 N88-27471
The calculation of the flow through a two-dimensional faired diffuser
[PNR90433] 22 p3076 N88-28259
Two-dimensional flow through a turbine cascade
[PDR/CFDU/IC/34] 22 p3076 N88-28264
Mass transport in flow of sources
[LRT-WE-9-FB-4(1987)] 22 p3077 N88-28268
Regular and chaotic motion of fluid particles in a two dimensional fluid
[PREPRINT-591] 22 p3078 N88-28278
Holographic flow visualization
[PNR90466] 22 p3079 N88-28283
Analysis and optimization of truncated scarf nozzles subject to external flow conditions
[NASA-TM-100955] 24 p3316 N88-29746
Numerical modelling of premixed flames in gaseous media 24 p3350 N88-29944

TWO DIMENSIONAL JETS
Techniques utilized in the simulated altitude testing of a 2D-CD vectoring and reversing nozzle
[NASA-TM-100872] 19 p2604 N88-25464

TWO DIMENSIONAL MODELS
Two-dimensional numerical modeling of the life cycle of fog 02 p0209 N88-11311
Two-dimensional static otolith model
10 p1367 N88-18167
Stability requirement FOT ignition and high gain implosion = 2-D simulation for high neutron yield experiment = 1F p2278 N88-23633
Theoretical study and numerical simulation of flame fronts
[PB88-122932] 22 p3051 N88-28104

TWO FLUID MODELS
A two-fluid model for solar wind fluid with higher order moments 01 p0116 N88-10739
International workshop on two-phase flow fundamentals
[DE88-001478] 06 p0699 N88-14287
Two-fluid turbulence models and reciprocating engines
[CFD/87/6] 14 p1918 N88-21449
ATHENA simulation of the 300 kW SP-100
17 p2414 N88-24357
Computer simulation of turbulent combustion in reciprocating engines
[CFDU/87/11] 18 p2482 N88-24725
The application of the two-fluid model of turbulence to the 3-D simulation of turbulent combustion in reciprocating engines
[PDR/CFDU/IC/37] 22 p3052 N88-28110

TWO PHASE FLOW
Thermal Control Working Group report
01 p0016 N88-10094
The numerical simulation of an idealised one-dimensional, steady monopropellant rocket
[PDR/CFDU/IC/31] 01 p0018 N88-10107
Research on one-dimensional two-phase flow. Theory on hydrodynamic balance in two fluid model and its application
[DE87-702615] 01 p0045 N88-10290
Two-phase non-Newtonian hydrodynamic modeling of slurries
[DE87-011519] 01 p0047 N88-10298
Problem specifications and collated solutions of the two-phase numerical-benchmark exercise 1986-7 — two phase flow
[CFDU/87/1] 01 p0047 N88-10300
Numerical simulation of transient two-phase flow
[CFDU/87/4] 02 p0171 N88-11077
Computer modeling of two-phase flow
[CFDU/87/5] 02 p0171 N88-11078
The dynamics of bubble growth for Rayleigh-Taylor unstable interfaces
[AD-A184752] 03 p0321 N88-12027
A study of two-phase flow in a reduced gravity environment
[NASA-CR-172035] 04 p0422 N88-12617
Geometric analysis of ensemble of solutions in two-phase flow and complete resolution of problem of choking
[DE88-001687] 04 p0445 N88-12764
Analysis of internal flows relative to the space shuttle main engine
[NASA-CR-179240] 06 p0674 N88-14125
International workshop on two-phase flow fundamentals
[DE88-001478] 06 p0699 N88-14287
Theoretical and numerical analysis of shock wave propagation through different dusty-gas mixture layers
06 p0699 N88-14292
An investigation into flow regimes for two-phase helium flow
[DE88-002834] 07 p0853 N88-15181
Influence of the friction coefficients, the power and the flowrate on the two-phase flow instabilities in natural circulation
[DE88-700036] 08 p0983 N88-15946
A review of two-phase flow-induced vibration
[DE88-001955] 09 p1160 N88-16955
Two-phase flow forms and pressure drop in horizontal T tube joints with vertical branch
[GKSS-87/E/12] 09 p1163 N88-16969
An analysis of the closure conditions for two-fluid models of two-phase flow
[DE88-003355] 09 p1164 N88-16982
An experiment to investigate Rankine cycle two-phase microgravity issues
[DE88-004197] 10 p1308 N88-17818
Boundary integral analysis of flow and deformation of long bubbles in capillaries
[DE88-002110] 10 p1326 N88-17927
Mechanistic model for void distribution in flashing flow
[DE88-002948] 10 p1326 N88-17928
Digital imaging techniques for single- and multi-phase reacting flowfields 10 p1327 N88-17933
A review of flow-induced vibration in two-phase flow
[DE88-002873] 10 p1329 N88-17946
Experimental investigation of low gravity two-phase flow behavior
[DE88-003779] 11 p1466 N88-18741
Diagnostics for research in atomization and turbulent two-phase flows
[AD-A187338] 11 p1482 N88-18843
Kinetic and turbulence models for granular and two-phase flows 11 p1484 N88-18862
To the problem of determining true volume steam content by measured values of mean density of a mixture in thermally unsteady two-phase flows
[DE88-700840] 12 p1626 N88-19726
Two-phase flows in the wake of in-cylinder projectiles
[AD-A189422] 13 p1765 N88-20559
Experimental and numerical study of liquid distribution in dispersive-annular flow
[DE88-700844] 14 p1909 N88-21406
Dense-spray structure and phenomena. Part 1. Turbulence/dispersed-phase interactions
[AD-A190606] 15 p2065 N88-22315
Noncondensing round turbulent gas jets in liquids
[AD-A191191] 16 p2208 N88-23179

Modeling of cavitation phenomena in homogeneous flow in transitory regimes in pipes
[ISAL-IDI1-87-15] 17 p2337 N88-23948
Pumped two-phase heat transfer loop
[NASA-CASE-MSC-20841-2] 17 p2339 N88-23958
Two-phase fluid management for a Rankine cycle isotope power system 17 p2405 N88-24303
An experiment to investigate Rankine cycle two-phase microgravity issues 17 p2409 N88-24322
ATHENA heat pipe transient model 17 p2412 N88-24344
Reduced-gravity two-phase flow experiments in the NASA KC-135 17 p2431 N88-24465
Analysis and interpretation of low gravity boiling experiments in the KC-135 17 p2432 N88-24466
Microgravity two-phase fluid flow pattern modeling 17 p2432 N88-24467
Experimental investigation of a microgravity separator for two phase mixtures containing small volumes of gas/vapor 17 p2432 N88-24468
Liquid phase decomposition in slurry fuels 19 p2624 N88-25564
Noise generation by air bubbles in water: An experimental study of creation and splitting
[AD-A192063] 19 p2664 N88-25839
An arranging method on L/D of two-phase closed thermosyphons 20 p2783 N88-26508
Characteristics of long size thermosyphons made of corrugated tube 20 p2784 N88-26511
Investigation of the quasi-steady approach used in transient two-phase flow analysis
[DE88-004303] 21 p2944 N88-27489
Mass flow rate influence on void fraction of two-phase helium flow
[DE88-702456] 21 p2945 N88-27495
Two phase flow in a rotating screw tube (screw tube pump). Investigation of the function and efficiency of the screw tube pump
[MPIS-16/1987] 23 p3222 N88-29178
Experimental and analytical study of two-phase flow in zero gravity
[AD-A195223] 24 p3358 N88-29993
Boltzmann equation approach to two-phase flow turbulence
[AD-A196153] 24 p3373 N88-30086

TWO PHASE SYSTEMS
U BINARY SYSTEMS (MATERIALS)

TWO PHOTON COHERENT STATES
U SQUEEZED STATES (QUANTUM THEORY)

TWO REFLECTOR ANTENNAS
Study of dual beam antenna systems for the data relay satellite, volume 1
[S-272-02-VOL-1] 09 p1152 N88-16905
Study of dual beam antenna systems for the data relay satellite. Volume 2: Executive summary
[S-272-03-VOL-2] 09 p1153 N88-16906

TWO-WAVELENGTH LASERS
Dye laser for holographic interferometry 07 p0920 N88-15588
Discussion of two-mode two-photon CW laser oscillation 16 p2187 N88-23042

TYPE 3 BURSTS
Small-scale structure in solar flare radio emission 08 p1097 N88-16598

TYPHOONS
Tropical cyclone intensity prediction based on empirical orthogonal function representation of wind and shear fields
[AD-A184699] 03 p0353 N88-12229
Annual tropical cyclone report, 1986
[AD-A184082] 04 p0470 N88-12903
Opportunities for tropical cyclone motion research in the Northwest Pacific region
[AD-A185068] 05 p0627 N88-13834
Typhoon structural evolution
[AD-A186090] 07 p0879 N88-15333

U

U BENDS
Laminar flow heat transfer downstream from U-bends 11 p1484 N88-18859
Numerical computation of three-dimensional turbulent flow in tightly curved ducts and spiral turbine casings
[ETN-88-92362] 21 p2948 N88-27511

U.S.S.R.
USSR report: Space
[JPRS-USP-87-003] 01 p0009 N88-10050
Errors associated with Russian name transliteration
[DE87-011717] 02 p0248 N88-11566
Assessment of the impacts of transferring certain nuclear reactor technologies to the Soviet Union and Eastern Europe
[DE87-014388] 02 p0249 N88-11576
USSR report: Engineering and equipment
[JPRS-UEQ-87-008] 04 p0423 N88-12621
USSR report: Earth sciences
[JPRS-UES-88-006] 04 p0458 N88-12831
Astrophysics observatory in Byurakan
[AD-A185144] 05 p0660 N88-14050
USSR report: Earth sciences
[JPRS-UES-87-004] 06 p0725 N88-14455
Polar Geophysical Institute's studies of magnetosphere, ionosphere 06 p0728 N88-14480
JPRS report: Science and technology. USSR: Life sciences
[JPRS-ULS-87-011] 06 p0749 N88-14601
USSR Space Life Sciences Digest index to issues 10-14
[NASA-CR-3922(17)] 07 p0883 N88-15361
Soviet state ergonomic standards (GOST)
[AD-A185537] 07 p0900 N88-15450
USSR report: Physics and mathematics
[JPRS-UPM-87-002] 07 p0918 N88-15575
USSR Space Life Sciences Digest, issue 14
[NASA-CR-3922(16)] 08 p1045 N88-16317
JPRS report: Science and technology. USSR: Physics and mathematics
[JPRS-UPM-87-009] 09 p1233 N88-17395
Proceedings of the First International Symposium on Physical and Technical Problems of Superconductivity Application in Power Generation
[DE88-700818] 11 p1559 N88-19332
Soviet high-technology restructuring drive: the MNTK network
[AD-A188138] 11 p1565 N88-19370
USSR report: Life sciences. Biomedical and behavioral sciences
[JPRS-UBB-87-010] 12 p1651 N88-19889
USSR report: Life sciences. Biomedical and behavioral sciences
[JPRS-UBB-87-008] 12 p1662 N88-19966
JPRS report: Science and technology. USSR: Life sciences
[JPRS-ULS-88-002] 12 p1665 N88-19982
Soviet military power, 1987 13 p1858 N88-21114
JPRS report: Science and technology. USSR: Materials science
[JPRS-UMS-87-009] 14 p1884 N88-21261
USSR Space Life Sciences Digest, issue 16
[NASA-CR-3922(19)] 15 p2101 N88-22515
Soviet remote sensing research and technology
[FASAC-TAR-3130] 17 p2369 N88-24108
Bibliography of Soviet laser developments, number 83, May - June 1986
[AD-A190969] 18 p2520 N88-24950
USSR space life sciences digest, issue 18
[NASA-CR-3922(21)] 19 p2707 N88-26096
Soviet dynamic fracture mechanics research
[FASAC-TAR-3140] 21 p2962 N88-27597
History of manned spaceflight
[CNES-NT-121] 21 p3032 N88-28000
Bibliography of Soviet laser developments, number 88, March - April 1987
[AD-A195978] 24 p3378 N88-30116

U.S.S.R. SPACE PROGRAM
Blagov commentary on Mir station, first manning 01 p0009 N88-10051
JPRS report: Science and technology. USSR: Life sciences
[JPRS-ULS-87-009] 04 p0473 N88-12915
JPRS report: Science and technology. USSR: Space
[JPRS-USP-87-006] 08 p1001 N88-16063
USSR Space Life Sciences Digest, issue 15
[NASA-CR-3922(18)] 10 p1368 N88-18175
Basic results of medical studies during prolonged manned flights on-board the Salyut-7/Soyuz-T orbital complex
[NASA-TT-20217] 10 p1369 N88-18182
Mediab: A project of a medical laboratory in space 12 p1660 N88-19946
JPRS report: Science and technology. USSR: Space
[JPRS-USP-88-002] 13 p1724 N88-20312
Soviet space transport systems 13 p1727 N88-20328
Features of Soyuz TM spacecraft 13 p1727 N88-20329
International manned flight, USSR-SAR
[NASA-TT-20260] 16 p2166 N88-22914
The USSR space systems for remote sensing of earth resources and the environment (sensor systems, processing techniques, applications) 17 p2356 N88-24035
USSR Space Life Sciences Digest, issue 17
[NASA-CR-3922(20)] 17 p2381 N88-24155
Soviet space program handbook
[AD-A194332] 22 p3046 N88-28077
The Soviet MIR space station
[AD-A194040] 23 p3184 N88-28951
JPRS report: Science and technology. USSR: Space
[JPRS-USP-88-001] 24 p3444 N88-30498

U-2 AIRCRAFT
First results from the Airborne Visible/Infrared Imaging Spectrometer (AVIRIS) 06 p0707 N88-14335

UH-1 HELICOPTER
Preliminary airworthiness evaluation of a UH-1 equipped with a terrain mapping receiver antenna
[AD-A186274] 07 p0819 N88-14980

UH-60A HELICOPTER
Analytic investigation of helicopter rotor blade appended aeroelastic devices
[NASA-CR-166525] 03 p0266 N88-11676
Preliminary airworthiness evaluation of the UH-60A with Advanced Digital Optical Control System (ADOCS)
[AD-A190674] 15 p2018 N88-22030
Airworthiness and flight characteristics test of a ski assembly for the UH-60A Black Hawk helicopter
[AD-A191414] 16 p2162 N88-22895

UHTREX (NUCLEAR REACTORS)
U HIGH TEMPERATURE NUCLEAR REACTORS

UK SATELLITES
Validate algorithms for the determination of rainfall rates from SSM/I microwave satellite imagery
[AD-A191337] 16 p2236 N88-23353
Validate algorithms for the determination of rainfall rates from SSM/I microwave satellite imagery
[AD-A195428] 24 p3404 N88-30270

UK SPACE PROGRAM
Developments in ocean colour research in the United Kingdom 08 p1043 N88-16306

ULLAGE
Development and evaluation of an airplane fuel tank ullage composition model. Volume 2: Experimental determination of airplane fuel tank ullage compositions
[AD-A190408] 15 p2017 N88-22025

ULTRAHIGH FREQUENCIES
A digital audio link to the Channel Islands in the UHF television band: Protection of television signals from digitally modulated interference
[BBC-RD-1987/7] 02 p0161 N88-11010
A digital audio link to the Channel Islands in the UHF television band: Preliminary experimental results
[BBC-RD-1987/9] 02 p0161 N88-11011
Performance of high power S-band klystrons focused with permanent magnet
[DE87-753024] 02 p0167 N88-11053
A conformal aircraft phased array antenna for airplane-satellite communication in the L band
[ESA-TT-1057] 03 p0305 N88-11926
Atomic frequency standards for ultra-high-frequency stability 04 p0433 N88-12685
Improvements to a UHF rebroadcast television link suffering tidal fading: Countisbury UHF relay station
[BBC-RD-1987/14] 05 p0573 N88-13495
Two-signal cross modulation effects, half-IF effects and interference criteria in land mobile sharing with UHF (Ultra High Frequency) television
[PB87-228037] 05 p0576 N88-13514
VHF/UHF propagation by diffraction: Calculation by numerical integration 12 p1615 N88-19659
A diffraction based theoretical model for prediction of UHF path loss in cities 12 p1616 N88-19661
Increasing the rate at which ceramic castings undergo preliminary heat-treatment in an ultra-high frequency magnetic field 14 p1886 N88-21275
IREPS (Integrated Refractive Effects Prediction System) 3.0, user's manual
[AD-A190398] 16 p2188 N88-23045
The AMSC mobile satellite system 19 p2643 N88-25681
Propagation effects by roadside trees measured at UHF and L-band for mobile satellite systems 19 p2644 N88-25693
Development of a mobile satellite communication unit 19 p2646 N88-25701
Technical characteristics of the OmniTRACS: The first operation mobile Ku-band satellite communications system 19 p2647 N88-25709
Omni-directional L-band antenna for mobile communications 19 p2648 N88-25717
A microstrip array feed for MSAT spacecraft reflector antenna 19 p2652 N88-25747

ULTRAHIGH VACUUM
The effect of additives on the reactivity of palladium surfaces for the chemisorption and hydrogenation of carbon monoxide: A surface science and catalytic study
[DE87-014685] 02 p0145 N88-10909
Ceramics thin film 04 p0403 N88-12505
Calculated sputtering and atomic displacement cross-sections for applications to medium voltage analytical electron microscopy
[DE88-002904] 09 p1168 N88-17006
In situ ultrahigh vacuum friction measurement and wear track analysis of ion implanted 304 stainless steel
[DE88-004537] 11 p1494 N88-18922

Mechanical design of a ultrahigh gravity UHV facility to launch and recover a low-speed projectile tested on board KC 135 14 p1877 N88-21216
Robotic joint experiments under ultravacuum 14 p1927 N88-21490
Analysis of the performance of the space ultravacuum research facility in attached and free-flyer mode [NASA-TM-100325] 20 p2763 N88-26387

ULTRALIGHT AIRCRAFT
Structural and material testing of a composite microlite wing model [BU-355] 14 p1923 N88-21461
Aeroacoustic investigation on the noise from ultralight aircraft [DFVLR-FB-88-03] 21 p3013 N88-27879

ULTRALOW FREQUENCIES
U EXTREMELY LOW RADIO FREQUENCIES

ULTRALOW TEMPERATURE
U CRYOGENIC TEMPERATURE

ULTRAPURE METALS
Center for the Space Processing of Engineering Materials 07 p0838 N88-15083

ULTRASHORT PULSED LASERS
Dynamic restructuring of pulsed CO2 laser frequency and multiple-peak generation in a cell with IR-absorbing gas in the resonator 07 p0919 N88-15580
A picosecond tunable ultrashort cavity dye laser 14 p1902 N88-21361
SDIO/IST ultrashort wavelength laser: Novel experimental schemes for observing the Mossbauer effect in long-lived nuclear levels [AD-A190275] 15 p2072 N88-22351
SDIO/IST ultrashort wavelength laser. Mossbauer effect in gamma-ray lasers [AD-A190306] 15 p2072 N88-22352

ULTRASONIC FLAW DETECTION
Ultrasonic examination of high performance polymer composites [DRIC-T-7862] 01 p0027 N88-10170
Nondestructive inspection of the pressure vessel in Stuttgart. ALOK part. Phase 1: ALOK combined with conventional probes [REPT-860113-TW] 01 p0057 N88-10367
Stationary reconstruction method. Development, test and comparison in ultrasonic testing [REPT-860125-TW] 01 p0057 N88-10368
Imaging of planar defects with synthetic aperture focusing technique (LSAFT) — ultrasonic inspection [VTT-468] 01 p0058 N88-10370
Method for the ultrasonic inspection of the soundness of the metal in weld joints in two-ply pipes [BLL-CE-TRANS-8265-(9022.09)] 04 p0453 N88-12805
Ultrasonic method of inspecting austenitic weld joints in nuclear power station equipment [BLL-CE-TRANS-8281-(9022.09)] 04 p0453 N88-12806
Nondestructive characterization of ceramic composite whiskers with neutron diffraction and ultrasonic techniques [DE88-003075] 08 p0965 N88-15844
Scattering of longitudinal wave normally incident on discal cavity in elastic body 08 p1077 N88-16492
Ultrasonic inspection of advanced CFRP structures by computer-controlled, pulse-echo technique [ETN-88-91665] 09 p1177 N88-17051
Focused ultrasonic backscatter technique for near-surface flaw detection in structural ceramics [DE88-003112] 09 p1183 N88-17091
Institute for Materials Science and Engineering, nondestructive evaluation: Technical activities 1987 [PB88-153655] 10 p1342 N88-18020
Backscatter from flaws in fiber-reinforced composites 11 p1450 N88-18639
Reference standards for nondestructive tests [AD-A187766] 11 p1497 N88-18936
STA-2A NDT testing [NASA-CR-179301] 11 p1497 N88-18937
Comparison of ultrasonic flaw detection analysis for spherical composite test specimens using two data acquisition techniques [DE88-005002] 12 p1634 N88-19782
Nondestructive testings of HTGR graphites 13 p1747 N88-20448
Ultrasonic inspection of irregular surfaces [AERE-R-12465] 13 p1780 N88-20648
A system to measure damage in composite materials by the ultrasonic method [ONERA-RT-2/7256-RY-061-R] 15 p2031 N88-22103
Ultrasonic characterization of ceramic joints [DE88-005844] 15 p2043 N88-22173
Manufacturing of ultrasonic focused probes [VTT-RR-487] 15 p2074 N88-22368
Nondestructive evaluation by acousto-ultrasonics 15 p2082 N88-22412
Characterization of sintered SiC by using NDE 15 p2082 N88-22413
Systems for ultrasonic scanning, analysis and imagery 15 p2082 N88-22414
Nondestructive testing using ultrahigh frequencies [CERT-5/1333-MO] 18 p2526 N88-24984
Design and implementation of contact ultrasonic sensors to assess internal damage [I-177/87] 21 p2906 N88-27247
Interface control using low frequency (3 to 20 MHz) acoustic microscopy [REPT-48-411/F] 21 p2959 N88-27577
Ultrasonic method and apparatus for determining crack opening load [NASA-CASE-LAR-13889-1] 24 p3385 N88-30160

ULTRASONIC RADIATION
Model for ultrasonic attenuation and elastic constant in chromium and its alloys [DE87-703478] 04 p0415 N88-12570
Anomalies in electromagnetic absorption of circularly polarized ultrasonic waves by tungsten within Doppler-shifted cyclotron resonance range 06 p0775 N88-14756
Imaging subtle microstructural variations in ceramics with precision ultrasonic velocity and attenuation measurements [NASA-TM-100129] 07 p0867 N88-15257
Ultrasonic testing of near-surface zones using scattered signals [ETN-88-90813] 07 p0929 N88-15642
Attenuation of ultrasonic waves in nonmagnetized magnetic fluids 09 p1234 N88-17398

ULTRASONIC SCANNERS
Ultrasonic inspection of irregular surfaces [AERE-R-12465] 13 p1780 N88-20648

ULTRASONIC TESTS
High precision ultrasonic scanning system and SAFT-UT development [DE87-010038] 01 p0008 N88-10044
Ultrasonic examination of high performance polymer composites [DRIC-T-7862] 01 p0027 N88-10170
Nonintrusive ultrasonic flow measurement techniques and their applications to BTU metering [DE87-011390] 01 p0045 N88-10286
Evaluation of mechanical and technological parameters of different steel states by nondestructive micro- and macromagnetic measuring quantities as well as ultrasonic techniques [MPA-810-079] 01 p0057 N88-10366
Stationary reconstruction method. Development, test and comparison in ultrasonic testing [REPT-860125-TW] 01 p0057 N88-10368
Model-based ultrasonic tomography [DE87-013786] 01 p0058 N88-10369
Needs assessment for NDT and characterization of ceramics: Assessment of inspection technology for green state and sintered ceramics [DE87-013550] 02 p0151 N88-10947
Ultrasonic mechanized checking of weld joints of nuclear power plant equipment 02 p0158 N88-10987
Transply crack density detection by acousto-ultrasonics [NASA-TM-100224] 03 p0279 N88-11758
Ultrasonic characterization of the nonlinear elastic properties of unidirectional graphite/epoxy composites [NASA-CR-4100] 03 p0281 N88-11767
Flaw imaging and ultrasonic techniques for characterizing sintered silicon carbide [NASA-TM-100177] 03 p0334 N88-12106
Real time analysis of the results from mechanized ultrasonic testing [DE87-752511] 03 p0334 N88-12107
Elastodynamic ray theory and asymptotic methods for direct and inverse scattering problems 03 p0335 N88-12108
Improvement of deep resolution in ultrasonic echographic nondestructive evaluation using signal processing methods [PB87-147658] 07 p0866 N88-15256
Ultrasonic testing of near-surface zones using scattered signals [ETN-88-90813] 07 p0929 N88-15642
A-scan ultrasound measurement of ocular changes during accommodation [AD-A186818] 09 p1198 N88-17181
Ultrasonic characterization of layered composite systems 10 p1404 N88-18374
Imaging methods for nondestructive materials testing [ETN-88-91477] 11 p1497 N88-18940
Ultrasonic characterization of non-uniform porosity distributions in SiC ceramic [DE88-004814] 13 p1749 N88-20459
Changes in the status of the human tibia during antiorthostatic hypokinesia [NASA-TT-20221] 13 p1810 N88-20813
Detection of bondline delaminations in multilayer structures with lossy components [NASA-CR-182716] 14 p1883 N88-21256
Nonlinear acoustic parameter and its application in ultrasonic imaging 14 p1902 N88-21364
A system to measure damage in composite materials by the ultrasonic method [ONERA-RT-2/7256-RY-061-R] 15 p2031 N88-22103
Ultrasonic beam distortion in transversely isotropic media [DE88-005937] 15 p2129 N88-22699
Ultrasonic Time-Of-Flight Diffraction (TOFD) measurements of crack depths in an acceleration reservoir of a high velocity research gun [DE88-006644] 16 p2164 N88-22907
Nondestructive evaluation of large scale composite components [AD-A190998] 16 p2173 N88-22954
Utility NDE personnel qualification/certification: Enhanced personnel qualification requirements for ASME (American Society for Mechanical Engineers) Code Section 11 examinations [DE88-006748] 16 p2216 N88-23222
Acousto-ultrasonic input-output characterization of unidirectional fiber composite plate by SV waves [NASA-CR-4152] 16 p2217 N88-23224
High frequency ultrasonic characterization of sintered SiC [NASA-TM-100825] 17 p2347 N88-23985
Input-output characterization of fiber composites by SH waves [NASA-CR-4153] 17 p2347 N88-23986
Characterization of noncontact piezoelectric transducer with conically shaped piezoelement [NASA-CR-4151] 17 p2347 N88-23987
Interaction of ultrasonic waves with composite plates [AD-A191879] 18 p2478 N88-24702
Knowledge based systems in nondestructive evaluation [DE88-006653] 18 p2525 N88-24981
Direct and inverse diffraction problems for QNDE (Quantitative Non-Destructive Evaluation) applications [AD-A194721] 22 p3085 N88-28322
Ultrasonic method and apparatus for determining crack opening load [NASA-CASE-LAR-13889-1] 24 p3385 N88-30160

ULTRASONIC WAVE TRANSDUCERS
The application of group radiators for the determination of tension crack corrosion [BAM-06264] 01 p0022 N88-10141
New wide-band transducer developed 14 p1901 N88-21353
In-flight measurement of ice growth on an airfoil using an array of ultrasonic transducers [AIAA-PAPER-87-0178] 17 p2293 N88-23717

ULTRASONIC WAVES
U ULTRASONIC RADIATION

ULTRASONIC WELDING
Modeling of laser ultrasound generation in a weld pool [DE88-005546] 13 p1834 N88-20971
Ultrasonic and video computerized data acquisition for automated welding [DE88-006741] 19 p2677 N88-25918

ULTRASONICS
Experimental investigation in a wind tunnel of the stability and vorticity of the vortex breakdown phenomenon above delta wings, using the ultrasonic laser method [DFVLR-FB-87-06] 01 p0003 N88-10017
High precision ultrasonic scanning system and SAFT-UT development [DE87-010038] 01 p0008 N88-10044
Computerized certification of digital ultrasonic instrumentation [DE88-000820] 04 p0488 N88-13008
Transport coefficients close to the mobility edge and nonlinear sigma model composite operators — electron transport [PREPRINT-541] 06 p0777 N88-14767
Wave propagation experiments on 22-bay lattice [AD-A186140] 07 p0824 N88-15002
Through-transmission/pulse-echo ultrasonic equipment evaluation [AD-A186340] 07 p0929 N88-15641
Low-g propellant gaging 08 p0982 N88-15937
A-scan ultrasound measurement of ocular changes during accommodation [AD-A186818] 09 p1198 N88-17181
Durability and damage tolerance of aluminum castings [AD-A186444] 10 p1341 N88-18013
Ultrasonic-velocity studies of composite and heterogeneous materials [AD-A189000] 12 p1604 N88-19595
Ultrasonic measurements research: Progress in 1987 [AD-A188506] 12 p1687 N88-20092

A continued study of optical sound generation and amplification
[AD-A188362] 12 p1691 N88-20116
Ultrasonic physical modeling of seismic wave propagation from graben-like structures
[AD-A189066] 13 p1796 N88-20744
Ultrasonic oxygen sensor
[AD-A189723] 15 p2105 N88-22537
Acousto-ultrasonic input-output characterization of unidirectional fiber composite plate by P waves
[NASA-CR-4162] 19 p2678 N88-25923
Quantitative particle characterization by scattered ultrasound 20 p2848 N88-26908
Ultrasonic studies of stresses and plastic deformation in steel during tension and compression
[AD-A192308] 21 p2912 N88-27280
New acousto-ultrasonic techniques applied to aerospace materials
[NASA-TM-101299] 22 p3086 N88-28323
Theory of acoustoplasticity and ultrasonic measurements of residual stresses 22 p3087 N88-28328
Combustion studies of acoustically suspended liquid droplets
[AD-A193892] 23 p3192 N88-28998
An investigation of acoustic cavitation produced by pulsed ultrasound
[AD-A193523] 23 p3278 N88-29516
Ultrasonic detection of diffusion and adhesion loss 24 p3354 N88-29967
In situ fault detection by the hybrid ray mode method
[AD-A195226] 24 p3381 N88-30137

ULTRAVIOLET ABSORPTION
Laboratory measurements of the ozone absorption coefficient in the wavelength region 339 to 362 nm at different temperatures
[NOTA-INTERNA-882] 07 p0878 N88-15324
Soluble polysilane derivatives: Chemistry and spectroscopy
[AD-A187889] 11 p1461 N88-18713
Temperature dependence of ultraviolet absorption cross sections of chlorofluoroethanes
[AERONOMICA-ACTA-A-325-1987] 18 p2482 N88-24726
Precise ultraviolet absorbance study of the interaction of amino acids and mononucleosides in aqueous solution
[ISAS-RN-356] 21 p2908 N88-27256
Ultraviolet absorption cross sections of chloro- and chlorofluoromethanes at stratospheric temperatures
[AERONOMICA-ACTA-A-324-1988] 23 p3231 N88-29228

ULTRAVIOLET ASTRONOMY
Diagnostics of solar coronal loops at interferometric angular resolution 01 p0098 N88-10642
Ultraviolet observations of cataclysmic variables: The IUE archive
[MPE-PREPRINT-91] 02 p0250 N88-11580
Ultraviolet observations of AM Her --- cataclysmic variable
[MPE-PREPRINT-92] 02 p0250 N88-11581
A comprehensive exploration of late-type stars in the far-ultraviolet 04 p0520 N88-13194
Optical photometer for the Tirgo telescope
[IFSI-87-5] 05 p0650 N88-13985
The EUV line flux variations and activity in Alpha Orionis 08 p1032 N88-16256
Solar ultraviolet spectrum obtained from a balloon gondola 08 p1032 N88-16258
Laser simulation of light and plasma action on comets and planets 09 p1237 N88-17413
Submillimeter and far infrared line observations of M17 SW: A clumpy molecular cloud penetrated by UV radiation
[NASA-CR-182866] 16 p2288 N88-23701
IUE evidence on the nature of the innermost broad-line region in Seyfert 1 galaxies 17 p2450 N88-24552
Detection of abundant molecular gas in the UV-excess quasar Mrk 1014 22 p3164 N88-28842
Beyond the visible: A decade of observations with the International Ultraviolet Explorer (IUE)
[ESA-F09] 24 p3331 N88-29828

ULTRAVIOLET DETECTORS
NT TOTAL OZONE MAPPING SPECTROMETER
NT ULTRAVIOLET SPECTROMETERS
NT ULTRAVIOLET SPECTROPHOTOMETERS

ULTRAVIOLET LASERS
JPRS Report: Science and Technology. China
[JPRS-CST-87-033] 03 p0326 N88-12062
Powerful picosecond ultraviolet laser output at 354.7 nanometers 03 p0327 N88-12063
Active medium formation in lasers using mixtures of inert gases and optical breakdown pumping 06 p0709 N88-14347
Efficiency of ionic noble gas and alkali metal molecules as ultraviolet and far-ultraviolet lasers 09 p1238 N88-17419
Research studies on extreme ultraviolet and soft X-ray lasers
[AD-A187506] 10 p1338 N88-17996
Research studies on extreme ultraviolet and soft X-ray lasers
[AD-A189163] 12 p1633 N88-19773
UV-Laser reactions of molecular adsorbates
[AD-A190796] 16 p2212 N88-23201
An investigation of 2-6 superlattice deposition by laser photochemical techniques
[AD-A191547] 18 p2581 N88-25336
A plasma ultraviolet source for short wavelength lasers
[AD-A192844] 21 p2952 N88-27537

ULTRAVIOLET LIGHT
U ULTRAVIOLET RADIATION

ULTRAVIOLET PHOTOGRAPHY
Global views of the aurora from the Viking satellite --- Swedish satellite 08 p1025 N88-16208
The calibration of photographic and spectroscopic films: The response of 2aO film to small dosages of alpha particles from 3/10th's rad to 8 rads at energy levels 153 MeV, 79 MeV and 47 MeV
[NASA-CR-177830] 13 p1773 N88-20608

ULTRAVIOLET PHOTOMETRY
Satellite UV image processing
[AD-A190466] 15 p2089 N88-22451

ULTRAVIOLET RADIATION
NT EXTREME ULTRAVIOLET RADIATION
NT FAR ULTRAVIOLET RADIATION
NT LYMAN ALPHA RADIATION
NT NEAR ULTRAVIOLET RADIATION
The largest white light flare ever observed: 25 April 1984, 0001 UT 01 p0111 N88-10714
Mathematical modelling of solar ultraviolet radiation induced optical degradation in anodized aluminum 02 p0135 N88-10846
LLE (Laboratory for Laser Energetics) review, volume 31
[DE87-013732] 03 p0328 N88-12072
DNA damage and repair in human skin in situ
[DE87-014288] 03 p0356 N88-12241
The onset of chromospheric activity among the A- and F- type stars 04 p0511 N88-13144
VLA observations of rapid 6 cm flux variations in alpha Ori 04 p0515 N88-13169
TOMS as a monitor of the ultraviolet radiation environment: Applications to photobiology 05 p0617 N88-13785
Radiation curing: Comparison of heat, UV, and radiation curing
[OEFZS-4393] 06 p0689 N88-14224
UV radiation: Human exposure to ultraviolet radiation
[PB87-137410] 06 p0752 N88-14619
Studies on nonlinear mechanisms of excimer laser propagation in fused silica fibers
[AD-A186822] 09 p1156 N88-16929
Tropospheric ultraviolet radiation: Assessment of existing data and effect on ozone formation
[PB88-130133] 10 p1354 N88-18095
Charge exchange in low energy (keV) and hyperthermal energy (10-100 eV) ion scattering
[AD-A187643] 11 p1543 N88-19222
Polar mesospheric cloud experiment
[AD-A188936] 12 p1648 N88-19872
X-ray lithographic research: A collection of NRL contributions
[AD-A188313] 12 p1695 N88-20140
Research on absorption of UV radiation in Venusian atmosphere from Vega-1 and Vega-2 landing modules 13 p1725 N88-20316
Energy transfer and non-linear optical properties at near ultraviolet wavelengths: Rare earth 4f yields 5d transitions in crystals and glasses
[DE88-005403] 13 p1840 N88-21012
Extension of free-electron lasers into the extreme ultraviolet
[DE88-005373] 15 p2070 N88-22341
NOAA-ERL-ARL (National Oceanic and Atmospheric Administration-Environmental Research Laboratories-Air Resources Laboratory) solar UV radiation and climate research project: Program description
[PB88-169396] 16 p2233 N88-23339
Determination of tropospheric H concentrations by a double-pulsed UV laser method 18 p2539 N88-25070
Investigation of the diffuse ultraviolet background with DE data
[NASA-CR-182863] 19 p2741 N88-26271
Ultraviolet imaging of hydrogen flames
[DE88-009152] 20 p2769 N88-26422
A plasma ultraviolet source for short wavelength lasers
[AD-A192844] 21 p2952 N88-27537
International ultraviolet explorer spectral atlas of planetary nebulae, central stars, and related objects
[NASA-RP-1203] 22 p3164 N88-28843

ULTRAVIOLET SPECTRA
Relations between chromospheric and coronal structure, flux-flux correlations and convective zone properties 04 p0510 N88-13138
Satellite observations of extreme ultraviolet radiation
[AD-A185043] 05 p0661 N88-14059
Short-term temporal variations of Nimbus-7 measurements of the solar UV spectral irradiance
[PB88-102132] 07 p0946 N88-15753
Ultraviolet rocket-spectra of a sunspot 08 p1032 N88-16257
Solar ultraviolet spectrum obtained from a balloon gondola 08 p1032 N88-16258
Ultraviolet absorption cross sections of methylbromide at stratospheric temperatures
[AERONOMICA-ACTA-A-320-1987] 15 p2036 N88-22132
Observation of injected silicon in heliotron E 17 p2441 N88-24524
IUE evidence on the nature of the innermost broad-line region in Seyfert 1 galaxies 17 p2450 N88-24552
Optical constants of minerals and other materials from the millimeter to the ultraviolet
[AD-A192210] 18 p2482 N88-24724
An investigation of 2-6 superlattice deposition by laser photochemical techniques
[AD-A191547] 18 p2581 N88-25336
Ultraviolet spectra of subluminous objects found in the Kiso Schmidt survey and systematic reanalysis of the archived ultraviolet spectra of white dwarfs observed with the IUE satellite under the Astrophysics Data Program (ADP)
[NASA-CR-182976] 18 p2592 N88-25406
Ultraviolet spectra of two magnetic white dwarfs and ultraviolet spectra of subluminous objects found in the Kiso Schmidt survey
[NASA-CR-183051] 18 p2593 N88-25408

ULTRAVIOLET SPECTROGRAPHS
U ULTRAVIOLET SPECTROMETERS

ULTRAVIOLET SPECTROMETERS
NT TOTAL OZONE MAPPING SPECTROMETER
LLE review
[DE87-014468] 02 p0178 N88-11110
Lyman alpha SMM/UVSP absolute calibration and geocoronal correction
[NASA-TM-100314] 03 p0389 N88-12446
Use of satellite data in volcano monitoring 05 p0618 N88-13797
Selection of optimum wavelengths for ozone mapping from satellites 05 p0619 N88-13798
Determination of total ozone from HIRS2/MSU sounding data 05 p0619 N88-13799
Complementary information between UV and IR for remote sensing of total ozone 05 p0619 N88-13800
Satellite observations of extreme ultraviolet radiation
[AD-A185043] 05 p0661 N88-14059
An advanced visible-UV spectrometer for atmospheric composition measurements 08 p1029 N88-16231
Satellite UV image processing
[AD-A190466] 15 p2089 N88-22451
Ultraviolet radiometry: Radiation sources and measuring methods 16 p2272 N88-23596

ULTRAVIOLET SPECTROPHOTOMETERS
NBS (National Bureau of Standards) measurement services: Spectral reflectance
[PB88-109905] 06 p0779 N88-14785
ROCOZ-A (improved rocket launched ozone sensor) for middle atmosphere ozone measurements 08 p1029 N88-16233

ULTRAVIOLET SPECTROSCOPY
What's needed in the UV and EUV 02 p0255 N88-11612
Extreme ultraviolet beam-foil spectroscopy of highly ionized neon and argon
[AD-A185197] 05 p0561 N88-13418
Two-photon (VUV and visible) resonant ionization spectroscopy of atoms and molecules
[DE88-004332] 10 p1407 N88-18388
Spectral radiometry: Methods, measuring techniques, and applications --- conference
[PTB-OPT-24] 16 p2271 N88-23585
Ion temperature measurement with spectroscopy in JT-60 17 p2439 N88-24513
Spectroscopic results from JET: Some examples of data comparison and data needs 17 p2440 N88-24517
Ion temperature profile measurement using charge exchange recombination spectroscopy on JIPP T-IIU 17 p2440 N88-24518

Spectroscopic measurements of ion temperature, rotation speed and beam deposition profile on DIII-D
17 p2440 N88-24519
Applications of charge transfer devices in spectroscopy
[AD-A194408] 23 p3192 N88-28992
High performance charge transfer device detectors
[AD-A194409] 23 p3192 N88-28993

ULTRAVIOLET TELESCOPES
International ultraviolet explorer observatory operations
[NASA-CR-180775] 22 p3145 N88-28708

ULYSSES MISSION
Media calibrations of the Doppler signal for a gravitational wave experiment — interplanetary medium
[IFSI-86-13] 05 p0625 N88-13825

UMBRAS
A near-earth optical communications terminal with a corevolving planetary sun shield
04 p0434 N88-12693

UNCONSCIOUSNESS
NT BLACKOUT (PHYSIOLOGY)

UNDER SURFACE BLOWING
Wind tunnel studies of circulation control elliptical airfoils 10 p1270 N88-17598
Analysis of a fixed-pitch X-wing rotor employing lower surface blowing 10 p1271 N88-17602
Analysis of a fixed-pitch X-wing rotor employing lower surface blowing
[AD-A187379] 24 p3321 N88-29779

UNDERGROUND EXPLOSIONS
Analysis of photopole data reduction models
05 p0593 N88-13616
Characteristics of seismic sources of some Asian earthquakes and Soviet underground explosions from Gauribidanur array records
[DE88-701233] 15 p2093 N88-22472
An approximation technique for solving a system of Fredholm integral equations for asymmetric detector response functions
[AD-A190577] 15 p2121 N88-22645
Research and development activities of the Seismology Section
[DE88-701235] 16 p2231 N88-23323
Effects of tectonic release on broadband regional distance bodywaves
[AD-A194247] 22 p3119 N88-28529

UNDERGROUND STORAGE
Protecting old oil tanks made of steel against internal corrosion using organic coatings
[DE88-751089] 11 p1459 N88-18698

UNDERGROUND STRUCTURES
Reinforced concrete arches under blast and shock environments 09 p1180 N88-17065
Finite element analysis of an underground structure
[AD-A191747] 18 p2527 N88-24991
Signal processing software for ground penetrating radar, user's manual
[AD-A194286] 23 p3203 N88-29059

UNDERGROUND TRANSMISSION LINES
Technology survey for a robot which will investigate the condition of underground pipe
[PB87-209979] 01 p0055 N88-10351

UNDERWATER ACOUSTICS
Geoacoustic models of the Hudson Canyon area
[AD-A183535] 01 p0073 N88-10465
A new method for determining acoustic properties of the seabed from the ambient noise field in the ocean
[RAE-TR-86035] 01 p0090 N88-10590
Proceedings of Conference on Vibrodiagnostics discussed 02 p0158 N88-10990
Underwater acoustic backscatter from a model of arctic ice open leads and pressure ridges
[AD-A184693] 03 p0354 N88-12234
The effect of ocean fluctuations on sound transmission in the ocean
[AD-A184382] 03 p0355 N88-12236
AFAR (Azores Fixed Acoustic Range) measurements of intensity and intensity moments
[AD-A184431] 03 p0355 N88-12237
Coupled acoustic and ocean thermodynamic model
[AD-A184357] 04 p0472 N88-12911
Multipath time-delay estimation via the EM algorithm
[PB88-106851] 07 p0845 N88-15124
FOR3D: A computer model for solving the LSS (Lee-Saad-Schultz) three-dimensional, wide angle wave equation
[AD-A186649] 08 p1080 N88-16511
High frequency acoustic underwater communication with low probability of being traced
[REPT-4-87] 09 p1242 N88-17447
An application of dimensionless Eigenvalues to underwater acoustic ducts
[AD-A188167] 11 p1542 N88-19219
The temporal and spatial acoustical response of a point-driven fluid-loaded plate
[AD-A188504] 12 p1636 N88-19794
Observations of waves and Langmuir circulation with Doppler sonars 13 p1805 N88-20790
Mathematical models of sound waves in fluids
[AD-A189270] 13 p1834 N88-20968
New wide-band transducer developed
14 p1901 N88-21353
A computerized investigation using the method of images to predict the sound field in a fluid wedge overlying a slow fluid half-space
[AD-A190013] 15 p2130 N88-22704
Low frequency ocean ambient noise: Measurements and theory
[AD-A191188] 16 p2237 N88-23362
Refraction in underwater acoustics --- navigation systems
[B8735053] 17 p2395 N88-24236
Construction of approximations to acoustic Green's functions for nonhomogeneous oceans using transmutation
[PB88-185384] 18 p2548 N88-25126
Evaluation of the biot coefficients
[AD-A191643] 18 p2570 N88-25265
ELIT: An autonomous underwater observation robot
19 p2699 N88-26048
A modal approach to Arctic noise modelling with implied vertical coherence
[AD-A192966] 20 p2850 N88-26916
Robust methods for array signal processing
[AD-A192854] 21 p3012 N88-27871
Vertical directionality of ambient noise at 32 deg N as a function of longitude: Tape number 86180
[AD-A193228] 21 p3012 N88-27872
Numerical modeling results for mode propagation in a wedge
[AD-A193998] 22 p3147 N88-28718
Polynomials with restricted coefficients and their applications
[AD-A192589] 23 p3202 N88-29055
Reflection and scattering of acoustic rays computed for parabolic ice keel models
[AD-A193898] 23 p3278 N88-29517
Acoustic pressure distribution on the bottom of a wedge-shaped ocean
[AD-A193961] 23 p3278 N88-29518

UNDERWATER COMMUNICATION
High frequency acoustic underwater communication with low probability of being traced
[REPT-4-87] 09 p1242 N88-17447
Long haul underwater fiber optic link
[AD-A194487] 23 p3282 N88-29542

UNDERWATER ENGINEERING
The nature of metallurgical reactions in underwater welding
[AD-A184464] 04 p0414 N88-12568
Design and preliminary evaluation of an underwater laser-based imaging system
[DE88-010560] 19 p2675 N88-25908

UNDERWATER EXPLOSIONS
Validation of the Underwater Shock Analysis (USA) program. Part 1: Theoretical considerations --- ship design
[REPT-5073713-86-01] 06 p0702 N88-14308

UNDERWATER OPTICS
The analytical exponential decay coefficient of the submarine light field
[AD-A187215] 11 p1548 N88-19261
Activities report of the Division of Optical Technology
[FOA-C-30477-3] 18 p2576 N88-25299
Design and preliminary evaluation of an underwater laser-based imaging system
[DE88-010560] 19 p2675 N88-25908
Underwater optical trajectography and video image mosaics 19 p2700 N88-26051
Methods for processing satellite images and their application to underwater operations
19 p2702 N88-26066

UNDERWATER PHYSIOLOGY
Experience in occupational medicine, derived from 16 operational deep saturation trimix 5 dives in GUSI from 150 to 600 m 19 p2695 N88-26018
Life in a hyperbaric environment. A new O2-H2 breathing mixture for industrial diving 19 p2695 N88-26019
Decompression procedures and accidents in space and sea 19 p2698 N88-26035
Monitoring of divers/astronauts during missions
19 p2698 N88-26036

UNDERWATER RESOURCES
Karst and submarine fresh water discharge in the Antalya area, southern Turkey 22 p3102 N88-28421

UNDERWATER SOUND
U UNDERWATER ACOUSTICS

UNDERWATER STRUCTURES
Detection of defects on structures
[EP-PATENT-0-210-794-A2] 04 p0453 N88-12807
Design and test of high performance composite tubes for use in deep water drilling and production systems
[SNIAS-872-430-107] 05 p0572 N88-13487
High performance composite tubes for offshore applications
[SNIAS-872-430-116] 05 p0572 N88-13488
Validation of the Underwater Shock Analysis (USA) program. Part 1: Theoretical considerations --- ship design
[REPT-5073713-86-01] 06 p0702 N88-14308
Retarded potential technique applied for shock wave loading of doubly symmetric submerged structures
09 p1179 N88-17058

UNDERWATER TESTS
NT NEUTRAL BUOYANCY SIMULATION
Experimental studies on the tripping behavior of narrow T-stiffened flat plates subjected to hydrostatic pressure and underwater shock 05 p0592 N88-13613
HERMES Program: Airlock swimming pool tests
12 p1591 N88-19525
Underwater simulation for space teleoperation
19 p2698 N88-26040
Study of human factors engineering criteria for Extra Vehicular Activity (EVA) systems, volume 2
[STF23-F87025-VOL-2] 24 p3409 N88-30293

UNDERWATER TRAJECTORIES
A feasibility study in path planning using optimization techniques
[AD-A193030] 21 p2894 N88-27177

UNDERWATER VEHICLES
NT SUBMARINES
A conceptual design of an inertial navigation system for an autonomous submersible testbed vehicle
[AD-A188038] 11 p1438 N88-18578
Design features of small Brayton cycles for autonomous underwater vehicles
[AD-A187799] 11 p1506 N88-18999
A feasibility study in path planning using optimization techniques
[AD-A193030] 21 p2894 N88-27177
A conceptual design study of a hovering system controller for an autonomous underwater vehicle
[AD-A193423] 21 p2930 N88-27399
Estimation forces acting on an underwater vehicle with G.P.S. (Global Positioning System) and Kalman filtering
[AD-A194339] 23 p3175 N88-28901
Remotely Operated Vehicle (ROV) reliability study, phase 1
[AD-A194367] 23 p3222 N88-29177

UNIAXIAL STRAIN
U AXIAL STRAIN

UNIFIED FIELD THEORY
A supersymmetric Lagrangian for Poincare gauge theories of gravity
[DE88-001670] 04 p0500 N88-13078
A review of two-phase flow-induced vibration
[DE88-001955] 09 p1160 N88-16955
Looking for new gravitational forces with antiprotons
[DE88-003154] 09 p1192 N88-17142
Ambiguity in determining the effective action for string-corrected Einstein gravity
[PB87-166153] 09 p1259 N88-17550

UNIFORM FLOW
NT BLASIUS FLOW
Conditions at infinity for theories of oscillating wings and propellers in subsonic flow
[NAL-TR-937] 11 p1434 N88-18556

UNIPHASE FLOW
U SINGLE-PHASE FLOW

UNIPOLAR TRANSISTORS
U FIELD EFFECT TRANSISTORS

UNIQUENESS THEOREM
On a class of similarity solutions of the equation u sub t = (absolute value of u sup m-1 u sub x) sub x with m greater than -1
[REPT-87-54] 14 p1963 N88-21713

UNITED KINGDOM
NT ENGLAND
NT SCOTLAND
Forecasting stratus over the British Isles
02 p0209 N88-11310
Time and cost reduction through computer integrated manufacture 12 p1703 N88-20191
A comparative assessment of US and UK explosives qualified as replacements for tetryl
[MRL-R-1094] 13 p1754 N88-20486
Managing and controlling change
[PNR90419] 22 p3159 N88-28801

UNITED KINGDOM SATELLITES
U UK SATELLITES

UNITED NATIONS
Current status of world weather service
06 p0725 N88-14459

Safety guidelines and procedures for bioscience-based industry and other applied microbiology
[PB87-140521] 08 p1045 N88-16316
System-wide medium-term environment programme for the period 1990-1995: Strategies of the United Nations system for the environment
[UNEP/GCSS.I/2] 12 p1641 N88-19826
United Nations deliberations of the use of nuclear power sources in space: 1978-1987 17 p2423 N88-24410
Discussions and agreements in the United Nations on important issues associated with nuclear power in space 17 p2423 N88-24411

UNITED STATES
NT ALABAMA
NT ALASKA
NT ARIZONA
NT CALIFORNIA
NT CONNECTICUT
NT DELAWARE
NT FLORIDA
NT HAWAII
NT ILLINOIS
NT KANSAS
NT KENTUCKY
NT MAINE
NT MASSACHUSETTS
NT MICHIGAN
NT MISSISSIPPI
NT NEVADA
NT NEW MEXICO
NT NEW YORK
NT NORTH CAROLINA
NT NORTH DAKOTA
NT TEXAS
NT WISCONSIN
NT WYOMING
Japanese industrial research on lean combustion: A case study: International Research Monitoring Program
[DE87-013839] 02 p0144 N88-10904
Assessment of the impacts of transferring certain nuclear reactor technologies to the Soviet Union and Eastern Europe
[DE87-014388] 02 p0249 N88-11576
Center for Electronics and Electrical Engineering Technical Progress Bulletin covering center programs, January to March 1987 with 1987 CEFE events calendar
[PB87-224648] 03 p0309 N88-11946
East coast gravity validation study
[AD-A184292] 03 p0351 N88-12217
Impacts of world development on selected characteristics of the atmosphere: An integrative approach. Volume 2: Appendices
[DE88-001496] 07 p0875 N88-15310
Aircraft accident reports: Brief format, US Civil and Foreign Aviation, Issue Number 5 of 1986 accidents
[PB87-916907] 08 p0952 N88-15780
Aircraft accident reports: Brief format, US Civil and Foreign Aviation, Issue Number 8 of 1986 accidents
[PB87-916910] 08 p0953 N88-15782
Advancing automation and robotics technology for the space station and for the US economy: Submitted to the United States Congress October 1, 1987
[NASA-TM-100777] 08 p0959 N88-15816
Advancing automation and robotics technology for the space station and for the US economy: Submitted to the United States Congress October 1, 1986
[NASA-TM-89190] 08 p0960 N88-15818
International role of US geoscience
[NASA-CR-182407] 08 p1035 N88-16281
Hurricane climatology for the Atlantic and Gulf coasts of the United States
[PB88-114657] 08 p1039 N88-16288
Recommendations for a US ice coring program
[PB88-115043] 09 p1185 N88-17102
America plans for space
[AD-A187485] 10 p1289 N88-17713
Proceedings of US-Japan Heliotron-Stellarator Workshop, volume 3
[DE88-004788] 11 p1554 N88-19299
Proceedings of US-Japan Heliotron-Stellarator Workshop, volume 2
[DE88-004789] 11 p1554 N88-19300
A comparative assessment of US and UK explosives qualified as replacements for tetryl
[MRL-R-1094] 13 p1754 N88-20486
Technology transfer to China. Volume 2: Working papers, part 1
[PB88-158704] 14 p1992 N88-21872
Technology transfer to China. Volume 2: Working papers, part 2
[PB88-158712] 14 p1992 N88-21873
Aircraft accident reports, brief format, US civil and foreign aviation, issue number 10 of 1986 accidents
[PB87-916912] 15 p2016 N88-22020
Monitoring space weaponry: Detection and verification issues
[DE88-008726] 20 p2847 N88-26900
Federal Council on Science, Engineering and Technology: Committee on Computer Research and Applications, Subcommittee on Science and Engineering Computing: The US Supercomputer Industry
[DE88-011262] 21 p2994 N88-27756
Potential use of SPOT satellite data for the national resources inventory 22 p3093 N88-28370
Factors influencing summer temperatures and precipitation in the southwest 22 p3124 N88-28565
On the modes of growing-season precipitation over central North America 22 p3124 N88-28567
Characteristics of regression equations for specifying monthly precipitation amounts over the United States from the field of concurrent mean 700 mb heights 22 p3127 N88-28591

UNITS OF MEASUREMENT
NT INTERNATIONAL SYSTEM OF UNITS

UNIVERSE
Our universe as an attractor in a superstring model
[DE87-703066] 02 p0251 N88-11585
Crucial cosmological observations
[DE87-703081] 02 p0251 N88-11587
Torsion as a source of expansion in a Bianchi type I universe in the self-consistent Einstein-Cartan theory of a perfect fluid with spin density
[AD-A184200] 03 p0322 N88-12037
Particle physics and cosmology
[DE87-005400] 03 p0387 N88-12432
Number count-redshift relation in universe models with nonzero cosmological constant
[DE87-703043] 03 p0388 N88-12435
New cosmological scenario
[DE87-703357] 04 p0520 N88-13198
Cosmological applications of singular hypersurfaces in general relativity 04 p0521 N88-13202
Galaxy formation by gravitational collapse in a universe dominated by cold dark matter 04 p0521 N88-13205
Laboratory and near-earth space plasma as a key to the plasma universe
[TRITA-EPP-87-09] 05 p0652 N88-13996
Cosmology in the plasma universe
[TRITA-EPP-87-07] 05 p0660 N88-14053
Model of earlier stage of universe's evolution 06 p0775 N88-14758
Evolution of perturbations in expanding universe 06 p0775 N88-14759
Number count-redshift relation in a perturbed Friedmann universe
[DE88-750302] 07 p0945 N88-15743
Post-Newtonian equations of motion in an expanding universe
[DE88-750303] 07 p0945 N88-15744
Evolution from pure states into mixed states in de Sitter space
[DE88-750316] 07 p0945 N88-15745
Existence of absolutely closed universe 08 p1080 N88-16509
The origin of the diffuse X-ray background and the formation of galaxies and voids 10 p1428 N88-18527
On the time delay of the ultrahigh-energy radiation signal from the source Cygnus X-3
[DE88-700649] 10 p1431 N88-18547
Early reheating and cosmic strings 13 p1855 N88-21103
Rotation of universe --- metagalaxies 14 p1974 N88-21780
Density perturbations in a rotating universe
[DE87-703036] 15 p2151 N88-22840
Cosmology for high energy physicists
[DE88-005705] 15 p2151 N88-22842
On the dynamics of the metagalaxy
[TRITA-EPP-88-05] 22 p3166 N88-28852
Time travel in the homogeneous Som-Raychaudhuri universe
[DE88-702220] 23 p3295 N88-29622
Non-linear scale invariance in a cold-dark-matter universe
[DE88-011725] 23 p3299 N88-29644

UNIVERSITIES
The British Technology Group
[ONRL-7-022-R] 01 p0107 N88-10698
Experiments: Test range facilities, part 1 03 p0304 N88-11920
The Black College satellite telecommunications network planning in support of energy-related collaborative research
[DE88-000182] 03 p0307 N88-11940
Calendar year 1985 solar and weather data for Austin, Texas
[PB87-220174] 03 p0352 N88-12219
National Center for Atmospheric Research
[PB87-228391] 04 p0470 N88-12901
A national model at Howard University demonstrating private sector interrelationships that facilitate research in predominantly Black colleges and universities
[DE88-000160] 04 p0502 N88-13089
University research initiative research program summaries
[AD-A184876] 05 p0658 N88-14035
A study of the minority college programs at the NASA Johnson Space Center 06 p0798 N88-14887
Activities report of the Technical University of Twente
[ETN-88-90620] 06 p0799 N88-14892
Research reports: 1987 NASA/ASEE Summer Faculty Fellowship Program
[NASA-CR-179219] 07 p0922 N88-15601
TABLET: The personal computer of the year 2000
[NASA-CR-182528] 10 p1384 N88-18267
Cumulative reports and publications through December 31, 1987
[NASA-CR-181624] 11 p1524 N88-19099
Institute for Computational Mechanics in Propulsion (ICOMP)
[NASA-TM-100790] 11 p1540 N88-19202
Experimental elementary particle physics at the University of Pittsburgh
[DE88-003542] 11 p1545 N88-19234
Experience with Berkeley UNIX interprocess communications
[AD-A188353] 12 p1680 N88-20041
Basic research in ceramic and semiconductor science at selected Japanese laboratories, based on a September 1986 visit: Highlights, summary and overview and detailed notes from selected Japanese laboratories
[DOE/ER-0314] 12 p1696 N88-20150
A project to transfer technology from NASA centers in support of industrial innovation in the midwest
[NASA-CR-180360] 12 p1708 N88-20224
Microvax networked computer system
[AD-A190308] 15 p2114 N88-22596
Structural ceramics research 17 p2324 N88-23878
Fiber waveguide sensors for intelligent materials
[NASA-CR-183028] 17 p2343 N88-23968
Transactions of the Fifth Symposium on Space Nuclear Power Systems
[DE88-006165] 17 p2417 N88-24374
RLE progress report, January 1 to December 31, 1987
[RLE-PR-130] 21 p3011 N88-27869

UNIVERSITY PROGRAM
University program management information system, fiscal year 1985
[NASA-TM-88381] 06 p0790 N88-14846

UNLOADING
Dislocation free zone model of fracture under reverse loading
[DE88-002676] 07 p0869 N88-15276

UNMANNED SPACECRAFT
NT GALILEO PROBE
NT GALILEO SPACECRAFT
NT GIOTTO MISSION
NT HEAO 2
NT HELIOS 1
NT HELIOS 2
NT HOTOL LAUNCH VEHICLE
NT MARS OBSERVER
NT MARS PROBES
NT PIONEER VENUS SPACECRAFT
NT SPACE PROBES
Expected value analysis for an unmanned expendable launch vehicle payload escape system
[AD-A189494] 13 p1728 N88-20337
Arguments for manned or unmanned spacecraft activities
[REPT-46/87] 17 p2309 N88-23813
Review of past and current trials and uses of unmanned vehicles
[AD-A194527] 22 p3084 N88-28311

UNSTEADY AERODYNAMICS
A supersonic potential gradient method for the calculation of unsteady aerodynamic pressures on harmonically oscillating wings
[ESA-TT-930] 03 p0259 N88-11631
The Green's function method for fully unsteady aerodynamics around three-dimensional bodies and its application to flutter analysis
[UTIAS-298] 03 p0260 N88-11639
Numerica calculation in the Laplace domain for subsonic unsteady aerodynamic forces acting on a finite wing 05 p0535 N88-13256
Unsteady aerodynamics of an oscillating cascade in a compressible flow field
[NASA-TM-100219] 05 p0549 N88-13346
Influence of the static deformation on a wing in the unsteady aerodynamic 05 p0551 N88-13357
Integration of a supersonic unsteady aerodynamic code into the NASA FASTEX system
[NASA-CR-182329] 06 p0663 N88-14068

Unsteady transonic algorithm improvements for realistic aircraft applications
[NASA-TM-100516] 08 p0949 N88-15760
Time accurate techniques using characteristic flux averaging with application to unsteady aerodynamics 08 p0985 N88-15957
Computational unsteady aerodynamics for aeroelastic analysis
[NASA-TM-100523] 09 p1112 N88-16668
Investigation of dynamic stall using LDV (Laser Doppler Velocimetry): Mean flow studies
[AD-A187629] 10 p1272 N88-17611
Effectiveness of various control surfaces in quasi-steady and unsteady conditions
[AGARD-R-735] 10 p1284 N88-17682
A semianalytical technique for sensitivity analysis of unsteady aerodynamic computations
[NASA-TM-100610] 11 p1503 N88-18976
Calculated unsteady aerodynamics of wings
[AD-A189608] 12 p1574 N88-19415
Unsteady transonic small-disturbance theory including entropy and vorticity effects
[NASA-TM-100568] 12 p1575 N88-19418
Steady and unsteady transonic small disturbance analysis of realistic aircraft configurations
[NASA-TM-100557] 13 p1717 N88-20269
Unsteady aerodynamics of a Wortmann FX-63-137 wing in a fluctuating wind field
[AD-A190128] 15 p2013 N88-22006
Bifurcations in unsteady aerodynamics-implications for testing
[NASA-TM-100083] 15 p2015 N88-22014
Methodology for matching experimental and computational aerodynamic data
[NASA-TM-100592] 17 p2295 N88-23728
Unsteady pressure and structural response measurements of an elastic supercritical wing
[NASA-TM-100591] 17 p2299 N88-23756
Calculations of unsteady aerodynamics for a full aircraft configuration using boundary element method 19 p2637 N88-25643
Experimental determination of aerodynamic damping in a three-stage transonic axial-flow compressor
[NASA-TM-100953] 21 p2897 N88-27200
Investigation of oscillating cascade aerodynamics by an experimental influence coefficient technique
[NASA-TM-101313] 22 p3039 N88-28041
Program user's manual for an unsteady helicopter rotor-fuselage aerodynamic analysis
[NASA-CR-181701] 22 p3039 N88-28047
An unsteady helicopter rotor: Fuselage interaction analysis
[NASA-CR-4178] 23 p3171 N88-28880
Accurate solutions, parameter studies and comparisons for the Euler and potential flow equations
[NASA-TM-100664] 23 p3173 N88-28892
Application of unsteady aerodynamic methods for transonic aeroelastic analysis
[NASA-TM-100665] 24 p3317 N88-29754
History of aeroelasticity in Germany from the beginning to 1945
[ESA-TT-1062] 24 p3319 N88-29767
Recent advances in transonic computational aeroelasticity
[NASA-TM-100663] 24 p3321 N88-29778
Aeroelastic response of metallic and composite propfan models in yawed flow
[NASA-TM-100964] 24 p3326 N88-29807

UNSTEADY FLOW
NT OSCILLATING FLOW
Advanced turboprop wing installation effects measured by unsteady blade pressure and noise
[NASA-TM-100200] 01 p0002 N88-10008
ARSPNS: A method to calculate steady and unsteady potential flow about fixed and rotational lifting and nonlifting bodies
[NLR-TR-85114-U] 01 p0044 N88-10282
Calculation of stationary and low frequency unsteady flows in a steam turbine end stage
[MITT-23] 01 p0057 N88-10364
Personal Computer (PC) based image processing applied to fluid mechanics
[NASA-TM-100024] 02 p0172 N88-11087
On the prediction of the aeroelastic behavior of lifting systems due to flow separation
[ESA-TT-1043] 03 p0259 N88-11633
The Green's function method for fully unsteady aerodynamics around three-dimensional bodies and its application to flutter analysis
[UTIAS-298] 03 p0260 N88-11639
Aerodynamic sensitivities from subsonic, sonic and supersonic unsteady, nonplanar lifting-surface theory
[NASA-TM-100502] 04 p0394 N88-12459
Application of Runge Kutta time marching scheme for the computation of transonic flows in turbomachines
[NASA-TM-86997] 04 p0394 N88-12461
Three-dimensional unsteady flow elicited by finite wings and complex configurations 04 p0395 N88-12468
Numerical simulation of unsteady separated flows
[AD-A184132] 04 p0442 N88-12741
An experimental investigation of unsteadiness in swept shock wave/turbulent boundary layer interactions 04 p0445 N88-12760
Driving mechanism of unsteady separation shock motion in hypersonic interactive flow 05 p0530 N88-13226
Numerica calculation in the Laplace domain for subsonic unsteady aerodynamic forces acting on a finite wing 05 p0535 N88-13256
The development of a computer code (U2DIIF) for the numerical solution of unsteady, inviscid and incompressible flow over an airfoil
[AD-A185033] 05 p0541 N88-13293
Unsteady aerodynamics of an oscillating cascade in a compressible flow field
[NASA-TM-100219] 05 p0549 N88-13346
Influence of the static deformation on a wing in the unsteady aerodynamic 05 p0551 N88-13357
Experimental study of the fluid mechanics of unsteady turbulent boundary layers
[AD-A184856] 05 p0560 N88-13536
Physical analysis and numerical simulation of coherent turbulent structures in mixed layers, jets, and wakes
[ETN-88-91183] 05 p0581 N88-13548
A numerical model of unsteady, subsonic aeroelastic behavior
[NASA-TM-100487] 06 p0663 N88-14064
Development of an unsteady wake theory appropriate for aeroelastic analyses of rotors in hover and forward flight
[NASA-CR-182357] 06 p0664 N88-14075
Methods for reducing computational costs of typical finite element unsteady hydrodynamic models
[AD-A185499] 06 p0702 N88-14312
Studies of unsteadiness in boundary layers
[AD-A185662] 06 p0703 N88-14315
An explicit Runge-Kutta method for unsteady rotor/stator interaction
[NASA-TM-100787] 07 p0816 N88-14967
Analysis of three-dimensional viscous internal flows
[AD-A186254] 07 p0849 N88-15155
Flow in Centrifugal Compressors — conference
[VKI-LS-1987-01] 07 p0850 N88-15160
Blade excitation due to unsteady flow phenomena 07 p0851 N88-15167
Numerical study of a centrifugal impeller response to a downstream static pressure perturbation 07 p0851 N88-15170
Programs for calculating transient Darcian flow through non-uniform materials
[DE88-001924] 07 p0852 N88-15177
An explicit method for the solution of the Euler equations, applied to unsteady two dimensional flows
[ETN-88-90807] 07 p0855 N88-15194
Unsteady three-dimensional flow separation
[NASA-CR-182412] 08 p0949 N88-15761
Three-dimensional unsteady flow elicited by finite wings and complex configurations
[AD-A186464] 08 p0951 N88-15770
Advanced propeller research 08 p0957 N88-15806
Time accurate techniques using characteristic flux averaging with application to unsteady aerodynamics 08 p0985 N88-15957
Modeling the unsteady flow found in axial turbomachinery
[ECL-87-07] 08 p0987 N88-15980
Computational unsteady aerodynamics for aeroelastic analysis
[NASA-TM-100523] 09 p1112 N88-16668
Mach number effects on transonic aeroelastic forces and flutter characteristics
[NASA-TM-100547] 09 p1113 N88-16675
Unsteady behavior of three-dimensional vortices relevant to turbulent boundary layers
[AD-A186767] 09 p1161 N88-16958
The unsteady gas flow through stator and rotor of a turbomachine 10 p1281 N88-17660
Parametric study of choke flutter with a linear theory 10 p1283 N88-17673
Ice-shelf response to ice-stream discharge fluctuation. Part 1: Unconfined ice tongues
[AD-A188147] 10 p1358 N88-18117
Well-posedness and spectral estimation for infinite dimensional systems
[AD-A187621] 10 p1401 N88-18354
Unsteady heat transfer in turbine blade ducts: Focus on combustor sources
[NASA-TM-100815] 11 p1486 N88-18870
Unsteady transonic small-disturbance theory including entropy and vorticity effects
[NASA-TM-100568] 12 p1575 N88-19418
To the problem of determining true volume steam content by measured values of mean density of a mixture in thermally unsteady two-phase flows
[DE88-700640] 12 p1626 N88-19726
Application of a flux vector splitting methodology towards the solution of unsteady transonic flows, with future emphasis on the blade flutter problem
[AD-A189500] 13 p1716 N88-20260
ARSPNSC: A method to calculate subsonic steady and unsteady potential flow about complex configurations
[NLR-TR-86122-U] 13 p1717 N88-20265
Discrete vortex analysis of unsteady flow about two-dimensional cambered plates
[DE88-006597] 14 p1909 N88-21407
An explicit method for the solution of the Euler equations applied to unsteady two-dimensional flows
[MBB/LKE-121/S/PUB/257] 14 p1910 N88-21411
Unsteady aerodynamics of a Wortmann FX-63-137 wing in a fluctuating wind field
[AD-A190128] 15 p2013 N88-22006
Oscillating airfoils: Achievements and conjectures
[AD-A190490] 15 p2014 N88-22008
Unsteady flow field measurements using LDV (Laser Doppler Velocimetry)
[AD-A189907] 15 p2063 N88-22298
Enhancement of data acquisition and numerical computation capabilities for unsteady fluid dynamics
[AD-A190115] 15 p2063 N88-22302
Bodies in unsteady flow
[AD-A190416] 15 p2064 N88-22308
Numerical study of unsteady viscous hypersonic blunt body flows with an impinging shock
[NASA-TM-100096] 15 p2122 N88-22650
Measurements of aerodynamic forces on unsteadily moving bluff parachute canopies 16 p2202 N88-23137
A non-invasive experimental technique for the measurement of unsteady velocity and vorticity fields 16 p2204 N88-23148
Structure of unsteady flows at leading- and trailing-edges: Flow visualization and its interpretation 16 p2205 N88-23154
Unsteady flow about cambered plates
[AD-A191226] 17 p2337 N88-23945
Development and improvement of a code to calculate small, three dimensional, unsteady transonic perturbations
[ONERA-RTS-31/3064-RY-062-R] 17 p2338 N88-23951
Accounting for the effects of unsteady, separated boundary layers in transonic two dimensional calculations
[ONERA-RT-30/3064-RY-063-R] 17 p2338 N88-23952
Research on aero-thermodynamic distortion induced structural dynamic response of multi-stage compressor blading
[AD-A192169] 18 p2456 N88-24584
Unsteady flow in a supercritical supersonic inlet 18 p2460 N88-24605
Forced response unsteady aerodynamics in a multistage compressor 18 p2512 N88-24903
Numerical simulation of nonlinear structural dynamics of large scale unsteady flow
[ETN-88-92156] 18 p2513 N88-24908
An implicit, high order accurate, upwind scheme for unsteady Euler equations 19 p2639 N88-25657
Pulsatile fluidic pump performance at elevated temperatures
[DE88-008046] 19 p2677 N88-25919
On the dynamic behavior of balloon during its launch; application of panel method and extension to unsteady problem
[ISAS-RN-622] 20 p2751 N88-26330
Calculation of 2-D unsteady transonic full potential flow about oscillating airfoils by two complementary approaches
[PB88-127519] 20 p2753 N88-26341
Control and use of unsteady flows: Insect use of various wing kinematics and related pressure measurements using a pitching airfoil 21 p2926 N88-27366
Coupled experimental and theoretical investigations of instability, chaos and turbulence in an axisymmetric jet flow
[AD-A192943] 21 p2942 N88-27476
Experimental study of unsteady separating turbulent boundary layers
[AD-A192997] 21 p2943 N88-27477
A computer model for the flow of a molten polymer in a narrow cavity
[NPL-DMA(A)-157] 22 p3058 N88-28146
Non-reflecting boundary conditions for computations of unsteady flows in turbomachines
[PNR90469] 22 p3079 N88-28284

The role of acoustic resonances in unsteady turbomachinery aerodynamics
[PNR90455] 22 p3147 N88-28720
An unsteady helicopter rotor: Fuselage interaction analysis
[NASA-CR-4178] 23 p3171 N88-28880
Unsteady water channel
[AD-A194231] 23 p3171 N88-28884
Unsteady flow past an NACA 0012 airfoil at high angles of attack
[AD-A194650] 23 p3172 N88-28886
An integral equation for the linearized unsteady supersonic flow over a wing
[AD-A193773] 23 p3172 N88-28887
Direct-solution techniques for viscous flows and their control
[AD-A194775] 23 p3211 N88-29114
Shock waves in unsteady flows
[NASA-TT-20329] 23 p3214 N88-29134
Numerical solutions of unsteady inviscid transonic turbine cascade flows
[AD-A196111] 24 p3316 N88-29748
An unconditionally stable Runge-Kutta method for unsteady flows
[NASA-TM-101347] 24 p3321 N88-29780
The effects of incoming boundary layer thickness on unsteady shock-induced turbulent separations induced by cylinders
[AD-A196190] 24 p3368 N88-30060
An analysis of finite-difference and finite-volume formulations of conservation laws
[NASA-CR-177416] 24 p3370 N88-30071
Numerical simulation of unsteady incompressible flow in a partially-filled rotating cylinder
[AD-A196001] 24 p3371 N88-30073
Numerical simulation of unsteady incompressible viscous flows in generalized coordinate systems
[NASA-TM-101016] 24 p3373 N88-30085
Studies of unsteady axial-compressor functioning
24 p3380 N88-30129

UNSTEADY STATE
Numerical and experimental investigation of the unsteady temperature distribution in solar central receivers
[ESA-TT-1050] 03 p0347 N88-12193
Aircraft dynamics: Aerodynamic aspects and wind tunnel techniques 05 p0545 N88-13320
Aircraft dynamics: Aerodynamic aspects and wind tunnel techniques 24 p3313 N88-29731

UP-CONVERTERS
Long duration coherent Lyman-alpha sources
16 p2268 N88-23571

UPDRAFTS
U VERTICAL AIR CURRENTS

UPGRADING
Effects of update and refresh rates on flight simulation visual displays
[NASA-TM-100415] 15 p2018 N88-22033

UPLINKING
A statistical rain attenuation prediction model with application to the advanced communication technology satellite project. Part 2: Theoretical development of a dynamic model and application to rain fade durations and tolerable control delays for fade countermeasures
[NASA-TM-100242] 03 p0308 N88-11945
X-band uplink ground systems development: Part 2
04 p0436 N88-12703
Tau ranging revisited 04 p0437 N88-12710
INPE position paper on the CCSDS standardized method of link budget computation
[INPE-4533-NTE/279] 15 p2148 N88-22820
Experimental radio frequency link for Ka-band communications applications
[NASA-TM-100824] 18 p2470 N88-24659
A statistical rain attenuation prediction model with application to the advanced communication technology satellite project. 1: Theoretical development and application to yearly predictions for selected cities in the United States
[NASA-CR-179498] 23 p3205 N88-29077

UPPER AIR
U UPPER ATMOSPHERE

UPPER ATMOSPHERE
NT D REGION
NT E REGION
NT EARTH IONOSPHERE
NT F REGION
NT F 2 REGION
NT LOWER IONOSPHERE
NT SPORADIC E LAYER
NT THERMOSPHERE
NT UPPER IONOSPHERE
Integrated systems with applications to the multi-phases of the ephemerides, physics and methematics of the upper atmosphere
[AD-A185748] 06 p0743 N88-14570
Holes in OI 130 nm emission fields of upper atmosphere during day 08 p1004 N88-16082
Lidar metal density measurements in the upper atmosphere 08 p1027 N88-16219
The influence of atmospheric thermal tides on diurnal variations in chemical constituents in the mesosphere
11 p1512 N88-19035
High resolution infrared absorption spectra of various trace gases present in the upper atmosphere of the Earth
[NASA-CR-182590] 12 p1642 N88-19829
Quality control of upper air conventional data (TEMP and PILOT)
[INPE-4223-RPE/546] 12 p1647 N88-19862
Measurement of rate constants of elementary gas reactions of importance to upper atmosphere and combustion systems
[AD-A189432] 13 p1737 N88-20386
Study of polyatomic dynamics in the atmosphere
[AD-A190964] 16 p2233 N88-23334
Fog, rain and aerosol attenuation in the atmosphere
[AD-A190867] 16 p2235 N88-23350
The precipitation of energetic heavy ions into the upper atmosphere of Jupiter
[NASA-TM-101155] 17 p2452 N88-24565
Observations of wave number dependent spectral line ratio fluctuations in the atmospheric emissions
[IRF-PREPRINT-101] 18 p2542 N88-25085
Components of an atmospheric lidar system
[AD-A193366] 21 p2953 N88-27539
Design, development, fabrication and launch support for a high altitude release of neodymium vapor
[AD-A194196] 22 p3118 N88-28527
Present state of knowledge of the upper atmosphere 1988: An assessment report
[NASA-RP-1208] 23 p3232 N88-29233
Approximation of atmospheric density by Chebyshev polynomials in predicting motion of low artificial earth satellites 24 p3445 N88-30503

UPPER IONOSPHERE
NT F REGION
NT F 2 REGION
Experimental proof of quasilongitudinal propagation of low-frequency waves in middle latitudes in upper ionosphere 24 p3447 N88-30516

UPPER STAGE ROCKET ENGINES
Altitude simulation testing of Ariane's second-stage engine 09 p1126 N88-16747
The HM-7 engine of Ariane's third stage
09 p1126 N88-16753
Centaur G Prime modal test 09 p1181 N88-17075
LGM-30B stage 2 disected motor test report
[AD-A190771] 15 p2027 N88-22079

UPPER SURFACE BLOWING
On the effect of leading edge blowing on circulation control airfoil aerodynamics 10 p1270 N88-17595
A potential flight evaluation of an upper-surface-blowing/circulation-control-wing concept
10 p1272 N88-17609

UPPER SURFACE BLOWN FLAPS
A numerical investigation on wing/nacelle interferences 05 p0535 N88-13258

UPPER VOLTA
U BURKINA

UPSTREAM
Relaxation method for the compressible Navier-Stokes equations using upwind schemes
05 p0539 N88-13283
Upwind formulations for the Euler equations
08 p0984 N88-15952
A survey of upwind principles for the multidimensional Euler equations 08 p0984 N88-15953

UPWELLING
U UPWELLING WATER

UPWELLING WATER
Satellite and synoptic studies of chemical fronts in the California current and coastal upwelling zone
[AD-A183909] 01 p0073 N88-10466
Biogeochemical cycling in the ocean. Part 1: Introduction to the effects of upwelling along the west coast of North America
[NASA-TM-88230] 07 p0882 N88-15349
North Pacific Ocean. Gulf of Alaska, R/V Thomas G. Thompson: 1 February - 8 March 1967. STD data report
[AD-A186569] 08 p1045 N88-16314
Circulation and exchange processes on the South Atlantic Bight Continental Shelf
[DE88-003330] 13 p1804 N88-20781
Biological processes in the water column of the South Atlantic bight: Zooplankton responses
[DE88-004811] 14 p1951 N88-21630
Changes in the California current system observed off northern California during July-August 1986
[AD-A190027] 15 p2100 N88-22510
Numerical simulation of coastal upwelling phenomena in Cabo Frio (RJ) through a two layer finite element model
[INPE-4502-RPE/561] 16 p2237 N88-23361
Observations of frontal instabilities on an upwelling filament
[AD-A191051] 17 p2375 N88-24122
Stability of a coastal upwelling front over topography
[AD-A192354] 20 p2829 N88-26784
Evolution of thermal structure of Benguela upswelling system according to satellite and shipboard data
24 p3449 N88-30525

URACIL
Photochemical conversion of nucleic acid components catalyzed by lunar soil 06 p0750 N88-14604

URANIUM
NT URANIUM ISOTOPES
NT URANIUM 238
Relation between shock strength and strain-rate plasticity at maximum deviatoric stress
[DE87-011736] 01 p0061 N88-10390
Hydrogen retention and release from uranium dioxide
[DE88-002042] 07 p0829 N88-15030
Phenomenological model of superconductivity of heavy fermions in U(sub 1-x)ThsubxBesub13
09 p1238 N88-17423
An irradiation performance data base for nitride fuels
17 p2427 N88-24438

URANIUM ALLOYS
Strain rate effects in fast-gas-cooled uranium-titanium and uranium-niobium alloys
[OUEL-1683/87] 02 p0149 N88-10937

URANIUM COMPOUNDS
NT URANIUM FLUORIDES
Uranium nitride fuel swelling and thermal conductivity correlations 17 p2409 N88-24327
Evaluation of UN fuel pin failure modes and motion of fuel during severe accidents for reactors in space
17 p2425 N88-24424
Material property and irradiation performance correlations for nitride fuels 17 p2434 N88-24483
A comparison of uranium nitride and mixed carbide fuels swelling 17 p2435 N88-24485

URANIUM FLUORIDES
Neutronics conceptual design of a UF6-fueled gasesous laser system 17 p2422 N88-24405

URANIUM ISOTOPES
NT URANIUM 238
High dose uranium ion implantation into silicon
[LBL-23509] 19 p2725 N88-26182

URANIUM 238
Diffusion bonding depleted uranium to copper
[RFP-3783-REV] 03 p0333 N88-12098

URANUS (PLANET)
Electrical conductivity and equation of state measurements on planetary fluids at high pressures and temperatures
[DE87-013787] 01 p0110 N88-10708
IUE program SUGSD: Varability time scale of H Ly-alpha from Uranus
[NASA-CR-182706] 13 p1856 N88-21107
Ultraviolet geometric albedo of Uranus
[NASA-CR-183099] 20 p2885 N88-27136

URANUS ATMOSPHERE
The solar radiation incident at the top of the atmosphere of Uranus and Neptune
[AERONOMICA-ACTA-A-317-1987]
07 p0878 N88-15323
Magnetic field of planet Uranus: Predictions, measurements, interpretations 08 p1005 N88-16094
Superthermal electron processes in the upper atmosphere of Uranus: Aurora and electroglow
[NASA-TM-101150] 18 p2594 N88-25417

URANUS RINGS
Discovery by Voyager-2 of predicted satellites which determine resonance nature of Uranian rings
08 p1006 N88-16095

URANUS SATELLITES
NT TITANIA
Discovery by Voyager-2 of predicted satellites which determine resonance nature of Uranian rings
08 p1006 N88-16095

URBAN AREAS
U CITIES

URBAN DEVELOPMENT
Department of Housing and Urban Development, and Certain Independent Agencies Appropriations, 1988, Part 2
[S-HRG-100-106-PT-2] 03 p0385 N88-12423
Orbital remote sensing: An instrument for monitoring urban growth
[INPE-4456-PRE/1287] 15 p2150 N88-22833
Earth resources: A continuing bibliography with indexes (issue 57)
[NASA-SP-7041(57)] 16 p2229 N88-23314

Applications of multitemporal compositions obtained from LANDSAT data in the study of urban growth
[INPE-4480-PRE/1246] 16 p2287 N88-23892

Four urban heliport case studies
[DOT/FAA/PM-87/32] 19 p2604 N88-25463

Remote sensing techniques applied to the study of metropolitan regions: The west sector of the Sao Paulo metropolitan area 19 p2681 N88-25941

Remote sensing applied to the monitoring of mineral extraction in the proximity of urban areas: Pros and cons 19 p2684 N88-25954

SPOT imagery for detecting residential expansion on the rural-urban fringe of Toronto, Canada 22 p3098 N88-28397

Spread of large tropical conurbations 22 p3098 N88-28398

Applications of SPOT data for urban real estate investment information systems 22 p3101 N88-28414

Utilization of SPOT multispectral data for urban planning 22 p3101 N88-28418

URBAN PLANNING

Adaptation of numerical SPOT data to an urban environment 03 p0342 N88-12158

Orbital remote sensing: An instrument for monitoring urban growth
[INPE-4456-PRE/1287] 15 p2150 N88-22833

Analyses of heliport system plans
[DOT/FAA/PM-87/31] 17 p2308 N88-23810

Low altitude remote sensing data in the implementation of a mathematical model for the planning of urban equipment networks 17 p2363 N88-24074

Four urban heliport case studies
[DOT/FAA/PM-87/32] 19 p2604 N88-25463

National Meeting on Remote Sensing Applied to Municipal Planning 19 p2681 N88-25939

Mapping of land use in Sao Jose dos Campos municipality by remote sensing, an aid for the elaboration of its PDDI 19 p2681 N88-25940

The impact of disorganized occupation of urban sub-basins: Sub-basin of the Cabucu River, metropolitan area of Sao Paulo (SP) 19 p2682 N88-25945

Remote sensing technique applied to vegetation as an aid to municipal planning 19 p2683 N88-25951

Monitoring urban land cover changes at the urban fringe from SPOT HRV imagery in south-east England 22 p3099 N88-28406

Utilization of SPOT multispectral data for urban planning 22 p3101 N88-28418

URBAN RESEARCH

Urban cartography: A book review 16 p2227 N88-23297

SPOT imagery for detecting residential expansion on the rural-urban fringe of Toronto, Canada 22 p3098 N88-28397

Utilization of remote sensing for the observation of urban populations. Ongoing research in Quito (Ecuador) 22 p3098 N88-28399

Monitoring urban land cover changes at the urban fringe from SPOT HRV imagery in south-east England 22 p3099 N88-28406

Mapping and urban multi-experimental assessment of SPOT: Urban results 22 p3101 N88-28415

Comparison of SPOT, LANDSAT TM and combined data for urban studies 22 p3101 N88-28417

Radiometric analysis and potential of SPOT HRV imagery for applications in urban environments and geology 22 p3112 N88-28486

URBAN TRANSPORTATION

Adiabatic diesel engine component development: Reference engine for on-highway applications
[NASA-CR-179531] 03 p0386 N88-12428

Electric vehicle demonstration project
[DE88-004076] 11 p1566 N88-19376

Digital maps for an electronic traffic guide 18 p2534 N88-25033

UREAS

Validation of maximum permissible concentration of urea in reclaimed potable water and evaluation of its biological effect 19 p2705 N88-26086

URETHANES

Stressed fabric abrasion test procedure for urethane coated fabric fuel tanks
[AD-A196327] 24 p3356 N88-29982

URINE

Human adaptation to various hypercapnic conditions in relation to salivary electrolyte dynamics and renal function 12 p1664 N88-19977

USA (UNITED STATES)

U UNITED STATES

USER MANUALS (COMPUTER PROGRAMS)

Space station integrated wall design and penetration damage control
[NASA-CR-179169] 01 p0013 N88-10070

Hanford Meteorological Station computer codes. Volume 1: The GEN computer code
[DE87-012816] 01 p0071 N88-10456

A user's guide for BIE3D: A boundary integral equation computer program for three-dimensional elastostatic analysis
[RAE-TM-MAT-STR-1078] 01 p0079 N88-10509

Manual for GetData version 3.1: A FORTRAN utility program for time history data
[NASA-TM-86288] 01 p0081 N88-10520

TIPS-1 user's manual: Cray-1 version
[DE87-013297] 01 p0081 N88-10522

EVA reference manual
[DE87-014073] 01 p0082 N88-10526

NOSTRADAMUS programmable translator user's manual and programmer's manual
[DE87-013414] 01 p0083 N88-10533

Blade loss transient dynamics analysis, volume 2. Task 2: TETRA 2 user's manual
[NASA-CR-179633] 02 p0126 N88-10792

RANDOM NUMBER: A syntax-directed package to produce random numbers in user-specified, univariate distributions. User's guide
[DE87-014278] 02 p0228 N88-11436

Numerical simulation of internal combustion engine flows: Development and users guide for MAGIC radial-azimuthal version
[DE87-014453] 03 p0332 N88-12091

The user's guide to the BACK system --- knowledge representation
[KIT-42] 03 p0367 N88-12310

Competition Analysis Model (CAM). Volume 2: Computer manual
[AD-A184017] 03 p0384 N88-12411

IDMS application documentation made easy
[DE88-000199] 03 p0384 N88-12416

Digital-flight-control-system software written in automated-engineering-design language: A user's guide of verification and validation tools
[NASA-TM-88313] 04 p0401 N88-12494

NACHOS 2: A finite element computer program for incompressible flow problems. Part 2: User's manual
[DE88-001451] 04 p0443 N88-12750

User's guide to NCAR (National Center for Atmospheric Research) CCM1
[PB87-224366] 04 p0469 N88-12899

SDVS (State Delta Verification System) 5 users' manual
[AD-A184339] 04 p0478 N88-12943

PROVER: A first-order logic system in Ada
[DE88-000220] 04 p0479 N88-12951

Guidelines for preparing software user documentation
[NASA-CR-181550] 04 p0480 N88-12959

SUSIE reference manual
[DE88-001462] 05 p0636 N88-13893

Diagnostic emulation: Implementation and user's guide
[NASA-CR-178391] 06 p0756 N88-14638

User manual for ATILA, a finite-element code for modeling piezoelectric transducers
[AD-A185948] 07 p0847 N88-15141

GENLPLOT: An interactive program for display and analysis of data, user's manual
[DE88-002292] 07 p0905 N88-15485

Attitude dynamics for satellites stabilized through spin
[INPE-4403-NTE/275] 08 p0963 N88-15833

User's guide to DIANE: A microcomputer program for modeling battery performance in electric vehicles
[DE88-003713] 08 p1068 N88-16456

Numerical arc segmentation algorithm for a radio conference-NASARC, version 2.0: User's manual
[NASA-TM-100161] 09 p1156 N88-16928

Guide for the program EXACT-NL — wave growth
[KNMI-TR-94] 09 p1163 N88-16971

Nimbus 7 Solar Backscatter Ultraviolet (SBUV) spectral scan solar irradiance and Earth radiance product user's guide
[NASA-RP-1199] 09 p1184 N88-17096

Voice technology using personal computers
[AD-A186743] 09 p1218 N88-17300

Handbook of the GEMS image processing system
[RAE-TR-86062] 09 p1219 N88-17310

General Rotorcraft Aeromechanical Stability Program (GRASP) version 1.03: User's manual
[NASA-TM-100043] 09 p1219 N88-17313

Operators manual for a computer controlled impedance measurement system
[AD-A187513] 10 p1324 N88-17917

MOAOPS and BOOM-MAP computer programs for sonic boom research, volume 1
[AD-A189548] 12 p1574 N88-19414

KREME (Knowledge Representation, Editing and Modeling Environment): A user's introduction, phase 1
[AD-A188906] 12 p1681 N88-20052

An interactive user-friendly approach to surface-fitting three-dimensional geometries
[NASA-CR-4126] 12 p1682 N88-20058

NFEARS (Nonlinear Finite Element Adaptive Research Solver): A nonlinear adaptive finite element solver. Part 2: User's manual
[AD-A189009] 12 p1684 N88-20070

Martian Clouds Data Workshop
[NASA-CR-182431] 12 p1711 N88-20238

Documentation and installation of the hypersonic arbitrary-body computer program (Mark 3 version) of A.E. Gentry on the IBM computer system
[MBB/LKE-127/S/PUB/256] 13 p1719 N88-20276

MOPAC manual: A general molecular orbital package, fourth edition
[AD-A188623] 13 p1733 N88-20362

MASPLT: A one-dimensional graphics post processor for wave propagation codes
[DE88-005506] 13 p1817 N88-20856

FLAP (Force and Loads Analysis Program) code development and validation
[DE88-001131] 15 p2075 N88-22371

Analysis of rotating flexible blades using MSC/NASTRAN 16 p2222 N88-23259

Integrated multidisciplinary analysis tool IMAT users' guide
[NASA-TM-100605] 16 p2223 N88-23273

COBOL Analysis System (CAS) users manual
[PB88-171442] 16 p2250 N88-23445

Fast Algorithm Simulation and Test (FAST) facility
[AD-A191183] 16 p2252 N88-23457

User's guide to the Fault Inferring Nonlinear Detection System (FINDS) computer program
[NASA-CR-178410] 18 p2462 N88-24619

SAM 2 data user's guide
[NASA-RP-1200] 18 p2543 N88-25094

Graphical Multiprocessing Analysis Tool (GMAT)
[DE88-008019] 19 p2715 N88-26116

A description of the reference frames and the coordinate transformations used in AMEER (Aero-Mechanical Equations Evaluations Routines)
[DE88-007960] 19 p2720 N88-26153

Axisymmetric liquid sloshing under low-g conditions: Numerical simulation method (reference manual)
[NLR-TR-86057-U] 20 p2802 N88-26627

PAX ECONOPACK economic analysis package users manual
[AD-A192949] 20 p2883 N88-27117

User's manual for C-HEMP: A two-dimensional wave propagation code. Volume 1: Description and derivations of the code
[AD-A193197] 21 p2944 N88-27486

DYNA3D (Nonlinear Dynamic Analysis of Structures in Three Dimensions) user's manual
[DE88-012242] 21 p2963 N88-27604

National air toxics information clearinghouse: NATICH data base users guide for data viewing, February 1988
[PB88-197470] 21 p2970 N88-27645

A PRELUDE (analysis and design of control systems-preliminary utilities depository). A data-based interactive system of control software, user's guid e
[DFVLR-MITT-88-12] 21 p3000 N88-27795

User's manual for the two-dimensional transputer graphics toolkit
[NASA-TM-100974] 21 p3001 N88-27799

Program user's manual for an unsteady helicopter rotor-fuselage aerodynamic analysis
[NASA-CR-181701] 22 p3039 N88-28047

Walter user's manual (Version 1.0)
[AD-A192542] 22 p3136 N88-28644

Loglisp programming system users manual
[AD-A193933] 22 p3142 N88-28682

Finite Element Composite Analysis Program (FECAP) for a microcomputer
[NASA-TM-100670] 23 p3190 N88-28982

Signal processing software for ground penetrating radar, user's manual
[AD-A194286] 23 p3203 N88-29059

Level 1 Ada/SQL (Structured Query Language) database language interface user's guide
[AD-A194480] 23 p3249 N88-29335

User's manual for three dimensional boundary layer (BL3-D) code
[NASA-CR-174899] 24 p3369 N88-30063

Supermap for Cray FORTRAN: A user's guide
[NASA-CR-177410] 24 p3412 N88-30308

The eivaN: A forward-looking interactive orbital trajectory plotting tool for use with proximity operations (PROX OPS) and other maneuvers: Description and user's manual
[NASA-CR-177490] 24 p3414 N88-30327

An operations manual for the digital data system
[NASA-CR-181688] 24 p3415 N88-30329

Aircraft noise prediction program propeller analysis system IBM-PC version user's manual version 2.0
[NASA-CR-181689] 24 p3428 N88-30399

USER REQUIREMENTS

Space station platforms 01 p0015 N88-10086

Spacecraft Systems Working Group report 01 p0015 N88-10091

Electrical Power Working Group report
01 p0016 N88-10095
Development of methods for the analysis of the frequency and voltage statics of electricity users and electrical networks
[ETN-87-90412] 01 p0043 N88-10271
Battery development and testing at ESA
02 p0164 N88-11027
Applications and benefits of short period weather forecasts 02 p0199 N88-11240
Tutorial and hands-on demonstration of a fluent interpreter for CARE 3
[NASA-TM-4011] 02 p0220 N88-11383
A general approach to error propagation
[DE87-014287] 02 p0224 N88-11412
Orbital Spacecraft Consumables Resupply System (OSCRS). Volume 4: Extended study results Part 1: Executive Summary
[NASA-CR-172012] 03 p0268 N88-11686
Optical laser technology, specifically CD-ROM (Compact Disc - Read Only Memory) and its application to the storage and retrieval of information
[AD-A184111] 03 p0330 N88-12086
An overview of remote sensing users' requirements
03 p0340 N88-12139
SDVS (State Delta Verification System): Program verification system development fiscal year 1986
[AD-A184338] 03 p0366 N88-12302
Concepts and techniques for support of real time distributed operating systems
[AD-A184491] 03 p0367 N88-12307
Guidelines for preparing software user documentation
[NASA-CR-181550] 04 p0480 N88-12959
User interface for a partially incompatible system software environment with non-ADP users
[DE88-001518] 04 p0482 N88-12968
On the next generation of reliability analysis tools
[NASA-CR-178380] 04 p0487 N88-13000
Small reactor power systems for manned planetary surface bases
[NASA-TM-100223] 04 p0524 N88-13209
Orbital Spacecraft Consumables Resupply System (OSCRS). Volume 1: Executive summary
[NASA-CR-172010] 05 p0553 N88-13368
File usage analysis and resource usage prediction: A measurement-based study
[NASA-CR-181553] 05 p0633 N88-13867
Usage analysis of user files in UNIX
[NASA-CR-181561] 05 p0633 N88-13868
Window system: A toolbox for interactive computer graphics
[PB87-234282] 06 p0756 N88-14637
Using user models and automatic expertise acquisition in data base interactions
[PB87-234357] 06 p0791 N88-14848
Scientific data manipulation in a relational database system
[PB87-124400] 06 p0791 N88-14850
FAA air traffic control operations concepts. Volume 5: ATCT/TCCC (Airport Traffic Control Tower/Tower Control Computer Complex) tower controllers
[AD-A185983] 07 p0818 N88-14977
An approach to validation and verification of the communications load model with supporting user's guide
[AD-A185926] 07 p0840 N88-15098
A multi user random access communication system for users with different priorities
[AD-A186041] 07 p0841 N88-15102
Using multiple dialog modes in a user-system interface to accomodate different levels of user experience: An experimental study
[AD-A186115] 07 p0899 N88-15444
TeXting the FORMULARY: A collection of examples of the use of TeX to produce ruled tables and displayed equations
[AD-A185920] 07 p0921 N88-15598
User interface devices for mission control
09 p1205 N88-17224
User engineering: A new look at system engineering
09 p1206 N88-17231
POCC capabilities document. Payload support capabilities description: MCC, JSC POCC, remote POCC interface
[NASA-TM-89708] 09 p1260 N88-17555
Shared workspaces for real-time collaboration in distributed networks: Concepts, techniques, problems
[AD-A188150] 10 p1394 N88-18315
Presentation of flight control design and handling quality commonality by separate surface stability augmentation for the family of commuter airplanes
[NASA-CR-182567] 12 p1583 N88-19471
Customer concerns regarding satellite servicing
12 p1587 N88-19503
Conceptual design and programmatics studies of space station accommodations for Life Sciences Research Facilities (LSRF)
[NASA-CR-179270] 12 p1598 N88-19567
User perceptions of side-arm flight control in rotary-wing aircraft
[AD-A188519] 12 p1672 N88-20009
A digital logic simulator with concurrent programming considerations
[AD-A188823] 12 p1678 N88-20032
A prototype for remotely shared textual workspaces
[AD-A188352] 12 p1679 N88-20040
An interactive user-friendly approach to surface-fitting three-dimensional geometries
[NASA-CR-4126] 12 p1682 N88-20058
A directory of databases available through SearchMAESTRO
[AD-A188813] 12 p1706 N88-20214
Orbital transfer vehicle concept definition and system analysis study. Volume 2: OTV concept definition and evaluation. Book 1: Mission and system requirements
[NASA-CR-179321] 13 p1729 N88-20339
Online aiding for human-computer interfaces
[AD-A189239] 13 p1815 N88-20842
Investigation of European remote sensing user needs in accessing MOS-1 payload
[ESA-CR(P)-2535] 14 p1940 N88-21580
DataViews: A personalizable, interactive, data display system for the decisionmaker
[AD-A188509] 14 p1991 N88-21868
Real-time flight test data distribution and display
[NASA-TM-100424] 15 p2022 N88-22050
ECP (Electrical Circuitry Program): A proposed program for electrical circuitry analysis
[AD-A190494] 15 p2060 N88-22280
CK-LOG system conversion (user's manual and user interface)
[AD-A190273] 15 p2111 N88-22577
Maps for tourists. A systematic approach to tourist cartography 16 p2227 N88-23296
WMO Region 2/Region 5 Training Seminar on Climate Data Management and User Services
[WCP-133] 16 p2234 N88-23344
Concurrency efficiency user's manual
[AD-A190884] 16 p2251 N88-23450
PPDS compas-primer
[DE88-701589] 16 p2266 N88-23554
Data management strategies in the industrial environment
[NLR-MP-87002-U] 16 p2286 N88-23684
Solid Earth mission end-to-end data system study
[C04825.08/FR] 17 p2309 N88-23811
Practical image analysis using personal computers: The Canadian experience 17 p2356 N88-24037
The SAGE geographic analysis system
17 p2361 N88-24063
Multimegawatt power conditioning requirements study
17 p2438 N88-24504
P-Plus: Polar Platform utilization study, executive summary
[BAE-TP-8391] 18 p2469 N88-24653
CIMAG2: The computer program to generate color images
[AD-A191847] 18 p2557 N88-25175
Department of Defense statement on the X-ray Lithography Program to the Research and Development Subcommittee of the House Armed Services Committee of 100th Congress, second session
[AD-A191854] 18 p2582 N88-25341
Advanced development of double-injection, deep-impurity semiconductor switches
[NASA-CR-182118] 18 p2583 N88-25346
Mars rover/sample return mission requirements affecting space station
[NASA-CR-172048] 18 p2594 N88-25414
Ocean satellite data and the needs of designers and operators of marine units 19 p2701 N88-26061
Flight Mechanics Panel Symposium on Rotorcraft Design for Operations: Technical evaluation report
[AGARD-AR-243] 20 p2758 N88-26362
Direct manipulation and the design of user interfaces
[PB88-126354] 20 p2834 N88-26810
SIMS: Single Interface to Multiple Systems
[AD-A192264] 20 p2837 N88-26832
Interaction management in CAD systems with a history mechanism
[CWI-CS-R8756] 20 p2840 N88-26851
Programmer-friendly LL(1) parser generator
[PB88-126933] 20 p2841 N88-26857
Engineering data compendium. Human perception and performance. User's guide
[LC-87-19560] 21 p2993 N88-27749
Software engineering guidelines for RASP and ANDECS: Requirements and architectural design
[DFVLR-MITT-88-07] 21 p3000 N88-27793
Capitalizing on experience with intelligence gateway software
[AD-A193362] 21 p3028 N88-27971
The management of software in airborne recording systems 22 p3035 N88-28019
Engineering data compendium. Human perception and performance, volume 2
[LC-87-19560] 22 p3134 N88-28631
Engineering data compendium. Human perception and performance, volume 3
[LC-87-19560] 22 p3134 N88-28632
Loglisp programming system users manual
[AD-A193933] 22 p3142 N88-28682
ADP (Automated Data Processing) requirements definition and documentation through user-developed prototypes
[AD-A194407] 23 p3248 N88-29332
An adaptive overlapping local grid refinement method for two-dimensional parabolic systems
[AD-A193560] 23 p3271 N88-29464
Central user and browse service --- ERS-1 ground segment
[CU-PG-MDA-SY-0005] 23 p3297 N88-29637
MANIP --- spacecraft modeling program
[MANIP-217A] 24 p3335 N88-29855
A static scheduler for the computer aided prototyping system: An implementation guide
[AD-A194340] 24 p3414 N88-30322
Integrated resource scheduling in a distributed scheduling environment 24 p3417 N88-30342

USER-COMPUTER INTERFACE
U MAN-COMPUTER INTERFACE

UTILITIES
Methodology for control and operation of wind arrays in utility systems
[DE87-013129] 01 p0039 N88-10248
The Environment for Application Software Integration and Execution (EASIE) version 1.0. Volume 4: System installation and maintenance guide
[NASA-TM-100576] 17 p2386 N88-24185
Phosphoric acid electric utility fuel cell technology development
[DE88-010187] 20 p2795 N88-26582

UTILITY AIRCRAFT
NT BO-105 HELICOPTER
NT DO-28 AIRCRAFT
NT U-2 AIRCRAFT
NT UH-1 HELICOPTER
NT UH-60A HELICOPTER

UTILIZATION
NT GEOTHERMAL ENERGY UTILIZATION
NT LASER APPLICATIONS
NT LASER CUTTING
NT LASER FUSION
NT REUSE
NT WASTE ENERGY UTILIZATION
NT WASTE UTILIZATION
NT WINDPOWER UTILIZATION
Photocurrent generation from basic metals, utilizing a short pulsed ArF excimer laser
[AD-A184928] 05 p0587 N88-13579
Disuse condition stimulates bone resorption in organ culture 12 p1656 N88-19926

UV CETI STARS
U FLARE STARS

UV LASERS
U ULTRAVIOLET LASERS

V

V BAND
U EXTREMELY HIGH FREQUENCIES

V/STOL AIRCRAFT
NT AH-64 HELICOPTER
NT BO-105 HELICOPTER
NT CH-46 HELICOPTER
NT COMPOUND HELICOPTERS
NT HEAVY LIFT HELICOPTERS
NT HELICOPTERS
NT MILITARY HELICOPTERS
NT OH-58 HELICOPTER
NT RIGID ROTOR HELICOPTERS
NT ROTARY WING AIRCRAFT
NT ROTOR SYSTEMS RESEARCH AIRCRAFT
NT SHORT TAKEOFF AIRCRAFT
NT TANDEM ROTOR HELICOPTERS
NT TILT ROTOR AIRCRAFT
NT UH-1 HELICOPTER
NT UH-60A HELICOPTER
NT VERTICAL TAKEOFF AIRCRAFT
NT XV-15 AIRCRAFT
Flight research at NASA Ames Research Center: A test pilot's perspective
[NASA-TM-100025] 02 p0125 N88-10788

Civil applications of high-speed rotorcraft and powered-lift aircraft configurations
[NASA-TM-100035] 03 p0261 N88-11643
V/STOL aircraft configurations and opportunities in the Pacific Basin
[NASA-TM-100005] 03 p0261 N88-11644
Test stand performance of a convertible engine for advanced V/STOL and rotorcraft propulsion
[NASA-TM-100211] 03 p0266 N88-11679
Flight propulsion control integration for V/STOL aircraft
[NASA-TM-100226] 03 p0267 N88-11680
Integrated control and display research for transition and vertical flight on the NASA V/STOL Research Aircraft (VSRA)
[NASA-TM-100029] 05 p0551 N88-13359
Full-envelope aerodynamic modeling of the Harrier aircraft
[NASA-TM-88376] 05 p0552 N88-13363
NASA supersonic STOVL propulsion technology program
[NASA-TM-100227] 06 p0668 N88-14093
A jet in a crossflow
[NASA-CR-182469] 09 p1113 N88-16674
A flight-test methodology for identification of an aerodynamic model for a V/STOL aircraft
[NASA-TM-100067] 09 p1117 N88-16694
Application of empirical and linear methods to VSTOL powered-lift aerodynamics
[NASA-TM-100048] 10 p1267 N88-17581
Recommendations for ground effects research for V/STOL and STOL aircraft and associated equipment for large scale testing
[NASA-CR-177429] 10 p1268 N88-17585
A computational study of thrust augmenting ejectors based on a viscous-inviscid approach
10 p1326 N88-17929
A review of technologies applicable to low-speed flight of high-performance aircraft investigated in the Langley 14- x 22-foot subsonic tunnel
[NASA-TP-2796] 13 p1717 N88-20264
Propulsion and airframe aerodynamic interactions of supersonic V/STOL configurations. Volume 1: Wind tunnel test pressure data report
[NASA-CR-177343-VOL-1] 16 p2157 N88-22866
Propulsion and airframe aerodynamic interactions of supersonic V/STOL configurations. Volume 2: Wind tunnel test force and moment data report
[NASA-CR-177343-VOL-2] 16 p2157 N88-22867
Propulsion and airframe aerodynamic interactions of supersonic V/STOL configurations. Volume 4: Summary
[NASA-CR-177343-VOL-4] 16 p2157 N88-22868
A numerical study of the hot gas environment around a STOVL aircraft in ground proximity
[NASA-TM-100895] 17 p2295 N88-23729
PAN AIR analysis of the NASA/MCAIR 279-3: An advanced supersonic V/STOL fighter/attack aircraft
[NASA-TM-86838] 17 p2298 N88-23750
Flight testing a V/STOL aircraft to identify a full-envelope aerodynamic model
[NASA-TM-100996] 17 p2301 N88-23762

VACANCIES (CRYSTAL DEFECTS)
Interaction between defects and the formation of dissipative structures in irradiated impure crystals
[DE87-703125] 02 p0246 N88-11552
Simulation of the layer-growth dynamics in silver films: Dynamics of adatom clusters and vacancy clusters on Ag(100)
[DE87-014764] 03 p0380 N88-12390
Evolution of radiation-induced voids and dislocations at low temperature
[DE88-700350] 07 p0939 N88-15704
Effect of irradiation on the diffusion evolution of void ensemble in crystals
[DE88-700558] 07 p0939 N88-15706
Structural properties of high-T/sub c/ oxide super conductors
[DE88-002974] 08 p1090 N88-16563
Electron diffraction evidence for the ordering of excess nickel atoms by relation to stoichiometry in nickel-rich beta'-NiAl formation of a nickel-aluminum (Ni2Al) superlattices
[NASA-TT-20177] 14 p1890 N88-21297
Abnormal diffusion of vacancies in metals
[DE88-701880] 20 p2773 N88-26441

VACUUM
NT HIGH VACUUM
NT LOW VACUUM
NT ULTRAHIGH VACUUM
Synergism of electroplating and vacuum processes
[DE87-013496] 01 p0033 N88-10211
Recovery of vacuum gaps after arcing
[DE87-013852] 01 p0039 N88-10250
Physics and device design of vacuum integrated circuits 01 p0039 N88-10251
Different ways of looking at the electromagnetic vacuum
[DE87-013150] 01 p0089 N88-10584
A new type of lamp and reflector for I.R. simulation
02 p0136 N88-10855
Vacuum ultraviolet electronic properties of liquids
[DE88-000165] 03 p0282 N88-11772
Cosmology with decaying vacuum energy
[DE88-000698] 03 p0389 N88-12443
Model of earlier stage of universe's evolution
06 p0775 N88-14758
Approximate method for predicting the permanent set in a beam in vacuo and in water subject to a shock wave 11 p1500 N88-18957
Molecular collision processes in gases and at surfaces
[AD-A189518] 13 p1836 N88-20982
A high field launch for electron cyclotron heating using an external window
[DE88-005350] 13 p1838 N88-21000
Vacuum-arc plasma centrifuge experiment
[INPE-4509-PRE/1263] 15 p2138 N88-22758
High frequency power distribution system
[NASA-CR-175071] 17 p2335 N88-23939
Propagation of neutralized ion beams
[AD-A191599] 18 p2574 N88-25289
Multiply stripped ion generation in the metal vapor vacuum arc
[DE88-008418] 19 p2725 N88-26179
A bibliography and author index for electrical discharges in vacuum (1897-1986)
[DE88-008744] 20 p2794 N88-26579
Theory and simulation of relaxed plasmoids
[AD-A192884] 21 p3032 N88-27997
Measurements of vacuum arc ion charge state distributions
[DE88-008249] 23 p3284 N88-29558

VACUUM APPARATUS
NT IONIZATION GAGES
NT VACUUM CHAMBERS
NT VACUUM GAGES
NT VACUUM PUMPS
Plasma centrifuge development at INPE
[INPE-4243-PRE/1117] 08 p1087 N88-16546
Three dimensional Monte Carlo simulation of molecular movement and heat radiation in vacuum devices: Computer code MOVAK3D --- fusion reactors
[KFK-4292] 09 p1246 N88-17471
Research and development of surface skimming bulk wave devices for sensor applications
[AD-A187504] 11 p1470 N88-18766
Planning, construction, and commissioning of a vacuum apparatus with a cold surface for the measurement of transistor functions at 20 K
[JUEL-SPEZ-397] 12 p1622 N88-19703
Low temperature storage container for transporting perishables to space station
[NASA-CASE-MFS-28248-1] 18 p2498 N88-24817
High temperature testing of C/C (Carbon/Carbon) composites
[AD-A193012] 20 p2768 N88-26411

VACUUM ARC SWITCHES
Measuring technical and mathematical investigation of multiple reignitions at the switching of a motor using vacuum circuit breakers
[ETN-87-90406] 01 p0042 N88-10270
Low-current behavior and current chopping of vacuum arcs
[ISBN-90-9001649-X] 05 p0578 N88-13529
The influence of ionization within a plasma opening switch
[AD-A193147] 21 p3017 N88-27906

VACUUM CHAMBERS
Meeting today's requirements for large thermal vacuum test facilities 02 p0134 N88-10840
Mobile test fixture system for use in a thermal vacuum facility 02 p0134 N88-10843
Test of the Hipparcos payload in the Liege vacuum facility focal 02 p0135 N88-10850
Evaluation and certification of heater assemblies developed for thermal vacuum acceptance testing
02 p0136 N88-10853
Thermal testing by internal IR heating of the FEP module 02 p0136 N88-10854
Chemical cleaning of metal surfaces in vacuum systems by exposure to reactive gases
[AD-A188588] 12 p1608 N88-19616
Ion generator and ion application system
[NASA-CASE-MFS-28122-1] 17 p2397 N88-24253
Conceptual design of the SP-100 GES test site
17 p2402 N88-24284

VACUUM DEPOSITION
Synthesis and characterization of thin films
[AD-A187335] 10 p1421 N88-18485
Deposition of device quality epitaxial layers of gallium nitride and indium nitride for electronic applications
[AD-A188001] 11 p1453 N88-18661
Design and demonstration of a system for the deposition of atomic-oxygen durable coatings for reflective solar dynamic power system concentrators
[NASA-CR-4158] 19 p2606 N88-25474
Laser measurement of particle velocities in vacuum plasma spray deposition
[DE88-007111] 19 p2728 N88-26198
Plasma deposition: Investigations on a new approach
[ETN-88-92619] 20 p2861 N88-26992
Growth and characterization of thin films of ZnSnP(sub)2
[DE88-001164] 20 p2874 N88-27060
Equipment for building and testing superconductive flux flow electronic devices
[AD-A192959] 21 p2936 N88-27436

VACUUM EFFECTS
Survival under space vacuum: Biochemical aspects
12 p1657 N88-19930
Ultraviolet (180 to 300 nm) action spectra for inactivation and DNA photoproduct formation of Bacillus subtilis spores under ultrahigh vacuum 12 p1657 N88-19931
Mechanical design of a ultrahigh gravity UHV facility to launch and recover a low-speed projectile tested on board KC 135 14 p1877 N88-21216

VACUUM GAGES
NT IONIZATION GAGES
Thermal vacuum sensors based on integrated silicon thermopiles
[ETN-88-92237] 16 p2210 N88-23190

VACUUM MELTING
Evaporation characteristics of elements during vacuum arc remelting of alloy A-286 15 p2055 N88-22248

VACUUM PUMPS
Vacuum pumps and systems: A review of current practice 02 p0134 N88-10839
Meeting today's requirements for large thermal vacuum test facilities 02 p0134 N88-10840
MPD (magnetoplasmadynamic) thruster advanced pumping system concepts
[AD-A190513] 15 p2138 N88-22756

VACUUM SYSTEMS
Meeting today's requirements for large thermal vacuum test facilities 02 p0134 N88-10840
Chemical cleaning of metal surfaces in vacuum systems by exposure to reactive gases
[AD-A188588] 12 p1608 N88-19616
Flotation processes
[PB88-180302] 18 p2540 N88-25075

VACUUM TESTS
NT THERMAL VACUUM TESTS
Outgassing data for selecting spacecraft materials
[NASA-RP-1124] 01 p0019 N88-10117
Altitude simulation testing of Ariane's second-stage engine 09 p1126 N88-16747
Robotic joint prototype for space applications
14 p1878 N88-21222
A test facility for the in-vacuo assessment of dry lubricants and small mechanisms at cryogenic temperatures 14 p1878 N88-21224
Separable electrical connectors for space: A tribological and electrical assessment 14 p1879 N88-21231

VACUUM TUBES
NT CATHODE RAY TUBES
NT CYCLOTRON RESONANCE DEVICES
NT KLYSTRONS
NT MAGNETRONS
NT MICROWAVE TUBES
NT TRAVELING WAVE TUBES

VACUUM ULTRAVIOLET RADIATION
U FAR ULTRAVIOLET RADIATION

VALENCE
Gaining control over rare earth valence fluctuations
[DE87-010116] 01 p0103 N88-10671
A quantum theoretical study of polyimides
[NASA-CR-181495] 03 p0292 N88-11831
The itinerant resonating-valence-bond model for superconductivity
[DE87-014794] 03 p0380 N88-12391
Superconductivity as a synchronous spatial alternation of valence bonds
[AD-A184208] 03 p0382 N88-12405
Valence bond theory and superconductivity
[AD-A184274] 04 p0496 N88-13052
Valence bond cluster studies of alkali metal/semiconductor bonding
[AD-A184276] 04 p0496 N88-13054
Atomic and electronic structure of surfaces and chemisorbed layers
[DE87-014987] 04 p0498 N88-13065
Electronic band structure and photoemission: A review and projection
[DE88-002236] 06 p0787 N88-14829
Electron Spin Resonance (ESR) measurements on intermediate-valence Cer compounds doped with paramagnetic ions: CeOs2:Gd ion and CePd3:Mn-ion
[ETN-88-91081] 09 p1256 N88-17526

Copper oxidation states, vacancy ordering and their effect on high temperature superconductivity
[DE88-003079] 09 p1258 N88-17542
Core-core and core-valence correlation
[NASA-CR-182552] 11 p1544 N88-19226
On the bond distance in methane
[NASA-CR-181436] 22 p3150 N88-28741

VALIDATION
U PROVING

VALKYRIE AIRCRAFT
U B-70 AIRCRAFT

VALLEYS
A real-data numerical study and four-dimensional data assimilation application for mesobeta-scale flow in complex terrain 02 p0212 N88-11329
Geological interpretation of a SPOT image over Kenya: The Gregory rift network of faults 03 p0343 N88-12164
Wind and temperature structure on the slopes of a mountain valley
[DE88-000080] 07 p0880 N88-15338
Cross flow in the Alps and flat foehn during the experiment MERKUR --- mesoscale experiment 08 p1013 N88-16142
The role of anabatic winds in the heating of valleys 08 p1014 N88-16144
Simulation of a typical flow in a broad valley 08 p1015 N88-16154
Groundwater sapping valleys: Experimental studies, geological controls and implications to the interpretation of valley networks on Mars
[NASA-CR-182718] 15 p2152 N88-22847
Application of remote sensing in the conservation of natural areas: Ribeira Valley 19 p2683 N88-25949
Intercrater plains deposits and the origin of Martian valleys 23 p3301 N88-29661

VALSALVA EXERCISE
The effect of orthostatic changes in central blood volume on the heart rate response to graded Valsalva maneuvers 12 p1653 N88-19904

VALSALVA MANEUVER
U VALSALVA EXERCISE

VALUE ENGINEERING
Value engineering --- space projects 22 p3160 N88-28817
Value analysis 22 p3161 N88-28819

VALVES
NT CONTROL VALVES
NT PRESSURE REGULATORS
Advanced natural gas fueled engine development. Part 2: Materials investigation
[PB87-223160] 03 p0331 N88-12088
Development, construction and testing of a novel internal combustion engine with conical rotating slide valve
[DE88-900071] 05 p0589 N88-13593
Gas feed system for the T-15 tokamak discharge chamber
[DE88-700351] 07 p0935 N88-15682
Influence of magnetic material on the transient of a controle electrovalve
[INPE-4418-PRE/1223] 12 p1624 N88-19713
Numerical methods in the resolution of control electrovalve model
[INPE-4154-RPE/540] 13 p1764 N88-20554

VAN ALLEN RADIATION BELTS
U RADIATION BELTS

VAN DE GRAAFF ACCELERATORS
Particle beam alignment system for single event upset-Van de Graaf experiments
[AD-A189695] 15 p2132 N88-22721

VAN DER WAAL FORCES
On the interaction of a planar metal surface with a charge and with a molecule
[DE87-703083] 02 p0147 N88-10920
The generalized van der Waals theory of pure fluids and mixtures
[DE88-002380] 07 p0855 N88-15192
Van der Waals clusters of aromatic molecules studied using supersonic molecular jet spectroscopy
[AD-A186087] 07 p0929 N88-15644
Half collision studies of inelastic energy transfer processes
[DE88-008096] 19 p2724 N88-26178
High resolution spectroscopy of dissociating molecules
[DE88-007959] 20 p2851 N88-26924

VANADIUM
Mechanical properties of an acicular ferrite steel microalloyed to niobium and vanadium
[DE87-703547] 04 p0415 N88-12574
Partial substitution of vanadium by niobium in AISI H13 steel
[DE87-703548] 04 p0415 N88-12575
Superconductivity and crystal structure of high-pressure phases in V-Ru-H system 09 p1239 N88-17426
Use of nonporous metals membranes for the separation of hydrogen from gas mixtures
[BMFT-FB-T-86-206] 14 p1888 N88-21280
Superconductivity of Cr/V superlattices 20 p2874 N88-27057
Constant amplitude fatigue life data for notched and unnotched annealed Ti-6Al-4V sheet
[AD-A193420] 21 p2913 N88-27287

VANADIUM ALLOYS
Investigation of creep crack growth in heat resistant tube steels
[ETN-87-90606] 03 p0288 N88-11813
Reduced-activation ferritic steels: A comparison with Cr-Mo steels
[DE88-000332] 03 p0290 N88-11826
The effect of neutron irradiation on the tensile properties and microstructure of several vanadium alloys
[DE88-001755] 06 p0682 N88-14176
Effect of overload ratios on fatigue crack growth behavior in Ti-6Al-4V alloy
[PB87-147062] 07 p0833 N88-15055
Experimental method for investigating helium effects in irradiated vanadium
[DE88-002891] 08 p0969 N88-15865
Influence of neutron irradiation on the Charpy impact properties of V-15Cr-5Ti
[DE88-003430] 11 p1458 N88-18692
Vibration spectra of oxygen and vanadium atoms in vanadium-oxygen disordered interstitial alloys
[DE87-703166] 13 p1740 N88-20404
Effect of hydrogen, deuterium and oxygen on the anelastic properties of refractory alloys
[DE88-007349] 18 p2484 N88-24736
The postirradiation tensile properties and microstructure of several vanadium alloys
[DE88-007140] 19 p2615 N88-25515
Low-chromium reduced-activation ferritic steels
[DE88-009060] 19 p2617 N88-25524
Stress relaxation of a titanium (Ti-6Al-4V) threaded joint
[DE88-010102] 21 p2961 N88-27590

VANADIUM COMPOUNDS
NT VANADIUM OXIDES

VANADIUM OXIDES
The development of a new and novel Hadamard transform infrared spectrometer for analytical chemistry
[DE87-014804] 02 p0175 N88-11094
Vibration spectra of oxygen and vanadium atoms in vanadium-oxygen disordered interstitial alloys
[DE87-703166] 13 p1740 N88-20404
Vanadic hot corrosion of gas turbine blade coating materials 17 p2321 N88-23864

VANES
NT GUIDE VANES
NT JET VANES
Turbine Engine Hot Section Technology, 1985
[NASA-CP-2405] 02 p0184 N88-11140
Development of heat flux sensors for turbine airfoils 02 p0184 N88-11143
Component specific modeling 02 p0187 N88-11166
Constitutive modeling for isotropic materials 02 p0188 N88-11172
Turbine airfoil deposition models and their hot corrosion implications 02 p0189 N88-11178
Fluid mass and thermal loading effects on the modal characteristics of space shuttle main engine liquid oxygen inlet splitter vanes 05 p0594 N88-13628
Examination of the development of a compressible turbulent boundary layer on a rough and porous wall
[PB87-148266] 07 p0815 N88-14964
Experimental evaluation of a translating nozzle sidewall radial turbine 10 p1280 N88-17656
Static performance of an axisymmetric nozzle with post-exit vanes for multiaxis thrust vectoring
[NASA-TP-2800] 13 p1719 N88-20280
Study on the heat resisting and cooling property of the ceramics-metal hybrid stator vanes
[DE88-753117] 20 p2810 N88-26668
Euler analysis of a swirl recovery vane design for use with an advanced single-rotation propfan
[NASA-TM-101357] 24 p3320 N88-29771

VANS
U TRUCKS

VAPOR DEPOSITION
NT VACUUM DEPOSITION
Equations for determining CVD tungsten-rhenium alloy composition and plating rate
[DE87-008831] 01 p0024 N88-10152
Laser chemically vapor deposited silicon-carbide: Growth features, topography, microstructure, and composition
[DE87-013767] 01 p0029 N88-10184
Ceramic composites by chemical vapor infiltration
[DE87-009128] 01 p0029 N88-10185
Chemical vapor deposition of B6P and B6As films
[DE87-009288] 02 p0151 N88-10942
Experimental verification of vapor deposition rate theory in high velocity burner rigs 02 p0189 N88-11179
The preparation of thin films for photovoltaic conversion by novel MOCVD techniques
[DE87-001185] 02 p0194 N88-11212
Preparation and properties of evaporated CdTe films
[DE87-012270] 02 p0195 N88-11216
Laser spectroscopy and gas-phase chemistry in CVD
[DE87-013715] 03 p0281 N88-11770
Ion plating: Fundamental processing studies and synthesis of high performance coatings
[AD-A184766] 03 p0303 N88-11908
Excimer laser-assisted deposition of GaAs, AlAs and (Al,Ga)As from Lewis acid-base adducts
[AD-A184588] 03 p0329 N88-12081
Inertial confinement fusion reactor cavity analysis
[DE88-000788] 04 p0492 N88-13028
Fabrication of composites by chemical vapor deposition
[DE87-014565] 05 p0559 N88-13408
Reactive sticking coefficients of silane on silicon
[DE88-000601] 05 p0570 N88-13473
Fundamental studies in the OM-CVD growth of Ga-In-As-Sb
[AD-A184822] 05 p0655 N88-14014
Bending properties of aluminum base composite with CVD-fiber
[PB87-130878] 06 p0678 N88-14156
An analysis of the effect of system variables on the quality of thin films and powders produced by laser-breakdown chemical vapor deposition
[DE88-001793] 06 p0708 N88-14342
Heteroepitaxial growth of 3-5 semiconductor compounds by metal-organic chemical vapor deposition for device applications
[NASA-CR-182346] 06 p0788 N88-14832
High-temperature electronics 08 p0956 N88-15797
TiN coatings on M2 steel produced by plasma assisted chemical vapor deposition
[DE88-003189] 08 p0970 N88-15867
Oxidation resistance of CVD coatings
[AD-A178337] 09 p1147 N88-16875
Superlattice photodetectors
[AD-A186956] 09 p1253 N88-17511
Microgravity research at the University of Mexico: Experiments in payload G-006 10 p1286 N88-17692
Metal modification for improved glass-ceramic to metal seals: 1. Auger results on ion implantation and vapor deposition films
[DE88-005244] 10 p1339 N88-18006
Fabrication and evaluation of transmissive multilayer optics for 8 keV X-rays
[DE88-003999] 10 p1409 N88-18402
Plasma deposition of silicon carbide thin films
[AD-A188093] 11 p1556 N88-19314
Preparation and characterization of Cu2Zn1-xMnxGeS4
[AD-A188113] 11 p1556 N88-19315
Feasibility studies of the growth of 3-5 compounds of boron by MOCVD
[NASA-CR-181622] 11 p1561 N88-19343
Preparation and characterization of thin films of alumina by metalorganic chemical vapor deposition
[AD-A188366] 12 p1608 N88-19614
Fundamental studies and device development in beta silicon carbide
[AD-A189540] 12 p1699 N88-20165
Research on mercury cadmium telluride
[AD-A189155] 13 p1845 N88-21039
Initial stages of silicon growth on the (100) surface of silicon by localized laser CVD
[DE88-005420] 13 p1848 N88-21059
Ball bearings with chemical vapor deposition (CVD)-TiC coated components 14 p1876 N88-21210
Chemical vapor deposited silica coatings for solar mirror protection
[NASA-TM-100834] 14 p1893 N88-21306
Measurements of optical nonlinearities in MOCVD-grown GaAs/GaAlAs multiple quantum wells 14 p1975 N88-21787
Numerical simulations of buoyancy driven flows in cylinders and cavities for vapor crystal growth 14 p1987 N88-21854
Oxide optical coatings prepared by metal-organic vapor deposition
[DE88-006809] 15 p2043 N88-22175
Investigation of laser diagnostics of PACVD processes for depositing hard face coatings
[DE88-007083] 15 p2043 N88-22176
Vapor phase deposition and growth of polyimide films on copper
[AD-A189969] 15 p2044 N88-22178

JPRS report: Science and technology. Japan
[JPRS-JST-88-002] 15 p2050 N88-22210
Single crystal growth by laser CVD
15 p2050 N88-22213
Fine grain development by laser CVD
15 p2050 N88-22214
Hard ceramic film by laser PVD
15 p2051 N88-22216
Laser evaporation studies
[AD-A189815] 15 p2071 N88-22346
Beam assisted fabrication of 3-5/Si monolithic devices
[AD-A189979] 15 p2142 N88-22785
Limited reaction processing for semiconductor device fabrication
[AD-A190913] 16 p2283 N88-23666
SiC fiber reinforced reaction-bonded Si3N4 composites 17 p2326 N88-23892
Studies of heat and mass transfer during chemical vapor deposition 17 p2338 N88-23953
Fabrication of SP-100 fuel barrier structures by chemical vapor deposition 17 p2416 N88-24371
Joint services electronics program research in electronics
[AD-A192206] 18 p2504 N88-24857
An investigation of 2-6 superlattice deposition by laser photochemical techniques
[AD-A191547] 18 p2581 N88-25336
Optical nonlinearities in GaAs/GaAlAs multiple quantum wells fabricated by metalorganic chemical vapor deposition for use in optical signal processing
[AD-A191558] 18 p2582 N88-25337
Strong fibers
[DE88-007798] 19 p2610 N88-25486
Hydrogenated amorphous silicon-germanium alloys
[DE88-001147] 19 p2620 N88-25546
Fabrication of a flexible conductor by vapor deposition
[DE88-007500] 19 p2661 N88-25826
Deposition techniques and properties of strain compensated LPCVD silicon nitride films
19 p2673 N88-25898
Hot electron transistors grown by MOCVD
20 p2861 N88-26996
On the electrical properties of carbon/carbon composites densified by chemical deposit in vapor phase
[SNIAS-881-430-117] 21 p2907 N88-27252
Laser probes and numerical modeling as process diagnostics in chemical vapor deposition
[DE88-011622] 21 p2911 N88-27275
PECVD of amorphous nickel--phosphorus films
[DE88-011086] 21 p2915 N88-27299
Superconducting thin films, composites and junctions
[AD-A193123] 21 p2937 N88-27440
Chemical vapor deposition of TiO2 thin films at room temperature
[DE88-008892] 21 p2953 N88-27542
Laser-heated CVD process for depositing thin films for low-cost solar-cell applications
[DE88-001162] 21 p2967 N88-27623
Low-band-gap, amorphous-silicon-based alloys by photochemical vapor deposition
[DE88-001165] 21 p3023 N88-27944
Chemistry of adhesion at the polyimide-metal interface
[AD-A194647] 22 p3058 N88-28143
Ultrafine microstructure composites prepared by chemical vapor deposition
[AD-A193849] 23 p3189 N88-28973
Low temperature film growth of the oxides of zinc, aluminum and vanadium (and related systems, oxides of gold and germanium, nitrides of aluminum and tungsten) by reactive sputter deposition
[AD-A193497] 23 p3191 N88-28986
Metal grid base heterojunction transistor operating at 60 and 94 GHz
[AD-A194763] 23 p3207 N88-29087
Laser induced chemical vapor epitaxial growth of gallium arsenide films
[AD-A194254] 23 p3291 N88-29595
Diamond film by hot filament CVD method
[NASA-TT-20335] 23 p3294 N88-29618
Iridium-coated rhenium thrusters by CVD
[NASA-TM-101309] 24 p3339 N88-29874
Processing technology research in composites
[AD-A195693] 24 p3341 N88-29890
A review of melt and vapor growth techniques for polydiacetylene thin films for nonlinear optical applications
[NASA-TM-100340] 24 p3430 N88-30412

VAPOR GENERATORS
U VAPORIZERS

VAPOR LIQUID EQUILIBRIUM
U LIQUID-VAPOR EQUILIBRIUM

VAPOR PHASE EPITAXY
Epitaxial reactor development for growth of silicon-on-insulator devices
[AD-A184758] 03 p0382 N88-12399
Research on single-crystal CdTe solar cells
[DE88-001115] 13 p1793 N88-20725
Zone crystallization experiments in mirror heating facilities
[BMFT-FB-W-86-023] 16 p2184 N88-23016
Initial stages of molecular beam heteroepitaxial growth in GaAs-(Ca,Sr)F2 and GaAs/Si systems
[LAAS-87-355] 16 p2281 N88-23658
The VPE-hydride technique with alloy source: Equilibrium analysis
[AD-A194036] 22 p3157 N88-28784

VAPOR PHASES
Low temperature deposition by laser induced breakdown in the vapor phase
[DE87-007509] 01 p0024 N88-10151
Kinetics investigations of atmospheric chemical reactions
[PB87-213351] 01 p0069 N88-10439
Application of new conformal solution of theories
[PB87-214557] 01 p0105 N88-10684
Laser spectroscopy and gas-phase chemistry in CVD
[DE87-013715] 03 p0281 N88-11770
Phase behavior in the Li-Al-O-H system at intermediate temperatures
[AD-A185732] 06 p0697 N88-14280
The kinetics and dynamics of iodine monofluoride formation in gas-phase collisions
[AD-A185715] 06 p0709 N88-14352
Van der Waals clusters of aromatic molecules studied using supersonic molecular jet spectroscopy
[AD-A186087] 07 p0929 N88-15644
High-temperature photoelectron spectroscopy. An increased sensitivity spectrometer for studying vapor-phase species produced at furnace temperatures greater than 2000K
[AD-A186542] 09 p1140 N88-16835
Gas phase pulse radiolysis
[DE88-002981] 10 p1296 N88-17751
Adhesion of vapour phase deposited ultra-thin polyimide films on polycrystalline silver
[AD-A187930] 10 p1306 N88-17810
Investigation of real-time two-dimensional visualization of fuel spray liquid/vapor distribution via exciplex fluorescence
[AD-A188268] 10 p1307 N88-17816
Gas-phase photoelectron spectroscopy of metals and metal oxides of importance in the upper atmosphere
[AD-A187771] 11 p1511 N88-19027
Gas phase reactions of electrons, negative ions and free-radicals with transition metal complexes
11 p1560 N88-19339
An interpretation of the ethylenic, carbidic, and graphite auger lineshapes of chemisorbed carbon species
[AD-A189092] 13 p1736 N88-20379
Measurement of rate constants of elementary gas reactions of importance to upper atmosphere and combustion systems
[AD-A189432] 13 p1737 N88-20386
Chemical kinetics modeling of HMX combustion
19 p2633 N88-25617
Thermostatistical estimations of vapor-state molecules affected by gravity in a heat pipe
20 p2783 N88-26505
On the electrical properties of carbon/carbon composites densified by chemical deposit in vapor phase
[SNIAS-881-430-117] 21 p2907 N88-27252
Electronic states of the Xe(sub n)HCl systems in gas and condensed phases
[AD-A193881] 23 p3192 N88-28997

VAPOR PRESSURE
Time-resolved measurements of shock-induced vapor-pressure profiles
[DE87-012972] 01 p0045 N88-10289
Prediction of high-temperature thermodynamic properties of mixed electrolyte solutions including solubility equilibria, vapor pressure depression and boiling point elevation
[DE88-006344] 13 p1849 N88-21069
Prediction of thermodynamic properties, including solubility equilibria and vapor pressures, for mixed aqueous electrolytes to high temperatures
[DE88-006317] 14 p1990 N88-21863
Study on shaft seals for potassium turbine
[EL-891] 15 p2074 N88-22364
The effect of weathering on octane quality for winter-grade and summer-grade gasolines
[AD-A190640] 16 p2183 N88-23012
Effects of moderate cold and heat stress on the potential work performance of industrial workers. Part 6: The effects of increasing vapour pressure at four air temperatures on the performance and physiology of white females
[PB88-124854] 18 p2550 N88-25137
Physical-chemical reactions at welding arc/molten pool interfaces
[DE88-007717] 20 p2808 N88-26662
Vapor Compression Distillation Subsystem (VCDS) component enhancement, testing and expert fault diagnostics development, volume 2
[NASA-CR-172076] 21 p2994 N88-27755

VAPORIZERS
NT EVAPORATORS
The design and development of mercury vaporisers for use with electron-bombardment ion engines
[RAE-TR-70042] 01 p0018 N88-10108
Evaluation of solder flux solvents in a vapor-degreasing application for hybrid microcircuits
[BDX-613-3638] 11 p1468 N88-18752
Development of a liquid-fed water resistojet
[NASA-TM-100927] 18 p2523 N88-24968
Flow characteristics of a model annular combustor
24 p3347 N88-29924

VAPORIZING
NT BOILING
NT EVAPORATION
NT EVAPOTRANSPIRATION
NT FILM BOILING
NT FLASHING (VAPORIZING)
NT NUCLEATE BOILING
NT SUBLIMATION
NT TRANSPIRATION
Energy balance in laser-irradiated vaporizing droplets
[DE88-000525] 04 p0449 N88-12782
Cohesive energies of transition metal silicides and phosphides --- Knudsen effusion
[AD-A186691] 09 p1254 N88-17519
Liquid sprays and flow studies in the direct-injection diesel engine under motored conditions
[NASA-TM-100135] 11 p1440 N88-18594
Impact-induced devolatilization and hydrogen isotopic fractionation of serpentine: Implications for planetary accretion
[NASA-CR-182877] 16 p2175 N88-22966
Photoionization dynamics and abundance patterns in laser vaporized tin and lead clusters
[AD-A191604] 18 p2482 N88-24722
High-energy laser-assisted imaging through vaporizing aerosols
[DE88-007911] 18 p2521 N88-24957
Fuel droplet vaporization and temperature distributions of axisymmetric unsteady sprays
19 p2626 N88-25579
Vaporization studies of plasma interactive materials in simulated plasma disruption events
[DE88-010100] 19 p2731 N88-26222
Investigation of annular flow at high evaporation rates in view of liquid film cooling
[DFVLR-FB-88-08] 21 p2949 N88-27517
Design, development, fabrication and launch support for a high altitude release of neodymium vapor
[AD-A194196] 22 p3118 N88-28527
Simulation study of spraying, streaming and vaporization phenomena associated with fuel injection
24 p3345 N88-29914

VAPORS
NT MERCURY VAPOR
NT METAL VAPORS
NT SODIUM VAPOR
NT WATER VAPOR
Experimental and theoretical study of condensation in multicomponent vapors
[DE87-013663] 02 p0145 N88-10907
Detection of vapors of flammable liquids in air by atmospheric sampling mass spectrometry/mass spectrometry
[DE88-000030] 02 p0196 N88-11227
Application of new conformal solution theories
[PB87-211934] 02 p0247 N88-11558
Experimental and theoretical study of condensation in multicomponent mixtures
[DE88-000897] 04 p0413 N88-12563
Investigation of the nature and concentration of vapor and mist during the cleaning of aircraft
[PML-1985-29] 05 p0623 N88-13817
Safety implications of onboard refueling vapor recovery systems
[PB88-102603] 07 p0839 N88-15088
Summary and analysis of comments on the recommended practice for the measurement of refueling emissions
[PB88-101530] 07 p0876 N88-15313
Zero-G thermodynamic vent system for shuttle/Centaur 08 p0983 N88-15943
Some investigations of electrical discharges at the surfaces of solid cathodes immersed in aqueous electrolyte solutions
[PB87-168209] 09 p1159 N88-16948
Computer modeling for optical waveguide sensors
[AD-A187702] 11 p1549 N88-19263
Discharge excitation of dye vapors
[AD-A188428] 12 p1632 N88-19770

Heat pipe transient analysis: Vapor dynamics
[DE88-005132] 13 p1767 N88-20568
Infrared differential absorption lidar for vapor detection
[AD-A190600] 15 p2098 N88-22497
Sensitivity of F-106B leading-edge-vortex images to flight and vapor-screen parameters
[NASA-TP-2818] 17 p2300 N88-23760
Theoretical studies of Resonance Enhanced Stimulated Raman Scattering (RESRS) of frequency doubled Alexandrite laser wavelength in cesium vapor
[NASA-CR-182871] 17 p2317 N88-23841
Method of evaporation
[NASA-CASE-NPO-15609-2] 17 p2318 N88-23846
Transient analysis of heat pipe vapor dynamics
17 p2412 N88-24341
A compressible vapor flux model for transient heat pipe analysis 17 p2412 N88-24343
Transient thermohydraulic heat pipe modeling
17 p2413 N88-24347
Heat pipe transient analysis: Vapor dynamics
17 p2421 N88-24397
Photoconductivity in carbon fibers
[AD-A191728] 18 p2492 N88-24782
Molecular-beam, mass-spectrometric studies of wood vapor and model compounds over HZSM-5 catalyst
18 p2535 N88-25044
Upgrading pyrolysis vapors to aromatic gasoline with zeolite catalysis at atmospheric pressure
18 p2536 N88-25045
Effect of long-term inhalation of acetic acid vapor on some functional parameters of man
19 p2705 N88-26084
Transport of organic vapors in multiphase polymer system
[AD-A194097] 23 p3198 N88-29033

VARACTOR DIODE CIRCUITS
GaAs varactor diode MMIC fabrication technology --- monolithic microwave integrated circuit (MMIC)
[RSRE-MEMO-4022] 09 p1158 N88-16943

VARIABILITY
A multiple-time-scale turbulence model based on variable partitioning of turbulent kinetic energy spectrum
[NASA-CR-179222] 04 p0444 N88-12754
Examination of the physical processes associated with the keyhole region of variable polarity plasma arc welds in aluminum alloy 2219 07 p0927 N88-15634
A method for designing robust multivariable feedback systems
[NASA-CR-182459] 09 p1225 N88-17341
Designing variable-length codes with good error-recovery properties
[BBC-RD-1987/19] 10 p1317 N88-17876
Implementing logical variables on a graph reduction architecture 10 p1382 N88-18252
Parallel access to synchronization variables
[DE88-003570] 10 p1392 N88-18306
A new algorithm for general multiobjective optimization
[NASA-TM-100536] 13 p1813 N88-20830
The atmosphere as a component of the climate system: Structure and variability 14 p1935 N88-21540
Wave propagation in locally isotropic turbulent medium with smoothly changing characteristics
[NASA-TT-20312] 20 p2800 N88-26617

VARIABLE AREA WINGS
U TRAILING EDGE FLAPS

VARIABLE GEOMETRY STRUCTURES
Test stand performance of a convertible engine for advanced V/STOL and rotorcraft propulsion
[NASA-TM-100211] 03 p0266 N88-11679
Solution of geometrically nonlinear problem for reinforced shell of revolution having arbitrary shape
04 p0426 N88-12637
Structurally tailorable non-linear snap-through spring system
[NASA-CASE-LAR-13729-1] 18 p2523 N88-24970
Techniques used in the F-14 variable-sweep transition flight experiment
[NASA-TM-100444] 24 p3374 N88-30093

VARIABLE LIFT
U LIFT

VARIABLE PITCH PROPELLERS
Analysis of possible transmission arrangements applicable for driving single or twin counterrotating fans on propfan engines 10 p1282 N88-17670
The effects of torque response and time delay on rotorcraft vertical axis handling qualities
[AD-A189873] 15 p2017 N88-22023
Structurally tailorable non-linear snap-through spring system
[NASA-CASE-LAR-13729-1] 18 p2523 N88-24970

VARIABLE STARS
NT CATACLYSMIC VARIABLES
NT CEPHEID VARIABLES
NT DWARF NOVAE
NT FLARE STARS
NT HERCULES NOVA
NT MIRA VARIABLES
NT NOVAE
NT SUPERNOVA 1987A
NT SUPERNOVAE
NT T TAURI STARS
Modes, masses, metallicities, and magnitudes of RR Lyrae variables
[DE87-013149] 01 p0109 N88-10703
The M-type stars
[NASA-SP-492] 02 p0252 N88-11592
Basic properties and variability
02 p0252 N88-11593
Differential B and V light curves of the bright BY Draconis star HD80715 04 p0509 N88-13130
Time series infrared spectroscopy of long period variables 04 p0516 N88-13172
A comprehensive exploration of late-type stars in the far-ultraviolet 04 p0520 N88-13194
The history and development of nonlinear stellar pulsation codes
[DE88-001828] 06 p0801 N88-14899
The distances and absolute magnitudes of RR Lyrae variable stars 11 p1568 N88-19386
A survey of the Ap stars for rapid variability
20 p2884 N88-27127
Analysis of emission features in IRAS LRS spectra
21 p2928 N88-27380
The ultrashort period dwarf nova SW Ursae Majoris
24 p3453 N88-30553

VARIABLE SWEEP WINGS
Variable sweep wings 10 p1309 N88-17823
Influence of unsteady aerodynamic forces on dynamic response of variable sweep aircraft
15 p2054 N88-22245
Pilot report: AFTI (Advanced Fighter Technology Integration) F-111
[AD-A192937] 21 p2895 N88-27184
Variable Sweep Transition Flight Experiment (VSTFE)-parametric pressure distribution boundary layer stability study and wing glove design task
[NASA-CR-3992] 23 p3173 N88-28894
Variable wing camber control systems for the future Airbus program
[MBB-UT-104/88] 23 p3180 N88-28932

VARIANCE (STATISTICS)
NT ANALYSIS OF VARIANCE
NT BIVARIATE ANALYSIS
NT COVARIANCE
NT MULTIVARIATE STATISTICAL ANALYSIS
NT REGRESSION ANALYSIS
A fully redundant double difference algorithm for obtaining minimum variance estimates from GPS observations
[NASA-CR-182363] 06 p0667 N88-14089
Nonparametric estimation of the generalized variance
[AD-A186029] 07 p0914 N88-15545
A note on extended quasi-likelihood
[AD-A186318] 07 p0915 N88-15555
Statistical evaluation of experimental results from fatigue strength tests on CFRP composite materials
11 p1449 N88-18635
Variances and higher order correlation coefficients: Continued
[RR-655-M] 18 p2563 N88-25219
Operational noise data for CH-47D and AH-64 army helicopters
[AD-A191059] 18 p2570 N88-25263
Definition of long ocean wave slope for radar applications
[AD-A193198] 21 p2933 N88-27412

VARIATION METHOD
U CALCULUS OF VARIATIONS

VARIATIONAL PRINCIPLES
Variational and nonvariational theory of frictionless adhesive contact between bodies
[REPT-87-11] 01 p0054 N88-10345
A mixed finite element method for the computation of stress in a composite with loaded holes
[ONERA-RT-34/4242-RY-054-R]
01 p0062 N88-10395
On the scheme dependency of the three-dimensional Euler solutions 03 p0318 N88-12010
A variational formulation of a hydrodynamic lubrication problem
[MEMO-642] 08 p0987 N88-15979
Transversely anisotropic curved optical fibres: Variational analysis of a nonstandard Eigenproblem
[PB88-112966] 08 p1083 N88-16528
Hypersonic blunt body computations including real gas effects
[NASA-TM-100074] 10 p1400 N88-18344
Flux coordinate studies of elongated plasmas at high Beta 12 p1694 N88-20134
Structural clearances and internal friction: Simulation by Eigen distortions
[ISSN-0208-5658] 13 p1779 N88-20640
Hamiltonian description of the interaction of surface waves with mixed-layer currents
13 p1806 N88-20799
A generalized variational method for solving stress intensity factors at cracks on the edge of holes in orthotropic plates
[IC-AERO-87-02] 17 p2348 N88-23992
Numerical simulation of the shock tube flows by TVD scheme 19 p2638 N88-25648
On the stationary solutions of three-dimensional Euler equations by the TVD difference schemes
19 p2639 N88-25660
Variational analysis of dielectrically loaded multidepth corrugated waveguides
[PB88-193602] 20 p2793 N88-26573
Theory and simulation of relaxed plasmoids
[AD-A192884] 21 p3032 N88-27997

VARIATIONS
NT ANNUAL VARIATIONS
NT DIURNAL VARIATIONS
NT GEOMAGNETIC MICROPULSATIONS
NT GEOMAGNETIC PULSATIONS
NT MAGNETIC VARIATIONS
NT NOCTURNAL VARIATIONS
NT PERIODIC VARIATIONS
NT SECULAR VARIATIONS
NT TWENTY-SEVEN DAY VARIATION
NT WIND VARIATIONS
The atomic weight and isotopic composition of nitrogen and their variation in nature
[DE87-012867] 02 p0144 N88-10902
Effects of pressure fluctuations on nickel electrodes
[AD-A184293] 03 p0311 N88-11967
The effect of ocean fluctuations on sound transmission in the ocean
[AD-A184382] 03 p0355 N88-12236
The atomic weight and isotopic composition of oxygen and their variation in nature
[DE87-014397] 04 p0413 N88-12558
Modes of surface circulation and climate over the tropical Atlantic, Eastern Pacific, and Indian Oceans
06 p0742 N88-14564
The EUV line flux variations and activity in Alpha Orionis 08 p1032 N88-16256
The advantage of variable geometry for turbine engines at low power 10 p1280 N88-17653
Ice-shelf response to ice-stream discharge fluctuation. Part 1: Unconfined ice tongues
[AD-A188147] 10 p1358 N88-18117
An investigation of terrain related variables for predicting the multipath fade depth distribution on terrestrial microwave lines 12 p1615 N88-19654
Evolution of poloidal variation of impurity density and ambipolar potential in rotating tokamak plasma, part 1
[DE88-006263] 13 p1842 N88-21022
The turbulent heat flux in low Mach number flows with large density variations
[DE88-006445] 14 p1911 N88-21419
Correlations of velocity and temperature fluctuations in the stagnation-point flow of circular cylinder in turbulent flow
[NASA-TM-100930] 19 p2597 N88-25435
Large-eddy simulations of concentration fluctuations
[DE88-009480] 21 p2973 N88-27660
On the estimation of a variance ratio
[AD-A193190] 21 p3009 N88-27854
The observed dynamical structure of low frequency variabilities 22 p3120 N88-28541
Climatology of various synoptic systems over the tropical North Pacific 22 p3121 N88-28542
Aspects of the 30-60 day oscillation in a GCM simulation 22 p3121 N88-28545
Modes of interannual climate variability and Sahel rainfall anomalies 22 p3121 N88-28547
Interannual variability in the Atlantic and Indian Oceans and its relationship to the southern oscillation
22 p3121 N88-28548
Low frequency variability of SST and its relationship to atmospheric forcing 22 p3122 N88-28554
Variations in the atmosphere associated with the 11-year solar cycle 22 p3122 N88-28557
The effects of changes in observation and data assimilation systems on CAC climate data sets
22 p3124 N88-28568
A method to adjust climatological time series for discontinuous inhomogeneities
22 p3124 N88-28570
Nonequilibrium flow of a radiating gas in a vertical channel with axial temperature variation
[DE88-702535] 23 p3212 N88-29120
Mathematical correlation between variations in solar radiation parameters. Part 1: Daily sums of global radiation and midday global radiation
[DE88-702742] 23 p3236 N88-29253
Improved time bounds for the maximum flow problem
[AD-A194034] 23 p3272 N88-29471

Fluctuations of order parameters in the high T(sub c) superconductors
[DE88-702549] 23 p3292 N88-29603
Nonequilibrium flow of a dissociating gas in a horizontal channel with axial temperature variation
[DE88-702536] 24 p3373 N88-30089

VARIOMETERS
NASA Marshall Space Flight Center solar observatory
[NASA-TM-100339] 24 p3332 N88-29832

VARISTORS
Metal oxide varistor polarization from an initial transient
[AD-A189012] 12 p1623 N88-19711
Electrical properties of medium field, chem-prep varistors
[DE88-006147] 13 p1762 N88-20540
Scale-up of a batch-type chemical powder preparation process for high field varistor fabrication
[DE88-006601] 13 p1762 N88-20541
The first synthesis of chem-prep varistor LAC (Lightning Arrestor Connector) granules
[DE88-008005] 21 p2936 N88-27438

VASCULAR SYSTEM
U CARDIOVASCULAR SYSTEM

VASOCONSTRICTION
The effects of acute cold exposure on exercise performance
[AD-A192650] 22 p3130 N88-28610
Alterations in cutaneous vasomotor regulation during acute and chronic hypoxia
[AD-A192653] 22 p3131 N88-28612

VASOCONSTRICTOR DRUGS
NT SEROTONIN

VASOMOTOR NERVOUS SYSTEM
U NERVOUS SYSTEM

VAX COMPUTERS
The VAXONLINE software system at Fermilab
[DE87-013565] 02 p0220 N88-11387
The MicroVAX-based data acquisition system for D0
[DE87-014475] 03 p0366 N88-12303
A new library of CAMAC routines for the control of the system CRATE by a microVAX in the VAXELN environment
[NOTA-INTERNA-893] 06 p0761 N88-14667
Introduction to the VMS (DEC) operating system
[ENST-87D006] 16 p2245 N88-23409
SAMS: The synchronization and monitoring system for ATF (Advanced Toroidal Facility) data acquisition provides unified data access for ATF data acquisition
[DE88-007268] 18 p2589 N88-25386
Effective communication between a microVAX and a specialized high-speed subprocessor
[DE88-007967] 19 p2714 N88-26115

VC-10 AIRCRAFT
A flight test investigation into flow separation and structural response for a transport aircraft at buffet onset
[RAE-TR-87006] 14 p1867 N88-21156

VCO
U VOLTAGE CONTROLLED OSCILLATORS

VECTOR ANALYSIS
NT COLLINEARITY
NT COPLANARITY
NT VORTICITY
Approximate polynomial preconditioning applied to biharmonic equations on vector supercomputers
[NASA-TM-100217] 01 p0087 N88-10563
Computational methods for problems in aerodynamics and large space structure using parallel and vector architectures
[AD-A185401] 05 p0541 N88-13294
Utilization of a high rate vector computer in computational fluid mechanics for aeronautics
[ETN-88-91171] 05 p0581 N88-13547
Asymptotic normality of poly-1 densities with Bayesian applications
[AD-A185718] 06 p0768 N88-14719
A vectorized Poisson solver over a spherical shell and its application to the quasi-geostrophic omega-equation
[NASA-CR-4116] 08 p1039 N88-16285
Series representations of infinitely divisible random vectors and a generalized shot noise in banach spaces
[AD-A186502] 08 p1073 N88-16474
Tensorial calibration. 2. Second order tensorial calibration
[AD-A186614] 09 p1167 N88-16994
The linear dependency structure of covariance nonstationary time series
[AD-A186548] 09 p1232 N88-17383
Estimation of gravity vector components from Bell gravity gradiometer and auxiliary data under consideration of topography and associated analytical upward continuation aspects
[AD-A188146] 10 p1355 N88-18099
An efficient sparse matrix multiplication scheme for the CYBER 205 computer
[NASA-TM-4028] 10 p1390 N88-18302
Vector bundles over real algebraic varieties
[PB88-126677] 10 p1398 N88-18335
Overview of multi-input frequency domain modal testing methods with an emphasis on sine testing
11 p1499 N88-18949
Measurement and analysis of memory conflicts on vector multiprocessors
[AD-A188206] 11 p1525 N88-19104
Deep water mass circulation in the Alboran Basin. Measurements - January to April 1982: ALBORAN 2
[AD-A189205] 13 p1803 N88-20777
Instrumentation for the characterization and development of millimeter wave components compatible with monolithic integration
[AD-A189724] 15 p2059 N88-22275
Martingale representation and the Malliavin calculus
[AD-A189721] 15 p2119 N88-22626
High speed transcendental elementary function architecture in support of the Vector Wave Equation (VWE)
[AD-A189746] 15 p2119 N88-22627
An FSK (Frequency Shift Keying) telemetry module for vector measuring current meters
[AD-A192142] 18 p2470 N88-24661
Improving the performance of a finite element method using vector analysis on CRAY 1
[ETN-88-92153] 18 p2513 N88-24907
Gram-Schmidt implementation of a linearly constrained adaptive array
[AD-A191651] 18 p2560 N88-25198
An investigation of the uses of time domain capable vector network analyzers as a diagnostic for helix traveling-wave circuits
[AD-A192460] 21 p2935 N88-27430
Parallel solutions to geometric problems on the scan model of computation
[AD-A192321] 21 p3004 N88-27819
A note on vector bimeasures
[AD-A192841] 21 p3009 N88-27849
Object discrimination via bulk temperature/velocity filtering, phase 1
[AD-A194533] 23 p3274 N88-29487
Limiting distributions of non-linear vector functions of stationary Gaussian processes
[AD-A194569] 23 p3274 N88-29488

VECTOR CALCULUS
U VECTOR SPACES

VECTOR CONTROL
U DIRECTIONAL CONTROL

VECTOR CURRENTS
Quantization of axial electrodynamics
[DE88-701498] 15 p2147 N88-22813
An FSK (Frequency Shift Keying) telemetry module for vector measuring current meters
[AD-A192142] 18 p2470 N88-24661

VECTOR SPACES
NT ADJOINTS
NT BANACH SPACE
NT CANONICAL FORMS
NT EIGENVALUES
NT EIGENVECTORS
NT HESSIAN MATRICES
NT HILBERT SPACE
NT MATRICES (MATHEMATICS)
NT STATE VECTORS
NT STIFFNESS MATRIX
NT VECTORS (MATHEMATICS)
NT VORTICITY
Division algebras and sphere fibrations
[ETN-87-90677] 01 p0087 N88-10566
Electromagnetic scattering problem in the wave-vector-time domain
[PB88-106083] 06 p0694 N88-14263
Analysis and synthesis of the Earth's gravity field variable in space and time using vector surface spherical functions
[SER-C-325] 07 p0878 N88-15328
An application of eigenspace methods to symmetric flutter suppression
[NASA-CR-181618] 10 p1284 N88-17684
The existence of smooth densities for the prediction filtering and smoothing problems
[AD-A189865] 15 p2119 N88-22629
An introduction to poloidal and toroidal fields
[MITT-54] 17 p2394 N88-24232
Linearization along invariant manifolds and a generalization of the Hartman-Grobman theorems for degenerate singularities of vector fields in R cubed
[REPT-87-80] 20 p2845 N88-26886
Cosmology in an N-dimensional vector space
[DE88-702550] 23 p3277 N88-29507

VECTORS (MATHEMATICS)
NT EIGENVECTORS
NT STATE VECTORS
NT VORTICITY
Implementation of a digital optical matrix-vector multiplier using a holographic look-up table and residue arithmetic
[NASA-CR-180431] 01 p0078 N88-10496
Vectorization of MHD equilibrium and stability codes
[DE87-753013] 02 p0240 N88-11516
Solution of some 3-D viscous and inviscid supersonic flow problems by finite-volume space-marching schemes
05 p0532 N88-13235
Multidimensional least squares fitting of fuzzy models
[AD-A185148] 05 p0640 N88-13916
Least squares for fuzzy vector data regression
[AD-A185156] 05 p0640 N88-13917
On detection of change points using mean vectors
[AD-A185581] 06 p0767 N88-14717
On hypercontractivity of alpha-stable random variables, 0 less than alpha less than 2
[AD-A186425] 07 p0915 N88-15559
Vector performance of register-to-register vector computers
[DE88-004013] 10 p1384 N88-18265
Implementation and analysis of a Navier-Stokes algorithm on parallel computers
[NASA-CR-181614] 10 p1390 N88-18301
Straightening and the Stanley decomposition for the (2;n)-nilpotent vectorfield
[PB88-126685] 10 p1398 N88-18336
Linear prediction of stationary vector sequences
[NASA-TM-100069] 10 p1403 N88-18366
New representation for kinematics of manipulator
[DE88-751446] 14 p1917 N88-21445
Vectorization of the odd-even hopscotch scheme and the alternating direction implicit scheme for the two-dimensional Burgers' equations
[CWI-NM-R8720] 16 p2249 N88-23440
Systolic algorithm for matrix-vector multiplication
[PB88-165394] 16 p2256 N88-23484
Vector graphics and raster data processing for spatial information systems 18 p2533 N88-25028
Electric field measurement by S-520-9 sounding rocket using the time of flight technique of lithium ion beam
[ISAS-RN-367] 18 p2543 N88-25095
Robust vector quantization for noisy channels
19 p2653 N88-25754
Analysis and improvement of the vector quantization in SELP (Stochastically Excited Linear Prediction)
19 p2653 N88-25756

VEGA PROJECT
Final phase of Project Vega 01 p0009 N88-10053
Space missions to Comets Halley and Giacobini-Zinner 03 p0272 N88-11712
JPRS report: Science and technology. USSR: Space
[JPRS-USP-88-002] 13 p1724 N88-20312
Vega-1 and Vega-2 automatic stations: Functioning of landing modules in Venusian atmosphere
13 p1725 N88-20313
Vega-1 and Vega-2 automatic stations: Functioning of flyby vehicles during encounter with Halley's comet
13 p1725 N88-20314
Thermal structure of Venusian Atmosphere determined from results of measurements from Vega-2 landing module 13 p1725 N88-20315
Research on absorption of UV radiation in Venusian atmosphere from Vega-1 and Vega-2 landing modules
13 p1725 N88-20316
Vertical structure of Venusian cloud layer at landing sites of Vega-1 and Vega-2 vehicles
13 p1725 N88-20317
Gas-chromatographic analysis of products of thermal reactions of aerosol in Venusian cloud layer on Vega-1 and Vega-2 automatic interplanetary stations
13 p1725 N88-20318
Roentgenoradiometric analysis of aerosol in Venusian clouds by Vega-1 and Vega-2 automatic interplanetary stations 13 p1726 N88-20319
Chemical composition and structure of Venusian clouds determined from results of roentgenoradiometric experiments carried out by landing modules of Vega-1 and Vega-2 automatic interplanetary stations
13 p1726 N88-20320
Determining chemical composition of aerosol in Venusian cloud layer on Vega-1 automatic interplanetary station using Malakhit mass spectrum analyzer
13 p1726 N88-20321
Elemental composition of Venusian rocks in northeastern part of Terra Aphrodite (determined using data from Vega-2 landing module)
13 p1726 N88-20322
Content of natural radioactive elements in Venusian rocks determined using data from Vega-1 and Vega-2 stations 13 p1726 N88-20323

Results of infrared spectrometer experiment. 2: Infrared radiometry of nucleus of Halley's Comet
13 p1727 N88-20326
Analysis of hydrocarbon band 3.35 in spectrum of Halley's Comet using data from infrared spectrometer on Vega-1 spacecraft 13 p1727 N88-20327
Variability of Comet Halley's coma: VEGA-1 and VEGA-2 magnetic field observations 14 p1995 N88-21891
Physical processes in the vicinity of the cometopause interpreted on the basis of plasma, magnetic field and plasma wave data measured on board VEGA-2 spacecraft --- Halley's comet 14 p1996 N88-21894
Some new features of plasma wave phenomena at Halley: APV-N observations --- VEGA
14 p1996 N88-21895
A comparison between wave observations performed in the environments of Comets Halley and Giacobini-Zinner 14 p1996 N88-21896
Plasma phenomena in the vicinity of the closest approach of VEGA-1, 2 spacecraft to the Comet Halley nucleus 14 p1996 N88-21899
Water vapor and hydroxyl distributions in the inner coma of Comet Halley measured by the VEGA-2 three channel spectrometer TKS 14 p1998 N88-21910
Color fluctuations in the inner coma of Comet Halley as measured from VEGA-2 14 p2000 N88-21925
Dust photometry in the near nucleus region of Comet Halley from VEGA-2 observations
14 p2001 N88-21930
Image processing on VEGA pictures
14 p2009 N88-21983
Determination of the Venus flyby orbits of the Soviet Vega probes using VLBI techniques
22 p3067 N88-28203

VEGETABLES
NT POTATOES

VEGETATION
NT CANOPIES (VEGETATION)
Enhancement of surface-atmosphere fluxes by desert-fringe vegetation through reduction of surface albedo and of soil heat flux
[NASA-CR-181442] 02 p0197 N88-11231
Vegetation classification, land systems and mapping using SPOT multispectral data: Preliminary results
03 p0342 N88-12160
Vegetation studies in the national Park of Comoe (Ivory Coast) using SPOT 1 satellite data
03 p0343 N88-12166
Electromagnetic wave probing of Earth's environment
[NASA-CR-182358] 06 p0690 N88-14232
Effects of fire on composition, biomass, and nutrients in oak scrub vegetation on John F. Kennedy Space Center, Florida
[NASA-TM-100305] 08 p1020 N88-16182
Physiological and ecological implications of coupled heat- and water-transport mechanisms of endotherms and vegetation
[DE88-004170] 10 p1352 N88-18081
Scattering and depolarization by random rough terrain and vegetation covered terrain-unified full wave approach 12 p1615 N88-19657
Research in remote sensing of vegetation
[NASA-CR-182663] 12 p1639 N88-19817
Measuring and modeling near surface reflected and emitted radiation fluxes at the FIFE site
[NASA-CR-182660] 12 p1640 N88-19818
Mesoscale monitoring of the soil freeze/thaw boundary from orbital microwave radiometry
[NASA-CR-182659] 12 p1645 N88-19855
Subsurface morphology and geoarchaeology revealed by spaceborne and airborne radar
17 p2353 N88-24022
Anomalies in the vegetation in the Alto Xingu - MT
17 p2357 N88-24043
Temporal analysis of the changes in Parque Estadual de Jacupiranga vegetation through digital treatment of LANDSAT imagery 17 p2367 N88-24094
An update on remote measurement of soil moisture over vegetation using infrared temperature measurements: A FIFE perspective
[NASA-CR-182926] 17 p2370 N88-24109
Monitoring biological impacts of space shuttle launches from Vandenberg Air Force Base: Establishment of baseline conditions
[NASA-TM-100982] 18 p2549 N88-25133
Propagation modeling for land mobile satellite systems
19 p2645 N88-25694
Sources of scattering in vegetarian and other surfaces and objects
[NASA-CR-182975] 20 p2816 N88-26710
SPOT-1 HRV data and vegetation amount
22 p3095 N88-28379
Topographic suppression and advances in classification for land cover mapping using SPOT-1 HRV imagery
22 p3099 N88-28404
Assessment of SPOT satellite based system in humid tropical vegetation identification, classification and monitoring 22 p3100 N88-28406
A comparison between SPOT and LANDSAT TM for mapping of vegetation and bedrock outcrops
22 p3100 N88-28409
Evaluation of SPOT imagery for discriminating vegetation communities associated with surficial and bedbrock geology and identifying anomalous and stressed vegetation associated with mineralization
22 p3103 N88-28426
Relevance of a thematic map (SPOT data) with regards to the real flora and structure of the vegetation covering of salt marshes (Mont Saint Michel Bay, France)
22 p3109 N88-28468
Assessment of SPOT imagery for topographic revision and vegetation mapping 22 p3111 N88-28477
Imaging instrument of the vegetation payload (SPOT 4)
[SNIAS-881-440-107] 24 p3386 N88-30169
Study of the spectral response of soybeans
[INPE-4592-PRE/1322] 24 p3387 N88-30174
Relief effect correction on LANDSAT imagery for forest applications using digital terrain models
[INPE-4611-PRE/1334] 24 p3388 N88-30179

VEGETATION GROWTH
NT CROP GROWTH
Controlled Ecological Life Support System: Regenerative Life Support Systems in Space
[NASA-CP-2480] 03 p0357 N88-12251
Progress in European CELSS activities
03 p0358 N88-12252
Design of an elemental analysis system for CELSS research 03 p0360 N88-12266
Study of the relationship between photosynthesis, respiration, transpiration, and mineral nutrition in wheat
03 p0360 N88-12268
Utilization of potatoes in bioregenerative life support systems 03 p0360 N88-12269
The effect of radiation on the long term productivity of a plant based CELSS 03 p0361 N88-12271
Mass balances for a biological life support system simulation model 03 p0361 N88-12272
Trickle water and feeding system in plant culture and light-dark cycle effects on plant growth
03 p0361 N88-12273
Disturbance and recovery of Arctic Alaskan tundra terrain. A review of recent investigations
[AD-A184442] 04 p0457 N88-12887
Comparative anatomic analysis of seedling organs of pisum sativum (fabaceae) cultivated under space flight conditions 06 p0749 N88-14603
Research on cotton plants grown in space
08 p1006 N88-16098
Species biology and potential for controlling four exotic plants (Ammophila arenaria, Carpobrotus edulis, Cortaderia jubata and Gasoul crystallinum) on Vandenberg Air Force Base, California
[NASA-TM-100980] 10 p1363 N88-18148

VEGETATIVE INDEX
Vegetation classification, land systems and mapping using SPOT multispectral data: Preliminary results
03 p0342 N88-12160
AIS-2 spectra of California wetland vegetation
05 p0613 N88-13763
Extension of the vegetation mission to thermal infrared spectral bands
[CNES-T-86/224-CT/DRT/TIT/IO]
16 p2227 N88-23299
Evaluation of a burned area and the vegetation regeneration affected by the burning in the Parque Nacional de Brazilia through TM/LANDSAT data
17 p2363 N88-24073
Use of LANDSAT images of vegetation cover to estimate effective hydraulic properties of soils
[NASA-CR-183185] 22 p3116 N88-28514
TM/LANDSAT-5 data to evaluate wheat and bean percent soil cover and leaf area index
[INPE-4609-PRE/1332] 24 p3385 N88-30165
LANDSAT TM and agrometeorological data for wheat yield estimation at the farm level
[INPE-4591-PRE/1321] 24 p3388 N88-30180

VEHICLE WHEELS
An investigation of the spray produced by a yawed wheel, including measurement of impact forces --- aircraft wheels
[BU-363] 14 p1866 N88-21150
Finding wheels of vehicles in stereo images
[AD-A194372] 22 p3080 N88-28292
Frequency dependent sliding coefficients for general three-dimensional rolling contact in high frequency range
[ILR-MITT-192] 22 p3085 N88-28318

VEHICLES
An efficient representation of spatial information for expert reasoning in robotic vehicles
09 p1214 N88-17278

VEINS
Operation Everest 2: Comparison of four instruments for measuring blood oxygen saturation
[AD-A186456] 08 p1049 N88-16337
Leg volume change under Lower Body Negative Pressure (LBNP) in dependence on stratification
[DFVLR-FB-87-47] 16 p2238 N88-23367

VELOCITY
NT ACOUSTIC VELOCITY
NT AIRSPEED
NT ANGULAR VELOCITY
NT CRITICAL VELOCITY
NT FLOW VELOCITY
NT GROUP VELOCITY
NT HIGH SPEED
NT HYPERSONIC SPEED
NT LIGHT SPEED
NT LOW SPEED
NT ORBITAL VELOCITY
NT PHASE VELOCITY
NT PROPAGATION VELOCITY
NT RADIAL VELOCITY
NT RELATIVISTIC VELOCITY
NT ROTOR SPEED
NT SOLAR WIND VELOCITY
NT SUBSONIC SPEED
NT SUPERSONIC SPEED
NT TERMINAL VELOCITY
NT TIP SPEED
NT TRANSONIC SPEED
NT WIND VELOCITY
Exact solutions to the governing dynamic equations of plasma armature electromagnetic railguns
[DE87-014442] 01 p0011 N88-10063
Fronts propagating with curvature dependent speed: Algorithms based on Hamilton-Jacobi formulations
[NASA-CR-178382] 01 p0077 N88-10495
Analytical modeling of helicopter static and dynamic induced velocity in GRASP
[NASA-TM-100026] 02 p0123 N88-10777
Rarefaction velocities in shocked lead
[DE87-013141] 02 p0146 N88-10917
Effects of injection of free electron lasers on axial velocity spread of beams 03 p0299 N88-11878
Ultimate velocities for induction launchers
[DE87-012360] 04 p0404 N88-12513
Use of a thermodynamic analog for pneumatic transport in horizontal pipes
[AD-A184076] 04 p0441 N88-12740
The velocity structure and turbulence at the center of the Orion Nebula 04 p0521 N88-13201
Hydrogen and deuterium in the local interstellar medium 04 p0521 N88-13204
Time-marching finite-difference methods for the three-dimensional Euler equations of contravariant velocity components 05 p0539 N88-13285
Velocity scaled aeroelastic testing of an unducted fan
[GTL-191] 05 p0548 N88-13337
Wing divergence of trimmed aircraft
05 p0550 N88-13354
Imaging subtle microstructural variations in ceramics with precision ultrasonic velocity and attenuation measurements
[NASA-TM-100129] 07 p0867 N88-15257
Velocity measurements in a 3D (three dimensional) shock wave laminar boundary layer interaction
[AD-A187334] 10 p1332 N88-17959
Velocity reversal and the arrows of time
[DE88-004237] 10 p1429 N88-18536
Splinter generator
[MBB-UA-1048/87] 11 p1491 N88-18897
Cramer-Rao bounds on the accuracy of location and velocity estimations using CCD optical sensors
[AD-A188481] 12 p1629 N88-19748
Quantization of quadratic friction revisited
[DE88-700839] 12 p1686 N88-20081
Erosion in dual-phase microstructures
[DE88-004507] 13 p1743 N88-20421
Reduction of erosion in elbows due to flow modifications, phase 1
[DE88-001028] 13 p1769 N88-20584
Some effects of heating on the wind-driven velocity in the upper ocean 13 p1805 N88-20792
Calibration of a hot-wire/hot-film anemometer over a range of temperatures, velocities and pressures
[AD-A189717] 14 p1913 N88-21430
Current velocity and hydrographic observations in the Straits of Florida, the Caribbean Sea and offshore of the Antillean Archipelago: Subtropical Atlantic Climate Studies (STACS) 1986
[PB88-160767] 14 p1951 N88-21628
Continuous measurements of in-bore projectile velocity
[DE88-006841] 15 p2023 N88-22056

Analytic solutions to dynamic equations of plasma armature railguns
[DE88-006842] 15 p2023 N88-22057
On new solvable many-body dynamical systems with velocity dependent forces
[PREPRINT-581] 15 p2127 N88-22683
Railgun rail gouging by hypervelocity sliding contact
[DE88-006866] 16 p2166 N88-22916
Effect of mass-velocity on liquid jet atomization in Mach 1 gasflow
[NASA-TM-100813] 16 p2211 N88-23194
Analysis of crack-tip fields in a viscoplastic material
17 p2349 N88-23996
Electrical pulse compression by traveling-wave photoconductivity 19 p2661 N88-25822
Analysis of the electrical harmonic characteristics of a slip recovery variable speed generating system for wind turbine applications
[DE88-001140] 19 p2687 N88-25972
Laser measurement of particle velocities in vacuum plasma spray deposition
[DE88-007111] 19 p2728 N88-26198
On linear relationship between shock velocity and particle velocity
[DE88-701827] 20 p2880 N88-27099
Prediction of velocity and temperature profiles in thermally driven gravity currents applied to stratified thermal storage tanks
[DE88-004452] 21 p2946 N88-27496
A method for determining absolute velocities from hydrographic data: The numerical code
[AD-A193997] 22 p3129 N88-28603
Object discrimination via bulk temperature/velocity filtering, phase 1
[AD-A194533] 23 p3274 N88-29487

VELOCITY DISTRIBUTION
An application of L1 to astronomy --- stellar velocity
[REPT-87-10] 01 p0108 N88-10702
Personal Computer (PC) based image processing applied to fluid mechanics
[NASA-TM-100024] 02 p0172 N88-11087
Experimental study of interacting vortex rings
03 p0318 N88-12007
Solar magnetic and velocity fields
[AD-A184360] 03 p0390 N88-12449
Comparative studies in the near-field of turbulent transports of heated and unheated jets normal to a cross stream 04 p0444 N88-12756
Hydrogen and deuterium in the local interstellar medium 04 p0521 N88-13204
Model-based motion estimation and its application to restoration and interpolation of motion pictures
[AD-A185054] 05 p0584 N88-13558
The new CP3 06 p0691 N88-14237
Highlights from a research program on a very highly loaded axial gas generator turbine
06 p0713 N88-14369
Models of sporadic meteor body distributions
06 p0739 N88-14543
Meteor velocity distribution and an optimum monitoring mathematical model 06 p0739 N88-14546
Lift distribution and velocity field measurements for a three-dimensional, steady blade/vortex interaction
[NASA-TM-100013] 07 p0815 N88-14962
The single particle and collective descriptions of the anomalous Doppler resonance and the role of ion dynamics
[INPE-4390-PRE/1210] 08 p0976 N88-15904
Absorption of electron cyclotron waves by superthermal electron velocity distributions in tokamak plasmas
[INPE-4385-PRE/1205] 08 p1086 N88-16539
The effect of asymmetric current-supporting electron velocity distributions on second harmonic electron cyclotron resonance heating: A ray-tracing treatment for the compass tokamak
[INPE-4389-PRE/1209] 08 p1087 N88-16549
A review of some flow visualization experiments carried out at the Institut Franco-Allemand de Recherches (ISL) shock tubes
[ISL-CO-243/86] 09 p1163 N88-16974
Corrections for the pseudorapidity gap correlation method --- particle correlations
[USIP-87-12] 09 p1245 N88-17463
Investigations of a circulation control airfoil flowfield using an advanced laser velocimeter
10 p1269 N88-17589
Boundary-layer and wake measurements on a swept, circulation-control wing 10 p1270 N88-17597
Transonic blade design on rotational stream surfaces
10 p1282 N88-17671
Implicit solution of the incompressible Navier-Stokes equations in primitive variables on non-staggered grids
10 p1326 N88-17930
A velocity-pressure integrated, mixed interpolation, Galerkin finite element method for high Reynolds number laminar flows
[NASA-CR-179264] 11 p1486 N88-18868
Correction of the wind field measured by the NCAR electra during FASINEX (Frontal Air-Sea Interaction Experiment) for inertial navigation system drifts
[AD-A187780] 11 p1514 N88-19045
Return stroke velocities and currents using a solid state silicon detector system 11 p1515 N88-19050
Coherent structure-reflective turbulent viscous flow modeling
[AD-A188339] 13 p1765 N88-20556
Numerical simulations of buoyancy driven flows in cylinders and cavities for vapor crystal growth
14 p1987 N88-21854
Selective growth velocity in needle crystals
14 p1988 N88-21858
High Reynolds number, low Mach number, steady flow field calculations over a NACA 0012 airfoil using Navier-Stokes and interactive boundary layer theory
[AD-A189871] 15 p2013 N88-22005
Unsteady aerodynamics of a Wortmann FX-63-137 wing in a fluctuating wind field
[AD-A190128] 15 p2013 N88-22006
Boundary-layer and wake measurements on a swept, circulation-control wing
[NASA-TM-89426] 15 p2014 N88-22013
Stochastic estimation of conditional eddies in turbulent channel flow 16 p2194 N88-23087
Big whorls carry little whorls 16 p2195 N88-23094
A statistical investigation of the single-point pdf of velocity and vorticity based on direct numerical simulations 16 p2196 N88-23101
On local approximations of the pressure-strain term in turbulence models 16 p2197 N88-23102
A non-invasive experimental technique for the measurement of unsteady velocity and vorticity fields
16 p2204 N88-23148
Measurements of the time dependent velocity field surrounding a model propeller in uniform water flow
16 p2205 N88-23155
Effect of initial tangential velocity distribution on the mean evolution of a swirling turbulent free jet
[NASA-TM-100934] 18 p2458 N88-24592
Theoretical investigation of the development of the normal fluid and superfluid velocity distributions during spin-up for a He2-filled cylinder
[MPIS-6/1987] 18 p2510 N88-24892
A single streamwise vortical structure and its instability in shear flows 18 p2515 N88-24921
Coal particle behaviour in a counter-current combustor
[TAE-606] 19 p2612 N88-25498
Driving of axial acoustic fields by side-wall stabilized premixed flames 19 p2629 N88-25592
Observations of electron cyclotron harmonic emissions associated with field-aligned electron beams
[SD-TR-87-33] 19 p2724 N88-26173
The velocity field of the outer galaxy
[B8681472] 20 p2885 N88-27132
Prediction of velocity and temperature profiles in thermally driven gravity currents applied to stratified thermal storage tanks
[DE88-004452] 21 p2946 N88-27496
Mass transport in sector and annular sector tubes
[LRT-WE-9-FB-9(1987)] 22 p3077 N88-28269
Application of acoustic-Doppler current profiler and expendable bathythermograph measurements to the study of the velocity structure and transport of the Gulf Stream
[NASA-CR-183188] 22 p3129 N88-28605
Rotation symmetric inside flow with diametric expansion resolution
[ILR-MITT-193] 23 p3213 N88-29123
Application of Particle Image Displacement Velocimetry (PIDV) to complex flows: Velocity field measurements in front of a heavy gas cloud
[VKI-TN-166] 23 p3213 N88-29125
Clustering of galaxies and clusters of galaxies in a decaying-particle cosmological model with a massive decay product
[DE88-753434] 23 p3298 N88-29642
The dynamics of SBO galaxies. Part 1: The data
[SER-C-PREPUBL-FASC-22] 24 p3455 N88-30567

VELOCITY FIELDS
U VELOCITY DISTRIBUTION

VELOCITY MEASUREMENT
NT WIND VELOCITY MEASUREMENT
An observer approach to the estimation of helicopter airspeed
[DFVLR-FB-87-13] 01 p0005 N88-10029
Jet formation and characterization of a conical shaped charge
[DE87-012102] 02 p0155 N88-10969
Three-dimensional calculation in high subsonic axial compressor rotor and its comparison with L2F velocity measurement 03 p0300 N88-11886
Particle velocity and stress gage measurements in spherical diverging flow
[DE87-007333] 03 p0321 N88-12033
Single-periodic multilayer grating laser Doppler vibrometer 03 p0327 N88-12066
Comparative studies in the near-field of turbulent transports of heated and unheated jets normal to a cross stream 04 p0444 N88-12756
Flow diagnostics and visualization in wind tunnels and flight 07 p0811 N88-14940
Pressure and mass velocity measurements in solids subjected to dynamic loadings 07 p0921 N88-15595
Velocity and density measurements in a turbulent nonpremixed flame with comparison to numerical model predictions
[DE87-014695] 08 p0967 N88-15854
EISCAT measurements of ion velocities during Coordinated Auroral Experiment using Scatter And Rockets (CAESAR) campaign 08 p1031 N88-16251
Velocity interferometry in shock tubes and shock tunnels
[ISL-CO-203/87] 09 p1122 N88-16713
Flow field measurements using hotwire anemometry
[AD-A187029] 09 p1160 N88-16951
An integration test for accelerometer evaluation
09 p1178 N88-17054
Development and application of oxygen flow tagging for velocity measurements and flow visualization in turbulent three-dimensional supersonic flows
[AD-A187982] 10 p1289 N88-17714
Measurement of forces and moments on, and velocity about a body of revolution with an attached fin at angles of attack
[AD-A187796] 11 p1433 N88-18554
Fluctuations and massive separation in three-dimensional shock-wave/boundary-layer interactions
[NASA-TM-89224] 11 p1434 N88-18559
Production by pyrolysis of diffusion particles for velocimetry in shock tubes
[ISL-R-119/86] 11 p1455 N88-18671
Measurement of velocity and temperature profiles in low-speed, turbulent non-isothermal flows
[PB88-155833] 11 p1486 N88-18872
New monostatic balanced Doppler velocimeter using a polarization preserving fiber
[PB88-130869] 11 p1490 N88-18895
Experiments on the flow of viscoelastic fluids between eccentric rotating cylinders 12 p1625 N88-19723
Laser Doppler velocimetry primer
[NASA-CR-177386] 12 p1631 N88-19761
Velocity and concentration measurements in flowing suspensions by nuclear magnetic resonance
[DE88-006225] 13 p1770 N88-20589
Observations of waves and Langmuir circulation with Doppler sonars 13 p1805 N88-20790
Combined aerodynamic size, charge-to-mass, and velocity measurements of aerosol particles
[ST-REPT-VOL-5-NO-4] 14 p1944 N88-21599
Continuous measurements of in-bore projectile velocity
[DE88-006841] 15 p2023 N88-22056
Instruments for use in experimental studies of complex turbulent shear flow: Three component LDVs
[AD-A190526] 15 p2065 N88-22312
New measurements of radial velocities in clusters of galaxies
[INPE-4527-PRE/1277] 15 p2152 N88-22845
Application of high speed holography to aerodynamic and hydrodynamic three-dimensional velocimetry
16 p2203 N88-23144
A non-invasive experimental technique for the measurement of unsteady velocity and vorticity fields
16 p2204 N88-23148
Gravity currents with heat transfer effects
[PB88-180047] 16 p2205 N88-23158
Inflow measurement made with a laser velocimeter on a helicopter model in forward flight. Volume 5: Tapered planform blades at an advance ratio of 0.23
[NASA-TM-100545] 17 p2299 N88-23755
Laser measurement of particle velocities in vacuum plasma spray deposition
[DE88-007111] 19 p2728 N88-26198
Position and velocity determination using a Global Positioning System: An outline
[B8735052] 20 p2757 N88-26355
Heterogeneous diffusion flame stabilization
[AD-A193014] 20 p2771 N88-26429
Crosslinking of two vortex rings side by side
20 p2782 N88-26502
Development of advanced flow simulation system by water flow model. New method of velocity measurement using cross-correlation
[DE88-753120] 20 p2799 N88-26608

Velocity-pressure integrated versus penalty finite element methods for high Reynolds number flows
[NASA-CR-179357] 20 p2803 N88-26635
Velocity measurements and flow visualization in turbulent three-dimensional supersonic flows using oxygen flow tagging
[AD-A192551] 21 p2892 N88-27165
Velocity measurements downstream of a sudden expansion using the Laser Doppler Velocimeters (LDV) technique. Part 1: Method of measurement and experimental facility
[FOA-C-20700-2.1-PT-1] 22 p3076 N88-28262
Calibration of a triple wire probe for turbulence measurements
[AD-A193956] 22 p3081 N88-28296
Hot-wire measurements of compressor blade wakes in a cascade wind tunnel
[AD-A194737] 23 p3181 N88-28936
A mapping of the viscous flow behavior in a controlled diffusion compressor cascade using laser Doppler velocimetry and preliminary evaluation of codes for the prediction of stall
[AD-A194490] 23 p3211 N88-29112
Application of Particle Image Displacement Velocimetry (PIDV) to complex flows: Velocity field measurements in front of a heavy gas cloud
[VKI-TN-166] 23 p3213 N88-29125
Application of optical correlation techniques to particle imaging velocimetry
[NASA-TM-101306] 23 p3218 N88-29152
Radial velocity measurements of a sample of northern metal-deficient stars
[SER-C-PREPUBL-FASC-25] 24 p3455 N88-30564

VELOCITY PROFILES
U VELOCITY DISTRIBUTION

VENTILATION
Hydride generation from the Exide load-leveling cells
[DE87-011361] 01 p0041 N88-10259
A plethysmograph for measuring pulmonary ventilation in small animals
[AD-A184978] 05 p0629 N88-13846
Plant Growth Module (PGM) conceptual design
05 p0631 N88-13855
Life-cycle cost analysis of residential heat pumps and alternative HVAC (Heating, Ventilating and Air-Conditioning) systems
[DE88-003701] 07 p0839 N88-15090
Load carriage induced alterations of pulmonary function
[AD-A186227] 07 p0889 N88-15386
Proceedings of the 19th DOE/NRC Airborne Waste Management and Air Cleaning Conference
[NUREG/CP-0086-VOL-1] 11 p1509 N88-19018
Proceedings of the 19th DOE/NRC Airborne Waste Management and Air Cleaning Conference
[NUREG/CP-0086-VOL-2] 11 p1509 N88-19019
Testing of the engine compartment fire extinguishing system in the F/EF-111 aircraft
[AD-A188801] 12 p1576 N88-19423
Liquid ventilation: New data and possible use in space medicine 12 p1654 N88-19908
Impact of control errors on the volume/weight demand of the Ventilation and Dryer (VAD) concept --- EURECA Botany Facility
[TN-RB524-006/87] 17 p2377 N88-24132
Evaluation of the toxicity of products from the thermal degradation of materials
[ETN-88-91995] 18 p2549 N88-25130
Model test of air-exchange efficiency
[DE88-752862] 23 p3201 N88-29049

VENTILATORS
Computer code simulations of explosions in flow networks and comparison with experiments
[DE88-001946] 05 p0573 N88-13491

VENTING
Zero-G thermodynamic vent system for shuttle/Centaur 08 p0983 N88-15943
Payload bay atmospheric vent airflow testing at the Vibration and Acoustic Test Facility
[NASA-TM-100460] 11 p1437 N88-18572
Enhanced emergency smoke venting
[DOT/FAA/CT-88/22] 20 p2756 N88-26350

VENTS
Zero-G thermodynamic vent system for shuttle/Centaur 08 p0983 N88-15943
Experimental and theoretical constraints on the origin of mid-ocean ridge geothermal fluids
13 p1804 N88-20784
Modification and development of the external tank hydrogen vent umbilical system for the space shuttle vehicle 14 p1928 N88-21496

VENUS (PLANET)
Final phase of Project Vega 01 p0009 N88-10053
Comparative plasma tails of Venus and comets
01 p0116 N88-10742
Interplanetary magnetic field effects on the interaction of the solar wind with Venus 06 p0805 N88-14910
To what extent is mass loading responsible for the Venus bowshock precursor?
[NASA-TM-89307] 12 p1711 N88-20239
Vega-1 and Vega-2 automatic stations: Functioning of landing modules in Venusian atmosphere
13 p1725 N88-20313
Elemental composition of Venusian rocks in northeastern part of Terra Aphrodite (determined using data from Vega-2 landing module)
13 p1726 N88-20322
Engineering planetary lasers for interstellar communication
[NASA-CR-180780] 17 p2311 N88-23825
Kinetics of thermochemical gas-solid reactions important in the Venus sulfur cycle
[NASA-CR-182963] 19 p2742 N88-26280
The rate of volcanism on Venus
[NASA-CR-183039] 19 p2742 N88-26281
A bibliography of dunes: Earth, Mars, and Venus
[NASA-CR-4149] 20 p2885 N88-27134

VENUS ATMOSPHERE
NT VENUS CLOUDS
Venusian surface and crust 01 p0010 N88-10054
Preliminary estimation of color inhomogeneities on the surface of Venus according to the television images obtained by the VENERA-13 and VENERA-14 automated space probes
[NASA-TT-20114] 02 p0254 N88-11608
Mechanisms of cloud layer formation in Venusian atmosphere 08 p1004 N88-16087
Atmosphere of Venus in southern polar area
08 p1005 N88-16088
Atmosphere of Venus in south polar area based on radio transmission data 08 p1005 N88-16089
Atmosphere of Venus in north polar area based on radio transmission data from Venera-15 and Venera-16 spacecraft 08 p1005 N88-16090
Peculiarities of daytime ionosphere of Venus during years of low and high solar activity
08 p1005 N88-16091
Distribution of electron concentration in nightime atmosphere of Venus based on radio transmission data
08 p1005 N88-16092
Applicability of extremely low frequency global resonances for study of Venusian storm activity
08 p1005 N88-16093
Vega-1 and Vega-2 automatic stations: Functioning of landing modules in Venusian atmosphere
13 p1725 N88-20313
Thermal structure of Venusian Atmosphere determined from results of measurements from Vega-2 landing module 13 p1725 N88-20315
Research on absorption of UV radiation in Venusian atmosphere from Vega-1 and Vega-2 landing modules
13 p1725 N88-20316
Vertical structure of Venusian cloud layer at landing sites of Vega-1 and Vega-2 vehicles
13 p1725 N88-20317
Gas-chromatographic analysis of products of thermal reactions of aerosol in Venusian cloud layer on Vega-1 and Vega-2 automatic interplanetary stations
13 p1725 N88-20318
Roentgenoradiometric analysis of aerosol in Venusian clouds by Vega-1 and Vega-2 automatic interplanetary stations 13 p1726 N88-20319
Chemical composition and structure of Venusian clouds determined from results of roentgenoradiometric experiments carried out by landing modules of Vega-1 and Vega-2 automatic interplanetary stations
13 p1726 N88-20320
Determining chemical composition of aerosol in Venusian cloud layer on Vega-1 automatic interplanetary station using Malakhit mass spectrum analyzer
13 p1726 N88-20321
Determination of the Venus flyby orbits of the Soviet Vega probes using VLBI techniques
22 p3067 N88-28203
Microphysical processes in cloud layers of Venus
24 p3448 N88-30522
Stability of Venusian ionopause
24 p3448 N88-30523

VENUS CLOUDS
Mechanisms of cloud layer formation in Venusian atmosphere 08 p1004 N88-16087
Roentgenoradiometric analysis of aerosol in Venusian clouds by Vega-1 and Vega-2 automatic interplanetary stations 13 p1726 N88-20319

VENUS RADAR ECHOES
Dike zones on Venus
[NASA-TT-20111] 02 p0254 N88-11607
Processing of radar images of Venus on the Magiscan-2 analyzer 08 p1009 N88-16117

VENUS SURFACE
Venusian surface and crust 01 p0010 N88-10054
Dike zones on Venus
[NASA-TT-20111] 02 p0254 N88-11607
Preliminary estimation of color inhomogeneities on the surface of Venus according to the television images obtained by the VENERA-13 and VENERA-14 automated space probes
[NASA-TT-20114] 02 p0254 N88-11608
Processing of radar images of Venus on the Magiscan-2 analyzer 08 p1009 N88-16117
Analysis of impact crater arrangement on the Venutian surface (from photographic materials of the Venera-15 and -16 spacecraft)
[NASA-TT-20211] 11 p1571 N88-19401
JPRS report: Science and technology. USSR: Space
[JPRS-USP-88-002] 13 p1724 N88-20312
Vega-1 and Vega-2 automatic stations: Functioning of landing modules in Venusian atmosphere
13 p1725 N88-20313
Elemental composition of Venusian rocks in northeastern part of Terra Aphrodite (determined using data from Vega-2 landing module)
13 p1726 N88-20322
Content of natural radioactive elements in Venusian rocks determined using data from Vega-1 and Vega-2 stations 13 p1726 N88-20323
Kinetics of thermochemical gas-solid reactions important in the Venus sulfur cycle
[NASA-CR-182963] 19 p2742 N88-26280
The rate of volcanism on Venus
[NASA-CR-183039] 19 p2742 N88-26281

VERBAL COMMUNICATION
Training in time interval discrimination using verbal feedback 12 p1665 N88-19985
Activities report of the Department of Systems and Communications
[ENST-87D004] 16 p2189 N88-23053
The representational code of the internal model of dynamic systems: An individual differences and dual task approach
[AD-A190876] 16 p2244 N88-23403
A review of workload measurement in relation to verbal comprehension 21 p2925 N88-27360

VERIFICATION (PROVING)
U PROVING

VERMICULITE
Activities report in metal manufacturing
[ISSN-0524-7705] 07 p0839 N88-15086

VERTEBRATES
NT AMPHIBIA
NT BIRDS
NT CATS
NT CHICKENS
NT DOGS
NT FISHES
NT FROGS
NT HUMAN BEINGS
NT MAMMALS
NT MICE
NT MONKEYS
NT PRIMATES
NT RATS
NT WATERFOWL
Functional plasticity of the nervous system of vertebrates 01 p0074 N88-10474
Proceedings and program draft in Gravitational Biology in the Federal Republic of Germany --- Effects of Weightlessness on the Human Organism
[ESA-TT-988] 07 p0884 N88-15363

VERTICAL AIR CURRENTS
Mesoscale density variability in the mesosphere and thermosphere: Effects of vertical flow accelerations
06 p0736 N88-14529
A Lagrangian model of dry thermals
[DM-50] 09 p1193 N88-17150
NASA wind shear model: Summary of model analyses
10 p1273 N88-17617
Windshear detection effect of static air temperature bias 10 p1274 N88-17621
Are windshear training aid recommendations appropriate for other than large jet transports? Pilot procedures: Shear models 10 p1275 N88-17635
Global vertical mass transport by clouds: A two-dimensional model study
[CM-74] 24 p3391 N88-30192

VERTICAL DISTRIBUTION
NT STAR DISTRIBUTION
ECC (Electrochemical Concentration Cell) ozonesonde observations at South Pole, Antarctica during 1986
[PB87-207502] 02 p0197 N88-11228
Hydrochemical structure of Gulf Stream frontal zone waters 06 p0727 N88-14476
Effect of neutral wind on the latitudinal variation of nighttime F-layer vertical movements
08 p1030 N88-16244

A comparison of multi-layer meso-alpha MLAM model results with surface and aircraft observations from CAPTEX
[DE88-000549] 09 p1188 N88-17118

Measurement of vertical distributions of halogenated hydrocarbons in the stratosphere
[ETN-88-91065] 09 p1191 N88-17135

Model investigations of atmospheric ammonia scavenging
[DE88-002337] 09 p1194 N88-17153

Vertical structure of Venusian cloud layer at landing sites of Vega-1 and Vega-2 vehicles
13 p1725 N88-20317

Forty-eight-inch lidar aerosol measurements taken at the Langley Research Center, May 1974 to December 1987
[NASA-RP-1209] 23 p3232 N88-29234

VERTICAL FINS
U FINS

VERTICAL FLIGHT
Integrated control and display research for transition and vertical flight on the NASA V/STOL Research Aircraft (VSRA)
[NASA-TM-100029] 05 p0551 N88-13359

The impact of vertical axis characteristics on helicopter handling qualities
[AD-A188964] 12 p1583 N88-19474

VERTICAL JUNCTION SOLAR CELLS
Three-dimensional models of conventional and vertical junction laser-photovoltaic energy converters
[NASA-TM-4039] 17 p2370 N88-24111

VERTICAL LANDING
GPS vertical axis performance enhancement for helicopter precision landing approach
[NASA-CR-177443] 04 p0397 N88-12477

Parametric study of supersonic STOVL flight characteristics
[NASA-CR-177330] 16 p2161 N88-22693

A numerical study of the hot gas environment around a STOVL aircraft in ground proximity
[NASA-TM-100895] 17 p2295 N88-23729

VERTICAL MOTION
Vertical ship motions and sea loads considering nonlinear effects
[TAE-592] 20 p2784 N88-26515

Utilization of a single clear-air Doppler radar beam to measure vertical divergence
[AD-A195543] 24 p3405 N88-30271

VERTICAL MOTION SIMULATORS
Status of NASA/Army rotorcraft research and development piloted flight simulation
09 p1110 N88-16651

VERTICAL ORIENTATION
Investigation of vertical axis handling qualities for helicopter hover and NOE flight
03 p0263 N88-11653

Effects of combining vertical and horizontal information into a primary flight display
[NASA-TP-2783] 04 p0399 N88-12487

Data acquisition and analysis system for the Sandia 34-meter Vertical Axis Wind Turbine
[DE88-002417] 09 p1187 N88-17112

Relationships between remotely-sensed surface properties and subsurface structure in the ocean
[AD-A189317] 12 p1650 N88-19881

A polarization diversity meteorological radar system
[AD-A189291] 13 p1758 N88-20515

The effects of torque response and time delay on rotorcraft vertical axis handling qualities
[AD-A189873] 15 p2017 N88-22023

Deflection of a circular liquid jet on a flat plate perpendicular to the flow direction
[NASA-TT-20279] 16 p2207 N88-23173

Single phase liquid immersion cooling of discrete heat sources in a vertical channel
[AD-A191224] 17 p2337 N88-23944

Observations of frontal instabilities on an upwelling filament
[AD-A191051] 17 p2375 N88-24122

The effect of a turbulent airstream on a vertically-launched missile at high angles of attack
[AD-A192408] 20 p2758 N88-26363

Stability of a coastal upwelling front over topography
[AD-A192354] 20 p2829 N88-26784

A modal approach to Arctic noise modelling with implied vertical coherence
[AD-A192966] 20 p2850 N88-26916

Vertical viewing ECE diagnostic for the D3-D tokamak
[DE88-010586] 20 p2860 N88-26987

Vertical directionality of ambient noise at 32 deg N as a function of longitude: Tape number 86180
[AD-A193228] 21 p3012 N88-27872

Nonequilibrium flow of a radiating gas in a vertical channel with axial temperature variation
[DE88-702535] 23 p3212 N88-29120

Possibilities of determining vertical profiles of microphysical characteristics of stratospheric aerosol using space measurements of transparency and solar halo 24 p3449 N88-30526

VERTICAL STABILIZERS
U STABILIZERS (FLUID DYNAMICS)

VERTICAL TAILS
U STABILIZERS (FLUID DYNAMICS)
U TAIL ASSEMBLIES

VERTICAL TAKEOFF
The ability of modified pavement quality concrete to resist ground erosion caused by VTOL aircraft
[BAE-ARG-238] 03 p0267 N88-11683

VERTICAL TAKEOFF AIRCRAFT
Propulsion-induced effects caused by out-of-ground effects
[NASA-TM-100032] 06 p0666 N88-14088

Development of a plenum chamber burner system for an advanced VTOL engine 10 p1281 N88-17664

Development of vertical takeoff aircraft with turbojet engines in Germany 10 p1309 N88-17822

VERTICAL TAKEOFF AND LANDING
U VERTICAL LANDING
U VERTICAL TAKEOFF

VERTOL MILITARY HELICOPTERS
U BOEING AIRCRAFT

VERY HIGH FREQUENCIES
Future developments of auroral D-region research using the EISCAT VHF incoherent scatter radar
08 p1035 N88-16278

VHF/UHF propagation by diffraction: Calculation by numerical integration 12 p1615 N88-19659

Some measurements of height gain at V.H.F.
12 p1617 N88-19671

Descriptions of HF and VHF Loran-C buoys and evaluations as potential datum marker buoys
[AD-A192069] 18 p2462 N88-24618

Theoretical basis for an experimental test with regard to the origin of VHF (Very High Frequency) radiation from natural lightning
[DE88-007535] 18 p2544 N88-25102

Mini-station for VHF reception: Argos system simplified description
[INPE-4551-NTE/279] 19 p2655 N88-25764

The VHF experimental radar LARA. A long-wavelength radar for helicopter detection 22 p3149 N88-28738

VERY HIGH SPEED INTEGRATED CIRCUITS
U VHSIC (CIRCUITS)

VERY LARGE ARRAY (VLA)
VLA observations of the X-ray bright Hyades M-dwarfs
04 p0512 N88-13147

IUE/Optical/VLA flares on AD Leo
04 p0512 N88-13152

Microwave observations of red dwarf flare stars
04 p0513 N88-13153

A VLA survey of dMe flare stars
04 p0513 N88-13154

VLA observations of rapid 6 cm flux variations in alpha Ori
04 p0515 N88-13169

Mars: High resolution VLA observations at wavelengths of 2 and 6 cm and derived properties
06 p0804 N88-14909

X-band system performance of the very large array
11 p1473 N88-18789

DSS 14 antenna calibrations for GSSR/VLA Saturn radar experiments 22 p3068 N88-28207

VERY LARGE SCALE INTEGRATION
Contribution to the development of smart design techniques for VLSI integrated circuits — CMOS
[LAAS-87-181] 02 p0221 N88-11395

The design plan of a VLSI single chip (255, 223) Reed-Solomon decoder 04 p0435 N88-12697

A simplified procedure for correcting both errors and erasures of a Reed-Solomon code using the Euclidean algorithm 04 p0435 N88-12698

On the VLSI design of a pipeline Reed-Solomon decoder using systolic arrays 04 p0436 N88-12700

A procedural method for the efficient implementation of full-custom VLSI designs 04 p0436 N88-12701

Research in VLSI (Very Large Scale Integration) systems
[AD-A184089] 04 p0438 N88-12721

A study of charged particles/radiation damage to VLSI device materials
[NASA-CR-172036] 05 p0577 N88-13518

New breakthrough in Chinese integrated circuits: Successful development of high-speed CMOS circuits
[AD-A185381] 05 p0578 N88-13525

Benchmarking and evaluation of hardware description languages for design of VLSI systems
[PB87-134557] 06 p0758 N88-14648

Very thin VLSI-layouts (Very Large Scale Integration-Layouts) of complete binary trees
[PB88-100847] 06 p0789 N88-14841

Correctness proofs for systolic algorithms: Palindromes and sorting
[PB88-106075] 07 p0912 N88-15534

Extraction of MOS VLSI (Very-Large-Scale-Integrated) circuit models including critical interconnect parasitics
[AD-A185847] 08 p0979 N88-15914

Application of parallel distributed processing to space based systems 08 p1059 N88-16393

High performance VLSI algorithms and architectures for digital signal processing 09 p1155 N88-16926

Formal multilevel hierarchical verification of synchronous MOS VLSI circuits
[AD-A187532] 10 p1324 N88-17918

Latent failures and coverage in fault-tolerant systems. A VLSI CMOS circuit design technique to aid test generation
[AD-A187615] 10 p1325 N88-17921

Signal processing studies program VLSI designs for unary functions
[AD-A188053] 10 p1325 N88-17922

The arithmetic cube and its associated algorithms
10 p1374 N88-18195

Wafer scale implementation of a GaAs systolic signal processor cell 10 p1381 N88-18247

A VLSI implementable block oriented data driven multiprocessor 10 p1381 N88-18249

On systolic architectures for interpolation and integration 10 p1382 N88-18250

Fuzzy logic inference processor for real time control: A second generation full custom design
[AD-A188155] 11 p1471 N88-18773

A comparison of VLSI architectures for time and transform domain decoding of Reed-Solomon codes
11 p1472 N88-18783

A simplified, general-purpose deep-space ranging correlator design 11 p1473 N88-18785

Description, analysis and simulation of a new realization of digital filters
[AD-A187763] 11 p1477 N88-18814

High bit rate serial input multipliers
[REPT-87-012] 11 p1530 N88-19140

On serial-input multipliers for two-complement numbers
[REPT-86-035] 11 p1536 N88-19181

Development of VLSI optical data link
[AD-A187883] 11 p1549 N88-19265

Development of VLSI optical data link
[AD-A187884] 11 p1549 N88-19266

Hercules: A power analyzer for MOS VLSI circuits
[AD-A188702] 12 p1623 N88-19706

VSLI design generators
[AD-A188706] 12 p1623 N88-19707

Computer aided fast turnaround laboratory for research in VLSI (Very Large Scale Integration)
[AD-A189451] 12 p1624 N88-19715

VLSI implementations for digital signal processing
[AD-A189612] 12 p1624 N88-19719

Gridless routing for generalized cell assemblies: Report and user manual
[EUT-87-E-180] 13 p1764 N88-20549

GM: A gate matrix layout generator
[EUT-87-E-179] 13 p1820 N88-20875

Applications of lasers to semiconductor studies
14 p1901 N88-21356

GADL: A gate array description language
[EUT-87-E-165] 14 p1907 N88-21396

Electron beam sensitive devices for controllability
[RR-658-I] 14 p1908 N88-21403

Higher levels of a silicon compiler
[EUT-86-E-163] 14 p1955 N88-21650

Generating layouts for random logic: Cell generation schemes
[EUT-86-E-164] 14 p1956 N88-21658

ESKISS: A program for optimal state assignment
[EUT-87-E-167] 14 p1956 N88-21659

Technology mapping from Boolean expressions to standard cells
[EUT-87-E-174] 14 p1963 N88-21709

Advanced packaging for VLSI/VHSIC (Very Large Scale Integrated Circuits/Very High Speed Integrated Circuits) applications: Electrical, thermal and mechanical considerations, an IR and D report
[AD-A189666] 14 p1965 N88-21724

An optimal CMOS structure for the design of a cell library
[EUT-87-E-166] 14 p1985 N88-21841

French Multiproject Chip (MPC) activity report, 1986
[RR-650-I] 15 p2059 N88-22273

Multiple-transform pipelines for image coding
[REPT-87-038] 15 p2108 N88-22561

Software structuring principles for VLSI CAD
[AD-A190386] 15 p2112 N88-22579

Design and implementation of VLSI prime factor algorithm processor
[AD-A190483] 15 p2112 N88-22580

Design of high yield microprocessors
[ETN-88-92184] 16 p2245 N88-23410
Automatic layout generation of data processing sections of VLSI microprocessor-like circuits
[ETN-88-92185] 16 p2245 N88-23411
HIFI: A design method for implementing signal processing algorithms on VLSI processor arrays
[ETN-88-92238] 16 p2247 N88-23421
Silicon compilers: Application to the compilation of the control area
[ETN-88-92188] 16 p2247 N88-23425
Correctness proofs for systolic algorithms: A palindrome recognizer
[CWI-CS-R8747] 16 p2248 N88-23434
Piecewise linear approach for timing simulation of VLSI (Very-Large-Scale-Integrated) circuits on serial and parallel computers
[AD-A191328] 16 p2252 N88-23462
A multigrid approach for the solution of a nonlinear diffusion equation in a time-dependent area using Cartesian coordinates
[GMD-STUDIEN-122] 16 p2257 N88-23491
Microelectronics the next fifteen years 17 p2305 N88-23792
Interfacing and integrating hardware and software design systems 17 p2306 N88-23796
Evolution of a family of image processing systems at INPE 17 p2361 N88-24065
Silicon-on-insulator electronics for a space nuclear power system 17 p2431 N88-24461
Defect detection and classification in VLSI pattern inspection 18 p2507 N88-24871
Some unsolved problems in modelling self-timed circuits using Petri Nets, series B, number 2
[PB88-181466] 18 p2507 N88-24872
SYMBL: A new Boolean compiler 18 p2554 N88-25160
An improved simulated annealing algorithm for standard cell placement
[NASA-CR-182952] 18 p2558 N88-25183
Mathematical models for VLSI device simulation
[AD-A191125] 18 p2562 N88-25212
Progress and challenges in HEMT LSI technology 19 p2656 N88-25779
Effects of cosmic rays on single event upsets
[NASA-CR-183053] 20 p2793 N88-26569
Research in VLSI computer systems
[AD-A192915] 20 p2835 N88-26816
Digital carrier demodulation for the DSN Advanced Receiver 22 p3064 N88-28183
Rule-based circuit optimization for CMOS VLSI 22 p3137 N88-28649
Performance analysis of k-ary n-cube interconnection networks
[AD-A195542] 24 p3361 N88-30010
Design of a self-timed VLSI multicomputer communication controller
[AD-A194567] 24 p3361 N88-30014

VERY LONG BASE INTERFEROMETRY
Extragalactic VLBI objects: Candidates for optical interferometry? 01 p0094 N88-10616
EVN (European VLBI network) and MERLIN observations of 5 superluminal radio sources
[PB87-110730] 04 p0520 N88-13193
Low-frequency VLBI in space and interstellar refraction
[PB87-127643] 06 p0696 N88-14267
Low frequency VLBI in space using GAS-Can satellites: Report on the May 1987 JPL Workshop
[NASA-CR-182362] 06 p0801 N88-14904
VLBI research on OH-maser IN W33 08 p1001 N88-16064
Crustal dynamics project data analysis, 1987. Volume 1: Fixed station VLBI geodetic results, 1979-1986
[NASA-TM-100682] 08 p1035 N88-16279
Crustal dynamics project data analysis, 1987. Volume 2: Mobile VLBI geodetic results, 1982-1986
[NASA-TM-100689-VOL-2] 08 p1035 N88-16280
Observation model and parameter partials for the JPL VLBI parameter estimation software MASTERFIT-1987
[NASA-CR-182524] 10 p1427 N88-18523
Source and event selection for radio-planetary frame-tie measurements using the Phobos Landers 11 p1471 N88-18775
A 2.3-GHz maser at Usuda, Japan, for TDRSS-orbiting VLBI experiment 11 p1472 N88-18779
Phase calibration generator 11 p1473 N88-18785
Deformations in VLBI antennas
[NASA-TM-100696] 11 p1502 N88-18970
Geodetic positioning by employment of the GPS-NAVSTAR satellites applying the techniques of VLBI and sequential recursive optimal estimation
[INPE-4438-TDL/311] 12 p1594 N88-19547
Polarization properties of SiO masers 13 p1858 N88-21113
The Spring 1985 high precision baseline test of the JPL GPS-based geodetic system
[NASA-CR-182686] 14 p1940 N88-21577
A 2.3-GHz low-noise cryo-FET amplifier 22 p3066 N88-28195
DSN very long baseline interferometry system Mark IV-88 22 p3067 N88-28199
Determination of the Venus flyby orbits of the Soviet Vega probes using VLBI techniques 22 p3067 N88-28203

VERY LOW FREQUENCIES
ELF/VLF/LF propagation and system design
[AD-A183261] 01 p0033 N88-10212
WAVFLD: A program to compute ionospheric height gain functions and field strengths at VLF
[AD-A191159] 16 p2191 N88-23066
WIPP (Wave Induced Particle Precipitation) experiment logistic support
[AD-A191184] 18 p2499 N88-24824
Outer zone electron precipitation produced by a VLF transmitter
[AD-A191944] 19 p2691 N88-25993
Airborne measurement of low frequency atmospheric noise ALFAN 1
[AD-A193056] 21 p2931 N88-27405
TE/TM (Transverse Electric/Transverse Magnetic) height profile measurements of transpolar VLF (Very Low Frequency) signals
[AD-A194503] 22 p3069 N88-28216
Influence of plasma parameters on VLF radiation in near-rocket region 24 p3448 N88-30518

VESTIBULAR NYSTAGMUS
Role of optokinetic stimulation in vesibulospinal reflexes 10 p1360 N88-18131

VESTIBULAR TESTS
Development of methods for the study of space motion sickness 07 p0892 N88-15408
Vestibular response to caloric stimulation during orbital flight 12 p1658 N88-19939
Facilitory effects of voluntary movements on vestibuiomotor reaction 12 p1664 N88-19976
Studies of the vestibulo-ocular reflex on STS 4, 5 and 6
[NASA-TM-100461] 12 p1666 N88-19987
Role of opioid peptides in pathogenesis of vestibulovegetative disorders 19 p2704 N88-26079
Motion evoked vestibular potentials 21 p2982 N88-27712

VESTIBULES
Motion and space sickness 04 p0404 N88-12510
Vestibular integrated function and microgravity 12 p1658 N88-19937
Significance of sensory signal phase mismatch in mechanisms of motion sickness development 20 p2830 N88-26787

VESTS
Fit evaluation of female body armor
[AD-A188721] 14 p1953 N88-21638

VFR (RULES)
U VISUAL FLIGHT RULES

VHSIC (CIRCUITS)
Interchange of electronic design through VHDL and EIS 09 p1205 N88-17222
A production-quality UNIX Very High Speed Integrated Circuit (VHSIC) Hardware Description Language (VHDL) subset analyzer
[AD-A188832] 12 p1623 N88-19710
Advanced packaging for VLSI/VHSIC (Very Large Scale Integrated Circuits/Very High Speed Integrated Circuits) applications: Electrical, thermal and mechanical considerations, an IR and D report
[AD-A189666] 14 p1965 N88-21724
Very High Speed Integrated Circuits (VHSIC)
[AD-A193225] 21 p2937 N88-27442

VIBRATION
NT BENDING VIBRATION
NT FLUTTER
NT FORCED VIBRATION
NT FREE VIBRATION
NT LATTICE VIBRATIONS
NT LINEAR VIBRATION
NT POGO EFFECTS
NT RANDOM VIBRATION
NT RESONANT VIBRATION
NT SELF INDUCED VIBRATION
NT STRUCTURAL VIBRATION
NT SUPERSONIC FLUTTER
NT TRANSONIC FLUTTER
Investigation of the excitation of turbine blade vibration in axial compressors in rotating stall
[ETN-87-90377] 01 p0007 N88-10035
Activities report of the Institute of Sound and Vibration Research
[ETN-87-90685] 01 p0090 N88-10589
The Shock and Vibration Digest, Volume 19, No. 11 03 p0265 N88-11673
The Shock and Vibration Digest, Volume 19, No. 10 03 p0335 N88-12112
Vibration and parametric excitation in rotating asymmetric circular plates 04 p0456 N88-12823
Initial dynamic load estimates during configuration design 05 p0593 N88-13621
The Shock and Vibration Digest, Volume 19, No. 12 05 p0610 N88-13746
Dynamics of cables and chains 05 p0610 N88-13747
Computation of natural frequencies of planar lattice structure
[AD-A185387] 05 p0641 N88-13920
Influence of general vertical vibration on relationships between mediators in various segments of brain 06 p0751 N88-14613
Vibrational properties of disordered solids. Far infrared studies: Performance report
[DE88-001474] 06 p0786 N88-14821
Methods of improving compacting quality of intricately shaped powder components
[BLL-M-37412-(5828.4)] 08 p0968 N88-15859
The Shock and Vibration Digest, Volume 20, No. 1 08 p0975 N88-15897
The Shock and Vibration Bulletin. Part 3: Isolation and damping, vibration test criteria, and vibration analysis and test
[AD-A186750] 08 p0997 N88-16040
The effects of rotor unbalance on the vertical response of a soft-mounted block 08 p1000 N88-16057
Investigation of vibration problems with heterodyne holographic interferometer 08 p1000 N88-16058
A summary of recent NASA/Army contributions to rotorcraft vibrations and structural dynamics technology 09 p1105 N88-16628
Geometric structure, pseudoband gaps, and surface vibrational resonances on metal surfaces
[AD-A187001] 09 p1143 N88-16851
Computational fluid dynamics and aerothermodynamics
[NASA-CR-182490] 09 p1166 N88-16989
An analytical study of the effects of transverse shear deformation and anisotropy on natural vibration frequencies of laminated cylinders
[NASA-TM-100554] 10 p1295 N88-17739
One-dimensional leakage-flow vibration instabilities
[DE88-002875] 10 p1330 N88-17947
Vibration and flutter characteristics of the SR7L large-scale propfan
[NASA-TM-100272] 10 p1344 N88-18036
Modal testing the EOLE
[DE88-003795] 10 p1350 N88-18066
Modal testing of a very flexible 110 m wind turbine structure
[DE88-003796] 10 p1351 N88-18072
The Shock and Vibration Digest, volume 20, no. 2 10 p1417 N88-18459
Dynamic analysis of plane frames by microcomputer 11 p1531 N88-19143
Vibrational, mechanical and thermal properties of 3-5 semiconductors
[AD-A187569] 11 p1556 N88-19316
Study of the vibrational modes of subsurface oxygen on Al (111) using diode laser infrared reflection-absorption spectroscopy
[AD-A188322] 12 p1632 N88-19769
Vibrations of shells containing fluid 12 p1635 N88-19787
Vibration spectra of oxygen and vanadium atoms in vanadium-oxygen disordered interstitial alloys
[DE87-703166] 13 p1740 N88-20404
Research on flow around bluff bodies, flow induced vibrations 14 p1864 N88-21135
The buckling and vibration of composite plates using the Levy method considering shear deformation and rotary inertia
[AD-A189743] 15 p2076 N88-22374
Effect of vibrational excitation on rate parameters of atmospheric reactions
[AD-A190464] 15 p2094 N88-22477
The nonlinear dynamics of a spacecraft coupled to the vibration of a contained fluid
[DE88-007035] 16 p2168 N88-22925
Periodic response of nonlinear systems 16 p2217 N88-23228
Modal forced response of propfans in yawed flow 16 p2221 N88-23253
Computer simulation of a motor pump unit to aid in interpreting vibration data
[DE88-004481] 16 p2223 N88-23270
The Shock and Vibration Digest, volume 20, no. 4 17 p2391 N88-24214
Low authority control of large space structures using a constrained threshold control formulation 18 p2472 N88-24667

A dynamic analysis of piezoelectric strained elements
[AD-A191478] 18 p2503 N88-24851
Effects of Coriolis acceleration on the vibrations of spinning structures 18 p2522 N88-24966
Vibration protection of inelastic structures by means of active and passive control 18 p2528 N88-25001
Vibrations of rotating thick or thin rings 18 p2529 N88-25003
Bimolecular reactions and energy-transfer processes of highly vibrationally excited molecules related to energetic materials
[AD-A189013] 18 p2571 N88-25270
Para-ortho abundance ratio of molecular hydrogen in NGC2023
[ISAS-RN-352] 18 p2573 N88-25286
Spectroscopy and energy transfer kinetics of the interhalogens
[AD-A192103] 18 p2583 N88-25344
Aircraft accident report: Air New Orleans, DBA continental express flight 962 British Aerospace 3101 (Jetstream 31), N331CY, New Orleans International Airport, Kenner, Louisiana, May 26, 1987
[PB88-910408] 19 p2601 N88-25450
Rare Gas Halide (RGH) kinetics
[AD-A192352] 20 p2770 N88-26425
A review of gear housing dynamics and acoustics literature
[NASA-CR-183110] 20 p2811 N88-26675
Vibration frequencies of tapered bars with nonclassical boundary conditions
[NASA-CR-183059] 20 p2813 N88-26688
FEB structural analysis, revision H
[AD-A192302] 20 p2814 N88-26698
Low energy molecular collisions
[ISAS-RN-366] 20 p2850 N88-26919
Enhancement of volume H(-) production by vibrationally pre-exciting the hydrogen molecules
[DE88-010783] 20 p2853 N88-26937
Aperiodic superlattices: Structured randomness 20 p2873 N88-27055
Vibrational impacts of hush house operation
[DE88-006983] 21 p2899 N88-27207
Nonlinear vibrations of periodically stiffened plates 21 p2963 N88-27598
Wave propagation and vibration of fibre reinforced laminates
[AD-A194144] 22 p3051 N88-28101
Power flow analysis of two coupled plates with arbitrary characteristics
[NASA-CR-183165] 22 p3075 N88-28251
Overview of computational vibro acoustics. State of the art and future development
[FFA-TN-1988-17] 23 p3279 N88-29521
Vibration spectra induced by impurities in 3-5-compounds semiconductors
[DE88-702730] 23 p3293 N88-29610
Containment of a silicone fluid free surface in reduced gravity using barrier coatings
[NASA-TM-101314] 24 p3371 N88-30072
Intramolecular dynamics: A study of molecules at high levels of vibrational excitation
[AD-A195285] 24 p3428 N88-30400

VIBRATION DAMPERS
U VIBRATION ISOLATORS

VIBRATION DAMPING
The effect of different packagings on the vibration behavior and the coupling factors of steam turbine blading
[ETN-87-90425] 01 p0056 N88-10357
Test of the Hipparcos payload in the Liege vacuum facility focal 02 p0135 N88-10850
On the root locus method applied to flexural vibration control systems 03 p0320 N88-12022
Combined problem of slew maneuver control and vibration suppression
[NASA-CR-181537] 04 p0455 N88-12817
The 58th Shock and Vibration Symposium, volume 1
[NASA-CP-2488-VOL-1] 05 p0592 N88-13609
Viscous damped space structure for reduced jitter 05 p0594 N88-13623
A system identification technique based on the random decrement signatures. Part 1: Theory and simulation 05 p0594 N88-13625
A system identification technique based on the random decrement signatures. Part 2: Experimental results 05 p0594 N88-13626
An efficient frequency response solution for nonproportionally damped systems 05 p0595 N88-13634
Shape optimization of damping layers 05 p0595 N88-13635
Advanced joining concepts for passive vibration control 05 p0596 N88-13638
Active control of flexural vibrations in beams 06 p0794 N88-14866
Experimental investigation of damping characteristics of bolted structural connections for plates and shells
[AD-A186075] 07 p0867 N88-15259
Identification and feedback control of machine tool vibrations
[PB88-109715] 08 p0976 N88-15902
The Shock and Vibration Bulletin. Part 1: Welcome, Keynote Address, Invited Papers, Nondevelopment Items Workshop and Pyrotechnic Shock Workshop
[AD-A186748] 08 p0997 N88-16034
Dynamic testing: Seven years later 08 p0997 N88-16035
The Shock and Vibration Bulletin. Part 3: Isolation and damping, vibration test criteria, and vibration analysis and test
[AD-A186750] 08 p0997 N88-16040
Dynamic analysis of a structure with sliding base 08 p0998 N88-16045
Rotorcraft flight research with emphasis on rotor systems 09 p1111 N88-16656
Rotorcraft technology at Boeing Vertol: Recent advances 09 p1111 N88-16658
Recent Sikorsky R and D progress 09 p1111 N88-16659
Launch vehicle vibration: Measures taken to avoid pogo on ESA's Ariane launch vehicle 09 p1123 N88-16727
Kinetic isolation tether experiment
[NASA-CR-182458] 09 p1135 N88-16810
A review of two-phase flow-induced vibration
[DE88-001955] 09 p1160 N88-16955
The dynamics of an oscillating four-bar linkage 09 p1181 N88-17074
Using frequency-domain methods to identify XV-15 aeroelastic modes
[NASA-TM-100033] 10 p1277 N88-17646
Sensitivity of active vibration control to structural changes and model reduction 10 p1284 N85-17683
Suspension design for a satellite transport container
[INPE-4352-TDL/296] 12 p1600 N88-19578
Experimental and analytical investigation on a proposed embedded fiber optic displacement sensor
[AD-A189030] 12 p1630 N88-19756
The Shock and Vibration Digest, volume 20, no. 3 12 p1635 N88-19786
Active vibration control of a cantilevered beam with three elastic coordinates
[AD-A188824] 12 p1636 N88-19797
Optimal placement of tuning masses for vibration reduction in helicopter rotor blades
[NASA-TM-100562] 13 p1782 N88-20665
Investigations on higher harmonic blade pitch control at helicopters
[DFVLR-FB-87-36] 14 p1868 N88-21165
Vibration isolation system for the Stratospheric Observatory For Infrared Astronomy (SOFIA) 14 p1926 N88-21483
Investigation of boundary layer disturbances caused by periodic heating of a thin ribbon
[AD-A190572] 15 p2065 N88-22314
Instrumentation to provide an active control capability for distributed parameter systems
[AD-A190043] 15 p2076 N88-22375
Vibrations of structures with parametric uncertainties
[AD-A190400] 15 p2076 N88-22378
Vibration control of large structures
[AD-A191358] 16 p2168 N88-22928
Lewis Structures Technology, 1988. Volume 1: Structural Dynamics
[NASA-CP-3003-VOL-1] 16 p2217 N88-23226
Survey of impact damper performance 16 p2217 N88-23227
Piezoelectric pushers for active vibration control of rotating machinery 16 p2218 N88-23229
Active control and system identification of rotordynamic structure 16 p2218 N88-23230
The LDCM actuator for vibration suppression
[NASA-CR-182898] 17 p2335 N88-23940
Vibration and control of flexible rotor supported by magnetic bearings
[NASA-TM-100688] 17 p2345 N88-23977
Experimental vibration damping characteristics of the third-stage rotor of a three-stage transonic axial-flow compressor
[NASA-TM-100948] 18 p2466 N88-24642
Electromagnetic damping and vibration isolation of space structures
[AD-A191492] 18 p2471 N88-24665
Experimental study of active vibration control
[AD-A191454] 18 p2526 N88-24989
Technologies for antenna shape and vibration control 19 p2652 N88-25748
Design of a controller to reduce residual vibration in the positioning control of flexible robotic manipulators 20 p2808 N88-26658
Experimental and theoretical investigation of passive damping concepts for member forced and free vibration
[NASA-CR-183082] 20 p2814 N88-26693
Vibration response of constrained viscoelastically damped plates: Analyses and experiments
[AD-A192329] 20 p2815 N88-26699
Vibration control of large structures
[AD-A193317] 21 p2961 N88-27587
Dual adaptive control: Design principles and applications
[NASA-CR-177485] 22 p3038 N88-28038
The effects of moisture loss and elevated temperature upon the material damping of fibre reinforced polymer matrix composites
[UTIAS-324] 23 p3188 N88-28970
Passive damping concepts for free and forced member and grillage vibration
[NASA-CR-183114] 23 p3225 N88-29196
Experimental investigation of the effects of underwater exposure on the damping characteristics of bolted structural connections for plates and shells
[AD-A194486] 23 p3226 N88-29200
Anti-aliasing filters for dynamics and control experiments
[AD-A193758] 23 p3226 N88-29203

VIBRATION EFFECTS
NT POGO EFFECTS
Nonsteady-state vibrations in acoustic medium of elastic elliptical shell subjected to instantaneously applied uniform pressure 02 p0160 N88-11000
Incipient fault detection study for advanced spacecraft systems
[NASA-CR-172014] 02 p0183 N88-11138
Development of rotorcraft interior noise control concepts. Phase 2: Full scale testing, revision 1
[NASA-CR-172594-REV-1] 06 p0777 N88-14769
Karyometric evaluation of neuronal reactions of rat cerebral cortex to the combined effect of ionizing radiation, longitudinal accelerations and vibration 07 p0890 N88-15396
Nystagmometric distinctions of individuals regularly exposed to vibration 07 p0891 N88-15401
A hybrid-stress finite element approach for stress and vibration analysis in linear anisotropic elasticity
[NASA-CR-179311] 12 p1634 N88-19784
Evaluation of chemical and atmospheric sciences research
[AD-A188468] 12 p1687 N88-20091
Vibration characteristics of pumped fluid systems (VCPFS) --- microgravity payloads
[ESA-CR(P)-2499] 14 p1895 N88-21310
Vibration testing of ACT fuselage 19 p2634 N88-25627
Effect of low-frequency whole-body vertical vibration on the serotoninergic system of the brain and spinal cord 19 p2704 N88-26081
Nonlinear hydroelastic vibrations in rectangular containers
[LRT-WE-9-FB-7(1987)] 22 p3088 N88-28340

VIBRATION ISOLATORS
Vibration-absorbing characteristics of metal-polymer shells 02 p0158 N88-10991
Controlling the dynamic environment during NOE flight 03 p0264 N88-11661
Modeling and control of large flexible vehicles in the atmosphere and space
[AD-A185368] 05 p0555 N88-13377
The 58th Shock and Vibration Symposium, volume 1
[NASA-CP-2488-VOL-1] 05 p0592 N88-13609
Optimal shock isolation with minimum settling time 05 p0595 N88-13633
A passive vibration-cancelling isolation mount 05 p0595 N88-13636
Microgravity isolation mount
[ESA-CR(P)-2480] 11 p1443 N88-18604
Suspension design for a satellite transport container
[INPE-4352-TDL/296] 12 p1600 N88-19578
Towards a practical microgravity environment --- isolation mount 14 p1878 N88-21223
The 22nd Aerospace Mechanisms Symposium
[NASA-CP-2506] 14 p1924 N88-21468
Vibration isolation system for the Stratospheric Observatory For Infrared Astronomy (SOFIA) 14 p1926 N88-21483
Development of a nitrile rubber for dynamic damping
[AD-A194060] 22 p3058 N88-28145

VIBRATION MEASUREMENT
USSR Report: Engineering and Equipment
[JPRS-UEQ-87-007] 02 p0157 N88-10985
Incipient fault detection study for advanced spacecraft systems
[NASA-CR-172014] 02 p0183 N88-11138
On the prediction of the aeroelastic behavior of lifting systems due to flow separation
[ESA-TT-1043] 03 p0259 N88-11633

Measurement of suspension and ride characteristics of the M1 main battle tank 05 p0596 N88-13637
Coupled elastic rotor/body vibrations with inplane degrees of freedom 05 p0596 N88-13643
Blade vibration problems in centrifugal compressors. Fundamental considerations 07 p0851 N88-15165
Modal analyses of the Kernville diagnostic canister [DE88-003268] 07 p0870 N88-15277
Parametric and experimental analysis using a power flow approach [NASA-CR-182460] 09 p1116 N88-16693
Spectral density estimates of coarsely quantized random vibration data 09 p1178 N88-17055
A reliable data collection/control system 10 p1289 N88-17708
Flaw identification from forced vibration testing [DE88-002641] 10 p1342 N88-18018
Low-cost optical data acquisition system for blade vibration measurement 16 p2219 N88-23240
Laboratory feasibility study of a composite embedded fiber optic sensor for measurement of structural vibrations [AD-A194270] 22 p3152 N88-28754
Use of holography in vibration and flutter study of fans [PNR90458] 24 p3375 N88-30098
Analytical and experimental studies of beam waveguide absorbers for structural damping [AD-A195085] 24 p3382 N88-30144
Vibrational power flow analysis of rods and beams [NASA-CR-183166] 24 p3383 N88-30151

VIBRATION METERS
NT SEISMOGRAPHS
Single-periodic multilayer grating laser Doppler vibrometer 03 p0327 N88-12066

VIBRATION MODE
Equivalent circuit consideration on the rotation of resonant modes of double resonant vibrators 07 p0839 N88-15092
Blade vibration due to different flow excitation 07 p0851 N88-15166
Modal analysis using frequency response measurement data 08 p0976 N88-15899
Overview of multi-input frequency domain modal testing methods with an emphasis on sine testing 11 p1499 N88-18949
A superelement component dynamic synthesis method 11 p1500 N88-18956
Method for finding principal modes of nonlinear vibration systems and their stabilities 14 p1899 N88-21340

VIBRATION PROTECTION
U VIBRATION ISOLATORS

VIBRATION SIMULATORS
NT VERTICAL MOTION SIMULATORS
Ultra-low frequency vibration data acquisition concerns in operating flight simulators [DE88-004795] 10 p1285 N88-17687

VIBRATION TESTING MACHINES
U VIBRATION SIMULATORS

VIBRATION TESTS
NT DAMPING TESTS
Surface scattering characteristics and the measurement of particulate contamination 02 p0137 N88-10862
Proceedings of Conference on Vibrodiagnostics discussed 02 p0158 N88-10990
Assessment of structural integrity from forced vibration testing [DE87-014642] 02 p0191 N88-11195
The Shock and Vibration Bulletin. Part 1: Welcome, Keynote Address, Invited Papers, Nondevelopment Items Workshop and Pyrotechnic Shock Workshop [AD-A186748] 08 p0997 N88-16034
Dynamic testing: Seven years later 08 p0997 N88-16035
Guidelines for qualifying non-development equipment to shock and vibration 08 p0997 N88-16036
Derivation of equipment vibration requirements for AV-8B 08 p0997 N88-16037
Designing electronics for pyrotechnic shock 08 p0997 N88-16038
TECOM's research efforts in the dynamic environments 08 p0999 N88-16048
The development of laboratory vibration test schedules: Philosophies and techniques 08 p0999 N88-16049
Laboratory vibration test schedules development beyond MIL-STD-810D 08 p0999 N88-16050
Comprehensive inflight vibration and acoustic testing 08 p0999 N88-16052
Evaluation of vibration specifications for acoustic environments 08 p0999 N88-16053
Fatigue effects of a swept sine test 08 p0999 N88-16054
Realization of the immediate objectives of the Aero-Gas Dynamics and Vibration Laboratory (LAGG) at the National Center for Research, Science and Technology (PUSPIPTEK) at Serpong, Java (Indonesia), Project TTA-79 [GG/QPR-10] 08 p1092 N88-16572
Failure of filament lamps subjected to vibration with special reference to the 26 volt 5 Watt tank lamp [EL-135] 09 p1158 N88-16938
Qualification by analysis of IUS plume deflectors 09 p1179 N88-17063
The dynamics of an oscillating four-bar linkage 09 p1181 N88-17074
Centaur G Prime modal test 09 p1181 N88-17075
Payload bay atmospheric vent airflow testing at the Vibration and Acoustic Test Facility [NASA-TM-100460] 11 p1437 N88-18572
NASDA's new test facilities for satellites and rockets 11 p1499 N88-18951
Design and dynamic testing of an instrumented spacecraft component 11 p1499 N88-18952
Random vibration (stress screening) of printed wiring assemblies 11 p1499 N88-18953
Development of a slip-ring system for energy transfer in space conditions. Space flight qualification and extended life tests [BMFT-FB-W-86-019] 16 p2169 N88-22932
Adjusting a finite element model using vibration type experimental data. Concept and error detection [ONERA-RT-7/3313-RY-060-R] 17 p2392 N88-24220
Vibration testing of ACT fuselage 19 p2634 N88-25627
Cross flow induced vibrations in tube bundle by displaced and misaligned tube configurations [ETN-88-92132] 20 p2801 N88-26621
Analytical and experimental studies of beam waveguide absorbers for structural damping [AD-A195085] 24 p3382 N88-30144

VIBRATIONAL FREQUENCIES (MOLECULAR)
U VIBRATIONAL SPECTRA

VIBRATIONAL FREQUENCIES (STRUCTURAL)
U RESONANT FREQUENCIES

VIBRATIONAL RELAXATION
U MOLECULAR RELAXATION

VIBRATIONAL SPECTRA
Picosecond CO2 laser interactions with polyatomic molecules [DE87-012072] 01 p0051 N88-10327
Diagnosis of flow channel in aircraft gas-turbine engines on basis of vibration spectrum characteristics 02 p0159 N88-10993
Kinetics of CO adsorption on nickel using time resolved vibration spectroscopy [ETN-87-90615] 03 p0289 N88-11814
Vibrational spectroscopy of shock-compressed fluid N2 and O2 [DE87-013138] 03 p0313 N88-11979
Ro-vibrational laser spectroscopy of ESD neutrals from chemisorbed species [DE87-013011] 04 p0447 N88-12770
Absorption of far IR-radiation by H2O-N2 complexes under atmospheric conditions 04 p0462 N88-12855
The delta upsilon = 1 fundamental bands of carbon monoxide in late-type stars 04 p0517 N88-13177
Pure dephasing of a vibrational adbond [AD-A185222] 05 p0609 N88-13740
Equilibrium retention in the nozzle of oxygen hydrogen propulsion systems 07 p0924 N88-15616
Fully turbulent internal flow excitation of pipe systems 08 p1000 N88-16056
Kinetic studies following state-selective laser excitation [DE88-004094] 10 p1335 N88-17981
Rovibrational spectroscopy of ArCO van der Waals complex [DE88-004291] 10 p1406 N88-18387
Coupling of vibrational modes of adsorbates: Application to field induced shifts for CO and CN on Cu(100) [AD-A187891] 11 p1453 N88-18659
In-situ vibrational spectroscopy of specifically adsorbed azide on silver electrodes [AD-A188511] 12 p1605 N88-19600
Advanced electron optics for vibrational spectroscopy [AD-A188469] 12 p1629 N88-19747
Stabilization and control problems in structural dynamics [AD-A190197] 15 p2073 N88-22361
Sequential excitation preparation of molecular energy levels with special structural and chemical properties [AD-A190041] 15 p2132 N88-22718
Time-resolved studies of free radicals and laser-initiated chain reactions [DE88-006569] 16 p2266 N88-23553
Vibrational spectroscopy of the hydrogen and hydrated hydronium cluster ions 16 p2268 N88-23566
Energy-transfer properties and mechanisms [DE88-007107] 18 p2571 N88-25272
Molecular characterization of structure and bonding in thin film materials [DE88-006811] 18 p2584 N88-25351
Polymeric electrolytes [AD-A193766] 23 p3198 N88-29031
Experimental investigation of the effects of underwater exposure on the damping characteristics of bolted structural connections for plates and shells [AD-A194486] 23 p3226 N88-29200
Measurements of XeF (Xenon Fluoride) ground state dissociation and vibrational equilibration [AD-A194611] 23 p3280 N88-29527
Analytical and experimental studies of beam waveguide absorbers for structural damping [AD-A195085] 24 p3382 N88-30144

VIBRATORY LOADS
Experimental determination of the oscillatory forces on two turbine blade profiles [ETN-87-90417] 01 p0007 N88-10037
Analytic investigation of helicopter rotor blade appended aeroelastic devices [NASA-CR-166525] 03 p0266 N88-11676
Resonant structures for integrated sensors 19 p2673 N88-25893

VIBROMETERS
U VIBRATION METERS

VICKERS VC-10 AIRCRAFT
U VC-10 AIRCRAFT

VICKERS 1100 AIRCRAFT
U VC-10 AIRCRAFT

VIDEO COMMUNICATION
Information technology to facilitate group interaction 24 p3438 N88-30463

VIDEO DATA
Fast, colour displays of digital terrain elevation data [AD-A185596] 06 p0729 N88-14485
A hybrid transform/DPCM encoder for data compression [DE88-003725] 09 p1154 N88-16919
Balance of X-ray radioscopy application to nondestructive tests of composite materials [SNIAS-881-430-110] 21 p2907 N88-27250
Use of optical disk technology at the Air Command and Staff College [AD-A192424] 21 p3027 N88-27969
More than a solar cycle of synoptic solar and coronal data: A video presentation [NASA-CR-181459] 23 p3308 N88-29708

VIDEO EQUIPMENT
Input devices for tasks using interactive video [NPL-DITC-87/87] 01 p0080 N88-10510
Health hazards of video display terminals. A comprehensive, annotated bibliography on a critical issue of workplace health and safety with sources for obtaining items and list of terminal suppliers [RSI-IAS-4] 03 p0355 N88-12240
Fiber optic video link [FOA-C-30444-3.1] 06 p0780 N88-14789
Issues associated with telerobotic systems in space 08 p1056 N88-16369
Reconfigurable work station for a video display unit and keyboard [NASA-CASE-MFS-26009-1-SB] 17 p2382 N88-24163
System overview: Teragon 4000, an image processing equipment at FOA 3 [FOA-C-30465-3.3] 18 p2557 N88-25179
Stereo and eye movement [AD-A193588] 22 p3142 N88-28681
Information technology to facilitate group interaction 24 p3438 N88-30463

VIDEO SIGNALS
Programmable real-time digital video image processing [PB87-104162] 04 p0430 N88-12661
Accommodating the residue of processed or computed digital video signals within the 8 bit CCIR recommendation 601 [BBC-RD-1987/12] 04 p0432 N88-12676
Digital video bit-rate reduction: DPCM for sub-Nyquist PAL [BBC-RD-1987/16] 05 p0573 N88-13494
Improvements to a UHF rebroadcast television link suffering tidal fading: Countisbury UHF relay station [BBC-RD-1987/14] 05 p0573 N88-13495
Two-signal cross modulation effects, half-IF effects and interference criteria in land mobile sharing with UHF (Ultra High Frequency) television [PB87-228037] 05 p0576 N88-13514
High-temperature photoelectron spectroscopy. An increased sensitivity spectrometer for studying vapor-phase species produced at furnace temperatures greater than 2000K [AD-A186542] 09 p1140 N88-16835

Limiting of YUV digital video signals
[BBC-RD-1987/22] 09 p1155 N88-16924
Simple high speed camera with CCD-sensor
[MPIS-8/1987] 18 p2518 N88-24940
Design and testing of a luminance and chrominance stabilization system for a computer-controlled color display
[AD-A191922] 18 p2554 N88-25159
Digital television routing systems: A survey of optical and electrical techniques
[BBC-RD-1988/3] 19 p2654 N88-25763
Underwater optical trajectography and video image mosaics 19 p2700 N88-26051
A 1/2-inch high-definition baseband VCR 21 p2930 N88-27393

VIDICONS
Characterization of new FPS (Focus Projection and Scale) vidicons for scientific imaging applications
[DE88-011213] 22 p3080 N88-28290

VIEW EFFECTS
Cloud cover determination in polar regions from satellite imagery
[NASA-CR-181544] 04 p0471 N88-12908
Surface reflectance factors derived from SPOT-1 HRV data at two view angles 22 p3113 N88-28492

VIEWING
NT FIELD OF VIEW
Vertical viewing ECE diagnostic for the D3-D tokamak
[DE88-010586] 20 p2860 N88-26987

VINEYARDS
Attempt to inventory vines using oblique SPOT images 22 p3095 N88-28380

VINYL COPOLYMERS
Group contribution analysis of the damping behavior of homopolymers, statistical copolymers and interpenetrating polymer networks based on acrylic, vinyl and styrenic mers
[AD-A185904] 07 p0836 N88-15070

VINYL CYANIDE
U ACRYLONITRILES

VINYL ETHYLENE
U BUTADIENE

VINYL POLYMERS
NT POLYVINYL FLUORIDE
NT VINYL COPOLYMERS
Novel conductive polymers
[EP-PATENT-0-182-548-A2] 01 p0026 N88-10163
Polyvinyl esters of omega-H-perfluoroacids and polyvinyl alcohol obtained from them
[AD-A184633] 03 p0279 N88-11755
High-molecular compounds (selected articles)
[AD-A184668] 03 p0293 N88-11842
Elementary fluorination of polymers
[ETN-88-90812] 07 p0836 N88-15075
Preparation of thin film polyvinylidene fluoride shock wave pressure transducers
[PB88-156070] 11 p1490 N88-18893
Piezoelectric polymer tactile sensor arrays for robotics
[AD-A188852] 12 p1634 N88-19780
Boundary layer measurements using hot-film sensors 17 p2297 N88-23743
Preferential surface adsorption in miscible blends of polystyrene and poly(vinyl methyl ether)
[AD-A191451] 18 p2490 N88-24769
Polymer-ceramic composites
[AD-A193244] 21 p2905 N88-27237
Alternative immersion accelerated testing of coating systems for Naval shoreline facilities 24 p3355 N88-29977

VINYLIDENE
Ferroelectric properties and impact behavior of the PVF2 polymer and the VF2/C2F3H polarized copolymers --- vinylidene polyfluorides
[ISL-CO-245/88] 08 p0971 N88-15876
NMR analysis of a fluorocarbon copolymer
[DE88-002364] 15 p2043 N88-22170
Interaction of vinylidene fluoride: Tetrafluoroethylene copolymer with ammonia
[NASA-TT-20292] 19 p2620 N88-25542

VIOLENCE
NT ATTACKING (ASSAULTING)

VIRGO GALACTIC CLUSTER
Molecular gas in Virgo cluster spiral galaxies 17 p2450 N88-24557

VIRGO STAR CLUSTER
U VIRGO GALACTIC CLUSTER

VIRIAL COEFFICIENTS
Optical determination of the virial coefficients of the gases C2H4, C2H6 and SF6
[ETN-87-90610] 03 p0282 N88-11776

VIRTUAL MEMORY SYSTEMS
Local concurrent error detection and correction in data structures using virtual backpointers
[NASA-CR-181432] 01 p0106 N88-10692
Memory systems for single bus multiprocessor architecture. Application to the SCQM system
[ENST-86E022] 02 p0219 N88-11379
Recovery using virtual memory
[AD-A187098] 09 p1217 N88-17296
Parallel garbage collection on a virtual memory system
[DE88-003567] 10 p1396 N88-18317

VIRTUAL PROPERTIES
Long-pulse, high-power vircator experiments
[DE88-011787] 21 p2940 N88-27458

VISCOELASTIC CYLINDERS
Buckling of viscoelastic columns 02 p0190 N88-11187
Calculation of rolling contact of two viscoelastic cylinders with application to the steady state normal contact problem
[ILR-MITT-188] 18 p2530 N88-25008

VISCOELASTIC DAMPING
Augmenting the control of a flexible manipulator with passive mechanical damping 01 p0055 N88-10350
Identification of linear structural models 03 p0337 N88-12121
Damping analysis of flexural waves in fluid-loaded single and constrained plates
[AD-A185116] 05 p0609 N88-13739
Investigation of constrained-layer technique using exact elasticity theory
[AD-A188664] 12 p1636 N88-19795
Feedback control of a hyperbolic partial-differential equation with viscoelastic damping
[AD-A192896] 21 p3003 N88-27810

VISCOELASTIC FLOW
U VISCOELASTICITY

VISCOELASTICITY
NT THERMOVISCOELASTICITY
Rheological behaviors of an elastomeric membrane
[DE87-013105] 01 p0061 N88-10392
Rheological and aging characterization of elastomers
[DE87-009598] 02 p0151 N88-10944
Interseismic deformation for normal fault earthquakes 03 p0349 N88-12207
Porosity influence on the strength and elasticity of first-year sea ice
[AD-A184493] 03 p0354 N88-12233
Explicit and implicit soil modelling for dynamic soil-structure interaction problems 04 p0428 N88-12650
Continuation finite element analysis of viscoelastic fluids 04 p0445 N88-12761
Exact finite element method analysis of viscoelastic tapered structures to transient loads 05 p0595 N88-13632
Bending of a bonded beam as a test method for adhesive properties
[AD-A184813] 05 p0609 N88-13736
Viscoelastic properties of EA951 adhesive: A source of creep deformations of a strongback
[DE88-001581] 06 p0685 N88-14197
Steady waves in a nonlinear theory of viscoelasticity
[AD-A185548] 06 p0723 N88-14448
The paradoxical asymptotic status of massless springs
[AD-A185625] 07 p0928 N88-15637
The properties of sound propagation in liquid constrained viscoelastic and polymeric structures
[AD-A185944] 07 p0929 N88-15640
Numerical solution methods for viscoelastic orthotropic materials
[NASA-CR-182381] 08 p0971 N88-15874
A finite element analysis of adhesively bonded composite joints including geometric nonlinearity, nonlinear viscoelasticity moisture diffusion and delayed failure
[AD-A187455] 10 p1296 N88-17747
Time delays and boundary feedback stabilization in one-dimensional viscoelasticity, appendices A through H
[AD-A187534] 10 p1401 N88-18353
A viscoelastic BEM (Boundary Element Method) for modeling oxidation
[AD-A187490] 11 p1452 N88-18653
Unstable elastic materials and the visco-elastic response of bars in tension
[AD-A187969] 11 p1498 N88-18946
Fracture characteristics of a viscoelastic polymer under constant load: Experiments and analysis 11 p1501 N88-18963
Experiments on the flow of viscoelastic fluids between eccentric rotating cylinders 12 p1625 N88-19723
On the energy release rate for dynamic transient anti-plane shear crack propagation in a general linear viscoelastic body
[AD-A188385] 12 p1635 N88-19791
On analysis of viscoelastic structures
[AD-A188445] 12 p1636 N88-19793
A continuum damage model for viscoelastic materials
[AD-A189426] 12 p1637 N88-19800
Viscoelastic behavior of a polyetheretherketone (PEEK) composite
[AD-A189545] 13 p1734 N88-20368
An analysis of large deformation axisymmetric inelastic problems by finite element and boundary element methods 13 p1782 N88-20664
Pressure induced ageing of polymers 14 p1929 N88-21504
Applications of elastic-viscoplastic constitutive models in dynamic analyses of crack run-arrest events 14 p1930 N88-21507
Thermoviscoelastic characterization and predictions of Kevlar/epoxy composite laminates
[NASA-CR-182878] 16 p2172 N88-22946
Effects of randomness of parameters on mean wave propagation in a viscoelastic medium
[REPT-87-60] 16 p2206 N88-23166
Effects of axial load on elastomeric isolation bearings
[PB88-179015] 16 p2223 N88-23269
Damage by creep fatigue: Influence of the visco-elasticity of the matrix
[PB88-124706] 18 p2528 N88-24998
Compression creep of filamentary composites
[NASA-CR-182550] 20 p2798 N88-26601
Vibration response of constrained viscoelastically damped plates: Analyses and experiments
[AD-A192329] 20 p2815 N88-26699
Thermo-viscoelastic analysis of composite materials, volume 1
[NASA-CR-183048-VOL-1] 21 p2904 N88-27230
Optimal design of viscoelastic structures 21 p2959 N88-27579
Finite element analysis of steady and transiently moving/rolling nonlinear viscoelastic structure. Part 1: Theory
[NASA-CR-179886] 23 p3273 N88-29480
Approximation of viscoelastic stresses from Newtonian turbulent kinematics
[AD-A194317] 24 p3371 N88-30077
Initial value problems in viscoelasticity
[AD-A196052] 24 p3382 N88-30145

VISCOMETERS
High intensity 5 eV O-atom exposure facility for material degradation studies 02 p0135 N88-10847

VISCOMETRY
Continual capillary viscosimetry using extrusiograph techniques
[PB88-166293] 15 p2046 N88-22195

VISCOPLASTIC FLOW
U VISCOPLASTICITY

VISCOPLASTICITY
Experimental determination of flow potential surfaces supporting a multiaxial formulation of viscoplasticity 02 p0187 N88-11167
Application of viscoplastic constitutive equations in finite element programs
[KFK-4254] 03 p0370 N88-12329
Ideal-viscoplastic extrusion model with application to deforming pistons in light-gas guns
[UTIAS-TN-266] 04 p0429 N88-12657
Steady shearing in a viscoplastic solid
[AD-A184341] 04 p0454 N88-12810
A critical review of the development of several viscoplastic constitutive theories
[AD-A185652] 07 p0867 N88-15262
A large strain thermomechanical forming model for elastic-viscoplastic behavior in metals 10 p1301 N88-17780
On stress collapse in adiabatic shear bands
[AD-A187185] 11 p1498 N88-18942
On the dissipative response due to discontinuous strains in bars of unstable elastic material
[AD-A188114] 11 p1498 N88-18947
Structure of a viscoplastic theory
[NASA-TM-100794] 11 p1501 N88-18968
Cyclic crack growth emanating at a round notch considering viscoplasticity
[AD-A189577] 13 p1781 N88-20655
A viscoplastic theory applied to copper
[NASA-TM-100831] 14 p1928 N88-21497
Nonlinear Constitutive Relations for High Temperature Applications, 1986
[NASA-CP-10010] 14 p1928 N88-21498
The viscoplasticity theory based on overstress applied to the modeling of a nickel base superalloy at 815 C 14 p1928 N88-21499
A viscoplastic constitutive theory for metal matrix composites at high temperature 14 p1929 N88-21500
Modeling the viscoplastic behavior of Inconel 718 at 1200 F 14 p1929 N88-21502
A simplified orthotropic formulation of the viscoplasticity theory based on overstress 14 p1929 N88-21505
Constitutive modeling and thermoviscoplasticity 14 p1930 N88-21506

A theory of viscoplasticity accounting for internal damage 14 p1930 N88-21508
Controlled-strain rate tests at very low strain rates of 2618 aluminum at 200 C 14 p1931 N88-21513
Cyclic uniaxial and biaxial hardening of type 304 stainless steel modeled by the viscoplasticity theory based on overstress 14 p1931 N88-21514
Some implications for cyclic plastic and viscoplastic equations based on nonproportional loading experiments 14 p1931 N88-21515
An experimental comparison of several current viscoplastic constitutive models at elevated temperature 14 p1931 N88-21516
On the global/local time incrementing for viscoplastic analysis 14 p1932 N88-21519
An automated procedure for material parameter evaluation for viscoplastic constitutive models 14 p1932 N88-21520
Nonlinear structural analysis of a turbine airfoil using the Walker viscoplastic material model for B1900 + Hf 14 p1932 N88-21522
Non-isothermal elastoviscoplastic analysis of planar curved beams 14 p1933 N88-21526
Effects of state recovery on creep buckling under variable loading 14 p1933 N88-21527
Evolution of hardening and damage during viscoplastic deformation
[AD-A190714] 15 p2077 N88-22381
Biaxial experiments supporting the development of constitutive theories for advanced high-temperature materials 15 p2078 N88-22386
Finite element (MARC) solution technologies for viscoplastic analyses 15 p2078 N88-22389
Heating at a propagating crack tip in a viscoplastic material
[AD-A190952] 16 p2224 N88-23274
Analysis of crack-tip fields in a viscoplastic material 17 p2349 N88-23996
Theory of viscoplasticity based on overstress with applications 18 p2529 N88-25007
Determination of multiaxial flow surfaces at elevated temperatures using the concept of dissipation potential
[ORNL/TM-10787] 24 p3383 N88-30149
An investigation of constitutive models for predicting viscoplastic response during cyclic loading
[AD-A194875] 24 p3385 N88-30163

VISCOSITY
NT EDDY VISCOSITY
NT GAS VISCOSITY
Viscosity measurements at high temperatures on a standard reference material supplied by BCR — Bureau Communite de Reference (BCR)
[NPL-DMA(A)-146] 01 p0020 N88-10126
Synthesis and characterization of processable polyimides with enhanced thermal stability
[NASA-CR-181447] 01 p0030 N88-10191
Two-phase non-Newtonian hydrodynamic modeling of slurries
[DE87-011519] 01 p0047 N88-10298
Effect of viscosity on a vertical cylinder due to surface waves
[ETN-87-90960] 02 p0171 N88-11075
The infiltration kinetics of aluminum in silicon carbide compacts
[AD-A184682] 03 p0290 N88-11823
Ion-matrix coupling in polymer electrolytes from relaxation time studies
[AD-A184632] 03 p0293 N88-11841
The axisymmetric sealing gap with variable viscosity. A variable hydraulic resistance
[ETN-87-90604] 03 p0314 N88-11987
In-situ characterization of the interface of glass reinforced composites
[AD-A185136] 05 p0557 N88-13391
Colloidal stability of oxidized silicon particles in ethanolic and aqueous media
[DE87-014783] 05 p0562 N88-13421
The effects of viscosity on resistive ballooning modes in line-tied coronal magnetic fields 08 p1097 N88-16599
Analysis of the spectral vanishing viscosity method for periodic conservation laws
[NASA-CR-181613] 09 p1231 N88-17378
Viscosity methods in optimal control of distributed systems
[AD-A188086] 10 p1401 N88-18357
Laser velocimeter measurements of solids in multiphase flow
[DE88-000196] 11 p1487 N88-18876
The effects of rotational flow, viscosity, thickness, and shape on transonic flutter dip phenomena
[NASA-TM-100811] 11 p1502 N88-18969
High shear rate rheometry of low-viscosity liquids
[AD-A188447] 12 p1627 N88-19733
Contrasting conductance/viscosity relations in liquid states of vitreous and polymer solid electrolytes
[AD-A189378] 13 p1748 N88-20452
A new method of measuring multigrade oil shear elasticity and viscosity at high shear rates
[AD-A190145] 15 p2064 N88-22304
A low dimensional dynamical system for the wall layer 16 p2194 N88-23088
Gravity currents with heat transfer effects
[PB88-180047] 16 p2205 N88-23158
Finite ion-relaxation and nonequilibrium radiation effects on laser-driven implosions 16 p2278 N88-23636
The viscosity of molten TNT
[MRL-R-1100] 19 p2622 N88-25553
Synthesis of model polymers and related structures in support of vinyl monomer grafting studies
[DE88-010245] 20 p2778 N88-26476
Optimal rheological characteristics in dynamic stability of polymer flow through porous media
[DE88-001225] 21 p2918 N88-27322
Fellowships in hypersonic aerodynamics
[AD-A194265] 23 p3172 N88-28885
A limiting viscosity approach to the Riemann problem for materials exhibiting change of phase
[AD-A193477] 23 p3210 N88-29103
Intraplate deformation, stress in the lithosphere and the driving mechanism for plate motions
[NASA-CR-183121] 23 p3231 N88-29231
Eruptive viscosity and volcano morphology 24 p3442 N88-30488

VISCOUS DAMPING
NT VISCOELASTIC DAMPING
Frequency domain identification of structural dynamic systems with general damping matrices 03 p0337 N88-12120
Viscous damped space structure for reduced jitter 05 p0594 N88-13623
Exact finite element method analysis of viscoelastic tapered structures to transient loads 05 p0595 N88-13632

VISCOUS DRAG
Viscous drag reduction of horizontal plates
[VKI-TN-159] 07 p0851 N88-15171
Boundary effects on the drag of a cylinder in axial motion at low Reynolds number 13 p1768 N88-20578
STARFIRE: Hypervelocity railgun development for high-pressure research
[DE88-008348] 19 p2605 N88-25469
Development and design of windtunnel and test facility for RPV (Remote Piloted Vehicle) enhancement devices
[AD-A194842] 24 p3329 N88-29822

VISCOUS FLOW
NT BOUNDARY LAYER FLOW
NT BOUNDARY LAYER SEPARATION
NT COUETTE FLOW
NT REATTACHED FLOW
NT SECONDARY FLOW
NT SEPARATED FLOW
NT STOKES FLOW
Locating parallel numerical tasks in the solution of viscous fluid flows
[DE87-013510] 02 p0169 N88-11064
FDM-FEM zonal method for viscous flow computations over multiple-bodies
[NAL-TR-925T] 02 p0170 N88-11069
Improved numerical methods for turbulent viscous recirculating flows 02 p0185 N88-11148
Mechanical and flow excited vibrations of elastic plates and cylindrical shells in dense fluids 03 p0316 N88-11996
Some experiences with the viscous-inviscid interaction approach
[NASA-TM-100015] 04 p0395 N88-12466
Total linearisation method for solving viscous free boundary flow problems by the finite element method
[PB87-222337] 04 p0441 N88-12737
Similar solutions for viscous hypersonic flow over a slender three-fourths-power body of revolution
[NASA-TM-100205] 04 p0443 N88-12752
Analytical studies of axially symmetric motion of an incompressible viscous fluid between two concentric rotating spheres 04 p0444 N88-12757
Low Reynolds number influence on aerodynamic performance of hypersonic lifting vehicles 05 p0531 N88-13230
Numerical simulation of the hypersonic flow around lifting vehicles 05 p0532 N88-13234
Numerical optimization of conical flow waveriders including detailed viscous effects 05 p0533 N88-13245
An analysis of the compressible-viscous flow field around a 3D-oscillating wing 05 p0535 N88-13254
Practical application of two-dimensional viscous flow computation 05 p0535 N88-13257
The role of computation fluid dynamics in aeronautical engineering (4). The development and applications of implicit TVD finite volume code 05 p0536 N88-13259
Computations of compressible viscous flows over multiple-bodies 05 p0539 N88-13282
A numerical study of the effects of curvature and convergence on dilution jet mixing
[NASA-TM-89878] 05 p0549 N88-13347
The simulation of the viscous flow around a cylinder by the random vortex method 05 p0579 N88-13534
Low thrust viscous nozzle flow fields prediction
[NASA-CR-182334] 05 p0582 N88-13551
Investigation of viscous/inviscid interaction in transonic flow over airfoils with suction 06 p0664 N88-14074
Implicit time dependent methods for inviscid and viscous compressible flows 06 p0701 N88-14304
Computation of free boundaries
[PB87-226023] 06 p0763 N88-14680
Rotation of magnetized particle in electrically conducting viscous medium 06 p0770 N88-14733
Viscous vortex flows 07 p0810 N88-14934
Wall turbulence control 07 p0812 N88-14943
Riblets for aircraft skin-friction reduction 07 p0814 N88-14955
Incompressible viscous flow simulations of the NFAC wind tunnel
[NASA-CR-177431] 07 p0816 N88-14969
Analysis of three-dimensional viscous internal flows
[AD-A186254] 07 p0849 N88-15155
Consistent boundary conditions for Reduced Navier-Stokes (RNS) scheme applied to 3-dimensional internal viscous flows
[NASA-CR-180874] 08 p0950 N88-15762
The simulation of three-dimensional viscous supersonic flow past blunt bodies with a hybrid implicit/explicit finite difference method
[DFVLR-FB-87-32] 08 p0950 N88-15765
Development of direct-inverse 3-D methods for applied aerodynamic design and analysis
[NASA-CR-182436] 08 p0950 N88-15767
Viscous flows, part 1 08 p0986 N88-15967
Viscous flows, part 2 08 p0986 N88-15968
Viscous flows. Part 3: Formulation of the Navier-Stokes equations by stream function vorticity methods 08 p0986 N88-15969
The viscous flow on surfaces with streamwise riblets
[DFVLR-FB-87-21] 09 p1162 N88-16961
Zonal solutions for viscous flow problems. Finite approximations in fluid mechanics
[MBB/LKE-122/S/PUB/226] 10 p1313 N88-17846
A three-dimensional dual potential procedure for rotational flows 10 p1329 N88-17942
Finite element methods of analysis for high speed viscous flows
[NASA-CR-182529] 11 p1483 N88-18852
Numerical analysis, computing and fundamental studies in fluid mechanics
[DE88-005343] 12 p1625 N88-19725
Mixing of viscous fluids: Behavior of microstructures and chaos
[DE88-006287] 13 p1766 N88-20566
Calculations of viscous flows with a multigrid method 13 p1769 N88-20580
Numerical analysis of three-dimensional viscous internal flows
[NASA-TM-100878] 14 p1861 N88-21116
Computational fluid dynamics drag prediction: Results from the Viscous Transonic Airfoil Workshop
[NASA-TM-100095] 15 p2014 N88-22009
Theoretical model and numerical solution for compressible viscous vortex cores 15 p2054 N88-22243
The numerical simulation of viscous flows with change of phase and chemical reaction
[DE88-003204] 15 p2062 N88-22292
Numerical study of unsteady viscous hypersonic blunt body flows with an impinging shock
[NASA-TM-100096] 15 p2122 N88-22650
High-resolution shock-capturing schemes for inviscid and viscous hypersonic flows
[NASA-TM-100097] 15 p2122 N88-22651
Coherent structures and dynamical systems 16 p2199 N88-23119
Numerical method for unsteady viscous-inviscid interaction to calculate buffeting
[ONERA-RSF-02/3617-AY-008-A] 17 p2309 N88-23949
Composite reduced Navier-Stokes procedures for flow problems with strong pressure interactions
[AD-A191127] 18 p2508 N88-24875
Theoretical investigation of 3-D shock wave-turbulent boundary layer interactions, part 6
[AD-A191546] 18 p2509 N88-24882

Axisymmetric viscid-inviscid interaction by a frozen vorticity approximation
[AD-A191743] 18 p2509 N88-24885
A variational finite element method for three-dimensional, steady, compressible, viscous flows 18 p2512 N88-24904
Development of a method of calculating unstable flows of cascades separated at the leading edge
[PB87-228714] 19 p2598 N88-25437
Improved numerical methods for turbulent viscous recirculating flows
[NASA-CR-180852] 19 p2599 N88-25445
Two-dimensional viscous flow computations of hypersonic scramjet nozzle flowfields at design and off-design conditions
[NASA-CR-182150] 19 p2603 N88-25459
Finite element analysis of incompressible viscous flow around multi-element aerofoils 19 p2635 N88-25634
Numerical calculation of supersonic flow by the PNS equations 19 p2636 N88-25636
Numerical simulation of viscous flows over transonic aircraft configurations 19 p2637 N88-25642
Numerical analysis of reconnection of vortex rings 20 p2782 N88-26500
Three-dimensional viscous flow computations of a circular jet in subsonic and supersonic cross flow
[NASA-CR-182153] 20 p2800 N88-26616
A study of flow separation in transonic flow using inviscid and viscous computational fluid dynamics (CFD) ischemes
[NASA-CR-183119] 20 p2801 N88-26618
Spectral resolution of the Navier-Stokes equations in multi-domain curved complex geometries
[ONERA-NT-1987-2] 20 p2802 N88-26631
Nonaxisymmetric viscous lower branch modes in axisymmetric supersonic flows
[NASA-CR-181687] 21 p2891 N88-27164
Prediction of velocity and temperature profiles in thermally driven gravity currents applied to stratified thermal storage tanks
[DE88-004452] 21 p2946 N88-27496
A fast vortex code for computing 2-D flow in a box
[DE88-011732] 21 p2946 N88-27498
Numerical methods for incompressible viscous flows with engineering applications
[NASA-CR-183143] 21 p2948 N88-27508
Plasma behavior in the boundary layer near a railgun isurface
[DE88-006889] 21 p3017 N88-27909
Field methods for computing high Reynolds number viscous flow
[FFA-TN-1988-01] 22 p3039 N88-28046
Numerical computation of space shuttle orbiter flow field
[NASA-CR-183193] 22 p3040 N88-28048
Boundary layer manipulation 23 p3170 N88-28877
Calculation of aerodynamic characteristics of airplane configurations at high angles of attack
[NASA-CR-4182] 23 p3172 N88-28891
A mapping of the viscous flow behavior in a controlled diffusion compressor cascade using laser Doppler velocimetry and preliminary evaluation of codes for the prediction of stall
[AD-A194490] 23 p3211 N88-29112
Direct-solution techniques for viscous flows and their control
[AD-A194775] 23 p3211 N88-29114
European research program on viscous flows
[DFVLR-AVA-IB-227-87-A-15] 23 p3214 N88-29129
Adaptive mesh generation for viscous flows using Delaunay triangulation
[NASA-CR-181699] 24 p3316 N88-29749
The viscous flow on surfaces with streamline riblets
[ESA-TT-1091] 24 p3370 N88-30067
Numerical simulation of unsteady incompressible viscous flows in generalized coordinate systems
[NASA-TM-101016] 24 p3373 N88-30085

VISCOUS FLUIDS
Effect of dissipation on propagation of spherical detonation shock wave 02 p0159 N88-10998
Locating parallel numerical tasks in the solution of viscous fluid flows
[DE87-013510] 02 p0189 N88-11064
Mechanical and flow excited vibrations of elastic plates and cylindrical shells in dense fluids 03 p0316 N88-11996
Numerical simulation of the interaction of vortex rings in viscous fluid 03 p0318 N88-12008
Dispersion equation for plane capillary-gravity wave on free surface of viscous incompressible fluid 04 p0459 N88-12842
Theoretical studies of multicomponent mixtures: Phase equilibrium and transport
[DE88-002717] 07 p0831 N88-15040
Properties of molecular solids and fluids at high pressure and temperature
[DE88-004195] 13 p1738 N88-20391
Implicit finite-difference simulation of an internal flow in a nozzle: An example of a physical application on a hypercube
[AD-A192475] 21 p2942 N88-27472
Heat transport in a parabolic tube of circular cross-section
[LRT-WE-9-FB-2(1988)] 22 p3078 N88-28274
Preliminary investigation of flow modeling during solid propellant processing
[AD-A196168] 24 p3357 N88-29987
Approximation of viscoelastic stresses from Newtonian turbulent kinematics
[AD-A194317] 24 p3371 N88-30077

VISIBILITY
NT LOW VISIBILITY
A preliminary taxonomy of visible surface algorithms
[DE87-013559] 02 p0220 N88-11386
Handling qualities criterion for very low visibility rotorcraft 03 p0263 N88-11654
ZEUS: A knowledge-based expert system that assists in predicting visibility at airbases
[AD-A184197] 05 p0626 N88-13829
Aerosol optical depth and ratios of diffuse-sky to total solar irradiance measured from aircraft following the eruption of El Chichon
[PB88-100789] 07 p0878 N88-15326
Visual evoked potentials
[AD-A187942] 11 p1519 N88-19071
The visiocelometer and its tactical applications
[AD-A188216] 12 p1647 N88-19866
Influence of hydrometeorological factors on visibility of objects detected by radar 13 p1790 N88-20707
Climatological data of the Netherlands lightvessels over the period 1949-1980 --- North Sea
[KNMI-WR-87-9] 14 p1947 N88-21613

VISIBLE INFRARED SPIN SCAN RADIOMETER
VISSR line number monitoring system 17 p2351 N88-24008

VISIBLE RADIATION
U LIGHT (VISIBLE RADIATION)

VISIBLE SPECTRUM
Visible free electron laser oscillator
[AD-A183871] 01 p0051 N88-10324
Spectrograms of the visible region in the JT-60 tokamak (wavelength range from 2210 A to 5250 A)
[DE87-753002] 02 p0240 N88-11513
An advanced visible-UV spectrometer for atmospheric composition measurements 08 p1029 N88-16231
Laser raman studies related to liquid propellants: Structural characteristics inferred from the nitrate anion spectra
[AD-A188462] 12 p1612 N88-19641
Synchronous measurements of effective photon path length in visible and near-IR spectral regions in real cloud systems 13 p1790 N88-20706
Global solar oscillations observed in the visible to near infrared continuum 13 p1858 N88-21110
On the interpretation of the 3 micron emission feature in the spectrum of Comet Halley: Abundances in Comet Halley and in interstellar matter 14 p2002 N88-21935
Comet P/Halley: Visual magnitude estimates and gas production 14 p2007 N88-21968
Spectrophotometric observations of Comet Halley 14 p2007 N88-21972
Laboratory amorphous carbon: A possible analog of cometary dust 14 p2009 N88-21981

VISION
NT BINOCULAR VISION
NT COLOR VISION
NT MONOCULAR VISION
NT NIGHT VISION
NT STEREOSCOPIC VISION
Vision of details in space and time
[B8711402] 06 p0753 N88-14624
Function-dependent plasticity in the nervous system 07 p0886 N88-15377
A directed method for locating the focus of expansion
[AD-A185840] 07 p0906 N88-15491
Solid modelling for the manipulative robot arm (power) and adaptive vision control for space station missions 08 p1061 N88-16409
A-scan ultrasound measurement of ocular changes during accommodation
[AD-A186818] 09 p1198 N88-17181
Image chunking: Defining spatial building blocks for scene analysis
[AD-A187072] 09 p1200 N88-17191
The relationship between vision carrier-to-noise ratio and picture signal-to-noise ratio in a System I television receiver
[BBC-RD-1987/23] 10 p1318 N88-17877
Hierachical object recognition using libraries of parameterized model sub-parts
[AD-A187476] 10 p1396 N88-18322
Computerised measurement of human horizontal smooth pursuit eye movements 13 p1811 N88-20819
Implementation of a visual servoing system for evaluation of robotic refueling applications
[AD-A189676] 14 p1954 N88-21645
A probabilistic approach to low-level vision
[AD-A189041] 15 p2107 N88-22553
Finding texture boundaries in images
[AD-A190554] 15 p2117 N88-22609
ROVER: A prototype active vision system
[AD-A189246] 15 p2133 N88-22722
Dissecting the visual and auditory pathways by means of the two-input technique 21 p2978 N88-27690
A study of sources in the human brain associated with stereopsis 21 p2979 N88-27695
Relation between VEP and visual function in lesions of the optic nerve and visual pathway 21 p2983 N88-27718
Vision research. A national plan: 1983-1987, 1987 evaluation and update
[PB88-192604] 21 p2985 N88-27726
A model for visual attention
[AD-A193061] 21 p2991 N88-27744
Distributed algorithms for probabilistic solution of computational vision problems
[AD-A193150] 21 p2997 N88-27773
Human performance and acute hypoxia, chapter 12
[AD-A192604] 23 p3238 N88-29270
Vision and visual protection in fast jet aircraft 23 p3241 N88-29292
Vision through aircraft transparencies 23 p3242 N88-29294

VISORS
Vision through aircraft transparencies 23 p3242 N88-29294

VISUAL ACCOMMODATION
Target size and luminance effects on accommodation and vergence
[AD-A185861] 08 p1051 N88-16343
Night Vision: Current Research and Future Directions, symposium proceedings
[PB88-132006] 11 p1550 N88-19274

VISUAL ACUITY
Eyesight trainer for pilots 03 p0355 N88-12239
The accommodative status in the dark of US Navy fighter pilots
[AD-A186188] 10 p1370 N88-18186
Laser flash effects on chromatic discrimination in monkeys
[AD-A187703] 11 p1517 N88-19061
Visual contrast sensitivity functions obtained from untrained observers using tracking and staircase procedures
[AD-A187715] 11 p1522 N88-19089
Measuring functional feasibility of human visual system 12 p1665 N88-19983
Laboratory equipment update
[AD-A189781] 15 p2102 N88-22522
Microesotropia patients performa well as military jet pilots 21 p2925 N88-27363
A model for visual attention
[AD-A193061] 21 p2991 N88-27744
A field study on soft contact lens wear in USAF military transport aircraft
[AD-A195962] 24 p3407 N88-30265
Functional assessment of laser irradiation
[AD-A195735] 24 p3408 N88-30287

VISUAL AIDS
Simulator evaluation of lineup visual landing aids for night carrier landing
[AD-A191212] 18 p2468 N88-24648

VISUAL DISCRIMINATION
Masking effects of fine and coarse grain pictorial noise
[IZF-1985-21] 01 p0076 N88-10485
Modulation transfer function --- SPOT 03 p0341 N88-12153
Latency differences and effects of selective attention to gratings in the central and right visual fields: 2
[DE87-014730] 04 p0473 N88-12918
Visual evoked responses to sinusoidal gratings presented in central and right visual fields: 1
[DE87-014731] 04 p0473 N88-12919
Visual attention effects on discrimination of line orientation and line arrangement
[AD-A187013] 09 p1200 N88-17190
Laser flash effects on chromatic discrimination in monkeys
[AD-A187703] 11 p1517 N88-19061

Visual contrast sensitivity functions obtained from untrained observers using tracking and staircase procedures
[AD-A187715] 11 p1522 N88-19089
Measuring functional feasibility of human visual system 12 p1665 N88-19983
Laboratory equipment update
[AD-A189781] 15 p2102 N88-22522
Perception of motion in statistically-defined displays
[AD-A193076] 21 p2991 N88-27745
Limits of pattern discrimination in human vision
[AD-A193449] 23 p3239 N88-29273
Functional assessment of laser irradiation
[AD-A195735] 24 p3408 N88-30287

VISUAL DISPLAYS
U DISPLAY DEVICES

VISUAL FIELDS
Latency differences and effects of selective attention to gratings in the central and right visual fields: 2
[DE87-014730] 04 p0473 N88-12918
Visual evoked responses to sinusoidal gratings presented in central and right visual fields: 1
[DE87-014731] 04 p0473 N88-12919
Target size and luminance effects on accommodation and vergence
[AD-A185861] 08 p1051 N88-16343
Influence of moving visual environment on saccadic eye movements and fixation 21 p2926 N88-27368

VISUAL FLIGHT
The role of adaptive supplemental visual cuing in flight simulation
[AD-A185932] 07 p0822 N88-14992
Task listing: Visually assisted and visually dependent tasks for fighter aircraft
[AD-A191041] 16 p2244 N88-23404

VISUAL FLIGHT RULES
Estimates of potential increases in airport capacity through ATC (Air Traffic Control) system improvements in the airport and terminal areas
[AD-A188533] 12 p1578 N88-19444

VISUAL OBSERVATION
Investigation of leaks in fiberglass-reinforced pressure vessels by direct observation of hollow fibers in glass cloth
[DE88-006936] 19 p2609 N88-25485

VISUAL PERCEPTION
NT SPACE PERCEPTION
NT VISUAL DISCRIMINATION
Computer-controlled testing of visual-spatial ability
[AD-A183971] 03 p0357 N88-12249
Effects of divided attention on identity and semantic priming
[AD-A184289] 03 p0357 N88-12250
An approach to object recognition: Aligning pictorial descriptions
[AD-A184462] 04 p0482 N88-12972
Learning a color algorithm from examples
[AD-A184385] 05 p0632 N88-13862
Interaction of different modules in depth perception: Stereo and shading
[AD-A185607] 06 p0759 N88-14655
The role of adaptive supplemental visual cuing in flight simulation
[AD-A185932] 07 p0822 N88-14992
Local versus global minima in visual pattern completion
[PB87-234803] 07 p0897 N88-15439
Image understanding by Image-Seeking Adaptive Networks (ISAN)
[AD-A186214] 07 p0906 N88-15492
Target size and luminance effects on accommodation and vergence
[AD-A185861] 08 p1051 N88-16343
Research on visual information processing with special reference to oculomotor behavior in the areas of exploration, recognition and search
[AD-A186598] 08 p1051 N88-16346
Considerations concerning the basic bandwidth reduction of high definition television systems (HDTV) component signals, based on psychophysiological properties of the eye
[IRT-B-83/87] 09 p1153 N88-16909
GAVID and ACQUIR, two Operations-Research (OR) models for visual detection
[FEL-1985-72] 09 p1200 N88-17194
Development of Moire machine vision
09 p1212 N88-17264
Perception and control of simulated self motion
[AD-A187444] 10 p1372 N88-18188
Measurement and effects of transport delays in a state-of-the-art F-16C flight simulator
[AD-A187367] 11 p1441 N88-18599
Visual contrast sensitivity functions obtained from untrained observers using tracking and staircase procedures
[AD-A187715] 11 p1522 N88-19089
Space vehicle approach velocity judgments under simulated visual space conditions
[NASA-TM-89437] 11 p1523 N88-19094
Night Vision: Current Research and Future Directions, symposium proceedings
[PB88-132006] 11 p1550 N88-19274
The visioceilometer and its tactical applications
[AD-A188216] 12 p1647 N88-19866
Neck receptor stimulation in 0 and 1 g
12 p1658 N88-19938
Mechanisms of early light and dark adaptations
12 p1663 N88-19972
Visual recognition training; Effectiveness of computer graphics
[AD-A188302] 12 p1669 N88-19997
Human efficiency for visual detection of targets on CRT displays using a two-level multiple channel time history format
[AD-A188419] 12 p1670 N88-20001
Computerised measurement of human horizontal smooth pursuit eye movements
13 p1811 N88-20819
Identification of visual evoked response parameters sensitive to pilot mental state
[NASA-CR-4140] 13 p1811 N88-20822
Mathematic modeling of visual perception problems
[INPE-4355-PRE/1186] 13 p1823 N88-20897
A comparison of visual evoked potential and behavioral measures of flashblindness in humans
[AD-A189757] 15 p2101 N88-22519
An evaluation of the effects of high visual taskload on the separate behaviors involved in complex monitoring performance
[AD-A190641] 15 p2105 N88-22538
Dynamic properties of human brightness perception
[ETN-88-92243] 16 p2238 N88-23366
Designing for design effectiveness of complex avionics systems 17 p2305 N88-23788
Image management research
17 p2380 N88-24150
Visual information processing in the perception of features and objects
[AD-A192026] 18 p2552 N88-25148
Shape from shading, occlusion and texture
[AD-A184840] 18 p2571 N88-25269
Biorhythms of binocular vision
20 p2830 N88-26788
The interaction of sensory and perceptual variables: Spatial, temporal and orientation response to figure and ground
[AD-A192897] 20 p2832 N88-26798
A new approach to machine-based perception of monocular images
[DE88-002418] 20 p2853 N88-26942
Three-dimensional scene analysis using stero based imaging
[AD-A193120] 21 p2894 N88-27178
Microesotropia patients performa well as military jet pilots 21 p2925 N88-27363
Assessments of maneuverability with the TeleOperated Vehicle (TOV)
[AD-A191584] 21 p2993 N88-27751
Models for motion perception
22 p3133 N88-28629
Natural object categorization
[AD-A194103] 22 p3139 N88-28662
Limits of pattern discrimination in human vision
[AD-A193449] 23 p3239 N88-29273
Visual motion perception and visual attentive processes
[AD-A193640] 23 p3241 N88-29288
Transformations of short-term visual memory
[AD-A193873] 23 p3241 N88-29290
Visual Effects in the High Performance Aircraft Cockpit
[AGARD-LS-156] 23 p3241 N88-29291
Visual related accidents/incidents
23 p3242 N88-29293
Multilevel computational theory of stereoscopic visual image processing
[AD-A195331] 24 p3408 N88-30288
Haptic exploration in humans and machines: Attribute integration and machine recognition/implementation
[AD-A193692] 24 p3410 N88-30299
Space station proximity operations windows: Human factors design guidelines
[NASA-TM-88233] 24 p3410 N88-30301
Dynamical systems and motion vision
[AD-A195932] 24 p3422 N88-30366

VISUAL PHOTOMETRY
Some ground-based optical observations of Comet Halley during its post-perihelion passage
08 p1033 N88-16259

VISUAL SIGNALS
Research on visual information processing with special reference to oculomotor behavior in the areas of exploration, recognition and search
[AD-A186598] 08 p1051 N88-16346
Helicopter external vision requirements and visual display characteristics: A report/bibliography, revision A
[AD-A187075] 10 p1276 N88-17641
A pyrotechnic delay ignition system for a submarine launched marine signal
[MRL-R-1079] 13 p1754 N88-20487
Analysis procedures and subjective flight results of a simulator validation and cue fidelity experiment
[NASA-TM-88270] 18 p2465 N88-24634

VISUAL STIMULI
Target size and luminance effects on accommodation and vergence
[AD-A185861] 08 p1051 N88-16343
Role of optokinetic stimulation in vesibulospinal reflexes 10 p1360 N88-18131
Visual contrast sensitivity functions obtained from untrained observers using tracking and staircase procedures
[AD-A187715] 11 p1522 N88-19089
Computerised measurement of human horizontal smooth pursuit eye movements
13 p1811 N88-20819
A systems engineering based methodology for analyzing human electrocortical responses
[AD-A190809] 18 p2550 N88-25135
Influence of moving visual environment on saccadic eye movements and fixation 21 p2926 N88-27368
Perception of motion in statistically-defined displays
[AD-A193076] 21 p2991 N88-27745
Human auditory and visual continuous evoked potentials 23 p3238 N88-29269
Visual motion perception and visual attentive processes
[AD-A193640] 23 p3241 N88-29288

VISUAL TRACKING
U OPTICAL TRACKING

VISUALIZATION OF FLOW
U FLOW VISUALIZATION

VITAMINS
NT NICOTINIC ACID

VITERBI DECODERS
The design plan of a VLSI single chip (255, 223) Reed-Solomon decoder 04 p0435 N88-12697
A simplified procedure for correcting both errors and erasures of a Reed-Solomon code using the Euclidean algorithm 04 p0435 N88-12698

VITREOUS MATERIALS
A-scan ultrasound measurement of ocular changes during accommodation
[AD-A186818] 09 p1198 N88-17181

VITRIFICATION
LFCM (Liquid-Fed Ceramic Melter) vitrification technology
[DE88-003441] 09 p1149 N88-16887
Remarks on solid state amorphizing transformations
[DE88-006452] 15 p2145 N88-22803
Influence of fiber reinforcement on the vitreous transition temperature of M 10 matrix composites
[ONERA-RT-44/7086-M] 17 p2316 N88-23835

VLASOV EQUATIONS
New directions in Vlasov plasma turbulence and anomalous transport
[DE87-014425] 02 p0238 N88-11500
Wave energy flow conservation for propagation in inhomogeneous Vlasov-Maxwell equilibria
[DE88-006705] 15 p2055 N88-22251

VLBI
U VERY LONG BASE INTERFEROMETRY

VLSI
U VERY LARGE SCALE INTEGRATION

VOCODERS
The design and performance of a real-time self excited vocoder 19 p2653 N88-25753
Development of an 8000 bps voice codec for AvSat
19 p2653 N88-25755

VOICE
Voice-stress measure of mental workload
16 p2240 N88-23381

VOICE COMMUNICATION
NT TELEPHONY
Integrated voice and visual systems research topics
[NASA-CR-177417] 03 p0356 N88-12246
Voice technology using personal computers
[AD-A186743] 09 p1218 N88-17300
Evaluating the performance of the LPC (Linear Predictive Coding) 2.4 kbps (kilobits per second) processor with bit errors using a sentence verification task
[AD-A188573] 12 p1620 N88-19686
Time-frequency representations for speech signals
[AD-A188861] 18 p2498 N88-24819

NASA's mobile satellite development program
19 p2643 N88-25682
Mobile satellite service for Canada
19 p2643 N88-25683
A satellite system for land-mobile communications in Europe 19 p2643 N88-25685
Developing a global aeronautical satellite system
19 p2644 N88-25687
World-wide aeronautical satellite communications
19 p2644 N88-25688
Satellite communications experiment for the Ontario air ambulance service 19 p2646 N88-25705
ACSB: A minimum performance assessment
19 p2649 N88-25731
A framework for implementing data services in multi-service mobile satellite systems
19 p2650 N88-25733
Speech coding at 4800 bps for mobile satellite communications 19 p2652 N88-25749
A 4.8 kbps code-excited linear predictive coder
19 p2652 N88-25750
Real-time speech encoding based on Code-Excited Linear Prediction (CELP) 19 p2653 N88-25751
Sinusoidal transform coding 19 p2653 N88-25752
The design and performance of a real-time self excited vocoder 19 p2653 N88-25753
Development of an 8000 bps voice codec for AvSat
19 p2653 N88-25755
Error performance of voice band data signals with an overloaded delta modulator
[FEL-1987-05] 20 p2792 N88-26562
A cockpit natural language study - selected transcripts
[AD-A192972] 20 p2834 N88-26608
Cockpit and cabin crew coordination
[AD-A192445] 21 p2993 N88-27752
A cockpit natural language study: Vocabulary and grammar analyses
[AD-A193289] 21 p2993 N88-27753
An overview of technology for spoken interaction with machines
[AD-A194153] 23 p3202 N88-29058

VOICE CONTROL
Integrated voice and visual systems research topics
[NASA-CR-177417] 03 p0356 N88-12246
Controlling robots with spoken commands
[DE88-000537] 04 p0452 N88-12801
Digital signal processing algorithms for automatic voice recognition 06 p0793 N88-14862
Voice/natural language interfacing for robotic control
[AD-A187765] 11 p1494 N88-18917

VOICE DATA PROCESSING
NT CEPSTRAL ANALYSIS
Activities report of the Department of Systems and Communications
[ENST-87D004] 16 p2189 N88-23053
Algorithms and architectures for acoustic phonetical detection of continuous speech
[ENST-87E016] 16 p2189 N88-23054
Experiments in isolated digit recognition using the multilayer perceptron
[RSRE-MEMO-4073] 17 p2333 N88-23927

VOICE OF AMERICA
Complementary satellite sound broadcasting systems: A NASA assessment for the Voice of America
[NASA-TM-100300] 10 p1321 N88-17899

VOID RATIO
Investigation of the inter-relationship between base pavement stiffness and asphalt overlay compaction
[DOT/FAA/ES-88/1] 14 p1869 N88-21170

VOIDS
The influence of microvoids on the electrical strength of glass fiber reinforced epoxy resins
[ETN-87-90443] 01 p0030 N88-10189
Effects of cure pressure on resin flow, voids, and mechanical properties
[AD-A184267] 03 p0295 N88-11853
Plastic strain localization between voids in shear deformation fields 04 p0427 N88-12648
A comparison of film-based tomography and computed tomography for advanced ceramic materials
[DE88-003114] 07 p0637 N88-15079
Evolution of radiation-induced voids and dislocations at low temperature
[DE88-700350] 07 p0939 N88-15704
Void formation in solidification
[DE88-003895] 11 p1452 N88-18650
A simulation of void lining during ductile fracture
[AD-A186404] 12 p1635 N88-19792
Material instabilities in solids
[AD-A189525] 13 p1738 N88-20388
Flaw characterization in structural ceramics using scanning laser acoustic microscopy
15 p2082 N88-22415
Vacancy ordering in the basal plane of YBa2Cu3O(sub)z
[DE88-004572] 18 p2583 N88-25348
Material void opening computation using particle method
[DE88-010950] 19 p2680 N88-25936
Mass flow rate influence on void fraction of two-phase helium flow
[DE88-702456] 21 p2945 N88-27495

VOLATILITY
Cost savings possible with Air Force conversion to JP-8 as its primary fuel
[AD-A183784] 01 p0030 N88-10192
Analysis of laser extracted volatiles in carbonaceous chondrites 06 p0793 N88-14861
Evaluation and prediction of Henry's law constants and aqueous solubilities for solvents and hydrocarbon fuel components. Volume 1: Technical discussion
[AD-A188571] 12 p1613 N88-19643
Martian geomorphology and its relation to subsurface volatiles
[NASA-CR-182428] 12 p1711 N88-20237
A mass spectrometer evolved gas analysis experiment for in-situ analysis of cometary dust volatiles
13 p1854 N88-21097
The effect of weathering on octane quality for winter-grade and summer-grade gasolines
[AD-A190640] 16 p2183 N88-23012
National ambient Volatile Organic Compounds (VOCs) data base update, documentation
[PB88-195631] 21 p2971 N88-27646

VOLATILIZATION
U VAPORIZING

VOLCANICS
U VOLCANOLOGY

VOLCANOES
NT MARS VOLCANOES
Solar Energy Meteorological Research and Training Site, Alaska
[DE87-013706] 01 p0069 N88-10440
Gravity and fault structures, Long Valley Caldera, California
[DE87-014117] 02 p0197 N88-11229
Volcanic eruption detection with TOMS
05 p0618 N88-13793
Analysis of SO2 signals in SBUV/TOMS data
05 p0618 N88-13794
Comparison of ground based and TOMS measurements of SO2 from volcanic emissions
05 p0618 N88-13795
TOMS and the NOAA/FAA volcano support plan
05 p0618 N88-13796
Use of satellite data in volcano monitoring
05 p0618 N88-13797
Interpretation of our present terrestrial climatic record
[DE88-000223] 06 p0744 N88-14573
Greatest volcanic eruptions in world during 17th-18th centuries and weather anomalies in Eurasian middle latitudes 08 p1012 N88-16134
Some evidence for a Northern Hemispheric extratropic trigger mechanism of ENSO events
22 p3123 N88-28558
Mars: Near-infrared comparative spectroscopy during the 1986 opposition 23 p3301 N88-29658
Early cratering rates and the nature of the Martian cratered uplands 23 p3306 N88-29694

VOLCANOLOGY
Volcanic eruption detection with TOMS
05 p0618 N88-13793
Mid-tertiary volcano-tectonic development of the Southwestern Cordillera of North America
06 p0797 N88-14879
Kinetics of thermochemical gas-solid reactions important in the Venus sulfur cycle
[NASA-CR-182963] 19 p2742 N88-26280
The rate of volcanism on Venus
[NASA-CR-183039] 19 p2742 N88-26281
SPOT imagery as an aid to understanding volcanism and tectonics: Examples from the Chilean Andes and the Tibetan Plateau 22 p3103 N88-28427
A review: Quantitative models for lava flows on Mars
23 p3301 N88-29656
Progress in determining the thickness and distribution of volcanic materials on Mars 23 p3302 N88-29670
Variability in spectral signatures of terrestrial volcanic rocks and implications for volcanology on Mars
23 p3303 N88-29672
The tectonic setting of Archean anorthosites
24 p3397 N88-30231
Physical processes in the growth of the continental crust 24 p3398 N88-30240
Volcanic contribution to crustal growth in the Central Andes: A new estimate and a discussion of uncertainties
24 p3401 N88-30255
NASA MEVTV Program Working Group Meeting: Volcanism on Mars
[NASA-CR-183074] 24 p3442 N88-30487
Eruptive viscosity and volcano morphology
24 p3442 N88-30488
Faulting and its relation to volcanism: Mars western equatorial region 24 p3443 N88-30489
Mars: Volcanism in the Valles Marineris overlooked
24 p3443 N88-30491
The Martian highland paterae: Evidence for explosive volcanism on Mars 24 p3443 N88-30492

VOLT-AMPERE CHARACTERISTICS
Analysis of the voltage-current characteristics of metal-isolator-tin-telluride sandwich structures
[ETN-88-91089] 09 p1256 N88-17528
Solid-state voltage standard performance and design guidelines
[PB88-123757] 10 p1322 N88-17905
Limiting efficiency of a thermionic diode
[DE88-700598] 11 p1479 N88-18830

VOLTAGE
U ELECTRIC POTENTIAL

VOLTAGE AMPLIFIERS
Arc lamp power supply using a voltage multiplier
[NASA-CASE-LAR-13202-1] 17 p2335 N88-23942

VOLTAGE BREAKDOWN
U ELECTRICAL FAULTS

VOLTAGE CONTROLLED OSCILLATORS
Spacecraft redesign to reduce microphonic response of a VCO component 11 p1499 N88-18955
Radio Frequency (RF) strain monitor
[NASA-CASE-LAR-13705-1] 18 p2530 N88-25011

VOLTAGE CONVERTERS (AC TO AC)
Voltage directive drive with claw pole motor and control without rotor position indicator
[ETN-88-93120] 24 p3366 N88-30047

VOLTAGE GENERATORS
Operation of the TEMPO machine
[DE87-011285] 01 p0038 N88-10241

VOLTAGE MEASUREMENT
U ELECTRICAL MEASUREMENT

VOLTAGE REGULATORS
Operation of multistage power supplies for electron beam welding installations 03 p0286 N88-11800

VOLTAGE VARIATION INDICATORS
U VOLTMETERS

VOLTERRA EQUATIONS
Experimental identification of nonlinear structural models
[DE88-001795] 09 p1184 N88-17094
New way to solve Volterra equations of the second kind
[PB88-148820] 13 p1828 N88-20931
Product-integrals and counting processes
[CWI-MS-R8707] 14 p1965 N88-21727
Computational sciences
[AD-A190826] 18 p2564 N88-25226
Numerical solution of a system of random Volterra integral equations. 1: Successive approximation method
18 p2564 N88-25227
Numerical solution to a system of random Volterra integral equations 18 p2565 N88-25230
Numerical solution of linear integral equations with random forcing terms 18 p2565 N88-25237

VOLTMETERS
Optical power line voltage and current measurement systems. Volume 1: Limits to the precision of electro-optic and magneto-optic sensors
[DE87-014558] 02 p0175 N88-11092

VOLUME
Evaluation of spare room in cerebrospinal system using noninvasive methods 10 p1361 N88-18137
Estimates of masses, volumes and densities of short-period comet nuclei 14 p2004 N88-21950
Mining volume measurement system
[NASA-CASE-LAR-13519-1] 17 p2342 N88-23963
A maximum entropy solution for the underdetermined electromagnetic field within a volume
[DE88-007020] 20 p2790 N88-26550
Progress in determining the thickness and distribution of volcanic materials on Mars 23 p3302 N88-29670

VOLUMETRIC ANALYSIS
On-line measurement of heat of combustion
[NASA-CR-183076] 19 p2738 N88-26255
Volumetric measurement of vorticity vectors by optical probe
[AD-A195997] 24 p3369 N88-30061

VOMITING
Gastric emptying assessment by echography after a stress (rotating chair) 12 p1661 N88-19955
Motion sickness: A study of its effects on human physiology
[AD-A188821] 12 p1667 N88-19995
Emetic mechanism in acute radiation sickness
[AD-A194102] 23 p3238 N88-29267

VON KARMAN EQUATION
Dynamics of the von Karman vortex street
03 p0316 N88-11998
Application of the Von Karman equation to the bifurcation theory
[NOTA-INTERNA-891] 05 p0642 N88-13927

Further study of relation of von Karman equation for elastic large deflection problem and Schrodinger equation for quantum eigenvalues problem
14 p1899 N88-21341

VON MISES THEORY
U STRESS FUNCTIONS

VORTEX ALLEVIATION
Computation of the turbulent boundary layer downstream of vortex generators
[AD-A191544] 18 p2508 N88-24881

VORTEX BREAKDOWN
Experimental investigation in a wind tunnel of the stability and vorticity of the vortex breakdown phenomenon above delta wings, using the ultrasonic laser method
[DFVLR-FB-87-06] 01 p0003 N88-10017
A note on the instability of a vortex sheet leaving a semi-infinite plate
[DFVLR-FB-87-16] 01 p0004 N88-10019
Breakdown of steady and unsteady interacting boundary layers
[NLR-MP-86047-U] 01 p0045 N88-10284
Analysis of the breakdown of the Antarctic circumpolar vortex using TOMS ozone data
05 p0615 N88-13779
A theory for the core flow of leading-edge vortices
07 p0810 N88-14935
Airfoil large eddy breakup devices for turbulent drag reduction 07 p0814 N88-14956
Control of vortical separation on conical bodies
10 p1267 N88-17580
Burst vortex/boundary layer interaction
[NASA-CR-182510] 10 p1268 N88-17583
Investigation on the movement of vortex burst position with dynamically changing angle of attack for a schematic deltawing in a watertunnel with correlation to similar studies in windtunnel 16 p2204 N88-23152
Rotation symmetric vortex in axiparallel flow
[ETN-88-92364] 21 p2948 N88-27512
Vortex flows 23 p3170 N88-28875

VORTEX COLUMNS
U VORTICES

VORTEX DISTURBANCES
U VORTICES

VORTEX FILAMENTS
Vortex filament simulation for the crosslinking rings
20 p2782 N88-26501

VORTEX FLAPS
On the pairing process in an excited, plane, turbulent mixing layer
[AD-A186355] 07 p0850 N88-15157

VORTEX FLOW
U VORTICES

VORTEX GENERATION
U VORTEX GENERATORS

VORTEX GENERATORS
The flow downstream of screens and the formation of longitudinal vortices in the stagnation point flow
[DFVLR-FB-87-27] 09 p1162 N88-16963
Burst vortex/boundary layer interaction
[NASA-CR-182510] 10 p1268 N88-17583
Transonic Navier-Stokes computations of strake-generated vortex interactions for a fighter-like configuration
[NASA-TM-100009] 15 p2014 N88-22010
Experimental studies of vortex flows
[NASA-CR-182874] 16 p2207 N88-23171
Computation of the turbulent boundary layer downstream of vortex generators
[AD-A191544] 18 p2508 N88-24881

VORTEX RINGS
The Proceedings of the Symposium on Mechanics for Space Flight
[ISAS-SP-5] 03 p0317 N88-12006
Experimental study of interacting vortex rings
03 p0318 N88-12007
Numerical simulation of the interaction of vortex rings in viscous fluid 03 p0318 N88-12008
Theory of dividing vortons 03 p0318 N88-12009
Numerical analysis of reconnection of vortex rings
20 p2782 N88-26500
Vortex filament simulation for the crosslinking rings
20 p2782 N88-26501
Crosslinking of two vortex rings side by side
20 p2782 N88-26502

VORTEX SHEDDING
A note on the instability of a vortex sheet leaving a semi-infinite plate
[DFVLR-FB-87-16] 01 p0004 N88-10019
The phenomenology of Karman vortex streets via sound in oscillatory flow
[MPIS-MITT-84-1987] 02 p0122 N88-10775
Vortex interaction with a leading-edge of finite thickness
[NASA-CR-182341] 05 p0543 N88-13307
Longitudinal mode combustion instabilities in air breathing engines 06 p0680 N88-14166
A study of rotor broadband noise mechanisms and helicopter tail rotor noise 06 p0777 N88-14766
Wall turbulence control 07 p0812 N88-14943
Meteosat tracks Karman vortex streets in the atmosphere 09 p1128 N88-16770
A numerical study of unsteady two-dimensional subsonic compressible base flow 10 p1327 N88-17931
On the prediction of highly vortical flows using an Euler equation model, part 2
[AD-A190245] 15 p2064 N88-22305
Bodies in unsteady flow
[AD-A190416] 15 p2064 N88-22308
Experiments to investigate the vortices shed from a submarine-like body of revolution
16 p2205 N88-23156
Stall flutter analysis of propfans
16 p2221 N88-23256
Theory of sound production by vortex-airfoil interaction
[AD-A193386] 21 p3012 N88-27875

VORTEX SHEETS
A note on the instability of a vortex sheet leaving a semi-infinite plate
[DFVLR-FB-87-16] 01 p0004 N88-10019
Coronal heating by means of helical magnetohydrodynamic turbulence
[AD-A187084] 10 p1410 N88-18413
Computational technique for compressible vortex flows using the integral equation solution
[NASA-CR-182695] 13 p1718 N88-20271
A multilifting line method and its application in design and analysis of nonplanar wing configurations
[DFVLR-FB-87-51] 16 p2155 N88-22860
Experimental study of vortex sheets in plane flow
16 p2203 N88-23142
A twin-mirrored galvanometer laser light sheet generator
[NASA-TM-100587] 19 p2674 N88-25901
Vortices on the world sheet and string's critical dynamics
[DE88-702116] 21 p3026 N88-27961
A study of the vortex sheet method for solving the Prandtl boundary layer equations
[DE88-011346] 22 p3074 N88-28249

VORTEX STREETS
NT KARMAN VORTEX STREET

VORTEX TUBES
U VORTICES

VORTEX-BLADE INTERACTION
U BLADE-VORTEX INTERACTION

VORTICES
NT WING TIP VORTICES
Mean flow structure of a turbulent junction vortex
[PB87-206231] 01 p0047 N88-10301
Vortex dynamics and transport to the wall in a crossed-field plasma sheath
[DE87-013286] 01 p0100 N88-10657
Vortex/boundary-layer interactions: Data report, volume 1
[NASA-CR-181462] 02 p0121 N88-10768
Vortex/boundary-layer interactions: Data report, volume 2
[NASA-CR-181463] 02 p0122 N88-10769
Numerical simulation of Toilmien-Schlichting waves by use of a modified vortex particle-in-cell method
[IC-AERO-85-02] 02 p0171 N88-11079
On the onset of three-dimensionality and time-dependence in the Goertler vortex problem
[NASA-CR-178404] 03 p0260 N88-11638
Analysis of the motions and effects of hairpin vortices
03 p0316 N88-11997
The diffusion-convection vortex method for solving two-dimensional incompressible Navier-Stokes equation
03 p0317 N88-12001
Momentum transport and particle dynamics in turbulent shear flows 03 p0317 N88-12002
Theory of dividing vortons 03 p0318 N88-12009
Structural characteristics of dean vortices in a curved channel
[AD-A184724] 03 p0320 N88-12024
Unsteady flow about cambered plates
[AD-A184725] 03 p0320 N88-12025
Numerical prediction of propeller performance by vortex lattice method
[UTIAS-TN-265] 04 p0400 N88-12489
Activities at government research laboratories reported 04 p0403 N88-12503
Some asymptotic modes of transonic vortex flow
04 p0425 N88-12632
Optical instrumentation and study of gas-solid suspension flows
[DE88-000147] 04 p0442 N88-12744
Blowup for a nonlinear evolution equation and self-reproducing strained shear layers
04 p0444 N88-12755
Equilibria, lattices and chaotic dynamics of point vortices 04 p0444 N88-12758
Turbulent mixing in a rotating, stratified fluid
04 p0445 N88-12759
Intensive synoptic eddies and quasigeostrophic approximation 04 p0460 N88-12844
Dynamics of isolated intrathermocline eddy
04 p0460 N88-12845
Influence of secondary eddy currents on scattering of admixture in zonal flow 04 p0460 N88-12846
Mesoscale eddy dynamics by the method of point vortices 04 p0463 N88-12863
Measurement of velocity and vorticity fields in the wake of an airfoil in periodic pitching motion
[NASA-TP-2780] 04 p0487 N88-13002
Vortex formation over delta, double-delta and wave rider configurations at supersonic speeds
05 p0533 N88-13243
The off-design performance of hypersonic waveriders
05 p0533 N88-13244
Application of discrete vortex method to analysis of separated flow around aerofoils
05 p0537 N88-13268
Three-dimensional flow past a two-dimensional body
05 p0539 N88-13280
Vortex interaction with a leading-edge of finite thickness
[NASA-CR-182341] 05 p0543 N88-13307
Nonlinear lift control at high speed and high angle of attack using vortex flow technology
05 p0545 N88-13319
Vortical Flows Research Program of the Fluid Dynamics Research Branch
[NASA-TM-88332] 05 p0582 N88-13549
Isentropic analysis and interpretation: Operational applications to synoptic and mesoscale forecast problems
[AD-A184814] 05 p0626 N88-13830
The production of turbulence in boundary layers: The role of microscale coherent motions
[AD-A185568] 06 p0703 N88-14313
Study of evolution of Gulf Stream cyclinic eddy
06 p0727 N88-14473
Viscous vortex flows 07 p0810 N88-14934
A theory for the core flow of leading-edge vortices
07 p0810 N88-14935
Vortex dynamics 07 p0812 N88-14945
Flow in volutes and the influence on the flow in centrifugal compressors 07 p0851 N88-15169
Typhoon structural evolution
[AD-A186090] 07 p0879 N88-15333
Acta Aerodynamica Sinica (selected articles)
[AD-A185723] 08 p0949 N88-15757
Calculation of symmetric and asymmetric vortex seperation on cones and tangent ogives based on discrete vortex models
[NASA-CR-4122] 08 p0950 N88-15768
Direct and large eddy simulation of turbulence. Summary of the state of art 1987 08 p0987 N88-15977
Computer program for the calculation of the profile-vortices interactions (two dimensional inviscid incompressible flow with point singularities)
[ISL-R-124/86] 08 p0987 N88-15982
The effect of eddy distribution on momentum and heat transfer near the wall in turbulent pipe flow
[NASA-TM-100257] 08 p0988 N88-15984
Cavitation inception scale effects. 1. Nuclei distributions in natural waters. 2. Cavitation inception in a turbulent shear flow
[AD-A186553] 08 p0988 N88-15987
Interaction of a vortex pair with a free surface
[AD-A186619] 08 p0988 N88-15988
Active control of jet flowfields
[AD-A186736] 08 p0989 N88-15989
Turbulence structure during high wind
08 p1014 N88-16149
A jet in a crossflow
[NASA-CR-182469] 09 p1113 N88-16674
Unsteady behavior of three-dimensional vortices relevant to turbulent boundary layers
[AD-A186767] 09 p1161 N88-16958
Numerical and physical aspects of large eddy simulation of turbulent flows
[ETN-88-91611] 09 p1162 N88-16965
Coherent vortex structures in the wake of a stationary disk and of a disk excited to vibration
[ESA-TT-994] 09 p1163 N88-16968
Mechanism of change of vortex structure orientation in type-2 superconductors 09 p1239 N88-17425
Investigation of the influence of wind shear on the aerodynamic characteristics of aircraft using a vortex-lattice method 10 p1274 N88-17619
Secondary flow measurements with L2F-technique in centrifugal compressors 10 p1283 N88-17676
Investigation of non-symmetric jets in cross flow
10 p1327 N88-17932
Instability and transition in curved channel flow
10 p1328 N88-17938

An analysis of the motion and effects of hairpin vortices
[AD-A187261] 10 p1331 N88-17958
Flow patterns induced by vortices
[NAL-TR-932] 10 p1332 N88-17963
Experimental study of two-dimensional vortex patterns for impulsively started bodies in comparison with other configurations 11 p1435 N88-18562
Structure of shear flow turbulence and its control
[AD-A187909] 11 p1482 N88-18846
The effects of rotational flow, viscosity, thickness, and shape on transonic flutter dip phenomena
[NASA-TM-100811] 11 p1502 N88-18969
Numerical analysis, computing and fundamental studies in fluid mechanics
[DE88-005343] 12 p1625 N88-19725
Rotational flow of rarefied gas between two coaxial cylinders with slip conditions
[INPE-4277-PRE/1149] 12 p1627 N88-19738
The international vortex flow experiment: A test case for compressible Euler codes
[NLR-MP-86076-U] 13 p1717 N88-20267
Control of structure in turbulent flows: Bifurcating and blooming jets
[AD-A189607] 13 p1766 N88-20562
An experimental investigation of decelerating flow about two-dimensional cambered plates
[DE88-006598] 13 p1766 N88-20567
Very large vortex calculations in two dimensions
[DE88-005748] 13 p1770 N88-20587
Mushroom-shaped currents (eddy dipoles) under rotation and stratification conditions
13 p1784 N88-20678
Dynamics of synoptic ocean eddies
13 p1786 N88-20689
Phenomenological description of eddy registered in Gulf Stream 13 p1787 N88-20694
Vortex flow over a delta wing with apex flaps using laser flow visualisation
[BU-356] 14 p1862 N88-21121
Incompressible theory of interaction between moving bodies and vorticity field: Force on moving bodies by vorticity field 14 p1863 N88-21132
Discrete vortex analysis of unsteady flow about two-dimensional cambered plates
[DE88-006597] 14 p1909 N88-21407
Mean flow structure in the near wake of a turbulent junction vortex
[PB88-150115] 14 p1910 N88-21416
Interaction of a strong vortex with decaying turbulence
[DE88-007102] 14 p1911 N88-21420
Ocean eddies 14 p1938 N88-21566
Alfven waves in plasma with finite ion temperatures
14 p1972 N88-21769
Experimental investigation of a spanwise forced mixing layer
[AD-A190136] 15 p2013 N88-22007
Transonic Navier-Stokes computations of strake-generated vortex interactions for a fighter-like configuration
[NASA-TM-100009] 15 p2014 N88-22010
Pressure measurements of impinging jet with asymmetric nozzle
[NASA-CR-182759] 15 p2014 N88-22011
Numerical simulation of turbulent flames using vortex methods
[AD-A189813] 15 p2034 N88-22116
Investigation of combustion in large vortices
[AD-A190408] 15 p2035 N88-22121
Theoretical model and numerical solution for compressible viscous vortex cores
15 p2054 N88-22243
Vortices in long Josephson junctions
[AD-A190338] 15 p2059 N88-22279
On the prediction of highly vortical flows using an Euler equation model, part 2
[AD-A190245] 15 p2064 N88-22305
Cavitation inception in rectangular two-dimensional slots
[AD-A190677] 15 p2066 N88-22318
The effects of time-dependent winds and ocean eddies on ice motion in a marginal ice zone
[AD-A190105] 15 p2100 N88-22511
A numerical model of unsteady, subsonic aeroelastic behavior
[NASA-TM-101126] 16 p2156 N88-22862
Stochastic estimation of conditional eddies in turbulent channel flow 16 p2194 N88-23087
Self similarity of two point correlations in wall bounded turbulent flows 16 p2195 N88-23089
EDQNM closure: A homogeneous simulation to support it. A quasi-homogeneous simulation to disprove it
16 p2195 N88-23091
Validation of EDQNM for subgrid and supergrid models 16 p2195 N88-23092
Big whorls carry little whorls 16 p2195 N88-23094
Conditionally-averaged structures in wall-bounded turbulent flows 16 p2198 N88-23112
Coherent structure 16 p2199 N88-23117
Coherent structures: Comments on mechanisms
16 p2199 N88-23118
Coherent structures and dynamical systems
16 p2199 N88-23119
Vortex breakdown and control experiments in the Ames-Dryden water tunnel 16 p2200 N88-23127
Flow visualization study of vortex manipulation on fighter configurations at high angles of attack
16 p2201 N88-23130
A comparative study of vortex flows in wind and water tunnels 16 p2204 N88-23151
Experimental studies of vortex flows
[NASA-CR-182874] 16 p2207 N88-23171
Random processes, turbulence and disordering fields
[AD-A191399] 16 p2209 N88-23181
The role of vortex structure in tropical cyclone motion
[AD-A190961] 16 p2235 N88-23351
Study of a system for reducing base drag by controlling vortices
[REPT-87/43] 17 p2295 N88-23730
Sensitivity of F-106B leading-edge-vortex images to flight and vapor-screen parameters
[NASA-TP-2818] 17 p2300 N88-23760
Unsteady flow around a profile subjected to pulsed motions
[ETN-88-92151] 18 p2458 N88-24594
Study of mixing and reaction in the field of a vortex
[AD-A191489] 18 p2508 N88-24878
The behavior of drop-containing turbulent eddies
[AD-A191669] 18 p2509 N88-24883
Fast algorithm development for large-eddy simulation of circular-jet turbulence
[AD-A192044] 18 p2509 N88-24887
Effects of Mach number on acoustic-vortex interactions in a ramjet 19 p2625 N88-25573
Numerical simulation of supersonic free-jets
19 p2636 N88-25639
Scaling laws for homogeneous turbulent shear flows in a rotating frame
[NASA-CR-181672] 19 p2665 N88-25847
Experimental and analytical studies of compressible vortices 19 p2665 N88-25848
Superfluid turbulence in counterflowing helium II
19 p2665 N88-25849
Numerical study of delta wing leading edge blowing
[NASA-CR-183101] 20 p2752 N88-26335
Vortex methods for separated flows
[NASA-TM-100068] 20 p2753 N88-26342
Evolution of hairpin vortices in a shear flow
[NASA-TM-100858] 20 p2845 N88-26885
Drift wave vortices and anomalous transport
[DE88-009562] 20 p2859 N88-26982
Theoretical and experimental investigations of a vortex drag behind a wing profile with spoiler
[ISL-PU-309/87] 21 p2892 N88-27169
A study of the interaction of diffusion flames with a vortex pair flowfield 21 p2908 N88-27258
Stream function-vorticity finite elements and the resolution of the Navier-Stokes equations
[DE88-702318] 21 p2945 N88-27494
A fast vortex code for computing 2-D flow in a box
[DE88-011732] 21 p2946 N88-27498
Higher order vortex methods with rezoning
[DE88-010777] 21 p2947 N88-27505
Rotation symmetric vortex in axiparallel flow
[ETN-88-92364] 21 p2948 N88-27512
Interactions between coherent structures and premixed flame fronts
[ETN-88-92885] 22 p3053 N88-28111
Flow dynamics stimulated by hairpin-like vortices in initially laminar boundary layers
[AD-A194253] 22 p3075 N88-28254
Vortex flows 23 p3170 N88-28875
Noise generation and boundary layer effects in vortex-airfoil interaction and methods of digital hologram analysis for these flow fields
[AD-A194191] 23 p3171 N88-28883
Unsteady flow past an NACA 0012 airfoil at high angles of attack
[AD-A194650] 23 p3172 N88-28886
Three-dimensional vortex interactions
[AD-A194066] 23 p3172 N88-28889
Vortex dynamics of coherent and chaotic structures (including algorithms for computer simulations and diagnosis)
[AD-A193580] 23 p3212 N88-29117
Construction of a laser Doppler anemometer and its use for the testing of a novel probe for the measurement of the variations of the lateral component of the vortex vector
[MPIS-13/1987] 23 p3217 N88-29147
Experiments on the dissipation of sound by separated flow at an edge
[ISVR-TR-151] 23 p3279 N88-29522
Vortex formation and particle transport in a cross-field plasma sheath
[DE88-008931] 23 p3284 N88-29553
Nonlinear Tollmien-Schlichting/vortex interaction in boundary layers
[NASA-CR-181698] 24 p3311 N88-29715
On the generation of mean flows by the interaction of Goertler vortices and Tollmien-Schlichting waves in curved channel flows
[NASA-CR-181690] 24 p3315 N88-29743
The present status and the future of missile aerodynamics
[NASA-TM-100063] 24 p3320 N88-29773
Computational methods for the problems of the tip vortex
[NASA-CR-181438] 24 p3320 N88-29775
The thermal behavior of film cooled turbulent boundary layers as affected by longitudinal vortices
[AD-A195155] 24 p3374 N88-30095
Vortex formation and particle transport in a cross-field plasma sheath
[AD-A194838] 24 p3432 N88-30425

VORTICITY

Description of NCAR (National Center for Atmospheric Research) Community Climate Model (CCM1)
[PB87-203782] 01 p0072 N88-10462
Measurement of velocity and vorticity fields in the wake of an airfoil in periodic pitching motion
[NASA-TP-2780] 04 p0487 N88-13002
Low-disturbance wind tunnels
07 p0811 N88-14937
The global balance of dynamic vorticity in relation to heat sources and sinks 07 p0876 N88-15316
Viscous flows. Part 3: Formulation of the Navier-Stokes equations by stream function vorticity methods
08 p0986 N88-15969
An introduction to single point closure methodology
08 p0986 N88-15973
Free-surface flow phenomena ahead of a two-dimensional body in a viscous fluid
10 p1329 N88-17944
Studies on homogeneous and heterogeneous reactive flows 11 p1484 N88-18861
Unsteady transonic small-disturbance theory including entropy and vorticity effects
[NASA-TM-100568] 12 p1575 N88-19418
Time-accurate simulations of a shear layer forced at a single frequency
[NASA-TM-100836] 12 p1628 N88-19740
Incompressible theory of interaction between moving bodies and vorticity field: Force on moving bodies by vorticity field 14 p1963 N88-21132
A low dimensional dynamical system for the wall layer
16 p2194 N88-23088
Ejection mechanisms in the sublayer of a turbulent channel 16 p2195 N88-23090
Direct numerical simulation of buoyantly driven turbulence 16 p2196 N88-23097
A statistical investigation of the single-point pdf of velocity and vorticity based on direct numerical simulations 16 p2196 N88-23101
Local structure of intercomponent energy transfer in homogeneous turbulent shear flow
16 p2197 N88-23103
Structure of turbulent shear flows
16 p2198 N88-23113
A non-invasive experimental technique for the measurement of unsteady velocity and vorticity fields
16 p2204 N88-23148
Crossflow vorticity sensor
[NASA-CASE-LAR-13436-1-CU]
17 p2300 N88-23759
Computation and characteristics of pulsatile multi-bifurcation flow 18 p2483 N88-24729
Axisymmetric viscid-inviscid interaction by a frozen vorticity approximation
[AD-A191743] 18 p2509 N88-24885
A single streamwise vortical structure and its instability in shear flows 18 p2515 N88-24921
The Proceedings of the Symposium on Mechanics for Space Flight 1987
[ISAS-SP-6] 20 p2782 N88-26499
The diffusion of vorticity from a plane boundary
[AD-A192706] 21 p2942 N88-27474
Cavitation inception in a turbulent shear flow
[DE88-011486] 21 p2946 N88-27497
Higher order vortex methods with rezoning
[DE88-010777] 21 p2947 N88-27505
Transonic blade-vortex interactions
22 p3037 N88-28035
On the energy source of 1982-83 ENSO episode simulated by the NCAR community climate model
22 p3122 N88-28558

Volumetric measurement of vorticity vectors by optical probe
[AD-A195997] 24 p3369 N88-30061
VORTICITY EQUATIONS
NT HELMHOLTZ VORTICITY EQUATION
Radial mixing in turbomachines
[AD-A188028] 11 p1482 N88-18847
VOYAGEUR HELICOPTER
U CH-46 HELICOPTER
VTOL
U VERTICAL LANDING
U VERTICAL TAKEOFF
VTOL AIRCRAFT
U VERTICAL TAKEOFF AIRCRAFT
VULCANIZATES
U VULCANIZED ELASTOMERS
VULCANIZED ELASTOMERS
Crosslinkable elastomeric materials
[EP-PATENT-0-181-735-A1] 01 p0026 N88-10165
VULCANIZING
Crosslinkable elastomeric materials
[EP-PATENT-0-181-735-A1] 01 p0026 N88-10165
Primerless RTV silicones
[BDX-613-3807] 24 p3356 N88-29980
VULNERABILITY
NT NUCLEAR VULNERABILITY
Performance evaluation of a half-wave resonant slot antenna over perfect ground using NEC (Numerical Electromagnetic Code)
[AD-A184004] 03 p0308 N88-11942
A methodology to assess the effects of high altitude electromagnetic pulse (HEMP) on electric power systems
[DE88-000338] 11 p1476 N88-18808
A computer graphics simulation of the endgame in aircraft combat survivability
[AD-A187826] 11 p1541 N88-19214
Defending secrets, sharing data: New locks and keys for electronic information
[PB88-143185] 12 p1706 N88-20210
The avionics software architecture impact on system architecture 17 p2303 N88-23778
The use of commercial off-the-shelf equipment and its impact on C3 (Command, Control and Communications EMP (electromagnetic pulse) survivability
[AD-A192614] 20 p2791 N88-26556
Fiber-optics used to record high-speed photographs inside a pressurized tank during lethality testing
[DE88-011283] 21 p2951 N88-27529
Defensive platform size and survivability
[DE88-011634] 23 p3184 N88-28948
Comparative analysis of passive communications satellites employing the SHF and HF spectrum for use in a strategic role
[AD-A194682] 24 p3362 N88-30019

W

W STARS
U WOLF-RAYET STARS
W WINGS
U VARIABLE SWEEP WINGS
W-R STARS
U WOLF-RAYET STARS
WAFERS
Hydrogen annealing of P(sub) b and E prime defect centers in oxidized silicon wafers
[DE87-014293] 02 p0152 N88-10951
Some 2-D WSI array architectures --- wafer scale integration (WSI)
[OUEL-1672/87] 02 p0219 N88-11381
Silicon microscale mechanisms from (110) oriented wafers
[DE88-002096] 06 p0787 N88-14825
Analytical investigations of bulk wave resonators in the piezoelectric thin film on gallium-arsenide configuration
[AD-A185716] 06 p0789 N88-14840
GaAs MMIC yield evaluation --- monolithic microwave integrated circuits (MMIC)
[ESA-CR(P)-2470] 08 p0979 N88-15916
Wafer scale implementation of a GaAs systolic signal processor cell 10 p1381 N88-18247
Corner compensation structures for (110) oriented silicon
[DE88-003300] 10 p1417 N88-18455
Fabrication and electrical characterization of multilevel aluminum interconnects used to achieve silicon-hybrid wafer-scale integration
[AD-A190519] 15 p2060 N88-22282
High-speed electron beam lithography devices discussed 16 p2185 N88-23023
A monolithic reduced-size Ku-Band SPOT (Single-Pole Double Throw) FET switch
[DE88-006273] 18 p2505 N88-24858
Determination of doping profiles in silicon from resistivity measurements via the four-point probe in combination with layer strippings via anodic oxidation 18 p2583 N88-25347
Chemical multisensors with selective encapsulation of ion-selective membranes 19 p2670 N88-25869
Stress modeling of microdiaphragm pressure sensors 19 p2670 N88-25873
Dissolution rates of polymers and copolymers based on methyl, ethyl and butyl methacrylate
[AD-A194713] 23 p3197 N88-29027
WAKEFULNESS
Sleep and wakefulness: Handbook for flight medical officers, second edition
[AGARD-AG-270(E)] 02 p0217 N88-11366
Effect of night watches and intermittent sleep on state of circadian rhythms of physiological functions of fishermen 06 p0750 N88-14610
Neurophysiological analysis of hypothalamic regulation mechanisms of primary sleep and hypobiosis 06 p0751 N88-14611
Pharmacological resetting of the Circadian sleep-wake cycle
[AD-A186194] 07 p0889 N88-15385
Exercise thermoregulation after prolonged wakefulness
[AD-A186224] 08 p1048 N88-16327
Role of adenosine analogs and growth hormone in waking and sleep
[AD-A187897] 11 p1519 N88-19070
Neurohumoral aspects of sleep
[AD-A188653] 12 p1667 N88-19992
Biological rhythms, sleep, and wakefulness in prolonged confinement 19 p2696 N88-26022
WAKES
NT AIRCRAFT WAKES
NT LAMINAR WAKES
NT NEAR WAKES
NT PROPELLER SLIPSTREAMS
NT SLIPSTREAMS
NT TURBULENT WAKES
Transverse focussing using plasma wake fields
[DE87-011503] 01 p0099 N88-10652
Investigations on a transonic airfoil with a 30 mm wide perforation/cavity arrangement
[ESA-TT-1072] 03 p0260 N88-11634
Unsteady flow about cambered plates
[AD-A184725] 03 p0320 N88-12025
The effect of object potentials on the wake of a flowing plasma
[AD-A184038] 03 p0379 N88-12385
A full potential flow analysis with realistic wake influence for helicopter rotor airload prediction
[NASA-CR-4007] 04 p0393 N88-12452
Measurement of velocity and vorticity fields in the wake of an airfoil in periodic pitching motion
[NASA-TP-2780] 04 p0487 N88-13002
An ultra-high-speed cinematographic method for the study of wakes in hypersonic ballistic ranges 05 p0531 N88-13228
Computational study of three-dimensional wake structures
[REPT-2] 05 p0539 N88-13281
Wakes of two dimensional bluff bodies in subsonic flow. Influence of a separating plate and of a pulsed injection of momentum
[IMFL-4200-86/75] 05 p0541 N88-13297
Development of an unsteady wake theory appropriate for aeroelastic analyses of rotors in hover and forward flight
[NASA-CR-182357] 06 p0664 N88-14075
Characteristics of a separating confluent boundary layer and the downstream wake
[NASA-TM-100046] 06 p0704 N88-14323
Observations of a midlatitude squall line boundary layer wake
[AD-A185609] 06 p0748 N88-14589
A qualitative study of wake fields for very short bunches
[DE88-002565] 09 p1164 N88-16980
Boundary-layer and wake measurements on a swept, circulation-control wing 10 p1270 N88-17597
SAR (Synthetic Aperture Radar) imaging of ship wakes in the Gulf of Alaska
[AD-A186554] 10 p1317 N88-17872
Emittance studies at the Los Alamos National Laboratory Free-Electron Laser (FEL)
[DE88-003146] 10 p1334 N88-17975
Wake effects in a Fayette 95-IIS wind turbine array
[DE88-001103] 10 p1349 N88-18063
Galileo probe parachute test program: Wake properties of the Galileo probe at Mach numbers from 0.25 to 0.95
[NASA-RP-1130] 11 p1488 N88-18884
Two-phase flows in the wake of in-cylinder projectiles
[AD-A189422] 13 p1765 N88-20559
Boundary-layer and wake measurements on a swept, circulation-control wing
[NASA-TM-89426] 15 p2014 N88-22013
Unsteady flow field measurements using LDV (Laser Doppler Velocimetry)
[AD-A189907] 15 p2063 N88-22298
Unsteady flow around a profile subjected to pulsed motions
[ETN-88-92151] 18 p2458 N88-24594
Supplements to the study of the wake of a Mirage G8 model at F2 --- wind tunnel
[CERT-RT-OA-20/5025-AYD] 18 p2458 N88-24596
Calibration of averaging total pressure flight wake rake and natural-laminar-flow airfoil drag certification
[NASA-CR-181630] 19 p2599 N88-25443
Analysis and modeling of complex non-stationary flows
[PB88-127188] 19 p2664 N88-25842
The diffusion of vorticity from a plane boundary
[AD-A192706] 21 p2942 N88-27474
A new method of calculating the boundary layer characteristics downstream of manipulators. Part 1: Boundary layer integral parameters
[PNR90455] 22 p3078 N88-28279
A new method of calculating the boundary layer characteristics downstream of manipulators. Part 2: Skin friction and net drag reduction
[PNR90456] 22 p3078 N88-28280
An examination of wake effects and power production for a group of large wind turbines
[DE88-009906] 22 p3117 N88-28518
Unsteady flow past an NACA 0012 airfoil at high angles of attack
[AD-A194650] 23 p3172 N88-28886
WALKING
Dynamics and stability of bipedal locomotion robots 03 p0333 N88-12096
Static standing and dynamic walking of a practical biped robot
[DE88-001367] 04 p0451 N88-12795
Determination of the effect of walking on the forced convective heat transfer coefficient using an articulated mannikin
[AD-A186452] 08 p1049 N88-16335
Morphological manifestations of primate adaptation to orthograde statics and walking erect 10 p1366 N88-18162
Force distribution and trajectory control for closed kinematic chains with applications to walking machines 13 p1779 N88-20642
Gastric emptying during walking and running: Effects of varied exercise intensity
[AD-A194025] 23 p3240 N88-29281
WALKING MACHINES
Correction of inertial navigation system drift errors for an autonomous land vehicle using optical radar terrain data
[AD-A184973] 05 p0544 N88-13311
A computer simulation study of an expert system for walking machine motion planning
[AD-A187907] 11 p1438 N88-18577
Space spider crane
[NASA-CASE-LAR-13411-1-SB] 17 p2312 N88-23828
Compliant robotic structures, part 3
[AD-A192426] 21 p2955 N88-27556
WALL FLOW
Wall interference tests of a CAST 10-2/DOA 2 airfoil in an adaptive-wall test section
[NASA-TM-4015] 02 p0122 N88-10772
Measurement of gas flow velocities near obstacles: Analysis and optimization of an optical barrier velocimeter. Associated signal processing
[ESA-TT-1056] 03 p0315 N88-11991
Analysis of the motions and effects of hairpin vortices 03 p0316 N88-11997
SCRAM JET (Supersonic Combustion Ramjet) combustion experiments 04 p0404 N88-12512
Time-dependent hypersonic viscous interactions
[AD-A185764] 06 p0665 N88-14082
A method for the approximate calculation of the skin friction coefficient of horizontal wavy plates
[VKI-TN-160] 07 p0851 N88-15172
Theoretical and experimental studies of the transonic flow field and associated boundary conditions near a longitudinally-slotted wind-tunnel wall
[NASA-CR-181169] 08 p0959 N88-15815
The effect of eddy distribution on momentum and heat transfer near the wall in turbulent pipe flow
[NASA-TM-100257] 08 p0988 N88-15984
Influence of the wall boundary layer on force measurements on half models in the transonic wind tunnel
[F+W-TF-1876] 09 p1122 N88-16715

A dynamical system/coherent structure approach to the fully developed turbulent wall layer
10 p1267 N88-17578
Navier-Stokes simulation of wind-tunnel flow using LU-ADI factorization algorithm
[NASA-TM-100042] 10 p1268 N88-17584
The influence of Mach number and heat transfer on the turbulent flow wall law
[NASA-TT-20230] 13 p1771 N88-20594
Wall interference assessment and corrections for transonic adaptive wall airfoil data
14 p1863 N88-21129
An efficient parallel algorithm for the simulation of three-dimensional compressible transition on a 20 processor Flex/32 multicomputer
[NASA-CR-178340] 17 p2337 N88-23943
Surface curvature and pressure gradient effects on turbulent flow: An assessment based on numerical solution of the Reynolds equations 17 p2338 N88-23954
Heat transfer from a negatively buoyant wall jet
[PB88-181953] 18 p2507 N88-24873
Hypersonic turbulent wall boundary layer computations
[NASA-CR-182147] 18 p2514 N88-24917
Wind tunnel wall interference (January 1980 - May 1988): A selected, annotated bibliography
[NASA-TM-4061] 19 p2604 N88-25466
Evolution of hairpin vortices in a shear flow
[NASA-TM-100858] 20 p2845 N88-26885
Supersonic wall adaptation in the rubber tube test section of the DFVLR Goettingen
[IB-222-87-A-08] 24 p3330 N88-29824

WALL JETS
Flow and heat transfer with impinging jets and rough surfaces
[DE87-014162] 02 p0169 N88-11065
Wall jet analysis for circulation control aerodynamics. Part 1: Fundamental CFD and turbulence modeling concepts 10 p1269 N88-17588
A theory for turbulent curved wall jets
10 p1269 N88-17590
Wall jet analysis for circulation control aerodynamics. Part 2: Zonal modeling concepts for wall jet/potential flow coupling 10 p1269 N88-17593
An experimental investigation of straight and curved annular wall jets
[NASA-CR-182546] 11 p1434 N88-18557
Heat transfer from a negatively buoyant wall jet
[NBS/GCR-88/541] 15 p2050 N88-22208
Variable Mach number wall jets for control/propulsion on hypervelocity projectiles/interceptors: Tests with an existing model
[AD-A192845] 21 p2892 N88-27167
Transition mixing study empirical model report
[NASA-CR-182139] 24 p3371 N88-30076

WALL PRESSURE
An engineering study of hybrid adaptation of wind tunnel walls for three-dimensional testing
[NASA-CR-178374] 07 p0814 N88-14957
Wavenumber - frequency structure of turbulent flow in a channel from a direct simulation
[AD-A189079] 12 p1627 N88-19737
Comparison of the wall pressure fluctuations in artificially generated turbulent spots, natural transition and turbulent boundary layers
[AD-A191777] 19 p2663 N88-25838
An experimental study of an adaptive-wall wind tunnel
[NASA-CR-183152] 24 p3329 N88-29821
The effects of incoming boundary layer thickness on unsteady shock-induced turbulent separations induced by cylinders
[AD-A196190] 24 p3368 N88-30060

WALL TEMPERATURE
Turbulent heat transfer and fluid flow measurements downstream of abrupt expansions and in a cavity of a circular tube at a uniform wall temperature
18 p2515 N88-24920
Plasma theory and simulation
[AD-A194674] 23 p3286 N88-29565
Radiative heat transfer to steady flow of a chemically reacting fluid in a horizontal porous channel with variable wall temperature
[DE88-702704] 24 p3372 N88-30081

WALLS
NT NOZZLE WALLS
NT POROUS WALLS
NT THIN WALLS
NT WIND TUNNEL WALLS
Space station integrated wall design and penetration damage control
[NASA-CR-179169] 01 p0013 N88-10070
Vortex dynamics and transport to the wall in a crossed-field plasma sheath
[DE87-013286] 01 p0100 N88-10657
A study of the optimal transition temperatue of PCM (Phase Change Material) wallboard for solar energy storage
[DE88-001522] 04 p0466 N88-12882
Aircraft interior noise reduction by alternate resonance tuning
[NASA-CR-181530] 04 p0488 N88-13005
The orientations of dipolar walls produced by cyclic deformation 05 p0598 N88-13655
Reversed field pinch plasmas with various boundary conditions
[DE88-000832] 05 p0653 N88-14004
The production of turbulence in boundary layers: The role of microscale coherent motions
[AD-A185568] 06 p0703 N88-14313
Geometrically nonlinear analysis of stiffened panels
06 p0722 N88-14440
Effect of plasma rotation in tokamak on stabilizing action of electrically conducting wall 06 p0773 N88-14748
Wall turbulence control 07 p0812 N88-14943
Examination of the development of a compressible turbulent boundary layer on a rough and porous wall
[PB87-148266] 07 p0815 N88-14964
Electromagnetic fields backscattered from an s-shaped inlet cavity with an absorber coating on its inner walls
[NASA-CR-182401] 07 p0845 N88-15130
Space station integrated wall damage and penetration damage control. Task 5: Space debris measurement, mapping and characterization system
[NASA-CR-179281] 10 p1285 N88-17688
One-dimensional leakage-flow vibration instabilities
[DE88-002875] 10 p1330 N88-17947
An analysis of the motion and effects of hairpin vortices
[AD-A187261] 10 p1331 N88-17958
Structural analyses of engine wall cooling concepts and materials 15 p2081 N88-22405
A low dimensional dynamical system for the wall layer
16 p2194 N88-23088
Self similarity of two point correlations in wall bounded turbulent flows 16 p2195 N88-23089
Conditionally-averaged structures in wall-bounded turbulent flows 16 p2198 N88-23112
Inflectional instabilities in the wall region of bounded turbulent shear flows 16 p2199 N88-23114
Active layer model for wall-bounded turbulence
16 p2199 N88-23115
Simulation of laminar-turbulent transition in the vicinity of a wall
[AD-A191380] 16 p2208 N88-23180
Research in electromagnetic shielding theory. Part1. Shielding by rectangular enclosures
[AD-A192881] 20 p2791 N88-26557
On the global radiation incident variously orientated surfaces on the South Coast of Finland
[FMI-5] 20 p2823 N88-26746
Aircraft interior noise reduction by alternate resonance tuning
[NASA-CR-182540] 20 p2849 N88-26909
Characterization of accelerating pipe flow
[AD-A193065] 21 p2943 N88-27481
Transverse resistive wall instability in a high-power, short-wavelength free-electron laser
[DE88-011730] 21 p2954 N88-27549
Solar energy absorption efficiency of an ellipsoidal receiver-reactor with specularly reflecting walls
[AD-A193726] 22 p3117 N88-28520
Experimental determination of drag modifications due to elastic compliant surfaces using quantitative visual techniques
[AD-A194785] 24 p3372 N88-30082
A parametric study of embedded cantilever retaining walls: The results of a finite element study
[RR-CE83] 24 p3383 N88-30152

WALSH FUNCTION
Estimation of multivariate binary density using orthonormal functions
[AD-A186386] 07 p0912 N88-15528
Solving singular systems using orthogonal functions
[AD-A190881] 16 p2260 N88-23512

WANKEL ENGINES
Performance and combustion characteristics of direct-injection stratified-charge rotary engines
[NASA-TM-100134] 04 p0400 N88-12490

WAR GAMES
Mapping a battlefield simulation onto message-passing parallel architectures
[NASA-CR-178396] 03 p0363 N88-12287
ADAM (Acquisition Deployment and Maneuvering): The space game
[AD-A189512] 12 p1685 N88-20078
Perfect knowledge and beyond --- chess endgames
[REPT-87-37] 14 p1967 N88-21738

WARFARE
NT ANTISUBMARINE WARFARE
NT CHEMICAL WARFARE
NT COMBAT
NT ELECTRONIC WARFARE
NT NUCLEAR WARFARE
Automation strategy and results for an airbase command and control information system
[NLR-MP-86031-U] 01 p0035 N88-10223
Performance evaluation of a half-wave resonant slot antenna over perfect ground using NEC (Numerical Electromagnetic Code)
[AD-A184004] 03 p0308 N88-11942
Assessment of physical activity intensity by heart rate during sleep limited military operations
[AD-A185913] 07 p0888 N88-15382
Relating service doctrine to space system requirements
[AD-A186620] 08 p1074 N88-16483
The evolution of naval warfare technology and the impact of space systems
[AD-A186900] 09 p1233 N88-17392
A strategy for space warfare
[AD-A186658] 09 p1233 N88-17394
Acta aeronautica et astronautica sinica (selected articles)
[AD-A191552] 18 p2455 N88-24575
Predicting Air Combat Maneuvering (ACM) performance: Fleet fighter ACM readiness program grades as performance criteria
[AD-A191605] 19 p2710 N88-26099
Computation of ECM (Electronic Counter-Measures) war reserve materiel spare requirements
[AD-A193301] 21 p2897 N88-27195
Proposal for a new aggressor aircraft
[AD-A194311] 22 p3041 N88-28056
Tactical air force night/adverse weather training
[AD-A194243] 22 p3133 N88-28625
The principles of mass and maneuver applied to space operations
[AD-A194037] 23 p3276 N88-29500

WARMING
U HEATING

WARNING DEVICES
U WARNING SYSTEMS

WARNING SIGNALS
U WARNING SYSTEMS

WARNING SYSTEMS
NT EARLY WARNING SYSTEMS
The flight evaluation of an advanced engine display and monitoring system 03 p0264 N88-11659
Techniques for fire detection
04 p0406 N88-12521
Annual tropical cyclone report, 1986
[AD-A184082] 04 p0470 N88-12903
Analytical study of the effect of early warning on optimal shock isolation 08 p0998 N88-16047
EUREX D: An expert system for failure diagnosis and recovery in the TCS of the European retrievable carrier EURECA 08 p1058 N88-16385
Airborne Wind Shear Detection and Warning Systems: First Combined Manufacturers' and Technologists' Conference
[NASA-CP-10006] 10 p1273 N88-17616
Response of wind shear warning systems to turbulence with implication of nuisance alerts
10 p1274 N88-17618
Windshear warning aerospatiale approach
10 p1274 N88-17620
Lidar windshear detection and avoidance: Performance and technical assessment 10 p1274 N88-17626
Infrared low-level wind shear work
10 p1275 N88-17628
Crew interface with windshear systems
10 p1275 N88-17631
Status of FAA terminal Doppler weather radar programs 10 p1275 N88-17632
The advanced low-level windshear alert system operational demonstration results, Summer, 1987, Denver Stapleton International Airport 10 p1275 N88-17633
Information transfer in the National Airspace System
10 p1275 N88-17634
Airworthiness considerations
10 p1276 N88-17636
Aviation weather: Status of FAA's (Federal Aviation Administration's) new hazardous weather detection and dissemination systems
[PB88-115910] 11 p1513 N88-19041
Rotorcraft TCAS (traffic alert and collision avoidance system) evaluation: Group 3 results
[AD-A191719] 18 p2461 N88-24614
An interagency working group on lightning threat warning
[DE88-009828] 20 p2826 N88-26767

Synoptic patterns related to tropical cyclone recurvature
[AD-A192338] 20 p2827 N88-26771
Helicopter Warning Sensor (HWS)
22 p3149 N88-28735

WASHING
NT BATHING
Analysis of water recovered after being used for washing by men and women 10 p1361 N88-18135

WASHOUT (RADIOACTIVITY)
U FALLOUT

WASTE DISPOSAL
NT HAZARDOUS MATERIAL DISPOSAL (IN SPACE)
The adaption and use of research codes for performance assessment
[DE88-000552] 06 p0756 N88-14639
Institute for Materials Science and Engineering, Metallurgy: Technical activities 1987
[PB88-157722] 11 p1460 N88-18702
Space reactor end of life issues
17 p2424 N88-24413
Review of numerical methods for radionuclide transport in three-dimensional porous media, at high Peclet numbers
[CFDU/87/10] 18 p2538 N88-25061
Optimization of mechanical/corrosion properties of TI-CODE 12 plate and sheet. Part 2: Thermomechanical processing effects
[DE88-007493] 19 p2616 N88-25517
Waste destruction by plasma
[SNIAS-881-430-113] 21 p2971 N88-27651
Advanced development waste processing unit for combat vehicles, phase 2
[AD-A193793] 23 p3243 N88-29302

WASTE ENERGY UTILIZATION
Use of natural gas diesel engines in mechanical pulp production: A preliminary study
[DE87-753065] 02 p0181 N88-11129
Organic Rankine-cycle power systems working fluids study. Topical report No. 1: Fluorinol 85
[DE87-014604] 02 p0195 N88-11217
Application of Organic Rankine Cycles (ORCs) to decentralized power generation, preliminary study
[DE87-753331] 03 p0347 N88-12197
Open-cycle centrifugal vapor-compression heat pump
[PB88-157391] 11 p1488 N88-18885
Alternative Energy in the Midwest: Research and Applications. Conference Proceedings, Rosemont, Illinois, March 19-20, 1987
[PB88-142278] 11 p1509 N88-19015
Overview of 1987 moonlight project
15 p2052 N88-22231
Application and technology requirements for heat pumps at the process industries
[DE88-006740] 15 p2062 N88-22293
An analysis of gas-steam total power recovery energy system 20 p2784 N88-26512
A comparative economic evaluation of industrial heat pumps. Part 2: Addendum
[DE88-011701] 22 p3117 N88-28519
Absorption heat pumps
[DE88-752820] 23 p3229 N88-29218

WASTE HEAT
Space vehicle/nuclear reactor thermal radiation integration issues 17 p2424 N88-24417
Experimental demonstrations of organic Rankine cycle waste heat rejection systems 17 p2432 N88-24469
An analysis of gas-steam total power recovery energy system 20 p2784 N88-26512

WASTE TREATMENT
Catalytic processes for space station waste conversion
[NASA-CR-177423] 01 p0077 N88-10491
Innovative and alternative technology projects
[PB87-230165] 05 p0623 N88-13818
Controlled Ecological Life Support Systems (CELSS) physiochemical waste management systems evaluation
[NASA-CR-177422] 06 p0754 N88-14626
Electrochemical processing of solid waste
[NASA-CR-182413] 08 p0967 N88-15852
Proceedings of the 19th DOE/NRC Airborne Waste Management and Air Cleaning Conference
[NUREG/CP-0086-VOL-1] 11 p1509 N88-19018
JPRS report: Science and technology. Japan
[JPRS-JST-87-030] 16 p2185 N88-23026

WASTE UTILIZATION
Catalytic processes for space station waste conversion
[NASA-CR-177423] 01 p0077 N88-10491
Operation of an experimental algal gas exchanger for use in a CELSS 03 p0358 N88-12255
A review of recent activities in the NASA CELSS program 03 p0359 N88-12259
Preliminary experimental results of gas recycling subsystems except carbon dioxide concentration
03 p0359 N88-12261
Mass balances for a biological life support system simulation model 03 p0361 N88-12272

WASTE WATER
Innovative and alternative technology projects
[PB87-230165] 05 p0623 N88-13818
Reclamation of water contaminated with fuel system icing inhibitor. Phase 1: Literature review and information compilation
[DE88-006575] 16 p2183 N88-23013
Vapor Compression Distillation Subsystem (VCDS) component enhancement, testing and expert fault diagnostics development, volume 1
[NASA-CR-172072] 22 p3134 N88-28634

WASTES
NT HUMAN WASTES
NT INDUSTRIAL WASTES
NT LIQUID WASTES
NT MANURES
NT RADIOACTIVE WASTES
NT URINE
NT WASTE WATER
Technology '87: Research and Development Laboratory Technology Transfer Program
[DE88-003142] 13 p1852 N88-21084
Overview of the TITAN-2 reversed-field pinch aqueous fusion power core design
[DE88-008170] 20 p2857 N88-26966

WATCHES
U CLOCKS

WATER
NT COASTAL WATER
NT COLD WATER
NT DEEP WATER
NT FRESH WATER
NT GROUND WATER
NT INLAND WATERS
NT POTABLE WATER
NT SEA WATER
NT SHALLOW WATER
NT SURFACE WATER
NT WASTE WATER
Cooling effect of a single evaporating droplet on a hot semi-infinite metal body
[PB87-201802] 01 p0046 N88-10294
The water permeability of multi-layer coatings
[BLL-M-37252-(5828.4)] 02 p0148 N88-10927
Trickle water and feeding system in plant culture and light-dark cycle effects on plant growth
03 p0361 N88-12273
Technical evaluation of a solar-powered absorption cooling system (LiBr-H2O)
[PB87-108254] 04 p0463 N88-12867
RRS DISCOVERY cruise 160, 30 June-25 July, 1986. Geochemical sampling over the Madeira and Porcupine Abyssal Plains
[PB87-222030] 04 p0471 N88-12910
Phase purity of NiCo2O4, a catalyst candidate for electrolysis of water
[NASA-TM-100239] 05 p0556 N88-13385
Operating envelopes of particle sizing instrumentation used for icing research
[NASA-CR-180870] 05 p0586 N88-13573
Observing effect of laser radiation of low-frequency Raman scattering of light 06 p0772 N88-14742
Experimental and theoretical study of condensation in multicomponent mixtures
[DE88-002715] 07 p0830 N88-15033
Vapor condensation on a turbulent liquid interface
08 p0982 N88-15939
Evidence for human adaptive response to dehydration: Increase of circulating protein mass
[AD-A186225] 08 p1048 N88-16328
Analysis of water recovered after being used for washing by men and women 10 p1361 N88-18135
Approximate method for predicting the permanent set in a beam in vacuo and in water subject to a shock wave 11 p1500 N88-18957
Emission of gamma rays from various materials pulsed with 14-MeV neutrons
[DE88-003837] 11 p1544 N88-19227
Optically stimulated sound from gas bubbles in water
12 p1686 N88-20087
Numerical experiments on the stability of controlled boundary layers
[NASA-CR-181649] 13 p1771 N88-20591
An investigation of the spray produced by a yawed wheel, including measurement of impact forces --- aircraft wheels
[BU-363] 14 p1866 N88-21150
The role of water in the thermal balance of the coma
14 p1999 N88-21916
Determination of the content of CO(+) and H2O(+) ions in the tail of Comet Giacobini-Zinner and Comet Halley 14 p2006 N88-21964
Mass transfer mechanisms for water adsorbed on silica gel
[DE88-005993] 15 p2032 N88-22107
Noncondensing round turbulent gas jets in liquids
[AD-A191191] 16 p2208 N88-23179
Development of a liquid-fed water resistojet
[NASA-TM-100927] 18 p2523 N88-24968
Direct determination of part-per-billion levels of volatile organics in water and soil samples using glow discharge mass spectrometry
[DE88-011389] 21 p2910 N88-27272
Structure and function of the manganese complex involved in photosynthetic oxygen evolution determined by X-ray adsorption spectroscopy and electron paramagnetic resonance spectroscopy
[DE88-010360] 21 p2985 N88-27725
Finite-rate water condensation in combustion-heated wind tunnels
[NASA-TP-2833] 22 p3046 N88-28075
Initiation of explosive molten aluminum-water interactions at wet or underwater surfaces
[DE88-004686] 23 p3194 N88-29006
Sub-kilometer rampart craters in the equatorial region of Mars: Possible implications for the state and distribution of regolith H2O 23 p3302 N88-29666
How dirty is Mars' North Polar cap, and why isn't it black 23 p3303 N88-29677
Coadsorption of H2O and CO2 on the Martian surface
23 p3307 N88-29702
General equations for the motions of ice crystals and water drops in gravitational and electric fields
[NASA-CR-183229] 24 p3370 N88-30070

WATER BALANCE
The influence of space flight on water-salt homeostasis in man and animals 12 p1659 N88-19943
Changes in blood conductivity during immersion
12 p1663 N88-19969
Human adaptation to various hypercapnic conditions in relation to salivary electrolyte dynamics and renal function 12 p1664 N88-19977
Climatology and space observations
[ISBN-2-85-428179-9] 14 p1935 N88-21536
Continental surface processes and water cycle
14 p1937 N88-21555
Hydrological models 14 p1937 N88-21559
The Hapex-Mobilhy program 14 p1938 N88-21560
Measurement of the water content of soil from space and application to the regional water balance
14 p1938 N88-21561

WATER CIRCULATION
NT COASTAL CURRENTS
NT EL NINO
NT GULF STREAM
NT LOMONOSOV CURRENT
NT OCEAN CURRENTS
NT WATER CURRENTS
Ocean model processor for climate studies
[PB87-224713] 03 p0353 N88-12226
North Pacific Ocean. Northeast Pacific Transition Zone, R/V Thomas G. Thompson: 1 November - 6 December 1989. STD data report
[AD-A186574] 09 p1195 N88-17161
Numerical model of Rayleigh instability and spin-off eddies on fronts 13 p1788 N88-20696
Ocean eddies 14 p1938 N88-21566

WATER COLOR
The influence of yellow substances on remote sensing of sea water constituents from space. Volume 1: Summary
[ESA-CR(P)-2443-VOL-1] 07 p0872 N88-15292
The influence of yellow substances on remote sensing of sea water constituents from space. Volume 2: Appendices
[ESA-CR(P)-2443-VOL-2] 07 p0873 N88-15293
Ocean Colour Workshop --- conference
[ESA-SP-1083] 08 p1042 N88-16292
Europe's position concerning ocean colour activities
08 p1042 N88-16293
Overview of ESA's activities in ocean colour remote sensing 08 p1042 N88-16294
Update of NASA's ocean colour activities
08 p1042 N88-16295
Remote sensing of ocean colour for studies of biological productivity and biochemical cycles
08 p1042 N88-16296
Ocean colour applications in ocean dynamics and coastal processes 08 p1042 N88-16297
Technical aspects of future ocean colour remote sensing 08 p1042 N88-16298
Federal Republic of Germany's interests, activities and goals in remote sensing of ocean colour/fluorescence from space 08 p1043 N88-16302
French activities in ocean colour observations
08 p1043 N88-16303
Italian activities in ocean colour remote sensing
08 p1043 N88-16304

National Remote Sensing Program (NRSP) of the Netherlands 08 p1043 N88-16305
Developments in ocean colour research in the United Kingdom 08 p1043 N88-16306

WATER CONTENT
U MOISTURE CONTENT

WATER COOLED REACTORS
NT BOILING WATER REACTORS
NT LIGHT WATER REACTORS
NT PRESSURIZED WATER REACTORS
NT ZERO POWER REACTORS

WATER COOLING
U LIQUID COOLING

WATER CURRENTS
NT COASTAL CURRENTS
NT EL NINO
NT GULF STREAM
NT LOMONOSOV CURRENT
NT OCEAN CURRENTS
Tide- and wind-forced currents in Buzzards Bay, Massachusetts
[PB88-110580] 07 p0882 N88-15350
Use of the thermodynamic evaporation formula of Hoffmann in energy balance models for flowing water 08 p1013 N88-16143
Model of hydrodynamic adjustment of temperature, salinity and current fields 13 p1789 N88-20700
Circulation and exchange processes on the South Atlantic Bight Continental Shelf
[DE88-003330] 13 p1804 N88-20781
FORTRAN programs for computation of time dependent sea levels and trajectory errors from satellite altimeter data
[BONN-MITT-73] 21 p2901 N88-27216

WATER CYCLE (HYDROLOGY)
U HYDROLOGICAL CYCLE

WATER DEPTH
Sea level changes
[DE87-014357] 04 p0472 N88-12913

WATER FLOW
Experimental evidence for modifying the current physical model for ice accretion on aircraft surfaces
[NASA-TM-87184] 04 p0397 N88-12473
Evaluation of the magnetic induction conductivity method for detecting frazil ice deposits
[AD-A186940] 09 p1194 N88-17157
Boundary-integral-equation method for computing the three-dimensional flow of groundwater
[PB88-126691] 10 p1330 N88-17951
Changes in the California current system observed off northern California during July-August 1986
[AD-A190027] 15 p2100 N88-22510
Evaluation of the floodable area of the canal of Sao Goncalo through TM-LANDSAT 5 imagery 17 p2364 N88-24078
Injection of drag reducing additives into turbulent water flows
[AD-A192072] 18 p2509 N88-24868
Noise generation by air bubbles in water: An experimental study of creation and splitting
[AD-A192063] 19 p2664 N88-25839
Development of advanced flow simulation system by water flow model. New method of velocity measurement using cross-correlation
[DE88-753120] 20 p2799 N88-26608
Mapping of streamflow and soil infiltration of a Sahelian catchment area by SPOT image interpretation: The Oursi pond catchment area in Burkino Faso 22 p3090 N88-28348

WATER HAMMER
Hydroacoustic pulsating jet generator
[MPIS-7/1987] 18 p2510 N88-24891

WATER HEATING
Development of an innovative, low-cost solar collector
[PB87-206819] 02 p0194 N88-11210
Actual performance and economic feasibility of residential solar water heaters
[INPE-4399-RPE/555] 08 p1023 N88-16191
Application of the estimation method to parameter performance date of solar water heating systems
[INPE-4268-PRE/1141] 11 p1508 N88-19007

WATER IMMERSION
Human thermoregulatory model for whole body immersion in water at 20 and 28 C
[AD-A185052] 05 p0629 N88-13849
Changes in regional and central hemodynamics during seven-day water immersion 07 p0895 N88-15421
Prediction of human thermoregulatory responses and endurance time in water at 20 and 24C
[AD-A186223] 08 p1048 N88-16326
Rational considerations for modelling human thermoregulation during cold water immersion
[AD-A186226] 08 p1048 N88-16329
Rapid hypothermia subsequent to oral nicotinic acid and immersion in warm (30C) water
[AD-A186458] 08 p1050 N88-16339
Respiratory and cardiovascular responses to cold stress following repeated cold water immersion
[AD-A186460] 08 p1050 N88-16340
Role of body fat in the prediction of the metabolic response for immersion in cold water
[AD-A186914] 09 p1198 N88-17182
Comparative evaluation of orthostatic stability following immersion in horizontal and vertical positions 10 p1363 N88-18143
Influence of a 6 hr head-out water immersion on different tests of endurance performance capacity 12 p1653 N88-19903
Changes in blood conductivity during immersion 12 p1663 N88-19969
Validation of mathematical model predictions of immersion survival times
[IAM-652] 14 p1952 N88-21635
Further development of a mathematical model for the specification of immersion clothing insulation
[IAM-653] 14 p1954 N88-21644
Experimental investigation of Hover flowfields in water at the McDonnell Douglas Research Laboratories 16 p2202 N88-23135
Human hemodynamics during water immersion as related to position during submersion 19 p2703 N88-26071

WATER INJECTION
Dense-spray structure and phenomena. Part 2: Pressure-atomized sprays
[AD-A190312] 15 p2064 N88-22307
Turbulence and flame propagation
[PB87-228912] 19 p2612 N88-25499

WATER JETS
U HYDRAULIC JETS

WATER LANDING
NT DITCHING (LANDING)

WATER MANAGEMENT
The use of SPOT images for water resources surveys. The examples of the Kasserine area (Tunisia) and the Jebel Amour (Algeria) 03 p0345 N88-12179
The world's water resources: A major neglect. A study in remote sensing in hydrology and water management
[ESA-BR-40] 22 p3116 N88-28511

WATER MASERS
Water masers associated with 2 carbon stars: EU Andromedae and V778 Cygni 04 p0517 N88-13176
The distance to the center of the galaxy: H2O maser proper motions in Sgr B2(N)
[MPE-PREPRINT-104] 16 p2288 N88-23702

WATER POLLUTION
NT OIL POLLUTION
Influence of surfactants on damping of gravity-capillary waves. 1: Frequency dependence 04 p0459 N88-12843
Uses of airborne laser Chayka-1 for probing water, land surfaces 06 p0725 N88-14461
Trace element geochemistry of the South Atlantic Bight
[DE88-003515] 10 p1356 N88-18108
Environmental projects. Volume 5, part 1: Study of subsurface contamination. Part 2: Guide to implement environmental compliance programs
[NASA-CR-182691] 13 p1796 N88-20741
Global mixed-layer natural and anthropogenic fluxes 13 p1807 N88-20803
Feasibility study for a 2nd generation system for airborne maritime pollution surveillance
[ETN-88-92108] 15 p2092 N88-22466
Study of reservoir water quality utilizing remote sensing techniques: Methodological concepts 17 p2364 N88-24076
Hydrocarbon fuel spill dispersion on water: Literature review
[AD-A192486] 21 p2922 N88-27346

WATER PURIFICATION
U WATER TREATMENT

WATER QUALITY
Rapid toxicity detection in water quality control utilizing automated multispecies biomonitoring for permanent space stations 02 p0135 N88-10848
Investigation of effect of silver compounds on microflora in water reclaimed from atmospheric moisture condensate in a closed environment 07 p0892 N88-15407
Two decades of achievement in the ocean, 1968-1988
[PB88-167077] 16 p2236 N88-23356
Satellite remote sensing of turbidity and sediment concentration in Lagoa dos Patos 17 p2355 N88-24032
Study of reservoir water quality utilizing remote sensing techniques: Methodological concepts 17 p2364 N88-24076
Validation of maximum permissible concentration of urea in reclaimed potable water and evaluation of its biological effect 19 p2705 N88-26086
Use of SPOT HRV data in the US Army Corps of Engineers dredging program 22 p3109 N88-28466

WATER RECLAMATION
Reclamation of water contaminated with fuel system icing inhibitor. Phase 1: Literature review and information compilation
[DE88-006575] 16 p2183 N88-23013
Cardiac rhythm of animals consuming reclaimed water differing in concentration of sodium and potassium ions 19 p2705 N88-26085
Validation of maximum permissible concentration of urea in reclaimed potable water and evaluation of its biological effect 19 p2705 N88-26086
Liquid-phase oxidation of acetone with hydrogen peroxide on oxide catalysts 19 p2706 N88-26091

WATER RECOVERY
U WATER RECLAMATION

WATER RESOURCES
NT AQUIFERS
The use of SPOT images for water resources surveys. The examples of the Kasserine area (Tunisia) and the Jebel Amour (Algeria) 03 p0345 N88-12179
Study of fractures as subsidiary research of ground water in the Sergipe state: An approach through remote sensing data
[INPE-4319-TDL/286] 12 p1639 N88-19813
Botany Facility: Problems of water supply, plant nutrients and soil in the Botany Facility
[SIRA-A/7373/WP220/RJS/003] 17 p2379 N88-24141
The use of SPOT images for water resources surveys in the Kasserine Basin (Tunisia) 22 p3090 N88-28349
Water resources and agricultural land use investigations in northeastern Gujarat (India) 22 p3091 N88-28355
Use of SPOT satellite in agrohydrology: Detection of spring water excess in a grassland region 22 p3091 N88-28357
The use of orbital remote sensing data for low cost ground-water survey
[INPE-4587-PRE/1318] 24 p3386 N88-30170

WATER RUNOFF
Groundwater sapping valleys: Experimental studies, geological controls and implications to the interpretation of valley networks on Mars
[NASA-CR-182718] 15 p2152 N88-22847
Reduce uncertainty in projection of future sea-level changes due to ice wastage
[DE88-009883] 22 p3129 N88-28601

WATER SPLITTING
DC conductivity studies in Li5AlO4 at intermediate temperatures and its possible application for the electrolysis of water
[AD-A185489] 06 p0697 N88-14276
Photosynthetic water splitting
[DE88-007809] 20 p2830 N88-26791

WATER TEMPERATURE
NT OCEAN TEMPERATURE
NT SEA SURFACE TEMPERATURE
Influence of stratification in near-surface water layer on intensity of gas exchange between atmosphere and water 04 p0459 N88-12841
Thermal instability and heat transfer characteristics in water/ice systems
[AD-A189627] 15 p2062 N88-22297
Observations of frontal instabilities on an upwelling filament
[AD-A191051] 17 p2375 N88-24122
Evaluating evaporation with satellite thermal data
[AD-A192042] 18 p2531 N88-25019
Study of human factors engineering criteria for Extra Vehicular Activity (EVA) systems, volume 2
[STF23-F87025-VOL-2] 24 p3409 N88-30293

WATER TREATMENT
Vapor compression distiller and membrane technology for water revitalization 03 p0359 N88-12262
An overview of Japanese CELSS research activities 03 p0360 N88-12267
Carbon dioxide treatment for scale removal and control in potable water systems
[AD-A184346] 04 p0412 N88-12556
Innovative and alternative technology projects
[PB87-230165] 05 p0623 N88-13818
Reverse osmosis treatment to remove inorganic contaminants from drinking water
[PB88-147780] 12 p1605 N88-19598
Review of selenium thermodynamic data
[DE88-006194] 13 p1849 N88-21068
Reclamation of water contaminated with fuel system icing inhibitor. Phase 1: Literature review and information compilation
[DE88-006575] 16 p2183 N88-23013
Vapor Compression Distillation Subsystem (VCDS) component enhancement, testing and expert fault diagnostics development, volume 1
[NASA-CR-172072] 22 p3134 N88-28634

WATER TUNNEL TESTS
Technical evaluation report on the Fluid Dynamics Panel Symposium on aerodynamic and related hydrodynamic studies using water facilities
[AGARD-AR-225] 03 p0312 N88-11968
High Reynolds number pump facility for cavitation research
[AD-A189310] 13 p1765 N88-20558
An experimental investigation of decelerating flow about two-dimensional cambered plates
[DE88-006598] 13 p1766 N88-20567
Water facilities in retrospect and prospect: An illuminating tool for vehicle design
16 p2200 N88-23126
Vortex breakdown and control experiments in the Ames-Dryden water tunnel 16 p2200 N88-23127
Qualification of a water tunnel for force measurements on aeronautical models 16 p2200 N88-23128
An experimental study to determine the flow and the subsonic static and dynamic stability characteristics of aircraft operating at high angles-of-attack
16 p2201 N88-23129
Oscillating flow over bluff bodies in a U-shaped water tunnel 16 p2201 N88-23131
The use of the NRC/NAE water facilities in Canadian aeronautical research and development
16 p2201 N88-23132
Short duration flow establishment on a profile in a Water-Ludwieg-Tunnel 16 p2201 N88-23134
Water tunnel measurements by an electrochemical method 16 p2203 N88-23146
Use of water towing tanks for aerodynamics and hydrodynamics 16 p2204 N88-23149
Investigation on the movement of vortex burst position with dynamically changing angle of attack for a schematic deltawing in a watertunnel with correlation to similar studies in windtunnel 16 p2204 N88-23152
Measurements of the time dependent velocity field surrounding a model propeller in uniform water flow
16 p2205 N88-23155
Unsteady water channel
[AD-A194231] 23 p3171 N88-28884

WATER TUNNELS
U HYDRAULIC TEST TUNNELS

WATER VAPOR
Millimeter-wave studies of moist air
[AD-A184681] 03 p0306 N88-11935
A method for remote sensing of precipitable water vapor and liquid in the atmosphere using a 22-ghz radiometer
[AD-A184204] 03 p0354 N88-12232
Absorption of far IR-radiation by H2O-N2 complexes under atmospheric conditions 04 p0462 N88-12855
Measurements of vapor flux, liquid water contents, precipitation rates and riming in a Utah mountain cloud system
[PB87-224945] 04 p0469 N88-12900
DC conductivity studies in Li5AlO4 at intermediate temperatures and its possible application for the electrolysis of water
[AD-A185489] 06 p0697 N88-14276
A critical review of measurements of water vapor absorption in the 840 to 1100 cm(-1) spectral region
[NASA-CR-182361] 06 p0742 N88-14565
Study of the vapor-liquid equilibria used in the fabrication process of hydrogen by thermochemistry
[DE88-900239] 07 p0830 N88-15035
Radiation absorption in the infrared spectral range: A comparison between laboratory measurements and theoretical calculation illustrated by a H2O 2.7 micrometer 08 p1018 N88-16170
In-situ stratospheric water vapor measurements on board long duration balloons 08 p1029 N88-16232
High-speed assembly language (80386/80387) programming for laser spectra scan control and data acquisition providing improved resolution water vapor spectroscopy
[NASA-CR-4117] 08 p1053 N88-16355
Concept, construction, and experimental testing of a polychromator for a Raman lidar for the simultaneous telemetering of carbon dioxide and water vapor, relative to oxygen
[GKSS-87/E/20] 09 p1191 N88-17134
Scattering of optical radiation by bursting water particles in fog 09 p1236 N88-17410
An experimental and theoretical study of the ice accretion process during artificial and natural icing conditions
[NASA-CR-182119] 14 p1865 N88-21143
Water vapor and hydroxyl distributions in the inner coma of Comet Halley measured by the VEGA-2 three channel spectrometer TKS 14 p1998 N88-21910
Mathematical modelling of the heat and water vapour transport in the human respiratory tract
17 p2382 N88-24160
Tracer water transport and subgrid precipitation variation within atmospheric general circulation models
[NASA-CR-182897] 20 p2823 N88-26745
Wavenumber spectra from THIR 6.7 micron water vapor data 20 p2824 N88-26756
Heat and mass transfer in laminar wavy film absorption with the presence of non-absorbable gases
21 p2947 N88-27502
On the energy source of 1982-83 ENSO episode simulated by the NCAR community climate model
22 p3122 N88-28556

WATER VEHICLES
NT AIRCRAFT CARRIERS
NT SHIPS
NT SUBMARINES
NT UNDERWATER VEHICLES
A comparative study of various electric propulsion systems and their impact on a nominal ship design
[AD-A187800] 11 p1477 N88-18816

WATER WAVES
Observations of wind waves on a reservoir
[IOS-234] 02 p0193 N88-11206
Breaking wave forces on vertical cylinders
[RR-CE71] 03 p0338 N88-12126
Studies of thin surface films aim at seeing deep ocean processes 04 p0460 N88-12847
Wave and wind data sources, environmental conditions committee report, International Ship and Offshore Structures Congress
[PB87-234902] 06 p0746 N88-14588
Far field of steady waves produced by local perturbation sources in stream of stratified fluid
06 p0771 N88-14736
Annual data summary and climatological evaluation, CERC (Coastal Engineering Research Center) field research facility, 1985, volume 2, appendix C
[AD-A185894] 07 p0881 N88-15344
Guide for the program EXACT-NL --- wave growth
[KNMI-TR-94] 09 p1163 N88-16971
Nearshore wave transformation study of sites near Port Canaveral Inlet, Florida
[AD-A186965] 09 p1195 N88-17159
Investigation of the quantitative determination of two dimensional sea surface wave spectra from shipborne radar measurements
[GKSS-87/E/10] 09 p1195 N88-17163
SAR (Synthetic Aperture Radar) imaging of ship wakes in the Gulf of Alaska
[AD-A186554] 10 p1317 N88-17872
Analysis of wind turbines on offshore support structures excited by random wind and random waves
[DE88-004772] 10 p1351 N88-18074
Variation of the wind stress related to frontal passages during FASINEX (Frontal Air-Sea Interaction Experiment) 1986
[AD-A187180] 11 p1514 N88-19042
Wave group analysis based on Kimura's method
[AD-A187610] 11 p1516 N88-19055
Effects of waves on the boundary layer of a surface-piercing flat plate: Experiment and theory
[AD-A188356] 12 p1626 N88-19731
Anisotropy of microstructural eddy motion in surface layer during calm 13 p1784 N88-20677
Numerical modeling of wave migration of seismic data
13 p1786 N88-20684
Invariant characteristics of acoustic field in stratified ocean 13 p1788 N88-20698
Study of spectra of sea waves on horizontally nonuniform current in rip zone 13 p1788 N88-20699
Dynamics of the Oceanic Surface Mixed Layer
[AD-A188348] 13 p1804 N88-20785
Wind forcing and observed oceanic wavenumber spectra 13 p1806 N88-20797
Energy and momentum fluxes through the sea surface
13 p1806 N88-20798
Hamiltonian description of the interaction of surface waves with mixed-layer currents
13 p1806 N88-20799
Evaluation of wave calculations using GONO in the period October 1985 - April 1986
[KNMI-TR-96] 13 p1807 N88-20804
Study of the dynamic topography of oceans by means of satellite altimetry 14 p1938 N88-21567
Climatological data of the Netherlands lightvessels over the period 1949-1980 --- North Sea
[KNMI-WR-87-9] 14 p1947 N88-21613
An improved wind input source term for third generation ocean wave modeling
[KNMI-WR-87-8] 14 p1950 N88-21624
Investigation of the imaging of ocean surface waves using a synthetic aperture radar
[SER-A-WISS-ABHANDL-84] 16 p2236 N88-23357
Research in nonlinear wave motion
[AD-A191686] 18 p2509 N88-24884
Definition of long ocean wave slope for radar applications
[AD-A193198] 21 p2933 N88-27412
Research on ocean forecasting and nonlinear wave propagation and numerical hydrodynamics in the ocean
[AD-A193363] 21 p2976 N88-27680
Nonlinear surface and internal waves on shear flow
[PREPRINT-584] 22 p3129 N88-28604
A singular perturbation analysis of the weakly nonlinear evolution of long and short water waves and waves in boundary layers 23 p3209 N88-29102
Mathematical problems of nonlinear wave propagation and of waves in heterogeneous media
[AD-A195970] 24 p3368 N88-30057
Impact force as a part of the total breaking wave force on a vertical cylinder
[RR-CE78] 24 p3384 N88-30154
A study of the feasibility of using sea and wind information from the ERS-1 satellite. Part 2: Use of scatterometer and altimeter data in wave modeling and assimilation
[ESA-CR(P)-2604-PT-2] 24 p3387 N88-30176
Analysis of environmental parameters from the Panama City tower radar experiment
[AD-A194994] 24 p3404 N88-30264

WATERFOWL
The suspended Japanese quail as an animal model for experiments related to microgravity
12 p1662 N88-19960

WATERPROOFING
Water disbondment characterization of organic Coating/metal substrate systems
[AD-A184847] 05 p0567 N88-13454
Improvement of the construction of protective clothing for better wearability and comfort — rainwear
[IZF-1986-26] 07 p0899 N88-15448

WATERSHEDS
Surface hydrology, sediment transport dynamics and remote sensing of disturbed watersheds in a humid temperate region
[DE88-008719] 20 p2817 N88-26715

WATERWAVE ENERGY
Survey on utility technology of a tidal and ocean current energy
[DE88-770148] 20 p2819 N88-26722

WATERWAVE ENERGY CONVERSION
Ocean, Wave, and Tidal Energy Systems: Current abstracts
[DE88-008299] 19 p2687 N88-25973

WATTMETERS
NBS (National Bureau of Standards) wideband sampling wattmeter
[PB87-210324] 03 p0323 N88-12041

WAVE AMPLIFICATION
Production-process CO2 laser with amplified pulse-repetition operation 06 p0771 N88-14739
Performance of linear vertical antenna in refractive multimode waveguide 08 p1076 N88-16489
Simulation and modeling of whistler mode wave growth through cyclotron resonance with energetic electrons in the magnetosphere 10 p1353 N88-18089

WAVE ATTENUATION
NT ACOUSTIC ATTENUATION
NT RADIO ATTENUATION
NT SHOCK WAVE ATTENUATION
Influence of surfactants on damping of gravity-capillary waves. 1: Frequency dependence
04 p0459 N88-12843
Experimental studies on acoustic emission monitoring of crack propagation in offshore structures: A literature survey 05 p0610 N88-13748
Imaging subtle microstructural variations in ceramics with precision ultrasonic velocity and attenuation measurements
[NASA-TM-100129] 07 p0867 N88-15257
Radar reflectivity and attenuation of radio waves in the melting layer of precipitation
[PB88-121553] 10 p1318 N88-17882
Numerical studies of propagation of Lg waves across ocean continent boundaries using the Representation Theorem (RT) 10 p1353 N88-18085
Regional wave attenuation and seismic moment from the inversion of NORESS spectra
[AD-A187399] 11 p1510 N88-19023
Investigation of constrained-layer technique using exact elasticity theory
[AD-A188664] 12 p1636 N88-19795
Attenuated direct and scattered wave propagation on simulated land mobile satellite service paths in the presence of trees 19 p2645 N88-25695

WAVE DEGRADATION
Aircraft field degradation and electromagnetic compatibility
[PB88-183975] 19 p2602 N88-25456

WAVE DIFFRACTION
Observation of instabilities in time during dynamic self-diffraction of light in anisotropic nonhomogeneous medium 06 p0769 N88-14730
New description of Lau effect based on theory of raster image forming process 06 p0772 N88-14744
Diffraction of sound at junction of two waveguides 08 p1076 N88-16491
Plane wave diffraction by a thin dielectric wedge [RSRE-MEMO-4045] 09 p1153 N88-16912
Calculation of noise in spatial speckle-field holograms under conditions of saturated photoresponse 09 p1235 N88-17403
VHF/UHF propagation by diffraction: Calculation by numerical integration 12 p1615 N88-19659
A diffraction based theoretical model for prediction of UHF path loss in cities 12 p1616 N88-19661
Complex space monofilar approximation of diffraction currents on a conducting half plane [NASA-CR-182883] 16 p2273 N88-23605
Diffraction by a simple deep phase object --- integrated circuit measurement [RSRE-MEMO-4039] 22 p3070 N88-28224
WAVE DISPERSION
Method for single-shot measurement of picosecond laser pulse-lengths without electronic time dispersion [DE87-013171] 02 p0178 N88-11107
Dispersion equation for plane capillary-gravity wave on free surface of viscous incompressible fluid 04 p0459 N88-12842
Effect of plasma resonance on properties of surface waves 06 p0773 N88-14749
Geometric structure, pseudoband gaps, and surface vibrational resonances on metal surfaces [AD-A187001] 09 p1143 N88-16851
Betatron oscillations in a free electron laser [DE88-004859] 10 p1337 N88-17990
Slow waves in waveguide with elliptical cross section [DE88-700159] 13 p1757 N88-20508
Basic physics of laser-plasma interactions [ETN-88-92055] 14 p1984 N88-21838
Range determination of pulsars, taking into account H2 regions [ETN-88-91492] 14 p1993 N88-21877
Plasma wave radiative damping of a new type in a relativistic one-dimensional plasma [DE88-701191] 15 p2135 N88-22739
Beam waves in random inhomogeneous media [DE88-701631] 16 p2190 N88-23058
Dispersive spectral apparatus 16 p2271 N88-23587
Numerical research of dispersion properties of plasma cylindrical waveguides located in magnetic field [DE87-703009] 16 p2275 N88-23615
Elastic wave dispersion in laminated composite plate [AD-A192289] 23 p3188 N88-28967
Wide band gyrotron traveling wave amplifier analysis [AD-A194269] 23 p3216 N88-29139
Kinetic theory for electrostatic waves due to transverse velocity shears [AD-A193404] 23 p3284 N88-29557
WAVE DRAG
NT INTERFERENCE DRAG
WAVE EQUATIONS
NT DIRAC EQUATION
NT EIKONAL EQUATION
NT KORTEWEG-DEVRIES EQUATION
NT SCHROEDINGER EQUATION
Inhomogeneous conditions at open boundaries for wave propagation problems [AD-A183847] 01 p0033 N88-10214
The polarization field for pulsed Raman transitions [DE87-013118] 01 p0035 N88-10227
An asymptotic theory for a class of initial-boundary value problems for weakly nonlinear wave equations with an application to a model of the galloping oscillations of overhead transmission lines [REPT-87-12] 01 p0086 N88-10556
Different ways of looking at the electromagnetic vacuum [DE87-013150] 01 p0089 N88-10584
Fundamentals of numerical magnetohydrodynamics [DE87-011769] 01 p0100 N88-10656
Large-aperture high-efficiency frequency doubling using tandem KDP crystals 03 p0301 N88-11894
Four-wave mixing used in optical amplitude encoding 03 p0376 N88-12366
Pulse-mode expansions and refractive indices in plane-wave propagation [DE88-001328] 04 p0437 N88-12714
On the wave excitation in the turbulent meteor trace 06 p0737 N88-14530
Coherence, propagation and fluctuations of light: A generalized ray approach [DE88-001669] 06 p0780 N88-14786
Statistical analyses of measured directional wave and current data [PB87-144523] 07 p0853 N88-15185
Equation of acoustic and gravitational waves in stratified moving medium 08 p1077 N88-16493
Equation of gravitational-gyroscopic waves: Angular potential and its applications 08 p1079 N88-16504
FOR3D: A computer model for solving the LSS (Lee-Saad-Schultz) three-dimensional, wide angle wave equation [AD-A186649] 08 p1080 N88-16511
Relation of wave energy and momentum with the plasma dispersion relation in an inhomogeneous plasma [DE88-002305] 08 p1084 N88-16530
Exact image principle in electromagnetic field computation [EL-57] 09 p1153 N88-16907
A project to experimentally and theoretically examine fluid interfacial wave phenomena in a rotating cylindrical geometry: Current results and future plans [DE88-003738] 09 p1165 N88-16984
Feedback stabilization of distributed systems [AD-A187111] 09 p1222 N88-17328
Note on boundary stabilization of wave equations [AD-A187113] 09 p1227 N88-17348
Analiticity in fourth order wave equations [DE88-700837] 12 p1686 N88-20080
A finite-amplitude analysis of the buoyant instability of a highly viscous film over a less viscous half-space 13 p1769 N88-20581
WKB theory of wave tunneling for Hermitian vector systems of integral equations [DE88-005332] 13 p1831 N88-20951
High speed transcendental elementary function architecture in support of the Vector Wave Equation (VWE) [AD-A189746] 15 p2119 N88-22627
Pointwise stabilization for coupled quasilinear and linear wave equations [AD-A190031] 15 p2120 N88-22632
Effects of randomness of parameters on mean wave propagation in a viscoelastic medium [REPT-87-60] 16 p2206 N88-23166
Nonlinear wave and diffusion equations [AD-A191421] 16 p2265 N88-23544
Asymptotics for a system of nonlinearly coupled wave equations with an application to the galloping oscillations of overhead transmission lines [REPT-87-78] 17 p2348 N88-23991
Nonlinear waves [AD-A192148] 18 p2510 N88-24889
MHD bending waves in a current sheet [NASA-TM-101149] 18 p2579 N88-25323
High spatial frequency thermal blooming instability: A linear stability analysis [DE88-010711] 20 p2807 N88-26655
Propagation of inernio-acoustic gravity waves in a rotating and radiating opaque atmosphere [DE88-701866] 20 p2823 N88-26750
Wave equations for pulse propagation [DE88-011760] 21 p2954 N88-27548
Research on ocean forecasting and nonlinear wave propagation and numerical hydrodynamics in the ocean [AD-A193363] 21 p2976 N88-27680
A numerical treatment of the fluid/elastic interface under range-dependent environments [AD-A192476] 21 p3005 N88-27821
Initial boundary value problems of nonlinear wave equations in an exterior domain [DE88-701883] 21 p3026 N88-27962
The construction of implicit and explicit solitary wave solutions of nonlinear partial differential equations [AD-A193475] 23 p3269 N88-29452
Solution of large order Fourier-Bessel equations [ARE-TM(UHA)-88504] 23 p3272 N88-29475
WAVE EXCITATION
NT ACOUSTIC EXCITATION
NT HARMONIC EXCITATION
Self-consistent modification of a fast tail distribution by resonant fields in nonuniform plasmas [AD-A183790] 01 p0099 N88-10650
Ultrafast intrinsic bistable devices [PB87-109310] 05 p0649 N88-13978
Lg wave excitation and propagation in the presence of one-, two-, and three-dimensional heterogeneities [AD-A187364] 11 p1510 N88-19022
Beam waves in random inhomogeneous media [DE88-701631] 16 p2190 N88-23058
Heating efficiency of beat wave excitation in a density gradient [AD-A193066] 21 p3017 N88-27905
Three-dimensional vortex interactions [AD-A194066] 23 p3172 N88-28889
WAVE FRONT DEFORMATION
Wavefront error sensing [NASA-CR-181504] 03 p0321 N88-12030
Calculation of the spatial-temporal deformation of laser pulses in multiple scattering [MBB-Z-111/87] 10 p1311 N88-17837
WAVE FRONT RECONSTRUCTION
Stationary reconstruction method. Development, test and comparison in ultrasonic testing [REPT-860125-TW] 01 p0057 N88-10368
Lasers with wavefront-reversing mirrors (review article) 06 p0709 N88-14349
Holographic phase correction [RSRE-MEMO-4036] 09 p1167 N88-17000
Reconstruction of wave distribution functions in warm plasmas [IRF-PREPRINT-104] 24 p3431 N88-30422
WAVE FRONTS
NT SHOCK FRONTS
Thermo-optical modeling of flashlamp-pumped zig-zag slabs [DE87-011878] 01 p0051 N88-10326
Fronts propagating with curvature dependent speed: Algorithms based on Hamilton-Jacobi formulations [NASA-CR-178382] 01 p0077 N88-10495
Analytical caustic surfaces [NASA-TM-87805] 02 p0168 N88-11060
Nonconventional optical techniques for optical wavefront processing [AD-A185099] 05 p0650 N88-13982
Compensation of small-scale phase distortions by means of a Fourier phase corrector 06 p0708 N88-14345
On connection between evolution of troposphere fronts and changes of circulation regime in meteor zone 06 p0735 N88-14519
A raytrace method for a laterally heterogeneous environment [AD-A186525] 08 p0978 N88-15912
Color shadow methods of analyzing reconstructed wave front 09 p1236 N88-17407
Theoretical investigation of the wave shaping process in a section of ladder fracture tape [MRL-R-1081] 13 p1771 N88-20595
Nonlinear optical phase conjugation techniques to reduce the physical size of lasers [AD-A196170] 24 p3379 N88-30122
WAVE FUNCTIONS
NT MOLECULAR ORBITALS
NT PAULI EXCLUSION PRINCIPLE
Local spectra and wave distribution functions --- space plasma [KGI-PREPRINT-099] 01 p0100 N88-10659
Asymptotics of the effective potentials and wave functions of a three-body problem in suitable coordinates [DE87-703323] 03 p0370 N88-12326
The finite element method for electronic structure [DE88-001708] 04 p0485 N88-12989
Final (n,l) state-resolved electron capture by multiply charged ions from neutral atoms [IPPJ-AM-54] 04 p0492 N88-13030
Development of a new method of measuring the characteristic impedance and complex wave number of a porous acoustic material [AD-A185038] 05 p0646 N88-13957
Coherence, propagation and fluctuations of light: A generalized ray approach [DE88-001669] 06 p0780 N88-14786
Modified quantum mechanics of small composite systems [NIKHEF-H/87-1] 06 p0790 N88-14845
Wave functions for bound states of relativistic electrons in a crystal at electron movement along crystallographic planes [DE88-700563] 07 p0939 N88-15708
On exact solutions of multidimensional Schroedinger equation with polynomial potentials [DE88-700460] 09 p1230 N88-17373
Surface and interface electronic structure [DE88-003363] 09 p1258 N88-17545
An overview of the transactional interpretation of quantum mechanics [DE88-004236] 10 p1423 N88-18497
Polarization of electrons in an electromagnetic wave field in the presence of magnetic field [DE88-700169] 13 p1757 N88-20509
WKB theory of wave tunneling for Hermitian vector systems of integral equations [DE88-005332] 13 p1831 N88-20951
Numerical simulations of multiphoton processes in many electron atoms [DE88-003293] 13 p1837 N88-20990
Dynamic and spectral properties of semiconductor lasers with quantum well, quantum wire, and quantum box structures 14 p1975 N88-21788
To the field theory with a fundamental mass [DE88-701159] 15 p2145 N88-22807

On 1/n-expansion and wave functions
[DE88-701639] 16 p2260 N88-23509
Quantum transport in an electron waveguide
20 p2864 N88-27010
To the twinning plane superconductivity theory
[DE88-702195] 20 p2874 N88-27058
Phenomenological approach to high T/sub c/ oxide superconductors
[DE88-701868] 20 p2876 N88-27074
Cosmic wavefunction with induced gravity
[DE88-701873] 20 p2884 N88-27129
Passage of relativistic magnetic dipole moments through magnetic fields
[DE88-702640] 23 p3295 N88-29624

WAVE GENERATION
The generation of nearly isotropic turbulence by means of grids
[PNR90411] 02 p0172 N88-11084
Magnetic flux tubes as sources of wave generation
04 p0505 N88-13108
HF sidebands in the ionosphere
05 p0574 N88-13497
A study of the mechanism of internal gravity wave generation by quasigeostrophic meteorological motions
06 p0735 N88-14520
Study of internal gravity waves in the meteor zone
06 p0735 N88-14521
Far field of steady waves produced by local perturbation sources in stream of stratified fluid
06 p0771 N88-14736
Dependence of acoustical characteristics of laser-induced breakdown in dielectric materials on shape of inelastic region 06 p0774 N88-14753
High repetition rate electron beam RF-acceleration and sub-millimeter wave generation via a free electron laser
[AD-A186066] 07 p0858 N88-15209
Microwave tubes: Literature study no. 8 comprising the year 1986
[FOA-C-30467-3] 09 p1159 N88-16944
Theoretical investigation of EM wave generation and radiation in the ULF, ELF and VLF bands by the electrodynamic orbiting tether
[NASA-CR-182720] 13 p1760 N88-20529
Nonlinear acoustic parameter and its application in ultrasonic imaging 14 p1902 N88-21364
Millimeter wave generation by relativistic electron beams
[AD-A195683] 24 p3362 N88-30016

WAVE INTERACTION
NT SHOCK WAVE INTERACTION
Generation of IR stimulated radiation, UV visible violet coherent radiation by two-photon resonance pumping in K vapor 03 p0301 N88-11892
Breaking wave forces on vertical cylinders
[RR-CE71] 03 p0338 N88-12126
Numerical experiments with hypersonic flows beneath a cone-delta-wing combination 05 p0532 N88-13238
Computation of flow past conical hypersonic wings using a second order Godunov method
05 p0533 N88-13241
On the interconnection of dynamic processes in the lower thermosphere with meteorological phenomena in the tropostratosphere 06 p0734 N88-14512
Simulation of effect on biological systems of impact wave from heavy charged particle track
07 p0896 N88-15429
Interaction of acoustic and electromagnetic waves involved in anomalous skin effect
08 p1079 N88-16503
Studies of nonlinear and chaotic phenomena in solid state systems
[DE88-002330] 09 p1254 N88-17515
Universal power spectra for wave turbulence: Applications to wind waves, flicker noise, solar wind spectrum and classical second sound
10 p1318 N88-17879
On the interaction of Tollmein-Schlichting waves in axisymmetric supersonic flows
[NASA-CR-181619] 10 p1331 N88-17955
Velocity measurements in a 3D (three dimensional) shock wave laminar boundary layer interaction
[AD-A187334] 10 p1332 N88-17959
Flow/acoustic interaction in duct inflow
[AD-A189264] 13 p1833 N88-20967
Wave interactions in a three-dimensional attachment line boundary layer
[NASA-CR-181653] 14 p1910 N88-21414
Three-wave parametric resonance in plasma of relativistic electron flux 14 p1972 N88-21772
Basic physics of laser-plasma interactions
[ETN-88-92055] 14 p1984 N88-21838
Nonlinear wave interactions in swept wing flows
[NASA-CR-4142] 16 p2206 N88-23160
Interaction of solitons in single model optical fibres
17 p2439 N88-24511
Electron-Rayleigh wave interaction in thin film carbons
[AD-A191727] 18 p2492 N88-24781
Guided wave interactions in millimeter-wave integrated circuits
[AD-A193017] 21 p2936 N88-27437
Interactions between air and ground sound at the Earth surface 22 p3149 N88-28733
Three-dimensional vortex interactions
[AD-A194066] 23 p3172 N88-28889
Interactions between synoptic and planetary scales of motion
[AD-A192328] 23 p3234 N88-29246
On the degenerate Ferrari-Ibanez solution for colliding plane gravitational waves
[MATH-REPT-209] 23 p3296 N88-29630
Nonlinear Tollmien-Schlichting/vortex interaction in boundary layers
[NASA-CR-181698] 24 p3311 N88-29715
The strong nonlinear interaction of Tollmien-Schlichting waves and Taylor-Goertler vortices in curved channel flow
[NASA-CR-181697] 24 p3311 N88-29716
Light-millimeter wave interactions in semiconductor devices
[AD-A195898] 24 p3432 N88-30428

WAVE MOTION
U WAVES

WAVE OSCILLATORS
U OSCILLATORS

WAVE PACKETS
Wavepacket propagation and current startup near the lower hybrid frequency in the torus
[IPPJ-840] 02 p0242 N88-11529
Quantum mechanics with spontaneous localization and the quantum theory of measurement
[DE87-703072] 02 p0247 N88-11559
A strategy to determine the transition state of an electron transfer reaction
[AD-A183976] 03 p0382 N88-12404
Evolution of acoustic gravity wave packet in spatially and temporally varying wind 11 p1469 N88-18760

WAVE PROPAGATION
NT ACOUSTIC PROPAGATION
NT DIFFRACTION PROPAGATION
NT GROUND WAVE PROPAGATION
NT HALOS
NT IONOSPHERIC PROPAGATION
NT LIGHT SCATTERING
NT SCATTER PROPAGATION
NT SHOCK WAVE PROPAGATION
NT TRANSEQUATORIAL PROPAGATION
Inhomogeneous conditions at open boundaries for wave propagation problems
[AD-A183847] 01 p0033 N88-10214
The polarization field for pulsed Raman transitions
[DE87-013118] 01 p0035 N88-10227
Geoacoustic models of the Hudson Canyon area
[AD-A183535] 01 p0073 N88-10465
Finite difference solution of a generic differential equation
[PB87-205878] 01 p0087 N88-10568
Fast wave injection into high temperature tokamak plasmas in the lower-hybrid-density regime of JIPP T-IIU
[ISSN-0469-4732] 01 p0099 N88-10649
Propagating shocks in the corona
01 p0112 N88-10718
Direct Absorption Receiver flow experiments
[DE87-014655] 02 p0196 N88-11221
Evaluation of a scale-model experiment to investigate long-range acoustic propagation
[NASA-TP-2748] 02 p0230 N88-11450
Wavepacket propagation and current startup near the lower hybrid frequency in the torus
[IPPJ-840] 02 p0242 N88-11529
Method estimating integral mean value of enhancement factor and path latitude for whistlers below magnetic latitude 10 deg 03 p0300 N88-11885
Target strength: An overview of some recent theoretical developments 03 p0303 N88-11910
Uniform geometrical theory of diffraction
03 p0303 N88-11911
A new method for measuring waveguide propagation losses
[DE87-011305] 03 p0307 N88-11938
Coupling and absorption phenomena in semiconductor-clad dielectric optical waveguides
[DE87-013446] 03 p0307 N88-11939
The effect of ocean fluctuations on sound transmission in the ocean
[AD-A184382] 03 p0355 N88-12236
General theory of radio propagation through a stratified atmosphere
[PB87-226197] 04 p0430 N88-12662
Pulse-mode expansions and refractive indices in plane-wave propagation
[DE88-001328] 04 p0437 N88-12714
High resolution finite volume methods on arbitrary grids via wave propagation
[NASA-CR-178397] 04 p0484 N88-12979
Boundary effects on the drag of an oscillating sphere: Applications to the magnetic sphere rheometer. Attenuation and dispersion of acoustic waves in nematic liquid crystals 04 p0488 N88-13007
The acceleration of winds by MHD waves in open magnetic structures 04 p0506 N88-13109
The dynamics of solar magnetic flux tubes subjected to resonant foot point shaking 04 p0507 N88-13118
Vortex interaction with a leading-edge of finite thickness
[NASA-CR-182341] 05 p0543 N88-13307
Measured characteristics of 800/900 MHz mobile radio channels with high-angle propagation through moderately dense foliage
[CRC-1398] 05 p0573 N88-13493
An investigation of millimeter wave propagation in the atmosphere: Measurement program
[AD-A184837] 05 p0574 N88-13498
Damping analysis of flexural waves in fluid-loaded single and constrained plates
[AD-A185116] 05 p0609 N88-13739
Theoretical and practical aspects of the functional absorber method of arranging sound absorbing panels
[BBC-RD-1987/15] 05 p0646 N88-13955
Propagation effects on satellite systems at frequencies below 10 GHz: A handbook for satellite systems design
[NASA-RP-1108/2] 06 p0690 N88-14226
Electromagnetic scattering problem in the wave-vector-time domain
[PB88-106083] 06 p0694 N88-14263
Tidal activity in the meteor zone over Budrio, Italy
06 p0734 N88-14517
Study of internal gravity waves in the meteor zone
06 p0735 N88-14521
Numerical modeling of troposphere-induced gravity wave propagation 06 p0735 N88-14522
Mesoscale density variability in the mesosphere and thermosphere: Effects of vertical flow accelerations
06 p0736 N88-14529
On the wave excitation in the turbulent meteor trace
06 p0737 N88-14530
A critical review of measurements of water vapor absorption in the 840 to 1100 cm(-1) spectral region
[NASA-CR-182361] 06 p0742 N88-14565
Effect of plasma resonance on properties of surface waves 06 p0773 N88-14749
Waves and vibrations in elastic superlattice composites 06 p0776 N88-14765
Coherence, propagation and fluctuations of light: A generalized ray approach
[DE88-001669] 06 p0780 N88-14786
Analytical investigations of bulk wave resonators in the piezoelectric thin film on gallium-arsenide configuration
[AD-A185716] 06 p0789 N88-14840
Solar-geophysical data number 515, July 1987. Part 1: (Prompt reports). Data for June 1987, May 1987 and late data
[PB87-233177] 06 p0805 N88-14912
Wave propagation experiments on 22-bay lattice
[AD-A186140] 07 p0824 N88-15002
Cage mode propagation experiments
[AD-A186019] 07 p0841 N88-15100
Microsecond beam propagation in air
[DE88-002221] 07 p0845 N88-15127
TRACKER: A 3-D radio ray tracing code
[DE88-003267] 07 p0847 N88-15137
Chapter 2: Threshold for Raman conversion of FEL laser pulses in the atmosphere
[DE88-002470] 07 p0859 N88-15215
Propagation of radiation along a constricting optical waveguide 07 p0920 N88-15590
Sound pressure distribution in front of a serrated boundary: Standing wave suppression and diffusion
07 p0928 N88-15639
Upwind formulations for the Euler equations
08 p0984 N88-15952
Fully turbulent internal flow excitation of pipe systems
08 p1000 N88-16056
Solar cosmic ray propagation in high-velocity solar wind stream 08 p1002 N88-16073
Interpretation of equatorial current meter data as internal waves
[PB88-108113] 08 p1044 N88-16309
Approximation of noncorrelated reflections in problem of sound propagation through waveguide with rough boundary 08 p1076 N88-16487
Mode pattern of field generated by parametric radiator in acoustic waveguide 08 p1076 N88-16488
Acoustic field in waveguide with sloping bed
08 p1076 N88-16490
Relativistic electromagnetic waves in an electron-ion plasma
[NASA-CR-182421] 08 p1085 N88-16532

Computational analysis of propagation properties of integrated-optical waveguides using a domain integral equation
[PB87-163358] 09 p1154 N88-16917
Guide for the program EXACT-NL — wave growth
[KNMI-TR-94] 09 p1163 N88-16971
Induced turbulence in aerosol-loaded atmospheres, Jun. 1987
[DE87-014724] 09 p1192 N88-17141
Attenuation of ultrasonic waves in nonmagnetized magnetic fluids 09 p1234 N88-17398
Propagation of creep waves around rough cylindrical surface 09 p1234 N88-17400
Parametric interaction of optical modes in fiber-optic light guide 09 p1235 N88-17406
Statistics of breakdown centers appearing during propagation of laser radiation through turbulent atmosphere 09 p1236 N88-17411
Flame propagation in the approximation of straight-line trajectories of burning products
[DE88-700675] 10 p1297 N88-17756
Diffusion description of flame propagation due to the translational motion of burning reaction products
[DE88-700676] 10 p1297 N88-17757
Time domain wave propagation in multilayered integrated circuits
[AD-A187462] 10 p1324 N88-17916
Numerical studies of propagation of Lg waves across ocean continent boundaries using the Representation Theorem (RT) 10 p1353 N88-18085
Simulation and modeling of whistler mode wave growth through cyclotron resonance with energetic electrons in the magnetosphere 10 p1353 N88-18089
Evolution of acoustic gravity wave packet in spatially and temporally varying wind 11 p1469 N88-18760
Research and development of surface skimming bulk wave devices for sensor applications
[AD-A187504] 11 p1470 N88-18766
Numerical simulation of the propagation and absorption due to air breakdown of long microwave pulses
[DE88-005227] 11 p1475 N88-18798
Unsteady heat transfer in turbine blade ducts: Focus on combustor sources
[NASA-TM-100815] 11 p1486 N88-18870
Applications and limitations of the spectral-analysis-of-surface-waves method
[PB88-136619] 11 p1513 N88-19038
Coherent VUV source at 130 nm: Theory and modeling
[DE88-003874] 11 p1549 N88-19269
Wave propagation in laminated composite plates
[AD-A188999] 12 p1604 N88-19594
Ultrasonic-velocity studies of composite and heterogeneous materials
[AD-A189000] 12 p1604 N88-19595
Terrestrial Propagation Characteristics in Modern Systems of Communications, Surveillance, Guidance and Control
[AGARD-CP-407] 12 p1614 N88-19653
An investigation of terrain related variables for predicting the multipath fade depth distribution on terrestrial microwave lines 12 p1615 N88-19654
A review of the role of surface reflection in multipath propagation over terrestrial microwave links 12 p1615 N88-19655
Development of a ground-conductivity map for the area of the Federal Republic of Germany from measured field-strength contours 12 p1615 N88-19656
Propagation in longitudinally varying ducts, with emphasis on guiding to antiguiding transitions 12 p1615 N88-19658
VHF/UHF propagation by diffraction: Calculation by numerical integration 12 p1615 N88-19659
Mono- and bistatic radar coverage diagrams including diffractive wave propagation 12 p1616 N88-19660
A program for the calculation of radio-wave transmission loss over the spherical earth and over obstacles 12 p1616 N88-19662
A propagation campaign in a marine environment utilizing a digital system at 36 GHz 12 p1618 N88-19675
Two-dimensional electron fluid computer calculations of nanosecond pulse, low pressure microwave air breakdown in a rectangular waveguide and their verification by experimental measurement
[DE88-004407] 12 p1618 N88-19678
Historical electromagnetic propagation condition database description
[AD-A189157] 12 p1621 N88-19695
Electromagnetic propagation in PEC and absorbing curved S-ducts
[NASA-TM-100833] 12 p1621 N88-19698
The temporal and spatial acoustical response of a point-driven fluid-loaded plate
[AD-A188504] 12 p1636 N88-19794
Dynamical and photometric studies of Saturn's rings 12 p1711 N88-20241
Slow waves in waveguide with elliptical cross section
[DE88-700159] 13 p1757 N88-20508
Detonation velocity of the hydrazinum nitrate-hydrazine water system
[NASA-TT-20213] 13 p1770 N88-20590
Numerical modeling of wave migration of seismic data 13 p1786 N88-20684
Invariant characteristics of acoustic field in stratified ocean 13 p1788 N88-20698
Ultrasonic physical modeling of seismic wave propagation from graben-like structures
[AD-A189066] 13 p1796 N88-20744
Method for determination of the wind velocity and direction
[NASA-TT-20233] 13 p1802 N88-20769
MASPLT: A one-dimensional graphics post processor for wave propagation codes
[DE88-005506] 13 p1817 N88-20856
HISPLT: A history graphics post processor for wave propagation codes
[DE88-005507] 13 p1817 N88-20857
CSQPLT: A graphics post processor for multidimensional wave propagation codes
[DE88-005508] 13 p1817 N88-20858
Mathematical models of sound waves in fluids
[AD-A189270] 13 p1834 N88-20988
Method for determining artillery position
[NASA-TT-20238] 13 p1834 N88-20973
Nonlinear acoustic parameter and its application in ultrasonic imaging 14 p1902 N88-21364
Numerical modeling of divergent detonation wave 14 p1903 N88-21373
Millimeter-wave properties of the atmosphere: Laboratory studies and propagation modeling
[PB88-164215] 14 p1905 N88-21387
An improved wind input source term for third generation ocean wave modeling
[KNMI-WR-87-8] 14 p1950 N88-21624
AGARD Highlights 88/1 14 p2012 N88-22001
Wave propagation and dynamics of lattice structures
[AD-A190037] 15 p2025 N88-22066
Wave propagation and dynamics of lattice structures
[AD-A190611] 15 p2025 N88-22069
Numerical and experimental research on propagation of elastic stress waves in conical shell under axial impulsive loading 15 p2053 N88-22238
Wave energy flow conservation for propagation in inhomogeneous Vlasov-Maxwell equilibria
[DE88-006705] 15 p2055 N88-22251
Generation and propagation of sound waves in a collapsing or anti-collapsing star with uniform density
[DE87-703034] 15 p2151 N88-22839
Propagation of acoustic gravity wave spectrum through vertical wind shear region 16 p2186 N88-23035
Beam waves in random inhomogeneous media
[DE88-701631] 16 p2190 N88-23058
Effects of randomness of parameters on mean wave propagation in a viscoelastic medium
[REPT-87-60] 16 p2206 N88-23166
Acousto-ultrasonic input-output characterization of unidirectional fiber composite plate by SV waves
[NASA-CR-4152] 16 p2217 N88-23224
Numerical simulation for particle acceleration and trapping by an electromagnetic wave 16 p2277 N88-23626
Microinstabilities in ion beam propagation 16 p2277 N88-23631
Investigation of intensity and phase fluctuations of an acoustic wave after crossing thermal turbulence
[ETN-88-92542] 17 p2395 N88-24238
Wave growth associated with turbulent spots in plane Poiseuille flow
[FFA-TN-1988-08] 18 p2457 N88-24587
Nonlinear wave propagation
[AD-A192104] 18 p2501 N88-24835
Research in nonlinear wave motion
[AD-A191686] 18 p2509 N88-24884
Nonlinear waves
[AD-A192148] 18 p2510 N88-24889
Atmospheric propagation of laser beams
[AD-A191447] 18 p2520 N88-24952
Evaluation of the biot coefficients
[AD-A191643] 18 p2570 N88-25265
Light propagation through gravitationally perturbed Friedmann universes 18 p2577 N88-25307
Numerical investigation of acoustic energy exchange through flow turning 19 p2629 N88-25593
On the propagating speed in difference approximations for conservation laws 19 p2639 N88-25658
Propagation effects by roadside trees measured at UHF and L-band for mobile satellite systems 19 p2644 N88-25693
Propagation modeling for land mobile satellite systems 19 p2645 N88-25694
Attenuated direct and scattered wave propagation on simulated land mobile satellite service paths in the presence of trees 19 p2645 N88-25695
Mobile satellite propagation measurements and modeling: A review of results for systems engineers 19 p2645 N88-25696
Propagation measurements for an Australian land mobile satellite system 19 p2645 N88-25697
Propagation effects on spread-spectrum mobile satellite systems 19 p2645 N88-25699
Mobilestar field test program 19 p2646 N88-25707
Electro-optic sampling of high-speed, InP-based integrated circuits 19 p2655 N88-25769
Multigigahertz logic based on InP-MISFET's exhibiting extremely high transconductance 19 p2656 N88-25771
Acousto-ultrasonic input-output characterization of unidirectional fiber composite plate by P waves
[NASA-CR-4162] 19 p2678 N88-25923
Propagation of linear gravity waves in a relativistic atmosphere
[DE88-702062] 19 p2691 N88-25995
Proceedings of the Array Signal Processing Symposium: Treaty Verification Program
[DE88-008346] 20 p2790 N88-26548
Variational analysis of dielectrically loaded multidepth corrugated waveguides
[PB88-193602] 20 p2793 N88-26573
Wave propagation in locally isotropic turbulent medium with smoothly changing characteristics
[NASA-TT-20312] 20 p2800 N88-26617
The propagation of irradiance moments of an aberrated, apodized FEL beam
[DE88-008972] 20 p2806 N88-26648
Propagation of inernio-acoustic gravity waves in a rotating and radiating opaque atmosphere
[DE88-701866] 20 p2823 N88-26750
Westward moving atmospheric wave disturbances over the African tropics: Dynamic and energetic aspects
[MITT-57] 20 p2827 N88-26774
XDATAP
[DE88-007161] 20 p2837 N88-26827
On the self-focusing of electric helicons
[DE88-701870] 20 p2848 N88-26905
An evaluation of two millimeter wave propagation models for horizontal atmospheric attenuation at 70-115 GHZ
[AD-A192699] 21 p2931 N88-27403
User's manual for C-HEMP: A two-dimensional wave propagation code. Volume 1: Description and derivations of the code
[AD-A193197] 21 p2944 N88-27486
Simulation and analysis of wave propagation through random media 21 p2947 N88-27503
Wave equations for pulse propagation
[DE88-011760] 21 p2954 N88-27548
On the small signal gain of free electron lasers in the low-current regime
[DFVLR-FB-88-10] 21 p2955 N88-27552
Research on ocean forecasting and nonlinear wave propagation and numerical hydrodynamics in the ocean
[AD-A193363] 21 p2976 N88-27680
Ion Bernstein modes in current-carrying plasmas 21 p3017 N88-27903
Magnetohydrodynamic wave propagation in the solar wind
[DE88-702411] 21 p3032 N88-27995
Wave propagation and vibration of fibre reinforced laminates
[AD-A194144] 22 p3051 N88-28101
Rapid-scanning Fourier transform spectrometer for studies of propagation of near-millimeter-wave radiation through clear air and fog
[AD-A193752] 22 p3070 N88-28219
Activities report of the Electromagnetic Environment Division
[FOA-C-30484-3.2/3.3/4.1/4.2] 22 p3071 N88-28233
Time domain wave propagation in multilayered integrated circuits
[AD-A193821] 22 p3073 N88-28241
Nonlinear surface and internal waves on shear flow
[PREPRINT-584] 22 p3129 N88-28604
Wave structures in thermospheric density from satellite electrostatic triaxial accelerometer measurements
[AD-A194134] 23 p3233 N88-29240
The acoustic field scattered from some approximate pressure release materials
[AD-A194768] 23 p3278 N88-29515
Waves and instabilities in an electron-positron plasma in an ultra-strong magnetic field 23 p3283 N88-29551
Plasmoid propagation
[AD-A192378] 23 p3284 N88-29555
Wave propagation and remote sensing 24 p3364 N88-30029

Mathematical problems of nonlinear wave propagation and of waves in heterogeneous media
[AD-A195970] 24 p3368 N88-30057
Determination of the specific area of liquid gas and the velocity of weak pressure waves in aqueous foams
[NASA-TT-20347] 24 p3373 N88-30087
Rossby waves in mid-latitude oceans
24 p3405 N88-30273
Consideration of plasma opening switches from a wave propagation perspective
[AD-A195681] 24 p3431 N88-30421
Experimental proof of quasilongitudinal propagation of low-frequency waves in middle latitudes in upper ionosphere 24 p3447 N88-30516

WAVE RADIATION
U ELECTROMAGNETIC RADIATION

WAVE REFLECTION
NT MACH REFLECTION
Multichannel deconvolution of P waves at seismic arrays and three component stations
[AD-A184450] 04 p0467 N88-12888
Nonlinear reflection of sound wave in gas mixture
06 p0769 N88-14728
Approximation of noncorrelated reflections in problem of sound propagation through waveguide with rough boundary 08 p1076 N88-16487
Comparison of the rough surface reflection coefficient with specularly scattered acoustic data
[AD-A187086] 09 p1242 N88-17444
A review of the role of surface reflection in multipath propagation over terrestrial microwave links
12 p1615 N88-19655
Correcting ray field failures caused by focusing in an inhomogeneous duct: A critical look at the Gaussian beam method 12 p1616 N88-19663
A propagation campaign in a marine environment utilizing a digital system at 36 GHz 12 p1618 N88-19675
Input-output characterization of fiber composites by SH waves
[NASA-CR-4153] 17 p2347 N88-23986
Reflection of sound in open ended ducts
[PB88-103478] 21 p3012 N88-27870
Electromagnetic wave incoherent reflection by a half-space of weakly-ionized plasma with an absorbing boundary
[DE88-702413] 21 p3019 N88-27917
Wave and fracture phenomena in impacted ceramics
[AD-A192946] 23 p3196 N88-29020

WAVE SCATTERING
NT ACOUSTIC SCATTERING
NT ATMOSPHERIC SCATTERING
NT ELECTROMAGNETIC SCATTERING
NT HALOS
NT LIGHT SCATTERING
NT MICROWAVE SCATTERING
NT MIE SCATTERING
NT RAMAN SPECTRA
NT RAYLEIGH SCATTERING
NT REVERBERATION
NT THOMSON SCATTERING
NT TROPOSPHERIC SCATTERING
NT X RAY SCATTERING
Parametrization in scattering models
03 p0304 N88-11916
Acoustic field in waveguide with sloping bed
08 p1076 N88-16490
Scattering of longitudinal wave normally incident on discal cavity in elastic body 08 p1077 N88-16492
Backscatter from flaws in fiber-reinforced composites
11 p1450 N88-18639
Lg wave excitation and propagation in the presence of one-, two-, and three-dimensional heterogeneities
[AD-A187364] 11 p1510 N88-19022
An efficient numerical algorithm for solving scattering and inverse scattering problems of electromagnetic waves
[AD-A188479] 12 p1619 N88-19684
Three-dimensional scattering of impulsive acoustic waves by a semi-infinite crack in the plane interface of a half space and a layer
[PB88-146998] 12 p1687 N88-20089
Transport and stability properties of free shear flows
13 p1768 N88-20577
Multiple scattering of waves in discrete random media
[AD-A191068] 18 p2499 N88-24823
Attenuated direct and scattered wave propagation on simulated land mobile satellite service paths in the presence of trees 19 p2645 N88-25695
Mobile satellite propagation measurements and modeling: A review of results for systems engineers
19 p2645 N88-25696
Staggered-grid finite element solution technique for the Maxwell's equations in the time domain
[DE88-011731] 21 p3007 N88-27838
Electromagnetic wave incoherent reflection by a half-space of weakly-ionized plasma with an absorbing boundary
[DE88-702413] 21 p3019 N88-27917
Mathematical problems of nonlinear wave propagation and of waves in heterogeneous media
[AD-A195970] 24 p3368 N88-30057

WAVEFORMS
NT PULSE AMPLITUDE
NT PULSE DURATION
NT SQUARE WAVES
Recording multiple signals on a single waveform recorder
[DE87-011632] 01 p0049 N88-10313
Computational methods and software for differential equations and their applications
[DE87-014601] 02 p0226 N88-11424
Experimental and analytic studies of the triggered lightning environment of the F106B
[NASA-CR-4104] 04 p0469 N88-12897
High frequency periodic time domain waveform measurement system
[PB87-225256] 06 p0695 N88-14264
Waveform for short-dwell-time meteorological Doppler radars
[PB88-102199] 07 p0845 N88-15126
Digital control of high frequency pulse-width modulated inverters
[ETN-87-90711] 09 p1157 N88-16936
Air gap testing using Trailing Wire Antenna (TWA) waveform
[AD-A187639] 11 p1477 N88-18812
Distortion of wideband carbon dioxide laser radar waveforms due to atmospheric dispersion and absorption
[AD-A188687] 12 p1632 N88-19771
MOSFET performance degradation due to hot carriers
13 p1848 N88-21063
Electron device probing in the femtosecond time scale
19 p2660 N88-25821
Time-Optimal Adaptive Shaped Torque (TOAST) technical note
[AD-A192719] 20 p2843 N88-26869
A numerically efficient digital matched filter for periodic and windowed periodic radar waveforms
[AD-A193132] 21 p2932 N88-27410
Picosecond optoelectronic sampling of electrical waveforms produced by an optically excited field effect transistor
[AD-A192384] 21 p2935 N88-27428
A deconvolution technique using least-squares model-fitting and its application to optical pulse measurement
[NPL-DES-87] 22 p3144 N88-28694
Effect of phase errors in stepped-frequency radar systems
[AD-A194476] 23 p3203 N88-29061
The 1983 direct strike lightning data, part 1
[NASA-TM-86426-PT-1] 23 p3237 N88-29259
The 1983 direct strike lightning data, part 2
[NASA-TM-86426-PT-2] 23 p3237 N88-29260
The 1983 direct strike lightning data, part 3
[NASA-TM-86426-PT-3] 23 p3237 N88-29261
Waveform analysis on the IBM PC
[AD-A194249] 23 p3248 N88-29330
Wigner distribution function: Relation to short-term spectral estimation, smoothing and performance in noise
[AD-A193865] 23 p3275 N88-29492
Waveform relaxation applied to transient device simulation
[AD-A194992] 24 p3432 N88-30429

WAVEGUIDE ANTENNAS
The wavenumber: An alternative to the directional coupler for multimode analysis in oversized waveguides
[IPF-87-2] 01 p0037 N88-10237
Current-drive on the Versator-2 tokamak with a slotted-waveguide fast-wave coupler
[DE88-006261] 15 p2136 N88-22743
Investigation of radiating and guiding structures in microstrip patch antennas
[AD-A191445] 16 p2193 N88-23082

WAVEGUIDE FILTERS
A study of scattering from E-plane circuit elements
[AD-A184473] 04 p0431 N88-12673

WAVEGUIDE LASERS
Investigation of BN CO2 wave guide laser
03 p0302 N88-11905
High power phased array and tailored gain semiconductor lasers 03 p0329 N88-12078
Coupled high power waveguide laser research
[AD-A189800] 15 p2071 N88-22345
Efficient narrow linewidth waveguide dye laser pumped by CuCl laser 16 p2187 N88-23038
UV-Laser reactions of molecular adsorbates
[AD-A190796] 16 p2212 N88-23201
Distributed feedback lasers
[NASA-CR-4154] 18 p2520 N88-24948

WAVEGUIDES
NT BEAM WAVEGUIDES
NT CIRCULAR WAVEGUIDES
NT OPTICAL FIBERS
NT OPTICAL WAVEGUIDES
NT PLASMAGUIDES
NT RECTANGULAR WAVEGUIDES
The wavenumber: An alternative to the directional coupler for multimode analysis in oversized waveguides
[IPF-87-2] 01 p0037 N88-10237
Design and analysis of a broadband TM(sub 01) mode generator in cylindrical waveguide
[DE87-011308] 01 p0038 N88-10243
Generalized coupled-mode equations, applications to fiber couplers 03 p0298 N88-11875
Coupling and absorption phenomena in semiconductor-clad dielectric optical waveguides
[DE87-013446] 03 p0307 N88-11939
Eigenmode analysis of parallel waveguide couplers
[PB87-132122] 06 p0693 N88-14254
ATF (Advanced Toroidal Facility) ECH (Electron Cyclotron Heating) waveguide component development and testing
[DE88-001432] 06 p0782 N88-14797
Propagation of radiation along a constricting optical waveguide 07 p0920 N88-15590
Low-g propellant gaging 08 p0982 N88-15937
Approximation of noncorrelated reflections in problem of sound propagation through waveguide with rough boundary 08 p1076 N88-16487
Mode pattern of field generated by parametric radiator in acoustic waveguide 08 p1076 N88-16488
Performance of linear vertical antenna in refractive multimode waveguide 08 p1076 N88-16489
Acoustic field in waveguide with sloping bed
08 p1076 N88-16490
Diffraction of sound at junction of two waveguides
08 p1076 N88-16491
Modeling of some coplanar waveguide discontinuities
[NASA-TM-100808] 10 p1318 N88-17880
Guided-wave approaches to spectrally selective energy absorption
[NASA-CR-182532] 10 p1320 N88-17892
First and second harmonic ECRH experience at gyrotron frequencies at LLNL
[DE88-003998] 10 p1413 N88-18430
Lg wave excitation and propagation in the presence of one-, two-, and three-dimensional heterogeneities
[AD-A187364] 11 p1510 N88-19022
Nonlinear optical waveguides containing a transition metal-based dye molecule
[DE88-003257] 11 p1550 N88-19275
Propagation in longitudinally varying ducts, with emphasis on guiding to antiguiding transitions
12 p1615 N88-19658
Two-dimensional electron fluid computer calculations of nanosecond pulse, low pressure microwave air breakdown in a rectangular waveguide and their verification by experimental measurement
[DE88-004407] 12 p1618 N88-19678
Transformation coefficient in wave-field acceleration scheme
[DE88-700158] 13 p1757 N88-20507
Slow waves in waveguide with elliptical cross section
[DE88-700159] 13 p1757 N88-20508
Multimode-waveguide laser beam deflector
[DE88-006222] 13 p1776 N88-20622
Low threshold ridge waveguide single quantum well lasers 13 p1777 N88-20631
Anisotropy of light absorption by color centers in waveguides produced on photochromic glasses by diffusion 14 p1896 N88-21320
Superconducting thin film vertex detector for SSC (Superconducting Super Collider) applications
[DE88-005951] 17 p2445 N88-24535
Nonlinear surface polaritons
[AD-A191046] 18 p2499 N88-24822
Signal processing with degenerate four-wave mixing
[AD-A191496] 18 p2499 N88-24825
Theoretical study of the folded waveguide
[DE88-007877] 19 p2654 N88-25759
Enhanced performance ultrabroadband distributed amplifiers 19 p2656 N88-25775
Characteristics and application of wideband guided-wave devices 19 p2660 N88-25817
Optical modulation above 20 GHz using a waveguide electrooptic switch 19 p2660 N88-25819
Variational analysis of dielectrically loaded multidepth corrugated waveguides
[PB88-193602] 20 p2793 N88-26573
Quantum transport in an electron waveguide
20 p2864 N88-27010

Experimental investigation of simplest inhomogeneities in cylindrical slit line
[DE88-702388] 21 p2933 N88-27418
Guided wave interactions in millimeter-wave integrated circuits
[AD-A193017] 21 p2936 N88-27437
An 8.4-GHz dual maser front end for Parkes reimplementation 22 p3066 N88-28197
Qualitative characteristics of open waveguide resonator spectra
[DE88-702387] 23 p3202 N88-29056
Confirmation of slow-waves in a crosstie overlay coplanar waveguide and its application to band-reject gratings and reflectors
[AD-A194981] 24 p3361 N88-30011
Dielectric millimeter waveguides: A feasibility study for a novel dielectric millimeter waveguide
[AD-A195104] 24 p3366 N88-30042
Analytical and experimental studies of beam waveguide absorbers for structural damping
[AD-A195085] 24 p3382 N88-30144

WAVELENGTH DIVISION MULTIPLEXING

Digital television routing systems: A survey of optical and electrical techniques
[BBC-RD-1988/3] 19 p2654 N88-25763

WAVELENGTHS

Spectrometric test of a linear array sensor
[NASA-TM-100676] 01 p0064 N88-10414
Selection of optimum wavelengths for ozone mapping from satellites 05 p0619 N88-13798
Collider constraints in the choices for wavelength and gradient scaling
[PB87-123691] 06 p0779 N88-14783
Modern pulsed wavemeters
[DE88-003875] 10 p1335 N88-17978
Study for the determination of general and specific properties of wide energy-band gap HgHdTe in the 1-2 micrometer wavelength range
[AD-A189177] 13 p1845 N88-21041
Theoretical studies of Resonance Enhanced Stimulated Raman Scattering (RESRS) of frequency-doubled Alexandrite laser wavelength in cesium vapor
[NASA-CR-182870] 15 p2036 N88-22133
SDIO/IST ultrashort wavelength laser. Mossbauer effect in gamma-ray lasers
[AD-A190306] 15 p2072 N88-22352
Dual wavelength holographic interferometry system
[NASA-CASE-MFS-28242-1] 17 p2341 N88-23960
Wavenumber spectra from THIR 6.7 micron water vapor data 20 p2824 N88-26756

WAVES

WKBJ method and strained coordinates for high frequency inertial wave filtering
[INPE-4214-PRE/1095] 11 p1537 N88-19186
Brunt-Doppler ducting of buoyancy waves in a temperature- and wind-stratified atmosphere 18 p2542 N88-25086

WEAK ENERGY INTERACTIONS

NT WEAK INTERACTIONS (FIELD THEORY)
Neutrinos in supernovae
[DE87-014295] 03 p0387 N88-12434
Few body hypernuclear systems: Weak decays
[DE87-014920] 04 p0488 N88-13010
The H5(+) potential energy hypersurface: Characterization of ten distinct energetically low-lying stationary points 16 p2267 N88-23561
Weak interaction physics: From its birth to the electroweak model
[DE88-702494] 23 p3280 N88-29531

WEAK INTERACTIONS (FIELD THEORY)

Summary and conclusions of the 6th Moriond workshop — standard electroweak model
[USIP-87-11] 01 p0092 N88-10602
An introduction to charm and heavy quark physics
[DE87-013589] 02 p0231 N88-11455
The standard theory group: Summary and conclusions
[PREPRINT-551] 06 p0778 N88-14776
Determination of the neutral current chiral coupling constants u sublsq, u subrsq, d sublsq and d subrsq from an (anti)neutrino-deuterium experiment
[B8715857] 06 p0779 N88-14780
Theory of elementary particle studies in weak iteration and grand unification and studies in accelerator design
[DE88-004261] 11 p1545 N88-19238
Semileptonic weak interactions in nuclei: A relativistic analysis
[CEBAF-PR-87-024] 11 p1547 N88-19249
Searches for forces weaker than gravity
[DE88-003579] 13 p1832 N88-20959
Intermediate energy neutrino physics
[DE88-005378] 13 p1836 N88-20984
The response of a small liquid scintillation counter for low energy (gamma, p) experiments
[NOTA-INTERNA-901] 14 p1980 N88-21819
Lattice QCD calculation of K yields pi nonleptonic weak transition and other hadronic weak parameters
[PREPRINT-580] 15 p2132 N88-22717
Weak interaction physics: From its birth to the electroweak model
[DE88-702494] 23 p3280 N88-29531

WEAPON SYSTEM MANAGEMENT

Contribution of expert systems to avionics advance. Application on AS30 laser weapon system
[SNIAS-881-320-103] 23 p3267 N88-29449

WEAPON SYSTEMS

NT LASER WEAPONS
NT MISSILE SYSTEMS
Design principles and practices for implementation of MIL-STD-1760 in aircraft and stores
[AD-A183724] 01 p0005 N88-10027
Current status of high power microwave effects and simulation
[DE87-004112] 06 p0751 N88-14615
Integrated diagnostics 09 p1111 N88-16655
A piloted simulation investigating handling qualities and performance requirements of a single-pilot helicopter in air combat employing a helmet-driven turreted gun
[AD-A188878] 09 p1116 N88-16689
Neural network based architectures for aerospace applications 09 p1204 N88-17218
Research and development. Technical-scientific publications (1956-1987): Retrospective view and prospects. Jubilee edition on the occasion of the 75th birthday of Dipl.-Engr. Dr.-Engr. E. H. Ludwig Boelkow
[ISSN-0931-9751] 10 p1309 N88-17819
Investigation of several spread shot conditions
[REPT-TR-164] 10 p1310 N88-17830
Development savings through parametric modeling of program costs 12 p1700 N88-20175
Systems analysis and simulation techniques: Essential tools for balanced complex weapon system designs in terms of performance and cost
12 p1702 N88-20187
AGARD Highlights 88/1 14 p2012 N88-22001
The Design, Development and Testing of Complex Avionics Systems
[AGARD-CP-417] 17 p2302 N88-23767
Architecture and role of the Sensor Subsystem in future aircraft weapon systems 17 p2302 N88-23770
The specification and design of a future maritime reconnaissance aircraft 17 p2303 N88-23772
A structured approach to weapon system design
17 p2303 N88-23773
A change in system design emphasis: From machine to man 17 p2304 N88-23782
Advanced development of a cockpit automation design support system 17 p2304 N88-23785
The electromagnetic threat to future avionic systems
17 p2305 N88-23790
Coherent functional development: Key to successful future system integration 17 p2307 N88-23803
Flight testing under extreme environmental conditions
[AGARD-AG-300-VOL-8] 21 p2951 N88-27525
Can CNV amplitude predict ability to accomplish a demanding task? 21 p2980 N88-27700
Inflight rearming
[AD-A193564] 23 p3176 N88-28909
Computers in weapons systems: A look at the F-15
[AD-A194498] 23 p3178 N88-28920

WEAPONS

NT ARTILLERY
NT GUNS (ORDNANCE)
NT LASER WEAPONS
NT MINES (ORDNANCE)
NT NUCLEAR WEAPONS
NT SPACE WEAPONS
The impact of environmental factors on the performance of millimeter wave seekers in smart munitions
[DE87-014277] 03 p0270 N88-11697
The evolution of naval warfare technology and the impact of space systems
[AD-A186900] 09 p1233 N88-17392
Computational studies of wave-shaping in a blast simulator by perforated plates in the driver
[AD-A188200] 11 p1483 N88-18850
Soviet military power, 1987 13 p1858 N88-21114
Free electron lasers in strategic defense
[DE88-007024] 17 p2394 N88-24231
On 3-5 transistors for MM-wave applications
[AD-A191580] 19 p2661 N88-25825
Dependence effects in unique signal transmission
[DE88-010331] 21 p2933 N88-27419
A method for estimating the susceptibility of electronic systems to HPM (High Power Microwave)
[DE88-012246] 21 p2934 N88-27422
Fiber-optics used to record high-speed photographs inside a pressurized tank during lethality testing
[DE88-011283] 21 p2951 N88-27529
The Soviet Stealth fighter: Check or checkmate
[AD-A195200] 24 p3323 N88-29791

WEAPONS DELIVERY

The evolution of naval warfare technology and the impact of space systems
[AD-A186900] 09 p1233 N88-17392
Investigation of several spread shot conditions
[REPT-TR-164] 10 p1310 N88-17830
Implementation and performance analysis of parallel assignment algorithms on a hypercube computer
[AD-A190678] 15 p2115 N88-22600

WEAR

Endurance testing of a natural gas-fueled rotary engine
[PB87-215703] 01 p0055 N88-10356
Wear of iron and nickel in corrosive liquid environments
[NASA-TM-100246] 03 p0289 N88-11817
The friction and wear of TPS fibers
[NASA-CR-181496] 03 p0291 N88-11830
Wear of hard steel in rolling lubricated contact
[RP-699] 03 p0332 N88-12094
Real-time Raman detection of molecular changes in ceramics undergoing sliding friction
[DE88-000558] 04 p0421 N88-12609
Analysis of wear metals in engine oils using the atomic absorption spectrophotometric method
[NAL-TM-MT-8704] 05 p0564 N88-13435
Fretting wear and fretting fatigue damage
05 p0603 N88-13697
Sliding-wear properties of retained austenite in carburized layer
[PB87-149092] 07 p0833 N88-15054
Evaluation of load tracks and wear of two sets of bearings from space shuttle main engine high pressure oxygen turbopumps
[NASA-CR-178969] 07 p0881 N88-15223
Technology developments for a compound cycle engine 09 p1107 N88-16637
Characterization of the arc/spark excitation sources used in the spectrometric oil analysis program
[AD-A187131] 10 p1297 N88-17758
Friction and wear of monolithic and fiber reinforced silicon-ceramics sliding against IN-718 alloy at 25 to 800 C in atmospheric air at ambient pressure
[NASA-TM-100294] 10 p1304 N88-17796
Tribology of ceramics: Report of the Committee on Tribology of Ceramics
[NASA-CR-182506] 10 p1305 N88-17802
Mechanisms of wear in single- and two-phase materials
[DE88-003846] 10 p1305 N88-17806
Synthesis and structure property studies of toughened epoxy resins via functionalized polysiloxanes. Friction and wear studies
[AD-A188258] 11 p1462 N88-18718
Characterization and fundamental studies on CuO sorbent materials to determine attrition mechanisms on substrate gamma alumina
[DE88-003674] 13 p1749 N88-20456
Corrosion-wear process under rolling-sliding motion
[AD-A189603] 13 p1778 N88-20635
Overview of the DOE-ECUT Tribology Program
[DE88-002878] 13 p1778 N88-20637
On the torque and wear behavior of selected thin film MOS2 lubricated gimbal bearings
14 p1926 N88-21485
Friction and wear of ceramics
17 p2323 N88-23874
Ceramic technology for advanced heat engines project
[DE88-008945] 21 p2919 N88-27323
Studies of dynamic contact of ceramics and alloys for advanced heat engines
[DE88-008996] 21 p2919 N88-27324
Friction, wear and electrical contact resistance of precious metal alloys
[DE88-011244] 21 p2938 N88-27450
Calibration of the portable wear metal analyzer
[AD-A192971] 21 p2950 N88-27524
Influence of dispersed additives reinforcement on the wear reinforcement mechanisms of the alumina-steel couple. Macroscopic and structural aspects
[ECL-88-01] 22 p3059 N88-28148
An investigation of some basic properties of hybrid composite materials
[AD-A194136] 23 p3189 N88-28975
Static and dynamic metal-metal friction at plastic stress levels
[DE88-011281] 23 p3222 N88-29176

WEAR INHIBITORS

The performance of thin solid films for satellite gears
14 p1876 N88-21209
Ball bearings with chemical vapor deposition (CVD)-TiC coated components 14 p1876 N88-21210

Influence of dispersed additives reinforcement on the wear reinforcement mechanisms of the alumina-steel couple. Macroscopic and structural aspects
[ECL-88-01] 22 p3059 N88-28148

WEAR RESISTANCE
NT ABRASION RESISTANCE
Ceramic technology for advanced heat engines project
[DE88-001520] 04 p0420 N88-12605
Corrosion control by composite material substitution with application to the M-939 5-ton truck
04 p0428 N88-12654
The tribological properties of MoS2 coatings in vacuum, low relative humidity and high relative humidity environments
[DE88-001611] 06 p0711 N88-14356
Sliding-wear properties of retained austenite in carburized layer
[PB87-149092] 07 p0833 N88-15054
Modification of properties of metals by high-power ion beams 08 p1079 N88-16507
Bias, internal stress and substrate effects on the microstructure and properties of PVD-wear resistant coatings
[AERE-R-12360] 10 p1304 N88-17798
Institute for Materials Science and Engineering, Metallurgy: Technical activities 1987
[PB88-157722] 11 p1460 N88-18702
Synthesis and structure property studies of toughened epoxy resins via functionalized polysiloxanes
[AD-A187984] 11 p1462 N88-18715
Standardization of lubricity test
[AD-A187776] 11 p1465 N88-18736
The effects of thin polymeric surface films in reducing fretting corrosion and wear
[AD-A188633] 12 p1611 N88-19634
Reduction of erosion in elbows due to flow modifications, phase 1
[DE88-001028] 13 p1769 N88-20584
Titanium carbide coatings for aerospace ball bearings
14 p1927 N88-21486
Reciprocating sliding wear characteristics of copper-carbon fiber composites
[NASA-TT-20176] 15 p2031 N88-22100
High temperature solid lubrication by catalytically generated carbon
[AD-A190804] 16 p2182 N88-23004
The performance of perfluoropolyalkylether oils under boundary lubrication conditions
[AD-A191057] 17 p2323 N88-23869
Characterization of coating wear phenomena in nitride and carbide coated tool inserts
[DE88-011196] 20 p2779 N88-26478
Basic mechanisms of diesel lubrication correlation of bench and engine tests
[AD-A193360] 21 p2956 N88-27561
Development of high temperature, high pressure rotating shaft seals
[DE88-001029] 23 p3221 N88-29172

WEAR TESTS
Hot piston ring/cylinder liner materials: Selection and evaluation
[NASA-TM-100276] 08 p0971 N88-15872
The WAFTER: A versatile wear and friction tester
[MRL-TN-519] 09 p1169 N88-17012
Characterization of coating wear phenomena in nitride and carbide coated tool inserts
[DE88-011196] 20 p2779 N88-26478

WEATHER
NT COLD WEATHER
Hanford Meteorological Station computer codes. Volume 2: The PROD computer code
[DE87-014807] 02 p0215 N88-11355
Short reference year
[PB87-107470] 03 p0352 N88-12221
Study of microburst detection performance during 1985 in Memphis, Tennessee
[AD-A184013] 03 p0354 N88-12231
Drought, solar activity link established by Leningrad geophysicists 04 p0458 N88-12835
Application of TOMS data to weather analysis models
05 p0617 N88-13787
The use of TOMS-modified VAS data for large-scale NWP 05 p0618 N88-13791
Use of satellite data in volcano monitoring
05 p0618 N88-13797
The global climate system: Autumn 1984 to spring 1986
[CSM-R84/86] 06 p0745 N88-14583
Greatest volcanic eruptions in world during 17th-18th centuries and weather anomalies in Eurasian middle latitudes 08 p1012 N88-16134
Mariners Weather Log, Volume 31, Number 3, Summer 1987
[PB87-234894] 08 p1039 N88-16284
North Pacific Ocean. Subtropical front north of Hawaii, R/V Thomas G. Thompson: 7 January - 10 February 1974. CTD data report
[AD-A186565] 08 p1044 N88-16310
North Pacific Ocean. Subarctic front central Pacific, R/V Thomas G. Thompson: 8 September - 9 October 1975. CTD data report
[AD-A186567] 08 p1044 N88-16312
North Pacific Ocean. Northwest Pacific Transition Zone, R/V Thomas G. Thompson: 19 March - 1 May 1971. STD data report
[AD-A186568] 08 p1044 N88-16313
The Meteosat operational program
09 p1127 N88-16759
Revised uniform summary of surface weather observations. Parts A-F: Carswell AFB, Texas
[AD-A186820] 09 p1192 N88-17144
North Pacific Ocean. Central Pacific Transition Zone, R/V Thomas G. Thompson: 25 March - 3 May 1968. STD data report
[AD-A186570] 09 p1195 N88-17160
Continental shelf processes affecting the oceanography of the South Atlantic Bight
[DE88-004102] 09 p1196 N88-17166
The structure and dynamics of monsoon depressions
10 p1355 N88-18102
Proceedings of the Forest-Atmosphere Interaction Workshop
[CONF-8510250] 12 p1641 N88-19824
Revised Uniform Summary of Surface Weather Observations, Loring AFB, Maine, Parts A - F
[AD-A188201] 14 p1947 N88-21610
Mariners weather log, volume 32, number 1, Winter 1988
[PB88-173869] 18 p2544 N88-25097
Meteorological and Environmental Inputs to Aviation Systems
[NASA-CP-2498] 18 p2545 N88-25105
TDWR (Terminal Doppler Weather Radar) PRF (Pulse Repetition Frequency) selection criteria
[AD-A193089] 21 p2932 N88-27407
Withstand voltage of slightly polluted insulator chains in humid weather conditions
[DE88-752818] 22 p3072 N88-28237
Prolonged periods of above-normal temperatures in Canada, 1986/87 22 p3120 N88-28538
Typical weather months in the past (1973-1983) in Central Europe
[AD-A194701] 23 p3235 N88-29249
Basic causes of amplitude modulation in climatic/weather parameters
[DE88-702743] 23 p3236 N88-29254

WEATHER CHARTS
U METEOROLOGICAL CHARTS

WEATHER CONDITIONS
U WEATHER

WEATHER CONTROL
U WEATHER MODIFICATION

WEATHER FORECASTING
NT LONG RANGE WEATHER FORECASTING
NT NOWCASTING
NT NUMERICAL WEATHER FORECASTING
NT STATISTICAL WEATHER FORECASTING
Tropical cyclone center locations from enhanced infrared satellite imagery
[PB87-213450] 01 p0071 N88-10455
Hanford Meteorological Station computer codes. Volume 1: The GEN computer code
[DE87-012816] 01 p0071 N88-10456
Applications and benefits of short period weather forecasts 02 p0199 N88-11240
COST-73 and its application in very short range forecasting 02 p0199 N88-11242
Mesoscale forecasting today and tomorrow: Problems and opportunities. A position paper
02 p0199 N88-11244
Improved geostationary satellite soundings for the mesoscale weather analysis/forecast operation
02 p0200 N88-11252
Analysis of thickness fields retrieved from NOAA-7 observations through the 3I (Improved Initialization Inversion) method. Interest for weather forecasting
02 p0201 N88-11255
Operational cloud-clearing techniques of VAS radiance data --- Visible and Infrared Spin Scan Radiometer Atmospheric Sounder (VAS) 02 p0201 N88-11256
The combined use of diagnosed mesoscale frontogenesis and satellite imagery in forecasting squall line formation 02 p0201 N88-11258
The role of low-level cooling in a conceptual model of the Australian summertime cool change: Implications for very-short-range forecasting 02 p0204 N88-11275
Meteorological systems support to critical shuttle requirements on the Eastern Test Range --- STS
02 p0205 N88-11281
Evaluation of the Rainsat precipitation analysis system in real-time use 02 p0205 N88-11283
The use of McIDAS as a Mesoscale forecasting tool during the Canadian Atlantic storms programs --- Man-computer Interactive Data Access System (McIDAS) 02 p0205 N88-11284
A short-range forecasting experiment conducted during the Canadian Atlantic storms program
02 p0205 N88-11285
The challenge of very short range forecasting in the tropics 02 p0205 N88-11287
Simplified models for use in an operational short range forecasting system 02 p0206 N88-11289
Use of time changes of surface data parameters in short range forecasting 02 p0206 N88-11291
Mesoscale thunderstorm forecasting using RAOB data, surface mesonet observations, and an expert system
02 p0206 N88-11293
A review of the analysis forecasting and research about severe local storms in Guangdong province (China)
02 p0207 N88-11298
Short-term forecasting of lightning based on the surface wind field at Kennedy Space Center
02 p0208 N88-11306
Forecasting stratus over the British Isles
02 p0209 N88-11310
Short range forecast of the daily maximum temperature 02 p0209 N88-11313
Short range forecasting of sea breeze generated thunderstorms at the Kennedy Space Center: A real-time experiment using a primitive equation mesoscale numerical model 02 p0211 N88-11324
Summary of 1987 Atlantic tropical cyclone activity and verification of author's seasonal forecast
02 p0215 N88-11356
Severe weather potential (SPOT) plotfile generator
[PB87-217717] 02 p0216 N88-11360
Convective cross section analys.s
[PB87-204566] 02 p0216 N88-11361
Kinds of bootstraps and kinds of jackknives, discussed in terms of a year of weather-related data
[AD-A184495] 03 p0353 N88-12227
Tropical cyclone intensity prediction based on empirical orthogonal function representation of wind and shear fields
[AD-A184699] 03 p0353 N88-12229
Progress in improving weather forecasting viewed
04 p0458 N88-12833
NWS (National Weather Service) watch/warning verification flash flood, winter storm and high wind, January 1980 - June 1986
[PB87-223053] 04 p0469 N88-12898
Annual tropical cyclone report, 1986
[AD-A184082] 04 p0470 N88-12903
Ozone, jet streaks and severe weather
05 p0616 N88-13781
ZEUS: A knowledge-based expert system that assists in predicting visibility at airbases
[AD-A184197] 05 p0626 N88-13829
Isentropic analysis and interpretation: Operational applications to synoptic and mesoscale forecast problems
[AD-A184814] 05 p0626 N88-13830
Mesoscale applications of high resolution imagery
[AD-A185039] 05 p0627 N88-13833
Opportunities for tropical cyclone motion research in the Northwest Pacific region
[AD-A185068] 05 p0627 N88-13834
USSR report: Earth sciences
[JPRS-UES-87-004] 06 p0725 N88-14455
Regional weather satellite data processing center opens in Tashkent 06 p0725 N88-14457
BARS-1M meteorological complex carried on IL-18 airplane 06 p0725 N88-14458
Current status of world weather service
06 p0725 N88-14459
Atmosphere dynamics in the equatorial meteor zone
06 p0733 N88-14508
Eighth Session of the Commission for Aeronautical Meteorology (abridged)
[WMO-673] 06 p0745 N88-14585
Verification of severe local storm forecasts issued by the National Severe Storms Forecast Center, 1986
[PB88-101407] 06 p0747 N88-14594
Objective prediction of monthly mean surface temperature and climatological relationships to mid-tropospheric heights
[DE88-000908] 07 p0880 N88-15340
Characterization of meteorological phenomena influencing aircraft operations 08 p0951 N88-15772
A study of finite difference and finite element vertical discretization schemes for baroclinic prediction equations
[AD-A186617] 08 p1040 N88-16291

Assessment of VAS-derived products created by a simultaneous algorithm on a convectively active day
[AD-A186158] 08 p1054 N88-16359
Numerical investigation of orographically enhanced instability
[AD-A186841] 09 p1189 N88-17125
Modification of a successive corrections objective analysis for improved higher order calculations
[NASA-CR-182467] 09 p1230 N88-17370
Prediction of polytomous events: Model description, algorithm development and methodological aspects, with an application
[AD-A186549] 09 p1232 N88-17384
Status of FAA terminal Doppler weather radar programs 10 p1275 N88-17632
AEV local verification for aviation, precipitation and temperature programs: AV, REL, TEM (September 1987 revision)
[PB88-115862] 10 p1355 N88-18101
Systematic errors of the FSU global spectral model 10 p1356 N88-18103
Aviation weather: Status of FAA's (Federal Aviation Administration's) new hazardous weather detection and dissemination systems
[PB88-115910] 11 p1513 N88-19041
Misty picture weather-watch and microbarograph project: Experiments 9412-14-18
[DE88-003949] 11 p1514 N88-19047
Optimal sampling to provide user-specific climate information 11 p1515 N88-19051
Model of limited area of 5 layers for numerical weather forcasting
[INPE-4324-RPE/551] 11 p1516 N88-19053
Effects of stress on judgement and decision making in dynamic tasks
[AD-A188203] 11 p1523 N88-19092
National Severe Storms Laboratory, fiscal year 1987
[PB88-140108] 12 p1647 N88-19863
Activities report in meteorology
[AR-86-87] 13 p1798 N88-20755
Wind shear as a predictor of severe weather for the eastern United States
[PB88-157144] 13 p1800 N88-20762
Adiabetic formation of large-scale models of the atmosphere 14 p1935 N88-21541
Baseline observing system experiments using the AFGL global data assimilation system
[AD-A188861] 15 p2024 N88-22062
Derivation of consistent surface fixed fields for use in a global NWP model
[AD-A190131] 15 p2093 N88-22475
Aircraft accident/incident summary reports: Modena, Pennsylvania, March 17, 1986; Redwater, Texas, April 4, 1986
[PB88-910403] 16 p2159 N88-22878
Very short range statistical forecasting of automated weather observations
[AD-A190803] 16 p2235 N88-23349
Fog, rain and aerosol attenuation in the atmosphere
[AD-A190867] 16 p2235 N88-23350
Spectroradiometry in meteorology 16 p2272 N88-23599
Adaptive grid refinement for numerical weather prediction
[AD-A192172] 18 p2544 N88-25101
Automation of surface observations program 18 p2545 N88-25106
Special observations 18 p2545 N88-25108
General-aviation's view of progress in the aviation weather system 18 p2546 N88-25110
National plans for aircraft icing and improved aircraft icing forecasts and associated warning services 18 p2546 N88-25113
Objective detection and forecasting of Clear-Air Turbulence (CAT): A status report 18 p2546 N88-25114
Denver ARTCC evaluation of PROFS (Prototype Regional Observations and Forecast System) mesoscale weather products 18 p2547 N88-25117
US participation in the TOGA (Tropical Ocean and the Global Atmosphere) Program: A research strategy
[DE88-010986] 19 p2681 N88-25938
ECMWF (European Centre for Medium Range Weather Forecasts) global analyses 1979-1986: Circulation statistics and data evaluation
[PB88-178165] 19 p2692 N88-26001
Suggested hurricane operational scenario for GOES I-M
[NASA-TM-89729] 19 p2692 N88-26002
Satellite observed Mesoscale Convective System (MCS) propagation characteristics and a 3-12 hour heavy precipitation forecast index
[PB88-180161] 19 p2692 N88-26004
BOLETIM: An expert system for weather forecasting
[INPE-4538-TDL/329] 19 p2693 N88-26011
Mariners weather log, volume 31, number 4, Fall 1987
[PB88-173851] 20 p2825 N88-26761
Synoptic patterns related to tropical cyclone recurvature
[AD-A192338] 20 p2827 N88-26771
Intercomparison of NMC (National Meteorological Center) and ECMWF (European Centre for Medium Range Weather Forecasts) global analyses: 1980-1986
[PB88-196548] 21 p2974 N88-27668
The Hanford meteorological data collection system and data base
[DE88-008632] 21 p2975 N88-27672
Modes of interannual climate variability and Sahel rainfall anomalies 22 p3121 N88-28547
Systematic behavior of NMC medium range forecasts and the effect of model changes 1985-87 22 p3125 N88-28575
The impact of the El Nino event on the ECMWF model performance 22 p3125 N88-28576
DERF forecasts of thickness 22 p3126 N88-28579
Analysis of the dynamic extended range forecast experiment 22 p3126 N88-28581
Investigations on the entropy of cloudy air
[ESA-TT-1060] 23 p3234 N88-29245
Typical weather months in the past (1973-1983) in Central Europe
[AD-A194701] 23 p3235 N88-29249
A study of the feasibility of using sea and wind information from the ERS-1 satellite. Part 1: Wind scatterometer data
[NASA-CR-182833] 24 p3386 N88-30167
A study of the feasibility of using sea and wind information from the ERS-1 satellite. Part 2: Use of scatterometer and altimeter data in wave modeling and assimilation
[ESA-CR(P)-2604-PT-2] 24 p3387 N88-30176
Temperature profile construction methods: An evaluation
[AD-A195919] 24 p3403 N88-30262

WEATHER FRONTS
U FRONTS (METEOROLOGY)

WEATHER MAPS
U METEOROLOGICAL CHARTS

WEATHER MODIFICATION
NT CLOUD DISPERSAL
NT CLOUD SEEDING
NT LIGHTNING SUPPRESSION
NT RAINMAKING
NT STORM ENHANCEMENT
NT STORM SUPPRESSION
Measurements of vapor flux, liquid water contents, precipitation rates and riming in a Utah mountain cloud system
[PB87-224945] 04 p0469 N88-12900
Altered and enhanced iodargyrite with bismuth triiodide for use in precipitation enhancement operations
[AD-A185229] 05 p0561 N88-13419
Electron acceleration by wave processes in the earth's ionosphere
[AD-A186110] 07 p0877 N88-15320
Cloud physics studies in SCPP (Sierra Cooperative Pilot Project) from 1977-87
[PB88-136924] 11 p1516 N88-19054
High altitude chemical release systems for project BIME (Brazilian Ionospheric Modification Experiments) project IMS (Ionospheric Modification Studies) project PIIE (Polar Ionospheric Irregularities Experiment) project polar arcs
[AD-A188299] 12 p1642 N88-19833
The Effect of the Ionosphere on Communication, Navigation and Surveillance Systems Based on Ionosph eric Effects Symposium held on 5-7 May 1987 in Springfield, Virginia
[AD-A191855] 18 p2541 N88-25081

WEATHER RADAR
U METEOROLOGICAL RADAR

WEATHER STATIONS
NT AUTOMATIC WEATHER STATIONS
Hanford Meteorological Station computer codes. Volume 1: The GEN computer code
[DE87-012816] 01 p0071 N88-10456
Hanford Meteorological Station computer codes. Volume 2: The PROD computer code
[DE87-014807] u2 p0215 N88-11355
Calendar year 1985 solar and weather data for Austin, Texas
[PB87-220174] 03 p0352 N88-12219
A single-station weather forecasting expert system
[AD-A184889] 05 p0627 N88-13832
Inventory of weather stations. Climatological data from Dutch stations, no. 26
[KNMI-150-26] 05 p0628 N88-13841
Hanford Meteorological Station computer codes. Volume 5: The TOWER computer code
[DE88-001610] 05 p0628 N88-13843
Mariners Weather Log, Volume 31, Number 3, Summer 1987
[PB87-234894] 08 p1039 N88-16284
Automatic data acquisition system utilizing microcomputers: Automatic Meteorological Stations (AMS)
[INPE-4215-PRE/1096] 12 p1646 N88-19859
Climatic summaries of ocean weather stations
[PB88-162920] 14 p1948 N88-21617

WEATHERING
The distribution of evaporitic weathering products on Antarctic meteorites 06 p0798 N88-14888
Application of inverse gas chromatography to fluidity studies
[DE88-002896] 10 p1296 N88-17750
A five year weathering experiment with solar collectors
[DE88-900369] 13 p1796 N88-20740
The effect of weathering on octane quality for winter-grade and summer-grade gasolines
[AD-A190640] 16 p2183 N88-23012
Investigation of the long term effects of aging on carbon epoxy composites exposed naturally to the weather under cyclic loads. (Results of sampling after 2.5 years). Test report M1-641300
[CEAT-39/M/79-C-M1-641300] 17 p2316 N88-23834
Effects of natural environment on first generation solid rocket booster thermal protection system materials
[NASA-TM-100329] 17 p2373 N88-24113
A sedimentological and mineralogical study of the Koogah Formation, New South Wales 18 p2542 N88-25087
Selective weathering of shocked minerals and chondritic enrichment of the Martian fines 23 p3301 N88-29660
Weathering of sulfides on Mars 23 p3301 N88-29662
Variability in spectral signatures of terrestrial volcanic rocks and implications for volcanology on Mars 23 p3303 N88-29672
Aqueous alteration in S-N-C meteorites and implications for weathering products on Mars 23 p3303 N88-29673
Some probable characteristics of the Martian regolith 23 p3303 N88-29678
What SNC meteorites tell us about Martian magmatism 23 p3303 N88-29679
Preliminary analysis of recent 2.2-4.2 micrometers teiescopic observations of Elysium, Mars: Implications for crystallinity and hydration state of surface materials 23 p3306 N88-29692
Photoacoustic Fourier transform infrared spectroscopy. An early detection technique for coatings degradation 24 p3354 N88-29968

WEAVING
Carbon-carbon composites and Aerospatiale. State of the art and prospects
[SNIAS-872-430-108] 05 p0559 N88-13401
Damage initiation and growth in sateen laminates under static and cyclic loading 11 p1449 N88-18634
An investigation of some basic properties of hybrid composite materials
[AD-A194136] 23 p3189 N88-28975

WEBS (MEMBRANES)
U MEMBRANES

WEDGE FLOW
Analytical investigation of reflection of a regular or mach reflection over a secondary wedge
[AD-A185690] 06 p0703 N88-14316
On the parabolized Navier-Stokes equations without sublayer assumptions
[AD-A186127] 07 p0849 N88-15152
Compressible flow in a pie-shaped cylinder rotating about the vertex 18 p2460 N88-24604
Navier-Stokes simulation of shock-tube flows over a wedge-type step by finite volume method
[ISAS-RN-628] 20 p2797 N88-26599

WEDGES
Eddy current density in wedge-shaped conducting cylinders with inhomogeneous conductivity
[ETN-87-90404] 01 p0042 N88-10268
Interior impedance wedge diffraction with surface waves
[NASA-CR-182405] 07 p0854 N88-15186
Plane wave diffraction by a thin dielectric wedge
[RSRE-MEMO-4045] 09 p1153 N88-16912
An interferometric investigation of the diffraction of planar shock waves over a half-diamond cylinder in air
[UTIAS-322] 13 p1768 N88-20575
Wind tunnel tests of the influence of airfoil-thickness on normal force and pitching moment of two slender wings at transonic and supersonic Mach numbers
[DFVLR-FB-88-17] 21 p2893 N88-27171
Experimental investigation of the reflection of a planar shock wave over a double wedge
[AD-A193078] 21 p2943 N88-27482

Numerical modeling results for mode propagation in a wedge
[AD-A193998] 22 p3147 N88-28718
Acoustic pressure distribution on the bottom of a wedge-shaped ocean
[AD-A193961] 23 p3278 N88-29518
WEIBULL DENSITY FUNCTIONS
A probabilistic model of brittle crack formation
[AD-A184423] 03 p0338 N88-12129
Static and dynamic determination of aluminum oxide toughness
[PB87-146999] 07 p0869 N88-15275
Statistical evaluation of experimental results from fatigue strength tests on CFRP composite materials
11 p1449 N88-18635
Tests for uniformity arising from a series of events
[AD-A189069] 13 p1828 N88-20935
Modeling failures of intermittently used machines
[AD-A190298] 15 p2074 N88-22367
Measurement and interpretation of North Atlantic Ocean marine radar sea scatter
[AD-A196239] 24 p3364 N88-30036
WEIERSTRASS FUNCTIONS
General solution of certain functional equations
[PREPRINT-554] 06 p0764 N88-14689
Mode 3 problems of doubly-periodic rhombic and rectangular array of equal cracks in an infinite plate
[PB87-144846] 08 p0996 N88-16031
WEIGHT
A class 2 weight assessment for the implementation of commonality and preliminary structural designs for the family of commuter airplanes
[NASA-CR-182565] 12 p1581 N88-19464
WEIGHT (MASS)
NT ATOMIC WEIGHTS
NT BIOMASS
NT BODY WEIGHT
NT STRUCTURAL WEIGHT
Shielding analysis of a small compact space nuclear reactor
[AD-A185566] 06 p0779 N88-14784
Alternative program approaches for the advanced satellite technology program
[AD-A188917] 12 p1600 N88-19576
Impact of control errors on the volume/weight demand of the Ventilation and Dryer (VAD) concept --- EURECA Botany Facility
[TN-RB524-006/87] 17 p2377 N88-24132
Ballistic evaluation of applique armours: Presentation and interpretation of ballistic data
[MRL-TN-527] 19 p2635 N88-25629
Spray automated balancing of rotors: Methods and materials
[NASA-CR-182151] 24 p3330 N88-29825
WEIGHT ANALYSIS
The initial calculation of range and mission fuel during conceptual design --- aircraft design
[LR-525] 16 p2161 N88-22889
WEIGHT FACTORS
U WEIGHT (MASS)
WEIGHT INDICATORS
Strain gage balance for half models 302-6. Calibration report --- wind tunnels
[F+W-FO-1803] 09 p1168 N88-17001
Strain gage sting balance 204-6. Calibration report --- wind tunnels
[F+W-FO-1838] 09 p1168 N88-17002
WEIGHT MEASUREMENT
Uniform laws and regulations as adopted by the National Conference on Weights and Measures (72nd), 1987
[PB88-123724] 06 p0689 N88-14225
Stability of uncapsulated weight cells with thin film elongation measurement bands under influence of humidity, temperature and operation voltage
[ETN-88-92383] 21 p2951 N88-27531
WEIGHT REDUCTION
The use of Kevlar on aero-engine fan containment casings
[PNR90410] 02 p0182 N88-11134
Rational reinforcement of cylindrical shells with variable stiffness frames subjected to external pressure
04 p0426 N88-12638
Corrosion control by composite material substitution with application to the M-939 5-ton truck
04 p0428 N88-12654
Making space nickel/hydrogen batteries lighter and less expensive
[DE88-000168] 05 p0578 N88-13530
Study on utilization of advanced composites in fuselage structures of large transports
[NASA-CR-172406] 07 p0827 N88-15014
Composite/metal jointing technology for vehicle weight reduction
[DE88-900228] 08 p0992 N88-16005
Operation Everest 2: Nutrition and body composition
[AD-A186449] 08 p1049 N88-16333
Rotorcraft weight trends in light of structural material characteristics
[AD-A186576] 10 p1276 N88-17642
Lightsats and their attraction to budget oriented Federal agencies 10 p1289 N88-17711
Modern materials for light constructions --- aircraft
[MBB-Z-136/86] 10 p1312 N88-17839
Minimum weight design of rectangular and tapered helicopter rotor blades with frequency constraints
[NASA-TM-100561] 12 p1582 N88-19465
Minimum weight design of rotorcraft blades with multiple frequency and stress constraints
[NASA-TM-100569] 16 p2161 N88-22892
The application of high temperature superconductors to space electrical power distribution components
[NASA-TM-100901] 16 p2171 N88-22939
Development of a lightweight structure with load bearing capability and high thermal conductance
17 p2420 N88-24393
Weight savings in aerospace vehicles through propellant scavenging
[NASA-TM-100900] 19 p2605 N88-25470
Performance of lightweight nickel electrodes
[NASA-TM-100958] 20 p2771 N88-26430
High power pulse energy system concept
[AD-A192440] 21 p2935 N88-27429
Variability in intake and dehydration in young men during a simulated desert walk
[AD-A192654] 22 p3131 N88-28613
WEIGHTING FUNCTIONS
The criterion of equal integrated quality: An improved method of planning DBS systems
[BBC-RD-1987/10] 02 p0161 N88-11012
Weighted decoding of block codes and some topics on decoding complexity
[ENST-87E005] 02 p0221 N88-11394
Finite element techniques 06 p0701 N88-14303
A weighting sequence approach to the analysis and design of multivariable control systems
[AD-A186086] 07 p0917 N88-15570
Finite element fundamentals, part 2
08 p0985 N88-15962
Boundary elements combined with singular fields for three-dimensional cracked solids
[RAE-TR-87038] 09 p1183 N88-17088
Five-diagonal weighting scheme for geoidal profiles
[AD-A188033] 10 p1347 N88-18054
On the dynamic estimation of relative weights for observation and forecast in numerical weather prediction
[NASA-CR-182531] 10 p1356 N88-18106
Two dimensional uncorrelated bias in fix algorithms
[NASA-CR-182683] 13 p1815 N88-20847
Robustifying the Kalman filter
[AD-A189240] 13 p1825 N88-20907
Weighted averaging method for image smoothing reported 14 p1901 N88-21352
On 2-D versus 3-D: Sine of squared angular error and weighted perpendicular fixing
[NASA-CR-182899] 16 p2252 N88-23458
Asymptotic theory for weighted least squares estimators in Aalen's additive risk model
[AD-A191085] 18 p2562 N88-25210
Wigner distribution function: Relation to short-term spectral estimation, smoothing and performance in noise
[AD-A193865] 23 p3275 N88-29492
A theoretical and experimental investigation into the use of SAW weighting techniques in optical diffraction gratings
[RSRE-MEMO-4128] 23 p3283 N88-29549
WEIGHTLESSNESS
Aquarack: Aims and Possible Research Projects
[DFVLR-MITT-87-01] 01 p0073 N88-10469
Long term investigations of the growth, metabolism, and reproduction of fish under conditions close to weightlessness 01 p0074 N88-10473
The influence of weightlessness on the metabolism of the Biomphalaria glabrata 01 p0074 N88-10475
Life support systems for biological experiments under weightlessness in the German and European space programs 01 p0074 N88-10477
Testing of heat pipes on SPAS-01
[BMFT-FB-W-86-014] 06 p0672 N88-14119
Proceedings and program draft in Gravitational Biology in the Federal Republic of Germany --- Effects of Weightlessness on the Human Organism
[ESA-TT-988] 07 p0884 N88-15363
The role of the DFVLR project management life sciences in the space program of the Federal Republic of Germany 07 p0884 N88-15364
A theoretical concept for state changes and shape changes in weightlessness 07 p0884 N88-15365
Some remarks on gravitational biology
07 p0884 N88-15366
Investigations of Paramecium cells analyzed under microgravity conditions 07 p0884 N88-15367
The origin of the spicule skeleton of fresh water sponges (Spongillides) 07 p0885 N88-15368
Limb regeneration in amphibians, a suitable model for investigations of the effects of weightlessness as regards evolution and modifications 07 p0885 N88-15369
Investigations of the reproductive physiology of the rainbow trout (Salmo gairdneri Richardson)
07 p0885 N88-15370
Changes in the morphological and molecular biological processes during early embryo development in amphibians under micro-g conditions 07 p0885 N88-15371
Xiphophorus: A system to recognize radiation-induced mutations and to study the effects of zero-gravity environment on embryo development
07 p0885 N88-15372
Hypoxic hypoxia as a stimulus of erythropoiesis in vivo and in vitro 07 p0885 N88-15373
A learning model as a basis for investigations of the effects of gravity on the learning processes and memory formulation 07 p0886 N88-15374
Long-term adaptation of the otolith organs
07 p0886 N88-15375
Functional development of gravity receptors in insects and amphibians 07 p0886 N88-15376
Function-dependent plasticity in the nervous system
07 p0886 N88-15377
Questions on the evolution of the development program of the vertebrate inner ear under long term zero-g conditions 07 p0886 N88-15379
Long duration confinement of aquatic organisms in weightlessness (aquaspace) 07 p0887 N88-15380
Program draft for a special field: Gravitational biology
07 p0887 N88-15381
JPRS report: Science and technology. USSR: Space Biology and Aerospace Medicine, volume 21, no. 3, May - June 1987
[JPRS-USB-88-001] 07 p0889 N88-15389
Cardiac contractility in weightlessness according to spatial ballistocardiography 07 p0890 N88-15393
Cosmonauts' hormonal responses after brief spaceflights 07 p0890 N88-15394
Mother-fetus system as object for investigation of mechanisms of physiological effect of weightlessness
07 p0891 N88-15402
Investigation of energy metabolism of biological systems in weightlessness 07 p0893 N88-15409
Brain morphogenesis in rats developing in weightlessness 07 p0894 N88-15415
Circulatory response of males 45-52 years of age to antiorthostatic hypokinesia 07 p0894 N88-15416
The effect of microgravity on flame spread over a thin fuel
[NASA-TM-100195] 08 p0967 N88-15853
Results of research with biological satellites
08 p1006 N88-16097
Research on cotton plants grown in space
08 p1006 N88-16098
White blood cells in space: An experiment for the first Spacelab mission 09 p1127 N88-16757
JPRS Report: Science and Technology. USSR: Space Biology and Aerospace Medicine, volume 21, no. 5, September - October 1987
[JPRS-USB-88-003] 10 p1359 N88-18122
Embryonic development of guppy in weightlessness
10 p1360 N88-18127
Histomorphometric analysis of rat bones after spaceflight aboard Cosmos-1667 biosatellite
10 p1360 N88-18128
Isotope methods of determining distribution and movement of blood in the body
10 p1362 N88-18138
Comparative evaluation of stress repsonse of rats to different methods of simulating some effects of weightlessness 10 p1363 N88-18144
Morphological study of early changes in rat bones in simulated weightlessness 10 p1365 N88-18158
New book on metabolic aspects of spaceflight stress
10 p1367 N88-18172
Genetic research in space
[NASA-TT-20216] 11 p1518 N88-19066
Ballistocardiography in weightlessness research
11 p1521 N88-19080
Central hemodynamics in antiorthostatic hypokinesia and immersion models of weightlessness
11 p1521 N88-19081
Summary of Payload Integration Plan (PIP) for Starlab-1 flight experiment, enclosure 3
[NASA-TM-89713] 11 p1522 N88-19086
Cytomorphology and ultrastructure of corn root meristem in weightlessness 12 p1651 N88-19891
The respiratory system under weightlessness
12 p1653 N88-19901
How does Physarum polycephalum perceive and use gravity? 12 p1655 N88-19918
Load and control of the cardiocirculatory system in weightlessness 12 p1656 N88-19922

Neck receptor stimulation in 0 and 1 g
12 p1658 N88-19938
Synopsis of the Spacelab D-1 frog statolith experiment STATEX
12 p1659 N88-19940
Cardiovascular effects of weightlessness and ground-based simulation
[NASA-TM-88314] 18 p2551 N88-25140
JPRS report: Science and technology. USSR: Space Biology and Aerospace Medicine, volume 22, no. 1, January - February 1988
[JPRS-USB-88-005] 19 p2702 N88-26069
Growth and differentiation of cells in organotypical rat embryo cerebellar culture developing in weightlessness
19 p2703 N88-26076
Axisymmetric liquid sloshing under low-g conditions: Numerical simulation method (reference manual)
[NLR-TR-86057-U] 20 p2802 N88-26627
Liquid motions in partially filled containers: Preliminary results of the D-1 mission — Spacelab
[NLR-MP-86042-U] 20 p2802 N88-26629
Effect of weightlessness on brain development (results of flight of pregnant rats on Kosmos-1514 biosatellite and study of subsequent development of their progeny on earth
20 p2829 N88-26786
Nonlinear oscillations of an inviscid liquid column under zero-gravity
[LRT-WE-9-FB-8(1987)] 22 p3063 N88-28173
Nonlinear oscillations of axially independent liquid column under zero-gravity environment
[LRT-WE-9-FB-12(1987)] 22 p3063 N88-28174
Nonlinear oscillations of a nonviscous cylindrical liquid system in weightlessness condition
[LRT-WE-9-FB-14(1987)] 22 p3063 N88-28175

WEIGHTLESSNESS SIMULATION
NT NEUTRAL BUOYANCY SIMULATION
Access to microgravity: A technical description of the NAE T-33 microgravity facility
[NAE-AN-47] 04 p0405 N88-12518
Morphology and development of the inner ear of Anurans
07 p0886 N88-15378
Skylark sounding rocket development-Skylark 8
08 p1035 N88-16274
Dynamic testing of a docking system — ground-based simulator
12 p1589 N88-19516
HERMES Program: Airlock swimming pool tests
12 p1591 N88-19525
Respratory parameters aboard an aircraft performing parabolic flights
12 p1653 N88-19902
Influence of a 6 hr head-out water immersion on different tests of endurance performance capacity
12 p1653 N88-19903
Lung function in simulated microgravity
12 p1654 N88-19907
Neuro-reflex mechanisms of circulation regulation in simulated microgravity
12 p1656 N88-19923
Physiological reactions upon controlled changes of blood distribution in humans
12 p1656 N88-19924
P-31 Magnetic Resonance Spectroscopy (MRS) of limb muscles during bedrest with exercise countermeasures
12 p1656 N88-19925
An in vitro model system to study the effect of microgravity and loading conditions on the mineralization and resorption of skeletal tissues
12 p1657 N88-19927
Does 7-day hindquarters unloading simulate 7 days of weightlessness exposure in rat trabecular bone?
12 p1657 N88-19928
The suspended Japanese quail as an animal model for experiments related to microgravity
12 p1662 N88-19960
Some reflections on the standardization of bed-rest procedures for weightlessness simulation (cardiovascular and endocrine apsects)
12 p1662 N88-19961
Regulation of hemodynamics upon imitation of the transition to weightlessness (mathematical modeling)
13 p1810 N88-20817
The relationship between preflight underwater training and space motion sickness
19 p2696 N88-26025
Underwater simulation for space teleoperation
19 p2696 N88-26040
Marintek's ocean basin, a training facility for extravehicular activity?
19 p2698 N88-26041
The Marshall Space Flight Center KC-135 microgravity test program for FY84-86
[NASA-TM-4059] 22 p3056 N88-28136
Study of human factors engineering criteria for Extra Vehicular Activity (EVA) systems, volume 2
[STF23-F87025-VOL-2] 24 p3409 N88-30293

WELD STRENGTH
Reserach on microprocessor controller for spot welding
[PB87-143913] 07 p0883 N88-15240
Characteristics of joint formation during friction welding of Ti alloys to Nb alloys
14 p1898 N88-21329
Optimum duration of steady-state stage in friction welding of metals without artificial braking
14 p1898 N88-21330
Ensuring higher stability of immersed-arc welding of structural aluminum alloys and magnesium alloys
14 p1898 N88-21331
Diffusion welding of aluminomagnesium alloys to ceramics
14 p1898 N88-21333
Distribution of weld quality in thin section stainless steel tube attachment welds
[PB88-109632] 21 p2955 N88-27555
The influence of weld metal properties, weld geometry and applied load on weld system performance
[AD-A193403] 21 p2961 N88-27588

WELD TESTS
Ultrasonic mechanized checking of weld joints of nuclear power plant equipment
02 p0158 N88-10987
Resistance of welded joints in high temperature Hastelloy N-type nickel alloy to hot crack formation
03 p0286 N88-11798
The mechanical properties of solid state diffusion bonds between Ti-6Al-4V and 304L stainless steel
[BAJ-TR-113-1987] 03 p0332 N88-12093
Detection of defects on structures
[EP-PATENT-0-210-794-A2] 04 p0453 N88-12807
Study on the cryogenic toughness of stainless steel weld metals
[PB87-143830] 07 p0834 N88-15057
Characteristics of welds joining parts of high-strength pipe steels and produced by beam of continuous-wave CO2-laser
14 p1897 N88-21325
Structure and properties of welded joints produced between niobium parts in controllable helium atmosphere
14 p1897 N88-21326
Ensuring higher stability of immersed-arc welding of structural aluminum alloys and magnesium alloys
14 p1898 N88-21331
Principles of a nondestructive evaluation process for damage location, damage profile, and damage extension in welded joints by radiometric measurements
[MPA-86-02] 20 p2812 N88-26683
Distribution of weld quality in thin section stainless steel tube attachment welds
[PB88-109632] 21 p2955 N88-27555

WELDABILITY
Welding and weldability of ductile intermetallic alloys
[DE87-014061] 04 p0416 N88-12582
Weldability of 2219-T851 and 2519-T87 aluminum armor alloys for use in Army vehicle systems
[AD-A184296] 04 p0451 N88-12792
The effect of temperature on the tensile properties of HSLA-100 steel
[AD-A184951] 05 p0565 N88-13441
Weldability of a leaded carbon steel
[PB88-110341] 07 p0861 N88-15225
Effects of sulfur content on the plain strain fracture toughness of inertia welds in 4340 steel
[AD-A188192] 11 p1458 N88-18689
Weldability of tritium-charged 304L stainless steel
[DP-1740] 12 p1607 N88-19611
Properties fo seals made with Li2O-Al2O3-SiO2-glass ceramics and aluminum-containing austenitic stainless steels
[DE88-004688] 12 p1633 N88-19776
Inertia welding with variable magnitude of impact load
14 p1897 N88-21328
The weldability of consolidated rapidly solidified Type 304 SS powders
[DE88-006738] 16 p2178 N88-22978
Weldability of general purpose heat source iridium capsules
17 p2426 N88-24429
Helium induced degradation in the weldability of an austenitic stainless steel
[DE88-009062] 20 p2773 N88-26443
Application of Auger electron spectroscopy to the study of trace element effects on weldability
[DE88-010457] 21 p2915 N88-27301

WELDED JOINTS
NT SPOT WELDS
Ultrasonic mechanized checking of weld joints of nuclear power plant equipment
02 p0158 N88-10987
Process and equipment capabilities materials joining laboratory, 1987
[DE87-014534] 02 p0180 N88-11122
Resistance of welded joints in high temperature Hastelloy N-type nickel alloy to hot crack formation
03 p0286 N88-11798
Stress state of welded joints of dissimilar materials obtained by diffusion welding
03 p0286 N88-11799
Microstructural characterization of irradiated PWR steels using the atom probe field-ion microscope
[DE88-000341] 03 p0291 N88-11828
Gas tungsten arc welding of Al-10Fe-5Ce
[AD-A184202] 03 p0334 N88-12104
Welding and weldability of ductile intermetallic alloys
[DE87-014061] 04 p0416 N88-12582
Development of an acoustic emission monitor and monitoring techniques for long-term monitoring of U-0.8Ti electron-beam weldments for postweld cracking
[DE88-000819] 04 p0453 N88-12804
Method for the ultrasonic inspection of the soundness of the metal in weld joints in two-ply pipes
[BLL-CE-TRANS-8265-(9022.09)]
04 p0453 N88-12805
Ultrasonic method of imspecting austenitic weld joints in nuclear power station equipment
[BLL-CE-TRANS-8281-(9022.09)]
04 p0453 N88-12806
Qualification of expansion and joint welding procedures of tube-to-tubesheet joints for heat exchangers in nuclear power plants
[DE87-703526] 05 p0589 N88-13592
Welded joint fatigue of a AISI 304 L type stainless steel
[DE87-703530] 05 p0592 N88-13607
Fatigue strength of alloy A286 at cryogenic temperature
05 p0603 N88-13695
Development of research on fatigue of spot-weld in automobile structures in Japan
05 p0608 N88-13728
Basic energy sciences research in the Metals and Ceramics Division of Oak Ridge National Laboratory
[DE87-013538] 06 p0681 N88-14171
Study on fracture behaviour of a joint with a crack in transverse hard layer: Effect of hard layer width on COD
[PB87-143855] 07 p0868 N88-15267
Study on characteristics of SCC propagation da/dt for welded joint
[PB87-143640] 07 p0869 N88-15270
Effects of fabrication on the fatigue capacity of welded steel structures
[PB87-144226] 08 p0995 N88-16021
Study on the fracture behavior of 9 percent Ni steel welded joint
[PB87-143863] 08 p0995 N88-16023
Microstructural modification during laser welding
[DE88-002344] 09 p1144 N88-16860
The role of composition and microstructure gradients on weld metal properties and behavior
[DE88-004956] 10 p1303 N88-17791
The influence of small defects on tensile specimen ductility and symmetry of deformation
[AD-A187983] 10 p1346 N88-18044
Effects of sulfur content on the plain strain fracture toughness of inertia welds in 4340 steel
[AD-A188192] 11 p1458 N88-18689
Joining of dissimilar materials with the pulsed Nd-YAG laser
[DE88-003757] 11 p1458 N88-18693
Reduction of residual stresses and distortion in girth welded pipes
[AD-A187728] 11 p1494 N88-18920
Transformation, metallurgical response and behavior of the weld fusion zone and heat affected zone in Cr-Mo steels for fossil energy application
[DE88-006037] 13 p1744 N88-20430
Influence of hydrogen on crack formation tendency in heat-affected zone with stress concentrator
14 p1887 N88-21276
Characteristics of welds joining parts of high-strength pipe steels and produced by beam of continuous-wave CO2-laser
14 p1897 N88-21325
Structure and properties of welded joints produced between niobium parts in controllable helium atmosphere
14 p1897 N88-21326
Inertia welding with variable magnitude of impact load
14 p1897 N88-21328
Characteristics of joint formation during friction welding of Ti alloys to Nb alloys
14 p1898 N88-21329
Optimum duration of steady-state stage in friction welding of metals without artificial braking
14 p1898 N88-21330
Ensuring higher stability of immersed-arc welding of structural aluminum alloys and magnesium alloys
14 p1898 N88-21331
The effect of surface tension in the weld pool on seam formation when welding thin sheet with light rays
14 p1898 N88-21334
Joints in fiber-reinforced aluminum alloys
[NASA-TT-20160] 15 p2031 N88-22104
Cracking tendencies of restrained welds in high strength low alloy steels under hyperbaric conditions
[AD-A190255] 15 p2039 N88-22150
Reduced thermal input by proper selection of YAG laser welding parameters
[DE88-000730] 15 p2072 N88-22356
Microstructural characterization and properties of 3Cr-1.5Mo-0.1V thick section electron beam welds
[DE88-004330] 16 p2486 N88-24747
Apparatus for pressure welding of titanium structures with a controlled rate of deformation
[RAE-TRANS-2161] 19 p2677 N88-25915

Principles of a nondestructive evaluation process for damage location, damage profile, and damage extension in welded joints by radiometric measurements
[MPA-86-02] 20 p2812 N88-26683
Distribution of weld quality in thin section stainless steel tube attachment welds
[PB88-109632] 21 p2955 N88-27555
Determination of the residual stresses in welded structures using the elastoplastodynamic method
[ETN-88-92745] 22 p3087 N88-28330
Qualification of expansion and welding procedures of tube-to-tubesheet joints for heat exchangers in nuclear power plants
[DE88-701621] 23 p3221 N88-29174
Development of graded reference radiographs for aluminum welds, phase 1
[AD-A195594] 24 p3381 N88-30140

WELDED STRUCTURES
NT STEEL STRUCTURES
Advanced radiator concepts utilizing honeycomb panel heat pipes
[NASA-CR-172017] 04 p0443 N88-12747
Evaluation method of the brittle fracture strength in structurally stress-concentrated regions
[PB87-129490] 06 p0721 N88-14435
Study of combination type CO2 laser welding system
[PB87-143764] 08 p0992 N88-16002
Effects of fabrication on the fatigue capacity of welded steel structures
[PB87-144226] 08 p0995 N88-16021
Computation of the tensile and bending restraint intensities of welded specimens by finite element method
[PB87-143798] 08 p0995 N88-16024
Crack opening displacement test in tension
[PB87-143848] 08 p0996 N88-16026
Acoustic emission measurements of PWR weld materials with inserted defects
[AERE-R-12386] 10 p1341 N88-18016
Microstructural characterization of HSLA-100 GMA-weldments
[AD-A187782] 11 p1457 N88-18683
Removal of out-of-plane distortion in mild steel panels using flame heating, volume 1
[AD-A187802] 11 p1457 N88-18684
Removal of out-of-plane distortion in mild steel panels using flame heating, volume 2
[AD-A187803] 11 p1457 N88-18685
Microstructural characterization of the heat affected zone of HSLA (High Strength Low Alloy)-100 steel GMA (Gas Metal Arc)-weldment
[AD-A187825] 11 p1457 N88-18686
Fracture toughness of steel weldments containing lack of penetration defects 11 p1501 N88-18965
Hydrogen induced cracks in armor steel weldments fabricated with austenitic filler alloys
[AD-A188733] 13 p1740 N88-20406
Plasma joining of metal matrix composites
[AD-A193939] 22 p3051 N88-28100

WELDING
NT ARC WELDING
NT BRAZING
NT DIFFUSION WELDING
NT ELECTRON BEAM WELDING
NT EXPLOSIVE WELDING
NT FRICTION WELDING
NT FUSION WELDING
NT GAS TUNGSTEN ARC WELDING
NT GAS WELDING
NT LASER WELDING
NT PLASMA ARC WELDING
NT PRESSURE WELDING
NT ULTRASONIC WELDING
Automatic seam welding with infrared sensor feedback
[DE87-013556] 01 p0055 N88-10352
Materials studies for magnetic fusion energy applications at low temperatures-X
[PB87-232575] 03 p0381 N88-12395
Effects of stress-relieving on the mechanical properties and the structure of specimens of high-temperature fine-grained structural steels heat-treated to simulate welding
[BLL-CE-TRANS-8258-(9022.09)] 04 p0417 N88-12586
The modelling of orientation in planar polymer welding flows
[AD-A184404] 04 p0451 N88-12793
Alignment and assembly tool for very large diameter cylinders
[NASA-CASE-MFS-28001-2] 06 p0711 N88-14360
Sulfur-induced ductility-dip cracking in weld metal of low-carbon steel
[PB87-143814] 07 p0833 N88-15051
Welding in high pressure CO2 atmosphere — underwater welding
[PB87-144044] 07 p0862 N88-15232
Study on automatic detection and identification of defects in weld by microcomputer
[PB87-143897] 07 p0863 N88-15237
Reserach on microprocessor controller for spot welding
[PB87-143913] 07 p0863 N88-15240
Transient welding strain measurement by Moire technique: A comparison between experimental measurement and numerical analysis for strain-stress cycles during GTA spot-welding
[PB87-143871] 07 p0868 N88-15269
A large strain thermomechanical forming model for elastic-viscoplastic behavior in metals 10 p1301 N88-17780
The role of composition and microstructure gradients on weld metal properties and behavior
[DE88-004956] 10 p1303 N88-17791
A collaborative program of research in engineering sciences
[DE88-003383] 10 p1423 N88-18504
Fracture toughness of steel weldments containing lack of penetration defects 11 p1501 N88-18965
Investigation of the use of horizontally polarised shear waves for TOFD studies on austenitic steel
[AERE-R-12145] 13 p1780 N88-20649
JPRS report: Science and technology. USSR: Materials science
[JPRS-UMS-87-009] 14 p1884 N88-21261
Metals. Preliminary study for an Innovation-Oriented research Program (IOP)
[ETN-88-91317] 14 p1889 N88-21290
Innovation-Oriented research Program (IOP) metals. Annexes
[ETN-88-91318] 14 p1889 N88-21291
JPRS report: Science and technology. USSR: Materials science
[JPRS-UMS-87-007] 14 p1895 N88-21312
Segregation effects in welded stainless steels
[DE88-701224] 15 p2037 N88-22139
Weldability of general purpose heat source iridium capsules 17 p2426 N88-24429
Frequency Analysis of Acoustic Emission - Application to machining and welding
[DE88-701478] 18 p2570 N88-25262
Finite elemertt welding computations using general purpose nonlinear analysis codes
[DE88-005398] 20 p2808 N88-26659
Milliwatt generator project
[DE88-011261] 20 p2853 N88-26939
High-speed, precision processing using an electron beam 21 p2929 N88-27391
The influence of weld metal properties, weld geometry and applied load on weld system performance
[AD-A193403] 21 p2961 N88-27588
Plasma joining of metal matrix composites
[AD-A193939] 22 p3051 N88-28100

WELDING MACHINES
Welding monitoring system
[NASA-CASE-MFS-29177-1] 06 p0712 N88-14362

WELLS
Status of the Magma Energy Project
[DE88-002413] 13 p1792 N88-20719
The use of orbital remote sensing data for low cost ground-water survey
[INPE-4587-PRE/1318] 24 p3386 N88-30170

WENTZEL-KRAMER-BRILLOUIN METHOD
WKB theory of wave tunneling for Hermitian vector systems of integral equations
[DE88-005332] 13 p1831 N88-20951

WEST COMET
Comet West: A view from the HELIOS zodiacal light photometers 01 p0117 N88-10749

WEST GERMANY
The history of aeroelasticity research in Germany from the beginning until 1945 — airframes
[DFVLR-MITT-86-25] 01 p0001 N88-10003
Observations of Earth tides by the German Geodetic Research Institute, division 1, in the period 1979-1985 at the Berchtesgaden and Wettzell stations
[SER-B-280] 07 p0872 N88-15291
The role of the DFVLR project management life sciences in the space program of the Federal Republic of Germany 07 p0884 N88-15364
German space policy on the threshold of the century. Analysis and proposals for the future
[ETN-88-90573] 07 p0943 N88-15734
The German scientific balloon and sounding rocket program 08 p1024 N88-16202
Federal Republic of Germany's interests, activities and goals in remote sensing of ocean colour/fluorescence from space 08 p1043 N88-16302
AZUR, the first German research satellite 625-A, 1964-1969 10 p1310 N88-17827
Protected areas with enhanced bird-aircraft collision risk in the Federal Republic of Germany
[GEOPHYSBDBW-FM-209] 11 p1437 N88-18576
Activities report in air traffic control
[ETN-88-91092] 11 p1438 N88-18581
Navigation experiment NAVEX. The reading differences between all ground station measuring clocks during each Spacelab pass of the D1 mission
[DFVLR-MITT-87-23] 16 p2159 N88-22880
Report on the cartographic activities of the Federal Republic of Germany in the period 1984 - 1987 16 p2225 N88-23280
Computer-assisted cartography research and development report of the Federal Republic of Germany 1984 - 1986 16 p2226 N88-23289
The atlas of regional development 16 p2226 N88-23291
West German Geodetic Working Group: Official topographic-cartographic information system (ATKIS), content description 18 p2533 N88-25026
West German Geodetic Working Group: Official topographic-cartographic information system (ATKIS), technical conception 18 p2533 N88-25027
Creation of digital topographic models with the ALK-GIAP. The DLM 25 as an example 18 p2534 N88-25031
State of development of ALK (October 1986) 18 p2534 N88-25035
Results of radiation measurements in West Germany and from special measurement series in the Meteorological Observatory of Hamburg
[REPT-11] 18 p2542 N88-25088
Space policy of common sense and moderation
[REPT-49/87] 20 p2883 N88-27118
Economic impact of space flight activities in West Germany. Influence of allocations of Bundesministerium fuer Forschung und Technologie
[ETN-88-92106] 21 p2901 N88-27215
Atmospheric turbulence research at DFVLR
[AGARD-R-752] 21 p2975 N88-27669
Organization of the TDF1/TDF2 program 22 p3161 N88-28827
Investigation of the large-scale impact of air pollution components on forest ecosystems in Bavaria
[ESA-TT-1087] 24 p3390 N88-30187

WETLANDS
Correlation between aircraft MSS and LIDAR remotely sensed data on a forested wetland in South Carolina
[NASA-TM-89643] 02 p0193 N88-11204
Compilation of 1986 annual reports of the Navy ELF (Extremely Low Frequency) communications system ecological monitoring program, volume 3
[AD-A184563] 03 p0306 N88-11932
AIS-2 spectra of California wetland vegetation 05 p0613 N88-13763
Remote sensing of wetlands: Applications overview
[DE88-010895] 21 p2966 N88-27618
An evaluation of SPOT imagery for wetland monitoring 22 p3091 N88-28353

WETNESS
U MOISTURE CONTENT

WETTABILITY
Adhesive bond strengths on aluminium alloys as a function of surface topographies and their wetting properties
[ARE-TM(UMM)-87403] 09 p1148 N88-16880
Correlations between wettability and structure in monolayers of alkanethiols adsorbed on gold
[AD-A194348] 23 p3191 N88-28991

WETTING
The infiltration kinetics of aluminum in silicon carbide compacts
[AD-A184682] 03 p0290 N88-11823
Adhesive bond strengths on aluminium alloys as a function of surface topographies and their wetting properties
[ARE-TM(UMM)-87403] 09 p1148 N88-16880
Thermodynamics of wetting by liquid metals
[DE88-003634] 11 p1563 N88-19360
Critical point wetting drop tower experiment
[NASA-CR-183062] 20 p2798 N88-26603
Depressed sweating during exercise at altitude
[AD-A192603] 22 p3130 N88-28609

WHARVES
Impact force as a part of the tctal breaking wave force on a vertical cylinder
[RR-CE78] 24 p3384 N88-30154

WHEAT
Study of the relationship between photosynthesis, respiration, transpiration, and mineral nutrition in wheat 03 p0360 N88-12268
Wheat production in controlled environments
[UAES-PAPER-3324] 03 p0361 N88-12270
Optimal sampling to provide user-specific climate information 11 p1515 N88-19051
Closed system physiology: Role of oxygen in the development of wheat 12 p1655 N88-19916

Use of energy emission for detecting the necessity of irrigation in wheat in field conditions
[INPE-4461-TDL/318] 16 p2229 N88-23315
Estimation of an area cultivated with wheat from LANDSAT data through a two-phase sampling method
17 p2357 N88-24041
Application of SPOT multidate data to wheat yield estimation in Beauce (France) 22 p3094 N88-28374
TM/LANDSAT-5 data to evaluate wheat and bean percent soil cover and leaf area index
[INPE-4609-PRE/1332] 24 p3385 N88-30165
LANDSAT TM and agrometeorological data for wheat yield estimation at the farm level
[INPE-4591-PRE/1321] 24 p3388 N88-30180

WHEELS
NT FLYWHEELS
NT REACTION WHEELS
NT TURBINE WHEELS
NT VEHICLE WHEELS

WHIRL
U ROTATION

WHIRL INSTABILITY
U ROTARY STABILITY

WHIRLING
U ROTATION

WHISKER COMPOSITES
Investigation of microstructural factors that cause low fracture toughness in silicon carbide whisker/Al alloy composites
[AD-A186443] 09 p1137 N88-16817
Microstructures and properties of SiC whisker-reinforced mullite composites
[DE88-002611] 09 p1139 N88-16826
Micro-mechanisms of deformation in SiC/Al composites
[AD-A188282] 10 p1296 N88-17749
Composites strengthening
[AD-A189258] 13 p1734 N88-20364
Interfacial chemistry-structure and fracture of ceramic composites
[DE88-005516] 13 p1750 N88-20461
The effect of strain rate on the strength and ductility of SiCw/2124 Al composite
[OUEL-1692/87] 14 p1924 N88-21466
Whisker-reinforced ceramic composites for heat engine components 15 p2082 N88-22410
Factors influencing the toughening behavior of whisker reinforced ceramics
[DE88-011396] 20 p2779 N88-26479
Theoretical and experimental analysis of the toughening behavior of whisker reinforcement in ceramic matrix composites
[DE88-011841] 21 p2906 N88-27241

WHISKERS (CRYSTALS)
Production of metallic monocrystals described
03 p0286 N88-11796
Nondestructive characterization of ceramic composite whiskers with neutron diffraction and ultrasonic techniques
[DE88-003075] 08 p0965 N88-15844
A laboratory study of tin whisker growth
[ESA-STR-223] 08 p1089 N88-16553
An organometallic route to micron-sized whiskers of zinc sulfide
[AD-A195889] 24 p3430 N88-30414

WHISTLERS
JPRS report: Science and technology. China
[JPRS-CST-87-031] 03 p0299 N88-11880
Method estimating integral mean value of enhancement factor and path latitude for whistlers below magnetic latitude 10 deg 03 p0300 N88-11885
Simulation and modeling of whistler mode wave growth through cyclotron resonance with energetic electrons in the magnetosphere 10 p1353 N88-18089
Observations and analyses of summer whistlers at the Great Wall Station of Antarctica
11 p1469 N88-18759
An analysis of whistler-mode radiation from the Spacelab-2 electron beam, revision
[AD-A188228] 11 p1552 N88-19287
Electrostatic whistler mode conversion at plasma resonance
[AD-A192951] 20 p2860 N88-26989

WHITE BLOOD CELLS
U LEUKOCYTES

WHITE DWARF STARS
PG 0308 + 096: A short-period white dwarf + dM binary with strongly modulated H-alpha emission
04 p0509 N88-13132
BE Ursae Majoris: A detached binary with a unique reprocessing spectrum
[NASA-CR-182419] 06 p1083 N88-16526
The X-ray properties of AM Her stars
[MPE-PREPRINT-106] 16 p2289 N88-23704
Ultraviolet spectra of subluminous objects found in the Kiso Schmidt survey and systematic reanalysis of the archived ultraviolet spectra of white dwarfs observed with the IUE satellite under the Astrophysics Data Program (ADP)
[NASA-CR-182976] 18 p2592 N88-25408
Ultraviolet spectra of two magnetic white dwarfs and ultraviolet spectra of subluminous objects found in the Kiso Schmidt survey
[NASA-CR-183051] 18 p2593 N88-25408

WHITE LIGHT HOLOGRAPHY
Rainbow holographic image reconstructed by spatially extended white light source 15 p2055 N88-22249

WHITE NOISE
NT THERMAL NOISE
White noise calculus for two-parameter filtering
[ENST-87C003] 01 p0088 N88-10578
Detection of signals by the digital integrate-and-dump filter with offset sampling 04 p0435 N88-12695

WICKS
Heat transfer of mesh-wick heat-pipes (bottom heat mode) 20 p2783 N88-26507
Polymeric heat pipe wick
[NASA-CASE-GSC-13019-1] 23 p3214 N88-29133

WIDE ANGLE LENSES
Treatment of systematic errors in the processing of wide angle sonar sensor data for robotic navigation
[DE88-008961] 20 p2756 N88-26352

WIDEBAND
U BROADBAND

WIDEBAND COMMUNICATION
The characteristics of two broadband (2 MHz to 10 MHz) switched vee antennas
[AD-A187874] 11 p1471 N88-18770
The Effect of the Ionosphere on Communication, Navigation and Surveillance Systems Based on Ionospheric Effects Symposium held on 5-7 May 1987 in Springfield, Virginia
[AD-A191855] 18 p2541 N88-25081

WIGGLER MAGNETS
Brightness and coherence of radiation from undulators and high-gain free electron lasers
[DE87-011093] 02 p0177 N88-11102
Sideband suppression by an intracavity optical filter in the Los Alamos free-electron laser oscillator
[DE87-011740] 02 p0177 N88-11103
Center for X-Ray Optics, 1986
[DE88-000715] 04 p0449 N88-12783
A long electromagnetic wiggler for the paladin free-electron laser experiments
[DE88-000970] 05 p0588 N88-13589
Development of a strong electromagnet wiggler
[DE88-000971] 05 p0645 N88-13952
Development of a laced electromagnetic wiggler
[DE88-000972] 05 p0646 N88-13953
Tapered wiggler analysis of high gain free electron laser oscillators
[AD-A187997] 10 p1338 N88-17997
Wiggler taper optimization for free-electron-laser amplifiers with moderate space-charge effects
[DE88-003758] 13 p1775 N88-20618
Research on variable-period wiggler type free electron lasers 14 p1902 N88-21360
Pulsed magnet fields for free-electron lasers
14 p1903 N88-21367
The free-electron laser: Theoretical innovations and gas-loaded experiment 20 p2806 N88-26646
On the small signal gain of free electron lasers in the low-current regime
[DFVLR-FB-88-10] 21 p2955 N88-27552
Free electron lasers with small period wigglers
[DE88-011627] 23 p3218 N88-29156

WIGHTMAN THEORY
U FIELD THEORY (PHYSICS)
U QUANTUM THEORY
U RELATIVISTIC THEORY

WIGNER COEFFICIENT
Wigner distribution function: Relation to short-term spectral estimation, smoothing and performance in noise
[AD-A193865] 23 p3275 N88-29492

WILDERNESS
History of wildland fires on Vandenberg Air Force Base, California
[NASA-TM-100983] 18 p2549 N88-25134

WIND (METEOROLOGY)
NT GEOSTROPHIC WIND
NT GROUND WIND
NT GUSTS
NT JET STREAMS (METEOROLOGY)
NT MONSOONS
NT SEA BREEZE
NT SQUALLS
NT WINDS ALOFT
Analysis of the bivariate parameter wind differences between Jimsphere and Windsonde
[NASA-TM-4014] 01 p0072 N88-10461
Global positioning satellite-based automatic landing system and wind estimated feedback for the AH-64 helicopter 02 p0124 N88-10784
Direct Absorption Receiver flow experiments
[DE87-014655] 02 p0196 N88-11221
Mesoscale MOS forecast support for 1988 winter Olympics ski events --- model output statistics (MOS)
02 p0209 N88-11312
NWS (National Weather Service) watch/warning verification flash flood, winter storm and high wind, January 1980 - June 1986
[PB87-223053] 04 p0469 N88-12898
Tropical easterly jet located using TOMS data
05 p0616 N88-13783
Studies in Aeolian geology
[NASA-CR-182328] 05 p0625 N88-13828
Radar observations of high-latitude lower-thermospheric and upper-mesospheric winds and their response to geomagnetic activity 06 p0742 N88-14563
Wave and wind data sources, environmental conditions committee report, International Ship and Offshore Structures Congress
[PB87-234902] 06 p0746 N88-14588
Middle atmospheric wind measurements using a medium frequency radar
[AD-A185931] 07 p0879 N88-15330
Research work at the Meteorological Institute of the University of Munich (Federal Republic of Germany)
[MITT-56] 08 p1013 N88-16141
The role of anabatic winds in the heating of valleys
08 p1014 N88-16144
North Pacific Ocean. Tradewind region east of Hawaii, R/V Thomas G Thompson: 25 September - 1 November 1972. STD data report
[AD-A186566] 08 p1044 N88-16311
North Pacific Ocean. Northeast Pacific Transition Zone, R/V Thomas G. Thompson: 1 November - 6 December 1969. STD data report
[AD-A186574] 09 p1195 N88-17161
Airborne Doppler radar technology for wind shear detection 10 p1274 N88-17622
Radar backscatter from airports and surrounding areas 10 p1274 N88-17623
Universal power spectra for wave turbulence: Applications to wind waves, flicker noise, solar wind spectrum and classical second sound
10 p1318 N88-17879
Remote sensing of atmospheric crosswinds by utilizing speckle-turbulence interaction and optical heterodyne detection
[AD-A187580] 10 p1347 N88-18052
The structure and dynamics of monsoon depressions
10 p1355 N88-18102
Systematic errors of the FSU global spectral model
10 p1356 N88-18103
Evolution of acoustic gravity wave packet in spatially and temporally varying wind 11 p1469 N88-18760
Caribbean and Central America wind energy assessment
[DE88-005134] 11 p1507 N88-19002
Site effects on wind characteristics at a turbine rotor
[DE88-005135] 11 p1507 N88-19003
Upper-thermospheric observations and neutral-gas dynamics at high latitudes during solar maximum
[AD-A188058] 11 p1512 N88-19031
Numerical simulation of near-surface environments and particulate clouds generated by large-area fires
[AD-A188375] 12 p1641 N88-19828
Retrieval of three-dimensional wind and temperature fields from single-Doppler radar data
12 p1646 N88-19858
Simulating high-resolution vertical plane array wind characteristics using lower-spatial-resolution wind measurements
[DE88-005626] 13 p1800 N88-20761
Circulation and exchange processes on the South Atlantic Bight Continental Shelf
[DE88-003330] 13 p1804 N88-20781
Monthly mean global climatology of temperature, wind, geopotential height, and pressure for 0 - 120 km
[NASA-TM-100697] 15 p2099 N88-22503
Global atmospheric circulation statistics, 1000-1 mb
[PB88-168240] 16 p2234 N88-23340
Report on project WIND: Preliminary experiments with the UK Meteorological Office mesoscale model, September 1987
[AD-A191621] 18 p2544 N88-25099
Estimation of balloon position from wind data
[DE88-008968] 19 p2597 N88-25434
A radar study of the interaction between lightning and precipitation
[DE88-009120] 20 p2827 N88-26770
Wind flow study: July 1987 and November-December 1987
[DE88-008969] 20 p2828 N88-26776

Zonal wind observations at Christmas Island (2 deg N, 157 deg W) during the 1986-1987 El-Nino
22 p3120 N88-28539
The observed dynamical structure of low frequency variabilities
22 p3120 N88-28541
The dynamics and thermodynamics of a 30-60 day oscillation
22 p3121 N88-28543
Complex EOF analysis of intraseasonal tropical wind fluctuations
22 p3121 N88-28544
Some diagnostic results concerning the tropical 40-50 day oscillation
22 p3121 N88-28546
Recent secular changes in the wintertime circulation of the Southern Hemisphere
22 p3122 N88-28555
Variations in the atmosphere associated with the 11-year solar cycle
22 p3122 N88-28557
Extratropical response to tropical heating as a function of period of model integrations
22 p3125 N88-28577
Doppler radar analysis of coastal marine atmospheric boundary layer structure during a cold air outbreak
[AD-A196023] 24 p3403 N88-30261
Analysis of environmental parameters from the Panama City tower radar experiment
[AD-A194994] 24 p3404 N88-30264

WIND CIRCULATION
U ATMOSPHERIC CIRCULATION

WIND DIRECTION
Coastal winds of the southeast Alaska Peninsula
[PB87-206173] 02 p0215 N88-11354
BARS-1M meteorological complex carried on IL-18 airplane
06 p0725 N88-14458
Remote sensing of atmospheric crosswinds by utilizing speckle-turbulence interaction and optical heterodyne detection
[AD-A187580] 10 p1347 N88-18052
Method for determination of the wind velocity and direction
[NASA-TT-20233] 13 p1802 N88-20769
Distribution of summertime lightning as a function of low-level wind flow in central Florida
[PB88-160759] 14 p1948 N88-21619
Parameterization of horizontal wind velocity variability
[AD-A190107] 15 p2097 N88-22493
The effects of time-dependent winds and ocean eddies on ice motion in a marginal ice zone
[AD-A190105] 15 p2100 N88-22511
Geostrophic flow in the central Bering Sea, Fall 1986 and Summer 1987
[PB88-174354] 16 p2237 N88-23360
A system for determination of wind fields using geostationary meterological satellites
17 p2360 N88-24056
Project wind, phase 4 (smoke test), Meadow Brook Valley, Red Bluff, California
[AD-A194742] 22 p3128 N88-28596
Analysis of environmental parameters from the Panama City tower radar experiment
[AD-A194994] 24 p3404 N88-30264

WIND EFFECTS
The effect of wind and currents on gas exchange in an estuarine system
[NASA-CR-181424] 01 p0073 N88-10468
Vertical profiles of wind-induced current --- North Sea
[IOS-238] 02 p0193 N88-11207
Direct Absorption Receiver flow experiments
[DE87-014655] 02 p0196 N88-11221
The application of divergence equation in the analysis of heavy rainfall
02 p0207 N88-11299
The effect of mass, wind angle and erection technique on the aeroelastic behaviour of a cable-stayed bridge model
[NAE-AN-46] 04 p0455 N88-12819
Theory of heat and moisture exchange between finely disperse storm-generated spray and turbulent air flow
04 p0461 N88-12851
Environmental processes and spectral reflectance characteristics associated with soil erosion in desert fringe regions
[NASA-CR-182332] 05 p0620 N88-13811
A comparison of the predicted and measured gravitational stresses in VAWT (Vertical Axis Wind Turbine) blades
[DE88-002113] 09 p1187 N88-17111
Site effects on wind characteristics at a turbine rotor
[DE88-005135] 11 p1507 N88-19003
Mesoscale coastal ocean dynamics
11 p1517 N88-19060
Study of spectra of sea waves on horizontally nonuniform current in rip zone
13 p1788 N88-20699
Circulation and exchange processes on the South Atlantic Bight Continental Shelf
[DE88-003330] 13 p1804 N88-20781
Dynamics of the Oceanic Surface Mixed Layer
[AD-A188348] 13 p1804 N88-20785
On the zonal momentum balance at the equator
13 p1805 N88-20788
The mixed layer of the western equatorial Pacific Ocean
[HIG-1861] 13 p1805 N88-20789
Unsteady shallowing mixed layer
13 p1805 N88-20791
Some effects of heating on the wind-driven velocity in the upper ocean
13 p1805 N88-20792
Mixed-layer shear related to wind stress in the central equatorial Pacific
13 p1805 N88-20793
Mixed-layer fronts in the California current
13 p1805 N88-20794
Horizontal scales of wind forced inertial motions
13 p1806 N88-20795
Wind forcing and observed oceanic wavenumber spectra
13 p1806 N88-20797
Energy and momentum fluxes through the sea surface
13 p1806 N88-20798
Hamiltonian description of the interaction of surface waves with mixed-layer currents
13 p1806 N88-20799
Monitoring ocean surface layer processes
13 p1806 N88-20801
An improved wind input source term for third generation ocean wave modeling
[KNMI-WR-87-8] 14 p1950 N88-21624
Experimental study on the influence of wind on acoustic pressure sensors
[ISL-R-121/86] 15 p2131 N88-22712
Use of energy emission for detecting the necessity of irrigation in wheat in field conditions
[INPE-4461-TDL/318] 16 p2229 N88-23315
Numerical model for the computation of radiance distributions in natural waters with wind-roughened surfaces
[PB88-192703] 20 p2826 N88-26765
Eigenmatrix representations of radiance distributions in layered natural waters with wind-roughened surfaces
[PB88-188701] 20 p2828 N88-26780
An examination of wake effects and power production for a group of large wind turbines
[DE88-009906] 22 p3117 N88-28518
Effects of precipitation on wind turbine performance
[DE88-001144] 23 p3228 N88-29211

WIND ENERGY
U WINDPOWER UTILIZATION

WIND MEASUREMENT
NT WIND VELOCITY MEASUREMENT
Analyses and assessments of span wise gust gradient data from NASA B-57B aircraft
[NASA-CR-178288] 01 p0002 N88-10007
Coastal winds of the southeast Alaska Peninsula
[PB87-206173] 02 p0215 N88-11354
Comparative testing of wind measuring equipment. Part 1: Inventory and selection
[R-814-D-PT-1] 03 p0325 N88-12053
Long-period variations of wind parameters in the mesopause region and the solar cycle dependence
06 p0733 N88-14509
Main results of atmospheric fine structure parameter observation in the lower thermosphere
06 p0735 N88-14518
Meteor detection on ST (MST) radars
06 p0740 N88-14554
Measurement in a wind tunnel of the modification of mean wind and turbulence characteristics due to induction effects near wind turbine rotors
[DE88-000249] 07 p0815 N88-14963
Middle atmospheric wind measurements using a medium frequency radar
[AD-A185931] 07 p0879 N88-15330
Development of a Doppler wind lidar system for atmospheric wind measurements
08 p1027 N88-16217
Project CONDOR: Middle atmosphere wind structure obtained with lightweight inflatable spheres near the equatorial electrojet
08 p1028 N88-16230
Wind measurements at high altitudes (150 m tower)
[BMFT-FB-T-86-169] 09 p1193 N88-17149
Minimum Energy Routing through Interactive Techniques (MERIT) modeling
[NASA-CR-182535] 10 p1356 N88-18105
Ground clutter processing for wind measurements with airport surveillance radars
[AD-A187708] 11 p1514 N88-19044
Correction of the wind field measured by the NCAR electra during FASINEX (Frontal Air-Sea Interaction Experiment) for inertial navigation system drifts
[AD-A187780] 11 p1514 N88-19045
A preliminary assessment of thunderstorm outflow wind measurement with airport surveillance radars
[AD-A189064] 13 p1799 N88-20757
Mixed-layer shear related to wind stress in the central equatorial Pacific
13 p1805 N88-20793
Optical properties of Southern Hemisphere aerosols: Report of the joint CSIRO/NASA study
[NASA-CR-179287] 14 p1945 N88-21605
Climatological data of the Netherlands lightvessels over the period 1949-1980 --- North Sea
[KNMI-WR-87-9] 14 p1947 N88-21613
Solar wind observation at the time of closest encounter with Comet Halley
14 p1995 N88-21890
Prospects of satellite wind sensing systems in the years 1995-2000
17 p2350 N88-24004
Comparison of surface current determined from satellite-tracked buoy with shipboard wind data during the 4th Brazilian antarctic expedition, 10-14 March, 1986
17 p2354 N88-24024
Overview of wind behavior research in the US Wind Energy Program
[DE88-005683] 18 p2537 N88-25057
Special observations
18 p2545 N88-25108
Aircraft/lidar turbulence comparison
18 p2546 N88-25111
The pneumatic wind shear sensor: A tool for meteorological investigations and flight management
22 p3036 N88-28024
A study of the feasibility of using sea and wind information from the ERS-1 satellite. Part 1: Wind scatterometer data
[NASA-CR-182833] 24 p3386 N88-30167
A study of the feasibility of using sea and wind information from the ERS-1 satellite. Part 2: Use of scatterometer and altimeter data in wave modeling and assimilation
[ESA-CR(P)-2604-PT-2] 24 p3387 N88-30176
Determining near-water wind speed using radar data from Cosmos-1500 artificial earth satellite
24 p3449 N88-30524

WIND PRESSURE
Typhoon structural evolution
[AD-A186090] 07 p0879 N88-15333
Determination of the ultimate loads for corrugated-steel, barrel-type shell structures
[AD-A187716] 11 p1498 N88-18944

WIND PROFILES
A real-time system for automatic single-Doppler wind field analysis
02 p0200 N88-11249
Statistical relationships between the mesoscale organization of convection and the large-scale wind profiles during GATE --- GARP Atlantic Tropical Experiment (GATE)
02 p0208 N88-11302
The importance of the lower level windshear profile in tornado/non-tornado discrimination
02 p0208 N88-11304
Short-term forecasting of lightning based on the surface wind field at Kennedy Space Center
02 p0208 N88-11306
Mesoscale surface field analysis from routine observations --- pressure, wind fields
02 p0209 N88-11315
High resolution determination of true surface winds at sea from wind and pressure data
02 p0210 N88-11316
A preliminary demonstration of the use of boundary-layer models of flow in complex terrain for high resolution surface wind forecasting
02 p0212 N88-11330
An improved method of analyzing surface geostrophic winds and pressure
02 p0212 N88-11334
Windfield simulations from a hierarchy of nested meso- and micrometeorological models
02 p0215 N88-11351
Middle Atmosphere Program. Handbook for MAP, volume 25
[NASA-CR-181571] 06 p0732 N88-14502
The climatic wind regime in the lower thermosphere from meteor radar observations
06 p0733 N88-14506
Meteor observation by the Kyoto meteor radar
06 p0733 N88-14507
Long-period variations of wind parameters in the mesopause region and the solar cycle dependence
06 p0733 N88-14509
The lower thermosphere wind regime from simultaneous observations over Euroasia (Collm, Dushanbe, Frunze)
06 p0733 N88-14510
Wind regime peculiarities in the lower thermosphere in the winter of 1983/84
06 p0733 N88-14511
On the interconnection of dynamic processes in the lower thermosphere with meteorological phenomena in the tropostratosphere
06 p0734 N88-14512
Tidal activity in the meteor zone over Budrio, Italy
06 p0734 N88-14517
On connection between evolution of troposphere fronts and changes of circulation regime in meteor zone
06 p0735 N88-14519
A study of the mechanism of internal gravity wave generation by quasigeostrophic meteorological motions
06 p0735 N88-14520
On the dependence of the lower thermospheric wind regime on the solar cycle
06 p0736 N88-14524
Lower thermosphere wind regime according to radiometeor measurements in Kazan
06 p0736 N88-14526

Some aspects of metallic ion chemistry and dynamics in the mesosphere and thermosphere
06 p0737 N88-14534
Observations of inertial period waves and vertical velocities in the tropical middle atmosphere using the MST radar technique 06 p0742 N88-14562
A method to obtain a wind model for the boundary layer in a representative tropical region
[R-818-D] 06 p0743 N88-14569
Improvements in profiler wind estimates using smoothed data in the spectrum finder algorithm
[PB88-102181] 07 p0881 N88-15342
Vertical sounding of th air layer close to a glacier on Mount Vernagferner in the Oetzal Alps, Tyrol (experiment LUZIVER 1983) 08 p1015 N88-16152
Simulation of a typical flow in a broad valley
08 p1015 N88-16154
Project CONDOR: Middle atmosphere wind structure obtained with lightweight inflatable spheres near the equatorial electrojet 08 p1028 N88-16230
Wind measurements at high altitudes (150 m tower)
[BMFT-FB-T-86-169] 09 p1193 N88-17149
Correction of the wind field measured by the NCAR electra during FASINEX (Frontal Air-Sea Interaction Experiment) for inertial navigation system drifts
[AD-A187780] 11 p1514 N88-19045
An analytical method for the determination of the average horizontal wind velocities across two-dimensional hills
[ISBN-3-923624-06-9] 11 p1515 N88-19048
Aerodynamic aspects of the Amazon Forest
[INPE-4445-TDL/313] 15 p2098 N88-22501
A system for determination of wind fields using geostationary meterological satellites
17 p2360 N88-24056
Special observations 18 p2545 N88-25108
Three-dimensional wind simulation
[DE88-009793] 21 p2975 N88-27671
Space shuttle natural environment analysis
[NASA-CR-179337] 21 p2976 N88-27676
A system for determination of wind fields from cloud tracks: INPE experiment
[INPE-4492-PRE/1256] 22 p3126 N88-28594
Wind measurements by electromagnetic probes
[NASA-TM-4066] 23 p3236 N88-29256

WIND SHEAR
Contributions to the modeling of wind shear for danger studies
[ETN-87-90442] 01 p0072 N88-10463
New nowcasting opportunities using modern meteorological radar 02 p0199 N88-11245
Nowcasting microbursts using Doppler radar in a forecaster-computer environment
02 p0200 N88-11246
The importance of the lower level windshear profile in tornado/non-tornado discrimination
02 p0208 N88-11304
Study of microburst detection performance during 1985 in Memphis, Tennessee
[AD-A184013] 03 p0354 N88-12231
Some aspects of metallic ion chemistry and dynamics in the mesosphere and thermosphere
06 p0737 N88-14534
Wind shear detection. Forward-looking sensor technology
[NASA-CP-10004] 07 p0817 N88-14970
Low altitude windshear threat to commercial aircraft
08 p0952 N88-15777
A comparison of multi-layer meso-alpha MLAM model results with surface and aircraft observations from CAPTEX
[DE88-000549] 09 p1186 N88-17118
Airborne Wind Shear Detection and Warning Systems: First Combined Manufacturers' and Technologists' Conference
[NASA-CP-10006] 10 p1273 N88-17616
NASA wind shear model: Summary of model analyses
10 p1273 N88-17617
Response of wind shear warning systems to turbulence with implication of nuisance alerts
10 p1274 N88-17618
Investigation of the influence of wind shear on the aerodynamic characteristics of aircraft using a vortex-lattice method 10 p1274 N88-17619
Windshear warning aerospatiale approach
10 p1274 N88-17620
Windshear detection effect of static air temperature bias 10 p1274 N88-17621
Airborne Doppler radar technology for wind shear detection 10 p1274 N88-17622
Radar backscatter from airports and surrounding areas 10 p1274 N88-17623
Wind shear radar simulation 10 p1274 N88-17625
Lidar windshear detection and avoidance: Performance and technical assessment 10 p1274 N88-17626
Airborne Doppler lidar detection of wind shear. Results of performance analysis 10 p1275 N88-17627
Infrared low-level wind shear work
10 p1275 N88-17628
Forward looking wind shear detection
10 p1275 N88-17629
Simulator investigation of wind shear recovery techniques 10 p1275 N88-17630
Crew interface with windshear systems
10 p1275 N88-17631
Status of FAA terminal Doppler weather radar programs 10 p1275 N88-17632
The advanced low-level windshear alert system operational demonstration results, Summer, 1987, Denver Stapleton International Airport 10 p1275 N88-17633
Are windshear training aid recommendations appropriate for other than large jet transports? Pilot procedures: Shear models 10 p1275 N88-17635
Airworthiness considerations
10 p1276 N88-17636
Windshear training aid. Volume 1: Overview, pilot guide, training program
[PB88-127196] 10 p1276 N88-17637
Variation of the wind stress related to frontal passages during FASINEX (Frontal Air-Sea Interaction Experiment) 1986
[AD-A187180] 11 p1514 N88-19042
Ground clutter processing for wind measurements with airport surveillance radars
[AD-A187708] 11 p1514 N88-19044
Wind shear as a predictor of severe weather for the eastern United States
[PB88-157144] 13 p1800 N88-20762
Power spectral density analysis of wind-shear turbulence for related flight simulations
[NASA-CR-182721] 13 p1802 N88-20773
Development and testing of the gust front algorithm
[AD-A189722] 14 p1949 N88-21622
Propagation of acoustic gravity wave spectrum through vertical wind shear region 16 p2186 N88-23035
Flight penetration of wind shear: Control strategies
17 p2294 N88-23727
The Federal Aviation Administration/Massachusetts Institute of Technology (FAA/MIT) Lincoln Laboratory Doppler weather radar program
18 p2547 N88-25118
Flight-management strategies for escape from microburst encounters
[NASA-TM-4057] 19 p2603 N88-25461
Influence of wind shear on the aerodynamic characteristics of airplanes
[NASA-TP-2827] 20 p2755 N88-26344
Intelligent guidance and control for wind shear encounter
[NASA-CR-183060] 20 p2755 N88-26347
The role played by FDRs in understanding the windshear phenomenon 22 p3036 N88-28023
The pneumatic wind shear sensor: A tool for meteorological investigations and flight management
22 p3036 N88-28024
Contributions to the modeling of wind shear for danger studies
[NASA-TT-20293] 23 p3174 N88-28900
Airborne radar technology for windshear detection
[NASA-CR-183203] 23 p3236 N88-29257
Cloud/mesoscale model development and application studies
[AFGL-TR-87-0219] 24 p3404 N88-30269

WIND TUNNEL APPARATUS
NT WIND TUNNEL DRIVES
A method for the calculation of transonic flows for the control of adaptive wind tunnels
[ETN-87-90411] 01 p0003 N88-10015
The generation of nearly isotropic turbulence by means of grids
[PNR90411] 02 p0172 N88-11084
Effect of a model support strut on measurement of aerodynamic longitudinal and lateral coefficients
[PB87-170288] 09 p1113 N88-16670
Strain gage balance for half models 302-6. Calibration report — wind tunnels
[F+W-FO-1803] 09 p1168 N88-17001
Strain gage sting balance 204-6. Calibration report — wind tunnels
[F+W-FO-1838] 09 p1168 N88-17002
Experimental evaluation of turning vane designs for high-speed and coupled fan-drive corners of 0.1-scale model of NASA Lewis Research Center's proposed altitude wind tunnel
[NASA-TP-2681] 10 p1285 N88-17686
Activities report of the Large Testing Facilities Department — aircraft/spacecraft
[ETN-88-91982] 13 p1724 N88-20311
The 5.5 m low speed wind tunnel. Introduction to the facilities
[ARG-205] 14 p1870 N88-21172
Main features of Warton (United Kingdom) 2.7 x 2.1 m low speed wind tunnel
[AXM-124] 14 p1870 N88-21173
Details of low speed intake test facility at the Warton (United Kingdom) 2.7m x 2.1m wind tunnel
[AXM-127] 14 p1870 N88-21174
Design of a supersonic wind tunnel
[ETN-88-92078] 14 p1870 N88-21176
Equipment for mass flow measurements in the low-speed wind tunnel at DFVLR in Brunswick, West Germany
[DFVLR-MITT-88-02] 21 p2900 N88-27212
Computer programs for calculation of sting pitch and roll angles required to obtain angles of attack and sideslip on wind tunnel models
[NASA-TM-100659] 24 p3329 N88-29820

WIND TUNNEL BALANCES
U WEIGHT INDICATORS
U WIND TUNNEL APPARATUS

WIND TUNNEL CALIBRATION
Calibration of a five hole probe and testing of an evaluation method for flow field measurements
[ESA-TT-1051] 03 p0325 N88-12051
Transonic wind tunnel calibration 1986: Force measurements on three ONERA-C5 models and three half sphere cylinder calibration bodies in the F+W transonic test section
[F+W-FO-1854] 09 p1122 N88-16714
Strain gage balance for half models 302-6. Calibration report — wind tunnels
[F+W-FO-1803] 09 p1168 N88-17001
Strain gage sting balance 204-6. Calibration report — wind tunnels
[F+W-FO-1838] 09 p1168 N88-17002
Reynolds number effects and the wind tunnel environment 23 p3168 N88-28862
Flow visualization on a small scale
[AD-A194728] 23 p3181 N88-28935
Hot-wire measurements of compressor blade wakes in a cascade wind tunnel
[AD-A194737] 23 p3181 N88-28936

WIND TUNNEL DRIVES
Analysis of 7- X 10-foot high speed wind tunnel shaft loads in support of fan blade failure investigation
[NASA-TM-100504] 04 p0402 N88-12496
Experimental evaluation of turning vane designs for high-speed and coupled fan-drive corners of 0.1-scale model of NASA Lewis Research Center's proposed altitude wind tunnel
[NASA-TP-2681] 10 p1285 N88-17686

WIND TUNNEL MODELS
Possibilities for the modeling of dynamically loaded cylindrical structural parts in the wind tunnel
[KU-SFB-210/T/24] 01 p0001 N88-10005
A transonic model representation for two-dimensional wall interference assessment
[NLR-TR-86026-U] 01 p0001 N88-10006
Flutter suppression and gust load alleviation. Part 1: Results of phase 1 to 3. Part 2: Description of the Garteur model
[MBB/LKE-292/S/PUB/191] 01 p0007 N88-10038
Comparison of wind tunnel and flight test afterbody and nozzle pressures for a twin-jet fighter aircraft at transonic speeds
[NASA-TP-2588] 02 p0121 N88-10765
Static Aeroelastic Effects on High Performance Aircraft
[AGARD-CP-403] 05 p0550 N88-13348
The use of aeroelastic wind tunnel models to prove structural design 05 p0551 N88-13355
Aerodynamic and propeller performance characteristics of a propfan-powered, semispan model
[NASA-TM-86705] 06 p0667 N88-14092
Status of magnetic suspension technology
07 p0811 N88-14939
Preliminary calibration and test results from the National Transonic Facility 07 p0811 N88-14941
Effect of a model support strut on measurement of aerodynamic longitudinal and lateral coefficients
[PB87-170288] 09 p1113 N88-16670
Testing of a schematic transport plane model in several European windtunnels
[PB87-170270] 09 p1113 N88-16671
Wind tunnel modeling techniques
[KU-SFB-210/E/33] 09 p1121 N88-16711
Influence of the wall boundary layer on force measurements on half models in the transonic wind tunnel
[F+W-TF-1876] 09 p1122 N88-16715
Ariane 4, long version: Pressure distribution measurements on two models of different scale of the Ariane 4 nose fairings in the transonic tunnel of F+W Emmen (Switzerland) with varying tunnel configurations. Comparison with measurements taken at Modane (France) and with calculations after the Euler method
[F+W-TF-1878] 09 p1122 N88-16716

Strain gage balance for half models 302-6. Calibration report --- wind tunnels
[F+W-FO-1803] 09 p1168 N88-17001
Strain gage sting balance 204-6. Calibration report --- wind tunnels
[F+W-FO-1838] 09 p1168 N88-17002
Effects of winglets on a first-generation jet transport wing. 7: Sideslip effects on winglet loads and selected wing loads at subsonic speeds for a full-span model
[NASA-TP-2619] 11 p1436 N88-18567
Acoustic measurements from a rotor blade-vortex interaction noise experiment in the German-Dutch Wind Tunnel (DNW)
[NASA-TM-4024] 11 p1542 N88-19218
Design of an aeroelastic composite wing wind tunnel model
[AD-A188855] 12 p1582 N88-19466
A wind tunnel model with dynamic control
[BU-352] 13 p1724 N88-20310
Activities report of the Large Testing Facilities Department --- aircraft/spacecraft
[ETN-88-91982] 13 p1724 N88-20311
Surface flow visualization of separated flows on the forebody of an F-18 aircraft and wind-tunnel model
[NASA-TM-100436] 14 p1863 N88-21127
Inflow measurement made with a laser velocimeter on a helicopter model in forward flight. Volume 2: Rectangular planform blades at an advance ratio of 0.23
[NASA-TM-100542] 14 p1864 N88-21139
Design, simulation and laboratory testing of an inertial system for measuring the attitude and narrow-spaced motions
[DFVLR-FB-87-42] 14 p1912 N88-21426
Inflow measurement made with a laser velocimeter on a helicopter model in forward flight. Volume 3: Rectangular planform blades at an advance ratio of 0.30
[NASA-TM-100543] 15 p2015 N88-22015
Acoustic characteristics of 1/20-scale model helicopter rotors
[NASA-CR-177355] 16 p2265 N88-23548
Inflow measurement made with a laser velocimeter on a helicopter model in forward flight. Volume 5: Tapered planform blades at an advance ratio of 0.23
[NASA-TM-100545] 17 p2299 N88-23755
Control law parameterization for an aeroelastic wind-tunnel model equipped with an active roll control system and comparison with experiment
[NASA-TM-100593] 17 p2308 N88-23807
Inflow measurements made with a laser velocimeter on a helicopter model in forward flight. Volume 1: Rectangular planform blades at an advance ration of 0.15
[NASA-TM-100541] 18 p2460 N88-24607
Heterogeneous diffusion flame stabilization
[AD-A193014] 20 p2771 N88-26429
An experimental investigation of two 15 percent-scale wind tunnel fan-blade designs
[NASA-TM-88256] 22 p3046 N88-28076
Techniques for boundary layer tripping and control
23 p3168 N88-28863
Experimental tools: The tunnel and the model
23 p3168 N88-28864
Computational tools for simulation methodologies
23 p3168 N88-28865
Technology for pressure-instrumented thin airfoil models
[NASA-CR-4173] 23 p3180 N88-28933
Test of an 0.8-scale model of the AH-64 Apache in the NASA Langley full-scale wind tunnel
[AD-A196129] 24 p3319 N88-29768
Computer programs for calculation of sting pitch and roll angles required to obtain angles of attack and sideslip on wind tunnel models
[NASA-TM-100659] 24 p3329 N88-29820

WIND TUNNEL STABILITY TESTS

Effects of the installation and operation of jet-exhaust yaw vanes on the longitudinal and lateral-directional characteristics of the F-14 airplane
[NASA-TP-2769] 04 p0393 N88-12455
A wind tunnel model with dynamic control
[BU-352] 13 p1724 N88-20310
Investigation of boundary layer disturbances caused by periodic heating of a thin ribbon
[AD-A190572] 15 p2065 N88-22314

WIND TUNNEL TESTS

Wind-tunnel investigation of a full-scale general aviation airplane equipped with an advanced natural laminar flow wing
[NASA-TP-2772] 01 p0002 N88-10009
Investigations of separated flow states on wings of medium aspect ratio taking into account the wind tunnel interference problem
[ETN-87-90437] 01 p0003 N88-10016
Investigation of the suitability of the 8ft x 6ft transonic wind-tunnel for aeroacoustic research on propellers
[RAE-TM-AERO-2093] 01 p0008 N88-10041
Analysis of free molecular effects on the attitude of satellites in geostationary transfer orbit. Part 2: Force and torque measurement in free molecular wind tunnel tests
[DFVLR-IB-222-86-A/07] 01 p0014 N88-10078
Experience about the application and valuation of roughness strips for boundary layer transition control in wind tunnel tests in the high-speed range
[ESA-TT-1028] 01 p0044 N88-10278
Comparison of wind tunnel and flight test afterbody and nozzle pressures for a twin-jet fighter aircraft at transonic speeds
[NASA-TP-2588] 02 p0121 N88-10765
Wall interference tests of a CAST 10-2/DOA 2 airfoil in an adaptive-wall test section
[NASA-TM-4015] 02 p0122 N88-10772
Intergration effects of D-shaped, underwing, aft-mounted, separate-flow, flow-through nacelles on a high-wing transport
[NASA-TM-4018] 02 p0122 N88-10773
A critical assessment of wind tunnel results for the NACA 0012 airfoil
[NASA-TM-100019] 03 p0260 N88-11636
An experimental evaluation of advanced rotorcraft airfoils in the NASA Ames eleven-foot transonic wind tunnel
[NASA-CR-166587] 03 p0261 N88-11640
Experimental aerothermodynamic research of hypersonic aircraft
[NASA-CR-181533] 04 p0399 N88-12483
Results of the 1986 NASA/FAA/DFVLR main rotor test entry in the German-Dutch wind tunnel (DNW)
[NASA-TM-100507] 04 p0487 N88-13003
European hypersonic wind tunnels
05 p0530 N88-13221
Turbulence measurement in hypersonic flow
05 p0530 N88-13224
The drag of slender axisymmetric cones in rarefied hypersonic flow
05 p0531 N88-13229
Low Reynolds number influence on aerodynamic performance of hypersonic lifting vehicles
05 p0531 N88-13230
Vortex formation over delta, double-delta and wave rider configurations at supersonic speeds
05 p0533 N88-13243
The RAE experimental data-base for missiles at high Mach number and its use in assessing CFD methods
05 p0534 N88-13250
Tip aerodynamics from wind tunnel test of semi-span wing
[NASA-TM-88253] 05 p0540 N88-13290
A swept wing panel in a low speed flexible walled test section
[NASA-CR-4106] 05 p0540 N88-13292
Study of the effect of mass transfer on a transonic boundary layer. Application to flow relaminarization
[ETN-88-91169] 05 p0541 N88-13296
Delta wing in incompressible flow. Experimental study in F2
[ONERA-RT-36/1147-AN-249-G]
05 p0541 N88-13298
Low speed wind tunnel investigation of propelier slipstream aerodynamic effects on different nacelle/wing combinations. Part 1: Total forces and moments and pressure distributions on nacelle/wing at different angles of attack and yaw and at different thrust coefficients
[FFA-TN-1987-22] 05 p0542 N88-13302
Aircraft dynamics: Aerodynamic aspects and wind tunnel techniques 05 p0545 N88-13320
Fundamentals of fighter aircraft design: Engine intake and afterbody 05 p0545 N88-13322
The role of experimental investigation and computational fluid dynamics during fighter aircraft design
05 p0546 N88-13326
Requirements and recommendations for the development of theoretical codes and experimental facilities in the near future 05 p0546 N88-13327
Static Aeroelastic Effects on High Performance Aircraft
[AGARD-CP-403] 05 p0550 N88-13348
The use of aeroelastic wind tunnel models to prove structural design 05 p0551 N88-13355
Measurement of model deformation in wind tunnels
05 p0551 N88-13358
Measurement of local convective heat transfer coefficients from a smooth and roughened NACA-0012 airfoil: Flight test data
[NASA-TM-100284] 05 p0582 N88-13552
Assessment of the reliability of a correction procedure for WGT (Wet Globe Thermometer) (Botsball) measurements of heat stress
[AD-A185193] 05 p0584 N88-13559
Wind tunnel results for a high-speed, natural laminar-flow airfoil designed for general aviation aircraft
[NASA-TM-87602] 06 p0665 N88-14078
Analysis and test evaluation of the dynamic stability of three advanced turboprop models at zero forward speed
[NASA-CR-175025] 06 p0668 N88-14095
Dutch-German wind tunnel's tenth anniversary
[ETN-88-91350] 06 p0670 N88-14105
An investigation of the effects of the propeller slipstream on a wing boundary layer 06 p0700 N88-14293
Flight and wind-tunnel measurements showing base drag reduction provided by a trailing disk for high Reynolds number turbulent flow for subsonic and transonic Mach numbers
[NASA-TP-2638] 06 p0701 N88-14299
Flow diagnostics and visualization in wind tunnels and flight 07 p0811 N88-14940
Riblets for aircraft skin-friction reduction
07 p0814 N88-14955
An engineering study of hybrid adaptation of wind tunnel walls for three-dimensional testing
[NASA-CR-178374] 07 p0814 N88-14957
Measurement in a wind tunnel of the modification of mean wind and turbulence characteristics due to induction effects near wind turbine rotors
[DE88-000249] 07 p0815 N88-14963
Incompressible viscous flow simulations of the NFAC wind tunnel
[NASA-CR-177431] 07 p0816 N88-14969
Static force and moment test of the Holloman narrow-gage rocket sled at Mach numbers from 3.5 to 5.5
[AD-A186291] 07 p0822 N88-14995
Thin film electret boundary layer transition detector: A feasibility study
[AD-A185675] 07 p0856 N88-15199
Supersonic boundary layer on a heated wall
[ETN-88-91617] 08 p0950 N88-15763
Effects of aircraft deicing/antiicing fluids on airfoil characteristics 08 p0952 N88-15776
Supersonic STOVL propulsion technology program: An overview 08 p0957 N88-15808
Theoretical and experimental studies of the transonic flow field and associated boundary conditions near a longitudinally-slotted wind-tunnel wall
[NASA-CR-181169] 08 p0959 N88-15815
Wind tunnel investigations of periodic vortex separation on rough-surface circular cylinders using acoustic measuring methods
[DFVLR-FB-87-24] 09 p1112 N88-16665
Testing of a schematic transport plane model in several European windtunnels
[PB87-170270] 09 p1113 N88-16671
Description of tests run in the T2 cryogenic wind tunnel
[PB87-170296] 09 p1113 N88-16672
Full scale and wind tunnel surface pressure measurements on the T.R.R.L. spray dispersion programme vehicles
[REPT-8623] 09 p1114 N88-16676
Airplane load drop and missile firing: Experimental methods for predicting trajectories
[PB87-170494] 09 p1117 N88-16695
Wind tunnel modeling techniques
[KU-SFB-210/E/33] 09 p1121 N88-16711
The wind tunnel as a yardstick for aircraft design
[NLR-MP-85032-U] 09 p1121 N88-16712
Flow field measurements using hotwire anemometry
[AD-A187029] 09 p1160 N88-16951
Techniques of flow visualization
[AGARD-AG-302] 09 p1164 N88-16977
Investigations of a circulation control airfoil flowfield using an advanced laser velocimeter
10 p1269 N88-17589
Prediction of aeroelastic response of a model X-wing rotor 10 p1271 N88-17603
Analysis of highspeed propellers aerodynamics
10 p1282 N88-17669
Experimental investigation of a supercritical compressor rotor blade section 10 p1284 N88-17680
Effectiveness of various control surfaces in quasi-steady and unsteady conditions
[AGARD-R-735] 10 p1284 N88-17682
An experimental investigation of pressure driven three-dimensional turbulent boundary layers
10 p1327 N88-17934
A three-dimensional dual potential procedure for rotational flows 10 p1329 N88-17942
La Recherche Aerospatiale, bimonthly bulletin, number 1987-2, 237/March-April
[ESA-TT-1074] 11 p1433 N88-18550
Pressure distributions from high Reynolds number transonic tests of an NACA 0012 airfoil in the Langley 0.3-meter transonic cryogenic tunnel
[NASA-TM-100526] 11 p1435 N88-18565
High Reynolds number transonic tests on a NACA 0012 airfoil in the Langley 0.3-meter transonic cryogenic tunnel
[NASA-TM-100527] 11 p1436 N88-18571

Store separation and missile firing from aircraft: Experimental methods for trajectory projection
[NASA-TT-20214] 11 p1439 N88-18589
Space shuttle phase B wind tunnel test database
[NASA-CR-4121] 11 p1444 N88-18611
Changes in the turbulent boundary layer structure associated with net drag reduction by outer layer manipulators
[NASA-CR-178152] 11 p1483 N88-18853
Acoustic measurements from a rotor blade-vortex interaction noise experiment in the German-Dutch Wind Tunnel (DNW)
[NASA-TM-4024] 11 p1542 N88-19218
A review of technologies applicable to low-speed flight of high-performance aircraft investigated in the Langley 14- x 22-foot subsonic tunnel
[NASA-TP-2796] 13 p1717 N88-20264
Tests on the AFWAL 65 deg delta wing at NLR: A study of vortex flow development between Mach = 0.4 and 4
[NLR-MP-86058-U] 13 p1717 N88-20266
The international vortex flow experiment: A test case for compressible Euler codes
[NLR-MP-86076-U] 13 p1717 N88-20267
The construction of a three-dimensional finite volume grid generator for a wing in a wind tunnel with application to Navier-Stokes flow solvers
[FFA-TN-1987-58] 13 p1719 N88-20277
Engine flow simulation for wind tunnel testing at NLR
[NLR-MP-87011-U] 13 p1723 N88-20305
Activities report of the Large Testing Facilities Department --- aircraft/spacecraft
[ETN-88-91962] 13 p1724 N88-20311
Activities report of the Aerodynamics Department
[ETN-88-91979] 14 p1862 N88-21123
Wall interference assessment and corrections for transonic adaptive wall airfoil data
14 p1863 N88-21129
Propagation of artificial disturbances immersed in thick turbulent boundary layer 14 p1864 N88-21136
An experimental and theoretical study of the ice accretion process during artificial and natural icing conditions
[NASA-CR-182119] 14 p1865 N88-21143
Determination of canopy loads for a light aircraft by wind tunnel testing and computer modelling
[BU-353] 14 p1869 N88-21167
Design of a sound neck in connection with the model-support system of a transonic wind tunnel test section
[ILR-MITT-186(1987)] 14 p1869 N88-21171
The 5.5 m low speed wind tunnel. Introduction to the facilities
[ARG-205] 14 p1870 N88-21172
Main features of Warton (United Kingdom) 2.7 x 2.1 m low speed wind tunnel
[AXM-124] 14 p1870 N88-21173
An experimental-computational investigation of transonic shock wave-turbulent boundary layer interaction in a curved test section
[CWI-NM-R8716] 14 p1900 N88-21408
Quick actuating closure and handling system
14 p1925 N88-21476
Development of drive mechanism for an oscillating airfoil 14 p1926 N88-21482
Procedures and requirements for testing in the Langley Research Center unitary plan wind tunnel
[NASA-TM-100529] 15 p2015 N88-22016
Porous wind tunnel corrections for counterrotation propeller testing
[NASA-TM-100873] 15 p2015 N88-22019
Design of an integrated control system for flutter margin augmentation and gust load alleviation, tested on a dynamic windtunnel model
[PB88-149885] 15 p2020 N88-22038
JPRS report: Science and technology. China
[JPRS-CST-87-043] 15 p2053 N88-22233
Investigation of side-wall effects in wind tunnel with supercritical airfoil testing 15 p2054 N88-22241
FLAP (Force and Loads Analysis Program) code development and validation
[DE88-001131] 15 p2075 N88-22371
Langley aerospace test highlights, 1987
[NASA-TM-100595] 15 p2153 N88-22853
Space directorate research and technology accomplishments for fiscal year 1987
[NASA-TM-100607] 15 p2153 N88-22854
Aerofoil testing in a self-streamlining flexible walled wind tunnel
[NASA-CR-4128] 16 p2156 N88-22865
Propulsion and airframe aerodynamic interactions of supersonic V/STOL configurations. Volume 2: Wind tunnel test force and moment data report
[NASA-CR-177343-VOL-2] 16 p2157 N88-22867
Qualification of a water tunnel for force measurements on aeronautical models 16 p2200 N88-23128
Study of the boundary layer of a flow pulsed by acoustic waves
[ETN-88-91998] 16 p2206 N88-23163
Propfan model wind tunnel aeroelastic research results 16 p2220 N88-23246
Methodology for matching experimental and computational aerodynamic data
[NASA-TM-100592] 17 p2295 N88-23728
High Reynolds number tests of a Douglas DLBA 032 airfoil in the Langley 0.3-meter transonic cryogenic tunnel
[NASA-TM-87663] 17 p2296 N88-23734
Full potential methods for analysis/design of complex aerospace configurations
[NASA-CR-3982] 17 p2296 N88-23736
Wind tunnel testing of low-drag airfoils
17 p2297 N88-23741
PAN AIR analysis of the NASA/MCAIR 279-3: An advanced supersonic V/STOL fighter/attack aircraft
[NASA-TM-86838] 17 p2298 N88-23750
Wind-tunnel investigation of actuated forebody strakes for yaw control at high angles of attack
17 p2299 N88-23754
Pressure distributions from subsonic tests of an advanced laminar-flow-control wing with leading- and trailing-edge flaps
[NASA-TM-4040-PT-1] 17 p2300 N88-23758
Thermal remote anemometer system
[NASA-CASE-LAR-13508-1] 17 p2342 N88-23962
Sources and levels of background noise in the NASA Ames 40- by 80-foot wind tunnel
[NASA-TM-100077] 17 p2395 N88-24239
Aerodynamic performance and pressure distributions for a NASA SC(2)-0714 airfoil tested in the Langley 0.3-meter transonic cryogenic tunnel
[NASA-TM-4044] 18 p2456 N88-24580
Experiment investigation on longitudinal characteristics of the forward swept wing
[AD-A191553] 18 p2456 N88-24582
Passive shock wave-boundary layer control for the Bell FX69-H-098 airfoil 18 p2457 N88-24588
Unsteady flow around a profile subjected to pulsed motions
[ETN-88-92151] 18 p2458 N88-24594
Supplements to the study of the wake of a Mirage G8 model at F2 --- wind tunnel
[CERT-RT-OA-20/5025-AYD] 18 p2458 N88-24596
Summary of low-speed wind tunnel results of several high-speed counterrotation propeller configurations
[NASA-TM-100945] 18 p2458 N88-24597
High speed and high angle of attack aerodynamic characteristics of winged space vehicle
[ISSN-0285-6808] 18 p2459 N88-24599
The experimental verification of wall movement influence coefficients for an adaptive walled test section
[NASA-CR-181681] 19 p2598 N88-25439
Wind tunnel wall interference (January 1980 - May 1988): A selected, annotated bibliography
[NASA-TM-4061] 19 p2604 N88-25466
High speed and high angle of attack wind tunnel test results of the winged space vehicle C-2
[ISAS-RN-623] 20 p2751 N88-26329
Propfan test assessment testbed aircraft stability and control/performance 1/9-scale wind tunnel tests
[NASA-CR-182121] 20 p2757 N88-26360
Low-speed wind-tunnel test of a STOL supersonic-cruise fighter concept
[NASA-TM-4050] 20 p2761 N88-26374
Wind tunnel study of atmospheric diffusion in unstable stratified boundary layer. Part 2: Characteristic scale and diffusion
[DE88-753109] 20 p2823 N88-26749
Helicopter main-rotor noise: Determination of source contributions using scaled model data
[NASA-TP-2825] 20 p2848 N88-26907
Aeroelastic characteristics of the AH-64 bearingless tail rotor 21 p2891 N88-27162
Theoretical and experimental investigations of a vortex drag behind a wing profile with spoiler
[ISL-PU-309/87] 21 p2892 N88-27169
Wind tunnel tests of the influence of airfoil-thickness on normal force and pitching moment of two slender wings at transonic and supersonic Mach numbers
[DFVLR-FB-88-17] 21 p2893 N88-27171
Space shuttle phase B wind tunnel model and test information. Volume 2: Orbiter configuration
[NASA-CR-178415-VOL-2-PT-2]
21 p2893 N88-27172
Hybrid procedure for dynamic measurements in transonic wind tunnels: Demonstrated by pitch oscillation
[DFVLR-FB-88-19] 21 p2900 N88-27211
Design of a mechanism to control wind tunnel turbulence 21 p2926 N88-27370
Determination of the local heat-transfer characteristics on glaze ice accretions on a cylinder and a NACA 0012 airfoil 21 p2946 N88-27500
Laser-Doppler measurements of turbulence structures in free streams behind flat and rotation symmetrical profiles
[ETN-88-92336] 21 p2948 N88-27510
Hypersonic flight testing
[DE88-001655] 21 p3015 N88-27894
Wind tunnel tests of elliptical missile body configurations at Mach numbers 0.4 to 5.0
[AD-A193525] 22 p3038 N88-28040
Wind tunnel investigation of wing and control panel loads at transonic and supersonic speeds on some schematic cruciform missile configurations
[FFA-TN-1986-43-SUPPL-1] 22 p3039 N88-28044
Missiles, fuselage and similar bodies
23 p3167 N88-28858
High-aspect-ratio wings 23 p3167 N88-28859
Complex configurations 23 p3167 N88-28861
Reynolds number effects and the wind tunnel environment 23 p3168 N88-28862
Techniques for boundary layer tripping and control
23 p3168 N88-28863
Experimental tools: The tunnel and the model
23 p3168 N88-28864
Empirical tools for simulation methodologies
23 p3168 N88-28866
Introduction and critical flow phenomena
23 p3169 N88-28870
Environmental effects on transition and boundary layer characteristics 23 p3170 N88-28876
Boundary layer manipulation 23 p3170 N88-28877
Effects of independent variation of Mach and Reynolds numbers on the low-speed aerodynamic characteristics of the NACA 0012 airfoil section
[NASA-TM-4074] 23 p3170 N88-28879
Space shuttle phase B wind tunnel model and test information. Volume 2: Orbiter configuration
[NASA-CR-178415-VOL-2-PT-1]
23 p3171 N88-28881
Aerodynamic data accuracy and quality: Requirements and capabilities in wind tunnel testing
[AGARD-AR-254] 23 p3173 N88-28893
Steady and unsteady transonic pressure measurements on a clipped delta wing for pitching and control-surface oscillations
[NASA-TP-2594] 23 p3173 N88-28895
Test results at transonic speeds on a contoured over-the-wing propfan model
[NASA-TM-88206] 23 p3177 N88-28918
Experimental and analytical evaluation of the effects of simulated engine inlets on the blade vibratory stresses of the SR-3 model prop-fan
[NASA-CR-174959] 23 p3179 N88-28927
Space shuttle phase B wind tunnel model and test information. Volume 3: Launch configuration
[NASA-CR-178416-VOL-3-PT-2]
24 p3315 N88-29744
Space shuttle phase B wind tunnel model and test information. Volume 1: Booster configuration
[NASA-CR-178414-VOL-1-PT-1]
24 p3315 N88-29745
Test of an 0.8-scale model of the AH-64 Apache in the NASA Langley full-scale wind tunnel
[AD-A196129] 24 p3319 N88-29768
Space shuttle phase B wind tunnel model and test information. Volume 1: Booster configuration
[NASA-CR-178414-VOL-1-PT-2]
24 p3320 N88-29770
Pressure distributions from subsonic tests of an advanced laminar-flow-control wing with leading- and trailing-edge flaps
[NASA-TM-4040-PT-2] 24 p3321 N88-29776
An experimental study of an adaptive-wall wind tunnel
[NASA-CR-183152] 24 p3329 N88-29821
Supersonic wall adaptation in the rubber tube test section of the DFVLR Goettingen
[IB-222-87-A-08] 24 p3330 N88-29824

WIND TUNNEL WALLS

A transonic model representation for two-dimensional wall interference assessment
[NLR-TR-86026-U] 01 p0001 N88-10006
Wall interference tests of a CAST 10-2/DOA 2 airfoil in an adaptive-wall test section
[NASA-TM-4015] 02 p0122 N88-10772
An analysis of sound absorbing linings for the interior of the NASA Ames 80 x 120-foot wind tunnel
[NASA-CR-177396] 04 p0488 N88-13006
A swept wing panel in a low speed flexible walled test section
[NASA-CR-4106] 05 p0540 N88-13292
Wind tunnel wall interference
07 p0811 N88-14938
An engineering study of hybrid adaptation of wind tunnel walls for three-dimensional testing
[NASA-CR-178374] 07 p0814 N88-14957
Supersonic boundary layer on a heated wall
[ETN-88-91617] 08 p0950 N88-15763

Theoretical and experimental studies of the transonic flow field and associated boundary conditions near a longitudinally-slotted wind-tunnel wall
[NASA-CR-181169] 08 p0959 N88-15815
Influence of the wall boundary layer on force measurements on half models in the transonic wind tunnel
[F+W-TF-1876] 09 p1122 N88-16715
Predictive wall adjustment strategy for two-dimensional flexible walled adaptive wind tunnel: A detailed description of the first one-step method
[NASA-CR-181635] 12 p1573 N88-19409
An evaluation in a modern wind tunnel of the transonic adaptive wall adjustment strategy developed by NPL in the 1940's
[NASA-CR-181623] 12 p1575 N88-19417
Flexiwall 3 SO: A second order predictive strategy for rapid wall adjustment in two-dimensional compressible flow
[NASA-CR-181662] 15 p2015 N88-22018
Porous wind tunnel corrections for counterrotation propeller testing
[NASA-TM-100873] 15 p2015 N88-22019
Investigation of side-wall effects in wind tunnel with supercritical airfoil testing 15 p2054 N88-22241
Aerofoil testing in a self-streamlining flexible walled wind tunnel
[NASA-CR-4128] 16 p2156 N88-22865
Flow quality of NAL two-dimensional transonic wind tunnel. Part 1: Mach number distributions, flow angularities and preliminary study of side wall boundary layer suction
[NASA-TT-20209] 16 p2165 N88-22911
The experimental verification of wall movement influence coefficients for an adaptive walled test section
[NASA-CR-181681] 19 p2598 N88-25439
Empty test section streamlining of the transonic self-streamlining wind tunnel fitted with new walls
[NASA-CR-181680] 19 p2598 N88-25442
Wind tunnel wall interference (January 1980 - May 1988): A selected, annotated bibliography
[NASA-TM-4061] 19 p2604 N88-25466
Wall interference assessment/correction of data from tests of a CAST 10-2/DOA 2 airfoil in the Langley 0.3-m transonic cryogenic tunnel 20 p2751 N88-26331
An experimental study of an adaptive-wall wind tunnel
[NASA-CR-183152] 24 p3329 N88-29821

WIND TUNNELS
NT BLOWDOWN WIND TUNNELS
NT CASCADE WIND TUNNELS
NT COMBUSTION WIND TUNNELS
NT CRYOGENIC WIND TUNNELS
NT HOTSHOT WIND TUNNELS
NT HYPERSONIC WIND TUNNELS
NT HYPERVELOCITY WIND TUNNELS
NT LOW SPEED WIND TUNNELS
NT RECTANGULAR WIND TUNNELS
NT SHOCK TUNNELS
NT SLOTTED WIND TUNNELS
NT SUBSONIC WIND TUNNELS
NT SUPERSONIC WIND TUNNELS
NT TRANSONIC WIND TUNNELS
NT TRISONIC WIND TUNNELS
Possibilities for the modeling of dynamically loaded cylindrical structural parts in the wind tunnel
[KU-SFB-210/T/24] 01 p0001 N88-10005
Theoretical and experimental study of flow-control devices for inlets of indraft wind tunnels 03 p0268 N88-11684
Analysis of 7- X 10-foot high speed wind tunnel shaft loads in support of fan blade failure investigation
[NASA-TM-100504] 04 p0402 N88-12496
Measured performance of the heat exchanger in the NASA icing research tunnel under severe icing and dry-air conditions
[NASA-TM-100116] 04 p0451 N88-12796
Rarefied gas numerical wind tunnel. 2: Two-dimensional and axially symmetric bodies 05 p0538 N88-13273
Dutch-German wind tunnel's tenth anniversary
[ETN-88-91350] 06 p0670 N88-14105
Low-disturbance wind tunnels 07 p0811 N88-14937
Realization of the immediate objectives of the Aero-Gas Dynamics and Vibration Laboratory (LAGG) at the National Center for Research, Science and Technology (PUSPIPTEK) at Serpong, Java (Indonesia), Project TTA-79
[GG/QPR-10] 08 p1092 N88-16572
Status of the special-purpose airfoil families
[DE88-001124] 11 p1506 N88-18998
Activities report of the Large Testing Facilities Department --- aircraft/spacecraft
[ETN-88-91982] 13 p1724 N88-20311
Quick actuating closure and handling system 14 p1925 N88-21476
Development of drive mechanism for an oscillating airfoil 14 p1926 N88-21482
Design and test of a new coaxial air joints
[DE88-751808] 16 p2164 N88-22908
Investigation on the movement of vortex burst position with dynamically changing angle of attack for a schematic deltawing in a watertunnel with correlation to similar studies in windtunnel 16 p2204 N88-23152
Sources and levels of background noise in the NASA Ames 40- by 80-foot wind tunnel
[NASA-TM-100077] 17 p2395 N88-24239
Rarefied gas numerical wind tunnel 3. Universal code for three dimensional bodies 19 p2637 N88-25644
An experimental investigation of two 15 percent-scale wind tunnel fan-blade designs
[NASA-TM-88256] 22 p3046 N88-28076
Development and design of windtunnel and test facility for RPV (Remote Piloted Vehicle) enhancement devices
[AD-A194842] 24 p3329 N88-29822

WIND TURBINES
ARSPNS: A method to calculate steady and unsteady potential flow about fixed and rotational lifting and nonlifting bodies
[NLR-TR-85114-U] 01 p0044 N88-10282
Results of a wind turbine/sealed lead-acid battery experiment
[DE87-012720] 02 p0166 N88-11044
The physics and mathematical description of the Achilles heel of stationary wind turbine aerodynamics: The tip flow
[R-812-D] 03 p0260 N88-11635
Linearized aeroelastic analysis of a wind turbine with a two-bladed rotor
[ETN-87-90600] 03 p0347 N88-12192
Dynamic response of a 330 KW horizontal axis wind turbine generator
[DE87-014867] 03 p0347 N88-12195
Application of ray theory to propagation of low frequency noise from wind turbines
[NASA-CR-178367] 03 p0373 N88-12349
Input turbulence features at a megawatt-size wind turbine, Medicine Bow, Wyoming
[DE88-000098] 04 p0464 N88-12873
Measurements and calculations of aerodynamic torques for a vertical-axis wind turbine
[DE88-001783] 04 p0465 N88-12876
Using a new characterization of turbulent wind for accurate correlation of wind turbine response with wind speed
[DE88-001453] 04 p0466 N88-12881
Variability of wind power near Oklahoma City and implications for siting of wind turbines
[DE88-000444] 04 p0470 N88-12902
An overview of the DOE/SANDIA/USDA vertical axis wind turbine Test Bed Project
[DE88-000604] 05 p0622 N88-13812
Accurate rotor loads prediction using the FLAP (Force and Loads Analysis Program) dynamics code
[DE88-001109] 05 p0623 N88-13815
Performance measurements of the Kolibrie and FACT rotor blades without tip vanes on the full-scale experimental wind turbine
[IW-R518] 06 p0665 N88-14077
Measurement in a wind tunnel of the modification of mean wind and turbulence characteristics due to induction effects near wind turbine rotors
[DE88-000249] 07 p0815 N88-14963
Data on existing wind energy converters in Denmark
[DE88-900199] 07 p0874 N88-15300
Realization and demonstration of a wind turbine of 200 kW demonstration project
[DE88-900207] 07 p0874 N88-15302
Collecting of new data on existing wind energy converters
[DE88-900221] 07 p0875 N88-15305
A proposed metric for assessing the potential of community annoyance from wind turbine low-frequency noise emissions
[DE88-001113] 08 p1022 N88-16187
Data acquisition and analysis system for the Sandia 34-meter Vertical Axis Wind Turbine
[DE88-002417] 09 p1187 N88-17112
Wind turbine acoustics research bibliography with selected annotation
[NASA-TM-100528] 09 p1243 N88-17450
Cape Blanco wind farm feasibility study
[DE88-003749] 10 p1349 N88-18060
Wake effects in a Fayette 95-IIS wind turbine array
[DE88-001103] 10 p1349 N88-18063
Modal testing the EOLE
[DE88-003795] 10 p1350 N88-18066
Preliminary results from the dynamic response testing of the Westinghouse 600-kW wind turbine
[DE88-001123] 10 p1350 N88-18070
Modal testing of a very flexible 110 m wind turbine structure
[DE88-003796] 10 p1351 N88-18072
Analysis of wind turbines on offshore support structures excited by random wind and random waves
[DE88-004772] 10 p1351 N88-18074
Turbulence loads on the Howden 26-m-diameter wind turbine
[DE88-001118] 10 p1351 N88-18075
Status of the special-purpose airfoil families
[DE88-001124] 11 p1506 N88-18998
Site effects on wind characteristics at a turbine rotor
[DE88-005135] 11 p1507 N88-19003
Testing of a one-bladed 30-meter-diameter rotor on the DOE/NASA Mod-O wind turbine
[NASA-TM-100274] 11 p1509 N88-19014
Fatigue load measurements and evaluation of the 25m Horizontal Axis Wind Turbine (HAWT) at Petten, The Netherlands
[NLR-MP-86054-U] 13 p1782 N88-20660
New airfoil sections for straight bladed turbine
[DE88-701075] 14 p1942 N88-21588
The 25 m horizontal-axis turbine as a test case for standard Dutch aerodynamic calculation methods for high-speed rotors
[R-762-D] 14 p1942 N88-21589
Comparison of pressure distributions on model and full-scale NACA 64-621 airfoils with ailerons for wind turbine application
[NASA-TM-100802] 14 p1943 N88-21593
FLAP (Force and Loads Analysis Program) code development and validation
[DE88-001131] 15 p2075 N88-22371
Lewis Structures Technology, 1988. Volume 3: Structural Integrity Fatigue and Fracture Wind Turbines HOST
[NASA-CP-3003-VOL-3] 15 p2081 N88-22408
Large-scale wind turbine structures 15 p2085 N88-22429
Lewis Structures Technology, 1988. Volume 1: Structural Dynamics
[NASA-CP-3003-VOL-1] 16 p2217 N88-23226
Variable speed optimal control of a wind turbine generator
[LAAS-87-358] 16 p2229 N88-23316
Aerodynamic noise of wind turbines
[PB88-165188] 16 p2265 N88-23546
Yaw dynamics of horizontal axis wind turbines
[DE88-001137] 18 p2537 N88-25055
The MOD-2 wind turbine: Aeroacoustical noise sources, emissions, and potential impact
[DE88-001132] 19 p2687 N88-25971
Analysis of the electrical harmonic characteristics of a slip recovery variable speed generating system for wind turbine applications
[DE88-001140] 19 p2687 N88-25972
Analysis of the electrical characteristics of a Westinghouse variable speed generating system for wind turbine applications
[DE88-001139] 20 p2818 N88-26721
Modal testing in the design evaluation of wind turbines
[DE88-010374] 21 p2968 N88-27632
Three-dimensional wind simulation
[DE88-009793] 21 p2975 N88-27671
Electromagnetic interference to radar and radio link systems caused by large scale wind turbines
[FOA-C-30486-3.2] 22 p3071 N88-28234
An examination of wake effects and power production for a group of large wind turbines
[DE88-009906] 22 p3117 N88-28518
Effects of precipitation on wind turbine performance
[DE88-001144] 23 p3228 N88-29211
Dynamic response of a 330-kW horizontal axis wind turbine generator
[DE88-001136] 23 p3228 N88-29212

WIND VARIATIONS
Parameterization of horizontal wind velocity variability
[AD-A190107] 15 p2097 N88-22493
Variable speed optimal control of a wind turbine generator
[LAAS-87-358] 16 p2229 N88-23316
Atmospheric angular momentum and length of day
[AD-A194505] 23 p3233 N88-29238

WIND VELOCITY
NT SOLAR WIND VELOCITY
Coastal winds of the southeast Alaska Peninsula
[PB87-206173] 02 p0215 N88-11354
A model for the convective atmospheric boundary layer during the winter in the Khartoum Region (Sudan)
[R-822-A] 03 p0353 N88-12225
Study of microburst detection performance during 1985 in Memphis, Tennessee
[AD-A184013] 03 p0354 N88-12231
Using a new characterization of turbulent wind for accurate correlation of wind turbine response with wind speed
[DE88-001453] 04 p0466 N88-12881
Variability of wind power near Oklahoma City and implications for siting of wind turbines
[DE88-000444] 04 p0470 N88-12902

The climatic wind regime in the lower thermosphere from meteor radar observations 06 p0733 N88-14506
Atmosphere dynamics in the equatorial meteor zone 06 p0733 N88-14508
The lower thermosphere wind regime from simultaneous observations over Euroasia (Collm, Dushanbe, Frunze) 06 p0733 N88-14510
Characteristics of atmospheric disturbances with a quasi-two day period 06 p0734 N88-14515
Tidal activity in the meteor zone over Budrio, Italy 06 p0734 N88-14517
Longitudinal peculiarities of meridional circulation in lower thermosphere and mesosphere 06 p0736 N88-14525
Atmosphere dynamic processes structure at 80-105 km altitude 06 p0736 N88-14527
Observations of inertial period waves and vertical velocities in the tropical middle atmosphere using the MST radar technique 06 p0742 N88-14562
Mean and peak wind load reduction on heliostats [DE87-012281] 07 p0873 N88-15296
Wind and temperature structure on the slopes of a mountain valley [DE88-000080] 07 p0880 N88-15338
Improvements in profiler wind estimates using smoothed data in the spectrum finder algorithm [PB88-102181] 07 p0881 N88-15342
Turbulence structure during high wind 08 p1014 N88-16149
Extrapolation of extremum values of the wind velocity 08 p1015 N88-16150
NASA wind shear model: Summary of model analyses 10 p1273 N88-17617
Caribbean and Central America wind energy assessment [DE88-005134] 11 p1507 N88-19002
Site effects on wind characteristics at a turbine rotor [DE88-005135] 11 p1507 N88-19003
Air temperature shield tests [AD-A187459] 11 p1514 N88-19043
Correction of the wind field measured by the NCAR electra during FASINEX (Frontal Air-Sea Interaction Experiment) for inertial navigation system drifts [AD-A187780] 11 p1514 N88-19045
An analytical method for the determination of the average horizontal wind velocities across two-dimensional hills [ISBN-3-923624-06-9] 11 p1515 N88-19048
Determining Langmuir circulation parameters on basis of similarity theory 13 p1785 N88-20680
Wind velocity measurement data. Zimbabwe, 4 measuring stations [R-845-D] 13 p1802 N88-20770
Study of passages of cross-equatorial current during southern monsoon 14 p1900 N88-21347
Unsteady aerodynamics of a Wortmann FX-63-137 wing in a fluctuating wind field [AD-A190128] 15 p2013 N88-22006
Parameterization of horizontal wind velocity variability [AD-A190107] 15 p2097 N88-22493
Describing the source created by turbulent flow over orifices and louvers [AD-A190254] 15 p2130 N88-22706
A system for determination of wind fields using geostationary meterological satellites 17 p2360 N88-24056
Overview of wind behavior research in the US Wind Energy Program [DE88-005683] 18 p2537 N88-25057
Wind flow study: July 1987 and November-December 1987 [DE88-008969] 20 p2828 N88-26776
Three-dimensional wind simulation [DE88-009793] 21 p2975 N88-27671
Project wind, phase 4 (smoke test), Meadow Brook Valley, Red Bluff, California [AD-A194742] 22 p3128 N88-28596
A review of measured gust responses in the light of modern analysis methods 24 p3312 N88-29724
A summary of atmospheric turbulence measurements with specially-equipped aircraft in the US 24 p3312 N88-29727
Re-assessment of gust statistics using CAADRP data 24 p3313 N88-29732
Analysis of environmental parameters from the Panama City tower radar experiment [AD-A194994] 24 p3404 N88-30264
A digital simulation technique for the Dryden atmospheric model [NASA-TT-20342] 24 p3404 N88-30266
Determining near-water wind speed using radar data from Cosmos-1500 artificial earth satellite 24 p3449 N88-30524

WIND VELOCITY MEASUREMENT
A 15 cm aperture LED scintillometer for C(n) squared and crosswind measurements [KNMI-WR-87-3] 01 p0070 N88-10448
A real-time system for automatic single-Doppler wind field analysis 02 p0200 N88-11249
Middle Atmosphere Program. Handbook for MAP, volume 25 [NASA-CR-181571] 06 p0732 N88-14502
A statistical study of variations of internal gravity wave energy characteristics in meteor zone 06 p0735 N88-14523
On the dependence of the lower thermospheric wind regime on the solar cycle 06 p0736 N88-14524
The Cyclone meteor radar system for routine wind measurements in the lower thermosphere 06 p0741 N88-14555
Collecting of new data on existing wind energy converters [DE88-900221] 07 p0875 N88-15305
Limiting accuracy of scatterometer determination of wind speed over ocean from satellite 08 p1007 N88-16107
Vertical sounding of th air layer close to a glacier on Mount Vernagferner in the Oetzal Alps, Tyrol (experiment LUZIVER 1983) 08 p1015 N88-16152
Remote measurement of aerosol stream velocity with continuous-wave CO2-laser 08 p1079 N88-16506
Convective wind fields as investigated with doppler lidar [PB88-115472] 09 p1193 N88-17151
Method for determination of the wind velocity and direction [NASA-TT-20233] 13 p1802 N88-20769
Wind velocity measurement data. Zimbabwe, 4 measuring stations [R-845-D] 13 p1802 N88-20770
Wind measurements by electromagnetic probes [NASA-TM-4066] 23 p3236 N88-29256

WINDING
NT FILAMENT WINDING
NT HELICAL WINDINGS
Tape wrapping apparatus and method [EP-PATENT-0-181-747-A2] 01 p0053 N88-10336
Departmental report on program EMTP-machine windings surge transients: Travelling wave method [PB87-123733] 04 p0438 N88-12719
High midplane accessibility stellarator windings for high current toroidal accelerators [AD-A186235] 07 p0933 N88-15665
Thermoplastic composite with continuous fibers [FOA-C-20707-2.6] 22 p3051 N88-28103

WINDMILLS (WINDPOWERED MACHINES)
Build, install and demonstrate a variable stroke pump control and windmill system [DE87-014656] 03 p0347 N88-12191

WINDOWS
Space station proximity operations windows: Human factors design guidelines [NASA-TM-88233] 24 p3410 N88-30301

WINDOWS (APERTURES)
Multilayered foils as radiation entrance windows and spectral filters for image converters in the ultrasoft X-ray wavelength region [MPE-PREPRINT-90] 02 p0176 N88-11099
A high field launch for electron cyclotron heating using an external window [DE88-005350] 13 p1838 N88-21000
Space station proximity operations and window design 17 p2380 N88-24149
Determination and application of bidirectional solar-optical properties of fenestration systems [DE88-010364] 20 p2820 N88-26727

WINDOWS (INTERVALS)
NT LASER WINDOWS

WINDPOWER UTILIZATION
Methodology for control and operation of wind arrays in utility systems [DE87-013129] 01 p0039 N88-10248
Variability of wind power near Oklahoma City and implications for siting of wind turbines [DE88-000444] 04 p0470 N88-12902
An overview of the DOE/SANDIA/USDA vertical axis wind turbine Test Bed Project [DE88-000604] 05 p0622 N88-13812
Wind measurements at high altitudes (150 m tower) [BMFT-FB-T-86-169] 09 p1193 N88-17149
Cape Blanco wind farm feasibility study [DE88-003748] 10 p1348 N88-18059
Caribbean and Central America wind energy assessment [DE88-005134] 11 p1507 N88-19002
8th Wind Energy Symposium [DE88-770028] 11 p1507 N88-19004
Alternative Energy in the Midwest: Research and Applications. Conference Proceedings, Rosemont, Illinois, March 19-20, 1987 [PB88-142278] 11 p1509 N88-19015
Wind energy resource survey of New Zealand: National resource assessment [PB88-139365] 12 p1640 N88-19822
Wind velocity measurement data. Zimbabwe, 4 measuring stations [R-845-D] 13 p1802 N88-20770
Activities report in flight and space travel [ISSN-0070-3966] 14 p2012 N88-22000
Energy from the wind [DE88-006897] 15 p2091 N88-22459
Overview of wind behavior research in the US Wind Energy Program [DE88-005683] 18 p2537 N88-25057
Analysis of the electrical characteristics of a Westinghouse variable speed generating system for wind turbine applications [DE88-001139] 20 p2818 N88-26721
Wind Energy Technology: Generating power from the wind, a current awareness bulletin [DE88-008292] 20 p2820 N88-26729

WINDPOWERED GENERATORS
Methodology for control and operation of wind arrays in utility systems [DE87-013129] 01 p0039 N88-10248
Results of a wind turbine/sealed lead-acid battery experiment [DE87-012720] 02 p0166 N88-11044
Data on existing wind energy converters in Denmark [DE88-900199] 07 p0874 N88-15300
Realization and demonstration of a wind turbine of 200 kW demonstration project [DE88-900207] 07 p0874 N88-15302
Optimal control of windpowered plants [FOA-C-20610-2.7] 08 p1022 N88-16188
Study on a rotor speed control system for a horizontal axis windmill [NAL-TR-931] 10 p1349 N88-18062
Wind energy resource survey of New Zealand: National resource assessment [PB88-139365] 12 p1640 N88-19822
Variable speed optimal control of a wind turbine generator [LAAS-87-358] 16 p2229 N88-23316
Overview of wind behavior research in the US Wind Energy Program [DE88-005683] 18 p2537 N88-25057
Analysis of the electrical characteristics of a Westinghouse variable speed generating system for wind turbine applications [DE88-001139] 20 p2818 N88-26721

WINDPOWERED PUMPS
Linear and nonlinear theories of flow through an actuator disk — windpowered pumps [R-803-A] 03 p0316 N88-11995
Pump rod forces due to hydrodynamic effects in piston pumps [PB88-164850] 16 p2214 N88-23212

WINDS ALOFT
NT GEOSTROPHIC WIND
NT JET STREAMS (METEOROLOGY)
Effect of neutral wind on the latitudinal variation of nighttime F-layer vertical movements 08 p1030 N88-16244

WINDSCREENS
U WINDSHIELDS

WINDSHIELDS
The deviation of light rays passing through a curved windscreen — aircraft [BAE-MSC.115] 01 p0093 N88-10610
Fracture study of windshield glass panes 06 p0799 N88-14891
Vision through aircraft transparencies 23 p3242 N88-29294

WING CAMBER
Variable wing camber control systems for the future Airbus program [MBB-UT-104/88] 23 p3180 N88-28932

WING FLAPS
NT LEADING EDGE FLAPS
NT TRAILING EDGE FLAPS
NT VORTEX FLAPS
Investigation into the effects of flap end modifications on the performance of a wing with a single slotted flap [BU-357] 14 p1866 N88-21148

WING LOADING
The RAE experimental data-base for missiles at high Mach number and its use in assessing CFD methods 05 p0534 N88-13250
Reduction of tilt rotor download using circulation control 10 p1271 N88-17605

Shape sensitivity analysis of wing static aeroelastic characteristics
[NASA-TP-2808] 15 p2018 N88-22031
Methodology for matching experimental and computational aerodynamic data
[NASA-TM-100592] 17 p2295 N88-23728
A summary of methods for establishing airframe design loads from continuous gust design criteria
24 p3312 N88-29721

WING NACELLE CONFIGURATIONS
A numerical investigation on wing/nacelle interferences 05 p0535 N88-13258
Computation of nacelle interference using boundary element method 05 p0537 N88-13267
Nacelle-wing interactions (studies 1986) development of a finite element code in a multi-domain version
[ONERA-RTS-10/3417-AY-308A]
08 p0950 N88-15764

WING OSCILLATIONS
An analysis of the compressible-viscous flow field around a 3D-oscillating wing 05 p0535 N88-13254
Computation of dynamic stall of NACA0012 airfoil by block pentadiagonal matrix scheme
05 p0535 N88-13255
Influence of the static deformation on a wing in the unsteady aerodynamic 05 p0551 N88-13357
ARSPNSC: A method to calculate subsonic steady and unsteady potential flow about complex configurations
[NLR-TR-86122-U] 13 p1717 N88-20265
Optimal control of the wing rock phenomenon
21 p2927 N88-27373

WING PANELS
Factors affecting the sticking of insects on modified aircraft wings
[NASA-CR-182451] 09 p1148 N88-16878
Accuracies of southwell and force/stiffness methods in the prediction of buckling strength of hypersonic aircraft wing tubular panels
[NASA-TM-88295] 09 p1183 N88-17090
Computational wing design studies relating to natural laminar flow 17 p2297 N88-23740
Fuel containment, lightning protection and damage tolerance in large composite primary aircraft structures
[NASA-CR-3875] 17 p2317 N88-23839

WING PLANFORMS
NT ARROW WINGS
NT DELTA WINGS
NT SWEPT FORWARD WINGS
NT SWEPTBACK WINGS
NT VARIABLE SWEEP WINGS
A discretization of the integral equation for the time dependent linearized subsonic potential flow over a wing
[AD-A188534] 12 p1574 N88-19411
Design of an aeroelastic composite wing wind tunnel model
[AD-A188855] 12 p1582 N88-19466
An integral equation for the linearized supersonic flow over a wing
[AD-A191408] 16 p2158 N88-22875
Computational wing design studies relating to natural laminar flow 17 p2297 N88-23740
Computational design of low aspect ratio wing-winglet configurations for transonic wind-tunnel tests
[NASA-CR-183021] 18 p2464 N88-24630
An integral equation for the linearized unsteady supersonic flow over a wing
[AD-A193773] 23 p3172 N88-28887

WING PROFILES
NT WING SPAN
Three-dimensional unsteady flow elicited by finite wings and complex configurations 04 p0395 N88-12468
Conical wing with maximum lift-to-drag ratio in supersonic gas flow 04 p0425 N88-12633
A numerical procedure for conformal mapping of the exterior of a circle onto the exterior of a wing profile with a spoiler
[ISL-R-110/86] 11 p1536 N88-19180
Wing flutter calculations with the CAP-TSD unsteady transonic small disturbance program
[NASA-TM-100580] 12 p1575 N88-19419
Shape sensitivity analysis of wing static aeroelastic characteristics
[NASA-TP-2808] 15 p2018 N88-22031
Improved potential flow computational methods with Euler corrections for airfoil and wing/body design
[AD-A192303] 20 p2752 N88-26334
Theoretical and experimental investigations of a vortex drag behind a wing profile with spoiler
[ISL-PU-309/87] 21 p2892 N88-27169

WING SPAN
Investigation of side-wall effects in wind tunnel with supercritical airfoil testing 15 p2054 N88-22241

WING TANKS
Fuel containment and damage tolerance in large composite primary aircraft structures. Phase 2: Testing
[NASA-CR-172519] 19 p2601 N88-25452

WING TIP VORTICES
Dispersion in the wake of aircraft: An investigation of the effects of a ground plane on trailing vortices. Literature survey
[IC-AERO-REP-86-04] 01 p0003 N88-10014
A study of rotor broadband noise mechanisms and helicopter tail rotor noise 06 p0777 N88-14766
Tip vortices of isolated wings and helicopter rotor blades
[AD-A191336] 16 p2158 N88-22874
Wave growth associated with turbulent spots in plane Poiseuille flow
[FFA-TN-1988-08] 18 p2457 N88-24587

WING TIPS
Analytic investigation of helicopter rotor blade appended aeroelastic devices
[NASA-CR-166525] 03 p0266 N88-11676
Tip aerodynamics from wind tunnel test of semi-span wing
[NASA-TM-88253] 05 p0540 N88-13290

WINGLETS
Effects of winglets on a first-generation jet transport wing. 7: Sideslip effects on winglet loads and selected wing loads at subsonic speeds for a full-span model
[NASA-TP-2619] 11 p1436 N88-18567
Investigation into the effects of flap end modifications on the performance of a wing with a single slotted flap
[BU-357] 14 p1866 N88-21148
Computational design of low aspect ratio wing-winglet configurations for transonic wind-tunnel tests
[NASA-CR-183021] 18 p2464 N88-24630
Theoretical-numerical study of feasibility of use of winglets on low aspect ration wings at subsonic and transonic Mach numbers at reduce drag
[NASA-CR-4174] 21 p2902 N88-27168

WINGS
NT AEROELASTIC RESEARCH WINGS
NT ARROW WINGS
NT BEARINGLESS ROTORS
NT CAMBERED WINGS
NT CIRCULATION CONTROL ROTORS
NT CRUCIFORM WINGS
NT DELTA WINGS
NT FIXED WINGS
NT LOW ASPECT RATIO WINGS
NT OBLIQUE WINGS
NT RIGID ROTORS
NT ROTARY WINGS
NT SLENDER WINGS
NT SUPERCRITICAL WINGS
NT SWEPT FORWARD WINGS
NT SWEPT WINGS
NT SWEPTBACK WINGS
NT THIN WINGS
NT TILTING ROTORS
NT VARIABLE SWEEP WINGS
NT X WING ROTORS
Advanced turboprop wing installation effects measured by unsteady blade pressure and noise
[NASA-TM-100200] 01 p0002 N88-10008
Wind-tunnel investigation of a full-scale general aviation airplane equipped with an advanced natural laminar flow wing
[NASA-TP-2772] 01 p0002 N88-10009
Computation of transonic separated wing flows using an Euler/Navier-Stokes zonal approach
[NASA-TM-88311] 02 p0173 N88-11089
AGARD standard aeroelastic configurations for dynamic response. Candidate configuration I.-wing 445.6
[NASA-TM-100492] 02 p0192 N88-11202
On the prediction of the aeroelastic behavior of lifting systems due to flow separation
[ESA-TT-1043] 03 p0259 N88-11633
On the scheme dependency of the three-dimensional Euler solutions 03 p0318 N88-12010
Reduced complexity structural modeling for automated airframe synthesis
[NASA-CR-177440] 04 p0393 N88-12453
Calculation of aerodynamic characteristics of three-dimensional finite span wings in potential incompressible flow 04 p0425 N88-12631
Numerica calculation in the Laplace domain for subsonic unsteady aerodynamic forces acting on a finite wing
05 p0535 N88-13256
Numerical analysis of supersonic flows using panel method 05 p0537 N88-13266
Navier-Stokes simulation of transonic transportation aircraft configurations. 1: Flow-field simulation over wing-fuselage combinations 05 p0540 N88-13288
Design of wings and wing/body configurations for transonic and supersonic speeds
05 p0545 N88-13318
An examination of coating failure on wing pivot fittings of f111 aircraft
[AD-A185028] 05 p0546 N88-13328
Nonlinear aerodynamic wing design
[NASA-CR-3950] 06 p0665 N88-14079
Design verification and fabrication of active control systems for the DAST ARW-2 high aspect ratio wing, part 1
[NASA-CR-177959-PT-1] 06 p0669 N88-14101
Design verification and fabrication of active control systems for the DAST ARW-2 high aspect ratio wing. Part 2: Appendices
[NASA-CR-177959-PT-2] 06 p0669 N88-14102
An investigation of the effects of the propeller slipstream on a wing boundary layer 06 p0700 N88-14293
Insect contamination protection for laminar flow surfaces 07 p0814 N88-14954
Unsteady stall penetration experiments at high Reynolds number
[AD-A186120] 07 p0814 N88-14958
Development of direct-inverse 3-D methods for applied aerodynamic design and analysis
[NASA-CR-182436] 08 p0950 N88-15767
Three-dimensional unsteady flow elicited by finite wings and complex configurations
[AD-A186464] 08 p0951 N88-15770
Effects of wing simulated ground frost on aircraft performance 08 p0952 N88-15775
Effect of an optimized fiber orientation on transonic flutter characteristics of a high-aspect-ratio composite wing
[NAL-TR-930] 09 p1120 N88-16709
Computational fluid dynamics and aerothermodynamics
[NASA-CR-182490] 09 p1166 N88-16989
Solution of the three-dimensional Navier-Stokes equations for transonic flow using a multigrid method
10 p1267 N88-17579
A transonic-small-disturbance wing design methodology
[NASA-TP-2806] 10 p1273 N88-17614
The intelligent wing. Aerodynamic development direction for future passenger aircraft
[MBB-UT-006/87] 10 p1313 N88-17848
Conditions at infinity for theories of oscillating wings and propellers in subsonic flow
[NAL-TR-937] 11 p1434 N88-18556
A discretization of the integral equation for the time dependent linearized subsonic potential flow over a wing
[AD-A188534] 12 p1574 N88-19411
Factors affecting the sticking of insects on modified aircraft wings
[NASA-CR-182615] 12 p1575 N88-19421
Computer aided deflection measurement of an aircraft wing
[AD-A187778] 12 p1581 N88-19461
Crack distribution and growth rates for critical fastener holes in Mirage wing RH79
[AD-A189080] 13 p1722 N88-20293
Constructing Gloved wings for aerodynamic studies
[NASA-TM-100440] 14 p1863 N88-21128
Scale model development for aeroelasticity studies
[ETN-88-91887] 14 p1868 N88-21164
Structural and material testing of a composite microlite wing model
[BU-355] 14 p1923 N88-21461
Control of laminar flow around of the wing in free-air conditions
[AD-A187479] 15 p2013 N88-22004
Unsteady aerodynamics of a Wortmann FX-63-137 wing in a fluctuating wind field
[AD-A190128] 15 p2013 N88-22006
A multilifting line method and its application in design and analysis of nonplanar wing configurations
[DFVLR-FB-87-51] 16 p2155 N88-22860
A numerical model of unsteady, subsonic aeroelastic behavior
[NASA-TM-101126] 16 p2156 N88-22862
Propulsive performance of a lifting flapping wing
17 p2295 N88-23733
Sensitivity of F-106B leading-edge-vortex images to flight and vapor-screen parameters
[NASA-TP-2818] 17 p2300 N88-23760
High speed and high angle of attack aerodynamic characteristics of winged space vehicle
[ISSN-0285-6808] 18 p2459 N88-24599
Applications of the Navier-Stokes equations to wings and complex configurations using a zonal approach
[NASA-TM-100080] 18 p2459 N88-24602
Investigation of the effect of minimum loads and compression of load spectra on the prediction capacities of the ONERA crack model --- wings
[ONERA-RTS-33/7169-RY-064-R]
18 p2527 N88-24994
On the stationary solutions of three-dimensional Euler equations by the TVD difference schemes
19 p2639 N88-25660

Numerical simulation of turbulent flow using the exponential expression of k-Epsilon equation
19 p2640 N88-25662
Development of direct-inverse 3-D methods for applied transonic aerodynamic wing design and analysis
[NASA-CR-183127] 22 p3037 N88-28033
Runge-Kutta finite-volume simulation of laminar transonic flow over the ONERA M6 wing using the Navier-Stokes equations
[FFA-TN-1987-06] 22 p3039 N88-28045
Transport-type configurations
23 p3169 N88-28867
An integral equation for the linearized unsteady supersonic flow over a wing
[AD-A193773] 23 p3172 N88-28887
Critical joints in large composite primary aircraft structures. Volume 2: Technology demonstration test report
[NASA-CR-172587] 23 p3177 N88-28915
Critical joints in large composite primary aircraft structures. Volume 3: Ancillary test results
[NASA-CR-172588] 23 p3177 N88-28916
Test results at transonic speeds on a contoured over-the-wing propfan model
[NASA-TM-88206] 23 p3177 N88-28918
Development of a glass fiber wing following the construction regulation FAR Part 23
[ETN-88-92966] 23 p3189 N88-28979
Critical joints in large composite primary aircraft structures. Volume 1: Technical summary
[NASA-CR-3914] 23 p3190 N88-28983

WINTER
Nowcasting rain/snow transitions and freezing rain
02 p0202 N88-11265
Forecasting the kind of precipitation in winter
02 p0202 N88-11266
Observational analysis of the interaction between fronts and the orography in Taiwan during the late winter monsoon season 02 p0203 N88-11270
A model for the convective atmospheric boundary layer during the winter in the Khartoum Region (Sudan)
[R-822-A] 03 p0353 N88-12225
NWS (National Weather Service) watch/warning verification flash flood, winter storm and high wind, January 1980 - June 1986
[PB87-223053] 04 p0469 N88-12898
Wind regime peculiarities in the lower thermosphere in the winter of 1983/84 06 p0733 N88-14511
Circulation in the mesosphere and lower thermosphere during the MAP (Middle Atmosphere Program)/WINE (Winter in the Northern Europe) period
06 p0734 N88-14514
The sodium layer at 69 N latitude in wintertime
06 p1027 N88-16218
Observational evidence for saturation of gravity waves and the production of turbulence in the mesosphere
06 p1028 N88-16229
Biorhythmic aspects of intercontinental Antarctic adaptation 06 p1046 N88-16321
Systematic errors of the FSU global spectral model
10 p1356 N88-18103
Aircraft and ground vehicle friction correlation test results obtained under winter runway conditions during joint FAA/NASA Runway Friction Program
[NASA-TM-100506] 11 p1438 N88-18582
Northern winter circulations for the period 1974-1983
[AD-A187779] 11 p1511 N88-19028
Estimates of ocean-atmosphere thermal interaction in Gulf Stream energy-active test range in winter of 1984
13 p1785 N88-20679
Analysis of winter season precipitation bands over the Southern Plains 14 p1947 N88-21609
Verification of regional climates of GISS GCM. Part 1: Winter
[NASA-TM-100695] 19 p2694 N88-26012
Recent secular changes in the wintertime circulation of the Southern Hemisphere 22 p3122 N88-26555
On the impact of low-latitude anomalous forcing on local and remote circulation: Winters(DJF) 1978/79 to 1986/87 22 p3123 N88-26560
Interannual variability of 850 mb temperatures during the Northern Hemisphere winter
22 p3123 N88-28562
Some screening experiments in objective prediction of monthly mean temperature over the United States during the winter season 22 p3127 N88-28589
One equatorial anomaly in nighttime ionospheric F region 24 p3447 N88-30517

WIRE
NT ELECTRIC WIRE
NT GUY WIRES
Wire interconnection reliability and moisture levels in hybrid microcircuits with epoxy-attached components
[DE87-012987] 01 p0039 N88-10247
Composite bearing materials containing solid lubricant in filamentary form, stages 3 and 4
[IRD-87/2] 01 p0054 N88-10344
Carbon-fiber reinforced aluminum
04 p0403 N88-12507
Small-diameter wire tensile testing
[DE88-000835] 04 p0455 N88-12815
Fracture analysis of drawn composite dual-phase steel wire
[DE88-001396] 06 p0681 N88-14173
Single wire drift chamber design
[DE87-011002] 07 p0857 N88-15205
MIG welding with pulsed wire feed
[PB87-143582] 07 p0863 N88-15234
Single-layer wire routing
[AD-A186990] 09 p1157 N88-16932
Composite ceramic superconducting filaments for superconducting cable
[AD-A187833] 11 p1556 N88-19312
High-T(sub c) superconducting wire fabrication and testing
[DE88-005989] 15 p2144 N88-22798
Corrosion and fatique properties of FeCrB/Si metallic glass wires in aqueous environments
17 p2320 N88-23855
Magnetization studies of multifilamentary Nb3Sn wires
[DE88-009103] 19 p2735 N88-26243
A model for insulated wires in the method of moments code NEC (Numerical Electromagnetics Code)
[DE88-008920] 20 p2794 N88-26577
Performance study of a unipole antenna with conventional and elevated radial wire ground screens
[AD-A193283] 21 p2933 N88-27413
Development of Nb-Ti multifilamentar superconducting wires
[DE88-702324] 23 p3290 N88-29592

WIRE CLOTH
Fatigue failure of regenerator screens in a high frequency Stirling engine 17 p2436 N88-24491

WIRE MESH
U WIRE CLOTH

WIRING
A design-philosophy for grounding and inter-unit wiring
[EMCR-20/85] 03 p0310 N88-11954
Discussions in support of the design-philosophy for grounding and inter-unit wiring
[EMCR-21/85] 03 p0310 N88-11955
Assessment of existing specifications against the design-philosophy for grounding and inter-unit wiring (EMCR 20/85)
[EMCR-22/85] 03 p0310 N88-11956
Alternatives to the techniques implicit in the design philosophy, and the penalties in performance associated with them --- grounding and wiring
[EMCR-31/85] 03 p0310 N88-11957
Summary record of presentations to the Federal Telecommunication Standards Committee/Fiber optics task group
[PB88-110853] 08 p0978 N88-15911
Gridless routing for generalized cell assemblies: Report and user manual
[EUT-87-E-180] 13 p1764 N88-20549
Locality, communication and interconnect length in multicomputers
[CWI-CS-R8706] 13 p1822 N88-20890
Characteristics of LSI-wiring expert system discussed
15 p2052 N88-22226
An improved simulated annealing algorithm for standard cell placement
[NASA-CR-182952] 18 p2558 N88-25183

WIRING SYSTEMS
U WIRING

WISCONSIN
GOES observations for the FIRE/SRB Wisconsin experiment region from October 11 through November 2, 1986
[NASA-TM-100485] 01 p0071 N88-10453

WKB APPROXIMATION
U WENTZEL-KRAMER-BRILLOUIN METHOD

WOLF-RAYET STARS
Grids of evolutionary models of massive stars with mass loss and overshooting. Properties of Wolf-Rayet stars sensitive to overshooting
[PUBL-SER-C-FASC-12] 03 p0388 N88-12437
The effects of rotation on the winds from hot stars
11 p1569 N88-19393
Colliding stellar winds in the eclipsing Wolf-Rayet binary V444 Cygni
[NASA-CR-182937] 17 p2451 N88-24563
Review of the theoretical changes of surface chemistry during massive star evolution
[SER-C-PREPUBL-FASC-17] 18 p2593 N88-25411

WOLFRAM
U TUNGSTEN

WOMEN
U FEMALES

WOOD
Use of natural gas diesel engines in mechanical pulp production: A preliminary study
[DE87-753065] 02 p0181 N88-11129
Method of radiographic inspection of wooden members
[NASA-CASE-LAR-13724-1] 17 p2346 N88-23983
Proceedings of the 1987 Biomass Thermochemical Conversion Contractors' Review Meeting
[DE88-006730] 18 p2535 N88-25041
An advanced extruder-feeder biomass liquefaction reactor system 18 p2535 N88-25042
Low pressure entrained flow pyrolysis of biomass to produce liquid fuels 18 p2535 N88-25043
Molecular-beam, mass-spectrometric studies of wood vapor and model compounds over HZSM-5 catalyst
18 p2535 N88-25044
Research on hydrotreating catalysts to hydrodeoxygenate biocrude oils
18 p2536 N88-25046
Bench-scale studies on fluid-bed pyrolysis of wood using different contact gases 18 p2536 N88-25049
A 3 MW wood fired gas turbine at Red Boiling Springs, Tennessee 18 p2536 N88-25051

WORD PROCESSING
An evaluation of WPS-Plus word processing software for the IBM PC and compatibles
[DE87-011972] 01 p0081 N88-10518
Electronic authoring tools
[DE87-011797] 02 p0248 N88-11567

WORDS (LANGUAGE)
NT SYLLABLES
Abregrams or deleweds: A forty-year view of acronyms
[DE87-010808] 01 p0106 N88-10690
Studies of the processing of single words using positron tomographic measures of cerebral blood flow change
[AD-A184058] 03 p0356 N88-12244
A two-stage isolated-word recognition system using discriminant analysis
[AD-A187425] 10 p1402 N88-18360
Auditory perception of complex sounds
[AD-A190528] 15 p2103 N88-22529
WORDNET: An electronic lexical reference system based on theories of lexical memory
[AD-A193086] 21 p3027 N88-27970
Exploiting lexical regularities in designing natural language systems
[AD-A195922] 24 p3423 N88-30375
Words: Keys or barriers to information transfer
24 p3438 N88-30464

WORK
NT PHYSICAL WORK
A comparison of plastic work energy and external input for fatigue crack propagation 05 p0607 N88-13722
Software-implemented fault insertion: An FTMP example
[NASA-CR-178423] 06 p0761 N88-14868
Risk of hypertension and functional cerebral laterality in oil expedition works in far north
12 p1665 N88-19980
Subsea approach to work systems development
17 p2379 N88-24146

WORK CAPACITY
Prediction of physical workload in reduced gravity environments 06 p0794 N88-14867
Cardiovascular and subjective measures of task demand in a low workload monitoring task
[REPT-8804] 10 p1368 N88-18176
Development of a coping strategies questionnaire to assess endurance performance
[AD-A188010] 11 p1520 N88-19074
Heat acclimatization under controlled hyperthermia
12 p1665 N88-19981
Hypnosis: Possible applications for cosmonauts
12 p1665 N88-19984
Efficiency of human workers and means to increase it
12 p1666 N88-19986
Psychophysical load of glider pilots on long-duration flights
[DFVLR-FB-87-38] 14 p1953 N88-21642
Experience in occupational medicine, derived from 16 operational deep saturation trimix 5 dives in GUSI from 150 to 600 m 19 p2695 N88-26018
A review of workload measurement in relation to verbal comprehension 21 p2925 N88-27360
Thermal stress and its effects on fine motor skill and decoding tasks 21 p2926 N88-27369

WORK FUNCTIONS
Question on the measurement of the metal work function in an electron spectrometer by the secondary-electron emission threshold method
[NASA-TT-20190] 16 p2178 N88-22979

WORK HARDENING
NT STRAIN HARDENING

Hardening of metal during production of bent shapes
[BLL-M-37250-(5828.4)] 02 p0148 N88-10928
Cyclic uniaxial and biaxial hardening of type 304 stainless steel modeled by the viscoplasticity theory based on overstress 14 p1931 N88-21514

WORK-REST CYCLE
Implications of shiftwork in space for human physiology experiments 12 p1659 N88-19942
Performance effectiveness and the work/rest cycle
[AD-A191448] 18 p2551 N88-25145

WORKING FLUIDS
Organic Rankine-cycle power systems working fluids study. Topical report No. 1: Fluorinol 85
[DE87-014604] 02 p0195 N88-11217
Pump assisted heat pipe 03 p0319 N88-12018
Working fluids for sorption heat pumps
[DE88-900203] 07 p0874 N88-15301
Design of a high-power-density Ljungstroem turbine using potassium as a working fluid
17 p2409 N88-24323
Low gravity thermal management using dielectrophoretic forces 17 p2432 N88-24470
Pressure drop and heat transfer in turbulent non-Newtonian pipe flow of advanced energy transmission fluids
[DE88-010021] 19 p2666 N88-25853
Heat transfer of mesh-wick heat-pipes (bottom heat mode) 20 p2783 N88-26507
The heat transfer and fluid dynamics of concave surface curvature
[AD-A193064] 21 p2943 N88-27479
Reaction-theoretical aspects of the thermal behavior of lubricating oils and working fluids
[NASA-TT-20304] 23 p3199 N88-29041
Radiative heat transfer to steady flow of a chemically reacting fluid in a horizontal porous channel with variable wall temperature
[DE88-702704] 24 p3372 N88-30081

WORKLOADS (PSYCHOPHYSIOLOGY)
Effect of motion cues during complex curved approach and landing tasks: A piloted simulation study
[NASA-TP-2773] 04 p0398 N88-12480
Research papers and publications (1981-1987): Workload research program
[NASA-TM-100016] 04 p0474 N88-12924
Taskomat, a task battery for information processing
[IZF-1987-2] 05 p0630 N88-13851
Prediction of physical workload in reduced gravity environments 06 p0794 N88-14867
Stability, reliability and cross-mode correlations of tests in a recommended 8-minute performance assessment battery
[NASA-CR-172039] 08 p1052 N88-16351
Proceedings of the DOD Workload Assessment Workshop on Workload Assessment Techniques and Tools held in Dayton, Ohio on 27-28 September 1986
[AD-A185650] 08 p1052 N88-16352
Helicopter human factors research 09 p1109 N88-16644
Identification and proposed control of helicopter transmission noise at the source 09 p1109 N88-16647
An integrated approach to rotorcraft human factors research 09 p1110 N88-16653
Crew procedures for microwave landing system operations
[NASA-CR-178359] 09 p1116 N88-16688
Measuring mental workload: A performance battery
[AD-A187118] 09 p1200 N88-17192
Trends in the distribution of tasks between commercial pilots and flight control systems
[MBB-UT-008/87] 10 p1314 N88-17851
Second All-Union Conference on Physiology of Extreme States and Individual Protection of Man 10 p1363 N88-18147
Cardiovascular and subjective measures of task demand in a low workload monitoring task
[REPT-8804] 10 p1368 N88-18176
Electromagnetic metrics of mental workload
[AD-A188205] 11 p1523 N88-19093
Identification of visual evoked response parameters sensitive to pilot mental state
[NASA-CR-4140] 13 p1811 N88-20822
Proceedings of the Workshop on the Assessment of Crew Workload Measurements Methods, Techniques and Procedures. Volume 1: Preliminary Selection of Measures
[AD-A189004] 13 p1812 N88-20827
A comparison of two chord keyboard coding systems for alphanumeric data entry
[AD-A189230] 13 p1813 N88-20834
Psychophysical load of glider pilots on long-duration flights
[DFVLR-FB-87-38] 14 p1953 N88-21642
Mental-State Estimation, 1987
[NASA-CP-2504] 16 p2239 N88-23370
Toward a mathematical formalism of performance, task difficulty, and activation 16 p2239 N88-23372
Predicting operator workload during system design 16 p2239 N88-23375
Pupil measures of alertness and mental load 16 p2239 N88-23378
Voice-stress measure of mental workload 16 p2240 N88-23381
Primary task event-related potentials related to different aspects of information processing 16 p2240 N88-23382
Defining and measuring pilot mental workload 16 p2240 N88-23383
POPEYE: A production rule-based model of multitask supervisory control (POPCORN) 16 p2240 N88-23384
Estimating the cost of mental loading in a bimodal divided-attention task: Combining reaction time, heart-rate variability and signal-detection theory 16 p2241 N88-23385
Information processing deficits in psychiatric populations: Implications for normal workload assessment 16 p2241 N88-23390
C3 generic workstation: Performance metrics and applications 16 p2242 N88-23397
NASA-Ames workload research program 17 p2380 N88-24151
An evaluation of three linear scale radar altimeter displays
[AD-A192173] 18 p2485 N88-24636
Timesharing performance as an indicator of pilot mental workload
[NASA-CR-182807] 18 p2552 N88-25150
Simultaneous multiple control force exertion capabilities of males and females versus helicopter control force design limits
[AD-A191653] 18 p2553 N88-25153
Proceedings of the Workshop on the Assessment of Crew Workload Measurement Methods, Techniques and Procedures. Volume 2: Library references
[AD-A191209] 19 p2710 N88-26101
Method for observing changes in functional state of human operator 20 p2830 N88-26789
A review of workload measurement in relation to verbal comprehension 21 p2925 N88-27360
Event-related brain potentials as indices of mental workload and attentional allocation 21 p2979 N88-27696
Event-related and steady potential changes in the brain related to workload during tracking 21 p2981 N88-27705
Behavioral effects of exposure to the tempo high-power microwave system
[AD-A193305] 21 p2987 N88-27738
Determinants of dual-task interference and resource theories in cognitive psychology
[DFVLR-FB-88-14] 21 p2992 N88-27748
Threat expert system technology advisor
[NASA-CR-177479] 24 p3328 N88-29816

WORKSTATIONS
A work station for EXELFS data acquisition and analysis
[USIP-87-10] 01 p0078 N88-10498
The use of McIDAS as a Mesoscale forecasting tool during the Canadian Atlantic storms programs — Man-computer Interactive Data Access System (McIDAS) 02 p0205 N88-11284
The challenge of very short range forecasting in the tropics 02 p0205 N88-11287
A scientific workstation operator-interface for accelerator control
[DE87-014689] 03 p0362 N88-12278
Some performance comparisons for a fluid dynamics code
[PB88-113709] 07 p0852 N88-15175
Facility design validation of the information systems laboratory
[AD-A186309] 07 p0906 N88-15488
An innovative workstation 08 p1063 N88-16421
Foundation: Transforming data bases into knowledge bases 08 p1063 N88-16423
A learning apprentice for software parts composition 08 p1065 N88-16436
MPAD MCC workstation system: ADDAM and EEVE 09 p1203 N88-17209
Development of a comprehensive software engineering environment 09 p1203 N88-17211
Simplifying the construction of domain-specific automatic programming systems: The NASA automated software development workstation project 09 p1204 N88-17212
Signal processing studies program VLSI designs for unary functions
[AD-A188053] 10 p1325 N88-17922
Shared workspaces for real-time collaboration in distributed networks: Concepts, techniques, problems
[AD-A188150] 10 p1394 N88-18315
Terrain Analyst Work Station (TAWS) demonstrations
[AD-A188139] 11 p1504 N88-18981
A prototype for remotely shared textual workspaces
[AD-A188352] 12 p1679 N88-20040
GM: A gate matrix layout generator
[EUT-87-E-179] 13 p1820 N88-20875
GADL: A gate array description language
[EUT-87-E-165] 14 p1907 N88-21396
Higher levels of a silicon compiler
[EUT-86-E-163] 14 p1955 N88-21650
Generating layouts for random logic: Cell generation schemes
[EUT-86-E-164] 14 p1956 N88-21658
ESKISS: A program for optimal state assignment
[EUT-87-E-167] 14 p1956 N88-21659
Software quality assurance workstation
[P-1124/RT-14791] 14 p1957 N88-21670
Technology mapping from Boolean expressions to standard cells
[EUT-87-E-174] 14 p1963 N88-21709
An optimal CMOS structure for the design of a cell library
[EUT-87-E-166] 14 p1985 N88-21841
Sigma system: Overview, prospects 15 p2052 N88-22230
Mental-State Estimation, 1987
[NASA-CP-2504] 16 p2239 N88-23370
Point accessibility and primary workspace of simple six-link robots 17 p2345 N88-23976
The geometric workstation, a new approach for geometric corrections of remotely sensed data 17 p2352 N88-24017
Reconfigurable work station for a video display unit and keyboard
[NASA-CASE-MFS-26009-1-SB] 17 p2382 N88-24163
Ergonomy and interior furnishing of the cabins of deep diving manned submarines: The Nautile example — couch 19 p2697 N88-26032
The high speed local area network 19 p2717 N88-26133
The MELCOM PSI 2 AI workstation 21 p2930 N88-27395
Assessing and enhancing human performance: Utility of a workstation network
[AD-A192840] 21 p2991 N88-27743
Research on wide area workstations
[AD-A192529] 22 p3136 N88-28643
Automated software development workstation 23 p3263 N88-29423

WORLD
U EARTH (PLANET)

WORLD DATA CENTERS
Wave and wind data sources, environmental conditions committee report, International Ship and Offshore Structures Congress
[PB87-234902] 06 p0746 N88-14588

WORLD METEOROLOGICAL ORGANIZATION
Current status of world weather service 06 p0725 N88-14459
Wave and wind data sources, environmental conditions committee report, International Ship and Offshore Structures Congress
[PB87-234902] 06 p0746 N88-14588
The World Climate Research Program 14 p1935 N88-21538
Activities report of the World Meteorological Organization
[WMO-689] 24 p3404 N88-30265

WRAPAROUND CONTACT SOLAR CELLS
U SOLAR CELLS

WRINKLING
Contribution to the study of wrinkling in metal stamping
[ISAL-IDI1-87-08] 08 p0976 N88-15900

WRIST
Causes and prevention of occupational Repetition Strain Injuries (RSI) 11 p1521 N88-19083
Real-time implementation of a kinematic optimization scheme for seven-degree-of-freedom redundant robots with spherical wrists
[DE88-006785] 18 p2524 N88-24974
Kinematics of Hooke universal joint robot wrists
[NASA-TM-100567] 20 p2843 N88-26870

WU-2 AIRCRAFT
U U-2 AIRCRAFT

WYOMING
Geological characterization and statistical comparison of outcrop and subsurface facies: Shannon Shelf sand ridges
[DE87-001243] 03 p0348 N88-12202

X

X BAND
U SUPERHIGH FREQUENCIES
X RAY ABSORPTION
L2,3 XANES of the high T sub c superconductor YBa2Cu3O7 with variable oxygen content
[NOTA-INTERNA-888] 06 p0788 N88-14837
Soft X-ray absorption and emission spectra and the electronic structure of the Ba2YCu3O/sub 7-x/ superconductor
[DE88-002609] 08 p1090 N88-16559
Variable spectra of active galaxies
[NASA-CR-182694] 13 p1853 N88-21091
EXAFS studies of the microstructure of semiconductor alloys, defects and semiconductor-metal interfaces 20 p2868 N88-27031
Structural studies of (Ga,In)(As,P) alloys and (InAs) sub m (GaAs) sub n strained-layer superlattices by fluorescence-detected EXAFS 20 p2872 N88-27051
X RAY ANALYSIS
NT X RAY SPECTROSCOPY
X-ray studies of strain, interface and impurity in semiconductors
[DE87-013856] 01 p0104 N88-10678
Cooperative analysis of zirconium and zirconium alloys by fluorescent X-ray method
[DE87-753011] 02 p0148 N88-10926
X-ray emission from high-Z spherical laser plasmas: Implications for plasma dynamics
[DE87-014722] 02 p0239 N88-11506
Flaw imaging and ultrasonic techniques for characterizing sintered silicon carbide
[NASA-TM-100177] 03 p0334 N88-12106
The Einstein survey of the young stars in the Orion Nebula 04 p0518 N88-13182
X-ray analysis of polycrystalline aluminium subjected to fatigue cycling
[NAL-TM-MT-8706] 05 p0564 N88-13434
X-ray fatigue failure prediction based on plasticity response to microcracks 05 p0607 N88-13725
X-ray structure analyses and molecular mechanics analyses of dense energetic materials
[AD-A185462] 06 p0779 N88-14781
X-ray microfluorescence analysis of thin- and thick-sectioned geologic materials
[DE87-009803] 09 p1189 N88-17126
High-resolution X-ray microstructural study of single crystals of YBa2Cu3O/sub 7-y/
[DE88-004856] 10 p1421 N88-18484
Advances in X-ray line profile analysis to determine microstructure information about ceramics
[DE88-003938] 13 p1750 N88-20465
The effects of normal and therapeutic baths on the central vascular organs of persons with healthy hearts, as measured by X-ray
[NASA-TT-20252] 13 p1811 N88-20818
Advances in geochemistry and cosmochemistry: Trace element microdistributions with the synchrotron X-ray fluorescence microprobe
[DE88-006355] 15 p2032 N88-22108
Detecting delaminations in CFRP specimens using X-ray techniques
[FFA-TN-1988-04] 18 p2479 N88-24704
Electrochemistry in liquid crystals
[AD-A191554] 18 p2481 N88-24719
On the reversion phenomena of Cu-3 percent Ti alloys
[NASA-TT-20170] 18 p2488 N88-24762
X-ray and optical analysis of surface properties of metal optics
[DE88-004033] 19 p2727 N88-26195
Photoconducting X-ray detectors for Z-pinch experiments
[DE88-007118] 19 p2728 N88-26199
X-ray response of GaAlAs/GaAs radiation hardened double Heterostructure photodiode compared to SiPIN photodiodes
[DE88-007425] 19 p2733 N88-26231
Development of an automated X-ray gauge for nondestructive quantitative analysis
[DE88-008633] 20 p2812 N88-26681
X-ray studies of strain, interface and impurities in semiconductors
[DE88-012460] 21 p3025 N88-27954
ZT imaging system for layered thin wall structures
[AD-A195466] 24 p3352 N88-29954
A method for the qua ltative determination of crystalline phases by X-ray
[NASA-TT-20324] 24 p3434 N88-30444
X RAY APPARATUS
NT X RAY TUBES
LLE Review, volume 30
[DE87-014469] 02 p0178 N88-11109
MAXIE-1 (Magnetospheric Atmospheric X-ray Imaging Experiment)
[AD-A192846] 21 p2902 N88-27221
X RAY ASTRONOMY
NT X RAY BINARIES
NT X RAY SOURCES
USSR report: Space
[JPRS-USP-87-003] 01 p0009 N88-10050
X-ray astronomy instruments to operate on Mir station 01 p0009 N88-10052
Multilayered foils as radiation entrance windows and spectral filters for image converters in the ultrasoft X-ray wavelength region
[MPE-PREPRINT-90] 02 p0176 N88-11099
The hard X-ray eclipse in the intermediate polar EX Hydrae
[MPE-PREPRINT-95] 02 p0251 N88-11582
Hard X-ray telescope HAPI-1 and its observation of Crab pulsar 03 p0269 N88-11692
A re-examination of the corona-wind dividing line: Diagnostics of non-coronal atmospheres 04 p0504 N88-13101
Recent X-ray observations of supernova remnants and their interpretation
[MPE-PREPRINT-96] 09 p1262 N88-17563
AXAF: The Advanced X-ray Astrophysics Facility
[NASA-EP-251(M)] 10 p1292 N88-17725
Investigation of nuclei of active galaxies as well as sources in the Large Magellanic Cloud using the X-ray astronomy satellite EXOSAT
[ETN-88-91494] 11 p1570 N88-19399
MAXIE 1
[AD-A189688] 14 p1882 N88-21247
Further development of a stellar camera following the rotation-modulation-collimator principle for balloon-borne observations in the X-ray range
[ETN-88-91496] 14 p1913 N88-21428
Measurements of the scintillation time constants of inorganic crystals for the development of a triple-Phoswich detector for high-energy X-ray quanta
[ETN-88-91501] 14 p1993 N88-21875
Data analysis of an observation of the quasar 3C 273 in the high-energy X-ray range, and the significance for astrophysical models
[ETN-88-91493] 14 p1993 N88-21878
EXOSAT observations of active galaxies in the medium-energy X-ray domain
[ETN-88-91499] 14 p1993 N88-21879
The X-ray properties of AM Her stars
[MPE-PREPRINT-106] 16 p2289 N88-23704
The thermal evolution of the jets in SS433 — galactic object
[MPE-PREPRINT-107] 16 p2289 N88-23705
SW UMa and V426 Oph: EXOSAT surprises 19 p2740 N88-26269
EXOSAT observations of Hercules X-1
[MPE-PREPRINT-119] 22 p3164 N88-28841
The high-throughput X-ray spectroscopy mission: The mission-science report
[ESA-SP-1097] 24 p3453 N88-30557
X RAY ASTROPHYSICS FACILITY
The Goddard Space Flight Center mechanical cooler program 08 p0983 N88-15944
AXAF: The Advanced X-ray Astrophysics Facility
[NASA-EP-251(M)] 10 p1292 N88-17725
X RAY BINARIES
EXOSAT guest observer program. Binary parameters of the X-ray Pulsar 4U1626-67
[NASA-CR-182374] 06 p0802 N88-14905
A 23 hour EXOSAT observation of the X-ray pulsar 1E2259+586 and the associated supernova remnant G109.1-1.0
[MPE-PREPRINT-99] 14 p1994 N88-21882
Spectral classification of Low Mass X-ray Binaries (LMXB) energy spectra with color-color diagrams
[MPE-PREPRINT-111] 22 p3163 N88-28837
The evolution of low-mass X-ray binaries
[MPE-PREPRINT-118] 22 p3165 N88-28851
X RAY DIFFRACTION
A generalized least-squares determination of triaxial stress states by X-ray diffraction and the associated errors
[AD-A183851] 01 p0058 N88-10371
The production of ultrasmall and superfine holographic diffraction gratings using synchrotron radiation and lithographic techniques
[AD-A185395] 05 p0585 N88-13562
Two digital X-ray imaging systems for applications in X-ray diffraction
[PB87-123683] 06 p0669 N88-14103
X-ray structure analyses and molecular mechanics analyses of dense energetic materials
[AD-A185462] 06 p0779 N88-14781
High temperature stability of superconducting YBa2Cu3O subx as characterized by X-ray diffraction
[DE88-001856] 06 p0787 N88-14824
X-ray diffraction study of thermotropic liquid crystalline polyesters and diester model compounds
[AD-A186788] 09 p1255 N88-17521
High-temperature charge-density studies of CeO/sub 2-x/ using X-ray and neutron diffraction techniques
[DE88-002988] 09 p1257 N88-17536
High resolution electron and ion microscopy
[AERE-R-12502] 10 p1297 N88-17754
Novel analytical X-ray Non-Destructive Evaluation (NDE) tool for quality control of energetic materials
[AD-A187737] 11 p1497 N88-18935
Advances in X-ray optics, 1987
[DE88-003298] 11 p1549 N88-19268
The synthesis, characterization and structural studies of In(C5H4Me) by X-ray diffraction and electron diffraction techniques and a reinvestigation of the crystalline state of In(C5H5) by X-ray diffraction studies
[AD-A189110] 13 p1844 N88-21038
X-ray diffraction study of a thin GaAs film on Si(100)
[DE88-005290] 13 p1847 N88-21055
Analysis of explosives. 1: Computer programs for processing of X-ray powder defiraction data
[PB88-156898] 14 p1894 N88-21309
An investigation of the crystalchemistry and thermochemistry of selected mineral systems
[AD-A189758] 15 p2142 N88-22781
The structural analysis of some crystalline and semi-crystalline substances using X-ray and neutron diffraction 17 p2445 N88-24540
Equation of state of solid neon from X-ray diffraction measurements to 110 GPa
[DE88-008723] 19 p2734 N88-26241
Precise rotational alignment of X-ray transmission diffraction gratings
[DE88-010599] 21 p2911 N88-27273
Superconducting oxides with high critical temperatures 21 p2930 N88-27392
Short pulse X-ray diffraction studies of shocked and annealed crystals using the JANUS research laser
[DE88-011329] 23 p3288 N88-29579
X-ray diffraction imaging (topography) of electroopticcrystals by synchrotron radiation
[NASA-CR-183266] 24 p3432 N88-30427
Applications of synchrotron radiation to materials science: Diffraction imaging (topography) and microradiography
[NASA-CR-183265] 24 p3434 N88-30440
Crystal structure and density of helium to 232 kbar 24 p3441 N88-30481
X RAY FLUORESCENCE
Cooperative analysis of zirconium and zirconium alloys by fluorescent X-ray method
[DE87-753011] 02 p0148 N88-10926
Stratiospheric particles: Synchrotron X-ray fluorescence determination of trace element contents
[DE87-012482] 02 p0198 N88-11234
Development of an X-ray fluorescence microprobe at the National Synchrotron Light Source, Brookhaven National Laboratory: Early results: Comparison with data from other techniques
[NASA-CR-181468] 02 p0236 N88-11486
Determination, by X-ray fluorescence, of platinum, palladium, ruthenium, iron and chromium in special steels
[PB87-132114] 06 p0683 N88-14183
X-ray microfluorescence analysis of thin- and thick-sectioned geologic materials
[DE87-009803] 09 p1189 N88-17126
Advances in geochemistry and cosmochemistry: Trace element microdistributions with the synchrotron X-ray fluorescence microprobe
[DE88-006355] 15 p2032 N88-22108
X RAY IMAGERY
X-ray tomography and nuclear magnetic resonance imaging applications for advanced ceramic materials
[DE87-011534] 01 p0027 N88-10171
Time-resolved ablation measurements of imploding targets
[DE87-014464] 02 p0178 N88-11111
Time-resolved absorption measurements on OMEGA
[DE87-014465] 02 p0179 N88-11112
Cineradiography
[DE87-013158] 03 p0324 N88-12045
Computer-aided X-ray image system design and evaluation
[DE88-000997] 04 p0481 N88-12965
X-ray imaging: Status and trends
[DE88-000756] 05 p0649 N88-13980
Two digital X-ray imaging systems for applications in X-ray diffraction
[PB87-123683] 06 p0669 N88-14103
Use of spherical optics in high resolution soft X-ray grating monochromators
[PB87-125191] 06 p0780 N88-14788
MAXIE 1 (Magnetospheric Atmospheric X-ray Imaging Experiment) Program
[AD-A185878] 07 p0877 N88-15317
Auroral X-ray images during a pulsation event 08 p1026 N88-16214

AURIO: A proposal for flying auroral imaging observatory on the Polar Platform in the Space Station/Columbus program 08 p1034 N88-16268
Recent X-ray observations of supernova remnants and their interpretation
[MPE-PREPRINT-96] 09 p1262 N88-17563
MAXIE 1
[AD-A189838] 14 p1882 N88-21247
Hot electron diagnostics using X-ray imaging on GAMMA10 17 p2443 N88-24530
The XRD (X-Ray Diode) array, the grazing incidence spectrometer and the X-ray imaging camera on PBFA 2
[DE88-007282] 19 p2728 N88-26200
Toroidal and poloidal soft X-ray imaging system on the D3-D tokamak
[DE88-010585] 20 p2860 N88-26986
MAXIE-1 (Magnetospheric Atmospheric X-ray Imaging Experiment)
[AD-A192846] 21 p2902 N88-27221
X-ray diffraction imaging (topography) of electroopticcrystals by synchrotron radiation
[NASA-CR-183266] 24 p3432 N88-30427

X RAY INSPECTION
Aviation security: FAA (Federal Aviation Administration) needs preboard passenger screening performance standards
[PB87-216800] 02 p0124 N88-10783
A comparison of film-based tomography and computed tomography for advanced ceramic materials
[DE88-003114] 07 p0837 N88-15079
Nondestructive testings of HTGR graphites 13 p1747 N88-20448
Damage in a perforated graphite-epoxy plate under monotonic, cyclic biaxial loading
[ONERA-NT-1987-5] 20 p2816 N88-26708
Balance of X-ray radioscopy application to nondestructive tests of composite materials
[SNIAS-881-430-110] 21 p2907 N88-27250
Optimization of nondestructive control of ceramic pieces for aeronautical turbines
[ETN-88-92884] 22 p3059 N88-28149

X RAY IRRADIATION
Variations in semiconductor device response in a medium-energy x-ray dose-enhancing environment
[DE87-012400] 02 p0243 N88-11538
The development of diagnostic fuses
[SAND-86-0395] 03 p0311 N88-11963
Late radiation damage in bone, bone marrow and brain vasculature, with particular emphasis upon fractionation models
[DE87-753039] 08 p1048 N88-16330
Practical constraints on sources for pulsed beam lithographies
[DE88-006594] 13 p1776 N88-20623
X-ray production in low energy proton stopping
[NASA-TM-100619] 16 p2270 N88-23582
The ratio of microwaves to X-rays in solar flares: The case for the thick target model
[NASA-CR-183102] 19 p2743 N88-26287

X RAY LASERS
XUV emission features from the Livermore soft X-ray laser experiments
[DE88-000420] 04 p0448 N88-12779
J = O Task Force
[DE88-001326] 04 p0450 N88-12788
The gamma-ray laser project
[AD-A184824] 05 p0587 N88-13578
Lawrence Livermore National Laboratory Soft X-ray Laser Program
[DE88-001888] 07 p0859 N88-15218
The application of photoconductive detectors to the measurement of X-ray production in laser produced plasmas
[DE88-001630] 07 p0934 N88-15671
Spatially resolved X-ray laser spectra and demonstration of gain in nickel-like systems
[DE88-003957] 10 p1335 N88-17979
Research studies on extreme ultraviolet and soft X-ray lasers
[AD-A187506] 10 p1338 N88-17996
Soft X-ray beamsplitters and highly dispersive multilayer mirrors for use as soft X-ray laser cavity components
[DE88-004003] 11 p1549 N88-19270
Research studies on extreme ultraviolet and soft X-ray lasers
[AD-A189163] 12 p1633 N88-19773
Wavelength scaling of lithium-like recombination scheme for X-UV gain production --- X-ray lasers
[ETN-88-92002] 13 p1778 N88-20634
X-ray lasers: State of art and prospect
[ETN-88-92003] 14 p1914 N88-21434
Progress in X-ray laser experiments
[ETN-88-92004] 14 p1915 N88-21442
Review of X-ray laser studies at the GRECO: Laser-matter interaction
[ETN-88-92005] 14 p1915 N88-21443
An elliptical spectrograph/gated microchannel plate detector for time-resolved spectral measurements in the X-ray region
[DE88-007590] 20 p2856 N88-26961
Target designs for plasma-implosion-driven, photoionization-pumped soft X-ray lasers
[DE88-011278] 21 p2954 N88-27547
LLE (Laboratory for Laser Energetics) review
[DE88-008065] 23 p3219 N88-29158
Modeling of atomic processes in X-ray laser plasmas
[AD-A194118] 23 p3286 N88-29567
Autoionization for lower level detrapping in X-ray lasers
[AD-A195845] 24 p3379 N88-30123

X RAY SCATTERING
Neutron- and X-ray-small angle scattering with Fe-base metallic glasses
[DE88-002538] 09 p1147 N88-16876
Neutron and X-ray scattering studies of layered solids 09 p1246 N88-17469
Grazing incidence X-ray scattering study of defect structures in MBE GaAs/Si using synchrotron radiation
[DE88-004556] 10 p1420 N88-18483
Structural analysis using X-ray scattering and neutron scattering on binary amorphous (Co,Cu)Ti alloys
[ETN-88-91487] 11 p1459 N88-18699
Tungsten-carbon multilayer system studied with X-ray scattering
[DE88-005749] 13 p1735 N88-20373

X RAY SOURCES
NT X RAY BINARIES
Soft X-ray observations of pre-main sequence stars in the chamaeleon dark cloud
[NASA-CR-181457] 02 p0250 N88-11579
A search for X-ray luminous late type stars in NIPSS data 04 p0511 N88-13143
Characteristics of laser-plasma X-radiation source (review) 09 p1239 N88-17428
Advances in X-ray optics, 1987
[DE88-003298] 11 p1549 N88-19268
Variable spectra of active galaxies
[NASA-CR-182694] 13 p1853 N88-21091
A model for the X-ray binary 4U1820-30
[NASA-TM-101143] 17 p2451 N88-24562
A coded mask telescope for observations of X and gamma ray sources in the southern sky
[INPE-4580-PRE/1314] 24 p3453 N88-30551
Activities in astrophysics
[INPE-4582-PRE/1316] 24 p3456 N88-30570

X RAY SPECTRA
Electron beam requirements for soft X-ray/XUV free-electron lasers
[DE87-011750] 01 p0051 N88-10325
Generating soft X-ray spectra using the SPEED pentaxial diode
[DE87-013591] 01 p0098 N88-10647
Fast wave injection into high temperature tokamak plasmas in the lower-hybrid-density regime of JIPP T-IIU
[ISSN-0469-4732] 01 p0099 N88-10649
Semiconductor detector performance for low-energy X-rays
[DE87-014132] 02 p0244 N88-11542
Relations between chromospheric and coronal structure, flux-flux correlations and convective zone properties 04 p0510 N88-13138
VLA observations of the X-ray bright Hyades M-dwarfs 04 p0512 N88-13147
Exosat results on the dMe flare Star Wolf 630AB and on VB 8 04 p0512 N88-13151
Singularities in X-ray spectra of metals
[DE88-001440] 06 p0681 N88-14174
Spatially resolved X-ray laser spectra and demonstration of gain in nickel-like systems
[DE88-003957] 10 p1335 N88-17979
Variable spectra of active galaxies
[NASA-CR-182694] 13 p1853 N88-21091
Smoothing technique to resolve X-ray spectra in laser nuclear fusion 15 p2053 N88-22235
Observation of injected silicon in heliotron E 17 p2441 N88-24524
Inner-shell X-ray line spectra of highly ionized titanium, chromium, iron and nickel and their appliation to laboratory plasmas
[PB87-225181] 19 p2730 N88-26212
The properties of solar coronal active regions deduced from X-ray line spectra
[AD-A193026] 20 p2886 N88-27141
Detection of absorption lines in the spectra of X-ray bursts from X1608-52
[ISAS-RN-360] 20 p2887 N88-27143

X RAY SPECTROGRAPHY
U X RAY SPECTROSCOPY

X RAY SPECTROMETRY
U X RAY SPECTROSCOPY

X RAY SPECTROSCOPY
Center for X-Ray Optics, 1986
[DE88-000715] 04 p0449 N88-12783
Review of X-ray spectroscopy from laser-produced plasmas
[DE88-000755] 04 p0494 N88-13043
Area detectors for X-ray spectroscopy
[DE88-001429] 06 p0679 N88-14163
Determination, by X-ray fluorescence, of platinum, palladium, ruthenium, iron and chromium in special steels
[PB87-132114] 06 p0683 N88-14183
First results of balloon-borne X-ray and electric field observations near the footprint of the Viking satellite 08 p1026 N88-16215
Application of a simple rotational spherical grating mounting to high resolution soft X-ray spectroscopy
[PB87-164836] 09 p1142 N88-16845
Recent X-ray observations of supernova remnants and their interpretation
[MPE-PREPRINT-96] 09 p1262 N88-17563
Durability and damage tolerance of aluminum castings
[AD-A186444] 10 p1341 N88-18013
S-glass analysis by X-ray spectroscopy
[DE88-004636] 11 p1454 N88-18666
UHV (Ultra-High Vacuum) double crystal monochromator design
[DE88-003904] 11 p1456 N88-18676
Ion temperature measurement with spectroscopy in JT-60 17 p2439 N88-24513
X-ray emission from tokamaks 17 p2439 N88-24514
X-ray spectroscopic diagnostics on JIPPT-IIU and HELIOTRON-E 17 p2440 N88-24515
Spectroscopic results from JET: Some examples of data comparison and data needs 17 p2440 N88-24517
The high-throughput X-ray spectroscopy mission E6889478 MN513835 --- ESA program
[ESA-SP-1092] 17 p2450 N88-24554
The XRD (X-Ray Diode) array, the grazing incidence spectrometer and the X-ray imaging camera on PBFA 2
[DE88-007282] 19 p2728 N88-26200
Time-resolved doubly bent crystal X-ray spectrometer
[DE88-007899] 20 p2805 N88-26637
The high-throughput X-ray spectroscopy mission: The mission-science report
[ESA-SP-1097] 24 p3453 N88-30557

X RAY STARS
The 35-day cycle of Hercules X-1
[MPE-204] 11 p1571 N88-19405

X RAY TELESCOPES
NT X RAY ASTROPHYSICS FACILITY
X-ray astronomy instruments to operate on Mir station 01 p0009 N88-10052
Hard X-ray telescope HAPI-1 and its observation of Crab pulsar 03 p0269 N88-11692
Some highlights on ROSAT mechanisms 14 p1874 N88-21195
Design, construction and performance of the ROSAT high resolution X-ray mirror assembly
[MPE-PREPRINT-101] 15 p2150 N88-22836

X RAY TUBES
Stabilized X-ray generator power supply
[DE88-700297] 07 p0830 N88-15034

X RAYS
NT COSMIC X RAYS
NT SOLAR X-RAYS
Saturn: A large area X-ray simulation accelerator
[DE87-012021] 02 p0233 N88-11472
X-ray pulsars: Accretion flow deceleration 03 p0390 N88-12451
The X-ray orbital lightcurves of AR Lac and TY Pyx 04 p0509 N88-13129
Solar-geophysical data number 515, July 1987. Part 2: (Comprehensive reports). Data for January 1987 and miscellanea
[PB87-233185] 06 p0805 N88-14913
Characterization of microstructure in metallic and composite materials
[AD-A186193] 07 p0826 N88-15012
Stabilized X-ray generator power supply
[DE88-700297] 07 p0830 N88-15034
Fabrication techniques used in the construction of a high resolution X-ray framing camera
[DE88-002653] 07 p0856 N88-15200
X-ray measurements of phason distortion in ion-implanted Al-Mn
[DE87-014566] 07 p0937 N88-15694
Energetics and dynamics of simple impulsive solar flares
[NASA-TM-87816] 07 p0947 N88-15755
Emission angles for soft X-ray coherent transition radiation
[AD-A186851] 09 p1151 N88-16898

The ISO narrow spectrum series of filtered X-radiations at NPL
[NPL-RS(EXT)-92] 09 p1245 N88-17462
The measurement of chemical compositon with high spatial resolution using a dedicated scanning transmission electron microscope
[AERE-R-12317] 10 p1297 N88-17753
Suppression of X-rays generated by runaway electrons in ATF
[DE88-004179] 10 p1414 N88-18440
Effects of X irradiation and high field electron injection on the electrical properties of rapid thermal oxides
[DE88-002642] 10 p1417 N88-18461
The origin of the diffuse X-ray background and the formation of galaxies and voids
10 p1428 N88-18527
An experimental measurement of metal multilayer X-ray reflectivity degradation due to intense X-ray flux
[LA-10989-T] 11 p1547 N88-19255
Advances in X-ray optics, 1987
[DE88-003298] 11 p1549 N88-19268
X-ray lithographic research: A collection of NRL contributions
[AD-A188313] 12 p1695 N88-20140
X-rays from z-pinches
[AD-A188911] 12 p1696 N88-20146
The imaging of extra-galactic low-energy gamma-ray sources prospects, techniques, and instrumentation
[NASA-CR-182536] 12 p1713 N88-20251
Solar-geophysical data number 519, November 1987. Part 2: (Comprehensive reports). Data for May 1987 and miscellanea
[PB88-158910] 14 p2011 N88-21997
Theory of interactions of intense light with nonlinear, inhomogeneous and periodic structures and its applications to optical bistability, optic gyroscopes, nonlinear spectroscopy, radiation protection, X-ray emission and related fields
[AD-A190040] 15 p2133 N88-22725
Computing X-ray effects in optics
[DE88-006722] 15 p2134 N88-22732
Preparing the Alcator C bolometer system for use on MTX (Microwave Tokamak Experiment)
[DE88-006724] 15 p2134 N88-22733
A model for the X-ray binary 4U1820-30
[NASA-TM-101143] 17 p2451 N88-24562
Progress toward a soft X-ray FEL
[DE88-007669] 19 p2675 N88-25905
Generation of coherent soft X-rays using a single-pass free-electron laser amplifier
[DE88-009137] 19 p2675 N88-25907
The solar flare of 18 August 1979: Incoherent scatter radar data and photochemical model comparisons
[DE88-007616] 19 p2743 N88-26286
Microfocus X-ray techniques for flaw location
[DE88-008636] 20 p2812 N88-26580
In-situ reactive of X-ray optics by glow discharge
[DE88-009840] 20 p2854 N88-26947
Properties of multilayers for soft X-ray optics
20 p2867 N88-27025
The hard X-ray burst spectrometer event listing 1980-1987
[NASA-TM-4036] 20 p2887 N88-27144
X- and gamma-ray background observations in Antarctic
[INPE-4583-PRE/1317] 24 p3459 N88-30578

X WING ROTORS
Rotorcraft designs for the year 2000
03 p0264 N88-11665
Proceedings of the Circulation-Control Workshop, 1986
[NASA-CP-2432] 10 p1268 N88-17586
Analysis of a fixed-pitch X-wing rotor employing lower surface blowing 10 p1271 N88-17602
Prediction of aeroelastic response of a model X-wing rotor 10 p1271 N88-17603
X-wing potential for Navy applications
10 p1271 N88-17604
Analysis of a fixed-pitch X-wing rotor employing lower surface blowing
[AD-A187379] 24 p3321 N88-29779

X-29 AIRCRAFT
An integrated study of structures, aerodynamics and controls on the forward swept wing X-29A and the oblique wing research aircraft
[NASA-CR-181548] 04 p0399 N88-12486
X-29A forward-swept-wing flight research program status
[NASA-TM-100413] 10 p1277 N88-17644
A correlation study of X-29A aircraft and associated analytical development
[NASA-CR-183103] 13 p1722 N88-20296
Development of a real-time aeroperformance analysis technique for the X-29A advanced technology demonstrator
[NASA-TM-100432] 14 p1866 N88-21151
Operational viewpoint of the X-29A digital flight control system
[NASA-TM-100434] 14 p1866 N88-21152

X-30 VEHICLE
National aero-space plane: A technology development and demonstration program to build the X-30
[GAO/NSIAD-88-122] 17 p2301 N88-23764

XANTHINES
NT CAFFEINE
Role of adenosine analogs and growth hormone in waking and sleep
[AD-A187897] 11 p1519 N88-19070

XB-70 AIRCRAFT
U B-70 AIRCRAFT

XENON
State parameters of pulse-discharge plasma in xenon-filled closed tube 06 p0773 N88-14747
Low-power photolytically pumped lasers
[DE88-002448] 08 p0991 N88-15998
Electron stimulated desorption and coherent electron scattering
[AD-A189091] 13 p1835 N88-20978
Theoretical calculations of XeF ground state kinetics
[AD-A191398] 16 p2270 N88-23580
Rare Gas Halide (RGH) kinetics
[AD-A192352] 20 p2770 N88-26425
Performance of 10-kW class xenon ion thrusters
[NASA-TM-101292] 22 p3049 N88-28088
Electronic states of the Xe(sub n)HCl systems in gas and condensed phases
[AD-A193881] 23 p3192 N88-28997

XENON CHLORIDE LASERS
XeCl excimer laser induced multiphoton ionization of ammonia molecule 03 p0299 N88-11883
Operational performance of repetitive KrF, XeCl excimer lasers 03 p0327 N88-12068
Gas flow effects in pulse avalanche discharge XeCl excimer lasers 03 p0328 N88-12070
Minimum necessary intensity of source of preionization for stabilization of a self-sustaining laser discharge with mean power raised by electron beam or X-rays
[PB87-178158] 09 p1171 N88-17024
Direct solar-pumped iodine laser amplifier
[NASA-CR-182674] 13 p1777 N88-20630
Folded long-pulse XeCl excimer laser described
14 p1901 N88-21357
XeCl laser-pumped nanosecond dye lasers
14 p1902 N88-21359
Emission characteristics of XeCl-laser excited by electron beam of microsecond duration
14 p1970 N88-21762
Effects of emission energy transient in periodic-pulse XeCl excimer laser of approximately 400 W average power 14 p1971 N88-21763
Controlling XeCl-laser by means of external signal with less than 2 W/cm (sup)2 intensity
14 p1972 N88-21768
Pulse duration control of XeCl*-laser by means of plasma shutter 14 p1973 N88-21774
Realization of an XeCl laser producing 100W on average
[ETN-88-92541] 17 p2344 N88-23970
Dynamics of a plasma produced under effect of the XeCl-laser radiation on metallic surface
[DE88-701983] 21 p3017 N88-27902

XENON FLUORIDE LASERS
XeF excimer laser pumped by high-intensity relativistic electron beam 14 p1901 N88-21355
Discharge excitation of the XeF C to A transition
[DE88-006448] 15 p2070 N88-22339
Optical coatings for high average power XeF lasers
[DE88-011356] 20 p2807 N88-26656
Measurements of XeF (Xenon Fluoride) ground state dissociation and vibrational equilibration
[AD-A194611] 23 p3280 N88-29527

XEROGRAPHY
Application of magnification xeroradiography to advanced ceramics
[DE88-009965] 20 p2778 N88-26473

XV-15 AIRCRAFT
Modeling XV-15 tilt-rotor aircraft dynamics by frequency and time-domain identification techniques
03 p0263 N88-11657
Using frequency-domain methods to identify XV-15 aeroelastic modes
[NASA-TM-100033] 10 p1277 N88-17646
Hover performance tests of baseline metal and Advanced Technology Blade (ATB) rotor systems for the XV-15 tilt rotor aircraft
[NASA-CR-177436] 20 p2759 N88-26367
Utilization of identification methods in the time and frequency domain for the determination of the XV-15 (tilt-rotor) dynamics for lateral motion in hover flight
20 p2787 N88-26532

Y

YAG (GARNET)
U YTTRIUM-ALUMINUM GARNET

YAG LASERS
JPRS report: Science and technology. China
[JPRS-CST-87-034] 03 p0301 N88-11897
Saturable absorbers for colliding pulse-locked Nd:YAG lasers 03 p0302 N88-11902
Physical design of parameters of Nd:YAG disk laser
03 p0302 N88-11904
Investigations of solid state slab lasers
[ETN-88-91055] 09 p1171 N88-17022
High-power periodic-pulse YAG:Nd3+-laser system with telescopic unstable resonator and two-stage amplifier
09 p1237 N88-17414
Airborne Doppler lidar detection of wind shear. Results of performance analysis 10 p1275 N88-17627
Diode pumped fiber laser
[AD-A187694] 11 p1491 N88-18902
Polarization effects in laser-pumped Nd:YAG lasers
[DE88-004019] 11 p1492 N88-18904
Radiation absorption in neodymium glasses during passage of strong laser pulse 14 p1969 N88-21757
Solid-state ring laser with acoustooptical phase nonreciprocity of opposing waves
14 p1970 N88-21761
Nonlinear stage of ultrashort-pulse formation in solid-state laser 14 p1971 N88-21765
Laser processing-status, perspectives
15 p2050 N88-22211
Reduced thermal input by proper selection of YAG laser welding parameters
[DE88-000730] 15 p2072 N88-22356
Observation of synchronously transient pumped mode-locking dye laser under negative cavity detuning
16 p2187 N88-23041
Process control improvements in pulsed Nd:YAG laser closure welding of electromechanical relays
[DE88-006275] 21 p2957 N88-27564

YANG-MILLS FIELDS
Ten dimensional N = 1 supergravity coupled to supersymmetric Yang-Mills fields in superspace
[DE87-703033] 15 p2146 N88-22808

YANG-MILLS THEORY
Chiral U(1) anomaly in D = 4 super Yang-Mills theory coupled to supergravity
[DE87-753022] 02 p0252 N88-11591

YARNS
Creep of carbon yarn and carbon-carbon composites at high temperatures and high stresses
[AD-A195224] 24 p3340 N88-29878

YAW
Low speed wind tunnel investigation of propeller slipstream aerodynamic effects on different nacelle/wing combinations. Part 1: Total forces and moments and pressure distributions on nacelle/wing at different angles of attack and yaw and at different thrust coefficients
[FFA-TN-1987-22] 05 p0542 N88-13302
An investigation of the spray produced by a yawed wheel, including measurement of impact forces --- aircraft wheels
[BU-363] 14 p1866 N88-21150
Modal forced response of propfans in yawed flow
16 p2221 N88-23253
Actuated forebody strakes
[NASA-CASE-LAR-13983-1] 18 p2464 N88-24628
Yaw dynamics of horizontal axis wind turbines
[DE88-001137] 18 p2537 N88-25055
Aeroelastic response of metallic and composite propfan models in yawed flow
[NASA-TM-100964] 24 p3326 N88-29807

YAWING MOMENTS
A comparison between theory and experiment for the yaw moment induced by a loose internal part
[AD-A187053] 09 p1131 N88-16787
Cornering characteristics of the main-gear tire of the space shuttle orbiter
[NASA-TP-2790] 11 p1438 N88-18583
Wind-tunnel investigation of actuated forebody strakes for yaw control at high angles of attack
17 p2299 N88-23754

YAWMETERS
U ATTITUDE INDICATORS
U YAW

YEAST
Survival and mutation induction of dehydrated yeast cells after UV exposure 12 p1657 N88-19932
Cellular effects of heavy ions: Experimental results and theoretical approaches --- space radiation
12 p1658 N88-19933

YEMEN
Topographic mapping with SPOT 1 data. A practical approach by the Ordnance Survey
22 p3111 N88-28479

YHU-1 HELICOPTER
U UH-1 HELICOPTER
YIELD
GaAs MMIC yield evaluation --- monolithic microwave integrated circuits (MMIC)
[ESA-CR(P)-2470] 08 p0979 N88-15916
YIELD POINT
Dugdale solutions for strain hardening materials
[FD-6/1985] 01 p0059 N88-10380
Long-range pulselength scaling of 351nm laser damage thresholds
[DE87-014754] 04 p0448 N88-12777
A finite element procedure for interference-fit and cold-working problems with limited yielding
[AR-004-517] 04 p0485 N88-12992
Fiber composite structural durability and damage tolerance: Simplified predictive methods
[NASA-TM-100179] 05 p0560 N88-13409
Optimized approach to damage tolerance --- spacecraft
[FOK-FSS-R-87-024] 09 p1134 N88-16806
Database of average-power damage thresholds at 1064 nm
[DE88-004352] 13 p1776 N88-20626
GARTEUR TP-037: Impact damage tolerance of carbon fiber and hybrid laminates
[RAE-TR-87057] 17 p2316 N88-23837
An experimental study of biaxial yield in modified 9Cr-1Mo steel at room temperature
[NASA-CR-175012] 24 p3385 N88-30164
YIELD STRENGTH
Face compression yield strength of the copper-Inconel composite specimen
[DE87-011974] 01 p0019 N88-10116
Wire interconnection reliability and moisture levels in hybrid microcircuits with epoxy-attached components
[DE87-012987] 01 p0039 N88-10247
Need for composites, new materials discussed
02 p0160 N88-11001
Corrosion-electrochemical and mechanical properties of composite graphite-carbide metal materials based on titanium and its alloys 03 p0285 N88-11794
The effect of strain rate on the yield behavior of iron-base LRO alloys at elevated temperatures
[DE87-014893] 03 p0288 N88-11808
Small-diameter wire tensile testing
[DE88-000835] 04 p0455 N88-12815
Analysis of end stresses in glass-metal bimaterial strips
[DE87-007848] 05 p0610 N88-13750
Effect of metal surface properties on the fatigue crack growth behavior 06 p0716 N88-14390
The relationship of tensile specimen size and geometry effects to unique constitutive parameters for ductile materials
[AD-A186020] 08 p0994 N88-16012
An experimental and numerical study of notch sensitivity of ARALL laminates
[CCMS-88-04] 11 p1450 N88-18644
Properties fo seals made with Li2O-Al2O3-SiO2-glass ceramics and aluminum-containing austenitic stainless steels
[DE88-004688] 12 p1633 N88-19776
A direct correlation of strength with impact velocity
[AD-A189251] 13 p1741 N88-20409
The effects of temperature and strain rate on the yielding behavior of the single crystal superalloy PWA 1480
14 p1931 N88-21517
Rapidly solidified lightweight durable disk material
[AD-A191697] 18 p2491 N88-24775
Geometric and material nonlinear analysis of structures comprising rectangular hollow sections
[CE-79] 24 p3382 N88-30141
YOUNG MODULUS
U MODULUS OF ELASTICITY
YTTERBIUM
Ytterbium monolayer diffusion barriers at Hg(1-x)Cd(x)Te/Al junctions
[AD-A188013] 10 p1299 N88-17768
YTTRIUM
Magnetic anomalies in the rare earth oxide superconductors GdBa2Cu3O(7-x) and YbBa2Cu3O(7-x)
[AD-A190713] 15 p2144 N88-22793
Synthesis and characterization of high-T(sub c) screen-printed Y-Ba-Cu-O films on alumina
[NASA-TM-100860] 15 p2146 N88-22805
Effects of 67.5 MeV electron irradiation on Y-Ba-Cu-O and Gd-Ba-Cu-O high-temperature superconductors
[AD-A191271] 16 p2283 N88-23669
Characterization of structural and magnetic order of Er/Y superlattices 20 p2873 N88-27056
Pure metallic bridge and point-contact tunneling into single- and polycrystal YBa2Cu3O(sub 7-y)
[DE88-010030] 20 p2878 N88-27084
The high temperature creep deformation of Si3N4-6Y2O3-2Al2O3
[NASA-CR-183204] 23 p3190 N88-28981
YTTRIUM COMPOUNDS
NT YTTRIUM OXIDES
NT YTTRIUM-ALUMINUM GARNET
400-nm photoluminescence of a color center in undoped YAG grown under reducing atmosphere
[DE88-001760] 07 p0858 N88-15213
Growth and characteristics of materials for tunable lasers in the near infrared spectral region
[NASA-CR-182501] 11 p1491 N88-18901
A sup 57 Fe Mossbauer study of the superconductor YBa sub 2 (Fe sub x Cu sub 1-x) sub 3 O sub y
[DE88-701543] 16 p2282 N88-23661
Effect of a weak magnetic field on high temperature superconductivity in Y-Ba-Cu-O ceramics
[DE88-702192] 19 p2733 N88-26235
All-electron local density theory of electronic structure and superconductivity in YBa2Cu3O7 and YBa2Cu3O6
[DE88-009944] 19 p2735 N88-26246
Anharmonic model for high-Tc superconductors
[DE88-702196] 21 p3020 N88-27924
Superconducting properties of LaBa2Cu3O(sub x) and YBa2Cu3O(sub y)
[DE88-012038] 21 p3024 N88-27952
YTTRIUM OXIDES
Synthesis of the monoclinic yttria by thermal plasma processing
[DE88-000496] 04 p0421 N88-12608
High temperature stability of superconducting YBa2Cu3O subx as characterized by X-ray diffraction
[DE88-001856] 06 p0787 N88-14824
Atomic-level studies of superconducting YBa2Cu3O sub 7-x
[DE88-002522] 06 p0788 N88-14831
Low field characterization of YBa2Cu3O sub 7-delta single crystals
[DE88-002895] 07 p0938 N88-15700
Fabrication of YBa2Cu3O7 superconducting ceramics
[DE88-003012] 07 p0938 N88-15701
Soft X-ray absorption and emission spectra and the electronic structure of the Ba2YCu3O/sub 7-x/ superconductor
[DE88-002609] 08 p1090 N88-16559
Advanced materials for solid oxide fuel cells
[DE88-002338] 10 p1350 N88-18071
The structure and properties of twin boundaries in superconducting YBa2Cu3O7
[DE88-003864] 10 p1418 N88-18468
Improved magnetization for YBa2Cu3O/sub 7-delta annealed in oxygen above 1000 C
[DE88-003934] 10 p1418 N88-18469
Freestanding films of YBa2Cu3O/sub 6.9/
[DE88-003995] 10 p1419 N88-18471
Grain boundaries, planar defects and superconducting properties of YBa2Cu3O7
[DE88-003477] 10 p1419 N88-18475
Superconducting properties and structural characterization of high T/sub c/ oxides
[DE88-003479] 10 p1420 N88-18477
Penetration depth measurements of YBa2Cu3O/sub 7-delta/ at 4 MHz
[DE88-003493] 10 p1420 N88-18478
The electronic structure of YBa2Cu3O/sub 7-delta/ above and below T/sub c/
[DE88-003495] 10 p1420 N88-18479
Simulation and processing of high resolution images of defects and interfaces in superconducting YBa2Cu3O7
[DE88-003856] 10 p1420 N88-18480
High-resolution X-ray microstructural study of single crystals of YBa2Cu3O/sub 7-y/
[DE88-004856] 10 p1421 N88-18484
The YAlO(sub 3):Er laser
[PB88-130877] 11 p1493 N88-18911
Atom probe microanalysis of superconducting YBa2Cu3O(sub 7-x)
[DE88-003203] 11 p1557 N88-19322
Processing relationships in YBa2Cu3O(7-x) superconductors
[DE88-005137] 11 p1559 N88-19330
Mass transport and chemical demixing of Y-Ba-Cu-O compounds during sintering in temperature gradients
[DE88-004887] 12 p1696 N88-20151
Ordered structures in YBa2Cu3O/sub 7-y/, La2Cu3O/sub 7-y/, La/sub 2-x/Sr/sub x/CuO/sub 4-par. delta/ and related perovskites
[DE88-006461] 14 p1987 N88-21851
Melt processing ceramic YBa2Cu3O(sub 6.9)
[DE88-007039] 15 p2047 N88-22199
Superconductivity and the tailoring of lattice parameters of the compound YBa2Cu3O(sub x)
[DE88-005904] 15 p2140 N88-22769
Vacancy ordering in the basal plane of YBa2Cu3O(sub)z
[DE88-004572] 18 p2583 N88-25348
Effects of grain boundary composition on properties of YBa2Cu3O/sub 7-x/
[DE88-007679] 20 p2875 N88-27064
The superconducting transition in oxygen deficient YBa2Cu3O(sub 7-Delta)
[DE88-009957] 20 p2877 N88-27079
Anisotropic characteristic lengths in single crystal YBa2Cu3O(sub 7-Delta)
[DE88-009959] 20 p2877 N88-27080
Anisotropy of the lower critical field in YBa2Cu3O(sub 7-Delta)
[DE88-009971] 20 p2877 N88-27081
Preparation of high-T(sub)c Y1Ba2Cu3O(sub 7-Delta) superconducting thin films by MBE (Molecular-Beam-Epitaxy) techniques
[DE88-009999] 20 p2877 N88-27082
Oxygen vacancy ordering and superconductivity in YBa2Cu3O(sub 7-x)
[DE88-010005] 20 p2877 N88-27083
Electron irradiation effects in YBa2Cu3O7-Delta single crystals
[DE88-010050] 20 p2878 N88-27085
Phase transformations and thermodynamic behavior of the YBa2Cu3O(sub)x system via EMF measurements
[DE88-010054] 20 p2878 N88-27086
Ceramic processing of high-T(sub)c superconductors
[DE88-010090] 20 p2878 N88-27087
Compilation of NRL publications on high temperature superconductivity
[AD-A189137] 21 p3019 N88-27921
Thermodynamics of oxygen-vacancy ordering in YBa2Cu3O(sub z)
[DE88-009816] 21 p3022 N88-27940
Preparation and characterization of isotopic oxygen-enriched yttrium barium copper oxide
[DE88-010939] 22 p3154 N88-28766
Superconducting properties of oxygen deficient YBa2Cu3O(sub 7-delta)
[DE88-009969] 22 p3155 N88-28774
Effect of neutron irradiation on critical magnetization current in single crystal YBa2Cu3O(sub 7-delta)
[DE88-009970] 22 p3156 N88-28775
Effects of metal substitutions (Fe and Ga) in YBa2Cu3O7 on its superconducting properties and microstructures
[DE88-007393] 23 p3287 N88-29572
Preparation of superconducting YBa2Cu3O(sub 7-x) films by magnetron sputtering
[DE88-009977] 23 p3289 N88-29583
YTTRIUM-ALUMINUM GARNET
Characterization of yttrium aluminum garnet/YAG/using 14 MeV neutron activation
[AD-A191925] 18 p2582 N88-25342
YUH-1 HELICOPTER
U UH-1 HELICOPTER
YUH-60A HELICOPTER
U UH-60A HELICOPTER

Z

ZEEMAN EFFECT
Laser induced fluorescent study of relativistic electron beams
[AD-A184456] 04 p0447 N88-12774
Measurements of stellar magnetic fields
04 p0503 N88-13093
Exploiting the IR: Solar and stellar spectroscopy in the IR 04 p0504 N88-13102
Magnetic fields on K and M stars
04 p0510 N88-13137
Observations and analysis of the photospheric magnetic fields on dwarf G, K and M stars
04 p0520 N88-13196
Nature of gigantic resistance fluctuations in metal-oxide-semiconductor wires
[DE88-002905] 09 p1256 N88-17533
ZENER DIODES
U AVALANCHE DIODES
ZEOLITES
Preliminary market analysis for large zeolite crystals
[NASA-CR-182882] 15 p2049 N88-22207
Upgrading pyrolysis vapors to aromatic gasoline with zeolite catalysis at atmospheric pressure
18 p2536 N88-25045
Studies of photochemically and electrochemically driven electron transport in zeolites
[DE88-008644] 22 p3155 N88-28769
ZERO CROSSINGS
U ROOTS OF EQUATIONS
ZERO GRAVITY
U WEIGHTLESSNESS
ZERO LIFT
Planform effects on the supersonic aerodynamics of multibody configurations
[NASA-TP-2762] 04 p0393 N88-12454

ZERO POWER REACTORS
Benchmark physics experiments for SP-100
17 p2429 N88-24453
ZETA PINCH
Analytic model of an imploding Z-pinch plasma colliding inelastically with a thin-shelled cylindrical target
[DE88-000051] 03 p0378 N88-12379
Magneto-Inertia Confinement Approach (MICA) to fusion in dynamic Z-pinch formed from a frozen deuterium-tritium tube
[IPPJ-856] 09 p1252 N88-17504
On selfsimilar thermonuclear ignition of a plasma in necks of zeta devices
[DE88-701640] 16 p2280 N88-23647
Photoconducting X-ray detectors for Z-pinch experiments
[DE88-007118] 19 p2728 N88-26199
Zero-dimensional calculation for ZT-H
[DE88-009175] 19 p2731 N88-26217
ZETA THERMONUCLEAR REACTOR
Zero-dimensional calculation for ZT-H
[DE88-009175] 19 p2731 N88-26217
ZIMBABWE
Wind velocity measurement data. Zimbabwe, 4 measuring stations
[R-845-D] 13 p1802 N88-20770
ZINC
Preparation and characterization of Cu2Zn1-xMnxGeS4
[AD-A188113] 11 p1556 N88-19315
Technology base research on zinc/air battery systems
[DE88-004893] 13 p1763 N88-20546
Influence of alternating magnetic fields on Zn-67 Moessbauer resonance in ZnO
[PB88-186432] 18 p2584 N88-25352
Laser fluorescence spectroscopy of zinc neutrals originating from laser-irradiated and ion-bombarded zinc sulfide and zinc surfaces
[DE88-008037] 20 p2769 N88-26418
Lattice-matched HgZnTe epitaxy development
[AD-A193677] 23 p3292 N88-29600
An electrochemical impedance spectroscopy study of reactions at the metal/coating interface
24 p3355 N88-29975
Zinc filled coatings 24 p3355 N88-29978
ZINC ALLOYS
Effect of Zr or Cr content on the fracture toughness of the high purity Al-Zn-Mg alloys
[NASA-TT-20294] 19 p2616 N88-25518
ZINC COATINGS
Adhesion properties of polyelectrolyte-chemisorbed zinc phosphate conversion coatings
[DE87-012489] 01 p0029 N88-10186
Studies on hot-dip zinc-aluminum coated sheet steels
[ETN-88-92217] 15 p2042 N88-22166
Polyacrylic acid electrolyte-modified zinc phosphate conversion coatings for corrosion protection of steel
[DE88-004878] 19 p2617 N88-25527
ZINC COMPOUNDS
NT ZINC OXIDES
NT ZINC SELENIDES
NT ZINC SULFIDES
NT ZINC TELLURIDES
Grace DAKASEP alkaline battery separator
02 p0164 N88-11031
Studies on estimation of nickel in zinc base die casting by D.C. polarography
[PD-MT-8729] 04 p0417 N88-12588
Resistivity of EuBa2(Cu/sub 1-y/Zn/sub y/)3O/sub x/ as a ffunction of temperature, magnetic field, pressure and Zn concentration
[DE87-014740] 04 p0499 N88-13069
ZINC NICKEL BATTERIES
U NICKEL ZINC BATTERIES
ZINC OXIDES
Sintering and densification of particulate composites: Inclusion size and clustering
[DE88-002230] 06 p0685 N88-14199
Model Cu/ZnO catalysts for methanol synthesis: The role of surface structure
[DE88-002354] 07 p0830 N88-15037
High temperature solar electrothermal processing-3. Zinc from zinc oxide at 1200-1675K using a non-consumable anode
[AD-A186600] 09 p1141 N88-16836
Improvements to Raney copper zinc methanol synthesis catalysts 17 p2318 N88-23844
Influence of alternating magnetic fields on Zn-67 Moessbauer resonance in ZnO
[PB88-186432] 18 p2584 N88-25352
Zinc-oxide thin films for integrated-sensor applications
19 p2673 N88-25896
The first synthesis of chem-prep varistor LAC (Lightning Arrestor Connector) granules
[DE88-008005] 21 p2936 N88-27438
Low temperature film growth of the oxides of zinc, aluminum and vanadium (and related systems, oxides of gold and germanium, nitrides of aluminum and tungsten) by reactive sputter deposition
[AD-A193497] 23 p3191 N88-28986
ZINC SELENIDES
Blue-green laser diode research program
[AD-A183517] 01 p0051 N88-10323
Physical vapor transport crystal growth
03 p0296 N88-11860
Preparation and characterization of members of the system (Zn,Se)1-xGaPx
[AD-A185073] 05 p0655 N88-14019
Inadequacies of EMI-seal material: A corrosion study
17 p2319 N88-23852
Growth and characterization of thin films of ZnSnP(sub)2
[DE88-001164] 20 p2874 N88-27060
Atomic layer epitaxy of ZnS and ZnSe
[AD-A192307] 21 p3020 N88-27928
Blue-green laser diode research program
[AD-A191980] 23 p3218 N88-29153
ZINC SULFIDES
Laser fluorescence spectroscopy of zinc neutrals originating from laser-irradiated and ion-bombarded zinc sulfide and zinc surfaces
[DE88-006033] 13 p1776 N88-20620
Laser fluorescence spectroscopy of zinc neutrals originating from laser-irradiated and ion-bombarded zinc sulfide and zinc surfaces
[DE88-008037] 20 p2769 N88-26418
Atomic layer epitaxy of ZnS and ZnSe
[AD-A192307] 21 p3020 N88-27928
The optical spectroscopy of copper-blue luminescence in zinc sulfide crystals. Zero-phonon line spectra under the influence of magnetic field, temperature and excitation intensity
[ETN-88-93122] 24 p3344 N88-29903
An organometallic route to micron-sized whiskers of zinc sulfide
[AD-A195889] 24 p3430 N88-30414
ZINC TELLURIDES
MBE (Molecular Beam Epitaxial) growth characterization and electronic device processing of HgCdTe, HgZnTe related heterojunctions and HgCdTe-CdTe superlattices
[AD-A187416] 11 p1555 N88-19307
CdZnTe as a wide-band-gap absorber for a tandem, thin-film solar cell
[DE88-001114] 13 p1793 N88-20724
ZINC-BROMIDE BATTERIES
Extended abstracts: Eighth Battery and Electrochemical Contractors' Conference
[DE88-000960] 06 p0730 N88-14489
ZINC-OXYGEN BATTERIES
Zinc-redox battery: A technology update
[DE87-010737] 01 p0040 N88-10256
A new concept in an electrically rechargeable zinc-air alkaline battery
[DE88-003858] 13 p1762 N88-20539
ZIRCONATES
Develop techniques for ion implantation of (lead-lanthanum-zirconate-titanate) for adaptive optics
[DE88-000642] 05 p0650 N88-13986
Refractory Materials of Zirconate. Part 2: Synthesis and some properties of strontium, zirconate, calcium zirconate and barium zirconate
[NASA-TT-20186] 20 p2779 N88-26483
Preparation and properties of high Q microwave dielectrics in the (CA, SR, BA) zirconate system
[AD-A193127] 21 p2918 N88-27317
ZIRCONIUM
Cooperative analysis of zirconium and zirconium alloys by fluorescent X-ray method
[DE87-753011] 02 p0148 N88-10926
The effect of sulfur and zirconium Co-doping on the oxidation of NiCrAl
[NASA-TM-100209] 02 p0150 N88-10940
Investigation by differential scanning calorimetry of microstructure in a superplastic Al-Mg-Zr alloy
[AD-A184902] 05 p0564 N88-13439
Creep behavior of tungsten/niobium and tungsten/niobium-1 percent zirconium composites
[NASA-TM-100804] 11 p1460 N88-18707
A case study of the development of a military specification - zirconium powder for thermal batteries
[AD-A188751] 13 p1792 N88-20717
A dense and strong ceramic material made from zirconium dioxide 14 p1886 N88-21274
Ion-beam mixing and amorphization in Au/Zr bilayers
[DE88-005999] 15 p2140 N88-22767
Characterization of precipitates in a niobium-zirconium-carbon alloy
[NASA-TM-100848] 16 p2178 N88-22981
Creep behavior of tungsten/niobium and tungsten/niobium-1 percent zirconium composites
17 p2425 N88-24427
Effect of Zr or Cr content on the fracture toughness of the high purity Al-Zn-Mg alloys
[NASA-TT-20294] 19 p2616 N88-25518
PLZT (Lead-Lathanium-Zirconium-Titanium) electro-optic photographic system
[AD-A193473] 23 p3215 N88-29137
Electrical properties of materials for elevated temperature resistance strain gage application
[NASA-CR-182214] 24 p3376 N88-30106
ZIRCONIUM ALLOYS
Cooperative analysis of zirconium and zirconium alloys by fluorescent X-ray method
[DE87-753011] 02 p0148 N88-10926
Microstructure of amorphous and crystalline zirconium alloys rapidly solidified
[DE87-703700] 05 p0564 N88-13432
Structural relaxation and mechanical properties of amorphous Fe-Zr alloys 07 p0840 N88-15094
Diffusion studies in amorphous NiZr alloys
[DE88-003009] 10 p1301 N88-17781
Crystallization and glass formation in electron and laser beam irradiated Cu-Zr alloys
[DE88-003390] 11 p1464 N88-18729
The precipitation processes of Cu-Zr-Cr alloys
[NASA-TT-20168] 18 p2488 N88-24758
Oxidation behavior and microstructural studies of melt-spun glassy Fe-Al-Zr metal
[DE88-009964] 19 p2617 N88-25526
ZIRCONIUM COMPOUNDS
NT ZIRCONATES
NT ZIRCONIUM NITRIDES
NT ZIRCONIUM OXIDES
Study of the micromechanical properties of fluor glasses based on ZrF4
[ISAL-ITC1-87-03] 09 p1148 N88-16882
Role of zircon in tracing crustal growth and recycling
24 p3394 N88-30211
The early archaean crustal history of West Greenland as recorded by detrital zircons 24 p3395 N88-30221
Growth of early archaean crust in the ancient Gneiss complex of Swaziland and adjacent Barberton Greenstone Belt, Southern Africa 24 p3396 N88-30223
ZIRCONIUM NITRIDES
Structure and properties of titanium nitride and zirconium nitride thin films prepared by reactive ion plating --- cutting tools
[ETN-88-92218] 15 p2042 N88-22167
ZIRCONIUM OXIDES
Effect of time and temperature on transformation toughened zirconias
[AD-A184356] 04 p0419 N88-12600
Studies of alumina additions in zirconia - magnesia
[DE87-703500] 04 p0419 N88-12602
Internal reforming development for solid oxide fuel cells
[DE87-006518] 04 p0464 N88-12871
On 1064 nm and 350 nm laser damage thresholds of high index oxide films deposited from organic solutions and sols
[DE88-001636] 07 p0859 N88-15217
Advanced materials for solid oxide fuel cells
[DE88-002338] 10 p1350 N88-18071
Perturbed angular correlations in zirconia ceramics
[DE88-004117] 11 p1464 N88-18731
The elastic properties of monoclinic ZrO2
[DE88-005920] 14 p1986 N88-21847
Stability limits in the monoclinic-tetragonal transformations of zirconia
[DE88-005924] 14 p1986 N88-21849
Superplastic flow of mullite-zirconia composites
[DE88-005905] 15 p2028 N88-22085
High-strength ceramic based on tetragonal ZrO2 with Al2O3 admixture 16 p2180 N88-22996
Mass spectrometric high temperature measurements of the barium oxide-zirconium dioxide system and the determination of thermodynamic data for barium zirconate. Clarification of the counter-stopping capacity of coated particles for solid fission products by zirconium dioxide addition
[NASA-TT-20187] 19 p2611 N88-25496
Preparation and characterization of ceramic materials based on Al2O3 reinforced with a ZrO2 dispersion
[ISAL-87-0041] 21 p2922 N88-27340
Comparison of sol-gel procedures for zircon and alumina
[REPT-881-430-108] 21 p2922 N88-27342
Preparation of superconducting YBa2Cu3O(sub 7-x) films by magnetron sputtering
[DE88-009977] 23 p3289 N88-29583
ZODIACAL DUST
Interaction mechanisms of comets with the zodiacal dust cloud 14 p2008 N88-21977
ZODIACAL LIGHT
Comet West: A view from the HELIOS zodiacal light photometers 01 p0117 N88-10749

Interaction mechanisms of comets with the zodiacal dust cloud 14 p2008 N88-21977
Doppler distortion of solar Fraunhofer lines in zodiacal light by reflection from interplanetary dust 19 p2740 N88-26270

ZONAL CIRCULATION
U ZONAL FLOW (METEOROLOGY)

ZONAL FLOW (METEOROLOGY)
Atmosphere dynamics in the equatorial meteor zone 06 p0733 N88-14508
Wind regime peculiarities in the lower thermosphere in the winter of 1983/84 06 p0733 N88-14511
Circulation in the mesosphere and lower thermosphere during the MAP (Middle Atmosphere Program)/WINE (Winter in the Northern Europe) period 06 p0734 N88-14514
A statistical study of variations of internal gravity wave energy characteristics in meteor zone 06 p0735 N88-14523
Lower thermosphere wind regime according to radiometeor measurements in Kazan 06 p0736 N88-14526
Atmosphere dynamic processes structure at 80-105 km altitude 06 p0736 N88-14527
JPRS report: Science and technology. China [JPRS-CST-87-042] 14 p1899 N88-21338
Physical processes for maintaining mean meridional and zonal circulation of atmosphere in middle latitudes, volume 1 14 p1900 N88-21343
Numerical simulation of generation of mesoscale convective systems in large-scale environment 14 p1900 N88-21344
Physical process for maintenance of mean meridional and zonal circulation of atmosphere in middle latitudes, volume 2 14 p1900 N88-21345
On regime selection in global atmospheric flow 17 p2374 N88-24119

ZONAL HARMONICS
The contraction of satellite orbits under the influence of air drag. Part 8: Orbital lifetime in an oblate atmosphere, when perigee distance is perturbed by odd zonal harmonics in the geopotential [RAE-TR-86069-PT-8] 01 p0010 N88-10058

ZONE MELTING
Elimination of subboundaries in 0.5-micron-thick Si-on-insulation films produced by ZMR [AD-A184590] 03 p0381 N88-12396

ZONE REFINING
U ZONE MELTING

ZONES
U REGIONS

ZOOM LENSES
A high-speed, eight-frame image intensified electro-optic camera with 200-800mm zoom objective capability [DE88-000229] 03 p0326 N88-12059
Zoom versus full-field sensitivity at the ETS (Experimental Test System) [AD-A188162] 12 p1628 N88-19742

ZPR REACTORS
U ZERO POWER REACTORS

VOLUME 26 NUMBERS 1-6

Scientific and Technical Aerospace Reports

Abstracts January—March 1988

TABLE OF CONTENTS

STAR Issue	Page
1	1
2	121
3	259
4	393
5	529
6	663

VOLUME 26 NUMBERS 7-12

Scientific and Technical Aerospace Reports

Abstracts April—June 1988

TABLE OF CONTENTS

STAR Issue	Page
7	809
8	949
9	1105
10	1267
11	1433
12	1573

VOLUME 26 NUMBERS 13-18

Scientific and Technical Aerospace Reports

Abstracts July—September 1988

TABLE OF CONTENTS

STAR Issue	Page
13	1715
14	1861
15	2013
16	2155
17	2293
18	2455

VOLUME 26 NUMBERS 19-24

Scientific and Technical Aerospace Reports

Abstracts October—December 1988

TABLE OF CONTENTS

STAR Issue	Page
19	2597
20	2745
21	2889
22	3033
23	3167
24	3311

*U.S. GOVERNMENT PRINTING OFFICE:1989-230-323

FEDERAL REGIONAL DEPOSITORY LIBRARIES

ALABAMA

AUBURN UNIV. AT MONTGOMERY LIBRARY
Documents Department
Montgomery, AL 36193
(205) 271-9650

UNIV. OF ALABAMA LIBRARY
Documents Dept.-Box S
University, AL 35486
(205) 348-6046

ARIZONA

DEPT. OF LIBRARY, ARCHIVES AND PUBLIC RECORDS
Third Floor—State Cap.
1700 West Washington
Phoenix, AZ 85007
(602) 255-4121

UNIVERSITY OF ARIZONA LIB.
Government Documents Dept.
Tucson, AZ 85721
(602) 621-6433

ARKANSAS

ARKANSAS STATE LIBRARY
One Capitol Mall
Little Rock, AR 72201
(501) 371-2326

CALIFORNIA

CALIFORNIA STATE LIBRARY
Govt. Publications Section
P.O. Box 2037
Sacramento, CA 95809
(916) 324-4863

COLORADO

UNIV OF COLORADO LIB.
Government Pub. Division
Campus Box 184
Boulder, CO 80309
(303) 492-8834

DENVER PUBLIC LIBRARY
Govt. Pub. Department
1357 Broadway
Denver, CO 80203
(303) 571-2131

CONNECTICUT

CONNECTICUT STATE LIBRARY
Government Documents Unit
231 Capitol Avenue
Hartford, CT 06106
(203) 566-7029

FLORIDA

UNIV. OF FLORIDA LIBRARIES
Library West
Documents Department
Gainesville, FL 32611
(904) 392-0367

GEORGIA

UNIV. OF GEORGIA LIBRARIES
Government Reference Dept.
Athens, GA 30602
(404) 542-8949

HAWAII

UNIV. OF HAWAII LIBRARY
Govt. Documents Collection
2550 The Mall
Honolulu, HI 96822
(808) 948-8230

IDAHO

UNIV. OF IDAHO LIBRARY
Documents Section
Moscow, ID 83843
(208) 885-6344

ILLINOIS

ILLINOIS STATE LIBRARY
Information Services Branch
Centennial Building
Springfield, IL 62756
(217) 782-5185

INDIANA

INDIANA STATE LIBRARY
Serials Documents Section
140 North Senate Avenue
Indianapolis, IN 46204
(317) 232-3686

IOWA

UNIV. OF IOWA LIBRARIES
Govt. Documents Department
Iowa City, IA 52242
(319) 353-3318

KANSAS

UNIVERSITY OF KANSAS
Doc. Collect—Spencer Lib.
Lawrence, KS 66045-2800
(913) 864-4662

KENTUCKY

UNIV. OF KENTUCKY LIBRARIES
Govt. Pub. Department
Lexington, KY 40506-0039
(606) 257-3139

LOUISIANA

LOUISIANA STATE UNIVERSITY
Middleton Library
Govt. Docs. Dept.
Baton Rouge, LA 70803
(504) 388-2570

LOUISIANA TECHNICAL UNIV. LIBRARY
Documents Department
Ruston, LA 71272-0046
(318) 257-4962

MAINE

UNIVERSITY OF MAINE
Raymond H. Fogler Library
Tri-State Regional Documents Depository
Orono, ME 04469
(207) 581-1680

MARYLAND

UNIVERSITY OF MARYLAND
McKeldin Lib.—Doc. Div.
College Park, MD 20742
(301) 454-3034

MASSACHUSETTS

BOSTON PUBLIC LIBRARY
Government Docs. Dept.
Boston, MA 02117
(617) 536-5400 ext.226

MICHIGAN

DETROIT PUBLIC LIBRARY
Sociology Department
5201 Woodward Avenue
Detroit, MI 48202-4093
(313) 833-1409

MICHIGAN STATE LIBRARY
P.O. Box 30007
Lansing, MI 48909
(517) 373-1593

MINNESOTA

UNIVERSITY OF MINNESOTA
Government Pubs. Division
409 Wilson Library
309 19th Avenue South
Minneapolis, MN 55455
(612) 373-7870

MISSISSIPPI

UNIV. OF MISSISSIPPI LIB.
Documents Department
University, MS 38677
(601) 232-5857

MONTANA

UNIV. OF MONTANA
Mansfield Library
Documents Division
Missoula, MT 59812
(406) 243-6700

NEBRASKA

UNIVERSITY OF NEBRASKA - LINCOLN
Love Library
Documents Department
Lincoln, NE 68588-0410
(402) 472-2562

NEVADA

UNIVERSITY OF NEVADA LIB.
Govt. Pub. Department
Reno, NV 89557-0044
(702) 784-6579

NEW JERSEY

NEWARK PUBLIC LIBRARY
5 Washington Street
Newark, NJ 07101-0630
(201) 733-7812

NEW MEXICO

UNIVERSITY OF NEW MEXICO
Zimmerman Library
Government Pub. Dept.
Albuquerque, NM 87131
(505) 277-5441

NEW MEXICO STATE LIBRARY
Reference Department
325 Don Gaspar Avenue
Santa Fe, NM 87503
(505) 827-3826

NEW YORK

NEW YORK STATE LIBRARY
Empire State Plaza
Albany, NY 12230
(518) 474-5563

NORTH CAROLINA

UNIVERSITY OF NORTH CAROLINA AT CHAPEL HILL
Davis Library
BA/SS Documents Division
Chapel Hill, NC 27515
(919) 962-1151

NORTH DAKOTA

UNIVERSITY OF NORTH DAKOTA
Chester Fritz Library
Documents Department
Grand Forks, ND 58202
(701) 777-4629
In cooperation with North Dakota State Univ. Library

OHIO

STATE LIBRARY OF OHIO
Documents Department
65 South Front Street
Columbus, OH 43266-0334
(614) 462-7051

OKLAHOMA

OKLAHOMA DEPT. OF LIB.
Government Documents
200 NE 18th Street
Oklahoma City, OK 73105
(405) 521-2502, ext. 252

OKLAHOMA STATE UNIV. LIB.
Documents Department
Stillwater, OK 74078
(405) 624-6546

OREGON

PORTLAND STATE UNIV. LIB.
Documents Department
P.O. Box 1151
Portland, OR 97207
(503) 229-3673

PENNSYLVANIA

STATE LIBRARY OF PENN.
Government Pub. Section
P.O. Box 1601
Harrisburg, PA 17105
(717) 787-3752

TEXAS

TEXAS STATE LIBRARY
Public Services Department
P.O. Box 12927—Cap. Sta.
Austin, TX 78711
(512) 475-2996

TEXAS TECH. UNIV. LIBRARY
Govt. Documents Department
Lubbock, TX 79409
(806) 742-2268

UTAH

UTAH STATE UNIVERSITY
Merrill Library, U.M.C. 30
Logan, UT 84322
(801) 750-2682

VIRGINIA

UNIVERSITY OF VIRGINIA
Alderman Lib.—Public Doc.
Charlottesville, VA 22903-2498
(804) 924-3133

WASHINGTON

WASHINGTON STATE LIBRARY
Documents Section
Olympia, WA 98504
(206) 753-4027

WEST VIRGINIA

WEST VIRGINIA UNIV. LIB.
Documents Department
Morgantown, WV 26506-6069
(304) 293-3640

WISCONSIN

MILWAUKEE PUBLIC LIBRARY
814 West Wisconsin Avenue
Milwaukee, WI 53233
(414) 278-3065

ST. HIST LIB. OF WISCONSIN
Government Pub. Section
816 State Street
Madison, WI 53706
(608) 262-4347

WYOMING

WYOMING STATE LIBRARY
Supreme Ct. & Library Bld.
Cheyenne, WY 82002
(307) 777-5919

National Aeronautics and
Space Administration
Code NTT-4
Washington, D.C.
20546

Official Business

Penalty for Private Use, $300

SPECIAL FOURTH-CLASS RATE
POSTAGE & FEES PAID
NASA
PERMIT No. G 27

NASA

POSTMASTER: If Undeliverable (Section 158
Postal Manual) Do Not Return